Scientific and Technical Aerospace Reports

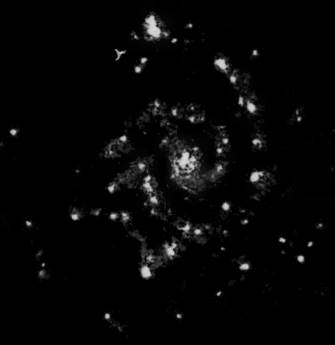

An Abstract Journal

Volume 32, Number 1
January 1994
N94-10001 to N94-12787

The NASA STI Program ... in Profile

Since its founding, NASA has been dedicated to the advancement of aeronautics and space science. The NASA Scientific and Technical Information (STI) Program plays a key part in helping NASA maintain this important role.

The NASA STI Program provides access to the NASA STI Database, the largest collection of aeronautical and space science STI in the world. The Program is also NASA's institutional mechanism for disseminating the results of its research and development activities.

Specialized services that help round out the Program's diverse offerings include creating custom thesauri, translating material to or from 34 foreign languages, building customized databases, organizing and publishing research results ... even providing videos.

For more information about the NASA STI Program, you can:

- **Phone** the NASA Access Help Desk at (301) 621-0390

- **Fax** your question to the NASA Access Help Desk at (301) 621-0134

- **E-mail** your question via the **Internet** to help@sti.nasa.gov

- **Write** to:

NASA Access Help Desk
NASA Center for AeroSpace Information
800 Elkridge Landing Road
Linthicum Heights, MD 21090-2934

Scientific and Technical Aerospace Reports

STAR

Scientific and Technical Aerospace Reports (STAR), is published each month as a major product of the International Aerospace Database, managed by the NASA Scientific and Technical Information (STI) Program.

Inside this issue you will find:

Front Matter
A typical citation and abstract sample explaining the standard format, which includes codes for ordering reports.

An Abstract Section
Citations and abstracts of reports and publications that provide comprehensive coverage of worldwide aerospace-related topics including aeronautics and space science technology. *STAR* lists published and publicly available reports entered into the NASA STI Database during the four weeks preceding publication of this issue. These citations and abstracts are listed by subject categories.

An Index Section
- Subject
- Personal author
- Corporate source
- Contract number
- Report number.

Appendix
A guide for ordering cited reports, registering with the NASA STI Program, and using the available products and services. Additionally, price schedules, phone numbers, and addresses are included in this information packed section.

NASA also sponsors companion journals, *International Aerospace Abstracts (IAA),* and *NASA Open Volumes on Aerospace (NOVA).* They list abstracts of the open literature on aerospace subjects available worldwide. IAA is available from the American Institute of Aeronautics and Astronautics (AIAA), and *NOVA* is for internal NASA use only, available from the NASA Center for AeroSpace Information (CASI).

Reports found in *STAR* are also available through the NASA online retrieval service, RECON, and the Aerospace Database through DIALOG.

The NASA STI Program gathers information through national and international agreements and exchanges and makes this information available to the NASA community and to the public in many forms through various outlets.

For additional information on the NASA STI Program, call the NASA Access Help Desk at (301) 621-0390, or write to:

NASA Center for AeroSpace Information
800 Elkridge Landing Road
Linthicum Heights, Maryland 21090-2934

US ISSN 0036-8741

This publication was prepared by the NASA Center for AeroSpace Information,
800 Elkridge Landing Road, Linthicum Heights, MD 21090-2934, (301) 621-0390.

Volume 32 Number 1 / January 1994

TABLE OF CONTENTS

AERONAUTICS For related information see also *Astronautics.*

01 AERONAUTICS (GENERAL) 1

02 AERODYNAMICS 2
Includes aerodynamics of bodies, combinations, wings, rotors, and control surfaces; and internal flow in ducts and turbomachinery. For related information see also *34 Fluid Mechanics and Heat Transfer.*

03 AIR TRANSPORTATION AND SAFETY 17
Includes passenger and cargo air transport operations; and aircraft accidents. For related information see also *16 Space Transportation* and *85 Urban Technology and Transportation.*

04 AIRCRAFT COMMUNICATIONS AND NAVIGATION 23
Includes digital and voice communication with aircraft; air navigation systems (satellite and ground based); and air traffic control. For related information see also *17 Space Communications, Spacecraft Communications, Command and Tracking* and *32 Communications and Radar.*

05 AIRCRAFT DESIGN, TESTING AND PERFORMANCE 25
Includes aircraft simulation technology. For related information see also *18 Spacecraft Design, Testing and Performance* and *39 Structural Mechanics.* For land transportation vehicles see *85 Urban Technology and Transportation.*

06 AIRCRAFT INSTRUMENTATION 27
Includes cockpit and cabin display devices; and flight instruments. For related information see also *19 Spacecraft Instrumentation* and *35 Instrumentation and Photography.*

07 AIRCRAFT PROPULSION AND POWER 27
Includes prime propulsion systems and systems components, e.g., gas turbine engines and compressors; and onboard auxiliary power plants for aircraft. For related information see also *20 Spacecraft Propulsion and Power, 28 Propellants and Fuels,* and *44 Energy Production and Conversion.*

08 AIRCRAFT STABILITY AND CONTROL 30
Includes aircraft handling qualities; piloting; flight controls; and autopilots. For related information see also *05 Aircraft Design, Testing and Performance.*

09 RESEARCH AND SUPPORT FACILITIES (AIR) 33
Includes airports, hangars and runways; aircraft repair and overhaul facilities; wind tunnels; shock tubes; and aircraft engine test stands. For related information see also *14 Ground Support Systems and Facilities (Space).*

ASTRONAUTICS For related information see also *Aeronautics.*

12 ASTRONAUTICS (GENERAL) 35
For extraterrestrial exploration see *91 Lunar and Planetary Exploration.*

13 ASTRODYNAMICS 38
Includes powered and free-flight trajectories; and orbital and launching dynamics.

14 GROUND SUPPORT SYSTEMS AND FACILITIES (SPACE) 39
Includes launch complexes, research and production facilities; ground support equipment, e.g., mobile transporters; and simulators. For related information see also *09 Research and Support Facilities (Air).*

15 LAUNCH VEHICLES AND SPACE VEHICLES 40
Includes boosters; operating problems of launch/space vehicle systems; and reusable vehicles. For related information see also *20 Spacecraft Propulsion and Power.*

16 SPACE TRANSPORTATION 40
Includes passenger and cargo space transportation, e.g., shuttle operations; and space rescue techniques. For related information see also *03 Air Transportation and Safety* and *18 Spacecraft Design, Testing and Performance.* For space suits see *54 Man/System Technology and Life Support.*

17 SPACE COMMUNICATIONS, SPACECRAFT COMMUNICATIONS, COMMAND AND TRACKING....41
Includes telemetry; space communications networks; astronavigation and guidance; and radio blackout. For related information see also *04 Aircraft Communications and Navigation* and *32 Communications and Radar.*

N.A.—No abstracts were assigned to this category for this issue.

18 SPACECRAFT DESIGN, TESTING AND PERFORMANCE 42
Includes satellites; space platforms; space stations; spacecraft systems and components such as thermal and environmental controls; and attitude controls. For life support systems see *54 Man/System Technology and Life Support.* For related information see also *05 Aircraft Design, Testing and Performance, 39 Structural Mechanics*, and *16 Space Transportation.*

19 SPACECRAFT INSTRUMENTATION .... N.A.
For related information see also *06 Aircraft Instrumentation* and *35 Instrumentation and Photography.*

20 SPACECRAFT PROPULSION AND POWER 45
Includes main propulsion systems and components, e.g., rocket engines; and spacecraft auxiliary power sources. For related information see also *07 Aircraft Propulsion and Power, 28 Propellants and Fuels, 44 Energy Production and Conversion*, and *15 Launch Vehicles and Space Vehicles.*

CHEMISTRY AND MATERIALS

23 CHEMISTRY AND MATERIALS (GENERAL) 55

24 COMPOSITE MATERIALS 56
Includes physical, chemical, and mechanical properties of laminates and other composite materials. For ceramic materials see *27 Nonmetallic Materials.*

25 INORGANIC AND PHYSICAL CHEMISTRY 75
Includes chemical analysis, e.g., chromatography; combustion theory; electrochemistry; and photochemistry. For related information see also *77 Thermodynamics and Statistical Physics.*

26 METALLIC MATERIALS 81
Includes physical, chemical, and mechanical properties of metals, e.g., corrosion; and metallurgy.

27 NONMETALLIC MATERIALS 87
Includes physical, chemical, and mechanical properties of plastics, elastomers, lubricants, polymers, textiles, adhesives, and ceramic materials. For composite materials see *24 Composite Materials.*

28 PROPELLANTS AND FUELS 97
Includes rocket propellants, igniters and oxidizers; their storage and handling procedures; and aircraft fuels. For related information see also *07 Aircraft Propulsion and Power, 20 Spacecraft Propulsion and Power*, and *44 Energy Production and Conversion.*

29 MATERIALS PROCESSING 99
Includes space-based development of products and processes for commercial application. For biological materials see *55 Space Biology:*

ENGINEERING For related information see also *Physics.*

31 ENGINEERING (GENERAL) 126
Includes vacuum technology; control engineering; display engineering; cryogenics; and fire prevention.

32 COMMUNICATIONS AND RADAR 131
Includes radar; land and global communications; communications theory; and optical communications. For related information see also *04 Aircraft Communications and Navigation* and *17 Space Communications, Spacecraft Communications, Command and Tracking.* For search and rescue see *03 Air Transportation and Safety*, and *16 Space Transportation.*

33 ELECTRONICS AND ELECTRICAL ENGINEERING 140
Includes test equipment and maintainability; components, e.g., tunnel diodes and transistors; microminiaturization; and integrated circuitry. For related information see also *60 Computer Operations and Hardware* and *76 Solid-State Physics.*

34 FLUID MECHANICS AND HEAT TRANSFER 147
Includes boundary layers; hydrodynamics; fluidics; mass transfer and ablation cooling. For related information see also *02 Aerodynamics* and *77 Thermodynamics and Statistical Physics.*

35 INSTRUMENTATION AND PHOTOGRAPHY 169
Includes remote sensors; measuring instruments and gauges; detectors; cameras and photographic supplies; and holography. For aerial photography see *43 Earth Resources and Remote Sensing.* For related information see also *06 Aircraft Instrumentation* and *19 Spacecraft Instrumentation.*

36 LASERS AND MASERS 172
Includes parametric amplifiers. For related information see also *76 Solid-State Physics.*

37 MECHANICAL ENGINEERING 177
Includes auxiliary systems (nonpower); machine elements and processes; and mechanical equipment.

38 QUALITY ASSURANCE AND RELIABILITY 183
Includes product sampling procedures and techniques; and quality control.

39 STRUCTURAL MECHANICS 184
Includes structural element design and weight analysis; fatigue; and thermal stress. For applications see *05 Aircraft Design, Testing and Performance* and *18 Spacecraft Design, Testing and Performance.*

GEOSCIENCES For related information see also *Space Sciences.*

42 GEOSCIENCES (GENERAL) 190

43 EARTH RESOURCES AND REMOTE SENSING 229
Includes remote sensing of earth resources by aircraft and spacecraft; photogrammetry; and aerial photography. For instrumentation see *35 Instrumentation and Photography.*

44 ENERGY PRODUCTION AND CONVERSION 262
Includes specific energy conversion systems, e.g., fuel cells; global sources of energy; geophysical conversion; and windpower. For related information see also *07 Aircraft Propulsion and Power, 20 Spacecraft Propulsion and Power,* and *28 Propellants and Fuels.*

45 ENVIRONMENT POLLUTION 264
Includes atmospheric, noise, thermal, and water pollution.

46 GEOPHYSICS 273
Includes aeronomy; upper and lower atmosphere studies; ionospheric and magnetospheric physics; and geomagnetism. For space radiation see *93 Space Radiation.*

47 METEOROLOGY AND CLIMATOLOGY 283
Includes weather forecasting and modification.

48 OCEANOGRAPHY 287
Includes biological, dynamic, and physical oceanography; and marine resources. For related information see also *43 Earth Resources and Remote Sensing.*

LIFE SCIENCES

51 LIFE SCIENCES (GENERAL) 299

52 AEROSPACE MEDICINE 303
Includes physiological factors; biological effects of radiation; and effects of weightlessness on man and animals.

53 BEHAVIORAL SCIENCES 313
Includes psychological factors; individual and group behavior; crew training and evaluation; and psychiatric research.

54 MAN/SYSTEM TECHNOLOGY AND LIFE SUPPORT 315
Includes human engineering; biotechnology; and space suits and protective clothing. For related information see also *16 Space Transportation.*

55 SPACE BIOLOGY 318
Includes exobiology; planetary biology; and extraterrestrial life.

MATHEMATICAL AND COMPUTER SCIENCES

59 MATHEMATICAL AND COMPUTER SCIENCES (GENERAL) 318

60 COMPUTER OPERATIONS AND HARDWARE 319
Includes hardware for computer graphics, firmware, and data processing. For components see *33 Electronics and Electrical Engineering.*

61 COMPUTER PROGRAMMING AND SOFTWARE 320
Includes computer programs, routines, algorithms, and specific applications, e.g., CAD/CAM.

62 COMPUTER SYSTEMS 335
Includes computer networks and special application computer systems.

63 CYBERNETICS 338
Includes feedback and control theory, artificial intelligence, robotics and expert systems. For related information see also *54 Man/System Technology and Life Support.*

64 NUMERICAL ANALYSIS 341
Includes iteration, difference equations, and numerical approximation.

65 STATISTICS AND PROBABILITY 347
Includes data sampling and smoothing; Monte Carlo method; and stochastic processes.

66 SYSTEMS ANALYSIS 348
Includes mathematical modeling; network analysis; and operations research.

67 THEORETICAL MATHEMATICS 348
Includes topology and number theory.

PHYSICS For related information see also *Engineering.*

70 PHYSICS (GENERAL) 350
For precision time and time interval (PTTI) see *35 Instrumentation and Photography*; for geophysics, astrophysics or solar physics see *46 Geophysics, 90 Astrophysics*, or *92 Solar Physics.*

71 ACOUSTICS 357
Includes sound generation, transmission, and attenuation. For noise pollution see *45 Environment Pollution.*

72 ATOMIC AND MOLECULAR PHYSICS 358
Includes atomic structure, electron properties, and molecular spectra.

73 NUCLEAR AND HIGH-ENERGY PHYSICS 370
Includes elementary and nuclear particles; and reactor theory. For space radiation see *93 Space Radiation.*

74 OPTICS 374
Includes light phenomena and optical devices. For lasers see *36 Lasers and Masers.*

75 PLASMA PHYSICS 384
Includes magnetohydrodynamics and plasma fusion. For ionospheric plasmas see *46 Geophysics.* For space plasmas see *90 Astrophysics.*

76 SOLID-STATE PHYSICS 394
Includes superconductivity. For related information see also *33 Electronics and Electrical Engineering* and *36 Lasers and Masers.*

77 THERMODYNAMICS AND STATISTICAL PHYSICS 408
Includes quantum mechanics; theoretical physics; and Bose and Fermi statistics. For related information see also *25 Inorganic and Physical Chemistry* and *34 Fluid Mechanics and Heat Transfer.*

SOCIAL SCIENCES

80 SOCIAL SCIENCES (GENERAL) 415
Includes educational matters.

81 ADMINISTRATION AND MANAGEMENT 416
Includes management planning and research.

82 DOCUMENTATION AND INFORMATION SCIENCE 418
Includes information management; information storage and retrieval technology; technical writing; graphic arts; and micrography. For computer documentation see *61 Computer Programming and Software.*

83 ECONOMICS AND COST ANALYSIS 422
Includes cost effectiveness studies.

84 LAW, POLITICAL SCIENCE AND SPACE POLICY 422
Includes NASA appropriation hearings; aviation law; space law and policy; international law; international cooperation; and patent policy.

85 URBAN TECHNOLOGY AND TRANSPORTATION 422
Includes applications of space technology to urban problems; technology transfer; technology assessment; and surface and mass transportation. For related information see *03 Air Transportation and Safety, 16 Space Transportation,* and *44 Energy Production and Conversion.*

SPACE SCIENCES For related information see also *Geosciences.*

88 SPACE SCIENCES (GENERAL) 423

89 ASTRONOMY 423
Includes radio, gamma-ray, and infrared astronomy; and astrometry.

90 ASTROPHYSICS 425
Includes cosmology; celestial mechanics; space plasmas; and interstellar and interplanetary gases and dust. For related information see also *75 Plasma Physics.*

91 LUNAR AND PLANETARY EXPLORATION 433
Includes planetology; and manned and unmanned flights. For spacecraft design or space stations see *18 Spacecraft Design, Testing and Performance.*

92 SOLAR PHYSICS 482
Includes solar activity, solar flares, solar radiation and sunspots. For related information see also *93 Space Radiation.*

93 SPACE RADIATION 484
Includes cosmic radiation; and inner and outer earth's radiation belts. For biological effects of radiation see *52 Aerospace Medicine.* For theory see *73 Nuclear and High-Energy Physics.*

GENERAL

Includes aeronautical, astronautical, and space science related histories, biographies, and pertinent reports too broad for categorization; histories or broad overviews of NASA programs.

99 GENERAL 485

SUBJECT INDEX I-1

PERSONAL AUTHOR INDEX I-179

CORPORATE SOURCE INDEX I-203

CONTRACT NUMBER INDEX I-235

REPORT NUMBER INDEX I-239

APPENDIX A-1

TYPICAL CITATION AND ABSTRACT

NASA SPONSORED
ON MICROFICHE
↓↓

ACCESSION NUMBER → **N94-12270*#** United Technologies Corp., West Palm Beach, FL. ← **CORPORATE SOURCE**
Pratt and Whitney.
TITLE → **ADVANCED CONTROL FOR AIRBREATHING ENGINES, VOLUME 1: PRATT AND WHITNEY**
AUTHOR → J. A. Ralph Jul. 1993 83 p ← **PUBLICATION DATE**
CONTRACT OR GRANT → (Contract NAS3-25952; RTOP 505-62-61)
REPORT NUMBERS → (NASA-CR-189203; E-8006; NAS 1.26:189203) Avail: CASI HC A05/MF A01 ← **AVAILABILITY SOURCE AND PRICE CODE**

The application of advanced control concepts to air breathing engines may yield significant improvements in aircraft/engine performance and operability. Screening studies of advanced control concepts for air breathing engines were conducted by three major domestic aircraft engine manufacturers to determine the potential impact of concepts on turbine engine performance and operability. The purpose of the studies was to identify concepts which offered high potential yet may incur high research and development risk. A target suite of proposed advanced control concepts was formulated and evaluated in a two phase study to quantify each concept's impact on desired engine characteristics. To aid in the evaluation specific aircraft/engine combinations were considered: a Military High Performance Fighter mission, a High Speed Civil Transport mission, and a Civil Tiltrotor mission. Each of the advanced control concepts considered in the study are defined and described. The concept potential impact on engine performance was determined. Relevant figures of merit on which to evaluate the concepts are determined. Finally, the concepts are ranked with respect to the target aircraft/engine missions. A final report describing the screening studies was prepared by each engine manufacturer. Volume 1 of these reports describes the studies performed by Pratt & Whitney. Author (revised)

VOLUME 32 NUMBER 1 / January 1994

Scientific and Technical Aerospace Reports

A Monthly Publication of the National Aeronautics and Space Administration

01 AERONAUTICS (GENERAL)

N94-10420* National Aeronautics and Space Administration, Washington, DC.
AERONAUTICAL ENGINEERING: A CONTINUING BIBLIOGRAPHY WITH INDEXES (SUPPLEMENT 293)
Jul. 1993 153 p
(NASA-SP-7037(293); NAS 1.21:7037(293)) Avail: CASI HC A08

This bibliography lists 476 reports, articles, and other documents introduced into the NASA scientific and technical information system in July, 1992. Subject coverage includes: design, construction and testing of aircraft and aircraft engines; aircraft components, equipment, and systems; ground support systems; and theoretical and applied aspects of aerodynamics and general fluid dynamics. Author

N94-10936*# National Aeronautics and Space Administration. Ames Research Center, Moffett Field, CA.
PERFORMANCE AND ROTOR LOADS MEASUREMENTS OF THE LYNX XZ170 HELICOPTER WITH RECTANGULAR BLADES
Benton H. Lau, Alexander W. Louie (Sterling Software, Inc., Palo Alto, CA.), Nicholas Griffiths (Westland Helicopters Ltd., Yeovil, England.), and Costantinos P. Sotiriou (Westland Helicopters Ltd., Yeovil, England.) May 1993 362 p
(RTOP 505-59-36)
(NASA-TM-104000; A-93039; NAS 1.15:104000) Avail: CASI HC A16/MF A03

This report presents the results of a series of flight tests on the Lynx XZ170 helicopter with rectangular blades. The test objectives were to explore the flight envelope and to measure the performance and structural loads of the Lynx main-rotor system. The tests were conducted as part of the British Experimental Rotor Program (BERP) under a contract with the Ministry of Defense in England. Data were acquired for steady-level flights at five weight coefficients. Some flight conditions were tested at beyond the retreating-blade stall boundary, which was defined by a predetermined limit on the pitchlink vibratory load. In addition to documenting the flight conditions and data, this report describes the aircraft, particularly the rotor system, in detail. Author

N94-11687* National Aeronautics and Space Administration, Washington, DC.
AERONAUTICAL ENGINEERING: A CONTINUING BIBLIOGRAPHY WITH INDEXES (SUPPLEMENT 289)
Mar. 1993 220 p
(NASA-SP-7037(289); NAS 1.21:7037(289)) Avail: CASI HC A10

This bibliography lists 792 reports, articles, and other documents introduced into the NASA scientific and technical information system in Mar. 1993. Subject coverage includes: design, construction and testing of aircraft and aircraft engines; aircraft components, equipment, and systems; ground support systems; and theoretical and applied aspects of aerodynamics and general fluid dynamics. Derived from text

N94-11690* National Aeronautics and Space Administration, Washington, DC.
AERONAUTICAL ENGINEERING: A CONTINUING BIBLIOGRAPHY WITH INDEXES (SUPPLEMENT 291)
May 1993 207 p
(NASA-SP-7037(291); NAS 1.21:7037(291)) Avail: CASI HC A10

This bibliography lists 757 reports, articles, and other documents introduced into the NASA scientific and technical information system in May. 1993. Subject coverage includes: design, construction and testing of aircraft and aircraft engines; aircraft components, equipment, and systems; ground support systems; and theoretical and applied aspects of aerodynamics and general fluid dynamics. Derived from text

N94-11691* National Aeronautics and Space Administration, Washington, DC.
AERONAUTICAL ENGINEERING: A CONTINUING BIBLIOGRAPHY WITH INDEXES (SUPPLEMENT 290)
Apr. 1993 376 p
(NASA-SP-7037(290); NAS 1.21:7037(290)) Avail: CASI HC A17

This bibliography lists 1396 reports, articles, and other documents introduced into the NASA Scientific and Technical Information System in Apr. 1993. Subject coverage includes: design, construction and testing of aircraft and aircraft engines; aircraft components, equipment, and systems; ground support systems; and theoretical and applied aspects of aerodynamics and general fluid dynamics. Derived from text

N94-11703*# National Aeronautics and Space Administration. Lewis Research Center, Cleveland, OH.
MICROGRAVITY VIBRATION ISOLATION TECHNOLOGY: DEVELOPMENT TO DEMONSTRATION Ph.D. Thesis - Case Western Reserve Univ.
Carlos M. Grodsinsky Sep. 1993 273 p
(RTOP 694-03-03)
(NASA-TM-106320; E-8067; NAS 1.15:106320) Avail: CASI HC A12/MF A03

The low gravity environment provided by space flight has afforded the science community a unique area for the study of fundamental and technological sciences. However, the dynamic environment observed on space shuttle flights and predicted for Space Station Freedom has complicated the analysis of prior 'microgravity' experiments and prompted concern for the viability of proposed space experiments requiring long term, low gravity environments. Thus, isolation systems capable of providing significant improvements to this random environment have been developed. This dissertation deals with the design constraints imposed by acceleration sensitive, microgravity experiment payloads in the unique environment of space. A theoretical background for the inertial feedback and feedforward isolation of a payload was developed giving the basis for two experimental active inertial isolation systems developed for the demonstration of these advanced active isolation techniques. A prototype six degree of freedom digital active isolation system was designed and developed for the ground based testing of an actively isolated payload in three horizontal degrees of freedom. A second functionally equivalent system was built for the multi-dimensional testing of an active inertial isolation system in a reduced gravity environment during low gravity aircraft trajectories. These multi-input multi-output control systems are discussed in detail with estimates on acceleration noise floor performance as well as the actual performance acceleration data. The attenuation performance is also given for both systems demonstrating the advantages between inertial and non-inertial control of a payload for both the ground base environment and the low gravity aircraft acceleration environment. A future goal for this area of research is to validate the technical approaches developed to the 0.01 Hz regime by demonstrating a functional active inertial feedforward/feedback isolation system during orbital flight. A NASA IN-STEP flight experiment has been proposed to accomplish this goal, and the expected selection for the IN-STEP program has been set for Jul. of 1993. Author (revised)

N94-12412# Federal Aviation Administration, Washington, DC.
US CIVIL AIRMEN STATISTICS FOR CALENDAR YEAR 1991
30 Jun. 1992 35 p
(AD-A266085) Avail: CASI HC A03/MF A01

This report furnishes detailed airmen statistics. It contains calendar year statistics on pilots and nonpilots and the number of certificates issued. DTIC

N94-12578# Federal Aviation Administration, Washington, DC. Office of Aviation Policy and Plans.
FEDERAL AVIATION ADMINISTRATION AVIATION FORECASTS FY 1993-2004
Feb. 1993 229 p
(AD-A265611; FAA-APO-93-1) Avail: CASI HC A11/MF A03

This report contains the Fiscal Years 1993-2004 Federal Aviation Administration (FAA) forecasts of aviation activity at FAA facilities. These include airports with FAA control towers, air route traffic control centers, and flight service stations. Detailed forecasts were made for the major users of the National Aviation System: air carriers, air taxi/commuters, military, and general aviation. The forecasts have been prepared to meet the budget and planning needs of the constituent units of the FAA and to provide information that can be used by state and local authorities, the aviation industry, and the general public. The lethargy of both the U.S. and world economies during the past several years has caused the aviation industry to experience continuing financial losses. However, the outlook for the 12-year forecast period is for moderate economic growth, stable real fuel prices, and modest inflation. Based on these assumptions, aviation activity for fiscal year 2004 is forecast to increase by 24.6 percent at towered airports and 27.0 percent at air route traffic control centers. The general aviation active fleet and hours flown are forecast to increase by 7.0 and 18.1 percent, respectively, during the same time period. Scheduled domestic revenue passenger miles (RPM's)are forecast to increase 58.3 percent, scheduled international RPM's are forecast to increase by 115.3 percent, and regional/commuter RPM's are forecast to increase by 145.1 percent. DTIC

02 AERODYNAMICS

Includes aerodynamics of bodies, combinations, wings, rotors, and control surfaces; and internal flow in ducts and turbomachinery.

For related information see also *34 Fluid Mechanics and Heat Transfer.*

N94-10350# National Aerospace Lab., Tokyo (Japan). Advanced Aircraft Research Group.
AN INVESTIGATION ON THE EFFECTIVENESS OF THE PIPING INTERFERENCE REMOVAL SYSTEM FOR STOL AIRCRAFT WIND TUNNEL TESTS [STOL ZENKI MOKEI HAIKAN KANSHOU JOKYU SOUCHI KOUKA SHIKEN]
Hitoshi Takahashi, Teruomi Nakaya, Masayoshi Noguti, Osamu Nonaka, Hideo Hoshino, and Takashi Inoue Apr. 1992 28 p In JAPANESE
(NAL-TM-647; JTN-93-80448) Avail: CASI HC A03/MF A01

The piping interference removal system, developed at the National Aerospace Laboratory (NAL) to reduce the interference on the balance caused by the high-pressure piping, was studied using force measurements from wind tunnel tests. A model was employed which utilized a simulated engine powered by high pressure air through the high pressure air hoses. It was founded that the interference effects on the measured forces were negligible; thus, no piping interference corrections were necessary for STOL aircraft wind tunnel tests used with the simulated engine. System usefulness was also confirmed since little difference occurred between the resultant aerodynamic coefficients and those obtained in tests using the previous high-pressure air hose system. Author (NASDA)

N94-10357 Toronto Univ. (Ontario).
NONLINEAR ASPECTS OF TRANSONIC AEROELASTICITY Ph.D. Thesis
Hema Sandhyarani Murty 1992 213 p
Avail: Univ. Microfilms Order No. DANN73808

Flutter analysis of airfoils in transonic flow has traditionally assumed linearity of the aerodynamic loads and moment with motion amplitude. However, the nonlinear nature of the mixed flow, incorporating large amplitude shock wave motion, may significantly invalidate the linearity assumption. The effect of nonlinear transonic aerodynamics on the flutter analysis is analyzed utilizing a simplified linear structural model. The aerodynamic conditions under which these effects are significant are determined for specific cases using the NACA 64A010 airfoil. In order to accurately determine the aerodynamic loads and moment, an unsteady full potential code was developed. This code was joined to an algorithm which integrates the structural equations of motion in time. A flutter analysis based on the assumption of linear aerodynamics was carried out to determine the neutral stability conditions defined by a set of structural and aerodynamic parameters. These neutral stability conditions were then used in the structural equations of motion with nonlinear aerodynamic loads and moment. These equations were then integrated in time to determine the response of the system. If the time response was not neutrally stable, then the structural parameter, Mu, the airfoil-to-air mass ratio was varied until the time response was neutrally stable. If the difference in the value of the 'nonlinear' Mu to 'linear' Mu was greater than 10 percent, then that case was considered to exhibit significant nonlinearities. Dissert. Abstr.

N94-10363# National Aerospace Lab., Tokyo (Japan). Airframe Div.
ESTIMATION OF CRITICAL VALUES AND VIBRATION CHARACTERISTICS ON SUPERSONIC DELTA WINGS. PART 1: ON-LINE TIME SERIES ANALYSIS OF STATIONARY RANDOM RESPONSE [CHOUONSOKU DERUTAYOKU NO SHINDOU TOKUSEI TO ANTEI GENKAI NO SUITEI. DAI 1 POU: TEIJOUNA FUKISOKU OUTOU NO ONRAIN JIKEIRETSU KAISEKI]
Yasukatsu Andou, Yuuji Matsuzaki, Masakatsu Minegishi, Hiroshi Ejiri, Seizou Sakakibara, Junichi Noda, and Kiyomichi Ishida Apr. 1992 20 p In JAPANESE
(NAL-TR-1153; JTN-93-80434; DE93-767977) Avail: CASI HC A03/MF A01

A personal computer based, on-line time series analysis system is described which estimates the flutter boundary and vibration-mode parameter of a flutter model. The system software is written in BASIC (Beginner's All-purpose Symbolic Instruction Code) and uses an autoregressive process. Ground vibration and wind tunnel flutter tests were conducted on supersonic delta wing models to enable system evaluation. Stationary random response of the wings was subsequently applied into the system and its practical use was confirmed using the estimated results. Author (NASDA)

N94-10421# Advisory Group for Aerospace Research and Development, Neuilly-Sur-Seine (France). Fluid Dynamics Panel.
THEORETICAL AND EXPERIMENTAL METHODS IN HYPERSONIC FLOWS [LES METHODES THEORIQUES ET EXPERIMENTALES POUR L'ETUDE DES ECOULEMENTS HYPERSONIQUES]
Apr. 1993 575 p Symposium held in Torino, Italy, 4-8 May 1992 Original contains color illustrations
(AGARD-CP-514; ISBN-92-835-0694-4) Copyright Avail: CASI HC A24/MF A04

Papers prepared for the AGARD Fluid Dynamics Panel Symposium on theoretical and experimental methods in hypersonic flows held on 4-8 May 1992 are presented. The objectives of the Symposium were to (1) report and assess the advances being made by the AGARD community on the development and application of theoretical methods and experimental techniques for simulating hypersonic flows over aerospace vehicles; (2) highlight outstanding problem areas; and (3) establish pointers to aid in the planning and implementation of future research programs. Major topics covered by the Symposium were testing techniques and instrumentation, computational methods and physical modeling, and validation and accuracy assessment. For individual titles, see N94-10422 through N94-10465.

N94-10422*# National Aeronautics and Space Administration. Ames Research Center, Moffett Field, CA.
CFD ANALYSIS OF HYPERSONIC, CHEMICALLY REACTING FLOW FIELDS
T. A. Edwards *In* AGARD, Theoretical and Experimental Methods in

Hypersonic Flows Apr. 1993 12 p (For primary document see N94-10421 01-02)
Copyright Avail: CASI HC A03/MF A04

Design studies are underway for a variety of hypersonic flight vehicles. The National Aero-Space Plane will provide a reusable, single-stage-to-orbit capability for routine access to low earth orbit. Flight-capable satellites will dip into the atmosphere to maneuver to new orbits, while planetary probes will decelerate at their destination by atmospheric aerobraking. To supplement limited experimental capabilities in the hypersonic regime, computational fluid dynamics (CFD) is being used to analyze the flow about these configurations. The governing equations include fluid dynamic as well as chemical species equations, which are being solved with new, robust numerical algorithms. Examples of CFD applications to hypersonic vehicles suggest an important role this technology will play in the development of future aerospace systems. The computational resources needed to obtain solutions are large, but solution adaptive grids, convergence acceleration, and parallel processing may make run times manageable.
Author

N94-10423# Avions Marcel Dassault, Saint-Cloud (France).
AERODYNAMIC AND AEROTHERMAL CHALLENGES FOR THE DESIGN OF THE HERMES SPACEPLANE **c16**
Pierre Perrier *In* AGARD, Theoretical and Experimental Methods in Hypersonic Flows Apr. 1993 10 p (For primary document see N94-10421 01-02)
Copyright Avail: CASI HC A02/MF A04

The Hermes spaceplane will represent a major step in the European space activities. It will be placed into orbit by the heavy-lift launcher Ariane 5. After completion of the mission, it will glide back from low earth orbit to its landing site. In order to take the different problems linked to the ascent and the reentry phases, an aerodynamic strategy was set up. A global review of this strategy will be made. It will contain elements on the available and necessary tools (experimental and theoretical) for the Hermes definition and qualification phases. Some aspects such as the design of the Hermes spaceplane will also be highlighted. It will review the different constraints that will be faced during the ascent and reentry phases. Constraints may come from mission requirements such as crossrange capability or from technology limits such as thermal limits on the thermal protection system or from guidance and control requirements. A new methodology was selected in order to take constraints and uncertainties into account in the design oriented towards qualification of the Hermes spaceplane. The main line of this methodology is the projection on a typical reentry trajectory of the uncertainties in the aerodynamic characteristics checked on control points.
Author

N94-10424# Messerschmitt-Boelkow-Blohm G.m.b.H., Munich (Germany).
EXPERIMENTAL RESULTS IN AERODYNAMIC STABILITY AND CONTROL OF A TSTO CONFIGURATION **c08**
T. Gottmann and G. Cucinelli *In* AGARD, Theoretical and Experimental Methods in Hypersonic Flows Apr. 1993 14 p (For primary document see N94-10421 01-02)
Copyright Avail: CASI HC A03/MF A04

A Winged Launcher Configuration (WLC) in a Two Stage To Orbit (TSTO) version has to fly through a wide range of angles-of-attack and Mach numbers (roughly -3 deg is less than or equal to alpha is less than or equal to 20 deg and 0.2 is less than or equal to Ma is less than or equal to 7.0). This and the requirements for horizontal take-off and landing in Central Europe, and the special separation maneuver at a hypersonic Mach number, causes a wide range of new aerodynamic and aerothermodynamic problems. Especially the problem of stability and control is increased by the wide alpha-Mach range and possibly strong engine effects. The main tasks of the experimental investigations of a TSTO configuration are to establish a data base to support the whole design process of Winged Launcher Configurations, to provide a validation base for CFD codes and to understand the very complicated problems which dominate stability, control, and stage separation aerodynamics. A generic baseline configuration of a TSTO was developed at MBB (lower and upper stage), which satisfies all requirements so far. To be able to test this configuration in all occurring speed regimes, a titanium model (size 1:160) was manufactured with an acceptable size to fit into most wind tunnels for sub-, super-, and hypersonic Mach numbers, especially at DLR in Germany and FFA in Sweden. The main part of the presentation deals with trends of the TSTO configuration in aerodynamic stability and control over the entire Mach regime, showing that some aerodynamic characteristics change significantly with increasing Mach number. Because all aerodynamic forces and moments must be balanced by the engine or aerodynamic controls to obtain reasonable flight conditions, statements regarding absolute stability and control features cannot be set up within this investigation, but tendencies can be given. Major emphasis is placed on the flap efficiency at high Mach numbers which exhibits a strongly nonlinear behavior. The separation of the upper stage was investigated in a special test phase, which shows the enormous changes in longitudinal characteristics caused by interference effects in close proximities between upper and lower stage.
Author (revised)

N94-10425# Alenia Aeronautica, Torino (Italy).
NUMERICAL SIMULATION OF THE FLOW THROUGH A SCRAMJET ENGINE **c07**
V. Selmin *In* AGARD, Theoretical and Experimental Methods in Hypersonic Flows Apr. 1993 13 p (For primary document see N94-10421 01-02)
Copyright Avail: CASI HC A03/MF A04

An inviscid numerical method was developed to simulate the flow through each component of a scramjet engine. Emphasis is on the effects due to non-ideal gas assumption and to H(sub 2)/air chemistry on the performance of air intakes and nozzles.
Author (revised)

N94-10426# Cranfield Inst. of Tech., Bedford (England). Coll. of Aeronautics.
CONTROL EFFECTIVENESS AT HYPERSONIC SPEEDS **c08**
J. L. Stollery, D. Kumar, P. A. Atcliffe, and H. Babinsky *In* AGARD, Theoretical and Experimental Methods in Hypersonic Flows Apr. 1993 10 p (For primary document see N94-10421 01-02)
Copyright Avail: CASI HC A02/MF A04

Two models equipped with trailing edge flaps were tested at a Mach number of 8.2. A simple flat plate model was used to understand how control effectiveness is influenced by transition, bluntness, and incidence, while a cropped-delta-wing spaceplane configuration has emphasized the important three-dimensional effects arising from the geometry chosen. Schlieren photographs were used to visualize the flow, and pressure measurements on the windward surface of the spaceplane model showed any regions of separation. Encapsulated liquid crystals were used to obtain an overall picture of the heat transfer distribution and to highlight the three-dimensional structure of the flow.
Author (revised)

N94-10427*# National Aeronautics and Space Administration. Hugh L. Dryden Flight Research Facility, Edwards, CA.
IN-FLIGHT EVALUATION OF AERODYNAMIC PREDICTIONS OF AN AIR-LAUNCHED SPACE BOOSTER
Robert E. Curry, Michael R. Mendenhall (Nielsen Engineering and Research, Inc., Mountain View, CA.), and Bryan Moulton (PRC Kentron, Inc., Edwards, CA.) *In* AGARD, Theoretical and Experimental Methods in Hypersonic Flows Apr. 1993 18 p Sponsored in part by DARPA and Orbital Sciences Corp. (For primary document see N94-10421 01-02)
Copyright Avail: CASI HC A03/MF A04

Several analytical aerodynamic design tools that were applied to the Pegasus air-launched space booster were evaluated using flight measurements. The study was limited to existing codes and was conducted with limited computational resources. The flight instrumentation was constrained to have minimal impact on the primary Pegasus missions. Where appropriate, the flight measurements were compared with computational data. Aerodynamic performance and trim data from the first two flights were correlated with predictions. Local measurements in the wing and wing-body interference region were correlated with analytical data. This complex flow region includes the effect of aerothermal heating magnification caused by the presence of a corner vortex and interaction of the wing leading edge shock and fuselage boundary layer. The operation of the first two missions indicates that the aerodynamic design approach for Pegasus was adequate, and data show that acceptable margins were available. Additionally, the correlations provide insight into the capabilities of these analytical tools for more complex vehicles in which design margins may be more stringent.
Author

N94-10428# Fluid Gravity Engineering Ltd., Witley (England).
PLANETARY ENTRY VEHICLE DESIGN FOR PLANNED AND POTENTIAL ESA MISSIONS TO TITAN, MARS, AND EARTH RETURN (FGE TN 51/92) **c18**
Arthur Smith *In* AGARD, Theoretical and Experimental Methods in Hypersonic Flows Apr. 1993 12 p (For primary document see N94-10421 01-02)
Copyright Avail: CASI HC A03/MF A04

Design of ballistic planetary entry probes for planned ESA/NASA Titan, Mars, and Earth-Return missions is discussed with emphasis on the common design constraints. The choice of aeroshell configuration and some of the simple design rules are outlined which are used initially at pre-feasibility stages. These include the influence of body dynamics, conventional aerodynamics, and aerothermodynamics. Prediction of the aerothermodynamic environment and influence of uncertainties in the basic physics and chemistry are seen to dominate. Analysis methodology and some of the ESA sponsored experimental program which was initiated to tackle the lack of basic chemistry data is discussed. Author (revised)

N94-10429# Office National d'Etudes et de Recherches Aerospatiales, Toulouse (France).
NEW HYPERSONIC TEST METHODS DEVELOPED AT ONERA: THE R5 AND F4 WIND TUNNELS [NOUVEAUX MOYENS D'ESSAIS HYPERSONIQUES DEVELOPPES A L'ONERA: LES SOUFFLERIES R5 ET F4] **c05**
B. Chanetz, M.-C. Coet, D. Nicout, T. Pot, P. Broussaud, G. Francois, A. Masson, and D. Vennemann (European Space Agency. Centre Spatial de Toulouse, France.) *In* AGARD, Theoretical and Experimental Methods in Hypersonic Flows Apr. 1993 12 p In FRENCH Previously announced in IAA as A92-48600 (For primary document see N94-10421 01-02)
Copyright Avail: CASI HC A03/MF A04

The R5 wind tunnel allows the simulation of hypersonic flows at low Reynolds numbers, corresponding to intake conditions encountered at altitudes of about 60 km. The F4 wind tunnel is projected to study the effects of actual gas and especially effects associated with chemical kinetics during atmospheric reentry. Attention is given to the performance, installation details, and description of the introduction of wind tunnel testing. Author

N94-10430# Deutsche Forschungs- und Versuchsanstalt fuer Luft- und Raumfahrt, Goettingen (Germany).
THE HIGH ENTHALPY FACILITIES HEG AND TH 2 IN GERMANY **c09**
G. Eitelberg and H. Olivier (Technische Hochschule, Aachen, Germany.) *In* AGARD, Theoretical and Experimental Methods in Hypersonic Flows Apr. 1993 14 p (For primary document see N94-10421 01-02)
Copyright Avail: CASI HC A03/MF A04

The two high enthalpy shock tunnels in Aachen and Gottingen, Germany are described. Both of these are shock tunnels operating in the reflected mode. The Aachen tunnel has a heated driver and the Gottingen tunnel has a free piston driver. The Aachen tunnel has been in operation for a number of years already and the characteristic operating conditions of this tunnel are described. The tunnel in Gottingen (HEG) is currently being established. The first commissioning results of this tunnel are being described. The Aachen tunnel TH2 covers a testing range in air from perfect gas behavior to real gas behavior with significant oxygen dissociation effects. The HEG was designed to operate in the flow regimes where also significant nitrogen dissociation dominates. Author (revised)

N94-10431# Aeronautica Macchi S.p.A., Varese (Italy). Aerodynamics Dept.
DESIGN AND PRODUCTION OF INSULATED WIND TUNNEL MODELS OF THE HERMES SHUTTLE FOR HEAT TRANSFER MEASUREMENTS AT HYPERSONIC SPEEDS **c09**
L. Visintini and C. Couedor (Dassault Aviation, Istres, France.) *In* AGARD, Theoretical and Experimental Methods in Hypersonic Flows Apr. 1993 9 p (For primary document see N94-10421 01-02)
Copyright Avail: CASI HC A02/MF A04

Among all kinds of wind tunnel experiments undertaken up to now by Dassault Aviation to develop the European HERMES shuttle, those relative to heat transfer measurements could be the last to be fully accomplished. To some extent, one could say that difficulties came from sensors themselves, from their integration conditions, and finally from additional similitude parameters not considered before. The paper introduces to Dassault Aviation so-called 'insulated models' and describes the ongoing activity developed with the collaboration of AerMacchi. The models have the purpose of making heat transfer measurements with correct simulation of surface temperatures due to its demonstrated effect on boundary layer transition. A number of pathfinder models were developed for this purpose: after a first attempt made by using a machinable ceramic, the second one was intended for surface temperatures up to 400 C and was made in a temperature resistant composite material, and the third one, able to sustain skin temperatures above 1000 C, is made by an insulating ceramic coating on a steel core. The fluid-dynamic and technological aspects related with the design and manufacture of these models are described.
Author (revised)

N94-10432# Deutsche Forschungs- und Versuchsanstalt fuer Luft- und Raumfahrt, Cologne (Germany).
THE UPGRADING OF THE ARC HEATED WIND TUNNEL OF THE DLR (LBK) WITH RESPECT TO ITS EFFECTS ON THE MATERIAL TESTING **c09**
A. Guelhan and K. Kindler *In* AGARD, Theoretical and Experimental Methods in Hypersonic Flows Apr. 1993 11 p (For primary document see N94-10421 01-02)
Copyright Avail: CASI HC A03/MF A04

The arc heated wind tunnel (LBK) of the DLR is a useful device for high enthalpy tests of thermal protection systems of spacecrafts. The facility is described concerning its capability in simulation of the gas-surface interaction phenomena at the stagnation point of space vehicles. The working area of the tunnel resulting from tests on SiC-samples is discussed and compared with other arc heated wind tunnels. To support experimental works on the LBK numerical computations including flow solutions based on chemical equilibrium, frozen chemistry, and chemical nonequilibrium were performed. It is shown that the flow field downstream the nozzle throat is nearly frozen. Finally, the upgrading concept and the proposed performance of the facility are discussed. Author

N94-10433*# National Aeronautics and Space Administration. Langley Research Center, Hampton, VA.
RECOMMENDATIONS FOR FUTURE RESEARCH IN HYPERSONIC INSTRUMENTATION
S. L. Ocheltree *In* AGARD, Theoretical and Experimental Methods in Hypersonic Flows Apr. 1993 2 p (For primary document see N94-10421 01-02)
Copyright Avail: CASI HC A01/MF A04

An overview of the NATO Advanced Research Workshop is presented. It describes the process followed to obtain a group consensus on the main technical recommendations for each of the five technical sessions of the Workshop and presents the general conclusions and recommendations for future research agreed upon by the workshop participants.
Author (revised)

N94-10434*# National Aeronautics and Space Administration. Langley Research Center, Hampton, VA.
LOCAL MEASUREMENT OF TEMPERATURES AND CONCENTRATIONS: A REVIEW FOR HYPERSONIC FLOWS
C. Dankert (Deutsche Forschungs- und Versuchsanstalt fuer Luft- und Raumfahrt, Goettingen, Germany.), R. Cattolica (California Univ., San Diego.), and W. Sellers *In* AGARD, Theoretical and Experimental Methods in Hypersonic Flows Apr. 1993 10 p (For primary document see N94-10421 01-02)
Copyright Avail: CASI HC A02/MF A04

The quality of reentry simulation for Shuttle, HERMES, Sanger, and NASP systematically suffers from the strong non-equilibrium of rotational and vibrational temperature due to the rapid acceleration of the test gas in the nozzle. Therefore the determination of temperatures is necessary and, if possible, preferable by a non-intrusive technique. The specific interests of this review are optical techniques such as electron beam fluorescence, laser-induced fluorescence, and coherent anti-Stokes Raman scattering. The capabilities available for local measurements with temporal resolution and quantitative accuracy are discussed for velocity, temperature, density, species concentrations, and fluctuations due to turbulence. The applicability of these methods of measurement is presented and discussed for the coming topic in aerothermodynamics: experimental techniques of hot gases in high enthalpy flows. Author

N94-10435*# National Aeronautics and Space Administration. Langley Research Center, Hampton, VA.

PRESSURE AND FORCE MEASUREMENTS ON MODELS SET IN HYPERSONIC FLOWS: A REVIEW

Charles G. Miller *In* AGARD, Theoretical and Experimental Methods in Hypersonic Flows Apr. 1993 11 p (For primary document see N94-10421 01-02)

Copyright Avail: CASI HC A03/MF A04

A review of measurement techniques used to obtain aerodynamic forces and moments and surface/flow field pressures for models tested in impulse hypersonic-hypervelocity facilities and in conventional-type hypersonic wind tunnels is presented. Although force and moment measurement techniques presently used in hypersonic wind tunnels are relatively unchanged from the 1960's and 1970's, significant advances have recently been made for impulse facilities. For both hypersonic wind tunnels and impulse facilities, the state-of-the-art has advanced via refinements, improved test techniques, and advances in semiconductor technology, data acquisition systems, and computers. The introduction of electronically scanned pressure systems over a decade ago 'revolutionized' pressure measurements in hypersonic wind tunnels and a second 'revolution' is impending with the development and application of optical, two-dimensional, global pressure measurement techniques. The development and continued refinement of miniature piezoresistive transducers has provided the capability to perform detailed surface pressure measurements on relatively small, complex models in impulse facilities; these transducers also provided the capability for intrusive flow field pressure measurements with miniature survey rakes. Author (revised)

N94-10436# Office National d'Etudes et de Recherches Aerospatiales, Paris (France).

VELOCITY MEASUREMENTS IN HYPERSONIC FLOWS: A REVIEW

Alain Boutier, William J. Yanta (Naval Surface Weapons Center, Silver Spring, MD.), and Gunter Smeets (Institut Franco-Allemand de Recherches, Saint-Louis, France.) *In* AGARD, Theoretical and Experimental Methods in Hypersonic Flows Apr. 1993 9 p (For primary document see N94-10421 01-02)

Copyright Avail: CASI HC A02/MF A04

With the renewed interest in hypersonics, there is a real need for accurate, detailed measurements of fluid flow and thermodynamic properties of high speed, high temperature flows. An analysis of the different means to measure the velocity is done; the relative merits of the particle based and the molecular based methods are evaluated, leading to a set of recommendations for future research. Papers presented at the NATO Advanced Research Workshop are reviewed and summarized. Derived from text

N94-10437# MetroLaser, Irvine, CA.

FLOW VISUALIZATION AND SPECTROSCOPY IN HYPERSONIC FLOWS: NEW TRENDS c74

James Trolinger, Georg Eitelberg (Deutsche Forschungsanstalt fuer Luft- und Raumfahrt, Goettingen, Germany.), and Marc Rapuc (Avions Marcel Dassault, Saint-Cloud, France.) *In* AGARD, Theoretical and Experimental Methods in Hypersonic Flows Apr. 1993 11 p (For primary document see N94-10421 01-02)

Copyright Avail: CASI HC A03/MF A04

This paper is based upon a session of the NATO Advanced Research Workshop, New Trends in Instrumentation for Hypersonic Research held at the ONERA La Fauga Facility in France during the week of 27 Apr. 1992. The discussion includes some of the frontiers of the technology of flow visualization and spectroscopy as well as a discussion of the current development needs and trends. Included in the discussion are optical integrated measurements such as resonance absorption, schlieren, interferometry, and holographic methods. The discussion shows that while the technology is mature in a broad sense, a significant number of new development areas exist such as resonant holography and phase shifting holographic interferometry. The maturity of the technology makes it immediately applicable to many problems and the untapped potential offers considerable room for improvement of existing capability. The methods which are described can be used in harsh environments and have the potential for becoming flight test diagnostics for the measurement of temperature, density, constituency, and velocity. Author (revised)

N94-10438# Von Karman Inst. for Fluid Dynamics, Rhode-Saint-Genese (Belgium).

THERMAL FLUX MEASUREMENTS IN HYPERSONIC FLOWS: A REVIEW c35

J. F. Wendt, D. Balageas (Office National d'Etudes et de Recherches Aerospatiales, Paris, France.), and R. D. Neumann (Dayton Univ. Research Inst., OH.) *In* AGARD, Theoretical and Experimental Methods in Hypersonic Flows Apr. 1993 5 p (For primary document see N94-10421 01-02)

Copyright Avail: CASI HC A01/MF A04

This contribution reviews the papers presented in the Session on 'Heat Flux' and 'Thermography' at a NATO Advanced Research Workshop entitled 'New Trends in Instrumentation for Hypersonic Research', 27 April-1 May, 1992, Le Fauga, France. The present status and problem areas associated with specific methods are discussed and recommendations for future research and development are presented. Author (revised)

N94-10439*# National Aeronautics and Space Administration. Ames Research Center, Moffett Field, CA.

A CFD VALIDATION ROADMAP FOR HYPERSONIC FLOWS c34

Joseph G. Marvin *In* AGARD, Theoretical and Experimental Methods in Hypersonic Flows Apr. 1993 16 p (For primary document see N94-10421 01-02)

Copyright Avail: CASI HC A03/MF A04

A roadmap for computational fluid dynamics (CFD) code validation is developed. The elements of the roadmap are consistent with air-breathing vehicle design requirements and related to the important flow path components: forebody, inlet, combustor, and nozzle. Building block and benchmark validation experiments are identified along with their test conditions and measurements. Based on an evaluation criteria, recommendations for an initial CFD validation data base are given and gaps identified where future experiments would provide the needed validation data. Author (revised)

N94-10440# Institut National de Recherche d'Informatique et d'Automatique, Valbonne (France).

SYNTHESIS OF THE WORKSHOP ON HYPERSONIC FLOWS FOR REENTRY PROBLEMS

Remi Abgrall, Jean-Antoine Desideri, Michel Mallet (Avions Marcel Dassault, Saint-Cloud, France.), Jacques Periaux (Avions Marcel Dassault, Saint-Cloud, France.), Pierre Perrier (Avions Marcel Dassault, Saint-Cloud, France.), and Bruno Stoufflet (Avions Marcel Dassault, Saint-Cloud, France.) *In* AGARD, Theoretical and Experimental Methods in Hypersonic Flows Apr. 1993 23 p Workshop held in Antibes, France, Jan. 1990 and Apr. 1991 (For primary document see N94-10421 01-02)

Copyright Avail: CASI HC A03/MF A04

One of the most challenging problems of modern aerospace engineering is undoubtedly the prediction of hypersonic flows around reentry vehicles. Indeed this challenge has many aspects: defining the appropriate physical model for these flows is the first difficulty since very complex physical and chemical phenomena take place during the reentry phase; moreover, temperature, velocity, and enthalpy are very high, density very low, making the reentry conditions very difficult to reproduce in ground-based experiments. Thus, in the past two decades, important efforts in computational fluid dynamics have been made employing supercomputers to simulate these complex flows. However, most simulation tools were originally designed for transonic or supersonic flow applications and later extended; these usually contain imperfect models, and also still have to be improved to permit the accurate prediction of hypersonic flows. This situation has motivated strong international cooperative efforts including three Europe/US Short Courses on Hypersonics and two sessions (Part 1 and 2) of the scientific workshop organized by INRIA and GAMNI which took place in Antibes, France. Part 1 brought together a group of experts active in hypersonics, and promoted direct comparisons of codes and experiments. The main objective of part 2 was to improve the quality of both experimental and computational results, and evaluate numerical codes by code-to-code or code-to-experiment comparisons, and permit a better confidence in the prediction tools to be used in the design of hypersonic vehicles. The presentation is aimed at reporting the main conclusions as

they were expressed at the meeting by experts, including some of their recommendations regarding the validation of numerical codes.
Derived from text

N94-10441# Texas Univ., Austin. Center for Aeromechanics Research.
PROBLEMS IN THE VALIDATION OF CFD CODES THROUGH COMPARISON WITH EXPERIMENT **c34**
David S. Dolling *In* AGARD, Theoretical and Experimental Methods in Hypersonic Flows Apr. 1993 15 p (For primary document see N94-10421 01-02)
Copyright Avail: CASI HC A03/MF A04

Accurate predictions of the effects of shock wave turbulent boundary layer interactions are of particular importance in the design of hypersonic vehicles. Such flows can generate intense heat transfer rates and pressure levels, complex large-scale unsteady separated flows, and large-amplitude fluctuating loads. With increased reliance on computation, it is critical that the predictions are accurate. Thus, it is imperative that such codes be validated and calibrated and deficiencies be identified and rectified. Comparison of the predictions of computational fluid dynamics (CFD) codes with experimental data is the key element of the validation process. However, drawing meaningful conclusions about the strengths and weaknesses of solution methodologies or of turbulence models from these comparisons is not a trivial task. As recently stated by Jameson, 'Simply comparing experimental data with numerical results provides no way to distinguish the source of the discrepancies, whether they are due to faulty numerical approximation or programming, or to deviations between the math model and true physics.' The conclusions drawn may be quite misleading if it is not clearly understood what the computations represent and what the experimental data represent. This paper discusses why it is important to know how experimental mean flowfield and surface data being used for comparison with CFD are generated. If the flowfields exhibit local or global large-scale unsteadiness, then such mean measurements, which form the bulk of the existing data base, may mask the underlying flow physics and be inappropriate for comparison with computation. Author (revised)

N94-10442# Toronto Univ., Downsview (Ontario). Inst. for Aerospace Studies.
FLOW DEVELOPMENT IN A CIRCULAR PIPE IN THE UTIAS/RPI M = 8.3 GUN TUNNEL
J. P. Sislian, Z. He, and R. L. Deschambault *In* AGARD, Theoretical and Experimental Methods in Hypersonic Flows Apr. 1993 13 p Sponsored in part by Natural Sciences and Engineering Research Council (For primary document see N94-10421 01-02)
(Contract F33615-87-C-2748)
Copyright Avail: CASI HC A03/MF A04

The investigation is concerned with the understanding of the structure of the hypersonic flow developed in a circular pipe. The experiments were conducted in the University of Toronto Institute for Aerospace Studies (UTIAS)/Ryerson Polytechnical Institute (RPI) gun tunnel at a freejet Mach number of 8.30 and Reynolds number based on the pipe diameter, Re = 2.44 x 10(exp 6). Wall static pressure, as well as in-stream static and pitot pressure measurements at several sections in the pipe, shed some light into the physical nature of the considered flow. The measurements indicate that shocks generated in the pipe flow are primarily oblique. Measurements near the pipe axis and in wave structures presented some difficulties. Further work is needed to clarify certain features of the investigated flow. The presented results may guide the development of computational fluid dynamic codes applicable to hypersonic pipe flows. Author (revised)

N94-10443# Wright Lab., Wright-Patterson AFB, OH.
EXPERIMENTAL AND COMPUTATIONAL COMPARISONS OF MACH 6 HIGH REYNOLDS NUMBER HEAT TRANSFER AND SKIN FRICTION
Lello Galassi and Norman E. Scaggs *In* AGARD, Theoretical and Experimental Methods in Hypersonic Flows Apr. 1993 14 p (For primary document see N94-10421 01-02)
Copyright Avail: CASI HC A03/MF A04

Wind tunnel measurements on a flat plate, ogive cylinder, and a compression ramp at zero angle-of-attack are compared to computational fluid dynamics (CFD) predictions of the flow parameters. These models provide a zero-pressure gradient, favorable-pressure gradient, and an adverse-pressure gradient flow condition, respectively. Results are presented for surface pressure and temperature distributions, boundary layer surveys, heat transfer rates, and local skin friction coefficients. Test conditions were varied over a free-stream Reynolds number range of 0.45-9.1 (10 exp 7) per meter, at a nominal Mach number of 6. Wind tunnel measurements on the three models were made using static pressure ports, embedded thermocouples, coaxial heat transfer gauges, slug calorimeters, Preston tube skin friction devices, and skin friction force balances. Boundary layer profiles were measured with total temperature and pitot pressure probes and with laser doppler velocimetry. Parabolized Navier-Stokes and full Navier-Stokes code predictions of the measured parameters are compared to experimental measurements. Results indicate surface pressure distributions are easily predicted by the CFD codes used and for the simple geometries modeled. For CFD codes which predict the surface heat transfer rate accurately, the local skin friction coefficient agrees to within 7-10 percent of the measured data for favorable-pressure gradient and zero-pressure gradient configurations. For adverse-pressure gradients, the code used did not predict skin friction values accurately, although heat transfer predictions matched the data. Large gradients in the hypersonic boundary layer require dense grids near the model surface in order for CFD codes to accurately predict the surface heat transfer rate and the local skin friction coefficient. Additionally, dense grids in the streamwise direction are necessary to properly resolve the boundary layer for adverse-pressure gradients. Author (revised)

N94-10444# Von Karman Inst. for Fluid Dynamics, Rhode-Saint-Genese (Belgium).
EXPERIMENTAL, ANALYTICAL, AND COMPUTATIONAL METHODS APPLIED TO HYPERSONIC COMPRESSION RAMP FLOWS
G. Simeonides, W. Haase (Dornier Luftfahrt G.m.b.H., Friedrichshafen, Germany.), and M. Manna *In* AGARD, Theoretical and Experimental Methods in Hypersonic Flows Apr. 1993 12 p (For primary document see N94-10421 01-02)
Copyright Avail: CASI HC A03/MF A04

Experimental data on fully laminar and transitional shock wave boundary layer interactions in two-dimensional compression corners are provided and used for the validation of two full Navier-Stokes solvers, as well as for checking the capabilities and limitations of simple analytical prediction methods. Viscous pressure interaction, free interaction, and inviscid oblique shock theory are found to predict well the pressure levels on the flat plate upstream of the interaction, within the separated region and downstream of the interaction, respectively. The reference temperature theory is found to perform well in attached flow regimes both upstream and downstream of the interaction region, and to provide the basis for a universal peak heating correlation law. Full Navier-Stokes computations are necessary, however, to predict the extent of the interaction region and the associated influence upon the pressure distribution (control effectiveness) as well as the detailed heat transfer distribution. To achieve this, very fine gridding coupled with the use of strict convergence criteria (based on the evolution of the location of the separation point rather than on standard density residuals) is shown to be necessary. It is finally shown that, although sophisticated turbulence models need to be further developed before the detailed characteristics of fully turbulent shock wave boundary layer interactions may be predicted, transitional interactions (where transition typically occurs in the neighborhood of reattachment) may be adequately handled by algebraic turbulence models 'switched on' just downstream of reattachment. Author

N94-10445# Sandia National Labs., Albuquerque, NM. Aerodynamics Dept.
JOINT COMPUTATIONAL AND EXPERIMENTAL AERODYNAMIC RESEARCH ON A HYPERSONIC VEHICLE
William L. Oberkampf, Daniel P. Aeschliman, and Mary McWherter Walker *In* AGARD, Theoretical and Experimental Methods in Hypersonic Flows Apr. 1993 11 p (For primary document see N94-10421 01-02)
(Contract DE-AC04-76DP-00789)
Copyright Avail: CASI HC A03/MF A04

A closely coupled computational and experimental aerodynamics research program was conducted on a hypersonic vehicle configuration at Mach 8. Aerodynamic force and moment measurements and flow visualization results were obtained in the Sandia National Laboratories hypersonic wind tunnel for laminar boundary layer conditions. Parabolized and iterative Navier-Stokes simulations were used to predict flow fields and forces and moments on the hypersonic configuration. The basic vehicle configuration is a spherically blunted 10 deg cone with a slice parallel with the axis of the vehicle. On the slice portion of the vehicle, a flap can be attached; flap deflection angles of 10 deg, 20 deg, and 30 deg were used. Comparisons are made between experimental and computational results to evaluate the quality of each and to identify areas where improvements are needed. This extensive set of high-quality experimental force and moment measurements is recommended for use in the calibration and validation of computational aerodynamics codes. Author (revised)

N94-10446*# National Aeronautics and Space Administration. Ames Research Center, Moffett Field, CA.

ISSUES AND APPROACH TO DEVELOP VALIDATED ANALYSIS TOOLS FOR HYPERSONIC FLOWS: ONE PERSPECTIVE

George S. Deiwert *In* AGARD, Theoretical and Experimental Methods in Hypersonic Flows Apr. 1993 10 p (For primary document see N94-10421 01-02)

Copyright Avail: CASI HC A02/MF A04

Critical issues concerning the modeling of low density hypervelocity flows where thermochemical nonequilibrium effects are pronounced are discussed. Emphasis is on the development of validated analysis tools, and the activity in the NASA Ames Research Center's Aerothermodynamics Branch is described. Inherent in the process is a strong synergism between ground test and real gas computational fluid dynamics (CFD). Approaches to develop and/or enhance phenomenological models and incorporate them into computational flowfield simulation codes are discussed. These models were partially validated with experimental data for flows where the gas temperature is raised (compressive flows). Expanding flows, where temperatures drop, however, exhibit somewhat different behavior. Experimental data for these expanding flow conditions is sparse and reliance must be made on intuition and guidance from computational chemistry to model transport processes under these conditions. Ground based experimental studies used to provide necessary data for model development and validation are described. Included are the performance characteristics of high enthalpy flow facilities, such as shock tubes and ballistic ranges. Author (revised)

N94-10447# Manchester Univ. (England). Dept. of Engineering.

COMPARISON OF COMPUTATION AND EXPERIMENT FOR A HIGH ENTHALPY, HEATED-DRIVER, SHOCK-TUBE ENVIRONMENT

S. Shahpar, A. Kennaugh, I. M. Hall, and D. I. A. Poll *In* AGARD, Theoretical and Experimental Methods in Hypersonic Flows Apr. 1993 26 p Sponsored by British Aerospace Aircraft Group (For primary document see N94-10421 01-02)

Copyright Avail: CASI HC A03/MF A04

A coordinated computational and experimental study was made of blunt-body flows with nonequilibrium chemistry. The temperature range was such that significant dissociation of oxygen was expected but very little dissociation of nitrogen. Both pure oxygen, O2 and O, and air, treated computationally using a five species (O2, N2, NO, N, and O) model were studied. Results obtained using different published values of the chemical rate coefficients were compared and assessed for a model problem. The effects of size (i.e., Damkohler number) and freestream velocity were also investigated. The flow computations used an explicit timemarching method based on a TVD version of the MacCormack predictor-corrector scheme. A point implicit TVD method was developed to deal with the stiffness problems introduced by the finite rate chemistry. Interferograms of the flow obtained in a shock tunnel are compared with the computational results. The bow shock wave shape and the shock detachment which are dependent on the degree of chemical reaction and thermal excitation of the gas show that the calculation method is promising. Author (revised)

N94-10448# European Space Agency. European Space Research and Technology Center, ESTEC, Noordwijk (Netherlands). Propulsion and Aerothermodynamics Div.

THERMODYNAMIC MODEL OF AIR IN CHEMICAL EQUILIBRIUM c77

D. Giordano and L. Marraffa *In* AGARD, Theoretical and Experimental Methods in Hypersonic Flows Apr. 1993 15 p (For primary document see N94-10421 01-02)

Copyright Avail: CASI HC A03/MF A04

A thermodynamic model of air in chemical equilibrium is described. The model includes 13 chemical components, namely N, O, Ar, e(-), NO, N2, 02, N(+), 0(+), Ar(+), NO(+), N2(+), O2(+), and is treated as a mixture of perfect gases. The constant pressure specific heats of the components constitute the basic information to be provided and they are assumed to be specified in the form of interpolating polynomials valid in assigned subranges of a given temperature range; the polynomial expressions were structured to preserve generality and flexibility with respect to temperature range subdivisions and polynomial coefficient data published by various sources. The set of the chemical reactions includes 47 reactions, of which only 9 are independent. The equilibrium composition is solved, in terms either of mass fractions or molar fractions, according to the method of the equilibrium constants and numerically computed by an iterative scheme which proves fast and accurate. A FORTRAN program was written to perform the numerical calculations of the thermodynamic properties and of the equilibrium composition. Temperature range subdivisions and polynomial coefficient data can be implemented at will. Presently, the program includes data from 3 US sources and 1 Soviet source. Discrepancies in the constant pressure specific heats of the components deriving from the choice of different data sources are put in evidence. The process to validate the program is described and validation evidence is given in the relevant diagrams. Author (revised)

N94-10449*# National Aeronautics and Space Administration. Langley Research Center, Hampton, VA.

THREE-DIMENSIONAL HYPERSONIC RAREFIED FLOW CALCULATIONS USING DIRECT SIMULATION MONTE CARLO METHOD

M. Cevdet Celenligil (Middle East Technical Univ., Ankara, Turkey.) and James N. Moss *In* AGARD, Theoretical and Experimental Methods in Hypersonic Flows Apr. 1993 12 p (For primary document see N94-10421 01-02)

Copyright Avail: CASI HC A03/MF A04

A summary of three-dimensional simulations on the hypersonic rarefied flows in an effort to understand the highly nonequilibrium flows about space vehicles entering the Earth's atmosphere for a realistic estimation of the aerothermal loads is presented. Calculations are performed using the direct simulation Monte Carlo method with a five-species reacting gas model, which accounts for rotational and vibrational internal energies. Results are obtained for the external flows about various bodies in the transitional flow regime. For the cases considered, convective heating, flowfield structure and overall aerodynamic coefficients are presented and comparisons are made with the available experimental data. The agreement between the calculated and measured results are very good. Author (revised)

N94-10450# Ohio State Univ., Columbus. Dept. of Mechanical Engineering.

STABILITY OF HYPERSONIC FLOW OVER A BLUNT BODY

Thorwald Herbert and Vahid Esfahanian (DynaFlow, Inc., Columbus, OH.) *In* AGARD, Theoretical and Experimental Methods in Hypersonic Flows Apr. 1993 12 p (For primary document see N94-10421 01-02) (Contracts F49620-87-K-0005; F49620-88-C-0082)

Copyright Avail: CASI HC A03/MF A04

A numerical method was developed to compute the axisymmetric flow over blunt slender bodies with high accuracy to enable reliable analysis of the stability properties. The flow field is obtained using the Beam-Warming method to solve the thin-layer Navier-Stokes equations. The code was thoroughly validated and applied to compute the laminar flow over a long blunt cone with 7 deg half-angle at M(sub infinity) = 8. The linear stability of this flow was analyzed with highly accurate finite-difference and spectral methods. The results are compared with previous numerical studies and the experimental data of Stetson et al. Author (revised)

N94-10451*# Arizona State Univ., Tempe. Dept. of Mechanical and Aerospace Engineering.

STABILITY OF HYPERSONIC BOUNDARY-LAYER FLOWS WITH CHEMISTRY

Helen L. Reed, Gregory K. Stuckert, and Timothy S. Haynes *In* AGARD, Theoretical and Experimental Methods in Hypersonic Flows Apr. 1993 13 p Sponsored by NASA. Langley Research Center; NASA. Ames Research Center; NSF; McDonnell-Douglas Corp.; and General Dynamics/Fort Worth (For primary document see N94-10421 01-02) (Contract F49620-88-C-0076)

Copyright Avail: CASI HC A03/MF A04

The effects of nonequilibrium chemistry and three dimensionality on

the stability characteristics of hypersonic flows are discussed. In two-dimensional (2-D) and axisymmetric flows, the inclusion of chemistry causes a shift of the second mode of Mack to lower frequencies. This is found to be due to the increase in size of the region of relative supersonic flow because of the lower speeds of sound in the relatively cooler boundary layers. Although this shift in frequency is present in both the equilibrium and nonequilibrium air results, the equilibrium approximation predicts modes which are not observed in the nonequilibrium calculations (for the flight conditions considered). These modes are superpositions of incoming and outgoing unstable disturbances which travel supersonically relative to the boundary-layer edge velocity. Such solutions are possible because of the finite shock stand-off distance. Their corresponding wall-normal profiles exhibit an oscillatory behavior in the inviscid region between the boundary-layer edge and the bow shock. For the examination of three-dimensional (3-D) effects, a rotating cone is used as a model of a swept wing. An increase of stagnation temperature is found to be only slightly stabilizing. The correlation of transition location (N = 9) with parameters describing the crossflow profile is discussed. Transition location does not correlate with the traditional crossflow Reynolds number. A new parameter that appears to correlate for boundary-layer flow was found. A verification with experiments on a yawed cone is provided.
Author (revised)

N94-10452# Manchester Univ. (England). Dept. of Engineering.
REAL GAS AND SURFACE TRANSPIRATION EFFECTS UPON SWEPT LEADING EDGE HIGH SPEED FLOW INCLUDING TRANSITION
D. I. A. Poll *In* AGARD, Theoretical and Experimental Methods in Hypersonic Flows Apr. 1993 16 p (For primary document see N94-10421 01-02)
Copyright Avail: CASI HC A03/MF A04

The extension of simple methods for the prediction of skin friction and heat transfer at an infinite-swept attachment line to cover the hypervelocity flight regime including the effects of surface transpiration is considered. The analysis is limited to the situation where the flow is in thermochemical equilibrium everywhere. Real gas effects are identified and their influence is quantified. The importance of freestream conditions and attachment-line inclination are assessed. Consideration is also given to the issue of boundary layer transition.
Author (revised)

N94-10453# Deutsche Forschungsanstalt fuer Luft- und Raumfahrt, Goettingen (Germany). Inst. of Theoretical Fluid Mechanics.
ON THE INSTABILITY OF HYPERSONIC FLOW PAST A POINTED CONE: COMPARISON OF THEORETICAL AND EXPERIMENTAL RESULTS AT MACH 8
Martin Simen (Dornier Luftfahrt G.m.b.H., Friedrichshafen, Germany.) and Uwe Dallmann *In* AGARD, Theoretical and Experimental Methods in Hypersonic Flows Apr. 1993 13 p Sponsored in part by BMFT (For primary document see N94-10421 01-02)
Copyright Avail: CASI HC A03/MF A04

In view of the prevailing discrepancies between experiment and theory with regard to instabilities in hypersonic flow, an extended theoretical approach is studied. For hypersonic flow past a pointed cone Thin Layer Navier Stokes solutions are compared to similarity solutions with different modeling of viscosity-temperature laws. The formulation of the stability equations in curvilinear coordinates allows a discussion of various representations of the local body metric. A systematic sensitivity study of basic state profiles and spatial amplification rates is performed. It is found that the improved agreement with the experiment in the viscous first mode region is equally due to the extended stability analysis, where cone metric is specified, and the extended mean flow solution as well. In the second mode region the major improvement results from the more complete basic state formulation, however, the close agreement with measured growth rates is only achieved when the stability analysis is based on conical metric.
Author (revised)

N94-10454# Imperial Coll. of Science and Technology, London (England). Dept. of Aeronautics.
STUDIES OF HYPERSONIC VISCOUS FLOWS
R. Hillier, D. C. Kirk, M. Sell, and S. Soltani *In* AGARD, Theoretical and Experimental Methods in Hypersonic Flows Apr. 1993 11 p Sponsored in part by Defence Research Agency (For primary document see N94-10421 01-02)
(Grant SRC-GR/G/57277)
Copyright Avail: CASI HC A03/MF A04

Results from current studies on slender bodies of revolution tested at a nominal Mach number of 9 are presented. It concentrates on the case of a spherically-blunted cone, providing kinetic heating data for laminar, turbulent, and transitional flow regimes. Nose blunting exerts a powerful control on the location of transition, and the quantitative measurements of this location using thin film gauge techniques are supported by flow visualization using liquid crystal thermography. We also discuss work and plans for two other studies which are in their early stages: these are a cavity-induced separation and the development of turbulent boundary layers under controlled pressure gradients. Preliminary computations using a high resolution Navier-Stokes code are also presented.
Author (revised)

N94-10455# Office National d'Etudes et de Recherches Aerospatiales, Paris (France).
CALCULATIONS OF VISCOUS NONEQUILIBRIUM FLOWS IN NOZZLES [CALCULS D'ECOULEMENTS VISQUEUX EN DESEQUILIBRE DANS DES TUYERES]
C. Marmignon, V. Joly, and F. Coquel *In* AGARD, Theoretical and Experimental Methods in Hypersonic Flows Apr. 1993 9 p In FRENCH Previously announced in IAA as A93-38574 (For primary document see N94-10421 01-02)
Copyright Avail: CASI HC A02/MF A04

An implicit finite-volume method for investigating viscous flows in a state of chemical and vibrational nonequilibrium in nozzles is presented. The ideal-fluid flux terms are calculated by a decentered Roe-type scheme that is second order in space, and the viscous fluxes are determined using a centered scheme. The numerical fluxes and the sources terms are coupled completely at the implicit stage. The proposed method is illustrated by application to two flow configurations: (1) a test case from the Antibes Workshop on hypersonic flows, and (2) a nozzle flow in the ONERA F4 wind tunnel.
AIAA

N94-10456# Office National d'Etudes et de Recherches Aerospatiales, Paris (France). Lab. IUSTI/SETT.
NONEQUILIBRIUM HYPERSONIC FLOW IN A WIND-TUNNEL NOZZLE
D. Zeitoun, E. Boccaccio, M. C. Druguet, M. Imbert, and R. Brun *In* AGARD. Theoretical and Experimental Methods in Hypersonic Flows Apr. 1993 9 p (For primary document see N94-10421 01-02)
Copyright Avail: CASI HC A02/MF A04

The interest in hypersonic flow was renewed through the Hermes European program. A better knowledge of chemical and thermodynamical nonequilibrium processes connected with aerodynamic aspects is needed to study the reentry phase of the shuttle Hermes. Around this research area, many numerical approaches, taking into account more or less complicated nonequilibrium models, were developed. In order to validate these computations, different hypersonic facilities were built or are being designed. In these facilities, the hypersonic air flow is obtained at the exit of a convergent-divergent nozzle in which the reservoir enthalpy level is such that dissociation of diatomic molecules occurs. It is of upmost importance to be able to compute the flowfield in these nozzles, in order to ascertain the upstream conditions in front of the model being studied. The aim is a numerical study of hypersonic laminar inviscid/viscous flows, taking into account, on one hand, a complete description of chemical and thermodynamical nonequilibrium processes in an inviscid flow and on the other hand, the viscous effects through solving the Navier-Stokes equations for a real gas mixture with a simplified model for the vibrational nonequilibrium effects of diatomic species.
Author (revised)

N94-10457# Centro Italiano Ricerche Aerospaziali, Naples.
SOME EXPERIMENTAL STUDY AND NUMERICAL SIMULATION IN WIND TUNNEL FLOW
S. Borrelli and E. Hettena (Alenia Aeronautica, Torino, Italy.) *In* AGARD, Theoretical and Experimental Methods in Hypersonic Flows Apr. 1993 12 p (For primary document see N94-10421 01-02)
Copyright Avail: CASI HC A03/MF A04

Some studies made during a collaboration between the Italian Aerospace Research Center (CIRA) and Alenia D.V.D., whose aim is to provide proper validation of CFD codes in hypersonic flow regime, are described. In fact, in our opinion, the combination of numerical and experimental tools should give a better theoretical understanding of such types of flow. Numerical methods able to give accurate prediction of hypersonic flows in hypersonic wind tunnels were developed and the results obtained by calculations are compared with experimental data gathered by CIRA. Alenia equilibrium three-dimensional Euler solver, originally developed to solve transonic flows and now extended to hypersonic ones, and a non-equilibrium two-dimensional Euler solver, developed by CIRA for the Hermes program, were used to get test chamber predictions. Author (revised)

N94-10458*# National Aeronautics and Space Administration. Langley Research Center, Hampton, VA.

A CFD-BASED AERODYNAMIC DESIGN PROCEDURE FOR HYPERSONIC WIND-TUNNEL NOZZLES **c09**

John J. Korte *In* AGARD, Theoretical and Experimental Methods in Hypersonic Flows Apr. 1993 10 p (For primary document see N94-10421 01-02)

Copyright Avail: CASI HC A02/MF A04

A new procedure which unifies the best of current classical design practices, computational fluid dynamics (CFD), and optimization procedures is demonstrated for designing the aerodynamic lines of hypersonic wind-tunnel nozzles. The new procedure can be used to design hypersonic wind tunnel nozzles with thick boundary layers where the classical design procedure has been shown to break down. An efficient CFD code, which solves the parabolized Navier-Stokes (PNS) equations using an explicit upwind algorithm, is coupled to a least-squares (LS) optimization procedure. A LS problem is formulated to minimize the difference between the computed flow field and the objective function, consisting of the centerline Mach number distribution and the exit Mach number and flow angle profiles. The aerodynamic lines of the nozzle are defined using a cubic spline, the slopes of which are optimized with the design procedure. The advantages of the new procedure are that it allows full use of powerful CFD codes in the design process, solves an optimization problem to determine the new contour, can be used to design new nozzles or improve sections of existing nozzles, and automatically compensates the nozzle contour for viscous effects as part of the unified design procedure. The new procedure is demonstrated by designing two Mach 15, a Mach 12, and a Mach 18 helium nozzles. The flexibility of the procedure is demonstrated by designing the two Mach 15 nozzles using different constraints, the first nozzle for a fixed length and exit diameter and the second nozzle for a fixed length and throat diameter. The computed flow field for the Mach 15 least squares parabolized Navier-Stokes (LS/PNS) designed nozzle is compared with the classically designed nozzle and demonstrates a significant improvement in the flow expansion process and uniform core region. Author (revised)

N94-10459# Messerschmitt-Boelkow-Blohm G.m.b.H., Munich (Germany). Military Aircraft Div.

NUMERICAL METHODS FOR AEROTHERMODYNAMIC DESIGN OF HYPERSONIC SPACE TRANSPORT VEHICLES **c16**

K. M. Wanie, A. Brenneis, A. Eberle, and S. Heiss *In* AGARD, Theoretical and Experimental Methods in Hypersonic Flows Apr. 1993 12 p (For primary document see N94-10421 01-02)

Copyright Avail: CASI HC A03/MF A04

The requirement of the design process of hypersonic vehicles to predict flow past entire configurations with wings, fins, flaps, and propulsion system represents one of the major challenges for aerothermodynamics. In this context computational fluid dynamics has come up as a powerful tool to support the experimental work. A couple of numerical methods developed at MBB designed to fulfill the needs of the design process are described. The governing equations and fundamental details of the solution methods are shortly reviewed. Results are given for both geometrically simple test cases and realistic hypersonic configurations. Since there is still a considerable lack of experience for hypersonic flow calculations an extensive testing and verification is essential. This verification is done by comparison of results with experimental data and other numerical methods. The results presented prove that the methods used are robust, flexible, and accurate enough to fulfill the strong needs of the design process. Author (revised)

N94-10460# Ecole Polytechnique Federale de Lausanne (Switzerland). Hydraulic Machines and Fluid Mechanics Inst.

HYPERSONIC MULTI BLOCK FLOW SIMULATIONS AROUND SPACE VEHICLES INCLUDING NON-EQUILIBRIUM CHEMISTRY

J. B. Vos, A. W. Rizzi (Aeronautical Research Inst. of Sweden, Bromma.), and C. M. Bergman (Royal Inst. of Tech., Stockholm, Sweden.) *In* AGARD, Theoretical and Experimental Methods in Hypersonic Flows Apr. 1993 11 p Sponsored in part by Commission Suisse d'Encouragement des Recherches Scientifiques (For primary document see N94-10421 01-02)

Copyright Avail: CASI HC A03/MF A04

An international collaboration on the development of multi block flow solvers using structured grids is presented. The flow equations are solved by the finite volume method using a space centered, explicit time marching scheme augmented by artificial dissipation terms. Implicit residual smoothing is used to accelerate convergence to steady state. The multi block flow solvers are written on top of the MEMCOM data base system which provides the data structure, and use a Dynamic Memory Manager to allocate the necessary storage for each block. The Euler solver EULMB can be used to simulate hypersonic flows including equilibrium and nonequilibrium air chemistry. Recently the Euler solver has been extended to solve the Navier Stokes equations for laminar caloric perfect gas flows (NSMB flow solver). Calculated results for the calculation of the flow over a double ellipsoid and over the HERMES space shuttle are presented. The inviscid calculations around HERMES showed that if one is only interested in the aerodynamic coefficients, equilibrium air calculations are sufficient. Parallel computations showed that the communication overhead between blocks is less than 0.5 percent, showing that the multi block concept is very promising for using parallel computers efficiently. Author

N94-10461*# Imperial Coll. of Science and Technology, London (England). Dept. of Aeronautics.

HYPERSONIC FLOW COMPUTATIONS AROUND RE-ENTRY VEHICLES

J. Peraire, J. Peiro, K. Morgan (Wales Univ., Swansea.), M. Vahdati, and R. C. Molina (European Space Agency. European Space Research and Technology Center, ESTEC, Noordwijk, Netherlands.) *In* AGARD, Theoretical and Experimental Methods in Hypersonic Flows Apr. 1993 13 p Sponsored in part by Dassault Aviation and British Aerospace Public Ltd. Co. (For primary document see N94-10421 01-02)
(Grant NAGw-1809)

Copyright Avail: CASI HC A03/MF A04

The development of an algorithm for the solution of the compressible Euler equations at high Mach numbers on unstructured tetrahedral meshes is described. The basic algorithm is constructed in the form of a central difference scheme plus an explicit added artificial viscosity based upon fourth order differences of the solution. The stability of the solution in the vicinity of strong gradients is preserved by the incorporation of an additional artificial viscosity based upon a second order difference. Higher order accuracy is regained by using the ideas of flux corrected transport to limit the amount of added viscosity. The solution is advanced to steady state by means of an explicit multi-stage time-stepping method. The computational efficiency of the complete process is improved by incorporating an unstructured multigrid acceleration procedure. A number of flows of practical interest are analyzed to demonstrate the numerical performance of the proposed approach. Author

N94-10462# Erlangen-Nuremberg Univ. (Germany). Lehrstuhl fuer Stroemungsmechanik.

ON THE ACCURACY AND EFFICIENCY OF CFD METHODS IN REAL GAS HYPERSONICS

D. Drikakis and S. Tsangaris (National Technical Univ., Athens, Greece.) *In* AGARD, Theoretical and Experimental Methods in Hypersonic Flows Apr. 1993 15 p (For primary document see N94-10421 01-02)

Copyright Avail: CASI HC A03/MF A04

A study of viscous and inviscid hypersonic flows, using generalized upwind methods, is presented. A new family of hybrid flux splitting methods is examined for hypersonic flows. A hybrid method is constructed by the superposition of the Flux Vector Splitting (FVS) method and second order artificial dissipation in the regions of the strong shock waves. The conservative variables on the cell faces are calculated by an upwind extrapolation scheme third order of accuracy. A second order accurate scheme is used for the discretization of the viscous terms. The solution of the system of equations is succeeded by an implicit unfactored method. In order to reduce the computational time a Local Adaptive Mesh Solution (LAMS) method is proposed. LAMS method combines the mesh sequencing technique and the local solution of the equations. Local solution of either Euler or Navier-Stokes equations is applied in the region of the flow field where numerical disturbances are died out slowly. Validation of the Euler and Navier-Stokes codes is obtained for hypersonic flows around blunt bodies. Real gas effects are introduced via a generalized equation of state. Extension of numerical methods in real gas hypersonics is presented for the hybrid FVS method and a Riemann solver. Author

N94-10463*# National Aeronautics and Space Administration. Lyndon B. Johnson Space Center, Houston, TX.

A COMPARISON OF HIGH RESOLUTION UPWIND SOLVERS ON 3-D INVISCID HYPERSONIC FLOWS

M. Manna (Von Karman Inst. for Fluid Dynamics, Rhode-Saint-Genese, Belgium.), H. Deconinck (Von Karman Inst. for Fluid Dynamics, Rhode-Saint-Genese, Belgium.), C. P. Li, and E. Ma *In* AGARD, Theoretical and Experimental Methods in Hypersonic Flows Apr. 1993 14 p (For primary document see N94-10421 01-02)

Copyright Avail: CASI HC A03/MF A04

A detailed comparison of numerical results obtained by solving the Euler equations for the inviscid flow over delta wings in reentry configurations is presented. The investigation involves a side-by-side comparison between independently developed upwind Euler solvers at VKI (M3D) and NASA Johnson Space Center (E3D) using identical grids. In both solvers the governing equations are integrated by means of time marching finite volume shock capturing methods, based on a cell centered upwind evaluation of the cell face fluxes and nonlinear limiters. High resolution schemes are obtained via MUSCL characteristic variable extrapolation to ensure total variation diminishing (TVD) properties and therefore monotonic discontinuity capturing. Further comparisons are made with several published results by other authors based on both upwind and central discretizations. The present results contribute in asserting the high resolution upwind TVD schemes as the most reliable numerical technique to handle the strong discontinuities typical of high speed flows. The performances of the two upwind solvers are satisfactory and the numerical results in good agreement. However, the important issue of reaching a grid converged solution for the present complex three-dimensional inviscid flow problems was not achieved. Author (revised)

N94-10464# Avions Marcel Dassault, Saint-Cloud (France).

LOCAL AEROTHERMAL PROBLEMS DURING HERMES RE-ENTRY

A. Naim, M. Mallet, P. Rostand, and J. M. Hasholder *In* AGARD, Theoretical and Experimental Methods in Hypersonic Flows Apr. 1993 16 p In FRENCH Original contains color illustrations (For primary document see N94-10421 01-02)

Copyright Avail: CASI HC A03/MF A04

The objective is to present results obtained with the Navier Stokes code used by Dassault Aviation for aerothermal reentry problems. We will emphasize the strategy employed and only give an outline of the numerical technique developed for each solver involved in the calculation. The method is designed to have a wide range of application. It involved a sequence of calculations using different modules and interfaces. This tool is not only multi-codes but also multi-computers. The preparation of the initial solution sets for computations were performed on our IBM ES 9000/820 with MVS ESA operating system, and most of the computation was done on a NEC SX3 (at NLR in the Nederlands) and on a CRAY YMP (at C.I.R.A. in Italy) with UNIX operating system. We shall present a validation case using the complete sequence, and afterwards a number of critical points of microaerothermodynamics. The validation test case is a Complete Hermes canopy of the 0.0 geometry (shape number 185 in Dassault catalog). A model of this shape was tested in R3CH ONERA wind tunnel yielding experimental results that are used for comparison. For the flight cases we plan to compute: various canopy shapes; a meteorite impact on the Hermes noze cap; and joint between tiles (in first tile position). Author (revised)

N94-10465# Rome Univ. (Italy). Dept. of Mechanics and Aeronautics.

THERMAL AND CHEMICAL NON EQUILIBRIUM HYPERSONIC FLOW COMPUTATIONS

F. Grasso and V. Bellucci *In* AGARD, Theoretical and Experimental Methods in Hypersonic Flows Apr. 1993 11 p (For primary document see N94-10421 01-02)

Copyright Avail: CASI HC A03/MF A04

A two-temperature model was developed for the description of thermal and chemical nonequilibrium viscous hypersonic flows. The model employs a vibrational coupling factor as proposed by Treanor and Marrone, and it uses a model based on a non-preferential removal of vibrational energy. The technique relies on a finite volume approach based on a second order accurate Total Variation Diminishing (TVD) formulation that accounts for thermal and chemical nonequilibrium effects. The stiffness due to the disparity in time scales is reduced by introducing a precondition matrix that allows a pointwise implicit solution of the source terms. Applications of the model to compute viscous hypersonic flows over a wedge and a cylinder showed that the postshock temperature plays a fundamental role in the achievement of thermal equilibrium and that the boundary layer is the most affected by thermal nonequilibrium. Author (revised)

N94-10466# National Aerospace Lab., Tokyo (Japan).

PROCEEDINGS OF THE 10TH NAL SYMPOSIUM ON AIRCRAFT COMPUTATIONAL AERODYNAMICS: CFD WORKSHOP ON GK AIRFOIL AND ONERA M5 GEOMETRY

Mar. 1993 111 p In JAPANESE Symposium held in Tokyo, Japan, 10-12 Jun. 1992

(NAL-SP-20) Avail: CASI HC A06/MF A02

The papers of the Computational Fluid Dynamics Workshop on the Garabedian-Korn airfoil and the ONERA M5 configuration are presented. Computational results from each of the Workshop contributors are summarized and compared. For individual titles, see N94-10467 through N94-10482.

N94-10467# National Aerospace Lab., Tokyo (Japan).

DESCRIPTION OF 2D PROBLEM: AERODYNAMIC ANALYSIS OF GARABEDIAN-KORN 75-06-12 AIRFOIL

Naoki Hirose *In its* Proceedings of the 10th NAL Symposium on Aircraft Computational Aerodynamics: CFD Workshop on GK Airfoil and ONERA M5 Geometry Mar. 1993 p 1-3 In JAPANESE (For primary document see N94-10466 01-02)

Avail: CASI HC A01/MF A02

Some 2D problems related to the analysis of the Garabedian-Korn 75-06-12 airfoil are addressed. The Problem A is to compute a shock-less flow of a Garabedian-Korn 75-06-12 airfoil at design conditions of Mach number, 0.75, C(sub 1), 0.63 and Reynolds number, 6 and 20 x 10(exp 6). Problem B is to obtain the aerodynamic characteristics of Mach number sweep and angle of attack sweep. The reference point is the same condition in Problem A. The output data format is described. Author (revised)

N94-10468# Nagoya Univ. (Japan). Dept. of Aeronautical Engineering.

AERODYNAMIC CHARACTERISTICS ANALYSIS OF GARABEDIAN-KORN 75-06-12 AIRFOIL

Andi Eka Sakya and Yoshiaki Nakamura *In* NAL, Proceedings of the 10th NAL Symposium on Aircraft Computational Aerodynamics: CFD Workshop on GK Airfoil and ONERA M5 Geometry Mar. 1993 p 5-6 In JAPANESE (For primary document see N94-10466 01-02)

(Paper-2D-2) Avail: CASI HC A01/MF A02

A Navier-Stokes code based on the implicit Yee-Harten TVD scheme is applied to compute the aerodynamic characteristics of Garabedian-Korn GK 75-06-12 airfoil at transonic speed. The algebraic turbulence model is employed to close the system of equations. Author

N94-10469# Fuji Heavy Industries Ltd., Utsunomiya (Japan).

AERODYNAMIC CHARACTERISTICS ANALYSIS OF GARABEDIAN-KORN 75-06-12 AIRFOIL

Kyoko Higaki, Yasuhiro Koshioka, and Kohei Tanaka *In* NAL, Proceedings of the 10th NAL Symposium on Aircraft Computational Aerodynamics: CFD Workshop on GK Airfoil and ONERA M5 Geometry Mar. 1993 p 7-8 In JAPANESE (For primary document see N94-10466 01-02)

(Paper-2D-3) Avail: CASI HC A01/MF A02

The flow field around a GK75-06-12 airfoil is analyzed by solving the two-dimensional compressible Navier-Stokes equations. The calculation was carried out, under the condition of Reynolds number 6 x 10(exp 6) and 2 x 10(exp 7), in each case CL (lift coefficient) was adjusted to 0.63. Author

N94-10470# Kawasaki Heavy Industries Ltd., Gifu (Japan). Technical Inst.

AERODYNAMIC CHARACTERISTICS ANALYSIS OF GARABEDIAN-KORN 75-06-12 AIRFOIL: COMPUTATION USING q-OMEGA 2 EQUATION TURBULENCE MODEL

Eiji Shima and Kouichi Egami *In* NAL, Proceedings of the 10th NAL Symposium on Aircraft Computational Aerodynamics: CFD Workshop on GK Airfoil and ONERA M5 Geometry Mar. 1993 p 9-10 In JAPANESE (For primary document see N94-10466 01-02)
(Paper-2D-4) Avail: CASI HC A01/MF A02

Reynolds-averaged Navier-Stokes equations for perfect gas are solved numerically for flow around GK75-06-12 airfoil at the design conditions. Coakley's 2 equation turbulence model is used. In order to solve the q-omega equations stably some improvements are added to the numerical scheme. Two turbulence models, the q-omega model in this paper, and the Baldwin-Lomax model in another paper, are used for this workshop, then some characteristics of each solutions are compared. It is found that (1) surface pressure distributions are almost identical; and (2) q-omega solution has larger skin friction that B-L solution and that causes thicker boundary layer and bigger drag. The effect of the difference of initial and boundary conditions of q and omega variables are shown.
Author (revised)

N94-10471# Kawasaki Heavy Industries Ltd., Gifu (Japan). Technical Inst.
AERODYNAMIC CHARACTERISTICS ANALYSIS OF GARABEDIAN-KORN 75-06-12 AIRFOILS: COMPUTATION USING BALDWIN-LOMAX TURBULENCE MODEL
Eiji Shima and Kouichi Egami *In* NAL, Proceedings of the 10th NAL Symposium on Aircraft Computational Aerodynamics: CFD Workshop on GK Airfoil and ONERA M5 Geometry Mar. 1993 p 11-12 In JAPANESE (For primary document see N94-10466 01-02)
(Paper-2D-5) Avail: CASI HC A01/MF A02

Flow around a Garabedian-Korn 75-06-12 Airfoil is simulated numerically using Navier-Stokes equations. Baldwin-Lomax's algebraic turbulence model is adopted, but wake modeling is not used because it was shown by the previous investigation that turbulence viscosity in wake region has only little influence on pressure distribution and boundary layer characteristics. The equations are computed by the cell centered finite volume method using an implicit upwind scheme. C-type grid, which is generated algebraicly by the transfinite interpolation, is used. The large linear equations arising from the implicit scheme are solved approximately using the multi-color Gauss-Seidel method. Numerical experiments show that optimum inner iteration for rapid convergence is about 10. Author (revised)

N94-10472# Chiba Univ. (Japan). Dept. of Mechanical Engineering.
AERODYNAMIC CHARACTERISTICS ANALYSIS OF GARABEDIAN-KORN 75-06-12 AIRCRAFT
Nobuhide Nishikawa and Noboru Mori *In* NAL, Proceedings of the 10th NAL Symposium on Aircraft Computational Aerodynamics: CFD Workshop on GK Airfoil and ONERA M5 Geometry Mar. 1993 p 13-14 In JAPANESE (For primary document see N94-10466 01-02)
(Paper-2D-7) Avail: CASI HC A01/MF A02

The flow structure of compressible flow around an aerofoil is numerically analyzed by TVD-MacCormack schemes. After calculating the Euler equations on transformed coordinates, the flow variables are interpolated for the fine mesh(AF mesh) for Navier-Stokes equations, and then calculation is continued for the case Re = 6 x 10(exp 6) with the Baldwin-Lomax turbulence model. Author (revised)

N94-10473# Fujitsu Ltd., Tokyo (Japan).
AERODYNAMIC CHARACTERISTICS ANALYSIS OF GARABEDIAN-KORN 75-06-12 AIRFOIL
Kisa Matsushima and Susumu Takanashi (National Aerospace Lab., Tokyo, Japan.) *In* NAL, Proceedings of the 10th NAL Symposium on Aircraft Computational Aerodynamics: CFD Workshop on GK Airfoil and ONERA M5 Geometry Mar. 1993 p 15-16 In JAPANESE (For primary document see N94-10466 01-02)
(Paper-2D-8) Avail: CASI HC A01/MF A02

The parametric study of Navier-Stokes computations has been performed to find an angle of attack which realizes a shockless pressure distribution over the Garabedian-Korn airfoil under the Mach number of 0.75. It would be almost impossible to realize a shockless solution by Navier-Stokes equations because of the viscous effect. A pressure distribution with weak shock has been attained, and it agrees with the theoretical pressure distribution quite well except in close vicinity to the location of a shock wave. In addition, a comparison has been made between computations using two different turbulence models. Author (revised)

N94-10474# Mitsubishi Heavy Industries Ltd., Tokyo (Japan).
AERODYNAMIC CHARACTERISTICS ANALYSIS OF GARABEDIAN-KORN 75-06-12 AIRFOIL
Takeshi Kaiden and Jun Ogino *In* NAL, Proceedings of the 10th NAL Symposium on Aircraft Computational Aerodynamics: CFD Workshop on GK Airfoil and ONERA M5 Geometry Mar. 1993 p 17-18 In JAPANESE (For primary document see N94-10466 01-02)
(Paper-2D-9) Avail: CASI HC A01/MF A02

Aerodynamic characteristics analysis of Garabedian-Korn 75-06-12 airfoil is presented. The governing equation is the thin layer Reynolds-averaged Navier-Stokes equation. The code is based on scalar pentadiagonal ADI scheme with a nonlinear artificial dissipation model and local time stepping. The turbulence modeling is added as the algebraic model of Baldwin-Lomax type. The grid system for the airfoil as C-type is generated solving the parabolic equation. The computations with 20,230 points are performed on a Convex 220. Author (revised)

N94-10475# National Aerospace Lab., Tokyo (Japan).
AERODYNAMIC CHARACTERISTICS ANALYSIS OF GARABEDIAN-KORN 75-06-12 AIRFOIL: COMPENDIUM OF RESULTS
Naoki Hirose *In its* Proceedings of the 10th NAL Symposium on Aircraft Computational Aerodynamics: CFD Workshop on GK Airfoil and ONERA M5 Geometry Mar. 1993 p 19-55 In JAPANESE (For primary document see N94-10466 01-02)
Avail: CASI HC A03/MF A02

A compendium of results of the 2D problem 'Garabedian-Korn Airfoil' is given. All of the submitted computation results were plotted on the respective figures to see the differences. Problem A: Design Point Computation was discussed significantly. Although pressure distribution gives fairly good agreement, turbulent boundary layer characteristics along chord, velocity profiles and eddy viscosity coefficient distributions in the boundary layer and wake disclosed scattered variation. The factors leading to the present results were discussed along with required future improvements.
Author (revised)

N94-10476# National Aerospace Lab., Tokyo (Japan).
DESCRIPTION OF 3D PROBLEM: FLOW ANALYSIS AROUND ONERA MODEL M5 CONFIGURATION
Jiro Nakamichi *In its* Proceedings of the 10th NAL Symposium on Aircraft Computational Aerodynamics: CFD Workshop on GK Airfoil and ONERA M5 Geometry Mar. 1993 p 57-61 In JAPANESE (For primary document see N94-10466 01-02)
Avail: CASI HC A01/MF A02

A description of the 3D Problem and Sub-problems A, B and C concerning flow analysis around the ONERA M5 configuration is presented. Problem A is to compute the flow at freestream conditions of Mach number 0.84, Reynolds number 1 x 10(exp 6), and angle of attack alpha = -1 degrees, with free transition condition. Problem B is to compute the flow at freestream conditions of Mach number 0.84, Reynolds number 6 x 10(exp 7), and angle of attack alpha = -1 degree with full turbulence condition. Problem C is to compute the aerodynamic characteristics of the model at freestream conditions of Mach number 0.84, Reynolds number 2 x 10(exp 6), and angles of attack, alpha = -3 degrees, -2 degrees and -1 degree, and to make plots of C(sub L)-alpha, C(sub L)-C(sub D) and C(sub L)-C(sub M) curves. The output formats are specified for all computed results.
Author (revised)

N94-10477# Fuji Heavy Industries Ltd., Utsunomiya (Japan).
FLOW ANALYSIS AROUND ONERA MODEL M5 CONFIGURATION
Tetsuo Yamazaki, Kyoko Higaki, Yasuhiro Koshioka, and Kohei Tanaka *In* NAL, Proceedings of the 10th NAL Symposium on Aircraft Computational Aerodynamics: CFD Workshop on GK Airfoil and ONERA M5 Geometry Mar. 1993 p 63-64 In JAPANESE (For primary document see N94-10466 01-02)
(Paper-3D-1) Avail: CASI HC A01/MF A02

Navier-Stokes code was used for flow analysis around the ONERA Model M5 configuration. This code utilizes the LU-ADI scheme and an algebraic turbulence model that was proposed by B.S. Baldwin and H. Lomax. The body surface grid used for this analysis was obtained by using the Master Dimension System, and the whole grid system was constructed in C-H type topology. The results of this analysis are in good agreement with wind tunnel test results. Author (revised)

N94-10478# Kawasaki Heavy Industries Ltd., Gifu (Japan). Technical Inst.
FLOW ANALYSIS AROUND ONERA MODEL M5 CONFIGURATION
Takuji Kishimoto *In* NAL, Proceedings of the 10th NAL Symposium on Aircraft Computational Aerodynamics: CFD Workshop on GK Airfoil and ONERA M5 Geometry Mar. 1993 p 65-66 In JAPANESE (For primary document see N94-10466 01-02)
(Paper-3D-2) Avail: CASI HC A01/MF A02

Numerical simulation of transonic flow around the ONERA model M5 configuration have been carried out by solving Navier-Stokes equations. The numerical grid used in this analysis is generated by an algebraic method with a multi-block transformation. The grid generation around the given configuration consists of more than 5 million points. We adopt as governing equations Reynolds-averaged thin-layer approximate Navier-Stokes equations with a q-omega two equation turbulence model for a turbulent viscous flow. These equations are solved by an implicit finite volume TVD upwind scheme with Roe's approximate Riemann solver to estimate convective fluxes. Author (revised)

N94-10479# Fujitsu Ltd., Tokyo (Japan).
FLOW ANALYSIS AROUND ONERA MODEL M5 CONFIGURATION
Yoko Takakura, Satoru Ogawa (National Aerospace Lab., Tokyo, Japan.), and Yasuhiro Wada (National Aerospace Lab., Tokyo, Japan.) *In* NAL, Proceedings of the 10th NAL Symposium on Aircraft Computational Aerodynamics: CFD Workshop on GK Airfoil and ONERA M5 Geometry Mar. 1993 p 67-68 In JAPANESE (For primary document see N94-10466 01-02)
(Paper-3D-3) Avail: CASI HC A01/MF A02

The numerical analysis of NAL transonic wind-tunnel flows around the ONERA aircraft model M5 has been tried to investigate the reliability of numerical simulation. The multi-domain technique is used to realize flow computations about the complicated configuration, and a simple modeling-method for the outflow/inflow through the perforated wall of a transonic wind-tunnel is presented. As a result it is known that this trial is successful since the numerical solutions agree with experiments well. Author (revised)

N94-10480# National Aerospace Lab., Tokyo (Japan).
FLOW ANALYSIS AROUND ONERA MODEL M5 CONFIGURATION
Susumu Takanashi, Ryozo Itoh, and Masakazu Tachibana *In its* Proceedings of the 10th NAL Symposium on Aircraft Computational Aerodynamics: CFD Workshop on GK Airfoil and ONERA M5 Geometry Mar. 1993 p 69-70 In JAPANESE (For primary document see N94-10466 01-02)
(Paper-3D-4) Avail: CASI HC A01/MF A02

Numerical simulation of the transonic flow about ONERA model M5 configuration has been carried out. The governing equations are the Reynolds-averaged thin-layer Navier-Stokes equations. The numerical algorithm used here is the implicit finite volume method based on the upwind TVD scheme. A computational grid with an O-C topology is generated by the point-charge distribution method. The computational results are also compared with the wind tunnel test data. Author (revised)

N94-10481# Mitsubishi Heavy Industries Ltd., Tokyo (Japan).
FLOW ANALYSIS AROUND ONERA MODEL M5 CONFIGURATION
Takeshi Kaiden and Jun Ogino *In* NAL, Proceedings of the 10th NAL Symposium on Aircraft Computational Aerodynamics: CFD Workshop on GK Airfoil and ONERA M5 Geometry Mar. 1993 p 71-72 In JAPANESE (For primary document see N94-10466 01-02)
(Paper-3D-5) Avail: CASI HC A01/MF A02

Flow analysis around the ONERA Model M5 Configuration is presented. The governing equation is the thin-layer Reynolds-averaged Navier-Stokes equation. The code is based on the scalar pentadiagonal ADI scheme with nonlinear artificial dissipation model and local time stepping. The turbulence modeling is also added as the algebraic model of Baldwin-Lomax type. The grid system for this configuration is generated utilizing the algebraic interpolation. The computations with 1,221,500 points are performed on a Fujitsu VP-2600. Author (revised)

N94-10482# National Aerospace Lab., Tokyo (Japan).
FLOW ANALYSIS AROUND ONERA MODEL M5 CONFIGURATION: COMPENDIUM OF RESULTS
Jiro Nakamichi *In its* Proceedings of the 10th NAL Symposium on Aircraft Computational Aerodynamics: CFD Workshop on GK Airfoil and ONERA M5 Geometry Mar. 1993 p 73-108 In JAPANESE (For primary document see N94-10466 01-02)
Avail: CASI HC A03/MF A02

A compendium of results of the 3D problem - flow analysis around ONERA M5 configuration - is given. All of the submitted computation results were compared to see the differences between the computed results and experimental data. In Problem A (flow analysis with freestream condition of Mach number 0.84, alpha = -1 degree, Reynolds number 1 x 10(exp 6), with free transition condition) and Problem B (flow analysis with freestream condition of Mach number 0.84, alpha = -1 degree, Reynolds number 6 x 10(exp 7) with fully turbulent conditions) the pressure distributions and Cp contours on the lifting surface and the fuselage were compared. Experimental data with Reynolds number 1 x 10(exp 6) were also shown. In Problem A, the computed transition lines of the main wing surface were compared. In Problem C (computation of aerodynamic characteristics of the Model aircraft) the C(sub L)-alpha, C(sub L)-C(sub D) and C(sub L)-C(sub M) curves are shown in comparison with experimental data. The factors leading to the present results were discussed along with necessary future improvements. Author (revised)

N94-10672*# National Aeronautics and Space Administration. Lewis Research Center, Cleveland, OH.
METHOD OF REDUCING DRAG IN AERODYNAMIC SYSTEMS Patent
Frank J. Hrach, inventor (to NASA) 17 Aug. 1993 6 p Filed 11 Sep. 1992 Supersedes N92-34243 (30 - 24, p 4111)
(NASA-Case-LEW-14791-1; US-Patent-5,236,155; US-Patent-Appl-SN-943659; US-Patent-Class-244-208; US-Patent-Class-244-130; US-Patent-Class-244-209; Int-Patent-Class-B64C-21/04) Avail: US Patent and Trademark Office

In the present method, boundary layer thickening is combined with laminar flow control to reduce drag. An aerodynamic body is accelerated enabling a ram turbine on the body to receive air at velocity V sub 0. The discharge air is directed over an aft portion of the aerodynamic body producing boundary layer thickening. The ram turbine also drives a compressor by applying torque to a shaft connected between the ram turbine and the compressor. The compressor sucks in lower boundary layer air through inlets in the shell of the aircraft producing laminar flow control and reducing drag. The discharge from the compressor is expanded in a nozzle to produce thrust. Official Gazette of the U.S. Patent and Trademark Office

N94-10673* National Aeronautics and Space Administration. Langley Research Center, Hampton, VA.
UNDERWING COMPRESSION VORTEX ATTENUATION DEVICE Patent
James C. Patterson, Jr., inventor (to NASA) 27 Jul. 1993 4 p Filed 22 May 1992 Supersedes N93-19053 (31 - 6, p 1408)
(NASA-Case-LAR-14744-1; US-Patent-5,230,486; US-Patent-Appl-SN-886998; US-Patent-Class-244-199; US-Patent-Class-244-198; Int-Patent-Class-B64C-23/06) Avail: US Patent and Trademark Office

A vortex attenuation device is presented which dissipates a lift-induced vortex generated by a lifting aircraft wing. The device consists of a positive pressure gradient producing means in the form of a compression panel attached to the lower surface of the wing and facing perpendicular to the airflow across the wing. The panel is located between the midpoint of the local wing cord and the trailing edge in the chord-wise direction and at a point which is approximately 55 percent of the wing span as measured from the fuselage center line in the spanwise direction. When deployed in flight, this panel produces a positive pressure gradient aligned with the final roll-up of the total vortex system which interrupts the axial flow in the vortex core and causes the vortex to collapse. Official Gazette of the U.S. Patent and Trademark Office

N94-10675*# National Aeronautics and Space Administration. Langley Research Center, Hampton, VA.
STATIC INTERNAL PERFORMANCE OF A SINGLE EXPANSION RAMP NOZZLE WITH MULTIAXIS THRUST VECTORING CAPABILITY

Francis J. Capone and Alberto W. Schirmer (George Washington Univ., Hampton, VA.) Washington Jul. 1993 272 p
(RTOP 505-62-30-01)
(NASA-TM-4450; L-17163; NAS 1.15:4450) Avail: CASI HC A12/MF A03

An investigation was conducted at static conditions in order to determine the internal performance characteristics of a multiaxis thrust vectoring single expansion ramp nozzle. Yaw vectoring was achieved by deflecting yaw flaps in the nozzle sidewall into the nozzle exhaust flow. In order to eliminate any physical interference between the variable angle yaw flap deflected into the exhaust flow and the nozzle upper ramp and lower flap which were deflected for pitch vectoring, the downstream corners of both the nozzle ramp and lower flap were cut off to allow for up to 30 deg of yaw vectoring. The effects of nozzle upper ramp and lower flap cutout, yaw flap hinge line location and hinge inclination angle, sidewall containment, geometric pitch vector angle, and geometric yaw vector angle were studied. This investigation was conducted in the static-test facility of the Langley 16-Foot Transonic Tunnel at nozzle pressure ratios up to 8.0.
Author (revised)

N94-10707*# National Aeronautics and Space Administration. Hugh L. Dryden Flight Research Facility, Edwards, CA.
EXTRACTION OF STABILITY AND CONTROL DERIVATIVES FROM ORBITER FLIGHT DATA
Kenneth W. Iliff and Mary F. Shafer Washington Jun. 1993 49 p Presented at the Orbiters Experiments (OEX) Aerothermodynamics Symposium, Williamsburg, VA, 27-30 Apr. 1993
(RTOP 505-68-50)
(NASA-TM-4500; H-1912; NAS 1.15:4500) Avail: CASI HC A03/MF A01

The Space Shuttle Orbiter has provided unique and important information on aircraft flight dynamics. This information has provided the opportunity to assess the flight-derived stability and control derivatives for maneuvering flight in the hypersonic regime. In the case of the Space Shuttle Orbiter, these derivatives are required to determine if certain configuration placards (limitations on the flight envelope) can be modified. These placards were determined on the basis of preflight predictions and the associated uncertainties. As flight-determined derivatives are obtained, the placards are reassessed, and some of them are removed or modified. Extraction of the stability and control derivatives was justified by operational considerations and not by research considerations. Using flight results to update the predicted database of the orbiter is one of the most completely documented processes for a flight vehicle. This process followed from the requirement for analysis of flight data for control system updates and for expansion of the operational flight envelope. These results show significant changes in many important stability and control derivatives from the preflight database. This paper presents some of the stability and control derivative results obtained from Space Shuttle flights. Some of the limitations of this information are also examined. Author

N94-10758*# Stanford Univ., CA. Dept. of Aeronautics and Astronautics.
NAVIER-STOKES FLOWFIELD COMPUTATION OF WING/ROTOR INTERACTION FOR A TILT ROTOR AIRCRAFT IN HOVER
Ian G. Fejtek Jul. 1993 156 p
(Contract NCC2-55)
(NASA-CR-4532; A-93096; NAS 1.26:4532) Avail: CASI HC A08/MF A02

The download on the wing produced by the rotor-induced downwash of a tilt rotor aircraft in hover is of major concern because of its severe impact on payload-carrying capability. A method has been developed to help gain a better understanding of the fundamental fluid dynamics that causes this download, and to help find ways to reduce it. In particular, the method is employed in this work to analyze the effect of a tangential leading edge circulation-control jet on download reduction. Because of the complexities associated with modeling the complete configuration, this work focuses specifically on the wing/rotor interaction of a tilt rotor aircraft in hover. The three-dimensional, unsteady, thin-layer compressible Navier-Stokes equations are solved using a time-accurate, implicit, finite difference scheme that employs LU-ADI factorization. The rotor is modeled as an actuator disk which imparts both a radical and an azimuthal distribution of pressure rise and swirl to the flowfield. A momentum theory blade element analysis of the rotor is incorporated into the Navier-Stokes solution method. Solution blanking at interior points of the mesh has been shown here to be an effective technique in introducing the effects of the rotor and tangential leading edge jet. Results are presented both for a rotor alone and for wing/rotor interaction. The overall mean characteristics of the rotor flowfield are computed including the flow acceleration through the rotor disk, the axial and swirl velocities in the rotor downwash, and the slipstream contraction. Many of the complex tilt rotor flow features are captured including the highly three-dimensional flow over the wing, the recirculation fountain at the plane of symmetry, wing leading and trailing edge separation, and the large region of separated flow beneath the wing. Mean wing surface pressures compare fairly well with available experimental data, but the time-averaged download/thrust ratio is 20-30 percent higher than the measured value. The discrepancy is due to a combination of factors that are discussed. Leading edge tangential blowing, of constant strength along the wing span, is shown to be effective in reducing download. The jet serves primarily to reduce the pressure on the wing upper surface. The computation clearly shows that, because of the three-dimensionality of the flowfield, optimum blowing would involve a spanwise variation in blowing strength. Author

N94-10820*# National Aeronautics and Space Administration. Hugh L. Dryden Flight Research Facility, Edwards, CA.
SPACE SHUTTLE HYPERSONIC AERODYNAMIC AND AEROTHERMODYNAMIC FLIGHT RESEARCH AND THE COMPARISON TO GROUND TEST RESULTS
Kenneth W. Iliff and Mary F. Shafer Jun. 1993 29 p Presented at the 17th Aerospace Ground Testing Conference, Nashville, TN, 6-8 Jul. 1992 Previously announced in IAA as A92-56812
(RTOP 506-69-50)
(NASA-TM-4499; H-1894; NAS 1.15:4499; AIAA Paper 92-3988) Avail: CASI HC A03/MF A01

Aerodynamic and aerothermodynamic comparisons between flight and ground test for the Space Shuttle at hypersonic speeds are discussed. All of the comparisons are taken from papers published by researchers active in the Space Shuttle program. The aerodynamic comparisons include stability and control derivatives, center-of-pressure location, and reaction control jet interaction. Comparisons are also discussed for various forms of heating, including catalytic, boundary layer, top centerline, side fuselage, OMS pod, wing leading edge, and shock interaction. The jet interaction and center-of-pressure location flight values exceeded not only the predictions but also the uncertainties of the predictions. Predictions were significantly exceeded for the heating caused by the vortex impingement on the OMS pods and for heating caused by the wing leading-edge shock interaction.
Author

N94-10855# National Aerospace Lab., Tokyo (Japan). Advanced Aircraft Research Group.
SIMULATED WAKE CHARACTERISTICS OF TAPERED ANNULAR WINGS BY A DISCRETE VORTEX METHOD [USUYOKU NIOKERU TEPA TSUKI ENKANYOKU NO KOURYUU TO USEI]
Masahiro Okuyama and Mitsuo Makino May 1992 18 p In JAPANESE
(NAL-TR-1156; JTN-93-80441) Avail: CASI HC A03/MF A01

This paper describes the wake characteristics of tapered annular wings which were numerically simulated by a discrete vortex method. In addition, two thin-wing models were employed to observe these characteristics using wind-tunnel tests. Author (NASDA)

N94-10856# National Aerospace Lab., Tokyo (Japan). Advanced Aircraft Research Group.
SIMULATED AND EXPERIMENTAL AERODYNAMIC CHARACTERISTICS OF TAPERED ANNULAR WINGS [USUYOKU NIOKERU TEPA TSUKI ENKANYOKU NO KUURIKI TOKUSEI]
Masahiro Okuyama and Mitsuo Makino May 1992 35 p In JAPANESE
(NAL-TR-1157; JTN-93-80442) Avail: CASI HC A03/MF A01

The longitudinal aerodynamic characteristics of Tapered Annular Wings (TAWs) were numerically simulated by extending the equations of the Quasi-Vortex Lattice Method (QVLM) for planar wings. Wind-tunnel experiments using two thin-wing models were also conducted to obtain the longitudinal and lateral characteristics of the TAW. The longitudinal aerodynamic characteristics of the experimental and calculational results were compared. As a result, the agreement was good except the drag coefficient. Author (NASDA)

N94-10860# National Aerospace Lab., Tokyo (Japan). Advanced Aircraft Research Group.

NEW AERODYNAMIC INFORMATION OBTAINED FROM THE SOLUTION OF THE INVERSE PROBLEM FOR AEROFOILS [YOKUGATA MAWARI NO NAGARE TO SONO KEISANHOU NI KANSHITE GYAKUMONDAI NO KAI KARA ERARERU KUUKIRIKIGAKU TEKINA CHIKEN]

Masashi Shigemi Jul. 1992 14 p In JAPANESE
(NAL-TR-1172; JTN-93-80446) Avail: CASI HC A03/MF A01

Direct and inverse problem solutions for an aerofoil are used for contrastive purposes, i.e., direct problems analyze flow around an aerofoil whose shape is prescribed, whereas inverse problems determine the aerofoil shape which realizes prescribed (and usually, idealized) flow conditions around it. In the present study, the solution of the inverse problem is applied differently because the flow input was measured in a wind tunnel experiment rather than being idealized. Investigation of the resultant aerofoil shape provided useful information on the real viscous flow characteristics around the aerofoil as well as on the feature of direct problem solution method to analyze it. The aerofoil shape from the inverse problem solution was found to be thicker than that of the one installed in the wind tunnel, with its trailing edge open. This difference is due to the boundary layer around the wind tunnel aerofoil, since inviscid flow was assumed in the computation and the actual fluid in the wind tunnel was viscous. The additional thickness of the converged aerofoil is of the same order as the displacement thickness of the boundary layer, hence, demonstrating the reliability of the popular approach to incorporate viscous effects into the inviscid analysis by solving the direct problem for an aerofoil with its shape modified by adding the displacement thickness of the boundary layer to the original shape. Inviscid flow analysis around the output shape showed that the applied inverse problem solution was quite accurate when the Reynolds number was 1.0 x 10(exp 5). Author (NASDA)

N94-10892*# National Aeronautics and Space Administration. Lewis Research Center, Cleveland, OH.

LASER VELOCIMETER MEASUREMENTS OF THE FLOW FIELD GENERATED BY A FORWARD-SWEPT PROPFAN DURING FLUTTER

Gary G. Podboy and Martin J. Krupar Jul. 1993 34 p Presented at the 24th AIAA Fluid Dynamics Conference, Orlando, FL, 6-9 Jul. 1993 Original contains color illustrations
(RTOP 535-03-10)
(NASA-TM-106195; E-7903; NAS 1.15:106195; AIAA Paper 93-2919)
Avail: CASI HC A03/MF A01; 12 functional color pages

Results are presented from an investigation to measure the flow field generated by a forward-swept propfan operating in flutter at a low forward velocity. For comparison to the flutter condition, flow field data are also presented for a slightly reduced rotational speed just below flutter. The forward-swept propfan was tested as the front rotor of a counterrotating pusher propeller. A laser Doppler velocimeter (LDV) was used to measure the velocity field in planes normal to the model centerline downstream of the rotor and in planes of constant radius within the blade passages at each operating condition. A comparison of the data taken at the two different operating conditions indicated that the mean, time-averaged flow about the blades did not change drastically as the propfan rotational speed was increased from the stable operating point to the flutter condition. No regions of flow separation could be identified in the data plots of the mean intrablade flow field. The data also indicate that the relative flow about the blades remained subsonic during flutter operation. The blades were found to have a higher than expected tip loading at both operating conditions. This is thought to have been caused by the outer blade sections twisting under load to higher than expected effective blade angles. This high tip loading resulted in strong vortices and a very nonuniform flow downstream of the tips of the forward-swept blades. This high tip loading may also have caused the blade flutter. Author

N94-11021*# National Aeronautics and Space Administration. Marshall Space Flight Center, Huntsville, AL.

PARACHUTE HAVING IMPROVED VENT LINE STACKING Patent Application.

John E. Hengel 29 Mar. 1993 12 p
(NASA-Case-MFS-28508-1; NAS 1.71:MFS-28508-1; US-Patent-Appl-SN-037877) Avail: CASI HC A03/MF A01

A parachute having an improved vent line stacking wherein the parachute is provided with a canopy having a central vent opening and a vent band secured to the canopy around the periphery of the vent opening, with a plurality of vent lines each lying on a diameter of the vent opening and having its ends secured to the vent band on opposite sides of the vent opening is described. The vent lines are sewed to the vent band in an order such that the end of a first vent line is sewed to the vent band at a starting point with the end of a second vent band then being sewed to the vent band adjacent to and counterclockwise from the first band. A third vent band is sewed to the vent band adjacent to and clockwise from the first band, with a fourth vent band being sewed to the vent band adjacent to and counterclockwise from the second vent band. It can be seen that, if the vent lines are numbered in the order of being sewed to the vent band, the odd numbered vent lines will run consecutively in a clockwise direction and the even numbered lines will run consecutively in a counterclockwise direction from the starting point. With this order of assembly, each and every vent line will be separated from adjacent vent lines by no more than one vent line in the center of the vent opening where the vent lines cross. Author (revised)

N94-11058 Princeton Univ., NJ.

THE EFFECTS OF SUCCESSIVE DISTORTIONS ON A TURBULENT BOUNDARY LAYER IN A SUPERSONIC FLOW Ph.D. Thesis

Douglas Robert Smith 1993 231 p
Avail: Univ. Microfilms Order No. DA9311228

Four experiments which investigate the effects of strong distortions on a supersonic turbulent boundary layer (Ma = 2.89, Re(sub theta) is approximately 80000) are discussed. The first two experiments include a boundary layer flow on a flat wall experiencing a pressure rise equivalent to 16 degrees of turning (Flat Plate Model 4), and a boundary layer flow encountering a 20 degrees expansion corner. In the first experiment, the pressure gradient matches the gradient on Donovans Model 4 curved wall (delta(sub 0)/R equals 0.08). In the second experiment, the nature of the expanded flow permits a calculation of the turbulence based upon Rapid Distortion Approximations. The second two experiments are an intensive study of the boundary layer response to successive distortions. In these two flows, the boundary layer experiences successive applications of compression and expansion on two forward-facing ramps with 20 degrees of turning. The first two studies investigate the influence of streamline curvature and pressure gradients on a supersonic turbulent boundary layer and demonstrate that compressibility effects arising from the pressure gradient dominate the flow response. The effect of curvature is small but not negligible. In the expansion corner flow, the evolution of the turbulence fields in the distortion is predicted surprisingly well with Rapid Distortion Approximations. The measurements in the compression-expansion flows provide some remarkable insight into the relaxation behavior of a strongly distorted boundary layer. In the middle of the relaxing boundary layer downstream of the distortions, the turbulence exhibits a second-order response, while near the boundary layer edge the response is first-order. The turbulent shear stress collapses throughout most of the boundary layer, and an overall destruction of the turbulence production mechanisms is apparent as the boundary layer exhibits a slow recovery.
Dissert. Abstr.

N94-11111# Sandia National Labs., Albuquerque, NM.

EXAMINATION OF WALL FUNCTIONS FOR A PARABOLIZED NAVIER-STOKES CODE FOR SUPERSONIC FLOW

T. H. Alsbrooks (New Mexico Univ., Albuquerque.) 1993 17 p Presented at the AIAA Region 4 Student Conference, Houston, TX, 1-3 Apr. 1993
(Contract DE-AC04-76DP-00789)
(DE93-011590; SAND-93-0878C; CONF-9304118-1) Avail: CASI HC A03/MF A01

Solutions from a Parabolized Navier-Stokes (PNS) code with an algebraic turbulence model are compared with wall functions. The wall functions represent the turbulent flow profiles in the viscous sublayer, thus removing many grid points from the solution procedure. The wall functions are intended to replace the computed profiles between the body surface and a match point in the logarithmic region. A supersonic adiabatic flow case was examined first. This adiabatic case indicates close agreement between computed velocity profiles near the wall and the wall function for a limited range of suitable match points in the logarithmic region. In an attempt to improve marching stability, a laminar to turbulent transition routine was implemented at the start of the PNS code. Implementing the wall function with the transitional routine in the PNS code is expected to reduce computational time while maintaining good accuracy in computed skin friction. DOE

N94-11133*# National Aeronautics and Space Administration. Lewis Research Center, Cleveland, OH.

LASER ANEMOMETER MEASUREMENTS AND COMPUTATIONS FOR TRANSONIC FLOW CONDITIONS IN AN ANNULAR CASCADE OF HIGH TURNING CORE TURBINE VANES

Louis J. Goldman Washington Jul. 1993 33 p

(RTOP 505-62-52)

(NASA-TP-3383; E-7662; NAS 1.60:3383) Avail: CASI HC A03/MF A01

An advanced laser anemometer (LA) was used to measure the axial and tangential velocity components in an annular cascade of turbine stator vanes operating at transonic flow conditions. The vanes tested were based on a previous redesign of the first-stage stator in a two-stage turbine for a high-bypass-ratio engine. The vanes produced 75 deg of flow turning. Tests were conducted on a 0.771-scale model of the engine-sized stator. The advanced LA fringe system employed an extremely small 50-micron diameter probe volume. Window correction optics were used to ensure that the laser beams did not uncross in passing through the curved optical access port. Experimental LA measurements of velocity and turbulence were obtained at the mean radius upstream of, within, and downstream of the stator vane row at an exit critical velocity ratio of 1.050 at the hub. Static pressures were also measured on the vane surface. The measurements are compared, where possible, with calculations from a three-dimensional inviscid flow analysis. Comparisons were also made with the results obtained previously when these same vanes were tested at the design exit critical velocity ratio of 0.896 at the hub. The data are presented in both graphical and tabulated form so that they can be readily compared against other turbomachinery computations. Author (revised)

N94-11154 Tennessee Univ., Knoxville.

WALL INTERFERENCE CORRECTION BASED ON INTERFACE MEASUREMENTS IN SUBSONIC WIND TUNNEL TESTING Ph.D. Thesis

Norbert Manfred Herm Ulbrich 1992 163 p

Avail: Univ. Microfilms Order No. DA9306700

Two types of wall interference correction methods in subsonic wind tunnel testing are investigated which are based on interface measurements of velocities or pressures in the flow field. The first method, called Two-Interface method, is derived from a small perturbation solution of the two-dimensional potential equation in subsonic flow. A surface pressure coefficient and angle of attack correction is calculated using axial velocity measurements on the first interface and vertical velocity measurements on the second interface in the wind tunnel. The method only requires the measurement of axial velocities on the first interface, if the solid wall of a wind tunnel is selected as the second interface. The method is applied to available experimental data. Corrected surface pressure coefficients show reasonable agreement with test data recorded in unconfined flow. The second method, called Wall Signature method, can be used to determine wall interference corrections in three-dimensional incompressible wind tunnel testing. Modifications of the Wall Signature method are presented. Pressure measurements on a limited number of wall locations are combined with influence functions to obtain an equivalent body representation of the test article and its wake in terms of surface panel elements. Blockage corrections in a wind tunnel with non-rectangular cross-section are computed using this equivalent body description and an existing three-dimensional panel code. A direct comparison of equivalent body and test article geometry is possible. The analysis of the symmetric part of the wall signature is improved by introducing a least squares fit based on a Gaussian. Advantages and disadvantages of Two-Interface and Wall Signature method are compared. The Two-Interface method is applicable in subsonic wind tunnel testing as long as the small perturbation assumption holds. This method uses explicit equations to compute wall interference corrections which makes it suited for on-line operation. The modified Wall Signature method is not restricted to slender bodies and can even be applied to high angle of attack tests. In its present form, however, the modified Wall Signature method is only applicable in post-test analysis as the method is computationally intensive. Dissert. Abstr.

N94-11195*# MCAT Inst., San Jose, CA.

PHYSICS OF FOREBODY FLOW CONTROL

Gabriel I. Font Aug. 1993 45 p

(Contract NCC2-729)

(NASA-CR-193626; NAS 1.26:193626; MCAT-93-12) Avail: CASI HC A03/MF A01

Performance in the high angle of attack regime is required by many different types of aircraft. Military aircraft, such as fighters, utilize flight in this regime to improve maneuverability. Civilian aircraft, such as supersonic or hypersonic transports, will also need to operate in this regime during take off and landing, due to their small highly swept wings. Flight at high angles of attack is problematic due to the vortices being created on the nose of the aircraft. The vortices tend to become asymmetric and produce side forces. At the same time, the rudders are less effective because they are becoming immersed in the flow separating from the wings and fuselage. Consequently, the side force produced by the vortices on the nose tend to destabilize the aircraft. This situation may be corrected through the use of a forebody flow control system such as tangential slot blowing. In this concept, a jet is blown from the nose in an effort to alter the flow field around the nose and diminish the destabilizing side force. Alternately, the jet may be used to create a side force which could be used to augment the rudders. This would allow the size of the rudders to be decreased which would, in turn, diminish the cruise drag. Therefore, the use of a tangential slot blowing system has the potential for improving both the maneuver performance and the cruise performance of an aircraft. The present study was conducted to explore the physics of forebody flow control. The study consisted of two major thrusts: (1) exploration of forebody flow control with tangential slot blowing; (2) investigation of flow and field response to a general perturbation. Author

N94-11203*# Toledo Univ., OH.

BLADING MODELS FOR TURBAN AND CSPAN TURBOMACHINE DESIGN CODES Final Report

Arthur J. Glassman Jul. 1993 9 p

(Grant NAG3-1165; RTOP 505-69-50)

(NASA-CR-191164; E-7997; NAS 1.26:191164) Avail: CASI HC A02/MF A01

Blading models added to TURBAN, an axial turbine meanline design code, and CSPAN, an axial compressor spanline design code, are presented. Calculations of blade chord length, blade axial length, and number of blades for each blade row are now provided by each code. In order to accomplish this, computational models for axial solidity and stagger angle were added to TURBAN. For a compressor, where solidity and chord were already available from input, the modeling additions to CSPAN were for stagger angle and for the blade angles to include incidence and deviation. All added computations utilized models already available in the literature. Author

N94-11857 Toronto Univ., Downsview (Ontario). Inst. for Aerospace Studies.

NONLINEAR ASPECTS OF TRANSONIC AEROELASTICITY Thesis, 1992

Hema Sandhyarani Murty Jan. 1993 212 p

(UTIAS-RN-345) Copyright Avail: CASI HC A10/MF A03

Flutter analysis of airfoils in transonic flow has traditionally assumed linearity of the aerodynamic loads and moment with motion amplitude. However, the nonlinear nature of the mixed flow, incorporating large amplitude shock wave motion, may significantly invalidate the linearity assumption. In this thesis, the effect of nonlinear transonic aerodynamics on the flutter analysis is analyzed utilizing a simplified linear structural model. The aerodynamic conditions under which these effects are significant are determined for specific cases using the NACA 64A010 airfoil. In order to accurately determine the aerodynamic loads and moment, an unsteady full potential code was developed. This code was joined to an algorithm which integrates the structural equations of motion in time. A flutter analysis based on the assumption of linear aerodynamics was carried out to determine the neutral stability conditions defined by a set of structural and aerodynamic parameters. These neutral stability conditions were then used in the structural equations of motion with nonlinear aerodynamic loads and moment. These equations were then integrated in time to determine the response of the system. If the time response was not neutrally stable, then the structural parameter, mu, the airfoil-to-air mass ratio was varied until the time response was neutrally stable. If the difference in the value of the 'nonlinear'mu to 'linear' mu was greater than 10 percent, then that case was considered to exhibit significant nonlinearities. Author (revised)

N94-11870# Army Research Lab., Aberdeen Proving Ground, MD.
COMPUTATION OF HYPERSONIC NOSETIP HEAT TRANSFER RATES FOR AN M829-LIKE PROJECTILE
Bernard J. Guidos and Walter B. Sturek Apr. 1993 28 p
(DA Proj. 1L1-62618-AH-80)
(AD-A263226; ARL-MR-52) Avail: CASI HC A03/MF A01

Computational predictions are presented of in-flight blunt nosetip heat transfer rates for an M829-like projectile configuration. Predictions are made for higher-than-conventional flight velocities up to 3 km/sec (Mach 8.8), for both laminar and turbulent flows. Comparisons are made between two predictive approaches: (1) a time-dependent Navier-Stokes numerical technique, and (2) a boundary-layer engineering analysis technique (known as ASCC). Additional comparison is made with wind-tunnel heat transfer measurements for a hemisphere-cylinder configuration at Mach 6.82. The Navier-Stokes predictions agree with the experimental data to within the estimated measurement accuracy. The comparisons between the two predictive approaches show agreement with 10 percent for laminar flow. For turbulent flow, the two codes agree within 10 percent at the stagnation point, and within about 30-40 percent further downstream. The heat transfer rates presented provide a boundary condition model for subsequent analysis of projectile transient thermal response. Author (revised)

N94-11888# Aircraft Research Association Ltd., Bedford (England).
THE MODELLING OF AERODYNAMIC FLOWS BY SOLUTION OF THE EULER EQUATIONS ON MIXED POLYHEDRAL GRIDS
A. J. Peace and J. A. Shaw Apr. 1992 44 p Previously announced in IAA as A93-21218
(Contract SLS41B/2437)
(ARA-84) Avail: CASI HC A03/MF A01

An algorithm for obtaining solutions to the compressible Euler equations on mixed polyhedral grids is described. These grids, which are in general composed of hexahedral, pentahedral, and tetrahedral elements are used in the modeling of aerodynamic flows over complex three-dimensional geometries. The hexahedra are grouped into regular blocks, while the other elements are part of irregular grid regions, giving rise to the term 'hybrid grid approach'. The interconnection of the grid elements is defined by an efficient data structure, which supplies the required information to drive the Euler algorithm. In fact, cell-vertex and cell-center spatial discretization variants of this algorithm are detailed, along with an explicit time-marching scheme for obtaining steady state solutions. Results on two geometrically simple configurations provide an evaluation of these solution techniques, while the focus on a third, complex configuration, demonstrates the potential of the method in addressing the flow over general aircraft geometries. Author (revised)

N94-11889# Florida Agricultural and Mechanical Univ., Tallahassee.
UNSTEADY FLOW PAST A NACA 0012 AIRFOIL PITCHING AT CONSTANT RATES Final Report, 1 Nov. 1988 - 31 Oct. 1992
Luiz M. Lourenco, A. Krothapalli, L. VanDommelen, and C. Shih 13 Apr. 1993 82 p
(Contract F49629-89-C-0014)
(AD-A265159; FMRL-TR-8; AFOSR-93-0363TR) Avail: CASI HC A05/MF A01

The dynamic stall process of a NACA 0012 airfoil undergoing a constant-rate pitching-up motion is studied experimentally in a water towing tank facility. This study focuses on the detailed measurement of the unsteady separated flow in the vicinity of the leading and trailing edges of the airfoil. The measurements are carried out using the Particle Image Velocimetry (PIV) technique. This technique provides the two-dimensional velocity and associated vorticity fields, at various instants in time, in the mid-span of the airfoil. Near the leading edge, large vortical structures emerge as a consequence of Van Dommelen and Shen type separation and a local vorticity accumulation. The interaction of these vortices with the reversing boundary layer vorticity initiates a secondary flow separation and the formation of a secondary vortex. The mutual induction of this counter-rotating vortex pair eventually leads to the ejection process of the dynamic stall vortex from the leading edge region. DTIC

N94-12377# Brown Univ., Providence, RI. Div. of Applied Mathematics.
COMPUTATIONAL METHODS FOR PROBLEMS IN AERODYNAMICS USING PARALLEL AND VECTOR ARCHITECTURES Final Report, 1 Dec. 1989 - 30 Nov. 1992
David Gottlieb 7 May 1993 12 p
(Grant AF-AFOSR-0093-90)
(AD-A265626; AFOSR-93-0404TR) Avail: CASI HC A03/MF A01

The effort to use spectral methods to simulate flows with shock waves is summarized in four published papers. In one of the papers, the authors study uniform high order spectral methods to solve multi-dimensional Euler equations for gas dynamics. Uniform high order spectral approximations with spectral accuracy in smooth regions of solutions are constructed by introducing the idea of the Essentially Non-Oscillatory (ENO) polynomial interpolations into the spectral methods. Based on the new approximations, nonoscillatory spectral methods which possess the properties of both upwinding difference schemes and spectral methods were proposed. Numerical results are presented for the inviscid Burger's equation, and for one dimensional Euler equations including the interactions between a shock wave and density disturbance, Sod's and Lax's shock tube problems, and the blast wave problem. Finally, the interaction between a Mach 3 two dimensional shock wave and a rotating vortex is simulated. DTIC

N94-12421*# National Aeronautics and Space Administration. Langley Research Center, Hampton, VA.
A DETERMINATION OF THE EXTERNAL FORCES REQUIRED TO MOVE THE BENCHMARK ACTIVE CONTROLS TESTING MODEL IN PURE PLUNGE AND PURE PITCH
Jonathan DCruz Jul. 1993 31 p
(RTOP 505-63-50-15)
(NASA-TM-107743; NAS 1.15:107743) Avail: CASI HC A03/MF A01

In view of the strong need for a well-documented set of experimental data which is suitable for the validation and/or calibration of modern Computational Fluid Dynamics codes, the Benchmark Models Program was initiated by the Structural Dynamics Division of the NASA Langley Research Center. One of the models in the program, the Benchmark Active Controls Testing Model, consists of a rigid wing of rectangular planform with a NACA 0012 profile and three control surfaces (a trailing-edge control surface, a lower-surface spoiler, and an upper-surface spoiler). The model is affixed to a flexible mount system which allows only plunging and/or pitching motion. An approximate analytical determination of the forces required to move this model, with its control surfaces fixed, in pure plunge and pure pitch at a number of test conditions is included. This provides a good indication of the type of actuator system required to generate the aerodynamic data resulting from pure plunging and pure pitching motion, in which much interest was expressed. The analysis makes use of previously obtained numerical results. Author (revised)

N94-12616# Meiji Univ., Kawasaki (Japan). School of Science and Technology.
FLUCTUATIONS OF LONGITUDINAL VORTICES ALONG A CONCAVE WALL [OUKYOKUMEN NI SOU TATEUZU NO YURAGI]
Akira Ito and Yasuyuki Fukutomi *In* NAL, Proceedings of the 9th and 10th NAL Workshop on Investigation and Control of Boundary-Layer Transition Nov. 1992 p 23-24 In JAPANESE (For primary document see N94-12611 01-34)
Avail: CASI HC A01/MF A02

N94-12621# Osaka Prefecture Univ., Sakai (Japan). Coll. of Engineering.
ON THE FORMATION PROCESS OF KARMAN VORTEX STREET [KARUMAN UZURETSU NO KEISEI KATEI NITSUITE]
Michio Nishioka *In* NAL, Proceedings of the 9th and 10th NAL Workshop on Investigation and Control of Boundary-Layer Transition Nov. 1992 p 41-45 In JAPANESE (For primary document see N94-12611 01-34)
Avail: CASI HC A01/MF A02

N94-12633# Gifu Univ. (Japan). Faculty of Engineering.
VISUAL STRUCTURE OF KARMAN VORTEX STREETS IN A ROUTE TO CHAOTIC STATES EXCITED BY OSCILLATION OF A CIRCULAR CYLINDER [KAOSU IKOU KATEI NIOKERU KARUMAN UZURETSU NO SHIKAKU KOUZOU]
Hiroshi Nagata and Takashi Ishimaru *In* NAL, Proceedings of the 9th and 10th NAL Workshop on Investigation and Control of Boundary-Layer Transition Nov. 1992 p 91-95 In JAPANESE (For primary document see N94-12611 01-34)
Avail: CASI HC A01/MF A02

03 AIR TRANSPORTATION AND SAFETY

Includes passenger and cargo air transport operations; and aircraft accidents.

For related information see also *16 Space Transportation* and *85 Urban Technology and Transportation.*

N94-10766# Federal Aviation Administration, Atlanta, GA.
PROCEEDINGS OF THE INTERNATIONAL CONFERENCE FOR THE PROMOTION OF ADVANCED FIRE RESISTANT AIRCRAFT INTERIOR MATERIALS
Richard G. Hill, Thor Eklund, Constantine P. Sarkos, and April Horner, comp. (Galaxy Scientific Corp., Pleasantville, NJ.) Mar. 1993 372 p Conference held in Atlantic City, NJ, 9-11 Feb. 1993
(DOT/FAA/CT-93/3) Avail: CASI HC A16/MF A03

This publication contains the proceedings of the International Conference for the Promotion of Advanced Fire Resistant Aircraft Interior Materials held in Atlantic City, New Jersey, 9-11 Feb. 1993. Presentations were made in the following areas: advanced fire resistant materials, advanced technology, test methods and modeling, and future needs and requirements. For individual titles, see N94-10767 through N94-10797.

N94-10767# American Technologies International, Clearwater, FL.
NEW THERMOPLASTIC LAMINATING ADHESIVES FOR THE AIRCRAFT INDUSTRY WITH LOW HEAT RELEASE AND LOW SMOKE EMISSION c27
Sarfraz A. Siddiqui *In* FAA, Proceedings of the International Conference for the Promotion of Advanced Fire Resistant Aircraft Interior Materials Mar. 1993 p 13-20 (For primary document see N94-10766 01-03)
Avail: CASI HC A02/MF A03

In Aeroplas '90 and Fire Safety '91, the flammability behavior of several aircraft substrates with different types of decorative laminates were discussed. We concluded that due to the substrate's own fire characteristics, aircraft decorative laminate manufacturers have substantial problems meeting current Heat Release and Smoke Emission requirements. To solve this problem, we decided to develop new thermoplastic adhesives which will help decorative laminates manufacturers meet current Federal Aviation Administration (FAA) flammability requirements on virtually all substrates. These adhesive films are tested on commercially available thermoplastic decorative laminate with a PVF surface, after bonding to crushed core substrate. All flammability tests are carried out in FAA-approved OSU Heat Release and NBS Smoke Emission Chambers. Toxicity tests are also carried out using the same NBS Smoke Chamber. The flammability test data of these new adhesives are discussed. Author (revised)

N94-10768# Gill (M. C.) Corp., El Monte, CA. Research and Development.
A NEW LOW SMOKE, LOW HEAT RELEASE STRUCTURAL FOAM c27
Martin I. Cohen and Melvin R. Kantz *In* FAA, Proceedings of the International Conference for the Promotion of Advanced Fire Resistant Aircraft Interior Materials Mar. 1993 p 21-28 (For primary document see N94-10766 01-03)
Avail: CASI HC A02/MF A03

Gillfoam was developed specifically to be a structural phenolic foam capable of providing increased cabin safety during a fire in an aircraft. This product meets current Federal Airworthiness Regulations pertaining to peak and total heat release, vertical and 45 deg flammability, smoke density, and toxic gas release. The NIST smoke density (D(sub s)) for the highest density foam (20 lbs/ft(sup 3)) is less than 50 when the product is tested in the flaming mode. Foams having densities ranging between 4.0 and 20.0 lbs/ft(sup 3) are currently being evaluated for a variety of potential applications. Some of these applications include: environmental control system (ECS) ducting; cores for partitions, bulkheads, and galley panels; and for close-outs in laminated honeycomb sidewall panels. Gillfoam, as sheet stock, is also conformable in crushed core applications so it can be laminated to produce contoured profiles. When fabricated into a duct, the low smoke foam product is lighter in weight than either a multi-layer prepreg duct or an aluminum duct of comparable size. Moreover, Gillfoam ducts may require no additional thermal insulation, depending on specific applications. Development issues, performance properties, and several applications of this state-of-the-art structural foam are described. Author (revised)

N94-10769# IMITECH, Inc., Elk Grove Village, IL.
POLYIMIDE FOAM INSULATION SYSTEMS: A MAJOR WEIGHT REDUCTION AND IMPROVEMENT IN FIRE RESISTANCE OF SIDEWALL SYSTEMS c27
Michael D. ODonnell *In* FAA, Proceedings of the International Conference for the Promotion of Advanced Fire Resistant Aircraft Interior Materials Mar. 1993 p 29-35 (For primary document see N94-10766 01-03)
Avail: CASI HC A02/MF A03

As a result of the 1967 Apollo fire, NASA started the Fireman Program. NASA's requirements for materials were for the lowest possible smoke, flame spread, toxicity, off-gassing, and out-gassing. The final NASA requirement was that weight should not exceed that of the existing materials. This resulted in the full development of polyimide foam. Solimide polyimide foam exceeds all of the stated requirements including weight, which is up to five times lighter in some applications than the materials it replaces. Commercial aircraft is a different situation. Today there are very limited fire requirements on insulation materials, or any material outside those requiring the O.S.U. Heat Release and Furnace Burners. However, there are several potential changes in requirements that would effect insulation in the future: (1) expansion of the fire test requirements such as O.S.U. Heat Release, Smoke Generation, etc. to include all non-metallic materials, structures, and systems from the skin in-board throughout the entire interior; and (2) burn-through requirements as discussed by the CAA and their proposed test and fire hardening of aircraft being developed by Darchem Engineering, Ltd. Additional testing or improved fire hardening has usually been considered as costly and unnecessary relative to benefits derived. Author (revised)

N94-10770# Illbruck, Inc., Minneapolis, MN.
A POLYIMIDE FOAM FOR ADVANCED FIRE RESISTANT AIRCRAFT APPLICATIONS c27
Amelia DeBaggis *In* FAA, Proceedings of the International Conference for the Promotion of Advanced Fire Resistant Aircraft Interior Materials Mar. 1993 p 37-48 (For primary document see N94-10766 01-03)
Avail: CASI HC A03/MF A03

A fire-proof, non-toxic, and lightweight modified polyimide foam was designed for advanced fire-resistant aircraft construction. The fire-resistant, thermal, mechanical, and water-repellency performance shows the insulation meets the needs of aerospace applications. Author (revised)

N94-10771# Gill (M. C.) Corp., El Monte, CA. Research and Development.
A REPAIR PATCHING SYSTEM FOR AIRCRAFT CARGO LINERS
Douglas F. Smith and Melvin R. Kantz *In* FAA, Proceedings of the International Conference for the Promotion of Advanced Fire Resistant Aircraft Interior Materials Mar. 1993 p 49-54 (For primary document see N94-10766 01-03)
Avail: CASI HC A02/MF A03

With the FAA's mandate that cargo liner repair patches must meet flame penetration requirements described in FAR 25, Appendix F, Part 3, several new repair systems were introduced to the airlines to meet this demanding application. Previously available patches consisted of liner material with a pressure sensitive adhesive. While easy to use, the adhesive could not withstand temperatures to 1800 F, as required by the flame penetration test. Consequently, the patch fell from the liner, allowing the flame to penetrate the damaged area. The currently available repair systems were developed to meet the flame penetration requirements; however, the patches are difficult and time-consuming to apply. Moreover, they are expensive. A new patching system was developed which can be applied in less than 5 minutes, depending on the extent of the damage. This system is designated Gillpatch 2 and meets all flammability and flame penetration resistance tests described in FAR 25.855. The patch and adhesive combinations will be available in kits for rapid, on-the-spot repairs. The installation criteria and technical approach to solving the repair patch needs of the airlines and maintenance stations are described. Author (revised)

N94-10772# Allied-Signal Corp., Morristown, NJ.
PRIMASET (TM): A SAFER MATERIAL FOR AIRCRAFT INTERIOR APPLICATIONS
Sajal Das *In* FAA, Proceedings of the International Conference for the Promotion of Advanced Fire Resistant Aircraft Interior Materials Mar. 1993 p 55-65 (For primary document see N94-10766 01-03)
Avail: CASI HC A03/MF A03

Aircraft interior designers favor plastics for their low weight, decorative effect, and functional strength. However, many plastics tend to emit smoke and toxic gases when they burn. Organic compounds such as hydrogen cyanide, hydrochloric acid, sulfur dioxide, carbon monoxide, and various oxides of nitrogen can be part of the lethal gaseous cocktail that modern laminates produce on combustion. Following a number of highly publicized accidents in which fatalities were primarily caused by fire on the ground, the Federal Aviation Administration (FAA) has moved to upgrade the fire performance of aircraft interiors, focusing on flammability. Faced with public horror and outrage over the years, airworthiness authorities have sought to make cabin interiors safer in fire. The underlying philosophy is simple: all concerned accept that, once established, a fire is likely to destroy the aircraft, but if the fire can be contained for a brief period, the occupants will be given time to evacuate. The realistic brief period has been determined to be two to five minutes in most of the Fire, Smoke, and Toxicity (FST) tests. A new non-volatile cure thermoset (Primaset) resin and some of its inherently good FST characteristics are discussed. In addition, a comparative study of cure characteristics of phenolic-triazine (PT) resin and phenol-formaldehyde (PF) resin is discussed. Author (revised)

N94-10773# RK Carbon Fibers, Inc., Philadelphia, PA.
A NEW FR WATER RESISTANT ACOUSTIC INSULATION MATERIAL FOR AIRCRAFT c24
Novis Smith and Geoff Gould *In* FAA, Proceedings of the International Conference for the Promotion of Advanced Fire Resistant Aircraft Interior Materials Mar. 1993 p 67-84 (For primary document see N94-10766 01-03)
Avail: CASI HC A03/MF A03

A new lightweight fire resistant thermal and acoustical insulation material was developed for weight critical applications such as aircraft. This new insulation is based on non melting microfibers of heat treated oxidized polyacrylonitrile fiber (OPF). The insulation material is in the form of light weight battings in the range of 0.2 to 0.4 lbs/ft. This material (Curlon) has outstanding fire blocking properties with an LOI of 58, nonconducting, high emissivity, and nonmelting. The flame burn through resistance of these battings significantly exceeds that of glass and polyimide insulation materials at 2000 F. The thermal, acoustical, and fire resistant properties of this new insulation are presented. Author (revised)

N94-10774# Great Lakes Chemical Corp., West Lafayette, IN.
NEW TECHNOLOGY FOR EFFECTIVE CONTROL OF FLAMMABILITY IN POLYOLEFIN FIBER/TEXTILES c27
Charles W. Yacomeni *In* FAA, Proceedings of the International Conference for the Promotion of Advanced Fire Resistant Aircraft Interior Materials Mar. 1993 p 85-91 (For primary document see N94-10766 01-03)
Avail: CASI HC A02/MF A03

The unsolved issue of how to effectively flame retard polyolefin (in particular polypropylene) fiber in order to impart inherent flame resistance to a finished textile is addressed. One product is used in substantial quantities world-wide to flame retard textiles (e.g. automotive and commercial upholstery) traditionally made from polyamide or polyester fiber; this product is applied in the form of a compounded latex back-coating. Polypropylene is difficult to flame retard. Substantial efforts have been made to incorporate some of the previously mentioned products into polypropylene fiber during the fiber extrusion process with some limited success. However most of these products are not melt blendable with polypropylene and therefore particle size of the flame retardant becomes a critical issue at the lower fiber deniers. There is also the necessity of antimony trioxide as a synergist which represents yet another incompatible particle present in the fiber cross section. Migration of an incompatible flame retardant to the fiber surface is also a possibility which could cause build-up on fiber processing equipment. Before discussion of flammability test results, it is appropriate to review the technical barriers that had to be overcome in order to offer a commercially viable product. The following issues had to be evaluated: spinnability, UV stability, corrosion, odor, coloration, and flammability. Each of these issues is addressed. Derived from text

N94-10775# Fokker B.V., Amsterdam (Netherlands). Design and Integration Dept.
APPLICATIONS OF CONTINUOUS FIBER REINFORCED THERMOPLASTICS IN AIRCRAFT INTERIORS c27
Robert G. Diehl *In* FAA, Proceedings of the International Conference for the Promotion of Advanced Fire Resistant Aircraft Interior Materials Mar. 1993 p 93-104 (For primary document see N94-10766 01-03)
Avail: CASI HC A03/MF A03

As part of a technology development program, actual aircraft interior parts were manufactured from polyetherimide (PEI) resin reinforced with woven glass fiber in the form of composite solid laminates and sandwich materials. These parts are evaluated against an aircraft manufacturer's design criteria, highlighting critical areas. The status of a number of the parts is given - technology proving, flying prototype part, serial production, etc. The materials have good fire safety properties, some unexpected mechanical properties, and an above average contribution to parts cost. The state of the art is such that the present interior applications for this material are restricted to areas with highly specific requirements. Further development to improve some mechanical properties and process control could quickly open up the field because of substantial savings in manufacturing costs. Author (revised)

N94-10776# SP Systems, Los Angeles, CA.
ADVANCED PHENOLIC SYSTEMS FOR AIRCRAFT INTERIORS c27
Herman Gupta and Mickey McCabe *In* FAA, Proceedings of the International Conference for the Promotion of Advanced Fire Resistant Aircraft Interior Materials Mar. 1993 p 105-119 (For primary document see N94-10766 01-03)
Avail: CASI HC A03/MF A03

Recent advances in the phenolic prepreg systems suitable for aircraft interior's applications are described. The current state of the art phenolic systems achieve a balance of properties and comfortably meet heat release and smoke emission requirements of various regulatory agencies such as FAR 25.853 and ATS 1000.001. A recent commercially available phenol formaldehyde resin based prepreg product SPH 2400 is reviewed. A single ply SPH 2400 sandwich laminates fabricated from Nomex honeycomb core and 7781 style fiberglass show Ohio State University (OSU) test peak heat release characteristics as low as 18 KW/M(sup 2) and an average OSU heat release of 15 KW-Min/M(sup 2) over a period of two minutes. The optical density of smoke emission measured by NBS method in naming mode was found to be only 6 when measured over four minutes. The product SPH 2400 can be processed by using a variety of techniques such as vacuum bag molding, multiple opening press (MOP) molding, and crushed core (CC) press molding. The prepreg system possesses outstanding self adhesive characteristics to a variety of core substrate and does not require an additional adhesive layer for core bonding. A proprietary latent catalysis technology enables rapid cures at temperature as low as 132 C (270 F) while maintaining excellent out time at room temperature. Author (revised)

N94-10777# Furane Plastics, Inc., Los Angeles, CA. Aerospace Product Group.
URALANE (TM) 5774-A/B: CIBA-GEIGY'S ADVANCED URETHANE ADHESIVE FOR THE AIRCRAFT INDUSTRY c27
Edwin C. Clark and Jose Salazar *In* FAA, Proceedings of the International Conference for the Promotion of Advanced Fire Resistant Aircraft Interior Materials Mar. 1993 p 121-135 (For primary document see N94-10766 01-03)
Avail: CASI HC A03/MF A03

In the aircraft industry, several trends in the fabrication of aircraft interiors have been observed in recent years. One development has been the application of new, flame resistant thermoplastics (i.e. Declar-T, Ultem, Kydex, Europlex, Radel, etc.) to the construction of aircraft interiors. Use of these advanced materials by aircraft manufacturers has created an accompanying need for new adhesives that can effectively bond the tough-to-join thermoplastics and also provide the required flame, smoke, and toxicity (FST) performance. In addition to these materials trends, is a heightened industry awareness of worker safety and the importance of minimizing worker exposure to chemicals. In response to industry demands generated by the above-mentioned factors, CIBA-GEIGY Corporation's Furane Aerospace Product Group initiated a new product development effort several years ago. The program was aimed at formulating an effective thermoplastic bonding adhesive that could be supplied in an environmentally improved package. The result was the creation of Uralane 5774-A/B urethane adhesive. Uralane 5774-A/B is a two-component urethane adhesive designed to bond the advanced thermoplastics used in fabricating aircraft interior components. The adhesive complies with the FST requirements of FAR 25.853 a. And, it is formulated with a 2 to 1 mix ratio by volume, permitting packaging in Accumix dual barrel cartridge kits. The kits are designed to accurately store, mix, and dispense Uralane 5774-A/B without the need for direct worker exposure to the adhesive. An additional safety benefit of Uralane 5774-A/B is that it can be applied to unabraded substrates and requires only minimal surface preparation, thereby reducing worker exposure to dust and harsh solvents. Several major airframe manufacturers, aircraft interior fabricators, and airlines have now specified this new adhesive for use in their shops. It is the intent to highlight the features and benefits of Uralane 5774-A/B as they apply to the aircraft industry. Author (revised)

N94-10778# Tomark Industries, Inc., Wilmington, DE.

THE FIRE PROPERTIES OF INSULATION BAGS, AS INSTALLED AND AFTER AIRCRAFT OPERATIONS **c27**

Robert F. Davis *In* FAA, Proceedings of the International Conference for the Promotion of Advanced Fire Resistant Aircraft Interior Materials Mar. 1993 p 137-143 (For primary document see N94-10766 01-03)
Avail: CASI HC A02/MF A03

Polymeric films and insulation bag materials made from these films were exposed to hydrolysis conditions and subjected to the 12 second Vertical Bunsen Burner Test. Despite a major weakening in mechanical strength of the polyester film samples, all the samples passed the test by shrinking away from the flame, immediately. Only by testing the samples in multiple layers were slight differences observed. Instead of developing a suitable accelerated aging program, it is recommended that the industry test used insulation bags when they are replaced during maintenance schedules, because the instability of polyester based materials may still be of concern. Author

N94-10779# National Inst. of Standards and Technology, Gaithersburg, MD. Building and Fire Research Lab.

COMPUTER-AIDED MOLECULAR DESIGN OF FIRE RESISTANT AIRCRAFT MATERIALS **c24**

Marc R. Nyden and James E. Brown *In* FAA, Proceedings of the International Conference for the Promotion of Advanced Fire Resistant Aircraft Interior Materials Mar. 1993 p 147-158 (For primary document see N94-10766 01-03)
Avail: CASI HC A03/MF A03

Molecular dynamic simulations and Cone Calorimeter measurements were used to assess the effects of electron beam irradiation and heat treatments on the flammability of the honeycomb composites used in the sidewalls, ceilings, and stowage bins of commercial aircraft. The irradiation of this material did not result in any measureable changes. A dramatic reduction in the peak rate of heat release, however, was observed in samples that had been heated overnight at 250 C. Author (revised)

N94-10780# Virginia Polytechnic Inst. and State Univ., Blacksburg. Dept. of Chemistry.

FIRE-RESISTANT HYDROLYTICALLY STABLE POLY(ARYLENE PHOSPHINE OXIDE) MATERIAL SYSTEMS **c27**

C. D. Smith, H. J. Grubbs, A. Gungor, J. Wescott, S. C. Liptak, P. A. Wood, and James E. McGrath *In* FAA, Proceedings of the International Conference for the Promotion of Advanced Fire Resistant Aircraft Interior Materials Mar. 1993 p 159-174 Sponsored by NSF (For primary document see N94-10766 01-03)
Avail: CASI HC A03/MF A03

Arylene ether phosphine oxide homopolymers were prepared via nucleophilic aromatic substitution step polymerization of bis (4-fluorophenyl)phenyl phosphine oxide (1) with various aromatic bisphenols in the presence of a weak base and an aprotic dipolar solvent. These thermoplastic materials with T(sub g) values in the range of about 200-285 C showed 5 percent weight loss in air around 500 C with substantial amounts (40-70 percent) of char yield at 700 C, in air, which suggests excellent self-extinguishing characteristics relative to other engineering thermoplastics. Additionally, the presence of high content phosphorus in the char after such high heating further implied a possible condensed phase mechanism. Nucleophilic substitution of (1) with m-aminophenyl oxide afforded the diamine, which was a key intermediate for thermoplastic polyimides, epoxy- and bismaleimide networks. These systems also showed extremely low amounts of etching in oxygen plasma when compared to other engineering polymers. The presence of phosphorus residues after either burning or etching with oxygen plasma suggests applications of commercial importance, including fire resistant materials. Qualitative burning experiments supports these conclusions. Author (revised)

N94-10781# National Inst. of Standards and Technology, Gaithersburg, MD. Building and Fire Research Lab.

A NON-HALOGENATED, FLAME RETARDED POLYCARBONATE **c27**

Takashi Kashiwagi, Thomas G. Cleary, Gary C. Davis (General Electric Co., Schenectady, NY.), and John H. Lupinski (General Electric Co., Schenectady, NY.) *In* FAA, Proceedings of the International Conference for the Promotion of Advanced Fire Resistant Aircraft Interior Materials Mar. 1993 p 175-189 Sponsored by GE (For primary document see N94-10766 01-03)
Avail: CASI HC A03/MF A03

Various flammability properties of a siloxane-containing bisphenol-A polycarbonate sample, with the siloxane as an additive or as a copolymer, were measured and compared with those of a pure polycarbonate sample. The results show that the peak heat release rate for the siloxane-containing polycarbonate sample is significantly reduced (less than half) compared to that for the pure polycarbonate sample with two different sizes of sample, 10cm x 10cm and 40cm x 40cm. However, the ignition delay time for the siloxane-containing sample is shorter than that for the pure polycarbonate sample. Also, the flame spread rate under an external radiant flux becomes faster for the siloxane-containing sample than that for the pure polycarbonate sample. The observed char behavior, such as char depth, physical nature and apparent combustibility, and its impact on flammability properties are discussed. Author (revised)

N94-10782# Darchem Engineering, Stillington (England).

AN INVESTIGATION INTO AIRCRAFT FUSELAGE FIRE HARDENING

Cliff T. M. Hall and Mark Snell *In* FAA, Proceedings of the International Conference for the Promotion of Advanced Fire Resistant Aircraft Interior Materials Mar. 1993 p 191-205 Sponsored by Civil Aviation Authority (For primary document see N94-10766 01-03)
Avail: CASI HC A03/MF A03

The current investigation into the development of a new test facility which can reproduce in a controlled manner the fire conditions that would be experienced by an aircraft fuselage following a fuel spillage incident is outlined. The early investigation work has led to the definition of a fire source based upon previous test work in the aircraft industry and industrial pool fires in general. This definition was then used to design a test facility which was built and commissioned. It can create a reproducible thermal insult of up to 1150 C and 210 Kw/m(sup 2). The commissioning program is now complete, however, one particular aspect proved to be of great interest. That is the increased burnthrough rate due to soot deposition during the first few seconds of a pool fire. This phenomena will prove to be very critical as the ultimate aim of the project is to enhance the burnthrough capabilities of aircraft fuselages. The program will look at the determination of burnthrough times of existing fuselages before moving onto investigating the burnthrough capabilities of both improved materials and systems. Author (revised)

N94-10783# Maryland Univ., College Park. Dept. of Fire Protection Engineering.

APPLICATIONS OF A MODEL TO PREDICT FLAME SPREAD OVER INTERIOR FINISH MATERIALS IN A COMPARTMENT **c25**

James G. Quintiere, Gerald Haynes, and Brian T. Rhodes *In* FAA, Proceedings of the International Conference for the Promotion of Advanced

Fire Resistant Aircraft Interior Materials Mar. 1993 p 207-224 (For primary document see N94-10766 01-03)
Avail: CASI HC A03/MF A03

Results from a mathematical model are investigated for fire growth on wall and ceiling combustible interior finish material in a compartment. A corner fire ignition source is maintained for 10 minutes at 100 kW and subsequently increased to 300 kW. For this scenario experimental results are available from the EURIFIC program, and are compared to the model. The time for the total rate of energy release rate to reach 1 MW is examined. In addition to the 11 EURIFIC materials, eight other materials are examined in this scenario by using the model. These materials represent the type of materials formerly and currently used as cabin interior finish materials in commercial aircraft. The model yields good results in most cases: in other cases, the model can be made to yield better agreement with the experimental results by making small changes in the property data. These changes are within the range of uncertainty of the property data. Author

N94-10784# National Research Council of Canada, Ottawa (Ontario). National Fire Lab.

THE OSU HEAT RELEASE RATE TEST USING THE OXYGEN CONSUMPTION PRINCIPLE **c25**

Yoshio Tsuchiya *In* FAA, Proceedings of the International Conference for the Promotion of Advanced Fire Resistant Aircraft Interior Materials Mar. 1993 p 225-232 (For primary document see N94-10766 01-03)
Avail: CASI HC A02/MF A03

The FAA Heat Release Rate (HRR) Test using the Ohio State University (OSU) apparatus can be improved by adopting the oxygen consumption principle. Using the present thermal method, the large heat input from the electrically-heated source of the radiative heat flux causes high baseline values in the output signals. The baseline value is easily and significantly changed by the thermal history of the apparatus and thermal disturbances. The heat absorbed by the apparatus and heat lost to the surroundings also cause errors. By using the oxygen consumption principle, these thermal errors can be eliminated. In Canada, a standard test method for measuring the HRR of low heat-releasing materials was developed. The method uses the OSU apparatus with the oxygen consumption principle. This method is useful for testing the heat release rate of airplane cabin materials. Only the addition of an oxygen analyzer is required for the present OSU apparatus and, thus, costs are minimized. Author

N94-10785# Benjamin/Clarke Associates, Inc., Kensington, MD.

PRACTICAL HAZARD ASSESSMENT: AN APPROACH TO THE FIRE SAFETY **c25**

Frederic B. Clarke and James R. Hoover (Du Pont de Nemours, E. I. and Co., Wilmington, DE.) *In* FAA, Proceedings of the International Conference for the Promotion of Advanced Fire Resistant Aircraft Interior Materials Mar. 1993 p 233-244 (For primary document see N94-10766 01-03)
Avail: CASI HC A03/MF A03

Fire hazard assessment, although a powerful technique, is usually complex and elaborate. A simplified approach for practical use is presented, which relies on simple, closed-form relationships to allow potential regulators and product designers to estimate the effects which material product fire and smoke properties would have on the developing fire hazard in aircraft interiors. The four steps in the process, scenario analysis, setting objectives, formulating a fire protection strategy, and test method selection and criteria setting are described and an illustrative example aircraft wire and cable is briefly discussed. (Most criteria involve more than one fire/smoke property, so that considerable flexibility in meeting the criteria is allowed.) Author (revised)

N94-10786# Georgia-Pacific Corp., Decatur, GA. Research and Development Lab.

FIRE RESISTANCE AND MECHANICAL PROPERTIES FOR PHENOLIC PREPREGS **c27**

Shahid P. Qureshi *In* FAA, Proceedings of the International Conference for the Promotion of Advanced Fire Resistant Aircraft Interior Materials Mar. 1993 p 245-253 (For primary document see N94-10766 01-03)
Avail: CASI HC A02/MF A03

Fire resistance performance, thermal analysis, and mechanical properties of glass fiber laminates prepared with four thermal cure phenol/formaldehyde resins are discussed. Prepregs for the laminates were produced by conventional solution process. This study was performed to optimize fire resistance (FR), and thermal and mechanical properties by changing formaldehyde/phenol (F/P) mole ratio. An optimum F/P ratio was identified for maximum fire resistance and thermal properties without any sacrifice in mechanical properties. The resins evaluated easily met Federal Aviation Administration (FAA) requirements for OSU heat release and NBS smoke tests. Also, all laminates exceeded the mechanical limits of MIL-R-9299C specifications. The resins are suitable for prepregs and honeycomb for aircraft interior applications. Author (revised)

N94-10787# National Inst. of Standards and Technology, Gaithersburg, MD. Building and Fire Research Lab.

DEVELOPMENTS NEEDED TO EXPAND THE ROLE OF FIRE MODELING IN MATERIAL FIRE HAZARD ASSESSMENT **c25**

Andrew J. Fowell *In* FAA, Proceedings of the International Conference for the Promotion of Advanced Fire Resistant Aircraft Interior Materials Mar. 1993 p 255-262 (For primary document see N94-10766 01-03)
Avail: CASI HC A02/MF A03

To assess the fire hazards associated with aircraft interior materials, prediction of how the materials perform under different fire scenarios is needed. This requires information on a variety of fire characteristics including thermal inertia, ease of ignition, rate of heat release, flame spread, products of combustion, and the response to suppressants. Exposure conditions such as location, orientation, ventilation, and proximity to other materials can influence some of those characteristics. Pass/fail test methods of the past cannot provide the information to assure fire safety under a variety of circumstances. Fire modeling in combination with new bench scale material flammability test methods can meet the need. National and international developments in model validation, documentation, and acceptance are presented. The transition to aircraft cabin fire hazard assessment using fire models requires a data base on material fire properties. The case is made for greater use of improved bench scale test methods which can provide data suitable for use in the fire models. Author (revised)

N94-10788# Factory Mutual Research Corp., Norwood, MA.

FLAMMABILITY PARAMETERS OF MATERIALS: IGNITION, COMBUSTION, AND FLAME SPREAD **c25**

A. Tewarson *In* FAA, Proceedings of the International Conference for the Promotion of Advanced Fire Resistant Aircraft Interior Materials Mar. 1993 p 263-281 (For primary document see N94-10766 01-03)
Avail: CASI HC A03/MF A03

Flammability parameters associated with the ignition, combustion, and flame spread processes and their usefulness for the advanced fire resistant aircraft interior materials are discussed. The flammability parameters discussed are: (1) critical heat flux (CHF) and thermal response parameter (TRP), associated with ignition, (2) heat release parameter (HRP) and fire propagation index (FPI), associated with combustion and flame spread. The CHF, TRP, and HRP values can be derived from the data measured in the most commonly used apparatuses: (1) the Ohio State University (OSU) Heat Release Apparatus, which is the Federal Aviation Administration's (FAA) standard apparatus, (2) the Factory Mutual Research Corporation (FMRC) Flammability Apparatus, and (3) the National Institute of Standards and Technology (NIST) Flame Spread Apparatus (LIFT) and the Cone Calorimeter. The OSU and FMRC Apparatuses and the Cone Calorimeter generate very similar data for ignition and heat release rate for small horizontal and vertical samples under ambient conditions. The NIST LIFT and the FMRC Apparatuses generate very similar data for lateral, upward, and downward flame spread for slabs and cylinders under ambient conditions. The FMRC Apparatus is also used to perform Flame Radiation Scaling experiments to determine the range of flame radiative and convective flame heat fluxes transferred to the surface during combustion in small- to large-scale fires, pertinent to the aircraft interior material fire scenarios leading to flashover. The flammability parameters in terms of the fundamental scientific principles is described. Numerous examples of data are presented in tables and graphs. Author (revised)

N94-10789# Du Pont de Nemours (E. I.) and Co., Wilmington, DE. Advanced Fiber Systems.

FACTORS THAT AFFECT OSU THERMAL PERFORMANCE OF AIRCRAFT INTERIOR MATERIALS **c25**

Steven D. Beare *In* FAA, Proceedings of the International Conference

for the Promotion of Advanced Fire Resistant Aircraft Interior Materials Mar. 1993 p 283-296 (For primary document see N94-10766 01-03)
Avail: CASI HC A03/MF A03

Decorative tapestries for interior vertical surfaces of aircraft are a complex system of materials of varying levels of flammability. This system can include face fiber, dyes and adjuvants, lubricants, backing, latex, adhesive, and rigid core materials, each of which can affect thermal performance. A new easily dyeable fiber, NOMEX THERMACOLOR aramid fiber, was recently developed and exceeds FAA OSU thermal performance requirements and provides additional styling capability and reduced cycle time over producer colored NOMEX CGF. The systematic study of the carpet variables of pile height and weight, backing type, and latex type and weight on OSU thermal performance of cut pile tapestry carpets containing yarns of NOMEX THERMACOLOR fibers is described. Author (revised)

N94-10790# Federal Aviation Administration, Atlanta, GA. Materials Fire Safety.
AIRCRAFT MATERIAL FIRE TESTING AND THE CREATION OF AN INTERNATIONAL WORKING GROUP c25
Richard G. Hill *In its* Proceedings of the International Conference for the Promotion of Advanced Fire Resistant Aircraft Interior Materials Mar. 1993 p 297-300 (For primary document see N94-10766 01-03)
Avail: CASI HC A01/MF A03

The Fire Safety Branch at the Technical Center in Atlantic City, New Jersey is The Federal Aviation Administration's (FAA) Research and Development (R&D) organization responsible for providing data to the regulatory organizations within the FAA for their use in developing, modifying, and/or interpreting rules and regulations pertaining to aircraft fire safety. In carrying out that responsibility, the Fire Safety Branch has developed a number of new or modified fire test methods for aircraft interior materials that were adopted as requirements by not only the FAA, but also the Joint Airworthiness Authority (JAA) and other regulatory airworthiness authorities around the world. As a result, the Fire Safety Branch has a responsibility to the world aviation community when questions or problems arise pertaining to those test methods. The Fire Safety Branch is a leader in aircraft fire safety R&D and is committed to improving aviation safety worldwide through international cooperation. Author

N94-10791# Wright Lab., Wright-Patterson AFB, OH. Materials Directorate.
DEVELOPMENT AND ANALYSIS OF INSULATION CONSTRUCTIONS FOR AEROSPACE WIRING APPLICATIONS c33
George A. Slenski and Lynn M. Woodford (McDonnell-Douglas Corp., Saint Louis, MO.) *In* FAA, Proceedings of the International Conference for the Promotion of Advanced Fire Resistant Aircraft Interior Materials Mar. 1993 p 303-312 (For primary document see N94-10766 01-03)
(Contract F33615-89-C-5605)
Avail: CASI HC A02/MF A03

The Wright Laboratory Materials Directorate at WPAFB, Ohio recently completed a research and development program under contract with the McDonnell Douglas Aerospace Company, St. Louis, Missouri. Program objectives were to develop wire insulation performance requirements, evaluate candidate insulations, and prepare preliminary specification sheets on the most promising candidates. Aircraft wiring continues to be a high maintenance item and a major contributor to electrically-related aircraft mishaps. Mishap data on aircraft show that chafing of insulation is the most common mode of wire failure. Improved wiring constructions are expected to increase aircraft performance and decrease costs by reducing maintenance actions. In the laboratory program, new insulation constructions were identified that had overall improved performance in evaluation tests when compared to currently available MIL-W-81381 and MIL-W-22759 wiring. These insulations are principally aromatic polyimide and crosslinked ethylene tetrafluoroethylene (ETFE), respectively. Candidate insulations identified in preliminary specification sheets were principally fluoropolymers with a polyimide inner layer. Examples of insulation properties evaluated included flammability, high temperature mechanical and electrical performance, fluid immersion, and susceptibility to arc propagation under applied power chafing conditions. Potential next generation wire insulation materials are also reviewed. Author (revised)

N94-10792# Boeing Commercial Airplane Co., Seattle, WA.
FUTURE MATERIAL DEVELOPMENT TRENDS FOR COMMERCIAL AIRPLANE INTERIORS c27
Peter S. Guard and James M. Peterson *In* FAA, Proceedings of the International Conference for the Promotion of Advanced Fire Resistant Aircraft Interior Materials Mar. 1993 p 313-319 (For primary document see N94-10766 01-03)
Avail: CASI HC A02/MF A03

Advances in airplane interiors in the past have, for the most part, been made by airplane manufacturers primarily through initiatives to improve safety, but also to update appearance and functionality. Recently, regulation has played a very large role in the design of airplane interiors. The Federal Aviation Administration (FAA) heat release rule was a major challenge to designers and materials suppliers, and required the development and incorporation of new materials on a very tight schedule. Industry was able to meet the rule, but the result was non-optimum solutions. It is suggested that all affected parties - regulatory and industry - work together in advance of regulation to continuously improve cabin furnishings. Strategic research and development programs involving all parties should be established, using an integrated material, design, and manufacturing philosophy. We have looked at how we can operate in a 'continuous improvement mode', and will share with how we are trying to incorporate this. Author (revised)

N94-10793# Maryland Univ., College Park. Dept. of Fire Protection Engineering.
DEVELOPMENT OF A HYPERMEDIA KNOWLEDGE BASE OF AIRCRAFT FIRE SAFETY REGULATIONS c82
Samuel A. Denny and Frederick W. Mowrer *In* FAA, Proceedings of the International Conference for the Promotion of Advanced Fire Resistant Aircraft Interior Materials Mar. 1993 p 321-331 (For primary document see N94-10766 01-03)
Avail: CASI HC A03/MF A03

A knowledge base of aircraft fire safety regulations is being developed using Hyperties, a hypermedia engine based on an encyclopedia metaphor. This knowledge base attempts to consolidate in one place the current fire safety regulations related to commercial aircraft promulgated by the Federal Aviation Administration (FAA), along with background information on the bases for these regulations and on the fire test methods adopted by the regulations. The use of a hypermedia engine permits the unprecedented storage, linkage, and retrieval of textual, graphic, audio, and video information. Electronic links between related topics in a knowledge base permit the user to rapidly transfer between topics in order to follow a common thread among different topics. Author (revised)

N94-10794# Deutsche Airbus G.m.b.H., Bremen (Germany).
FUTURE NEEDS IN THE DEVELOPMENT OF MATERIALS FOR AIRCRAFT INTERIORS AND EQUIPMENT c27
Hans-Dieter Berg *In* FAA, Proceedings of the International Conference for the Promotion of Advanced Fire Resistant Aircraft Interior Materials Mar. 1993 p 333-337 (For primary document see N94-10766 01-03)
Avail: CASI HC A01/MF A03

The presentation starts with information on the state of the art of the materials for interior furnishings and equipment of the current Airbus Program. The second part deals with the intentions of Deutsche Aerospace Airbus with regard to further development of materials for interior furnishings and equipment. A very important criterion for interior materials development is the improvement of fire safety. In addition, aspects like human toxicity, environmental protection, repairability, costs and weight are important criteria for future new materials. Author (revised)

N94-10795# Boeing Co., Seattle, WA.
HEALTH AND SAFETY ISSUES FOR AEROSPACE WORKERS IN THE USE OF ADVANCED MATERIALS c52
James M. Peterson and Wilfrid L. Cameron (International Association of Machinists and Aerospace Workers, Washington, DC.) *In* FAA, Proceedings of the International Conference for the Promotion of Advanced Fire Resistant Aircraft Interior Materials Mar. 1993 p 339-344 (For primary document see N94-10766 01-03)
Avail: CASI HC A02/MF A03

The Boeing Company is committed to providing a safe and healthy working environment for its employees. Furthermore, the Company is committed to the well-being of communities in which the employees live and work. Wherever possible, hazardous materials and processes in the work place are being substituted with less hazardous materials and processes in the manufacture of aircraft. This change of substituting materials and processes must be achieved efficiently and cost effectively. Author

N94-10796# Federal Aviation Administration, Atlanta, GA.
ADVANCED AIRCRAFT MATERIALS RESEARCH AND DEVELOPMENT PLAN c24
Richard Lyon and Thor Eklund *In its* Proceedings of the International Conference for the Promotion of Advanced Fire Resistant Aircraft Interior Materials Mar. 1993 p 345-364 (For primary document see N94-10766 01-03)
Avail: CASI HC A03/MF A03

The DOT/FAA Long-Range Fire Safety Research Plan is outlined and a preliminary strategy for developing advanced, fire-resistant, aircraft materials as an integral component of the program is discussed. Long-range research thrusts are also proposed in fire modeling, aircraft vulnerability analysis, improved systems, advanced suppression, and fuel safety. The research plan anticipates fire safety needs for next-generation aircraft and attempts to identify emerging materials and systems technologies where a focused, sustained research effort could lead to order-of-magnitude improvements in air transportation fire safety over the next two decades. The FAA's role in the proposed framework is to initiate and maintain a balanced program of basic university research, private-sector advanced development, and in house applied research to facilitate technology insertion. The FAA Fire Safety Research Plan describes programmatic opportunities for the public from the increased research funding sought by the FAA for this activity. Leveraging of research dollars will be accomplished through collaboration and cost-sharing with government agencies having similar fire safety requirements. Technology transfer will occur through FAA-sponsored meetings, scientific publications, industrial liaisons, and student internships at the FAA Technical Center. It is expected that fire safety needs of the construction, manufacturing, and chemical process industries will provide opportunities for the utilization of advanced fire safety technology beyond commercial aviation. Author (revised)

N94-10797# Federal Aviation Administration, Atlanta, GA. Materials Fire Safety.
THE FUTURE OF AIRCRAFT CABIN FIRE SAFETY
Richard G. Hill and Nick J. Povey (Civil Aviation Authority, Gatwick, England.) *In its* Proceedings of the International Conference for the Promotion of Advanced Fire Resistant Aircraft Interior Materials Mar. 1993 p 365-369 (For primary document see N94-10766 01-03)
Avail: CASI HC A01/MF A03

The Fire Safety Branch at the Technical Center in Atlantic City, New Jersey, is the Federal Aviation Administration's (FAA) Research and Development (R&D) organization responsible for providing data to the regulatory organizations within the FAA for their use in developing, modifying, and/or interpreting rules and regulations pertaining to aircraft fire safety. The Fire Safety Branch has developed many of the fire safety standards adopted by civil aviation authorities throughout the world and is presently involved in R&D for future improvements. The Safety Regulation Group of the United Kingdom Civil Aviation Authority (CAA) initiates and funds research which is conducted by agencies external to the Authority. The research is 'Project Managed' by CAA staff working as a team involving technical experts, certification and regulatory specialists, and a project manager. There are programs of work in which the CAA together with other Authorities jointly manage complementary studies, an example is the research into Cabin Water Spray Systems which has involved the CAA, FAA, Transport Canada, DGAC of France, and the European Commission. In the future, it is expected that CAA research activities will increasingly involve other European Joint Aviation Authorities (JAA) as partners and become integrated into a JAA-wide program of research. Author (revised)

N94-11044# National Transportation Safety Board, Washington, DC.
AIRCRAFT ACCIDENT/INCIDENT SUMMARY REPORT: LOSS OF CONTROL. BUSINESS EXPRESS, INC., BEECHCRAFT 1900C N811BE NEAR BLOCK ISLAND, RHODE ISLAND, DECEMBER 28, 1991
27 Apr. 1993 77 p
(PB93-910405; NTSB/AAR-93/01/SUM) Avail: CASI HC A05/MF A01

The crash of N811BE into the Rhode Island Sound is explained. The safety issues discussed include the use of flight simulators rather than airplanes for training, the adequacy of FAA surveillance of Part 135 pilot training, and the adequacy of management oversight of pilot training for Part 135 commuter operators. Author (revised)

N94-12384# Federal Aviation Administration, Atlantic City, NJ.
PROCEEDINGS OF THE INTERNATIONAL CONFERENCE FOR THE PROMOTION OF ADVANCED FIRE RESISTANT AIRCRAFT INTERIOR MATERIALS
11 Feb. 1993 293 p Conference held in Atlantic City, NJ, 9-11 Feb. 1993
(AD-A266057; DOT/FAA/93/3) Avail: CASI HC A13/MF A03

This publication contains the proceedings of the International Conference for the Promotion of Advanced Fire Resistant Aircraft Interior Materials held in Atlantic City, New Jersey, 9-11 Feb. 1993. Presentations were made in the following areas: advanced fire resistant materials, advanced technology, test methods and modeling, and future needs and requirements. DTIC

N94-12397# Federal Aviation Administration, Washington, DC.
FAA AIR TRAFFIC ACTIVITY Statistical Report, 1 Oct. 1991 - 30 Sep. 1992
Nancy Trembley 1992 252 p
(AD-A266043) Avail: CASI HC A12/MF A03

This FAA publication furnishes terminal and en route air traffic activity information of the National Airspace System. The data were reported by the FAA-operated Airport Traffic Control Towers (ATCT's), Air Route Traffic Control Centers (ARTCC's), Flight Service Stations, Approach Control Facilities, and FAA-contracted ATCT's. These reports are used as a guide in determining the need for larger or additional facilities, upgraded equipment at particular facilities, and possible increases in personnel at existing facilities. DTIC

N94-12575# Federal Aviation Administration, Atlantic City, NJ. Technical Center.
ANALYTICAL METHOD FOR WATER VAPOR COLLECTION AND ANALYSIS IN AIRCRAFT CABIN FIRES
Louise C. Speitel Aug. 1993 22 p
(DOT/FAA/CT-TN93/33) Avail: CASI HC A03/MF A01

The purpose of this work is to develop a method of quantifying water vapor in the presence of a complex mixture of airborne combustion products, to verify that this method is relatively free of interferences, and to demonstrate the applicability of this method to measure water vapor as a function-of-time in an aircraft cabin fire with and without water spray. This data was used to access whether there is an additional thermal inhalation hazard from the water vapor generated by water mist suppression of aircraft cabin fires. Author

N94-11333# Deutsche Forschungs- und Versuchsanstalt fuer Luft- und Raumfahrt, Munich (Germany). Aircraft Div.
IN-FLIGHT AIRCRAFT STRUCTURE HEALTH MONITORING BASED ON SMART STRUCTURES TECHNOLOGY
C. Boller and R. Dilger *In* AGARD, Smart Structures for Aircraft and Spacecraft Apr. 1993 19 p (For primary document see N94-11317 01-24)
Copyright Avail: CASI HC A03/MF A04

N94-11334# British Aerospace Aircraft Group, Kingston-upon-Thames (England).
STRUCTURAL HEALTH MONITORING USING EMBEDDED FIBRE OPTIC SENSORS
P. A. Tutton and F. M. Underwood *In* AGARD, Smart Structures for Aircraft and Spacecraft Apr. 1993 10 p (For primary document see N94-11317 01-24)
Copyright Avail: CASI HC A02/MF A04

04 AIRCRAFT COMMUNICATIONS AND NAVIGATION

Includes digital and voice communication with aircraft; air navigation systems (satellite and ground based); and air traffic control.

For related information see also *17 Space Communications, Spacecraft Communications, Command and Tracking* and *Communications and Radar.*

N94-10933# Computer Resource Management, Inc., Herndon, VA.
NATIONAL AIRSPACE SYSTEM OPERATIONAL CONCEPT Final Report
William Trent and Thomas Pickerell Jun. 1993 567 p
(Contract DTFA01-91-Y-01004)
(DOT/FAA/SE-93/1; NAS-SR-130) Avail: CASI HC A24/MF A04

The Federal Aviation Administration (FAA) has established specific goals for modernization of the National Airspace System (NAS) over the next decade. These goals include the replacement and modernization of aging air traffic control and navigation equipment and the development of a more comprehensive and coordinated system design to reflect specific needs of the user and specialist communities, to enhance safety, to improve efficiency and capacity, and to reduce operating costs. The programs to achieve these objectives are documented in the Capital Investment Plan (CIP). In conjunction with the CIP, the FAA has prepared system engineering management documents to assist in the orderly development and integration of CIP programs. The NAS Systems Requirements Specification (NASSRS) is a compilation of requirements which describe the operational capabilities for the NAS as envisioned to exist by the year 2000. The organization of this NAS Operational Concept corresponds to the major paragraphs of the NASSRS and provides an in-depth discussion of the higher level descriptions found in the NASSRS. This operational concept provides an overview of the NAS along with operational sequence diagrams and operational scenario diagrams to amplify the eight major sections of the NASSRS.
Author (revised)

N94-11103 Massachusetts Inst. of Tech., Cambridge. Lexington Lincoln Lab.
THE MEMPHIS PRECISION RUNWAY MONITOR PROGRAM INSTRUMENT LANDING SYSTEM FINAL APPROACH STUDY Project Report
Martha R. Owen 24 May 1993 120 p Limited Reproducibility: More than 20% of this document may be affected by microfiche quality
(Contracts F19628-90-C-0002; DTFA01-93-Z-02012)
(AD-A266035; ATC-194; DOT/FAA/NR-92/11) Avail: Issuing Activity (Defense Technical Information Center (DTIC))

This report documents the study of the lateral positions of aircraft on Instrument Landing System (ILS) approaches during the Memphis, Tennessee, Precision Runway Monitor (PRM) demonstration. The PRM is an advanced radar monitoring system that improved the arrival capacity of closely spaced parallel runways in poor weather conditions. The results of this study are used to assist in determining the minimum runway spacing that will be authorized for PRM. The objective of this study was to quantify the lateral character of ILS arrivals and the consequent impact on independent simultaneous ILS arrival on closely spaced parallel runways. The sensitivity of the arriving aircrafts' lateral positions to different variables such as visibility, wind runway, aircraft type, autopilot performance, and localizer beam width was determined. Also, the Memphis arrival data were compared to FAA Technical Center Chicago O'Hare approach data. The analysis was primarily based on surveillance reports of 4,000 ILS arrivals into Memphis International Airport, collected with the PRM AMPS sensor (ATCRBS Monopulse Processing System). A major result of the study was that lateral aircraft positions will not hamper independent arrivals to parallel runways spaced 3,400 feet apart, but will impede operations at 3,000 feet or smaller unless approach modifications are introduced. Lateral deviations were found to be most sensitive to reduced visibility and certain autopilots. Lateral deviations were also found to be somewhat more at Memphis relative to Chicago O'Hare. Recommendations for further data analysis and collection are discussed.
DTIC

N94-11177*# Texas Univ., Austin. Center for Space Research.
PRECISION GPS EPHEMERIDES AND BASELINES Final Report, 1 Jan. 1991 - 30 Jun. 1992
1992 81 p
(Grant NAGw-2717)
(NASA-CR-194171; NAS 1.26:194171) Avail: CASI HC A05/MF A01

The emphasis of this grant was focused on precision ephemerides for the Global Positioning System (GPS) satellites for geodynamics applications. During the period of this grant, major activities were in the areas of thermal force modeling, numerical integration accuracy improvement for eclipsing satellites, analysis of GIG '91 campaign data, and the Southwest Pacific campaign data analysis.
Derived from text

N94-11525*# Ohio State Univ., Columbus. Dept. of Electrical Engineering.
PERFORMANCE OF TRAFFIC-ALERT COLLISION AVOIDANCE (TCAS) ANTENNAS IN THE PRESENCE OF SCATTERERS
K. S. Sampath, R. G. Rojas, and W. D. Burnside Jul. 1993 142 p
(Grant NAG1-1058)
(NASA-CR-193569; NAS 1.26:193569; TR-722792-5) Avail: CASI HC A07/MF A02

The performance of two TCAS systems is studied in the presence of electromagnetic scatterers. TCAS is an aircraft mounted angle of arrival (AOA) system, which estimates the bearing of a signal transmitted from a mode-S transponder on another nearby aircraft (intruder). Two systems are studied: (1) Comparison of Relative Amplitude system (CRA), and (2) Spiral Phase Antenna (SPA). The CRA antenna receives the reply via four switched beams. The bearing is estimated by comparing the amplitudes of the received signal. The SPA is based on the phase interferometer, which utilizes the received phase via sum and difference beams. The AOA is computed by comparing the reply with similar values on a calibration table, which is generated by modeling the TCAS antenna on the bare fuselage of a Boeing 727-200. The antenna patterns for the TCAS are found via high frequency methods based on the Uniform Geometric theory of Diffraction (UTD). By minimizing the standard deviation of the bearing error in a specified angular sector, optimal locations for top and bottom mounted TCAS antennas are found on the Boeing 727-200, 737-300 and 747-200 airframes. It will be shown that the overall bearing errors of the amplitude system are consistently smaller than the spiral phase TCAS. The effect of two types of nearby scatterers--antennas, and engine inlets--is studied. The AT741 L-band blade, DMC60-1 VHF Communication antenna were chosen as being representative antenna interference examples. Models are derived for the blades via a moment method analysis followed by a least squares procedure to synthesize the scattering patterns. Studies were conducted to estimate the minimum separation between the two antennas for acceptable operation. It will be shown that the spiral phase TCAS is adversely affected by the presence of a blade antenna. The amplitude system does not suffer from this limitation, especially for the forward look angles which are of most interest here. A model to represent the inlet scattering is based on the multiple scattering method and UTD. The engine on top of the B727-200 fuselage is modeled by a terminated circular waveguide. Then, the effect of moving the antenna forward on the fuselage is studied. It is again shown that the performance of the amplitude system is superior.
Author

N94-11626# Department of Transportation, Cambridge, MA. National Transportation Systems Center.
IMPACT OF SHUTTING DOWN EN ROUTE PRIMARY RADARS WITHIN CONUS INTERIOR Final Report, Jun. 1992 - Feb. 1993
Janis Vilcans Jun. 1993 43 p
(DOT-VNTSC-FAA-93-1; DOT/FAA/NR-93-1) Avail: CASI HC A03/MF A01

The impact on the Air Traffic Control (ATC) operations resulting from the shutdown of all en route primary radars (except for ARSR-4s) within the CONUS interior will result in loss of real-time weather data and aircraft skin tracking over 33 percent primary surveillance loss of coverage in the CONUS and an increase in the accident rate of one accident in 11 years as predicted on recent statistics. The report concludes that real-time weather data while of limited quality must be retained until it can be replaced by data from the NEXRAD weather radar or other weather data source. Ability to track non-transponder equipped aircraft is significant but less critical and can be minimized by other system improvements. These include: better beacon radar (Mode S) in combination with Traffic Alert and Collision Avoidance System (TCAS) and Automatic Dependent Surveillance (ADS); increased transponder equipage; reduced altitude for non-transponder equipped aircraft to 10,000 feet; increased DF network to 370 sites; and better siting of beacon-only antennas. Based on current availability projections (derived from Capital Investment PLan (CIP) schedules) the most feasible en route primary radar shutdown date is the year 2008. If weather data from external sources can be made available on controllers displays before that time (for example by 1998 when ISSS is installed) that data can be advanced. Author (revised)

N94-11863# Massachusetts Inst. of Tech., Lexington.
EVALUATION OF THE CAPACITY AND DELAY BENEFITS OF TERMINAL AIR TRAFFIC CONTROL AUTOMATION
Steven B. Boswell 14 Apr. 1993 76 p
(Contracts F19628-90-C-0002; DTFA01-88-Z-0200)
(AD-A265323; ATC-192) Avail: CASI HC A05/MF A01

The benefits that the Center/TRACON Automation System (CTAS) component of the FAA Terminal Air Traffic Control Automation program (TATCA) offers to aviation users are reviewed. In particular, the prospects that exist for increasing arrival capacity during Instrument Meteorological Conditions (IMC) by introducing CTAS functionality into current operations are reported. The impact of anticipated capacity gains on air traffic delays is analyzed. Savings in delay are translated into dollar savings using FAA statistics on the fleet-weighted direct cost of delay to domestic air carriers. Also, the value of passenger time is considered. Economic impacts are estimated and reported on an annualized, nationwide basis. Adopting FAA projections of future traffic growth, estimates of delay and attendant cost savings to air carriers and their passengers are provided for fiscal years 1995-2015. Taking the nominal estimate of a 12% gain in IMC arrival capacity, a nationwide implementation of CTAS would be estimated to save an average of 412,000 hours of air carrier delay annually over this 21-year period, and 273 million gallons of fuel per year. With current fuel and labor costs, this amounts to average direct operating savings to air carriers of $1.5 billion per year, and value to passengers of over $3 billion per year, in constant 1988 dollars. There may be factors outside the scope of this study that restrict the implementation of CTAS to certain sites, or that limit the weather conditions in which CTAS is effective. Methods are discussed for modifying benefits estimates in response to such considerations. DTIC

N94-11879# Aeronautical Systems Div., Wright-Patterson AFB, OH.
EVALUATION OF THE C/EC/KC-135 GROUND COLLISION AVOIDANCE SYSTEM (GCAS), STUDY 2 Final Report, 1 Feb. - 30 Apr. 1992
Justin D. Rueb, Jordan R. Kriss, and John A. Hassoun Mar. 1993 150 p
(AD-A265193; ASC-TR-93-5004) Avail: CASI HC A07/MF A02

This report represents the second of a two-study evaluation program. The first study evaluated the original Cubic GCAS algorithm in four distinct phases. Throughout the four phases, concerns and recommendations were forwarded to the System Program Office and to the Cubic Corporation. This resulted in modification of the algorithm prior to the next phase of the evaluation. Phase 1 efforts focused on the verification and validation of the algorithm. This phase simply established how well the algorithm predicted altitude loss based on current inputs. Phase 2 was the robot pilot model phase. During this phase, a computer pilot model tested the GCAS under different aircraft configurations and environmental conditions. The man-in-the-loop phase, Phase 3, used a subset of the configuration in Phase 2 in addition to a series of Instrument Landing System (ILS) runs to determine algorithm ability to accurately predict under realistic conditions (human reaction times). In the final phase, current operational pilots flew mission scenarios based on selected CFIT mishaps. This phase permitted an evaluation of the Cubic GCAS algorithm under real-world conditions. Study 2 used the same four-phase approach as that used during Study 1. However, the evaluation was performed on the newly revised Cubic algorithm. The revised algorithm incorporated more extensive changes than those conducted after each of the Study 1 phases. Additionally, Study 2 evaluated Phase 1-Phase 4 without any delay. Unlike Study 1, the algorithm was not returned to Cubic for modification prior to the next phases. DTIC

N94-12355*# California Polytechnic State Univ., San Luis Obispo.
HELICOPTER APPROACH CAPABILITY USING THE DIFFERENTIAL GLOBAL POSITIONING SYSTEM
David N. Kaufmann Aug. 1993 58 p
(Contract NCC2-775)
(NASA-CR-177618; A-93110; NAS 1.26:177618) Avail: CASI HC A04/MF A01

The results of flight tests to determine the feasibility of using the Global Positioning System (GPS) in the differential mode (DGPS) to provide high accuracy, precision navigation and guidance for helicopter approaches to landing are presented. The airborne DGPS receiver and associated equipment is installed in a NASA UH-60 Black Hawk helicopter. The ground-based DGPS reference receiver is located at a surveyed test site and is equipped with a real-time VHF data link to transmit correction information to the airborne DGPS receiver. The corrected airborne DGPS information, together with the preset approach geometry, is used to calculate guidance commands which are sent to the aircraft's approach guidance instruments. The use of DGPS derived guidance for helicopter approaches to landing is evaluated by comparing the DGPS data with the laser tracker truth data. Both standard (3 degrees) and steep (6 degrees and 9 degrees) glidescope straight-in approaches were flown. DGPS positioning accuracy based on a time history analysis of the entire approach was 0.2 m (mean) +/- 1.8 m (2 sigma) laterally and -2.0 m (mean) +/- 3.5 m (2 sigma) vertically for 3 degree glidescope approaches, -0.1 m (mean) +/- 1.5 m (2 sigma) laterally and -1.1 m (mean) +/- 3.5 m (2 sigma) vertically for 6 degree glidescope approaches, and 0.2 m (mean) +/- 1.3 m (2 sigma) laterally and -1.0 m (mean) +/- 2.8 (2 sigma) vertically for 9 degree glidescope approaches. DGPS positioning accuracy at the 200 ft decision height on a standard 3 degree glidescope approach was 0.3 m (mean) +/- 1.5 m (2 sigma) laterally and -2.3 m (mean) +/- 1.6 m (2 sigma) vertically. These errors indicate that the helicopter position based on DGPS guidance satisfies the International Civil Aviation Organization Category 1 lateral and vertical accuracy requirements. Author

N94-10964*# ITT Aerospace/Communications Div., Clifton, NJ.
THE TIME KEEPING SYSTEM FOR GPS BLOCK IIR
H. C. Rawicz, M. A. Epstein, and J. A. Rajan *In* NASA. Goddard Space Flight Center, The 24th Annual Precise Time and Time Interval (PTTI) Applications and Planning Meeting Jun. 1993 p 5-16 (For primary document see N94-10963 01-70)
Avail: CASI HC A03/MF A04

N94-10965*# Bureau International des Poids et Mesures, Sevres (France).
PROGRESS ON GPS STANDARDIZATION
C. Thomas *In* NASA. Goddard Space Flight Center, The 24th Annual Precise Time and Time Interval (PTTI) Applications and Planning Meeting Jun. 1993 p 17-30 (For primary document see N94-10963 01-70)
Avail: CASI HC A03/MF A04

N94-10966*# Coast Guard, Washington, DC. GPS Information Center.
US COAST GUARD GPS INFORMATION CENTER (GPSIC) AND ITS FUNCTION WITHIN THE CIVIL GPS SERVICE (CGS)
In NASA. Goddard Space Flight Center, The 24th Annual Precise Time and Time Interval (PTTI) Applications and Planning Meeting Jun. 1993 p 31-46 (For primary document see N94-10963 01-70)
Avail: CASI HC A03/MF A04

N94-10967*# Bureau International des Poids et Mesures, Sevres (France).
COMPARISON OF GPS AND GLONASS COMMON-VIEW TIME TRANSFERS
W. Lewandowski, G. Petit, C. Thomas, G. T. Cherenkov (All-Union Research Inst. for Physical and Radiotechnical Measurements, Mendeleevo, USSR.), N. B. Koshelyaevsky (All-Union Research Inst. for Physical and Radiotechnical Measurements, Mendeleevo, USSR.), and S. B. Pushkin (All-Union Research Inst. for Physical and Radiotechnical Measurements, Mendeleevo, USSR.) *In* NASA. Goddard Space Flight Center, The 24th Annual Precise Time and Time Interval (PTTI) Applications and Planning Meeting Jun. 1993 p 47-58 (For primary document see N94-10963 01-70)
Avail: CASI HC A03/MF A04

05 AIRCRAFT DESIGN, TESTING AND PERFORMANCE

Includes aircraft simulation technology.

For related information see also *18 Spacecraft Design, Testing and Performance* and *39 Structural Mechanics.*For land transportation vehicles see *85 Urban Technology and Transportation.*

N94-10344*# Oregon State Univ., Corvallis. Dept. of Electrical and Computer Engineering.

NONLINEAR STABILITY AND CONTROL STUDY OF HIGHLY MANEUVERABLE HIGH PERFORMANCE AIRCRAFT Final Report

R. R. Mohler 20 Jul. 1993 118 p
(Grant NAG1-1081)
(NASA-CR-193480; NAS 1.26:193480; OSU-ECE-NASA-93-03) Avail: CASI HC A06/MF A02

This project is intended to research and develop new nonlinear methodologies for the control and stability analysis of high-performance, high angle-of-attack aircraft such as HARV (F18). Past research (reported in our Phase 1, 2, and 3 progress reports) is summarized and more details of final Phase 3 research is provided. While research emphasis is on nonlinear control, other tasks such as associated model development, system identification, stability analysis, and simulation are performed in some detail as well. An overview of various models that were investigated for different purposes such as an approximate model reference for control adaptation, as well as another model for accurate rigid-body longitudinal motion is provided. Only a very cursory analysis was made relative to type 8 (flexible body dynamics). Standard nonlinear longitudinal airframe dynamics (type 7) with the available modified F18 stability derivatives, thrust vectoring, actuator dynamics, and control constraints are utilized for simulated flight evaluation of derived controller performance in all cases studied. Author (revised)

N94-10728# National Aerospace Lab., Tokyo (Japan). STOL Aircraft Project Group.

AERODYNAMIC MODEL IDENTIFICATION OF QUIET STOL EXPERIMENTAL AIRCRAFT ASKA FROM DYNAMIC FLIGHT TEST DATA [TEISOUON STOL JIKKENKI ASUKA NO DOUTEKI HIKOU SHIKEN NIYORU KUURIKI MODERU DOUTEI]

Masaaki Yanagihara and Toshio Bandou Jan. 1992 34 p In JAPANESE
(DE93-767967; NAL-TR-1138; JTN-93-80424) Avail: CASI HC A03/MF A01

A method to identify an aircraft aerodynamic model using dynamic flight tests was investigated by National Aerospace Laboratory (NAL). This method is subsequently being applied to flight test data of the Quiet Short Take-Off and Landing (QSTOL) experimental aircraft 'ASKA' to obtain its nonlinear non-dimensional aerodynamic model. Estimated static parameters were evaluated by comparing results from steady/quasi-steady state tests, whereas estimated dynamic parameters were compared with theoretical ones. In addition, an overall evaluation was performed by calculating simulated time histories using the identified model and comparing the results with recorded test data. Good correlations were obtained, except for configurations in which limited flight tests had been conducted, thereby demonstrating the effectiveness of this method. Author (NASDA)

N94-10935*# National Aeronautics and Space Administration. Ames Research Center, Moffett Field, CA.

DETERMINING XV-15 AEROELASTIC MODES FROM FLIGHT DATA WITH FREQUENCY-DOMAIN METHODS

C. W. Acree, Jr. and Mark B. Tischler May 1993 68 p Prepared in cooperation with Army Aviation Systems Command, Moffett Field, CA
(RTOP 505-61-51)
(NASA-TP-3330; A-91002; NAS 1.60:3330; USAATCOM-TR-93-A-004)
Avail: CASI HC A04/MF A01

The XV-15 tilt-rotor wing has six major aeroelastic modes that are close in frequency. To precisely excite individual modes during flight test, dual flaperon exciters with automatic frequency-sweep controls were installed. The resulting structural data were analyzed in the frequency domain (Fourier transformed). All spectral data were computed using chirp z-transforms. Modal frequencies and damping were determined by fitting curves to frequency-response magnitude and phase data. The results given in this report are for the XV-15 with its original metal rotor blades. Also, frequency and damping values are compared with theoretical predictions made using two different programs, CAMRAD and ASAP. The frequency-domain data-analysis method proved to be very reliable and adequate for tracking aeroelastic modes during flight-envelope expansion. This approach required less flight-test time and yielded mode estimations that were more repeatable, compared with the exponential-decay method previously used. Author

N94-10945 Aeronautical Systems Div., Wright-Patterson AFB, OH.

AN ENVIRONMENTAL STUDY OF THE NATIONAL AEROSPACE PLANE Final Report, 1 Dec. 1991 - 30 Dec. 1992

Charles Brown, Ted Wierzbanowski, Helmut Reda, and Gregory T. Duecker Dec. 1992 39 p Limited Reproducibility: More than 20% of this document may be affected by microfiche quality
(AD-A266071; ASC-TR-93-5007) Avail: CASI HC A03

The overall objective of the United States (US) National Aero-Space Plane (NASP) Program is to develop the hypersonic technologies required for future military and civilian aerospace plane systems to reduce payload cost to orbit and provide for flexible-responsive space operations. If successful, the NASP Program will be the stimulus for developing a whole new class of airbreathing hypersonic aircraft powered by clean-burning scramjet engines using liquid hydrogen as the primary fuel. As part of this development, the potential environmental impacts from these vehicles must be considered and analyzed. This process has been initiated using the NASP Program's proposed X-30 flight research vehicle and flight test program as a basis for analysis. Environmental issues addressed include the following: noise and sonic booms, stratospheric ozone depletion, public health and safety, hazardous materials/waste, air quality, biological and cultural resources, geology and soils, and water use. Although this study is not yet complete, preliminary analysis has determined that the X-30 vehicle and flight test program would have minimal environmental impact. DTIC

N94-11056 Syracuse Univ., NY.

ADVANCED ROTORCRAFT FLIGHT SIMULATION: MODEL DEVELOPMENT, VALIDATION AND PARALLEL IMPLEMENTATION Ph.D. Thesis

Sriprakash Partha Sarathy 1992 243 p
Avail: Univ. Microfilms Order No. DA9312589

The development of parallel algorithms for the real-time rotorcraft flight simulation is addressed. The objective is to employ more refined models that better predict helicopter behavior. A new Rotating Blade Element (RBE) model is developed, implemented, and validated. The new model includes coupled blade flap, lag, and pitch motions. The development of a parallel version of this model, together with appropriate parallel algorithms, is discussed for all phases of the flight simulation model. The 14 processor Encore Multimax (shared memory MIMD) parallel computer is used to implement the parallel flight simulation code. Results for the sequential and parallel implementations are provided. The RBE formulation is compared with results from CAMRAD for the OH-6 helicopter. The fully coupled nonlinear forward flight trim results compare well with those of CAMRAD. The coupled blade response is validated against Runge-Kutta integration. The timing results from the parallel code demonstrated speed up factors between 10 and 12 for the trim and response tasks. Dissert. Abstr.

N94-11150*# MCAT Inst., San Jose, CA.

SUPERSONIC AIRPLANE STUDY AND DESIGN

Samson Cheung Jun. 1993 17 p Original contains color illustrations
(Contract NCC2-617)
(NASA-CR-193219; NAS 1.26:193219; MCAT-93-10) Avail: CASI HC A03/MF A01; 3 functional color pages

A supersonic airplane creates shocks which coalesce and form a classical N-wave on the ground, forming a double bang noise termed sonic boom. A recent supersonic commercial transport (the Concorde) has a loud sonic boom (over 100 PLdB) and low aerodynamic performance (cruise lift-drag ratio 7). To enhance the U.S. market share in supersonic transport, an airframer's market risk for a low-boom airplane has to be reduced. Computational fluid dynamics (CFD) is used to design airplanes to meet the dual constraints of low sonic boom and high aerodynamic performance. During the past year, a research effort was focused on three main topics. The first was to use the existing design tools, developed in past years, to design one of the low-boom wind-tunnel configurations (Ames Model 3) for testing at Ames Research Center in April 1993. The second was to use a Navier-Stokes code (Overflow) to support the Oblique-All-Wing (OAW) study at Ames. The third was to study an optimization technique applied on a Haack-Adams body to reduce aerodynamic drag. Author (revised)

N94-11233*# National Aeronautics and Space Administration. Hugh L. Dryden Flight Research Facility, Edwards, CA.

GROUND VIBRATION AND FLIGHT FLUTTER TESTS OF THE SINGLE-SEAT F-16XL AIRCRAFT WITH A MODIFIED WING

David F. Voracek Jun. 1993 60 p
(RTOP 533-02-35)
(NASA-TM-104269; H-1906; NAS 1.15:104269) Avail: CASI HC A04/MF A01

The NASA single-seat F-16XL aircraft was modified by the addition of a glove to the left wing. Vibration tests were conducted on the ground to assess the changes to the aircraft caused by the glove. Flight Luther testing was conducted on the aircraft with the glove installed to ensure that the flight envelope was free of aeroelastic or aeroservoelastic instabilities. The ground vibration tests showed that above 20 Hz, several modes that involved the control surfaces were significantly changed. Flight test data showed that modal damping levels and trends were satisfactory where obtainable. The data presented in this report include estimated modal parameters from the ground vibration and flight flutter test. Author

N94-11464# Howell (J. R.), Bradenton, FL.

COMPARING AIRCRAFT AGILITY USING MAHALANOBIS DISTANCES Final Report

J. R. Howell and Norman E. Howell 2 Dec. 1992 6 p
(PB93-175446; AGILITY-1) Avail: CASI HC A02/MF A01

Suppose a set of p agile maneuvers is executed and measured N1 times on an aircraft of one type, and N2 times on an aircraft of another type. Based on these agility measurements, the paper shows how to calculate a generalized Mahalanobis agility distance between the two aircraft. If there are more than two types of aircraft, the agility distance between each pair can be calculated and compared. NTIS

N94-11587*# National Aeronautics and Space Administration. Langley Research Center, Hampton, VA.

FURTHER STUDIES USING MATCHED FILTER THEORY AND STOCHASTIC SIMULATION FOR GUST LOADS PREDICTION

Robert C. Scott, Anthony S. Pototzky (Lockheed Engineering and Sciences Co., Hampton, VA.), and Boyd III Perry Jul. 1993 15 p Presented at the AIAA 34th Structures, Structural Dynamics, and Materials Conference, La Jolla, CA, 19-21 Apr. 1993 Previously announced in IAA as N93-33932
(RTOP 505-63-50-15)
(NASA-TM-109010; NAS 1.15:109010) Avail: CASI HC A03/MF A01

This paper describes two analysis methods -- one deterministic, the other stochastic -- for computing maximized and time-correlated gust loads for aircraft with nonlinear control systems. The first method is based on matched filter theory; the second is based on stochastic simulation. The paper summarizes the methods, discusses the selection of gust intensity for each method and presents numerical results. A strong similarity between the results from the two methods is seen to exist for both linear and nonlinear configurations. Author

N94-11858# Kansas Univ., Lawrence. Flight Research Lab.

GENERAL AVIATION AIRCRAFT-NORMAL ACCELERATION DATA ANALYSIS AND COLLECTION PROJECT Final Report

James E. Locke, Howard W. Smith, Edward A. Gabriel, and Thomas DeFlore Feb. 1993 341 p
(AD-A265055; KR-FRL-926-1; DOT/FAA/CT-91/20) Avail: CASI HC A15/MF A03

The analysis and condensation of repeated flight loads obtained from 77 airplanes that participated in the NASA VGH General Aviation Program are reported. In addition, the load spectra for 98 airplanes in the NASA VGH data base are presented as plotted and tabulated data. Curve fit equations are listed for the original data and for extrapolation, which was used in the statistical analysis. Airspeed, normal load factor, and altitude were recorded continuously during flight. The load factor data were separated into gust and maneuver normal accelerations. The reduced data are presented as cumulative number of occurrences per nautical mile versus acceleration fraction (incremental normal acceleration divided by incremental limit load factor). For statistical analysis, the airplanes were grouped into seven single and twin-engine operational usage groups. The mean (weighted by flight time); weighted mean plus one, two, and three standard deviation spectra; and the 90% probability/95% confidence spectra were determined for each operational usage group and for several of the groups combined. An estimate of the scatter associated with groups having small sample size was determined by computing a pooled variance and pooled standard deviation. The resulting load spectra are to be used for wing fatigue test or safe-life estimation. DTIC

N94-11872# Naval Postgraduate School, Monterey, CA.

LIFT ENHANCEMENT OF A WING/STRAKE USING PNEUMATIC BLOWING M.S. Thesis

Craig J. Zgraggen Mar. 1993 92 p
(AD-A265074) Avail: CASI HC A05/MF A01

A low-speed wind-tunnel study to quantitatively measure the lift and drag effects of pneumatically controlling strake and leading-edge vortices generated by a half-span, generic-fighter model was conducted. The study measured the increase in lift and drag on the model throughout a range of angles of attack. The study utilized various blowing tubes of different geometries and orientations. Results showed that blowing produced changes in lift with minimal effect on drag. Blowing appeared to reattach flow during the initial stages of stall. Blowing increased lift a maximum of 9 percent at an angle of attack of 20 degrees, and up to 7 percent at angles of attack greater than 20 degrees. Blowing rates were varied from C(sub mu) of 0.0094 to C(sub mu) of 0.022. Near axial blowing produced the largest increases in lift. It was found that lift increases were directly proportional to changes in blowing rate. DTIC

N94-11892# Naval Aerospace Medical Research Lab., Pensacola, FL.

AIRCRAFT WINDSCREENS ENHANCE VISUAL SEARCH DISRUPTION PRODUCED BY LASER GLARE Interim Report

J. A. DAndrea, R. N. Shull, and J. C. Knepton, Jr. Dec. 1992 16 p
(AD-A265167; NAMRL-1380) Avail: CASI HC A03/MF A01

Naval aircrews may be exposed to laser radiation that is used for a variety of purposes. Consequently, there is high probability of both deliberate and accidental exposure of personnel to laser radiation. One deliberate use of laser radiation may be as a mission deterrent to disrupt aircrew visual performance. The purpose of this study was to determine how low-intensity laser glare interacts with an aircraft windscreen and if flat or wraparound aircraft windscreens differentially enhance glare and disrupt visual search performance. In addition, we evaluated the effectiveness of laser glare in high ambient light. Visual search time to locate target disks viewed through either a flat or curved windscreen under laser glare conditions was significantly longer compared to a no glare control. The glare pattern and disruption of visual search under low ambient light, simulating dawn or dusk, was more extensive when viewed through a wraparound F/A-18 windscreen than a flat A/4 windscreen. Detection of targets also depended on their location relative to the center of the laser glare pattern. Visual search performance returned to baseline levels under daytime ambient lighting conditions. The results of this experiment illustrate that aircraft windscreens can significantly increase laser-produced glare as measured by a visual search performed under low levels of ambient lighting. Eye protection is needed to prevent mission disruption, even at laser intensities that are not harmful to the eye. DTIC

N94-10429# Office National d'Etudes et de Recherches Aerospatiales, Toulouse (France).

NEW HYPERSONIC TEST METHODS DEVELOPED AT ONERA: THE R5 AND F4 WIND TUNNELS [NOUVEAUX MOYENS D'ESSAIS HYPERSONIQUES DEVELOPPES A L'ONERA: LES SOUFFLERIES R5 ET F4]

B. Chanetz, M.-C. Coet, D. Nicout, T. Pot, P. Broussaud, G. Francois, A. Masson, and D. Vennemann (European Space Agency. Centre Spatial de Toulouse, France.) *In* AGARD, Theoretical and Experimental Methods in Hypersonic Flows Apr. 1993 12 p In FRENCH Previously announced in IAA as A92-48600 (For primary document see N94-10421 01-02)
Copyright Avail: CASI HC A03/MF A04

N94-11318# Deutsche Forschungs- und Versuchsanstalt fuer Luft- und Raumfahrt, Munich (Germany). Military Aircraft Div.
SMART STRUCTURES: A TECHNOLOGY FOR NEXT GENERATION AIRCRAFT
W. Schmidt and C. Boller *In* AGARD, Smart Structures for Aircraft and Spacecraft Apr. 1993 14 p (For primary document see N94-11317 01-24)
Copyright Avail: CASI HC A03/MF A04

N94-11321# Eurocopter Deutschland G.m.b.H., Munich (Germany).
SMART MATERIALS FOR HELICOPTER ROTOR ACTIVE CONTROL
H. Strehlow and H. Rapp *In* AGARD, Smart Structures for Aircraft and Spacecraft Apr. 1993 16 p (For primary document see N94-11317 01-24)
Copyright Avail: CASI HC A03/MF A04

N94-11341*# National Aeronautics and Space Administration. Langley Research Center, Hampton, VA.
THE IMPACT OF ACTIVE CONTROLS TECHNOLOGY ON THE STRUCTURAL INTEGRITY OF AERONAUTICAL VEHICLES
Thomas E. Noll, Edward Austin (Army Aviation Research and Technology Activity, Hampton, VA.), Shawn Donley (Naval Air Development Center, Warminster, PA.), George Graham (National Defence Headquarters, Ottawa, Ontario.), Terry Harris (Wright Lab., Wright-Patterson AFB, OH.), Ian Kaynes (Defence Research Agency, Farnborough, England.), Ben Lee (Institute for Aerospace Research, Ottawa, Ontario.), and James Sparrow (Aeronautical Research Labs., Melbourne, Australia.) *In* AGARD, Smart Structures for Aircraft and Spacecraft Apr. 1993 10 p (For primary document see N94-11317 01-24)
Copyright Avail: CASI HC A02/MF A04

N94-11345# Stirling Dynamics Ltd., Bristol (England).
ACTIVE LANDING GEAR CONTROL FOR IMPROVED RIDE QUALITY DURING GROUND ROLL
Tyrone F. Catt, David Cowling (Bristol Univ., England.), and Alan Shepherd *In* AGARD, Smart Structures for Aircraft and Spacecraft Apr. 1993 11 p Sponsored in part by British Aerospace Public Ltd. Co. (For primary document see N94-11317 01-24)
Copyright Avail: CASI HC A03/MF A04

N94-11347# Wright Lab., Wright-Patterson AFB, OH.
MULTIDIMENSIONAL INTELLIGENT CONTROL FOR SUPERLIGHT AIR VEHICLES
Aivars Smitchens, Anthony DeThomas, Kurt Grevstad (Boeing Co., Seattle, WA.), and Doug Moore (Rockwell International Corp., El Segundo, CA.) *In* AGARD, Smart Structures for Aircraft and Spacecraft Apr. 1993 12 p (For primary document see N94-11317 01-24)
Copyright Avail: CASI HC A03/MF A04

N94-12630# Institute of Flow Research, Tokyo (Japan).
IDEA OF UNDERGROUND AIRPLANE [CHICHUU HIKOUKI NO AIDEIA]
Hiroshi Satou *In* NAL, Proceedings of the 9th and 10th NAL Workshop on Investigation and Control of Boundary-Layer Transition Nov. 1992 p 79-81 In JAPANESE (For primary document see N94-12611 01-34)
Avail: CASI HC A01/MF A02

06 AIRCRAFT INSTRUMENTATION

Includes cockpit and cabin display devices; and flight instruments.

For related information see also *19 Spacecraft Instrumentation* and *35 Instrumentation and Photography.*

N94-10664*# Lockheed Engineering and Sciences Co., Houston, TX.
AN ANALYSIS OF THE MODES AND STATES FOR GENERIC AVIONICS
Richard B. Wray Jul. 1993 57 p
(Contract NAS9-17900)
(NASA-CR-188253; NAS 1.26:188253; LESC-30749) Avail: CASI HC A04/MF A01

The objective of this study was to develop a topology for describing the behavior of mission, vehicle and system/substem entities in new flight vehicle designs based on the use of open standards. It also had to define and describe the modes and states which may be used in generic avionics behavioral descriptions, describe their interrelationships, and establish a method for applying generic avionics to actual flight vehicle designs.
Derived from text

07 AIRCRAFT PROPULSION AND POWER

Includes prime propulsion systems and systems components, e.g., gas turbine engines and compressors; and onboard auxilliary power plants for aircraft.

For related information see also *20 Spacecraft Propulsion and Power, 28 Propellants and Fuels,* and *44 Energy Production and Conversion.*

N94-10367# National Aerospace Lab., Kakuda (Japan).
STUDIES ON SCRAMJET NOZZLES. PART 1: PERFORMANCE OF TWO DIMENSIONAL NOZZLES [SUKURAMU JETTO NOZURU NO KENKTUU. SONO 1: NIJIGEN NOZURU NO SEINOU]
Hiroshi Miyajima, Tooru Mitani, Shigeru Satou, Shuuichi Ueda, Kouichirou Tani, Tetsuo Hiraiwa, Katsuhiro Itou, Kazuo Kusaka, Muneo Izumikawa, and Atsushige Tanaka et al Apr. 1992 54 p In JAPANESE
(NAL-TR-1149; JTN-93-80438; DE93-793617) Avail: CASI HC A04/MF A01

A series of experiments was conducted for studying scramjet nozzle performance under Mach 8 flight conditions using high temperature gas flow with Mach 2.5. MonoMethyl Hydrazine (MMH) and Nitrogen TetraOxide (NTO) were adopted to produce high temperature gas flow. The stagnation temperature was designed to be 3,170 K, and the stagnation pressure to be 1 MPa. A simple configuration by plane walls was selected for the scramjet nozzle. Thrust by the scramjet nozzles with expansion ratios of 3 (EN3) and 5 (EN5) was examined. The experiments were performed using a thrust measuring system installed in a high altitude test facility. Delivered specific impulse I(sub sp) by MMH/NTO combustion was found to be 17.3 sec (EN3) to 26.1 sec (EN5). These small increments of I(sub sp) in the scramjet nozzles, however, correspond to I(sub sp) gains of about 1,100 sec for H2 fueled scramjets. Performances of nozzles were predicted using computer codes, and energy release loss, kinetic loss, and two-dimensional loss were identified. The two-dimensional loss was predicted to be 16.5 percent in the EN3 nozzle and to decrease to 7.0 percent in the EN5 nozzle. The kinetic loss due to chemical freezing was found to be 4.4 percent (EN3) and 3.0 percent (EN5). The nozzle performance could be compared with the experimental results. A friction loss (12.4 percent) measured by thrusts suggested laminar flow in the scramjet nozzle used in the MMH/NTO experiments. Measured heat flux on nozzles also supported the laminar boundary layer.
Author (NASDA)

N94-10370# National Aerospace Lab., Tokyo (Japan). Computational Sciences Div.
NUMERICAL CALCULATION OF SCRAMJET INLET FLOW
Tomiko Ishiguro, Satoru Ogawa, and Yasuhiro Wada Jul. 1992 31 p
(NAL-TR-1174T; JTN-93-80447; DE93-793626) Avail: CASI HC A03/MF A01

A numerical procedure to analyze flowfields through and around the Langley-type scramjet engine inlet is proposed. To accurately treat boundary conditions (walls, edges, etc.), all boundaries are mapped onto certain parts of the faces of three rectangular parallelepipeds. A computational space is made by connecting them. The three dimensional full Navier-Stokes equations which include the Baldwin-Lomax algebraic turbulent model are solved by applying the TVD (Total Variation Diminishing) scheme to the uniform mesh points of the space. To exhibit capability of the numerical procedure, parametric studies on flow simulations were carried out by fixing freestream Reynolds number Re = rho(sub infinity) x c(sub infinity) x L/mu(sub infinity) = 5.3 x 10(exp 5) under various trios of a freestream Mach number M(sub infinity), a sweep angle of leading edge of side plate beta and an entrance/throat contraction ratio R (M(sub infinity) approximately equals 2 to 10, beta approximately equals 0 deg to 60 deg, R approximately equals 3 to 10). The influence of the parameters on inlet performances (a mass capture ratio, a total pressure recovery ratio, and possibility of starting) is discussed. The results are in good agreements with the experiments under M(sub infinity) = 4 in starting cases, where iterated reflective oblique shock waves made by wedges of side panels decelerate and compress air. Unstarting phenomenon was analyzed in cases either of low M(sub infinity) or high R. Author (NASDA)

N94-10816*# Purdue Univ., West Lafayette, IN.

DEVELOPMENT OF AN UNSTRUCTURED SOLUTION ADAPTIVE METHOD FOR THE QUASI-THREE-DIMENSIONAL EULER AND NAVIER-STOKES EQUATIONS

Yi-Tsann Jiang Jul. 1993 267 p
(Grant NAG3-1127; RTOP 505-62-10)
(NASA-CR-191161; E-7967; NAS 1.26:191161) Avail: CASI HC A12/MF A03

A general solution adaptive scheme-based on a remeshing technique is developed for solving the two-dimensional and quasi-three-dimensional Euler and Favre-averaged Navier-Stokes equations. The numerical scheme is formulated on an unstructured triangular mesh utilizing an edge-based pointer system which defines the edge connectivity of the mesh structure. Jameson's four-stage hybrid Runge-Kutta scheme is used to march the solution in time. The convergence rate is enhanced through the use of local time stepping and implicit residual averaging. As the solution evolves, the mesh is regenerated adaptively using flow field information. Mesh adaptation parameters are evaluated such that an estimated local numerical error is equally distributed over the whole domain. For inviscid flows, the present approach generates a complete unstructured triangular mesh using the advancing front method. For turbulent flows, the approach combines a local highly stretched structured triangular mesh in the boundary layer region with an unstructured mesh in the remaining regions to efficiently resolve the important flow features. One-equation and two-equation turbulence models are incorporated into the present unstructured approach. Results are presented for a wide range of flow problems including two-dimensional multi-element airfoils, two-dimensional cascades, and quasi-three-dimensional cascades. This approach is shown to gain flow resolution in the refined regions while achieving a great reduction in the computational effort and storage requirements since solution points are not wasted in regions where they are not required. Author (revised)

N94-11022# Advisory Group for Aerospace Research and Development, Neuilly-Sur-Seine (France). Structures and Materials Panel.

A RECOMMENDED METHODOLOGY FOR QUANTIFYING NDE/NDI BASED ON AIRCRAFT ENGINE EXPERIENCE [LE PROJET DE METHODOLOGIE POUR L'EVALUATION DU CONTROLE NON-DESTRUCTIF FONDE SUR L'EXPERIENCE ACQUISE SUR LES MOTEURS D'AVIONS]

Apr. 1993 85 p Lectures held in Ankara, Turkey, 26-27 Apr. 1993, in Lisbon, Portugal, 29-30 Apr. 1993, in Patras, Greece, 4 May 1993, and in Ottawa, Canada, 3-4 Jun. 1993
(AGARD-LS-190; ISBN-92-835-0707-X) Copyright Avail: CASI HC A05/MF A01

Methods to quantify nondestructive inspection (NDI) reliability and capability have been evolving for over twenty-five years. Initial attempts were qualitative rather than quantitative. With the advent of damage tolerance methodologies, it has become imperative to express more accurately probability of detection for a given inspection method and inspection system. This Lecture Series is aimed at providing a methodology to quantify probability of detection. This methodology includes, but is not limited to, design of experiments, specimen generation and maintenance, statistical analyses, data reduction and presentation, evaluation of inspection results in retirement for cause decisions, and the procedure required to establish a reliable probability based inspection for detecting anomalies in engine parts. The material to be presented is applicable to civil as well as military aircraft and turbine engine manufacturing and maintenance organizations. The lectures will examine the detection capabilities of fluorescent penetrant inspection, eddy current, ultrasonic, and magnetic particle inspection. This Lecture Series incorporates lessons learned in the design of experiments to validate nondestructive evaluation (NDE)/NDI systems and in the interpretation of the results of these experiments. Samples of specimens used in NDE/NDI reliability programs will be available for inspection by attendees. The Lecture Series also includes examples to help with the understanding of design of experiments and the statistical modeling for probability of detection analyses. This Lecture Series, sponsored by the Structures and Materials Panel of AGARD, was implemented by the Consultant and Exchange Program. Author (revised)

N94-11205*# National Aeronautics and Space Administration. Hugh L. Dryden Flight Research Facility, Edwards, CA.

PRELIMINARY SUPERSONIC FLIGHT TEST EVALUATION OF PERFORMANCE SEEKING CONTROL

John S. Orme and Glenn B. Gilyard Washington Jun. 1993 20 p Presented at the 29th AIAA/SAE/ASME/ASEE Joint Propulsion Conference, Monterey, CA, 28-30 Jun. 1993
(RTOP 533-02-34)
(NASA-TM-4494; H-1909; NAS 1.15:4494; AIAA Paper 93-1821) Avail: CASI HC A03/MF A01

Digital flight and engine control, powerful onboard computers, and sophisticated controls techniques may improve aircraft performance by maximizing fuel efficiency, maximizing thrust, and extending engine life. An adaptive performance seeking control system for optimizing the quasi-steady state performance of an F-15 aircraft was developed and flight tested. This system has three optimization modes: minimum fuel, maximum thrust, and minimum fan turbine inlet temperature. Tests of the minimum fuel and fan turbine inlet temperature modes were performed at a constant thrust. Supersonic single-engine flight tests of the three modes were conducted using varied after burning power settings. At supersonic conditions, the performance seeking control law optimizes the integrated airframe, inlet, and engine. At subsonic conditions, only the engine is optimized. Supersonic flight tests showed improvements in thrust of 9 percent, increases in fuel savings of 8 percent, and reductions of up to 85 deg R in turbine temperatures for all three modes. The supersonic performance seeking control structure is described and preliminary results of supersonic performance seeking control tests are given. These findings have implications for improving performance of civilian and military aircraft. Author (revised)

N94-11234*# National Aeronautics and Space Administration. Lewis Research Center, Cleveland, OH.

APPLICATION OF JET-SHEAR-LAYER MIXING AND EFFERVESCENT ATOMIZATION TO THE DEVELOPMENT OF A LOW-NO(x) COMBUSTOR Ph.D. Thesis - Purdue Univ.

Renato Olaf Colantonio Jun. 1993 72 p
(RTOP 535-05-10)
(NASA-TM-105888; E-7353; NAS 1.15:105888) Avail: CASI HC A04/MF A01

An investigation was conducted to develop appropriate technologies for a low-NO(x), liquid-fueled combustor. The combustor incorporates an effervescent atomizer used to inject fuel into a premixing duct. Only a fraction of the combustion air is used in the premixing process to avoid autoignition and flashback problems. This fuel-rich mixture is introduced into the remaining combustion air by a rapid jet-shear-layer-mixing process involving radial fuel-air jets impinging on axial air jets in the primary combustion zone. Computational analysis was used to provide a better understanding of the fluid dynamics that occur in jet-shear-layer mixing and to facilitate a parametric analysis appropriate to the design of an optimum low-NO(x) combustor. A number of combustor configurations were studied to assess the key combustor technologies and to validate the modeling code. The results from the experimental testing and computational analysis indicate a low-NO(x) potential for the jet-shear-layer combustor. Key parameters found to affect NO(x) emissions are the primary combustion zone fuel-air ratio, the number of axial and radial jets, the aspect ratio and radial location of the axial air jets, and the radial jet inlet hole diameter. Each of these key parameters exhibits a low-NO(x) point from which an optimized combustor was developed. Using the parametric analysis, NO(x) emissions were reduced by a factor of 3 as compared with the emissions from conventional, liquid-fueled combustors operating at cruise conditions. Further development promises even lower NO(x) with high combustion efficiency. Author (revised)

N94-11238*# National Aeronautics and Space Administration. Lewis Research Center, Cleveland, OH.

ON THE COMBUSTION OF A LAMINAR SPRAY

Yeshayahou Levy (Technion - Israel Inst. of Tech., Haifa.) and Daniel L. Bulzan Jul. 1993 24 p Presented at the Fifth International Conference on Liquid Atomization and Spray System, Gaithersburg, MD, 15-18 Jul. 1991 Original contains color illustrations

(RTOP 505-62-11)
(NASA-TM-106210; E-7920; NAS 1.15:106210) Avail: CASI HC
A03/MF A01; 5 functional color pages

A spray combustor, with flow velocities in the laminar range, exhibits a unique operating mode where large amplitude, self-induced oscillations of the flame shape occur. The phenomenon, not previously encountered, only occurs when fuel is supplied in the form of fine liquid droplets and does not occur when fuel is supplied in gaseous form. Several flow mechanisms are coupled in such a fashion as to trigger and maintain the oscillatory motion of the flame. These mechanisms include heat transfer and evaporation processes, dynamics of two-phase flows, and effects of gravity (buoyancy forces). An interface volume, lying above the fuel nozzle and below the flame was found to be the most susceptible to gravity effects and postulated to be responsible for inducing the oscillatory motion. Heptane fuel was used in the majority of the tests. Tests performed with iso-octane also showed similar results. Author (revised)

N94-11255*# National Aeronautics and Space Administration. Lewis Research Center, Cleveland, OH.
A COMPARISON BETWEEN NUMERICALLY MODELLED AND EXPERIMENTALLY MEASURED LOSS MECHANISMS IN WAVE ROTORS
Daniel E. Paxson Jun. 1993 13 p Presented at the 29th Joint Propulsion Conference and Exhibit, Monterey, CA, 28-20 Jun. 1993; sponsored by AIAA, SAE, ASME, and ASEE
(RTOP 505-62-50)
(NASA-TM-106279; AIAA Paper 93-2522; E-8018; NAS 1.15:106279)
Avail: CASI HC A03/MF A01

A numerical model has been developed which is capable of predicting the performance of a wave rotor (pressure exchanger) of specified geometry over a wide range of operating conditions. The model can account for the major loss mechanisms of leakage from the tube ends, fluid viscosity, heat transfer to the tube walls, finite tube opening time, shock waves, and non-uniform port flows. It is a one dimensional flow model which follows a single tube as it rotates past the various stationary ports. Since the model is relatively simple (i.e. one dimensional) it uses little computer time. This makes it suitable for design as well as analytical purposes. This paper will present a brief description of the model then discuss a comparison between the model predictions and several wave rotor experiments. Author (revised)

N94-12270*# United Technologies Corp., West Palm Beach, FL. Pratt and Whitney.
ADVANCED CONTROL FOR AIRBREATHING ENGINES, VOLUME 1: PRATT AND WHITNEY
J. A. Ralph Jul. 1993 83 p
(Contract NAS3-25952; RTOP 505-62-61)
(NASA-CR-189203; E-8006; NAS 1.26:189203) Avail: CASI HC
A05/MF A01

The application of advanced control concepts to air breathing engines may yield significant improvements in aircraft/engine performance and operability. Screening studies of advanced control concepts for air breathing engines were conducted by three major domestic aircraft engine manufacturers to determine the potential impact of concepts on turbine engine performance and operability. The purpose of the studies was to identify concepts which offered high potential yet may incur high research and development risk. A target suite of proposed advanced control concepts was formulated and evaluated in a two phase study to quantify each concept's impact on desired engine characteristics. To aid in the evaluation specific aircraft/engine combinations were considered: a Military High Performance Fighter mission, a High Speed Civil Transport mission, and a Civil Tiltrotor mission. Each of the advanced control concepts considered in the study are defined and described. The concept potential impact on engine performance was determined. Relevant figures of merit on which to evaluate the concepts are determined. Finally, the concepts are ranked with respect to the target aircraft/engine missions. A final report describing the screening studies was prepared by each engine manufacturer. Volume 1 of these reports describes the studies performed by Pratt & Whitney. Author (revised)

N94-12271*# General Electric Co., Cincinnati, OH. Aircraft Engines.
ADVANCED CONTROL FOR AIRBREATHING ENGINES, VOLUME 2: GENERAL ELECTRIC AIRCRAFT ENGINES
Indar Bansal Jul. 1993 112 p
(Contract NAS3-25951; RTOP 505-62-41)
(NASA-CR-189204; E-8005; NAS 1.26:189204) Avail: CASI HC
A06/MF A02

The application of advanced control concepts to air breathing engines may yield significant improvements in aircraft/engine performance and operability. Screening studies of advanced control concepts for air breathing engines were conducted by three major domestic aircraft engine manufacturers to determine the potential impact of concepts on turbine engine performance and operability. The purpose of the studies was to identify concepts which offered high potential yet may incur high research and development risk. A target suite of proposed advanced control concepts was formulated and evaluated in a two phase study to quantify each concept's impact on desired engine characteristics. To aid in the evaluation specific aircraft/engine combinations were considered: a Military High Performance Fighter mission, a High Speed Civil Transport mission, and a Civil Tiltrotor mission. Each of the advanced control concepts considered in the study are defined and described. The concept potential impact on engine performance was determined. Relevant figures of merit on which to evaluate the concepts are determined. Finally, the concepts are ranked with respect to the target aircraft/engine missions. A final report describing the screening studies was prepared by each engine manufacturer. Volume 2 of these reports describes the studies performed by GE Aircraft Engines. Author (revised)

N94-12272*# General Motors Corp., Indianapolis, IN. Allison Gas Turbine Div.
ADVANCED CONTROLS FOR AIRBREATHING ENGINES, VOLUME 3: ALLISON GAS TURBINE
R. M. Bough Jul. 1993 43 p
(Contract NAS3-25459; RTOP 505-62-41)
(NASA-CR-189205; E-8007; NAS 1.26:189205) Avail: CASI HC
A03/MF A01

The application of advanced control concepts to airbreathing engines may yield significant improvements in aircraft/engine performance and operability. Screening studies of advanced control concepts for airbreathing engines were conducted by three major domestic aircraft engine manufacturers to determine the potential impact of concepts on turbine engine performance and operability. The purpose of the studies was to identify concepts which offered high potential yet may incur high research and development risk. A target suite of proposed advanced control concepts was formulated and evaluated in a two-phase study to quantify each concept's impact on desired engine characteristics. To aid in the evaluation specific aircraft/engine combinations were considered: a Military High Performance Fighter mission, a High Speed Civil Transport mission, and a Civil Tiltrotor mission. Each of the advanced control concepts considered in the study are defined and described. The concept potential impact on engine performance was determined. Relevant figures of merit on which to evaluate the concepts are determined. Finally, the concepts are ranked with respect to the target aircraft/engine missions. A final report describing the screening studies was prepared by each engine manufacturer. Volume 3 of these reports describes the studies performed by the Allison Gas Turbine Division. Author (revised)

N94-12274# Army Cold Regions Research and Engineering Lab., Hanover, NH.
ICING OF TURBINE INTAKE LOUVERS Special Report
Michael R. Walsh, Donald E. Garfield, James S. Morse, Kurt V. Knuth, and Nathan D. Mulherin Apr. 1993 43 p
(AD-A265714; CRREL-SR-93-4) Avail: CASI HC A03/MF A01

Superstructure icing is a phenomenon that can have debilitating effects on the operation of any ship. When designing ships that will operate in environments where icing may occur, careful consideration must be given to minimizing the accumulation and effect of superstructure icing. Such consideration was given to the U.S. Navy DDG-51-class destroyer when new turbine intake louvers were proposed. To ensure that sufficient air would be available to the vessel's gas turbines and ventilation system during an icing event, the Navy asked the U.S. Army Cold Regions Research and Engineering Laboratory (CRREL), through Advanced Marine Enterprises, Inc., (AME) of Arlington, Virginia, to conduct a series of comparative icing tests between standard intake louvers and a new louver design. DTIC

N94-10425# Alenia Aeronautica, Torino (Italy).
NUMERICAL SIMULATION OF THE FLOW THROUGH A SCRAMJET ENGINE
V. Selmin *In* AGARD, Theoretical and Experimental Methods in Hypersonic Flows Apr. 1993 13 p (For primary document see N94-10421 01-02)
Copyright Avail: CASI HC A03/MF A04

08 AIRCRAFT STABILITY AND CONTROL

Includes aircraft handling qualities; piloting; flight controls; and autopilots.

For related information see also *05 Aircraft Design, Testing and Performance.*

N94-10734# National Aerospace Lab., Tokyo (Japan). Flight Research Div.
IN-FLIGHT SIMULATION OF BACKSIDE OPERATING MODELS USING DIRECT LIFT CONTROLLER [DLC WO MOCHIITA BAKKUSAIDO MODERU NO IN FURAITO SHIMYURESHON]
Yuukichi Tsukano and Toshiharu Inagaki Apr. 1992 18 p In JAPANESE
(NAL-TR-1152; JTN-93-80433; DE93-767976) Avail: CASI HC A03/MF A01

Effectiveness of a Direct Lift Controller (DLC) for in-flight simulation is discussed. A DLC device has been shown to be indispensable for in-flight simulation of backside operating models, hence quick-moving flaps were installed on the Variable Stability and Response Airplane (VSRA) of the National Aerospace Laboratory (NAL) of Japan. After tailoring feedback and feed-forward gains, a model-following system was constructed to simulate backside operating mother aircraft. Flight verification test results are included and indicate that a DLC is helpful but not required for simulating frontside operating models, whereas it is mandatory to obtain acceptable model following errors necessary to simulate backside operating models. Flight test results for a simulated landing approach in the backside region are also presented. Author (NASDA)

N94-10895*# Purdue Univ., West Lafayette, IN. School of Aeronautics and Astronautics.
A FEASIBILITY STUDY REGARDING THE ADDITION OF A FIFTH CONTROL TO A ROTORCRAFT IN-FLIGHT SIMULATOR Final Report, 1 Jun. 1990 - 31 May 1991
Simon Turner and Dominick Andrisani, II Jul. 1992 143 p
(Contract NCC2-671)
(NASA-CR-193240; NAS 1.26:193240) Avail: CASI HC A07/MF A02

The addition of a large movable horizontal tail surface to the control system of a rotorcraft in-flight simulator being developed from a Sikorsky UH-60A Black Hawk Helicopter is evaluated. The capabilities of the control surface as a trim control and as an active control are explored. The helicopter dynamics are modeled using the Generic Helicopter simulation program developed by Sikorsky Aircraft. The effect of the horizontal tail on the helicopter trim envelope is examined by plotting trim maps of the aircraft attitude and controls as a function of the flight speed and horizontal tail incidence. The control power of the tail surface relative to that of the other controls is examined by comparing control derivatives extracted from the simulation program over the flight speed envelope. The horizontal tail's contribution as an active control is evaluated using an explicit model following control synthesis involving a linear model of the helicopter in steady, level flight at a flight speed of eighty knots. The horizontal tail is found to provide additional control flexibility in the longitudinal axis. As a trim control, it provides effective control of the trim pitch attitude at mid to high forward speeds. As an active control, the horizontal tail provides useful pitching moment generating capabilities at mid to high forward speeds. Author (revised)

N94-11134*# National Aeronautics and Space Administration. Ames Research Center, Moffett Field, CA.
CRITERIA FOR DESIGN OF INTEGRATED FLIGHT/PROPULSION CONTROL SYSTEMS FOR STOVL FIGHTER AIRCRAFT
James A. Franklin Apr. 1993 34 p Sponsored by NASA. Washington
(RTOP 533-02-37)
(NASA-TP-3356; A-93038; NAS 1.60:3356) Avail: CASI HC A03/MF A01

As part of NASA's program to develop technology for short takeoff and vertical landing (STOVL) fighter aircraft, control system designs have been developed for a conceptual STOVL aircraft. This aircraft is representative of the class of mixed-flow remote-lift concepts that was identified as the preferred design approach by the U.S./U.K. STOVL Joint Assessment and Ranking Team. The control system designs have been evaluated throughout the powered-lift flight envelope on the Vertical Motion Simulator (VMS) at Ames Research Center. Items assessed in the control system evaluation were: maximum control power used in transition and vertical flight, control system dynamic response associated with thrust transfer for attitude control, thrust margin in the presence of ground effect and hot-gas ingestion, and dynamic thrust response for the engine core. Effects of wind, turbulence, and ship airwake disturbances are incorporated in the evaluation. Results provide the basis for a reassessment of existing flying-qualities design criteria applied to STOVL aircraft. Author

N94-11251*# National Aeronautics and Space Administration. Lewis Research Center, Cleveland, OH.
APPLICATION OF CONTROLLER PARTITIONING OPTIMIZATION PROCEDURE TO INTEGRATED FLIGHT/PROPULSION CONTROL DESIGN FOR A STOVL AIRCRAFT
Sanjay Garg and Phillip H. Schmidt (Akron Univ., OH.) Jul. 1993 11 p Prepared for presentation at the AIAA Guidance, Navigation, and Control Conference, Monterey, CA, 9-11 Aug. 1993; sponsored by AIAA
(RTOP 505-62-50)
(NASA-TM-106265; AIAA Paper 93-3766; E-7992; NAS 1.15:106265)
Avail: CASI HC A03/MF A01

A parameter optimization framework has earlier been developed to solve the problem of partitioning a centralized controller into a decentralized, hierarchical structure suitable for integrated flight/propulsion control implementation. This paper presents results from the application of the controller partitioning optimization procedure to IFPC design for a Short Take-Off and Vertical Landing (STOVL) aircraft in transition flight. The controller partitioning problem and the parameter optimization algorithm are briefly described. Insight is provided into choosing various 'user' selected parameters in the optimization cost function such that the resulting optimized subcontrollers will meet the characteristics of the centralized controller that are crucial to achieving the desired closed-loop performance and robustness, while maintaining the desired subcontroller structure constraints that are crucial for IFPC implementation. The optimization procedure is shown to improve upon the initial partitioned subcontrollers and lead to performance comparable to that achieved with the centralized controller. This application also provides insight into the issues that should be addressed at the centralized control design level in order to obtain implementable partitioned subcontrollers. Author (revised)

N94-11259*# National Aeronautics and Space Administration. Ames Research Center, Moffett Field, CA.
MOVING-BASE SIMULATION EVALUATION OF THRUST MARGINS FOR VERTICAL LANDING FOR THE NASA YAV-8B HARRIER AIRCRAFT
James A. Franklin and Michael W. Stortz Mar. 1993 26 p
(RTOP 505-59-36)
(NASA-TM-104008; A-93051; NAS 1.15:104008) Avail: CASI HC A03/MF A01

A simulation experiment was conducted on Ames Research Center's Vertical Motion Simulator to evaluate the thrust margin for vertical landing required for the YAV-8B Harrier. Two different levels of ground effect were employed, representing the aircraft with or without lift improvement devices installed. In addition, two different inlet temperature profiles were included to cover a wide range of hot gas ingestion. For each ground effect and hot gas ingestion variant, vertical landings were performed at successively heavier weights, with the pilot assessing the acceptability of the operation in each case. Results are presented as a function of hover weight ratio and a metric of the mean ground effect and ingestion that reflect the increase in thrust margin required to provide acceptable control of sink rate during the descent to touchdown with increasing suck down and hot gas ingestion. Author (revised)

N94-11489# Advisory Group for Aerospace Research and Development, Neuilly-Sur-Seine (France). Guidance and Control Panel.
STABILITY IN AEROSPACE SYSTEMS [LA STABILITE DANS LES SYSTEMES AEROSPATIAUX]
Feb. 1993 233 p Workshop held in Toulouse, France, 23-25 Jun. 1992
(AGARD-R-789; ISBN-92-835-0702-9) Copyright Avail: CASI HC A11/MF A03

This volume contains the 18 unclassified papers presented at the Guidance and Control Panel Workshop. The presented papers cover topics under the following headings: fundamental aspects of stability with examples; basic theoretical aspects and chaos; and applications of aerospace techniques. For individual titles, see N94-11490 through N94-11504.

N94-11490# GEC Hirst Research Centre, Wembley (England). Long Range Research Lab.
CHAOTIC TIME SERIES ANALYSIS **c70**
Jaroslav Stark *In* AGARD, Stability in Aerospace Systems Feb. 1993 11 p (For primary document see N94-11489 01-08)
Copyright Avail: CASI HC A03/MF A03

This paper begins with a brief description of the basic theoretical framework for analyzing chaotic time series and then goes on to discuss recent work in this area in the Long Range Research Laboratory. As a particular example, we shall show how the ability to make short term predictions of chaotic time series can be used to extract small signals from a complex deterministic background. Experiments with simulated data have shown that it is possible to recover signals to a reasonable accuracy in situations where the ratio of amplitudes of signal to chaotic background is as low as 10(exp -5):1. Derived from text

N94-11491# Universite Catholique de Louvain (Belgium).
STABILITY ANALYSIS AND AEROSPACE VEHICLE DYNAMICS
Pierre Y. Willems *In* AGARD, Stability in Aerospace Systems Feb. 1993 10 p Sponsored by Belgian State Science Policy Programming Office (For primary document see N94-11489 01-08)
Copyright Avail: CASI HC A02/MF A03

This paper presents stability analysis results which can be used to analyze the behavior of aerospace vehicles. A certain number of definitions are recalled. Liapunov stability criteria are given for autonomous systems described by ordinary differential equations and discrete-time equations. Particular attention is paid to the stability of mechanical systems around equilibrium configurations. Derived from text

N94-11492# Max-Planck-Inst. fuer Aeronomie, Katlenburg-Lindau (Germany).
ON NON-LINEAR LONGITUDINAL STABILITY OF AN AIRCRAFT IN A DIVE IN THE PRESENCE OF ATMOSPHERIC DISTURBANCES
L. M. B. C. Campos (Instituto Superior Tecnico, Lisbon, Portugal.) and A. A. Fonseca (Instituto Superior Tecnico, Lisbon, Portugal.) *In* AGARD, Stability in Aerospace Systems Feb. 1993 19 p (For primary document see N94-11489 01-08)
Copyright Avail: CASI HC A03/MF A03

We consider the nonlinear longitudinal stability problem of aircraft starting a dive from an initial velocity far removed from the steady dive speeds: the aim is to find a pitch control law, which will keep the aircraft in a constant glide slope, compensating for the phugoid mode. The problem is extended to account for the presence of arbitrary atmospheric winds, e.g., windshears. The theoretical stability curves are compared with flight test data, obtained using the BAFR (Basic aircraft for flight research) in Portugal. The model includes a number of effects, and has also some restrictions, which do not affect its suitability for the present application: (1) it includes compensation of the phugoid, but not short-period, mode i.e., neglects rotational inertia; (2) it accounts for boundary-layer and induced drag, but not wave drag, i.e., applies at low Mach numbers, typical of approach to land; (3) it neglects lateral motion, but allows for non-linear effects on longitudinal motion; and (4) it leads to a free-flying control law, in stall free conditions, and in the absence of autopilot or active control. These additional effects would be relevant to other applications, and would require extension or modification of the present model. Derived from text

N94-11493# Universite Catholique de Louvain (Belgium). Mecanique Appliquee.
STABILITY OF VISCOELASTIC FLOW: PHYSICAL AND NUMERICAL CONSIDERATIONS **c34**
M. J. Crochet and C. Bodart *In* AGARD, Stability in Aerospace Systems Feb. 1993 16 p (For primary document see N94-11489 01-08)
Copyright Avail: CASI HC A03/MF A03

The topics are presented in viewgraph form and include the following: viscoelastic flow; numerical difficulties -- the high Weissenberg number problem; efficient algorithms for smooth problems; efficient algorithms for singular problems; experimental evidence of instability; numerical procedure for verifying stability; and numerical results. CASI

N94-11494*# Cornell Univ., Ithaca, NY.
DYNAMICS AND CONTROL OF COHERENT STRUCTURES IN THE TURBULENT WALL LAYER: AN OVERVIEW
Gal Berkooz, Philip Holmes, and John Lumley *In* AGARD, Stability in Aerospace Systems Feb. 1993 5 p Sponsored by NASA. Langley Research Center; AFOSR; ONR; and NSF (For primary document see N94-11489 01-08)
Copyright Avail: CASI HC A01/MF A03

We expand the velocity field in the vicinity of the wall in empirical eigenfunctions obtained from experiment. Truncating our system and using Galerkin projection, we obtain a closed set of non-linear ordinary differential equations with ten degrees of freedom. We find a rich dynamical behavior, including in particular a heteroclinic attracting orbit giving rise to intermittency. The intermittent jump from one attracting point to the other resembles in many respects the bursts observed in experiments. Specifically, the time between jumps and the duration of the jumps, is approximately that observed in a burst; the jump begins with the formation of a narrowed and intensified updraft, like the ejection phase of a burst, and is followed by a gentle, diffuse downdraft like the sweep phase of a burst. The magnitude of the Reynolds stress spike produced during a burst is limited by our truncation. The behavior is quite robust, much of it being due to the symmetries present (Aubry's group has examined dimensions up to 128 with persistence of the global behavior). We have examined eigenvalues and coefficients obtained from experiment, and from exact simulation, which differ in magnitude. Similar behavior is obtained in both cases; in the latter case, the heteroclinic orbits connect limit cycles instead of fixed points, corresponding to cross-stream waving of the streamwise rolls. The bifurcation diagram remains structurally similar, but somewhat distorted. The role of the pressure term is made clear - it triggers the intermittent jumps, which otherwise would occur at longer and longer intervals, as the system trajectory is attracted closer and closer to the heteroclinic cycle. The pressure term results in the jumps occurring at essentially random times, and the magnitude of the signal determines the average timing. Stretching of the wall region shows that the model is consistent with observations of polymer drag reduction. Change of the third order coefficients, corresponding to acceleration or deceleration of the mean flow, changes the heteroclinic cycles from attracting to repelling, increasing or decreasing the stability, in agreement with observations. The existence of fixed points is an artifact introduced by the projection; however, a decoupled model still displays the rich dynamics. Numerous assumptions made in Aubry et al. (1988) can now be proved exactly. Feeding back eigenfuncitons with the proper phase can delay the bursting, (the heteroclinic jump to the other fixed point), decreasing the drag. It is also possible to speed up the bursting, increasing mixing to control separation. Our approach is optimal for short time tracking in control. Author

N94-11495# Office National d'Etudes et de Recherches Aerospatiales, Paris (France). Directiondes Etudes de Synthese.
CHAOS, ENTROPY, AND REVERSIBILITY: A SIMPLE EXAMPLE **c70**
C. Marchal *In* AGARD, Stability in Aerospace Systems Feb. 1993 3 p (For primary document see N94-11489 01-08)
Copyright Avail: CASI HC A01/MF A03

The contradiction between mathematical reversibility and physical irreversibility has traditionally led to the suspicion of 'hidden correlations' that will allow, in some cases, the decrease of the entropy of isolated systems. This idea seems wrong, as shown by a very simplified model. The true reason of the physical irreversibility is certainly the very large number of parameters of irreversible systems. Derived from text

N94-11496# Office National d'Etudes et de Recherches Aerospatiales, Paris (France).

NONLINEAR AND DYNAMIC ANALYSIS OF FLIGHT [ANALYSE NON LINEAIRE ET DYNAMIQUE DU VOL]

P. Guicheteau *In* AGARD, Stability in Aerospace Systems Feb. 1993 12 p In FRENCH (For primary document see N94-11489 01-08)

Copyright Avail: CASI HC A03/MF A03

In a rigorous manner, aircraft motion can be described by a set of nonlinear differential equations, depending of parameters, associating the state vector (angle of attack, sideslip angle, speed ...) with the control vector (motivators) through flight dynamics equations, aerodynamic aircraft model, and flight control system. The communication presents some works which aim at a better understanding and at the precise prediction of aircraft behavior in particular flight phases for which classical linearized analysis of differential equations is insufficient or not valid. Author

N94-11497# Wright Lab., Wright-Patterson AFB, OH.

DECOUPLING OF AIRCRAFT RESPONSES

David J. Moorhouse *In* AGARD, Stability in Aerospace Systems Feb. 1993 9 p (For primary document see N94-11489 01-08)

Copyright Avail: CASI HC A02/MF A03

The theory of aircraft stability is at least as old as powered flight. The original impetus was to design the configuration to have acceptable characteristics. Flight control technology was next applied to tailor, i.e. improve, the classical response characteristics: a yaw damper being a simple example. More recent flight control technology has provided the means to change the character of the aircraft response so that it no longer exhibits the classical behavior of a short period, a phugoid, a Dutch roll, a roll mode, and a spiral. With additional control effectors and the use of feedback there is an infinite number of ways to change the basic stability and response characteristics. Pilot preferences are also well established, however, so that care is needed in implementing any theoretical improvements. The technology exists to provide the pilot with the capability to individually control all six degrees of freedom. Obviously, a requirement for a pilot to integrate six different control effectors would be likely to increase his workload. In that sense, decoupling all six axes would be detrimental. Conversely, any unwanted coupling that can be eliminated should reduce the pilot task. The Wright Laboratory has had a series of flight demonstration programs that have evaluated new technologies in the most realistic tasks. First, an F-16 was provided with the additional control effectors to allow independent control of all six degrees of freedom. A variety of control modes was mechanized, so that the pilot could evaluate both coupled and decoupled modes. Following a subjective in-flight assessment, a ground-based piloted simulation experiment was performed to evaluate all modes for both offensive and defensive combat use. Second, an F-15 was modified to facilitate precise landing in adverse conditions. A special short landing mode was implemented to feature decoupling of airspeed and glideslope responses plus the integrated coupling of direct lift and sideforce control. This paper presents results from both these programs to illustrate the benefits of either decoupling or new coupling of aircraft responses. Derived from text

N94-11498# Centre d'Etudes et de Recherches, Toulouse (France). Aerothermodynamics Dept.

BOUNDARY LAYER TRANSITION: PREDICTION AND WIND TUNNEL SIMULATION **c34**

D. Arnal *In* AGARD, Stability in Aerospace Systems Feb. 1993 12 p (For primary document see N94-11489 01-08)

Copyright Avail: CASI HC A03/MF A03

This paper gives a survey of theoretical and experimental results related to the problem of boundary layer transition; emphasis is given on applications of practical prediction methods. In the first part of the paper, it is shown that the linear stability theory can provide a good estimate of the transition location if the free stream disturbance level is low enough; the difficulties to properly simulate free flight conditions in ground facilities is underlined. The second part of the paper is devoted to the problem of boundary layer tripping in the presence of large external disturbances; in this case, the linear theory no longer applies and empirical criteria need to be developed. Derived from text

N94-11499# Wright Lab., Wright-Patterson AFB, OH.

MODELING NONLINEAR AERODYNAMIC LOADS FOR AIRCRAFT STABILITY AND CONTROL ANALYSIS

Jerry E. Jenkins and James H. Myatt *In* AGARD, Stability in Aerospace Systems Feb. 1993 10 p Sponsored by AFOSR and Dept. of National Defence (For primary document see N94-11489 01-08)

Copyright Avail: CASI HC A02/MF A03

Results from systematic wind tunnel tests of the dynamic roll behavior of a 65 degree swept delta wing at moderate (15 to 35 degree) angles of attack are reviewed. These tests, conducted in both the IAR 2 x 3 m low-speed wind tunnel and the 7 x 10 ft SARL facility at WPAFB, included static, forced oscillation and free-to-roll experiments with flow visualization. Multiple stable trim points (attractors) for body-axis rolling motions and other hard-to-explain dynamic behavior were observed. These data are examined in light of the nonlinear indicial response theory advanced by Tobak and his colleagues. The current analysis shows that force and moment, free-to-roll motion, and flow visualization data all confirm the existence of 'critical states' with respect to the static roll angle. When these singularities are encountered in a dynamic situation, large and persistent transients are induced. Conventional means of representing the nonlinear force and moments in the equations of motion are shown to be inadequate in these cases. Alternative approaches based on simplification of the nonlinear indicial model are briefly discussed. Derived from text

N94-11500# Technische Univ., Brunswick (Germany). Inst. fuer Flugfuehrung.

STABILITY MODEL OF THE ATMOSPHERE **c46**

Andreas Knueppel, Daniel Martens, and Andreas Siemer (Technische Univ., Hamburg, Germany.) *In* AGARD, Stability in Aerospace Systems Feb. 1993 17 p (For primary document see N94-11489 01-08)

Copyright Avail: CASI HC A03/MF A03

The atmosphere of the earth is a very complex system covering a wide range of interacting scales. The concept of stability is applied to subsystems thereof where the quantities involved in a stability analysis depend on the particular question to be answered. But all stability considerations share a common basic structure. After giving a short account to the nature of stability investigations, some examples of stability related atmospheric phenomena are presented which are relevant for flight operation. Finally, the impact of atmospheric instability on aircraft performance with special regard to flight safety is illustrated. Author

N94-11501# Air Force Inst. of Tech., Wright-Patterson AFB, OH.

UTILIZING QUANTITATIVE FEEDBACK THEORY DESIGN TECHNIQUE FOR FLIGHT CONTROL SYSTEM

Constantine H. Houpis *In* AGARD, Stability in Aerospace Systems Feb. 1993 10 p (For primary document see N94-11489 01-08)

Copyright Avail: CASI HC A02/MF A03

Quantitative feedback theory (QFT) has achieved the status as a very powerful design technique for the achievement of assigned performance tolerances over specific ranges of plant uncertainties without and with control effector failures. This paper presents a brief overview of QFT and its applications to advanced multi-input multi-output (MIMO) flight control systems. Desired performance over varied flight conditions may be achieved with fixed compensators (controllers), despite failures of effectors. QFT is the only design technique that has been able to make considerable progress in improving the design of an overall flight control system taking into account the man-in-the-loop specifications. Author

N94-11502# State Univ. of New York, Binghamton. Dept. of Electrical Engineering.

ADAPTIVE RECONFIGURABLE FLIGHT CONTROLS FOR HIGH ANGLE OF ATTACK AIRCRAFT AGILITY

T. Sadeghi, M. Tascillo, A. Simons, and K. Lai *In* AGARD, Stability in Aerospace Systems Feb. 1993 13 p (For primary document see N94-11489 01-08)

Copyright Avail: CASI HC A03/MF A03

Two control technologies have been developed and integrated towards the definition of an Integrated Flight Control for the year 2000 (IFC2000) aircraft. The control technologies considered for IFC2000 are flight control reconfiguration and post stall maneuvering. The reconfiguration technique allows an aircraft to utilize the inherent redundancy among its control effectors for maintaining aircraft's controllability after loss (or degradation in effectiveness) of one or more of its control effectors. The reconfiguration technique used in this paper consisted of redistribution of control signals after identification of a control effector failure (first stage adaptation). This technique is based on utilizing a pseudo-inverse algorithm and minimizing a performance index to redistribute pilot's commands to the remaining control effectors. Two control laws were developed for controlling the aircraft in the post stall region where the aircraft is flying at high angle of attack (HAOA) while allowing reconfiguration in the event of surface damage or actuator failure. A self-tuning adaptive control law was developed for parameter estimation and control gain tuning (second stage adaptation). The control law utilizes the Bierman's algorithm for estimating aircraft parameters, and a linear quadratic regulator for tuning the gains. A neural net control law was developed to account for nonlinearity, parameter uncertainties, and disturbances in the flight control system. The reconfiguration, adaptive, and neural net control laws have been partially integrated; the results are reported in this paper. Post-stall maneuvering is configuration sensitive requiring a high performance aircraft with relaxed static stability, thrust vectoring, and/or additional surfaces (such as canard). A generic high performance aircraft model was modified to incorporate thrust vectoring for generating pitch and yaw moments. A control structure was developed to fly the aircraft with high angle of attack at low speed. The control structure can track alpha, phi, and beta commands from pilot's longitudinal and lateral sticks and rudder pedal, respectively. The control laws were designed to give steady state tracking for fuselage pointing. Thrust vectoring was used to produce pitch and yaw moments at HAOA. The control signal distribution function of the control laws was modified to facilitate aircraft transition from and to post-stall region. Author

N94-11503*# Princeton Univ., NJ. Dept. of Mechanical and Aerospace Engineering.

TOWARD INTELLIGENT FLIGHT CONTROL

Robert F. Stengel *In* AGARD, Stability in Aerospace Systems Feb. 1993 22 p Sponsored in part by FAA (For primary document see N94-11489 01-08)
(Contract NGL-31-001-252; DAAL03-89-K-0092)
Copyright Avail: CASI HC A03/MF A03

Flight control systems can benefit by being designed to emulate functions of natural intelligence. Intelligent control functions fall in three categories: declarative, procedural, and reflexive. Declarative actions involve decision-making, providing models for system monitoring, goal planning, and system/scenario identification. Procedural actions concern skilled behavior and have parallels in guidance, navigation, and adaptation. Reflexive actions are more-or-less spontaneous and are similar to inner-loop control and estimation. Intelligent flight control systems will contain a hierarchy of expert systems, procedural algorithms, and computational neural networks, each expanding on prior functions to improve mission capability to increase the reliability and safety of flight and to ease pilot workload. Author

N94-11504# Wright Lab., Wright-Patterson AFB, OH.

X-29: LONGITUDINAL INSTABILITY AT HIGH ANGLE-OF-ATTACK

Lawrence A. Walchli *In* AGARD, Stability in Aerospace Systems Feb. 1993 13 p (For primary document see N94-11489 01-08)
Copyright Avail: CASI HC A03/MF A03

Relaxed static stability (RSS) was chosen as one of the primary technologies to be flight demonstrated on the forward swept wing X-29 aircraft. Development experiences and performance benefits of this technology in the high angle-of-attack (AOA) regime of flight are described. Flight test results validate the X-29's wind tunnel database and the updated piloted simulation is used for parameter variations to thoroughly explore the potential performance of an aircraft with high levels of static instability. Author

N94-12769*# Technion Research and Development Foundation Ltd., Haifa (Israel). Dept. of Project Promotion and R/D Administration.

IMPROVEMENT OF METHOD FOR EXPERIMENTAL DETERMINATION OF FLUTTER SPEED BY PARAMETER IDENTIFICATION Final Report

E. Nissim 5 Aug. 1993 7 p
(Grant NAGw-3201)
(NASA-CR-193555; NAS 1.26:193555) Avail: CASI HC A02/MF A01

The method investigated in the current research work is based on the identification of the equations of motion during test flights, followed by the solution of these identified equations to numerically compute the flutter dynamic pressure. The current research work is aimed at overcoming two main difficulties which arise when: (1) A continuous system is truncated into a system with a finite number of degrees of freedom. (2) The desired range of frequencies is wide; in the latter case, numerical difficulties occur that can only partly be overcome by giving relatively more weight to the high frequency modes. Results pertaining to the above first point will be presented under section entitled 'Truncation Effects', and results pertaining to the above second point will be presented under section entitled 'Frequency Range Effects'. The numerical example used herein consists of a continuous simply supported beam. It is further assumed that the object of the identification procedure is to identify the beam's first seven modes. Derived from text

N94-10424# Messerschmitt-Boelkow-Blohm G.m.b.H., Munich (Germany).

EXPERIMENTAL RESULTS IN AERODYNAMIC STABILITY AND CONTROL OF A TSTO CONFIGURATION

T. Gottmann and G. Cucinelli *In* AGARD, Theoretical and Experimental Methods in Hypersonic Flows Apr. 1993 14 p (For primary document see N94-10421 01-02)
Copyright Avail: CASI HC A03/MF A04

N94-10426# Cranfield Inst. of Tech., Bedford (England). Coll. of Aeronautics.

CONTROL EFFECTIVENESS AT HYPERSONIC SPEEDS

J. L. Stollery, D. Kumar, P. A. Atcliffe, and H. Babinsky *In* AGARD, Theoretical and Experimental Methods in Hypersonic Flows Apr. 1993 10 p (For primary document see N94-10421 01-02)
Copyright Avail: CASI HC A02/MF A04

09 RESEARCH AND SUPPORT FACILITIES (AIR)

Includes airports, hangars and runways; aircraft repair and overhaul facilities; wind tunnels; shock tubes; and aircraft engine test stands.

For related information see also *14 Ground Support Systems and Facilities (Space).*

N94-10669* National Aeronautics and Space Administration. Marshall Space Flight Center, Huntsville, AL.

DYNAMIC TESTER FOR ROTOR SEALS AND BEARINGS Patent

George L. vonPragenau, inventor (to NASA) 31 Aug. 1993 7 p Filed 1 Apr. 1991 Supersedes N91-25155 (29 - 17, p 2737)
(NASA-Case-MFS-28493-1; US-Patent-5,239,864; US-Patent-Appl-SN-678780; US-Patent-Class-73-118.1; US-Patent-Class-73-119R; US-Patent-Class-73-865.9; Int-Patent-Class-G01M-15/00; Int-Patent-Class-G01N-19/00) Avail: US Patent and Trademark Office

A dynamic tester for testing vibration damping seals and bearings is constructed having a hollow shaft extending through the seal or bearing, with the shaft internally supported at each end by fluid bearings on hollow bosses connected to an interior of an enclosure, with no rolling members connected to the shaft is described. A high pressure working fluid is forced through the hollow bosses to operate the bearings. Additionally, the shaft is provided with a reaction turbine that angularly vents a portion of the high pressure working fluid in order to rotate the shaft at high speed, up to 40,000 rpm. The seal or bearing is mounted in a bushing, in turn supported by rods to a shaking device that vibrates the seal or bearing as the shaft is rotated. A plurality of proximity sensors are mounted from outside the enclosure to sense shaft and seal bushing vibrations, and a plurality of pressure ports are disposed in the enclosure to allow sensing of dynamic and static pressures of the testing apparatus.
Official Gazette of the U.S. Patent and Trademark Office

N94-10733# National Aerospace Lab., Tokyo (Japan). Control Systems Div.

FLIGHT SIMULATOR EXPERIMENT OF THE COCKPIT ADVISORY SYSTEM [KOKKUPITTO ADOBAIZARI SHISUTEMU NO SHIMYURETA HYOUKA JIKKEN]

Keiji Tanaka, Hiroyasu Kawahara, Koutarou Matsumoto, and Hideo Masuzawa Apr. 1992 34 p In JAPANESE Original contains color illustrations

(NAL-TR-1151; JTN-93-80432; DE93-767975) Avail: CASI HC A03/MF A01

This paper describes the flight simulation experiment of a cockpit human-interface system which monitors aircraft utility systems and provides timely displays of aircraft conditions, warnings, and suggestions of initial actions, as well as operational procedures. This 'Cockpit Advisory System' is a kind of intelligent display which functions as a real-time flight manual. The current system was developed using the utility systems of 'ASKA', a Short Take-Off and Landing (STOL) experimental aircraft of the National Aerospace Laboratory (NAL). The system has two displays controlled by a real-time expert system, i.e., one for conditions and procedures and the other for various messages. Two pilots participated in flight simulator tests in which various emergency situations were encountered. Results indicate that the system: (1) remarkably reduced pilot workload; (2) enhanced crew coordination and situation awareness due to looking at color graphic displays instead of reading written checklists; (3) created a different cockpit environment since reading checklists is not necessary; and (4) is proved to be especially useful for pilot training. Author (NASDA)

N94-10894# Aircraft Research Association Ltd., Bedford (England).

IMPROVEMENT OF THE FLOW QUALITY IN THE ARA TRANSONIC TUNNEL BY MEANS OF A LONG CELL HONEYCOMB

D. R. Stanniland, C. A. McHugh, and J. E. Green Aug. 1992 13 p Presented at the Conference on Wind Tunnels and Wind Tunnel Test Techniques, Southampton, England, 14-17 Sep. 1992 Original contains color illustrations
(ARA-Memo-375) Avail: CASI HC A03/MF A01

In August 1990, the flow smoothing screen in the ARA 9' x 8' Transonic Wind Tunnel was replaced by a honeycomb with a high ratio of cell length to diameter. Investigations into a suitable honeycomb design is described and the resulting changes in flow quality in the wind tunnel are presented. Detailed surveys of the total pressure, steady and unsteady flow angularity, and turbulence show that a high degree of flow uniformity was achieved in the test section. Turbulence levels of 0.05 percent longitudinally and 0.18 percent laterally were derived from measurements in the working section. These are in good agreement with values derived from settling chamber measurements and compare well with the estimates of minimum longitudinal and lateral turbulence levels (0.06 percent and 0.15 percent) achievable with the chosen design of honeycomb. Author (revised)

N94-10930*# National Aeronautics and Space Administration. Ames Research Center, Moffett Field, CA.

ARCJET EXPLORATORY TESTS OF ARC OPTICAL WINDOW DESIGN FOR THE AFE VEHICLE Final Report, 14 Dec. 1990 - 6 Mar. 1991

Ellis E. Whiting (Eloret Corp., Moffett Field, CA.), Imelda Terrazas-Salinas (Eloret Corp., Moffett Field, CA.), Roger A. Craig (Eloret Corp., Moffett Field, CA.), Charles K. Sobeck, George L. Sarver, III, Louis J. Salerno, Wendell Love, Scott Maa, and Al Covington Apr. 1991 86 p
(Contract NCC2-653)
(NASA-CR-192655; NAS 1.26:192655; AFE-9004-003) Avail: CASI HC A05/MF A01

Tests were made in the 20 MW arc jet facility at the NASA ARC to determine the suitability of sapphire and fused silica as window materials for the Aeroassist Flight Experiment (AFE) entry vehicle. Twenty nine tests were made; 25 at a heating rate about 80 percent of that expected during the AFE entry and 4 at approximately the full, 100 percent AFE heating rate profile, that produces a temperature of about 2900 F on the surface of the tiles that protect the vehicle. These tests show that a conductively cooled window design using mechanical thermal contacts and sapphire is probably not practical. Cooling the window using mechanical thermal contacts produces thermal stresses in the sapphire that cause the window to crack. An insulated design using sapphire, that cools the window as little as possible, appears promising although some spectral data in the vacuum-ultra-violet (VUV) will be lost due to the high temperature reached by the sapphire. The surface of the insulated sapphire windows, tested at the 100 percent AFE heating rate, showed some slight ablation, and cracks appeared in two of three test windows. One small group of cracks were obviously caused by mechanical binding of the window in the assembly, which can be eliminated with improved design. Other cracks were long, straight, thin crystallographic cracks that have very little effect on the optical transmission of the window. Also, the windows did not fall apart along these crystallographic cracks when the windows were removed from their assemblies. Theoretical results from the thermal analysis computer program SINDA indicate that increasing the window thickness from 4 to 8 mm may enable surface ablation to be avoided. An insulated design using a fused silica window tested at the nominal AFE heating rate experienced severe ablation, thus fused silica is not considered to be an acceptable window material. Author (revised)

N94-11041 Tokyo Univ., Tanashi (Japan). Inst. for Nuclear Study.

DEVELOPMENT OF MICROSTRIP GAS CHAMBER AND APPLICATION TO IMAGING GAMMA-RAY DETECTOR

T. Tanimori, S. Minami (Tokyo Inst. of Tech., Japan.), T. Nagae, T. Takahashi, and T. Miyagi Jul. 1992 11 p Limited Reproducibility: More than 20% of this document may be affected by microfiche quality
(DE93-754294; INS-939) Avail: Issuing Activity (Department of Energy (DOE))

Microstrip Gas Chamber (MSGC) was developed by using Multi-Chip technology which enables high-density assembly of bare Large Scale Integration (LSI) chips on a silicon board. Our MSGC was operated steadily with approximately 10(exp 3) gain more than one week. An energy resolution of 15% (FWHM) for 5.9 keV x-ray of Fe-55 was obtained. With very thin polyimide substrate of 16 microns thickness, two interesting phenomena were observed; one is a strong dependence of gains on the back plane potential, and the other is little time variation of gains. New type of MSGC with a guarding mask of a thin polyimide layer on the cathode edges was examined to reduce incidental electrical discharges between anode and cathode strips. Furthermore, a new approach to reduce the resistivity of the substrate was examined. By these approaches, the stability of the high gain operation of approximately 10(exp 4) was drastically improved. In addition, the possibility of the application of MSGC to the coded mask x-ray imaging detector for astrophysics is discussed. DOE

N94-11869*# National Aeronautics and Space Administration, Washington, DC.

OVERVIEW OF THE 1989 WIND TUNNEL CALIBRATION WORKSHOP

Arthur Henderson, Jr. (Futron Corp., Washington, DC.) and L. Wayne McKinney Aug. 1993 45 p Workshop held in Hampton, VA, 19-20 Apr. 1989
(NASA-TP-3393; NAS 1.60:3393) Avail: CASI HC A03/MF A01

An overview of the 1989 Wind Tunnel Calibration Workshop held at NASA LaRC in Hampton, VA on 19-20 Apr. 1989 is presented. The purpose of the Workshop was to explore wind tunnel calibration requirements as they relate to test quality and data accuracy, with the ultimate goal of developing wind tunnel calibration requirements for the major NASA wind tunnels at ARC, LaRC, and LeRC. The two sessions addressed the following topics: (1) what constitutes a properly calibrated wind tunnel; and (2) the status of calibration of NASA's major wind tunnels. The most significant contributions to the stated goals are highlighted, and the consensus of the Workshop's conclusions and recommendations regarding formulation and implementation of that goal are presented. Author (revised)

N94-12436# Aircraft Research Association Ltd., Bedford (England).

A UNIQUE FACILITY TO SUPPORT CRYOGENIC WIND TUNNEL OPERATIONS

R. Porter Sep. 1992 11 p Presented at the Conference on Wind Tunnels and Wind Tunnel Test Techniques, Southampton, England, 14-17 Sep. 1992
(ARA-Memo-377) Avail: CASI HC A03/MF A01

The cryogenic environmental room at Aircraft Research Association (ARA) is designed to support research activities related to the design of cryogenic wind tunnel models and to provide a means of checking out a fully instrumented wind tunnel model, at relatively low cost in preparation for a test campaign at cryogenic temperatures. The facility is essentially a large thermally insulated room which houses a low speed open return wind tunnel circuit. Cooling is achieved by the direct injection of liquid nitrogen into the circuit. A centrifugal fan generates moderate forced convection velocities of up to 10 m/s over a model which is located in the exit section of the circuit. The room is constructed in a modular form such that modifications can readily be performed and the tunnel circuit can be reconfigured for alternative working section arrangements. The installation of the environmental room and associated systems is complete and a commissioning phase is at an advanced stage. To date, the facility has been successfully operated at temperatures down to 123K. Author

N94-12562# Naval Civil Engineering Lab., Port Hueneme, CA.
THREE-DIMENSIONAL FINITE ELEMENT ANALYSIS OF EXPLOSIVE SAFETY FACILITIES: A TECHNOLOGY ASSESSMENT Interim Report, FY90 - FY92
T. A. Shugar, T. J. Holland, L. J. Malvar, and D. A. Doi Dec. 1992 152 p
(AF Proj. RM3-3-F-60)
(AD-A265700; NCEL-TN-1856) Avail: CASI HC A08/MF A02

To establish research requirements for the development of modern, specialized software for computational structural dynamics in support of Navy explosive safety facilities, NCEL conducted baseline studies to assess commercial or currently available general purpose computer programs. Two widely available general purpose computer programs for three-dimensional nonlinear dynamic finite element analysis were applied to three types of reinforced concrete structures of interest to Navy explosive safety facility designers: (1) a novel cylindrical missile test cell concept; (2) flat slabs with variable shear steel; and (3) a soil-covered roof slab for a new high performance magazine concept. Results from codified single-degree-of-freedom (SDOF) methods for design of explosive safety structures were also considered and compared with finite element technology. This report provides an overview of these baseline studies. DTIC

N94-10430# Deutsche Forschungs- und Versuchsanstalt fuer Luft- und Raumfahrt, Goettingen (Germany).
THE HIGH ENTHALPY FACILITIES HEG AND TH 2 IN GERMANY
G. Eitelberg and H. Olivier (Technische Hochschule, Aachen, Germany.) *In* AGARD, Theoretical and Experimental Methods in Hypersonic Flows Apr. 1993 14 p (For primary document see N94-10421 01-02)
Copyright Avail: CASI HC A03/MF A04

N94-10431# Aeronautica Macchi S.p.A., Varese (Italy). Aerodynamics Dept.
DESIGN AND PRODUCTION OF INSULATED WIND TUNNEL MODELS OF THE HERMES SHUTTLE FOR HEAT TRANSFER MEASUREMENTS AT HYPERSONIC SPEEDS
L. Visintini and C. Couedor (Dassault Aviation, Istres, France.) *In* AGARD, Theoretical and Experimental Methods in Hypersonic Flows Apr. 1993 9 p (For primary document see N94-10421 01-02)
Copyright Avail: CASI HC A02/MF A04

N94-10432# Deutsche Forschungs- und Versuchsanstalt fuer Luft- und Raumfahrt, Cologne (Germany).
THE UPGRADING OF THE ARC HEATED WIND TUNNEL OF THE DLR (LBK) WITH RESPECT TO ITS EFFECTS ON THE MATERIAL TESTING
A. Guelhan and K. Kindler *In* AGARD, Theoretical and Experimental Methods in Hypersonic Flows Apr. 1993 11 p (For primary document see N94-10421 01-02)
Copyright Avail: CASI HC A03/MF A04

N94-10458*# National Aeronautics and Space Administration. Langley Research Center, Hampton, VA.
A CFD-BASED AERODYNAMIC DESIGN PROCEDURE FOR HYPERSONIC WIND-TUNNEL NOZZLES
John J. Korte *In* AGARD, Theoretical and Experimental Methods in Hypersonic Flows Apr. 1993 10 p (For primary document see N94-10421 01-02)
Copyright Avail: CASI HC A02/MF A04

N94-11535*# National Aeronautics and Space Administration. Ames Research Center, Moffett Field, CA.
MEASURES FOR SIMULATOR EVALUATION OF A HELICOPTER OBSTACLE AVOIDANCE SYSTEM
Joe DeMaio (Army Aviation Systems Command, Moffett Field, CA.), Thomas J. Sharkey (Monterey Technologies, Inc., Carmel, CA.), David Kennedy (Monterey Technologies, Inc., Carmel, CA.), Micheal Hughes (CAE Electronics Ltd., Saint Laurent, Quebec.), and Perry Meade (CAE Electronics Ltd., Saint Laurent, Quebec.) *In* NASA. Johnson Space Center, Sixth Annual Workshop on Space Operations Applications and Research (SOAR 1992), Volume 2 Feb. 1993 p 507-511 (For primary document see N94-11527 01-99)
Avail: CASI HC A01/MF A03

12 ASTRONAUTICS (GENERAL)

For extraterrestrial exploration see *91 Lunar and Planetary Exploration.*

N94-10676# Science and Technology Agency, Tokyo (Japan).
SPACE ACTIVITIES IN THE ASIA PACIFIC REGION
16 Nov. 1992 92 p Transl. into ENGLISH of Pure Ajia Taiheiyou Kokusa Conference held in Tokyo, Japan, 23-25 Mar. 1992 Original language document was announced as NASDA-CM-174 Prepared in cooperation with the Inst. of Space and Astronautical Science, Tokyo, Japan; NASDA, Tokyo, Japan; and Japan International Space Year Association, Tokyo, Japan
(JTN-93-80421) Avail: CASI HC A05/MF A01

The following topics were discussed: space programs of countries in the Asia Pacific Region, remote sensing, satellite observation, earth resources survey, monitoring of earth environment, global change, land management, water management, ocean observation, satellite communication, and spaceborne experiments. For individual titles, see N94-10677 through N94-10695.

N94-10677# National Space Development Agency, Tokyo (Japan). SAFISY Program Office.
CURRENT STATUS OF SPACE ACTIVITIES IN ASIA PACIFIC REGION
Tasuku Tanaka and Akiko Suzuki *In* Science and Technology Agency, Space Activities in the Asia Pacific Region 16 Nov. 1992 p 2-13 (For primary document see N94-10676 01-12)
Avail: CASI HC A03/MF A01

An overview of the space activities in the Asia Pacific Region in the following fields is presented: (1) utilization of meteorological satellite data from Geostationary Meteorological Satellites (GMSs) and NOAA satellites; (2) application of data from earth observing satellites, including LANDSAT, SPOT, and Marine Observation Satellite-1 (MOS-1); (3) satellite communication network, domestic communication satellites, and the Japanese Pan-Pacific Regional Telecommunication Network Experiment and Research Satellite (PARTNERS) project; (4) space science projects; and (5) launch vehicle projects. Space activity organizations of the countries in this region are outlined. Author (NASDA)

N94-10678# National Space Development Agency, Tokyo (Japan). SAFISY Program Office.
CONSIDERATIONS FOR FUTURE REGIONAL SPACE COOPERATION Abstract Only **c84**
Tasuku Tanaka and Akiko Suzuki *In* Science and Technology Agency, Space Activities in the Asia Pacific Region 16 Nov. 1992 p 14 (For primary document see N94-10676 01-12)
Avail: CASI HC A01/MF A01

Necessity of the international cooperation in space technology field in the Asia Pacific Region is mentioned. It is pointed out that fostering experts and technology transfer are the two key elements for enhancing space activities in the region. Author (NASDA)

N94-10679# Bangladesh Space Research and Remote Sensing Organization, Dhaka.
SPACE RESEARCH AND REMOTE SENSING PROGRAMMES IN BANGLADESH **c43**
A. K. M. Fariduddin Bhuiyan *In* Science and Technology Agency, Space Activities in the Asia Pacific Region 16 Nov. 1992 p 20-23 Original language document was announced as N93-21271 (For primary document see N94-10676 01-12)
Avail: CASI HC A01/MF A01

Major remote sensing research, development, and utilization activities in SPARRSO (Space Research and Remote Sensing Organization) of Bangladesh in the following areas are presented: (1) measurement of crop and land utilization patterns, soil characteristics pattern, and so forth in agriculture; (2) meteorological observation; (3) surface water analysis, seasonal change in lake and reservoir water-level, and so forth in water resources; (4) monitoring of forestation and new deforestation; (5) quantitative data acquisition on suspended solids, ocean current, sea surface temperature, and so forth in oceanography; and (6) production of maps indicating surface characteristics in cardiography. Author (NASDA)

N94-10680# State Science and Technology Commission, Beijing (China). Dept. of Fundamental Research and High Technology.
INTERNATIONAL SPACE YEAR IN CHINA **c84**
Quan Lin *In* Science and Technology Agency, Space Activities in the Asia Pacific Region 16 Nov. 1992 p 24-26 Original language document was announced as N93-21272 (For primary document see N94-10676 01-12)
Avail: CASI HC A01/MF A01

The status of remote sensing activities conducted by China are presented. Topics discussed are as follows: (1) publication of land utilization and classification maps; (2) monitoring of flood and drought, and detection and recording all processes of forest fires; and (3) monitoring experiments on forestation and deforestation, survey on land erosion, desertification, industrial waste pollution, and cartography of desert distribution maps in northern China. Study on space science such as research on solar-terrestrial energy transfer systems for the International Solar-Terrestrial Energy Program and other research activities in space science, and events scheduled to be conducted for the International Space Year (ISY) are outlined.
Author (NASDA)

N94-10681# Indonesian National Inst. of Aeronautics and Space, Jakarta.
SPACE PROGRAM IN INDONESIA
I. H. Wiryosumarto *In* Science and Technology Agency, Space Activities in the Asia Pacific Region 16 Nov. 1992 p 27-29 Original language document was announced as N93-21273 (For primary document see N94-10676 01-12)
Avail: CASI HC A01/MF A01

Space programs and development entrusted by the government to the Indonesian National Inst. of Aeronautics and Space (LAPAN) in the fields of remote sensing, and climate prediction are outlined. Indonesian International Space Year (ISY) activities in 1992 are as follows: (1) high school essay contest on space; (2) proposal on regional center for space education in Indonesia; (3) conference on space science and technology; (4) seminar on communications; (5) campaign on remote sensing application; and (6) public awareness on space science and technology. Indonesian observation facilities are shown. Author (NASDA)

N94-10682# Science and Technology Agency, Tokyo (Japan). International Space-Affairs Div.
JAPANESE SPACE ACTIVITIES
Tsuyoshi Maruyama *In its* Space Activities in the Asia Pacific Region 16 Nov. 1992 p 30-32 Original language document was announced as N93-21274 (For primary document see N94-10676 01-12)
Avail: CASI HC A01/MF A01

The following subjects concerning Japanese space activities are presented: (1) fundamental policy and principles; (2) major objectives; (3) space activity classification; (4) space science; (5) common technologies for satellites; (6) space transportation; (7) communication and broadcasting; (8) earth observation; (9) space environment utilization, including drop experiment facilities, rockets, space shuttle and satellites, and the Space Station Freedom; and (10) information concerning the International Space Year (ISY), such as its concept and purposes, Space Agency Forum on ISY, Japan ISY Association, related organizations, publicity, and activities.
Author (NASDA)

N94-10683# Korea Advanced Inst. of Science and Technology, Seoul (Republic of Korea). Satellite Technology and Research Center.
OVERVIEW OF KITSAT **c18**
Dal Choi Soon *In* Science and Technology Agency, Space Activities in the Asia Pacific Region 16 Nov. 1992 p 33-35 Original language document was announced as N93-21275 (For primary document see N94-10676 01-12)
Avail: CASI HC A01/MF A01

An overview of the roles and plans of the Satellite Technology and Research Center in the space activities in Korea are presented. The following items about the Korea Institute of Technology Satellite-A (KITSAT-A) launched simultaneously with the Topography Experiment for Ocean Circulation (TOPEX) by an ESA ARIANE launch vehicle are presented: (1) major missions such as space technology acquisition and experiencing of designing, structuring, and operating minisatellites; (2) specifications for orbit, power budget, frequency allocation, attitude control, machinery, onboard data systems, and module structure; and (3) experiments with KITSAT borne equipment on data transmission, Charge Coupled Device (CCD) earth imaging, digital signal processing, and cosmic radiation measuring. The KITSAT project time schedule is also presented.
Author (NASDA)

N94-10684# Korea Aerospace Research Inst., Taejon (Republic of Korea). Space Research and Development Div.
KOREA SPACE PROGRAM
Jang-Soo Ryoo *In* Science and Technology Agency, Space Activities in the Asia Pacific Region 16 Nov. 1992 p 36-37 (For primary document see N94-10676 01-12)
Avail: CASI HC A01/MF A01

An overview of the missions, history, and organization of the Korea Aerospace Research Institute (KARI) is presented. The following three projects included in the Korean space program are presented: (1) KOREASAT procurement project to procure multipurpose satellites and have them launched through international tenders to be used for communication and broadcasting in Korea; (2) exploration rocket project, Korea's self-developed rocket project, conducted by KARI to observe the ozone concentration and ionosphere over the country, and conduct microgravity experiment; and (3) KITSAT (Korea Institute of Technology Satellite-A) minisatellite project undergoing joint development with the UK Surrey University to be launched by a ARIANE launch vehicle.
Author (NASDA)

N94-10685# Malayan Centre for Remote Sensing, Kuala-Lampur.
SPACE PROGRAMME IN MALAYSIA
Nik Nasruddin Mahmood *In* Science and Technology Agency, Space Activities in the Asia Pacific Region 16 Nov. 1992 p 38-40 (For primary document see N94-10676 01-12)
Avail: CASI HC A01/MF A01

An overview of space activities in Malaysia in the following areas is presented: (1) utilization of the INTELSAT system including INTELSAT Business Service (IBS); (2) introduction of mobile satellite communication, INMARSAT service, and improvement of communication by the use of the domestic and regional satellite Malaysian East Asian Satellite-1 (MEASAT-1) and -2; (3) reception and processing of image data from the TIROS-N and Geostationary Meteorological Satellites (GMSs); and (4) National Remote Sensing Program (NRSP) started to promote establishment of the Malaysian Center for Remote Sensing (MACRES) and other activities related to remote sensing. Author (NASDA)

N94-10686# National Remote Sensing Centre, Ulaanbaatar (Mongolia).
NATIONAL SPACE PROGRAMMES AND APPLICATION OF THE REMOTE SENSING DATA IN MONGOLIA
Mendbayariin Badarch *In* Science and Technology Agency, Space Activities in the Asia Pacific Region 16 Nov. 1992 p 41-44 Original language document was announced as N93-21278 (For primary document see N94-10676 01-12)
Avail: CASI HC A01/MF A01

An overview of the remote sensing satellite data application in Mongolia is presented. The application area is as follows: (1) the operation of meteorological satellite data acquisition station in receiving data from the U.S. and former USSR satellites; (2) establishment and operation of the meteorological rocket exploration station; and (3) establishment of the National Remote Sensing Center. An overview of the activities of the Center in the following areas is presented: (1) development of domestic capability to examine, classify, and monitor the natural resources; (2) monitoring of natural disasters such as cyclones, drought, forest fires, hurricanes, and air pollution; and (3) examples of remote sensing data application to natural disaster monitoring, geology, hydrology, and environment control. Author (NASDA)

N94-10687# Department of Environment and Natural Resources, Quezon City (Philippines).
STATUS OF REMOTE SENSING AND GEOGRAPHIC INFORMATION SYSTEM (GIS) APPLICATIONS IN THE ENVIRONMENT AND NATURAL RESOURCES (ENR) SECTOR **c43**
Ricardo M. Umali *In* Science and Technology Agency, Space Activities in the Asia Pacific Region 16 Nov. 1992 p 45-47 Original language

document was announced as N93-21279 (For primary document see N94-10676 01-12)
Avail: CASI HC A01/MF A01

Remote sensing and Geographic Information Systems (GIS) will play a vital role in the coming years when the Philippines seriously pursues its decentralization and countryside programs. As a very useful tool in resource assessment and monitoring, remote sensing is gradually gaining popularity as a commercial technology both nationally and internationally mainly because of its increasing resolution, the declining cost of computer hardware and software, and the increasing popularity of the GIS which needs remote sensing data. The topics covered include the following: the role and functions of the National Mapping and Resource Information Authority (NAMRIA); major accomplishments; and present capabilities. Author (NASDA)

N94-10688# Academy of Sciences (USSR), Moscow. Inst. of Radio Engineering and Electronics.
RUSSIAN SPACE SYSTEM FOR THE EARTH REMOTE SENSING c43
Neon A. Armand *In* Science and Technology Agency, Space Activities in the Asia Pacific Region 16 Nov. 1992 p 48-51 Original language document was announced as N93-21280 (For primary document see N94-10676 01-12)
Avail: CASI HC A01/MF A01

An overview of the major characteristics of the Russian short-term earth observing systems such as follows is presented: (1) meteorological satellites METEOR-2 and 3, and Geostationary Operational Meteorological Satellite (GOMS); (2) oceanographical satellite OKEAN and OKEAN satellite sensor KOSMO-1500; (3) practical land resources satellite RESURS-1, 2, and F; (4) ALAMAZ mission; (5) PRIRODA mission for developing remote sensing technology to assess global changes, and to combine visible, infrared, and microwave measurements for simultaneous examination of natural environments of selected regions; and (6) ECOS-A mission. Author (NASDA)

N94-10689# National Univ. of Singapore. Dept. of Physics.
SUN-SYNCHRONOUS AND GEO-SYNCHRONOUS SATELLITE DATA UTILIZATION FOR ENVIRONMENTAL STUDIES
Yean-Joo Chong *In* Science and Technology Agency, Space Activities in the Asia Pacific Region 16 Nov. 1992 p 52-53 Original language document was announced as N93-21281 (For primary document see N94-10676 01-12)
Avail: CASI HC A01/MF A01

The remote sensing activities in Singapore are presented. Activities explained are as follows: (1) the satellite ground station that are receiving data from the Geostationary Meteorological Satellite-4 (GMS-4), NOAA-11, and 12 satellites on a real-time basis; (2) data processing systems of Singapore University that are being used for resource mapping of the Organism and Coastal Resources Project under the Asian-Australia Oceanography Joint Program; and (3) trials have been conducted to utilize the combination of the radiometer data from GMS-4 satellite, the Indian National Satellite System (INSAT), and NOAA satellites with the high-resolution data from the Marine Observation Satellite (MOS), the Infrared Astronomical Satellite (IRAS), the ERS, and the Japanese Earth Resources Satellite-1 (JERS-1). Author (NASDA)

N94-10690# National Research Council, Bangkok (Thailand).
THAILAND ISY ACTIVITIES
Suvit Vibulsresth *In* Science and Technology Agency, Space Activities in the Asia Pacific Region 16 Nov. 1992 p 54-55 Original language document was announced as N93-21282 (For primary document see N94-10676 01-12)
Avail: CASI HC A01/MF A01

An overview of the past participation of Thailand in international cooperation in remote sensing activities especially in Association of Southeast Asian Nations (ASEAN) region is presented. An overview of Thailand International Space Year (ISY) activities such as follows is presented: (1) improvement of the ERS-1 ground station; (2) Japan-Thailand remote sensing improvement project to provide satellite data for global change research and tropical forest survey; (3) ASEAN remote sensing cooperation project for promoting joint study and engineer exchange; and (4) ocean environment information project to provide fundamental data on Thailand Bay environment. Author (NASDA)

N94-10691# Embassy of Australia, Tokyo (Japan).
NATIONAL SPACE PROGRAM IN AUSTRALIA
G. M. Brennan *In* Science and Technology Agency, Space Activities in the Asia Pacific Region 16 Nov. 1992 p 56-59 Original language document was announced as N93-21283 (For primary document see N94-10676 01-12)
Avail: CASI HC A01/MF A01

An overview of the Australian space activity history and present status is presented in the following aspects: (1) full-scale space activities since the establishment of the Australian Space Board in 1987 and the start of governmental budgetary support to national space program; (2) cooperation with NASA and ESA through satellite ground stations in satellite communication and ground support; (3) Australian private enterprises contract to provide launch support for INTERSAT and other satellites and schedule to start mobile satellite communication all over the country; and (4) supporting the second ground station construction to facilitate acquisition of the southern Pacific Ocean data of the wide area covering from the end of Antarctic continent to the eastern end of New Zealand. The remote sensing equipment development, launch service business plan, present status of supersonic technology in Australia and Australian space policy are outlined. Author (NASDA)

N94-10692# Embassy of Canada, Tokyo (Japan).
CANADA'S LONGTERM SPACE PLAN AND ISY ACTIVITIES
B. Carl Kuhnke *In* Science and Technology Agency, Space Activities in the Asia Pacific Region 16 Nov. 1992 p 60-62 Original language document was announced as N93-21284 (For primary document see N94-10676 01-12)
Avail: CASI HC A01/MF A01

An overview of Canada's long-term space plan and International Space Year (ISY) activities is presented. An outline of the following is presented: the responsibilities and fiscal year's expenditures (including those for the Space Station Freedom, RADARSAT, Canada's Synthetic Aperture Radar (SAR) satellite, etc.); five major space programs implemented by the Canadian Space Agency (CSA); Canadian space industry's activities; Canada's space science programs (in the fields of fluid physics, combustion, materials research, and life sciences); and technology programs (including the space station, Mission to Planet Earth, and communication). Canada's major contribution for ISY Canadian 'Global Change Encyclopedia', named 'GOESCOPE' and led by the CSA and the Canadian Center for Remote Sensing (CCRS) and other ISY activities are outlined. Author (NASDA)

N94-10693# Embassy of Pakistan, Tokyo (Japan).
PAKISTAN SPACE AND UPPER ATMOSPHERE RESEARCH COMMISSION
Mian Suhail Aslam *In* Science and Technology Agency, Space Activities in the Asia Pacific Region 16 Nov. 1992 p 63-65 Original language document was announced as N93-21285 (For primary document see N94-10676 01-12)
Avail: CASI HC A01/MF A01

An overview of the major activities conducted by Pakistan Space and Upper Atmosphere Research Commission (SUPARCO) is presented. Subjects of the activities are as follows: (1) atmosphere research; (2) ionosphere and radio wave propagation; (3) remote sensing application; (4) measurement of meteorological, hydrological and oceanographic parameters by ARGOS data collection system; (5) operation of satellite ground station; (6) satellite aided search and rescue project; (7) air pollution monitoring; (8) geomagnetic field observation; (9) Pakistan communication satellite PAKSAT; and (10) international cooperation of SUPARCO with European, American, and Asian countries. Major space related facilities, such as the Space Research Council, Remote Sensing Application Center, and Aerospace Engineering Laboratory, of the SUPARCO are introduced. Author (NASDA)

N94-10694# National Space Activities Council, Tokyo (Japan).
PANEL DISCUSSION: ROLE OF SPACE PROGRAM IN THE ASIA PACIFIC REGION
Tamiya Nomura *In* Science and Technology Agency, Space Activities in the Asia Pacific Region 16 Nov. 1992 p 66-82 Original language document was announced as N93-21286 (For primary document see N94-10676 01-12)
Avail: CASI HC A03/MF A01

The dialogue from the panel discussion on the role of space exploration in the Asia Pacific Region is presented. The purpose of the panel discussion is to identify ways and means to best promote the welfare of this region through the space exploitation. The topics discussed include remote sensing and what kind of observation data and cooperation are required to promote the benefits of remote sensing. Author (NASDA)

N94-10695# Ministry of Posts and Telecommunications, Tokyo (Japan). Communications Policy Bureau.
PARTNERS c84
Kiyoshi Ooida *In* Science and Technology Agency, Space Activities in the Asia Pacific Region 16 Nov. 1992 p 83-84 Original language document was announced as N93-21287 (For primary document see N94-10676 01-12)
Avail: CASI HC A01/MF A01

An overview of the PARTNERS (Pan-Pacific Regional Telecommunication Network Experiment and Research Satellite) Project conducted for the purpose of promoting technical cooperation in the area of satellite communication with Asia Pacific countries through joint experimentation using the Engineering Test Satellite-5 (ETS-5) on the following subjects is presented: (1) validation test for educational and medical utilization; (2) joint research for developing rural satellite network with small mobile ground stations; and (3) joint measurement of radio wave propagation characteristics. Author (NASDA)

N94-11461# European Space Agency. European Space Research and Technology Center, ESTEC, Noordwijk (Netherlands). Publications Div.
SPAIN: SUCCESS STORY IN SPACE [ESPANA EN EL ESPACIO: HACIA LA CONQUISTA DE NUEVAS FRONTERAS]
Norman Longdon, ed. 1992 30 p In ENGLISH and SPANISH LIMITED REPRODUCIBILITY: More than 20% of this document may be affected by color photographs Original contains color illustrations
(ESA-BR-81; ISBN-92-9092-103-X) Avail: CASI HC A03/MF A01

From the early 1960's, European governments were aware that they had to take part in the exploration, and potential exploitation, of space, or be left behind in a field of high-technology that had far-reaching possibilities. It was also realized that financial and manpower constraints would limit the extent to which individual nations could carry out their own national programs. They, therefor, joined forces in two organizations: the European Space Research Organization (ESRO) and the European Launcher Development Organization (ELDO). By 1975, when the potential of space development had been more fully appreciated, the two organizations were merged into the Europeans Space Agency (ESA) of which Spain was a founding member. ESA looks after the interest of 13 member states, one associated member state (Finland), and one cooperating state (Canada) in the peaceful uses of space. Its programs center around a mandatory core of technological research and space science to which member states contribute on the basis of their Gross National Product. Spain in 1992 contributes 6.46% to this mandatory program budget. The member states then have the chance to join optional programs that include telecommunications, observation of the earth and its environment, space transportation systems, microgravity research, and participation in the European contribution to the International Space Station Freedom. Each government decides whether it is in its interest to join a particular optional program, and the percentage that it wishes to contribute to the budget. Although in the early days of ESA, Spain participated in only a few optional programs, today Spain makes a significant contribution to nearly all of ESA's optional programs. This document presents Spain's contributions to particular ESA Programs and discusses Spain's future involvement in ESA. Derived from text

N94-12567# Federal Aviation Administration, Oklahoma City, OK. Civil Aeromedical Inst.
SATORI: SITUATION ASSESSMENT THROUGH THE RE-CREATION OF INCIDENTS Final Report
Mark D. Rodgers and Duane A. Duke Jul. 1993 13 p
(DOT/FAA/AM-93/12) Avail: CASI HC A03/MF A01

A system was developed that graphically re-creates the radar data recorded at En Route air traffic control (ATC) facilities. Each facility records data sent to the displays associated with the airspace under its control on a System Analysis Report (SAR) tape. SATORI (Situation Assessment Through Re-creation of Incidents) overlays the SAR data on the appropriate sector maps using map data from the Adaptation Control Environmental System (ACES) database. The analog switch display settings of the plan view display (PVD) are not recorded; however, subroutines were written for SATORI that allow the display to be set up with the settings reported to have been used by a given controller. In addition, SATORI has the capability to display the high and low weather intensity that was displayed on a given PVD. All software routines written for SATORI use Open Systems Foundation (OSF) technology. Similar data to those available from En Route facilities are recorded at Terminal Radar Approach Control (TRACON) facilities and should allow for the development of a re-creation tool much like the one discussed. Once SATORI is developed and evaluated, it will be possible to accomplish the goals of evaluating system designs, over-the-shoulder appraisals, training outcomes, procedures, airspace design, and measuring controller performance. Not only will the capabilities and features of SATORI provide those interested in air traffic with a valuable tool for assessing the dynamics of the air traffic situation, but additionally, and more importantly, the Agency will be in a better position to bring about effective change in future ATC systems. Author (revised)

N94-11565*# Air Force Human Resources Lab., Wright-Patterson AFB, OH.
ON-ORBIT REFUELING Abstract Only
Pospisil *In* NASA. Johnson Space Center, Sixth Annual Workshop on Space Operations Applications and Research (SOAR 1992), Volume 2 Feb. 1993 p 635 (For primary document see N94-11527 01-99)
Avail: CASI HC A01/MF A03

N94-11566*# National Aeronautics and Space Administration. Lyndon B. Johnson Space Center, Houston, TX.
ON-ORBIT REFUELING Abstract Only
James S. Moore and Shelby L. Owens (Hernandez Engineering, Inc., Houston, TX.) *In its* Sixth Annual Workshop on Space Operations Applications and Research (SOAR 1992), Volume 2 Feb. 1993 p 636 (For primary document see N94-11527 01-99)
Avail: CASI HC A01/MF A03

N94-11567*# Air Force Logistics Command, Kelly AFB, TX.
PRELIMINARY ANALYSIS OF THE BENEFITS DERIVED TO US AIR FORCE SPACECRAFT FROM ON-ORBIT REFUELING
Scott Smith *In* NASA. Johnson Space Center, Sixth Annual Workshop on Space Operations Applications and Research (SOAR 1992), Volume 2 Feb. 1993 p 637-655 (For primary document see N94-11527 01-99)
Avail: CASI HC A03/MF A03

13 ASTRODYNAMICS

Includes powered and free-flight trajectories; and orbital and launching dynamics.

N94-10359 Texas Univ., Austin.
TOPEX ORBIT DETERMINATION USING GPS TRACKING SYSTEM Ph.D. Thesis
Hyung Jin Rim 1992 243 p
Avail: Univ. Microfilms Order No. DA9309265

An extensive simulation study was performed to analyze several aspects of Topex Precise Orbit Determination (POD) using the Global Positioning System (GPS). Since the error modeling is the key to such an experiment, extensive investigation was performed based on real GPS data processing experience to create realistic measurement and dynamic error models for GPS. Double-differenced Topex-GPS phase measurements were evaluated in relation to improving the Earth geopotential model, which is the dominant error source for Topex POD. The effect of model errors on the Topex orbit and gravity recovery accuracies was evaluated. Long arc and short arc gravity solutions were compared to understand the effect of the model errors in using the long arc and the short arc solutions for the gravity recovery. Limiting factors for the long arc and the short arc gravity recovery were identified. The effect of ambiguity parameters on the gravity recovery was analyzed. Since the number of ambiguity parameters are quite large, an algorithm was developed to handle the ambiguity parameters more efficiently. Subarc parameters and empirical parameters were tested to find an optimal set of parameters to be estimated for the gravity recovery. Several gravity models were obtained by combining Topex-GPS information with a nominal geopotential information. These combined gravity models were evaluated by the statistical comparison of the recovered geopotential model parameters and by the Topex orbit analysis. Significant improvement in the nominal geopotential model, especially for the low degree harmonics, was achieved. More than a factor of three improvement in Topex orbit accuracy was demonstrated using the recovered gravity model. Analysis associated with predicted Topex radial orbit errors using the solution covariance indicates error estimates for the orbit accuracy is realistic.

Dissert. Abstr.

N94-10659*# National Aeronautics and Space Administration. Goddard Space Flight Center, Greenbelt, MD.

SATELLITE SITUATION REPORT, VOLUME 31, NO. 4

31 Dec. 1991 353 p

(NASA-TM-109232; NAS 1.15:109232) Avail: CASI HC A16/MF A03

This report consists of data computed at the U.S. Space Command, GSFC, or provided by satellite owners. A space objects box score table is presented with data under the following headings: source/organization, objects in orbit, and decayed objects. The objects in orbit and decayed objects headings have payload, debris, and total as subheadings. The bulk of the document is objects-in-orbit tables with data under the following headings: international designation, name, catalog number, source, launch date, period minutes, inclination, apogee (km), perigee (km), and notes.

CASI

N94-10764*# National Aeronautics and Space Administration. Lewis Research Center, Cleveland, OH.

A COMPARATIVE STUDY OF FULL NAVIER-STOKES AND REDUCED NAVIER-STOKES ANALYSES FOR SEPARATING FLOWS WITHIN A DIFFUSING INLET S-DUCT

B. H. Anderson, D. R. Reddy, and K. Kapoor Jun. 1993 18 p Presented at the 29th AIAA Joint Propulsion Conference and Exhibit, Monterey, CA, 28-30 Jun. 1993; sponsored by AIAA, SAE, ASME, and ASEE

(RTOP 505-62-52)

(NASA-TM-106250; E-7972; NAS 1.15:106250; AIAA Paper 93-2154)

Avail: CASI HC A03/MF A01

A three-dimensional implicit Full Navier-Stokes (FNS) analysis and a 3D Reduced Navier-Stokes (RNS) initial value space marching solution technique has been applied to a class of separate flow problems within a diffusing S-duct configuration characterized as vortex-liftoff. Both Full Navier-Stokes and Reduced Navier-Stokes solution techniques were able to capture the overall flow physics of vortex lift-off, however more consideration must be given to the development of turbulence models for the prediction of the locations of separation and reattachment. This accounts for some of the discrepancies in the prediction of the relevant inlet distortion descriptors, particularly circumferential distortion. The 3D RNS solution technique adequately described the topological structure of flow separation associated with vortex lift-off.

Author

N94-12530# Observatoire de la Cote d'Azur, Nice (France).

REGIONAL ORBIT PRECISION IN THE MEDITERRANEAN AREA

P. Bonnefond, P. Exertier, F. Barlier, and Y. Boudon *In* ESA, Proceedings of 1st ERS-1 Symposium on Space at the Service of Our Environment, Volume 2 Mar. 1993 p 889-891 (For primary document see N94-12471 01-43)

Copyright Avail: CASI HC A01/MF A03; EPD, ESA, ESTEC, Noordwijk, Netherlands, HC

14 GROUND SUPPORT SYSTEMS AND FACILITIES (SPACE)

Includes launch complexes, research and production facilities; ground support equipment, e.g., mobile transporters; and simulators.

For related information see also *09 Research and Support Facilities (Air).*

N94-10118# Societe Anonyme Belge de Constructions Aeronautiques, Brussels.

DESCRIPTION OF THE LIQUID STRUCTURE FACILITY ARCHITECTURE AND EXPERIMENTAL DEMONSTRATION OF THE DIAGNOSTIC CAPABILITIES

G. Bekaert, Olivier Dupont (Brussels Univ., Belgium.), Olivier Rousselle (Brussels Univ., Belgium.), J. C. Legros (Brussels Univ., Belgium.), Alain Gonfalone (European Space Agency. European Space Research and Technology Center, ESTEC, Noordwijk, Netherlands.), A. Verga (European Space Agency. European Space Research and Technology Center, ESTEC, Noordwijk, Netherlands.), P. Holbrouck (Verhaert Design and Development, Kruibeke, Belgium.), V. Zolesi (Kayser Italia, Livorno.), and J. L. VanEck (Brussels Univ., Belgium.) *In* ESA, Proceedings of the 8th European Symposium on Materials and Fluid Sciences in Microgravity, Volume 1 Aug. 1992 p 325-330 (For primary document see N94-10070 01-29)

Copyright Avail: CASI HC A02/MF A04; ESA, EPD, ESTEC, Noorwijk, Netherlands, HC

N94-10119# Dornier System G.m.b.H., Friedrichshafen (Germany).

ADVANCED PROTEIN, CRYSTALLIZATION FACILITY AND ASSOCIATED NEW DEVELOPMENTS

R. Bosch, P. Lautenschlager, Lothar Potthast, and J. Stapelmann *In* ESA, Proceedings of the 8th European Symposium on Materials and Fluid Sciences in Microgravity, Volume 1 Aug. 1992 p 331-336 (For primary document see N94-10070 01-29)

Copyright Avail: CASI HC A02/MF A04; ESA, EPD, ESTEC, Noordwijk, Netherlands, HC

N94-10134# Microgravity Advanced Research and Support Center, Naples (Italy).

TOLS (TELESCIENCE ON-LINE SIMULATOR): AN ESSENTIAL INSTRUMENT FOR MICRO-GRAVITY INTERACTIVE EXPERIMENT

Raimondo Fortezza and Rodolfo Monti (Naples Univ., Italy.) *In* ESA, Proceedings of the 8th European Symposium on Materials and Fluid Sciences in Microgravity, Volume 1 Aug. 1992 p 407-411 (For primary document see N94-10070 01-29)

Copyright Avail: CASI HC A01/MF A04; ESA, EPD, ESTEC, Noordwijk, Netherlands, HC

N94-10136# European Space Agency. European Space Research and Technology Center, ESTEC, Noordwijk (Netherlands). Microgravity Div.

THE ADVANCED FLUID PHYSICS MODULE: HOW TO ACHIEVE SCIENTIFIC GOALS FOR SPACELAB D2

V. Pletser, A. Verga, F. Klinkhamer (Netherlands Organization for Applied Scientific Research TNO, Delft.), and N. Janning (Netherlands Organization for Applied Scientific Research TNO, Delft.) *In its* Proceedings of the 8th European Symposium on Materials and Fluid Sciences in Microgravity, Volume 1 Aug. 1992 p 419-424 (For primary document see N94-10070 01-29)

Copyright Avail: CASI HC A02/MF A04; ESA, EPD, ESTEC, Noordwijk, Netherlands, HC

N94-11433*# IBM Federal Systems Div., Gaithersburg, MD.

A RECENT CLEANROOM SUCCESS STORY: THE REDWING PROJECT

Philip A. Hausler *In* NASA. Goddard Space Flight Center, Proceedings of the Seventeenth Annual Software Engineering Workshop Dec. 1992 30 p (For primary document see N94-11422 01-61)

Avail: CASI HC A03/MF A04

15 LAUNCH VEHICLES AND SPACE VEHICLES

Includes boosters; operating problems of launch/space vehicle systems; and reusable vehicles.

For related information see also *20 Spacecraft Propulsion and Power.*

N94-10640*# National Aeronautics and Space Administration. Lewis Research Center, Cleveland, OH.

ACHIEVEMENTS AND CHALLENGES OF SPACE STATION FREEDOM'S SAFETY REVIEW PROCESS

David W. Robinson Jul. 1993 17 p Proposed for presentation at the 11th International System Safety Conference, Cincinnati, OH, 28 Jul. - 2 Aug. 1993; sponsored by the System Safety Society

(RTOP 474-17-10)

(NASA-TM-106199; E-7959; NAS 1.15:106199) Avail: CASI HC A03/MF A01

The most complex space vehicle in history, Space Station Freedom, is well underway to completion, and System Safety is a vital part of the program. The purpose is to summarize and illustrate the progress that over one-hundred System Safety engineers have made in identifying, documenting, and controlling the hazards inherent in the space station. To date, Space Station Freedom has been reviewed by NASA's safety panels through the first six assembly flights, when Freedom achieves a configuration known as Man Tended Capability. During the eight weeks of safety reviews spread out over a year and a half, over 200 preliminary hazard reports were presented. Along the way NASA and its contractors faced many challenges, made much progress, and even learned a few lessons. Author

N94-11637 Texas Univ., Austin.

INVESTIGATION OF MULTIPHASE RAILGUN SYSTEMS Ph.D. Thesis

Sunil Keshava Murthy 1992 206 p

Avail: Univ. Microfilms Order No. DA9309240

Multiphase railguns (electromagnetic launchers) powered by multiphase compensated pulsed alternators (compulsators) is examined. The impediments to implementing multiphase railguns are identified and solutions to the problems are presented. Methods for improving the acceleration profile of the multiphase railgun system are also detailed. Several options of a single element multiphase compulsator powered railgun system are discussed. Comparison of the multiphase railgun system with the existing state of the art single phase compulsator driven railgun system is also included. Dissert. Abstr.

N94-11893# National Transportation Safety Board, Washington, DC.

SPECIAL INVESTIGATION REPORT: COMMERCIAL SPACE LAUNCH INCIDENT, LAUNCH PROCEDURE ANOMALY ORBITAL SCIENCES CORPORATION PEGASUS/SCD-1, 80 NAUTICAL MILES EAST OF CAPE CANAVERAL, FLORIDA, FEBRUARY 9, 1993

1993 109 p

(PB93-917003; NTSB/SIR-93/02) Avail: CASI HC A06/MF A02

This report explains the procedural anomaly that occurred during the launch sequence of an Orbital Sciences Corporation Pegasus expendable launch vehicle, which was subsequently deployed successfully from an NB-52B airplane, on 9 Feb. 1993. The safety issues discussed in the report include command, control and communications responsibility, launch crew fatigue, launch interphone procedures, efficiency of launch constraints, and the lack of common launch documents. Safety recommendations concerning these issues were made to the Department of Transportation, the National Aeronautics and Space Administration, and the Orbital Sciences Corporation. Author (revised)

N94-11576*# Air Force Systems Command, Norton AFB, CA. National Launch System Joint Program Office.

THE NATIONAL LAUNCH SYSTEM ADVANCED DEVELOPMENT PROGRAM: A BRIEF OVERVIEW

J. A. Battenburg *In* NASA. Johnson Space Center, Sixth Annual Workshop on Space Operations Applications and Research (SOAR 1992), Volume 2 Feb. 1993 p 716-717 (For primary document see N94-11527 01-99) Avail: CASI HC A01/MF A03

16 SPACE TRANSPORTATION

Includes passenger and cargo space transportation, e.g., shuttle operations; and space rescue techniques.

For related information see also *03 Air Transportation and Safety* and *18 Spacecraft Design, Testing and Performance.* For space suits see *54 Man/System Technology and Life Support.*

N94-10147# Rockwell International Corp., Canoga Park, CA. Rocketdyne Div.

THE 40 kWe S-PRIME THERMIONIC DESIGN AND TECHNOLOGY DEMONSTRATION PROGRAM

1992 535 p Program held in Washington, DC, 8-9 Dec. 1992

(Contract DE-AC03-92SF-19138)

(DE93-004738; CONF-921244) Avail: CASI HC A23/MF A04 (US Sales Only)

This quarterly program review provides a status of the 40 kWe S-Prime Design and Technology Demonstration Program. Viewgraphs are presented. DOE

N94-10805*# National Aeronautics and Space Administration. John F. Kennedy Space Center, Cocoa Beach, FL.

DEBRIS/ICE/TPS ASSESSMENT AND INTEGRATED PHOTOGRAPHIC ANALYSIS FOR SHUTTLE MISSION STS-57 Final Report, 18 Jun. - 2 Jul. 1993

Gregory N. Katnik, Barry C. Bowen, and J. Bradley Davis Jul. 1993 131 p Original contains color illustrations

(NASA-TM-107562; NAS 1.15:107562) Avail: CASI HC A07/MF A02; 47 functional color pages

A Debris/Ice/Thermal Protection System (TPS) assessment and integrated photographic analysis was conducted for Shuttle mission STS-57. Debris inspections of the flight elements and launch pad were performed before and after launch. Ice/frost conditions on the External Tank were assessed by the use of computer programs, nomographs, and infrared scanner data during cryogenic loading of the vehicle followed by on-pad visual inspection. High speed photography was analyzed after launch to identify ice/debris sources and evaluate potential vehicle damage and/or in-flight anomalies. The debris/ice/TPS conditions and integrated photographic analysis of Shuttle mission STS-57, and the resulting effect on the Space Shuttle Program are documented. Author (revised)

N94-10811*# National Aeronautics and Space Administration. Lewis Research Center, Cleveland, OH.

SPACE TRANSPORTATION ALTERNATIVES FOR LARGE SPACE PROGRAMS: THE INTERNATIONAL SPACE UNIVERSITY SUMMER SESSION, 1992

Bryan A. Palaszewski Jun. 1993 25 p Presented at the 29th Joint Propulsion Conference and Exhibit, Monterey, CA, 28-30 Jun. 1993; sponsored by AIAA, SAE, ASME, and ASEE

(RTOP 506-42-72)

(NASA-TM-106271; E-7999; NAS 1.15:106271; AIAA Paper 93-2278) Copyright Avail: CASI HC A03/MF A01

In 1992, the International Space University (ISU) held its Summer Session in Kitakyushu, Japan. This paper summarizes and expands upon some aspects of space solar power and space transportation that were considered during that session. The issues discussed in this paper are the result of a 10-week study by the Space Solar Power Program design project members and the Space Transportation Group to investigate new paradigms in space propulsion and how those paradigms might reduce the costs for large space programs. The program plan was to place a series of power satellites in Earth orbit. Several designs were studied where many kW, MW, or GW of power would be transmitted to Earth or to other spacecraft in orbit. During the summer session, a space solar power system was also detailed and analyzed. A high-cost space transportation program is potentially the most crippling barrier to such a space power program. At ISU, the focus of the study was to foster and develop some of the new paradigms that may eliminate the barriers to low cost for space exploration and exploitation. Many international and technical aspects of a large multinational program were studied. Environmental safety, space construction and maintenance, legal and policy issues of frequency allocation, technology transfer and control and many other areas were addressed. Over 120

students from 29 countries participated in this summer session. The results discussed in this paper, therefore, represent the efforts of many nations.
Author

N94-10826*# General Dynamics/Astronautics, San Diego, CA.
TRANSPORTATION SYSTEMS ANALYSES: VOLUME 1: EXECUTIVE SUMMARY Semiannual Report
6 May 1993 21 p
(Contract NAS8-39209)
(NASA-CR-192583; NAS 1.26:192583) Avail: CASI HC A03/MF A01

The principal objective of this study is to accomplish a systems engineering assessment of the nation's space transportation infrastructure. This analysis addresses the necessary elements to perform man delivery and return, cargo transfer, cargo delivery, payload servicing, and the exploration of the Moon and Mars. Specific elements analyzed, but not limited to, include the Space Exploration Initiative (SEI), the National Launch System (NLS), the current expendable launch vehicle (ELV) fleet, ground facilities, the Space Station Freedom (SSF), and other civil, military and commercial payloads. The performance of this study entails maintaining a broad perspective on the large number of transportation elements that could potentially comprise the U.S. space infrastructure over the next several decades. To perform this systems evaluation, top-level trade studies are conducted to enhance our understanding of the relationships between elements of the infrastructure. This broad 'infrastructure-level perspective' permits the identification of preferred infrastructures. Sensitivity analyses are performed to assure the credibility and usefulness of study results. This executive summary of the transportation systems analyses (TSM) semi-annual report addresses the SSF logistics resupply. Our analysis parallels the ongoing NASA SSF redesign effort. Therefore, there could be no SSF design to drive our logistics analysis. Consequently, the analysis attempted to bound the reasonable SSF design possibilities (and the subsequent transportation implications). No other strategy really exists until after a final decision is rendered on the SSF configuration.
Derived from text

N94-10827*# General Dynamics Corp., San Diego, CA. Space Systems Div.
TRANSPORTATION SYSTEMS ANALYSES. VOLUME 2: TECHNICAL/PROGRAMMATICS Semiannual Report
6 May 1993 71 p
(Contract NAS8-39209)
(NASA-CR-192582; NAS 1.26:192582; Rept-93H-C-009-0-Vol-2) Avail: CASI HC A04/MF A01

The principal objective of this study is to accomplish a systems engineering assessment of the nation's space transportation infrastructure. This analysis addresses the necessary elements to perform man delivery and return, cargo transfer, cargo delivery, payload servicing, and the exploration of the Moon and Mars. Specific elements analyzed, but not limited to, include the Space Exploration Initiative (SEI), the National Launch System (NLS), the current expendable launch vehicle (ELV) fleet, ground facilities, the Space Station Freedom (SSF), and other civil, military and commercial payloads. The performance of this study entails maintaining a broad perspective on the large number of transportation elements that could potentially comprise the U.S. space infrastructure over the next several decades. To perform this systems evaluation, top-level trade studies are conducted to enhance our understanding of the relationships between elements of the infrastructure. This broad 'infrastructure-level perspective' permits the identification of preferred infrastructures. Sensitivity analyses are performed to assure the credibility and usefulness of study results. This report documents the three principal transportation systems analyses (TSA) efforts during the period 7 November 92 - 6 May 93. The analyses are as follows: Mixed-Fleet (STS/ELV) strategies for SSF resupply; Transportation Systems Data Book - overview; and Operations Cost Model - overview/introduction.
Derived from text

N94-10423# Avions Marcel Dassault, Saint-Cloud (France).
AERODYNAMIC AND AEROTHERMAL CHALLENGES FOR THE DESIGN OF THE HERMES SPACEPLANE
Pierre Perrier *In* AGARD, Theoretical and Experimental Methods in Hypersonic Flows Apr. 1993 10 p (For primary document see N94-10421 01-02)
Copyright Avail: CASI HC A02/MF A04

N94-10459# Messerschmitt-Boelkow-Blohm G.m.b.H., Munich (Germany). Military Aircraft Div.
NUMERICAL METHODS FOR AEROTHERMODYNAMIC DESIGN OF HYPERSONIC SPACE TRANSPORT VEHICLES
K. M. Wanie, A. Brenneis, A. Eberle, and S. Heiss *In* AGARD, Theoretical and Experimental Methods in Hypersonic Flows Apr. 1993 12 p (For primary document see N94-10421 01-02)
Copyright Avail: CASI HC A03/MF A04

17 SPACE COMM., SPACECRAFT COMM., COMMAND & TRACKING

Includes telemetry; space communications networks; astronavigation and guidance; and radio blackout.

For related information see also *04 Aircraft Communications and Navigation* and *32 Communications and Radar.*

N94-10512*# Booz-Allen and Hamilton, Inc., McLean, VA.
POTENTIAL MARKETS FOR ADVANCED SATELLITE COMMUNICATIONS Final Report, Jun. 1993
Steven Adamson, David Roberts, LeRoy Schubert, Brian Smith, Robert Sogegian, and Daniel Walters Sep. 1993 372 p
(Contract NAS3-26387; RTOP 144-50-50)
(NASA-CR-191145; NAS 1.26:191145) Avail: CASI HC A16/MF A03

This report identifies trends in the volume and type of traffic offered to the U.S. domestic communications infrastructure and extrapolates these trends through the year 2011. To describe how telecommunications service providers are adapting to the identified trends, this report assesses the status, plans, and capacity of the domestic communications infrastructure. Cable, satellite, and radio components of the infrastructure are examined separately. The report also assesses the following major applications making use of the infrastructure: (1) Broadband services, including Broadband Integrated Services Digital Network (BISDN), Switched Multimegabit Data Service (SMDS), and frame relay; (2) mobile services, including voice, location, and paging; (3) Very Small Aperture Terminals (VSAT), including mesh VSAT; and (4) Direct Broadcast Satellite (DBS) for audio and video. The report associates satellite implementation of specific applications with market segments appropriate to their features and capabilities. The volume and dollar value of these market segments are estimated. For the satellite applications able to address the needs of significant market segments, the report also examines the potential of each satellite-based application to capture business from alternative technologies.
Author (revised)

N94-11282# EG and G Rocky Flats, Inc., Golden, CO.
REMOTE SURFACE WATER MONITORING RADIO BASED TELEMETRY SYSTEM
W. L. Goodwin and D. Baxter Feb. 1993 12 p Presented at the Thematic Conference of Geologic Remote Sensing, Pasadena, CA, 15 Mar. 1993
(Contract DE-AC34-90DP-62349)
(DE93-009643; RFP-4718; CONF-9303121-1) Avail: CASI HC A03/MF A01

The Environmental Protection Department of EG&G Rocky Flats has designed and developed a unique Remote Surface Water Monitoring System using radio telemetry hardware and computer control software. The system is based on new technologies in microelectronics and environmental monitoring sensors. An engineering team, headed up by the Surface Water Division at EG&G, has proven that with careful evaluation of new technologies and hardware components, a reliable, cost effective and graphical user interface (GUI) system can be designed and installed. The network utilizes standard industrial control hardware and off-the-shelf components in order to meet several time requirements outlined by an Interagency Agreement (IAG) between the Department of Energy, the U.S. Environmental Protection Agency, and state and local authorities. In addition, the system had to meet tight environmental specifications and procedures. The Rocky Flats Plant is part of the U.S. Department of Energy Weapons Complex and is located near the Denver metropolitan area. The plant is required by law, and Interagency Agreement, to maintain strict environmental standards for surface water monitoring and discharge characteristics, including the requirement for utilization of best available technology. DOE

N94-11297*# New Mexico State Univ., Las Cruces. Dept. of Electrical Engineering.

TELEMETERING AND TELECOMMUNICATIONS RESEARCH

William Osborne, Robert Paz, Michael Ross, Brian Kopp, and Norm Ashley 1993 58 p

(Grant NAG5-1491)

(NASA-CR-193235; NAS 1.26:193235) Avail: CASI HC A04/MF A01

The New Mexico State University (NMSU) Center for Space Telemetering and Telecommunications systems is engaged in advanced communications systems research. Four areas of study that are being sponsored concern investigations into the use of trellis-coded modulation (TCM). In particular, two areas concentrate on carrier synchronization research in TCM M-ary phase shift key (MPSK) systems. A third research topic is the study of interference effects on TCM, while the fourth research area is in the field of concatenated TCM systems. Author (revised)

N94-10974*# Rockwell International Corp., Downey, CA. Space Systems Div.

PTTI-AIDED EPHEMERIS CALCULATION AND RAPID DATA LINK ACQUISITION FOR MANNED SPACE FLIGHT

Alfred Anderman *In* NASA. Goddard Space Flight Center, The 24th Annual Precise Time and Time Interval (PTTI) Applications and Planning Meeting Jun. 1993 p 137-152 (For primary document see N94-10963 01-70)

Avail: CASI HC A03/MF A04

18 SPACECRAFT DESIGN, TESTING AND PERFORMANCE

Includes satellites; space platforms; space stations; spacecraft systems and components such as thermal and environmental controls; and attitude controls.

For life support systems see *54 Man/System Technology and Life Support.* For related information see also *05 Aircraft Design, Testing and Performance, 39 Structural Mechanics,* and *16 Space Transportation.*

N94-10366# National Aerospace Lab., Tokyo (Japan). Space Technology Research Group.

ESTIMATION OF THE ATTITUDE MOTION OF THE SMALL SATELLITE ORIZURU [KOGATA JIKKEN EISEI ORIZURU NO SHISEI UNDOU]

Atsushi Nakajima, Fuyuto Terui, Kazuto Ishii, and Hiroaki Habe Apr. 1992 31 p In JAPANESE

(NAL-TR-1145; JTN-93-80437) Avail: CASI HC A03/MF A01

The attitude motion of the small experimental satellite, ORIZURU, was estimated by comparing flight data with computer simulation results from its dynamic model. ORIZURU was ejected from the 2nd stage of an H-1 launch vehicle by a separation mechanism having a single coil-spring whose mechanical characteristics possess a certain degree of uncertainty. Since ORIZURU only transmits attitude information using its sun sensors, both the initial angular momentum added to the satellite at separation from the launcher and its steady motion during in-orbit experimentation were estimated to evaluate release mechanism characteristics and to perform experimental data analysis. Author (NASDA)

N94-10493# Naval Postgraduate School, Monterey, CA.

EXERGY DECREASE IN SHOCK WAVES AND BOUNDARY LAYERS OF SPACE LAUNCH VEHICLES M.S. Thesis

Benjamin F. Roper Mar. 1993 61 p

(AD-A265272) Avail: CASI HC A04/MF A01

The exergy method of analysis uses both the First and Second laws of Thermodynamics to determine where losses occur. This method has been shown to be superior to conventional heat balance analyzes. A primary contributor to the exergy decrease is the production of entropy. Entropy is produced in shock waves and boundary layers, as well as in other regions of the flowfield. A method of analysis is presented to quantify the entropy that is produced in the bow shock wave and the boundary layer of a space launch vehicle for Mach numbers between 1.1 and 10. DTIC

N94-10520# Sandia National Labs., Albuquerque, NM.

PROTON TRANSPORT METHODS FOR SATELLITE SHIELD MODELING

C. R. Drumm Mar. 1993 45 p

(Contract DE-AC04-76DP-00789)

(DE93-013602; SAND-93-0200) Avail: CASI HC A03/MF A01

Satellite electronics may be subjected to a large fluence of protons from the Van Allen belt and from solar flares. To determine if unhardened electronics will survive a radiation environment, the total ionizing dose and displacement damage to the electronics must be determined. Several computer codes are available for modeling proton transport. The codes range in complexity from a very-efficient straight-line approximation to general-geometry, time-dependent Monte Carlo transport, with corresponding increase in computer run time. For most satellite applications, neutrons can be neglected in the analysis. However, neutrons may be important for modeling heavily shielded compartments for personnel and electronics. DOE

N94-10562*# National Aeronautics and Space Administration. Goddard Space Flight Center, Greenbelt, MD.

SATELLITE SITUATION REPORT, VOLUME 32, NO. 1

31 Mar. 1992 97 p

(NASA-TM-109233; NAS 1.15:109233) Avail: CASI HC A05/MF A02

This report consists of data computed at the U.S. Space Command, GSFC, or provided by satellite owners. A space objects box score table is presented with data under the following headings: source/organization, objects in orbit, and decayed objects. The objects in orbit and decayed objects headings have payload, debris, and total as subheadings. The bulk of the document is objects-in-orbit tables with data under the following headings: international designation, name, catalog number, source, launch date, period minutes, inclination, apogee (km), perigee (km), and notes. CASI

N94-10563*# National Aeronautics and Space Administration. Goddard Space Flight Center, Greenbelt, MD.

SATELLITE SITUATION REPORT, VOLUME 32, NO. 2

30 Jun. 1992 97 p

(NASA-TM-109234; NAS 1.15:109234) Avail: CASI HC A05/MF A02

This report consists of data computed at the U.S. Space Command, GSFC, or provided by satellite owners. A space objects box score table is presented with data under the following headings: source/organization, objects in orbit, and decayed objects. The objects in orbit and decayed objects headings have payload, debris, and total as subheadings. The bulk of the document is objects-in-orbit tables with data under the following headings: international designation, name, catalog number, source, launch date, period minutes, inclination, apogee (km), perigee (km), and notes. CASI

N94-10663*# National Aeronautics and Space Administration, Washington, DC.

SPACE STATION REDESIGN TEAM: FINAL REPORT TO THE ADVISORY COMMITTEE ON THE REDESIGN OF THE SPACE STATION

Jun. 1993 300 p

(NASA-TM-109241; NAS 1.15:109241) Avail: CASI HC A13/MF A03

This report is the result of the Space Station Redesign Team's activity. Its purpose is to present without bias, and in appropriate detail, the characteristics and cost of three design and management approaches for the Space Station Freedom. It was presented to the Advisory Committee on the Redesign of the Space Station on 7 Jun. 1993, in Washington, D.C. Derived from text

N94-10665*# POD Associates, Inc., Albuquerque, NM.

DIMENSIONAL SCALING FOR IMPACT CRATERING AND PERFORATION

Alan Watts, Dale Atkinson, and Steve Rieco 16 Mar. 1993 174 p

Sponsored by NASA. Johnson Space Center

(NASA-CR-188259; NAS 1.26:188259) Avail: CASI HC A08/MF A02

This report summarizes the development of two physics-based scaling laws for describing crater depths and diameters caused by normal incidence impacts into aluminum and TFE Teflon. The report then describes equations for perforations in aluminum and TFE Teflon for normal impacts. Lastly, this report also studies the effects of non-normal incidence on cratering and perforation. Derived from text

N94-10666*# POD Associates, Inc., Albuquerque, NM.
THE MAGNITUDE OF IMPACT DAMAGE ON LDEF MATERIALS Final Report
Martha Allbrooks and Dale Atkinson 11 Jul. 1992 89 p Original contains color illustrations
(Contracts NAS9-17900; SC-02N0165768; POD Proj. 960-12-171)
(NASA-CR-188258; NAS 1.26:188258) Avail: CASI HC A05/MF A01; 40 functional color pages

The purpose of this report is to document the magnitude and types of impact damage to materials and systems on the LDEF. This report will provide insights which permit NASA and industry space-systems designers to more rapidly identify potential problems and hazards in placing a spacecraft in low-Earth orbit (LEO). This report is structured to provide (1) a background on LDEF, (2) an introduction to the LEO meteoroid and debris environments, and (3) descriptions of the types of damage caused by impacts into structural materials, and contamination caused by spallation and ejecta from impact events. Derived from text

N94-10699*# National Aeronautics and Space Administration, Washington, DC.
TOPEX/POSEIDON: A UNITED STATES/FRANCE MISSION. OCEANOGRAPHY FROM SPACE: THE OCEANS AND CLIMATE
1992 23 p Original contains color illustrations
(NASA-TM-108253; NAS 1.15:108253) Avail: CASI HC A03/MF A01; 17 functional color pages

The TOPEX/POSEIDON space mission, sponsored by NASA and France's space agency, the Centre National d'Etudes Spatiales (CNES), will give new observations of the Earth from space to gain a quantitative understanding of the role of ocean currents in climate change. Rising atmospheric concentrations of carbon dioxide and other 'greenhouse gases' produced as a result of human activities could generate a global warming, followed by an associated rise in sea level. The satellite will use radar altimetry to measure sea-surface height and will be tracked by three independent systems to yield accurate topographic maps over the dimensions of entire ocean basins. The satellite data, together with the Tropical Ocean and Global Atmosphere (TOGA) program and the World Ocean Circulation Experiment (WOCE) measurements, will be analyzed by an international scientific team. By merging the satellite observations with TOGA and WOCE findings, the scientists will establish the extensive data base needed for the quantitative description and computer modeling of ocean circulation. The ocean models will eventually be coupled with atmospheric models to lay the foundation for predictions of global climate change. Derived from text

N94-10756*# National Aeronautics and Space Administration. Lewis Research Center, Cleveland, OH.
EXPERIMENTAL MEASUREMENT OF THE PLASMA CONDUCTIVITY OF Z93 AND Z93P THERMAL CONTROL PAINT
G. Barry Hillard Sep. 1993 77 p
(RTOP 506-41-52)
(NASA-TM-106284; E-8022; NAS 1.15:106284) Avail: CASI HC A05/MF A01

Two samples each of Z93 and Z93P thermal control paint were exposed to a simulated space environment in a plasma chamber. The samples were biased through a series of voltages ranging from -200 volts to +300 volts and electron and ion currents measured. By comparing the currents to those of pure metal samples of the same size and shape, the conductivity of the samples was calculated. Measured conductivity was dependent on the bias potential in all cases. For Z93P, conductivity was approximately constant over much of the bias range and we find a value of 0.5 micro-mhos per square meter for both electron and ion current. For Z93, the dependence on bias was much more pronounced but conductivity can be said to be approximately one order of magnitude larger. In addition to presenting these results, this report documents all of the experimental data as well as the statistical analyses performed. Author

N94-10808*# National Aeronautics and Space Administration. Marshall Space Flight Center, Huntsville, AL.
SPACE STATION REDESIGN OPTION A: MODULAR BUILDUP CONCEPT
10 Jun. 1993 85 p
(NASA-TM-108415; NAS 1.15:108415) Avail: CASI HC A05/MF A01

In early 1993, President Clinton mandated that NASA look at lower cost alternatives to Space Station Freedom. He also established an independent advisory committee - the Blue Ribbon Panel - to review the redesign work and evaluate alternatives. Daniel Goldin, NASA Administrator, established a Station Redesign Team that began operating in late March from Crystal City, Virginia. NASA intercenter teams - one each at Marshall Space Flight Center, Johnson Space Center, and Langley Research Center provided engineering and other support. The results of the Option A study done at Marshall Space Flight Center are summarized. Two configurations (A-1 and A-2) are covered. Additional data is provided in the briefing package MSFC SRT-001, Final System Review to SRT-002, Space Station Option A Modular Buildup Concept, Volumes 1-5, Revision B, June 10, 1993. In June 1993, President Clinton decided to proceed with a modular concept consistent with Option A, and asked NASA to provide an Implementation Plan by September. All data from the Option A redesign activity was provided to NASA's Transition Team for use in developing the Implementation Plan. Author (revised)

N94-10859# National Aerospace Lab., Tokyo (Japan). Thermofluid Dynamics Div.
IN-ORBIT PERFORMANCE TESTS AND TELE-COMMAND SYSTEMS OF THE UMBRELLA TEST SATELLITE (DEBUT) ['ORIZURU' (DEBUT) NO UCHUU JIKKEN UNYOU]
Takao Kumagai, Atsushi Nakajima, and Yoshio Sakurai Jun. 1992 27 p In JAPANESE
(NAL-TR-1165; JTN-93-80445) Avail: CASI HC A03/MF A01

In February 1990, an H-1 launch vehicle was launched which successfully put DEBUT (Deployable Boom and Umbrella Test Satellite), MOS-1b (Marine Observation Satellite), and JAS-1b (Japan Amateur Radio Satellite) into each orbits. DEBUT is the small satellite (50 kg) having deployable and retractable boom and umbrella systems which are important subsystems to be used on the Tether/Boomeran Satellite. All the mission and telemetry/command (tele-command) systems functioned well, and all the planned, in-orbit performance tests were successfully completed. These tests and DEBUT's tele-command systems are described. Author (NASDA)

N94-10944 RADEX, Inc., Bedford, MA.
ANALYSIS OF GEOPHYSICAL MEASUREMENTS AND SPACECRAFT INTERACTIONS Final Report, Jun. 1989 - Jan. 1993
J. N. Bass, K. H. Bhavnani, N. A. Bonito, K. H. Bounar, and P. L. Grady 29 Jan. 1993 286 p Limited Reproducibility: More than 20% of this document may be affected by microfiche quality
(Contract F19628-89-C-0068)
(AD-A266064; RXR-93011; PL-TR-93-2031) Avail: Issuing Activity (Defense Technical Information Center (DTIC))

Investigations were supported to analyze geophysical measurements with integrated applications of ephemerides physics and mathematics of the ionosphere and near space. The projects undertaken included analytical and computational simulation of the interactive spacecraft processes associated with the following: charging, contamination, liquid venting, and critical ionization velocity; data based and analytical investigations of trapped particles, dosage, magnetic fields, and instrumentation for the CRRES experiment; and data based studies of auroral electron and ion precipitation including neural network techniques, ionospheric scintillation and OTH backscatter, and atmospheric density and orbital decay. Systems were developed and applied for calibration and processing of the CRRES and APEX magnetometers, and for generation of satellite attitude and ephemeris. Techniques employed for applying coordinate systems, depicting vehicle and astronomical circumstances, and interactively presenting data in conventional and color formats are also described. DTIC

N94-11223# Weight (Thomas H.) and Associates, Long Beach, CA.
FUZZIFICATION OF ASAT'S RULE BASED AIMPOINT SELECTION Final Report, 2 Nov. 1992 - 15 Jun. 1993
Thomas H. Weight 15 Jun. 1993 69 p
(Contract DASG60-93-C-0005)
(AD-A266068) Avail: CASI HC A04/MF A01

The aimpoint algorithms being developed at Dr. Weight and Associates are based on the concept of fuzzy logic. This approach does not require a particular type of sensor data or algorithm type, but allows the user to develop a fuzzy logic algorithm based on existing aimpoint algorithms and models. This provides an opportunity for the user to upgrade an existing system design to achieve higher performance at minimal cost. Many projects have aimpoint algorithms which are based on 'crisp' logic rule based algorithms. These algorithms are sensitive to glint, corner reflectors, or intermittent thruster firings, and to uncertainties in the a priori estimates of angle of attack. If these projects are continued through to a demonstration involving a launch to hit a target, it is quite possible that the crisp logic approaches will need to be upgraded to handle these important error sources. DTIC

N94-11462# European Space Agency. European Space Research and Technology Center, ESTEC, Noordwijk (Netherlands). Publications Div.
ESRO'S FIRST SCIENTIFIC SATELLITE PROGRAMME, 1961 - 1966
M. DeMaria (Rome Univ., Italy.), J. Krige (European Univ. Inst., Florence, Italy.), and Arturo Russo (Palermo Univ., Italy.) Oct. 1992 51 p Original contains color illustrations
(ESA-HSR-2) Avail: CASI HC A04/MF A01

The European Space Agency (ESA) History Study Reports are preliminary reports of studies carried out within the framework of an ESA contract. As such they will form the basis of a comprehensive study of European Space activities covering the period from 1959 to 1987. The early development of ESRO's satellite program is addressed. The process which led to the definition of ESRO's eight year scientific program is analyzed. The organizational structure by which proposals coming from the scientific community were discussed within ESRO in order to arrive at definite choices about mission objectives and satellite payloads is described. The painful process of revision of the original program undertaken in the first three-year period of ESRO (1964-1966) is addressed. Derived from text

N94-12280# National Space Development Agency, Ibaraki (Japan). Thermal and Structural Engineering Lab.
THE TRIAL MANUFACTURE AND TEST OF CRITICAL COMPONENTS IN DOCKING MECHANISM Technical Progress Report, FY 1991 [DOKKINGO KIKOU: KURITIKARU YOUSO SHISAKU SHIKEN]
31 Mar. 1993 106 p In JAPANESE
(NASDA-TMR-930005; TK-ST0467; JTN-93-80480) Avail: CASI HC A06/MF A02

An overview of the trial manufacture and test of critical elements for rendezvous and docking mechanism is presented. The following aspects of the research and development are outlined: (1) overall scheme of the research and development; (2) progress of the research and development from FY (Fiscal Year) 1976 through FY 1991; (3) the trial manufacture and test of critical elements, including the system design, design studies on mechanism section and driving circuit, the manufacture and test, docking mechanism system test, and simulation analysis; and (4) docking mechanism for ETS-7 (Engineering Test Satellite-7), including development specifications for ETS-7 docking mechanism, study on the development program and schedule, and microgravity simulation test equipment. Author (NASDA)

N94-12356# Instituto de Pesquisas Espaciais, Sao Jose dos Campos (Brazil).
PROJECT OF AN ATTITUDE CONTROL SYSTEM (THREE AXIS) OF A SATELLITE USING THE LQG/LTR METHODOLOGY M.S. Thesis [PROJETO DE UM SISTEMA DE CONTROLE DE ATITUDE (TRES EIXOS) DE SATELITES UTILIZANDO A METODOLOGIA LQG/LTR]
Ney Ricardo Moscati Feb. 1992 239 p In PORTUGESE
(INPE-5473-TDI/504) Avail: CASI HC A11/MF A03

In Earth remote sensing satellites, an Attitude Control System (ACS) is necessary for stabilization, due to the fact that even if the vehicle is precisely oriented in launch, it can deviate from this orientation due the influence of ambiental torques, internal changes and coupling between attitude dynamics and a satellite's orbital and flexible dynamics. The configuration adopted for the ACS (a momentum wheel and two reaction wheels) exhibits a strong coupling between roll and yaw, hence it is a multivariable system, while the pitch axis is practically decoupled. The linear model for the attitude dynamics of this satellite exhibits uncertainties due to non-modeled dynamics of the flexible panels and giroscopic coupling variations, caused by momentum wheel velocity changes. The LQG/LTR methodology is used to project the ACS operating on the normal mode. This methodology is inherently a multivariable tool, where the compensator's structure is known as MBC, the same structure as LQG compensators. It is based on both time and frequency domain approaches, and has the great advantage of treating the robustness at project level. The frequency project specifications, usually used for SISO systems such as gain and phase margins, bandwidth, disturbance rejection characteristics and insensitivity to parameter variations are extended to the MIMO case through the singular value concept. The LQG/LTR methodology provides, basically, the recovery of the excellent robustness characteristics of systems with LQR regulators when the state is completely measured. On the other hand, specifications on the time domain are difficult to deal with. In view of the easy usage of the methodology and good simulations results obtained, it has been concluded that the LQG/LTR methodology is an attractive option to project ACS when the model is a MIMO type. Author (revised)

N94-12387# Virginia Polytechnic Inst. and State Univ., Blacksburg. Dept. of Engineering Science and Mechanics.
CONTROL OF LARGE SPACE STRUCTURES WITH VARYING CONFIGURATION Final Report, 15 Apr. 1989 - 31 Aug. 1992
Leonard Meirovitch 12 Mar. 1993 9 p
(Contract F49620-89-C-0045)
(AD-A265764; AFOSR-93-0387TR) Avail: CASI HC A02/MF A01

The research has produced significant advances in the state of the art on the following subjects: (1) a mathematical formulation for the maneuvering and control of flexible articulated multibody systems; (2) a theory for the modeling of flexible multibody structures; and (3) a perturbation theory for the maneuvering and control of articulated flexible multibody systems. DTIC

N94-12394# Aerospace Corp., El Segundo, CA. Technology Operations.
LESSONS LEARNED FROM THE LONG DURATION EXPOSURE FACILITY
Wayne K. Stuckey 15 Feb. 1993 20 p
(Contract F04701-88-C-0089)
(AD-A266026; TR-93(3935)-7; SMC-TR-93-23) Avail: CASI HC A03/MF A01

The Long Duration Exposure Facility (LDEF) was launched by the Space Shuttle in Apr. 1984 and recovered in Jan. 1990. There were 57 experiments containing over 10,000 specimens to test the effects of the space environment on materials, components, and systems. Originally planned for one year, the exposure actually lasted almost six years. While many LDEF investigations are continuing, results to date have given valuable information on long-term performance in orbit. Results from the LDEF investigators and the Special Investigation Groups are briefly summarized along with potential benefits from LDEF for future missions. DTIC

N94-12541# Wright Lab., Wright-Patterson AFB, OH.
SPACE TRUSS ZERO GRAVITY DYNAMICS Final Report, Mar. 1989 - Feb. 1990
Andrew D. Swanson, Wayne Yuen, and John R. Mackaman Mar. 1993 49 p
(AF Proj. 2401)
(AD-A266130; WL-TR-92-3030) Avail: CASI HC A03/MF A01

This technical report describes two truss experiments flown on the NASA KC-135 Reduced Gravity Aircraft. The purpose of these experiments was to investigate large space structure dynamics, ground test methods, and passive and active damping. A 2-meter truss was first flown to determine the rigid body dynamics in the aircraft during zero-gravity. The second flight's objective was to measure structural modes of a 12-meter truss, which represented a space structure component. Typically five to ten seconds of zero gravity data were recorded for each parabolic arc. Flight test results are compared with ground testing in which a low restraint spring mechanism was used to suspend the truss. Good correlation between ground and flight test results was achieved; the major differences were caused by suspension system friction, which coupled the frame modes with the bending and torsion modes. DTIC

N94-10250# European Space Agency. European Space Research and Technology Center, ESTEC, Noordwijk (Netherlands).
THE CRITICAL FACILITY ON IML-1
T. Dewandre, M. Cork, and Alain Gonfalone *In its* Proceedings of the 8th European Symposium on Materials and Fluid Sciences in Microgravity, Volume 2 Aug. 1992 p 917-919 (For primary document see N94-10171 01-29)

Copyright Avail: CASI HC A01/MF A04; ESA, EPD, ESTEC, Noordwijk, Netherlands, HC

N94-10428# Fluid Gravity Engineering Ltd., Witley (England).
PLANETARY ENTRY VEHICLE DESIGN FOR PLANNED AND POTENTIAL ESA MISSIONS TO TITAN, MARS, AND EARTH RETURN (FGE TN 51/92)
Arthur Smith *In* AGARD, Theoretical and Experimental Methods in Hypersonic Flows Apr. 1993 12 p (For primary document see N94-10421 01-02)
Copyright Avail: CASI HC A03/MF A04

N94-10683# Korea Advanced Inst. of Science and Technology, Seoul (Republic of Korea). Satellite Technology and Research Center.
OVERVIEW OF KITSAT
Dal Choi Soon *In* Science and Technology Agency, Space Activities in the Asia Pacific Region 16 Nov. 1992 p 33-35 Original language document was announced as N93-21275 (For primary document see N94-10676 01-12)
Avail: CASI HC A01/MF A01

N94-11319# Phillips Lab., Edwards AFB, CA.
ADAPTIVE STRUCTURES FOR SPACECRAFT: A USAF PERSPECTIVE
Alok Das, Glenn Ormbrek (Wright Lab., Wright-Patterson AFB, OH.), and Michael Obal (Strategic Defense Initiative Organization, Washington, DC.) *In* AGARD, Smart Structures for Aircraft and Spacecraft Apr. 1993 13 p (For primary document see N94-11317 01-24)
Copyright Avail: CASI HC A03/MF A04

N94-11320*# National Aeronautics and Space Administration. Langley Research Center, Hampton, VA.
DYNAMIC TESTS ON THE NASA LANGLEY CSI EVOLUTIONARY MODEL
H. Troidl (Industrieanlagen-Betriebsgesellschaft m.b.H., Ottobrunn, Germany.) and K. B. Elliott *In* AGARD, Smart Structures for Aircraft and Spacecraft Apr. 1993 9 p (For primary document see N94-11317 01-24)
Copyright Avail: CASI HC A02/MF A04

N94-11323# Strategic Defense Initiative Organization, Washington, DC.
THE SATELLITE ATTACK WARNING AND ASSESSMENT FLIGHT EXPERIMENT (SAWAFE)
Michael Obal, Bill Saylor, Hugh S. Murray, Martin R. Sweet, Dan Holden, and Calvin Moss *In* AGARD, Smart Structures for Aircraft and Spacecraft Apr. 1993 13 p (For primary document see N94-11317 01-24)
Copyright Avail: CASI HC A03/MF A04

N94-11342# Rome Univ. (Italy). Dipt. Aerospaziale.
ON POSSIBLE APPLICATIONS OF SMART STRUCTURES TO CONTROL OF SPACE SYSTEMS
F. Betti, P. Gasbarri, P. Gaudenzi, F. Persiani (Bologna Univ., Italy.), G. M. Saggiani (Istituto Studi e Applicazioni Scienze Aeronautiche Spaziali, Forli, Italy.), and P. Santini *In* AGARD, Smart Structures for Aircraft and Spacecraft Apr. 1993 14 p Sponsored in part by Ist. Studi e Applicazioni Scienze Aeronautiche Spaziali (For primary document see N94-11317 01-24)
(Grant 293/62)
Copyright Avail: CASI HC A03/MF A04

N94-11559*# National Aeronautics and Space Administration. Lyndon B. Johnson Space Center, Houston, TX.
RADIATION CONSIDERATIONS FOR INTERPLANETARY MISSIONS Abstract Only
Gautam D. Badwar, Patrick M. ONeill (National Aeronautics and Space Administration. Langley Research Center, Hampton, VA.), and Francis A. Cucinotta (National Aeronautics and Space Administration. Langley Research Center, Hampton, VA.) *In its* Sixth Annual Workshop on Space Operations Applications and Research (SOAR 1992), Volume 2 Feb. 1993 p 611 (For primary document see N94-11527 01-99)
Avail: CASI HC A01/MF A03

N94-11579*# National Aeronautics and Space Administration. Goddard Space Flight Center, Greenbelt, MD.
ROBOTIC SERVICING ON EARTH ORBITING SATELLITES Abstract Only
Stanford Ollendorf *In* NASA. Johnson Space Center, Sixth Annual Workshop on Space Operations Applications and Research (SOAR 1992), Volume 2 Feb. 1993 p 733 (For primary document see N94-11527 01-99)
Avail: CASI HC A01/MF A03

19 SPACECRAFT INSTRUMENTATION

For related information see also *06 Aircraft Instrumentation* and *35 Instrumentation and Photography.*

No abstracts in this category.

20 SPACECRAFT PROPULSION AND POWER

Includes main propulsion systems and components, e.g., rocket engines; and spacecraft auxilliary power sources.

For related information see also *07 Aircraft Propulsion and Power, 28 Propellants and Fuels, 44 Energy Production and Conversion,* and *15 Launch Vehicles and Space Vehicles.*

N94-10282# Sandia National Labs., Albuquerque, NM.
SPACE NUCLEAR THERMAL PROPULSION NUCLEAR ELEMENT TESTS AT SANDIA NATIONAL LABORATORIES
G. W. Mitchell 1992 6 p Presented at the 10th Symposium on Space Nuclear Power and Propulsion, Albuquerque, NM, 10-14 Jan. 1993
(Contract DE-AC04-76DP-00789)
(DE93-002301; SAND-92-1350C; CONF-930103-13) Avail: CASI HC A02/MF A01 (US Sales Only)

Nuclear Element Tests (NET) which are being performed as part of the US Air Force Space Nuclear Thermal Propulsion (SNTP) Program to evaluate high performance fuel elements intended for use in future nuclear propulsion systems are described. The NET experiments are to be performed at the Sandia National Laboratories (SNL's) Annular Core Research Reactor (ACRR). Objectives of these experiments are to provide engineering validation and demonstration of critical-fuel-element-related technologies and an experimental data base to support analytical design methods for the SNTP Program. Currently, hardware for the first two fueled NET experiments was fabricated, and cold flow tests were accomplished with a representative set of hardware to assure the experimental capability to achieve test objectives in-reactor. Assembly of the first NET experiment to test a representative nuclear fuel elements is in progress, and planned operational sequences were defined. DOE

N94-10299# Sandia National Labs., Albuquerque, NM.
SPACE NUCLEAR TECHNOLOGY
J. V. Walker 1 Dec. 1992 21 p
(Contract DE-AC04-76DP-00789)
(DE93-010184; DOE/FTR-93010184) Avail: CASI HC A03/MF A01 (US Sales Only)

Member of Industry-Lab-Government delegation invited to visit the Commonwealth of Independent States (CIS) to attend Nuclear Rocket Engines Conference in Semipalatinsk-21, Kazakhstan; visit a number of nuclear facilities; participate in technical discussions at several Russian organizations involved with space nuclear technology; discuss possibilities of Sandia participation in US/CIS programs. Significant programs exist in the CIS in these areas, but appear to have slowed due to funding difficulties and national priorities. The CIS possesses valuable technologies of significant relevance to current US interests and programs which they seem willing to make available to the US as relations between the US and the CIS improve. DOE

N94-10700*# Tennessee Univ. Space Inst., Tullahoma. Center for Laser Applications.
ARCJET SPACE THRUSTERS Final Technical Report, Mar. 1990 - May 1993
Dennis Keefer and Robert Rhodes May 1993 7 p
(Grant NAG3-1159)
(NASA-CR-193191; NAS 1.26:193191) Avail: CASI HC A02/MF A01

Electrically powered arc jets which produce thrust at high specific impulse could provide a substantial cost reduction for orbital transfer and station keeping missions. There is currently a limited understanding of the complex, nonlinear interactions in the plasma propellant which has hindered the development of high efficiency arc jet thrusters by making it difficult to predict the effect of design changes and to interpret experimental results. A computational model developed at the University of Tennessee Space Institute (UTSI) to study laser powered thrusters and radio frequency gas heaters has been adapted to provide a tool to help understand the physical processes in arc jet thrusters. The approach is to include in the model those physical and chemical processes which appear to be important, and then to evaluate our judgement by the comparison of numerical simulations with experimental data. The results of this study have been presented at four technical conferences. The details of the work accomplished in this project are covered in the individual papers included in the appendix of this report. We present a brief description of the model covering its most important features followed by a summary of the effort. Derived from text

N94-10761*# National Aeronautics and Space Administration. Lewis Research Center, Cleveland, OH.
CHARACTERIZATION OF IN-FLIGHT PERFORMANCE OF ION PROPULSION SYSTEMS
James S. Sovey and Vincent K. Rawlin Jun. 1993 15 p Presented at the 29th AIAA Joint Propulsion Conference and Exhibit, Monterey, CA, 28-30 Jun. 1993; sponsored by AIAA, SAE, ASME, and ASEE
(RTOP 506-42-31)
(NASA-TM-106283; E-8021; NAS 1.15:106283; AIAA Paper 93-2217)
Avail: CASI HC A03/MF A01

In-flight measurements of ion propulsion performance, ground test calibrations, and diagnostic performance measurements were reviewed. It was found that accelerometers provided the most accurate in-flight thrust measurements compared with four other methods that were surveyed. An experiment has also demonstrated that pre-flight alignment of the thrust vector was sufficiently accurate so that gimbal adjustments and use of attitude control thrusters were not required to counter disturbance torques caused by thrust vector misalignment. The effects of facility background pressure, facility enhanced charge-exchange reactions, and contamination on ground-based performance measurements are also discussed. Vacuum facility pressures for inert-gas ion thruster life tests and flight qualification tests will have to be less than 2 mPa to ensure accurate performance measurements. Author

N94-10763*# National Aeronautics and Space Administration. Lewis Research Center, Cleveland, OH.
AXISYMMETRIC SINGLE SHEAR ELEMENT COMBUSTION INSTABILITY EXPERIMENT
Kevin J. Breisacher Jun. 1993 13 p Presented at the 29th Joint Propulsion Conference and Exhibit, Monterey, CA, 28-30 Jun. 1993; sponsored by AIAA, SAE, ASME, and ASEE
(RTOP 584-03-11)
(NASA-TM-106327; E-8082; NAS 1.15:106327; AIAA Paper 93-1953)
Avail: CASI HC A03/MF A01

The combustion stability characteristics of a combustor consisting of a single shear element and a cylindrical chamber utilizing LOX and gaseous hydrogen as propellants are presented. The combustor geometry and the resulting longitudinal mode instability are axisymmetric. Hydrogen injection temperature and pyrotechnic pulsing were used to determine stability boundaries. Mixture ratio, fuel annulus gap, and LOX post configuration were varied. Performance and stability data are presented for chamber pressures of 300 and 1000 psia. Author

N94-10765*# National Aeronautics and Space Administration. Lewis Research Center, Cleveland, OH.
SPECIFICATION AND TESTING FOR POWER BY WIRE AIRCRAFT
Irving G. Hansen and Barbara H. Kenney Aug. 1993 8 p Presented at the 28th Intersociety Energy Conversion Engineering Conference, Atlanta, GA, 8-13 Aug. 1993; sponsored by American Chemical Society
(RTOP 538-01-11)
(NASA-TM-106232; E-7951; NAS 1.15:106232) Avail: CASI HC A02/MF A01

A power by wire aircraft is one in which all active functions other than propulsion are implemented electrically. Other nomenclature are 'all electric airplane,' or 'more electric airplane.' What is involved is the task of developing and certifying electrical equipment to replace existing hydraulics and pneumatics. When such functions, however, are primary flight controls which are implemented electrically, new requirements are imposed that were not anticipated by existing power system designs. Standards of particular impact are the requirements of ultra-high reliability, high peak transient bi-directional power flow, and immunity to electromagnetic interference and lightning. Not only must the electromagnetic immunity of the total system be verifiable, but box level tests and meaningful system models must be established to allow system evaluation. This paper discusses some of the problems, the system modifications involved, and early results in establishing wiring harness and interface susceptibility requirements. Author (revised)

N94-10911*# Lamar Univ., Beaumont, TX. Coll. of Engineering.
INVESTIGATION OF ALTERNATE POWER SOURCE FOR SPACE SHUTTLE ORBITER HYDRAULIC SYSTEM Final Technical Report
William E. Simon and Fred M. Young 26 May 1993 95 p
(Grant NAG9-626)
(NASA-CR-193229; NAS 1.26:193229) Avail: CASI HC A05/MF A01

This investigation consists of a short-term feasibility study to determine whether or not an alternate electrical power source would trade favorably from a performance, reliability, safety, operation, and weight standpoint in replacing the current auxiliary power unit subsystems with its attendant components (water spray boiler, hydrazine fuel and tanks, feed and vent lines, controls, etc.), operating under current flight rules. Results of this feasibility study are used to develop recommendations for the next step (e.g., to determine if such an alternate electrical power source would show an advantage given that the current operational flight mode of the system could be modified in such a way as not to constrain the operational capability and safety of the vehicle). However, this next step is not within the scope of this investigation. This study does not include a cost analysis, nor does it include investigation of the integration aspects involved in such a trade, except in a qualitative sense for the determination of concept feasibility. Derived from text

N94-10934*# Computational Fluid Dynamics Research Corp., Huntsville, AL. Research and Development Services and Software.
COMBUSTION CHAMBER ANALYSIS CODE Final Report, Dec. 1989 - Jun. 1993
A. J. Przekwas, Y. G. Lai, A. Krishnan, R. K. Avva, and M. G. Giridharan May 1993 93 p
(Contract NAS8-37824)
(NASA-CR-192585; NAS 1.26:192585; CFDRC-4105/6) Avail: CASI HC A05/MF A01

A three-dimensional, time dependent, Favre averaged, finite volume Navier-Stokes code has been developed to model compressible and incompressible flows (with and without chemical reactions) in liquid rocket engines. The code has a non-staggered formulation with generalized body-fitted-coordinates (BFC) capability. Higher order differencing methodologies such as MUSCL and Osher-Chakravarthy schemes are available. Turbulent flows can be modeled using any of the five turbulent models present in the code. A two-phase, two-liquid, Lagrangian spray model has been incorporated into the code. Chemical equilibrium and finite rate reaction models are available to model chemically reacting flows. The discrete ordinate method is used to model effects of thermal radiation. The code has been validated extensively against benchmark experimental data and has been applied to model flows in several propulsion system components of the SSME and the STME. Author

N94-10938*# TRW Space Technology Labs., Redondo Beach, CA. Applied Technology Div.
SPACE STORABLE ROCKET TECHNOLOGY PROGRAM (SSRT). OPTION 1 PROGRAM Final Report
Melvin L. Chazen, Thomas Mueller, and Thomas Rust 5 Aug. 1993

95 p
(Contract NAS3-26246)
(NASA-CR-191171; NAS 1.26:191171) Avail: CASI HC A05/MF A01

The Space Storable Rocket Technology (SSRT) Option 1 Program was initiated in October 1991 after completion of the Basic Program. The program was restructured in mid-July 1992 to incorporate a Rhenium Technology Task and reduce the scope of the LO2-N2H4 engine development. The program was also extended to late February 1993 to allow for the Rhenium Technology Task completion. The Option 1 Program was devoted to evaluation of two new injector elements, evaluation of two different methods of thermal protection of the injector, evaluation of high temperature material properties of rhenium and evaluation of methods of joining the rhenium thrust chamber to the columbium injector and nozzle extension. In addition, critical experiments were conducted (Funded by Option 2) to evaluate mechanisms to understand the effects of GO2 injection into the chamber, helium injection into the main LO2, effect of the splash plate and effect of decreasing the aspect ratio of the 120-slot (-13a) element. The performance and thermal models were used to further correlate the test results with analyses. The results of the work accomplished are summarized. Derived from text

N94-11053*# National Aeronautics and Space Administration, Washington, DC.

APPLYING DESIGN PRINCIPLES TO FUSION REACTOR CONFIGURATIONS FOR PROPULSION IN SPACE

Scott A. Carpenter (California Univ., Berkeley. Lawrence Berkeley Lab.), Marc E. Deveny (Deveny, Marc E., Corona, CA.), and Norman R. Schulze 1993 20 p Presented at the AIAA/SAE/ASME/ASEE 29th Joint Propulsion Conference and Exhibit, Monterey, CA, 28-30 Jun. 1993
(NASA-TM-108247; NAS 1.15:108247; AIAA Paper 93-2027) Copyright
Avail: CASI HC A03/MF A01

The application of fusion power to space propulsion requires rethinking the engineering-design solution to controlled-fusion energy. Whereas the unit cost of electricity (COE) drives the engineering-design solution for utility-based fusion reactor configurations; initial mass to low earth orbit (IMLEO), specific jet power (kW(thrust)/kg(engine)), and reusability drive the engineering-design solution for successful application of fusion power to space propulsion. We applied three design principles (DP's) to adapt and optimize three candidate-terrestrial-fusion-reactor configurations for propulsion in space. The three design principles are: provide maximum direct access to space for waste radiation, operate components as passive radiators to minimize cooling-system mass, and optimize the plasma fuel, fuel mix, and temperature for best specific jet power. The three candidate terrestrial fusion reactor configurations are: the thermal barrier tandem mirror (TBTM), field reversed mirror (FRM), and levitated dipole field (LDF). The resulting three candidate space fusion propulsion systems have their IMLEO minimized and their specific jet power and reusability maximized. We performed a preliminary rating of these configurations and concluded that the leading engineering-design solution to space fusion propulsion is a modified TBTM that we call the Mirror Fusion Propulsion System (MFPS). Author (revised)

N94-11122# Sandia National Labs., Albuquerque, NM.

AD100/ADSIM, ACSL, AND MATLAB OUTPUT COMPARISONS USING FREQUENCY-RESPONSE ANALYSIS

R. S. Edmunds 1992 6 p Presented at the Summer Computer Simulation Conference, Boston, MA, 19-21 Jul. 1993
(Contract DE-AC04-76DP-00789)
(DE93-009640; SAND-92-2526C; CONF-930765-1) Avail: CASI HC A02/MF A01

Control system design and design verification make use of a variety of simulation tools, often including both nonreal-time and hardware-in-the-loop simulation. Additionally, the design process often uses linear analysis tools. This paper discusses the use of frequency-response analysis to assist in verifying that the different design and verification tools are consistent, and to help uncover and understand inconsistancies should they exist. The control system design example considered is for an elastic sounding-rocket thrust-vector control system. DOE

N94-11252*# National Aeronautics and Space Administration. Lewis Research Center, Cleveland, OH.

A LABORATORY MODEL OF A HYDROGEN/OXYGEN ENGINE FOR COMBUSTION AND NOZZLE STUDIES

Sybil Huang Morren, Roger M. Myers (Sverdrup Technology, Inc., Brook Park, OH.), Stephen E. Benko, Lynn A. Arrington (Sverdrup Technology, Inc., Brook Park, OH.), and Brian D. Reed Jun. 1993 35 p Presented at the 29th Joint Propulsion Conference and Exhibit, Monterey, CA, 28-30 Jun. 1993; sponsored by AIAA, SAE, ASME, and ASEE
(RTOP 506-42-31)
(NASA-TM-106281; AIAA Paper 93-1825; E-7813; NAS 1.15:106281)
Avail: CASI HC A03/MF A01

A small laboratory diagnostic thruster was developed to augment present low thrust chemical rocket optical and heat flux diagnostics at the NASA Lewis Research Center. The objective of this work was to evaluate approaches for the use of temperature and pressure sensors for the investigation of low thrust rocket flow fields. The nominal engine thrust was 110 N. Tests were performed at chamber pressures of about 255 kPa, 370 kPa, and 500 kPa with oxidizer to fuel mixture ratios between 4.0 and 8.0. Two gaseous hydrogen/gaseous oxygen injector designs were tested with 60 percent and 75 percent fuel film cooling. The thruster and instrumentation designs were proven to be effective via hot fire testing. The thruster diagnostics provided inner wall temperature and static pressure measurements which were compared to the thruster global performance data. For several operating conditions, the performance data exhibited unexpected trends which were correlated with changes in the axial wall temperature distribution. Azimuthal temperature distributions were found to be a function of operating conditions and hardware configuration. The static pressure profiles showed that no severe pressure gradients were present in the rocket. The results indicated that small differences in injector design can result in dramatically different thruster performance and wall temperature behavior, but that these injector effects may be overshadowed by operating at a high fuel film cooling rate. Author (revised)

N94-11307*# National Aeronautics and Space Administration. Lewis Research Center, Cleveland, OH.

HIGH EFFICIENCY DIRECT THERMAL TO ELECTRIC ENERGY CONVERSION FROM RADIOISOTOPE DECAY USING SELECTIVE EMITTERS AND SPECTRALLY TUNED SOLAR CELLS

Donald L. Chubb, Dennis J. Flood, and Roland A. Lowe (Cleveland State Univ., OH.) Aug. 1993 16 p Prepared for presentation at the Third European Space Power Conference, Graz, Austria, 23-27 Aug. 1993; sponsored by ESA and ASA
(RTOP 506-41-11)
(NASA-TM-106227; E-7945; NAS 1.15:106227) Avail: CASI HC A03/MF A01

Thermophotovoltaic (TPV) systems are attractive possibilities for direct thermal-to-electric energy conversion, but have typically required the use of black body radiators operating at high temperatures. Recent advances in both the understanding and performance of solid rare-earth oxide selective emitters make possible the use of TPV at temperatures as low as 1200K. Both selective emitter and filter system TPV systems are feasible. However, requirements on the filter system are severe in order to attain high efficiency. A thin-film of a rare-earth oxide is one method for producing an efficient, rugged selective emitter. An efficiency of 0.14 and power density of 9.2 W/KG at 1200K is calculated for a hypothetical thin-film neodymia (Nd_2O_3) selective emitter TPV system that uses radioisotope decay as the thermal energy source. Author (revised)

N94-11354*# Stuttgart Univ. (Germany). Inst. fuer Raumfahrtsysteme.

DEVELOPMENT OF A HIGH SPECIFIC 1.5 TO 5 kW THERMAL ARCJET Interim Report No. 2, Nov. 1992 - Apr. 1993

M. Riehle, B. Glocker, M. Auweter-Kurtz, and H. Kurtz May 1993 21 p
(Grant NAGw-1736)
(NASA-CR-193133; NAS 1.26:193133; IRS-93-P7) Avail: CASI HC A03/MF A01

A research and development project on the experimental study of a 1.5-5 kW thermal arcjet thruster was started in 1992 at the IRS. Two radiation cooled thrusters were designed, constructed, and adapted to the test facilities, one at each end of the intended power range. These thrusters are currently subjected to an intensive test program with main emphasis on the exploration of thruster performance and thruster behavior at high specific enthalpy and thus high specific impulse. Propelled by simulated hydrazine and ammonia, the thruster's electrode configuration such as constrictor diameter and cathode gap was varied in order to investigate their influence and to optimize these parameters. In addition, test runs with pure hydrogen were performed for both thrusters. Author

N94-11372# New Mexico Univ., Albuquerque. Inst. for Space Nuclear Power Studies.
EXPERIMENTAL AND THEORETICAL INVESTIGATIONS OF Cs-Ba VAPOR TACITRON INVERTER FOR POWER CONDITIONING IN SPACE POWER SYSTEMS
M. El-Genk, C. Murray, and B. Wernsman Jan. 1993 53 p
(Contract DE-FG02-92ER-75708)
(DE93-012971; DOE/ER-75708/T1; UNM-ISNPS-1-1993) Avail: CASI HC A04/MF A01

The operational characteristics of the Cs-Ba tacitron as a switch are investigated experimentally in three modes: (1) breakdown mode, (2) 1-5 mode, and (3) current modulation mode. The switching frequency, grid potentials for ignition and extinguishing of discharge, and the Cs pressure and emission conditions (Ba pressure and emitter temperature) for stable current modulation are determined. The experimental data is also used to determine the off-time required for successful ignition, and the effects of the aforementioned operational parameters on the ignition duty cycle threshold for stable modulation. The measured operational parameters include the following: switching frequency up to 20 kHz, hold-off voltage up to 180 V, current densities in excess of 15 A/sq cm, switch power density of 1 kW/sq cm, and a switching efficiency in excess of 90% at collector C. The voltage drop strongly depends on the Cs pressure and to a lesser extent on the emission conditions. Increasing the Cs pressure and/or the emission current lowers the voltage drop, however, for the same initial Cs pressure and emission conditions, the voltage drop in the 1-5 mode is usually lower than that during current modulation. As long as the discharge current is kept lower that the emission current, the voltage drop during stable current modulation could be as low as 3 V. DOE

N94-11380*# National Aeronautics and Space Administration. Lewis Research Center, Cleveland, OH.
PROCEEDINGS OF THE 12TH SPACE PHOTOVOLTAIC RESEARCH AND TECHNOLOGY CONFERENCE (SPRAT 12)
Washington May 1993 351 p Conference held in Cleveland, OH, 20-22 Oct. 1992
(RTOP 506-41-11)
(NASA-CP-3210; E-7551; NAS 1.55:3210) Avail: CASI HC A16/MF A03

The Twelfth Space Photovoltaic Research and Technology conference was held at the NASA Lewis Research Center from 20 to 22 Oct. 1992. The papers and workshops presented in this volume report substantial progress in a variety of areas in space photovoltaics. Topics covered include: high efficiency GaAs and InP solar cells, GaAs/Ge cells as commercial items, flexible amorphous and thin film solar cells (in the early stages of pilot production), high efficiency multiple bandgap cells, laser power converters, solar cell and array technology, heteroepitaxial cells, betavoltaic energy conversion, and space radiation effects in InP cells. Space flight data on a variety of cells were also presented. For individual titles, see N94-11381 through N94-11419.

N94-11381*# Naval Research Lab., Washington, DC.
A DETAILED STUDY OF THE PHOTO-INJECTION ANNEALING OF THERMALLY DIFFUSED InP SOLAR CELLS
R. J. Walters, G. P. Summers, and J. Bruening (Naval Postgraduate School, Monterey, CA.) *In* NASA. Lewis Research Center, Proceedings of the 12th Space Photovoltaic Research and Technology Conference (SPRAT 12) May 1993 p 1-7 (For primary document see N94-11380 01-20)
Avail: CASI HC A02/MF A03

A detailed analysis of the annealing of thermally diffused InP solar cells fabricated by the Nippon Mining Co. is presented. The cells were irradiated with 1 MeV electrons, and the induced degradation is measured using deep level transient spectroscopy and low temperature (86 K) IV measurements. Clear recovery of the photovoltaic parameters is observed during low temperature (T is less than 300 K) solar illuminations (1 sun, AMO) with further recovery at higher temperatures (300 less than T less than 500 K). For example, the output of a cell which was irradiated up to a fluence of 1 x 10(exp 16) cm(sup -2) was observed to recover to within 5 percent of the pre-irradiation output. An apparent correlation between the recovery of I(sub sc) and the annealing of the H4 defect and of the minority carrier trapping centers is observed. An apparent correlation between the recovery of VO, and the annealing of the H5 defect is also observed. These apparent correlations are used to develop a possible model for the mechanism of the recovery of the solar cells. Author (revised)

N94-11382*# SFA, Inc., Landover, MD.
HIGH TEMPERATURE ANNEALING OF MINORITY CARRIER TRAPS IN IRRADIATED MOCVD n(+)p InP SOLAR CELL JUNCTIONS
S. R. Messenger, R. J. Walters (Naval Research Lab., Washington, DC.), and G. P. Summers (Maryland Univ. Baltimore County, Catonsville.) *In* NASA. Lewis Research Center, Proceedings of the 12th Space Photovoltaic Research and Technology Conference (SPRAT 12) May 1993 p 8-15
(For primary document see N94-11380 01-20)
Avail: CASI HC A02/MF A03

Deep level transient spectroscopy was used to monitor thermal annealing of trapping centers in electron irradiated n(+)p InP junctions grown by metalorganic chemical vapor deposition, at temperatures ranging from 500 up to 650K. Special emphasis is given to the behavior of the minority carrier (electron) traps EA (0.24 eV), EC (0.12 eV), and ED (0.31 eV) which have received considerably less attention than the majority carrier (hole) traps H3, H4, and H5, although this work does extend the annealing behavior of the hole traps to higher temperatures than previously reported. It is found that H5 begins to anneal above 500K and is completely removed by 630K. The electron traps begin to anneal above 540K and are reduced to about half intensity by 630K. Although they each have slightly different annealing temperatures, EA, EC, and ED are all removed by 650K. A new hole trap called H3'(0.33 eV) grows as the other traps anneal and is the only trap remaining at 650K. This annealing behavior is much different than that reported for diffused junctions. Author (revised)

N94-11383*# National Aeronautics and Space Administration. Lewis Research Center, Cleveland, OH.
RADIATION EFFECTS IN HETEROEPITAXIAL InP SOLAR CELLS
I. Weinberg, H. B. Curtis, C. K. Swartz, D. J. Brinker, and C. Vargas-Aburto (Kent State Univ., OH.) *In its* Proceedings of the 12th Space Photovoltaic Research and Technology Conference (SPRAT 12) May 1993 p 16-22
(For primary document see N94-11380 01-20)
Avail: CASI HC A02/MF A03

Heteroepitaxial InP solar cells, with GaAs substrates, were irradiated by 0.5 and 3 MeV protons and their performance, temperature dependency, and carrier removal rates determined as a function of fluence. The radiation resistance of the present cells was significantly greater than that of non-heteroepitaxial InP cells at both proton energies. A clear difference in the temperature dependency of V(sub oc), was observed between heteroepitaxial and homoepitaxial InP cells. The analytically predicted dependence of dV(sub oc)/dT on Voc was confirmed by the fluence dependence of these quantities. Carrier removal was observed to increase with decreasing proton energy. The results obtained for performance and temperature dependency were attributed to the high dislocation densities present in the heteroepitaxial cells while the energy dependence of carrier removal was attributed to the energy dependence of proton range. Author (revised)

N94-11384*# National Aeronautics and Space Administration. Lewis Research Center, Cleveland, OH.
PROGRESS IN p(+)n InP SOLAR CELLS FABRICATED BY THERMAL DIFFUSION
D. J. Flood, D. J. Brinker, I. Weinberg, C. Vargas, Mircea Faur (Cleveland State Univ., OH.), Maria Faur (Cleveland State Univ., OH.), C. Goradia (Cleveland State Univ., OH.), M. Goradia (Cleveland State Univ., OH.), and N. S. Fatemi (Sverdrup Technology, Inc., Cleveland, OH.) *In its* Proceedings of the 12th Space Photovoltaic Research and Technology Conference (SPRAT 12) May 1993 p 23-32 (For primary document see N94-11380 01-20)
Avail: CASI HC A02/MF A03

The performance results of our most recently thermally diffused InP solar cells using the p(+)n (Cd,S) structures are presented. We have succeeded in fabricating cells with measured AMO, 25 C V(sub oc) exceeding 880 mV (bare cells) which to the best of our knowledge is higher than previously reported V(sub oc) values for any InP homojunction solar cells.

The cells were fabricated by thinning the emitter, after Au-Zn front contacting, from its initial thickness of about 4.5 microns to about 0.6 microns. After thinning, the exposed surface of the emitter was passivated by a thin (approximately 50A) P-rich oxide. Based on the measured EQY and J(sub sc)-V(sub oc) characteristics of our experimental high V(sub oc) p(+)n InP solar cells, we project that reducing the emitter thickness to 0.3 microns, using an optimized AR coating, maintaining the surface hole concentration of 3 x 10(exp 18)cm(sup -3), reducing the grid shadowing from actual 10.55 percent to 6 percent and reducing the contact resistance will increase the actual measured 12.57 percent AMO 25 C efficiency to about 20.1 percent. By using our state-of-the-art p(+)n structures which have a surface hole concentration of 4 x 10(exp 18)cm(sup -3) and slightly improving the front surface passivation, an even higher practically achievable AMO, 25 C efficiency of 21.3 percent is projected. Author (revised)

N94-11385*# National Aeronautics and Space Administration. Lewis Research Center, Cleveland, OH.

ELECTROCHEMICAL CHARACTERIZATION OF p(+)n AND n(+)p DIFFUSED InP STRUCTURES **c76**

David M. Wilt, Maria Faur (Cleveland State Univ., OH.), Mircea Faur (Cleveland State Univ., OH.), M. Goradia (Cleveland State Univ., OH.), and Carlos Vargas-Aburto (Kent State Univ., OH.) *In its* Proceedings of the 12th Space Photovoltaic Research and Technology Conference (SPRAT 12) May 1993 p 33-42 (For primary document see N94-11380 01-20)
Avail: CASI HC A02/MF A03

The relatively well documented and widely used electrolytes for characterization and processing of Si and GaAs-related materials and structures by electrochemical methods are of little or no use with InP because the electrolytes presently used either dissolve the surface preferentially at the defect areas or form residual oxides and introduce a large density of surface states. Using an electrolyte which was newly developed for anodic dissolution of InP, and was named the 'FAP' electrolyte, accurate characterization of InP related structures including nature and density of surface states, defect density, and net majority carrier concentration, all as functions of depth was performed. A step-by-step optimization of n(+)p and p(+)n InP structures made by thermal diffusion was done using the electrochemical techniques, and resulted in high performance homojunction InP structures. Author (revised)

N94-11386*# National Aeronautics and Space Administration. Lewis Research Center, Cleveland, OH.

ACTIVATION ENERGY AND CAPTURE CROSS SECTION OF MAJORITY CARRIER TRAPS IN Zn DOPED InP **c76**

George Rybicki and Wendell Williams (Case Western Reserve Univ., Cleveland, OH.) *In its* Proceedings of the 12th Space Photovoltaic Research and Technology Conference (SPRAT 12) May 1993 p 43-53 (For primary document see N94-11380 01-20)
Avail: CASI HC A03/MF A03

Schottky barrier diodes were fabricated on Zn doped InP Wafers. The diodes were radiation damaged with 2 MeV protons to a dose of 2 x 10(exp 12)cm(sup -2). The damage was analyzed by DLTS (deep level transient spectroscopy) using the double correlation technique. Capture cross sections were measured directly. Two major defects were observed in the DLTS spectra. The first defect, was H4 at Ev + 0.29 eV, with capture cross section 1.1 x 10(exp -17)cm(sup 2). The second defect, was H5 at Ev + 0.53 eV. Its capture cross section varied with temperature as described by the relationship sigma = sigma(sub 0) exp(delta(E)/kT) where sigma(sub 0) = 1.3 x 10(exp -19)cm(sup 2) and delta(E) = .08 eV. This relationship yields a sigma of 5.9 x 10(exp -21)cm(sup 2) at room temperature. The surprisingly small capture cross section of H5 and its temperature dependence are discussed in terms of the multiphonon emission process for carrier capture at the defect. The advantages of the improved experimental techniques used are also discussed. Author (revised)

N94-11387*# National Aeronautics and Space Administration. Lewis Research Center, Cleveland, OH.

EFFECTS OF SOLAR CELL ENVIRONMENT ON CONTACT INTEGRITY

Victor G. Weizer and Navid S. Fatemi (Sverdrup Technology, Inc., Cleveland, OH.) *In its* Proceedings of the 12th Space Photovoltaic Research and Technology Conference (SPRAT 12) May 1993 p 54-63 (For primary document see N94-11380 01-20)
Avail: CASI HC A02/MF A03

The III-V semiconductors react extremely rapidly with most commonly used contact metallizations. This precludes the use of elevated temperatures in the contact formation process for solar cells and other shallow junction devices. These devices must rely upon contact metallizations that are sufficiently conductive in their 'as-fabricated' state. However, while there are a number of non-sintered metallizations that have acceptable characteristics, the lack of a sintering step makes them vulnerable to a variety of environmentally induced degradation processes. The degrading effects resulting from the exposure of unsintered devices to a humid environment and to a vacuum (space) environment are described. It is shown, further, that these effects are magnified by the presence of mechanical damage in the contact metallization. The means to avoid or prevent these degrading interactions are presented. Author (revised)

N94-11388*# National Aeronautics and Space Administration. Lewis Research Center, Cleveland, OH.

MEASUREMENT OF THE MINORITY CARRIER DIFFUSION LENGTH AND EDGE SURFACE-RECOMBINATION VELOCITY IN InP **c76**

Sheila G. Bailey and Roshanak Hakimzadeh (Sverdrup Technology, Inc., Brook Park, OH.) *In its* Proceedings of the 12th Space Photovoltaic Research and Technology Conference (SPRAT 12) May 1993 p 64-77 (For primary document see N94-11380 01-20)
Avail: CASI HC A03/MF A03

A scanning electron microscope (SEM) was used to measure the electron (minority carrier) diffusion length (L(sub n)) and the edge surface-recombination velocity (V(sub s)) in zinc-doped Czochralski-grown InP wafers. Electron-beam-induced current (EBIC) profiles were obtained in specimens containing a Schottky barrier perpendicular to the scanned (edge) surface. An independent technique was used to measure V(sub s), and these values were used in a theoretical expression for normalized EBIC. A fit of the experimental data with this expression enabled us to determine L(sub n). Author (revised)

N94-11389*# National Aeronautics and Space Administration. Lewis Research Center, Cleveland, OH.

SURFACE PASSIVATION OF InP SOLAR CELLS WITH InAlAs LAYERS **c76**

Raj K. Jain, Dennis J. Flood, and Geoffrey A. Landis (Sverdrup Technology, Inc., Brook Park, OH.) *In its* Proceedings of the 12th Space Photovoltaic Research and Technology Conference (SPRAT 12) May 1993 p 78-87 (For primary document see N94-11380 01-20)
Avail: CASI HC A02/MF A03

The efficiency of indium phosphide solar cells is limited by high values of surface recombination. The effect of a lattice-matched In(0.52)Al(0.48)As window layer material for InP solar cells, using the numerical code PC-1D is investigated. It was found that the use of InAlAs layer significantly enhances the p(+)n cell efficiency, while no appreciable improvement is seen for n(+)p cells. The conduction band energy discontinuity at the heterojunction helps in improving the surface recombination. An optimally designed InP cell efficiency improves from 15.4 percent to 23 percent AMO for a 10 nm thick InAlAs layer. The efficiency improvement reduces with increase in InAlAs layer thickness, due to light absorption in the window layer. Author (revised)

N94-11390*# Iowa Thin Film Technologies, Inc., Ames.

POLYIMIDE BASED AMORPHOUS SILICON SOLAR MODULES

Frank R. Jeffrey, Derrick P. Grimmer, Steven A. Martens, Khaled Abudagga, Michael L. Thomas, and Max Noak (Iowa State Univ. of Science and Technology, Ames.) *In* NASA. Lewis Research Center, Proceedings of the 12th Space Photovoltaic Research and Technology Conference (SPRAT 12) May 1993 p 88-97 (For primary document see N94-11380 01-20)
(Contract NAS3-26244)
Avail: CASI HC A02/MF A03

Requirements for space power are increasingly emphasizing lower costs and higher specific powers. This results from new fiscal constraints, higher power requirements for larger applications, and the evolution toward longer distance missions such as a Lunar or Mars base. The polyimide based a-Si modules described are being developed to meet these needs. The modules consist of tandem a-Si solar cell material deposited directly on a roll of polyimide. A laser scribing/printing process subdivides the deposition into discrete cell strips which are series connected to produce the required voltage without cutting the polymer backing. The result is a large, monolithic, blanket type module approximately 30 cm wide and variable in length depending on demand. Current production modules have a specific power slightly over 500 W/Kg with room for significant improvement. Costs for the full blanket modules range from $30/Watt to $150/Watt depending on quantity and engineering requirements. Work to date focused on the modules themselves and adjusting them for the AMO spectrum. Work is needed yet to insure that the modules are suitable for the space environment. Author (revised)

N94-11391*# Wayne State Univ., Detroit, MI. Dept. of Electrical and Computer Engineering.

INVESTIGATION OF THE RADIATION RESISTANCE OF TRIPLE-JUNCTION a-Si:H ALLOY SOLAR CELLS IRRADIATED WITH 1.00 MeV PROTONS

Kenneth R. Lord, II, Michael R. Walters, and James R. Woodyard *In* NASA. Lewis Research Center, Proceedings of the 12th Space Photovoltaic Research and Technology Conference (SPRAT 12) May 1993 p 98-107 Sponsored in part by TRW (For primary document see N94-11380 01-20)
(Grant NAG3-833)
Avail: CASI HC A02/MF A03

The effect of 1.00 MeV proton irradiation on hydrogenated amorphous silicon alloy triple-junction solar cells is reported for the first time. The cells were designed for radiation resistance studies and included 0.35 cm(sup 2) active areas on 1.0 by 2.0 cm(sup 2) glass superstrates. Three cells were irradiated through the bottom contact at each of six fluences between 5.10E12 and 1.46E15 cm(sup -2). The effect of the irradiations was determined with light current-voltage measurements. Proton irradiation degraded the cell power densities from 8.0 to 98 percent for the fluences investigated. Annealing irradiated cells at 200 C for two hours restored the power densities to better than 90 percent. The cells exhibited radiation resistances which are superior to cells reported in the literature for fluences less than 1E14 cm(sup -2). Author (revised)

N94-11392*# Jet Propulsion Lab., California Inst. of Tech., Pasadena.

RESULTS OF SOME INITIAL SPACE QUALIFICATION TESTING ON TRIPLE JUNCTION a-Si AND CuInSe2 THIN FILM SOLAR CELLS

Robert L. Mueller and Bruce E. Anspaugh *In* NASA. Lewis Research Center, Proceedings of the 12th Space Photovoltaic Research and Technology Conference (SPRAT 12) May 1993 p 108-117 Sponsored by USAF Phillips Lab. (For primary document see N94-11380 01-20)
Avail: CASI HC A02/MF A03

A series of environmental tests were completed on one type of triple junction a-Si and two types of CuInSe2 thin film solar cells. The environmental tests include electron irradiation at energies of 0.7, 1.0, and 2.0 MeV, proton irradiation at energies of 0.115, 0.24, 0.3, 0.5, 1.0, and 3.0 MeV, post-irradiation annealing at temperatures between 20 C and 60 C, long term exposure to air mass zero (AM0) photons, measurement of the cells as a function of temperature and illumination intensity, and contact pull strength tests. As expected, the cells are very resistant to electron and proton irradiation. However, when a selected cell type is exposed to low energy protons designed to penetrate to the junction region, there is evidence of more significant damage. A significant amount of recovery was observed after annealing in several of the cells. However, it is not permanent and durable, but merely a temporary restoration, later nullified with additional irradiation. Contact pull strengths measured on the triple junction a-Si cells averaged 667 grams, and pull strengths measured on the Boeing CuInSe2 cells averaged 880 grams. Significant degradation of all cell types was observed after exposure to a 580 hour photon degradation test, regardless of whether the cells had been unirradiated or irradiated (electrons or protons). Although one cell from one manufacturer lost approximately 60 percent of its power after the photon test, several other cells from this manufacturer did not degrade at all. Author (revised)

N94-11393*# Martin Marietta Aerospace, Denver, CO. Astronautics Group.

FLEXIBLE POLYCRYSTALLINE THIN-FILM PHOTOVOLTAICS FOR SPACE APPLICATIONS Abstract Only

J. H. Armstrong, B. R. Lanning, M. S. Misra, V. K. Kapur (International Solar Electric Technology, Inglewood, CA.), and B. M. Basol (International Solar Electric Technology, Inglewood, CA.) *In* NASA. Lewis Research Center, Proceedings of the 12th Space Photovoltaic Research and Technology Conference (SPRAT 12) May 1993 p 118 (For primary document see N94-11380 01-20)
Avail: CASI HC A01/MF A03

Polycrystalline thin-film photovoltaics (PV), such as CIS and CdTe, have received considerable attention recently with respect to space power applications. Their combination of stability, efficiency, and economy from large-scale monolithic-integration of modules can have significant impact on cost and weight of PV arrays for spacecraft and planetary experiments. An added advantage, due to their minimal thickness (approximately 6 microns sans substrate), is the ability to manufacture lightweight, flexible devices (approximately 2000 W/kg) using large-volume manufacturing techniques. The photovoltaic effort at Martin Marietta and ISET is discussed, including large-area, large-volume thin-film deposition techniques such as electrodeposition and rotating cylindrical magnetron sputtering. Progress in the development of flexible polycrystalline thin-film PV is presented, including evaluation of flexible CIS cells. In addition, progress on flexible CdTe cells is presented. Finally, examples of lightweight, flexible arrays and their potential cost and weight impact is discussed. Author (revised)

N94-11394*# Spire Corp., Bedford, MA.

InGaAs CONCENTRATOR CELLS FOR LASER POWER CONVERTERS AND TANDEM CELLS

S. Wojtczuk, S. Vernon, and E. Gagnon *In* NASA. Lewis Research Center, Proceedings of the 12th Space Photovoltaic Research and Technology Conference (SPRAT 12) May 1993 p 119-128 (For primary document see N94-11380 01-20)
(Contracts NAS1-19258; NAS1-19592)
Avail: CASI HC A02/MF A03

In(0.53)Ga(0.47)As N-on-P concentrator cells were made as part of an effort to develop 1.315 micron laser power converters. The 1.315 micron laser power conversion efficiency was estimated as 29.4 percent (at 5.57 W/cm(sup 2)) based on an 86 percent measured external quantum efficiency at 1.315 microns, and a measured open circuit voltage (484 mV), and fill-factor (67 percent) at the equivalent AM0 short-circuit photocurrent (5.07 A/cm(sup 2)). A 13.5 percent percent AMO efficiency was achieved at 89 suns and 25 C. Measured one-sun and 100-sun AMO efficiency, log I-V analysis, and quantum efficiency are presented for InGaAs cells with and without InP windows to passivate the front surface. Windowed cells performed better at concentration than windowless cells. Lattice mismatch between InGaAs epilayers and InP substrate was less than 800 ppm. Theoretical efficiency is estimated for 1.315 microns laser power converters versus the bandgap energy. Adding aluminum to InGaAs to form In(x)Al(y)Ga(1-x-y)As is presented as a way to achieve an optimal bandgap for 1.315 microns laser power conversion. Author (revised)

N94-11395*# Cleveland State Univ., OH.

THE EFFICIENCY OF PHOTOVOLTAIC CELLS EXPOSED TO PULSED LASER LIGHT

R. A. Lowe, G. A. Landis (Sverdrup Technology, Inc., Brook Park, OH.), and P. Jenkins (Sverdrup Technology, Inc., Brook Park, OH.) *In* NASA. Lewis Research Center, Proceedings of the 12th Space Photovoltaic Research and Technology Conference (SPRAT 12) May 1993 p 129-146 (For primary document see N94-11380 01-20)
Avail: CASI HC A03/MF A03

Future space missions may use laser power beaming systems with a free electron laser (FEL) to transmit light to a photovoltaic array receiver. To investigate the efficiency of solar cells with pulsed laser light, several types of GaAs, Si, CuInSe2, and GaSb cells were tested with the simulated pulse format of the induction and radio frequency (RF) FEL. The induction pulse format was simulated with an 800-watt average power copper vapor laser and the RF format with a frequency-doubled mode-locked Nd:YAG laser. Averaged current vs bias voltage measurements for each cell were taken at various optical power levels and the efficiency measured at the maximum power point. Experimental results show that the conversion efficiency for the cells tested is highly dependent on cell minority carrier lifetime, the width and frequency of the pulses, load impedance, and the average incident power. Three main effects were found to decrease the efficiency of solar cells exposed to simulated FEL illumination: cell series resistance, LC 'ringing', and output inductance. Improvements in efficiency were achieved by modifying the frequency response of the cell to match the spectral energy content of the laser pulse with external passive components. Author (revised)

N94-11396*# National Aeronautics and Space Administration. Marshall Space Flight Center, Huntsville, AL. Information and Electronic Systems Lab.

RESPONSE OF SILICON SOLAR CELL TO PULSED LASER ILLUMINATION

D. Willowby, D. Alexander, T. Edge, and K. Herren *In* NASA. Lewis Research Center, Proceedings of the 12th Space Photovoltaic Research and Technology Conference (SPRAT 12) May 1993 p 147-154 (For primary document see N94-11380 01-20)

Avail: CASI HC A02/MF A03

The response of silicon solar cell(s) to pulsed laser illumination is discussed. The motivation was due to the interest of Earth to space/Moon power beaming applications. When this work began, it was not known if solar cells would respond to laser light with pulse lengths in the nanosecond range and a repetition frequency in the kHz range. This is because the laser pulse would be shorter than the minority carrier lifetime of silicon. A 20-nanosecond (ns) full width half max (FWHM) pulse from an aluminum-gallium/arsenide (Al-Ga-As) diode laser was used to illuminate silicon solar cells at a wavelength of 885 nanometers (nm). Using a high-speed digital oscilloscope, the response of the solar cells to individual pulses across various resistive loads was observed and recorded. Author (revised)

N94-11397*# National Aeronautics and Space Administration. Lewis Research Center, Cleveland, OH.

APPROACHES TO SOLAR CELL DESIGN FOR PULSED LASER POWER RECEIVERS

Raj K. Jain and Geoffrey A. Landis (Sverdrup Technology, Inc., Brook Park, OH.) *In its* Proceedings of the 12th Space Photovoltaic Research and Technology Conference (SPRAT 12) May 1993 p 155-166 (For primary document see N94-11380 01-20)

(Contract NAS3-25266)

Avail: CASI HC A03/MF A03

Using a laser to beam power from Earth to a photovoltaic receiver in space could be a technology with applications to many space missions. Extremely high average-power lasers would be required in a wavelength range of 700-1000 nm. However, high-power lasers inherently operate in a pulsed format. Existing solar cells are not well designed to respond to pulsed incident power. To better understand cell response to pulsed illumination at high intensity, the PC-1D finite-element computer model was used to analyze the response of solar cells to continuous and pulsed laser illumination. Over 50 percent efficiency was calculated for both InP and GaAs cells under steady-state illumination near the optimum wavelength. The time-dependent response of a high-efficiency GaAs concentrator cell to a laser pulse was modeled, and the effect of laser intensity, wavelength, and bias point was studied. Three main effects decrease the efficiency of a solar cell under pulsed laser illumination: series resistance, L-C 'ringing' with the output circuit, and current limiting due to the output inductance. The problems can be solved either by changing the pulse shape or designing a solar cell to accept the pulsed input. Cell design possibilities discussed are a high-efficiency, light-trapping silicon cell, and a monolithic, low-inductance GaAs cell. Author (revised)

N94-11398*# Applied Solar Energy Corp., City of Industry, CA.

EOL PERFORMANCE COMPARISON OF GaAs/Ge AND Si BSF/R SOLAR ARRAYS

Thomas J. Woike *In* NASA. Lewis Research Center, Proceedings of the 12th Space Photovoltaic Research and Technology Conference (SPRAT 12) May 1993 p 167-176 (For primary document see N94-11380 01-20)

Avail: CASI HC A02/MF A03

EOL power estimates for solar array designs are significantly influenced by the predicted degradation due to charged particle radiation. New radiation-induced power degradation data for GaAs/Ge solar arrays applicable to missions ranging from low earth orbit (LEO) to geosynchronous earth orbit (GEO) and compares these results to silicon BSF/R arrays. These results are based on recently published radiation damage coefficients for GaAs/Ge cells. The power density ratio (GaAs/Ge to Si BSF/R) was found to be as high as 1.83 for the proton-dominated worst-case altitude of 7408 km medium Earth orbit (MEO). Based on the EOL GaAs/Ge solar array power density results for MEO, missions which were previously considered infeasible may be reviewed based on these more favorable results. The additional life afforded by using GaAs/Ge cells is an important factor in system-level trade studies when selecting a solar cell technology for a mission and needs to be considered. The data presented supports this decision since the selected orbits have characteristics similar to most orbits of interest. Author (revised)

N94-11399*# AEC-Able Engineering Co., Inc., Goleta, CA.

A HIGH SPECIFIC POWER SOLAR ARRAY FOR LOW TO MID-POWER SPACECRAFT

P. Alan Jones, Stephen F. White, T. Jeffery Harvey, and Brian S. Smith (Spectrolab, Inc., Sylmar, CA.) *In* NASA. Lewis Research Center, Proceedings of the 12th Space Photovoltaic Research and Technology Conference (SPRAT 12) May 1993 p 177-187 (For primary document see N94-11380 01-20)

Avail: CASI HC A03/MF A03

UltraFlex is the generic term for a solar array system which delivers on-orbit power in the 400 to 6,000 watt per wing sizes with end-of-life specific power performance ranging to 150 watts-per-kilogram. Such performance is accomplished with off-the-shelf solar cells and state-of the-art materials and processes. Much of the recent work in photovoltaics is centered on advanced solar cell development. Successful as such work has been, no integrated solar array system has emerged which meets NASA's stated goals of 'increasing the end-of-life performance of space solar cells and arrays while minimizing their mass and cost.' This issue is addressed; namely, is there an array design that satisfies the usual requirements for space-rated hardware and that is inherently reliable, inexpensive, easily manufactured and simple, which can be used with both advanced cells currently in development and with inexpensive silicon cells? The answer is yes. The UltraFlex array described incorporates use of a blanket substrate which is thermally compatible with silicon and other materials typical of advanced multi-junction devices. The blanket materials are intrinsically insensitive to atomic oxygen degradation, are space rated, and are compatible with standard cell bonding processes. The deployment mechanism is simple and reliable and the structure is inherently stiff (high natural frequency). Mechanical vibration modes are also readily damped. The basic design is presented as well as supporting analysis and development tests. Author (revised)

N94-11400*# Boeing Defense and Space Group, Seattle, WA.

TAB INTERCONNECTS FOR SPACE CONCENTRATOR SOLAR CELL ARRAYS

J. Avery, J. S. Bauman, P. Gallagher, and J. W. Yerkes *In* NASA. Lewis Research Center, Proceedings of the 12th Space Photovoltaic Research and Technology Conference (SPRAT 12) May 1993 p 188-195 (For primary document see N94-11380 01-20)

Avail: CASI HC A02/MF A03

The Boeing Company has evaluated the use of Tape Automated Bonding (TAB) and Surface Mount Technology (SMT) for a highly reliable, low cost interconnect for concentrator solar cell arrays. TAB and SMT are currently used in the electronics industry for chip interconnects and printed circuit board assembly. TAB tape consists of sixty-four 3-mil/1-oz tin-plated copper leads on 8-mil centers. The leads are thermocompression gang bonded to GaAs concentrator solar cell with silver contacts. This bond, known as an Inner Lead Bond (ILB), allows for pretesting and sorting capability via nondestruct wire bond pull and flash testing. Destructive wire pull tests resulted in preferred mid-span failures. Improvements in fill factor were attributed to decreased contact resistance on TAB bonded cells. Preliminary thermal cycling and aging tests were shown excellent bond strength and metallurgical results. Auger scans of bond sites reveals an Ag-Cu-Tin composition. Improper bonds are identified through flash testing as a performance degradation. On going testing of cells are underway at Lewis Research Center. SMT techniques are utilized to excise and form TAB leads post ILB. The formed leads' shape isolates thermal mismatches between the cells and the flex circuit they are mounted on. TABed cells are picked and placed with a gantry x-y-z positioning system with pattern recognition. Adhesives are selected to avoid thermal expansion mismatch and promote thermal transfer to the flex circuit. TAB outer lead bonds are parallel gap welded (PGW) to the flex circuit to finish the concentrator solar cell subassembly. Author

N94-11401*# National Aeronautics and Space Administration. Langley Research Center, Hampton, VA.

SPACE STATION FREEDOM ADVANCED PHOTOVOLTAICS AND BATTERY TECHNOLOGY DEVELOPMENT PLANNING

Karen D. Brender, Spruce M. Cox (Boeing Defense and Space Group, Huntsville, AL.), Mark T. Gates (Boeing Defense and Space Group, Seattle, WA.), and Scott A. Verzwyvelt (Boeing Defense and Space Group, Seattle, WA.) *In* NASA. Lewis Research Center, Proceedings of the 12th Space Photovoltaic Research and Technology Conference (SPRAT 12) May 1993 p 196-205 (For primary document see N94-11380 01-20) (Contract NAS1-19247)

Avail: CASI HC A02/MF A03

Space Station Freedom (SSF) usable electrical power is planned to be built up incrementally during assembly phase to a peak of 75 kW end-of-life (EOL) shortly after Permanently Manned Capability (PMC) is achieved in 1999. This power will be provided by planar silicon (Si) arrays and nickel-hydrogen (NiH2) batteries. The need for power is expected to grow from 75 kW to as much as 150 kW EOL during the evolutionary phase of SSF, with initial increases beginning as early as 2002. Providing this additional power with current technology may not be as cost effective as using advanced technology arrays and batteries expected to develop prior to this evolutionary phase. A six-month study sponsored by NASA Langley Research Center and conducted by Boeing Defense and Space Group was initiated in Aug. 1991. The purpose of the study was to prepare technology development plans for cost effective advanced photovoltaic (PV) and battery technologies with application to SSF growth, SSF upgrade after its arrays and batteries reach the end of their design lives, and other low Earth orbit (LEO) platforms. Study scope was limited to information available in the literature, informal industry contacts, and key representatives from NASA and Boeing involved in PV and battery research and development. Ten battery and 32 PV technologies were examined and their performance estimated for SSF application. Promising technologies were identified based on performance and development risk. Rough order of magnitude cost estimates were prepared for development, fabrication, launch, and operation. Roadmaps were generated describing key issues and development paths for maturing these technologies with focus on SSF application. Author (revised)

N94-11402*# National Aeronautics and Space Administration. Lewis Research Center, Cleveland, OH.

RECENT DEVELOPMENTS IN REFRACTIVE CONCENTRATORS FOR SPACE PHOTOVOLTAIC POWER SYSTEMS

Michael F. Piszczor and Mark J. ONeill (ENTECH Corp., Dallas-Fort Worth Airport, TX.) *In its* Proceedings of the 12th Space Photovoltaic Research and Technology Conference (SPRAT 12) May 1993 p 206-216 (For primary document see N94-11380 01-20)

Avail: CASI HC A03/MF A03

Since SPRAT 11, significant progress has been made in the development of refractive concentrator elements and components designed specifically for space applications. The status of the mini-dome Fresnel lens concentrator array is discussed and then the results of work recently completed in the area of prismatic cell covers for concentrator systems are summarized. This is followed by a brief discussion of some work just starting in the area of line-focus refractive concentrators for space. Author (revised)

N94-11403*# Space Systems/Loral, Palo Alto, CA.

NEW EXPERIMENTAL TECHNIQUES FOR SOLAR CELLS

R. Lenk *In* NASA. Lewis Research Center, Proceedings of the 12th Space Photovoltaic Research and Technology Conference (SPRAT 12) May 1993 p 217-225 (For primary document see N94-11380 01-20)

Avail: CASI HC A02/MF A03

Solar cell capacitance has special importance for an array controlled by shunting. Experimental measurements of solar cell capacitance in the past have shown disagreements of orders of magnitude. Correct measurement technique depends on maintaining the excitation voltage less than the thermal voltage. Two different experimental methods are shown to match theory well, and two effective capacitances are defined for quantifying the effect of the solar cell capacitance on the shunting system. Author

N94-11404*# Naval Research Lab., Washington, DC.

RADIATION EFFECTS IN Ga(0.47)In(0.53)As SOLAR CELLS c76

R. J. Walters, G. J. Shaw, G. P. Summers, and S. R. Messenger (SFA, Inc., Landover, MD.) *In* NASA. Lewis Research Center, Proceedings of the 12th Space Photovoltaic Research and Technology Conference (SPRAT 12) May 1993 p 226-234 (For primary document see N94-11380 01-20)

Avail: CASI HC A02/MF A03

The effects of irradiating Ga(0.47)In(0.53)As p-i-n junctions with 1 MeV electrons were measured using Deep Level Transient Spectroscopy (DLTS) and both dark and illuminated (1 sun, air mass zero (AM0)) current-voltage (I-V) measurements. The I-V measurements were made over the range 100K less than T less than 350K. Temperature coefficients of the Ga(0.47)In(0.53)As photovoltaic parameters are presented which follow the same general behavior as other solar cell materials (e.g. Si and GaAs). Fits of the dark I-V data to the two term diode equation before irradiation were satisfactory, yielding an estimated band-gap energy of 0.79 eV. The recombination component of the dark current was found to increase linearly with fluence. DLTS detected two radiation-induced defect levels one shallow (E(sub c)-0.10 eV) and one near mid-gap (E(sub c)-0.29 eV), and it is the near mid-gap level which is expected to be the cause of the dark current increase. The radiation-induced degradation of the open circuit voltage is shown to be accurately predicted from the dark I-V measurements. The degradation of the open circuit voltage dominated the radiation response of the photovoltaic parameters while the short circuit current was only moderately degraded. This behavior is qualitatively explained in terms of the base thickness and dopant level. Appropriate changes in the device structure are suggested which should increase the radiation resistance. Isochronal thermal annealing induced recovery in the photovoltaic parameters at approximately 400K, coinciding with an annealing stage of the near mid-gap defect level. Author (revised)

N94-11405*# Washington State Univ., Richland.

INVESTIGATION OF ZnSe-COATED SILICON SUBSTRATES FOR GaAs SOLAR CELLS c76

Daniel A. Huber, Larry C. Olsen, Glen Dunham, and F. William Addis *In* NASA. Lewis Research Center, Proceedings of the 12th Space Photovoltaic Research and Technology Conference (SPRAT 12) May 1993 p 235-248 Sponsored by USAF Phillips Lab. (For primary document see N94-11380 01-20)

Avail: CASI HC A03/MF A03

Studies are being carried out to determine the feasibility of using ZnSe as a buffer layer for GaAs solar cells grown on silicon. This study was motivated by reports in the literature indicating ZnSe films had been grown by metallorganic chemical vapor deposition (MOCVD) onto silicon with EPD values of 2 x 10(exp 5) cm(sup -2), even though the lattice mismatch between silicon and ZnSe is 4.16 percent. These results combined with the fact that ZnSe and GaAs are lattice matched to within 0.24 percent suggest that the prospects for growing high efficiency GaAs solar cells onto ZnSe-coated silicon are very good. Work to date has emphasized development of procedures for MOCVD growth of (100) ZnSe onto (100) silicon wafers, and subsequent growth of GaAs films on ZnSe/Si substrates. In order to grow high quality single crystal GaAs with a (100) orientation, which is desirable for solar cells, one must grow single crystal (100) ZnSe onto silicon substrates. A process for growth of (100) ZnSe was developed involving a two-step growth procedure at 450 C. Single crystal, (100) GaAs films were grown onto the (100) ZnSe/Si substrates at 610 C that are adherent and specular. Minority carrier diffusion lengths for the GaAs films grown on ZnSe/Si substrates were determined from photoresponse properties of Al/GaAs Schottky barriers. Diffusion lengths for n-type GaAs films are currently on the order of 0.3 microns compared to 2.0 microns for films grown simultaneously by homoepitaxy. Author (revised)

N94-11406*# English Electric Valve Co. Ltd., Chelmsford (England).

HETEROEPITAXIAL InP, AND ULTRATHIN, DIRECTLY GLASSED, GaAs 3-5 SOLAR CELLS c76

C. M. Hardingham and T. A. Cross *In* NASA. Lewis Research Center, Proceedings of the 12th Space Photovoltaic Research and Technology Conference (SPRAT 12) May 1993 p 249-255 (For primary document see N94-11380 01-20)

Avail: CASI HC A02/MF A03

The commercial application of Indium Phosphide solar cells in practical space missions is crucially dependent upon achieving a major cost reduction which could be offered by heteroepitaxy on cheaper, more rugged substrates. Furthermore, significant mass reduction, compatibility with mechanically stacked multijunction cells, and elimination of the current loss through glue discoloration, is possible in III-V solar cells by the development of ultrathin, directly glassed cells. The progress of a UK collaborative program to develop high efficiency, homojunction InP solar cells, grown by MOCVD on Si substrates, is described. Results of homoepitaxial cells (is greater than 17 percent 1 Sun AM0) are presented, together with progress in achieving low dislocation density heteroepitaxy. Also, progress in a UK program to develop ultrathin directly-glassed GaAs cells is described. Ultrathin (5 micron) GaAs cells, with 1 Sun AM0 efficiencies up to 19.1 percent, are presented, together with progress in achieving a direct (adhesive-less) bond between the cell and coverglass. Consequential development to, for example, cell grids, are also discussed. Author (revised)

N94-11407*# Washington State Univ., Richland.

REVIEW OF BETAVOLTAIC ENERGY CONVERSION

Larry C. Olsen *In* NASA. Lewis Research Center, Proceedings of the 12th Space Photovoltaic Research and Technology Conference (SPRAT 12) May 1993 p 256-267 (For primary document see N94-11380 01-20)

Avail: CASI HC A03/MF A03

Betavoltaic energy conversion refers to the generation of power by coupling a beta source to a semiconductor junction device. The theory of betavoltaic energy conversion and some past studies of the subject are briefly reviewed. Calculations of limiting efficiencies for semiconductor cells versus bandgap are presented along with specific studies for Pm-147 and Ni-63 fueled devices. The approach used for fabricating Pm-147 fueled batteries by the author in the early 1970's is reviewed. Finally, the potential performance of advanced betavoltaic power sources is considered. Author (revised)

N94-11408*# Communications Satellite Corp., Clarksburg, MD.

UV TESTING OF SOLAR CELLS: EFFECTS OF ANTIREFLECTIVE COATING, PRIOR IRRADIATION, AND UV SOURCE **c44**

A. Meulenberg *In* NASA. Lewis Research Center, Proceedings of the 12th Space Photovoltaic Research and Technology Conference (SPRAT 12) May 1993 p 268-279 Sponsored in part by COMSAT Corporation (For primary document see N94-11380 01-20)

Avail: CASI HC A03/MF A03

Short-circuit current degradation of electron irradiated double-layer antireflective-coated cells after 3000 hours ultraviolet (UV) exposure exceeds 3 percent; extrapolation of the data to 10(exp 5) hours (11.4 yrs.) gives a degradation that exceeds 10 percent. Significant qualitative and quantitative differences in degradation were observed in cells with double- and single-layer antireflective coatings. The effects of UV-source age were observed and corrections were made to the data. An additional degradation mechanism was identified that occurs only in previously electron-irradiated solar cells since identical unirradiated cells degrade to only 6 +/- 3 percent when extrapolated 10(exp 5) hours of UV illumination. Author (revised)

N94-11409*# Defence Research Agency, Farnborough (England). Space Technology Dept.

THE UoSAT-5 SOLAR CELL EXPERIMENT: FIRST YEAR IN ORBIT **c44**

C. Goodbody *In* NASA. Lewis Research Center, Proceedings of the 12th Space Photovoltaic Research and Technology Conference (SPRAT 12) May 1993 p 280-288 (For primary document see N94-11380 01-20)

Avail: CASI HC A02/MF A03

The results for the first year in orbit of the DRA solar cell experiment flying on the Surrey University UoSAT-5 satellite are described. Several problems were identified with the measured data, which are discussed along with the techniques used to remove or minimize the effect of the problems. After 1 year in orbit the majority of the cells flying on the experiment have undergone little or no degradation. The exception to this are all the ITO/InP cells, supplied by two different manufacturers, they are showing more degradation than the GaAs cells. This result is unexpected and currently unexplainable. It will be necessary to retrieve data from the experiment for several years to obtain the best results due to the relatively benign radiation environment. Author (revised)

N94-11410*# National Aeronautics and Space Administration. Lewis Research Center, Cleveland, OH.

RESULTS OF THERMAL VACUUM TESTS FOR THE PASP+ FLIGHT MODULES

Henry Curtis, Michael Piszczor, Don Guidice (Phillips Lab., Hanscom AFB, MA.), and Paul Severance (Phillips Lab., Hanscom AFB, MA.) *In its* Proceedings of the 12th Space Photovoltaic Research and Technology Conference (SPRAT 12) May 1993 p 289-297 (For primary document see N94-11380 01-20)

Avail: CASI HC A02/MF A03

The PASP PLUS (Photovoltaic Array Space Power Plus Diagnostics) program is a photovoltaic experiment which will be flown on the Air Force satellite APEX (Advanced Photovoltaic And Electronic Experiment). APEX will be launched with a Pegasus during the summer of 1993. There are two other small experiments on APEX but PASP+ is the largest, uses the most power, and accounts for over 90 percent of the data requirements. The orbit is elliptical with apogee and perigee of 1050 and 190 nautical miles respectively. The inclination is 70 deg. The two main objectives of PASP+ are to determine the interactions between high voltage arrays and the space plasma environment and to determine the radiation damage characteristics of several newer types of solar cells. In order to determine the interactions with the space plasma, several of the individual cell strings will be biased to voltages up to plus or minus 500 V, and leakage currents and arcing rates will be measured. The radiation degradation characteristics will be determined by the continuous monitoring of I-V data for all of the cell strings. As part of an overall testing program, the PASP+ panels and controller were put through a thermal vacuum test in order to check the thermal analysis, obtain temperature coefficients for the individual modules, and have an end-to-end test of the entire PASP+ experiment. This thermal vacuum test is described briefly and the results obtained during that testing are discussed. Author (revised)

N94-11411*# Florida Solar Energy Center, Cape Canaveral.

COMPUTATION OF PHOTOVOLTAIC PARAMETERS UNDER LUNAR TEMPERATURE VARIATION

Neelkanth G. Dhere and James V. Santiago *In* NASA. Lewis Research Center, Proceedings of the 12th Space Photovoltaic Research and Technology Conference (SPRAT 12) May 1993 p 298-306 (For primary document see N94-11380 01-20)

Avail: CASI HC A02/MF A03

Photovoltaic (PV) arrays with regenerative-fuel-cell energy storage is a prime, power-system candidate for lunar photo-power. The PV module performance decreases at higher temperatures. Surface temperature variations of the moon are extreme, the maximum (noon) temperature being 384 K. The present work utilizes detailed computations of photovoltaic parameters with computer program developed earlier for the computation of optimum bandgaps of single- and two-junction solar cells at different temperatures, and calculates the power output of single and two-junction solar modules under different configurations which constitutes an improvement over the assumption of a linear variation of efficiency with temperature. The program also calculates the necessary PV-array size to satisfy stipulated levels of day- and night-time power consumption. Author

N94-11412*# Defence Research Agency, Farnborough (England). Space Technology Dept.

AN OVERVIEW OF THE DEFENCE RESEARCH AGENCY PHOTOVOLTAIC PROGRAMME

C. Goodbody and M. A. H. Davies *In* NASA. Lewis Research Center, Proceedings of the 12th Space Photovoltaic Research and Technology Conference (SPRAT 12) May 1993 p 307-317 (For primary document see N94-11380 01-20)

Avail: CASI HC A03/MF A03

The Defense Research Agency (DRA) has been active in the photovoltaic field since the early 1960's, then as the Royal Aircraft Establishment (RAE). The early work was aimed at developing silicon cells, solar panels, and light-weight flexible arrays in support of the 'UK' and 'X' series of British scientific and technology satellites, for which the RAE was either the design authority or technical advisor. The X3 satellite - Prospero, launched in 1971 test flew 50 micron wrap-round silicon cells. The X4 satellite -

Miranda, launched in 1974 test flew a deployable flexible silicon array which was developed at the DRA. During this period an extensive range of test equipment was developed which was maintained, modernized, and extended to date. Following a period of reduced activity in the late 1970's and early 1980's the current program evolved. The programs that have been undertaken since 1983 are briefly summarized. These range from various cell developments, new types of coverglasses, flight experiments, radiation testing, primary cell calibration, and environmental testing. The current photovoltaic program is mainly funded by the UK Ministry of Defence and by the Department of Trade and Industry through the British National Space Center (BNSC). The program is aimed at research and development, both internally and with industry, to meet the customer's technical objectives and requirements and to provide them with technical advice. The facilities are also being used on contract work for various national and international organizations. Author (revised)

N94-11413*# Tsukuba Space Center (Japan).
NASDA ACTIVITIES IN SPACE SOLAR POWER SYSTEM RESEARCH, DEVELOPMENT AND APPLICATIONS
Sumio Matsuda, Yasunari Yamamoto, and Masato Uesugi *In* NASA. Lewis Research Center, Proceedings of the 12th Space Photovoltaic Research and Technology Conference (SPRAT 12) May 1993 p 318-325 (For primary document see N94-11380 01-20)
Avail: CASI HC A02/MF A03

NASDA activities in solar cell research, development, and applications are described. First, current technologies for space solar cells such as Si, GaAs, and InP are reviewed. Second, future space solar cell technologies intended to be used on satellites of 21st century are discussed. Next, the flight data of solar cell monitor on ETS-V is shown. Finally, establishing the universal space solar cell calibration system is proposed. Author (revised)

N94-11414*# National Aeronautics and Space Administration. Lewis Research Center, Cleveland, OH.
WORKSHOP ON HETEROEPITAXIAL InP SOLAR CELLS c76
I. Weinberg and R. W. Walters (Naval Research Lab., Washington, DC.) *In its* Proceedings of the 12th Space Photovoltaic Research and Technology Conference (SPRAT 12) May 1993 p 326-328 (For primary document see N94-11380 01-20)
Avail: CASI HC A01/MF A03

In a generic sense, the justification for any sort of InP solar cell research applies, i.e. to take advantage of the inherently high radiation resistance and efficiency of InP solar cells. To be more specific, the approach is justified by its potential for significant cost reduction and the availability of greatly increased cell area afforded by substrates such as Si and Ge. The use of substrates, such as the latter two, would result in increased ruggedness, ease of handling, and improved manufacturability. The use of more rugged substrates would lead to a greatly increased capability for cell thinning leading to the desirable feature of reduced array weight. Author (revised)

N94-11415*# Martin Marietta Aerospace, Denver, CO.
THIN FILM SOLAR CELL WORKSHOP c44
Joe Armstrong and Frank Jeffrey (Iowa Thin Film Technologies, Inc., Ames.) *In* NASA. Lewis Research Center, Proceedings of the 12th Space Photovoltaic Research and Technology Conference (SPRAT 12) May 1993 p 329-330 (For primary document see N94-11380 01-20)
Avail: CASI HC A01/MF A03

A summation of responses to questions posed to the thin-film solar cell workshop and the ensuing discussion is provided. Participants in the workshop included photovoltaic manufacturers (both thin film and crystalline), cell performance investigators, and consumers. Author (revised)

N94-11416*# National Aeronautics and Space Administration. Lewis Research Center, Cleveland, OH.
WORKSHOP ON SOLAR ELECTRIC PROPULSION
David Bents and Dean Marvin (Aerospace Corp., El Segundo, CA.) *In its* Proceedings of the 12th Space Photovoltaic Research and Technology Conference (SPRAT 12) May 1993 p 331-333 (For primary document see N94-11380 01-20)
Avail: CASI HC A01/MF A03

A summary of the discussion at the workshop on solar electric propulsion (SEP) is presented. The purpose of ELITE SEP flight experiment is to demonstrate operation of solar array powered electric thrusters for raising spacecraft from parking orbit to higher altitudes, leading to definition of an operational SEP orbit transfer vehicles (OTV) for Air Force missions. Many of the problems or potential problems that may be associated with SEP are not well understood nor clearly identified, and system level phenomena such as interaction of thruster plume with the solar arrays cannot be simulated in a ground test. Therefore, an end-to-end system flight test is required to demonstrate solar electric propulsion. Derived from text

N94-11417*# Communications Satellite Corp., Clarksburg, MD.
WORKSHOP SUMMARY: NEW SILICON CELLS c44
A. Meulenberg and P. A. Iles (Applied Solar Energy Corp., City of Industry, CA.) *In* NASA. Lewis Research Center, Proceedings of the 12th Space Photovoltaic Research and Technology Conference (SPRAT 12) May 1993 p 334-336 (For primary document see N94-11380 01-20)
Avail: CASI HC A01/MF A03

The workshop on new silicon cells held during SPRAT12 is summarized. A smaller than average group attended this workshop reflecting the reduction in research dollars available to this portion of the photovoltaics community. Despite the maturity of the silicon technology, a core of the group maintained an excitement about new developments and potential opportunities. The group addressed both the implications and the applications of recent developments. Topics discussed include: light trapping and ultrathin silicon cells; different uses for silicon cells; new silicon cell developments; and radiation tolerant high efficiency cells. Author (revised)

N94-11418*# Research Triangle Inst., Research Triangle Park, NC.
MULTI-BAND GAP AND NEW SOLAR CELL OPTIONS WORKSHOP c44
J. Hutchby, M. Timmons, and J. M. Olson (Midwest Research Inst., Golden, CO.) *In* NASA. Lewis Research Center, Proceedings of the 12th Space Photovoltaic Research and Technology Conference (SPRAT 12) May 1993 p 337-339 (For primary document see N94-11380 01-20)
Avail: CASI HC A01/MF A03

Discussions of the multi-band gap (MBG) and new solar cell options workshop are presented. Topics discussed include: greater than 2 terminal cells; radiation damage preventing development of MBG cells for space; lattice matching; measurement of true performance; future of II-VI materials in MBG devices; and quaternaries. CASI

N94-11419*# Sverdrup Technology, Inc., Brook Park, OH.
WORKSHOP SUMMARY: RECEIVERS FOR LASER POWER BEAMING
Geoffrey A. Landis *In* NASA. Lewis Research Center, Proceedings of the 12th Space Photovoltaic Research and Technology Conference (SPRAT 12) May 1993 p 340-343 (For primary document see N94-11380 01-20)
Avail: CASI HC A01/MF A03

At the Space Photovoltaics Research and Technology (SPRAT) conference at NASA Lewis Research Center, a workshop session was held to discuss issues involved in using photovoltaic arrays ('solar cells') to convert laser power into electrical power for use as receiving elements for beamed power. Author (revised)

N94-11643# Naval Research Lab., Washington, DC.
ULTRAVIOLET PLUME INSTRUMENT DESCRIPTION AND PLUME DATA REDUCTION METHODOLOGY Interim Report
H. W. Smathers, D. M. Horan, J. G. Cardon, E. R. Malaret, and M. R. Corson 12 May 1993 65 p
(AD-A266141; NRL/FR/8121-93-9531) Avail: CASI HC A04/MF A01

The Ultraviolet Plume Instrument (UVPI) is a small plume-tracking instrument flown on the Naval Research Laboratory's Low-power Atmospheric Compensation Experiment (LACE) satellite, which was launched on 14 February 1990. The UVPI's mission is to collect images of rocket plumes. Missile tracking in the ultraviolet range is advantageous because of extremely low Earth and solar background, extremely sensitive photodetectors that do not require cryogenic cooling, and very high optical resolution that is possible with optics of relatively modest size. The two cameras of the instrument use filters, image intensifiers, and charge-coupled device (CCD) detectors to observe sources in the ultraviolet, a tracker camera for target acquisition, a plume camera with a narrow field of view (0.184 deg by 0.137 deg), and four filters for data acquisition. Filters have passbands of 195 to 295 nm, 220 to 320 nm, 235 to 350 nm, and 300 to 320 nm. Rocket stages reaching 110-km altitude have been successfully detected and tracked by the UVPI from a range of 450 to 550 km for about 30 seconds. The spectral radiance and spectral radiant intensities of the plumes were extracted for the data by using a reference spectrum characteristic of micron-sized alumina particles at the melting-point temperature. DTIC

N94-11675# International Space Univ., Inc., Kitakyushu (Japan).
SPACE SOLAR POWER PROGRAM Final Report
Humayun Arif, Hugo Barbosa, Christophe Bardet, Michel Baroud, Alberto Behar, Keith Berrier, Phillippe Berthe, Reinhold Bertrand, Irene Bibyk, and Joel Bisson et al Aug. 1992 527 p
(Contract DE-FG02-92ER-75839)
(DE93-011750; DOE/ER-75839/1) Avail: CASI HC A23/MF A04

Information pertaining to the Space Solar Power Program is presented on the following topics: energy analysis; markets; overall development plan; organizational plan; environmental and safety issues; power systems; space transportation; space manufacturing, construction, and operations; design examples; and finance. DOE

N94-12283# Aircraft Research Association Ltd., Bedford (England).
AN OVERVIEW OF THE CAPABILITIES OF ARA FOR THE MEASUREMENT OF NOZZLE DISCHARGE AND THRUST
R. S. Sale, M. Elliott, and I. F. Burns Aug. 1992 12 p Presented at the European Forum on Wind Tunnels and Wind Tunnel Testing Techniques, Southampton, England, 14-17 Sep. 1992
(ARA-Memo-378) Avail: CASI HC A03/MF A01

Details are given of the present nozzle thrust and discharge measuring ability of Aircraft Research Association (ARA) and the practical application of the measurements explained. Two major facilities for the measurement of thrust and discharge, the Mach Simulation Tank (MST) and the Large Scale Thrust Measuring Rig (LSTMR) are described in detail. The history of the development of these facilities is discussed and present data quality standards illustrated. Special emphasis is placed on the need for high precision mass flow measurements. The use of reference nozzles for qualification tests is described and possible future evolution of both facilities presented. Author

N94-12569*# National Aeronautics and Space Administration. Lewis Research Center, Cleveland, OH.
HOT-GAS-SIDE HEAT TRANSFER CHARACTERISTICS OF SUBSCALE, PLUG-NOZZLE ROCKET CALORIMETER CHAMBER
Richard J. Quentmeyer (Sverdrup Technology, Inc., Brook Park, OH.) and Elizabeth A. Roncace Washington Jul. 1993 14 p
(RTOP 584-03-11)
(NASA-TP-3380; E-7614; NAS 1.60:3380) Avail: CASI HC A03/MF A01

An experimental investigation was conducted to determine the hot-gas-side heat transfer characteristics for a liquid-hydrogen-cooled, subscale, plug-nozzle rocket test apparatus. This apparatus has been used since 1975 to evaluate rocket engine advanced cooling concepts and fabrication techniques, to screen candidate combustion chamber liner materials, and to provide data for model development. In order to obtain the data, a water-cooled calorimeter chamber having the same geometric configuration as the plug-nozzle test apparatus was tested. It also used the same two showerhead injector types that were used on the test apparatus: one having a Rigimesh faceplate and the other having a platelet faceplate. The tests were conducted using liquid oxygen and gaseous hydrogen as the propellants over a mixture ratio range of 5.8 to 6.3 at a nominal chamber pressure of 4.14 MPa abs (600 psia). The two injectors showed similar performance characteristics with the Rigimesh faceplate having a slightly higher average characteristic-exhaust-velocity efficiency of 96 percent versus 94.4 percent for the platelet faceplate. The throat heat flux was 54 MW/m(sup 2) (33 Btu/in.(sup 2)-sec) at the nominal operating condition, which was a chamber pressure of 4.14 MPa abs (600 psia), a hot-gas-side wall temperature of 730 K (1314 R), and a mixture ratio of 6.0. The chamber throat region correlation coefficient C(sub g) for a Nusselt number correlation of the form Nu =C(sub g)Re(sup 0.8)Pr(sup 0.3) averaged 0.023 for the Rigimesh faceplate and 0.026 for the platelet faceplate. Author (revised)

23 CHEMISTRY AND MATERIALS (GENERAL)

N94-10513*# Virginia Polytechnic Inst. and State Univ., Blacksburg.
NEW AROMATIC ACTIVATED DIHALIDES AND BISPHENOL MONOMERS FOR THE PREPARATION OF NOVEL POLY(ARYLENE ETHERS)
James F. Wolfe 7 Jun. 1993 8 p
(Grant NAG1-1250)
(NASA-CR-193190; NAS 1.26:193190) Avail: CASI HC A02/MF A01

The goal of this research program was to synthesize a series of unique monomers of type I to be utilized at NASA-Langley in the preparation of new poly(arylene ether ketones), poly(arylene ether ketosulfones), and poly(arylene ether ketophosphine oxides). These A-A and A-B monomer systems, which possess activated aryl halide and/or phenolic end groups, are accessible via condensation reactions of appropriately substituted aryl acetonitrile carbanions with activated aryl dihalides followed by oxidative decyanation. Author

N94-10947*# Boeing Defense and Space Group, Seattle, WA.
SPACE ENVIRONMENTAL EFFECTS ON THE INTEGRITY OF CHROMIC ACID ANODIZED COATINGS Special Report, Oct. 1989 - Feb. 1992
W. L. Plagemann May 1993 189 p
(Contracts NAS1-18224; NAS1-19247; RTOP 506-43-61-02)
(NASA-CR-191468; NAS 1.26:191468) Avail: CASI HC A09/MF A02

This report describes the condition of chromic acid anodized aluminum subsequent to a 69-month exposure to low Earth orbit (LEO) on the Long Duration Exposure Facility. Optical properties and the condition of anodized coating are reported. This material was exposed to each environmental parameter present in LEO. Only slight changes in the material were observed. Author

N94-11362*# National Aeronautics and Space Administration. Lewis Research Center, Cleveland, OH.
TRIBOLOGICAL CHARACTERISTICS OF SPUTTERED Au/Cr FILMS ON ALUMINA SUBSTRATES AT ELEVATED TEMPERATURES Final Report
P. A. Benoy and C. DellaCorte May 1993 15 p Presented at the International Conference on Metallurgical Coatings and Thin Films, San Diego, CA, 17-21 Apr. 1993; sponsored by the American Vacuum Society
(Contract DE-AI01-91CE-50306; RTOP 505-63-1A)
(NASA-TM-106078; DOE/NASA/50306-3; E-7692; NAS 1.15:106078)
Avail: CASI HC A03/MF A01

Research to evaluate the tribological properties of alumina pins sliding against thin sputtered gold films deposited on alumina disk substrates is described. A 250 A thick chromium interlayer was first deposited onto the alumina test disks to enhance adhesion and high temperature wetting of the gold films. The Au/Cr films were tribotested in pure sliding in a pin-on-disk tribometer under a 4.9 N load at 1m/s. The test atmosphere was room air at temperatures of 25, 500, and 800 C and the test duration varied from 60 to 540 min. The use of the Au/Cr films reduced friction by about a factor of two compared to the unlubricated alumina sliding couple. The coatings prevented wear of the alumina substrate disks and reduced pin wear by one to two orders of magnitude. In addition, wear lives in excess of 200,000 sliding passes (9 hr) were observed during sliding at 800 C. The results suggest that these films show promise for the practical lubrication of many high temperature sliding components. Author (revised)

N94-12011 Pennsylvania Univ., Philadelphia. Dept. of Chemistry.
STUDIES IN BIOORGANIC CHEMISTRY Final Report
Jeffrey D. Winkler 2 Jun. 1993 3 p Limited Reproducibility: More than 20% of this document may be affected by microfiche quality
(Contract N00014-91-J-1886)
(AD-A265532) Avail: CASI HC A01

The grant addressed two issues of fundamental importance in biomimetic chemistry that had not been successfully imitated in a non-enzymatic system at the time at which this project started: the conformational flexibility of the enzyme active site and the consequences of such mobility for catalysis, and the stereoselective formation of carbon-carbon bonds using compounds that are based on the ubiquitous biological methylating agent S-adenosylmethionine. The photodynamic macrocycles that were originally proposed are not only fascinating molecules because of their unique structural effects, but were designed to be useful in the active transport of both metals and organic molecules which would have obvious implications in processes like the extraction of metals and organic molecules from aqueous solutions. The mimics of S-adenosylmethionine that were proposed in the original contract were to be applied to a variety of alkylation reactions and could ultimately be applied to the development of site-specific reagents for DNA functionalization, thereby providing an important control mechanism for gene expression. DTIC

N94-12588*# Alabama Univ., Huntsville. Center for Microgravity and Materials Research.
PROCESS MODELLING FOR MATERIALS PREPARATION EXPERIMENTS Semiannual Progress Report No. 8, 1 Feb. - 31 Jul. 1993
Franz Rosenberger and J. Iwan D. Alexander 1993 30 p
(Grant NAG8-790)
(NASA-CR-193556; NAS 1.26:193556) Avail: CASI HC A03/MF A01

The main goals of the research consist of the development of mathematical tools and measurement of transport properties necessary for high fidelity modeling of crystal growth from the melt and solution, in particular for the Bridgman-Stockbarger growth of mercury cadmium telluride (MCT) and the solution growth of triglycine sulphate (TGS). Of the tasks described in detail in the original proposal, two remain to be worked on: development of a spectral code for moving boundary problems, and diffusivity measurements on concentrated and supersaturated TGS solutions. During this eighth half-year period, good progress was made on these tasks. Author (revised)

24 COMPOSITE MATERIALS

Includes physical, chemical, and mechanical properties of laminates and other composite materials.

For ceramic materials see *27 Nonmetallic Materials.*

N94-10001# European Space Agency, Paris (France).
ADVANCED MATERIALS FOR LIGHTWEIGHT STRUCTURES
W. R. Burke, comp. Oct. 1992 405 p In ENGLISH and FRENCH Symposium held in Noordwijk, Netherlands, 25-27 Mar. 1992; sponsored by Commission of the European Communities and EUREKA
(ESA-SP-336; ISBN-92-9092-186-2; ETN-93-93943) Copyright Avail: CASI HC A18/MF A04

Papers covering a wide range of emerging materials and applications, presented at a symposium which recognized the importance of interdisciplinary interests in any structural materials development, are presented. The consolidation of work in reinforced plastics, which has seen widespread use for satellite payloads and structures, together with use in launch vehicle construction, is reflected. A strong interest in thermoplastics is evident. There is also a clear realization that further exploitation of isotropic metals is achievable; the development of aluminum/lithium alloys is used as a typical example. Aspects related to the need for materials resistant to high temperature and whose structural integrity can be assured, and to the need for materials which can perform effectively at cryogenic temperatures, are reflected. For individual titles, see N94-10002 through N94-10069.

N94-10002# European Research Coordination Agency, Brussels (Belgium).
THE EUREKA PROJECT PORTFOLIO IN NEW MATERIALS
Olaf Meyer *In* ESA, Advanced Materials for Lightweight Structures Oct. 1992 p 3-6 (For primary document see N94-10001 01-24)
Copyright Avail: CASI HC A01/MF A04

The bottom up character of the EUREKA initiative invites project participants to propose and carry out cooperative research and development projects that develop all conceivable technologies and aim at all but military applications. The function and result of the initiative are described. An overview of the project portfolio in the area of 'new materials' is provided with emphasis on lightweight structures. ESA

N94-10003# Deutsche Forschungsanstalt fuer Luft- und Raumfahrt, Stuttgart (Germany). Structures and Design Inst.
HIGH TEMPERATURE MATERIALS FOR HYPERSONIC TRANSPORT
R. Kochendoerfer *In* ESA, Advanced Materials for Lightweight Structures Oct. 1992 p 7-13 (For primary document see N94-10001 01-24)
Copyright Avail: CASI HC A02/MF A04

The requirements of high temperature materials for a hypersonic transport are discussed. The challenging structural requirements of hypersonic vehicles and the available materials for these high temperature structures are discussed. The critical issues for ceramic matrix composite materials are discussed. At present there is no alternative to these materials for lightweight structures operating over 1000 C. A fast silicon infiltration process for the fabrication of ceramic matrix composite structures and the implication this has for the designer are described. ESA

N94-10004# Messerschmitt-Boelkow-Blohm G.m.b.H., Bremen (Germany).
SPINFORMING CHARACTERISTICS OF A NET SHAPE FORMING PROCESS
D. Mueller-Wiesner (Erno Raumfahrttechnik G.m.b.H., Bremen, Germany.) and E. Sieger (Zeppelin-Metallwerke G.m.b.H., Friedrichshafen, Germany.) *In* ESA, Advanced Materials for Lightweight Structures Oct. 1992 p 15-18 (For primary document see N94-10001 01-24)
Copyright Avail: CASI HC A01/MF A04

The characteristics of the (near) net shape spin forming process are discussed. In addition to the description of process parameters and the machining, interdependencies between the process and properties of materials are indicated. Examples of the application of the spin forming process to hemispheres and domes for spacecraft propellant tasks, fabricated out of aluminum and steel alloys, are given. Aspects of future developments with respect to titanium beta and aluminum lithium alloys are addressed. ESA

N94-10005# Deutsche Forschungsanstalt fuer Luft- und Raumfahrt, Stuttgart (Germany). Structures and Design Inst.
LIGHTWEIGHT CFRP FRAME STRUCTURES FOR A ROTEX-DERIVED MANIPULATOR SYSTEM
Hermann Hald *In* ESA, Advanced Materials for Lightweight Structures Oct. 1992 p 21-27 (For primary document see N94-10001 01-24)
Copyright Avail: CASI HC A02/MF A04

A lightweight manipulator system is under development which is derived from the German Robotic Technology Experiment (Rotex). It is realized by combining ultralight CFRP (Carbon Fiber Reinforced Plastic) frame structures, which are fabricated by filament winding on a lost core, and powerful joint driving units of a new design concept. The overall modular system concept is discussed, and the chosen frame structure design and its geometry, load introduction, joint integration and fabrication method, are described. Results of a successful static loading test under a combined torsion/bending worst case loading are compared with load assumptions and calculated strain and deflection distributions evaluated by a detailed finite element analysis. Calculated results on the influence of material anisotropy combined with slightly curved truss beam elements due to the fabrication method are discussed as well as sensitivity due to local impact. ESA

N94-10006# Short Bros. and Harland Ltd., Belfast (Northern Ireland).
APPLICATION OF COMPOSITE MATERIALS FOR PRODUCTION NACELLE STRUCTURES
W. McGarel *In* ESA, Advanced Materials for Lightweight Structures Oct. 1992 p 29-31 (For primary document see N94-10001 01-24)
Copyright Avail: CASI HC A01/MF A04

The manufacturing of a number of aircraft nacelle components from composite materials is reported. The selected components are characterized by special features including acoustic performance, fireproof capability, and the ability to contain fanblades in the event of a failure. The choice of composite materials and manufacturing techniques used offer substantial weight savings at an economic cost. ESA

N94-10007# Construcciones Aeronauticas S.A., Madrid (Spain). Space Div.
DESIGN AND DEVELOPMENT OF A CFRP CENTRAL CYLINDER FOR SATELLITES
A. Jimenez, V. Diaz, F. Cespedosa, and W. J. Rits (European Space Agency. European Space Research and Technology Center, ESTEC, Noordwijk, Netherlands.) *In* ESA, Advanced Materials for Lightweight

Structures Oct. 1992 p 33-38 (For primary document see N94-10001 01-24)
Copyright Avail: CASI HC A02/MF A04

The central cylinder of a satellite is the element of the structure that transmits all the loads acting on the structure subsystem to the launcher interface and with its stiffness influences the natural frequencies of the satellite. The high performance demanded of spacecraft structures makes it necessary to use materials with a high stiffness/mass ratio in order to obtain the lightest structure, since the mass is one of the most important parameters in space structures. For this reason, it is almost mandatory to use carbon fiber technology for these structures. The development of a central cylinder with the main objective of establishing appropriate and cost effective design and manufacturing techniques is described. ESA

N94-10008# Construcciones Aeronauticas S.A., Madrid (Spain). Space Div.
AN APPROACH TO HIGH PRECISION ANTENNA STRUCTURES BY A CFRP CORE SANDWICH CONCEPT
A. Alonso, A. Cuadrado, A. Bonet, and H. Stark (European Space Agency. European Space Research and Technology Center, ESTEC, Noordwijk, Netherlands.) *In* ESA, Advanced Materials for Lightweight Structures Oct. 1992 p 39-44 (For primary document see N94-10001 01-24)
Copyright Avail: CASI HC A02/MF A04

High precision antenna structures such as the one foreseen for the FIRST (Far Infrared and Submillimeter Telescope) project require very high manufacturing accuracy, ultrahigh assembling precision, and obviously, very stable materials. A sandwich concept is thought to be one of the feasible options for the manufacturing of the FIRST project antenna, provided that the core has a low coefficient of thermal expansion. The development of an adequate core is thereby needed. A study was carried out in which a low cost and reliable CFRP (Carbon Fiber Reinforced Plastic) core was designed, analyzed, manufactured, and tested for mechanical and thermomechanical behavior. A double curvature sandwich panel having a CFRP core was manufactured as a feasibility concept model, and its thermal stability is being measured. ESA

N94-10009# Dornier System G.m.b.H., Friedrichshafen (Germany).
LOW COST AND THERMALLY STABLE SANDWICH DESIGN FOR FIRST
G. Helwig, R. Sippel, and H. Stark (European Space Agency. European Space Research and Technology Center, ESTEC, Noordwijk, Netherlands.) *In* ESA, Advanced Materials for Lightweight Structures Oct. 1992 p 45-49 (For primary document see N94-10001 01-24)
Copyright Avail: CASI HC A01/MF A04

The technical approach for the small version of the FIRST (Far Infrared and Submillimeter Space Telescope) antenna system is guided by the idea of showing the feasibility of a simple and consequently lower cost design which can meet the stringent requirement for proper operation of 7 microns of overall RSS deformation. The concept is a 'panel only' design which needs no additional supporting framework for the reflector surface. The reflector is an all CFRP (Carbon Fiber Reinforced Plastic) sandwich construction having such a low coefficient of thermal expansion that deformations under even large temperature changes are very small. Manufacturing accuracy has to be very precise. Different specimens and a reflector with the size of 500 by 500 mm were built and thermally tested (coefficient of thermal expansion measurements). Measured deformations were compared with analysis results. ESA

N94-10010# Stork Product Engineering, Amsterdam (Netherlands).
DESIGN AND MANUFACTURING OF FILAMENT WOUND THRUST CYLINDER
C. A. L. Kemper, S. R. Birjmohan, Bastiaan Visser (Ultra Centrifuge Nederland, Almelo.), and W. Rits (European Space Agency. European Space Research and Technology Center, ESTEC, Noordwijk, Netherlands.) *In* ESA, Advanced Materials for Lightweight Structures Oct. 1992 p 51-56 (For primary document see N94-10001 01-24)
Copyright Avail: CASI HC A02/MF A04

The study on the feasibility of a CFRP (Carbon Fiber Reinforced Plastic) filament wound central cylinder for spacecraft applications is presented. Apart from design, much emphasis is given on the manufacturing of this structural element as filament winding is considered as a promising manufacturing technology in terms of mass, cost, and reliability. ESA

N94-10011# Westland Aerostructures Ltd., East Cowes (England).
THE APPLICATION OF ADVANCED MATERIALS TO AIRCRAFT NACELLE STRUCTURES
M. J. Curran and N. C. Eaton *In* ESA, Advanced Materials for Lightweight Structures Oct. 1992 p 57-62 (For primary document see N94-10001 01-24)
Copyright Avail: CASI HC A02/MF A04

The application of fiber reinforced plastic composites in the nacelle structures designed and manufactured over the last twelve years is traced. The design, development, and manufacturing techniques which have evolved to meet the requirements of aerospace quality structural composites, are highlighted. ESA

N94-10012# Dornier System G.m.b.H., Friedrichshafen (Germany).
DESIGN CONCEPTS FOR LOAD-CARRYING HOT STRUCTURES FOR REENTRY BODIES
Ulrich Trabandt and Joerg Heitzer *In* ESA, Advanced Materials for Lightweight Structures Oct. 1992 p 65-70 (For primary document see N94-10001 01-24)
Copyright Avail: CASI HC A02/MF A04

Carbon/Carbon (C/C) and Carbon/Silicon Carbide (C/SiC) panels were manufactured for a reusable load carrying heat shield. Investigations of design concepts led to the application of cost efficient manufacturing and assembling methods. Via C/C and niobium screws, the individual panels are easily joinable to complex structures. Thermomechanical analysis and high temperature tests of joining elements confirmed the feasibility of two different design concepts: the double wall version and the resin transfer molding stringer stiffened concept. ESA

N94-10013# Technische Univ., Delft (Netherlands). Structures and Materials Lab.
HYBRID MATERIALS FOR USE AT ELEVATED TEMPERATURES
C. A. J. R. Vermeeren, J. Sinke, and M. J. L. vanTooren *In* ESA, Advanced Materials for Lightweight Structures Oct. 1992 p 71-77 (For primary document see N94-10001 01-24)
Copyright Avail: CASI HC A02/MF A04

The hybrid materials developed are named fiber metal laminates (ARALL). These materials are built up from thin metal alloy sheets that alternate with unidirectional or cross ply prepregs. Various fibers are applied in this concept, such as aramid, R glass, and carbon fiber materials. These fibers offer outstanding mechanical and fatigue properties as well as fracture toughness. Fiber metal laminates with titanium (alloy) sheets are primarily developed for space applications. Structural applications up to 250 C are possible while preserving good mechanical and fatigue strength. The mechanical properties of fiber metal laminates, in general, and laminates with titanium alloy sheets and carbon fibers, in particular, are discussed and compared with other materials. Epoxy and thermoplastic (PEEK) adhesives were tested. Limitations on formability in manufacturing processes are discussed. An example of a space application of GLARE in the Hermes space suit is shown regarding production and forming techniques. ESA

N94-10014# Stuttgart Univ. (Germany). Inst. for Statics and Dynamics of Aerospace Structures.
DISTORTIONS AND STRESSES IN THIN SHELLS DUE TO ANISOTROPIC THERMAL EXPANSION c39
Manfred Koenig *In* ESA, Advanced Materials for Lightweight Structures Oct. 1992 p 79 Submitted for publication (For primary document see N94-10001 01-24)
Copyright Avail: CASI HC A01/MF A04

The considerable interest in the application of refractory anisotropic materials to the design of shell components, which are used in the very hot regions of future hypersonic flight and reusable reentry vehicle structures, is discussed. These materials are often homogeneous in the macroscopic scale but anisotropic. Typical examples are pyrolytic graphite (obtained by vapor deposition) and more recently, carbon fiber reinforced carbon (C/C) and carbon fiber reinforced silicon carbide (C/SiC). The carbon fiber reinforcement of C/C and C/SiC often consists of layers of fabrics (0/90 deg), resulting in a behavior that is nearly isotropic in the plane of the shell but differs in the perpendicular (thickness) direction. The study focuses on such transversely isotropic materials and deals with distortions and residual stresses in shells made of such materials and resulting from uniform temperature changes. ESA

N94-10015# Rome Univ. (Italy). Dipt. Aerospaziale.
NUMERICAL SIMULATION AND EXPERIMENTAL RESULTS OF FILAMENT WOUND CFRP TUBES TESTED UNDER BIAXIAL LOAD **c39**
A. Amaldi, M. Giannuzzi (Ente Nazionale per l'Energia Elettrica, Rome, Italy.), M. Marchetti, and A. Miliozzi (Ente Nazionale per l'Energia Elettrica, Rome, Italy.) *In* ESA, Advanced Materials for Lightweight Structures Oct. 1992 p 81-86 (For primary document see N94-10001 01-24)
Copyright Avail: CASI HC A02/MF A04

The analysis of angle ply carbon/epoxy laminated composites when subjected to uniaxial and biaxial stresses is presented. Three classes of interwoven pattern filament wound cylindrical specimens are studied in order to compare the influence of angle on the mechanical behavior of the laminate. Three dimensional finite element and thin shell analyses were first applied to the problem in order to predict global elastic behavior of specimens subjected to uniaxial loads. Different failure criteria were then adopted to investigate specimens' failure and experimental tests were carried out for a comparison with numerical results. Biaxial stress conditions were produced by applying combinations of internal pressure and axial tensile and compressive loads to the specimens. ESA

N94-10016# Maschinenfabrik Augsburg-Nuernberg A.G., Munich (Germany).
ANALYTICAL PREDICTION AND TEST VERIFICATION OF THE MULTIAXIAL BEHAVIOUR OF HIGH-STRENGTH STEEL FOR LIGHTWEIGHT STRUCTURES **c39**
P. Agatonovic and U. Clormann *In* ESA, Advanced Materials for Lightweight Structures Oct. 1992 p 87-92 (For primary document see N94-10001 01-24)
Copyright Avail: CASI HC A02/MF A04

Within the Ariane 5 booster case development, combined pressure and axial load tests were carried out on tubes of the booster material 48 CrMoNiV 4 10 to determine the yield and burst criteria under biaxial loading conditions. The tests showed a burst type failure. At the intermediate stress ratios of 1:2 and 2:1 the results fall in between the von Mises and Tresca criteria. Based on this examination, the J2 based von Mises criterion can be a good first approximation of the biaxial behavior when prediction of yielding is required. In the calculation of the fracture, the (J2, J3) based Drucker theory is more appropriate. Based on the unified approach in this work, all named criteria can be simulated using simple generalized relationship. The coefficient necessary for the application are fitted based on the experimental results. ESA

N94-10017# Technical Research Centre of Finland, Espoo. Metals Lab.
DESIGN WITH HIGH STRENGTH STEEL: A CASE OF FAILURE AND ITS IMPLICATIONS **c39**
Klaus Rahka *In* ESA, Advanced Materials for Lightweight Structures Oct. 1992 p 93-99 (For primary document see N94-10001 01-24)
Copyright Avail: CASI HC A02/MF A04

A recent proof test failure of a high strength steel pressure vessel is scrutinized. Apparent deficiencies in the procedures to account for elasto-plastic local strain are indicated for the applicable routine (code) strength calculations. Tentative guidance is given for the use of material tensile fracture strain and its strain state (plane strain) correction in fracture margin estimation. A hypothesis that the calculated local strain is comparable with a gauge length weighted tensile ductility for fracture to initiate at a notch root is given. A discussion about the actual implications of the failure case and the suggested remedy in the light of the ASME Boiler and Pressure Vessel Code section 3 and 8 is presented. Further needs for research and development are delineated. Possible yield and ductility related design limits and their use as material quality indices are discussed. ESA

N94-10018# Societe Nationale de Construction Aeronautique, Gosselies (Belgium).
DEVELOPMENT OF A FATIGUE ANALYSIS APPROACH FOR CFRP STRUCTURES UNDER ACOUSTIC LOADING **c39**
S. Costantini *In* ESA, Advanced Materials for Lightweight Structures Oct. 1992 p 101-106 (For primary document see N94-10001 01-24)
Copyright Avail: CASI HC A02/MF A04

The evaluation of acoustic fatigue problems on aerospace structural elements is considered through finite element modeling of their dynamic behavior. A computer code was developed for this purpose. In order to validate the approach, RMS (Root Mean Square) computed stresses were compared with corresponding tests recorded on different structural components. S-N curves were established from representative coupon tests of typical panel junctions and stiffener sections at different levels of RMS deformation. These results were used to determine an estimated fatigue life for the full size component, to be correlated by fullscale test. ESA

N94-10019# Tampere Univ. of Technology (Finland). Inst. of Materials Science.
COMPARISON OF Al-Fe ALLOYS PRODUCED BY PFC AND USGA TECHNIQUES **c26**
T. K. Lepisto, P. Kettunen, and J. Rautiola *In* ESA, Advanced Materials for Lightweight Structures Oct. 1992 p 109-112 Sponsored by Technology Development Center and USGA (For primary document see N94-10001 01-24)
Copyright Avail: CASI HC A01/MF A04

An UltraSonic Gas Atomization (USGA) unit was built. Based on experiences in planar flow casting (PFC), melt dpinning (MS), and first test runs with USGA, the chamber construction and melting unit were strongly modified and a PC based control and data collection system was built up. In the final test runs Al-8Fe, Al-12Fe, and Al-12Fe-2V-2.5Si alloys were gas atomized in patches of 1 kg. Ribbons produced by PFC technique and chopped into flakes were used as reference materials. Microstructure of powders was finer and more homogeneous than that of flakes. Powders and flakes were extruded into rods, and their mechanical and hardness values were tested at different temperatures. ESA

N94-10020# Centro Sviluppo Materiali S.p.A., Rome (Italy).
THE MICROSTRUCTURE AND MECHANICAL PROPERTIES OF HOT WORKED FeAl INTERMETALLIC ALLOYS **c26**
O. Tassa, C. Testani, and A. Lefort (CEREM, Grenoble, France.) *In* ESA, Advanced Materials for Lightweight Structures Oct. 1992 p 113-118 (For primary document see N94-10001 01-24)
Copyright Avail: CASI HC A02/MF A04

The iron-rich iron aluminides are highly oxidation and sulfidation resistant and display good mechanical stength combined with low density. Two alloys, prepared by vacuum casting, were worked by compression in order to study the recrystallization conditions. After high temperature compression tests, two types of microstructure were observed: an equiaxed structure and a bimodal structure. Toughness tests were carried out on the compressed materials at 20 C. For the homogeneous structures with coarse grains, the energy values are lower than 37 J/sq cm; for the bimodal structures, these values are higher than 50 J/sq cm. Two deformation temperatures were studied in tensile tests: 950 and 1100 C. The strain rate was shown to be the critical parameter which controls the ductility of FeAl at a defined temperature. ESA

N94-10021# BHP Labs. Ltd., Limerick (Ireland).
ALUMINIUM-LITHIUM FORGINGS: PROPERTIES AND POTENTIAL SATELLITE APPLICATIONS **c26**
B. OBrien and A. Pradier (European Space Agency. European Space Research and Technology Center, ESTEC, Noordwijk, Netherlands.) *In* ESA, Advanced Materials for Lightweight Structures Oct. 1992 p 119-124 (For primary document see N94-10001 01-24)
Copyright Avail: CASI HC A02/MF A04

A tradeoff study demonstrated that up to 17 percent weight savings could be obtained on a selected ring component. The study indicated that in order to benefit fully from the advantages of Al-Li alloys, components for redesign must have a stiffness critical element. In order to determine the mechanical suitability, a test program was performed on an Al-Li forging. Tensile, compression, fracture toughness, and fatigue crack growth behavior was evaluated. In general, all properties are promising, though fracture toughness and fatigue crack growth in the ST orientation are relatively poor. In conclusion, the project findings have been promising, and application of Al-Li on satellites and other spacecraft structures must now be seriously considered. ESA

N94-10022# Southampton Univ. (England). Engineering Materials.
MECHANICAL AND FATIGUE PROPERTIES OF FIBRE REINFORCED ALUMINIUM-LITHIUM ALLOY AND ALUMINIUM-LITHIUM MMC BASED LAMINATES **c26**

E. P. Hunt, P. J. Gregson, R. Moreton (Defence Research Agency, Farnborough, England.), and C. J. Peel (Defence Research Agency, Farnborough, England.) *In* ESA, Advanced Materials for Lightweight Structures Oct. 1992 p 125-128 (For primary document see N94-10001 01-24)
Copyright Avail: CASI HC A01/MF A04

Continuous fiber reinforced laminates offer excellent resistance to fatigue crack growth and are potentially attractive for thin sheet damage tolerant aerospace applications. The current work set out to investigate the mechanical and fatigue properties of Al-Li alloy and Al-Li MMC (Metal Matrix Composites) laminates reinforced by carbon, aramid, and glass fibers. The low density of the lithium containing alloy and MMC causes the laminates to exhibit excellent specific strength and stiffness. For the fiber reinforcement to be beneficial to fatigue strength, the stiffness of the fibers must exceed that of the metallic components; in the present laminates, carbon fibers are shown to be advantageous. Fatigue crack growth rates are low and decrease with increasing fiber stiffness and increasing R ratio (increasing crack length). These effects are attributed to the influence of fiber bridging of the fatigue crack. ESA

N94-10023# Deutsche Airbus G.m.b.H., Bremen (Germany).
INVESTIGATIONS ON ALUMINIUM-LITHIUM ALLOYS FOR DAMAGE TOLERANT APPLICATION **c26**
W. Zink, Y. Barbaux (Aerospatiale, Suresnes, France.), A. Camacho (Construcciones Aeronauticas S.A., Madrid, Spain.), H. Price (British Aerospace Public Ltd. Co., Bristol, England.), G. Vaessen (Fokker B.V., Amsterdam, Netherlands.), L. Tirilly (Pechiney Co., Paris, France.), S. Schwantes (Dornier System G.m.b.H., Friedrichshafen, Germany.), N. Bernicot (Dassault Aviation, Istres, France.), S. Pantelakis (Patras Univ., Greece.), and R. Grimes (British Aluminum Co. Ltd., London, England.) et al *In* ESA, Advanced Materials for Lightweight Structures Oct. 1992 p 129-134 (For primary document see N94-10001 01-24)
Copyright Avail: CASI HC A02/MF A04

The Al-Li damage tolerant alloys now becoming available do not cover the whole range of properties required by the aircraft industry; for successful application on aerospace structures in the future, a full understanding of the material behavior will be necessary. Therefore a development program was initiated in 1990 by the European airframe industry and aerospace institutes with the following objectives: improving the properties of existing alloys as compared to conventional alloys; and evaluating the existing damage tolerant Al-Li alloys from a fundamental point of view, giving confidence in terms of all safety and reliability aspects for real aircraft applications. A survey of this project and some initial results are presented. ESA

N94-10024# Office National d'Etudes et de Recherches Aerospatiales, Paris (France). Direction des Materiaux.
MECHANICAL PROPERTIES OF MAGNESIUM/CARBON COMPOSITES DEVELOPED BY HOT PRESSING UNDER MEDIUM PRESSURE [PROPRIETES MECANIQUES DE COMPOSITES MAGNESIUM/CARBONE ELABORES PAR PRESSAGE A CHAUD SOUS MOYENNE PRESSION]
M. Rabinovitch, J. C. Daux, J. L. Raviart, M. H. Vidal-Setif, R. Mevrel, H. Abiven (Aerospatiale, Les Mureaux, France.), and J. F. Peltier (Aerospatiale, Les Mureaux, France.) *In* ESA, Advanced Materials for Lightweight Structures Oct. 1992 p 135-139 In FRENCH (For primary document see N94-10001 01-24)
Copyright Avail: CASI HC A01/MF A04

Several C/Mg unidirectional composite systems were investigated: AZ61 alloy (Mg, 6Al, 1Zn, wt) as the matrix and various high modulus fibers, M40, M40J, Teijin, E105, FT700. On a laboratory scale, tensile stengths as high as 1400 MPa were obtained with a M40J/AZ61 composite. Longitudinal Young's Modulus of 200 GPa with M40J/AZ61 and 320 GPa with FT 700/AZ61 were measured. The first tensile tests with the industrial composite are encouraging. A tensile strengh of 968 MPa was obtained on a FT700/AZ61 composite. ESA

N94-10025# Construcciones Aeronauticas S.A., Madrid (Spain).
DESIGN AND MANUFACTURING OF CFRP RINGS BY RTM
A. Jimenez, A. Ayuso, P. Rodriguez (Escuela Tecnica Superior de Ingenieros Aeronauticos, Madrid, Spain.), A. Sanz (Escuela Tecnica Superior de Ingenieros Aeronauticos, Madrid, Spain.), I. Gonzalez (Escuela Tecnica Superior de Ingenieros Aeronauticos, Madrid, Spain.), Henri Girardy (Brochier S.A., Dagneux, France.), R. Gallet (Brochier S.A., Dagneux, France.), and B. LaMotte (Brochier S.A., Dagneux, France.) *In* ESA, Advanced Materials for Lightweight Structures Oct. 1992 p 143-148 (For primary document see N94-10001 01-24)
Copyright Avail: CASI HC A02/MF A04

A development program aimed at exploring the feasibility of the Resin Transfer Molding (RTM) process to produce space structural parts is reported. A description is given of the different aspects of work: design of the piece to be manufactured by RTM taking into account all the constraints derived from the process, study of the process in order to establish materials and equipment, development of preforms, determination of process parameters by means of a test campaign which includes the manufacturing and testing of different types of pieces, and design and manufacturing of molds. Test results are presented and a qualification test for the ring is outlined. ESA

N94-10026# Dornier Luftfahrt G.m.b.H., Friedrichshafen (Germany).
SPF/DB: A MANUFACTURING TECHNIQUE FOR LIGHTWEIGHT STRUCTURES **c31**
G. Broden *In* ESA, Advanced Materials for Lightweight Structures Oct. 1992 p 149-153 (For primary document see N94-10001 01-24)
Copyright Avail: CASI HC A01/MF A04

The principles of SPF/DB (Super Plastic Forming/Diffusion Bonding) facilities and the SPF/DB process are presented. Recently developed SPF/DB structures, five wall components and a precooler exhaust, made from Ti6Al4V intended for serial production are presented. The advanced structural concept for a leading edge manufactured with a modified four sheet technology is addressed. For aluminum structures the process is restricted to pure superplastic forming up to now because of the difficult joining technique for aluminum alloys. Large high strength aluminum structures formed with the membrane technique are presented. The use of membrane technique in comparison to conventional SPF technique is discussed. An overview of the work on developing a joining technique for aluminum and aluminum-lithium alloys compatible with the SPF process is given with results of fundamental work on diffusion bonding. Some results from the determination of SPF properties and from DB process parameter evaluation are presented. ESA

N94-10027# Dornier Luftfahrt G.m.b.H., Friedrichshafen (Germany).
UNIVERSAL ADJUSTABLE MOULD FOR ANTENNA REFLECTORS **c31**
Ulrich Trabandt and Rafael GarciaPrieto (European Space Agency. European Space Research and Technology Center, ESTEC, Noordwijk, Netherlands.) *In* ESA, Advanced Materials for Lightweight Structures Oct. 1992 p 155-160 (For primary document see N94-10001 01-24)
Copyright Avail: CASI HC A02/MF A04

The investigation of a concept to produce solid reflectors with different shapes for space application with very good surface accuracy is reported. The adjustable mold should be used for curing composite materials by autoclave treatment under heat and pressure. The result of the concept selection investigation was the bed of nails concept together with a thermoplast mold skin. Backed by creep behavior tests of the thermoplast and trials on the model mold, the appropriate parameters were found to form the thermoplast mold skin over the contour-giving nailheads. Once formed at a temperature of around 200C, the mold skin remains stable during the reflector curing process. The requirement for the contour accuracy can be fully met. The root mean square values of the formed thermoplast mold skin were between 20 and 40 micrometers and for the elegant breadboard reflector panel less than 44 micrometers. ESA

N94-10028# Slovak Technical Univ., Trnava (Czechoslovakia). Dept. of Welding.
WELDABILITY OF MARAGING STEELS **c26**
Ryban Dusan *In* ESA, Advanced Materials for Lightweight Structures Oct. 1992 p 161-164 (For primary document see N94-10001 01-24)
Copyright Avail: CASI HC A01/MF A04

Metallurgical weldability of martensitic hardenable steels and the applicable welding technologies are addressed. The martensitic hardenable steels are the alloys of iron and nickel designed in such a way to provide high strength and high fracture toughness simultaneously. These properties are attained by hardening of the low carbon martensite, which is formed on the austenitization temperatures. Martensite is formed regardless of the cooling rate and is relatively soft, but by ageing at 480C it hardens due to precipitation of intermetallic phases. The welded joints show three characteristic heat affected zones, whereas the central narrowest one (heated approximately at 600 to 730C) is the weakest point of the weld. The most suitable technologies seem to be welding in shielding gases, friction welding, plasma arc and electron beam welding. ESA

N94-10029# Brush Wellman, Inc., Cleveland, OH.
ALUMINUM-BERYLLIUM ALLOYS FOR AEROSPACE APPLICATIONS **c26**
D. Hashiguchi, A. N. Ashurst, F. C. Grensing, and J. M. Marder *In* ESA, Advanced Materials for Lightweight Structures Oct. 1992 p 165-169 (For primary document see N94-10001 01-24)
Copyright Avail: CASI HC A01/MF A04

A family of low density, high elastic modulus aluminum-beryllium alloys is under development in order to meet the requirements of advanced aerospace designs. These alloys are aluminum based with 10 to 75 percent beryllium and combine the high specific stiffness of beryllium with the ductility and ease of fabrication of aluminium. Densities ranging from 2.0 to 2.58 g/cc with excellent strength and ductility have been achieved. The family of Albemet (Trademark) alloys under development was manufactured by both powder and ingot metallurgy techniques. Property characterization of extruded bar and rolled sheet included tensile, fatigue and fracture mechanics evaluation. The dependence of microstructure and properties upon composition and fabrication method, as well as upon third element additions is described. ESA

N94-10030# Integrated Aerospace Sciences Corp., Athens (Greece).
DEFORMATION MECHANISMS OF CONTINUOUS FIBRE-REINFORCED THERMOPLASTIC COMPOSITES DURING MANUFACTURING: A PROBABILISTIC APPROACH
Dimitri A. Bofilios and C. A. M. vandenEnde (Keuring van Electrotechnische Materialen N.V., Arnhem, Netherlands.) *In* ESA, Advanced Materials for Lightweight Structures Oct. 1992 p 173-177 (For primary document see N94-10001 01-24)
(Contract BE-3062-89/BREU-268)
Copyright Avail: CASI HC A01/MF A04

The flow mechanism that takes place during consolidation, under constant load, of a unidirectional thermoplastic composite laminate, is modeled. The application of normal force results in a pressure gradient within the material, thus inducing transverse flow. In a deformation process, the fibers constrain the flow of the resin but are themselves convected with the resin. It was observed that during consolidation, a resin rich layer is formed between successive plies. The thickness of each of these resin layers is defined by the variability and non uniformity of the consolidation process. The analysis uses the concept of an incompressible viscous Newtonian fluid to describe the behavior of the resin layers while plies are modeled according to the theory of highly anisotropic imcompressible viscous fluids. ESA

N94-10031# Integrated Aerospace Sciences Corp., Athens (Greece).
HEAT ANALYSIS OF THERMOPLASTIC COMPONENTS DURING THE INITIAL STAGES OF MANUFACTURING: A PROBABILISTIC APPROACH **c27**
Dimitri A. Bofilios and J. H. vanLochem (Keuring van Electrotechnische Materialen N.V., Arnhem, Netherlands.) *In* ESA, Advanced Materials for Lightweight Structures Oct. 1992 p 179-183 (For primary document see N94-10001 01-24)
(Contract BE-3062-89/BREU-268)
Copyright Avail: CASI HC A01/MF A04

Analytical models describing the preheating and the unsteady state conduction phenomena during the initial stages of manufacturing are presented. To expedite the process, the semi-product is preheated dielectrically (microwave heating), followed by stamping at a temperature below the T(sub g) of the matrix. The model developed to describe the microwave heating process is based on the notion of the Poynting vector which represents the energy flow per unit area in an electromagnetic wave. The analytical model used for predicting the temperature profiles in the specimen during stamping is based on transient heat conduction principles. In order to analyze the effects of process variability, simulation models were developed. These models allow for probabilistic inputs of either the processing variables or geometrical/material parameters. ESA

N94-10032# Dornier Luftfahrt G.m.b.H., Friedrichshafen (Germany).
COST EFFECTIVENESS OF STRUCTURAL APPLICATIONS OF FIBRE REINFORCED THERMOPLASTICS **c27**
Winfried Werner *In* ESA, Advanced Materials for Lightweight Structures Oct. 1992 p 185-190 (For primary document see N94-10001 01-24)
Copyright Avail: CASI HC A02/MF A04

In the past years, graphite fiber reinforced thermoplastics were investigated for their possible application in structural components on aircrafts. Initially, cost savings were expected from the known advantages of these materials compared to graphite fiber reinforced epoxy resins. Since thermoplastics, as opposed to thermosets, do not cure but solidify during the cooling process of the melt, very short manufacturing cycles can be achieved. On account of the saving potential of fiber reinforced thermoplastics studies were carried out to investigate and evaluate several manufacturing concepts. ESA

N94-10033# Fokker Special Products B.V., Hoogeveen (Netherlands).
APPLICATION OF ADVANCED THERMOPLASTICS **c27**
Arnt R. Offringa *In* ESA, Advanced Materials for Lightweight Structures Oct. 1992 p 191-195 (For primary document see N94-10001 01-24)
Copyright Avail: CASI HC A01/MF A04

Continuous fiber reinforced thermoplastic composites are maturing and moving into series production. The main driver for the application of thermoplastics is reduced part cost. Products can be produced cost effectively by applying certain innovative manufacturing processes. A number of these have been developed, among others: thermofolding, pressforming, hot dimpling and welding. The amount of processes is expanding rapidly. Development is often carried out jointly with partners, for example with material suppliers. In this manner, development efforts are speeded up, each party bringing in its own expertise. Government supported cooperation programs offer an extra incentive for industrial teamwork. Examples of products which are in series production are aircraft ice protection plates and wing panels as well as medical patient support panels. Applications outside the aerospace market are high end niche products such as medical support tables and robot arms. Thermoplastics are a young growth market with plenty of potential. ESA

N94-10034# DSM/nv Nederlandse Staatsmijnen, Geleen.
LOW COST THERMOPLASTIC COMPOSITES FOR STRUCTURAL APPLICATIONS: DESIGN CONCEPTS USING NEW MATERIALS AND PROCESSES **c27**
L. E. P. Wenmakers, A. E. Gaalman, and R. Marissen *In* ESA, Advanced Materials for Lightweight Structures Oct. 1992 p 197-202 (For primary document see N94-10001 01-24)
Copyright Avail: CASI HC A02/MF A04

Processing techniques and application examples, for example the automotive industry for PETP (Polyethylen Terephtalate) glass industrial composites, which fulfill the cost requirements, are described. A case study on a TPC (Thermo Plastic Composite) bumper beam is presented in order to show the potential of this material for weight reduction in automotive parts. Compared to an aluminum bumper beam, a TPC bumper beam will show an equivalent mechanical performance combined with a significant weight reduction (2.7 kg in the example considered) at a similar costs level. ESA

N94-10035# Tampere Univ. of Technology (Finland). Inst. of Plastics Technology.
TAPE WINDING OF THERMOPLASTIC COMPOSITES **c27**
K. Lahteenkorva, P. Peltonen, P. Jarvela, and P. Tormala *In* ESA, Advanced Materials for Lightweight Structures Oct. 1992 p 203-206 (For primary document see N94-10001 01-24)
Copyright Avail: CASI HC A01/MF A04

The effects of process parameters in thermoplastic tape winding are addressed. Analysis of processing parameters included: mandrell temperature, prepreg tension, roller compression on in situ consolidation, prepreg and wound surface warming, and winding speed. The effect of processing parameters on the wound part was evaluated by several different mechanical tests. Axial strength was the best indicator of wound part quality. Mandrell temperature and consolidation pressure effected mechanical properties most. In addition, suitability of the Taguchi method for this kind of application was studied. Results suggest the method is useful in limited circumstance for thermoplastic composite winding. ESA

N94-10036# Politecnico di Milano (Italy). Dept. of Aerospace Engineering.

SPECIAL PROBLEMS OF 3-D ULTRASONIC QNDI TECHNIQUES AND APPLICATIONS TO COMPOSITES AEROSPACE STRUCTURES c38

G. Sala, M. Anghileri, and A. Antoniazzi (Centro Sviluppo Applicazioni, Milan, Italy.) *In* ESA, Advanced Materials for Lightweight Structures Oct. 1992 p 209-215 (For primary document see N94-10001 01-24)
Copyright Avail: CASI HC A02/MF A04

A theoretical and experimental research activity carried out in order to set up a three dimensional (3D) ultrasonic QNDI (Quantitative Non Destructive Inspection) technique able to assess damage state of composite laminates is summarized. The role played by surface roughness, laminate thickness, fiber orientation, damage location and defect superposition were investigated. Signal acquisition and optimization processes were considered: ultrasonic spectroscopy has proven to be a suitable technique, consisting in the study of ultrasonic waveforms resolved into their Fourier frequency components; quantitative information can be extracted from the spectrum of the received ultrasonic signal and time of flight of ultrasounds. Various signal processing techniques were evaluated, relevant to complete waveform analysis: digital and analog filtering procedures, sampling, smoothing, fast Fourier transform, convolution and deconvolution. ESA

N94-10037# Indian Space Research Organization, Ahmedabad. Space Applications Center.

DESIGN OF INSPECTION AND ACCEPTANCE TEST METHODOLOGY FOR TIG WELDED ALUMINUM-ALLOY BRACKET FOR CAMERA HOUSINGS FOR IRS-1A SPACE CRAFT AND EXECUTING IT c38

V. K. Manglik, Rajeev Vaghmare, and A. K. Shah *In* ESA, Advanced Materials for Lightweight Structures Oct. 1992 p 217-221 (For primary document see N94-10001 01-24)
Copyright Avail: CASI HC A01/MF A04

The Indian Remote Sensing Satellite (IRS) 1A was the first indigenously developed operational remote sensing satellite. The most critical element in the satellite was the remote sensing camera. The camera was mounted on aluminum alloy bracket which was fabricated by TIG welding. The methodology of acceptance and inspection of the TIG welded bracket is presented and discussed. These efforts not only provided the confidence in reliable welded joint but also provided trouble free operation of the camera on board the satellite for its whole life. ESA

N94-10038# Robert Gordon's Inst. of Tech., Aberdeen (Scotland). School of Applied Sciences.

QUANTIFYING DISBOND AREA c38

D. W. Lowden *In* ESA, Advanced Materials for Lightweight Structures Oct. 1992 p 223-228 (For primary document see N94-10001 01-24)
Copyright Avail: CASI HC A02/MF A04

Disbonds simulated in a composite helicopter rotor blade were profiled using eddy currents. The method is inherently accurate and reproducible. An algorithm is described for calculating disbond margin. Disbond area is estimated assuming in-service disbondments exhibit circular geometry. ESA

N94-10039# Bundesanstalt fuer Materialpruefung, Berlin (Germany).

NEW X RAY SCANNING TOPOGRAPHIC APPROACHES TO NONDESTRUCTIVE EVALUATION OF COMPOSITES c38

M. P. Hentschel, W. Harbich, and A. Lange *In* ESA, Advanced Materials for Lightweight Structures Oct. 1992 p 229-232 (For primary document see N94-10001 01-24)
Copyright Avail: CASI HC A01/MF A04

In research, processing and application of composite materials, a strong demand for nondestructive characterization has developed. For several years it has continuously been stated in material science conferences that the performance of nondestructive techniques is dissatisfying in the case of composites. In attempting to bridge this technological gap, methods of nondestructive characterization of composites by X-ray scanning topography were created. They are capable of imaging microstructural properties by crystallographic contrast, interface sensitivity and orientational selectivity. ESA

N94-10040# Societe Nationale de Construction Aeronautique, Gosselies (Belgium).

APPLICATION OF THE INFRARED PHOTOACOUSTIC SPECTROSCOPY TO THE STUDY OF THE CURE MECHANISMS OF STRUCTURAL EPOXY ADHESIVES c25

J. L. Coppee *In* ESA, Advanced Materials for Lightweight Structures Oct. 1992 p 233-238 (For primary document see N94-10001 01-24)
Copyright Avail: CASI HC A02/MF A04

An interesting application of photoacoustic detection is the study of curing process of epoxy resins. Using this technique combined with thermal analysis method, differential scanning calorimetry and dynamic mechanical spectroscopy, the polymerization of two structural adhesives, designated A and B was studied. Fourier transform infrared spectroscopy photoacoustics was the only way to investigate the cure of the adhesive films with their carrier. In the adhesive A, the dicyandiamide, one of the curing agents, participates in reactions at the end of the cure, when the consumption of the epoxide groups stops. Those reactions, which are not exothermic, seem to increase the glass transition temperature and to homogenize the network. The cure mechanisms of the adhesive B consists of consecutive reactions: at the beginning of the cure, the exothermic reactions occur without consumption of epoxide groups and with a weak increase of T(sub G), in a second step, the epoxide groups participate in etherification reactions. ESA

N94-10041# Dornier System G.m.b.H., Friedrichshafen (Germany).

FIBRE-REINFORCED CERAMIC COMPONENTS BY FILAMENT WINDING FOR INTERMEDIATE TEMPERATURE APPLICATIONS

R. Ostertag and U. Trabandt *In* ESA, Advanced Materials for Lightweight Structures Oct. 1992 p 241-243 Sponsored in part by BMFT and ESA (For primary document see N94-10001 01-24)
Copyright Avail: CASI HC A01/MF A04

Filament winding techniques were combined with Si-polymer pyrolysis to establish a cost effective method for the fabrication of fiber reinforced ceramic structures. The thermomechanical properties of this material allow for a use as structural materials or hot gas ducts. Sandwich structures, shingles for re-entry vehicles and hot gas nozzles for turboprop engines were fabricated and the hot gas nozzles were successfully tested inflight. ESA

N94-10042# Tampere Univ. of Technology (Finland). Inst. of Materials Science.

AN ULTRALIGHT CARBON-CARBON COMPOSITE WITH AMORPHOUS MATRIX

Pentti O. Kettunen, Quancheng Gu, and Toivo K. Lepisto *In* ESA, Advanced Materials for Lightweight Structures Oct. 1992 p 245-248 (For primary document see N94-10001 01-24)
Copyright Avail: CASI HC A01/MF A04

The methods of controlled porosity are applied to pyrolization of carbon fiber reinforced phenolic thermosets in order to avoid the cracking of the matrix during pyrolization and to get the formed matrix into amorphous state. As based on results of optical microscopy, X-ray and selected area electron diffraction, TEM, and HREM, the goals are reached successfully. As compared to pure amorphous carbon, the carbon fiber reinforced modification has at room temperature bending strength values about four times higher, and exhibits quasi ductile fracture behavior. At 1500C, the composite reaches bending strength values from 550 N/sq mm to about 1000 N/sq mm. As the density of the structure is 1.25 to 1.35 g/cu cm, the specific bending strengths of the structure is less than or equal to 800,000 Nmm/g. ESA

N94-10043# Maschinenfabrik Augsburg-Nuernberg A.G., Munich (Germany).

NEW PROCESSES FOR LIGHTWEIGHT CERAMIC MATRIX COMPOSITES c27

A. Muehlratzer, K. Handrick, H. Koeberle, and K. Peetz *In* ESA, Advanced Materials for Lightweight Structures Oct. 1992 p 249-254 (For primary document see N94-10001 01-24)
Copyright Avail: CASI HC A02/MF A04

The current status of the industrial development of a thermal and pressure gradient CVI (Chemical Vapor Infiltration) process for the manufacture of CMC (Ceramic Matrix Composites) parts with SiC matrix is described. The short periods of time required for CVI densification with this process (in the order of several ten hours) makes the process cost effective and allows for short development cycles. Tensile strengths of up to 320 MPa for C/SiC and over 200 MPa for SiC/SiC together with strain tolerance were obtained. Within the German Hypersonics Technology Program the process is applied for the development of a CMC demonstrator part. A sol-gel derived alumina CMC is used for a newly developed insulation in the thermal protection system of the European Spaceplane Hermes. Thin alumina fiber reinforced alumina foils obtained by sol impregnation of fiber fleeces and coated with noble metal thin films are applied as reflective screens. ESA

N94-10044# GEC Alsthom, Stafford (England). Engineering Research Centre.
CERAMIC MATRIX COMPOSITES: HIGH PERFORMANCE MATERIALS FOR SPACE APPLICATION c27
Andrew R. Hyde *In* ESA, Advanced Materials for Lightweight Structures Oct. 1992 p 255-260 Sponsored by Commission of the European Communities (For primary document see N94-10001 01-24)
Copyright Avail: CASI HC A02/MF A04

The properties of carbon and silicon carbide fiber reinforced Ceramic Matrix Composites (CMC's) are reported and discussed and these are related to their potential applications. These materials are attractive for applications requiring zero, or controlled thermal expansion, low density, high stiffness, refractoriness, damage tolerance and high strength to low mass ratio. The development of CMC's and component fabrication technology is reported. This development encompassed design methods, component performance, production routes and materials. The fabrication of large complex geometry, multidirectional fiber, reinforced CMC's to near net size and shape is discussed. ESA

N94-10045# Maschinenfabrik Augsburg-Nuernberg A.G., Munich (Germany).
SPIN-ROLLING, WELDING, AND HEAT TREATMENT OF ALUMINIUM 2219 FOR ARIANE 5 GAM HIGH PRESSURE VESSEL LINERS c31
W. Radtke *In* ESA, Advanced Materials for Lightweight Structures Oct. 1992 p 263-266 (For primary document see N94-10001 01-24)
Copyright Avail: CASI HC A01/MF A04

Cylindrical liners made of Al 2219 may be spinrolled if both recrystallization and metastable precipitates can be avoided during forging or preparatory heat treatment. So welding is to be limited to circumferential joints. Pore-free welds are attainable immediately after hydroxide layer removal by diamond cutting without grease application. The EB vacuum is favorable to porosity suppression. A complete heat treatment of the liner incorporating solutionizing, water quenching and ageing leads to 100 percent weld efficiency. Pressure stabilization avoids buckling. Subsequent carbon fiber winding, curing and plastic prestressing of the liner results in an efficient high pressure vessel for hydrogen service. ESA

N94-10046# Maschinenfabrik Augsburg-Nuernberg A.G., Munich (Germany).
STRESS RELAXATION FORMING OF ARIANE 5 FRONT SKIRT OUTER SKIN PANELS c39
W. Radtke *In* ESA, Advanced Materials for Lightweight Structures Oct. 1992 p 267-269 (For primary document see N94-10001 01-24)
Copyright Avail: CASI HC A01/MF A04

The integrally milled Ariane 5 front skirt axial load reaction structure panels are being formed successfully by stress relation of fully averaged Al 7075 T7351. The special features of the well known age forming process, such as smoothness of contours, reproductiveness, formability of complicated integrally stiffened parts and favorable residual stresses, were combined with an extraordinarily flexible choice of forming parameters, namely clamping radius and time at temperature. During the process the T7351 material properties are preserved. ESA

N94-10047# Construcciones Aeronauticas S.A., Madrid (Spain). Space Div.
DEVELOPMENT TESTS FOR A HIGH STABILITY OPTICAL BENCH c74
E. Ozores, F. Arevalo, A. Ayuso, A. Bonet, S. Lareo, and A. Pradier (European Space Agency. European Space Research and Technology Center, ESTEC, Noordwijk, Netherlands.) *In* ESA, Advanced Materials for Lightweight Structures Oct. 1992 p 271-276 (For primary document see N94-10001 01-24)
Copyright Avail: CASI HC A02/MF A04

The optical communications in satellites and some other optical experiments, require supporting baseplates to attach highly precise and sensitive optical equipments. A concept of baseplate based on a sandwich construction with both, faces and core, made of CFRP (Carbon Fiber Reinforced Plastic) was designed, accomplishing with very stringent requirements as follows: very high dimensional stability (deformations lower than 0.1 micrometers and rotations lower than 0.1 arcsec), very high stiffness to mass ratio (first natural frequency higher than 160 Hz and a total mass lower than 3 Kg), and availability of a great number of hard points to attach the different equipments placed in several configurations. The development test campaign carried out to demonstrate the capabilities of the outstanding baseplate design for high stability applications, the manufacturing activities to get a fully representative first prototype and the initial approach to a complete performances verification program, is presented. ESA

N94-10048# Erno Raumfahrttechnik G.m.b.H., Bremen (Germany).
ON THE MECHANICAL DEVELOPMENT OF THE FLEXIBLE EXTERNAL INSULATION (FEI) FOR HERMES SPACEPLANE
J. Bolz *In* ESA, Advanced Materials for Lightweight Structures Oct. 1992 p 277-283 (For primary document see N94-10001 01-24)
Copyright Avail: CASI HC A02/MF A04

The Flexible External Insulation (FEI) is a thermal protection system which covers large areas of the Hermes spaceplane. Under nominal reentry conditions the thermal loading of these areas is moderate (650 C). Targeting for minimum weight, the fibrous FEI blanket has to ensure that the temperature of the 'cold' Hermes structure remains below 175 C. As critical mechanical design driver the high acoustic loading was identified. This noise results from the boundary layer during ascent of the Ariane 5. Additionally, a dynamic excitation (flutter) of the outer cover fabric of the FEI by the airflow may occur. An overview on the structurally related aspects of the FEI development is presented, concentrating on the performed test program and on the achieved results and their influence on the development process. ESA

N94-10049# Erno Raumfahrttechnik G.m.b.H., Bremen (Germany).
MATERIAL ADVANCES FOR LIGHTWEIGHT TPS c27
U. Rieck and L. Kampmann *In* ESA, Advanced Materials for Lightweight Structures Oct. 1992 p 285-289 Sponsored by Dassault Aviation and Centre Spatial Dassault (For primary document see N94-10001 01-24)
Copyright Avail: CASI HC A01/MF A04

Amongst the various Thermal Protection Systems (TPS) the Hermes Flexible External Insulation (FEI) represents a novel solution combining attractive lightweight properties with adaptability to more complex substrate shapes, possibility for the extension to higher service temperatures and increased structural load bearing capabilities. Consisting of a microfiber insulation core embedded between silica/glass fabrics and sewn together using a silica/glass thread system, the structural integrity of the FEI TPS strongly depends on the proper performance of each single component. The investigation program performed so far included the determination of the specific interaction mechanisms of the different components, especially under certain aging conditions. ESA

N94-10050# British Aerospace Public Ltd. Co., Bristol (England).
VECTRA INSULATIVE SUPPORT STRUCTURES WITHIN SPACECRAFT c27
G. H. F. Nayler *In* ESA, Advanced Materials for Lightweight Structures Oct. 1992 p 291-298 (For primary document see N94-10001 01-24)
Copyright Avail: CASI HC A02/MF A04

Vectra A130 is a 30% glass fiber reinforced liquid crystal polymer which can be molded reliably, has a low thermal conductivity, and adequate strength and stiffness. The reaction control system support and insulation requirements of the ESA Cluster spacecraft gave the necessary impetus for evaluation of Vectra in a real environment. As space usage was unknown, it was necessary to perform acceptance tests before proceeding to flight hardware. ESA

N94-10051# Fokker B.V., Schipol-Oost (Netherlands). Stress Research Group.

DESIGN EVALUATION OF GLARE LAMINATE LAY-UPS

A. I. Pendus, P. T. Elangovan, and P. Minderhoud *In* ESA, Advanced Materials for Lightweight Structures Oct. 1992 p 301-306 (For primary document see N94-10001 01-24)

Copyright Avail: CASI HC A02/MF A04

The initial buckling shear strength of flat rectangular panels is determined for various GLARE (Glass Aluminum Reinforced) laminate configurations to evolve an optimum design layup for shear panels. It is shown possible to simplify the laminate anisotropy to special orthotropy for which the readily available solutions for elastic buckling can be employed. If the calculated elastic buckling stresses are above the value of linear limit, a plasticity correction is applied on those stresses. The correction process is iterative; the load redistribution among the layers has to be accounted for as the iteration proceeds. The design evaluation of GLARE laminates entails a number of design parameters such as laminate layup, fiber orientation, panel size, and the type of loading. ESA

N94-10052# BNF-Fulmer, Wantage (England).

JOINTS BETWEEN DISSIMILAR METALLIC AND CERAMIC MATERIALS

David P. Bashford *In* ESA, Advanced Materials for Lightweight Structures Oct. 1992 p 307-314 (For primary document see N94-10001 01-24)

Copyright Avail: CASI HC A02/MF A04

The joining of dissimilar metallic and ceramic materials requires an understanding of the implications of dissimilar properties on the integrity of the joint configuration. The joints may be classified in two ways: either fused and permanent or mechanical interconnections, which allow disassembly. Wherever possible, the physical and mechanical properties of the dissimilar materials should be matched as closely as is practically feasible. In particular, stiffness and coefficients of thermal expansion are the most significant properties. The materials of interest include alloys, metal matrix composites, monolithic ceramics, and ceramic and carbon-carbon composites. Where radically different materials need to be joined, then graded structures or functionally gradient materials can provide a realistic means of achieving a transition joint. Integrity and inspection of joints is important and mechanical joints tend to provide greater confidence on these counts than do fused joints. Reference is made to jointing in thrusters and nozzles plus experience with thermal protection systems. ESA

N94-10053# BNF-Fulmer, Wantage (England).

INTRODUCING SMaSE: AN AIDE MEMOIRE ON STRUCTURAL MATERIALS AND SPACE ENGINEERING

Josephine Wilson *In* ESA, Advanced Materials for Lightweight Structures Oct. 1992 p 315-319 (For primary document see N94-10001 01-24)

Copyright Avail: CASI HC A01/MF A04

A document produced in response to a need identified by ESTEC, which brings together in one source all those factors which require evaluation by the designers of all space structures, is introduced. It provides basic information on the use of metal alloys and fiber reinforced plastic composite materials and is an 'aide memoire' for the whole design process. It cannot, for reasons of usable size, present a detailed analysis of each topic. However, a comprehensive referencing system directs the reader to the source documents, design guides, manuals, ESA PSS documents, and verification tools, including recognized Test Specifications and nondestructive testing techniques for manufacturing and in-service use. ESA

N94-10054# Oulu Univ. (Finland). Engineering Mechanics Lab.

A NEW AND EFFICIENT WAY TO JOIN COMPOSITE PIPES c31

H. Lahtinen, M. Autio, S.-G. Sjolind, and A. Pramila *In* ESA, Advanced Materials for Lightweight Structures Oct. 1992 p 321-324 (For primary document see N94-10001 01-24)

Copyright Avail: CASI HC A01/MF A04

Most of the European standards and norms applied by the pressure vessel authorities require testing of the structure by a pressure ten times the design pressure. One of the goals during the course of a referenced work was to show that the burst pressure in fact is ten times the design pressure. All the joints in the structure were of traditional hand laminated butt joint type. Several tests were carried out but the goal pressure was never reached. The reason was always the same: leakage of joints. Because of this, a new type of joint was created. The joint is the cylindrical analogy of a scarf joint. The target pressure was reached during the first test. ESA

N94-10055# Maschinenfabrik Augsburg-Nuernberg A.G., Munich (Germany).

STRUCTURAL MATERIAL, MANUFACTURE, AND DESIGN REQUIREMENTS FOR HIGH-TEMPERATURE FASTENERS FOR SPACE PLANE TECHNOLOGIES c37

P. Agatanovic and M. Dogigli *In* ESA, Advanced Materials for Lightweight Structures Oct. 1992 p 325-332 (For primary document see N94-10001 01-24)

Copyright Avail: CASI HC A02/MF A04

The design of high temperature refractory alloy fasteners for Hermes is addressed. Principles of fastener design, implications of material selection and processing, and requirements for coating selection are reviewed. Methods for calculation of fastener preload and the possible sources of preload loss (including thermal expansion mismatch) are discussed. In particular, the need for a systems approach to the development of the whole joint concept is stressed, and the potential of numerical analysis techniques, such as finite elements, to support such an approach is illustrated. ESA

N94-10056# Ceskoslovenska Akademie Ved, Prague. Central Lab. for Experimental Mechanics.

PERFORATED PLATES FOR THIN-WALLED STRUCTURES c39

M. Drdacky and J. Lesak *In* ESA, Advanced Materials for Lightweight Structures Oct. 1992 p 333-337 Sponsored by Ministry for Economy and Industries (For primary document see N94-10001 01-24)

Copyright Avail: CASI HC A01/MF A04

Perforated plates, that is, plates with a high density of small openings, as a suitable sheet material for thin walled plated structures are presented. Perforations enable to increase a wall thickness of thin walled structures and thus, also, their load carrying capacity at the same material consumption. Results of experimental research concerning the stability behavior of such perforated webs compressed at two opposite edges are described. The influence of the plate thickness, the perforation extent, shapes of holes, and support conditions were studied. A simple semi-empirical method for estimating critical loads of perforated webs is presented. A utilization of perforated webs in search of optimum mass distribution in compressed thin walls is demonstrated. ESA

N94-10057# Nauchno-Issledovatelskii Inst. Grafit, Moscow (Russia).

ADVANCED METHODS OF PERMANENTLY JOINING CARBON MATERIALS c39

L. T. Anikin, A. V. Demin, G. A. Kravetskiy, and V. I. Kostikov *In* ESA, Advanced Materials for Lightweight Structures Oct. 1992 p 339-342 Prepared in cooperation with Nauchno-Issledovatelskii Inst. Grafit USA Corp. and Nauchno-Issledovatelskii Inst. Grafit-Europa G.m.b.H., Germany (For primary document see N94-10001 01-24)

Copyright Avail: CASI HC A01/MF A04

The most promising method of joining large sized articles and structures of an intricate configuration is by glueing using high temperature carbonizable adhesives. Due to low hardening temperature (20 to 110 C) of such adhesives, there is no need to use fluxes or protective atmospheres, energy consumption is reduced, the stress problem in the joint is favorably solved, and the serviceability of the joint is ensured at high temperatures in various media. When joining dissimilar materials such as carbon or metal, a serviceable structure can be generally formed by combining different ways of decreasing stresses. On the basis of stressed state investigation in graphite-metal joints, recommendations were developed on the stepwise production of a friction pair involving the preparation of a soldered member having a joint line on the side surface, followed by its welding to a metal case. ESA

N94-10058# Fraunhofer-Inst. fuer Chemische Technologie, Pfinztal (Germany).

INVESTIGATION OF THE REASON FOR THE SOFTENING BEHAVIOUR OF FILLED POLYMERS c27

N. Aksel and C. Huebner *In* ESA, Advanced Materials for Lightweight

Structures Oct. 1992 p 345-349 (For primary document see N94-10001 01-24)
Copyright Avail: CASI HC A01/MF A04

An investigation to develop methods to characterize filled polymers and to determine the different contributions to the softening behavior is described. The softening of crosslinked, unfilled and filled polybutadienes as an effect of a mechanical load and the subsequent recovery was examined at small strains. The contributing factors to the softening are discussed in terms of macroscopic observable phenomena and microscopic and molecular mechanisms which cause those phenomena. It is shown that most of the softening is recoverable because it is due to stress relaxation at the test conditions used. ESA

N94-10059# Fraunhofer-Inst. fuer Angewandte Material Forschung, Bremen (Germany).
PM TECHNOLOGY AND MECHANICAL PROPERTIES OF METALLIC FOAMS **c27**
J. Baumeister, J. Banhart, M. Weber, and B. Guenther *In* ESA, Advanced Materials for Lightweight Structures Oct. 1992 p 351-353 (For primary document see N94-10001 01-24)
Copyright Avail: CASI HC A01/MF A04

A powder technological method for manufacturing lightweight materials is described. Aluminum or aluminum based alloy powder and an appropriate foaming agent are processed into a semifinished product which can be made to expand in order to form a metallic foam of very low density. Mechanical, electrical, thermal, and technological properties in general are discussed. ESA

N94-10060# Maschinenfabrik Augsburg-Nuernberg A.G., Munich (Germany).
CONSTITUTIVE LAWS FOR DESCRIBING THE SERVICE RELEVANT CREEP BEHAVIOUR OF METALLIC MATERIALS **c26**
P. Agatonovic, J. M. Church (Joint Research Centre of the European Communities, Petten, Netherlands.), and R. Hurst (Joint Research Centre of the European Communities, Petten, Netherlands.) *In* ESA, Advanced Materials for Lightweight Structures Oct. 1992 p 355-360 Sponsored by Commission of the European Communities (For primary document see N94-10001 01-24)
Copyright Avail: CASI HC A02/MF A04

The optimum design of a structure for operation in the high temperature creep regime conventionally relies on in-built safety features applied to stress rupture data. As considerable inaccuracy is intrinsic and conservative design inevitable using such design rules, lightweight structures are unlikely to benefit from such an approach. Based on the results of the BRITE P-1209 program, it is demonstrated that advanced modeling methods exhibit significant advantage over conventional methods. Design of lightweight structure involves various aspects which a successful model has to handle; focus is on the two of the most important. The first is the ability to interpolate with confidence between data from a limited high quality data set and the second is the extension potential from uniaxial data to more complex multiaxial stress conditions. ESA

N94-10061# Ecole Nationale Superieure de Ceramique Industrielle, Limoges (France). Lab. Materiaux Ceramiques.
STUDY OF THE TRIBOLOGICAL BEHAVIOR OF SiC AND Si3N4 CERAMIC COUPLES IN TERMS OF TEMPERATURE: THE REALITY [ETUDE DU COMPORTEMENT TRIBOLOGIQUE DE COUPLE CERAMIQUES SiC ET Si3N4 EN FONCTION DE LA TEMPERATURE: LA REALITE] **c37**
F. Platon and Y. Berthier (Institut National des Sciences Appliquees, Lyon, France.) *In* ESA, Advanced Materials for Lightweight Structures Oct. 1992 p 361-366 In FRENCH Sponsored by Commission of the European Communities (For primary document see N94-10001 01-24)
Copyright Avail: CASI HC A02/MF A04

Tribological analysis of ceramic couples (SiC and Si3N4) was carried out by identifying Velocity Accommodation Mechanisms (VAM) activated in different conditions. Results obtained in the temperature region 20 to 1000 C show raised values of friction and flow interest. To reduce these values, three artificial bodies, of solid lubricant type, such as cerium fluoride powder and 'plasma' coatings, are used. ESA

N94-10062# Aerospatiale Aquitaine, Saint-Medard en Jalles (France). Espace et Defense.
HIGH TEMPERATURE COMPOSITES IN AEROSPATIALE ACTIVITIES
J. L. Macret and P. Lautissier *In* ESA, Advanced Materials for Lightweight Structures Oct. 1992 p 367-372 (For primary document see N94-10001 01-24)
Copyright Avail: CASI HC A02/MF A04

A review of activities in the development of high temperature composites for use in aerospace transportation systems is presented. A wide range of temperature is needed for structural materials and for thermal protection. The emergence of thermal resistant fibers like carbon and ceramics was the basis for the development of advanced materials. For very high temperatures up to 2000 C, the use of carbon-carbon is effective and improvement has been achieved regarding coating protection systems in order to face oxidation reaction of carbon above 500C. Oxidation resistant carbon-carbon is currently the baseline solution for the nose cap and the wing leading edges, hottest parts of Hermes, the European Spaceplane. Growing interest has appeared for the use of glass ceramic composites with availability of suitable ceramics fibers (mainly SiC fibers) and potentiality of cost effective processing due to glass ceramic. The objective operating temperature of glass ceramic fibers is above 1000 C and a large area of the outer surface of future winged transportation systems is aimed at as nominal application. ESA

N94-10063# Norges Tekniske Hoegskole, Trondheim. Dept. of Metallurgy.
STRUCTURE AND PROPERTIES OF AN RS Al-Si-Ni-Mn-Zr ALLOY FOR HIGH TEMPERATURE APPLICATIONS **c27**
H. J. Roven, I. Johansen (Technical Univ. of Norway, Trondheim.), B. Jensen, and O. Jensrud (Raufoss Ammunisjonsfabrikker, Norway.) *In* ESA, Advanced Materials for Lightweight Structures Oct. 1992 p 373-378 Sponsored by Royal Norweigan Council for Scientific and Industrial Research (For primary document see N94-10001 01-24)
Copyright Avail: CASI HC A02/MF A04

Rapidly Solidified (RS) aluminum alloys may have a high benefit/cost factor and can effectively be produced in the industrial scale. This type of lightweight alloy is attractive for applications in dynamically loaded structures operating at temperatures up to approximately 300 C. The microstructure and properties of an alloy rich in Si, Ni, and Mn are presented. Efforts are directed towards establishing detailed knowledge about the microstructure and properties in order to form a knowledge base which can be used in designing materials for specific applications. Among the beneficial properties of the RS aluminum alloys, high values for the E modulus, fatigue strength, and tensile properties are demonstrated. Some data giving an indication of the thermal stability, thermal expansion behavior, and cyclic stress response are presented. ESA

N94-10064# Deutsche Forschungsanstalt fuer Luft- und Raumfahrt, Brunswick (Germany). Structural Engineering Inst.
FIBRE REINFORCED STRUCTURES WITH GLASS MATRIX **c27**
Malte Froevel *In* ESA, Advanced Materials for Lightweight Structures Oct. 1992 p 379-381 (For primary document see N94-10001 01-24)
Copyright Avail: CASI HC A01/MF A04

The development of a method for the fabrication of long fiber reinforced composites with glass matrix is reported. The new technology enables the fabrication of fiber reinforced glass without the fabrication step of hot pressing. Composite structures of a large scale and complex shape can be fabricated in an economic way. The matrix material will be obtained by a sol-gel process. The used mixture is a low viscosity dispersion of inorganic colloids in water, that allows the infiltration of fibers in a way analogous to that used in the fabrication of composites with polymeric matrix, for example filament winding and tape lay up processing. ESA

N94-10065# Southampton Univ. (England). Dept. of Electronics.
MULTIPLEXED AND DISTRIBUTED OPTICAL FIBRE SENSORS **c74**
J. P. Dakin *In* ESA, Advanced Materials for Lightweight Structures Oct. 1992 p 385-392 (For primary document see N94-10001 01-24)
Copyright Avail: CASI HC A02/MF A04

The basic concepts of multiplexing and distributed fiber sensing methods are outlined and a number of methods which show promise for space applications are addressed. The optical sensor is initially assumed to be a simple amplitude modulation device, incorporated in a fiber path, although most sensors tend to be more complex in practice. For space applications, multiplexing offers reduced weight. The way in which new systems may provide attractive possibilities for future space systems is suggested. ESA

N94-10066# Strathclyde Univ., Glasgow (Scotland).

FIBRE OPTIC STRAIN AND TEMPERATURE MEASUREMENT IN COMPOSITE MATERIALS: A REVIEW OF THE OSTIC PROGRAMME **c39**

Brian Culshaw and Craig Michie *In* ESA, Advanced Materials for Lightweight Structures Oct. 1992 p 393-398 Sponsored in part by Commission of the European Communities (For primary document see N94-10001 01-24)

Copyright Avail: CASI HC A02/MF A04

OSTIC (Optical Sensing Technologies for Intelligent Composites) is a recently completed European collaborative project which represents the first concerted effort in Europe on fiber optic sensing technologies for use in carbon and glass fiber reinforced plastic material. The scope of the project embraced both the characterization of material interactions and the derivation of fiber optic sensing techniques for use within these materials. The project demonstrated successfully that optical fibers may be embedded within 1 mm thick composite samples without any degradation in the mechanical performance of the composite panel. Fiber optic sensing in composite materials was also demonstrated showing distributed measurement of dynamic strain over a sample of the order of 1 m in length with linear spatial resolution of the stain measurement of approximately 20 cm. Additionally, the successful simultaneous measurement of temperature and quasi-static strain over similar gauge lengths were experimentally demonstrated. ESA

N94-10067# Ministry of Economic Affairs, The Hague (Netherlands). Materials Technology Dept.

THE NETHERLANDS INNOVATION ORIENTED RESEARCH PROGRAMME ON POLYMER COMPOSITES AND SPECIAL POLYMERS 1985-1993 **c27**

C. J. G. vanHalen *In* ESA, Advanced Materials for Lightweight Structures Oct. 1992 p 401-402 (For primary document see N94-10001 01-24)

Copyright Avail: CASI HC A01/MF A04

Innovation is often initiated by research carried out by universities or scientific institutions. Therefore, IOP (Innovation Oriented research Programs) support of these research activities is considered to be of great importance for the industry. Most IOP can be situated at the lower end of the well known S curve which models the generation of technological knowledge. The precompetitive IOP activities include mission oriented fundamental and strategic applied research. IOP are created on selected areas of stategic technology. Their main goals are generation of new technology, enhancement of promising research activities, and clustering of research groups. ESA

N94-10068# CAE-FEM Engineering, Stuttgart (Germany).

SOLVING THE ESSENTIALS OF AN INNOVATIVE TENNIS RACKET PRODUCT: FUNCTIONALITY, SIMPLICITY, AND SUPER-LIGHTWEIGHT TECHNOLOGY **c61**

E. Schlenker *In* ESA, Advanced Materials for Lightweight Structures Oct. 1992 p 403-405 (For primary document see N94-10001 01-24)

Copyright Avail: CASI HC A01/MF A04

In trying to profit from the benefits of aerospace technologies for sporting goods enjoyed by people day by day, a new bi-frame tennis racket '2-rac' was developed. Mainly to minimize potential problems with the tennis elbow and to optimize playing characteristics, some basic questions were addressed and carefully answered in to what is and should be a tennis racket, prior to studying the state of the art and the market conditions. From problem reduction, an idea and consequent step by step solution technique with proof of concept analysis, handmade functional models, many simple then more detailed computer simulations, and also high speed camera tests, the final acceptable solution was obtained. The remaining problem was to overcome optical and real weight restrictions by a super lightweight design. Problems and steps are summarized. ESA

N94-10069# Oulu Univ. (Finland). Engineering Mechanics Lab.

LAMINV: A COMPUTER CODE FOR CREATING LAMINATES HAVING PRESCRIBED PROPERTIES

M. Autio, M. Laitinen, and A. Pramila *In* ESA, Advanced Materials for Lightweight Structures Oct. 1992 p 407-411 (For primary document see N94-10001 01-24)

Copyright Avail: CASI HC A01/MF A04

A computer program for creating composite structures with prescribed thermomechanical properties is presented. The problem of this type can be called an inverse one. The problem is formulated as a constrained nonlinear minimization problem where ply orientations and/or thicknesses are selected to be design variables. The formulation of the inverse problem and the laminate theory used are described. The prescribed thermomechanical properties are used as objective function and constraints, and the values of the properties are derived from the classical lamination theory. ESA

N94-10740 Los Alamos National Lab., NM.

SILICON-BASED ELEMENTARY PARTICLE TRACKING SYSTEM: MATERIALS SCIENCE AND MECHANICAL ENGINEERING DESIGN

W. O. Miller, M. T. Gamble, T. C. Thompson, and J. A. Hanlon 1993 9 p Presented at the 9th International Conference on Composite Materials, Madrid, Spain, 12-16 Jul. 1993 Limited Reproducibility: More than 20% of this document may be affected by microfiche quality

(Contract W-7405-eng-36)

(DE93-012630; LA-UR-93-1162; CONF-930758-1) Avail: CASI HC A02

Research and development of the mechanical, cooling, and structural design aspects of a silicon detector-based elementary particle tracking system has been performed. Achieving stringent system precision, stability, and mass requirements necessitated the use of graphite fiber-reinforced cyanate-ester (C-E) resins. Mechanical test results of the effects of butane, ionizing radiation, and a combination of both on the mechanical properties of these materials are presented, as well as progress on developing compression molding of an ultralightweight graphite composite ring structure and TV holography-based noninvasive evaluation. DOE

N94-10812*# Thiokol Corp., Brigham City, UT. Space Operations.

LEVEL 3 MATERIAL CHARACTERIZATION OF NARC HRPF, HRHU, HRHF, AND HRPU Final Report

Mark E. Tobias Apr. 1993 926 p

(Contract NAS8-38100)

(NASA-CR-192579; NAS 1.26:192579; TWR-60736; Publ-931333) Avail: CASI HC A99/MF A10

The North American Rayon Corporation (NARC) precursor was developed, qualified, and characterized for Space Shuttle nozzle carbon-cloth phenolic ablative materials in three distinct phases. The characterization phase includes thermal and structural material property analysis and comparisons. This report documents the thermal and structural material property characterization performed by Southern Research Institute (SRI) on the two NARC baseline and two crossover materials. Author (revised)

N94-10857# National Aerospace Lab., Tokyo (Japan). Airframe Div.

EVALUATION OF TEST SPECIMEN SHAPE EFFECTS ON THE FLEXURAL FATIGUE OF CFRP LAMINATES [CHOKKOU SEKISOU CFRP NO MAGE TSUKARE SHIKEN NIOKERU SHIKENHEN KEIJOU NO HYOUKA NI KANSURU KENKYUU]

Yoshio Noguchi May 1992 19 p In JAPANESE

(NAL-TR-1159; JTN-93-80443; DE93-793622) Avail: CASI HC A03/MF A01

The flexural fatigue behavior and strength characteristics of cross-ply Carbon Fiber Reinforced Plastic (CFRP) laminate composites were investigated using three different PolyAcryloNitrile (PAN) based carbon fiber composite test specimens, i.e., Medium Strength (MS), InterMedium Strength (IMS), and High Strength (HS) types. Flexural fatigue tests employed four-points plane bending operations under a complete reversal frequency of 30 Hz. The effects of using test specimens having a coupon or side-curved shape were experimentally evaluated, with flexural fatigue strength results indicating that IMS and HS cross-ply CFRP laminates are effected more by the shape and generally have a greater S-N (Stress amplitude versus Number of cycles to failure) curves in the slope than MS ones. After being subjected to 10(exp 7) cycles, the resultant ratio of flexural fatigue strength to static flexural strength was found to be 0.50, 0.42, and 0.40 for MS, IMS, and HS cross-ply CFRP laminates, respectively. Author (NASDA)

N94-10858# National Aerospace Lab., Tokyo (Japan). Space Technology Research Group.
TRIBOLOGICAL CHARACTERISTICS OF HOT-PRESSED SELF-LUBRICATING COMPOSITES [HOTTOPURESU HOU DE SAKUSEISHITA JIKO JUNKATSUSEI FUKUGOU ZAIRYOU NO TORAIBOROJI TOKUSEI NI KANSURU KENKYUU]
Mineo Suzuki and Makoto Nishimura May 1992 51 p In JAPANESE
(NAL-TR-1160; JTN-93-80444; DE93-793623) Avail: CASI HC A04/MF A01

Tribological characteristics of hot-pressed self-lubricating composites were investigated to develop new high performance tribo-materials for space applications. The composites consisted of molybdenum disulfide (MoS2), refractory metal oxide (MoO3, MoO2, WO3, WO2, Ta2O5, or Nb2O5), and refractory metal (Mo, W, Ta, or Nb). Friction tests were performed in a vacuum, in nitrogen, and in air atmospheres using ring-on-disk type friction testers. The best material composition under the applied test conditions (contact pressures of from 0.5 to 4 MPa and sliding speeds of from 0.11 to 0.55 m/sec) was found to be composition of MoS2 80 percent plus MoO2 10 percent plus Nb 10 percent. In a vacuum, this composite showed a coefficient of friction of less than 0.07 and a specific wear rate of less than 10(exp -11) cu mm/(N x mm). Good tribological performance was also obtained with composition of MoS2 80 percent plus Nb2O5 10 percent plus Nb 10 percent, MoS2 80 percent plus MoO2 10 percent plus Mo 10 percent and MoS2 80 percent plus MoO2 20 percent. For the composites showing good tribological performance, a thin, uniform transfer film was formed on the steel ring surface. X-ray diffraction results showed that Mo2S3 was present in almost all the composites, thereby, suggesting that MoS2 partially dissociated into Mo2S3 during the hot-press process. It was also found that the addition of the refractory metal oxide and/or metal promoted both the dissociation of MoS2 and the chemical reaction among the involved species. Author (NASDA)

N94-10902 California Univ., Los Angeles.
RESPONSE OF COMPOSITE LAMINATES TO DYNAMIC SURFACE LOADS Ph.D. Thesis
Shyh-Shiuh Lih 1992 200 p
Avail: Univ. Microfilms Order No. DA9310963

The quantitative features of the elastodynamic field produced in unidirectional and multilayered graphite/epoxy composite laminates by surface loads are studied. Each layer is assumed to be transversely isotropic and dissipative with arbitrarily oriented symmetry axis, and characterized by five complex and frequency dependent constants. The dissipative property of the material is modeled approximately through the introduction of a frequency dependent damping function. A new nondestructive ultrasonic technique is developed for the determination of the material constants. A multiple transform technique involving time and spatial Fourier transforms is used to formulate the response problem due to a transient surface load. A global matrix method is used to solve the resulting boundary problem; the solution for a half space with the same loading conditions is obtained as a special case. The integrals involving the spatial inverse transforms are evaluated by a modified version of the Clenshaw-Curtis quadrature scheme for the two dimensional problem and by an adaptive surface-fitting integration scheme for the three dimensional problem. Time inversion is carried out by means of the Fast Fourier transform (FFT) algorithm. The response of a laminate to different transient loads including concentrated loads and distributed loads is presented. In addition, approximate solutions based on the classical plate bending theory and the modified shear deformation plate theory are obtained and the range of validity of the approximate solutions are determined through comparison with the exact results. The multiple transform technique is shown to be a practical alternative to finite element and other numerically intensive computational schemes for wave-field calculations in composite laminates. Dissert. Abstr.

N94-11085# Deutsche Forschungsanstalt fuer Luft- und Raumfahrt, Cologne (Germany). Inst. fuer Werkstoff-Forschung.
FIBRE REINFORCED POLYMER MATRIX COMPOSITES: MICROSTRUCTURE AND MECHANICAL PROPERTIES [FASERVERBUNDWERKSTOFFE MIT POLYMERMATRIX: AUFBAU UND MECHANISCHE EIGENSCHAFTEN]
Karl Schulte May 1992 317 p In GERMAN Sponsored by DFG
(DLR-FB-92-28; ETN-93-93959) Avail: CASI HC A14/MF A03; DLR, Zentrale Allgemeine Dienst, Versand, Postfach 90 60 58, 5000 Cologne, Germany, HC

The increasing interest in fiber reinforced polymer composites for technical application because of their superior properties, which requires a deepened knowledge of their microstructure and mechanical properties, is addressed. Based on a literature survey and investigations, an overview is given concerning the microstructure of composites. The influence of the microstructure on the mechanical properties under static and fatigue loading is given, together with the various damage mechanisms that occur. While the various damage mechanisms that occur during loading can be described quite sufficiently, there remains a lack in knowledge and understanding of what finally determines composite failure. Via a systematic description of composite damage mechanisms, an attempt to understand the interactions that lead to composite failure is made. Various nondestructive and destructive test methods to detect damage mechanisms are introduced. ESA

N94-11135*# National Aeronautics and Space Administration. Lewis Research Center, Cleveland, OH.
DAMPING MECHANISMS IN CHEMICALLY VAPOR DEPOSITED SIC FIBERS
James A. DiCarlo and Jon C. Goldsby Jul. 1993 11 p Presented at the International Symposium on Damping of Multiphase Inorganic Materials, Chicago, IL, 2-5 Nov. 1992; sponsored by PMCC
(RTOP 510-01-50)
(NASA-TM-106334; E-7697; NAS 1.15:106334) Avail: CASI HC A03/MF A01

Evaluating the damping of reinforcement fibers is important for understanding their microstructures and the vibrational response of their structural composites. In this study the damping capacities of two types of chemically vapor deposited silicon carbide fibers were measured from -200 C to as high as 800 C. Measurements were made at frequencies in the range 50 to 15000 Hz on single cantilevered fibers. At least four sources were identified which contribute to fiber damping, the most significant being thermoelastic damping and grain boundary sliding. The mechanisms controlling all sources and their potential influence on fiber and composite performance are discussed. Author (revised)

N94-11143 Academy of Sciences of the Ukraine, Kharkov. Fiziko-Tekhnicheskij Inst.
THE POSSIBILITY OF USING CARBON-GRAPHITE MATERIALS FOR MICROWAVE PLASMA DIAGNOSTICS IN LARGE FUSION DEVICES
A. I. Skibenko, V. V. Vasilev, V. S. Vojtsenya, S. V. Gozhenko, Y. F. Konotop, R. O. Pavlichenko, V. E. Strelnitskij, and I. P. Fomin 1992 12 p Limited Reproducibility: More than 20% of this document may be affected by microfiche quality
(DE93-621609; KFTI-92-40) Avail: CASI HC A03 (US Sales Only)

The possibility of replacing the plasma-facing elements of microwave diagnostics (antennae, mirrors), which are usually made of metals, by elements made of carbon-graphite materials was studied. The results of our comparison indicate that the main working characteristics of some metallic and carbon-graphite units (conical antennae, two-plate antennae, mirrors) are rather similar. DOE

N94-11202*# Sverdrup Technology, Inc., Brook Park, OH.
INTERFACE CONSIDERATIONS IN Al2O3/NiAl COMPOSITE Final Report
Ajay K. Misra Jul. 1993 33 p
(Contract NAS3-25266; RTOP 510-01-50)
(NASA-CR-191167; E-8032; NAS 1.26:191167) Avail: CASI HC A03/MF A01

The fiber-matrix interface requirements in an Al2O3/NiAl composite were examined from theoretical considerations. Several factors that influence the interface bonding requirements were analyzed. These include: (1) residual stresses due to fiber-matrix coefficient of thermal expansion (CTE) mismatch; (2) matrix cracking stress at room temperature; (3) fracture toughness at room temperature; (4) load transfer from the matrix to the fiber and ultimate tensile strength at the use temperature; and (5) creep resistance at high temperature. A relatively weak fiber-matrix bond, with an interfacial shear strength of approximately 15-20 MPa, might be sufficient for attaining the desired mechanical properties in the fiber direction at the use temperature. A weak fiber-matrix bond is also beneficial for increasing the fracture toughness of the composite at room temperature. In contrast, a strong fiber-matrix bond is required to withstand some of the residual stresses resulting from the fiber-matrix CTE mismatch, which are not likely to be reduced significantly by interface coatings. A relatively strong bond is also beneficial in increasing the matrix cracking stress at room temperature. Various interface coating options to accommodate the conflicting bonding requirements were reviewed. One viable coating option is to incorporate a thick, ductile interface layer well bonded to both the fiber and the matrix. Author (revised)

N94-11221# North Coast Innovation, Inc., Cleveland, OH.
DRY IN-LINE THERMOPLASTIC MATRIX IMPREGNATION, PHASE 1 Final Report, Aug. 1992 - Jan. 1993
L. S. Duncan Apr. 1993 49 p
(Contract DAAL04-92-C-0011)
(AD-A265016; NCI/93-07-Phase-1; ARL-CR-55-Phase-1) Avail: CASI HC A03/MF A01

The objective of this program is to develop an in-line thermoplastic impregnation module which can be used with existing automated manufacturing systems, such as filament winding equipment, which were originally designed for use with thermoset materials. During Phase 1, the ability to melt impregnate non-woven glass tow with polyphenylene sulfide (PPS), nylon, and polycarbonate resins has been demonstrated at the breadboard level by using a laboratory injection molding press to feed resins to a melt coating module. The tow was preheated prior to coating by means of a convection heating tunnel. Key parameters governing melt penetration included incoming tow temperature and melt viscosity. Further development of the process would allow the creation of composite shapes and structures which could be post processed by thermoforming techniques and would have the desirable performance characteristics of thermoplastics such as damage tolerance (impact resistance) and repairability. DTIC

N94-11237*# National Aeronautics and Space Administration. Lewis Research Center, Cleveland, OH.
ASSESSMENT OF DAMAGE IN CERAMICS AND CERAMIC MATRIX COMPOSITES USING ULTRASONIC TECHNIQUES
Y. C. Chu (Ohio State Univ., Columbus.), G. Y. Baaklini, and S.I. Rokhlin (Ohio State Univ., Columbus.) May 1993 12 p
(RTOP 510-01-50)
(NASA-TM-106121; E-7785; NAS 1.15:106121) Avail: CASI HC A03/MF A01

This paper addresses the application of ultrasonic sensing to damage assessment in ceramics and ceramic matrix composites. It focuses on damage caused by thermal shock or oxidation at elevated temperatures, which often results in elastic anisotropy. This damaged-induced anisotropy is determined by measuring the velocities of ultrasonic waves in different propagation directions. Thermal shock damage is assessed in ceramic samples of reaction bonded silicon nitride (RBSN). Thermal shock treatment from different temperatures up to 1000 C is applied to produce the microcracks. Results indicate that most microcracks produced by thermal shock are located near sample surfaces. Ultrasonic measurements using the surface wave method are found to correlate well with measurements of degradation of mechanical properties obtained independently by other authors using destructive methods. Oxidation damage is assessed in silicon carbide fiber/reaction bonded silicon nitride matrix (SCS-6/RBSN) composites. The oxidation is done by exposing the samples in a flowing oxygen environment at elevated temperatures, up to 1400 C, for 100 hr. The Youngs' modulus in the fiber direction as obtained from ultrasonic measurements decreases significantly at 600 C but retains its original value at temperatures above 1200 C. This agrees well with the results of destructive tests by other authors. On the other hand, the transverse moduli obtained from ultrasonic measurements decrease continually until 1200 C. Measurements on the shear stiffnesses show behavior similar to the transverse moduli. The results of this work show that the damage-induced anisotropy in both ceramics and ceramic matrix composites can be determined successfully by ultrasonic methods. This suggests the possibility of assessing damage severity using ultrasonic techniques. Author (revised)

N94-11260 Florida Univ., Gainesville. Dept. of Chemistry.
IONIZATION POTENTIALS OF SMALL CARBON CLUSTERS Technical Report, Sep. 1991 - Aug. 1992
Ragulan Ramanathan, Jeffrey A. Zimmerman, and John R. Eyler 5 May 1993 30 p Prepared in cooperation with IBM Technology Lab., Endicott, NY Limited Reproducibility: More than 20% of this document may be affected by microfiche quality
(Contract N00014-87-J-1248)
(AD-A264379; TR-40) Avail: CASI HC A03

Ionization potentials (IP's) of small carbon clusters (C(sub n), n = 3-6) have been bracketed with an uncertainty of a few tenths of an eV by charge-transfer methods in a Fourier transform ion cyclotron resonance mass spectrometer. Values obtained are compared to previously determined experimental and theoretical values. Several interesting reactions other than charge-transfer were observed between the carbon cluster ions and the charge-transfer reference compounds. The products of these reactions are reported and discussed. DTIC

N94-11276*# National Aeronautics and Space Administration. Langley Research Center, Hampton, VA.
AN ANALYSIS OF FIBER-MATRIX INTERFACE FAILURE STRESSES FOR A RANGE OF PLY STRESS STATES
J. H. Crews, R. A. Naik (Analytical Services and Materials, Inc., Hampton, VA.), and S. J. Lubowinski Jul. 1993 43 p
(RTOP 505-63-50-04)
(NASA-TM-108999; NAS 1.15:108999) Avail: CASI HC A03/MF A01

A graphite/bismaleimide laminate was prepared without the usual fiber treatment and was tested over a wide range of stress states to measure its ply cracking strength. These tests were conducted using off-axis flexure specimens and produced fiber-matrix interface failure data over a correspondingly wide range of interface stress states. The absence of fiber treatment, weakened the fiber-matrix interfaces and allowed these tests to be conducted at load levels that did not yield the matrix. An elastic micromechanics computer code was used to calculate the fiber-matrix interface stresses at failure. Two different fiber-array models (square and diamond) were used in these calculations to analyze the effects of fiber arrangement as well as stress state on the critical interface stresses at failure. This study showed that both fiber-array models were needed to analyze interface stresses over the range of stress states. A linear equation provided a close fit to these critical stress combinations and, thereby, provided a fiber-matrix interface failure criterion. These results suggest that prediction procedures for laminate ply cracking can be based on micromechanics stress analyses and appropriate fiber-matrix interface failure criteria. However, typical structural laminates may require elastoplastic stress analysis procedures that account for matrix yielding, especially for shear-dominated ply stress states. Author (revised)

N94-11315 Missouri Univ., Rolla.
CREEP DEFORMATION AND MECHANICAL PROPERTIES OF SINTERED GLASS AND POLYCRYSTALLINE MATRIX COMPOSITES Ph.D. Thesis
Rollie Eugene Dutton 1992 126 p
Avail: Univ. Microfilms Order No. DA9311026

It was observed that the free sintering of ceramic particulate composites is reduced significantly, even at modest volume fractions of the dispersed inclusions. The decrease in the sintering rate might reside in a decrease in the driving force for sintering, a modification of the kinetic factors, or a combination of these. Realistic physical models indicate that the reduction in the driving force is small. The first task of the research was to determine how dispersed inclusions influenced the creep viscosity of the composite. The results of this phase of the research are described. The effect of spherical nickel inclusions on the sintering, creep, and electrical conductivity of a glass matrix composite was investigated. Glass was chosen as the matrix phase in order to eliminate the complications of grain growth. The effects of zirconia inclusions on the sintering and creep of a polycrystalline matrix (for which grain growth occurs) are reported. A combination of this work and other studies indicated that the main factors responsible for the sintering difficulty are the packing of the matrix phase and interactions between the inclusions. A method for alleviating the difficulty associated with these factors was developed and used to form particulate composites with nearly full density. The second task of this research was to measure the mechanical properties of the composites formed by the improved method and to compare the data with those for similar composites formed by more conventional methods. The mechanical properties of the sintered composites are reported. Dissert. Abstr.

N94-11317# Advisory Group for Aerospace Research and Development, Neuilly-Sur-Seine (France). Structures and Materials Panel.
SMART STRUCTURES FOR AIRCRAFT AND SPACECRAFT [LES STRUCTURES INTELLIGENTES POUR LES AERONEFS ET LES VAISSEAUX SPATIAUX]
Apr. 1993 387 p The 75th meeting was held in Lindau, Germany, 5-7 Oct. 1992
(AGARD-CP-531; ISBN-92-835-0701-X) Copyright Avail: CASI HC A17/MF A04

An overview of the state-of-the-art of 'Smart Structures' technology as well as detailed descriptions of specific applications is presented. This technology offers extremely attractive advantages in the design, development, and operation of aerospace structures. For individual titles, see N94-11318 through N94-11347.

N94-11318# Deutsche Forschungs- und Versuchsanstalt fuer Luft- und Raumfahrt, Munich (Germany). Military Aircraft Div.
SMART STRUCTURES: A TECHNOLOGY FOR NEXT GENERATION AIRCRAFT **c05**
W. Schmidt and C. Boller *In* AGARD, Smart Structures for Aircraft and Spacecraft Apr. 1993 14 p (For primary document see N94-11317 01-24)
Copyright Avail: CASI HC A03/MF A04

Performance of aircraft structures has progressed in a sequence of steps during the past. Since composite materials have gained broad application because of significant technological improvement, it is timely to look for the next step in improvement of aircraft performance. It is very likely that this step is related to smart structures technology. Smart structures technology is able to meet various aircraft design objectives such as improved military aircraft effectiveness through improved aircraft capabilities and reduced life cycle cost or reduced direct operating cost of civil aircraft through improvement in performance, fuel consumption, and aircraft maintainability. Active/adaptive structures, structure health monitoring, and structure integrated avionics are the three areas which are felt to be the areas where smart structures technology is most beneficial. Ways for cooperation between various engineering and natural sciences, being a major driving force for the success of smart structures, are described as well as some laboratory scale experiments which were recently performed. It is felt that an increased effort in engineers in various fields towards realization of smart structures can be a new rewarding challenge for the aircraft industry in developing next generation aircraft. Author (revised)

N94-11319# Phillips Lab., Edwards AFB, CA.
ADAPTIVE STRUCTURES FOR SPACECRAFT: A USAF PERSPECTIVE **c18**
Alok Das, Glenn Ormbrek (Wright Lab., Wright-Patterson AFB, OH.), and Michael Obal (Strategic Defense Initiative Organization, Washington, DC.) *In* AGARD, Smart Structures for Aircraft and Spacecraft Apr. 1993 13 p (For primary document see N94-11317 01-24)
Copyright Avail: CASI HC A03/MF A04

The precise pointing/shape control needs of future space systems coupled with a 10-20 year life requirement and very stringent limitation on system weight has motivated a new approach in control system design. This approach, referred to as 'adaptive structures,' exploits recent breakthroughs in advanced composite materials, sensors and actuators, and intelligent control concepts to provide an integrated structure/controller. Author (revised)

N94-11320*# National Aeronautics and Space Administration. Langley Research Center, Hampton, VA.
DYNAMIC TESTS ON THE NASA LANGLEY CSI EVOLUTIONARY MODEL **c18**
H. Troidl (Industrieanlagen-Betriebsgesellschaft m.b.H., Ottobrunn, Germany.) and K. B. Elliott *In* AGARD, Smart Structures for Aircraft and Spacecraft Apr. 1993 9 p (For primary document see N94-11317 01-24)
Copyright Avail: CASI HC A02/MF A04

A modal analysis study, representing one of the anticipated 'Cooperative Spacecraft Structural Dynamics Experiments on the NASA Langley CSI Evolutionary Model', was carried out as a sub-task under the NASA/DLR collaboration in dynamics and control of large space systems. The CSI evolutionary testbed (CEM) is designed for the development of Controls-Structures Interaction (CSI) technology to improve space science platform pointing. For orbiting space structures like large flexible trusses, new identification challenges arise due to their specific dynamic characteristics (low frequencies and high modal density) on the one hand, and the limited possibilities of exciting such structures and measuring their responses on orbit on the other. The main objective was to investigate the modal identification potential of several different types of forcing functions that could possibly be realized with on-board excitation equipment using a minimum number of exciter locations as well as response locations. These locations were defined in an analytical test prediction process used to study the implications of measuring and analyzing the responses thus produced. It turned out that broadband excitation is needed for a general modal survey, but if only certain modes are of particular interest, combinations of exponentially decaying sine functions provide favorable excitation conditions as they allow to concentrate the available energy on the modes being of special interest. From a practical point-of-view structural nonlinearities as well as noisy measurements make the analysis more difficult, especially in the low frequency range and when the modes are closely spaced. Author (revised)

N94-11321# Eurocopter Deutschland G.m.b.H., Munich (Germany).
SMART MATERIALS FOR HELICOPTER ROTOR ACTIVE CONTROL **c05**
H. Strehlow and H. Rapp *In* AGARD, Smart Structures for Aircraft and Spacecraft Apr. 1993 16 p (For primary document see N94-11317 01-24)
Copyright Avail: CASI HC A03/MF A04

A major improvement of helicopter performance and comfort can be achieved by the implementation of rotor active control technology (RACT). The introduction of individual blade control (IBC) is a subject of current research activities. But the breakthrough of this technology is still missing due to the lack of appropriate rotating blade actuation systems. Smart materials may open a new possibility for the realization of rotor active control. A survey of current hydraulic individual blade actuation systems shows that these are very complicated and heavy. Blade actuation by smart materials offers the change for an electrical system integrated into the blade itself. A study of different blade actuation systems shows that in principle there is the possibility of achieving this goal. But, today the available materials are not ready for real 'smart' applications. The preferred materials - piezoceramics - show a too low tension strength and very low active strains. Therefore, at this time the only feasible blade actuation system for individual blade control seems to be a hinged flap at the outer third of a rotor blade. This flap can be controlled by a smart (piezoelectric) actuator. Estimations show that such a system will work on the desired yaw. Author (revised)

N94-11322# Massachusetts Inst. of Tech., Cambridge. Space Engineering Research Center.
INTELLIGENT STRUCTURES: A TECHNOLOGY OVERVIEW AND ASSESSMENT
Edward F. Crawley and Mac Vicar *In* AGARD, Smart Structures for Aircraft and Spacecraft Apr. 1993 16 p (For primary document see N94-11317 01-24)
Copyright Avail: CASI HC A03/MF A04

A topical review of a decade of work toward the development of intelligent structures is presented, i.e., structures with highly distributed actuators, sensors, and processors. The background and status of the research in this area are covered, as are the evolution of the technology components: strain actuators, acceleration and strain sensors, processors and signal conditioning, and control algorithms. The results of several system level experimental implementations are presented, as are the challenges for further development. Author

N94-11323# Strategic Defense Initiative Organization, Washington, DC.
THE SATELLITE ATTACK WARNING AND ASSESSMENT FLIGHT EXPERIMENT (SAWAFE) **c18**
Michael Obal, Bill Saylor, Hugh S. Murray, Martin R. Sweet, Dan Holden, and Calvin Moss *In* AGARD, Smart Structures for Aircraft and Spacecraft Apr. 1993 13 p (For primary document see N94-11317 01-24)
Copyright Avail: CASI HC A03/MF A04

A program to develop an advanced satellite health and status monitoring subsystem for detecting and discriminating hostile threats is described. The threats considered are laser, radio frequency, and x-rays. The subsystem uses lightweight electronics and sensors that are imbedded in the satellite structure to minimize the integration impact on the host satellite. The sensor materials are described. The first of a series of flight experiments is also described. Author

N94-11324# Strathclyde Univ., Glasgow (Scotland). Optoelectronics Div.

OPTICAL FIBRE TECHNIQUES FOR STRUCTURAL MONITORING IN COMPOSITES

W. Craig Michie, B. Culshaw, and D. Uttamchandani *In* AGARD, Smart Structures for Aircraft and Spacecraft Apr. 1993 9 p Sponsored in part by BRITE/OSTIC (For primary document see N94-11317 01-24)

Copyright Avail: CASI HC A02/MF A04

The sensor technology to be used in smart structures must be compatible both operationally and mechanically with the material and the functional specification of the smart structure system. Fiber optic sensors are particularly attractive since they are mechanically robust and flexible. An overview of work which was carried out within the University of Strathclyde concerning the development of fiber optic sensing techniques for use in structural monitoring applications for composite material systems is presented. Author (revised)

N94-11325# Strathclyde Univ., Glasgow (Scotland). Smart Structures Research Inst.

SMART PROCESSING OF COMPOSITE MATERIALS FOR ENHANCED PERFORMANCE AND PROPERTIES

A. McDonach, R. Pethrick, and P. Gardiner *In* AGARD, Smart Structures for Aircraft and Spacecraft Apr. 1993 6 p (For primary document see N94-11317 01-24)

Copyright Avail: CASI HC A02/MF A04

There have been a large number of technologies described whose purpose is to aid in the control of composite manufacture. The aim of this paper is to readdress the requirements of composite manufacture to assess which features of the various techniques are best suited to providing improved processing. To start with, the requirements of quality in manufacture and the hidden costs associated with incorrect processing are considered. This will allow us to rank the aspects of processing which it would be attractive to improve. Following this, a range of monitoring processes and their ability to deliver on these improvements and at what cost in terms of expense and complexity are considered. Monitoring processes considered include fiber-optic (optical) methods, dielectrometry, and ultrasonic methods. Author

N94-11326# Aastra Aerospace, Inc., Downsview (Ontario).

SMART STRUCTURES AT AASTRA CORPORATION

D. R. Uffen, H. Scholaert, and G. Schmid *In* AGARD, Smart Structures for Aircraft and Spacecraft Apr. 1993 8 p Sponsored in part by Canadian Space Agency and Defence Research Establishment (For primary document see N94-11317 01-24)

Copyright Avail: CASI HC A02/MF A04

Aastra Advanced Ceramics is a major manufacturer of piezoelectric ceramic materials. Aastra Aerospace is involved in the development of smart structures technology based on these materials. Piezoelectric ceramics as actuators offer high mechanical stiffness, large output stress, and good linearity. As strain sensors, piezoceramics offer very high sensitivity. Initial research into the use of externally-bonded or embedded piezoceramic strain sensors and actuators has lead to the development of in-line sensor-actuator systems for use in truss-type smart structures. The target applications for these units are large flexible space structures, but the technology is applicable to earth-based truss structures as well. Similarly, Aastra is investigating the use of piezoelectric materials for the active damping of aircraft structures, with the goal of reducing structure-borne cabin noise with minimum additional weight. The development of Aastra's piezoceramic research activities and an overview of present work in the field of smart structures is presented. Author (revised)

N94-11327# Toronto Univ., Downsview (Ontario). Inst. for Aerospace Studies.

FIBER OPTIC SENSING FOR COMPOSITE SMART STRUCTURES

Raymond M. Measures *In* AGARD, Smart Structures for Aircraft and Spacecraft Apr. 1993 43 p Sponsored in part by Ontario Laser and Lightwave Research Centre; Natural Sciences and Engineering Research Council; Inst. for Space and Terrestrial Science; and Ontario Centre for Materials Research (For primary document see N94-11317 01-24)

Copyright Avail: CASI HC A03/MF A04

Structurally integrated fiber optic sensors (SIFORS) will form a necessary part of future Smart Structures and strain sensing will provide valuable information on the use and loading of such structures and also determine the response of the structure to these loads. Strain measurements may be used to check structural integrity and in the case of Smart Adaptive Structure they would provide the deformation information required by the structurally integrated actuation control system. Continuous monitoring of the applied loads could also be used to determine the actual fatigue life of the structure at any point in its operation. In the case of composite materials improved quality control during fabrication may be possible from such a built-in sensing system and this could lead to a more consistent and reliable product. Overall the introduction of an embedded fiber optic strain sensing system to composite structures may enhance confidence in their use and lead to an expansion in the range of application, especially as primary structures in the aerospace field. The types of fiber optic sensors are reviewed and it is shown that the intracore Bragg grating and the intrinsic Fabry-Perot interferometer appear to qualify for continued consideration as the universal sensor for the broad range of potential Smart Structures. The key elements of strain sensing with both types of structurally integrated fiber optic sensors are reviewed and issues such as thermally induced apparent strain are discussed. It is shown that although both sensors now have good methods of demodulation, the Bragg grating sensor has the greatest potential to satisfy the requirements demanded of the ideal sensor for Smart Structures due to the recently developed radiometric wavelength demodulation system. This system promises the fabrication of a robust, simple, absolute measurement, low cost multisensor system that could be integrated onto an optoelectronic chip that can form part of the interface to any structure and in essence solve the critical interconnect problem. Two important questions, however, remain to be addressed: can the intracore Bragg grating sensor perform all of the tasks required, and can Bragg gratings of 'sufficient quality' be fabricated in an automated process. Author (revised)

N94-11328# Alenia Spazio S.p.A., Turin (Italy).

STRAIN MEASUREMENT OF CARBON/EPOXY COMPOSITE WITH FIBRE OPTICS WHITE LIGHT QUASI DISTRIBUTED POLARIMETRIC SENSOR

B. Fornari, J. J. Guerin (Bertin et Cie., Aix-les-Milles, France.), P. Sansonetti (Bertin et Cie., Aix-les-Milles, France.), M. Lequime (Bertin et Cie., Aix-les-Milles, France.), and G. Romeo (Politecnico di Torino, Italy.) *In* AGARD, Smart Structures for Aircraft and Spacecraft Apr. 1993 3 p (For primary document see N94-11317 01-24)
(BRITE/EURAM-0173)

Copyright Avail: CASI HC A01/MF A04

The results obtained in measuring the static and dynamic strain of carbon/epoxy composites with embedded or bonded fiber optics white light quasi-distributed polarimetric sensor are reported. Linear and accurate measurements were obtained and up to six sensing zones were parallely interrogated along a single optical fiber. Author (revised)

N94-11329# Technische Hogeschool, Twente (Netherlands). Lab. for Material Science.

ON THE STABILITY OF SHAPE MEMORY MATERIALS AND THEIR PROPERTIES IN STATIC AND DYNAMIC APPLICATIONS

J. Beyer and M. Chandrasekaran *In* AGARD, Smart Structures for Aircraft and Spacecraft Apr. 1993 7 p (For primary document see N94-11317 01-24)

Copyright Avail: CASI HC A02/MF A04

Shape memory materials form one group of 'smart materials' which are of current interest. The sensing and actuating performance of these shape memory materials have been used in diverse industrial applications. These applications involve either the one-way or two-way effect, pseudoelasticity, recovery forces or damping characteristics of the SM-alloy. Each of these characteristics is associated with its unique response to thermal-mechanical forces. Besides these material parameters, the operating conditions and design parameters have to be taken into account when structures, in which SM elements are incorporated, are to be considered. The processing as well as subsequent operating conditions are relevant to the reproducible

(stable) behavior and life time of the material and are discussed.
Author (revised)

N94-11330# Pisa Univ. (Italy). Faculty of Engineering.
SMART POLYMERIC SYSTEM FOR ELECTROMECHANICAL TRANSDUCTION **c27**
P. Chiarelli, D. DeRossi, and Kayo Umezawa *In* AGARD, Smart Structures for Aircraft and Spacecraft Apr. 1993 3 p (For primary document see N94-11317 01-24)
Copyright Avail: CASI HC A01/MF A04

The various mechanisms eliciting electromechanical response, in polymer gels and conducting polymers, which have been exploited to eventually develop electrically driven gel actuators are briefly reviewed. A few approaches undertaken to eventually obtain electrochemomechanical systems with better performance are indicated. Author (revised)

N94-11331# Martin Marietta Corp., Denver, CO. Astronautics Group.
ADAPTIVE STRUCTURE DESIGN EMPLOYING SHAPE MEMORY ACTUATORS
Mohan S. Misra, Bernie Carpenter, and Brian Maclean *In* AGARD, Smart Structures for Aircraft and Spacecraft Apr. 1993 6 p (For primary document see N94-11317 01-24)
Copyright Avail: CASI HC A02/MF A04

Shape memory alloy wire 'tendons' can be used as embedded actuator elements to control the level of facesheet strain in adaptive structural components which utilize sandwich panel construction. As facesheet strain is varied, the degree of curvature and magnitude of tip deflection of a panel section can be controlled. Methods for modeling and conditioning shape memory materials and their subsequent integration into composite structures are described along with related control system and feedback sensor development. Finally, an adaptive antenna application employing 'flex-biased' actuation and an attitude control surface based on 'antagonistic' actuation are described. Author (revised)

N94-11332# Pennsylvania State Univ., University Park. Materials Research Lab.
RECENT DEVELOPMENTS IN PIEZOELECTRIC AND ELECTROSTRICTIVE SENSORS AND ACTUATORS FOR SMART STRUCTURES **c35**
L. Eric Cross *In* AGARD, Smart Structures for Aircraft and Spacecraft Apr. 1993 33 p (For primary document see N94-11317 01-24)
Copyright Avail: CASI HC A03/MF A04

Piezoelectricity will be defined phenomenologically and discussed pictorially to underscore the distinction between single crystal piezoelectrics and the poled ceramics which form the basis for most practical sensor and actuator systems. The classical lead zirconate: lead titanate (PZT) family is the most widely used. Recent advances in the understanding of the conventional morphotropic phase boundary (MPB) compositions are discussed with particular emphasis upon the nature and the control of fatigue at high strain levels. Phase switching compositions in the lead zirconate stannate titanate PZSnT system exhibit very high switching volume strain, shape memory, and controlled induced piezoelectric response. Electrostrictors in the lead magnesium niobate: lead titanate and lead lanthanum zirconate titanate (PMN:PT and PLZT) families form most interesting spin glass states at lower temperature in which precise reproducible elastic strain may be induced by electric field. In PMN:PT the strain is free from aging and other domain related problems, the thermal expansion is very low, and these materials are ideal for very precise actuation. Polarization biased electrostrictors have exceedingly high induced piezoelectric d(sub 33), d(sub 31), and d(sub h) coefficients and can be used as agile transducers in which both the magnitude and phase of the response is under DC field control. Both spin glass and phase switching systems can be tuned in composition to optimize performance at 100 K and provide low power 'dial-a-displacement' capability. Recent advances in the fabrication of highly perfect thin films of PZT type compositions on silicon, by both vapor and liquid phase techniques provides a new high force electromechanical power source for microelectromechanical (MEMS) systems. The current status of the evaluation of electromechanical response in PZT, PMN:PT and PbSnZT thin films on silicon is briefly reviewed and possible applications in MEMS systems discussed. Author (revised)

N94-11333# Deutsche Forschungs- und Versuchsanstalt fuer Luft- und Raumfahrt, Munich (Germany). Aircraft Div.
IN-FLIGHT AIRCRAFT STRUCTURE HEALTH MONITORING BASED ON SMART STRUCTURES TECHNOLOGY **c03**
C. Boller and R. Dilger *In* AGARD, Smart Structures for Aircraft and Spacecraft Apr. 1993 19 p (For primary document see N94-11317 01-24)
Copyright Avail: CASI HC A03/MF A04

Aircraft are known to be highly complex systems requiring an extensive amount of monitoring because of their safety criticality. To reduce direct operating or life cycle cost a lot of effort was spent on automated monitoring systems. On-board loads monitoring systems for aircraft as well as built in test equipment in avionics systems are already available nowadays. On-board loads monitoring systems however do not monitor damage in-situ and on-board. This still has to be performed on-ground by manual nondestructive testing (NDT) inspection. Smart structures technology is a means which can support development towards automated in-situ monitoring of damage even on-board the aircraft. The paper starts with a brief view on aircraft maintenance cost, describes existing aircraft health and usage monitoring systems as well as NDT procedures, and explains how these procedures could be combined to a smart system using smart materials and structures technology. A strategy is proposed how gradual introduction of smart structures technology into structure health monitoring systems can make this new technology beneficial for aircraft operators in short term.
Author (revised)

N94-11334# British Aerospace Aircraft Group, Kingston-upon-Thames (England).
STRUCTURAL HEALTH MONITORING USING EMBEDDED FIBRE OPTIC SENSORS **c03**
P. A. Tutton and F. M. Underwood *In* AGARD, Smart Structures for Aircraft and Spacecraft Apr. 1993 10 p (For primary document see N94-11317 01-24)
Copyright Avail: CASI HC A02/MF A04

Structural health monitoring on military aircraft is currently carried out via strain gauges attached to the surface of the aircraft structure. A parametric system based exclusively on flight parameters is being developed for use on EFA. Both of these systems monitor the airframe fatigue life. With the emergence of Smart Structures technology, a new method of structural health monitoring is feasible that has perceived advantages over the current technology. How fiber optics embedded within a composite laminate can be used to monitor strains within the aircraft structure, and hence its fatigue life is described. Embedded fiber optics can be used to monitor sustained damage - battle or low velocity impact damage, give a full flight history and, with diagnostic capability, unconditioned maintenance would be available. Author (revised)

N94-11335# Manchester Univ. (England). Dynamics Research Group.
FAULT LOCATION IN STRUCTURES USING NEURAL NETWORKS **c38**
K. Worden, A. D. Ball, and G. R. Tomlinson *In* AGARD, Smart Structures for Aircraft and Spacecraft Apr. 1993 19 p Sponsored in part by BRITE/EURAM (For primary document see N94-11317 01-24)
Copyright Avail: CASI HC A03/MF A04

A neural network is trained to report the position of a fault in a framework structure. It is shown that a network trained on data from finite element simulation of the structure can successfully locate faults in the framework itself. Author (revised)

N94-11336# Westland Aerostructures Ltd., East Cowes (England).
FACTORS AFFECTING THE EMBEDDING OF OPTICAL FIBRE SENSORS IN ADVANCED COMPOSITE STRUCTURES
N. C. Eaton, M. J. Curran, J. P. Dakin (Southampton Univ., England.), and H. Geiger (Southampton Univ., England.) *In* AGARD, Smart Structures for Aircraft and Spacecraft Apr. 1993 14 p (For primary document see N94-11317 01-24)
Copyright Avail: CASI HC A03/MF A04

Composite materials offer tremendous benefits for engineering applications and are now specified for use in several safety critical structures. However, despite extensive materials research and development, they do have a number of areas where their behavior is still not fully understood. This is particularly so with the more complex mechanical parameters in larger structures. Current structural design attempts to allow for these unknowns by over-designing, extensive testing, and frequent inspection. Embedded optical fiber sensors offer the potential to monitor many of these parameters, and are additionally of a similar physical and mechanical nature to the reinforcement fibers used in advanced composites. Westland Aerospace was involved in the development of fiber sensors for composite monitoring for over five years, and pioneered the application of embedded fiber sensors in thermoplastic composites during earlier joint research projects with the United Technologies Research Center. Previous programmers showed that research and development into both optical fiber sensors and materials is a key to the success of 'smart structures' technologies. The BRITE sponsored Optical Sensing Techniques in Composites (OSTIC) program represents the largest European research program to date. Similar research is underway at several centers worldwide, mainly in the USA and Canada. It was decided to set up a joint sensors/materials project under the UK Government supported LINK Structural Composites collaborative research program. The project will be performed by Westland Aerospace and the Optical Fibre Sensors Group at the UK Optoelectronics Research Centre. Factors relating to the development and application of optical fiber strain sensors for the monitoring of composite structures, and in particular the factors relating to the embedding of these optical fibers in composite laminates are addressed. Author (revised)

N94-11337# Canadian Marconi Co. Ltd., Montreal (Quebec).
FIBER-OPTIC SENSOR SYSTEMS FOR MEASURING STRAIN AND THE DETECTION OF ACOUSTIC EMISSIONS IN SMART STRUCTURES
F. A. Blaha and S. L. McBride (Acoustic Emission Monitoring Services, Inc., Montreal, Quebec.) *In* AGARD, Smart Structures for Aircraft and Spacecraft Apr. 1993 11 p Sponsored in part by Dept. of Defence and Canadair Ltd. (For primary document see N94-11317 01-24)
Copyright Avail: CASI HC A03/MF A04

The requirements of a fiber-optic strain sensor system for aircraft smart structures are outlined, and an experimental system developed by Canadian Marconi Company for this application is reported. Fiber-optic strain sensors were mounted on an aircraft undergoing full-scale durability and damage tolerance tests, the results of which are presented. Tests were also carried out to verify the response of fiber-optic sensors to acoustic impulse signals. Input signals, similar to the ones encountered in damaged materials under stress, were used to evaluate the response of the sensor to bulk, surface, and plate waves. This was done in order to assess the performance of fiber-optic sensors employed in the acoustic detection of damage in materials. Author (revised)

N94-11338# Deutsche Forschungs- und Versuchsanstalt fuer Luft- und Raumfahrt, Munich (Germany). Inst. of Aeroelasticity.
ADAPTIVE ALGORITHMS FOR USE WITH DIGITAL FILTERS IN VIBRATION CONTROL c61
R. Wimmel *In* AGARD, Smart Structures for Aircraft and Spacecraft Apr. 1993 5 p (For primary document see N94-11317 01-24)
Copyright Avail: CASI HC A01/MF A04

Digital filters can easily be used to alter signal flows. As long as the desired transfer function of the filter is causal, a great variety of responses is made possible by appropriate choice of filter coefficients. To make use of this property in vibration control, algorithms should automatically change the filter coefficients to meet any given objective. A class of adaptive algorithms which search the gradient of a given performance function is described. In order to illustrate the requirements of adaptive structures, such as structurally conformed design, the feed-forward control environment serves as an example for applying these algorithms. Author (revised)

N94-11339# Deutsche Forschungs- und Versuchsanstalt fuer Luft- und Raumfahrt, Munich (Germany). Inst. of Aeroelasticity.
STRUCTURAL ANALYSIS AND OPTIMIZATION OF ADAPTIVE STRUCTURES BY USE OF THE FINITE ELEMENT METHOD c39
R. Lammering *In* AGARD, Smart Structures for Aircraft and Spacecraft Apr. 1993 11 p (For primary document see N94-11317 01-24)
Copyright Avail: CASI HC A03/MF A04

New finite elements which allow for the analysis and optimization of adaptive structures are presented. Two finite elements accounting for integrated piezo-electric devices are formulated: a shell element for the analysis of shallow shell structures with piezo-electric polymers bonded to the surfaces and a truss element with an integrated piezo-electric ceramic. Test cases are presented to illustrate the potential of the finite elements. The shell element is used to compute the vibration excitation of a thin plate as well as the vibration control of a cantilever beam. The truss element is applied to the problem of optimal actuator placement in adaptive truss structures. For the solution of this problem, objective functions for the minimization of the control effort and the spillover energy are formulated. The second part is concerned with the finite element analysis of the behavior of shape memory alloys. A non-linear one-dimensional finite truss element and a non-linear beam element are used for the analysis of a composite beam with embedded shape memory alloy wires, of which the temperature is varied in order to tune the eigenfrequencies. Author (revised)

N94-11340# Deutsche Forschungs- und Versuchsanstalt fuer Luft- und Raumfahrt, Brunswick (Germany). Inst. for Flight Guidance.
FIBER-OPTIC INTERFEROMETRIC STRAIN GAUGE FOR SMART STRUCTURES APPLICATIONS: FIRST FLIGHT TESTS c35
N. Fuerstenau, D. D. Janzen, and W. Schmidt *In* AGARD, Smart Structures for Aircraft and Spacecraft Apr. 1993 6 p (For primary document see N94-11317 01-24)
Copyright Avail: CASI HC A02/MF A04

Initial flight tests of a fiber-optic strain gauge (OSG) based on a double-polarization Michelson interferometer with incremental readout via fringe counting were performed. The passive quadrature demodulation technique allows for balanced interferometer arms, exhibiting partial self temperature compensation. A bent reference (R) arm approach for the sake of isolation of the R-arm from the strain to be measured was tested for the first time. The sensor was surface adhered on a carbon fiber reinforced plastic plate which, in turn, was screwed to the main wing spar of a Cessna C207A aircraft. Strain was measured under different flight conditions and compared to the readout of a conventional resistive strain gauge (ESG). Good agreement with the theoretical predictions as well as with the readout of the ESG was observed for short term (of the order of minutes) quasistatic strain measurements despite large vibration induced noise. The Fourier spectra of the time series exhibited also good agreement between ESG and OSG with respect to the dynamical response up to at least 250 Hz. The measurement range and stability of the present experimental setup is limited by polarization instabilities which partly are due to anisotropic transverse stress effects at the adhered fiber sections. Longer term dc strain measurements require carefully controlled isotropic adhesion conditions and miniaturized optomechanical components with improved mechanical stability. Author

N94-11341*# National Aeronautics and Space Administration. Langley Research Center, Hampton, VA.
THE IMPACT OF ACTIVE CONTROLS TECHNOLOGY ON THE STRUCTURAL INTEGRITY OF AERONAUTICAL VEHICLES c05
Thomas E. Noll, Edward Austin (Army Aviation Research and Technology Activity, Hampton, VA.), Shawn Donley (Naval Air Development Center, Warminster, PA.), George Graham (National Defence Headquarters, Ottawa, Ontario.), Terry Harris (Wright Lab., Wright-Patterson AFB, OH.), Ian Kaynes (Defence Research Agency, Farnborough, England.), Ben Lee (Institute for Aerospace Research, Ottawa, Ontario.), and James Sparrow (Aeronautical Research Labs., Melbourne, Australia.) *In* AGARD, Smart Structures for Aircraft and Spacecraft Apr. 1993 10 p (For primary document see N94-11317 01-24)
Copyright Avail: CASI HC A02/MF A04

The findings of an investigation conducted under the auspices of The Technical Cooperation Program (TTCP) to assess the impact of active controls technology on the structural integrity of aeronautical vehicles and to evaluate the present state-of-the-art for predicting loads caused by a flight-control system modification and the resulting change in the fatigue life of the flight vehicle are summarized. Important points concerning structural technology considerations implicit in applying active controls technology in new aircraft are summarized. These points are well founded and based upon information received from within the aerospace industry and government laboratories, acquired by sponsoring workshops which brought together experts from contributing and interacting technical disciplines, and obtained by conducting a case study to independently assess the state of the technology. The paper concludes that communication between technical disciplines is absolutely essential in the design of future high performance aircraft. Author (revised)

N94-11342# Rome Univ. (Italy). Dipt. Aerospaziale.
ON POSSIBLE APPLICATIONS OF SMART STRUCTURES TO CONTROL OF SPACE SYSTEMS **c18**
F. Betti, P. Gasbarri, P. Gaudenzi, F. Persiani (Bologna Univ., Italy.), G. M. Saggiani (Istituto Studi e Applicazioni Scienze Aeronautiche Spaziali, Forli, Italy.), and P. Santini *In* AGARD, Smart Structures for Aircraft and Spacecraft Apr. 1993 14 p Sponsored in part by Ist. Studi e Applicazioni Scienze Aeronautiche Spaziali (For primary document see N94-11317 01-24)
(Grant 293/62)
Copyright Avail: CASI HC A03/MF A04

The general equations for a multi-body space system with internal control forces are written. Single body, or 'local', equations of motion are written and then they are transformed into global equations, associated with a sufficient number of 'internal' equations describing the relative motions of the various parts of the system. In such a transformation, quantities of two orders of magnitude arise: the first group is associated with the Earth's equatorial radius, and the second group is associated with a characteristic length of the spacecraft. The two groups are separated in order to avoid round-off errors. Furthermore, a law of control associated with deformations of the connections between the elements of the system is introduced, in such a way that efficient control of instability phenomena may be possible. Numerical examples complete the work. Author

N94-11343# Wright Lab., Wright-Patterson AFB, OH. Structures Div.
AIRCRAFT SMART STRUCTURES RESEARCH IN THE USAF WRIGHT LABORATORY
Gregory S. Agnes and Kevin Silva *In* AGARD, Smart Structures for Aircraft and Spacecraft Apr. 1993 9 p (For primary document see N94-11317 01-24)
Copyright Avail: CASI HC A02/MF A04

For several years, the Air Force Wright Laboratory has been investigating smart structures technologies. Smart structures incorporate active materials into structural components. Active materials either sense their environment or change in response to an external stimulus or both, and also should be able to carry loads. A smart structure is thus capable of sensing and/or reacting to its environment. Smart structures research at Wright Laboratory has mainly concentrated on aircraft sensory structures and multi-functional structures, such as integrated antennae (i.e., smart skins). Several major programs were initiated to apply and demonstrate these technologies. Recently, the ability of active materials (piezoceramics, for example) to control aircraft structures for improved performance and longevity, has received attention as well. The smart structures technologies are categorized as sensory, active, or multi-functional. The current state of the art for each area and programs aimed at exploiting smart technologies for aircraft applications are described. Gaps in the current technology are identified.
Author (revised)

N94-11344*# Jet Propulsion Lab., California Inst. of Tech., Pasadena.
ADVANCES IN ADAPTIVE STRUCTURES AT JET PROPULSION LABORATORY
Ben K. Wada and John A. Garba *In* AGARD, Smart Structures for Aircraft and Spacecraft Apr. 1993 13 p Sponsored by NASA, Washington (For primary document see N94-11317 01-24)
Copyright Avail: CASI HC A03/MF A04

Future proposed NASA missions with the need for large deployable or erectable precision structures will require solutions to many technical problems. The Jet Propulsion Laboratory (JPL) is developing new technologies in Adaptive Structures to meet these challenges. The technology requirements, approaches to meet the requirements using Adaptive Structures, and the recent JPL research results in Adaptive Structures are described. Author (revised)

N94-11345# Stirling Dynamics Ltd., Bristol (England).
ACTIVE LANDING GEAR CONTROL FOR IMPROVED RIDE QUALITY DURING GROUND ROLL **c05**
Tyrone F. Catt, David Cowling (Bristol Univ., England.), and Alan Shepherd *In* AGARD, Smart Structures for Aircraft and Spacecraft Apr. 1993 11 p Sponsored in part by British Aerospace Public Ltd. Co. (For primary document see N94-11317 01-24)
Copyright Avail: CASI HC A03/MF A04

Active control of an aircraft landing gear can give improved passenger ride quality during take-off and landing. The active control system studied uses feedback from airframe mounted sensors to modify rigid body and structural response. The system is based primarily on modifying the damping characteristics in the nose gear oleo. This is achieved by reducing the damping orifice area, with active control of the area about this new datum value. In addition, the benefits of a fully active nose gear using a separate supply of high pressure hydraulic fluid are evaluated. Significant benefits are demonstrated with the active damping control system compared with the basic landing gear. Responses to general runway roughness and discrete runway bumps are considered. The active damping control system is shown to be effective in reducing peak and rms passenger normal accelerations at all fuselage stations, particularly nose and tail. Good improvement can be obtained from active damping control of the nose gear, with no modification to the main gear. The first fuselage bending mode response can be reduced by active damping control. The benefits from the fully active system are marginal, considering the additional system complication. These effects are illustrated for a typical transport aircraft configuration.
Author

N94-11346# Institut Superieur de Technologie (Luxembourg).
ACTIVE DAMPING AUGMENTATION OF ELASTOMECHANICAL SYSTEMS USING PIEZOELECTRIC SENSORS AND ACTUATORS
Raymond Freymann and Edmond Stuemper *In* AGARD, Smart Structures for Aircraft and Spacecraft Apr. 1993 12 p (For primary document see N94-11317 01-24)
Copyright Avail: CASI HC A03/MF A04

It will be shown how use can be made of piezoelectric elements, integrated as sensors and actuators in a closed control loop, to improve the modal damping behavior of elastomechanical systems. Focus is pointed on some special characteristics of piezoelectric elements, such as their dynamic behavior, their energy transfer capabilities when being used as actuators, and their geometric filtering possibilities when being used as sensors. The experimental part of the work concentrates on the active damping augmentation in the low frequency range of a flexible beam-shaped structural system with a total length of 4 meters. Author (revised)

N94-11347# Wright Lab., Wright-Patterson AFB, OH.
MULTIDIMENSIONAL INTELLIGENT CONTROL FOR SUPERLIGHT AIR VEHICLES **c05**
Aivars Smitchens, Anthony DeThomas, Kurt Grevstad (Boeing Co., Seattle, WA.), and Doug Moore (Rockwell International Corp., El Segundo, CA.) *In* AGARD, Smart Structures for Aircraft and Spacecraft Apr. 1993 12 p (For primary document see N94-11317 01-24)
Copyright Avail: CASI HC A03/MF A04

Flexible wing technology was explored in a number of design studies. Wind tunnel experiments generally affirm the results of these studies that a flexible, variable twist wing holds the potential for dramatic air vehicle performance improvements. However, the attendant control reversal, increase in control parameter nonlinearities, and the need for an active control system to suppress flutter has discouraged the application of this technology in production designs. Advancement of a robust control capability for damping structural modes; embedded sensors to provide required inputs to the control system for active flutter control and, possibly, battle damage tolerance; high-speed on-board computation; and other technologies promise the capability to exploit the benefits promised by more flexible structures. Current proposals to reduce air vehicle structural weight are briefly reviewed and implications on the control system are assessed. Even though control system concerns exist, they are resolvable and it may be timely to undertake the development and demonstration of an actively controlled flexible wing.
Author (revised)

N94-11368# Oak Ridge National Lab., TN.
HIGH-TEMPERATURE CORROSION OF CERAMIC-CERAMIC COMPOSITES IN A WASTE INCINERATOR ENVIRONMENT
J. R. Keiser, J. I. Federer, T. J. Henson, and D. L. Hindman (Babcock and Wilcox Co., Lynchburg, VA.) Jan. 1993 60 p
(Contract DE-AC05-84OR-21400)
(DE93-012430; ORNL/M-12212) Avail: CASI HC A04/MF A01

Three types of ceramic composite were exposed to the flue gases of a hazardous waste incinerator to assess their corrosion behavior. One composite consisted of continuously wound filaments of Al2O3-23 wt % ZrO2 in an alumina matrix. This composite was tested, both uncoated and coated, with zirconia on the outer surface. The second composite type consisted of the same fiber but in a zirconia matrix. The third composite consisted of an alumina matrix strengthened with silicon carbide particles. Tubes of these materials were exposed in the waste incinerator at about 900 C for up to six months. Two principal results of exposure were revealed by optical microscopy and electron microprobe examinations: flue gas constituents either penetrated the uncoated alumina matrix of the filament-wound composite, apparently through porosity in the matrix, or deposited on the surfaces of the other composite types where reaction and bonding occurred. Neither event caused significant microstructural degradation although the reaction in the composite with a zirconia matrix suggests that degradation could be a problem under more severe conditions. Apparently, the concentration of penetrating species was too small to form a significant amount of new compounds that could cause degradation within the alumina matrix of the filament-wound composite, and the temperature was too low for the deposits on the surface of the other two types of composites to react significantly with the materials during the longest exposure of 6 months. The zirconia coating on the alumina matrix composite was not adherent enough to permit an assessment of its effect. DOE

N94-11446# Army Research Lab., Watertown, MA.
STRAIN CONCENTRATION ASSESSMENT OF LAMINATES SUBJECTED TO LOW VELOCITY IMPACT Final Report
Robert F. Anastasi and Steven M. Serabian Apr. 1993 20 p
(AD-A264497; ARL-TR-91) Avail: CASI HC A03/MF A01

Low velocity impact upon composite laminates can lead to both apparent and non-apparent damage zones that result in structural strain concentrations. The strain concentrations can be, or grow to be, larger than permissible design levels through static or cyclic loading conditions. This can drastically reduce the structural integrity of the composite component. In this paper, glass/epoxy composite coupons in three laminate orientations were damaged by low velocity impact that create a damage zone consisting of local fiber breakage and delamination. Conventional moire was then used to measure strain concentration as a function of applied tensile load. Correlations were made between impact energy, delamination area, strain concentration, and laminate orientation. DTIC

N94-11484*# Camber Corp., Huntsville, AL.
PROPERTY CHANGES INDUCED BY THE SPACE ENVIRONMENT IN COMPOSITE MATERIALS ON LDEF: SOLAR ARRAY MATERIALS PASSIVE LDEF EXPERIMENT A0171 (SAMPLE)
Apr. 1993 18 p
(Contract NAS8-38978)
(NASA-CR-192572; NAS 1.26:192572) Avail: CASI HC A03/MF A01

Surface modifications to composite materials induced by long term exposure in low earth orbit (LEO) were dominated by atomic oxygen erosion and micrometeoroid and space debris impacts. As expected, calculated erosion rates were peculiar to material type and within the predicted order of magnitude. Generally, about one ply of the carbon fiber composites was eroded during the 70 month LDEF experiment. Matrix erosion was greater than fiber erosion and was more evident for a polysulfone matrix than for epoxy matrices. Micrometeoroid and space debris impacts resulted in small (less than 1mm) craters and splattered contaminants on all samples. Surfaces became more diffuse and darker with small increases in emissivity and absorption. Tensile strength decreased roughly with thickness loss, and epoxy matrices apparently became slightly embrittled, probably as a result of continued curing under UV and/or electron bombardment. However, changes in the ultimate yield stress of the carbon reinforced epoxy composites correlate neither with weave direction nor fiber type. Unexpected developments were the discovery of new synergistic effects of the space environment in the interaction of atomic oxygen and copious amounts of contamination and in the induced luminescence of many materials. Author

N94-11612# Pacific Northwest Lab., Richland, WA.
THE EFFECTS OF AN AGGRESSIVE ENVIRONMENT ON THE SUBCRITICAL CRACK GROWTH OF A CONTINUOUS-FIBER CERAMIC COMPOSITE
C. H. Henager, Jr. and R. H. Jones Jan. 1993 10 p Presented at the 16th Annual Conference on Composites, Materials, and Structures, Cocoa Beach, FL, 13-16 Jan. 1992
(Contract DE-AC06-76RL-01830)
(DE93-011690; PNL-SA-19958; CONF-920144-6) Avail: CASI HC A02/MF A01

Time-dependent crack growth measurements of ceramic composites in aggressive environments are being conducted on materials consisting of CVI SiC reinforced with Nicalon fibers (SiC/SiC(sub f)) having C and BN fiber-matrix interfaces. Crack velocities are determined as a function of applied stress intensity. Results have been obtained for crack velocity-stress intensity relationships in pure Ar and in Ar plus 2000 ppM O2 atmospheres at 1100 C. A 2D micromechanics model is used to represent the time-dependence of observed crack bridging events and is able to rationalize the observed phenomena. DOE

N94-11686 Michigan Univ., Ann Arbor. Dept. of Civil Engineering.
MECHANICAL INTERACTION BETWEEN SYNTHETIC FIBER AND CEMENT BASE MATRIX IN FRC COMPOSITES Final Report, 1 Jul. 1990 - 31 Oct. 1992
Victor C. Li and Yin-Wen Chan Feb. 1993 26 p Limited Reproducibility: More than 20% of this document may be affected by microfiche quality
(Grant AF-AFOSR-0328-90)
(AD-A265310; AFOSR-93-0364TR) Avail: CASI HC A03

In cement-based materials, cement is usually employed to bind other materials together. Different interfaces are thus generated between various media in the resulted materials. It has been well recognized that the interfacial microstructure between cement binder and inclusions is of the greatest importance for the mechanical properties of the composite. Specifically, in fiber reinforced cementitious composites, the composite material properties are especially predominated by the fiber-cement interface due to its influence on the mechanical interactions between fibers and cement matrix. This report summarizes research investigations and findings of a study of the fiber-cement interfacial debond mode, namely strength-based or fracture-based debond modes and on an issue of interfacial bond property control. These studies have been done with the help of fiber pull-out experiments using an MTS digitally controlled load frame and micromechanical modeling, accompanied by environmental scanning electron microscopy. We expect that such investigations will provide physical insights into the break-down processes occurring at the interphase levels of fiber reinforced cementitious composites. The knowledge, in turn, many serve to achieve fiber reinforced cementitious composites with higher performance. DTIC

N94-12013 Toronto Univ. (Ontario). Inst. for Aerospace Studies.
LOCALIZED AND DISTRIBUTED FIBER-OPTIC STRAIN SENSORS EMBEDDED IN COMPOSITE MATERIALS Thesis
Tomas Valis Sep. 1992 301 p Sponsored by Ontario Laser and Lightwave Research Centre; Natural Sciences and Engineering Research Council; and Inst. for Space and Terrestrial Science
(UTIAS-346; AD-B172623L) Copyright Avail: Issuing Activity

Fiber-optic sensors capable of being surface-adhered, or embedded within advanced composite materials to measure local strain are developed. Three types of strain sensors -- polarimeter, Michelson interferometer, and Fabry-Perot interferometer -- are built and tested in both uniaxial and rosette configurations. These are embedded in graphite/PEEK thermoplastic and Kevlar/epoxy thermoset composite laminates. Parameters that are experimentally determined include: response linearity, strain sensitivity, transverse-strain sensitivity, temperature cross-sensitivity, and maximum elongation. The fiber-optic strain rosettes demonstrated in situ strain-tensor measurement. Issues related to the compatibility and interaction of optical fibers with composite materials are addressed. A passive-quadrature phase-demodulation scheme for the Michelson interferometer is reported. The fiber-optic strain sensor with the most desirable properties is determined to be the Fabry-Perot interferometer. A technique for distributed strain-sensing based on counterpropagating waves coupled through backward stimulated-Raman-scattering is treated theoretically. Author (revised)

N94-12344# Integrated System Assemblies Corp., Woburn, MA.
LIQUID COOLED HEAT SINK WITH THROUGH VIAS (LCHS) Interim Report, Dec. 1992 - May 1993
Charles W. Eichelberger and J. Patrick Kusior 31 May 1993 13 p
(Contract N00014-91-C-0219; ARPA Order 8021)
(AD-A266008) Avail: CASI HC A03/MF A01

This document presents the results of the Liquid Cooled Heat Sink with Through Vias (LCHS) Program. The goal of the program was to fabricate a structure with microchannels and through vias. The microchannels allow a heat dissipating liquid to flow through the structure while the vias provide an electrical pathway from the top of the structure to the bottom. A series of electrical and thermal tests were performed. The results of these tests have been interpreted. Recommendations to improve the current design were addressed. DTIC

N94-12347# Universal Technology Corp., Dayton, OH.
ANALYTICAL MODELS FOR DESCRIBING THE MECHANICAL BEHAVIOR OF FIBER REINFORCED COMPOSITES Final Report, Jun. - Sep. 1992
James M. Whitney Sep. 1992 44 p
(Contract F33615-89-C-5609)
(AD-A265906; WL-TR-93-4060) Avail: CASI HC A03/MF A01

This report covers three topics in mechanics of advanced composites: effect of fiber cross-section on stiffness and strength of laminated composites; failure criteria for composites under combined loading; and stress analysis models for thick composites. In the area of fiber cross-sectional effect, micromechanics analysis addresses the effect of elliptical fibers on the stiffness and in-plane stress concentrations. Numerical results show that fiber cross-sectional geometry has only a modest influence on laminate elastic constants. The second topic addresses the interaction between longitudinal compression and transverse loading (tension and compression). Data obtained with a mini-sandwich beam are used to generate failure stresses. Classical lamination theory, including thermal residual stresses due to cure, is utilized for determining play stresses. Experimental results reveal little interaction between longitudinal compression and transverse stresses as long as the transverse load is below uniaxial transverse failure. Under the topic of thick composites, the effect of shear deformation and transverse normal stress on the cylindrical bending of laminated, anisotropic plates subjected to a uniform lateral load is investigated. Closed form solutions indicate that the effect of transverse normal stress on maximum deflection is small, even for relatively thick plates. DTIC

N94-12401# Cincinnati Univ., OH. Dept. of Aerospace Engineering and Engineering Mechanics.
ULTRASONIC WAVE INTERACTION WITH ADVANCED COMPLEX MATERIALS FOR NONDESTRUCTIVE EVALUATION APPLICATIONS Final Report, 15 Dec. 1988 - 15 Dec. 1992
Adnan H. Nayfeh 15 Dec. 1992 74 p
(Grant AF-AFOSR-0177-89)
(AD-A265704; AFOSR-93-0394TR) Avail: CASI HC A04/MF A01

During the period of the grant we continued our modeling and analysis of the mechanical behavior of complex composite materials. Analytical and numerical modeling techniques of the influence of general composite laminate orientation on the ultrasonic behavior of anisotropic plates and substrates were developed. In the second phase piezoelectric effects were introduced into our modeling. In the final phase, the dynamic response of the layered composite to transient-loadings in the form of time-dependent source loads were studied. Complete documentation of the results of the first two phases were submitted to the AFOSR in the form of yearly reports. Since these reports contained completed items which also appeared in the literature as archival publications, we need not rereport them. Results for the recently completed works were also prepared for journal publication. Description of these works are included in detail. DTIC

N94-12431*# National Aeronautics and Space Administration. Lewis Research Center, Cleveland, OH.
PROTECTIVE COATINGS FOR HIGH-TEMPERATURE POLYMER MATRIX COMPOSITES
David R. Harding (Sverdrup Technology, Inc., Brook Park, OH.), James K. Sutter, and Demetrios S. Papadopoulos (Case Western Reserve Univ., Cleveland, OH.) Jul. 1993 16 p Proposed for presentation at the 25th International SAMPE Technical Conference, Philadelphia, PA, 26-28 Oct. 1993; sponsored by the Society for the Advancement of Material and Process Engineering
(RTOP 510-01-50)
(NASA-TM-106276; E-8013; NAS 1.15:106276) Avail: CASI HC A03/MF A01

Plasma-enhanced chemical vapor deposition was used to deposit silicon nitride on graphite-fiber-reinforced polyimide composites to protect against oxidation at elevated temperatures. The adhesion and integrity of the coating were evaluated by isothermal aging (371 C for 500 hr) and thermal cycling. The amorphous silicon nitride (a-SiN:H) coating could withstand stresses ranging from approximately 0.18 GPa (tensile) to -1.6 GPa (compressive) and provided a 30 to 80 percent reduction in oxidation-induced weight loss. The major factor influencing the effectiveness of a-SiN:H as a barrier coating against oxidation is the surface finish of the polymer composite. Author

N94-12449*# National Aeronautics and Space Administration. Lewis Research Center, Cleveland, OH.
PROPOSED FRAMEWORK FOR THERMOMECHANICAL LIFE MODELING OF METAL MATRIX COMPOSITES
Gary R. Halford, Bradley A. Lerch, and James F. Saltsman Washington Jul. 1993 15 p
(RTOP 505-63-52)
(NASA-TP-3320; E-7483; NAS 1.60:3320) Avail: CASI HC A03/MF A01

The framework of a mechanics of materials model is proposed for thermomechanical fatigue (TMF) life prediction of unidirectional, continuous-fiber metal matrix composites (MMC's). Axially loaded MMC test samples are analyzed as structural components whose fatigue lives are governed by local stress-strain conditions resulting from combined interactions of the matrix, interfacial layer, and fiber constituents. The metallic matrix is identified as the vehicle for tracking fatigue crack initiation and propagation. The proposed framework has three major elements. First, TMF flow and failure characteristics of in situ matrix material are approximated from tests of unreinforced matrix material, and matrix TMF life prediction equations are numerically calibrated. The macrocrack initiation fatigue life of the matrix material is divided into microcrack initiation and microcrack propagation phases. Second, the influencing factors created by the presence of fibers and interfaces are analyzed, characterized, and documented in equation form. Some of the influences act on the microcrack initiation portion of the matrix fatigue life, others on the microcrack propagation life, while some affect both. Influencing factors include coefficient of thermal expansion mismatch strains, residual (mean) stresses, multiaxial stress states, off-axis fibers, internal stress concentrations, multiple initiation sites, nonuniform fiber spacing, fiber debonding, interfacial layers and cracking, fractured fibers, fiber deflections of crack fronts, fiber bridging of matrix cracks, and internal oxidation along internal interfaces. Equations exist for some, but not all, of the currently identified influencing factors. The third element is the inclusion of overriding influences such as maximum tensile strain limits of brittle fibers that could cause local fractures and ensuing catastrophic failure of surrounding matrix material. Some experimental data exist for assessing the plausibility of the proposed framework. Author

N94-12594*# Battelle Memorial Inst., Columbus, OH.
ISOTHERMAL FATIGUE MECHANISMS IN Ti-BASED METAL MATRIX COMPOSITES Final Report
Bhaskar S. Majumdar and Golam M. Newaz Sep. 1993 62 p
(Contract NAS3-26494; RTOP 510-01-50)
(NASA-CR-191181; E-8086; NAS 1.26:191181) Avail: CASI HC A04/MF A01

Stress-controlled isothermal fatigue experiments were performed at room temperature (RT) and 548 C (in argon) on (0)8 SCS6/Ti 15-3 metal matrix composites (MMC's) with 15 and 41 volume percent SCS6 (SiC) fibers. The primary objectives were to evaluate the mechanical responses, and to obtain a clear understanding of the damage mechanisms leading to failure of the MMC's. The mechanical data indicated that strain ranges attained fairly constant values in the stress-controlled experiments at both RT and 538 C, and remained so for more than 85 percent of life. The fatigue data for MMC's with different volume fraction fibers showed that MMC life was controlled by the imposed strain range rather than the stress range. At RT, and at low and intermediate strain ranges, the dominant fatigue mechanism was matrix fatigue, and this was confirmed metallurgically from fractographic evidence as well as from observations of channel type dislocation structures in the matrix of fatigued MMC specimens. Reaction-zone cracks acted as important crack initiating sites at RT, with their role being to facilitate slip band formation and consequent matrix crack initiation through classical fatigue mechanisms. MMC life agreed with

matrix life at the lower strain ranges, but was smaller than matrix life at higher strain ranges. Unlike the case of monotonic deformation, debonding damage was another major damage mechanism during fatigue at RT, and it increased for higher strain ranges. At high strain ranges at RT, fractography and metallography showed an absence of matrix cracks, but long lengths of debonds in the outer layers of the SCS6 fibers. Such debonding and consequent rubbing during fatigue is believed to have caused fiber damage and their failure at high strain ranges. Thus, whereas life was matrix dominated at low and intermediate strain ranges, it was fiber dominated at high strain ranges. At 538 C, the mean stain constantly increased (ratchetting) with the number of cycles. At high strain ranges, such ratchetting led to overload failure of the fibers, and debonding of the type at RT was very small. At intermediate strain ranges, fractography showed large areas of matrix cracks. However, in spite of this matrix dominated mechanism, the MMC life at elevated temperatures was significantly less than the matrix fatigue life at all strain ranges. The reason for this difference is still unclear, although metallographic and fractographic evidences suggest that internal crack initiation sites at Mo-ribbons and reaction-zone cracks may have played a critical role, with the former tending to dominate.
Author (revised)

N94-10186# Katholieke Univ. te Leuven (Belgium). Dept. of Metallurgy and Materials Engineering.
TEM STUDY OF A SPACE PROCESSED Al-Al2O3 METALLIC COMPOSITE
H. Zou (Wuhan Univ., China.), L. Froyen, L. Delaey, and A. Deruyttere *In* ESA, Proceedings of the 8th European Symposium on Materials and Fluid Sciences in Microgravity, Volume 2 Aug. 1992 p 549-554 (For primary document see N94-10171 01-29)
Copyright Avail: CASI HC A02/MF A04; ESA, EPD, ESTEC, Noordwijk, Netherlands, HC

N94-10773# RK Carbon Fibers, Inc., Philadelphia, PA.
A NEW FR WATER RESISTANT ACOUSTIC INSULATION MATERIAL FOR AIRCRAFT
Novis Smith and Geoff Gould *In* FAA, Proceedings of the International Conference for the Promotion of Advanced Fire Resistant Aircraft Interior Materials Mar. 1993 p 67-84 (For primary document see N94-10766 01-03)
Avail: CASI HC A03/MF A03

N94-10779# National Inst. of Standards and Technology, Gaithersburg, MD. Building and Fire Research Lab.
COMPUTER-AIDED MOLECULAR DESIGN OF FIRE RESISTANT AIRCRAFT MATERIALS
Marc R. Nyden and James E. Brown *In* FAA, Proceedings of the International Conference for the Promotion of Advanced Fire Resistant Aircraft Interior Materials Mar. 1993 p 147-158 (For primary document see N94-10766 01-03)
Avail: CASI HC A03/MF A03

N94-10796# Federal Aviation Administration, Atlanta, GA.
ADVANCED AIRCRAFT MATERIALS RESEARCH AND DEVELOPMENT PLAN
Richard Lyon and Thor Eklund *In its* Proceedings of the International Conference for the Promotion of Advanced Fire Resistant Aircraft Interior Materials Mar. 1993 p 345-364 (For primary document see N94-10766 01-03)
Avail: CASI HC A03/MF A03

N94-12320*# Stanford Univ., CA. Center for Turbulence Research.
TENSORAL: A SYSTEM FOR POST-PROCESSING TURBULENCE SIMULATION DATA
Eliot Dresselhaus *In its* Annual Research Briefs, 1992 Jan. 1993 p 455-460 (For primary document see N94-12284 01-34)
Avail: CASI HC A02/MF A04

25 INORGANIC AND PHYSICAL CHEMISTRY

Includes chemical analysis, e.g., chromatography; combustion theory; electrochemistry; and photochemistry.

For related information see also *77 Thermodynamics and Statistical Physics.*.

N94-10337# General Management Associates, Abingdon, MD.
AEROSOL SAMPLING MODELS SURVEY Final Report, Jun. - Dec. 1990
Dennis Metz and Paul Harvey Mar. 1993 151 p
(Contract DAAA15-87-D-0021)
(AD-A265903; ERDEC-CR-019) Avail: CASI HC A08/MF A02

The Obscuration Sciences Branch of the Physics Division, Research Directorate at the U.S. Army Chemical Research, Development, and Engineering Center, has undertaken a research project. This effort is aimed at identifying a comprehensive algorithm, computer program, or theory that might already exist and could be used to design aerosol sampling and transport systems. Initially, a literature survey was performed by the Obscuration Sciences Branch which began with several hundred potential articles and has been distilled to four candidate reports. This report evaluates the four candidate aerosol sampling models for self consistency and compares the numerical calculations resulting from four models. Finally a comparison of these model-derived results is made to the experimentally-derived results.
Author (DTIC)

N94-10338# Brookhaven National Lab., Upton, NY.
A NEW MATRIX FOR THE AGELESS 21.6-keV Eu-151 NUCLEAR GAMMA RAY MOESSBAUER SOURCE
C. I. Wynter (Nassau Community Coll., Garden City, NY.), P. E. Haustein, H. Stadelmaier (North Carolina State Univ., Raleigh.), A. Thorpe (Howard Univ., Washington, DC.), J. J. Spijkerman (Ranger Scientific, Burleson, TX.), and I. Nowik (Hebrew Univ. of Jerusalem, Rehovot, Israel.) 1993 4 p Presented at the Second Nassau Moessbauer Conference, Garden City, NY, 8 Jan. 1993
(Contract DE-AC02-76CH-00016)
(DE93-009795; BNL-48628; CONF-930195-1) Avail: CASI HC A01/MF A01

Moessbauer spectroscopy has been used over the past two decades to advance the study of europium compounds and alloys, primarily utilizing the 21.6-keV gamma ray emitted from beta decaying Sm-151. This isotope, which has a 87 year half-life, has been used in either a samarium fluoride (SmF3) or samarium oxide (Sm2O3) matrix. We now report a study involving, europium oxalate decahydrate (Eu2(C2O) (center dot) 10(H2O)), europium fluoride EuF3, and EuBe13 as absorbers at known thicknesses. Our data supports the view that Sm2(C2O4)(sub 3)(center dot) H2O will provide a better source matrix than either the fluoride or oxide due to the narrower linewidth and comparable 'f' factor to (Sm-151)F(sub 3). DOE

N94-10380# Department of the Navy, Washington, DC.
ELECTROCHEMICAL PROCESS AND PRODUCT THEREFROM Patent Application
Michael J. Marachyke, inventor (to Navy) 31 Dec. 1992 23 p
(AD-D015767; US-Patent-Appl-SN-999629) Avail: CASI HC A03/MF A01

An object of this invention is a simple, cheap, selective and clean electrochemical removal of non-diamond carbon from a surface at below or above room temperature. Another object of this invention is to electrochemically pattern a substrate with non-diamond carbon with high resolution and relatively undamaged exposed surface. These and other objects of this invention are realized by a process which comprises disposing a surface with a non-diamond carbon layer in an electrolyte and subjecting the surface to sufficient electric field. The selective removal of non-diamond carbon is achieved by the addition of a mask on the non-diamond carbon layer. These and other objects of this invention are also realized by patterned diamond products made by the procedure disclosed herein. DTIC

N94-10519# Rochester Univ., NY. Dept. of Physics and Astronomy.
COHERENCE EFFECTS IN RADIOMETRY AND IN SPECTROSCOPY
E. Wolf 1992 9 p Presented at the 10th Symposium on Energy Engineering Sciences: Synergism of Analysis, Modeling, and Experiment,

Argonne, IL, 11-13 May 1992
(Contract DE-FG02-90ER-14119)
(DE93-013437; CONF-9205147-5) Avail: CASI HC A02/MF A01

Recent research concerning the effects of the state of coherence of a source on the spatial and the spectral distributions of energy generated by the source is described. The research has elucidated the foundations of radiometry and it has also revealed some unexpected new phenomena relating to spectral changes which can be induced by source correlations and also by scattering on random media. DOE

N94-10653# Washington Univ., Seattle. Dept. of Physics.
X RAY AND GAMMA RAY SPECTROSCOPY OF SOLIDS UNDER PRESSURE
R. L. Ingalls 30 Apr. 1993 13 p
(Contract DE-FG06-84ER-45163)
(DE93-014847; DOE/ER-45163/33) Avail: CASI HC A03/MF A01

The described studies were either completed or underway during this 3-year period: XAFS study of pressure-induced transition in Rb-W bronze (Rb(0.31)WO3); XAFS study of bcc-hcp transition in Fe; XAFS search for valence change in thallium perhenate (TlReO4) at high pressure; XANES analysis of alkali halides; pair potentials in alkali halides studied via EXAFS; EXAFS determination of bond angles in ReO3; XAFS study of mixed-valence transition in SmSe; Moessbauer studies of Fe hydride at high pressure; and Moessbauer and x-ray studies of Fe silicate spinel at high pressure. DOE

N94-10713*# Hampton Univ., VA. Dept. of Physics.
HYDROGEN PARTITIONING AND TRANSPORT IN TITANIUM ALUMINIDES Final Report, 1 Mar. 1990 - 28 Aug. 1993
Kwang S. Han and Weon S. Lee 28 Aug. 1993 40 p
(Grant NAG1-1110)
(NASA-CR-194117; NAS 1.26:194117) Avail: CASI HC A03/MF A01

This report gives the final summary of the research work perfomed from March 1, 1990 to August 28, 1993. Brief descriptions of the research findings are given on the surface variation of Ti-14Al-21Nb as a function of temperature under ultrahigh vacuum conditions; titanium aluminides: surface composition effects as a function of temperature; Auger electron intensity variation in oxygen-charged silver; and segregation of sulfur on a titanium surface studied by Auger electron spectroscopy. Each description details one or more of the attached corresponding figures. Published journal documents are provided as appendices to give further detail. CASI

N94-10854# Rice Univ., Houston, TX.
APPLICATION OF SPIN-SENSITIVE ELECTRON SPECTROSCOPIES TO INVESTIGATIONS OF ELECTRONIC AND MAGNETIC PROPERTIES OF SOLID SURFACES AND EPITAXIAL SYSTEMS
G. K. Walters and F. B. Dunning Apr. 1993 5 p
(Contract DE-FG05-86ER-45233)
(DE93-015079; DOE/ER-45233/8) Avail: CASI HC A01/MF A01

Research during this year focused on the angular dependence of polarization of electrons backscattered from metallic surfaces, as a function of energy loss, using spin-polarized electron energy loss spectroscopy (SPEELS), and on dynamics of metastable He deexcitation at Xe-covered metallic surfaces using spin-polarized metastable deexcitation spectroscopy (SPMDS). In the SPEELS study, the data from Au, Ag, Mo, and Fe surfaces suggest that all inelastically scattered electrons underwent small-angle inelastic scattering either preceded or followed by large-angle elastic scattering that redirects the incident electron away from the target. The SPMDS study was extended from other gases to include rare gas adsorbates on Cu(100) and Au(100) surfaces; the spectra from the Xe-metal systems are unlike those from other systems and may provide new insights into metastable atoms. DOE

N94-11075# Lawrence Livermore National Lab., CA.
PROGRESS IN ZIRCONIUM RESONANCE IONIZATION SPECTROSCOPY
R. H. Page, S. C. Dropinski, E. F. Worden, Jr., and J. A. D. Stockdale 29 Dec. 1992 17 p Presented at the OE/LASE 1993 International Society for Optical Engineering Conference, Los Angeles, CA, 16-23 Jan. 1993
(Contract W-7405-eng-48)
(DE93-011881; UCRL-JC-112518; CONF-930159-25) Avail: CASI HC A03/MF A01

We have examined the stepwise-resonant free-photon-ionization spectrum of neutral zirconium atoms using three separately-tunable pulsed visible dye lasers. The ground-level (first-step) transitions were chosen on the basis of demonstrated Zr-91 selectivity. Lifetimes of even-parity levels around 36000/cm, measured with the delayed-photoionization technique, range from 10 to 100 ns. Direct ionization cross sections appear to be less than 10(exp -17) sq cm; newly-detected autoionizing levels give peak ionization cross sections (inferred from saturation fluences) up to 10(exp -15) sq cm. Portions of Rydberg series converging to the 315 and 763/cm levels of Zr(+) were identified. 'Clumps' of auto-ionizing levels are thought to be due to Rydberg-valence mixing. DOE

N94-11140# Edgerton, Germeshausen and Grier, Inc., Idaho Falls, ID.
IN SITU SECONDARY ION MASS SPECTROMETRY ANALYSIS
G. S. Groenewold, A. D. Applehans, J. C. Ingram, J. E. Delmore, and D. A. Dahl Jan. 1993 31 p
(Contract DE-AC07-76ID-01570)
(DE93-012185; EGG-WTD-10507) Avail: CASI HC A03/MF A01

The direct detection of tributyl phosphate (TBP) on rocks using molecular beam surface analysis (MBSA or in situ secondary ion mass spectrometry (SIMS)) is demonstrated. Quantities as low as 250 ng were detected on basalt and sandstone with little or no sample preparation. Detection of TBP on soil has proven to be more problematic and requires further study. Ethylene- diamine- tetra- acetic acid (EDTA) is more difficult to detect because it is very reactive with surfaces of interest. Nevertheless, it is possible to detect EDTA if the acidity of the surface is controlled. The detection of EDTA-metal complexes is currently an open question, but evidence is presented for the detection of ions arising from a EDTA-lead complex. Carboxylic acids (i.e., citric, ascorbic, malic, succinic, malonic, and oxalic) give characteristic SIM spectra, but their detection on sample surfaces awaits evaluation. DOE

N94-11216 Institute of Sound and Vibration Research, Southampton (England). Fluid Dynamics and Acoustics Group.
A THEORY OF MEMBRANE ABSORBERS
M. J. Fisher Mar. 1993 33 p
(ISVR-TR-217) Copyright Avail: Issuing Activity (Institute of Sound and Vibration Research, University of Southampton, Southampton SO9 5NH, England)

The use of membrane absorbers, traditionally considered as a combination of a baffle resonator and Helmholtz resonator, are finding applications in an increasingly wide field of industrial noise control applications. Previous theoretical work in this area appears to have assumed that each resonator acts independently of the other; each controlling the absorption in its own frequency range. We consider them as two coupled oscillators, the coupling arising through the fluctuation of pressure in the absorber cavity which drives both the membrane and air through the Helmholtz resonator exit. The coupling is demonstrated to yeild a number of important effects which should be included in a rational design procedure for membrane absorbers. Author (revised)

N94-11244# Virginia Polytechnic Inst. and State Univ., Blacksburg.
PHASE EQUILIBRIA AND VOLUMETRIC PROPERTIES FOR THE SYSTEM NaCl-CaCl2-H2O Ph.D. Thesis
Charles Steger Oakes 1993 119 p
(Contracts DE-FG05-89ER-14065; DE-AC05-84OR-21400)
(DE93-013590; DOE/ER-14065/T1) Avail: CASI HC A06/MF A02

Low temperature phase relations in the ice-stable field of the system NaCl-CaCl2-H2O were determined under 1 atm. total pressure along the NaCl-H2O and CaCl2-H2O binaries and along five pseudobinaries with constant NaCl/(NaCl + CaCl2) weight ratios. The results are in excellent agreement with published data along the NaCl-H2O binary but show large discrepancies when compared to previous determinations of the ice liquidus alone, the CaCl2-H2O binary and in the NaCl-CaCl2-H2O ternary. At moderate to high salinities, isotherms cross the ice sub-field at lower total salt concentrations than previously reported. In addition, NaCl(NaCl + CaCl2) weight ratios estimated from hydrohalite- and ice-melting temperatures may be low by as much as 15%. Relative densities were measured for NaCl(aq) and CaCl2(aq) solutions to 250 C and 400 bars and over the range of ionic strengths 0.2-5.5 and 0.2-19.2 mol (center dot)/kg, respectively. The results span the pressure and temperature of earlier volumetric studies and extend to higher molalities than reported previously. The relative densities have been fitted as apparent molar volumes (V(sub phi)) using the Pitzer ion-interaction treatment, with appropriate expressions chosen for the temperature- and pressure-dependence of the virial coefficients of the model. The results presented for NaCl(aq) are in good agreement with published results to 250 C. The results presented for CaCl2(aq) are in good agreement with published values to approximately 125 C. DOE

N94-11249# Los Alamos National Lab., NM.
KIVA-3: A KIVA PROGRAM WITH BLOCK-STRUCTURED MESH FOR COMPLEX GEOMETRIES
A. A. Amsden Mar. 1993 97 p
(Contract W-7405-eng-36)
(DE93-011986; LA-12503-MS) Avail: CASI HC A05/MF A02

This report describes the KIVA-3 computer program for numerical calculation of transient, two- and three-dimensional chemically reactive fluid flows with sprays. KIVA-3 is an extension of the earlier KIVA-2, uses the same numerical solution procedure, and solves the same set of equations. The full generality of KIVA-II has been retained; thus KIVA-3 is applicable to laminar or turbulent flows, subsonic or supersonic flows, and single-phase or dispersed two-phase flows. KIVA-3 differs from KIVA-2 in that it uses a block-structured mesh with connectivity defined through indirect addressing. The departure from a single rectangular structure in (i,j,k) logical space allows complex geometries to be modeled with significantly greater efficiency than was previously possible because large regions of deactivated cells are no longer necessary. Cell-face boundary conditions permit greater flexibility and simplification in the application of boundary conditions. This report discusses those features of KIVA-3 that differ from KIVA-2, the input required from a mesh generation preprocessor, and the output provided to a graphics postprocessor. Basic pre- and post-processors are included in the KIVA-3 package, and are also described. DOE

N94-11264# California Univ., Los Angeles. Dept. of Chemistry and Biochemistry.
SIZE DEPENDENCE OF CHEMICAL REACTIVITY OF GASEOUS METAL CLUSTERS: A NEW MECHANISTIC PROBE
M. A. El-Sayed 17 May 1993 17 p
(Contract N00014-89-J-1350)
(AD-A264690; TR-75) Avail: CASI HC A03/MF A01

The determination of the mechanisms of chemical reactions leading to the formation of different types of materials is one of the principal occupations of many chemists today. To accomplish this, the dependence of the observed transformation is studied as a function of a number of intensive variables such as temperature, pressure, concentration of reactants as well as the Hydrogen ion concentration of the solution. In this account, we summarize recent studies in which the observed changes of the chemical reactivity of gaseous niobium clusters with size was used as a new degree of freedom that assists in deducing the mechanism of the chemical reactions studied. DTIC

N94-11265# Cincinnati Univ., OH. Dept. of Chemistry.
X RAY ABSORPTION SPECTROSCOPY OF ELECTROCHEMICALLY GENERATED SPECIES
William R. Heineman and Richard C. Elder 19 Feb. 1993 22 p
(Grant AF-AFOSR-0089-88)
(AD-A264749; AFOSR-93-0209TR) Avail: CASI HC A03/MF A01

X-ray absorption fine structure (EXAFS) spectroscopy has been combined with electrochemistry to enable the measurement of coordination numbers, donor atom types, and bond lengths of metal ions in multiple oxidation states which are generated electrochemically. We have demonstrated the applicability of this technique to study the redox coordination chemistry of metal ions in aqueous and nonaqueous solvents, ionically conducting polymer films, electroactive films on conducting metals, and electrically conducting polymers. Our objectives were to conduct research in the following areas: (1) electrostatic cross-linking of ionic polymer films and their effects on the structures of charged coordination compounds immobilized in the film; (2) cation charge transport and its effects on the structures of electroactive films such as Prussian blue deposited on electrodes; (3) metal ions incorporated in electrically conducting polymers; (4) development of a flow cell which enables EXAFS spectroelectrochemistry to be performed in a controlled atmosphere environment; (5) structure determination for metals and intermetallic compounds in mercury solvent; and (6) evaluation of spectroelectrochemical nernstian plots. DTIC

N94-11359# Pittsburgh Univ., PA. Dept. of Chemistry.
CHARACTERIZATION OF GAS-AEROSOL INTERACTION KINETICS USING MORPHOLOGY DEPENDENT STIMULATED RAMAN SCATTERING
P. M. Aker 30 Jan. 1993 20 p
(Contract DE-FG02-92ER-61480)
(DE93-012324; DOE/ER-61480/1) Avail: CASI HC A03/MF A01

This study is aimed at characterizing the influence of aerosol surface structure on the kinetics of gas-aerosol interactions. Changes in gas phase chemical reaction rates as a function of exposure to a specific aerosol are measured with aerosols having different surface properties due to the composition and/or temperature of the material making up the aerosol. The kinetic data generated can be used directly in atmospheric modeling calculations. The surface structure of the aerosol is determined using morphology-dependent enhancement of simulated Raman scattering (MDSRS). Detailed dynamics of gas-aerosol interactions can be obtained by correlating the change in the reaction rate with change in surface structure and by monitoring the change in aerosol surface structure during, the course of the reaction. This dynamics information can be used to generate kinetic data for systems which are similar in nature to those studied, but are not amenable to laboratory investigation. We show here that increased MDSRS sensitivity is achieved by using an excitation laser source that has a narrow linewidth and we have been able to detect sulfate anion concentrations much lower than previously reported. We have shown that the linewidth of the MDSRS mode excited in a droplet is limited by the laser linewidth. This result suggests that MDSRS signal size should be independent of droplet size, and preliminary experiments confirm this hypothesis. DOE

N94-11370# Sandia National Labs., Albuquerque, NM.
A MODEL OF ELEMENTARY CHEMISTRY AND FLUID MECHANICS IN THE COMBUSTION OF HYDROGEN ON PLATINUM SURFACES
J. Warnatz (Stuttgart Univ., Germany.), M. D. Allendorf, R. J. Kee, and M. E. Coltrin Apr. 1993 21 p
(Contract DE-AC04-76DP-00789)
(DE93-012767; SAND-93-8228) Avail: CASI HC A03/MF A01

Using computational methods, we consider the catalyzed combustion of lean hydrogen-oxygen mixtures in a stagnation flow over a platinum surface and in a flat-plate boundary layer. The analysis includes elementary chemistry in the gas phase as well as on the surface. The stagnation flow is modeled using a similarity transformation that leads to a one-dimensional boundary-value problem, whereas the flat-plate boundary layer is modeled by use of the boundary-layer assumption. Predictions of each model are compared with experimental measurements of catalytic ignition and combustion of hydrogen-oxygen mixtures at low pressure (100 mTorr) and OH concentration profiles in catalytically supported combustion at atmospheric pressure. The paper proposes reaction mechanisms and interprets the catalytic behavior in terms of the chemistry models. DOE

N94-11602 Lawrence Livermore National Lab., CA.
THE SOLUBILITY OF EPSILON-CL-20 IN SELECTED MATERIALS
E. vonHoltz, D. Ornellas, M. F. Foltz, and J. E. Clarkson Aug. 1992 31 p Presented at the Energetic Materials for Munitions Conference, China Lake, CA, 22-24 Sep. 1992 Limited Reproducibility: More than 20% of this document may be affected by microfiche quality
(Contract W-7405-eng-48)
(DE93-009304; UCRL-JC-111005; CONF-9209326-1) Avail: CASI HC A03 (US Sales Only)

Solubility of the epsilon polymorph of CL-20 was determined in thirteen liquids over temperature range ambient to 74C using high performance liquid chromatography. The experiments included epsilon-CL-20 produced by two different synthesis routes; one lot contained a higher level of polymorphic impurity, the other lot contained a higher level of non-CL-20 impurity. In general, the epsilon-CL-20 was found to be highly soluble in the solvents with carbonyl groups, and relatively insoluble in hydrocarbons and materials containing ether linkages. The amount of phase conversion to gamma-CL-20 which occurred during the solubility testing was measured using FRIR, and ranged from essentially zero to approximately 10%

conversion. It appears that the presence of Beta-CL-20 in the virgin epsilon-CL-20 lots will affect the amount of gamma-phase present in the final residue. DOE

N94-11622# Oak Ridge National Lab., TN.
THERMOGRAPHIC PROPERTIES OF EIGHT BLUE-EMITTING PHOSPHORS
D. M. Cunningham, S. W. Allison, and D. B. Smith Jan. 1993 47 p
(Contract DE-AC05-84OR-21400)
(DE93-011459; ORNL/ATD-70) Avail: CASI HC A03/MF A01

We examined the effect of temperature on the light emission and absorption properties of eight phosphorescent compounds. The phosphors are commercially produced powders that emit mainly in the blue region when illuminated with ultraviolet light (220 to 400 nm). Excitation and emission spectra taken over the temperature range of 20 to 350 C are presented for these phosphors. Data from the spectra indicate a strong temperature dependence over this temperature range. Maximum relative intensity changed as a function of temperature in every phosphor examined. In some samples, spectral band shifts and bandwidths also changed with temperature. Of these phosphors, BaMg2Al16O27:Eu and (Ba3PO4)(sub 2):Eu are candidates for higher-temperature studies. DOE

N94-11683# Duke Univ., Durham, NC. Dept. of Chemistry.
ALUMINUM-PHOSPHORUS CHEMISTRY: PREPARATION AND STRUCTURAL CHARACTERIZATION OF (Et2AlP(SiMe3)2)2, Et(Cl)2Al(DOT)P(SiMe3)3, AND i-Bu2(Cl)Al(DOT)P(SiMe3)3
Richard L. Wells, Andrew T. McPhail, and Mark F. Self 24 Mar. 1993 31 p
(Contract N00014-89-J-1545)
(AD-A265268; DU/DC/TR-35) Avail: CASI HC A03/MF A01

Reactions of R2AlCl (R = Et, i-Bu) and EtAlCl2 with P(SiMe3)3 and LiP(SiMe3)2 were studied to investigate the potential use of dehalosilylation and lithium chloride elimination reactions for the preparation of compounds containing either Al-P-Al-P or Al-P-Al-Cl core rings. The dimeric compound Et2AlP(SiMe3)22 (1) was isolated from the 1:1 reaction of Et2AlCl and LiP(S iMe3)2 at -78 C, as a result of LiCl elimination. The 1:1 reaction of EtAlCl2 and P(SiMe3)3 yields Et(Cl)2Al(dot)P(SiMe3)3 (2). Interestingly, a similar reaction between Et2AlCl and P(SiMe3)3 in a 2:1 mole ratio also affords (2), in moderate yield, suggesting a rearrangement of the original aluminum alkylhalide. However, when Et2AlCl was reacted with P(SiMe3)3 in a 1:1 mole ratio, the expected adduct Et2(Cl)Al(dot)P (SiMe3)3 (3) results. Unlike the Et2AlCl reaction, the analogous 2:1 mole reaction of i-Bu2AlCl and P(SiMe3)3 forms the mono-chloro adduct, i-Bu2AlCl(dot)P(SiMe3)3 (4), rather than a rearrangement product. DTIC

N94-11699# Surface/Interface, Inc., Mountain View, CA.
CHARGE DISTRIBUTION ANALYSIS OF CATALYSTS UNDER SIMULATED REACTION CONDITIONS Technical Progress Report, 1 Oct. - 31 Dec. 1992
Friedemann Freund 1992 5 p
(Contract DE-AC22-92PC-92106)
(DE93-013604; DOE/PC-92106/T1) Avail: CASI HC A01/MF A01

Charge Distribution Analysis (CDA) is a technique for measuring mobile charge carriers in dielectric materials. CDA is based on dielectric polarization in an electric field gradient. The CDA apparatus is now under construction. DOE

N94-11855# Cambridge Univ. (England). Cavendish Lab.
DIELECTRIC BREAKDOWN AND ITS INFLUENCE ON IGNITION Final Report
M. M. Chaudhri, F. A. Al-Ramadhan, and I. U. Haq Mar. 1993 74 p
(Contract MOD-D/ER1/9/4/2029/RARDE)
(AD-A264925) Avail: CASI HC A04/MF A01

Electrical conduction, dielectric breakdown, and the consequent ignition of small pellets, 0.2 to 5 mm in thickness and 5 to 7 mm in diameter, of MTV compositions SR886B, SR886E, and SR886E have been investigated. The investigations were made using d.c fields and high-speed photography at framing rates of up to one million frames per second was employed to follow the breakdown and ignition behavior. It was found that under suitable conditions, the dielectric breakdown of the samples led to their ignition and the delay time between the breakdown and ignition could be as small as 20-25 microseconds. Furthermore, a special circuit was designed and constructed for determining the minimum ignition energies of samples of different thicknesses. It was found that for samples of thickness of approximately 0.2 mm, the minimum electrostatic energy which could cause ignition was as low as approximately 1 mJ. Moreover, the minimum ignition energy was found to increase with the sample thickness. A model, based on our previous model for the electrical ignition of silver azide, has been proposed. According to this, the dielectric breakdown leads to the formation of high conductivity filaments in which Joule heating-results in the formation of high temperature hot spots. Ignition initiates at these hot spots. An essential feature of this model is that the dielectric breakdown is a prerequisite for electrical ignition. DTIC

N94-11873# York Univ. (Ontario). Dept. of Chemistry.
PUBLICATIONS/PATENTS/PRESENTATIONS/HONORS/STUDENT REPORT Final Report
A. B. Lever 1993 7 p
(Contract N00014-91-J-1910)
(AD-A265136) Avail: CASI HC A02/MF A01

Electrochemical studies are carried out in three main areas. Phthalocyanine electrochemistry: emphasis is placed on the chemistry of phthalocyanine modified electrodes for the study of electrocatalytic processes ultimately leading to chemical sensors. These studies include polymeric phthalocyanine conductive species. We also seek a comprehensive understanding of phthalocyanine electrochemistry to benefit all phthalocyanine redox applications. This work is extended to include Langmuir Blodgett (LB) surface (monolayer) phthalocyanine films with spectroelectrochemical studies being undertaken in situ on the trough surface. Redox active ligands and electronic structure: A broad range of chemical techniques (uv/vis/FTIR/resonance Raman/PES/X-ray/ Electrochemistry/solvatochromism/ ab initio calcs, are brought into play to understand the electronic structure, spectroscopy and electrochemistry of ruthenium (mainly) complexes of quinonoid ligands (including derivatives such as quinonediimines) where oxidation states are non-integral. In situ LB electrochemistry: studies of the interactions of surface films with subphase redox species, in situ, in an LB trough. This is exploratory work aimed at developing methods for creating arrays of molecules and studying them through electronic spectra and electrochemistry - towards nanotechnology. DTIC

N94-12009 Defence Research Establishment Suffield, Ralston (Alberta).
TANDEM MASS SPECTROMETRIC ANALYSIS OF PHOSPHATE ESTERS
Paul A. DAgostino and Lionel R. Provost Mar. 1993 45 p Limited Reproducibility: More than 20% of this document may be affected by microfiche quality
(AD-A265483; DRES-SR-581) Avail: CASI HC A03

A homologous series of phosphate esters (trimethyl phosphate, triethyl phosphate, tripropyl phosphate, and tributyl phosphate), which are often employed as chemical simulants for chemical warfare agents, were characterized by tandem mass spectrometry under EI conditions. The daughter spectra for the principal EI ions of each phosphate ester were acquired by stepping the collisional activated dissociation cell energy from 1 eV to 100 eV (laboratory scale) in 1 eV increments with residual air and argon target gases. A standardized MS/MS setup procedure was established and the reproducibility of daughter scanning over the long and short term was evaluated. The sensitivity of capillary column GC-MS/MS was excellent and approximated that achieved during full scanning capillary column GC-MS analysis under EI conditions. Author (DTIC)

N94-12273# Wyoming Univ., Laramie. Dept. of Chemistry.
A VIBRATIONAL SPECTROSCOPIC STUDY OF THE STRUCTURE OF ELECTROACTIVE SELF-ASSEMBLED MONOLAYERS OF VIOLOGEN DERIVATIVES Technical Report, Jun. 1992 - May 1993
Xiaoyan Tang, Thomas Schneider, and Daniel A. Buttry 12 May 1993 24 p
(Contract N00014-90-J-1167)
(AD-A265705; TR-20) Avail: CASI HC A03/MF A01

Surface Enhanced Raman and glancing angle FTIR are used to characterize the structure of self-assembled monolayers of viologen derivatives at electrode surfaces. Both techniques rely on the surface selection rules. These monolayers were found to have some degree of order, with the long axis of the viologen group found to be along the surface normal. DTIC

N94-12351# Washington Univ., Seattle. Dept. of Physiology and Biophysics.

ROLE OF SPATIALLY DISTRIBUTED ION CHANNELS IN SINGLE NEURON COMPUTATION Final Report, 1 Mar. 1990 - 15 Dec. 1992

Peter C. Schwindt 17 May 1993 5 p
(Contract N00014-90-J-1627)
(AD-A265972) Avail: CASI HC A01/MF A01

Towards the overall goal of making an accurate mathematical model of a neocortical pyramidal neuron, (1) the electrical properties of Na+ and Ca2+ channel subtypes were measured in sufficient detail to construct a quantitative empirical model, and (2) antibodies were raised against the a1 subunits of these channel subtypes in order to determine their spatial distribution and relative density using quantitative immunocytochemistry. DTIC

N94-12373# Bowling Green State Univ., OH. Center for Photochemical Sciences.

VIBRATIONAL OVERTONE ACTIVATION OF METHYLCYCLOPROPENE

Geoff Snavely, Salah Hassoon, and D. L. Snavely 27 May 1993 10 p
(Contract N00014-83-K-4130)
(AD-A265588; TR-12) Avail: CASI HC A02/MF A01

The photoisomerization of 1-methylcyclopropene (MCPene) was studied at specific internal energies accessed by laser vibrational overtone activation. The vibrational overtone spectrum of the 6-0 and 5-0 CH stretches were observed for our synthesized mixture of 75% MCPene and 25% methylenecyclopropane (MCPane). The overtone spectrum of neat MCPane was determined in the spectral regions. The transition wavenumbers were compared to the previously known members of the vinyl, methylenic, and methyl vibrational progressions. Product yields from activation through the 5-0 vinyl and methyl CH stretches were determined using gas chromotography. Product ratios of 1,3-butadiene to 2-butyne were measured as a function of pressure and compared to the RRKM predicted yields. After careful measurements we conclude that at these photolysis energies methylcyclopropene does not produce methylenecyclopropane. DTIC

N94-12378# Cornell Univ., Ithaca, NY.

MAPPING CLOSURES FOR TURBULENT COMBUSTION Annual Report, 15 Feb. 1992 - 14 Feb. 1993

Stephen B. Pope 31 Mar. 1993 11 p
(Grant AF-AFOSR-0184-91)
(AD-A265671; AFOSR-93-0380TR) Avail: CASI HC A03/MF A01

The overall objective of the research program is to develop and test an improved model for the process of molecular diffusion in turbulent reactive flows. In application to turbulent combustion, a major shortcoming of existing models is that they are non-local in composition. A model based on the construction of a Euclidean minimum spanning tree (EMST) has been developed. This model is inspired by the mapping closure and reduces to it in the case of a single composition. In general, the model is asymptotically local and hence, overcomes a major flaw in previous models. Additionally, studies have been made of stochastic Lagrangian models for turbulent reactive flows, and an exact expression has been obtained for the probability density function of temperature (or other random quantities) in statistically stationary turbulence. DTIC

N94-12403# California Univ., San Diego, La Jolla.

THEORIES OF TURBULENT COMBUSTION IN HIGH SPEED FLOWS Annual Report, Apr. 1992 - Apr. 1993

P. A. Libby and F. A. Williams 9 Apr. 1993 7 p
(Contract F49620-92-J-0184)
(AD-A265735; AFOSR-93-0382TR) Avail: CASI HC A02/MF A01

This research involves theoretical studies of the chemical and fluid mechanical phenomena which make turbulent combustion in high-speed flows different from such combustion in low-speed flows. Finite-rate chemistry plays a significant role in high-speed flows because of the small ratios of flow times to chemical times. The study addresses ignition and extinction phenomena in the nonpremixed turbulent combustion of hydrogen-air systems by both numerical and asymptotic methods. Attention also is paid to the effects of compressibility in high-speed turbulent combustion, with consideration given to interdispersal configurations of shocklets and flamelets. Efforts are made to provide a firmer foundation for the modeling of high-speed turbulent reacting flows, to aid in the development of a formulation which gives results that can be compared with experiments, and on turbulent combustion. DTIC

N94-12415# Naval Research Lab., Washington, DC.

METHANOL PAN FIRES IN AN ENCLOSED SPACE: EFFECT OF PRESSURE AND OXYGEN CONCENTRATION

J. L. Bailey, F. W. Williams, and P. A. Tatem 24 Mar. 1993 55 p
(AD-A266108; NRL/MR/6180-93-7310) Avail: CASI HC A04/MF A01

A series of fire tests was conducted in FIRE I, a large-scale pressurizable fire test chamber, to investigate the effect of pressure and oxygen concentration on methanol pan fires. As the oxygen concentration decreased from 21 vol-% to 13.5 vol-% throughout the experiments, the mass loss rate linearly decreased from 10 kg/hr to 6.6 kg/hr. Below 13.5 vol-% oxygen concentration, the mass loss rate rapidly declined. The fire self-extinguished when the oxygen concentration level approached 12 vol-%. An increase in initial chamber pressure from 14.7 psi to 23.9 psi (at 21 vol-% initial oxygen concentration) increased the burning rate by 34%. Experiments are planned at combinations of higher than ambient pressures and lower than ambient oxygen concentrations in order to quantify the combined effect of these variables on the mass loss rate of methanol. Experiments are also planned to determine the effect of pressure and oxygen concentration on the burning rates of other fuels. DTIC

N94-12534# Oregon Univ., Eugene. Dept. of Chemistry.

NONLINEAR OPTICAL SPECTROSCOPY OF Ag(111) IN ELECTROLYTE AND IN VACUUM Technical Report No. 2, May 1992 - May 1993

R. Bradley, R. Georgiadis, S. D. Kevan, and G. L. Richmond 27 May 1993 43 p
(Contract N00014-89-J-1261)
(AD-A265622) Avail: CASI HC A03/MF A01

In this paper, we investigate the electronic structure of a metal surface in the presence of aqueous electrolyte and an applied potential by optical second harmonic generation (SHG). We have obtained the detailed wavelength dependence (lambda(sub SH) = 300-350 nm) of the SH response from Ag(111) in both an aqueous electrolyte and in ultrahigh vacuum (UHV) and find that, when the Ag(111) electrode is biased at the potential of zero charge (PZC), the SH response is strongly correlated with the SH response in UHV. For the surface in both environments there is a sharp peak near 3.82 eV. Possible contributing factors to this peak are discussed. In the electrochemical environment, the effect of applied potential on the SH response at longer wavelengths, (nonresonant regime), is consistent both with previous observations at fixed frequencies and predictions of the surface charge density (SCD) model. At resonant wavelengths, there is a dramatic deviation from behavior predicted by the SCD model, a result consistent with previous experiments at discrete wavelengths. DTIC

N94-12538# Pittsburgh Univ., PA. Surface Science Center.

THE ADSORPTION AND SURFACE REACTION OF SiCl4 ON Si(100)-(2X1) Technical Report No. 57

Q. Geo, Z. Dohnalek, C. C. Cheng, W. J. Choyke, and J. T. Yates, Jr. 26 May 1993 30 p
(Contract N00014-82-0280)
(AD-A266124) Avail: CASI HC A03/MF A01

The adsorption and surface reaction of SiCl4 on Si(100)-(2x1) have been investigated in the temperature range of 100K-1000K. Adsorption of monolayer SiCl4 and multilayer SiCl4 are observed by temperature programmed desorption (TPD), high resolution electron energy loss spectroscopy (HREELS), and electron stimulated desorption ion angular distribution (ESDIAD). Upon heating to approx. 200K and above, Si-Cl bond scission in adsorbed SiCl4 occurs, depositing SiCl(x) species. Heating to 673K leaves the surface with only silicon monochloride species, SiCl(a), exhibiting Si-Cl stretching mode, vSiCl, at approx. 560 cm/cm, and a Cl(+) ESDIAD pattern indicative of inclined Si-Cl bond directions from Cl adsorbed on Si2 dimer sites. Silicon substrate etching occurs above 800K producing SiCl2(g) as the desorption product. Author (DTIC)

N94-10040# Societe Nationale de Construction Aeronautique, Gosselies (Belgium).

APPLICATION OF THE INFRARED PHOTOACOUSTIC SPECTROSCOPY TO THE STUDY OF THE CURE MECHANISMS OF STRUCTURAL EPOXY ADHESIVES

J. L. Coppee *In* ESA, Advanced Materials for Lightweight Structures Oct. 1992 p 233-238 (For primary document see N94-10001 01-24)
Copyright Avail: CASI HC A02/MF A04

N94-10228# Technische Univ., Berlin (Germany). Iwan-N. Stranski Inst.
STUDIES OF CRITICAL POINT PHENOMENA OF FLUIDS: BULK FLUIDS, FLUIDS IN PORES, AND AT INTERFACES
Gerhard H. Findenegg, M. Thommes, and T. Michalski *In* ESA, Proceedings of the 8th European Symposium on Materials and Fluid Sciences in Microgravity, Volume 2 Aug. 1992 p 795-800 (For primary document see N94-10171 01-29)
Copyright Avail: CASI HC A02/MF A04; ESA, EPD, ESTEC, Noordwijk, Netherlands, HC

N94-10248# McGill Univ., Montreal (Quebec).
MICROGRAVITY COMBUSTION OF DUST SUSPENSION IN A SPHERICAL CHAMBER
John H. S. Lee, Olivier Peraldi, Rom Knystautas, and Robert Thirsk (Canadian Space Agency, Ottawa, Ontario.) *In* ESA, Proceedings of the 8th European Symposium on Materials and Fluid Sciences in Microgravity, Volume 2 Aug. 1992 p 905-908 (For primary document see N94-10171 01-29) (Contract CSA-9F007-1-80-22)
Copyright Avail: CASI HC A01/MF A04; ESA, EPD, ESTEC, Noordwijk, Netherlands, HC

N94-10783# Maryland Univ., College Park. Dept. of Fire Protection Engineering.
APPLICATIONS OF A MODEL TO PREDICT FLAME SPREAD OVER INTERIOR FINISH MATERIALS IN A COMPARTMENT
James G. Quintiere, Gerald Haynes, and Brian T. Rhodes *In* FAA, Proceedings of the International Conference for the Promotion of Advanced Fire Resistant Aircraft Interior Materials Mar. 1993 p 207-224 (For primary document see N94-10766 01-03)
Avail: CASI HC A03/MF A03

N94-10784# National Research Council of Canada, Ottawa (Ontario). National Fire Lab.
THE OSU HEAT RELEASE RATE TEST USING THE OXYGEN CONSUMPTION PRINCIPLE
Yoshio Tsuchiya *In* FAA, Proceedings of the International Conference for the Promotion of Advanced Fire Resistant Aircraft Interior Materials Mar. 1993 p 225-232 (For primary document see N94-10766 01-03)
Avail: CASI HC A02/MF A03

N94-10785# Benjamin/Clarke Associates, Inc., Kensington, MD.
PRACTICAL HAZARD ASSESSMENT: AN APPROACH TO THE FIRE SAFETY
Frederic B. Clarke and James R. Hoover (Du Pont de Nemours, E. I. and Co., Wilmington, DE.) *In* FAA, Proceedings of the International Conference for the Promotion of Advanced Fire Resistant Aircraft Interior Materials Mar. 1993 p 233-244 (For primary document see N94-10766 01-03)
Avail: CASI HC A03/MF A03

N94-10787# National Inst. of Standards and Technology, Gaithersburg, MD. Building and Fire Research Lab.
DEVELOPMENTS NEEDED TO EXPAND THE ROLE OF FIRE MODELING IN MATERIAL FIRE HAZARD ASSESSMENT
Andrew J. Fowell *In* FAA, Proceedings of the International Conference for the Promotion of Advanced Fire Resistant Aircraft Interior Materials Mar. 1993 p 255-262 (For primary document see N94-10766 01-03)
Avail: CASI HC A02/MF A03

N94-10788# Factory Mutual Research Corp., Norwood, MA.
FLAMMABILITY PARAMETERS OF MATERIALS: IGNITION, COMBUSTION, AND FLAME SPREAD
A. Tewarson *In* FAA, Proceedings of the International Conference for the Promotion of Advanced Fire Resistant Aircraft Interior Materials Mar. 1993 p 263-281 (For primary document see N94-10766 01-03)
Avail: CASI HC A03/MF A03

N94-10789# Du Pont de Nemours (E. I.) and Co., Wilmington, DE. Advanced Fiber Systems.
FACTORS THAT AFFECT OSU THERMAL PERFORMANCE OF AIRCRAFT INTERIOR MATERIALS
Steven D. Beare *In* FAA, Proceedings of the International Conference for the Promotion of Advanced Fire Resistant Aircraft Interior Materials Mar. 1993 p 283-296 (For primary document see N94-10766 01-03)
Avail: CASI HC A03/MF A03

N94-10790# Federal Aviation Administration, Atlanta, GA. Materials Fire Safety.
AIRCRAFT MATERIAL FIRE TESTING AND THE CREATION OF AN INTERNATIONAL WORKING GROUP
Richard G. Hill *In its* Proceedings of the International Conference for the Promotion of Advanced Fire Resistant Aircraft Interior Materials Mar. 1993 p 297-300 (For primary document see N94-10766 01-03)
Avail: CASI HC A01/MF A03

N94-12045*# Lockheed Engineering and Sciences Co., Houston, TX.
MINERALOGY OF CHONDRITIC INTERPLANETARY DUST PARTICLE IMPACT RESIDUES FROM LDEF Abstract Only
R. A. Barrett, M. E. Zolensky (National Aeronautics and Space Administration. Lyndon B. Johnson Space Center, Houston, TX.), and R. Bernhard *In* Lunar and Planetary Inst., Twenty-fourth Lunar and Planetary Science Conference. Part 1: A-F 1993 p 65-66 (For primary document see N94-12015 01-91)
Avail: CASI HC A01/MF A06

N94-12051*# Minnesota Univ., Minneapolis. School of Physics and Astronomy.
NITROGEN AND NOBLE GASES IN A GLASS SAMPLE FROM LEW88516 Abstract Only
R. H. Becker and R. O. Pepin *In* Lunar and Planetary Inst., Twenty-fourth Lunar and Planetary Science Conference. Part 1: A-F 1993 p 77-78 (For primary document see N94-12015 01-91)
Avail: CASI HC A01/MF A06

N94-12052*# California Inst. of Tech., Pasadena. Div. of Geological and Planetary Sciences.
THE STABILITY OF HIBONITE AND OTHER ALUMINOUS PHASES IN SILICATE MELTS: IMPLICATIONS FOR THE ORIGIN OF HIBONITE-BEARING INCLUSIONS Abstract Only
J. R. Beckett and E. Stolper *In* Lunar and Planetary Inst., Twenty-fourth Lunar and Planetary Science Conference. Part 1: A-F 1993 p 79-80 (For primary document see N94-12015 01-91)
Avail: CASI HC A01/MF A06

N94-12082*# National Aeronautics and Space Administration. Lyndon B. Johnson Space Center, Houston, TX.
NOBLE GASES IN LEW88516 SHERGOTTITE: EVIDENCE FOR EXPOSURE AGE PAIRING WITH ALH77005 Abstract Only
D. D. Bogard and D. H. Garrison *In* Lunar and Planetary Inst., Twenty-fourth Lunar and Planetary Science Conference. Part 1: A-F 1993 p 139-140 (For primary document see N94-12015 01-91)
Avail: CASI HC A01/MF A06

N94-12087*# Sandia National Labs., Albuquerque, NM.
SI-29 NMR SPECTROSCOPY OF NATURALLY-SHOCKED QUARTZ FROM METEOR CRATER, ARIZONA: CORRELATION TO KIEFFER'S CLASSIFICATION SCHEME Abstract Only
M. B. Boslough, R. T. Cygan, and R. J. Kirkpatrick (Illinois Univ., Urbana.) *In* Lunar and Planetary Inst., Twenty-fourth Lunar and Planetary Science Conference. Part 1: A-F 1993 p 149-150 (For primary document see N94-12015 01-91)
Avail: CASI HC A01/MF A06

N94-12096*# Arizona Univ., Tucson. Lunar and Planetary Lab.
TRACE-ELEMENT ABUNDANCES IN SEVERAL NEW UREILITES Abstract Only
William V. Boynton and Dolores H. Hill *In* Lunar and Planetary Inst., Twenty-fourth Lunar and Planetary Science Conference. Part 1: A-F

1993 p 167-168 (For primary document see N94-12015 01-91)
Avail: CASI HC A01/MF A06

N94-12099*# MVA, Inc., Norcross, GA.
CARBON ANALYSES OF IDP'S SECTIONED IN SULFUR AND SUPPORTED ON BERYLLIUM FILMS Abstract Only
J. P. Bradley, L. Keller (National Aeronautics and Space Administration. Lyndon B. Johnson Space Center, Houston, TX.), K. L. Thomas (Lockheed Corp., Houston, TX.), T. B. VanderWood, and D. E. Brownlee (Washington Univ., Seattle.) *In* Lunar and Planetary Inst., Twenty-fourth Lunar and Planetary Science Conference. Part 1: A-F 1993 p 173-174 (For primary document see N94-12015 01-91)
Avail: CASI HC A01/MF A06

N94-12110*# Arizona Univ., Tucson. Lunar and Planetary Lab.
THE SPECTRAL EFFECTS OF SUBSOLIDUS REDUCTION OF OLIVINE AND PYROXENE Abstract Only
D. T. Britt *In* Lunar and Planetary Inst., Twenty-fourth Lunar and Planetary Science Conference. Part 1: A-F 1993 p 195-196 (For primary document see N94-12015 01-91)
Avail: CASI HC A01/MF A06

N94-12156*# Arizona State Univ., Tempe. AX646679
THERMAL-INFRARED EMISSION SPECTROSCOPY OF NATURAL SURFACES: APPLICATION TO COATED SURFACES Abstract Only
Philip R. Christensen, Stephanie T. Harrison (National Aeronautics and Space Administration. Goddard Space Flight Center, Greenbelt, MD.), Paul Barbera, and Steve Ruff *In* Lunar and Planetary Inst., Twenty-fourth Lunar and Planetary Science Conference. Part 1: A-F 1993 p 287-288 (For primary document see N94-12015 01-91)
Avail: CASI HC A01/MF A06

N94-12214*# Academy of Sciences (USSR), Moscow.
THE CORRELATION OF ALKALIS AND ALUMINUM DURING HIGH-TEMPERATURE VOLATILIZATION OF ALBITE AND NEPHELINE Abstract Only
Yu. P. Dikov, M. V. Gerasimov, O. I. Yakovlev, and F. Wlotzka (Max-Planck-Inst. fuer Chemie, Mainz, Germany.) *In* Lunar and Planetary Inst., Twenty-fourth Lunar and Planetary Science Conference. Part 1: A-F 1993 p 403-404 (For primary document see N94-12015 01-91)
Avail: CASI HC A01/MF A06

N94-12256*# Academy of Sciences (USSR), Moscow. Inst. of Geochemistry and Analytical Chemistry.
THE FRACTIONATION OF NOBLE GASES IN DIAMONDS OF CV3 EFREMOVKA CHONDRITE Abstract Only
A. V. Fisenko, A. B. Verchovsky, L. F. Semjonova, and Yu. A. Shukolyukov *In* Lunar and Planetary Inst., Twenty-fourth Lunar and Planetary Science Conference. Part 1: A-F 1993 p 487-488 (For primary document see N94-12015 01-91)
Avail: CASI HC A01/MF A06

N94-12258*# Stanford Univ., CA. Dept. of Geology.
NMR SPECTROSCOPY OF EXPERIMENTALLY SHOCKED SINGLE CRYSTAL QUARTZ: A REEXAMINATION OF THE NMR SHOCK BAROMETER Abstract Only
P. S. Fiske, A. J. Gratz (Lawrence Livermore National Lab., CA.), and W. J. Nellis (Lawrence Livermore National Lab., CA.) *In* Lunar and Planetary Inst., Twenty-fourth Lunar and Planetary Science Conference. Part 1: A-F 1993 p 491-492 (For primary document see N94-12015 01-91)
Avail: CASI HC A01/MF A06

N94-12316*# Stanford Univ., CA. Center for Turbulence Research.
THE EVOLUTION EQUATION FOR THE FLAME SURFACE DENSITY IN TURBULENT PREMIXED COMBUSTION
Arnaud Trouve *In its* Annual Research Briefs, 1992 Jan. 1993 p 393-409 (For primary document see N94-12284 01-34)
Avail: CASI HC A03/MF A04

N94-12317*# Stanford Univ., CA. Center for Turbulence Research.
STUDY AND MODELING OF FINITE RATE CHEMISTRY EFFECTS IN TURBULENT NON-PREMIXED FLAMES
Luc Vervisch *In its* Annual Research Briefs, 1992 Jan. 1993 p 411-429 (For primary document see N94-12284 01-34)
Avail: CASI HC A03/MF A04

N94-12319*# Stanford Univ., CA. Center for Turbulence Research.
WHY DOES PREFERENTIAL DIFFUSION STRONGLY AFFECT PREMIXED TURBULENT COMBUSTION?
Vadim R. Kuznetsov (Izdatelstvo Nauka, Moscow, USSR.) *In its* Annual Research Briefs, 1992 Jan. 1993 p 443-453 (For primary document see N94-12284 01-34)
Avail: CASI HC A03/MF A04

26 METALLIC MATERIALS

Includes physical, chemical, and mechanical properties of metals, e.g., corrosion; and metallurgy.

N94-10297# Metals Information Analysis Center, West Lafayette, IN.
BIBLIOGRAPHY ON HOT ISOSTATIC PRESSING (HIP) TECHNOLOGY
B. F. Gilp, P. D. Desai, J. F. Radavich, and C. Y. Ho Nov. 1992 325 p
(Contract DLA900-90-D-0305)
(AD-A265668; MIAC-1) Avail: CASI HC A14/MF A03

This report contains an annotated bibliography of 950 documents on the Hot Isostatic Pressing (HIP) Technology dealing with metals, alloys, and intermetallic compounds and covers over 450 materials. Documents published from 1966 to early 1992 are covered. Bibliographic information reported here are divided into three broad categories. The first category includes an annotated bibliography dealing with HIP technology as applied to powder metallurgy. The second category deals with casting and the third deals with miscellaneous materials which either are not properly identified or have a limited number of bibliographic citations. Within each category, bibliographic information is organized according to major alloy groups, e.g., aluminum alloys, beryllium alloys, cobalt alloys, etc., followed by bibliographies for miscellaneous alloys which are alloys either not properly identified or not having enough data to warrant a separate category. Each alloy group is further subdivided into individual commercial alloys, e.g., aluminum alloys AA 2024, AA 7075, AA 7090, etc., followed by miscellaneous aluminum alloys. DTIC

N94-10504*# National Aeronautics and Space Administration. Goddard Space Flight Center, Greenbelt, MD.
FRACTOGRAPHY HANDBOOK OF SPACEFLIGHT METALS
Rebecca J. Derro Washington Jun. 1993 126 p
(NASA-RP-1291; Rept-93B00019; NAS 1.61:1291) Avail: CASI HC A07/MF A02

This handbook was produced with the intention of providing failure analysts who work with space flight metals a reference of scanning electron microscope (SEM) fractographs of fracture surfaces produced under known condition. The metals and the fracture conditions were chosen to simulate situations that are encountered in spaceflight applications. This includes tensile overload at both room temperature and liquid nitrogen temperature, and fatigue at room temperature. Author

N94-10522# Lawrence Livermore National Lab., CA.
MONTE CARLO SIMULATIONS OF PHASE TRANSFORMATIONS IN Fe-Cr ALLOYS
L. Reinhard and P. E. A. Turchi 1 Dec. 1992 8 p Presented at the 16th Material Research Society International Symposium on the Scientific Basis for Nuclear Waste Management Fall Meeting, Boston, MA, 30 Nov. - 5 Dec. 1992
(Contract W-7405-eng-48)
(DE93-013847; UCRL-JC-111004; CONF-921101-117) Avail: CASI HC A02/MF A01

Phase stability properties of bcc based Fe-Cr alloys are examined in the framework of the first-principles KKR-CPA-GPM formalism and Monte Carlo simulations. For Fe-rich alloys, ordered configurations are found stable with respect to the random state of the alloy, but unstable with respect to the pure Fe and Cr metals. Results are compared with the ones obtained by using energy parameters extracted from experimental diffuse scattering data. DOE

N94-10732# National Aerospace Lab., Tokyo (Japan). Space Technology Research Group.
EFFECT OF SURFACE CLEANLINESS OF BEARING STEEL ON ADHESIVE STRENGTH AND TRIBOLOGICAL PROPERTIES OF SPUTTER-DEPOSITED GOLD FILMS [KINMAKU NO FUCHAKU KYOUDO OYOBI JUNKATSU TOKUSEI NI OYOBOSU JIKUUKEKOU KIBAN HYOUMEN SEIJOUDO NO EIKYOU]
Makoto Nishimura and Akihiko Matsui Apr. 1992 22 p In JAPANESE
(DE93-767974; NAL-TR-1148; JTN-93-80431) Avail: CASI HC A03/MF A01

The tribological responses of gold films sputtered on bearing steel and the effects of surface cleanliness on the film's adhesive strength were studied using X-ray Photoelectron Spectroscopy (XPS). To eliminate air contamination, a sputtering apparatus was built in the spectrometer and the gold film was directly deposited on characterized steel surfaces. The adhesion strength was evaluated by an epoxy resin adhesion strength measuring and also by a sliding friction test method conducted in nitrogen using a pin-on-disc type tester. Results showed the adhesive strength measuring method can effectively determine the existence of several tenth-layer to a monolayer of anti-rust agent. A sliding friction test indicated that the film's wear life was sensitive to the presence of oxygen and carbon following anti-rust agent removal by ion-bombardment. In addition, a monolayer of anti-rust agent, remaining on the surface after solvent cleaning, was found to lower the friction coefficient in the first ten repeated traverses under the test conditions employed. Author (NASDA)

N94-10804*# Compressor Components Textron, Inc., Cleveland, OH. Materials and Manufacturing Technology Center.
APPLICATION OF POWDER METALLURGY TECHNIQUES TO PRODUCE IMPROVED BEARING ELEMENTS FOR LIQUID ROCKET ENGINES Final Report, Feb. 1982 - Aug. 1992
D. J. Moracz, R. J. Shipley, V. S. Moxson, R. J. Killman, and H. E. Munson Aug. 1992 115 p
(Contract NAS8-34763)
(NASA-CR-193731; NAS 1.26:193731; EER-1041) Avail: CASI HC A06/MF A02

The objective was to apply powder metallurgy techniques for the production of improved bearing elements, specifically balls and races, for advanced cryogenic turbopump bearings. The materials and fabrication techniques evaluated were judged on the basis of their ability to improve fatigue life, wear resistance, and corrosion resistance of Space Shuttle Main Engine (SSME) propellant bearings over the currently used 440C. An extensive list of candidate bearing alloys in five different categories was considered: tool/die steels, through hardened stainless steels, cobalt-base alloys, and gear steels. Testing of alloys for final consideration included hardness, rolling contact fatigue, cross cylinder wear, elevated temperature wear, room and cryogenic fracture toughness, stress corrosion cracking, and five-ball (rolling-sliding element) testing. Results of the program indicated two alloys that showed promise for improved bearing elements. These alloys were MRC-2001 and X-405. 57mm bearings were fabricated from the MRC-2001 alloy for further actual hardware rig testing by NASA-MSFC. Author (revised)

N94-10842 Academy of Sciences of the Ukraine, Kiev. Inst. Yadernykh Issledovanij.
ON PROBLEM ABOUT NATURE OF PORTEVIN-LE CHATELIER EFFECT IN IRRADIATED ALUMINIUM ALLOYS [K VOPROSU O PRIRODE EHFFEKTA PORTEVENA-LE-SHATEL'E V OBLUCHENNYKH ALYUMINIEVYKH SPLAVAKH]
V. N. Drobyazin, S. P. Polovneva, Y. S. Podzirej, G. A. Soldatenko, and V. G. Vorobev 1991 15 p In RUSSIAN Limited Reproducibility: More than 20% of this document may be affected by microfiche quality
(DE93-617200; KIYal-91-14) Avail: CASI HC A03 (US Sales Only)

The influence of hardening return, deformation ageing, and gamma-irradiation on the Portevin-le-Chatelier effect in aluminum alloys (D16, D95, AK4, and AK6) was investigated. It was shown that the hardening temperature slightly influences on the discontinuous current nature, whereas the temperature and ageing on return causes the considerable changes of Portevin-le-Chatelier. It was shown that the irradiation of gamma-quantum low doses causes the Portevin-le-Chatelier effect in natural-aged state of alloy and disappearance of its effect during the subsequent ageing or during the irradiation with high doses. DOE

N94-10957# Ames Lab., IA.
PARTICLE ATTRACTION EFFECTS ON THE CENTRIFUGAL CASTING AND EXTRUSION OF ALUMINA
C. H. Schilling, L. Bergstroem (Stockholm Univ., Sweden.), H. L. Ker (Princeton Univ., NJ.), and I. A. Aksay (Princeton Univ., NJ.) 1993 17 p Presented at the 95th Annual Meeting of the American Ceramic Society, Cincinnati, OH, 18-22 Apr. 1993
(Contract W-7405-eng-82)
(DE93-011559; IS-M-744; CONF-930438-4) Avail: CASI HC A03/MF A01

Interparticle attraction forces were empirically related to the centrifugal casting and extrusion behavior of flocculated alumina suspensions. Attractive forces were altered by two approaches: salt flocculation, which entails regulating the electrical double-layer thickness through electrolyte additions; and screening of van der Waals attraction by steric interactions of surface-adsorbed fatty acids. Specimens produced by both methods exhibited a shift from high to low compressibility at a critical maximum density that increased with decreasing interparticle attraction. Gradients in packing density during centrifugal casting were alleviated using both methods as long as spatial variations of the effective stress were within the low-compressibility range. We hypothesized that the reduced interparticle attraction in both methods may also raise the threshold packing density at which ductile-to-brittle transitions occur during plastic shear. Specimens prepared with oleic acid adlayers were highly plastic and easily extrudable at solids contents of up to 59 vol%, although salt-flocculated samples at 55 vol% density extruded at creeping flow rates that were insensitive to the applied pressure. Results suggested that particle rearrangement during shear is a rate-limiting process, with an average relaxation time that is lowered by reducing interparticle attraction. DOE

N94-11008# Missouri Univ., Rolla. Rock Mechanics and Explosives Research Center.
TITANIUM ALLOYS MILLING ASSISTANCE BY HIGH PRESSURE LUBRICOOLANT JET
M. Mazurkiewicz 12 Nov. 1992 9 p
(Contract DE-FG01-90CE-15467)
(DE93-013302; DOE/CE-15467/T1) Avail: CASI HC A02/MF A01

The study of high pressure lubricooling jet injection into tool/chip interface showed good results by decreasing friction, tool forces, and temperature at tool/chip interface. Tool wear vs time using different cooling conditions at 1.52 mm depth of cut is shown. Surface roughness generated is in lower range for water jet assisted tool. A test chart is given for visualization of chip formation. DOE

N94-11076# Lawrence Livermore National Lab., CA.
DAMPING MEASUREMENTS FOR ULTRA-HIGH CARBON STEEL/BRASS LAMINATES
B. P. Bonner, D. R. Lesuer, C. K. Syn, A. E. Brown, and O. D. Sherby (Stanford Univ., CA.) 26 Oct. 1992 7 p Presented at the Minerals, Metals, and Materials Society/American Society for Metals Materials Week 1992, Chicago, IL, 2-5 Nov. 1992
(Contract W-7405-eng-48)
(DE93-011886; UCRL-JC-110334; CONF-9211117-6) Avail: CASI HC A02/MF A01

Damping measurements were made at high and low frequencies to investigate laminated metal composites (LMC's) consisting of ultrahigh carbon steel and brass for use in applications that require high damping capacity while maintaining strength and toughness. Properties of such laminates can be tailored through the selection of the component materials, volume percentage of the materials, layer thickness, interface strength, and microstructural control. Damping was measured in the ultrasonic range (2.25 MHz) with pulse-echo torsional oscillator from 2 to 40 Hz in shear strain range 10(exp -7) to 10(exp -6). Results at low frequencies indicate that Q(sub s)(exp -1) is 2 to 3 times higher than that of the highest damping component (brass). Damping is also independent of the layer orientation. Ultrasonic attenuation is much larger than for the component materials, with insertion losses approximately 100 dB/m greater than either component. Microstructure (metallography, SEM) and correlations between laminate structure and damping behavior are discussed. DOE

N94-11108# Oak Ridge National Lab., TN.
A HISTORY OF TUNGSTEN- AND MOLYBDENUM-BASE ALLOYS

R. L. Heestand 1993 9 p Presented at the Annual Meeting of The Metallurgical Society, Denver, CO, 21-25 Feb. 1993
(Contract DE-AC05-84OR-21400)
(DE93-010283; CONF-930202-8) Avail: CASI HC A02/MF A01

The development of tungsten and molybdenum alloys was initiated in the early 1900s in search of a better electric lamp filament with tantalum, tungsten, rhenium, and osmium being the prime candidates. The efforts required for accomplishment of the task led to refining oxides to high purity, reduction of the oxides to metal powders, forming green product forms by extrusion or pressing, and finally sintering by electric furnace and self-heating by direct current almost to the melting point. The technology required for producing lamp filaments led to the development of the powder metallurgy field and early research on high-melting-temperature metals. During the period 1909 through 1959, most of the tungsten-molybdenum, high-melting-temperature element alloys were developed and produced in almost any product form required. DOE

N94-11127# Xform, Inc., Cohoes, NY.
PRODUCTION OF REACTIVE SINTERED NICKEL ALUMINIDE
R. M. Cooper 1993 8 p
(Contract DE-FG01-91CE-15492)
(DE93-014434; DOE/CE-15492/T4) Avail: CASI HC A02/MF A01

Our efforts over the past 3 months were directed at increasing manufacturing capacity (ball milling) and improving product quality. Orders for the powder have increased, mainly for plasma spray powders. NiAl is an excellent coat between a metal and a ceramic, and its use, instead of cobalt, should extend operating range for carbide tools. The feather phase in the sintered Ni3Al was identified to be a Ni-rich phase nucleated on the grain boundaries with 10 wt % Al composition. The ductile to brittle temperature of powder extruded NiAl was found to be between 500 and 600 C and shows a 50% elongation at 600 C. DOE

N94-11141# Edgerton, Germeshausen and Grier, Inc., Idaho Falls, ID.
PROCESSING, PROPERTIES, AND WEAR RESISTANCE OF ALUMINIDES
R. N. Wright, B. H. Rabin, and J. K. Wright Mar. 1993 42 p
(Contract DE-AC07-76ID-01570)
(DE93-012186; EGG-MS-10441) Avail: CASI HC A03/MF A01

Fully dense alloys based on Fe3Al were produced by reaction synthesis from low cost elemental powders using hot pressing, hot isostatic pressing, or the Ceracon process. The reaction proceeds by outward spreading of a transient liquid phase from the initial aluminum particle site and precipitation of the compound phase from the liquid. Combustion synthesized material has a very fine grain size that is resistant to coarsening at high temperature because of a high density of fine oxides from the prior particle boundaries. The fine grain size results in approximately twice the yield strength in the reaction synthesized material compared to hot extruded pre-alloyed powder. Combustion synthesis has also been successfully applied to joining Fe3Al and to forming coatings on carbon steel substrates. Combustion synthesis has been shown to be viable for fabricating trialuminides from elemental powder compacts. Al3Ti, Al73Ti24Cr3, and Al67Ti25Cr8 were examined. Fully dense, homogeneous materials exhibiting an equiaxed grain structure were produced by conducting reaction and homogenization under pressure, or in a furnace at ambient pressure and subsequently densifying the porous preform by hot consolidation. The tetragonal DO22 structure was the primary reaction product for all compositions. Most of the Cr remained undissolved after reaction and a homogenization heat treatment at 1200 C or above was used to put the Cr into solution and form the desired L1(sub 2) phase. DOE

N94-11250# Westinghouse Savannah River Co., Aiken, SC.
A SURVEY OF TECHNIQUES FOR CORROSION MONITORING
J. I. Mickalonis Oct. 1992 10 p
(Contract DE-AC09-89SR-18035)
(DE93-012131; WSRC-TR-92-472) Avail: CASI HC A02/MF A01

Corrosion monitoring techniques have improved with advances in instrumentation technology and corrosion research. Older techniques, such as coupon immersion, generally provide historical information. The new electrochemical techniques, which have not been used widely at SRS, allow on-line monitoring and correlation with process changes. These techniques could improve the corrosion assessment of the waste tanks to be used for In-Tank Precipitation and Extended Sludge Processing. A task was initiated to place an electrochemical probe into tank 48 for testing the utility of this technique for waste tank applications. DOE

N94-11316 Pennsylvania State Univ., University Park.
EXPERIMENTAL PROOF OF THE NEW IR-INDUCED MECHANISM OF CREVICE CORROSION AND ITS CONSEQUENCES REGARDING PROTECTION SCHEMES Ph.D. Thesis
Kyehyun Cho 1992 164 p
Avail: Univ. Microfilms Order No. DA9311610

Recent results have shown that crevice corrosion of iron occurs solely by a shift of the local electrode potential into the active region of the polarization curve, this shift of potential to the less oxidizing direction is caused by the IR drop in the crevice electrolyte. Thus, crevice corrosion occurs when IR greater than IR*, where IR is the voltage drop in the electrolyte between the cathodic site at the outer surface (where oxygen is plentiful) and the crevicing site, and IR* is the potential difference between the electrode potential at the outer surface (cathodic site) established by the oxidant (or power supply) and the electrode potential of the active/passive transition of the crevice electrolyte. The local electrode potential inside the crevice and the pH of the crevice solution were measured and correlated to visually observed changes occurring within the crevice of an iron sample during the crevicing process in various electrolytes. It has been known that acidification and build-up of chloride inside the crevice are not prerequisite conditions for crevicing to occur. But acidification and chloride anions have been known to promote crevice corrosion. Therefore, acidification and chloride ions were investigated for their roles in promoting the IR greater than IR* criterion. Also, the roles of oxidizing power of the electrolyte, anodic inhibitors, solution resistance, and electrolyte temperature were studied in order to confirm the IR drop mechanism and apply it in engineering design. Acidification and chloride ions promote crevicing by a shift of the passivation potential to more noble potentials (IR decreases) and by increasing the active loop currents (IR increases), thereby facilitating the IR greater than IR* condition. Finally, based on the IR greater than IR* criterion, crevice corrosion can be suppressed by (1) shifting the surface potential (corrosion potential) in the more noble direction (increasing IR*), (2) adding inhibitors to the electrolyte that significantly shift E(sub pass) to less noble values (increasing IR*) and decrease I(sub max) (decrease IR), (3) increasing the solution conductivity (decreasing IR), and (4) decreasing the electrolyte temperature since lower temperatures decrease the active loop on the polarization curve. Dissert. Abstr.

N94-11363 Academy of Sciences of the Ukraine, Kharkov. Fiziko-Tekhnicheskij Inst.
A METHOD OF INFLUENCE REGIONS IN THE THEORY OF VACANCY SWELLING OF METALS [METOD OBLASTEJ VLIYANIYA V TEOTII VAKANSIONNOGO RASPUKHANIYA METALLOV]
P. N. Ostapchuk and V. V. Slezov 1992 64 p In RUSSIAN Limited Reproducibility: More than 20% of this document may be affected by microfiche quality
(DE93-620579; KFTI-92-14) Avail: CASI HC A04 (US Sales Only)

A new method is developed to calculate point defect fluxes for various sinks. The method takes into account the volume fraction of sinks similar to the well known effective medium approach. But in contrast to the latter in our method, we introduce sink-free regions around each sink. The sizes of the sinks are determined self-consistently. As an illustration, the defect fluxes to a void and an edge dislocation are found. The vacancy swelling of metals under irradiation is discussed in terms of results obtained. DOE

N94-11445# Army Research Lab., Watertown, MA.
EFFECT OF POWDER PROCESSING ON SLIP CASTING PARAMETERS AND SINTERING OF Si3N4-Y2O3-SiO2 Final Report
Gary Gilde and George Gazza Apr. 1993 16 p
(AD-A264474; ARL-TR-93) Avail: CASI HC A03/MF A01

A procedure was developed for slip casting Si3N4(-)Y2O3(-)SiO2 compositions. The silicon nitride was oxidized to supply the silica. The procedure resulted in 65 w/o slips with viscosities of 35 mPa(dot)s which, when cast, yielded compacts which were 56% of theoretical density. Slips with 70 w/o solids loading were also prepared having viscosities of 120 mPa(dot)s. The properties of the slips were influenced by the starting silicon nitride powder, dispersant, and milling media. The resulting compacts could be gas pressure sintered to full density, at temperatures as low as

1850 C, using nitrogen pressures as low as 4 MPa. Strengths as high as 750 MPa were achieved and the initial results show good creep resistance at 1350 C. DTIC

N94-11459# Brookhaven National Lab., Upton, NY.
IN SITU XANES STUDIES OF THE PASSIVE FILM ON Fe AND Fe-26Cr
A. J. Davenport, H. S. Isaacs, J. A. Bardwell (National Research Council of Canada, Ottawa, Ontario.), and B. MacDougall (National Research Council of Canada, Ottawa, Ontario.) 1993 10 p Presented at the European Symposium on Passive Films, Paris, France, 15-19 Feb. 1993
(Contract DE-AC02-76CH-00016)
(DE93-010869; BNL-48620; CONF-930271-2) Avail: CASI HC A02/MF A01

In situ x-ray absorption near edge structure (XANES) has been used to study the passive film on iron and Fe-Cr-26 thin films under potential control in borate buffer. The technique enables information on both valence state and the amount of material lost through dissolution to be determined. The passive films on both Fe and Fe-Cr are formed with negligible dissolution. On reduction, iron is lost from both films due to reductive dissolution. In the case of Fe, it has been determined that some of the iron in the film is reduced back to-the-metallic state. Concurrent monitoring of the Fe and Cr edges has shown that in the case of Fe-Cr, loss of iron leads to enrichment of Cr in the film. DOE

N94-11488# General Electric Co., Schenectady, NY.
THE EFFECT OF PROCESSING ON THE MICROSTRUCTURE AND TENSILE PROPERTIES OF A (GAMMA)-TiAl BASED ALLOY
G. E. Fuchs Feb. 1993 15 p Presented at the 7th World Conference and Exhibition on Titanium, San Diego, CA, 28 Jun. - 2 Jul. 1992
(Contract DE-AC12-76SN-00052)
(DE93-013221; KAPL-4737; CONF-920604-4) Avail: CASI HC A03/MF A01

Compositional and microstructural control, and alloying additions have been the primary methods used to increase the low temperature ductility of TiAl-based alloys. However, very little has been done to characterize the effect of processing on ductile gamma-TiAl alloys. The effect of processing on microstructure and properties of cast, wrought and powder metallurgy TiAl-based alloys with a similar nominal composition is examined. The alloy was Ti-48Al-2Nb-2Cr (at. %). After processing, all of the samples were heat treated in the alpha + gamma phase field. Microstructures were characterized by optical, scanning electron, and transmission electron microscopy. Tensile properties were evaluated in the temperature range 25-1000 C in air. The powder processed alloys exhibited the highest strength and ductility at test temperatures up to 850 C. All of the alloys exhibited similar tensile properties at 1000 C. Examination of fracture surfaces indicated that tensile failure occurred by predominantly transgranular cleavage at temperatures below 700 C. However, above 850 C, significant plastic deformation was observed, particularly in the powder metallurgy samples. The inter-relationships of processing-microstructure-mechanical properties of Ti-48Al-2Nb-2Cr (at. %) are discussed. DOE

N94-11593 Japan Atomic Energy Research Inst., Tokyo.
FACILITY FOR STRESS CORROSION CRACKING TEST OF IRRADIATED MATERIAL IN HIGH TEMPERATURE WATER
Takashi Tsukada (Japan Atomic Energy Research Inst., Tokai.), Kiyoyuki Shiba (Japan Atomic Energy Research Inst., Tokai.), Hajime Nakajima (Japan Atomic Energy Research Inst., Tokai.), Minoru Kizaki (Japan Atomic Energy Research Inst., Tokai.), Kenji Sudo (Japan Atomic Energy Research Inst., Tokai.), G. E. C. Bell, Masao Ohmi, and Ichiro Goto Jun. 1992 35 p Limited Reproducibility: More than 20% of this document may be affected by microfiche quality
(DE93-753189; JAERI-M-92-081) Avail: CASI HC A03

Irradiation assisted stress corrosion cracking (IASCC) is a synergistic effect of neutron irradiation, aqueous environment, and stress on nuclear core materials. In order to investigate the IASCC, a facility for stress corrosion cracking tests of irradiated materials was developed. The slow strain rate technique (SSRT) in high temperature and pressure water environment was employed. The post irradiation SSRT test facility consists of an SSRT test machine and a water circulation and purification system. In the design of the facility, attentions were paid to safe and reliable remote operation of heavily irradiated materials in hot cell. Main specification of the facility is as follows; maximum load capacity: 30 kN, strain rate range: 10(exp -7) s(sup -1) approximately 10(exp -3) s(sup -1), test temperature/pressure: 300 C and 10 MPa in maximum, water supply rate: 5 1/h, controllable range of dissolved oxygen (DO): 0.01 approximately 32 ppm. Water chemistry is monitored on DO, electric conductivity, and pH. Electrochemical potential and electric current are monitored and controlled on specimen. A preliminary test was carried out on the type 316 stainless steel irradiated up to 8 dpa in Oak Ridge Research Reactor under spectrally tailored condition. As a result of the test an occurrence of IASCC and a good performance of the facility were confirmed. DOE

N94-11668# Lawrence Livermore National Lab., CA.
PLATING UNDER REDUCED PRESSURE
J. W. Dini, T. G. Beat, W. C. Cowden, L. E. Ryan, and W. B. Hewitt (TRW, Inc., Redondo Beach, CA.) Jun. 1992 21 p Presented at the 1992 American Electroplaters and Surface Finishers Society Conference, Atlanta, GA, 22-25 Jun. 1992
(Contract W-7405-eng-48)
(DE93-011896; UCRL-JC-109782; CONF-9206129-4) Avail: CASI HC A03/MF A01

Plating under reduced pressure was evaluated for both electroless nickel and electrodeposited copper systems. The objective was to reduce pitting of these coatings thereby further enhancing their usage for diamond turning applications. Cursory experiments with electroless nickel showed reduced porosity when deposition was done at around 500 torr. Detailed experiments with electrodeposited copper at around 100 torr provided similar results. Scanning tunneling microscopy was effectively used to show the improvement in the copper deposits plated under reduced pressure. Benefits included reduced surface roughness and finer and denser grain structure. DOE

N94-11816# Lehigh Univ., Bethlehem, PA. Energy Research Center.
WELD OVERLAY COATINGS FOR EROSION CONTROL
B. Levin, J. N. DuPont, and A. R. Marder 3 Mar. 1993 22 p
(Contract DE-FG22-92PC-92542)
(DE93-013592; DOE/PC-92542/T1) Avail: CASI HC A03/MF A01

A literature review was made. In spite of similarities between abrasive wear and solid particle erosion, weld overlay hardfacing alloys that exhibit high abrasion resistance may not necessarily have good erosion resistance. The performance of weld overlay hardfacing alloys in erosive environments has not been studied in detail. It is believed that primary-solidified hard phases such as carbides and intermetallic compounds have a strong influence on the erosion resistance of weld overlay hardfacing alloys. However, relationships between size, shape, and volume fraction of hard phases in hardfacing alloys and erosion resistance were not established. Almost all hardfacing alloys can be separated into two major groups based upon chemical compositions of the primary solidified hard phases: (1) carbide hardening alloys (Co-base/carbide, WC-Co, and some Fe base superalloys); and (2) intermetallic hardening alloys (Ni-base alloys, austenitic steels, iron-aluminides). DOE

N94-12361 International Centre for Theoretical Physics, Trieste (Italy).
GRAIN BOUNDARY CREEP IN COPPER
A. Ayensu (Cape Coast Univ., Ghana.), G. K. Quainoo (Cape Coast Univ., Ghana.), and S. K. Adjepong (Cape Coast Univ., Ghana.) Oct. 1992 12 p Limited Reproducibility: More than 20% of this document may be affected by microfiche quality
(DE93-610974; IC-92/327) Avail: CASI HC A03 (US Sales Only)

Hard-drawn polycrystalline copper wires of 99.9% purity and grain size ranging from 90 to 125 microns produced by Kabelmetal (Ghana) Ltd. were creep tested within the temperature range of 0.42 to 0.57 T(sub m) at atmospheric pressure under uniaxial stress of 7.08 to 21.24 MPa. The stress exponent, n, determined ranges from 2.0 to 2.4 and the activation energy, delta(H), ranges from 61.3 to 63.2 kJ/mol. It was observed that n decreased with temperature and delta(H) decreased with stress. The deformation mechanism is attributed to grain boundary sliding and the self-diffusion of copper atoms within the grain boundary calculated on the Cobble model ranges from 2.2 x 10(exp -11) sq cm/s to 2.2 x 10(exp -10) sq cm/s. DOE

N94-12393# George Washington Univ., Washington, DC. Dept. of Chemistry.
CORROSION CONTROL BY VITREOUS FILMS ON ALUMINUM AND HIGH T(SUB c) SUPERCONDUCTORS Final Report, 1 Jan. 1991 - 31 Dec. 1992
David E. Ramaker 31 Dec. 1992 7 p
(Contract N00014-91-J-1896)
(AD-A266016) Avail: CASI HC A02/MF A01

Electron spectroscopy has become one of our most important tools for the study of electronic structure of solids and at surfaces. The passivation and inhibition of corrosion, utilizing the spectroscopic techniques of x-ray photoelectron spectroscopy (XPS), Auger electron spectroscopy (AES), and NEXAFS were studied. In particular, the passivation of Al and Al-alloys towards attack by Cl(-), and the utility of Zr-Ir alloys to serve as diffusion/reaction barriers on silicon and carbon at elevated temperatures was studied. DTIC

N94-12404# Texas Univ., Austin. Dept. of Mechanical Engineering.
CORROSION BEHAVIOR OF METAL MATRIX COMPOSITES Final Report, 1 Jul. 1989 - 30 Sep. 1992
Harovel G. Wheat 29 Jan. 1993 80 p
(Contract N00014-89-J-3116)
(AD-A265352) Avail: CASI HC A05/MF A01

A research program was conducted to assess the corrosion behavior of two categories of copper metal matrix composites: commercially available composites and composites in development. The commercially available composite studied was dispersion strengthened copper (2.7 vol % Al2O3/Cu) which was found to possess comparable corrosion resistance to copper. In addition, it did not appear to be susceptible to stress corrosion cracking when U-bend specimens were tested in 3.5 wt % NaCl or artificial seawater for a period of 4 months. Stress corrosion cracking was also not observed under proof ring loading in 3.5 wt % NaCl for a period of 8 months at an applied stress of 95% of the yield stress. The composites in development studied were HEHR Gr(sub p)/Cu composites containing 1.2, 5, 15, 25, and 40 vol % graphite; 50 vol % GR (sub f) Cu; and 70 vol % W (sub f) Cu. These composites experienced varying degrees of galvanic corrosion during polarization. Benzotriazole, however, offers excellent potential as a corrosion inhibitor for these composites. DTIC

N94-12418# United Technologies Corp., West Palm Beach, FL.
FATIGUE IN SINGLE CRYSTAL NICKEL SUPERALLOYS Technical Progress Report, 16 Mar. - 15 Apr. 1993
Daniel P. DeLuca and Charles Annis 15 Apr. 1993 6 p
(Contract N00014-91-C-0124)
(AD-A266116; PW/GESP-FR21998-18) Avail: CASI HC A02/MF A01

This program investigates the seemingly unusual behavior of single crystal airfoil materials. The fatigue initiation processes in single crystal (SC) materials are significantly more complicated and involved than fatigue initiation and subsequent behavior of a (single) macrocrack in conventional, isotropic materials. To understand these differences is the major goal of this project. DTIC

N94-12426 Southwest Research Inst., San Antonio, TX.
MICROSTRUCTURE-BASED FATIGUE LIFE PREDICTION METHODS FOR NAVAL STEEL STRUCTURES Quarterly Report
K. S. Chan, R. C. McClung, and T. Y. Torng 30 Jan. 1993 17 p
Limited Reproducibility: More than 20% of this document may be affected by microfiche quality
(Contract N00014-91-C-0214)
(AD-A265429) Avail: CASI HC A03

The ongoing development of new HSLA (high-strength, low alloy) steels for use in ship and submarine structures permits increases in design stress levels, which may in turn increase the significance of fatigue cracking as a threat to structural integrity. The subject program was motivated by the desire for improved understandings of the relationships between microstructure and fatigue damage in naval steel structures, with particular application to the prediction of fatigue life. Among the intended products of the study are improved methods for fatigue life prediction which give appropriate attention to different potential microstructures and associated microstructural influences on fatigue crack initiation and growth rates. The methods could be used to provide guidance in optimizing alloy chemistry, processing, and welding protocols for improved fatigue resistance, while also expediting improved fitness-for-service assessments of actual or postulated cracking. DTIC

N94-12447*# Pennsylvania State Univ., University Park. Dept. of Materials Science and Engineering.
NiAl ALLOYS FOR STRUCTURAL USES Final Report, 27 Oct. 1987 - 31 Dec. 1991
D. A. Koss 31 Dec. 1991 33 p
(Grant NAG3-827)
(NASA-CR-194113; NAS 1.26:194113) Avail: CASI HC A03/MF A01

Alloys based on the intermetallic compound NiAl are of technological interest as high temperature structural alloys. These alloys possess a relatively low density, high melting temperature, good thermal conductivity, and (usually) good oxidation resistance. However, NiAl and NiAl-base alloys suffer from poor fracture resistance at low temperatures as well as inadequate creep strength at elevated temperatures. This research program explored macroalloying additions to NiAl-base alloys in order to identify possible alloying and processing routes which promote both low temperature fracture toughness and high temperature strength. Initial results from the study examined the additions of Fe, Co, and Hf on the microstructure, deformation, and fracture resistance of NiAl-based alloys. Of significance were the observations that the presence of the gamma-prime phase, based on Ni3Al, could enhance the fracture resistance if the gamma-prime were present as a continuous grain boundary film or 'necklace'; and the Ni-35Al-20Fe alloy was ductile in ribbon form despite a microstructure consisting solely of the B2 beta phase based on NiAl. The ductility inherent in the Ni-35Al-20Fe alloy was explored further in subsequent studies. Those results confirm the presence of ductility in the Ni-35Al-20Fe alloy after rapid cooling from 750 - 1000 C. However exposure at 550 C caused embrittlement; this was associated with an age-hardening reaction caused by the formation of Fe-rich precipitates. In contrast, to the Ni-35Al-20Fe alloy, exploratory research indicated that compositions in the range of Ni-35Al-12Fe retain the ordered B2 structure of NiAl, are ductile, and do not age-harden or embrittle after thermal exposure. Thus, our recent efforts have focused on the behavior of the Ni-35Al-12Fe alloy. A second parallel effort initiated in this program was to use an alternate processing technique, mechanical alloying, to improve the properties of NiAl-alloys. Mechanical alloying in the conventional sense requires ductile powder particles which, through a cold welding and fracture process, can be dispersion strengthened by submicron-sized oxide particles. Using both the Ni-35Al-Fe alloys to contain approx. 1 v/o Y2O3. Preliminary results indicate that mechanically alloyed and extruded NiAl-Fe + Y2O3 alloys when heat treated to a grain-coarsened condition, exhibit improved creep resistance at 1000 C when compared to NiAl; oxidation resistance comparable to NiAl; and fracture toughness values a factor of three better than NiAl. As a result of the research initiated on this NASA program, a subsequent project with support from Inco Alloys International is underway. Derived from text

N94-12532# Naval Surface Warfare Center, Bethesda, MD. Ship Materials Engineering Dept.
ADVANCES IN LOW CARBON, HIGH STRENGTH FERROUS ALLOYS Research and Development Report
E. J. Czyryca and M. G. Vassilaros Apr. 1993 51 p
(AD-A265264; CDNSWC/SME-92/64) Avail: CASI HC A04/MF A01

Carderock Division, Naval Surface Warfare Center participated in the Indo-US Pacific Rim Workshop on 'Advances in Low Carbon, High Strength Ferrous Alloys' held in New Delhi, India, 25 to 28 March 1992. E.J. Czyryca and M.G. Vassilaros gave invited presentations on the status of Navy program on steel plate and weld metal research and development, respectively. The workshop was jointly sponsored by Office of Naval Research, Naval Research Laboratory, US Army Research Office - Far East, and the National Metallurgical Laboratory of India. This report contains papers based on the two presentations. Paper 1 - 'Advances in High Strength Steel Technology for Naval Hull Construction,' covers an overview of US Navy steel plate research programs. Paper 2 - 'The Development of High-Strength, Cooling-Rate Insensitive Ultra-Low-Carbon Weld Metals,' presents the status of research in high-strength steel weld metal systems based on ultra-low carbon bainitic (ULCB) metallurgy. ULCB weld metals show a potential for wire electrode formulations for HSLA steel welding, where the as deposited weld metal strength is independent of weld metal cooling rate with a good low-temperature toughness. DTIC

N94-10019# Tampere Univ. of Technology (Finland). Inst. of Materials Science.
COMPARISON OF Al-Fe ALLOYS PRODUCED BY PFC AND USGA TECHNIQUES
T. K. Lepisto, P. Kettunen, and J. Rautiola *In* ESA, Advanced Materials for Lightweight Structures Oct. 1992 p 109-112 Sponsored by Technology Development Center and USGA (For primary document see N94-10001 01-24)
Copyright Avail: CASI HC A01/MF A04

N94-10020# Centro Sviluppo Materiali S.p.A., Rome (Italy).
THE MICROSTRUCTURE AND MECHANICAL PROPERTIES OF HOT WORKED FeAl INTERMETALLIC ALLOYS
O. Tassa, C. Testani, and A. Lefort (CEREM, Grenoble, France.) *In* ESA, Advanced Materials for Lightweight Structures Oct. 1992 p 113-118 (For primary document see N94-10001 01-24)
Copyright Avail: CASI HC A02/MF A04

N94-10021# BHP Labs. Ltd., Limerick (Ireland).
ALUMINIUM-LITHIUM FORGINGS: PROPERTIES AND POTENTIAL SATELLITE APPLICATIONS
B. OBrien and A. Pradier (European Space Agency. European Space Research and Technology Center, ESTEC, Noordwijk, Netherlands.) *In* ESA, Advanced Materials for Lightweight Structures Oct. 1992 p 119-124 (For primary document see N94-10001 01-24)
Copyright Avail: CASI HC A02/MF A04

N94-10022# Southampton Univ. (England). Engineering Materials.
MECHANICAL AND FATIGUE PROPERTIES OF FIBRE REINFORCED ALUMINIUM-LITHIUM ALLOY AND ALUMINIUM-LITHIUM MMC BASED LAMINATES
E. P. Hunt, P. J. Gregson, R. Moreton (Defence Research Agency, Farnborough, England.), and C. J. Peel (Defence Research Agency, Farnborough, England.) *In* ESA, Advanced Materials for Lightweight Structures Oct. 1992 p 125-128 (For primary document see N94-10001 01-24)
Copyright Avail: CASI HC A01/MF A04

N94-10023# Deutsche Airbus G.m.b.H., Bremen (Germany).
INVESTIGATIONS ON ALUMINIUM-LITHIUM ALLOYS FOR DAMAGE TOLERANT APPLICATION
W. Zink, Y. Barbaux (Aerospatiale, Suresnes, France.), A. Camacho (Construcciones Aeronauticas S.A., Madrid, Spain.), H. Price (British Aerospace Public Ltd. Co., Bristol, England.), G. Vaessen (Fokker B.V., Amsterdam, Netherlands.), L. Tirilly (Pechiney Co., Paris, France.), S. Schwantes (Dornier System G.m.b.H., Friedrichshafen, Germany.), N. Bernicot (Dassault Aviation, Istres, France.), S. Pantelakis (Patras Univ., Greece.), and R. Grimes (British Aluminum Co. Ltd., London, England.) et al *In* ESA, Advanced Materials for Lightweight Structures Oct. 1992 p 129-134 (For primary document see N94-10001 01-24)
Copyright Avail: CASI HC A02/MF A04

N94-10028# Slovak Technical Univ., Trnava (Czechoslovakia). Dept. of Welding.
WELDABILITY OF MARAGING STEELS
Ryban Dusan *In* ESA, Advanced Materials for Lightweight Structures Oct. 1992 p 161-164 (For primary document see N94-10001 01-24)
Copyright Avail: CASI HC A01/MF A04

N94-10029# Brush Wellman, Inc., Cleveland, OH.
ALUMINUM-BERYLLIUM ALLOYS FOR AEROSPACE APPLICATIONS
D. Hashiguchi, A. N. Ashurst, F. C. Grensing, and J. M. Marder *In* ESA, Advanced Materials for Lightweight Structures Oct. 1992 p 165-169 (For primary document see N94-10001 01-24)
Copyright Avail: CASI HC A01/MF A04

N94-10060# Maschinenfabrik Augsburg-Nuernberg A.G., Munich (Germany).
CONSTITUTIVE LAWS FOR DESCRIBING THE SERVICE RELEVANT CREEP BEHAVIOUR OF METALLIC MATERIALS
P. Agatonovic, J. M. Church (Joint Research Centre of the European Communities, Petten, Netherlands.), and R. Hurst (Joint Research Centre of the European Communities, Petten, Netherlands.) *In* ESA, Advanced Materials for Lightweight Structures Oct. 1992 p 355-360 Sponsored by Commission of the European Communities (For primary document see N94-10001 01-24)
Copyright Avail: CASI HC A02/MF A04

N94-10190# Deutsche Forschungsanstalt fuer Luft- und Raumfahrt, Cologne (Germany). Space Simulation Inst.
THERMOPHYSICAL PROPERTIES OF UNDERCOOLED LIQUID METALS
Ivan Egry and Berndt Feuerbacher *In* ESA, Proceedings of the 8th European Symposium on Materials and Fluid Sciences in Microgravity, Volume 2 Aug. 1992 p 569-575 (For primary document see N94-10171 01-29)
Copyright Avail: CASI HC A02/MF A04; ESA, EPD, ESTEC, Noordwijk, Netherlands, HC

N94-10194# Academia Sinica, Beijing (China). Inst. of Physics.
SOLIDIFICATION OF UNDERCOOLED Ni-32.5 WT PERCENT Sn EUTECTIC ALLOY
L. Q. Xing, D. Q. Zhao, X. C. Chen, X. S. Chen, G. C. Yang (Northwestern Polytechnical Univ., Xian, China.), and Y. H. Zhou (Northwestern Polytechnical Univ., Xian, China.) *In* ESA, Proceedings of the 8th European Symposium on Materials and Fluid Sciences in Microgravity, Volume 2 Aug. 1992 p 597-602 (For primary document see N94-10171 01-29)
Copyright Avail: CASI HC A02/MF A04; ESA, EPD, ESTEC, Noordwijk, Netherlands, HC

N94-10195# Commissariat a l'Energie Atomique, Grenoble (France). Section d'Etudes de la Solidification et de la Cristallogenese.
UNDERCOOLED W-Re AND Mo-Re DROPS IN AN ULTRA HIGH VACUUM DROP TUBE
E. Cini, B. Vinet, L. Cortella, and J. Bletry *In* ESA, Proceedings of the 8th European Symposium on Materials and Fluid Sciences in Microgravity, Volume 2 Aug. 1992 p 603-607 (For primary document see N94-10171 01-29)
(Contract ESTEC-9638/91/NL/JSC)
Copyright Avail: CASI HC A01/MF A04; ESA, EPD, ESTEC, Noordwijk, Netherlands, HC

N94-10196# Deutsche Forschungsanstalt fuer Luft- und Raumfahrt, Cologne (Germany). Inst. fuer Raumsimulation.
NON-EQUILIBRIUM SOLIDIFICATION IN UNDERCOOLED Ni-B ALLOYS
Klaus Eckler, R. F. Cochrane (Leeds Univ., England.), M. Jurisch (Zentralinstitut fuer Festkoerperphysik und Werkstofforschung, Dresden, German D.R..), D. M. Herlach, and Berndt Feuerbacher *In* ESA, Proceedings of the 8th European Symposium on Materials and Fluid Sciences in Microgravity, Volume 2 Aug. 1992 p 609-614 (For primary document see N94-10171 01-29)
Copyright Avail: CASI HC A02/MF A04; ESA, EPD, ESTEC, Noordwijk, Netherlands, HC

N94-10197# Commissariat a l'Energie Atomique, Grenoble (France). Section d'Etudes de la Solidification et le la Cristallogenese.
GROUND RESULTS OF THE MEPHISTO PROGRAM: BENEFITS AND SPACE EXPERIMENTS ORIENTATION
Andre Rouzaud, J. Comera, P. Contamin, and Jean-Jacques Favier *In* ESA, Proceedings of the 8th European Symposium on Materials and Fluid Sciences in Microgravity, Volume 2 Aug. 1992 p 615-618 (For primary document see N94-10171 01-29)
Copyright Avail: CASI HC A01/MF A04; ESA, EPD, ESTEC, Noordwijk, Netherlands, HC

N94-10199# Technische Univ., Munich (Germany). Inst. for Materials and Processing Sciences.
EUSO-D2-EXPERIMENT: UNIDIRECTIONAL SOLIDIFICATION WITH QUENCHING OF AN AlSi11 ALLOY
Hans M. Tensi and Raimund Roesch *In* ESA, Proceedings of the 8th European Symposium on Materials and Fluid Sciences in Microgravity, Volume 2 Aug. 1992 p 629-633 Sponsored by BMFT (For primary document see N94-10171 01-29)
Copyright Avail: CASI HC A01/MF A04; ESA, EPD, ESTEC, Noordwijk, Netherlands, HC

N94-10202# Deutsche Forschungsanstalt fuer Luft- und Raumfahrt, Cologne (Germany). Space Simulation Inst.
OSTWALD RIPENING OF SOLID COBALT PARTICLES IN LIQUID COPPER
W. Bender, L. Ratke, and Berndt Feuerbacher *In* ESA, Proceedings of the 8th European Symposium on Materials and Fluid Sciences in Microgravity, Volume 2 Aug. 1992 p 645-649 (For primary document see N94-10171 01-29)
Copyright Avail: CASI HC A01/MF A04; ESA, EPD, ESTEC, Noordwijk, Netherlands, HC

N94-10204# Zentralinstitut fuer Festkoerperphysik und Werkstofforschung, Dresden (German D.R.). Inst. fuer Metallische Werkstoffe.
SOLIDIFICATION AND METASTABLE PHASE FORMATION OF HIGHLY UNDERCOOLED Fe-Cr-Ni ALLOY MELTS
W. Loeser, T. Volkmann (Deutsche Forschungsanstalt fuer Luft- und Raumfahrt, Cologne, Germany.), and Dieter M. Herlach (Deutsche Forschungsanstalt fuer Luft- und Raumfahrt, Cologne, Germany.) *In* ESA, Proceedings of the 8th European Symposium on Materials and Fluid Sciences in Microgravity, Volume 2 Aug. 1992 p 655-663 Sponsored by DLR (For primary document see N94-10171 01-29)
Copyright Avail: CASI HC A02/MF A04; ESA, EPD, ESTEC, Noordwijk, Netherlands, HC

N94-10231# Deutsche Forschungsanstalt fuer Luft- und Raumfahrt, Cologne (Germany). Inst. fuer Raumsimulation.
MEASUREMENTS OF HEAT CAPACITY IN UNDERCOOLED METALS
A. Bewersdorff, G. P. Goerler, Rainer Willnecker, Klaus Wittmann, R. Kuhl (Deutsche Agentur fuer Raumfahrtangelegenheiten G.m.b.H., Bonn, Germany.), R. Roestel, M. Guenter (Humboldt Univ., Berlin, German D.R..), and Genevieve Kell (Humboldt Univ., Berlin, German D.R..) *In* ESA, Proceedings of the 8th European Symposium on Materials and Fluid Sciences in Microgravity, Volume 2 Aug. 1992 p 817-819 (For primary document see N94-10171 01-29)
Copyright Avail: CASI HC A01/MF A04; ESA, EPD, ESTEC, Noordwijk, Netherlands, HC

N94-12086*# Max-Planck-Inst. fuer Chemie, Mainz (Germany).
THE SOLUBILITY OF GOLD IN SILICATE MELTS: FIRST RESULTS Abstract Only
A. Borisov, H. Palme, and B. Spettel *In* Lunar and Planetary Inst., Twenty-fourth Lunar and Planetary Science Conference. Part 1: A-F 1993 p 147-148 (For primary document see N94-12015 01-91)
Avail: CASI HC A01/MF A06

N94-12240*# Bern Univ. (Switzerland). Physikalisches Inst.
ON THE ORIGIN OF (4)He AND (40)Ar IN NATURAL GOLD Abstract Only
O. Eugster, B. Hofmann, S. Niedermann, and Ch. Thalmann *In* Lunar and Planetary Inst., Twenty-fourth Lunar and Planetary Science Conference. Part 1: A-F 455-456 (SEE N94-12015 01-91) 1993 (For primary document see N94-12015 01-91)
Avail: CASI HC A01/MF A06

27 NONMETALLIC MATERIALS

Includes physical, chemical, and mechanical properties of plastics, elastomers, lubricants, polymers, textiles, adhesives, and ceramic materials.

For composite materials see *24 Composite Materials.*

N94-10271# Lawrence Livermore National Lab., CA.
ZERODUR POLISHING PROCESS FOR HIGH SURFACE QUALITY AND HIGH EFFICIENCY
A. Tesar and B. Fuchs Aug. 1992 6 p Presented at the OPTCON 1992: Optical Fabrication and Testing Workshop, Boston, MA, 17 Nov. 1992
(Contract W-7405-eng-48)
(DE93-012596; UCRL-JC-111396; CONF-9211104-8) Avail: CASI HC A02/MF A01

Zerodur is a glass-ceramic composite of technical importance in applications where temperature instabilities influence optical and mechanical performance, such as in earthbound and spaceborne telescope mirror substrates. Polished Zerodur surfaces of high quality have been required for laser gyro mirrors. Polished surface quality of substrates affects performance of high reflection coatings. Thus, the interest in improving Zerodur polished surface quality has become more general. Beyond eliminating subsurface damage, high quality surfaces are produced by reducing the amount of hydrated material redeposited on the surface during polishing. With the proper control of polishing parameters, such surfaces exhibit roughnesses of less than 1 A rms. Zerodur polishing was studied to recommend a high surface quality polishing process which could be easily adapted to standard planetary continuous polishing machines and spindles. This summary contains information on a polishing process developed at LLNL which reproducibly provides high quality polished Zerodur surfaces at very high polishing efficiencies. DOE

N94-10295# Pacific Northwest Lab., Richland, WA.
SENSING GLASS TRANSITIONS IN THIN POLYMER FILMS ON ACOUSTIC WAVE MICROSENSORS
J. W. Grate Mar. 1993 24 p Presented at the American Society of Testing and Materials Meeting on Glass Transition, Atlanta, GA, 4-5 Mar. 1993
(Contract DE-AC06-76RL-01830)
(DE93-010805; PNL-SA-21812; CONF-930398-2) Avail: CASI HC A03/MF A01

Acoustic wave microsensors are capable of sensing transition behaviors of homogeneous amorphous polymers applied as thin films to the surface of the sensors. The device and wave characteristics of four such microsensors, and examples of their uses in monitoring polymer properties, are described. The devices are the thickness-shear mode (TSM), surface acoustic wave (SAW), flexural plate wave (FPW), and shear horizontal acoustic plate mode (SH-APM) devices. Using the FPW device, the change in the polymer coefficient of thermal expansion at the static glass transition temperature is sensed as a change in slope of the frequency-temperature plot. This behavior reflects the fact that the frequency measures acoustic velocity, which decreases as the polymer modulus decreases. Modulus decreases as the polymer volume increases. Frequency-dependent relaxation properties are detected with a sigmoidal change in slope of the frequency-temperature plot and a maximum in signal amplitude. The minimum in signal amplitude is analogous to the maximum in the loss tangent in dynamic mechanical analysis, or the maximum in sound damping in bulk-wave ultrasonic studies. DOE

N94-10508# Massachusetts Univ., Lowell. Dept. of Plastics Engineering.
PHYSICAL PROPERTIES OF INJECTION MOLDED LIQUID CRYSTAL POLYMERS AND HIGH TEMPERATURE ENGINEERING POLYMERS Final Report, Jan. - Dec. 1992
Robert R. Schott, Robert E. Nienn, Mifta Rahman, and Sudesh Appaji Mar. 1993 177 p
(Contract F04611-91-M-0149)
(AD-A264912; PL-TR-92-3056; AD-E201507) Avail: CASI HC A09/MF A02

This experimental study investigated the System Molding of Four Liquid Crystal Polymers, Vectra A 950, Vectra B 950, HX 4000, and Xydar SRT 500 and two high temperature engineering polymers, polyetherimide (Ultem) and polyphenylene sulfide (Fortran). It also investigated the evaluation of mechanical properties, tensile, flexural, and compression of molded samples. DTIC

N94-10510 Texas Univ., Austin. Dept. of Chemical Engineering.
AMPEROMETRIC BIOSENSORS BASED ON 3-DIMENSIONAL HYDROGEL-FORMING EPOXY NETWORKS Technical Report, Oct. 1992 - May 1993
Ruben Maidan, Dan-Li Wang, and Adam Heller 24 May 1993 12 p Sponsored by ONR; NIH; NSF; and Robert A. Welch Foundation Limited Reproducibility: More than 20% of this document may be affected by microfiche quality
(AD-A265528; TR-004) Avail: CASI HC A03

Proteins and glycoproteins of enzymes behave with respect to electron transport, but not ion transport, as good electrical insulators. We have shown that these insulators can be made sufficiently electron conducting to allow the flow of a current between reaction centers of redox enzymes and electrodes equaling or exceeding the current associated with the turnover of the enzymes. In order for such a current to flow, it is necessary to introduce into the enzyme proteins of glycoproteins fast electron relaying centers, so as to reduce the electron transfer distances. DTIC

N94-10527# Oak Ridge National Lab., TN.
MICROANALYSIS OF DIRECTIONALLY SOLIDIFIED COBALT OXIDE-ZIRCONIA EUTECTIC
J. Bentley, S. McKernan (Paris-Sud Univ., Orsay, France.), C. B. Carter (Paris-Sud Univ., Orsay, France.), and A. Revcolevschi (Paris-Sud Univ., Orsay, France.) 1993 2 p Presented at the 27th Microbeam Analysis Society Meeting, Los Angeles, CA, 11-16 Jul. 1993
(Contracts DE-AC05-84OR-21400; DE-AC05-76OR-00033)
(DE93-013207; CONF-930783-1) Avail: CASI HC A01/MF A01

Analytical electron microscopy (AEM) was performed with an AEM system equipped with a field emission gun, an electron energy-loss spectrometer, and an energy-dispersive x-ray spectrometer. The microstructure consists of alternating lamellae of CoO and Ca-stabilized cubic-ZrO2, each up to 1 micron wide, and a thin (100-200 nm) irregular layer of Co3O4 spinel extending into the CoO from the flat ZrO2 interface. DOE

N94-10710 Pennsylvania State Univ., University Park. Dept. of Materials Science and Engineering.
FRACTURE BEHAVIOR OF SURFACE-MODIFIED CERAMICS
D. J. Green Apr. 1993 9 p Limited Reproducibility: More than 20% of this document may be affected by microfiche quality
(Contract DE-FG02-86ER-45252)
(DE93-013707; DOE/ER-45252/6) Avail: CASI HC A02

Research was performed in 3 areas: fracture behavior of ion-exchanged glasses, fracture of SiC-coated graphite, and subcritical crack growth in ion-exchanged glasses. DOE

N94-10749# Kansas Univ., Lawrence.
IMPROVING RESERVOIR CONFORMANCE USING GELLED POLYMER SYSTEMS
D. W. Green and G. P. Willhite Apr. 1993 6 p
(Contract DE-AC22-92BC-14881)
(DE93-014532; DOE/BC-14881/2) Avail: CASI HC A02/MF A01

The general objectives are as follows: (1) to identify and develop gelled polymer systems which have potential to improve reservoir conformance of fluid displacement processes; (2) to determine the performance of these systems in bulk and in porous media; and (3) to develop methods to predict the capability of these systems to recover oil from petroleum reservoirs. This work focuses on three types of gel systems: an aqueous polysaccharide (KUSPI) system that gels as a function of pH, the chromium-based system where polyacrylamide and xanthan are crosslinked by CR(3), and an organic crosslinked system. Development of the KUSPI system and evaluation and identification of a suitable organic crosslinked system will be done. The laboratory research is directed at the fundamental understanding of the physics and chemistry of the gelation process in bulk form and in porous media. This knowledge will be used to develop conceptual and mathematical models of the gelation process. Mathematical models will then be extended to predict the performance of gelled polymer treatments in oil reservoirs. Accomplishments for this period are presented for the following tasks: development and selection of gelled polymer systems, physical and chemical characterization of gel systems; and mathematical modeling of gel systems. DOE

N94-10863# Bioelastics Research Ltd., Birmingham, AL.
DEVELOPMENT OF BIOELASTIC MATERIALS FOR THE PREVENTION OF ADHESIONS: POLYPENTA- AND POLYTETRAPEPTIDES Final Report, 15 Sep. 1989 - 14 Mar. 1993
14 Mar. 1993 162 p
(Contract N00014-89-C-0282)
(AD-A264851) Avail: CASI HC A08/MF A02

The purpose of the contract was the development of bioelastic materials for the application of preventing post-surgical and post-trauma adhesions by preparing compliant sheets which can be placed between repair sites and which act as barriers to the formation of adhesions between the repairing sites. Specifically to be prepared were quantities of a series of polypentapeptides and polytetrapeptides which were gamma-irradiation cross-linked to form elastomeric sheets and which were supplied to the Naval Medical Research and Development Command, Combat Casualty Care Unit for the animal model efficacy studies carried out at the Naval Medical Research Institute. In addition, in the process of carrying out the specific objectives, considerations of further applications was stimulated and these stimuli, coming from interactions with Navy personnel and others, have resulted in the development of intellectual property with the support of this contract. DTIC

N94-10864*# National Aeronautics and Space Administration. Lewis Research Center, Cleveland, OH.
THE PROPERTIES OF PERFLUOROPOLYETHERS USED FOR SPACE APPLICATIONS
William R. Jones, Jr. Jul. 1993 16 p
(RTOP 505-53-1A)
(NASA-TM-106275; E-8010; NAS 1.15:106275) Avail: CASI HC A03/MF A01

The perfluoropolyether (PFPE) class of liquid lubricants has been used for space applications for over two decades. At first, these fluids performed satisfactorily as early spacecraft placed few demands on their performance. However, as other spacecraft components have become more reliable and lifetimes have been extended, PFPE lubricant deficiencies have been exposed. Therefore, the objective of this paper is to review the PFPE properties that are important for successful long term operation in space. Author

N94-10877# Technische Univ., Delft (Netherlands). Faculty of Mechanical Engineering.
SOME ENVIRONMENTAL ASPECTS OF THE APPLICATION OF FIBRE REINFORCED PLASTICS IN STRUCTURES
R. Marissen 28 Jan. 1993 13 p
(LM-998; ETN-93-94334) Copyright Avail: CASI HC A03/MF A01

The savings on resource consumption and the associated waste production concerning the recycling of glass fiber composites are discussed. Recycling can be understood literally in a sense that, after completing its life cycle, a product is reprocessed to an identical product. A broader perception of recycling allows the reprocessing of waste products to less valuable products. Considering recycling aspects only, neglects the use of resources and waste production related to the use of the product during its life time. Some of these aspects are discussed. It is demonstrated that the application of composites in transport may reduce the use of resources and the production of waste, to an extent which is potentially much larger than that of the involved composite material itself. ESA

N94-10891# Brookhaven National Lab., Upton, NY.
ADVANCED ZINC PHOSPHATE CONVERSION AND PRE-CERAMIC POLYMETALLOSILOXANE COATINGS FOR CORROSION PROTECTION OF STEEL AND ALUMINUM, AND CHARACTERISTICS OF POLYPHENYLETHERETHERKETONE-BASED MATERIALS
T. Sugama and N. R. Carciello Jul. 1992 14 p Prepared for Army Research Office, Research Triangle Park, NC
(Contract DE-AC02-76CH-00016)
(DE93-008717; BNL-48106) Avail: CASI HC A03/MF A01 (US Sales Only)

Anhydrous zinc phosphate (Zn(center dot)Ph) coatings deposited by immersing the steel in transition Co, Ni, and Mn cation-incorporated phosphating solutions were investigated. Two features for the anhydrous 340C-heated (Zn(center dot)Ph) were addressed; one was to determine if electron trapping of adsorbed CO(sup 2+) and Ni(sup 2+) ions acts to inhibit the cathodic reaction on the (Zn(center dot)Ph), and the second was to determine the less susceptibility of the (alpha)-Zn(sub 3)(PO(sub 4))(sub 2) phase to alkali-induced dissolution. The factors governing film-forming of pre-ceramic polymetallosiloxane (PMS) coatings for Al substrates were investigated. Four factors were important in obtaining a good film: (1) formation of organopolymetallosiloxane at sintering temperatures of 150C; (2) pyrolytic conversion at 350C into an amorphous PMS network structure in which the Si-O-M linkage were moderately enhanced; (3) noncrystalline phases; and (4) formation of interfacial oxane bond between PMS and Al oxide. Formation of well-crystallized polyphenyletheretherketone (PEEK) in vicinity of silica aggregates was found in the molted body made in N2. Crystalline PEEK contributed to thermal and hydrothermal stabilities of mortar specimens at temperatures up to 200C, and resistance in 5 wt % H2SO4 solution at 80C. DOE

N94-10958# Sandia National Labs., Albuquerque, NM.
PREPARATION OF CARBON MONOLITHS HAVING TAILORED PORE STRUCTURE FROM POROUS POLYMER PRECURSORS
R. R. Lagasse 1993 3 p Presented at the Biennial Conference on Carbon, Buffalo, NY, 13-18 Jun. 1993
(Contract DE-AC04-76DP-00789)
(DE93-011576; SAND-93-0825C; CONF-930615-1) Avail: CASI HC A01/MF A01

This work concerns preparing tailored porous carbon monoliths by pyrolyzing porous polymer precursors. Prior work in this laboratory demonstrated that a low density (0.05 g/cu cm), high void fraction (97 vol%) carbon monolith could be prepared by pyrolyzing a porous poly(acrylonitrile) (PAN) precursor. A higher density, more robust carbon material is preferred for certain applications, such as electrodes for electrochemical devices. The present work demonstrates that porous carbon monoliths having mass density of 0.7 g/cu cm can be prepared from a porous PAN precursor if the pyrolysis is controlled carefully. The macropore structure of the carbon is adjusted by changing the pore structure of the PAN precursor, and the finer scale structure (such as the crystallite size L(sub c)) is adjusted by varying the pyrolysis or heat treatment temperature. DOE

N94-11007# State Univ. of New York, Stony Brook. Dept. of Materials Science and Engineering.
DETERMINATION OF CONCENTRATION PROFILES AT INTERFACES AND SURFACES OF PARTIALLY MISCIBLE POLYMER BLENDS
M. Rafailovich and J. Sokolov 30 Apr. 1993 6 p
(Contract DE-FG02-90ER-45437)
(DE93-013140; DOE/ER-45437/2) Avail: CASI HC A02/MF A01

The research is divided among several topics: wetting of thin liquid polyethylene-propylene films, Fourier reconstruction of density profiles of thin films using anomalous x-ray reflectivity, and temperature and concentration effects on grafted polymers in the melt. DOE

N94-11106# Oak Ridge National Lab., TN.
LOW-EXPANSION CERAMICS INITIATIVE
D. P. Stinton and D. W. Richerson 1992 5 p Presented at the Annual Automotive Development Technology Contractors' Coordination Meeting, Dearborn, MI, 2-5 Nov. 1992
(Contract DE-AC05-84OR-21400)
(DE93-011860; CONF-9211101-9) Avail: CASI HC A01/MF A01

The U.S. Department of Energy and the Ceramic Technology Project support research into low-thermal-expansion ceramics for application in advanced diesel and turbine engines. New activities are being initiated to accelerate the development of these materials. The strength of this program includes the integration of efforts of engine companies, ceramic manufacturers, and universities. This paper briefly describes the application of the low-expansion sodium-zirconium-phosphate (NZP) class of materials in engines and summarizes a 2-year program plan for this area. DOE

N94-11107 Materials Research Labs., Ascot Vale (Australia).
THERMAL STABILITY OF SEALANTS FOR MILITARY AIRCRAFT: MODIFICATION OF POLYSULFIDE PREPOLYMERS WITH ETHER AND THIOETHER MONOMERS
P. J. Hanhela and W. Mazurek Feb. 1993 25 p Limited Reproducibility: More than 20% of this document may be affected by microfiche quality
(AD-A264079; MRL-TR-92-2; DODA-AR-006-864) Avail: Issuing Activity (Defense Technical Information Center (DTIC))

The effect of modifying Thiokol polysulfide prepolymers with dimercapto diethyl ether and dimercapto diethyl sulfide on the resistance to heat aging has been examined together with a commercially modified (PR-1770 B-2) and an unmodified equivalent sealant (PR-1750 13-2). Mechanical test performed on specimens, after heat aging at 182 C, indicated that the modifications did not improve the best resistance of polysulfide sealants. DTIC

N94-11145# Imagination Resources, Inc., Dublin, OH.
MEASUREMENT OF VISCOSITY, DENSITY AND GAS SOLUBILITY OF REFRIGERANT BLENDS
R. C. Cavestri and J. Munk Apr. 1993 22 p Prepared in cooperation with Air-Conditioning and Refrigeration Technology Inst., Inc., Arlington
(Contract DE-FG02-91CE-23810)
(DE93-014772; DOE/CE-23810/11B) Avail: CASI HC A03/MF A01

Liquid/liquid miscibilities of four different 32 ISO VG polyolesters and one alkylbenzene at three concentrations were determined. Also a full vapor lubricant equilibrium (VLE) viscosity reduction of a 32 ISO VG mineral oil with HCFC-22 is complete. Partial viscosity reduction information by the fractionate components from R-502 in 32 ISO VG mineral oil is presented from 40C (104F) and 70C (158F) isotherms. DOE

N94-11146# Illinois Univ., Urbana-Champaign.
ACCELERATED SCREENING METHODS FOR PREDICTING LUBRICANT PERFORMANCE IN REFRIGERANT COMPRESSORS
C. Cusano Mar. 1993 11 p Prepared in cooperation with Air-Conditioning and Refrigeration Technology Inst., Inc., Arlington
(Contract DE-FG02-91CE-23810)
(DE93-014773; DOE/CE-23810/11C) Avail: CASI HC A03/MF A01

As the result of a thorough literature search and consultation with manufacturers of compressors, a specimen testing program is proposed to simulate specific contacts in components of compressors. Specimen testing will be conducted using a high pressure tribometer. Specific components to be simulated, with their approximate operating and environmental conditions, are identified. A list of references, related to compressors lubrication, friction and wear, is given in the Appendix. DOE

N94-11151# Lawrence Livermore National Lab., CA.
POLYMERIC NITROGEN
C. Mailhiot, L. H. Yang, and A. K. McMahan Aug. 1992 7 p Presented at the 1992 Air Force High Energy Density Materials Contractors Meeting, Lancaster, CA, 12-14 Apr. 1992 Revised
(Contract W-7405-eng-48)
(DE93-012600; UCRL-JC-110049-Rev-1; CONF-9204235-2-Rev-1) Avail: CASI HC A02/MF A01

Ab initio local-density functional total-energy calculations indicate that a polymeric form should be the stable phase of nitrogen above approximately 35 GPa, and that such a polymeric phase is likely to be both energetic and metastable at atmospheric pressure. These results also suggest that such a polymeric form of nitrogen may survive metastably at atmospheric pressure as an energetic, high-melting temperature, insulating solid, with a specific enthalpy of 6.7-14.1 MJ/kg. While this does not exceed the Air Force HEDM goal of 15 MJ/kg, such a material may nevertheless compare favorably with existing monopropellants. DOE

N94-11175*# National Aeronautics and Space Administration. Marshall Space Flight Center, Huntsville, AL.
THERMAL TESTING OF ALUMINIZED MYLAR
D. L. Lowe, II and D. L. Edwards Jun. 1993 8 p
(NASA-TM-108414; NAS 1.15:108414) Avail: CASI HC A02/MF A01

The effect of heat on aluminized Mylar film is summarized. A summary of the procedure used in testing the material, background information describing the physical properties of the material, and the experimental results of heating the material at various temperatures are included. It is revealed that aluminized Mylar film is thermally stable within the temperature range of 50 to 200 C. The information compiled will be used to determine if aluminized Mylar can be useful in space applications. Author (revised)

N94-11204*# National Aeronautics and Space Administration. Lewis Research Center, Cleveland, OH.
LOW TEMPERATURE SYNTHESIS OF MONOLITHIC TRANSPARENT Ta2O5 GELS FROM HYDROLYSIS OF METAL ALKOXIDE
Narottam P. Bansal Jul. 1993 20 p
(RTOP 510-01-50)
(NASA-TM-106246; E-7966; NAS 1.15:106246) Avail: CASI HC A03/MF A01

Tantalum oxide gels in the form of transparent monoliths and powder were prepared from hydrolysis of tantalum pentaethoxide under controlled conditions using different mole ratios of Ta(OC2H5)5:C2H50H:H20:HCl. Alcohol acts as the mutual solvent and HCl as the deflocculating agent. For a fixed alkoxide:water:HCl ratio, time of gel formation increased with the alcohol to alkoxide mole ratio. Thermal evolution of the physical and structural changes in the gel was monitored by differential thermal analysis, thermogravimetric analysis, x-ray diffraction, and infrared spectroscopy. On heating to approximately 400 C, the amorphous gel crystallized into the low temperature orthorhombic phase Beta-Ta2O5, which transformed into the high temperature tetragonal phase Alpha-Ta2O5 when further heated to approximately 1450 C. The volume fraction of the crystalline phase increased with the firing temperature. The Alpha-Ta205 converted back into the low temperature phase, Beta-Ta2O5, on slow cooling through the transformation temperature of 1360 C indicating a slow but reversible transformation. Author (revised)

N94-11222# Institute for Productivity Research, New York, NY.
ADVANCED MODEL OF GRADUAL WEAR OF VISCOELASTIC SURFACE FILM Final Report
Apr. 1993 43 p
(Contract N00014-92-C-0101)
(AD-A265130) Avail: CASI HC A03/MF A01

This final report of project, Advanced Model of Gradual Wear of Viscoelastic Surface Film, under Office of Naval Research Contract N00014-92-C-0101, contains three tabs: Tab A Manuscript of the paper, 'On the Prediction of Gradual Wear Life of Solid Lubricating Films' - this is to be presented at, and published by the 6th International Congress on Tribology, August 30-September 2, 1993, Budapest, Hungary; Tab B Manuscript of the paper, 'Theory of Gradual Wear Life Prediction of Viscoelastic Lubricating Surface Film' - this has been submitted for presentation at the 1993 Joint Tribology Conference, and publication in the STLE Tribology Transactions; and Tab C Report on a requisite task element of the contract: a method of verifying the results experimentally. DTIC

N94-11230# Lawrence Livermore National Lab., CA.
DAMAGE THRESHOLDS OF FLUORIDE MULTILAYERS AT 355 nm
R. Chow, M. R. Kozlowski, G. E. Loomis, and F. Rainer Oct. 1992 12 p Presented at the Symposium on Optical Materials for High-Power Lasers, Boulder, CO, 28-30 Oct. 1992
(Contract W-7405-eng-48)
(DE93-009523; UCRL-JC-111482; CONF-921047-1) Avail: CASI HC A03/MF A01

Fluoride multilayer coatings were evaluated for use in 355 nm high reflector applications. The LaF3/Na3AlF6, NdF3/Na3AlF6, and GdF3/Na3AlF6 multilayers had laser damage thresholds of 20, 17.9, and 7.4 (measured at 10-ns pulsewidths), respectively. High tensile stresses in the coatings restricted this evaluation to only 5-layer-pair partial reflectors (49-52%). The LaF3/Na3AlF6, NdF3/Na3Al6, and GdF3/Na3AlF6 multilayers had tensile stresses of approximately 1.1 x 10(exp 9), 1.3 x 10(exp 9), and 9.3 x 10(exp 8) dynes/sq cm, respectively. Substrate material and glow-discharge processing of the substrates were found to influence the density of stress-induced coating fractures and damage thresholds in some cases. If stress fracturing and scatter can be controlled, these fluoride material combinations are suited for 3(omega) applications. DOE

N94-11257*# National Aeronautics and Space Administration. Lewis Research Center, Cleveland, OH.
SYNTHESIS AND THERMAL EVOLUTION OF STRUCTURE IN ALKOXIDE-DERIVED NIOBIUM PENTOXIDE GELS
Narottam P. Bansal Jul. 1993 21 p
(RTOP 510-01-50)
(NASA-TM-106259; E-7984; NAS 1.15:106259) Avail: CASI HC A03/MF A01

Niobium pentoxide gels in the form of transparent monoliths and powder have been synthesized from the controlled hydrolysis and polycondensation of niobium pentaethoxide under different experimental conditions using various mole ratios of Nb(OC2H5)5:H2O:C2H5OH:HCl. Alcohol acted as the mutual solvent and HCl as the deflocculating agent. In the absence of HCl, precipitation of colloidal particles was encountered on the addition of any water to the alkoxide. The gels were subjected to various thermal treatments and characterized by differential thermal analysis, thermogravimetric analysis, x-ray diffraction, and infrared spectroscopy. After drying at 400 C, the gels were amorphous to x-rays. The amorphous powder crystallized into the low-temperature orthorhombic form of Nb2O5 at approximately 500 C, which transformed irreversibly into the high-temperature monoclinic alpha-Nb2O5 between 900 to 1000 C. The kinetics of crystallization of the amorphous niobium pentoxide have been investigated by non-isothermal differential scanning calorimetry. The crystallization activation energy was determined to be 399 kJ/mol. Author (revised)

N94-11281 Minnesota Univ., Minneapolis. Dept. of Chemical Engineering and Materials Science.
STRUCTURAL DEVELOPMENT IN CERAMIC PRECURSOR SOLS AND GELS Final Report, 15 Mar. 1989 - 14 Mar. 1992
Martha L. Mecartney Mar. 1993 52 p Limited Reproducibility: More than 20% of this document may be affected by microfiche quality
(Contract F49620-89-C-0050)
(AD-A264354; AFOSR-93-0218TR) Avail: Issuing Activity (Defense Technical Information Center (DTIC))

The effect of water of hydrolysis on nucleation, crystallization, and microstructural development of sol-gel derived single phase LiNbO3 thin films has been studied using transmission electron microscopy (TEM), atomic force microscopy (AFM), x-ray diffraction (XRD), and differential scanning calorimetry (DSC). A percursor solution of double ethoxides of lithium and niobium in ethanol was used for the preparation of sol. DSC results indicated that adding water to the solution for hydrolysis of the double ethoxides lowered the crystallization temperature from 500 deg C (no water) to 390 deg C (2 moles water per mole ethoxide). The amount of water has no effect on the short range order in amorphous LiNbO3 gels but rendered significant microstructural variations for the crystallized films. AFM studies indicated that surface roughness of dip coated films increased with increasing water of hydrolysis. DTIC

N94-11292# Pennsylvania State Univ., University Park. Dept. of Chemistry.
RING-OPENING POLYMERIZATION OF PHOSPHAZENES
Harry R. Allcock 18 May 1993 27 p
(Contract N00014-91-J-1194)
(AD-A265000; TR-8-ONR) Avail: CASI HC A03/MF A01

Phosphazenes comprise a broad range of cyclic or linear small-molecules and high polymers that occupy and important place in the chemistry of heterocyclic compounds and new macromolecules. Typical structures are shown. In these molecules the side groups, R, attached to phosphorus can vary broad range, from halogen or pseudohalogen units such as fluorine, chlorine, bromine, iodine, cyano, or isothiocyano, to simple or complex organic groups such as alkoxy-, arylox-, amino-, alkyl-, aryl-, sugar units, amino acid ester groups, oligopeptides, transition metal complexes, porphyrins, phthalocyanines, organosilicon units, liquid crystalline, nonlinear optical, and photosensitive side groups, and a whole range of biologically active side groups. DTIC

N94-11302# Materials Research Labs., Ascot Vale (Australia).
FORMULATING INFRARED COATINGS FOR DEFENCE APPLICATIONS
L. V. Wake and R. F. Brady Mar. 1993 38 p
(MRL-RR-1-93; AR-008-254) Avail: CASI HC A03/MF A01

Relevant physical laws governing the response of coatings to solar and infrared radiation were reviewed. The reflection of infrared radiation by a paint is controlled primarily by the refractive index and particle size of the pigments in the coating. Pigments were evaluated for reflectance, transparence and hiding power in the near infrared region, and guidelines for pigment selection for various applications given in terms of their optical properties in the near infrared region. Raw materials selection, manufacture, and evaluation of coatings were discussed with respect to tailoring infrared reflectance. By employing the principles developed and using pigments with appropriate properties, organic coatings were developed which are consistent with the visible color requirements of the Australian and US Navies. Significant increases in the reflection of infrared radiation were demonstrated by the new formulations. The need for a very clear understanding of the threat systems and the operational conditions of service platforms was emphasized. It is only with this understanding that optimum paint schemes can be devised. However, it can be stated that the use of the solar infrared reflecting paints described would reduce conspicuity of isolated platforms to surveillance and seeker systems operating in the mid and far infrared without detriment to visual camouflage characteristics. Author (revised)

N94-11311 Aeronautical Research Labs., Melbourne (Australia).
FIELD EVALUATION OF SIX PROTECTIVE COATINGS APPLIED TO T-56 TURBINE BLADES AFTER 2500 HOURS OF ENGINE USE
S. G. Russo Apr. 1993 25 p Original contains color illustrations
(ARL-TR-27; AR-008-336) Copyright Avail: Issuing Activity

An assessment of the performance of six different aluminide coatings applied to Allison T-56 high-pressure turbine blades after 2500 hours of engine operation is outlined. The results confirm the superior resistance of the precious metal (platinum and platinum/rhodium) modified aluminide coatings to high temperature oxidation and hot-corrosion, as previously indicated by the earlier progressive evaluations at 500, 1500 and 2000 hour intervals. Special attention was given to the use of qualitative analysis using energy dispersive x ray spectroscopy. This technique identified substantial residue quantities of precious metal (Pt and Pt/Rh) in their respective aluminide coated surfaces. The results show that the precious-metal modified aluminides are capable of affording protection to the T-56 substrate superalloy designated IN-738LC up to, and hopefully beyond, the desired 3000 hour interval. Author (revised)

N94-11350*# National Aeronautics and Space Administration. Lyndon B. Johnson Space Center, Houston, TX.
VACUUM STABILITY REQUIREMENTS OF POLYMERIC MATERIAL FOR SPACECRAFT APPLICATION
J. W. Craig 24 Feb. 1994 63 p Revised
(NASA-TM-109216; NAS 1.15:109216; SP-R-0022A) Avail: CASI HC A04/MF A01

The purpose of this document is to establish outgassing requirements and test guidelines for polymeric materials used in the space thermal/vacuum environment around sensitive optical or thermal control surfaces. The scope of this document covers the control of polymeric materials used near or adjacent to optical or thermal control surfaces that are exposed to the thermal/vacuum environment of space. This document establishes the requirements and defines the test method to evaluate polymeric materials used in the vicinity of these surfaces in space applications.
Derived from text

N94-11487# Aerospace Corp., El Segundo, CA. Technology Operations.
CRYSTALLINITY AND DIELECTRIC PROPERTIES OF PEEK, A THERMOPLASTIC POLY(ETHER ETHER KETONE) Technical Report
Thomas W. Giants 1 May 1993 33 p
(Contract F04701-88-C-0089)
(AD-A266027; TR-93(3935)-10; SMC-TR-93-29) Avail: CASI HC A03/MF A01

The overall objective was to investigate the interdependence of specific dielectric properties of polymers on their fundamental molecular parameters in order to optimize the application of these polymeric materials in critical SMC systems. SMC systems utilize polymeric materials in applications involving high voltage (HV) insulation in systems aboard DSCS, Nilstar, and several classified spacecraft. Studies of polymer dielectrics have shown that changes in polymer morphology can influence fundamental electrical properties leading to premature breakdown. This investigation focused on the effect of polymer morphology on the electrical characteristics of PEEK, a high temperature insulating thermoplastic, as part of an effort in understanding the causes of dielectric breakdown. This amorphous material was thermally annealed to produce a range of crystallinities. The results of this effort showed that as the crystalline/amorphous ratio of the polymer increases, the dielectric breakdown strength is reduced. Electrical conductivity of the material was also shown to decrease. When translated to resins, blends, and advanced composites where environmental aging or thermal cycling can influence the morphology of the material, any reliance on the maintenance of stable electrical properties may have to be carefully considered. The introduction of advanced materials with tailored properties that involve different families of polymers will require a sophisticated understanding of the morphology of materials and the processes by which it varies. This will not only be important for enhancing mechanical properties of materials but also for recognizing the subtle influences that affect electrical properties of materials. DTIC

N94-11665# Sandia National Labs., Albuquerque, NM.
FINITE ELEMENT SIMULATION OF THE 2D COLLAPSE OF A POLYELECTROLYTE GEL DISK
D. Segalman, W. Witkowski, R. Rao, D. Adolf, and M. Shahinpoor (New Mexico Univ., Albuquerque.) 1993 8 p Presented at the SPIE Smart Structures and Materials 1993 Meeting, Albuquerque, NM, 31 Jan. - 4 Feb. 1993
(Contract DE-AC04-76DP-00789)
(DE93-010693; SAND-92-2239C; CONF-930171-3) Avail: CASI HC A02/MF A01

Theoretical models describing the dynamic behavior of the expansion and contraction of polyelectrolyte gels present numerically challenging problems. This paper describes how a method of weighted residuals approach has been used to solve the two-dimensional governing system of equations by finite element analysis. The modulation of the imbibition/expulsion of solvent by a gel disk is studied as an example.
DOE

N94-11672# Oak Ridge National Lab., TN.
CERAMICS TECHNOLOGY PROJECT DATABASE Report, Sep. 1991
B. L. P. Keyes Jun. 1992 125 p
(Contract DE-AC05-84OR-21400)
(DE93-012431; ORNL/M-1862) Avail: CASI HC A06/MF A02

The piston ring-cylinder liner area of the internal combustion engine must withstand very-high-temperature gradients, highly-corrosive environments, and constant friction. Improving the efficiency in the engine requires ring and cylinder liner materials that can survive this abusive environment and lubricants that resist decomposition at elevated temperatures. Wear and friction tests have been done on many material combinations in environments similar to actual use to find the right materials for the situation. This report covers tribology information produced from 1986 through Jul. 1991 by Battelle columbus Laboratories, Caterpillar Inc., and Cummins Engine Company, Inc. for the Ceramic Technology Project (CTP). All data in this report were taken from the project's semiannual and bimonthly progress reports and cover base materials, coatings, and lubricants. The data, including test rig descriptions and material characterizations, are stored in the CTP database and are available to all project participants on request. The objective of this report is to make available the test results from these studies, but not to draw conclusions from these data. DOE

N94-11673# Oak Ridge National Lab., TN.
CERAMIC TECHNOLOGY PROJECT DATABASE Report, Mar. 1990
B. L. P. Keyes Jul. 1992 145 p
(Contract DE-AC05-84OR-21400)
(DE93-012432; ORNL/M-1860) Avail: CASI HC A07/MF A02

This report is the fifth in a series of semiannual data summary reports on information being stored in the Ceramic Technology Project (CTP) database. The overall system status as of 31 Mar. 1990 is summarized, and the latest additions of ceramic mechanical properties data are given for zirconia, silicon carbide, and silicon nitride ceramic mechanical properties data including some properties on brazed specimens. DOE

N94-11698# Massachusetts Inst. of Tech., Cambridge. Dept. of Materials Science and Engineering.
RADIATION-INDUCED APERIODICITY IN IRRADIATED CERAMICS
L. W. Hobbs Feb. 1993 5 p
(Contract DE-FG02-89ER-45396)
(DE93-013335; DOE/ER-45396/4) Avail: CASI HC A01/MF A01

The experimental program is designed to reveal details of the metamict (amorphization, or crystal-to-glass) transformation in irradiated ceramics (silica compounds, less-connected lead phosphates). The silica compounds were amorphized using electrons, neutrons, and ions, while the phosphates were amorphized using ions (primarily) and neutrons. Energy-filtered electron microdiffraction, high-resolution transmission electron microscopy, and high-performance liquid-phase chromatography are being used. DOE

N94-11830# Texas Univ., Austin.
POLYMER-POLYMER INTERACTIONS Final Report, 15 Sep. 1989 - 14 Nov. 1992
Isaac C. Sanchez and Donald R. Paul May 1993 16 p
(Grant AF-AFOSR-0479-89)
(AD-A265304; AFOSR-93-0358TR) Avail: CASI HC A03/MF A01

Our approach for understanding polymer-polymer interactions is to measure heats of mixing of small molecule analogs. In particular, focus was on small molecule analogs of polystyrene (PS) and poly (2, 6 dimethyl phenylene oxide) (PPO). This well-known system is miscible, but the origin of its miscibility has perplexed investigators for over 25 years. Our measurements and associated molecular mechanics/Monte Carlo calculations firmly established that the two methyl groups on PPO play a significant role in affecting miscibility. Two equation of state models for hydrogen bonding interactions were developed. They represent a significant advance in our understanding of hydrogen bonding interactions in both polymeric and non-polymeric systems. The models were successfully applied to a variety of systems that include supercritical fluids. Solubility of gases in liquid polymers was treated theoretically using the lattice-fluid model. Author (DTIC)

N94-11847# Pennsylvania State Univ., University Park. Dept. of Chemistry.

SYNTHESIS, CHARACTERIZATION, AND MODIFICATION OF POLY(ORGANOPHOSPHAZENES), THAT BEAR BOTH 2,2,2-TRIFLUOROETHOXY AND PHENOXY GROUPS

Harry R. Allcock and Young B. Kim 18 May 1993 51 p
(Contract N00014-91-J-1194)
(AD-A264913; TR-12) Avail: CASI HC A04/MF A01

High molecular weight polyphosphazenes that bear varying ratios of phenoxy and 2,2,2-trifluoroethoxy groups were synthesized by the reactions of (NPC12)n with sodium phenoxide, PhO(-)Ne, and sodium 2,2,2-trifluoroethoxide, CF3CH2O(-)Na(+), using either competitive or sequential exposure to the two nucleophiles. The relative amounts of NP(OCH2CF3)(sub 2), NP(OCH2CF3)(OPh), and NP(OPh)(sub 2) units in the polymer are dependent on both the synthesis method and the amounts of CF3CH2O(-)Na(+) and PhO(-)Na(+) used for the synthesis. The sequential reaction of poly(dichlorophosphazene), (NPC12)(sub n), with CF3CH2O(-)Na(+) followed by PhO(-)Na(+) yields mixtures of polymers that have very different compositions depending on the presence or absence of tetra-n-butyl ammonium bromide or 15-crown-5 ether. The reactions are complicated by the fact that phenoxy groups in NP(OCH2CF3)(OPh) units are replaced by 2,2,2-trifluoroethoxy groups at elevated temperatures or at 25 C in the presence of either 15-crown-5 ether or tetra-n-butyl ammonium bromide. The sodium salt of 3-hydroxypropanol replaces both 2,2,2-trifluoroethoxy and phenoxy groups in these polymers at room temperature in the presence of either tetra-n-butyl ammonium bromide or 15-crown-5 ether. These side group exchange reactions are affected by steric effects. The mechanisms of these reactions are interpreted from the perspective that the reaction of CF3CH2O(-) Na+ alone with the small molecule model compound, (NPCl2)(sub 3), yields significant amounts of geminally substituted products in the presence of either tetra-n-butyl ammonium bromide or 15-crown-5 ether. DTIC

N94-11848# Pennsylvania State Univ., University Park. Dept. of Chemistry.

RADIATION-INDUCED MODIFICATIONS OF ALLYLAMINO-SUBSTITUTED POLYPHOSPHAZENES

M. F. Welker, H. R. Allcock, G. L. Grune, R. T. Chern, and V. T. Stannett 18 May 1993 17 p
(Contract N00014-91-J-1194)
(AD-A264914; TR-9) Avail: CASI HC A03/MF A01

A collaborative effort to synthesize amino-substituted polyphosphazenes and examine their sensitivity to radiation has recently been undertaken. The objective was to determine the value of using such polymers as new and better resist materials for microlithographic applications. An initial study was carried out using elastomeric phenoxy-substituted polyphosphazenes as models for radiation and grafting. However, it became necessary to synthesize several new amino-substituted polyphosphazenes for several reasons. First, the usefulness of elastomeric polymers for resist applications is severely limited by their inability to remain dimensionally stable at normal temperatures. Glassy polymers have been shown to provide the necessary thermal properties required for resist films deposited on SiO2 wafers. Second, the amino-substituted polyphosphazenes are excellent film-forming polymers with high molecular weights. Finally, it seemed possible that these polymers would exhibit similar reactive ion etching resistance to those of a phenoxy-substituted counterpart, and experimental work was performed to determine reactive ion etching values for the most radiation-sensitive of the new polymer candidates. DTIC

N94-11849# Pennsylvania State Univ., University Park. Dept. of Chemistry.

THE SYNTHESIS OF PHOTOCROSSLINKABLE CHALCONE-BEARING POLYPHOSPHAZENES

Harry R. Allcock and Charles G. Cameron 18 May 1993 27 p
(Contract N00014-91-J-1194)
(AD-A264915; TR-13) Avail: CASI HC A03/MF A01

Cyclic and high polymeric phosphazenes that bear 3-(4-oxyphenyl)-1-phenyl- 2-propen-1-one (4-oxychalcone) side groups have been prepared in order to study their photochemical behavior. Small molecule cyclic trimers of the general formula N3P3R5R' where R = phenoxy, 2,2,2-trifluoroethoxy, chloro, and 4-oxychalcone and R'= 4-oxychalcone were synthesized in order to model the crosslinking reactions at the high polymer level. Single-substituent and cosubstituent polymeric phosphazenes NPRR'2n' where R= phenoxy, 2,2,2-trifluoroethoxy, or 4-oxychalcone, and R'= 4-oxychalcone were also prepared. Their photolytic crosslinking was followed by ultraviolet spectroscopy. DTIC

N94-11862# Maryland Univ., Baltimore. Dept. of Mathematics.

A SIMPLE MODEL OF MELT FRACTURE Final Technical Report, 1 Sep. 1991 - 31 Dec. 1992

James Greenberg 31 Dec. 1992 60 p
(Grant AF-AFOSR-0352-91)
(AD-A265311; AFOSR-93-0323TR) Avail: CASI HC A04/MF A01

The PI produced an excellent explanation of the unpleasant shark-skinning observed in certain polymer extrusion processes. This work was brought to the attention of researchers at Corning and Hoechst Celanese and Greenberg and Demay will work this summer with members of the Materials Sciences Center at the Ecole Nationale Superieure des Mines de Paris led by J.F. Agassant. One goal of this work is to see if the same oscillatory phenomena is present when one replaces the slip boundary condition by a no slip one and looks instead at materials whose shear stress-strain rate constitutive equation has a spinodal type nonlinearity. A difficult question also worth pursuing is whether now understanding the nature of the flow instability - a switch from a slip to a no slip boundary condition at the wall of the capillary tube - if it is possible to control the inlet flow to the capillary in the unstable regime in such a way as to reduce the oscillations and shark skinning of the final product. DTIC

N94-11866# Materials Research Society, Pittsburg, PA.

CHEMICAL VAPOR DEPOSITION OF REFRACTORY METALS AND CERAMICS 2. MATERIALS RESEARCH SOCIETY SYMPOSIUM PROCEEDINGS

Theodore M. Besmann, Bernard M. Gallois, and James W. Warren Apr. 1993 386 p Symposium held in Boston, MA, 4-6 Dec. 1991
(AF Proj. 2306)
(AD-A265072; AFOSR-93-0267TR) Avail: CASI HC A17/MF A04

The production of thin or thick films of metals or ceramics by chemical vapor deposition has often been achieved by the use of halide gas precursors. In certain cases, this choice was made purely for reasons of simplicity. Experience has subsequently shown, however, that this choice can give rise to significant changes in the nature and proportions of deposited phases. These are highly dependent upon the following: the value of the oxidiser:reducer ratio in the gas phase; the degree of metal oxidation in the halide considered; and possible competition between two reducing agents designed to reduce the halide. These factors, among others, strongly influence the thermochemistry of the deposition reaction. Their roles must therefore be clearly understood, interpreted and predicted by the thermochemical analysis. Based on examples relating to silicide, nitride, and boride deposits, an attempt will be made to determine sensitive parameters and deduce selection criteria. DTIC

N94-11876# United Technologies Research Center, East Hartford, CT.

PROCESSING AND PROPERTIES OF COATED HPZ FIBER REINFORCED GLASS-CERAMIC MATRIX COMPOSITES Final Report, May 1988 - Jan. 1993

John Brennan, William Allen, Philip McCluskey, and David Jarmon 31 Mar. 1993 124 p
(Contract F49620-88-C-0062)
(AD-A265177; R93-970104-2; AFOSR-93-0362TR) Avail: CASI HC A06/MF A02

The main objective of this program was to utilize fiber coatings to tailor, or 'engineer,' the chemistry and bonding characteristics of the fiber/matrix interface in glass-ceramic matrix composites reinforced with Dow Corning's polymer derived Si-N-C-O 'HPZ' fibers such that relatively weak bonding exists at the interface to allow matrix crack deflection to occur, thus increasing the toughness and damage tolerance of the composite, while at the same time maintaining the high temperature oxidative stability of the matrix/coating/fiber interfacial region. In addition, for this particular system which is inherently reactive, the fiber coating must also act as a barrier to interdiffusion and reaction. A secondary objective of this program is to investigate advanced composite processing methods other than the traditional hot-pressing, such as hot isostatic pressing (HIP) and glass matrix transfer molding into integrally woven fiber preforms. During the performance of this contract, the microstructure and properties of HPZ fibers, CVD/BN, and SiC/BN coatings on HPZ fibers and barium magnesium aluminosilicate (BMAS) glass-ceramic composites fabricated with these coated fibers were investigated. DTIC

N94-12330# Department of the Navy, Washington, DC.
CERAMICS FORMED BY PYROLYSIS OF EITHER LINEAR OR THERMOSETTING CARBORANE (SILOXANE OR SILANE) ACETYLENE BASED PRECURSOR POLYMERS Patent Application
Leslie J. Hnderson, inventor (to Navy) and Teddy M. Keller, inventor (to Navy) 8 Feb. 1993 35 p
(AD-D015747; US-Patent-Appl-SN-014928; Navy-Case-75190) Avail: CASI HC A03/MF A01

This invention relates to a new class of novel ceramic materials that are formed from linear inorganic-organic hybrid polymers of varying molecular weight. These new ceramics are formed from oxidatively stable thermosetting polymers which, in turn, are formed from linear polymeric material having repeating units that contain at least one alkynl group for cross-linking purposes and at least one bis (silyl or siloxanyl) carboranyl group. The thermosetting polymers are converted into the novel ceramics, the subject of the present invention, at elevated temperatures. DTIC

N94-12331 Pennsylvania State Univ., University Park. Applied Research Lab.
CERAMIC ACTUATORS FOR SMART MATERIALS Final Report, 1 Jul. 1991 - 30 Jun. 1992
L. E. Cross 30 Jun. 1992 44 p Limited Reproducibility: More than 20% of this document may be affected by microfiche quality
(Contract N00014-91-J-1922)
(AD-A265664) Avail: CASI HC A03

In earlier studies a number of phase switching systems had been explored which permit the switching of large electric polarization and the associated high elastic strain. The question to be resolved was whether these large polarization values could be repeatedly switched without associated mechanical or electrical fatigue. Early fatigue was shown to be an electrode problem, and with care in electrode application, density control, grain size control, and field homogeneity it was shown that full switching lifetimes, with no fatigue of more than 10(exp 9) cycles, were achievable. In polymer-ceramic composite transducers, the 1:3 type connectivity is highly desirable. A new theoretical approach has been made to calculate the inhomogeneous stress profiles in both piezoceramic and polymer phases. The predictions have been tested using the MRL ultra-dilatometer and good agreement is shown between predicted and observed strain profiles. A new type of 1:3 composite making use of radially poled ceramic tubes has been explored and shown to offer unusually attractive possibilities for the control of piezoelectric, elastic, and electric impedance characteristics and to offer a vehicle for the new electrostrictive agile piezoelectrics. DTIC

N94-12340# Connecticut Univ., Storrs.
INTERFACIAL MODIFICATION THROUGH END GROUP COMPLEXATION IN POLYMER BLENDS Technical Report, 1992 - 1993
C. A. Fleischer, A. R. Morales, and J. T. Koberstein 4 Jun. 1993 35 p
(Contract N00014-91-J-1786)
(AD-A265887; TR-1) Avail: CASI HC A03/MF A01

The concept of interpolymer complexation is applied to develop a new method for interfacial modification of immiscible binary homopolymer blends. In this method, end-functional homopolymers terminated with acid and base groups are added to the blend to promote in situ end-complexation of the immiscible materials across the interface. The interpolymer complex that forms between acid and base groups creates a 'block-copolymer-like' structure that spans across the interface. Pendant drop tensiometry is applied to measure the interfacial tension reduction afforded by this complexation. The interfacial tension data show behavior similar to that observed for block copolymer addition to homopolymer blends. In difference to the behavior of block copolymers, however, the formation of interpolymer complexes is dependent on the equilibrium between associated and dissociated functional groups. That is, the ultimate plateau value for interfacial tension reduction is dependent on the functional group stoichiometry. A reaction model for end-complexation is developed including the effects of carboxylic acid dimerization in order to reproduce the interfacial reduction data. Fourier transform infrared spectroscopy is applied to determine the appropriate rate constants. Finally it is shown that the overall interfacial tension behavior is consistent with that predicted by current statistical thermodynamic theories developed for block copolymers. DTIC

N94-12353# Oregon Univ., Eugene. Dept. of Chemistry.
A NOVEL PHOTOSENSITIVE POLYIMIDE RESIST CONSISTING OF A SOLUBLE POLYIMIDE AND A BIS(PERFLUOROPHENYL AZIDE) AS A CROSS-LINKER Technical Report, Mar. 1992 - Jun. 1993
Sui X. Cai, M. N. Wybourne, and John F. Keana 10 Jun. 1993 15 p
(Contract N00014-92-J-1412)
(AD-A265998; UO-JFWK-MNW-04) Avail: CASI HC A03/MF A01

A photosensitive polyimide resist that consists of a soluble polyimide 5 and bisPFPA 6 as a cross-linker has been formulated. Polyimide 5 containing 11 wt% of bisPFPA has a deep-UV sensitivity of 30-35 mJ sq cm while polyimide 5 itself has a deep-UV sensitivity of 350-400 mJ sq cm. Under our present conditions, features of about 0.5 microns could be resolved with this resist system. DTIC

N94-12354# New Mexico Inst. of Mining and Technology, Socorro. Energetic Material Research and Test Center.
DYNAMIC HIGH-PRESSURE SHOCK COMPACTION OF DIAMOND POWDERS Final Report, May 1991 - 25 May 1993
N. N. Thadhani, P. A. Persson, A. Grebe, V. S. Joshi, and T. J. Arhens 25 May 1993 86 p Prepared in cooperation with CalTech, Pasadena, CA
(Contract N00014-91-C-2173)
(AD-A266004; EMRTC-FR-93-12) Avail: CASI HC A05/MF A01

The present report summarizes investigations carried out on shock consolidation of diamond powders for fabrication of compacts for electronic substrate applications. Consolidation of various types of commercially available natural and synthetic diamond powders has been performed in this study. The type of diamond and morphology of the powder particles affects the consolidation mechanisms as well as the diamond compact characteristics. It is shown that with the use of appropriate particle size distribution, and therefore a high initial packing density, compacts with optimum physical characteristics crack-free and better than 90% of theoretical maximum density can be obtained. However, about 3-5% transformed graphite and extensive residual strain in the compacts has been detected, both of which severely limit the thermal conductivity. The work contained in this report provides an extensive series of experimental results and mechanistic studies discussing the consolidation behavior of diamond powders by the shock compression technique. Author (DTIC)

N94-12380# Massachusetts Univ., Lowell. Dept. of Chemistry.
A RELAXATION STUDY OF POLED NONLINEAR OPTICAL POLYMERS BY INFRARED REFLECTION-ABSORPTION SPECTROSCOPY Technical Report, 1 Jun. 1992 - 31 May 1993
J. I. Chen, S. Marturunkakul, Y. M. Chen, J. Kumar, and S. K. Tripathy 31 May 1993 24 p
(Contract N00014-90-J-1148)
(AD-A265797; TR-93-01) Avail: CASI HC A03/MF A01

The relaxation of poled nonlinear optical (NLO) chromophores in polymer films was characterized by infrared reflection-absorption spectroscopy. Both a guest-host system and a photocrosslinkable polymer system were investigated. Polymethylmethacrylate (PMMA) doped with either 2-methyl-4-nitroaniline (MNA) or 4(4'-nitrophenylazo) phenylamine (DO3) was studied. The photocrosslinkable polymer system, polyvinylcinnamate (PVCN) doped with xy-phenylazo-nitrobenzene (CNNB-R) was also investigated. Doped NLO active molecules were aligned using the corona poling technique. Infrared spectra as a function of time were used to monitor the relaxation behavior of the oriented dyes after poling. Relaxation of NLO molecules was followed at various characteristic vibrational frequencies. The relaxation of MNA was found to be faster than that of DO3. The NLO dye molecule, CNNB-R was covalently bonded to the host polymer and formed a three dimensional crosslinked network after ultraviolet (UV) irradiation. Relaxation of NLO molecules in pristine and UV treated samples were compared. The

UV light induced crosslinking provided better temporal stability of molecular alignment in this system. DTIC

N94-12381# University of Southern Mississippi, Hattiesburg. Dept. of Polymer Science.

THE 13C AND 15N SOLID-STATE NMR OF COPOLYMERS OF NYLON 6 AND 7: OBSERVATION OF A STABLE PSEUDOHEXAGONAL PHASE Technical Report, 1 Jun. 1992 - 31 May 1993

C. G. Johnson and L. J. Mathias 7 Jun. 1993 20 p
(Contract N00014-89-J-1225)
(AD-A265799; TR-54) Avail: CASI HC A03/MF A01

We have synthesized and characterized a series of nylon copolymers based on the even-odd A-B monomer combination, caprolactam, and enantholactam. The nylon 6-co-7 samples obtained were found to possess physical properties which directly correlate with copolymer composition. We have determined degrees and types of crystallinity for these materials using a combination of thermal, NMR, and X-ray measurements. The homopolymers each display highly ordered alpha-crystallites while the copolymers possess less-ordered domains that decrease in alpha-like characteristics down to the 1:1 copolymer which possesses a thermodynamically stable pseudohexagonal ordered phase. The 13C T1 values determined for the annealed 1:1 copolymer were shorter than those of crystalline regions of homopolymers, comparable to those observed for amorphous domains in melt quenched nylon 6 and nylon 7 homopolymers, and significantly longer than the values for precipitated and annealed 1:1 nylon 11-co-12 sample. DTIC

N94-12396# Oregon Univ., Eugene.

POLYMERS FOR MICROELECTRONICS Technical Report, Mar. 1992 - Jun. 1993

S. X. Cai, M. N. Wybourne, and J. F. Keana 10 Jun. 1993 11 p
(Contract N00014-92-J-1412)
(AD-A266036; UO-JFWK-MNW-02) Avail: CASI HC A03/MF A01

A comparative study of polystyrene (PS) with bis(perfluorophenyl) azides 1-2 and the corresponding non-fluorinated bisazides 3-4 as deep-UV resists is reported. Inclusion of as low as 1.2 wt-% of 1 in PS led to 70% retention of film thickness after photolysis and development. PS containing 2.4 wt-% of 1 is greater than 100 times more sensitive as a deep-UV negative resist than PS itself. The presence of 1 in PS also increased the contrast of the resist. On a molar basis, 1 was about 10 times as effective as non-fluorinated bisazide 3 in cross-linking PS while 2 was about 6 times as effective as 4. PS containing 2.4 wt-% of 1 was found to have a deep-UV sensitivity of 5-10 mJ/sq cm and resolution of about 0.5 micrometer. DTIC

N94-12399# Department of the Navy, Washington, DC.

SYNTHESIS AND POLYMERIZATION OF OLIGOMERIC MULTIPLE AROMATIC ETHER-CONTAINING PHTHALONITRILES Patent Application

Teddy M. Keller, inventor (to Navy) 18 Feb. 1993 29 p
(AD-D015729; US-Patent-Appl-SN-019373; Navy-Case-73258) Avail: CASI HC A03/MF A01

Oligomeric monomers are produced by reaction of a bisphenol compound with either a dihalobenzophenone or a (2,2) bis (4-halophenyl) hexafluoropropane and any other activated halogen containing aromatic compounds in the presence of a base and an appropriate solvent. The resulting oligomeric product, a dialkaline bisphenate terminated salt, is then reacted with 4-nitrophthalonitrile to form an oligomer-based phthalonitrile. These oligomers, in the presence or absence of a curing agent, may then be heated to form high temperature thermosetting polymers. These polymers can potentially be used as advanced materials for composites, as adhesives, and for microelectronic applications. DTIC

N94-12407# Rutgers - The State Univ., Piscataway, NJ. Dept. of Mechanics and Materials Science.

FRACTURE BEHAVIOR OF IONOMERS AND IONOMERIC BLENDS

Masanori Hara 27 Feb. 1993 3 p
(Contract DAAL03-89-K-0044)
(AD-A265379; ARO-25424.15-MS) Avail: CASI HC A01/MF A01

We have elucidated the deformation/fracture behavior of ionomers and correlated them to their microstructure. We have also found important molecular variables to achieve enhanced fracture properties of ionomers: high ion content above a critical value, divalent counterions, and excess neutralizing agent. We have elucidated the structural changes associated with the change of each molecular variable. Subsequently, we have produced unique blends made of small amounts of ionomers and large amounts of unmodified polymers. They show synergistic mechanical behavior, retention of transparency of the unmodified polymer, good processability, and excellent cost performance. We have elucidated the structural characteristics responsible for these behavior. Author (DTIC)

N94-12425# Texas Univ., Austin. Dept. of Chemical Engineering.

GLUCOSE ELECTRODES BASED ON CROSS-LINKED (Os(bpy)2Cl)(SUP +/2+) COMPLEXED POLY(1-VINYLIMIDAZOLE) FILMS Technical Report, Oct. 1992 - May 1993

Timothy J. Ohara and Adam Heller 24 May 1993 30 p
(AD-A265404) Avail: CASI HC A03/MF A01

Enzyme electrodes based on a redox hydrogel formed upon complexing water-soluble poly(1-vinylimidazole) ('PVI') with (Os(bpy)2Cl)(+)('Os') and cross-linked with water-soluble poly(ethylene glycol) diglycidyl ether (molecular weight 400, peg 400) are described. The properties of the electrodes depended on their polymers' osmium content, its extent of cross-linking, on the pH, and the ionic strength in which they were used. The redox hydrogels' electron diffusion coefficients (D(sub e)) increased with the osmium content of their polymers. DTIC

N94-12450*# Old Dominion Univ., Norfolk, VA. Dept. of Physics.

MOLECULAR PROPERTIES OF POLYMERIC MATERIALS FOR SPACE APPLICATIONS Final Report, period ending 15 Apr. 1992

Wynford L. Harries, Kristen T. Kern, and Phillip C. Stancil May 1992 13 p
(Contract NCC1-139)
(NASA-CR-194370; NAS 1.26:194370; ODU-TR-PTR-92-1) Avail: CASI HC A03/MF A01

This cooperative agreement was intended to investigate the effects of a space environment on the properties of polymeric materials. In addition, efforts have been made to understand and investigate environment simulation techniques and test methodology. The results identified the changes in the properties of six aerospace structural adhesives, three neat high polymers, and two fiber-reinforced polymers, as caused by exposure to four simulated space environmental conditions. Significant property changes occurred for several of the systems as a result of one or more of the exposures. A summary of the research follows a list of related publications and presentations. CASI

N94-12536# Southeastern Oklahoma State Univ., Durant. Dept. of Physical Sciences.

NMR CHARACTERIZATION OF POLYMERS FORMED IN DIAZOTIZING MIXTURES OF LUMINOL AND 3-AMINO-L-TYROSINE Final Report, 1 Apr. 1992 - 31 Mar. 1993

John R. Wright 24 May 1993 52 p
(AF Proj. 2312)
(AD-A266093; AFOSR-93-0418TR) Avail: CASI HC A04/MF A01

A melanin-like polymer was prepared by diazotizing luminol (5-amino-2,3-dihydro-1, 4-phthalazinedione) and 3-amino-L-tyrosine in a mixed water/dimethylsulfoxide solvent; this was followed by acetone precipitation and aging of the solid residue for a month (the polymer forms slowly in the solid residue). An aqueous solution containing 0.50 F NaOH, 0.0011 M luminol, 0.010 F potassium formate and the polymer at a concentration of 0.050 mg/mL was observed to undergo an instantaneous seven-fold increase of chemiluminescence when the solution was subjected to a 0.5 Watt/mL irradiation with 20 kHz acoustic energy. This sonochemiluminescent property suggests that earlier reports of strobes of luminescense induced by pulsed microwave irradiations of aqueous solutions of the polymer might have an origin in the microwave acoustic effect. Since the sonochemiluminescent effect is marked and easily detected, the polymer may be applicable as a dosimeter for studying acoustic effects in pulsed, high-powered microwave irradiations, especially where the target geometry is complex. Further insight into the observed properties will depend on a characterization of the structure of the polymer, which is currently not known. Attempts at a structural characterization have been hampered thus far by a lack of suitable polymer fragments, i.e., a reliable means for fragmenting the polymer or limiting its DPn has not been found. DTIC

N94-12577# Cornell Univ., Ithaca, NY. Dept. of Chemistry.
PREPARATION OF STABLE PHOTOPATTERNABLE POLYMERIC MATERIALS FOR NON-LINEAR OPTICS
Jean M. Frechet, Jody E. Beecher, Tony Durst, and Adelheid Godt 12 May 1993 14 p
(Contract N00014-91-J-1338)
(AD-A265359; TR-12) Avail: CASI HC A03/MF A01

Several new functionalized chromophores have been prepared and tested in the preparation of optically stable, photopatternable, NLO polymers for second harmonic generation at the diode laser wavelength of 820 nm. In particular, chromophores containing the sulfonamide or sulfonate ester functionalities have been found to be extremely versatile as they allow attachment of a polymerizable group at the electron-poor end of NLO chromophores. The results of model studies confirm that the sulfonamide groups do not have a deleterious effect on NLO properties. Several new monomers containing 4-alkoxy-4'- sulfonamido-stilbene moieties have been prepared. The 4-alkoxy end of the chromophore is designed to allow its incorporation into a linear polymer backbone. The sulfonamido end of the chromophore has a polymerizable double bond that can be photocrosslinked after poling of the chromophores. As it is extremely important to carry out the photopatterning step without affecting the NLO chromophore or introducing any color into the imaged polymer, novel photoinitiators were tested and found to be suitable. The radiation induced photo-patterning step can be done without causing isomerization of the stilbene chromophores, or introducing any color into the patterned coating. DTIC

N94-12585# Cornell Univ., Ithaca, NY. Dept. of Chemistry.
PHOTOGENERATED BASE IN POLYMER IMAGING. SYNTHESIS AND PHOTOPATTERNING OF POLY(2-CYANO-2-(P-VINYLPHENYL) BUTANOIC ACID)
Man-Kit Leung, Jean M. Frechet, James F. Cameron, and C. G. Willson 12 May 1993 14 p
(Contract N00014-91-J-1338)
(AD-A265288; TR-10-ONR) Avail: CASI HC A03/MF A01

Since the concept of chemical amplification was first introduced by us more that twelve years ago, a number of new resists based on acid-catalyzed thermolysis have been developed and commercialized. This report describes the first chemically amplified resist operating through photogenerated base. The concept is demonstrated with poly(2-cyano-2-(p-vinylphenyl) butanoic acid) which decarboxylates readily under basic conditions. A resist system consisting of this polymer and an amine photogenerator bis(2,6-dinitrobenzyloxy) carbonylhexan-1,6-diamine has been formulated and tested in microlithography. The sensitivity of this resist is extremely high (1.4 mJ/sq cm) with a very high contrast of 13.7. This very high sensitivity confirms that chemical amplification is achieved as the photogenerated base is not consumed in the overall decarboxylation process. The mechanistic insights gained from the study of the decarboxylation process may be used in the design of other resists involving more readily accessible polymers. DTIC

N94-12596# Oak Ridge National Lab., TN.
IN-SITU CRYSTALLIZATION OF SILICATE GLASS FILMS DEPOSITED ON ALPHA- Al2O3
M. P. Mallamaci (Minnesota Univ., Minneapolis.), C. B. Carter (Minnesota Univ., Minneapolis.), and J. Bentley 1993 3 p Presented at the Annual Meeting of the Electron Microscopy Society of America, Cincinnati, OH, 1-6 Aug. 1993
(Contracts DE-AC05-84OR-21400; DE-FG02-92ER-45465; DE-AC05-76OR-00033)
(DE93-012969; CONF-930822-4) Avail: CASI HC A01/MF A01

Ca aluminosilicate glass films were grown on single-crystal alpha-Al2O3 at less than 950 C by pulsed-laser deposition. The films were then heated in an electron microscope to determine the effect of alpha-Al2O3 crystallography on crystallization of Ca-aluminosilicate glasses. DOE

N94-12602# Lawrence Livermore National Lab., CA.
DAMAGE THRESHOLD STUDY OF ION BEAM SPUTTERED COATINGS FOR A VISIBLE HIGH-REPETITION LASER AT LLNL
C. J. Stolz and J. R. Taylor Oct. 1992 11 p Presented at the Symposium on Optical Materials for High-Power Lasers, Boulder, CO, 28-30 Oct. 1992
(Contract W-7405-eng-48)
(DE93-013430; UCRL-JC-111388; CONF-921047-4) Avail: CASI HC A03/MF A01

Ion Beam Sputtered (IBS) coatings offer some distinct advantages over electron beam deposited (e-beam) coatings, namely environmental stability and extremely low total losses. Initial IBS coatings had excessive stress and low laser damage thresholds. For these reasons, a study was initiated to examine potential laser damage thresholds and stress of IBS coatings. A material study was conducted of IBS coatings produced in industry, and a variety of design techniques were explored to increase laser damage thresholds. A post annealing process and backside coatings were developed to reduce the coating stress. DOE

N94-12610# Los Alamos National Lab., NM.
PREDICTION OF ALUMINA PENETRATION
D. A. Mandell Feb. 1993 30 p
(Contract W-7405-eng-36)
(DE93-014017; LA-12520) Avail: CASI HC A03/MF A01

The MESA hydrocode was used to predict two-dimensional tests of L/D 10 and L/D 15 tungsten rods impacting AD 90 alumina with a steel backing. The residual penetration into the steel is the measured quantity in these experiments conducted at the Southwest Research Institute (SWR). The interface velocity as a function of time between an alumina target and a lithium fluoride window, impacted by an alumina disk at velocities between 544 m/s and 2329 m/s, was also predicted. These one-dimensional flyer plate experiments were conducted at Sandia National Laboratories using Coors AD 995 alumina. The material strength and fracture models are important in the prediction of ceramic experiments. The models used in these predictions are discussed. The penetrations in the two-dimensional tests were predicted to 11.4 percent or better. In five of the six experiments, the predicted penetration depth was deeper than the measured value. This trend is expected since the calculation is based on ideal conditions. The results show that good agreement between the 1-D flyer plate data and the MESA predictions exists at the lower impact velocities, but the maximum velocity is overpredicted as the flyer plate velocity increases. At a flyer plate velocity of 2329 m/s the code overpredicted the data by 12.3 percent. DOE

N94-10031# Integrated Aerospace Sciences Corp., Athens (Greece).
HEAT ANALYSIS OF THERMOPLASTIC COMPONENTS DURING THE INITIAL STAGES OF MANUFACTURING: A PROBABILISTIC APPROACH
Dimitri A. Bofilios and J. H. vanLochem (Keuring van Electrotechnische Materialen N.V., Arnhem, Netherlands.) *In* ESA, Advanced Materials for Lightweight Structures Oct. 1992 p 179-183 (For primary document see N94-10001 01-24)
(Contract BE-3062-89/BREU-268)
Copyright Avail: CASI HC A01/MF A04

N94-10032# Dornier Luftfahrt G.m.b.H., Friedrichshafen (Germany).
COST EFFECTIVENESS OF STRUCTURAL APPLICATIONS OF FIBRE REINFORCED THERMOPLASTICS
Winfried Werner *In* ESA, Advanced Materials for Lightweight Structures Oct. 1992 p 185-190 (For primary document see N94-10001 01-24)
Copyright Avail: CASI HC A02/MF A04

N94-10033# Fokker Special Products B.V., Hoogeveen (Netherlands).
APPLICATION OF ADVANCED THERMOPLASTICS
Arnt R. Offringa *In* ESA, Advanced Materials for Lightweight Structures Oct. 1992 p 191-195 (For primary document see N94-10001 01-24)
Copyright Avail: CASI HC A01/MF A04

N94-10034# DSM/nv Nederlandse Staatsmijnen, Geleen.
LOW COST THERMOPLASTIC COMPOSITES FOR STRUCTURAL APPLICATIONS: DESIGN CONCEPTS USING NEW MATERIALS AND PROCESSES
L. E. P. Wenmakers, A. E. Gaalman, and R. Marissen *In* ESA, Advanced Materials for Lightweight Structures Oct. 1992 p 197-202 (For primary document see N94-10001 01-24)
Copyright Avail: CASI HC A02/MF A04

N94-10035# Tampere Univ. of Technology (Finland). Inst. of Plastics Technology.
TAPE WINDING OF THERMOPLASTIC COMPOSITES
K. Lahteenkorva, P. Peltonen, P. Jarvela, and P. Tormala *In* ESA, Advanced Materials for Lightweight Structures Oct. 1992 p 203-206 (For primary document see N94-10001 01-24)
Copyright Avail: CASI HC A01/MF A04

N94-10043# Maschinenfabrik Augsburg-Nuernberg A.G., Munich (Germany).
NEW PROCESSES FOR LIGHTWEIGHT CERAMIC MATRIX COMPOSITES
A. Muehlratzer, K. Handrick, H. Koeberle, and K. Peetz *In* ESA, Advanced Materials for Lightweight Structures Oct. 1992 p 249-254 (For primary document see N94-10001 01-24)
Copyright Avail: CASI HC A02/MF A04

N94-10044# GEC Alsthom, Stafford (England). Engineering Research Centre.
CERAMIC MATRIX COMPOSITES: HIGH PERFORMANCE MATERIALS FOR SPACE APPLICATION
Andrew R. Hyde *In* ESA, Advanced Materials for Lightweight Structures Oct. 1992 p 255-260 Sponsored by Commission of the European Communities (For primary document see N94-10001 01-24)
Copyright Avail: CASI HC A02/MF A04

N94-10049# Erno Raumfahrttechnik G.m.b.H., Bremen (Germany).
MATERIAL ADVANCES FOR LIGHTWEIGHT TPS
U. Rieck and L. Kampmann *In* ESA, Advanced Materials for Lightweight Structures Oct. 1992 p 285-289 Sponsored by Dassault Aviation and Centre Spatial Dassault (For primary document see N94-10001 01-24)
Copyright Avail: CASI HC A01/MF A04

N94-10050# British Aerospace Public Ltd. Co., Bristol (England).
VECTRA INSULATIVE SUPPORT STRUCTURES WITHIN SPACECRAFT
G. H. F. Nayler *In* ESA, Advanced Materials for Lightweight Structures Oct. 1992 p 291-298 (For primary document see N94-10001 01-24)
Copyright Avail: CASI HC A02/MF A04

N94-10058# Fraunhofer-Inst. fuer Chemische Technologie, Pfinztal (Germany).
INVESTIGATION OF THE REASON FOR THE SOFTENING BEHAVIOUR OF FILLED POLYMERS
N. Aksel and C. Huebner *In* ESA, Advanced Materials for Lightweight Structures Oct. 1992 p 345-349 (For primary document see N94-10001 01-24)
Copyright Avail: CASI HC A01/MF A04

N94-10059# Fraunhofer-Inst. fuer Angewandte Material Forschung, Bremen (Germany).
PM TECHNOLOGY AND MECHANICAL PROPERTIES OF METALLIC FOAMS
J. Baumeister, J. Banhart, M. Weber, and B. Guenther *In* ESA, Advanced Materials for Lightweight Structures Oct. 1992 p 351-353 (For primary document see N94-10001 01-24)
Copyright Avail: CASI HC A01/MF A04

N94-10063# Norges Tekniske Hoegskole, Trondheim. Dept. of Metallurgy.
STRUCTURE AND PROPERTIES OF AN RS Al-Si-Ni-Mn-Zr ALLOY FOR HIGH TEMPERATURE APPLICATIONS
H. J. Roven, I. Johansen (Technical Univ. of Norway, Trondheim.), B. Jensen, and O. Jensrud (Raufoss Ammunisjonsfabrikker, Norway.) *In* ESA, Advanced Materials for Lightweight Structures Oct. 1992 p 373-378 Sponsored by Royal Norweigan Council for Scientific and Industrial Research (For primary document see N94-10001 01-24)
Copyright Avail: CASI HC A02/MF A04

N94-10064# Deutsche Forschungsanstalt fuer Luft- und Raumfahrt, Brunswick (Germany). Structural Engineering Inst.
FIBRE REINFORCED STRUCTURES WITH GLASS MATRIX
Malte Froevel *In* ESA, Advanced Materials for Lightweight Structures Oct. 1992 p 379-381 (For primary document see N94-10001 01-24)
Copyright Avail: CASI HC A01/MF A04

N94-10067# Ministry of Economic Affairs, The Hague (Netherlands). Materials Technology Dept.
THE NETHERLANDS INNOVATION ORIENTED RESEARCH PROGRAMME ON POLYMER COMPOSITES AND SPECIAL POLYMERS 1985-1993
C. J. G. vanHalen *In* ESA, Advanced Materials for Lightweight Structures Oct. 1992 p 401-402 (For primary document see N94-10001 01-24)
Copyright Avail: CASI HC A01/MF A04

N94-10767# American Technologies International, Clearwater, FL.
NEW THERMOPLASTIC LAMINATING ADHESIVES FOR THE AIRCRAFT INDUSTRY WITH LOW HEAT RELEASE AND LOW SMOKE EMISSION
Sarfraz A. Siddiqui *In* FAA, Proceedings of the International Conference for the Promotion of Advanced Fire Resistant Aircraft Interior Materials Mar. 1993 p 13-20 (For primary document see N94-10766 01-03)
Avail: CASI HC A02/MF A03

N94-10768# Gill (M. C.) Corp., El Monte, CA. Research and Development.
A NEW LOW SMOKE, LOW HEAT RELEASE STRUCTURAL FOAM
Martin I. Cohen and Melvin R. Kantz *In* FAA, Proceedings of the International Conference for the Promotion of Advanced Fire Resistant Aircraft Interior Materials Mar. 1993 p 21-28 (For primary document see N94-10766 01-03)
Avail: CASI HC A02/MF A03

N94-10769# IMITECH, Inc., Elk Grove Village, IL.
POLYIMIDE FOAM INSULATION SYSTEMS: A MAJOR WEIGHT REDUCTION AND IMPROVEMENT IN FIRE RESISTANCE OF SIDEWALL SYSTEMS
Michael D. ODonnell *In* FAA, Proceedings of the International Conference for the Promotion of Advanced Fire Resistant Aircraft Interior Materials Mar. 1993 p 29-35 (For primary document see N94-10766 01-03)
Avail: CASI HC A02/MF A03

N94-10770# Illbruck, Inc., Minneapolis, MN.
A POLYIMIDE FOAM FOR ADVANCED FIRE RESISTANT AIRCRAFT APPLICATIONS
Amelia DeBaggis *In* FAA, Proceedings of the International Conference for the Promotion of Advanced Fire Resistant Aircraft Interior Materials Mar. 1993 p 37-48 (For primary document see N94-10766 01-03)
Avail: CASI HC A03/MF A03

N94-10774# Great Lakes Chemical Corp., West Lafayette, IN.
NEW TECHNOLOGY FOR EFFECTIVE CONTROL OF FLAMMABILITY IN POLYOLEFIN FIBER/TEXTILES
Charles W. Yacomeni *In* FAA, Proceedings of the International Conference for the Promotion of Advanced Fire Resistant Aircraft Interior Materials Mar. 1993 p 85-91 (For primary document see N94-10766 01-03)
Avail: CASI HC A02/MF A03

N94-10775# Fokker B.V., Amsterdam (Netherlands). Design and Integration Dept.
APPLICATIONS OF CONTINUOUS FIBER REINFORCED THERMOPLASTICS IN AIRCRAFT INTERIORS
Robert G. Diehl *In* FAA, Proceedings of the International Conference for the Promotion of Advanced Fire Resistant Aircraft Interior Materials Mar. 1993 p 93-104 (For primary document see N94-10766 01-03)
Avail: CASI HC A03/MF A03

N94-10776# SP Systems, Los Angeles, CA.
ADVANCED PHENOLIC SYSTEMS FOR AIRCRAFT INTERIORS
Herman Gupta and Mickey McCabe *In* FAA, Proceedings of the International Conference for the Promotion of Advanced Fire Resistant Aircraft Interior Materials Mar. 1993 p 105-119 (For primary document

see N94-10766 01-03)
Avail: CASI HC A03/MF A03

N94-10777# Furane Plastics, Inc., Los Angeles, CA. Aerospace Product Group.
URALANE (TM) 5774-A/B: CIBA-GEIGY'S ADVANCED URETHANE ADHESIVE FOR THE AIRCRAFT INDUSTRY
Edwin C. Clark and Jose Salazar *In* FAA, Proceedings of the International Conference for the Promotion of Advanced Fire Resistant Aircraft Interior Materials Mar. 1993 p 121-135 (For primary document see N94-10766 01-03)
Avail: CASI HC A03/MF A03

N94-10778# Tomark Industries, Inc., Wilmington, DE.
THE FIRE PROPERTIES OF INSULATION BAGS, AS INSTALLED AND AFTER AIRCRAFT OPERATIONS
Robert F. Davis *In* FAA, Proceedings of the International Conference for the Promotion of Advanced Fire Resistant Aircraft Interior Materials Mar. 1993 p 137-143 (For primary document see N94-10766 01-03)
Avail: CASI HC A02/MF A03

N94-10780# Virginia Polytechnic Inst. and State Univ., Blacksburg. Dept. of Chemistry.
FIRE-RESISTANT HYDROLYTICALLY STABLE POLY(ARYLENE PHOSPHINE OXIDE) MATERIAL SYSTEMS
C. D. Smith, H. J. Grubbs, A. Gungor, J. Wescott, S. C. Liptak, P. A. Wood, and James E. McGrath *In* FAA, Proceedings of the International Conference for the Promotion of Advanced Fire Resistant Aircraft Interior Materials Mar. 1993 p 159-174 Sponsored by NSF (For primary document see N94-10766 01-03)
Avail: CASI HC A03/MF A03

N94-10781# National Inst. of Standards and Technology, Gaithersburg, MD. Building and Fire Research Lab.
A NON-HALOGENATED, FLAME RETARDED POLYCARBONATE
Takashi Kashiwagi, Thomas G. Cleary, Gary C. Davis (General Electric Co., Schenectady, NY.), and John H. Lupinski (General Electric Co., Schenectady, NY.) *In* FAA, Proceedings of the International Conference for the Promotion of Advanced Fire Resistant Aircraft Interior Materials Mar. 1993 p 175-189 Sponsored by GE (For primary document see N94-10766 01-03)
Avail: CASI HC A03/MF A03

N94-10786# Georgia-Pacific Corp., Decatur, GA. Research and Development Lab.
FIRE RESISTANCE AND MECHANICAL PROPERTIES FOR PHENOLIC PREPREGS
Shahid P. Qureshi *In* FAA, Proceedings of the International Conference for the Promotion of Advanced Fire Resistant Aircraft Interior Materials Mar. 1993 p 245-253 (For primary document see N94-10766 01-03)
Avail: CASI HC A02/MF A03

N94-10792# Boeing Commercial Airplane Co., Seattle, WA.
FUTURE MATERIAL DEVELOPMENT TRENDS FOR COMMERCIAL AIRPLANE INTERIORS
Peter S. Guard and James M. Peterson *In* FAA, Proceedings of the International Conference for the Promotion of Advanced Fire Resistant Aircraft Interior Materials Mar. 1993 p 313-319 (For primary document see N94-10766 01-03)
Avail: CASI HC A02/MF A03

N94-10794# Deutsche Airbus G.m.b.H., Bremen (Germany).
FUTURE NEEDS IN THE DEVELOPMENT OF MATERIALS FOR AIRCRAFT INTERIORS AND EQUIPMENT
Hans-Dieter Berg *In* FAA, Proceedings of the International Conference for the Promotion of Advanced Fire Resistant Aircraft Interior Materials Mar. 1993 p 333-337 (For primary document see N94-10766 01-03)
Avail: CASI HC A01/MF A03

N94-11330# Pisa Univ. (Italy). Faculty of Engineering.
SMART POLYMERIC SYSTEM FOR ELECTROMECHANICAL TRANSDUCTION
P. Chiarelli, D. DeRossi, and Kayo Umezawa *In* AGARD, Smart Structures for Aircraft and Spacecraft Apr. 1993 3 p (For primary document see N94-11317 01-24)
Copyright Avail: CASI HC A01/MF A04

N94-12029*# Washington Univ., Saint Louis, MO. Center for the Space Sciences and the Physics Dept.
INTERSTELLAR GRAPHITE IN MURCHISON: CONTINUED SEARCH FOR ISOTOPICALLY DISTINCT COMPONENTS Abstract Only
Sachiko Amari, Ernst Zinner, and Roy S. Lewis (Chicago Univ., IL.) *In* Lunar and Planetary Inst., Twenty-fourth Lunar and Planetary Science Conference. Part 1: A-F 1993 p 29-30 (For primary document see N94-12015 01-91)
Avail: CASI HC A01/MF A06

N94-12039*# Academy of Sciences (USSR), Moscow. Inst. of Geochemistry and Analytical Chemistry.
VAPORIZATION BY SHOCK LOADING OF ALBITE, JADEITE, AND PYREX GLASS: EXPERIMENTAL STUDY Abstract Only
D. D. Badjukov and T. L. Petrova (Institute of Lithosphere, Moscow, Russia.) *In* Lunar and Planetary Inst., Twenty-fourth Lunar and Planetary Science Conference. Part 1: A-F 1993 p 51-52 (For primary document see N94-12015 01-91)
Avail: CASI HC A01/MF A06

N94-12040*# Academy of Sciences (USSR), Moscow. Inst. of Geochemistry and Analytical Chemistry.
SHOCK TRANSFORMATIONS IN QUARTZITE Abstract Only
D. D. Badjukov, E. A. Koslov (Institute of Technical Physics, Chelyabinsk, Russia.), Yu. N. Zhugin (Institute of Technical Physics, Chelyabinsk, Russia.), and E. V. Abakshin (Institute of Technical Physics, Chelyabinsk, Russia.) *In* Lunar and Planetary Inst., Twenty-fourth Lunar and Planetary Science Conference. Part 1: A-F 1993 p 53-54 (For primary document see N94-12015 01-91)
Avail: CASI HC A01/MF A06

28 PROPELLANTS AND FUELS

Includes rocket propellants, igniters, and oxidizers; their storage and handling procedures; and aircraft fuels.

For related information see also *07 Aircraft Propulsion and Power, 20 Spacecraft Propulsion and Power,* and *44 Energy Production and Conversion.*

N94-10294# Los Alamos National Lab., NM.
TEMPERATURE EFFECTS ON FAILURE THICKNESS AND DEFLAGRATION-TO-DETONATION TRANSITION IN PBX 9502 AND TATB
B. W. Asay and J. B. McAfee 1993 14 p Presented at the 10th Detonation Symposium, Boston, MA, 12-16 Jul. 1993
(Contract W-7405-eng-36)
(DE93-010742; LA-UR-93-1119; CONF-930713-6) Avail: CASI HC A03/MF A01

The deflagration-to-detonation (DDT) behavior of TATB has been investigated at high temperatures and severe confinement. Comparison is made to other common explosives under similar confinement. TATB did not DDT under these conditions. The failure thickness of PBX 9502 at 250 C has also been determined. Two (2) mm appears to be the limiting value at this temperature. DOE

N94-10489# Army Research Lab., Aberdeen Proving Ground, MD.
TIME-TEMPERATURE SHIFT FACTORS FOR GUN PROPELLANTS Final Report, Jun. - Oct. 1992
Robert J. Lieb and Michael G. Leadore May 1993 29 p
(DA Proj. 1L1-61102-AH-43)
(AD-A264979; ARL-TR-131) Avail: CASI HC A03/MF A01

To estimate the response of gun propellants at higher rates than can be easily reached within the laboratory, stress relaxation measurements have been made in compression for single- (M14), double- (JA2), and triple-based (M30) propellants, as well as a nitramine composite (M43) gun propellant, over the temperature range of -40 to 60 C. Master curves were generated and shift factors were calculated which were used to determine the time-temperature shift factors for each of the propellants over these temperatures. DTIC

N94-10751# Lawrence Livermore National Lab., CA.
SENSITIVITIES OF CALCULATED RESIDUAL STRESS TO SEPARATION DISTANCES OF TWO SIMULTANEOUS EVENTS
J. T. Rambo and W. C. Moss Feb. 1992 20 p Presented at the 6th Symposium on Containment of Underground Nuclear Explosions, Reno, NV, 24-26 Sep. 1991
(Contract W-7405-eng-48)
(DE92-019571; UCRL-JC-109645; CONF-9109114-12) Avail: CASI HC A03/MF A01 (US Sales Only)

LLNL has developed calculational capabilities to model simultaneous explosions of different yields with DYNA2D. Past experimental experience suggests that double events are contained when the work points are separated by no less than twice the sum of the final radii of the two cavities with the higher yield device buried at a safe depth and above the lower yield device. In the past, this non-optimal use of the drill hole was chosen to ensure safe containment and to provide cost savings. Although additional savings can be realized by placing the lower yield device above the higher yield device, there is no really relevant experimental experience. Given current and projected funding levels for the nuclear testing program, study (calculationally) of the feasibility of a low-over-high emplacement could make possible significant savings. In this study we examine the sensitivity of the residual stress field to work point separation for a one kiloton device placed above a ten kiloton device. The geometry is cylindrically symmetric. Work point separations were varied between 50 and 300 m. The depth of burial for the upper device was fixed at 270 m so that overburden would not be a sensitivity factor in the residual stress calculation. Results show that unanticipated weaknesses in the residual stress of the lower yield device occur at some work point separations. DOE

N94-10844 Texas Univ., Austin. Center for Transportation Research.
VEHICULAR FLEET OPERATION ON NATURAL GAS AND PROPANE: AN OVERVIEW Final Report
Dean B. Taylor, Hani Mahmassani, and Mark A. Euritt Nov. 1992 116 p See also PB92-218049 Limited Reproducibility: More than 20% of this document may be affected by microfiche quality
(PB93-194603; CTR-3-4-90/2-983-5F; TX-93+983-5F) Avail: CASI HC A06

The report attempts to contribute to the timely area of alternative vehicular fuels. It addresses the analysis of fleet operation on alternative fuels, specifically compressed natural gas (CNG) and propane, in terms of both fleet economics and societal impacts. Comprehensive information on engine technology, fueling infrastructure design, and societal impacts are presented. An evaluation framework useful for decisions between any vehicular fuels is developed. The comprehensive fleet cost-effectiveness analysis framework used in previous Project 983 reports is discussed in great detail. This framework/model is flexible enough to allow substantial sensitivity and scenario analysis. The model is used to perform sample analyses of both fleet economic and societal impacts. NTIS

N94-10901 Pennsylvania State Univ., University Park.
COMBUSTION-INDUCED CRACK PROPAGATION PROCESS IN A SOLID-PROPELLANT CRACK CAVITY Ph.D. Thesis
Yeu-Cherng Lu 1992 155 p
Avail: Univ. Microfilms Order No. DA9311683

The presence of flaws in a burning solid-propellant rocket motor grain could potentially cause anomalous burning leading to unexpectedly high pressure and subsequent failure of the motor. Present understanding of the combustion and fracture processes in such flaws is limited by the difficulty of instrumenting a full-scale burning grain. Thus, the problem was attacked by taking measurement in a labscale fracture/combustion test rig as well as by developing a coupled finite-element/finite-difference computer code. Emphasis was placed on the investigation of the effects of propellant type, pressurization rate, and boundary confinement on combustion-induced crack propagation in the damaged zone of a propellant grain. Both crack and debond samples were tested. Two types of propellant were studied: AP/PBAN/Al composite and polyester-based high-elongation propellants. A windowed test chamber was designed and fabricated for use in crack and debond test runs. Data acquisition systems include high-speed cameras and pressure transducers. A theoretical model was established for simulating crack combustion process in solid propellants. The interrelated structural deformation and combustion process were simulated by integrating the following analyses: (1) transient, one-dimensional mass, momentum, and energy conservation equations for the gas phase; (2) a transient, one-dimensional heat conduction equation for the solid phase; (3) stress and strain calculations for a two-dimensional, linear viscoelastic, homogeneous, isotropic, thermorheologically simple solid propellant; and (4) fracture analysis for the propellant crack under dynamic pressure loading. The gas- and solid-phase governing equations were solved numerically using a finite differencing technique. Stress and strain calculations were performed with a commercially available finite element code (ANSYS). Quasi-elastic approximation was used to simplify the viscoelastic constitutive equations. J-integral was calculated for the determination of fracture initiation. A useful correlation for crack propagation speed was obtained by combining the information of experimentally observed crack speed and numerically calculated J-integral at different pressurization rates. Reasonably good agreement of crack contour and crack propagation speed between experimental and theoretical results was obtained. Dissert. Abstr.

N94-11017# Runzheimer International, Rochester, WI.
BUSINESS FLEET REFUELING ASSESSMENT Final Report, Mar. - Nov. 1992
A. Chaudier Jan. 1993 73 p
(Contract GRI-5092-810-2365)
(PB93-189892; GRI-93/0026) Avail: CASI HC A04/MF A01

The report investigates refueling characteristics and capabilities for the light-duty market sector, particularly business automobile fleets. It develops a profile of the characteristics of light-duty and automobile business fleets in 22 designated non-attainment areas, as well as Pittsburgh and Salt Lake City. Reliable data on these subjects will enable better analysis of the market potential for natural gas in the surveyed areas. NTIS

N94-11269# Lawrence Livermore National Lab., CA.
ENERGY TRANSFER DYNAMICS AND IMPACT SENSITIVITY
L. E. Fried and A. J. Ruggiero Dec. 1992 8 p Presented at the 16th Material Research Society International Symposium on the Scientific Basis for Nuclear Waste Management Fall Meeting, Boston, MA, 30 Nov. - 5 Dec. 1992
(Contract W-7405-eng-48)
(DE93-009551; UCRL-JC-111995; CONF-921101-101) Avail: CASI HC A02/MF A01

In this paper we focus on the relation between impact sensitivity and energy transfer rates. When a crystal receives an impact, low frequency lattice vibrations (called phonons) are excited. Typical phonon frequencies are 0-200 cm(exp -1). This energy must then be converted to vibron frequencies (1000-2000 cm(exp -1)) before bond breaking can occur. We derive a simple formula for the energy transfer rate in terms of the density of vibrational states and the vibron-phonon coupling. We are able to estimate the phonon upconversion rate in widely varying energetic materials such as TATB, HMX, and Pb styphnate by examining existing inelastic neutron scattering data. We find that the estimated energy transfer rates in pure unreacted material are strongly correlated with impact sensitivity. DOE

N94-11303# Materials Research Labs., Maribyrnong (Australia).
SUBMARINE INTERNAL WAVES
E. O. Tuck (Adelaide Univ., Australia.) Jan. 1993 64 p
(MRL-GD-0049; AR-008-256) Avail: CASI HC A04/MF A01

Details are provided of research directed towards the development of the computer program WAKE for predicting the internal waves produced by the passage of a submarine in a density stratified ocean. The research was undertaken within DSTO during the period Feb.-Mar. 1992. The report takes the form of a series of appendices (presented in chronological order), which provide a record of the progress of the research during that period. Results are presented which indicate that a representative submarine produces internal waves which have a velocity magnitude of about one millimeter per second. Author (revised)

N94-11366# Sandia National Labs., Albuquerque, NM.
ADVANCED DIAGNOSTICS FOR IN SITU MEASUREMENT OF PARTICLE FORMATION AND DEPOSITION IN THERMALLY STRESSED JET FUELS

T. J. OHern, W. M. Trott, S. J. Martin, and E. A. Klavetter 1993 12 p Presented at the 31st AIAA Aerospace Sciences Meeting, Reno, NV, 11-14 Jan. 1993 Previously announced in IAA as A93-23045
(Contract DE-AC04-76DP-00789)
(DE93-009798; SAND-92-1168C; CONF-930108-6; AIAA Paper 93-0363)
Avail: CASI HC A03/MF A01

Two techniques have been developed and applied for in situ monitoring of the processes involved in thermal degradation and solids deposition when several different aviation fuels are thermally stressed. Photon correlation spectroscopy is a dynamic light scattering technique that has proven to be a valuable tool for both real-time and post-test analysis of thermally stressed jet fuels. In situ measurements of post-stressed fuels have shown that significant particle formation can occur at temperatures as low as 120 C, and that relatively large particles (greater than 200 nm mean hydrodynamic diameter) are formed at temperatures less than 200 C. Particle size tends to increase with increasing stress temperature over the range 125-180 C, with substantial changes in the mean particle size occurring over ranges of only 10-20 C. Real-time measurements indicate that the mean particle diameter increases with increased exposure time at fixed temperature. An induction time is also evident in the real-time data, as an increasingly shorter exposure time is needed for particles to form in detectable size and concentration as the stress temperature is increased. The particle diameters measured post-test, when the fuel has cooled to room temperature, are larger than those measured at elevated temperatures, demonstrating the need for real-time measurements. A complementary experimental system using a quartz crystal microbalance has proven valuable for in situ determination of mass deposition rates during thermal stress tests. These data can be used to determine such kinetic factors as the global activation energies for the tested fuels and for quantitative evaluation of fuel thermal stability. DOE

N94-11444# Musashi Inst. of Tech., Tokyo (Japan).
PREPRINTS OF THE 13TH HYDROGEN ENERGY SYSTEM SYMPOSIUM
Masaru Hiruma, Hiromasa Hashimoto (National Space Development Agency, Ibaraki, Japan.), and Yasuharu Hosono 17 Nov. 1992 56 p Symposium held in Tokyo, Japan, 17 Nov. 1992
(DE93-781115; ETDE/JP-mf-93781115) Avail: CASI HC A04/MF A01

Twelve preprints, which were given originally at the 13th Hydrogen Energy System Symposium, are presented. The preprints cover the following topics: a study on a hydrogen engine with direct injection before TDC; a study on the combustion of hydrogen jet in hydrogen engine; tests of a hydrogen-oxygen combusted gas turbine with inert-gas recirculation; flow analysis of a scramjet engine combustor; a study of the structure of a liquid hydrogen pump;the fuel vessel of an LNG vehicle; magnetic field effects on metal hydride electrode potential; absorbing-desorbing characterization of Ti-V-Fe alloy system; the effects of measurement condition and method on cyclic hydriding and dehydriding property of hydrogen storage alloys; studies on the match between the PV array and S.P.E. electrolyzer; cost estimate of photovoltaic hydrogen production; and a catalyst study on liquid-phase dehydrogenation of cyclohexane for thermo-regenerative fuel cell. DOE

N94-12275# Advanced Fuel Research, Inc., East Hartford, CT.
A NOVEL TEST METHOD FOR FUEL THERMAL STABILITY Final Report, 13 Apr. 1992 - 13 Jan. 1993
Michael A. Serio, David S. Pines, Erik Kroo, Kim S. Knight, and Peter R. Solomon Feb. 1993 84 p
(Contract F33615-92-C-2213)
(AD-A265853; AFR-526021; WL-TR-93-2032) Avail: CASI HC A05/MF A01

The object of this work was to demonstrate that an FT-IR fiber optic probe and a quartz crystal microbalance (QCM) probe could be used to measure deposit formation from thermal stressing of jet fuels in a high-temperature, high pressure flow system. These probes were designed, constructed, and tested in an existing Fuel Stability Test System (FSTS) which had an FT-IR Attenuated Total Reflectance (ATR) circle cell monitoring the stressed fuel after cooling to ambient temperature. Shell Jet A and Sun Jet A-1 fuel were tested. It was demonstrated that both the FT-IR fiber optic probe and the QCM probe could successfully differentiate between a 'stable' and an 'unstable' fuel. The results from the QCM probe tests indicate that the drop in frequency for this particular probe results from viscosity dampening and not the mass of the film. The changes in the bulk fuel composition from thermal stressing were measured with the ATR circle cell and were found to be significantly different from the changes in the deposit layer composition measured by the fiber-optic probe. DTIC

N94-12282# Pennsylvania State Univ., University Park. Dept. of Materials Science and Engineering.
ADVANCED THERMALLY STABLE COAL-DERIVED JET FUELS: COMPOSITIONAL FACTORS AFFECTING THERMAL DEGRADATION OF JET FUELS Annual Report, 1 Aug. 1991 - 31 Jul. 1992
C. Song, S. Eser, H. H. Schobert, P. G. Hatcher, and M. M. Coleman Dec. 1992 177 p
(Contract MIPR-FY1455-91N-0638; AF Proj. 3048)
(AD-A265842; WL-TR-93-2007) Avail: CASI HC A09/MF A02

This project focuses on the compositional factors affecting the high temperature thermal stability of coal-derived and petroleum-based jet fuels in the pyrolytic regime. Thermal stability refers to the resistance of fuel to chemical decomposition at high temperatures to cause the solid deposition and liquid depletion. There are four broad objectives in this project, and the research work is divided into four tasks. The first task clarifies the chemistry of fuel degradation and mechanisms of solid formation, identifies thermally stable classes of hydrocarbon compounds, and provides information for enhancing intrinsic stability of jet fuels. The second task involves characterization of the solids including deposits, sediments, and gums produced from fuels and model compounds at high temperatures. The third task is to explore the means to enhance the thermal stability of fuels by examining the effects of various additives. The fourth task is a newly initiated exploratory study on conversion of coals to thermally stable jet fuels. DTIC

N94-12564# Brigham Young Univ., Provo, UT. Dept. of Chemical Engineering.
DISTRIBUTED COMBUSTION IN SOLID PROPELLANTS Final Report, 1 Feb. 1991 - 1 Feb. 1992
M. W. Beckstead and K. P. Brooks Mar. 1993 58 p
(Grant AF-AFOSR-0152-91)
(AD-A265727; AFOSR-93-0401TR) Avail: CASI HC A04/MF A01

This report summarizes work on a research program to quantify the effect of distributed combustion of metal particles in a Rijke burner. Under a previous contract, experimental data were obtained with the Rijke burner, and a mathematical model of the burner was developed. To improve the model, the McIntosh flame model, based on large activation energy asymptotics, has been coupled to the acoustic model. Results have been compared to experimental data showing that the McIntosh transfer function is an improvement over previous models. Law's model of aluminum combustion has been modified to include the effects of multiple oxidizers and their products, oxide accumulation on the surface of the burning aluminum particle, and convection. There are no adjustable parameters in the improved aluminum combustion model, and both transport and thermodynamic properties are calculated internally. Results indicate that the modified model compares more favorably to experimental data than a simple liquid droplet model. The aluminum combustion model has also been coupled to the Rijke acoustic model. Calculations show a sensitivity to the size of the region of influence surrounding a particle and to the time lag between the particle response and the acoustic pressure. The results show reasonable agreement with available data for aluminum particles burning in the Rijke burner. DTIC

29 MATERIALS PROCESSING

Includes space-based development of products and processes for commercial applications.

For biological materials see *55 Space Biology.*

N94-10070# European Space Agency, Paris (France).
PROCEEDINGS OF THE 8TH EUROPEAN SYMPOSIUM ON MATERIALS AND FLUID SCIENCES IN MICROGRAVITY, VOLUME 1
Brigitte Kaldeich, ed. Aug. 1992 445 p Symposium held in Brussels, Belgium, 12-16 Apr. 1992; sponsored by NASA; ESA; CNES; Deutsche Agentur fuer Raumfahrtangelegenheiten; Italian Space Agency; EEC; Brussels Univ.; and the Science Policy Office of Belgium

(ESA-SP-333-Vol-1; ISBN-92-9092-174-9; ETN-93-93949) Copyright
Avail: CASI HC A19/MF A04; ESA, EPD, ESTEC, Noordwijk, Netherlands, HC

Papers presented at the 8th European Symposium on Materials and Fluid Sciences in Microgravity are published. In this volume, the following aspects are discussed: liquid bridge configuration; Marangoni flow, heat, and mass transfer; technology and new facilities used in the study of materials; and fluid sciences in microgravity. For individual titles, see N94-10071 through N94-10143.

N94-10071# Kodak Ltd., Harrow (England).
THE FORMATION AND BREAKAGE OF LIQUID BRIDGES UNDER MICROGRAVITY
John F. Padday *In* ESA, Proceedings of the 8th European Symposium on Materials and Fluid Sciences in Microgravity, Volume 1 Aug. 1992 p 41-49 (For primary document see N94-10070 01-29)
Copyright Avail: CASI HC A02/MF A04; ESA, EPD, ESTEC, Noordwijk, Netherlands, HC

The formation and breakage of liquid bridges under microgravity was analyzed experimentally from data obtained in parabolic flight, and it is shown that all such formation and breakages take place in at least two stages. With respect to breakage, the first stage, the bifurcation process, is shown to be slow and is driven slowly by diminution in surface free energy. The energy is, however, sufficiently large to increase the capillary pressure inside the bridge. The second stage may follow one of two paths depending on the capillary number of the liquid. At low capillary number, the neck of the bridge forms a rod of liquid which then breaks at each end to form a satellite drop, while the two liquid caps recoil under inertial forces. At high capillary number, the rod diameter decreases successively until it becomes threadlike and finally microscopic. Under these conditions no visible satellite drop is formed and no recoil occurs. Some experiments were performed which followed the merging of two spherical caps of liquid to form a stable unified zone. The process of merging is shown to require a small capillary pressure to bring the surface molecules into contact. Thereafter, the equilibrium shape is reached only after minimum area is reached. Again, liquids with high capillary number reach equilibrium quiescently whereas those with a low capillary number undergo traumatic union. When the two caps are composed of immiscible liquids the merging process is not as traumatic but is greatly slowed down as the new liquid-liquid interface is generated. The breakage follows the same pattern as with a single liquid, but the liquid of lowest surface tension is the phase in which breakage occurs. ESA

N94-10072# Escuela Tecnica Superior de Ingenieros Aeronauticos, Madrid (Spain). Lab. de Aerodinamica.
EXPERIMENTAL STUDY OF AXISYMMETRIC THERMOCAPILLARY FLOWS
Jesus Lopez-Diez *In* ESA, Proceedings of the 8th European Symposium on Materials and Fluid Sciences in Microgravity, Volume 1 Aug. 1992 p 51-55 Sponsored by Comision Interministerial de Ciencia y Tecnologia, Spain (For primary document see N94-10070 01-29)
Copyright Avail: CASI HC A01/MF A04; ESA, EPD, ESTEC, Noordwijk, Netherlands, HC

The steady small amplitude thermocapillary driven convection and deformation of the free surface in a floating zone held by capillary forces between two circular concentric solids is experimentally analyzed when the temperature is not constant along the interface and the gravitational effects can be neglected. The technique of diagnosis implemented in order to analyze the induced Marangoni convection is presented. The aim of these combined techniques is to determine the interface deformation and the velocity field inside a floationg zone, heated from above and cooled from below, at the same time. An experimental set up was devised and a number of experiments with different liquids and slenderness, using millimetric floating zones in order to simulate reduced gravity conditions, were carried out. Results of these experiments related both in the interface deformation and in the velocity field are presented. The shape of the free surface is determined using a high contrasted illumination of the float zone and acquiring and analyzing the image in real time. The particle displacement tracking technique is used to estimate the induced velocity field inside the float zone. ESA

N94-10073# Erlangen-Nuremberg Univ. (Germany). Kristallabor.
THE USE OF MAGNETIC FIELDS FOR DAMPING UNSTEADY MARANGONI CONVECTION IN GaAs FLOATING ZONES UNDER MICROGRAVITY
F. M. Herrmann, Johannes Baumgartl, T. Feulner, and Georg Mueller *In* ESA, Proceedings of the 8th European Symposium on Materials and Fluid Sciences in Microgravity, Volume 1 Aug. 1992 p 57-60 (For primary document see N94-10070 01-29)
Copyright Avail: CASI HC A01/MF A04; ESA, EPD, ESTEC, Noordwijk, Netherlands, HC

Experiments which investigated the occurrence of Marangoni Convection (MC) in GaAs Floating Zones (FZ) are presented. Previous results obtained in TEXUS flights, terrestrial crystal growth (with small diameters), and numerical calculations showed that the Marangoni convection causes unsteady flow conditions in the melt during crystal growth. As a result, the FZ grown GaAs crystals contain doping striations. The possibility of establishing steady growth conditions using magnetic fields was consequently investigated. A series of results of terrestrial FZ GaAs experiments under the influence of magnetic fields is presented. It is shown that the formation of striations due to unsteady MC can be avoided during FZ growth of (d approximately equal to 6 mm) GaAs crystals by using axial or transverse magnetic fields of a certain strength. The values of the critical induction, B(sup c) are in the range of B(sup C) is approximately 120 mT (h/d = 1.0) and B(sup C) is approximately 140 mT (h/d = 1.2). The experimental set up of the permanent pole magnet device to be used in the mirror furnace Parelli during the D2 mission is shown. Results of a numerical modeling of the MC under the conditions of these inhomogeneous field conditions are presented. ESA

N94-10074# Cambridge Univ. (England). Dept. of Applied Mathematics and Theoretical Physics.
NON-LINEAR LIQUID BRIDGE DYNAMICS **c34**
R. M. S. M. Schulkes *In* ESA, Proceedings of the 8th European Symposium on Materials and Fluid Sciences in Microgravity, Volume 1 Aug. 1992 p 61-65 (For primary document see N94-10070 01-29)
(Contract B/SC1-900617)
Copyright Avail: CASI HC A01/MF A04; ESA, EPD, ESTEC, Noordwijk, Netherlands, HC

The complete set of nonlinear equations which govern the motion of an inviscid liquid column is studied by means of an integral formulation of the problem. Viscous effects were neglected, and the liquid column was assumed to be rotationally symmetric, but otherwise no restrictions were imposed. This integral formulation is particularly advantageous in an axisymmetric configuration, since it yields a one dimensional problem with unknowns restricted to the free boundary. The evolution of the capillary surface can be traced beyond the point at which the liquid column breaks. ESA

N94-10075# Seville Univ. (Spain). Dept. de Electronica y Electromagnetismo.
DIELECTRIC LIQUID BRIDGE STABILIZATION IN MICROGRAVITY BY MEANS OF ELECTRIC FIELDS
Antonio Castellanos, Antonio Ramos, and Francois Gonzalez *In* ESA, Proceedings of the 8th European Symposium on Materials and Fluid Sciences in Microgravity, Volume 1 Aug. 1992 p 67-71 (For primary document see N94-10070 01-29)
(Contract DGICYT-PB-90-0905)
Copyright Avail: CASI HC A01/MF A04; ESA, EPD, ESTEC, Noordwijk, Netherlands, HC

The role of the different parameters affecting the stability of dielectric liquid bridges subjected to electric fields is presented. Two approaches were used to solve the governing electromechanical equations. First, the Lyapunov-Schmidt reduction was applied to obtain the local bifurcation nature and stability criteria of cylinders and quasicylinders (with residual gravity). Secondly, the Galerkin/finite element method was implemented to extend this study for a wider range of parameters for nonrotating bridges. The differences in electrical permittivites, the volume of the zone, and gravitational and centrifugal force effects upon the critical slenderness as a function of the applied electric field were taken into account. Results show that the electric field has a stabilizing effect somewhat similar to the inverse of the slenderness. ESA

N94-10076# Aix-Marseilles Univ. (France). Inst. de Mecanique des Fluides.

INSTABILITY OF THERMOCAPILLARY CONVECTION IN FLOATING ZONES c76

G. Chen and Bernard Roux *In* ESA, Proceedings of the 8th European Symposium on Materials and Fluid Sciences in Microgravity, Volume 1 Aug. 1992 p 73-78 Sponsored by CNES (For primary document see N94-10070 01-29)

Copyright Avail: CASI HC A02/MF A04; ESA, EPD, ESTEC, Noordwijk, Netherlands, HC

Bifurcation theory combined with the finite difference method is applied to investigate the instability of thermocapillary convection in a model of the floating zone crystal growth process. Both axisymmetric (n = 0) and nonaxisymmetric (n greater than or equal to 1) disturbances for an axisymmeric steady state of thermocapillary convection in a floating zone of O(1) aspect ratio (length/radius) are considered. The critical Marangoni number, the associated oscillatory frequency and the convective flow at the bifurcation are predicted by solving an extended system of steady equations. The critical values of the Marangoni number for the bifurcation from the steady thermocapillary convection to periodic one in time are found very dependent on the Prandtl number of the fluid and the aspect ratio of the floating zone. The variation with these parameters of the threshold for oscillations is obtained by continuation method. ESA

N94-10077# Bremen Univ. (Germany). Center of Applied Space Technology and Microgravity.

THERMOCAPILLARY INSTABILITIES IN CYLINDRICAL LIQUID BRIDGES: MECHANISMS AND TRANSITION BOUNDARIES c34

Hendrik C. Kuhlmann *In* ESA, Proceedings of the 8th European Symposium on Materials and Fluid Sciences in Microgravity, Volume 1 Aug. 1992 p 79-83 (For primary document see N94-10070 01-29)

Copyright Avail: CASI HC A01/MF A04; ESA, EPD, ESTEC, Noordwijk, Netherlands, HC

The stability of steady two dimensional thermocapillary flow in a differentially heated cylindrical liquid bridge of unit aspect ratio is investigated numerically. The basic state is calculated by a Galerkin tau method and the linear stability equations are solved by Galerkin collocation tau. For small Prandtl numbers a new symmetry breaking hydrodynamic instability is found, which is stationary, whereas the supercritical flow for larger Prandtl numbers is identified as a superposition of two hydrothermal waves. In both cases the azimuthal wave number of the critical mode is one. Heat loss of the liquid bridge stabilizes or destabilizes the base state depending on the Prandtl number. ESA

N94-10078# Battelle Inst., Frankfurt am Main (Germany).

STABILITY OF LIQUID BRIDGES BETWEEN PARALLEL PLATES c34

Dieter Langbein *In* ESA, Proceedings of the 8th European Symposium on Materials and Fluid Sciences in Microgravity, Volume 1 Aug. 1992 p 85-93 (For primary document see N94-10070 01-29)

Copyright Avail: CASI HC A02/MF A04; ESA, EPD, ESTEC, Noordwijk, Netherlands, HC

The shape and stability of liquid bridges between parallel plates is investigated. The axisymmetric solutions of the capillary equation under microgravity conditions are nodoids, catenoids, and unduloids. The unduloids fit between parallel plates; if the slope at their inflection point falls short of the contact angle of the liquid with the two plates. Depending on whether the inflection points lie inside or outside the plates, several families of axisymmetric solutions arise. In the case of equal contact angles at both plates, the unduloids become unstable if the slope at the inflection point equals the contact angle. A second stability limit arises from the minimum volume conditions, that is, if two surface shapes enclosing the same liquid volume show up within a family of solutions of the capillary equation. Both kinds of instabilities coincide, if the contact angle equals 31.15 deg. If the contact angles at the two plates differ, the families of unduloids split up accordingly. Their stability is limited by the minimum volume condition. Respective stability diagrams are presented. Another well known asymmetry between the two plates arises from gravity. The stability limits in dependence on Bond number and liquid volume are also given. ESA

N94-10079# Technische Univ., Munich (Germany). Lehrstuhl A fuer Thermodynamik.

TRANSIENT THREE-DIMENSIONAL NUMERICAL SIMULATION OF MARANGONI FLOW IN A LIQUID COLUMN UNDER MICROGRAVITY c34

Johannes Straub and Rudi Marek *In* ESA, Proceedings of the 8th European Symposium on Materials and Fluid Sciences in Microgravity, Volume 1 Aug. 1992 p 95-101 (For primary document see N94-10070 01-29)

Copyright Avail: CASI HC A02/MF A04; ESA, EPD, ESTEC, Noordwijk, Netherlands, HC

The interaction of buoyancy and Marangoni flow in a vertical cylindrical floating zone of aspect ratio 1 with an adiabatic free lateral surface and isothermal top and bottom walls is studied numerically in a transient three dimensional simulation under zero, micro, and Earth gravity conditions. In zero gravity, a rotationally symmetric toroidal flow pattern evolves. The flow mode and the corresponding isotherms remain qualitatively unchanged in all gravity environments. Although natural convection itself forms a single roll, no significant distortion of the symmetric toroidal flow mode occurs, when buoyancy and surface tension driven flows interact. In this study, not only the flow field but also the heat transfer in the liquid bridge is investigated. The enhancement of the steady state heat transfer is examined for Marangoni and buoyancy convection acting in the same or in the opposite direction. The dependence of the overall heat transfer rate on the strength of the thermocapillary convection is established. In a range of Ma greater than or equal to 1 and less than or equal to 10(exp 7), no transition from the steady thermocapillary flow to stable oscillations is observed. ESA

N94-10080# Wisconsin Univ., Madison. Dept. of Materials Science and Engineering.

EFFECT OF ROTATION ON MICROGRAVITY FLOATING-ZONE CRYSTAL GROWTH c76

C. W. Lan, Sindo Kou, and B. C. Liao *In* ESA, Proceedings of the 8th European Symposium on Materials and Fluid Sciences in Microgravity, Volume 1 Aug. 1992 p 103-108 (For primary document see N94-10070 01-29)

(Grant NSF CTS-90-15217)

Copyright Avail: CASI HC A02/MF A04; ESA, EPD, ESTEC, Noordwijk, Netherlands, HC

Computer simulation of heat transfer and fluid flow was conducted to study the effect of rotation on microgravity floating zone crystal growth. The feed rod and the growing crystal were counterrotated at different, as well as the same, speeds ranging from 0 to 400 rpm. A high Prandtl number material NaNO3 (Pr = 9.12) and a low Prandtl number material Si (Pr = 0.01) were examined. The effect of rotation on the convection pattern in the melt and the shapes of the melt/solid interfaces was studied. It was found that rotation helps reduce thermocapillary convection and control the growth front shape very effectively in the case of NaNO3 but less so in Si. ESA

N94-10081# Canadian Space Agency, Ottawa (Ontario).

MARANGONI AND BUOYANT CONVECTIONS IN ZONE MELTING OF GaAs WITH LIQUID ENCAPSULATION c76

Jing Li (Aix-Marseilles Univ., France.) and M. Ziad Saghir *In* ESA, Proceedings of the 8th European Symposium on Materials and Fluid Sciences in Microgravity, Volume 1 Aug. 1992 p 109-113 (For primary document see N94-10070 01-29)

Copyright Avail: CASI HC A01/MF A04; ESA, EPD, ESTEC, Noordwijk, Netherlands, HC

Buoyant and thermocapillary flow in liquid bridges of GaAs melt and its encapsulant B2O3 are studied numerically. Half zone configurations are considered. The influence of buoyant flow on velocity and temperature distributions in the melt as well as in the encapsulant are studied. It is observed that the interfacial deformation is mainly caused by the hydrostatic pressure, however, with the increase of temperature difference, the dynamic effect can become strong enough to totally reverse the deformation of the interface when the bridges is heated at the top. The presence of encapsulant decreases significantly the thermocapillary convection in the melt. ESA

N94-10082# Perm State Univ. (Russia).

COUPLED THERMOVIBRATIONAL AND THERMOCAPILLARY CONVECTION IN LIQUID BRIDGE (FLOATING ZONE SYSTEM) c76

Grigory Z. Gershuni, Tatiana P. Lyubimova (Academy of Sciences, USSR, Perm.), D. V. Lyubimov (Academy of Sciences, USSR, Perm.), and Bernard Roux (Aix-Marseilles Univ., France.) *In* ESA, Proceedings of the 8th European Symposium on Materials and Fluid Sciences in Microgravity, Volume 1 Aug. 1992 p 117-122 Sponsored by Academy of Sciences, Perm, Russia, and CNES (For primary document see N94-10070 01-29)
Copyright Avail: CASI HC A02/MF A04; ESA, EPD, ESTEC, Noordwijk, Netherlands, HC

Numerical simulation of time averaged thermovibrational convection, with or without thermocapillary effect, in a wide range of vibrational Rayleigh number, is addressed. The aim was to use axial vibration to damp thermocapillary convection and improve the crystal growth in the floating zone in weightlessness conditions. The numerical simulation showed that the vibration effect induces a flow that tends to make the isotherms perpendicular to vibration direction. The present results show that the thermocapillary flow is strongly reduced by the effect of axial vibrations. Thus, axial vibration appears to be a very effective way to dynamically control the convection in melts during crystal growth by floating zone techniques. Furthermore, it was shown that the efficiency of this dynamic control should be quite general for any other crystal growth technique, if the direction of vibration is perpendicular to the crystallization front. ESA

N94-10083# Universidad Politecnica de Madrid (Spain). Escuela Tecnica Superior de Ingenieros Navales.

EFFECTS OF AXIAL AND CENTRIFUGAL FORCES ON THE STABILITY OF LIQUID BRIDGES **c34**

I. Martinez, J. M. Perales, and M. Gomez *In* ESA, Proceedings of the 8th European Symposium on Materials and Fluid Sciences in Microgravity, Volume 1 Aug. 1992 p 123-130 Sponsored by Comision Interministerial de Ciencia y Tecnologia, Spain (For primary document see N94-10070 01-29)
Copyright Avail: CASI HC A02/MF A04; ESA, EPD, ESTEC, Noordwijk, Netherlands, HC

The equilibrium and stability equations for liquid bridges are well known, but they are nonlinear and it is difficult to guess real behavior, such as the sensitivity of the shape to axial and rotational forces (measured by Bond and Weber numbers, respectively) or to the geometry of the solid supports that support the bridge. A parametric study by numerical methods of the different effects and the analytical solutions at the bifurcation points in the stability diagrams is presented. The well known shooting method to numerically compute equilibrium shapes of liquid bridges, and their stability limits, is applied to a five parameter case, when different disc sizes (measured by H), bridge lengths (Lr), liquid volumes (Vr), residual axial acceleration (Bo), and solid body centrifugation (We) are contemplated. The bundle of diagrams presented give an idea of the complexities of such a multiparametric analysis and may help in further research to delimitate other forms of instability. The numerical results were used to check the validity of several analytical asymptotic expressions, with perfect agreement over the range of interest (long liquid bridges), but these models only take into consideration the subset (Lr, Vr = 1, H = 0, Bo, We) of the five parameter family. These results will be of great help to plan future space experiments on liquid columns and floating zones in space and in particular will show a method to easily measure very weak residual forces in microgravity platforms. ESA

N94-10084# Splav Technical Center, Moscow (Russia).

ON SHAPE OF SINGLE CRYSTALS GROWN BY FZM IN MICROGRAVITY **c76**

Alexander S. Senchenkov and I. G. Smirnova *In* ESA, Proceedings of the 8th European Symposium on Materials and Fluid Sciences in Microgravity, Volume 1 Aug. 1992 p 131-134 (For primary document see N94-10070 01-29)
Copyright Avail: CASI HC A01/MF A04; ESA, EPD, ESTEC, Noordwijk, Netherlands, HC

The shape of a crystal grown in space by Floating Zone Melting (FZM) is studied theoretically for the axisymmetric case. The effects of the growth angle, the longitudinal acceleration, and the zone length variations are shown. It is found that the growth angle and the zone length variations are of importance. ESA

N94-10085# Universidad Politecnica de Madrid (Spain). Escuela Tecnica Superior de Ingenieros Navales.

LIQUID BRIDGES AND FLOATING ZONES **c34**

I. Martinez and A. Croell (Freiburg Univ., Germany.) *In* ESA, Proceedings of the 8th European Symposium on Materials and Fluid Sciences in Microgravity, Volume 1 Aug. 1992 p 135-142 Sponsored by Comission Interministerial de Ciencia y Tecnologia, Spain (For primary document see N94-10070 01-29)
Copyright Avail: CASI HC A02/MF A04; ESA, EPD, ESTEC, Noordwijk, Netherlands, HC

Fluid science research in float zones, and more specifically on the mechanical stability of the liquid bridge model, is addressed. A liquid bridge spanning between two sharply edged coaxial solids represents a fluid interface configuration of the highest interest, both to basic fluid science and to materials science, particularly as a model of the molten bridge in the floating zone technique of crystal growth and high melting point refining. The float zone process is described, and differences between liquid bridges and float zones are given with regard to statics, dynamics, convection, diffusion, phase changes, electric and magnetic effects, and reactive processes. The conditions under which the liquid bridge model may be applied to real float zone processes are analyzed in detail. The application of this model to the real processing of silicon rods is presented. ESA

N94-10086# Aix-Marseilles Univ. (France).

EVAPORATION UNDER MICROGRAVITY CONDITIONS

A. Steinchen, A. Sanfeld (Brussels Univ., Belgium.), M. Lallemant (Bourgogne Univ., France.), D. Stuerga (Bourgogne Univ., France.), J. Pantaloni (Provence Univ., Marseille, France.), and L. Tadrist (Provence Univ., Marseille, France.) *In* ESA, Proceedings of the 8th European Symposium on Materials and Fluid Sciences in Microgravity, Volume 1 Aug. 1992 p 145-150 (For primary document see N94-10070 01-29)
Copyright Avail: CASI HC A02/MF A04; ESA, EPD, ESTEC, Noordwijk, Netherlands, HC

A review of the hydrodynamic instabilities observed on Earth during the evaporation of various liquids under constraint, for a plane surface or for drops evaporating in another immiscible liquid, is given. The constraints used are mainly an overheating of the liquid above the equilibrium temperature corresponding to the vapor pressure or a constraint of depression under the equilibrium pressure corresponding to the temperature of the liquid. On the basis of the theoretical analysis of the stability of the evaporating systems, the complexity of the coupling between volume (Rayleigh-Benard) instability and surface instabilies (Marangoni and Hickman instability) is highlighted. The role of gravity on these couplings is discussed through the dimensionless parameters of the problem. ESA

N94-10087# Naples Univ. (Italy).

TOWARDS REAL TIME NUMERICAL STIMULATION OF MARANGONI CONVECTION: A HELP FOR TELESCIENCE MICROGRAVITY EXPERIMENTS

Rodolfo Monti, Raimondo Fortezza (Microgravity Advanced Research and Support Center, Naples, Italy.), Gianfranco Desiderio (Microgravity Advanced Research and Support Center, Naples, Italy.), M. K. Ermakov (Academy of Sciences, USSR, Moscow.), Vladimir L. Griaznov (Academy of Sciences, USSR, Moscow.), S. A. Nikitin (Academy of Sciences, USSR, Moscow.), D. S. Pavlovsky (Academy of Sciences, USSR, Moscow.), and V. I. Polezhaev (Academy of Sciences, USSR, Moscow.) *In* ESA, Proceedings of the 8th European Symposium on Materials and Fluid Sciences in Microgravity, Volume 1 Aug. 1992 p 151-156 (For primary document see N94-10070 01-29)
Copyright Avail: CASI HC A02/MF A04; ESA, EPD, ESTEC, Noordwijk, Netherlands, HC

Results of the application of the PC based COMGA (Convection in Microgravity) code for numerical simulation of fluid dynamic experiments are presented. The global system which is called TOLS (Telescience On Line numerical Simulator) and which consists of hardware and software tools that simulate the process in real time and provide all the information to help the experimenter take appropriate decisions during the course of experiments is described. An example of a microgravity experiment on Marangoni convection in axisymmetric liquid bridge is used for calculations. The possibilities of calculation in real time are shown and discussed. It was shown that the PC-TOLS system COMGA is able to model regimes of Marangoni convection for telescience floating zone experiment conditions.

Modifications of COMGA system were carried out to accelerate the program and to use Intel-i860, and to change boundary conditions according to experimental data. A new improved version of COMGA for telescience real time calculation can qualitatively predict unsteady axisymmetrical Marangoni convection for floating zone experiments. It is necessary to introduce appropriate schemes in order to control numerical diffusion and to ensure accuracy of the computed values. It is suggested that the next versions of the simulator should allow input from the experiment of not only the boundary condition but also the measured temperature and velocity field. ESA

N94-10088# Academy of Sciences (USSR), Novosibirsk. Lavrentyev Inst. of Hydrodynamics.

MODEL OF CONVECTIVE MOTION UNDER LOW GRAVITY

V. V. Pukhnachov *In* ESA, Proceedings of the 8th European Symposium on Materials and Fluid Sciences in Microgravity, Volume 1 Aug. 1992 p 157-160 (For primary document see N94-10070 01-29)

Copyright Avail: CASI HC A01/MF A04; ESA, EPD, ESTEC, Noordwijk, Netherlands, HC

It is shown that the classic model of Oberbeck-Boussinesq is not applicable for the description of a liquid motion at very low gravity. Another model which is adequate to the investigated phenomenon is proposed. It is assumed that: the liquid density depends only on its temperature; the potential energy of liquid in the field of gravity is essentially less than its inner energy; the dissipation of the kinetic liquid energy during the motion is negligible; and the dynamic coefficient of liquid viscosity, the thermoconductivity coefficient and the heat capacity of liquid as well as their relation are constant. ESA

N94-10089# Erlangen-Nuremberg Univ. (Germany). Lehrstuhl Werkstoffe der Elektrotechnik.

CALCULATION OF THE EFFECTS OF MAGNETIC FIELD DAMPING IN FLUID FLOW: COMPARISON OF MAGNETOHYDRODYNAMIC MODELS OF DIFFERENT COMPLEXITY

Johannes Baumgartl and Georg Mueller *In* ESA, Proceedings of the 8th European Symposium on Materials and Fluid Sciences in Microgravity, Volume 1 Aug. 1992 p 161-164 (For primary document see N94-10070 01-29)

(Grant BMFT-01-QC-85229)

Copyright Avail: CASI HC A01/MF A04; ESA, EPD, ESTEC, Noordwijk, Netherlands, HC

Magnetohydrodynamic equations were applied in three different commonly used approximations to a model system of a zone melting technique. Magnetic fields (B fields) can be used under microgravity conditions in order to suppress unsteady thermocapillary (Marangoni) convection and the disturbances occurring from steady as well as unsteady (g jitter) residual accelerations. A numerical modeling which is as close to reality as possible would be a valuable help for predicting experimental results and in designing the experiments. In the literature there are different approximations used to describe the magnetohydrodynamic interaction. The results of three commonly used approximations of a three dimensional numerical simulation of flow configurations and their time dependence are presented. The simulations were carried out for a terrestrial g level in order to compare them with experimental results published in an earlier paper. ESA

N94-10090# Liege Univ. (Belgium). Inst. of Physics.

SURFACE-TENSION DRIVEN CONVECTION IN FINITE-SIZE CONTAINERS

G. Lebon (Louvain Univ., Belgium.) and Pierre C. Dauby *In* ESA, Proceedings of the 8th European Symposium on Materials and Fluid Sciences in Microgravity, Volume 1 Aug. 1992 p 165-168 (For primary document see N94-10070 01-29)

Copyright Avail: CASI HC A01/MF A04; ESA, EPD, ESTEC, Noordwijk, Netherlands, HC

When a thin layer of fluid is heated from below and placed in a microgravity environment, surface tension effect is the single motor of convective instability (Marangoni effect). Although several works have been devoted to this subject, most of them concern fluid layers with lateral dimensions very much larger than their thickness. In the present note, this constraint is removed and finite size containers are considered. The critical Marangoni number and the critical wave number are calculated in the case of rectagular boxes. The influence of the dimensions of the boxes on the onset of convection is analyzed. The privileged planform is also determined. The numerical procedure is based on a variational principle. ESA

N94-10091# Bremen Univ. (Germany). Center of Applied Space Technology and Microgravity.

GAS-LIQUID JETS UNDER REDUCED GRAVITY CONDITIONS

Olaf Pamperin and Hans J. Rath *In* ESA, Proceedings of the 8th European Symposium on Materials and Fluid Sciences in Microgravity, Volume 1 Aug. 1992 p 169-172 (For primary document see N94-10070 01-29)

Copyright Avail: CASI HC A01/MF A04; ESA, EPD, ESTEC, Noordwijk, Netherlands, HC

Experimental drafts for the investigation of the behavior of gas-liquid jets under microgravity conditions and a conception of a facility to use inside the capsule of the drop tower Bremen are presented. Gas-liquid jets are very important subjects of fluid dynamic science with many applications in nature and industrial technique. In many cases of two phase flow it is possible to simulate the behavior of immiscible fluids with the help of gas-liquid systems, for example. The disturbance free investigation of two phase jets described by low inertial velocity and by clear density difference between the jet components, is almost impossible under normal gravity conditions. To realize gas-liquid jets without any disturbances and phase separating phenomena affected by convective mass transport a microgravity environment allows interesting experiments. Furthermore, surface tension can be observed much better under zero gravity conditions. Interesting experimental drafts in this field are the variation of nozzle design and shape, the effects of clearly defined disturbances on jet flow, and the interaction of two or more jets. ESA

N94-10092# Academy of Sciences (USSR), Perm. Inst. of Continuous Media Mechanics.

HEAT AND MASS TRANSFER MECHANISMS OF THE POLYMERIZATION UNDER TERRESTRIAL AND MICROGRAVITY CONDITIONS

L. G. Bogatyreva, Vladimir A. Briskman, K. G. Kostarev, V. B. Leontyev (Academy of Sciences of the Uzbek SSR, Tashkent.), M. G. Levkovich (Academy of Sciences of the Uzbek SSR, Tashkent.), Tatiana P. Lyubimova, A. L. Mashinsky (Institute of Biomedical Problems, Moscow, USSR.), G. S. Nechitailo (Energia, Inc., Moscow, Russia.), and P. G. Righetti (Milan Univ., Italy.) *In* ESA, Proceedings of the 8th European Symposium on Materials and Fluid Sciences in Microgravity, Volume 1 Aug. 1992 p 173-178 (For primary document see N94-10070 01-29)

Copyright Avail: CASI HC A02/MF A04; ESA, EPD, ESTEC, Noordwijk, Netherlands, HC

Heat and mass transfer mechanisms of Poly Acryl Amide gels (PAA gels) photopolymerization are investigated in terrestrial experiments and with the help of numerical methods. Experiments include photoregistration of convective flows with the help of light scattering particles, investigation of the temperature and concentration fields by shadow and interferometer methods and viscoelastic measurements. Mathematical modeling is developed for describing heat and mass transfer in a polymerizing mixture under terrestrial and orbital conditions taking into account the main features of the kinetics and the rheology of the process. It is found that the buoyancy convective flows caused by the reaction exothermality and the appearance of a new more dense phase may exert marked influence on the polymerization process characteristics and on the structure of gels obtained on Earth. Under microgravity conditions the intensity of bouyancy convection is markedly less, however nongravitational types of convection might be important. The role of time averaged flows induced by high frequency vibrations is studied numerically. ESA

N94-10093# Academy of Sciences of the Moldavian SSR, Kishinev. Inst. of Applied Physics.

TWO-PHASE FLOW HEAT TRANSFER AND HYDRODYNAMICS IN AN ELECTRIC FIELD c34

M. K. Bologa, S. M. Klimov, and S. I. Chuchkalov *In* ESA, Proceedings of the 8th European Symposium on Materials and Fluid Sciences in Microgravity, Volume 1 Aug. 1992 p 181-186 (For primary document see N94-10070 01-29)

Copyright Avail: CASI HC A02/MF A04; ESA, EPD, ESTEC, Noordwijk, Netherlands, HC

The experimental investigation results of boiling heat transfer, mechanism and internal characteristics during R-113 boiling in narrow flat ducts and annuli under an applied electric field are presented. The influence of a direct current electric field on the two phase flow heat transfer and hydrodynamics during R-113 flow boiling and condensation in vertical narrow annuli is also investigated. Boiling heat transfer intensification in an electric field is found to be caused by a liquid microlayer thining resulting from an increase of the interface movement velocity and is accompanied by the reduction of 'dry spots'. The enhancement of low condensation heat transfer is provided by the augmentation of the vapor flow influence on the condensate film and by the additional interaction of vapor flow and the jet droplet cross flow of the liquid dispersed by the electric field. ESA

N94-10094*# National Aeronautics and Space Administration. Lewis Research Center, Cleveland, OH.
MARANGONI INSTABILITY INDUCED CONVECTION IN AN EVAPORATING LIQUID DROPLET **c34**
An-Ti Chai, N. Rashidnia, and V. S. Arpaci (Michigan Univ., Ann Arbor.) *In* ESA, Proceedings of the 8th European Symposium on Materials and Fluid Sciences in Microgravity, Volume 1 Aug. 1992 p 187-192 (For primary document see N94-10070 01-29)
Copyright Avail: CASI HC A02/MF A04; ESA, EPD, ESTEC, Noordwijk, Netherlands, HC

The processes occurring when a liquid drop undergoes evaporation are described. When a liquid drop undergoes evaporation, its surface temperature decreases. If the droplet is free floating in a microgravity environment, the heat transfer process inside the droplet is initially condition controlled. As the process continues, a radial temperature gradient builds up at the free surface until the critical Marangoni number is exceeded. Then the onset of instability induces thermocapillary convective flows, which in turn speed up the evaporation. The convective flows will subside when the interior of the droplet reaches a certain equilibrium temperature, and the process will return to the diffusion controlled mode. Both preliminary modeling and recent laboratory data have confirmed that Marangoni instability induced convection can and does occur in the droplet evaporation process. Mathematical models representing Marangoni instability in an evaporating liquid drop are presented. An ideal space experiment to study and characterize the onset of Marangoni instability in an evaporating liquid droplet and to establish the effect of Marangoni instability induced convection on the droplet evaporation rate is outlined and the need for conducting such experiments in space is highlighted. However, before an opportunity to conduct experiments in space arises, ground based experiments have to be conducted to study feasibility issues and proof of concept. A ground based experiment of this type is outlined. ESA

N94-10095# Escuela Tecnica Superior de Ingenieros Industriales, Madrid (Spain). Dept. of Ingenieria Energetica y Fluidomecanica.
THERMOCAPILLARY MIGRATION OF BUBBLES: A SEMI-ANALYTICAL SOLUTION FOR LARGE MARANGONI NUMBERS **c34**
A. Crespo and J. Jimenez-Fernandez *In* ESA, Proceedings of the 8th European Symposium on Materials and Fluid Sciences in Microgravity, Volume 1 Aug. 1992 p 193-196 (For primary document see N94-10070 01-29)
(Contracts DGICYT-PS-90-0011; CICYT-ESP88-0586-C02-02)
Copyright Avail: CASI HC A01/MF A04; ESA, EPD, ESTEC, Noordwijk, Netherlands, HC

The thermocapillary motion of bubbles in a liquid environment induced by temperature gradients in the continuous phase is studied. The problem is analyzed under conditions where convective heat transfer is important, that is, for large Marangoni numbers and vanishing Reynolds number, by assuming a thermal boundary layer around the bubble. The temperature and velocity fields are determined, and the corresponding value for the terminal velocity is evaluated by an iterative procedure. The temperature field obtained is given in a form valid for arbitrary Reynolds number; this provides a more direct procedure for further numerical works. ESA

N94-10096# Colorado Univ., Boulder. Low-Gravity Center.
HIGH PRANDTL NUMBER FLUIDS IN A MULTILAYERED SYSTEM UNDER 1-g OR MICRO-g ENVIRONMENT
J.-P. Fontaine and R. L. Sani *In* ESA, Proceedings of the 8th European Symposium on Materials and Fluid Sciences in Microgravity, Volume 1 Aug. 1992 p 197-202 Sponsored in part by ESA, and Center for Low-Gravity Fluid Mechanics and Transport Phenomena, Boulder, CO (For primary document see N94-10070 01-29)
Copyright Avail: CASI HC A02/MF A04; ESA, EPD, ESTEC, Noordwijk, Netherlands, HC

The combined effects of thermocapillary and buoyancy forces in an open cavity heated from one side is modeled numerically. The configuration is that of two shallow, immiscible superposed liquid layers. High Prandtl number fluids are considered under both 1 g and microgravity environments. The interfaces are considered deformable. It is shown that a microgravity environment significantly reduces the flow in the lower layer. ESA

N94-10097# Naples Univ. (Italy). Facolta di Ingegneria.
MARANGONI FLOWS IN OPEN CAVITIES WITH DIFFERENTIALLY HEATED END WALLS **c34**
C. Golia, Antonio Viviani, and Dario Castagnolo (Microgravity Advanced Research and Support Center, Naples, Italy.) *In* ESA, Proceedings of the 8th European Symposium on Materials and Fluid Sciences in Microgravity, Volume 1 Aug. 1992 p 203-210 (For primary document see N94-10070 01-29)
Copyright Avail: CASI HC A02/MF A04; ESA, EPD, ESTEC, Noordwijk, Netherlands, HC

Surface tension driven flows, induced by imposed temperature differences, in plane cavities with differentially heated end walls are considered. This configuration is connected to processes of crystal growth from melt by the open boat horizontal technique. The field equations are numerically solved and the free surface shape is computed under the assumption of small capillary number. Attention is focused on the influence on the flow field structure and behavior of the aspect ratio $A = H/L$, with H and L, respectively, the height and the length of the cavity. Stream lines, isotherms, velocity profiles, and surface shapes are given and discussed; in particular, the maximum of the surface velocity, the maximum of the surface deformation and the bulk heat transfer coefficient (Nusselt number) are reported as functions of the aspect ratio and of the Peclet number. ESA

N94-10098# Naples Univ. (Italy). Facolta di Ingegneria.
BUBBLES AND DROPS BEHAVIOUR UNDER LOW-GRAVITY: A SPACE EXPERIMENT FOR THE IML-2 MISSION
C. Golia, Antonio Viviani, and Raimondo Fortezza (Microgravity Advanced Research and Support Center, Naples, Italy.) *In* ESA, Proceedings of the 8th European Symposium on Materials and Fluid Sciences in Microgravity, Volume 1 Aug. 1992 p 211-216 (For primary document see N94-10070 01-29)
Copyright Avail: CASI HC A02/MF A04; ESA, EPD, ESTEC, Noordwijk, Netherlands, HC

The experiment, that will be flown onboard Spacelab IML-2 (International Microgravity Laboratory) mission to investigate bubble and drop dynamics in a non uniform temperature field under low gravity, is presented and discussed. The experimental configuration, liquid matrix, injection liquids and experimental runs are described and the onground research activities are illustrated. Onground experiments are limited to low values of the Reynolds and Peclet number due to restrictions imposed by gravity both on particle size and temperature gradient. Microgravity offers a unique opportunity to quantitatively investigate the migration of bubbles and drops of different sizes at higher transport numbers. ESA

N94-10099# Academy of Sciences (USSR), Moscow. Inst. for Problems in Mechanics.
SPACE AND TEMPORAL BEHAVIOR AND CONTROL OF THE RESIDUAL CONVECTION IN MICROGRAVITY
Vladimir Griaznov, M. K. Ermakov, S. A. Nikitin, D. S. Pavlovsky, and V. I. Polezhaev *In* ESA, Proceedings of the 8th European Symposium on Materials and Fluid Sciences in Microgravity, Volume 1 Aug. 1992 p 217-220 (For primary document see N94-10070 01-29)
Copyright Avail: CASI HC A01/MF A04; ESA, EPD, ESTEC, Noordwijk, Netherlands, HC

Mathematical models of convection were developed: a three Dimensional (3D) direct simulation based on Navier-Stokes equations, and a new PC based system COMGA (Convection in Microgravity) for multiparametrical study of two dimensional convection problems. The possibility of eliminating lateral macroinhomogeneities in an ampoule in semiconductor melts by slow rotation in microgravity is shown using the dialog system COMGA. A slow rotation of microacceleration vector should be used also for the elimination of longitudinal inhomogeneities in the sample. The study of convection in microgravity shows numerous opportunities of eliminating macroinhomogeneities in microgravity due to a slow rotation which should be used also in terrestrial environments as alternative control opportunities. A multiparametrical study with specialized analysis models is needed to obtain conclusions in each case of space processing. ESA

N94-10100*# Colorado Univ., Boulder.

BENARD AND MARANGONI CONVECTION IN MULTIPLE LIQUID LAYERS **c34**

Jean N. Koster, A. Prakash, D. Fujita, and T. Doi (National Space Development Agency, Tokyo, Japan.) *In* ESA, Proceedings of the 8th European Symposium on Materials and Fluid Sciences in Microgravity, Volume 1 Aug. 1992 p 221-226 (For primary document see N94-10070 01-29)

(Grant NAG3-1094)

Copyright Avail: CASI HC A02/MF A04; ESA, EPD, ESTEC, Noordwijk, Netherlands, HC

Convective fluid dynamics of immiscible double and triple liquid layers are considered. First results on multilayer convective flow, in preparation for spaceflight experiment aboard IML-2 (International Microgravity Laboratory), are discussed. Convective flow in liquid layers with one or two horizontal interfaces with heat flow applied parallel to them is one of the systems investigated. The second system comprises two horizontally layered immiscible liquids heated from below and cooled from above, that is, heat flow orthogonal to the interface. In this system convection results due to the classical Benard instability. ESA

N94-10101# Aix-Marseilles Univ. (France). Inst. de Mecanique des Fluides.

COUPLED THERMOGRAVITATIONAL AND THERMOCAPILLARY CONVECTION IN A TWO-LAYER FLUID SYSTEM **c34**

Q. S. Liu, G. Chen, and Bernard Roux *In* ESA, Proceedings of the 8th European Symposium on Materials and Fluid Sciences in Microgravity, Volume 1 Aug. 1992 p 227-231 Sponsored by CNES (For primary document see N94-10070 01-29)

Copyright Avail: CASI HC A01/MF A04; ESA, EPD, ESTEC, Noordwijk, Netherlands, HC

Steady thermogravitational and thermocapillary driven flow of two immiscible liquid layers is considered in the case of a cavity subjected to a horizontal temperature gradient. The Navier-Stokes equations with Boussinesq approximation are solved numerically by a finite different method in a staggered grid. Convective patterns were emphasized numerically. They depend on property ratios of the two liquid layers and on depth fractions of the layers. Reduction of convection in the lower (encapsulated) layer can be achieved by a proper choice of the parameters. Both situations with rigid or with free top surface were considered. This latter configuration is similar to that of an encalpsulated crystal growth. The computations were performed for flat interfaces, liquid-liquid and liquid-gas. Most of them were limited to a cavity of aspect ratio A = 2 (length/height). ESA

N94-10102# Space Technology Corp., Tokyo (Japan).

MEASUREMENT OF THE THERMAL CONDUCTIVITY OF MOLTEN InSb IN A DROP SHAFT

Shin Nakamura and Taketoshi Hibiya *In* ESA, Proceedings of the 8th European Symposium on Materials and Fluid Sciences in Microgravity, Volume 1 Aug. 1992 p 233-236 (For primary document see N94-10070 01-29)

Copyright Avail: CASI HC A01/MF A04; ESA, EPD, ESTEC, Noordwijk, Netherlands, HC

The thermal conductivity of molten InSb was measured under microgravity in a drop shaft by the transient hot wire method using the Thermal Conductivity Measurement Facility (TCMF). Convective heat transfer was confirmed to be sufficiently suppressed during free fall, whereas measurements before dropping were affected by convection due to wire heating. The thermal conductivity of molten InSb was 16.7 W/m.K at 850K and 17.5 W/m.K at 870K. Thermal conductivity values obtained in a drop shaft showed the same temperature dependence as those obtained on board the TEXUS rocket. These thermal conductivities were consistent with estimations using the Wiedemann-Franz law, indicating that molten InSb is metallic. ESA

N94-10103*# National Inst. of Standards and Technology, Gaithersburg, MD.

THE EFFECT OF GRAVITY MODULATION ON THERMOSOLUTAL CONVECTION

Bonita V. Saunders, Bruce T. Murray, G. B. McFadden, S. R. Coriell, and A. A. Wheeler *In* ESA, Proceedings of the 8th European Symposium on Materials and Fluid Sciences in Microgravity, Volume 1 Aug. 1992 p 237-241 Sponsored by NASA and DARPA (For primary document see N94-10070 01-29)

Copyright Avail: CASI HC A01/MF A04; ESA, EPD, ESTEC, Noordwijk, Netherlands, HC

In a gravitational field, the opposing effects of components of different diffusivities, for example, temperature and solute, in the density profile in a fluid may produce convective instabilities that exhibit a broad range of dynamical behavior. The effect of time periodic vertical gravity modulation on the onset of these instabilities in an infinite horizontal layer with stress free boundaries is examined. This work is viewed as a first step in expanding previous results in solidification to the full problem of characterizing the effects of gravity modulation in thermosolutal convection during the directional solidification of binary alloys. Calculations carried out both with and without steady background acceleration are presented, the latter results being relevant to microgravity conditions. ESA

N94-10104# Goettingen Univ. (Germany). Inst. fuer Angewandte Mechanik und Stroemungsphysik.

THERMOCAPILLARY SLUG FLOW IN A CAPILLARY TUBE **c34**

Martin Schaefer, Heinz Lang (Max-Planck-Inst. fuer Stroemungsforschung, Goettingen, Germany.), and Helmut Eckelmann *In* ESA, Proceedings of the 8th European Symposium on Materials and Fluid Sciences in Microgravity, Volume 1 Aug. 1992 p 243-246 (For primary document see N94-10070 01-29)

Copyright Avail: CASI HC A01/MF A04; ESA, EPD, ESTEC, Noordwijk, Netherlands, HC

The thermocapillary motion of a liquid slug in a horizontally mounted capillary tube filled with a matrix liquid was investigated theoretically and experimentally. It was found that the slug velocity U depends on the square of the film thickness h between the capillary wall and the slug, linearly on the temperature gradient dT/dx and is inversely proportional to the dynamic viscosity mu(sub 1) of the matrix liquid. A further result of the present investigations is that a critical Bond number can be defined, which is constant and a measure for the starting of the motion of the slug. Furthermore, a theory by Goldsmith and Mason, describing the influence of buoyancy on slug flow, was modified for the case of thermocapillary motion. A good agreement between experiment and theory was found. ESA

N94-10105# Bremen Univ. (Germany). Center of Applied Space Technology and Microgravity.

SEPARATION OF GRAVITATIONAL EFFECTS ON THE FLOW OF SUSPENSION IN TUBES BY MEASUREMENTS IN WEIGHTLESSNESS

Bernhard Schwark-Werwach and Hans J. Rath *In* ESA, Proceedings of the 8th European Symposium on Materials and Fluid Sciences in Microgravity, Volume 1 Aug. 1992 p 247-251 (For primary document see N94-10070 01-29)

Copyright Avail: CASI HC A01/MF A04; ESA, EPD, ESTEC, Noordwijk, Netherlands, HC

Under microgravity the influence of gravity disappears and therefore sedimentation effects are eliminated. In this case it is possible to separate effects of gravity from the interaction between solid particles, fluid and wall. A suspension of glass spheres in water was chosen as a model suspension. The pressure drop for different flow rates, tube diameters, particle diameters and concentrations of particles was measured in the turbulent region. Measurements were made under microgravity in the drop tower Bremen and during parabolic flights of aeroplanes. They were completed by measurements under Earth gravity. The method to measure the pressure drop without sedimentation of a suspension, which is heterogeneous under terrestrial gravity conditions, was successfully tested. The additional pressure drop by the particles differs from other homogeneous suspensions and depends on the tube diameter, Reynolds number and concentration. A reduction of turbulent energy dissipation was demonstrated. ESA

N94-10106# Gesamthochschule, Essen (Germany).
LABORATORY STUDY ON THE NATURAL MODES OF A ROTATING TWO-PHASE FLUID SYSTEM SUBJECT TO AXIAL EXCITATION **c34**
Julius Siekmann and Dieter Raake *In* ESA, Proceedings of the 8th European Symposium on Materials and Fluid Sciences in Microgravity, Volume 1 Aug. 1992 p 253-256 Sponsored in part by Ministerium fuer Wissenschaft und Forschung des Landes Nordrhein-Westfalen, Germany (For primary document see N94-10070 01-29)
Copyright Avail: CASI HC A01/MF A04; ESA, EPD, ESTEC, Noordwijk, Netherlands, HC

A series of experiments was carried out to investigate the natural modes and the natural frequencies of a rotating two phase fluid system which is subject to a axial excitation. The fluid system air/silicon oil AK-0.65, enclosed in a right circular cylinder rotating about a vertical axis, was studied by specifying the rotational frequency and applying a freely selected axial frequency. A plot of the test data with logarithmic scales in both axes shows a linear relationship between the Weber and the Bond number. ESA

N94-10107# Technische Univ., Munich (Germany). Lehrstuhl A fuer Thermodynamik.
NUMERICAL SIMULATION OF MARANGONI CONVECTION AROUND GAS BUBBLES IN A LIQUID MATRIX **c34**
Johannes Straub, Johann Betz, and Rudi Marek *In* ESA, Proceedings of the 8th European Symposium on Materials and Fluid Sciences in Microgravity, Volume 1 Aug. 1992 p 257-264 (For primary document see N94-10070 01-29)
(Grant DFG-Str-117/29-1)
Copyright Avail: CASI HC A02/MF A04; ESA, EPD, ESTEC, Noordwijk, Netherlands, HC

Transient Marangoni convection under micro and Earth gravity conditions around a gas bubble floating in a liquid filled rectangular box with adiabatic side walls, while the bottom and top walls are maintained at different temperatures, is simulated with a two dimensional model. Employing two numerical methods, a finite difference scheme with explicit time steps and a fully implicit control volume finite element method, the enhancement of the heat transfer in the liquid matrix due to Marangoni convection is investigated in parallel. To simplify the calculations, the bubble is fixed at a certain location in the container, while the necessary transient force to hold the bubble in place is determined. For a test fluid with Prandtl number equal to 1.93, the transient overall heat transfer and fluid flow are examined for several configurations of bubble and container in terms of the dimensionless numbers Nusselt number and Marangoni number. Contrary to the very common view that the gas bubble would reduce the heat transfer due to its insulating behavior, the energy transport is rather augmented by the Marangoni convection acting on the free surface of the bubble. The numerical simulations show that Marangoni convection can fully replace buoyancy induced heat transfer mechanisms in a microgravity environment. In contrast to former assumptions, Marangoni flow is, in general, not negligible. The transient development of fluid flow and heat transfer was calculated; only the final steady state results are presented. ESA

N94-10108# Naples Univ. (Italy). Facolta di Ingegneria.
BOUNDARY LAYERS ALONG HORIZONTAL FREE SURFACES DUE TO COMBINED EFFECTS OF TEMPERATURE AND CONCENTRATION GRADIENTS **c34**
Antonio Viviani and R. Savino *In* ESA, Proceedings of the 8th European Symposium on Materials and Fluid Sciences in Microgravity, Volume 1 Aug. 1992 p 265-272 (For primary document see N94-10070 01-29)
Copyright Avail: CASI HC A02/MF A04; ESA, EPD, ESTEC, Noordwijk, Netherlands, HC

Boundary layers along horizontal free surfaces due to buoyancy forces and surface tension gradients, arising from combined effects of temperature and concentration gradients are considered. A similarity analysis is performed in combination with a nondimensional order of magnitude analysis that give, at the same time, the a priori conditions for the existence and characterization of all possible flow regimes, and the conditions for the existence of similar solutions. The numerical results are presented for Prandtl and Schmidt numbers ranging from liquid metals to silicon oils and different values of the similarity parameters. In the more general case of double diffusive boundary layers, the computed profiles are discussed for typical Prandtl and Schmidt numbers of interest in melt crystal growth, in both the cases of aiding or opposing thermal and solutal driving actions. ESA

N94-10109# Gesamthochschule, Essen (Germany).
EXPERIMENTAL ANALYSIS OF BENARD-CONVECTION BY THE COMBINED APPLICATION OF LIQUID CRYSTALS AND PIV **c34**
Klaus Wozniak and G. Wozniak *In* ESA, Proceedings of the 8th European Symposium on Materials and Fluid Sciences in Microgravity, Volume 1 Aug. 1992 p 273-278 (For primary document see N94-10070 01-29)
Copyright Avail: CASI HC A02/MF A04; ESA, EPD, ESTEC, Noordwijk, Netherlands, HC

A flow visualization technique, which combines Particle Image Velocimetry (PIV) and the liquid crystal tracer technique, for the simultaneous measurement of temperature and velocity fields of thermoconvective liquid flows, is introduced. This technique was applied to the so called Benard convection between two horizontal plates. Additionally, laser doppler velocimetry measurements were performed for the verification of experimental and theoretical predictions. Experimental techniques and results are discussed. ESA

N94-10110# MATRA Marconi Space, Toulouse (France).
PROPELLANT MANAGEMENT IN SURFACE TENSION TANKS
Eric Ducret (Altran Technologies, Toulouse, France.) and L. LeMoullec *In* ESA, Proceedings of the 8th European Symposium on Materials and Fluid Sciences in Microgravity, Volume 1 Aug. 1992 p 281-287 (For primary document see N94-10070 01-29)
Copyright Avail: CASI HC A02/MF A04; ESA, EPD, ESTEC, Noordwijk, Netherlands, HC

Software models and experimental benches for studying some of the physical aspects of the fluid motion in a zero gavity environment are described. These tools are used in the design, development and testing of Propellant Management Devices (PMD's) which provide gas free propellant from the tanks to the thrusters during the life of a spacecraft. PMD's and their validation in simulated low gravity using bubble point measurements and neutral buoyancy tests are addressed. ESA

N94-10111# Freiburg Univ. (Germany). Kristallographisches Inst.
CdTe CRYSTAL GROWTH IN THE SOVIET FACILITY ZONA 4 **c76**
Manfred Salk, B. Lexow, K. W. Benz, D. G. Matioukhin (Scientific Research Inst. for Radioisotope Apparatus, Riga, Latvia.), Y. M. Gelfgat (Academy of Sciences of the Latvian SSR, Riga.), M. Z. Sorkin (Academy of Sciences of the Latvian SSR, Riga.), Alexander S. Senchenkov (Splav Technical Center, Moscow, Russia.), A. V. Egorov (Splav Technical Center, Moscow, Russia.), I. V. Barmin (Splav Technical Center, Moscow, Russia.), and Peter Sickinger (Kayser Threde G.m.b.H., Munich, Germany.) et al *In* ESA, Proceedings of the 8th European Symposium on Materials and Fluid Sciences in Microgravity, Volume 1 Aug. 1992 p 289-291 Sponsored by BMFT (For primary document see N94-10070 01-29)
Copyright Avail: CASI HC A01/MF A04; ESA, EPD, ESTEC, Noordwijk, Netherlands, HC

Two CdTe crystal growth experiments which were successfully performed during the unmanned Photon 7 mission in Oct. 1991 are described. CdTe crystals were grown by the traveling heater method under 1 g and microgravity conditions with and without a rotating magnetic field. All experiments were accompanied by theoretical modeling of temperature profiles, phase boundaries, and flow patterns in the solution zone. ESA

N94-10112# European Space Agency. European Space Research and Technology Center, ESTEC, Noordwijk (Netherlands). Electrical Systems Dept.
PROTEIN, GLASS, AEROSOL RESEARCH, CONTAINERLESS PROCESSING AND DIAGNOSTICS TECHNOLOGY FOR MICROGRAVITY APPLICATION
Matthias Dieckmann *In its* Proceedings of the 8th European Symposium on Materials and Fluid Sciences in Microgravity, Volume 1 Aug. 1992 p 293-296 (For primary document see N94-10070 01-29)
Copyright Avail: CASI HC A01/MF A04; ESA, EPD, ESTEC, Noordwijk, Netherlands, HC

An overview of instrumentation and technologies developed under the European Space Agency's Technology Research Program is given. The initiation phase of a gas film positioning system for processing glasses at advanced temperatures above 700C was completed. Acoustic levitation and containerless processsing were performed with proteins and glasses. Diagnostic techniques, appropriate cuvette and window designs enabling interactions according to the investigated process status and experiment requirements during fluid dynamic and solution growth experiments are intended and latest results are included. Light scattering techniques, similar to those applied to monitor protein crystal growth, are identified as a potential useful microgravity research tool for glasses and aerosols. Developments of appropriate diagnostic instruments dedicated to such applications under microgravity are planned and an overview of technology approaches is given. ESA

N94-10113# Centro Informazioni Studi Esperienze, Milan (Italy).
THE PYRENE LASER INDUCED FLUORESCENCE TECHNIQUE AS A DIAGNOSTIC TOOL FOR COMBUSTION THERMOMETRY IN MICROGRAVITY
Iva Gianinoni, U. Perini, R. Pozzi, Zhou Fuxin (International Centre for Theoretical Physics, Trieste, Italy.), G. Zizak (Consiglio Nazionale delle Ricerche, Milan, Italy.), and A. Lundstroem (European Space Agency. European Space Research and Technology Center, ESTEC, Noordwijk, Netherlands.) *In* ESA, Proceedings of the 8th European Symposium on Materials and Fluid Sciences in Microgravity, Volume 1 Aug. 1992 p 297-300 Sponsored by ESA and Dornier (For primary document see N94-10070 01-29)
Copyright Avail: CASI HC A01/MF A04; ESA, EPD, ESTEC, Noordwijk, Netherlands, HC

A simple instrument technique for temperature measurements around a burning droplet in microgravity conditions was developed. To this purpose the 'anomalous' Laser Induced Fluorescence (LIF) of pyrene was tested in the case of liquid hydrocarbon fuels. The pyrene spectrum exhibits two bands (350 and 395 nm) whose ratio is sensitive to the temperature. A rugged Nd:YAG laser case was used for the excitation of pyrene vapor at 266 nm in seeded flames. Spectral investigations were performed with an optical multichannel detector. Temperatures of flames generated by a porous sphere burner fed with liquid fuel were measured and compared with the corresponding thermocouple measurements. The results indicate that the pyrene LIF technique is suitable for temperature measurements of n-octane flames in the 700 to 1200K range with less than +/- 100K data spread on single measurement points from shot to shot. Future developments might involve the use of a charge coupled device camera to perform single shot two dimensional imaging of the temperature fields in different kinds of flames. ESA

N94-10114# Technische Univ., Munich (Germany). Lehrstuhl A fuer Thermodynamik.
A NEW METHOD FOR HYSTERESIS MEASUREMENTS DEVELOPED FOR C(SUB v) MEASUREMENTS AT THE CRITICAL POINT DURING THE D2-MISSION **c35**
Johannes Straub, Axel Haupt, K. Nitsche, and Kurt Kemmerle (Kayser Threde G.m.b.H., Munich, Germany.) *In* ESA, Proceedings of the 8th European Symposium on Materials and Fluid Sciences in Microgravity, Volume 1 Aug. 1992 p 301-308 Sponsored by BMFT (For primary document see N94-10070 01-29)
Copyright Avail: CASI HC A02/MF A04; ESA, EPD, ESTEC, Noordwijk, Netherlands, HC

The method and design of the High Precision Thermostat (HPT) calorimeter, used for the study of the hysteresis of the specific heat capacity C(sub v) between heating and cooling ramps, are described. The HPT used during the D1 mission is now modified for the D2 mission. The new design provides the possibility to measure C(sub v) in the critical region both during heating and cooling runs at an enlarged temperature range. The unexpected results of the first microgravity measurements of C(sub v) performed during the D1 mission can be explained by an asymmetrical mass distribution in the cell. There the sample was heated electrically, which provides highest accuracy in measuring caloric data, that is, C(sub v), but only measurements from the two phase region into the one phase region are possible. Even at smallest temperature ramps (D1:+3.6 mK/h) the thermodynamic equilibrium can not be reached, which is seen as the reason for the unexpected results of the D1 mission. The new calorimeter is constructed in such a way, that the measurements start in the homogeneous density region above critical temperature, and the sample is cooled down into the two phase region. In microgravity the density will remain homogeneous down to critical temperature and it is anticipated that the real value of C(sub v) can be observed not being influenced by density stratification. A fluid sample of SF6 at the critical density is enclosed in a spherical cell; the energy transport between it and the surrounding shell, which can be heated and cooled continuously, takes place by radiation. By measuring the temperature difference between them as well as the temperature ramp of the sample cell itself, the heat capacity C(sub v) is determined. ESA

N94-10115# Ishikawajima-Harima Heavy Industries Co. Ltd., Tokyo (Japan). Applied Science Dept.
CONCEPT AND DESIGN OF AMPOULE FOR MELT GROWTH OF GALLIUM ARSENIDE IN FIRST MISSION OF SPACE FLYER UNIT
Satoshi Adachi, K. Takahashi, M. Watanabe, Y. Ikegami, J. Ochiai, M. Kuribayashi, and H. Sakai (Institute for Unmanned Space Experiments Free Flyer, Tokyo, Japan.) *In* ESA, Proceedings of the 8th European Symposium on Materials and Fluid Sciences in Microgravity, Volume 1 Aug. 1992 p 311-314 Sponsored by New Energy Development Organization, Tokyo, Japan (For primary document see N94-10070 01-29)
Copyright Avail: CASI HC A01/MF A04; ESA, EPD, ESTEC, Noordwijk, Netherlands, HC

The experimental set up to be installed in the first mission of the space flyer unit for melt growth experiments of gallium arsenide is described. The aim of the experiments is to obtain crystals with uniform concentration of dopant. In order to obtain such crystals, sufficient suppression of the Marangoni convection is required. The design of the gradient heat furnace and ampoules is described. The present design of the ampoule for the crystal growth consists of three parts, that is, the crucible, the vacuum seal, and the sample case. Although an arsenic vapor source is not employed in this ampoule, the stoichiometric change in the melt is negligibly small due to the elimination of the excessive space in the ampoule. The crucible would well reduce the Marangoni convection by covering the melt with the rigid wall. In the case of the melting zone length of 35 mm, the length of the uniform concentration is obtained as about 20 mm from the results of numerical calculation of the diffusion equation. ESA

N94-10116# Splav Technical Center, Moscow (Russia).
CdTe CRYSTAL GROWTH BY THM WITH A ROTATING MAGNETIC FIELD **c76**
I. V. Barmin, A. V. Egorov, G. Filatov, Alexander S. Senchenkov, K. W. Benz (Freiburg Univ., Germany.), B. Lexow (Freiburg Univ., Germany.), Manfred Salk (Freiburg Univ., Germany.), Peter Hofmann (Kayser Threde G.m.b.H., Munich, Germany.), Peter Sickinger (Kayser Threde G.m.b.H., Munich, Germany.), and J. M. Gelfgat (Academy of Sciences of the Latvian SSR, Riga.) et al *In* ESA, Proceedings of the 8th European Symposium on Materials and Fluid Sciences in Microgravity, Volume 1 Aug. 1992 p 315-320 (For primary document see N94-10070 01-29)
Copyright Avail: CASI HC A02/MF A04; ESA, EPD, ESTEC, Noordwijk, Netherlands, HC

To ensure axisymmetric growth conditions and to accelerate mass transfer from the dissolving to the growing interface the experiment on CdTe crystal growth employing the Travelling Heater Method (THM) and a rotating magnetic field was carried out during the Photon 7 mission in the Zona 4 facility in Oct. 1991. The ampoule had an inner diameter of 15 mm. To prepare the flight experiment, a mathematical modeling of the physico-chemical processes in the solution zone, the processes of a dissolving and growth was performed. It is shown that the magnetic field has great influence on the growth conditions. Studies of the grown crystal are being caried out. ESA

N94-10117# Genoa Univ. (Italy). DISTER.
THE SENSITIVITY OF AN OPTICAL FIBER HOLOGRAPHIC INTERFEROMETER **c35**
F. Bedarida, Gian Antonio DallAglio, L. Gatti (Alenia Spazio S.p.A., Turin, Italy.), and F. Solitro (Alenia Spazio S.p.A., Turin, Italy.) *In* ESA, Proceedings of the 8th European Symposium on Materials and Fluid Sciences in Microgravity, Volume 1 Aug. 1992 p 321-323 (For primary document see N94-10070 01-29)
(Contract ESTEC-8822/90/NL/PB(SC))
Copyright Avail: CASI HC A01/MF A04; ESA, EPD, ESTEC, Noordwijk, Netherlands, HC

A sensitivity check of a fiber optic holographic interferometer, which is to be used to study crystal growth and the concentration or thermal gradients in transparent inorganic and biological solution, for the detection of the refractive index, is described. The sensitivity concerning the measurement of the change in refractive index was evaluated by using different glasses with known refractive indices in a series of holograms. Limited by the test pieces it is stated that the sensitivity of the change in refractive index can be at least 0.0001/mm. ESA

N94-10118# Societe Anonyme Belge de Constructions Aeronautiques, Brussels.

DESCRIPTION OF THE LIQUID STRUCTURE FACILITY ARCHITECTURE AND EXPERIMENTAL DEMONSTRATION OF THE DIAGNOSTIC CAPABILITIES **c14**

G. Bekaert, Olivier Dupont (Brussels Univ., Belgium.), Olivier Rousselle (Brussels Univ., Belgium.), J. C. Legros (Brussels Univ., Belgium.), Alain Gonfalone (European Space Agency. European Space Research and Technology Center, ESTEC, Noordwijk, Netherlands.), A. Verga (European Space Agency. European Space Research and Technology Center, ESTEC, Noordwijk, Netherlands.), P. Holbrouck (Verhaert Design and Development, Kruibeke, Belgium.), V. Zolesi (Kayser Italia, Livorno.), and J. L. VanEck (Brussels Univ., Belgium.) *In* ESA, Proceedings of the 8th European Symposium on Materials and Fluid Sciences in Microgravity, Volume 1 Aug. 1992 p 325-330 (For primary document see N94-10070 01-29)
Copyright Avail: CASI HC A02/MF A04; ESA, EPD, ESTEC, Noorwijk, Netherlands, HC

An overview of the Liquid Structure Facility (LSF) architecture, a multiuser multimission experimental facility capable of performing fluid sciences experiments related to surface tension, thermal behavior diffusion, concentration and surface deformation phenomena is given. The LSF was preliminary designed for a Spacelab mission, however, the design analysis takes into account the accommodation on future Columbus missions. The diagnostics fit in the facility is described from a theoretical and experimental point of view. Since the idea of a real multiuser facility dedicated to the fluid physics community has been initiated, the LSF has gone through an evolutive process which now can produce for the scientists a tool dedicated to its specific needs. This is achieved thanks to the modularity of its set of diagnosis tools and to the choice of a standard link to control and to monitor the intelligent cell module. The last development and technical choices related to the LSF made possible the experimental evaluation of the diagnosis performances in terms of feasibility, application range, accuracy, and sensitivity. ESA

N94-10119# Dornier System G.m.b.H., Friedrichshafen (Germany).

ADVANCED PROTEIN, CRYSTALLIZATION FACILITY AND ASSOCIATED NEW DEVELOPMENTS **c14**

R. Bosch, P. Lautenschlager, Lothar Potthast, and J. Stapelmann *In* ESA, Proceedings of the 8th European Symposium on Materials and Fluid Sciences in Microgravity, Volume 1 Aug. 1992 p 331-336 (For primary document see N94-10070 01-29)
Copyright Avail: CASI HC A02/MF A04; ESA, EPD, ESTEC, Noordwijk, Netherlands, HC

The facility concept, reactor design, and latest developments of the Advanced Protein Crystallization Facility (APCF), a multiuser facility for protein crytallization experiments under microgravity, are described. First space flights are planned for 1993 (Spacelab) and 1994 (IML-2 (International Microgravity Laboratory)). In the APCF, 48 experiments can be accommodated under controlled temperature conditions and partly under video observation of the crytallization process. Three types of protein reactors were developed. These allow protein crystallization according to the methods liquid-liquid diffusion, dialysis, and vapor diffusion (hanging drop). New developments include another type of hanging drop reactor with active controlled diffusion and the upgrade of the APCF for the diagnostic methods. ESA

N94-10120*# Space Hardware Optimization Technology, Inc., Floyds Knobs, IN.

DESIGN OF MULTISAMPLE, MULTISTEP PHASE PARTITIONING APPARATUS FOR USE ON SPACE SHUTTLE SPACELAB, AND SPACELAB MISSIONS **c51**

Mark S. Deuser, James M. VanAlstine (Alabama Univ., Huntsville.), John C. Vellinger, Francis C. Wessling (Alabama Univ., Huntsville.), and Charles A. Lundquist (Alabama Univ., Huntsville.) *In* ESA, Proceedings of the 8th European Symposium on Materials and Fluid Sciences in Microgravity, Volume 1 Aug. 1992 p 337-341 (For primary document see N94-10070 01-29)
(Grants NAGw-812; NAGw-1196)
Copyright Avail: CASI HC A01/MF A04; ESA, EPD, ESTEC, Noordwijk, Netherlands, HC

Traditional separation techniques are inadequate for many new bioprocessing challenges. Innovative separation methods such as aqueous two phase partitioning are needed to perpetuate bioprocess commercialization. Aqueous two phase polymer partitioning systems provide a process for separating biological materials when combined with microgravity. An innovative space qualified apparatus developed for carrying out separations by partitioning in immiscible polymer systems under mirogravity conditions is described. The apparatus offers an innovative approach to low gravity bioseparations in general and phase partitioning in particular. These capabilities support NASA's interest in serving the biotechnology research community and providing quantitative data in the gravity dependent components of separation processes. ESA

N94-10121# Bremen Univ. (Germany). Center of Applied Space Technology and Microgravity.

CALIBRATION OF ACCELEROMETERS ON DROP TOWER BREMEN **c35**

U. Kaczmarczik, Hansjorg Dittus, and Hans J. Rath *In* ESA, Proceedings of the 8th European Symposium on Materials and Fluid Sciences in Microgravity, Volume 1 Aug. 1992 p 343-347 (For primary document see N94-10070 01-29)
Copyright Avail: CASI HC A01/MF A04; ESA, EPD, ESTEC, Noordwijk, Netherlands, HC

Accuracy of accelerometer calibration under normal Earth gravity has a limit of about 0.001 m/sq s approximately equal to 0.0001 g(sub 0) in resolution (g(sub 0) acceleration of normal Earth gravity). The most important error influence is the accelerometer cross sensitivity that produces an additional bias error. Under microgravity conditions disturbing cross sensitivities can be neglected. The new ZARM (Center of Applied Space Technology and Microgravity, University of Bremen, Germany) accelerometer calibration device uses the excellent microgravity conditions of drop tower 'Bremen' to achieve better calibration accuracy. The device is specially designed to calibrate the well known quartz flexure sensors for navigation purposes. Other sensor types can be easily adapted by changing the mounting frame and the amplifier. The quality of this device will be shown by testing a high performance quartz flexure sensor (type JA 5L14). ESA

N94-10122# Commissariat a l'Energie Atomique, Grenoble (France). Section d'Etudes de la Solification et de la Cristallogenese.

GAS FILM LEVITATOR FOR CONTAINERLESS PROCESSING OF GLASSES IN MICROGRAVITY CONDITIONS: EARLY CONCEPT AND TECHNOLOGY DEMONSTRATION

Jean Granier, M. Daniel, C. Parayre, J. Bancillon, and J. P. Bugeat (Societe Europeenne de Propulsion, Moissy-Cramayel, France.) *In* ESA, Proceedings of the 8th European Symposium on Materials and Fluid Sciences in Microgravity, Volume 1 Aug. 1992 p 349-356 (For primary document see N94-10070 01-29)
Copyright Avail: CASI HC A02/MF A04; ESA, EPD, ESTEC, Noordwijk, Netherlands, HC

The overall design and main features of a gas film levitator foreseen for containerless processing of glasses in microgravity conditions are presented. The scientific motivations in favor of the development of this multiuser facility and the scientific requirements in stimuli/performances are reviewed. A high temperature mock up of the foreseen facility was designed, manufactured, and tested in order to establish: the feasibility of the overall design concept and of the most critical technologies; and the feasibility of containerless processing of bulk glass samples in the tubular gas film levitator. Large cylindrical glass samples (diameter 15 mm, length 10 mm) were containerlessly processed up to 1250C on ground in this facility. Even larger samples (up to 60 mm length) will be processed in microgravity conditions up to 1500 to 1600C. ESA

N94-10123# Kayser Threde G.m.b.H., Munich (Germany).

HOLOGRAPHIC INTERFEROMETRY FOR MICROGRAVITY APPLICATIONS **c35**

Peter Hofmann, J. Winter (Technische Univ., Munich, Germany.), J.

Engelsberger (Labor Dr. Steinbichler, Neubeuern, Germany.), and Hans Steinbichler (Labor Dr. Steinbichler, Neubeuern, Germany.) *In* ESA, Proceedings of the 8th European Symposium on Materials and Fluid Sciences in Microgravity, Volume 1 Aug. 1992 p 357-359 (For primary document see N94-10070 01-29)
Copyright Avail: CASI HC A01/MF A04; ESA, EPD, ESTEC, Noordwijk, Netherlands, HC

Recent instruments and activities in the field of holographic interferometry for microgravity applications are presented. The work described is a result of close cooperation between industry, institutes, and various universities based upon integrated optical measurement techniques. The following are presented: a holographic interferometer for measurements during parabolic flights in an aircraft; a project study for a universal modular optical system which shall be adaptable to several carriers for microgravity missions; HOLOP, a state of the art holographic interferometer for the German D2 Spacelab mission with emphasis on future improvements; and advanced video and holographic techniques presently developed for industrial applications. ESA

N94-10124# Kayser Threde G.m.b.H., Munich (Germany).
THE HIGH PRECISION THERMOSTAT HPT-HYDRA **c35**
Kurt Kemmerle, H.-G. Bernhardt, Johannes Straub (Technische Univ., Munich, Germany.), Axel Haupt (Technische Univ., Munich, Germany.), and K. Nitsche (Technische Univ., Munich, Germany.) *In* ESA, Proceedings of the 8th European Symposium on Materials and Fluid Sciences in Microgravity, Volume 1 Aug. 1992 p 361-366 (For primary document see N94-10070 01-29)
(Contract BMFT-01-QV-8873)
Copyright Avail: CASI HC A02/MF A04; ESA, EPD, ESTEC, Noordwijk, Netherlands, HC

During the D1 mission the HPT (High Precision Thermostat) produced surprising results regarding the behavior of C(sub v) of SF6 at its critical point. One-g reference tests with the flight unit proved the microgravity origin of the observed phenomenon. It was hypothesized that these results may be due to nonequilibrium and hysteresis effects. Thus the demand for a modified experiment measuring the hysteresis of the specific heat of SF6 at its critical point arose. Additionally, the measuring range around the critical point should be enlarged considerably. This experiment is known as HYDRA (Hysteresis of the specific heat During heating And cooling through the critical point) and will fly on the D2 mission. The necessity of this modified experiment had impacts on the functional concept and on the set up of the HPT. The modifications which had to be installed and the new performance data are described in detail. ESA

N94-10125# Dornier System G.m.b.H., Friedrichshafen (Germany).
TEMPUS: AN ELECTROMAGNETIC LEVITATION FACILITY FOR CONTAINERLESS PROCESSING UNDER MICRO-g IN SPACELAB
Richard Knauf, J. Piller, A. Seidel, and W. Dreier (Deutsche Agentur fuer Raumfahrtangelegenheiten G.m.b.H., Bonn, Germany.) *In* ESA, Proceedings of the 8th European Symposium on Materials and Fluid Sciences in Microgravity, Volume 1 Aug. 1992 p 367-372 (For primary document see N94-10070 01-29)
Copyright Avail: CASI HC A02/MF A04; ESA, EPD, ESTEC, Noorwijk, Netherlands, HC

TEMPUS, an electromagnetic levitator with inductive heating and positioning that allows containerless processing of metallic samples up to 2400C under ultraclean environmental conditions, is presented. Containerless processing under microgravity is one key technology in microgravity materials science research which allows study of the formation of metastable phases, nucleation phenomena, as well as important thermophysical properties like heat capacity, surface tension, and viscosity of high melting materials. A Spacelab version of TEMPUS that is based on an already built laboratory model (which was also tested on parabolic KC 135 flights) and a sounding rocket payload flown within the TEXUS program is being developed. This Spacelab model is a payload element of the U.S. microgravity Spacelab mission IML-2 (International Microgravity Laboratory) to be launched in Jun. 1994. Main features are the nearly independent control of the RF heating and positioning power down to lowest values and the extensive diagnostic devices in the visual and infrared regime, combined with elaborate sample stimulation capability. Comfortable commanding and reprogramming capabilities allow telescience experiments as well as quasi-automatic processing. ESA

N94-10126# Stuttgart Univ. (Germany). Inst. fuer Kerntechnik und Energiewandlung.
THE ELECTRON BEAM FURNACE: A NEW FACILITY FOR MATERIALS SCIENCE RESEARCH
C. Krass, H.-G. Mayer, Michael Braun (Dornier System G.m.b.H., Friedrichshafen, Germany.), H. Lenski (Dornier System G.m.b.H., Friedrichshafen, Germany.), and Christian Stenzel (Dornier System G.m.b.H., Friedrichshafen, Germany.) *In* ESA, Proceedings of the 8th European Symposium on Materials and Fluid Sciences in Microgravity, Volume 1 Aug. 1992 p 373-378 (For primary document see N94-10070 01-29)
(Contract ESTEC-7337/87/NL/PB(SC))
Copyright Avail: CASI HC A02/MF A04; ESA, EPD, ESTEC, Noordwijk, Netherlands, HC

The development and the test results of an electron beam furnace for the utilization in a microgravitational environment are reported. The furnace hardware which can be divided into three major parts is described: electron beam gun, electron optics and diagnostics, and a process chamber including sample and optical sensor system. The optical sensor and control system are described. By just varying the deflection pattern by means of the electron optical components two different types of thermal profiles, a gradient profile with a slope of 200 K/cm, and a hot zone profile with a maximum zone temperature of 1520 K could be established and maintained. A beam power of 550 W had to be applied to a sample out of massive Ta for the gradient profile; for creating a hot zone profile, an input power of only 250 W onto a sample with a ceramic core was sufficient. A continuous pyrometric measurement system with a high local and time resolution has been realized. Temperature sensing with this system reflected an intrinsic feature of electron beam heating: the sharply localized energy deposition at the sample surface. ESA

N94-10127*# Vanderbilt Univ., Nashville, TN. Dept. of Mechanical Engineering.
DESIGN OF A CVD REACTOR FOR THE DEPOSITION OF DIAMOND IN A MICROGRAVITY ENVIRONMENT
Michael L. Languell, J. L. Davidson, and A. M. Strauss *In* ESA, Proceedings of the 8th European Symposium on Materials and Fluid Sciences in Microgravity, Volume 1 Aug. 1992 p 379-381 (For primary document see N94-10070 01-29)
(Grant NAGw-2540)
Copyright Avail: CASI HC A01/MF A04; ESA, EPD, ESTEC, Noordwijk, Netherlands, HC

There is a growing body of theoretical and experimental evidence suggesting that the uniformity, rate, adhesion, quality, and other key properties of Chemical Vapor Deposition (CVD) diamond coatings are influenced by the gas mixing kinetics in the thermal plasma environment of the reaction chamber. The implementation of, for example, Microwave Plasma Enhanced Chemical Vapor Deposition (MPECVD) process in microgravity has, thus, been suggested. Such a diamond deposition system, which overcomes the limitations of present systems and which is distiguishable from them by the use of high pressure MPECVD and recirculation of the would be effluent hydrogen and carbon, is described. Given the key fact that there is nothing in the effluent of the MPECVD process that is truly a byproduct or 'waste', the system can, at least in principle, lend itself to being closed loop yet dynamic. The exhaust contains hydrogen and carbon species which can be recirculated to the plasma reactor, that is, since there are no unusable reaction byproducts, the effluent can be fed back to the reaction chamber with no detriment, thus allowing deployment in a microgravity environment. ESA

N94-10128# Swedish Space Corp., Solna.
MICROGRAVITY APPLICATIONS FURNACE FACILITY (MAFF) FOR PARABOLIC FLIGHTS
Christian Lockowandt, K. Loeth, Lars Ekbom (Royal Inst. of Tech., Stockholm, Sweden.), A. Eliasson (Royal Inst. of Tech., Stockholm, Sweden.), and Anders E. W. Jarfors (Royal Inst. of Tech., Stockholm, Sweden.) *In* ESA, Proceedings of the 8th European Symposium on Materials and Fluid Sciences in Microgravity, Volume 1 Aug. 1992 p 383-386 Sponsored by Swedish Board for Space Activities, and ESA (For primary document see N94-10070 01-29)
Copyright Avail: CASI HC A01/MF A04; ESA, EPD, ESTEC, Noordwijk, Netherlands, HC

The Microgravity Applications Furnace Facility (MAFF), which is used for high temperature microgravity processing metals, alloys, and composites in parabolic flights, is addressed and its applications are given. The facility is able to melt, maintain the temperature, and solidify a sample during the microgravity periods of 20 seconds given during a parabolic flight. MAFF is equipped with six IR heated furnaces. The radiation from halogen lamps is focused on the sample with ellipsoid mirrors. A cooling system enables active cooling of the samples. Data is collected and the furnaces are controlled by a computer (PC). An experiment to study the dissolution of solid aluminum carbide particles and precipitation of solid titanium carbide particles in liquid aluminum is reported. The study of precipitation morphologies, under normal gravity conditions, is impossible due to large convective motions. The effect of both temperature and composition were investigated. A further experiment which investigated liquid phase sintering of tunsgten composites in microgravity is reported. ESA

N94-10129# Deutsche Forschungsanstalt fuer Luft- und Raumfahrt, Cologne (Germany). Space Simulation Inst.

FORCE AND POWER EFFICIENCY OF MICRO-g ELECTROMAGNETIC LEVITATION COILS

Georg Lohoefer *In* ESA, Proceedings of the 8th European Symposium on Materials and Fluid Sciences in Microgravity, Volume 1 Aug. 1992 p 387-390 (For primary document see N94-10070 01-29)
Copyright Avail: CASI HC A01/MF A04; ESA, EPD, ESTEC, Noordwijk, Netherlands, HC

The study of undercooled liquids requires containerless sample handling to avoid nucleation at container walls. For electrically conductuing bulk samples this can be obtained by using the electromagnetic levitation technique, where the material is contactlessly positioned and heated in one or several alternating magnetic fields. An efficiency optimized microgravity coil system, which is also used in the microgravity levitation facility TEMPUS is presented. Data on its heating efficiency and force-power relation depending on the sample conductivity is also given. ESA

N94-10130# European Space Agency. European Space Research and Technology Center, ESTEC, Noordwijk (Netherlands). Electrical Systems Dept.

HIGH TEMPERATURE PROCESSING AND DIAGNOSTIC TECHNOLOGIES FOR MICROGRAVITY APPLICATIONS

A. Lundstroem and Matthias Dieckmann *In its* Proceedings of the 8th European Symposium on Materials and Fluid Sciences in Microgravity, Volume 1 Aug. 1992 p 391-394 (For primary document see N94-10070 01-29)
Copyright Avail: CASI HC A01/MF A04; ESA, EPD, ESTEC, Noordwijk, Netherlands, HC

An overview of high temperature processing techniques and diagnostic instrumentation for materials science developed under the European Space Agency's Technological Research Program is given. On the space processing side, electron beam and induction heating are investigated together with resistance furnaces with 2000 C capability. The integration of magnets in furnaces to achieve magnetic damping of residual flows is being studied at breadboard level for crystal growth applications. Studies on new cartridge technologies compatible with these developments were also initiated. On the diagnostic side, pyrometry was improved by avoiding window contamination. Thin film thermocouples are under development allowing miniaturized arrays for high density of instrumentation with minimal disturbances for the experiments. Ultrasound techniques are explored for flow field mapping and solid-liquid interface detection in opaque melts. ESA

N94-10131*# West Virginia Univ., Morgantown.

DETERMINATION OF THE VISCOUS ACOUSTIC FIELD FOR LIQUID DROP POSITIONING/FORCING IN AN ACOUSTIC LEVITATION CHAMBER IN MICROGRAVITY

Margaret J. Lyell *In* ESA, Proceedings of the 8th European Symposium on Materials and Fluid Sciences in Microgravity, Volume 1 Aug. 1992 p 395-397 (For primary document see N94-10070 01-29)
(Contract NAG3-1005)
Copyright Avail: CASI HC A01/MF A04; ESA, EPD, ESTEC, Noordwijk, Netherlands, HC

The development of acoustic levitation systems has provided a technology with which to undertake droplet studies as well as do containerless processing experiments in a microgravity environment. Acoustic levitation chambers utilize radiation pressure forces to position/manipulate the drop. Oscillations can be induced via frequency modulation of the acoustic wave, with the modulated acoustic radiation vector acting as the driving force. To account for tangential as well as radial forcing, it is necessary that the viscous effects be included in the acoustic field. The method of composite expansions is employed in the determination of the acoustic field with viscous effects. ESA

N94-10132# Swedish Space Corp., Solna.

MUZO: THE PROGRAMMABLE MULTI ZONE FURNACE FOR GAS PAYLOADS AND SOUNDING ROCKETS

Henrik Malmstroem and Torbjorn Carlberg (Sundsvall Univ., Sweden.) *In* ESA, Proceedings of the 8th European Symposium on Materials and Fluid Sciences in Microgravity, Volume 1 Aug. 1992 p 399-402 Sponsored by Swedish Board for Space Activities (For primary document see N94-10070 01-29)
Copyright Avail: CASI HC A01/MF A04; ESA, EPD, ESTEC, Noordwijk, Netherlands, HC

The Multi Zone (MUZO) furnace, developed for high temperature experiments in a Get Away Special (GAS) payload, is presented. MUZO is also suitable for use in sounding rockets such as MASER and MAXUS (7 to 14 minutes microgravity). The furnace is built around a ceramic tube with five independent heating elements and a gas cooling system. A sophisticated computer control system was developed consisting of five separate regulators using information from 15 thermocouples. In order to characterize the furnace performance, in terms of convection level in the melt, axial concentration profiles in germanium crystal doped with gallium were studied under 1 g conditions. ESA

N94-10133# Officine Galileo S.p.A., Florence (Italy).

THE SURFACE PLASMON SPECTROSCOPY AS DIAGNOSTIC TECHNIQUE IN MICROGRAVITY EXPERIMENTS

G. Margheri, Matteo Tacconi, and P. G. Falciani *In* ESA, Proceedings of the 8th European Symposium on Materials and Fluid Sciences in Microgravity, Volume 1 Aug. 1992 p 403-405 (For primary document see N94-10070 01-29)
Copyright Avail: CASI HC A01/MF A04; ESA, EPD, ESTEC, Noordwijk, Netherlands, HC

The performance of an experimental apparatus using the Surface Plasmon Spectroscopy (SPS) with a Kretschmann like coupling configuration is analyzed. The growing film deposited in a metal film (whose dielectric constant and thickness have to be accurately measured before the deposition process) is directly evaporated on the face of a glass prism. The method is very helpful to resolve interfacial deposition layers of the order to some A. Simultaneously, the SPS equations allow the very precise determination of the characteristics of the metal layer in which the deposition occurs (thickness, dielectric constant). It is shown that with a coupling configuration using conical beams and an area array (Charge Coupled Device (CCD)) as sensor, it is possible to design very compact and simple experimental modules with minimum optomechanical moving parts. ESA

N94-10134# Microgravity Advanced Research and Support Center, Naples (Italy).

TOLS (TELESCIENCE ON-LINE SIMULATOR): AN ESSENTIAL INSTRUMENT FOR MICRO-GRAVITY INTERACTIVE EXPERIMENT c14

Raimondo Fortezza and Rodolfo Monti (Naples Univ., Italy.) *In* ESA, Proceedings of the 8th European Symposium on Materials and Fluid Sciences in Microgravity, Volume 1 Aug. 1992 p 407-411 (For primary document see N94-10070 01-29)
Copyright Avail: CASI HC A01/MF A04; ESA, EPD, ESTEC, Noordwijk, Netherlands, HC

The telescience operative mode represents for the investigator the capability to perform a scientific interactive experiment directly from the ground. Interaction means that the scientist is able to take appropriate actions and to modify the experiment execution on the basis of the data, video, and, more in general, information that he receives directly from the onboard facility. The scientific knowledge and expertise of the investigator ensures a more intelligent control, guarantees best results, and limits the involvement of the crew onboard (if any). The capability to perform the experiment directly from a ground based facility, with an approach similar to that used to carry out the research in an on ground laboratory, represents the final objective. To reach this goal it is required to establish communication links that are completely transparent to the scientist and to design specific devices able to provide support in the experiment control and management. Some such devices developed to support several experiments performed, using telescience approach, on sounding rockets are illustrated. These consist of hardware and software tools that simulate the experimental processes in real or quasi-real-time, visualize in a quick look format the relevant data, and help the investigators to take the appropriate decisions during the course of the experiments. The future development of these tools is also considered. ESA

N94-10135# Centro Informazioni Studi Esperienze, Milan (Italy).
LASER BEAM DEFLECTION: A DIAGNOSTIC TOOL FOR VAPOUR GROWTH EXPERIMENTS IN MICROGRAVITY
Sergio Musazzi, A. Torinesi, F. Trespidi, and Michael Braun (Dornier System G.m.b.H., Friedrichshafen, Germany.) *In* ESA, Proceedings of the 8th European Symposium on Materials and Fluid Sciences in Microgravity, Volume 1 Aug. 1992 p 413-417 (For primary document see N94-10070 01-29)
(Contract ESTEC-7337/87/NL/PB(SC))
Copyright Avail: CASI HC A01/MF A04; ESA, EPD, ESTEC, Noordwijk, Netherlands, HC

While the growth of bulk crystals and thin layers from vapor is a method with increasing importance and great potential, the theoretical understanding of this technique is quite limited. In particular, the influence of impurities and natural convection on the transport mechanism is not well understood. Density gradients in the vapor phase can be measured by the deflection of a laser beam traversing the growth cell perpendicular to the main direction of material transport. The suitability of this method was demonstrated in a laboratory set up using iodine as reference material. Optical gradients dn/dz less than 0.000001/cm can be detected over a 1 cm depth region of transport. The results of the first experiments are in the range predicted by theory. Since the beam deflection apparatus can be tailored to fit a quite small volume and does not require exhaustive diagnostics instrumentation or data processing, it can easily be adapted to a spaceflight experiment. ESA

N94-10136# European Space Agency. European Space Research and Technology Center, ESTEC, Noordwijk (Netherlands). Microgravity Div.
THE ADVANCED FLUID PHYSICS MODULE: HOW TO ACHIEVE SCIENTIFIC GOALS FOR SPACELAB D2 **c14**
V. Pletser, A. Verga, F. Klinkhamer (Netherlands Organization for Applied Scientific Research TNO, Delft.), and N. Janning (Netherlands Organization for Applied Scientific Research TNO, Delft.) *In its* Proceedings of the 8th European Symposium on Materials and Fluid Sciences in Microgravity, Volume 1 Aug. 1992 p 419-424 (For primary document see N94-10070 01-29)
Copyright Avail: CASI HC A02/MF A04; ESA, EPD, ESTEC, Noordwijk, Netherlands, HC

The general design of the Advanced Fluid Physics Module (AFMP), a multipurpose multiuser facility dedicated to research on basic phenomena of fluid behavior in a microgravity environment, is introduced. Its accommodation for the Spacelab D2 mission is described. In the course of the AFMP technical development, the performance of the instrument was upgraded to ensure that scientific objectives set for the five experiments on board Spacelab D2 could be met. In addition, specific experimental equipment, in the form of discs and a cell, were developed to be mounted on the AFMP for the experiment realization to provide superior experimental capabilities to the AFPM facility. ESA

N94-10137# Escuela Tecnica Superior de Ingenieros Aeronauticos, Madrid (Spain). Lab. de Aerodinamica.
PARTICLE IMAGE VELOCIMETRY TECHNIQUE: CALIBRATION TESTS
A. Sanz and J. L. Espino *In* ESA, Proceedings of the 8th European Symposium on Materials and Fluid Sciences in Microgravity, Volume 1 Aug. 1992 p 425-428 Sponsored by Comision Interministerial de Ciencia y Tecnologia, Spain (For primary document see N94-10070 01-29)
(Contract ESTEC-7337/87/NL/PB)
Copyright Avail: CASI HC A01/MF A04; ESA, EPD, ESTEC, Noordwijk, Netherlands, HC

Activities carried out to assess the performance of a nonintrusive diagnostic technique (Particle Image Velocimetry (PIV)), which is used to study combustion problems relevant to microgravity research, are described. A setup for production of suitable flames and an instrument to implement PIV was previously developed. To assess the performance of this instrument, a calibration device was used. The calibration device consists of a disk with a flat front surface, on which tracers are deposited. This surface is illuminated by a time modulated light sheet. The disk is made to rotate at a controlled speed. An error analysis is presented concerning the calibration device and the Young fringe analysis involved. This error analysis is supported by a set of trials, which also give an estimation of both the systematic and random errors involved as well as the dynamic range of the instrument. ESA

N94-10138# Deutsche Forschungsanstalt fuer Luft- und Raumfahrt, Cologne (Germany). Space Simulation Inst.
RESULTS OF MISSION PREPARATION SUPPORT TO MICROGRAVITY EXPERIMENTS ON BOARD OF EURECA 1
H. P. Schmidt, M. Exner, W. Koerver, C. Krug, C. Lindberg, B. Paetz, T. Neuhausen, and K. Strauch *In* ESA, Proceedings of the 8th European Symposium on Materials and Fluid Sciences in Microgravity, Volume 1 Aug. 1992 p 429-432 (For primary document see N94-10070 01-29)
Copyright Avail: CASI HC A01/MF A04; ESA, EPD, ESTEC, Noordwijk, Netherlands, HC

Concept and facilities of the experiment preparation and the mission support program for Eureca 1, given by the Microgravity Support Center (MUSC) in Cologne (Germany), are discussed. Eureca will be used to conduct experiments in microgravity. The support covers essential parts of the experiment preparation and the experiment execution during the mission. The engineering models of the experiment facilities were used to run simulation experiments for development and verification of experiment control parameters and procedures. During the mission, the user support center will take care of the processing of telemetry data generated by the experiment facilities in space. It will also support the investigators in the control of the experiment performance. ESA

N94-10139# Kayser Threde G.m.b.H., Munich (Germany).
MISSION SUPPORT FOR CRYSTAL GROWTH EXPERIMENTS IN RUSSIAN UNMANNED CARRIERS **c76**
Peter Sickinger, Peter Hofmann, K. Kemmerle, E. Wulf, R. Klett, Alexander S. Senchenkov (Splav Technical Center, Moscow, Russia.), A. V. Egorov (Splav Technical Center, Moscow, Russia.), I. V. Barmin (Splav Technical Center, Moscow, Russia.), D. G. Matioukhin (Scientific Research Inst. for Radioisotope Apparatus, Riga, Latvia.), and Manfred Salk (Freiburg Univ., Germany.) et al *In* ESA, Proceedings of the 8th European Symposium on Materials and Fluid Sciences in Microgravity, Volume 1 Aug. 1992 p 433-434 (For primary document see N94-10070 01-29)
Copyright Avail: CASI HC A01/MF A04; ESA, EPD, ESTEC, Noordwijk, Netherlands, HC

The ground and flight support activities for two CdTe crystal growth experiments performed during the Photon 7 mission in Oct. 1991 are described. The activities include: sample preparation, furnace selection, scheduling, safety and contractual matters, as well as the actual mission support. Technical data of crystal growth facilities are given. ESA

N94-10140# National Aerospace Lab., Emmeloord (Netherlands).
ANALYSIS OF THE ALIGNMENT OF A SCHLIEREN SYSTEM FOR TELE-OPERATION
F. H. P. Spaan and A. J. Kramer *In* ESA, Proceedings of the 8th European Symposium on Materials and Fluid Sciences in Microgravity, Volume 1 Aug. 1992 p 435-440 (For primary document see N94-10070 01-29)
(Contract NIVR-02905N)
Copyright Avail: CASI HC A02/MF A04; ESA, EPD, ESTEC, Noordwijk, Netherlands, HC

A theory for alignment of the gratings of the multiple source schlieren system, which can be used in microgravity experiments, was developed and verified by experiments. The results indicate the feasibility of reliable teleoperated or automated alignment for fast and accurate alignment. Due to hardware limitations, some minor problems were identified in the region very close to optimal alignment. Analysis of the so called bright spot intensity profile of Prototype Optical Diagnostic Instrument (PODI) revealed a slight suboptimal position of the lens (unsharp imaging). It was shown that a teleoperated/automated alignment procedure for the sharp focusing schlieren system can be operated successfully. It encourages further development of tools for teleoperation or automation assistance for optimization of parameters of (spaceborne) diagnostical instruments. It is suggested that future work may include studies on tools for schlieren lens adjustment and focusing. ESA

N94-10141# Technische Univ., Munich (Germany). Inst. for Materials and Processing Sciences.

AGF (AUTOMATIC GRADIENT FURNACE): A PROPOSED MICROGRAVITY FACILITY

Hans M. Tensi and Raimund Roesch *In* ESA, Proceedings of the 8th European Symposium on Materials and Fluids Sciences in Microgravity, Volume 1 Aug. 1992 p 441-446 (For primary document see N94-10070 01-29)

Copyright Avail: CASI HC A02/MF A04; ESA, EPD, ESTEC, Noordwijk, Netherlands, HC

The Automatic Gradient Furnace (AGF) with quenching device, proposed in Mar. 1991 as a facility development for the Columbus precursor flights especially for Eureca missions, is presented. The experimental selection of these microgravity missions is still pending. The proposed AGF is planned for unidirectional solidification of metallic and nonmetallic samples with quenching of the solidification front and the residual melt in a microgravity environment. The furnace is automatically regulated to the parameter requirements of the experimenter, automatically comparing the actual (measured and calculated) crystallization parameters (solidification rate and thermal gradient in liquid ahead of the solidification front) with the nominal values. After quenching, the specimen is automatically changed. ESA

N94-10142# National Space Development Agency, Tokyo (Japan). Space Experiment Group.

MICROGRAVITY EXPERIMENTS USING TR-1A ROCKET

Schinichi Yoda, T. Nakamura, S. Yoshitomi, and M. Saito *In* ESA, Proceedings of the 8th European Symposium on Materials and Fluid Sciences in Microgravity, Volume 1 Aug. 1992 p 447-453 (For primary document see N94-10070 01-29)

Copyright Avail: CASI HC A02/MF A04; ESA, EPD, ESTEC, Noordwijk, Netherlands, HC

The objectives, hardware development, and microgravity experiments performed during the first flight of the TR-1A are addressed. Six experiment systems were developed for the first flight experiment: the crystal growth experiment equipment; the fluid dynamics technology experiment equipment; the bubble generation; dynamics and handling experiment equipment; the isothermal furnace; and the high temperature heating furnace. The TR-1A was launched on 16 Sep. 1991 to study Marangoni convection flow, bubble gerneration mechanisms, crystal growth from solution, melting and solidifying of particle dispersion strengthened alloy with different wettability between the particle and matrix, and high temperature oxide superconductors using the above equipment. All experiment sequences were performed satisfactorily for each system. Video cameras properly recorded the behavior such as melting of materials, liquid flow, bubble formation and combinations, and crystal growth behavior. ESA

N94-10143# Augsburg Univ. (Germany). Inst. fuer Physik.

EXPERIMENTAL APPROACH TO NON-CONTACT CALORIMETRY IN SPACE

Rainer K. Wunderlich, Angelika Diefenbach (Deutsche Forschungsanstalt fuer Luft- und Raumfahrt, Cologne, Germany.), Rainer Willnecker (Deutsche Forschungsanstalt fuer Luft- und Raumfahrt, Cologne, Germany.), and Hans-Jorg Fecht *In* ESA, Proceedings of the 8th European Symposium on Materials and Fluid Sciences in Microgravity, Volume 1 Aug. 1992 p 455-460 (For primary document see N94-10070 01-29)
(Contracts DARA-50-WM-9110-5; DARA-50-QV-9101)

Copyright Avail: CASI HC A02/MF A04; ESA, EPD, ESTEC, Noordwijk, Netherlands, HC

Ground based experiments were performed to verify the applicability of noncontact calorimetry in space for the determination of the thermodynamic properties of undercooled liquid metals and alloys with relatively high melting temperatures. In this method, a sample is exposed to an amplitude modulated radio frequency heating field and the dynamic temperature response of the sample is detected by noncontact temperature measurements. The experimental set up used for the ground based experiments is described. The first results on solid niobium samples demonstrating the validity of this new method are given. ESA

N94-10171# European Space Agency, Paris (France).

PROCEEDINGS OF THE 8TH EUROPEAN SYMPOSIUM ON MATERIALS AND FLUID SCIENCES IN MICROGRAVITY, VOLUME 2

Brigitte Kaldeich, ed. (European Space Agency. European Space Research and Technology Center, ESTEC, Noordwijk, Netherlands.) Aug. 1992 453 p Symposium held in Brussels, Belgium, 12-16 Apr. 1992; sponsored by NASA; ESA; CNES; Deutsche Agentur fuer Raumfahrtangelegenheiten; Italian Space Agency; Commission of the European Communities; Brussels Univ.; and Science Policy Office of Belgium
(ESA-SP-333-Vol-2; ISBN-92-9092-174-9; ETN-93-93950) Copyright

Avail: CASI HC A20/MF A04; ESA, EPD, ESTEC, Noordwijk, Netherlands, HC

Papers concerning materials and fluid sciences in microgravity are presented. In this volume, volume 2, the following topics are discussed: interactions between flow and crystallization; crystallization and solidification; flow instabilities; basic physics and physical chemistry; and preliminary results of the International Microgravity Laboratory (IML-1). For individual titles, see N94-10172 through N94-10250.

N94-10172*# Georgia Inst. of Tech., Atlanta. School of Mechanical Engineering.

THERMOCAPILLARY CONVECTION INSTABILITY IN MICROGRAVITY CRYSTAL GROWTH

G. P. Neitzel, D. F. Jankowski (Arizona State Univ., Tempe.), Y. Shen (Arizona State Univ., Tempe.), C. C. Law (Arizona State Univ., Tempe.), K.-T. Chang (Arizona State Univ., Tempe.), and H. D. Mittelmann (Arizona State Univ., Tempe.) *In* ESA, Proceedings of the 8th European Symposium on Materials and Fluid Sciences in Microgravity, Volume 2 Aug. 1992 p 463-467 (For primary document see N94-10171 01-29)
(Grants NAG3-1221; AF-AFOSR-0080-90)

Copyright Avail: CASI HC A01/MF A04; ESA, EPD, ESTEC, Noordwijk, Netherlands, HC

Energy and linear stability theories are applied to study the stability properties of thermocapillary convection in a half zone model of the float zone crystal growth process. The analyses yield results which provide sufficient conditions for both stability and instability, respectively, and therefore, lower and upper bounds for the Marangoni numbers at which oscillatory thermocapillary convection will appear. The results of the analyses are compared with available experimental and numerical data. ESA

N94-10173# Brussels Univ. (Belgium). Dept. of Chemical Physics.

ON THE ROLE OF SORET EFFECT IN CONCENTRATION DISTRIBUTION IN CRYSTALS GROWING FROM THE MELT c76

Stefan VanVaerenbergh, J. C. Legros, and Marcel Hennenberg *In* ESA, Proceedings of the 8th European Symposium on Materials and Fluid Sciences in Microgravity, Volume 2 Aug. 1992 p 469-474 (For primary document see N94-10171 01-29)

Copyright Avail: CASI HC A02/MF A04; ESA, EPD, ESTEC, Noordwijk, Netherlands, HC

The nonconvective transport processes which may govern the concentration profile in the liquid phase near a crystallization front are considered. Such transport processes may govern, for example, in absence of buoyancy and surface tension forces or when the diffusion boundary layer is large enough. The concentration profiles are then governed not only by rejection and diffusion processes, but also by thermodiffusion. In such situations, there are significant couplings between thermal and solutal variations, near and at the interface, that influence the concentration distribution near the solidification front and consequently, in the solidified phase. This problem is analyzed for a crystal growing from the melt. The conditions of existence of oscillatory regime are deduced from a model with a semi-infinite liquid phase. ESA

N94-10174*# Alabama Univ., Birmingham.

SOLIDIFICATION IN IMMISCIBLE SYSTEMS: THE INFLUENCE OF PROCESSING CONDITIONS ON RESULTING MICROSTRUCTURES

J. Barry Andrews, R. A. Merrick, and A. L. Schmale (National Academy of Sciences - National Research Council, Washington, DC.) *In* ESA, Proceedings of the 8th European Symposium on Materials and Fluid Sciences in Microgravity, Volume 2 Aug. 1992 p 475-480 Sponsored by NASA. Marshall Space Flight Center and NSF (For primary document see N94-10171 01-29)

Copyright Avail: CASI HC A02/MF A04; ESA, EPD, ESTEC, Noordwijk, Netherlands, HC

Research carried out over the past two decades in which attempts have been made to produce desirable microstructures in immiscible alloys is reviewed. Factors affecting the formation of desirable microstructures in immiscible alloys are addressed and some of the techniques that have been successful in controlling these factors in order to produce useful structures are discussed. Some of the intended applications of these alloys require a dispersion of one phase in the other, while other applications favor the use of aligned, fibrous microstructures with continuity of both phases. The microstructures obtained in immiscible alloys are often strongly influenced by processing conditions. Perhaps the most well known effect is gravity induced sedimentation of the denser immiscible phase during solidification. This difficulty with sedimentation led to low gravity processing in attempts to produce dispersed microstructures. However, experimentation under low gravity conditions soon revealed that many other factors, including wetting of the crucible walls and surface tension driven flows, often resulted in complete separation and coalescence of the two immiscible phases. The production of aligned fibrous microstructures in hypermonotectic alloys appears to be even more difficult than the formation of a dispersion. Here, in addition to sedimentation and crucible wetting, convective and interfacial instabilities must be considered as well. Calculation of the limits of stability during directional solidification were carried out but require experimental verification. ESA

N94-10175*# National Aeronautics and Space Administration. Goddard Space Flight Center, Greenbelt, MD.

STARDUST: A SIMULATION EXPERIMENT OF COSMIC DUST ANALOGUES PRODUCTION IN MICROGRAVITY CONDITIONS

Frank Ferguson (Virginia Univ., Charlottesville.), Lembit U. Lilleleht (Virginia Univ., Charlottesville.), J. Nuth, J. R. Stephens (Matrix Corp., Santa Fe, NM.), E. Bussoletti (Naples Univ., Italy.), L. Carotenuto (Microgravity Advanced Research and Support Center, Naples, Italy.), L. Colangeli (Cassino Univ., Italy.), P. DellAversana (Microgravity Advanced Research and Support Center, Naples, Italy.), F. Mele (Microgravity Advanced Research and Support Center, Naples, Italy.), and V. Mennella (Osservatorio Astronomico, Capodimonte, Naples, Italy.) et al *In* ESA, Proceedings of the 8th European Symposium on Materials and Fluid Sciences in Microgravity, Volume 2 Aug. 1992 p 481-488 Sponsored by Italian Space Agency (For primary document see N94-10171 01-29)

Copyright Avail: CASI HC A02/MF A04; ESA, EPD, ESTEC, Noordwijk, Netherlands, HC

The aim, activity, and some preliminary results of the STARDUST program are presented. The condensation of solid materials from the vapor phase is important in several scientific fields such as chemical vapor deposition, air pollution, and the formation of refractory cosmic dust around stars. Conventional studies of refractory grain formation, using high temperature furnace and shock tube techniques, are restricted to short time scales and suffer from buoyancy induced convection that limit their accuracy. In order to simulate more accurately the condensation of refractory grains near stars and to investigate the advantages of performing condensation studies in microgravity conditions, an experimental investigation of vapor phase condensation in microgravity was undertaken. The experimental equipment currently used is reported. The results from the first flight series and particle aggregation modeling efforts are presented. ESA

N94-10176# Mitsubishi Research Inst., Inc., Tokyo (Japan).

SOLIDIFICATION FROM SUPERCOOLED MELT UNDER MICROGRAVITY

Masamichi Ishikawa, S. Kamei, A. Iwasaki (Electrotechnical Lab., Ibaraki, Japan.), S. Hosokawa (Electrotechnical Lab., Ibaraki, Japan.), M. Tanimoto (Electrotechnical Lab., Ibaraki, Japan.), and I. Kudo (Electrotechnical Lab., Ibaraki, Japan.) *In* ESA, Proceedings of the 8th European Symposium on Materials and Fluid Sciences in Microgravity, Volume 2 Aug. 1992 p 489-494 Sponsored by Ministry of International Trade and Industry; Mechanical Social Systems Foundation; Society of Japanese Aerospace Co., Inc.; and Ishikawajimi-Harima Heavy Industries Co., Ltd. (For primary document see N94-10171 01-29)

Copyright Avail: CASI HC A02/MF A04; ESA, EPD, ESTEC, Noordwijk, Netherlands, HC

To clarify the contribution of thermal convection on the growth rate in supercooled melts, an experimental study of the unidirectional solidification of a liquid crystal was executed under normal and microgravity conditions. The Laser Interferometric Observation System (LIOS) launched by MASER 4 in Mar. 1990 was employed. The liquid crystal, 4-cyano-4'-5-alkoxy biphenyl (Merck), was used as a model material. Two kinds of phase change, isotropic-nematic and nematic-solid phase changes, were observed in the same run under the conditions of normal and microgravity. Microconvection in the supercooled melt was observed at the nematic-solid interface on the ground and disappeared under microgravity. Unknown oscillation of the growth rate was confirmed as a result of enhanced supercooling in the absence of microconvection. It is confirmed that the microconvection induced by latent heat diminishes supercooling and suppresses the growth rate of solid phase on the ground. The observed phenomena were modeled using Landau-Ginzburg type potential. ESA

N94-10177# Deutsche Forschungsanstalt fuer Luft- und Raumfahrt, Cologne (Germany). Space Simulation Inst.

MARANGONI MOTION DURING MELTING OF A HYPERMONOTECTIC ALLOY: NUMERICAL SIMULATIONS FOR THE D2 EXPERIMENT IHF04

c76

L. Ratke, S. Diefenbach, B. Prinz (Metallgesellschaft A.G., Frankfurt am Main, Germany.), H. Ahlborn (Technische Univ., Hamburg, Germany.), and Berndt Feuerbacher *In* ESA, Proceedings of the 8th European Symposium on Materials and Fluid Sciences in Microgravity, Volume 2 Aug. 1992 p 495-501 (For primary document see N94-10171 01-29)

Copyright Avail: CASI HC A02/MF A04; ESA, EPD, ESTEC, Noordwijk, Netherlands, HC

The scientific objectives, experimental procedure, numerical simulation, and expected results of the D2 experiment IHF-04, in which the Marangoni transport of Bi droplets in an Al-Si melt will be investigated by directional melting of sandwich like samples of Al-Si-Bi alloys, are addressed. The sandwich like samples consist of periodically arranged cylinders of an Al-Si alloy in which 5 wt percent Bi are distributed as droplets and cylinders of an Al-Si-Bi alloy of exact monotectic composition and being thus free of Bi droplets at the processing temperature. Ahead of the melting front there exists a temperature gradient which leads to a motion of the droplets within the Al-Si matrix melt. Bi droplets move from the cylinder with hypermonotectic composition into the droplets free one as soon as the melting front moves into it in a controlled way. At the end of an experiment a large number of droplets will be located within the molten zone. From the spatial arrangement of the droplets and a comparison with computer simulations of the whole process, conclusions are drawn concerning the Marangoni motion of Bi droplets. The investigations are relevant for the improvement of terrestrial industrial casting processes of bearing alloys. ESA

N94-10178*# National Inst. of Standards and Technology, Gaithersburg, MD.

THE EFFECT OF GRAVITATIONAL MODULATION ON CONVECTION IN VERTICAL BRIDGMAN GROWTH

Bruce T. Murray, S. R. Coriell, G. B. McFadden, and A. A. Wheeler (Bristol Univ., England.) *In* ESA, Proceedings of the 8th European Symposium on Materials and Fluid Sciences in Microgravity, Volume 2 Aug. 1992 p 503-506 Sponsored by NASA, Washington (For primary document see N94-10171 01-29)

Copyright Avail: CASI HC A01/MF A04; ESA, EPD, ESTEC, Noordwijk, Netherlands, HC

During vertical directional solidification of a binary alloy at constant velocity, buoyancy driven solutal convection may occur due to the solute gradient associated with the solidification process. This problem is further complicated if time periodic forcing is considered, which is relevant to materials processing in a microgravity environment or as a means of dynamic control of flow instabilities. The effect of time periodic modulation is studied by introducing a gravitational acceleration which is a sinusoidal function of time. The onset of solutal convection is treated by a stability analysis of the linearized governing equations and boundary conditions. Solutions are obtained numerically by employing two distinct computational implementations of Floquet theory. Results for materials with large Schmidt number are presented, and an analysis for large frequency and large Schmidt number yields a more complete description of the behavior in this relevant limit. ESA

N94-10179# Ishikawajima-Harima Heavy Industries Co. Ltd., Tokyo (Japan). Applied Science Dept.

NUMERICAL CALCULATION OF THE GROWTH OF InP BY THE TRAVELLING HEATER METHOD IN THE FIRST MISSION OF THE SPACE FLYER UNIT **c76**

K. Takahashi, Satoshi Adachi, M. Watanabe, Y. Ikegami, J. Ochiai, M. Kuribayashi, and H. Sakai (Institute for Unmanned Space Experiments Free Flyer, Tokyo, Japan.) *In* ESA, Proceedings of the 8th European Symposium on Materials and Fluid Sciences in Microgravity, Volume 2 Aug. 1992 p 507-511 Sponsored by New Energy and Industrial Technology Development Organization (For primary document see N94-10171 01-29)

Copyright Avail: CASI HC A01/MF A04; ESA, EPD, ESTEC, Noordwijk, Netherlands, HC

The possibility of constitutional supercooling occurring in InP crystals grown in space and on the ground by the Travelling Heater Method (THM) was determined by numerical computation. This was done in preparation for the growth of these crystals using the image mirror furnace on the first mission of the Space Flyer Unit in 1994. In THM the quality of the crystals depends on whether or not constitutional supercooling occurs. For this purpose, thermal convection, Marangoni convection, diffusion, solute (posphrous) transport, and isotherms in solution zone of InP were calculated using the model of cylindrical coordination. It was anticipated that a free surface would appear in the center of the solvent surface and a linear pattern would be assumed for that temperature distribution at the solvent surface. ESA

N94-10180# Commissariat a l'Energie Atomique, Grenoble (France). Section d'Etudes de la Solidification et de la Cristallogenese.

SCIENTIFIC SPECIFICATIONS FOR AN AUTOMATED FACILITY FOR GROWING LARGE SEMICONDUCTING CRYSTALS FROM THE MELT IN SPACE

Thierry Duffar, J. P. Nabot, C. Barat, Jean-Jacques Favier, and G. Cambon (Centre National d'Etudes Spatiales, Toulouse, France.) *In* ESA, Proceedings of the 8th European Symposium on Materials and Fluid Sciences in Microgravity, Volume 2 Aug. 1992 p 513-517 (For primary document see N94-10171 01-29)

Copyright Avail: CASI HC A01/MF A04; ESA, EPD, ESTEC, Noordwijk, Netherlands, HC

Scientific specifications of a new facility, called Sesame (a Bridgeman machine), are given in order to get the best possible large crystals (5 by 25 cm) of ternary semiconductors in space. Optimal growth conditions (growth rate, thermal gradients) are determinated to minimize dislocations density, interface destabilization, and convection. The gravity levels, interface curvature, and thermal and pulling stability are computed in order to get chemical heterogeneities less than 1 percent (both longitudinal and radial). It is shown that use of a magnetic field during an unmanned mission is necessary to achieve this goal. ESA

N94-10181# Aachener Centrum fuer Erstarrung unter Schwerelosigkeit e.V. (Germany).

VARIATIONS OF THE TEMPERATURE PROFILE IN THE GRADIENT FURNACE GFQ WITHIN A CYLINDRICAL SAMPLE USED FOR DIRECTIONAL SOLIDIFICATION **c76**

Martin Stehle and S. Rex *In* ESA, Proceedings of the 8th European Symposium on Materials and Fluid Sciences in Microgravity, Volume 2 Aug. 1992 p 521-526 (For primary document see N94-10171 01-29)

Copyright Avail: CASI HC A02/MF A04; ESA, EPD, ESTEC, Noordwijk, Netherlands, HC

In preparation for the Spacelab Mission D-2, the temperature profile within samples of the alloy Cu-Mn inserted in the gradient furnace GFQ was determined as a function of the heater temperature, the atmosphere within the furnace chamber, the relative sample position, and the pulling speed. These furnace parameters determine the steady state temperature profile in the sample as well as the shape and the relative position of the solid-liquid interface during the directional solidification. The experiments result in a set of parameters by which the solid-liquid interface is located on Earth close to the nominal position. Also, in microgravity this parameter set will guarantee a plane solidification front and a sufficiently high cooling rate to fix the interface at the actual position by quenching. ESA

N94-10182# Deutsche Forschungsanstalt fuer Luft- und Raumfahrt, Cologne (Germany).

NUMERICAL SIMULATION OF MULTI-DROPLET HYDRODYNAMIC INTERACTIONS IN LIQUID DISPERSIONS **c34**

S. Diefenbach, X. Zhang (Colorado Univ., Boulder.), R. H. Davis (Colorado Univ., Boulder.), and L. Ratke *In* ESA, Proceedings of the 8th European Symposium on Materials and Fluid Sciences in Microgravity, Volume 2 Aug. 1992 p 527-532 (For primary document see N94-10171 01-29)

Copyright Avail: CASI HC A02/MF A04; ESA, EPD, ESTEC, Noordwijk, Netherlands, HC

The velocities and trajectories of three and four droplets interacting hydrodynamically were determined theoretically using asymptotic solutions for two droplet arrangements and a pairwise addition scheme describing the disturbance velocities, in the case of buoyancy driven motion. The numerical calculations are compared with dedicated experiments. The agreement between theoretical predictions and experimental data is very good, though decreasing with increasing number of particles. The calculation procedure developed is applicable to the case of real multiparticle dispersion, found in immiscible alloys. ESA

N94-10183*# Aix-Marseilles Univ. (France). Inst. de Mecanique des Fluides.

FLOW TRANSITIONS IN A 2D DIRECTIONAL SOLIDIFICATION MODEL **c76**

Philippe Larroude, Jalil Ouazzani (Alabama Univ., Birmingham.), and J. Iwan D. Alexander (Alabama Univ., Birmingham.) *In* ESA, Proceedings of the 8th European Symposium on Materials and Fluid Sciences in Microgravity, Volume 2 Aug. 1992 p 533-538 Sponsored by NASA, Washington; Alabama Supercomputer Network; Alabama Univ.; CNES; and Inst. Mediterraneen de Technologie (For primary document see N94-10171 01-29)

Copyright Avail: CASI HC A02/MF A04; ESA, EPD, ESTEC, Noordwijk, Netherlands, HC

Flow transitions in a Two Dimensional (2D) model of crystal growth were examined using the Bridgman-Stockbarger me thod. Using a pseudo-spectral Chebyshev collocation method, the governing equations yield solutions which exhibit a symmetry breaking flow tansition and oscillatory behavior indicative of a Hopf bifurcation at higher values of Ra. The results are discussed from fluid dynamic viewpoint, and broader implications for process models are also addressed. ESA

N94-10184# Deutsche Forschungsanstalt fuer Luft- und Raumfahrt, Cologne (Germany). Materials Research Inst.

TEXUS 28 EXPERIMENT: CONVECTIONS AND CRYSTAL GROWTH OF Ge:Ga. ANALYSIS OF TEMPERATURE MEASUREMENTS **c76**

Uwe Moeller, B. O. Hildmann, and G. Baehr *In* ESA, Proceedings of the 8th European Symposium on Materials and Fluid Sciences in Microgravity, Volume 2 Aug. 1992 p 539-543 (For primary document see N94-10171 01-29)

Copyright Avail: CASI HC A01/MF A04; ESA, EPD, ESTEC, Noordwijk, Netherlands, HC

A TEXUS sounding rocket experiment in which a Ga doped germanium crystal was directionally solidified under different acceleration states is presented. The solidification process was started on Earth (1g) and was continued during lift off of the rocket (up to 12g) and the microgravity period (0.0001g) until the reentry phase. The aim of this experiment was to analyze the effects of resulting convections in the melt on the grown crystal. For characterization of the different convectional states, temperatures were measured with three thermocouples at different positions in the melt. An analysis of the thermocouple data is presented. The results are compared to corresponding experiments in the Earth laboratory. The temperatures signals measured in the melt can be assigned to the different acceleration states during the flight. The fast Fourier transform analyses of these signals on Earth, and under microgravity conditions, show that low frequent disturbances up to 0.3 Hz are more pronounced under 1g than under microgravity. Whereas frequencies at about 1.1 Hz are more pronounced under microgravity than under 1g. The measured axial concentration profile agrees well with model calculations known from literature. ESA

N94-10185# Commissariat a l'Energie Atomique, Grenoble (France). Section d'Etudes de la Solification et de la Cristallogenese.

CONVECTION RELATED RADIAL SEGREGATION IN AN IDEALIZED HORIZONTAL BRIDGMAN CONFIGURATION **c76**

J. P. Garandet, Thierry Duffar, and Jean-Jacques Favier *In* ESA, Proceedings of the 8th European Symposium on Materials and Fluid Sciences in Microgravity, Volume 2 Aug. 1992 p 545-547 (For primary document see N94-10171 01-29)

Copyright Avail: CASI HC A01/MF A04; ESA, EPD, ESTEC, Noordwijk, Netherlands, HC

The influence of natural convection on the maximum radial concentration difference along a solid-liquid interface is estimated in an horizontal Bridgman growth configuration. This mechanism has to be considered along with interface curvature for a careful design of a space experiment. ESA

N94-10186# Katholieke Univ. te Leuven (Belgium). Dept. of Metallurgy and Materials Engineering.

TEM STUDY OF A SPACE PROCESSED Al-Al2O3 METALLIC COMPOSITE **c24**

H. Zou (Wuhan Univ., China.), L. Froyen, L. Delaey, and A. Deruyttere *In* ESA, Proceedings of the 8th European Symposium on Materials and Fluid Sciences in Microgravity, Volume 2 Aug. 1992 p 549-554 (For primary document see N94-10171 01-29)

Copyright Avail: CASI HC A02/MF A04; ESA, EPD, ESTEC, Noordwijk, Netherlands, HC

The microstructure of space processed Al-Al2O3 metallic composite was studied with Transmission Electron Microscopy (TEM) and compared with the microstructures of the starting material and the material remelted on Earth. The alumina particles are flat, ellipsoid-like, and have dimensions of about 0.2 micrometers in diameter and about 0.03 micrometers in thickness. The alumina particle agglomerates distribute densely in bands in the starting material. No significant difference in the distribution of particles was found between the samples that were liquid phase processed in space and those processed on Earth. No sedimentation of particles in the material remelted on Earth was observed. These findings are explained in terms of Brownian motion. The alumina particles are identified with electron diffraction mainly as gamma alumina. After remelting at 800 C for 3 minutes, a few alpha alumina particles were observed. A crystallographic relationship between gamma and alpha alumina was found with electron microscopy. ESA

N94-10187# Academia Sinica, Beijing (China). Inst. of Physics.

IN SITU OBSERVATION OF TEMPERATURE DEPENDENCE OF CONCENTRATION FIELD DURING GROWTH OF KB5 CRYSTALS BY HOLOGRAPHIC INTERFEROMETRY **c76**

W. C. Chen, Y. X. Shen, and M. Y. Ma *In* ESA, Proceedings of the 8th European Symposium on Materials and Fluid Sciences in Microgravity, Volume 2 Aug. 1992 p 555-558 (For primary document see N94-10171 01-29)

Copyright Avail: CASI HC A01/MF A04; ESA, EPD, ESTEC, Noordwijk, Netherlands, HC

The growth of potassium pentaborate tetrahydrate crystals was studied by both gel and low temperature solution methods for simulation of crystal growth in space. A set of in situ experiments concerning the temperature dependence of KB5 crystal growth were carried out by holographic interferometry. The experimental results showed that the concentration distribution during cooling is quite different than that in heating, and that, the influence of temperature on the concentration of KB5 in a free solution is more sensitive than that in the gelled medium. The findings will benefit the design of the facility which could be used for crystal growth in space and on the Earth. ESA

N94-10188*# National Inst. of Standards and Technology, Gaithersburg, MD.

PULSATILE INSTABILITY IN RAPID DIRECTIONAL SOLIDIFICATION: STRONGLY-NONLINEAR ANALYSIS **c76**

Richard J. Braun, G. J. Merchant (Stanford Univ., CA.), K. Brattkus (California Inst. of Tech., Pasadena.), and S. H. Davis (Northwestern Univ., Evanston, IL.) *In* ESA, Proceedings of the 8th European Symposium on Materials and Fluid Sciences in Microgravity, Volume 2 Aug. 1992 p 559-562 Sponsored by NASA, Washington (For primary document see N94-10171 01-29)

Copyright Avail: CASI HC A01/MF A04; ESA, EPD, ESTEC, Noordwijk, Netherlands, HC

In models of rapid directional solidification, non-equilibrium interfacial conditions are employed. As a result, there is an oscillatory mode of instability, as well as the steady cellular mode, found in the equilibrium model of Mullins and Sekerka. When the temperature field is decoupled from the problem, the preferred wave number for the oscillatory mode is zero, and the interface pulsates in time while remaining spatially uniform. Results from multiple scale analyses in the two limiting cases of the parameters are reported. In these limits, it is found that the instability is a bifurcation to relaxation oscillations; these nonlinear oscillations may be related to the observed microstructure that results from rapid solidification processes such as laser surface remelting. ESA

N94-10189# Centre National de la Recherche Scientifique, Meudon-Bellevue (France). Lab. d'Aerothermique.

WETTING EFFECTS ON NYLON SPHERES ENGULFMENT IN ICE **c76**

M. Yemmou, M. A. Azouni, C. Allain (Paris-Sud Univ., Orsay, France.), and G. Petre (Brussels Univ., Belgium.) *In* ESA, Proceedings of the 8th European Symposium on Materials and Fluid Sciences in Microgravity, Volume 2 Aug. 1992 p 563-566 (For primary document see N94-10171 01-29)

Copyright Avail: CASI HC A01/MF A04; ESA, EPD, ESTEC, Noordwijk, Netherlands, HC

The capture of particles during crystal growth, which is determined not only by the crystallization process but also by transport phenomena and the whole complex of surface properties, is considered here in terms of wetting. Conclusive proof of the importance of surface properties in particle engulfing is offered by the experimental investigation of treated and untreated small polyamide spheres ahead of an upward-moving, planar, horizontal ice-water interface. The surface state of the particles is characterized for each experiment by the measurement of the contact angle of a sessile water drop. A clear correlation is established between the contact angle values and the properties of engulfment. For very high angles (approximately 80 deg), the particle is always captured, whereas for low angles, there is a critical velocity of the freezing front below which the particle is rejected. ESA

N94-10190# Deutsche Forschungsanstalt fuer Luft- und Raumfahrt, Cologne (Germany). Space Simulation Inst.

THERMOPHYSICAL PROPERTIES OF UNDERCOOLED LIQUID METALS **c26**

Ivan Egry and Berndt Feuerbacher *In* ESA, Proceedings of the 8th European Symposium on Materials and Fluid Sciences in Microgravity, Volume 2 Aug. 1992 p 569-575 (For primary document see N94-10171 01-29)

Copyright Avail: CASI HC A02/MF A04; ESA, EPD, ESTEC, Noordwijk, Netherlands, HC

Recent developments and results relating to specific heat, thermal conductivity, surface tension, and viscosity of undercooled liquid metals are surveyed. Undercooling plays a major role in any solidification process. In fact, it is the driving force for solidification and determines not only the growth velocity, but also phase selection and formation of metastable phases. In this regime, the knowledge of the thermophysical properties, such as specific heat, thermal conductivity, viscosity, is of particular importance. Convective instabilities, nucleation rates, and solidification velocities are all governed by these parameters. With the advent of containerless processing techniques, in particular electromagnetic levitation, it is now possible to study the undercooled melt in situ and apply sophisticated noncontact diagnostics, such as pyrometry and high speed videography. Electromagnetic levitation is especially suited for studying bulk properties of metallic samples. ESA

N94-10191# Parma Univ. (Italy). Dept. of Physics.

CRYSTAL GROWTH FROM LOW TEMPERATURE VAPOUR PHASE **c76**

Carlo Paorici (Consiglio Nazionale delle Ricerche, Parma, Italy.) *In* ESA, Proceedings of the 8th European Symposium on Materials and Fluid Sciences in Microgravity, Volume 2 Aug. 1992 p 577-583 Sponsored by Italian Space Agency and CNR (For primary document see N94-10171 01-29)

Copyright Avail: CASI HC A02/MF A04; ESA, EPD, ESTEC, Noordwijk, Netherlands, HC

Fundamental aspects and techniques relevant to vapor crystal growth are reviewed. The emphasis is on the low temperature vapor growth, with particular reference to model substances (mercuric iodide, urea, and some organic materials for nonlinear optical applications) and growth techniques suitable for experiments in microgravity environment. As regards the techniques, the role of semiopen configurations is stressed and their principal advantages and drawbacks are discussed with respect to the more traditional closed configurations. ESA

N94-10192# Deutsche Forschungsanstalt fuer Luft- und Raumfahrt, Cologne (Germany).

NEW MECHANISM OF OSTWALD RIPENING IN LORENTZ-FORCE STABILIZED Cu-Pb DISPERSIONS **c76**

Dirk Uffelmann, L. Ratke, W. Bender, and Berndt Feuerbacher *In* ESA, Proceedings of the 8th European Symposium on Materials and Fluid Sciences in Microgravity, Volume 2 Aug. 1992 p 585-589 (For primary document see N94-10171 01-29)

Copyright Avail: CASI HC A01/MF A04; ESA, EPD, ESTEC, Noordwijk, Netherlands, HC

Measurements and theoretical investigations on Ostwald ripening of Cu particles in a liquid Pb-Cu melt with low volume content of the phase dispersed are presented. For this purpose, a novel technique that is able to suppress sedimentation of particles in an electrically conducting matrix was invented. The experiments on solid-liquid Cu-Pb dispersions in a low volume fraction range, which is not accessible by conventional experimental techniques, reveal the existence of stationary particle size distributions. The particle growth differs significantly from the growth law of the Lifshitz, Slyozov, and Wagner theory (the basic theory for particle coarsening) for diffusion controlled Ostwald ripening indicating that in this system the particle coarsening is not only diffusion limited. A new growth model that is based on the assumption of preferred places for the trapping of Cu atoms at dislocation sites emerging at the particle surface is presented. The new theoretical approach describes the experimental results excellently. ESA

N94-10193# Splav Technical Center, Moscow (Russia).

RESULTS OF CRYSTAL GROWTH EXPERIMENTS BY FZM ON ZONA FACILITIES IN MICROGRAVITY

I. V. Barmin, A. V. Egorov, and Alexander S. Senchenkov *In* ESA, Proceedings of the 8th European Symposium on Materials and Fluid Sciences in Microgravity, Volume 2 Aug. 1992 p 591-596 (For primary document see N94-10171 01-29)

Copyright Avail: CASI HC A02/MF A04; ESA, EPD, ESTEC, Noordwijk, Netherlands, HC

Some results of the experiments on crystal growth by Floating Zone Method (FZM), which were carried out onboard photon satellites, are presented. The description of the ampoule design and the list of the samples used are given. It is shown that heat transfer between a heater and a sample differ in space and on the ground. Consequently, it is insufficient to determine the heater temperature experimentally on Earth, but the theoretical analysis of heat transfer in space and on Earth is indispensable. The data on macro- and microinhomogeneity and dislocation density are presented. The presence of growth striations in the grown crystals testifies to the oscillating regime of the thermocapillary convection. To eliminate this defect, the axial static and rotating magnetic fields are used. ESA

N94-10194# Academia Sinica, Beijing (China). Inst. of Physics.

SOLIDIFICATION OF UNDERCOOLED Ni-32.5 WT PERCENT Sn EUTECTIC ALLOY **c26**

L. Q. Xing, D. Q. Zhao, X. C. Chen, X. S. Chen, G. C. Yang (Northwestern Polytechnical Univ., Xian, China.), and Y. H. Zhou (Northwestern Polytechnical Univ., Xian, China.) *In* ESA, Proceedings of the 8th European Symposium on Materials and Fluid Sciences in Microgravity, Volume 2 Aug. 1992 p 597-602 (For primary document see N94-10171 01-29)

Copyright Avail: CASI HC A02/MF A04; ESA, EPD, ESTEC, Noordwijk, Netherlands, HC

Bulk Ni-32.5 wt percent Sn eutectic alloy was undercooled by electromagnetic levitation processing. The recoalescence event was observed by using high speed cinematography. The dendrite tip velocities were measured and calculated. The solidification mechanism and the microstructural change from regular eutectic to anomalous eutectic were studied. It was found that the dendrite tip velocity of Ni3Sn phase was greatly larger than that of Ni(alpha) phase, as a result, Ni3Sn dendrites grew primarily into the undercooled melt in a 'dendritic cluster' morphology. The 'dendrite clusters' developed into 'anomalous eutectic' microstructures by ripening of Ni3Sn dendrites and growing of Ni(alpha) phase between the Ni3Sn arms. ESA

N94-10195# Commissariat a l'Energie Atomique, Grenoble (France). Section d'Etudes de la Solidification et de la Cristallogenese.

UNDERCOOLED W-Re AND Mo-Re DROPS IN AN ULTRA HIGH VACUUM DROP TUBE **c26**

E. Cini, B. Vinet, L. Cortella, and J. Bletry *In* ESA, Proceedings of the 8th European Symposium on Materials and Fluid Sciences in Microgravity, Volume 2 Aug. 1992 p 603-607 (For primary document see N94-10171 01-29)

(Contract ESTEC-9638/91/NL/JSC)

Copyright Avail: CASI HC A01/MF A04; ESA, EPD, ESTEC, Noordwijk, Netherlands, HC

Millimetric W-Re and Mo-Re droplets were undercooled and solidified under ultra high vacuum conditions in a 48 m high drop tube. The first observations and experimental results concerning the microstructures and the phases that were obtained are presented. For the most part, the W-Re and Mo-Re droplets exhibited cellular to dendritic microstructures. One solidification velocity was estimated at 3 m/s. Both the observations and the estimation agree with the usual cooling rates measured in high drop tubes under vacuum conditions (about 500 K/s). However, solidification microstructures may be altered during cooling in the solid state (namely by grain coarsening and ripening). The expected contraction of the (W) lattice parameter with the addition of Re was measured. The microstructural features of some W-Re droplets together with porosity measurements suggested two typical solidification regimes for droplets: one with a 'shell' solidification front for small relative undercoolings, and one with a 'quasi-planar' front for large relative undercoolings prior to nucleation. Some results obtained by numerical simulation provided qualitative agreement. Two Mo-Re droplets yielded a supersaturated (Mo) solid solution containing 59 wt. percent (i.e. 43 at. percent) Re. This seems to indicate a compositional metastability, which could be expected from the Mo-Re phase diagram. ESA

N94-10196# Deutsche Forschungsanstalt fuer Luft- und Raumfahrt, Cologne (Germany). Inst. fuer Raumsimulation.

NON-EQUILIBRIUM SOLIDIFICATION IN UNDERCOOLED Ni-B ALLOYS **c26**

Klaus Eckler, R. F. Cochrane (Leeds Univ., England.), M. Jurisch (Zentralinstitut fuer Festkoerperphysik und Werkstofforschung, Dresden, German D.R..), D. M. Herlach, and Berndt Feuerbacher *In* ESA, Proceedings of the 8th European Symposium on Materials and Fluid Sciences in Microgravity, Volume 2 Aug. 1992 p 609-614 (For primary document see N94-10171 01-29)

Copyright Avail: CASI HC A02/MF A04; ESA, EPD, ESTEC, Noordwijk, Netherlands, HC

Dendrite growth velocities were measured as a function of undercooling in droplets of dilute alloys of B in Ni undercooled by up to 306 K using an electromagnetic levitation technique. At a critical undercooling, depending strongly on the B concentration, a steep rise of the dendrite growth velocity was observed. The analysis of the results within current theories of dendrite growth gives evidence for a transition from diffusion limited to purely thermally controlled growth with the consequence of partitionless solidification. The consequences of such a transition were investigated with respect to the microstructure evolution. ESA

N94-10197# Commissariat a l'Energie Atomique, Grenoble (France). Section d'Etudes de la Solidification et le la Cristallogenese.

GROUND RESULTS OF THE MEPHISTO PROGRAM: BENEFITS AND SPACE EXPERIMENTS ORIENTATION **c26**

Andre Rouzaud, J. Comera, P. Contamin, and Jean-Jacques Favier *In* ESA, Proceedings of the 8th European Symposium on Materials and Fluid Sciences in Microgravity, Volume 2 Aug. 1992 p 615-618 (For primary document see N94-10171 01-29)

Copyright Avail: CASI HC A01/MF A04; ESA, EPD, ESTEC, Noordwijk, Netherlands, HC

The main goal of the Mephisto first flight is the study of the morphological instability of a plane front. The Mephisto space device is the result of a collaboration between the French atomic and space agencies. Operational since 1988, this advanced solidification furnace is scheduled to fly in the Space Shuttle on Sep. 1992. Its main feature consists in following the real solidification interface temperature by means of a thermoelectric measurement. Interesting results already obtained on the ground are presented. The results concern the following topics: macro and micro segregations real time supervision; and check of theoretical models predicting the solute layer extension versus the hydrodynamic state of the liquid bulk. The lessons of the ground experiments and their impact on the flight program are discussed. ESA

N94-10198# California Univ., Riverside. Dept. of Biochemistry.

EFFECTS OF A MICROGRAVITY ENVIRONMENT ON THE CRYSTALLIZATION OF BIOLOGICAL MACROMOLECULES

Alexander McPherson *In* ESA, Proceedings of the 8th European Symposium on Materials and Fluid Sciences in Microgravity, Volume 2 Aug. 1992 p 619-626 (For primary document see N94-10171 01-29)
Copyright Avail: CASI HC A02/MF A04; ESA, EPD, ESTEC, Noordwijk, Netherlands, HC

Macromolecules crystals are indispensable intermediates in the analysis of macromolecular structure, are essential for the application of X-ray diffraction methods, and are at the same time the greatest obstacle to success. Protein crystals are generally difficult to grow, often of imperfect form or small size, and frequently lack sufficient order. Their growth has become the rate limiting step in X-ray crystallography. Evidence has emerged from protein crystallization experiments carried out in space that suggest macromolecular crystals of improved order and quality can be grown in a microgravity environment. Presumably the absence of density driven convection and sedimentation permits a more deliberate and graceful entry of individual molecules into the crystal lattice. This in turn results in improvements in both morphology and the diffraction patterns of the crystals. The precise mechanisms for these improvements and the means for their optimization are, however, not understood at more than a rudimentary level. Microgravity effects that may play a role in protein crystal growth, sedimentation, convection and surface contact are reviewed and suggestions as to their possible mechanisms are made. ESA

N94-10199# Technische Univ., Munich (Germany). Inst. for Materials and Processing Sciences.

EUSO-D2-EXPERIMENT: UNIDIRECTIONAL SOLIDIFICATION WITH QUENCHING OF AN AlSi11 ALLOY c26

Hans M. Tensi and Raimund Roesch *In* ESA, Proceedings of the 8th European Symposium on Materials and Fluid Sciences in Microgravity, Volume 2 Aug. 1992 p 629-633 Sponsored by BMFT (For primary document see N94-10171 01-29)
Copyright Avail: CASI HC A01/MF A04; ESA, EPD, ESTEC, Noordwijk, Netherlands, HC

The experimental technique and scientific goal of the experiment EUSO (Eutectic Solidification under microgravity) which will be carried out during the German Spacelab D2 mission in Jan. 1993, are addressed. The solidification experiments with quenching of the solidification front are planned with a close eutectic AlSi11 alloy to investigate the influence of microgravity on the dendritic growth of the aluminum solid solution and on the interdendritic AlSi eutectic. The experiments will be processed in the gradient furnace with quenching device which is a Bridgman type furnace. The investigation continues the experiments of the German Spacelab D1 mission with an AlSi7 alloy. ESA

N94-10200# Queens Univ., Kingston (Ontario). Dept. of Metallurgical Engineering.

RIPENING OF IMMISCIBLE LIQUID DROPLETS IN MICROGRAVITY WITH CONSTRAINED MARANGONI DRIFT

S. Goodman and Reginald W. Smith *In* ESA, Proceedings of the 8th European Symposium on Materials and Fluid Sciences in Microgravity, Volume 2 Aug. 1992 p 635-640 (For primary document see N94-10171 01-29)
Copyright Avail: CASI HC A02/MF A04; ESA, EPD, ESTEC, Noordwijk, Netherlands, HC

In order to investigate droplet growth phenomena in immiscible alloy systems, experiments are currently being performed with the binary system of aluminum-indium. The experiments are performed during the reduced gravity periods available in parabolic aircraft trajectories and sounding rocket flights. These experiments, as well as ground based work consitute the QUIMAL (Queen's University Experiments in Immiscible Alloys) program. The aim of the program is to restrain Stokes' flow as well as Marangoni convection in order to measure the rate of droplet growth due to Ostwald ripening alone. In order to restrain these forces a small amount of iron is added to the system. Upon cooling the addition of iron results in the nucleation of intermetallic FeAl3 blades prior to the separation of indium droplets. Preliminary experiments aboard NASA's KC-135 have shown that 4 wt percent iron is effective in reducing Marangoni drift. Results of all QUIMAL tests done to date are given and an overview of experiment preparations and hardware design is provided. ESA

N94-10201# Aix-Marseilles Univ. (France). Inst. de Mecanique des Fluides.

CONDUCTIVE-RADIATIVE MODEL FOR PREDICTING THE SHAPE OF HgI2 CRYSTAL GROWN IN THE LTVG FURNACE c76

A. Roux, A. Fedoseyev (Institute of Biomedical Problems, Moscow, USSR.), and Bernard Roux *In* ESA, Proceedings of the 8th European Symposium on Materials and Fluid Sciences in Microgravity, Volume 2 Aug. 1992 p 641-644 Sponsored by Conseil Regional PACA (For primary document see N94-10171 01-29)
(Contract ESTEC-8431/89/F/BZ)
Copyright Avail: CASI HC A01/MF A04; ESA, EPD, ESTEC, Noordwijk, Netherlands, HC

The modeling of heat exchanges in a sealed ampoule in the LTVG (Low Temperature Vapor Growth) furnace is focused upon, in order to compute temperature fields and control the growth of HgI2 crystals from vapor phase at low temperatures. A coupled conductive radiative model was used to determine the shape of the source and the crystal at different equilibrium states (that is, without growth rate). The model involves conductivity anisotropy in the crystal and radiative exchanges between grey and diffuse surfaces (source and crystal interfaces, pyrex walls), which are considered as opaque. Internal buoyancy effect is not taken into account as the pressure inside the ampoule is very small. The source temperature is fixed. For different undercoolings, that is, for different cold finger temperatures, the 'equilibrium' isotherm between the source/gas and crystal/gas interfaces was numerically obtained. This 'equilibrium' isotherm, which is associated with the stop of the growing process, gives a crystal shape. This shape is compared with experimental results given by the ETH-Zurich group. The model would permit a better understanding and control of the future HgI2 crystal growth experiment. The computations are performed using a finite element package (FIDAP). ESA

N94-10202# Deutsche Forschungsanstalt fuer Luft- und Raumfahrt, Cologne (Germany). Space Simulation Inst.

OSTWALD RIPENING OF SOLID COBALT PARTICLES IN LIQUID COPPER c26

W. Bender, L. Ratke, and Berndt Feuerbacher *In* ESA, Proceedings of the 8th European Symposium on Materials and Fluid Sciences in Microgravity, Volume 2 Aug. 1992 p 645-649 (For primary document see N94-10171 01-29)
Copyright Avail: CASI HC A01/MF A04; ESA, EPD, ESTEC, Noordwijk, Netherlands, HC

The coarsening of solid cobalt particles in a liquid copper matrix during annealing at 1200C was investigated experimentally using volume fractions of cobalt between 30 and 50 percent. This is possible on Earth, since the density difference between both phases is small. Sedimentation was negligible in the alloys used. The experimental results are compared with the theory of Ostwald ripening for diffusional transport of matter. Generally the experimental results agree well with the theory of Voorhees and Glicksman. At higher volume concentrations and after long coarsening times there are small but significant differences between the theoretical predictions and the experimental results. They indicate that experiments under microgravity conditions would be needed to extend the range of volume fractions down to a few percent which would be desirable theoretically, and to suppress all effects stemming from buoyancy. ESA

N94-10203# Aix-Marseilles Univ. (France). Lab. de Physique Cristalline.

EFFECT OF EXPERIMENTAL PROCEDURE ON PATTERN FORMATION AND ARRAY DISORDER IN CELLULAR SOLIDIFICATION c76

Henri Nguyen Thi, Haik Jamgotchian, and B. Billia *In* ESA, Proceedings

of the 8th European Symposium on Materials and Fluid Sciences in Microgravity, Volume 2 Aug. 1992 p 651-654 Sponsored by CNES and CNRS (For primary document see N94-10171 01-29)
Copyright Avail: CASI HC A01/MF A04; ESA, EPD, ESTEC, Noordwijk, Netherlands, HC

Cellular arrays in Bridgman directional solidification of Pb-Tl are investigated. By using two different experimental procedures, the response of the planar interface to a sudden change in pulling velocity is examined. It is shown that the final pattern characteristics (average wavelength, level of disorder) are independent of experimental conditions even if the system reaches its steady state by different transients. It is found that in both cases, the solid-liquid front velocity significantly overshoots. ESA

N94-10204# Zentralinstitut fuer Festkoerperphysik und Werkstofforschung, Dresden (German D.R.). Inst. fuer Metallische Werkstoffe.
SOLIDIFICATION AND METASTABLE PHASE FORMATION OF HIGHLY UNDERCOOLED Fe-Cr-Ni ALLOY MELTS **c26**
W. Loeser, T. Volkmann (Deutsche Forschungsanstalt fuer Luft- und Raumfahrt, Cologne, Germany.), and Dieter M. Herlach (Deutsche Forschungsanstalt fuer Luft- und Raumfahrt, Cologne, Germany.) *In* ESA, Proceedings of the 8th European Symposium on Materials and Fluid Sciences in Microgravity, Volume 2 Aug. 1992 p 655-663 Sponsored by DLR (For primary document see N94-10171 01-29)
Copyright Avail: CASI HC A02/MF A04; ESA, EPD, ESTEC, Noordwijk, Netherlands, HC

Nonequilibrium solidification behavior and the expected phase formation of ferrite (bcc) and austenitic (fcc) primary solidification type Fe-Cr-Ni alloys are theoretically analyzed. Using current theories the nucleation probability and the dendrite growth velocity are investigated as a function of melt undercooling and concentration for both types of the alternative phases. The results of the calculations are compared with measured dendrite growth velocities revealing an agreement between theory and experiment. Microgravity aspects of the experiments are highlighted with respect to an extension of the attainable undercooling towards the hypercooling limit where critical effects are expected to occur in the formation of metastable phases and in the growth behavior. ESA

N94-10205# Aachener Centrum fuer Erstarrung unter Schwerelosigkeit e.V. (Germany).
CONTAINERLESS PROCESSING OF EQUIATOMIC Mn50Bi50 IN A DROP TUBE
J. Laakmann, K. Hoffmann, H. Koenig, and S. Ruellenrath *In* ESA, Proceedings of the 8th European Symposium on Materials and Fluid Sciences in Microgravity, Volume 2 Aug. 1992 p 665-667 Sponsored by BMFT and Deutsche Agentur fuer Raumfahrtangelegenheiten G.m.b.H. (For primary document see N94-10171 01-29)
Copyright Avail: CASI HC A01/MF A04; ESA, EPD, ESTEC, Noordwijk, Netherlands, HC

A drop tube providing a free fall time of approximately 0.7 s which is capable of containerless melting and resolidification of small samples with diameters of less than 500 micrometers, is described. Processing can be done in UHV (less than 0.000001 Pa) or in a clean gas atmosphere (He, purity 99.9996 percent). First results on the creation of the intermetallic compound Mn50Bi50 are presented. The system MnBi exhibits a miscibility gap in the liquid. The equiatomic compound of 1:1 stoichiometry is built at 719K by means of a peritectic transformation. As a consequence of the Bi sedimentation Mn is lacking for this peritectic reaction to the gravity of Earth. Thus the final reaction product is a relatively coarse mixture of Mn, Bi and MnBi, the latter having only a portion of less than 20 percent by weight. A way to solve this problem is containerless melting and resolidification in microgravity. ESA

N94-10206# Ames Lab., IA.
COUPLED GROWTH OF CELLS AND BUBBLES IN DIRECTIONAL SOLIDIFICATION OF SUCCINONITRILE-ACETONE ALLOYS **c76**
Haik Jamgotchian (Iowa State Univ. of Science and Technology, Ames.), R. Trivedi (Iowa State Univ. of Science and Technology, Ames.), and B. Billia (Aix-Marseilles Univ., France.) *In* ESA, Proceedings of the 8th European Symposium on Materials and Fluid Sciences in Microgravity, Volume 2 Aug. 1992 p 669-672 Sponsored by CNRS-NSF and NATO (For primary document see N94-10171 01-29)
Copyright Avail: CASI HC A01/MF A04; ESA, EPD, ESTEC, Noordwijk, Netherlands, HC

During the directional solidification of succinonitrile-acetone mixtures, acetone bubbles are nucleated in the intercellular grooves. Then bubbles grow with elongated bodies the tip position being a function of the growth parameters and bubble size. Solid envelopes get attached to the bubbles to form duplex structures. The interaction of such localized duplex structures with the solidification front, which depends on the experimental control parameters, was investigated. In the beginning of the cellular range, finite amplitude cells are observed only a distance from the bubbles. At higher acetone concentration, highly correlated sidebranches appear and amplify on the duplex structure, which means that a duplex structure can undergo an oscillatory dendritic transition. ESA

N94-10207# Royal Inst. of Tech., Stockholm (Sweden). Dept. of Casting of Metals.
LIQUID PHASE SINTERING OF TUNGSTEN COMPOSITES UNDER MICROGRAVITY. EFFECT OF MATRIX COMPOSITION
Lars B. Ekbom and A. Eliasson *In* ESA, Proceedings of the 8th European Symposium on Materials and Fluid Sciences in Microgravity, Volume 2 Aug. 1992 p 673-678 Sponsored by ESA and Swedish Board for Space Activities (For primary document see N94-10171 01-29)
Copyright Avail: CASI HC A02/MF A04; ESA, EPD, ESTEC, Noordwijk, Netherlands, HC

Tungsten heavy metals containing 90 to 95 percent W, Ni and Fe, were produced from powders by liquid phase sintering. The resulting composite consists of tungsten particles in a Ni-Fe-W-matrix. Eight different compositions were studied. TEXUS flights (10, 19, 26, 27) and parabolic flights were used for liquid phase sintering microgravity experiments. Liquid phase sintering includes a liquid penetration of agglomerates and tungsten particle growth. Cobalt was found to facilitate the separation of agglomerates and increases the growth rate. The particle growth rate of a W-Ni-alloy is higher than for the W-Ni-Fe-alloys. Calculations show that the surface energy is 5 times larger for the W-Ni alloy. ESA

N94-10208# Victoria Univ. (British Columbia). Dept. of Mechanical Engineering.
EFFECT OF GRAVITY ON THE DISSOLUTION AND LIQUID PHASE EPITAXIAL GROWTH PROCESSES IN A HORIZONTAL SANDWICH SYSTEM
Sadik Dost, S. Erbay, H. A. Erbay, and N. Djilali *In* ESA, Proceedings of the 8th European Symposium on Materials and Fluid Sciences in Microgravity, Volume 2 Aug. 1992 p 679-684 Sponsored by Canadian Space Agency (For primary document see N94-10171 01-29)
Copyright Avail: CASI HC A02/MF A04; ESA, EPD, ESTEC, Noordwijk, Netherlands, HC

Results of a numerical study of the dissolution and growth processes of silicon in a sandwich system are presented. The governing equations and the associate boundary and interface conditions of the system under isothermal conditions are given for a nominally two dimensional model. The numerical results for the concentration distribution, the dissolution depth and the growth thickness are in good general agreement with experimental observations. It is concluded that convective effects must be accounted for in order to reproduce experimentally observed features such as differences between the dissolution depths or the growth thicknesses of the upper and lower substrates. ESA

N94-10209# Freiburg Univ. (Germany). Kristallographisches Inst.
THM-GROWTH OF III-V-SEMICONDUCTORS IN THE MAGNETIC FIELD **c76**
A. N. Danilewsky, P. Dold, and K. W. Benz *In* ESA, Proceedings of the 8th European Symposium on Materials and Fluid Sciences in Microgravity, Volume 2 Aug. 1992 p 685-689 Sponsored by BMFT (For primary document see N94-10171 01-29)
Copyright Avail: CASI HC A01/MF A04; ESA, EPD, ESTEC, Noordwijk, Netherlands, HC

III-V semiconductor crystals were grown by the traveling heater method in a homogeneous axial magnetic field. First results demonstrate an influence not only on transport phenomena but also on growth kinetics and morphological stability. An interpretation of the growth results is given by an order of magnitude analysis using the dimensionless Rayleigh and Hartmann numbers. ESA

N94-10210# Ecole Nationale Superieure de Chimie, Montpellier (France). Lab. de Chimie Organique Physique et Cinetique Chimique Appliquees.
CRYSTALLIZATION OF ZEOLITES IN THE MICROGRAVITY ENVIRONMENT OF SPACE
F. DiRenzo, R. Dutartre, P. Espiau, F. Fajula, and M. A. Nicolle *In* ESA, Proceedings of the 8th European Symposium on Materials and Fluid Sciences in Microgravity, Volume 2 Aug. 1992 p 691-695 Sponsored by CNES, ELF Aquitaine, and and Michelin (For primary document see N94-10171 01-29)
Copyright Avail: CASI HC A01/MF A04; ESA, EPD, ESTEC, Noordwijk, Netherlands, HC

Several zeolites were prepared in microgravity conditions during the Casimir 1 flight in Sep. 1990. The effects of reduced gravity on the crystal size, composition and crystallinity of an analcime, mordenite, gismondine and zeolite beta were studied. Microgravity affected crystal size in a significant way in the case of zeolite synthesis from a clear aluminosilicate solution. A lower crystallization rate was observed in microgravity experiments, probably due to a slower mass transfer in the solution. ESA

N94-10211# Bulgarian Academy of Sciences, Sofia. Space Research Inst.
A STUDY OF THE QUASIBINARY Al-W-Mo SYSTEM. PART 1: PRELIMINARY INVESTIGATIONS AND PREPARATION FOR MICROGRAVITY EXPERIMENTS
Stavri Stavrev and V. Atanasova *In* ESA, Proceedings of the 8th European Symposium on Materials and Fluid Sciences in Microgravity, Volume 2 Aug. 1992 p 697-698 (For primary document see N94-10171 01-29)
Copyright Avail: CASI HC A01/MF A04; ESA, EPD, ESTEC, Noordwijk, Netherlands, HC

Some problems connected with the fabrication of composite materials are discussed and the main problems to be investigated are formulated. A quasibinary composite of approximate composition 70Al:20W:10Mo is of special interest because the binary systems W:Mo, W:Al and Mo:Al have already been well studied. The sample preparation technique is described as well as the multipurpose technological plant with electron beam heater. The experiments described were to be carried out on the Space Station Mir. ESA

N94-10212# Bulgarian Academy of Sciences, Sofia. Space Research Inst.
A STUDY OF THE QUASIBINARY Al-Mo-W SYSTEM. PART 2: A PHYSICO-MECHANICAL INVESTIGATION OF THE SYSTEM FABRICATED UNDER THE GRAVITYLESSNESS CONDITIONS
Stavri Stavrev and V. Atanasova *In* ESA, Proceedings of the 8th European Symposium on Materials and Fluid Sciences in Microgravity, Volume 2 Aug. 1992 p 699-702 (For primary document see N94-10171 01-29)
Copyright Avail: CASI HC A01/MF A04; ESA, EPD, ESTEC, Noordwijk, Netherlands, HC

The investigation of a quasibinary Al-W-Mo system formed under weightlessness conditions at different temperature gradients are described. The samples were fabricated using the onboard 'Yantar 2' crystallization plant on board the Space Station Mir. Such methods as X-ray, SEM (Scanning Electron Microscopy), microprobe, metallographic microscopy and chemical analysis were used to estimate conditions necessary for fabrication of this promising composite. It was found that the greater temperature gradient (greater overcooling) results in more homogeneous and fine structure of the composite. ESA

N94-10213# Freiburg Univ. (Germany). Kristallographisches Inst.
CRYSTAL GROWTH IN THE ZONE MELTING FACILITY (ZMF) c76
Ralf Schwarz, A. N. Danilewsky, G. Bischopink, and K. W. Benz *In* ESA, Proceedings of the 8th European Symposium on Materials and Fluid Sciences in Microgravity, Volume 2 Aug. 1992 p 703-707 Sponsored by BMFT (For primary document see N94-10171 01-29)
Copyright Avail: CASI HC A01/MF A04; ESA, EPD, ESTEC, Noordwijk, Netherlands, HC

The resistivity heater ZMF was developed to examine the influence of the temperature gradient on crystal growth. The ZMF in the present configuration is described. It is a ten zone resistance heater for growth experiments by the Travelling Heater Method (THM). The furnace is built up as a modular crystal growth facility for accommodation onboard of Spacelab and Space Station Freedom. One advantage of the furnace is the possibility to change the temperature gradient at the phase boundaries over a wide range. Temperature characteristics of the furnace are specified, which show a high accuracy of the temperature field. Growth experiments are described and the results confirm the appropriate heater concept. Single crystals in the II-VI semiconductor CdTe and of the ternary compound (Al,Ga)Sb with the size of one inch in the diamater and a length of 28 mm are grown. ESA

N94-10214# IFLYSIB, La Plata (Argentina).
MARANGONI-DRIVEN SOLITARY WAVES c34
Alfredo N. Garazo and Manuel G. Velarde (Universidad Nacional de Educacion a Distancia, Madrid, Spain.) *In* ESA, Proceedings of the 8th European Symposium on Materials and Fluid Sciences in Microgravity, Volume 2 Aug. 1992 p 711-715 (For primary document see N94-10171 01-29)
(Grants CICYT-PB86-651; CICYT-PB90-264)
Copyright Avail: CASI HC A01/MF A04; ESA, EPD, ESTEC, Noordwijk, Netherlands, HC

The quasi two dimensional Kadomtsev-Petsviashvili theory together with the corresponding one dimensional Korteweg-de Vries equation for solitary waves in open shallow (thin) liquid layers is generalized to account for viscous and heat dissipation, and energy supply provided by interfacial tension forces. Specific attention is paid to Benard convection when the driving force is the thermally induced Marangoni effect. ESA

N94-10215# Ecole Centrale de Lyon (France). Lab. de Mecanique des Fluides et d'Acoustique.
MARANGONI BENARD INSTABILITIES IN LIQUID MIXTURES WITH SORET EFFECT
Daniel Henry, H. Benhadid, Stefan VanVaerenbergh (Brussels Univ., Belgium.), J.-C. Legros (Brussels Univ., Belgium.), and Bernard Roux (Aix-Marseilles Univ., France.) *In* ESA, Proceedings of the 8th European Symposium on Materials and Fluid Sciences in Microgravity, Volume 2 Aug. 1992 p 717-722 (For primary document see N94-10171 01-29)
Copyright Avail: CASI HC A02/MF A04; ESA, EPD, ESTEC, Noordwijk, Netherlands, HC

In relation with microgravity experiments, numerical simulations of pure Marangoni flows in binary mixtures are presented. The concentration gradient is induced via Soret effect by the heat flux applied across the layer. The simulations are performed in large two dimensional cavities for slightly supercritical situations. They concern steady situations (pure thermal flows or with a destabilizing concentration contribution), as well as oscillatory situations (stabilizing concentration contribution). The results are analyzed through symmetry considerations and flow characterizations. ESA

N94-10216# Brussels Univ. (Belgium). Microgravity Research Center.
TRANSIENT EFFECTS IN THE BENARD INSTABILITIES: COUPLING BETWEEN CAPILLARY AND GRAVITY EFFECTS
Olivier Dupont, Pierre Colinet, Philippe Georis, and J.-C. Legros *In* ESA, Proceedings of the 8th European Symposium on Materials and Fluid Sciences in Microgravity, Volume 2 Aug. 1992 p 723-728 (For primary document see N94-10171 01-29)
Copyright Avail: CASI HC A02/MF A04; ESA, EPD, ESTEC, Noordwijk, Netherlands, HC

Theoretical and experimental analyses of the coupling between thermogravitational and thermocapillary instabilities in pure liquids are presented. Focus is on transient effects appearing in horizontal liquid layers open to an inert gas, and submitted to heat fluxes several times higher than the critical heat flux necessary to induce convection. In this case, infinitesimal perturbations are amplified and evolve towards a stationary convective state. It is shown that this can happen through a process of damped oscillations, especially when gravity induced convection plays the dominating role, or when the injected heat flux is high enough (which is shown to be equivalent). This is explained by the creation of a stabilizing thermal gradient in the bulk of the liquid, where the buoyancy force acts. Experiments also show the possibility to correlate the relative phase displacement between mean temperature drop and mean surface velocity curves, with the ratio between the driving forces. This is qualitatively confirmed by the initial conditions approach. The limits of velocity of the classical frozen time linear stability method, are also discussed and compared with the initial conditions method. ESA

N94-10217# Perm State Univ. (Russia). Inst. of Pedagogy.

NUMERICAL INVESTIGATIONS ON MARANGONI-BENARD INSTABILITY IN MULTI LAYER SYSTEMS

Illya B. Simanovskii, Philippe Georis (Brussels Univ., Belgium.), Marcel Hennenberg (Brussels Univ., Belgium.), Stefan VanVaerenbergh (Brussels Univ., Belgium.), I. Wertgeim (Academy of Sciences, USSR, Perm.), and J.-C. Legros (Brussels Univ., Belgium.) *In* ESA, Proceedings of the 8th European Symposium on Materials and Fluid Sciences in Microgravity, Volume 2 Aug. 1992 p 729-734 (For primary document see N94-10171 01-29)

Copyright Avail: CASI HC A02/MF A04; ESA, EPD, ESTEC, Noordwijk, Netherlands, HC

The study of the Marangoni-Benard and Rayleigh-Benard instability is extended to a system of three superposed immiscible layers submitted to an external temperature gradient perpendicular to the free interfaces. Under microgravity conditions, a symmetrical system consisting of a fluid A sandwiched between two layers of a fluid B is considered. The crucial role of diffusivity ratio (kappa = kappa(sub B)/kappa(sub A) on the kind of instability is shown. When the thermal diffusivities are very different (kappa not equal to 1), monotonous mode of instability driven by one interface is observed. When kappa is close to one, the monotonous critical Marangoni number becomes infinite and an overstable solution results from the coupling of both interfaces as a flip-flop oscillating mechanism. An experimental three layer was then taken, consisting of Fluorinert FC70, Silicone Oil 50 CS and air which is stable with respect to the density on ground. Different instability mechanisms were recorded. For moderate values of the Rayleigh number, the threshold of instability depends on the value of Marangoni number only, when the Rayleigh number is increased both thermocapillary and gravitational mechanisms collaborate, reminiscent of the famous Nield's theory. For pure thermocapillary convection, mechanical coupling between the layers can exist, and the appearance of thermal coupling for gravitational convection is explained in term of a nonlinear coupling. ESA

N94-10218# Aix-Marseilles Univ. (France). Inst. de Mecanique des Fluides.

INSTABILITY OF THERMOCAPILLARY CONVECTION IN MULTIPLE SUPERPOSED IMMISCIBLE LIQUID LAYERS c34

Q. S. Liu and Bernard Roux *In* ESA, Proceedings of the 8th European Symposium on Materials and Fluid Sciences in Microgravity, Volume 2 Aug. 1992 p 735-740 (For primary document see N94-10171 01-29)

Copyright Avail: CASI HC A02/MF A04; ESA, EPD, ESTEC, Noordwijk, Netherlands, HC

The linear and nonlinear instabilities analyses of multiple (two or three) immiscible liquid layers heated from below under microgravity conditions was studied by means of small perturbation method and a finite difference method, respectively. The lower wall is considered as a rigid perfectly conducting boundary. Either rigid or free top surface and planar interfaces are considered. The mode of instability is induced purely by surface tension gradient at each of the two or three interfaces (liquid-liquid and liquid-air). This may have application in space experiments. Marangoni-Benard instability in a three layer system in gravitational field is also studied. ESA

N94-10219# Academy of Sciences (USSR), Moscow. Inst. for Problems in Mechanics.

CONVECTIVE MOTION IN A MULTI-LAYERED SYSTEM WITH A FREE SURFACE c34

Valentina M. Shevtsova and A. E. Indeikina *In* ESA, Proceedings of the 8th European Symposium on Materials and Fluid Sciences in Microgravity, Volume 2 Aug. 1992 p 741-746 (For primary document see N94-10171 01-29)

Copyright Avail: CASI HC A02/MF A04; ESA, EPD, ESTEC, Noordwijk, Netherlands, HC

The problem of thermocapillary motion in a two layered system, due to the existence of temperature gradient, is considered. The problem is considered both by asymptotic method at the approximation of small Marangoni numbers and numerically. The free surface and boundary between liquids are assumed deformable. ESA

N94-10220# Perm State Univ. (Russia). Inst. of Pedagogy.

VIBRATIONAL-THERMOCAPILLARY PARALLEL FLOWS AND STABILITY c34

R. Birikh, Vladimir Briskman (Academy of Sciences, USSR, Perm.), V. Myznikov, Bernard Roux (Aix-Marseilles Univ., France.), and Manuel G. Velarde (Universidad Nacional de Educacion a Distancia, Madrid, Spain.) *In* ESA, Proceedings of the 8th European Symposium on Materials and Fluid Sciences in Microgravity, Volume 2 Aug. 1992 p 747-752 (For primary document see N94-10171 01-29)

Copyright Avail: CASI HC A02/MF A04; ESA, EPD, ESTEC, Noordwijk, Netherlands, HC

The influence of high frequency linear polarized vibrations of the plane liquid layer or liquid cylinder on Marangoni convection developed due to a temperature gradient is considered. Situations which may give rise to thermocapillary parallel closed flows in a liquid layer subject to harmonic high frequency vibrations are examined. The layer is bounded by cylindrical or plane interfaces. In case of a plane layer one or both boundaries are assumed to be free and vibration has arbitrary orientation. For liquid cylinder vibrations are supposed longitudinal. The flow is described by the averaged equations of convection. The flow structure and its intensity depend on three dimensionless parameters: Marangoni, q and Q numbers which define longitudinal and inclined vibration effects. It is shown that intensity of convective flow may be effectively controlled by an appropriate choice of vibration parameters. ESA

N94-10221# Ruhr Univ., Bochum (Germany). Lehrstuhl fuer Physikalische Chemie 2.

APPEARANCE OF CONVECTIVE INSTABILITIES CAUSED BY LIQUID-LIQUID PHASE SEPARATION UNDER SMALL BUOYANCY FORCES c34

Roland Zander and G. M. Schneider *In* ESA, Proceedings of the 8th European Symposium on Materials and Fluid Sciences in Microgravity, Volume 2 Aug. 1992 p 755-759 Sponsored by BMFT (For primary document see N94-10171 01-29)

Copyright Avail: CASI HC A01/MF A04; ESA, EPD, ESTEC, Noordwijk, Netherlands, HC

The far critical liquid-liquid phase decomposition that is induced in a horizontal fluid layer being exposed to a vertical temperature gradient and which can generate dissipative structures is investigated during ground based experiments using samples of near isopycnic components. The dissipative structures generated appear as a bulk fluid convection that is closely related to the two component Rayleigh-Benard instability. The convection is mainly driven by the concentration gradient which occurs in consequence of the demixing under the influence of the temperature gradient. Because comparatively small buoyancy forces are sufficient to trigger the instability, it is expected to appear also under reduced gravity down to an order of magnitude that is in praxi about 0.00001 g. Additionally, even in the presence of gradients which do not suffice to support such a bulk liquid convection, a regular organization of the floating precipitate is found. This phenomenon could result from an instability of the two phase liquid layer that is caused by the Marangoni driven migration of the droplets. ESA

N94-10222# Strathclyde Univ., Glasgow (Scotland). Dept. of Mathematics.

THE EFFECT OF A UNIFORM MAGNETIC FIELD ON THE ONSET OF STEADY MARANGONI CONVECTION IN A LAYER OF CONDUCTING FLUID c34

S. K. Wilson *In* ESA, Proceedings of the 8th European Symposium on Materials and Fluid Sciences in Microgravity, Volume 2 Aug. 1992 p 761-765 (For primary document see N94-10171 01-29)

Copyright Avail: CASI HC A01/MF A04; ESA, EPD, ESTEC, Noordwijk, Netherlands, HC

A combination of analytical and numerical techniques are used to analyze the effect of a uniform vertical magnetic field on the onset of steady Marangoni convection in a horizontal layer of quiescent electrically conducting fluid subject to a uniform vertical temperature gradient. It was concluded that the presence of the magnetic field always has a stabilizing effect on the flow, but that there will always be certain ranges of unstable wave numbers however strong the magnetic field is. ESA

N94-10223# Perm State Univ. (Russia). Inst. of Pedagogy.

THE COMBINED INFLUENCE OF ANTICONVECTIVE AND THERMOCAPILLARY MECHANISMS ON THE STABILITY OF SYSTEMS WITH INTERFACE c34

Illya B. Simanovskii, Alexander A. Nepomnyashchy (Technion - Israel Inst. of Tech., Haifa.), P. Colinet (Brussels Univ., Belgium.), J.-C. Legros (Brussels Univ., Belgium.), and Stefan VanVaerenbergh (Brussels Univ., Belgium.) *In* ESA, Proceedings of the 8th European Symposium on Materials and Fluid Sciences in Microgravity, Volume 2 Aug. 1992 p 767-770 (For primary document see N94-10171 01-29)
Copyright Avail: CASI HC A01/MF A04; ESA, EPD, ESTEC, Noordwijk, Netherlands, HC

A theoretical analysis of the combined influence of anticonvective and thermocapillary mechanisms in a two layer system is presented. The lower fluid has a significantly larger value of heat diffusivity than the upper one, and the upper fluid gas a significantly lower value of heat expansion coefficient than the lower one. These are necessary conditions for the anticonvective mechanisms to manifest, when heating the system from above. Both linear and nonlinear situations are analyzed. Linearly, the threshold value of the Grashoff number across the layers is foreseen to decrease with the increasing effect of destabilizing Marangoni-Benard mechanism. In the nonlinear case, when both mechanisms are destabilizing, numerical simulations predict multiple stationary solutions, which can be obtained starting from different initial conditions. ESA

N94-10224# Warsaw Technical Univ. (Poland). Inst. of Heat Engineering.

INFLUENCE OF NEUTRAL PARTICLES CONCENTRATION ON FLAME PROPAGATION IN METHANE-AIR MIXTURES AT ZERO AND NORMAL GRAVITY CONDITIONS

M. M. Gieras *In* ESA, Proceedings of the 8th European Symposium on Materials and Fluid Sciences in Microgravity, Volume 2 Aug. 1992 p 773-777 (For primary document see N94-10171 01-29)
Copyright Avail: CASI HC A01/MF A04; ESA, EPD, ESTEC, Noordwijk, Netherlands, HC

Results of investigation of flame propagation and extinction in methane-air mixtures in the presence of chemically neutral particles are presented. Standard vertical tube 1.2 m long and square cross section 0.05 by 0.05 sq m was used in the tests. The experiments were conducted at normal gravity and microgravity conditions, using a special stand. Profiles of velocity, temperature and thickness of flame front as well as changes in the flame structure in relation to methane and neutral particles concentration were determined. The experiments allowed conditions at which addition of neutral particles could cause extinction or acceleration of flame to also be determined. It was indicated that particles cause development of microturbulence and intensify combustion process by increase of burning surfaces and by increase of heat exchange by radiation. ESA

N94-10225# Consiglio Nazionale delle Ricerche, Genoa (Italy). Ist. di Chimica Fisica Applicata dei Materiali.

SURFACE TENSION AND ADSORPTION KINETICS IN IMMISCIBLE LIQUID SYSTEMS AT MICROGRAVITY

Libero Liggieri, Francesca Ravera, Alberto Passerone, and Annie Steinchen (Aix-Marseilles Univ., France.) *In* ESA, Proceedings of the 8th European Symposium on Materials and Fluid Sciences in Microgravity, Volume 2 Aug. 1992 p 779-782 Sponsored in part by ESA (For primary document see N94-10171 01-29)
Copyright Avail: CASI HC A01/MF A04; ESA, EPD, ESTEC, Noordwijk, Netherlands, HC

A new theory of adsorption kinetics at fluid-fluid interfaces was developed, taking into account both the energetics of the adsorption-desorption mechanism and the diffusion in the bulk phases. This theory allows the activation adsorption and desorption energies to be evaluated by using dynamic interfacial tension data determined by an extension of the pressure derivative method. ESA

N94-10226# Pisa Univ. (Italy). Dipt. di Energetica.

GRAVITY AND ELECTRIC FIELD EFFECTS ON POOL BOILING HEAT TRANSFER

W. Grassi and Paolo DiMarco *In* ESA, Proceedings of the 8th European Symposium on Materials and Fluid Sciences in Microgravity, Volume 2 Aug. 1992 p 783-788 (For primary document see N94-10171 01-29)
Copyright Avail: CASI HC A02/MF A04; ESA, EPD, ESTEC, Noordwijk, Netherlands, HC

A review was carried out to investigate the effects of gravity and electric fields on pool boiling heat transfer. The electric field proved to enhance the boiling performance in on Earth applications. In absence of gravity, phenomena generally neglected in Earth theories, may have a fundamental role in the boiling process. Besides, the boiling crisis is probably not governed by the hydrodynamic instability in such conditions. As far as known, the effect of an electic field on boiling in microgravity has never been investigated experimentally. The main features of the pool boiling heat transfer with and without an imposed electric field, and the expected modifications in a microgravity environment, are stressed. The areas in which further investigation and experimentation is needed are reported. An experimental campaign in microgravity conditions is expected to yield advances both in the understanding of the basic boiling mechanisms and in space heat transfer applications. ESA

N94-10227# Max-Planck-Inst. fuer Ernaehrungsphysiologie, Dortmund (Germany).

CHEMICAL PATTERN FORMATION UNDER MICROGRAVITY

Stefan C. Mueller and Axel Bewersdorff (Deutsche Forschungsanstalt fuer Luft- und Raumfahrt, Cologne, Germany.) *In* ESA, Proceedings of the 8th European Symposium on Materials and Fluid Sciences in Microgravity, Volume 2 Aug. 1992 p 789-793 (For primary document see N94-10171 01-29)
Copyright Avail: CASI HC A01/MF A04; ESA, EPD, ESTEC, Noordwijk, Netherlands, HC

Chemical structures which arise spontaneously on a macroscopic scale in certain reaction systems with autocatalytic steps evolving far from thermodynamic equilibrium are considered. In these systems, symmetry is broken as a consequence of the nonlinear coupling of chemical kinetics with transport processes such as diffusion or convection. Interesting applications lie in the understanding of pattern formation in biology. The formation and dynamics of the patterns depend delicately on the precise experimental conditions. They can be disturbed by sedimentation which, under normal gravity, can be caused by global and local heat production by the reaction itself. Regular and irregular structure formation is illustrated for a few examples and the relevance of microgravity research is substantiated by proposing several ideas for microgravity experiments. ESA

N94-10228# Technische Univ., Berlin (Germany). Iwan-N. Stranski Inst.

STUDIES OF CRITICAL POINT PHENOMENA OF FLUIDS: BULK FLUIDS, FLUIDS IN PORES, AND AT INTERFACES c25

Gerhard H. Findenegg, M. Thommes, and T. Michalski *In* ESA, Proceedings of the 8th European Symposium on Materials and Fluid Sciences in Microgravity, Volume 2 Aug. 1992 p 795-800 (For primary document see N94-10171 01-29)
Copyright Avail: CASI HC A02/MF A04; ESA, EPD, ESTEC, Noordwijk, Netherlands, HC

The adsorption behavior of a near critical fluid (sulfur hexafluoride) on a graphitized carbon black (V3G) and in Controlled Pore Glasses (CPG-10) was studied. The surface excess amount Gamma of SF6 on V3G was measured by approaching the critical point along the critical isochor from the one phase region using a new volumetric technique. Results of experiments to investigate the critical behavior of SF6 in narrow pores (CPG-10) of mean pore diameters 7.7 nm and 24.2 nm are also reported. ESA

N94-10229# Ecole Superieure de Physique et de Chimie Industrielles, Paris (France). Lab. de Physique et de Mecanique des Milieux Heterogenes.

FLUID-FLUID INTERFACIAL INSTABILITIES INDUCED BY GRAVITY

M. Fermigier, P. Jenffer (Paris-Sud Univ., Orsay, France.), L. Limat, and J. E. Wesfreid *In* ESA, Proceedings of the 8th European Symposium on Materials and Fluid Sciences in Microgravity, Volume 2 Aug. 1992 p 801-806 (For primary document see N94-10171 01-29)
Copyright Avail: CASI HC A02/MF A04; ESA, EPD, ESTEC, Noordwijk, Netherlands, HC

The instabilities induced by gravity on the interface separating two fluids of different densities (Rayleigh-Taylor instability), one of the two fluids being confined in a thin layer spread on a solid surface, is studied. In the simplest geometry (liquid films hanging below solid surfaces, the second fluid being a gas), pattern formations in two dimensions are observed involving competition between different symmetries, front propagation phenomena, nonlinear pattern selection, etc. When the unstable film is continuously supplied with 'fresh' liquid by an external source, different regimes of liquid emission are observed: periodic arrays of dripping sites, periodic arrays of liquid columns, and liquid sheets. The arrays of liquid columns exhibit a spatiotemporal behavior suggesting a possible transition towards chaos (oscillations, wave propagation, pairing or nucleation of cells, etc.). ESA

N94-10230# Paris VIII Univ., Villetaneuse (France). Inst. Galilee.
TRANSPORT OF HEAT AND MASS IN NEAR-CRITICAL FLUIDS c77
Yves Garrabos, B. LeNeindre, P. Guenoun (Commissariat a l'Energie Atomique, Gif-sur-Yvette, France.), F. Perrot (Commissariat a l'Energie Atomique, Gif-sur-Yvette, France.), and Daniel Beysens (Commissariat a l'Energie Atomique, Gif-sur-Yvette, France.) *In* ESA, Proceedings of the 8th European Symposium on Materials and Fluid Sciences in Microgravity, Volume 2 Aug. 1992 p 807-813 Sponsored by CNES and ESA (For primary document see N94-10171 01-29)
Copyright Avail: CASI HC A02/MF A04; ESA, EPD, ESTEC, Noordwijk, Netherlands, HC

In order to investigate some aspects of heat and mass transport in fluids in the absence of gravity, thermal cycles were performed near the liquid-phase critical point of CO2 and SF6 in the TEXUS 25 rocket and during the International Microgravity Laboratory (IML-1) Spacelab mission. In the absence of gravity driven convection, the heat transport is expected to be diffusive and very slow. Experimentally, although the local density and temperature gradients indeed relax by a diffusive process, clear evidence is found of fast and uniform thermal equilibration. This new mechanism is a 'piston effect'. ESA

N94-10231# Deutsche Forschungsanstalt fuer Luft- und Raumfahrt, Cologne (Germany). Inst. fuer Raumsimulation.
MEASUREMENTS OF HEAT CAPACITY IN UNDERCOOLED METALS c26
A. Bewersdorff, G. P. Goerler, Rainer Willnecker, Klaus Wittmann, R. Kuhl (Deutsche Agentur fuer Raumfahrtangelegenheiten G.m.b.H., Bonn, Germany.), R. Roestel, M. Guenter (Humboldt Univ., Berlin, German D.R..), and Genevieve Kell (Humboldt Univ., Berlin, German D.R..) *In* ESA, Proceedings of the 8th European Symposium on Materials and Fluid Sciences in Microgravity, Volume 2 Aug. 1992 p 817-819 (For primary document see N94-10171 01-29)
Copyright Avail: CASI HC A01/MF A04; ESA, EPD, ESTEC, Noordwijk, Netherlands, HC

Details of the experiment TES (German acronym for thermodynamic properties of undercooled melts) and the developed experiment hardware equipment are given. TES is scheduled for flight on the German-Russian mission Mir '92, and is aimed at the determination of the heat capacity of undercooled metals and alloys. It is realized by two probes, which will be processed in the furnace CSK-1, and by a dedicated data acquisition unit. A differentional method is applied comparing the thermal behavior of the sample under study with that of a reference sample of well known properties. The experimental device allows the measurement of absolute temperatures within the range 0 to 1000 C with a resolution of 0.25 K and of temperature differences with a resolution of 2.5 mK. It is noted that the thermophysical data of metallic melts are fundamental in characterizing the liquid state and analyzing the thermodynamics and kinetics of the liquid-solid phase transition. Within the regime of the undercooled melt, the heat capacity as the most important property is generally not available. ESA

N94-10232# Technische Univ., Munich (Germany). Lehrstuhl A fuer Thermodynamik.
STUDY OF VAPOR BUBBLE GROWTH IN A SUPERSATURATED LIQUID c34
Johannes Straub, J. Winter, G. Picker, H. Merte (Michigan Univ., Ann Arbor.), and Ayahiko Kono (JGC Corp., Yokohama, Japan.) *In* ESA, Proceedings of the 8th European Symposium on Materials and Fluid Sciences in Microgravity, Volume 2 Aug. 1992 p 820-825 (For primary document see N94-10171 01-29)
Copyright Avail: CASI HC A02/MF A04; ESA, EPD, ESTEC, Noordwijk, Netherlands, HC

Preparation experiments performed in laboratory and during parabolic flights for a major experiment in nucleation, bubble growth, interfacial phenomena, and evaporation/condensation kinetics forseen for BDPU on the International Microgravity Laboratory (IML-2) are presented. The intention was to get first scientific results and to reduce the technological uncertainties on the development of the BDPU test container. The process starts at a high system pressure to deactivate the nuclei at the walls of a test cell. The pressure is reduced below saturation by a quasi-isothermal expansion. The bubble growth is initiated by a short heating pulse of a thermistor in the liquid. The volume of the growing bubble is compensated by a pressure control system. After this cycle, the pressure is increased again and recondensation is observed. The test of the experimental set up was successful. Only small vapor bubbles can be observed under normal gravity, under reduced gravity<; however, vapor bubbles up to 1 cm in diameter can be produced. Nevertheless, the system is very sensitive to gravity disturbances. ESA

N94-10233# Deutsche Forschungsanstalt fuer Luft- und Raumfahrt, Cologne (Germany). Inst. fuer Raumsimulation.
PHASE SEPARATION AT GAS-LIQUID CRITICAL POINTS
Gerd Schmitz, H. Klein, Berndt Feuerbacher, and D. Woermann (Cologne Univ., Germany.) *In* ESA, Proceedings of the 8th European Symposium on Materials and Fluid Sciences in Microgravity, Volume 2 Aug. 1992 p 826-828 (For primary document see N94-10171 01-29)
Copyright Avail: CASI HC A01/MF A04; ESA, EPD, ESTEC, Noordwijk, Netherlands, HC

Results of two TEXUS experiments on phase separation at the gas-liquid critical point under reduced gravity conditions are reported. In the initial stages of phase separation, ring shaped light scattering patterns appear and temperature propagation through the sample slows down markedly. The scattering rings are analyzed in terms of the theory of spinodal decomposition. ESA

N94-10234# Toulouse Univ. (France). Lab. de Genie Chimique et Electrochimie.
ELECTROHYDRODYNAMIC EFFECTS IN CONTINUOUS FLOW ELECTROPHORESIS OBSERVATIONS ON EARTH AND IN MICROGRAVITY
H. Roux-deBalmann, Michael J. Clifton, and V. Sanchez *In* ESA, Proceedings of the 8th European Symposium on Materials and Fluid Sciences in Microgravity, Volume 2 Aug. 1992 p 829-832 Sponsored by CNES (For primary document see N94-10171 01-29)
Copyright Avail: CASI HC A01/MF A04; ESA, EPD, ESTEC, Noordwijk, Netherlands, HC

The study of electrohydrodynamics, which is one of the transport phenomena involved in continuous flow electrophoresis, is considered. An experimental study was performed using a visualization system that allows to follow in real time the sample stream in a cross section of the separation chamber. Both ground based and flight results obtained on board TEXUS sounding rockets are reported and discussed together with theoretical calculations concerning the influence of electrohydrodynamic effects on the sample distorsion. ESA

N94-10235*# National Aeronautics and Space Administration. Marshall Space Flight Center, Huntsville, AL.
GRANULAR INSTABILITY IN FLUIDIZED BEDS: A SMALL-OVER-LARGE INSTABILITY c34
David A. Noever *In* ESA, Proceedings of the 8th European Symposium on Materials and Fluid Sciences in Microgravity, Volume 2 Aug. 1992 p 833-837 (For primary document see N94-10171 01-29)
Copyright Avail: CASI HC A01/MF A04; ESA, EPD, ESTEC, Noordwijk, Netherlands, HC

For different particle diameters arranged in a gas fluidized bed, a new gravitational instability is predicted. The first order stability analysis yields conditions for growth of the most unstable wavenumber both as a function of particle diameter and dimensionless Bond number. Gravity acts to distribute the greater fluid mass associated with smaller particles, while surface tension stabilizes the entire bed against accelerations. The phenomenon, called the 'Small-over-Large' (SL) instability, evolves somewhat akin to a Rayleigh-Taylor mechanism and in addition to fundamental interest, carries implications for predicting solute redistribution and gravitational alignments in particle beds and chemical separation columns. ESA

N94-10236*# National Aeronautics and Space Administration. Goddard Space Flight Center, Greenbelt, MD.

COLUMBUS PROTO-PLANETESIMAL DUST AGGREGATION EXPERIMENT

H. U. Keller (Max-Planck-Inst. fuer Aeronomie, Katlenburg-Lindau, Germany.), J. Blum (Max-Planck-Inst. fuer Kernphysik, Heidelberg, Germany.), B. Donn, A. ElGoresy (Max-Planck-Inst. fuer Kernphysik, Heidelberg, Germany.), H. Fechtig (Max-Planck-Inst. fuer Kernphysik, Heidelberg, Germany.), Berndt Feuerbacher (Deutsche Forschungsanstalt fuer Luft- und Raumfahrt, Cologne, Germany.), E. Gruen (Max-Planck-Inst. fuer Kernphysik, Heidelberg, Germany.), W.-H. Ip (Max-Planck-Inst. fuer Aeronomie, Katlenburg-Lindau, Germany.), H. Kochan (Deutsche Forschungsanstalt fuer Luft- und Raumfahrt, Cologne, Germany.), and I. Mann (Max-Planck-Inst. fuer Aeronomie, Katlenburg-Lindau, Germany.) et al *In* ESA, Proceedings of the 8th European Symposium on Materials and Fluid Sciences in Microgravity, Volume 2 Aug. 1992 p 839-844 (For primary document see N94-10171 01-29)
Copyright Avail: CASI HC A02/MF A04; ESA, EPD, ESTEC, Noordwijk, Netherlands, HC

A microgravity experiment to study the growth of dust particles which has been proposed to be flown on one of the Columbus precursor flights is described. The microgravity environment will allow for low collision velocities (of order of mm/s) of the dust grains and for a large Knudsen number of the embedding gas; conditions expected in the early solar nebula. The outcome of the experiment will yield estimates of the sticking efficiency and the critical velocity for agglomeration. The values of these two parameters will provide substantial improvements in the constraints for models of the formation of planetesimals. In particular, the questions related to growth rate and mode of the aggregation process will be answered. The range of material type, collision velocities, properties of the environment in which growth takes place, and other factors permit a natural extension of this experiment to take advantage of the capabilities of the Space Station Columbus. Other astrophysical applications, such as processes in Saturnian rings, with somewhat different regimes could also be investigated. ESA

N94-10237# Politecnico di Torino (Italy). Dipt. di Scienza dei Materiali e Ingegneria Chimica.

INTERFACE REACTIONS OF (NI3AI) RIBBONS/AI-MMC IN GROUND PREPARATION AS PRELIMINARY TEST FOR MICROGRAVITY EXPERIMENTS c76

P. Appendino, C. Badini, M. Ferraris (Fiat Research Center, Orbassano, Turin, Italy.), and F. Marino (Trento Univ., Italy.) *In* ESA, Proceedings of the 8th European Symposium on Materials and Fluid Sciences in Microgravity, Volume 2 Aug. 1992 p 845-847 (For primary document see N94-10171 01-29)
Copyright Avail: CASI HC A01/MF A04; ESA, EPD, ESTEC, Noordwijk, Netherlands, HC

The preparation and characterization of an aluminum Metal Matrix Composite (MMC) reinforced with Ni3Al rapidly solidified intermetallic ribbons prepared with melt spinning technique is considered. The manufacturing of these composites presents some difficulties for the high reactivity between matrix and intermetallic and their different density. For this reason a space manufacturing is proposed. With the purpose of studying chemical reactions at the interface and preparing a reference material, ground experiments were performed. They confirm the high reactivity of this system and the difficulties in obtaining a homogeneous dispersion in a short time. Preliminary mechanical tests show an almost ductile behavior of this composite. ESA

N94-10238# Royal Inst. of Tech., Stockholm (Sweden).

THE REACTION BETWEEN TITANIUM CARBIDE AND ALUMINIUM CARBIDE IN LIQUID ALUMINIUM; A MICROGRAVITY STUDY

Anders E. W. Jarfors and Hasse Fredriksson *In* ESA, Proceedings of the 8th European Symposium on Materials and Fluid Sciences in Microgravity, Volume 2 Aug. 1992 p 849-854 Sponsored by Swedish Board for Space Activities (For primary document see N94-10171 01-29)
Copyright Avail: CASI HC A02/MF A04; ESA, EPD, ESTEC, Noordwijk, Netherlands, HC

The reaction between aluminum carbide and liquid aluminum containing titanium was studied in normal gravity and microgravity. Microgravity was obtained using parabolic aircraft flights. The temperature-time cycle for both normal gravity and microgravity were similar, the samples were preheated to 873 K during a 1.8 g phase and melt when g levels were well below 0.1 g. The heat treatment in liquid state was done at three different temperatures 973, 1173, and 1373 K. A rapid quenching was obtained using a jet of air. Two samples of different composition, one aluminum alloy containing titanium and one aluminum alloy containing carbon, were brought together in the liquid state. Diffusion of titanium and carbon was established. The precipitation process of titanium carbide and the dissolution of aluminum carbide was analyzed. ESA

N94-10239*# National Aeronautics and Space Administration. Lewis Research Center, Cleveland, OH.

THE KINEMATICS OF BUOYANCY INDUCED MIXING c34

Walter M. B. Duval *In* ESA, Proceedings of the 8th European Symposium on Materials and Fluid Sciences in Microgravity, Volume 2 Aug. 1992 p 855-861 (For primary document see N94-10171 01-29)
Copyright Avail: CASI HC A02/MF A04; ESA, EPD, ESTEC, Noordwijk, Netherlands, HC

A model problem to study mixing driven by buoyancy flow fields due to a time dependent body force which consists of a steady and an oscillatory component is considered. Flow fields generated by a time dependent body force, which consists of a steady and an oscillatory component from vibrations or g-jitter, mix two fluids inside a cavity by stretching and folding the interface into various morphological patterns. These patterns show two basic structures depending on the dominant components of the body force. These structures are whirls and tendrils, corresponding to the dominance of either the steady or oscillatory component, respectively. A combination of these structures also occurs in the interaction region. In this region the effect of the steady component opposes the oscillatory component and the result is to smooth the interface, and prevent breakup of the interface. For the parametric range considered, two basic flow regimes occur: convective and chaotic. In the convective regime, the morphological patterns are topological. In the chaotic regime, mixing occurs by a repetitive sequence of bubble formation, necking, and breakup which spreads the concentration field throughout the cavity. The length stretch of the interface increases exponentially with time. The dynamical system characteristics show that in the convective regime, at a point in space, the flow field is oscillatory with elliptical phase space trajectories, and its power spectrum indicates that the flow field responds to the corresponding input frequency. Whereas, in the chaotic regime, the flow field is aperiodic, the phase space trajectories show irregular patterns, and the power spectrum shows a broadband distribution. ESA

N94-10240# Centre National de la Recherche Scientifique, Meudon-Bellevue (France). Lab. d'Aerothermique.

INFLUENCE OF GRAVITY AND AMBIENT PRESSURE VARIATIONS ON THE BEHAVIOR OF BUOYANT LAMINAR DIFFUSION FLAMES

Daniel Durox, Tao Yuan, and E. Villermaux (Grenoble-1 Univ., France.) *In* ESA, Proceedings of the 8th European Symposium on Materials and Fluid Sciences in Microgravity, Volume 2 Aug. 1992 p 863-868 (For primary document see N94-10171 01-29)
Copyright Avail: CASI HC A02/MF A04; ESA, EPD, ESTEC, Noordwijk, Netherlands, HC

The buoyant laminar diffusion flames were studied theoretically and experimentally to observe the flame dynamic behaviors as global shape and flame flickering in function of gravity and ambient pressure. The mechanisms of gravity effects and ambient pressure effects acting on these flame behaviors are discussed. The apparent power laws of flame surface for steady flames and of flame flickering frequency for oscillating flames as a function of gravity and ambient pressure were theoretically predicted; the experimental results for these power laws as functions of ambient pressures are in a good agreement with the theoretical predictions. The experiments also showed that both for diffusion flames and premixed flames, the flame flickering frequencies are in the same order of absolute value and possess the same power law as a function of ambient pressure. ESA

N94-10241# Microgravity Advanced Research and Support Center, Naples (Italy).

LASER COOLING AND TRAPPING OF ATOMS IN MICROGRAVITY: ULTRACOLD ATOMS COLLISIONS

Carlo Albanese, Raimond Fortezza, M. Inguscio (Florence Univ., Italy.), and G. M. Tino (Naples Univ., Italy.) *In* ESA, Proceedings of the 8th European Symposium on Materials and Fluid Sciences in Microgravity, Volume 2 Aug. 1992 p 869-871 (For primary document see N94-10171 01-29)

Copyright Avail: CASI HC A01/MF A04; ESA, EPD, ESTEC, Noordwijk, Netherlands, HC

An experiment to investigate the collisional processes in molasses, such as collisions between cold atoms and cold atom surface interactions, in a drastically simplified environment in which the effect of gravity is negligible, is proposed. One of the most interesting areas in the contemporary physical research involves the investigation on atoms and ions in conditions of controlled density, position, and velocity. An outstanding interest is dedicated to atoms slowing down by laser radiation pressure and their localization by magnetic and optical traps. But, the gravitational force in Earth based laboratories reduces the observation time during the experiment, as the slowed atoms fall down out of the region of observation. So a privileged environment for the research on atom trapping by laser radiation pressure is the microgravitational one. Due to the development of diode laser technology, the drawbacks present on Earth may be divided and a very compact experimental facility may be obtained to perform the experiments in a space laboratory. Attention is given to the compactness and energy requisites of the facility and to the possibility of telescience utilization. ESA

N94-10242# Academy of Sciences (USSR), Moscow. Space Research Inst.

USE OF INERT IMMISCIBLE LIQUID FOR CRYSTAL SEPARATION OUT OF ITS FEEDING SOLUTION IN WEIGHTLESSNESS

A. A. Vedernikov, Patrick Queeckers (Brussels Univ., Belgium.), and J. C. Legros (Brussels Univ., Belgium.) *In* ESA, Proceedings of the 8th European Symposium on Materials and Fluid Sciences in Microgravity, Volume 2 Aug. 1992 p 873-878 (For primary document see N94-10171 01-29)

Copyright Avail: CASI HC A02/MF A04; ESA, EPD, ESTEC, Noordwijk, Netherlands, HC

The theory behind the use of an inert immiscible liquid for crystal separation out of its feeding solution in weightlessness is discussed. Experiments to test this procedure are described. The preservation of monocrystals after production in microgravity could be reached by pushing away slowly the feeding solution out of the cell. The introduction of an inert liquid leads to the formation of a bridge with two contact lines: one on the inner side of the cell and the other on the crystal. The bridge evolution is analyzed in the framework of quasistationary motion of equilibrium surfaces and compared with the results of separation simulations using two isodense immiscible liquids. Numerical analysis revealed a wide range of parameters for which an increasing liquid volume does not lead to the motion of contact line on the crystal in the direction of its tip. Hysteresis of both contact angles plays an important role in evolution of liquid-liquid interface. ESA

N94-10243# Technische Univ., Munich (Germany). Lehrstuhl A fuer Thermodynamik.

SINGLE BUBBLE EXPERIMENTS IN POOL BOILING: RESULTS FROM TEXUS 26

Bernd Vogel and Johannes Straub *In* ESA, Proceedings of the 8th European Symposium on Materials and Fluid Sciences in Microgravity, Volume 2 Aug. 1992 p 879-886 Sponsored by Deutsche Agentur fuer Raumfahrtangelegenheiten G.m.b.H. (For primary document see N94-10171 01-29)

Copyright Avail: CASI HC A02/MF A04; ESA, EPD, ESTEC, Noordwijk, Netherlands, HC

Single bubble experiments performed on a TEXUS flight to investigate heat transport mechanisms in pool boiling are described. During the series of experiment runs in subcooled boiling, data about bubble growth, heater temperature distributions, and temperature profiles close to the bubble were gained and evaluated. As a result, it can be stated that the main heat transport mechanism is evaporation at the heater wall. Condensation together with Marangoni flow serve as secondary mechanisms for the heat transport from the vapor bubble further on into the bulk liquid. ESA

N94-10244# Bulgarian Academy of Sciences, Sofia. Inst. for Mechanics and Biomechanics.

SOME ASPECTS OF COMBUSTION MODELLING BY LOW AND NORMAL GRAVITY

I. Petrova Nikolova *In* ESA, Proceedings of the 8th European Symposium on Materials and Fluid Sciences in Microgravity, Volume 2 Aug. 1992 p 887-890 (For primary document see N94-10171 01-29)

Copyright Avail: CASI HC A01/MF A04; ESA, EPD, ESTEC, Noordwijk, Netherlands, HC

An overview of combustion modeling approach by convection is given and comparison with communications in a recently published paper is also given. The accent is put on investigation of flame spreading from a 'hot spot' by normal and low gravity. Some numerical results of flame kernel deformation and evolution as well as some characteristics curves and flow fields are presented. ESA

N94-10245# Georgia Tech Research Inst., Atlanta. Zeolite Research Program.

SYNTHESIS OF MOLECULAR SIEVES FROM CLEAR SOLUTION c76

Rosemarie Szostak, Rosario Aiello (Calabria Univ., Arcavacta di Rende, Italy.), Flaviano Testa (Calabria Univ., Arcavacta di Rende, Italy.), and Alfonso Nasrto (Calabria Univ., Arcavacta di Rende, Italy.) *In* ESA, Proceedings of the 8th European Symposium on Materials and Fluid Sciences in Microgravity, Volume 2 Aug. 1992 p 891-893 Sponsored by Italian Space Agency (For primary document see N94-10171 01-29)

Copyright Avail: CASI HC A01/MF A04; ESA, EPD, ESTEC, Noordwijk, Netherlands, HC

In order to offer a contribution to the identification of synthesis suitable for a systematical investigation on the influence of microgravity on zeolite crystallization, a series of molecular sieves was synthesized from unconventional, very diluted, synthesis mixtures characterized by the initial absence of solid, gel like, phases (clear solutions). Aluminophosphate (AlPO4) and silicate (silicate-1) molecular sieves were obtained in this way and the role of the chemical composition of the system is discussed. ESA

N94-10246# Bremen Univ. (Germany). Center of Applied Space Technology and Microgravity.

PHOTOINITIATED RADICAL POLYMERIZATION OF LIQUID MONOMERS IN MICROGRAVITY

Dieter Sturm, R. Mueller, and Hans-J. Rath *In* ESA, Proceedings of the 8th European Symposium on Materials and Fluid Sciences in Microgravity, Volume 2 Aug. 1992 p 895-899 Sponsored by BMFT (For primary document see N94-10171 01-29)

Copyright Avail: CASI HC A01/MF A04; ESA, EPD, ESTEC, Noordwijk, Netherlands, HC

The role of gravity sensitive mechanisms in the processing of polymers is analyzed on the basis of comparative study of polymerization under terrestrial and microgravitational conditions. The investigations mainly focus on the influence on the molecular weight, polymer tacticity, particle size dispersivity, and on the influence of wall effects on the polymerization behavior. Research is concentrated on the photoinitiated radical polymerization of mono- and multi-functional monomers. ESA

N94-10247# Bremen Univ. (Germany). Center of Applied Space Technology and Microgravity.

A METHOD FOR DETERMINATION OF THE ELONGATIONAL VISCOSITY OF VISCOELASTIC FLUIDS WITHOUT BODY FORCES c34

S. Berg, A. Delgado, R. Kroeger, and Hans J. Rath *In* ESA, Proceedings of the 8th European Symposium on Materials and Fluid Sciences in Microgravity, Volume 2 Aug. 1992 p 901-904 Sponsored by BMFT and the Senator for Education and Arts of the State of Bremen (For primary document see N94-10171 01-29)

Copyright Avail: CASI HC A01/MF A04; ESA, EPD, ESTEC, Noordwijk, Netherlands, HC

The elongational viscosity of elastic fluids depends on the actual elongation stress as well as on the stress history. In order to perform an accurate determination of the elongational viscosity of polymer liquids, a pure extensional flow with a constant strain rate and a zero stress history is required. Both requirements can not be provided under terrestrial conditions but under conditions of microgravity. For this purpose a new experimental set up was developed, which realizes the classical tension experiment under conditions of microgravity but fluids are used as the sample. An arrangement like this enables the direct measurement of the arising elastic forces during extension of the fluid bridge. However, this leads to significant requirements of fluid management, especially because the experimental set up is designed for short time operation in drop tower facilities. ESA

N94-10248# McGill Univ., Montreal (Quebec).
MICROGRAVITY COMBUSTION OF DUST SUSPENSION IN A SPHERICAL CHAMBER **c25**
John H. S. Lee, Olivier Peraldi, Rom Knystautas, and Robert Thirsk (Canadian Space Agency, Ottawa, Ontario.) *In* ESA, Proceedings of the 8th European Symposium on Materials and Fluid Sciences in Microgravity, Volume 2 Aug. 1992 p 905-908 (For primary document see N94-10171 01-29)
(Contract CSA-9F007-1-00-22)
Copyright Avail: CASI HC A01/MF A04; ESA, EPD, ESTEC, Noordwijk, Netherlands, HC

Experiments in constant volume combustion of dust in air in a 4 liter spherical vessel were carried out in 1 g and microgravity environments. The diagnostics involved exclusively piezoelectric pressure transducers to measure the pressure-time history of the combustion process. Different delay times between dust dispersion and ignition were generated to assess the effect of dispersion turbulence on the combustion process. Highest pressures were achieved with delay times of the order of 200 ms in both the 1 g and microgravity experiments. This peak pressure was of the order of the theoretically calculated constant volume pressure (approximately 12 bar). In the 1 g case, the peak combustion pressure decreased to nothing as the delay times approached 600 ms. For microgravity experiments, long delay times (up to 20 sec) could be generated. The peak pressure asymptotically levelled out to about 4 bar (one third of peak constant volume pressure) for delay times larger than about 600 ms. ESA

N94-10249*# National Aeronautics and Space Administration. Marshall Space Flight Center, Huntsville, AL.
THE INTERNATIONAL MICROGRAVITY LABORATORY, A SPACELAB FOR MATERIALS AND LIFE SCIENCES
Robert S. Snyder *In* ESA, Proceedings of the 8th European Symposium on Materials and Fluid Sciences in Microgravity, Volume 2 Aug. 1992 p 911-915 (For primary document see N94-10171 01-29)
Copyright Avail: CASI HC A01/MF A04; ESA, EPD, ESTEC, Noordwijk, Netherlands, HC

The material science experiments performed on the International Microgravity Laboratory (IML-1), which is used to perform investigations which require the low gravity environment of space, are discussed. These experiments, the principal investigator, and associated organization are listed. Whether the experiment was a new development or was carried on an earlier space mission, such as the third Spacelab (SL-3) or the Shuttle Middeck, is also noted. The two major disciplines of materials science represented on IML-1 were the growth of crystals from the melt, solution, or vapor and the study of fluids (liquids and gases) in a reduced gravity environment. The various facilities on board IML-1 and their related experiments are described. The facilities include the Fluids Experiment System (FES) Vapor Crystal Growth System (VCGS) Organic Crystal Growth Facility (OCGF), Cryostat (CRY), and the Critical Point Facility (CPF). ESA

N94-10250# European Space Agency. European Space Research and Technology Center, ESTEC, Noordwijk (Netherlands).
THE CRITICAL FACILITY ON IML-1 **c18**
T. Dewandre, M. Cork, and Alain Gonfalone *In its* Proceedings of the 8th European Symposium on Materials and Fluid Sciences in Microgravity, Volume 2 Aug. 1992 p 917-919 (For primary document see N94-10171 01-29)
Copyright Avail: CASI HC A01/MF A04; ESA, EPD, ESTEC, Noordwijk, Netherlands, HC

Some technical highlights of the Critical Point Facility (CPF), an instrument dedicated to the study of transparent fluids around their critical point which was successfully flown on the International Microgravity Laboratory (IML-1) launched in Jan. 1992 are presented. The following are considered: the downlink of data and video images in real time; the downlink of digital video images; the CPF commanding capability; and the commercial photocamera to acquire high resolution images of interferometric patterns. ESA

N94-10730# National Aerospace Lab., Tokyo (Japan). Space Technology Research Group.
LARGE AMPLITUDE SHAPE OSCILLATIONS IN A MERCURY DROP USING A DROP TOWER [RAKKATOU WO MOCHIITA EKITEKI NO DAISHINPUKU SHINDOU JIKKEN]
Shouichi Yoshihara and Hisao Azuma Mar. 1992 18 p In JAPANESE
(DE93-767972; NAL-TR-1143; JTN-93-80429) Avail: CASI HC A03/MF A01

The application of an AC (Alternate Current) electric field to a mercury drop resulted in large-amplitude shape oscillations due to variations in its surface tension. Quasi-two-dimensional (2-D) oscillation patterns were identified from the 2nd to 16th modes for flattened drops under a pressure of 1 G. In addition, three dimensional oscillations were observed in low-gravity using a drop tower, with several polyhedra patterns being clearly identified, e.g., a tetrahedron, hexahedron, octahedron, and dodecahedron. Author (NASDA)

N94-11235*# National Aeronautics and Space Administration. Lyndon B. Johnson Space Center, Houston, TX.
PROJECT ARGO: GAS PHASE FORMATION IN SIMULATED MICROGRAVITY
Michael R. Powell, James M. Waligora, William T. Norfleet, and K. Vasantha Kumar (Krug Life Sciences, Inc., Houston, TX.) Jul. 1993 96 p
(NASA-TM-104762; S-711; NAS 1.15:104762) Avail: CASI HC A05/MF A01

The ARGO study investigated the reduced incidence of joint pain decompression sickness (DCS) encountered in microgravity as compared with an expected incidence of joint pain DCS experienced by test subjects in Earth-based laboratories (unit gravity) with similar protocols. Individuals who are decompressed from saturated conditions usually acquire joint pain DCS in the lower extremities. Our hypothesis is that the incidence of joint pain DCS can be limited by a significant reduction in the tissue gas micronuclei formed by stress-assisted nucleation. Reductions in dynamic and kinetic stresses in vivo are linked to hypokinetic and adynamic conditions of individuals in zero g. We employed the Doppler ultrasound bubble detection technique in simulated microgravity studies to determine quantitatively the degree of gas phase formation in the upper and lower extremities of test subjects during decompression. We found no evidence of right-to-left shunting through pulmonary vasculature. The volume of gas bubble following decompression was examined and compared with the number following saline contrast injection. From this, we predict a reduced incidence of DCS on orbit, although the incidence of predicted mild DCS still remains larger than that encountered on orbit. Author (revised)

N94-11483*# Auburn Univ., AL. Dept. of Aerospace Engineering.
REDUCED GRAVITY MULTIBODY DYNAMICS TESTING Final Report
Meija Sillanpaa 30 Jun. 1993 3 p
(Contract NAS8-39131)
(NASA-CR-192589; NAS 1.26:192589) Avail: CASI HC A01/MF A01

The Final Report on reduced gravity multibody dynamics testing is presented. Tests were conducted on board the NASA KC-135 RGA in Houston, Texas. The objective was to analyze the effects of large angle rotations on flexible, multi-segmented structures. The flight experiment was conducted to provide data which will be compared to the data gathered from ground tests of the same configurations. The flight and ground tested data will be used to validate the TREETOPS software, software which models dynamic multibody systems, and other multibody codes. The flight experiment consisted of seven complete flights on board the KC-135 RGA during two one-week periods. The first period of testing was 4-9 Apr. 1993. The second period of testing was 13-18 Jun. 1993. CASI

31 ENGINEERING (GENERAL)

Includes vacuum technology; control engineering; display engineering; cryogenics; and fire prevention.

N94-10293# Los Alamos National Lab., NM.
MATERIAL REMOVAL PROCESSES: ENGINEERING MECHANICS CONSIDERATION
C. A. Anderson 1993 6 p Presented at the 1993 ASPE Spring Topical Meeting, Tucson, AZ, 13-15 Apr. 1993
(Contract W-7405-eng-36)
(DE93-010733; LA-UR-93-1025; CONF-9304106-2) Avail: CASI HC A02/MF A01

In the material removal process called machining, a layer of material of constant thickness is removed from the workpiece by a wedge-shaped tool that travels parallel to the workpiece at a preselected depth. Even though the speed of relative movement between workpiece and tool is low (typical 1-10 m/s), the strain-rates in the workpiece near the tool can be high, on the order of 10(exp 4)-10(exp 5) /s. When machining brittle materials or unlubricated ductile materials at low speed, the removed metal (or chip) will be discontinuous and made up of small fractured segments. On the other hand, when machining ductile material under lubricated conditions, the removed material forms a continuous coil. In this case, we can represent the material removal process as a steady-state process. In this presentation, we will restrict ourselves to orthogonal machining where the cutting edge is perpendicular to the relative motion--a situation also approximated by other material removal processes such as planing and broaching, and turning on a lathe. DOE

N94-10613# Advisory Group for Aerospace Research and Development, Neuilly-Sur-Seine (France). Structures and Materials Panel.
ENVIRONMENTALLY SAFE AND EFFECTIVE PROCESSES FOR PAINT REMOVAL [LES PROCEDES EFFICACES ET ECOLOGIQUES POUR L'ENLEVEMENT DES PEINTURES]
Mar. 1993 133 p The 75th meeting was held in Lindau, Germany, 7-8 Oct. 1992
(AGARD-R-791; ISBN-92-835-0705-3) Copyright Avail: CASI HC A07/MF A02

Paint stripping and repainting of aircraft surfaces are required periodically during the operating lifetime of an aircraft. Historically, paint removal has been achieved with chemical strippers. These materials often contain toxic components and create hazardous working conditions. It is necessary to ensure that alternate paint removal techniques are available that can be performed in a cost effective, environmentally safe manner without causing damage to aircraft surfaces. For individual titles, see N94-10614 through N94-10629.

N94-10614# Naval Air Warfare Center, Warminster, PA. Aircraft Div.
PAINT REMOVAL ACTIVITIES IN THE US NAVY
Joseph Kozol *In* AGARD, Environmentally Safe and Effective Processes for Paint Removal Mar. 1993 5 p (For primary document see N94-10613 01-31)
Copyright Avail: CASI HC A01/MF A02

Use of methylene chloride and phenol based chemical strippers for aircraft paint removal generates large quantities of hazardous waste and creates health and safety problems for operating personnel. This paper presents an overview of the U.S. Navy's activities in the investigation and implementation of alternate paint stripping methods which will minimize or eliminate hazardous waste and provide a safe operating environment. Alternate paint removal methods under investigation by the Navy at the present time include use of non-hazardous chemical paint removers, xenon flashlamp/CO2 pellets, lasers and plastic media. Plastic media blasting represents a mature technology in current usage for aircraft paint stripping and is being investigated for determination of its effects on Navy composite aircraft configurations. Author (revised)

N94-10615# Defence Research Establishment Pacific, Victoria (British Columbia).
PAINT REMOVAL ACTIVITIES IN CANADA
Terry Foster *In* AGARD, Environmentally Safe and Effective Processes for Paint Removal Mar. 1993 3 p (For primary document see N94-10613 01-31)
Copyright Avail: CASI HC A01/MF A02

Paint removal activities currently under way in Canada include: research and development of laser paint stripping; development and commercialization of a new blasting medium based on wheat starch; commercialization of a new blasting medium and process using crystalline ice blasting for paint removal and surface cleaning; and the development of automated and robotic systems for paint stripping applications. A specification for plastic media blasting (PMB) of aircraft and aircraft components is currently being drafted by NDHQ for use by the Canadian Armed Forces (CAF) and contractors involved in coating removal for the CAF. Defense Research Establishment Pacific (DREP) is studying the effects of various blast media on coating removal rates, and minimizing the possibility of damage to substrates other than aluminum such as graphite epoxy composite and Kevlar. The effects of plastic media blasting on liquid penetrant detection of fatigue cracks is also under investigation. Author (revised)

N94-10616# Delegation Generale de l'Armement, Toulouse (France).
PROCEDURES WITHOUT DANGER TO THE ENVIRONMENT AND EFFICIENCY (PSDEE) FOR THE REMOVAL OF PAINT. POINT ON THE FRENCH ACTIVITIES CONCERNING THE REMOVAL OF PAINT [PROCEDES SANS DANGER POUR L'ENVIRONNEMENT ET EFFICACES (PSDEE) POUR L'ENLEVEMENT DES PEINTURES. POINT SUR LES ACTIVITIES FRANCAISES CONCERNANT L'ENLEVEMENT DES PEINTURES]
Pierre Gauthier *In* AGARD, Environmentally Safe and Effective Processes for Paint Removal Mar. 1993 6 p In ENGLISH and FRENCH (For primary document see N94-10613 01-31)
Copyright Avail: CASI HC A02/MF A02

The text presents a synthesis of the activities and subjects of French interest in new techniques for the removal of paint in the civil and military air transport sector. Transl. by FLS

N94-10617# Dornier Luftfahrt G.m.b.H., Friedrichshafen (Germany).
PAINT REMOVAL ACTIVITIES IN GERMANY
R. Holbein and G. Arnolds-Mayer *In* AGARD, Environmentally Safe and Effective Processes for Paint Removal Mar. 1993 5 p (For primary document see N94-10613 01-31)
Copyright Avail: CASI HC A01/MF A02

To replace paint removing chemicals containing chlorinated hydrocarbons several alternative paint stripping methods have been developed or are under study in Germany: high pressure water stripping; plastic media blasting; use of alcalic and acid activated softeners; CO2 pellet blasting; and laser application. Author (revised)

N94-10618# Royal Air Force, Harrogate (England). Surface Finish Support Authority.
THE DEVELOPMENT OF ALTERNATIVE PAINT REMOVAL TECHNIQUES IN THE RAF
M. Hartley and M. Weeding *In* AGARD, Environmentally Safe and Effective Processes for Paint Removal Mar. 1993 8 p (For primary document see N94-10613 01-31)
Copyright Avail: CASI HC A02/MF A02

Personnel safety and environmental legislation is forcing the removal of chemical removers. The RAF chose the Plastic Media Stripping process as their alternative. During testing of the process a number of problem areas and additional advantages were highlighted. Solution to the problems are discussed and the advantages quantified. Author (revised)

N94-10619# Fokker B.V., Amsterdam (Netherlands).
OPERATIONAL ASPECTS OF F.16 PLASTIC MEDIA BLASTING, AS CARRIED OUT BY FOKKER AIRCRAFT SERVICES
Frank Pot *In* AGARD, Environmentally Safe and Effective Processes for Paint Removal Mar. 1993 3 p (For primary document see N94-10613 01-31)
Copyright Avail: CASI HC A01/MF A02

In 1987, Fokker Aircraft Services started F.16 air-intake paint removal by means of Plastic Media Blasting (PMB). Especially for this process, a robot has been developed. In a later stage, complete exterior PMB-paint removal has been tested and successfully adopted. The paint removal is carried out in the scope of a thorough corrosion control program. The requirement that all the paint must be removed in order to allow this control program to be carried out properly, leads to severe masking complications. The process parameters are relatively conservative, because of the requirement that absolutely no anodic layer damage is permitted. Following PMB paint removal, corrosion is removed using aluminum oxide blasting. Finally, a highly flexible polyurethane paint system is applied, based upon TT-P-2760 Koroflex primer. To summarize the process, it can be stated that the plastic media blasting itself is straightforward. Proper masking is difficult to perform though, compounded by special customer requirements such as open panel edges. Author (revised)

N94-10620# Aerospatiale, Toulouse (France).

USE OF ROBOTS FOR AIRCRAFT DRY STRIPPING VIA PLASTIC MEDIA BLASTING

E. Gillard *In* AGARD, Environmentally Safe and Effective Processes for Paint Removal Mar. 1993 6 p (For primary document see N94-10613 01-31)

Copyright Avail: CASI HC A02/MF A02

In order to meet constant financial and reliability concerns, European manufacturers have introduced more and more composite materials on their aircraft. In addition to fairings for which the use of composites has become absolutely necessary, composites are used on each new program for structures which are more and more highly loaded and sophisticated. Similarly to metallic structures, an external paint scheme is applied to these composite structures to protect them from ultraviolet rays, provide general corrosion resistance and allow the airlines to customize their aircraft. Conventional stripping methods using chemical strippers cannot be used as many impregnation resins do not resist chemical strippers. Aerospatiale has endeavored to find new efficient methods that are easy to implement, cause no damage and are applicable both to metallic and composite structures. Dry stripping via plastic media blasting has formed the subject of many tests. These tests proved that such stripping was compatible with the objectives but required automation of the process for large airframe stripping. Author

N94-10621# German Air Force, Cologne (Germany). Support Command.

GERMAN AIR FORCES EXPERIENCES WITH PLASTIC MEDIA BLASTING AND FUTURE REQUIREMENTS

Matthias Stoermer *In* AGARD, Environmentally Safe and Effective Processes for Paint Removal Mar. 1993 14 p (For primary document see N94-10613 01-31)

Copyright Avail: CASI HC A03/MF A02

German Air Force (GAF) has been researching a method of paint removal for a couple of years to replace the chemical method still in use. This is to improve corrosion prevention, environmental protection and health care. With the support of German aerospace company MBB and the University of the Armed Forces in Munich GAF selected Plastic Media Blasting (PMB) as the most suitable method. Having a stripping facility for the entire aircraft at MBB Manching already in existence, GAF decided that the next step forward to gain more experiences is to establish a smaller 'stripping cabin' at an air force base. This cabin is suitable for stripping removable parts and components of aircraft and equipment with the max. size of a half dismantled TORNADO wing. With these gained experiences GAF will be in position to formulate the specific requirements for an entire on-base aircraft stripping plant which will be suitable for F-4's, TORNADO's and EFA's, too. Author (revised)

N94-10622# Air Force Logistics Command, Hill AFB, UT.

PLASTIC MEDIA BLASTING ACTIVITIES AT HILL AIR FORCE BASE

J. D. Christensen *In* AGARD, Environmentally Safe and Effective Processes for Paint Removal Mar. 1993 2 p (For primary document see N94-10613 01-31)

Copyright Avail: CASI HC A01/MF A02

Hill Air Force Base in Utah developed plastic media blasting (PMB) paint removal process for removing paint from Air Force aircraft. The development of the process involved extensive testing of various abrasives and subsequent parameters to end up with an approved production process. Hill AFB has been using PMB in a production mode since 1985, and completely discontinued chemical stripping of airframes in 1989. We have recently installed and began operating a fully automated PMB facility that utilizes two nine-axis robots to strip an aircraft. This system has enabled us to further reduce the manhours required to strip an aircraft, and also allowed us to remove the employee from the blasting atmosphere into a control room. We have, and will continue to realize, significant environmental and economic savings by using PMB. Hill is also actively involved with the development of future paint stripping technologies. Derived from text

N94-10623# Wright Lab., Eglin AFB, FL. Manufacturing Technology Directorate.

LARGE AIRCRAFT ROBOTIC PAINT STRIPPING (LARPS) SYSTEM AND THE HIGH PRESSURE WATER PROCESS

David W. See, Scott A. Hofacker (United Technologies Corp., Huntsville, AL.), M. Anthony Stone (United Technologies Corp., Huntsville, AL.), and Darcy Harbaugh (United Technologies Corp., Huntsville, AL.) *In* AGARD, Environmentally Safe and Effective Processes for Paint Removal Mar. 1993 21 p (For primary document see N94-10613 01-31)

(Contract F33615-91-C-5708)

Copyright Avail: CASI HC A03/MF A02

The aircraft maintenance industry is beset by new Environmental Protection Agency (EPA) guidelines on air emissions, Occupational Safety and Health Administration (OSHA) standards, dwindling labor markets, Federal Aviation Administration (FAA) safety guidelines, and increased operating costs. In light of these factors, the USAF's Wright Laboratory Manufacturing Technology Directorate and the Aircraft Division of the Oklahoma City Air Logistics Center initiated a MANTECH/REPTECH effort to automate an alternate paint removal method and eliminate the current manual methylene chloride chemical stripping methods. This paper presents some of the background and history of the LARPS program, describes the LARPS system, documents the projected operational flow, quantifies some of the projected system benefits and describes the High Pressure Water Stripping Process. Certification of an alternative paint removal method to replace the current chemical process is being performed in two phases: Process Optimization and Process Validation. This paper also presents the results of the Process Optimization for metal substrates. Data on the coating removal rate, residual stresses, surface roughness, preliminary process envelopes, and technical plans for process Validation Testing will be discussed. Author (revised)

N94-10624# International Technical Associates, Inc., Santa Clara, CA.

AUTOMATED LASER PAINT STRIPPING (ALPS) UPDATE

Paul Lovoi *In* AGARD, Environmentally Safe and Effective Processes for Paint Removal Mar. 1993 12 p (For primary document see N94-10613 01-31)

Copyright Avail: CASI HC A03/MF A02

To date, the DoD has played a major role in funding a number of paint stripping programs. Some technologies have proven less effective than contemplated. Others are still in the validation phase. Paint stripping is one of the hottest issues being addressed by the finishing industry since the Environmental Protection Agency (EPA) has mandated that chemical stripping using methylene chloride/phenolic type strippers be stopped. The DoD and commercial aircraft companies are hard-pressed to find an alternative. Automated laser paint stripping has been identified as a technique for removing coatings from aircraft surfaces. International Technical Associates (InTA) was awarded a Navy contract for an automated laser paint stripping system (ALPS) that will remove paint from metallic and composite substrates. For the program, which will validate laser paint stripping, InTA will design, build, test, and install a system for fighter-sized aircraft at both the Norfolk and North Island (San Diego) Aviation Depots. Derived from text

N94-10625# Deutsche Lufthansa A.G., Hamburg (Germany). Structural Engineering Dept.

AQUASTRIP (TM): AN INNOVATIVE PAINT REMOVAL TECHNOLOGY

J. Volkmar *In* AGARD, Environmentally Safe and Effective Processes for Paint Removal Mar. 1993 10 p (For primary document see N94-10613 01-31)

Copyright Avail: CASI HC A02/MF A02

Environmental, safety and health issues, forced operators to search for an alternative paint removal process. High pressure water jetting and new integrated paint and stripper systems are Lufthansa's answer to this challenge. AQUASTRIP complies with the specification requirements. In order to receive approval from airframe manufacturers and authorities the process has undergone an extensive research program since 1988. An operation window was established, to enable maximum of safety during operation on metal and composite surfaces. Even though AQUASTRIP is a hybrid process and requires technological investment, it is well on the way to prove its innovative, ecological and economical character in first large scale applications under realistic conditions. Its potential has already been reflected by patents and trademarks, which were registered in conjunction with the development of AQUASTRIP and the vital interest for cooperative work on the process development and other potential utilization. Author (revised)

N94-10626# Defence Research Establishment Pacific, Victoria (British Columbia).
PAINT REMOVAL AND SURFACE CLEANING USING ICE PARTICLES
Terry Foster and S. Visaisouk (Ice Blast International Corp., Victoria, British Columbia.) *In* AGARD, Environmentally Safe and Effective Processes for Paint Removal Mar. 1993 10 p (For primary document see N94-10613 01-31)
Copyright Avail: CASI HC A02/MF A02

Research into the possibility of using ice particles as a blast medium was first initiated at Defence Research Establishment Pacific (DREP) in an effort to develop a more environmentally acceptable paint removal method. A paint removal process was also required that could be used in areas where normal grit blasting could not be used due to the possibility of the residual blasting grit contaminating machinery and other equipment. As a result of this research a commercial ice blasting system was developed by RETECH. This system is now being used to remove paint from substrates that cannot be easily blasted by conventional techniques and also to clean soiled or contaminated surfaces. The problems involved in the development of an ice blast system, and its components and their functions are described. Due to the complexity of paint removal using ice blasting, parameters such as air pressure, ice particle size and ice particle flow rate were studied and adjusted to suit the nature of the particular coating and substrate of interest. The mechanism of paint removal by ice particles has also been investigated. A theoretical model has been developed to explain the different paint removal mechanisms such as erosion by abrasion and erosion by fracture as they relate to ice blasting. Finally, the use of ice blasting to removal paint from a variety of substrates is presented as well as examples of surface cleaning and surface decontamination. Author

N94-10627# Defence Research Establishment Pacific, Victoria (British Columbia).
PAINT REMOVAL USING WHEAT STARCH BLAST MEDIA
Terry Foster and John Oestreich (Ogilvie Mills Ltd., Montreal, Quebec.) *In* AGARD, Environmentally Safe and Effective Processes for Paint Removal Mar. 1993 9 p (For primary document see N94-10613 01-31)
Copyright Avail: CASI HC A02/MF A02

A review of the Wheat Starch Blasting technology is presented. Laboratory evaluations covering Almen Arc testing on bare 2024-T3 aluminum and magnesium, as well as crack detection on 7075-T6 bare aluminum, are discussed. Comparisons with Type V plastic media show lower residual stresses are achieved on aluminum and magnesium with wheat starch media. Dry blasting effects on the detection of cracks confirms better crack visibility with wheat starch media versus Type V or Type II plastic media. Testing of wheat starch media in several composite test programs, including fiberglass, Kevlar, and graphite-epoxy composites, showed no fiber damage. Process developments and production experience at the first U.S. aircraft stripping facility are also reviewed. Corporate and regional aircraft are being stripped in this three nozzle dry blast hanger. Author

N94-10628# KLM Aerocarto, Schiphol (Netherlands). Central Engineering Dept.
IATA TASKFORCE: PAINTSTRIPPING
Thomas Mooy *In* AGARD, Environmentally Safe and Effective Processes for Paint Removal Mar. 1993 5 p (For primary document see N94-10613 01-31)
Copyright Avail: CASI HC A01/MF A02

In 1990 the International Air Transport Association (IATA) established a task force to stimulate the development of alternatives for chemical stripping of commercial aircraft. The IATA TaskForce Paintstripping objectives are: to identify the most promising, current alternatives for short term implementation; to prepare a document containing requirements for the development of alternatives; to stimulate the information exchange. After the September 1992 meeting the TaskForce will report back to IATA. The most tangible result of the TaskForce is the IATA Guidelines containing requirements for the qualification of stripping processes. Author (revised)

N94-10629# Imperial Chemical Industries Ltd., Duesseldorf (Germany). Aerospace Coatings.
SELECTIVELY STRIPPABLE PAINT SCHEMES
R. Stein, D. Thumm, and Roger W. Blackford (Imperial Chemical Industries Ltd., Slough, England.) *In* AGARD, Environmentally Safe and Effective Processes for Paint Removal Mar. 1993 4 p (For primary document see N94-10613 01-31)
Copyright Avail: CASI HC A01/MF A02

In order to meet the requirements of more environmentally acceptable paint stripping processes many different removal methods are under evaluation. These new processes can be divided into mechanical and chemical methods. ICI has developed a paint scheme with intermediate coat and fluid resistant polyurethane topcoat which can be stripped chemically in a short period of time with methylene chloride free and phenol free paint strippers. Author

N94-11028# Martin Marietta Energy Systems, Inc., Piketon, OH.
ENGINEERING PERFORMANCE METRICS
R. DeLozier and N. Snyder (Portsmouth Gaseous Diffusion Plant, OH.) 31 Mar. 1993 9 p Presented at the 3rd Annual International Symposium of the National Council on Systems Engineering, Arlington, VA, 26-28 Jul. 1993
(Contract DE-AC05-76OR-00001)
(DE93-012084; POEF-T-3605; CONF-930768-1) Avail: CASI HC A02/MF A01

Implementation of a Total Quality Management (TQM) approach to engineering work required the development of a system of metrics which would serve as a meaningful management tool for evaluating effectiveness in accomplishing project objectives and in achieving improved customer satisfaction. A team effort was chartered with the goal of developing a system of engineering performance metrics which would measure customer satisfaction, quality, cost effectiveness, and timeliness. The approach to developing this system involved normal systems design phases including, conceptual design, detailed design, implementation, and integration. The lessons teamed from this effort will be explored in this paper. These lessons learned may provide a starting point for other large engineering organizations seeking to institute a performance measurement system accomplishing project objectives and in achieving improved customer satisfaction. To facilitate this effort, a team was chartered to assist in the development of the metrics system. This team, consisting of customers and Engineering staff members, was utilized to ensure that the needs and views of the customers were considered in the development of performance measurements. The development of a system of metrics is no different than the development of any type of system. It includes the steps of defining performance measurement requirements, measurement process conceptual design, performance measurement and reporting system detailed design, and system implementation and integration. DOE

N94-11161# Los Alamos National Lab., NM.
THE SUPERFLUID STIRLING REFRIGERATOR, A NEW METHOD FOR COOLING BELOW 0.5 K
J. G. Brisson, V. Kotsubo, and G. W. Swift Apr. 1993 4 p Presented at the Conference of the International Union of Pure and Applied Physics on Low Temperature Physics (LT 20), Eugene, OR, 1-11 Aug. 1993
(Contract W-7405-eng-36)
(DE93-012672; LA-UR-93-1420; CONF-930801-1) Avail: CASI HC A01/MF A01

A new subkelvin refrigerator, the superfluid Stirling cycle refrigerator, uses a working fluid of He-3/He-4 mixture in a Stirling cycle. The thermodynamically active components of the mixture are the He-3, which behaves like a Boltzman gas, and the phonon-proton gas in the He-4. The superfluid component of the liquid is inert. Two refrigerators have been built and temperatures of 340 mK have been achieved. DOE

N94-11304# Materials Research Labs., Melbourne (Australia). Scientific Services Div.
DYNAMIC LOADING IN MANUFACTURING AND SERVICE: AUSTRALIA'S SHOCK TESTING CAPABILITY

P. Elischer and J. Howe 11 Feb. 1993 8 p
Avail: CASI HC A02/MF A01

Australia's involvement in shock testing to evaluate the structural response of Naval vessels and ships' equipment to transient dynamic loads began in late 1970. It commenced with gaining the necessary understanding of underwater blast phenomena and culminated in the successful shock testing of an Australian designed and constructed, glass reinforced plastic (GRP) minehunter. Since then we have maintained an active role in conducting full scale shock trials to evaluate the vulnerability of vessels and equipment supporting mine countermeasure operations. We also conduct smaller scale trials to support the submarine construction program and the various research tasks undertaken by DSTO. An overview of the shock trials conducted to date, together with a brief description of facilities available and considerations which needed to be addressed when conducting such tests in shallow water is presented. Author (revised)

N94-11456# Oak Ridge Associated Universities, Inc., Washington, DC.
DEPARTMENT OF ENERGY FUNDAMENTALS HANDBOOK: ENGINEERING SYMBOLOGY, PRINTS, AND DRAWINGS
Jan. 1993 88 p
(DE93-012181; DOE-HDBK-1016/2-93) Avail: CASI HC A05/MF A01

The Engineering Symbology, Prints, and Drawings Handbook was developed to assist nuclear facility operating contractors in providing operators, maintenance personnel, and technical staff with the necessary fundamental training to ensure a basic understanding of engineering prints, their use, and their function. The handbook includes information on the following: engineering fluid drawings and prints; piping and instrument drawings; major symbols and conventions; electronic diagrams and schematics; logic circuits and diagrams; and fabrication, construction, and architectural drawings. This information will provide personnel with a foundation for reading, interpreting, and using the engineering prints and drawings that are associated with various DOE nuclear facility operations and maintenance. DOE

N94-11606# Sandia National Labs., Albuquerque, NM.
ADVANCED SOLDERING PROCESSES
J. L. Jellison, J. Golden, D. R. Frear, F. M. Hosking, D. M. Keicher, and F. G. Yost 20 Feb. 1993 40 p Presented at the 122nd Annual Tool-Made Sample Meeting and Exhibition, Denver, CO, 24 Feb. 1993
(Contract DE-AC04-76DP-00789)
(DE93-009856; SAND-92-2029C; CONF-9302101-1) Avail: CASI HC A03/MF A01

Advanced soldering processes are discussed in a complete manner. The ability to meet the needs of electronic manufacturing, while addressing the environmental issues are challenging goals. Government regulations mandate the elimination of most solvents in solder flux removal. Alternative approaches to promoting wetting are discussed. Inert atmosphere soldering, acid vapor fluxless soldering, atomic and ionic hydrogen as reactive atmospheres, fluxless laser soldering in a controlled atmosphere are offered as soldering mechanisms for the future. Lasers are discussed as alternate heat sources. Various types of lasers, advantages of lasers, and fiber optic beam delivery are considered. DOE

N94-11670# Department of Defense, Washington, DC.
DEPARTMENT OF ENERGY FUNDAMENTALS HANDBOOK: ENGINEERING SYMBOLOGY, PRINTS, AND DRAWINGS
Jan. 1993 112 p
(DE93-012220; DOE-HDBK-1016/1-93) Avail: CASI HC A06/MF A02

The Engineering Symbology, Prints, and Drawings Handbook was developed to assist nuclear facility operating contractors in providing operators, maintenance personnel, and technical staff with the necessary fundamental training to ensure a basic understanding of engineering prints, their use, and their function. The handbook includes information on engineering fluid drawings and prints; piping and instrument drawings; major symbols and conventions; electronic diagrams and schematics; logic circuits and diagrams; and fabrication, construction, and architectural drawings. This information will provide personnel with a foundation for reading, interpreting, and using the engineering prints and drawings that are associated with various DOE nuclear facility operations and maintenance. DOE

N94-11831# National Space Development Agency, Ibaraki (Japan).
THE SECOND WORKSHOP ON REFRIGERATING SYSTEM UTILIZATION ONBOARD THE JEM [DAI 2 KAI JEM TOUSAI REITOUKI RIYOU NI KANSURU WAKU SHOPPU]
31 Mar. 1993 182 p In JAPANESE Workshop held in Ibaraki, Japan, 28 Mar. 1991
(NASDA-CON-930001; JTN-93-80473) Avail: CASI HC A09/MF A02

The following topics were discussed: the JEM (Japanese Experiment Module), spacecraft equipment cooling systems, refrigerators, coolers, cryogenic cooling and equipment, thermodynamic cycles (Gifford-MacMahon cycle, Stirling cycle), spaceborne experiments, cooling requirements for spaceborne instruments, SIS (Superconductor Insulator Superconductor) based devices, and IR (infrared) telescopes, For individual titles, see N94-11832 through N94-11843.

N94-11832# National Space Development Agency, Tokyo (Japan).
SUMMARY OF THE PRE-AO OF THE JEM ONBOARD SCIENTIFIC AND ENGINEERING EXPERIMENTS FOR REFRIGERATOR UTILIZATION [JEM RIKOUGAKU JIKKEN NO PURE AO SOUDATSU]
Yoshinori Fujimori *In its* The Second Workshop on Refrigerating System Utilization Onboard the JEM 31 Mar. 1993 p 1-22 In JAPANESE
(For primary document see N94-11831 01-31)
Avail: CASI HC A03/MF A02

Topics discussed include: AO (Announcement of Opportunity); JEM (Japanese Experiment Module); the number of proposals for small missions; the list of small missions on the exposed facility; the results of the study on the candidate common experiment equipment; present status of the candidate equipment specifications; study on research systemization; the scenario for research systemization; study on experiment scenarios; the results of the case studies from the study options (focusing on infrastructure construction and basic science); and examples of the draft experiment scenarios. This presentation is represented by viewgraphs only. NASDA

N94-11833# Hitachi Ltd., Tokyo (Japan).
DEVELOPMENT OF SPACE REFRIGERATOR [UCHUUYOU REIKYAKUKI NO KAIHATSU]
Satoshi Sugawara, Tsunehiko Takakusaki, Tamio Fukuda, and Ikuhiro Saitou *In* NASDA, The Second Workshop on Refrigerating System Utilization Onboard the JEM 31 Mar. 1993 p 23-39 In JAPANESE
(For primary document see N94-11831 01-31)
Avail: CASI HC A03/MF A02

Topics discussed include: the target specifications (development needs) for refrigerator body; development problems; study subjects concerning the components; development schedule, the design features of the BBM2 (Breadboard Model 2); schematic drawing; exterior appearance; the electromagnetic bearing (displacer section) element test equipment; electromagnetic controller; refrigerator cooler body structure for feasibility verification; various evaluation tests; the comparison of refrigerator cooler body BBM1 (Breadboard Model 1); and feasibility of the BBM1 and BBM2 structure for the JEM (Japanese Experiment Module) onboard refrigerator. This presentation is represented by viewgraphs only. NASDA

N94-11834# National Space Development Agency, Tokyo (Japan).
STUDIES ON REFRIGERATOR SENSORS AND COOLING SECTION INTERFACE [REIKYAKUKI SENSA TO INTAFESU NO KENTOU]
Yoshirou Miyazaki *In its* The Second Workshop on Refrigerating System Utilization Onboard the JEM 31 Mar. 1993 p 40-60 In JAPANESE
(For primary document see N94-11831 01-31)
Avail: CASI HC A03/MF A02

The results of a patents examination are outlined including the following items: (1) examination methods and their results concerning the cooling type photoelectric conversion devices; (2) the infrared ray receiver with cooler radiation detector; (3) cryogenic container; (4) the expansion cylinder device; (5) the vibration isolation device for cooling a focal plane; and (6) an infrared detector. The results of users' opinion survey for JEM (Japanese Experiment Module) utilization are summarized as follows: (1) the development of cryogenic (4 K) coolers are strongly desired; (2) pointing device is indispensable for observation system users; (3) vibration condition requirements range from ten micrometer to less than 1 micrometer; (4) miniaturization is strongly desired; and (5) cooler interface is not the image of direct cooling of the sensor but overall cooling of the system. This presentation is represented by viewgraphs only. Author (NASDA)

N94-11835# National Space Development Agency, Tokyo (Japan).
TREND OF MINIATURE REFRIGERATOR UTILIZATION IN EARTH OBSERVATION AREA [CHIKYUU KANSOKU BUNYA NI OKERU KOGATA REITOUKI NO RIYOU DOUDOU NI TSUITE]
Takashi Moriyama *In its* The Second Workshop on Refrigerating System Utilization Onboard the JEM 31 Mar. 1993 p 61-75 In JAPANESE (For primary document see N94-11831 01-31)
Avail: CASI HC A03/MF A02

Topics discussed include: the algebraic equation showing the relation between the detector element area; equivalent noise band width; instantaneous view angle; optical system aperture area; detector detectability; mirror reflectance and integrated permeability of the optical system; detector limit and performance; wavelength via detector detectability relationship; the processes for studying the effects of increasing elements; cryogenic cooling missions in space; cooling effect / operating temperature relationship; system weight / cooling temperature; flight examples of space coolers; coolers under development; tendency of cooler service life; ESA cryo-requirements; JPL (Jet Propulsion Laboratory)/AIRS 55 K Stirling cooler overall performance requirements; and Japanese mission instrument using mechanical cryocoolers. This presentation is represented by viewgraphs only. NASDA

N94-11836# National Inst. for Environmental Studies, Tsukuba (Japan).
SATELLITE OBSERVATION OF ATMOSPHERIC TRACER COMPONENTS: JEM/POP [TAIKI BIRYOU SEIBUN NO EISEI KANSOKU: JEM/POP] c45
Makoto Suzuki *In* NASDA, The Second Workshop on Refrigerating System Utilization Onboard the JEM 31 Mar. 1993 p 76-88 In JAPANESE (For primary document see N94-11831 01-31)
Avail: CASI HC A03/MF A02

Topics discussed include: NIMBUS-7 TOMS (Total Ozone Mapping Spectrometer) data; JEM (Japanese Experiment Module); POP (Polar Orbit Platform); observation subjects of the ILAS (Improved Limb Atmospheric Spectrometer); total, H2O, NO2, and continuum transmissions via wavelength relationship; limb emission coverage and maximum solar occultation coverage; solar occultation limb absorption; remote sensing of atmosphere with the ADEOS (Advanced Earth Observing Satellite) limb instruments; the observation of atmospheric trace components; and the necessity of cooling. This presentation is represented by viewgraphs only. NASDA

N94-11837# Nobeyema Solar Radio Observatory (Japan).
SUBMILLIMETER WAVE OBSERVATION EXPERIMENT OF EARTH ATMOSPHERE WITH SIS MIXER [SIS MIKISA NI YORU SABUMIRIHA KANSOKU JIKKEN] c43
Junji Inatani, Suguru Noguchi, Kentarou Kawaguchi, Harunobu Masuko (Ministry of Posts and Telecommunications, Tokyo, Japan.), and Satoshi Ochiai (Ministry of Posts and Telecommunications, Tokyo, Japan.) *In* NASDA, The Second Workshop on Refrigerating System Utilization Onboard the JEM 31 Mar. 1993 p 89-103 In JAPANESE (For primary document see N94-11831 01-31)
Avail: CASI HC A03/MF A02

The feasibility of submillimeter wave observation from satellites with SIS (Superconductor Insulator Superconductor) mixers, for which the JEM (Japanese Experiment Module) was expected to provide the experiment opportunities before launching a full scale observation satellite, was studied. The following objectives are presented: (1) to check the operation behavior and stability of space refrigerators; (2) to verify the receiving performance and anti-space environment properties of the submillimeter wave SIS mixers; and (3) to verify the effectiveness of earth atmosphere observation and astronomical observation by such a system. Candidate refrigerators, observation frequency of SIS mixer receivers, observation subjects for the earth atmosphere observation and astronomical observation, and major characteristics of experiment equipment are outlined. NASDA

N94-11838# Nagoya Univ. (Japan). School of Science.
REFRIGERATOR UTILIZATION IN INFRARED ASTRONOMY [SEKIGAISEN TENMONGAKU NI OKERU REITOUKI NO RIYOU] c89
Toshio Matsumoto *In* NASDA, The Second Workshop on Refrigerating System Utilization Onboard the JEM 31 Mar. 1993 p 104-114 In JAPANESE (For primary document see N94-11831 01-31)
Avail: CASI HC A03/MF A02

Topics discussed include: the necessity of cooling in IR (infrared) astronomy; sensitivity limits due to thermal background of a telescope operated at its diffraction limit; steady orbital temperature and flow rate conditions; advantages of using coolers; schematic drawing of the telescope with refrigerators; major characteristics of and problems with the cooled telescope to be carried onboard the JEM (Japanese Experiment Module); and light coming to the earth from extragalactic and galactic systems and the zodiacal light. This presentation is represented by viewgraphs only. NASDA

N94-11839# Nihon Univ., Funabashi (Japan). Atomic Energy Research Inst.
STUDY ON VARIOUS CRYOGENIC REFRIGERATION CYCLES USING ALL PURPOSE REFRIGERATORS [HANYOU REITOUKI O RIYOU SHITA KAKUSHU GOKUTEION REITOU SAIKURU NO KENTOU]
Youichi Matsubara *In* NASDA, The Second Workshop on Refrigerating System Utilization Onboard the JEM 31 Mar. 1993 p 115-119 In JAPANESE (For primary document see N94-11831 01-31)
Avail: CASI HC A01/MF A02

The establishment of and the candidate systems for the following three case study subjects on the cryogenic refrigerating cycles using all-purpose refrigerators are outlined: (1) cryogenic circulation loop and electric power plus 80 K heat radiation; (2) thermal compressor and 30 K heat absorption plus 80 K heat radiation; and (3) application of high compression ratio, 1,000 K heat absorption plus 300 K and 80 K heat radiation. The merits and demerits of the heat displacer type refrigerator and microturbo-systems for below 40 K and examples of the case two study results are also outlined. This presentation is represented by viewgraphs only. NASDA

N94-11840# Nippon Electric Co. Ltd., Yokohama (Japan).
DEVELOPMENT TEST ON 2 K COOLING SYSTEMS [2 K REIDYAKU SHISUTEMU NO KAIHATSU SHIKEN]
Toshiaki Okudaira and Genshirou Fujii *In* NASDA, The Second Workshop on Refrigerating System Utilization Onboard the JEM 31 Mar. 1993 p 120-135 In JAPANESE (For primary document see N94-11831 01-31)
Avail: CASI HC A03/MF A02

Topics discussed include: the detail of proposal; configuration of the laboratory dilution refrigerator; the adiabatic vacuum section of the dilution refrigerator; the relationship between refrigerating capability and cooling temperature; phase diagram and vapor pressure curves of the He-3 and He-4; the fractionation chamber and dilution chamber; separation control by electric field of He-3 rich and He-4 rich phases; mixer utilizing electric field; restriction of liquid; the mixture cell; and continuous operation type dilution type refrigerator. This presentation is represented by viewgraphs only. NASDA

N94-11841# Mitsubishi Electric Corp., Amagasaki (Japan). Central Research Lab.
GENERATION OF SUPERFLUID He BY G-M CYCLE CRYOGENIC REFRIGERATOR [G-M REIKYAKUKI NI YORU CHOU RYUUDOU HERIUMU NO HASSEI]
Hideto Yoshimura, Masashi Nagao, and Takashi Inaguchi *In* NASDA, The Second Workshop on Refrigerating System Utilization Onboard the JEM 31 Mar. 1993 p 136-146 In JAPANESE (For primary document see N94-11831 01-31)
Avail: CASI HC A03/MF A02

The external view and schematic drawing of the three stage expansion G-M (Gifford-MacMahon) refrigerator are outlined. Topics discussed include: displacer section of G-M refrigerator; the specific heat characteristics of rare earth metal compounds used for the experiments for generating superfluid helium; schematic drawing of superfluid He generation experiment; superfluid He container; refrigerating capability characteristics of three stage G-M refrigerator; and amplitude of temperature oscillation in refrigeration stage. This presentation is represented by viewgraphs only. NASDA

N94-11842# Toshiba Corp., Kawasaki (Japan). Energy Science and Technology Lab.
DEVELOPMENT OF 4 K REFRIGERATOR USING HIGHLY EFFICIENT HEAT ACCUMULATING RESERVOIR [KOU KOURITSU CHIKUREIKI O MOCHIITA 4 K REITOUKI NO KAIHATSU]
Hideki Nakagome *In* NASDA, The Second Workshop on Refrigerating

System Utilization Onboard the JEM 31 Mar. 1993 p 147-161 In JAPANESE (For primary document see N94-11831 01-31)
Avail: CASI HC A03/MF A02

Topics discussed include: the schematic drawings of the refrigerator; relationship between temperature and specific heat; refrigerator efficiency; reciprocating speed; refrigeration capacity; comparison of operation frequency and pressure; and refrigeration capacity dependency. This presentation is represented by viewgraphs only. NASDA

N94-11843# National Space Development Agency, Tokyo (Japan).
UTILIZATION OF SUPERCONDUCTIVITY IN THE AREA OF SPACE [UCHUU BUNYA NI OKERU CHOUDENDOU RIYOU NI TSUITE]
Atsuo Tsuiki *In its* The Second Workshop on Refrigerating System Utilization Onboard the JEM 31 Mar. 1993 p 162-173 In JAPANESE (For primary document see N94-11831 01-31)
Avail: CASI HC A03/MF A02

The objectives, research subjects, and the methods of the space superconductivity technology research are outlined. Topics discussed include: the operation of the external magnetic field MPD (magnetoplasmadynamics) thruster; AOTV (Automatic Orbit Transfer Vehicle); system concepts applying superconducting magnets for AOTV; basic composition of the SIS (Superconductor Insulator Superconductor) receiver system; possibility of the JEM (Japanese Experiment Module) utilization of superconductivity technology; experiments of space superconductivity technology aiming at bringing the techniques to practical use; and the refrigeration measures in superconductivity technology utilization. This presentation is represented by viewgraphs only. NASDA

N94-10026# Dornier Luftfahrt G.m.b.H., Friedrichshafen (Germany).
SPF/DB: A MANUFACTURING TECHNIQUE FOR LIGHTWEIGHT STRUCTURES
G. Broden *In* ESA, Advanced Materials for Lightweight Structures Oct. 1992 p 149-153 (For primary document see N94-10001 01-24)
Copyright Avail: CASI HC A01/MF A04

N94-10027# Dornier Luftfahrt G.m.b.H., Friedrichshafen (Germany).
UNIVERSAL ADJUSTABLE MOULD FOR ANTENNA REFLECTORS
Ulrich Trabandt and Rafael GarciaPrieto (European Space Agency. European Space Research and Technology Center, ESTEC, Noordwijk, Netherlands.) *In* ESA, Advanced Materials for Lightweight Structures Oct. 1992 p 155-160 (For primary document see N94-10001 01-24)
Copyright Avail: CASI HC A02/MF A04

N94-10045# Maschinenfabrik Augsburg-Nuernberg A.G., Munich (Germany).
SPIN-ROLLING, WELDING, AND HEAT TREATMENT OF ALUMINIUM 2219 FOR ARIANE 5 GAM HIGH PRESSURE VESSEL LINERS
W. Radtke *In* ESA, Advanced Materials for Lightweight Structures Oct. 1992 p 263-266 (For primary document see N94-10001 01-24)
Copyright Avail: CASI HC A01/MF A04

N94-10054# Oulu Univ. (Finland). Engineering Mechanics Lab.
A NEW AND EFFICIENT WAY TO JOIN COMPOSITE PIPES
H. Lahtinen, M. Autio, S.-G. Sjolind, and A. Pramila *In* ESA, Advanced Materials for Lightweight Structures Oct. 1992 p 321-324 (For primary document see N94-10001 01-24)
Copyright Avail: CASI HC A01/MF A04

N94-12026*# National Aeronautics and Space Administration. Lyndon B. Johnson Space Center, Houston, TX.
COLD PRESS SINTERING OF SIMULATED LUNAR BASALT Abstract Only
D. A. Altemir *In* Lunar and Planetary Inst., Twenty-fourth Lunar and Planetary Science Conference. Part 1: A-F 1993 p 23-24 Sponsored by NASA. Washington (For primary document see N94-12015 01-91)
Avail: CASI HC A01/MF A06

N94-12027*# National Aeronautics and Space Administration. Lyndon B. Johnson Space Center, Houston, TX.
GENERAL OVERVIEW OF AN INTEGRATED LUNAR OXYGEN PRODUCTION/BRICKMAKING SYSTEM Abstract Only
D. A. Altemir *In* Lunar and Planetary Inst., Twenty-fourth Lunar and Planetary Science Conference. Part 1: A-F 1993 p 25-26 Sponsored by NASA. Washington (For primary document see N94-12015 01-91)
Avail: CASI HC A01/MF A06

32 COMMUNICATIONS AND RADAR

Includes radar; land and global communications; communications theory; and optical communications.

For related information see also *04 Aircraft Communications and Navigation* and *17 Space Communications, Spacecraft Communications, Command and Tracking.* For search and rescue see *03 Air Transportation and Safety,* and *16 Space Transportation.*

N94-10165# Universiteit Twente, Enschede (Netherlands). Tele-Informatics and Open Systems Group.
AN EFFICIENT MEDIUM ACCESS CONTROL STRATEGY FOR HIGH SPEED WDM MULTIACCESS NETWORKS
J. H. Laarhuis and A. M. J. Koonen 1992 41 p
(Memo-INF-92-74; TIOS-92/31; ETN-93-94322) Copyright Avail: CASI HC A03/MF A01

A medium access control strategy and a supporting physical layer design, which maximize the network throughput at given constraints on transceiver tunability, and which maintain the transparancy of the network, are proposed. The main requirements of multichannel networks are described. The wavelength demultiplexer (WDM) is one of the most attractive techniques to create multichannel networks. The physical layer architecture and the medium access control strategy are presented. Full interconnectivity, contention free access, and a high value of concurrency are achieved by dividing the network into disjunct subnetworks on a wave length basis and by reconfigurating these subnetworks on a time basis. Each subnetwork allows for simplified access to be implemented with fast tunable transceivers each accessing only a moderate number of wavelengths. A performance analysis shows that this concept is most efficient when applied to a high level broadband interconnection metropolitan area communications networks. ESA

N94-10270# Oak Ridge National Lab., TN.
MULTIPLE ANTENNA IMPLEMENTATION SYSTEM (MAntIS)
M. D. Carter, D. B. Batchelor, and E. F. Jaeger Jan. 1993 33 p
(Contract DE-AC05-84OR-21400)
(DE93-012515; ORNL/TM-12264) Avail: CASI HC A03/MF A01

The MAntIS code was developed as an aid to the design of radio frequency (RF) antennas for fusion applications. The code solves for the electromagnetic fields in three dimensions near the antenna structure with a realistic plasma load. Fourier analysis is used in the two dimensions that are tangential to the plasma surface and backwall. The third dimension is handled analytically in a vacuum region with a general impedance match at the plasma-vacuum interface. The impedance tensor is calculated for a slab plasma using the ORION-1D code with all three electric field components included and warm plasma corrections. The code permits the modeling of complicated antenna structures by superposing currents that flow on the surfaces of rectangular parallelepipeds. Specified current elements have feeders that continuously connect the current flowing from the ends of the strap to the feeders. The elements may have an arbitrary orientation with respect to the static magnetic field. Currents are permitted to vary along the length of the current strap and feeders. Parameters that describe this current variation can be adjusted to approximately satisfy boundary conditions on the current elements. The methods used in MAntIS and results for a primary loop antenna design are presented. DOE

N94-10280# Universiteit Twente, Enschede (Netherlands). Tele-Informatics and Open Systems Group.
FORMAL SPECIFICATION OF THE PLAIN UCN LAYER IN LOTOS
Jan Willem vanHeerde, Harro Kremer, and Hans Pasch Dec. 1992 167 p
(Memo-INF-92-83; TIOS-92/32; ETN-93-94324) Copyright Avail: CASI HC A08/MF A02

A new high speed local area network design that can be made to behave either like a token ring or a slotted ring, is presented. The name of the new proposal is Universal Channel Network (UCN). The UCN layer protocol and the formal specification of the UCN layer are summarized. While the token ring outperforms the slotted ring for long messages, a slotted ring performs significantly better for short messages. The factor that causes this difference is the number of tokens on the ring. In UCN, the number of tokens is adaptive, resulting in a network that can be made to behave like a token ring and a slotted ring or anything in between. The UCN performs optimally for any given message length. The reference model of UCN consists of the following layers: the medium layer, the basic slot layer, the UCN layer, and the UCN adaptation layer. The formal specification of UCN uses the specification language LOTOS. The service of the basic slot layer, which is used by the UCN layer, is described informally and formally. ESA

N94-10315# Instituto de Pesquisas Energeticas e Nucleares, Sao Paulo (Brazil).

THE THEORY FOR, AND DEMONSTRATION OF, INFORMATION THEORY APPLIED TO RADAR TARGET IDENTIFICATION Ph.D. Thesis

S. D. Briles Jan. 1993 216 p
(Contract W-7405-eng-36)
(DE93-006393; LA-12480-T) Avail: CASI HC A10/MF A03 (US Sales Only)

The desire for a radar system to be able to identify a target under interrogation has motivated a long standing interest in determining the best possible performance of such radar target identification systems. With the advent of Ultra-Wideband radar, radar target identification became a more feasible task. Experimental performance has usually been presented without relationships to the difficulty of the problem, and design has primarily taken a trial and error approach. Tools are developed that can aid in the design of identification systems by applying information theory to the radar target identification problem. Specifically, by using the Bayes rate-distortion function, the minimum probability of error can be determined for the radar system in use and for the level of noise the system operates under. Performance changes, with such parameters as bandwidth, can be determined by using the Bayes rate-distortion function and calculations of mutual information for the various parameters. Proofs of the theoretical bases for using information theory for radar target identification are included. The continuous channel, inherent to the radar problem, is used in developing all proofs presented. An intuitive basis for using information theory is also presented from a signal detection theory background. Validity of the theory is demonstrated by using experimental radar target signatures of different bandwidths in Monte Carlo simulations. In addition, a method for computing mutual information is derived and performed on the experimental radar signatures to support the theory. DOE

N94-10382# Department of the Navy, Washington, DC.

INTERFERENCE PHOTOCATHODE Patent Application

John F. Seely, inventor (to Navy) and William R. Hunter, inventor (to Navy) 26 May 1992 26 p
(AD-D015770; US-Patent-Appl-SN-888083) Avail: CASI HC A03/MF A01

It is an object of the present invention to selectively reduce sensitivity to radiation of one wavelength while selectively enhancing sensitivity to radiation of a second wavelength, different from the first wavelength, in a photocathode. To achieve this and other objects made apparent hereinafter, the invention concerns a photocathode having a reflector for reflecting incident electromagnetic radiation, and an interference means for causing interference of electromagnetic radiation reflected from the reflector and incident electromagnetic radiation. The reflector and the interference means are adapted to cause the interference to result in an electromagnetic field zero at or near the surface of the interference means for incident electromagnetic radiation at a first selected wavelength, and to cause an electromagnetic field maximum at or near the surface for a second preselected electromagnetic wavelength. DTIC

N94-10401 International Centre for Theoretical Physics, Trieste (Italy).

WAVE FUNCTION COLLAPSE: AN UNNECESSARY CONDITION FOR THE DYNAMICAL DESCRIPTION OF THE ZENO AND PARTIAL ZENO EFFECT

G. Crespo, H. A. Cerdeira, and A. N. Proto Sep. 1992 19 p Limited Reproducibility: More than 20% of this document may be affected by microfiche quality
(DE93-612970; IC-92/298) Avail: Issuing Activity (Department of Energy (DOE)) (US Sales Only)

A model Hamiltonian of a three-level system coupled to an electromagnetic field, whose associated dynamics successfully explains the Zeno and 'partial' Zeno effect without resorting to the concept of the wave function collapse, is presented. DOE

N94-10497 Air Force Inst. of Tech., Wright-Patterson AFB, OH.

THE RADAR EYE BLINDED: THE USAF AND ELECTRONIC WARFARE, 1945-1955 Ph.D. Thesis

Daniel T. Kuehl 1992 279 p Limited Reproducibility: More than 20% of this document may be affected by microfiche quality
(AD-A265494; AFIT/CI/CIA-92-033D) Avail: CASI HC A13

This study concentrates on the doctrinal and operational elements of the Air Force's use of ECM to support offensive combat operations. It does not directly address such factors as intelligence gathering or technology development except as they pertain to the primary topic. As a result, the study focuses closely on the activities of the Air Force's two primary combat commands, the Strategic Air Command (SAC), and Tactical Air Command (TAC). DTIC

N94-10514# Varian Associates of Canada Ltd., Georgetown (Ontario). Microwave Products Div.

WIDE BAND 140 GHz TWTA Research Report, 1 Jan. - 30 Jun. 1992

16 Jul. 1992 26 p
(Contract DAAL01-92-C-0217)
Avail: CASI HC A03/MF A01

A single section low gain 140 GHz 200 watt travelling wave tube has been designed. The design uses the biperiodic ladder circuit of the 140 GHz extended interaction klystron amplifier developed on a previous Laboratory Command (LABCOM) contract. Circuit properties were obtained using X band models and the length of circuit needed for 20dB small signal gain was calculated as 0.9 inches (2.3 cm). Using X band models also, the required circuit to waveguide transitions were developed with voltage standing wave ratios of less than 1.3:1 within the operating band 137.5 to 142.5 GHz. The first experimental tube is expected to be tested in October 1992. Author (revised)

N94-10518# Lawrence Livermore National Lab., CA.

CHARACTERIZATION OF HIGH-POWER RF STRUCTURES USING TIME-DOMAIN FIELD CODES

C. C. Shang, J. F. DeFord, and T. L. Swatloski 21 Aug. 1992 3 p Presented at the 16th International LINAC Conference, Ottawa, Ontario, 23-28 Aug. 1992
(Contract W-7405-eng-48)
(DE93-013416; UCRL-JC-110202; CONF-9208109-82) Avail: CASI HC A01/MF A01

We have modeled gyrotron windows and gyrotron amplifier structures for TE modes in the 100-150 GHz range. Additionally, we have computed the reflection and transmission characteristics from the field data. Good agreement with frequency domain codes and analytic analysis was obtained for some simple geometries. We present results for realistic structures with lousy coatings. Finally, we describe implementation of microwave diagnostics. DOE

N94-10560 Japan Broadcasting Corp., Tokyo. Science and Technical Research Lab.

A NEW HMM LEARNING ALGORITHM FOR CONTINUOUS SPEECH RECOGNITION

Toru Imai and Akio Ando Mar. 1993 10 p
(NHK-Serial-413) Copyright Avail: Issuing Activity (NHK Science and Technical Research Laboratories, 1-10-11, Kinuta, Setagaya, Tokyo, 157 Japan)

Recently, hidden Markov models (HMMs) have been widely researched as an effective way of speech recognition. This paper describes a new HMM learning algorithm to obtain model parameters which appropriately describe training speech data. It is experimentally shown that the algorithm yields better recognition results than other training algorithms, and gives a good performance to a continuous speech recognition system for superimposing TV captions. Author

N94-10660 Scripps Institution of Oceanography, La Jolla, CA. Marine Physical Lab.
WIDEBAND BEAMFORMING FOR A SPARSE NONUNIFORM SPACED SENSOR ARRAY Final Report
Jeffrey Krolik Apr. 1993 6 p Limited Reproducibility: More than 20% of this document may be affected by microfiche quality
(Contract N00014-89-D-0142)
(AD-A265909; MPL-U-20/93) Avail: CASI HC A02

This project concerns the continued development and evaluation of a computationally-efficient wideband adaptive beamformer for a large non-uniformly-spaced sensor array which effectively extends its operation to wavelengths which are considerably smaller than the average inter-element spacing. DTIC

N94-10709# Stanford Linear Accelerator Center, CA.
OPTIMAL ROUTING OF IP PACKETS TO MULTI-HOMED SERVERS
K. L. Swartz Aug. 1992 9 p Presented at the 6th Usenix Systems Administration Conference on Large Installation System Administration, Long Beach, CA, 19-23 Oct. 1992
(Contract DE-AC03-76SF-00515)
(DE93-010949; SU-SLAC-PUB-5895; CONF-9210331-2) Avail: CASI HC A02/MF A01

Multi-homing, or direct attachment to multiple networks, offers both performance and availability benefits for important servers on busy networks. Exploiting these benefits to their fullest requires a modicum of routing knowledge in the clients. Careful policy control must also be reflected in the routing used within the network to make best use of specialized and often scarce resources. While relatively straightforward in theory, this problem becomes much more difficult to solve in a real network containing often intractable implementations from a variety of vendors. This paper presents an analysis of the problem and proposes a useful solution for a typical campus network. Application of this solution at the Stanford Linear Accelerator Center is studied and the problems and pitfalls encountered are discussed, as are the workarounds used to make the system work in the real world. DOE

N94-10960# Superconducting Super Collider Lab., Dallas, TX.
DILUTE: A CODE FOR STUDYING BEAM EVOLUTION UNDER RF NOISE
H. J. Shih (Superconducting Super Collider Lab., Dallas, TX.), J. Ellison (New Mexico Univ., Albuquerque.), and W. Schiesser (Lehigh Univ., Bethlehem, PA.) Apr. 1993 9 p Presented at the Computational Accelerator Physics Conference (CAP93), Pleasanton, CA, 22-26 Feb. 1993
(Contract DE-AC35-89ER-40486)
(DE93-011605; SSCL-Preprint-220; CONF-930269-12) Avail: CASI HC A02/MF A01

Longitudinal beam dynamics under RF noise have been modeled using a diffusion-inaction PDE. If the primary interest is the evolution of the beam in action, it is much simpler to integrate the model PDE than to undertake tracking simulations. Here we describe the code that we developed to solve the model PDE using the numerical Method of Lines. Features of the code include the following: (1) computation of the distribution in action for the initial beam from a Gaussian or user-supplied distribution in longitudinal phase space; (2) computation of the diffusion coefficient for white noise or from a user-supplied spectral density for non-white noise; (3) discretization of the model PDE using finite-difference or Galerkin finite-element approximations with a uniform or non-uniform grid; and (4) integration of the system of ODE's in time by the solver RKF45 or a user-supplied ODE solver. DOE

N94-11023 British Broadcasting Corp., Kingswood (England). Engineering Div.
MEASUREMENT OF DISPLAY TRANSFER CHARACTERISTICS USING TEST PICTURES
A. Roberts 1992 11 p
(BBC-RD-1992/13) Copyright Avail: BBC, Kingswood Warren, Tadworth, Surrey, England

There are three basic parameters which define the transfer characteristic of monitors: contrast, flare, and gamma. Each of these can be measured, with varying degrees of accuracy, by a variety of methods. This Report attempts to clarify the definitions of the terms and to specify methods of measurement which give unique and repeatable results. Test pictures are described which permit measurements to be made precisely and rapidly. The test picture for gamma measurement can be used both subjectively and objectively, and gives results which compare well with those produced by the classical method of making point-by-point measurement of the transfer function. The test pictures for flare and contrast give results which are specific to those test pictures only, these results can be used only for making relative assessments of monitors and cannot be used to make accurate predictions of the color performance of a monitor. Author

N94-11024 British Broadcasting Corp., Kingswood (England). Engineering Div.
BUILDING PENETRATION LOSS MEASUREMENTS FOR DAB SIGNALS AT 211 MHz
J. A. Green 1992 18 p
(BBC-RD-1992/14) Copyright Avail: BBC, Kingswood Warren, Tadworth, Surrey, England

Digital Audio Broadcasting (DAB) is being considered as a future method of transmitting radio programs to the public. Some of the advantages of DAB over conventional Frequency Modulation (FM) include its resistance to multipath and its ruggedness in the presence of interference. Because of these qualities it is ideally suited for reception by mobile and portable receivers. It is proposed that a DAB service will be planned to be effective for use by fixed, portable, and mobile receivers. But many problems have to be overcome, to allow accurate planning of suitable transmitter sites and powers, if the desired coverage is to be obtained economically. This Report gives the results of one aspect of this work, namely the signal level received within a building compared to the level received outside. This is generally termed building penetration loss. Several different frequency bands are being considered for DAB transmission in the UK. The work reported concentrates on one of the proposed bands: Band III. The two broad aims of the work were: (1) by measuring the field strength both inside and outside buildings, determine a Building Penetration Loss figure; and (2) using first generation prototype Coded Orthogonal Frequency Division Modulation (COFDM) equipment, find the relationship between field strength and some particular values of Bit Error Ratio (BER). A mean building penetration loss of approximately 8 dB was measured for the whole of the ground floor of brick-built houses. Using first generation prototype DAB transmitting and receiving equipment, in the absence of interference, a field strength of the order of 39 dB (microV/m) will provide the receiver with an adequate signal. Further work is essential to quantify the lower limit of felt strength in which a trial specification receiver will work. There is a potential saving of up to 5 dB on transmitter powers, depending on the particular levels of ambient man-made noise. Author (revised)

N94-11030 Gosudarstvennyi Komitet po Ispolzovaniyu Atomnoi Energii, Moscow (USSR).
TO THE THEORY OF IRREGULAR AUTO MODULATION IN ELECTRON BEAM-BACKWARD ELECTROMAGNETIC WAVE DYNAMIC SYSTEM [KTEORII NEREGULYARNOJ AVTOMODULYATSII V DINAMICHESKOJ SISTEME EHLEKTRONNYJ PUCHOK-OBRATNAYA EHLEKTROMAGNITNAYA VOLNA]
A. O. Ostrovskij and Y. V. Tkach 1991 11 p In RUSSIAN Limited Reproducibility: More than 20% of this document may be affected by microfiche quality
(DE93-620982; KFTI-91-7) Avail: CASI HC A03 (US Sales Only)

Nonlinear dynamics of auto vibration processes in a distributed electron beam - backward electromagnetic wave system is described. It was shown that depending on the correlation between the wave complification parameter and initial electron beam energy, the considered system may demonstrate different mechanisms of transition to autostochastic vibrations. In particular, it was established that such a transition may be realized through the sequence of period doubling bifurcations. The efficiency of irregular auto vibration excitations is determined. DOE

N94-11034 Gosudarstvennyi Komitet po Ispolzovaniyu Atomnoi Energii, Moscow (USSR).
ABOUT EXCITATION OF ROUND WAVEGUIDE BY A POINT CURRENT SOURCE [O VOZBUZHDENII KRUGLOGO VOLNOVODA TOCHECHNYM ISTOCHNIKOM TOKA]
S. D. Prijmenko, V. G. Papkovich, and N. A. Khizhnyak 1991 15 p In

RUSSIAN Limited Reproducibility: More than 20% of this document may be affected by microfiche quality
(DE93-621352; KFTI-91-27) Avail: CASI HC A03 (US Sales Only)

The problem of tensor Green function formulation for electric vector potential G(sub e)(r-vector,r'-vector) is solved as a problem of tensor spheric wave diffraction on inner surface of a round waveguide. It is shown that G(sub e)(r-vector,r'-vector) is a superposition of tensor Green-function of free space and a regular Green function of round waveguide G(sub e)(sup (0))(r-vector,r'-vector) being a solution of homogeneous Helmholz equation which satisfy unhomogeneous boundary conditions on waveguide surface. The obtained results may be applied in design of UHF installations and accelerating technique in which charged round waveguides are used. DOE

N94-11035 Gosudarstvennyi Komitet po Ispolzovaniyu Atomnoi Energii, Moscow (USSR).

LINEAR ANTENNA OF AN ARBITRARY ORIENTATION AND POSITION IN CYLINDRIC SCREEN [LINEJNAYA ANTENNA PROIZVOL'NOJ ORIENTASII I POLOZHENIYA V TSILINDRICHESKOM EHKRANE]

S. D. Prijmenko, V. G. Papkovich, and N. A. Khizhnyak 1991 9 p In RUSSIAN Limited Reproducibility: More than 20% of this document may be affected by microfiche quality
(DE93-621353; KFTI-91-29) Avail: CASI HC A02 (US Sales Only)

An equation of the linear antenna in cylindric screen is formulated. Using the averaging method a solution of this equation for the antenna of arbitrary orientation which does not contact the screen walls or contacts them in one or two ends is received. The obtained asymptotic expression for stream permits to describe in a single manner the case of resonance and non-resonance scattering. These results may be applied in design of UHF and accelerating installations using cylindric screens charged with linear vibrators. DOE

N94-11037 Academy of Sciences of the Ukraine, Kharkov. Fiziko-Tekhnicheskij Inst.

TO THE COMPLEXITY OF DYNAMIC SYSTEM PROBLEM [K VOPROSU O SLOZHNOSTI DINAMICHESKIKH SISTEM]

V. A. Buts, N. M. Zemlyanskij, and A. P. Tolstoluzhskij 1991 12 p In RUSSIAN Limited Reproducibility: More than 20% of this document may be affected by microfiche quality
(DE93-621355; KFTI-91-51) Avail: CASI HC A03 (US Sales Only)

On the basis of the Hausdorf dimension concept, a dynamic system complexity is defined as a minimal dimension of the phase volume in which its attractor may be included. A procedure of such a dimension determination according to timely realization of one variable is proposed. The dimensions of some experimental realizations and that of one mathematical model are found. DOE

N94-11038 Academy of Sciences of the Ukraine, Kharkov. Fiziko-Tekhnicheskij Inst.

ASYMPTOTIC EXPRESSIONS FOR REGULAR GREEN FUNCTIONS OF A ROUND CYLINDRICAL SCREEN [ASIMPTOTICHESKIE VYRAZHENIYA FUNKTSIJ GRINA KRUGOVOGO TSILINDRICHESKOGO EHKRANA]

S. D. Prijmenko and N. A. Khizhnyak 1992 16 p In RUSSIAN Limited Reproducibility: More than 20% of this document may be affected by microfiche quality
(DE93-621356; KFTI-92-4) Avail: CASI HC A03 (US Sales Only)

Asymptotic expressions of tensor regular Green functions for electric vector potential G(sub e)(sup (o) and magnetic vector potential G(sub mu)(sup o) of a round cylindric screen are obtained. In low-frequency approximation G(sub e)(sup o) and G(sub mu)(sup o) for a synphase linear current source are described by Green function of the secondary source with an addition in the form of finite series. In high-frequency approximation: at internal excitation by a synphase linear current source asymptotic correlations are represented by an infinite sum of secondary current source Green functions; at external excitation G(sub mu)(sup o) for a synphase linear current source and G(sub e)(sup o) for a point current source have a form of closed expressions. The obtained results may be applied in design of UHF, antenna and accelerating installations using charged cylindric screen. DOE

N94-11060 National Astronomy and Ionosphere Center, Arecibo, Puerto Rico.

PROPAGATION EFFECTS IN SPACE VLBI

Leonid I. Gurvits, ed. (Academy of Sciences, USSR, Moscow.) Arecibo Ionospheric Observatory 1993 109 p Workshop held in Leningrad, Russia, 28-30 May 1990 Sponsored by NSF; Academy of Sciences (USSR); and Special Astrophysical Observatory
Copyright Avail: Issuing Activity

Very Long Baseline Interferometry (VLBI) leads all other kinds of astronomical techniques in achieving the highest angular resolution. The main purpose of the workshop was to discuss some possible complications of VLBI experiments with baselines longer than the Earth's diameter due to propagation phenomena in the various media. Papers presented at the workshop are included. For individual titles, see N94-11061 through N94-11071.

N94-11051# Academy of Sciences (USSR), Moscow. Physical Inst.

RADIOWAVES PROPAGATION THROUGH INHOMOGENEOUS INTERSTELLAR PLASMA

V. I. Shishov *In* National Astronomy and Ionosphere Center, Propagation Effects in Space VLBI 1993 p 1-12 (For primary document see N94-11060 01-32)
Avail: Issuing Activity

Data on measurements of the effects of scattering, short-period and long-period scintillation of pulsars and quasars which are caused by modulation of radiowaves propagating through interstellar plasmas with turbulent inhomogeneities are analyzed. Arguments are stated in favor of piecewise power form of spatial spectrum of electron density with sharp decrease of level on scale of 1 = 10(exp 13)cm. The estimation of the angle of scattering, specific temporal and frequency scales of scintillations for an extragalactic source, located in the vicinity of galaxy pole, is presented. Author (revised)

N94-11062# Academy of Sciences of the Ukraine, Kharkov. Inst. of Radio Astronomy.

THE INFLUENCE OF THE PROPAGATION MEDIUM ON THE SENSITIVITY AND RESOLUTION OF METER WAVELENGTH APERTURE SYNTHESIS SYSTEMS

A. V. Kukushkin *In* National Astronomy and Ionosphere Center, Propagation Effects in Space VLBI 1993 p 13-22 (For primary document see N94-11060 01-32)
Avail: Issuing Activity

Among the effects restricting the sensitivity and resolution of radio interferometers stands out scattering in the medium where the waves propagate, i.e., the ionosphere, the interplanetary or interstellar plasma. In a majority of papers dedicated to the problem, the weak scattering approximation is considered and proves sufficient owing to the frequency range employed. The currently existing aperture synthesis systems and radio interferometers operate, for the most part, at the centimeter wavelengths, in which band scattering effects are reasonably weak both in the interplanetary plasma (IPM) and the ionosphere. Representative scales of wave front pertubations owing to the interstellar plasma exceed the maximum size of the synthesized apertures of Earth based systems. A more detailed theoretical analysis of the scattering effects with an application to the characteristics of the aperture synthesis systems is suggested. Author (revised)

N94-11063# Virginia Polytechnic Inst. and State Univ., Blacksburg. Dept. of Physics.

INTERSTELLAR SCATTERING AND THE SELECTION OF EXTRAGALACTIC RADIOSOURCES WITH HIGHLY COMPACT COMPONENTS

Brian Dennison, R. L. Fiedler (Naval Research Lab., Washington, DC.), K. J. Johnston (Naval Research Lab., Washington, DC.), and R. L. Simon (Naval Research Lab., Washington, DC.) *In* National Astronomy and Ionosphere Center, Propagation Effects in Space VLBI 1993 p 23-32 (For primary document see N94-11060 01-32)
Avail: Issuing Activity

Interstellar scattering of radiowaves imposes strong constraints upon the resolution of fine scale intrinsic structure in compact sources. Depending upon frequency and galactic latitude, some high resolution observations will probably be dominated by scattering. Nevertheless, orbiting VLBI will provide opportunities to observe directly refractive distortions, especially those connected with extreme scattering events. An additional consequence of the similarity of the putative refractive angular scale and RADIOASTRON resolution is that observations of refractive scintillation provide rudimentary information on the compact flux on these scales. Author

N94-11064# Max-Planck-Inst. fuer Radioastronomie, Bonn (Germany).

INTRADAY VARIABILITY AND THE COMPACTNESS OF EXTRAGALACTIC RADIO SOURCES

A. Witzel and A. Quirrenbach *In* National Astronomy and Ionosphere Center, Propagation Effects in Space VLBI 1993 p 33-44 (For primary document see N94-11060 01-32)

Avail: Issuing Activity

Recent advances in the technology of radio interferometry have led to a substantial improvement of the resolution achievable in observations of extragalactic objects. By proceeding from cm wavelengths into the mm regime and leaving the ground to form earth-satellite baselines, submilliarcsecond resolution has become feasible. Since both mm-VLBI and space projects are maturing from 'first fringes' to scientifically productive techniques, the quest for ultra-compact sources, which are potential candidates for high-resolution studies, has become an increasingly important issue. Historically, it was the flux density variability of extragalactic compact sources on the timescale of weeks to several months that triggered the development of VLBI in the late sixties: The existence of compact structures inferred from the variations on the basis of light travel time arguments (and more indirectly from the shape of the synchrotron spectra) gave the scientific justification to build instruments with a resolving power in the milliarcsecond range. The successful direct observations of the small-scale structures of strong sources, the detection of apparent superluminal motion, and later the detailed images obtained by hybrid mapping procedures led to an excellent confirmation of the predictions and to numerous refinements of the earlier theories on compact sources. Specifically, it could be shown that flux density variations in the cm and mm ranges are frequently accompanied by structural variations, thus showing that the former are really intrinsic to the sources. However, the apparent consistency of the picture of compact radio sources was challenged by the extremely high brightness temperatures derived from low frequency variability. Therefore, Shapirovskaya's suggestion that interstellar scintillation should play a significant role at least in some sources was widely accepted; and separating propagation effects from intrinsic variability became an important and difficult issue in the analyses of light curves, except at very high frequencies. The importance of scattering in the interstellar medium even at cm wavelengths was reinforced by the detection of unusual 'high amplification events' at 3.6 and 11 cm. Also small-amplitude flickering on the timescale of a few days can be readily explained by refractive interstellar scintillation. Flux density variability on time scales of a day or even less in extragalactic radio sources had not been convincingly demonstrated before intraday variability was found in several high-declination flat spectrum sources. Although the physical origin of these variations has not yet been indisputably identified, a very high degree of compactness can be inferred for short-timescale variables, making them prime targets for ultra-high resolution studies. Clearly, there is also an important impact of short time scale variations on interferometry by its influence on aperture synthesis. The present status of our observations on intraday variability is reported and some ideas on their interpretation are discussed. Author (revised)

N94-11065# Cornell Univ., Ithaca, NY. Dept. of Astronomy.

INTERSTELLAR SCATTERING AND THE PULSAR STUDIES WITH SPACE VLBI c93

James M. Cordes *In* National Astronomy and Ionosphere Center, Propagation Effects in Space VLBI 1993 p 45-56 Sponsored by National Astronomy and Ionosphere Center (For primary document see N94-11060 01-32)

Avail: Issuing Activity

Observable interstellar scattering phenomena (angular broadening, temporal broadening, diffractive scintillations, angle of arrival variations, and time of arrival variations) are used to show that: (1) the wave number spectrum of electron density fluctuations is Kolmogorov in form over at least five orders of magnitude in wave number; there may be an implied inner scale of approximately few x 10(exp 7) cm. All observables yield an implied scattering measure (SM, the line of sight integral of the spectral coefficient C(sup 2)(sub n) that varies by at least 5 orders of magnitude between lines of sight; and (3) the Galactic distribution of scattering material, as inferred from analysis of SM, displays both large scale systematic structure and localized enhancements. A fit of an axisymmetric model shows two components with scale heights of 0.05 and 0.5 kpc and galactrocentric radial scales approximately greater than 20 kpc and 7 kpc. The small scale height component is stronger than the other by a factor approximately 2000. From the model fit, predictions for angular broadening as a function of galactic coordinates l,b are given for extragalactic sources at the four frequencies of interest to RADIOASTRON. Several projects are suggested for RADIOASTRON that will enhance our understanding of the galactic turbulence that causes scattering and that aim at resolving pulsar magnetospheres. These include: angular broadening of nearby pulsars; angular broadening of extra galactic sources for the absolute value of b is approximately less than 1 deg toward the galactic anticenter; and interferometry of pulsars using very large baselines, b is approximately 0.1-1 AU. The first two projects require a one day orbit, the last an interplanetary orbit. Author (revised)

N94-11066# Iowa Univ., Iowa City. Dept. of Physics.

VLBI AND THE DETECTION OF INTERSTELLAR MAGNETOHYDRODYNAMIC WAVES c75

Steven R. Spangler *In* National Astronomy and Ionosphere Center, Propagation Effects in Space VLBI 1993 p 57-67 (For primary document see N94-11060 01-32)

Avail: Issuing Activity

The capability of Very Long Baseline Interferometry (VLBI) for measuring plasma turbulence in the interstellar medium on interestingly small scales is discussed. These scales are sufficiently small that the irregularities should be part of plasma waves which partake in processes such as resonant interaction with cosmic rays. VLBI results to date show that intense scattering can occur in regions of small spatial extent. Specific regions such as supernova remnants and interstellar bubbles, which are good candidates for generation of plasma density fluctuations are examined. The capacity of Radioastron to further this area of research is discussed. With longer baselines, Radioastron will be capable of detecting regions with smaller scattering measure than can presently be detected. This might produce important new observational results in plasma astrophysics.
Author (revised)

N94-11067# Academy of Sciences (USSR), Moscow. Physical Inst.

GENERALIZATION OF DYSON CRITERION FOR THE AMPLITUDE-PHASE FLUCTUATIONS CASE AND FOR THE SYSTEM OF INTERFEROMETERS

V. I. Tatarskii *In* National Astronomy and Ionosphere Center, Propagation Effects in Space VLBI 1993 p 68-78 (For primary document see N94-11060 01-32)

Avail: Issuing Activity

It is well known that due to the medium parameters fluctuations some restrictions on the resolution of the Very Long Baseline Interferometry (VLBI) arise. Some special methods to compensate this effect are developed. The adaptive systems and processing of signals are the examples of such methods. In fact both are two different ways to realize the same ideas. For the adaptive optical systems, some different criteria C(sup i) were suggested, that condition C(sub i) = max, corresponds to elimination of phase fluctuations on the input aperture. Some of these criteria are based on the difference in the time scales and spatial behavior of fluctuations which are caused by source properties and by medium properties. For example, if the source fluctuations have a very short correlation time and spatial scale in comparison with the corresponding values of medium fluctuations, it is possible to distinguish them using this difference. To use such methods it is not necessary to have the reference point source. Thus, such methods are rather universal. One such method is considered. The model of source, then the interferometrical measurements in the homogeneous medium is analyzed. The well known Dyson criterion for the phase fluctuations is derived. It is shown, that this criterion is valid only for the small enough angle sizes of source. Two generalizations are made: it is shown how it is possible to use the Dyson criterion in the presence of intensity fluctuations (including the case of strong and saturate fluctuations) and how to formulate it if the field is measured only for the discrete system of observation points (telescopes). The corresponding algorithm of the signal processing is formulated. The influence of the

additive noise on the Dyson criterion is analyzed. It is shown also that Dyson criterion is useless, if the angle size of source is not small enough.
Author (revised)

N94-11068# Academy of Sciences (USSR), Moscow. Physical Inst.
THE POSSIBILITY OF IMAGE RESTORATION UNDER OBSERVATION IN A REGIME OF STRONG SCATTERING **c74**
V. U. Zavorotny *In* National Astronomy and Ionosphere Center, Propagation Effects in Space VLBI 1993 p 79-85 (For primary document see N94-11060 01-32)
Avail: Issuing Activity

The statistical theory of interferometric imaging of extended incoherent sources in a random medium is developed. It is shown that the small enough objects can be resolved in a regime of strong scattering. Author

N94-11069# Academy of Sciences (USSR), Moscow.
THE SUPERRESOLUTION EFFECT OBSERVED THROUGH A RANDOM MEDIUM **c74**
M. I. Charnotskii, V. U. Zavorotny, and V. A. Myakinin *In* National Astronomy and Ionosphere Center, Propagation Effects in Space VLBI 1993 p 86-89 (For primary document see N94-11060 01-32)
Avail: Issuing Activity

It is well known that the angular resolution of a telescope is limited by diffraction on the aperture and the solution of an interferometer is defined by the length of its base. In fact, due to atmospheric turbulence (if long-exposure images are recorded), the resolution of large telescopes and long base interferometers is determined not so much by diffraction as by medium-induced wave front perturbations. But in the case of short exposure when image averaging does not take place, one can observe details with diffraction limited resolution. This property of short exposure images was used by Labeyrie as the basis for the speckle interferometric method. Nowadays there are many modifications of this method, allowing restoration of an image with diffraction-limited resolution by computer processing of short-exposure images and interferometric signals. It seems obvious that turbulence is a disturbing noise factor. But under certain conditions it may produce a positive effect; however paradoxical it sounds, it may lead to an increase in the resolution beyond the diffraction limit. Theoretical and experimental results concerning this phenomenon are described elsewhere. A theoretical description of this effect for interferometric imaging is given. Author (revised)

N94-11070# Harvard-Smithsonian Center for Astrophysics, Cambridge, MA.
TROPOSPHERIC AND IONOSPHERIC EFFECTS ON DIFFERENTIAL ASTROMETRY WITH A GROUND-SPACE BASED VLBI ARRAY
Norbert Bartel *In* National Astronomy and Ionosphere Center, Propagation Effects in Space VLBI 1993 p 90-101 (For primary document see N94-11060 01-32)
(Grant NSF AST-89-02087)
Avail: Issuing Activity

The effects of the troposphere and the ionosphere on the interferometric delay in differential ground-based astrometric VLBI observations are analytically and empirically investigated and compared with other effects influencing the accuracy of such observations. The results from this investigation are then used to estimate the tropospheric and ionospheric effects in ground space based VLBI observations such as those anticipated with RADIOASTRON, VSOP, and IVS. It is found that tropospheric effects can most likely be corrected easily with standard methods and with sufficient accuracy not to dominate the error budget of position determinations. Ionospheric effects at frequencies approximately greater than 1.7 GHz are also not likely to dominate such error budget if the standard errors of the components of the baseline vectors are approximately greater than 10 m. In contrast, if the components of the ground-space baseline vectors have standard errors approximately less than 1 m, ionospheric effects at frequencies are approximately less than 2 GHz could still be a significant contribution to such an error budget, even if more elaborate correction methods are applied. Author (revised)

N94-11071# Radio Research Inst. (USSR).
ELIMINATION OF THE INFLUENCE OF THE ATMOSPHERE ON THE ACCURACY OF SOLUTIONS TO ASTROMETRIC PROBLEMS BY MEANS OF A GROUND-SPACE VLBI NETWORK
V. A. Alexeev *In* National Astronomy and Ionosphere Center, Propagation Effects in Space VLBI 1993 p 102-104 (For primary document see N94-11060 01-32)
Avail: Issuing Activity

The elimination of the influence of the atmosphere on the accuracy of solutions to astrometric problems by means of a ground-space Very Large Baseline Interferometry (VLBI) network is discussed. The feasibility of ground-space VLBI projects (RadioAstron, VSOP, and IVS) requires that the possibility of organizing from them a ground-space radio VLBI system with essentially greater potential for solving astrometric problems than each two-element radio interferometer taken separately is examined. The algorithm for processing information in a ground-space radiointerferometer which consists of a minimum of two space-based stations is examined. CASI

N94-11084*# Michigan Univ., Ann Arbor. Radiation Lab.
RADIATION AND SCATTERING BY CAVITY-BACKED ANTENNAS ON A CIRCULAR CYLINDER Semiannual Report, Feb. - Aug. 1993
Leo C. Kempel and John L. Volakis Jul. 1993 69 p
(Grant NAG1-1478)
(NASA-CR-193409; NAS 1.26:193409; UM-030601-1-T) Avail: CASI HC A04/MF A01

Conformal arrays are popular antennas for aircraft and missile platforms due to their inherent low weight and drag properties. However, to date there has been a dearth of rigorous analytical or numerical solutions to aid the designer. In fact, it has been common practice to use limited measurements and planar approximations in designing such non-planar antennas. The finite element-boundary integral method is extended to scattering and radiation by cavity-backed structures in an infinite, metallic cylinder. In particular, the formulation specifics such as weight functions, dyadic Green's function, implementation details, and particular difficulties inherent to cylindrical structures are discussed. Special care is taken to ensure that the resulting computer program has low memory demand and minimal computational requirements. Both scattering and radiation parameters are computed and validated as much as possible.
Author (revised)

N94-11158# Naval Postgraduate School, Monterey, CA.
DESIGN OF A MATCHING NETWORK FOR DIPOLE ANTENNAS M.S. Thesis
Jennifer Park Mar. 1993 55 p
(AD-A265115) Avail: CASI HC A04/MF A01

The input impedance of an antenna is highly dependent on the frequency range in which it operates. For an electrically small antenna to operate in a broad frequency range, the antenna must be properly matched. This thesis presents the design of a matching network for a 1-meter monopole antenna, operating over 30-90 MHz using the real frequency method (RFM). It outlines the mathematical steps needed to determine the equalizer function, which ultimately leads to the circuit design. The goal of the RFM, given the real frequency data, is to optimize the Transducer Power Gain (TPG) and minimize the reflection coefficient or power lost due to the impedance mismatch. Complete design including network realization is given. However, no experimental results are presented. DTIC

N94-11206*# SRI International Corp., Menlo Park, CA. Geoscience and Engineering Center.
TELESCIENCE CAPABILITY FOR THE SONDRE STROMFJORD, GREENLAND, INCOHERENT-SCATTER RADAR FACILITY Final Report, 15 Aug. 1991 - 14 Jan. 1993
Yadunath B. Zambre Jan. 1993 13 p
(Grant NAG5-1728; SRI Proj. 2724)
(NASA-CR-193683; NAS 1.26:193683) Avail: CASI HC A03/MF A01

SRI International (SRI) operates an upper-atmospheric research facility in Sondre Stromfjord (Sondrestrom), Greenland. In the past, the facility's remote location and limited logistical support imposed constraints on the research that could be carried out at the site. Campaigns involving multiple instruments were often constrained due to limited space, and experiments requiring coordination with other geographically separated facilities, though possible, were difficult. To provide greater access to the facility, an electronic connection between Sondrestrom and the mainland U.S.A. was established, providing access to the National Science Internet. SRI developed telescience software that sends data from the incoherent scatter radar at the Sondrestrom facility to SRI's offices in Menlo Park, California. This software uses the transmission control protocol (TCP/IP) to transmit the data in near real time between the two locations and the X window system to generate displays of the data in Menlo Park. This is in contrast to using the X window system to display data remotely across a wide-area network. Using CP to transport data over the long distance network has resulted in significantly improved network throughput and latency. While currently used to transport radar data, the telescience software is designed and intended for simultaneous use with other instruments at Sondrestrom and other facilities. Work incorporating additional instruments is currently in progress. Author (revised)

N94-11357*# Texas A&M Univ., College Station. Center for Space Power.

CONSTRUCTION AND TESTING OF A SPACE READY RECTENNA Final report

Alan M. Brown 1993 37 p
(Grant NAG3-1368)
(NASA-CR-193310; NAS 1.26:193310) Avail: CASI HC A03/MF A01

In Feb. 1993, the Solar Power Satellite (SPS) Working Group from ISAS, Japan will launch a sounding rocket into low earth orbit to perform two activities: collect scientific information on the high power microwave-ionosphere interaction, and demonstrate microwave power transmission in space at 2.45 GHz. The SPS Working Group announced an open invitation to international agencies willing to collaborate with the Microwave Energy Transmission in Space (METS) experiment in a number of categories. Under the sponsorship of the NASA's Lewis Research Center, the Center for Space Power located at Texas A&M University joined the experiment by producing a microwave rectifying receiving antenna (rectenna). The rectenna is a special type of receiving antenna with unique properties and characteristics. The rectenna's main purpose is to efficiently convert microwave power into DC power. The rectenna is an advanced component in microwave power beaming technology developed for 2.45 GHz. The state-of-the-art rectenna for this frequency consists of dipole antennas, filter circuits, and transmission lines etched on a thin layer of Kapton film. The format of the thin film rectenna is ideally suited for space applications. Thin film rectennas have a low specific mass of approximately 1 kg/kW. The main component of the rectenna is the rectifying diode. High conversion efficiencies (90 percent) in microwave to DC power are capable with special Schottky barrier diodes correctly located in the rectenna circuitry. The theory of operation of the 2.45 GHz rectenna is explained. Experimental test results on the METS rectenna are presented. The packaging of the rectenna is also discussed to meet space qualifications. Author (revised)

N94-11453# General Atomic Co., San Diego, CA.

CONVERSION OF THE FOUR-STRAP ARRAY IN D3-D TO A TUNABLE TRAVELING WAVE ANTENNA

D. A. Phelps, C. P. Moeller, C. C. Petty, R. I. Pinsker, P. M. Ryan, R. H. Goulding, and D. J. Hoffman (Oak Ridge Associated Universities, Inc., TN.) Apr. 1993 4 p Presented at the 10th Topical Conference on Radio Frequency Power in Plasmas, Boston, MA, 1-3 Mar. 1993
(Contracts DE-AC03-89ER-51114; DE-AC05-84OR-21400)
(DE93-012085; GA-A-21264; CONF-9303130-1) Avail: CASI HC A01/MF A01

The in situ conversion of the two-standing wave resonator driven four-strap array in D3-D to a new type of traveling wave antenna (TWA) is introduced. First observations are reported on the following: (1) broad frequency range turnability; (2) narrow frequency band phase control; (3) single pass transmission loss and modification caused by resistive and reactive sheet simulators of plasma loading; and (4) recirculating power resonance and gain in a traveling wave resonator (TWR) driven TWA. DOE

N94-11466# Lawrence Livermore National Lab., CA.

ONE-DIMENSIONAL CALCULATION OF HIGH-POWER MICROWAVE PULSE COMPRESSION BY THE EARTH'S IONOSPHERE

D. J. Mayhall, J. H. Yee, and G. E. Sieger (Sieger, G. E., Woodland, CA.) Aug. 1992 4 p Presented at the 6th National Conference on High Power Microwave Technologies, Lackland AFB, TX, 24-28 Aug. 1992
(Contract W-7405-eng-48)
(DE93-009517; UCRL-JC-110117; CONF-9208127-7) Avail: CASI HC A01/MF A01

In propagating significant distances in the ionosphere, a short microwave pulse will undergo strong dispersion from the ambient electrons it encounters. The pulse will be extended in time with dramatic reductions in peak amplitude and power. This undesirable dispersive reduction may be counteracted by transmission of a frequency-chirped pulse. In principle, with the proper initial pulse and a sufficient knowledge of the ionospheric electron density distribution, compressed pulses are possible at many points in the ionosphere. We use two computational methods to examine ionospheric compression of plane-wave pulses with several waveforms. DOE

N94-11621# Los Alamos National Lab., NM.

ON THE COUPLING OF ELECTROMAGNETIC RADIATION INTO CAVITIES

T. J. T. Kwan Mar. 1993 13 p
(Contract W-7405-eng-36)
(DE93-011406; LA-12493-MS) Avail: CASI HC A03/MF A01

We present a comprehensive report of time-resolved reflectivity and transmission measurements of the superconducting system Pr(x)Y(1-x)Ba2Cu3O(7-delta). For a fixed photon energy (1.98 eV), varying the Pr content permits optical probing of energy states both above and below the Fermi level where a superconducting gap is expected to occur. We find qualitatively different behavior in the sign, magnitude, and temporal responses as a function of Pr fraction. Our results indicate that a simple two-fluid model interpretation cannot account for the observed response and that the intrinsic band structure of Pr(x)Y(1-x)Ba2Cu3O(7-delta) plays a significant role in the dynamics of these systems. DOE

N94-11636 California Univ., Los Angeles.

PO/PTD DIFFRACTION SYNTHESIS OF ARRAY-FED REFLECTOR ANTENNAS FOR SATELLITE AND RADAR APPLICATIONS Ph.D. Thesis

Dah-Weih Duan 1992 252 p
Avail: Univ. Microfilms Order No. DA9310918

Reflector antennas find wide applications in satellite communications, direct broadcast satellite (DBS) communications, radar systems, radio astronomy, and deep space telemetry. The ever increasingly stringent requirements on the antenna performance have demanded the development of sophisticated synthesis/analysis techniques. For this purpose, a diffraction synthesis methodology, which combines the optimization techniques and the diffraction analysis techniques of Physical Optics (PO) and Physical Theory of Diffraction (PTD,) is developed. This methodology is used to solve the problems of synthesizing single and dual-reflector antennas with an arbitrarily configured array feed. In the analysis, the PTD technique is reformulated using a general approach, and a singularity analysis is performed. The inaccuracy of the PO field in the far-angular regions and cross-polarized field predictions are effectively corrected by the PTD fringe field. In the synthesis, reflector shaping is achieved by adjusting the coefficients of a Jacobi-Fourier global surface expansion, which yields reflectors that are characterized by smooth surfaces, well defined boundaries, and continuous surface derivatives. The edge diffraction and the near-field effects are automatically taken into account in the synthesis. The reflector aperture is allowed to vary from an ellipse (circle) to a rectangle (square) using the superquadric function, and the array feed may consist of point sources or aperture type of feeds (horns). Alternative reflector antenna configurations and concepts developed using the PO/PTD diffraction synthesis/analysis technique are demonstrated through example applications such as high gain dual-reflector antennas, reflector surface distortion compensation, High Power Microwave (HPM) antenna systems, and contoured-beam satellite antennas. Dissert. Abstr.

N94-11639 Texas Univ., Austin.

BOUNDARY INTEGRAL SOLUTION TO THE ELECTROMAGNETIC SCATTERING FROM COATED SURFACES CONTAINING EDGES, GAPS, AND PERIODIC GRATINGS Ph.D. Thesis

John Thomas Moore 1992 103 p
Avail: Univ. Microfilms Order No. DA9309235

A boundary integral approach is used to investigate the electromagnetic scattering from three types of coated structures: the isolated gap in a coating, the semi-infinite coated edge, and the coated periodic grating. For the gap in the coating, the numerical implementation of the solution is facilitated by removing the specular fields and the surface wave contributions from the boundary integral equation. Consequently the discretization domain of the infinite structure can be reduced to a localized region near the gap.

Numerical diffraction coefficients and surface wave launch coefficients are extracted from the scattered field. The results of this approach are validated against a spectral integral solution to the gap, and excellent agreement is observed. For the semi-infinite edge, an exact boundary integral formulation is used without resorting to the impedance boundary condition approximation. As is done for the coated gap, numerical diffraction coefficients and surface wave launch coefficients are extracted from the scattered field. Solutions to several finite sized coated strips are constructed using the numerical diffraction coefficients and are shown to be valid for a variety of strip configurations. The solution to a coated strip with a gap is constructed one mechanism at a time via a high frequency ray framework. This numerical 'building block' approach provides a clear physical picture of the complex scattering mechanisms in coated structures. Finally, a boundary integral formulation is presented for computing the scattering from material coated periodic gratings under oblique incidence. Periodic boundary conditions and expansion of the fields in terms of Floquet harmonics allow the boundary integral formulation to treat just a single period of the infinite grating. Numerical results for etched conducting gratings designed for use at infrared wavelengths are presented and shown to be in good agreement with a series of measurements. Results for a number of dielectric gratings for both normal and oblique incidence also agree well with other published data. The conductor-backed coated grating is also studied, and it is shown that the groove profile can be used to significantly alter the absorbing characteristics for lossy material coatings. Dissert. Abstr.

N94-11655# Naval Research Lab., Washington, DC.
HF-OTH RADAR PERFORMANCE RESULTS
J. M. Hudnall and S. W. Der 31 May 1993 26 p
(AD-A266106; NRL/MR/5325-93-7326) Avail: CASI HC A03/MF A01

Radar performance forecasts for Navy Relocatable Over-the-Horizon Radars (ROTHR) using computer program RADARC Version 1.0 for Beeville, Texas and Northwest, Virginia are presented. Computer instructions to run RADARC on VMS are given to obtain data files for a location of interest. Instructions on personal computers to generate graphs for noise levels, forecast graphs and tables of availability predictions are provided. DTIC

N94-11883# Naval Command, Control and Ocean Surveillance Center, San Diego, CA. RDT and E Div.
DISTURBANCE IMPACT ASSESSMENT SYSTEM (DIAS), VERSION 2.0. SYSTEM DESIGN DOCUMENT Final Report, 1990 - 1992
R. B. Rose and D. R. Lambert Feb. 1993 260 p
(AD-A265251; NCCOSC/RDT/E-TD-2452) Avail: CASI HC A12/MF A03

This technical document, actually a system design document or functional description document, covers the Disturbance Impact Assessment System (DIAS). This system is a computer software package designed to assess the effects of solar flares on HF radio communications. The document describes its software functions and their interrelationships. Specifically, the document provides background information on the effects of high levels of solar activity on high-latitude HF missions, outlines the architecture of DIAS, and defines the product that DIAS provides to the user. DTIC

N94-11891# Naval Command, Control and Ocean Surveillance Center, San Diego, CA.
FEATURE ASSOCIATION WITHOUT A MOTION ESTIMATE
R. L. Ricks Apr. 1993 3 p
(AD-A265162) Avail: CASI HC A01/MF A01

The problem of associating the features of a moving object in sequential images without estimates of object motion or structure (relative position of features) is addressed. A method is presented and analyzed for associating features even if some of the features are occluded (not visible in one or more of the images of interest). The method models the object as a rigid set of point reflectors each with independent reflectivity that is correlated from image to image. Object motion is modeled as a circular trajectory in a known plane. It requires measurements of position plus Doppler. Such measurements are available from monopulse radar and some sonar and laser imaging systems. The method assumes all possible associations and minimizes the least trimmed squares (LTS) of error residuals to remove erroneous associations. Byproducts of the minimization include estimates of object motion and feature structure. DTIC

N94-12281# Naval Postgraduate School, Monterey, CA. Dept. of Electrical and Computer Engineering.
DESIGN OF A CONTINUOUS RESISTIVELY LOADED MONOPOLE ANTENNA Interim Report, 1 Jan. - 1 May 1993
Darwish A. Mohamed and Ramakrishna Janaswamy 1 May 1993 34 p
(AD-A265852; NPSEC-93-011) Avail: CASI HC A03/MF A01

Hallen's integral equation with continuous resistive loading is used to design a broadband monopole antenna. The resistive profile is different from that of the well known Wu-King profile and results in a higher efficiency compared to the latter. An optimization function for determining the optimal continuous resistive load of the monopole antenna in order to satisfy the broadband property is constructed. The simplex method is used to perform the optimization. The integral equation is solved by the moment method to determine the current distribution, the efficiency, and the radiation pattern of the monopole. DTIC

N94-12338# Connecticut Univ., Storrs. Dept. of Electrical and Systems Engineering.
ESTIMATION WITH MULTISENSOR/MULTISCAN DETECTION FUSION Final Report, 1 Mar. 1992 - 28 Feb. 1993
Fadil Santosa 28 Feb. 1993 6 p
(Contract F49620-92-J-0150)
(AD-A265673; AFOSR-93-0391TR) Avail: CASI HC A02/MF A01

This first topic deals with a new procedure to carry out nonlinear transformations commonly encountered in practical surveillance systems. The procedure eliminates the bias and provides a correct (rather than optimistic) covariance matrix. The topics covered in sections 2, 5 and 6 deal with discrete optimization (assignment) techniques applied to various multisensor-multitarget problems including ballistic missile track initiation from a passive orbiting sensor. Section 3 presents some new efficient factorization algorithms that improve the numerical accuracy for several advanced state estimation filters used in practice. Section 4 deals with evaluation of performability measure of complex manufacturing systems. DTIC

N94-12406# Naval Postgraduate School, Monterey, CA.
COMPARISON OF MULTIRESOLUTION TECHNIQUES FOR DIGITAL SIGNAL PROCESSING M.S. Thesis
Neil A. Hamlett Mar. 1993 239 p
(AD-A265364) Avail: CASI HC A11/MF A03

A comprehensive study of multiresolution techniques is conducted. Background material in functional analysis and Quadrature Mirror Filter (QMF) banks is presented. The development of Mallat's algorithm for multiresolution decomposition and reconstruction is outlined and demonstrated to be equivalent to QMF banks. The Laplacian pyramid and the a trous algorithm are described and demonstrated. General multiresolution structures are constructed from cascades of QMF and pseudo-QMF banks and are demonstrated for applications in signal decomposition and reconstruction and for signal detection and identification. DTIC

N94-12409# Army Electronic Proving Ground, Fort Huachuca, AZ.
FR/GE/US RADAR RECEIVER PULSE COMPRESSION RATIO Final Report
31 Mar. 1993 10 p
(AD-A265391; ITOP-6-2-531) Avail: CASI HC A02/MF A01

This ITOP describes procedures for measuring radar receiver pulse compression ratio. Procedures described are limited to measuring the performance of the radar receiver under test as a major component. Receiver pulse compression ratio must be measured with the total radar system. DTIC

N94-12440 Naval Command, Control and Ocean Surveillance Center, San Diego, CA. Research, Development, Test and Evaluation Div.
ISAR MOTION COMPENSATION USING THE BURST DERIVATIVE MEASURE AS A FOCAL QUALITY INDICATOR Professional Paper
Richard P. Bocker and Scott A. Jones Apr. 1993 2 p Sponsored by ONR Limited Reproducibility: More than 20% of this document may be affected by microfiche quality
(AD-A265647) Avail: CASI HC A01

Inverse synthetic aperture radar (ISAR) is an imaging technique that shows great promise in classifying airborne targets in realtime, under all weather conditions. The success of classifying targets using ISAR is predicated upon forming highly focused radar images of these targets. Efforts to develop highly focused imaging computer software have been challenging, mainly because the imaging depends on and is affected by the motion of the target. Computationally intensive motion compensation algorithms have been developed to remove the unwanted degrading effects of target motion. Those particular motion compensation algorithms which require the use of a space-domain focal quality indicator, e.g., entropy, to determine image sharpness as processing proceeds pay a severe computational penalty due to the large number of two-dimensional fast Fourier transforms (2D-FFT's) which must be computed. This is due to the fact that the actual processing of ISAR data is primarily done in the spatial frequency domain and not in the space-domain where the final ISAR image is displayed. If a focal quality indicator could be developed to measure image sharpness in the spatial frequency domain, then the computational burden introduced by the numerous 2D-FFT's could be greatly relaxed. This paper describes the use of a new focal quality indicator called the burst derivative measure for determining ISAR image sharpness in the spatial frequency domain. Tests have been performed on simulated as well as actual ISAR data using both the burst derivative measure and the entropy measure. DTIC

N94-12778*# Kansas Univ. Center for Research, Inc., Lawrence. Radar Systems and Remote Sensing Lab.
FUNDAMENTAL STUDIES OF RADAR SCATTERING FROM WATER SURFACES: THE LAKE WASHINGTON EXPERIMENT Preliminary Report
A. Salam, D. Bush, S. Gogineni, and A. Zaide Dec. 1991 298 p
(Grant NAGw-1278)
(NASA-CR-194030; NAS 1.26:194030; RSL-TR-7970-2) Avail: CASI HC A13/MF A03

The University of Kansas and the University of Washington conducted a series of experiments during July and August of 1989, and July and August of 1990, to study the effects of various geophysical parameters on radar backscatter. The experiments were conducted from a platform in Lake Washington. Measurements of backscattered power and radar range were made by the University of Kansas, and environmental data such as wind speed, wind direction, and air and water temperature were measured by the University of Washington. Results of preliminary data processing are described. Radar data were acquired using two radars, one that operated at C and X bands and another at Ka band. Measurements were made at W and HH antenna polarizations, at different angles of incidence and under various wind conditions. Plots of backscattered power, normalized radar cross section, and wave height, and the Modulation Transfer Functions of selected data are presented. Author (revised)

N94-10984*# Instituto Elettrotecnico Nazionale, Galileo Ferraris, Turin (Italy).
PERFORMANCES OF A DATE DISSEMINATION CODE ON TELEPHONE LINES USING COMMERCIAL MODEMS
F. Cordara, V. Pettiti, R. Quasso (Politecnico di Torino, Italy.), and E. Rubiola (Politecnico di Torino, Italy.) *In* NASA. Goddard Space Flight Center, The 24th Annual Precise Time and Time Interval (PTTI) Applications and Planning Meeting Jun. 1993 p 243-254 (For primary document see N94-10963 01-70)
Avail: CASI HC A03/MF A04

N94-10989*# Nippon Telegraph and Telephone Public Corp., Yokosuka (Japan). Transmission Systems Labs.
TIME SIGNAL DISTRIBUTION IN COMMUNICATION NETWORKS BASED ON SYNCHRONOUS DIGITAL HIERARCHY
Atsushi Imaoka and Masami Kihara *In* NASA. Goddard Space Flight Center, The 24th Annual Precise Time and Time Interval (PTTI) Applications and Planning Meeting Jun. 1993 p 303-312 (For primary document see N94-10963 01-70)
Avail: CASI HC A02/MF A04

N94-10990*# Telecom Solutions Ltd., San Jose, CA.
SYNOPSIS OF TIMING MEASUREMENT TECHNIQUES USED IN TELECOMMUNICATIONS
George Zampetti *In* NASA. Goddard Space Flight Center, The 24th Annual Precise Time and Time Interval (PTTI) Applications and Planning Meeting Jun. 1993 p 313-326 (For primary document see N94-10963 01-70)
Avail: CASI HC A03/MF A04

N94-10991*# Bell Telephone Labs., Inc., Holmdel, NJ.
TIMING IN PRIVATE DIGITAL TELECOMMUNICATION NETWORKS
J. E. Abate, C. D. Near, and M. S. Russo *In* NASA. Goddard Space Flight Center, The 24th Annual Precise Time and Time Interval (PTTI) Applications and Planning Meeting Jun. 1993 p 327-336 (For primary document see N94-10963 01-70)
Avail: CASI HC A02/MF A04

N94-10996*# Computer Sciences Corp., Patrick AFB, FL.
ANALYSIS OF THE EASTERN RANGE MULTIPLEXED FIBER OPTIC IRIG B120 DISTRIBUTION SYSTEM
Michael J. Duncan, John S. Martell, and James L. Wright *In* NASA. Goddard Space Flight Center, The 24th Annual Precise Time and Time Interval (PTTI) Applications and Planning Meeting Jun. 1993 p 375-384 (For primary document see N94-10963 01-70)
Avail: CASI HC A02/MF A04

N94-11000*# Jet Propulsion Lab., California Inst. of Tech., Pasadena.
SPACECRAFT SIGNAL SOURCES PORTABLE TEST SYSTEM
Albert Kirk, Paul Kuhnle, Richard Sydnor, William Diener, and David Stowers *In* NASA. Goddard Space Flight Center, The 24th Annual Precise Time and Time Interval (PTTI) Applications and Planning Meeting Jun. 1993 p 427-438 (For primary document see N94-10963 01-70)
Avail: CASI HC A03/MF A04

N94-11902 Ministry of Posts and Telecommunications, Okinawa (Japan). Okinawa Radio Observatory.
HF OCEAN RADAR SYSTEM AT OKINAWA RADIO OBSERVATORY
Hiroshi Kuroiwa, Yuuichi Oono, Yukiharu Hisaki, and Akitsugu Nadai *In* Scientific Organizing Committee of PORSEC, Proceedings of the PORSEC 1992 in Okinawa: Conference for Pacific Ocean Environments and Probing, Volume 1 25 Aug. 1992 p 47-52 (For primary document see N94-11894 01-42)
Copyright Avail: Issuing Activity (Scientific Organizing Committee of PORSEC, P.O. Box 10, Shimizu, Shizuoka 424, Japan, HC)

N94-11905 Ministry of Posts and Telecommunications, Okinawa (Japan). Okinawa Radio Observatory.
STATISTICAL STUDY OF HF OCEAN RADAR ECHO
Akitsugu Nadai *In* Scientific Organizing Committee of PORSEC, Proceedings of the PORSEC 1992 in Okinawa: Conference for Pacific Ocean Environments and Probing, Volume 1 25 Aug. 1992 p 65-70 (For primary document see N94-11894 01-42)
Copyright Avail: Issuing Activity (Scientific Organizing Committee of PORSEC, P.O. Box 10, Shimizu, Shizuoka 424, Japan, HC)

N94-11906 James Cook Univ. of North Queensland, Townsville (Australia). Dept. of Physics.
GROUNDWAVE HF OCEAN SURFACE RADAR
M. L. Heron and N. R. McLaren *In* Scientific Organizing Committee of PORSEC, Proceedings of the PORSEC 1992 in Okinawa: Conference for Pacific Ocean Environments and Probing, Volume 1 25 Aug. 1992 p 71-75 (For primary document see N94-11894 01-42)
Copyright Avail: Issuing Activity (Scientific Organizing Committee of PORSEC, P.O. Box 10, Shimizu, Shizuoka 424, Japan, HC)

N94-11917 Japan Marine Science and Technology Center, Tokyo.
STUDY ON COLOR VIDEO PICTURES TRANSMISSION BY DIGITAL ACOUSTIC SIGNAL
Hiroshi Ochi, Toshio Tsuchiya, Yasutaka Amitani, Michiya Suzuki (Nippon Electric Co. Ltd., Japan.), and Satoru Negishi (Nippon Electric Co. Ltd., Japan.) *In* Scientific Organizing Committee of PORSEC, Proceedings of the PORSEC 1992 in Okinawa: Conference for Pacific Ocean Environments and Probing, Volume 1 25 Aug. 1992 p 132-137 (For primary document see N94-11894 01-42)
Copyright Avail: Issuing Activity (Scientific Organizing Committee of PORSEC, P.O. Box 10, Shimizu, Shizuoka 424, Japan, HC)

N94-11965 Japan Marine Science and Technology Center, Tokyo.
DEVELOPMENT OF SHIPBOARD OCEAN LIDAR
Ichio Asanuma, Kei Muneyama, and Motoaki Kishino (Institute of Physical and Chemical Research, Tokyo, Japan.) *In* Scientific Organizing Committee of PORSEC, Proceedings of the PORSEC 1992 in Okinawa: Conference for Pacific Ocean Environments and Probing, Volume 1 25 Aug. 1992 p 413-418 (For primary document see N94-11894 01-42)
Copyright Avail: Issuing Activity (Scientific Organizing Committee of PORSEC, P.O. Box 10, Shimizu, Shizuoka 424, Japan, HC)

N94-12706 Komatsu Ltd. (Japan). Research Div.
RESISTIVITY AND RADAR VOID DETECTORS FOR TUNNELING MACHINES
A. Khan, T. Abe, K. Shibatani, H. Yamaguchi, T. Shinbo, S. Sakanishi, and A. Okamoto *In* Scientific Organizing Committee of PORSEC, Proceedings of the PORSEC 1992 in Okinawa: Conference for Pacific Ocean Environments and Probing, Volume 2 25 Aug. 1992 p 958-963 Original contains color illustrations (For primary document see N94-12635 01-42)
Copyright Avail: Issuing Activity (Scientific Organizing Committee of PORSEC, P.O. Box 10, Shimizu, Shizuoka 424, Japan, HC)

33 ELECTRONICS AND ELECTRICAL ENGINEERING

Includes test equipment and maintainability; components, e.g., tunnel diodes and transistors; microminiaturization; and integrated circuitry.

For related information see also *60 Computer Operations and Hardware* and *76 Solid-State Physics.*

N94-10300# Brookhaven National Lab., Upton, NY.
FABRICATION AND TEST OF A SUPERCONDUCTING RFQ
A. Jain, H. Wang, I. Ben-Zvi, P. Paul, J. W. Noe, and A. Lombardi (Istituto Nazionale di Fisica Nucleare, Legnaro, Italy.) 1992 4 p Presented at the 1992 International Conference of Applications of Particle Accelerators, Denton, TX, Oct. 1992
(Contract DE-AC02-76CH-00016)
(DE93-010860; BNL-48570; CONF-9210337-1) Avail: CASI HC A01/MF A01

The fabrication and first performance tests of a prototype superconducting radio-frequency quadrupole resonator (SRFQ) are described. The SRFQ operates at 57 MHz and is optimized for a particle velocity of beta = 0.033. It is constructed of copper electroplated with a lead-tin alloy. An accelerating field gradient of 1.25 MV/m was achieved with about 7 watts of helium dissipation. This corresponds to an energy gain of 700 keV per unit charge over the 56 cm overall diameter of the resonator. DOE

N94-10309# Lawrence Livermore National Lab., CA.
EFFECTS OF AQUEOUS SOLUTION COMPOSITIONS ON AEROCAPACITOR ENERGY DENSITY
S. T. Mayer, J. L. Kaschmitter, and R. W. Pekala Nov. 1992 7 p Presented at the Electrochemical Society Meeting, Honolulu, HI, 16-21 May 1993
(Contract W-7405-eng-48)
(DE93-013431; UCRL-JC-112177; CONF-930571-12) Avail: CASI HC A02/MF A01

The Aerocapacitor is an electrochemical double-layer energy-storage device that utilizes carbon aerogels as electrodes. In this paper, the effect of 1M electrolyte composition on the Aerocapacitor's average-integral (AIC) and differential capacitance is investigated. The AIC values range from 7.2 to 22.5 F/cc for the electrode formulation used in this study. Typically, the AIC increase by a factor of two, and the differential capacitance by a factor of four, between 0 and 1.2 V. DOE

N94-10377# Department of the Navy, Washington, DC.
THIN-FILM EDGE FIELD EMITTER DEVICE AND METHOD OF MANUFACTURE THEREFORE Patent Application
Henry F. Gray, inventor (to Navy) and David S. Hsu, inventor (to Navy) 31 Mar. 1993 36 p
(AD-D015764; US-Patent-Appl-SN-040944) Avail: CASI HC A03/MF A01

It is therefore an object of the present invention to provide a field emitter device which substantially eliminates the need for the use of high spatial resolution lithography in its fabrication. It is another object of the present invention to provide a field emitter device having inherent advantages over previous electron sources, including higher emission currents, lower power requirements, less expensive fabrication costs and ease of integration with other circuitry. It is a further object of the present invention to fabricate gated and ungated thin-film edge field emitter devices wherein the spacing between the elements is small enough to enable low voltage operation. It is a further object of the present invention to fabricate FEA's over a large area in a manner which is inexpensive, yet results in an equal or greater degree of precision and reproducibility when compared with other prior art processes. DTIC

N94-10384# Department of the Navy, Washington, DC.
CONTINUOUS-TIME ADAPTIVE LEARNING CIRCUIT Patent Application
Francis J. Kub, inventor (to Navy) and Eric A. Justh, inventor (to Navy) 31 Dec. 1992 13 p
(AD-D015773; US-Patent-Appl-SN-984111) Avail: CASI HC A03/MF A01

This patent application discloses a continuous-time multiplier-integrator-multiplier circuit in which the integrator is a transconductance-C circuit. This permits the integrators to have long time constants despite being tightly fabricated on the integrated semiconductor chip. The multipliers can preferably be Gilbert multipliers to improve circuit frequency response. DTIC

N94-10389# Department of the Navy, Washington, DC.
MICROWAVE MULTIPLEXER WITH CHANNELS OF VARYING FRACTIONAL BANDWIDTHS Patent Application
Christen Rauscher, inventor (to Navy) 29 Jan. 1993 27 p
(AD-D015754; US-Patent-Appl-SN-010948) Avail: CASI HC A03/MF A01

A multiplexer includes a first channel segment having first components derived from a first log-periodically scaled prototype. The first channel segment receives a composite signal from a composite-signal port, selects a first channel having a first bandwidth and first center frequency from the composite signal, and directs a first channelized signal to the first channelized-signal port responsive to the first channel. In addition, the multiplexer includes a second channel segment, connected to the first channel segment and having second components derived from a second log-periodically scaled prototype. The second channel segment receives the portions of the composite signal from the composite-signal port via the first segment, selects a second channel having a second bandwidth and second center frequency from the composite signal, and directs a second channelized signal to a second channelized-signal port responsive to the second channel. DTIC

N94-10390# Department of the Navy, Washington, DC.
ALUMINUM BASED ALKALINE BATTERY Patent Application
James R. Moden, inventor (to Navy) and Zoe Adamedes, inventor (to Navy) 26 Feb. 1993 11 p
(AD-D015775; US-Patent-Appl-SN-017918) Avail: CASI HC A02/MF A01

A battery is provided comprising an aluminum anode, an alkali aqueous solution of controlled concentration and temperature and a second electrode operates with high anode efficiency. DTIC

N94-10505*# Sverdrup Technology, Inc., Brook Park, OH.
LIGHTWEIGHT LINEAR ALTERNATORS WITH AND WITHOUT CAPACITIVE TUNING
Janis M. Niedra Jun. 1993 58 p
(Contract NAS3-25266; RTOP 583-02-21)
(NASA-CR-185273; E-7929; NAS 1.26:185273) Avail: CASI HC A04/MF A01

Permanent magnet excited linear alternators rated tens of kW and coupled to free-piston Stirling engines are presently viewed as promising candidates for long term generation of electric power in both space and terrestrial applications. Series capacitive cancellation of the internal inductive reactance of such alternators was considered a viable way to both increase power extraction and to suppress unstable modes of the thermodynamic oscillation. Idealized toroidal and cylindrical alternator geometries are used for a comparative study of the issues of specific mass and capacitive tuning, subject to stability criteria. The analysis shows that the stator mass of an alternator designed to be capacitively tuned is always greater than the minimum achievable stator mass of an alternator designed with no capacitors, assuming equal utilization of materials ratings and the same frequency and power to a resistive load. This conclusion is not substantially altered when the usually lesser masses of the magnets and of any capacitors are added. Within the reported stability requirements and under circumstances of normal materials ratings, this study finds no clear advantage to capacitive tuning. Comparative plots of the various constituent masses are presented versus the internal power factor taken as a design degree of freedom. The explicit formulas developed for stator core, coil, capacitor, and magnet masses and for the degree of magnet utilization provide useful estimates of scaling effects. Author (revised)

N94-10509 Range Commanders Council, White Sands Missile Range, NM. Telemetry Group.
THE 17TH TRANSDUCER WORKSHOP
Jun. 1993 296 p Workshop held in San Diego, CA, 22-24 Jun. 1993 Limited Reproducibility: Document partially illegible
(AD-A265526) Avail: Issuing Activity (Defense Technical Information Center (DTIC))

This committee apprises the Telemetry Group (TG) of significant progress in the field of transducers used in telemetry systems; maintains any necessary liaison between the TG and the National Institute of Standards and Technology and their transducers' program or other related telemetry transducer efforts; coordinates TG activities with other professional technical groups; collects and passes on information on techniques of measurement, evaluation, reliability, calibration, reporting, and manufacturing; recommends uniform practices for calibration, testing, and evaluation of vehicular instrumentation components; and contributes to standards in the area of vehicular instrumentation. DTIC

N94-10521# Sandia National Labs., Albuquerque, NM.
APPLICATION OF NORMALIZED GRAY-SCALE CORRELATION
M. Yee, F. M. Dickey, K. T. Stalker, and B. A. Kast (Spectra Research Inst., Albuquerque, NM.) 1993 11 p Presented at the Society of Photo-Optical Instrumentation Engineers (SPIE) OE/Aerospace Science and Sensing Meeting, Orlando, FL, 11-16 Apr. 1993
(Contract DE-AC04-76DP-00789)
(DE93-013765; SAND-93-0539C; CONF-930445-12) Avail: CASI HC A03/MF A01

Real-time gray-scale correlation in the spatial domain has been demonstrated previously using an acousto-optical (AO) correlator. This work demonstrates normalized gray-scale correlation as implemented on an AO correlator system capable of operating at real-time video rates. The motivation for using normalized gray-scale correlation is presented. The normalized correlation algorithm as implemented on the AO correlator is detailed. The entire real-time AO correlator system is described including the electronic support hardware and the user interface. Since normalization requires a division operation, system numerical precision issues are addressed. Test results obtained in non-real time experiments are presented. DOE

N94-10533 Joint Inst. for Nuclear Research, Dubna (USSR). Lab. of Nuclear Problems.
DIRECT CURRENT TRANSDUCER [DATCHIK POSTOYANNOGO TOKA]
E. G. Batmanova, G. G. Kazakova, and V. V. Kalinichenko 1991 10 p In RUSSIAN Limited Reproducibility: More than 20% of this document may be affected by microfiche quality
(DE92-644548; JINR-R-13-91-282) Avail: CASI HC A02 (US Sales Only)

A direct current transducer based on magnetic comparison of direct currents is discussed. The principle of operation of the transducer is considered, its blockdiagram, circuit diagram, and technical solutions for some of its units are given. General zero drift of the transducer, reduced to the current measured, does not exceed 0.1 A. The output voltage of the transducer is 10 V at the rated value of the current measured. DOE

N94-10543 Academy of Sciences of the Ukraine, Kharkov. Fiziko-Tekhnicheskij Inst.
ON THE STABILITY OF STATIONARY REGIMES IN A DISTRIBUTED AUTOVIBRATION SYSTEM WITH EXTERNAL FEEDBACK [OB USTOJCHIVOSTI STATSIONARNYKH REZHIMOV V RASPREDELENNOJ AVTOKOLEBATEL'NOJ SISTEME S VNESHNEJ SVYAZ'YU]
N. I. Ajzatskij and A. O. Ostrovskij 1991 15 p In RUSSIAN Limited Reproducibility: More than 20% of this document may be affected by microfiche quality
(DE93-620979; KFTI-91-39) Avail: CASI HC A03 (US Sales Only)

A numerical investigation of the distributed autogenerator stationary state stability is described. It was shown that the realization of stable stationary excitation of resonance frequency vibrations strongly depends on the normalized nonlinear amplifier length (l). At small l-values such a regime is unstable, but with increasing of this parameter, the autovibration system becomes stable. Linear characteristics of stationary regime instability are found. It was shown that in the considered range of dynamic system non-equilibrium parameter changes, two stationary generation regimes on different frequencies correspond to the same autogenerator transmitting characteristics. DOE

N94-10656* National Aeronautics and Space Administration. Pasadena Office, CA.
METHOD FOR PRODUCING A HYBRIDIZATION OF DETECTOR ARRAY AND INTEGRATED CIRCUIT FOR READOUT Patent
Eric R. Fossum, inventor (to NASA) (Jet Propulsion Lab., California Inst. of Tech., Pasadena.) and Frank J. Grunthaner, inventor (to NASA) (Jet Propulsion Lab., California Inst. of Tech., Pasadena.) 17 Aug. 1993 7 p Filed 29 Apr. 1992 Supersedes N92-305542 (30 - 21, p 3623)
(NASA-Case-NPO-18062-1-CU; US-Patent-5,236,871;
US-Patent-Appl-SN-877966; US-Patent-Class-437-195;
US-Patent-Class-437-3; US-Patent-Class-437-5; US-Patent-Class-437-203;
US-Patent-Class-437-234; US-Patent-Class-148-DIG.80;
Int-Patent-Class-H01L-21/44) Avail: US Patent and Trademark Office

A process is explained for fabricating a detector array in a layer of semiconductor material on one substrate and an integrated readout circuit in a layer of semiconductor material on a separate substrate in order to select semiconductor material for optimum performance of each structure, such as GaAs for the detector array and Si for the integrated readout circuit. The detector array layer is lifted off its substrate, laminated on the metallized surface on the integrated surface, etched with reticulating channels to the surface of the integrated circuit, and provided with interconnections between the detector array pixels and the integrated readout circuit through the channels. The adhesive material for the lamination is selected to be chemically stable to provide electrical and thermal insulation and to provide stress release between the two structures fabricated in semiconductor materials that may have different coefficients of thermal expansion.
Official Gazette of the U.S. Patent and Trademark Office

N94-10668 Department of the Army, Washington, DC.
DIELECTRIC RESONATOR Patent
Arthur Ballato, inventor (to Army) 1 Apr. 1986 5 p Filed 11 Feb. 1985 Supersedes AD-D011573
(US-Patent-4,580,116; US-Patent-Appl-SN-699990;
US-Patent-Class-333-234; US-Patent-Class-333-219;
US-Patent-Class-333-235; Int-Patent-Class-H01P-7/10) Avail: US Patent and Trademark Office

This invention relates generally to signal oscillators and more particulary to microwave and millimeter wave oscillators comprised of dielectric resonators. A method and means for producing a zero temperature coefficient for providing frequency stabilization as well as adjusting the frequency at a particular temperature of a dielectric resonator element mounted on a substrate and having a dielectric disc affixed to the top of the resonator element is discussed. A zero temperature coefficient is obtained by selectively choosing the thickness of the dielectric disc depending upon the temperature coefficients of the constituent material of both the disc and resonator element. The operating frequency at a given temperature is furthermore adjusted by including two mutually contiguous patterns of metallization on the top surface of the resonator element and the bottom surface of the dielectric disc and thereafter rotating the disc so that a predetermined percentage of overlap between the two patterns exists.
DTIC

N94-10799 International Centre for Theoretical Physics, Trieste (Italy).
EFFECT OF EFFECTIVE MASS DIFFERENCES ON THE TUNNELING CURRENT-VOLTAGE BEHAVIOUR OF A RESONANT DIODE IN THE PRESENCE OF SPACE CHARGE BUILD-UP
F. B. Sigalo and S. Y. Mensah Sep. 1992 14 p Limited Reproducibility: More than 20% of this document may be affected by microfiche quality
(DE93-613817; IC-92/300) Avail: Issuing Activity (Department of Energy (DOE)) (US Sales Only)

A theoretical study of the effect of differences in effective masses for electrodes and well, on the characteristics of tunneling current against bias voltage, in the presence of charge build-up was conducted. It is observed that balanced effective mass (i.e M(sup *)(sub l) = m(sup *)(sub r)), where m(sup *)(sub l) and m(sup *)(sub r) are the effective masses for electrode and well, respectively, results in the normal expected behaviour of rising current with increased bias voltage. Whereas, a positive difference causes charge saturation and zero current change, while a negative difference invokes excess current flow. DOE

N94-10818 Hughes Aircraft Co., Torrance, CA. Electron Dynamics Div.
RF VACUUM MICROELECTRONICS Quarterly Technical Report No. 4, 1 Jan. - 31 Mar. 1993
31 Mar. 1993 14 p Limited Reproducibility: More than 20% of this document may be affected by microfiche quality
(Contract MDA972-92-C-0034; ARPA Order 8162)
(AD-A266066) Avail: CASI HC A03

All layers of mask set 2 were received prior to Feb. 1. A photograph of the overall reticle layout is shown. There are 16 reticles per 1 in. wafer and 9 different chips per reticle for a total of 149 chips of which about 120 are expected to be usable (about 30 chips are too close to the wafer edge). On this mask set, we concentrated on straightforward arrays of tips of different sizes oriented in such a way that they could be conveniently packaged onto TO-8 headers. In the previous experiments, we found the most significant impediment to consistency in testing was the bonding, die-attaching, and packaging. DTIC

N94-10931*# Toledo Univ., OH. Dept. of Electrical Engineering.
A STUDY OF DC-DC CONVERTERS WITH MCTS FOR ARCJET POWER SUPPLIES
Thomas A. Stuart, Roger J. King, and Brian J. Masserant Jan. 1993 78 p
(Grant NAG3-1102)
(NASA-CR-193457; NAS 1.26:193457) Avail: CASI HC A05/MF A01

Many arcjet DC power supplies use PWM full bridge converters with large arrays of parallel FET's. This report investigates an alternative supply using a variable frequency series resonant converter with small arrays of parallel metal oxide semiconductor controlled thyristors (MCT's). The reasons for this approach are to: increase reliability by reducing the number of switching devices; and decrease the surface mounting area of the switching arrays. The variable frequency series resonant approach is used because the relatively slow switching speed of the MCT precludes the use of PWM. The 10 KW converter operated satisfactorily with an efficiency of over 91 percent. Test results indicate this efficiency could be increased further by additional optimization of the series resonant inductor. Author (revised)

N94-10951 Argonne National Lab., IL. Materials and Components Technology Div.
DEVELOPMENT OF COMMERCIALLY VIABLE HIGH-T(SUB c) Bi-2223 SUPERCONDUCTOR TAPES
U. Balachandran, C. A. Youngdahl, P. Haldar (Intermagnetics General Corp., Guilderland, NY.), and L. R. Motowidlo (IGC/Advanced Supercomputers, Inc., Waterbury, CT.) Feb. 1993 9 p Presented at the 5th Annual International Superconductor Applications Conference, San Jose, CA, 1-3 Feb. 1993 Limited Reproducibility: More than 20% of this document may be affected by microfiche quality
(Contract W-31-109-eng-38)
(DE93-009966; ANL/MCT/CP-78926; CONF-930235-1) Avail: CASI HC A02

Long lengths of flexible Ag-clad Bi-2223 Superconductors have been fabricated by the powder-in-tube technique using prereacted, poly-phase, Pb-doped Bi-Sr-Ca-Cu-O powders. At the temperature of liquid helium (4.2 K), improved process conditions yielded transport critical current density (J(sub c)) values greater than 10(exp 5) A/sq cm at zero field; at the temperature of liquid nitrogen (77K), the J(sub c) values of short tape samples exceeded 4(10)(exp 4) A/sq cm. Rolled tapes are cut into lengths up to 2 m in length and are used in parallel to fabricate small superconducting pancake coils by the 'wind-and-react' technique. The coils are characterized at 77 K and 4.2 K. The J(sub c) of the coils are up to 80% of the short, rolled sample result at 77 K. The coils exhibited these results even after being cooled and warmed several times between ambient, 77 K, and 4.2 K indicating their stability following thermal cycling. DOE

N94-11009# Lawrence Livermore National Lab., CA.
ELECTROMECHANICAL BATTERIES AND THE ELECTRIC LOCOMOTIVE
R. F. Post 21 Sep. 1992 4 p
(Contract W-7405-eng-48)
(DE93-013311; UCRL-ID-111855) Avail: CASI HC A01/MF A01

This technical note describes an electromechanical battery to be used as an electrical storage system for powering locomotives instead of traditional diesel-electric generators. The electromechanical battery would entail a high-speed rotor, supported by a magnetic suspension/bearing system, and carrying an integrally mounted generator/motor; the whole operating in an evacuated enclosure. The concept also includes the concept of modularity, i.e. using many relatively small units to build up a battery bank, in the same manner that ordinary batteries are used. This note emphasizes the rotor, its material, and its volumetric energy storage density. DOE

N94-11050# Lawrence Livermore National Lab., CA.
A PICOSECOND HIGH PRESSURE GAS SWITCH
W. R. Cravey, P. P. Poulsen, and P. A. Pincosy Jun. 1992 6 p Presented at the 20th International Power Modulator Symposium, Myrtle Beach, SC, 23-25 Jun. 1992
(Contract W-7405-eng-48)
(DE93-011897; UCRL-JC-110977; CONF-920671-14) Avail: CASI HC A02/MF A01

Work is being done to develop a high pressure gas switch (HPGS) with picosecond risetimes for UWB applications. Pulse risetimes on the order of 200 picoseconds have been observed at 1 kHz prf and 1 atmosphere. Calculations show that switching closure times on the order of tens of picoseconds can be achieved at high pressures and higher electric fields. A voltage hold-off of 1 MV/cm has been measured at 10 atmospheres and several MV/cm appears possible with the HPGS. With these high electric field levels, energy storage of tens of Joules in a reasonably sized package is achievable. Initial HPGS performance has been characterized on the WASP pulse generator at LLNL. A detailed description of the switch used for initial testing is given. Switch recovery times of 1-ms have been measured at 1 atmosphere. Data on the switching uniformity, voltage hold-off recovery, and pulse repeatability, is presented. In addition, a physics switch model is described and results are compared with lab data. DOE

N94-11094# North Carolina Univ., Chapel Hill. Dept. of Chemistry.
ELLIPSOMETRY STUDIES OF SEMICONDUCTORS SURFACE CLEANING
E. A. Irene and Y. Z. Hu 4 May 1993 8 p
(Contract N00014-89-J-1178)
(AD-A265150; TR-55) Avail: CASI HC A02/MF A01

Ellipsometry is shown to provide a sensitive evaluation of the surface cleaning process based on in-situ and ex-situ studies of the cleaning of Si, Ge, and InP surfaces. Both single wavelengths and spectroscopic ellipsometry are shown to be applicable. The essentials of the measurement and sample results are discussed. DTIC

N94-11131*# Computer Technology Associates, Inc., Hampton, VA.
NODE ASSIGNMENT IN HETEROGENEOUS COMPUTING Report, May - Aug. 1992
Sukhamoy Som Washington Aug. 1993 39 p
(Contract NAS1-18936; RTOP 586-03-11)
(NASA-CR-4534; NAS 1.26:4534; Rept-038-3524-150-93-1) Avail: CASI HC A03/MF A01

A number of node assignment schemes, both static and dynamic, are explored for the Algorithm to Architecture Mapping Model (ATAMM). The architecture under consideration consists of heterogeneous processors and implements dataflow models of real-time applications. Terminology is developed for heterogeneous computing. New definitions are added to the ATAMM for token and assignment classifications. It is proved that a periodic execution is possible for dataflow graphs. Assignment algorithms are developed and proved. A design procedure is described for satisfying an objective function in an heterogeneous architecture. Several examples are provided for illustration. Author

N94-11159# North Carolina Univ., Chapel Hill. Dept. of Chemistry.
APPLICATIONS OF SPECTROSCOPIC ELLIPSOMETRY TO MICROELECTRONICS Technical Report
E. A. Irene 4 May 1993 43 p
(Contract N00014-89-J-1178)
(AD-A265148) Avail: CASI HC A03/MF A01

Ellipsometry has been applied to problems in the microelectronics industry from the beginning in the 1960's. More recently spectroscopic ellipsometry has been introduced. In-situ during process ellipsometry offers great promise for monitoring and control of a wide variety of microelectronics processes. This review covers some applications in silicon technology such as oxidation, chemical vapor deposition, etching, interfaces, and new processing techniques such as plasma, ion beam, and rapid thermal, in an effort to demonstrate the kinds of crucial microelectronics information and processes that modern ellipsometry can access. The conclusion is that single wavelength ellipsometry alone is not sufficient; spectroscopic ellipsometry is required to establish the optimum ellipsometry measurement conditions. The future of ellipsometry in microelectronics is assessed. DTIC

N94-11160# North Carolina Univ., Chapel Hill. Dept. of Chemistry.
CHARACTERIZATION OF THE SI/SIO2 INTERFERE MORPHOLOGY FROM QUANTUM OSCILLATIONS IN FOWLER-NORDHEIM TUNNELING CURRENTS Technical Report
J. C. Poler, K. K. McKay, and E. A. Irene 4 May 1993 41 p
(Contract N00014-89-J-1178)
(AD-A265149; TR-52) Avail: CASI HC A03/MF A01

As design rules shrink to conform with ULSI device dimensions, gate dielectrics for MOSFET structures are required to be scaled to below-60A where some properties of the device, such as interface roughness, that are negligible for thicker films become critical. Microroughness at the interface of ultrathin MOS capacitors has been shown to degrade these devices. DTIC

N94-11271# Sandia National Labs., Albuquerque, NM.
EFFECT OF SWITCHED-BIAS BAKES ON THE POSTIRRADIATION ELECTRICAL RESPONSE OF MOS DEVICES
D. M. Fleetwood, M. R. Shaneyfelt, L. C. Riewe, and P. S. Winokur 1993 5 p Presented at the Nuclear and Space Radiation Effects Conference, Snowbird, UT, 19-23 Jul. 1993
(Contract DE-AC04-76DP-00789)
(DE93-009629; SAND-93-0346C; CONF-930704-7) Avail: CASI HC A01/MF A01

Qualitatively different trends in postirradiation electrical response are observed in MOS devices after very long (up to 2.75-year) switched-bias bakes. A revised defect nomenclature is introduced, and implications for MOS defect models are discussed. DOE

N94-11273# Lawrence Livermore National Lab., CA.
RADIATION HARDNESS OF Mo/Si MULTILAYERS DESIGNED FOR USE IN A SOFT X RAY PROJECTION LITHOGRAPHY SYSTEM
D. P. Gaines, R. C. Spitzer, N. M. Ceglio, M. Krumrey, and G. Ulm Sep. 1992 21 p Presented at the Soft X Ray Projection Lithography Topical Meeting, Monterey, CA, 6-8 Apr. 1992
(Contract W-7405-eng-48)
(DE93-011879; UCRL-JC-111725; CONF-9204120-6) Avail: CASI HC A03/MF A01

A molybdenum silicon multilayer was irradiated with 13.4 nm radiation to investigate changes in multilayer performance under simulated Soft X-ray Projection Lithography (SXPL) conditions. The wiggler/undulator at the Berlin electron storage ring BESSY was used as a quasi-monochromatic source of calculable spectral radiant intensity and was configured to simulate an incident SXPL x-ray spectrum. The test multilayer received a radiant exposure of 240 J/sq mm in an exposure lasting 8.9 hours. The corresponding average incident power density was 7.5 mW/sq mm. The absorbed dose of 7.8 x 10(exp 10) J/kg (7.8 x 10(exp 12) rd) is equivalent to 1.2 times the dose that would be absorbed by a multilayer coating on the first imaging optic in a hypothetical SXPL system during one year of operation. Surface temperature increases did not exceed 2 C during the exposure. Normal incidence reflectance measurements at lambda(sub 0) = 13.4 nm performed prior to radiation exposure were in agreement with measurements performed after the exposure, indicating that no significant damage had occurred. DOE

N94-11285# Sandia National Labs., Albuquerque, NM.
RELATIONSHIP BETWEEN IBICC IMAGING AND SEU IN CMOS ICs
F. W. Sexton, K. M. Horn, B. L. Doyle, J. S. Laird (Melbourne Univ., Parkville, Australia.), M. Cholewa (Melbourne Univ., Parkville, Australia.), A. Saint (Melbourne Univ., Parkville, Australia.), and G. J.F. Legge (Melbourne Univ., Parkville, Australia.) 1993 4 p Presented at the Nuclear and Space Radiation Effects Conference, Snowbird, UT, 19-23 Jul. 1993
(Contract DE-AC04-76DP-00789)
(DE93-009854; SAND-93-0595C; CONF-930704-8) Avail: CASI HC A01/MF A01

Ion-beam-induced charge-collection (IBICC) images of the TA670 16K-bit CMOS SRAM are analyzed and compared to previous SEU images. Enhanced charge collection was observed in the n-source/drains regions consistent with bipolar amplification or shunting. DOE

N94-11298 Prins Maurits Lab. TNO, Rijswijk (Netherlands).
CHARACTERIZATION OF THE PULSE TRANSFORMER Final Report
W. H. Mosterdijk Dec. 1992 32 p In DUTCH Limited Reproducibility: More than 20% of this document may be affected by microfiche quality
(AD-A263414; ISL-PML-1992-73) Avail: Issuing Activity (Defense Technical Information Center (DTIC))

This report treats characterization of the pulse transformer at TNO PML Pulse Physics, Delft. The pulse transformer constitutes the final step of an energy compression system, called the Kapitza facility, and is able to amplify the current up to 24 times. The pulse transformer consists of a primary single layer winding of 24 turns which is enclosed by an aluminium secondary winding, consisting of one inner- and one outer which are coupled in parallel. Characterization means: determination of the electrical quantities, such as the ohmic resistance and the inductance of the primary and secondary windings. A current source able to deliver single-wave currents with adjustable frequencies was used. From the measurement it appears that the main inductances decrease and the ohmic resistances increase with increasing frequency. This is caused by differential currents, skin and proximity effect, and parasitic induced currents in aluminum secondary winding. DTIC

N94-11365 Academy of Sciences of the Ukraine, Kharkov. Fiziko-Tekhnicheskij Inst.
NON-LINEAR DYNAMICS OF AUTOMODULATION PROCESSES IN COUPLED DISTRIBUTED AUTOVIBRATION SYSTEMS WITH DELAY [NELINEJNAYA DINAMIKA AVTOMODULYATSIONNYKH PROTSESSOV V SVYAZANNYKH RASPREDELENNYKH AVTOKOLEBATEL'NYKH SISTEMAKH S ZAPAZDYVANIEM]
A. O. Ostrovskij and Y. V. Tkach 1991 20 p In RUSSIAN Limited Reproducibility: More than 20% of this document may be affected by microfiche quality
(DE93-620976; KFTI-91-30) Avail: CASI HC A03 (US Sales Only)

The dynamics of autovibration processes in a system of narrow-band autogenerators coupled in a distributive manner with delayed feedback is considered. A system of self-consistent equations describing the space-time dynamics of HF field excitation in coupled electrodynamic delaying structures is obtained. Numerical modelling shows that the coupling of the autogenerators leads to a decrease in the non-equilibrium parameter in a dynamic system compared with an isolated autogenerator. The effectiveness of electron beam energy transfer into electromagnetic radiation energy is defined. DOE

N94-11454# Argonne National Lab., IL.
ASSESSMENT OF THE IMPACT OF HTSC'S ON SUPERCONDUCTING FAULT-CURRENT LIMITERS
R. F. Giese and M. Runde (Electric Power Research Inst., Trondheim, Norway.) 1993 8 p Presented at the 55th Annual American Power Conference, Chicago, IL, 13-15 Apr. 1993 Prepared in cooperation with

Energiforsyningens Forskningsinstitutt A/S, Trondheim, Norway
(Contract W-31-109-eng-38)
(DE93-009986; ANL/ES/CP-78917; CONF-930433-4) Avail: CASI HC A02/MF A01

The possible impact of nitrogen-cooled superconductors on the design and cost of superconducting fault-current limiters is assessed by considering the technical specifications such devices must meet and by comparing material properties of 77K and 4K superconductors. The main advantages of operating superconductors at 77K are that the refrigeration operating cost is reduced by a factor of up to 25 and the refrigeration capital cost is reduced by a factor of up to 10. The heat capacity is several orders of magnitude larger at 77K and at 4K. This phenomenon increases conductor stability against flux jumps but makes switching from the superconducting to the normal state slow and difficult. Therefore, a high critical current density, probably at least 10(exp 5) A/sq cm, is required. DOE

N94-11478# Allied-Signal Aerospace Co., Kansas City, MO.
ENSAFE FIRESET FLEX CIRCUIT ANALYSIS
W. R. Freeman Apr. 1993 47 p
(Contract DE-AC04-76DP-00613)
(DE93-013106; KCP-613-5113) Avail: CASI HC A03/MF A01

Finite element analysis (FEA) was used to investigate the possibility of mechanical damage or failure of an exceptionally flexible circuit design during assembly or thermal cycling. The circuit components are soldered to the flexible circuit while it is flat, then the circuit is wrapped into a partial cylinder shape for packaging purposes. Foam potting is applied, and the assembly is subjected to temperature changes. Analysis indicates that no mechanical problems should be expected during the wrapping process or because of thermal changes in the potting. DOE

N94-11479# Allied-Signal Aerospace Co., Kansas City, MO.
PROGRAMMABLE LOGIC DEVICES
J. L. Jacobs Apr. 1993 23 p
(Contract DE-AC04-76DP-00613)
(DE93-013117; KCP-613-5042) Avail: CASI HC A03/MF A01

Erasable programmable logic devices (EPLD's) were investigated to determine their advantages and/or disadvantages in Test Equipment Engineering applications. It was found that EPLD's performed as well as or better than identical circuits using standard transistor transistor logic (TTL). The chip count in these circuits was reduced, saving printed circuit board space and shortening fabrication and prove-in time. Troubleshooting circuits of EPLD's was also easier with 10 to 100 times fewer wires needed. The reduced number of integrated circuits (IC's) contributed to faster system speeds and an overall lower power consumption. In some cases changes to the circuit became software changes using EPLD's instead of hardware changes for standard logic. Using EPLD's was fairly easy; however, as with any new technology, a learning curve must be overcome before EPLD's can be used efficiently. The many benefits of EPLD's outweighed this initial inconvenience. DOE

N94-11508 Tokyo Univ., Tanashi (Japan). Inst. for Nuclear Study.
PERFORMANCE CHARACTERISTICS OF THE INS 25.5-MHz SPLIT COAXIAL RFQ
N. Tokuda, S. Arai, A. Imanishi, T. Morimoto, S. Shibuya, and E. Tojyo Apr. 1992 4 p Limited Reproducibility: More than 20% of this document may be affected by microfiche quality
(DE93-753168; INS-920) Avail: CASI HC A01

The performance of the INS 25.5-MHz split coaxial RFQ was clarified through high-power and acceleration tests. The cavity operates stably at a duty factor of 20% and a peak power of 80 kW, generating an intervane voltage of 109.3 kV, the design value for ions with a charge-to-mass ratio of 1/30. Acceleration tests were conducted to study the performance of the vanes machined by means of the two-dimensionally cutting technique. The results show that the A(sub 10) coefficient of the electric field will be close to the one calculated by Crandall, and that the field in the radial matching section might be different from the designed one. DOE

N94-11516 Wright State Univ., Dayton, OH. Dept. of Electrical Engineering.
GaAs SIGMA-DELTA MODULATOR MODELING FOR ANALOG TO DIGITAL CONVERTERS (ADC'S) Interim Report, 1 Jun. - 29 Dec. 1992
Eric Mahurin and Ray Siford Dec. 1992 18 p Limited Reproducibility: More than 20% of this document may be affected by faint or broken type
(Contract F33615-90-C-1405)
(AD-A263419; WL-TR-93-5006) Avail: Issuing Activity (Defense Technical Information Center (DTIC))

In this project a sigma-delta modulator has been designed. The circuit was designed and simulated using model parameters corresponding to the Vitesse 1.2 micron GaAs MESFET technology. The clock rate of the circuit is 512-MHz, and preliminary results show that it can be used for a 9-10 bit A/D converter accepting a 4-MHz input signal. This bandwidth could be used for video signals such as television. DTIC

N94-11607# Argonne National Lab., IL. Materials and Components Technology Div.
IMPROVEMENT OF AZIMUTHAL HOMOGENEITY IN PERMANENT-MAGNET BEARING ROTORS
J. R. Hull, T. D. Rossing, T. M. Mulcahy, and K. L. Uherka 23 Oct. 1992 3 p Presented at the International Magnetics Conference, Stockholm, Sweden, 13-16 Apr. 1993
(Contract W-31-109-eng-38)
(DE93-009954; ANL/MCT/CP-77835; CONF-930416-2) Avail: CASI HC A01/MF A01

Permanent magnets that are levitated and rotating over a bulk high-temperature superconductor (HTS) form the basis of many superconducting bearing designs. Experiments have shown that the rotational-loss 'coefficient of friction' for thrust bearings of this type can be as low as 8 x 10(exp -6). While the loss mechanisms of such bearings are not well understood, the azimuthal homogeneity of the rotating permanent magnet is believed to play an important role in determining the loss. One possible loss mechanism is magnetic hysteresis in the HTS, where the energy loss E per cycle is derived from the critical state model and given by E = K (Delta B)(sup 3)/J(sub c) where K is a geometric coefficient, Delta B is the variation in magnetic field at the surface of the HTS experienced during a rotation of the levitated magnet, and J(sub c) is the critical current density of the HTS. It is clear that a small decrease in Delta B (i.e., decreasing the azimuthal inhomogeneity of the rotating magnetic field) could have profound effects on decreasing E and the rotational coefficient of friction. The role of Delta B is also expected to be significant in reducing losses from eddy currents and other mechanisms. Low rotational losses in HTS bearings have been demonstrated only for levitated masses of several grams. For practical bearings, it is important to obtain these low losses with larger levitated masses. There are two main routes toward decreasing Delta B. The first is to improve the alignment of the magnetic particles during fabrication and to maintain close tolerances on grinding angles during manufacture of the permanent magnet. The second, the subject of this paper, is to provide correctional procedures after the magnet is fabricated. DOE

N94-11609# Kansas State Univ., Manhattan.
ELECTRIC AND HYBRID VEHICLE SITE OPERATORS PROGRAM: THINKING OF THE FUTURE
1993 31 p
(Contract DE-FC07-91ID-13074)
(DE93-011231; DOE/ID-13074/T7) Avail: CASI HC A03/MF A01

Kansas State University, with support from federal, state, public, and private companies, is participating in the Department of Energy's Electric Vehicle Site Operator Program. Through participation in this program, Kansas State is displaying, testing, and evaluating electric or hybrid vehicle technology. This participation will provide organizations the opportunity to examine the latest EHV prototypes under actual operating conditions. KSU proposes to purchase one electric or hybrid van and two electric cars during the first two years of this five-year program. KSU has purchased one G-Van built by Conceptor Industries, Toronto, Canada and has initiated a procurement order to purchase two Soleq 1993 Ford EVcort station wagons. The G-Van has been signed in order for the public to be aware that this is an electric drive vehicle. Financial participants' names have been stenciled on the back door of the van. This vehicle is available for short term loan to interested utilities and companies. When other vehicles are obtained, the G-Van will be maintained on K-State's campus. DOE

N94-11624# Sandia National Labs., Albuquerque, NM.
A THERMAL IONIZATION MODEL FOR THE SUSTAINING PHASE OF LOCK-ON IN GaAs

H. P. Hjalmarson, F. J. Zutavern, G. M. Loubriel, M. T. Buttram, A. G. Baca, and L. A. Romero 1992 10 p Presented at the OE/LASE 1993: International Society for Optical Engineering (SPIE) Conference, Los Angeles, CA, 16-23 Jan. 1993
(Contract DE-AC04-76DP-00789)
(DE93-011558; SAND-92-2857C; CONF-930159-28) Avail: CASI HC A02/MF A01

Thermal ionization of electrons and holes is proposed as an explanation for the sustained phase of lock-on in semi-insulating GaAs. In this mechanism, thermal ionization leads to a current instability which drives the formation of current filaments. The model predicts bistable states: either a highly conductive on-state or weakly conductive off-state. The model predicts that a transition from the off-state to a filamentary-current on-state can be triggered by illumination in agreement with experiments using photoexcitation. DOE

N94-11645# Maryland Univ., College Park. Lab. for Plasma Research.
THREE-CAVITY CIRCUIT STUDIES OF THE MARYLAND GYROKLYSTRON
C. D. Striffler, S. Tantawi, W. Main, B. Hogan, P. E. Latham, W. Lawson, U. V. Koc, H. W. Matthews, G. S. Nusinovich, and V. L. Granatstein 1992 4 p Presented at the 16th International LNAC Conference, Ottawa, Canada, 23-28 Aug. 1992
(Contract DE-FG05-91ER-40642)
(DE93-010173; CONF-9208109-80) Avail: CASI HC A01/MF A01

At the University of Maryland we have examined an X-Band TE(sub 01) mode three-cavity gyroklystron circuit that includes a tunable buncher cavity. The system parameters are: 425 kV, 100-200 A, pulse length approximately 1 (mu)s, operating frequency 9.85 GHz, and a beam alpha, upsilon(perpendicular)/upsilon(sub z), in the range 0.7-1.0. This circuit produced a maximum power of 27 MW at 32% efficiency and a gain of 36 dB. We will summarize the major results of the three-cavity systems, including recent output cavity configurations that were to affect the post-cavity interaction. DOE

N94-11819# Cornell Univ., Ithaca, NY. Dept. of Chemistry.
RESIST MATERIALS DESIGN: BASE-CATALYZED CHEMICAL AMPLIFICATION
C. G. Willson, J. F. Cameron, S. A. MacDonald, C. P. Niesert, and J. M. Frechet 12 May 1993 16 p
(Contract N00014-91-J-1338)
(AD-A265286; TR-11-ONR) Avail: CASI HC A03/MF A01

The search for advanced resists that can provide the high density of circuits and high throughput required for the new generations of microelectronic devices requires that highly stable chemically amplified materials be developed. In view of the high susceptibility of resists, based on photoacid generation, to environmental contamination, resulting in lessened performance, a program aimed at the development of chemically amplified resists utilizing photobase generation has been undertaken. In a first approach, the photogenerated amines we developed in the first stage of this project were used as catalysts for the decarboxylation of totally new resist systems containing active carboxylic acid pendant groups. The resist materials could be developed to afford negative tone images through wet development in aqueous base, or positive tone images through dry development using a gas-phase silylation reaction followed by oxygen plasma etching. The first patterning experiments carried out with two new resists utilizing photogenerated base have confirmed the validity of the approach. DTIC

N94-11884# Naval Command, Control and Ocean Surveillance Center, San Diego, CA.
STATISTICAL PROCESS CONTROL IN THE HYBRID MICROELECTRONICS MANUFACTURING INDUSTRY: A NAVY VIEW POINT
Charles C. Azu, Jr. Apr. 1993 12 p
(AD-A265164) Avail: CASI HC A03/MF A01

The U.S. Navy is concerned with receiving high quality hybrid microelectronic circuits. The Navy recognizes that in order to obtain high quality circuits a manufacturer must have an effective statistical process control (SPC) program implemented. The implementation of effective SPC programs is an objective of the military hybrid microelectronics industry. Often the smaller sized manufacturers in the industry have little SPC implementation, while the larger manufacturers have practices originally developed for the control of other product lines outside the hybrid technology area. The industry recognizes that SPC programs will result in high quality hybrid microcircuits which the U.S. Navy requires. In the past, the goal of the industry had not been to put in effective process control methods, but to merely meet the government military standards on the quality of the hybrids they produce. This practice, at best, resulted in a 'hit or miss' situation when it comes to hybrid microcircuit assemblies meeting military standards. The U.S. Navy through its MicroCIM program has been challenging and working with the industry in the area of SPC practice methods. The major limitations so far have been a lack of available sensors for the real-time collection of effective SPC data on the factory floor. This paper will discuss the Navy's efforts in bringing about effective SPC programs in the military hybrid manufacturing industry. DTIC

N94-12322# Department of the Navy, Washington, DC.
LIMITED BANDWIDTH MICROWAVE FILTER Patent Application
Christen Rauscher, inventor (to Navy) 26 Feb. 1993 41 p
(AD-D015744; US-Patent-Appl-SN-025210; Navy-Case-74067) Avail: CASI HC A03/MF A01

A limited-bandwidth microwave transversal or recursive filter, compatible with microwave monolithic integrated circuit (MMIC) design requirements is described. The device comprises a means to split an incident signal into multiple parts for distribution among a plurality of input ports of frequency-selective feedforward and feedback network branches comprising filter elements and active devices so designed as to provide a desired degree and type of signal filtration. After filtration, the resulting signals from these branches are combined to form a composite filter output signal. DTIC

N94-12333 Hypress, Inc., Elmsford, NY.
SUPERCONDUCTING SQUID AMPLIFIERS FOR IR DETECTORS AND OTHER APPLICATIONS, PHASE 2 Final Report
David Osterman 1 May 1993 23 p Limited Reproducibility: More than 20% of this document may be affected by microfiche quality
(Contract N00014-91-C-0264)
(AD-A265447) Avail: CASI HC A03

The subject is a completed Phase 2 SBIR project to develop a superconducting analog multiplexer circuit. The intended application of the multiplexer is as a component of processing circuitry for a superconducting infrared focal plane array (IR FPA). Development of the IR FPA is in progress under a separate contract. Among the accomplishments that are described below is the fabrication and testing of a functioning, superconducting, 20-input multiplexer, appropriate for use with an IR FPA. The motivation for developing a superconducting multiplexer circuit derives primarily from the significant potential advantages of an all-superconducting IR FPA system, i.e. a system in which the detectors, as well as the associated processing circuitry, are superconducting. Section 3 reviews the subject of superconducting IR FPA's. Chief among the advantages of such systems is the potential for larger arrays with greater numbers of detectors than is now possible. DTIC

N94-12405# Stanford Univ., CA. Center for Integrated Systems.
LOW VOLTAGE ELECTRON BEAM LITHOGRAPHY Monthly Report
R. Browning and R. F. Pease Feb. 1993 10 p
(AD-A265358) Avail: CASI HC A02/MF A01

The contract is presented in three parts, each of which discusses aspects of high precision electron beam lithography: (1) comprehensive computer modeling of the electron beam tool; (2) experimental determination of the properties of sources, columns, and targets; and (3) the use of silicon single crystals as straightness and orthogonality standards using orientation dependent etching techniques. DTIC

N94-12424# Naval Research Lab., Washington, DC.
NONLINEAR ANALYSIS OF A MAGNICON OUTPUT CAVITY Interim Report
B. Hafizi, S. H. Gold, P. Sprangle, and W. M. Manheimer 9 Apr. 1993 49 p
(AD-A265342; NRL/MR/6790-93-7300) Avail: CASI HC A03/MF A01

A nonlinear analysis of the wave-particle interaction in the output cavity of a frequency-doubling magnicon amplifier is presented. The cavity is immersed in an axial magnetic field wherein electronics interact with a rotating TM210 mode via a gyro-resonant mechanism. The electron equations of motion and the wave equation for the radio-frequency field are derived and expressed in terms of scaled variables in order to study the general scaling of the output cavity. Single-electron, time-dependent simulation of the interaction in the cavity is performed to assess the accessibility and stability of high-efficiency states for an x-band magnicon. Results from multi-electron, steady-state simulation are presented to show the effect of spreads in electron beam radius, energy, and transverse momentum on the efficiency. DTIC

N94-12433*# Harris Corp., Melbourne, FL. Government Communications Systems Div.
FLEXIBLE HIGH-SPEED CODEC Final Report
Greg P. Segallis, Jim V. Wernlund, and Glen Corry Aug. 1993 54 p
(Contract NAS3-25087; RTOP 506-72-21)
(NASA-CR-191169; E-8041; NAS 1.26:191169) Avail: CASI HC A04/MF A01

This report is prepared by Harris Government Communication Systems Division for NASA Lewis Research Center under contract NAS3-25087. It is written in accordance with SOW section 4.0 (d) as detailed in section 2.6. The purpose of this document is to provide a summary of the program, performance results and analysis, and a technical assessment. The purpose of this program was to develop a flexible, high-speed CODEC that provides substantial coding gain while maintaining bandwidth efficiency for use in both continuous and bursted data environments for a variety of applications. Author (revised)

N94-12565# Aerospace Corp., El Segundo, CA. Engineering and Technology Group.
TIN WHISKERS IN ELECTRONIC CIRCUITS
Gary W. Stupian 20 Dec. 1992 24 p
(Contract F04701-88-C-0089)
(AD-A265917; TR-92(2925)-7; SMC-TR-93-18) Avail: CASI HC A03/MF A01

Fibrous, conducting 'whiskers' often grow on pure tin plating. These tin whiskers have, for many years, been known to pose a reliability problem in electronic circuitry; therefore, the use of pure tin coatings in any critical electronic application is not recommended. Despite the warnings of the experts, tin plating is still found on electronic and mechanical components and problems with whiskers still arise. This document summarizes what is known about the growth of tin whiskers. A number of factors (e.g., coating thickness, plating conditions) are thought to be important in determining whether whiskers will grow. Although tin whiskers have been investigated from some decades, there is still disagreement on the effects of virtually every coating parameter. There is no disagreement, however, on the essential fact that it is very difficult to predict with certainty whether whiskers will grow on any specific tin-plated component, which of course is the basis of the 'experts' advice not to use pure tin plating. If tin-plated components are found in an electronic system, replacement is the safest policy. Some additional recommendations to minimize risk are presented here that may be of use in situations in which replacement of all suspect components is not the option of choice because of cost or schedule constraints. DTIC

N94-12584# California Univ., San Diego, La Jolla. Dept. of Chemistry.
SYNTHESIS AND ELECTRONIC PROPERTIES OF NANOPHASE SEMICONDUCTOR MATERIALS Report, 1 Jun. 1992 - 31 May 1993
Michael J. Sailor 25 May 1993 13 p
(Contract N00014-92-J-1810)
(AD-A265287) Avail: CASI HC A03/MF A01

The objective of the research effort is to understand and learn to control the morphologic and electronic properties of electrodeposited nanophase semiconductors. The initial work has focused on electrodeposition of nanophase CdSe, using a sequential monolayer deposition technique that we are developing. We are currently extending the synthesis phase of this project into silicon, silicon carbide, and phosphor materials. This work also encompasses studying semiconductor electrodeposition into materials with restricted dimensions, such as microporous alumina and porous silicon membranes. By growing films with very small grain sizes, we hope to produce and study materials that display unusual electronic or luminescent effects. We are primarily interested in the electronic properties of the II-VI and group IV materials, for potential applications in nanoscale electronics and optical detector technologies. The phosphors are being studied for their potential as efficient high-resolution display materials. DTIC

N94-12603# Fermi National Accelerator Lab., Batavia, IL.
UPGRADED D(O) CALORIMETER ELECTRONICS FOR SHORT TEVATRON BUNCH SPACE AND THE EFFECT OF PILE-UP ON THE W MASS MEASUREMENT
S. Lokos Nov. 1992 4 p Presented at the Meeting of the Division of Particles and Fields of the American Physical Society, Batavia, IL, 10-14 Nov. 1992
(Contract DE-AC02-76CH-03000)
(DE93-013566; FNAL/C-93/053-E; CONF-921122-56) Avail: CASI HC A01/MF A01

The high luminosity and short bunch spacing time of the upgraded Tevatron force the calorimeter to replace a significant part of the present electronics. The W mass measurement was used to study the pile-up effects. DOE

N94-12773*# Microwave Monolithics, Inc., Simi Valley, CA.
LOW COST HIGH EFFICIENCY GaAs MONOLITHIC RF MODULE FOR SARSAT DISTRESS BEACONS Final Report, 11 Jul. 1989 - 10 Nov. 1991
W. C. Petersen, D. P. Siu, and H. F. Cook Dec. 1991 101 p
(Contract NAS3-25712; SBIR-14.03-6642)
(NASA-CR-194235; NAS 1.26:194235) Avail: CASI HC A06/MF A02

Low cost high performance (5 Watts output) 406 MHz beacons are urgently needed to realize the maximum utilization of the Search and Rescue Satellite-Aided Tracking (SARSAT) system spearheaded in the U.S. by NASA. Although current technology can produce beacons meeting the output power requirement, power consumption is high due to the low efficiency of available transmitters. Field performance is currently unsatisfactory due to the lack of safe and reliable high density batteries capable of operation at -40 C. Low cost production is also a crucial but elusive requirement for the ultimate wide scale utilization of this system. Microwave Monolithics Incorporated (MMInc.) has proposed to make both the technical and cost goals for the SARSAT beacon attainable by developing a monolithic GaAs chip set for the RF module. This chip set consists of a high efficiency power amplifier and a bi-phase modulator. In addition to implementing the RF module in Monolithic Microwave Integrated Circuit (MMIC) form to minimize ultimate production costs, the power amplifier has a power-added efficiency nearly twice that attained with current commercial technology. A distress beacon built using this RF module chip set will be significantly smaller in size and lighter in weight due to a smaller battery requirement, since the 406 MHz signal source and the digital controller have far lower power consumption compared to the 5 watt power amplifier. All the program tasks have been successfully completed. The GaAs MMIC RF module chip set has been designed to be compatible with the present 406 MHz signal source and digital controller. A complete high performance low cost SARSAT beacon can be realized with only additional minor iteration and systems integration. Derived from text

N94-10791# Wright Lab., Wright-Patterson AFB, OH. Materials Directorate.
DEVELOPMENT AND ANALYSIS OF INSULATION CONSTRUCTIONS FOR AEROSPACE WIRING APPLICATIONS
George A. Slenski and Lynn M. Woodford (McDonnell-Douglas Corp., Saint Louis, MO.) *In* FAA, Proceedings of the International Conference for the Promotion of Advanced Fire Resistant Aircraft Interior Materials Mar. 1993 p 303-312 (For primary document see N94-10766 01-03)
(Contract F33615-89-C-5605)
Avail: CASI HC A02/MF A03

N94-10999*# Stanford Univ., CA. Experimental Physics Lab.
A MULTI-VARIANCE ANALYSIS IN THE TIME DOMAIN
Todd Walter *In* NASA. Goddard Space Flight Center, The 24th Annual Precise Time and Time Interval (PTTI) Applications and Planning Meeting Jun. 1993 p 413-426 (For primary document see N94-10963 01-70)
Avail: CASI HC A03/MF A04

34 FLUID MECHANICS AND HEAT TRANSFER

Includes boundary layers; hydrodynamics; fluidics; mass transfer; and ablation cooling.

For related information see also *02 Aerodynamics* and *77 Thermodynamics and Statistical Physics.*

N94-10252# Sandia National Labs., Albuquerque, NM.
AN EXPERIMENTAL INVESTIGATION OF HIGH-SPEED WATER-ENTRY FOR FULL-SIZE AND SCALE-MODEL POINTED NOSE VEHICLES
J. K. Cole, C. E. Hailey, W. T. Gutierrez, and M. T. Ferrario (Sandia National Labs., Livermore, CA.) Feb. 1993 29 p
(Contract DE-AC04-76DP-00789)
(DE93-008491; SAND-92-2579) Avail: CASI HC A03/MF A01 (US Sales Only)

A full-scale water-entry test of a pointed nose penetrator was conducted at the Kauai Test Facility in February 1991. The vehicle was rocket boosted to enter the water at a velocity of 301 m/s and an impact angle of -29 deg from the horizontal. During the test, triaxial accelerations and base pressures were recorded by a rugged, onboard data acquisition system. In June 1991, a scale-model water-entry test program was conducted at the Naval Surface Warfare Center's (NSWC) Hydroballistics Facility. Each scale model contained an onboard, miniature, data acquisition system which recorded axial acceleration and base pressure during water entry. The data acquisition system was specially designed to survive high-speed water entry and to fit inside models with base diameters as small as 3.81 cm. The NSWC test program was conducted for impact velocities ranging from 96-319 m/s and impact angles of -27 deg and -35 deg. This report compares the full-scale and scale-model acceleration histories and minimum cavity pressures. The validity of using Froude scaling is discussed and relationships are presented for minimum cavity pressure and maximum deceleration as a function of entry velocity and angle. DOE

N94-10275# Universiteit Twente, Enschede (Netherlands). Faculty of Applied Mathematics.
UNI-DIRECTIONAL WAVES OVER SLOWLY VARYING BOTTOM. PART 1: DERIVATION OF A KdV-TYPE OF EQUATION
E. W. C. vanGroesen and S. R. Pudjaprasetya (Bandung Inst. of Tech., Indonesia.) 29 Nov. 1992 27 p
(MEMO-1098; ETN-93-94311) Avail: CASI HC A03/MF A01

A new version of forced Korteweg-de Vries (KdV) equation for undirectional surface over an uneven bottom is derived. The Hamiltonian formulation of the exact equations for surface waves are reviewed. The approximation leading to the bidirectional Boussinesq equation is described. The KdV equation for the ease of constant bottom is derived in suitable way for the generalization to uneven bottom. The linear, lowest order equation, which also shows the special properties of the spatial dependent map gamma(x), is investigated. The forced KdV equation is derived for the elevation itself and the forcing is investigated in the case of localized bottom variations. The forcing equation derived allows precise estimation for its order of magnitude when compared to the usual KdV equation. In part 2 of the investigation, the distortion of solitary waves is studied. ESA

N94-10307# Lawrence Livermore National Lab., CA.
FLOW VISUALIZATION OF SHOCK PROPAGATION IN BAFFLE SYSTEMS
A. L. Kuhl and H. Reichenbach (Ernst-Mach-Inst., Freiburg, Germany.) Sep. 1992 18 p
(Contract W-7405-eng-48)
(DE93-013312; UCRL-ID-111898) Avail: CASI HC A03/MF A01

There is renewed interest in blast propagation in multi-chamber systems, related to the vulnerabilities of buried bunker systems to conventional weapons effects. In this short report, the authors suggest some idealized test problems that can be used to evaluate the accuracy of computer code calculations of such problems. The generic problem selected was that of shock wave propagation through a baffle system -- either aligned baffles or staggered baffles -- as shown schematically in a figure. Here results of shock tube experiments performed previously in the Ernst-Mach-Institut are reported. DOE

N94-10320# California Univ., San Diego.
LATTICE GAS HYDRODYNAMICS: THEORY AND SIMULATIONS
B. Hasslacher 1993 10 p
(Contract DE-FG03-89ER-13991)
(DE93-013297; DOE/ER-13991/2) Avail: CASI HC A02/MF A01

The first successful application of a microscopic analogy to create a skeleton cellular automaton and analyze it with statistical mechanical tools, was the work of Frisch, Hasslacher and Pomeau on the Navier-Stokes equation in two and three dimensions. This has become a very large research area with lattice gas models and methods being used for both fundamental investigations into the foundations of statistical mechanics and a large number of diverse applications. This present research was devoted to enlarging the fundamental scope of lattice gas models and proved successful. Since the beginning of this proposal, cellular automata have been constructed for statistical mechanical models, fluids, diffusion and shock systems in fundamental investigations. In applied areas, there are now excellent lattice gas models for complex flows through porous media, chemical reaction and combustion dynamics, multiphase flow systems, and fluid mixtures with natural boundaries. With extended cellular fluid models, one can do problems with arbitrary pairwise potentials. Recently, these have been applied to such problems as non-newtonian or polymeric liquids and a mixture of immiscible fluids passing through fractal or spongelike media in two and three dimensions. This proposal has contributed to and enlarged the scope of this work. DOE

N94-10364# National Aerospace Lab., Tokyo (Japan). Computational Sciences Div.
A GRID GENERATION METHOD TO CALCULATE THE FLOW FIELD IN A THREE-DIMENSIONAL CASCADE OF BLADES [SANJIGEN YOKURETSU NAGARE KEISAN NO TAMENO KOUSHI KEISEI]
Kenji Inoue May 1992 10 p In JAPANESE
(NAL-TR-1158; JTN-93-80435; DE93-767978) Avail: CASI HC A02/MF A01

A method is described for generating boundary fitted grids to calculate the flow field across a three dimensional cascade of blades placed radially in the axially symmetric space between the hub and casing. Successive application of a series of stretching and conformal transformation maps one-period domain of the cascade onto a box in computational space. The grid in physical space is then obtained by inverse transformation of the grid points in computational space, being an H-type grid and having a periodicity which includes the inclination of grid lines at the periodic boundary. Author (NASDA)

N94-10365# National Aerospace Lab., Tokyo (Japan). Computational Sciences Div.
SOLVING THE INVERSE PROBLEM FOR INCOMPRESSIBLE POTENTIAL FLOW THROUGH TWO-DIMENSIONAL CASCADES [NIJIGEN YOKURETSU WO SUGIRU HIASSHUKU POTENSHARU NAGARE NO GYAKUMONDAI]
Kenji Inoue Jun. 1992 12 p In JAPANESE
(NAL-TR-1162; JTN-93-80436; DE93-767979) Avail: CASI HC A03/MF A01

A method to solve the inverse problem for incompressible potential flow through two-dimensional cascades is described. This method enables the determination of blade profiles which realize a flow possessing the prescribed surface speed distribution, solidity, and incident angle. The employed method reduces the problem to one for conformal mappings, with the unknown coefficients used in the mappings being determined by computational numerical iterations. A sample calculation is conducted for a representative compressor cascade having known flow conditions, and the cascade's original configuration is well simulated. In addition, the method is also applied to obtain blade profiles for the same surface speed distribution but at a different solidity or incident angle. Author (NASDA)

N94-10383# Department of the Navy, Washington, DC.
CORNER VORTEX SUPPRESSOR Patent Application
Promode R. Bandyopadhyay, inventor (to Navy) 22 Feb. 1993 12 p
(AD-D015772; US-Patent-Appl-SN-020940) Avail: CASI HC A03/MF A01

The general purpose and object of this invention is to provide means for suppressing corner vortex generation and/or growth without the necessity for applying continuous suction at the corner and/or by providing structural faring or filleting at the corner. Another object of the invention is to provide a passive structure for alleviating the adverse effects of a corner vortex, and providing a means for accomplishing this result that is amenable to retrofitting and which does not require substantial changes in the cross sectional configuration of the structure as would be the case in faring or filleting the corner. This technique is passive and thus involves no suction of the fluid. DTIC

N94-10391 Tel-Aviv Univ. (Israel). Dept. of Fluid Mechanics and Heat Transfer.

HYGROSCOPIC ABSORPTION TO FALLING FILMS: THE EFFECTS OF THE CONCENTRATION LEVEL M.S. Thesis

Genick Meyerson Dec. 1991 137 p
(ITN-93-85198) Copyright Avail: Issuing Activity (Tel-Aviv Univ., Exact Sciences Library, Ramat Aviv 69978, Israel)

The aim was to investigate analytically the influence of the concentration of the absorbate in a liquid film on the process of vapor absorption into the film. The theoretical approach is an extension of earlier work on isothermal absorption and on non-isothermal absorption under conditions of low concentration and short contact time. Following presentation of a model for isothermal absorption, a model for non-isothermal absorption is developed which considers simultaneous heat and mass transfer. The main assumptions in the model are short exposure time, uniform film thickness and constant physical properties. In contrast to the low-concentration case, the governing diffusion equation is nonlinear with respect to absorbate concentration; an analytical solution for the equation was established; it leads to a pair of algebraic equations for isothermal absorption and to a set of four algebraic equations for non-isothermal absorption. Computer-calculated numerical solutions are presented for both cases. Theories based on the assumption of low concentration can lead to inaccurate mass-transer rate estimation; it was found that the mass-transfer rate increases with concentration, so that boundary layer growth is faster in a high-concentration film than in one with low concentration. Coupling between heat transfer and mass transfer leads to reduced mass transfer in the non-isothermal case. ISA

N94-10530 International Centre for Theoretical Physics, Trieste (Italy).

ON THE SOBOLEV SYSTEMS WITH ELLIPSOID CAVITIES

A. Bohigas (Instituto de Cibernetica, Matematica y Fisica, Havanna, Cuba.) and R. Felipe (Instituto de Cibernetica, Matematica y Fisica, Havanna, Cuba.) Jun. 1992 16 p Limited Reproducibility: More than 20% of this document may be affected by microfiche quality
(DE92-641290; IC-92/94) Avail: Issuing Activity (Department of Energy (DOE)) (US Sales Only)

In this paper, one studies the possible number of instability zones of a Sobolev system having n inner cavities each one being an ellipsoid of revolution completely filled with an ideal fluid of constant density rho(sub k), k+1,..., n. One proves that this number is at most n+1. This sort of mechanical system appears frequently in different applications and has lately received (nonlinear case) attention since it constitutes completely integrable systems. DOE

N94-10644*# National Aeronautics and Space Administration. Langley Research Center, Hampton, VA.

SCHLIEREN PHOTOGRAPHS AND INTERNAL PRESSURE DISTRIBUTIONS FOR THREE-DIMENSIONAL SIDEWALL-COMPRESSION SCRAMJET INLETS AT A MACH NUMBER OF 6 IN CF4

Scott D. Holland Washington Aug. 1993 143 p
(RTOP 506-40-41-02)
(NASA-TM-4479; L-17206; NAS 1.15:4479) Avail: CASI HC A07/MF A02

Three-dimensional sidewall-compression scramjet inlets with leading-edge sweeps of 30 deg and 70 deg were tested in the Langley Hypersonic CF4 Tunnel at a Mach number of 6 and a free-stream ratio of specific heats of 1.2. The parametric effects of leading-edge sweep, cowl position, contraction ratio, and Reynolds number were investigated. The models were instrumented with static pressure orifices distributed on the sidewalls, baseplate, and cowl. Schlieren movies were made of selected tunnel runs for flow visualization of the entrance plane and cowl region. Although these movies could not show the internal flow, the effect of the internal flow on the external flow was evident by way of spillage. The purpose is to provide a preliminary data release for the investigation. The models, facility, and testing methods are described, and the test matrix and a tabulation of tunnel runs are provided. Line plots highlighting the stated parametric effects and a representative set of schlieren photographs are presented without analysis. Author (revised)

N94-10703 Wright Lab., Wright-Patterson AFB, OH.

VISCOUS FLOW SIMULATION USING AN UPWIND METHOD FOR HEXAHEDRAL BASED ADAPTIVE MESHES Final Report, Apr. 1992 - Jan. 1993

Michael J. Aftosmis 1 Mar. 1993 70 p Limited Reproducibility: More than 20% of this document may be affected by microfiche quality
(AF Proj. 2404)
(AD-A265901; WL-TR-93-3015) Avail: CASI HC A04

Details of an adaptive, high resolution, upwind algorithm for the simulation of viscous flows on unstructured hexahedral meshes are presented. The method used a TVD scheme for modeling the inviscid terms while the viscous terms rely upon central differencing. Grid adaptation is achieved through directional division of hexahedral cells in response to flow features. The discussion focuses primarily on details of the new viscous discretization and evaluates it through example problems, analysis, and mathematical proof. Several issues facing the development of upwind schemes on adaptive, unstructured meshes are prominently discussed. The test cases examine issues of consistency and mesh convergence of the adaptive methodology and the ability of the adaptation to accurately resolve flows which require detailed resolution of subtle flow features. These examples point out several general issues regarding the interaction of the upwind inviscid discretization with the centrally differenced viscous terms, especially near inviscid stagnation points, and within the boundary layer itself. A technique for avoiding the appearance of anomalous solutions in such regions is presented and discussed. DTIC

N94-10717 Academy of Sciences of the Ukraine, Kiev. Inst. Teoreticheskoj Fiziki.

ON THE DOUBLING OF HYDRODYNAMIC THEOREMS IN RELATIVISTIC THEORY OF SUPERFLUIDITY [OB UDVOENII GIDRODINAMICHESKIKH TEOREM V RELYATIVISTSKOJ TEORII SVERKHTEKUCHESTI]

P. I. Fomin and S. I. Vilchinskij 1991 15 p In RUSSIAN Limited Reproducibility: More than 20% of this document may be affected by microfiche quality
(DE93-617895; ITF-91-74) Avail: Issuing Activity (Department of Energy (DOE)) (US Sales Only)

Using the relativistic equations of the theory of superfluidity, we consider the basic hydrodynamic theorems for two-component superfluon systems in the non-dissipative approximation. We show that the number of basic theorems is doubled as compared to that in one-component relativistic hydrodynamics. DOE

N94-10727# National Aerospace Lab., Tokyo (Japan). Thermofluid Dynamics Div.

ATOMIZATION CHARACTERISTICS OF A PREFILMING AIRBLAST ATOMIZER [JITSUYOU KIRYUU BIRYUUKA NENRYOU NOZURU NO BIRYUUKA TOKUSEI]

Shigeru Hayashi, Atsushi Koito, and Manabu Hishiki Jan. 1992 14 p In JAPANESE
(NAL-TM-644; JTN-93-80422) Avail: CASI HC A03/MF A01

The size distribution of water test sprays generated by a prefilming airblast atomizer used for aeroengines was measured in swirling and non-swirling flows with the well established laser scattering particle sizing technique. Atomizing air velocity (or pressure difference) was varied in a range wider than the conditions of actual engines. The Sauter Mean Diameter (SMD) decreased at approximately a 1.5 power of the atomizing air velocity, being a higher velocity index than the previously reported values of 1 to 1.2. It was unexpectedly found that the effect of the liquid/air flow ratio was small. Since swirling flow increased the SMD at lower air velocities yet decreased it at higher ones, it is suggested that the reverse flow near the nozzle pintle adversely affects atomization. Author (NASDA)

N94-10810*# Institute for Computer Applications in Science and Engineering, Hampton, VA.

THE NONLINEAR EVOLUTION OF MODES ON UNSTABLE STRATIFIED SHEAR LAYERS Final Report

Nicholas Blackaby (Manchester Univ., England.), Andrew Dando (Manchester Univ., England.), and Philip Hall (Manchester Univ., England.) Washington NASA Jun. 1993 45 p Submitted for publication Sponsored in part by Science Research Council

(Contract NAS1-19480; RTOP 505-90-52-01)

(NASA-CR-191492; NAS 1.26:191492; ICASE-93-36) Avail: CASI HC A03/MF A01

The nonlinear development of disturbances in stratified shear flows (having a local Richardson number of value less than one quarter) is considered. Such modes are initially fast growing but, like related studies, we assume that the viscous, non-parallel spreading of the shear layer results in them evolving in a linear fashion until they reach a position where their amplitudes are large enough and their growth rates have diminished sufficiently so that amplitude equations can be derived using weakly nonlinear and non-equilibrium critical-layer theories. Four different basic integro-differential amplitude equations are possible, including one due to a novel mechanism; the relevant choice of amplitude equation, at a particular instance, being dependent on the relative sizes of the disturbance amplitude, the growth rate of the disturbance, its wavenumber, and the viscosity of the fluid. This richness of choice of possible nonlinearities arises mathematically from the indicial Frobenius roots of the governing linear inviscid equation (the Taylor-Goldstein equation) not, in general, differing by an integer. The initial nonlinear evolution of a mode will be governed by an integro-differential amplitude equations with a cubic nonlinearity but the resulting significant increase in the size of the disturbance's amplitude leads on to the next stage of the evolution process where the evolution of the mode is governed by an integro-differential amplitude equations with a quintic nonlinearity. Continued growth of the disturbance amplitude is expected during this stage, resulting in the effects of nonlinearity spreading to outside the critical level, by which time the flow has become fully nonlinear. Author (revised)

N94-10824 Princeton Univ., NJ.

DEVELOPMENT OF A DELAUNAY-BASED ADAPTION SCHEME WITH APPLICATIONS TO COMPLEX THREE-DIMENSIONAL ROTATIONAL FLOWS Ph.D. Thesis

Todd Jay Mitty 1993 139 p

Avail: Univ. Microfilms Order No. DA9311205

In order to compute accurate numerical solutions, it is necessary to maintain a small discretization error. This error may be controlled by adjusting the spacing between discrete points. However, it is preferable to selectively choose locations for such alterations rather than affect the entire domain. This leads to the notion of solution adaptation. A new solution adaptive technique was developed for solving the Euler equations within Delaunay tessellated, three dimensional, computational domains possessing planar boundaries. Mesh generation and solution adaptive mesh enrichment were achieved through application of the Bowyer/Watson algorithm, and resolution criteria were explored to determine the set of adapted points. The example of a reflecting oblique shock wave flow was used to validate the method. The other aspect of this research involved the application of the solution adaption method to supersonic inviscid rotational flows modeled by introducing vorticity through an inlet flow velocity distribution. The extent to which this model represents shock wave/boundary layer interactions was examined by comparing the solution adapted predictions with corresponding experimental data and published viscous computations for a 20 deg fin at nominal Mach numbers of both 3 and 4. The solution adaptation provided well resolved inviscid solutions which were sufficiently accurate to allow testing of the hypothesis that inviscid rotational features dominate the shock wave/boundary layer interaction flows. Dissert. Abstr.

N94-10838 Academy of Sciences of the Ukraine, Kiev. Inst. Teoreticheskoj Fiziki.

THE HEAT TRANSFER BY RADIATION BETWEEN TWO MEDIA [TEPLOOBMEN IZLUCHENIEM MEZHDU DVUMYA SREDAMI]

A. G. Zagorodnij, A. S. Usenko, and I. P. Yakimenko 1991 48 p In RUSSIAN Limited Reproducibility: More than 20% of this document may be affected by microfiche quality

(DE93-617820; ITF-91-75) Avail: CASI HC A03 (US Sales Only)

The electromagnetic field generated by arbitrary distributed sources all over the whole space is obtained for the case of semi-bounded plasma with specular and random scattering of charged plasma particles by a boundary surface. The spectrum distribution of thermal radiation by plasma half-space into external medium with non-zero temperature is calculated. DOE

N94-10851 Maryland Univ., College Park. Dept. of Mechanical Engineering

EXPERIMENTAL STUDY OF MULTIPLE DROPLET EVAPORATIVE COOLING Final Report, Dec. 1992

H. Dawson and M. diMarzo Apr. 1993 115 p Limited Reproducibility: More than 20% of this document may be affected by microfiche quality

(Grant NANB1H1173)

(PB93-198463; REPT-92-1; NIST/GCR-93/624) Avail: Issuing Activity (National Technical Information Service (NTIS))

The purpose of the experimental study was to quantify the transient evaporative cooling of a radiantly heated, low thermal conductivity material subject to a random impingement of water droplets. Specifically, the transient behavior and spatial distribution of the surface temperature were investigated over a range of initial surface temperatures and impinging mass fluxes. Additionally, it was desired to draw some conclusions about the important parameters in the evaporative cooling phenomenon and about evaporative cooling generally. A concurrent goal of the research was to continue development of the infrared thermography and digital image analysis techniques and equipment employed in the data acquisition system. NTIS

N94-10861# National Aerospace Lab., Tokyo (Japan). Aircraft Aerodynamics Div.

NUMERICAL WIND TUNNEL PROJECT AND COMPUTATIONAL FLUID DYNAMICS AT NATIONAL AEROSPACE LABORATORY, JAPAN

Naoki Hirose Jul. 1992 13 p

(NAL-TM-648T; JTN-93-80449; DE93-793615) Avail: CASI HC A03/MF A01

The National Aerospace Laboratory (NAL) is the only research organization under the Science and Technology Agency which performs aerospace research in Japan, with NAL being actively involved in conducting Computational Fluid Dynamic (CFD) and supercomputer research and development. This paper summarizes the Numerical Wind Tunnel Project and associated CFD work carried out by NAL. Author (NASDA)

N94-10896 Iowa State Univ. of Science and Technology, Ames.

A DYNAMICALLY ADAPTIVE MESH METHOD FOR INTERNAL FLOWS Ph.D. Thesis

John William Slater 1992 204 p

Avail: Univ. Microfilms Order No. DA9311535

A dynamic solution adaptive mesh method was implemented into a finite-volume numerical method for solving unsteady flow fields described by the two-dimensional, unsteady, Navier-Stokes and Euler equations. The objective was to improve the resolution and accuracy of solutions which contained flow gradients which varied in strength and position with time. Variational principles were used to formulate the mesh equations with which meshes were generated to have the desired smoothness, orthogonality, and volume adaption qualities. The adaption of the mesh to the flow solution was driven by the presence of flow gradients. The dynamics of the mesh was accounted for in the flow equations through the mesh speeds. A comparison was made between one approach which computed the mesh speeds from a backwards time differences of the mesh and another approach which computed the mesh speeds from a system of mesh speed equations which were derived from the time differentiation of the mesh equations. The dynamically adaptive mesh method was demonstrated for model problems involving solution and boundary dynamics, inviscid flows in a converging-diverging noble, viscous boundary-layer flows over flat plates, and viscous flows in a transonic diffuser. It was found that the approach using the mesh speed equations was more accurate than the approach using the time-differenced mesh speeds. There was difficulty is obtaining proper clustering of the meshes for viscous flows. Dissert. Abstr.

N94-10899 Pennsylvania State Univ., University Park.

FLOWFIELD STRUCTURE OF SWEPT SHOCK WAVE/TURBULENT

BOUNDARY-LAYER INTERACTIONS Ph.D. Thesis
Farrukh Sabbah Alvi 1992 270 p
Avail: Univ. Microfilms Order No. DA9311584

A parametric experimental study was conducted to investigate the flowfield structure of sharp fin-generated swept shock wave/turbulent boundary-layer interactions. Two sets of experiments utilizing the conical shadowgraphy and PLS (Planar Laser Scattering) techniques were used to nonintrusively study the flowfield. This study was unique in that both these techniques took advantage of the natural quasiconical symmetry of these interactions. A broad range of interaction strengths, from barely separated to very strongly separated, was covered in both sets of experiments. The conical shadowgraphy experiments covered freestream Mach numbers of 2.5, 3, 3.5, and 4, while the PLS experiments were conducted at freestream Mach numbers of 3 and 4. The flowfield structure was visualized with a high degree of resolution and several new flowfield features were observed. By combining the results from these two experiments with previous results (mainly consisting of surface flowfield studies), a detailed physical model was constructed for the present class of interactions in the appropriate conical reference frame. This physical model is presented and discussed in terms of six detailed flowfield maps. Several new flowfield regime boundaries associated with the newly observed features were also defined. Finally, scaling laws, correlating the interaction growth to the appropriate interaction strength parameters, are also presented. Dissert. Abstr.

N94-10912*# California Polytechnic State Univ., San Luis Obispo.
EVALUATION OF DUAL FLOW THRUST VECTORED NOZZLES WITH EXHAUST STREAM IMPINGEMENT MS Thesis Final Technical Report, Oct. 1990 - Jul. 1991
Thomas W. Carpenter 1991 106 p
(Contract NCC2-686)
(NASA-CR-193292; NAS 1.26:193292) Avail: CASI HC A06/MF A02

The main objective of this project was to predict the expansion wave/oblique shock wave structure in an under-expanded jet expanding from a convergent nozzle. The shock structure was predicted by combining the calculated curvature of the free pressure boundary with principles and governing equations relating to oblique shock wave and expansion wave interaction. The procedure was then continued until the shock pattern repeated itself. A mathematical model was then formulated and written in FORTRAN to calculate the oblique shock/expansion wave structure within the jet. In order to study shock waves in expanding jets, Schlieren photography, a form of flow visualization, was employed. Thirty-six Schlieren photographs of jets from both a straight and 15 degree nozzle were taken. An iterative procedure was developed to calculate the shock structure within the jet and predict the non-dimensional values of Prandtl primary wavelength (w/rn), distance to Mach Disc (Ld) and Mach Disc radius (rd). These values were then compared to measurements taken from Schlieren photographs and experimental results. The results agreed closely to measurements from Schlieren photographs and previously obtained data. This method provides excellent results for pressure ratios below that at which a Mach Disc first forms. Calculated values of non-dimensional distance to the Mach Disc (Ld) agreed closely to values measured from Schlieren photographs and published data. The calculated values of non-dimensional Mach Disc radius (rd), however, deviated from published data by as much as 25 percent at certain pressure ratios. Derived from text

N94-10939*# National Aeronautics and Space Administration. Lewis Research Center, Cleveland, OH.
NEW DEVELOPMENTS IN THE METHOD OF SPACE-TIME CONSERVATION ELEMENT AND SOLUTION ELEMENT: APPLICATIONS TO THE EULER AND NAVIER-STOKES EQUATIONS
Sin-Chung Chang Jun. 1993 99 p Presented at the second US National Congress on Computational Mechanics, 16-18 Aug. 1993; sponsored by the US Association for Computational Mechanics
(RTOP 505-62-52)
(NASA-TM-106226; E-7943; NAS 1.15:106226) Avail: CASI HC A05/MF A02

A new numerical framework for solving conservation laws is being developed. This new approach differs substantially in both concept and methodology from the well-established methods--i.e., finite difference, finite volume, finite element, and spectral methods. It is conceptually simple and designed to avoid several key limitations to the above traditional methods. An explicit model scheme for solving a simple 1-D unsteady convection-diffusion equation is constructed and used to illuminate major differences between the current method and those mentioned above. Unexpectedly, its amplification factors for the pure convection and pure diffusion cases are identical to those of the Leapfrog and the DuFort-Frankel schemes, respectively. Also, this explicit scheme and its Navier-Stokes extension have the unusual property that their stabilities are limited only by the CFL condition. Moreover, despite the fact that it does not use any flux-limiter or slope-limiter, the Navier-Stokes solver is capable of generating highly accurate shock tube solutions with shock discontinuities being resolved within one mesh interval. An accurate Euler solver also is constructed through another extension. It has many unusual properties, e.g., numerical diffusion at all mesh points can be controlled by a set of local parameters. Author

N94-11014# Rutgers - The State Univ., New Brunswick, NJ. Dept. of Mechanical and Aerospace Engineering.
THEORETICAL INVESTIGATION OF 3-D SHOCK WAVE TURBULENT BOUNDARY LAYER INTERACTIONS Interim Report, 1 Mar. - 30 Sep. 1992
Doyle D. Knight 30 Nov. 1993 56 p
(Grant AF-AFOSR-0266-86)
(AD-A265275; RU-TR-MAE-184-F; AFOSR-93-0357TR) Avail: CASI HC A04/MF A01

The research concerns the understanding of 3-D shock wave/turbulent boundary-layer interactions. The research effort during the current period focused on the following areas: (1) the 3-D double fin (crossing shock) interaction at Mach 8.3 for symmetric 15 deg fins; (2) the 3-D crossing shock interaction at Mach 4 for symmetric 15 deg fins; and (3) the 3-D triple (triple shock) interaction at Mach 8.3 for 10 deg fins. DTIC

N94-11026# Lawrence Livermore National Lab., CA.
INVERTING ULTRASONIC DATA ON SOLID/FLUID MIXTURES FOR BIOT-GASSMANN PARAMETERS
J. G. Berryman and D. E. Lumley (Stanford Univ., CA.) Feb. 1993 12 p Presented at the 2nd International Conference on Mathematical and Numerical Aspects of Wave Propagation (SIAM), Newark, DE, 7-10 Jun. 1993
(Contract W-7405-eng-48)
(DE93-011952; UCRL-JC-112052; CONF-9306142-1) Avail: CASI HC A03/MF A01

Although the Biot-Gassmann equations are known to predict acoustic data for water-saturated glass bead packings very well, these equations often seem to give anomalous results for naturally occurring rocks. The theory shows that, as the compressibility of the pore fluid increases, the inverse of the coefficients C and M in Biot's equations should increase linearly, and the theory also gives definite predictions about the values of the slope and intercept of the resulting lines. Although the anticipated linear behavior is observed in real data, the values of the slopes are smaller than expected for some rocks. Therefore, the process of inverting this data for the desired coefficients must incorporate other physical constraints and then produces, not a single value but rather, a range of possible values for each coefficient. DOE

N94-11072# Argonne National Lab., IL.
FORCE2: A STATE-OF-THE-ART TWO-PHASE CODE FOR HYDRODYNAMIC CALCULATIONS
Jianmin Ding, R. W. Lyczkowski, and S. W. Burge (Babcock and Wilcox Co., Alliance, OH.) Feb. 1993 9 p Presented at the 12th International Conference on Fluidized-Bed Combustion, San Diego, CA, 8-13 May 1993
(Contract W-31-109-eng-38)
(DE93-010661; ANL/MCT/CP-76429; CONF-930521-5) Avail: CASI HC A02/MF A01

A three-dimensional computer code for two-phase flow named FORCE2 has been developed by Babcock and Wilcox (B & W) in close collaboration with Argonne National Laboratory (ANL). FORCE2 is capable of both transient as well as steady-state simulations. This Cartesian coordinates computer program is a finite control volume, industrial grade and quality embodiment of the pilot-scale FLUFIX/MOD2 code and contains features such as three-dimensional blockages, volume and surface porosities to account for various obstructions in the flow field, and distributed resistance modeling to account for pressure drops caused by baffles, distributor plates and large tube banks. Recently computed results demonstrated the significance of and necessity for three-dimensional models of hydrodynamics and erosion. This paper describes the process whereby ANL's pilot-scale FLUFIX/MOD2 models and numerics were implemented into FORCE2. A description of the quality control to assess the accuracy of the new code and the validation using some of the measured data from Illinois Institute of Technology (UT) and the University of Illinois at Urbana-Champaign (UIUC) are given. It is envisioned that one day, FORCE2 with additional modules such as radiation heat transfer, combustion kinetics and multi-solids together with user-friendly pre- and post-processor software and tailored for massively parallel multiprocessor shared memory computational platforms will be used by industry and researchers to assist in reducing and/or eliminating the environmental and economic barriers which limit full consideration of coal, shale and biomass as energy sources, to retain energy security, and to remediate waste and ecological problems. DOE

N94-11144# Lawrence Livermore National Lab., CA.
TURBULENT WALL JET IN BLAST WAVE PRECURSOR
A. L. Kuhl Jan. 1993 38 p Presented at the 1993 National Symposium on Shock Waves, Sendai, Japan, 11-15 Jan. 1993
(Contract W-7405-eng-48)
(DE93-011955; UCRL-JC-112713; CONF-9301100-1) Avail: CASI HC A03/MF A01

Numerical simulations of the turbulent dusty flow induced by an explosion over a ground surface were performed with a second-order Godunov code. Adaptive Mesh Refinement was used to capture the convective mixing processes on the computational grid. The most prominent feature of the flow was a turbulent wall jet that was induced by the precursor shock refraction into a thermal layer on the surface. Dust lofting occurred because the rotational structures of the boundary layer entrained dust from the ground surface. Scaling methods were defined in order to evaluate the mean and r.m.s. profiles of the wall jet. The profiles were shown to be similar to the profiles calculated for self-similar wall jets propagating over dust layers, and agreed with experimental profiles of a dusty boundary layer behind a shock. The Convective Mixing Model described here can be applied to a wide spectrum of fluid-dynamic mixing problems. DOE

N94-11192*# National Aeronautics and Space Administration. Lewis Research Center, Cleveland, OH.
A GALILEAN AND TENSORIAL INVARIANT k-EPSILON MODEL FOR NEAR WALL TURBULENCE
Z. Yang and T. H. Shih Jul. 1993 12 p Presented at the 24th Fluid Dynamics Conference, Orlando, FL, 6-9 Jul. 1993; sponsored by AIAA
(Contract NCC3-233; RTOP 505-62-21)
(NASA-TM-106263; AIAA Paper 93-3105; ICOMP-93-24; CMOTT-93-10; E-7990; NAS 1.15:106263) Avail: CASI HC A03/MF A01

A k-epsilon model is proposed for wall bounded turbulent flows. In this model, the eddy viscosity is characterized by a turbulent velocity scale and a turbulent time scale. The time scale is bounded from below by the Kolmogorov time scale. The dissipation rate equation is reformulated using this time scale and no singularity exists at the wall. A new parameter R = k/S(nu) is introduced to characterize the damping function in the eddy viscosity. This parameter is determined by local properties of both the mean and the turbulent flow fields and is free from any geometry parameter. The proposed model is then Galilean and tensorial invariant. The model constants used are the same as in the high Reynolds number Standard k-epsilon Model. Thus, the proposed model will also be suitable for flows far from the wall. Turbulent channel flows and turbulent boundary layer flows with and without pressure gradients are calculated. Comparisons with the data from direct numerical simulations and experiments show that the model predictions are excellent for turbulent channel flows and turbulent boundary layers with favorable pressure gradients, good for turbulent boundary layers with zero pressure gradients, and fair for turbulent boundary layer with adverse pressure gradients. Author (revised)

N94-11253*# National Aeronautics and Space Administration. Lewis Research Center, Cleveland, OH.
HIGH ORDER ACCURATE SOLUTIONS OF VISCOUS PROBLEMS
M. Ehtesham Hayder and Eli Turkel (Tel-Aviv Univ., Israel.) Jul. 1993 13 p Presented at the 24th Fluid Dynamics Conference, Orlando, FL, 6-9 Jul. 1993; sponsored by AIAA
(RTOP 505-62-21)
(NASA-TM-106267; AIAA Paper 93-3074; ICOMP-93-26; E-7994; NAS 1.15:106267) Avail: CASI HC A03/MF A01

We consider a fourth order extension to MacCormack's scheme. The original extension was fourth order only for the inviscid terms but was second order for the viscous terms. We show how to modify the viscous terms so that the scheme is uniformly fourth order in the spatial derivatives. Applications are given to some boundary layer flows. In addition, for applications to shear flows the effect of the outflow boundary conditions are very important. We compare the accuracy of several of these different boundary conditions for both boundary layer and shear flows. Stretching at the outflow usually increases the oscillations in the numerical solution but the addition of a filtered sponge layer (with or without stretching) reduces such oscillations. The oscillations are generated by insufficient resolution of the shear layer. When the shear layer is sufficiently resolved then oscillations are not generated and there is less of a need for a nonreflecting boundary condition. Author (revised)

N94-11256*# National Aeronautics and Space Administration. Lewis Research Center, Cleveland, OH.
A RESEARCH PROGRAM FOR IMPROVING HEAT TRANSFER PREDICTION FOR THE LAMINAR TO TURBULENT TRANSITION REGION OF TURBINE VANES/BLADES
Frederick F. Simon Aug. 1993 35 p Presented at the Workshop on End-State Boundary Layer Transition, Blue Mountain Lake, NY, 15-18 Aug. 1993; sponsored by Syracuse Univ.
(RTOP 505-62-52)
(NASA-TM-106278; E-8015; NAS 1.15:106278) Avail: CASI HC A03/MF A01

A program sponsored by NASA for the investigation of the heat transfer in the transition region of turbine vanes and blades with the objective of improving the capability for predicting heat transfer is described. The accurate prediction of gas-side heat transfer is important to the determination of turbine longevity, engine performance, and developmental costs. The need for accurate predictions will become greater as the operating temperatures and stage loading levels of advanced turbine engines increase. The present methods for predicting transition shear stress and heat transfer on turbine blades are based on incomplete knowledge and are largely empirical. To meet the objective of the NASA program, a team approach consisting of researchers from government, universities, a research institute, and a small business is presented. The research is divided into the areas of experiments, direct numerical simulations (DNS), and turbulence modeling. A summary of the results to date is given for the above research areas in a high-disturbance environment (bypass transition) with a discussion of the model development necessary for use in numerical codes. Author (revised)

N94-11272# Lawrence Livermore National Lab., CA.
QUALITY FACTORS AND LOCAL ADAPTION (WITH APPLICATIONS IN EULERIAN HYDRODYNAMICS)
W. P. Crowley 17 Jun. 1992 9 p Presented at the 7th IMACS International Conference on Computer Methods for Partial Differential Equations, New Brunswick, NJ, 22-24 Jun. 1992
(Contract W-7405-eng-48)
(DE93-010502; UCRL-JC-110862; CONF-9206185-12) Avail: CASI HC A02/MF A01

Adapting the mesh to suit the solution is a technique commonly used for solving both ODE's and PDE's. For Lagrangian hydrodynamics, ALE and Free-Lagrange are examples of structured and unstructured adaptive methods. For Eulerian hydrodynamics the two basic approaches are the macro-unstructuring technique and the micro-unstructuring technique. Here, we will describe a new micro-unstructuring technique, LAM, (for Local Adaptive Mesh) as applied to Eulerian hydrodynamics. The LAM technique consists of two independent parts: (1) the time advance scheme is a variation on the artificial viscosity method; and (2) the adaption scheme uses a micro-unstructured mesh with quadrilateral mesh elements. The adaption scheme makes use of quality factors and the relation between these and truncation errors is discussed. The time advance scheme; the adaption strategy; and the effect of different adaption parameters on numerical solutions are described. DOE

N94-11371# Sandia National Labs., Albuquerque, NM.
CRESLAF. VERSION 4.0: A FORTRAN PROGRAM FOR MODELING LAMINAR, CHEMICALLY REACTING, BOUNDARY-LAYER FLOW IN CYLINDRICAL OR PLANAR CHANNELS
M. E. Coltrin, H. K. Moffat, R. J. Kee, and F. M. Rupley Apr. 1993 50 p
(Contract DE-AC04-76DP-00789)
(DE93-012835; SAND-93-0478) Avail: CASI HC A03/MF A01

CRESLAF is a Fortran program that predicts the velocity, temperature, and species profiles in two-dimensional (planar or axisymmetric) channels. The program accounts for finite-rate gas-phase and surface chemical kinetics and molecular transport. The model employs the boundary-layer approximations for the fluid-flow equations, coupled to gas-phase and surface species continuity equations. The program runs in conjunction with the Chemkin preprocessors for the gas-phase and surface chemical reaction mechanisms and the transport properties. This report presents the equations defining the model, the method of solution, the input parameters to the program, and a sample problem illustrating its use. Applications of CRESLAF include chemical vapor deposition (CVD) reactors, heterogeneous catalysis on reactor walls, and corrosion processes. DOE

N94-11376*# National Aeronautics and Space Administration. Lewis Research Center, Cleveland, OH.
MARANGONI INSTABILITY IN A LIQUID LAYER WITH TWO FREE SURFACES
Robert J. Deissler, Alxander Oron (Technion - Israel Inst. of Tech., Haifa.), and J. C. Duh (Sverdrup Technology, Inc., Brook Park, OH.) Jul. 1993 26 p
(Contract NCC3-233; RTOP 505-90-5K)
(NASA-TM-106166; ICOMP-93-15; E-7862; NAS 1.15:106166) Avail: CASI HC A03/MF A01

The onset of the Marangoni instability in a liquid layer with two free nearly insulating surfaces heated from below is studied. Linear stability analysis yields a condition for the emergence of a longwave or a finite wavelength instability from the quiescent equilibrium state. Using the method of asymptotic expansions, a weakly nonlinear evolution equation describing the spatiotemporal behavior of the velocity and temperature fields at the onset of the longwave instability is derived. The latter is given by delta(M) = 24, delta(M) being the difference between the upper and the lower Marangoni numbers. It is shown that in some parametric range one convective cell forms across the layer, while in other parametric domains two convective cells emerge between the two free surfaces. Author (revised)

N94-11377*# National Aeronautics and Space Administration. Lewis Research Center, Cleveland, OH.
ON NONLINEAR TOLLMIEN-SCHLICHTING/VORTEX INTERACTION IN THREE-DIMENSIONAL BOUNDARY LAYERS
Dominic A. R. Davis and Frank T. Smith (University Coll., London, England.) May 1993 29 p
(Contract NCC3-233; RTOP 505-62-21)
(NASA-TM-106184; ICOMP-93-17; E-7889; NAS 1.15:106184) Avail: CASI HC A03/MF A01

The instability of an incompressible three-dimensional boundary layer (that is, one with cross-flow) is considered theoretically and computationally in the context of vortex/wave interactions. Specifically the work centers on two low amplitude, lower-branch Tollmien-Schlichting waves which mutually interact to induce a weak longitudinal vortex flow; the vortex motion, in turn, gives rise to significant wave-modulation via wall-shear forcing. The characteristic Reynolds number is taken as a large parameter and, as a consequence, the waves' and the vortex motion are governed primarily by triple-deck theory. The nonlinear interaction is captured by a viscous partial-differential system for the vortex coupled with a pair of amplitude equations for each wave pressure. Three distinct possibilities were found to emerge for the nonlinear behavior of the flow solution downstream - an algebraic finite-distance singularity, far downstream saturation or far-downstream wave-decay (leaving pure vortex flow) - depending on the input conditions, the wave angles, and the size of the cross-flow. Author (revised)

N94-11448# Naval Command, Control and Ocean Surveillance Center, San Diego, CA. Research, Development, Technology and Evaluation Div.
SHEAR FLOW CONTROL OF GAS JETS IN LIQUIDS
T. G. Ogden, L. A. Parnell, E. W. Hendricks, and W. M. Schieber Mar. 1993 10 p
(AD-A264673) Avail: CASI HC A02/MF A01

Passive control of shear flow is used to control the rate of mixing and stability of submerged gaseous jets in liquids. The object is to evaluate the effectiveness of recently developed shear flow control techniques for application to gaseous jets injected into liquids and ultimately to apply these techniques to gaseous oxidants injected into liquid metal fuels. These control techniques have been initially tested in nonreacting gas/liquid systems. A large increase in the degree of mixing and jet stability occurs when non-axisymmetric nozzles are used as injectors relative to injection by axisymmetric Fanno tube type nozzles. Jet volume spreading rate is increased by a factor of 4. A characteristic instability (the 'reverse shock' or reverse flow effect) occurring in such two-phase systems is greatly reduced by passive control of the shear flow. A simple passive technique of controlling entrainment is described which is effective in eliminating the reverse flow effect. The relevance of these control techniques to liquid metal combustion is discussed. DTIC

N94-11481*# National Aeronautics and Space Administration. Lewis Research Center, Cleveland, OH.
VISCOUS ANALYSIS OF THREE-DIMENSIONAL ROTOR FLOWS USING A MULTIGRID METHOD
A. Arnone (Florence Univ., Italy.) Jul. 1993 36 p
(Contract NCC3-233; RTOP 505-90-5K)
(NASA-TM-106266; ICOMP-93-25; E-7993; NAS 1.15:106266) Avail: CASI HC A03/MF A01

A three-dimensional code for rotating blade-row flow analysis was developed. The space discretization uses a cell-centered scheme with eigenvalues scaling for the artificial dissipation. The computational efficiency of a four-stage Runge-Kutta scheme is enhanced by using variable coefficients, implicit residual smoothing, and a full-multigrid method. An application is presented for the NASA rotor 67 transonic fan. Due to the blade stagger and twist, a zonal, non-periodic H-type grid is used to minimize the mesh skewness. The calculation is validated by comparing it with experiments in the range from the maximum flow rate to a near-stall condition. A detailed study of the flow structure near peak efficiency and near stall is presented by means of pressure distribution and particle traces inside boundary layers. Author (revised)

N94-11519# Sigma Research, Inc., Westford, MA.
A FOUR-DIMENSIONAL, MESOSCALE, NON-GAUSSIAN MULTISPECTRAL SMOKE MODEL. PHASE 1: FEASIBILITY STUDY Final Report
R. J. Yamartino, D. G. Strimaitis, J. S. Scire, and E. M. Insley Dec. 1992 70 p
(Contract DAAD07-91-C-0133)
(AD-A264805; ARL-CR-15) Avail: CASI HC A04/MF A01

The feasibility of developing a four-dimensional, non-Gaussian mesoscale multispectral smoke model that could run on a personal computer is investigated. Several of the model components are formulated, coded, and tested. This included the main driver program for accessing and interpolating the mesoscale winds and generating particle trajectories, a sub-grid-scale velocity field generator based on the kinematic simulation approach, and a dry deposition model for particle deposition velocities. Current understanding of flow and turbulence modeling is reviewed and can be applied to developing appropriate kinematic simulation fields. Technical approaches to account for the height and particle size dependent probability of particle removal and to compute the point and path average particle concentrations are also presented. Conclusions and recommendations for future work are included. DTIC

N94-11526*# Pennsylvania State Univ., University Park. Dept. of Mechanical Engineering.
SHEAR COAXIAL INJECTOR ATOMIZATION PHENOMENA FOR COMBUSTING AND NON-COMBUSTING CONDITIONS
S. Pal, M. D. Moser, H. M. Ryan, M. J. Foust, and R. J. Santoro 1992 39 p

(Contract NAS8-38862; NAGw-1356)
(NASA-CR-193339; NAS 1.26:193339) Avail: CASI HC A03/MF A01

Measurements of LOX drop size and velocity in a uni-element liquid propellant rocket chamber are presented. The use of the Phase Doppler Particle Analyzer in obtaining temporally-averaged probability density functions of drop size in a harsh rocket environment has been demonstrated. Complementary measurements of drop size/velocity for simulants under cold flow conditions are also presented. The drop size/velocity measurements made for combusting and cold flow conditions are compared, and the results indicate that there are significant differences in the two flowfields. Author

N94-11601# Los Alamos National Lab., NM.
MASSIVELY PARALLEL HYDRODYNAMICS ON UNSTRUCTURED GRIDS
M. S. Sahota and H. E. Trease 1993 5 p Presented at the 1993 International Simulators Conference on High Performance Computing, Arlington, VA, 29 Mar. - 1 Apr. 1993
(Contract W-7405-eng-36)
(DE93-007325; LA-UR-93-435; CONF-930372-4) Avail: CASI HC A01/MF A01 (US Sales Only)

We investigate the feasibility of using massively parallel Single Instruction Multiple Data (SIMD) and Multiple Instruction Multiple Data (MIMD) computer architectures for explicit three-dimensional unstructured-grid finite-element Lagrange and finite-volume free-Lagrange hydrodynamics. We compare the Cray-YMP, Connection Machine 200 (CM-200), and CM-5 computational times required for the foregoing algorithms. Although we observe very large global communication penalty (approximately 40-95% depending upon the problem) on the CM for these algorithms, moderate to good speedups over a single-processor Cray-YMP are obtained. Also, when the FORTRAN 90 code written for the CM is ported back to the Cray, we observe approximately 30-40% speedups over the original vectorized Cray coding. To reduce the global communication cost, we investigate the possibility of using an automatic generalized domain decomposition technique for MIMD architectures (CM-5) currently under development at the Thinking Machines Corporation. DOE

N94-11604 International Centre for Theoretical Physics, Trieste (Italy).
ON TEMPERATURE DISTRIBUTION IN NON-PARTICIPATING MEDIUM WITH RADIATION BOUNDARY CONDITION
A. Naseem Nov. 1992 8 p Limited Reproducibility: More than 20% of this document may be affected by microfiche quality
(DE93-619375; IC-92/374) Avail: CASI HC A02 (US Sales Only)

Flow of Walters liquid B model is considered to obtain temperature distribution and the Nusselt number in non-participating medium with radiation boundary condition. The influence of visco-elasticity on the Nusselt number is discussed. DOE

N94-11615 Texas Univ., Austin.
ACCRETION DISK VISCOSITY AND INTERNAL WAVES IN DISKS Ph.D. Thesis
Min Huang 1992 185 p
Avail: Univ. Microfilms Order No. DA9309192

Recently, Vishniac, Jin and Diamond suggested that internal waves in accretion disks play a critical role in generating magnetic fields, and consequently are indirectly responsible for angular momentum transfer in thin, conducting, and non-self-gravitational disk systems. A project in which we will construct a quantitative model of the internal wave spectrum in accretion disks is started. It includes two aspects of work. The physical properties of the waves in a thin, non-self-gravitational, and non-magnetized accretion disk with realistic vertical structure is cataloged and examined. Besides the low frequency internal waves discovered by Vishniac and Diamond, it was found that sound waves with low frequency and low axisymmetry (with small absolute value of m) are capable of a driving dynamo because they are (1) well confined in a layer with thickness 2(absolute value of m)H where H is the disk scale height; (2) highly dispersive so they may survive the strong dissipation caused by the coherent nonlinear interaction their high frequency partners experience; and (3) elliptically polarized because they are confined in the z-direction. As a first step towards constructing a quantitative theory of this dynamo effect, a framework of calculating resonant nonlinear interaction among waves in disk is established. We are developing a numerical code which will compute the steady spectrum of the wave field in this framework. For simplicity, we only include the low frequency internal waves suggested by Vishniac and Diamond in the present stage. In the vicinity of the static state, the time step whose length is determined by the evolution of the modes with the largest amplitudes is too large for the modes with smaller amplitudes and overshooting occurs. Through nonlinear coupling, this overshooting is amplified and appears as a numerical instability affecting the evolution of the large amplitude modes. Shorter time steps may delay the appearance of the instability but not cure it. Additionally, shorter and shorter time steps make the computation more and more inefficient. Two ways to improve the codes are suggested. Dissert. Abstr.

N94-11616 McGill Univ., Montreal (Quebec).
MODELLING QUASI-TWO-DIMENSIONAL TURBULENT SHEAR FLOW Ph.D. Thesis
Sofia Babarutsi 1991 223 p
Avail: Univ. Microfilms Order No. DANN72131

A two-length-scale turbulence model is introduced for the computation of quasi-two-dimensional turbulent shear flow with two distinct length scales of motion. In the model, the turbulence motions of the two distinct length scales are computed separately. The small-scale turbulence is treated as a background component locally in equilibrium while the large-scale turbulence is simulated using a second order closure procedure. The development of the turbulent shear flows depends on the rate of energy transfer from the large-scale to the small scale turbulence. Two mechanisms are identified to have a significant effect on the rate of this energy transfer. On one hand, the rate is reduced due to the confinement of the large-scale turbulence to two dimensional motion, since the nonlinear energy cascade process is less efficient in two-dimensional turbulent motion. On the other hand, the rate is enhanced due to the work done by the large-scale turbulent motion against the friction forces. The energy transfer rate due to friction is derived in the model using a two-step averaging procedure, whereas the transfer rate due to nonlinear cascade process is determined using a model equation. The data from a number of experimental investigations of quasi-two-dimensional turbulent shear flows are analyzed. These data support the notion of the two-length-scale turbulence model, that (1) the maintenance of the turbulent motion depends on the transfer of energy from the large-scale turbulence to the small-scale turbulence, and (2) the transfer rate is subjected to confinement and friction influences as specified in the model. Numerical computations are conducted using the two-length-scale model and a single-length-scale model. The results are compared with the experimental data. The two-length-scale model is superior in performance compared with the single-length-scale model, particularly in the intermediate region of the flow where both length scales of the turbulent motion are equally important. Dissert. Abstr.

N94-11635 California Univ., Los Angeles.
NUMERICAL SIMULATIONS OF THERMAL CONVECTION IN RAPIDLY ROTATING SPHERICAL FLUID SHELLS Ph.D. Thesis
Zi-Ping Sun 1992 286 p
Avail: Univ. Microfilms Order No. DA9310954

Numerical simulations of thermal convection in rapidly rotating spherical shells of Boussinesq fluid were carried out with a nonlinear, three-dimensional, time-dependent spectral-transform code. The basic state is hydrostatic, spherically symmetric, and independent of time. The numerical methods, the numerical stability, and the adequacy of the spatial resolution were examined by a benchmarking study. A sequence of bifurcations from the onset of a steadily propagating convective state, to a periodic state, to a quasi-periodic state and thence a chaotic state was found. Convective solutions at each stage along the route to chaos were studied. The emphases are on the three dimensional and time-dependent convective structures and associated mean zonal flow. The spherical shell is heated from both below and within. The boundaries are isothermal and stress-free. The consequences of imposing a spatially varying temperature anomaly on the upper surface of a spherical shell on thermal convection in the shell was also explored. The spherical shell is heated from below and cooled from above. The lower boundary is isothermal and both boundaries are rigid and impermeable. The results show that the patterns and amplitudes of the convective motions and associated mean zonal and meridional flows depend largely on the pattern and amplitude of the imposed thermal anomaly. The purpose is to illustrate the influence of thermal conditions in the lower mantle on motions in the Earth's liquid outer core. Finally, numerical

simulations at both high Taylor and Rayleigh numbers were carried out. The spherical shell is heated from below and cooled from above. The boundaries are isothermal and stress-free. Columnar rolls that are quasi-layered in cylindrical radius and associated banded mean zonal flow are obtained. The quasi-layered convective structure and the banded zonal wind are consequent upon both the high Taylor and Rayleigh numbers. The numerical results confirm the theory that cylindrically multilayered columnar thermal convection occurs in rapidly rotating systems and can result in a banded zonal surface flow thereby providing an explanation in principle for the remarkable bandings of Jupiter and Saturn.
Dissert. Abstr.

N94-11641# Nielsen Engineering and Research, Inc., Mountain View, CA.
TURBULENCE MODELING FOR THRUST REVERSER FLOW FIELD PREDICTION METHODS Final Report, 30 Apr. 1990 - 31 Dec. 1992
Robert E. Childs, Laura C. Rodman, and Peter Bradshaw Dec. 1992 70 p
(Contract F33615-90-C-3002)
(AD-A266139; NEAR-TR-457; WL-TR-92-3121) Avail: CASI HC A04/MF A01

The use of thrust reversing on aircraft operating in ground effect produces complex flow fields, for which conventional turbulence models are inadequate. The main objective of the work was to produce an improved turbulence model. The work included experimental measurements of an impinging jet inclined 45 degrees into the crossflow. Large eddy simulation (LES) was used to identify the dominant turbulent physics in these flows and to guide the development of an improved k-epsilon model for Reynolds-averaged calculations. Modifications to the k-epsilon model for the effects of streamline curvature and vortex stretching (lateral divergence) were used. Compared to the original k-epsilon model, the modified model reduced by as much as 70 percent the errors in predicting the ground vortex location.
DTIC

N94-11814# Pittsburgh Univ., PA.
THE PHYSICS OF PATTERN FORMATION OF LIQUID INTERFACES
1993 26 p
(Contract DE-FG02-84ER-45131)
(DE93-013333; DOE/ER-45131/T2) Avail: CASI HC A03/MF A01

Energy consumption in fabrication of materials for all applications is process dependent. Improvements in the ability to process materials are of great importance to the DOE mission. This project addresses basic science questions related to the processing of materials and is aimed at understanding growth of interfaces and evolution of patterns on interfaces, both macroscopic and microscopic. Three laboratory experiments are proposed: A study of the changes in patterns available to the growth of a macroscopic interface when that interface is grown over one of a variety of 'microscopic' lattices; a study of reversible aggregation of colloidal particles in a mixed solvent, and of the interactions and relaxations of both solvent and suspended particles when thermodynamic conditions are changed for a liquid matrix with suspended particles or fibres; and an investigation of the sedimentation of particles in a quasi-two-dimensional viscous fluid, with attention both to the dynamics of the flow and to the roughness of the resulting surface of settled particles.
DOE

N94-11824 Texas Univ., Austin.
GRID OPTIMIZATION AND MULTIGRID TECHNIQUES FOR FLUID FLOW AND TRANSPORT PROBLEMS Ph.D. Thesis
Anand L. Pardhanani 1992 215 p
Avail: Univ. Microfilms Order No. DA9309251

Special numerical techniques for the efficient and accurate solution of fluid flow and certain other transport processes are investigated. These include adaptive redistribution and optimization of computational grids, multigrid techniques for convection-diffusion problems, and multigrid time-marching methods for non-stationary and nonlinear problems. The grid optimization strategy is based on constructing and minimizing a mathematical objective function which defines the desired grid properties. For convection-diffusion problems, it is demonstrated that standard multigrid techniques fail when the coarse grids violate mesh-size restrictions. A variety of alternate multigrid strategies are explored, including artificial dissipation, fine grid pre-elimination, self-adjoint formulation, defect correction, and combination with grid redistribution. Multilevel techniques are also developed for time-dependent problems, including evolution problems with non-steady or transient solutions, and steady-state problems solved with artificial time-marching. Both explicit and implicit integration schemes are investigated, and it is shown that significant performance improvements can be gained with the use of multigrid. These techniques are implemented and tested on representative model problems as well as practical applications of current research interest. The grid investigations involve optimization in model problems, and in large-scale 3-D aircraft wing-body configurations. The multigrid applications range from model convection-diffusion problems, to time-dependent problems, to coupled nonlinear problems in two major application areas. The first application involves simulating spatio-temporal patterns in a coupled, nonlinear, reaction-diffusion problem that models the behavior of the Belousov-Zhabotinskii reaction. This multi-species reaction, which exhibits intricate patterns in laboratory experiments, has attracted considerable interest in the field of nonlinear dynamics. The numerical simulation of this problem is carried out using the above multigrid strategies, and it is shown that considerable speed up can be achieved. The other main application involves the simulation of submicron semiconductor devices using a new hydrodynamic transport model. This is a very complex application, and many of its modeling and simulation aspects remain a subject of ongoing research. The present work has yielded preliminary results, including significant performance gains for a representative MOSFET structure in 1-D. The software for these applications is optimized to yield high performance on vector supercomputers such as the Cray Y-MP. This is demonstrated, in particular, for the applications involving timestepping, where computational efficiency is of crucial importance.
Dissert. Abstr.

N94-11859# Aircraft Research Association Ltd., Bedford (England).
SAUNA: A SYSTEM FOR GRID GENERATION AND FLOW SIMULATION USING HYBRID STRUCTURED/UNSTRUCTURED GRIDS
P. N. Childs, J. A. Shaw, A. J. Peace, and J. M. Georgala May 1992 9 p Presented at the First European Computational Fluid Dynamics Conference, Brussels, Belgium, 7-11 Sept. 1992 Original contains color illustrations
(Contract SLS41B/2437)
(ARA-Memo-370) Avail: CASI HC A02/MF A01

The development of a flow simulation facility for predicting the aerodynamics of complex configurations wherein the grid is composed of both structured and unstructured regions is described. Issues relating to the generation and analysis of such grids and to the accurate and efficient computation of both inviscid and viscous flows thereon are considered. Further the development of a comprehensive post-processing and visualization facility is explored. Techniques are illustrated throughout by application to realistic aircraft geometries.
Author (revised)

N94-11865# Woods Hole Oceanographic Inst., MA.
VORTEX-INDUCED FORCES ON OSCILLATING BLUFF CYLINDERS Ph.D. Thesis
Ramnarayan Gopalkrishnan Feb. 1993 254 p
(Contracts N00014-89-C-0179; N00014-92-J-1726; NSF OCE-85-11431; NA90AA-D-SG424)
(AD-A265056; WHOI-92-38) Avail: CASI HC A12/MF A03

Vortex-induced forces and the consequent vibration of long cylindrical structures are important for a large number of engineering applications; the complexity of the underlying physical mechanisms is such that this is one of the canonical problems of fluid mechanics. Vortex shedding force varies in frequency and magnitude along the length of the structure causing the response at any point to be amplitude-modulated in space and time. The focus is on the measurement, via forced-oscillation experiments, of the vortex-induced lift and drag forces acting on circular cylinders undergoing sinusoidal and amplitude-modulated oscillations. Basic concepts on vortex formation and vortex-induced vibrations, a review of the existing literature, and details of the experimental apparatus and data processing methods are presented. Stationary and sinusoidal oscillation tests are presented. Several novel properties are described, among them the role of the lift force phase angle in causing the amplitude-limited nature of VIV, and use of the lift force excitation region in contrast with the often-quoted but quite different lift force lock-in region. Next, a comprehensive data error analysis and a simple VIV prediction scheme are described. New data on amplitude-modulated oscillations are presented. The concept of control of the mean wake velocity profile via the control of the major vortical feature is explored with possible applications being the reduction of the in-line wake velocity and alteration of the wake signature. DTIC

N94-12284*# Stanford Univ., CA. Center for Turbulence Research.
ANNUAL RESEARCH BRIEFS, 1992 Progress Reports
Debra Spinks, comp. Jan. 1993 449 p Sponsored in part by AFOSR and ONR
(Contract NCC2-460)
(NASA-CR-194389; NAS 1.26:194389) Avail: CASI HC A19/MF A04

This report contains the 1992 annual progress reports of the Research Fellows and students of the Center for Turbulence Research. Considerable effort was focused on the large eddy simulation technique for computing turbulent flows. This increased activity has been inspired by the recent predictive successes of the dynamic subgrid scale modeling procedure which was introduced during the 1990 Summer Program. Several Research Fellows and students are presently engaged in both the development of subgrid scale models and their applications to complex flows. The first group of papers in this report contain the findings of these studies. They are followed by reports grouped in the general areas of modeling, turbulence physics, and turbulent reacting flows. The last contribution in this report outlines the progress made on the development of the CTR post-processing facility. For individual titles, see N94-12285 through N94-12320.

N94-12285*# Stanford Univ., CA. Center for Turbulence Research.
A LOCAL DYNAMIC MODEL FOR LARGE EDDY SIMULATION
Sandip Ghosal, Thomas S. Lund, and Parviz Moin *In its* Annual Research Briefs, 1992 Jan. 1993 p 3-25 (For primary document see N94-12284 01-34)
Avail: CASI HC A03/MF A04

The dynamic model is a method for computing the coefficient C in Smagorinsky's model for the subgrid-scale stress tensor as a function of position from the information already contained in the resolved velocity field rather than treating it as an adjustable parameter. A variational formulation of the dynamic model is described that removes the inconsistency associated with taking C out of the filtering operation. This model, however, is still unstable due to the negative eddy-viscosity. Next, three models are presented that are mathematically consistent as well as numerically stable. The first two are applicable to homogeneous flows and flows with at least one homogeneous direction, respectively, and are, in fact, a rigorous derivation of the ad hoc expressions used by previous authors. The third model in this set can be applied to arbitrary flows, and it is stable because the C it predicts is always positive. Finally, a model involving the subgrid-scale kinetic energy is presented which attempts to model backscatter. This last model has some desirable theoretical features. However, even though it gives results in LES that are qualitatively correct, it is outperformed by the simpler constrained variational models. It is suggested that one of the constrained variational models should be used for actual LES while theoretical investigation of the kinetic energy approach should be continued in an effort to improve its predictive power and to understand more about backscatter. Derived from text

N94-12286*# Stanford Univ., CA. Center for Turbulence Research.
PARAMETERIZATION OF SUBGRID-SCALE STRESS BY THE VELOCITY GRADIENT TENSOR
Thomas S. Lund and E. A. Novikov (California Univ., San Diego.) *In its* Annual Research Briefs, 1992 Jan. 1993 p 27-43 Sponsored in part by DOE (For primary document see N94-12284 01-34)
(Contracts N00014-91-J-4072; F49620-92-J-0003)
Avail: CASI HC A03/MF A04

The objective of this work is to construct and evaluate subgrid-scale models that depend on both the strain rate and the vorticity. This will be accomplished by first assuming that the subgrid-scale stress is a function of the strain and rotation rate tensors. Extensions of the Caley-Hamilton theorem can then be used to write the assumed functional dependence explicitly in the form of a tensor polynomial involving products of the strain and rotation rates. Finally, use of this explicit expression as a subgrid-scale model will be evaluated using direct numerical simulation data for homogeneous, isotropic turbulence. Derived from text

N94-12287*# Stanford Univ., CA. Center for Turbulence Research.
LARGE EDDY SIMULATIONS OF TIME-DEPENDENT AND BUOYANCY-DRIVEN CHANNEL FLOWS
William H. Cabot *In its* Annual Research Briefs, 1992 Jan. 1993 p 45-60 (For primary document see N94-12284 01-34)
Avail: CASI HC A03/MF A04

The primary goal of this work has been to assess the performance of the dynamic SGS model in the large eddy simulation (LES) of channel flows in a variety of situations, viz., in temporal development of channel flow turned by a transverse pressure gradient and especially in buoyancy-driven turbulent flows such as Rayleigh-Benard and internally heated channel convection. For buoyancy-driven flows, there are additional buoyant terms that are possible in the base models, and one objective has been to determine if the dynamic SGS model results are sensitive to such terms. The ultimate goal is to determine the minimal base model needed in the dynamic SGS model to provide accurate results in flows with more complicated physical features. In addition, a program of direct numerical simulation (DNS) of fully compressible channel convection has been undertaken to determine stratification and compressibility effects. These simulations are intended to provide a comparative base for performing the LES of compressible (or highly stratified, pseudo-compressible) convection at high Reynolds number in the future. Derived from text

N94-12288*# National Aeronautics and Space Administration. Ames Research Center, Moffett Field, CA.
A NORMAL STRESS SUBGRID-SCALE EDDY VISCOSITY MODEL IN LARGE EDDY SIMULATION
K. Horiuti (Tokyo Univ., Japan.), N. N. Mansour, and John J. Kim *In* Stanford Univ., Annual Research Briefs, 1992 Jan. 1993 p 61-71 Sponsored in part by Tokyo Univ. (For primary document see N94-12284 01-34)
Avail: CASI HC A03/MF A04

The Smagorinsky subgrid-scale eddy viscosity model (SGS-EVM) is commonly used in large eddy simulations (LES) to represent the effects of the unresolved scales on the resolved scales. This model is known to be limited because its constant must be optimized in different flows, and it must be modified with a damping function to account for near-wall effects. The recent dynamic model is designed to overcome these limitations but is compositionally intensive as compared to the traditional SGS-EVM. In a recent study using direct numerical simulation data, Horiuti has shown that these drawbacks are due mainly to the use of an improper velocity scale in the SGS-EVM. He also proposed the use of the subgrid-scale normal stress as a new velocity scale that was inspired by a high-order anisotropic representation model. The testing of Horiuti, however, was conducted using DNS data from a low Reynolds number channel flow simulation. It was felt that further testing at higher Reynolds numbers and also using different flows (other than wall-bounded shear flows) were necessary steps needed to establish the validity of the new model. This is the primary motivation of the present study. The objective is to test the new model using DNS databases of high Reynolds number channel and fully developed turbulent mixing layer flows. The use of both channel (wall-bounded) and mixing layer flows is important for the development of accurate LES models because these two flows encompass many characteristic features of complex turbulent flows. Derived from text

N94-12289*# Stanford Univ., CA. Center for Turbulence Research.
LARGE EDDY SIMULATION OF SHOCK TURBULENCE INTERACTION
Sangsan Lee *In its* Annual Research Briefs, 1992 Jan. 1993 p 73-84 (For primary document see N94-12284 01-34)
Avail: CASI HC A03/MF A04

A nonconservative formulation of the energy equation (solving for internal energy) was used to perform large eddy simulations of compressible turbulence in Moin et al. due to its simplicity in implementing SGS models compared to the conservative formulation (solving for total energy). In problems with shocks in the domain, however, the total energy formulation is preferred due to its conservative nature. A conservative set of equations for the LES were derived from the nonconservative equations derived by Moin et al. Performance of the conservative formulation was compared with the experiment on decaying grid-generated turbulence as well as with the filtered DNS field. Various shock-capturing schemes were tested, and an ENO shock-capturing scheme of Shu and Osher was chosen for the simulation of shock/turbulence interaction. The scheme was tested and validated against the data base generated by DNS of weak shock waves. The results obtained with the essentially nonoscillatory (ENO) scheme were within 5 percent from the DNS results, and used less than 25 percent of the CPU time used in the DNS. Derived from text

N94-12290*# Stanford Univ., CA. Center for Turbulence Research.
APPLICATION OF A DYNAMIC SUBGRID-SCALE MODEL TO TURBULENT RECIRCULATING FLOWS
Y. Zang, R. L. Street, and J. R. Koseff *In its* Annual Research Briefs, 1992 Jan. 1993 p 85-95 (For primary document see N94-12284 01-34)
(Grant NSF CTS-87-19509)
Avail: CASI HC A03/MF A04

The dynamic subgrid-scale model of Germano et al. is implemented in a finite volume formulation and applied to the simulation of turbulent flow in a three-dimensional lid-driven cavity at Reynolds number of 7500. The filtering operation is carried out in physical space, and the model coefficient is calculated locally. The computed mean and rms velocities as well as the Reynolds stress are compared with experimental data. It is shown that backscatter from small to large scales is necessary to sustain turbulent fluctuations. The model is being applied to the simulation of turbulent flows in a stratified and rotating environment in complex geometries. Derived from text

N94-12291*# Stanford Univ., CA. Center for Turbulence Research.
LARGE-EDDY SIMULATION OF TURBULENT FLOW WITH A SURFACE-MOUNTED TWO-DIMENSIONAL OBSTACLE
Kyung-Soo Yang and Joel H. Ferziger *In its* Annual Research Briefs, 1992 Jan. 1993 p 97-111 (For primary document see N94-12284 01-34)
(Contract N00014-89-J-1343)
Avail: CASI HC A03/MF A04

In this paper, we perform a large eddy simulation (LES) of turbulent flow in a channel containing a two-dimensional obstacle on one wall using a dynamic subgrid-scale model (DSGSM) at Re = 3210, based on bulk velocity above the obstacle and obstacle height; the wall layers are fully resolved. The low Re enables us to perform a DNS (Case 1) against which to validate the LES results. The LES with the DSGSM is designated Case 2. In addition, an LES with the conventional fixed model constant (Case 3) is conducted to allow identification of improvements due to the DSGSM. We also include LES at Re = 82,000 (Case 4) using conventional Smagorinsky subgrid-scale model and a wall-layer model. The results will be compared with the experiment of Dimaczek et al. Derived from text

N94-12292*# Stanford Univ., CA. Center for Turbulence Research.
SIMILARITY STATES OF HOMOGENEOUS STABLY-STRATIFIED TURBULENCE AT INFINITE FROUDE NUMBER
Jeffrey R. Chasnov *In its* Annual Research Briefs, 1992 Jan. 1993 p 113-127 (For primary document see N94-12284 01-34)
Avail: CASI HC A03/MF A04

We present evidence of similarity states which may develop inhomogeneous stably-stratified flows if a dimensionless group in addition to the Reynolds number, the so-called Froude number, is sufficiently large. Here, we define the Froude number as the ratio of the internal wave time-scale to the turbulence time-scale. We examine three different similarity states which may develop depending on the initial conditions of the velocity and density fields. Theoretical arguments and results of large-eddy simulations will be presented. We will conclude this report with some speculative thoughts on similarity states which may develop in stably-stratified turbulence at arbitrary Froude number as well as our future research plans in this area. Derived from text

N94-12293*# Stanford Univ., CA. Center for Turbulence Research.
APPLICATION OF INCREMENTAL UNKNOWNS TO THE BURGERS EQUATION
Haecheon Choi and Roger Temam (Paris-Sud Univ., Orsay, France.) *In its* Annual Research Briefs, 1992 Jan. 1993 p 129-138 (For primary document see N94-12284 01-34)
Avail: CASI HC A02/MF A04

In this article, we make a few remarks on the role that attractors and inertial manifolds play in fluid mechanics problems. We then describe the role of incremental unknowns for approximating attractors and inertial manifolds when finite difference multigrid discretizations are used. The relation with direct numerical simulation and large eddy simulation is also mentioned. Derived from text

N94-12294*# Stanford Univ., CA. Center for Turbulence Research.
DIRECT SIMULATION OF COMPRESSIBLE WALL-BOUNDED TURBULENCE
Gary N. Coleman *In its* Annual Research Briefs, 1992 Jan. 1993 p 139-144 (For primary document see N94-12284 01-34)
Avail: CASI HC A02/MF A04

When analyzing many turbulent flows, the effects of compressibility can be neglected. Even some relatively high-speed flows, such as boundary layers generated by a supersonic aircraft, produce turbulent statistics that are similar to those found for the incompressible case. There are other situations, however, in which the non-zero divergence of the turbulence leads to behavior that is fundamentally different from that found at constant density. Examples include flows created by internal combustion engines, hypersonic flight, and supersonic combustion. It is with instances such as these that this project is concerned. In particular, we are interested in the effects of compressibility on turbulence near a smooth solid constant temperature surface; our primary objective is an increased physical understanding that can be used to improve turbulence models of wall-bounded compressible flows. With this in mind, we have begun a direct numerical simulation (DNS) study of turbulence in a plane channel. Because all of the relevant spatial and temporal scales are to be resolved, the simulations require no subgrid scale parameterization. The DNS code developed by Buell to study compressible plane Couette flow was modified to solve the compressible Navier-Stokes equations in the plane channel. The channel was chosen over the Couette flow for two reasons: (1) to avoid using the very large streamwise domains needed to adequately capture the large Couette vortical structures; and (2) to make use of previous experience by considering the compressible version of a well established case and isolate finite Mach number effects by comparing to the incompressible channel. Author (revised)

N94-12295*# Stanford Univ., CA. Center for Turbulence Research.
DIRECT NUMERICAL SIMULATION OF HOT JETS
Marc C. Jacob *In its* Annual Research Briefs, 1992 Jan. 1993 p 145-160 (For primary document see N94-12284 01-34)
Avail: CASI HC A03/MF A04

The ultimate motivation of this work is to investigate the stability of two dimensional heated jets and its implications for aerodynamic sound generation from data obtained with direct numerical simulations (DNS). As pointed out in our last report, these flows undergo two types of instabilities, convective or absolute, depending on their temperature. We also described the limits of earlier experimental and theoretical studies and explained why a numerical investigation could give us new insight into the physics of these instabilities. The aeroacoustical interest of these flows was also underlined. In order to reach this goal, we first need to succeed in the DNS of heated jets. Our past efforts have been focused on this issue which encountered several difficulties. Our numerical difficulties are directly related to the physical problem we want to investigate since these absolutely or almost absolutely unstable flows are by definition very sensitive to the smallest disturbances and are very likely to reach nonlinear saturation through a numerical feedback mechanism. As a result, it is very difficult to compute a steady laminar solution using a spatial DNS. A steady state was reached only for strongly co-flowed jets, but these flows are almost equivalent to two independent mixing layers. Thus they are far from absolute instability and have much lower growth rates. Author (revised)

N94-12296*# Stanford Univ., CA. Center for Turbulence Research.
DIRECT NUMERICAL SIMULATION OF TURBULENT FLOW OVER A BACKWARD-FACING STEP
Hung Le and Parviz Moin *In its* Annual Research Briefs, 1992 Jan. 1993 p 161-173 Sponsored in part by NSF (For primary document see N94-12284 01-34)
Avail: CASI HC A03/MF A04

The objectives of this study are as follows: (1) to conduct a direct numerical simulation of turbulent backward facing step flow using inflow and outflow conditions; and (2) to provide data in the form of Reynolds stress budgets for Reynolds averaged modeling. The report presents the basic statistical data and comparisons with the concurrent experiments of Jovic and Driver and budgets of turbulent kinetic energy. Author (revised)

N94-12297*# Stanford Univ., CA. Center for Turbulence Research.

NUMERICAL SIMULATION USING VORTICITY-VECTOR POTENTIAL FORMULATION

Hiroshi Tokunaga *In its* Annual Research Briefs, 1992 Jan. 1993 p 175-184 (For primary document see N94-12284 01-34)
Avail: CASI HC A02/MF A04

An accurate and efficient computational method is needed for three-dimensional incompressible viscous flows in engineering applications. On solving the turbulent shear flows directly or using the subgrid scale model, it is indispensable to resolve the small scale fluid motions as well as the large scale motions. From this point of view, the pseudo-spectral method is used so far as the computational method. However, the finite difference or the finite element methods are widely applied for computing the flow with practical importance since these methods are easily applied to the flows with complex geometric configurations. However, there exist several problems in applying the finite difference method to direct and large eddy simulations. Accuracy is one of most important problems. This point was already addressed by the present author on the direct simulations on the instability of the plane Poiseuille flow and also on the transition to turbulence. In order to obtain high efficiency, the multi-grid Poisson solver is combined with the higher-order, accurate finite difference method. The formulation method is also one of the most important problems in applying the finite difference method to the incompressible turbulent flows. The three-dimensional Navier-Stokes equations have been solved so far in the primitive variables formulation. One of the major difficulties of this method is the rigorous satisfaction of the equation of continuity. In general, the staggered grid is used for the satisfaction of the solenoidal condition for the velocity field at the wall boundary. However, the velocity field satisfies the equation of continuity automatically in the vorticity-vector potential formulation. From this point of view, the vorticity-vector potential method was extended to the generalized coordinate system. In the present article, we adopt the vorticity-vector potential formulation, the generalized coordinate system, and the 4th-order accurate difference method as the computational method. We present the computational method and apply the present method to computations of flows in a square cavity at large Reynolds number in order to investigate its effectiveness. Author (revised)

N94-12298*# Stanford Univ., CA. Center for Turbulence Research.

REYNOLDS STRESS CLOSURE MODELING IN WALL-BOUNDED FLOWS

Paul A. Durbin *In its* Annual Research Briefs, 1992 Jan. 1993 p 185-197 (For primary document see N94-12284 01-34)
Avail: CASI HC A03/MF A04

This report describes two projects. Firstly, a Reynolds stress closure for near-wall turbulence is described. It was motivated by the simpler k-epsilon-(v-bar(exp 2)) model described in last year's annual research brief. Direct Numerical Simulation of three-dimensional channel flow shows a curious decrease of the turbulent kinetic energy. The second topic of this report is a model which reproduces this effect. That model is described and used to discuss the relevance of the three dimensional channel flow simulation to swept wing boundary layers. Author (revised)

N94-12299*# Stanford Univ., CA. Center for Turbulence Research.

APPLICATION OF A REYNOLDS STRESS MODEL TO SEPARATING BOUNDARY LAYERS

Sung Ho Ko *In its* Annual Research Briefs, 1992 Jan. 1993 p 199-211 (For primary document see N94-12284 01-34)
Avail: CASI HC A03/MF A04

Separating turbulent boundary layers occur in many practical engineering applications. Nonetheless, the physics of separation/reattachment of flows is poorly understood. During the past decade, various turbulence models were proposed and their ability to successfully predict some types of flows was shown. However. prediction of separating/reattaching flows is still a formidable task for model developers. The present study is concerned with the process of separation from a smooth surface. Features of turbulent separating boundary layers that are relevant to modeling include the following: the occurrence of zero wall shear stress, which causes breakdown of the boundary layer approximation; the law of the wall not being satisfied in the mean back flow region; high turbulence levels in the separated region; a significant low-frequency motion in the separation bubble; and the turbulence structure of the separated shear layer being quite different from that of either the mixing layers or the boundary layers. These special characteristics of separating boundary layers make it difficult for simple turbulence models to correctly predict their behavior. Author (revised)

N94-12300*# Stanford Univ., CA. Center for Turbulence Research.

PROGRESS IN MODELING HYPERSONIC TURBULENT BOUNDARY LAYERS

Otto Zeman *In its* Annual Research Briefs, 1992 Jan. 1993 p 213-225 (For primary document see N94-12284 01-34)
Avail: CASI HC A03/MF A04

A good knowledge of the turbulence structure, wall heat transfer, and friction in turbulent boundary layers (TBL) at high speeds is required for the design of hypersonic air breathing airplanes and reentry space vehicles. This work reports on recent progress in the modeling of high speed TBL flows. The specific research goal described here is the development of a second order closure model for zero pressure gradient TBL's for the range of Mach numbers up to hypersonic speeds with arbitrary wall cooling requirements. Author (revised)

N94-12301*# Stanford Univ., CA. Center for Turbulence Research.

RECEPTIVITY IN PARALLEL FLOWS: AN ADJOINT APPROACH

D. Christopher Hill *In its* Annual Research Briefs, 1992 Jan. 1993 p 227-236 (For primary document see N94-12284 01-34)
Avail: CASI HC A02/MF A04

Linear receptivity studies in parallel flows are aimed at understanding how external forcing couples to the natural unstable motions which a flow can support. The vibrating ribbon problem models the original Schubauer and Skramstad boundary layer experiment and represents the classic boundary layer receptivity problem. The process by which disturbances are initiated in convectively-unstable jets and shear layers has also received attention. Gaster was the first to handle the boundary layer analysis with the recognition that spatial modes, rather than temporal modes, were relevant when studying convectively-unstable flows that are driven by a time-harmonic source. The amplitude of the least stable spatial mode, far downstream of the source, is related to the source strength by a coupling coefficient. The determination of this coefficient is at the heart of this type of linear receptivity study. The first objective of the present study was to determine whether the various wave number derivative factors, appearing in the coupling coefficients for linear receptivity problems, could be reexpressed in a simpler form involving adjoint eigensolutions. Secondly, it was hoped that the general nature of this simplification could be shown; indeed, a rather elegant characterization of the receptivity properties of spatial instabilities does emerge. The analysis is quite distinct from the usual Fourier-inversion procedures, although a detailed knowledge of the spectrum of the Orr-Sommerfeld equation is still required. Since the cylinder wake analysis proved very useful in addressing control considerations, the final objective was to provide a foundation upon which boundary layer control theory may be developed. Author (revised)

N94-12302*# Stanford Univ., CA. Center for Turbulence Research.

LOCAL ISOTROPY IN HIGH REYNOLDS NUMBER TURBULENT SHEAR FLOWS

Seyed G. Saddoughi *In its* Annual Research Briefs, 1992 Jan. 1993 p 237-262 (For primary document see N94-12284 01-34)
Avail: CASI HC A03/MF A04

This is a report on the continuation of experiments, which Dr. Srinivas Veeravalli and the present author started in 1991, to investigate the hypothesis of local isotropy in shear flows. This hypothesis, which states that at sufficiently high Reynolds numbers the small-scale structures of turbulent motions are independent of large-scale structures and mean deformations, has been used in theoretical studies of turbulence and computational methods like large-eddy simulation. The importance of Kolmogorov's ideas arises from the fact that they create a foundation for turbulence theory. Author (revised)

N94-12303*# Stanford Univ., CA. Center for Turbulence Research.

AN INVESTIGATION OF SMALL SCALES OF TURBULENCE IN A BOUNDARY LAYER AT HIGH REYNOLDS NUMBERS

James M. Wallace (Maryland Univ., College Park.), L. Ong (Maryland Univ., College Park.), and J.-L. Balint (Maryland Univ., College Park.) *In its* Annual Research Briefs, 1992 Jan. 1993 p 263-268 (For primary

document see N94-12284 01-34)
(Grant NSF CTS-92-17505)
Avail: CASI HC A02/MF A04

The assumption that turbulence at large wave-numbers is isotropic and has universal spectral characteristics which are independent of the flow geometry, at least for high Reynolds numbers, has been a cornerstone of closure theories as well as of the most promising recent development in the effort to predict turbulent flows, viz. large eddy simulations. This hypothesis was first advanced by Kolmogorov based on the supposition that turbulent kinetic energy cascades down the scales (up the wave-numbers) of turbulence and that, if the number of these cascade steps is sufficiently large (i.e. the wave-number range is large), then the effects of anisotropies at the large scales are lost in the energy transfer process. Experimental attempts were repeatedly made to verify this fundamental assumption. However, Van Atta has recently suggested that an examination of the scalar and velocity gradient fields is necessary to definitively verify this hypothesis or prove it to be unfounded. Of course, this must be carried out in a flow with a sufficiently high Reynolds number to provide the necessary separation of scales in order unambiguously to provide the possibility of local isotropy at large wave-numbers. An opportunity to use our 12-sensor hot-wire probe to address this issue directly was made available at the 80'x120' wind tunnel at the NASA Ames Research Center, which is normally used for full-scale aircraft tests. An initial report on this high Reynolds number experiment and progress toward its evaluation is presented. Author (revised)

N94-12304*# Stanford Univ., CA. Center for Turbulence Research.

PROBABILITY DENSITY DISTRIBUTION OF VELOCITY DIFFERENCES AT HIGH REYNOLDS NUMBERS

Alexander A. Praskovsky (Tsentralni Aerogidrodinamicheskii Inst., Moscow, USSR.) *In its* Annual Research Briefs, 1992 Jan. 1993 p 269-276 (For primary document see N94-12284 01-34)
Avail: CASI HC A02/MF A04

Recent understanding of fine-scale turbulence structure in high Reynolds number flows is mostly based on Kolmogorov's original and revised models. The main finding of these models is that intrinsic characteristics of fine-scale fluctuations are universal ones at high Reynolds numbers, i.e., the functional behavior of any small-scale parameter is the same in all flows if the Reynolds number is high enough. The only large-scale quantity that directly affects small-scale fluctuations is the energy flux through a cascade. In dynamical equilibrium between large- and small-scale motions, this flux is equal to the mean rate of energy dissipation epsilon. The pdd of velocity difference is a very important characteristic for both the basic understanding of fully developed turbulence and engineering problems. Hence, it is important to test the findings: (1) the functional behavior of the tails of the probability density distribution (pdd) represented by P(delta(u)) is proportional to exp(-b(r) absolute value of delta(u)/sigma(sub delta(u))) and (2) the logarithmic decrement b(r) scales as b(r) is proportional to r(sup 0.15) when separation r lies in the inertial subrange in high Reynolds number laboratory shear flows. Author (revised)

N94-12305*# Stanford Univ., CA. Center for Turbulence Research.

THE IDEAL KOLMOGOROV INERTIAL RANGE AND CONSTANT

Ye Zhou *In its* Annual Research Briefs, 1992 Jan. 1993 p 277-283 (For primary document see N94-12284 01-34)
Avail: CASI HC A02/MF A04

The energy transfer statistics measured in numerically simulated flows are found to be nearly self-similar for wavenumbers in the inertial range. Using the measured self-similar form, an 'ideal' energy transfer function and the corresponding energy flux rate were deduced. From this flux rate, the Kolmogorov constant was calculated to be 1.5, in excellent agreement with experiments. Author (revised)

N94-12306*# Stanford Univ., CA. Center for Turbulence Research.

THE HELICAL DECOMPOSITION AND THE INSTABILITY ASSUMPTION

Fabian A. Waleffe *In its* Annual Research Briefs, 1992 Jan. 1993 p 285-289 (For primary document see N94-12284 01-34)
Avail: CASI HC A01/MF A04

Direct numerical simulations show that the triadic transfer function T(k,p,q) peaks sharply when q (or p) is much smaller than k. The triadic transfer function T(k,p,q) gives the rate of energy input into wave number k from all interactions with modes of wave number p and q, where k, p, q form a triangle. This observation was thought to suggest that energy is cascaded downscale through non-local interactions with local transfer and that there was a strong connection between large and small scales. Both suggestions were in contradiction with the classical Kolmogorov picture of the energy cascade. The helical decomposition was found useful in distinguishing between kinematically independent interactions. That analysis has gone beyond the question of non-local interaction with local transfer. In particular, an assumption about the statistical direction of triadic energy transfer in any kinematically independent interaction was introduced (the instability assumption). That assumption is not necessary for the conclusions about non-local interactions with local transfer recalled above. In the case of turbulence under rapid rotation, the instability assumption leads to the prediction that energy is transferred in spectral space from the poles of the rotation axis toward the equator. The instability assumption is thought to be of general validity for any type of triad interactions (e.g. internal waves). The helical decomposition and the instability assumption offer detailed information about the homogeneous statistical dynamics of the Navier-Stokes equations. The objective was to explore the validity of the instability assumption and to study the contributions of the various types of helical interactions to the energy cascade and the subgrid-scale eddy-viscosity. This was done in the context of spectral closures of the Direct Interaction or Quasi-Normal type. Author (revised)

N94-12307*# Stanford Univ., CA. Center for Turbulence Research.

SUPERFLUID TURBULENCE

David C. Samuels *In its* Annual Research Briefs, 1992 Jan. 1993 p 291-301 (For primary document see N94-12284 01-34)
Avail: CASI HC A03/MF A04

At low temperatures (below 5 Kelvin), helium is a liquid with a very low kinematic viscosity. It was proposed that wind tunnels could be built using liquid helium as the test fluid. The primary advantages of such wind tunnels would be a combination of large Reynolds numbers and a relatively small apparatus. It is hoped that this combination will allow the study of high Reynolds number flows in an academic setting. There are two basic types of liquid helium wind tunnels that can be built, corresponding to the two phases of liquid helium. The high temperature phase (between approximately 2 to 5 Kelvin) is called helium 1 and is a Navier-Stokes fluid. There are no unanswered scientific questions about the design or operation of a wind tunnel in the helium 1 phase. The low temperature phase (below approximately 2 Kelvin) of liquid helium is called helium 2. This is a quantum fluid, meaning that there are some properties of helium 2 which are directly due to quantum mechanical effects and which are not observed in Navier-Stokes fluids. The quantum effects that are relevant to this paper are: (1) helium 2 is well described as a superposition of two separate fluids called the superfluid and the normal fluid. The normal-fluid component is a Navier-Stokes fluid and the superfluid is an irrotational Euler fluid; and (2) circulation in the superfluid exists only in quantized vortex filaments. All quantized vortex filaments have identical circulations kappa and core size a. The objective of the research at CTR was to develop an understanding of the microscopic processes responsible for the observed Navier-Stokes behavior of helium 2 flows. Author (revised)

N94-12308*# Stanford Univ., CA. Center for Turbulence Research.

REGENERATION OF NEAR-WALL TURBULENCE STRUCTURES

James M. Hamilton, John J. Kim, and Fabian A. Waleffe *In its* Annual Research Briefs, 1992 Jan. 1993 p 303-315 (For primary document see N94-12284 01-34)
Avail: CASI HC A03/MF A04

An examination of the regeneration mechanisms of near-wall turbulence and an attempt to investigate the critical Reynolds number conjecture of Waleffe & Kim is presented. The basis is an extension of the 'minimal channel' approach of Jimenez and Moin which emphasizes the near-wall region and further reduces the complexity of the turbulent flow. Reduction of the flow Reynolds number to the minimum value which will allow turbulence to be sustained has the effect of reducing the ratio of the largest scales to the smallest scales or, equivalently, of causing the near-wall region to fill more of the area between the channel walls. In addition, since each wall may have an active near-wall region, half of the channel is always somewhat redundant. If a plane Couette flow is instead chosen as the base flow, this redundancy is eliminated: the mean shear of a plane Couette flow has a single sign, and at low Reynolds numbers, the two wall regions share a single set of structures. A minimal flow with these modifications possesses, by construction, the strongest constraints which allow sustained turbulence, producing a greatly simplified flow in which the regeneration process can be examined. Author (revised)

N94-12309*# Stanford Univ., CA. Center for Turbulence Research.
EXPERIMENTS ON NEAR-WALL STRUCTURE OF THREE-DIMENSIONAL BOUNDARY LAYERS
Karen A. Flack and J. P. Johnston *In its* Annual Research Briefs, 1992 Jan. 1993 p 317-324 (For primary document see N94-12284 01-34)
Avail: CASI HC A02/MF A04

Investigations of three-dimensional turbulent boundary layers have shown basic differences between two- and three-dimensional flows. These differences can significantly impact the modeling of three-dimensional flows since many flow models are based on results from two-dimensional boundary layers. In many cases the shear stress vector direction has been shown to lag relative to the direction of the mean velocity gradient as the cross flow grows downstream. Coincidence of these vectors is necessary for a scalar eddy viscosity modeling assumption. A second effect is a reduction in magnitude of the shear stress and/or the shear stress to turbulence energy ratio, a(sub 1). This reduction has been observed in several experiments. Recent numerical simulations also indicate wall-layer structural differences between two- and three-dimensional boundary layers. The differences in structure between two- and three-dimensional boundary layers was also addressed in the experiment of Littell & Eaton. The experiment used two-point correlations to investigate the vortical structures in a three dimensional boundary layer on a spinning disk. It was found that each sign of longitudinal vortex is equally likely to exist, but one sign of vorticity is associated with a structure which is better at producing ejections. The goal of the current investigation is to study the structure of the inner layers. Among other questions, the differences between the effects deduced from the three-dimensional flow simulations and the effects seen in experiments can be examined. The research concentrates on the structure of the wall-layer through flow visualization and direct turbulence measurements down to y(+) = 5. Author (revised)

N94-12310*# National Aeronautics and Space Administration. Ames Research Center, Moffett Field, CA.
THE THREE-DIMENSIONAL EVOLUTION OF A PLANE WAKE
H. Maekawa (University of Electro-Communications, Chofu, Japan.), R. D. Moser, and N. N. Mansour *In* Stanford Univ., Annual Research Briefs, 1992 Jan. 1993 p 325-334 (For primary document see N94-12284 01-34)
Avail: CASI HC A02/MF A04

In the past three decades, linear stability analysis has led to a comprehensive understanding of the linear stages of transition in plane wakes. Our understanding of the nonlinear and turbulent stages is less developed. Nonlinear theory developed by Papageorgiou and Smith was used to study the long-wavelength regime in wakes. The nonlinear and turbulent stages were investigated experimentally, and few numerical studies examined the early nonlinear stages of forced wakes. The evolution of three dimensional disturbances in an incompressible wake is investigated using direct numerical simulations. The instantaneous three-dimaensional structures and corresponding statistics are presented. Author (revised)

N94-12311*# Stanford Univ., CA. Center for Turbulence Research.
MIXING IN A STRATIFIED SHEAR FLOW: ENERGETICS AND SAMPLING
G. N. Ivey (University of Western Australia, Nedlands.), J. R. Koseff, D. A. Briggs, and J. H. Ferziger *In its* Annual Research Briefs, 1992 Jan. 1993 p 335-344 (For primary document see N94-12284 01-34)
(Contract N00014-92-J-1611)
Avail: CASI HC A02/MF A04

Direct numerical simulations of the time evolution of homogeneous stably stratified shear flows have been performed for Richardson numbers from 0 to 1 and for Prandtl numbers between 0.1 and 2. The results indicate that mixing efficiency R(sub f) varies with turbulent Froude number in a manner consistent with laboratory experiments performed with Prandtl numbers of 0.7 and 700. However, unlike the laboratory results, for a particular Froude number, the simulations do not show a clear dependence on the magnitude of R(sub f) on Pr. The observed maximum value of R(sub f) is 0.25. When averaged over vertical length scales of an order of magnitude greater than either the overturning or Ozmidov scales of the flow, the simulations indicate that the dissipation rate epsilon is only weakly lognormally distributed with an intermittency of about 0.01 whereas estimated values in the ocean are 3 to 7. Author (revised)

N94-12312*# Stanford Univ., CA. Center for Turbulence Research.
LIF MEASUREMENTS OF SCALAR MIXING IN TURBULENT SHEAR LAYERS
Paris S. Karasso and M. G. Mungal *In its* Annual Research Briefs, 1992 Jan. 1993 p 345-356 (For primary document see N94-12284 01-34)
Avail: CASI HC A03/MF A04

The structure of shear layer flows at high Reynolds numbers remains a very interesting problem. Straight mixing layers have been studied and yielded information on the probability density function (pdf) of a passive scalar across the layer. Konrad and Koochesfahani & Dimotakis measured the pdf of the mixture fraction for mixing layers of moderate Reynolds numbers, each about 25,000 (Re based on velocity difference and visual thickness). Their measurements showed a 'non-marching' pdf (central hump which is invariant from edge to edge across the layer), a result which is linked to the visualizations of the spanwise Kelvin-Helmholtz (K-H) instability mode, which is the primary instability for plane shear layer flows. A secondary instability mode, the Taylor-Gortler (T-G) instability, which is associated with streamwise vortical structures, has also been observed in shear layers. Image reconstruction by Jimenez et al. and volume renderings by Karasso & Mungal at low Re numbers have demonstrated that the K-H and the T-G instability modes occur simultaneously in a non-mutually destructive way, evidence that supports the quasi two-dimensional aspect of these flows and the non-marching character of the pdf at low Reynolds numbers. At higher Re numbers though, the interaction of these two instability modes is still unclear and may affect the mixing process. In this study, we perform measurements of the concentration pdf of plane mixing layers for different operating conditions. At a speed ratio of r = U(sub 1)/U(sub 2) = 4:1, we examine three Reynolds number cases: Re = 14,000, Re = 31,000, and Re = 62,000. Some other Re number cases' results, not presented in detail, are invoked to explain the behavior of the pdf of the concentration field. A case of r = 2.6:1 at Re = 20,000 is also considered. The planar laser-induced fluorescence technique is used to yield quantitative measurements. The different Re are obtained by changing the velocity magnitudes of the two streams. The question of resolution of these measurements is addressed. In order to investigate the effects of the initial conditions on the development and the structure of the mixing layer, the boundary layer on the high-speed side of the splitter plate is tripped. The average concentration and the average mixed fluid concentration are also calculated to further understand the changes in the shear layer for the different cases examined. Derived from text

N94-12313*# Stanford Univ., CA. Center for Turbulence Research.
PLANE MIXING LAYER VORTICAL STRUCTURE KINEMATICS
Richard L. LeBoeuf *In its* Annual Research Briefs, 1992 Jan. 1993 p 357-371 (For primary document see N94-12284 01-34)
Avail: CASI HC A03/MF A04

The objective of the current project was to experimentally investigate the structure and dynamics of the streamwise vorticity in a plane mixing layer. The first part of this research program was intended to clarify whether the observed decrease in mean streamwise vorticity in the far-field of mixing layers is due primarily to the 'smearing' caused by vortex meander or to diffusion. Two-point velocity correlation measurements have been used to show that there is little spanwise meander of the large-scale streamwise vortical structure. The correlation measurements also indicate a large degree of transverse meander of the streamwise vorticity which is not surprising since the streamwise vorticity exists in the inclined braid region between the spanwise vortex core regions. The streamwise convection of the braid region thereby introduces an apparent transverse meander into measurements using stationary probes. These results corroborated with estimated secondary velocity profiles in which the streamwise vorticity produces a signature which was tracked in time. Derived from text

N94-12314*# Stanford Univ., CA. Center for Turbulence Research.
NUMERICAL SIMULATION OF THE NON-NEWTONIAN MIXING LAYER
Jalel Azaiez and G. M. Homsy *In its* Annual Research Briefs, 1992 Jan. 1993 p 373-380 (For primary document see N94-12284 01-34)
Avail: CASI HC A02/MF A04

This work is a continuing effort to advance our understanding of the effects of polymer additives on the structures of the mixing layer. In anticipation of full nonlinear simulations of the non-Newtonian mixing layer, we examined in a first stage the linear stability of the non-Newtonian mixing layer. The results of this study show that, for a fluid described by the Oldroyd-B model, viscoelasticity reduces the instability of the inviscid mixing layer in a special limit where the ratio (We/Re) is of order 1 where We is the Weissenberg number, a measure of the elasticity of the flow, and Re is the Reynolds number. In the present study, we pursue this project with numerical simulations of the non-Newtonian mixing layer. Our primary objective is to determine the effects of viscoelasticity on the roll-up structure. We also examine the origin of the numerical instabilities usually encountered in the simulations of non-Newtonian fluids. Derived from text

N94-12315*# Stanford Univ., CA. Center for Turbulence Research.
PDF APPROACH FOR TURBULENT SCALAR FIELD: SOME RECENT DEVELOPMENTS
Feng Gao *In its* Annual Research Briefs, 1992 Jan. 1993 p 381-391 (For primary document see N94-12284 01-34)
Avail: CASI HC A03/MF A04

The probability density function (PDF) method has been proven a very useful approach in turbulence research. It has been particularly effective in simulating turbulent reacting flows and in studying some detailed statistical properties generated by a turbulent field There are, however, some important questions that have yet to be answered in PDF studies. Our efforts in the past year have been focused on two areas. First, a simple mixing model suitable for Monte Carlo simulations has been developed based on the mapping closure. Secondly, the mechanism of turbulent transport has been analyzed in order to understand the recently observed abnormal PDF's of turbulent temperature fields generated by linear heat sources. Derived from text

N94-12316*# Stanford Univ., CA. Center for Turbulence Research.
THE EVOLUTION EQUATION FOR THE FLAME SURFACE DENSITY IN TURBULENT PREMIXED COMBUSTION c25
Arnaud Trouve *In its* Annual Research Briefs, 1992 Jan. 1993 p 393-409 (For primary document see N94-12284 01-34)
Avail: CASI HC A03/MF A04

The mean reaction rate in flamelet models for turbulent premixed combustion depends on two basic quantities: a mean chemical rate, called the flamelet speed, and the flame surface density. Our previous work had been primarily focused on the problem of the structure and topology of turbulent premixed flames, and it was then determined that the flamelet speed, when space-averaged, is only weakly sensitive to the turbulent flow field. Consequently, the flame surface density is the key quantity that conveys most of the effects of the turbulence on the rate of energy release. In flamelet models, this quantity is obtained via a modeled transport equation called the Sigma-equation. Past theoretical work has produced a rigorous approach that leads to an exact but unclosed formulation for the turbulent Sigma-equation. In the exact Sigma-equation, it appears that the dynamical properties of the flame surface density are determined by a single parameter, namely the turbulent flame stretch. Unfortunately, the turbulent flame stretch as well as the flame surface density is not available from experiments, and, in the absence of experimental data, little is known on the validity of the closure assumptions used in current flamelet models. Direct Numerical Simulation (DNS) is the alternative approach to get basic information on these fundamental quantities. In the present work, three-dimensional DNS of premixed flames in isotropic turbulent flow is used to estimate the different terms appearing in the Sigma-equation. A new methodology is proposed to provide the source and sink terms for the flame surface density, resolved both temporally and spatially throughout the turbulent flame brush. Using this methodology, our objective is to extract the turbulent flame stretch from the DNS data base and then perform extensive comparisons with flamelet models. Thanks to the detailed information produced by the DNS-based analysis, it is expected that this type of comparison will not only underscore the shortcomings of current models, but also suggest ways to improve them. Derived from text

N94-12317*# Stanford Univ., CA. Center for Turbulence Research.
STUDY AND MODELING OF FINITE RATE CHEMISTRY EFFECTS IN TURBULENT NON-PREMIXED FLAMES c25
Luc Vervisch *In its* Annual Research Briefs, 1992 Jan. 1993 p 411-429 (For primary document see N94-12284 01-34)
Avail: CASI HC A03/MF A04

The development of numerical models that reflect some of the most important features of turbulent reacting flows requires information about the behavior of key quantities in well defined combustion regimes. In turbulent flames, the coupling between turbulent and chemical processes is so strong that it is extremely difficult to isolate the role played by one individual physical phenomenon. Direct numerical simulation (hereafter DNS) allows us to study in detail the turbulence-chemistry interaction in some restricted but completely defined situations. Globally, non-premixed flames are controlled by two limiting regimes: the fast chemistry case, where the turbulent flame can be pictured as a random distribution of local chemical equilibrium problems; and the slow chemistry case, where the chemistry integrates in time the turbulent fluctuations. The Damkoehler number, ratio of a mechanical time scale to chemical time scale, is used to distinguish between these regimes. Today most of the industrial computer codes are able to perform predictions in the hypothesis of local equilibrium chemistry using a presumed shape for the probability density function (pdt) of the conserved scalar. However, the finite rate chemistry situation is of great interest because industrial burners usually generate regimes in which, at some points, the flame is undergoing local extinction or at least non-equilibrium situations. Moreover, this variety of situations strongly influences the production of pollutants. To quantify finite rate chemistry effect, the interaction between a non-premixed flame and a free decaying turbulence is studied using DNS. The attention is focused on the dynamic of extinction, and an attempt is made to quantify the effect of the reaction on the small scale mixing process. The unequal diffusivity effect is also addressed. Finally, a simple turbulent combustion model based on the DNS observations and tractable in real flow configurations is proposed. Derived from text

N94-12318*# Stanford Univ., CA. Center for Turbulence Research.
GENERATION OF TWO-DIMENSIONAL VORTICES IN A CROSS-FLOW
Jean-Michel Samaniego *In its* Annual Research Briefs, 1992 Jan. 1993 p 431-441 (For primary document see N94-12284 01-34)
Avail: CASI HC A03/MF A04

The present report is concerned with an experimental study on the generation of plane two-dimensional vortices in a cross-flow. The purpose of this work is to address the problem of the feasibility of a two-dimensional experiment of flame-vortex interactions. Derived from text

N94-12319*# Stanford Univ., CA. Center for Turbulence Research.
WHY DOES PREFERENTIAL DIFFUSION STRONGLY AFFECT PREMIXED TURBULENT COMBUSTION? c25
Vadim R. Kuznetsov (Izdatelstvo Nauka, Moscow, USSR.) *In its* Annual Research Briefs, 1992 Jan. 1993 p 443-453 (For primary document see N94-12284 01-34)
Avail: CASI HC A03/MF A04

Combustion of premixed reactants in a turbulent flow is a classical but unresolved problem. The key problem is to explain the following data: the maximal turbulent and laminar burning velocities u(sub t) and u(sub L) occur at different equivalence ratios Phi. It is known that the equivalence ratio varies along a curved flame if molecular diffusivity D(sub fuel) does not equal D(sub oxygen). However, the mean flame radius of curvature is much larger than the laminar flame thickness delta-L. Therefore, significant influence of preferential diffusion should occur only if the flame propagation speed varies with flame curvature. This conclusion agrees with Zel'dovich's long-standing idea about the important role of leading points of a flame. The main objective of this paper is to prove Zel'dovich's hypothesis. An equation for the mean flame surface area density (MFSAD) is employed for this purpose. The second objective of this paper is to suggest a different approach to the derivation of the equation for MFSAD. It is based on the pdf equation for the reaction progress variable C and the relation between the pdf and MFSAD. This treatment suggests an entirely different closure assumption. Derived from text

N94-12320*# Stanford Univ., CA. Center for Turbulence Research.
TENSORAL: A SYSTEM FOR POST-PROCESSING TURBULENCE SIMULATION DATA c24
Eliot Dresselhaus *In its* Annual Research Briefs, 1992 Jan. 1993 p 455-460 (For primary document see N94-12284 01-34)
Avail: CASI HC A02/MF A04

Many computer simulations in engineering and science -- and especially in computational fluid dynamics (CFD) -- produce huge quantities of numerical data. These data are often so large as to make even relatively simple post-processing of this data unwieldy. The data, once computed and quality-assured, is most likely analyzed by only a few people. As a result, much useful numerical data is under-utilized. Since future state-of-the-art simulations will produce even larger datasets, will use more complex flow geometries, and will be performed on more complex supercomputers, data management issues will become increasingly cumbersome. My goal is to provide software which will automate the present and future task of managing and post-processing large turbulence datasets. My research has focused on the development of these software tools -- specifically, through the development of a very high-level language called 'Tensoral'. The ultimate goal of Tensoral is to convert high-level mathematical expressions (tensor algebra, calculus, and statistics) into efficient low-level programs which numerically calculate these expressions given simulation datasets. This approach to the database and post-processing problem has several advantages. Using Tensoral the numerical and data management details of a simulation are shielded from the concerns of the end user. This shielding is carried out without sacrificing post-processor efficiency and robustness. Another advantage of Tensoral is that its very high-level nature lends itself to portability across a wide variety of computing (and supercomputing) platforms. This is especially important considering the rapidity of changes in supercomputing hardware. Derived from text

N94-12342# Scripps Institution of Oceanography, La Jolla, CA. Marine Physical Lab.

TOPICS IN PATTERN FORMATION AND CHAOTIC SYSTEMS Final Report

H. D. Abarbanel May 1993 5 p
(Contract N00014-89-D-0142)
(AD-A265922; MPL-U-24/93) Avail: CASI HC A01/MF A01

This project was a Joint Research Project in the study of Pattern Formation and Chaotic Dynamics by members of the Institute for Applied Physics (IPFAN) in Gorky, USSR and the Marine Physical Laboratory, at the University of California, San Diego, USA. This project involved both experimental and theoretical research in the topic of interest. At both IPFAN and UCSD the scientists have investigated the creation of patterns in spatio-temporal systems and the chaotic dynamics of these systems in several specific examples: (1) Dynamics of Surface Waves, Variation on the classical Faraday experiment; (2) Surface tension induced convection, Benard-Marangoni Convection; (3) Vortex eneration in the wakes of bluff bodies; and (4) Boundary layer chaos and transition in turbulence. DTIC

N94-12352# Pennsylvania State Univ., University Park. Applied Research Lab.

SUPPRESSION OF THE NEAR WALL BURST PROCESS OF A FULLY DEVELOPED TURBULENT PIPE FLOW

A. A. Fontaine and S. Deutsch May 1993 229 p
(Contracts N00014-91-J-1064; N00014-91-J-1608)
(AD-A265995; TR-93-06) Avail: CASI HC A11/MF A03

A local suppression of the near wall region burst process is achieved by modifying the buffer region and sublayer (Y+ less than 30) of a fully developed turbulent pipe flow with a 16.4 wall unit high, wall-mounted bump. A downstream converging flow field is produced by the divergence of the approaching mean flow around the bump. In addition, a pair of counter-rotating vortices are generated by the bump and convected downstream. The vortices have a circulation which produces a common wall directed flow between them, which also contributes to the flow convergence. These vortices are 10 to 15 wall units in diameter and persist for more than 174 wall units downstream. The investigation is conducted in the ARL/PSU glycerin tunnel at a Reynolds number, based on pipe diameter, of approximately 10,000. The momentum thickness Reynolds number is 730. Multicomponent, multi-point, time resolved laser Doppler velocimetry measurements are made in both the undisturbed and modified boundary layers. The measurements include single-point three-component velocity profiles, two-point multi-component velocity correlations and velocity spectral estimates. DTIC

N94-12437# Aircraft Research Association Ltd., Bedford (England).

TOWARDS A CELL-VERTEX NAVIER-STOKES ALGORITHM FOR THREE-DIMENSIONAL STRUCTURED/UNSTRUCTURED MESHES

A. J. Peace Apr. 1992 10 p Presented at the ICFD Conference on Numerical Methods for Fluid Dynamics, Reading, England, 7-10 Apr. 1992
(Contract SLS41B/2437)
(ARA-Memo-366) Avail: CASI HC A02/MF A01

The achievements made in the move towards an efficient Navier-Stokes algorithm for three-dimensional structured/unstructured meshes are described. These achievements can be divided into three main areas - a three-dimensional Euler algorithm for general meshes, a multi-grid technique for block-structured meshes, and a Navier-Stokes algorithm for two-dimensional general meshes. Outlines of the methods used, demonstration examples, and a discussion of remaining problems are included. Author (revised)

N94-12547# National Space Development Agency, Ibaraki (Japan).

THE THIRD WORKSHOP ON TWO PHASE FLUID EXPERIMENT IN THE SPACE ENVIRONMENT [DAI 3 KAI UCHUU KANKYOUKA NI OKERU NISOU RYUUTAI JIKKEN NI KANSURU WAKU SHOPPU]

31 Mar. 1993 102 p In JAPANESE Workshop held in Hyogo, Japan, 23 Jul. 1991
(NASDA-CON-930002; JTN-93-80474) Avail: CASI HC A06/MF A02

The following topics were discussed: Japanese spacecraft, JEM (Japanese Experiment Module), spaceborne experiments, space technology experiments, spacecraft equipment, microgravity, aerospace environments, two phase fluid, two phase flow, thermal control, flow stability, flow characteristics, heat transfer coefficient, heat flux, heat radiators, cold plate, heat pipes, boiling, evaporation, condensation, liquid-air separation, pressure losses, void ratio, drop towers, air-borne experiments, users requirements, mission planning, and equipment specifications. For individual titles, see N94-12548 through N94-12556.

N94-12548# National Space Development Agency, Tokyo (Japan).

SUMMARY OF STUDIES ON JEM UTILIZATION EXPERIMENT PROJECTS [JEM RIYOU JIKKEN KEIKAKU KENTOU GAIYOU]

Tadashi Matsushita *In its* The Third Workshop on Two Phase Fluid Experiment in the Space Environment 31 Mar. 1993 p 1-12 In JAPANESE (For primary document see N94-12547 01-34)
Avail: CASI HC A03/MF A02

The outlines of the international Space Station Freedom Program, configuration of JEM (Japanese Experiment Module), JEM utilization plan and its development schedule, and plan and configuration of the two phase fluid experiment system are introduced. Topics discussed include: schematic drawing of JEM; the original and revised space station structures; overall schedule; the progress of two phase fluid experiment equipment study; the common experiment equipment and infrastructure construction experiment equipment; JEM technology missions and space infrastructure; proposed themes by Tsukuba Space Center, NASDA (National Space Development Agency of Japan); two phase liquid common experiment configuration; and actions to be taken in the future. This presentation is represented by viewgraphs only. Author (NASDA)

N94-12549# Ibaraki Univ., Hitachi (Japan).

COMPILATION OF PROPOSALS FOR BOILING AND EVAPORATION EXPERIMENTS IN SPACE ENVIRONMENTS AND PROPOSALS CONCERNING EXPERIMENT PROJECTS [UCHUU KANKYOUKA NI OKERU FUTTOU JOUHATSU JIKKEN TEIAN NO SEIRI TO JIKKEN KEIKAKU NI KANSURU TEIAN]

Humito Kaminaga and Kouichi Chiba (Ishikawajima-Harima Heavy Industries Co. Ltd., Tokyo, Japan.) *In its* The Third Workshop on Two Phase Fluid Experiment in the Space Environment 31 Mar. 1993 p 14-17 In JAPANESE Sponsored in cooperation with Boiling Evaporation Group, Japan (For primary document see N94-12547 01-34)
Avail: CASI HC A01/MF A02

An overview of the results of the compilation of proposals for boiling and vaporization experiments in the space environment and experiment plans is presented. The results of boiling an vaporization experiment in space proposal compilation, proposals on the experiments, and items to be considered in conducting the experiments are outlined. In utilizing boiling heat transmission in space, some kinds of forced flow patterns are necessary. Items which must be made clear in boiling phenomena in microgravity are as follows: (1) developed nuclear boiling heat transmission and burnout thermal flux; (2) boiling and vaporization heat transmission when convection effects are not so large due to comparatively low flow rate; and (3) unstable boiling phenomena such as flushing. The following activities are deemed necessary to boil down the experiment projects: (1) equipment requiring forced heat rejection and its structure; (2) thermal conditions; (3) appropriate working fluid; and (4) appropriate heat transmission. Author (NASDA)

N94-12550# Mechanical Engineering Lab., Tsukuba (Japan). Thermal Engineering Div.
CONDENSATION PHENOMENA [GYOUSHUKU GENSHOW NI TSUITE]
Akira Yabe and Yuujirou Hayashi (Kanazawa Univ., Japan.) *In* NASDA, The Third Workshop on Two Phase Fluid Experiment in the Space Environment 31 Mar. 1993 p 18-20 In JAPANESE (For primary document see N94-12547 01-34)
Avail: CASI HC A01/MF A02

The results of theoretical consideration about condensation phenomena in microgravity are described. Methods of condensation heat transfer promotion in microgravity by rejecting condensed fluid from the heat transfer surfaces to make condensed liquid films are described. Characteristics of condensers as components of two liquid phase systems (compatibility with gas and liquid separator after exiting from the condenser), and a method of equipment temperature control are outlined. The system requirements are shown. Author (NASDA)

N94-12551# Tokyo Inst. of Tech. (Japan).
DEVELOPMENTAL RESEARCH OF THERMAL CONTROL SYSTEM IN SPACE ENVIRONMENT [UCHUU KANKYOUKA NO NETSU SEIGYO SHISUTEMU NO KAIHATSU KENKYUU]
Masanori Aritomi and Terushige Fujii (Kobe Univ., Japan.) *In its* The Third Workshop on Two Phase Fluid Experiment in the Space Environment 31 Mar. 1993 p 21-25 In JAPANESE Sponsored in cooperation with Two Phase Flow System Group, Japan (For primary document see N94-12547 01-34)
Avail: CASI HC A01/MF A02

An overview of the objectives and significance of the research on boiling two phase flow is presented. The essential functions for the system and research subjects are discussed. Topics discussed include: circulation; gas and liquid separation; condensation; heat rejection; pressure control; load heat rejection; void ratio; flow pattern transient; pressure loss; gas and liquid separation; boiling heat transmission rate and transmission limit; condensing heat transmission and transmission promotion; recombination of liquid phases; flow distribution in multi-group parallel flow channels and flow stability; flow characteristics in two phase header; and integrated test. Author (NASDA)

N94-12552# Kobe Univ. (Japan). Dept. of Mechanical Engineering.
TWO PHASE FLOW AND ISOPYCNIC LIQUID-LIQUID TWO PHASE FLUID IN REDUCED GRAVITY FIELD [TEI JUURYOKUBA NO NISOURYUU TO TOUMITSUDO EKI EKI NISOURYUU]
Terushige Fujii and Junichi Oota *In* NASDA, The Third Workshop on Two Phase Fluid Experiment in the Space Environment 31 Mar. 1993 p 26-38 In JAPANESE (For primary document see N94-12547 01-34)
Avail: CASI HC A03/MF A02

The possibility of applying the existent gas-liquid two phase flow behavior diagrams in the earth gravity to those in reduced gravity are described. Outlines of the results of free drop tower experiments, airplane experiments, free drop tower experiment and airplane experiment are reviewed. The result of the isopycnic two phase liquid flow experiments on the ground simulating the reduced gravity effects using silicone oil and water of the same specific gravity are outlined. Author (NASDA)

N94-12553# Tokyo Univ. of Agriculture and Technology (Japan).
DEVICES RELATED FOR THERMAL CONTROL SYSTEMS USED IN MICROGRAVITY [UCHUU KANKYOUKA NO NETSU KANRI SHISUTEMU NI OKERU KANREN DEBAISU]
E. Boelman and Tetsurou Oogushi (Mitsubishi Electric Corp., Tokyo, Japan.) *In* NASDA, The Third Workshop on Two Phase Fluid Experiment in the Space Environment 31 Mar. 1993 p 39-44 In JAPANESE (For primary document see N94-12547 01-34)
Avail: CASI HC A02/MF A02

The following aspects of activities to search for the system requirements for devices (including heat pipe, control unit, pump, separator, and accumulator) for high performance thermal control system used in microgravity are outlined: (1) collection of the related information from experiment proposals concerned with the devices, researchers on subsystems (such as two phase liquid loop, radiator, evaporator and condenser), and industrial circles; (2) coordinating the experiment proposals and the research and development needs; and (3) study of the system requirements to clarify the requirements, scopes, and problems of the proposed experiments and to grasp the needs of the user of the JEM (Japanese Experiment Module) in the different areas. This presentation is represented by viewgraphs only. Author (NASDA)

N94-12554# Osaka Univ., Suita (Japan). Faculty of Engineering.
RESEARCH ON TWO PHASE FLOW IN MICROGRAVITY [BISHOU JUURYOKUKA NI OKERU NISOURYUU NI KANSURU KENKYUU]
Masaki Saitou *In* NASDA, The Third Workshop on Two Phase Fluid Experiment in the Space Environment 31 Mar. 1993 p 46-65 In JAPANESE (For primary document see N94-12547 01-34)
Avail: CASI HC A03/MF A02

An overview of the results of the study on two phase flow in microgravity is described. Topics discussed include: estimation of air-water two phase flow characteristics in microgravity based on the conventional flow regime maps; two phase flow simulation using two liquids of the same specific gravity; two phase flow experiment in microgravity using free drop towers and airplanes; and the results of the experiments for assessing pressure losses and heat transmission properties in two phase flows. Various microgravity flow regime maps are introduced. Author (NASDA)

N94-12555# Kawasaki Heavy Industries Ltd., Kobe (Japan).
RESEARCH AND DEVELOPMENT OF COLD PLATE FOR TWO PHASE FLUID LOOP THERMAL CONTROL SYSTEM [NISOU RYUUTAI RUPU HOUSHIKI NETSU SEIGYO SHISUTEMUYOU KORUDO PURETO NO KENKYUU KAIHATSU NI TSUITE]
Tatsusaburou Nakamura and Hiroyuki Yamada *In* NASDA, The Third Workshop on Two Phase Fluid Experiment in the Space Environment 31 Mar. 1993 p 66-89 In JAPANESE (For primary document see N94-12547 01-34)
Avail: CASI HC A03/MF A02

Topics discussed include: the concept of two phase fluid thermal control system; requirements for the cold plate; classification of cold plates resulting from seeking for measures to upgrade heat transmission characteristics in microgravity; types of cold plate including heat pipe type, plate type, and swirl type; experiment system onboard NASA microgravity experiment plane; drop tower; examples of flow in microgravity; gas-liquid two phase flow regime maps in a swirl tube in microgravity; and the loop structure of the airborne experiment equipment. This presentation is represented by viewgraphs only. Author (NASDA)

N94-12556# National Space Development Agency, Ibaraki (Japan).
ORGANIZATION AND MANAGEMENT POLICY FOR TWO PHASE FLUID EXPERIMENT IN SPACE ENVIRONMENT [UCHUU KANKYOUKA NI OKERU NISOU RYUUTAI JIKKEN NI KANSURU SOSHIKI OYOBI UNEI HOUSHIN]
Masao Furukawa *In its* The Third Workshop on Two Phase Fluid Experiment in the Space Environment 31 Mar. 1993 p 91-95 In JAPANESE (For primary document see N94-12547 01-34)
Avail: CASI HC A01/MF A02

Outline of the two phase fluid experiment group is described. The following topics are mentioned: the purpose of establishment, the objectives, the roles, the organizational structure, the constituents, the missions of the executive committee, the way of outside negotiation, ownership of the research results, and the way of handling the materials of the experiment group. Author (NASDA)

N94-12571*# National Aeronautics and Space Administration. Langley Research Center, Hampton, VA.
HYPERSONIC, NONEQUILIBRIUM FLOW OVER A CYLINDRICALLY BLUNTED 6 DEG WEDGE
Peter A. Gnoffo Aug. 1993 39 p
(RTOP 506-40-91-02)
(NASA-TM-108994; NAS 1.15:108994) Avail: CASI HC A03/MF A01

The numerical simulation of hypersonic flow in chemical nonequilibrium over cylindrically blunted 6 degree wedge is described. The simulation was executed on a Cray C-90 with Program LAURA 92-vl. Code setup procedures and sample results, including grid refinement studies and variations of species number are discussed. This simulation relates to a study of wing leading edge heating on transatmospheric vehicles. Author

N94-12576*# National Aeronautics and Space Administration. Lewis Research Center, Cleveland, OH.
MODELING VOID GROWTH AND MOVEMENT WITH PHASE CHANGE IN THERMAL ENERGY STORAGE CANISTERS
Douglas Darling, David Namkoong, and J. Raymond Lee Skarda Jul. 1993 12 p Presented at the 28th AIAA Thermophysics Conference, Orlando, FL, 6-9 Jul. 1993; sponsored by AIAA Previously announced in IAA as A93-46569
(RTOP 506-41-31)
(NASA-TM-106288; E-8026; NAS 1.15:106288; AIAA Paper 93-2832)
Avail: CASI HC A03/MF A01

A scheme was developed to model the thermal hydrodynamic behavior of thermal energy storage salts. The model included buoyancy, surface tension, viscosity, phases change with density difference, and void growth and movement. The energy, momentum, and continuity equations were solved using a finite volume formulation. The momentum equation was divided into two pieces. The void growth and void movement are modeled between the two pieces of the momentum equations. Results showed this scheme was able to predict the behavior of thermal energy storage salts. Author

N94-12604# Edgerton, Germeshausen and Grier, Inc., Idaho Falls, ID.
PERFORMANCE ASPECTS OF DE LAVAL SPRAY-FORMING NOZZLES
K. M. McHugh and J. F. Key 1993 10 p Presented at the Multiphase Flow Problems in Manufacturing and Productive Technology, Bethesda, MD, Jun. 1993
(Contract DE-AC07-76ID-01570)
(DE93-013671; EGG-M-92696; CONF-9306165-1) Avail: CASI HC A02/MF A01

Spray forming is a multiphase fabrication technology in which a spray of finely atomized liquid droplets is directed onto a suitably shaped substrate or pattern to produce a coherent, near-net-shape deposit. The technology can simplify materials processing where simultaneously improving product quality. Researchers at the Idaho National Engineering Laboratory (INEL) are developing spray-forming technology for producing near-net-shape solids and coatings of a variety of metals, polymers, and composite materials using de Laval nozzles. Here we briefly describe the flow field characterization and atomization behavior of liquid metals in linear de Laval nozzles, and illustrate their versatility by summarizing results from three spray-forming programs. In one program, low-carbon steel strip greater than 0.75 mm was produced. In another program, polymer membranes approximately 5 microns thick were spray formed. Finally, recent results in spray forming molds, dies, and related tooling for rapid prototyping are described. DOE

N94-12611# National Aerospace Lab., Tokyo (Japan).
PROCEEDINGS OF THE 9TH AND 10TH NAL WORKSHOP ON INVESTIGATION AND CONTROL OF BOUNDARY-LAYER TRANSITION [KYOUKAISOU SENI NO KAIMEI TO SEIGYO KENKYUUKAI KOUEN RONBUNSHUU (DAI KAI TO DAI 10 KAI)]
Nov. 1992 100 p In ENGLISH and JAPANESE Workshop held in Tokyo, Japan, 24-25 Sep. 1991, 16-18 Mar. 1992
(NAL-SP-18; JTN-93-80498) Avail: CASI HC A05/MF A02

Research results on the following were discussed: nonlinear stability calculations of pipe flow; turbulence modeling and compressibility; interaction between free shear layer and the leading edge of a parallel flat plate; longitudinal vortices along a concave wall; the wake behind a high speed train; the formation process of Karman vortex street; curvature effects in three-dimensional boundary layers; a numerical experiment of boundary layer transition; turbulent boundary layer interacting with spanwise periodic longitudinal vortex arrays; coherent structure in near wall turbulence with riblets; growth and breakdown of Taylor-Goertler vortices; and visual structure of Karman vortex streets in a route to chaotic states. For individual titles, see N94-12612 through N94-12634.

N94-12612# National Aerospace Lab., Tokyo (Japan).
NONLINEAR STABILITY CALCULATIONS OF PIPE FLOW [ENKANRYUU NO HISENKEI ANTEI KEISAN]
Nobutake Itoh and Hiroshi Kadota (University of Electro-Communications, Chofu, Japan.) *In its* Proceedings of the 9th and 10th NAL Workshop on Investigation and Control of Boundary-Layer Transition Nov. 1992 p 1-4 In JAPANESE (For primary document see N94-12611 01-34)
Avail: CASI HC A01/MF A02

Fully nonlinear computations with an iterative method are made to investigate the stability of Poiseuille pipe flow to axisymmetric and non-axisymmetric disturbances. Numerical results indicate that the weakly nonlinear theory cannot predict nonlinear development of disturbances, and that there is no equilibrium amplitude of monochromatic-type disturbances in the wavenumber and Reynolds number range concerned. Author (NASDA)

N94-12613# National Aerospace Lab., Tokyo (Japan).
DNS ON CONTROL OF LAMINAR-TURBULENT TRANSITION IN CHANNEL FLOW WITH SUCTION AND BLOWING [SUIKOMI FUKIDASHI NIYORU CHANNERURYUU SENI SEIGYO NO DNS]
Kiyoshi Yamamoto, Takeo Murase (Fujitsu Ltd., Tokyo, Japan.), and J. M. Floryan (University of Western Ontario, London.) *In its* Proceedings of the 9th and 10th NAL Workshop on Investigation and Control of Boundary-Layer Transition Nov. 1992 p 5-9 In JAPANESE (For primary document see N94-12611 01-34)
Avail: CASI HC A01/MF A02

Numerical simulation of laminar-turbulent transition in channel flow with spatially periodic suction/blowing from its channel walls is conducted with a spectral method based on the Fourier spectral method. Reynolds number is fixed on a subcritical value, 5,000, and the influence of both amplitude and wave number of the suction/blowing on the transition is investigated. When the amplitude is small, the transition does not occur because the suction/blowing gives only a slight effect to the basic flow and the resulted flow remains stable to all three-dimensional small disturbances. On the other hand, when the amplitude is a large value, the transition occurs in a finite time, and finally it is obtained instantaneously with a huge value of the amplitude. It is found that the suction/blowing makes the separation ridges on the wall, which may simulate a wall roughness. The transition times are obtained for the moderately large amplitudes and wave numbers, obey nearly a minus two power law dependence on the ratio of amplitude to wave number. Author (NASDA)

N94-12614# Tokyo Univ. (Japan). Inst. of Industrial Science.
TURBULENCE MODELING AND COMPRESSIBILITY [RANRYUU MODERU TO ASSHUKUSEI]
Akira Yoshizawa *In* NAL, Proceedings of the 9th and 10th NAL Workshop on Investigation and Control of Boundary-Layer Transition Nov. 1992 p 11-13 In JAPANESE (For primary document see N94-12611 01-34)
Avail: CASI HC A01/MF A02

Some prominent features of compressibility effects are discussed from the viewpoint of turbulence modeling. The difference between the ensemble and mass-weighted averagings is also referred to in relation to the feasibility of incorporating compressibility effects. Author (NASDA)

N94-12615# Hiroshima Univ. (Japan). School of Engineering.
AERODYNAMIC SOUND DUE TO INTERACTION BETWEEN A TWO-DIMENSIONAL FREE SHEAR LAYER AND THE LEADING EDGE OF A PARALLEL FLAT PLATE [NIJIGEN SENDANSOU TO HEIBAN NO KANSHOU NIYORU HASSHIN TO KUURIKION] c71
Fujihiko Sakao *In* NAL, Proceedings of the 9th and 10th NAL Workshop on Investigation and Control of Boundary-Layer Transition Nov. 1992 p 15-22 In JAPANESE (For primary document see N94-12611 01-34)
Avail: CASI HC A02/MF A02

Sound is generated aerodynamically when the leading edge of a flat plate is set in the middle of a free shear layer. The mechanism for it is a self-maintaining oscillation based on a feedback loop including perturbation of the shear layer by sound at the nozzle lip, developments of the perturbation downstream, and sound generation at the edge by passing of the perturbed vorticity. Due to absence of acoustic resonance in the present set up, any change in parameters results in smooth, continuous, and wide-ranged changes in the outcome, unlike in previous experiments, where changes are often sticky, discontinuous, and with hysteresis. It seems that there are more than two different mechanisms, and either of them appears according to the conditions. Among the conditions is whether the shear

layer from the nozzle to the edge is laminar or turbulent is very important.
Author (NASDA)

N94-12616# Meiji Univ., Kawasaki (Japan). School of Science and Technology.
FLUCTUATIONS OF LONGITUDINAL VORTICES ALONG A CONCAVE WALL [OUKYOKUMEN NI SOU TATEUZU NO YURAGI] **c02**
Akira Ito and Yasuyuki Fukutomi *In* NAL, Proceedings of the 9th and 10th NAL Workshop on Investigation and Control of Boundary-Layer Transition Nov. 1992 p 23-24 In JAPANESE (For primary document see N94-12611 01-34)
Avail: CASI HC A01/MF A02

The fluctuations of the longitudinal vortices along a concave wall of one m in radius were visualized by smoke and measured by hot-wire anemometer at a free air stream velocity ranging from two to five m/sec. It was shown that the magnitude of such fluctuations increased as the length of straight channel set in front of the concave channel increased. The experiments were carried out by three straight channels of 200 mm, 800 mm, and 1,600 mm in length. The relation between the fluctuation behavior and the turbulence intensity of the free stream flow in the straight channel were investigated. Author (NASDA)

N94-12617# Tohoku Univ., Sendai (Japan). Faculty of Engineering.
EXPERIMENT ON A HIGH REYNOLDS NUMBER TURBULENT BOUNDARY LAYER [KOU REINORUZUSUU RANRYUU KYOUKAISOU NO JIKKEN]
Yuu Fukunishi, Yasuaki Kohama, and Ryouji Kobayashi *In* NAL, Proceedings of the 9th and 10th NAL Workshop on Investigation and Control of Boundary-Layer Transition Nov. 1992 p 25-28 In JAPANESE (For primary document see N94-12611 01-34)
Avail: CASI HC A01/MF A02

A smooth roof of a high-speed train was used to investigate turbulent boundary layers at high Reynolds number. A total of 19 hot-wire probes were used simultaneously to obtain data. Conditional sampling technique was applied to the data in order to investigate the features of coherent structures in turbulent boundary layers at high Reynolds numbers.
Author (NASDA)

N94-12618# Meijo Univ., Nagoya (Japan). Faculty of Science and Technology.
ON THE WAKE BEHIND A HIGH SPEED TRAIN [KOUSOKU SOUKOU SHARYOU NO HANRYUU]
Muneshige Okude, Hidetoshi Hayafuji, and Tatsuya Matsui (Gifu Univ., Japan.) *In* NAL, Proceedings of the 9th and 10th NAL Workshop on Investigation and Control of Boundary-Layer Transition Nov. 1992 p 29-32 In JAPANESE (For primary document see N94-12611 01-34)
Avail: CASI HC A01/MF A02

The velocity distributions in the boundary layer on the side wall of a high speed train were measured by using two rakes of the multiple hot-wires. One was set on the wall of the last car of a train which was running at 320 km/hr on the downway railroad, the other was set on the nose of the first car of a train which was at rest on the upway railroad. The instant the two rakes of multiple hot-wire came in a straight line, and the velocity distribution throughout the boundary layer could be obtained. After that instant, the velocity distributions in the outer part of the wake behind the running train were measured by the stationary hot-wire rake set on the car at rest. The thickness of the boundary layer on the wall of the last car was about 2.5 m. The spectrum of the velocity fluctuations in the wake had strong intensity at about 1.5 and 3.5 Hz in its distribution. The flow pattern in the wake was visualized by using the smoke generated by smoke markers. Recording of the wake flow by a video camera was not successful, but the naked eye observation noticed the alternating vortex shedding from the rear surface of the last car as in the case of an automobile. The flow patterns on the rear surface of the last car visualized by the tuft method also showed the alternating vortex shedding. The shedding frequency could be roughly about two to five Hz. Author (NASDA)

N94-12619# National Research Lab. of Metrology, Tokyo (Japan).
CALIBRATION OF ANEMOMETERS AT LOW SPEED BY MEANS OF TOWING CARRIAGE [SOUKOU DAISHA WO MOCHIITA TEISOKUIKI DENO FUUSOKUKEI NO KOUSEI] **c35**
Yoshiya Terao *In* NAL, Proceedings of the 9th and 10th NAL Workshop on Investigation and Control of Boundary-Layer Transition Nov. 1992 p 33-35 In JAPANESE (For primary document see N94-12611 01-34)
Avail: CASI HC A01/MF A02

A towing carriage system for anemometers in the range below one m/sec is described. Anemometers under calibration are set on the carriage which moves on the 45 meter long rails through stationary air at a constant speed between 0.05 and 1.00 m/sec. The output of the anemometers are calibrated against the carriage velocity. Author (NASDA)

N94-12620# Tohoku Univ., Sendai (Japan). Faculty of Engineering.
CRITERIA FOR ONSET OF BOUNDARY-LAYER TRANSITION ON SPINNING BODIES [KAITENTAI MAWARI NO SANJIGEN KYOUKAISOU NO FUANTEISEI NITSUITE]
Yasuaki Kohama *In* NAL, Proceedings of the 9th and 10th NAL Workshop on Investigation and Control of Boundary-Layer Transition Nov. 1992 p 37-40 In JAPANESE (For primary document see N94-12611 01-34)
Avail: CASI HC A01/MF A02

Boundary-Layers on spinning axisymmetric bodies become unstable much earlier than two-dimensional cases owing to centrifugal or crossflow instabilities. There is no reliable parameter up to now with which the onset condition of turbulent transition is predicted. Considering local flow conditions on a spinning cone, together with Goertler instability condition on a concave wall, criteria for the onset condition on spinning bodies is discussed.
Author (NASDA)

N94-12621# Osaka Prefecture Univ., Sakai (Japan). Coll. of Engineering.
ON THE FORMATION PROCESS OF KARMAN VORTEX STREET [KARUMAN UZURETSU NO KEISEI KATEI NITSUITE] **c02**
Michio Nishioka *In* NAL, Proceedings of the 9th and 10th NAL Workshop on Investigation and Control of Boundary-Layer Transition Nov. 1992 p 41-45 In JAPANESE (For primary document see N94-12611 01-34)
Avail: CASI HC A01/MF A02

An experimental study is conducted on the formation process of a Karman vortex street. The growth of wave-disturbances into the vortex street is examined by introducing initially small-amplitude disturbances using a loud-speaker, at a cylinder Reynolds number, R = 3.2 x 10(exp 3). On the basis of the results of mu-fluctuation measurements and stability calculations, it is shown that the formation process is initially controlled by wave-disturbances similar to those of symmetric mu, which evolve into the antisymmetric type downstream and eventually into the vortex street. Thus, the process is quite complex, and a further careful and detailed study is required to obtain a better understanding of the mechanism of vortex formation, especially in terms of the absolute instability. Author (NASDA)

N94-12622# Kyoto Inst. of Tech. (Japan).
NONLINEAR INSTABILITY OF A LAMINAR FLOW IN A RECTANGULAR DUCT AND GENERATION OF THE TURBULENT SECONDARY FLOW [CHOUHOUKEI KANNAI NO SOURYUU NO HISENKEI FUANTEISEI TO RANRYUU NIJIRYUU NO HASSEI]
Tomomasa Tatsumi and Takahiro Yoshimura (Hitachi Ltd., Tokyo, Japan.) *In* NAL, Proceedings of the 9th and 10th NAL Workshop on Investigation and Control of Boundary-Layer Transition Nov. 1992 p 47-49 In JAPANESE (For primary document see N94-12611 01-34)
Avail: CASI HC A01/MF A02

The generation of the turbulent secondary flow in a rectangular duct is investigated in the framework of hydrodynamical nonlinear instability of the corresponding laminar flow. The secondary flow is obtained as an equilibrium state of growing unstable disturbances. Author (NASDA)

N94-12623*# Arizona State Univ., Flagstaff. Dept. of Mechanical and Aerospace Engineering.
CURVATURE EFFECTS IN THREE-DIMENSIONAL BOUNDARY LAYERS
R.-S. Lin and H. L. Reed (Tohoku Univ., Sendai, Japan.) *In* NAL, Proceedings of the 9th and 10th NAL Workshop on Investigation and Control of Boundary-Layer Transition Nov. 1992 p 51-53 Sponsored by NASA. Langley Research Center (For primary document see N94-12611 01-34)
Avail: CASI HC A01/MF A02

The effect of including wall and streamline curvature terms in swept-wing boundary-layer stability calculations is studied. The linear disturbance equations are cast on a fixed, body-intrinsic, curvilinear coordinate system.

Those nonparallel terms which contribute mainly to the streamline-curvature effect are retained in this formulation and approximated by their local finite-difference values. Convex wall curvature has a stabilizing effect, while streamline curvature is destabilizing. Author (NASDA)

N94-12624# Tokyo Inst. of Tech. (Japan). Faculty of Engineering.

SIMULTANEOUS 3D TURBULENT LARGE-SCALE STRUCTURES IN A FLOOD FLOW BY MULTI-CHANNELS MEASURING SYSTEM [KOUZUIJI NO JITSU KASEN DENO MIDARE NO SHUNKANZOU NO KEISOKU]

Mikio Hino, Yang Meng, and Nobuyoshi Murayama *In* NAL, Proceedings of the 9th and 10th NAL Workshop on Investigation and Control of Boundary-Layer Transition Nov. 1992 p 55-58 In JAPANESE (For primary document see N94-12611 01-34)

Avail: CASI HC A01/MF A02

Field measurements on turbulent large-scale structure of a flood flow in the Hinuma river at a high Reynolds number of the order of 10(exp 6) were conducted with 16-channel electromagnetic velocimeters. The turbulent velocity components (u, v) at eight points in a plane perpendicular to the mean flow have been sampled and recorded simultaneously by a A/D converter. The quasi-instantaneous 3D images of coherent structures in the flood flow were reconstructed from these data by using a new method of data analysis. These structures detected near the river bed are low-velocity lumps of fluid and generate intermittently peaks of the high positive Reynolds stress. The high concentration of the suspended load in the flood flow may be explained by these structures. Near the water surface, the coherent structure has also been found and they generated small-scale boils. Author (NASDA)

N94-12625# Osaka Prefecture Univ., Sakai (Japan). Coll. of Engineering.

A NUMERICAL EXPERIMENT OF BOUNDARY LAYER TRANSITION AT SUBCRITICAL REYNOLDS NUMBERS [ARINKAI KYOUKAISOU SENI NO SUUCHI JIKKEN]

Makoto Asai *In* NAL, Proceedings of the 9th and 10th NAL Workshop on Investigation and Control of Boundary-Layer Transition Nov. 1992 p 59-62 In JAPANESE (For primary document see N94-12611 01-34)

Avail: CASI HC A01/MF A02

In order to clarify the mechanism of wall turbulence generation, the response of boundary layer to strong disturbances at subcritical Reynolds numbers is investigated through a direct numerical simulation. To trigger the subcritical transition, a discrete vortex is initially introduced upstream of the leading edge of boundary-layer plate. The preliminary results on the excited vortical flow structures and on the deformation and viscous damping of vortices are presented. Author (NASDA)

N94-12626# Yamaguchi Univ., Ube (Japan). Dept. of Mechanical Engineering.

TURBULENT BOUNDARY LAYER INTERACTING WITH SPANWISE PERIODIC LONGITUDINAL VORTEX ARRAYS [SUPAN HOUKOU SHUUKI KAKURAN NIYORU RANRYUU KYOUKAISOU NO SEIGYO]

Hideo Oosaka and Chiharu Fukushima *In* NAL, Proceedings of the 9th and 10th NAL Workshop on Investigation and Control of Boundary-Layer Transition Nov. 1992 p 63-65 In JAPANESE (For primary document see N94-12611 01-34)

Avail: CASI HC A01/MF A02

Detailed mean and turbulent flow measurements have been made to investigate the development of turbulent boundary layer interacting with artificially generated trailing vortex arrays in a free stream. Two parameters, the spanwise period of the longitudinal vortex arrays (L/S) and the ratio of the longitudinal vortex scale to the boundary layer scale (b/delta(sub 0)), were varied for five cases. Author (NASDA)

N94-12627# Yamaguchi Univ., Ube (Japan). Dept. of Mechanical Engineering.

TURBULENT DRAG REDUCTION OF A d-TYPE ROUGH WALL BOUNDARY LAYER WITH LONGITUDINAL RIBS PLACED WITHIN THE GROOVES [TATERIBU NIYORU D-GATA SOMEN RANRYUU KYOUKAISOU NO TEIKOU GENSHOU]

Hideo Oosaka and Shinsuke Mochizuki *In* NAL, Proceedings of the 9th and 10th NAL Workshop on Investigation and Control of Boundary-Layer Transition Nov. 1992 p 67-70 In JAPANESE (For primary document see N94-12611 01-34)

Avail: CASI HC A01/MF A02

In order to control the turbulent energy production and transport processes due to the coherent vortices associated with the bursting phenomenon in a d-type rough wall turbulent boundary layer, longitudinal thin ribs were placed within the transverse grooves with a suitable spanwise spacing. Direct measurements of the local skin friction coefficient evidently show the effectiveness of drag reduction using the longitudinal ribs. Maximum drag reduction rates to d-type rough wall flow and to smooth wall flow are minus 10 percent and minus 3 percent, respectively. The drag reduction rate can be reasonably expressed in terms of the rib Reynolds number. Comparisons of some mean flow properties between the modified flow and the d-type rough wall flow provide evidence that the present passive control device reduces the turbulent energy production rate. Author (NASDA)

N94-12628# Tokuyama Coll. of Technology (Japan).

COHERENT STRUCTURE IN NEAR WALL TURBULENCE WITH RIBLETS [RIBURETTO SOMEN RANRYUU KYOUKAISOU NO SOSHIKI KOUZOU]

Hirofumi Oonari *In* NAL, Proceedings of the 9th and 10th NAL Workshop on Investigation and Control of Boundary-Layer Transition Nov. 1992 p 71-74 In JAPANESE (For primary document see N94-12611 01-34)

Avail: CASI HC A01/MF A02

Coherent structures in near-wall region of turbulent boundary layer with riblets are investigated using the technique of flow visualization. The results indicate that the pattern of low speed streaks near the riblet wall is a straight line at Reynolds number 4,240 and is different from the streaky structure near the smooth wall of turbulent boundary layer. Author (NASDA)

N94-12629# Nihon Univ., Tokyo (Japan). Dept. of Aerospace Engineering.

INSTABILITY AROUND AN ISOLATED ROUGHNESS ELEMENT [KORITSU SODO MAWARI NO FUANTEISEI]

Tatsuo Motohashi *In* NAL, Proceedings of the 9th and 10th NAL Workshop on Investigation and Control of Boundary-Layer Transition Nov. 1992 p 75-77 In JAPANESE (For primary document see N94-12611 01-34)

Avail: CASI HC A01/MF A02

Detailed measurements were made of the flow field around an isolated roughness element. High shear layers generated in the near wake of the roughness element were disclosed through the hot wire measurements. In the region immediate behind the roughness, the shear stress in the vertical direction is responsible for the instability. On the other hand, the spanwise distribution of shear stress begins to play a dominant role in the transition process in the downstream region. Author (NASDA)

N94-12630# Institute of Flow Research, Tokyo (Japan).

IDEA OF UNDERGROUND AIRPLANE [CHICHUU HIKOUKI NO AIDEIA] c05

Hiroshi Satou *In* NAL, Proceedings of the 9th and 10th NAL Workshop on Investigation and Control of Boundary-Layer Transition Nov. 1992 p 79-81 In JAPANESE (For primary document see N94-12611 01-34)

Avail: CASI HC A01/MF A02

An underground airplane is proposed as a rapid transit system between large cities. A large-diameter tunnel is constructed and medium-size airplanes are operated at around 600 km/hr. The tunnel can be used also for storage and transportation of material, energy, and information. Author (NASDA)

N94-12631# Keio Univ., Yokahama (Japan). Dept. of Mechanical Engineering.

GROWTH AND BREAKDOWN OF TAYLOR-GOERTLER VORTICES IN ROTATING BLASIUS BOUNDARY LAYER [KORIORIRYOKU BA NIOKERU TERA-GERUTORA UZU NO SEICHOU TO HOUKAI]

Masaharu Matsubara and Shigeaki Masuda *In* NAL, Proceedings of the 9th and 10th NAL Workshop on Investigation and Control of Boundary-Layer Transition Nov. 1992 p 83-86 In JAPANESE (For primary document see N94-12611 01-34)

Avail: CASI HC A01/MF A02

The Coriolis force normal to the wall causes Taylor-Goertler vortices in a boundary layer rotating around the spanwise axis. These vortices distort the basic Blasius boundary layer into an inflectional distribution that should be inviscidly unstable. The experimental results showed that the pitch of Taylor-Goertler vortices are independent of the given initial disturbance, and suggested some mechanisms to select the spanwise pitch. The velocity fluctuation was rounded near the inflectional point of the spanwise velocity distribution, though it was not clear whether it was caused by the inviscid inflectional instability or by the spanwise fluctuation of the Taylor-Goertler vortex itself. Author (NASDA)

N94-12632# Tohoku Univ., Sendai (Japan). Faculty of Engineering.
TRAVELING DISTURBANCES APPEARING IN YAWED CYLINDER BOUNDARY LAYER TRANSITION [KEISHA ENCHUU KYOUKAISOU SENI NIOKERU SHINKOUHA FUANTEISEI NITSUITE]
Yasuaki Kohama *In* NAL, Proceedings of the 9th and 10th NAL Workshop on Investigation and Control of Boundary-Layer Transition Nov. 1992 p 87-89 In JAPANESE (For primary document see N94-12611 01-34)
Avail: CASI HC A01/MF A02

Unsteady disturbances with two different frequency f(sub 1) and f(sub 2) were detected in the boundary layer transition process on a yawed cylinder surface. Detailed velocity field measurement were performed using rotatable hot wire system. It was found that the high frequency(f(sub 2)) disturbance seems to be a streamwise inflectional instability that appears locally over the top of each of the crossflow vortices and drives the flow field directly into a full turbulent state. Directions and phase velocities of these disturbances were measured and it was found that the high frequency disturbance (f(sub 2)) is the secondary instability which was visualized by smoke previously. Author (NASDA)

N94-12633# Gifu Univ. (Japan). Faculty of Engineering.
VISUAL STRUCTURE OF KARMAN VORTEX STREETS IN A ROUTE TO CHAOTIC STATES EXCITED BY OSCILLATION OF A CIRCULAR CYLINDER [KAOSU IKOU KATEI NIOKERU KARUMAN UZURETSU NO SHIKAKU KOUZOU] **c02**
Hiroshi Nagata and Takashi Ishimaru *In* NAL, Proceedings of the 9th and 10th NAL Workshop on Investigation and Control of Boundary-Layer Transition Nov. 1992 p 91-95 In JAPANESE (For primary document see N94-12611 01-34)
Avail: CASI HC A01/MF A02

The structure of Karman vortex streets formed behind a circular cylinder oscillated in the streamwise direction was studied by using flow visualization and hot-film anemometry. The spectra of the velocity fluctuation at one point, which is located immediately downstream of the absolute instability region, were found to correspond intimately to the global structure of the vortex street. The chaotic vortex streets appear in the two ranges both around the lower and the upper boundaries of the lock-in range for the frequency of the cylinder oscillation. In the ranges outside the lock-in and the chaotic ranges, the velocity fluctuations become quasi-periodic states. The variation of the structure of the vortex streets can be interpreted as a result of nonlinear interaction between the pattern created by the oscillation of the cylinder and the pattern formed by natural shedding of the vortices. The chaotic vortex streets are considered to develop under the unsteady states in a competition between these two patterns. Author (NASDA)

N94-12634# Tokyo Univ. (Japan). Dept. of Physics.
BOUNDARY CONDITIONS AND BIFURCATIONS IN PLANE POISEUILLE FLOW [HEIMEN POAZUIYURYUU NO BUNKI TO KYOUKAI JOUKEN]
Makoto Umeki *In* NAL, Proceedings of the 9th and 10th NAL Workshop on Investigation and Control of Boundary-Layer Transition Nov. 1992 p 97-99 In JAPANESE Prepared in cooperation with Hitachi Ltd., Tokyo, Japan (For primary document see N94-12611 01-34)
Avail: CASI HC A01/MF A02

Effects of boundary conditions on bifurcation structures of two-dimensional steady progressive waves in plane Poiseuille flows are considered. There may exists a Hopf bifurcation on the upper branch of the progressive waves. In terms of the spectral method, the dimension of evolution equations of modes with a constant pressure gradient is larger by one than that with a constant flux. Author (NASDA)

N94-12774*# Remtech, Inc., Huntsville, AL.
THE 1991 VERSION OF THE PLUME IMPINGEMENT COMPUTER PROGRAM. VOLUME 2: USER'S INPUT GUIDE
Robert L. Bender, Richard E. Somers, Maurice J. Prendergast, Joseph P. Clayton, and Sheldon D. Smith (SECA, Inc., Huntsville, AL.) Oct. 1991 69 p
(Contract NAS8-38423; SBIR-02.08-8581A)
(NASA-CR-194191; NAS 1.26:194191; RTR-214-01-Vol-2) Avail: CASI HC A04/MF A01

The Plume Impingement Program (PLIMP) is a computer code used to predict impact pressures, forces, moments, heating rates, and contamination on surfaces due to direct impingement flowfields. Typically, it has been used to analyze the effects of rocket exhaust plumes on nearby structures from ground level to the vacuum of space. The program normally uses flowfields generated by the MOC, RAMP2, SPF/2, or SFPGEN computer programs. It is capable of analyzing gaseous and gas/particle flows. A number of simple subshapes are available to model the surfaces of any structure. The original PLIMP program has been modified many times of the last 20 years. The theoretical bases for the referenced major changes, and additional undocumented changes and enhancements since 1988 are summarized in volume 1 of this report. This volume is the User's Input Guide and should be substituted for all previous guides when running the latest version of the program. This version can operate on VAX and UNIX machines with NCAR graphics ability. Derived from text

N94-12775*# Remtech, Inc., Huntsville, AL.
THE 1991 VERSION OF THE PLUME IMPINGEMENT COMPUTER PROGRAM. VOLUME 1: DESCRIPTION
Robert L. Bender, Richard E. Somers, Maurice J. Prendergast, Joseph P. Clayton, and Sheldon D. Smith (SECA, Inc., Huntsville, AL.) Oct. 1991 146 p Original contains color illustrations
(Contract NAS8-38423; SBIR-02.08-8581A)
(NASA-CR-194192; NAS 1.26:194192; RTR-214-01-Vol-1) Avail: CASI HC A07/MF A02; 9 functional color pages

The objective of this contract was to continue development of a vacuum plume impingement evaluator to provide an analyst with a capability for rapid assessment of thruster plume impingement scenarios. The research was divided into three areas: Plume Impingement Computer Program (PLIMP) modification/validation; graphics development; and documentation in the form of a Plume Handbook and PLIMP Input Guide. Derived from text

N94-12777# Cambridge Univ. (England). Dept.of Engineering.
VIB3D: METHOD FOR CALCULATING 3-D UNSTEADY FLOW THROUGH TURBOMACHINERY BLADES
Li He and J. D. Denton Jan. 1993 43 p
(CUED/A-TURBO/TR.128) Avail: CASI HC A03/MF A01

This report consists of two parts. In the first part, the brief features and user's guide for the basic version of VIB3D are presented. In the second part, the features and user's guide for STAG3D, a program for a rotor-stator stage solution are described. Author (revised)

N94-12779# Cambridge Univ. (England). Dept. of Engineering.
VIB2D: QUASI 3-D UNSTEADY VISCOUS FLOW METHOD FOR BLADE FLUTTER CALCULATION
Li He Feb. 1993 43 p
(CUED/A-TURBO/TR.129) Avail: CASI HC A03/MF A01

VIB2D is a computer program developed for calculating quasi three dimensional unsteady flows through vibrating turbomachinery blades. The brief features and user's guide for the basic single blade passage version of VIB2D are first presented. VIB2D-MP, a multiple blade-passage version of VIB2D with an aerodynamic/structural coupled model is then described. Finally, the user's guide for VIB2D-MP is presented, Derived from text

N94-10074# Cambridge Univ. (England). Dept. of Applied Mathematics and Theoretical Physics.
NON-LINEAR LIQUID BRIDGE DYNAMICS
R. M. S. M. Schulkes *In* ESA, Proceedings of the 8th European Symposium on Materials and Fluid Sciences in Microgravity, Volume 1 Aug. 1992 p 61-65 (For primary document see N94-10070 01-29)
(Contract B/SC1-900617)
Copyright Avail: CASI HC A01/MF A04; ESA, EPD, ESTEC, Noordwijk, Netherlands, HC

N94-10077# Bremen Univ. (Germany). Center of Applied Space Technology and Microgravity.
THERMOCAPILLARY INSTABILITIES IN CYLINDRICAL LIQUID BRIDGES: MECHANISMS AND TRANSITION BOUNDARIES
Hendrik C. Kuhlmann *In* ESA, Proceedings of the 8th European Symposium on Materials and Fluid Sciences in Microgravity, Volume 1 Aug. 1992 p 79-83 (For primary document see N94-10070 01-29)
Copyright Avail: CASI HC A01/MF A04; ESA, EPD, ESTEC, Noordwijk, Netherlands, HC

N94-10078# Battelle Inst., Frankfurt am Main (Germany).
STABILITY OF LIQUID BRIDGES BETWEEN PARALLEL PLATES
Dieter Langbein *In* ESA, Proceedings of the 8th European Symposium on Materials and Fluid Sciences in Microgravity, Volume 1 Aug. 1992 p 85-93 (For primary document see N94-10070 01-29)
Copyright Avail: CASI HC A02/MF A04; ESA, EPD, ESTEC, Noordwijk, Netherlands, HC

N94-10079# Technische Univ., Munich (Germany). Lehrstuhl A fuer Thermodynamik.
TRANSIENT THREE-DIMENSIONAL NUMERICAL SIMULATION OF MARANGONI FLOW IN A LIQUID COLUMN UNDER MICROGRAVITY
Johannes Straub and Rudi Marek *In* ESA, Proceedings of the 8th European Symposium on Materials and Fluid Sciences in Microgravity, Volume 1 Aug. 1992 p 95-101 (For primary document see N94-10070 01-29)
Copyright Avail: CASI HC A02/MF A04; ESA, EPD, ESTEC, Noordwijk, Netherlands, HC

N94-10083# Universidad Politecnica de Madrid (Spain). Escuela Tecnica Superior de Ingenieros Navales.
EFFECTS OF AXIAL AND CENTRIFUGAL FORCES ON THE STABILITY OF LIQUID BRIDGES
I. Martinez, J. M. Perales, and M. Gomez *In* ESA, Proceedings of the 8th European Symposium on Materials and Fluid Sciences in Microgravity, Volume 1 Aug. 1992 p 123-130 Sponsored by Comision Interministerial de Ciencia y Tecnologia, Spain (For primary document see N94-10070 01-29)
Copyright Avail: CASI HC A02/MF A04; ESA, EPD, ESTEC, Noordwijk, Netherlands, HC

N94-10085# Universidad Politecnica de Madrid (Spain). Escuela Tecnica Superior de Ingenieros Navales.
LIQUID BRIDGES AND FLOATING ZONES
I. Martinez and A. Croell (Freiburg Univ., Germany.) *In* ESA, Proceedings of the 8th European Symposium on Materials and Fluid Sciences in Microgravity, Volume 1 Aug. 1992 p 135-142 Sponsored by Comission Interministerial de Ciencia y Tecnologia, Spain (For primary document see N94-10070 01-29)
Copyright Avail: CASI HC A02/MF A04; ESA, EPD, ESTEC, Noordwijk, Netherlands, HC

N94-10093# Academy of Sciences of the Moldavian SSR, Kishinev. Inst. of Applied Physics.
TWO-PHASE FLOW HEAT TRANSFER AND HYDRODYNAMICS IN AN ELECTRIC FIELD
M. K. Bologa, S. M. Klimov, and S. I. Chuchkalov *In* ESA, Proceedings of the 8th European Symposium on Materials and Fluid Sciences in Microgravity, Volume 1 Aug. 1992 p 181-186 (For primary document see N94-10070 01-29)
Copyright Avail: CASI HC A02/MF A04; ESA, EPD, ESTEC, Noordwijk, Netherlands, HC

N94-10094*# National Aeronautics and Space Administration. Lewis Research Center, Cleveland, OH.
MARANGONI INSTABILITY INDUCED CONVECTION IN AN EVAPORATING LIQUID DROPLET
An-Ti Chai, N. Rashidnia, and V. S. Arpaci (Michigan Univ., Ann Arbor.) *In* ESA, Proceedings of the 8th European Symposium on Materials and Fluid Sciences in Microgravity, Volume 1 Aug. 1992 p 187-192 (For primary document see N94-10070 01-29)
Copyright Avail: CASI HC A02/MF A04; ESA, EPD, ESTEC, Noordwijk, Netherlands, HC

N94-10095# Escuela Tecnica Superior de Ingenieros Industriales, Madrid (Spain). Dept. of Ingenieria Energetica y Fluidomecanica.
THERMOCAPILLARY MIGRATION OF BUBBLES: A SEMI-ANALYTICAL SOLUTION FOR LARGE MARANGONI NUMBERS
A. Crespo and J. Jimenez-Fernandez *In* ESA, Proceedings of the 8th European Symposium on Materials and Fluid Sciences in Microgravity, Volume 1 Aug. 1992 p 193-196 (For primary document see N94-10070 01-29)
(Contracts DGICYT-PS-90-0011; CICYT-ESP88-0586-C02-02)
Copyright Avail: CASI HC A01/MF A04; ESA, EPD, ESTEC, Noordwijk, Netherlands, HC

N94-10097# Naples Univ. (Italy). Facolta di Ingegneria.
MARANGONI FLOWS IN OPEN CAVITIES WITH DIFFERENTIALLY HEATED END WALLS
C. Golia, Antonio Viviani, and Dario Castagnolo (Microgravity Advanced Research and Support Center, Naples, Italy.) *In* ESA, Proceedings of the 8th European Symposium on Materials and Fluid Sciences in Microgravity, Volume 1 Aug. 1992 p 203-210 (For primary document see N94-10070 01-29)
Copyright Avail: CASI HC A02/MF A04; ESA, EPD, ESTEC, Noordwijk, Netherlands, HC

N94-10100*# Colorado Univ., Boulder.
BENARD AND MARANGONI CONVECTION IN MULTIPLE LIQUID LAYERS
Jean N. Koster, A. Prakash, D. Fujita, and T. Doi (National Space Development Agency, Tokyo, Japan.) *In* ESA, Proceedings of the 8th European Symposium on Materials and Fluid Sciences in Microgravity, Volume 1 Aug. 1992 p 221-226 (For primary document see N94-10070 01-29)
(Grant NAG3-1094)
Copyright Avail: CASI HC A02/MF A04; ESA, EPD, ESTEC, Noordwijk, Netherlands, HC

N94-10101# Aix-Marseilles Univ. (France). Inst. de Mecanique des Fluides.
COUPLED THERMOGRAVITATIONAL AND THERMOCAPILLARY CONVECTION IN A TWO-LAYER FLUID SYSTEM
Q. S. Liu, G. Chen, and Bernard Roux *In* ESA, Proceedings of the 8th European Symposium on Materials and Fluid Sciences in Microgravity, Volume 1 Aug. 1992 p 227-231 Sponsored by CNES (For primary document see N94-10070 01-29)
Copyright Avail: CASI HC A01/MF A04; ESA, EPD, ESTEC, Noordwijk, Netherlands, HC

N94-10104# Goettingen Univ. (Germany). Inst. fuer Angewandte Mechanik und Stroemungsphysik.
THERMOCAPILLARY SLUG FLOW IN A CAPILLARY TUBE
Martin Schaefer, Heinz Lang (Max-Planck-Inst. fuer Stroemungsforschung, Goettingen, Germany.), and Helmut Eckelmann *In* ESA, Proceedings of the 8th European Symposium on Materials and Fluid Sciences in Microgravity, Volume 1 Aug. 1992 p 243-246 (For primary document see N94-10070 01-29)
Copyright Avail: CASI HC A01/MF A04; ESA, EPD, ESTEC, Noordwijk, Netherlands, HC

N94-10106# Gesamthochschule, Essen (Germany).
LABORATORY STUDY ON THE NATURAL MODES OF A ROTATING TWO-PHASE FLUID SYSTEM SUBJECT TO AXIAL EXCITATION
Julius Siekmann and Dieter Raake *In* ESA, Proceedings of the 8th European Symposium on Materials and Fluid Sciences in Microgravity, Volume 1 Aug. 1992 p 253-256 Sponsored in part by Ministerium fuer Wissenschaft und Forschung des Landes Nordrhein-Westfalen, Germany (For primary document see N94-10070 01-29)
Copyright Avail: CASI HC A01/MF A04; ESA, EPD, ESTEC, Noordwijk, Netherlands, HC

N94-10107# Technische Univ., Munich (Germany). Lehrstuhl A fuer Thermodynamik.
NUMERICAL SIMULATION OF MARANGONI CONVECTION AROUND GAS BUBBLES IN A LIQUID MATRIX
Johannes Straub, Johann Betz, and Rudi Marek *In* ESA, Proceedings of the 8th European Symposium on Materials and Fluid Sciences in Microgravity, Volume 1 Aug. 1992 p 257-264 (For primary document see N94-10070 01-29)
(Grant DFG-Str-117/29-1)
Copyright Avail: CASI HC A02/MF A04; ESA, EPD, ESTEC, Noordwijk, Netherlands, HC

N94-10108# Naples Univ. (Italy). Facolta di Ingegneria.
BOUNDARY LAYERS ALONG HORIZONTAL FREE SURFACES DUE TO COMBINED EFFECTS OF TEMPERATURE AND CONCENTRATION GRADIENTS
Antonio Viviani and R. Savino *In* ESA, Proceedings of the 8th European Symposium on Materials and Fluid Sciences in Microgravity, Volume 1 Aug. 1992 p 265-272 (For primary document see N94-10070 01-29)
Copyright Avail: CASI HC A02/MF A04; ESA, EPD, ESTEC, Noordwijk, Netherlands, HC

N94-10109# Gesamthochschule, Essen (Germany).
EXPERIMENTAL ANALYSIS OF BENARD-CONVECTION BY THE COMBINED APPLICATION OF LIQUID CRYSTALS AND PIV
Klaus Wozniak and G. Wozniak *In* ESA, Proceedings of the 8th European Symposium on Materials and Fluid Sciences in Microgravity, Volume 1 Aug. 1992 p 273-278 (For primary document see N94-10070 01-29)
Copyright Avail: CASI HC A02/MF A04; ESA, EPD, ESTEC, Noordwijk, Netherlands, HC

N94-10182# Deutsche Forschungsanstalt fuer Luft- und Raumfahrt, Cologne (Germany).
NUMERICAL SIMULATION OF MULTI-DROPLET HYDRODYNAMIC INTERACTIONS IN LIQUID DISPERSIONS
S. Diefenbach, X. Zhang (Colorado Univ., Boulder.), R. H. Davis (Colorado Univ., Boulder.), and L. Ratke *In* ESA, Proceedings of the 8th European Symposium on Materials and Fluid Sciences in Microgravity, Volume 2 Aug. 1992 p 527-532 (For primary document see N94-10171 01-29)
Copyright Avail: CASI HC A02/MF A04; ESA, EPD, ESTEC, Noordwijk, Netherlands, HC

N94-10214# IFLYSIB, La Plata (Argentina).
MARANGONI-DRIVEN SOLITARY WAVES
Alfredo N. Garazo and Manuel G. Velarde (Universidad Nacional de Educacion a Distancia, Madrid, Spain.) *In* ESA, Proceedings of the 8th European Symposium on Materials and Fluid Sciences in Microgravity, Volume 2 Aug. 1992 p 711-715 (For primary document see N94-10171 01-29)
(Grants CICYT-PB86-651; CICYT-PB90-264)
Copyright Avail: CASI HC A01/MF A04; ESA, EPD, ESTEC, Noordwijk, Netherlands, HC

N94-10218# Aix-Marseilles Univ. (France). Inst. de Mecanique des Fluides.
INSTABILITY OF THERMOCAPILLARY CONVECTION IN MULTIPLE SUPERPOSED IMMISCIBLE LIQUID LAYERS
Q. S. Liu and Bernard Roux *In* ESA, Proceedings of the 8th European Symposium on Materials and Fluid Sciences in Microgravity, Volume 2 Aug. 1992 p 735-740 (For primary document see N94-10171 01-29)
Copyright Avail: CASI HC A02/MF A04; ESA, EPD, ESTEC, Noordwijk, Netherlands, HC

N94-10219# Academy of Sciences (USSR), Moscow. Inst. for Problems in Mechanics.
CONVECTIVE MOTION IN A MULTI-LAYERED SYSTEM WITH A FREE SURFACE
Valentina M. Shevtsova and A. E. Indeikina *In* ESA, Proceedings of the 8th European Symposium on Materials and Fluid Sciences in Microgravity, Volume 2 Aug. 1992 p 741-746 (For primary document see N94-10171 01-29)
Copyright Avail: CASI HC A02/MF A04; ESA, EPD, ESTEC, Noordwijk, Netherlands, HC

N94-10220# Perm State Univ. (Russia). Inst. of Pedagogy.
VIBRATIONAL-THERMOCAPILLARY PARALLEL FLOWS AND STABILITY
R. Birikh, Vladimir Briskman (Academy of Sciences, USSR, Perm.), V. Myznikov, Bernard Roux (Aix-Marseilles Univ., France.), and Manuel G. Velarde (Universidad Nacional de Educacion a Distancia, Madrid, Spain.) *In* ESA, Proceedings of the 8th European Symposium on Materials and Fluid Sciences in Microgravity, Volume 2 Aug. 1992 p 747-752 (For primary document see N94-10171 01-29)
Copyright Avail: CASI HC A02/MF A04; ESA, EPD, ESTEC, Noordwijk, Netherlands, HC

N94-10221# Ruhr Univ., Bochum (Germany). Lehrstuhl fuer Physikalische Chemie 2.
APPEARANCE OF CONVECTIVE INSTABILITIES CAUSED BY LIQUID-LIQUID PHASE SEPARATION UNDER SMALL BUOYANCY FORCES
Roland Zander and G. M. Schneider *In* ESA, Proceedings of the 8th European Symposium on Materials and Fluid Sciences in Microgravity, Volume 2 Aug. 1992 p 755-759 Sponsored by BMFT (For primary document see N94-10171 01-29)
Copyright Avail: CASI HC A01/MF A04; ESA, EPD, ESTEC, Noordwijk, Netherlands, HC

N94-10222# Strathclyde Univ., Glasgow (Scotland). Dept. of Mathematics.
THE EFFECT OF A UNIFORM MAGNETIC FIELD ON THE ONSET OF STEADY MARANGONI CONVECTION IN A LAYER OF CONDUCTING FLUID
S. K. Wilson *In* ESA, Proceedings of the 8th European Symposium on Materials and Fluid Sciences in Microgravity, Volume 2 Aug. 1992 p 761-765 (For primary document see N94-10171 01-29)
Copyright Avail: CASI HC A01/MF A04; ESA, EPD, ESTEC, Noordwijk, Netherlands, HC

N94-10223# Perm State Univ. (Russia). Inst. of Pedagogy.
THE COMBINED INFLUENCE OF ANTICONVECTIVE AND THERMOCAPILLARY MECHANISMS ON THE STABILITY OF SYSTEMS WITH INTERFACE
Illya B. Simanovskii, Alexander A. Nepomnyashchy (Technion - Israel Inst. of Tech., Haifa.), P. Colinet (Brussels Univ., Belgium.), J.-C. Legros (Brussels Univ., Belgium.), and Stefan VanVaerenbergh (Brussels Univ., Belgium.) *In* ESA, Proceedings of the 8th European Symposium on Materials and Fluid Sciences in Microgravity, Volume 2 Aug. 1992 p 767-770 (For primary document see N94-10171 01-29)
Copyright Avail: CASI HC A01/MF A04; ESA, EPD, ESTEC, Noordwijk, Netherlands, HC

N94-10232# Technische Univ., Munich (Germany). Lehrstuhl A fuer Thermodynamik.
STUDY OF VAPOR BUBBLE GROWTH IN A SUPERSATURATED LIQUID
Johannes Straub, J. Winter, G. Picker, H. Merte (Michigan Univ., Ann Arbor.), and Ayahiko Kono (JGC Corp., Yokohama, Japan.) *In* ESA, Proceedings of the 8th European Symposium on Materials and Fluid Sciences in Microgravity, Volume 2 Aug. 1992 p 820-825 (For primary document see N94-10171 01-29)
Copyright Avail: CASI HC A02/MF A04; ESA, EPD, ESTEC, Noordwijk, Netherlands, HC

N94-10235*# National Aeronautics and Space Administration. Marshall Space Flight Center, Huntsville, AL.
GRANULAR INSTABILITY IN FLUIDIZED BEDS: A SMALL-OVER-LARGE INSTABILITY
David A. Noever *In* ESA, Proceedings of the 8th European Symposium on Materials and Fluid Sciences in Microgravity, Volume 2 Aug. 1992 p 833-837 (For primary document see N94-10171 01-29)
Copyright Avail: CASI HC A01/MF A04; ESA, EPD, ESTEC, Noordwijk, Netherlands, HC

N94-10239*# National Aeronautics and Space Administration. Lewis Research Center, Cleveland, OH.
THE KINEMATICS OF BUOYANCY INDUCED MIXING
Walter M. B. Duval *In* ESA, Proceedings of the 8th European Symposium on Materials and Fluid Sciences in Microgravity, Volume 2 Aug. 1992 p 855-861 (For primary document see N94-10171 01-29)
Copyright Avail: CASI HC A02/MF A04; ESA, EPD, ESTEC, Noordwijk, Netherlands, HC

N94-10247# Bremen Univ. (Germany). Center of Applied Space Technology and Microgravity.
A METHOD FOR DETERMINATION OF THE ELONGATIONAL VISCOSITY OF VISCOELASTIC FLUIDS WITHOUT BODY FORCES
S. Berg, A. Delgado, R. Kroeger, and Hans J. Rath *In* ESA, Proceedings of the 8th European Symposium on Materials and Fluid Sciences in Microgravity, Volume 2 Aug. 1992 p 901-904 Sponsored by BMFT and the Senator for Education and Arts of the State of Bremen (For primary document see N94-10171 01-29)
Copyright Avail: CASI HC A01/MF A04; ESA, EPD, ESTEC, Noordwijk, Netherlands, HC

N94-10439*# National Aeronautics and Space Administration. Ames Research Center, Moffett Field, CA.
A CFD VALIDATION ROADMAP FOR HYPERSONIC FLOWS
Joseph G. Marvin *In* AGARD, Theoretical and Experimental Methods in Hypersonic Flows Apr. 1993 16 p (For primary document see N94-10421 01-02)
Copyright Avail: CASI HC A03/MF A04

N94-10441# Texas Univ., Austin. Center for Aeromechanics Research.
PROBLEMS IN THE VALIDATION OF CFD CODES THROUGH COMPARISON WITH EXPERIMENT
David S. Dolling *In* AGARD, Theoretical and Experimental Methods in Hypersonic Flows Apr. 1993 15 p (For primary document see N94-10421 01-02)
Copyright Avail: CASI HC A03/MF A04

N94-11493# Universite Catholique de Louvain (Belgium). Mecanique Appliquee.
STABILITY OF VISCOELASTIC FLOW: PHYSICAL AND NUMERICAL CONSIDERATIONS
M. J. Crochet and C. Bodart *In* AGARD, Stability in Aerospace Systems Feb. 1993 16 p (For primary document see N94-11489 01-08)
Copyright Avail: CASI HC A03/MF A03

N94-11498# Centre d'Etudes et de Recherches, Toulouse (France). Aerothermodynamics Dept.
BOUNDARY LAYER TRANSITION: PREDICTION AND WIND TUNNEL SIMULATION
D. Arnal *In* AGARD, Stability in Aerospace Systems Feb. 1993 12 p (For primary document see N94-11489 01-08)
Copyright Avail: CASI HC A03/MF A03

N94-11944 Taisei Corp., Yokohama (Japan).
THE FLOW STRUCTURE AROUND A CYLINDRICAL PIER FOR THE FLOW OF TRANSCRITICAL REYNOLDS NUMBER
Kazuo Ishino, Hideo Ootani, Ryouta Okada (Honshu Shikoku Bridge Authority, Kobe, Japan.), and Yoshitaka Nakagawa (Akashi Kaikyo Ohashi Substructure Construction, Kobe, Japan.) *In* Scientific Organizing Committee of PORSEC, Proceedings of the PORSEC 1992 in Okinawa: Conference for Pacific Ocean Environments and Probing, Volume 1 25 Aug. 1992 p 293-298 (For primary document see N94-11894 01-42)
Copyright Avail: Issuing Activity (Scientific Organizing Committee of PORSEC, P.O. Box 10, Shimizu, Shizuoka 424, Japan, HC)

N94-12044*# Brown Univ., Providence, RI. Dept. of Geological Sciences.
BEHAVIOR OF VORTICES GENERATED BY AN ADVANCING EJECTA CURTAIN IN THEORY, IN THE LABORATORY, AND ON MARS
Abstract Only
O. S. Barnouin and P. H. Schultz *In* Lunar and Planetary Inst., Twenty-fourth Lunar and Planetary Science Conference. Part 1: A-F 1993 p 63-64 (For primary document see N94-12015 01-91)
Avail: CASI HC A01/MF A06

N94-12728 Academy of Sciences (USSR), Vladivostok. Pacific Oceanological Inst.
THE THERMODYNAMICS OF THE NONLINEAR SHEAR FLOWS
S. V. Simonenko *In* Scientific Organizing Committee of PORSEC, Proceedings of the PORSEC 1992 in Okinawa: Conference for Pacific Ocean Environments and Probing, Volume 2 25 Aug. 1992 p 1079-1084 (For primary document see N94-12635 01-42)
Copyright Avail: Issuing Activity (Scientific Organizing Committee of PORSEC, P.O. Box 10, Shimizu, Shizuoka 424, Japan, HC)

35 INSTRUMENTATION AND PHOTOGRAPHY

Includes remote sensors; measuring instruments and gages; detectors; cameras and photographic supplies; and holography.

For aerial photography see *43 Earth Resources and Remote Sensing.* For related information see also *06 Aircraft Instrumentation,* and *19 Spacecraft Instrumentation.*

N94-10326# Argonne National Lab., IL. Reactor Engineering Div.
DEMONSTRATION PROTOTYPE GAMMA-RAY HODOSCOPE ALTERNATIVE TO CARGOSCAN FOR ROCKET STAGE MONITORING
C. E. Dickerman, R. E. Boyar, J. P. Regis, and D. J. Travis Nov. 1992 57 p
(Contract W-31-109-eng-38)
(DE93-006908; ANL/ACTV-92/2) Avail: CASI HC A04/MF A01 (US Sales Only)

The potential of the gamma-ray hodoscope as a less expensive and less intrusive alternate to CARGOSCAN for rocket stage monitoring was demonstrated in measurements with a full-scale prototype gamma-ray hodoscope system. After preliminary tests at Argonne and other laboratories, the system was shipped to the Technical On-Site Inspection (TOSI) simulation facility at Albuquerque NM, and used for a series of 'blind' tests conducted under the supervision of Sandia and Brookhaven personnel. A low-level Co-60 source was adequate for hodoscope determination of the locations of the diameter and end edges of the rocket motor items inside a missile-shipping railcar. The system was not fooled by the 'simple spoofing' attempts made during the TOSI runs. However, most of the 'complex spoofing' attempts were successful with this low-resolution system. Although not optimized for portable service, the prototype was unpacked and set up by the three-person ANL team within four hours, and taken down and packed by the same team within four hours. The prototype was returned to Argonne, where the detector arrays were reconfigured and used successfully to detect a complex spoofing simulation in which an SS-20 is loaded inside an SS-25 shell, and the annulus outside the SS-20 is packed with material at solid-fuel density. The hodoscope uses a technology proven by over twenty-five years experience; it does not require a complex accelerator or large expensive gamma-ray detectors. As a result of its modular, commercial, off-the-shelf technology, the hodoscope is expected to be more reliable, much lower in cost, and less intrusive than the CARGOSCAN (trademark) as applied to either fixed portal monitoring or portable on-site inspection of rockets and other treaty-limited items. The level of hodoscope resolution may be adjusted, in a trade-off between intrusiveness and resistance to complex spoofing attempts, as part of a suitably defined inspection system. DOE

N94-10526# Lawrence Livermore National Lab., CA.
SURFACE AND NEAR-SURFACE ATOM IMAGING WITH PHOTOELECTRON HOLOGRAPHY
L. J. Terminello, J. J. Barton (IBM Research Lab., Yorktown Heights, NY.), and D. A. Lapiano-Smith (IBM Research Lab., Yorktown Heights, NY.) Jul. 1992 8 p Presented at the 10th International Conference on Vacuum Ultraviolet Radiation Physics, Paris, France, 27-31 Jul. 1992
(Contracts W-7405-eng-48; DE-AC02-76CH-00016)
(DE93-013197; UCRL-JC-111627; CONF-920735-6) Avail: CASI HC A02/MF A01

Near-surface atoms from a Cu(001) surface were imaged using 3p photoelectron holograms. The angle-dependent electron diffraction patterns that constitute an electron hologram were Fourier transformed to create a three dimensional, real-space image of the scattering atoms. We have made use of a multiple-wavenumber, phased summing method to improve the atom imaging capabilities of experimental photoelectron holography using the Cu(001) prototype system. DOE

N94-10630 Melbourne Univ., Parkville (Australia). School of Physics.
TEST OF A METHOD FOR PHASE RETRIEVAL IN HRTEM
M. J. Beeching and A. E. C. Spargo 1992 2 p Presented at the 27th Annual Meeting of the Microbeam Analysis Society and the 19th Annual Meeting of the Microscopial Society of Canada, Boston, MA, 1 Aug. 1992 Limited Reproducibility: More than 20% of this document may be affected by microfiche quality
(DE93-612641; UM-P-92/21; CONF-9208150) Avail: CASI HC A01 (US Sales Only)

Several methods of phase retrieval from the high resolution transmission electron microscopy image intensity distributions have been proposed but no standard method has emerged. The results achieved using a technique based on a development of the focus variation method, are reported. The dependence of the retrieved wavefunction on various experimental parameters is investigated and the method tested using computer simulated images. The method is shown to be useful in finding the complex wavefield at the exit surface of the specimen but the relationship of this to the specimen structure is considered as a separate issue. DOE

N94-10667*# National Aeronautics and Space Administration. Goddard Space Flight Center, Greenbelt, MD.
NASA'S FIRST IN-SPACE OPTICAL GYROSCOPE: A TECHNOLOGY EXPERIMENT ON THE X RAY TIMING EXPLORER SPACECRAFT
Glenn Unger, David M. Kaufman, Michael Krainak, Glenn Sanders (Honeywell, Inc., Phoenix, AZ.), Bill Taylor (Honeywell, Inc., Clearwater, FL.), and Norman R. Schulze (National Aeronautics and Space Administration, Washington, DC.) [1993] 7 p
(NASA-TM-109242; Rept-1953-09; NAS 1.15:109242) Avail: CASI HC A02/MF A01

A technology experiment on the X-ray Timing Explorer spacecraft to determine the feasibility of Interferometric Fiber Optic Gyroscopes for space flight navigation is described. The experiment consists of placing a medium grade fiber optic gyroscope in parallel with the spacecraft's inertial reference unit. The performance of the fiber optic gyroscope will be monitored and compared to the primary mechanical gyroscope's performance throughout the two-year mission life. Author (revised)

N94-10704 Scripps Institution of Oceanography, La Jolla, CA. Marine Physical Lab.
LOW POWER DIGITAL RECORDER DEVELOPMENT Final Report
William S. Hodgkiss Jan. 1993 4 p Limited Reproducibility: More than 20% of this document may be affected by microfiche quality
(Contract N00014-89-D-0142)
(AD-A265921; MPL-U-5/93) Avail: CASI HC A01

The objective of this program was to assist NOSC (Now NRaD, San Diego) in the development and testing of a digital recorder suitable for extended low-power remote operations where low frequency acoustic or engineering data must be recorded. DTIC

N94-10873 Army Engineer Waterways Experiment Station, Vicksburg, MS. Structures Lab.
DESIGN AND DEVELOPMENT OF A MINIATURE COLUMN-BASED INTERFACE (MCBI) STRESS GAGE Final Report, Jan. - Nov. 1988
Denis D. Rickman Apr. 1993 145 p Limited Reproducibility: More than 20% of this document may be affected by microfiche quality
(Contract DNA-MIPR-88-503)
(AD-A266054; WES/TR/SL-93-3) Avail: CASI HC A07

Tests are routinely conducted to evaluate the survivability, under simulated battlefield conditions, of buried military structures subjected to high-explosive loadings. The survivability assessments require the measurement of dynamic normal stresses induced at soil/structure interfaces. Stresses in excess of 10,000 psi and accelerations greater than 100,000 g's may be applied at interface locations. Normal-incidence interface stress gages currently used in such tests are incapable of accurately measuring stresses above 5,000 psi, and are sensitive to lateral accelerations and structure-transmitted stresses which distort the measurement. This study explores the design, development, and testing of a miniature, column-based, interface (MCBI) stress gage. The MCBI gage is designed to measure normal stresses up to 35,000 psi. Laboratory tests indicate that the gage produces a linear output due to applied pressure and is virtually insensitive to lateral stresses. Explosive tests have shown the MCBI gage compares favorably to commonly-used interface stress gages at stresses up to 3,000 psi and is survivable at stresses up to 25,000 psi. DTIC

N94-10948*# Christopher Newport Coll., Newport News, VA.
DEVELOPMENT AND TESTING OF A SUPERCONDUCTING LINK FOR AN IR DETECTOR Final Technical Report, Jul. 1989 - Apr. 1991
R. Caton and R. Selim 1991 10 p
(Grant NAG1-1042)
(NASA-CR-193674; NAS 1.26:193674) Avail: CASI HC A02/MF A01

The development and testing of a ceramic superconducting link for an infrared detector is summarized. Areas of study included the materials used, the electrical contacts, radiation and temperature cycling effects, aging, thermal conductivity, and computer models of an ideal link. Materials' samples were processed in a tube furnace at temperatures of 840 C to 865 C for periods up to 17 days and transition temperatures and critical current densities were recorded. The project achieved better quality high superconducting transition temperature material through improved processing and also achieved high quality electrical contacts. Studies on effects of electron irradiation, temperature cycling, and aging on superconducting properties indicate that the materials will be suitable for space applications. Various presentations and publications on the study's results are reported. CASI

N94-11267# Lawrence Livermore National Lab., CA.
DESIGN OF CCD CAMERA SYSTEM FOR USE INSIDE ELECTRON BEAM FURNACE
J. S. Sze Oct. 1992 16 p Presented at the Electron Beam Melting and Refining Conference, Reno, NV, 25-27 Oct. 1992
(Contract W-7405-eng-48)
(DE93-009525; UCRL-JC-111578; CONF-9210282-2) Avail: CASI HC A03/MF A01

The design of a wide dynamic range camera system for use inside Electron Beam furnaces is presented. The camera system is designed for use in high vacuum and in a high radiant heat flux environment looking directly into a high metallic vapor flux. In addition, the camera is designed to have a dynamic range that can provide a good image in both low light level conditions as well as in high brightness situations such as when the electron beam is impinging on the melt surface. An analysis is given for estimating the dynamic range of the camera imaging system and the camera cooling requirements. Techniques for capturing and recording video images are also presented. The application of various optical filters and liquid crystal variable attenuators for the camera imaging system is discussed. DOE

N94-11310*# National Aeronautics and Space Administration. Lewis Research Center, Cleveland, OH.
HEAT FLUX MEASUREMENTS ON CERAMICS WITH THIN FILM THERMOCOUPLES
Raymond Holanda, Robert C. Anderson, and Curt H. Liebert Nov. 1993 15 p Proposed for presentation at the SEM Fall Conference Structural Testing Technology at High Temperature, Ojai, CA, 8-10 Nov. 1993; sponsored by the Society for Experimental Mechanics
(RTOP 505-62-50)
(NASA-TM-106305; E-7963; NAS 1.15:106305) Avail: CASI HC A03/MF A01

Two methods were devised to measure heat flux through a thick ceramic using thin film thermocouples. The thermocouples were deposited on the front and back face of a flat ceramic substrate. The heat flux was applied to the front surface of the ceramic using an arc lamp Heat Flux Calibration Facility. Silicon nitride and mullite ceramics were used; two thicknesses of each material was tested, with ceramic temperatures to 1500 C. Heat flux ranged from 0.05-2.5 MW/m2(sup 2). One method for heat flux determination used an approximation technique to calculate instantaneous values of heat flux vs time; the other method used an extrapolation technique to determine the steady state heat flux from a record of transient data. Neither method measures heat flux in real time but the techniques may easily be adapted for quasi-real time measurement. In cases where a significant portion of the transient heat flux data is available, the calculated transient heat flux is seen to approach the extrapolated steady state heat flux value as expected. Author (revised)

N94-11420# Foster-Miller Associates, Inc., Waltham, MA.
HOLOGRAPHIC MULTIPLEXING FOR 3D OPTICAL MEMORY Final Report
V. R. Domash Jun. 1993 26 p
(Contract F49620-92-C-0077)
(AD-A266099; AFB-0077-FM-9566-624; AFOSR-93-0414TR) Avail: CASI HC A03/MF A01

The increasing demand for larger memory capacity has led to the exploration of volume data storage in optical materials with theoretical capacities of 10 to the 13th power bits/cm cubed. However, an important technical barrier is the design of an input/output architecture to read and write to the optical 3D memory at very high speed. During Phase 1 of this effort, we have experimentally demonstrated the operation of a unique optical lock-in instrument that can play a key role in accessing optical memories at high data rates. This optical lock-in detector is capable of demultiplexing a highly complex wavefront consisting of a number of holograms that have been combined on a single light beam. Using the optical lock-in detector, it is possible to demultiplex and recover any individual hologram using optical mixing in a photorefractive medium with the appropriate modulation applied to the reference optical beam. For Phase 2 a prototype optical memory system is proposed, including highly parallel input/output techniques, a cache memory for faster access, and a unique photorefractive material for optical data storage. At least one key component of this optical memory system, an optical beamlet array generator, is a likely candidate for Phase 3 development by Foster-Miller and Polaroid Corporation. DTIC

N94-12335 Army War Coll., Carlisle Barracks, PA.
INTEGRATING THE SERVICES' IMAGERY ARCHITECTURES Study Project Report
John F. Mader 15 Apr. 1993 137 p Limited Reproducibility: More than 20% of this document may be affected by microfiche quality
(AD-A265487) Avail: CASI HC A07

Any military organization requiring imagery must deal with one or more of several architectures: the tactical architectures of the three military departments, the theater architectures, and their interfaces to a separate national architecture. A seamless, joint, integrated architecture must meet today's imagery requirements. The CIO's vision of 'the right imagery to the right people in the right format at the right time' would serve well as the objective of a joint, integrated architecture. A joint imagery strategy should be initially shaped by the four pillars of the National Military Strategy of the United States: strategic deterrence; forward presence; crisis response; and reconstitution. In a macro view, it must consist of a series of sub-strategies to include science and technology and research and development, maintenance of the imagery related industrial base, acquisition, resource management, and burden sharing. Common imagery doctrine must follow the imagery strategy. Most of all, control, continuity, and direction must be maintained with regard to organizations and systems development as the architecture evolves. These areas and more must be addressed to reach the long term goal of a joint, integrated imagery architecture. This will require the services and theaters to relinquish some sovereignty over at least systems development and acquisition. Nevertheless, the goal of a joint, integrated imagery architecture is feasible. The author presents arguments and specific recommendations to orient the imagery community in the direction of a joint, integrated imagery architecture. DTIC

N94-12362# Army Engineer Waterways Experiment Station, Vicksburg, MS. Structures Lab.
ANALYSIS OF HOPKINSON BAR PRESSURE GAGE Final Report
James T. Baylot Jan. 1993 68 p
(AD-A262366; WES/TR/SL-93-1) Avail: CASI HC A04/MF A01

In order to fully understand the results of experiments on buried structures subjected to high intensity airblast that simulates nuclear weapons effects, an accurate measurement of the airblast pressure time-history must be made. Quite often, the peak airblast pressures in these tests are above what commercially-available air-pressure gages are capable of measuring. Hopkinson bar pressure gages remain elastic while measuring these very high airblast pressures. These bar gages also have the advantage that the sensing element of the gage is placed at a distance down the bar from the high pressure airblast. Thus the sensing element and the wires attached to it stand a much better chance of surviving the environment created by the simulator. The U.S. Army Engineer Waterways Experiment Station (WES) has developed a bar gage, designed to measure the airblast for tests in which airblast-induced ground shock is simulated. The primary objective of this study was to determine the accuracy of the WES bar gage and the possible effects the water and water seal have on the measured waveforms. Other objectives are to evaluate the differences in measured stresses between the WES and NMERI bars in the DET test, and to determine if modifications to the WES bar gage design are needed. Derived from text

N94-12391# Colorado Univ., Boulder.
AN OPTOELECTRONIC GRAPHICS DISPLAY PROCESSOR Quarterly Report, 15 Mar. - 14 Jun. 1993
Vincent P. Heuring 14 Jun. 1993 2 p
(Contract N00014-93-1-0419)
(AD-A266011) Avail: CASI HC A01/MF A01

The first three months of this grant period have seen significant progress toward the project goals. A one bit optoelectronic counter has been constructed as prototypical of an optoelectronic control unit. The counter runs at 305 MHz, and provided us much information on the timing and synchronization of such processors. We are beginning our work on developing or acquiring the optoelectronic integrated circuits and holographic optical elements that are necessary to the development of the optoelectronic graphic display processor, OGDP. We have also begun work on a CAD system for designing and constructing such processors. The CAD efforts have begun with development of algorithms for computing bit error rate in these systems. We are also in the midst of developing the logical architecture for the OGDP, including control unit and front end processor design. DTIC

N94-12533 Virginia Polytechnic Inst. and State Univ., Blacksburg. Dept. of Aerospace and Ocean Engineering.
DEVELOPMENT OF THE ONE-COMPONENT DIODE-ARRAY VELOCIMETER Final Report
Jun. 1993 91 p Limited Reproducibility: More than 20% of this document may be affected by microfiche quality
(Contract N00014-92-J-1292)
(AD-A265552; VPI-AOE-201) Avail: CASI HC A05

A new optical flow measurement technique, the diode array velocimeter (DAV), has been proposed. A DAV works by timing the passage of seed particles through a small section of a light beam. This is achieved by imaging light scattered by the particles on to one or more photodiode arrays. The arrays have a few carefully shaped elements, the shapes and positions of the elements are used to control the measurement volume geometry and thus select the measurement made. Measurement volumes sensitive to velocity, position, and acceleration may be designed. Measurements in highly turbulent and reversing flows are possible. A DAV for one-component velocity measurements has been developed to demonstrate this concept. This device uses a single laser beam to illuminate particles and a photodiode array with two rectangular elements to sense their motion. The sensitivity of this device to electrical noise in the photodiode circuitry is analyzed and found to decrease with reduction in measurement volume size. The angle response is also studied and, depending on the signal processing used, found to be closely cosinusoidal to about 60 deg. Changes to the photodiode array design could substantially increase this limit. DTIC

N94-10114# Technische Univ., Munich (Germany). Lehrstuhl A fuer Thermodynamik.
A NEW METHOD FOR HYSTERESIS MEASUREMENTS DEVELOPED FOR C(SUB v) MEASUREMENTS AT THE CRITICAL POINT DURING THE D2-MISSION
Johannes Straub, Axel Haupt, K. Nitsche, and Kurt Kemmerle (Kayser Threde G.m.b.H., Munich, Germany.) *In* ESA, Proceedings of the 8th European Symposium on Materials and Fluid Sciences in Microgravity, Volume 1 Aug. 1992 p 301-308 Sponsored by BMFT (For primary document see N94-10070 01-29)
Copyright Avail: CASI HC A02/MF A04; ESA, EPD, ESTEC, Noordwijk, Netherlands, HC

N94-10117# Genoa Univ. (Italy). DISTER.
THE SENSITIVITY OF AN OPTICAL FIBER HOLOGRAPHIC INTERFEROMETER
F. Bedarida, Gian Antonio DallAglio, L. Gatti (Alenia Spazio S.p.A., Turin, Italy.), and F. Solitro (Alenia Spazio S.p.A., Turin, Italy.) *In* ESA, Proceedings of the 8th European Symposium on Materials and Fluid Sciences in Microgravity, Volume 1 Aug. 1992 p 321-323 (For primary document see N94-10070 01-29)
(Contract ESTEC-8822/90/NL/PB(SC))
Copyright Avail: CASI HC A01/MF A04; ESA, EPD, ESTEC, Noordwijk, Netherlands, HC

N94-10121# Bremen Univ. (Germany). Center of Applied Space Technology and Microgravity.
CALIBRATION OF ACCELEROMETERS ON DROP TOWER BREMEN
U. Kaczmarczik, Hansjorg Dittus, and Hans J. Rath *In* ESA, Proceedings of the 8th European Symposium on Materials and Fluid Sciences in Microgravity, Volume 1 Aug. 1992 p 343-347 (For primary document see N94-10070 01-29)
Copyright Avail: CASI HC A01/MF A04; ESA, EPD, ESTEC, Noordwijk, Netherlands, HC

N94-10123# Kayser Threde G.m.b.H., Munich (Germany).
HOLOGRAPHIC INTERFEROMETRY FOR MICROGRAVITY APPLICATIONS
Peter Hofmann, J. Winter (Technische Univ., Munich, Germany.), J. Engelsberger (Labor Dr. Steinbichler, Neubeuern, Germany.), and Hans Steinbichler (Labor Dr. Steinbichler, Neubeuern, Germany.) *In* ESA, Proceedings of the 8th European Symposium on Materials and Fluid Sciences in Microgravity, Volume 1 Aug. 1992 p 357-359 (For primary document see N94-10070 01-29)
Copyright Avail: CASI HC A01/MF A04; ESA, EPD, ESTEC, Noordwijk, Netherlands, HC

N94-10124# Kayser Threde G.m.b.H., Munich (Germany).
THE HIGH PRECISION THERMOSTAT HPT-HYDRA
Kurt Kemmerle, H.-G. Bernhardt, Johannes Straub (Technische Univ., Munich, Germany.), Axel Haupt (Technische Univ., Munich, Germany.), and K. Nitsche (Technische Univ., Munich, Germany.) *In* ESA, Proceedings of the 8th European Symposium on Materials and Fluid Sciences in Microgravity, Volume 1 Aug. 1992 p 361-366 (For primary document see N94-10070 01-29)
(Contract BMFT-01-QV-8873)
Copyright Avail: CASI HC A02/MF A04; ESA, EPD, ESTEC, Noordwijk, Netherlands, HC

N94-10438# Von Karman Inst. for Fluid Dynamics, Rhode-Saint-Genese (Belgium).
THERMAL FLUX MEASUREMENTS IN HYPERSONIC FLOWS: A REVIEW
J. F. Wendt, D. Balageas (Office National d'Etudes et de Recherches Aerospatiales, Paris, France.), and R. D. Neumann (Dayton Univ. Research Inst., OH.) *In* AGARD, Theoretical and Experimental Methods in Hypersonic Flows Apr. 1993 5 p (For primary document see N94-10421 01-02)
Copyright Avail: CASI HC A01/MF A04

N94-11332# Pennsylvania State Univ., University Park. Materials Research Lab.
RECENT DEVELOPMENTS IN PIEZOELECTRIC AND ELECTROSTRICTIVE SENSORS AND ACTUATORS FOR SMART STRUCTURES
L. Eric Cross *In* AGARD, Smart Structures for Aircraft and Spacecraft Apr. 1993 33 p (For primary document see N94-11317 01-24)
Copyright Avail: CASI HC A03/MF A04

N94-11340# Deutsche Forschungs- und Versuchsanstalt fuer Luft- und Raumfahrt, Brunswick (Germany). Inst. for Flight Guidance.
FIBER-OPTIC INTERFEROMETRIC STRAIN GAUGE FOR SMART STRUCTURES APPLICATIONS: FIRST FLIGHT TESTS
N. Fuerstenau, D. D. Janzen, and W. Schmidt *In* AGARD, Smart Structures for Aircraft and Spacecraft Apr. 1993 6 p (For primary document see N94-11317 01-24)
Copyright Avail: CASI HC A02/MF A04

N94-11916 Japan Marine Science and Technology Center, Tokyo.
ACOUSTIC CHARACTERISTICS OF SIDE SCAN SONAR AND SUB-BOTTOM PROFILER FOR 10,000 m CLASS ROV
Toshiaki Nakamura, Toshio Tsuchiya, Yasutaka Amitani, and Hideharu Morimatsu (Furuno Electric Co. Ltd., Nishinomiya, Japan.) *In* Scientific Organizing Committee of PORSEC, Proceedings of the PORSEC 1992 in Okinawa: Conference for Pacific Ocean Environments and Probing, Volume 1 25 Aug. 1992 p 126-131 (For primary document see N94-11894 01-42)
Copyright Avail: Issuing Activity (Scientific Organizing Committee of PORSEC, P.O. Box 10, Shimizu, Shizuoka 424, Japan, HC)

N94-11966 Xian Inst. of Optics and Precision Mechanics (China).
ON RESOLUTION OF UNDERWATER STEREO PHOTOGRAMMETRY
Jianguo Wu *In* Scientific Organizing Committee of PORSEC, Proceedings of the PORSEC 1992 in Okinawa: Conference for Pacific Ocean Environments and Probing, Volume 1 25 Aug. 1992 p 419-424 (For primary document see N94-11894 01-42)
Copyright Avail: Issuing Activity (Scientific Organizing Committee of PORSEC, P.O. Box 10, Shimizu, Shizuoka 424, Japan, HC)

N94-11968 Electrotechnical Lab., Ibaraki (Japan).
OCEAN MEASURING EXPERIMENTS USING OPTICAL FIBER DISTRIBUTED TEMPERATURE SENSOR
Hiroshi Iitaka, Soujun Satou, Yukio Fujinawa, Yoshikazu Murata (Sumitomo Electric Industries Ltd., Osaka, Japan.), Satoshi Terakubo (Sumitomo Electric Industries Ltd., Osaka, Japan.), and Masayoshi Yamaguchi (Sumitomo Electric Industries Ltd., Osaka, Japan.) *In* Scientific Organizing Committee of PORSEC, Proceedings of the PORSEC 1992 in Okinawa: Conference for Pacific Ocean Environments and Probing, Volume 1 25 Aug. 1992 p 430-435 Sponsored by Science and Technology Agency (For primary document see N94-11894 01-42)
Copyright Avail: Issuing Activity (Scientific Organizing Committee of PORSEC, P.O. Box 10, Shimizu, Shizuoka 424, Japan, HC)

N94-12038*# Los Alamos National Lab., NM. Space Science and Technology Div.
THE LOS ALAMOS NEUTRON SPECTROMETER FOR THE LUNAR SCOUT-1 MISSION Abstract Only
George Auchampaugh, Bruce Barraclough, Roger Byrd, Darrell Drake, William Feldman, Calvin Moss, and Robert Reedy *In* Lunar and Planetary Inst., Twenty-fourth Lunar and Planetary Science Conference. Part 1: A-F 1993 p 49-50 (For primary document see N94-12015 01-91)
Avail: CASI HC A01/MF A06

N94-12619# National Research Lab. of Metrology, Tokyo (Japan).
CALIBRATION OF ANEMOMETERS AT LOW SPEED BY MEANS OF TOWING CARRIAGE [SOUKOU DAISHA WO MOCHIITA TEISOKUIKI DENO FUUSOKUKEI NO KOUSEI]
Yoshiya Terao *In* NAL, Proceedings of the 9th and 10th NAL Workshop on Investigation and Control of Boundary-Layer Transition Nov. 1992 p 33-35 In JAPANESE (For primary document see N94-12611 01-34)
Avail: CASI HC A01/MF A02

36 LASERS AND MASERS

Includes parametric amplifiers.
For related information see also *76 Solid-State Physics.*

N94-10150# Naval Research Lab., Washington, DC. Computational Physics and Fluids Dynamics Div.
START-UP IMPRINTING AND SHOCK DYNAMICS IN LASER-TARGET INTERACTION
M. H. Emery 10 Dec. 1992 27 p
(Contract DE-AI03-79DP-40092)
(DE93-008051; NRL/MR-6440-92-7174) Avail: CASI HC A03/MF A01 (US Sales Only)

Improved uniformity of the laser focal spot profile is a necessary criterion for the success of high intensity laser fusion and to improve the quality of data from moderate intensity laser driven shock experiments in solids. Recently developed laser smoothing techniques rely on both temporal smoothing and thermal smoothing to produce uniform ablation pressures on the target surface. Thermal smoothing is not effective during the low intensity portion of a laser pulse and the resultant shock structure mirrors the residual laser nonuniformities. The impact of the first (nonuniform) shock can be diminished by using foam layers, a precursor x-ray flash, shallow angles of incidence, and by adiabatically compressing the target with a temporally long, slowly rising laser pulse. DOE

N94-10160# Oak Ridge National Lab., TN.
OPTIMIZATION OF A CO2 LASER THOMSON SCATTERING ALPHA PARTICLE DIAGNOSTIC
R. K. Richards, D. P. Hutchinson, and C. H. Ma Jan. 1993 21 p
(Contract DE-AC05-84OR-21400)
(DE93-012782; ORNL/TM-12219) Avail: CASI HC A03/MF A01

The optimization of a CO2 laser Thomson scattering system for measurement of the velocity distribution of fusion product alpha particles is studied. It is found that for the International Thermonuclear Experimental Reactor (ITER) plasma, the optimal system conditions are a 20-MW source laser and a receiver bandwidth of 15 GHz. DOE

N94-10255# Oak Ridge National Lab., TN.
LASER SPECTROSCOPY
J. M. Ramsey 23 Dec. 1992 10 p
(Contract DE-AC05-84OR-21400)
(DE93-009403; ORNL/FTR-4513) Avail: CASI HC A02/MF A01 (US Sales Only)

The primary purpose of this trip was to present two invited lectures at the Second Venezuelan Workshop on Laser Spectroscopy. This conference included essentially all of the Venezuelan researchers active in this area. In addition, four speakers from outside of Venezuela were invited to this meeting; two from the USA and two from the former Soviet Union (FSU). The primary topics of the meeting were fluorescence spectroscopy, photothermal spectroscopy, and laser - material interactions. Prior to the conference, three institutions in Caracas were visited (IVIC, USB, and UCV) and a presentation was given at UCV. The group of scientists and students attending the conference were interested in establishing collaborations with scientists in the USA. DOE

N94-10287# Brookhaven National Lab., Upton, NY.
DYNAMICS OF DISSOCIATION VERSUS IONIZATION IN STRONG LASER FIELDS
L. F. DiMauro and B. Yang 1993 10 p Presented at the Third SILAP Conference, Hansui, Belgium, 8-14 Jan. 1993
(Contract DE-AC02-76CH-00016)
(DE93-009261; BNL-48611; CONF-930184-2) Avail: CASI HC A02/MF A01

In this paper, experimental results are presented which clearly demonstrate the effectiveness that an external field has in altering the dissociation dynamics. The experiment examines the strong-field dissociation dynamics of molecular hydrogen ions and its deuterated isotopes. These studies involve multiphoton excitation in the intensity regime of 10(exp 11)-10(exp 14) W/sq cm with the fundamental and second harmonic of a ND:YAG or ND:YLF laser system. Measurements include energy resolved electron and mass spectroscopy which provide useful probes in elucidating the interaction dynamics predicted by existing models. The example this in this paper, examines the strong-field dissociation of H2(+), HD(+), and D2(+) at green (0.5 micron) and infrared (1 micron) frequencies. The diatomic ions are formed via multiphonon ionization of the neutral precursor which is physically separable from the dissociation process. This study provides the first observation of the dynamics associated with the above threshold dissociation (ATD) process and analogies will be made with the more familiar above threshold ionization (ATI) phenomenon. DOE

N94-10371# Department of the Navy, Washington, DC.
LASER SYNCHROTRON SOURCE (LSS) Patent Application
Philip Sprangle, inventor (to Navy), Antonio Ting, inventor (to Navy), Eric Esarey, inventor (to Navy), Amon Fisher, inventor (to Navy), and Gerald Mourou, inventor (to Navy) 19 Feb. 1993 19 p
(AD-D015755; US-Patent-Appl-SN-020158) Avail: CASI HC A03/MF A01

The Laser Synchrotron Source (LSS) utilizes a high peak power or high average power laser to generate within a vacuum chamber a laser beam travelling in one direction to interact with an electron beam traveling in an opposite direction in order to generate high-power x-rays. A ring resonator formed by a plurality of mirrors directs the laser beam in a closed loop to impact with the electron beam to produce x-rays. Concave mirrors in the ring resonator focus the laser beam upon the point where the laser beam interacts with the electron beam to intensify the laser energy at that point. When a Radio Frequency Linear Accelerator (RF linac) is used to produce the electron beam, x-rays having a short pulse length are generated. When a betatron is used as an electron source, x-rays having a long pulse length are generated. DTIC

N94-10483# China Nuclear Information Centre, Beijing.
NUMERICAL SIMULATION OF SIDEBANDS IN FREE ELECTRON LASER OSCILLATORS
Xiaojian Shu, Wengui Ji, and Taichun Wang Mar. 1992 16 p
(DE93-612675; CNIC-00605; IAPCM-0020) Avail: CASI HC A03/MF A01 (US Sales Only)

A computer code named GOFEL-P for studying sidebands of free electron laser (FEL) oscillators was developed. Simulation results from this code are in agreement with experiments and the FELP code developed by others. The mechanism about the generation, development, hopping process, spiking mode and chaos of sidebands as well as the chirp of optical frequency has been investigated. The effect of sidebands on optical output is studied with a uniform wiggler or tapered wiggler. Methods to suppress sidebands with reducing optical cavity length or with optical filter are proposed. DOE

N94-10746 Sandia National Labs., Albuquerque, NM.
HIGH POWER z PINCHES AS X RAY LASER PHOTOPUMPS
T. J. Nash, R. B. Spielman, L. Ruggles, and M. Vargas 1992 15 p Presented at the 3rd International Conference on Dense z-Pinches, London, England, 19-23 Apr. 1993 Limited Reproducibility: More than 20% of this document may be affected by microfiche quality
(Contract DE-AC04-76DP-00789)
(DE93-012842; SAND-92-2804C; CONF-9304126-6) Avail: CASI HC A03

Using Saturn as a driver, we are pursuing both photoresonantly pumped and photoionization/recombination lasers. Our lasing targets are gas cells with thin windows that are pumped by a z pinch 2 cm away radiating 10 TW. In both schemes the lasant and gas fill is neon. To increase our chances of measuring the resonantly photopumped lasing transition we have introduced potassium into a sodium z pinch and have eliminated oxygen from the gas cell windows. We have measured the spatial dependence of ionization balance across the gas cell, and this measurement is consistent with propagation of a shock front across the gas cell target. We have measured blue-shifted satellites to several Li-like neon transitions that may indicate return-current driven jetting a high 1.5e8 cm/sec velocity. Using a gold z-pinch we have shown that key radiation is necessary to excite the He-like lines of neon. An attempt at a single shot gain measurement also indicates that radiation is not the only source of gas cell heating. DOE

N94-10755 Lawrence Livermore National Lab., CA.
SECOND AND THIRD ORDER NONLINEAR OPTICAL PROPERTIES OF CRYSTALLINE INORGANIC/ORGANIC COMPLEXES
H. O. Marcy (Rockwell International Corp., Thousand Oaks, CA.), L. F. Warren (Rockwell International Corp., Thousand Oaks, CA.), L. E. Davis, M. S. Webb, and S. P. Velsko Jul. 1992 8 p Presented at the 1991 Spring Materials Research Society (MRS) Meeting, Baltimore, MD, May 1991 Limited Reproducibility: More than 20% of this document may be affected by microfiche quality
(Contract W-7405-eng-48)
(DE93-011883; UCRL-JC-105732; CONF-9105418-1) Avail: CASI HC A02

Properties for members of a new class of nonlinear optical (NLO) materials which stoichiometrically incorporate organic and inorganic constituents into a single crystalline lattice are reported. Recent results for our synthetic, crystal growth, and optical studies suggest that a number of these relatively transparent 'semiorganic' compounds have significant second and/or third order NLO responses and often display favorable crystal growth morphologies. The prototype material of this class zinc tris(thiourea) sulfate, or ZTS, has a UV cutoff at about 325 nm, can be readily grown to cm(sup 3) sizes, and has been shown to be a highly efficient Type II frequency doubler for 1064 nm Nd:Yag laser radiation. ZTS also processes a moderate third order nonlinear optical response (ca. 0.1 x CS(sub 2)) which occurs on at least a picosecond time scale as determined by degenerate four-wave mixing (DFWM) experiments at 532 nm. Refractive index, second harmonic generation, and DFWM data for a number of these new compounds are presented. DOE

N94-10870# North Texas Research and Development Inst., Denton.
[CONTROLLING CHAOTIC BEHAVIOR IN CO2 AND OTHER LASERS]
Progress Report No. 1, 16 Mar. - 15 Apr. 1991
26 Apr. 1993 5 p
(Contract N00014-93-C-0051)
(AD-A264811) Avail: CASI HC A01/MF A01

Significant progress has been made in the first month in setting up the equipment in preparation for producing chaotic behavior in a CO2 laser. The project goal is to synchronize and control chaos in a CO2 and other lasers, and thereby increase the power in ensembles of coupled laser sources. One method of inducing chaotic behavior in a CO2 laser is to modulate the beam in the cavity with a frequency between 50 and 100 kHz. The project has designed two schemes to achieve this modulation. These are through the modulation of the high voltage by inductive coupling and the modulation of the beam by a CdTe electro-optic modulator (EOM). Modulation of the beam using modulation of the high voltage has been achieved in the laboratory this month. This was accomplished by modulating the high voltage on the laser using an inductor connected to the anode of the laser. Modulation of the laser plasma was confirmed by detecting modulation of the plasma with a light by using a photomultiplier tube. Analysis of the chaotic regime awaits arrival and check-out of the HgCdTe detector. DTIC

N94-10904# Groningen Rijksuniv. (Netherlands). Computing Science Section.
FFT-BASED METHODS FOR NONLINEAR IMAGE RESTORATION IN CONFOCAL MICROSCOPY
J. B. T. M. Roerdink 1993 17 p
(CS-9301; ETN-93-94348) Copyright Avail: CASI HC A03/MF A01

A new method for attenuation correction in three dimensional imaging by a Confocal Scanning Laser Microscope (CSLM) in the (epi)fluorescence mode was developed. The fundamental element in the approach consisted in multiplying the measured fluorescent intensity by a correction factor involving a convolution integral of this intensity, which can be computed efficiently by the Fast Fourier Transform (FFT). The resulting algorithm is one or two orders of magnitude faster than an existing iterative method, but has smaller accuracy. This latter point is improved by reformulating the problem as a statistical estimation problem. First order moment and cumulant estimators are derived leading to a nonlinear integral equation for the unknow fluorescent density which is solved by an iterative method where in each step a discrete convolution is performed using the FFT. Only a few iterations are needed. It is shown that the estimators proposed are more accurate than the existing iterative method, while retaining the advantage in computational efficiency of the FFT based approach. ESA

N94-10959# Sandia National Labs., Albuquerque, NM.
CHARACTERIZATION OF A SCANNERLESS LADAR SYSTEM
P. Garcia, J. Anthes, J. T. Pierce, P. Dressendorfer, I. K. Evans, B. D. Bradley, J. T. Sackos, and M. M. LeCavalier 1993 8 p Presented at the Society of Photo-Optical Instrumentation Engineers OE/Aerospace Science and Sensing Meeting, Orlando, FL, 11-16 Apr. 1993
(Contract DE-AC04-76DP-00789)
(DE93-011582; SAND-93-0937C; CONF-930445-5) Avail: CASI HC A02/MF A01

Performance projections based on the analytical model of a scannerless laser radar system are compared to laboratory simulations and to field data measurements. Data and characteristics of the system including camera response, image spatial resolution, and contributions to the signal-to-noise ratio are presented. A discussion of range resolution for this system will also be presented, and finally, the performance characteristics of the prototype benchtop system will be summarized. DOE

N94-11005# Sandia National Labs., Albuquerque, NM.
SEMICONDUCTOR RING LASERS
J. P. Hohimer, G. R. Hadley, G. A. Vawter, and D. C. Craft Mar. 1993 41 p
(Contract DE-AC04-76DP-00789)
(DE93-012386; SAND-92-2760) Avail: CASI HC A03/MF A01

Semiconductor ring lasers are being developed for use as direct-waveguide-coupled sources for photonic integrated circuits. This report describes the results of our research and development of this new class of diode lasers. We have fabricated and characterized semiconductor ring lasers which operate continuous-wave at room temperature with a single-frequency output of several milliwatts. Our work has led to an increased understanding of the operating behavior of these lasers and to the development of two new types of advanced devices. The interferometric ring diode laser uses a coupled-cavity structure to improve the level of single-frequency performance. And, the unidirectional ring diode laser uses an active crossover waveguide to promote lasing in a single ring direction with up to 96% of the output emitted in the preferred lasing direction. DOE

N94-11095# North Carolina Univ., Chapel Hill. Dept. of Chemistry.
THERMAL-OPTICAL SWITCHING OF A SILICON BASED INTERFERENCE FILTER
B. H. Augustine, S. T. Feng, and E. A. Irene 4 May 1993 13 p
(Contract N00014-89-J-1178)
(AD-A265152; TR-54) Avail: CASI HC A03/MF A01

We report thermal-optical switching using a silicon based interference filter fabricated by plasma enhanced chemical vapor deposition. A five film structure using high index films of amorphous Si and low index films of SiO2 comprised the device which yielded detector limited 40 ns rise time switching. Operation is in the near infrared spectral region with probe wavelengths of 810 nm and 1.152 micrometers. A 56% contrast ratio is reported when pumped by a 10.6 micrometers CO2 pulsed laser. Lower contrast switching-was also demonstrated with a Nd:YAG pumped dye laser tunable from 600-700 nm. In addition, we have demonstrated that atomic layer thickness precision is not necessary, and suggest several improvements which can further enhance device performance. DTIC

N94-11126# Lawrence Livermore National Lab., CA.
AN ANALYTIC MODEL FOR CALCULATING PUMP-INDUCED WAVEFRONT DISTORTIONS IN LASER SLABS
M. D. Rotter, A. C. Erlandson, and R. W. McCracken Mar. 1993 16 p Presented at the Society for Optical and Quantum Electronics Conference, McLean, VA, 7-11 Dec. 1992
(Contract W-7405-eng-48)
(DE93-011953; UCRL-JC-111193; CONF-921268-1) Avail: CASI HC A03/MF A01

We have developed an analytical model to predict the pump-induced wavefront distortions in flashlamp-pumped, Nd:glass, Brewster-angle slab amplifiers. The model is based on analytically solving the time-dependent bi-harmonic equation for a thin plate to obtain the spatially and time-varying surface distortions. These distortions are then directly related to the uneven heating of the laser slab by pumping processes. Experimental verification for the model was obtained by measuring the time-dependent deflections of a small-diameter CW probe beam that had been passed through our multi-segment amplifier. Good agreement between the model and experiment was obtained. DOE

N94-11132*# National Aeronautics and Space Administration. Lewis Research Center, Cleveland, OH.
A PRELIMINARY STUDY ON ICE SHAPE TRACING WITH A LASER LIGHT SHEET
Carolyn R. Mercer, Mario Vargas, and John R. Oldenburg Aug. 1993 11 p
(RTOP 505-68-10)
(NASA-TM-105964; E-7375-1; NAS 1.15:105964) Avail: CASI HC A03/MF A01

Preliminary work towards the development of an automated method of measuring the shape of ice forming on an airfoil during wind tunnel tests has been completed. A thin sheet of light illuminated the front surfaces of rime, glaze, and mixed ice shapes and a solid-state camera recorded images of each. A maximum intensity algorithm extracted the profiles of the ice shapes and the results were compared to hand tracings. Very good general agreement was found in each case. Author

N94-11266# Lawrence Livermore National Lab., CA.
DEMONSTRATION DESIGNS FOR OPTICAL-FIELD-IONIZED PLASMA X-RAY LASERS
P. A. Amendt, D. C. Eder, R. A. London, B. M. Penetrante, and M. D. Rosen Feb. 1993 13 p Presented at the International Society for Optical Engineering (SPIE) Conference, Los Angeles, CA, 16-23 Jan. 1993
(Contract W-7405-eng-48)
(DE93-009227; UCRL-JC-112924; CONF-930159-24) Avail: CASI HC A03/MF A01

Previous studies of recombination x-ray lasers based on optical-field-induced ionization have stressed the conditions necessary for high gain and high output energy efficiency in Li-like Neon. Unfortunately, the higher electron density n(sub e) necessary to realize efficient generation of 98.26 A x-rays in Li-like Neon also demands serious consideration of ionization-induced refractive defocussing. We propose a demonstration experiment of optical-field-ionized plasma x-ray lasing at 247 A in Nitrogen which can tolerate strong refractive defocussing. The relatively low ionization potential energy of approximately 98 eV in Nitrogen should result in correspondingly low residual electron temperature T(sub e) which, in turn, allows large gain at lower values of electron density. The use of low electron density provides less collisional heating as well as reduced refractive defocussing. In addition to using low electron density to mitigate refraction, we also propose the use of a wide UV laser-driver focus to give reduced transverse intensity gradients near the laser axis. Milder transverse intensity gradients lead to longer refraction lengths which effectively define the volume of x-ray lasing. These two techniques for avoiding excessive refraction are used in tandem to identify an experimental regime where x-ray lasing dominates spontaneous noise by an unambiguous margin associated with a gain-length product of five. Such a margin is predicted to be exceeded for a Li-like Nitrogen plasma with n(sub e) approximately 5 x 10(exp 19)cm(exp -3), T(sub e) approximately 10 eV, and a UV laser-driver intensity of 3 x 10(exp 16)W/sq cm with 0.25 micron wavelength and 30 microns waist radius. DOE

N94-11283# Sandia National Labs., Albuquerque, NM.
MULTIPLE LASER BEAM COMBINING AND PHASING USING CLOSED-LOOP CONTROL
D. R. Neal, T. G. Smith, G. R. Eisler, J. L. Wilcoxen, and R. R. Rosenthal 1992 11 p Presented at the SPIE Smart Structures and Materials Meeting, Albuquerque, NM, 31 Jan. - 4 Feb. 1993
(Contract DE-AC04-76DP-00789)
(DE93-009830; SAND-92-1896C; CONF-930171-2) Avail: CASI HC A03/MF A01

One method for scaling lasers to higher power is to build several separate amplifier chains, and then coherently combine the individual beams together. To combine the beams the pathlengths must be matched to an integer number of waves, and the tip and tilt of each beam must be the same. Since optical tolerances are fractional micrometers, a sophisticated control system must be employed to actively measure tip/tilt and piston errors, and apply real time corrections. We have developed a test bed that allows us to develop the required control algorithms for two to four beams and then scale to a larger numbers. DOE

N94-11468# Stanford Linear Accelerator Center, CA.
LCLS OPTICS: SELECTED TECHNOLOGICAL ISSUES AND SCIENTIFIC OPPORTUNITIES
R. Tatchyn Mar. 1993 27 p Presented at the Workshop on Scientific Application of Short Wavelength Coherent Light Source, Stanford, CA, United States, 21 Oct. 1992
(Contract DE-AC03-76SF-00515)
(DE93-010953; SU-SLAC-Pub-6064; SU-SLAC/SSRL-0010; CONF-9210278-1) Avail: CASI HC A03/MF A01

The Stanford Linac Coherent Light Source (LCLS) promises to generate photon pulses of unprecedented brevity and peak brightness in the soft x-ray range. In this presentation selected limitations and novel opportunities for technology and science associated with the availability of such pulses will be briefly assessed. Special emphasis will be placed on possible techniques for extending the peak power density and the temporal and spectral regimes of the LCLS output radiation by orders of magnitude beyond their nominal (calculated) values and to the associated instrumentation for processing this radiation. DOE

N94-11633# International Centre for Theoretical Physics, Trieste (Italy).
THE LASER SECOND THRESHOLD: ITS EXACT ANALYTICAL DEPENDENCE ON DETUNING AND RELAXATION RATES
A. A. Bakasov and N. B. Abraham Nov. 1992 79 p
(DE93-619706; IC-92/390) Avail: CASI HC A05/MF A01 (US Sales Only)

An exact analysis was carried out for general analytical expressions for the second threshold of a single-mode homogeneously broadened laser and for the initial pulsation frequency at the second threshold for arbitrary physical values of the relaxation rates, and at arbitrary detuning between the cavity frequency and the atomic resonance frequency. These expressions also give correspondingly exact forms for asymptotic cases that were previously studied with some approximations. Earlier approximate results are partly confirmed and partly improved by these more general expressions. The physical status of various expressions and approximations is re-considered and specified more clearly, including an analysis of which reasonably can be attained in lasers or masers. A general analytical proof is given that for larger detuning of the laser cavity from resonance a higher value of the laser excitation is required to destabilize the steady state solution (the second threshold). Results for the minimum value of the second threshold at fixed detuning as a function of the other parameters of the system and on the dependence of the ratio of the second threshold to the first threshold as a function of detuning are presented. Minima of the second threshold and of the threshold ratio occur only if the population relaxation rate is equal to zero. The minima of the threshold ratio are shown to be bounded from above as well as from below (as functions of the relaxation rates, so long as the second threshold exists). The upper bound on the threshold ratio is equal to 17. The variation of the second threshold in the semi-infinite parameter space of the decay rates is shown at various detunings in plots with a finite domain by normalizing the material relaxation rates to the cavity decay rate. DOE

N94-11634 International Centre for Theoretical Physics, Trieste (Italy).
ANALYTICAL DETAILS OF THE INSTABILITY THRESHOLD OF THE LASER-LORENZ MODEL
A. A. Bakasov and N. B. Abraham (Bryn Mawr Coll., PA.) Nov. 1992 14 p Limited Reproducibility: More than 20% of this document may be affected by microfiche quality
(DE93-619707; IC-92/391) Avail: CASI HC A03 (US Sales Only)

An exact analysis of the second threshold of a single-mode homogeneously broadened laser is given for the most general operating conditions. A general analytical proof that increasing the detuning increases the second threshold is given. An analysis of the second threshold at a fixed detuning and of the ratio of the second threshold to the first threshold reveals that the smallest values occur when the population relaxation rate is minimized. DOE

N94-12012 Puerto Rico Univ., Rio Piedras. Dept. of Chemistry.
THE LASER ABLATION OF GOLD FILMS AT THE ELECTRODE SURFACE OF A QUARTZ CRYSTAL MICROBALANCE
James Perez and Brad R. Weiner May 1993 16 p Limited Reproducibility: More than 20% of this document may be affected by microfiche quality
(Contract N00014-89-J-1829)
(AD-A265535; TR-4) Avail: CASI HC A03

We report in this letter the amount of gold removed by ablation with a pulsed laser operating at 532 and 355 nm. The removed gold was measured by using a quartz crystal microbalance as a mass detector. The results indicate that for the 532 and 355 nm pulsed laser ablation of gold thin films, 10(exp 13)-10(exp 15) atom per pulse are removed over the fluence range of 0.5-5.0 J/sq cm. The amount of ablated material is found to depend on the fluence at constant wavelength and on the wavelength at constant fluence. In addition, the mass sensitivity distribution across the quartz crystal microbalance electrode has been characterized by using the laser ablation technique. DTIC

N94-12321# Department of the Navy, Washington, DC.
A 1.94 MICRON LASER APPARATUS, SYSTEM, AND METHOD USING A THULIUM-DOPED YTTRIUM-LITHIUM-FLUORIDE LASER CRYSTAL PUMPED WITH A DIODE LASER Patent Application
Leon Esterowitz, inventor (to Navy) and Robert C. Stoneman, inventor (to Navy) 28 Jan. 1993 16 p
(AD-D015740; US-Patent-Appl-SN-010253; Navy-Case-72490) Avail: CASI HC A03/MF A01

A laser apparatus, system, and method include a laser crystal formed of thulium-doped yttrium-lithium-fluoride, and a laser diode arranged in proximity to the laser crystal. The laser diode is capable of emitting a first laser light which is suitable for use as a pump beam for causing lasing to occur in the laser crystal. In response to the first laser light from the laser diode, the laser crystal emits a second laser light at a wavelength which is relatively highly-absorbed by organic tissue and/or water. The second laser light is therefore well-suited to medical applications, for example, and can be used to irradiate organic tissue for medical treatment. Author (DTIC)

N94-12329# Department of the Navy, Washington, DC.
IMPROVED SUPER LUMINESCENT LIGHT SOURCE SPECIFICATION Patent Application
Elias Snitzer, inventor (to Navy), William K. Burns, inventor (to Navy), and Robert P. Moeller, inventor (to Navy) 29 Jan. 1993 17 p
(AD-D015746; US-Patent-Appl-SN-010944; Navy-Case-73675) Avail: CASI HC A03/MF A01

A fiber superfluorescent light source is disclosed which suppresses laser oscillations without interfering with the pump light or the super luminescence. In a preferred embodiment of the invention, the fiber superfluorescent light source comprises a laser diode array for providing a pump beam at a wavelength of 0.81 microns, a first fiber doped with neodymium activator ions and being responsive to the pump beam for providing a spontaneous emission at a wavelength of 1.06 microns, and a second fiber optically coupled between the laser diode arrays and the first fiber for passing the pump beam therethrough to the first fiber to enable the first fiber to spontaneously emit light at the 1.06 micron wavelength and for suppressing backemissions of the 1.06 micron wavelength from the first fiber toward the laser diode array to prevent oscillations in the laser diode array. DTIC

N94-12337# Department of the Navy, Washington, DC.
SUBMICROSECOND, SYNCHRONIZABLE X RAY SOURCE Patent Application
Robert Whitlock, inventor (to Navy) 31 Mar. 1993 19 p
(AD-D015745; US-Patent-Appl-SN-041388; Navy-Case-74582) Avail: CASI HC A03/MF A01

In the submicrosecond, synchronizable x-ray source a high intensity pulsed laser is focused onto negatively biased laser target, at high irradiance in a vacuum, producing high temperature plasma from which electrons are emitted. The emitted electrons are accelerated in a electric field formed by impressing a potential difference across a laser target-electron target gap. The positively biased electron collects the emitted electrons, which upon impact with the electron target cause x-rays to be emitted synchronously with the incident laser pulse. DTIC

N94-12372# North Texas Research and Development Inst., Denton.
[CONTROLLING CHAOTIC BEHAVIOR IN A CO2 AND OTHER LASERS] Progress Report No. 2, 16 Apr. - 15 May 1993
26 May 1993 5 p
(Contract N00014-93-C-0051)
(AD-A265458) Avail: CASI HC A01/MF A01

Substantial progress was made in the second month of the project in setting up the equipment and testing for the production of chaotic behavior by a CO2 laser. The project goal is to synchronize and control chaos in CO2 and other lasers and thereby, to increase the power in ensembles of coupled laser sources. Weekly Coordination Meetings of the project team were held. These meetings were well attended by the project members. Significant technical discussions regarding approaches to the data analysis and theoretical analysis have occurred. The successful experimental results described later have provided stimulus regarding theoretical considerations. Analysis of the chaotic regime in detail is awaiting the next set of experiments, and additional care is to be taken in recording data for subsequent analysis. A second CO2 laser is in the initial stages of assembly. Initial checkout of components indicates a working system should result. DTIC

N94-12382 Multilayer Optics and X-ray Technology, Inc., Orem, UT.
INEXPENSIVE CAPILLARY DISCHARGE X-RAY LASER DRIVER Final Report, 30 Sep. 1992 - 31 Mar. 1993
Alexander M. Panin 28 May 1993 35 p Limited Reproducibility: More than 20% of this document may be affected by microfiche quality
(Contract N00014-92-C-2218)
(AD-A265932) Avail: Issuing Activity (Defense Technical Information Center (DTIC))

In Phase 1 of the research, we computationally modelled a capillary discharge device capable of producing the necessary plasma conditions to demonstrate ASE in argon at a wavelength of about 700 A. Phase 2 of the research will involve the development and diagnosis of the experimental apparatus necessary to demonstrate ASE in argon. The scaling and modification of that apparatus to demonstrate ASE at shorter wavelengths using higher-Z materials will also be investigated. Future work will involve the development of robust multilayer cavity mirrors for shorter wavelengths to increase the overall intensity and usefulness of soft x-ray lasers. DTIC

N94-12402# University of South Florida, Tampa. Dept. of Physics.
SHORT WAVELENGTH CRYSTAL FIBER DEVICES Final Report, 1 Mar. 1989 - 28 Feb. 1993
N. Djeu Apr. 1993 24 p
(Grant AF-AFOSR-0263-89)
(AD-A265716; AFOSR-93-0396TR) Avail: CASI HC A03/MF A01

The potential of crystal fibers for the generation of short wavelength visible laser radiation was explored under this program. There were two major thrusts to this work. One of them was the search for a suitable technique to produce low loss crystal fibers. Implantation cladding of bare crystal fibers with high energy ion beams was investigated for this purpose. The other was the identification of a suitable upconversion process which would be amenable for implementation in the crystal fiber form. The upconversion laser potential of Tm:YAG was explored in this area. DTIC

N94-12590# Lawrence Livermore National Lab., CA.
SPATIAL COHERENCE OF SOFT X RAY LASERS
J. Trebes 3 Aug. 1992 5 p Presented at the Third International Colloquium on X Ray Lasers, Schliersee, Germany, 18-22 May 1992
(Contract W-7405-eng-48)
(DE93-012497; UCRL-JC-111392; CONF-920523-11) Avail: CASI HC A01/MF A01

Experiments to measure the spatial coherence of soft x ray lasers conducted at RAL are briefly described. Preliminary results are summarized. DOE

N94-12784# Lawrence Livermore National Lab., CA.
LASER SYSTEM DESIGN FOR THE GENERATION OF A SODIUM-LAYER LASER GUIDE STAR
H. W. Friedman Jan. 1993 12 p Presented at the OE/LASE 1993: International Society for Optical Engineering (SPIE) Conference, Los Angeles, CA, 16-23 Jan. 1993
(Contract W-7405-eng-48)
(DE93-014127; UCRL-JC-111173; CONF-930159-32) Avail: CASI HC A03/MF A01

The design considerations for a laser system used to generate a sodium-layer guide star are presented. Laser technology developed for the Atomic Vapor Laser Isotope Separation (AVLIS) Program is shown to be directly relevant to this problem and results of a demonstration using the AVLIS laser to generate such a guide star are shown. The design of a compact laser suitable for use at a large telescope such as the Keck is also presented. DOE

N94-10982*# National Physical Lab., Teddington (England).
DEVELOPMENT OF A CRYOGENIC HYDROGEN MASER AT THE NPL
R. Mossavati *In* NASA. Goddard Space Flight Center, The 24th Annual Precise Time and Time Interval (PTTI) Applications and Planning Meeting Jun. 1993 p 221-230 (For primary document see N94-10963 01-70)
Avail: CASI HC A02/MF A04

N94-12722 Academy of Sciences (USSR), Moscow. Inst. of Oceanology.
POLARISATION OF BACKSCATTERING RADIATION AT REMOTE SENSING OF OCEAN WITH IMPULSE LASER BEAM
Alexander P. Vasilkov, Timothy V. Kondranin, and Yegeny V. Myasnikov *In* Scientific Organizing Committee of PORSEC, Proceedings of the PORSEC 1992 in Okinawa: Conference for Pacific Ocean Environments and Probing, Volume 2 25 Aug. 1992 p 1058-1062 (For primary document see N94-12635 01-42)
Copyright Avail: Issuing Activity (Scientific Organizing Committee of PORSEC, P.O. Box 10, Shimizu, Shizuoka 424, Japan, HC)

N94-12732 Academy of Sciences (USSR), Vladivostok. Inst. of Oceanology.
LASER PHOTOHETERODYNE INTERFEROMETERS FOR OCEANOGRAPHIC INVESTIGATIONS
V. L. Vlassov *In* Scientific Organizing Committee of PORSEC, Proceedings of the PORSEC 1992 in Okinawa: Conference for Pacific Ocean Environments and Probing, Volume 2 25 Aug. 1992 p 1101-1106 (For primary document see N94-12635 01-42)
Copyright Avail: Issuing Activity (Scientific Organizing Committee of PORSEC, P.O. Box 10, Shimizu, Shizuoka 424, Japan, HC)

N94-12755 Moscow State Univ. (Russia). Physics Dept.
LASER FLUORESCENT MONITORING OF DISSOLVED ORGANIC MATTER IN NATURAL WATER
Elena M. Filippova, Svetlana V. Patsayeva, Vasily V. Chubarov, Victor V. Fadeev, and Victor I. Yuzhakov *In* Scientific Organizing Committee of PORSEC, Proceedings of the PORSEC 1992 in Okinawa: Conference for Pacific Ocean Environments and Probing, Volume 2 25 Aug. 1992 p 1225-1230 (For primary document see N94-12635 01-42)
Copyright Avail: Issuing Activity (Scientific Organizing Committee of PORSEC, P.O. Box 10, Shimizu, Shizuoka 424, Japan, HC)

37 MECHANICAL ENGINEERING

Includes auxiliary systems (nonpower); machine elements and processes; and mechanical equipment.

N94-10269# Oak Ridge National Lab., TN.
POSITION AND FORCE CONTROL OF A VEHICLE WITH TWO OR MORE STEERABLE DRIVE WHEELS
D. B. Reister and M. A. Unseren Oct. 1992 34 p
(Contract DE-AC05-84OR-21400)
(DE93-012512; ORNL/TM-12193) Avail: CASI HC A03/MF A01

When a vehicle with two or more steerable drive wheels is traveling in a circle, the motion of the wheels is constrained. The wheel translational velocity divided by the radius to the center of rotation must be the same for all wheels. When the drive wheels are controlled independently using position control, the motion of the wheels may violate the constraints and the wheels may slip. Consequently, substantial errors can occur in the orientation of the vehicle. A vehicle with N drive wheels has (N - 1) constraints and one degree of freedom. We have developed a new approach to the control of a vehicle with N steerable drive wheels. The novel aspect of our approach is the use of force control. To control the vehicle, we have one degree of freedom for the position on the circle and (N - 1) forces that can be used to reduce errors. Recently, Kankaanranta and Koivo developed a control architecture that allows the force and position degrees of freedom to be decoupled. In the work of Kankaanranta and Koivo, the force is an exogenous input. We have made the force endogenous by defining the force in terms of the errors in satisfying the rigid body kinematic constraints. We have applied the control architecture to the HERMIES-3 robot and have measured a dramatic reduction in error (more than a factor of 20) compared to motions without force control. DOE

N94-10322# Lawrence Livermore National Lab., CA.
THE INTENSITY OF KNOCK IN AN INTERNAL COMBUSTION ENGINE: AN EXPERIMENTAL AND MODELING STUDY
J. S. Cowart, M. Haghooie, C. E. Newman, G. C. Davis, W. J. Pitz, and C. K. Westbrook Sep. 1992 9 p Presented at the International Fuels and Lubricants Meeting and Exposition, San Francisco, CA, 19-22 Oct. 1992
(Contract W-7405-eng-48)
(DE93-013089; UCRL-JC-110069-Rev-1; CONF-9210140-2-Rev-1) Avail: CASI HC A02/MF A01

Experimental data have been obtained that characterize knock occurrence times and knock intensities in a spark ignition engine operating on indolene and 91 primary reference fuel, as spark timing and inlet temperature were varied. Individual, in-cylinder pressure histories measured under knocking conditions were conditioned and averaged to obtain representative pressure traces. These averaged pressure histories were used as input to a reduced and detailed chemical kinetic model. The time derivative of CO concentration and temperature were correlated with the measured knock intensity and percent cycles knocking. The goal was to evaluate the potential of using homogeneous, chemical kinetic models as predictive tools for knock intensity. DOE

N94-10341*# Grumman Aerospace Corp., Bethpage, NY.
PRELIMINARY SYSTEM DESIGN OF A THREE ARM CAPTURE MECHANISM (TACM) FLIGHT DEMONSTRATION ARTICLE
Otto Schaefer and Bill Stasi Apr. 1993 83 p
(Contract NAS8-36641)
(NASA-CR-192573; NAS 1.26:192573; ATS-92-2) Avail: CASI HC A05/MF A01

The overall objective of the Three Arm Capture Mechanism (TACM) is to serve as a demonstration of capability for capture of objects in space. These objects could be satellites, expended boosters, pieces of debris, etc.; anything of significant size. With this capability we can significantly diminish the danger of major collisions of debris with valuable space assets and with each other, which would otherwise produce many smaller, high velocity pieces of debris which also become concerns. The captured objects would be jettisoned into the atmosphere, relocated in 'parking' orbits, or recovered for disposition or refurbishment. The dollar value of satellites launched into space continues to grow along with the cost of insurance; having a capture capability takes a positive step towards diminishing this added cost. The effort covered is a planning step towards a flight demonstration of the satellite capture capability. Based on the requirement to capture a communication class satellite, its associated booster, or both, a preliminary system definition of a retrieval kit is defined. The objective of the flight demonstration is to demonstrate the techniques proposed to perform the mission and to obtain data on technical issues requiring an in situ space environment. The former especially includes issues such as automated image recognition techniques and control strategies that enable an unmanned vehicle to rendezvous and capture a satellite, contact dynamics between the two bodies, and the flight segment level of automation required to support the mission. A development plan for the operational retrieval capability includes analysis work, computer and ground test simulations, and finally a flight demonstration. A concept to perform a selected mission capturing a precessing communications satellite is described. Further development efforts using analytical tools and laboratory facilities are required prior to reaching the point at which a full commitment to the flight demonstration design can be made. Derived from text

N94-10348# Sandia National Labs., Albuquerque, NM.
EXTENSIONS OF SOME GUIDELINES FOR THE MECHANICAL DESIGN OF COAXIAL COMPRESSION PIN SEALS
R. S. Chambers and S. N. Burchett Mar. 1993 29 p
(Contract DE-AC04-76DP-00789)
(DE93-012385; SAND-93-0306) Avail: CASI HC A03/MF A01

Compression seals are commonly used in electronic components. Because glass has such a low fracture toughness, tensile residual stresses must be kept low to avoid cracks. A variety of compression pin seals were analyzed to identify mechanically optimal configurations when work hardened Alloy 52 conductor pins are sealed in a 304 stainless steel housing with a Kimble TM-9 glass insulator. Mechanical property tests on Alloy 52, have shown that the heat treatments encountered in a typical glass sealing cycle are capable of annealing the Alloy 52 pins, increasing ductility, and lowering the yield strength. Since most seal analyses are routinely based on unannealed Alloy 52 properties, a limited study was performed to determine the design impact of lowering the yield strength of the pins in a typical compression seal. Thermal residual stresses were computed in coaxial compression seals with annealed pins, and the results then were used to reconstruct design guidelines following the procedures employed by Miller and Burchett. Annealing was found to significantly narrow the optimal design range (as defined by a dimensionless geometric parameter). The Miller-Burchett analyses which were based on very coarse finite element meshes and a 50 ksi yield strength fortuitously predicted an overly conservative design range that is a subset of the narrow design window prevalent when the yield strength is assumed to be 34 ksi. This may not remain true for lower yield strengths. The presence of pin wetting was shown to exacerbate the glass stress state. The time is right to develop a modern and enhanced set of design guidelines which could address new material systems, three dimensional geometries, and viscoelastic effects. DOE

N94-10369# National Aerospace Lab., Kakuda (Japan).
DURABILITY OF A CARBON SEGMENTED CIRCUMFERENTIAL SEAL FOR A LIQUID OXYGEN TURBOPUMP [EKITAI SANSO TABO PONPU YOU KABON SEGUMENTO SHIRU NO TAIKYUU SEINOU]
Masataka Kikuchi, Mamoru Oike, Masataka Nosaka, and Yoshiaki Watanabe May 1992 17 p In JAPANESE
(NAL-TR-1155; JTN-93-80440; DE93-793619) Avail: CASI HC A03/MF A01

A carbon segmented circumferential seal with Rayleigh steps, designed as a helium purge seal for the liquid oxygen turbopump of the LE-7 rocket engine, was experimentally studied to improve its durability over a wide range of operating conditions. Five combinations of sealing materials were tested for long durations using helium purged pressures from 0.3 to 0.8 MPa and speeds from 52 to 105 m/sec. Friction tests of the sealing materials were also performed to enable comparisons with the seal test results. The effects of the operating conditions and the use of carbon materials, hard coating materials on the runner, and MoS_2 lubricating films were examined to enable the tribological performance of the sealing surfaces. The test seal having a MoS_2 lubrication film sprayed on the carbon sealing surface and a runner coated with a Cr_2O_3 plasma-sprayed film demonstrated sufficient durability over a wide range of operating conditions. Author (NASDA)

N94-10375# Department of the Navy, Washington, DC.
EXTERNAL COMBUSTION ENGINE HAVING A COMBUSTION EXPANSION CHAMBER Patent Application
Anthony W. Duva, inventor (to Navy) 23 Mar. 1993 15 p
(AD-D015761; US-Patent-Appl-SN-035862) Avail: CASI HC A03/MF A01

This patent application discloses an external combustion engine having a combustion expansion chamber. The engine includes a combustion chamber for generating a high-pressure, energized gas from a monopropellant fuel, and a cylinder for receiving the energized gas through a rotary valve to perform work on a cylinder disposed therein. A baffle plate is positioned between the combustion area and expansion area for reducing the pressure of the gas. The combustion area and expansion area are separated by a baffle plate having a flow area which is sufficiently large to eliminate the transmission of pressure pulsations from the combustion area to the expansion area while being small enough to provide for substantially complete combustion in the combustion area. The engine is particularly well suited for use in a torpedo. DTIC

N94-10378# Department of the Navy, Washington, DC.
HEAT REGENERATIVE EXTERNAL COMBUSTION ENGINE Patent Application
Anthony W. Duva, inventor (to Navy) 23 Mar. 1993 15 p
(AD-D015765; US-Patent-Appl-SN-035867) Avail: CASI HC A03/MF A01

It is an object of the invention to provide an external combustion expander-type engine having improved efficiency. It is another object of the invention to provide an external combustion engine in which afterburning in the exhaust channel is substantially prevented. Yet another object of the invention is to provide an external combustion engine which is less noisy than an external combustion engine of conventional design. These and other objects of the invention will become more apparent from the following description. The above objects of the invention are realized by providing a heat regenerative external combustion engine. The heat regenerative external combustion engine of the invention comprises a combustion chamber for combusting a monopropellant fuel in order to form an energized gas. The energized gas is then passed through a rotary valve to a cylinder having a reciprocating piston disposed therein. The gas is spent in moving the piston, thereby driving a drive shaft. DTIC

N94-10379# Department of the Navy, Washington, DC.
DUAL VALVE PLATE TWO-WAY PRESSURE RELIEF VALVE Patent Application
Robert J. Angeli, inventor (to Navy) 23 Feb. 1993 15 p
(AD-D015766; US-Patent-Appl-SN-023426) Avail: CASI HC A03/MF A01

This patent application discloses a two-way valve which includes dual valve plates to be positioned between first and second chambers having varying pressure therein, to relieve excess pressure in either chamber by permitting fluid flow from one chamber to the other. The valve includes a body portion having disposed therein dual valve plates. In the equilibrium state, the first valve plate is spring biased against the valve body in the direction of the first chamber to seal off any flow through the valve. The second valve plate is separately spring biased against the first valve plate in the direction of the second chamber, sealing off flow between the valve plates. When the pressure of the first chamber is greater than the pressure of the second chamber by a predetermined amount, the first and second valve plates move away from the valve body permitting fluid flow from the first chamber to the second chamber. When the pressure of the second chamber exerted on the second valve plate through apertures in the first valve plate is greater than the pressure of the first chamber by a predetermined amount, the second valve plate moves away from the face of the first valve plate permitting fluid flow from the second chamber to the first chamber. DTIC

N94-10381# Department of the Navy, Washington, DC.
VIBRATION ISOLATION MOUNT WITH LOCKING MEANS Patent Application
Stuart C. Dickinson, inventor (to Navy) 29 Mar. 1993 10 p
(AD-D015769; US-Patent-Appl-SN-037878) Avail: CASI HC A02/MF A01

A vibration isolation mount comprises a frame adapted for attachment to a support member, a spring device mounted on the fame and adapted for attachment to a protected device, the spring device being movable on the frame to permit movement of the protected device relative to the support member, and a locking mechanism for limiting movement of the spring device on the frame, thereby to limit movement of the protected device relative to the support member. DTIC

N94-10385# Department of the Navy, Washington, DC.
SELF LOCKING SET SCREW Patent Application
Michael A. Tucchio, inventor (to Navy) 3 Feb. 1993 12 p
(AD-D015774; US-Patent-Appl-SN-012837) Avail: CASI HC A03/MF A01

A threaded, locking set screw with standard outer dimensions having a threaded body, an expansion plug, and a retaining wedge. The threaded body has a tapered cavity at its bottom end. The expansion plug and retaining wedge are inserted into the cavity in the body. The base of the plug extends from the cavity, and the plug is held in place by a force fit between the wedge and a retaining slot in the body. When the set screw is tightened against a part, the plug is forced into the cavity. Because of a locking taper between the plug and the cavity, the plug exerts an outward force on the inner surface of the cavity causing the set screw body to expand radially, thus, locking the set screw in place. DTIC

N94-10393 Tel-Aviv Univ. (Israel). Dept. of Industrial Engineering.
OBJECT RECOGNITION IN INDUSTRIAL ENVIRONMENT BY MEANS OF TACTILE SENSOR M.S. Thesis
Michael Fainstein Oct. 1993 140 p In ENGLISH and HEBREW
(ITN-93-85200) Copyright Avail: Issuing Activity (Tel-Aviv Univ., Exact Sciences Library, Ramat Aviv 69978, Israel)

The practicability of using a tactile sensor for object recognition in an industrial environment was investigated. Towards this aim, two algorithms were developed for dynamic feature selection in object recognition, and a combination of statistical object recognition and template-matching was applied to the images generated by the tactile sensor. The algorithms which were developed were based on the observation that each feature can be tested and graded independently of other features on the basis of the analysis of variations statistical test. A further basic consideration was that, if two features are correlated, only one need be used for object recognition. The system's recognition success rate was about 15 percent better than that of a method based on the Karhunen-Loeve expansion. A success rate of 95-99 percent could be achieved by changing the problem to that of reducing a large set of objects to a small set of two or three candidates for a more complex and more costly recognition procedure. Problems requiring further research include the integration of an additional sensor, such as a video camera, for a second stage of object recognition; and the development of a selection procedure for identifying one out of a group of two or three candidates. ISA

N94-10400*# Pratt and Whitney Aircraft, East Hartford, CT.
AGBT ADVANCED COUNTER-ROTATING GEARBOX DETAILED DESIGN REPORT Report, Aug. 1984 - Jan. 1987
D. C. Howe, C. V. Sundt, and A. H. McKibbon Oct. 1988 164 p
(Contract NAS3-24342; RTOP 535-03-22)
(NASA-CR-180883; NAS 1.26:180883) Avail: CASI HC A08/MF A02

An Advanced Counter-Rotating (CR) Gearbox was designed and fabricated to evaluate gearbox efficiency, durability and weight characteristics for emerging propfan-powered airplanes. Component scavenge tests showed that a constant volume collector had high scavenge effectiveness, which was uneffected by added airflow. Lubrication tests showed that gearbox losses could be reduced by controlling the air/oil mixture and by directing the oil jets radially, with a slight axial component, into the sun/planet gears. Author

N94-10654* National Aeronautics and Space Administration. Pasadena Office, CA.
FORCE REFLECTION WITH COMPLIANCE CONTROL Patent
Won S. Kim, inventor (to NASA) (Jet Propulsion Lab., California Inst. of Tech., Pasadena.) 24 Aug. 1993 18 p Filed 8 Jul. 1991 Supersedes N92-29765 (30 - 20, p 3479)
(NASA-Case-NPO-18668-1-CU; US-Patent-5,239,246;
US-Patent-Appl-SN-912955; US-Patent-Class-318-568.11;
US-Patent-Class-318-560; US-Patent-Class-318-568.21;
US-Patent-Class-318-568.17; US-Patent-Class-318-568.12;
US-Patent-Class-901-9; US-Patent-Class-901-19) Avail: US Patent and Trademark Office

Two types of systems for force-reflecting control, which enables high force-reflection gain, are presented: position-error-based force reflection and low-pass-filtered force reflection. Both of the systems are combined with shared compliance control. In the position-error-based class, the position error between the commanded and the actual position of a compliantly controlled robot is used to provide force reflection. In the low-pass-filtered force reflection class, the low-pass-filtered output of the compliance control is used to provide force reflection. The increase in force reflection gain can be more than 10-fold as compared to a conventional high-bandwidth pure force reflection system, when high compliance values are used for the compliance control.
Official Gazette of the U.S. Patent and Trademark Office

N94-10655* National Aeronautics and Space Administration. Lyndon B. Johnson Space Center, Houston, TX.
CHECK VALVE WITH POPPET DAMPING MECHANISM Patent
Brian G. Morris, inventor (to NASA) 3 Aug. 1993 5 p Filed 22 Jun. 1992 Supersedes N92-30101 (30 - 20, p 3480)
(NASA-Case-MSC-21903-1; US-Patent-5,232,013;
US-Patent-Appl-SN-902266; US-Patent-Class-137-514.7;
Int-Patent-Class-F16K-15/06) Avail: US Patent and Trademark Office

An inline check valve for a flow line is presented where the valve element is guided for inline travel forward and rearward of a valve sealing member and is spring biased to a closed sealing condition. One of the guides for the valve element includes a dashpot bore and plunger member to control the rate of travel of the valve element in either direction as well as provided a guiding function. The dashpot is not anchored to the valve body so that the valve can be functional even if the plunger member becomes jammed in the dashpot.
Official Gazette of the U.S. Patent and Trademark Office

N94-10658* National Aeronautics and Space Administration. Lyndon B. Johnson Space Center, Houston, TX.
CHECK VALVE WITH POPPET DASHPOT/FRICTIONAL DAMPING MECHANISM Patent
Brian G. Morris, inventor (to NASA) 31 Aug. 1993 5 p Filed 22 Jun. 1992 Supersedes N92-34242 (30 - 24, p 4189)
(NASA-Case-MSC-21950-1; US-Patent-5,240,036;
US-Patent-Appl-SN-902265; US-Patent-Class-137-514.7;
US-Patent-Class-137-514; Int-Patent-Class-F16K-15/06) Avail: US Patent and Trademark Office

An inline check valve for a flow line where the valve element is guided for inline travel forward and rearward of a valve sealing member and is spring biased to a closed sealing condition is presented. One of the guides for the valve element includes a dashpot housing with a bore and plunger member to control the rate of travel of the valve element in either direction, providing a guiding function. The plunger member is arranged with a dashpot ring to frictionally contact the dashpot bore and has an interior tortuous flow path from one side to the other side of the dashpot ring. The dashpot housing is not anchored to the valve body so that the valve can be functional even if the dashpot ring becomes jammed in the dashpot housing.
Official Gazette of the U.S. Patent and Trademark Office

N94-10670* National Aeronautics and Space Administration. Pasadena Office, CA.
TELEROBOT CONTROL SYSTEM Patent
Paul G. Backes, inventor (to NASA) (Jet Propulsion Lab., California Inst. of Tech., Pasadena.) and Kam S. Tso, inventor (to NASA) (Jet Propulsion Lab., California Inst. of Tech., Pasadena.) 27 Jul. 1993 8 p Filed 9 May 1991 Supersedes N91-32509 (29 - 24, p 4028)
(NASA-Case-NPO-18116-1-CU; US-Patent-5,231,693;
US-Patent-Appl-SN-699299; US-Patent-Class-395-99;
US-Patent-Class-395-84; US-Patent-Class-395-905;
US-Patent-Class-318-568.1; Int-Patent-Class-G06F-15/00;
Int-Patent-Class-G06F-15/46; Int-Patent-Class-G05B-19/24) Avail: US Patent and Trademark Office

This invention relates to an operator interface for controlling a telerobot to perform tasks in a poorly modeled environment and/or within unplanned scenarios. The telerobot control system includes a remote robot manipulator linked to an operator interface. The operator interface includes a setup terminal, simulation terminal, and execution terminal for the control of the graphics simulator and local robot actuator as well as the remote robot actuator. These terminals may be combined in a single terminal. Complex tasks are developed from sequential combinations of parameterized task primitives and recorded teleoperations, and are tested by execution on a graphics simulator and/or local robot actuator, together with adjustable time delays. The novel features of this invention include the shared and supervisory control of the remote robot manipulator via operator interface by pretested complex tasks sequences based on sequences of parameterized task primitives combined with further teleoperation and run-time binding of parameters based on task context.
Official Gazette of the U.S. Patent and Trademark Office

N94-10674* National Aeronautics and Space Administration. Lyndon B. Johnson Space Center, Houston, TX.
COOLED SPOOL PISTON COMPRESSOR Patent
Brian G. Morris, inventor (to NASA) 24 Aug. 1993 11 p Filed 29 Dec. 1992 Supersedes N93-19331 (31 - 6, p 1550)
(NASA-Case-MSC-22020-1; US-Patent-5,238,372;
US-Patent-Appl-SN-998062; US-Patent-Class-417-393;
US-Patent-Class-417-404; Int-Patent-Class-F04B-35/00) Avail: US Patent and Trademark Office

A hydraulically powered gas compressor receives low pressure gas and outputs a high pressure gas. The housing of the compressor defines a cylinder with a center chamber having a cross-sectional area less than the cross-sectional area of a left end chamber and a right end chamber, and a spool-type piston assembly is movable within the cylinder and includes a left end closure, a right end closure, and a center body that are in sealing engagement with the respective cylinder walls as the piston reciprocates. First and second annual compression chambers are provided between the piston enclosures and center housing portion of the compressor, thereby minimizing the spacing between the core gas and a cooled surface

of the compressor. Restricted flow passageways are provided in the piston closure members and a path is provided in the central body of the piston assembly, such that hydraulic fluid flows through the piston assembly to cool the piston assembly during its operation. The compressor of the present invention may be easily adapted for a particular application, and is capable of generating high gas pressures while maintaining both the compressed gas and the compressor components within acceptable temperature limits.
Official Gazette of the U.S. Patent and Trademark Office

N94-10706 Mechanical Technology, Inc., Latham, NY.
DEVELOPMENT OF PASSIVE SUPERCONDUCTING BEARINGS. PHASE 3 Final Report
Dantam K. Rao 14 May 1993 100 p Limited Reproducibility: More than 20% of this document may be affected by microfiche quality
(Contract SDIO84-89-C-0043)
(AD-A266050; MTI-93TR26) Avail: CASI HC A05

This report documents the development of a passive superconducting bearing that is used to levitate relatively heavy rotors. This bearing was used to levitate a 7 lb rotor and spin at speeds of up to 12,000 rpm. The success of this effort indicates that the superconducting bearings have the potential for transition from a mere laboratory curiosity to a functional bearing component in a wider range of practical applications such as cryoturbopumps, miniature cryocoolers, and magnetic refrigerators. In addition, several configurations using superconductors to support loads along a single axis were investigated. The effort was directed to identify a specific configuration that offers a very high stiffness. DTIC

N94-10760*# National Aeronautics and Space Administration. Lewis Research Center, Cleveland, OH.
A SOFT-START CIRCUIT FOR ARCJET IGNITION
John A. Hamley and John M. Sankovic Jun. 1993 24 p Presented at the 29th AIAA Joint Propulsion Conference and Exhibit, Monterey, CA, 28-30 Jun. 1993; sponsored by AIAA, SAE, ASME, and ASEE
(RTOP 506-42-31)
(NASA-TM-106287; E-8025; NAS 1.15:106287; AIAA Paper 93-2396)
Avail: CASI HC A03/MF A01

The reduced propellant flow rates associated with high performance arcjets have placed new emphasis on electrode erosion, especially at startup. A soft-start current profile was defined which limited current overshoot during the initial 30 to 50 ms of operation, and maintained significantly lower than the nominal arc current for the first eight seconds of operation. A 2-5 kW arcjet PPU was modified to provide this current profile, and a 500 cycle test using simulated fully decomposed hydrazine was conducted to determine the electrode erosion during startup. Electrode geometry and mass flow rates were selected based on requirements for a 600 second specific impulse mission average arcjet system. The flow rate was varied throughout the test to simulate the blow down of a flight propellant system. Electrode damage was negligible at flow rates above 33 mg/s, and minor chamfering of the constrictor occurred at flow rates of 33 to 30 mg/s, corresponding to flow rates expected in the last 40 percent of the mission. Constrictor diameter remained unchanged and the thruster remained operable at the completion of the test. The soft-start current profile significantly reduced electrode damage when compared to state of the art starting techniques. Author

N94-10803 Naval Command, Control and Ocean Surveillance Center, San Diego, CA.
SENSOR ABSTRACTIONS TO SUPPORT MANY-ROBOT SYSTEMS
Douglas W. Gage Apr. 1993 14 p Limited Reproducibility: More than 20% of this document may be affected by microfiche quality
(AD-A265907) Avail: CASI HC A03

The rapid evolution of micromechanical fabrication techniques and other sensor, effector, and processing technologies will soon make it possible to employ large numbers of very inexpensive autonomous mobile robots with fairly limited sensor capabilities to perform real-world missions in ground, air, space, and underwater environments. One approach to such a system is to realize desired emergent collective group behaviors with simple sensor-based reactive planners. The initial thrust of this effort has been to develop generic ensemble behaviors, such as blanket, barrier, and sweep coverage, and various deployment and recovery modes, which can address a broad spectrum of generic applications, both military and civilian. However, while different applications may require similar group behaviors, the sensor, information, and communications resources available to the participating individual robots may be very different. This paper outlines the many-robot approach to real-world problems solving and discusses the various roles that different types of sensors can play in such systems. Analysis and simulation results are presented to show how useful behavioral algorithms can be designed to make use of diverse information resources, and the area search problem is analyzed to derive both system measures of effectiveness and system design considerations. DTIC

N94-10815*# Alabama Univ., Huntsville. Dept. of Electrical and Computer Engineering.
ENHANCEMENTS TO THE ENGINE DATA INTERPRETATION SYSTEM (EDIS) Final Report, 16 Apr. 1992 - 15 Apr. 1993
Martin O. Hofmann Jul. 1993 124 p
(Contract NAS8-38609)
(NASA-CR-192593; NAS 1.26:192593) Avail: CASI HC A06/MF A02

The Engine Data Interpretation System (EDIS) expert system project assists the data review personnel at NASA/MSFC in performing post-test data analysis and engine diagnosis of the Space Shuttle Main Engine (SSME). EDIS uses knowledge of the engine, its components, and simple thermodynamic principles instead of, and in addition to, heuristic rules gathered from the engine experts. EDIS reasons in cooperation with human experts, following roughly the pattern of logic exhibited by human experts. EDIS concentrates on steady-state static faults, such as small leaks, and component degradations, such as pump efficiencies. The objective of this contract was to complete the set of engine component models, integrate heuristic rules into EDIS, integrate the Power Balance Model into EDIS, and investigate modification of the qualitative reasoning mechanisms to allow 'fuzzy' value classification. The result of this contract is an operational version of EDIS. EDIS will become a module of the Post-Test Diagnostic System (PTDS) and will, in this context, provide system-level diagnostic capabilities which integrate component-specific findings provided by other modules. Author (revised)

N94-10821*# Tulane Univ., New Orleans, LA. Dept. of Electrical Engineering.
MOMENTUM MANAGEMENT IN REDUNDANT MANIPULATORS FOR VIBRATION SUPPRESSION Final Report, 1 Jun. 1992 - 31 Aug. 1993
Enrique Barbieri 31 Aug. 1993 5 p
(Grant NAG1-1270)
(NASA-CR-194112; NAS 1.26:194112) Avail: CASI HC A01/MF A01

This research project dealt with the development of control methodologies which would effectively use existing inertial devices as control actuators in the manipulation of Remote Manipulator System (RMS)-type robotic arms. The existing devices proposed to be investigated are the Torque-Wheel (TW) and the Proof-Mass actuator (PM). This report presents a succinct summary of our results. Derived from text

N94-11155 Concordia Univ., Montreal (Quebec).
COMPREHENSIVE DYNAMIC ANALYSIS OF A BLADED DISK-TURBOROTOR-BEARING SYSTEM Ph.D. Thesis
Ashok Kaushal 1992 310 p
(ISBN-0-315-73646-1) Avail: Univ. Microfilms Order No. DANN73646

The dynamic behavior of a bladed disk-turborotor-bearing system is studied employing analytical, numerical, and experimental methods. The system consists of several subsystems such as turbine disk, blades, bearings, support pedestals etc. In order to completely understand the dynamic behavior of the turborotor system an appropriate model for each individual component of the system is first developed. The individual components are modeled to include various design parameters and the effect of these parameters on the vibrational behavior is studied. The vibration studies on the individual components are carried out using Rayleigh-Ritz method boundary characteristic orthogonal polynomials as assumed shape functions. The individual components are then assembled using the finite element technique. The turborotor system is studied from a system point of view and the natural frequencies and mode shapes are obtained for various rotational speeds. The results show that the natural frequencies of the system are different from those obtained by analyzing individual components, suggesting that a system approach must be adopted for proper design of a turborotor system. The amplitude of vibration and stresses due to harmonic and centrifugal loading on the blades and the disk are also obtained. The results indicate that for the turborotor speed of operation, the centrifugal loading is the major factor in determining the critical stresses in comparison to the gas forces on the blade modeled as harmonic loading. Experimental validation of the analytical model is carried out and suggestions for future work are given. Dissert. Abstr.

N94-11156 McGill Univ., Montreal (Quebec).
MECHANICAL ANALYSIS OF PARALLEL MANIPULATORS WITH SIMULATION, DESIGN, AND CONTROL APPLICATIONS Ph.D. Thesis
Ou Ma 1991 278 p
(ISBN-0-315-72013-1) Avail: Univ. Microfilms Order No. DANN72013

The kinematics and dynamics for the purposes of analysis, control, simulation, and design of general platform-type parallel manipulators are discussed. Two new methods of direct kinematics for displacement analysis are proposed. Velocity and acceleration analyses for general kinematic architectures are fully studied. Furthermore, kinematic singularities are classified based on their nature. Architecture singularities and architecture conditioning are deeply studied and incorporated into design strategies, along with design examples. Moreover, formulation singularities are also given due attention with case studies. In dynamics modeling, the method of the natural orthogonal complement is applied such that the resulting models are structurally algorithmic, computationally efficient, and numerically robust - essential properties for the implementation of more sophisticated control strategies. Efficient inverse and direct dynamics algorithms are developed based on the dynamics models in both joint space and Cartesian space. The algorithms were implemented with a general software package that is available for dynamics control and motion simulation of platform manipulators. As practical applications, the dynamics modeling and simulation of some commercial flight simulators are included. Finally, the concept of dynamic isotropy is introduced, which allows one to evaluate the motion/force performance of a manipulator with respect to control and simulation. Application strategies of this concept to some robotics problems such as design, trajectory planning, and inverse kinematics are discussed along with examples. Dissert. Abstr.

N94-11157*# Cincinnati Univ., OH. Mechanical, Industrial and Nuclear Engineering.
COMPUTATIONAL GEARING MECHANICS Final Report
Ronald L. Huston 23 Nov. 1992 10 p
(Grant NsG-3188)
(NASA-CR-193666; NAS 1.26:193666) Avail: CASI HC A02/MF A01

The Final Report on computational gear mechanics is presented. This is an expository report summarizing the research efforts and results. Research on gear geometry, gear stress, and gear dynamics is discussed. Current research and planned future efforts are also discussed. A comprehensive bibliography is presented. Author (revised)

N94-11219 State Univ. of New York, Stony Brook.
TRAJECTORY PATTERN INVERSE DYNAMICS AND CONTROL OF NONLINEAR DYNAMICS SYSTEMS WITH APPLICATION TO FLEXIBLE STRUCTURES Ph.D. Thesis
Qing Tu 1992 257 p
Avail: Univ. Microfilms Order No. DA9309990

A new approach to the study of the inherent characteristics of the nonlinear dynamics of mechanical systems, path and motion planning for systems with joint and structural flexibility, and kinematic and dynamic synthesis of such systems is presented. The investigations are based on a new method, which was referred to as the trajectory pattern method. In this method, the inherent characteristics of the nonlinear dynamics of a system is determined by selecting a trajectory pattern (i.e., the time history of motion), and examining the structure of the resulting inverse dynamics equations (models). The trajectory patterns are described in parametric form in terms of the variables of the differential equations of motion. The corresponding inverse dynamics equations can then be derived in terms of the trajectory pattern and system parameters. Each trajectory pattern produces an inverse dynamics model with a specific structure. The structure of the resulting inverse dynamics models and the fact that they can be derived in parametric form for any selected trajectory pattern, makes them ideal for investigating the inherent characteristics of the dynamics of nonlinear mechanical systems. The primary objective is the development of systematic methods for the design of a number of classes of nonlinear dynamics systems with superior dynamic characteristics; and optimal path and trajectory synthesis for tracking and point to point motions, such as for minimal vibrational excitation, minimum time with minimal residual vibration, and/or minimal sensitivity to certain system parameters and their variations. The study of the dynamic characteristics of robot manipulators includes the study of effects of the operating speed on the dynamic behavior of robot manipulators with rigid links in the presence and absence of gravitational acceleration; and the study of the effects of the payload mass, size, and end-effector holding locations. The systems considered are mechanical systems with rigid elements or with flexible joints and structures. A number of examples including computer simulation of the effectiveness of the developed method and some experimental results are presented. Dissert. Abstr.

N94-11228# Westinghouse Savannah River Co., Aiken, SC.
WELDING TRITIUM AGED STAINLESS STEEL
W. R. Kanne, Jr. 1993 5 p Presented at the DOE Compatibility, Aging and Service Life Conference, Aiken, SC, 20-22 Apr. 1993
(Contract DE-AC09-89SR-18035)
(DE93-011782; WSRC-MS-93-090; CONF-9304103-5) Avail: CASI HC A01/MF A01

Stainless steels exposed to tritium become unweldable by conventional methods due to He buildup within the metal matrix. With longer service lives expected for new weapon systems, and service life extensions of older systems, methods for welding/repair on tritium-exposed material will become important. Results are reported that indicate that both solid-state resistance welding and low-heat gas metal arc overlay welding are promising methods for repair or modification of tritium-aged stainless steel. DOE

N94-11247# Lawrence Livermore National Lab., CA.
PULSED PLASMA PROCESSING FOR CONTROL OF DIESEL ENGINE EMISSIONS
G. E. Vogtlin, E. K. Freytag, J. N. Bardsley, and H. Wallman 12 Feb. 1993 8 p Presented at the Annual Automotive Development Technology Contractors' Coordination Meeting, Dearborn, MI, 2-5 Nov. 1992
(Contract W-7405-eng-48)
(DE93-011884; UCRL-JC-111555; CONF-9211101-8) Avail: CASI HC A02/MF A01

Electrical discharges can be used as an after treatment for diesel exhaust. We are presently involved in research to determine the feasibility of this process. These discharges have been shown to remove nitric oxide, sulfur dioxide, particulates, and many organic compounds. A key issue is the efficiency of this removal since it effects both capital and operating costs. These discharges must be of short duration, less than one microsecond, to avoid energy losses due to heating of bulk gas molecules. The voltage must be kept below the voltage breakdown limit where ion heating creates an arc discharge. The basic process is the acceleration of electrons which then collide with gas molecules to form radicals such as O and OH. These radicals then react with and eliminate pollutants. Two basic electrode geometries are used to generate these discharges. The barrier discharge is when one or both of the electrodes is insulated and the pulse length is limited by charging of the insulator. This discharge must be driven by alternating current to permit alternating charging of the insulator. The other geometry is when one electrode has a peak voltage stress five or more times the average stress. We have been investigating the high stress geometry which uses a small wire inside a pipe. The principal experimental apparatus utilized by this effort uses a closed loop gas system. This system permits the production of various gas combinations prior to testing. Analysis can be conducted during or after these tests. The recirculated gas can be heated up to 400 F. This system can measure the energy used and the pollutant removal to determine efficiency. Our primary goal is the simultaneous removal of nitric oxide and particulates typical of diesel exhaust. This is expected to be accomplished in one or more metal tubes no larger than two inches in diameter and 36 inches long. DOE

N94-11290# Naval Command, Control and Ocean Surveillance Center, San Diego, CA. Research, Development, Test and Evaluation Div.
A PORTABLE CONTROLLER FOR UNMANNED GROUND VEHICLES
A. Y. Umeda, T. W. Hughes, A. H. Koyamatusu, B. N. Nobunaga, and K. K. Yamada Mar. 1993 6 p
(AD-A264963) Avail: CASI HC A02/MF A01

The portable remote vehicle controller (PRVC), recently developed at the Naval Command, Control and Ocean Surveillance Center's Research, Development, Test and Evaluation Division (NRaD) Detachment, Kailua, Hawaii, provides a lightweight, compact, teleoperator control station that allows remote, high speed control of unmanned ground vehicles (UGV). This ruggedized UGV operator control unit is configurable to work in any operating environment. Test drivers rated PRVC's ergonomically designed steering, brake and throttle controls superior to other driving configurations. All functional vehicle controls are easily accessible and can be manipulated by feel-without the need to look at physical buttons or levers. Graphic overlays displayed on the video image inform the UGV operator of critical system conditions and obviate the need to concentrate on other visual displays. Fiber optic data communications to the UGV, and RF audio communication to the military networks are fully supported by the PRVC. DTIC

N94-11438# Engineering Systems Management, Inc., Gaithersburg, MD.
LIFE-CYCLE COST ANALYSIS OF CONVENTIONAL AND FUEL CELL/BATTERY POWERED URBAN PASSENGER VEHICLES
30 Nov. 1992 248 p
(Contract DE-AC02-91CH-10491)
(DE93-010770; DOE/CH-10491/1) Avail: CASI HC A11/MF A03

This Final Report summarizes the work on the life cycle cost (LCC) analysis of conventional and fuel cell/battery powered urban passenger vehicles. The purpose of the work is to support the Division in making sound economic comparisons between conventional and fuel cell/battery powered buses, passenger vans, and cars for strategic analysis of programmatic R&D goals. The LCC analysis can indicate whether paying a relatively high initial capital cost for advanced technology with low operating and/or environmental costs is advantageous over paying a lower initial cost for conventional technology with higher operating and/or environmental costs. While minimizing life cycle cost is an important consideration, it does not always result in technology penetration in the marketplace. The LCC analysis model developed under this contract facilitates consideration of all perspectives. Over 100 studies have been acquired and analyzed for their applicability. Drawing on prior work by JPL and Los Alamos National Laboratory as primary sources, specific analytical relationships and cost/performance data relevant to fuel cell/battery and internal combustion engine (ICE) powered vehicles were selected for development of an LCC analysis model. The completed LCC model is structured around twelve integrated modules. Comparative analysis is made between conventional gasoline and diesel vehicles and fuel cell/battery vehicles using either phosphoric acid fuel cells or proton-exchange membrane fuel cells. In all, seven base vehicle configuration cases with a total of 21 vehicle class/powertrain/fuel combinations are analyzed. The LCC model represents a significant advance in comparative economic analysis of conventional and fuel cell/battery powered vehicle technologies embodying several unique features which were not included in prior models. DOE

N94-11625# Argonne National Lab., IL.
INSTANTANEOUS ENGINE FRICTIONAL TORQUE: ITS COMPONENTS AND PISTON ASSEMBLY FRICTION
Fred A. Nichols, ed. and N. A. Henein (Wayne State Univ., Detroit, MI.) May 1992 197 p
(Contract W-31-109-eng-38)
(DE93-011639; ANL/OTM/CR-1) Avail: CASI HC A09/MF A03

The overall goal of this report is to document the work done to determine the instantaneous frictional torque of an internal combustion engine by using a new approach known as the P-(omega) method developed at Wayne State University. The emphasis has been to improve the accuracy of the method, and apply it to both diesel and gasoline engines under different operating conditions. Also work included an investigation to determine the effect of using advanced materials and techniques to coat the piston rings on the instantaneous engine frictional torque and the piston assembly friction. The errors in measuring the angular velocity, omega, have been determined and found to be caused by variations in the divisions within one encoder, encoder-to-encoder variations, misalignment within the encoder itself, and misalignment between the encoder and crankshaft. The errors in measuring the cylinder gas pressure, P, have been determined and found to be caused by transducer-to-transducer variations, zero drift, thermal stresses and lack of linearity. The ability of the (P-(omega)) method in determining the frictional torque of many engine components has been demonstrated. These components include valve train, fuel injection pump with and without fuel injection, and piston with and without different ring combinations. The emphasis in this part of the research program has been on the piston-ring assembly friction. The effects of load and other operating variables on IFT have been determined. The motoring test, which is widely used in industry to measure engine friction has been found to be inaccurate. The errors have been determined at different loads. DOE

N94-12374# Virginia Univ., Charlottesville. School of Engineering and Applied Science.
PROPERTIES OF INTERFACIAL TRIBO-FILMS Final Report, 15 Mar. 1992 - 28 Feb. 1993
D. D. Makel and D. Kuhlmann-Wilsdorf Jun. 1993 239 p
(Contract N00014-92-J-1505)
(AD-A265591; UVA/525755/MSE93/101) Avail: CASI HC A11/MF A03

Research has been conducted on the properties of interfacial films of the kind formed in the course of sliding wear, named 'tribo-films.' Using specialized instrumentation, in particular the so-called Hoop Apparatus and a Bridgman-Anvil Device, we have found many new insights into the fundamental mechanisms responsible for the phenomena observed during sliding. In particular, advances have been made in the following areas: (1) the understanding of lubrication through adsorbed films; (2) the fundamental understanding of stick-slip; (3) the deformation mechanisms at high strains, pertinent to tribo-films and sub-surface regions; (4) micromechanisms of MoS2 lubrication; (5) understanding the implications of various material properties for possible solid lubricants; and (6) the formation of amorphous tribo-material by high strains. The results from this contract have been documented in 14 refereed publications. DTIC

N94-12605# Georgetown Univ., Washington, DC.
RESEARCH DEVELOPMENT AND DEMONSTRATION OF A FUEL CELL/BATTERY POWERED BUS SYSTEM
S. Romano and R. Wimmer Feb. 1993 218 p
(Contract DE-AC02-87NV-10649)
(DE93-013778; DOE/NV-10649/T1) Avail: CASI HC A10/MF A03

During 1992, the design of the three test bed buses evolved. Georgetown participated in all the working meetings and the preliminary design review of the Test Bed Bus (TBB). Throughout the Year, Georgetown provided input on system design and integration issues, transit industry requirements, and bus performance. GU also attended technical seminars, presenting papers at two. The computer simulation 'HYBRID', developed by Georgetown, was used to assess performance of different bus designs and system control algorithms. GU also modified the simulation to be more flexible and allow easier evaluation of designs. Georgetown had Exhibitgroup design and construct, to our specifications, a fuel cell bus display with a 1/10 scale model of the TBB for use at trade shows and exhibits. Energy Partners of West Palm Beach, Florida completed their subcontract for the engineering design study of a hydrogen fueled, fuel-cell-powered multi-passenger vehicle. Georgetown performed a study to determine the size of the US bus fleet and expected new bus deliveries over the next 10 years. Trojan Battery Company of Santa Fe Springs, California conducted a study to determine the specific design characteristics required of a lead acid battery to meet the special requirements posed by hybrid vehicle operation. Finally, GU assisted the prime contractor with the design of the system controller and its control algorithms. DOE

N94-10055# Maschinenfabrik Augsburg-Nuernberg A.G., Munich (Germany).
STRUCTURAL MATERIAL, MANUFACTURE, AND DESIGN REQUIREMENTS FOR HIGH-TEMPERATURE FASTENERS FOR SPACE PLANE TECHNOLOGIES
P. Agatanovic and M. Dogigli *In* ESA, Advanced Materials for Lightweight Structures Oct. 1992 p 325-332 (For primary document see N94-10001 01-24)
Copyright Avail: CASI HC A02/MF A04

N94-10061# Ecole Nationale Superieure de Ceramique Industrielle, Limoges (France). Lab. Materiaux Ceramiques.
STUDY OF THE TRIBOLOGICAL BEHAVIOR OF SiC AND SI3N4 CERAMIC COUPLES IN TERMS OF TEMPERATURE: THE REALITY [ETUDE DU COMPORTEMENT TRIBOLOGIQUE DE COUPLE CERAMIQUES SIC ET SI3N4 EN FONCTION DE LA TEMPERATURE: LA REALITE]
F. Platon and Y. Berthier (Institut National des Sciences Appliquees, Lyon,

France.) *In* ESA, Advanced Materials for Lightweight Structures Oct. 1992 p 361-366 In FRENCH Sponsored by Commission of the European Communities (For primary document see N94-10001 01-24)
Copyright Avail: CASI HC A02/MF A04

N94-11577*# Jet Propulsion Lab., California Inst. of Tech., Pasadena.
SUPERVISED AUTONOMOUS CONTROL, SHARED CONTROL, AND TELEOPERATION FOR SPACE SERVICING
Paul G. Backes *In* NASA. Johnson Space Center, Sixth Annual Workshop on Space Operations Applications and Research (SOAR 1992), Volume 2 Feb. 1993 p 720-731 Sponsored by NASA, Washington (For primary document see N94-11527 01-99)
Avail: CASI HC A03/MF A03

38 QUALITY ASSURANCE AND RELIABILITY

Includes product sampling procedures and techniques; and quality control.

N94-10170# Technische Univ., Eindhoven (Netherlands). Dept. of Mathematics and Computing Science.
BAYESIAN RELIABILITY ANALYSIS WITH IMPRECISE PRIOR PROBABILITIES
F. P. A. Coolen and M. J. Newby Dec. 1992 31 p
(MEMO-COSOR-92-50; ETN-93-94329) Copyright Avail: CASI HC A03/MF A01

An extension of the standard Bayesian approach based on the theory of imprecise probabilities and intervals of measures is developed. The Bayesian framework for statistical inference offers the possibility of taking expert opinions into account. It is attractive in practical problems concerning reliability of technical systems. Probability is the only language in which uncertainty can be consistently expressed, and this requires the use of prior distributions for reporting expert opinions. It is shown that it is necessary to take the nature of experts knowledge into account. The application of this approach in reliability theory is outlined. ESA

N94-10847 International Atomic Energy Agency, Vienna (Austria).
REPORT OF THE IAEA CONSULTANTS' MEETING ON REAL-TIME NONDESTRUCTIVE MONITORING OF WEAR AND CORROSION USING THE THIN LAYER ACTIVATION TECHNIQUE
Jan. 1993 73 p Meeting held in Vienna, Austria, 15-18 May 1990 Limited Reproducibility: More than 20% of this document may be affected by microfiche quality
(DE93-617422; INIS-MF-13441; CONF-9005440) Avail: CASI HC A04 (US Sales Only)

The report includes 5 papers presented by the participants and conclusions and recommendations of the meeting. A separate abstract was prepared for each paper. The papers cover the following: thin layer activation techniques in research and industry, thin layer activation with charged particles -- applications and remarks, thin layer activation technique applications in the USSR, activation technique for industry at the Debrecan Cyclotron Laboratory, and radionuclide technique in mechanical engineering in Germany. DOE

N94-11110# Ames Lab., IA.
ULTRASONIC INSPECTION, MATERIAL NOISE AND SURFACE ROUGHNESS
M. Bilgen, J. H. Rose, and P. B. Nagy (Ohio State Univ., Columbus.) 1992 9 p Presented at the Review of Progress in Quantitative Nondestructive Evaluation, La Jolla, CA, 19-24 Jul. 1992
(Contract W-7405-eng-82)
(DE93-011560; IS-M-741; CONF-920799-7) Avail: CASI HC A02/MF A01

The phase-screen approximation (PSA) can be used to model interaction of ultrasound with rough surfaces if the height variation is small and correlation length is large relative to wavelength. Material noise is enhanced for early times and decreased for late times. PSA can calculate ultrasound transmission through random rough surfaces; as a numerical method, it will be most appropriate for complicated problems such as rough curved surfaces, where the Boundary Integral Equation is too time-consuming. PSA can serve as a starting point for analyzing the physics of transmission through rough surfaces. However, it needs corrections to the amplitude of the transmitted wave. Nonetheless, it can serve as the basic engineering model for the effects of surface roughness on ultrasonic inspections. DOE

N94-11167*# National Aeronautics and Space Administration. Lewis Research Center, Cleveland, OH.
ACARA USER'S MANUAL
Dale K. Stalnaker Aug. 1993 128 p
(RTOP 474-12-10)
(NASA-TM-106277; E-8014; NAS 1.15:106277) Avail: CASI HC A07/MF A02

ACARA (Availability, Cost, and Resource Allocation) is a computer program which analyzes system availability, lifecycle cost (LCC), and resupply scheduling using Monte Carlo analysis to simulate component failure and replacement. This manual was written to: (1) explain how to prepare and enter input data for use in ACARA; (2) explain the user interface, menus, input screens, and input tables; (3) explain the algorithms used in the program; and (4) explain each table and chart in the output. Author (revised)

N94-11168 Japan Atomic Energy Research Inst., Tokyo.
DBTT MEASUREMENT BY USE OF SMALL PUNCH (SP) TEST
Masahide Suzuki (Japan Atomic Energy Research Inst., Tokai.), Kiyoshi Fukaya (Japan Atomic Energy Research Inst., Tokai.), Yutaka Nishiyama (Japan Atomic Energy Research Inst., Tokai.), and Motokuni Eto (Japan Atomic Energy Research Inst., Tokai.) Jun. 1992 50 p Limited Reproducibility: More than 20% of this document may be affected by microfiche quality
(DE93-753188; JAERI-M-92-086) Avail: CASI HC A03

Microhardness and SP tests were conducted to improve the reliability of ductile-brittle transition temperature (DBTT) shift evaluation caused by aging (thermal aging, neutron irradiation, cold rolling) using several model alloys (Fe-0.15C alloys and 2 1/4 Cr-1Mo steels). Although evaluation of DBTT by the SP test was overall good, intergranular brittleness could not be detected by SP DBTT measurement only. By combining other measurements like fractographic observation, however, material degradation can be evaluated more properly. DOE

N94-11586# Sandia National Labs., Albuquerque, NM.
POTENTIAL TECHNIQUES FOR NON-DESTRUCTIVE EVALUATION OF CABLE MATERIALS
Kenneth T. Gillen, Roger L. Clough, Bengt Mattson (Royal Inst. of Tech., Stockholm, Sweden.), Bengt Stenberg (Royal Inst. of Tech., Stockholm, Sweden.), and Erik Oestman (Skega A.B., Ersmark, Sweden.) 1993 13 p Presented at the EPRI Workshop on Power Plant Cable Condition Monitoring, San Francisco, CA, 9-11 Feb. 1993
(Contract DE-AC04-76DP-00789)
(DE93-008350; SAND-93-0308C; CONF-930254-3) Avail: CASI HC A03/MF A01

This paper describes the connection between mechanical degradation of common cable materials, in radiation and elevated temperature environments, and density increases caused by the oxidation which leads to this degradation. Two techniques based on density changes are suggested as potential non-destructive evaluation (NDE) procedures which may be applicable to monitoring the mechanical condition of cable materials in power plant environments. The first technique is direct measurement of density changes, via a density gradient column, using small shavings removed from the surface of cable jackets at selected locations. The second technique is computed X-ray tomography, utilizing a portable scanning device. DOE

N94-11647# Oak Ridge National Lab., TN.
QUALITY ASSURANCE IN BASIC RESEARCH AND R/D
P. B. Hoke 1993 7 p Presented at the 4th Annual Workshop on Management in Basic Applied Research and R/D Environment, Stanford, CA, 3-4 Mar. 1993
(Contract DE-AC05-84OR-21400)
(DE93-010825; CONF-9303111-3) Avail: CASI HC A02/MF A01

Oak Ridge National Laboratory (ORNL) is one of the nation's largest and most widely diversified federal multipurpose research and development centers. The Laboratory is operated by Martin Marietta Energy Systems Inc. for the U.S. DOE. Its mission embraces non-nuclear as well as nuclear energy development together with a wide range of supporting research in engineering, physical sciences, and life sciences, as well as social sciences and economics. The Laboratory's program is dominated by four major areas of development that are approximately equal in size: nuclear (fission) energy development; basic physical sciences research; biomedical and environmental; and magnetic fusion energy development. This document outlines ORNL's quality assurance (QA) program in response to the ten criteria of DOE order 5700.6C. Guidance for implementation comes both from Attachment 1 of 5700.6C and DOE-ER-STD-6001-92. The bases for the program, integration of DOE orders, program architecture, assessment activities, and financial restraints are discussed. DOE

N94-10036# Politecnico di Milano (Italy). Dept. of Aerospace Engineering.
SPECIAL PROBLEMS OF 3-D ULTRASONIC QNDI TECHNIQUES AND APPLICATIONS TO COMPOSITES AEROSPACE STRUCTURES
G. Sala, M. Anghileri, and A. Antoniazzi (Centro Sviluppo Applicazioni, Milan, Italy.) *In* ESA, Advanced Materials for Lightweight Structures Oct. 1992 p 209-215 (For primary document see N94-10001 01-24)
Copyright Avail: CASI HC A02/MF A04

N94-10037# Indian Space Research Organization, Ahmedabad. Space Applications Center.
DESIGN OF INSPECTION AND ACCEPTANCE TEST METHODOLOGY FOR TIG WELDED ALUMINUM-ALLOY BRACKET FOR CAMERA HOUSINGS FOR IRS-1A SPACE CRAFT AND EXECUTING IT
V. K. Manglik, Rajeev Vaghmare, and A. K. Shah *In* ESA, Advanced Materials for Lightweight Structures Oct. 1992 p 217-221 (For primary document see N94-10001 01-24)
Copyright Avail: CASI HC A01/MF A04

N94-10038# Robert Gordon's Inst. of Tech., Aberdeen (Scotland). School of Applied Sciences.
QUANTIFYING DISBOND AREA
D. W. Lowden *In* ESA, Advanced Materials for Lightweight Structures Oct. 1992 p 223-228 (For primary document see N94-10001 01-24)
Copyright Avail: CASI HC A02/MF A04

N94-10039# Bundesanstalt fuer Materialpruefung, Berlin (Germany).
NEW X RAY SCANNING TOPOGRAPHIC APPROACHES TO NONDESTRUCTIVE EVALUATION OF COMPOSITES
M. P. Hentschel, W. Harbich, and A. Lange *In* ESA, Advanced Materials for Lightweight Structures Oct. 1992 p 229-232 (For primary document see N94-10001 01-24)
Copyright Avail: CASI HC A01/MF A04

N94-11335# Manchester Univ. (England). Dynamics Research Group.
FAULT LOCATION IN STRUCTURES USING NEURAL NETWORKS
K. Worden, A. D. Ball, and G. R. Tomlinson *In* AGARD, Smart Structures for Aircraft and Spacecraft Apr. 1993 19 p Sponsored in part by BRITE/EURAM (For primary document see N94-11317 01-24)
Copyright Avail: CASI HC A03/MF A04

N94-11563*# Aeronautical Radio, Inc., Annapolis, MD. Advanced Research and Development Group.
DESIGN FOR TESTABILITY AND DIAGNOSIS AT THE SYSTEM-LEVEL
William R. Simpson and John W. Sheppard *In* NASA. Johnson Space Center, Sixth Annual Workshop on Space Operations Applications and Research (SOAR 1992), Volume 2 Feb. 1993 p 627-632 (For primary document see N94-11527 01-99)
Avail: CASI HC A02/MF A03

39 STRUCTURAL MECHANICS

Includes structural element design and weight analysis; fatigue; and thermal stress.

For applications see *05 Aircraft Design, Testing and Performance* and *18 Spacecraft Design, Testing and Performance.*

N94-10155# Oak Ridge National Lab., TN.
HEAVY-SECTION STEEL TECHNOLOGY PROGRAM
D. E. McCabe 16 Oct. 1992 17 p
(Contract DE-AC05-84OR-21400)
(DE93-009222; ORNL/FTR-4398) Avail: CASI HC A03/MF A01 (US Sales Only)

The objective of this travel was to spend a 3-month work period at GKSS-Forschungzentrum in Geesthact, Germany, to work on the development of an American Society for Testing and Materials (ASTM) standard practice for transition range testing of pressure vessel steels. A side trip was made to the Technical Research Center of Finland (VTT). As a result of this work experience, a GKSS report has been produced that covers background research performed, and a proposed test standard has been prepared. This standard will be made available to the Nuclear Regulatory Commission (NRC) in the form of a NUREG report. DOE

N94-10161# Universiteit Twente, Enschede (Netherlands). Systems and Control Group.
PAYLOAD SENSITIVITY IN COUPLED BENDING AND TORSIONAL VIBRATIONS IN FLEXIBLE BEAMS
M. Vajta Nov. 1992 135 p
(MEMO-1102; ETN-93-94315) Avail: CASI HC A07/MF A02

The sensitivity of coupled bending and torsional vibrations in flexible robot arms to the payload parameters is analyzed. The coupling is usually disregarded but it is ultimately present due to the asymmetricity of a realistic payload. The coupling is shown to modify the system dynamics, most dominantly in mid-frequency range. The kinematic equations are given assuming an Euler Bernoulli model with Voigt type of internal damping and with an asymmetric tip body. Different damping coefficients in bending and in torsional vibrations are applied. The exact frequency response in the frequency domain is given. Based on a frequency function, a sensitivity analysis regarding the payload parameters is provided. A computer package was developed to calculate the frequency responses, the sensitivity functions, and their pole zero configurations. Properties of the sensitivity functions and of their pole zero configurations are given. ESA

N94-10264# Oak Ridge National Lab., TN.
HYDROSTATIC TESTING OF THICK LAMINATED COMPOSITE CYLINDERS FOR PERFORMANCE MODEL VALIDATION
H. W. Blake and J. M. Starbuck Mar. 1993 225 p
(Contract DE-AC05-84OR-21400)
(DE93-012728; ORNL/ATD-67) Avail: CASI HC A10/MF A03

This report details the design, fabrication, and testing of four S-GLASS cylinders and an all circ-wound graphite cylinder. The results of an extensive parametric design study are presented. The study formed the foundation for the test article constructions. Included are the details of the cylinder constructions, the design calculations for stress and buckling, and the cylinder failure predictions. Analytical results are presented for both closed-form elasticity solutions and finite element methods. The test data and observations from the five hydrotests are summarized and correlated with the analytical results. Also provided are the details of a performance model for thick composites in compression, validated by the results of the experimental/analytical correlation. The predicted first-ply failure pressures from the performance model were within 10% of the experimentally measured pressures with the exception of the 2:1 hoop:axial ply ratio S-GLASS cylinder. The performance of this cylinder was underpredicted by 25%. DOE

N94-10288# Oak Ridge National Lab., TN.
POTENTIAL CHANGE IN FLAW GEOMETRY DURING PRESSURIZED-THERMAL-SHOCK TRANSIENTS
D. K. M. Shum, J. W. Bryson, J. G. Merkle, J. Keeney-Walker, T. L. Dickson, and B. R. Bass 1993 42 p Presented at the Pressure Vessel and Piping Conference, Denver, CO, 25-29 Jul. 1993
(Contract DE-AC05-84OR-21400)
(DE93-009709; CONF-930702-12) Avail: CASI HC A03/MF A01

This study presents preliminary estimates on the potential change in flaw geometry of an initially shallow, axially oriented, inner-surface finite-length flaw in a PWR-RPV during the course of a postulated PTS transient. Specifically, the question being addressed is whether a shallow, axially oriented, finite-length surface flaw would tend to elongate in the axial direction and/or deepen into the wall of the vessel during the transient. In the first part of the study, estimates are obtained based on the assumptions of linear-elastic material response. The thermo-elastic properties of the cladding and base material are explicitly considered. The flaw geometry corresponds to a family of modified-elliptical flaws characterized by the flaw's half-length to maximum depth (aspect ratio). Requirements for numerical convergence of the finite element results are examined. In the second part of the study, the sensitivity of the numerical results and conclusions obtained in the first part of the study to the following three analysis assumptions are evaluated: (1) Reference flaw geometry along the entire crack front and especially within the cladding region; (2) Linear-elastic versus elastic-plastic description of material response; and (3) Base-material-only vs bi-material cladding-base vessel-model assumption. DOE

N94-10306# Lawrence Livermore National Lab., CA.
COMPUTATIONAL PROCEDURES FOR DETERMINING PARAMETERS IN RAMBERG-OSGOOD ELASTOPLASTIC MODEL BASED ON MODULUS AND DAMPING VERSUS STRAIN
Tzou-Shin Ueng and Jian-Chu Chen Jul. 1992 18 p
(Contract W-7405-eng-48)
(DE93-013309; UCRL-ID-111487) Avail: CASI HC A03/MF A01

A computer code, RAMBO, is developed for obtaining the values of parameters in the Ramberg-Osgood elastoplastic model based on data of shear modulus and damping ratio at various shear strains. The basis and procedures for finding the parameters for the best fit of the data or relations defining modulus and damping ratios versus shear strain are given in this report. The Ramberg-Osgood relationship is rearranged so that the results can best fit data of both modulus and damping ratio. Constraints of data in the model are also discussed. DOE

N94-10342*# Alabama Univ., Huntsville. Materials Processing Lab.
MATERIAL CHARACTERIZATION AND MODELING WITH SHEAROGRAPHY Final Report
Gary L. Workman and Virginia Callahan 7 Jun. 1993 66 p
(Contract NAS8-38609)
(NASA-CR-192576; NAS 1.26:192576) Avail: CASI HC A04/MF A01

Shearography has emerged as a useful technique for nondestructible evaluation and materials characterization of aerospace materials. A suitable candidate for the technique is to determine the response of debonds on foam-metal interfaces such as the TPS system on the External Tank. The main thrust is to develop a model which allows valid interpretation of shearographic information on TPS type systems. Confirmation of the model with shearographic data will be performed. Author (revised)

N94-10361*# National Aeronautics and Space Administration. Lewis Research Center, Cleveland, OH.
PROBABILISTIC EVALUATION OF UNCERTAINTIES AND RISKS IN AEROSPACE COMPONENTS
A. R. Shah (Sverdrup Technology, Inc., Cleveland, OH.), M. C. Shiao (Sverdrup Technology, Inc., Cleveland, OH.), V. K. Nagpal (Sverdrup Technology, Inc., Cleveland, OH.), and C. C. Chamis Mar. 1992 48 p
(RTOP 505-63-53)
(NASA-TM-105603; E-6240; NAS 1.15:105603) Avail: CASI HC A03/MF A01

This paper summarizes a methodology developed at NASA Lewis Research Center which computationally simulates the structural, material, and load uncertainties associated with Space Shuttle Main Engine (SSME) components. The methodology was applied to evaluate the scatter in static, buckling, dynamic, fatigue, and damage behavior of the SSME turbo pump blade. Also calculated are the probability densities of typical critical blade responses, such as effective stress, natural frequency, damage initiation, most probable damage path, etc. Risk assessments were performed for different failure modes, and the effect of material degradation on the fatigue and damage behaviors of a blade were calculated using a multi-factor interaction equation. Failure probabilities for different fatigue cycles were computed and the uncertainties associated with damage initiation and damage propagation due to different load cycle were quantified. Evaluations on the effects of mistuned blades on a rotor were made; uncertainties in the excitation frequency were found to significantly amplify the blade responses of a mistuned rotor. The effects of the number of blades on a rotor were studied. The autocorrelation function of displacements and the probability density function of the first passage time for deterministic and random barriers for structures subjected to random processes also were computed. A brief discussion was included on the future direction of probabilistic structural analysis. Author (revised)

N94-10671* National Aeronautics and Space Administration. Langley Research Center, Hampton, VA.
METHOD OF RECERTIFYING A LOADED BEARING MEMBER USING A PHASE POINT Patent
Joseph S. Heyman, inventor (to NASA) 17 Aug. 1993 13 p Filed 19 Jun. 1991 Supersedes N92-11384 (29 - 2, p 249)
(NASA-Case-LAR-14741-1; US-Patent-5,237,516; US-Patent-Appl-SN-720153; US-Patent-Class-364-508; US-Patent-Class-73-761; US-Patent-Class-73-862.59; US-Patent-Class-364-571.03; Int-Patent-Class-G01H-1/00; Int-Patent-Class-G01N-29/16) Avail: US Patent and Trademark Office

A method of recertifying a load on a bearing member using a pulsed phase locked loop (P2L2) system is disclosed. A first tone burst signal with a corresponding first phase signal is generated in the bearing member in a first load condition. The sample/hold of the P2L2 is adjusted to a determined phase point on the first phase signal and then the P2L2 is locked at this phase period to determine a first load measurement. Next, the phase sample point is correlated with a corresponding position, w, on the first tone burst signal. A second tone burst with a corresponding second phase signal is then generated at some later time in the bearing member in a second load condition. The sample/hold is adjusted to the sample/hold phase point as before and then the output frequency of the P2L2 is adjusted until the sample/hold is positioned at the previously determined phase point corresponding to position w on the second tone burst signal. The P2L2 is then locked at this phase point to determine a frequency indicative of the load of the second loading condition.
Official Gazette of the U.S. Patent and Trademark Office

N94-10712*# Georgia Inst. of Tech., Atlanta. School of Mechanical Engineering.
ELASTIC PLASTIC FRACTURE MECHANICS METHODOLOGY FOR SURFACE CRACKS Semiannual Report No. 2
Hugo A. Ernst, D. W. Boatwright, W. J. Curtin, and D. M. Lambert Aug. 1993 114 p
(Grant NAG8-243)
(NASA-CR-194129; NAS 1.26:194129) Avail: CASI HC A06/MF A02

The Elastic Plastic Fracture Mechanics (EPFM) Methodology has evolved significantly in the last several years. Nevertheless, some of these concepts need to be extended further before the whole methodology can be safely applied to structural parts. Specifically, there is a need to include the effect of constraint in the characterization of material resistance to crack growth and also to extend these methods to the case of 3D defects. As a consequence, this project was started as a 36 month research program with the general objective of developing an EPFM methodology to assess the structural reliability of pressure vessels and other parts of interest to NASA containing defects. This report covers a computer modelling algorithm used to simulate the growth of a semi-elliptical surface crack; the presentation of a finite element investigation that compared the theoretical (HRR) stress field to that produced by elastic and elastic-plastic models; and experimental efforts to characterize three dimensional aspects of fracture present in 'two dimensional', or planar configuration specimens. Derived from text

N94-10715*# Purdue Univ., West Lafayette, IN. School of Mechanical Engineering.
FATIGUE-LIFE BEHAVIOR AND MATRIX FATIGUE CRACK SPACING IN UNNOTCHED SCS-6/TIMETAL 21S METAL MATRIX COMPOSITES
G. T. Ward, D. J. Herrmann, and B. M. Hillberry Jul. 1993 27 p
(Grant NAG1-1316; RTOP 763-23-45-85)
(NASA-CR-191467; NAS 1.26:191467) Avail: CASI HC A03/MF A01

Fatigue tests of the SCS-6/Timetal 21S composite system were performed to characterize the fatigue behavior for unnotched conditions. The stress-life behavior of the unnotched (9/90)2s laminates was investigated for stress ratios of R = 0.1 and R = 0.3. The occurrence of matrix cracking was also examined in these specimens. This revealed multiple matrix crack initiation sites throughout the composite, as well as evenly spaced surface cracks along the length of the specimens. No difference in fatigue lives were observed for stress ratios of R = 0.1 and R = 0.3 when compared on a stress range basis. The unnotched

SCS-6/Timetal 21S composites had shorter fatigue lives than the SCS-6/Ti-15-3 composites, however the neat Timetal 21S matrix material had a longer fatigue life than the neat Ti-15-3. Author (revised)

N94-10762*# National Aeronautics and Space Administration. Lewis Research Center, Cleveland, OH.
COMPUTATIONAL SIMULATION OF HOT COMPOSITE STRUCTURES
C. C. Chamis, P. L. N. Murthy, and S. N. Singhal (Sverdrup Technology, Inc., Brook Park, OH.) Sep. 1993 16 p Presented at the 10th Biennial Conference on Reliability, Stress Analysis and Failure Prevention, Albuquerque, NM, 19-22 Sep. 1993; sponsored by ASME
(RTOP 510-01-50)
(NASA-TM-106200; E-7908; NAS 1.15:106200) Avail: CASI HC A03/MF A01

Computational procedures are described to simulate the thermal and mechanical behavior of high temperature metal matrix composites (HT-MMC) in the following three broad areas: (1) Behavior of HT-MMC's from micromechanics to laminate via Metal Matrix Composite Analyzer (METCAN), (2) tailoring of HT-MMC behavior for optimum specific performance via Metal Matrix Laminate Tailoring (MMLT), and (3) HT-MMC structural response for hot structural components via High Temperature Composite Analyzer (HITCAN). Representative results from each area are presented to illustrate the effectiveness of computational simulation procedures. The sample case results show that METCAN can be used to simulate material behavior such as strength, stress-strain response, and cyclic life in HTMMC's; MMLT can be used to tailor the fabrication process for optimum performance such as that for in-service load carrying capacity of HT-MMC's; and HITCAN can be used to evaluate static fracture and fatigue life of hot pressurized metal matrix composite rings. Author

N94-10879# Technische Univ., Delft (Netherlands). Faculty of Aerospace Engineering.
IMPERFECTION SENSITIVITY OF THE BRAZIER EFFECT FOR ORTHOTROPIC CYLINDRICAL SHELLS
Menahem Baruch, Johann Arbocz, and G. Q. Zhang 1990 24 p
(LR-687; ETN-93-94415) Avail: NTIS HC A03/MF A01

The sensitivity to imperfections of the Brazier effect for orthotropic circular shells is investigated. Cylindrical tubes are subjected to a bending moment loose stability for a certain value of the moment and buckle. Using an elegant (but somewhat approximate) approach, Brazier determined the limit moment for infinitely long circular tubes subjected to pure bending. It is shown that the limit point of the external critical bending moment of an orthotropic cylindrical tube is sensitive but not very sensitive to initial imperfections. Both the critical moment and the critical longitudinal stresses are reduced by the initial imperfections. ESA

N94-10897 Wayne State Univ., Detroit, MI.
NONLINEAR RESPONSE OF A CLAMPED-CLAMPED BEAM WITH INTERNAL RESONANCE UNDER SINUSOIDAL EXCITATION Ph.D. Thesis
Abdul-Hafiz Ahmed Afaneh 1992 219 p
Avail: Univ. Microfilms Order No. DA9310614

The nonlinear response characteristics of a clamped-clamped beam is investigated analytically, numerically, and experimentally. The beam is under an initial static axial load and subjected to a harmonic excitation of its support. Two ranges of the axial load are considered. These are below (the beam is initially straight) and above Euler buckling load (the beam is initially buckled). Hamilton's principle is used to derive a fourth order partial differential equation of motion which is descritized and reduced to a set of second order ordinary differential equations by applying Galerkin's method. Under certain values of the static load, the normal modes are nonlinearly coupled and this coupling results in a fourth order internal resonance condition between the first three modes when the beam is initially straight. Second and third order internal resonance conditions occur between the first two modes for the case of initially buckled beam. The multiple scales method showed the significant effects of these internal resonance conditions on the system behavior. In the straight beam case, the third mode which is externally excited transfers energy to the first two modes within a small range of internal detuning. Outside this region, the response is governed by a unimodal response of the third mode. In the neighborhood of 1:1 internal resonance, it is found that within the region of two mode interaction, the solution is either stationary or nonstationary depending on the excitation level and system parameters. Saturation and jump phenomena are found to take place in the case of two mode interaction with 2:1 internal resonance. Numerical simulation and experimental testing confirmed these predictions and revealed the occurrence of multifurcation, snap-through (escaping from one well to the other in an irregular manner), and chaotic motion. Dissert. Abstr.

N94-10900 Illinois Inst. of Tech., Chicago.
AN ELECTRO-OPTICAL SYSTEM FOR THE MEASUREMENT OF STRAINS Ph.D. Thesis
Gopalakrishna K. Bhat 1992 240 p
Avail: Univ. Microfilms Order No. DA9311927

Optical techniques for whole field displacement measurement, such as moire, holography, and speckle interferometry are attractive within the engineering industry in a variety of areas ranging from nondestructive testing and quality control to research and development. However, these techniques were restricted to research laboratories because of the specialized equipment and the laborious photographic process needed to record the images, and the skillful personnel needed to interpret the images. The major objective was to develop the basic principles of operation of an electro-optical system which can be used for the stress analysis of structures in the field. This objective was accomplished by means of three stages. The first stage was interfacing optical systems with the digital imaging system for the real time observation of whole field displacement patterns. Images of test objects are recorded using a TV camera (instead of a photographic film) and processed using a digital image processing system. The second stage was development of digital techniques for the analysis of interferometric fringes. Two dimensional Fourier transform techniques (spatial heterodyning and local heterodyning are developed to obtain the displacement and strain fields from the interferometric fringes. Techniques to minimize the errors introduced by the sharp object boundaries and to compute the strain field without obtaining the displacement field are also introduced. The third stage was application to study the feasibility of the system. The electro-optical system is employed to measure displacements and strains: under static and dynamic conditions, at normal and elevated temperatures and at the macro and micro levels. The applications include: measurement of strains in a disk subjected diametral compression, strain measurement at high temperatures, modal analysis of turbine blades, contact stress analysis; and measurement of the displacement field in the vicinity of a crack tip. Dissert. Abstr.

N94-10937*# California Univ., San Diego, La Jolla. Dept. of Applied Mechanics and Engineering Sciences.
NASTRAN MODELING OF FLIGHT TEST COMPONENTS FOR UH-60A AIRLOADS PROGRAM TEST CONFIGURATION Final Report
Florentino R. Idosor and Frieder Seible Feb. 1993 173 p Original contains color illustrations
(Contract NCC2-712)
(NASA-CR-193614; NAS 1.26:193614; SSRP-93/03) Avail: CASI HC A08/MF A02; 9 functional color pages

Based upon the recommendations of the UH-60A Airloads Program Review Committee, work towards a NASTRAN remodeling effort has been conducted. This effort modeled and added the necessary structural/mass components to the existing UH-60A baseline NASTRAN model to reflect the addition of flight test components currently in place on the UH-60A Airloads Program Test Configuration used in NASA-Ames Research Center's Modern Technology Rotor Airloads Program. These components include necessary flight hardware such as instrument booms, movable ballast cart, equipment mounting racks, etc. Recent modeling revisions have also been included in the analyses to reflect the inclusion of new and updated primary and secondary structural components (i.e., tail rotor shaft service cover, tail rotor pylon) and improvements to the existing finite element mesh (i.e., revisions of material property estimates). Mode frequency and shape results have shown that components such as the Trimmable Ballast System baseplate and its respective payload ballast have caused a significant frequency change in a limited number of modes while only small percent changes in mode frequency are brought about with the addition of the other MTRAP flight components. With the addition of the MTRAP flight components, update of the primary and secondary structural model, and imposition of the final MTRAP weight distribution, modal results are computed representative of the 'best' model presently available. Author

N94-11055 California Univ., Los Angeles.
MULTILEVEL COMPUTER-AIDED OPTIMUM DESIGN OF STRUCTURAL SYSTEMS USING MULTIPLE BASIS VECTORS Ph.D. Thesis
Kang-Seon Seomun 1992 312 p
Avail: Univ. Microfilms Order No. DA9310868

A new alternative multilevel structural optimization method using multiple basis vectors for each substructure is presented. The system level design task is formulated using multiple design space basis vectors for each substructure and the corresponding participation coefficients (system level design variables). In the system level design problem the total structural weight is minimized, subject to the system level constraints, namely static displacement limitations and natural frequency constraints. At the end of a system level optimization stage, the weight of each substructure is evaluated and used to establish an updated upper bound weight cap constraint for each upcoming substructure optimization procedure. At the subsystem level the structure is decomposed into a number of small substructures each one of which contains multiple design space basis vectors. A buffer (slack) variable is selected as the objective function for each substructure. Stress and member buckling constraints are incorporated at the subsystem level. The design modification problem at the subsystem level is formulated in a manner such that maximization of the buffer variable drives the substructure design vector away; from all of the constraints except the side constraints. After completing the subsystem level optimization task, the final values of buffer variables, local behavior constraints, and local design variables are obtained and used to evaluate lower limit values for the upcoming system level design variables. At both the system level and the subsystem level, design modification is carried out by solving a sequence of explicit approximate problems. The new alternative multilevel method which introduces multiple basis vectors for each substructure leads to greater flexibility when constructing and solving design optimization models for large structural systems. Dissert. Abstr.

N94-11096# Southwest Research Inst., San Antonio, TX.
MICROMECHANISMS OF FATIGUE CRACK GROWTH AND FRACTURE TOUGHNESS IN METAL MATRIX COMPOSITES Final Report, 27 Apr. 1985 - 15 Apr. 1993
D. L. Davidson 15 Apr. 1993 14 p
(Contract N00014-85-C-0206)
(AD-A265153; SWRI-06-8602/8) Avail: CASI HC A03/MF A01

This final report summarizes research in the fatigue and fracture toughness of a large number of materials ranging from metallic and ceramic matrix composites reinforced with ceramic particulates to aluminum, titanium, and glass matrix composites reinforced with continuous fibers. The purpose of this report is to summarize and draw conclusions about the state of knowledge of fatigue and fracture mechanisms from the past several years of research sponsored mainly by ONR. DTIC

N94-11169# Oak Ridge National Lab., TN.
FRACTURE MECHANICS AND FULL SCALE PIPE BREAK TESTING FOR THE DEPARTMENT OF ENVIRONMENT'S NEW PRODUCTION REACTOR-HEAVY WATER REACTOR
A. B. Poole 1992 33 p Presented at the 24th National American Society for Testing and Materials Symposium on Fracture Mechanics, Gatlinburg, TN, 30 Jun. - 2 Jul. 1992
(Contract DE-AC05-84OR-21400)
(DE93-005428; CONF-920672-4) Avail: CASI HC A03/MF A01 (US Sales Only)

Oak Ridge National Laboratory (ORNL) is completing a major task for the Department of Energy (DOE) in the demonstration that the primary piping of the New Production Heavy Water Reactor (NPR-HWR), with its relatively moderate temperature and pressure, should not suffer an instantaneous Double-Ended-Guillotine-Break (DEGB) under design basis loadings and conditions. The growth of possible small preexisting defects in the piping wall was estimated over a plant life of 60 years. This worst case flaw was then evaluated using fracture mechanics methods. J estimation methods and tearing instability approximations used in this analysis are discussed in this paper. It was established that this worst case flaw would increase in size by at least 14 times before pipe instability during an earthquake would even begin to be possible. The fatigue crack growth analysis is discussed in this paper. DOE

N94-11190*# Texas A&M Univ., College Station. Dept. of Civil Engineering.
FAILURE PREDICTION OF THIN BERYLLIUM SHEETS USED IN SPACECRAFT STRUCTURES Final Technical Report, 1 Jul. 1990 - 30 Jun. 1991
Paul N. Roschke, Edward Mascorro, Photios Papados, and Oscar R. Serna 1991 260 p
(Grant NAG9-280)
(NASA-CR-194164; NAS 1.26:194164) Avail: CASI HC A12/MF A03

The primary objective of this study is to develop a method for prediction of failure of thin beryllium sheets that undergo complex states of stress. Major components of the research include experimental evaluation of strength parameters for cross-rolled beryllium sheet, application of the Tsai-Wu failure criterion to plate bending problems, development of a high order failure criterion, application of the new criterion to a variety of structures, and incorporation of both failure criteria into a finite element code. A Tsai-Wu failure model for SR-200 sheet material is developed from available tensile data, experiments carried out by NASA on two circular plates, and compression and off-axis experiments performed in this study. The failure surface obtained from the resulting criterion forms an ellipsoid. By supplementing experimental data used in the the two-dimensional criterion and modifying previously suggested failure criteria, a multi-dimensional failure surface is proposed for thin beryllium structures. The new criterion for orthotropic material is represented by a failure surface in six-dimensional stress space. In order to determine coefficients of the governing equation, a number of uniaxial, biaxial, and triaxial experiments are required. Details of these experiments and a complementary ultrasonic investigation are described in detail. Finally, validity of the criterion and newly determined mechanical properties is established through experiments on structures composed of SR200 sheet material. These experiments include a plate-plug arrangement under a complex state of stress and a series of plates with an out-of-plane central point load. Both criteria have been incorporated into a general purpose finite element analysis code. Numerical simulation incrementally applied loads to a structural component that is being designed and checks each nodal point in the model for exceedance of a failure criterion. If stresses at all locations do not exceed the failure criterion, the load is increased and the process is repeated. Failure results for the plate-plug and clamped plate tests are accurate to within 2 percent. Author (revised)

N94-11218 Utah Univ., Salt Lake City.
UNDERSTANDING CRACKING FAILURES OF COATINGS: A FRACTURE MECHANICS APPROACH Ph.D. Thesis
Sung-Ryong Kim 1993 223 p
Avail: Univ. Microfilms Order No. DA9311236

A fracture mechanics analysis of coating (paint) cracking was developed. A strain energy release rate (G(sub c)) expression due to the formation of a new crack in a coating was derived for bending and tension loadings in terms of the moduli, thicknesses, Poisson's ratios, load, residual strain, etc. Four-point bending and instrumented impact tests were used to determine the in-situ fracture toughness of coatings as functions of increasing baking (drying) time. The system used was a thin coating layer on a thick substrate layer. The substrates included steel, aluminum, polycarbonate, acrylonitrile-butadiene-styrene (ABS), and Noryl. The coatings included newly developed automotive paints. The four-point bending configuration promoted nice transversed multiple coating cracks on both steel and polymeric substrates. The crosslinked type automotive coatings on steel substrates showed big cracks without microcracks. When theoretical predictions for energy release rate were compared to experimental data for coating/steel substrate samples with multiple cracking, the agreement was good. Crosslinked type coatings on polymeric substrates showed more cracks than theory predicted and the G(sub c)'s were high. Solvent evaporation type coatings on polymeric substrates showed clean multiple cracking and the G(sub c)'s were higher than those obtained by tension analysis of tension experiments with the same substrates. All the polymeric samples showed surface embrittlement after long baking times using four-point bending tests. The most apparent surface embrittlement was observed in the acrylonitrile-butadiene-styrene (ABS) substrate system. The impact properties of coatings as a function of baking time were also investigated. These experiments were performed using an instrumented impact tester. There was a rapid decrease in G(sub c) at short baking times and convergence to a constant value at long baking times. The surface embrittlement conditions and an embrittlement toughness were found upon impact loading. This analysis provides a basis for a quantitative approach to measuring coating toughness. Measuring toughness can be used to develop new coating systems. With these results the cracking behavior of baked coatings can be used to predict the durability or long time cracking behavior of those coatings. Dissert. Abstr.

N94-11254*# National Aeronautics and Space Administration. Lewis Research Center, Cleveland, OH.
FUNCTIONAL APPROXIMATION USING ARTIFICIAL NEURAL NETWORKS IN STRUCTURAL MECHANICS
Javed Alam (Youngstown State Univ., OH.) and Laszlo Berke Jul. 1993 18 p
(RTOP 505-63-5B)
(NASA-TM-105820; E-7251; NAS 1.15:105820) Avail: CASI HC A03/MF A01

The artificial neural networks (ANN) methodology is an outgrowth of research in artificial intelligence. In this study, the feed-forward network model that was proposed by Rumelhart, Hinton, and Williams was applied to the mapping of functions that are encountered in structural mechanics problems. Several different network configurations were chosen to train the available data for problems in materials characterization and structural analysis of plates and shells. By using the recall process, the accuracy of these trained networks was assessed. Author (revised)

N94-11275*# National Aeronautics and Space Administration. Marshall Space Flight Center, Huntsville, AL.
A STUDY OF STRENGTH EVALUATIONS OF EDNI/EDCu/NARloy-Z BONDED JOINTS
J. B. Min and K. L. Spanyer Jul. 1993 27 p
(NASA-TM-108418; NAS 1.15:108418) Avail: CASI HC A03/MF A01

Dissimilar material interfaces can be found in many materials and structural bonds such as composite materials, welded parts, inclusion in matrix, bond between metallic and ceramic materials, and so forth. One of such structural bonds can be seen in the main combustion chamber (MCC) of the Space Shuttle Main Engine (SSME). In this study, from a practical sense, the primary concern is to understand the systems response of EDNi/EDCu/NARloy-Z bonded joints using stress values approximated by the finite element method to determine an influence of the variation of structural bond parameters on the bonded joints, and consequently main combustion chamber of the Space Shuttle Main Engine. The results presented in this study could be an appropriate indicator for a good bond of EDNi/DECu/NARloy-Z layers with the desired thickness of copper deposition in the SSME MCC manufacturing process. Furthermore, the results from this study appear to be applicable to any bonded joints that can be characterized by the parameters and assumptions used in this analysis. Author (revised)

N94-11364 Gosudarstvennyi Komitet po Ispolzovaniyu Atomnoi Energii, Moscow (USSR).
ELASTIC DEFORMATIONS AND SOUND IN ANISOTROPE SUPERCONDUCTORS NEAR CRITICAL TEMPERATURE [UPRUGIE DEFORMATSII I ZVUK V ANIZOTROPNYKH SVERKHPROVODNIKAKH VBLIZI KRITICHESKOJ TEMPERATURY]
Y. M. Poluehktov 1991 20 p In RUSSIAN Limited Reproducibility: More than 20% of this document may be affected by microfiche quality
(DE93-620636; KFTI-91-17) Avail: CASI HC A03 (US Sales Only)

The influence of elastic deformations on the characteristics of anisotropic superconductors was investigated within the framework of elasticity theory and Ginsburg-Landau theory. Propagation and damping of sound in these superconductors near the critical temperature T(sub c) was considered. Sound velocity makes a jump and damping increases at T(sub c) point. It was shown that the magnetic field decreases in value and changes in direction when it penetrates an anisotropic superconductor. DOE

N94-11367# Oak Ridge National Lab., TN.
TEST SPECIFICATIONS, SPECIMEN DESIGN AND INSTRUMENTATION TEST DATA INTERPRETATION
T. J. Theiss 1992 23 p Presented at the Oak Ridge National Laboratory Biaxial Shallow-Flaw Fracture Toughness Testing Program, Oak Ridge, TN, 17 Dec. 1992
(Contract DE-AC05-84OR-21400)
(DE93-012338; CONF-921267-1) Avail: CASI HC A03/MF A01

The following document discusses uniaxial three-point bend beams and ORNL biaxial cruciform specimens. DOE

N94-11460# Allied-Signal Aerospace Co., Kansas City, MO.
SINE AND RANDOM VIBRATION PROGRAM EVALUATION ON VIBRATION CONTROL SYSTEMS
R. R. Hubert and A. Hsiung Apr. 1993 35 p
(Contract DE-AC04-76DP-00613)
(DE93-011974; KCP-613-5040) Avail: CASI HC A03/MF A01

The software used to perform sinusoidal and random vibration analysis has been evaluated. The effects of changing the parameters in the test setups were studied. In doing this, the capabilities and limitations of the software have been noted and documented in the operating procedures for the systems. By documenting the software capabilities and limitations, the operation has been improved by avoiding operations that are not possible with the current software. The operation has also been improved through a better understanding of the effects of test parameter changes. The procedure for performing random vibration analysis has been updated. A procedure for performing sinusoidal vibration analysis has been issued. DOE

N94-11482*# National Aeronautics and Space Administration. Lewis Research Center, Cleveland, OH.
A MODELING INVESTIGATION OF THERMAL AND STRAIN INDUCED RECOVERY AND NONLINEAR HARDENING IN POTENTIAL BASED VISCOPLASTICITY
S. M. Arnold, A. F. Saleeb (Akron Univ., OH.), and T. E. Wilt (Toledo Univ., OH.) Mar. 1993 23 p
(RTOP 510-01-50)
(NASA-TM-106122; E-7786; NAS 1.15:106122) Avail: CASI HC A03/MF A01

Specific forms for both the Gibb's and the complementary dissipation potentials were chosen such that a complete potential based multiaxial, isothermal, viscoplastic model was obtained. This model in general possesses three internal state variables (two scalars associated with dislocation density and one tensor associated with dislocation motion) both thermal and dynamic recovery mechanisms, and nonlinear kinematic hardening. This general model, although possessing associated flow and evolutionary laws, is shown to emulate three distinct classes of theories found in the literature, by modification of the driving threshold function F. A parametric study was performed on a specialized nondimensional multiaxial form containing only a single tensorial internal state variable (i.e., internal stress). The study was conducted with the idea of examining the impact of including a strain-induced recovery mechanism and the compliance operator, derived from the Gibb's potential, on the uniaxial and multiaxial response. One important finding was that inclusion of strain recovery provided the needed flexibility in modeling stress-strain and creep response of metals at low homologous temperatures, without adversely affecting the high temperature response. Furthermore, for nonproportional loading paths, the inclusion of the compliance operator had a significant influence on the multiaxial response, but had no influence on either uniaxial or proportional load histories. Author

N94-11617 State Univ. of New York, Stony Brook.
INTEGRAL EQUATION METHODS FOR MIXED BOUNDARY PROBLEM OF FRACTURE MECHANICS Ph.D. Thesis
Jianhua Li 1992 84 p
Avail: Univ. Microfilms Order No. DA9310044

A mathematical model to study a mixed boundary value problem of fracture mechanics, embedding the interface crack in a nonhomogeneous boundary layer, is developed. A general solution for a nonhomogeneous finite strip is found. The boundary value problem is reduced to a pair of 'dual integral equations'. Using the Hankel transform or the Fourier transform, the dual integral equations are reduced to a Fredholm integral equation of the second kind with a weakly singular kernel and a Cauchy integral equation (CSIE) of the first kind with a strong singular kernel, respectively. The Fredholm weakly singular integral equation (WSIE) is solved approximately by the product integral method. In order to develop a numerical method to solve CSIE with variable coefficients, the singular weight function technique is extended, as a complement to constant coefficient case. The discrete system of nonlinear equations to determine the exponents of the singular weight function is constructed through Gauss-Lobatta-Chebyshev method (GLCM) or Stengers formula. Using Newtons method, the nonlinear system is solved numerically. The convergence of the Newton iterative process is proved. Furthermore, employing the orthogonality property of the solution spaces of Cauchy type integral operator and its adjoint operator, a new direct numerical method for solving nonhomogeneous CSIE with variable coefficient is found and implemented. The numerical simulations of these methods gave excellent results for computing stress intensity factor and crack energy of the mixed boundary value problems and for a number of interesting examples. The numerical results are tabulated and shown graphically. Dissert. Abstr.

N94-11823 Pennsylvania State Univ., University Park.

ACTIVE VIBRATION CONTROL OF ADAPTIVE FLEXIBLE STRUCTURES USING PIEZOELECTRIC SMART SENSORS AND ACTUATORS Ph.D. Thesis

Suk-Yoon Hong 1992 176 p

Avail: Univ. Microfilms Order No. DA9311652

The active control of vibrations and radiated noise from structures is studied. The emphasis of the theoretical and experimental study is the use of a minimum number of discrete piezoelectric wafer type sensors and actuators and optimal control algorithms. One of the major objectives is to effect control without substantially changing the structural dynamics of the original system. Canonical structures such as a cantilever beam and an all-clamped square plate, as well as practical structures such as fuel tanks, are investigated to cover a wide range of structural vibration control problems. For the suppression of a single mode as well as for multi-mode structural motions, velocity feedback and coupled model steady-state quadratic optimal control methods are applied using both analog and digital control systems with the various types of PZT (Lead-Zirconate-Titanate) transducers. The advantages of circular disc type PZT wafers are explained and a uni-disc type co-located sensor and actuator system was proposed. For more efficient filtering of the structural mode signal, a smart filtering idea was developed considering the mode shape and poling direction of the sensor. To convert the signals from a partially distributed sensor and actuator to a point displacement and forcing signal, respectively, efficient conversion methods are developed. From the experimental and theoretical studies on the optimum selection of actuator positions, a coupled mode optimal control simulations is executed. On the basis of all the related theories and the developed ideas and control systems, a variety of adaptive structural vibration control experiments are performed verifying the potential of PZT transducers as sensors and actuators. Both single mode and multimode control of structural vibration and radiated noise was achieved in all cases. Using at the most 1-4 small disc or ring-shaped actuators, the original vibration levels were reduced by 12-25 dB. Successful vibration control of the automobile fuel tank indicates that the ideas proposed and implemented can be applied to several practical structures such as the passenger compartments of ground and airborne vehicles. Such structures which adapt themselves to different types of sources and environments can be called 'Smart Structures'.
Dissert. Abstr.

N94-12359# Tokyo Univ., Sagamihara (Japan).

LABORATORY STUDIES ON THE VELOCITY OF FRAGMENTS FROM IMPACT DISRUPTIONS Report No. 651

Akiko M. Nakamura Jul. 1993 94 p

Avail: CASI HC A05/MF A01

The velocity distribution of fragments from impact disruption was experimentally determined as a step toward better understanding of the collisional evolution of planetary bodies. Ejection velocity and rotational frequency of fragments larger than approximately 1 mm were investigated by taking 16 mm pictures. Basalt, alumina, and gypsum spheres of 4 cm to approximately 8 cm in diameter were shattered by nylon spheres 7 mm in diameter at velocity of 1 km sec(exp -1) to approximately 4 km sec(exp -1). In order to investigate the velocity of fine fragments 1 micrometer to approximately 100 micrometers in size, new impact disruption experiments of basalt blocks were performed, where thin films and foils were exposed to the ejecta as a secondary target. The velocity of fragments was estimated by the size distribution of holes perforated on the secondary target. A comprehensive compilation of velocity data is proposed. The results are reported with emphasis on the relation to the dimension of the fragments. For large fragments of the three target materials, similar relations between the velocity in the center of mass system and the size are obtained. The velocity dispersion of a given fragment size is within about one order of magnitude. The slopes of log-log relations of the velocity versus the size range from -1 to -1/2. Although the size-velocity relation of smaller fragments depends on the ejection angle, the results suggest that the systematic relation of mm- to approximately cm-sized fragments can be extrapolated to smaller sized fragments. The rotational frequency decreases with increasing size of the fragment. It is shown that the laboratory data and data on the crate ring on the Moon can be conformed to a single dimensionless size-velocity relation, V(s) = V* (Y,rho,C) (s/a)(exp -xi) (1/2 less than or equal to xi less than or equal to 1), where V(s), V* (Y,rho,C), Y, rho, C, and a denote the representative velocity of fragments of size s, a function with dimension of velocity, strength of the target, target density, sound velocity of the target, and the size of the projectile, respectively.
Author

N94-10014# Stuttgart Univ. (Germany). Inst. for Statics and Dynamics of Aerospace Structures.

DISTORTIONS AND STRESSES IN THIN SHELLS DUE TO ANISOTROPIC THERMAL EXPANSION

Manfred Koenig *In* ESA, Advanced Materials for Lightweight Structures Oct. 1992 p 79 Submitted for publication (For primary document see N94-10001 01-24)

Copyright Avail: CASI HC A01/MF A04

N94-10015# Rome Univ. (Italy). Dipt. Aerospaziale.

NUMERICAL SIMULATION AND EXPERIMENTAL RESULTS OF FILAMENT WOUND CFRP TUBES TESTED UNDER BIAXIAL LOAD

A. Amaldi, M. Giannuzzi (Ente Nazionale per l'Energia Elettrica, Rome, Italy.), M. Marchetti, and A. Miliozzi (Ente Nazionale per l'Energia Elettrica, Rome, Italy.) *In* ESA, Advanced Materials for Lightweight Structures Oct. 1992 p 81-86 (For primary document see N94-10001 01-24)

Copyright Avail: CASI HC A02/MF A04

N94-10016# Maschinenfabrik Augsburg-Nuernberg A.G., Munich (Germany).

ANALYTICAL PREDICTION AND TEST VERIFICATION OF THE MULTIAXIAL BEHAVIOUR OF HIGH-STRENGTH STEEL FOR LIGHTWEIGHT STRUCTURES

P. Agatonovic and U. Clormann *In* ESA, Advanced Materials for Lightweight Structures Oct. 1992 p 87-92 (For primary document see N94-10001 01-24)

Copyright Avail: CASI HC A02/MF A04

N94-10017# Technical Research Centre of Finland, Espoo. Metals Lab.

DESIGN WITH HIGH STRENGTH STEEL: A CASE OF FAILURE AND ITS IMPLICATIONS

Klaus Rahka *In* ESA, Advanced Materials for Lightweight Structures Oct. 1992 p 93-99 (For primary document see N94-10001 01-24)

Copyright Avail: CASI HC A02/MF A04

N94-10018# Societe Nationale de Construction Aeronautique, Gosselies (Belgium).

DEVELOPMENT OF A FATIGUE ANALYSIS APPROACH FOR CFRP STRUCTURES UNDER ACOUSTIC LOADING

S. Costantini *In* ESA, Advanced Materials for Lightweight Structures Oct. 1992 p 101-106 (For primary document see N94-10001 01-24)

Copyright Avail: CASI HC A02/MF A04

N94-10046# Maschinenfabrik Augsburg-Nuernberg A.G., Munich (Germany).

STRESS RELAXATION FORMING OF ARIANE 5 FRONT SKIRT OUTER SKIN PANELS

W. Radtke *In* ESA, Advanced Materials for Lightweight Structures Oct. 1992 p 267-269 (For primary document see N94-10001 01-24)

Copyright Avail: CASI HC A01/MF A04

N94-10056# Ceskoslovenska Akademie Ved, Prague. Central Lab. for Experimental Mechanics.

PERFORATED PLATES FOR THIN-WALLED STRUCTURES

M. Drdacky and J. Lesak *In* ESA, Advanced Materials for Lightweight

Structures Oct. 1992 p 333-337 Sponsored by Ministry for Economy and Industries (For primary document see N94-10001 01-24)
Copyright Avail: CASI HC A01/MF A04

N94-10057# Nauchno-Issledovatelskii Inst. Grafit, Moscow (Russia).
ADVANCED METHODS OF PERMANENTLY JOINING CARBON MATERIALS
L. T. Anikin, A. V. Demin, G. A. Kravetskiy, and V. I. Kostikov *In* ESA, Advanced Materials for Lightweight Structures Oct. 1992 p 339-342 Prepared in cooperation with Nauchno-Issledovatelskii Inst. Grafit USA Corp. and Nauchno-Issledovatelskii Inst. Grafit-Europa G.m.b.H., Germany (For primary document see N94-10001 01-24)
Copyright Avail: CASI HC A01/MF A04

N94-10066# Strathclyde Univ., Glasgow (Scotland).
FIBRE OPTIC STRAIN AND TEMPERATURE MEASUREMENT IN COMPOSITE MATERIALS: A REVIEW OF THE OSTIC PROGRAMME
Brian Culshaw and Craig Michie *In* ESA, Advanced Materials for Lightweight Structures Oct. 1992 p 393-398 Sponsored in part by Commission of the European Communities (For primary document see N94-10001 01-24)
Copyright Avail: CASI HC A02/MF A04

N94-11339# Deutsche Forschungs- und Versuchsanstalt fuer Luft- und Raumfahrt, Munich (Germany). Inst. of Aeroelasticity.
STRUCTURAL ANALYSIS AND OPTIMIZATION OF ADAPTIVE STRUCTURES BY USE OF THE FINITE ELEMENT METHOD
R. Lammering *In* AGARD, Smart Structures for Aircraft and Spacecraft Apr. 1993 11 p (For primary document see N94-11317 01-24)
Copyright Avail: CASI HC A03/MF A04

N94-12178*# POD Associates, Inc., Albuquerque, NM.
MODELLING HYPERVELOCITY IMPACTS INTO ALUMINUM STRUCTURES BASED ON LDEF DATA Abstract Only
C. R. Coombs, D. R. Atkinson, A. J. Watts, J. R. Wagner, M. K. Allbrooks, and C. J. Hennessy *In* Lunar and Planetary Inst., Twenty-fourth Lunar and Planetary Science Conference. Part 1: A-F 1993 p 331-332 (For primary document see N94-12015 01-91)
Avail: CASI HC A01/MF A06

42 GEOSCIENCES (GENERAL)

N94-11079# Meteorological Satellite Center, Tokyo (Japan).
METEOROLOGICAL SATELLITE CENTER Technical Note No. 26
Mar. 1993 62 p In ENGLISH and JAPANESE Original contains color illustrations
(MSC-TN-26) Avail: CASI HC A04/MF A01

Meteorological Satellite Center technical note is presented. Topics covered include: fine tuning of stretched-VISSR image mapping; simulation of images of 'water vapor channel' and 'infrared split channel'; statistical study on the regional and seasonal distribution of fog in the Far East region by using GMS imagery; and an overview of training seminar for the use of Japanese Earth Resources Satellite-1 (JERS-1) data. For individual titles, see N94-11080 through N94-11083.

N94-11080# Meteorological Satellite Center, Tokyo (Japan).
FINE TUNING OF STRETCHED-VISSR IMAGE MAPPING **c43**
Seiichiro Kigawa *In its* Meteorological Satellite Center Mar. 1993 p 1-10 (For primary document see N94-11079 01-42)
Avail: CASI HC A02/MF A01

Stretched-VISSR (Visible and Infrared Spin Scan Radiometer) image mapping error may increase after satellite orbit control (station-keeping maneuver) or satellite attitude control (attitude maneuver). To solve this problem, a fine tuning technique of the Stretched-VISSR image for user's computer systems was developed. This technique can be applied to both full disc images and half disc (Northern Hemisphere) images. The applicable theory and sample fine tuning programs written in FORTRAN are presented. Author (revised)

N94-11081# Meteorological Satellite Center, Tokyo (Japan).
SIMULATION OF IMAGES OF WATER VAPOR CHANNEL AND INFRARED SPLIT CHANNEL **c43**
Masami Tokuno *In its* Meteorological Satellite Center Mar. 1993 p 11-34 In JAPANESE (For primary document see N94-11079 01-42)
Avail: CASI HC A03/MF A01

An attempt to produce images of temperature fields simulated by the radiative transfer model (LOWTRAN-6) is performed. Two different types of images are produced. One is the water vapor image (Simulated Water Vapor, SWV image) based on temperatures calculated in the same wavelength as the water vapor channel (channel 12) of HIRS/2, and the other is the infrared split image (Simulated Split Pseudo color,SSP image) based on temperature difference (channel 4-5) calculated in the same wavelengths as the infrared split channels (channel 4 and 5) of Advanced Very High Resolution Radiometer (AVHRR) on NOAA-11. In the computation of the radiative transfer model, the following assumptions are made. Atmospheric vertical data (height, temperature, and humidity) provided by the numerical forecast division, JMA, are utilized. The lowest vertical level (1000 hPa) is assumed as the surface of the earth and its emissivity equal to unity. The filter functions of NOAA-11 HIRS channel 12, AVHRR channel 4 and 5 are assumed. Zenith angle is zero degrees. The following results are obtained by the comparison of the simulated images with the observed HIRS channel 12 (WV) image and AVHRR temperature difference (channel 4-5,SP) image. Warm regions relating to the dryness on the mid tropospheric layer are relatively well expressed on the SWV image. The boundary of temperature difference relating to the surface front and the regions with large temperature difference inferred to the moist regions of lower tropospheric layer are also relatively well expressed on the image. Author (revised)

N94-11082# Meteorological Satellite Center, Tokyo (Japan).
STATISTICAL STUDY ON THE REGIONAL AND SEASONAL DISTRIBUTION OF FOG IN THE FAR EAST REGION BY USING GMS IMAGERY **c47**
Motoi Matukawa *In its* Meteorological Satellite Center Mar. 1993 p 35-47 In JAPANESE (For primary document see N94-11079 01-42)
Avail: CASI HC A03/MF A01

Statistical investigation was made on the frequency of fog formations in the Far East region. The higher frequency regions are (1) the vicinity of Hokkaido and its eastern sea area, and (2) the southern part of China and the coastal area of middle China. In the region 1 it shows an annual variation (increasing in warm half year and decreasing in cold half year), but in region 2 peaks of the frequency appear in May, August, and December. Author (revised)

N94-11083# Meteorological Satellite Center, Tokyo (Japan).
OVERVIEW OF TRAINING SEMINAR FOR THE USE OF JAPANESE EARTH RESOURCES SATELLITE-1 (JERS-1) DATA **c43**
Haruo Taguchi *In its* Meteorological Satellite Center Mar. 1993 p 49-59 In JAPANESE (For primary document see N94-11079 01-42)
Avail: CASI HC A03/MF A01

The outline of the training seminar on the applications of JERS-1 data, which was held in Remote Sensing Technology Center of Japan (RESTEC) from 14-23 Oct. 1992 is shown. Author (revised)

N94-11674# California Univ., San Diego, La Jolla.
CENTRAL EQUATORIAL PACIFIC EXPERIMENT (CEPEX)
1993 182 p
(Contract DE-FG03-91ER-61198)
(DE93-011656; DOE/ER-61198/T2) Avail: CASI HC A09/MF A02

The Earth's climate has varied significantly in the past, yet climate records reveal that in the tropics, sea surface temperatures seem to have been remarkably stable, varying by less than a few degrees Celsius over geologic time. Today, the large warm pool of the western Pacific shows similar characteristics. Its surface temperature always exceeds 27 C, but never 31 C. Heightened interest in this observation has been stimulated by questions of global climate change and the exploration of stabilizing climate feedback processes. Efforts to understand the observed weak sensitivity of tropical sea surface temperatures to climate forcing has led to a number of competing ideas about the nature of this apparent thermostat. Although there remains disagreement on the processes that regulate tropical sea surface temperature, most agree that further progress in resolving these differences requires comprehensive field observations of three-dimensional water vapor concentrations, solar and infrared radiative fluxes, surface fluxes of heat and water vapor, and cloud microphysical properties. This document describes the Central Equatorial Pacific Experiment (CEPEX) plan to collect such observations over the central equatorial Pacific Ocean during March of 1993. DOE

N94-11894 Scientific Organizing Committee of PORSEC, Shizuoka (Japan).

PROCEEDINGS OF THE PORSEC 1992 IN OKINAWA: CONFERENCE FOR PACIFIC OCEAN ENVIRONMENTS AND PROBING, VOLUME 1

25 Aug. 1992 572 p Conference held in Okinawa, Japan, 25-31 Aug. 1992; sponsored by NASA, Intergovernmental Oceanographic Commission, Scientific Committee on Ocean Research, International Association of Meteorology and Atmospheric Physics, International Association for (JTN-93-80418) Copyright Avail: Issuing Activity (Scientific Organizing Committee of PORSEC, P.O. Box 10, Shimizu, Shizuoka 424, Japan, HC)

The following topics were discussed: remote sensing, ocean observation, satellite imagery, radar observations, satellite altimetry, sea states, sea roughness, ocean color, wind profiles, ocean temperature, ocean waves, ocean currents, streamers, air sea interactions, hydrological cycles, heat budgets, water vapors, heat flux, latent heat, suspended solids, phytoplankton, chlorophylls, oil slicks, atmospheric correction, cloud cover, ocean surface scattering, backscattering, radar cross section, underwater photogrammetry, underwater communication, numerical analysis, mathematical models, optical fibers, ocean color scanner, spectrometers, radiometers, echo sounders, Acoustic Doppler Current Profiler, and solar radiation. For individual titles, see N94-11895 through N94-11990.

N94-11895 Science Council of Japan, Tokyo.

REMOTE SENSING AND GLOBAL ENVIRONMENT c43

Jirou Kondou *In* Scientific Organizing Committee of PORSEC, Proceedings of the PORSEC 1992 in Okinawa: Conference for Pacific Ocean Environments and Probing, Volume 1 25 Aug. 1992 p 1-8 (For primary document see N94-11894 01-42)

Copyright Avail: Issuing Activity (Scientific Organizing Committee of PORSEC, P.O. Box 10, Shimizu, Shizuoka 424, Japan, HC)

Remote sensing is utilized extensively to monitor the global environment which is presently a big international issue. This paper discusses the application of remote sensing to obtain the data for various aspects of the global environment. This paper is intending to indicate as many examples as possible. Author (NASDA)

N94-11896 Tohoku Univ., Sendai (Japan). Dept. of Geophysics.

REMOTE SENSING AND THE AIR-SEA BOUNDARY LAYERS c43

Yoshiaki Toba *In* Scientific Organizing Committee of PORSEC, Proceedings of the PORSEC 1992 in Okinawa: Conference for Pacific Ocean Environments and Probing, Volume 1 25 Aug. 1992 p 9-14 (For primary document see N94-11894 01-42)

Copyright Avail: Issuing Activity (Scientific Organizing Committee of PORSEC, P.O. Box 10, Shimizu, Shizuoka 424, Japan, HC)

A review is given on characteristics of pure wind waves, which are coupling processes of the air and water turbulent boundary layers. A special reference is given to the dependence of the aerodynamic roughness length on sea state: a question to be solved in the near future for better remote sensing of the air-sea boundary. Author (NASDA)

N94-11897 Chiba Univ. (Japan). Dept. of Information and Computer Sciences.

A STATISTICAL METHOD TO DETERMINE AEROSOL PATH RADIANCE AND ITS APPLICATION TO ATMOSPHERIC CORRECTION FOR CZCS IMAGERY c46

Hua Qi, Kazuhiko Oonuma, and Yoshizumi Yasuda *In* Scientific Organizing Committee of PORSEC, Proceedings of the PORSEC 1992 in Okinawa: Conference for Pacific Ocean Environments and Probing, Volume 1 25 Aug. 1992 p 15-20 (For primary document see N94-11894 01-42)

Copyright Avail: Issuing Activity (Scientific Organizing Committee of PORSEC, P.O. Box 10, Shimizu, Shizuoka 424, Japan, HC)

An accurate method to eliminate the large signal component due to the atmospheric scattering is required to obtain quantitative ocean color measurement in remote sensing. The most widely used atmospheric correction for CZCS (Coastal Zone Color Scanner) sensor, proposed by Gordon et al. (1983, 1988), utilizes the 'clear water radiance concept' to determine the aerosol parameters which is the most important parameter. However, the 'clear water radiance concept' has been reported to be useless against a significant portion of Japanese CZCS data sets. This is considered to be due to a generally turbid atmosphere in the region. This paper is to examine a statistical method to obtain the aerosol parameter epsilon (lambda, 670) based on an idea that the aerosol scattering pattern has no correlation with the ocean color pattern. The method is applied to a sequence of CZCS imagery around Japan and the results are compared with the results given by the clear water method. The wavelength dependency of aerosol parameters is also discussed. Author (NASDA)

N94-11898 Fuyo Ocean Development and Engineering Co. Ltd., Tokyo (Japan).

EFFECTS OF WIND-ROUGHENED SEA SURFACE ON OCEAN COLOR REMOTE SENSING: NOISE DERIVED FROM REFLECTED LIGHT AND WHITECAPS c48

Susumu Kanno *In* Scientific Organizing Committee of PORSEC, Proceedings of the PORSEC 1992 in Okinawa: Conference for Pacific Ocean Environments and Probing, Volume 1 25 Aug. 1992 p 21-26 (For primary document see N94-11894 01-42)

Copyright Avail: Issuing Activity (Scientific Organizing Committee of PORSEC, P.O. Box 10, Shimizu, Shizuoka 424, Japan, HC)

Some problems in atmospheric correction of ocean color remote sensing which derived from reflection of incoming light by wind-roughened sea surface are discussed. Reflectance of ocean surface is calculated with the aid of wave slope distribution and effective reflectance of whitecaps. These effects are estimated as the error in retrievals of waterleaving radiance and phytoplankton pigment concentration. The error in retrieval increase with wind speed, solar position, and pigment concentration. Airborne remote sensing data is processed with the atmospheric correction algorithm including the effects of ruffled sea surface and compared with conventional one. The difference from the image of waterleaving radiance retrieved by conventional algorithm is clearly shown although little difference of phytoplankton pigment concentration appeared in each image. The proposed algorithm is particularly suited for the condition that wind speed, solar position, and pigment concentration are relatively high. Author (NASDA)

N94-11899 Institute of Ocean Sciences, Sidney (British Columbia).

SATELLITE OBSERVATIONS OF RED TIDE EVENTS: PLANS FOR EESI c48

J. F. R. Gower *In* Scientific Organizing Committee of PORSEC, Proceedings of the PORSEC 1992 in Okinawa: Conference for Pacific Ocean Environments and Probing, Volume 1 25 Aug. 1992 p 27-33 (For primary document see N94-11894 01-42)

Copyright Avail: Issuing Activity (Scientific Organizing Committee of PORSEC, P.O. Box 10, Shimizu, Shizuoka 424, Japan, HC)

A recent occurrence of a major red tide event on the west coast of Canada demonstrated the value of satellite images for mapping their occurrence and extent, but also showed the need for an improved satellite sensor. The EESI (Earth Environment Space Initiative) satellite, designed in Canada as part of the national space program, meets many of the requirements for studying such events. It is being designed to give wide-swath visible imagery having a spatial resolution intermediate between the AVHRR (Advanced Very High Resolution Radiometer) and the TM (Thematic Mapper), with near-daily coverage. Spectral band positions and sensitivities would be more suitable for water observations than those of either the TM or AVHRR. Author (NASDA)

N94-11900 Commission of the European Communities, Ispra (Italy). Inst. for Remote Sensing Applications.

AN ALGORITHM FOR THE DETECTION OF MUCILAGE (GREEN SLIME) IN THE ADRIATIC SEA c48

Stelvio Tassan *In* Scientific Organizing Committee of PORSEC, Proceedings of the PORSEC 1992 in Okinawa: Conference for Pacific Ocean Environments and Probing, Volume 1 25 Aug. 1992 p 34-39 (For primary document see N94-11894 01-42)

Copyright Avail: Issuing Activity (Scientific Organizing Committee of PORSEC, P.O. Box 10, Shimizu, Shizuoka 424, Japan, HC)

In the summer of 1989, an exceptional production of mucilaginous matter occurred in the Adriatic Sea, forming slimy patches driven around by winds and currents. The presence of this 'mucilage' spoiled the tourist season. The phenomenon, which depends on a combination of favorable meteorological conditions, is not rare in the area. Its identification by remote sensing techniques, beside being clearly useful for the timely organization of appropriate safeguard measures, may also help to identify the still unknown cause of the phenomenon. The Advanced Very High Resolution Radiometers (AVHRR) on board NOAA-10 and 11 cover the same zone of the earth twice a day (in daylight), providing time series of considerable value. This paper summarizes the results obtained in setting up an algorithm for mucilage monitoring which uses AVHRR data. An algorithm for mucilage detection using AVHRR data and including a cloud-screening routine was developed and tested versus sea truth provided by a TM (Thematic Mapper) scene. The algorithm seems to meet the prescribed reliability requirement over a large variety of atmospheric conditions. Apart from providing for mucilage identification, the algorithm also yields information on the mucilage density. The small computational effort required for the data analysis makes the procedure suitable for operational use. Author (NASDA)

N94-11901 Qingdao Inst. of Oceanology (China). Ocean Remote Sensing and Optics Lab.

REMOTE SENSING OF THE SUSPENDED MATTER DISTRIBUTION WITH HIGH CONCENTRATION IN CHINA SEA c48

Jun Ma, Xiao-Sheng Huang, Mao-Chong Shi, and Zhi-Shen Liu *In* Scientific Organizing Committee of PORSEC, Proceedings of the PORSEC 1992 in Okinawa: Conference for Pacific Ocean Environments and Probing, Volume 1 25 Aug. 1992 p 40-46 Sponsored by China National Foundation of Natural Science (For primary document see N94-11894 01-42)

Copyright Avail: Issuing Activity (Scientific Organizing Committee of PORSEC, P.O. Box 10, Shimizu, Shizuoka 424, Japan, HC)

The pattern recognition method has been successfully applied to remote sensing the suspended matter distribution with high concentration. Using multispectral radiance, the characteristic signature of suspended matter with characteristic vectors, and concentration of suspended matter with eigenvalues were depicted. This paper describes a characteristic vector analysis of 38 sea surface water reflectance spectra acquired from a ship in the mouth of Yellow River, China. Four vectors are sufficient to account for over 4 percent of the variance in all cases. Linear combinations of the scalar multipliers can be used to estimate the suspended matter content. A good correlation (correlation coefficient = 0.91) is obtained between them. Thematic Mapper data were analyzed for mapping the suspended matter distribution. The first vector appears to be dominated by the backscatter effects and the atmosphere effect is removed. Author (NASDA)

N94-11902 Ministry of Posts and Telecommunications, Okinawa (Japan). Okinawa Radio Observatory.

HF OCEAN RADAR SYSTEM AT OKINAWA RADIO OBSERVATORY c32

Hiroshi Kuroiwa, Yuuichi Oono, Yukiharu Hisaki, and Akitsugu Nadai *In* Scientific Organizing Committee of PORSEC, Proceedings of the PORSEC 1992 in Okinawa: Conference for Pacific Ocean Environments and Probing, Volume 1 25 Aug. 1992 p 47-52 (For primary document see N94-11894 01-42)

Copyright Avail: Issuing Activity (Scientific Organizing Committee of PORSEC, P.O. Box 10, Shimizu, Shizuoka 424, Japan, HC)

An HF (High Frequency) ocean radar has been developed at Okinawa Radio Observatory. This radar is the first ocean radar aiming at to be used for a remote sensor for the oceanography in Japan. The radar is the groundwave, narrow beam radar. The radar is FMICW (Frequency Modulated Interrupted Continuous Wave) radar with peak power 100 W. After 1988, several performance test observations have been done and it is confirmed that this HF ocean radar has a potential to measure the ocean current about 80 km range, the wave height up to about 30 km range, and wind direction. Another HF ocean radar having almost the same performance as the first radar has been developed for the precise measurement of the ocean current vector. Author (NASDA)

N94-11903 Ministry of Posts and Telecommunications, Okinawa (Japan). Okinawa Radio Observatory.

MEASUREMENT OF WAVE PARAMETERS BY HF OCEAN RADAR c48

Yukiharu Hisaki and Masayuki Tokuda (Kokusai Kogyo Co. Ltd., Tokyo, Japan.) *In* Scientific Organizing Committee of PORSEC, Proceedings of the PORSEC 1992 in Okinawa: Conference for Pacific Ocean Environments and Probing, Volume 1 25 Aug. 1992 p 53-58 (For primary document see N94-11894 01-42)

Copyright Avail: Issuing Activity (Scientific Organizing Committee of PORSEC, P.O. Box 10, Shimizu, Shizuoka 424, Japan, HC)

An approximate method to estimate wave parameters by HF (High Frequency) radar is investigated. The validity of the approximate method is examined by comparing the estimated wave parameters with in-situ observation. Wave height and period can be estimated with sufficient accuracy. But it is difficult to estimate wave direction precisely. Author (NASDA)

N94-11904 Ministry of Posts and Telecommunications, Okinawa (Japan). Okinawa Radio Observatory.

KUROSHIO OBSERVATIONS BY THE HF OCEAN RADAR c48

Yuuichi Oono and Masayuki Tokuda (Kokusai Kogyo Co. Ltd., Tokyo, Japan.) *In* Scientific Organizing Committee of PORSEC, Proceedings of the PORSEC 1992 in Okinawa: Conference for Pacific Ocean Environments and Probing, Volume 1 25 Aug. 1992 p 59-64 (For primary document see N94-11894 01-42)

Copyright Avail: Issuing Activity (Scientific Organizing Committee of PORSEC, P.O. Box 10, Shimizu, Shizuoka 424, Japan, HC)

Ocean currents observations in the Tokara strait were carried out at Yakushima and Tanegashima from October to December in 1990, using the HF (High Frequency) ocean radar which was developed by the Okinawa Radio Observatory of Communications Research Laboratory (CRL). It can measure the line-of-sight velocities of surface currents over the range of 50 km. Kuroshio are investigated from the time series of the current velocities over two months. The changes of the current velocities which might be caused by the moving of the location of Kuroshio are detected by the ocean radar. Author (NASDA)

N94-11905 Ministry of Posts and Telecommunications, Okinawa (Japan). Okinawa Radio Observatory.

STATISTICAL STUDY OF HF OCEAN RADAR ECHO c32

Akitsugu Nadai *In* Scientific Organizing Committee of PORSEC, Proceedings of the PORSEC 1992 in Okinawa: Conference for Pacific Ocean Environments and Probing, Volume 1 25 Aug. 1992 p 65-70 (For primary document see N94-11894 01-42)

Copyright Avail: Issuing Activity (Scientific Organizing Committee of PORSEC, P.O. Box 10, Shimizu, Shizuoka 424, Japan, HC)

The difference of surface velocities extracted from two first order echoes backscattered by approaching and leaving wave is studied statistically. The result is that the difference is smaller than the resolving power of HF (High Frequency) ocean radar, but some data shows a large difference. The studying of Doppler spectrum shows that the splitting of first-order echo is the reason of this large difference. Simple calculation shows the probability that the broadening and splitting of first-order echo is produced by the distribution of surface velocity in radar target cells. Author (NASDA)

N94-11906 James Cook Univ. of North Queensland, Townsville (Australia). Dept. of Physics.

GROUNDWAVE HF OCEAN SURFACE RADAR c32

M. L. Heron and N. R. McLaren *In* Scientific Organizing Committee of PORSEC, Proceedings of the PORSEC 1992 in Okinawa: Conference for Pacific Ocean Environments and Probing, Volume 1 25 Aug. 1992 p 71-75 (For primary document see N94-11894 01-42)

Copyright Avail: Issuing Activity (Scientific Organizing Committee of PORSEC, P.O. Box 10, Shimizu, Shizuoka 424, Japan, HC)

This paper reviews the performance of the James Cook University Coastal Ocean Surface Radar (COSRAD) system. COSRAD is an HF (High Frequency) ocean surface radar and has the advantage of a narrow steerable beam for both the transmit and receive functions. The operator can focus all the radar energy onto one sector. The transportable 30 MHz COSRAD system has been used in many locations and this is discussed showing measured currents in a coastal area where water quality is a concern. A long range groundwave radar has been tested in Australia. This system can observe surface currents and wave data beyond 200 km from the shore-based radar site. Design trade-offs in this system require a longer integration time on each viewing direction in order to achieve a constant resolution of surface current as lower HF radar frequencies are used to obtain longer ranges. Both of the existing systems, at 30 MHz and 6.77

MHz operating frequencies, have relatively coarse spatial resolution of approximately 2 km and 15 km respectively. The need often arises for a current mapping radar with finer spatial resolution to around 100 m. The Marine Radar Group at James Cook University are developing a VHF radar operating in the 150-200 MHz range. This system has a spatial resolution down to 100 m and an operating range of a few kilometers for observing surface currents. The Bragg resonant sea waves for this system are 0.75-1.0 m and the echo spectra are heavily modulated by swell and wing waves. Author (NASDA)

N94-11907 National Remote Sensing Agency, Hyderabad (India).

SATELLITE DERIVED SEA SURFACE TEMPERATURE APPLICATIONS FOR INDIAN OCEAN RESOURCES DEVELOPMENT **c48**

B. L. Deekshatulu, A. Narendra Nath, and M. V. Rao *In* Scientific Organizing Committee of PORSEC, Proceedings of the PORSEC 1992 in Okinawa: Conference for Pacific Ocean Environments and Probing, Volume 1 25 Aug. 1992 p 76-82 Sponsored by Dept. of Ocean Development (For primary document see N94-11894 01-42)

Copyright Avail: Issuing Activity (Scientific Organizing Committee of PORSEC, P.O. Box 10, Shimizu, Shizuoka 424, Japan, HC)

This paper describes the processing procedures of NOAA-AVHRR (Advanced Very High Resolution Radiometer) data for the retrieval of SSTs (Sea Surface Temperatures), validation of the satellite derived SSTs, and their oceanographic and fishery applications. In order to study the activities of monsoons, the oceanic response has been realized in the recent past. The very long coast line of India stretching about 7,500 km in length provides a unique opportunity for exploring the use of remote sensing technology for identifying Potential Fishing Zones (PFZs). The use of NOAA-AVHRR data by way of retrieving SSTs on near real time basis for forecasting PFZs is made operational during the fishing seasons along east and west coasts of India. The SST information is also being used to study the Indian summer monsoon vagaries. Satellite based potential fishing zones have resulted in three to four fold increase in the fish catch during the lean periods. The Somali current with its associated upwelling and the formation of two gyre system along Somali coast during summer monsoon 1991 have been discussed in relation to the variations of summer monsoonal rains over India. The NOAA-AVHRR derived SST information is found to be useful in identification of potential fishing zones and to study the monsoon vagaries over India. Author (NASDA)

N94-11908 Tohoku Univ., Sendai (Japan). Disaster Control Research Center.

EXCHANGE OF BAY WATER WITH OCEAN CURRENT MONITORED BY THE NOAA SATELLITE **c48**

Masayuki Nagao, N. Hashimoto, F. Imamura, and N. Shutou *In* Scientific Organizing Committee of PORSEC, Proceedings of the PORSEC 1992 in Okinawa: Conference for Pacific Ocean Environments and Probing, Volume 1 25 Aug. 1992 p 83-88 Sponsored by Ministry of Education, Science and Culture and Shizugawa Town Office (For primary document see N94-11894 01-42)

Copyright Avail: Issuing Activity (Scientific Organizing Committee of PORSEC, P.O. Box 10, Shimizu, Shizuoka 424, Japan, HC)

Sudden decreases in the water temperature at the bay head are explained as a result of the movement of ocean currents outside the bay, which is monitored by NOAA images and is confirmed to be more effective than other factors. Author (NASDA)

N94-11909 Nihon Univ., Tokyo (Japan). Dept. of Fisheries.

A CONSIDERATION ON PRINCIPAL COMPONENT ANALYSIS OF SATELLITE IR DATA **c43**

H. Shinomiya, F. Inoue (Nihon Univ., Funabashi, Japan.), A. Itou (Nihon Univ., Funabashi, Japan.), Hideo Tameishi (Japan Fisheries Information Service Center, Tokyo.), Hiromichi Yamamoto (National Aerospace Lab., Tokyo, Japan.), and Masao Naka (National Aerospace Lab., Tokyo, Japan.) *In* Scientific Organizing Committee of PORSEC, Proceedings of the PORSEC 1992 in Okinawa: Conference for Pacific Ocean Environments and Probing, Volume 1 25 Aug. 1992 p 89-94 (For primary document see N94-11894 01-42)

Copyright Avail: Issuing Activity (Scientific Organizing Committee of PORSEC, P.O. Box 10, Shimizu, Shizuoka 424, Japan, HC)

In the field of fisheries, NOAA/AVHRR (Advanced Very High Resolution Radiometer) imageries have become widely used for detecting fishing grounds through fishery-aid charts. However, more expert knowledge and experience are needed to complete a more detailed chart. A computer-processed fishery and oceanographic condition chart using satellite information have been studied. In this paper, the use of PCA (Principal Component Analysis) for IR (Infrared) data is discussed. First, calculate the SST (Sea Surface Temperature) gradients in four directions per pixel in AVHRR imagery. Then, obtain four values for all pixels in an area and carry out a PCA using these data. The maximum eigenvector of first principal component should signify the direction and value of major SST gradients in the area. Thus, the key vector can provide with a distribution of major water masses for some area data and their continuity or movement for time-series area data. Furthermore, the first principal component score chart for each pixel must enable us to estimate the oceanographic characteristics in the area. These features are considered to be useful for modeling oceanographic conditions from satellite imagery data using AI (Artificial Intelligence). Author (NASDA)

N94-11910 Ryukyu Univ., Okinawa (Japan).

TROUBLE AREAS IN THE IRT MEASUREMENT OF THE EARTH SURFACE TEMPERATURE **c43**

Suguru Ishijima *In* Scientific Organizing Committee of PORSEC, Proceedings of the PORSEC 1992 in Okinawa: Conference for Pacific Ocean Environments and Probing, Volume 1 25 Aug. 1992 p 95-99 (For primary document see N94-11894 01-42)

Copyright Avail: Issuing Activity (Scientific Organizing Committee of PORSEC, P.O. Box 10, Shimizu, Shizuoka 424, Japan, HC)

Trouble areas encountered when measuring the earth surface temperature by using the Infrared Radiation Thermometer (IRT) from a low elevation near the ground are described. The result of some testing cases of the sea surface temperature using a spot type IRT is presented and the trouble areas involved in verifying the observed result are discussed. Author (NASDA)

N94-11911 Japan Marine Science and Technology Center, Tokyo.

CURRENT STRUCTURES IN THE WESTERN EQUATORIAL PACIFIC DURING JAPACS CRUISES **c48**

Yoshifumi Kuroda, Kentarou Andou, Kei Muneyama, and Michael J. McPhaden (National Oceanic and Atmospheric Administration, Seattle, WA.) *In* Scientific Organizing Committee of PORSEC, Proceedings of the PORSEC 1992 in Okinawa: Conference for Pacific Ocean Environments and Probing, Volume 1 25 Aug. 1992 p 100-105 Sponsored by Science and Technology Agency (For primary document see N94-11894 01-42)

Copyright Avail: Issuing Activity (Scientific Organizing Committee of PORSEC, P.O. Box 10, Shimizu, Shizuoka 424, Japan, HC)

The RV (Research Vessel) Natsushima of Japan Marine Science and Technology Center (JAMSTEC) made two cruises in the equatorial Pacific in January-February 1989 and in January-February 1990 as part of the Japanese Pacific Climate Study (JAPACS) program. These cruises spanned the central and western Pacific along the equator to sample conditions in both the equatorial cold tongue east of the dateline and conditions in the warm pool west of the dateline. Cruise in 1989 was performed during predominant La Nina conditions in which the SOI (Southern Oscillation Index) showed largest positive anomaly since 1976, and cruise in 1990 during El Nino like conditions in which the SOI showed extremely negative. The surface wind, temperature, salinity, and current data set along the equator obtained in these cruises enabled us to depict uniquely the oceanic response in the context of El Nino and Southern Oscillation. Author (NASDA)

N94-11912 National Inst. of Oceanography, Goa (India).

ACOUSTIC WAVEGUIDE CHARACTERISTICS OF THE INDIAN OCEAN NORTH OF EQUATOR **c48**

S. Prasanna Kumar, T. V. Ramana Murty, Y. K. Somayajulu, and C. S. Murty *In* Scientific Organizing Committee of PORSEC, Proceedings of the PORSEC 1992 in Okinawa: Conference for Pacific Ocean Environments and Probing, Volume 1 25 Aug. 1992 p 106-111 Sponsored by Dept. of Ocean Development (For primary document see N94-11894 01-42)

Copyright Avail: Issuing Activity (Scientific Organizing Committee of PORSEC, P.O. Box 10, Shimizu, Shizuoka 424, Japan, HC)

The acoustic characteristics of the waters of the Arabian Sea and Bay of Bengal, constituting the northern Indian Ocean, are analyzed based on a climatological mean sound speed field. In the upper 30-40 m in the Bay of Bengal, a weak surface duct is noticed. The depth of the SOFAR (Sound Fixing and Ranging) axis varies from 1,400-1,950 m in the Arabian Sea and from 1,100-1,750 m in the Bay of Bengal. While the depth of the SOFAR axis increases towards the northern latitudes in the Arabian Sea, it decreases in the Bay of Bengal. The axial sound speed varies from 1,492-1,496 m/s in the Arabian Sea and from 1,492-1,494 m/s in the Bay of Bengal. A feature important and common to both Arabian Sea and Bay of Bengal is the depth limited nature of the sound speed profile. As a consequence the effective waveguide lies much below the sea surface (100-300 m). The acoustic ray arrival pattern, obtained from ray computations, reveals that rays with emergence angles between 6.5 and 7.5 deg in the Arabian Sea reach the receiver first followed by the flat angle rays and steep RBR (Refracted Bottom-Reflected) rays. In the Bay of Bengal, flat angle rays reach faster than the purely refracted steep angle rays. This arrival pattern is, due to the presence of a weak acoustic waveguide in the northern Indian Ocean, contrary to the arrival sequences reported for the Atlantic and the Pacific Oceans. Author (NASDA)

N94-11913 Hiroshima Univ. (Japan). Faculty of Engineering.

ONE-YEAR MOORING OF AN ADCP IN THE CENTRAL REGION OF THE KUROSHIO WEST OF OKINAWA **c48**

Hideo Nakajima, Arata Kaneko, Noriaki Gouda, Kazuo Kawatate (Kyushu Univ., Fukuoka, Japan.), and Shinjirou Mizuno (Kyushu Univ., Fukuoka, Japan.) *In* Scientific Organizing Committee of PORSEC, Proceedings of the PORSEC 1992 in Okinawa: Conference for Pacific Ocean Environments and Probing, Volume 1 25 Aug. 1992 p 112-115 (For primary document see N94-11894 01-42)

Copyright Avail: Issuing Activity (Scientific Organizing Committee of PORSEC, P.O. Box 10, Shimizu, Shizuoka 424, Japan, HC)

A first long-term profiling measurement of the Kuroshio has been carried out by using a moored ADCP (Acoustic Doppler Current Profiler) in the central region of the Kuroshio west of Okinawa during the period of December 1989 to November 1990. A clear spectral peak related to the cross-streamwise movement of the Kuroshio axis was found to form at the period of 15 days. The monthly mean currents showed a remarkable slackening of magnitude in the surface layer especially in the period of August to November in 1990. On the basis of the EOF (Empirical Orthogonal Function) analysis, it is suggested that the slackening of the Kuroshio in the surface layer is replaced by the generation of wind-driven currents in this layer. Author (NASDA)

N94-11914 Hiroshima Univ. (Japan). Faculty of Engineering.

ACOUSTIC DOPPLER CURRENT PROFILING OF THE KUROSHIO OVER THE EAST CHINA SEA SHELF SLOPE **c48**

Noriaki Gouda, Arata Kaneko, Kazuo Kawatate (Kyushu Univ., Fukuoka, Japan.), and Shinjirou Mizuno (Kyushu Univ., Fukuoka, Japan.) *In* Scientific Organizing Committee of PORSEC, Proceedings of the PORSEC 1992 in Okinawa: Conference for Pacific Ocean Environments and Probing, Volume 1 25 Aug. 1992 p 116-119 (For primary document see N94-11894 01-42)

Copyright Avail: Issuing Activity (Scientific Organizing Committee of PORSEC, P.O. Box 10, Shimizu, Shizuoka 424, Japan, HC)

A bottom-moored ADCP (Acoustic Doppler Current Profiler) was recovered successfully after continuous use during December 1990 to November 1991 in the Kuroshio on the East China Sea shelf slope. The raw ADCP data sampled every one hour with a depth bin of 8 m were smoothed through a filter of one month. The current flowing to the northeast along the isobathes showed vertical profiles of decreasing linearly from the surface to bottom. In August, the northeast current was confined to the upper 200 m of water and the weak reverse current formed in the deeper water. The near-bottom current perpendicular to the isobathes was directed to climb down the East China Sea shelf slope. Author (NASDA)

N94-11915 University of Electro-Communications, Chofu (Japan).

MEASUREMENT OF THE SURFACE LAYER CURRENT AVERAGED VERTICALLY USING MULTIPATHS INVERTED ECHOSOUNDER **c48**

Tomoyoshi Takeuchi and Keisuke Taira (Tokyo Univ., Japan.) *In* Scientific Organizing Committee of PORSEC, Proceedings of the PORSEC 1992 in Okinawa: Conference for Pacific Ocean Environments and Probing, Volume 1 25 Aug. 1992 p 120-125 (For primary document see N94-11894 01-42)

Copyright Avail: Issuing Activity (Scientific Organizing Committee of PORSEC, P.O. Box 10, Shimizu, Shizuoka 424, Japan, HC)

A Multipaths Inverted Echo Sounder (MIES) was developed and tested for measuring vertical average currents by accurately measuring time differences for sound wave to travel in two opposite directions along a path in the ocean. The acoustic path's 'sing around' vertical triangle, with a base of approximately 10 km long, and the time differences determine the horizontal component of velocity averaged through the water column. The field tests were conducted by using two MIES. Each MIES provides the function of transponder and records all data. The results of the field tests are presented and discussed. Author (NASDA)

N94-11916 Japan Marine Science and Technology Center, Tokyo.

ACOUSTIC CHARACTERISTICS OF SIDE SCAN SONAR AND SUB-BOTTOM PROFILER FOR 10,000 m CLASS ROV **c35**

Toshiaki Nakamura, Toshio Tsuchiya, Yasutaka Amitani, and Hideharu Morimatsu (Furuno Electric Co. Ltd., Nishinomiya, Japan.) *In* Scientific Organizing Committee of PORSEC, Proceedings of the PORSEC 1992 in Okinawa: Conference for Pacific Ocean Environments and Probing, Volume 1 25 Aug. 1992 p 126-131 (For primary document see N94-11894 01-42)

Copyright Avail: Issuing Activity (Scientific Organizing Committee of PORSEC, P.O. Box 10, Shimizu, Shizuoka 424, Japan, HC)

A side scan sonar, a sub-bottom profiler system for the 10,000 m class ROV (Remotely Operated Vehicle), was developed to observe both surface and sedimentary layers of several thousand meters in depth. The side scan sonar has two transducers with the frequency of 38 and 42 kHz in each side of the ROV. Acoustic imaging of the sea bottom of 1 km width in each side was obtained with the use of 2 deg beam width transducer. Using a parametric array, a technology of the nonlinear acoustics in the sub-bottom profiler, we realized a very narrow beam width of 5 degrees with the frequency of 3.5 kHz. In this report, acoustic characteristics of this equipment are measured in a water tank and experimental results in shallow water are shown. Author (NASDA)

N94-11917 Japan Marine Science and Technology Center, Tokyo.

STUDY ON COLOR VIDEO PICTURES TRANSMISSION BY DIGITAL ACOUSTIC SIGNAL **c32**

Hiroshi Ochi, Toshio Tsuchiya, Yasutaka Amitani, Michiya Suzuki (Nippon Electric Co. Ltd., Japan.), and Satoru Negishi (Nippon Electric Co. Ltd., Japan.) *In* Scientific Organizing Committee of PORSEC, Proceedings of the PORSEC 1992 in Okinawa: Conference for Pacific Ocean Environments and Probing, Volume 1 25 Aug. 1992 p 132-137 (For primary document see N94-11894 01-42)

Copyright Avail: Issuing Activity (Scientific Organizing Committee of PORSEC, P.O. Box 10, Shimizu, Shizuoka 424, Japan, HC)

A high-speed and reliable video transmission system of color pictures from an underwater vehicle to a sea surface vessel by digital acoustic signal has been developed for real-time deep-sea viewing on the support vessel. The color video picture transmission by a digital acoustic signal has been studied, and it achieved good results in the transmission from 3,500 m depth in 1988. Then based on these studies, Japan Marine Science and Technology Center (JAMSTEC) has produced the practical system for the deep-sea submergible 'Shinkai 6500' and its support vessel 'Yokosuka' (6.5 K system). A sea trial of the system was carried out at the Ryukyu trench (about 6,500 m depth) in March 1992, and the clear video picture of the sea bottom on 'Yokosuka' was succeeded to receive at a rate of 8 seconds per a frame. Author (NASDA)

N94-11918 Florida State Univ., Tallahassee. Mesoscale Air-Sea Interaction Group.

VARIABILITY OF WIND STRESS, AND SENSIBLE AND LATENT HEAT FLUX IN THE NORTH ATLANTIC DURING SEASAT **c48**

David M. Legler and James J. OBrien *In* Scientific Organizing Committee of PORSEC, Proceedings of the PORSEC 1992 in Okinawa: Conference for Pacific Ocean Environments and Probing, Volume 1 25 Aug. 1992 p 138-143 (For primary document see N94-11894 01-42)

Copyright Avail: Issuing Activity (Scientific Organizing Committee of PORSEC, P.O. Box 10, Shimizu, Shizuoka 424, Japan, HC)

The focus of this research is on utilizing all available data (remotely sensed and in-situ) to objectively produce ocean-atmosphere fluxes of momentum and latent and sensible heat to serve as forcing fields as well as guides for model products and by-products. A variational objective analysis technique is used to operate on all available in-situ as well as remotely sensed wind, temperature, and humidity data to calculate surface flux fields of wind stress and sensible and latent heat flux during the SEASAT mission. The technique forces interdependencies amongst the fluxes so that the resultant fields of winds, temperatures, humidity, and momentum as well as heat fluxes are consistent with the bulk formulations as well as with each other. Thus, the resulting maps not only include fluxes, but the component fields as well. This analysis has been completed for the north Atlantic region during the 5 day SEASAT mission. Results from the investigation of the temporal and spatial variability of the wind stress and heat flux fields are presented. Author (NASDA)

N94-11919* Jet Propulsion Lab., California Inst. of Tech., Pasadena.
EVAPORATION AND THERMAL/HYDROLOGIC BALANCE IN THE PACIFIC
W. Timothy Liu *In* Scientific Organizing Committee of PORSEC, Proceedings of the PORSEC 1992 in Okinawa: Conference for Pacific Ocean Environments and Probing, Volume 1 25 Aug. 1992 p 144-149 Sponsored by NASA, Washington (For primary document see N94-11894 01-42)
Copyright Avail: Issuing Activity (Scientific Organizing Committee of PORSEC, P.O. Box 10, Shimizu, Shizuoka 424, Japan, HC)

Spaceborne microwave radiometers have provided accurate observations of water vapor over the oceans. Water vapor is an important greenhouse gas. At periods longer than a week, the column-integrated water vapor is found to be closely related to surface level humidity which is needed to compute evaporation from the ocean. Evaporation and precipitation derived from satellite data were combined to approximate hydrologic forcing on the ocean. The forcing was found to agree with the climatological seasonal distribution of surface salinity. Sea surface temperature as a determining factor in evaporation change was examined but no significant positive contemporary correlation was found: higher sea surface temperature does not necessarily correspond to high evaporation. However, significant negative lag correlations were found: increase in evaporation lowers sea surface temperature a few months later in most of the ocean. There is a strong relation between greenhouse effect and the water vapor in the atmosphere over most of the tropical and mid-latitude oceans, but the relation is not as simple as previously prescribed. Exceptions were found in the equatorial regions where temporal correlations between water vapor and sea surface temperature are low, and in high latitudes where the annual cycles of greenhouse effect are out of phase with sea surface temperature. Author (NASDA)

N94-11920 National Centre for Science Information Systems, Tokyo (Japan).
A NEW EXPRESSION FOR THE PRODUCTION RATE OF SEA WATER DROPLETS ON THE SEA SURFACE **c48**
Noriko Iida, Yoshiaki Toba (Tohoku Univ., Sendai, Japan.), and Masaaki Chaen (Kagoshima Univ., Japan.) *In* Scientific Organizing Committee of PORSEC, Proceedings of the PORSEC 1992 in Okinawa: Conference for Pacific Ocean Environments and Probing, Volume 1 25 Aug. 1992 p 150-155 (For primary document see N94-11894 01-42)
Copyright Avail: Issuing Activity (Scientific Organizing Committee of PORSEC, P.O. Box 10, Shimizu, Shizuoka 424, Japan, HC)

A new set of empirical formulas for the production rate and the number concentration of seawater droplets on the sea surface are proposed, synthesizing past observation data of sea-salt particles in the sea and water droplets in wind-wave tanks. A new level z(sub c) is introduced as the effective wind-sea surface where sea-water droplets are produced. The new formulas are expressed in linear functions in logarithmic scales of u(sub *)(exp 2)/nu sigma(sub p), a parameter to describe overall conditions of air-sea boundary processes, where u(sub *) is the friction velocity of air, nu the kinematic viscosity of air, and sigma(sub p) the peak angular frequency of wind-wave part of wave spectra. A model of coexistence of spray droplets and suspended particles near the sea surface is proposed. As for the independent parameter, a comparison between the uses of u(sub *)(exp 2)/nu sigma(sub p) and u(sub *)(exp 3), which was the traditional way of parameterization excluding wave measure, shows that the advantage of using u(sub *)(exp 2)/nu sigma(sub p) is statistically significant with a confidence limit of 89% in F-test. Author (NASDA)

N94-11921 Tokyo Univ. (Japan). Center for Climate System Research.
EVALUATION OF ECMWF LATENT HEAT FLUX IN TOGA CD-ROM **c48**
Riko Yamane and Akimasa Sumi *In* Scientific Organizing Committee of PORSEC, Proceedings of the PORSEC 1992 in Okinawa: Conference for Pacific Ocean Environments and Probing, Volume 1 25 Aug. 1992 p 156-160 (For primary document see N94-11894 01-42)
Copyright Avail: Issuing Activity (Scientific Organizing Committee of PORSEC, P.O. Box 10, Shimizu, Shizuoka 424, Japan, HC)

A feature of latent heat flux data in TOGA (Tropical Ocean Global Atmosphere) CD-ROM which was given by the ECMWF (European Center for Medium Range Weather Forecasts) has been investigated for different time scales with emphasis on the tropical ocean. For a monthly-mean time scale, the magnitude is smaller than climatology in the Pacific Ocean, probably because wind fields of the ECMWF model is weaker than the nature. For a synoptic time scale, it can qualitatively represent the fluctuations associated with tropical disturbances of 2,000 km scale. It is concluded that latent heat flux estimated by numerical models can be used in a qualitative sense for studying a behavior of disturbances over the tropical ocean. Author (NASDA)

N94-11922* Jet Propulsion Lab., California Inst. of Tech., Pasadena.
AIR-SEA FLUXES AND UNIVERSAL CONSTANTS IN WEAK-TURBULENCE THEORY OF SURFACE GRAVITY WAVES **c46**
Roman E. Glazman *In* Scientific Organizing Committee of PORSEC, Proceedings of the PORSEC 1992 in Okinawa: Conference for Pacific Ocean Environments and Probing, Volume 1 25 Aug. 1992 p 161-165 Sponsored by NASA, Washington and ONR (For primary document see N94-11894 01-42)
Copyright Avail: Issuing Activity (Scientific Organizing Committee of PORSEC, P.O. Box 10, Shimizu, Shizuoka 424, Japan, HC)

For a statistically stationary wave field, analysis of wind-to-wave energy and momentum exchanges is carried out by employing integrated equations of wave action, energy, and momentum transfer. Equilibrium range of wave spectra is presented by a power law in which the effective exponent and the Phillips constant depend on the wave age. Two regimes of wind-wave interactions are identified: the regime in which the direct energy cascade through the wave spectrum is a dominant factor of wave dynamics and that in which the inverse cascade dominates. For the latter case, the present understanding of wave dynamics appears to be insufficient. Finally, the drag coefficient is inferred from the momentum balance equation and shown to exhibit the wave-age dependence observed in field experiments. Energy and momentum transfer coefficients from wind to waves are estimated indirectly by comparing theoretical behavior with field observations. One of the conclusions is that the main sink of energy and momentum may be associated with larger-scale motions excited by the wave field, rather than with small scale breaking waves. Author (NASDA)

N94-11923 Ryukyu Univ., Okinawa (Japan). Dept. of Marine Sciences.
SEA SURFACE HEAT FLUX IN THE BEGINNING OF THE KUROSHIO **c48**
Momoki Koga *In* Scientific Organizing Committee of PORSEC, Proceedings of the PORSEC 1992 in Okinawa: Conference for Pacific Ocean Environments and Probing, Volume 1 25 Aug. 1992 p 166-170 Sponsored by Ministry of Education, Science and Culture (For primary document see N94-11894 01-42)
Copyright Avail: Issuing Activity (Scientific Organizing Committee of PORSEC, P.O. Box 10, Shimizu, Shizuoka 424, Japan, HC)

The direct measurement of the sea surface heat flux was started in October 1990 using automatic weather-station system. The measuring system is set on a ferryboat between Okinawa and Taiwan (the beginning region of the Kuroshio). Using the measured data (one year) and additional data from the logbook of the ferryboat in recent five years (1986-1990), the seasonal and spatial (mesoscale) variability of the surface heat flux in this region is discussed. The GMS (Geostationary Meteorological Satellite)-visible image data is also used in conjunction with the field data to estimate the spatial distribution of the solar radiation. Author (NASDA)

N94-11924 Tokyo Univ. (Japan). Ocean Research Inst.
SEASONAL VARIATION OF THE SURFACE MIXED LAYER IN THE SUBTROPICAL RE-CIRCULATION AREA OF THE NORTH PACIFIC DURING OMLET **c48**

Hirotaka Otobe, Keisuke Taira, and Tomio Asai *In* Scientific Organizing Committee of PORSEC, Proceedings of the PORSEC 1992 in Okinawa: Conference for Pacific Ocean Environments and Probing, Volume 1 25 Aug. 1992 p 171-176 (For primary document see N94-11894 01-42)
Copyright Avail: Issuing Activity (Scientific Organizing Committee of PORSEC, P.O. Box 10, Shimizu, Shizuoka 424, Japan, HC)

Seasonal variation of the heat balance in the surface mixed layer in the vicinity of the former OWS-T (Ocean Weather Station 'Tango') south of Japan where a large amount of heat transported by the Kuroshio is distributed by three dimensional processes in the sea and transferred to the atmosphere was studied during OMLET (Ocean Mixed Layer Experiment) which is an oceanographic component of the Japanese WCRP (World Climate Research Program). Four time series, total 669 days, of temperature and currents data in the upper ocean were collected from a surface moored buoy system for the periods of April 18, 1988 to November 2, 1988 (OMLET88), August 12, 1989 to February 26, 1990 (OMLET89), April 18, 1990 to September 8, 1990 (OMLET901), and September 9, 1990 to January 15, 1991 (OMLET902). In this paper, the moored data of upper 100 m for the later three time series (OMLET89, 901, 902) were analyzed and the heat balances were discussed. A large fluctuation of oceanic convergence/divergence, 200-300 Watt/sq m in amplitude and predominant periodicity of 20-30 days, occurred in the early half period of OMLET89 when it was early in the formation process of a large meander path of the Kuroshio. A large amount of heat convergence of 60, 71, and 15 Watt/sq m in the average over each period was estimated, respectively. It was found that those variations of oceanic heat convergence in this region were closely related to the behavior of the Kuroshio axis south of Japan.
Author (NASDA)

N94-11925 Tokai Univ., Shizuoka (Japan). School of Marine Sciences and Technology.
MIXED LAYER HEAT BUDGET OF KUROSHIO-TANGO TRIANGLE USING SATELLITE AND SHIP OBSERVATIONS c48
Pankajakshan Thadathil (National Inst. of Oceanography, Goa, India.), Masatoshi Akiyama, Yasuhiro Sugimori, Jun Suwa, Y. Okada, and A. Siripong *In* Scientific Organizing Committee of PORSEC, Proceedings of the PORSEC 1992 in Okinawa: Conference for Pacific Ocean Environments and Probing, Volume 1 25 Aug. 1992 p 177-183 Sponsored by Ministry of Education, Science and Culture (For primary document see N94-11894 01-42)
Copyright Avail: Issuing Activity (Scientific Organizing Committee of PORSEC, P.O. Box 10, Shimizu, Shizuoka 424, Japan, HC)

Using a three dimensional heat flux model, variation of heat storage in the mixed layer of a triangular oceanic area, embedded in the Kuroshio has been studied for a period of a few days in the month of November, 1983. For the estimation of vertical heat flux across the air-sea boundary, both satellite (NIMBUS-7 SMMR (Scanning Multichannel Microwave Radiometer)) and ship observations are used. The advective fluxes across the lateral boundaries of the system are derived from sequential images of AVHRR (Advanced Very High Resolution Radiometer). The net heat divergence of the triangular system is obtained as the residual of these computed estimates of vertical and advective fluxes. The net heat loss of the system from heterogeneous data sets (ship and satellite) is found to be 4.8 times 10(exp 13) W. Whereas, using only ship observations, the net heat loss is found to be 2.3 times 10(exp 13) W. It is presumed that this observed difference in the two separate budgets is imparted through the better spatial resolution of SMMR derived wind speed and precipitable water.
Author (NASDA)

N94-11926 Kunsan National Fisheries Junior Coll. (Republic of Korea).
ESTIMATION OF SOLAR RADIATION AT THE SEA SURFACE WITH GEOSTATIONARY METEOROLOGICAL SATELLITE DATA c46
Young Seup Kim and Ryuuji Kimura (Tokyo Univ., Japan.) *In* Scientific Organizing Committee of PORSEC, Proceedings of the PORSEC 1992 in Okinawa: Conference for Pacific Ocean Environments and Probing, Volume 1 25 Aug. 1992 p 184-188 (For primary document see N94-11894 01-42)
Copyright Avail: Issuing Activity (Scientific Organizing Committee of PORSEC, P.O. Box 10, Shimizu, Shizuoka 424, Japan, HC)

Two methods to estimate solar radiation over oceans near Japan with Japanese Geostationary Meteorological Satellite (GMS) are presented. One is the estimate by means of cloud amount derived from cloud imagery by GMS. An empirical formula that connects the solar radiation at the sea surface with cloud amount estimated by the satellite is proposed. The other is the estimate based on histogram data of T(sub BB) (Blackbody Temperature) at cloud top. It was found that reduction rate due to high-level clouds is greater than that due to low-level clouds, suggesting that information of cloud height is needed in addition to total cloud amount to make better estimates of solar radiation at the surface. Author (NASDA)

N94-11927 National Aeronautics and Space Inst., Bandung (Indonesia).
THE USE OF REMOTE SENSING DATA FOR COASTAL ZONE MANAGEMENT AND ENVIRONMENT IN INDONESIA c48
Suharso Martadiwirya and Bidawi Hasyim *In* Scientific Organizing Committee of PORSEC, Proceedings of the PORSEC 1992 in Okinawa: Conference for Pacific Ocean Environments and Probing, Volume 1 25 Aug. 1992 p 189-192 (For primary document see N94-11894 01-42)
Copyright Avail: Issuing Activity (Scientific Organizing Committee of PORSEC, P.O. Box 10, Shimizu, Shizuoka 424, Japan, HC)

As an archipelagic country, Indonesia has a total coastline length of 81,000 km consisting of mangrove forest and potential areas for fishponds which plays an important role in the economical aspect of the National Development Program. By using LANDSAT-MSS (Multi Spectral Scanner) data from the existing ground station, studies on coastal resources and mangrove forest change and their impact on coastal environment have been conducted.
Author (NASDA)

N94-11928 National Center for Scientific Research of Vietnam, Hanoi.
SHORELINE CHANGE DETECTION USING REMOTE SENSING AND GIS IN VIETNAM c43
Pham Trung Luong and To Quang Thinh *In* Scientific Organizing Committee of PORSEC, Proceedings of the PORSEC 1992 in Okinawa: Conference for Pacific Ocean Environments and Probing, Volume 1 25 Aug. 1992 p 193-198 Prepared in cooperation with State Dept. for Geodesy and Cartography, Vietnam (For primary document see N94-11894 01-42)
Copyright Avail: Issuing Activity (Scientific Organizing Committee of PORSEC, P.O. Box 10, Shimizu, Shizuoka 424, Japan, HC)

Vietnam has more than 3,200 km of shoreline, the problems of coastal and marine management are of major concern. The objectives of this study is to develop technology procedure of application of remote sensing and GIS (Global Information System) to shoreline change detection and to shoreline change map for entire Vietnam coastline as well as for most important estuaries in Red and Mekong river plains for period from 1930 to present. The multidate Vietnam shoreline maps on scale 1/250,000 produced from remote sensing data such as LANDSAT, SPOT, and Soyuz combined with other data sources and national topographic maps established in 1930 and other time at scale 1/100,000 were digitized and brought in to GIS, which is developed by Remote Sensing Application Division, for PC (Personal Computer) based system. The shoreline change analysis for period 1930-1965, 1965-1986 was carried out with some quantitative estimations by GIS-multilayer overlay technique. Based on obtained analysis results, all Vietnam shoreline has been classified as the following: accretion, erosion, mixed and permanent. The obtained results are not only used for a scientific purpose but are also used as data base components for coastal management in Vietnam. They show that shoreline problems could be successfully solved by using remote sensing and GIS. Author (NASDA)

N94-11929 Allan (T. D.) Associates, Godalming (England).
THE REQUIREMENT FOR GLOBAL TRAINING PROGRAMMES TO MEET THE NEW REMOTE SENSING TECHNOLOGY c43
T. D. Allan *In* Scientific Organizing Committee of PORSEC, Proceedings of the PORSEC 1992 in Okinawa: Conference for Pacific Ocean Environments and Probing, Volume 1 25 Aug. 1992 p 199-204 (For primary document see N94-11894 01-42)
Copyright Avail: Issuing Activity (Scientific Organizing Committee of PORSEC, P.O. Box 10, Shimizu, Shizuoka 424, Japan, HC)

An overview of the offshore application of satellite data (for such purposes as monitoring and protecting marine environment), the development of marine science training to produce highly-skilled specialists, access to satellite data, necessity of in-situ measurement by ships and buoys to enhance the effectiveness of the remote sensing, and remote sensing educational programs in the developing countries is presented. The conclusions are as follows: (1) oceanographers familiar with remote sensing should communicate their progress to others; (2) up-to-date, in-country

teaching and training applicable to the region should be implemented; (3) training should not be limited to professional maritime scientists but should also aim to make the administrators and program managers be aware of potential benefits of remote sensing; (4) space agencies should cooperate with science agencies to create a proper structure to widen the 'user community' of satellite data; and (5) a small fraction of financial commitment for current space missions should be dedicated to studying the ocean.
Author (NASDA)

N94-11930 Qingdao Inst. of Oceanology (China). Ocean Remote Sensing and Ocean Optics Lab.

ANALYSIS OF THE CHARACTERISTIC AND MECHANISM OF SUSPENDED MATTER TRANSPORTATION IN HUANGHE DELTA SEA AREA USING REMOTE SENSING TECHNIQUES **c48**

Maochong Shi, Wei Huang, Ge Chen, and Mingxia He *In* Scientific Organizing Committee of PORSEC, Proceedings of the PORSEC 1992 in Okinawa: Conference for Pacific Ocean Environments and Probing, Volume 1 25 Aug. 1992 p 205-210 (For primary document see N94-11894 01-42)
Copyright Avail: Issuing Activity (Scientific Organizing Committee of PORSEC, P.O. Box 10, Shimizu, Shizuoka 424, Japan, HC)

In this paper, the distribution and transportation of surface suspended matter in the area from Bohai Bay to Laizhou Bay are analyzed using satellite data and in-situ currents data. It is concluded that in the summer the distribution of surface suspended matter has a close relationship with the residual currents in this sea area. In windless weather, the suspended matter brought by the runoff of the Huanghe River doesn't move toward northeast directly by the inertia but diffuses along the seashore. The nearby Wuhaozhuang is the only way for suspended matter to be transported to the outer sea. In the north of Dongfeng Port of Shandong Province, special eddies make clear water extend to the coast so that there is a fine condition for port-building. Author (NASDA)

N94-11931 Nagasaki Univ., Bunkyo (Japan). Graduate School of Marine Science and Engineering.

THE EXTRACTION OF BOTTOM CHARACTERISTICS AND MAPPING IN KIN BAY, OKINAWA MAIN ISLAND, JAPAN, USING LANDSAT-5/TM AND SPOT-1/HRV DATA **c48**

Byungdug Jun, Keinosuke Gotou, Yoshihiko Tanabashi, and Sam Wouthuyzen *In* Scientific Organizing Committee of PORSEC, Proceedings of the PORSEC 1992 in Okinawa: Conference for Pacific Ocean Environments and Probing, Volume 1 25 Aug. 1992 p 211-216 (For primary document see N94-11894 01-42)
Copyright Avail: Issuing Activity (Scientific Organizing Committee of PORSEC, P.O. Box 10, Shimizu, Shizuoka 424, Japan, HC)

In bathymetric study, if there are many bottom features in the study areas, it is necessary to analyze the information of the bottom characteristics in order to get accurate measurement on water depth. In the present study, the bottom features effect in Kin Bay, Okinawa Main Island, Japan, are analyzed using LANDSAT-5/TM (Thematic Mapper) and SPOT-1/HRV (High Resolution Visible Instrument) data. A bathymetry model was developed considering four types of the bottom features, namely, coral, sand, sand with a little of mud, and mud with a little of sand. According to the proposed model in this paper, the correlation coefficients of each bottom features between depth and digital counts are 0.40, 0.90, 0.57, 0.54 and 0.42, 0.95, 0.75, 0.07 for LANDSAT-5/TM and SPOT-1/HRV data, respectively. Author (NASDA)

N94-11932 Sydney Univ. (Australia). Ocean Technology Group.

OCEAN WAVE DETECTION BY SAR **c43**

Ian S. F. Jones *In* Scientific Organizing Committee of PORSEC, Proceedings of the PORSEC 1992 in Okinawa: Conference for Pacific Ocean Environments and Probing, Volume 1 25 Aug. 1992 p 217-222 (For primary document see N94-11894 01-42)
Copyright Avail: Issuing Activity (Scientific Organizing Committee of PORSEC, P.O. Box 10, Shimizu, Shizuoka 424, Japan, HC)

The physical processes involved in radar sensing of ocean waves are reviewed. A model for normalized radar cross sections of the sea surface based on surface wave number spectra is described, and the processes important in SAR (Synthetic Aperture Radar) imaging are reviewed.
Author (NASDA)

N94-11933 James Cook Univ. of North Queensland, Townsville (Australia). Dept. of Physics.

ON THE DETERMINATION OF THE SAR OCEAN SURFACE SCATTERING PATCH SIZE

I. Amadou and M. L. Heron *In* Scientific Organizing Committee of PORSEC, Proceedings of the PORSEC 1992 in Okinawa: Conference for Pacific Ocean Environments and Probing, Volume 1 25 Aug. 1992 p 223-228 (For primary document see N94-11894 01-42)
Copyright Avail: Issuing Activity (Scientific Organizing Committee of PORSEC, P.O. Box 10, Shimizu, Shizuoka 424, Japan, HC)

This paper discusses the imaging of ocean features by SAR (Synthetic Aperture Radar) through a variety of mechanisms. Fundamental to the derivation of the complex SAR images from the ocean is the identification of scattering points on the surface. The size of the scattering patch depends on the interactions of radar waves and ocean dynamics. The received signal from each point on a frozen (terrestrial) target is determined by the Doppler frequency shift corresponding to the approach velocity of that point. For a complicated moving target (oceanic) the point aperture becomes spread by additional velocity components within the target plane. The amplitude aperture thus formed, produces a self-interfering bundle of rays towards the receiver. Model calculations show that at low altitudes (air-borne) the image observed by the SAR receiver has a linear (or refraction) relationship with the ocean surface. However, at high altitude (satellite) and rough seas the image is nonlinear. It is shown that the scattering patch size is dependent upon look-angle, wave amplitude, platform altitude and velocity. Author (NASDA)

N94-11934 Qingdao Inst. of Oceanology (China). Ocean Remote Sensing and Ocean Optics Lab.

THE OPTICAL/COMPUTER HYBRID PROCESSING OF EXTRACTING OCEAN WAVE DIRECTIONAL SPECTRUM BY AIRBORNE PHOTOGRAPH **c43**

Ming Xia He, Chao Fang Zhao, Xiao Dong Zhang, and Hui Fang *In* Scientific Organizing Committee of PORSEC, Proceedings of the PORSEC 1992 in Okinawa: Conference for Pacific Ocean Environments and Probing, Volume 1 25 Aug. 1992 p 229-236 (For primary document see N94-11894 01-42)
Copyright Avail: Issuing Activity (Scientific Organizing Committee of PORSEC, P.O. Box 10, Shimizu, Shizuoka 424, Japan, HC)

An optics/computer hybrid processing method to extract the ocean wave directional spectrum from a diffusion photograph is presented in detail. A thorough discussion of a remote sensing model, proposed by Stilwell, used to obtain the ocean wave directional spectrum is presented. The ocean wave directional spectra acquired by this method agree well with theory and in-situ data and are superior to those put forth in previous literature. The application research has been carried out in various sea areas of China. This method can be used as a validation of satellite SAR (Synthetic Aperture Radar)/ocean wave direction and can also be applied to theoretical studies of ocean waves, verification of an ocean wave forecasting model, and ocean engineering. Author (NASDA)

N94-11935* National Aeronautics and Space Administration. Goddard Space Flight Center, Greenbelt, MD.

OCEAN-ICE INTERACTION STUDY OF WAVES AND MESOSCALE FEATURES **c48**

Antony K. Liu and Chih Y. Peng (Science Systems and Applications, Inc., Lanham, MD.) *In* Scientific Organizing Committee of PORSEC, Proceedings of the PORSEC 1992 in Okinawa: Conference for Pacific Ocean Environments and Probing, Volume 1 25 Aug. 1992 p 237-242 (For primary document see N94-11894 01-42)
Copyright Avail: Issuing Activity (Scientific Organizing Committee of PORSEC, P.O. Box 10, Shimizu, Shizuoka 424, Japan, HC)

Ocean-ice interaction processes in the Marginal Ice Zone (MIZ) by waves and mesoscale features, such as upwelling and eddies, are studied using Synthetic Aperture Radar (SAR) imagery and wave-ice interaction models. Satellite observations of mesoscale features can play a crucial role in ocean-ice interaction study. Author (NASDA)

N94-11936 Kyoto Univ., Sakyoku (Japan). Dept. of Geophysics.

TIME EVOLUTION OF CROSS-STREAM EXCHANGE ASSOCIATED WITH THE VARIATIONS IN THE KUROSHIO **c48**

Toshiyuki Awaji, Kazunori Akimoto, and Norihisa Imasato *In* Scientific

Organizing Committee of PORSEC, Proceedings of the PORSEC 1992 in Okinawa: Conference for Pacific Ocean Environments and Probing, Volume 1 25 Aug. 1992 p 243-248 (For primary document see N94-11894 01-42)
(Grant MOE-01646010)
Copyright Avail: Issuing Activity (Scientific Organizing Committee of PORSEC, P.O. Box 10, Shimizu, Shizuoka 424, Japan, HC)

The Lagrangian water motion and the resultant water exchange processes driven by variations in the Kuroshio, south of Japan, are studied by numerically tracking numerous labeled particles with the Euler-Lagrangian method. Temporal evolution of the fluid particle motion clearly shows that remarkable cross-stream exchange takes place in association with the formation and eastward progression of the Kuroshio meander: in particular, when the Kuroshio grows into a large-meander path, the cross-stream exchange is most striking. A close examination of temporal change in the vorticity balance along the stream reveals the generation mechanism. A growing meander mainly controlled by vorticity advection from the no-slip coast of Japan produces the regions with a negative minimum (positive maximum) value of temporal change in vorticity on the offshore (coastal) side of the Kuroshio axis near the apex of the meander. This drives local anticyclonic-motion (cyclonic-motion) of fluid particles across the stream, and eventually causes intense cross-stream exchange. The resultant particle distribution shows a fairly good similarity to thermal infrared pictures. These facts indicate that the cross-stream exchange driven by the Kuroshio path variation is one of the major factors that control the mass and heat transport processes in the ocean south of Japan. Author (NASDA)

N94-11937 Tokyo Univ. (Japan). Ocean Research Inst.
APPEARANCE, BEHAVIOR, AND OCEANIC STRUCTURES OF WARM STREAMERS IN THE KUROSHIO OYASHIO FRONTAL REGION **c48**
Takashige Sugimoto, Kenji Morinaga (Seikai Regional Fisheries Research Lab., Nagasaki, Japan.), and Yoshiharu Endou (Tohoku Univ., Sendai, Japan.) *In* Scientific Organizing Committee of PORSEC, Proceedings of the PORSEC 1992 in Okinawa: Conference for Pacific Ocean Environments and Probing, Volume 1 25 Aug. 1992 p 249-254 (For primary document see N94-11894 01-42)
Copyright Avail: Issuing Activity (Scientific Organizing Committee of PORSEC, P.O. Box 10, Shimizu, Shizuoka 424, Japan, HC)

Formation process, frequency, and horizontal and vertical structures of giant warm streamers associated with warm-core rings in the Kuroshio-Oyashio transitional region are described. The study is based on the field observation made by using satellite thermal images of the sea surface, hydrographic observations with a CTD (Conductivity, Temperature, and Depth) meter and a ADCP (Acoustic Doppler Current Profiler), and a time series of current and water temperature with mooring systems and ferry boats. Author (NASDA)

N94-11938 Japan Fisheries Information Service Center, Tokyo.
WARM STREAMERS EXTENDED FROM WARM CORE RINGS (WCRS) AND THEIR ROLE ON FISH MIGRATION AND FISHING GROUND FORMATION **c48**
Hideo Tameishi and Takashige Sugimoto (Tokyo Univ., Japan.) *In* Scientific Organizing Committee of PORSEC, Proceedings of the PORSEC 1992 in Okinawa: Conference for Pacific Ocean Environments and Probing, Volume 1 25 Aug. 1992 p 255-260 (For primary document see N94-11894 01-42)
Copyright Avail: Issuing Activity (Scientific Organizing Committee of PORSEC, P.O. Box 10, Shimizu, Shizuoka 424, Japan, HC)

It was recognized that Warm Streamers (WSs) often branch out toward the north or northwest from Warm Core Rings (WCRs), in satellite thermal imageries. They become migration paths toward the north and from offshore to nearshore. In this study, the relationship between these fine structures and fishing grounds, are investigated, using NOAA AVHRR (Advanced Very High Resolution Radiometer) data with assistance of aircraft data and fisheries information. Obtained results are as follows: (1) NOAA AVHRR imageries with spatial resolution of 1.1 km well represent the structures of the WSs of about 10 km in width around the WCRs; (2) by using the simultaneous aircraft data, many sardine's schools are recognized at the head of WS, in which coastal region sardine's fishing grounds are often formed; (3) it seems that WS is useful for the transfer of schools toward the coast; and (4) schools of sardine, mackerel, and other species make zonation across the front of WCRs. Author (NASDA)

N94-11939 Ehime Univ., Matsuyama (Japan). Dept. of Civil and Ocean Engineering.
THE KYUCHO EVENTS IN SUKUMO BAY INDUCED BY KUROSHIO FRONT DISTURBANCES **c48**
Hideki Akiyama and Sei-Ichi Saitou (Japan Weather Association, Tokyo.) *In* Scientific Organizing Committee of PORSEC, Proceedings of the PORSEC 1992 in Okinawa: Conference for Pacific Ocean Environments and Probing, Volume 1 25 Aug. 1992 p 261-266 (For primary document see N94-11894 01-42)
Copyright Avail: Issuing Activity (Scientific Organizing Committee of PORSEC, P.O. Box 10, Shimizu, Shizuoka 424, Japan, HC)

The swift current with a sudden increase in temperature has been often observed in a coastal region, south of Japan, exposed to the north Pacific Ocean. Such phenomena are called the Kyucho in Japan. The Kyucho event also frequently occurs in Sukumo Bay, southwest of Shikoku. The causes of occurrence of the Kyucho event in the bay, however, have not been clarified yet. Seasonal variability of the Kyucho event in the bay are investigated to analyze surface temperature data obtained in and out of the bay from March 1990 to February 1991. The Kyucho event periodically occurs in the bay during the warming and cooling periods. Its average reoccurrence period is approximately ten and eight days during the two observation periods, respectively. Thermal infrared images obtained by the NOAA-11 in the sea off to the east of Kyushu are also analyzed. It is found that a warm filament derived from the Kuroshio is advected northeast to Cape Ashizuri-misaki along the Kuroshio, then it collides against the southwest coast of Shikoku, inducing the Kyucho event by the warm water intrusion in the bay. Author (NASDA)

N94-11940 Science Univ. of Tokyo, Chiba (Japan).
THE COHERENT STRUCTURE IN THE OCEANIC TURBULENCE AROUND JAPAN ISLANDS CHAIN FORCED BY AN AIR, SEA, AND SOLID EARTH INTERACTION **c48**
Tsukasa Nishimura, Soutarou Tanaka (Remote Sensing Technology Center, Tokyo, Japan.), Toshirou Sugimura (Remote Sensing Technology Center, Tokyo, Japan.), Yuuji Hatakeyama (Asia Air Survey Co. Ltd., Suita, Japan.), I. Hisano, and M. Tazuke *In* Scientific Organizing Committee of PORSEC, Proceedings of the PORSEC 1992 in Okinawa: Conference for Pacific Ocean Environments and Probing, Volume 1 25 Aug. 1992 p 267-272 (For primary document see N94-11894 01-42)
Copyright Avail: Issuing Activity (Scientific Organizing Committee of PORSEC, P.O. Box 10, Shimizu, Shizuoka 424, Japan, HC)

Based on a daily monitoring by the NOAA/AVHRR (Advanced Very High Resolution Radiometer), the coherent structure of extremely deterministic substances inside the oceanic turbulence fields around the Japan Islands Chain has been detected and researched. The satellite remote sensing and also the coherent structure concept are applied as the flow visualization technique and as the analyzing tool of turbulence. For the sea truth of the satellite survey, a series of hydrodynamical experiments are run in the rotating system. The site has some characteristics noticeable in the air, in the sea, and in the solid earth. In the atmosphere, extratropical lows sequentially pass through and typhoons approach sometimes. In the ocean, the Kuroshio mixes with the Arctic water and produces high energy of turbulence. The most characteristic nature of the solid earth is the periodic geometry of the sea basin. The cusped capes and arched bays succeed with a regular interval of about 100 miles. In this paper, it is discussed that the mechanical interactions among these elements in the air, in the sea, and in the solid earth reinforces the deterministic substances of the coherent structure remarkably. It is shown that the frequent passes of the atmospheric lows feed the turbulent energy and the cusped capes give tight locks on the eddy structure, and that the mechanisms result from the chaotic substances of the turbulence in the rotating system. Author (NASDA)

N94-11941 Kyushu Univ., Fukuoka (Japan). Research Inst. for Applied Mechanics.
WESTWARD PROPAGATION OF SEA SURFACE ANOMALIES IN THE WESTERN NORTH PACIFIC AS SEEN BY THE ALTIMETER AND RADIOMETER **c48**
Shigeru Aoki, Shirou Imawaki, and Kaoru Ichikawa (Kyoto Univ., Sakyoku, Japan.) *In* Scientific Organizing Committee of PORSEC, Proceedings of the PORSEC 1992 in Okinawa: Conference for Pacific Ocean Environments and Probing, Volume 1 25 Aug. 1992 p 273-278 (For primary

document see N94-11894 01-42)
Copyright Avail: Issuing Activity (Scientific Organizing Committee of PORSEC, P.O. Box 10, Shimizu, Shizuoka 424, Japan, HC)

Satellite radar altimeter data of GEOSAT during the first year of the Exact Repeat Mission are analyzed to estimate anomalies of the Sea Surface Dynamic Topography (SSDT) for the western north Pacific. They are compared with anomalies of the Sea Surface Temperature (SST) derived from NOAA Advanced Very High Resolution Radiometer (AVHRR). At mid-latitude, SSDT anomalies clearly show persistent westward propagation of both cyclonic and anticyclonic eddies. SST anomalies also reveal westward propagation, and this fact shows that these features are baroclinic. The propagation speeds of these features are roughly equal to those of the first mode baroclinic long Rossby waves, but the observed phase speeds differ from the phase speeds of Rossby waves, considerably at some latitudes. In the western part (140 deg E to 160 deg E), the observed westward speeds are slightly faster than the speeds of Rossby waves at all latitudes except for around 20 deg N, while in the eastern part (160 deg E to 180 deg E), they are slower at around 20 deg N and 28 deg N, and much faster at around 30 deg N. In the Kuroshio Extension region, SSDT anomalies show relatively constant propagation in the downstream region, while their propagations are complex in the upstream region.
Author (NASDA)

N94-11942 National Defense Medical Coll., Saitama (Japan). Dept. of Physics.

COASTAL PROCESSES DUE TO NEARSHORE CURRENT AROUND AN UPHEAVING ISLAND **c48**

Masahiro Hashima and Yasuhiro Sugimori (Tokai Univ., Shizuoka, Japan.) *In* Scientific Organizing Committee of PORSEC, Proceedings of the PORSEC 1992 in Okinawa: Conference for Pacific Ocean Environments and Probing, Volume 1 25 Aug. 1992 p 279-286 (For primary document see N94-11894 01-42)
Copyright Avail: Issuing Activity (Scientific Organizing Committee of PORSEC, P.O. Box 10, Shimizu, Shizuoka 424, Japan, HC)

This paper concerns with the coastal processes of upheaving island due to near-shore currents. It is a well known phenomena that cusps form at the behind of a small island. If the island uplifts, coastal sands are transported by the littoral currents and cusps or sand spits are formed at the beach of the island. These phenomena have been observed remarkably at the upheaving island of Iwo-jima. In order to prove the mechanism that such cusps are formed, the longshore circulation due to waves breaking are calculated by numerical simulation. These currents are confirmed by experiments using a model and assumed by using air photographs. Then coastal processes of Iwo-jima are discussed. Author (NASDA)

N94-11943 Science Univ. of Tokyo, Chiba (Japan). Faculty of Science and Technology.

CHARACTERISTIC SCALES AND VORTEX FEATURES OF MESOSCALE VORTICES OBSERVED BY THE SATELLITES DURING THE WINTER **c43**

Yuuichi Miura *In* Scientific Organizing Committee of PORSEC, Proceedings of the PORSEC 1992 in Okinawa: Conference for Pacific Ocean Environments and Probing, Volume 1 25 Aug. 1992 p 287-292 Sponsored by Tokyo Univ. (For primary document see N94-11894 01-42)
Copyright Avail: Issuing Activity (Scientific Organizing Committee of PORSEC, P.O. Box 10, Shimizu, Shizuoka 424, Japan, HC)

The spiral precipitation bands that encircle mesoscale vortices and the thermal structure of the center domain are studied by satellite remote sensing data and radar. From the structure and environmental atmosphere of the vortices, it is confirmed that vortices form where three spiral precipitation bands around a vortex are successively intensified counter-clockwise. This occurs with increasing cyclonic curvature and moist convection in the convergence zone induced by cold air outbreaks.
Author (NASDA)

N94-11944 Taisei Corp., Yokohama (Japan).

THE FLOW STRUCTURE AROUND A CYLINDRICAL PIER FOR THE FLOW OF TRANSCRITICAL REYNOLDS NUMBER **c34**

Kazuo Ishino, Hideo Ootani, Ryouta Okada (Honshu Shikoku Bridge Authority, Kobe, Japan.), and Yoshitaka Nakagawa (Akashi Kaikyo Ohashi Substructure Construction, Kobe, Japan.) *In* Scientific Organizing Committee of PORSEC, Proceedings of the PORSEC 1992 in Okinawa: Conference for Pacific Ocean Environments and Probing, Volume 1 25 Aug. 1992 p 293-298 (For primary document see N94-11894 01-42)
Copyright Avail: Issuing Activity (Scientific Organizing Committee of PORSEC, P.O. Box 10, Shimizu, Shizuoka 424, Japan, HC)

The flow structure around a cylindrical pier is studied for the flow where Reynolds number is over 10(exp 8). The field measurement around Akashi Kaikyo Ohashi bridge pier was performed. The occurrence period of the shed vortex of the pier was about 30 seconds. In the rear side of the pier, large Karman vortices which had four times the occurrence period as that of the shed vortex could be seen. From the period of Karman Vortices, the Strouhal number in the region of transcritical Reynolds number is found to be 0.21. The flow was also simulated numerically by the three-dimensional flow analysis program, 'Flow 3D'. The result of the numerical simulation agreed well with the measurement. Author (NASDA)

N94-11945 Japan Marine Science and Technology Center, Tokyo.

AN APPLICATION OF REDUCED GRAVITY MODEL TO MESOSCALE EDDIES **c48**

T. Kawano, Kei Muneyama, and S. Nakamoto (Sanyo Techno Marine Co. Ltd., Tokyo, Japan.) *In* Scientific Organizing Committee of PORSEC, Proceedings of the PORSEC 1992 in Okinawa: Conference for Pacific Ocean Environments and Probing, Volume 1 25 Aug. 1992 p 299-303 (For primary document see N94-11894 01-42)
Copyright Avail: Issuing Activity (Scientific Organizing Committee of PORSEC, P.O. Box 10, Shimizu, Shizuoka 424, Japan, HC)

In order to predict parcel paths for cold eddies as well as warm eddies, an f-plane reduced gravity model with upper-layer thickness and velocity fields was developed. This model reduced to eight dimensional system of nonlinear coupled ordinary differential equations, which describe time-evolution of kinematic differential parameters and eddy shape parameters. Although this eight-dimensional system of nonlinear coupled time-evolution equations can be solved numerically, exact solutions for a steady rotating mode of both warm and cold eddies were found. For warm eddies, the rigidly rotating ellipse mode solution is a generalization of the 'rodon' solution for lens-like warm eddies. The corresponding rigidly rotating mode solution for cold eddies shows triangular path with abrupt change of direction. Elliptical paths for warm eddies and triangular paths for cold eddies were observed in the drifter tracking data of the Western Pacific Ocean Circulation Experiment (WEPOCS) 3. It may be interpreted to be a manifestation of the rotating mode solutions predicted in this study.
Author (NASDA)

N94-11946 Office de la Recherche Scientifique et Technique Outre-Mer, Noumea (New Caledonia). FLUPAC Group.

THE USE OF CZCS FOR PRIMARY PRODUCTION ESTIMATE IN THE PACIFIC **c43**

C. Dupouy, H. Oiry, A. LeBouteiller, and M. Rodier *In* Scientific Organizing Committee of PORSEC, Proceedings of the PORSEC 1992 in Okinawa: Conference for Pacific Ocean Environments and Probing, Volume 1 25 Aug. 1992 p 305-312 (For primary document see N94-11894 01-42)
Copyright Avail: Issuing Activity (Scientific Organizing Committee of PORSEC, P.O. Box 10, Shimizu, Shizuoka 424, Japan, HC)

NIMBUS-7 CZCS (Coastal Zone Color Scanner) DSP Level 2 images from NASA/GSFC (Goddard Space Flight Center) are used to form quarterly global chlorophyll fields over the western equatorial region (15 deg N to 15 deg S, 140 deg E to 170 deg W) for 1981 and 1982. Ocean color analysis combined with in-situ chlorophyll data from ORSTOM (Office de la Recherche Scientifique et Technique Outre-Mer) cruises (1988-1991) is successful in retrieving the variability of the phytoplankton enrichment due to the equatorial upwelling. The feasibility of a production estimation is analyzed from ORSTOM in-situ data. Author (NASDA)

N94-11947 Tokai Univ., Shizuoka (Japan). School of Marine Science and Technology.

CZCS DERIVED CHLOROPHYLL DISTRIBUTION IN ANTARCTIC WATER DURING AUSTRAL SUMMER **c48**

Kedarnath Mahapatra, Yoshihiro Okada, and Yasuhiro Sugimori *In* Scientific Organizing Committee of PORSEC, Proceedings of the PORSEC 1992 in Okinawa: Conference for Pacific Ocean Environments and Probing, Volume 1 25 Aug. 1992 p 313-318 Sponsored in part by Matsumae International Foundation (For primary document see N94-11894 01-42)

Copyright Avail: Issuing Activity (Scientific Organizing Committee of PORSEC, P.O. Box 10, Shimizu, Shizuoka 424, Japan, HC)

Near-surface chlorophyll concentrations derived from CZCS (Coastal Zone Color Scanner) imageries covering the area between the south Drake passage and the Antarctic peninsula are broadly in agreement with in-situ values obtained during FIBEX (First Biomass Experiment) investigations in the same area during austral summer in 1981. The results validate the applicability of satellite data to identify mesoscale pigment distribution patterns in the south polar region. Author (NASDA)

N94-11948 National Inst. for Resources and Environment, Ibaraki (Japan).

SEASONAL CHANGES OF PHYTOPLANKTON DISTRIBUTIONS IN THE NORTHWEST PACIFIC DETECTED BY COASTAL ZONE COLOR SCANNER **c48**

J. Ishizaka and K. Nakata *In* Scientific Organizing Committee of PORSEC, Proceedings of the PORSEC 1992 in Okinawa: Conference for Pacific Ocean Environments and Probing, Volume 1 25 Aug. 1992 p 319-324 (For primary document see N94-11894 01-42)

Copyright Avail: Issuing Activity (Scientific Organizing Committee of PORSEC, P.O. Box 10, Shimizu, Shizuoka 424, Japan, HC)

Seasonal changes of phytoplankton distributions in the Pacific Ocean was described by simple statistics of 7-8 year monthly averages of Coastal Zone Color Scanner (CZCS) data. September data was also compared with ship-observed vertical chlorophyll distributions along 175 deg E. These data showed regional differences of the seasonal changes of phytoplankton concentrations. Subarctic front and coastline are the two major factors in determining the seasonal changes of surface phytoplankton pigment concentrations. Author (NASDA)

N94-11949 Kinki Univ., Osaka (Japan).

SATELLITE-DERIVED OCEANIC FEATURES **c43**

Itaru Sano and Sonoyo Mukai *In* Scientific Organizing Committee of PORSEC, Proceedings of the PORSEC 1992 in Okinawa: Conference for Pacific Ocean Environments and Probing, Volume 1 25 Aug. 1992 p 325-329 (For primary document see N94-11894 01-42)

Copyright Avail: Issuing Activity (Scientific Organizing Committee of PORSEC, P.O. Box 10, Shimizu, Shizuoka 424, Japan, HC)

This paper proposes that ocean color-temperature relationship is a useful tool in analyzing the oceanic feature. Edge detection and clustering work with two-dimensional feature space is attempted to map chlorophyll and thermal patterns derived from CZCS (Coastal Zone Color Scanner) data. It is found that a synoptic set of ocean color and temperature data provided by satellite allows the spatial distribution of oceanic features. Author (NASDA)

N94-11950 Tokyo Univ. (Japan). Ocean Research Inst.

PARTICLE DYNAMICS IN THE WESTERN SUBARCTIC PACIFIC: IMPLICATIONS FROM CZCS IMAGERY **c48**

Toshirou Saino *In* Scientific Organizing Committee of PORSEC, Proceedings of the PORSEC 1992 in Okinawa: Conference for Pacific Ocean Environments and Probing, Volume 1 25 Aug. 1992 p 330-335 (For primary document see N94-11894 01-42)

Copyright Avail: Issuing Activity (Scientific Organizing Committee of PORSEC, P.O. Box 10, Shimizu, Shizuoka 424, Japan, HC)

Four regions are identified in the western subarctic Pacific in the seasonal variability of the pigments field obtained by CZCS (Coastal Zone Color Scanner). Spring blooms appear in the offshore of northern Japan in April and shift to northeastward in May and June. In the Oyashio region, southeast of the Kuril Islands, pigment concentration is high in June, and September through November. High pigment concentration appears in the western subarctic gyre from October to December. Pigment concentration in the Kuroshio extension region shows moderate annual maxima in spring and fall. Author (NASDA)

N94-11951 Tokai Univ., Shizuoka (Japan). School of High-Technology for Human Welfare.

HIGH-REFLECTANCE WATER MASS IN OFF-SANRIKU AREA OBSERVED BY CZCS **c43**

Hajime Fukushima *In* Scientific Organizing Committee of PORSEC, Proceedings of the PORSEC 1992 in Okinawa: Conference for Pacific Ocean Environments and Probing, Volume 1 25 Aug. 1992 p 336-340 (For primary document see N94-11894 01-42)
(Grant MOE-03248216)

Copyright Avail: Issuing Activity (Scientific Organizing Committee of PORSEC, P.O. Box 10, Shimizu, Shizuoka 424, Japan, HC)

Patches of high reflectance water are often observed in CZCS (Coastal Zone Color Scanner) data covering Off-Sanriku area, a northeastern part of marginal seas of Japan. The study is to investigate the spatial and temporal extent of the high reflectance waters as well as to validate the hypothesis that the phenomena is due to coccolithophore bloom. Eighty-nine of the total 301 CZCS scenes which covers the study area (35 deg N to 43 deg N, 140 deg E to 151 deg E) were selected in terms of low cloud coverage, with most of them obtained in 1979-1981. Atmospheric correction was done to all the selected scenes, applying a simple spatial filtering on the channel 4 image to avoid the effects of non-zero water-leaving radiance at 670 nm. The magnitude of resulting spectral reflectance was found to be at the same level as reported for coccolithophore blooms elsewhere in the world, suggesting the high reflectance patches were caused by detached coccoliths. The 'blooms' are popularly seen in May-August imageries with the length scale of several tens to 100 km. Author (NASDA)

N94-11952 Tohoku Univ., Sendai (Japan). Dept. of Geophysics.

PHYSICAL PROCESSES OF MICROWAVE BACKSCATTERING FROM LABORATORY WIND-WAVE SURFACES **c43**

Naoto Ebuchi, Hiroshi Kawamura, and Yoshiaki Toba *In* Scientific Organizing Committee of PORSEC, Proceedings of the PORSEC 1992 in Okinawa: Conference for Pacific Ocean Environments and Probing, Volume 1 25 Aug. 1992 p 341-346 (For primary document see N94-11894 01-42)

Copyright Avail: Issuing Activity (Scientific Organizing Committee of PORSEC, P.O. Box 10, Shimizu, Shizuoka 424, Japan, HC)

Physical processes of microwave backscattering from laboratory wind-wave surfaces are investigated using an x-band (9.6 GHz) scatterometer. Time series of the displacement of water surface, the backscattered intensity, and the Doppler spectrum are observed and analyzed to study the relationship between the microwave backscattering and fine structures of the wind-wave surfaces. At large incident angles, the backscattered intensity is in phase with wave profile. Variation of the Doppler spectra also corresponds to the phase of the individual waves. High Doppler velocity observed at the crests of the individual waves coincides with the propagating speed of the crests. It is concluded that the fine structures of wind-wave surfaces, which are trapped near the crests and are propagating with the crests, mainly contribute to microwave backscattering. At the normal incidence, variation of the scattered intensity with the phase of the dominant waves is consistent with the specular point scattering. Author (NASDA)

N94-11953 Consiglio Nazionale delle Ricerche, Venice (Italy). Ist. Studio Dinamica Grandi Masse.

EXPERIMENT AND RESULTS OF THE ITALIAN ACTIVITY IN THE FIELD OF OCEAN MICROWAVE BACKSCATTERING **c43**

Stefano Zecchetto and Paolo Trivero (Consiglio Nazionale delle Ricerche, Turin, Italy.) *In* Scientific Organizing Committee of PORSEC, Proceedings of the PORSEC 1992 in Okinawa: Conference for Pacific Ocean Environments and Probing, Volume 1 25 Aug. 1992 p 347-352 Sponsored by Agenzia Spaziale Italiana (For primary document see N94-11894 01-42)

Copyright Avail: Issuing Activity (Scientific Organizing Committee of PORSEC, P.O. Box 10, Shimizu, Shizuoka 424, Japan, HC)

This paper describes the experimental results of two campaigns carried out on board of the Italian National Research Council (CNR (Consiglio Nazionale delle Ricerche)) oceanographic platform in the northern Adriatic Sea. The aim of these as well as of the future campaigns is to measure the geophysical parameters influencing the radar backscattering from the sea surface, i.e. the wind speed and the sea surface elevation, and the radar backscatter itself. The radars used are three band (L, S, C) and single band (C) scatterometers. The sea surface elevation was measured, up to 26 Hz, by a microwave interferometric probe and the wind speed by a K-Gill two propeller anemometer. Results show the potentialities of the combined use of these instruments in studying the radar cross section sigma(sub 0) modulation due to the gravity waves and the low period (approximately 40 s) wind fluctuations, and the damping of sigma(sub 0) due to the presence of surface slicks. The examples reported here correspond to light wind conditions around 4 to 6 m/s. Author (NASDA)

N94-11954 Ministry of Posts and Telecommunications, Kashima (Japan). Kashima Space Research Center.

MEASUREMENTS OF OCEAN CROSS-SECTION WITH A SIDE-LOOKING AIRBORNE RADAR c43

Hiroaki Horie and Kenji Nakamura *In* Scientific Organizing Committee of PORSEC, Proceedings of the PORSEC 1992 in Okinawa: Conference for Pacific Ocean Environments and Probing, Volume 1 25 Aug. 1992 p 353-356 (For primary document see N94-11894 01-42)
Copyright Avail: Issuing Activity (Scientific Organizing Committee of PORSEC, P.O. Box 10, Shimizu, Shizuoka 424, Japan, HC)

A result of measurements of ocean cross-section using an airborne real aperture side-looking radar is described. The radar cross section measurement is one of the objectives of the radar. In an observation of rain over ocean, an interesting phenomenon that the sea surface echo fluctuates with a shorter time scale in rain is found. It seems to be the interference of the rain echo and sea surface echo. Author (NASDA)

N94-11955 Washington Univ., Seattle. Dept. of Atmospheric Sciences.

AIR-SEA INTERACTION: FLUXES, A REVIEW c46

Robert A. Brown *In* Scientific Organizing Committee of PORSEC, Proceedings of the PORSEC 1992 in Okinawa: Conference for Pacific Ocean Environments and Probing, Volume 1 25 Aug. 1992 p 357-362 (For primary document see N94-11894 01-42)
Copyright Avail: Issuing Activity (Scientific Organizing Committee of PORSEC, P.O. Box 10, Shimizu, Shizuoka 424, Japan, HC)

Air-sea interaction (ASI) should propably be a category, like oceanography and atmospheric science. At least for the purpose of funding. Too often, the problems and solutions for the interface between these two fluids is neglected. Perhaps it is always assumed by those in charge of one domain that it will be taken care of by the other. Another reason for the neglect of air-sea interaction is that not much is known about it. Measurements and theory are extremely difficult. The generation of waves inhibits both. The theoretical problem of wave generation has occupied some of the best fluid dynamics minds, and it cannot be said to be solved yet. A short review is made of research methods for air-sea interaction, their problems, and current status. Author (NASDA)

N94-11956 Washington Univ., Seattle. Dept. of Atmospheric Sciences.

SCATTEROMETER OBSERVATIONS: REVIEW c43

Robert A. Brown *In* Scientific Organizing Committee of PORSEC, Proceedings of the PORSEC 1992 in Okinawa: Conference for Pacific Ocean Environments and Probing, Volume 1 25 Aug. 1992 p 363-368 (For primary document see N94-11894 01-42)
Copyright Avail: Issuing Activity (Scientific Organizing Committee of PORSEC, P.O. Box 10, Shimizu, Shizuoka 424, Japan, HC)

The application of a new class of data such as that furnished by a satellite scatterometer requires a basic understanding of the nature of the data. The assumptions and techniques required to translate backscatter cross-section into surface stress, air-sea fluxes, wind profiles, and pressure fields are mentioned here. Although these involve a mixture of theory and parameterization, the results are convincing and rewarding. Author (NASDA)

N94-11957 Remote Sensing Systems, Inc., Santa Rosa, CA.

DEPENDENCE OF OCEANIC MICROWAVE EMISSION ON WIND DIRECTION c43

Frank J. Wentz *In* Scientific Organizing Committee of PORSEC, Proceedings of the PORSEC 1992 in Okinawa: Conference for Pacific Ocean Environments and Probing, Volume 1 25 Aug. 1992 p 369-374 (For primary document see N94-11894 01-42)
Copyright Avail: Issuing Activity (Scientific Organizing Committee of PORSEC, P.O. Box 10, Shimizu, Shizuoka 424, Japan, HC)

Ocean observations taken by the satellite microwave radiometer SSM/I (Special Sensor Microwave Imager) show a variation that is correlated with the direction of the wind relative to the observation direction. For moderate wind speeds, the vertically polarized upwind brightness temperature T(sub B) is about 2 K higher than the downwind T(sub B). For horizontally polarized observations, the T(sub B) maximum occurs at crosswind rather than upwind and is approximately 3.5 K higher than the minimum at downwind. This SSM/I wind direction signal is used to make global, low-resolution maps of the monthly mean oceanic wind vector. These results indicate that it may be feasible to measure wind direction from space using a two-look microwave radiometer. Author (NASDA)

N94-11958 Kyoto Univ., Sakyoku (Japan). Geophysical Inst.

SURFACE ROUGHNESS VARIATIONS ACROSS THE ICELAND-FAROES FRONTAL REGION OBSERVED BY THE GEOSAT ALTIMETER AND NOAA AVHRR c43

Kaoru Ichikawa, John P. Matthews (University Coll. of North Wales, Bangor.), and Stephen B. Groom (Natural Environmental Research Council, Swindon, England.) *In* Scientific Organizing Committee of PORSEC, Proceedings of the PORSEC 1992 in Okinawa: Conference for Pacific Ocean Environments and Probing, Volume 1 25 Aug. 1992 p 375-380 (For primary document see N94-11894 01-42)
Copyright Avail: Issuing Activity (Scientific Organizing Committee of PORSEC, P.O. Box 10, Shimizu, Shizuoka 424, Japan, HC)

Surface roughness variations across the Iceland-Faroes frontal region have been studied using NOAA AVHRR (Advanced Very High Resolution Radiometer) imagery and GEOSAT altimeter microwave echo intensity, sigma(sub 0). From the atmospheric boundary layer stability theory, substantial decrease of surface roughness is naively expected on the cold side. The frontal area was covered by an atmospheric high pressure system during May 21-25, 1987 and hence, the calm weather condition was satisfied. A synoptic view of surface roughness variation derived from the sunglint intensity variation in the visible bands of NOAA-9 AVHRR imagery within the calm weather period confirms the existence of the anticipated substantial roughness variation across the front. The profile of sigma(sub 0) along the GEOSAT track observed closest in time to the imagery also indicate flat surface on the cold water. In general, however, sigma(sub 0) profiles along GEOSAT tracks do not exhibit clear signatures at the front. One considered reason for this is that weather conditions to produce roughness changes observable by altimeter were severe in this region. It is also suggested from the image of sunglint variations that the intermittent presence of regions of anomalously flat surfaces play a role in masking the expected behavior at the front. Author (NASDA)

N94-11959 Kyushu Univ., Fukuoka (Japan). Research Inst. for Applied Mechanics.

THE MICROWAVE BACKSCATTERING FROM WIND WAVES c43

H. Mitsuyasu, T. Kusaba, K. Marubayashi, and M. Ishibashi *In* Scientific Organizing Committee of PORSEC, Proceedings of the PORSEC 1992 in Okinawa: Conference for Pacific Ocean Environments and Probing, Volume 1 25 Aug. 1992 p 381-386 (For primary document see N94-11894 01-42)
Copyright Avail: Issuing Activity (Scientific Organizing Committee of PORSEC, P.O. Box 10, Shimizu, Shizuoka 424, Japan, HC)

Microwave backscattering from wind wave surface has been measured simultaneously with winds and waves in a large wind-wave tank by using a x-band scatterometer at .6 GHz with horizontal polarization. Various relations among the backscattered microwave power, incidence angle theta, characteristic wind speeds, u(sub *) and U(sub 10), and wind wave spectrum have been studied within the ranges -35 deg less than or equal to theta less than or equal to 35 deg and 3.5 m/s less than or equal to U(sub 10) less than or equal to 20.5 m/s, where u(sub *) is the friction velocity of the wind and U(sub 10) is the wind speed at the height z = 10 m, which is obtained by extrapolating logarithmic profiles of the wind. It is shown that the friction velocity depends on various quantities such as the wind speed U(sub 10), the backscattered microwave power, and the high frequency wave spectrum changes near the wind speed u(sub *) = 0.2 m/s and that these changing patterns are quite similar. The results show a close connection among the high frequency wave spectrum, the wind structure, and the backscattered microwave power. Author (NASDA)

N94-11960 Tohoku Univ., Sendai (Japan). Center for Atmospheric and Oceanic Studies.

ON THE VARIABILITY OF WIND SPEEDS IN THE NORTH WESTERN PACIFIC OBSERVED BY ALTIMETER/GEOSAT AND SSM/I/DMSP c43

Hiroshi Kawamura *In* Scientific Organizing Committee of PORSEC, Proceedings of the PORSEC 1992 in Okinawa: Conference for Pacific Ocean Environments and Probing, Volume 1 25 Aug. 1992 p 387-391

(For primary document see N94-11894 01-42)
Copyright Avail: Issuing Activity (Scientific Organizing Committee of PORSEC, P.O. Box 10, Shimizu, Shizuoka 424, Japan, HC)

Wind speed field in the north western Pacific is observed by using the GEOSAT altimeter and the SSM/I (Special Sensor Microwave Imager) of DMSP (Defense Meteorological Satellite Program) during the summer 1987 to 1988. Both sets of data are examined by the ocean data buoys near Japan and are validated. Characteristics of the wind velocity field in this area are investigated in detail and presented. Author (NASDA)

N94-11961 Tohoku Univ., Sendai (Japan). Dept. of Geophysics.
OBSERVATION OF WIND AND WAVES BY GEOSAT ALTIMETER c43
Naoto Ebuchi, Hiroshi Kawamura, and Yoshiaki Toba *In* Scientific Organizing Committee of PORSEC, Proceedings of the PORSEC 1992 in Okinawa: Conference for Pacific Ocean Environments and Probing, Volume 1 25 Aug. 1992 p 392-397 (For primary document see N94-11894 01-42)
Copyright Avail: Issuing Activity (Scientific Organizing Committee of PORSEC, P.O. Box 10, Shimizu, Shizuoka 424, Japan, HC)

The wind speeds and significant wave heights derived from the GEOSAT altimeter are validated by comparing with the data obtained at Japanese ocean data buoy stations. A systematic error is found in the altimeter wind speeds at high winds. An experimental equation is derived in order to correct this error. By using the corrected wind speeds and the wave heights, growth of wind waves with fetch in the Sea of Japan under winter monsoon is investigated. The altimeter derived non-dimensional significant wave height and non-dimensional fetch show good agreement with the empirical fetch graph formulas. Author (NASDA)

N94-11962 Tokai Univ., Shizuoka (Japan). School of Marine Science and Technology.
AVAILABILITY OF WIND FIELD OVER THE NORTH PACIFIC DERIVED FROM DATA ON SHIPS-OF-OPPORTUNITY AND ANALYSIS OF LONG-TERM VARIABILITIES c47
Kunio Kutsuwada *In* Scientific Organizing Committee of PORSEC, Proceedings of the PORSEC 1992 in Okinawa: Conference for Pacific Ocean Environments and Probing, Volume 1 25 Aug. 1992 p 398-403 (For primary document see N94-11894 01-42)
Copyright Avail: Issuing Activity (Scientific Organizing Committee of PORSEC, P.O. Box 10, Shimizu, Shizuoka 424, Japan, HC)

Wind(-stress) fields on the sea surface over the north Pacific are derived from winds measured on ships-of-opportunity supplied by the Japan Meteorological Agency (JMA). Since the density of the ships-of-opportunity data is inhomogeneous in space, pseudo-stress data in the FSU (Florida State University) data set are supplemented in the poor-data area. Using time series of the zonal and meridional components in this data set covering a period of 27 years of 1961-1987, interannual variabilities are investigated. On time scales of several years, two dominant signals are found. These have periods of three to four years and about two years. The spatial coherences of the two signals are much different from each other. On a decadal time scale, gradual increasings of the stress magnitudes are found in the westerly and trade wind areas. The wind field based on ships-of-opportunity data is compared with that derived from satellite data (SSM/I (Special Sensor Microwave Imager)). The SSM/I winds are about 20 percent smaller in the mid-latitude area than the ship winds. Causes for these discrepancies are discussed. Author (NASDA)

N94-11963 Tokyo Univ. (Japan). Center for Climate System Research.
WIND FIELD ESTIMATE BY USING ONE HOUR GMS DATA c47
Akimasa Sumi and Tetsuo Nakazawa (Meteorological Research Inst., Tsukuba, Japan.) *In* Scientific Organizing Committee of PORSEC, Proceedings of the PORSEC 1992 in Okinawa: Conference for Pacific Ocean Environments and Probing, Volume 1 25 Aug. 1992 p 404-407 (For primary document see N94-11894 01-42)
Copyright Avail: Issuing Activity (Scientific Organizing Committee of PORSEC, P.O. Box 10, Shimizu, Shizuoka 424, Japan, HC)

Preliminary results of the study on obtaining wind data by using one hour Geostationary Meteorological Satellite (GMS) data are presented. The study was conducted to supplement the limited spacial scale of the Integrated Sounding System (ISS), which will be implemented around the Intensive Flux Area (IFA) for the Tropical Ocean and Global Atmosphere (TOGA) Coupled Ocean Atmosphere Response Experiment (COARE) to investigate an air-sea interaction for various temporal and horizontal scales. Comparable number of wind data were obtained by using one hour and 30 minutes GMS data, and the quality of the data from both GMS data seemed to be similar. These results support a possibility to obtain wind fields by using one hour GMS images. Author (NASDA)

N94-11964* Jet Propulsion Lab., California Inst. of Tech., Pasadena.
THE PACIFIC RESPONSES EXHIBITED BY AN OGCM TO VARIOUS WIND FIELDS c47
Wenqing Tang and W. Timothy Liu *In* Scientific Organizing Committee of PORSEC, Proceedings of the PORSEC 1992 in Okinawa: Conference for Pacific Ocean Environments and Probing, Volume 1 25 Aug. 1992 p 408-412 Sponsored by NASA, Washington (For primary document see N94-11894 01-42)
Copyright Avail: Issuing Activity (Scientific Organizing Committee of PORSEC, P.O. Box 10, Shimizu, Shizuoka 424, Japan, HC)

While ocean circulation is mainly forced by surface wind stress, in-situ observations of ocean surface wind stress have been sparse. In the studies of ocean circulation through numerical models, climatological wind fields derived from ship reports and wind fields produced by operational weather forecast models have been used. Recently, a new wind data set was produced by R. Atlas by combining the wind speed measured by a spaceborne microwave radiometer and wind direction from in-situ measurements and models through a variational method. These wind fields were compared as forcings on the ocean. The responses of the ocean to these forcings were studied through the Ocean General Circulation Model (OGCM) developed at the Geophysical Fluid Dynamic Laboratory. The model was first forced by wind stress climatology. After a spin-up period, various wind fields were applied and the outputs of the model were compared with outputs from a controlled run using climatological forcing. As expected the OGCM shows temporal variations and reproduces El Nino anomalies when forced by ECMWF (European Center for Medium Range Forecasts) and SSM/I (Special Sensor Microwave Imager) winds which are absent from the response to climatological wind forcing. The SSM/I winds were found to cause more rapid cooling at the end of El Nino episode than the ECMWF winds. Author (NASDA)

N94-11965 Japan Marine Science and Technology Center, Tokyo.
DEVELOPMENT OF SHIPBOARD OCEAN LIDAR c32
Ichio Asanuma, Kei Muneyama, and Motoaki Kishino (Institute of Physical and Chemical Research, Tokyo, Japan.) *In* Scientific Organizing Committee of PORSEC, Proceedings of the PORSEC 1992 in Okinawa: Conference for Pacific Ocean Environments and Probing, Volume 1 25 Aug. 1992 p 413-418 (For primary document see N94-11894 01-42)
Copyright Avail: Issuing Activity (Scientific Organizing Committee of PORSEC, P.O. Box 10, Shimizu, Shizuoka 424, Japan, HC)

A multi-parametric shipboard ocean lidar was developed and has been used to observe a vertical cross section of phytoplanktons and suspended solids in the upper layer of the water. This ocean lidar measures three parameters simultaneously, which include returns from the water surface, lights scattered by suspended solids, and fluorescent lights from phytoplankton. The returns from the surface were applied to evaluate the effects of the water surface for signals from the water. Through an experiment from the equator to the mid-latitude, this shipboard ocean lidar was operated to observe fluorescence and lights scattered with conventional measurements. The results showed the validity of this system to detect the change of phytoplanktons as a function of concentration of chlorophyll-a. Author (NASDA)

N94-11966 Xian Inst. of Optics and Precision Mechanics (China).
ON RESOLUTION OF UNDERWATER STEREO PHOTOGRAMMETRY c35
Jianguo Wu *In* Scientific Organizing Committee of PORSEC, Proceedings of the PORSEC 1992 in Okinawa: Conference for Pacific Ocean Environments and Probing, Volume 1 25 Aug. 1992 p 419-424 (For primary document see N94-11894 01-42)
Copyright Avail: Issuing Activity (Scientific Organizing Committee of PORSEC, P.O. Box 10, Shimizu, Shizuoka 424, Japan, HC)

Underwater photogrammetry using a low cost camera system is capable of measuring the fine details of seafloor for sedimentation analysis. The system can be calibrated and the stereo models can incorporate the camera distortions. The resolution of the image in underwater situations is important

for photogrammetric measurement. One major factor which affects the image quality of an underwater object, as opposed to one in the atmosphere, is the water turbidity. In this paper, several experimental results of underwater stereo photogrammetry obtained in four different locations around Australia are presented. A technique to measure water turbidity was developed. Simple relationships between image quality and turbidity and image quality and the resolution of stereo system may be derived respectively.
Author (NASDA)

N94-11967 Electrotechnical Lab., Ibaraki (Japan). Life Electronics Research Center.
THE DEVELOPMENT OF PHYTOPLANKTON SENSING SYSTEM WITH OPTICAL FIBER c74
T. Saitou, A. Nishimoto, Y. Kakui, R. Tsuda (Kinki Univ., Osaka, Japan.), M. Kumagai (Lake Biwa Research Inst., Shiga, Japan.), M. Ichihara (Mitsubishi Cable Industries Ltd., Amagasaki, Japan.), K. Yamazaki (Mitsubishi Cable Industries Ltd., Amagasaki, Japan.), M. Kimura (Mitsubishi Cable Industries Ltd., Amagasaki, Japan.), and K. Suzuki (Mitsubishi Cable Industries Ltd., Amagasaki, Japan.) *In* Scientific Organizing Committee of PORSEC, Proceedings of the PORSEC 1992 in Okinawa: Conference for Pacific Ocean Environments and Probing, Volume 1 25 Aug. 1992 p 425-429 (For primary document see N94-11894 01-42)
Copyright Avail: Issuing Activity (Scientific Organizing Committee of PORSEC, P.O. Box 10, Shimizu, Shizuoka 424, Japan, HC)

A system that measures size distribution and spatial profile of phytoplankton has been developed. The phytoplankton can be measured by the system even though the other suspended matters such as inorganic particles and zooplankton exist. This system consists of a laser, a signal processor, and an optical sensor unit. To transmit the light among these, optical fibers are employed. When the phytoplankton in the water flow is irradiated by a laser, chlorophyll-a is excited and emits fluorescence pulse. This pulse is measured as a pulse height distribution of fluorescence. The size distributions of the phytoplankton can be obtained from the computational processing of the pulse height distribution. In the field where multiple plankton species exist, this system allows the size distribution of phytoplankton to be acquired without water sampling. Author (NASDA)

N94-11968 Electrotechnical Lab., Ibaraki (Japan).
OCEAN MEASURING EXPERIMENTS USING OPTICAL FIBER DISTRIBUTED TEMPERATURE SENSOR c35
Hiroshi Iitaka, Soujun Satou, Yukio Fujinawa, Yoshikazu Murata (Sumitomo Electric Industries Ltd., Osaka, Japan.), Satoshi Terakubo (Sumitomo Electric Industries Ltd., Osaka, Japan.), and Masayoshi Yamaguchi (Sumitomo Electric Industries Ltd., Osaka, Japan.) *In* Scientific Organizing Committee of PORSEC, Proceedings of the PORSEC 1992 in Okinawa: Conference for Pacific Ocean Environments and Probing, Volume 1 25 Aug. 1992 p 430-435 Sponsored by Science and Technology Agency (For primary document see N94-11894 01-42)
Copyright Avail: Issuing Activity (Scientific Organizing Committee of PORSEC, P.O. Box 10, Shimizu, Shizuoka 424, Japan, HC)

A new phase of ocean research can be expected by making a practical application of a distributed optical fiber sensor to ocean temperature measurement. The distributed optical fiber sensor has been developed for the purpose of continuous measurement of vertical temperature profile in the ocean. The new type of sensor cable, in which the optical fiber of going and returning configuration is encapsulated, was designed and the test cable was fabricated. Experimental measurement was conducted in the Toyama Bay for 16 days from July to August in 1990. In order to estimate the accuracy of the optical fiber sensor, a CTD (conductivity, temperature, and depth) meter was used as a standard instrument. Temperature accuracy at a successive depth spatial interval of 1 m was analyzed. In a representative case, by applying the proposed correction technique to the new sensor system, the accuracy of the ocean temperature spatial profile measurements has increased by about 30 percent compared with non-corrected profile and the average value of the accuracy index proposed for the estimation of the distributed temperature measurements turned out to be about 0.43 C. Author (NASDA)

N94-11969 Electrotechnical Lab., Ibaraki (Japan). Life Electronics Research Center.
AUTOMATIC CLASSIFICATION SYSTEM FOR ZOOPLANKTON Abstract Only c51
H. Nakano and T. Sasaki *In* Scientific Organizing Committee of PORSEC, Proceedings of the PORSEC 1992 in Okinawa: Conference for Pacific Ocean Environments and Probing, Volume 1 25 Aug. 1992 p 436 (For primary document see N94-11894 01-42)
Copyright Avail: Issuing Activity (Scientific Organizing Committee of PORSEC, P.O. Box 10, Shimizu, Shizuoka 424, Japan, HC)

To understand marine ecosystem structure, it is necessary to know marine organism population. Since zooplankton is the secondary producer in the ocean and is a basic link in the food chain, it is important to know the spatial distribution and temporal variation of zooplankton. For this purpose, zooplankton should be collected frequently at various points. Then, these samples should be identified and counted. For rapid processing of many samples, the automatic classification and counting system has been developed. Features, including sizes, extracted from digital images of plankton for classification are used. Geometric features (for example, maximum length, area, and perimeter of plankton) are extracted as numerical values from images of some samples for one taxonomic group of plankton. The geometric features and non-dimensional features constitute the feature vector and it is taken as a specific characteristic of that group. The accuracy of classification to taxonomic groups of zooplankton depends greatly on image processing and the selection of features. Optimum features for classification with the interclass variance and the interclass variance of the features are found. Effective techniques for the classification are selected between the discriminant analysis and the neural network. The developed classification system consists of microscope, TV (Television) camera, magneto-optical disk, image processor, engineering workstation (EWS), and file server with Ethernet. Images are obtained with the TV camera attached to the microscope. They are digitized and processed through binarization. The EWS is used for extraction of features, classification, and counting of zooplankton. Author (NASDA)

N94-11970 Qingdao Inst. of Oceanology (China). Ocean Remote Sensing and Ocean Optics Lab.
REMOTE SENSING OF SUBSURFACE WATER TEMPERATURE PROFILE AND BACKSCATTERING COEFFICIENT IN THE CHINA SEA BY OCEAN LIDAR (OLIDAR) c43
Zhi-Shen Liu, Jin-Long Zhang, Wen-Zhong Chen, Xiao-Sheng Huang, and Jun Ma *In* Scientific Organizing Committee of PORSEC, Proceedings of the PORSEC 1992 in Okinawa: Conference for Pacific Ocean Environments and Probing, Volume 1 25 Aug. 1992 p 437-443 Sponsored by China National Foundation of Natural Science (For primary document see N94-11894 01-42)
(Grant SSTC-75760605)
Copyright Avail: Issuing Activity (Scientific Organizing Committee of PORSEC, P.O. Box 10, Shimizu, Shizuoka 424, Japan, HC)

In this paper, the optical attenuation coefficient and the sea temperature profile measured by Ocean Lidar (OLIDAR) are presented. A concurrent Raman scattering signal is used as a calibrating signal for reducing the influence of the random sea surface. From the return signal, the backscattering coefficient, which is about 0.11 in this area, is obtained. The temperature profile of the sea is extracted from the Raman spectrum with different depths detected using the OLIDAR system. The accuracy of temperature measurement is 0.5-1.0 C in-situ, and the depth of detection is about three attenuation lengths with +/- 1.5 m resolution.
Author (NASDA)

N94-11971 Paris VI Univ., Villefranche-sur-Mer (France). Lab. de Physique et Chimie Marines.
BI-DIRECTIONAL REFLECTANCE BY OCEANIC WATERS STUDIED VIA MONTE-CARLO SIMULATIONS c43
Andre Morel and Bernard Gentili *In* Scientific Organizing Committee of PORSEC, Proceedings of the PORSEC 1992 in Okinawa: Conference for Pacific Ocean Environments and Probing, Volume 1 25 Aug. 1992 p 444-445 (For primary document see N94-11894 01-42)
Copyright Avail: Issuing Activity (Scientific Organizing Committee of PORSEC, P.O. Box 10, Shimizu, Shizuoka 424, Japan, HC)

An overview of the algorithms of Monte-Carlo simulations used for processing ocean color remotely sensed data is derived and a systematic study via Monte-Carlo simulations are carried out with varying chlorophyll concentrations, commonly encountered in oceanic waters, for the main wavelengths involved in the ocean color remote sensing, and also for various atmospheric turbidities (allowing the ocean to be seen from space,

however). The particularly geometrical conditions (sun angle and viewing angle) considered are those typical of a satellite-borne ocean color sensor operated on a sun synchronous polar orbit. The possible variations of the geometrical factor Q (theta, phi, theta(sub O)) along the track and within the swath (+/- 45 deg) are predicted for various waters. When the algorithms are used to process the ocean color signals and derive the pigment (chlorophyll, C) concentration, the factor f (irradiance ratio/backscattering coefficient/sum of backscattering and absorption coefficients) and Q geometrical factors generally interfere via their ratio of f/Q. Because of similar trends of f and Q variation, their ratio is less varying. Since these residual variations are predictable, iterative schemes can be imagined to improve the accuracy of the computations leading to the pigment concentration from the ocean color remotely sensed data.
Author (NASDA)

N94-11972 Institute of Physical and Chemical Research, Saitama (Japan).
OPTICAL CHARACTERISTICS IN TOKYO BAY **c48**
Motoaki Kishino and Shigehiko Sugihara *In* Scientific Organizing Committee of PORSEC, Proceedings of the PORSEC 1992 in Okinawa: Conference for Pacific Ocean Environments and Probing, Volume 1 25 Aug. 1992 p 446-451 (For primary document see N94-11894 01-42)
Copyright Avail: Issuing Activity (Scientific Organizing Committee of PORSEC, P.O. Box 10, Shimizu, Shizuoka 424, Japan, HC)

An understanding of the optical characteristics in the sea is essential for the study of primary production by means of ocean color remote sensing. Measurements of underwater spectral irradiance, and absorption coefficient and water quality parameters of surface seawater were carried out at various stations and various seasons during three years in Tokyo Bay. Obtained relationships between spectral irradiance, optical properties, and water quality parameters are discussed. Author (NASDA)

N94-11973 Jawaharlal Nehru Technological Univ., Hyderabad (India).
REMOTE SENSING FOR NUMERICAL MODELLING OF RADIATIVE TRANSFER PROCESSES IN OCEAN ENVIRONMENT **c43**
I. V. Muralikrishna *In* Scientific Organizing Committee of PORSEC, Proceedings of the PORSEC 1992 in Okinawa: Conference for Pacific Ocean Environments and Probing, Volume 1 25 Aug. 1992 p 452-459 (For primary document see N94-11894 01-42)
Copyright Avail: Issuing Activity (Scientific Organizing Committee of PORSEC, P.O. Box 10, Shimizu, Shizuoka 424, Japan, HC)

In order to develop the data reduction and pigment retrieval algorithms from remote sensing data it is imperative to adopt a sort of simulation of radiative transfer processes and related bio-optical properties. This paper deals primarily with the radiative transfer simulation using numerical techniques. Remote sensing techniques are used for deriving boundary conditions for simulation of radiative transfer processes. The ocean waters are considered to be partially stratified and the optical properties are not homogeneous in the vertical direction. The influence of factors concerned with the heterogeneous environment is found to be considerable. The simulation study included the influence of fluorescence on radiative processes. The factors concerned with horizontal spatial variability needed greater attention and thus, demonstrated the gaps and inconsistencies in the existing bio-optical models. The results are compared with in-situ radiometric observations as well as airborne six channel ocean color radiometer data. A detailed analysis of optical data along with biochemical parameters provided bio-optical models for pigment estimation. The absorption coefficients calculated based on water constituents concentration helped in numerical simulation of radiative transfer processes.
Author (NASDA)

N94-11974 Hokkaido Univ., Sapporo (Japan).
A DEVELOPMENT ON ESTIMATION METHOD OF UNDERSEA LIGHT **c48**
Masaaki Fukuda *In* Scientific Organizing Committee of PORSEC, Proceedings of the PORSEC 1992 in Okinawa: Conference for Pacific Ocean Environments and Probing, Volume 1 25 Aug. 1992 p 460-464 (For primary document see N94-11894 01-42)
Copyright Avail: Issuing Activity (Scientific Organizing Committee of PORSEC, P.O. Box 10, Shimizu, Shizuoka 424, Japan, HC)

A method to estimate the extinction coefficient, a fundamental parameter for marine optics, using particle size, density, and transmittance has been developed. It is assumed that particles are spherical-shaped suspended matter and polygonal particles are spherical with an equivalent volume. In case of different sized particles, the extinction coefficient is calculated for each particle size that is individually estimated and summed up for all sizes after discriminating by size. A numerical method for calculating a multiple volume scattering function has been developed, assuming that primary scattering is caused by the cleanest sea water. The secondary volume scattering function was calculated by integration in all directions for particles which scattered twice. The second order volume scattering function is the sum of the secondary volume scattering function and the primary scattering function. The higher order volume scattering functions can be calculated by repeating the same procedures. This newly developed parameter could be a strong tool for marine optics analysis.
Author (NASDA)

N94-11975* Miami Univ., Coral Gables, FL. Dept. of Physics.
ATMOSPHERIC CORRECTION PLANS FOR SeaWiFS **c43**
Howard R. Gordon *In* Scientific Organizing Committee of PORSEC, Proceedings of the PORSEC 1992 in Okinawa: Conference for Pacific Ocean Environments and Probing, Volume 1 25 Aug. 1992 p 465-470 (For primary document see N94-11894 01-42)
(Contracts NAS5-30911; NAS5-31363; NAS5-31734; NAGw-273)
Copyright Avail: Issuing Activity (Scientific Organizing Committee of PORSEC, P.O. Box 10, Shimizu, Shizuoka 424, Japan, HC)

The ocean color sensor SeaWiFS (Sea Wide-Field Sensor) on the SeaStar satellite is scheduled to be launched in the Fall of 1993. Studies are now under way to develop a new atmospheric correction algorithm to process the imagery. SeaWiFS will have significantly higher radiometric sensitivity than CZCS (Coastal Zone Color Scanner), and because of this the CZCS algorithm is not accurate enough to provide a correction that will enable utilization of the full increases in sensitivity. The goal of the correction is that the atmospheric radiance be removed with an error that is no more than the noise equivalent spectral radiance of the sensor. The specific plans for the SeaWiFS correction algorithm are described. The discussion centers on a modification of the CZCS algorithm to account for the interaction between Rayleigh and aerosol scattering. However, other requirements such as the need for the surface wind speed and surface atmospheric pressure are discussed. Author (NASDA)

N94-11976 Hokkaido Univ., Sapporo (Japan). Dept. of Marine Sciences and Technology.
DISTRIBUTION OF MINERAL AEROSOLS OVER THE NORTH PACIFIC **c43**
Mitsuo Uematsu and Sei-Ichi Saitou (Japan Weather Association, Tokyo.) *In* Scientific Organizing Committee of PORSEC, Proceedings of the PORSEC 1992 in Okinawa: Conference for Pacific Ocean Environments and Probing, Volume 1 25 Aug. 1992 p 471-475 (For primary document see N94-11894 01-42)
Copyright Avail: Issuing Activity (Scientific Organizing Committee of PORSEC, P.O. Box 10, Shimizu, Shizuoka 424, Japan, HC)

In this paper, temporal and spatial variations of atmospheric dust concentration over the North Pacific are compared with the monthly composites of aerosol radiance around Japan. The atmospheric dust events observed by the aerosol sampling at Sapporo, Japan and Vladivostok, CIS (Common-wealth of Independent States) are also determined by the satellite images from NOAA and GMS (Geostationary Meteorological Satellite). From the Level 3 CZCS (Coastal Zone Color Scanner) products in the NASA video browse discs, the images in every spring (April and May) show high values over the Sea of Japan, the east China Sea, and the western North Pacific in the mid-latitude band (20 deg N to 40 deg N). This distribution pattern agrees well with the results from the consecutive measurements of mineral aerosol concentrations and their probability and travel time maps calculated based on the back air trajectory analysis during the Bai (Asian dust storm) events observed at the island stations in the central North Pacific. Pronounced Bai events recognized by the satellite images of GMS and NOAA are observed at both the sampling stations in late April, 1990 and May, 1991. The results of chemical analysis confirm the dust clouds from the satellite images. Author (NASDA)

N94-11977 Tokyo Univ. (Japan). Center for Climate System Research.
STUDY OF CLIMATIC EFFECTS OF CLOUD-AEROSOL INTERACTION **c45**

Teruyuki Nakajima *In* Scientific Organizing Committee of PORSEC, Proceedings of the PORSEC 1992 in Okinawa: Conference for Pacific Ocean Environments and Probing, Volume 1 25 Aug. 1992 p 476-477 (For primary document see N94-11894 01-42)
Copyright Avail: Issuing Activity (Scientific Organizing Committee of PORSEC, P.O. Box 10, Shimizu, Shizuoka 424, Japan, HC)

This paper discusses a possible climate change resulting from modification of cloud microphysics through interacting low level clouds with aerosols, which will increase as a result of global scale pollution. Recent study has shown several examples of large scale contamination of low level clouds due to increasing anthropogenic SO2 emission and it is pointed out that such cloud modification may partly compensate for the global warming. Two cases of anthropogenic cloud modification are studied to assess the magnitude of their climate effects. Semi-empirical relationships between effective droplet radius and cloud water path for marine stratocumulus clouds off California and for cumulus clouds over Amazon area are determined. Global average surface temperature changes, associated with the cloud modification are estimated by a simple assumption of climatic sensitivity of 0.7 K (W/sq m)(exp -1) and that 1 percent of cloud cover undergoes cloud modification. Since the increase of aerosol concentration is much lower for the maritime cloud case than the Amazon case, the cooling effect will dominate over the heating effect in the global scale average. Author (NASDA)

N94-11978 Kinki Univ., Osaka (Japan).
IMPLICATIONS OF AEROSOL RETRIEVAL AND ATMOSPHERIC CORRECTION IN REMOTE SENSING **c43**
Sonoyo Mukai and Itaru Sano *In* Scientific Organizing Committee of PORSEC, Proceedings of the PORSEC 1992 in Okinawa: Conference for Pacific Ocean Environments and Probing, Volume 1 25 Aug. 1992 p 478-482 (For primary document see N94-11894 01-42)
Copyright Avail: Issuing Activity (Scientific Organizing Committee of PORSEC, P.O. Box 10, Shimizu, Shizuoka 424, Japan, HC)

This paper describes two algorithms for aerosol retrieval. One involves vertical structure inversion, which provides the profile of atmospheric extinction from the ADEOS (Advanced Earth Observing Satellite)-ILAS (Improved Limb Atmospheric Spectrometer) data, and the iterative routine in respect of comparison of the simulated results with the measurements in order to estimate the optical thickness of stratospheric aerosols. The other is an algorithm to set up an appropriate aerosol model suitable for the NIMBUS-7 CZCS (Coastal Zone Color Scanner) image of interest to pursue an accurate atmospheric correction. Author (NASDA)

N94-11979 Kagoshima Univ. (Japan). Faculty of Education.
OVERWATER ATMOSPHERIC DISPERSION OF VOLCANIC SMOKES FROM MT. SAKURAJIMA OBSERVED IN NOAA-AVHRR DATA **c45**
K. Kinoshita, S. Hosoyamada, Sei-Ichi Saitou (Japan Weather Association, Tokyo.), and Azumi Shirasawa (Japan Weather Association, Tokyo.) *In* Scientific Organizing Committee of PORSEC, Proceedings of the PORSEC 1992 in Okinawa: Conference for Pacific Ocean Environments and Probing, Volume 1 25 Aug. 1992 p 483-488 (For primary document see N94-11894 01-42)
Copyright Avail: Issuing Activity (Scientific Organizing Committee of PORSEC, P.O. Box 10, Shimizu, Shizuoka 424, Japan, HC)

Twenty NOAA-AVHRR (Advanced Very High Resolution Radiometer) data sets between March and July 1990 were analyzed to see the dispersion of volcanic ash clouds from Mt. Sakurajima in Kyushu Island, Japan, in conjunction with the ground observation. The extension of ash clouds was found to be more than 100 km in some cases when the activity of the volcano is relatively high. The pattern of the horizontal diffusion of the ash clouds was found to be most sensitive to the vertical shear of the winds around 1-3 km above the sea level. For the extraction of volcanic clouds, multi-level slice classification using AVHRR Channel 3 and 4 is found to be useful. False color composites (Channel 3, 4, and 5) are also simple and useful. Author (NASDA)

N94-11980 Kanazawa Inst. of Tech. (Japan). Information Science Lab.
THE EVALUATION OF RADIATIVE PROCESS IN THE ATMOSPHERE-GROUND SYSTEM BY MONTE CARLO METHOD **c46**
Yoshiyuki Kawata and A. Hatakeyama *In* Scientific Organizing Committee of PORSEC, Proceedings of the PORSEC 1992 in Okinawa: Conference for Pacific Ocean Environments and Probing, Volume 1 25 Aug. 1992 p 489-494 (For primary document see N94-11894 01-42)
Copyright Avail: Issuing Activity (Scientific Organizing Committee of PORSEC, P.O. Box 10, Shimizu, Shizuoka 424, Japan, HC)

The radiances impinging on a ground target point in mountainous terrain can be divided into three radiance components, namely: (1) the direct solar radiance component; (2) the diffusely transmitted radiance component by the atmosphere; and (3) the diffusely reflected radiance by adjacent slopes. These radiances are evaluated quantitatively for various sun positions and target slope orientations by using the backward Monte Carlo method. The evaluation of the adjacency effect due to multiple reflections of light by surrounding slopes for realistic topographic conditions is, for the first time, in this study. Author (NASDA)

N94-11981 Meteorological Research Inst., Tsukuba (Japan).
THE UPWELLING RADIATION AT THE TOP OF THE ATMOSPHERE IN COASTAL REGION **c46**
Tsutomu Takashima and Kazuhiko Masuda *In* Scientific Organizing Committee of PORSEC, Proceedings of the PORSEC 1992 in Okinawa: Conference for Pacific Ocean Environments and Probing, Volume 1 25 Aug. 1992 p 495-500 (For primary document see N94-11894 01-42)
Copyright Avail: Issuing Activity (Scientific Organizing Committee of PORSEC, P.O. Box 10, Shimizu, Shizuoka 424, Japan, HC)

For a precise atmospheric correction on the ocean color data near the coastal region, a numerical method of evaluating the upwelling radiation at the top of the atmosphere bounded by the two half semi-infinite surfaces is developed. The present method would be able to apply to the case of hazy atmosphere and/or large albedo of the surface. Author (NASDA)

N94-11982 Hirosaki Univ. (Japan). Dept. of Earth Science.
INCIDENT SHORTWAVE AND LONGWAVE RADIATIONS OVER THE WESTERN NORTH PACIFIC AND THE SEA OF OKHOTSK DERIVED FROM GMS-WEFAX IMAGES **c43**
Yasumasa Kodama *In* Scientific Organizing Committee of PORSEC, Proceedings of the PORSEC 1992 in Okinawa: Conference for Pacific Ocean Environments and Probing, Volume 1 25 Aug. 1992 p 501-504 (For primary document see N94-11894 01-42)
Copyright Avail: Issuing Activity (Scientific Organizing Committee of PORSEC, P.O. Box 10, Shimizu, Shizuoka 424, Japan, HC)

Clouds developed over ocean are considered to effect oceanic boundary layer through a radiative process. A model to estimate incident shortwave and longwave radiations at sea surface using GMS (Geostationary Meteorological Satellite)-WEFAX (Weather Facsimile) visible images are developed and the radiative effects of clouds developed over the western North Pacific and the Sea of Okhotsk during the summer are discussed. Author (NASDA)

N94-11983 Japan Consulting Engineers Association.
A STUDY OF POLLUTION COURSES OF SPILLED OIL FLOATATION IN THE OUTER OCEAN **c45**
Anshin Ishimine *In* Scientific Organizing Committee of PORSEC, Proceedings of the PORSEC 1992 in Okinawa: Conference for Pacific Ocean Environments and Probing, Volume 1 25 Aug. 1992 p 505-509 (For primary document see N94-11894 01-42)
Copyright Avail: Issuing Activity (Scientific Organizing Committee of PORSEC, P.O. Box 10, Shimizu, Shizuoka 424, Japan, HC)

Because oil spill incidents, both accidental and intentional, will likely become more frequent in the future, it is of grave importance to be able to determine the oil spill floatation courses in the oceans. Taking into consideration that most Japanese tankers shuttling between Japan and the Persian Gulf pass through the surrounding waters of the Okinawa Islands, research has been conducted to determine the course that oil spills originating in the lower latitudes of the western Pacific Ocean will take. The research results are based on the findings of: (1) drift bottles; (2) GEK (Geomagnetic Electrokinetograph); (3) routes of drifting ships; (4) distribution of wind speed in the north Pacific Ocean; (5) flotation of Pumice stones; and (6) other related findings. Author (NASDA)

N94-11984 Academy of Sciences (USSR), Moscow. Inst. of Oceanology.
OBSERVATIONS OF THE FRACTAL PROPERTIES OF THE JAPAN SEA SURFACE TEMPERATURE PATTERNS **c43**
Leonid A. Bunimovich (Georgia Inst. of Tech., Atlanta.), Alexander G.

Ostrovskii (Kyushu Univ., Fukuoka, Japan.), and Shin-Ichirou Umatani (Kyushu Univ., Fukuoka, Japan.) *In* Scientific Organizing Committee of PORSEC, Proceedings of the PORSEC 1992 in Okinawa: Conference for Pacific Ocean Environments and Probing, Volume 1 25 Aug. 1992 p 510-515 Sponsored in part by Japan Society for the Promotion of Science (For primary document see N94-11894 01-42)
Copyright Avail: Issuing Activity (Scientific Organizing Committee of PORSEC, P.O. Box 10, Shimizu, Shizuoka 424, Japan, HC)

Calculations of isotherms lengths at the NOAA AVHRR (Advanced Very High Resolution Radiometer) infrared images for the Japan sea from April 1990 provide experimental evidence of the fractal properties of the SST (Sea Surface Temperature) patterns as being tracers of sea mesoscale turbulence. The isotherms fractal dimension is found to be 1.27 plus or minus 0.07 for space scales from at least 4 km to approximately 120 km. Estimation of sequences of mass exponents shows that the SST patterns exhibit rather monofractal than multifractal behavior. Analysis of the AVHRR images shows that self-similar turbulent structures-chains of vortices consist of vortex pairs and anticyclonic eddies. Their evolution and possible mechanism of formation are discussed. Author (NASDA)

N94-11985 Tokai Univ., Shizuoka (Japan). Faculty of Oceanography.
CIRCULATION OF NORTH PACIFIC INTERMEDIATE WATER c48
Masao Fukasawa, Naoki Hagiwara, and Yasuhiro Sugimori *In* Scientific Organizing Committee of PORSEC, Proceedings of the PORSEC 1992 in Okinawa: Conference for Pacific Ocean Environments and Probing, Volume 1 25 Aug. 1992 p 516-520 (For primary document see N94-11894 01-42)
Copyright Avail: Issuing Activity (Scientific Organizing Committee of PORSEC, P.O. Box 10, Shimizu, Shizuoka 424, Japan, HC)

This paper describes a geostrophic transport field in NPIW (North Pacific Intermediate Water). The circulation pattern of the NPIW became clear using Levitus's climatological data as a data source for the inverse model. NPIW circulation is composed of four main branches. Three of them recirculate in the sub-tropical region and the other branch recirculates in sub-polar region. The most eastward going branch in the sub-tropical region continues to the eastward flow of salinity minimum layer in the lower latitude, of which specific volume anomaly is 150 cl/ton, but main circulation of NPIW is confined to the region of higher latitude than 25 deg N and will coincide with the distribution of NPIW (i.e., the salinity minimum of 125 cl/ton). The source region of NPIW may be identified around the sub-polar region adjacent to the Sea of Okhotsk and from the western end of the disturbed area. The inverse model used in this study did not include boundary areas, so the heat and volume transferred across the Pacific were not clear. Also, mesh size was too coarse to identify the process of NPIW change along the easternmost branch and to distinguish waters from the Sea of Okhotsk and those from the western region of the disturbed area. Author (NASDA)

N94-11986 Tokyo Univ. (Japan). Ocean Research Inst.
SOFAR FLOAT TRACKING IN THE SHIKOKU BASIN c48
Daigo Yanagimoto, Keisuke Taira, and Shouji Kitagawa *In* Scientific Organizing Committee of PORSEC, Proceedings of the PORSEC 1992 in Okinawa: Conference for Pacific Ocean Environments and Probing, Volume 1 25 Aug. 1992 p 521-526 (For primary document see N94-11894 01-42)
Copyright Avail: Issuing Activity (Scientific Organizing Committee of PORSEC, P.O. Box 10, Shimizu, Shizuoka 424, Japan, HC)

The mid-depth circulation of the Shikoku basin was measured using twelve neutral SOFAR (Sound Fixing and Ranging) floats released at five layers ranging from 1,000 m to 4,000 m. Some trajectories of the floats tracked from April 1988 to January 1991 indicate the clockwise circulation associated with the dominant warm water mass in the Shikoku basin. The mean drift speed was 7.6 cm/s above 1,500 m depth and 3.2 cm/s under 2,000 m. The eddy diffusivities were 10(exp 6) to 10(exp 7) sq cm/s and the values decreased with depth. Author (NASDA)

N94-11987 National Inst. of Oceanography, Goa (India).
ON AN UPWELLING FRONT, PROPAGATION OF UPWELLING AND VERTICAL VELOCITY IN THE EASTERN ARABIAN SEA DURING MONSOON, 1987 c48
M. K. Antony and A. S. Unnikrishnan *In* Scientific Organizing Committee of PORSEC, Proceedings of the PORSEC 1992 in Okinawa: Conference for Pacific Ocean Environments and Probing, Volume 1 25 Aug. 1992 p 527-532 (For primary document see N94-11894 01-42)
Copyright Avail: Issuing Activity (Scientific Organizing Committee of PORSEC, P.O. Box 10, Shimizu, Shizuoka 424, Japan, HC)

A coastal upwelling front parallel to the coast and identifiable up to a depth of 75 m was observed between 12.5 and 16 deg N along the eastern Arabian Sea in September, 1987 from closely spaced digital BT (Brightness Temperature) data. With a north-south slope in the thermocline, the front has a temperature gradient of about 6 C over a distance of 30-50 km and appears to be closer to the coast on the northern side than the southern side. Information derived from data during July, 1987 shows no such front at a depth of up to 30 m at this location. An estimate based on the positions of isotherms indicates offshore movement of surface water at a rate of about 1-2 km/day from July to September. Vertical velocities computed in the frontal region using the conservation equation of temperature show an average value of -2.77 times 10(exp -2) cm/sec which is indicative of upwelling. A comparison of offshore volume transport and a temperature anomaly near the coast did not show good correlation. These observations suggest that upwelling along this coast propagates from south to north in the form of a coastally trapped wave. Author (NASDA)

N94-11988 National Inst. of Oceanography, Goa (India).
SEA SURFACE TEMPERATURE ANOMALIES IN THE ARABIAN SEA c48
M. R. Ramesh Kumar *In* Scientific Organizing Committee of PORSEC, Proceedings of the PORSEC 1992 in Okinawa: Conference for Pacific Ocean Environments and Probing, Volume 1 25 Aug. 1992 p 533-537 (For primary document see N94-11894 01-42)
Copyright Avail: Issuing Activity (Scientific Organizing Committee of PORSEC, P.O. Box 10, Shimizu, Shizuoka 424, Japan, HC)

The sea surface temperature anomalies over the various study areas, namely, the northern, western, central, eastern, and southern Arabian Sea areas have been studied for the period 1948-1972. There were about 105, 87, 2, 74, and 87 sea surface temperature anomalies for the above regions, respectively. An analysis has shown that most of the short duration anomalies (i.e., anomalies with periods less than four months) are driven by the surface heat fluxes. The medium duration anomalies (i.e., anomalies with periods between five and ten months) are driven by advection (both horizontal and vertical) and other oceanic processes. The causative factor of large duration anomalies (with periods greater than ten months) cannot be pinpointed to any particular factor. Further analysis has shown that the sea surface anomalies are well correlated to the anomalies of air temperature and latent heat flux values; whereas, they are least correlated to the anomalies of wind stress and net radiation values, except over the northern Arabian Sea where they are negatively and significantly correlated with the net radiation values. Author (NASDA)

N94-11989 Remote Sensing Applications Centre, Jakarta (Indonesia).
FLOOD MONITORING IN NORTHERN PART OF CENTRAL JAVA BY REMOTE SENSING TECHNIQUE. CASE STUDY: THE FLOODING OF SEMARANG IN JANUARY, 1990 c43
Sumardjo, Dede Dirgahayu, and Ratih Dewanti *In* Scientific Organizing Committee of PORSEC, Proceedings of the PORSEC 1992 in Okinawa: Conference for Pacific Ocean Environments and Probing, Volume 1 25 Aug. 1992 p 538-549 (For primary document see N94-11894 01-42)
Copyright Avail: Issuing Activity (Scientific Organizing Committee of PORSEC, P.O. Box 10, Shimizu, Shizuoka 424, Japan, HC)

In the western part of Indonesia, January is the beginning of rainy season. This season is caused by the pressure difference between Asia (high pressured) and Australia (low pressured), in which wet air masses flow from the Indian Ocean to the eastern part of West Java, producing a very high intensity of precipitation in the northern part of Central Java. This precipitation influences flooding in Semarang, because of the amount of surplus soil water greater than Water Holding Capacity (WHC). Author (NASDA)

N94-11990 Academia Sinica, Beijing (China). Inst. of Oceanology.
ROLES OF THE NEC AND MC IN THE FORMATION AND EVOLUTION OF THE EQUATORIAL PACIFIC WARM POOL c48
Ming Feng, Dunxin Hu, and Yongxiang Li *In* Scientific Organizing Committee of PORSEC, Proceedings of the PORSEC 1992 in Okinawa: Conference

for Pacific Ocean Environments and Probing, Volume 1 25 Aug. 1992 p 550-554 (For primary document see N94-11894 01-42)
Copyright Avail: Issuing Activity (Scientific Organizing Committee of PORSEC, P.O. Box 10, Shimizu, Shizuoka 424, Japan, HC)

The volumes of the warm water flowing into the western Pacific Warm Pool through the MC (Mindanao Current) are estimated on the basis of the existing CTD (conductivity, temperature, and depth) data from western Pacific cruises of R/V (Research Vessel) Science 1 of Academia Sinica Institute of Oceanology in the fall of the recent four years and recent results from other scientists upon the western Pacific region are analyzed to assure the idea that NEC (North Equatorial Current) and MC may be important in the formation and seasonal and annual variation of the Pacific Warm Pool. It can be seen that despite the temporal variation of the surface heat flux, the convergence of the main currents in this area such as the MC and SEC (Southern Equatorial Current) may be important in the variation of the Warm Pool and that the warm water transport in the NEC may be important in the warm water balance in the Warm Pool area.
Author (NASDA)

N94-12635 Scientific Organizing Committee of PORSEC, Shizuoka (Japan).
PROCEEDINGS OF THE PORSEC 1992 IN OKINAWA: CONFERENCE FOR PACIFIC OCEAN ENVIRONMENTS AND PROBING, VOLUME 2
25 Aug. 1992 752 p Conference held in Okinawa, Japan, 25-31 Aug. 1992; sponsored by NASA, Intergovernmental Oceanographic Commission, Scientific Committee on Ocean Research, International Association of Meteorology and Atmospheric Physics, International Association for Original contains color illustrations
(JTN-93-80419) Copyright Avail: Issuing Activity (Scientific Organizing Committee of PORSEC, P.O. Box 10, Shimizu, Shizuoka 424, Japan, HC)

The following topics were discussed: remote sensing, ocean observation, satellite observation, satellite imagery, satellite altimetry, ocean models, ocean surface, sea states, sea roughness, oceanographic parameters, ocean temperature, ocean waves, ocean currents, streamers, eddies, wind profiles, air sea interactions, energy budgets, water vapors, atmospheric correction, suspended solids, phytoplankton, chlorophylls, water pollution, fisheries, cloud cover, backscattering, aerial photography, statistical analysis, numerical analysis, mathematical models, algorithms, spectrometers, radiometers, echo sounders, numerical flow visualization, sea ice, edge detection, snow cover, data processing, image analysis, image processing, and underwater vehicles. For individual titles, see N94-12636 through N94-12766.

N94-12636 Tokai Univ., Shizuoka (Japan). School of Marine Science and Technology.
ANALYSIS OF GEOSAT WIND DATA c47
Masahisa Kubota *In* Scientific Organizing Committee of PORSEC, Proceedings of the PORSEC 1992 in Okinawa: Conference for Pacific Ocean Environments and Probing, Volume 2 25 Aug. 1992 p 555-561 (For primary document see N94-12635 01-42)
Copyright Avail: Issuing Activity (Scientific Organizing Committee of PORSEC, P.O. Box 10, Shimizu, Shizuoka 424, Japan, HC)

The GEOSAT wind data within a 2 deg by 2 deg grid over the North Pacific was analyzed for each month. Then, the monthly GEOSAT wind data was compared with other wind data, i.e., ship wind (COADS (Comprehensive Ocean Atmosphere Data Set)), satellite wind (SSM/I (Special Sensor Microwave Imager)), and model output wind (ECMWF (European Center for Medium Range Weather Forecast)) data. Cross correlation coefficients between them are fairy high, and show remarkable seasonal variation such that those show higher values in winter and lower values in summer. The similarity between GEOSAT and SSM/I wind data is remarkable.
Author (NASDA)

N94-12637* Jet Propulsion Lab., California Inst. of Tech., Pasadena. Earth and Space Sciences Div.
SSMI WIND SPEED VARIABILITY OVER THE PACIFIC OCEAN c47
David Halpern and William Knauss *In* Scientific Organizing Committee of PORSEC, Proceedings of the PORSEC 1992 in Okinawa: Conference for Pacific Ocean Environments and Probing, Volume 2 25 Aug. 1992 p 562-571 (For primary document see N94-12635 01-42)
(RTOP 578-22-26-40; RTOP 578-22-29-40)
Copyright Avail: Issuing Activity (Scientific Organizing Committee of PORSEC, P.O. Box 10, Shimizu, Shizuoka 424, Japan, HC)

Annual and interannual variability of upper ocean circulation is primarily caused by surface wind, yet little is known about the surface wind field because of difficulties in making adequately sampled in-situ wind observations. Since July 1987, the Remote Sensing Systems (RSS) routinely computes from first principles the wind speed from the intensity of microwave radiation emitted at the ocean surface by the Special Sensor Microwave Imager (SSM/I). Annual and interannual variations of monthly-mean RSS SSM/I 10 m height wind speed were analyzed during the July 1987 to December 1990 period over selected regions and at selected sites of the Pacific Ocean. The annual cycle amplitude and annual mean value were not the same in the northern and southern hemispheres. No multi-year trend was observed. The largest interannual variations were associated with the 1987 El Nino and 1988 La Nina, and only in the equatorial zone.
Author (NASDA)

N94-12638 Toyama National Coll. of Maritime Technology, Shinminato (Japan).
OBSERVATION OF WAVE CRESTS BY SATELLITE REMOTE SENSED DATA c43
Shigeki Ishimori and Masashi Kawai *In* Scientific Organizing Committee of PORSEC, Proceedings of the PORSEC 1992 in Okinawa: Conference for Pacific Ocean Environments and Probing, Volume 2 25 Aug. 1992 p 572-575 (For primary document see N94-12635 01-42)
Copyright Avail: Issuing Activity (Scientific Organizing Committee of PORSEC, P.O. Box 10, Shimizu, Shizuoka 424, Japan, HC)

The wave-coming direction is of vital concern to ship's navigator, especially in rough seas. Wave crests and troughs are clearly visible in the satellite imagery. Some information on wave features are taken from such remotely sensed data. On 22 June 1987, LANDSAT TM (Thematic Mapper) image was taken over the coastal region of Miyagi, Japan, where storm-driven large waves were prevailing. Wave crests appear to be discontinuous and short offshore and become less broken and longer towards the shore. In this paper, the evolution of wave crests is studied by an FFT (Fast Fourier Transform) technique and inspection of computer processed imageries. Some interesting facts directly observed or derived from the TM images are as follows: (1) depths at which shoaling effects begin to appear can be determined; (2) lengths to which wave crest grow as they continue to move shoreward can be estimated; and (3) wave convergence zones where the wave crests are broken can be specified and monitored.
Author (NASDA)

N94-12639 Tokai Univ., Shizuoka (Japan). School of Marine Science and Technology.
OBSERVATIONS OF EDDY FIELDS IN THE NORTHWEST PACIFIC BY GEOSAT ALTIMETRY c43
Jun Suwa, Akira Mukaida, and Yasuhiro Sugimori *In* Scientific Organizing Committee of PORSEC, Proceedings of the PORSEC 1992 in Okinawa: Conference for Pacific Ocean Environments and Probing, Volume 2 25 Aug. 1992 p 576-581 (For primary document see N94-12635 01-42)
Copyright Avail: Issuing Activity (Scientific Organizing Committee of PORSEC, P.O. Box 10, Shimizu, Shizuoka 424, Japan, HC)

The purpose of this study is to estimate the space and time characteristics of the sea level variability in the Northwest Pacific, including the Kuroshio extension region, from November 1986 to December 1987, based on the GEOSAT data. A collinear differences method was applied to only data along ascending passes. In processing the raw altimeter data, all the environmental corrections were applied. A mean profile of each pass is constructed from each individual profile to eliminate time-independent effects of the gravity field and quasi-permanent mean circulations. Orbit error can be removed by substructing the quadratic trend from each pass using a least square fit. The orbit error removal is performed using the passes with a length of about 2,000 km. Thus, any oceanic temporal variabilities of wavelengths 2,000 km or longer are significantly altered, while only those of wavelengths shorter than 1,000 km remain, and then these data are interpolated to a 0.5 degrees latitude and longitude grid. Sea height variability can be estimated simply by computing the standard deviation at each grid point. The method to calculate the wave propagation speed and the equations used for the computation are presented.
Author (NASDA)

N94-12640 Japan Marine Science and Technology Center, Tokyo.
VARIABILITY OF SEA LEVEL AND SEA SURFACE TEMPERATURE ANOMALIES IN THE EQUATORIAL PACIFIC **c48**
K. Yoneyama, K. Andou, Ichirou Asanuma, and Kei Muneyama *In* Scientific Organizing Committee of PORSEC, Proceedings of the PORSEC 1992 in Okinawa: Conference for Pacific Ocean Environments and Probing, Volume 2 25 Aug. 1992 p 582-586 (For primary document see N94-12635 01-42)
Copyright Avail: Issuing Activity (Scientific Organizing Committee of PORSEC, P.O. Box 10, Shimizu, Shizuoka 424, Japan, HC)

Using GEOSAT altimeter data, sea level variability are analyzed in the equatorial Pacific Ocean during November 1986 to February 1989. SST (Sea Surface Temperature) from NOAA/AVHRR (Advanced Very High Resolution Radiometer) and temperature from the ATLAS (Atmospheric Laboratory for Application and Science) buoy array deployed by PMEL (Pacific Marine Environmental Laboratory) are also analyzed over the same area and the same period, respectively. Positive SLA (Sea Level Anomaly) and SSTA (SST Anomaly) were formed near 160 deg W on the equator and then propagated eastward from the end of 1986 through the beginning of 1987, respectively. But time lag was found for about 20 days of SLA precedence. Variation of SLA corresponds with that of the thermocline depth with the correlation coefficient of 0.7. Author (NASDA)

N94-12641* Jet Propulsion Lab., California Inst. of Tech., Pasadena.
THEORY AND OCEANOGRAPHIC APPLICATIONS OF SATELLITE ALTIMETER MEASUREMENTS **c43**
Roman E. Glazman *In* Scientific Organizing Committee of PORSEC, Proceedings of the PORSEC 1992 in Okinawa: Conference for Pacific Ocean Environments and Probing, Volume 2 25 Aug. 1992 p 587-590 (For primary document see N94-12635 01-42)
Copyright Avail: Issuing Activity (Scientific Organizing Committee of PORSEC, P.O. Box 10, Shimizu, Shizuoka 424, Japan, HC)

Altimeter measurements of wind speed, significant wave height, and sea level are based on empirical Geophysical Model Functions (GMF) relating satellite Level 1 data products to oceanographic parameters of interest. However, analysis of altimeter measurements show that the Level 1 data (i.e., the radar cross section, the travel time of the return pulse and the wave form) are affected by oceanographic factors, particularly the wave age, which are not directly accounted for in the GMFs. As a result, satellite measurements of sea level height and wind speed contain systematic errors correlated with the wave age. Such errors would introduce geographically and seasonally related biases into satellite-based global maps. Hence, new GMFs which account for effects of the wave age are desirable. In the present work, the improved GMFs developed at Jet Propulsion Laboratory (JPL) are described. Author (NASDA)

N94-12642 Sydney Univ. (Australia).
ANALYSIS OF COLLINEAR PASSES OF SATELLITE ALTIMETER DATA **c43**
Richard Coleman, Herman VanGysen (Natal Univ., Durban, South Africa.), Rosemary Morrow, and Neil White (Commonwealth Scientific and Industrial Research Organization, Sydney, Australia.) *In* Scientific Organizing Committee of PORSEC, Proceedings of the PORSEC 1992 in Okinawa: Conference for Pacific Ocean Environments and Probing, Volume 2 25 Aug. 1992 p 591-596 Sponsored by Australian Research Council, Belconnen, Australia (For primary document see N94-12635 01-42)
Copyright Avail: Issuing Activity (Scientific Organizing Committee of PORSEC, P.O. Box 10, Shimizu, Shizuoka 424, Japan, HC)

The analysis of altimetry measurements along repeated satellite ground tracks provides an excellent way of determining temporal variability in the sea surface height. A new unified analysis method has been proposed for the simultaneous estimation of orbit error, mean sea surface height, and residual sea surface heights (variability) with respect to each pass. All passes are treated in exactly the same way; the consequent rank or datum defect in the model can be overcome by appending a minimal set of conditions, chosen either to give no overall distortion of the orbits or otherwise a best fit to a reference profile, such as the geoid. Gaps in the altimeter data are easily accommodated. Numerical results of the simultaneous method are shown using data from the GEOSAT Exact Repeat Mission (ERM). Some consideration is given to the choice of a suitable radial orbit error model. The results indicate that for removing the time-varying portion of the orbit error, a sinusoid model is the most appropriate over a one revolution cycle. Author (NASDA)

N94-12643 Sydney Univ. (Australia). Marine Studies Centre.
SURFACE EDDY FLUXES FROM THE GEOSAT SATELLITE ALTIMETER **c43**
Rosemary Morrow, John Church (Commonwealth Scientific and Industrial Research Organization, Sydney, Australia.), Richard Coleman, Dudley Chelton (Oregon State Univ., Corvallis.), and Neil White (Commonwealth Scientific and Industrial Research Organization, Sydney, Australia.) *In* Scientific Organizing Committee of PORSEC, Proceedings of the PORSEC 1992 in Okinawa: Conference for Pacific Ocean Environments and Probing, Volume 2 25 Aug. 1992 p 597-602 Sponsored by Australian Research Council, Belconnen, Australia (For primary document see N94-12635 01-42)
Copyright Avail: Issuing Activity (Scientific Organizing Committee of PORSEC, P.O. Box 10, Shimizu, Shizuoka 424, Japan, HC)

The Southern Ocean is known to have a vigorous eddy field with large geographical variations. However, quantitative measurements of these eddies have been limited by the difficulty and expense in maintaining long term observational arrays. This study uses GEOSAT satellite altimeter data in the Southern Ocean to resolve anisotropic eddy kinetic energy and horizontal eddy momentum flux on fine space and time scales. The resultant eddy variability ellipses compare favorably with surface drifter data in the Tasman Sea, and with in-situ current meter observations. The complex spatial distribution of surface eddy momentum flux is strongly influenced by bottom topography, and the position of the mean current. In general, the horizontal eddy fluxes tend to converge momentum towards the defined mean flow, with limited regions of divergence. In regard to the momentum balance, the results show the circumpolar average of horizontal eddy momentum flux from transient eddies to be an order of magnitude too small and in the wrong direction to directly balance the eastward momentum input by the wind. The altimeter data cannot resolve the standing eddy component, and transient and standing eddies may still be important in transporting momentum downwards, to be balanced by bottom friction and topographic form drag. Author (NASDA)

N94-12644* Jet Propulsion Lab., California Inst. of Tech., Pasadena.
COMPARISON OF GEOSAT SEA SURFACE HEIGHT AND MODEL-SIMULATED SURFACE DYNAMIC HEIGHT Abstract Only **c43**
Y. Chao (California Univ., Los Angeles.) and D. Halpern *In* Scientific Organizing Committee of PORSEC, Proceedings of the PORSEC 1992 in Okinawa: Conference for Pacific Ocean Environments and Probing, Volume 2 25 Aug. 1992 p 603 (For primary document see N94-12635 01-42)
Copyright Avail: Issuing Activity (Scientific Organizing Committee of PORSEC, P.O. Box 10, Shimizu, Shizuoka 424, Japan, HC)

The OGCM (Tropical Pacific Ocean General Circulation Model) simulated surface dynamic height is compared with the sea surface height derived from the GEOSAT Exact Repeat Mission. Good agreement was found between the GEOSAT data and OGCM simulation in describing an equatorial Kelvin wave pulse generated by westerly wind bursts in December 1986, 1987 El Nino, and 1988 La Nina. Both data sets are validated against in-situ sea level measurements at 12 stations in the equatorial Pacific Ocean, and found to be in good agreement with the in-situ data with correlation coefficients of approximately 0.7. The standard deviations of the GEOSAT data and OGCM simulation are 7.7 cm and 7.1 cm, which capture 79 percent and 72 percent of the variance observed by in-situ measurements (the standard deviation of the in-situ data is .8 cm), respectively. The model sensitivity experiment on two different wind products showed that the FSU (Florida State University) winds are about 30 percent stronger than the winds from European Center for Medium Range Weather Forecast (ECMWF), and that these differences in surface wind forcing produce significantly different OGCM simulated dynamic height as compared with the in-situ and GEOSAT data. Author (NASDA)

N94-12645 Japan Marine Science and Technology Center, Tokyo.
PSEUDO MAGNETIC ANOMALY DERIVED FROM SATELLITE ALTIMETRY AND ITS APPLICATION TO THE TECTONICS IN THE NORTH FUJI BASIN **c43**
Takeshi Matsumoto *In* Scientific Organizing Committee of PORSEC, Proceedings of the PORSEC 1992 in Okinawa: Conference for Pacific

Ocean Environments and Probing, Volume 2 25 Aug. 1992 p 604-607 Sponsored by Science and Technology Agency, Tokyo, Japan (For primary document see N94-12635 01-42)
Copyright Avail: Issuing Activity (Scientific Organizing Committee of PORSEC, P.O. Box 10, Shimizu, Shizuoka 424, Japan, HC)

The pseudo-magnetic anomaly in NFB (North Fuji Basin) was calculated from GEOS-3, SEASAT, and GEOSAT altimetric gravity data by the assumption that both gravity and magnetic anomalies were caused by a certain common source material. The distribution of the calculated pseudo-magnetic anomaly is compared with the observed one in order to verify the parameters characterizing the geomagnetic structure in this area. The pattern of positive and negative magnetic anomaly coincides well with that of the pseudo-magnetic anomaly in the southern part of the NFB where the opening has been in progress since 0.7 MaBP; whereas, these patterns are quite different from each other in the northwestern part of NFB where the opening occurred from 10 MaBP to 3 MaBP. Author (NASDA)

N94-12646 Hamburg Univ. (Germany). Inst. fuer Meereskunde.
PRINCIPAL OSCILLATION PATTERN ANALYSIS OF SEA LEVEL VARIATIONS IN THE TROPICAL PACIFIC MEASURED BY THE GEOSAT ALTIMETER **c48**
Jiansheng Zou *In* Scientific Organizing Committee of PORSEC, Proceedings of the PORSEC 1992 in Okinawa: Conference for Pacific Ocean Environments and Probing, Volume 2 25 Aug. 1992 p 608-613 (For primary document see N94-12635 01-42)
Copyright Avail: Issuing Activity (Scientific Organizing Committee of PORSEC, P.O. Box 10, Shimizu, Shizuoka 424, Japan, HC)

From November 1986 to January 1989, sea level variations in the tropical Pacific (30 deg S to 30 deg N) have been derived from GEOSAT ERM (Exact Repeat Mission) data using methods of both crossover and collinear analysis. The Principal Oscillation Pattern (POP) analysis is applied to analyze the altimetrically derived sea level variations in order to identify the dominant patterns present in the observational field. One dominant POP pair describes the eastward propagating equatorial Kelvin waves with the period of 110 days. This Kelvin mode is considered as a random force acting on the coupled ocean-atmosphere system. On the other hand, an individual Kelvin wave is not the precursor of the El Nino event. However, strong Kelvin waves can very likely result in an El Nino event. The second POP pair delineates the north-south oscillation of the sea level between two zonal bands 4 deg N to 10 deg N and 2 deg S to 4 deg N with a period of one year. This oscillation pattern results from the meridional Ekman transports of the upper layer associated with the seasonal migration of the Intertropical Convergence Zone (ITCZ). This meridional oscillation in the annual cycle is in phase with the onset and decay of the 1986-1987 El Nino event. Furthermore, the upper layer seems to move more rapidly from the equator to the northern hemisphere (five months) than from the northern hemisphere to the equator (seven months). Author (NASDA)

N94-12647 Institute of Ocean Sciences, Sidney (British Columbia).
MEASUREMENT OF EDDY STRUCTURE AND MOVEMENT IN THE NORTH-EAST PACIFIC WITH THE GEOSAT ALTIMETER **c43**
J. F. R. Gower and S. Tabata *In* Scientific Organizing Committee of PORSEC, Proceedings of the PORSEC 1992 in Okinawa: Conference for Pacific Ocean Environments and Probing, Volume 2 25 Aug. 1992 p 614-621 (For primary document see N94-12635 01-42)
Copyright Avail: Issuing Activity (Scientific Organizing Committee of PORSEC, P.O. Box 10, Shimizu, Shizuoka 424, Japan, HC)

Movement of sea surface height anomalies can be studied using GEOSAT altimetry data and may provide useful new information on large scale ocean circulation. A cross-correlation analysis of anomaly maps of the north-east Pacific (approximately 0 deg N to 60 deg N, 110 deg W to 160 deg W) compiled from 48 of the 17 day cycles of GEOSAT data, mapped mean drift speeds of 0.5 to 3.5 cm/s for the 2.2 year period with a spatial resolution of 600 km. The velocity variation with latitude is consistent with the motion of baroclinic Rossby waves and advection by the large scale ocean circulation. Author (NASDA)

N94-12648* Jet Propulsion Lab., California Inst. of Tech., Pasadena.
PRELIMINARY RESULTS FROM A SATELLITE ALTIMETRIC DATA ASSIMILATION USING A KALMAN FILTER AND SMOOTHER **c43**
Ichirou Fukumori, Lee-Lueng Fu, and Robert N. Miller (Oregon State Univ., Corvallis.) *In* Scientific Organizing Committee of PORSEC, Proceedings of the PORSEC 1992 in Okinawa: Conference for Pacific Ocean Environments and Probing, Volume 2 25 Aug. 1992 p 622-626 (For primary document see N94-12635 01-42)
Copyright Avail: Issuing Activity (Scientific Organizing Committee of PORSEC, P.O. Box 10, Shimizu, Shizuoka 424, Japan, HC)

GEOSAT altimeter data is analyzed in the tropical Pacific Ocean by assimilating the observations with an ocean circulation model. The assimilation method, a time-invariant Kalman filter, is novel and its results are compared with that of the full Kalman filter. Author (NASDA)

N94-12649 Kyushu Univ., Fukuoka (Japan). Research Inst. for Applied Mechanics.
FLUCTUATIONS OF THE KUROSHIO EXTENSION DETECTED BY THE GEOSAT ALTIMETRY DATA **c43**
Shirou Imawaki, Kaoru Ichikawa, and Shigeru Aoki *In* Scientific Organizing Committee of PORSEC, Proceedings of the PORSEC 1992 in Okinawa: Conference for Pacific Ocean Environments and Probing, Volume 2 25 Aug. 1992 p 627-632 (For primary document see N94-12635 01-42)
Copyright Avail: Issuing Activity (Scientific Organizing Committee of PORSEC, P.O. Box 10, Shimizu, Shizuoka 424, Japan, HC)

Fluctuations of the Sea Surface Dynamic Topography (SSDT) are studied for the Kuroshio extension region during the first year of the GEOSAT Exact Repeat Mission (ERM) in 1986-1987. A set of successive maps of the temporal fluctuation of SSDT derived from the GEOSAT altimetry data shows that a pair of cyclonic disturbances moved westward at a fairly constant speed over 200 days and finally coalesced into a stronger single cyclonic disturbance. In the field of approximated total SSDT (the climatological mean SSDT plus the present temporal fluctuation SSDT), the same phenomenon can be understood as a westward propagation of a southward meander of the Kuroshio extension followed by pinching-off of the amplified meander accompanied with formation of a cyclonic eddy south to the stream. Those fluctuations found in the approximated SSDT field are confirmed by conventional oceanographic observation data and NOAA Advanced Very High Resolution Radiometer (AVHRR) imageries, although the latter are fragmental. Author (NASDA)

N94-12650 Woods Hole Oceanographic Inst., MA. Dept. of Physical Oceanography.
MEAN FLOW AND VARIABILITY IN THE KUROSHIO EXTENSION FROM GEOSAT ALTIMETRY DATA **c43**
Bo Qiu, Kathryn A. Kelly, and Terrence M. Joyce *In* Scientific Organizing Committee of PORSEC, Proceedings of the PORSEC 1992 in Okinawa: Conference for Pacific Ocean Environments and Probing, Volume 2 25 Aug. 1992 p 633-638 (For primary document see N94-12635 01-42)
Copyright Avail: Issuing Activity (Scientific Organizing Committee of PORSEC, P.O. Box 10, Shimizu, Shizuoka 424, Japan, HC)

This study presents a method that estimates the mean surface height field in a boundary current region from residual height data of altimetric observations. Applying this method to the Kuroshio Extension (KE) region revealed that the mean and the instantaneous height fields estimated in this manner compared well with the available hydrographic data and the Sea Surface Temperature (SST) patterns from NOAA satellites. Based on 2.5 years of the GEOSAT Exact Repeat Mission (ERM) data, it was found that the mean surface height difference across the KE attains its maximum around 146 deg E between the two quasi-stationary meanders, and its decrease thereafter is mainly due to large-scale recirculations on the southern side of the KE. Propagation of mesoscale fluctuations in the height fields is generally westward except for the upstream region of the KE. Effects of deep mean flow and baroclinic shear are found to be important in explaining the observed propagation speeds. In the upstream region of 141 deg E and 154 deg E, annual variations in the surface height difference across the KE (delta h) have a September maximum with an average amplitude of 0.2 m. For large-scale interannual fluctuations, anomalies in delta h are found to be significantly correlated with those of the current axis positions: a larger surface height difference corresponds to a more northerly position of the KE. The interannual changes in delta h are possibly related to the ENSO (El Nino and Southern Oscillation) event during 1986 to 1987 in the low-latitude Pacific Ocean. Author (NASDA)

N94-12651* National Aeronautics and Space Administration. Goddard Space Flight Center, Greenbelt, MD.
PACIFIC RIM SEA ICE AS OBSERVED WITH THE NIMBUS-7 SMMR **c43**
Per Gloersen, William J. Campbell (Geological Survey, Tacoma, WA.), Donald J. Cavalieri, Josefino C. Comiso, Claire L. Parkinson, and H. Jay Zwally *In* Scientific Organizing Committee of PORSEC, Proceedings of the PORSEC 1992 in Okinawa: Conference for Pacific Ocean Environments and Probing, Volume 2 25 Aug. 1992 p 639-644 (For primary document see N94-12635 01-42)
Copyright Avail: Issuing Activity (Scientific Organizing Committee of PORSEC, P.O. Box 10, Shimizu, Shizuoka 424, Japan, HC)

Data collected by the Scanning Multichannel Microwave Radiometer (SMMR), flown on the NIMBUS-7 spacecraft have been analyzed to provide spatial and temporal coverage of sea ice in the polar regions from October 28, 1978, through August 20, 1987. The region selected for discussion here is of particular interest to the Pacific-rim countries. This region includes the Seas of Japan and Okhotsk, as well as the Bering Sea and, in the South Pacific, the Amundsen, Bellingshausen, and Ross Seas. Monthly averages of the sea ice concentrations in all of these seas are presented, as are time series of single-day records, obtained every other day on the average, of the area enclosed by the ice boundaries, the areal coverage of ocean by ice, and the open water area within the ice boundaries. Interannual variability and the 8.8 year trends are also described, as well as the contribution of the Pacific-rim regions to the overall negative trend of ice coverage in the Arctic, and the lack of trend in the Antarctic, during this period. Author (NASDA)

N94-12652 Kyoto Univ., Sakyoku (Japan). Dept. of Geophysics.
A NUMERICAL STUDY OF DEEP CONVECTION AT HIGH LATITUDES **c48**
Kazunori Akitomo, Toshiyuki Awaji, and Norihisa Imasato *In* Scientific Organizing Committee of PORSEC, Proceedings of the PORSEC 1992 in Okinawa: Conference for Pacific Ocean Environments and Probing, Volume 2 25 Aug. 1992 p 645-650 (For primary document see N94-12635 01-42)
Copyright Avail: Issuing Activity (Scientific Organizing Committee of PORSEC, P.O. Box 10, Shimizu, Shizuoka 424, Japan, HC)

Numerical experiments have been carried out to investigate the formation process and the properties of deep convection in the Weddell Sea. The thermobaric effect, i.e., an increase in value of the thermal expansion coefficient of sea water with pressure (depth) at low temperatures, makes the mixed layer unstable and deep convection catastrophically occurs as a 'thermal' plume. As the colder (less-saline) mixed-layer water intrudes into the warmer (more-saline) underlying layer, the thermocline (halocline) at the base of the mixed layer gradually ascends to disappear at the sea surface. It takes only a few days for the thermocline (halocline) to disappear if the sea surface is not covered with ice. On the other hand, it takes more than 20 days, owing to the reduction of cooling rate, if the sea surface is covered with ice. The latter implies that the vertical transport of heat and materials will be modified in the interannual time scale by such a moderate overturning process. Author (NASDA)

N94-12653 Nansen Environmental and Remote Sensing Center, Solheimsvik (Norway).
ICE STUDIES IN THE BARENTS SEA BY ERS-1 DURING SIZEX 1992 **c43**
Stein Sandven and Ola M. Johannessen *In* Scientific Organizing Committee of PORSEC, Proceedings of the PORSEC 1992 in Okinawa: Conference for Pacific Ocean Environments and Probing, Volume 2 25 Aug. 1992 p 651-657 (For primary document see N94-12635 01-42)
Copyright Avail: Issuing Activity (Scientific Organizing Committee of PORSEC, P.O. Box 10, Shimizu, Shizuoka 424, Japan, HC)

The Seasonal Ice Zone Experiment (SIZEX) 1992 was a post-launch ERS-1 field experiment carried out in the Barents Sea in March 1992. The overall objective is to estimate and validate ice parameters derived from ERS-1 SAR (Synthetic Aperture Radar) such as ice edge location, ice motion, ice concentration, and ice type classification. The SAR images provide a promising tool to classify ice regions based on different ice characteristics such as floe size, leads, ice types, shear zones, wave penetration in the ice edge region, and areas of new-frozen ice. Author (NASDA)

N94-12654 Hokkaido Univ. of Education, Kushiro (Japan).
DISINTEGRATING ICE FRONT OF SHIRASE GLACIER, EAST ANTARCTICA **c43**
Fumihiko Nishio and Kohei Chou (Remote Sensing Technology Center, Tokyo, Japan.) *In* Scientific Organizing Committee of PORSEC, Proceedings of the PORSEC 1992 in Okinawa: Conference for Pacific Ocean Environments and Probing, Volume 2 25 Aug. 1992 p 658-662 (For primary document see N94-12635 01-42)
Copyright Avail: Issuing Activity (Scientific Organizing Committee of PORSEC, P.O. Box 10, Shimizu, Shizuoka 424, Japan, HC)

Mass balance in the Shirase Glacier drainage basin in the Queen Maud Land ice sheet, East Antarctica, has been studied using the accumulated data of snow stake measurements, density, flow rate of ice, and ice thickness, and could suggest a small negative value with a large error estimated more than 30 percent. Due to the most uncertainty of snow accumulation in the drainage area for mass balance calculation, the regional snow accumulation measured will be compared with the amount of snow deposition estimated by satellite image data and discussed on mass balance trends of Shirase Glacier drainage basin in the Antarctic Ice Sheet. Author (NASDA)

N94-12655 Indian Inst. of Tech., Kanpur. Dept. of Civil Engineering.
MICROWAVE RADIOMETRY OF ICE COVER IN POLAR REGIONS **c43**
Ashok K. Keshari, Ramesh P. Singh, and Anupma Rastogi *In* Scientific Organizing Committee of PORSEC, Proceedings of the PORSEC 1992 in Okinawa: Conference for Pacific Ocean Environments and Probing, Volume 2 25 Aug. 1992 p 663-668 Sponsored by Ministry of Human Resource Development, New Delhi, India (For primary document see N94-12635 01-42)
Copyright Avail: Issuing Activity (Scientific Organizing Committee of PORSEC, P.O. Box 10, Shimizu, Shizuoka 424, Japan, HC)

In the polar regions, ocean and land are covered by ice of different thickness. Due to the intrusion of ocean water in the coastal areas, the salinity of ice changes. In the present paper, detailed numerical calculations have been carried out to study the microwave remote sensing response over various models representative of polar regions consisting of ice covering of different physical characteristics. Effect of the physical, chemical, and electrical characteristics of the ice and ice thickness on the radiometer response has been found to be significant. Author (NASDA)

N94-12656 National Inst. for Resources and Environment, Ibaraki (Japan).
THE SEASONAL CHANGE OF PHYTOPLANKTON SIZE DISTRIBUTION USING OPTICAL FIBER SENSOR **c51**
Kisaburou Nakata, Fumio Horiguchi, and Tooru Nakane (Biological Research Inst., Ibaraki, Japan.) *In* Scientific Organizing Committee of PORSEC, Proceedings of the PORSEC 1992 in Okinawa: Conference for Pacific Ocean Environments and Probing, Volume 2 25 Aug. 1992 p 669-676 (For primary document see N94-12635 01-42)
Copyright Avail: Issuing Activity (Scientific Organizing Committee of PORSEC, P.O. Box 10, Shimizu, Shizuoka 424, Japan, HC)

Phytoplankton size spectrum in Hunka Bay is measured using an optical fiber sensor developed by Kakui et al. The time variation of size spectra throughout a year is also presented. The major feature is that the phytoplankton that are 40-45 micrometers in diameter dominate in the spring bloom, which corresponds to chain form Chaetoceros. In other seasons, remarkable phytoplankton does not appear. With regard to zooplankton, the microzooplankton population peak coincides with the phytoplankton blooming period, while net zooplankton population grow after the termination of spring bloom. Author (NASDA)

N94-12657 Hokkaido Tokai Univ., Tokyo (Japan).
A SURFACE WATER MONITORING SYSTEM: A DEVICE FOR THE SEA-TRUTH OBSERVATIONS **c48**
Hiroshi Hattori, Atsuhiro Yanagisawa, and Mitsuo Fukuchi (National Inst. of Polar Research, Tokyo, Japan.) *In* Scientific Organizing Committee of PORSEC, Proceedings of the PORSEC 1992 in Okinawa: Conference for Pacific Ocean Environments and Probing, Volume 2 25 Aug. 1992 p 677-681 (For primary document see N94-12635 01-42)
Copyright Avail: Issuing Activity (Scientific Organizing Committee of PORSEC, P.O. Box 10, Shimizu, Shizuoka 424, Japan, HC)

A surface water monitoring system was developed to continuously measure water temperature, conductivity, dissolved oxygen, fluorescence intensity, and plankton size composition in the sea surface layer. The system consists of three units, sensors unit, navigation information unit, and control unit. Water pumped up from a haul intake is led into the sensors unit to measure the variables mentioned above as well as the flow rate of water running through the system. Analog signals from the sensors unit and digital data from navigation information are transferred into the control unit at one minute intervals. These data are displayed and stored in a computer system. The system is expected to provide useful data for the sea-truth observations in satellite observing area. Field experiments made in various areas revealed the usefulness of this system for detecting fine scale spatial variation of the oceanographic variables. The relation between the sea surface temperature observed by this system and the thermal image from NOAA-11 is examined. Author (NASDA)

N94-12658 National Research Inst. of Far Seas Fisheries, Shizuoka (Japan).

PRIMARY PRODUCTIVITY IN THE OYASHIO AREA IN THE SPRING AND SUMMER OF 1990 c48

Akihiro Shiomoto, Katsuyuki Sasaki (National Research Inst. of Fisheries Science, Tokyo, Japan.), Satsuki Matsumura, and Tooru Shimoda (National Research Inst. of Fisheries Science, Tokyo, Japan.) *In* Scientific Organizing Committee of PORSEC, Proceedings of the PORSEC 1992 in Okinawa: Conference for Pacific Ocean Environments and Probing, Volume 2 25 Aug. 1992 p 682-687 (For primary document see N94-12635 01-42)
Copyright Avail: Issuing Activity (Scientific Organizing Committee of PORSEC, P.O. Box 10, Shimizu, Shizuoka 424, Japan, HC)

Primary productivity within the euphotic zone was measured with C-13 method and daily primary production was estimated. Daily primary production was in the range of 372 to 633 mgC(m sup -2)(d sup -1) in the spring and 384 to 2109 mgC(m sup -2)(d sup -1) in the summer. Excluding the largest one, the values in the summer were within the range of those in spring. To cancel the difference of light condition during observation, light utilization efficiency and quantum yield were calculated. From these results, the factors affecting primary production are discussed. Author (NASDA)

N94-12659 Tokai Univ., Shizuoka (Japan). School of Marine Science and Technology.

CHARACTERIZATION OF DISSOLVED ORGANIC MATTER IN THE OCEAN BY USING THE FLUORESCENCE EXCITATION-EMISSION MATRIX c48

Yasuhiro Senga and Naoya Tomii *In* Scientific Organizing Committee of PORSEC, Proceedings of the PORSEC 1992 in Okinawa: Conference for Pacific Ocean Environments and Probing, Volume 2 25 Aug. 1992 p 688-691 (For primary document see N94-12635 01-42)
Copyright Avail: Issuing Activity (Scientific Organizing Committee of PORSEC, P.O. Box 10, Shimizu, Shizuoka 424, Japan, HC)

Three dimensional fluorescence matrices (EEM (Excitation-Emission Matrix)) has been obtained for characterizing Dissolved Organic Matters (DOM) in the ocean. DOM was concentrated from the filtered sea water by using the gel adsorption chromatography, where ion-exchange gel or hydrophobic gel was used. EEMs of the concentrated sea water sampled at Suruga Bay reveal at least four characteristic fluorophores. Two of them are suggested to be a humic acid and a carbohydrate. Author (NASDA)

N94-12660 Nagoya Univ. (Japan). Water Research Inst.

THE PHYTOPLANKTON BLOOM IN THE KINU-URA BAY, JAPAN IN THE RAINY SEASON c51

Junko Hama and Nobuhiko Handa *In* Scientific Organizing Committee of PORSEC, Proceedings of the PORSEC 1992 in Okinawa: Conference for Pacific Ocean Environments and Probing, Volume 2 25 Aug. 1992 p 692-697 (For primary document see N94-12635 01-42)
Copyright Avail: Issuing Activity (Scientific Organizing Committee of PORSEC, P.O. Box 10, Shimizu, Shizuoka 424, Japan, HC)

Biomass, chemical composition, and production rate of phytoplankton populations are studied at Kinu-ura Bay, Japan, which is semi-closed eutrophic bay. The study took place during the rainy season from late May to early July in 1983, at intervals from one to five days. Considerable amounts of nutrients were frequently supplied from rivers into the surface layer of the bay in the experimental period. These appeared to be a major direct nutrient source for phytoplankton blooms in this season. Renewal of water mass with frequent river influx largely affected occurrence and disappearance of phytoplankton bloom. The protein/carbohydrate ratio of particulate matter at the surface layer was generally greater than or equal to three, which indicated high growth activities of phytoplankton populations at the surface layer throughout this period. Mean and total production rate for the experimental period were about 2 and 90 gC(m sup -2)(d sup -1), respectively. The importance of the production in the rainy season to an annual production is suggested by this study. Author (NASDA)

N94-12661 Nagoya Univ. (Japan). Water Research Inst.

VARIATION OF THE PHOTOSYNTHETIC PRODUCTS IN THE REGIONAL UPWELLING AREA AROUND THE IZU ISLANDS, JAPAN c51

Takeo Hama *In* Scientific Organizing Committee of PORSEC, Proceedings of the PORSEC 1992 in Okinawa: Conference for Pacific Ocean Environments and Probing, Volume 2 25 Aug. 1992 p 698-703 (For primary document see N94-12635 01-42)
Copyright Avail: Issuing Activity (Scientific Organizing Committee of PORSEC, P.O. Box 10, Shimizu, Shizuoka 424, Japan, HC)

This study is carried out to assess the relation between the photosynthetic products and nutrient availability of the phytoplankton population. A combined C-13 tracer and Gas Chromatography-Mass Spectrometry (GC-MS) method was applied to determine the composition of photosynthetic products inside and outside of regional upwelling waters around the Izu Islands, Japan. This method can measure the monosaccharide and amino acid composition of carbohydrate and protein/amino acid of photosynthetic products, respectively. Production rate of protein/amino acid (sum of the production rates of 12 amino acids) was highest in the nutrient-rich 'maturing' upwelling water, where higher concentrations of nutrients were measured than in the non-upwelling and nutrient-depleted 'aged' upwelling waters. Production rate of carbohydrate (sum of the production rates of eight monosaccharides), on the other hand, showed the highest value in the 'aged' upwelling water and this was exclusively due to the high production rate of glucose; the production rate of glucose accounted for 90 percent of the total carbohydrate production, whereas glucose accounted for 50 percent in 'maturing' upwelling water. These results demonstrated that composition of photosynthetic products significantly varied through the 'aging' of upwelling, probably due to the change in the nutrient availability. Author (NASDA)

N94-12662 National Oceanic and Atmospheric Administration, Camp Springs, MD. Ocean Products Center.

AN INTEGRATED APPROACH TO TOTAL END-TO-END QUALITY CONTROL OF OCEAN DATA IN THE REAL-TIME ENVIRONMENT c82

Walton B. Campbell and Marshall P. Waters *In* Scientific Organizing Committee of PORSEC, Proceedings of the PORSEC 1992 in Okinawa: Conference for Pacific Ocean Environments and Probing, Volume 2 25 Aug. 1992 p 704-708 (For primary document see N94-12635 01-42)
Copyright Avail: Issuing Activity (Scientific Organizing Committee of PORSEC, P.O. Box 10, Shimizu, Shizuoka 424, Japan, HC)

In Jan. 1985, the NOAA created the Ocean Products Center (OPC) to formalize the realization that marine data sets are scientifically useful only when quality controlled and then integrated with relative measurements to provide multidisciplinary information. The OPC is a unique cooperative center housing elements of the National Weather Service, National Ocean Service, and the National Environmental Satellite, Data, and Information Service. The contributing offices work closely together to provide a tightly coupled, integrated approach of end-to-end quality control and distribution of forecasts, analyses, observation, data products, and imagery. This body of real-time, quality controlled in situ data, satellite remotely-sensed data and model output is made available through the OPC-managed NOAA Ocean Communications Network (NOCN) to users world-wide. This paper describes the end-to-end quality control of ocean data in the real-time environment conducted at OPC. Author (NASDA)

N94-12663 Meteorological Research Inst., Tsukuba (Japan).

WORLDWIDE MAP OF RAINFALL AMOUNT OVER THE OCEAN DERIVED FROM PASSIVE MICROWAVE RADIOMETER c47

Akira Shibata *In* Scientific Organizing Committee of PORSEC, Proceedings of the PORSEC 1992 in Okinawa: Conference for Pacific Ocean Environments and Probing, Volume 2 25 Aug. 1992 p 709-714 (For primary document see N94-12635 01-42)

Copyright Avail: Issuing Activity (Scientific Organizing Committee of PORSEC, P.O. Box 10, Shimizu, Shizuoka 424, Japan, HC)

The method of retrieving liquid water content by considering water vapor content as a substitute parameter is presented. A comparison of the retrieved liquid water content is made with an amount of rain measured on the Chichijima Island. A worldwide map of liquid water content is shown for several months in 1987 and 1988. Author (NASDA)

N94-12664 Science Univ. of Tokyo, Chiba (Japan). Dept. of Civil Engineering.

STUDY ON DIFFUSION PHENOMENA OF RIVER EFFLUENTS ISSUED INTO SEA AROUND JAPAN WITH SATELLITE REMOTE SENSING DATA c43

Sotoaki Oonishi and Hiroyasu Kawai *In* Scientific Organizing Committee of PORSEC, Proceedings of the PORSEC 1992 in Okinawa: Conference for Pacific Ocean Environments and Probing, Volume 2 25 Aug. 1992 p 715-720 (For primary document see N94-12635 01-42)

Copyright Avail: Issuing Activity (Scientific Organizing Committee of PORSEC, P.O. Box 10, Shimizu, Shizuoka 424, Japan, HC)

Hydraulic behaviors of river effluents are discussed in a qualitative manner with LANDSAT data. An analytical method to obtain the distribution of water turbidity and temperature with satellite data using a personal computer is proposed. The method is applied to the effluents from the Shingu and Nahari rivers. Author (NASDA)

N94-12665 Muroran Inst. of Tech., Mizumoto (Japan). Dept. of Computer Science and Systems Engineering.

A BASIC CONSIDERATION FOR REMOTE SENSING USING MICROWAVE RADARS ON A SATELLITE c43

Masahiko Hatanaka, Masayuki Hikichi, and Akira Nishitsuji *In* Scientific Organizing Committee of PORSEC, Proceedings of the PORSEC 1992 in Okinawa: Conference for Pacific Ocean Environments and Probing, Volume 2 25 Aug. 1992 p 721-726 (For primary document see N94-12635 01-42)

Copyright Avail: Issuing Activity (Scientific Organizing Committee of PORSEC, P.O. Box 10, Shimizu, Shizuoka 424, Japan, HC)

In order to analyze remote sensing data from microwave radar on a satellite, it is necessary to remove the effects of microwave attenuation and reflection caused by precipitation. Generally, the attenuation and reflective coefficients depend on precipitation rate, kinds of precipitation, raindrop/snowflake size-distributions, and temperature. In the case of satellite observation, precipitation structure models from snowflake to raindrop along a slant path have to be considered. In this paper, one of the precipitation structure models and its evaluated parameters using ETS-2 (Engineering Test Satellite-2) satellite experiment data at Kashima, Japan in 1977 is reviewed, and a trial was made to simulate the radar echo observed from a meteorological satellite based upon the calculated precipitation model. This kind of approach will be useful in performing a feasibility study of active satellite radar and to design a meteorological satellite system. Author (NASDA)

N94-12666 National Oceanic and Atmospheric Administration, Washington, DC. National Ocean Service.

MIGRATION OF OPERATIONAL ICE ANALYSIS AND FORECASTING TO A WORKSTATION PLATFORM AT THE JOINT ICE CENTER c43

Robert Andrew Warner and Franklin E. Kniskern *In* Scientific Organizing Committee of PORSEC, Proceedings of the PORSEC 1992 in Okinawa: Conference for Pacific Ocean Environments and Probing, Volume 2 25 Aug. 1992 p 727-730 (For primary document see N94-12635 01-42)

Copyright Avail: Issuing Activity (Scientific Organizing Committee of PORSEC, P.O. Box 10, Shimizu, Shizuoka 424, Japan, HC)

The Joint Ice Center (JIC) is responsible for producing global, regional, and local ice analyses and forecasts for the Arctic, Antarctic, and the Great Lakes. Traditional hard copy/grease pencil methods of manual analysis have been the principal mode of ice analysis until recently. The JIC now has a prototype Digital Ice Analysis and Forecast System (DIFAS-version 0) that has been used to demonstrate the applicability of computer science as a tool for the interactive production of ice analyses. This paper discusses the suite of products produced at the JIC, the interim use of manual drafting techniques blended with DIFAS-0, and the future plans for integration of interactive digital techniques as well as the computer systems necessary to meet these goals. Author (NASDA)

N94-12667 MATRA Marconi Space, Toulouse (France). System and Instrumentation Div.

METEOSAT SECOND GENERATION PROGRAMME SEVIRI: AN ENHANCED VISIBLE AND IR RADIOMETER FOR METEOROLOGY c43

J. Jouan, P. Hollier, F. Pasternak, and Kunkle (Messerschmitt-Boelkow-Blohm G.m.b.H., Ottobrunn, Germany.) *In* Scientific Organizing Committee of PORSEC, Proceedings of the PORSEC 1992 in Okinawa: Conference for Pacific Ocean Environments and Probing, Volume 2 25 Aug. 1992 p 731-741 Sponsored by ESA, Paris, France (For primary document see N94-12635 01-42)

Copyright Avail: Issuing Activity (Scientific Organizing Committee of PORSEC, P.O. Box 10, Shimizu, Shizuoka 424, Japan, HC)

After a presentation of the METEOSAT first generation program, the new missions foreseen for the second generation of METEOSAT are given. They include a continuity of Earth imaging with improved performances and a sounding capability necessary to monitor instability processes. The paper presents the new generation instrument SEVIRI (Spinning Enhanced Visible and Infrared Imager) with its unique features for sounding from a spinning geostationary spacecraft. The instrument spatial, temporal, radiometric, and spectral resolutions will be shown to fit the rapid development of weather prediction numerical models. Emphasis is on instrument characteristics directly relevant to meteorological applications and corresponding processing, including: (1) convective phenomena evolution monitoring on local scale; (2) wind data and cloud motion vector measurements; and (3) surface data and derivation of thermodynamic surface temperature, etc. The conclusion will enlighten the improvements that can be expected from better vertical information at a high repeat cycle. Author (NASDA)

N94-12668 National Inst. of Agro-Environmental Science, Ibaraki (Japan). Div. of Changing Earth and Agro-Environment.

EVALUATING THE SPREAD OF RED SOIL WITH LANDSAT TM DATA IN CORAL REEFS OF OKINAWA MAIN ISLAND, SOUTHWESTERN JAPAN c43

Katsuo Okamoto, Ichirou Yamada, Toshiaki Imagawa, and Michikazu Fukuhara *In* Scientific Organizing Committee of PORSEC, Proceedings of the PORSEC 1992 in Okinawa: Conference for Pacific Ocean Environments and Probing, Volume 2 25 Aug. 1992 p 742-747 Prepared in cooperation with Okinawa Prefecture Agricultural Experimental Station, Okinawa, Japan Original contains color illustrations (For primary document see N94-12635 01-42)

Copyright Avail: Issuing Activity (Scientific Organizing Committee of PORSEC, P.O. Box 10, Shimizu, Shizuoka 424, Japan, HC)

The purpose of this paper is to clarify the distribution of red soil which is deposited over the coral reefs at the periphery of Katabaru located on the eastern coast of the northern part of Okinawa Island, by grasping the degree of contamination based on the relationship between the TM (Thematic Mapper) data and the amount of Fe2O3 contained in the red soil. As a result, the facts stated below are revealed: (1) there is a high-correlation between the interchannel ratio of the TM data and the amount of Fe2O3 contained in the red soil; thus, the interchannel ratio is an effective index for analyzing the distribution of the sedimented red soil; (2) the distribution of red soil was estimated using the interchannel ratio of the TM data, and a remarkably large amount of red soil was found to be deposited near the estuary, and other sedimented areas were recognized inside the reef crests and along the coast, as well; and (3) the distribution area of red soil off the coast of Katabaru was almost identical from 1984 to 1989. This is consistent with the fact that large-scale construction work, which involved major topographic alterations to the basins of rivers flowing into this area of the coast, was concentrated in the period up to and including the early 1980's, and that there was only a small number of construction projects after 1984. Author (NASDA)

N94-12669 Qingdao Inst. of Oceanology (China).

SIMPLE AND LOW COST IMAGE PROCESSING SYSTEM FOR SATELLITE REMOTE SENSING DATA c82

Ting-Lu Zhang, Zhi-Sheng Liu, and Huang-Tao et al *In* Scientific Organizing Committee of PORSEC, Proceedings of the PORSEC 1992 in Okinawa: Conference for Pacific Ocean Environments and Probing, Volume 2 25 Aug. 1992 p 748-750 (For primary document see N94-12635 01-42)

Copyright Avail: Issuing Activity (Scientific Organizing Committee of PORSEC, P.O. Box 10, Shimizu, Shizuoka 424, Japan, HC)

A special image processing system for satellite remote sensing was developed. The system is provided with many advantages, such as powerful hardware functions, abundant software, high performance to cost ratio, etc. The hardware of the system consists of an image processing board with integrated microcomputer, a tape recorder, an optical disc, a video signal source (TV (Television) camera), a plotter, a paint jet, and an image monitor. The software of the image processing system includes an image data base management system which is a simplified command language to invoke application programs and a library of tens of image processing application programs. The features, configuration, and each part function of the image processing board and detail of the software are outlined.

Author (NASDA)

N94-12670 Iwate Univ., Morioka (Japan).

VALIDATION TEST SYSTEM FOR SEA SURFACE TEMPERATURE DETECTED BY SATELLITES IN MUTSU BAY **c43**

S. Tanba, T. Souma, M. Konda, I. Yoshida, T. Watanabe, R. Yokoyama, Hironori Maejima, and Korehiro Maeda *In* Scientific Organizing Committee of PORSEC, Proceedings of the PORSEC 1992 in Okinawa: Conference for Pacific Ocean Environments and Probing, Volume 2 25 Aug. 1992 p 751-756 Prepared in cooperation with NASDA, Tokyo, Japan (For primary document see N94-12635 01-42)

Copyright Avail: Issuing Activity (Scientific Organizing Committee of PORSEC, P.O. Box 10, Shimizu, Shizuoka 424, Japan, HC)

An accuracy validation test project for the Sea Surface Temperature (SST) estimation by satellite data was undertaken in Mutsu Bay. The sea and air truth data are provided by the four observation systems operated by independent organizations: (1) Mutsu Bay Automatic Buoy System (MBABS); (2) Automatic Meteorological Data Acquisition System (AMeDAS); (3) Sea Surface Temperature Profiler Buoy (SSTPB); and (4) Radio Sonde Observation System (RSOS). The satellite SST is combined with the sea truth SST by MBABS to form match-ups for the validation test. Their temporal and spatial coincidences are guaranteed to be within 30 minutes and one pixel resolution, respectively. The data of AMeDAS, SSTPB, and RSOS can be effectively referred in the error analysis of the SST estimation.

Author (NASDA)

N94-12671 Tokyo Metropolitan Fisheries Experiment Station (Japan).

SEA SURFACE TEMPERATURE IMAGES OF GEOSTATIONARY METEOROLOGICAL SATELLITE (GMS) AND SEA TRUTH DATA FROM FERRY BOATS **c43**

Tsutomu Chino *In* Scientific Organizing Committee of PORSEC, Proceedings of the PORSEC 1992 in Okinawa: Conference for Pacific Ocean Environments and Probing, Volume 2 25 Aug. 1992 p 757-761 (For primary document see N94-12635 01-42)

Copyright Avail: Issuing Activity (Scientific Organizing Committee of PORSEC, P.O. Box 10, Shimizu, Shizuoka 424, Japan, HC)

Since May 1989, Hachijo branch of the Tokyo Metropolitan Fisheries Experiment Station has been using satellite imagery and computer technology to get sea surface temperature images of north-west Pacific Ocean to assist the fishermen at Hachijo Island. Hachijo branch can obtain the sea surface temperatures on the ferries' course along the Izu Archipelago and it's eastern area within a one day time interval. It is very difficult to get information about sea surface temperatures of the western area, every day, so infrared images from Geostationary Meteorological Satellite (GMS) are useful in providing the western sea surface temperatures during the early spring when the bonito fishing starts. On March 23, 1990, the range of the temperature front on the ferries' course was from 17 to 19 C, and the position of the front in the image on the line of Izu Archipelago and it's eastern area was almost equal to the position of the temperature front provided by the ferries' observations. The western temperature contour lines could be drawn as the pattern of the Kuroshio which was meandering offshore the southern mainland of Japan.

Author (NASDA)

N94-12672 Kyoto Univ., Sakyoku (Japan). Dept. of Geophysics.

MEASUREMENT OF THE SEA SURFACE EMISSIVITY **c43**

Masanori Konda, Norihisa Imasato, Katsuya Nishi, and Takashi Toda (Shiga Prefecture Board of Education, Japan.) *In* Scientific Organizing Committee of PORSEC, Proceedings of the PORSEC 1992 in Okinawa: Conference for Pacific Ocean Environments and Probing, Volume 2 25 Aug. 1992 p 762-767 (For primary document see N94-12635 01-42)

Copyright Avail: Issuing Activity (Scientific Organizing Committee of PORSEC, P.O. Box 10, Shimizu, Shizuoka 424, Japan, HC)

Sea surface emissivity is determined by observation data analyses, considering surface reflection of atmospheric downward radiation. Radiation balance and other meteorological variables are measured almost throughout a year at the oceanographic observatory tower in Tanabe Bay. It is found that the cool skin on sea surface is disturbed and temperature difference across the cool skin vanishes under the condition of large wind speed over 5 m/s. Reliable emissivity values are computed under a condition such as 0.984 +/- 0.004. Consequently, half of the temperature difference between SST (Sea Surface Temperature) and the temperature retrieved from surface radiation are found to be reduced, in comparison with our results for the case in which we assume the sea surface to be a black body.

Author (NASDA)

N94-12673 Tokai Univ., Shizuoka (Japan). School of Marine Science and Technology.

EVALUATION OF THE METHOD OF GEOSTROPHIC FLOW USING NOAA-AVHRR DATA **c48**

Masatoshi Akiyama and Yasuhiro Sugimori *In* Scientific Organizing Committee of PORSEC, Proceedings of the PORSEC 1992 in Okinawa: Conference for Pacific Ocean Environments and Probing, Volume 2 25 Aug. 1992 p 768-773 (For primary document see N94-12635 01-42)

Copyright Avail: Issuing Activity (Scientific Organizing Committee of PORSEC, P.O. Box 10, Shimizu, Shizuoka 424, Japan, HC)

Near surface velocities in the Kuroshio extension area are derived from a single scene of NOAA-6 AVHRR (Advanced Very High Resolution Radiometer) imagery supplementing the satellite observed SST (Sea Surface Temperature) with synchronized hydrographic observations. The geostrophic equation is approximated to derive the surface velocities. The flow field obtained is compared with GEK (Geomagnetic Electrokinetograph) current vectors and also with the geostrophic surface currents. It is found that the geostrophic approximation, used in this study, resolved the salient features of the flow patterns in this region. The fairly good agreement of the approximated geostrophic currents with the GEK and geostrophic currents supports the validity of geostrophic approximation in the regions where the surface topography can be expressed as a function of sea surface temperature. Since the AVHRR infrared images are vulnerable to cloud contamination, the availability of cloud-free sequential-image pairs sometimes occurs as a limitation to obtain surface currents using sequential-image pairs. In such cases, the method presented in this study can be considered as an option.

Author (NASDA)

N94-12674 Qingdao Inst. of Oceanology (China). Ocean Remote Sensing and Ocean Optics Lab.

FURTHER STUDY OF THE NON-REGRESSION-COEFFICIENT SST RETRIEVAL METHOD **c65**

Ming Xia He, Yun Yue Yu, and Wei Huang *In* Scientific Organizing Committee of PORSEC, Proceedings of the PORSEC 1992 in Okinawa: Conference for Pacific Ocean Environments and Probing, Volume 2 25 Aug. 1992 p 774-779 Sponsored by NSF, Beijing, China (For primary document see N94-12635 01-42)

Copyright Avail: Issuing Activity (Scientific Organizing Committee of PORSEC, P.O. Box 10, Shimizu, Shizuoka 424, Japan, HC)

Further study of NOAA satellite SST (Sea Surface Temperature) measurement has been done based on the Non-Regression Coefficient SST (NRCSST) method presented. Instead of a set of regression coefficients, the NRCSST method requires a brightness temperature ratio (R(sub 54)) of T(sub 5) to T(sub 4) which can be determined from a scatterogram of the brightness temperatures. The method is practiced and demonstrated in the north, east and south of the China Sea. The retrieved SSTs are compared with the ones derived from the MCSST (Multi-Channel SST) algorithm provided by NOAA/NESDIS (National Environmental Satellite, Data, and Information Service). It is shown that both the NRCSST and MCSST methods give the same SST distributions. A main difficulty in the NRCSST method is to determine the ratio R(sub 54) accurately. A complementary method is to make an off-set on one of the brightness temperatures, which may modify the SST output. As an example, the NRCSSTs will be 0.4 K higher than the MCSSTs when the off-set on T(sub 4) is -0.1 K. This result is satisfied since the MCSSTs are normally about 0.5 K lower than the in-situ measurements in the China Sea.

Author (NASDA)

N94-12675 Academia Sinica, Beijing (China). Inst. of Atmospheric Physics.

DELINEATION OF MESOSCALE FEATURES OF OCEAN ON SATELLITE IR IMAGE **c43**

Jun Li and Fengxian Zhou *In* Scientific Organizing Committee of PORSEC, Proceedings of the PORSEC 1992 in Okinawa: Conference for Pacific Ocean Environments and Probing, Volume 2 25 Aug. 1992 p 780-785 (For primary document see N94-12635 01-42)
Copyright Avail: Issuing Activity (Scientific Organizing Committee of PORSEC, P.O. Box 10, Shimizu, Shizuoka 424, Japan, HC)

An GCSED (Generalized Cluster Shade Edge Detection) algorithm and a series of post processing techniques are discussed for automatic delineation of mesoscale structure of the ocean on digital IR (infrared) images. The popular derivative based edge operators are shown to be too sensitive to edge fine structure and to weak gradients. The new edge detection algorithm is GCSED method, and it is found to be an excellent edge detector that exhibits the characteristic of fine structure rejection while retaining edge sharpness. This characteristic is highly desirable for analyzing oceanographic satellite images. This procedure is evaluated on an AVHRR (Advanced Very High Resolution Radiometer) image with the Kuroshio. Error rate criterion is used to statistically evaluate the performance of GCSED algorithm and other edge detectors for both noise free and noise contaminated images. Results and analyses show that the mesoscale features of the Kuroshio can be well identified by using GCSED method. Author (NASDA)

N94-12676 Remote Sensing Technology Center, Tokyo (Japan).

OBSERVATION OF WARM CURRENT AT THE BOUNDARY FROM NORTH EQUATORIAL CURRENT TO KUROSHIO BY NOAA/AVHRR **c48**

Toshirou Sugimura, Soutarou Tanaka, Tsukasa Nishimura (Tokyo Science Univ., Japan.), and Masataka Hishida (Maritime Safety Agency, Tokyo, Japan.) *In* Scientific Organizing Committee of PORSEC, Proceedings of the PORSEC 1992 in Okinawa: Conference for Pacific Ocean Environments and Probing, Volume 2 25 Aug. 1992 p 786-789 (For primary document see N94-12635 01-42)
Copyright Avail: Issuing Activity (Scientific Organizing Committee of PORSEC, P.O. Box 10, Shimizu, Shizuoka 424, Japan, HC)

It is verified that the subtraction image of twice Channel 4 minus Channel 5 data of NOAA/AVHRR (Advanced Very High Resolution Radiometer) expresses the sea surface temperature pattern in the subtropical ocean well. Using this image, the next two phenomena were found. One is the existence of sharp straight edge between the northward flowing warm current and the stationary or southward flowing colder water at the sea area from about 200 km east of Batan Islands. Another phenomenon is a sea surface temperature front existing at about 23 deg N latitude line zone, and this front line coincides with the density front which was observed previously by Hakuhomaru Cruise in 1974 and also by Takuyo in WESTPAC (Tropical Western Pacific Ocean). Author (NASDA)

N94-12677 Deutsche Forschungsanstalt fuer Luft- und Raumfahrt, Oberpfaffenhofen (Germany).

INFORMATION CAPABILITY OF NOAA-AVHRR DATA FOR MONITORING OCEANOGRAPHIC AND ATMOSPHERIC POLLUTION **c45**

Hans-Joachim Lotz-Iwen, Stefan Werner Dech, Ruediger Glaser (Wuerzburg Univ., Germany.), and Andrea Holz (Mainz Univ., Germany.) *In* Scientific Organizing Committee of PORSEC, Proceedings of the PORSEC 1992 in Okinawa: Conference for Pacific Ocean Environments and Probing, Volume 2 25 Aug. 1992 p 790-795 (For primary document see N94-12635 01-42)
Copyright Avail: Issuing Activity (Scientific Organizing Committee of PORSEC, P.O. Box 10, Shimizu, Shizuoka 424, Japan, HC)

The potential of NOAA-AVHRR (Advanced Very High Resolution Radiometer) data for monitoring large-scale pollution phenomena is demonstrated by means of two case studies. The first study focuses on the polluting effects of smoke plumes from burning oilfields in Kuwait as a consequence of the Gulf War. Beyond the analysis of spatial distribution, height thickness, and dynamic aspects of the smoke plumes, the effects of fallout in the southern Mesopotamian region have been investigated. During and after the Gulf War, DLR's (Deutsche Forschungsanstalt fuer Luft- und Raumfahrt) DFD (German Remote Sensing Data Center) acquired NOAA-11 passes over the Gulf region showing smoke plume phenomena and surface contamination effects both in desert and vegetated areas. Qualitative information with respect to spatial distribution, height, thickness, and dynamic aspects of the smoke plumes were derived. In addition, processing of satellite imagery from April, May, and June confirmed that large vegetated areas in the Mesopotamian region have been obviously affected by fallout. As this region belongs to the most important agricultural areas in Iraq, a fundamental lack of food supply must be expected. Sea surface contamination in the Black Sea has been detected and monitored during late summer 1990 by evaluating multispectral data from NOAA-AVHRR. Analysis of sea surface temperature and surface currents results in conclusions with respect to sediment transport from the Danube as well as to algae plumes growth forced by nutrient supply and suitable climatic conditions. Author (NASDA)

N94-12678 National Inst. of Oceanography, Goa (India).

SATELLITE OBSERVATIONS OF THE NORTHEAST MONSOON COASTAL CURRENT **c43**

S. S. C. Shenoi, A. D. Gouveia, S. R. Shetye, and L. V. G. Rao *In* Scientific Organizing Committee of PORSEC, Proceedings of the PORSEC 1992 in Okinawa: Conference for Pacific Ocean Environments and Probing, Volume 2 25 Aug. 1992 p 796-801 (For primary document see N94-12635 01-42)
Copyright Avail: Issuing Activity (Scientific Organizing Committee of PORSEC, P.O. Box 10, Shimizu, Shizuoka 424, Japan, HC)

Satellite infrared observations from the Advanced Very High Resolution Radiometer (AVHRR), during November 1987 to February 1988 and hydrographic data from the eastern Arabian Sea are used to describe the poleward flowing coastal current in the eastern Arabian Sea during the northeast monsoon. The current, identified by a band of warm water, forms in November in the south, and is best developed during December to January when it can be traced along the entire coast of the eastern Arabian Sea. Off the southwest coast of India (10 deg N), the current was approximately 400 km wide. At about 22 deg N, the flow was restricted mainly to the vicinity of the continental slope and the current was a narrow jet of about 150 km width. Further north the core of the current narrowed down to about 50 km and turned west following the shelf off Pakistan. The current carried warmer waters (greater than 29 C) of southern origin to the north Arabian Sea. In the northern half of the coastline (north of 15 deg N), the temperature within the core of the current was about 1 C above the ambient temperatures. Author (NASDA)

N94-12679 Department of Scientific and Industrial Research, Lower Hutt (New Zealand). Image Processing Section.

ASPECTS OF APPLYING A RELAXATION METHOD TO COMPUTING SEA SURFACE VELOCITIES FROM SEA SURFACE TEMPERATURE IMAGES **c48**

Q. X. Wu, D. Pairman, and E. J. Barnes *In* Scientific Organizing Committee of PORSEC, Proceedings of the PORSEC 1992 in Okinawa: Conference for Pacific Ocean Environments and Probing, Volume 2 25 Aug. 1992 p 802-807 Sponsored by New Zealand Foundation for Research, Science and Technology, New Zealand (For primary document see N94-12635 01-42)
Copyright Avail: Issuing Activity (Scientific Organizing Committee of PORSEC, P.O. Box 10, Shimizu, Shizuoka 424, Japan, HC)

There has been increasing interest in computing sea surface advective velocities from sequential satellite thermal infrared images in recent years. Computational methods include those based either on Maximum Cross Correlation (MCC) or on inversion models, and the recently developed iterative approach termed the relaxation technique. Two aspects of the relaxation technique are discussed in this paper with regards to its practical implementation. One of them is concerned with employing different numbers of thermal feature points, and the other is related to the use of the Discrete Compatibility Functions (DCF) and the Continuous Compatibility Functions (CCF). It is shown that using a large number of feature points gives better results but at a cost of increased computation time. Similarly, CCF is advantageous in performance but not in speed compared to DCF. A major limitation of the relaxation method is its weakness in the treatment of strong shearing motion. The current research strategy towards overcoming the limitation is outlined. Author (NASDA)

N94-12680 Kagoshima Univ. (Japan). Faculty of Fisheries.
SEA SURFACE TEMPERATURE DIFFERENCE BETWEEN NOAA/AVHRR AND IN-SITU OBSERVATION c48
Hiroshi Ichikawa, Katsutoshi Nishimura, and Masaaki Chaen *In* Scientific Organizing Committee of PORSEC, Proceedings of the PORSEC 1992 in Okinawa: Conference for Pacific Ocean Environments and Probing, Volume 2 25 Aug. 1992 p 808-813 (For primary document see N94-12635 01-42)
Copyright Avail: Issuing Activity (Scientific Organizing Committee of PORSEC, P.O. Box 10, Shimizu, Shizuoka 424, Japan, HC)

In order to elucidate the origin of the large difference between sea surface skin temperature (Temp/Sat) estimated by MCSST (Multi-Channel Sea Surface Temperature) technique and the subsurface in-situ bulk water temperature (Temp/in-situ), the vertical gradients of water temperature near the sea surface were measured by a CTD (conductivity, temperature, and depth) meter lowerings at 18 stations across the Kuroshio in the Tokara Strait south of Japan in December 1989. The Temp/Sat were estimated by MCSST technique utilizing brightness temperature of Channel 3 and 4 of AVHRR (Advanced Very High Resolution Radiometer) on NOAA-10 together with the 18 Temp/in-situ measured at ship bottom of 5 m depth. It is found that the standard deviation of Temp/Sat from Temp/in-situ is reduced about one half by correction using the in-situ vertical gradient of temperature. The corrected temperature difference is well correlated with the heat flux from the ocean. Author (NASDA)

N94-12681 Japan Fisheries Information Service Center, Tokyo.
APPLICATION OF NOAA AVHRR DATA TO FISHERIES c43
Hideo Tameishi, Shin Fujita, and Katsuya Saitou *In* Scientific Organizing Committee of PORSEC, Proceedings of the PORSEC 1992 in Okinawa: Conference for Pacific Ocean Environments and Probing, Volume 2 25 Aug. 1992 p 814-819 (For primary document see N94-12635 01-42)
Copyright Avail: Issuing Activity (Scientific Organizing Committee of PORSEC, P.O. Box 10, Shimizu, Shizuoka 424, Japan, HC)

Presently, JAFIC (Japan Fisheries Information Service Center) makes the satellite aided oceanographic condition charts with NOAA AVHRR (Advanced Very High Resolution Radiometer) data and sends these charts to fishing boats in ocean. It was shown that the NOAA AVHRR data were applicable to fishing ground forecasting, and with the use of NOAA AVHRR data or imagery, a fishing and oceanographic condition chart with fishing information about current, front, intrusion of warm or cold water, and eddies can be produced by using JAFIC image processing system. It turns out that the expert system was useful and effective for extraction of ocean conditions from sea surface temperature data. Now, according to the communication between JAFIC and fishing boats operated offshore of east Hokkaido, Japan, it is shown that fishing grounds of saury, skipjack, squid, and sardine are highly correlated with the above mentioned environment. Author (NASDA)

N94-12682 National Research Inst. of Far Seas Fisheries, Shizuoka (Japan).
STATISTICAL FEATURES OF MESOSCALE EDDIES AT THE KUROSHIO FRONT c43
Kiyoshi Kawasaki *In* Scientific Organizing Committee of PORSEC, Proceedings of the PORSEC 1992 in Okinawa: Conference for Pacific Ocean Environments and Probing, Volume 2 25 Aug. 1992 p 821-823 (For primary document see N94-12635 01-42)
Copyright Avail: Issuing Activity (Scientific Organizing Committee of PORSEC, P.O. Box 10, Shimizu, Shizuoka 424, Japan, HC)

Two types of mesoscale eddies are observed using NOAA AVHRR (Advanced Very High Resolution Radiometer) infrared images. The eddy propagates along the Kuroshio front at a speed about 30 miles per day. It makes it difficult to trace mesoscale eddies with only intermittently taken images. This propagation speed is several times faster than that of the small Kuroshio meander. Author (NASDA)

N94-12683 Yosu National Fisheries Coll. (Republic of Korea). Dept. of Oceanography.
INTRUSION OF KUROSHIO WARM WATER INTO SAGAMI BAY c48
Hyo Sang Choo, Takashige Sugimoto (Tokyo Univ., Japan.), and Hideo Tameishi (Japan Fisheries Information Service Center, Tokyo.) *In* Scientific Organizing Committee of PORSEC, Proceedings of the PORSEC 1992 in Okinawa: Conference for Pacific Ocean Environments and Probing, Volume 2 25 Aug. 1992 p 824-828 (For primary document see N94-12635 01-42)
Copyright Avail: Issuing Activity (Scientific Organizing Committee of PORSEC, P.O. Box 10, Shimizu, Shizuoka 424, Japan, HC)

Warm water intrusions from Kuroshio into coastal waters are investigated focusing on Sagami Bay. Satellite AVHRR (Advanced Very High Resolution Radiometer) thermal images were used, combined with hydrographic observations and moored current meters. The results indicate that not only the branched current of the Kuroshio from the western channel but also warm streamers or intermittent intrusions of the warm water from ridges of the meandered Kuroshio front through the eastern channel are essentially important in the formation of the cyclonic circulation in Sagami Bay. Author (NASDA)

N94-12684 Taiwan Fisheries Research Inst., Tungkang.
A STUDY OF FRONT DYNAMICS OFF NORTHEASTERN TAIWAN BASED ON THE NOAA-AVHRR SATELLITE REMOTE SENSING DATA c43
Chung-Zen Shyu, Wen-Hung Shih, and Chi-Yuan Lin *In* Scientific Organizing Committee of PORSEC, Proceedings of the PORSEC 1992 in Okinawa: Conference for Pacific Ocean Environments and Probing, Volume 2 25 Aug. 1992 p 829-834 (For primary document see N94-12635 01-42) (Grant NSC-80-0209-M056-01)
Copyright Avail: Issuing Activity (Scientific Organizing Committee of PORSEC, P.O. Box 10, Shimizu, Shizuoka 424, Japan, HC)

Two years (October 1989 to September 1991) of NOAA AVHRR (Advanced Very High Resolution Radiometer) imageries were derived to analyze the surface dynamics in the waters off northeastern Taiwan. The observed area is 285 km by 356 km with the center point at 26 deg N, 123 deg E. The location and type of Kuroshio front was distinctly different in different seasons. The greatest extending of the front appeared in winter and had about a 4 C/100 km gradient, while the least was in summer with about a 2 C/100 km gradient. In May, October, and November, the Kuroshio anticurrent which formed an anticlockwise front was prevalent and had a life span of two to seven days. The location and feature of eddies also varied in different seasons. It was located near Taiwan in winter, moved away from Taiwan, and extended northeastward in summer. In autumn, the eddy was easily influenced by the Kuroshio anticurrent. Its life span was about 10 to 16 days. Author (NASDA)

N94-12685 Kyoto Univ., Sakyoku (Japan). Oceanographic Observatory.
SATELLITE THERMAL VARIATIONS OF KUROSHIO IN RELATION TO STORM FLOODS c48
Shigehisa Nakamura *In* Scientific Organizing Committee of PORSEC, Proceedings of the PORSEC 1992 in Okinawa: Conference for Pacific Ocean Environments and Probing, Volume 2 25 Aug. 1992 p 835-840 Sponsored by Ministry of Education, Science and Culture, Tokyo, Japan (For primary document see N94-12635 01-42)
Copyright Avail: Issuing Activity (Scientific Organizing Committee of PORSEC, P.O. Box 10, Shimizu, Shizuoka 424, Japan, HC)

The sea surface thermal patterns of Kuroshio around the Shirahama Oceanographic Observatory were derived using a real time imagery of NOAA APT (Automatic Picture Transmission) system. Variations of the thermal pattern indicate variations of Kuroshio as those that have been surveyed and studied intensively in relation to weather prediction, ocean prediction, or storm floods. Interrelations of Kuroshio variations and storm floods around the tower have been studied. A simple notice about a trigger of the Kuroshio variations are given. Storms may effect the minor variations on the sea surface. Some of the episodic examples could be introduced with a descriptive notice in the scope of geophysical hydrodynamics. Author (NASDA)

N94-12686 First Inst. of Oceanography, Qingdao (China). First Inst. of Oceanography.
ADCP EVIDENCE FOR UPPER LAYER CIRCULATION IN NORTHEAST OF THE SOUTH CHINA SEA c48
Shuzhen Pu, Huiling Yu, and Songnian Jiang (National Marine Date and Information, Tianjin, China.) *In* Scientific Organizing Committee of PORSEC, Proceedings of the PORSEC 1992 in Okinawa: Conference for Pacific Ocean Environments and Probing, Volume 2 25 Aug. 1992 p 841-845 (For primary document see N94-12635 01-42)

Copyright Avail: Issuing Activity (Scientific Organizing Committee of PORSEC, P.O. Box 10, Shimizu, Shizuoka 424, Japan, HC)

Branching of the Kuroshio into Bashi Channel or the warm current in Taiwan Strait are associated with the top layer circulation in the northeast of the South China Sea. This paper goes over the previous research results, and then uses the ADCP (Acoustic Doppler Current Profiler) observations to discuss the top layer circulation in Bashi Channel and the northeast of the South China Sea. As it is indicated from the ADCP measurements: (1) Kuroshio indeed branches into the northeast of the South China Sea through Bashi Channel. The branch of Kuroshio flows northwestward as it is measured many times, and the width and strength of the Kuroshio branch varies in time; (2) the branch of Kuroshio getting into the South China Sea might bifurcate again into the northward current off the west coast of Taiwan and the westward current in the northwest of the South China Sea; (3) the strength of the westward current in the northeast of South China Sea varies in time; (4) there is some structure like an eddy to the south of the westward current in the northeast of the South China Sea; and (5) there might be an eastward current or a northward current to the onshore side of the westward current. Author (NASDA)

N94-12687 Academy of Sciences (USSR), Moscow. Inst. of Oceanology.

FRONTAL ZONES IN PACIFIC OCEAN: SATELLITE AND SHIP DATA ANALYSIS c48

A. S. Kazmin *In* Scientific Organizing Committee of PORSEC, Proceedings of the PORSEC 1992 in Okinawa: Conference for Pacific Ocean Environments and Probing, Volume 2 25 Aug. 1992 p 846-850 (For primary document see N94-12635 01-42)

Copyright Avail: Issuing Activity (Scientific Organizing Committee of PORSEC, P.O. Box 10, Shimizu, Shizuoka 424, Japan, HC)

The results of frontal zones research in the Pacific, based on the combined analysis of ship-borne and satellite data, are presented. Both large scale oceanic frontal zones and mesoscale fronts in marginal seas have been investigated. The main types of frontal zones thermal structure have been distinguished, and comparative characteristics of frontal zones are discussed. Author (NASDA)

N94-12688 Universidad Catolica del Norte, Coquimbo (Chile). Facultad Ciencias del Mar.

SWORDFISH (XIPHIAS GLADIUS) CATCH DISTRIBUTIONS RELATIVE TO ENVIRONMENTAL FEATURES OBSERVED FROM SATELLITES OFF COQUIMBO, CHILE (30 DEG S) c48

Eduardo Uribe and Claudio Salazar (Pesquera Santa Lucia, Valpariso, Chile.) *In* Scientific Organizing Committee of PORSEC, Proceedings of the PORSEC 1992 in Okinawa: Conference for Pacific Ocean Environments and Probing, Volume 2 25 Aug. 1992 p 851-857 (For primary document see N94-12635 01-42)

Copyright Avail: Issuing Activity (Scientific Organizing Committee of PORSEC, P.O. Box 10, Shimizu, Shizuoka 424, Japan, HC)

The commercial swordfish fishery started in Chile in 1983, but the waters off the coast of Coquimbo have not been fished on account of the colder superficial waters (13 C), as a result of the intensive upwelling that occur in this area. Analyzing the satellite temperature images of NOAA-H from 1985 to 1989 and the sea surface color images of NIMBUS-7 during 1980 to 1991, it was determined that beside the upwelling there is an oceanic plume of 15 C water, with low phytoplankton biomass (0.5 mg/cu m of chlorophyll-a) that approaches the coast. This environmental condition would theoretically allow the presence of the swordfish in the zone of Coquimbo. This hypothesis was presented to Santa Lucia fishery, which sent the F/V (Fishing Vessel) Vamas 2 for a survey during August 1989, when the fishing season for this species had finished in Chile, to test it. Nineteen swordfish were caught in three days, proving that this oceanographic structure produces the concentration of this fish. With these preliminary studies, fishing was planned in the waters off Coquimbo during 1990, and the results of those activities are presented. Author (NASDA)

N94-12689 Korea Ocean Research and Development Inst., Seoul (Republic of Korea).

OBSERVATION OF COLD COASTAL WATER WITH HIGH TURBIDITY AROUND THE SOUTHWESTERN TIP OF KOREAN PENINSULA c48

Heung-Jae Lie, Hong-Rhyong Yoo, and Sang Sup Yuk *In* Scientific Organizing Committee of PORSEC, Proceedings of the PORSEC 1992 in Okinawa: Conference for Pacific Ocean Environments and Probing, Volume 2 25 Aug. 1992 p 858-863 (For primary document see N94-12635 01-42)

Copyright Avail: Issuing Activity (Scientific Organizing Committee of PORSEC, P.O. Box 10, Shimizu, Shizuoka 424, Japan, HC)

The Simpson-Hunter criterion predicts the occurrence of strong tidal mixing off the midwest coast and around the southwestern tip of the Korean Peninsula. Surface coastal water in the two areas during the summer is colder than the surrounding water. The boundary between coastal mixed and offshore stratified regions is clearly marked by a thermal front on NOAA infrared imagery. Strong tidal stirring causes high concentration of suspended matter throughout the year in the study area, which is evident on LANDSAT visible images. The turbidity front formed around the southwestern corner of Korea generally is concordant with the thermal front in summer. Author (NASDA)

N94-12690 Iwate Univ., Morioka (Japan).

ON THE ERROR CHARACTERISTICS OF THE SEA SURFACE TEMPERATURE OBSERVED BY SATELLITE c48

Sumio Tanba, Takashi Souma, Yukifumi Iwakuma, Isao Yoshida, Takashi Watanabe, and Ryuuzou Yokoyama *In* Scientific Organizing Committee of PORSEC, Proceedings of the PORSEC 1992 in Okinawa: Conference for Pacific Ocean Environments and Probing, Volume 2 25 Aug. 1992 p 864-867 (For primary document see N94-12635 01-42)

Copyright Avail: Issuing Activity (Scientific Organizing Committee of PORSEC, P.O. Box 10, Shimizu, Shizuoka 424, Japan, HC)

The accuracy of the sea surface temperature estimated by a split-window function was validated by the total data set with 390 match-ups, which were composed of the brightness temperatures by NOAA-9/AVHRR (Advanced Very High Resolution Radiometer) and the sea surface temperature by fixed buoys in Mutsu Bay. The temporal and spatial coincidence in each match-up is within 30 minutes and one pixel resolution. The standard deviation of residues by the regression analysis was 0.59 C. By referring to the meteorological data, several match-ups having large residue were found. Those were estimated to be caused by the air-sea interaction effects. By removing the match-ups with larger errors, a selected data set with 328 match-ups was prepared and the SST (Sea Surface Temperature) estimation function was recalculated. The standard deviation of residues reduced to 0.34 C. Author (NASDA)

N94-12691 Scripps Institution of Oceanography, La Jolla, CA.

THE WOCE/TOGA SURFACE VELOCITY PROGRAMME (SVP) c48

Pearn P. Niiler, Laurence Sombardier, and Andrew Sybrandy *In* Scientific Organizing Committee of PORSEC, Proceedings of the PORSEC 1992 in Okinawa: Conference for Pacific Ocean Environments and Probing, Volume 2 25 Aug. 1992 p 868-875 (For primary document see N94-12635 01-42)

Copyright Avail: Issuing Activity (Scientific Organizing Committee of PORSEC, P.O. Box 10, Shimizu, Shizuoka 424, Japan, HC)

Measurements of surface velocity, sea surface temperature, and sea-level barometric pressure on ocean basin space scales and seasonal time scales are required in the World Climate Research Program. The scientific rationale is to obtain a global description of the mean state of these variables, to map their variability, and with this data to study processes of momentum and heat transport in the upper ocean and improve ocean circulation models. A global Surface Velocity Program (SVP) has been organized in thirteen countries to obtain these measurements from low cost ARGOS tracked Lagrangian drifters, 350 of which are now deployed in the Pacific and Atlantic Oceans. SST (Sea Surface Temperature) and barometer data from drifters are used by operational agencies in real time for improving weather forecasts and modeling and predicting short term climate change. A global population of 900-1,000 drifters will be needed by 1997 in support of the Global Climate Observing System (GCOS). Since 1985, Scripps Institution of Oceanography (SIO) has been a center for drifter technology development and deployments. This is a report of the technical and scientific progress in SVP and ACCP (Atlantic Climate Change Program) organized in support of the WOCE (World Ocean Circulation Experiment)/TOGA (Tropical Ocean and Global Atmosphere Program) in the U.S. since 1988. Author (NASDA)

N94-12692 Tokai Univ., Shizuoka (Japan). Graduate School of Marine Science and Technology.

DEVELOPMENT OF A SHUTTLE AUV FOR OCEANOGRAPHIC MEASUREMENT **c48**

Katsuyoshi Kawaguchi, Tamaki Ura, Yoshibumi Tomoda, and Heihachirou Kobayashi *In* Scientific Organizing Committee of PORSEC, Proceedings of the PORSEC 1992 in Okinawa: Conference for Pacific Ocean Environments and Probing, Volume 2 25 Aug. 1992 p 876-880 (For primary document see N94-12635 01-42)

Copyright Avail: Issuing Activity (Scientific Organizing Committee of PORSEC, P.O. Box 10, Shimizu, Shizuoka 424, Japan, HC)

A prototype of a shuttle type Autonomous Underwater Vehicle (AUV), which is named 'ALBAC', was designed and constructed for oceanographic measurement of the water column from the surface to the seabed. The ALBAC mainly consists of a cylindrical body and a pair of wings that provide lift force to let the vehicle glide horizontally without consuming energy from batteries. Therefore, the mother ship is not obliged to be shifted above the measuring point for it's deploy. The constructed ALBAC (1.4 m in length, and 45 kgf in dry weight) is able to glide 20 degrees down from horizontal plane and dive to the depth of 300 m. To make the total system reliable, major equipments except some ultrasonic apparatuses are installed in one pressure chamber. For scientific measurement devices, 3 liter payload space is available in this chamber. The attitude of the vehicle in gliding is controlled automatically using two balance actuators that displace the center of gravity longitudinally and laterally.

Author (NASDA)

N94-12693 Taisei Corp., Tokyo (Japan).

INTEGRATED MARINE SURVEY SYSTEM **c48**

Tadashi Kanzaki *In* Scientific Organizing Committee of PORSEC, Proceedings of the PORSEC 1992 in Okinawa: Conference for Pacific Ocean Environments and Probing, Volume 2 25 Aug. 1992 p 881-885 (For primary document see N94-12635 01-42)

Copyright Avail: Issuing Activity (Scientific Organizing Committee of PORSEC, P.O. Box 10, Shimizu, Shizuoka 424, Japan, HC)

Many of the large construction projects currently in progress in Japan are under water. The actual sites, however, vary greatly in terms of water depth, geology, wave action, tidal currents, and other characteristics. For example, in the cases of the Trans-Tokyo Bay Highway and Kansai International Airport, large artificial islands have been constructed on an extremely soft seabed where the water depth is in excess of 20 m. In the case of the Honshu-Shikoku Bridges project, the world's largest suspension bridge is presently being constructed over water 50 m deep in an area where tidal currents reach 8 knots. To carry out construction work under such complex marine conditions, it is extremely important that prudent surveys and planning is implemented in advance and that adequate construction management is performed. The system described in this paper allows marine information to be collected over a wide area in a continuous and quick vessel-based process using ultrasonics. It has already been applied to many phases of the construction procedure ranging from surveys to construction management, and the more than 20 projects which have made use of the system so far include the large projects described above.

Author (NASDA)

N94-12694 Japan Weather Association, Tokyo.

DEVELOPMENT OF A BUOY SYSTEM FOR MONITORING MARINE WEATHER AND MARINE LIFE ABUNDANCE **c48**

Masafumi Ichikawa, Mamoru Shimanuki, Kouzou Okada, Harumi Yamada (Japan Marine Fishery Resources Research Center, Tokyo.), and Tadahiko Noda (Japan Meteorological Agency, Tokyo.) *In* Scientific Organizing Committee of PORSEC, Proceedings of the PORSEC 1992 in Okinawa: Conference for Pacific Ocean Environments and Probing, Volume 2 25 Aug. 1992 p 886-891 Original contains color illustrations (For primary document see N94-12635 01-42)

Copyright Avail: Issuing Activity (Scientific Organizing Committee of PORSEC, P.O. Box 10, Shimizu, Shizuoka 424, Japan, HC)

A buoy system for monitoring marine weather and marine life abundance at the Yamato Bank in the Sea of Japan has been developed. The system observes marine weather parameters and acoustic echo under the buoy every three hours. The data is transmitted in real time to the receiving center of the Japan Meteorological Agency via the GMS (Geostationary Meteorological Satellite). The buoy was moored at a site with a depth of 305 m on 9 March, 1990, and the observation was carried out until the end of March 1991. The data obtained of wave height and wave direction were reasonably accurate. An installed echo sounder recorded some typical changes of marine life abundance. The buoy system has been practically completed.

Author (NASDA)

N94-12695 Concepcion Univ. (Chile). Oceanography Dept.

REMOTE SENSING OF POLLUTING FOCAL POINTS AND COASTAL DISTURBANCES IN THE GULF OF ARAUCO AND ADJACENT BAYS, CENTRAL CHILE **c43**

J. Stuardo, C. Valdovinos, and C. Pampaloni *In* Scientific Organizing Committee of PORSEC, Proceedings of the PORSEC 1992 in Okinawa: Conference for Pacific Ocean Environments and Probing, Volume 2 25 Aug. 1992 p 892-897 (For primary document see N94-12635 01-42)

Copyright Avail: Issuing Activity (Scientific Organizing Committee of PORSEC, P.O. Box 10, Shimizu, Shizuoka 424, Japan, HC)

An image-processing system available at the Center EULA for Environmental Studies, University of Concepcion, and the microcomputer software packages RESOURCE and DRAGON to display and manipulate images, were used to process LANDSAT TM (Thematic Mapper) and SPOT images covering the Gulf of Arauco, Bay of San Vicente, Bay of Concepcion and adjacent areas in central Chile, all largely affected by environmental constraints, the impact of population growth and multiple industrial development. Individual bands or their combination were used to localize and measure the extension of the effect of pollution due to suspended particles, and/or thermal inputs along the coast, with a resolution of 30 by 30 m for Band 1 to 5 and 7 and of 120 by 120 m for Band 6 (thermal). Panchromatic SPOT images and aerial orthophotographs taken with a ROLLEY metric camera also permitted the study of the dispersion of particulate-suspended material and sediment in estuarine areas with less than 10 by 10 m resolution. The general dynamics of coastal oceanographic processes in the area of study is discussed regarding local upwelling events, the effects of rivers, sedimentation pattern and, local estuarine input into coastal areas. The identification and degree of comparative pollution is correlated with areas of concentrated industrial or urban effluents, corroborating in-situ measurements and observations. Author (NASDA)

N94-12696 Taisei Corp., Narashino (Japan).

STUDY ON SEA WATER PURIFICATION USING A SUBSTRATUM OF MARINE ORGANISMS **c48**

Fumio Kaneko, Norio Katakura, and Tetsuo Yagura *In* Scientific Organizing Committee of PORSEC, Proceedings of the PORSEC 1992 in Okinawa: Conference for Pacific Ocean Environments and Probing, Volume 2 25 Aug. 1992 p 898-903 (For primary document see N94-12635 01-42)

Copyright Avail: Issuing Activity (Scientific Organizing Committee of PORSEC, P.O. Box 10, Shimizu, Shizuoka 424, Japan, HC)

In recent years, artificial shore protection works and embankments, which are concrete structures, have been increased as a result of active water front development, and natural sea shores have almost disappeared. The organisms living in the sea are disturbed, so the water front development that includes the protective and landscape function is desired to increase the existence of organisms living in the sea. The experiments were made using porous concrete that has large contact area with sea water. The experiments were made with piled concrete aggregates under sea surface and the relationship between the number of species and amount of organism and changes of water quality were examined. As a result, the number of species and amount of organisms were found to depend on the size of aggregate, and the transmissivity was improved by using porous concrete aggregate compared with natural stone. Author (NASDA)

N94-12697 Indian Inst. of Remote Sensing, Dehra Dun.

ROLE OF REMOTE SENSING AND ITS COST EFFECTIVENESS IN SITE SELECTION FOR COASTAL AQUACULTURE **c43**

R. Sudarshana and M. S. Siddiqui *In* Scientific Organizing Committee of PORSEC, Proceedings of the PORSEC 1992 in Okinawa: Conference for Pacific Ocean Environments and Probing, Volume 2 25 Aug. 1992 p 904-909 (For primary document see N94-12635 01-42)

Copyright Avail: Issuing Activity (Scientific Organizing Committee of PORSEC, P.O. Box 10, Shimizu, Shizuoka 424, Japan, HC)

Coastal aquaculture in brackish water expanses of the tropical zone has gained importance as a means of supplementing food production for the ever increasing demands of multiplying populations. Nevertheless, the process is very slow due to lack of inventory of aquaculturable areas in the coast, and there are not many reliable field methods that can produce comprehensive surveys. In view of this, some experiments were made in India to delineate aquaculturable areas using the indigenous data of Indian remote sensing satellite. Termed as the Weighted Index Scheme (WIS), the approach was developed on the incidence of natural processes in determining the potentiality of estuarine brackish water areas. Initially, three estuaries on the west coast were critically analyzed using WIS. Further, the whole of about 6,400 km of Indian coast line was considered and in the background of available statistics on yield, turn over, and profits, projections for the whole coastline in terms of production and yield were made. The cost of remote sensing efforts has also been calculated and it has been demonstrated that the use of remote sensing techniques would only amount to about 0.4 percent of the profits that are obtainable from country-wide exercise. A balance sheet of expenditure and profits in using modern techniques is presented, and the paper upholds that remote sensing can substantially enhance the food production and earnings from coastal aquaculture. Author (NASDA)

N94-12698 Center for Oceanology Research and Development, Jakarta (Indonesia).

SEASONAL VARIABILITY OF SURFACE OCEAN COLOR IN THE OMURA BAY USING MULTITEMPORAL LANDSAT-5 TM DATA c48

Sam Wouthuyzen, Keinosuke Gotou (Nagasaki Univ., Japan.), and Shirou Uno (Seikai Regional Fisheries Research Lab., Nagasaki, Japan.) *In* Scientific Organizing Committee of PORSEC, Proceedings of the PORSEC 1992 in Okinawa: Conference for Pacific Ocean Environments and Probing, Volume 2 25 Aug. 1992 p 910-915 (For primary document see N94-12635 01-42)

Copyright Avail: Issuing Activity (Scientific Organizing Committee of PORSEC, P.O. Box 10, Shimizu, Shizuoka 424, Japan, HC)

The aim of this study is to discuss the seasonal variability of surface ocean color in the Omura Bay, Nagasaki Prefecture, Japan, using multitemporal LANDSAT-5 TM (Thematic Mapper) data. For this purpose, thirteen sets of sea-truth data collected near-simultaneously with LANDSAT-5 TM overpass, consisting of five data sets in autumn, three data sets in winter, three data sets in spring, and two data sets in summer were used to develop the seasonal estimation models using simple linear regression. Among the algorithms, the ratio of atmospheric corrected Digital Count (DC) TM-2 to TM-1 (TM-2/TM-1) consistently correlated best with chlorophyll-a for each season. Weak correlation was found for total pigments, and no correlation for Total Suspended Solid (TSS). Based on this result, it could be concluded that the water of the Omura Bay is optically dominated by living phytoplankton. Validation of the models yielded the Root Mean Square (rms) error of 1.5, 1.0, 0.8 and 0.5 microgram/l within the chlorophyll-a ranges of 1 to 8, 1 to 9, 1 to 8, and 0 to 4 microgram/l for autumn, winter, spring, and summer, respectively. Author (NASDA)

N94-12699 Tokyo Univ. (Japan). Ocean Research Inst.

ACOUSTIC ESTIMATION OF PLANKTON BIOMASS c51

Tadashi Inagaki, Ichirou Aoki, and Takeo Ishii *In* Scientific Organizing Committee of PORSEC, Proceedings of the PORSEC 1992 in Okinawa: Conference for Pacific Ocean Environments and Probing, Volume 2 25 Aug. 1992 p 916-921 (For primary document see N94-12635 01-42)

Copyright Avail: Issuing Activity (Scientific Organizing Committee of PORSEC, P.O. Box 10, Shimizu, Shizuoka 424, Japan, HC)

The around-the-world cruise of R/V (Research Vessel) Hakuho-maru was performed by Ocean Research Institute, University of Tokyo during 130 days. Acoustic measurements at four frequencies with small organisms sampling were carried out 43 times at 19 stations. The biomass represented by settling volume was compared with acoustic volume scattering strength (SV in decibels) at each frequency. The relationship between biomass (transformed into logarithm) and SV was obtained as linear regression equations. Slopes of the regression equations for four frequencies were all close to one. There was a decreasing tendency of SV with increasing frequency. This result suggests that resonance phenomenon occurs in scattering process of the small organisms. Author (NASDA)

N94-12700 Ryukyu Univ., Okinawa (Japan). Coll. of Agriculture.

PROPERTIES OF SPECTRAL REFLECTANCE OF CROWN AND CROWN STRUCTURE OF MANGROVE SPECIES IN OKINAWA c43

Kazuhiro Satou, Dwi Setyono, Osmar DeMoraes (Empresa Brasileira de Pesquisa Agropecuaria, Santa Catarina.), and Takashi Hoshi (Ibaraki Univ., Hitachi, Japan.) *In* Scientific Organizing Committee of PORSEC, Proceedings of the PORSEC 1992 in Okinawa: Conference for Pacific Ocean Environments and Probing, Volume 2 25 Aug. 1992 p 922-927 (For primary document see N94-12635 01-42)

Copyright Avail: Issuing Activity (Scientific Organizing Committee of PORSEC, P.O. Box 10, Shimizu, Shizuoka 424, Japan, HC)

The fundamental data of this study is spectral reflectance measurements above the crown layer of a mangrove stand with three mixed species. Several indexes related with the shape of spectral reflectance curve, and several combinations among these indexes were examined to separate mangrove species. Comparatively good results were found out as combinations of a ratio of reflectance at 850 nm divided by reflectance at 650 nm, and two gradients calculated from reflectances at 850 nm and 650 nm or 550 nm. It was considered that spectral reflectance properties of the mangrove crown related closely with the structure of crown. Author (NASDA)

N94-12701 Diponegoro Univ., Jepara (Indonesia). Coastal Region Eco-Development Lab.

APPLICATION OF REMOTE SENSING FOR COASTAL MANAGEMENT IN THE NORTH COAST OF JAVA c43

A. Hartoko and D. Suprapto *In* Scientific Organizing Committee of PORSEC, Proceedings of the PORSEC 1992 in Okinawa: Conference for Pacific Ocean Environments and Probing, Volume 2 25 Aug. 1992 p 928-935 (For primary document see N94-12635 01-42)

Copyright Avail: Issuing Activity (Scientific Organizing Committee of PORSEC, P.O. Box 10, Shimizu, Shizuoka 424, Japan, HC)

The study is intended to explore possibilities of applications and uses of remote sensing/satellite data for coastal management program holistically. The study itself is a part of a five year research program. The purpose of first year study is to map and monitor the growth of a mangrove area, a brackish water pond area, and the seasonal pattern of sedimentation, sea surface temperature, and primary productivity. The approach used LANDSAT satellite data, MSS (Multi Spectral Scanner) channel 4, 5, 6, and 7. The means was a principal component transformation of channel 1, 2, 3, and 4. The software used is a CCRS (Canadian Center for Remote Sensing) computer package. The sea surface temperature was derived from NOAA/AVHRR (Advanced Very High Resolution Radiometer) satellite data. Sampling for the sea truth data for suspended solids (mg/lit), primary productivity (chlorophyll content, mg/cu m), and sea surface temperature have been done simultaneously in 1991. The first year study program revealed a significant increase of suspended solid during the west monsoon (November-February) due to the pattern of the predominant wind direction. Sea surface temperature in dry monsoon ranged from 22.5 to 30 C, and from 22.5 to 28 C in wet monsoon. The study on the image on mangrove area of Cilacap Bay revealed that mangrove coverage in 1986 was denser than the following year. Author (NASDA)

N94-12702 National Defense Medical Coll., Saitama (Japan). Dept. of Physics.

STUDY OF GROWING PROCESSES OF A TOMBOLO USING AN AIR PHOTOGRAPH c48

Masahiro Hashima and Yasuhiro Sugimori (Tokai Univ., Shizuoka, Japan.) *In* Scientific Organizing Committee of PORSEC, Proceedings of the PORSEC 1992 in Okinawa: Conference for Pacific Ocean Environments and Probing, Volume 2 25 Aug. 1992 p 936-939 (For primary document see N94-12635 01-42)

Copyright Avail: Issuing Activity (Scientific Organizing Committee of PORSEC, P.O. Box 10, Shimizu, Shizuoka 424, Japan, HC)

A sand spit had been developed on the coast of the volcanic island of Iwo Jima (sulfur island). The distribution of median size of this spit's sand and an air photograph are used in order to make clear the growing processes of this spit. The distribution curves of median size show the predominant maximum and minimum looks periodically, and many remarkable wavy patterns are visible in an air photograph. If such two distribution curves will be laid on, the frequency domain of these two curves can be found to coincide well with each other. The fact that these wavy patterns are overlapped so well, enables the prediction of the growing processes of this spit more clearly. Author (NASDA)

N94-12703 Kitami Inst. of Tech., Hokkaido (Japan). Dept. of Developmental Engineering.
ESTIMATION OF AREAL EVAPOTRANSPIRATION USING LANDSAT TM DATA: KITAMI CITY, HOKKAIDO, JAPAN **c43**
Kimiteru Sado *In* Scientific Organizing Committee of PORSEC, Proceedings of the PORSEC 1992 in Okinawa: Conference for Pacific Ocean Environments and Probing, Volume 2 25 Aug. 1992 p 940-945 Original contains color illustrations (For primary document see N94-12635 01-42)
Copyright Avail: Issuing Activity (Scientific Organizing Committee of PORSEC, P.O. Box 10, Shimizu, Shizuoka 424, Japan, HC)

The land cover classification in Kitami which covers an area of 12 by 9.5 km is done after geometric correction, and the monthly mean albedo is estimated for seven land cover categories. The monthly mean of Kitami's areal evapotranspiration (ET) is obtained by Kojima's equation in winter and by Morton's equation in other seasons. The annual change in estimated ET which reach its maximum value in July correlates reasonably well with ET in an observation field. The influence of both slope solar radiation and housing land development on ET are examined. Author (NASDA)

N94-12704 Plan and Budget Organization, Teheran (Iran). Remote Sensing Center.
LAND USE/LAND COVER MAPPING OF CENTRAL WATER SHED OF IRAN AREA BASED ON SATELLITE DATA INTERPRETATION **c43**
Kiadokhi Ahmadi Soroush *In* Scientific Organizing Committee of PORSEC, Proceedings of the PORSEC 1992 in Okinawa: Conference for Pacific Ocean Environments and Probing, Volume 2 25 Aug. 1992 p 946-951 (For primary document see N94-12635 01-42)
Copyright Avail: Issuing Activity (Scientific Organizing Committee of PORSEC, P.O. Box 10, Shimizu, Shizuoka 424, Japan, HC)

An area of 2,125 sq km located in the northwestern part of the Iranian Central Plateau, which is a sub-basin of Iranian internal watershed, was selected for this investigation. The main objectives of this investigation are: (1) construction of a land use map and land cover map; and (2) measurment of the area coverage in all units. On the basis of LANDSAT imagery and available data which were interpreted, the final map was prepared at scale of 1:1,000,000. In the land use map, several major units such as agricultural lands, forest lands, range lands, wet lands, barren lands, water resources, and urban areas have been recognized. Results obtained in this investigation indicate LANDSAT imagery could be used for land use and land cover mapping in an area and undoubtedly could be considered as an essential tool for this type of investigation in the country. Author (NASDA)

N94-12705 Nippon Koei Co. Ltd., Tokyo (Japan).
A METHOD TO MINIMIZE REFERENCE DATA IN CLASSIFYING SATELLITE REMOTE SENSING DATA INTO LAND COVER CLASSES **c43**
L. Samarakoon, H. Ohara (Saga Univ., Japan.), R. Lapitan (Ehime Univ., Matsuyama, Japan.), S. Inoue (Ehime Univ., Matsuyama, Japan.), N. Ebisu (Ehime Univ., Matsuyama, Japan.), S. Ogawa (Ehime Univ., Matsuyama, Japan.), and N. Kishihara (Saga Univ., Japan.) *In* Scientific Organizing Committee of PORSEC, Proceedings of the PORSEC 1992 in Okinawa: Conference for Pacific Ocean Environments and Probing, Volume 2 25 Aug. 1992 p 952-957 (For primary document see N94-12635 01-42)
Copyright Avail: Issuing Activity (Scientific Organizing Committee of PORSEC, P.O. Box 10, Shimizu, Shizuoka 424, Japan, HC)

The use of reference data in statistical algorithms is the standard pattern recognition technique in satellite remote sensing, although it is costly. This paper presents a method that minimizes the quantity and quality of reference data in classifying spectral data into land cover classes. With this method, the reference data is limited to land cover maps, which could be easily obtainable for any geographical location. The method uses cluster analysis and factor analysis for classification. The spectral classes or the natural grouping in a satellite image is identified by clustering. Factor analysis is carried out with these spectral classes, and physical properties of the factors are interpreted on factor loadings. Using factor interpretation, land cover classes of these spectral classes are estimated. Typical spectral response patterns of land cover and band ratios are used as supporting data in spectral classes interpretation. Samples that belonged to each estimated land cover class are used as the true reference data of the particular class and the whole scene is classified using a maximum likelihood algorithm. Application of the above method was attempted in two different cases such as mapping severity of forest fire damage, and estimating the land cover classes, using LANDSAT Thematic Mapper (TM) data. It was found that the accuracy of severity of fire damage mapping was 78 percent and land cover mapping was 80 percent, when compared with aerial photographs. Author (NASDA)

N94-12706 Komatsu Ltd. (Japan). Research Div.
RESISTIVITY AND RADAR VOID DETECTORS FOR TUNNELING MACHINES **c32**
A. Khan, T. Abe, K. Shibatani, H. Yamaguchi, T. Shinbo, S. Sakanishi, and A. Okamoto *In* Scientific Organizing Committee of PORSEC, Proceedings of the PORSEC 1992 in Okinawa: Conference for Pacific Ocean Environments and Probing, Volume 2 25 Aug. 1992 p 958-963 Original contains color illustrations (For primary document see N94-12635 01-42)
Copyright Avail: Issuing Activity (Scientific Organizing Committee of PORSEC, P.O. Box 10, Shimizu, Shizuoka 424, Japan, HC)

Resistivity and UHF radar based surface collapse detection systems for Pressurized Slurry Shield Tunneling Machines (PSSTM) have been developed and are discussed. Author (NASDA)

N94-12707 National Taiwan Univ., Taipei. Inst. of Oceanography.
THE CIRCULATION NEAR LUZON **c48**
Cho-Teng Liu, Su-Cheng Pai, Gil Jacinto (University of the Philippines, Quezon City.), and Israel Bentillo (University of the Philippines, Quezon City.) *In* Scientific Organizing Committee of PORSEC, Proceedings of the PORSEC 1992 in Okinawa: Conference for Pacific Ocean Environments and Probing, Volume 2 25 Aug. 1992 p 964-968 (For primary document see N94-12635 01-42)
Copyright Avail: Issuing Activity (Scientific Organizing Committee of PORSEC, P.O. Box 10, Shimizu, Shizuoka 424, Japan, HC)

During the two WOCE (World Ocean Circulation Experiment) PR21 cruises and the Joint Sino-Philippino cruises, hydrographic surveys were made around the northern part of Luzon Island. Both CTD (conductivity, temperature, and depth) and chemical water samples were taken for studying the coastal hydrography and Kuroshio near Luzon. In the region northeast of Luzon, both the geostrophic calculation and the Acoustic Doppler Current Profiler (ADCP) data suggest that the Kuroshio transport in June 1991 contributes only part of the Kuroshio transport further downstream near southeast of Taiwan, where a significant portion of Kuroshio water comes from the westward current between 18 deg N - 22 deg N. In the region west of Luzon, the on-shore current splits at 15 deg N. It forms northward coastal current (against the NE (Northeast) winter monsoon) north of 15 deg N, and southward coastal current south of 15 deg N where monsoonal wind is relatively weaker than the northern region. To balance the fresh water and salt, a counter clockwise gyre in the South China Sea north of 15 deg N is suggested. Author (NASDA)

N94-12708 National Taiwan Univ., Taipei. Inst. of Oceanography.
CURRENT VARIABILITY ON THE SHELF BREAK NORTHEAST OF TAIWAN **c48**
T. Y. Tang, Y. J. Yang, and D. Lee *In* Scientific Organizing Committee of PORSEC, Proceedings of the PORSEC 1992 in Okinawa: Conference for Pacific Ocean Environments and Probing, Volume 2 25 Aug. 1992 p 969-974 (For primary document see N94-12635 01-42)
(Grant NCS-81-0209-M-002A-08)
Copyright Avail: Issuing Activity (Scientific Organizing Committee of PORSEC, P.O. Box 10, Shimizu, Shizuoka 424, Japan, HC)

A buoy-mounted Acoustic Doppler Current Profiler (ADCP) was deployed on the shelf-break off the northeast coast of Taiwan to monitor current variation in the upper ocean. The acquired data was used to study the variations of low-frequency current and semidiurnal tidal current. The low-frequency flow in the upper water column was initially southwest and then abruptly turned northwest. This abrupt change occurred in mid-October, starting from the surface layer and then gradually extending to the deeper layer. In contrast with this flow, the low-frequency flow in the lower water column was over the entire record. The abrupt change of current from southwest to northwest is related to the intrusion of Kuroshio. Examination of the wind record at Pengchiayu showed that the local wind and current were incoherent. The intrusion of Kuroshio appears to be induced by remote factors. Both barotropic and first baroclinic tides were found to be important in this area. The intrusion of Kuroshio had relative small impact on the barotropic tide but large impact on the baroclinic tide. The speed of barotropic and baroclinic tides were comparable before the intrusion. After the Kuroshio intruded, the baroclinic tidal speed was enlarged. The intrusion also changed the orientation and the ratio of two axes of ellipse for both barotropic and baroclinic tides, but the later one has more significant change. The change of local water stratification and background low-frequency current may be responsible for the variation of the semidiurnal tide. Author (NASDA)

N94-12709 National Sun Yat-Sen Univ., Kaohsiung (China). Inst. of Marine Geology.

SEDIMENTATION RATES AND PARTICULATE FLUXES IN THE SLOPE AND DEEP SEA AREAS OFF EASTERN TAIWAN **c48**

G. W. Hung and Y. Chung *In* Scientific Organizing Committee of PORSEC, Proceedings of the PORSEC 1992 in Okinawa: Conference for Pacific Ocean Environments and Probing, Volume 2 25 Aug. 1992 p 975-981 (For primary document see N94-12635 01-42)
Copyright Avail: Issuing Activity (Scientific Organizing Committee of PORSEC, P.O. Box 10, Shimizu, Shizuoka 424, Japan, HC)

Th-230 and Pb-210 were measured for sedimentation rate and flux determinations from several cores collected from the East China Sea continental slope and the deep-sea areas off eastern Taiwan. In the East China Sea slope area, the sedimentation rate as determined by the Pb-210 method was 0.28 cm/year for the past 100 years. In the deep sea areas off eastern Taiwan, the rates as determined by the Th-230 method from two cores were similar at about 2 to 3 cm/k year. Another core was located to the southeast of Taiwan, the rate was 0.6 cm/k year. These results suggest that the river input and runoff from the east coast of Taiwan have contributed a significant amount of sediments into the deep sea off the east coast. The sedimentation rate obtained in the East China Sea Continental Slope is about 100 times greater than that in the deep sea off the east coast, suggesting that additional major source from mainland China may be responsible for such high sedimentation rate. There are indications that the output of sediments from both the Yangtze and Yellow Rivers may be transported southward by coastal current before deviating eastward to the north of Taiwan. Sediment traps deployed repeatedly near the coring site in the East China Sea yield an apparent particulate flux of about 2.5 gm(sup -2)d(sup -1). The flux is at least five times as great as the above value. As the current speed is quite high in the area, the trapping efficiency may have been significantly reduced. Author (NASDA)

N94-12710 Tohoku Univ., Sendai (Japan). Center for Atmospheric and Oceanic Studies.

STUDY ON AIR-SEA INTERACTIONS IN THE OMLET (OCEAN MIXED LAYER EXPERIMENT) AREA USING SATELLITE REMOTE SENSING **c46**

Hiroshi Kawamura, Shouichi Kizu, Futoki Sakaida, Naoto Ebuchi, and Yoshiaki Toba *In* Scientific Organizing Committee of PORSEC, Proceedings of the PORSEC 1992 in Okinawa: Conference for Pacific Ocean Environments and Probing, Volume 2 25 Aug. 1992 p 982-987 (For primary document see N94-12635 01-42)
Copyright Avail: Issuing Activity (Scientific Organizing Committee of PORSEC, P.O. Box 10, Shimizu, Shizuoka 424, Japan, HC)

Air-sea interaction in the OMLET (Ocean Mixed Layer Experiment) area has been studied to understand mechanisms of variation of a layer in the vicinity of the ocean surface, which covers a wide area and has a time scale on the order of a day. Remote sensing data of several satellite sensors are employed for estimation of the air-sea fluxes together with in-situ observations of the OMLET. The OMLET region is investigated during April to May, 1988, when the OMLET cruise KH88-2 was performed. Author (NASDA)

N94-12711 Qingdao Inst. of Oceanology (China). Ocean Remote Sensing and Optics Lab.

INVESTIGATION OF MESO-SCALE FRONTS, EDDIES AND UPWELLINGS IN CHINA SEAS WITH AVHRR DATA **c48**

Ming Xia He, Ge Chen, and A. S. Kazmin *In* Scientific Organizing Committee of PORSEC, Proceedings of the PORSEC 1992 in Okinawa: Conference for Pacific Ocean Environments and Probing, Volume 2 25 Aug. 1992 p 989-998 (For primary document see N94-12635 01-42)
Copyright Avail: Issuing Activity (Scientific Organizing Committee of PORSEC, P.O. Box 10, Shimizu, Shizuoka 424, Japan, HC)

Using Sea Surface Temperature (SST) images derived from Advanced Very High Resolution Radiometer (AVHRR) data, a number of meso-scale ocean phenomena such as fronts, eddies, and upwellings have been investigated in the China Seas. Firstly, five kinds of temperature fronts have been observed and their generating causes have been studied, they are shelf-break front, tidal mixing front, estuarine discharge front, coastal upwelling front, and a front formed in the junction of two currents with different natures. A general map indicating the locations and types of eight main frontal zones in the eastern China Seas has been presented. Secondly, several meso-scale eddies have been found, their causes and evolution processes have been examined, among which a cyclonic cold eddy with a lifetime of nearly one month in the northern Yellow Sea is reported and analyzed for the first time. In-situ measurements of some of the eddies have shown good agreement with satellite observations. Thirdly, behavior of the famous Zhejiang coastal upwelling has been identified and studied. Author (NASDA)

N94-12712 Joint Research Centre of the European Communities, Ispra (Italy). Inst. for Remote Sensing Applications.

COASTAL UPWELLING MONITORED BY SATELLITE DATA: METHODOLOGIES AND RESULTS **c48**

Leo Nykjaer, Lieve VanCamp, Trevor Barker, and Nick Jewell *In* Scientific Organizing Committee of PORSEC, Proceedings of the PORSEC 1992 in Okinawa: Conference for Pacific Ocean Environments and Probing, Volume 2 25 Aug. 1992 p 999-1003 (For primary document see N94-12635 01-42)
Copyright Avail: Issuing Activity (Scientific Organizing Committee of PORSEC, P.O. Box 10, Shimizu, Shizuoka 424, Japan, HC)

A total of 3400 NOAA GAC (Global Area Coverage) satellite images covering the northwest African upwelling area have been processed to Sea Surface Temperature (SST) maps. An SST upwelling index has been extracted from the SST maps and is analyzed for seasonal and spatial variabilities and compared to an Ekman upwelling index computed from the large scale wind field. Author (NASDA)

N94-12713 Nihon Univ., Funabashi (Japan). Coll. of Science and Technology.

THE WARM EDDY DETECTION FROM NOAA/AVHRR THERMAL IMAGES USING THE HOUGH TRANSFORMATION **c48**

Fumio Inoue, Akiyoshi Itou, Hiroshi Shinomiya (Nihon Univ., Tokyo, Japan.), Hideo Tameishi (Japan Fisheries Information Service Center, Tokyo.), Hiromichi Yamamoto (National Aerospace Lab., Tokyo, Japan.), and Masao Naka (National Aerospace Lab., Tokyo, Japan.) *In* Scientific Organizing Committee of PORSEC, Proceedings of the PORSEC 1992 in Okinawa: Conference for Pacific Ocean Environments and Probing, Volume 2 25 Aug. 1992 p 1004-1009 (For primary document see N94-12635 01-42)
Copyright Avail: Issuing Activity (Scientific Organizing Committee of PORSEC, P.O. Box 10, Shimizu, Shizuoka 424, Japan, HC)

Satellite infrared images enable us to recognize ocean phenomena such as current, eddy, front, and others as macroscopic patterns. However, the recognition has still remained ambiguous in minute parts. A theoretical method to extract warm eddies from NOAA/AVHRR (Advanced Very High Resolution Radiometer) images is investigated. Based on an assumption that the shape of an eddy is approximately ellipse, the detections of the size, location, and orientation of an eddy were examined by using a generalized Hough transformation. As a result, ellipses in various types were detected from images. One of them could be along an eddy and the other overlaid on fronts close to an eddy. As a warm eddy possibly causes a cold streamer as well as fronts, the detection of ellipses overlapped on an eddy and front leads to a prediction of a cold streamer. Author (NASDA)

N94-12714 Central Research Inst. of Electric Power Industry, Tokyo (Japan).

APPLICABILITY OF SATELLITE INFRARED DATA FOR THE MONITORING OF COASTAL ENVIRONMENTS **c43**

Shinichi Sakai, Masafumi Mizutori, and Norikazu Nakashiki *In* Scientific Organizing Committee of PORSEC, Proceedings of the PORSEC 1992 in Okinawa: Conference for Pacific Ocean Environments and Probing, Volume 2 25 Aug. 1992 p 1010-1015 (For primary document see N94-12635

01-42)
Copyright Avail: Issuing Activity (Scientific Organizing Committee of PORSEC, P.O. Box 10, Shimizu, Shizuoka 424, Japan, HC)

In recent years, large power stations have been constructed close to each other on the coast of Japan. The need of monitoring more widely and immediately the sea adjacent to power stations has been increasing. The satellites observation has been applied as an effective method for this purpose. The objective of this study is to estimate the applicability of the satellite data for the monitoring of coastal environments. First, the applicability of the LANDSAT/TM (Thematic Mapper) data for the monitoring of warm water discharged from power stations was examined. The distribution of the Sea Surface Temperature (SST) was estimated by the regression analysis with the field data measured with the thermometer. The measuring ratio of the available LANDSAT/TM data for the monitoring was evaluated at 57 power stations in 1987 and 1988. Second, the template method, which computes the velocity of surface water mass displacement using the temporal change of the SST distribution estimated by the NOAA/AVHRR (Advanced Very High Resolution Radiometer) data, was applied to three oceanic areas in Japan. The controversial points in applying the template method are discussed. Author (NASDA)

N94-12715 Japan Weather Association, Tokyo. Meteorological Information Center.

SATELLITE AND MOORED BUOY OBSERVATIONS OF POLAR FRONTAL SYSTEM OVER THE YAMATO RISE IN THE JAPAN SEA **c43**

Seiichi Saitou, Masafumi Ichikawa, Kouzou Okada, and Yutaka Isoda *In* Scientific Organizing Committee of PORSEC, Proceedings of the PORSEC 1992 in Okinawa: Conference for Pacific Ocean Environments and Probing, Volume 2 25 Aug. 1992 p 1016-1021 (For primary document see N94-12635 01-42)
Copyright Avail: Issuing Activity (Scientific Organizing Committee of PORSEC, P.O. Box 10, Shimizu, Shizuoka 424, Japan, HC)

Time series satellite infrared observations of NOAA-11 AVHRR (Advanced Very High Resolution Radiometer) were carried out around the Yamato Rise in the Japan Sea from October 1990 to January 1991. In the same period, a ocean buoy system moored over the Yamato Rise has been gathering sea surface temperature and other marine meteorological parameters. Buoy observation is useful to grasp the movement of a polar front in the Japan Sea. On the other hand, satellite observation is applied to understand spatial variabilities of the polar frontal system. As a result, movement of the polar front is connected to variabilities of SST (Sea Surface Temperature) observed by the moored buoy. A warm eddy existing on the western side of the Yamato Rise is an important phenomenon in understanding the variabilities of the polar frontal system over the Yamato Rise. Author (NASDA)

N94-12716 Colorado Univ., Boulder.

THE RELATIONSHIP BETWEEN SKIN AND BULK SEA SURFACE TEMPERATURES **c48**

W. J. Emery, L. Kantha, G. A. Wick, and Peter Schluessel (Hamburg Univ., Germany.) *In* Scientific Organizing Committee of PORSEC, Proceedings of the PORSEC 1992 in Okinawa: Conference for Pacific Ocean Environments and Probing, Volume 2 25 Aug. 1992 p 1022-1027 (For primary document see N94-12635 01-42)
Copyright Avail: Issuing Activity (Scientific Organizing Committee of PORSEC, P.O. Box 10, Shimizu, Shizuoka 424, Japan, HC)

Historically, sea surface temperatures were measured from bucket samples or engine cooling water samples that measure the temperature of the upper meter of the ocean. Known as the bulk sea surface temperature, this measurement has been used to compute air-sea heat fluxes using empirical formulae. Infrared satellite sensors collect radiation emitted from the millimeter thin skin of the ocean. Depending on atmospheric and oceanic conditions, this skin temperature differs from the bulk temperature on average by about 0.5 C. Maximum bulk-skin differences can be as large as 1.4 or -1.2 C. Measurements of the skin temperature from ship-mounted radiometers are used with coincident measurements of bulk temperature to study these differences and their correlations in time and space. A one-dimensional numerical model is used to simulate both skin and bulk temperatures as a function of surface heat fluxes and wind stress. Author (NASDA)

N94-12717 Institute of Disaster and Earth Sciences, Ibaraki (Japan).

VARIABILITY OF THE KUROSHIO OBSERVED FROM SATELLITE THERMAL IMAGERY **c48**

Takashi Toda, Atsushi Takeda, and Norihisa Imasato (Kyoto Univ., Japan.) *In* Scientific Organizing Committee of PORSEC, Proceedings of the PORSEC 1992 in Okinawa: Conference for Pacific Ocean Environments and Probing, Volume 2 25 Aug. 1992 p 1028-1033 (For primary document see N94-12635 01-42)
Copyright Avail: Issuing Activity (Scientific Organizing Committee of PORSEC, P.O. Box 10, Shimizu, Shizuoka 424, Japan, HC)

A sharp front is found at the northern edge of the warmest area along the Kuroshio in each thermal image (hereafter, the 'surface Kuroshio front'). The relationship between the Kuroshio axis and the surface Kuroshio front was analyzed. It was found that the surface Kuroshio front always coincides with the Kuroshio axis in the area of the Pacific Ocean, east of Japan, whereas it tends to coincide with the northern edge of the strong flow of the Kuroshio in the East China Sea and the area of the Pacific Ocean near Japan. In other words, the relationship depends on the area. Therefore, it was ensured that the surface Kuroshio front is a good measure of the location of the Kuroshio axis. Then, the location of the surface Kuroshio front was analyzed statistically to examine the variability of the Kuroshio. The transition of the type of the Kuroshio meander in August 1990 was successfully identified. It was also found that the standard deviation of the variation in the location of the surface Kuroshio front is the smallest (less than 20 km) in the regions off Shikoku Island and Boso Peninsula, Japan; therefore, the Kuroshio path is the most stable here. Author (NASDA)

N94-12718 Delaware Univ., Newark. Coll. of Marine Studies.

VARIABILITY OF THE MIXED LAYER DEPTH IN THE NORTH PACIFIC OCEAN AS CALCULATED BY A 3-D SEMI-ANALYTICAL MIXED LAYER REMOTE SENSING MODEL **c48**

Xiao-Hai Yan and Akira Okubo (State Univ. of New York, Stony Brook.) *In* Scientific Organizing Committee of PORSEC, Proceedings of the PORSEC 1992 in Okinawa: Conference for Pacific Ocean Environments and Probing, Volume 2 25 Aug. 1992 p 1034-1039 Sponsored by NASA, Washington (For primary document see N94-12635 01-42)
(Contracts N00014-88-K-0207; N00014-91-J-1052; NSF OCE-91-16020)
Copyright Avail: Issuing Activity (Scientific Organizing Committee of PORSEC, P.O. Box 10, Shimizu, Shizuoka 424, Japan, HC)

A three-dimensional (3-D) semi-analytical mixed layer remote sensing model which includes the horizontal advection and diffusion processes in previous one-dimensional (1-D) model have been recently developed. The 3-D model can be used as a supplement to the 1-D model in the area where advection is important and for a finer resolution grid prediction. The 3-D thermal inertia model is based on the 3-D thermal energy conservation equation. Using sine transformation and inverse sine transformation methods, the solution for mixed layer thermal inertia which, in turn, can be used to calculate mixed layer depth using a similar method, was obtained. In the solution, the thermal inertia, which is proportional to the mixed layer depth, is expressed as functions of Sea Surface Temperature (SST) changes (delta SST), heat flux (Q), and surface layer velocity (u and v). The vertical entrainment and wind effects are accounted for in the model by changes of delta SST, e.g., if vertical entrainment is larger, delta SST will be smaller and vice versa. The model was tested using the data from AVHRR (Advanced Very High Resolution Radiometer)-MCSST (Multi-Channel SST) data set and COADS (Comprehensive Ocean Atmosphere Data Set) for the North Pacific Ocean. The model predicted mixed layer depths compared favorably with the mixed layer depths calculated from fourteen years of VOS (Vehicle on Stand)-XBT (Expandable Bathy Thermograph) observation data. The model/data comparison also exhibited a number of mesoscale features of seasonal changes and anomalies of the mixed layer depth. Author (NASDA)

N94-12719 Consiglio Nazionale delle Ricerche, Venice (Italy). Ist. per lo Studio della Dinamica delle Grandi Masse.

SST ASSIMILATION: EASTERN MEDITERRANEAN CASE STUDY **c48**

A. Bergamasco, W. Thacker, R. Long (National Oceanic and Atmospheric Administration, Miami, FL.), and P. Malanotte Rizzoli (Massachusetts Inst. of Tech., Cambridge.) *In* Scientific Organizing Committee of PORSEC, Proceedings of the PORSEC 1992 in Okinawa: Conference for Pacific Ocean Environments and Probing, Volume 2 25 Aug. 1992

p 1040-1043 (For primary document see N94-12635 01-42)
Copyright Avail: Issuing Activity (Scientific Organizing Committee of PORSEC, P.O. Box 10, Shimizu, Shizuoka 424, Japan, HC)

The adjoint method is an elegant data assimilation technique to find the solution to the numerical model equations best reproducing all available physical observations wherever located in space and time. The desired numerical model solution is the one which minimizes the cost function defining the extent to which the model results fail to reproduce the data. In searching for the minimum of the cost, the variables of the model cannot be adjusted independently because they are related by the model equations. These constraints are incorporated into the optimization problem via a Lagrange function that has a saddle point which corresponds to the constrained minimum of the cost. The GFDL (Geophysical Fluid Dynamics Laboratory)-GCM (General Ocean Circulation Model), a nonlinear, primitive equation model that has excellent numerical conservation properties, was used to build a model fitting procedure to assimilate the Eastern Mediterranean climatological data. Seasonal steady state general circulation induced by T (temperature), S (salinity), and wind data are already assimilated and used to start the time dependent data assimilation of Sea Surface Temperature (SST) from AVHRR (Advanced Very High Resolution Radiometer) imagery. Author (NASDA)

N94-12720 Seikai Regional Fisheries Research Lab., Nagasaki (Japan).
MAPPING OF HIGH DENSITY AREA OF BENTHIC DIATOM IN ARIAKE SEA **c43**
Shirou Uno *In* Scientific Organizing Committee of PORSEC, Proceedings of the PORSEC 1992 in Okinawa: Conference for Pacific Ocean Environments and Probing, Volume 2 25 Aug. 1992 p 1045-1050 Sponsored by Science and Technology Agency, Tokyo, Japan (For primary document see N94-12635 01-42)
Copyright Avail: Issuing Activity (Scientific Organizing Committee of PORSEC, P.O. Box 10, Shimizu, Shizuoka 424, Japan, HC)

Application of near infrared data for monitoring of a benthic diatom in a tidal area was examined in Ariake Sea, western Kyushu. CCT (computer compatible tape) count on the dense area was apparently different from that on the other area and indicated about half the value of paddy fields. Images taken by the spectral slice method using the near infrared band was effective in monitoring the high density area of a benthic diatom. For detection of the dense area, it is necessary to be at a lower tidal level. However, the dense area occupied a small portion of the tidal area at low tide. The dense area was found in the west coast and never found in the east coast of the Ariake Sea. As this tendency of distribution of dense area well coincided to that of bivalve production, the detected area in this procedure should indicate potential productivity in the tidal area. Author (NASDA)

N94-12721 National Inst. of Oceanography, Goa (India).
ADVECTIVE SURFACE VELOCITY IN THE NORTH WEST PACIFIC DERIVED FROM NOAA AVHRR IMAGES **c48**
Pankajakshan Thadathil, Masatoshi Akiyama (Tokai Univ., Tokyo, Japan.), Y. Okada (Tokai Univ., Tokyo, Japan.), and Yasuhiro Sugimori (Tokai Univ., Tokyo, Japan.) *In* Scientific Organizing Committee of PORSEC, Proceedings of the PORSEC 1992 in Okinawa: Conference for Pacific Ocean Environments and Probing, Volume 2 25 Aug. 1992 p 1051-1057 (For primary document see N94-12635 01-42)
Copyright Avail: Issuing Activity (Scientific Organizing Committee of PORSEC, P.O. Box 10, Shimizu, Shizuoka 424, Japan, HC)

Using sequential AVHRR (Advanced Very High Resolution Radiometer) images in November 1983, near-surface advective velocities in the region Kuroshio south of Japan are derived. For deriving the velocities two methods are used. One is the Method of Cross Correlation (MCC), using image pair, and the other is geostrophic approximation, using single image. Both of the velocity vectors are found to be comparable in magnitude and direction. While the approximated geostrophic velocities exhibit the Kuroshio large meander, the MCC velocities failed to derive any velocity vectors associated with the large meander. The vector fields off Kii Peninsula demonstrated an onshore intrusion of Kuroshio water. Near the Bungo Sidan channel, the MCC velocities appeared to be the geostrophic surface currents perturbed by south easterly winds. Author (NASDA)

N94-12722 Academy of Sciences (USSR), Moscow. Inst. of Oceanology.
POLARISATION OF BACKSCATTERING RADIATION AT REMOTE SENSING OF OCEAN WITH IMPULSE LASER BEAM **c36**
Alexander P. Vasilkov, Timothy V. Kondranin, and Yegeny V. Myasnikov *In* Scientific Organizing Committee of PORSEC, Proceedings of the PORSEC 1992 in Okinawa: Conference for Pacific Ocean Environments and Probing, Volume 2 25 Aug. 1992 p 1058-1062 (For primary document see N94-12635 01-42)
Copyright Avail: Issuing Activity (Scientific Organizing Committee of PORSEC, P.O. Box 10, Shimizu, Shizuoka 424, Japan, HC)

The problem determining polarized backscattering radiation in a highly anisotropic scattering medium illuminated by impulse laser beam is solved. The expressions for the Stokes vector of the backscattering radiation are obtained in a small angle approximation of the vector radiative transfer equation. The influence of the optical properties of the water and remote sensing geometry on the temporal dependence of the degree of polarization is investigated. The obtained solution also allowed for the analysis of the effect of optical property stratification on the time dependence of linear polarization of backscattering. A method for the determination of the light scattering coefficient vertical distribution from the measurement of the linear polarization time dependence of the backscattering radiation is proposed. The experimental verification of this method is reported. Author (NASDA)

N94-12723 Academy of Sciences (USSR), Moscow. Inst. of Oceanology.
THE METHOD OF INVESTIGATION OF THE HORIZONTAL STRUCTURE OF THE THERMAL FRONTS **c48**
L. I. Koprova and Ju. A. Romanov *In* Scientific Organizing Committee of PORSEC, Proceedings of the PORSEC 1992 in Okinawa: Conference for Pacific Ocean Environments and Probing, Volume 2 25 Aug. 1992 p 1063-1065 (For primary document see N94-12635 01-42)
Copyright Avail: Issuing Activity (Scientific Organizing Committee of PORSEC, P.O. Box 10, Shimizu, Shizuoka 424, Japan, HC)

Data are presented on the space-time variability of SST (Sea Surface Temperature) in the northwest Atlantic (45 deg N-53 deg N, 36 deg W-45 deg W), which were obtained in accordance with the WOCE (World Ocean Circulation Experiment) Program on the 50th cruise of the scientific vessel, the Akademik Kurchatov. Author (NASDA)

N94-12724 Academy of Sciences (USSR), Moscow. Inst. of Oceanology.
ON A NONSTATIONARY DYNAMICS OF THE NORTH-WEST PACIFIC OCEAN **c48**
A. I. Ginzburg *In* Scientific Organizing Committee of PORSEC, Proceedings of the PORSEC 1992 in Okinawa: Conference for Pacific Ocean Environments and Probing, Volume 2 25 Aug. 1992 p 1066-1069 (For primary document see N94-12635 01-42)
Copyright Avail: Issuing Activity (Scientific Organizing Committee of PORSEC, P.O. Box 10, Shimizu, Shizuoka 424, Japan, HC)

Analysis of satellite visible band and infrared images of the northwest Pacific Ocean reveals typical mesoscale elements of nonstationary dynamics (vortices, jets, and their combinations) and areas of their intensive generation. The main processes, which condition is a nonstationary dynamics in the region such as velocity shear of different kinds, regulating of various non-organized disturbances, processes in a marginal ice zone, eddy evolution, and eddy-front interaction are indicated. Interactions of eddies with the Kuroshio and Oyashio fronts are shown to condition the near-surface circulation in the subarctic frontal zone frequently at distances up to 300 km from the initial eddy. The possiblity of decoupling the near-surface dynamics with the deeper one is considered. Author (NASDA)

N94-12725 Academy of Sciences (USSR), Saint Petersburg. Inst. of Oceanology.
PROPAGATION OF LIGHT PULSES THROUGH A THREE-LAYER MEDIUM (CLOUD, PURE AIR, AND OCEAN WATER) **c74**
V. M. Greysukh and I. M. Levin *In* Scientific Organizing Committee of PORSEC, Proceedings of the PORSEC 1992 in Okinawa: Conference for Pacific Ocean Environments and Probing, Volume 2 25 Aug. 1992 p 1070-1072 (For primary document see N94-12635 01-42)
Copyright Avail: Issuing Activity (Scientific Organizing Committee of PORSEC, P.O. Box 10, Shimizu, Shizuoka 424, Japan, HC)

Monte-Carlo simulations of total energy and the delay and width of a pulse transmitted through a three-layer medium (i.e., cloud, pure atmosphere, and ocean water) are compared with a simple model developed for computing these parameters. The model showed high accuracy for optically thick clouds (with optical depth greater than or equal to 15). Author (NASDA)

N94-12726 Academy of Sciences (USSR), Saint Petersburg. Inst. of Oceanology.

OPTIMUM SELECTION OF SPECTRAL CHANNELS IN THE PROBLEM OF REMOTE SENSING OF PHYTOPLANKTON CONCENTRATION IN OCEAN WATER **c51**

V. P. Kozlov, J. M. Levin, and L. V. Zolotukhin *In* Scientific Organizing Committee of PORSEC, Proceedings of the PORSEC 1992 in Okinawa: Conference for Pacific Ocean Environments and Probing, Volume 2 25 Aug. 1992 p 1073-1074 (For primary document see N94-12635 01-42)
Copyright Avail: Issuing Activity (Scientific Organizing Committee of PORSEC, P.O. Box 10, Shimizu, Shizuoka 424, Japan, HC)

A new method is proposed to estimate phytoplankton (chlorophyll) concentration in ocean water at the maximum accuracy by measurements of the upwelling radiation spectra conducted by a ship or satellite. The method is based on the results of the mathematical theory of experimental design. The accuracy can be strongly increased by optimum selection of spectral channels for the measurements. A convergent iterative algorithm is proposed for searching for optimum channels and corresponding time intervals. The algorithm is realized as a routine in the PASCAL language. The input data for this algorithm are correlation characteristics of the system: spectrum of upwelling radiation to chlorophyll concentration (C). Increasing the number of both joint and separate measurements of the upwell radiation and C from a ship and satellite will make it possible to improve the accuracy of defining optimum spectral channels and consequently accuracy of the C estimate. The method of statistical simulation can also be used to determine the correlation characteristics needed for searching for optimum channels. Author (NASDA)

N94-12727 Marine Hydrophysical Inst., Sevastopol (USSR).

FIELD RESEARCH OF WIND WAVE SPECTRUM VARIABILITY **c47**

V. V. Efimov and A. V. Babanin *In* Scientific Organizing Committee of PORSEC, Proceedings of the PORSEC 1992 in Okinawa: Conference for Pacific Ocean Environments and Probing, Volume 2 25 Aug. 1992 p 1075-1078 (For primary document see N94-12635 01-42)
Copyright Avail: Issuing Activity (Scientific Organizing Committee of PORSEC, P.O. Box 10, Shimizu, Shizuoka 424, Japan, HC)

The report is devoted to the research into the spatial-temporal spectrum of wind waves and group characteristics of the wave disturbances related to it. The study is based on the field in-situ data. Results of the research on the variability of one-dimensional frequency spectra of waves, and functions of the directional distribution of the energy of wind waves are described. The investigations of the equilibrium range of wave spectrum and the kinematic characteristics of the groups of wind waves related to the initial wave spectrum were also reported. Author (NASDA)

N94-12728 Academy of Sciences (USSR), Vladivostok. Pacific Oceanological Inst.

THE THERMODYNAMICS OF THE NONLINEAR SHEAR FLOWS **c34**

S. V. Simonenko *In* Scientific Organizing Committee of PORSEC, Proceedings of the PORSEC 1992 in Okinawa: Conference for Pacific Ocean Environments and Probing, Volume 2 25 Aug. 1992 p 1079-1084 (For primary document see N94-12635 01-42)
Copyright Avail: Issuing Activity (Scientific Organizing Committee of PORSEC, P.O. Box 10, Shimizu, Shizuoka 424, Japan, HC)

The consideration of the energy balance in the strongly nonlinear shear flow of ideal fluid in internal hydraulic jump requires that the first principle of thermodynamics for ideal fluids should be modified. The dependence of entropy and internal energy on the velocity of deformation is supposed. Author (NASDA)

N94-12729 Academy of Sciences (USSR), Vladivostok. Pacific Oceanological Inst.

THE ACOUSTIC ARRANGEMENT FOR MEASURING VERTICAL STRUCTURE OF SEA CURRENT **c48**

V. Ya. Kogan, A. A. Voronin, Y. V. Petrova, and V. A. Bannov *In* Scientific Organizing Committee of PORSEC, Proceedings of the PORSEC 1992 in Okinawa: Conference for Pacific Ocean Environments and Probing, Volume 2 25 Aug. 1992 p 1085-1088 (For primary document see N94-12635 01-42)
Copyright Avail: Issuing Activity (Scientific Organizing Committee of PORSEC, P.O. Box 10, Shimizu, Shizuoka 424, Japan, HC)

A three-component acoustic device for measuring the current velocity in the sea is considered. The procedure of carrying out the studies from aboard the drifting vessel is presented. The arrangement which has been used and the construction are described. For illustrating the studies, the results obtained in the course of the experiments are given. Author (NASDA)

N94-12730 Academy of Sciences (USSR), Moscow. Inst. of Oceanology.

TURBULENCE GENERATION IN THE PACIFIC UNDERCURRENT BY SHEAR **c48**

Konstantin A. Korotenko *In* Scientific Organizing Committee of PORSEC, Proceedings of the PORSEC 1992 in Okinawa: Conference for Pacific Ocean Environments and Probing, Volume 2 25 Aug. 1992 p 1089-1094 (For primary document see N94-12635 01-42)
Copyright Avail: Issuing Activity (Scientific Organizing Committee of PORSEC, P.O. Box 10, Shimizu, Shizuoka 424, Japan, HC)

The second-order closure model is used to estimate kinetic energy of turbulence, its dissipation rate, and turbulent fluxes of density in the Pacific equatorial undercurrent. Numerical solutions are presented as adaptive adjustment of turbulence parameters to corresponding profiles of density and velocity. The latter were collected during the 51st cruise of the R/V (Research Vessel) Academic Kurchatov in the central part of the undercurrent on October, 1990. Simulations showed that active turbulence is mainly concentrated above and below velocity maximum within high-shear layers. Magnitudes of dissipation rate found there approach the level of about 2 times 10(exp -3) Wm(exp -3). Comparison of the modeling results for the dissipation rate with ones obtained in direct measurements proved to be in close agreement. Author (NASDA)

N94-12731 Academy of Sciences (USSR), Vladivostok. Pacific Oceanological Inst.

THE PACIFIC SUBARCTIC FRONTAL ZONE: STRUCTURE AND DYNAMICS **c48**

T. R. Kilmatov and V. A. Kuzmin *In* Scientific Organizing Committee of PORSEC, Proceedings of the PORSEC 1992 in Okinawa: Conference for Pacific Ocean Environments and Probing, Volume 2 25 Aug. 1992 p 1095-1100 (For primary document see N94-12635 01-42)
Copyright Avail: Issuing Activity (Scientific Organizing Committee of PORSEC, P.O. Box 10, Shimizu, Shizuoka 424, Japan, HC)

Some new aspects of the structure and dynamics of the thermocline, halocline, and density fronts in the Subarctic Frontal Zone (SFZ) are presented. Joint analysis of the horizontal distribution of temperature, salinity, and density on meridional hydrographic routes crossing the Subarctic Front (SF) has been conducted to illustrate the peculiarities of the horizontal distribution of those parameters in the upper 500 m layer in the SF. Several correlation types can be used to determine structural boundaries, for example, of eddies and jets. The changes of the horizontal temperature-density and salinity-density relationships may be used to determine the position of the SF. The seasonal variation of the caballing process at the SF and the structure of intermediate water of lowered salinity are discussed. The experimental observation in the North Pacific confirm indirectly that the interannual periodicity of the caballing effect plays an important role at the SF. Influence of stratification on the cross-structure of the density front are mathematically described. Author (NASDA)

N94-12732 Academy of Sciences (USSR), Vladivostok. Inst. of Oceanology.

LASER PHOTOHETERODYNE INTERFEROMETERS FOR OCEANOGRAPHIC INVESTIGATIONS **c36**

V. L. Vlassov *In* Scientific Organizing Committee of PORSEC, Proceedings of the PORSEC 1992 in Okinawa: Conference for Pacific Ocean Environments and Probing, Volume 2 25 Aug. 1992 p 1101-1106 (For primary document see N94-12635 01-42)
Copyright Avail: Issuing Activity (Scientific Organizing Committee of PORSEC, P.O. Box 10, Shimizu, Shizuoka 424, Japan, HC)

The method is developed to measure the rho, S, T, and P (Density, Salinity, Temperature, and Pressure) parameters in the ocean via the measurement of the only thermodynamic parameter, namely the refractive index n(S, T, P) of sea water. The method is based on the differential optical compensation of the measured refraction index in regard with any two out of three measured parameters (S, T, P). The precision measurement is made by a multichannel photoheterodyne interferometer. On the basis of this method, a set of oceanological devices, which do not have analogs in the world, was constructed: (1) a laser interference refractometer; (2) the optical nSTD (Refractive index, Salinity, Temperature and Depth)-probe without S, T, D sensors with a resolution of delta n = 3 times 10(exp -7), delta S = 1.5 times 10(exp -3) percent, delta T = 3 times 10(exp -3) C, and delta P = 0.2 dbar (delta P is independent on depth); and (3) the optical sensor for the sea surface level supplied with a thermocompensation system. It has resolution of a 2-3 mm water column. This resolution does not depend on the depth. The sensor is intended for exploration in the oceanic bottom moored stations and in the systems prediction of tsunami. Author (NASDA)

N94-12733 Academy of Sciences (USSR), Moscow. Inst. of Oceanology.

A DETAILED INVESTIGATION OF THE BENTHIC REGIME IN THE CLARION-CLIPPERTON PROVINCE OF THE PACIFIC AND A FORECAST OF CONSEQUENCES OF MANGANESE NODULE MINING **c48**

Evgeny A. Kontar, Gleb N. Baturin, and Tatiana A. Demidova *In* Scientific Organizing Committee of PORSEC, Proceedings of the PORSEC 1992 in Okinawa: Conference for Pacific Ocean Environments and Probing, Volume 2 25 Aug. 1992 p 1107-1112 (For primary document see N94-12635 01-42)

Copyright Avail: Issuing Activity (Scientific Organizing Committee of PORSEC, P.O. Box 10, Shimizu, Shizuoka 424, Japan, HC)

Features of bottom currents in the Clarion-Clipperton province of the Pacific should be one of the most important components defining the consequences of future mining of deep water manganese nodule deposits. The problem of bottom layer disturbance, its scales, and peculiarities due to mining, have been forecasted on the basis of the available data on benthic current activity in the region. Both published data and that obtained in experiments with pop-up self contained bottom stations were employed. As an example, features of the benthic currents circulation of one detailed area of the province which is rich in high grade nodules are discussed. This includes observed 'benthic storms'. Bottom relief, the oceanological and sedimentary situation, physical properties of the bottom sediments and nodules, the capability of benthic currents of different velocities in reworking and redepositing mining wastes, as well as different excavation schemes are taken into account in estimating future disturbance of the area. This has obvious relevance to environmental protection policies. Author (NASDA)

N94-12734 Academy of Sciences (USSR), Moscow. Inst. of Oceanology.

BOTTOM CURRENTS AND POSSIBILITIES FOR NEAR BOTTOM LAYER ENVIRONMENTAL INVESTIGATIONS IN THE PACIFIC BY MEANS OF SELF CONTAINED BOTTOM STATIONS **c48**

Evgeny A. Kontar and Tatiana A. Demidova *In* Scientific Organizing Committee of PORSEC, Proceedings of the PORSEC 1992 in Okinawa: Conference for Pacific Ocean Environments and Probing, Volume 2 25 Aug. 1992 p 1113-1117 (For primary document see N94-12635 01-42)

Copyright Avail: Issuing Activity (Scientific Organizing Committee of PORSEC, P.O. Box 10, Shimizu, Shizuoka 424, Japan, HC)

Circulation of bottom currents in the Pacific is presently believed to be one of the most important components defining consequences of increasing ocean pollution. Wastes of differing nature are accumulated in deep depressions in the ocean as well as, in different forms, in near bottom ocean water and in bottom sediments. Taking into account the evident importance of the problem, pop-up self-contained bottom stations designed at the Shirshov Inst. of Oceanology, Moscow, are equipped with one to five 'Potoc' current and temperature meters which are located 2 to 35 m above the sea floor, as well as several sediment traps and hydrochemical sensor modules for recording the time variation of dissolved oxygen. On the basis of experimental data obtained synchronously from three to ten of the stations deployed on the bottom for several months, the distances, directions, and paths of mass transport are calculated; the possible zones both of stagnation and of active oxygen exchange due to hydrodynamic peculiarities are mapped; and the flow of suspended particles coming down from the ocean-surface which defines contamination of the bottom are estimated. Other features of bottom currents relating to bottom pollution are discussed. Author (NASDA)

N94-12735 Academy of Sciences (USSR), Moscow. Inst. of Oceanology.

AUTONOMOUS SELF CONTAINED BOTTOM POP-UP STATIONS FOR STUDY OF THE BENTHIC LAYER AND SEISMICITY OF THE OCEAN'S BOTTOM **c48**

Evgeny A. Kontar *In* Scientific Organizing Committee of PORSEC, Proceedings of the PORSEC 1992 in Okinawa: Conference for Pacific Ocean Environments and Probing, Volume 2 25 Aug. 1992 p 1118-1121 (For primary document see N94-12635 01-42)

Copyright Avail: Issuing Activity (Scientific Organizing Committee of PORSEC, P.O. Box 10, Shimizu, Shizuoka 424, Japan, HC)

Outline of the autonomous self-contained bottom pop-up stations designed at the Shirshov Inst. of Oceanology, Russian Academy of Sciences is described. The stations are provided with an analog and digital magnetic recorder designed for continuous work during 45 days which enables storage of seismic information by six channels. For measurements, the stations are equipped with a three-component block of geophones of chemotron type which are used to measure variations of the oceanic bed within a frequency range from 0.3 to 20 Hz. The pop-up carrier of the stations has two individual instrument containers. The measuring complex also comprises a hydrophone channel and some other autonomously functioning devices; for instance, a bottom current and temperature meter, etc. Author (NASDA)

N94-12736 Academy of Sciences (USSR), Moscow. Inst. of Oceanology.

REMOTE SENSING OF LIGHT SCATTERING COEFFICIENT OF SEA WATER VERTICAL DISTRIBUTION BY THE MEANS OF AIRBORNE LIDAR **c43**

Alexander P. Vasilkov, Yuri A. Goldin, and Boris A. Gureev *In* Scientific Organizing Committee of PORSEC, Proceedings of the PORSEC 1992 in Okinawa: Conference for Pacific Ocean Environments and Probing, Volume 2 25 Aug. 1992 p 1122-1126 (For primary document see N94-12635 01-42)

Copyright Avail: Issuing Activity (Scientific Organizing Committee of PORSEC, P.O. Box 10, Shimizu, Shizuoka 424, Japan, HC)

It has been theoretically shown that light scattering coefficient (B) dependence on depth (Z) can be derived from temporal dependence of backscattered pulse polarization degree when sounding sea water by linear polarized light pulses. Experimental examination of the method is carried out by using an airborne lidar at the altitude 300 m (5 mW of sounding pulse power, 5 nsec in pulse duration, 532 nm in radiation wavelength, and 10-40 mrad in field of view). Backscattered pulse depolarization degree variation from 0 to 6 percent at the interval 0-200 nsec was determined. Qualitative agreement of the determined dependence B(Z) with that measured by an underwater device from the research vessel, good reproduction of B(Z) for different return signals at the same region, and clear distinctions for different regions are obtained. Author (NASDA)

N94-12737 Academy of Sciences (USSR), Vladivostok. Pacific Research Inst. of Fisheries and Oceanography.

INFLUENCE OF THE KUROSHIO WARM-CORE RINGS ON HYDROGRAPHIC AND FISHERY CONDITIONS OFF SOUTHERN KURIL ISLANDS **c48**

N. V. Bulatov and V. B. Lobanov *In* Scientific Organizing Committee of PORSEC, Proceedings of the PORSEC 1992 in Okinawa: Conference for Pacific Ocean Environments and Probing, Volume 2 25 Aug. 1992 p 1127-1131 (For primary document see N94-12635 01-42)

Copyright Avail: Issuing Activity (Scientific Organizing Committee of PORSEC, P.O. Box 10, Shimizu, Shizuoka 424, Japan, HC)

Behavior of the Kuroshio Warm-Core Rings (KWCR) in the southern Kurils area is studied using NOAA satellite infrared (IR) images for the period of 1986-1991. Six rings were traced entering the area and moving northeastward along the coastline. It was found that they can reach the traverse of Urup Island preserving a core of modified Kuroshio water.

Hydrographic fronts and warm and cold water streamers associated with rings are supposed to determine the Pacific saury and sardine distribution. A stable accumulation of fish schools is shown at the northern edge of a ring and in a low temperature interior part. Ring influence on a position and intensity of cold water offshore intrusions and branches of the Oyashio current, which control the fish migration routes, are supposed to be an important point in understanding a variability of conditions for commercial fishing in the area. Author (NASDA)

N94-12738 Academy of Sciences (USSR), Moscow. All-Union Scientific Research Inst. of Fisheries and Oceanography.

VERIFICATION OF THE ATMOSPHERE-OCEAN RADIATIVE TRANSFER PARAMETRIC MODELS **c46**

Andrey V. Belokhvostikov, Andrey A. Ioltukhovski, and Vladimir M. Orlov *In* Scientific Organizing Committee of PORSEC, Proceedings of the PORSEC 1992 in Okinawa: Conference for Pacific Ocean Environments and Probing, Volume 2 25 Aug. 1992 p 1132-1137 (For primary document see N94-12635 01-42)

Copyright Avail: Issuing Activity (Scientific Organizing Committee of PORSEC, P.O. Box 10, Shimizu, Shizuoka 424, Japan, HC)

Three parametric models are compared with ascending atmosphere-ocean radiance numerically computed by the iteration method of characteristics. Computations are carried out under similar illumination and viewing conditions for all models. It is found out that the different parametric models have the lowest errors under different illumination and viewing conditions. Author (NASDA)

N94-12739 Academy of Sciences (USSR), Vladivostok. Pacific Inst. of Oceanology.

CONVECTIVE AND DYNAMIC INSTABILITY IN MERIDIONAL TRENCHES **c48**

L. F. Muratov *In* Scientific Organizing Committee of PORSEC, Proceedings of the PORSEC 1992 in Okinawa: Conference for Pacific Ocean Environments and Probing, Volume 2 25 Aug. 1992 p 1138-1144 (For primary document see N94-12635 01-42)

Copyright Avail: Issuing Activity (Scientific Organizing Committee of PORSEC, P.O. Box 10, Shimizu, Shizuoka 424, Japan, HC)

The possibility of Rayleigh convection on the rotating earth in the deep-sea basins of the ocean has been theoretically studied using some observations. The study resulted in the following conclusions: (1) the resonance interaction of two modes of perturbation in abyssal trenches can lead to nonlinear instability which varies at different locations; (2) shift flux determined by a meridional temperature gradient is a destabilizing factor in Rayleigh instability; (3) meridionally oriented trenches are more 'dangerous' for instability initiation than those oriented latitudinally; (4) the calculated profiles of velocity components of tidal flux in the bottom layer is consistent with real observations; (5) vertical profiles of friction tensions happen to be nearly linear downward; (6) conditions of dynamic stability of bottom layer waters of the trenches are rather tidal cycle sensitive; (7) a complicated dynamic interaction in trenches should change critical parameters of 'convection with velocity shift' in tidal cycle than in the case of Rayleigh convection on rotating earth; (8) advective shift flux induced by meridional temperature gradient influence a dynamic stability in bottom layers of meridionally oriented trenches and results in change of periodicity in Richardson number temporal variability; and (9) presence of well-pronounced and determined component and variability of dynamic stability of bottom waters of trenches suggests a possibility of forecasting fine structure development in them by this method. It is believed that the above result will be applicable for describing tidal phenomena and can solve disputable problems concerning the scales of bottom convection development and determining its critical parameters. Author (NASDA)

N94-12740 Academy of Sciences (USSR), Vladivostok. Pacific Oceanological Inst.

SPATIAL VARIABILITY OF THE OCEAN UNDERWATER DYNAMIC NOISE FROM SATELLITE RADAR SENSING DATA **c43**

L. M. Mitnik and M. L. Mitnik *In* Scientific Organizing Committee of PORSEC, Proceedings of the PORSEC 1992 in Okinawa: Conference for Pacific Ocean Environments and Probing, Volume 2 25 Aug. 1992 p 1145-1150 (For primary document see N94-12635 01-42)

Copyright Avail: Issuing Activity (Scientific Organizing Committee of PORSEC, P.O. Box 10, Shimizu, Shizuoka 424, Japan, HC)

The ocean surface state, changing mainly because of wind action, determines the intensity of the scattered radar signals and makes the basic contribution in the underwater noise level. Dimensions of a ground resolution of the OKEAN satellite side looking radar operating at X band and a listening area of the ocean noising surface at kilohertz frequencies are commensurable with each other. These features permit estimates of the noise intensity by the satellite radar data. The radar images of regions with strong winds, sharp wind speed gradients, and mesoscale regulated structures are used to analyze the spatial distribution of ambient noise. Author (NASDA)

N94-12741 Academy of Sciences (USSR), Nizhny Novgorod. Inst. of Applied Physics.

OBSERVATIONS OF FILM SLICKS AND INTERNAL WAVES WITH Ka-BAND SCATTEROMETER **c43**

S. A. Ermakov, L. V. Lubjako, and S. G. Salashin *In* Scientific Organizing Committee of PORSEC, Proceedings of the PORSEC 1992 in Okinawa: Conference for Pacific Ocean Environments and Probing, Volume 2 25 Aug. 1992 p 1151-1154 (For primary document see N94-12635 01-42)

Copyright Avail: Issuing Activity (Scientific Organizing Committee of PORSEC, P.O. Box 10, Shimizu, Shizuoka 424, Japan, HC)

Remote sensing of the surface manifestation of internal waves and film slicks were carried out by Ka-band radar with a frequency 37 GHz. Observations of the radar backscattering were accompanied by measurements of the wavenumber spectrum of wind waves within the 6-120 cm wavelength range. Variability of the radar signals due to internal waves and slicks has been shown to exceed variability of the spectrum of short wind waves with decimeter-centimeter (dm-cm) wavelengths. This effect can be interpreted on the base of mechanism of 'parasitic' capillary ripple generated by dm-cm waves near their crests. Author (NASDA)

N94-12742 Academy of Sciences (USSR), Moscow. Inst. of Applied Mathematics.

OPTICAL TRANSFER OPERATOR OF THE ATMOSPHERE-OCEAN SYSTEM **c74**

T. A. Suchkevich *In* Scientific Organizing Committee of PORSEC, Proceedings of the PORSEC 1992 in Okinawa: Conference for Pacific Ocean Environments and Probing, Volume 2 25 Aug. 1992 p 1155-1159 (For primary document see N94-12635 01-42)

Copyright Avail: Issuing Activity (Scientific Organizing Committee of PORSEC, P.O. Box 10, Shimizu, Shizuoka 424, Japan, HC)

Improved accuracy and quality of interpretation of satellite imagery in the marine observation may be obtained by using the Optical Transfer Operator (OTO) of the Atmosphere-Ocean System (AOS) illuminated by a solar beam. Solar radiation transfer is described by two models, the atmosphere-surface model and the atmosphere-ocean model with reflective and refractive interface. Operators to express reflection and refraction of the interface are defined. Three problems of radiative transfer are considered for calculating the sunlight intensity field in the atmosphere-ocean system: the ocean-surface, atmosphere-ocean system with later homogeneous interface, and the atmosphere-ocean with later homogeneous interface, including the effects of the ocean waves. In the first stage, the atmosphere influence functions are defined. In the second stage, the optical transfer operator, which establishes the obvious connection with the radiation interaction law at the boundary, is calculated. Basic theoretical tools needed to solve the three-dimensional radiative transfer with the reflective and refractive interface is obtained in form of the linear vector-functional equation. Author (NASDA)

N94-12743 Academy of Sciences (USSR), Vladivostok. Pacific Oceanological Inst.

CLOUD LIQUID WATER CONTENT OVER THE PACIFIC OCEAN TROPICAL ZONE DERIVED FROM SHIP MICROWAVE RADIOMETRIC MEASUREMENT **c47**

L. M. Mitnik, M. L. Mitnik, and M. Yu. Shoom *In* Scientific Organizing Committee of PORSEC, Proceedings of the PORSEC 1992 in Okinawa: Conference for Pacific Ocean Environments and Probing, Volume 2 25 Aug. 1992 p 1160-1165 (For primary document see N94-12635 01-42)

Copyright Avail: Issuing Activity (Scientific Organizing Committee of PORSEC, P.O. Box 10, Shimizu, Shizuoka 424, Japan, HC)

Measurements of the brightness temperatures from the research vessels at wavelengths 2.3 cm and 1.35 cm during ten cruises permitted investigation of the spatial variability of total cloud liquid water content Q. Values of Q were estimated by the brightness temperature difference of the cloudy and cloudless atmosphere delta T(sub B). The microwave measurements were accompanied by hydrometeorological and radar ones and radiosonde sounding. The delta T(sub B) and Q profiles obtained at crossing of a tropical depression are analyzed. Ship data for the atmospheric front and radiative transfer model are used to simulate future multichannel microwave measurements from the orbital station MIR ('Priroda' project) and to investigate the effect of antenna smoothing. Author (NASDA)

N94-12744 Academy of Sciences (USSR), Moscow. Inst. of Oceanology.

VARIABILITY OF SPECTRAL REFLECTANCE IN COASTAL WATERS NEAR THE RIVER PLUMES **c43**

Vladimir I. Burenkov and Alexander P. Vasilkov *In* Scientific Organizing Committee of PORSEC, Proceedings of the PORSEC 1992 in Okinawa: Conference for Pacific Ocean Environments and Probing, Volume 2 25 Aug. 1992 p 1166-1170 (For primary document see N94-12635 01-42)
Copyright Avail: Issuing Activity (Scientific Organizing Committee of PORSEC, P.O. Box 10, Shimizu, Shizuoka 424, Japan, HC)

Because of great difference in optical properties of river and sea waters, optical remote sensing is very effective for investigation of river plumes and their dynamics. The results of shipboard measurements of spectral reflectance in coastal waters near mouths of different rivers are described. Vertical profiles of the beam attenuation coefficient are also considered. Due to the high concentration of suspended matter in river waters, the value of spectral reflectance in blue and green regions of the spectrum in river plumes was anomalous and came to 20 percent. River waters were separated from surrounding sea waters by intensive fronts in which the value of spectral reflectance diminished by three-four times. This reduction was greater in red and green parts of the spectrum than in blue. Sometimes diffusive zones of mixing of river and sea waters existed. Spatial distribution of spectral reflectance inside the river plumes was very heterogeneous. Often the system of internal fronts was observed. Also, quasiperiodic structures connected with short-period internal waves took place. Vertical profiles of water transparency showed that the thickness of the turbid water layer inside the river plume was about a few meters. Below the layer of turbid water, optical properties inside and outside the river plumes, essentially, didn't differ. Author (NASDA)

N94-12745 Academy of Sciences (USSR), Moscow. Space Research Inst.

WIND-WAVE AND FOAM DYNAMICS FROM OPTICAL AND RADAR AIRBORNE OBSERVATIONS **c43**

V. Yu. Raizer and V. S. Etkin *In* Scientific Organizing Committee of PORSEC, Proceedings of the PORSEC 1992 in Okinawa: Conference for Pacific Ocean Environments and Probing, Volume 2 25 Aug. 1992 p 1171-1174 (For primary document see N94-12635 01-42)
Copyright Avail: Issuing Activity (Scientific Organizing Committee of PORSEC, P.O. Box 10, Shimizu, Shizuoka 424, Japan, HC)

The results of airborne optical and radar observations of a large-scale ocean surface structure and storm surges are discussed. Special image processing is used for the investigation of ocean surface dynamics. The existence of quantitative correlation between two-dimensional wavenumber spectrum and foam coverage characteristics is shown. Author (NASDA)

N94-12746 Academy of Sciences (USSR), Moscow. Space Research Inst.

OBSERVATIONS OF SURFACE SIGNATURES IN THE NORTH-WEST PACIFIC OCEAN WITH THE SPACEBORNE SAR **c43**

Konstantin T. Litovchenko, Andre V. Smirnov, and Valentin S. Etkin *In* Scientific Organizing Committee of PORSEC, Proceedings of the PORSEC 1992 in Okinawa: Conference for Pacific Ocean Environments and Probing, Volume 2 25 Aug. 1992 p 1175-1177 (For primary document see N94-12635 01-42)
Copyright Avail: Issuing Activity (Scientific Organizing Committee of PORSEC, P.O. Box 10, Shimizu, Shizuoka 424, Japan, HC)

The results of a spaceborne Synthetic Aperture Radar (SAR) mission at an S-band (10 cm) wavelength for oceanological investigations in the northwest Pacific are presented. The problems of SAR application for surface and internal waves, fronts, and bottom feature indication are discussed. Author (NASDA)

N94-12747 Academy of Sciences (USSR), Moscow. Space Research Inst.

RADAR OBSERVATION OF INTERNAL WAVES FIELD IN THE NORTH-WEST PACIFIC **c43**

Andre V. Smirnov and Valentin S. Etkin *In* Scientific Organizing Committee of PORSEC, Proceedings of the PORSEC 1992 in Okinawa: Conference for Pacific Ocean Environments and Probing, Volume 2 25 Aug. 1992 p 1178-1183 (For primary document see N94-12635 01-42)
Copyright Avail: Issuing Activity (Scientific Organizing Committee of PORSEC, P.O. Box 10, Shimizu, Shizuoka 424, Japan, HC)

This study represents the remote sensing investigation of surface manifestations of internal waves in the northwest Pacific in different seasons. Two radars were involved in the experiments: aircraft Real Aperture Radar (RAR) (2 cm in wavelength) and satellite Synthetic Aperture Radar (SAR) ALMAZ-1 (10 cm in wavelength). The analysis of RAR-images on two polarizations and SAR-image on only Horizontal Transmission Horizontal Reception Mode (HH)-polarization permitted interesting physical phenomena on images which may be visible or invisible, depending on radio wavelength, the angle of incidence, polarizations, and velocity of sensor's carrier. The investigation of the surface manifestations and of the interaction between internal and surface waves using radar and optical surveys are discussed. The oceanic waveguide propagation of short internal waves in seasonal thermocline and the waveguide's conversion in an open resonator with the aid of internal waves in the main thermocline are assumed. Some ideas are discussed about a possible increase in the Q-factor of the resonator, about the amplification of internal waves in the seasonal thermocline, and their surface manifestations. Author (NASDA)

N94-12748 Moscow Physical-Engineering Inst. (Russia).

TRAJECTORY CURVING IN UNDERWATER PROPAGATION OF LIGHT **c74**

V. S. Remizovich, D. B. Rogozkin, and Sh. A. Shekhmametyev *In* Scientific Organizing Committee of PORSEC, Proceedings of the PORSEC 1992 in Okinawa: Conference for Pacific Ocean Environments and Probing, Volume 2 25 Aug. 1992 p 1184-1188 (For primary document see N94-12635 01-42)
Copyright Avail: Issuing Activity (Scientific Organizing Committee of PORSEC, P.O. Box 10, Shimizu, Shizuoka 424, Japan, HC)

A problem of the optical radiation transmission through a thick layer of the ocean water is considered. An analytical description of the radiance distribution taking into account features of the oceanic phase functions is developed. The small-angle solution of the radiative transfer equation is modified by a self-consistent calculation procedure of the photon diffusion coefficient. The new parametric forms for the in-water radiance distribution parameters are found. The obtained solution provides good quantitative agreement with the experimental and numerical data. Author (NASDA)

N94-12749 Academy of Sciences (USSR), Vladivostok. Inst. for Automation and Control Processes.

DISTERM: A SHIPBOARD DATA SYSTEM FOR SATELLITE MONITORING OF OCEAN AND ATMOSPHERE **c82**

E. E. Gherbek, Ju. G. Proshyants, Ju. V. Naumkin, and I. I. Gorin *In* Scientific Organizing Committee of PORSEC, Proceedings of the PORSEC 1992 in Okinawa: Conference for Pacific Ocean Environments and Probing, Volume 2 25 Aug. 1992 p 1189-1193 (For primary document see N94-12635 01-42)
Copyright Avail: Issuing Activity (Scientific Organizing Committee of PORSEC, P.O. Box 10, Shimizu, Shizuoka 424, Japan, HC)

The shipboard computer system, designed for acquiring and processing satellite and in-situ hydrometeorological data and being operated on board R/V (Research Vessel) AKADEMIK KOROLEV is outlined. The system is composed of subsystems for processing the medium and high resolution data from NOAA satellites, Meteorological Satellite (METEOR), the Geostationary Meteorological Satellite-4 (GMS-4) and so forth, in-situ aerological probing data, and in-situ hydrological probing data, and meteorological data. Wide experience of Automatic Picture Transmission (APT)-data processing for calculating the Sea Surface Temperature (SST) fields and for reconstructing the currents by sea marker tracing were planned, and during two marine expeditions, the experiments laying out the system on a ship compactly and subsurface eddy observation were carried out successfully. Recent activities for utilization of the system are introduced. Author (NASDA)

N94-12750 Academy of Sciences (USSR), Vladivostok. Inst. of Automation and Control Processes.

ATMOSPHERIC CORRECTION FOR DETERMINATION OF AVERAGE SST FIELDS BASED ON AVHRR DATA **c46**

Alexander V. Kazansky *In* Scientific Organizing Committee of PORSEC, Proceedings of the PORSEC 1992 in Okinawa: Conference for Pacific Ocean Environments and Probing, Volume 2 25 Aug. 1992 p 1194-1199 (For primary document see N94-12635 01-42)
Copyright Avail: Issuing Activity (Scientific Organizing Committee of PORSEC, P.O. Box 10, Shimizu, Shizuoka 424, Japan, HC)

An atmospheric attenuation model is derived for average conditions and used to determine an optimal form of SST (Sea Surface Temperatures) retrieval algorithms for AVHRR (Advanced Very High Resolution Radiometer) data depending on region and season. Since multi-viewing angle SST measurements are found to be important for accurate SST retrieval, a statistical method of obtaining this information from collection of AVHRR imagery for about 10 days is described. As on the same data set, an extrapolation to zero cloudiness by means of quantile estimators is also possible. A combined technique is suitable for average SST field determination in cloudy conditions common to the North Pacific in winter. Author (NASDA)

N94-12751 Academy of Sciences (USSR), Vladivostok. Pacific Oceanological Inst.

THE STRUCTURE OF HYDROPHYSICAL MEASURING SYSTEMS OF VERTICAL SOUNDING AND SELF-CONTAINED STATIONS **c82**

G. V. Smirnov, V. V. Gorbachev, A. G. Starikov, and N. A. Shmyrov *In* Scientific Organizing Committee of PORSEC, Proceedings of the PORSEC 1992 in Okinawa: Conference for Pacific Ocean Environments and Probing, Volume 2 25 Aug. 1992 p 1200-1204 (For primary document see N94-12635 01-42)
Copyright Avail: Issuing Activity (Scientific Organizing Committee of PORSEC, P.O. Box 10, Shimizu, Shizuoka 424, Japan, HC)

Microprocessing and computer-based instrumentation have recently become more prevalent in oceanological studies. Specific features of deep-water measurements make it necessary to find an adequate telemetry system structure which has to satisfy the whole group of contradictory demands. This paper is dedicated to some aspects of elaboration on the hydrophysical measuring systems structure. The structure can be applicable for the data acquisition and processing of vertical sounding and of self-contained stations. Particular care has been taken in designing underwater devices. Two types of hydrophysical instruments were built upon the structure base: a multichannel sonde and a self-contained current meter. Author (NASDA)

N94-12752 Academy of Sciences (USSR), Moscow. Inst. of Oceanology.

COUPLED NUMERICAL MODEL FOR ALTIMETRIC DATA ASSIMILATION AND VELOCITY FIELD ANALYSIS **c48**

A. L. Berestov and A. D. Marushkevich *In* Scientific Organizing Committee of PORSEC, Proceedings of the PORSEC 1992 in Okinawa: Conference for Pacific Ocean Environments and Probing, Volume 2 25 Aug. 1992 p 1205-1210 (For primary document see N94-12635 01-42)
Copyright Avail: Issuing Activity (Scientific Organizing Committee of PORSEC, P.O. Box 10, Shimizu, Shizuoka 424, Japan, HC)

A coupled barotropic model of the South China Sea (SCS) is presented. The first part includes a geostrophic model which was used to study emerging or changing large-scale organized currents under the influence of stochastic excitation to simulate the wind action on the surface and some other physical mechanisms. The second part is based on the shallow water equations. It can be used for assimilating altimetric data simulated with the first part and for calculating the velocity field. This part of the model was also used for independent analysis of wind driven circulation in the SCS. Author (NASDA)

N94-12753 Academy of Sciences (USSR), Vladivostok. Pacific Oceanological Inst.

COMPLEX (HYDRODYNAMIC, SATELLITE) MONITORING OF DYNAMIC STRUCTURES IN THE WESTERN PACIFIC WITH THE AIM OF FORECASTING THE MARINE ECOSYSTEMS BEHAVIOUR **c43**

A. S. Vasiliev *In* Scientific Organizing Committee of PORSEC, Proceedings of the PORSEC 1992 in Okinawa: Conference for Pacific Ocean Environments and Probing, Volume 2 25 Aug. 1992 p 1211-1218 (For primary document see N94-12635 01-42)
Copyright Avail: Issuing Activity (Scientific Organizing Committee of PORSEC, P.O. Box 10, Shimizu, Shizuoka 424, Japan, HC)

Based on ocean-surface-temperature and atmospheric-pressure satellite data, the main physical fields of the western Pacific are reconstructed with the help of mathematical models. Statistics of subsequent scripts created for medium state are used for forecasting the thermodynamic structures and biota behavior with the help of adaptive learning models. Mathematical formulation of the problem is given. Results of numerical experiments in the western Pacific and the subarctic front area are analyzed. Author (NASDA)

N94-12754 Academy of Sciences (USSR), Vladivostok. Pacific Oceanological Inst.

MESOSCALE DYNAMIC STRUCTURES OF THE SUBARCTIC FRONTAL ZONE IN THE PACIFIC OCEAN **c48**

A. S. Vasiliev and V. P. Makashin *In* Scientific Organizing Committee of PORSEC, Proceedings of the PORSEC 1992 in Okinawa: Conference for Pacific Ocean Environments and Probing, Volume 2 25 Aug. 1992 p 1219-1224 (For primary document see N94-12635 01-42)
Copyright Avail: Issuing Activity (Scientific Organizing Committee of PORSEC, P.O. Box 10, Shimizu, Shizuoka 424, Japan, HC)

Dynamic structures of the subarctic zone in the western Pacific are studied on the base of a quasi-geostrophic baroclinic model with the help of satellite data on the ocean surface temperature. The calculated fields of zonal components for full fluxes and the transport stream function are used to diagnose and recognize the variability of the Subarctic Front (SF) and Kuroshio Front (KF) on synoptical time scales with decadal discreteness. It is shown that the characteristic peculiarity of the Subarctic Frontal Zone (SAFZ) is the horizontal alternation of zonal countercurrents, on the margins of which the conditions are created for generating the baroclinic vortices and fronts; the thermal SF is more vividly exposed on the Kuroshio northern branch periphery and in the place of the subarctic current adjoining the Emperor Mounts. It is stated that the temperature field of the SAFZ water surface preserves the information on the bottom relief of the region. Author (NASDA)

N94-12755 Moscow State Univ. (Russia). Physics Dept.

LASER FLUORESCENT MONITORING OF DISSOLVED ORGANIC MATTER IN NATURAL WATER **c36**

Elena M. Filippova, Svetlana V. Patsayeva, Vasily V. Chubarov, Victor V. Fadeev, and Victor I. Yuzhakov *In* Scientific Organizing Committee of PORSEC, Proceedings of the PORSEC 1992 in Okinawa: Conference for Pacific Ocean Environments and Probing, Volume 2 25 Aug. 1992 p 1225-1230 (For primary document see N94-12635 01-42)
Copyright Avail: Issuing Activity (Scientific Organizing Committee of PORSEC, P.O. Box 10, Shimizu, Shizuoka 424, Japan, HC)

Important problems of environment control demand elaboration of remote methods for Dissolved Organic Matter (DOM) diagnostics in natural water. Currently, fluorescent methods using a Raman scattering signal as an internal standard are widely applied for environment control DOM in water. The most difficult problems arising during fluorescent monitoring of natural sea and river water are: (1) the correlation between fluorescent intensity (I(sub fl)) and DOM concentration (C); (2) taking into account the natural temperature variations and ultraviolet sunlight radiation; and (3) the influence of Ultraviolet (UV) laser excitation on DOM fluorescence. This paper represents the results of a study of the fluorescence of natural DOM. Experimental study of the influence of temperature and sunlight UV irradiation on the fluorescence signal of DOM has been carried out in this study. The features of fluorescence spectra of DOM under UV laser excitation (the effect of fluorescence saturation and photo-chemical destructions) have been observed. The optimal regime of spectra detection is under consideration. The recommendations on laser remote sensing of organic pollutions in water have been given (wavelength of excitation and experimental conditions). Author (NASDA)

N94-12756 Moscow State Univ. (Russia). Physics Dept.

ECOLOGICAL APPLICATION OF SURFACE ENHANCED RAMAN SPECTROSCOPY **c43**

O. A. Aktsipetrov, A. M. Klevtsov, and A. F. Pasternak *In* Scientific Organizing Committee of PORSEC, Proceedings of the PORSEC 1992 in

Okinawa: Conference for Pacific Ocean Environments and Probing, Volume 2 25 Aug. 1992 p 1231-1234 (For primary document see N94-12635 01-42)
Copyright Avail: Issuing Activity (Scientific Organizing Committee of PORSEC, P.O. Box 10, Shimizu, Shizuoka 424, Japan, HC)

Surface Enhanced Raman Scattering (SERS) for organic molecules dissolved in the sea water has been reviewed for the first time. An increase in the intensity of Raman lines by a factor of 10(exp 6), in the case of the surface enhancement, gives the new sensitive method of pollution monitoring. SERS spectra for aqueous solutions of oil components in the sea water were observed. Dependence of SERS intensity on concentration of pollution has been obtained. SERS intensity of the H2O band as an internal standard for measurement of pollution concentration has been used.
Author (NASDA)

N94-12757 Academy of Sciences (USSR), Vladivostok. Pacific Research Inst.
A POSSIBILITY TO DEFINE THE LOCATION OF EPIPELAGIC FISH CONCENTRATIONS WITH ASSISTANCE OF SATELLITE SENSING **c43**
Yury I. Zuenko, Sergey Yu. Shershenkov, Nafanail V. Bulatov, and Valentina I. Lapshina *In* Scientific Organizing Committee of PORSEC, Proceedings of the PORSEC 1992 in Okinawa: Conference for Pacific Ocean Environments and Probing, Volume 2 25 Aug. 1992 p 1235-1239 (For primary document see N94-12635 01-42)
Copyright Avail: Issuing Activity (Scientific Organizing Committee of PORSEC, P.O. Box 10, Shimizu, Shizuoka 424, Japan, HC)

Possibile formation of fish concentrations on the north and south divisions of the polar front (NPF (Northern Polar Front) and SPF (Southern Polar Front)) is investigated according to the data of vertical water structure, plankton community state, and epipelagic fish distribution using the acoustic method in the North Korean and Russian exclusive zone. Both NPF and SPF had considerable inclination. Downwelling was observed near the surface front and upwelling was in the back part of these zones. The productivity of plankton in the NPF and SPF zones was higher than that in subarctic and interfrontal zones. The sparse fish concentrations (sardine, Japanese anchovy, pacific mackerel, Japanese pearlside, round-herring, and squids) were arranged as almost continuous striples in the back parts of both frontal zones, increasing from one to five shoals per nautical mile in the areas of meandering NPF and SPF. It is supposed that high productivity of plankton due to nutrients influx in upwellings is the reason for fish concentrations in the SPF and NPF zones. This concentration forms on the warm sides of thermal fronts. The location of these fronts may be rather easily defined on the satellite infrared images of the ocean surface.
Author (NASDA)

N94-12758 Academy of Sciences (USSR), Vladivostok. Pacific Research Inst. of Fisheries and Oceanography.
HIGH BIOLOGICAL PRODUCTION OF THE TIDAL MIXING ZONES ON JAPAN SEA SHELF **c51**
Yury I. Zuenko *In* Scientific Organizing Committee of PORSEC, Proceedings of the PORSEC 1992 in Okinawa: Conference for Pacific Ocean Environments and Probing, Volume 2 25 Aug. 1992 p 1240-1244 (For primary document see N94-12635 01-42)
Copyright Avail: Issuing Activity (Scientific Organizing Committee of PORSEC, P.O. Box 10, Shimizu, Shizuoka 424, Japan, HC)

The seasonal variation of summary plankton production is considered according to the observational data from summer-autumn 1989-1990 in the northwestern part of the Sea of Japan. In stratificated offshore waters, the low productivity (P/B (Daily Production per a Unit of Biomass) 0.2 d(exp -1)) was observed in July-August. It grew in September, especially in October (to 1 to 3 d(exp -1)). In the tidal mixing zones on shelf with weakened stratification, the period of low productivity was shorter: from the middle of July to the middle of August. The reason for these peculiar tidal mixed zones is an uninterrupted nutrient influx to the euphotic layer, that becomes weak in the time of the highest heating only. Everywhere in the north-western part of the sea, the autumn bloom of phytoplankton begins in September, owing to a wind-wave stirring, with addition of an upwelling effect near the Prymorye Coast in October-November. When the plankton production is low offshore but still (or already) high in the tidal mixing zones, plankton-eating fishes (such as sardine) concentrate in this zone on the shelf.
Author (NASDA)

N94-12759 Academy of Sciences (USSR), Moscow. Inst. of Oceanology.
STUDY OF THE ADMIXTURE DIFFUSION IN THE SEA USING REMOTE TECHNIQUES **c43**
Rostislav V. Ozmidov *In* Scientific Organizing Committee of PORSEC, Proceedings of the PORSEC 1992 in Okinawa: Conference for Pacific Ocean Environments and Probing, Volume 2 25 Aug. 1992 p 1245-1250 (For primary document see N94-12635 01-42)
Copyright Avail: Issuing Activity (Scientific Organizing Committee of PORSEC, P.O. Box 10, Shimizu, Shizuoka 424, Japan, HC)

Study of the admixture diffusion in the Black Sea using aerial photography techniques is performed. Wide variability of the sizes and shapes of the admixture patches during diffusion is observed. Some relationships between peculiarities of the diffusion and background hydrometeorological conditions are established.
Author (NASDA)

N94-12760 Academy of Sciences (USSR), Moscow. Inst. of Oceanology.
MIXING OF DRIFTER ENSEMBLE BY MESOSCALE CURRENTS **c48**
Tatyana G. Sazhina, Nikolay A. Maksimenko, and Natalya M. Mardashkina *In* Scientific Organizing Committee of PORSEC, Proceedings of the PORSEC 1992 in Okinawa: Conference for Pacific Ocean Environments and Probing, Volume 2 25 Aug. 1992 p 1251-1256 (For primary document see N94-12635 01-42)
Copyright Avail: Issuing Activity (Scientific Organizing Committee of PORSEC, P.O. Box 10, Shimizu, Shizuoka 424, Japan, HC)

This paper presents the results of a study on drifter paths calculated from a simplified kinematic model. The problem of horizontal diffusion, stirring, and mixing processes parameterization in open ocean mesoscale currents is under discussion. Appropriate formulas are proposed from the model. It is shown that the most effective diffusion corresponds to instationarity regime when eddies evolution time is comparable with time of half of particle circuit around eddy center. It is also learned that believing intervals of diffusion coefficient K are always greater than K itself; hence, its traditional parameterization can be used only when the roughness of the K definition cannot influence the study results. The original approach formulates a task for stirring exponent definition. In the presence of molecular diffusion, the balance between stirring and mixing results in filaments of stable scale in the tracer field. Mathematical modeling of drifter ensemble spreading over a large-scale basin shows that the most homogeneous drifter set can be obtained by their initial deployment in frontal and vortical active areas.
Author (NASDA)

N94-12761 Academy of Sciences (USSR), Moscow. Inst. of Oceanology.
THE ALGORITHM OF PRIMARY PRODUCTION DETERMINATION **c43**
Olga J. Koblentz-Mishke, Vadim N. Pelevin, and Bogdan Wozniak (Polish Academy of Sciences, Gdansk.) *In* Scientific Organizing Committee of PORSEC, Proceedings of the PORSEC 1992 in Okinawa: Conference for Pacific Ocean Environments and Probing, Volume 2 25 Aug. 1992 p 1257-1262 (For primary document see N94-12635 01-42)
Copyright Avail: Issuing Activity (Scientific Organizing Committee of PORSEC, P.O. Box 10, Shimizu, Shizuoka 424, Japan, HC)

The algorithm for primary production determination from satellite data is proposed. The algorithm consists of the steps such as the following: (1) data acquisition of the upwelling radiance spectrum from satellite data; (2) atmospheric correction; (3) estimation of approximate chlorophyll content in the surface sea layer by means of solving the 'inverse problem of hydro-optics'; (4) more precise determination of chlorophyll using relations between this one, pigment index, and light absorption by phytoplankton pigments; (5) determination of underwater fields of irradiance by means of optical classifications of the ocean waters; (6) estimation of light energy absorbed by phytoplankton using typical profiles of chlorophyll, its relation to light absorption by pigments, and taking into account other light-absorbing components of sea water; (7) determination of primary production, based on preliminary study of light dependence of the quantum yield of marine photosynthesis and parameters obtained according to points five and six; and (8) verification, integration of results, and their correction. The structure of the algorithm makes it possible to modify relevant relationships in response to the experimental information.
Author (NASDA)

N94-12762 Central Aerological Observatory, Moscow (USSR). Inst. of Physics, Technology, and Oceanology.
NON-IMAGE VISIBLE POLARIZATION REMOTE SENSING OF THE OCEAN c43
Nikolay A. Krotkov, Tymothy V. Kondranin, and Alexander P. Vasilkov *In* Scientific Organizing Committee of PORSEC, Proceedings of the PORSEC 1992 in Okinawa: Conference for Pacific Ocean Environments and Probing, Volume 2 25 Aug. 1992 p 1263-1268 (For primary document see N94-12635 01-42)
Copyright Avail: Issuing Activity (Scientific Organizing Committee of PORSEC, P.O. Box 10, Shimizu, Shizuoka 424, Japan, HC)

A new parametric model has been developed to calculate Stokes parameters of scattered solar radiation in the atmosphere above the ocean surface. Mathematical modeling is used to examine angular variations of the degree of polarization above the ocean surface and at the top of the atmosphere as well. The effectiveness of the polarization measurements for the different techniques of optical passive remote sensing of the ocean have been studied. Author (NASDA)

N94-12763 Academy of Sciences (USSR), Vladivostok. Pacific Oceanological Inst.
GENERATION OF INTERNAL WAVES NEAR THE SHELF BOUNDARY c48
V. V. Navrotsky and S. V. Simonenko *In* Scientific Organizing Committee of PORSEC, Proceedings of the PORSEC 1992 in Okinawa: Conference for Pacific Ocean Environments and Probing, Volume 2 25 Aug. 1992 p 1269-1274 (For primary document see N94-12635 01-42)
Copyright Avail: Issuing Activity (Scientific Organizing Committee of PORSEC, P.O. Box 10, Shimizu, Shizuoka 424, Japan, HC)

A three layer model of Internal Hydraulic Jump (IHJ) is proposed and the KdV (Korteweg-de Vries) equation is used to explain the observed peculiarities of the thermocline structure and generation of short internal wave packets near the shelf boundary of the Sea of Japan. Author (NASDA)

N94-12764 Academy of Sciences (USSR), Vladivostok. Pacific Oceanological Inst.
EXPERIMENTAL AND THEORETICAL INVESTIGATION OF UNDULAR BORE FORMATION UPSTREAM THE BANK c48
S. V. Simonenko and V. Ya. Kogan *In* Scientific Organizing Committee of PORSEC, Proceedings of the PORSEC 1992 in Okinawa: Conference for Pacific Ocean Environments and Probing, Volume 2 25 Aug. 1992 p 1275-1280 (For primary document see N94-12635 01-42)
Copyright Avail: Issuing Activity (Scientific Organizing Committee of PORSEC, P.O. Box 10, Shimizu, Shizuoka 424, Japan, HC)

A theoretical and experimental investigation of upstream disturbance is made for two-layer tidal flow over the bank on the north shelf of the Okhotsk Sea. A comparison is made between theoretical predictions and observation when the upper fluid has a depth less than that of the lower fluid. The results indicate quantitative agreement between theory and observations. Author (NASDA)

N94-12765 Academy of Sciences (USSR), Novosibirsk.
MODEL OF KUROSHIO REGION CIRCULATION c48
V. I. Kuzin, E. N. Golubeva, A. V. Martynov, and V. M. Moiseyev *In* Scientific Organizing Committee of PORSEC, Proceedings of the PORSEC 1992 in Okinawa: Conference for Pacific Ocean Environments and Probing, Volume 2 25 Aug. 1992 p 1281-1287 (For primary document see N94-12635 01-42)
Copyright Avail: Issuing Activity (Scientific Organizing Committee of PORSEC, P.O. Box 10, Shimizu, Shizuoka 424, Japan, HC)

The influence of the bottom topography near Izu-Ogasavara ridge and features of the coastline in this region on the Kuroshio current is studied using a 2-D model. Diagnostic and adaptational calculations of the currents for 12 months are carried out on the basis of a 3-D version of the model. Simulated currents show remarkable seasonal changes in their structures from July to December. Author (NASDA)

N94-12766 Academy of Sciences (USSR), Moscow. Inst. of Computational Mathematics.
PROBLEM OF CLIMATE CHANGE PREDICTABILITY AND SATELLITE RADIATION BUDGET OBSERVATIONS c47
Vladimir V. Kozoderov *In* Scientific Organizing Committee of PORSEC, Proceedings of the PORSEC 1992 in Okinawa: Conference for Pacific Ocean Environments and Probing, Volume 2 25 Aug. 1992 p 1288-1292 (For primary document see N94-12635 01-42)
Copyright Avail: Issuing Activity (Scientific Organizing Committee of PORSEC, P.O. Box 10, Shimizu, Shizuoka 424, Japan, HC)

The predictability problem for climate change is considered as that of signal to noise ratio calculated using satellite temporal data sets of the earth radiation budget components. In these ratios, the signal is characterized by cross-correlations of outgoing longwave radiation anomalies and noise by the standard deviations of the anomalies. To develop such a scientific approach, a concept of energy active zones of the world ocean has been elaborated based on results of monitoring and modeling. The approach using principal component techniques and climate indices enables satellite remote sensing data and measurements from scientific vessels to be linked in order to develop dynamical models of the ocean. Author (NASDA)

43 EARTH RESOURCES AND REMOTE SENSING

Includes remote sensing of earth resources by aircraft and spacecraft; photogrammetry; and aerial photography.

For instrumentation see *35 Instrumentation and Photography.*

N94-10417# Naval Surface Warfare Center, Silver Spring, MD.
A METHOD FOR CALCULATING EXACT GEODETIC LATITUDE AND ALTITUDE
Isaac Sofair Mar. 1993 18 p
(AD-A265783; NSWC-TR-85-85-Rev) Avail: CASI HC A03/MF A01

This report derives a new and improved technique for computing the geodetic latitude and altitude of an arbitrary point in space assuming the Earth is an ellipsoid of revolution. This method theoretically computes the exact values of the geodetic latitude and altitude. All the programs currently in use utilize approximation techniques for computing the quantities mentioned above. The method is simple and efficient and is strongly recommended for implementation. DTIC

N94-10702*# Texas Univ., Austin. Center for Space Research.
TOWARD 10(EXP 9) GPS GEODESY: VECTOR BASELINES, EARTH ROTATION AND REFERENCE FRAMES Annual Progress Report, 1 Jan. - 31 Dec. 1992
Bob E. Schutz 1 Jun. 1993 23 p
(Grant NAG5-1936)
(NASA-CR-193184; NAS 1.26:193184) Avail: CASI HC A03/MF A01

The University of Texas Center for Space Research research efforts under NASA Grant No. NAG-1936 from 1 Jan. 1992 - 31 Dec. 1992 were in the following areas: GPS orbit accuracy assessments and efforts to improve the accuracy; analysis of global GPS data collected during the first three months of the IGS campaign, and analysis of regional data. A brief summary of each of the above activities is presented in the following. Derived from text

N94-10714 McGill Univ., Montreal (Quebec).
RETRIEVAL OF RADIATION BUDGETS IN THE ARCTIC FROM SATELLITE MEASUREMENTS Ph.D. Thesis
Zhanqing Li 1991 200 p
Avail: Univ. Microfilms Order No. DANN72022

This study addresses the problems associated with each step of the process of retrieving radiation budgets at the top of atmosphere (TOA) and at the surface from satellite measurements in the Arctic. The data used are from the Earth Radiation Budget Experiment (ERBE) radiometer and Advanced Very High Resolution Radiometer (AVHRR), together with radiative transfer calculations. The limitations of the ERBE scene identification algorithm when applied to observations in the Arctic are investigated by comparing the scenes identified by ERBE with simultaneous and colocated AVHRR-based scenes. Considerable discrepancies are found, especially the misidentification by the ERBE scene identification method of clear fractional ice as being partly cloudy skies over open water. More accurate TOA fluxes and cloud forcing in the Arctic are derived by taking advantage of the broadband radiance measurements made by the ERBE radiometer and the more reliable scene identification deduced from narrow band multi spectral measurements made by the AVHRR. Comparisons of the cloud forcing determined from the two scene identification methods show differences as large as 50 Wm(exp -2) in some regions of the Arctic. The validity of the ERBE angular dependence models (ADMs) is also evaluated in the Arctic. It is found that the ADM for clear ice/snow is not reliable when applied in the Arctic during summer. The ADM for overcast skies contains systematic errors when applied to overcast conditions over ice/snow surfaces. The systematic error is removed by modifying the ADM. To estimate the surface absorbed flux from reflected flux at the TOA, a simple parameterized model is developed based on comprehensive radiative simulations. The model is independent of cloud optical thickness, surface type, and has only a moderate dependence on the presence or absence of cloud, cloud type and water vapor, but a strong dependence on solar zenith angle (SZA). Surface absorbed fluxes determined by radiative transfer calculations may generally be estimated to within 10 W m(exp -2) by the simple model from TOA reflected fluxes with knowledge of the SZA and precipitable water. Finally, narrowband-to-broadband reflectance conversion is carried out with careful attention paid to a particular statistical problem, namely, regression analysis with spatially autocorrelated satellite measurements. Both scene-dependent and scene-independent regressional models are developed to estimate broadband reflectance from the narrow band reflectances in channels 1 and 2 of AVHRR. The RMS errors in the percentage reflectances from the scene-dependent models are 1.0, 1.8, 2.0 and 3.1 for the ocean, land, ice/snow and cloud, respectively. Except for land, the scene-independent model does virtually as good a job as the scene-dependent models. Author

N94-10953*# Scripps Institution of Oceanography, La Jolla, CA.
STUDIES OF THE NET SURFACE RADIATIVE FLUX FROM SATELLITE RADIANCES DURING FIFE Final Report
Robert Frouin 14 Jun. 1993 146 p
(Grant NAG5-900)
(NASA-CR-193150; NAS 1.26:193150) Avail: CASI HC A07/MF A02

Studies of the net surface radiative flux from satellite radiances during First ISLSCP Field Experiment (FIFE) are presented. Topics covered include: radiative transfer model validation; calibration of VISSR and AVHRR solar channels; development and refinement of algorithms to estimate downward solar and terrestrial irradiances at the surface, including photosynthetically available radiation (PAR) and surface albedo; verification of these algorithms using in situ measurements; production of maps of shortwave irradiance, surface albedo, and related products; analysis of the temporal variability of shortwave irradiance over the FIFE site; development of a spectroscopy technique to estimate atmospheric total water vapor amount; and study of optimum linear combinations of visible and near-infrared reflectances for estimating the fraction of PAR absorbed by plants. For individual titles, see N94-10954 through N94-10955.

N94-10954*# Scripps Institution of Oceanography, La Jolla, CA.
SATELLITE-DERIVED PHOTOSYNTHETICALLY AVAILABLE AND TOTAL SOLAR IRRADIANCE AT THE SURFACE DURING FIFE'S INTENSIVE FIELD CAMPAIGNS
Robert Frouin and J. McPherson *In its* Studies of the Net Surface Radiative Flux from Satellite Radiances During FIFE 14 Jun. 1993 31 p (For primary document see N94-10953 01-43)
Avail: CASI HC A03/MF A02

Satellite-derived photosynthetically available and total solar irradiance at the surface during First International Satellite Land Surface Climatology Project (ISLSCP) Field Experiment's (FIFE) intensive field compaigns are addressed. Graphs showing photosynthetically available radiation (PAR) vs. Julian Day and insolation vs. Julian Day are included. CASI

N94-10955*# Scripps Institution of Oceanography, La Jolla, CA.
ESTIMATING PHOTOSYNTHETICALLY AVAILABLE RADIATION (PAR) AT THE EARTH'S SURFACE FROM SATELLITE OBSERVATIONS
Robert Frouin *In its* Studies of the Net Surface Radiative Flux from Satellite Radiances During FIFE 14 Jun. 1993 p 28 Submitted for publication (For primary document see N94-10953 01-43)
Avail: CASI HC A03/MF A02

Current satellite algorithms to estimate photosynthetically available radiation (PAR) at the earth' s surface are reviewed. PAR is deduced either from an insolation estimate or obtained directly from top-of-atmosphere solar radiances. The characteristics of both approaches are contrasted and typical results are presented. The inaccuracies reported, about 10 percent and 6 percent on daily and monthly time scales, respectively, are useful to model oceanic and terrestrial primary productivity. At those time scales variability due to clouds in the ratio of PAR and insolation is reduced, making it possible to deduce PAR directly from insolation climatologies (satellite or other) that are currently available or being produced. Improvements, however, are needed in conditions of broken cloudiness and over ice/snow. If not addressed properly, calibration/validation issues may prevent quantitative use of the PAR estimates in studies of climatic change. The prospects are good for an accurate, long-term climatology of PAR over the globe. Author (revised)

N94-11129# Mitsubishi Electric Corp., Tokyo (Japan).
PRE-OPERATION ANALYSIS OF ERS-1 TRACKING AND OPERATION, PART 2-A [ERS-1 TSUISEKI KANSEI UNYOU JUNBI]
National Space Development Agency 31 Mar. 1993 51 p In JAPANESE
(NASDA-CNT-930001-Pt-2-A; JTN-93-80455) Avail: CASI HC A04/MF A01

A summary of the system engineering and pre-operation analysis conducted on the JERS-1 (Japanese Earth Resources Satellite-1) tracking and operation and their results are presented. The following items are included in the system engineering: (1) updating the operation analysis to make the tracking and control operation conditions and operation limits clear; (2) updating the tracking and control data base and construction of JERS-1 SOP (Spacecraft Operation Procedure); (3) supporting the interface coordination with non-Japanese organization; and (4) updating the tracking and control system development documentations. Included items in the tracking and control preparation are as follows: (1) supporting computer software integration test; (2) supporting GDST (Ground Data System Test); (3) supporting operation procedure preparation; (4) supporting the training; and (5) supporting rehearsal operation. Author (NASDA)

N94-11130# Mitsubishi Space Software Corp. (Japan).
PRE-OPERATION ANALYSIS OF ERS-1 TRACKING AND OPERATION, PART 2-F [ERS-1 TSUISEKI KANSEI UNYOU JUNBI]
National Space Development Agency 31 Mar. 1993 15 p In JAPANESE
(NASDA-CNT-930002-Pt-2-F; JTN-93-80456) Avail: CASI HC A03/MF A01

A summary of the results of the pre-operation analysis is presented and includes the following: (1) detailed analysis of ground station antenna pointing errors at the tracking and data acquisition stations in and out of the country and overseas portable tracking stations during the satellite's critical phase; and (2) the launch and early orbit phase and RSP (Receiver Signal Processor) maintenance analysis during the satellite mission duration of the JERS-1 (Japanese Earth Resources Satellite-1). The result of both analyses, azimuth to elevation and azimuth to time errors for each station for the former and the RSP maintenance limits, eccentricity maintenance limits, number of controls, and propellant weight required in four cases of atmospheric model error estimation are shown. Author (NASDA)

N94-11179# Instituto de Pesquisas Espaciais, Sao Jose dos Campos (Brazil).
TOVS SOUNDINGS: IMPACT ON THE SYNOPTIC ANALYSIS OVER THE SOUTH AND SOUTHEAST REGIONS OF BRAZIL FROM MARCH 18 TO MARCH 19, 1991 M.S. Thesis [SONDAGENS TOVS: IMPACTO NA ANALISE SINOTICA ENTRE 18 E 19 DE MARCO DE 1991 NA REGIAO SUL E SUDESTE DO BRASIL]
Jojhy Sakuragi Nov. 1992 151 p In PORTUGESE
(INPE-5497-TDI/512) Avail: CASI HC A08/MF A02

This report explores the impact of temperature and humidity profiles retrieved from radiances obtained by TIROS Operational Vertical Sounder (TOVS) on the synoptic analysis over South and Southeast of Brazil. The radiance data obtained by the TOVS sounder which operates on board of the TIROS-N/NOAA polar orbiting meteorological satellites were processed with the aid of the International TOVS Processing Package-4 (ITPP-4), numerical analyses from National Meteorological Center (NMC), and conventional meteorological data. From the temperature and humidity profiles initially obtained, temperature, geopotential height, precipitable water, instability index, and advection fields were generated at constant pressure levels. A case study of the occurrence of intense precipitation during 19 March, 1991, in the Greater Sao Paulo and nearby coastal regions, was so formed. The results were compared with the NMC analyses and the meteorological conditions observed in the satellite imagery. Based on these results, it is generally concluded that the impact of satellite data is positive, especially due to its availability over the oceanic regions, and by the high spatial resolution and high temporal frequency. The good agreement between the TOVS results and the observed meteorological conditions from satellite images supports this conclusion. Author (revised)

N94-11236*# JJM Systems, Inc., Arlington, VA.
AN EXPERT SYSTEM SHELL FOR INFERRING VEGETATION CHARACTERISTICS: PROTOTYPE HELP SYSTEM (TASK 1)
Jul. 1993 24 p
(Contract NAS5-30127)
(NASA-CR-193411; NAS 1.26:193411; C931032-U-2R08) Avail: CASI HC A03/MF A01

The NASA Vegetation Workbench (VEG) is a knowledge based system that infers vegetation characteristics from reflectance data. A prototype of the VEG subgoal HELP.SYSTEM has been completed and the Help System has been added to the VEG system. It is loaded when the user first clicks on the HELP.SYSTEM option in the Tool Box Menu. The Help System provides a user tool to support needed user information. It also provides interactive tools the scientist may use to develop new help messages and to modify existing help messages that are attached to VEG screens. The system automatically manages system and file operations needed to preserve new or modified help messages. The Help System was tested both as a help system development and a help system user tool. Author (revised)

N94-11309*# George Washington Univ., Washington, DC. Dept. of Electrical Engineering and Computer Science.
ENHANCEMENT EFFECTS IN POLARIMETRIC RADAR RETURNS: PHASE DIFFERENCE STATISTICS
R. H. Lang and N. Khadr 1993 4 p
(Grant NAG5-1807)
(NASA-CR-193408; NAS 1.26:193408) Avail: CASI HC A01/MF A01

The probability density functions (pdfs) of the co- and cross-polarized phase differences are derived for backscatter from vegetation using the coherent and incoherent scattering theories. Unlike previous derivations, no assumptions or observations other than the applicability of the Central Limit Theorem (CLT), the low fractional volume of the medium, the reciprocity of the scatterers, and the azimuthal symmetry of the scatterer's orientation statistics are employed. Everything else follows logically via the mathematics. The difference between the coherent theory and the incoherent theory is referred to as the backscatter enhancement effect. The influence of this enhancement effect on the phase difference pdfs is examined and found to be important under combined conditions of scatterer anisotropy and appropriate reflection coefficient values. Author (revised)

N94-11378*# National Aeronautics and Space Administration. Ames Research Center, Moffett Field, CA.
APPLICATION OF THE AIRBORNE OCEAN COLOR IMAGER FOR COMMERCIAL FISHING
Robert C. Wrigley Mar. 1993 81 p Original contains color illustrations
(RTOP 142-20-37)
(NASA-TM-103986; A-93005; NAS 1.15:103986) Avail: CASI HC A05/MF A01; 8 functional color pages

The objective of the investigation was to develop a commercial remote sensing system for providing near-real-time data (within one day) in support of commercial fishing operations. The Airborne Ocean Color Imager (AOCI) had been built for NASA by Daedalus Enterprises, Inc., but it needed certain improvements, data processing software, and a delivery system to make it into a commercial system for fisheries. Two products were developed to support this effort: the AOCI with its associated processing system and an information service for both commercial and recreational fisheries to be created by Spectro Scan, Inc. The investigation achieved all technical objectives: improving the AOCI, creating software for atmospheric correction and bio-optical output products, georeferencing the output products, and creating a delivery system to get those products into the hands of commercial and recreational fishermen in near-real-time. The first set of business objectives involved Daedalus Enterprises and also were achieved: they have an improved AOCI and new data processing software with a set of example data products for fisheries applications to show their customers. Daedalus' marketing activities showed the need for simplification of the product for fisheries, but they successfully marketed the current version to an Italian consortium. The second set of business objectives tasked Spectro Scan to provide an information service and they could not be achieved because Spectro Scan was unable to obtain necessary venture capital to start up operations. Author

N94-11485*# National Aeronautics and Space Administration. Goddard Space Flight Center, Greenbelt, MD.
[GLOBAL MONITORING OF ATMOSPHERIC PROPERTIES BY THE EOS MODIS] Semiannual Technical Report, Jan. - Jun. 1993
Michael D. King 1993 20 p Original contains color illustrations
(NASA-TM-109237; NAS 1.15:109237) Avail: CASI HC A03/MF A01; 2 functional color pages

The Moderate Resolution Imaging Spectroradiometer (MODIS) being developed for the Earth Observing System (EOS) is well suited to the global monitoring of atmospheric properties from space. Among the atmospheric properties to be examined using MODIS observations, clouds are especially important, since they are a strong modulator of the shortwave and longwave components of the earth's radiation budget. A knowledge of cloud properties (such as optical thickness and effective radius) and their variation in space and time, which are our task objectives, is also crucial to studies of global climate change. In addition, with the use of related airborne instrumentation, such as the Cloud Absorption Radiometer (CAR) and MODIS Airborne Simulator (MAS) in intensive field experiments (both national and international campaigns, see below), various types of surface and cloud properties can be derived from the measured bidirectional reflectances. These missions have provided valuable experimental data to determine the capability of narrow bandpass channels in examining the Earth's atmosphere and to aid in defining algorithms and building an understanding of the ability of MODIS to remotely sense atmospheric conditions for assessing global change. Therefore, the primary task objective is to extend and expand our algorithm for retrieving the optical thickness and effective radius of clouds from radiation measurements to be obtained from MODIS. The secondary objective is to obtain an enhanced knowledge of surface angular and spectral properties that can be inferred from airborne directional radiance measurements. Author

N94-11521*# Minnesota Univ., Saint Paul. Dept. of Forest Resources.
SATELLITE INVENTORY OF MINNESOTA FOREST RESOURCES Final Report
Marvin E. Bauer, Thomas E. Burk, Alan R. Ek, Pol R. Coppin, Stephen D. Lime, Terese A. Walsh, David K. Walters, William Befort (Minnesota Dept. of Natural Resources, Grand Rapids.), and David F. Heinzen (Minnesota Dept. of Natural Resources, Grand Rapids.) Jul. 1993 27 p Original contains color illustrations
(Grant NAGw-1431)
(NASA-CR-193565; NAS 1.26:193565; NRA-87-106) Avail: CASI HC A03/MF A01; 3 functional color pages

The methods and results of using Landsat Thematic Mapper (TM) data to classify and estimate the acreage of forest covertypes in northeastern Minnesota are described. Portions of six TM scenes covering five counties with a total area of 14,679 square miles were classified into six forest and five nonforest classes. The approach involved the integration of cluster sampling, image processing, and estimation. Using cluster sampling, 343 plots, each 88 acres in size, were photo interpreted and field mapped as a source of reference data for classifier training and calibration of the TM data classifications. Classification accuracies of up to 75 percent were achieved; most misclassification was between similar or related classes. An inverse method of calibration, based on the error rates obtained from the classifications of the cluster plots, was used to adjust the classification class proportions for classification errors. The resulting area estimates for total forest land in the five-county area were within 3 percent of the estimate made independently by the USDA Forest Service. Area estimates for conifer and hardwood forest types were within 0.8 and 6.0 percent respectively, of the Forest Service estimates. A trial of a second method of estimating the same classes as the Forest Service resulted in standard errors of 0.002 to 0.015. A study of the use of multidate TM data for change detection showed that forest canopy depletion, canopy increment, and no change could be identified with greater than 90 percent accuracy. The project results have been the basis for the Minnesota Department of Natural Resources and the Forest Service to define and begin to implement an annual system of forest inventory which utilizes Landsat TM data to detect changes in forest cover. Author

N94-11524# Instituto de Pesquisas Espaciais, Sao Jose dos Campos (Brazil).
LANDSAT AS A COMMERCIAL ENTERPRISE M.S. Thesis
Maria Carmen deMello Lemos 1992 62 p
(INPE-5477-TAE/019) Avail: CASI HC A04/MF A01

In 1985 the government of the United States signed a contract with the Earth Observation Satellite Company (EOSAT) transferring the operation and future development of the country's earth resources observation system, the Landsat. The objective of this study is to discuss the commercialization of the Landsat system in light of its economical and political implications, mainly concerning international relations, security and the U.S. leadership in space technology. The commercialization allegedly goals were mainly to establish a strong market for Landsat data and to cut government's support for operations and construction costs. So far neither goal was satisfactorily met. The general conclusion of this study is that the Landsat transfer to the private sector was much more motivated by budget cuts than by the real possibilities of Landsat surviving as a private enterprise. As a consequence, the Landsat program has been seriously threatened of termination in the past 5 years with dramatic political, social and economical consequences to the United States. Author

N94-11623# Sandia National Labs., Albuquerque, NM.
SPACEBORNE SAR STUDY: LDRD 1992 Final Report
D. L. Bickel, B. C. Brock, and C. T. Allen (Allied-Signal Aerospace Co., Kansas City, MO.) Mar. 1993 116 p
(Contract DE-AC04-76DP-00789)
(DE93-011485; SAND-93-0731) Avail: CASI HC A06/MF A02

This is the final report for a study performed for the 1992 LDRD spaceborne SAR (Synthetic Aperture Radar) study. This report presents an overview of some of the issues that must be considered for design and implementation of a SAR on a spaceborne platform. The issues addressed in this report include the following: a survey of past, present, and future spaceborne SARs; pulse-repetition frequency (PRF); general image processing issues; transmitter power requirements; the ionosphere; antennas; two case studies; and an appendix with a simplified presentation on geometry and orbits. DOE

N94-11704# European Space Agency, Paris (France).
PROCEEDINGS OF FIRST ERS-1 SYMPOSIUM ON SPACE AT THE SERVICE OF OUR ENVIRONMENT, VOLUME 1
Brigitte Kaldeich, ed. Mar. 1993 483 p Symposium held in Cannes, France, 4-6 Nov. 1992
(ESA-SP-359-Vol-1; ISBN-92-9092-278-8; ETN-93-94634) Copyright
Avail: CASI HC A21/MF A04; EPD, ESA, ESTEC, Noordwijk, Netherlands, HC

Papers from the first ERS-1 symposium are presented in two volumes. The first volume is subdivided into the following topics: wind and wave validation; oceanography; SAR (Synthetic Aperture Radar) calibration; SAR interferometry; glaciology and ice sheet monitoring; sea ice studies; and radar altimeter. For individual titles, see N94-11705 through N94-11786.

N94-11705# Technical Univ. of Denmark, Lyngby. Remote Sensing Unit.
SEA ICE: A CLIMATE COMPONENT **c48**
P. Gudmandsen *In* ESA, Proceedings of First ERS-1 Symposium on Space at the Service of Our Environment, Volume 1 Mar. 1993 p 9-13 (For primary document see N94-11704 01-43)
Copyright Avail: CASI HC A01/MF A04; EPD, ESA, ESTEC, Noordwijk, Netherlands, HC

Some of the features of the air sea ice interaction processes and the characteristics of sea ice relative to applications of remote sensing techniques are described qualitatively. The polar regions play an important role in the global climate mechanisms since generally they act as heat sinks in the large scale atmospheric circulation. In this context the polar oceans interact with the atmosphere in the way that sea ice forms over large areas and thereby, reduces the heat exchange between the ocean surface and the atmosphere. Sea ice also interacts with the ocean in a number of ways so that we are faced with a rather complex air sea ice interaction problem. This is subject to research in order to be able to arrive at a good understanding of the phenomena observed with a view to applications in global climate studies including numerical modeling. Remote sensing is used extensively and at an increased rate after the launch of ERS-1 which offers fine resolution SAR (Synthetic Aperture Radar) data independent of cloud and light conditions. Examples of observations are given and the role of ERS-1 in polar ocean research is discussed. ESA

N94-11706# European Space Agency, Paris (France).
CALIBRATION AND VALIDATION OF THE ERS-1 WIND SCATTEROMETER
P. Lecomte and E. P. W. Attema *In its* Proceedings of First ERS-1 Symposium on Space at the Service of Our Environment, Volume 1 Mar. 1993 p 19-29 (For primary document see N94-11704 01-43)
Copyright Avail: CASI HC A03/MF A04; EPD, ESA, ESTEC, Noordwijk, Netherlands, HC

In a period of 8 months after the launch of the ERS-1 satellite, the wind scatterometer has been calibrated to an absolute level of 0.2 dB, using transponders and the stable backscattering of the tropical rain forest. With the support of the scientific user community, a program of geophysical validation and model tuning was carried out based on meteorological model analysis and high quality surface observations. After one year in orbit, the ERS-1 wind product has achieved a high level of accuracy. Supporting work on ice mapping is reported. ESA

N94-11707# Physics and Electronics Lab. TNO, The Hague (Netherlands).
VALIDATION OF DIRECTIONAL WAVE SPECTRA FROM THE ERS-1 DURING THE ESA CAL/VAL CAMPAIGN
J. C. M. Kleijweg and H. Greidanus *In* ESA, Proceedings of First ERS-1 Symposium on Space at the Service of Our Environment, Volume 1 Mar. 1993 p 31-34 (For primary document see N94-11704 01-43)
Copyright Avail: CASI HC A01/MF A04; EPD, ESA, ESTEC, Noordwijk, Netherlands, HC

The 1991 ESA experimental campaign 'RENE91' was meant to calibrate and validate (Cal/Val) ERS-1 ocean data and geophysical products. For a number of days during this campaign, directional ocean wave spectra were measured concurrently by the ERS-1 in AMI (Active Microwave Instrument) image mode; by the airborne SAR (Synthetic Aperture Radar), 'PHARS' (Phased Array SAR); by the shipborne radar 'SHIRA'; and by a Datawell wave buoy. The results of these instruments are compared and qualitatively interpreted on the basis of SAR ocean wave imaging theory. It is found that: very short (less than 70 m) waves are not seen by ERS-1, nor by PHARS; roughly half the wave occurrences are detected by both ERS-1 and PHARS, the remaining are missed by either or both; peak wavelength and direction of the same wave component can differ considerably as imaged by the various sensors; and ERS-1 has more difficulty detecting wave systems than the other sensors, especially azimuth traveling ones. All these effects can be understood in terms of the elements of the SAR ocean wave imaging process, viz scanning distortion, velocity bunching, and defocussing. ESA

N94-11708*# National Aeronautics and Space Administration. Wallops Flight Center, Wallops Island, VA.
THE GRAND BANKS ERS-1 SAR WAVE SPECTRA VALIDATION EXPERIMENT **c48**
P. W. Vachon (Canada Centre for Remote Sensing, Ottawa, Ontario.), F. W. Dobson (Bedford Inst. of Oceanography, Dartmouth, Nova Scotia.), S. D. Smith (Bedford Inst. of Oceanography, Dartmouth, Nova Scotia.), R. J. Anderson (Bedford Inst. of Oceanography, Dartmouth, Nova Scotia.), J. R. Buckley (Royal Roads Military Coll., Victoria, British Columbia.), M. Allingham (Royal Roads Military Coll., Victoria, British Columbia.), D. Vandemark, E. J. Walsh, M. Khandekar (Atmospheric Environment Service, Downsview, Ontario.), and R. Lalbeharry (Atmospheric Environment Service, Downsview, Ontario.) et al *In* ESA, Proceedings of First ERS-1 Symposium on Space at the Service of Our Environment, Volume 1 Mar. 1993 p 35-40 (For primary document see N94-11704 01-43)
Copyright Avail: CASI HC A02/MF A04; EPD, ESA, ESTEC, Noordwijk, Netherlands, HC

As part of the ERS-1 validation program, the ERS-1 Synthetic Aperture Radar (SAR) wave spectra validation experiment was carried out over the Grand Banks of Newfoundland (Canada) in Nov. 1991. The principal objective of the experiment was to obtain complete sets of wind and wave data from a variety of calibrated instruments to validate SAR measurements of ocean wave spectra. The field program activities are described and the rather complex wind and wave conditions which were observed are summarized. Spectral comparisons with ERS-1 SAR image spectra are provided. The ERS-1 SAR is shown to have measured swell and range traveling wind seas, but did not measure azimuth traveling wind seas at any time during the experiment. Results of velocity bunching forward mapping and new measurements of the relationship between wind stress and sea state are also shown. ESA

N94-11709# European Centre for Medium-Range Weather Forecasts, Reading (England).

ERS-1 SCATTEROMETER DATA CHARACTERISTICS AND WIND RETRIEVAL SKILL

Ad Stoffelen and David L. T. Anderson (Oxford Univ., England.) *In* ESA, Proceedings of First ERS-1 Symposium on Space at the Service of Our Environment, Volume 1 Mar. 1993 p 41-47 (For primary document see N94-11704 01-43)

Copyright Avail: CASI HC A02/MF A04; EPD, ESA, ESTEC, Noordwijk, Netherlands, HC

Calibration and validation activities for the ERS-1 scatterometer have been carried out at ECMWF (European Center for Medium range Weather Forecasting), where a wealth of verifying data is available both in time and space for satellite instrument calibration and validation. It is shown that measurement noise is sufficiently low that a solution surface is generally well defined in three dimensional measurement space except at the inner edge of the swath and a low wind speed. Based on the ECMWF analyses, ESA's prelaunch transfer model CMOD2 was reformulated (denoted CMOD3 by ESA) and some further improvements in bias and wind direction sensitivity subsequently made (CMOD4). Based on the new transfer function, a revision of the existing wind retrieval scheme used by ESA is proposed. ESA

N94-11710# Norwegian Meteorological Inst., Blindern.

VALIDATION OF ERS-1 WIND AND WAVE DATA BY USE OF OPERATIONAL FORECAST MODELS

Lars-Anders Breivik and Magnar Reistad (Norwegian Meteorological Inst., Bergen.) *In* ESA, Proceedings of First ERS-1 Symposium on Space at the Service of Our Environment, Volume 1 Mar. 1993 p 49-53 (For primary document see N94-11704 01-43)

Copyright Avail: CASI HC A01/MF A04; EPD, ESA, ESTEC, Noordwijk, Netherlands, HC

Since the launch of ERS-1 in Jul. 1991 scatterometer wind information and altimeter wave information from the North Atlantic has been received in real time at the Norwegian Meteorological Institute. The data has been collocated with and evaluated against operational numerical weather forecast model and sea wave model data. The wind scatterometer data are found to be capable of observing the surface wind field with high accuracy. The main problem is connected to obtaining the right wind direction in cases of rapid spatial variations in the wind field. The altimeter wave height data are good. Routines for assimilating the data in the numerical models were developed and are currently running in parallel with the operational routines. The average impact is modest, but there are cases of significant positive impact. ESA

N94-11711# Hamburg Univ. (Germany). Inst. fuer Meereskunde.

A C-BAND WIND SCATTEROMETER MODEL DERIVED FROM THE DATA OBTAINED DURING THE ERS-1 CALIBRATION/VALIDATION CAMPAIGN

Volkmar Wismann *In* ESA, Proceedings of First ERS-1 Symposium on Space at the Service of Our Environment, Volume 1 Mar. 1993 p 55-59 (For primary document see N94-11704 01-43)

(Grant BMFT-01-QS-90144)

Copyright Avail: CASI HC A01/MF A04; EPD, ESA, ESTEC, Noordwijk, Netherlands, HC

The geophysical calibration and validation campaign for the first European Remote Sensing Satellite (ERS-1) took place in the Norwegian Sea between 15 Sep. - 10 Dec. 1991. Ocean surface wind measurements were carried out with the airborne C band scatterometer RACS of the University of Hamburg during 46 underflights of the satellite. The wind was measured by the navigational system of the Do-228 aircraft during low level (6 to 150 m) flights. A high quality subset of these data was used to tune the proposed wind scatterometer model function which differs from the ERS-1 prelaunch CMOD-2 formulation by an azimuth dependance of the wind speed exponent. A wind retrieval test demonstrates that the proposed model satisfies the ESA specifications for the ERS-1 wind scatterometer model. ESA

N94-11712# Institut Francais de Recherche pour l'Exploitation de la Mer, Brest. Dept. d'Oceanographie Spatiale.

ERS-1 STUDIES AT THE DEPARTMENT OF OCEANOGRAPHY FROM SPACE, IFREMER/BREST (FRANCE) c48

Kristina B. Katsaros, Abderrahim Bentamy, Alain Cavanie, Bertrand Chapron, Robert Ezraty, Patrick Farcy, Francis Gohin, Pierre Queffeulou, Yves Quilfen, and Jean Tournadre *In* ESA, Proceedings of First ERS-1 Symposium on Space at the Service of Our Environment, Volume 1 Mar. 1993 p 61-66 (For primary document see N94-11704 01-43)

Copyright Avail: CASI HC A02/MF A04; EPD, ESA, ESTEC, Noordwijk, Netherlands, HC

The contribution to calibration and validation of ERS-1 data products and scatterometer model function development is described and an overview of current scientific studies is given. The latter includes studies on air sea interaction and sea ice. The scatterometer provides vector wind fields over the 500 km wide swath, which allows analysis of frontal weather systems and tropical cyclones over the sea. ESA

N94-11713# Consiglio Nazionale delle Ricerche, Venice (Italy). Ist. Studio Dinamica Grandi Masse.

THE ACTIVITY OF THE ERS-1 VENICE (ITALY) GROUP ON SCATTEROMETRY

Stefano Zecchetto and Piero Pavese (Consiglio Nazionale delle Ricerche, Turin, Italy.) *In* ESA, Proceedings of First ERS-1 Symposium on Space at the Service of Our Environment, Volume 1 Mar. 1993 p 71-73 (For primary document see N94-11704 01-43)

Copyright Avail: CASI HC A01/MF A04; EPD, ESA, ESTEC, Noordwijk, Netherlands, HC

An account of the status of the project 'Aspects of ERS-1 LBR validation in the Mediterranean Sea' is given. The project is composed of two complementary activities: one devoted to experiments in the open sea measuring the C band radar backscattering, wind stress, and high frequency sea surface elevation; the other devoted to the scatterometer and altimeter data validation. The aim is to assess the dependences of the radar backscattering from the sea wave parameters using both the satellite and the platform data on one hand, and to validate the ERS-1 scatterometer wind fields in studying their mesoscale characteristics. Results of the experimental activity are only quoted; the reported examples of the ERS-1 scatterometer wind fields show that they are unsuitable to be used without a deep and systematic correction of the directions selected by the fast delivery algorithm. ESA

N94-11714# SACLANT ASW Research Center, La Spezia (Italy).

USE OF ERS-1 DATA AT SACLANT UNDERSEA RESEARCH CENTRE c48

H.-H. Essen *In* ESA, Proceedings of First ERS-1 Symposium on Space at the Service of Our Environment, Volume 1 Mar. 1993 p 75-77 (For primary document see N94-11704 01-43)

Copyright Avail: CASI HC A01/MF A04; EPD, ESA, ESTEC, Noordwijk, Netherlands, HC

During a number of cruises to the Iceland-Faeroe frontal area suface meteorological data (wind velocity, air and sea surface temperature etc.) were collected. Data covering about eight weeks of different seasons and meteorological conditions are available and in situ winds are intended for comparison with scatterometer derived ones. Appropriate satellite data are not yet received. Five SAR (Synthetic Aperture Radar) images from Mar. 1992 were investigated for mesoscale variability. From CTD profiles, a correlation between dynamic height at the sea surface and the amplitudes of empirical orthogonal eigenfunctions of sound velocity profiles were found, which in principle, allows to observe subsurface sound velocity by altimetry. ESA

N94-11715*# Oregon State Univ., Corvallis.

A PRELIMINARY C-BAND SCATTEROMETER MODEL FUNCTION FOR THE ERS-1 AMI INSTRUMENT

M. H. Freilich and R. S. Dunbar (Jet Propulsion Lab., California Inst. of Tech., Pasadena.) *In* ESA, Proceedings of First ERS-1 Symposium on

Space at the Service of Our Environment, Volume 1 Mar. 1993 p 79-83 (For primary document see N94-11704 01-43)
(Contracts NAGw-3062; JPL-959294; JPL-959351)
Copyright Avail: CASI HC A01/MF A04; EPD, ESA, ESTEC, Noordwijk, Netherlands, HC

Backscatter cross section (sigma(sub 0)) measurements from the ERS-1 scatterometer are collocated with surface wind velocity data from operational Numerical Weather Prediction (NWP) analyses to yield a fully empirical C band model function. The empirical model does not obey a power law at speeds less than 5 m/s, and upwind/crosswind ratios are small for all incidence angles at low wind speeds and for small incidence angles at all wind speeds. Downwind sigma(sub 0) exceeds upwind values for incidence angles below approximately 28 degrees. The full ERS-1 scatterometer data set has been reprocessed using the NWP model function. ESA

N94-11716# Aston Univ., Birmingham (England). Dept. of Computer Science and Applied Mathematics.
CALIBRATION OF ERS-1 ALTIMETRY OVER THE NORTH SEA
C. W. Lam, P. Moore, and P. L. Woodworth (Proudman Oceanographic Lab., Birkenhead, England.) *In* ESA, Proceedings of First ERS-1 Symposium on Space at the Service of Our Environment, Volume 1 Mar. 1993 p 85-90 (For primary document see N94-11704 01-43)
Copyright Avail: CASI HC A02/MF A04; EPD, ESA, ESTEC, Noordwijk, Netherlands, HC

A calibration exercise utilizing seven ascending repeat passes over the English Channel in conjunction with precise orbits, GPS (Global Positioning System) measurement, local levelling, tide gauge data, and geoid/ocean tide/storm surge models was carried out for Jan. - Mar. 1992. Precise orbits of +/- 5 cm radial accuracy was achieved due to the satellite flying near overhead of the Herstmonceux laser ranger. From a total of 76 calibration points, a mean height residual of -46.0 cm with a standard deviation of 10.8 cm was observed. The derived electronic bias of -46.0 cm +/- 11 cm can be compared to -19.2 cm as estimated from the dedicated calibration validation based on the Venice Tower experiment and -60 cm to -70 cm from various long-arc studies. ESA

N94-11717# Commonwealth Scientific and Industrial Research Organization, Hobart (Australia). Oceanography Div.
MAPPING OF THE EAST AUSTRALIAN CURRENT WITH THE ERS-1 SAR AND SHIPBORNE STUDIES c48
C. S. Nilsson, P. Tildesley, and J. Peterson *In* ESA, Proceedings of First ERS-1 Symposium on Space at the Service of Our Environment, Volume 1 Mar. 1993 p 95-100 (For primary document see N94-11704 01-43)
Copyright Avail: CASI HC A02/MF A04; EPD, ESA, ESTEC, Noordwijk, Netherlands, HC

Seven ERS-1 SAR (Synthetic Aperture Radar) passes were acquired during the first two weeks of Nov. and three in Dec. 1991 over the western Tasman Sea and East Australian Current (EAC) area. The EAC is a strongly flowing western boundary current that displays strong baroclinic instability and is the principal dynamic feature in the study area. The principal aim of this experiment was to evaluate the usefulness of ERS-1 C-band SAR in mapping ocean currents. An Airborne Expendable Bathythermograph (AXBT) survey and research ship cruise provided surface truth data. In most of the SAR swaths studied to date, the current flow shows, to varying degrees, some sharp ridges of enhanced backscatter that are assumed to be related to current shear-wave interaction. The data show clear evidence of SAR sensitivity to natural surface organic films. In one instance, a cool stream of Southern Ocean water images in great detail on the SAR and it is deduced that natural surfactants are the controlling mechanism, given uniform wind conditions. Thus, ERS-1 SAR will probably correlate with ocean color and prove a useful tool for studies of oceanic mixing, particularly at higher latitudes. ESA

N94-11718# Institute of Ocean Sciences, Sidney (British Columbia).
WIND AND SURFACE FEATURES IN SAR IMAGES: THE CANADIAN PROGRAM
J. F. R. Gower *In* ESA, Proceedings of First ERS-1 Symposium on Space at the Service of Our Environment, Volume 1 Mar. 1993 p 101-106 (For primary document see N94-11704 01-43)
Copyright Avail: CASI HC A02/MF A04; EPD, ESA, ESTEC, Noordwijk, Netherlands, HC

The program plans to use data from the ERS-1 SAR (Synthetic Aperture Radar), together with surface data, to show coastal circulation, mixing, and other features in regions of the east, west, and Hudson Bay coasts of Canada. Sufficient coverage is planned to assess the variation of feature visibility with season, and to determine the influence of wind speed and surfactants. The extent of the Canadian program is described, and sample images are presented. The variation of SAR signal level with wind speed and direction is discussed, based on images of a Vancouver Island study area. The present ESA model of wind induced C band backscatter appears to overestimate variation with wind direction at ERS-1 SAR incidence angles. Surfactant slicks are visible for wind speeds less than about 5 m/s. Internal wave patterns are visible at higher speeds. ESA

N94-11719# Indian Space Research Organization, Ahmedabad. Space Applications Center.
PRELIMINARY ANALYSIS OF CIRCULATIONS OVER THE INDIAN OCEAN AND ADJOINING REGIONS USING ERS-1 SURFACE WINDS IN THE NCMRWF DATA ASSIMILATION SYSTEM c48
P. C. Joshi, B. Simon, M. S. Narayanan, S. R. H. Rizvi (National Centre for Medium Range Weather Forecasting, New Delhi, India.), and R. K. Bansal (National Centre for Medium Range Weather Forecasting, New Delhi, India.) *In* ESA, Proceedings of First ERS-1 Symposium on Space at the Service of Our Environment, Volume 1 Mar. 1993 p 107-111 (For primary document see N94-11704 01-43)
Copyright Avail: CASI HC A01/MF A04; EPD, ESA, ESTEC, Noordwijk, Netherlands, HC

ESR-1 C band scatterometer winds for five days of Nov. 1991 were analyzed to study its impact on the analysis. The data was examined in association with the climatological information, synoptic charts, as well as the ship data from the GTS network. It is observed that the wind data distribution over the Indian Ocean, where no other data exists, is good. There are many locations having opposite wind directions which calls for improved data quality evaluation. Data of 28 Nov. was found to be the most consistent and was used in the Global Data Assimilation System (GDAS). ESA

N94-11720# Nansen Remote Sensing Center, Bergen (Norway).
COASTAL OCEAN STUDIES WITH ERS-1 SAR DURING NORCSEX 1991 c48
J. A. Johannessen, R. A. Shuchman (Environmental Research Inst. of Michigan, Ann Arbor.), K. Davidson (Naval Postgraduate School, Monterey, CA.), O. Frette, G. Digranes, and O. M. Johannessen *In* ESA, Proceedings of First ERS-1 Symposium on Space at the Service of Our Environment, Volume 1 Mar. 1993 p 113-117 Sponsored by Norwegian Space Center; Bergen Univ.; ESA; Norwegian Navy; and NATO (For primary document see N94-11704 01-43)
Copyright Avail: CASI HC A01/MF A04; EPD, ESA, ESTEC, Noordwijk, Netherlands, HC

The Norwegian Continental Shelf Experiment (NORCSEX 91) was conducted between 6-29 Nov. 1991 during the commissioning phase of ERS-1. In this period about 30 SAR (Synthetic Aperture Radar) scenes were obtained at a regular interval of three days. Complementary in situ observations of wind wave current and their interaction were collected from ship and moorings. The integrated data base reveal that SAR images express features associated with: mesoscale ocean current circulation pattern including frontal boundaries and eddies; slicks; internal waves; and rapid mesoscale wind field variations. The expressions of oceanic circulation features and slicks are limited by both high and low wind speed. These preliminary results are presented and discussed. ESA

N94-11721# Southampton Univ. (England). Dept. of Oceanography.
SAR IMAGING OF DYNAMICAL FEATURES IN THE ENGLISH CHANNEL c48
Alison Scoon and Ian S. Robinson *In* ESA, Proceedings of First ERS-1 Symposium on Space at the Service of Our Environment, Volume 1 Mar. 1993 p 119-124 Sponsored in part by Natural Environmental Research Council (For primary document see N94-11704 01-43)
Copyright Avail: CASI HC A02/MF A04; EPD, ESA, ESTEC, Noordwijk, Netherlands, HC

ERS-1 Synthetic Aperture Radar (SAR) images of a study area in the central English Channel were examined in relation to the information which they contain about dynamical ocean features. After compression to 8 bits and block averaging to reduce speckle, the mean radar return from an offshore region with uniform backscatter was related to the wind and tidal conditions. Repeat images of inshore areas show that fronts between inshore and offshore and offshore water can be seen in many tidal states. Their location is consistent with numerical model predictions of tidal residual flows. Smooth slicks, regions of low backscatter, also appear to correlate with discharges from rivers and coastal outfalls. By examining several images, permanent bathymetric signatures can be distinguished from the quasi-permanent dynamical and ephemeral features, pointing to a useful role for routine SAR monitoring for coastal management studies. ESA

N94-11722# Chilworth Research Centre, Southampton (England). Remote Sensing Applications Development Unit.
EFFECTS OF WAVE NONLINEARITY ON ERS-1 RADAR ALTIMETER RETURNS: A PRELIMINARY INVESTIGATION **c48**
M. A. Srokosz and G. D. Quartly *In* ESA, Proceedings of First ERS-1 Symposium on Space at the Service of Our Environment, Volume 1 Mar. 1993 p 125-130 (For primary document see N94-11704 01-43)
Copyright Avail: CASI HC A02/MF A04; EPD, ESA, ESTEC, Noordwijk, Netherlands, HC

A preliminary look at the sea state bias (due to wave nonlinearity) in ERS-1 radar altimeter measurements of sea surface topography is given. Using the limited amount of ERS-1 data available, the approach adopted is to choose occasions when the significant wave height changes over a short distance and to examine the corresponding change in the residual sea surface heights (obtained from the altimeter height measurements after applying various corrections and removing the orbit error and mean sea surface topography). The bias, as a percentage of significant waveheight, is found to vary from -1.7% to 9.4% with a mean value of 5.0%. The application of these results, to the correction of sea state bias in the ERS-1 altimeter height measurements, must be treated with caution due to the small number of cases studied here. ESA

N94-11723# Ocean Research and Engineering, Pasadena, CA.
SAR OCEAN IMAGING IN THE GULF OF ALASKA **c48**
O. H. Shemdin, D. W. Hayt, and D. P. Kasilingam *In* ESA, Proceedings of First ERS-1 Symposium on Space at the Service of Our Environment, Volume 1 Mar. 1993 p 131-134 (For primary document see N94-11704 01-43)
Copyright Avail: CASI HC A01/MF A04; EPD, ESA, ESTEC, Noordwijk, Netherlands, HC

Radar images of portions of the Gulf of Alaska acquired by the Synthetic Aperture Radar (SAR) aboard the ERS-1 platform are analyzed to extract qualitative and quantitative geophysical information. The primary objectives of this study are to investigate the imaging of ocean surface waves, ship wakes, and oil slicks. A preliminary version of a SAR image inversion model is used to obtain surface wave spectral information from the SAR images. Significant wave heights obtained from this technique agree well with in situ data obtained from buoys located near the image site. The images of ship wakes and oil slicks also provide useful qualitative information. ESA

N94-11724*# Jet Propulsion Lab., California Inst. of Tech., Pasadena.
EVALUATION OF TWO JANUARY - JUNE 1992 ERS-1 AMI WIND VECTOR DATA SETS
D. Halpern, M. H. Freilich (Oregon State Univ., Corvallis.), and R. S. Dunbar *In* ESA, Proceedings of First ERS-1 Symposium on Space at the Service of Our Environment, Volume 1 Mar. 1993 p 135-139 (For primary document see N94-11704 01-43)
(Contracts NAGw-3062; RTOP 578-22-26-40; JPL-959294; JPL-959351)
Copyright Avail: CASI HC A01/MF A04; EPD, ESA, ESTEC, Noordwijk, Netherlands, HC

A Jan. - Jun. 1992 10 m height wind vector field was computed with the CMOD2 model function. Freilich and Dunbar used ESA measurements of AMI (Active Microwave Instrument) sigma-naught to derive a refined model function and to produce an alternate Jan. - Jun. 1992 10 m height wind vector field, named FD data. The ESA and FD model functions and algorithms were substantially different. The FD wind vectors were in better agreement with the climatological mean wind field and with moored buoy wind measurements. The average correlation coefficients between monthly mean and daily averaged FD and moored buoy matchups of the Cartesian wind components were 0.84 and 0.74, respectively. The average root mean square differences between the monthly mean and daily averaged FD and moored buoy matchups of the Cartesian wind components were 1.25 and 3.0 m/s, respectively. ESA

N94-11725# Chilworth Research Centre, Southampton (England). Center for Ocean Circulation.
COMPARISONS OF ERS-1 ALTIMETER HEIGHT DATA AND THE FINE RESOLUTION ANTARCTIC MODEL (FRAM)
H. M. Snaith and D. J. Webb (Institute of Oceanographic Sciences, Wormley, England.) *In* ESA, Proceedings of First ERS-1 Symposium on Space at the Service of Our Environment, Volume 1 Mar. 1993 p 141-146 (For primary document see N94-11704 01-43)
Copyright Avail: CASI HC A02/MF A04; EPD, ESA, ESTEC, Noordwijk, Netherlands, HC

Improvement in the understanding of the dynamics of the Southern Ocean is discussed. The Fine Resolution Antarctic Model (FRAM) was designed to help explain some of the dynamic mechanisms of the region and satellite altimetry offers a method of verifying the mesoscale activity of this large scale model. The study focuses on the Agulhas region. Comparisons of the FRAM surface dynamic height fields with historical data show that the major current systems are represented with reasonable accuracy. Geosat altimeter data were processed using a collinear technique to obtain sea surface height variability. The FRAM surface pressure fields were sampled as if by an altimeter and processed using the same collinear technique in order to gain an insight into errors involved in the method. The resultant variability fields are here compared with Geosat height variability and bathymetry. The same collinear technique was applied to ERS-1 altimeter data from the commissioning phase. ESA

N94-11726# European Space Agency. European Space Research and Technology Center, ESTEC, Noordwijk (Netherlands). Earth Observation Dept.
ERS-1 SAR CALIBRATION STRATEGY
Jean Pierre Guignard *In its* Proceedings of First ERS-1 Symposium on Space at the Service of Our Environment, Volume 1 Mar. 1993 p 151-156 (For primary document see N94-11704 01-43)
Copyright Avail: CASI HC A02/MF A04; EPD, ESA, ESTEC, Noordwijk, Netherlands, HC

The main elements defining the ESA strategy in view of calibrating SAR (Synthetic Aperture Radar) images are reviewed. The stability of the satellite itself is mentioned as allowing for a proper use of the ESA developed active targets (transponders) and/or the use of corner reflectors. A reference processor (verification mode processor) was specifically developed for calibration activities. ESA

N94-11727# Deutsche Forschungsanstalt fuer Luft- und Raumfahrt, Oberpfaffenhofen (Germany). Inst. fuer Hochfrequenztechnik.
ERS-1 PRELIMINARY ANTENNA ELEVATION PATTERN MEASURED BY GROUND-RECEIVERS
Pedro Seifert, Manfred Zink, and Harald Lentz (Stuttgart Univ., Germany.) *In* ESA, Proceedings of First ERS-1 Symposium on Space at the Service of Our Environment, Volume 1 Mar. 1993 p 157-159 (For primary document see N94-11704 01-43)
Copyright Avail: CASI HC A01/MF A04; EPD, ESA, ESTEC, Noordwijk, Netherlands, HC

An approach to measure a SAR (Synthetic Aperture Radar) antenna elevation diagram which uses a greater number of high precision calibration receivers, lined up in cross track direction, to record azimuth slices of the antenna pattern, is described. The coregistration of the time of receipt, together with precise orbit and attitude data of the satellite, allows correlation of the azimuth cuts and calculation of adequate antenna elevation angles. As each of the received radar pulses is sampled 16 times, an examination of the pulse shape is also possible. The principle system is described and the preliminary result of the ERS-1 antenna elevation pattern measurement is presented. ESA

N94-11728# Bari Univ. (Italy).
PRELIMINARY RESULTS OF THE EXPERIMENT I-7
C. Cafforio, G. DeCarolis (Consiglio Nazionale delle Ricerche, Bari, Italy.), F. Mattia (Consiglio Nazionale delle Ricerche, Bari, Italy.), A. Moccia (Naples Univ., Italy.), S. Ponte (Naples Univ., Italy.), F. Posa, V. D. Schena (CORISTA, Naples, Italy.), R. Sergi (CORISTA, Naples, Italy.), P. Smacchia (Consiglio

Nazionale delle Ricerche, Matera, Italy.), and V. Sozzi et al *In* ESA, Proceedings of First ERS-1 Symposium on Space at the Service of Our Environment, Volume 1 Mar. 1993 p 161-166 (For primary document see N94-11704 01-43)
(Contracts ASI-91-RS-70; ASI-91-RS-63)
Copyright Avail: CASI HC A02/MF A04; EPD, ESA, ESTEC, Noordwijk, Netherlands, HC

The preliminary results related to the ERS-1 AMI (Active Microwave Instrument) image mode data analysis carried out in the framework of the experiment I-7 are described. The SAR (Synthetic Aperture Radar) data was acquired during the 23 Oct. 1991 night pass over the Salento peninsula and the 21 Jun. and 7 Jul. 1992 day passes over the Matera area in southern Italy. In this experimental phase, the main objectives are the SAR image quality evaluation and calibration. To accomplish this, two active radar calibrators and several trihedral corner reflectors were deployed on both sites. A preliminary comparison with an available SAR omega-k processor is presented. ESA

N94-11729# Canada Centre for Remote Sensing, Ottawa (Ontario).
THE ERS-1/CV 580 SAR CROSS-CALIBRATION EXPERIMENT: SAULT STE MARIE, OCTOBER 26 - NOVEMBER 2, 1991
C. E. Livingstone, D. Maxwell (Waterloo Univ., Ontario.), and J. R. C. Lafontaine (INTERA Technologies Ltd., Ottawa, Ontario.) *In* ESA, Proceedings of First ERS-1 Symposium on Space at the Service of Our Environment, Volume 1 Mar. 1993 p 167-171 (For primary document see N94-11704 01-43)
Copyright Avail: CASI HC A01/MF A04; EPD, ESA, ESTEC, Noordwijk, Netherlands, HC

During the period 26 Oct. - 2 Nov. 1991 a series of five consecutive ERS-1 SAR (Synthetic Aperture Radar) passes were underflown by the Canada Center for Remote Sensing CV 580 SAR system. In the airborne component of the experiment grids of nadir mode, C band VV polarized strip images were acquired along the ERS-1 SAR azimuth and range directions. The three coincident sets of ERS-1 and airborne SAR data acquired were analyzed to derive calibration functions for the Gatineau SGF products. The measured ERS-1 SAR antenna pattern is in good agreement with that reported by ESA. The calibration constant for the Gatineau SGF images was 61.3 +/- 0.45 dB with a residual uncertainly of +/- 1 dB. ESA

N94-11730# Chalmers Univ. of Technology, Goeteborg (Sweden). Dept. Radio and Space Science.
CALIBRATION OF THE ERS-1 SAR FAST-DELIVERY IMAGES
L. M. H. Ulander *In* ESA, Proceedings of First ERS-1 Symposium on Space at the Service of Our Environment, Volume 1 Mar. 1993 p 173-178 (For primary document see N94-11704 01-43)
Copyright Avail: CASI HC A02/MF A04; EPD, ESA, ESTEC, Noordwijk, Netherlands, HC

The possibility of performing absolute radiometric calibration of ERS-1 SAR (Synthetic Aperture Radar) Fast Delivery (FD) images is investigated. A 1.5 month time series during the first ice phase included fourteen satellite overpasses and showed that the radiometric stability of the SAR FD images was better than 0.3 dB (root mean square). A comparison with the average ESA calibration constant showed an average difference of 0.2 dB. The average difference obtained from a second calibration experiment during the commissioning phase was 0.9 dB, but included only two overpasses. It is pointed out that the FD product header does not provide sufficient information to determine the image geometry for across track calibration. Methods to solve this problem are suggested, but more work is needed to evaluate their performance. ESA

N94-11731# Physics and Electronics Lab. TNO, The Hague (Netherlands).
CALIBRATION RESULTS FOR THE ERS-1, AIRSAR, AND PHARS
A. C. vandenBroek and J. S. Groot *In* ESA, Proceedings of First ERS-1 Symposium on Space at the Service of Our Environment, Volume 1 Mar. 1993 p 179-190 (For primary document see N94-11704 01-43)
Copyright Avail: CASI HC A03/MF A04; EPD, ESA, ESTEC, Noordwijk, Netherlands, HC

Satellite SAR (Synthetic Aperture Radar) data (ERS-1) and airborne SAR data (AIRSAR and PHARS) of the agriculture test site Flevoland in the Netherlands on coincident dates are studied. AIRSAR can be calibrated with an accuracy of about 1 dB and PHARS data with an accuracy of about 2 dB. The calibration accuracy for the ERS-1 data is on average 0.3 dB. The results show that these satellite and airborne SAR data can give consistent results despite their differences in resolution and speckle (number of looks). ESA

N94-11732# Joint Research Centre of the European Communities, Ispra (Italy). Remote Sensing Applications Inst.
THE USE OF ACTIVE DEVICES IN THE ERS-1 RADIOMETRIC CALIBRATION
Carlo Lavalle *In* ESA, Proceedings of First ERS-1 Symposium on Space at the Service of Our Environment, Volume 1 Mar. 1993 p 191-194 (For primary document see N94-11704 01-43)
Copyright Avail: CASI HC A01/MF A04; EPD, ESA, ESTEC, Noordwijk, Netherlands, HC

The main objective of the investigations carried out on images acquired during the commissioning phase of the ERS-1 life, was the quality assessment and calibration of image data. This required the availability of a set of targets of known radar scattering behavior, distributed over the imaged area in such a way to allow accurate analysis and calibration of the system response. The Institute for Remote Sensing Applications of the Joint Research Centre, in the frame of the International Forest Investigation project, selected the area of Freiburg Black Forest (Germany) as calibration site for the ERS-1 data. During the satellite commissioning phase, a set of three active radar calibrators were deployed on five dates, four weeks apart approximately, with location accuracy of 5 m. The first results achieved in the radiometric calibration and quality analysis of the ERS-1 images over the Black Forest show good agreement with the expected theoretical values of the impulse response function characteristics for the precision image product while the single look complex data sets processed presented saturation phenomena. ESA

N94-11733# Defence Research Agency, Farnborough (England).
AN EXPERIMENT FOR THE RADIOMETRIC CALIBRATION OF THE ERS-1 SAR
P. J. Bird, G. E. Keyte, and D. R. D. Kenward *In* ESA, Proceedings of First ERS-1 Symposium on Space at the Service of Our Environment, Volume 1 Mar. 1993 p 195-200 Sponsored by British National Space Centre (For primary document see N94-11704 01-43)
Copyright Avail: CASI HC A02/MF A04; EPD, ESA, ESTEC, Noordwijk, Netherlands, HC

The performance of 4 precision corner reflectors and a radome cover are assessed. Measurements made on the reflectors indicate a very rigid, accurate construction. From an analysis of ERS-1 SAR imagery, it is shown that the reflectors provide a calibration target of similar stability to that of the DRA ground based scatterometer transponder. Variations in the reflector image response were found, which are related to changes in the replica pulse power. The cause of the replica power changes are not known. A number of other reflectors were deployed and are used, together with the precision reflectors and transponder to demonstrate the good SAR (Synthetic Aperture Radar) system linearity. Grass and bare soil backgrounds are compared. It is shown that grass provides the more suitable calibration site. A good agreement between SAR and ground based scatterometer data is found. ESA

N94-11734*# Zurich Univ. (Switzerland). Remote Sensing Labs.
TECHNIQUES AND APPLICATIONS OF SAR INTERFEROMETRY FOR ERS-1: TOPOGRAPHIC MAPPING, CHANGE DETECTION, AND SLOPE MEASUREMENT
Charles L. Werner, Scott Hensley (Jet Propulsion Lab., California Inst. of Tech., Pasadena.), Richard M. Goldstein (Jet Propulsion Lab., California Inst. of Tech., Pasadena.), Paul A. Rosen (Jet Propulsion Lab., California Inst. of Tech., Pasadena.), and Howard A. Zebker (Jet Propulsion Lab., California Inst. of Tech., Pasadena.) *In* ESA, Proceedings of First ERS-1 Symposium on Space at the Service of Our Environment, Volume 1 Mar. 1993 p 205-210 Sponsored by NASA, Washington (For primary document see N94-11704 01-43)
Copyright Avail: CASI HC A02/MF A04; EPD, ESA, ESTEC, Noordwijk, Netherlands, HC

SAR (Synthetic Aperture Radar) interferometry allows the measurement of high resolution topography of terrain from repeat orbit SAR data sets obtained by the ERS-1 AMI (Active Microwave Instrument). The system parameters which affect the accuracy of the topographic maps are errors in determination of the interferometric baseline, non parallel orbit tracks, decorrelation caused by baseline length, thermal noise, and surface change. Surface change can be observed in the interferograms either through decorrelation of the interferometric phase, or coherent phase shifts caused by locally uniform surface displacements. Phase gradient maps can be derived directly from the complex interferograms and can be transformed into surface slopes mapped onto a geometrically corrected grid. ESA

N94-11735# Politecnico di Milano (Italy). Dipt. di Elettronica.
SAR INTERFEROMETRY EXPERIMENTS WITH ERS-1
C. Prati, F. Rocca, and A. MontiGuarnieri *In* ESA, Proceedings of First ERS-1 Symposium on Space at the Service of Our Environment, Volume 1 Mar. 1993 p 211-218 (For primary document see N94-11704 01-43)
Copyright Avail: CASI HC A02/MF A04; EPD, ESA, ESTEC, Noordwijk, Netherlands, HC

Synthetic Aperture Radar (SAR) is a microwave coherent imaging system which has day, night and all weather capabilities. SAR coherence can be exploited for applications of repeated surveys like digital elevation map generation, improvement of ground range resolution, measurement of small changes of the terrain. ERS-1 SAR mission represents a good opportunity for testing these applications. The first experiments carried out with ERS-1 SAR Image mode on coherent multitemporal imaging applications are reported. ESA

N94-11736# Stuttgart Univ. (Germany). Inst. fuer Navigation.
SAR-INTERFEROMETRY APPLYING ERS-1: SOME PRELIMINARY TEST RESULTS
P. Hartl, M. Reich, K.-H. Thiel, and Y. Xia *In* ESA, Proceedings of First ERS-1 Symposium on Space at the Service of Our Environment, Volume 1 Mar. 1993 p 219-222 (For primary document see N94-11704 01-43)
Copyright Avail: CASI HC A01/MF A04; EPD, ESA, ESTEC, Noordwijk, Netherlands, HC

The ERS-1 mission with its different orbit modes and excellent SAR (Synthetic Aperture Radar) performance offers particularly good opportunities to test and to promote the methods of SAR interferometry. Preliminary results are reported. For the Bonn (Germany) area it could be shown that the method of differential SAR interferometry allows very small height changes to be detected. The SAR interferometry allows, under proper physical conditions, both, the determination of the three dimensional topography and of the heights of forests, of buildings in settlements, and of other fine structured natural and man made targets. The preliminary results from the Antarctica show that the degree of correlation, and therefore of the coherence of the signals from an image pair can be used as a new measure for surface feature classification, and for change detection. ESA

N94-11737# Innsbruck Univ. (Austria). Inst. fuer Meteorologie und Geophysik.
SIGNATURES OF ANTARCTIC FIRN BY MEANS OF ERS-1 AMI AND BY FIELD MEASUREMENTS
H. Rott, K. Sturm, and H. Miller (Alfred-Wegener-Inst. for Polar Research, Bremerhaven, Germany.) *In* ESA, Proceedings of First ERS-1 Symposium on Space at the Service of Our Environment, Volume 1 Mar. 1993 p 227-233 (For primary document see N94-11704 01-43)
(Contract FWF-P8476)
Copyright Avail: CASI HC A02/MF A04; EPD, ESA, ESTEC, Noordwijk, Netherlands, HC

Backscattering coefficients sigma(naught), measured by ERS-1 AMI (Active Microwave Instrument) in scatterometer mode, show significant regional variations over Antarctica. The angular dependence and magnitude of sigma(naught) are related to the morphology of the snow, enabling the discrimination of different snow regimes. Field measurements on backscattering signatures and on snow properties in Antarctica provide the basis for the interpretation of the ERS-1 scatterometer data. Examples of field data and satellite measurements are presented for refrozen firn on the ice shelves, homogeneous snow in high accumulation zones, and strongly stratified snow at the high plateaus. ESA

N94-11738# Mullard Space Science Lab., Dorking (England).
ANALYSIS OF ERS-1 ALTIMETER DATA OVER THE POLAR ICE SHEETS
C. G. Rapley, J. L. Bamber, J. G. Morley, J. K. Ridley, S. W. Laxon, D. Mantripp, J. A. D. Mansley, and D. J. Wingham *In* ESA, Proceedings of First ERS-1 Symposium on Space at the Service of Our Environment, Volume 1 Mar. 1993 p 235-240 (For primary document see N94-11704 01-43)
Copyright Avail: CASI HC A02/MF A04; EPD, ESA, ESTEC, Noordwijk, Netherlands, HC

The use of ERS-1 altimeter fast delivery data to derive height maps of Greenland and Antarctica is reported. Without the off line waveform data it is not possible to correct these for tracker bias. However, over large areas of the ice sheets, this introduces an error which is small compared with the height resolution of our displays. Errors in the orbits and preliminary atmospheric corrections used were reduced by averaging data over multiple repeat cycles. For Greenland, a slope induced error correction was applied. The maps are the most accurate yet of the regions beyond +/- 72 deg. Preliminary results include the delineation of drainage basins on the Greenland ice sheet, and the observation of glaciologically interesting surface features in Antarctica. ESA

N94-11739# Institut fuer Angewandte Geodaesie, Leipzig (Germany).
SOME RESULTS OF THE DERIVATION OF ICE SHEET ELEVATIONS IN ANTARCTICA FROM ERS-1 ALTIMETER DATA
Johannes Ihde, Uwe Schirmer, Andreas Reinhold, and Juergen Eck *In* ESA, Proceedings of First ERS-1 Symposium on Space at the Service of Our Environment, Volume 1 Mar. 1993 p 241-245 (For primary document see N94-11704 01-43)
Copyright Avail: CASI HC A01/MF A04; EPD, ESA, ESTEC, Noordwijk, Netherlands, HC

Investigations aimed at the derivations of orthometric heights (sea heights) along a mean three day repeat cycle and the estimation of the reproduceable accuracy of the ERS-1 fast delivery altimeter heights are reported. For more than 55 the accuracy of derived ellipsoidal ice sheet elevations is better than 1 m. The OSU91A geoid was introduced as level surface for the orthometric heights. Comparisons of the altimeter heights with GPS and trigonometric heights indicate an agreement of better than 0.5 m on flat ice sheets. ESA

N94-11740# Institut fuer Angewandte Geodaesie, Frankfurt am Main (Germany).
UTILISATION OF ERS-1 DATA FOR MAPPING OF ANTARCTICA
J. Sievers, R. Hartmann (Joint Publications Research Service, Arlington, VA.), D. Kosmann (Deutsche Forschungsanstalt fuer Luft- und Raumfahrt, Oberpfaffenhofen, Germany.), A. Reinhold (Institut fuer Angewandte Geodaesie, Leipzig, Germany.), and K.-H. Thiel (Stuttgart Univ., Germany.) *In* ESA, Proceedings of First ERS-1 Symposium on Space at the Service of Our Environment, Volume 1 Mar. 1993 p 247-251 (For primary document see N94-11704 01-43)
Copyright Avail: CASI HC A01/MF A04; EPD, ESA, ESTEC, Noordwijk, Netherlands, HC

Mapping of Antarctica by the ERS-1 satellite is described. Remote sensing data of spaceborne sensors are able to give a multitude of geoscientific information on regions difficult or inaccessible at all for terrestrial survey programs. This is particularly true for Antarctica because of its geographic isolation and its environment, in general hostile towards life. Here ERS-1 and in particular its microwave sensors give reason to expect new and better research possibilities. Apart from the suitability of radar sensors for penetrating clouds, it will for the first time be possible to observe continuously the southern polar region during the austral winter. ESA

N94-11741*# National Aeronautics and Space Administration. Goddard Space Flight Center, Greenbelt, MD.
MONITORING OF THE GREENLAND ICE SHEET USING ERS-1 SYNTHETIC APERTURE RADAR IMAGERY
Robert Bindschadler, Mark Fahnestock, and Ron Kwok (Jet Propulsion Lab., California Inst. of Tech., Pasadena.) *In* ESA, Proceedings of First ERS-1 Symposium on Space at the Service of Our Environment, Volume 1 Mar. 1993 p 253-257 (For primary document see N94-11704 01-43)
(RTOP 578-35-02-20)
Copyright Avail: CASI HC A01/MF A04; EPD, ESA, ESTEC, Noordwijk, Netherlands, HC

ERS-1 Synthetic Aperture Radar (SAR) imagery is shown to be suitable for monitoring the climate of the Greenland ice sheet and for measuring changes in its marginal position. Four distinct hydrologic zones are easily recognized. Zone boundaries align closely with elevation. Seasonal changes in at least one of these zones indicate that late Winter is a better time than late Summer for the collection of images intended for long term monitoring. Subtle variations of the backscatter intensity from the highest portions of the ice sheet where melting never occurs are believed to indicate surface topography. ESA

N94-11742# British Antarctic Survey, Cambridge (England).
PRELIMINARY EVALUATION OF ERS-1 ALTIMETRY OVER FILCHNER-RONNE ICE SHELF, ANTARCTICA
Christopher Doake, David Vaughan, David Mantripp (Mullard Space Science Lab., Dorking, England.), Joern Sievers (Institut fuer Angewandte Geodaesie, Frankfurt am Main, Germany.), and Franz Thyssen (Forschungsstelle fuer Physikalische Glaziologie, Muenster, Germany.) *In* ESA, Proceedings of First ERS-1 Symposium on Space at the Service of Our Environment, Volume 1 Mar. 1993 p 259-261 (For primary document see N94-11704 01-43)
Copyright Avail: CASI HC A01/MF A04; EPD, ESA, ESTEC, Noordwijk, Netherlands, HC

Accurate surface elevation data over the Antarctic ice sheet are needed to understand how the ice sheet is changing at present and to help determine how it might respond to future global climate change. Range measurements from the ERS-1 fast delivery data product were used to construct a preliminary map of surface elevation for Filchner-Ronne ice shelf. The map shows several important features related to processes controlling the movement of the ice shelf and its interaction with the underlying ocean. Elevation data over Berkner Island was compared to a digital elevation model constructed from airborne data and show slope induced errors of up to 50 m. Analysis of waveforms derived from raw data suggest that there is little tracker bias. ESA

N94-11743# Scott Polar Research Inst., Cambridge (England).
INVESTIGATIONS OF ARCTIC ICE-SHEETS AND GLACIERS USING ERS-1 SAR
W. G. Rees, J. A. Dowdeswell, and A. D. Diament *In* ESA, Proceedings of First ERS-1 Symposium on Space at the Service of Our Environment, Volume 1 Mar. 1993 p 263-268 (For primary document see N94-11704 01-43)
(Grants NERC-GR3/ERS-1/1-3; NERC-GR3/8507)
Copyright Avail: CASI HC A02/MF A04; EPD, ESA, ESTEC, Noordwijk, Netherlands, HC

Qualitative and quantitative analysis of several geocoded, precision and low resolution SAR (Synthetic Aperture Radar) images from a number of sites in Greenland, Svalbard and Franz Josef Land, are described. These images were acquired as part of ESA's program for the study of ice sheets and glaciers using ERS-1 data, and they will ultimately be compared with a wide variety of validating datasets in order to assess and model the response of a SAR system to the changing conditions of these elements of the Earth's surface. Preliminary analyses of these images are described, assessing their potential for mapping the two dimensional geometry of glacier fronts and of different surface facies (dry snow, wet snow, superimposed ice and bare glacier ice); for the detection of seasonal change in the position of the snow line; and for confirming the variation of the backscatter coefficient with incidence angle over snow covered surfaces. The drift velocities of icebergs calving from ice sheet outlet glaciers on Greenland can also be monitored. ESA

N94-11744*# Ohio State Univ., Columbus. Polar Research Center.
SPATIAL PATTERNS IN BACKSCATTER STRENGTH ACROSS THE GREENLAND ICE SHEET
K. C. Jezek *In* ESA, Proceedings of First ERS-1 Symposium on Space at the Service of Our Environment, Volume 1 Mar. 1993 p 269-272 Sponsored by NASA, Washington (For primary document see N94-11704 01-43)
Copyright Avail: CASI HC A01/MF A04; EPD, ESA, ESTEC, Noordwijk, Netherlands, HC

The relationship between the physical properties of the Greenland ice sheet and Synthetic Aperture Radar (SAR) data collected from aircraft and from ERS-1 is addressed. Limited aircraft data are combined with a description of the glacier surface to predict qualitatively the spatial and seasonal variation in backscatter strength across the ice sheet. In particular the model predicts relatively low backscatter near the ice edge where scattering is dominated by rough surface effects. Backscatter increases through the lake zone as volume scattering becomes important. Strongest backscatter is found in the percolation facies where volume scatter from snow grains and volume scatter from large, buried ice bodies becomes important. Backscatter weakens in the interior ice sheet where fine grained snow is the only mechanism producing backscatter. ESA

N94-11745# Nansen Ocean and Remote Sensing Center, Solheimsvik (Norway).
ICE STUDIES IN THE BARENTS SEA BY ERS-1 SAR DURING SIZEX 92
Ola M. Johannessen, Stein Sandven, William J. Campbell (Geological Survey, Tacoma, WA.), and Robert Shuchmann (Environmental Research Inst. of Michigan, Ann Arbor.) *In* ESA, Proceedings of First ERS-1 Symposium on Space at the Service of Our Environment, Volume 1 Mar. 1993 p 277-282 (For primary document see N94-11704 01-43)
Copyright Avail: CASI HC A02/MF A04; EPD, ESA, ESTEC, Noordwijk, Netherlands, HC

The Seasonal Ice Zone Experiment (SIZEX 92) is a sea ice validation program for ERS-1 SAR (Synthetic Aperture Radar). The main field experiment was carried out in the Barents Sea in Mar. 1992 using an ice strengthened vessel, a helicopter and a research vessel which operated in thin ice outside the main ice edge. In situ measurements, aerial photographs and video records were obtained from different ice types such as multiyear, firstyear, refrozen leads, pancake ice, grease ice and icebergs. Approximately 50 low resolution SAR scenes (100 m) and 5 full resolution SAR scenes (25 m) were obtained from ERS-1 during the experiment. The experiment showed that multiyear ice, which was more than 4 m thick, had generally higher SAR backscatter values than the firstyear ice in the interior of the ice pack. On the other hand, firstyear ice which dominated in a 30 to 40 km wide zone inside the ice edge had similar backscatter values as the multiyear ice. The lowest backscatter values were found in refrozen leads and in areas outside the ice edge where grease was formed. In addition to ice type classification the SAR images from ERS-1 were useful to characterize the ice edge, estimate ice concentration, locate leads/polynyas, find shear zones in the ice pack, quantify ice motion and map areas of new ice formation. ESA

N94-11746# Scott Polar Research Inst., Cambridge (England).
USE OF ERS-1 SAR TO MEASURE ICE FLUX IN THE EAST GREENLAND CURRENT
P. Wadhams, E. Aldworth, and F. Parmiggiani (Istituto per lo Studio delle Metodologie Geofische Ambientali, Modena, Italy.) *In* ESA, Proceedings of First ERS-1 Symposium on Space at the Service of Our Environment, Volume 1 Mar. 1993 p 283-287 (For primary document see N94-11704 01-43)
Copyright Avail: CASI HC A01/MF A04; EPD, ESA, ESTEC, Noordwijk, Netherlands, HC

A joint project among several European institutions is in progress to measure ice flux across the 79th and the 75th parallels of latitude, and hence estimate the fresh water flux into the northern Greenland sea. At 75 deg north a line of three upward looking moored sonars have been in place since Aug. 1991, renewed for a further year in Aug. 1992. ERS-1 SAR (Synthetic Aperture Radar) imagery is being used in conjunction with AVHRR (Advanced Very High Resolution Radiometer) to measure north-south ice velocity components across the width of east Greenland Current at 75 deg north with averaging of three days (Jan. to Mar. 1992) and a slightly longer, variable period after Mar. 1992 when the satellite entered a 35 day repeat orbit. By combining velocities and 3 day averaged ice thickness, both interpolated across the width of the current, it is possible to estimate the ice flux in an unbiased way. Initial results of the satellite work are reported, since the upward sonar thickness data are not yet available. ESA

N94-11747# Chalmers Univ. of Technology, Goeteborg (Sweden). Dept. of Radio and Space Science.
VALIDATION OF ERS-1 SAR MEASUREMENTS OF SEA ICE DURING ARCTIC-1991
J. Askne, L. M. H. Ulander, A. Carlstroem, Y. Sun, and D. Birkeland *In* ESA, Proceedings of First ERS-1 Symposium on Space at the Service of Our Environment, Volume 1 Mar. 1993 p 289-294 Sponsored by

Swedish Board for Space Activities and Knut and Alice Wallenberg Foundation (For primary document see N94-11704 01-43)
Copyright Avail: CASI HC A02/MF A04; EPD, ESA, ESTEC, Noordwijk, Netherlands, HC

Results from ARCTIC-91, the first field experiments to the high Arctic with simultaneous coverage of the ERS-1 SAR (Synthetic Aperture Radar) satellite, are reported. Results from the advanced melt period and early freeze-up period are given. Average sigma deg values as well as Delta-sigma deg/Delta-Theta over the image for different ice classification are given. Methods to derive ice concentration and the uncertainties in the procedure are investigated. Accuracy within a few percent seems to be possible during the late melt period, and results are in good agreement with the less good ship reports. Ice concentration estimates are important for climate change studies and for comparison with passive microwave sensors. An example illustrating complex ice motion phenomena derived from automatic routines is given. ESA

N94-11748*# National Aeronautics and Space Administration. Goddard Space Flight Center, Greenbelt, MD.

ARCTIC COASTAL POLYNYA OBSERVATIONS WITH ERS-1 SAR AND DMSP SSM/I

D. J. Cavalieri and R. G. Onstott (Environmental Research Inst. of Michigan, Ann Arbor.) *In* ESA, Proceedings of First ERS-1 Symposium on Space at the Service of Our Environment, Volume 1 Mar. 1993 p 295-299 (For primary document see N94-11704 01-43)
Copyright Avail: CASI HC A01/MF A04; EPD, ESA, ESTEC, Noordwijk, Netherlands, HC

Work to improve the characterization of the distribution of new and young sea ice types and open water amount within Arctic coastal polynyas through the combined use of ERS-1 SAR (Synthetic Aperture Radar) and DMSP SSM/I (Defense Meteorological Satellite Program Special Sensor Microwave/Imager) data is described. Two St. Lawrence Island polynya events are studied using low resolution, geocoded SAR images and coincident SSM/I data. The SAR images are analyzed in terms of polarization and spectral gradient ratios. Results of the combined analysis show that the SAR ice type classification is consistent with that from SSM/I and that the combined use of SAR and SSM/I can improve the characterization of thin ice better than either data set can do alone. ESA

N94-11749# Washington Univ., Seattle. Polar Science Center.

SEA ICE DEFORMATION OBSERVED WITH ERS-1 SAR

D. A. Rothrock and H. L. Stern *In* ESA, Proceedings of First ERS-1 Symposium on Space at the Service of Our Environment, Volume 1 Mar. 1993 p 301-306 (For primary document see N94-11704 01-43)
Copyright Avail: CASI HC A02/MF A04; EPD, ESA, ESTEC, Noordwijk, Netherlands, HC

The material properties of the sea ice cover are exhibited in the spatial structure of the field of ice motion. This structure is well sampled by sea ice displacements computed by a geophysical processor system at the Alaska SAR (Synthetic Aperture Radar) facility. Each pair of images can give rise to as many as 400 displacement vectors on a 5 km grid, with an average of about 200 vectors per pair. The data from about 1700 such image pairs was analyzed, and histograms of the average velocity derivatives and deformation invariants are shown. The estimate of mean vorticity in the Beaufort Gyre, for example, agrees with published results derived from buoy and ice station data. Values of divergence are found to have a mean of -0.002 and a standard deviation of 0.022/day. Mosaics of motion data some 1500 km long show the piece-like structure of field of motion. ESA

N94-11750# Helsinki Univ. (Finland). Dept. of Geophysics.

FINNISH ERS-1 BALTIC SEA ICE EXPERIMENT IN WINTER 1992

M. Lepparanta, M. Hallikainen (Helsinki Univ. of Technology, Espoo, Finland.), E.-A. Herland (Technical Research Centre of Finland, Espoo.), M. Simila (Marine Research Inst., Helsinki, Finland.), R. Berglund (Technical Research Centre of Finland, Espoo.), M. Lensu (Marine Research Inst., Helsinki, Finland.), T. Manninen (Marine Research Inst., Helsinki, Finland.), and M. Toikka (Helsinki Univ. of Technology, Espoo, Finland.) *In* ESA, Proceedings of First ERS-1 Symposium on Space at the Service of Our Environment, Volume 1 Mar. 1993 p 307-312 Sponsored by Marine Research Inst.; Helsinki Univ. of Technology; Technical Research Centre of Finland; McGill Univ.; Scott Polar Research Inst.; Lulea Univ.; and LLNL (For primary document see N94-11704 01-43)
Copyright Avail: CASI HC A02/MF A04; EPD, ESA, ESTEC, Noordwijk, Netherlands, HC

PIPOR (Program for International Polar Oceans Research) Finland project examines the use of ERS-1 SAR (Synthetic Aperture Radar) in sea ice mapping in the Baltic Sea through geophysical validation and demonstration. The experimental part was performed in Jan. - Mar. 1992. The winter was very mild which caused restrictions in all planned activities. Two expeditions were made with an airborne program and ground truth. In the demonstration phase, near real time SAR imagery was provided to users. ERS-1 SAR data are also used in ice dynamics modeling. The first results show that ERS-1 SAR is an excellent complement to the existing ice mapping routine. ESA

N94-11751# Swedish Meteorological and Hydrological Inst., Norkoeping.

EXPERIENCES FROM THE SWEDISH SEA ICE PROGRAMME DURING BEERS-1992

Thomas Thompson, Bertil Haakansson, Lars Ulander (Chalmers Univ. of Technology, Goeteborg, Sweden.), and Anders Carlstrom (Chalmers Univ. of Technology, Goeteborg, Sweden.) *In* ESA, Proceedings of First ERS-1 Symposium on Space at the Service of Our Environment, Volume 1 Mar. 1993 p 313-318 (For primary document see N94-11704 01-43)
Copyright Avail: CASI HC A02/MF A04; EPD, ESA, ESTEC, Noordwijk, Netherlands, HC

During the period Jan. - Mar. 1992 the Baltic Experiment for ERS-1 (BEERS-92) was carried out in the Gulf of Bothnia. The purpose of the experiment was: to carry out field measurements on various types of ice in time for ERS-1 over passes; to demonstrate the usefulness of ERS-1 SAR (Synthetic Aperture Radar) images in an operational Sea Ice Service; and for icebreaker operations. For the experiment a BDDN (Broadband Data Dissemination Network) receive station was installed where SAR images were processed, disseminated, and stored. The field program, carried out from an icebreaker, consisted of in situ sea ice measurements and of helicopter photography. The emphasis was on sea ice parameters relevant for radar scattering investigations, i.e surface roughness, ice, and snow physics. Preliminary analysis of the SAR images shows a wide range of radar signatures mainly related to surface roughness variations. The demonstration experiment included the use of SAR images by the operational Sea Ice Service and the transmission of processed SAR images to icebreakers in near real time. ESA

N94-11752# Technical Univ. of Denmark, Lyngby. Remote Sensing Unit.

GREENLAND SEA OBSERVATIONS

P. Gudmandsen, H. Buch Mortensen, L. Toudal Pedersen, H. Skriver, and P. Minnett (Brookhaven National Lab., Upton, NY.) *In* ESA, Proceedings of First ERS-1 Symposium on Space at the Service of Our Environment, Volume 1 Mar. 1993 p 319-323 Sponsored by BNL and Danish Space Research Inst. (For primary document see N94-11704 01-43) (Grant NSF DPP-91-13962)
Copyright Avail: CASI HC A01/MF A04; EPD, ESA, ESTEC, Noordwijk, Netherlands, HC

ERS-1 SAR (Synthetic Aperture Radar) data was acquired over the Greenland Sea and Fram Strait during two periods, the ice phase of three day repeat cycle from Jan. to Mar. 1992 and a one month period in the 35 day repeat cycle from 16 Jul. to 15 Aug. 1992. Most data became available by way of the Broadband Data Dissemination System, with a spatial resolution of about 100 m. With these data various algorithms were tested to derive sea ice parameters such as ice extent, ice concentration and ice displacement. In the latter period data were collected to support the activities of a research vessel in the area mainly related to the large polynyas that form east and north of Greenland. The formation of polynyas could clearly be outlined but other phenomena were also observed related to the influence of wind streets and gravity waves associated with the atmospheric boundary layer. The data will have to be studied further, including full resolution data to substantiate the conclusions. ESA

N94-11753# Alfred-Wegener-Inst. for Polar Research, Bremerhaven (Germany).

AIR-SEA-ICE INTERACTIONS IN THE WEDDELL SEA

T. Viehoff, P. Lemke, W. Dierking, and M. Schmidt-Groettrup *In* ESA, Proceedings of First ERS-1 Symposium on Space at the Service of Our

Environment, Volume 1 Mar. 1993 p 325-327 (For primary document see N94-11704 01-43)
Copyright Avail: CASI HC A01/MF A04; EPD, ESA, ESTEC, Noordwijk, Netherlands, HC

As part of the Program for International Polar Oceans Research (PIPOR), ground measurements were carried out during two cruises to the Weddell Sea. These ground based data together with several remote sensing techniques (SAR (Synthetic Aperture Radar), AVHRR (Advanced Very High Resolution Radiometer), SSMI (Special Sensor Microware Images)) and coupled ocean ice atmosphere models are to be used for the geophysical interpretation of the sea ice dynamics in the Weddell Sea. ESA

N94-11754*# Environmental Research Inst. of Michigan, Ann Arbor. Earth Sciences Center.
ARCTIC SEA ICE MICROWAVE SIGNATURE AND GEOPHYSICAL PROCESSES STUDY
Robert G. Onstott and Robert A. Shuchman *In* ESA, Proceedings of First ERS-1 Symposium on Space at the Service of Our Environment, Volume 1 Mar. 1993 p 329-332 (For primary document see N94-11704 01-43)
(Contracts NAG2-543; N00014-90-C-0148; N00014-92-C-0140)
Copyright Avail: CASI HC A01/MF A04; EPD, ESA, ESTEC, Noordwijk, Netherlands, HC

Studies on the validation and utilization of ERS-1 SAR (Synthetic Aperture Radar) derived liquid and solid ocean information and the study of the interregional, regional, and temporal variation of the microwave signatures of sea ice and snow, are reported. Initial interests are focused on the accuracy of the estimates of ice type, ice form, deformation state, or thickness, and the ability to retrieve ice physical property information. Two in situ campaigns were conducted for the purpose of 'truth' ERS-1 SAR products and to gather data in support of the above science studies. ESA

N94-11755# National Space Development Agency, Saitama (Japan). Earth Observation Center.
C-BAND SAR BACKSCATTER FROM ICE ON SHALLOW TUNDRA LAKES: OBSERVATIONS AND MODELLING
H. Wakabayashi, M. O. Jeffries (Alaska Univ., Fairbanks.), and W. F. Weeks (Alaska Univ., Fairbanks.) *In* ESA, Proceedings of First ERS-1 Symposium on Space at the Service of Our Environment, Volume 1 Mar. 1993 p 333-337 (For primary document see N94-11704 01-43)
Copyright Avail: CASI HC A01/MF A04; EPD, ESA, ESTEC, Noordwijk, Netherlands, HC

The pronounced backscatter variations observed in sequential ERS-1 SAR (Synthetic Aperture Radar) images of tundra lakes near Barrow, Alaska are investigated. Earlier work suggested that weak returns could be attributed to attenuation of the radar signal where the ice was frozen to the lake bed, and strong returns to forward scattering off bubbles in the ice in combination with a near specular ice water interface. Field measurements in Apr. 1992 confirmed this hypothesis. At the locations sampled, grounded ice was less than 1 m thick while free floating ice exceeded 2 m. As long as the ice remained bubble free, backscatter values were low (-20 dB). When tubular bubbles appeared, these values rose to -9 to -10 dB and then gradually increased to values as high as -6 dB. Where the ice froze to the lake bed, values dropped to -18 dB. A numerical model of C band backscatter from such lake ice covers was also developed. A preliminary comparison between the modeled and observed backscatter is presented. ESA

N94-11756*# Jet Propulsion Lab., California Inst. of Tech., Pasadena.
SEA ICE RADAR SIGNATURES FROM ERS-1 SAR DURING LATE SUMMER AND FALL IN THE BEAUFORT AND CHUKCHI SEAS
Benjamin Holt, Glenn Cunningham, and Ron Kwok *In* ESA, Proceedings of First ERS-1 Symposium on Space at the Service of Our Environment, Volume 1 Mar. 1993 p 339-342 Sponsored by NASA, Washington (For primary document see N94-11704 01-43)
Copyright Avail: CASI HC A01/MF A04; EPD, ESA, ESTEC, Noordwijk, Netherlands, HC

A study which examines ERS-1 C band SAR (Synthetic Aperture Radar) imagery of sea ice obtained in the Beaufort and Chukchi Seas from mid Summer through Fall freeze up and early Winter in 1991 is presented. Radar backscatter statistics of sea ice were obtained from the imagery, using common floes tracked through consecutive repeat images whenever possible. During the Summer months, strong fluctuations in ice signatures of several dB are observed over 2 to 3 day periods, which are found to be closely related to air temperature excursions above and below freezing that alters the phase of the ice surface. As air temperatures drop steadily below freezing in the Fall, the signatures of the pack ice increase in brightness and become more stable with time. Multiyear ice is distinguished from rough and smooth first year ice. There are also variations in the multiyear signatures with latitude. Large variations are seen in new ice and open water contained within leads which results in ambiguous classification. ESA

N94-11757*# National Aeronautics and Space Administration. Goddard Space Flight Center, Greenbelt, MD.
WAVES AND MESOSCALE FEATURES IN THE MARGINAL ICE ZONE
Antony K. Liu and Chih Y. Peng (Science Systems and Applications, Inc., Greenbelt, MD.) *In* ESA, Proceedings of First ERS-1 Symposium on Space at the Service of Our Environment, Volume 1 Mar. 1993 p 343-348 Sponsored by ONR (For primary document see N94-11704 01-43)
Copyright Avail: CASI HC A02/MF A04; EPD, ESA, ESTEC, Noordwijk, Netherlands, HC

Ocean-ice interaction processes in the Marginal Ice Zone (MIZ) by waves and mesoscale features, such as upwelling and eddies, are studied using ERS-1 Synthetic Aperture Radar (SAR) imagery and wave-ice interaction models. Satellite observations of mesoscale features can play a crucial role in ocean-ice interaction study. ESA

N94-11758# Waterloo Univ. (Ontario). Earth Observations Lab.
THE SEASONAL SEA ICE MONITORING AND MODELLING SITE (SIMMS): USING ERS-1 IN CLIMATE RESEARCH Abstract Only
Ellsworth F. LeDrew and David G. Barber *In* ESA, Proceedings of First ERS-1 Symposium on Space at the Service of Our Environment, Volume 1 Mar. 1993 p 349 (For primary document see N94-11704 01-43)
Copyright Avail: CASI HC A01/MF A04; EPD, ESA, ESTEC, Noordwijk, Netherlands, HC

The Seasonal Sea Ice Monitoring and Modeling Site (SIMMS) experiment is introduced and the use of ERS-1 data to develop a better understanding of radiative, turbulent, and conductive fluxes which operate at the ocean-sea ice-atmosphere interface, is described. The objective is to understand the magnitude and rate of change of the major physical fluxes which occur between the ocean, sea ice, and atmosphere. ERS-1 data are the primary remote sensing data being used in the SIMMS experiment. The rationale for selection of ERS-1 data, the scales over which the surface validations are being conducted, and the theory behind how microwavelength radiance can be linked to climatological shortwave interaction and hence be of value in numerical studies of climate processes, are described. Preliminary results showing how the relative scattering cross section can be used to infer the climatological shortwave albedo over the seasonally varying snow covered sea ice surface are given in conclusion. ESA

N94-11759# Bedford Inst. of Oceanography, Dartmouth (Nova Scotia). Physical and Chemical Sciences.
OCEAN CIRCULATION REVEALED BY ICE FLOE TRACKING c48
M. Ikeda and S. Prinsenberg *In* ESA, Proceedings of First ERS-1 Symposium on Space at the Service of Our Environment, Volume 1 Mar. 1993 p 351-353 (For primary document see N94-11704 01-43)
Copyright Avail: CASI HC A01/MF A04; EPD, ESA, ESTEC, Noordwijk, Netherlands, HC

ERS-1 SAR (Synthetic Aperture Radar) images and airborne SAR and SLAR (Side Looking AR) images were collected from the ice covered region over the Labrador and Newfoundland (Canada) shelves in Feb. and Mar. 1992. In the ERS-1 SAR images, very new ice (grease ice) is shown dark, and open water filled with wind waves is very bright. Airborne electromagnetic measurements combined with a laser and an altimeter clearly demonstrate ice thicknesses variable in space and may provide calibration data for the SAR data. Once ice floes are tracked between two images, ice velocity field will be constructed and used for detecting ocean currents under the ice cover. ESA

N94-11760# Atmospheric Environment Service, Downsview (Ontario).

PRELIMINARY EVALUATION OF ERS-1 SAR DATA FOR OPERATIONAL USE IN THE CANADIAN SEA ICE MONITORING PROGRAM

Mohammed E. Shokr, Bruce Ramsay (Ice Centre Environment Canada, Ottawa, Ontario.), and John C. Falkingham (Ice Centre Environment Canada, Ottawa, Ontario.) *In* ESA, Proceedings of First ERS-1 Symposium on Space at the Service of Our Environment, Volume 1 Mar. 1993 p 355-360 (For primary document see N94-11704 01-43)

Copyright Avail: CASI HC A02/MF A04; EPD, ESA, ESTEC, Noordwijk, Netherlands, HC

A preliminary evaluation of ERS-1 SAR (Synthetic Aperture Radar) data for operational use in the Canadian ice monitoring program was conducted. The analysis was based on manual image interpretation by ice analysts in the Ice Center Environment Canada. A potential for operational use of SAR data exists although it was not fully demonstrated. Ice types and surface features can be extracted successfully from images of fully consolidated ice. Image interpretation is not easy for summer ice and open pack ice. The frequency of satellite coverage does not match frequency of events in ice. Limitations on the use of data are presented along with recommendations to relax them. ESA

N94-11761*# Colorado Univ., Boulder. Cooperative Inst. for Research in Environmental Sciences.

SEA ICE FEATURE AND TYPE IDENTIFICATION IN MERGED ERS-1 SAR AND LANDSAT THEMATIC MAPPER IMAGERY

K. Steffen, J. Heinrichs, J. Maslanik, and J. Key *In* ESA, Proceedings of First ERS-1 Symposium on Space at the Service of Our Environment, Volume 1 Mar. 1993 p 361-365 (For primary document see N94-11704 01-43)

(Grant NAGw-2598)

Copyright Avail: CASI HC A01/MF A04; EPD, ESA, ESTEC, Noordwijk, Netherlands, HC

LANDSAT Thematic Mapper (TM) and ERS-1 SAR (Synthetic Aperture Radar) C band images were acquired for the same area in the Beaufort Sea, 18 Apr. 1992. The two images were co-located to the same grid (25 m resolution) and supervised classification was performed on the TM channel 3 scene in order to classify open water, nilas, grey ice, first year ice, and multiyear ice. Comparison of the LANDSAT classification and the corresponding dB values from the SAR scene showed that, under the given circumstances (high surface winds), open water/nilas/grey ice as defined by a single ice category by the SAR classifier could not be distinguished from first year ice. Surface roughening due to wind appears to be a major problem for the SAR classifier, as the range of the dB values is large enough to overlap all the other ice categories. Additional information, such as surface wind speed is necessary to overcome part of this problem. ESA

N94-11762*# National Aeronautics and Space Administration. Goddard Space Flight Center, Greenbelt, MD.

SUMMER ARCTIC ICE CONCENTRATIONS AND CHARACTERISTICS FROM SAR AND SSM/I DATA

Joey C. Comiso and Ron Kwok (Jet Propulsion Lab., California Inst. of Tech., Pasadena.) *In* ESA, Proceedings of First ERS-1 Symposium on Space at the Service of Our Environment, Volume 1 Mar. 1993 p 367-372 (For primary document see N94-11704 01-43)

Copyright Avail: CASI HC A02/MF A04; EPD, ESA, ESTEC, Noordwijk, Netherlands, HC

The extent and concentration of the Summer minima provide indirect information about the long term ability of the perennial portion of the ice pack to survive the Arctic atmosphere and ocean system. Both active and passive microwave data were used with some success for monitoring the ice cover during the Summer, but they both suffer from similar problems caused by the presence of meltponding, surface wetness, flooding, and freeze/thaw cycles associated with periodic changes in surface air temperatures. A comparative analysis of ice conditions in the Arctic region using coregistered ERS-1 SAR (Synthetic Aperture Radar) and SSM/I (Special Sensor Microwave/Imager) data was made. The analysis benefits from complementary information from the two systems, the good spatial resolution of SAR data, and the good time resolution of and global coverage by SSM/I data. The results show that in many areas ice concentrations derived from SAR data are significantly different (usually higher) than those derived from passive microwave data. Additional insights about surface conditions can be inferred depending on the nature of the discrepancies. ESA

N94-11763# Naval Ocean Research and Development Activity, Bay Saint Louis, MS. Remote Sensing Applications Branch.

EVALUATING ERS-1 ICE MOTION AND CLASSIFICATION PRODUCTS

F. Fetterer and D. Gineris (Sverdrup Technology, Inc., Bay Saint Louis, MS.) *In* ESA, Proceedings of First ERS-1 Symposium on Space at the Service of Our Environment, Volume 1 Mar. 1993 p 373-375 Sponsored by NRL (For primary document see N94-11704 01-43)

Copyright Avail: CASI HC A01/MF A04; EPD, ESA, ESTEC, Noordwijk, Netherlands, HC

ERS-1 Synthetic Aperture Radar (SAR) imagery from the Alaska SAR Facility is available to operational ice analysts at the Joint Ice Center. Analysts can use the imagery directly through manual interpretation. One such use would be to provide information on ice conditions for a field expedition. In addition, analysts can run automated algorithms which produce estimates of ice type and ice motion from SAR images. Such automated analysis will become increasingly important if SAR is to be used to improve climatologies of ice characteristics and to improve the performance of dynamic ice models. The ice classification and ice motion algorithms developed for ERS-1 SAR imagery are evaluated and results presented. ESA

N94-11764# European Space Agency. European Space Research and Technology Center, ESTEC, Noordwijk (Netherlands).

THE HEIGHT CALIBRATION OF THE ERS-1 RADAR ALTIMETER

C. R. Francis *In its* Proceedings of First ERS-1 Symposium on Space at the Service of Our Environment, Volume 1 Mar. 1993 p 381-393 (For primary document see N94-11704 01-43)

Copyright Avail: CASI HC A03/MF A04; EPD, ESA, ESTEC, Noordwijk, Netherlands, HC

During Aug. and Sep. 1991 a coordinated campaign of many different types of measurements was made in order to perform a height calibration of the ERS-1 Radar Altimeter (RA). This followed extensive preparatory campaigns over the previous years. The basic scenario required the satellite to overfly a small oceanographic research platform in the northern Adriatic Sea, off the shore from Venice. This was surveyed into the same network as a set of European Satellite Laser Ranging (SLR) stations, by a series of GPS campaigns. Additionally a new site for a mobile SLR station was established in the area. Local measurements of sea level were made at the platform during the overflights, together with additional environmental measurements. Following the measurement campaign all of the data sets, including the altimeter data themselves, were carefully processed and cross checked against other data sources, where possible, to ensure consistency. Eventually it was possible to determine the bias in the altimeter measurements to a high level of accuracy. ESA

N94-11765# Bonn Univ. (Germany). Inst. for Theoretical Geodesy.

FIRST RESULTS FOR THE SIMULTANEOUS ESTIMATION OF THE GEOID AND THE SEA SURFACE TOPOGRAPHY BY ERS-1 ALTIMETER DATA

N. Arent, G. Hueckelheim, and K. R. Koch *In* ESA, Proceedings of First ERS-1 Symposium on Space at the Service of Our Environment, Volume 1 Mar. 1993 p 395-399 (For primary document see N94-11704 01-43)

(Contract BMFT-01-QS-8901)

Copyright Avail: CASI HC A01/MF A04; EPD, ESA, ESTEC, Noordwijk, Netherlands, HC

The geoid and the sea surface topography are simultaneously estimated by ERS-1 altimeter data in an area of the North Atlantic containing the Gulf stream east of the coast of the U.S. The method is based on a quasi-geostrophic model by which the sea surface topography is represented. Orbital errors are accounted for by a bias and tilt for each arc running through the area of investigation. Prior information is introduced for all unknown parameters, for the geoid undulations, for the streamfunctions of the quasi-geostrophic model and for the biases and tilts, which leads to a Kalman filter for estimating the parameters. Two steps of the Kalman filter are applied to analyze 35 days of ERS-1 data. The results indicate improvements of the geoid in the area of investigation. ESA

N94-11766# Stuttgart Univ. (Germany). Geodaetisches Inst.
SEPARATION OF GEOID AND SEA SURFACE TOPOGRAPHY IN SHALLOW WATER REGIONS: A FIRST ERS-1 RADAR ALTIMETER DATA EVALUATION
Margitta Metzner (Hamburg Univ., Germany.) and Erik W. Grafarend *In* ESA, Proceedings of First ERS-1 Symposium on Space at the Service of Our Environment, Volume 1 Mar. 1993 p 401-406 Sponsored by DFG (For primary document see N94-11704 01-43)
Copyright Avail: CASI HC A02/MF A04; EPD, ESA, ESTEC, Noordwijk, Netherlands, HC

Regional mesoscale marine geoids of horizontal scales between x(sub h) greater than or equal to 60 km and less than or equal to 100 km using ERS-1 radar altimeter data were analyzed. For this investigation three different sea areas, the North Sea, the Baltic Sea, and the Indonesian waters are selected. To point out the main characteristics causing sea level changes in the three study areas, an overview is given. A proposed analysis scheme is presented. Due to this concept, instantaneous sea surface heights and predicted geoid heights are required. A first statistical analysis of ERS-1 ocean product altimeter data is given, due to the relative sparse coverage of the study areas during the 3 day repeat cycle. This analysis supplies selection criteria which are needed to avoid measurement biases influencing the data quality. ESA

N94-11767# Technische Hochschule, Darmstadt (Germany). Inst. of Physical Geodesy.
A STOCHASTIC-DETERMINISTIC APPROACH AS AN ALTERNATIVE TO CLASSICAL CROSS-OVER TECHNIQUES IN SMALL OCEAN BASINS
L. Fenoglio and E. Groten *In* ESA, Proceedings of First ERS-1 Symposium on Space at the Service of Our Environment, Volume 1 Mar. 1993 p 407-411 (For primary document see N94-11704 01-43)
(Contract DFG-GR-361/30-1)
Copyright Avail: CASI HC A01/MF A04; EPD, ESA, ESTEC, Noordwijk, Netherlands, HC

A stochastic deterministic approach to sea surface determination combining altimetry and tide gauge data is discussed. These two methods were combined to improve upon the poor performance of stand-alone altimetry methods. The method is applied to Geosat real data. One repeat cycle of 17 days is considered. The test area chosen is the western Mediterranean Sea because the sea surface height values for a set of tide gauges stations were available. The geometrical stability of the solution is tested using simulated Geosat data. A solution for the sea surface topography and its estimated accuracy are presented. ESA

N94-11768# Copenhagen Univ. (Denmark). Geofysisk Inst.
AN ANALYSIS OF THE GRAVITY FIELD IN THE NORWEGIAN SEA AND MAPPING OF THE ICE CAP OF GREENLAND USING ERS-1 ALTIMETER MEASUREMENTS
C. C. Tscherning, P. Knudsen (National Survey of Denmark, Copenhagen.), S. Ekholm (National Survey of Denmark, Copenhagen.), and O. Baltazar Andersen (National Survey of Denmark, Copenhagen.) *In* ESA, Proceedings of First ERS-1 Symposium on Space at the Service of Our Environment, Volume 1 Mar. 1993 p 413-418 Sponsored by Danish Space Board (For primary document see N94-11704 01-43)
Copyright Avail: CASI HC A02/MF A04; EPD, ESA, ESTEC, Noordwijk, Netherlands, HC

Recent ERS-1 altimeter data were used to recover the gravity field in the Norwegian Iceland Greenland Sea. The spectral characteristics of the gravity field were investigated from 18 arcs of 3 day repeat period data. The recovered gravity field correlates exclusively with the major geological structures. This clearly demonstrates the potential of the new ERS-1 altimeter data. For land applications, ERS-1 altimetry has completed a monitoring of the ice sheet in Greenland up to 82 deg. The first digital elevation model was constructed from altimeter data with an almost complete coverage of the ice sheet. ESA

N94-11769# Centre National d'Etudes Spatiales, Toulouse (France). Groupe de Recherche de Geodesie Spatiale.
SPACE AND TIME VARIABILITY OF THE GULF STREAM USING ERS-1 ALT-OPR02 DATA **c48**
J.-F. Minster, C. Brossier, M.-C. Gennero, S. Houry, and P. Vincent *In* ESA, Proceedings of First ERS-1 Symposium on Space at the Service of Our Environment, Volume 1 Mar. 1993 p 419-423 (For primary document see N94-11704 01-43)
Copyright Avail: CASI HC A01/MF A04; EPD, ESA, ESTEC, Noordwijk, Netherlands, HC

The ERS-1 OPR-02 (Ocean Product) altimeter data from 1 Sep. - 9 Dec. 1991 was analyzed. In the North Atlantic Ocean, along-track wavenumber spectra of the mesoscale variability are very consistent with those derived from 2 years of Geosat data. They indicate a noise of 4 to 4.5 cm and a space resolution from 90 to 150 km. In the Gulf Stream area, the height variability derived from 3 months of ERS-1 3 day repeat data is comparable to that derived from 2 years of Geosat 17 day repeat data, while it is slightly lower elsewhere. Indeed, ERS-1 samples more of the high frequency variability of the Gulf Stream but less of the lower frequency mesoscale signal elsewhere. This is confirmed by 3, 6, and 9 day isocorrelation maps. ESA

N94-11770# Indian Space Research Organization, Ahmedabad. Meteorology and Oceanography Div.
REMOVAL OF ORBITAL ERROR AND THE LOCAL GEOID EFFECTS FROM ERS-1 ALTIMETER DATA
M. M. Ali and Rashmi Sharma *In* ESA, Proceedings of First ERS-1 Symposium on Space at the Service of Our Environment, Volume 1 Mar. 1993 p 425-430 (For primary document see N94-11704 01-43)
Copyright Avail: CASI HC A02/MF A04; EPD, ESA, ESTEC, Noordwijk, Netherlands, HC

Sea surface height data, obtained from the altimeters, are subject to many sources of errors, unlike the other two parameters: wind speed and the significant wave height. Orbital error can be removed by subtracting the individual satellite heights from the quadratic fit. The fluctuations remaining after this are due to the local geoid effects and can be removed by subtracting the individual passes from a reference pass over the same track. ERS-1 altimeter data was analyzed. The maximum radial orbital error is found to be about 80 m. ESA

N94-11771# European Space Agency. European Space Operations Center, Darmstadt (Germany).
ERS-1 PRECISE ORBITS AND ALTIMETRY ANALYSIS
J. M. Dow, M. Romay-Merino (Grupo de Mecanica del Vuelo S.A., Madrid, Spain.), P. Duque, R. Piriz (Grupo de Mecanica del Vuelo S.A., Madrid, Spain.), and R. Zandbergen (Logica Ltd., London, England.) *In its* Proceedings of First ERS-1 Symposium on Space at the Service of Our Environment, Volume 1 Mar. 1993 p 431-437 (For primary document see N94-11704 01-43)
Copyright Avail: CASI HC A02/MF A04; EPD, ESA, ESTEC, Noordwijk, Netherlands, HC

In parallel with the routine operational orbit determination and control activities associated with the ERS-1 Mission Management and Control Center (MMCC), a precise orbit solution based on laser tracking and altimetry is generated at ESOC. This provides a valuable check on the quality of the MMCC orbit and is also compared from time to time with the D-PAF (German Processing and Archiving Facility) preliminary orbit. A comprehensive history since launch of all three solutions is presented. Both MMCC and laser solutions include continuous monitoring of the unmodeled altimeter bias, the results of which are consistent and stable to within a few cm. Work on improving the modeling of the altimetry as a tracking type has concentrated on determining a mean sea surface model (with respect to an adopted geoid). Of special interest is the extent of coherency of these solutions with respect to time. ESA

N94-11772# Technische Univ., Delft (Netherlands). Dept. of Aerospace Engineering.
ERS-1 RADAR ALTIMETRY OVER THE NORTH ATLANTIC **c48**
K. F. Wakker, E. Wisse, M. C. Naeije, R. Scharroo, P. N. A. M. Visser, and B. A. C. Ambrosius *In* ESA, Proceedings of First ERS-1 Symposium on Space at the Service of Our Environment, Volume 1 Mar. 1993 p 439-444 Sponsored by Space Research Organization Netherlands and Beleidscommissie Remote Sensing (For primary document see N94-11704 01-43)
Copyright Avail: CASI HC A02/MF A04; EPD, ESA, ESTEC, Noordwijk, Netherlands, HC

Recent ERS-1 (35 day repeat) altimetric measurements over the north Atlantic were processed to study the mean sea surface and the sea surface currents. Some details on the processing techniques used and on the results obtained are presented. The large scale semi-permanent circulation is determined from a least squares parameter adjustment method in which a number of gravity field coefficients and a low degree and order dynamic ocean topography model are solved simultaneously. After radial orbit error reduction by crossover difference residuals minimization, the variable mesoscale circulation is obtained from analyzing the temporal variation of the local sea surface. In addition, mean wavenumber spectra were computed for two areas in the north atlantic. ESA

N94-11773# Chilworth Research Centre, Southampton (England). Center for Ocean Circulation.

THE EFFECT OF RAIN ON ERS-1 ALTIMETER DATA

T. H. Guymer and G. D. Quartly *In* ESA, Proceedings of First ERS-1 Symposium on Space at the Service of Our Environment, Volume 1 Mar. 1993 p 445-450 (For primary document see N94-11704 01-43)
Copyright Avail: CASI HC A02/MF A04; EPD, ESA, ESTEC, Noordwijk, Netherlands, HC

Atmospheric liquid water, particularly in the form of rain, can produce anomalies in altimeter data. A preliminary investigation into such features in the ERS-1 dataset was conducted using sudden, large changes in radar backscatter as a means of identification. Most occurred in tropical latitudes. It is found that there is a close relationship between the existence of altimeter anomalies and a liquid water correction derived from the passive microwave instrument on ERS-1. However, the correction accounts for only 20 percent of the observed effects. Some of the altimeter passes exhibit enhanced backscatter and waveheight features which are probably caused by distortion of the pulse shape. One pass through Hurricane Andrew was also examined in which heavy rain appears to have caused the altimeter to lose lock. ESA

N94-11774# Deutsche Forschungsanstalt fuer Luft- und Raumfahrt, Oberpfaffenhofen (Germany). German Processing and Archiving Facility.

OPERATIONAL ERS-1 ORBIT DETERMINATION AT D-PAF

F.-H. Massmann, C. Reigber, R. Koenig, J. C. Raimondo, and C. Rajasenan *In* ESA, Proceedings of First ERS-1 Symposium on Space at the Service of Our Environment, Volume 1 Mar. 1993 p 451-455 Prepared in cooperation with Academy of Sciences, Potsdam, Germany (For primary document see N94-11704 01-43)
Copyright Avail: CASI HC A01/MF A04; EPD, ESA, ESTEC, Noordwijk, Netherlands, HC

The German Processing and Archiving Facility for ERS-1 (D-PAF) is in charge of computing Preliminary (PRL) and Precise (PRC) orbits. These tasks have been performed since the launch of ERS-1 on 17 Jul. 1991. The precision orbit determinations are mainly based on Satellite Laser Ranging (SLR) data from a global tracking network. To enable the SLR stations to track ERS-1, orbit predictions have to be generated and distributed, which is also done by D-PAF. On a weekly basis PRL orbits are computed from laser quick look and radar altimeter fast delivery data and disseminated within one week. The PRC orbits are generated after reception of the laser full rate data. For the three different orbit types, the status is presented and quality estimates are shown. ESA

N94-11775# Centre National d'Etudes Spatiales, Toulouse (France). Groupe de Recherche de Geodesie Spatiale.

PRELIMINARY GEOPHYSICAL INVESTIGATION WITH ERS-1 35-DAY ALTIMETER DATA

A. Cazenave, S. Houry, K. Dominh, and M. C. Gennero *In* ESA, Proceedings of First ERS-1 Symposium on Space at the Service of Our Environment, Volume 1 Mar. 1993 p 457-462 Sponsored by CNES (For primary document see N94-11704 01-43)
Copyright Avail: CASI HC A02/MF A04; EPD, ESA, ESTEC, Noordwijk, Netherlands, HC

ERS-1 altimeter data of the first 35 day cycle provided by the National Ocean Service at NOAA were interpolated and gridded at a global scale to recover mean sea surface heights. A regional analysis was also performed over the south central Pacific combining ERS-1 and Geosat profiles to increase the coverage. Some geoid features are discussed. ESA

N94-11776*# California Univ., Santa Barbara. Dept. of Physics.

ARCTIC GEODYNAMICS: CONTINENTAL SHELF AND DEEP OCEAN GEOPHYSICS. ERS-1 SATELLITE ALTIMETRY: A FIRST LOOK

Allen Joel Anderson, David T. Sandwell (Scripps Institution of Oceanography, La Jolla, CA.), Gabriele Marquart (Uppsala Univ., Sweden.), and Hans-Georg Scherneck (Onsala Space Observatory, Sweden.) *In* ESA, Proceedings of First ERS-1 Symposium on Space at the Service of Our Environment, Volume 1 Mar. 1993 p 463-468 Sponsored by NASA, Washington and Swedish Delegation for Space Research (For primary document see N94-11704 01-43)
Copyright Avail: CASI HC A02/MF A04; EPD, ESA, ESTEC, Noordwijk, Netherlands, HC

An overall review of the Arctic Geodynamics project is presented. A composite gravity field model of the region based upon altimetry data from ERS-1, Geosat, and Seasat is made. ERS-1 altimetry covers unique Arctic and Antarctic latitudes above 72 deg. Both areas contain large continental shelf areas, passive margins, as well as recently formed deep ocean areas. Until ERS-1 it was not possible to study these areas with satellite altimetry. Gravity field solutions for the Barents sea, portions of the Arctic ocean, and the Norwegian sea north of Iceland are shown. The gravity anomalies around Svalbard (Spitsbergen) and Bear island are particularly large, indicating large isostatic anomalies which remain from the recent breakup of Greenland from Scandinavian. Recently released gravity data from the Armed Forces Topographic Service of Russia cover a portion of the Barents and Kara seas. A comparison of this data with the ERS-1 produced gravity field is shown. ESA

N94-11777# Deutsche Forschungsanstalt fuer Luft- und Raumfahrt, Oberpfaffenhofen (Germany). German Processing and Archiving Facility.

QUICK-LOOK MONITORING OF THE SEA SURFACE WITH ERS-1 FAST DELIVERY ALTIMETER DATA

T. Spoecker, M. Anzenhofer, W. Bosch (Deutsches Geodaetisches Forschungsinst., Munich, Germany.), and T. Gruber *In* ESA, Proceedings of First ERS-1 Symposium on Space at the Service of Our Environment, Volume 1 Mar. 1993 p 469-472 Prepared in cooperation with Academy of Sciences, Potsdam, Germany (For primary document see N94-11704 01-43)
Copyright Avail: CASI HC A01/MF A04; EPD, ESA, ESTEC, Noordwijk, Netherlands, HC

For the ERS-1 mission, ESA provides altimeter fast delivery products that are available within three hours after measurement. The data consist of time tagged altimeter altitude, wind speed, and significant wave height completed by atmospheric corrections. Use and analysis at the German Processing and Archiving Facility (D-PAF) indicate that the altimeter data, when combined with preliminary satellite ephemerides, can be very well used for a quick look monitoring of the sea surface. For this purpose a preliminary orbit, generated at D-PAF by means of globally acquired laser tracking data is merged into the fast delivery altimeter data. In addition, Earth and ocean tides are computed, atmospheric corrections are improved, orbit error adjustment and digital sampling techniques are used to generate a series of quick look sea surface height models. These new products span a time period of 35 days (one repeat cycle) and are processed every week. They compile sea surface heights, an estimate of the rate of change of the sea surface as well as resampled wind speed and wave heights averaged for the same period of time. ESA

N94-11778# Deutsche Forschungsanstalt fuer Luft- und Raumfahrt, Oberpfaffenhofen (Germany). German Processing and Archiving Facility.

THE EARTH'S GRAVITY MODEL FOR THE ERS-1 COMMISSIONING PHASE

P. Schwintzer, C. Reigber, A. Bode, Z. Chen, F.-H. Massmann, J. C. Raimondo, R. Biancale (Centre National d'Etudes Spatiales, Toulouse, France.), G. Balmino (Centre National d'Etudes Spatiales, Toulouse, France.), J. M. Lemoine (Centre National d'Etudes Spatiales, Toulouse, France.), and B. Moynot (Centre National d'Etudes Spatiales, Toulouse, France.) et al *In* ESA, Proceedings of First ERS-1 Symposium on Space at the Service of Our Environment, Volume 1 Mar. 1993 p 473-476 Prepared in cooperation with Academy of Sciences, Potsdam, Germany (For primary document see N94-11704 01-43)
Copyright Avail: CASI HC A01/MF A04; EPD, ESA, ESTEC, Noordwijk, Netherlands, HC

The German ERS-1 Processing and Archiving Facility (D-PAF) is charged by ESA to provide the global Earth's gravity field model for ERS-1 precise orbit determination and altimeter data reduction. The just delivered ERS-1 Gravity Model, EGM1, which is dedicated to the ERS-1 commissioning phase (Jul. - Dec. 1991), is based on the most recent non-ERS-1 GRIM4 satellite-only model. The GRIM4 gravity models are elaborated within the long term German/French cooperation. The accuracy of the EGM1 gravity model is estimated in terms of geoid undulations and crossover differences. The quality is evaluated by satellite test arc computations. ESA

N94-11779# Technische Univ., Delft (Netherlands). Faculty of Aerospace Engineering.

ERS-1 PRECISE ORBIT DETERMINATION

R. Scharroo, K. F. Wakker, B. A. C. Ambrosius, R. Noomen, W. J. vanGaalen, and G. J. Mets *In* ESA, Proceedings of First ERS-1 Symposium on Space at the Service of Our Environment, Volume 1 Mar. 1993 p 477-482 (For primary document see N94-11704 01-43)

Copyright Avail: CASI HC A02/MF A04; EPD, ESA, ESTEC, Noordwijk, Netherlands, HC

Various aspects of the computation of ERS-1 orbits incorporated on the NOAA ERS-1 IGDR's, the effects of selecting an improved gravity model, the ways to assess the orbit accuracy, and the orbit improvements to be obtained from incorporating altimeter range data in the orbit computation, are addressed. The operational ERS-1 orbits using the NASA/GSFC GEM-T2 gravity model appear to have a radial accuracy of about 140 cm, whereas the GSFC PGS-4591 model already delivers orbits with a radial accuracy of about 35 cm. The best SLR (Satellite Laser Ranging) solutions obtained so far, however, have a radial precision of about 22 cm, and they are based on the GSFC PGS-4988 gravity model including the estimation of a 1 cpr along track acceleration. Incorporating altimeter range measurements as tracking data in the orbit determination can bring this figure down to 19 cm. ESA

N94-11780# Mullard Space Science Lab., Dorking (England).

VALIDATING THE UK-PAF LAND ICE PRODUCT SURFACE ELEVATION

D. R. Mantripp and J. K. Ridley *In* ESA, Proceedings of First ERS-1 Symposium on Space at the Service of Our Environment, Volume 1 Mar. 1993 p 483-488 (For primary document see N94-11704 01-43)

Copyright Avail: CASI HC A02/MF A04; EPD, ESA, ESTEC, Noordwijk, Netherlands, HC

The UK-PAF (Processing and Archiving Facility) ERS1.ALT.LIR product is designed to provide users with measurements of geophysical parameters over continental ice sheets. The PAF philosophy of providing fully calibrated and validated products extends to these data, and as part of this process a series of field experiments were carried out in Jan./Feb. 1992 on Filchner Ice Shelf, Antarctica. The objectives of the fieldwork were to obtain calibrating/validation data for ice shelf elevation and radar backscatter. The preliminary work towards establishing a method for external calibration of surface elevation is discussed. Two subsatellite track test areas were established, one on the ice shelf itself nearby Berkner Island, and one on the Coats Land plateau, at 500 m above sea level. Surface profiles were obtained from GPS (Global Positioning System) kinematic surveying. One GPS profile from Filchner ice shelf, coinciding with a subsatellite track from the 35 day repeat mission, was compared with ERS-1 Radar Altimeter 3 day repeat raw data and 35 day repeat URA products. Altimeter derived surface elevation was calculated using restituted orbit data. The GPS elevation data are found to lie within 1 m of the URA data and within 5 m of the 3 day repeat raw elevation data. While the results are not yet good enough to provide validation data to targeted accuracies, they will be improved significantly with more sophisticated analysis and further field data. ESA

N94-11781# Institute of Oceanographic Sciences, Wormley (England). Deacon Lab.

GLOBAL WAVE HEIGHT CLIMATOLOGIES FROM ERS-1 ALTIMETER DATA, AND COMPARISONS WITH THOSE FROM GEOSAT

D. J. T. Carter *In* ESA, Proceedings of First ERS-1 Symposium on Space at the Service of Our Environment, Volume 1 Mar. 1993 p 489-492 (For primary document see N94-11704 01-43)

Copyright Avail: CASI HC A01/MF A04; EPD, ESA, ESTEC, Noordwijk, Netherlands, HC

Global monthly mean significant wave height data (H(sub s)) in 2 deg latitude by 2 deg longitude bins are estimated from Geosat and from the ERS-1 altimeter. The data are analyzed to see whether a cross calibration of the two altimeters can be obtained. The ERS-1 fast delivery data from Jan. - Jun. 1992 are used. The principal component fits for the same months of different years indicate a consistent difference between the data sets from the two satellites, from which a linear relationship between Geosat and ERS-1 estimates of H(sub s) is derived. A preliminary check of monthly mean H(sub s) values from ERS-1 against buoy data suggests an inconsistency, which can only be resolved by further validation. ESA

N94-11782# Chilworth Research Centre, Southampton (England). Center for Ocean Circulation.

SPATIAL SCALES OF WAVE HEIGHT c48

Peter G. Challenor *In* ESA, Proceedings of First ERS-1 Symposium on Space at the Service of Our Environment, Volume 1 Mar. 1993 p 493-498 Sponsored by Health and Safety Executive (For primary document see N94-11704 01-43)

Copyright Avail: CASI HC A02/MF A04; EPD, ESA, ESTEC, Noordwijk, Netherlands, HC

Using Geosat data it is shown that the along-track spectrum of significant wave height is invariant across the world oceans. This spectrum can be represented by three (or possibly two) power laws. When spectra from Geosat ERS-1 fast delivery and ERS-1 offline data are examined, there are differences particularly between Geosat and ERS-1. These differences are examined and it is hypothesized that they are due to differences in the trackers onboard the satellites. The offline data is reprocessed on the ground and therefore does not contain the effect of any tracker. It thus should give the 'true' spectrum. ESA

N94-11783*# Scripps Institution of Oceanography, La Jolla, CA.

LATENT AND SENSIBLE HEAT FLUX ESTIMATED FROM ERS-1 DATA

S. F. Iacobellis and C. Gautier (California Univ., Santa Barbara.) *In* ESA, Proceedings of First ERS-1 Symposium on Space at the Service of Our Environment, Volume 1 Mar. 1993 p 499-503 Sponsored by NASA, Washington and California Univ. (For primary document see N94-11704 01-43)

Copyright Avail: CASI HC A01/MF A04; EPD, ESA, ESTEC, Noordwijk, Netherlands, HC

Two issues regarding surface latent and sensible heat flux are addressed: its value in low wind speed conditions over the tropical oceans,and its determination solely from satellite observations. The investigation is performed with an oceanic mixed layer model operated in an 'inverse' mode. The 'normal' model is forced with the surface heat and radiative fluxes and produces the SST evolution, whereas the 'inverse' model produces the latent sensible heat flux given the SST and surface radiative flux as input. The results indicate that at low wind speeds there exists a minimum latent sensible heat flux of about 80 to 100 W/sq m. Sensitivity studies show that the latent sensible heat flux is very sensitive to random errors in the forcing SST time series. The implications of this strong sensitivity in regards to the use of satellite measurements to supply the forcing SST are discussed. ESA

N94-11784# National Ocean Survey, Rockville, MD.

THE 1992 EL NINO VIEWED BY ERS-1 ALTIMETRY c48

Robert Cheney and John Lillibridge *In* ESA, Proceedings of First ERS-1 Symposium on Space at the Service of Our Environment, Volume 1 Mar. 1993 p 505-510 (For primary document see N94-11704 01-43)

Copyright Avail: CASI HC A02/MF A04; EPD, ESA, ESTEC, Noordwijk, Netherlands, HC

The ERS-1 altimeter has provided more than 1 year of precise, global observations of sea level. These data are being used to monitor tropical Pacific sea level in near real time. A combination of ERS-1 data and existing Geosat altimetry have provided a comprehensive view of the 1992 El Nino. ESA

N94-11785# Rutherford Appleton Lab., Chilton (England). Space Radar Group.

USING TRANSPONDERS WITH THE ERS-1 ALTIMETER TO MEASURE ORBIT ALTITUDE TO +/- 3 cm

R. J. Powell, A. R. Birks, W. J. Bradford, C. L. Wrench, and J. Biddiscombe *In* ESA, Proceedings of First ERS-1 Symposium on Space at the Service of Our Environment, Volume 1 Mar. 1993 p 511-516 (For primary document see N94-11704 01-43)

Copyright Avail: CASI HC A02/MF A04; EPD, ESA, ESTEC, Noordwijk, Netherlands, HC

Analysis suggests that, by deploying an active transponder on land beneath a satellite altimeter it should be possible to make a measurement of the height of the satellite as it passes over the transponder with an accuracy equal to or better than that with which the altimeter can measure the range to the sea surface, +/- 1 to 3 cm. Early progress in successfully demonstrating the basic altimeter to transponder measurement technique by deploying transponders beneath the ERS-1 satellite is reported, preliminary experiments to assess the technique are described, and some potential applications are identified. ESA

N94-11786# Bedford Inst. of Oceanography, Dartmouth (Nova Scotia). Physical and Chemical Sciences.
OCEAN CIRCULATION REVEALED BY ALTIMETER DATA
M. Ikeda *In* ESA, Proceedings of First ERS-1 Symposium on Space at the Service of Our Environment, Volume 1 Mar. 1993 p 517-518 (For primary document see N94-11704 01-43)
Copyright Avail: CASI HC A01/MF A04; EPD, ESA, ESTEC, Noordwijk, Netherlands, HC

ERS-1 altimeter data at the Fast Delivery Copy (FDC) format from the 3 day repeat mission were analyzed to demonstrate mesoscale eddy features around the Gulf Stream. The analysis procedure is: to interpolate sea surface height at regular grids; to remove time average mean heights at the grids; and to remove a quadratic curve fit to height structures on an approximately 2000 km long arc. It was shown that the FDC may be useful for observing energetic mesoscale features at mid latitudes. A striking feature is a high anomaly captured on the track only for 10 days. Since the data from the descending tracks are clean, ERS-1 data will give cross track resolution higher than Goesat in the Gulf Stream and the Kuroshio regions. ESA

N94-11851# Phillips Lab., Hanscom AFB, MA.
EFFECTS OF SATELLITE SPECTRAL RESOLUTION AND ATMOSPHERIC WATER VAPOR ON RETRIEVAL OF NEAR-GROUND TEMPERATURES
Alan E. Lipton 28 Apr. 1993 12 p
(AD-A264920; AD-E201523; PL-TR-93-2101) Avail: CASI HC A03/MF A01

One of the challenges in remote sensing of surface temperatures for meteorological applications is to distinguish clearly the influence of the ground surface on the measured radiances from the influence of the overlaying atmosphere. It is common, particularly in cloud-free situations, to have large differences in temperature over very short vertical distances from the ground up through the lowest kilometer of the atmosphere. The research to be presented focused on the vertical resolution capabilities of the VISSR Atmospheric Sounder (VAS) and the proposed GOES High-Resolution Interferometer Sounder (GHIS) in this lowest part of the temperature profile. Results of simulated retrievals and experiments on the sensitivity of radiances to profile perturbations indicated that, for a moderately moist atmosphere, ground surface temperature errors of about 1 C and low-level air temperature errors of about 3 C can occur in VAS retrievals due specifically to vertical resolution limitations and instrument noise. For a drier atmosphere the surface temperature errors tend to be smaller and the low-level air temperature errors tend to be larger. These values do not account for other sources of retrieval error, such as interference by clouds, uncertainty of the ground surface emittance, or deficiencies in the radiative transfer computation method. DTIC

N94-11885*# National Aeronautics and Space Administration. Goddard Space Flight Center, Greenbelt, MD.
EFFECT OF SPECIES STRUCTURE AND DIELECTRIC CONSTANT ON C-BAND FOREST BACKSCATTER
R. H. Lang (George Washington Univ., Washington, DC.), R. Landry (Canada Centre for Remote Sensing, Ottawa, Ontario.), O. Kilic (George Washington Univ., Washington, DC.), N. Chauhan, N. Khadr (George Washington Univ., Washington, DC.), and D. Leckie (Petawawa National Forestry Inst., Chalk River, Ontario.) 1993 4 p
(NASA-TM-109219; NAS 1.15:109219) Avail: CASI HC A01/MF A01

A joint experiment between Canadian and USA research teams was conducted early in Oct. 1992 to determine the effect of species structure and dielectric variations on forest backscatter. Two stands, one red pine and one jack pine, in the Petawawa National Forestry Institute (PNFI) were utilized for the experiment. Extensive tree architecture measurements had been taken by the Canada Centre for Remote Sensing (CCRS) several months earlier by employing a Total Station surveying instrument which provides detailed information on branch structure. A second part of the experiment consisted of cutting down several trees and using dielectric probes to measure branch and needle permittivity values at both sites. The dielectric and the tree geometry data were used in the George Washington University (GWU) Vegetation Model to determine the C band backscattering coefficients of the individual stands for VV polarization. The model results show that backscatter at C band comes mainly from the needles and small branches and the upper portion of the trunks acts only as an attenuator. A discussion of variation of backscatter with specie structure and how dielectric variations in needles for both species may affect the total backscatter returns is provided. Author (revised)

N94-12279# Mitsubishi Electric Corp., Tokyo (Japan).
FLIGHT DATA ANALYSIS OF JAPANESE EARTH RESOURCES SATELLITE-1 (JERS-1) [CHIKYUU SHIGEN EISEI 1 GOU (JERS-1) TSUISEKI KANSEI GIJUTSU SHIEN OYOBI HYOUKA KAISEKI]
National Space Development Agency 31 Mar. 1993 19 p In JAPANESE
(NASDA-CNT-930004; JTN-93-80458) Avail: CASI HC A03/MF A01

A summary of the satellite operation conditions in the launch and early orbit operation phase and the results of the launch and early orbit phase operation and functional verification on the following subsystems of the JERS-1 (Japanese Earth Resources Satellite-1) is presented: (1) C & DH (Communication and Data Handling Subsystem); (2) EPS (Electrical Power Subsystem); (3) AOCS (Attitude and Orbit Control Subsystem); (4) RCS (Reaction Control Subsystem); (5) TCS (Thermal Control Subsystem); (6) SAR (Synthetic Aperture Radar); (7) OPS (Optical Sensor); (8) MDT (Mission Data Transmitter); and (9) MDR (Mission Data Recorder). Author (NASDA)

N94-12432*# National Aeronautics and Space Administration. Langley Research Center, Hampton, VA.
SAMPLING AND POSITION EFFECTS IN THE ELECTRONICALLY STEERED THINNED ARRAY RADIOMETER (ESTAR)
Stephen J. Katzberg Aug. 1993 17 p
(RTOP 476-14-15-01)
(NASA-TM-108998; NAS 1.15:108998) Avail: CASI HC A03/MF A01

A simple engineering level model of the Electronically Steered Thinned Array Radiometer (ESTAR) is developed that allows an identification of the major effects of the sampling process involved with this technique. It is shown that the ESTAR approach is sensitive to aliasing and has a highly non-uniform sensitivity profile. It is further shown that the ESTAR approach is strongly sensitive to position displacements of the low-density sampling antenna elements. Author

N94-12471# European Space Agency, Paris (France).
PROCEEDINGS OF 1ST ERS-1 SYMPOSIUM ON SPACE AT THE SERVICE OF OUR ENVIRONMENT, VOLUME 2
Brigitte Kaldeich, ed. Mar. 1993 376 p In ENGLISH and FRENCH
Symposium held in Cannes, France, 4-6 Nov. 1992
(ESA-SP-359-Vol-2; ISBN-92-9092-278-8; ETN-93-94635) Copyright
Avail: CASI HC A17/MF A03; EPD, ESA, ESTEC, Noordwijk, Netherlands, HC

Papers from the first ERS-1 symposium are presented in two volumes. The second volume is subdivided into the following topics: land use, topography and geology; hydrology; vegetation and crop monitoring; forest monitoring; meteorology; ocean and wave imaging mechanisms; Along Track Scanning Radar (ATSR) applications; operational Synthetic Aperture Radar (SAR) applications; coastal phenomena; focus on the Mediterranean Sea; and the TREES (Tropical Ecosystem Environment Monitoring by Satellites) Project. For individual titles, see N94-12472 through N94-12531.

N94-12472# Technische Univ., Munich (Germany). Lehrsthul fuer Geographie und Geographische Fernerkundung.
SEGMENTED LAND USE CLASSIFICATION OF MULTITEMPORAL ERS-1 SAR DATA USING A MAJORITY FILTER
J. Kellndorfer, R. Schadt, and W. Mauser *In* ESA, Proceedings of 1st ERS-1 Symposium on Space at the Service of Our Environment, Volume 2 Mar. 1993 p 523-526 (For primary document see N94-12471 01-43)
Copyright Avail: CASI HC A01/MF A03; EPD, ESA, ESTEC, Noordwijk, Netherlands, HC

Twenty-eight ERS-1 single look complex scenes of the commissioning phase of ERS-1 in the time period 17 Aug. to 30 Nov. 1991 of the Freiburg test site (Upper Rhine Valley (Germany)) were converted to greyvalue images that were speckle reduced using a Lee filter and geometrically matched. A maximum likelihood classification of the testsite (approximately 50 sq km) was performed. The classes, buildings/villages, water, forest, corn, and meadows/fallow fields were compared with a digital land use map resulting from the 1991 ground data collection. As can be expected, speckle still influences the classification results. To overcome this problem the classification result was fitted to the digital field boundary map. This enabled a fieldwise postclassification using the majority rule which considerably improved the result of the multitemporal land use classification. ESA

N94-12473# Winand Staring Centre, Wageningen (Netherlands).
LAND COVER MONITORING WITH MULTI-TEMPORAL ERS-1 SAR OBSERVATIONS IN THE NETHERLANDS
G. J. A. Nieuwenhuis and C. G. J. Schotten *In* ESA, Proceedings of 1st ERS-1 Symposium on Space at the Service of Our Environment, Volume 2 Mar. 1993 p 527-531 (For primary document see N94-12471 01-43)
Copyright Avail: CASI HC A01/MF A03; EPD, ESA, ESTEC, Noordwijk, Netherlands, HC

Since the launch of the ERS-1 satellite in Jul. 1991, Synthetic Aperture Radar (SAR) C band images have been obtained on a regular basis. A calibrated SAR image taken on 7 Sep. 1991 was evaluated. It was found that for different land cover types, reliable backscatter values were obtained. Multitemporal images, acquired during the first three months after the launch of the satellite, were applied to perform a land cover mapping experiment. To solve the speckle problem of the applied SAR images, a field based classification method was used. The first results are very promising and they show the great potential of ERS-1 SAR images to monitor land cover. Crop classification accuracy varied from 60 to 90% for spring barley (already harvested at the acquisition dates) and potatoes, respectively. Fruit trees, often difficult to classify with images taken in the shortwave range of the spectrum, were classified correctly for about 75%. Following the land cover mapping experiment in a later stage, land cover information will be combined with crop growth simulation results to forecast crop yield. ESA

N94-12474# Reading Univ. (England). NERC Unit for Thematic Information Systems.
MAPPING A DYNAMIC PLAYA SURFACE USING MULTITEMPORAL ERS-1 SAR DATA: FIRST RESULTS
G. Wadge, A. C. Millington, and D. J. Archer *In* ESA, Proceedings of 1st ERS-1 Symposium on Space at the Service of Our Environment, Volume 2 Mar. 1993 p 533-538 Sponsored by Natural Environmental Research Council, United Kingdom (For primary document see N94-12471 01-43)
Copyright Avail: CASI HC A02/MF A03; EPD, ESA, ESTEC, Noordwijk, Netherlands, HC

The mapping of Chott el Djerid in north central Tunisia, a flat salt playa whose surface composition and micromorphology are highly dynamic, is considered. The ERS-1 Active Microwave Instrument (AMI) Synthetic Aperture Radar (SAR) is sensitive to temporal changes in roughness and moisture, and geocoded images from May and Aug. 1992 show within and between scene changes in backscatter of the order of 10 dB. These changes are the result of the interplay of the processes of temporary lake formation and evaporation, capillary evaporation, surface water flow, and aeolian transport and deposition. A multitemporal sequence of SAR images with a field monitoring program of roughness and moisture measurement will provide a quantitative test of the ability to understand backscatter change in terms of these processes. ESA

N94-12475# Mullard Space Science Lab., Dorking (England).
ERS-1 ALTIMETRY OF INLAND WATER AND LAND
C. G. Rapley, S. G. Baker, C. M. Birkett, S. W. Laxon, J. K. Ridley, R. F. Scott, and F. Strawbridge *In* ESA, Proceedings of 1st ERS-1 Symposium on Space at the Service of Our Environment, Volume 2 Mar. 1993 p 539-542 (For primary document see N94-12471 01-43)
Copyright Avail: CASI HC A01/MF A03; EPD, ESA, ESTEC, Noordwijk, Netherlands, HC

In order to extract useful information from satellite radar altimeter data acquired over inland water and land, considerable insight into the response of a pulse limited altimeter to a complex, topographic surface is required. Also, except over continuous water surfaces, it is essential to process the echo waveforms, both to eliminate erroneous data points, and to match the data analysis technique to the echo characteristics of the surface. The use of ERS-1 altimeter fast delivery (non-echo) data to provide an initial overview of the global data set is described. The work relies on a new data filtering scheme designed to eliminate erroneous data points. Preliminary results using a limited quantity of waveform data are reported. ESA

N94-12476# University Coll., London (England).
PRELIMINARY STUDIES ON THE APPLICATION OF ERS-1 DATA TO TOPOGRAPHIC MAPPING
I. Dowman, M. Upton, J. deKnecht, and C. Davison *In* ESA, Proceedings of 1st ERS-1 Symposium on Space at the Service of Our Environment, Volume 2 Mar. 1993 p 543-549 (For primary document see N94-12471 01-43)
Copyright Avail: CASI HC A02/MF A03; EPD, ESA, ESTEC, Noordwijk, Netherlands, HC

A geocoding system was developed and used to geocode ERS-1 Synthetic Aperture Radar (SAR) images with the aim of using the data for topographical applications. The results are presented. A validation scheme is part of the system and this includes the production of shadow, layover, and energy conservation maps. Cultural features were extracted from the data and compared to existing maps. The use of speckle reduction filters was investigated and the results indicate that the level of information which can be extracted is low without supporting map data. If existing data is used then new features can be identified and mapped. Height was extracted from ERS-1 data using stereoscopic methods. Stereoscopic data were obtained from overlapping scenes from adjacent orbits and from the roll tilt mode. Preliminary results are presented showing that stereo matching can be applied on the overlapping images with the same incidence angle at the scene center and from images with different incidence angles from the roll tilt mode. ESA

N94-12477# Deutsche Forschungsanstalt fuer Luft- und Raumfahrt, Oberpfaffenhofen (Germany).
RADARMAP OF GERMANY: FIRST MOSAIC AND CLASSIFICATION
R. Winter, D. Kosmann, B.-S. Schulz (Institut fuer Angewandte Geodaesie, Frankfurt am Main, Germany.), M. Sties (Karlsruhe Univ., Germany.), and M. Wiggenhagen (Technische Univ., Hanover, Germany.) *In* ESA, Proceedings of 1st ERS-1 Symposium on Space at the Service of Our Environment, Volume 2 Mar. 1993 p 551-554 (For primary document see N94-12471 01-43)
Copyright Avail: CASI HC A01/MF A03; EPD, ESA, ESTEC, Noordwijk, Netherlands, HC

First results of the project to produce a radarmap of Germany are described. Specific software was developed to fulfill the special requirements for interpretation of Synthetic Aperture Radar (SAR) images. A new approach was developed and implemented on a Stardent computer. A mosaiking tool, the Mosaiking Mask Editor (MME), was designed and realized on a SUN computer together with an expert system shell. With this software it is possible to combine different ERS-1 scenes. The standard input images are SUN raster image files. This software was tested with different Seasat and ERS-1 images. Various data sources are in use for this project. The main input data are terrain corrected ERS-1 SAR data. To extract special auxiliary information, a digital terrain model was integrated into the classification system. Different cartographic parameters are used by the MME. The results of the Col's are integrated. ESA

N94-12478# Food and Agriculture Organization of the United Nations, Rome (Italy). Remote Sensing Center.
COMBINED ANALYSIS OF ERS-1 SAR AND VISIBLE/INFRARED REMOTE SENSING DATA FOR LAND COVER/LAND USE MAPPING IN A TROPICAL ZONE: A CASE STUDY IN GUINEA
J. F. Dallemand, J. Lichtenegger (European Space Agency. ESRIN, Frascati, Italy.), V. Kaufmann (Technische Univ., Graz, Austria.), D. Paudyal (Asian Inst. of Tech., Bangkok, Thailand.), and P. Reichert *In* ESA, Proceedings of 1st ERS-1 Symposium on Space at the Service of Our Environment, Volume 2 Mar. 1993 p 555-561 (For primary document see N94-12471 01-43)
Copyright Avail: CASI HC A02/MF A03

Preliminary results of an assessment of the use of ERS-1 SAR (Synthetic

Aperture Radar) data for land use mapping in a savannah zone of West Africa are presented. Optical data (LANDSAT, SPOT) were compared with microwave data (SIR-A, ERS-1). LANDSAT Thematic Mapper data were initially geocoded with a Digital Terrain Model (DTM) and then registered to ERS-1 data. Standard and adaptive filters were applied to SAR data and the results compared. Two methods of optical/microwave data integration were tested. It appeared that land use classes identification was not satisfactory using single date ERS-1 data. Good results were obtained in the case of a multitemporal SAR approach and particularly when combining dry season optical data with rainy season SAR data.
ESA

N94-12479# ISTAR, Valbonne (France).
EXAMPLE OF SPOT/ERS-1 COMPLEMENTARITY
Frederic P. Perlant *In* ESA, Proceedings of 1st ERS-1 Symposium on Space at the Service of Our Environment, Volume 2 Mar. 1993 p 563-568 (For primary document see N94-12471 01-43)
Copyright Avail: CASI HC A02/MF A03; EPD, ESA, ESTEC, Noordwijk, Netherlands, HC

With the many optical data available from various remote sensing platforms (LANDSAT, SPOT) and the recent ERS-1 Synthetic Aperture Radar (SAR) satellite data, it is critical to be able to register, compare and analyze these different data if full advantage is to be made from the multiplicity of information sources. An example of SPOT/ERS-1 complementarity is given. The main differences between SPOT and ERS-1 are described and a practical application illustrated by a project called 'production of SPOT/ERS image maps on a scale of 1/50,000' is developed. Focus is on the technical aspects of the specific geocoded products generation process, in particular, the radiometry and geometry. Limitations and constraints are discussed.
ESA

N94-12480# Faculte des Sciences Agronomiques de l'Etat, Gembloux (Belgium).
THE USE OF ERS-1 SAR DATA TO STUDY SURFACE STATES [UTILISATION DES DONNEES SAR D'ERS-1 POUR L'ETUDE DES ETATS DE SURFACE]
Arnaud Dewez and Sylvia Dautrebande *In* ESA, Proceedings of 1st ERS-1 Symposium on Space at the Service of Our Environment, Volume 2 Mar. 1993 p 569-571 In FRENCH (For primary document see N94-12471 01-43)
Copyright Avail: CASI HC A01/MF A03; EPD, ESA, ESTEC, Noordwijk, Netherlands, HC

A study to determine the potential use of ERS-1 Synthetic Aperture Radar (SAR) data for agrohydrological applications, based on the relation between the radar response and superficial soil moisture, is reported. The study is based on the comparison of satellite data with measurements done in the field and other catographic information. The remote sensing radar was combined with other sources of geographical information, to locate regions susceptible to drought and to flooding and to determine the morphology of the land. In order to be integrated into the geographic information system, the ERS-1 images were geometrically rectified. Details of the material and method used and first data analysis results and conclusions are given.
ESA

N94-12481# Innsbruck Univ. (Austria). Inst. fuer Meteorologie und Geophysik.
SNOW AND GLACIER INVESTIGATIONS BY ERS-1 SAR: FIRST RESULTS
H. Rott and Th. Nagler *In* ESA, Proceedings of 1st ERS-1 Symposium on Space at the Service of Our Environment, Volume 2 Mar. 1993 p 577-582 Sponsored by Oesterreichische Akademie der Wissenschaften (For primary document see N94-12471 01-43)
Copyright Avail: CASI HC A02/MF A03; EPD, ESA, ESTEC, Noordwijk, Netherlands, HC

The backscattering behavior of snow and glacier ice was investigated using 12 ERS-1 Synthetic Aperture Radar (SAR) scenes acquired over the test site Otztal in the Austrian Alps between Apr. and Oct. 1992. Significant temporal changes of the backscattering coefficient were observed, which were mainly caused by variations in liquid water content of the snowpack and in the roughness of snow and ice surfaces, as confirmed by field measurements of structural and dielectric properties. Corner reflectors deployed on the firn areas of the glaciers, provide useful reference for geometric corrections and for radiometric calibration. ERS-1 SAR images show good capabilities for monitoring the areal extent of wet snow on glaciers and ice free areas and for detecting the snowline on glaciers. Digital techniques for snow and glacier mapping by means of ERS-1 SAR data are in progress.
ESA

N94-12482# Zurich Univ. (Switzerland). Remote Sensing Labs.
MONITORING OF SNOWCOVER IN HIGH MOUNTAIN TERRAIN WITH ERS-1 SAR
Harold Haefner, Francesco Holecz, Erich Meier, and Daniel Nueesch *In* ESA, Proceedings of 1st ERS-1 Symposium on Space at the Service of Our Environment, Volume 2 Mar. 1993 p 583-588 (For primary document see N94-12471 01-43)
Copyright Avail: CASI HC A02/MF A03; EPD, ESA, ESTEC, Noordwijk, Netherlands, HC

A method was developed to make ERS-1 Synthetic Aperture Radar (SAR) a suitable, operational tool for high mountain geoecological studies. It is based on a very precise geocoding using a high resolution Digital Elevation Model (DEM); on radiometric corrections to minimize topographic effects by a pixelwise computation of the local incidence angle, using various backscatter models; and by creating a new synthetic ERS-1 product, containing the fully interpretable SAR information by combining the interpretable parts of an ascending scene with the one of a timely close descending path. For the classification of snow, snowpack, and snow water equivalent and additional geoecological units, correlations with optical satellite data and ground measurements applying data fusion techniques are performed. The evaluation of the results will reveal the possibilities and limitations of ERS-1 for snowpack monitoring in mountainous terrain.
ESA

N94-12483# Helsinki Univ. of Technology, Espoo (Finland). Space Technology Lab.
APPLICATION OF ERS-1 SAR DATA TO SNOW MAPPING
M. Hallikainen, V. Jaeaeskelaeinen, L. Kurvonen, J. Koskinen, E.-A. Herland (Technical Research Centre of Finland, Espoo.), and J. Peraelae (National Board of Waters and the Environment, Helsinki, Finland.) *In* ESA, Proceedings of 1st ERS-1 Symposium on Space at the Service of Our Environment, Volume 2 Mar. 1993 p 589-594 (For primary document see N94-12471 01-43)
Copyright Avail: CASI HC A02/MF A03; EPD, ESA, ESTEC, Noordwijk, Netherlands, HC

Preliminary results from a 3 year program to investigate the feasibility of the ERS-1 Synthetic Aperture Radar (SAR) to remote sensing of snow are presented. The main goals of the program are to determine: the capability of the ERS-1 SAR to map snow cover, especially melting snow; the effect of forest canopies to SAR snow mapping; and the usefulness of complementing SAR data with other satellite and airborne data types (microwave radiometer and optical data).
ESA

N94-12484# Waterloo Univ. (Ontario).
METHODOLOGICAL CONSIDERATIONS FOR USE OF ERS-1 IMAGERY FOR THE DELINEATION OF RIVER NETWORKS IN TROPICAL FOREST AREAS
S. I. Solomon *In* ESA, Proceedings of 1st ERS-1 Symposium on Space at the Service of Our Environment, Volume 2 Mar. 1993 p 595-600 (For primary document see N94-12471 01-43)
Copyright Avail: CASI HC A02/MF A03; EPD, ESA, ESTEC, Noordwijk, Netherlands, HC

Reasons why the use of spaceborne radar imagery would lead to more detailed mapping of a river network in a tropical forest region than other methods (aerial photography and LANDSAT Thematic Mapper) are discussed and a future project to do this in Venezuela is mentioned. No results of this project were present at the time of printing. Basic principles of ERS-1 Synthetic Aperture Radar (SAR) imagery interpretation to delineation of river networks are outlined and further development of the methodology of the project are addressed.
ESA

N94-12485# Katholieke Univ. te Leuven (Belgium). Inst. for Land and Water Management.
PER-FIELD FILTERING AND CLASSIFICATION OF MULTITEMPORAL ERS-1 SAR IMAGERY
Annick Grillet, Herman Eerens, and Roland Gombeer *In* ESA, Proceedings

of 1st ERS-1 Symposium on Space at the Service of Our Environment, Volume 2 Mar. 1993 p 605-609 Prepared in cooperation with Service de la Programmation de la Politique Scientifique, Brussels, Belgium (For primary document see N94-12471 01-43)
Copyright Avail: CASI HC A01/MF A03; EPD, ESA, ESTEC, Noordwijk, Netherlands, HC

The heavy speckle noise intrinsic to ERS-1 SAR-imagery strengthens the need for spatial smoothing filters. This pilot study departs from external information on the parcel boundaries in order to apply a per-field filtering. Three different per-pixel classifiers are evaluated: decision tree, maximum likelihood, and nonparametric Bayes. When applied on preliminary filtered image data, the maximum likelihood yields an accuracy of 83% well classified pixels. ESA

N94-12486# Canada Centre for Remote Sensing, Ottawa (Ontario).
PRELIMINARY ERS-1 ASSESSMENT FOR CANADIAN AGRICULTURE AND FORESTRY APPLICATIONS
R. J. Brown, B. Brisco (INTERA Technologies Ltd., Nepean, Ontario.), F. Ahern, S. Yatabe (Petawawa National Forestry Inst., Chalk River, Ontario.), and J. Drieman (Drieman Curtis, Inc., Corner Brook, Newfoundland.) *In* ESA, Proceedings of 1st ERS-1 Symposium on Space at the Service of Our Environment, Volume 2 Mar. 1993 p 611-616 (For primary document see N94-12471 01-43)
Copyright Avail: CASI HC A02/MF A03; EPD, ESA, ESTEC, Noordwijk, Netherlands, HC

The use of ERS-1 data for agriculture and forestry applications in Canada is addressed. The preliminary results demonstrate the imagery can be used to separate crop types for a test site in Manitoba. The ERS-1 data of a test site in Ontario also contain information about variable soil moisture but surface roughness effects are still present at the steep incidence angle and must be accounted for. Forestry test sites in Ontario and Alberta demonstrate confusion of clear cuts and forested areas on ERS-1 data but good separability on Almaz and airborne Synthetic Aperture Radar (SAR) data. This was attributed to the steep incidence angle of ERS-1 rather than the polarization or frequency differences of the sensors. Promising results in detecting burned areas with ERS-1 data of a test site in Labrador were obtained. ESA

N94-12487# Sheffield Univ. (England).
SEGMENTATION AND CHANGE DETECTION IN ERS-1 IMAGES OVER EAST ANGLIA
S. Quegan, R. G. Caves, K. D. Grover, and R. G. White (Defence Research Agency, Malvern, England.) *In* ESA, Proceedings of 1st ERS-1 Symposium on Space at the Service of Our Environment, Volume 2 Mar. 1993 p 617-622 (For primary document see N94-12471 01-43)
Copyright Avail: CASI HC A02/MF A03; EPD, ESA, ESTEC, Noordwijk, Netherlands, HC

ERS-1 images gathered two months apart from an agricultural region near Feltwell (UK) were analyzed using automatic segmentation based on an iterative edge detection and segment growing method which progressively learns the structure in the image. The images show great structural change, though there is little corresponding variation on the ground; the apparent change in structure is because of large relative changes in the backscatter of fields. Results of segmentation were compared with visual inspection and indicate that the algorithms appear to preserve all the relevant features present in the original data. Over segmentation is more of a problem, which is combatted by removing edges from the original segmentation on the basis of a measure of confidence in the existence of an edge. The segmented images provide a quantitative assessment of the structure in the image, which can be used for comparison and change detection purposes. The striking changes between images serve to emphasize that only by combining images and/or other data sources will a reliable picture of true ground structures be built up. Modifications in order to improve segmentation performance are much clarified by this initial study. ESA

N94-12488# Defence Research Agency, Farnborough (England).
ERS-1 SAR CROP MONITORING EXPERIMENT IN EAST ANGLIA, UK
P. J. Bird, R. A. Cordey (GEC-Marconi Electronic Systems Corp., Wayne, NJ.), A. Diament (Cambridge Univ., England.), M. R. Gorman (Cambridge Univ., England.), M. G. Holmes (Cambridge Univ., England.), D. R. D. Kenward, G. E. Keyte, M. Wooding (Remote Sensing Applications Consultants, Farnborough, England.), and P. A. Wright (GEC-Marconi Electronic Systems Corp., Wayne, NJ.) *In* ESA, Proceedings of 1st ERS-1 Symposium on Space at the Service of Our Environment, Volume 2 Mar. 1993 p 623-624 (For primary document see N94-12471 01-43)
Copyright Avail: CASI HC A01/MF A03; EPD, ESA, ESTEC, Noordwijk, Netherlands, HC

The first experimental phase of the crop monitoring experiment, whose aim is to examine the feasibility of large area crop monitoring by Synthetic Aperture Radar (SAR) by studying the imaging of a restricted range of crops on a variety of soil types, is addressed. Four agricultural experiment sites in East Anglia (UK) were monitored by the ERS-1 SAR through the 1992 growing season. In situ data were collected on the structural and moisture properties of crops and soil in selected fields, concentrating particularly on wheat and sugar beet. A C band ground based scatterometer was used to monitor the backscatter variations of a particular wheat field with a temporal spacing finer than that provided by ERS-1. Statistical analyses of the radar and in situ data are about to commence. A further experiment will be planned for the 1993 growing season. ESA

N94-12489# Technische Univ., Berlin (Germany). Fachgebiet Regionale Bodenkunde.
GEOECOLOGICAL MONITORING OF AN AGRICULTURAL AREA
Corinna Prietzsch *In* ESA, Proceedings of 1st ERS-1 Symposium on Space at the Service of Our Environment, Volume 2 Mar. 1993 p 625-628 (For primary document see N94-12471 01-43)
(Contract DARA-FKZ-50-EE-9115/22)
Copyright Avail: CASI HC A01/MF A03; EPD, ESA, ESTEC, Noordwijk, Netherlands, HC

The geoecological monitoring of a biosphere reserve near Berlin (Germany), using ERS-1 Synthetic Aperture Radar (SAR) data and LANDSAT Thematic Mapper data in order to gain information about land suitability for agricultural purposes or protection needs, is addressed. Land use changes and soil physical parameters are determined each month using speckle filtered images in order to provide planning information for the local biosphere reserve administration. ESA

N94-12490# SCOT Conseil, Ramonville (France).
INTEGRATION OF ERS-1 DATA INTO THE EUROPEAN PROJECT OF AGRICULTURE STATISTICS
Jochen Harms *In* ESA, Proceedings of 1st ERS-1 Symposium on Space at the Service of Our Environment, Volume 2 Mar. 1993 p 629-630 (For primary document see N94-12471 01-43)
Copyright Avail: CASI HC A01/MF A03; EPD, ESA, ESTEC, Noordwijk, Netherlands, HC

The possibility of integrating ERS-1 data into the European project of agriculture statistics (Action 4) is investigated. The objective of Action 4 is the rapid estimation of crop surface and potential yield at European level. The estimation of surface and production of crops (within the whole season) is performed with the help of high resolution satellite data of LANDSAT or SPOT over 53 selected sites (40 by 40 km) representing the Commission for the European Community agriculture. In order to test the use of ERS-1 data, three data sets were used over Seville (Spain), one of the Action 4 test sites. A visual interpretation of mono/multitemporal data sets is shown. First results of SPOT/ERS-1 merge are presented. ESA

N94-12491# Technische Univ., Munich (Germany). Lehrstuhl fuer Geographie und Geographische Fernerkundung.
EXTRACTION OF PLANT AND SOIL PARAMETERS FROM MULTITEMPORAL ERS-1 SLC DATA OF THE FREIBURG TEST SITE
A. Demircan, M. Rombach, and W. Mauser *In* ESA, Proceedings of 1st ERS-1 Symposium on Space at the Service of Our Environment, Volume 2 Mar. 1993 p 631-634 (For primary document see N94-12471 01-43)
Copyright Avail: CASI HC A01/MF A03; EPD, ESA, ESTEC, Noordwijk, Netherlands, HC

During the Summer season 1991 intensive ground data collection was carried out on 7 fields within a test site in the Upper Rhine valley (Germany) to continuously record soil moisture in 4 different depths and to weekly measure agricultural plant parameters (leaf area index, biomass, height) of different crops. The high temporal resolution of the ERS-1 Single Look Complex (SLC) radar data of almost 3 days during the commissioning phase in the period of 17 Aug. to 30 Nov. 1991 enabled the continuous documentation of the change of radar backscatter with changing surface features. Correlations between the different plant and soil parameters and the averaged backscatter from the fields under investigation were calculated. ESA

N94-12492# Indian Space Research Organization, Ahmedabad. Space Applications Center.

ASSESSMENT OF ERS-1 SAR DATA FOR SOIL MOISTURE ESTIMATION

S. Mohan, N. S. Mehta, R. L. Mehta, Parul Patel, D. Rajak, Hari Shanker Srivastava, D. K. Das (Indian Agricultural Research Inst., New Delhi.), Sunder Sharma (Indian Agricultural Research Inst., New Delhi.), C. M. Saxena (Indian Agricultural Research Inst., New Delhi.), and A. K. Sutrodhar (Indian Agricultural Research Inst., New Delhi.) *In* ESA, Proceedings of 1st ERS-1 Symposium on Space at the Service of Our Environment, Volume 2 Mar. 1993 p 635-639 (For primary document see N94-12471 01-43)

Copyright Avail: CASI HC A01/MF A03; EPD, ESA, ESTEC, Noordwijk, Netherlands, HC

The ability of C band ERS-1 Synthetic Aperture Radar (SAR) data to detect near surface soil moisture was examined over parts of Agra district (U.P. State, India). The ERS-1 SAR data of 9 Dec. 1991 (orbit No. 2081) was evaluated for this purpose. The SAR derived DN (backscatter) values were linearly correlated with near surface soil moisture (0 to 5 cm depth) for bare soil, mustard crop covered soil and combined data set. The value of correlation coefficient was 0.82 for bare soil, 0.89 for mustard covered soil and 0.79 for combined data set. The models were applied to Kiraoli taluka to map the soil moisture distribution. ESA

N94-12493# Remote Sensing Applications Consultants, Farnborough (England).

TEMPORAL MONITORING OF SOIL MOISTURE USING ERS-1 SAR DATA

M. G. Wooding, G. H. Griffiths, R. Evans, P. J. Bird (Defence Research Agency, Farnborough, England.), D. R. D. Kenward (Defence Research Agency, Farnborough, England.), and G. E. Keyte (Defence Research Agency, Farnborough, England.) *In* ESA, Proceedings of 1st ERS-1 Symposium on Space at the Service of Our Environment, Volume 2 Mar. 1993 p 641-648 (For primary document see N94-12471 01-43)

Copyright Avail: CASI HC A02/MF A03; EPD, ESA, ESTEC, Noordwijk, Netherlands, HC

A program of soil and crop measurements, undertaken during the ERS-1 commissioning phase as part of the UK Synthetic Aperture Radar (SAR) calibration experiment on the test site at Romney Marsh, Kent, is addressed. On 9 overpass days detailed measurements of soil moisture and surface roughness were made in 3 bare soil and 3 grass fields used for corner reflector deployment. Surveys were also undertaken on 5 of these days to record crop type and soil conditions in another 150 agricultural fields. A total of 18 ERS-1 precision images acquired during the 3 day repeat orbit were used. These images were coregistered with a digital map of field boundaries to extract the mean backscatter for sample fields. Accurate calibration of the backscatter measurements was achieved using correction factors derived from the analysis of corner reflector target responses. Analysis of ERS-1 backscatter for the bare soil fields with corner reflectors shows very high positive correlation with volumetric soil moisture over the range 10 to 40 percent. In contrast, there is no correlation between ERS-1 backscatter and the soil moisture for the 3 grass fields with corner reflectors. Temporal backscatter profiles for the sample fields over the 18 imaging dates show large changes in backscatter. Overall trends in ERS-1 backscatter are dominated by moisture effects. Daily and hourly rainfall data are used in conjunction with the detailed soil moisture measurements to explain the temporal profiles for different cover types. Between field variation in ERS-1 backscatter on individual dates is shown to be related to cover type and surface roughness conditions. ESA

N94-12494# Environmental Research Inst. of Michigan, Ann Arbor. Center for Earth Sciences.

OBSERVATIONS OF ERS-1 SAR SENSITIVITIES TO CHANGES IN ABOVEGROUND BIOMASS IN YOUNG LOBLOLLY PINE FORESTS

E. S. Kasischke, N. L. Christensen, Jr. (Duke Univ., Durham, NC.), L. L. Bourgeau-Chavez, and E. Haney (Duke Univ., Durham, NC.) *In* ESA, Proceedings of 1st ERS-1 Symposium on Space at the Service of Our Environment, Volume 2 Mar. 1993 p 653-656 (For primary document see N94-12471 01-43)

Copyright Avail: CASI HC A01/MF A03; EPD, ESA, ESTEC, Noordwijk, Netherlands, HC

The sensitivity of the microwave return recorded by the ERS-1 C band Synthetic Aperture Radar (SAR) to changes in above ground woody biomass in young loblolly pine forests (dry weight biomass less than 6 kg/sq m) was evaluated. Radar backscattering coefficients were derived from ERS-1 SAR imagery collected over 11 test stands near Durham, North Carolina. Ground truth data were collected in order to characterize the aboveground biomass of the pine trees in the test stands. A significant (at $p = 0.001$) linear correlation (r) was found between the radar backscattering and the various components of biomass (both wet and dry weight) within the pine canopy (for example, bole biomass, stem biomass, needle biomass, canopy biomass and total biomass). The linear correlation coefficients ranged between 0.87 and 0.93. ESA

N94-12495# Joint Research Centre of the European Communities, Ispra (Italy). Remote Sensing Applications Inst.

SEEING THE BLACK FOREST BY ERS-1 AND AIRSAR: A COMPARISON

Carlo Lavalle and Alois J. Sieber *In* ESA, Proceedings of 1st ERS-1 Symposium on Space at the Service of Our Environment, Volume 2 Mar. 1993 p 657-660 (For primary document see N94-12471 01-43)

Copyright Avail: CASI HC A01/MF A03; EPD, ESA, ESTEC, Noordwijk, Netherlands, HC

During the Summer and the Autumn of 1991 the Black Forest (Germany) was surveyed by two unique Synthetic Aperture Radar (SAR) systems: the C band SAR on board the ERS-1 and the polarimetric SAR on board the AIRSAR. This provided the opportunity to monitor the area for a long period, from Jun. to Nov. 1991. Although the two sensors present sensible differences in the basic imaging characteristics, the collected images were useful in the study of the temporal evolution of the radar backscattering from forested and non forested areas of the region. The forest return showed a dynamic range of about 5 dB over the seven months period, but in the Oct. survey the range was reduced to about 2 dB. The unforested areas, either agricultural fields or clear cut areas, showed a large variation over the observed period and it resulted that the discrimination forest/non forest was not always possible. ESA

N94-12496# VEGA Space Systems Engineering Ltd., Harpenden (England).

THE TREES PROJECT: PRE-PROCESSING AND GENERATION OF TERRAIN DATA FOR INCLUSION IN AN ERS-1 SAR CLASSIFICATION SCHEME

A. Sowter, H. DeGroof (Joint Research Centre of the European Communities, Ispra, Italy.), and A. J. Sieber (Joint Research Centre of the European Communities, Ispra, Italy.) *In* ESA, Proceedings of 1st ERS-1 Symposium on Space at the Service of Our Environment, Volume 2 Mar. 1993 p 665-670 Sponsored by Joint Research Center of the European Communities (For primary document see N94-12471 01-43)

Copyright Avail: CASI HC A02/MF A03; EPD, ESA, ESTEC, Noordwijk, Netherlands, HC

Within the TREES (Tropical Ecosystem Environment monitoring by Satellites) project, there is a high probability of encountering areas of terrain variations of such an extent that routine classifications of the corresponding Synthetic Aperture Radar (SAR) imagery will be severely limited. In recognition of this, a minimal number of desirable sets of information relating to the topography was identified. The generation of the data sets was shown to be clear when a digital elevation model is available, using a three dimensional simulation of sensor/target geometry to derive them; when no terrain information is available, an attempt must be made to generate the information by other means or risk a higher failure rate of the classification. A method to derive some of the data sets using SAR interferometry is outlined and the results generated using ERS-1 data taken over Sardinia (Italy) are presented. ESA

N94-12497# Joint Research Centre of the European Communities, Ispra (Italy).

TREES PROJECT: A CASE STUDY ON THE USE OF MULTI-TEMPORAL ERS-1 SAR DATA AND SPOT DATA FOR MONITORING TROPICAL ECOSYSTEMS

A. D. Soekeland, H. DeGroof, J. Conway (National Remote Sensing Centre,

Farnborough, England.), and A. J. Sieber *In* ESA, Proceedings of 1st ERS-1 Symposium on Space at the Service of Our Environment, Volume 2 Mar. 1993 p 671-677 (For primary document see N94-12471 01-43)
Copyright Avail: CASI HC A02/MF A03; EPD, ESA, ESTEC, Noordwijk, Netherlands, HC

Within the TREES (Tropical Ecosystem Environment monitoring by Satellites) project multitemporal ERS-1 Synthetic Aperture Radar (SAR) data of West Africa were used to investigate their information content for monitoring tropical ecosystems. Classification methodology to exploit both the tonal and textural characteristics of ERS-1 SAR imagery is described. A visual interpretation and supervised classifications were carried out for a forest/nonforest discrimination. The results are presented visually as images and as confusion matrices. It was found that the classification accuracies for the ERS-1 SAR data are in general low, but can be improved using multitemporal data and texture information. ESA

N94-12498# National Remote Sensing Centre, Farnborough (England).
TREES PROJECT: A SUITE OF TOOLS FOR INFORMATION EXTRACTION FROM ERS-1 SAR DATA
J. A. Conway, H. DeGroof (Joint Research Centre of the European Communities, Ispra, Italy.), and A. J. Sieber (Joint Research Centre of the European Communities, Ispra, Italy.) *In* ESA, Proceedings of 1st ERS-1 Symposium on Space at the Service of Our Environment, Volume 2 Mar. 1993 p 679-684 (For primary document see N94-12471 01-43)
Copyright Avail: CASI HC A02/MF A03; EPD, ESA, ESTEC, Noordwijk, Netherlands, HC

A prototype suite of software tools, developed for the TREES (Tropical Ecosystem Environment monitoring by Satellites) project for the post processing of ERS-1 Synthetic Aperture Radar (SAR) data, with the aim of monitoring the tropical rainforests, is described. An overview of the toolbox is given and each of the tools is described in detail. These tools include methods for filtering SAR data, segmentation and classification using both the tonal and texture information contained in the imagery. Examples of the outputs of these tools using ERS-1 SAR imagery of a test site in West Africa are also given. The current status of the toolbox is described and plans for its future development are outlined. ESA

N94-12499# Joint Research Centre of the European Communities, Ispra (Italy).
TREES PROJECT: OVERVIEW AND STATUS OF THE ERS-1 SAR CONTRIBUTION
H. DeGroof, A. Sowter (VEGA Space Systems Engineering Ltd., Harpenden, England.), A. Soekeland, J. A. Conway (National Remote Sensing Centre, Farnborough, England.), and A. J. Sieber *In* ESA, Proceedings of 1st ERS-1 Symposium on Space at the Service of Our Environment, Volume 2 Mar. 1993 p 685-689 (For primary document see N94-12471 01-43)
Copyright Avail: CASI HC A01/MF A03; EPD, ESA, ESTEC, Noordwijk, Netherlands, HC

An overview of the ERS-1 part of the multi-annual TREES (Tropical Ecosystem Environment monitoring by Satellites) project is given. Objectives, strategies and major milestones of the project are reviewed. The status reports on first developments and results obtained during the initial research and development phase of the TREES project in the 1991 to 1992 timeframe. The interpretation of these first results led to a first tuning of the initially devised strategies and data processing concepts. ESA

N94-12500# Norwegian Meteorological Inst., Blindern.
IMPACT OF ERS-1 WIND/WAVE/ICE DATA ON OPERATIONAL OCEAN FORECASTING c48
Johannes Guddal *In* ESA, Proceedings of 1st ERS-1 Symposium on Space at the Service of Our Environment, Volume 2 Mar. 1993 p 695-699 (For primary document see N94-12471 01-43)
Copyright Avail: CASI HC A01/MF A03; EPD, ESA, ESTEC, Noordwijk, Netherlands, HC

ERS-1 data for winds, waves and sea ice were applied close to the frontline of operational ocean forecasting. The potential end user benefit of the ERS-1 contribution to ocean sensoring, and the relation to the operational forecasting/nowcasting service itself are highlighted. ESA

N94-12501# British Antarctic Survey, Cambridge (England).
A FIRST ASSESSMENT OF THE VALUE OF ERS-1 SCATTEROMETER WINDS FOR METEOROLOGICAL STUDIES IN THE POLAR REGIONS
J. Turner and J. P. Thomas *In* ESA, Proceedings of 1st ERS-1 Symposium on Space at the Service of Our Environment, Volume 2 Mar. 1993 p 701-704 (For primary document see N94-12471 01-43)
Copyright Avail: CASI HC A01/MF A03; EPD, ESA, ESTEC, Noordwijk, Netherlands, HC

ERS-1 scatterometer winds for the Southern Ocean were examined in conjunction with conventional surface meteorological analyses to assess their value in investigations of the meso and synoptic scale structure of high latitude weather systems. Fast delivery surface wind vectors for Jan. to Jul. 1992 were examined. Early data showed significant problems with ambiguity removal, although later data were improved and only occasional directional errors were encountered. The resolution of the winds appeared variable with constant directions and speeds being found occasionally over large areas. Early case studies show the potential of the data with good resolution of flow in the vicinity of fronts and around isolated islands. ESA

N94-12502# Meteorological Office, Bracknell (England).
USE OF ERS-1 WIND AND WAVE PRODUCTS IN OPERATIONAL METEOROLOGY c47
Stuart Bell and Martin Holt *In* ESA, Proceedings of 1st ERS-1 Symposium on Space at the Service of Our Environment, Volume 2 Mar. 1993 p 705-710 (For primary document see N94-12471 01-43)
Copyright Avail: CASI HC A02/MF A03; EPD, ESA, ESTEC, Noordwijk, Netherlands, HC

Statistics from validations of altimeter and scatterometer data are presented. The scatterometer winds were processed from the sigma O's in house and dealiased with the help of U.K. Meteorological Office (UKMO) operational global model background winds. The altimeter data were obtained directly from the ESA fast delivery product. Winds derived from the scatterometer were assimilated into the UKMO atmospheric forecast model and preliminary results from these assimilations are presented. The derived wind fields from atmospheric assimilations were used to drive a global wave model to measure their impact on analyzed wave fields. Preliminary experiments to assimilate the altimeter wave data directly into the wave model are reported. Further work to optimize the use of these new data sources is anticipated. ESA

N94-12503# MeteorMer, Puget sur Argens (France).
USE OF SAR-WAVE, ALTIMETER, AND WIND-SCATTEROMETER DATA IN AN OPERATIONAL SWELL FORECASTING SYSTEM
P. Lasnier, P. Charriez, H. Hajji, and F. Cauneau (Ecole Nationale Superieure des Mines, Sophia-Antipolis, France.) *In* ESA, Proceedings of 1st ERS-1 Symposium on Space at the Service of Our Environment, Volume 2 Mar. 1993 p 711-720 (For primary document see N94-12471 01-43)
Copyright Avail: CASI HC A02/MF A03; EPD, ESA, ESTEC, Noordwijk, Netherlands, HC

The first phase of a pilot project whose aim was to evaluate the quality improvement of marine meteorological forecast and analysis, using the information provided on sea state by the three instruments of the ESA ERS-1 satellite (Synthetic Aperture Radar (SAR) in wave mode, wind scatterometer, and radar altimeter) is reported. The mastery in the domains of data acquisition (fast delivery), via a server installed at the French meteorological office, and in the domain of data management and archiving (applied to the site climatology study) was given. This implied the first handling of visualization softwares, and permitted a first visual evaluation of the data. The first analysis and controls for the data quality were achieved. ESA

N94-12504# Atmospheric Environment Service, Toronto (Ontario).
USE OF ERS-1 SCATTEROMETER WINDS IN CANADIAN FORECAST CENTRES c47
Patrick King *In* ESA, Proceedings of 1st ERS-1 Symposium on Space at the Service of Our Environment, Volume 2 Mar. 1993 p 721-724 (For primary document see N94-12471 01-43)
Copyright Avail: CASI HC A01/MF A03; EPD, ESA, ESTEC, Noordwijk, Netherlands, HC

The current and future use of ERS-1 scatterometer data at the Canadian Meteorological Centre (CMC) in Montreal and at regional forecast centers is described. Scatterometer data are received at CMC, decoded, filtered, and retransmitted as pseudo ship codes to weather forecast centers. Each office plots the data on maps which are then used in conjunction with conventional data. Forecasters record their first impressions on the supplementary chart. They then make a systematic comparison of the scatterometer data with the latest analysis done using conventional data. In the Spring of 1993 a systematic evaluation of the effect that the scatterometer data has made on analyses and forecasts will be made. A systematic comparison is being made between CMC model winds and scatterometer winds. Experiments are planned in assimilating scatterometer data into both global and regional models. ESA

N94-12505# Johns Hopkins Univ., Laurel, MD. Applied Physics Lab.
ERS-1 AND ALMAZ SAR OCEAN WAVE IMAGING OVER THE GULF STREAM AND THE GRAND BANKS **c48**
David George Tilley and Robert Carl Beal *In* ESA, Proceedings of 1st ERS-1 Symposium on Space at the Service of Our Environment, Volume 2 Mar. 1993 p 729-734 (For primary document see N94-12471 01-43)
Copyright Avail: CASI HC A02/MF A03; EPD, ESA, ESTEC, Noordwijk, Netherlands, HC

Initial assessments of both Almaz and ERS-1 image quality were compared with a similar Seasat Synthetic Aperture Radar (SAR) evaluation. ERS-1 and Almaz spectral estimates were collected nearly simultaneously and coincidentally in the Labrador Sea (Canada), and then compared with both aircraft SAR and directional buoy spectra. Similarly to Seasat, ERS-1 spectra were found to be substantially attenuated in the azimuth (along crack) direction, with typical falloff wavelengths of 250 m or more. The Almaz SAR responded well to wavelengths as short as 100 m. The SAR signal to noise response, however, was about a factor of four lower for Almaz than for ERS-1. ERS-1 imagery of the Gulf Stream was examined in four passes. Linear features in the SAR imagery were compared with satellite IR imagery, and were found to agree with the thermal fronts within 5 km. The results so far support the idea that a future wide swath scansar will be a valuable tool for monitoring large scale ocean dynamics at high resolution. ESA

N94-12506# Sydney Univ. (Australia). Ocean Technology Group.
REAL TIME PROCESSING WAVE SPECTRA FROM SATELLITE SAR **c48**
Ian S. F. Jones *In* ESA, Proceedings of 1st ERS-1 Symposium on Space at the Service of Our Environment, Volume 2 Mar. 1993 p 735-737 Sponsored by Esso-BHP (For primary document see N94-12471 01-43)
Copyright Avail: CASI HC A01/MF A03; EPD, ESA, ESTEC, Noordwijk, Netherlands, HC

A scheme under development to exploit a remote sensing technique to provide real time, deep ocean wave spectra at a significant number of points below a satellite track is reported. Real time is taken to mean within four hours of reception and will be achieved by retransmission at 1/10 the original rate (that is transmitted at 10 Mbits/sec) from a tape recorder. The processing system and computer program used are described. After a short delay the program WASP (Wave Spectral Program) produces 4 spectra per swath continuously. Synthetic Aperture Radar (SAR) signals from the ERS-1 were used in the tests to date and an intercomparison between a pass across Bass Strait (Australia) during a storm and the directional wave gauge installed on an offshore platform is presented. A number of critical elements in a 'real time' ocean wave spectra delivery system and the outstanding issues were identified. The first example used to test those components that are in place employed the ERS-1 satellite as it traversed Bass Strait. This was the occasion when there was a typical storm in progress below the satellite. The wind waves however were traveling in a nearly azimuth direction and as expected this did not produce a strong wave image. ESA

N94-12507# Institut Francais de Recherche pour l'Exploitation de la Mer, Brest. Dept. d'Oceanographie Spatiale.
A STATISTICAL ANALYSIS OF SEA STATE SURFACE ERS-1 SAR-WAVE MODE IMAGETTES **c48**
B. Chapron, R. Garello (Ecole Nationale Superieure des Telecommunicatons, Brest, France.), and G. Engen (Forut, Tromsoe, Norway.) *In* ESA, Proceedings of 1st ERS-1 Symposium on Space at the Service of Our Environment, Volume 2 Mar. 1993 p 739-742 (For primary document see N94-12471 01-43)
Copyright Avail: CASI HC A01/MF A03; EPD, ESA, ESTEC, Noordwijk, Netherlands, HC

The statistical properties of ERS-1 Synthetic Aperture Radar (SAR) wave mode imagettes are presented. Acknowledging the different mechanisms affecting the imaging processes of the ocean surface with a SAR, the aim of such analysis is to extract relevant parameters to complete the traditional spectral information. The statistical properties of the images depend on the roughness of the sea, the underlying long wave system, the instrument characteristics, and the space-time variation of the surface. Following previous studies on the application of non-gaussian noise model, the use of K distribution and Gamma probability law to describe different SAR images is discussed. Based on the analysis of ERS-1 imagettes, the use of such models helps not only in the classification of the products, but also for their possible physical interpretation and link with the nonlinear ocean SAR integral transform widely used to interpret the distorted mapping commonly observed with SAR instruments. ESA

N94-12508# James Cook Univ. of North Queensland, Townsville (Australia). Dept. of Physics.
A NEW MODEL FOR SYNTHETIC APERTURE RADAR (SAR) IMAGES FROM OCEAN SCATTER **c48**
M. L. Heron and I. Amadou *In* ESA, Proceedings of 1st ERS-1 Symposium on Space at the Service of Our Environment, Volume 2 Mar. 1993 p 743-745 Sponsored by DSTO, Adelaide, Australia (For primary document see N94-12471 01-43)
Copyright Avail: CASI HC A01/MF A03; EPD, ESA, ESTEC, Noordwijk, Netherlands, HC

A project to produce a model which will incorporate dynamic features of the ocean surface to determine instantaneous scattering points, and calculate the complex image by conventional Kirchoff integral is introduced. In this calculation all the known effects of modulation of the short wavelengths Bragg scatterers like tilting, straining, and velocity bunching will be taken into account. The Doppler shift for each scattering facet is therefore made up from that due to the motion of the satellite plus that due to the surface dynamics. Initial calculations using this model indicate that the scattering patch size depends on look angle, wave parameters, platform, and altitude. A validation experiment was proposed using the NASA DC-8 AirSAR flying with synthetic aperture radars operating simultaneously in the X band, C band and in L band and flying along the same track at the same time and with the same look angle as ERS-1, at a site instrumented for wave directional spectra. ESA

N94-12509# Hamburg Univ. (Germany). Inst. fuer Meereskunde.
ON THE EXTRACTION OF OCEAN WAVE SPECTRA FROM ERS-1 SAR WAVE MODE IMAGE SPECTRA **c48**
C. Bruening, S. Hasselmann (Max-Planck-Inst. fuer Meteorologie, Hamburg, Germany.), K. Hasselmann (Max-Planck-Inst. fuer Meteorologie, Hamburg, Germany.), S. Lehner (Max-Planck-Inst. fuer Meteorologie, Hamburg, Germany.), and T. Gerling (Johns Hopkins Univ., Laurel, MD.) *In* ESA, Proceedings of 1st ERS-1 Symposium on Space at the Service of Our Environment, Volume 2 Mar. 1993 p 747-752 (For primary document see N94-12471 01-43)
(Contract BMFT-01-QS-9014)
Copyright Avail: CASI HC A02/MF A03; EPD, ESA, ESTEC, Noordwijk, Netherlands, HC

The ERS-1 Synthetic Aperture Radar (SAR) wave mode data contain valuable global information on the full two dimensional ocean wave spectrum. This must be extracted, however, from nonlinearly distorted images. Wave spectra were derived from SAR wave mode image spectra using Hasselmann's inversion scheme based on their closed nonlinear spectral integral transform relation describing the mapping of a wave spectrum into a SAR image spectrum. The scheme uses a first guess (WAM) model wave spectrum as regularization term. The optimally fitted wave spectra yield simulated SAR image spectra in good agreement with measured SAR spectra. The wave spectra provide significant wave heights to the same accuracy as ERS-1 radar altimeter. The separation of the SAR derived wave spectra into individual wave systems using a partitoning technique showed excellent overall agreement with modeled wave spectra while demonstrating the complexity of typical wave spectra in the open ocean. ESA

N94-12510# Hamburg Univ. (Germany). Inst. fuer Meereskunde.
TIDE-GENERATED NONLINEAR INTERNAL WAVE PACKETS IN THE STRAIT OF GIBRALTAR OBSERVED BY THE SYNTHETIC APERTURE RADAR ABOARD THE ERS-1 SATELLITE **c48**
W. Alpers and P. E. LaViolette (Mississippi State Univ., Mississippi State.) *In* ESA, Proceedings of 1st ERS-1 Symposium on Space at the Service of Our Environment, Volume 2 Mar. 1993 p 753-758 (For primary document see N94-12471 01-43)
(Contract BMFT-01-QS-9014)
Copyright Avail: CASI HC A02/MF A03; EPD, ESA, ESTEC, Noordwijk, Netherlands, HC

Thirteen radar images acquired over the Strait of Gibraltar by the Synthetic Aperture Radar (SAR) aboard the ERS-1 satellite in the period from Jan. to Mar. 1992 were analyzed. Most of them show surface manifestations of nonlinear internal waves in the way theory predicts. In addition, the SAR images display features in the surface roughness pattern that were not known before. For the first time, internal waves propagating southward from Gibraltar across the Strait were detected. ESA

N94-12511# Centre de Recherches en Physique de l'Environnement, Velizy (France).
VALIDATION OF THE ATSR/M MICROWAVE RADIOMETER DATA
Laurence Eymard, Luc Tabary, and Alain LeCornec *In* ESA, Proceedings of 1st ERS-1 Symposium on Space at the Service of Our Environment, Volume 2 Mar. 1993 p 763-766 (For primary document see N94-12471 01-43)
Copyright Avail: CASI HC A01/MF A03; EPD, ESA, ESTEC, Noordwijk, Netherlands, HC

The validation of the ERS-1 Along Track Scanning Radiometer (ATSR) data is described. This microwave radiometer was designed to correct the altimeter tropospheric path for the delay due to humidity. The data quality assessment consisted of verifying the instrument calibration, then of comparing the retrieved geophysical products with available observations. The inflight calibration included control of gain stability and long term survey of internal and brightness temperature variations, as well as footprint location verification. No anomaly was detected after one year. Data validation was performed by comparing routine radiosonde measurements with the retrieved water vapors and altimeter path corrections. There is no routine measurement of cloud water content, so this retrieval cannot be simply tested. The water vapor content and altimeter tropospheric path correction retrievals were validated. ESA

N94-12512# Indian Space Research Organization, Ahmedabad. Meteorology and Oceanography Div.
MULTICHANNEL DUAL ANGLE APPROACH FOR SEA SURFACE TEMPERATURE RETRIEVAL IN CONTEXT OF ERS-1 SCENARIO
Aloke K. Mathur and Vijay K. Agarwal *In* ESA, Proceedings of 1st ERS-1 Symposium on Space at the Service of Our Environment, Volume 2 Mar. 1993 p 767-771 (For primary document see N94-12471 01-43)
Copyright Avail: CASI HC A01/MF A03; EPD, ESA, ESTEC, Noordwijk, Netherlands, HC

An algorithm to retrieve Sea Surface Temperature (SST) based on the simulated Along Track Scanning Radiometer (ATSR) data over the Indian Ocean with the help of radiative transfer models is described. Details of the atmospheric profiles used for ATSR data simulation representing the Indian tropical conditions are given. Error estimate, advantages and disadvantages of such retrieval are discussed. It was found that observations from the ATSR and Microwave Sounder (MWS) onboard the first European Remote Sensing Satellite (ERS-1) enabled retrieval of SST within an accuracy of 0.3K because dual angle capability by ATSR accompanied by total water vapor content retrieved by MWS is expected to reduce the existing ambiguities due to atmospheric stratifications especially in tropics. ESA

N94-12513# Indian Space Research Organization, Ahmedabad. Meteorology and Oceanography Div.
ESTIMATIONS OF THE SURFACE FLUXES FROM SATELLITE OBSERVATIONS OF BOUNDARY LAYER AND THE SURFACE
Vijay K. Agarwal, Aloke K. Mathur, and S. Ilanthirayan *In* ESA, Proceedings of 1st ERS-1 Symposium on Space at the Service of Our Environment, Volume 2 Mar. 1993 p 773-778 (For primary document see N94-12471 01-43)
Copyright Avail: CASI HC A02/MF A03; EPD, ESA, ESTEC, Noordwijk, Netherlands, HC

Innovative methods to obtain information about the boundary layer and the interfacial layer at the Earth-atmosphere boundary, which is essential for the understanding of the energy exchange processes, are addressed. A possible method for these calculations based on the data from ERS-1 ATSR/M (Along Track Scanning Radiometer/M), scatterometer, and the NOAA Tiros Operational Vertical Sounder (TOVS) is described. The NOAA-TOVS can provide information about the vertical structures of the humidity and the temperature at coarse levels. The oblique view angles of the ERS-1 ATSR/M observations in the thermal spectral bands have capability to detect the stratifications in the boundary layer. These combined with NOAA inferences are found to provide adequate representation of the lower boundary layer. ESA

N94-12514# Hamburg Univ. (Germany). Meteorologisches Inst.
ATSR CORRELATIVE SKIN MEASUREMENTS OF SEA SURFACE TEMPERATURE **c48**
Peter Schluessel and Jens Meywerk *In* ESA, Proceedings of 1st ERS-1 Symposium on Space at the Service of Our Environment, Volume 2 Mar. 1993 p 779-784 Sponsored by DFG, and BMFT (For primary document see N94-12471 01-43)
Copyright Avail: CASI HC A02/MF A03; EPD, ESA, ESTEC, Noordwijk, Netherlands, HC

Case studies which showed that Sea Surface Temperature (SST) as derived from Along Track Scanning Radiometer (ATSR) with different retrieval algorithms match the surface skin temperatures which were measured with a precisely calibrated radiation thermometer within few tenths of a degree are discussed. Partly cloudy ATSR data was used too and showed to be of value for SST retrievals within 0.5 to 1K accuracy. Retrieval coefficients that are designed for the use with Advanced Very High Resolution Radiometer (AVHRR) data are inadequate for the use with ATSR measurements. The cloud detection scheme of SADIST (Synthesis of ATSR Data Into Sea surface Temperature) properly rejects cloudy pixels but also cloud free measurements in areas with strong SST gradients. The colocation of nadir and forward view measurements as given from the SADIST processing needs a further improvement for a better match up. A further validation of ATSR derived sea surface temperatures is essential in order to get statistically significant conclusions about the accuracy of the derived products. ESA

N94-12515# Meteorological Office, Farnborough (England). Remote Sensing Instrumentation.
VALIDATION OF ATSR-1 USING AIRCRAFT RADIOMETER MEASUREMENTS OVER THE SOUTH ATLANTIC
A. H. Smith and R. W. Saunders *In* ESA, Proceedings of 1st ERS-1 Symposium on Space at the Service of Our Environment, Volume 2 Mar. 1993 p 785-790 (For primary document see N94-12471 01-43)
Copyright Avail: CASI HC A02/MF A03; EPD, ESA, ESTEC, Noordwijk, Netherlands, HC

The first Along Track Scanning Radiometer (ATSR) tropical experiment, carried out in Nov. 1991 to validate the ATSR measurements of Sea Surface Temperature (SST) in the tropics is reported. A multichannel radiometer which had channels spectrally matched to those at 11 and 12 micrometers on the ATSR was flown around the tropics (8 deg South, 14 deg West) on a C130 aircraft and used to make radiance and brightness temperature measurements at a number of different altitudes. An attempt to quantify the absorption/emission effect of any stratospheric aerosol due to the eruption of Mount Pinatubo in Jun. 1991 was made. ATSR sea surface temperature retrievals (using both nadir and forward instrument views) were compared with low level measurements of radiative sea surface temperature. Brightness temperature profiles of the atmosphere were obtained for comparison with those obtained from the Rutherford Appleton Laboratory radiative transfer model which was used to generate the ATSR SST retrieval coefficients. ESA

N94-12516# Meteorological Office, Bracknell (England).
A USER APPRAISAL OF ATSR NEAR-REAL-TIME PRODUCTS
Dawn L. Harrison and Clive P. Jones *In* ESA, Proceedings of 1st ERS-1 Symposium on Space at the Service of Our Environment, Volume 2 Mar. 1993 p 791-795 (For primary document see N94-12471 01-43)

Copyright Avail: CASI HC A01/MF A03; EPD, ESA, ESTEC, Noordwijk, Netherlands, HC

The Along Track Scanning Radiometer (ATSR) Near Real Time (NRT) demonstration project, which was established to address the needs of meteorological centers for Fast Delivery (FD) data, is reported. The ATSR NRT products consist of 0.5 deg. by 0.5 deg. Average Sea Surface Temperatures (ASST) plus ancillary data. The aim of the project was to show that the data processing and transmission system devised can provide data, of high quality and in near real time, to an end user. If this can be achieved then it is hoped that the system will eventually be adopted by ESA as part of the ERS-1 FD service. The NRT ASST's were assessed by comparison with coincident SST's derived from the U.K. meteorological office operational global SST analysis and with collocated, high quality drifting buoy observations. The evaluation was further subdivided into day and nighttime observations and those resulting from the use of single and dual view data because different algorithms are used for the SST retrieval under these conditions. It was found that a bias of around -0.4 K exists. This can largely be attributed to the genuine difference between the temperature of the ocean's radiative skin, as measured by ATSR, and the sub-surface bulk temperature measured by buoy sensors. ESA

N94-12517# Oxford Univ. (England). Dept. of Atmospheric, Oceanic and Planetary Physics.

CLOUD STUDIES USING ATSR DATA c47

C. I. Rice and E. J. Williamson *In* ESA, Proceedings of 1st ERS-1 Symposium on Space at the Service of Our Environment, Volume 2 Mar. 1993 p 797-799 (For primary document see N94-12471 01-43)

Copyright Avail: CASI HC A01/MF A03; EPD, ESA, ESTEC, Noordwijk, Netherlands, HC

The two angle measurement technique of the Along Track Scanning Radiometer (ATSR) provides the opportunity to determine cloud characteristics. It is shown how a simple one layer model of a cloud can be used to determine the cloud top temperature and cloud optical depth from ATSR radiances in the nadir and forward views. Results in which optically thick and optically thin clouds are identified using an interactive image display system are presented. ESA

N94-12518# British Antarctic Survey, Cambridge (England).

A COMPARISON OF ATSR AND SHIPBOARD RADIOMETER SST MEASUREMENTS ALONG TRANSECTS BETWEEN THE UK AND THE ANTARCTIC c48

J. P. Thomas, J. Turner, and C. J. Symon *In* ESA, Proceedings of 1st ERS-1 Symposium on Space at the Service of Our Environment, Volume 2 Mar. 1993 p 801-805 (For primary document see N94-12471 01-43)

Copyright Avail: CASI HC A01/MF A03; EPD, ESA, ESTEC, Noordwijk, Netherlands, HC

A campaign made between Oct. 1991 and May 1992 to make in situ Sea Surface Temperature (SST) measurements to validate the Along Track Scanning Radiometer (ATSR) SST product is reported. The campaign was carried out on a ship as it sailed from the U.K. to Antarctica and back. The ship carried an infrared radiometer, a temperature sensor trailed from the side, and a hull thermistor. The results showed that the present ATSR SST product gives results cooler than the in situ measurements. In the tropics the difference was less than or equal to 1K except in the one case where the forward view was used in the retrieval, when agreement was within 0.1K. ESA

N94-12519# Chilworth Research Centre, Southampton (England). Center for Ocean Circulation.

PRELIMINARY VALIDATION OF ATSR SEA SURFACE TEMPERATURES NEAR THE FAEROES c48

T. N. Forrester, T. H. Guymer, and P. G. Challenor *In* ESA, Proceedings of 1st ERS-1 Symposium on Space at the Service of Our Environment, Volume 2 Mar. 1993 p 807-811 (For primary document see N94-12471 01-43)

Copyright Avail: CASI HC A01/MF A03; EPD, ESA, ESTEC, Noordwijk, Netherlands, HC

Measurements of sea surface temperature made with a thermosalinograph on a cruise near the Faeroes (Norwegian sea) were compared with those derived from the Along Track Scanning Radiometer (ATSR) on ERS-1. Qualitatively, the temperature fields are very similar and show that the area was under the influence of the Iceland-Faeroes Front. Although the presence of significant horizontal gradients and of appreciable amounts of cloud complicated the analysis, it was demonstrated that the accuracy of the ERS-1 temperatures is within their design specification of 0.5K. The ERS-1 values are a few tenths of a Kelvin colder than the in situ data, this is consistent with the skin effect. ESA

N94-12520# Ministry of Posts and Telecommunications, Tokyo (Japan). Communications Research Lab.

ARTIFICIAL OIL POLLUTION DETECTION AND WAVE OBSERVATION IN THE SEA ADJACENT TO JAPAN BY ERS-1 SAR c45

Kenichi Okamoto, Harunobu Masuko, Satoshi Ochiai, Seiho Uratsuka, Kenji Nakamura, Hiroaki Horie, Masaharu Fujita, Masanobu Shimada (National Space Development Agency, Tokyo, Japan.), Masao Nakai (National Space Development Agency, Tokyo, Japan.), and Akira Shibata (Meteorological Research Inst., Tsukuba, Japan.) *In* ESA, Proceedings of 1st ERS-1 Symposium on Space at the Service of Our Environment, Volume 2 Mar. 1993 p 817-821 (For primary document see N94-12471 01-43)

Copyright Avail: CASI HC A01/MF A03; EPD, ESA, ESTEC, Noordwijk, Netherlands, HC

On 10 and 13 Nov. 1991, an experiment to detect artificial oil pollution and ocean waves was performed using the C band Synthetic Aperture Radar (SAR) of ERS-1. An artificial oil slick was made by spilling oleyl alcohol from a small vessel in the Pacific ocean about 100 km off the coast of Omaezaki, Shizuoka prefecture (Japan). Sea truth data were gathered from a research vessel and from another small vessel. Synchronous observation by X band, VV polarization airborne real aperture Side Looking Airborne Radar (SLAR) was made together with the observation by SAR. In the 10 Nov. 1991 SAR image, the artificial oil spill, which appeared to be dark because of capillary wave action, was clear. The decrement of the scattering cross section was about 2.5 dB at the maximum. ESA

N94-12521# Norwegian Defence Research Establishment, Kjeller.

SHIP TRAFFIC MONITORING USING THE ERS-1 SAR

Terje Wahl, Knut Eldhuset, and Aage Skoeelv *In* ESA, Proceedings of 1st ERS-1 Symposium on Space at the Service of Our Environment, Volume 2 Mar. 1993 p 823-828 Sponsored in part by Norwegian Space Center (For primary document see N94-12471 01-43)

Copyright Avail: CASI HC A02/MF A03; EPD, ESA, ESTEC, Noordwijk, Netherlands, HC

A fast processing and distribution chain for ERS-1 Synthetic Aperture Radar (SAR) images was developed in Norway. Large quantities of ERS-1 images were used to assess the ship detection and wake imaging capability of ERS-1. Also, there is an ongoing campaign for detection of oil spill from ships along the Norwegian coast. Automatic detection and analysis of ships and ship wakes using the 30 m resolution SAR fast delivery product was demonstrated. For oil spill detection, 100 m resolution images of high radiometric quality are used. Ships above 120 m in length are generally seen in ERS-1 images under most weather conditions. Ships smaller than 100 m may sometimes become practically invisible in the SAR images because of the strong backscatter from the sea surface at some wind speeds. The main cause of this detection problem is the rather steep incidence angle of ERS-1. Ship wake signatures in ERS-1 images are very similar to those in Seasat images. The most frequent wake feature is the dark turbulent wake. Several confirmed observations of oil slicks have been reported. At low wind speed, natural surface slicks may in some cases be classified as oil slicks. ESA

N94-12522# Oceanor, Trondheim (Norway).

OIL SPILL DETECTION USING SATELLITE-BASED SAR: EXPERIENCE FROM A FIELD EXPERIMENT c45

Tom-Ivar Bern, Terje Wahl (Norwegian Defence Research Establishment, Kjeller.), Tom Anderssen (Oslo Univ., Kjeller, Norway.), and Richard Olsen (Satlantic, Inc., Halifax, Nova Scotia.) *In* ESA, Proceedings of 1st ERS-1 Symposium on Space at the Service of Our Environment, Volume 2 Mar. 1993 p 829-834 Previously announced in IAA as A93-28143 Sponsored by ESSO Norge A/S, Norway; Statoil Norge S/A, Norway; Marine Spill Response Corp.; Norwegian Space Center; Norwegian State Pollution Control Authority; ESA; DEC Norge A/S; and OCEANOR A/S (For primary document see N94-12471 01-43)

Copyright Avail: CASI HC A02/MF A03; EPD, ESA, ESTEC, Noordwijk, Netherlands, HC

The aim of this project is to develop and demonstrate a system for early oil spill detection using satellite based Synthetic Aperture Radar (SAR). During the Dedicated Oil Spill Experiment in Aug. 1991 (DOSE-91), three slicks, each 20 tons of stabilized crude oil, were released in phase with the passages of the ERS-1 satellite. Sea truthing, oil slick tracking using drifting buoys, and aircraft surveillance using various remote sensing techniques to compare and verify satellite observations were performed. The observations gathered during the experiment are presented with emphasis on the SAR imagery of oil slicks under certain environmental conditions. Image enhancement techniques used to process the imagery are also discussed. ESA

N94-12523# Paris VI Univ. (France).

PILOT PROJECT PPF12. COASTAL AND FLUVIAL ENVIRONMENT IN FRENCH GUIANA: FIRST RESULTS OF ERS-1 SAR DATA ANALYSIS **c45**

Jean-Paul Rudant, J. P. Cautru (Bureau de Recherches Geologiques et Minieres, Cayenne, France.), Marc Lointier (Institut Francais de Recherche Scientifique pour le Developpement en Cooperation, Cayenne.), Christophe Charron (Institut Francais de Recherche Scientifique pour le Developpement en Cooperation, Cayenne.), M. Dechambre (Centre de Recherches en Physique de l'Environnement, Velizy, France.), B. Deffontaines, J. P. Deroin (Bureau de Recherches Geologiques et Minieres, Cayenne, France.), M. T. Prost (Institut Francais de Recherche Scientifique pour le Developpement en Cooperation, Cayenne.), D. Raymond, and O. Vanderhaeghe (Bureau de Recherches Geologiques et Minieres, Cayenne, France.) *In* ESA, Proceedings of 1st ERS-1 Symposium on Space at the Service of Our Environment, Volume 2 Mar. 1993 p 835-845 (For primary document see N94-12471 01-43)

Copyright Avail: CASI HC A03/MF A03; EPD, ESA, ESTEC, Noordwijk, Netherlands, HC

A few Synthetic Aperture Radar (SAR) scenes, acquired in Apr. (roll tilt mode, 35 deg. incidence angle) and May 1992 (normal mode, 23 deg. incidence) and available since early Oct. 1992 were evaluated in the following principal thematic applications: morphotectonics, coastal geomorphology, mapping of surficial deposits, and hydrology. The first analysis showed that SAR ERS-1 imagery can contribute, in an original way, to the applications mentioned above, in inland, where the main structural lineaments and lithological units can be easily detected under heavy canopy, as well as in coastal zones where the image resolution is well adapted to the study of erosion and progradation zones, characteristic to the area, and to estimate flood plains during rain periods (during which 'optical' images can not be used). ESA

N94-12524# Liege Univ. (Belgium). Lab. de Geomorphologie et de Geologie du Quatenaire.

COASTAL MORPHODYNAMICS AND ENERGETIC CHARACTERISTICS OF SWELL STUDIED WITH ERS-1 SAR [MORPHODYNAMIQUE DES COTES ET CARACTERISTIQUES ENERGETIQUES DE LA HOULE ETUDIEE GRACE AU SAR DE ERS-1] **c48**

A. Ozer, Y. Cornet, and A. L. Comhaire *In* ESA, Proceedings of 1st ERS-1 Symposium on Space at the Service of Our Environment, Volume 2 Mar. 1993 p 851-855 In FRENCH (For primary document see N94-12471 01-43)

Copyright Avail: CASI HC A01/MF A03; EPD, ESA, ESTEC, Noordwijk, Netherlands, HC

A study of the correlation between meteomarine conditions and the sediment on several beaches in the Mediterranean and in the North Sea is reported. The textural and morphological characteristics of a beach test which resulted from several in situ measurement campaigns are presented. The data processing and production of ERS-1 Synthetic Aperture Radar (SAR) images are described. Correlations with wavelength, swell height, and width are presented. ESA

N94-12525# Rijkswaterstaat, Rijswijk (Netherlands).

MAPPING OF SEA BOTTOM TOPOGRAPHY WITH ERS-1 C-BAND SAR **c48**

J. Vogelzang, G. J. Wensink (Delft Hydraulics Lab., Emmeloord, Netherlands.), M. W. A. vanderKooij (Physics and Electronics Lab. TNO, The Hague, Netherlands.), and G. vanderBurg (National Aerospace Lab., Emmeloord, Netherlands.) *In* ESA, Proceedings of 1st ERS-1 Symposium on Space at the Service of Our Environment, Volume 2 Mar. 1993 p 857-860 (For primary document see N94-12471 01-43)

Copyright Avail: CASI HC A01/MF A03; EPD, ESA, ESTEC, Noordwijk, Netherlands, HC

The mapping of sea bottom topography with ERS-1 C band Synthetic Aperture Radar (SAR) was investigated giving particular attention to the range of hydrometeo parameters under which bottom topography can be observed as well as the optimum parameters. Practical application for monitoring sand waves was considered. A number of ERS-1 C band SAR images of a test area off the Dutch coast were collected. Hydrometeo data were measured on a fixed platform close to the test area. The surface current is obtained from a quasi-three dimensional flow model. Images showing bottom topography were compared with a detailed bathymetric map of the test area and with predictions from state of the art models of the imaging mechanism. ESA

N94-12526# International Inst. for Aerospace Survey and Earth Sciences, Enschede (Netherlands).

ERS-1 IMAGING RADAR OVER THE WADDENSEA-NORTH NETHERLANDS **c48**

B. N. Koopmans and Wang Yiman (Academia Sinica, Beijing, China.) *In* ESA, Proceedings of 1st ERS-1 Symposium on Space at the Service of Our Environment, Volume 2 Mar. 1993 p 861-865 Sponsored by Beleidscommissie Remote Sensing Board, Delft, Netherlands (For primary document see N94-12471 01-43)

Copyright Avail: CASI HC A01/MF A03; EPD, ESA, ESTEC, Noordwijk, Netherlands, HC

A project area was selected in the northern part of the Dutch Waddensea between the island of Vlieland and the town of Harlingen, to investigate the usefulness of ERS-1 radar imaging data for mapping and monitoring. With the radar data, use will be made of the fundamental properties of this area; the dynamics of the tidal cycle and the waterlines which are examples of these properties. A mapping procedure was established on the basis of existing LANDSAT data, consisting of landwater classification, filtering procedures for smoothing the waterline, construction of water surface models at time of data acquisition, defining height elevations along the waterline, and error evaluation on basis of a ground truth mapping digital elevation model. For satellite radar observations a similar procedure will be followed. Before the radar waterline method may be applied, a fundamental question as to whether or not the water-land boundaries on ERS-1 C band radar are clearly mappable under different weather and seastate conditions has to be answered. Meteo and sea state observations were obtained during ERS-1 data acquisition, which may give an answer after the radar data have been processed in future. ESA

N94-12527# City of London Polytechnic (England).

SAR IMAGING OF GEOLOGY AND BATHYMETRY: KENT COASTAL AREA - SOUTHERN NORTH SEA **c48**

B. DOlier (City of London Polytechnic, England.) and N. Lynn (Royal Naval Coll., Greenwich, London, England.) *In* ESA, Proceedings of 1st ERS-1 Symposium on Space at the Service of Our Environment, Volume 2 Mar. 1993 p 867-871 (For primary document see N94-12471 01-43)

Copyright Avail: CASI HC A01/MF A03; EPD, ESA, ESTEC, Noordwijk, Netherlands, HC

A preliminary account of studies linking offshore field work, carried out since 1968 and continuing at present, with Synthetic Aperture Radar (SAR) images obtained in 1978 (Seasat) and with ERS-1, which are being used to determine the value of the system for shallow water geological mapping is given. In addition, changes in the morphology of large mobile sand bedforms are being monitored in order to aid in decisions affecting coastal environmental and protection management. This in particular concerns monitoring changes to coastal sedimentological pathways and 'cells.' ESA

N94-12528# Army Cold Regions Research and Engineering Lab., Hanover, NH.

APPLICATIONS OF ERS-1 SAR DATA FOR ANALYZING RIVERINE AND COASTAL PROCESSES AND GEOMORPHOLOGY **c48**

L. W. Gatto, D. J. Calkins, E. F. Chacho, D. E. Lawson, and R. A. Melloh *In* ESA, Proceedings of 1st ERS-1 Symposium on Space at the Service of Our Environment, Volume 2 Mar. 1993 p 873-878 (For primary document see N94-12471 01-43)

Copyright Avail: CASI HC A02/MF A03; EPD, ESA, ESTEC, Noordwijk, Netherlands, HC

Initial analyses of ERS-1 Synthetic Aperture Radar (SAR) images of geomorphic features around Alaska are summarized. Tha aim of this analysis was to determine the utility of such images in monitoring environmental conditions and processes important for managing water resources. Patterns on SAR images were compared to those on LANDSAT images, and data from ground penetrating radar and field observations were used to interpret the SAR images. These comparisons showed that the ERS-1 SAR can do the following: locate unfrozen water beneath river and lake ice on the Sagavanirktok River floodplain; determine the general ice, snow, and sediment conditions along the Matanuska Glacier; show general nearshore ice conditions and coastal geomorphology along Alaska's north shore; and delineate coastal wetlands vegetation along Knik Arm. These results suggest that the ERS-1 SAR imagery will be a valuable source of environmental data for addressing water supply in cold regions, for glacial monitoring, for coastal navigation, and for assessing wetland conditions. ESA

N94-12529# Consejo Superior de Investigaciones Cientificas, Barcelona (Spain). Inst. de Ciencies del Mar.

COMPARISON OF ERS-1 SAR IMAGES OF THE WESTERN MEDITERRANEAN TO IN SITU OCEANOGRAPHIC DATA: PRIM-1 CRUISE (MAY 1992) **c48**

J. Font, A. Martinez, E. G. Gorriz, E. Garcia (Universidad de Palma de Mallorca, Spain.), A. Castellon, A. Julia, M. Manriquez, A. Viudez (Universidad de Palma de Mallorca, Spain.), and M. R. Vitria *In* ESA, Proceedings of 1st ERS-1 Symposium on Space at the Service of Our Environment, Volume 2 Mar. 1993 p 883-887 Sponsored by Spanish National Program on Marine Resources and INISEL Espacio (For primary document see N94-12471 01-43)

Copyright Avail: CASI HC A01/MF A03; EPD, ESA, ESTEC, Noordwijk, Netherlands, HC

An ERS-1 project to evaluate the ERS-1 microwave sensors capability in the study of oceanic fronts which aimed at observing the location and evolution of surface density structures in the western Mediterranean by using Synthetic Aperture Radar (SAR) imagery and altimetry is addressed. The mesoscale dynamics related to salinity gradients play a major role in delineating the regional general circulation. Mesoscale eddies were observed in ERS-1 SAR images in Nov. 1991, and a comparison of in situ data to SAR scenes in a shelf/slope area of the north west Mediterranean was made. Complex structures were observed to be related to the influence of a submarine canyon on an alongslope flow. ESA

N94-12530# Observatoire de la Cote d'Azur, Nice (France).

REGIONAL ORBIT PRECISION IN THE MEDITERRANEAN AREA **c13**

P. Bonnefond, P. Exertier, F. Barlier, and Y. Boudon *In* ESA, Proceedings of 1st ERS-1 Symposium on Space at the Service of Our Environment, Volume 2 Mar. 1993 p 889-891 (For primary document see N94-12471 01-43)

Copyright Avail: CASI HC A01/MF A03; EPD, ESA, ESTEC, Noordwijk, Netherlands, HC

The determination, with the best possible accuracy, of the orbit of an oceanographic satellite like ERS-1 with an onboard altimeter is discussed. The tracking system is the laser network. The radial component of the position vector of the satellite is of particular importance. In the Mediterranean area for ERS-1 an accuracy better than 10 cm can be obtained, and in some cases, for which the geometry of the tracking network is favorable, this accuracy can be of the order of 5 cm. ESA

N94-12531# Chilworth Research Centre, Southampton (England). Centre for Ocean Circulation.

TOPOGRAPHY OF THE WESTERN MEDITERRANEAN FROM THE ERS-1 ALTIMETER

T. H. Guymer and R. T. Tokmakian *In* ESA, Proceedings of 1st ERS-1 Sympsoium on Space at the Service of Our Environment, Volume 2 Mar. 1993 p 893-898 (For primary document see N94-12471 01-43)

Copyright Avail: CASI HC A02/MF A03; EPD, ESA, ESTEC, Noordwijk, Netherlands, HC

A preliminary analysis of ERS-1 altimeter height data in the western Mediterranean was conducted using all available off line data in the Algero-Provencale Basin. Sea level variability is shown to be 5 cm or less and it is suggested, in line with previous work, that the region is suitable for calibration of the altimeter height measurements. Further examination of the height residuals, however, showed that they may contain oceanographic information. In particular, features were found in the southern portion of the Basin which are consistent with the migration of mesoscale eddies from the Algerian Current, as is known to happen. The observed features cannot be explained by errors in the altimeter corrections. ESA

N94-10679# Bangladesh Space Research and Remote Sensing Organization, Dhaka.

SPACE RESEARCH AND REMOTE SENSING PROGRAMMES IN BANGLADESH

A. K. M. Fariduddin Bhuiyan *In* Science and Technology Agency, Space Activities in the Asia Pacific Region 16 Nov. 1992 p 20-23 Original language document was announced as N93-21271 (For primary document see N94-10676 01-12)

Avail: CASI HC A01/MF A01

N94-10687# Department of Environment and Natural Resources, Quezon City (Philippines).

STATUS OF REMOTE SENSING AND GEOGRAPHIC INFORMATION SYSTEM (GIS) APPLICATIONS IN THE ENVIRONMENT AND NATURAL RESOURCES (ENR) SECTOR

Ricardo M. Umali *In* Science and Technology Agency, Space Activities in the Asia Pacific Region 16 Nov. 1992 p 45-47 Original language document was announced as N93-21279 (For primary document see N94-10676 01-12)

Avail: CASI HC A01/MF A01

N94-10688# Academy of Sciences (USSR), Moscow. Inst. of Radio Engineering and Electronics.

RUSSIAN SPACE SYSTEM FOR THE EARTH REMOTE SENSING

Neon A. Armand *In* Science and Technology Agency, Space Activities in the Asia Pacific Region 16 Nov. 1992 p 48-51 Original language document was announced as N93-21280 (For primary document see N94-10676 01-12)

Avail: CASI HC A01/MF A01

N94-11080# Meteorological Satellite Center, Tokyo (Japan).

FINE TUNING OF STRETCHED-VISSR IMAGE MAPPING

Seiichiro Kigawa *In its* Meteorological Satellite Center Mar. 1993 p 1-10 (For primary document see N94-11079 01-42)

Avail: CASI HC A02/MF A01

N94-11081# Meteorological Satellite Center, Tokyo (Japan).

SIMULATION OF IMAGES OF WATER VAPOR CHANNEL AND INFRARED SPLIT CHANNEL

Masami Tokuno *In its* Meteorological Satellite Center Mar. 1993 p 11-34 In JAPANESE (For primary document see N94-11079 01-42)

Avail: CASI HC A03/MF A01

N94-11083# Meteorological Satellite Center, Tokyo (Japan).

OVERVIEW OF TRAINING SEMINAR FOR THE USE OF JAPANESE EARTH RESOURCES SATELLITE-1 (JERS-1) DATA

Haruo Taguchi *In its* Meteorological Satellite Center Mar. 1993 p 49-59 In JAPANESE (For primary document see N94-11079 01-42)

Avail: CASI HC A03/MF A01

N94-11837# Nobeyema Solar Radio Observatory (Japan).

SUBMILLIMETER WAVE OBSERVATION EXPERIMENT OF EARTH ATMOSPHERE WITH SIS MIXER [SIS MIKISA NI YORU SABUMIRIHA KANSOKU JIKKEN]

Junji Inatani, Suguru Noguchi, Kentarou Kawaguchi, Harunobu Masuko (Ministry of Posts and Telecommunications, Tokyo, Japan.), and Satoshi Ochiai (Ministry of Posts and Telecommunications, Tokyo, Japan.) *In* NASDA, The Second Workshop on Refrigerating System Utilization Onboard the JEM 31 Mar. 1993 p 89-103 In JAPANESE (For primary document see N94-11831 01-31)

Avail: CASI HC A03/MF A02

N94-11895 Science Council of Japan, Tokyo.

REMOTE SENSING AND GLOBAL ENVIRONMENT

Jirou Kondou *In* Scientific Organizing Committee of PORSEC, Proceedings

of the PORSEC 1992 in Okinawa: Conference for Pacific Ocean Environments and Probing, Volume 1 25 Aug. 1992 p 1-8 (For primary document see N94-11894 01-42)
Copyright Avail: Issuing Activity (Scientific Organizing Committee of PORSEC, P.O. Box 10, Shimizu, Shizuoka 424, Japan, HC)

N94-11896 Tohoku Univ., Sendai (Japan). Dept. of Geophysics.
REMOTE SENSING AND THE AIR-SEA BOUNDARY LAYERS
Yoshiaki Toba *In* Scientific Organizing Committee of PORSEC, Proceedings of the PORSEC 1992 in Okinawa: Conference for Pacific Ocean Environments and Probing, Volume 1 25 Aug. 1992 p 9-14 (For primary document see N94-11894 01-42)
Copyright Avail: Issuing Activity (Scientific Organizing Committee of PORSEC, P.O. Box 10, Shimizu, Shizuoka 424, Japan, HC)

N94-11909 Nihon Univ., Tokyo (Japan). Dept. of Fisheries.
A CONSIDERATION ON PRINCIPAL COMPONENT ANALYSIS OF SATELLITE IR DATA
H. Shinomiya, F. Inoue (Nihon Univ., Funabashi, Japan.), A. Itou (Nihon Univ., Funabashi, Japan.), Hideo Tameishi (Japan Fisheries Information Service Center, Tokyo.), Hiromichi Yamamoto (National Aerospace Lab., Tokyo, Japan.), and Masao Naka (National Aerospace Lab., Tokyo, Japan.) *In* Scientific Organizing Committee of PORSEC, Proceedings of the PORSEC 1992 in Okinawa: Conference for Pacific Ocean Environments and Probing, Volume 1 25 Aug. 1992 p 89-94 (For primary document see N94-11894 01-42)
Copyright Avail: Issuing Activity (Scientific Organizing Committee of PORSEC, P.O. Box 10, Shimizu, Shizuoka 424, Japan, HC)

N94-11910 Ryukyu Univ., Okinawa (Japan).
TROUBLE AREAS IN THE IRT MEASUREMENT OF THE EARTH SURFACE TEMPERATURE
Suguru Ishijima *In* Scientific Organizing Committee of PORSEC, Proceedings of the PORSEC 1992 in Okinawa: Conference for Pacific Ocean Environments and Probing, Volume 1 25 Aug. 1992 p 95-99 (For primary document see N94-11894 01-42)
Copyright Avail: Issuing Activity (Scientific Organizing Committee of PORSEC, P.O. Box 10, Shimizu, Shizuoka 424, Japan, HC)

N94-11928 National Center for Scientific Research of Vietnam, Hanoi.
SHORELINE CHANGE DETECTION USING REMOTE SENSING AND GIS IN VIETNAM
Pham Trung Luong and To Quang Thinh *In* Scientific Organizing Committee of PORSEC, Proceedings of the PORSEC 1992 in Okinawa: Conference for Pacific Ocean Environments and Probing, Volume 1 25 Aug. 1992 p 193-198 Prepared in cooperation with State Dept. for Geodesy and Cartography, Vietnam (For primary document see N94-11894 01-42)
Copyright Avail: Issuing Activity (Scientific Organizing Committee of PORSEC, P.O. Box 10, Shimizu, Shizuoka 424, Japan, HC)

N94-11929 Allan (T. D.) Associates, Godalming (England).
THE REQUIREMENT FOR GLOBAL TRAINING PROGRAMMES TO MEET THE NEW REMOTE SENSING TECHNOLOGY
T. D. Allan *In* Scientific Organizing Committee of PORSEC, Proceedings of the PORSEC 1992 in Okinawa: Conference for Pacific Ocean Environments and Probing, Volume 1 25 Aug. 1992 p 199-204 (For primary document see N94-11894 01-42)
Copyright Avail: Issuing Activity (Scientific Organizing Committee of PORSEC, P.O. Box 10, Shimizu, Shizuoka 424, Japan, HC)

N94-11932 Sydney Univ. (Australia). Ocean Technology Group.
OCEAN WAVE DETECTION BY SAR
Ian S. F. Jones *In* Scientific Organizing Committee of PORSEC, Proceedings of the PORSEC 1992 in Okinawa: Conference for Pacific Ocean Environments and Probing, Volume 1 25 Aug. 1992 p 217-222 (For primary document see N94-11894 01-42)
Copyright Avail: Issuing Activity (Scientific Organizing Committee of PORSEC, P.O. Box 10, Shimizu, Shizuoka 424, Japan, HC)

N94-11934 Qingdao Inst. of Oceanology (China). Ocean Remote Sensing and Ocean Optics Lab.
THE OPTICAL/COMPUTER HYBRID PROCESSING OF EXTRACTING OCEAN WAVE DIRECTIONAL SPECTRUM BY AIRBORNE PHOTOGRAPH
Ming Xia He, Chao Fang Zhao, Xiao Dong Zhang, and Hui Fang *In* Scientific Organizing Committee of PORSEC, Proceedings of the PORSEC 1992 in Okinawa: Conference for Pacific Ocean Environments and Probing, Volume 1 25 Aug. 1992 p 229-236 (For primary document see N94-11894 01-42)
Copyright Avail: Issuing Activity (Scientific Organizing Committee of PORSEC, P.O. Box 10, Shimizu, Shizuoka 424, Japan, HC)

N94-11943 Science Univ. of Tokyo, Chiba (Japan). Faculty of Science and Technology.
CHARACTERISTIC SCALES AND VORTEX FEATURES OF MESOSCALE VORTICES OBSERVED BY THE SATELLITES DURING THE WINTER
Yuuichi Miura *In* Scientific Organizing Committee of PORSEC, Proceedings of the PORSEC 1992 in Okinawa: Conference for Pacific Ocean Environments and Probing, Volume 1 25 Aug. 1992 p 287-292 Sponsored by Tokyo Univ. (For primary document see N94-11894 01-42)
Copyright Avail: Issuing Activity (Scientific Organizing Committee of PORSEC, P.O. Box 10, Shimizu, Shizuoka 424, Japan, HC)

N94-11946 Office de la Recherche Scientifique et Technique Outre-Mer, Noumea (New Caledonia). FLUPAC Group.
THE USE OF CZCS FOR PRIMARY PRODUCTION ESTIMATE IN THE PACIFIC
C. Dupouy, H. Oiry, A. LeBouteiller, and M. Rodier *In* Scientific Organizing Committee of PORSEC, Proceedings of the PORSEC 1992 in Okinawa: Conference for Pacific Ocean Environments and Probing, Volume 1 25 Aug. 1992 p 305-312 (For primary document see N94-11894 01-42)
Copyright Avail: Issuing Activity (Scientific Organizing Committee of PORSEC, P.O. Box 10, Shimizu, Shizuoka 424, Japan, HC)

N94-11949 Kinki Univ., Osaka (Japan).
SATELLITE-DERIVED OCEANIC FEATURES
Itaru Sano and Sonoyo Mukai *In* Scientific Organizing Committee of PORSEC, Proceedings of the PORSEC 1992 in Okinawa: Conference for Pacific Ocean Environments and Probing, Volume 1 25 Aug. 1992 p 325-329 (For primary document see N94-11894 01-42)
Copyright Avail: Issuing Activity (Scientific Organizing Committee of PORSEC, P.O. Box 10, Shimizu, Shizuoka 424, Japan, HC)

N94-11951 Tokai Univ., Shizuoka (Japan). School of High-Technology for Human Welfare.
HIGH-REFLECTANCE WATER MASS IN OFF-SANRIKU AREA OBSERVED BY CZCS
Hajime Fukushima *In* Scientific Organizing Committee of PORSEC, Proceedings of the PORSEC 1992 in Okinawa: Conference for Pacific Ocean Environments and Probing, Volume 1 25 Aug. 1992 p 336-340 (For primary document see N94-11894 01-42)
(Grant MOE-03248216)
Copyright Avail: Issuing Activity (Scientific Organizing Committee of PORSEC, P.O. Box 10, Shimizu, Shizuoka 424, Japan, HC)

N94-11952 Tohoku Univ., Sendai (Japan). Dept. of Geophysics.
PHYSICAL PROCESSES OF MICROWAVE BACKSCATTERING FROM LABORATORY WIND-WAVE SURFACES
Naoto Ebuchi, Hiroshi Kawamura, and Yoshiaki Toba *In* Scientific Organizing Committee of PORSEC, Proceedings of the PORSEC 1992 in Okinawa: Conference for Pacific Ocean Environments and Probing, Volume 1 25 Aug. 1992 p 341-346 (For primary document see N94-11894 01-42)
Copyright Avail: Issuing Activity (Scientific Organizing Committee of PORSEC, P.O. Box 10, Shimizu, Shizuoka 424, Japan, HC)

N94-11953 Consiglio Nazionale delle Ricerche, Venice (Italy). Ist. Studio Dinamica Grandi Masse.
EXPERIMENT AND RESULTS OF THE ITALIAN ACTIVITY IN THE FIELD OF OCEAN MICROWAVE BACKSCATTERING
Stefano Zecchetto and Paolo Trivero (Consiglio Nazionale delle Ricerche,

Turin, Italy.) *In* Scientific Organizing Committee of PORSEC, Proceedings of the PORSEC 1992 in Okinawa: Conference for Pacific Ocean Environments and Probing, Volume 1 25 Aug. 1992 p 347-352 Sponsored by Agenzia Spaziale Italiana (For primary document see N94-11894 01-42)
Copyright Avail: Issuing Activity (Scientific Organizing Committee of PORSEC, P.O. Box 10, Shimizu, Shizuoka 424, Japan, HC)

N94-11954 Ministry of Posts and Telecommunications, Kashima (Japan). Kashima Space Research Center.
MEASUREMENTS OF OCEAN CROSS-SECTION WITH A SIDE-LOOKING AIRBORNE RADAR
Hiroaki Horie and Kenji Nakamura *In* Scientific Organizing Committee of PORSEC, Proceedings of the PORSEC 1992 in Okinawa: Conference for Pacific Ocean Environments and Probing, Volume 1 25 Aug. 1992 p 353-356 (For primary document see N94-11894 01-42)
Copyright Avail: Issuing Activity (Scientific Organizing Committee of PORSEC, P.O. Box 10, Shimizu, Shizuoka 424, Japan, HC)

N94-11956 Washington Univ., Seattle. Dept. of Atmospheric Sciences.
SCATTEROMETER OBSERVATIONS: REVIEW
Robert A. Brown *In* Scientific Organizing Committee of PORSEC, Proceedings of the PORSEC 1992 in Okinawa: Conference for Pacific Ocean Environments and Probing, Volume 1 25 Aug. 1992 p 363-368 (For primary document see N94-11894 01-42)
Copyright Avail: Issuing Activity (Scientific Organizing Committee of PORSEC, P.O. Box 10, Shimizu, Shizuoka 424, Japan, HC)

N94-11957 Remote Sensing Systems, Inc., Santa Rosa, CA.
DEPENDENCE OF OCEANIC MICROWAVE EMISSION ON WIND DIRECTION
Frank J. Wentz *In* Scientific Organizing Committee of PORSEC, Proceedings of the PORSEC 1992 in Okinawa: Conference for Pacific Ocean Environments and Probing, Volume 1 25 Aug. 1992 p 369-374 (For primary document see N94-11894 01-42)
Copyright Avail: Issuing Activity (Scientific Organizing Committee of PORSEC, P.O. Box 10, Shimizu, Shizuoka 424, Japan, HC)

N94-11958 Kyoto Univ., Sakyoku (Japan). Geophysical Inst.
SURFACE ROUGHNESS VARIATIONS ACROSS THE ICELAND-FAROES FRONTAL REGION OBSERVED BY THE GEOSAT ALTIMETER AND NOAA AVHRR
Kaoru Ichikawa, John P. Matthews (University Coll. of North Wales, Bangor.), and Stephen B. Groom (Natural Environmental Research Council, Swindon, England.) *In* Scientific Organizing Committee of PORSEC, Proceedings of the PORSEC 1992 in Okinawa: Conference for Pacific Ocean Environments and Probing, Volume 1 25 Aug. 1992 p 375-380 (For primary document see N94-11894 01-42)
Copyright Avail: Issuing Activity (Scientific Organizing Committee of PORSEC, P.O. Box 10, Shimizu, Shizuoka 424, Japan, HC)

N94-11959 Kyushu Univ., Fukuoka (Japan). Research Inst. for Applied Mechanics.
THE MICROWAVE BACKSCATTERING FROM WIND WAVES
H. Mitsuyasu, T. Kusaba, K. Marubayashi, and M. Ishibashi *In* Scientific Organizing Committee of PORSEC, Proceedings of the PORSEC 1992 in Okinawa: Conference for Pacific Ocean Environments and Probing, Volume 1 25 Aug. 1992 p 381-386 (For primary document see N94-11894 01-42)
Copyright Avail: Issuing Activity (Scientific Organizing Committee of PORSEC, P.O. Box 10, Shimizu, Shizuoka 424, Japan, HC)

N94-11960 Tohoku Univ., Sendai (Japan). Center for Atmospheric and Oceanic Studies.
ON THE VARIABILITY OF WIND SPEEDS IN THE NORTH WESTERN PACIFIC OBSERVED BY ALTIMETER/GEOSAT AND SSM/I/DMSP
Hiroshi Kawamura *In* Scientific Organizing Committee of PORSEC, Proceedings of the PORSEC 1992 in Okinawa: Conference for Pacific Ocean Environments and Probing, Volume 1 25 Aug. 1992 p 387-391 (For primary document see N94-11894 01-42)
Copyright Avail: Issuing Activity (Scientific Organizing Committee of PORSEC, P.O. Box 10, Shimizu, Shizuoka 424, Japan, HC)

N94-11961 Tohoku Univ., Sendai (Japan). Dept. of Geophysics.
OBSERVATION OF WIND AND WAVES BY GEOSAT ALTIMETER
Naoto Ebuchi, Hiroshi Kawamura, and Yoshiaki Toba *In* Scientific Organizing Committee of PORSEC, Proceedings of the PORSEC 1992 in Okinawa: Conference for Pacific Ocean Environments and Probing, Volume 1 25 Aug. 1992 p 392-397 (For primary document see N94-11894 01-42)
Copyright Avail: Issuing Activity (Scientific Organizing Committee of PORSEC, P.O. Box 10, Shimizu, Shizuoka 424, Japan, HC)

N94-11970 Qingdao Inst. of Oceanology (China). Ocean Remote Sensing and Ocean Optics Lab.
REMOTE SENSING OF SUBSURFACE WATER TEMPERATURE PROFILE AND BACKSCATTERING COEFFICIENT IN THE CHINA SEA BY OCEAN LIDAR (OLIDAR)
Zhi-Shen Liu, Jin-Long Zhang, Wen-Zhong Chen, Xiao-Sheng Huang, and Jun Ma *In* Scientific Organizing Committee of PORSEC, Proceedings of the PORSEC 1992 in Okinawa: Conference for Pacific Ocean Environments and Probing, Volume 1 25 Aug. 1992 p 437-443 Sponsored by China National Foundation of Natural Science (For primary document see N94-11894 01-42)
(Grant SSTC-75760605)
Copyright Avail: Issuing Activity (Scientific Organizing Committee of PORSEC, P.O. Box 10, Shimizu, Shizuoka 424, Japan, HC)

N94-11971 Paris VI Univ., Villefranche-sur-Mer (France). Lab. de Physique et Chimie Marines.
BI-DIRECTIONAL REFLECTANCE BY OCEANIC WATERS STUDIED VIA MONTE-CARLO SIMULATIONS
Andre Morel and Bernard Gentili *In* Scientific Organizing Committee of PORSEC, Proceedings of the PORSEC 1992 in Okinawa: Conference for Pacific Ocean Environments and Probing, Volume 1 25 Aug. 1992 p 444-445 (For primary document see N94-11894 01-42)
Copyright Avail: Issuing Activity (Scientific Organizing Committee of PORSEC, P.O. Box 10, Shimizu, Shizuoka 424, Japan, HC)

N94-11973 Jawaharlal Nehru Technological Univ., Hyderabad (India).
REMOTE SENSING FOR NUMERICAL MODELLING OF RADIATIVE TRANSFER PROCESSES IN OCEAN ENVIRONMENT
I. V. Muralikrishna *In* Scientific Organizing Committee of PORSEC, Proceedings of the PORSEC 1992 in Okinawa: Conference for Pacific Ocean Environments and Probing, Volume 1 25 Aug. 1992 p 452-459 (For primary document see N94-11894 01-42)
Copyright Avail: Issuing Activity (Scientific Organizing Committee of PORSEC, P.O. Box 10, Shimizu, Shizuoka 424, Japan, HC)

N94-11975* Miami Univ., Coral Gables, FL. Dept. of Physics.
ATMOSPHERIC CORRECTION PLANS FOR SeaWiFS
Howard R. Gordon *In* Scientific Organizing Committee of PORSEC, Proceedings of the PORSEC 1992 in Okinawa: Conference for Pacific Ocean Environments and Probing, Volume 1 25 Aug. 1992 p 465-470 (For primary document see N94-11894 01-42)
(Contracts NAS5-30911; NAS5-31363; NAS5-31734; NAGw-273)
Copyright Avail: Issuing Activity (Scientific Organizing Committee of PORSEC, P.O. Box 10, Shimizu, Shizuoka 424, Japan, HC)

N94-11976 Hokkaido Univ., Sapporo (Japan). Dept. of Marine Sciences and Technology.
DISTRIBUTION OF MINERAL AEROSOLS OVER THE NORTH PACIFIC
Mitsuo Uematsu and Sei-Ichi Saitou (Japan Weather Association, Tokyo.) *In* Scientific Organizing Committee of PORSEC, Proceedings of the PORSEC 1992 in Okinawa: Conference for Pacific Ocean Environments and Probing, Volume 1 25 Aug. 1992 p 471-475 (For primary document see N94-11894 01-42)
Copyright Avail: Issuing Activity (Scientific Organizing Committee of PORSEC, P.O. Box 10, Shimizu, Shizuoka 424, Japan, HC)

N94-11978 Kinki Univ., Osaka (Japan).
IMPLICATIONS OF AEROSOL RETRIEVAL AND ATMOSPHERIC CORRECTION IN REMOTE SENSING
Sonoyo Mukai and Itaru Sano *In* Scientific Organizing Committee of PORSEC, Proceedings of the PORSEC 1992 in Okinawa: Conference for

Pacific Ocean Environments and Probing, Volume 1 25 Aug. 1992 p 478-482 (For primary document see N94-11894 01-42)
Copyright Avail: Issuing Activity (Scientific Organizing Committee of PORSEC, P.O. Box 10, Shimizu, Shizuoka 424, Japan, HC)

N94-11982 Hirosaki Univ. (Japan). Dept. of Earth Science.
INCIDENT SHORTWAVE AND LONGWAVE RADIATIONS OVER THE WESTERN NORTH PACIFIC AND THE SEA OF OKHOTSK DERIVED FROM GMS-WEFAX IMAGES
Yasumasa Kodama *In* Scientific Organizing Committee of PORSEC, Proceedings of the PORSEC 1992 in Okinawa: Conference for Pacific Ocean Environments and Probing, Volume 1 25 Aug. 1992 p 501-504 (For primary document see N94-11894 01-42)
Copyright Avail: Issuing Activity (Scientific Organizing Committee of PORSEC, P.O. Box 10, Shimizu, Shizuoka 424, Japan, HC)

N94-11984 Academy of Sciences (USSR), Moscow. Inst. of Oceanology.
OBSERVATIONS OF THE FRACTAL PROPERTIES OF THE JAPAN SEA SURFACE TEMPERATURE PATTERNS
Leonid A. Bunimovich (Georgia Inst. of Tech., Atlanta.), Alexander G. Ostrovskii (Kyushu Univ., Fukuoka, Japan.), and Shin-Ichirou Umatani (Kyushu Univ., Fukuoka, Japan.) *In* Scientific Organizing Committee of PORSEC, Proceedings of the PORSEC 1992 in Okinawa: Conference for Pacific Ocean Environments and Probing, Volume 1 25 Aug. 1992 p 510-515 Sponsored in part by Japan Society for the Promotion of Science (For primary document see N94-11894 01-42)
Copyright Avail: Issuing Activity (Scientific Organizing Committee of PORSEC, P.O. Box 10, Shimizu, Shizuoka 424, Japan, HC)

N94-11989 Remote Sensing Applications Centre, Jakarta (Indonesia).
FLOOD MONITORING IN NORTHERN PART OF CENTRAL JAVA BY REMOTE SENSING TECHNIQUE. CASE STUDY: THE FLOODING OF SEMARANG IN JANUARY, 1990
Sumardjo, Dede Dirgahayu, and Ratih Dewanti *In* Scientific Organizing Committee of PORSEC, Proceedings of the PORSEC 1992 in Okinawa: Conference for Pacific Ocean Environments and Probing, Volume 1 25 Aug. 1992 p 538-549 (For primary document see N94-11894 01-42)
Copyright Avail: Issuing Activity (Scientific Organizing Committee of PORSEC, P.O. Box 10, Shimizu, Shizuoka 424, Japan, HC)

N94-12030*# Arizona State Univ., Tempe. Dept. of Geology.
FOURIER DOMAIN TARGET TRANSFORMATION ANALYSIS IN THE THERMAL INFRARED Abstract Only
D. L. Anderson *In* Lunar and Planetary Inst., Twenty-fourth Lunar and Planetary Science Conference. Part 1: A-F 1993 p 31-32 (For primary document see N94-12015 01-91)
Avail: CASI HC A01/MF A06

N94-12097*# Washington Univ., Saint Louis, MO. Dept. of Earth and Planetary Sciences.
COMPOSITIONAL AND TEXTURAL INFORMATION FROM THE DUAL INVERSION OF VISIBLE, NEAR AND THERMAL INFRARED REMOTELY SENSED DATA Abstract Only
Robert A. Brackett and Raymond E. Arvidson *In* Lunar and Planetary Inst., Twenty-fourth Lunar and Planetary Science Conference. Part 1: A-F 1993 p 169-170 (For primary document see N94-12015 01-91)
Avail: CASI HC A01/MF A06

N94-12638 Toyama National Coll. of Maritime Technology, Shinminato (Japan).
OBSERVATION OF WAVE CRESTS BY SATELLITE REMOTE SENSED DATA
Shigeki Ishimori and Masashi Kawai *In* Scientific Organizing Committee of PORSEC, Proceedings of the PORSEC 1992 in Okinawa: Conference for Pacific Ocean Environments and Probing, Volume 2 25 Aug. 1992 p 572-575 (For primary document see N94-12635 01-42)
Copyright Avail: Issuing Activity (Scientific Organizing Committee of PORSEC, P.O. Box 10, Shimizu, Shizuoka 424, Japan, HC)

N94-12639 Tokai Univ., Shizuoka (Japan). School of Marine Science and Technology.
OBSERVATIONS OF EDDY FIELDS IN THE NORTHWEST PACIFIC BY GEOSAT ALTIMETRY
Jun Suwa, Akira Mukaida, and Yasuhiro Sugimori *In* Scientific Organizing Committee of PORSEC, Proceedings of the PORSEC 1992 in Okinawa: Conference for Pacific Ocean Environments and Probing, Volume 2 25 Aug. 1992 p 576-581 (For primary document see N94-12635 01-42)
Copyright Avail: Issuing Activity (Scientific Organizing Committee of PORSEC, P.O. Box 10, Shimizu, Shizuoka 424, Japan, HC)

N94-12641* Jet Propulsion Lab., California Inst. of Tech., Pasadena.
THEORY AND OCEANOGRAPHIC APPLICATIONS OF SATELLITE ALTIMETER MEASUREMENTS
Roman E. Glazman *In* Scientific Organizing Committee of PORSEC, Proceedings of the PORSEC 1992 in Okinawa: Conference for Pacific Ocean Environments and Probing, Volume 2 25 Aug. 1992 p 587-590 (For primary document see N94-12635 01-42)
Copyright Avail: Issuing Activity (Scientific Organizing Committee of PORSEC, P.O. Box 10, Shimizu, Shizuoka 424, Japan, HC)

N94-12642 Sydney Univ. (Australia).
ANALYSIS OF COLLINEAR PASSES OF SATELLITE ALTIMETER DATA
Richard Coleman, Herman VanGysen (Natal Univ., Durban, South Africa.), Rosemary Morrow, and Neil White (Commonwealth Scientific and Industrial Research Organization, Sydney, Australia.) *In* Scientific Organizing Committee of PORSEC, Proceedings of the PORSEC 1992 in Okinawa: Conference for Pacific Ocean Environments and Probing, Volume 2 25 Aug. 1992 p 591-596 Sponsored by Australian Research Council, Belconnen, Australia (For primary document see N94-12635 01-42)
Copyright Avail: Issuing Activity (Scientific Organizing Committee of PORSEC, P.O. Box 10, Shimizu, Shizuoka 424, Japan, HC)

N94-12643 Sydney Univ. (Australia). Marine Studies Centre.
SURFACE EDDY FLUXES FROM THE GEOSAT SATELLITE ALTIMETER
Rosemary Morrow, John Church (Commonwealth Scientific and Industrial Research Organization, Sydney, Australia.), Richard Coleman, Dudley Chelton (Oregon State Univ., Corvallis.), and Neil White (Commonwealth Scientific and Industrial Research Organization, Sydney, Australia.) *In* Scientific Organizing Committee of PORSEC, Proceedings of the PORSEC 1992 in Okinawa: Conference for Pacific Ocean Environments and Probing, Volume 2 25 Aug. 1992 p 597-602 Sponsored by Australian Research Council, Belconnen, Australia (For primary document see N94-12635 01-42)
Copyright Avail: Issuing Activity (Scientific Organizing Committee of PORSEC, P.O. Box 10, Shimizu, Shizuoka 424, Japan, HC)

N94-12644* Jet Propulsion Lab., California Inst. of Tech., Pasadena.
COMPARISON OF GEOSAT SEA SURFACE HEIGHT AND MODEL-SIMULATED SURFACE DYNAMIC HEIGHT Abstract Only
Y. Chao (California Univ., Los Angeles.) and D. Halpern *In* Scientific Organizing Committee of PORSEC, Proceedings of the PORSEC 1992 in Okinawa: Conference for Pacific Ocean Environments and Probing, Volume 2 25 Aug. 1992 p 603 (For primary document see N94-12635 01-42)
Copyright Avail: Issuing Activity (Scientific Organizing Committee of PORSEC, P.O. Box 10, Shimizu, Shizuoka 424, Japan, HC)

N94-12645 Japan Marine Science and Technology Center, Tokyo.
PSEUDO MAGNETIC ANOMALY DERIVED FROM SATELLITE ALTIMETRY AND ITS APPLICATION TO THE TECTONICS IN THE NORTH FUJI BASIN
Takeshi Matsumoto *In* Scientific Organizing Committee of PORSEC, Proceedings of the PORSEC 1992 in Okinawa: Conference for Pacific Ocean Environments and Probing, Volume 2 25 Aug. 1992 p 604-607 Sponsored by Science and Technology Agency, Tokyo, Japan (For primary document see N94-12635 01-42)
Copyright Avail: Issuing Activity (Scientific Organizing Committee of PORSEC, P.O. Box 10, Shimizu, Shizuoka 424, Japan, HC)

N94-12647 Institute of Ocean Sciences, Sidney (British Columbia).
MEASUREMENT OF EDDY STRUCTURE AND MOVEMENT IN THE NORTH-EAST PACIFIC WITH THE GEOSAT ALTIMETER
J. F. R. Gower and S. Tabata *In* Scientific Organizing Committee of PORSEC, Proceedings of the PORSEC 1992 in Okinawa: Conference for Pacific Ocean Environments and Probing, Volume 2 25 Aug. 1992 p 614-621 (For primary document see N94-12635 01-42)
Copyright Avail: Issuing Activity (Scientific Organizing Committee of PORSEC, P.O. Box 10, Shimizu, Shizuoka 424, Japan, HC)

N94-12648* Jet Propulsion Lab., California Inst. of Tech., Pasadena.
PRELIMINARY RESULTS FROM A SATELLITE ALTIMETRIC DATA ASSIMILATION USING A KALMAN FILTER AND SMOOTHER
Ichirou Fukumori, Lee-Lueng Fu, and Robert N. Miller (Oregon State Univ., Corvallis.) *In* Scientific Organizing Committee of PORSEC, Proceedings of the PORSEC 1992 in Okinawa: Conference for Pacific Ocean Environments and Probing, Volume 2 25 Aug. 1992 p 622-626 (For primary document see N94-12635 01-42)
Copyright Avail: Issuing Activity (Scientific Organizing Committee of PORSEC, P.O. Box 10, Shimizu, Shizuoka 424, Japan, HC)

N94-12649 Kyushu Univ., Fukuoka (Japan). Research Inst. for Applied Mechanics.
FLUCTUATIONS OF THE KUROSHIO EXTENSION DETECTED BY THE GEOSAT ALTIMETRY DATA
Shirou Imawaki, Kaoru Ichikawa, and Shigeru Aoki *In* Scientific Organizing Committee of PORSEC, Proceedings of the PORSEC 1992 in Okinawa: Conference for Pacific Ocean Environments and Probing, Volume 2 25 Aug. 1992 p 627-632 (For primary document see N94-12635 01-42)
Copyright Avail: Issuing Activity (Scientific Organizing Committee of PORSEC, P.O. Box 10, Shimizu, Shizuoka 424, Japan, HC)

N94-12650 Woods Hole Oceanographic Inst., MA. Dept. of Physical Oceanography.
MEAN FLOW AND VARIABILITY IN THE KUROSHIO EXTENSION FROM GEOSAT ALTIMETRY DATA
Bo Qiu, Kathryn A. Kelly, and Terrence M. Joyce *In* Scientific Organizing Committee of PORSEC, Proceedings of the PORSEC 1992 in Okinawa: Conference for Pacific Ocean Environments and Probing, Volume 2 25 Aug. 1992 p 633-638 (For primary document see N94-12635 01-42)
Copyright Avail: Issuing Activity (Scientific Organizing Committee of PORSEC, P.O. Box 10, Shimizu, Shizuoka 424, Japan, HC)

N94-12651* National Aeronautics and Space Administration. Goddard Space Flight Center, Greenbelt, MD.
PACIFIC RIM SEA ICE AS OBSERVED WITH THE NIMBUS-7 SMMR
Per Gloersen, William J. Campbell (Geological Survey, Tacoma, WA.), Donald J. Cavalieri, Josefino C. Comiso, Claire L. Parkinson, and H. Jay Zwally *In* Scientific Organizing Committee of PORSEC, Proceedings of the PORSEC 1992 in Okinawa: Conference for Pacific Ocean Environments and Probing, Volume 2 25 Aug. 1992 p 639-644 (For primary document see N94-12635 01-42)
Copyright Avail: Issuing Activity (Scientific Organizing Committee of PORSEC, P.O. Box 10, Shimizu, Shizuoka 424, Japan, HC)

N94-12653 Nansen Environmental and Remote Sensing Center, Solheimsvik (Norway).
ICE STUDIES IN THE BARENTS SEA BY ERS-1 DURING SIZEX 1992
Stein Sandven and Ola M. Johannessen *In* Scientific Organizing Committee of PORSEC, Proceedings of the PORSEC 1992 in Okinawa: Conference for Pacific Ocean Environments and Probing, Volume 2 25 Aug. 1992 p 651-657 (For primary document see N94-12635 01-42)
Copyright Avail: Issuing Activity (Scientific Organizing Committee of PORSEC, P.O. Box 10, Shimizu, Shizuoka 424, Japan, HC)

N94-12654 Hokkaido Univ. of Education, Kushiro (Japan).
DISINTEGRATING ICE FRONT OF SHIRASE GLACIER, EAST ANTARCTICA
Fumihiko Nishio and Kohei Chou (Remote Sensing Technology Center, Tokyo, Japan.) *In* Scientific Organizing Committee of PORSEC, Proceedings of the PORSEC 1992 in Okinawa: Conference for Pacific Ocean Environments and Probing, Volume 2 25 Aug. 1992 p 658-662 (For primary document see N94-12635 01-42)
Copyright Avail: Issuing Activity (Scientific Organizing Committee of PORSEC, P.O. Box 10, Shimizu, Shizuoka 424, Japan, HC)

N94-12655 Indian Inst. of Tech., Kanpur. Dept. of Civil Engineering.
MICROWAVE RADIOMETRY OF ICE COVER IN POLAR REGIONS
Ashok K. Keshari, Ramesh P. Singh, and Anupma Rastogi *In* Scientific Organizing Committee of PORSEC, Proceedings of the PORSEC 1992 in Okinawa: Conference for Pacific Ocean Environments and Probing, Volume 2 25 Aug. 1992 p 663-668 Sponsored by Ministry of Human Resource Development, New Delhi, India (For primary document see N94-12635 01-42)
Copyright Avail: Issuing Activity (Scientific Organizing Committee of PORSEC, P.O. Box 10, Shimizu, Shizuoka 424, Japan, HC)

N94-12664 Science Univ. of Tokyo, Chiba (Japan). Dept. of Civil Engineering.
STUDY ON DIFFUSION PHENOMENA OF RIVER EFFLUENTS ISSUED INTO SEA AROUND JAPAN WITH SATELLITE REMOTE SENSING DATA
Sotoaki Oonishi and Hiroyasu Kawai *In* Scientific Organizing Committee of PORSEC, Proceedings of the PORSEC 1992 in Okinawa: Conference for Pacific Ocean Environments and Probing, Volume 2 25 Aug. 1992 p 715-720 (For primary document see N94-12635 01-42)
Copyright Avail: Issuing Activity (Scientific Organizing Committee of PORSEC, P.O. Box 10, Shimizu, Shizuoka 424, Japan, HC)

N94-12665 Muroran Inst. of Tech., Mizumoto (Japan). Dept. of Computer Science and Systems Engineering.
A BASIC CONSIDERATION FOR REMOTE SENSING USING MICROWAVE RADARS ON A SATELLITE
Masahiko Hatanaka, Masayuki Hikichi, and Akira Nishitsuji *In* Scientific Organizing Committee of PORSEC, Proceedings of the PORSEC 1992 in Okinawa: Conference for Pacific Ocean Environments and Probing, Volume 2 25 Aug. 1992 p 721-726 (For primary document see N94-12635 01-42)
Copyright Avail: Issuing Activity (Scientific Organizing Committee of PORSEC, P.O. Box 10, Shimizu, Shizuoka 424, Japan, HC)

N94-12666 National Oceanic and Atmospheric Administration, Washington, DC. National Ocean Service.
MIGRATION OF OPERATIONAL ICE ANALYSIS AND FORECASTING TO A WORKSTATION PLATFORM AT THE JOINT ICE CENTER
Robert Andrew Warner and Franklin E. Kniskern *In* Scientific Organizing Committee of PORSEC, Proceedings of the PORSEC 1992 in Okinawa: Conference for Pacific Ocean Environments and Probing, Volume 2 25 Aug. 1992 p 727-730 (For primary document see N94-12635 01-42)
Copyright Avail: Issuing Activity (Scientific Organizing Committee of PORSEC, P.O. Box 10, Shimizu, Shizuoka 424, Japan, HC)

N94-12667 MATRA Marconi Space, Toulouse (France). System and Instrumentation Div.
METEOSAT SECOND GENERATION PROGRAMME SEVIRI: AN ENHANCED VISIBLE AND IR RADIOMETER FOR METEOROLOGY
J. Jouan, P. Hollier, F. Pasternak, and Kunkle (Messerschmitt-Boelkow-Blohm G.m.b.H., Ottobrunn, Germany.) *In* Scientific Organizing Committee of PORSEC, Proceedings of the PORSEC 1992 in Okinawa: Conference for Pacific Ocean Environments and Probing, Volume 2 25 Aug. 1992 p 731-741 Sponsored by ESA, Paris, France (For primary document see N94-12635 01-42)
Copyright Avail: Issuing Activity (Scientific Organizing Committee of PORSEC, P.O. Box 10, Shimizu, Shizuoka 424, Japan, HC)

N94-12668 National Inst. of Agro-Environmental Science, Ibaraki (Japan). Div. of Changing Earth and Agro-Environment.
EVALUATING THE SPREAD OF RED SOIL WITH LANDSAT TM DATA IN CORAL REEFS OF OKINAWA MAIN ISLAND, SOUTHWESTERN JAPAN
Katsuo Okamoto, Ichirou Yamada, Toshiaki Imagawa, and Michikazu Fukuhara *In* Scientific Organizing Committee of PORSEC, Proceedings of the PORSEC 1992 in Okinawa: Conference for Pacific Ocean Environments and Probing, Volume 2 25 Aug. 1992 p 742-747 Prepared

in cooperation with Okinawa Prefecture Agricultural Experimental Station, Okinawa, Japan Original contains color illustrations (For primary document see N94-12635 01-42)
Copyright Avail: Issuing Activity (Scientific Organizing Committee of PORSEC, P.O. Box 10, Shimizu, Shizuoka 424, Japan, HC)

N94-12670 Iwate Univ., Morioka (Japan).
VALIDATION TEST SYSTEM FOR SEA SURFACE TEMPERATURE DETECTED BY SATELLITES IN MUTSU BAY
S. Tanba, T. Souma, M. Konda, I. Yoshida, T. Watanabe, R. Yokoyama, Hironori Maejima, and Korehiro Maeda *In* Scientific Organizing Committee of PORSEC, Proceedings of the PORSEC 1992 in Okinawa: Conference for Pacific Ocean Environments and Probing, Volume 2 25 Aug. 1992 p 751-756 Prepared in cooperation with NASDA, Tokyo, Japan (For primary document see N94-12635 01-42)
Copyright Avail: Issuing Activity (Scientific Organizing Committee of PORSEC, P.O. Box 10, Shimizu, Shizuoka 424, Japan, HC)

N94-12671 Tokyo Metropolitan Fisheries Experiment Station (Japan).
SEA SURFACE TEMPERATURE IMAGES OF GEOSTATIONARY METEOROLOGICAL SATELLITE (GMS) AND SEA TRUTH DATA FROM FERRY BOATS
Tsutomu Chino *In* Scientific Organizing Committee of PORSEC, Proceedings of the PORSEC 1992 in Okinawa: Conference for Pacific Ocean Environments and Probing, Volume 2 25 Aug. 1992 p 757-761 (For primary document see N94-12635 01-42)
Copyright Avail: Issuing Activity (Scientific Organizing Committee of PORSEC, P.O. Box 10, Shimizu, Shizuoka 424, Japan, HC)

N94-12672 Kyoto Univ., Sakyoku (Japan). Dept. of Geophysics.
MEASUREMENT OF THE SEA SURFACE EMISSIVITY
Masanori Konda, Norihisa Imasato, Katsuya Nishi, and Takashi Toda (Shiga Prefecture Board of Education, Japan.) *In* Scientific Organizing Committee of PORSEC, Proceedings of the PORSEC 1992 in Okinawa: Conference for Pacific Ocean Environments and Probing, Volume 2 25 Aug. 1992 p 762-767 (For primary document see N94-12635 01-42)
Copyright Avail: Issuing Activity (Scientific Organizing Committee of PORSEC, P.O. Box 10, Shimizu, Shizuoka 424, Japan, HC)

N94-12675 Academia Sinica, Beijing (China). Inst. of Atmospheric Physics.
DELINEATION OF MESOSCALE FEATURES OF OCEAN ON SATELLITE IR IMAGE
Jun Li and Fengxian Zhou *In* Scientific Organizing Committee of PORSEC, Proceedings of the PORSEC 1992 in Okinawa: Conference for Pacific Ocean Environments and Probing, Volume 2 25 Aug. 1992 p 780-785 (For primary document see N94-12635 01-42)
Copyright Avail: Issuing Activity (Scientific Organizing Committee of PORSEC, P.O. Box 10, Shimizu, Shizuoka 424, Japan, HC)

N94-12678 National Inst. of Oceanography, Goa (India).
SATELLITE OBSERVATIONS OF THE NORTHEAST MONSOON COASTAL CURRENT
S. S. C. Shenoi, A. D. Gouveia, S. R. Shetye, and L. V. G. Rao *In* Scientific Organizing Committee of PORSEC, Proceedings of the PORSEC 1992 in Okinawa: Conference for Pacific Ocean Environments and Probing, Volume 2 25 Aug. 1992 p 796-801 (For primary document see N94-12635 01-42)
Copyright Avail: Issuing Activity (Scientific Organizing Committee of PORSEC, P.O. Box 10, Shimizu, Shizuoka 424, Japan, HC)

N94-12681 Japan Fisheries Information Service Center, Tokyo.
APPLICATION OF NOAA AVHRR DATA TO FISHERIES
Hideo Tameishi, Shin Fujita, and Katsuya Saitou *In* Scientific Organizing Committee of PORSEC, Proceedings of the PORSEC 1992 in Okinawa: Conference for Pacific Ocean Environments and Probing, Volume 2 25 Aug. 1992 p 814-819 (For primary document see N94-12635 01-42)
Copyright Avail: Issuing Activity (Scientific Organizing Committee of PORSEC, P.O. Box 10, Shimizu, Shizuoka 424, Japan, HC)

N94-12682 National Research Inst. of Far Seas Fisheries, Shizuoka (Japan).
STATISTICAL FEATURES OF MESOSCALE EDDIES AT THE KUROSHIO FRONT
Kiyoshi Kawasaki *In* Scientific Organizing Committee of PORSEC, Proceedings of the PORSEC 1992 in Okinawa: Conference for Pacific Ocean Environments and Probing, Volume 2 25 Aug. 1992 p 821-823 (For primary document see N94-12635 01-42)
Copyright Avail: Issuing Activity (Scientific Organizing Committee of PORSEC, P.O. Box 10, Shimizu, Shizuoka 424, Japan, HC)

N94-12684 Taiwan Fisheries Research Inst., Tungkang.
A STUDY OF FRONT DYNAMICS OFF NORTHEASTERN TAIWAN BASED ON THE NOAA-AVHRR SATELLITE REMOTE SENSING DATA
Chung-Zen Shyu, Wen-Hung Shih, and Chi-Yuan Lin *In* Scientific Organizing Committee of PORSEC, Proceedings of the PORSEC 1992 in Okinawa: Conference for Pacific Ocean Environments and Probing, Volume 2 25 Aug. 1992 p 829-834 (For primary document see N94-12635 01-42) (Grant NSC-80-0209-M056-01)
Copyright Avail: Issuing Activity (Scientific Organizing Committee of PORSEC, P.O. Box 10, Shimizu, Shizuoka 424, Japan, HC)

N94-12695 Concepcion Univ. (Chile). Oceanography Dept.
REMOTE SENSING OF POLLUTING FOCAL POINTS AND COASTAL DISTURBANCES IN THE GULF OF ARAUCO AND ADJACENT BAYS, CENTRAL CHILE
J. Stuardo, C. Valdovinos, and C. Pampaloni *In* Scientific Organizing Committee of PORSEC, Proceedings of the PORSEC 1992 in Okinawa: Conference for Pacific Ocean Environments and Probing, Volume 2 25 Aug. 1992 p 892-897 (For primary document see N94-12635 01-42)
Copyright Avail: Issuing Activity (Scientific Organizing Committee of PORSEC, P.O. Box 10, Shimizu, Shizuoka 424, Japan, HC)

N94-12697 Indian Inst. of Remote Sensing, Dehra Dun.
ROLE OF REMOTE SENSING AND ITS COST EFFECTIVENESS IN SITE SELECTION FOR COASTAL AQUACULTURE
R. Sudarshana and M. S. Siddiqui *In* Scientific Organizing Committee of PORSEC, Proceedings of the PORSEC 1992 in Okinawa: Conference for Pacific Ocean Environments and Probing, Volume 2 25 Aug. 1992 p 904-909 (For primary document see N94-12635 01-42)
Copyright Avail: Issuing Activity (Scientific Organizing Committee of PORSEC, P.O. Box 10, Shimizu, Shizuoka 424, Japan, HC)

N94-12700 Ryukyu Univ., Okinawa (Japan). Coll. of Agriculture.
PROPERTIES OF SPECTRAL REFLECTANCE OF CROWN AND CROWN STRUCTURE OF MANGROVE SPECIES IN OKINAWA
Kazuhiro Satou, Dwi Setyono, Osmar DeMoraes (Empresa Brasileira de Pesquisa Agropecuaria, Santa Catarina.), and Takashi Hoshi (Ibaraki Univ., Hitachi, Japan.) *In* Scientific Organizing Committee of PORSEC, Proceedings of the PORSEC 1992 in Okinawa: Conference for Pacific Ocean Environments and Probing, Volume 2 25 Aug. 1992 p 922-927 (For primary document see N94-12635 01-42)
Copyright Avail: Issuing Activity (Scientific Organizing Committee of PORSEC, P.O. Box 10, Shimizu, Shizuoka 424, Japan, HC)

N94-12701 Diponegoro Univ., Jepara (Indonesia). Coastal Region Eco-Development Lab.
APPLICATION OF REMOTE SENSING FOR COASTAL MANAGEMENT IN THE NORTH COAST OF JAVA
A. Hartoko and D. Suprapto *In* Scientific Organizing Committee of PORSEC, Proceedings of the PORSEC 1992 in Okinawa: Conference for Pacific Ocean Environments and Probing, Volume 2 25 Aug. 1992 p 928-935 (For primary document see N94-12635 01-42)
Copyright Avail: Issuing Activity (Scientific Organizing Committee of PORSEC, P.O. Box 10, Shimizu, Shizuoka 424, Japan, HC)

N94-12703 Kitami Inst. of Tech., Hokkaido (Japan). Dept. of Developmental Engineering.
ESTIMATION OF AREAL EVAPOTRANSPIRATION USING LANDSAT TM DATA: KITAMI CITY, HOKKAIDO, JAPAN
Kimiteru Sado *In* Scientific Organizing Committee of PORSEC, Proceedings of the PORSEC 1992 in Okinawa: Conference for Pacific Ocean

Environments and Probing, Volume 2 25 Aug. 1992 p 940-945 Original contains color illustrations (For primary document see N94-12635 01-42)
Copyright Avail: Issuing Activity (Scientific Organizing Committee of PORSEC, P.O. Box 10, Shimizu, Shizuoka 424, Japan, HC)

N94-12704 Plan and Budget Organization, Teheran (Iran). Remote Sensing Center.
LAND USE/LAND COVER MAPPING OF CENTRAL WATER SHED OF IRAN AREA BASED ON SATELLITE DATA INTERPRETATION
Kiadokhi Ahmadi Soroush *In* Scientific Organizing Committee of PORSEC, Proceedings of the PORSEC 1992 in Okinawa: Conference for Pacific Ocean Environments and Probing, Volume 2 25 Aug. 1992 p 946-951 (For primary document see N94-12635 01-42)
Copyright Avail: Issuing Activity (Scientific Organizing Committee of PORSEC, P.O. Box 10, Shimizu, Shizuoka 424, Japan, HC)

N94-12705 Nippon Koei Co. Ltd., Tokyo (Japan).
A METHOD TO MINIMIZE REFERENCE DATA IN CLASSIFYING SATELLITE REMOTE SENSING DATA INTO LAND COVER CLASSES
L. Samarakoon, H. Ohara (Saga Univ., Japan.), R. Lapitan (Ehime Univ., Matsuyama, Japan.), S. Inoue (Ehime Univ., Matsuyama, Japan.), N. Ebisu (Ehime Univ., Matsuyama, Japan.), S. Ogawa (Ehime Univ., Matsuyama, Japan.), and N. Kishihara (Saga Univ., Japan.) *In* Scientific Organizing Committee of PORSEC, Proceedings of the PORSEC 1992 in Okinawa: Conference for Pacific Ocean Environments and Probing, Volume 2 25 Aug. 1992 p 952-957 (For primary document see N94-12635 01-42)
Copyright Avail: Issuing Activity (Scientific Organizing Committee of PORSEC, P.O. Box 10, Shimizu, Shizuoka 424, Japan, HC)

N94-12714 Central Research Inst. of Electric Power Industry, Tokyo (Japan).
APPLICABILITY OF SATELLITE INFRARED DATA FOR THE MONITORING OF COASTAL ENVIRONMENTS
Shinichi Sakai, Masafumi Mizutori, and Norikazu Nakashiki *In* Scientific Organizing Committee of PORSEC, Proceedings of the PORSEC 1992 in Okinawa: Conference for Pacific Ocean Environments and Probing, Volume 2 25 Aug. 1992 p 1010-1015 (For primary document see N94-12635 01-42)
Copyright Avail: Issuing Activity (Scientific Organizing Committee of PORSEC, P.O. Box 10, Shimizu, Shizuoka 424, Japan, HC)

N94-12715 Japan Weather Association, Tokyo. Meteorological Information Center.
SATELLITE AND MOORED BUOY OBSERVATIONS OF POLAR FRONTAL SYSTEM OVER THE YAMATO RISE IN THE JAPAN SEA
Seiichi Saitou, Masafumi Ichikawa, Kouzou Okada, and Yutaka Isoda *In* Scientific Organizing Committee of PORSEC, Proceedings of the PORSEC 1992 in Okinawa: Conference for Pacific Ocean Environments and Probing, Volume 2 25 Aug. 1992 p 1016-1021 (For primary document see N94-12635 01-42)
Copyright Avail: Issuing Activity (Scientific Organizing Committee of PORSEC, P.O. Box 10, Shimizu, Shizuoka 424, Japan, HC)

N94-12720 Seikai Regional Fisheries Research Lab., Nagasaki (Japan).
MAPPING OF HIGH DENSITY AREA OF BENTHIC DIATOM IN ARIAKE SEA
Shirou Uno *In* Scientific Organizing Committee of PORSEC, Proceedings of the PORSEC 1992 in Okinawa: Conference for Pacific Ocean Environments and Probing, Volume 2 25 Aug. 1992 p 1045-1050 Sponsored by Science and Technology Agency, Tokyo, Japan (For primary document see N94-12635 01-42)
Copyright Avail: Issuing Activity (Scientific Organizing Committee of PORSEC, P.O. Box 10, Shimizu, Shizuoka 424, Japan, HC)

N94-12736 Academy of Sciences (USSR), Moscow. Inst. of Oceanology.
REMOTE SENSING OF LIGHT SCATTERING COEFFICIENT OF SEA WATER VERTICAL DISTRIBUTION BY THE MEANS OF AIRBORNE LIDAR
Alexander P. Vasilkov, Yuri A. Goldin, and Boris A. Gureev *In* Scientific Organizing Committee of PORSEC, Proceedings of the PORSEC 1992 in Okinawa: Conference for Pacific Ocean Environments and Probing, Volume 2 25 Aug. 1992 p 1122-1126 (For primary document see N94-12635 01-42)
Copyright Avail: Issuing Activity (Scientific Organizing Committee of PORSEC, P.O. Box 10, Shimizu, Shizuoka 424, Japan, HC)

N94-12740 Academy of Sciences (USSR), Vladivostok. Pacific Oceanological Inst.
SPATIAL VARIABILITY OF THE OCEAN UNDERWATER DYNAMIC NOISE FROM SATELLITE RADAR SENSING DATA
L. M. Mitnik and M. L. Mitnik *In* Scientific Organizing Committee of PORSEC, Proceedings of the PORSEC 1992 in Okinawa: Conference for Pacific Ocean Environments and Probing, Volume 2 25 Aug. 1992 p 1145-1150 (For primary document see N94-12635 01-42)
Copyright Avail: Issuing Activity (Scientific Organizing Committee of PORSEC, P.O. Box 10, Shimizu, Shizuoka 424, Japan, HC)

N94-12741 Academy of Sciences (USSR), Nizhny Novgorod. Inst. of Applied Physics.
OBSERVATIONS OF FILM SLICKS AND INTERNAL WAVES WITH Ka-BAND SCATTEROMETER
S. A. Ermakov, L. V. Lubjako, and S. G. Salashin *In* Scientific Organizing Committee of PORSEC, Proceedings of the PORSEC 1992 in Okinawa: Conference for Pacific Ocean Environments and Probing, Volume 2 25 Aug. 1992 p 1151-1154 (For primary document see N94-12635 01-42)
Copyright Avail: Issuing Activity (Scientific Organizing Committee of PORSEC, P.O. Box 10, Shimizu, Shizuoka 424, Japan, HC)

N94-12744 Academy of Sciences (USSR), Moscow. Inst. of Oceanology.
VARIABILITY OF SPECTRAL REFLECTANCE IN COASTAL WATERS NEAR THE RIVER PLUMES
Vladimir I. Burenkov and Alexander P. Vasilkov *In* Scientific Organizing Committee of PORSEC, Proceedings of the PORSEC 1992 in Okinawa: Conference for Pacific Ocean Environments and Probing, Volume 2 25 Aug. 1992 p 1166-1170 (For primary document see N94-12635 01-42)
Copyright Avail: Issuing Activity (Scientific Organizing Committee of PORSEC, P.O. Box 10, Shimizu, Shizuoka 424, Japan, HC)

N94-12745 Academy of Sciences (USSR), Moscow. Space Research Inst.
WIND-WAVE AND FOAM DYNAMICS FROM OPTICAL AND RADAR AIRBORNE OBSERVATIONS
V. Yu. Raizer and V. S. Etkin *In* Scientific Organizing Committee of PORSEC, Proceedings of the PORSEC 1992 in Okinawa: Conference for Pacific Ocean Environments and Probing, Volume 2 25 Aug. 1992 p 1171-1174 (For primary document see N94-12635 01-42)
Copyright Avail: Issuing Activity (Scientific Organizing Committee of PORSEC, P.O. Box 10, Shimizu, Shizuoka 424, Japan, HC)

N94-12746 Academy of Sciences (USSR), Moscow. Space Research Inst.
OBSERVATIONS OF SURFACE SIGNATURES IN THE NORTH-WEST PACIFIC OCEAN WITH THE SPACEBORNE SAR
Konstantin T. Litovchenko, Andre V. Smirnov, and Valentin S. Etkin *In* Scientific Organizing Committee of PORSEC, Proceedings of the PORSEC 1992 in Okinawa: Conference for Pacific Ocean Environments and Probing, Volume 2 25 Aug. 1992 p 1175-1177 (For primary document see N94-12635 01-42)
Copyright Avail: Issuing Activity (Scientific Organizing Committee of PORSEC, P.O. Box 10, Shimizu, Shizuoka 424, Japan, HC)

N94-12747 Academy of Sciences (USSR), Moscow. Space Research Inst.
RADAR OBSERVATION OF INTERNAL WAVES FIELD IN THE NORTH-WEST PACIFIC
Andre V. Smirnov and Valentin S. Etkin *In* Scientific Organizing Committee of PORSEC, Proceedings of the PORSEC 1992 in Okinawa: Conference for Pacific Ocean Environments and Probing, Volume 2 25 Aug. 1992 p 1178-1183 (For primary document see N94-12635 01-42)
Copyright Avail: Issuing Activity (Scientific Organizing Committee of PORSEC, P.O. Box 10, Shimizu, Shizuoka 424, Japan, HC)

N94-12753 Academy of Sciences (USSR), Vladivostok. Pacific Oceanological Inst.

COMPLEX (HYDRODYNAMIC, SATELLITE) MONITORING OF DYNAMIC STRUCTURES IN THE WESTERN PACIFIC WITH THE AIM OF FORECASTING THE MARINE ECOSYSTEMS BEHAVIOUR

A. S. Vasiliev *In* Scientific Organizing Committee of PORSEC, Proceedings of the PORSEC 1992 in Okinawa: Conference for Pacific Ocean Environments and Probing, Volume 2 25 Aug. 1992 p 1211-1218 (For primary document see N94-12635 01-42)

Copyright Avail: Issuing Activity (Scientific Organizing Committee of PORSEC, P.O. Box 10, Shimizu, Shizuoka 424, Japan, HC)

N94-12756 Moscow State Univ. (Russia). Physics Dept.

ECOLOGICAL APPLICATION OF SURFACE ENHANCED RAMAN SPECTROSCOPY

O. A. Aktsipetrov, A. M. Klevtsov, and A. F. Pasternak *In* Scientific Organizing Committee of PORSEC, Proceedings of the PORSEC 1992 in Okinawa: Conference for Pacific Ocean Environments and Probing, Volume 2 25 Aug. 1992 p 1231-1234 (For primary document see N94-12635 01-42)

Copyright Avail: Issuing Activity (Scientific Organizing Committee of PORSEC, P.O. Box 10, Shimizu, Shizuoka 424, Japan, HC)

N94-12757 Academy of Sciences (USSR), Vladivostok. Pacific Research Inst.

A POSSIBILITY TO DEFINE THE LOCATION OF EPIPELAGIC FISH CONCENTRATIONS WITH ASSISTANCE OF SATELLITE SENSING

Yury I. Zuenko, Sergey Yu. Shershenkov, Nafanail V. Bulatov, and Valentina I. Lapshina *In* Scientific Organizing Committee of PORSEC, Proceedings of the PORSEC 1992 in Okinawa: Conference for Pacific Ocean Environments and Probing, Volume 2 25 Aug. 1992 p 1235-1239 (For primary document see N94-12635 01-42)

Copyright Avail: Issuing Activity (Scientific Organizing Committee of PORSEC, P.O. Box 10, Shimizu, Shizuoka 424, Japan, HC)

N94-12759 Academy of Sciences (USSR), Moscow. Inst. of Oceanology.

STUDY OF THE ADMIXTURE DIFFUSION IN THE SEA USING REMOTE TECHNIQUES

Rostislav V. Ozmidov *In* Scientific Organizing Committee of PORSEC, Proceedings of the PORSEC 1992 in Okinawa: Conference for Pacific Ocean Environments and Probing, Volume 2 25 Aug. 1992 p 1245-1250 (For primary document see N94-12635 01-42)

Copyright Avail: Issuing Activity (Scientific Organizing Committee of PORSEC, P.O. Box 10, Shimizu, Shizuoka 424, Japan, HC)

N94-12761 Academy of Sciences (USSR), Moscow. Inst. of Oceanology.

THE ALGORITHM OF PRIMARY PRODUCTION DETERMINATION

Olga J. Koblentz-Mishke, Vadim N. Pelevin, and Bogdan Wozniak (Polish Academy of Sciences, Gdansk.) *In* Scientific Organizing Committee of PORSEC, Proceedings of the PORSEC 1992 in Okinawa: Conference for Pacific Ocean Environments and Probing, Volume 2 25 Aug. 1992 p 1257-1262 (For primary document see N94-12635 01-42)

Copyright Avail: Issuing Activity (Scientific Organizing Committee of PORSEC, P.O. Box 10, Shimizu, Shizuoka 424, Japan, HC)

N94-12762 Central Aerological Observatory, Moscow (USSR). Inst. of Physics, Technology, and Oceanology.

NON-IMAGE VISIBLE POLARIZATION REMOTE SENSING OF THE OCEAN

Nikolay A. Krotkov, Tymothy V. Kondranin, and Alexander P. Vasilkov *In* Scientific Organizing Committee of PORSEC, Proceedings of the PORSEC 1992 in Okinawa: Conference for Pacific Ocean Environments and Probing, Volume 2 25 Aug. 1992 p 1263-1268 (For primary document see N94-12635 01-42)

Copyright Avail: Issuing Activity (Scientific Organizing Committee of PORSEC, P.O. Box 10, Shimizu, Shizuoka 424, Japan, HC)

44 ENERGY PRODUCTION AND CONVERSION

Includes specific energy conversion systems, e.g., fuel cells; global sources of energy; geophysical conversion; and windpower.

For related information see also *07 Aircraft Propulsion and Power, 20 Spacecraft Propulsion and Power,* and *28 Propellants and Fuels.*

N94-10258# Midwest Research Inst., Golden, CO. National Renewable Energy Lab.

DEPARTMENT OF ENERGY SOLAR PROCESS HEAT PROGRAM: FY 1991 SOLAR PROCESS HEAT PREFEASIBILITY STUDIES ACTIVITY

R. Hewett Nov. 1992 4 p Presented at the SOLAR 1993 ASME American Solar Energy Society Joint Solar Energy Conference, Washington, DC, 22-28 Apr. 1993

(Contract DE-AC02-83CH-10093)

(DE93-010010; NREL/TP-432-5068; CONF-930435-8) Avail: CASI HC A01/MF A01

During fiscal year (FY) 1991, the US Department of Energy (DOE) Solar Process Heat Program implemented a Solar Process Heat Prefeasibility Studies activity. For Program purposes, a prefeasibility study is an engineering assessment that investigates the technical and economic feasibility of a solar system for a specific application for a specific end-user. The study includes an assessment of institutional issues (e.g., financing, availability of insurance, etc.) that impact the feasibility of the proposed solar project. Solar process heat technology covers solar thermal energy systems (utilizing flat plate or concentrating solar collectors) for water heating, water preheating, cooling/refrigeration, steam generation, ventilation air heating/preheating, etc., for applications in industry, commerce, and government. The studies are selected for funding through a competitive solicitation. For FY-91, six projects were selected for funding. As of 31 Aug. 1992, three teams had completed their studies. This paper describes the prefeasibility studies activity, presents the results from the study performed by United Solar Technologies, and summarizes the conclusions from the studies that have been completed to date and their implications for the Solar Process Heat Program. DOE

N94-10498# Agency of Industrial Science and Technology, Tokyo (Japan).

JAPAN'S SUNSHINE PROJECT

Jul. 1992 528 p

(DE93-767980; ETDE/JP-mf-93767980) Avail: CASI HC A23/MF A04

The 1991 results of the Sunshine Project/solar energy research and development are described. As for solar energy utilization, R and D are made on types of advanced, high-efficiency, and amorphous solar cells. Photovoltaic hydrogen production and CO2 fixation are also studied. For commercialization of the photovoltaic power generation system, technologies for thin substrate solar cells and tandem solar cells are studied. Research is made on integration of amorphous solar cells for electric power use, layer formation using new raw material gas, and production technology for high reliability and high quality. Studies are made on a new production method for ultra-high efficiency solar cells and compound semiconductor solar cells. Evaluation technology and peripheral technology for the photovoltaic power generation system are studied. As for the photovoltaic power generation utilization system, a photovoltaic-wind power generation hybrid system and a photovoltaic-thermal hybrid system are studied. The analysis/evaluation method is studied for commercialization of the photovoltaic power generation system. Concerning solar heat utilization, research is conducted on equipment, materials, elementary technology for commercialization of the industrial use solar system, solar heat refrigeration, the passive solar system, etc. International cooperation is also referred to. DOE

N94-11051# Pacific Northwest Lab., Richland, WA.

US AREAL WIND RESOURCE ASSESSMENT

M. N. Schwartz and D. L. Elliott Mar. 1993 5 p Presented at the Alternate Fuels and the Environment Symposium, Denver, CO, 28 Mar. - 2 Apr. 1993

(Contract DE-AC06-76RL-01830)

(DE93-011905; PNL-SA-21606; CONF-9303133-1) Avail: CASI HC A01/MF A01

Estimates of the electricity that could potentially be generated by wind power and of the land area available for wind energy development have been calculated for the contiguous United States, in support of the US Department of Energy's National Energy Strategy. These estimates were based on the wind resource data published in a national resource atlas. Estimates of the wind resource in this atlas are expressed in wind power classes ranging from class 1 to class 7, with each class representing a range of mean wind power density or equivalent mean speed at specified heights above the ground. Areas designated class 4 or greater are suitable for most wind turbine applications. Power class 3 areas are suitable for wind energy development using tall (50m hub height) turbines. Class 2 areas are marginal, and class 1 areas are unsuitable for wind energy development. A map of the areal (percentage of land area) distribution of the wind resource digitized in grid cells (1/4 deg latitude by 1/3 deg longitude) shows that exposed areas with moderate to high wind resource (class 3 and greater) are dispersed throughout much of the contiguous United States. DOE

N94-11116# Akron Univ., OH. Dept. of Chemistry.
DYNAMICS OF CHARGE-TRANSFER EXCITED STATES RELEVANT TO PHOTOCHEMICAL ENERGY CONVERSION
E. C. Lim 1993 5 p
(Contract DE-FG02-89ER-14024)
(DE93-013981; DOE/ER-14024/4) Avail: CASI HC A01/MF A01

A systematic study of intramolecular photoassociation and photoinduced charge transfer (CT) was initiated in bichromophoric systems of M-X-M, where two identical aromatic hydrocarbons, M, are joined by X = CH2, O, NH, etc. Dinaphthylamines, dinaphthylethers, and dinaphthylmethanes in nonpolar solvents form triplet excimers, following intersystem crossing of singlets to the triplet manifold; in polar solvents, the molecule forms an intramolecular CT state. The interchromophore interaction study was extended to N-phenyl-2-naphthylamine. The lowest excited singlet states of the dinaphthylamines were studied by semiempirical quantum chemical methods. Exciplex formation was studied in excited states of jet-cooled van der Waals complexes, such as fluorene/substituted benzenes and 1-cyanonaphthalene-aliphatic amines. DOE

N94-11173# Sandia National Labs., Albuquerque, NM.
FATIGUE LIFE PREDICTION FOR WIND TURBINES: A CASE STUDY ON LOADING SPECTRA AND PARAMETER SENSITIVITY
H. J. Sutherland, P. S. Veers, and T. D. Ashwill 1992 39 p Presented at the 5th ASTM Symposium on Composite Materials: Fatigue and Fracture, Atlanta, GA, 4-6 May 1993
(Contract DE-AC04-76DP-00789)
(DE93-011597; SAND-92-0501C; CONF-930532-2) Avail: CASI HC A03/MF A01

Wind turbines are fatigue-critical machines used to produce electrical energy from the wind. These rotating machines are subjected to environmental loadings that are highly irregular in nature. Historical examples of fatigue problems in both research and commercial wind turbine development are presented. Some example data on wind turbine environments, loadings and material properties are also shown. Before a description of how the authors have chosen to attack the cumulative damage assessment, questions are presented for the reader's reflection. The solution technique used by the authors is then presented, followed by a case study applying the procedures to an actual wind turbine blade joint. The wind turbine is the 34-meter diameter vertical axis wind turbine (VAWT) erected by Sandia National Laboratories near Bushland, Texas. The case study examines parameter sensitivities for realistic uncertainties in inputs defining the turbine environment, stress response and material properties. The fatigue lifetimes are calculated using a fatigue analysis program, called LIFE2, which was developed at Sandia. The LIFE2 code, described in some detail in an appendix, is a PC-based, menu-driven package that leads the user through the steps required to characterize the loading and material properties, then uses Miner's rule or a linear crack propagation rule to numerically calculate the time to failure. Only S-n based cumulative damage applications are illustrated here. The LIFE2 code is available to educational institutions for use as a case study in describing complicated loading histories and for use by students in examining, hands on, parameter sensitivity of fatigue life analysis. DOE

N94-11313 Missouri Univ., Rolla.
THIN FILM PREPARATION AND INTERFACIAL REACTION STUDY OF SOLID OXIDE FUEL CELL MATERIALS
Chieh-Cheng Chen 1992 148 p
Avail: Univ. Microfilms Order No. DA9311023

Solid oxide fuel cells (SOFC's) operate at 1000 C and their components are processed at even higher temperatures. It is generally desirable to reduce the operating and processing temperatures of SOFC's to make them competitive with other types of fuel cells and to avoid the interactions and interdiffusion between cell components. This can be achieved by either developing a technology to produce thin film electrolytes, or by developing new electrolyte and electrode materials with reduced interaction, lower interfacial resistance. The synthesis and characterization of (Ce-O2)0.8(Sm01.5)0.2 thin films from polymeric precursors is discussed. The reaction mechanism of the precursors and important parameters for making dense, crack-free films were investigated. The cathode/electrolyte interactions and their expected impact on SOFC performance are addressed. The cathode characteristics and cathode/electrolyte interaction of various perovskites are studied. The impact of interfacial reactions on cell performance is investigated. The electrode characteristics of dense La0.6Sr0.4Co0.2Fe0.8O3 (LSCF) thin film produced by polymeric precursors are presented. The electrode resistance and characteristics of the electrode (dense)/electrolyte interface are studied. The effect of reactions and interdiffusion on interfacial resistance are discussed. A potential method for making dense ZrO2 films at relatively low temperatures by plasma-enhanced chemical vapor deposition is presented. The deposition parameters and characterization of ZrO2 film are reported. Dissert. Abstr.

N94-11505# Czechoslovak Solar Energy Society, Prague.
RENEWABLE ENERGY SOURCES 1991, PART 3
L. Michalicka 1991 100 p Conference held in Prague, Czechoslovakia, 1-4 Jul. 1991 Prepared in cooperation with Technical Univ. of Prague, Czechoslovakia
(DE93-605594; INIS-mf-13363-Pt-3; CONF-9107237) Avail: CASI HC A05/MF A02 (US Sales Only)

The Fourth International Conference on Renewable Energy Sources was held at Prague Technical University from 1-4 Jul. 1991. Part 3 of the proceedings contains a report on the conference and 10 contributions, of which 2 were inputted in INIS: one deals with the economic problems of wind-, solar- and oil-driven water pumps, the other deals with the decrease in sunshine brought about by the operation of Czechoslovak nuclear power plants. DOE

N94-11506# Czechoslovak Solar Energy Society, Prague.
RENEWABLE ENERGY SOURCES 1991, PART 2
L. Michalicka 1991 121 p Conference held in Prague, Czechoslovakia, 1-4 Jul. 1991 Prepared in cooperation with Technical Univ. of Prague, Czechoslovakia
(DE93-605634; INIS-mf-13362-Pt-2; CONF-9107237) Avail: CASI HC A06/MF A02 (US Sales Only)

The International Conference on Renewable Energy Sources was held in Prague on 1-4 Jul. 1991. Part 2 of the proceedings is devoted to the use of the energy of wind, biogas, and small hydroelectric sources. The publication contains 14 contributions, of which 3 were inputted in INIS. Topics covered include: a wind power plant in Sweden and its environmental impacts, economic aspects of the introduction of alternative energy sources in Czechoslovakia, and the efficiency of application of a Fresnel lens-based solar collector. DOE

N94-11638 Princeton Univ., NJ.
MEASUREMENT AND MODELING OF THE STABILITY OF HYDROGENATED AMORPHOUS SILICON SOLAR CELLS AND FILMS AFTER INTENSE ILLUMINATION Ph.D. Thesis
Xiao-Rui Li 1993 117 p
Avail: Univ. Microfilms Order No. DA9311203

Hydrogenated amorphous silicon p-i-n solar cells were aged under high-intensity illumination at 50 to approximately 60 C, well into saturation of their conversion efficiency. The cell characteristics were measured at intervals, and also modeled numerically with the model for Analysis of Microelectronic and Photonic Structures (AMPS). The light-induced degradation in the isolated i-layer films, grown under identical conditions to the cells, were also studied using the Constant Photocurrent Method. The

CPM-measured defect density was fitted to strenched exponential form, which become input parameters for the modeling. The model results agree with the experimental data very well, suggesting that the light-induced defect density in the bulk i-layer is primarily responsible for the cell degradation under light. Model results also suggested that a new degradation mechanism - the p/i interfacial defects might exist, contributing to the cell degradation as well. The defect density at the p/i interface rise with illumination time. However, this needs to be verified experimentally. The modeling results predict that the cells with thickness of 200nm have the best long term stability. The a-Si:H material with the saturated defect density of approximately 10(exp 16) cm(sup -3) is the target for improving stability of solar cells. The material with this saturated defect density will give a cell with stabilized conversion efficiency of 90 percent of initial value. This shows that growing stable a-Si:H films with low defects is the key for a stable a-Si:H p-i-n solar cell with high conversion efficiency.
Dissert. Abstr.

N94-11666# Los Alamos National Lab., NM.
POLYMER ELECTROLYTE FUEL CELLS: POTENTIAL TRANSPORTATION AND STATIONARY APPLICATIONS
S. Gottesfeld 1993 13 p Presented at the EPRI/GRI Fuel Cell Review Meeting, New Orleans, LA, 12-14 Apr. 1993
(Contract W-7405-eng-36)
(DE93-010734; LA-UR-93-1018; CONF-9304108-1) Avail: CASI HC A03/MF A01

The application of the polymer electrolyte fuel cell (PEFC) as a primary power source in electric vehicles has received increasing attention during the last few years. This increased attention is the result of a combination of significant technical advances in this fuel cell technology and the initiation of some projects for the demonstration of a complete, PEFC-based power system in a bus or in a passenger car. Such demonstration projects reflect an increase in industry's faith in the potential of this technology for transportation applications, or, at least, in the need for a detailed evaluation of this potential. Nevertheless, large scale transportation applications of PEFC's require a continued concerted effort of research on catalysis, materials, and components, combined with the engineering efforts addressing the complete power system. This is required to achieve a cost effective, highly performing PEFC stack and power system. A related set of technical and cost challenges arises in the context of potential applications of PEFC's for stationary power applications; although, there are clearly some differences in their nature, particularly, having to do with the different types of fuels to be employed for each of these applications. We describe in this contribution some recent results of work performed by the Core Research PEFC Program at Los Alamos National Laboratory, which has addressed materials, components, and single cell testing of PEFC's. Also included are some recent observations and some insights regarding the potential of this fuel cell technology for stationary power generation. DOE

N94-11408*# Communications Satellite Corp., Clarksburg, MD.
UV TESTING OF SOLAR CELLS: EFFECTS OF ANTIREFLECTIVE COATING, PRIOR IRRADIATION, AND UV SOURCE
A. Meulenberg *In* NASA. Lewis Research Center, Proceedings of the 12th Space Photovoltaic Research and Technology Conference (SPRAT 12) May 1993 p 268-279 Sponsored in part by COMSAT Corporation
(For primary document see N94-11380 01-20)
Avail: CASI HC A03/MF A03

N94-11409*# Defence Research Agency, Farnborough (England). Space Technology Dept.
THE UoSAT-5 SOLAR CELL EXPERIMENT: FIRST YEAR IN ORBIT
C. Goodbody *In* NASA. Lewis Research Center, Proceedings of the 12th Space Photovoltaic Research and Technology Conference (SPRAT 12) May 1993 p 280-288 (For primary document see N94-11380 01-20)
Avail: CASI HC A02/MF A03

N94-11415*# Martin Marietta Aerospace, Denver, CO.
THIN FILM SOLAR CELL WORKSHOP
Joe Armstrong and Frank Jeffrey (Iowa Thin Film Technologies, Inc., Ames.) *In* NASA. Lewis Research Center, Proceedings of the 12th Space Photovoltaic Research and Technology Conference (SPRAT 12) May 1993 p 329-330 (For primary document see N94-11380 01-20)
Avail: CASI HC A01/MF A03

N94-11417*# Communications Satellite Corp., Clarksburg, MD.
WORKSHOP SUMMARY: NEW SILICON CELLS
A. Meulenberg and P. A. Iles (Applied Solar Energy Corp., City of Industry, CA.) *In* NASA. Lewis Research Center, Proceedings of the 12th Space Photovoltaic Research and Technology Conference (SPRAT 12) May 1993 p 334-336 (For primary document see N94-11380 01-20)
Avail: CASI HC A01/MF A03

N94-11418*# Research Triangle Inst., Research Triangle Park, NC.
MULTI-BAND GAP AND NEW SOLAR CELL OPTIONS WORKSHOP
J. Hutchby, M. Timmons, and J. M. Olson (Midwest Research Inst., Golden, CO.) *In* NASA. Lewis Research Center, Proceedings of the 12th Space Photovoltaic Research and Technology Conference (SPRAT 12) May 1993 p 337-339 (For primary document see N94-11380 01-20)
Avail: CASI HC A01/MF A03

45 ENVIRONMENT POLLUTION

Includes atmospheric, noise, thermal, and water pollution.

N94-10256# Oak Ridge National Lab., TN.
PRESENTATIONS TO THE MEXICAN PHYSICS SOCIETY ON ENVIRONMENTAL CONTAMINATION
R. B. Gammage 25 Nov. 1992 12 p
(Contract DE-AC05-84OR-21400)
(DE93-009565; ORNL/FTR-4479) Avail: CASI HC A03/MF A01 (US Sales Only)

The author attended the 35th Annual Congress of the Mexican Physics Society. A presentation at a roundtable on environmental contamination focused on groundwater and soil contamination problems at Department of Energy facilities. Another invited presentation to the general public and staff of the University of Puebla was about radon in indoor environments and the associated risks of lung cancer. Discussions were held with National Autonomous University of Mexico (UNAM) staff on aspects of environmental contamination monitoring that are of mutual concern. Plans were made to develop joint proposals under the new cooperative research agreement between UNAM and Oak Ridge National Laboratory (ORNL). Arrangements were also made for two UNAM staff members to work at ORNL in 1993.
DOE

N94-10650# Oak Ridge National Lab., TN.
ENVIRONMENTAL SCIENCES DIVISION Annual Progress Report, period ending 30 Sep. 1992
Apr. 1993 287 p
(Contract DE-AC05-84OR-21400)
(DE93-013865; ORNL-6733; ESDP-4034) Avail: CASI HC A13/MF A03

This progress report summarizes the research and development activities conducted in the Environmental Sciences Division of Oak Ridge National Laboratory during FY-92, which extended from 1 Oct. 1991, through 30 Sep. 1992. This report is structured to provide descriptions of current activities and accomplishments in each of the division's major organizational units. Section activities are described in the Earth and Atmospheric sciences, ecosystem studies, Environmental analysis, environmental biotechnology, and division operations. DOE

N94-10836 Environmental Protection Agency, Washington, DC. Office of Pollution, Prevention, and Toxics.
TOXIC CHEMICAL RELEASE INVENTORY REPORTING FORM R AND INSTRUCTIONS. REVISED 1992 VERSION. SECTION 313 OF THE EMERGENCY PLANNING AND COMMUNITY RIGHT-TO-KNOW ACT
Jan. 1993 121 p See also 1988 version, PB89-164248 Limited Reproducibility: More than 20% of this document may be affected by microfiche quality
(PB93-194140; EPA/745/K-93/001) Avail: Issuing Activity (National Technical Information Service (NTIS))

Reporting is required to provide the public with information on the releases of listed toxic chemicals in their communities and to provide EPA with release information to assist the Agency in determining the need for future regulations. Facilities must report the quantities of both routine and accidental releases of listed toxic chemicals, as well as the maximum amount of the listed toxic chemical on-site during the calendar year and the amount contained in wastes transferred off-site. These instructions supplement and elaborate on the requirements in the reporting rule (40 CFR Part 372). Together with the reporting rule, they constitute the reporting requirements. All references in these instructions are to sections in the reporting rule unless otherwise indicated. NTIS

N94-10841 Environmental Protection Agency, Cincinnati, OH. Risk Reduction Engineering Lab.

ENVIRONMENTAL PROTECTION AGENCY'S LIFE CYCLE METHODOLOGY: GUIDELINES FOR USE IN DEVELOPMENT OF PACKAGING

Mary Ann Curran 1992 13 p See also PB93-194207 Limited Reproducibility: More than 20% of this document may be affected by microfiche quality

(PB93-194199; EPA/600/A-93/112) Avail: CASI HC A03

Approaches to reducing the environmental effects of products and processes have moved steadily upstream over the years from end-of-pipe controls to source reduction and recycling of hazardous waste, and more recently, toward multimedia pollution prevention. Life Cycle Assessment (LCA) continues the trend of expanding the authors view and approach to environmental protection. An informal review of the open literature found 29 references to product life cycle studies, 17 of which are related to packaging materials or packaging systems. Beverage containers (cans, bottles, and cartons) are the focus of ten of these studies. These packaging-related studies are provided in the bibliography at the end of the paper. The paper includes discussion of the history of LCA's SETAC's involvement in LCA, the EPA's guidance on life cycle inventory methodology, life cycle design, and the future of LCA. NTIS

N94-10846 Environmental Protection Agency, Washington, DC.

SUMMARY OF IMPLEMENTATION AND DEMONSTRATION PROJECTS IN BAYS AND ESTUARIES

Nov. 1992 139 p See also PB91-168385 Limited Reproducibility: More than 20% of this document may be affected by microfiche quality

(PB93-194637; EPA/842/B-92/009) Avail: CASI HC A07

The projects investigated include demonstration projects as well as unique programmatic initiatives of 15 bays and estuaries and are divided into 11 separate project categories: Boat and Marine Wastes; Contaminated Sediments; Land Use and Development Controls; Local Government and Community Involvement; Nutrient Loading; On-site Disposal Systems; Public Outreach and Education; Shellfish Bed Protection and Restoration; Stormwater Controls; Toxic Waste Reduction; and Wetlands/Habitat Protection and Restoration. NTIS

N94-11015# Naval Energy and Environmental Support Activity, Port Hueneme, CA.

IMMEDIATE RESPONSE TO FREE PRODUCT DISCOVERY Remedial Action Tech Data Sheet

Nov. 1992 13 p

(PB93-182970; NEESA-20.2-051.4) Avail: CASI HC A03/MF A01

Underground storage of petroleum products such as gasoline, diesel oil, fuel oil, and aviation fuel can be a significant source of contamination of ground water and soil. Estimates by the Environmental Protection Agency (EPA) indicate that nearly 25% of all steel underground storage tanks (UST) are leaking. The need to initiate remedial measures as soon as leaking is detected is of paramount importance. For any migrating fuel plume problem, the first priority must be to gain control of the migrating product to prevent further soil and ground water contamination. Proper immediate response can significantly reduce the ultimate cleanup cost, increase the efficiency of the cleanup, and mitigate further environmental damage. NTIS

N94-11016# Sigma Research, Inc., Concord, MA.

USER'S MANUAL FOR THE PLUME VISIBILITY MODEL PLUVUE 2 (REVISED) Final Report

Oct. 1992 108 p See also PB84-158302 Sponsored by EPA, Research Triangle Park, NC

(Contract EPA-68-D9-0067)

(PB93-188233; EPA/454/B-92/008) Avail: CASI HC A06/MF A02

The document provides a description for the restructured and revised version of the Plume Visibility Model (PLUVUE 2). The model was restructured in order to improve the user interface and computing requirements and revised to remove several errors in the original code. The objective of the PLUVUE 2 model is to calculate visual range reduction and atmospheric discoloration caused by plumes consisting of primary particles, nitrogen oxides, and sulfur oxides emitted by a single emission source. NTIS

N94-11018# Environmental Protection Agency, Washington, DC.

GULF OF MEXICO SALES 147 AND 150: CENTRAL AND WESTERN PLANNING AREAS. DRAFT ENVIRONMENTAL IMPACT STATEMENT. VOLUME 1: SECTIONS 1 THROUGH 4.C

Apr. 1993 310 p See also PB93-190312 and PB93-127850 Sponsored by EPA

(PB93-190304; OCS/EIS/EA/MMS-93-0012-Vol-1) Avail: CASI HC A14/MF A03

The Draft Environmental Impact Statement (EIS) covers the proposed 1994 Gulf of Mexico OCS oil and gas lease sales (Central Gulf of Mexico Sale 147 (March 1994) and Western Gulf of Mexico Sale 150 (August 1994)). The document includes the purpose and background of the proposed actions, the alternatives, the description of the affected environment, and the potential environmental impacts of the proposed actions and alternatives. Proposed mitigating measures and their effects are analyzed, in addition to potential cumulative impacts resulting from proposed activities. NTIS

N94-11019# Minerals Management Service, New Orleans, LA.

GULF OF MEXICO SALES 147 AND 150: CENTRAL AND WESTERN PLANNING AREAS. DRAFT ENVIRONMENTAL IMPACT STATEMENT. VOLUME 2: SECTIONS 4.D THROUGH 9

Apr. 1993 629 p See also PB93-190304 and PB93-127868 Sponsored by EPA

(PB93-190312; OCS/EIS/EA/MMS-93-0012-Vol-2) Avail: CASI HC A99/MF A06

Contents: Environmental Impacts of the Proposed Actions and Alternatives; Proposed Central Gulf Sale 147; Proposed Western Gulf Sale 150; Analysis of a Large Oil Spill; Consultation and Coordination; Bibliography and Special References; Glossary; and Appendices. NTIS

N94-11189 Pennsylvania State Univ., University Park.

NUMERICAL SIMULATIONS ON THE REDISTRIBUTION OF ATMOSPHERIC TRACE CHEMICALS THROUGH CLOUD PROCESSES Ph.D. Thesis

Jen-Ping Chen 1992 360 p

Avail: Univ. Microfilms Order No. DA9311607

The redistribution of atmospheric trace substances through cloud processes is investigated using a detailed microphysical and chemical cloud model. A multi-component categorization scheme is used in the model to group cloud particles into different bins according to their various properties. Cloud drops are categorized in both their water mass and solute mass components. An extra 'shape' component is included in the ice-phase particle framework to describe the distribution of ice-phase particles. Special efforts are paid to develop the theory and parameterization for the change of the growth habits for ice particles. In dealing with a model that inevitably has a large dimension, a hybrid bin-method is applied so that it can maintain the conservation of all properties and, at the same time, perform fast and accurate calculations for transferring various properties between categories in the multi-component systems. With a minimum of parameterization, this model is capable of simulating detailed microphysical and chemical processes that occurred during cloud and precipitation formations. Using the multi-component model, it is shown that the drop number concentration is a function of both the water mass and the solute mass in the drops, a phenomenon that cannot be resolved by conventional cloud models. Applying a full set of liquid- and ice-phase microphysics, it is also shown that the number concentration of ice particles is indirectly controlled by the number concentration of cloud condensation nuclei. Bulk water models that can not treat the in-cloud supersaturation are not able to properly simulate such processes. The concept of the relative removal efficiency was introduced and tested in a simple particle model in the earlier stage of the study. An extended test on the relative removal efficiencies was done by simulating a wintertime, orographic cloud in a two-dimensional, steady-state model. Satisfactory results for both the microphysical and chemical behavior of the cloud are produced in the simulation. It is shown that the redistribution of atmospheric trace substances is controlled by their microphysical pathways. Dissert. Abstr.

N94-11374*# Michigan Univ., Ann Arbor. Dept. of Electrical Engineering and Computer Science.

EXTENDED ECOSYSTEM SIGNATURES WITH APPLICATION TO Eos SYNERGISM REQUIREMENTS Final Report

Fawwaz T. Ulaby, M. Craig Dobson, and Kamal Sarabandi Jul. 1993 24 p
(Grant NAGw-1101)
(NASA-CR-193398; NAS 1.26:193398; UMICH-024557-1-F) Avail: CASI HC A03/MF A01

The primary objective is to define the advantages of synergistically combining optical and microwave remote sensing measurements for the determination of biophysical properties important in ecosystem modeling. This objective was approached in a stepwise fashion starting with ground-based observations of controlled agricultural and orchard canopies and progressing to airborne observations of more natural forest ecosystems. This observational program is complemented by a parallel effort to model the visible reflectance and microwave scattering properties of composite vegetation canopies. The goals of the modeling studies are to verify our basic understanding of the sensor-scene interaction physics and to provide the basis for development of inverse models optimized for retrieval of key biophysical properties. These retrieval algorithms can then be used to simulate the expected performance of various aspects of Eos including the need for simultaneous SAR and HIRIS observations or justification for other (non-synchronous) relative timing constraints and the frequency, polarization, and angle of incidence requirements for accurate biophysical parameter extractions. This program completed a very successful series of truck-mounted experiments, made remarkable progress in development and validation of optical reflectance and microwave scattering models for vegetation, extended the scattering models to accommodate discontinuous and periodic canopies, developed inversion approaches for surface and canopy properties, and disseminated these results widely through symposia and journal publications. In addition, the third generation of the computer code for the microwave scattering models was provided to a number of other US, Canadian, Australian, and European investigators who are currently presenting and publishing results using the MIMICS research code.
Author (revised)

N94-11451 Miami Univ., FL. Rosenstiel School of Marine and Atmospheric Science.

BISCAYNE BAY: A BIBLIOGRAPHY OF THE MARINE ENVIRONMENT

K. K. Hale Apr. 1993 121 p See also COM-75-11043 Sponsored by National Sea Grant Coll. Program, Silver Spring, MD Prepared in cooperation with Florida Sea Grant Coll. Program, Gainesville Limited Reproducibility: More than 20% of this document may be affected by microfiche quality
(Grant NA-89-AA-D-SG053)
(PB93-184802; TP-67) Avail: CASI HC A06

The history of Miami and Biscayne Bay are intimately related. In addition to food, industry, transportation, and recreation, the Bay provides a constant source of aesthetic satisfaction for those who live and work along its shores. Information on the marine environment of Biscayne Bay includes pollution, monitoring, conservation and protection, coastal and resource management, artificial reefs, fishery assessments, park and marina construction, estuarine dynamics, and sampling. This bibliographic database containing over 1,700 entries was compiled using PROCITE software.
NTIS

N94-11471# Science Applications International Corp., Durham, NC.

METHODOLOGIES FOR ESTIMATING AIR EMISSIONS FROM THREE NON-TRADITIONAL SOURCE CATEGORIES: OIL SPILLS, PETROLEUM VESSEL LOADING AND UNLOADING, AND COOLING TOWERS Final Report, Oct. 1991 - Mar. 1993

W. Ramadan, S. Sleva, K. Dufner, S. Snow, and S. L. Kersteter Apr. 1993 119 p Sponsored by EPA, Research Triangle Park, NC Prepared in cooperation with Southern Research Inst., Durham, NC, and TRC Environmental Corp., Chapel Hill, NC
(Contract EPA-68-D9-0173)
(PB93-181592; EPA/600/R-93/063) Avail: CASI HC A06/MF A02

The report discusses part of EPA's program to identify and characterize emissions sources not currently accounted for by either the existing Aerometric Information Retrieval System (AIRS) or State Implementation Plan (SIP) area source methodologies and to develop appropriate emissions estimation methodologies and emission factors for a group of these source categories. Based on the results of the identification and characterization portions of this research, three source categories were selected for methodology and emission factor development: oil spills, petroleum vessel loading and unloading, and cooling towers. The report describes the category selection process and presents emissions estimation methodologies and emission factor data for the selected source categories. The discussions for each category include general background information, emissions generation activities, pollutants emitted, sources of activity and pollutant data, emissions estimation methodologies and data issues. The information used in these discussions was derived from various sources including available literature, industrial and trade association publications and contracts, experts on the category and activity, and knowledgeable federal and state personnel. NTIS

N94-11472# Naval Energy and Environmental Support Activity, Port Hueneme, CA.

CATALYTIC OXIDATION OF ORGANICS IN VAPOR STREAMS AT REMEDIATION SITES Remedial Action Tech Data Sheet

Jan. 1993 10 p
(PB93-182962; NEESA-20.2-051.5) Avail: CASI HC A02/MF A01

Leaks from underground fuel storage tanks and associated piping have resulted in contamination of soil and ground water. Navy-wide, more than 350 sites are in need of remediation to remove fuel contamination from soil and ground water. These sites are located at about 80 different Navy activities (including Marine Corps installations). As a result of remedial activities to clean these contaminated soils and ground water, contaminated air streams are often generated. Available alternatives for the treatment of these air streams include carbon adsorption and incineration. The Tech Data Sheet describes catalytic oxidation, a third alternative that has the potential to be effective at a lower cost. NTIS

N94-11584# Advisory Commission on Intergovernmental Relations, Washington, DC.

INTERGOVERNMENTAL DECISIONMAKING FOR ENVIRONMENTAL PROTECTION AND PUBLIC WORKS

D. R. Mandelker, M. C. Rubino, and K. I. Rubin Nov. 1992 96 p
(PB93-176824; A-122) Avail: CASI HC A05/MF A01

The purpose of the study is to identify conflicts between state and local provision of public works and the federal environmental decisions concerning these proposed public works. The federal environmental decision-making process includes federal agency permitting, licensing, review (approval/disapproval), and veto of state and local public works projects. Where conflicts are defined and appear unmanageable, the study will propose and assess alternative solutions that could improve the efficiency and timeliness of public works processes while protecting the environment.
NTIS

N94-11671# Clarkson Univ., Potsdam, NY. Dept. of Chemistry.

STUDY OF THE ATMOSPHERIC CHEMISTRY OF RADON PROGENY IN LABORATORY AND REAL INDOOR ATMOSPHERES

P. K. Hopke Jul. 1992 12 p
(Contract DE-FG02-90ER-61029)
(DE93-012236; DOE/ER-61029/13) Avail: CASI HC A03/MF A01

This report describes studies on the chemical and physical behavior of the Po-218 atom immediately following its formation by the alpha decay of radon. Because small changes in size for activity in the sub-10 nm size range result in large changes in the delivered dose per unit exposure, this behavior must be understood if the exposure to radon progeny and its dose to the cells in the respiratory tract are to be fully assessed. The specific tasks of the controlled laboratory studies are to determine the formation rates of (center dot)OH radicals formed by the radiolysis of air following radon decay, to examine the formation of particles by the radiolytic oxidation of substances like SO2 ethylene, and H2S to lower vapor pressure compounds and determine the role of gas phase additives such as H2O and NH3 in determining the particle size, to measure the rate of ion-induced nucleation using a thermal diffusion cloud chamber, and to measure the neutralization rate of Po-218(x)(+) in O2 at low radon concentrations.

Tasks of the exposure studies in occupied indoor spaces are to initiate measurements of the activity size distributions in actual homes with occupants present so that the variability of the indoor activity size distributions can be assessed with respect to indoor aerosol sources and general lifestyle variations of the occupants, to initiate a prospective study of the utility of measurement of deposited Pb-210 embedded in glass surfaces as a measure of the long-term, integrated exposure of the population to radon, and to develop the methodology to determine the hygroscopicity of the indoor aerosol so that the changes in deposition efficiency of the radioactive indoor aerosol with hygroscopic growth in the respiratory tract can be assessed. DOE

N94-11697# Alaska Univ., Fairbanks. Inst. of Northern Engineering.
ENERGY FLOW IN AN ARCTIC AQUATIC ECOSYSTEM
D. M. Schell 1993 8 p
(Contract DE-FG06-84ER-60265)
(DE93-013178; DOE/ER-60265/T1) Avail: CASI HC A02/MF A01

This project has been using natural isotope abundances to trace major pathways of energy flow to consumers in Imnavait Creek and the tundra ecosystem of the R4D watershed with comparative work in the coastal tundra. We are processing samples collected at the R4D intensive site over the past three years and are comparing these data with similar samples collected from the coastal plain. Our approach is as follows: to determine if carbon is accumulating in upland and coastal tundra; to determine the role of eroded peat carbon in the aquatic ecosystem; and to determine the distribution of carbon and nitrogen isotopes in the tundra-pond ecosystem to establish the feasibility of using natural differences as tracers. DOE

N94-11845# Brookhaven National Lab., Upton, NY.
COPROCESSING OF FOSSIL FUELS AND BIOMASS FOR CO2 EMISSION REDUCTION IN THE TRANSPORTATION SECTOR Report, Apr. 1991 - Jul. 1992
Meyer Steinberg, Yuan-Ji Dong (Hydrocarb Corp., New York, NY.), and Robert H. Borgwardt (Environmental Protection Agency, Research Triangle Park, NC.) 1993 10 p Presented at the IEA Carbon Dioxide Disposal Symposium, Oxford, England, 29-31 Mar. 1993
(Contract EPA-IAG-DW-89934598)
(PB93-194165; EPA/600/A-93/109) Avail: CASI HC A02/MF A01

The paper discusses an evaluation of the Hydrocarb process for conversion of carbonaceous raw material to clean carbon and methanol products. As fuel, methanol and carbon can be used economically, either independently or in slurry form, in efficient heat engines (turbines and internal combustion engines) for both mobile and stationary single and combined cycle power plants. When considering carbon dioxide (CO2) emission control in the utilization of fossil fuels, the coprocessing of those fossil fuels with biomass (which may include wood, municipal solid waste, and sewage sludge) is a viable mitigation approach. By coprocessing both types of feedstock to produce methanol and carbon, while sequestering all or part of the carbon, a significant net CO2 reduction is achieved if the methanol is substituted for petroleum fuels in the transportation sector. Biomass removes CO2 from the atmosphere by photosynthesis and is thus a prime feedstock for mitigation of CO2 emission from mobile sources. Since the availability of biomass will, in most cases, determine the amount of petroleum that can be displaced, it is essential to obtain maximum yield of fuel in the conversion process. NTIS

N94-11864# Coastal Environmental Services, Inc., Linthicum, MD.
DATA MANAGEMENT STRATEGY FOR THE TAMPA BAY NATIONAL ESTUARY PROGRAM: RECOMMENDATIONS AND IMPLEMENTATION PLAN Final Technical Report
Sara Cairns Aug. 1992 200 p
(Contract T-91-11)
(PB93-191633; TBNEP-08-92) Avail: CASI HC A09/MF A03

One goal of the Tampa Bay National Estuary Program (TBNEP) is to identify and develop the plans for a data management system that meets the needs of potential users who can benefit from improved access to information that is pertinent to resource management. As part of the project, the needs and goals of data users in the Tampa Bay area were investigated by means of a survey, followed by a workshop at which participants discussed how the DMS could improve on existing information resources. The recommendations resulting from the survey and workshop discussions focused on the following: (1) developing a Central Subject Directory (CSD) for existing data, (2) standardizing data management forms and protocols used by different agencies, and (3) providing data management services for the TBNEP throughout its tenure. NTIS

N94-12269 Iowa State Univ. of Science and Technology, Ames.
THE GLOBAL POTENTIAL ENERGY SURFACES OF THE LOWEST TWO 1A' STATES OF THE OZONE MOLECULE: THEORETICAL DETERMINATION AND ANALYSIS Ph.D. Thesis
Gregory John Atchity 1992 271 p
Avail. Univ. Microfilms Order No. DA9311473

The two lowest 1A' potential energy surfaces (PES) of the ozone molecule are determined and analyzed using accurate ab-initio MCSCF calculations. As appropriate internal coordinates, the shape-scale perimetric coordinates for triatomic molecules are discussed and further developed. Because the previously determined intersection between these two surfaces of like symmetry is unusual, much of the present work involves this intersection. The relevant theory of intersections is reviewed, and a method for characterizing intersections according to the topology of the surfaces in their vicinity is developed. Furthermore, the reasons for this particular crossing in ozone are investigated. The analysis is based on a method for transforming the adiabatic states produced by quantum chemical calculations into diabatic states. The method is founded on the idea that a diabatic state should be dominated throughout coordinate space by a single set of configurations. Accordingly, the transformation to diabatic states is derived by maximizing the contribution of these configurations to their respective states. It is shown that the crossing in ozone is due to an additional exchange in dominance of configurations within each diabatic state. The intersection point in C(sub 2v) symmetry is part of a larger, 1-dimensional intersection seam in C(sub s) symmetry. This seam is shown to consist of four branches, one of which is a closed loop. The three other branches lie entirely in C(sub 2v) restricted subspaces and connect to the first branch at nodes. Additional intersections must exist. A new method for determining an intersection point in a two-dimensional coordinate space, based on the wave function phase-change theorem of Herzberg-Longuet-Higgins, is also developed. Finally, global mappings of the two potential energy surfaces in the scale-shape perimetric coordinates are determined. The minima of the two surfaces, their dissociation and rearrangement paths, and the map of the energy difference between them are all discussed. It is shown that direct formation of the ring structure of ozone from O2 and O is improbable and that there is no rearrangement pathway on the ground state representing the interchange of two atoms. Dissert. Abstr.

N94-12451*# New Hampshire Univ., Durham. Inst. for the Study of Earth, Oceans and Space.
TERMINAL DECOMPOSITION AND GASEOUS SULFUR RELEASE FROM TIDAL WETLANDS Final Technical Report, 1 Oct. 1983 - 31 May 1992
Mark E. Hines 1992 137 p
(Grant NAGw-0512)
(NASA-CR-193466; NAS 1.26:193466) Avail: CASI HC A07/MF A02

A summary of the results of a multi-year project which studied the release of biogenic sulfur gases from wetland habitats is reported. This project also included an initial study of factors that control terminal decomposition in temperate salt marsh sediments. This preliminary research was used as a biogeochemical foundation for the interpretation of data collected during other aspects of the work. As time progressed the research moved greatly into freshwaters since it became clear that these habitats had a greater influence on regional and global processes and these habitats were grossly understudied with respect to their role as producers and consumers of atmospheric S compounds. More detailed information is provided as appendices. For individual titles, see N94-12452 through N94-12470.

N94-12452*# New Hampshire Univ., Durham.
A PRELIMINARY STUDY OF THE VARIABILITY AND MAGNITUDE OF THE FLUX OF BIOGENIC SULFUR GASES FROM A NEW HAMPSHIRE SALT MARSH M.S. Thesis
Michael Cope Morrison *In its* Terminal Decomposition and Gaseous Sulfur Release from Tidal Wetlands 1992 2 p (For primary document see N94-12451 01-45)
Avail: CASI HC A01/MF A02

Salt marshes have highly variable spatial and temporal fluxes of hydrogen sulfide, carbonyl sulfide, methane thiol, dimethyl sulfide, and carbon disulfide (H2S, COS, MeSH, DMS, and CS2, respectively). This variability was tested at nine emission sites in a New Hampshire, USA salt marsh: three replicates in each of three vegetation zones, Spartina alterniflora, S. patens, and a transition zone. Three sites were sampled simultaneously, either within or across vegetation zones, using a dynamic flux chamber technique. Difficulties with calibration and field equipment resulted in fluxes with maximum absolute uncertainties of greater than plus or minus 200 percent. However, the relative uncertainty between subsequent samples was closer to plus or minus 20 percent. Chambers are expected to affect the natural flux of gases by altering the humidity, temperature, and composition of the gas inside the chamber. Summertime fluxes are highest for all gases except COS which demonstrated evidence of a springtime peak. A summertime background flux of 5 to 100 x 10(exp -9) g S/m(sup -2) min was observed for all gases, while S alternifora fluxes of MeSH and DMS were approximately 8 fold and approximately 100 fold higher than S. patens, respectively. DMS and MeSH fluxes were higher during the day than at night. Evidence of COS uptake by plants was observed. CS2 appeared to be the quantitatively least important sulfur gas emitted. Improved laboratory and sample collection techniques and further data collection in the field will yield information on the details of salt marsh variability, will improve estimates of the error associated with single flux measurements, and will allow a more accurate estimation of sulfur fluxes from salt marshes based on vegetation and area coverage data. Inability to control the temperature and humidity inside of the chamber remain significant problems with the chamber design. Author (revised)

N94-12453*# New Hampshire Univ., Durham.

SULFATE REDUCTION AND OTHER SEDIMENTARY BIOGEOCHEMISTRY IN A NORTHERN NEW ENGLAND SALT MARSH

Mark E. Hines, Stephen L. Knollmeyer, and Joyce B. Tugel *In its* Terminal Decomposition and Gaseous Sulfur Release from Tidal Wetlands 1992 23 p (For primary document see N94-12451 01-45)
(Grant NAGw-512)
Avail: CASI HC A03/MF A02

Sulfate reduction rates, dissolved iron and sulfide concentrations, and titration alkalinity were measured in salt marsh soils along a transect that included areas inhabited by both the tall and short forms of Spartina alterniflora and by Spartina patens. Pore waters were collected with in situ 'sippers' to acquire temporal data from the same location without disturbing plant roots. During 1984, data collected at weekly intervals showed rapid temporal changes in belowground biogeochemical processes that coincided with changes in S. alterniflora physiology. Rates of SO4(-2) reduction increased fivefold (to greater than 2.5 micromol ml(sup -1)d(sup -1)) when plants began elongating aboveground yet decreased fourfold upon plant flowering. This rapid increase in rates of SO4(-2) reduction must have been fueled by dissolved organic matter released from roots only during active growth. Once plants flowered, the supply of oxidants to the soil decreased and sulfide and alkalinity concentrations increased despite decreases in SO4(-2) reduction and increases in SO4(-2):Cl(-) ratios. Sulfide concentrations were highest in soils inhabited by tallest plants. During 1985, S. alterniflora became infested with fly larvae (Chaetopsis apicalis John) and aboveground growth ceased in late June. This cessation was accompanied by decreased rates of SO4(-2) reduction similar to those noted during the previous year when flowering occurred. After the fly infestation, the pore-water chemical profiles of these soils resembled profiles of soils inhabited by the short form of S. alterniflora. The SO4(-2) reduction rates in S. patens soils are the first reported. Rates were similar to those in S. alterniflora except that they did not increase greatly when S. patens was elongating. Tidal and rainfall events produced desiccation-saturation cycles that altered redox conditions in the S. patens soils, resulting in rapid changes in the dissolution and precipitation of iron and in the magnitude and spatial distribution of SO4(-2) reduction. Author (revised)

N94-12454*# New Hampshire Univ., Durham. Inst. for the Study of Earth, Oceans and Space.

THE ROLE OF CERTAIN INFAUNA AND VASCULAR PLANTS IN THE MEDIATION OF REDOX REACTIONS IN MARINE SEDIMENTS

Mark E. Hines *In its* Terminal Decomposition and Gaseous Sulfur Release from Tidal Wetlands 1992 12 p (For primary document see N94-12451 01-45)
(Grants NAGw-512; NSF OCE-80-18460; NSF OCE-82-14863; NSF OCE-85-15639)
Avail: CASI HC A03/MF A02

The mechanisms by which certain animals and plants affect redox processes in sediments was examined by studying three environments: (1) subtidal sediments dominated by the deposit-feeding polychaete Heteromastus filiformis; (2) a saltmarsh inhabited by the tall form of Spartina alterniflora; and (3) tropical carbonate sediments inhabited by three species of seagrasses. S-35-sulfide production rates were compared to pool sizes of dissolved sulfide and dissolved iron. In all of the sediments studied, rates of sulfide reduction were enhanced by macroorganisms while the rate of turnover of dissolved sulfide increased. The polychaete enhanced microbial activity and redox cycling primarily by subducting particles of organic matter and oxidized iron during sediment reworking. The Spartina species enhanced anaerobic activity by transporting primarily dissolved organic matter and oxidants. Although the final result of both animal and plant activities was the enhancement of sub-surface cycling of sulfur and iron, decreased dissolved sulfide and increased dissolved iron concentrations, the mechanisms which produced these results differed dramatically. Author (revised)

N94-12455*# New Hampshire Univ., Durham. Inst. for the Study of Earth, Oceans and Space.

EMISSIONS OF BIOGENIC SULFUR GASES FROM ALASKAN TUNDRA

Mark E. Hines and Michael C. Morrison *In its* Terminal Decomposition and Gaseous Sulfur Release from Tidal Wetlands 1992 5 p (For primary document see N94-12451 01-45)
(Grant NAGw-512)
Avail: CASI HC A01/MF A02

Fluxes of the biogenic sulfur gases carbonyl sulfide (COS), dimethyl sulfide (DMS), methyl mercaptan (MeSH), and carbon disulfide (CS2) were determined for several freshwater and coastal marine tundra habitats using a dynamic enclosure method and gas chromatography. In the freshwater tundra sites, highest emissions, with a mean of 6.0 nmol/m(sup -2)H(sup -1) (1.5-10) occurred in the water-saturated wet meadow areas inhabited by grasses, sedges, and Sphagnum mosses. In the drier upland tundra sites, highest fluxes occurred in areas inhabited by mixed vegetation and labrador tea at 3.0 nmol/m(sup -2)h(sup -1) (0-8.3) and lowest fluxes were from lichen-dominated areas at 0.9 nmol/m(sup -2)h(sup -1). Sulfur emissions from a lake surface were also low at 0.8 nmol/m(sup -2)h(sup -1). Of the compounds measured, DMS was the dominant gas emitted from all of these sites. Sulfure emissions from the marine sites were up to 20-fold greater than fluxes in the freshwater habitats and were also dominated by DMS. Emissions of DMS were highest from intertidal soils inhabited by Carex subspathacea (150-250 nmol/m(sup -2)h(sup -1)). This Carex sp. was grazed thoroughly by geese and DMS fluxes doubled when goose feces were left within the flux chamber. Emissions were much lower from other types of vegetation which were more spatially dominant. Sulfure emissions from tundra were among the lowest reported in the literature. When emission data were extrapolated to include all tundra globally, the global flux of biogenic sulfur from this biome is 2-3 x 10(exp 8) g/yr. This represents less than 0.001 percent of the estimated annual global flux (approximately 50 Tg) of biogenic sulfur and less than 0.01 percent of the estimated terrestrial flux. The low emissions are attributed to the low availability of sulfate, certain hydrological characteristics of tundra, and the tendency for tundra to accumulate organic matter. Author (revised)

N94-12456*# New Hampshire Univ., Durham.

FACTORS CONTROLLING FLUXES OF VOLATILE SULFUR COMPOUNDS IN SPHAGNUM PEATLANDS Ph.D. Thesis

William Zamboni deMello *In its* Terminal Decomposition and Gaseous Sulfur Release from Tidal Wetlands 1992 2 p (For primary document see N94-12451 01-45)
Avail: CASI HC A01/MF A02

Exchange of DMS and OCS between the surface of Sphagnum peatlands and the atmosphere were measured with dynamic (S-free sweep air) and static enclosures. DMS emission rates determined by both methods were comparable. The dynamic method provided positive OCS flux rates (emission) for measurements performed at sites containing Sphagnum. Conversely, data from the static method indicated that OCS was consumed from the atmosphere. Short and long-term impacts of increased S deposition on fluxes of volatile S compounds (VSC's) from Sphagnum peatlands were

investigated in a poor fen (Mire 239) at the Experimental Lakes Area, Ontario, Canada. Additional experiments were conducted in a poor fen (Sallie's Fen in Barrington, NH, USA). At Mire 239, emissions of VSC's were monitored, before and after acidification, at control and experimental sections within two major physiographic areas of the mire (oligotrophic and minerotrophic). DMS was the predominant VSC released from Mire 239 and varied largely with time and space. Sulfur addition did not affect DMS emissions in a period of hours to a few days. DMS emissions in the experimental oligotrophic area of the mire was approximately 3-fold greater than in the control oligotrophic area, and approximately 10-fold greater than in the minerotrophic zones. These differences could be due to a combination of differences in types of vegetation, nutritional status, and S input. At Sallie's Fen, DMS fluxes were not significantly affected by sulfate amendments, while DMS and MSH concentrations increased greatly with time in the top 10 cm of the peat column. The major environmental factors controlling fluxes of DMS in a Sphagnum-dominated peatland were investigated in Sallie's Fen, NH. DMS emissions from the surface of the peatland varied greatly over 24 hours and seasonally. Temperature seemed to be the major environmental factor controlling these variabilities. Concentrations of dissolved VSC's varied with time and space throughout the fen. Dissolved DMS, MSH, and OCS in the surface of the water table were supersaturated with respect to their concentrations in the atmosphere. Sphagnum mosses did not appear to be a direct source of VSC's, however they increase transport of DMS from the peat surface to the atmosphere.
Author (revised)

N94-12457*# National Aeronautics and Space Administration. John C. Stennis Space Center, Bay Saint Louis, MS.

EMISSIONS OF SULFUR GASES FROM MARINE AND FRESHWATER WETLANDS OF THE FLORIDA EVERGLADES: RATES AND EXTRAPOLATION USING REMOTE SENSING

Mark E. Hines (New Hampshire Univ., Durham.), Ramona E. Pelletier, and Patrick M. Crill (New Hampshire Univ., Durham.) *In* New Hampshire Univ., Terminal Decomposition and Gaseous Sulfur Release from Tidal Wetlands 1992 8 p Sponsored by NASA. Washington (For primary document see N94-12451 01-45)
(Grants NAGw-512; NAGw-2771)
Avail: CASI HC A02/MF A02

Rates of emissions of the biogenic sulfur (S) gases carbonyl sulfide (COS), methyl mercaptan (MSH), dimethyl sulfide (DMS), and carbon disulfide (CS2) were measured in a variety of marine and freshwater wetland habitats in the Florida Everglades during a short duration period in October using dynamic chambers, cryotrapping techniques, and gas chromatography. The most rapid emissions of greater than 500 nmol/m(sup -2)h(sup -1) occurred in red mangrove-dominated sites that were adjacent to open seawater and contained numerous crab burrows. Poorly drained red mangrove sites exhibited lower fluxes of approximately 60 nmol/m(sup -2)h(sup -1) which were similar to fluxes from the black mangrove areas which dominated the marine-influenced wetland sites in the Everglades. DMS was the dominant organo-S gas emitted especially in the freshwater areas. Spectral data from a scene from the Landsat thematic mapper were used to map habitats in the Everglades. Six vegetation categories were delineated using geographical information system software and S gas emission were extrapolated for the entire Everglades National Park. The black mangrove-dominated areas accounted for the largest portion of S gas emissions to the area. The large area extent of the saw grass communities (42 percent) accounted for approximately 24 percent of the total S emissions.
Author (revised)

N94-12458*# New Hampshire Univ., Durham. Inst. for the Study of Earth, Oceans and Space.

EMISSIONS OF SULFUR GASES FROM WETLANDS

Mark E. Hines *In its* Terminal Decomposition and Gaseous Sulfur Release from Tidal Wetlands 1992 21 p (For primary document see N94-12451 01-45)
Avail: CASI HC A03/MF A02

Data on the emissions of sulfur gases from marine and freshwater wetlands are summarized with respect to wetland vegetation type and possible formation mechanisms. The current data base is largest for salt marshes inhabited by Spartina alterniflora. Both dimethyl sulfide (DMS) and hydrogen sulfide (H2S) dominate emissions from salt marshes, with lesser quantities of methyl mercaptan (MeSH), carbonyl sulfide (COS), carbon disulfide (CS2) and dimethyl disulfide (DMDS) being emitted. High emission rates of DMS are associated with vegetation that produces the DMS precursor dimethylsulfonionpropionate (DMSP). Although large quantities of H2S are produced in marshes, only a small percentage escapes to the atmosphere. High latitude marshes emit less sulfur gases than temperate ones, but DMS still dominates. Mangrove-inhabited wetlands also emit less sulfur than temperate S. alterniflora marshes. Few data are available on sulfur gas emissions from freshwater wetlands. In most instances, sulfur emissions from temperate freshwater sites are low. However, some temperate and subtropical freshwater sites are similar in magnitude to those from marine wetlands which do not contain vegetation that produces DMSP. Emissions are low in Alaskan tundra but may be considerably higher in some bogs and fens.
Author

N94-12459*# New Hampshire Univ., Durham. Inst. for the Study of Earth, Oceans and Space.

ACETATE CONCENTRATIONS AND OXIDATION IN SALT MARSH SEDIMENTS

In its Terminal Decomposition and Gaseous Sulfur Release from Tidal Wetlands 1992 32 p (For primary document see N94-12451 01-45)
(Grants NAGw-512; NSF OCE-85-18491; NSF OCE-84-15687; NSF OCE-86-15055)
Avail: CASI HC A03/MF A02

Acetate concentrations and rates of acetate oxidation and sulfate reduction were measured in S. alterniflora sediments in New Hampshire and Massachusetts. Pore water extracted from cores by squeezing or centrifugation contained in greater than 0.1 mM acetate and, in some instances, greater than 1.0 mM. Pore water sampled nondestructively contained much less acetate, often less than 0.01 mM. Acetate was associated with roots, and concentrations varied with changes in plant physiology. Acetate turnover was very low whether whole core or slurry incubations were used. Radiotracers injected directly into soils yielded rates of sulfate reduction and acetate oxidation not significantly different from core incubation techniques. Regardless of incubation method, acetate oxidation did not account for a substantial percentage of sulfate reduction. These results differ markedly from data for unvegetated coastal sediments where acetate levels are low, oxidation rate constants are high, and acetate oxication rates greatly exceed rates of sulfate reduction. The discrepancy between rates of acetate oxidation and sulfate reduction in these marsh soils may be due either to the utilization of substrates other than acetate by sulfate reducers or artifacts associated with measurements of organic utilization by rhizosphere bacteria. Care must be taken when interpreting data from salt marsh sediments since the release of material from roots during coring may affect the concentrations of certain compounds as well as influencing results obtained when sediment incubations are employed.
Author (revised)

N94-12460*# New Hampshire Univ., Durham. Inst. for the Study of Earth, Oceans and Space.

APPLICATION OF STATIC AND DYNAMIC ENCLOSURES IN DETERMINING DMS AND OCS FLUXES IN SPHAGNUM PEATLANDS
Abstract Only

William Zamboni deMello and Mark E. Hines *In its* Terminal Decomposition and Gaseous Sulfur Release from Tidal Wetlands 1992 1 p Submitted for publication (For primary document see N94-12451 01-45)
Avail: CASI HC A01/MF A02

A static enclosure method was applied to determine the exchange of dimethyl sulfide (DMS) and OCS between the surface of Sphagnum peatlands and the atmosphere. Measurements were performed concurrently with dynamic enclosure measurements with S-free air used as sweep gas. DMS emission rates determined by both methods were comparable between 5 and 500 nmol/m(sup -2)h(sup -1). The dynamic method provided positive OCS flux rates (emission) for measurements performed at sites containing Sphagnum. Conversely, data from the static method indicated that OCS was consumed from the atmosphere. Measurements using both techniques at a site devoid of vegetation showed that peat is a source of both DMS and OCS. Results suggested that OCS is produced in surface peat but it is taken up from the atmosphere by Sphagnum mosses. However, the net effect of both processes is that OCS uptake exceeds emission. The dynamic enclosure technique is adequate to measure rates of emissions of S gases which are produced in peatlands but not consumed, as long as attention is paid to the rate of sweep flow.
Author

N94-12461*# New Hampshire Univ., Durham. Inst. for the Study of Earth, Oceans and Space.

EFFECTS OF INORGANIC SULFUR ADDITION ON FLUXES OF VOLATILE SULFUR COMPOUNDS IN SPHAGNUM PEATLANDS Abstract Only

William Zamboni deMello, Mark E. Hines, and Suzanne E. Bayley (Alberta Univ., Edmonton.) *In its* Terminal Decomposition and Gaseous Sulfur Release from Tidal Wetlands 1992 1 p Submitted for publication (For primary document see N94-12451 01-45)

Avail: CASI HC A01/MF A02

Short and long-term impacts of increased S deposition on fluxes of volatile S compounds (VSC's) from Sphagnum peatlands were investigated in an artificially acidified (sulfuric and nitric acids) poor fen (Mire 239) at the Experimental Lakes Area (ELA), Ontario, Canada. Additional experiments were conducted in a poor fen (Sallie's Fen) in Barrington, NH, USA. At Mire 239, emissions of VSC's were monitored, before and after acidification, at control (unacidified) and experimental sections within two major physiographic zones of the mire (oligotrophic and minerotrophic). The experimental segments of the mire received S amendments since 1983, in amounts equivalent to the annual S deposition in the highest polluted areas of Canada and U.S. Dimethyl sulfide (DMS) was the predominant VSC released from the mire and varied largely with time and space (i.e., from 2.5 to 127 nmol/m(sup -2)h(sup -1)). Sulfur addition did not affect DMS emissions in a period of hours to a few days, although it stimulated production of DMS and MSH in the anoxic surficial regions of the peat. DMS emissions in the experimental oligotrophic segment of the mire was approximately 3-fold greater than in the control oligotrophic segment, and approximately 10-fold greater than in the minerotrophic zones. These differences could be due to a combination of differences in types of vegetation, nutritional status, and S input. At Sallie's Fen, DMS fluxes were approximately 8 times higher from a Sphagnum site than from a bare peat site. Fluxes of VSC's were not significantly affected by sulfate amendments at both sites, while DMS and MSH concentrations increases greatly with time in the top 10 cm of the peat column. Our data indicated that although Sphagnum is not the direct source of DMS released from Sphagnum peatlands, it might play a role in regulating DMS emissions to the atmosphere. Author (revised)

N94-12462*# New Hampshire Univ., Durham. Inst. for the Study of Earth, Oceans and Space.

ENVIRONMENTAL FACTORS CONTROLLING FLUXES OF DIMETHYL SULFIDE IN A NEW HAMPSHIRE FEN Abstract Only

William Zamboni deMello and Mark E. Hines *In its* Terminal Decomposition and Gaseous Sulfur Release from Tidal Wetlands 1992 2 p Submitted for publication (For primary document see N94-12451 01-45)
(Grant NAGw-0512)

Avail: CASI HC A01/MF A02

The major environmental factors controlling fluxes of dimethyl sulfide (DMS) in a Sphagnum-dominated peatland were investigated in a poor fen in New Hampshire. DMS emissions from the surface of the peatland varied greatly over 24 hours and seasonally. Maximum DMS emissions occurred in summer with minima in the late fall. Temperature was the major environmental factor controlling these variabilities. There was also some evidence that the changes in water table height might have contributed to the seasonable variability in DMS emission. The influence of the water table was greater during periods of elevated temperature. DMS and MSH were the most abundant dissolved volatile sulfur compound (VSC) in the surface of the water table. Concentrations of dissolved VSC's varied with time and space throughout the fen. Dissolved MDS, MSH, and OCS in the surface of the water table were supersaturated with respect to their concentrations in the atmosphere suggesting that the peat surface was a source of VSC's in the peatland. VCS in peatlands seemed to be produced primarily by microbial processes in the anoxic surface layers of the peat rich in organic matter and inorganic sulfide. Sphagnum mosses were not a direct source of VSC's. However, they increased transport of DMS from the peat surface to the atmosphere. Author (revised)

N94-12463*# New Hampshire Univ., Durham. Estuarine Lab.

SULFUR TRANSFORMATIONS IN THE SEDIMENTS OF A NEW HAMPSHIRE SALT MARSH Abstract Only

Mark E. Hines, S. L. Knollmeyer, A. Eldridge, D. Luken, Joyce B. Tugel, and W. Berry Lyons *In its* Terminal Decomposition and Gaseous Sulfur Release from Tidal Wetlands 1992 1 p (For primary document see N94-12451 01-45)

Avail: CASI HC A01/MF A02

Summer sulfate reduction and sulfide and iron chemistry were monitored in marsh soils along a gradient from a creekside Spartina alterniflora region to an inland area dominated by S. patens. Sulfate reduction rates measured using S-35 increased from 0.4 in June to as much as 4.5 micro-mole/ml(sup -1)d(sup -1) in July in S. alterniflora soils with most rapid rates occurring in the upper few cm. Rates in S. patens soils were approximately equal to 5-8 fold slower with the most rapid rates occurring generally in soils deeper than 10 cm. The recovery percentage of reduced S-35 sulfur varied with depths at both locations; dissolved and acid-volatile sulfides dominating S. alterniflora regions while chromium-reducible solid phases were abundant in S. patens soils. Dissolved sulfide in S. alterniflora soils increased throughout the summer to approximately equal to 2.8 mM while sulfide in S. patens soils was abundant only in soils deeper than 15 cm. Dissolved sulfide covaried inversely with iron. Diel studies demonstrated that sulfide and iron varied approximately equal to two-fold in response to a semi-diurnal tide. Dissolved sulfide turnover was most rapid during periods of active plant growth. Author (revised)

N94-12464*# New Hampshire Univ., Durham. Inst. for the Study of Earth, Oceans and Space.

BIOGEOCHEMICAL FACTORS WHICH REGULATE THE FORMATION AND FATE OF SULFIDE IN WETLANDS

Mark E. Hines, W. Berry Lyons, and H. E. Gaudette *In its* Terminal Decomposition and Gaseous Sulfur Release from Tidal Wetlands 1992 12 p Submitted for publication (For primary document see N94-12451 01-45)

Avail: CASI HC A03/MF A02

Coastal wetland areas occupy a small percentage of the terrestrial environment yet are extremely productive regions which support rapid rates of belowground bacterial activity. Wetlands appear to be significant as biogenic sources of gaseous sulfur, carbon, and nitrogen. These gases are important as tracers of man's activities, and they influence atmospheric chemistry. The interactions among wetland biogeochemical processes regulate the anaerobic production of reduced gases and influence the fate of these volatiles. Therefore, spatial and temporal variations in hydrology, salinity, temperature and specification, and growth of vegetation affect the type and magnitude of gas emissions thus hindering predictive estimates of gas flux. Our research is divided into two major components, the first is the biogeochemical characterization of a selected tidal wetland area in terms of factors likely to regulate sulfide flux; the second is a direct measurement of gaseous sulfur flux as related to changes in these biogeochemical conditions. Presently, we are near completion of phase one. Author (revised)

N94-12465*# New Hampshire Univ., Durham. Inst. for the Study of Earth, Oceans and Space.

THE EFFECTS OF ACID DEPOSITION ON SULFATE REDUCTION AND METHANE PRODUCTION IN PEATLANDS Abstract Only

Georgia L. Murray, Mark E. Hines, and Suzanne E. Bayley (Alberta Univ., Edmonton.) *In its* Terminal Decomposition and Gaseous Sulfur Release from Tidal Wetlands 1992 1 p Presented at the Gordon Research Conference on Hydrological/Geological/Biological Interactions in Forested Catchments, Plymouth, NH, 1991 (For primary document see N94-12451 01-45)

Avail: CASI HC A01/MF A02

Peatlands, as fens and bods, make up a large percentage of northern latitude terrestrial environments. They are organic rich and support an active community of anaerobic bacteria, such as methanogenic and sulfate-reducing bacteria. The end products of these microbial activities, methane and hydrogen sulfide, are important components in the global biogeochemical cycles of carbon and sulfur. Since these two bacterial groups compete for nutritional substrates, increases in sulfate deposition due to acid rain potentially can disrupt the balance between these processes leading to a decrease in methane production and emission. This is significant because methane is a potent greenhouse gas that effects the global heat balance. A section of Mire 239 in the Experimental Lakes Area, in Northwestern Ontario, was artificially acidified and rates of sulfate reduction and methane production were measured with depth. Preliminary results suggested that methane production was not affected immediately after acidification. However, concentrations of dissolved methane decreased and dissolved sulfide increased greatly after acidification and both took several days to recover. The exact mechanism for the decrease in methane was not determined. Analyses are under way which will be used to determine rates of sulfate reduction. These results will be available by Spring and will be discussed. Author

N94-12466*# New Hampshire Univ., Durham. Inst. for the Study of Earth, Oceans and Space.

DMS EMISSIONS FROM SPHAGNUM-DOMINATED WETLANDS Abstract Only

Mark E. Hines, William Zamboni deMello, and Suzanne E. Bayley *In its* Terminal Decomposition and Gaseous Sulfur Release from Tidal Wetlands 1992 1 p (For primary document see N94-12451 01-45)

Avail: CASI HC A01/MF A02

The role of terrestrial sources of biogenic S and their effect on atmospheric chemistry remain as major unanswered questions in our understanding of the natural S cycle. The role of northern wetlands as sources and sinks of gaseous S was investigated by measuring rates of S gas exchange as a function of season, hydrologic conditions, and gradients in trophic status. Experiments were conducted in wetlands in New Hampshire (NH), and in Mire 239, a poor fen at the Experimental Lakes Area (ELA) in Ontario. Emissions were determined using Teflon enclosures, gas cryotrapping methods, and GC with flame photometric detection. Emissions of DMS dominated fluxes. In NH, DMS fluxes were greater than 1.6 micromol/m(sup -2)d(sup -1) in early summer, 1989 when temperatures were warm and the water table was approximately 5 cm below the surface. These rates are several-fold faster than average oceanic rates of DMS emission. A rapid drop in the water table resulted in a 6-fold decrease in DMS emissions in late July. In 1990, a new beaver dam kept water levels above the surface and S emissions were much lower than during 1989. The elimination of the beaver and a drop in the water table in August produced a rapid increase in S gas emissions. Emissions of DMS were highest in the most oligotrophic areas. Mire 239 (ELA) was irrigated with sulfuric and nitric acids to simulate acid rain. S emissions were determined before and after an acidification event in control and experimental areas in both minerotrophic and oligotrophic regions. Emissions of DMS were higher in the acidified areas compared to unacidified controls. Emissions were also much higher in the oligotrophic regions compared to the minerotrophic ones. Despite the wide differences in S gas fluxes (20-fold), it was difficult to determine whether acidification or variations in trophic status was not responsible for differences in S gas emissions. DMS emitted into the atmosphere was not derived from the water table but originated in peat in the unsaturated zone. Author (revised)

N94-12467*# New Hampshire Univ., Durham. Inst. for the Study of Earth, Oceans and Space.

EMISSIONS OF BIOGENIC SULFUR GASES FROM NORTHERN BOGS AND FENS Abstract Only

William Zamboni deMello, Mark E. Hines, and Suzanne E. Bayley (Alberta Univ., Edmonton.) *In its* Terminal Decomposition and Gaseous Sulfur Release from Tidal Wetlands 1992 1 p (For primary document see N94-12451 01-45)

Avail: CASI HC A01/MF A02

Sulfur gases are important components of the global cycle of S. They contribute to the acidity of precipitation and they influence global radiation balance and climate. The role of terrestrial sources of biogenic S and their effect on atmospheric chemistry remain as major unanswered questions in our understanding of the natural S cycle. The role of northern wetlands as sources and sinks of gaseous S by measuring rates of S gas exchange as a function of season, hydrologic conditions, and gradients in tropic status was investigated. Experiments were conducted in wetlands in New Hampshire, particularly a poor fen, and in Mire 239, a poor fen at the Experimental Lakes Area (ELA) in Ontario. Emissions were determined using Teflon enclosures, gas cryotrapping methods and gas chromatography (GC) with flame photometric detection. Dynamic (sweep flow) and static enclosures were employed which yielded similar results. Dissolved S gases and methane were determined by gas stripping followed by GC. Author (revised)

N94-12468*# New Hampshire Univ., Durham. Inst. for the Study of Earth, Oceans and Space.

ELEVATED ACETATE CONCENTRATIONS IN THE RHIZOSPHERE OF SPARTINA ALTERNIFLORA AND POTENTIAL INFLUENCES ON SULFATE REDUCTION

Mark E. Hines, Joyce B. Tugel, A. E. Giblin (Marine Biological Lab., Woods Hole, MA.), G. T. Banta (Marine Biological Lab., Woods Hole, MA.), and J. E. Hobbie (Marine Biological Lab., Woods Hole, MA.) *In its* Terminal Decomposition and Gaseous Sulfur Release from Tidal Wetlands 1992 1 p (For primary document see N94-12451 01-45)

Avail: CASI HC A01/MF A02

Acetate is important in anaerobic metabolism of non-vegetated sediments but its role in salt marsh soils was not investigated thoroughly. Acetate concentrations, oxidation (C-14) and SO4(2-) reduction (S-35) were measured in S. alterniflora soils in NH and MA. Pore water from cores contained greater than 0.1 mM acetate and in some instances greater than 1.0 mM. Non-destructive samples contained less than 0.01 mM. Acetate was associated with roots and concentrations were highest during vegetative growth and varied with changes in plant physiology. Acetate turnover was very low whether whole core or slurry incubations were used. Radiotracers injected directly into soils yielded rates of SO4(2-) reduction and acetate oxidation not significantly different from core incubation techniques. Regardless of incubation method, acetate oxidation did not account for a significant percentage of SO4(2-) reduction. These results differ markedly from data for non-vegetated coastal sediments where acetate levels are low, oxidation rate constants are high and acetate oxidation rates greatly exceed rates of SO4(2-) reduction. The discrepancy between rates of acetate oxidation and SO4(2-) reduction in marsh soils may be due either to the utilization of substrates other than acetate by SO4(2-) reducers or artifacts associated with measurements of organic utilization by rhizosphere bacteria. Author (revised)

N94-12469*# New Hampshire Univ., Durham. Inst. for the Study of Earth, Oceans and Space.

FACTORS CONTROLLING SULFUR GAS EXCHANGE IN SPHAGNUM-DOMINATED WETLANDS

William Zamboni deMello, Mark E. Hines, and Suzanne E. Bayley (Alberta Univ., Edmonton.) *In its* Terminal Decomposition and Gaseous Sulfur Release from Tidal Wetlands 1992 1 p (For primary document see N94-12451 01-45)

Avail: CASI HC A01/MF A02

Atmosphere-peatland exchange of reduced sulfur gases was determined seasonally in fen in NH, and in an artificially-acidified fen at the Experimental Lakes Area (ELA) in Canada. Dimethyl sulfide (DMS) dominated gas fluxes at rates as high as 400 nmol/m(sup -2)hr(sup -1). DMS fluxes measured using enclosures were much higher than those calculated using a stagnant-film model, suggesting that Sphagnum regulated efflux. Temperature controlled diel and seasonal variability in DMS emissions. Use of differing enclosure techniques indicated that vegetated peatlands consume atmospheric carbonyl sulfide. Sulfate amendments caused DMS and methane thiol concentrations in near-surface pore waters to increase rapidly, but fluxes of these gases to the atmosphere were not affected. However, emission data from sites experiencing large differences in rates of sulfate deposition from the atmosphere suggested that chronic elevated sulfate inputs enhance DMS emissions from northern wetlands. Author (revised)

N94-12470*# New Hampshire Univ., Durham. Inst. for the Study of Earth, Oceans and Space.

SULFUR GAS EXCHANGE IN SPHAGNUM-DOMINATED WETLANDS

Mark E. Hines, William Zamboni deMello, and Carolyn A. Porter *In its* Terminal Decomposition and Gaseous Sulfur Release from Tidal Wetlands 1992 1 p (For primary document see N94-12451 01-45)

Avail: CASI HC A01/MF A02

Sulfur gases are important components of the global cycle of S. They contribute to the acidity of precipitation and they influence global radiation balance and climate. The role of terrestrial sources of biogenic S and their effect on atmospheric chemistry remain as major unanswered questions in our understanding of the natural S cycle. The role of northern wetlands as sources and sinks of gaseous S was investigated by measuring rates of S gas exchange as a function of season, hydrologic conditions, and gradients in trophic status. The effects of inorganic S input on the production and emission of gaseous S were also investigated. Experiments were conducted in wetlands in New Hampshire, particularly a poor fen, fens within the Experimental Lakes Area (ELA) in Ontario, Canada and in freshwater and marine tundra. Emissions were determined using Teflon enclosures, gas cryotrapping methods, and gas chromatography (GC) with flame photometric detection. Dynamic (sweep flow) and static enclosures were employed. Dissolved gases were determined by gas stripping followed by GC.

Author (revised)

N94-12592# Lawrence Livermore National Lab., CA.

COMMENTS ON POSSIBLE CAUSES OF RECENT GLOBAL WARMING

P. B. Duffy 24 Sep. 1992 9 p Presented at the 73rd AMS Meeting, Anaheim, CA, 17-22 Jan. 1992

(Contract W-7405-eng-48)

(DE93-010501; UCRL-JC-110846; CONF-9201148-1) Avail: CASI HC A02/MF A01

The researcher shows that recent global temperature changes cannot be due to solar luminosity variations coincident with changes in solar cycle amplitudes, since this would violate causality. In addition, a related suggestion using solar cycle lengths instead of amplitudes appears highly unlikely, since time lags between changes in the cycle lengths and observed temperatures are very different from those calculated with a climate model. Finally, lag correlations between historical land and sea temperates indicate that ocean temperatures follow land temperatures by 15 or 20 yr. This means that the oceans' response time must be at least this long, if these temperature changes are due to some change in external forcing. It also suggests that this is in fact the case, since 'natural' climate variations might well entail SST's changing beforeLAT's, which is not observed.

DOE

N94-12780# Los Alamos National Lab., NM.

QUALITY ASSURANCE FOR ENVIRONMENTAL CHEMISTRY: 1991, VOLUME 2

M. A. Gautier, E. S. Gladney, E. A. Jones, N. L. Koski, B. T. OMalley, G. H. Brooks, and W. D. Moss Dec. 1992 473 p

(Contract W-7405-eng-36)

(DE93-011792; LA-12436-MS-Vol-2) Avail: CASI HC A20/MF A04

This report documents the continuing quality assurance efforts of the Environmental Chemistry Group (EM-9) at the Los Alamos National Laboratory. The philosophy, methodology, computing resources, and laboratory information management system used by the quality assurance program to encompass the diversity of analytical chemistry practiced in the group are described. Included in the report are all quality assurance reference materials used, along with their certified or consensus concentrations, and all analytical chemistry quality assurance measurements made by EM-9 during 1991. This volume contains figures and tables related to analytical results and the computer software QA CHECK. DOE

N94-12783# SRI International Corp., Menlo Park, CA.

NOVEL MASS SPECTROMETRIC INSTRUMENT FOR GASEOUS AND PARTICULATE CHARACTERIZATION AND MONITORING

M. J. Coggiola Feb. 1993 15 p

(Contract DE-AC21-92MC-29116)

(DE93-014093; DOE/MC-29116/3355) Avail: CASI HC A03/MF A01

SRI International will develop a unique new instrument that will be capable of providing real-time, quantitative, chemical characterization of gaseous and particulate pollutants generated from DOE waste cleanup activities. The instrument will be capable of detecting and identifying volatile organic compounds, polynuclear aromatic hydrocarbons, heavy metals, and transuranic species released during waste cleanup activities. The instrument will be unique in its ability to detect and quantify in real-time these diverse pollutants in both vapor and particulate form. The function of the sampler is to obtain a sufficient and representative quantity of air pollutants from a wide range of waste cleanup activities, both vapor and particulate. In addition, the sampler must deliver the vapors and particles to the detection instrument with minimal material loss. DOE

N94-11836# National Inst. for Environmental Studies, Tsukuba (Japan).

SATELLITE OBSERVATION OF ATMOSPHERIC TRACER COMPONENTS: JEM/POP [TAIKI BIRYOU SEIBUN NO EISEI KANSOKU: JEM/POP]

Makoto Suzuki *In* NASDA, The Second Workshop on Refrigerating System Utilization Onboard the JEM 31 Mar. 1993 p 76-88 In JAPANESE (For primary document see N94-11831 01-31)

Avail: CASI HC A03/MF A02

N94-11977 Tokyo Univ. (Japan). Center for Climate System Research.

STUDY OF CLIMATIC EFFECTS OF CLOUD-AEROSOL INTERACTION

Teruyuki Nakajima *In* Scientific Organizing Committee of PORSEC, Proceedings of the PORSEC 1992 in Okinawa: Conference for Pacific Ocean Environments and Probing, Volume 1 25 Aug. 1992 p 476-477 (For primary document see N94-11894 01-42)

Copyright Avail: Issuing Activity (Scientific Organizing Committee of PORSEC, P.O. Box 10, Shimizu, Shizuoka 424, Japan, HC)

N94-11979 Kagoshima Univ. (Japan). Faculty of Education.

OVERWATER ATMOSPHERIC DISPERSION OF VOLCANIC SMOKES FROM MT. SAKURAJIMA OBSERVED IN NOAA-AVHRR DATA

K. Kinoshita, S. Hosoyamada, Sei-Ichi Saitou (Japan Weather Association, Tokyo.), and Azumi Shirasawa (Japan Weather Association, Tokyo.) *In* Scientific Organizing Committee of PORSEC, Proceedings of the PORSEC 1992 in Okinawa: Conference for Pacific Ocean Environments and Probing, Volume 1 25 Aug. 1992 p 483-488 (For primary document see N94-11894 01-42)

Copyright Avail: Issuing Activity (Scientific Organizing Committee of PORSEC, P.O. Box 10, Shimizu, Shizuoka 424, Japan, HC)

N94-11983 Japan Consulting Engineers Association.

A STUDY OF POLLUTION COURSES OF SPILLED OIL FLOATATION IN THE OUTER OCEAN

Anshin Ishimine *In* Scientific Organizing Committee of PORSEC, Proceedings of the PORSEC 1992 in Okinawa: Conference for Pacific Ocean Environments and Probing, Volume 1 25 Aug. 1992 p 505-509 (For primary document see N94-11894 01-42)

Copyright Avail: Issuing Activity (Scientific Organizing Committee of PORSEC, P.O. Box 10, Shimizu, Shizuoka 424, Japan, HC)

N94-12520# Ministry of Posts and Telecommunications, Tokyo (Japan). Communications Research Lab.

ARTIFICIAL OIL POLLUTION DETECTION AND WAVE OBSERVATION IN THE SEA ADJACENT TO JAPAN BY ERS-1 SAR

Kenichi Okamoto, Harunobu Masuko, Satoshi Ochiai, Seiho Uratsuka, Kenji Nakamura, Hiroaki Horie, Masaharu Fujita, Masanobu Shimada (National Space Development Agency, Tokyo, Japan.), Masao Nakai (National Space Development Agency, Tokyo, Japan.), and Akira Shibata (Meteorological Research Inst., Tsukuba, Japan.) *In* ESA, Proceedings of 1st ERS-1 Symposium on Space at the Service of Our Environment, Volume 2 Mar. 1993 p 817-821 (For primary document see N94-12471 01-43)

Copyright Avail: CASI HC A01/MF A03; EPD, ESA, ESTEC, Noordwijk, Netherlands, HC

N94-12522# Oceanor, Trondheim (Norway).

OIL SPILL DETECTION USING SATELLITE-BASED SAR: EXPERIENCE FROM A FIELD EXPERIMENT

Tom-Ivar Bern, Terje Wahl (Norwegian Defence Research Establishment, Kjeller.), Tom Anderssen (Oslo Univ., Kjeller, Norway.), and Richard Olsen (Satlantic, Inc., Halifax, Nova Scotia.) *In* ESA, Proceedings of 1st ERS-1 Symposium on Space at the Service of Our Environment, Volume 2 Mar. 1993 p 829-834 Previously announced in IAA as A93-28143 Sponsored by ESSO Norge A/S, Norway; Statoil Norge S/A, Norway; Marine Spill Response Corp.; Norwegian Space Center; Norwegian State Pollution Control Authority; ESA; DEC Norge A/S; and OCEANOR A/S (For primary document see N94-12471 01-43)

Copyright Avail: CASI HC A02/MF A03; EPD, ESA, ESTEC, Noordwijk, Netherlands, HC

N94-12523# Paris VI Univ. (France).

PILOT PROJECT PPF12. COASTAL AND FLUVIAL ENVIRONMENT IN FRENCH GUIANA: FIRST RESULTS OF ERS-1 SAR DATA ANALYSIS

Jean-Paul Rudant, J. P. Cautru (Bureau de Recherches Geologiques et Minieres, Cayenne, France.), Marc Lointier (Institut Francais de Recherche Scientifique pour le Developpement en Cooperation, Cayenne.), Christophe Charron (Institut Francais de Recherche Scientifique pour le Developpement en Cooperation, Cayenne.), M. Dechambre (Centre de Recherches en

Physique de l'Environnement, Velizy, France.), B. Deffontaines, J. P. Deroin (Bureau de Recherches Geologiques et Minieres, Cayenne, France.), M. T. Prost (Institut Francais de Recherche Scientifique pour le Developpement en Cooperation, Cayenne.), D. Raymond, and O. Vanderhaeghe (Bureau de Recherches Geologiques et Minieres, Cayenne, France.) *In* ESA, Proceedings of 1st ERS-1 Symposium on Space at the Service of Our Environment, Volume 2 Mar. 1993 p 835-845 (For primary document see N94-12471 01-43)
Copyright Avail: CASI HC A03/MF A03; EPD, ESA, ESTEC, Noordwijk, Netherlands, HC

N94-12677 Deutsche Forschungsanstalt fuer Luft- und Raumfahrt, Oberpfaffenhofen (Germany).
INFORMATION CAPABILITY OF NOAA-AVHRR DATA FOR MONITORING OCEANOGRAPHIC AND ATMOSPHERIC POLLUTION
Hans-Joachim Lotz-Iwen, Stefan Werner Dech, Ruediger Glaser (Wuerzburg Univ., Germany.), and Andrea Holz (Mainz Univ., Germany.) *In* Scientific Organizing Committee of PORSEC, Proceedings of the PORSEC 1992 in Okinawa: Conference for Pacific Ocean Environments and Probing, Volume 2 25 Aug. 1992 p 790-795 (For primary document see N94-12635 01-42)
Copyright Avail: Issuing Activity (Scientific Organizing Committee of PORSEC, P.O. Box 10, Shimizu, Shizuoka 424, Japan, HC)

46 GEOPHYSICS

Includes aeronomy; upper and lower atmosphere studies; ionospheric and magnetospheric physics; and geomagnetism.

For space radiation see *93 Space Radiation.*

N94-10151# Lawrence Livermore National Lab., CA.
AMIP: THE ATMOSPHERIC MODEL INTERCOMPARISON PROJECT
W. L. Gates Dec. 1992 20 p
(Contract W-7405-eng-48)
(DE93-007400; UCRL-ID-111532-Rev-1; PCMDI-7) Avail: CASI HC A03/MF A01

The Atmospheric Model Intercomparison Project (AMIP) is an international effort to determine the systematic climate errors of atmospheric models under realistic conditions. The AMIP requires the simulation of the climate of the decade 1979-1988 using the observed monthly-averaged distributions of sea-surface temperature and sea ice as boundary conditions. Organized by the Working Group on Numerical Experimentation (WGNF) as a contribution to the World Climate Research Programme, AMIEP involves the international atmospheric modeling community in a major test and intercomparison of model performance; in addition to an agreed-to set of monthly-averaged output variables, each of the participating models will generate a daily history of state. These data will be stored and made available in standard format by the Program for Climate Model Diagnosis and Intercomparison (PCMDI) at the Lawrence Livermore National Laboratory. Following completion of the computational phase of AMIP in 1993, emphasis will shift to a series of diagnostic subprojects, now being planned, for the detailed examination of model performance and the simulation of specific physical processes and phenomena. AMIP offers an unprecedented opportunity for the comprehensive evaluation and validation of current atmospheric models and is expected to provide valuable information for model improvement. DOE

N94-10152# Lawrence Livermore National Lab., CA.
AMIP: THE ATMOSPHERIC MODEL INTERCOMPARISON PROJECT
W. L. Gates Sep. 1992 20 p
(Contract W-7405-eng-48)
(DE93-007413; UCRL-ID-111532) Avail: CASI HC A03/MF A01

The Atmospheric Model Intercomparison Project (AMIP) is an international effort to determine the systematic climate errors of atmospheric models under realistic conditions. The AMIP requires the simulation of the climate of the decade 1979-1988 using the observed monthly-averaged distributions of sea-surface temperature and sea ice as boundary conditions. Organized by the Working Group on Numerical Experimentation (WGNE) of the World Climate Resource Programme, AMIP involves the international atmospheric modeling community in a major test and intercomparison of model performance; in addition to an agreed-to set of monthly averaged output variables, each of the participating models will generate a daily history of state. These data will be stored and made available in standard format by the Program for Climate Model Diagnosis and Intercomparison (PCMDI) at the Lawrence Livermore National Laboratory. Following completion of the computational phase of AMIP in 1993, emphasis will shift to a series of diagnostic subprojects, now being formed, for the detailed examination of model performance and the simulation of specific physical processes and phenomena. AMIP offers an unprecedented opportunity for the comprehensive evaluation and validation of current atmospheric models, and is expected to provide valuable information for model improvement. DOE

N94-10285# Los Alamos National Lab., NM.
THE LATHROP WELLS VOLCANIC CENTER: STATUS OF FIELD AND GEOCHRONOLOGY STUDIES
B. Crowe, R. Morley, S. Wells (California Univ., Riverside.), J. Geissman, E. McDonald, L. McFadden, and F. Perry (New Mexico Univ., Albuquerque.) 1993 16 p
(Contract W-7405-eng-36)
(DE93-008917; LA-Sub-93-51) Avail: CASI HC A03/MF A01

The Lathrop Wells volcanic center is located 20 km south of the potential Yucca Mountain site, at the south end of the Yucca Mountain range. It has long been recognized as the youngest basalt center in the region. However, determination of the age and eruptive history of the center has proven problematic. The purpose of this paper is to describe the status of field and geochronology studies of the Lathrop Wells center. Our perspective is that it is critical to assess all possible methods for obtaining cross-checking data to resolve chronology and field problems. It is equally important to consider application of the range of chronology methods available in Quaternary geologic research. Such an approach seeks to increase the confidence in data interpretations through obtaining convergence among separate isotopic, radiogenic, and age-correlated methods. Finally, the assumptions, strengths, and weaknesses of each dating method need to be carefully described to facilitate an impartial evaluation of results. DOE

N94-10305# Alaska Univ., Fairbanks.
A STUDY OF THE MAGNETIC FIELD ANNIHILATION PROCESS IN THE MAGNETOSPHERE AND SOME GEOTECHNICAL APPLICATIONS
1993 8 p
(Contract DE-FG06-86ER-13530)
(DE93-013249; DOE/ER-13530/5; GI-91-75) Avail: CASI HC A02/MF A01

This paper describes significant progress made in the study of magnetic field reconnection and plasma processes in the magnetosphere in the past three years. A total of 43 research and review papers have been completed under the DOE support. In this paper, some of the most important results obtained in the past three-years are described. DOE

N94-10319# Alaska Univ., Fairbanks. Geophysical Inst.
A STUDY OF THE MAGNETIC FIELD ANNIHILATION PROCESS IN THE MAGNETOSPHERE AND SOME GEOTECHNICAL APPLICATIONS
1993 7 p
(Contract DE-FG06-86ER-13530)
(DE93-013248; DOE/ER-13530/6; GI-91-75a) Avail: CASI HC A02/MF A01

Our proposed project is to study the magneto reconnection processes in the Earth's magnetosphere by using both analytical methods and computer simulations. The three-dimensional (3-D) topology of the reconnected field lines and the kinetic aspects of magnetic reconnection in the collisionless magnetosphere are emphasized in the present study. At the dayside magnetopause magnetic flux ropes can form as a result of multiple X-line reconnection. Our 3-D MHD simulation shows that for an appropriate extent and location of two neighboring X-lines, a simple magnetic topology can be expected, in which the major amount of magnetic flux of the rope is connected at each end to only one side of the current sheet. This simple rope is different from the 'frayed' rope which has a complicated field topology. For a sufficient relative shift of the X-lines magnetic flux may enter a flux rope from the magnetosphere and exit into the magnetosphere, leading to the formation of magnetic flux ropes which contain a considerable amount of magnetosheath plasma on closed magnetospheric field lines. This process may provide a possible explanation for the formation of fossil

flux transfer events in the magnetosphere and the formation of the low latitude boundary layer.
DOE

N94-10323# Pacific Northwest Lab., Richland, WA.
DEVELOPMENT OF A BALLOON-BORNE STABILIZED PLATFORM FOR MEASURING RADIATIVE FLUX PROFILES IN THE ATMOSPHERIC BOUNDARY LAYER
C. D. Whiteman, J. M. Alzheimer, G. A. Anderson, and W. J. Shaw Mar. 1993 7 p Presented at the 3rd ARM Science Team Meeting, Norman, OK, 1-5 Mar. 1993, 1-5 Mar. 1993
(Contract DE-AC06-76RL-01830)
(DE93-013186; PNL-SA-21966; CONF-9303122-2) Avail: CASI HC A02/MF A01

A stabilized platform has been developed to carry broadband short-wave and long-wave radiometric sensors on the tetherline of a small tethered balloon that ascends through atmospheric depths of up to 1.5 km to obtain vertical profiles of radiative flux and flux divergence for evaluating atmospheric radiative transfer models. The Sky Platform was designed to keep the radiometers level despite unpredictable movements of the balloon and tetherline occasioned by turbulence and wind shear. The automatic control loop drives motors, gears, and pulleys located on two of the vertices of the triangular frame to climb the harness lines to keep the platform level. Radiometric sensors, an electronic compass, and an on-board data acquisition system make up the remainder of the Sky Platform. Because knowledge of the dynamic response of the tether line-platform system is essential to properly close the automatic control loop on the Sky Platform, a Motion Sensing Platform (MSP) was developed to fly in place of the Sky Platform on the tetherline to characterize the Sky Platform's operating environment. This unstabilized platform uses an array of nine solid-state linear accelerometers to measure the lateral and angular accelerations, velocities, and displacements that the Sky Platform will experience. This paper presents field performance tests of the Sky and Motion Sensing Platforms, as conducted at Richland, Washington, on February 17, 1993. The tests were performed primarily to characterize the stabilization system on the Sky Platform. Test flights were performed on this cold winter day from 1400 to 1800 Pacific Standard Time (PST). During this period, temperature profiles were near the dry adiabatic lapse rate. Flights were made through a jet wind speed profile having peak wind speeds of 7 m/s at a height of 100 m AGL. Wind directions were from the northwest. All flights were performed as continuous ascents, rather than ascending in discrete steps with halts at set altitudes.
DOE

N94-10407# Geological Survey of Canada, Ottawa (Ontario).
RADIOGENIC AGE AND ISOTOPIC STUDIES
1992 259 p
(DE93-610548; GSCAN-P-91-2) Avail: CASI HC A12/MF A03 (US Sales Only)

This is one of an annual collection of reports presenting data from the Geochronology Section of the Continental Geoscience Division of the Geological Survey of Canada (GSC). The main purpose of this collection is to make geochronological and other radiogenic isotope data produced by the section available promptly to the geological community. Reports make full presentation of the data, relate these to field settings, and make comparatively short interpretations. Other geochronological and isotope data produced in the laboratory but published in outside journals or separate GSC publications are summarized at the end of this report. Report 5 contains 24 papers from most regions of Canada, but particularly from British Columbia. The Geochronology Laboratory has, over the years, provided substantial U-Pb dating for the Cordilleran Division of the Geological Survey of Canada in Vancouver, and the results of a number of these studies are presented this year. A compilation of K-Ar ages is given.
DOE

N94-10496 Aerospace Corp., El Segundo, CA. Technology Operations.
REVIEW OF SHARC 2.0 O3 KINETICS AND SPECTROSCOPY
Valerie I. Lang 1 Apr. 1993 28 p Limited Reproducibility: More than 20% of this document may be affected by microfiche quality
(Contract F04701-88-C-0089)
(AD-A265481; TOR-93(3078)-1) Avail: CASI HC A03

A critical review of rate constants assigned to vibrational excitation and de-excitation processes for O3 in the Strategic High Altitude Atmospheric Radiance Code (SHARC 2.0) is presented. A complete list of O3 pure rotational and rovibrational band parameters, based on the 1991/92 version of the HITRAN data base, is included. Modifications to specific energy transfer processes used in the SHARC 2.0 scheme have been recommended based on recent experimental literature data and on recent atmospheric observations.
DTIC

N94-10698 Environmental Protection Agency, Washington, DC.
COMPUTER MODELS USED TO SUPPORT CLEANUP DECISION-MAKING AT HAZARDOUS AND RADIOACTIVE WASTE SITES Final Report
Mar. 1993 113 p Prepared in cooperation with DOE, Washington, DC, and Nuclear Regulatory Commission, Washington, DC Limited Reproducibility: More than 20% of this document may be affected by microfiche quality
(PB93-183333; EPA/402/R-92/005) Avail: Issuing Activity (National Technical Information Service (NTIS))

To identify computer models actually being used to support decision-making at hazardous and radioactive waste sites, the EPA, DOE, and NRC jointly funded a study. The purpose was to identify models being used for hazardous and radioactive waste site assessment and describe and classify these models. Approximately 550 surveys were mailed to people engaged in cleanups at hazardous and radioactive waste sites. Responses were received from 87. The respondents identified 127 computer models used at EPA Superfund, DOE, and NRC sites. The models included multi-media models, ground water models, air models, engineering models, surface water models, geochemical models, and utility models. The responses revealed that few models were used across a large number of sites. In contrast, the results suggested that most cleanup efforts employed site-specific models.
NTIS

N94-10701*# Pennsylvania State Univ., University Park. Dept. of Meteorology.
IN SITU DETECTION OF TROPOSPHERIC OH, HO2, NO2, AND NO BY LASER-INDUCED FLUORESCENCE IN DETECTION CHAMBERS AT REDUCED PRESSURES Final Report, 1 Oct. 1989 - 31 Mar. 1993
William H. Brune 24 Jun. 1992 60 p
(Grant NAG1-1057)
(NASA-CR-193189; NAS 1.26:193189) Avail: CASI HC A04/MF A01

For detection of OH and HO2, we have met or exceeded most of the goals of the proposal for this grant. We have succeeded in building a prototype instrument for the detection of OH and HO2 that has a detection sensitivity of about 2 x 10 exp 4 (OH molecules/cc)/(ct/s), about five times greater than proposed. The current minimum detectable OH of 1.4 x 10 exp 5 OH molecules/cc (S/N=2; 30 second integration) is less than half that proposed, and will be much lower once scattered light levels are reduced. The instrument displays other important properties. First, interfering signals from other gases and OH losses on the inlet appear to be small under laboratory and field conditions. Second, three different calibration methods, two external to the inlet, give similar results, to within 30 percent. Third, the chemical conversion efficiency of HO2 to OH by addition of reagent NO is better than 90 percent. All of these factors give us great confidence that this technique works. The instrument has gone through several variations that have not affected its potential performance but have affected its use. We were able to undergo the first field trials away from State College in June 1992, when we were able to participate informally in the ROSE experiment in rural Alabama, a year ahead of the proposed schedule for field studies. Because this field experiment was our first and the data analysis was complicated by instrument instabilities, we have not yet released the observations. None-the-less, we have gained insight into instrument design. We have not yet completed all of the proposed work. The calibration systems need to be improved to reduce the 50 percent to 100 percent uncertainties to less than 30 percent. Interference signals from ambient gases and possible losses on the inlet under field conditions need to be quantified. Finally, the detection of NO2 and NO with laser induced fluorescence is only now being seriously pursued.
Derived from text

N94-10726*# Georgia Inst. of Tech., Atlanta. School of Electrical Engineering.
INVESTIGATION OF PASSIVE ATMOSPHERIC SOUNDING USING MILLIMETER AND SUBMILLIMETER WAVELENGTH CHANNELS Semiannual Status Report No. 5, 1 Jan. - 30 Jun. 1993

A. J. Gasiewski, L. K. Adelberg, D. B. Kunkee, and D. M. Jackson 1993 69 p
(Grant NAG5-1490)
(NASA-CR-193627; NAS 1.26:193627) Avail: CASI HC A04/MF A01

Progress by investigators at the Georgia Institute of Technology in the development of techniques for passive microwave retrieval of water vapor, cloud, and precipitation parameters using millimeter- and sub-millimeter wavelength channels is reviewed. Channels of particular interest are in the tropospheric transmission windows at 90, 166, 220, 340, and 410 GHz and centered around the water vapor lines at 183 and 325 GHz. Collectively, these channels have potential application in high-resolution mapping (e.g., from geosynchronous orbit), remote sensing of cloud and precipitation parameters, and retrieval of water vapor profiles. During the period from 1 Jan. 1993 through 30 Jun. 1993 the Millimeter-wave Imaging Radiometer (MIR) completed data flights during a two-month long deployment in conjunction with TOGA/COARE. Coincident data was collected from several other ground-based, airborne, and satellite sensors, including the NASA/MSFC AMPR, MIT MTS, DMSP SSM/T-2 satellite, collocated radiosondes, ground- and aircraft-based radiometers and cloud lidars, airborne infrared imagers, solar flux probes, and airborne cloud particle sampling probes. Author

N94-10742 Los Alamos National Lab., NM.
IMAGING OF MAGNETOSPHERIC DYNAMICS USING LOW ENERGY NEUTRAL ATOM DETECTION
H. O. Funsten, D. J. McComas, K. R. Moore, and E. E. Scime 1993 19 p Presented at the AGU Monograph/Solar System Plasma Physics Meeting on Resolution of Processes in Space and Time, Yosemite, CA, Feb. 1993 Limited Reproducibility: More than 20% of this document may be affected by microfiche quality
(Contract W-7405-eng-36)
(DE93-012656; LA-UR-93-1241; CONF-9302115-1) Avail: CASI HC A03

Recent advances in low energy neutral atom (LENA) detection technology show that magnetospheric imaging is achievable with 4(sub o)(times)4(sub o) resolution and can distinguish numerous features of the magnetosphere. A critical factor in detecting low energy neutrals is their removal from the ambient UV background. One technique to accomplish this is by ionizing the neutrals by their transmission through an ultrathin charge modification foil and subsequent electrostatic deflection. In this type of instrument, the driving factor for resolution and sensitivity is scattering in the foil and the ionization probability of transiting neutrals. We describe results of a prototype LENA imager using a collimated beam of 10 keV H. Additionally, we illustrate model results of anticipated LENA images of the magnetosphere based on the Rice Convection Model and show that plasma variations resulting from geomagnetic storm disturbances can be observed using a LENA imager. DOE

N94-10798 International Centre for Theoretical Physics, Trieste (Italy).
CLASSICAL GRAVITY COUPLED TO LIOUVILLE THEORY
F. D. Mazzitelli and N. Mohammedi (Bonn Univ., Germany.) Sep. 1992 22 p Limited Reproducibility: More than 20% of this document may be affected by microfiche quality
(DE93-613049; IC-92/292) Avail: Issuing Activity (Department of Energy (DOE)) (US Sales Only)

The two dimensional Jackiw-Teitelboim model of gravity is considered. We first couple the model to the Liouville action and c scalar fields and show, treating the combined system as a nonlinear sigma model, that the resulting theory can be interpreted as a critical string moving in a target space of dimension $D = c + 2$. We then analyze perturbatively a generalized model containing a kinetic term and an arbitrary potential for the auxiliary field. We use the background field method and work covariant gauges. We show that the renormalizability of the theory depends on the form of the potential. For a general potential, the theory can be renormalized as a nonlinear sigma model. In the particular case of a Liouville-like potential, the theory is renormalized in the usual sense. DOE

N94-10950*# Scripps Institution of Oceanography, La Jolla, CA. Inst. of Geophysics and Planetary Physics.
STATISTICAL DESCRIPTION OF TECTONIC MOTIONS Final Technical Report, 15 Apr. 1987 - 31 Jan. 1993
Duncan Carr Agnew 1993 6 p
(Grant NAG5-905)
(NASA-CR-193701; NAS 1.26:193701) Avail: CASI HC A02/MF A01

This report summarizes investigations regarding tectonic motions. The topics discussed include statistics of crustal deformation, Earth rotation studies, using multitaper spectrum analysis techniques applied to both space-geodetic data and conventional astrometric estimates of the Earth's polar motion, and the development, design, and installation of high-stability geodetic monuments for use with the global positioning system. CASI

N94-11013# Phillips Lab., Hanscom AFB, MA.
EFFECTS OF ENERGETIC PARTICLE EVENTS ON VLF/LF PROPAGATION PARAMETERS/1989 Interim Report
W. I. Klemetti, J. E. Rasmussen, and P. A. Kossey 4 Dec. 1992 41 p
(AD-A265266; AD-E201543; PL-TR-92-2329; ERP-1112) Avail: CASI HC A03/MF A01

This report is a summary of disturbance effects of three major energetic particle events (PCA's) on VLF/LF propagation parameters as observed by the Phillips Laboratory High Resolution Oblique VLF/LF Ionosounder located in Northern Greenland. Disturbance effects on ionospheric reflectivity parameters, including deduced reflection heights and plane wave reflection coefficients, are presented along with riometer, magnetometer, and satellite particle detector data. DTIC

N94-11052# Lawrence Livermore National Lab., CA.
A SELF-CONSISTENT MODEL OF NON-LINEAR PARAMETERIZATION OF TURBULENT DIFFUSION IN ATMOSPHERIC BOUNDARY LAYER
V. P. Gavrilov (Institute of Experimental Meteorology, Obninsk, USSR.), N. V. Klepikova (Institute of Experimental Meteorology, Obninsk, USSR.), H. C. Rodean, and P. H. Gudiksen Nov. 1992 4 p Presented at the 10th Symposium on Turbulence and Diffusion, Portland, OR, 29 Sep. - 2 Oct. 1992
(Contract W-7405-eng-48)
(DE93-011950; UCRL-JC-110558; CONF-9209158-12) Avail: CASI HC A01/MF A01

The paper presents a self-consistent model for pollutant dispersal in the atmosphere in which coefficients of turbulent diffusion are determined through concentration distribution function. Boundary and initial conditions, which are considered for real meteorological information and real conditions of dispersal, relate field measurements to concentration distribution function and thereby to diffusion coefficient. DOE

N94-11101# Naval Command, Control and Ocean Surveillance Center, San Diego, CA.
SOME RESULTS WITH THE NEW DIGITAL IONOSONDE IN SAN DIEGO
A. K. Paul and R. A. Sprague Jan. 1993 3 p
(AD-A265178) Avail: CASI HC A01/MF A01

The new digital ionosonde (Dynasonde) became operational in early March 1992. The system takes ionograms in five minute intervals and the data are processed, extracting F-region profile and propagation parameters on a routine basis. The data verify earlier findings that a minimum sampling rate of twelve ionograms per hour is necessary to avoid aliasing. The most surprising result to date is the observation of large variations of the height of the F-region maximum (of the order of 100 km) during the nighttime hours of otherwise undisturbed days in late March and early April. The observed height variations are quasi-periodic, with periods of two to three hours and appear to have little effect on the F-region maximum electron density. DTIC

N94-11102 Pennsylvania State Univ., University Park. Dept. of Geosciences.
WAVE PROPAGATION CHARACTERISTICS OF SHORT-PERIOD CRUSTAL PHASES NEAR ARCESS AND NORESS Final Report, 1 May 1991 - 31 Oct. 1992
Kristin S. Vogfjord and Charles A. Langston Feb. 1993 54 p Limited Reproducibility: More than 20% of this document may be affected by microfiche quality
(Contract F19628-90-K-0044)
(AD-A265959; PL-TR-93-2034) Avail: CASI HC A04

Wave propagation of crustal phases near the ARCESS array is examined and compared to characteristics near the NORESS array, with emphasis on Lg and its composition. An f-k analysis is applied to the data to identify arrivals in the records. Then a composite of array beams is used to approximate each event. Record sections of composite-seismograms are constructed for different directions from ARCESS, to study propagational characteristics with distance and azimuth. Near surface velocity under NORESS and ARCESS is obtained through inversion of Rg wave dispersion curves. A composite ARCESS record section is compared to a NORESS record section of events located in the Caledonides. The differences that emerge are that Lg in the Caledonian region, north of NORESS, is dominated by discrete arrivals representing Moho reflections, with the order of reflection increasing with distance. In the Archean ARCESS region, however, Lg is dominated by turning waves, also with the order of reverberation increasing with distance, but with each confined to a small distance range. Rg wave propagation in the ARCESS region is much more efficient than in the Caledonian NORESS region, as Rg is observed to 400 km distance at ARCESS, but only to 200 km distance at NORESS. Synthetic record sections are constructed by wavenumber integration in order to model the observed character of Lg and Rg in the two regions. The dominating factor in the difference of Lg characteristics turns out to be the velocity gradient in the lower crust. A few earthquakes near ARCESS are also studied. Their depths can be constrained on the basis of phase velocities and depth phases. For reliable phase identification, however, the composition of Lg in the region needs to be accurately known. DTIC

N94-11138# Argonne National Lab., IL. Mathematics and Computer Sciences Div.

A TOOLKIT FOR BUILDING EARTH SYSTEM MODELS

I. Foster Mar. 1993 7 p

(Contract W-31-109-eng-38)

(DE93-012147; ANL/MCS-TM-171) Avail: CASI HC A02/MF A01

An earth system model is a computer code designed to simulate the interrelated processes that determine the earth's weather and climate, such as atmospheric circulation, atmospheric physics, atmospheric chemistry, oceanic circulation, and biosphere. I propose a toolkit that would support a modular, or object-oriented, approach to the implementation of such models. DOE

N94-11165# Instituto de Pesquisas Espaciais, Sao Jose dos Campos (Brazil).

A STUDY ON THE MAGNETOSPHERIC ACTIVITY USING THE AE, ap, AND Dst GEOMAGNETIC INDICES M.S. Thesis [ESTUDO DA ATIVIDADE MAGNETOSFERICA ATRAVES DOS INDICES GEOMAGNETICOS AE, AP E DST]

Marcelo MagalhaesFaresSaba Nov. 1992 123 p In PORTUGESE

(INPE-5470-TDI/501) Avail: CASI HC A06/MF A02

The usage of the geomagnetic indices AE, Dst and Kp (and its linear form ap) in studies of the earth's magnetic field variability is vast. However the relationship between them has been poorly studied. In this work different averages and correlations are done with these indices for the years 1974 (near solar minimum) and 1979 (solar maximum). A better understanding of magnetospheric activity monitoring, the relationships between these indices as well as of their uses and limitations is achieved. The correlations apx-Dst, AEx-Dst, apxAE and, for the first time, a multiple correlation apxAEx-Dst are done for different time intervals and levels of geomagnetic activity. In general, better correlations are found for the year 1974 and for the periods of geomagnetic storms. Furthermore, a study on the value of the minimum Dst and the correspondent maximum ap for storms and on two previous studies on the behavior of AE during the main phase of major magnetic storms are done. These studies make possible a better understanding of the storm/substorm relations and the estimation of indices when one of them is missing. Author (revised)

N94-11227# Lawrence Livermore National Lab., CA.

THE IMPACT OF HORIZONTAL RESOLUTION ON MOIST PROCESSES IN THE ECMWF MODEL

T. J. Phillips, L. C. Corsetti, and S. L. Grotch Jan. 1993 39 p

(Contract W-7405-eng-48)

(DE93-011718; UCRL-ID-112719; PCMDI-8) Avail: CASI HC A03/MF A01

Summer and winter climates simulated at spectral scales T21, T42, T63 and T106 with the ECMWF model are analyzed to determine the impact of changes in horizontal resolution on atmospheric water vapor, clouds, convection, and precipitation. Qualitative changes in Pi many moist processes occur in the transition from spectral T21 to T42, especially in the tropics where atmospheric convection plays a central role. However, the seasonal climate simulations do not show evidence of convergence to an asymptotic climate state at high resolution. Global convective precipitation increases monotonically with resolution, but frontal precipitation, precipitable water, and cloud cover display a qualitatively different pattern; after undergoing abrupt reductions in the transition from T21 to T42, their global averages show relative increases at finer resolutions. Precipitable water and cloud cover also display a seasonal asymmetry in their responses to increasing resolution. The comparative insensitivity of global cloud cover to resolution is mainly a consequence of compensating tendencies of clouds in different regions. With increasing resolution, decreases in low latitude clouds that result from drying of the tropical atmosphere are partially offset by increases in high-latitude clouds associated with enhanced relative humidity in response to an intensifying extratropical cold bias. The large-scale tropical moist processes are modeled more realistically at T21 than in the finer-resolution simulations, wherein anomalous seasonal climatic features such as a double ITCZ and underdeveloped summer monsoon circulation are evident. Although some of these anomalies might ameliorate if the physical parameterizations were suitably 'tuned,' these deficiencies may reflect more fundamental problems related to a mismatch between the resolution of the model and the implicit spatial and temporal scales of the parameterizations. DOE

N94-11241# Lawrence Livermore National Lab., CA.

A MODELING PERSPECTIVE ON CLOUD RADIATIVE FORCING

G. L. Potter, L. Corsetti, J. M. Slingo, and J. J. Morcrette (European Centre for Medium-Range Weather Forecasts, Reading, England.) Feb. 1993 24 p

(Contract W-7405-eng-48)

(DE93-012383; UCRL-ID-108158; PCMDI-9) Avail: CASI HC A03/MF A01

Radiation fields from a perpetual July integration of a T106 version of the ECM-WF operational model are used to identify the most appropriate way to diagnose cloud radiative forcing in a general circulation model, for the purposes of intercomparison between models. Differences between the Methods 1 and 2 of Cess and Potter and a variant method are addressed. Method 1 is shown to be the least robust of all methods, due to the potential uncertainties related to persistent cloudiness, length of the sampling period and biases in retrieved clear-sky quantities due to insufficient sampling of the diurnal cycle. Method 2 is proposed as an unambiguous way to produce consistent radiative diagnostics for intercomparing model results. The impact of the three methods on the derived sensitivities and cloud feedbacks following an imposed change in sea surface temperature is discussed. The sensitivity of the results to horizontal resolution is considered by using the diagnostics from parallel integrations with T21 version of the model. DOE

N94-11355*# West Virginia State Coll., Charleston. Community Coll. Div.

MAGNETIC EARTH IONOSPHERE RESONANT FREQUENCIES (MEIRF) PROJECT Semiannual Progress Report, Sep. 1992 - Mar. 1993

Craig Spaniol Jun. 1993 69 p

(Grant NAG5-1267)

(NASA-CR-193182; NAS 1.26:193182) Avail: CASI HC A04/MF A01

The West Virginia State College Community College Division NASA Magnetic Earth Ionosphere Resonant Frequencies (MEIRF) study is described. During this contract period, the two most significant and professionally rewarding events were the presentation of the research activity at the Sir Isaac Newton Conference in St. Petersburg, Russia, and the second Day of Discovery Conference, focusing on economic recovery in West Virginia. An active antenna concept utilizing a signal feedback principle similar to regenerative receivers used in early radio was studied. The device has potential for ELF research and other commercial applications for improved signal reception. Finally, work continues to progress on the development of a prototype monitoring station. Signal monitoring, data display, and data storage are major areas of activity. In addition, we plan to continue our dissemination of research activity through presentations at seminars and other universities. CASI

N94-11463 Aerospace Corp., El Segundo, CA. Technology Operations.

DATA PROCESSING UNITS FOR EIGHT MAGNETOSPHERIC PARTICLE AND FIELD SENSORS

R. Koga, S. S. Immamoto, N. Katz, and S. D. Pinkerton 29 Jan. 1993 10 p Limited Reproducibility: More than 20% of this document may be affected by microfiche quality
(Contract F04701-88-C-0089)
(AD-A264403; TR-0091(6940-05)-05; SMC-TR-93-20) Avail: CASI HC A02

The DPUA, DPUB, and DPU57 data processing units associated with eight CRRES particle and field experiments are described. Operation of the experiments is controlled by the data processing units (DPU's), which constitute the interface between the spacecraft and the sensors subserving the individual experiments. All data to and from the sensors pass through the associated DPU's. Each DPU consists of a microprocessor, power supply, signal handler, and various peripherals such as input/output buffers and specialized data processing hardware. In addition to experiment control and data processing functions, DPU software performs such tasks as loading the system software from ROM into RAM, writing the memory-resident look-up tables utilized by the DPU hardware, checking the system RAM's for memory retention faults, outputting system memory to the telemetry stream, and outputting a fixed pattern of telemetry. To maximize the available telemetry bandwidth, much of the raw sensor data is analyzed by the DPU's, using various onboard processing schemes, and then compressed prior to being output in telemetry. DTIC

N94-11465 Colorado State Univ., Fort Collins.

LARGE EDDY SIMULATIONS OF THE ATMOSPHERIC BOUNDARY LAYER EAST OF THE COLORADO ROCKIES Ph.D. Thesis

Keeley Rochelle Costigan 1992 150 p
Avail: Univ. Microfilms Order No. DA9311367

Large eddy simulation, LES, has often been carried out for the idealized situation of a simple convective boundary layer. Studies of dual Doppler radar and aircraft data from the Phoenix 2 experiment indicate that the boundary layer of the Colorado High Plains is not a purely convective boundary layer and it is influenced by the mountains to the west. The purpose is to investigate the atmospheric boundary layer on one particular day on the Colorado High Plains. This research applies a LES nested within larger grids, which contain realistic topography and can simulate the larger-scale circulations initiated by the presence of the mountain barrier. How and to what extent the atmospheric boundary layer of the Colorado High Plains is influenced by larger scale circulations and other phenomena associated with the mountain barrier to the west is investigated. Comparison of the model produced fields and turbulence statistics to the observations of the Phoenix 2 experiment shows that the nested grid LES reproduces the characteristics of the atmosphere for the case study day reasonably well. Further comparison of the model results to other LES for a purely convective, horizontally homogeneous boundary layer indicates that the mountains influence the atmospheric boundary layer over the plains to the east in several ways. The mountains contribute to the vertical shear of the horizontal winds through the thermally-induced mountain-plains circulation. As a consequence of the wind shear, the boundary layer that develops over the mountains is advected eastward over the top of the plains boundary layer, which is developing separately. This layer is marked by a mixture of gravity waves and turbulence and is atypical of a purely convective boundary layer. Just below this layer, the capping inversion of the plains boundary layer is weak and poorly defined compared to the inversions capping purely convective boundary layers. Gravity waves, triggered by the obstacle of the Rocky Mountains and by convection in the mountain boundary layer, also influence the atmosphere above the Colorado High Plains. These influences are found to have significant effects on the turbulence statistics and the energy spectra. Dissert. Abstr.

N94-11480 Colorado State Univ., Fort Collins.

THE IMPACT OF VEGETATION ON THE ATMOSPHERIC BOUNDARY LAYER AND CONVECTIVE STORMS Ph.D. Thesis

Tsengdar John Lee 1992 155 p
Avail: Univ. Microfilms Order No. DA9311386

The impact of vegetation on atmospheric boundary layer and convective storms is examined through the construction and testing of a soil-vegetation-atmosphere transfer (SVAT) model. The Land Ecosystem-Atmosphere (LEAF) model is developed using an elevated canopy structure, an above-canopy aerodynamic resistance, two in-canopy aerodynamic resistances, and one stomatal conductance functions. The air temperature and humidity are assumed to be constant in the canopy whereas the wind and radiation follow a specified vertical profile. A simple dump-bucket method is used to parameterize the interception of precipitation and a multi-layer soil model is utilized to handle the vertical transfer of soil water. Evaporation from soil and wet leaves and transpiration from dry leaves are evaluated separately. The solid water uptake is based on soil water potential rather than on the length of roots. Separate energy budgets for vegetation and for the soil are used in order to remove unnecessary assumptions on energy partition between the vegetation and the substrate. Primary parameters are LAI, maximum stomatal conductance, and albedo. Secondary parameters include displacement height and environmental controls on stomatal resistance function. Due to the complexity of the LEAF model, statistical methods are used to improve LEAF model performance. The Multi-response Randomized Bock Permutation (MRBP) procedure is used to guide the choice of model parameter values. The Fourier Amplitude Sensitivity Test (FAST) is applied to better understand the model behavior in response to the changes in model parameters. Finally, LEAF is used to study the growth of boundary layer and the local thermal circulations generated by surface inhomogeneities. Results show the atmospheric boundary layer is substantially cooler and more moist over unstressed vegetation than over bare dry soil. Thermally forced circulation can result from the juxtaposition of two vegetation types due to different biophysical characteristics. Results from three-dimensional simulations show that the surface spatial heterogeneities made by vegetation play an important role in generating local convective storms.
Dissert. Abstr.

N94-11585 California Univ., Los Angeles.

A MODEL FOR THE SUBDUCTION MECHANICS OF FLEXIBLE LITHOSPHERE AND ITS VISCOUS COUPLING TO THE MANTLE USING POWER-LAW RHEOLOGIES Ph.D. Thesis

David VanDyke Kemp 1992 266 p
Avail: Univ. Microfilms Order No. DA9310859

Plate subduction plays a fundamental role in mantle convection due to the localization of negative buoyancy and the plate's role as a stress guide. Convection studies have demonstrated subduction's dynamic significance, but the subduction mechanics of plates that have enhanced strength relative to the asthenosphere and self-consistently defined trajectories have not been previously investigated. In this study, I seek the steady-state plate profile which is consistent with loads acting on the plate and its rheological response; the plate profile is not prescribed a priori. The plate has a uniform, rate-dependent rheology, allowing continuous bending from the open ocean to a depth of 670 km. Loads acting to define the plate shape include body forces, static pressure anomalies, shear contact with the overriding plate, and dynamic pressures and shear stresses resulting from viscous coupling to the mantle. These loads are in turn coupled to the plate shape, with the mantle responses described by a power-law rheology. In addition, the slabs may meet resistance at the top of the lower mantle and may experience a depth-independent lateral pressure drop. Numerical experiments have been conducted using a combination of spectral methods and nonlinear optimization. The plate's flexural strength is found capable of making a significant contribution to slab support, allowing more shallow stable dips than previous corner-flow models. Dynamic pressures do not provide 'unbending stresses' to plates, however. Weak plates unbend beneath the forearc load and also downdip from the arc under their own weight. Stronger plates may not unbend at all without weakening as they subduct. Preferred models have trenches no deeper than 12.5 km and do not overturn in the upper mantle. Although one each is 40, 60 and 80-km thick, a constant in the moment/curvature relationship for these matches to within 20 percent. A factor of five variation would result from the thickness variation without compensating adjustment of the plate rheology. Support at depth may increase the dynamic pressures by making the mantle wedge more narrow, but does not appear to significantly alter the forearc shape, and thus the static pressures there. Modest depth-independent pressure drops across the weak slabs are capable of significantly decreasing their dip in the upper mantle and reducing the slab pull. Author

N94-11603 International Centre for Theoretical Physics, Trieste (Italy).

AN OVERVIEW OF INTERTROPICAL CONVERGENCE AND INTERTROPICAL DISCONTINUITY

E. C. Adibe Sep. 1992 27 p Limited Reproducibility: More than 20%

of this document may be affected by microfiche quality
(DE93-619229; IC-92/286) Avail: CASI HC A03 (US Sales Only)

In its simplest form, the general circulation of the atmosphere may be regarded as two meridional circulation in opposite directions and separated by what is sometimes known as the 'meteorological equator'. The meteorological equator, as a planetary entity, divides the troposphere into two meteorological hemispheres, ensuring energy equilibrium in them, and corresponding to what are known as intertropical convergence zone, intertropical discontinuity, intertropical front, monsoon front, etc. The meteorological equator moves from the south towards the north and then from the north towards the south in harmony with the apparent movement of the Sun. DOE

N94-11702*# Maxwell Labs., Inc., La Jolla, CA. S-Cubed Div.
NASCAP PROGRAMMER'S REFERENCE MANUAL Final Report
M. J. Mandell, P. R. Stannard, and I. Katz May 1993 549 p
(Contract NAS3-22826; RTOP 506-41-52)
(NASA-CR-191044; E-7850; NAS 1.26:191044) Avail: CASI HC A23/MF A04

The NASA Charging Analyzer Program (NASCAP) is a computer program designed to model the electrostatic charging of complicated three-dimensional objects, both in a test tank and at geosynchronous altitudes. This document is a programmer's reference manual and user's guide. It is designed as a reference to experienced users of the code, as well as an introduction to its use for beginners. All of the many capabilities of NASCAP are covered in detail, together with examples of their use. These include the definition of objects, plasma environments, potential calculations, particle emission and detection simulations, and charging analysis. Author (revised)

N94-11828# Johns Hopkins Univ., Laurel, MD. Applied Physics Lab.
AN INVESTIGATION OF THE NEAR EARTH SPACE ENVIRONMENTS Annual Progress Report, 1 Jan. - 31 Dec. 1992
Ching I. Meng Jan. 1993 12 p
(Contract F49620-92-J-0196)
(AD-A265295; AFOSR-93-0261TR) Avail: CASI HC A03/MF A01

Progress was made in four areas: (1) mapping the different regions of the magnetosphere into the ionosphere under varying solar wind conditions; this research is relevant to future USAF operational systems needs in that the environment experienced by a spacecraft differs greatly depending on the region being transited; (2) understanding the convection surge mechanism in the magnetotail; (3) determining the plasma source region for dayside auroral emissions through coordinated satellite imagery and particle data; and (4) creating a new interpretation of dayside auroral transients, involving directly driven ionospheric response to magnetosheath changes. DTIC

N94-11852# Atmospheric and Environmental Research, Inc., Cambridge, MA.
FFTSCAN: A PROGRAM FOR SPECTRAL SMOOTHING USING FOURIER TRANSFORMS
W. O. Gallery and S. A. Clough 19 May 1992 24 p
(Contract F19628-89-C-0150)
(AD-A264921; PL-TR-92-2131; AD-E201529) Avail: CASI HC A03/MF A01

FFTSCAN is a computer program which uses Fourier Transforms to convolve a spectrum with an instrument spectral scanning function. This technique mimics the operation of Fourier transform spectroscopy and preserves the full extent of the scanning function, which is particularly important for functions with large side lobes, like sin(x)/x. Five scanning functions commonly used in Fourier transform spectroscopy are available: sinc, sinc2, Beer, Hamming, and Hanning, plus triangle and gauss. The program is specifically adapted to process spectra created by the atmospheric transmittance/radiance program FASCODE. A special, disk-based Fourier transform routine allows FFTSCAN to handle spectra of any size. FFTSCAN is more accurate and as, or more, efficient that the existing equivalent FASCODE routines. This report describes the mathematical basis for spectral smoothing in the Fourier domain and gives the user instructions for FFTSCAN. It gives examples of spectral smoothing, including estimates of error limits and computational times, and provides guidance on implementing the program on different computers. DTIC

N94-11871# Naval Command, Control and Ocean Surveillance Center, San Diego, CA.
RESULTS FROM A YEAR-LONG AURORAL-E MEASUREMENT CAMPAIGN
Robert B. Rose, R. D. Hunsucker, and Gus K. Lott Apr. 1993 8 p
(AD-A265059) Avail: CASI HC A02/MF A01

The Disturbance Impact Assessment System (DIAS) was developed to make qualitative assessments of the impact of solar flares on high latitude HF propagation. The system employed new techniques in expert system technology to describe some of the vaguer aspects in high latitude disturbance phenomenology. In developing the rulesets for the different high latitude disturbances, it was obvious that there was some confusion regarding the occurrence characteristics of sporadic-E, auroral sporadic-E, and just plain auroral-E. It was very difficult to determine the type of sporadic ionization being described in different studies. In order to gain better insight on the characteristics of auroral-E so an accurate ruleset for DIAS could be developed, it was decided to conduct a year-long measurement campaign. The results of the first year of measurements are described, theories on the generation of sporadic ionization at E-region ionospheric heights are presented, and finally an attempt to correlate the observations to the theories is made. DTIC

N94-11886*# Massachusetts Inst. of Tech., Cambridge. Dept. of Earth, Atmospheric, and Planetary Sciences.
ANALYSIS OF GRAVITY, MAGNETIC, AND SEISMIC REFLECTION DATA FROM TIBET AND NEIGHBORING REGIONS OF CHINA Semiannual Report, Mar. - Aug. 1993
Marcia McNutt Aug. 1993 8 p
(Grant NAGw-2629)
(NASA-CR-193405; NAS 1.26:193405) Avail: CASI HC A02/MF A01

Our principal effort was devoted to completing the analysis of the new gravity data over the Tibet plateau and its margins. A paper was completed discussing the statistical relationship between gravity and topography over the plateau. A paper on the structure of the Tarim Basin as constrained by Love wave dispersion is also under completion. This research project has also supported research on the newly-released gravity data from the former Soviet Union. Author (revised)

N94-12277# Boston Coll., Chestnut Hill, MA. Dept. of Physics.
A NEW DATA COLLECTION SYSTEM FOR IONOSPHERIC MODELLING AND RELATED TOPICS Final Report, 7 Nov. 1988 - 30 Sep. 1992
Robert E. Sheehan 15 Apr. 1993 100 p
(Contract F19628-89-K-0001)
(AD-A265893; PL-TR-92-2263) Avail: CASI HC A05/MF A02

Work performed under this contract can be divided into the following areas: (1) development and testing of a PC based Scintillation Data Recording System (SDRS) and related analysis software, (2) updating and extending D. Anderson's global ionospheric model for studies concerning the generation and transport of polar cap patches, and (3) implementation of existing and new software utilities on the PC and SUN workstation in support of Phillips Laboratory. Beginning in Nov. 1990, SDRS has been installed at 5 field sites from Thule, Greenland to Ascension Island in the South Atlantic. Modified systems have also become TEC receiving stations for a tomography project and a remote access system designed to report scintillation activity at field sites. New software was developed to extract and display SDRS and TEC phase data on the PC. Two important additions were made to the Anderson model; the Hardy statistical model describes electron precipitation patterns, and production caused by precipitating electrons is based on a parameterized version of Strickland's flux transport model provided by R. Daniel. DTIC

N94-12392# Cornell Univ., Ithaca, NY.
STUDIES OF ELECTROSTATIC WAVES AND VLF-WAVE PARTICLE INTERACTION IN THE IONOSPHERE Final Report
Paul M. Kintner 3 Jun. 1993 5 p
(Contract N00014-90-C-0003)
(AD-A266013) Avail: CASI HC A01/MF A01

Under this contract a HF plasma wave receiver was delivered for the Swedish spacecraft Freja and subsequently launched in Oct. 1992. The receiver was designed to sense short wavelength intermittent plasma waves in the frequency range characterized by the electroplasma and gyrofrequency. The receiver is operating nominally and preliminary data

analysis indicates the common occurrence of coherent and modulated Langmuir waves with amplitudes of several to greater than 20 mV/m.
DTIC

N94-12419# Michigan Univ., Ann Arbor.
OBSERVING AND MODELLING F-REGION IONOSPHERIC DYNAMICS USING THE (O2) 7320A EMISSION Ph.D. Thesis
Stephen S. Carr 1992 330 p
(AD-A265407; AFIT/CI/CIA-92-031D) Avail: CASI HC A15/MF A03

Limb-scan observations of Doppler line profiles from the (OII) lambda 7320A emission at F-Region altitudes, made with the Fabry-Perot interferometer (FPI) on the Dynamics Explorer-2 (DE-2) spacecraft, have been analyzed to provide measurements of the meridional component of the ion convection velocity along the instrument line-of-sight. The DE-2 results presented here demonstrate the first spaceborne use of the remote-sensing Doppler techniques for measurements of ionospheric convection. The FPI meridional ion drift measurements have been compared with nearly simultaneous in situ ion drift measurements from the Retarding Potential Analyzer (RPA) on DE-2. Once allowance is made for the temporal lag between the in situ and remote measurements, the results from the two techniques are found to be in good agreement, within specified experimental errors, giving confidence in the FPI measurements. DTIC

N94-12422# Sigma Research, Inc., Concord, MA.
AN ATMOSPHERIC BOUNDARY LAYER STABILITY ESTIMATOR FOR URBAN AREAS Final Report
J. S. Scire and S. R. Hanna Dec. 1992 86 p
(Contract DAAD07-91-C-0135)
(AD-A265189; ARL-CR-10) Avail: CASI HC A05/MF A01

In most U.S. Army atmospheric dispersion models, the Pasquill methodology is used to estimate stability in the boundary layer. As a result, there are discontinuities in calculated dispersion among the six stability classes. Furthermore, corrections for surface conditions (i.e., fields, urban areas, or forests) are also discrete functions. Recent theoretical developments provide the basis for revising this methodology using principles of Monin-Obukhov and convective similarity theory. A model is described which predicts stability indicators in a continuous manner. The procedure consists of three components: a soil moisture module to predict surface moisture; a meteorological module, based on an energy balance method, to predict surface energy fluxes and boundary layer parameters; and a set of similarity relations to estimate atmospheric stability and plume dispersion parameters. The model is designed for PC use and requires only routinely available meteorological and land use data. DTIC

N94-12560*# Texas A&M Univ., College Station. Coll. of Geosciences and Maritime Studies.
STUDIES OF DYNAMICAL PROCESSES AFFECTING THE DISTRIBUTION OF STRATOSPHERIC OZONE Final Report, 1 Jan. 1990 - 30 Jun. 1993
Kenneth P. Bowman (Illinois Univ., Urbana.) 27 Jul. 1993 3 p
(Grant NAGw-992)
(NASA-CR-193477; NAS 1.26:193477) Avail: CASI HC A01/MF A01

The purpose of the research was to understand large-scale tracer transport processes in the stratosphere. Two approaches were taken. The first is analysis of tracer observations, especially satellite observations of ozone concentration and total column ozone. The second is numerical simulation of tracer transport processes. Topics researched include: quasi-biennial oscillation (QBO) and stratospheric ozone; mixing in the polar vortices; polar stratospheric clouds (PSC) properties from Antarctic lidar data; and statistical methods for numerical experiments. Author (revised)

N94-12561# Utah State Univ., Logan. Space Dynamics Labs.
POLAR MESOSPHERIC WAVES AND STRUCTURE Final Report
James C. Ulwick May 1993 18 p
(Contract N00014-91-J-1883)
(AD-A265360; SDL/93-039) Avail: CASI HC A03/MF A01

This report discusses a quantitative comparison of rocket observations of electron density fluctuations and simultaneous 53.5 MHz radar measurements that were obtained during the MAC/SINE campaign in Northern Norway. Two of the three rockets launched during the Turbulence/Gravity Wave salvo were flown during conditions that allowed a detailed investigation. A large part of the data from these rocket flights indicate that the radar reflectivity is about 10 dB enhanced over what would be expected from the rocket observations in the case of isotropic electron density fluctuations. The observations can be reconciled under the assumption of an anisotropic turbulence. Assuming a simple model spectrum for the electron density fluctuations, we derive a relation between the rocket and radar observation that covers the whole range from isotropic turbulent scatter to Fresnel-scatter at horizontal density stratifications. For the observed data set, an anisotropy which typically corresponds to a ratio of horizontal to the vertical coherence length of about 10 is consistent with the comparison of rocket and radar observations. A similar anisotropy is found in the observed aspect sensitivity of the radar echoes. The variation of the anisotropy with height and time shows an anticorrelation with the turbulence level of the mesosphere as deduced from the spectral width of the radar echoes. The anisotropy is found to maximize in heights where density displays deep 'bite-outs'. These depletion in the electron density were independently observed by a Langmuir and an admittance probe on board the rocket. DTIC

N94-12568# National Science Foundation, Washington, DC. Div. of Polar Programs.
FACTS ABOUT THE US ANTARCTIC PROGRAM
Oct. 1992 28 p
(NSF-92-134) Avail: CASI HC A03/MF A01

Approximately 2,500 Americans work in and around Antarctica each year in the U.S. Antarctic Program. This National program involves the operation of ships, aircraft, stations, and camps, and it draws upon the resources and scientists of numerous U.S. universities, a number of Federal agencies, and several commercial firms. A digest of the operation is provided: facilities in Antarctica, objectives, Federal responsibilities, the substantial international aspects, and a brief history of prior U.S. activities. A final section provides sources of further information. Author (revised)

N94-12572*# Aerodyne Research, Inc., Billerica, MA.
STRATOSPHERIC AIRCRAFT EXHAUST PLUME AND WAKE CHEMISTRY
R. C. Miake-Lye, M. Martinez-Sanchez, R. C. Brown, C. E. Kolb, D. R. Worsnop, M. S. Zahniser, G. N. Robinson, J. M. Rodriguez (Atmospheric and Environmental Research, Inc., Cambridge, MA.), M. K. W. Ko (Atmospheric and Environmental Research, Inc., Cambridge, MA.), and R-L. Shia (Atmospheric and Environmental Research, Inc., Cambridge, MA.) et al Jul. 1993 65 p
(Contract NAS1-19161; RTOP 537-01-20-01)
(NASA-CR-191495; NAS 1.26:191495; ARI-RR-1006) Avail: CASI HC A04/MF A01

Progress to date in an ongoing study to analyze and model emissions leaving a proposed High Speed Civil Transport (HSCT) from when the exhaust gases leave the engine until they are deposited at atmospheric scales in the stratosphere is documented. A kinetic condensation model was implemented to predict heterogeneous condensation in the plume regime behind an HSCT flying in the lower stratosphere. Simulations were performed to illustrate the parametric dependence of contrail droplet growth on the exhaust condensation nuclei number density and size distribution. Model results indicate that the condensation of water vapor is strongly dependent on the number density of activated CN. Incorporation of estimates for dilution factors into a Lagrangian box model of the far-wake regime with scale-dependent diffusion indicates negligible decrease in ozone and enhancement of water concentrations of 6-13 times background, which decrease rapidly over 1-3 days. Radiative calculations indicate a net differential cooling rate of the plume about 3K/day at the beginning of the wake regime, with a total subsidence ranging between 0.4 and 1 km. Results from the Lagrangian plume model were used to estimate the effect of repeated superposition of aircraft plumes on the concentrations of water and NO(y) along a flight corridor. Results of laboratory studies of heterogeneous chemistry are also described. Kinetics of HCl, N2O5 and ClONO2 uptake on liquid sulfuric acid were measured as a function of composition and temperature. Refined measurements of the thermodynamics of nitric acid hydrates indicate that metastable dihydrate may play a role in the nucleation of more stable trihydrates PSC's. Author (revised)

N94-12581*# Alabama Univ., Huntsville. Dept. of Chemistry.
CHEMICAL RELEASE AND RADIATION EFFECTS (CRRES) DATA DIRECTORY Final Report, 24 Feb. 1993 - 24 Apr. 1993

George P. Miller 24 Apr. 1993 5 p
(Contract NAS8-38609)
(NASA-CR-192551; NAS 1.26:192551; UAH-5-33180) Avail: CASI HC A01/MF A01

The following tasks were completed under this contract: a revision and update of the Chemical Release and Radiation Effects (CRRES) data directory was performed taking into account the corrections and suggests for improvements obtained from the participants at the final CRRES IWG meeting held at SAIC on 14-16 Dec. 1992. A draft copy of the report was then circulated to as many as possible of the relevant CRRES Principal Investigators, co-Investigators, and technicians with a request for a final check on accuracy and completion. A copy of the mailing list is given in Appendix A. All corrections and updates received were implemented. A hard copy together with a floppy disk version was forwarded to Richard Howard, NASA Headquarters, who is arranging for the archiving of the CRRES Data Summary at NSSDC. Final copies were sent where possible. Author

N94-12582*# Oregon Univ., Eugene.
ATMOSPHERIC AND SPECTROSCOPIC RESEARCH IN THE FAR INFRARED Final Technical Report, 23 Feb. 1989 - 22 Feb. 1992
Kwangjai Park and James V. Radostitz 1992 6 p
(Grant NAG1-963)
(NASA-CR-193551; NAS 1.26:193551) Avail: CASI HC A02/MF A01

The University of Oregon (UO) has been a major participant in the development of far infrared spectroscopic research of the stratosphere for the purpose of understanding the ozone layer processes. The UO has had a 15-year collaboration with the Italian group of B. Carli, and have participated in the 1978/79 Sub-millimeter Infrared Balloon Experiment (SIBEX), in the Balloon Intercomparison Campaign, (BIC), in the Infrared Balloon Experiment (IBEX), and in the recently concluded Far Infrared Experiment for UARS Correlative Measurements (FIREX). Both IBEX and FIREX programs were conducted in collaboration with NASA Langley, and were designed as validation flights in support of the Upper Atmosphere Research Satellite (UARS) Program. The technique of atmospheric far infrared spectroscopy offers two important advantages. First, many chemically important species can be measured simultaneously and co-spatially in the atmosphere. Second, far infrared atmospheric spectra can be obtained in thermal emission without reference to the sun's position, enabling full diurnal and global coverage. Recent improvements in instrumentation, field measurements, and molecular concentration retrieval techniques are now making the far infrared a mature measurement technology. This work to date has largely focused on balloon-based studies, but the future efforts will focus also on satellite-based experiments. A program of research in the following general areas was proposed: Laboratory Pressure broadening coefficient studies; specialized detector system assembly and testing; and consultation and assistance with instrument and field support. The proposal was approved and a three-year research grant titled 'Atmospheric and Spectroscopic Research in the Far Infrared' was awarded. A summary of technical accomplishments attained during the grant period are presented. Author (revised)

N94-12583*# Massachusetts Inst. of Tech., Westford. Atmospheric Sciences Group.
MID-LATITUDE IONOSPHERIC RESPONSE TO ACTIVE EXPERIMENTS Final Report, 1 May 1990 - 30 Apr. 1992
John C. Foster 1992 5 p
(Grant NAG5-669)
(NASA-CR-193549; NAS 1.26:193549) Avail: CASI HC A01/MF A01

Understanding the ion chemistry and conditions leading to the formation of ionospheric depletions (ionospheric holes) was an important objective of the NASA active ionospheric experiment program. Millstone Hill radar observations were used to monitor the magnitude and temporal extent of the plasma holes produced under varying conditions. The major objective of the completed project was to provide radar diagnostic support for individual NASA rocket campaigns flown from Wallops Island. Two rocket programs, NICARE and REDAIR 2, were selected by NASA for radar support during the proposal period and pre-launch and in-flight radar observations were provided for each as well as basic reduction of the acquired data for scientific analysis. Radar operations and analysis for both of these experiments were performed as proposed and the work on these projects at M.I.T. was completed. Author (revised)

N94-11500# Technische Univ., Brunswick (Germany). Inst. fuer Flugfuehrung.
STABILITY MODEL OF THE ATMOSPHERE
Andreas Knueppel, Daniel Martens, and Andreas Siemer (Technische Univ., Hamburg, Germany.) *In* AGARD, Stability in Aerospace Systems Feb. 1993 17 p (For primary document see N94-11489 01-08)
Copyright Avail: CASI HC A03/MF A03

N94-11897 Chiba Univ. (Japan). Dept. of Information and Computer Sciences.
A STATISTICAL METHOD TO DETERMINE AEROSOL PATH RADIANCE AND ITS APPLICATION TO ATMOSPHERIC CORRECTION FOR CZCS IMAGERY
Hua Qi, Kazuhiko Oonuma, and Yoshizumi Yasuda *In* Scientific Organizing Committee of PORSEC, Proceedings of the PORSEC 1992 in Okinawa: Conference for Pacific Ocean Environments and Probing, Volume 1 25 Aug. 1992 p 15-20 (For primary document see N94-11894 01-42)
Copyright Avail: Issuing Activity (Scientific Organizing Committee of PORSEC, P.O. Box 10, Shimizu, Shizuoka 424, Japan, HC)

N94-11922* Jet Propulsion Lab., California Inst. of Tech., Pasadena.
AIR-SEA FLUXES AND UNIVERSAL CONSTANTS IN WEAK-TURBULENCE THEORY OF SURFACE GRAVITY WAVES
Roman E. Glazman *In* Scientific Organizing Committee of PORSEC, Proceedings of the PORSEC 1992 in Okinawa: Conference for Pacific Ocean Environments and Probing, Volume 1 25 Aug. 1992 p 161-165 Sponsored by NASA, Washington and ONR (For primary document see N94-11894 01-42)
Copyright Avail: Issuing Activity (Scientific Organizing Committee of PORSEC, P.O. Box 10, Shimizu, Shizuoka 424, Japan, HC)

N94-11926 Kunsan National Fisheries Junior Coll. (Republic of Korea).
ESTIMATION OF SOLAR RADIATION AT THE SEA SURFACE WITH GEOSTATIONARY METEOROLOGICAL SATELLITE DATA
Young Seup Kim and Ryuuji Kimura (Tokyo Univ., Japan.) *In* Scientific Organizing Committee of PORSEC, Proceedings of the PORSEC 1992 in Okinawa: Conference for Pacific Ocean Environments and Probing, Volume 1 25 Aug. 1992 p 184-188 (For primary document see N94-11894 01-42)
Copyright Avail: Issuing Activity (Scientific Organizing Committee of PORSEC, P.O. Box 10, Shimizu, Shizuoka 424, Japan, HC)

N94-11955 Washington Univ., Seattle. Dept. of Atmospheric Sciences.
AIR-SEA INTERACTION: FLUXES, A REVIEW
Robert A. Brown *In* Scientific Organizing Committee of PORSEC, Proceedings of the PORSEC 1992 in Okinawa: Conference for Pacific Ocean Environments and Probing, Volume 1 25 Aug. 1992 p 357-362 (For primary document see N94-11894 01-42)
Copyright Avail: Issuing Activity (Scientific Organizing Committee of PORSEC, P.O. Box 10, Shimizu, Shizuoka 424, Japan, HC)

N94-11980 Kanazawa Inst. of Tech. (Japan). Information Science Lab.
THE EVALUATION OF RADIATIVE PROCESS IN THE ATMOSPHERE-GROUND SYSTEM BY MONTE CARLO METHOD
Yoshiyuki Kawata and A. Hatakeyama *In* Scientific Organizing Committee of PORSEC, Proceedings of the PORSEC 1992 in Okinawa: Conference for Pacific Ocean Environments and Probing, Volume 1 25 Aug. 1992 p 489-494 (For primary document see N94-11894 01-42)
Copyright Avail: Issuing Activity (Scientific Organizing Committee of PORSEC, P.O. Box 10, Shimizu, Shizuoka 424, Japan, HC)

N94-11981 Meteorological Research Inst., Tsukuba (Japan).
THE UPWELLING RADIATION AT THE TOP OF THE ATMOSPHERE IN COASTAL REGION
Tsutomu Takashima and Kazuhiko Masuda *In* Scientific Organizing Committee of PORSEC, Proceedings of the PORSEC 1992 in Okinawa: Conference for Pacific Ocean Environments and Probing, Volume 1 25 Aug. 1992 p 495-500 (For primary document see N94-11894 01-42)
Copyright Avail: Issuing Activity (Scientific Organizing Committee of PORSEC, P.O. Box 10, Shimizu, Shizuoka 424, Japan, HC)

N94-12032*# Iowa Geological Survey, Iowa City.
DESCRIPTIONS AND PRELIMINARY INTERPRETATIONS OF CORES RECOVERED FROM THE MANSON IMPACT STRUCTURE (IOWA) Abstract Only
R. R. Anderson, B. J. Witzke, J. B. Hartung, E. M. Shoemaker (Geological Survey, Flagstaff, AZ.), and D. J. Roddy (Geological Survey, Flagstaff, AZ.) *In* Lunar and Planetary Inst., Twenty-fourth Lunar and Planetary Science Conference. Part 1: A-F 1993 p 35-36 (For primary document see N94-12015 01-91)
Avail: CASI HC A01/MF A06

N94-12041*# National Aeronautics and Space Administration, Washington, DC.
RECONSTRUCTION OF THE DYNAMICS OF THE 1800-1801 HUALALAI ERUPTION: IMPLICATIONS FOR PLANETARY LAVA FLOWS Abstract Only
Stephen Baloga and Paul Spudis (Lunar and Planetary Inst., Houston, TX.) *In* Lunar and Planetary Inst., Twenty-fourth Lunar and Planetary Science Conference. Part 1: A-F 1993 p 55-56 (For primary document see N94-12015 01-91)
Avail: CASI HC A01/MF A06

N94-12042*# Jet Propulsion Lab., California Inst. of Tech., Pasadena.
HORIZONTAL STRESSES INDUCED BY VERTICAL PROCESSES IN PLANETARY LITHOSPHERES Abstract Only
W. B. Banerdt *In* Lunar and Planetary Inst., Twenty-fourth Lunar and Planetary Science Conference. Part 1: A-F 1993 p 57-58 (For primary document see N94-12015 01-91)
Avail: CASI HC A01/MF A06

N94-12055*# National Aeronautics and Space Administration. Ames Research Center, Moffett Field, CA.
CHANGES IN HAWAIIAN PALAGONITE FE MINERALOGY ASSOCIATED WITH THERMAL ALTERATION: IMPLICATIONS FOR MARS Abstract Only
James F. Bell, III, Richard V. Morris (National Aeronautics and Space Administration. Lyndon B. Johnson Space Center, Houston, TX.), and John B. Adams (Washington Univ., Seattle.) *In* Lunar and Planetary Inst., Twenty-fourth Lunar and Planetary Science Conference. Part 1: A-F 1993 p 85-86 Sponsored by NASA. Washington (For primary document see N94-12015 01-91)
Avail: CASI HC A01/MF A06

N94-12056*# Iowa Univ., Iowa City. Dept. of Geology.
PETROGRAPHY AND PRELIMINARY INTERPRETATIONS OF THE CRYSTALLINE BRECCIAS FROM THE MANSON M-1 CORE Abstract Only
M. S. Bell, M. K. Reagan, R. R. Anderson, and C. T. Foster, Jr. *In* Lunar and Planetary Inst., Twenty-fourth Lunar and Planetary Science Conference. Part 1: A-F 1993 p 87-88 (For primary document see N94-12015 01-91)
Avail: CASI HC A01/MF A06

N94-12072*# Lancaster Univ. (England). Environmental Science Div.
STABLE ISOTOPE ANALYSES OF THE PERALKALINE VOLCANICS GREGORY RIFT VALLEY, KENYA Abstract Only
S. Black, R. Macdonald, A. E. Fallick (Scottish Research Reactor Centre, East Kilbride.), and M. Kelly *In* Lunar and Planetary Inst., Twenty-fourth Lunar and Planetary Science Conference. Part 1: A-F 1993 p 119-120 (For primary document see N94-12015 01-91)
Avail: CASI HC A01/MF A06

N94-12073*# Lancaster Univ. (England). Environmental Science Div.
TH-230 - U-238 SERIES DISEQUILIBRIUM OF THE OLKARIA BASALTS GREGORY RIFT VALLEY, KENYA Abstract Only
S. Black, R. Macdonald, and M. Kelly *In* Lunar and Planetary Inst., Twenty-fourth Lunar and Planetary Science Conference. Part 1: A-F 1993 p 121-122 (For primary document see N94-12015 01-91)
Avail: CASI HC A01/MF A06

N94-12074*# Lancaster Univ. (England). Environmental Science Div.
TH-230 - U-238 SERIES DISEQUILIBRIUM OF THE OLKARIA BASALTS GREGORY RIFT VALLEY, KENYA: PETROGENESIS Abstract Only
S. Black, R. Macdonald, and M. Kelly *In* Lunar and Planetary Inst., Twenty-fourth Lunar and Planetary Science Conference. Part 1: A-F 1993 p 123-124 (For primary document see N94-12015 01-91)
Avail: CASI HC A01/MF A06

N94-12075*# Lancaster Univ. (England). Environmental Science Div.
TH-230 - U-238 SERIES DISEQUILIBRIUM OF THE OLKARIA RHYOLITES GREGORY RIFT VALLEY, KENYA: PETROGENESIS Abstract Only
S. Black, R. Macdonald, and M. Kelly *In* Lunar and Planetary Inst., Twenty-fourth Lunar and Planetary Science Conference. Part 1: A-F 1993 p 125-126 (For primary document see N94-12015 01-91)
Avail: CASI HC A01/MF A06

N94-12076*# Lancaster Univ. (England). Environmental Science Div.
TH-230 - U-238 SERIES DISEQUILIBRIUM OF THE OLKARIA RHYOLITES GREGORY RIFT VALLEY, KENYA: RESIDENCE TIMES Abstract Only
S. Black, R. Macdonald, and M. Kelly *In* Lunar and Planetary Inst., Twenty-fourth Lunar and Planetary Science Conference. Part 1: A-F 1993 p 127-128 (For primary document see N94-12015 01-91)
Avail: CASI HC A01/MF A06

N94-12080*# Dartmouth Coll., Hanover, NH. Dept. of Earth Sciences.
STRONTIUM AND OXYGEN ISOTOPE STUDY OF M-1, M-3 AND M-4 DRILL CORE SAMPLES FROM THE MANSON IMPACT STRUCTURE, IOWA: COMPARISON WITH HAITIAN K-T IMPACT GLASSES Abstract Only
Joel D. Blum, C. Page Chamberlain, Michael P. Hingston, and Christian Koeberl (Wien Univ., Austria.) *In* Lunar and Planetary Inst., Twenty-fourth Lunar and Planetary Science Conference. Part 1: A-F 1993 p 135-136 (For primary document see N94-12015 01-91)
Avail: CASI HC A01/MF A06

N94-12081*# Rutgers Univ., New Brunswick, NJ. Dept. of Geological Sciences.
PRELIMINARY RESULTS OF Mn PARTITIONING EXPERIMENTS ON MURCHISON ANALOGUES Abstract Only
Joseph S. Boesenberg and Jeremy S. Delaney *In* Lunar and Planetary Inst., Twenty-fourth Lunar and Planetary Science Conference. Part 1: A-F 1993 p 137-138 (For primary document see N94-12015 01-91)
Avail: CASI HC A01/MF A06

N94-12083*# National Aeronautics and Space Administration. Lyndon B. Johnson Space Center, Houston, TX.
Ar-39 - Ar-40 AGES OF ACAPULCOITES AND LODRANITES: EVIDENCE FOR EARLY PARENT BODY HEATING Abstract Only
D. D. Bogard, D. H. Garrison, T. J. McCoy (Hawaii Univ., Honolulu.), and K. Keil (Hawaii Univ., Honolulu.) *In* Lunar and Planetary Inst., Twenty-fourth Lunar and Planetary Science Conference. Part 1: A-F 1993 p 141-142 (For primary document see N94-12015 01-91)
Avail: CASI HC A01/MF A06

N94-12084*# Geological Survey, Denver, CO.
ARROYO EL MIMBRAL, MEXICO, K/T UNIT: ORIGIN AS DEBRIS FLOW/TURBIDITE, NOT A TSUNAMI DEPOSIT Abstract Only
Bruce F. Bohor and William J. Betterton *In* Lunar and Planetary Inst., Twenty-fourth Lunar and Planetary Science Conference. Part 1: A-F 1993 p 143-144 (For primary document see N94-12015 01-91)
Avail: CASI HC A01/MF A06

N94-12085*# Geological Survey, Denver, CO.
K/T SPHERULES FROM HAITI AND WYOMING: ORIGIN, DIAGENESIS, AND SIMILARITY TO SOME MICROTEKTITES Abstract Only
B. F. Bohor, B. P. Glass (Delaware Univ., Newark.), and W. J. Betterton *In* Lunar and Planetary Inst., Twenty-fourth Lunar and Planetary Science Conference. Part 1: A-F 1993 p 145-146 (For primary document see N94-12015 01-91)
Avail: CASI HC A01/MF A06

N94-12091*# California Univ., Los Angeles. Inst. of Geophysics and Planetary Physics.
IMPACT MINERALOGY AND CHEMISTRY OF THE CRETACEOUS-TERTIARY BOUNDARY AT DSDP SITE 576 Abstract Only
Jennifer A. Bostwick and Frank T. Kyte *In* Lunar and Planetary Inst., Twenty-fourth Lunar and Planetary Science Conference. Part 1: A-F 1993 p 157-158 (For primary document see N94-12015 01-91)
Avail: CASI HC A01/MF A06

N94-12093*# Toronto Univ. (Ontario).
AGE OF POPIGAI IMPACT EVENT USING THE Ar-40 - Ar-39 METHOD Abstract Only
R. J. Bottomley and R. A. F. Grieve (Geological Survey of Canada, Ottawa, Ontario.) *In* Lunar and Planetary Inst., Twenty-fourth Lunar and Planetary Science Conference. Part 1: A-F 1993 p 161-162 (For primary document see N94-12015 01-91)
Avail: CASI HC A01/MF A06

N94-12102*# Witwatersrand Univ., Johannesburg (South Africa). Dept. of Geology.
A STRUCTURAL AND PETROGRAPHIC INVESTIGATION OF THE PRETORIA SALTPAN IMPACT STRUCTURE Abstract Only
D. Brandt and W. U. Reimold *In* Lunar and Planetary Inst., Twenty-fourth Lunar and Planetary Science Conference. Part 1: A-F 1993 p 179-180 Sponsored in part by the Barringer Crater Co. (For primary document see N94-12015 01-91)
Avail: CASI HC A01/MF A06

N94-12103*# Witwatersrand Univ., Johannesburg (South Africa). Dept. of Geology.
GEOPHYSICAL SIGNATURE OF THE PRETORIA SALTPAN IMPACT STRUCTURE AND A POSSIBLE SATELLITE CRATER Abstract Only
D. Brandt, R. J. Durrheim, and W. U. Reimold *In* Lunar and Planetary Inst., Twenty-fourth Lunar and Planetary Science Conference. Part 1: A-F 1993 p 181-182 Sponsored in part by the Barringer Crater Co. (For primary document see N94-12015 01-91)
Avail: CASI HC A01/MF A06

N94-12104*# New Mexico Univ., Albuquerque. Dept. of Earth and Planetary Sciences.
CARBONACEOUS CHONDRITE CLASTS IN THE KAPOETA HOWARDITE Abstract Only
Adrian J. Brearley and J. J. Papike *In* Lunar and Planetary Inst., Twenty-fourth Lunar and Planetary Science Conference. Part 1: A-F 1993 p 183-184 (For primary document see N94-12015 01-91)
(Grant NAG9-497)
Avail: CASI HC A01/MF A06

N94-12116*# Hawaii Univ., Honolulu. Dept. of Geology and Geophysics.
QUANTIFYING THE EFFECT OF RHEOLOGY ON PLAN-VIEW SHAPES OF LAVA FLOWS Abstract Only
B. C. Bruno, G. J. Taylor, and R. M. C. Lopes-Gautier (Jet Propulsion Lab., California Inst. of Tech., Pasadena.) *In* Lunar and Planetary Inst., Twenty-fourth Lunar and Planetary Science Conference. Part 1: A-F 1993 p 207-208 (For primary document see N94-12015 01-91)
Avail: CASI HC A01/MF A06

N94-12121*# Academy of Sciences (USSR), Moscow.
YANA RING STRUCTURE, NORTH-EASTERN SIBERIA: A POSSIBLE COUNTERPART OF CORONAE ON VENUS Abstert Only
G. A. Burba *In* Lunar and Planetary Inst., Twenty-fourth Lunar and Planetary Science Conference. Part 1: A-F 1993 p 217-218 (For primary document see N94-12015 01-91)
Avail: CASI HC A01/MF A06

N94-12123*# Academy of Sciences (USSR), Moscow. Geographical Dept.
LANDSCAPE AND GEOMORPHIC SURVEY OF ZHAMANSHIN AREA, NORTHERN KAZAKHSTAN: PRELIMINARY REPORT ON 1992 FIELD TRIP DATA
G. G. Burba, Jr. and V. A. Meshcherskaya *In* Lunar and Planetary Inst., Twenty-fourth Lunar and Planetary Science Conference. Part 1: A-F 1993 p 221-222 (For primary document see N94-12015 01-91)
Avail: CASI HC A01/MF A06

N94-12138*# Rhode Island Univ., Narragansett. Graduate School of Oceanography.
STRATIGRAPHY AND SEDIMENTOLOGY OF THE K/T BOUNDARY DEPOSIT IN HAITI Abstract Only
S. Carey, H. Sigurdsson, S. DHondt, and J. M. Espindola (Universidad Nacional Autonoma de Mexico, Mexico City.) *In* Lunar and Planetary Inst., Twenty-fourth Lunar and Planetary Science Conference. Part 1: A-F 1993 p 251-252 (For primary document see N94-12015 01-91)
Avail: CASI HC A01/MF A06

N94-12141*# Field Museum of Natural History, Chicago, IL. Dept. of Geology.
DISTRIBUTION OF VANADIUM AND MELTING OF OPAQUE ASSEMBLAGES IN EFREMOVKA CAI'S Abstract Only
I. Casanova and L. Grossman (Chicago Univ., IL.) *In* Lunar and Planetary Inst., Twenty-fourth Lunar and Planetary Science Conference. Part 1: A-F 1993 p 257-258 (For primary document see N94-12015 01-91)
Avail: CASI HC A01/MF A06

N94-12149*# California Inst. of Tech., Pasadena. Lab. of Experimental Geophysics.
SHOCK INDUCED REACTION IN CHICXULUB TARGET MATERIALS (CaSO4 AND SIO2) AND THEIR RELATION TO EXTINCTIONS Abstract Only
Guangqing Chen and Thomas J. Ahrens *In* Lunar and Planetary Inst., Twenty-fourth Lunar and Planetary Science Conference. Part 1: A-F 1993 p 273-274 (For primary document see N94-12015 01-91)
Avail: CASI HC A01/MF A06

N94-12161*# California Univ., Davis. Dept. of Geology.
KT BOUNDARY IMPACT GLASSES FROM THE GULF OF MEXICO REGION Abstract Only
Philippe Claeys, Walter Alvarez (California Univ., Berkeley.), Jan Smit (Vrije Univ., Amsterdam, Netherlands.), A. R. Hildebrand (Geological Survey of Canada, Ottawa, Ontario.), and Alessandro Montanari (Osservatorio Geologico di Coldigioco, Aprio, Italy.) *In* Lunar and Planetary Inst., Twenty-fourth Lunar and Planetary Science Conference. Part 1: A-F 1993 p 297-298 (For primary document see N94-12015 01-91)
Avail: CASI HC A01/MF A06

N94-12188*# New Mexico Univ., Albuquerque. Dept. of Earth and Planetary Sciences.
POST-IMPACT ALTERATION OF THE MANSON IMPACT STRUCTURE Abstract Only
L. J. Crossey and P. McCarville *In* Lunar and Planetary Inst., Twenty-fourth Lunar and Planetary Science Conference. Part 1: A-F 1993 p 351-352 (For primary document see N94-12015 01-91)
Avail: CASI HC A01/MF A06

N94-12197*# Hawaii Univ., Honolulu. Dept. of Geology and Geophysics.
THE GRANULITE SUITE: IMPACT MELTS AND METAMORPHIC BRECCIAS OF THE EARLY LUNAR CRUST Abstract Only
J. A. Cushing, G. J. Taylor, M. D. Norman, and K. Keil *In* Lunar and Planetary Inst., Twenty-fourth Lunar and Planetary Science Conference. Part 1: A-F 1993 p 369-370 (For primary document see N94-12015 01-91)
Avail: CASI HC A01/MF A06

N94-12199*# Chicago Univ., IL.
IRON AND NICKEL ISOTOPIC MASS FRACTIONATION IN DEEP-SEA SPHERULES Abstract Only
Andrew M. Davis and Donald E. Brownlee (Washington Univ., Seattle.) *In* Lunar and Planetary Inst., Twenty-fourth Lunar and Planetary Science Conference. Part 1: A-F 1993 p 373-374 (For primary document see N94-12015 01-91)
Avail: CASI HC A01/MF A06

N94-12210*# State Univ. of New York, Albany. Dept. of Geological Sciences.
OXIDATION STATE OF THE EARTH'S UPPER MANTLE DURING THE LAST 3800 MILLION YEARS: IMPLICATIONS FOR THE ORIGIN OF LIFE Abstract Only
J. W. Delano *In* Lunar and Planetary Inst., Twenty-fourth Lunar and Planetary Science Conference. Part 1: A-F 1993 p 395-396 (For primary document see N94-12015 01-91)
Avail: CASI HC A01/MF A06

N94-12217*# Lunar and Planetary Inst., Houston, TX.
DOES THE THERMAL WIND EXIST NEAR THE EARTH'S CORE BOUNDARY? Abstract Only
A. Z. Dolginov *In its* Twenty-fourth Lunar and Planetary Science Conference. Part 1: A-F 1993 p 409-410 (For primary document see N94-12015 01-91)
Avail: CASI HC A01/MF A06

N94-12219*# Lunar and Planetary Inst., Houston, TX.
POLARITY REVERSALS AND TILT OF THE EARTH'S MAGNETIC DIPOLE Abstract Only
A. Z. Dolginov *In its* Twenty-fourth Lunar and Planetary Science Conference. Part 1: A-F 1993 p 413-414 (For primary document see N94-12015 01-91)
Avail: CASI HC A01/MF A06

N94-12236*# Ottawa Univ. (Ontario). Dept. of Geology.
GIANT RADIATING DYKE SWARMS ON EARTH AND VENUS Abstract Only
Richard E. Ernst, James W. Head (Brown Univ., Providence, RI.), Elisabeth Parfitt (Brown Univ., Providence, RI.), Lionel Wilson (Brown Univ., Providence, RI.), and Eric Grosfils (Brown Univ., Providence, RI.) *In* Lunar and Planetary Inst., Twenty-fourth Lunar and Planetary Science Conference. Part 1: A-F 1993 p 447-448 (For primary document see N94-12015 01-91)
Avail: CASI HC A01/MF A06

N94-12249*# Arizona Univ., Tucson. Dept. of Geosciences.
TRANSMANTLE FLUX TECTONICS Abstract Only
V. J. Finn, A. Z. Dolginov (Lunar and Planetary Inst., Houston, TX.), and V. R. Baker *In* Lunar and Planetary Inst., Twenty-fourth Lunar and Planetary Science Conference. Part 1: A-F 1993 p 473-474 (For primary document see N94-12015 01-91)
Avail: CASI HC A01/MF A06

N94-12710 Tohoku Univ., Sendai (Japan). Center for Atmospheric and Oceanic Studies.
STUDY ON AIR-SEA INTERACTIONS IN THE OMLET (OCEAN MIXED LAYER EXPERIMENT) AREA USING SATELLITE REMOTE SENSING
Hiroshi Kawamura, Shouichi Kizu, Futoki Sakaida, Naoto Ebuchi, and Yoshiaki Toba *In* Scientific Organizing Committee of PORSEC, Proceedings of the PORSEC 1992 in Okinawa: Conference for Pacific Ocean Environments and Probing, Volume 2 25 Aug. 1992 p 982-987 (For primary document see N94-12635 01-42)
Copyright Avail: Issuing Activity (Scientific Organizing Committee of PORSEC, P.O. Box 10, Shimizu, Shizuoka 424, Japan, HC)

N94-12738 Academy of Sciences (USSR), Moscow. All-Union Scientific Research Inst. of Fisheries and Oceanography.
VERIFICATION OF THE ATMOSPHERE-OCEAN RADIATIVE TRANSFER PARAMETRIC MODELS
Andrey V. Belokhvostikov, Andrey A. Ioltukhovski, and Vladimir M. Orlov *In* Scientific Organizing Committee of PORSEC, Proceedings of the PORSEC 1992 in Okinawa: Conference for Pacific Ocean Environments and Probing, Volume 2 25 Aug. 1992 p 1132-1137 (For primary document see N94-12635 01-42)
Copyright Avail: Issuing Activity (Scientific Organizing Committee of PORSEC, P.O. Box 10, Shimizu, Shizuoka 424, Japan, HC)

N94-12750 Academy of Sciences (USSR), Vladivostok. Inst. of Automation and Control Processes.
ATMOSPHERIC CORRECTION FOR DETERMINATION OF AVERAGE SST FIELDS BASED ON AVHRR DATA
Alexander V. Kazansky *In* Scientific Organizing Committee of PORSEC, Proceedings of the PORSEC 1992 in Okinawa: Conference for Pacific Ocean Environments and Probing, Volume 2 25 Aug. 1992 p 1194-1199 (For primary document see N94-12635 01-42)
Copyright Avail: Issuing Activity (Scientific Organizing Committee of PORSEC, P.O. Box 10, Shimizu, Shizuoka 424, Japan, HC)

47 METEOROLOGY AND CLIMATOLOGY

Includes weather forecasting and modification.

N94-10290# Lawrence Livermore National Lab., CA.
THE CLOUD RADIATIVE FEEDBACK OF A MIDLATITUDE SQUALL LINE SYSTEM AND IMPLICATION FOR CLIMATE STUDY
H. N. S. Chin 1 May 1992 12 p Presented at the 11th International Conference on Clouds and Precipitation, Montreal, Ontario, 17-21 Aug. 1992
(Contract W-7405-eng-48)
(DE93-010511; UCRL-JC-110400; CONF-920881-2) Avail: CASI HC A03/MF A01

The main objectives of this study are as follows: (1) to study the impact of longwave and shortwave radiation on the thermodynamic and kinematic structure of a midlatitude squall line; and (2) to explore the influence of specifically including the ice phase in the cloud-radiation feedback mechanism for climate models. DOE

N94-10336# Hughes STX, Inc., Lexington, MA.
DATABASE BLENDING FOR THE CLIMATOLOGY OF CLOUD STATISTICS PROGRAM Final Report, 26 Apr. 1988 - 25 Nov. 1992
James H. Willand 26 Feb. 1993 66 p
(Contract F19628-88-C-0089)
(AD-A265034; PL-TR-92-2344) Avail: CASI HC A04/MF A01

This report describes data sources, data processing activities, compression, prediction, and blending of the climatological databases chosen to represent realistic global cloud amount statistics within the C Cloud S program. DTIC

N94-10561# World Meteorological Organization, Geneva (Switzerland). World Climate Programme Applications and Services.
TECHNICAL CONFERENCE ON TROPICAL URBAN CLIMATES: EXTENDED ABSTRACTS
Jan. 1993 107 p Conference held in Dhaka, Bangladesh, 28 Mar. - 2 Apr. 1993
(WMO/TD-538; WCASP-24) Avail: CASI HC A06/MF A02; print copy available at WMO, Geneva, Switzerland

Abstracts for the Technical Conference on Tropical Urban Climates (held March 28 - April 2, 1993) that were available by January 1993 are presented within the ouline of its 6 working sessions. The topics include 'Urban Systems in a Large-scale Climate Context'; 'The Impact of Natural Disasters on Urban Systems'; 'Urban Climate, Comfort and Human Health'; 'The Impact of Climate on Planning and Architecture'; 'Urban Design and Climate'; and 'TRUCE-related Activities.' CASI

N94-10725*# California Univ., Los Angeles. Dept. of Atmospheric Sciences.
LEE WAVES: BENIGN AND MALIGNANT
M. G. Wurtele, A. Datta, and R. D. Sharman Jun. 1993 30 p Sponsored by NASA. Dryden Flight Research Facility
(Contract NCC2-0374; RTOP 505-68-50)
(NASA-CR-186024; H-1890; NAS 1.26:186024) Avail: CASI HC A03/MF A01

The flow of an incompressible fluid over an obstacle will produce an oscillation in which buoyancy is the restoring force, called a gravity wave. For disturbances of this scale, the atmosphere may be treated as dynamically incompressible, even though there exists a mean static upward density gradient. Even in the linear approximation - i.e., for small disturbances - this model explains a great many of the flow phenomena observed in the lee of mountains. However, nonlinearities do arise importantly, in three ways: (1) through amplification due to the decrease of mean density with height; (2) through the large (scaled) size of the obstacle, such as a mountain range; and (3) from dynamically singular levels in the fluid field. These effects produce a complicated array of phenomena - large departure of the streamlines from their equilibrium levels, high winds, generation of small scales, turbulence, etc. - that present hazards to aircraft and to lee surface areas. The nonlinear disturbances also interact with the larger-scale flow in such a manner as to impact global weather forecasts and the climatological momentum balance. If there is no dynamic barrier, these waves can penetrate vertically into the middle atmosphere (30-100 km), where recent observations show them to be of a length scale that must involve the coriolis force in any modeling. At these altitudes, the amplitude of the waves is very large, and the phenomena associated with these wave dynamics are being studied with a view to their potential impact on high performance aircraft, including the projected National Aerospace Plane (NASP). The presentation shows the results of analysis and of state-of-the-art numerical simulations, validated where possible by observational data, and illustrated with photographs from nature. Author (revised)

N94-10739 Lawrence Livermore National Lab., CA.

PRELIMINARY VALIDATION OF THE LOW FREQUENCY VARIABILITY OF TROPOSPHERIC TEMPERATURE AND CIRCULATION SIMULATED FOR THE AMIP BY THE ECMWF MODEL

J. S. Boyle Apr. 1993 22 p Limited Reproducibility: More than 20% of this document may be affected by microfiche quality

(Contract W-7405-eng-48)

(DE93-012382; UCRL-ID-113623; PCMDI-11) Avail: CASI HC A03

The ECMWF global model is used to simulate the climate from 1979 to 1988. This integration is in support of the WGNE Atmospheric Model Intercomparison Project (AMIP). The model uses the observed monthly sea surface temperature for the ten year period during the integration. Anomaly correlation and RMS calculations are carried out between monthly mean observed circulation and the model results, although the use of monthly mean data restricts the conclusions to the low frequency variability. The variables and regions considered are the 500 hPa geopotential and MSU temperatures for the Northern Hemisphere (30N to 70N), the 200 hPa zonal wind and MSU temperatures for the equatorial belt (15S to 15N), and the 1000 hPa zonal wind for the equatorial Pacific (15N to 15S and 120E to 100W). The results show: (1) For the midlatitude 500 hPa geopotential there is a signal in the model results for the ENSO events of 1982/1983 and 1986/1987; (2) the model underestimates the midlatitude 500 hPa geopotential interannual variability as measured by the RMS but overestimates the MSU temperature variability in this region; (3) in general, outside of the ENSO periods, there is little correlation between the model and observed data anomalies of midlatitude 500 hPa geopotential; (4) in the tropics the variables evince a stronger correlation with observations, with the 200 hPa winds yielding greater agreement than the MSU temperatures and the 1000 hPa zonal wind showing a significant correlation with observations in the interannual variation; (5) in the tropics the model underestimates the variability of the 200 hPa wind and MSU temperature; (6) the model, although non-interacting with the ocean, produces a credible simulation of the low frequency variability of the equatorial JPacific low level zonal wind. DOE

N94-10822 State Univ. of New York, Albany.

ON THE IMPORTANCE OF MESOSCALE POTENTIAL VORTICITY ANOMALIES AND TOPOGRAPHIC FORCING DURING CYCLONE REDEVELOPMENT ACROSS THE APPALACHIANS: A GALE CASE STUDY Ph.D. Thesis

Christopher OHandley 1992 446 p

Avail: Univ. Microfilms Order No. DA9311872

The evolution of the structure of cyclones and cold fronts over the eastern United States is investigated observationally. Two primary goals of the research are to understand the mechanisms controlling cyclone and frontal evolution across the Appalachian mountains, and to document the presence and importance of mesoscale disturbances during cyclogenesis. The research was accomplished in two phases. First, a climatological survey of seven winter seasons of cyclones and fronts was performed. This study revealed that cold fronts are slowed and deformed by the Appalachians, with the cross-frontal pressure and thermal contrasts enhanced considerably across the mountains. In addition, cyclones generally curve northward and dissipate over the mountains while secondary development occurs further south over the lee region. Both upper-level 'forcing' and lower-level thermal structure are important in determining the exact location of redevelopment. Second, a detailed case study was conducted of a cyclone observed during the Genesis of Atlantic Lows Experiment (GALE). The primary cyclone dissipated over the northern Appalachians while a secondary lower tropospheric (800-900 mb) cyclone formed over eastern North Carolina. However, strong low-level static stability prevented this disturbance from penetrating to the surface. Instead, cyclogenesis occurred offshore when two mesoscale mid-tropospheric (500 mb) PV maxima, one of which represented an upper level frontal zone, moved over a series of quasi-stationary shallow cloud clusters over the Gulf Stream. Meanwhile, the primary surface cold front was blocked west of the Appalachians, but the mid-level (700-850 mb) front progressed unimpeded across the mountains. Later, a new surface front formed east of the mountains through diabatic processes. Both surface heating and evaporation played important roles in the frontal redevelopment. These results indicate that future mesoscale models will need to incorporate topography and diabatic processes with increased accuracy. In addition, observing and analysis systems must be capable of resolving mesoscale disturbances of the type identified here. Further research is suggested to determine the prevalence of such features, their impact on cyclogenesis, and the degree of resolution required for successful prediction. Author

N94-10871# Army Research Lab., White Sands Missle Range, NM.

SELECTED UPPER-AIR WIND SPEED DISTRIBUTIONS Final Report

Elton P. Avara Dec. 1992 106 p

(AD-A264822; ARL-TR-38) Avail: CASI HC A06/MF A02

Some weapon systems are sensitive to winds in the lower part of the atmosphere. Wind speed distributions and random wind speeds derived from the distributions are often required to help determine the operational capabilities of these systems. A literature survey revealed that investigators usually used either a log-normal or a Weibull distribution as the model for the distribution of wind speeds independent of direction. In addition to these two distributions, a gamma distribution is also evaluated in this report. Wind speeds observed in three different geographical regions at 10 altitudes up to 5 km 3 diurnal time periods, and 5 seasonal time periods were evaluated. This report contains the results of the wind speed analysis for some of the combinations of altitude, diurnal time periods, and seasonal time periods for each of the three geographical regions--European Lowlands, European Highlands, and Mideast Desert. The observed wind speed distributions were adequately represented by the analytical distributions. DTIC

N94-10940*# National Aeronautics and Space Administration. Goddard Space Flight Center, Greenbelt, MD.

DESIGN OF A GLOBAL SOIL MOISTURE INITIALIZATION PROCEDURE FOR THE SIMPLE BIOSPHERE MODEL

G. E. Liston (Universities Space Research Association, Columbia, MD.), Y. C. Sud, and G. K. Walker (General Sciences Corp., Laurel, MD.) Aug. 1993 130 p

(RTOP 039-09-01-25)

(NASA-TM-104590; NAS 1.15:104590; Rept-93B00092) Avail: CASI HC A07/MF A02

Global soil moisture and land-surface evapotranspiration fields are computed using an analysis scheme based on the Simple Biosphere (SiB) soil-vegetation-atmosphere interaction model. The scheme is driven with observed precipitation, and potential evapotranspiration, where the potential evapotranspiration is computed following the surface air temperature-potential evapotranspiration regression of Thomthwaite (1948). The observed surface air temperature is corrected to reflect potential (zero soil moisture stress) conditions by letting the ratio of actual transpiration to potential transpiration be a function of normalized difference vegetation index (NDVI). Soil moisture, evapotranspiration, and runoff data are generated on a daily basis for a 10-year period, January 1979 through December 1988, using observed precipitation gridded at a 4 deg by 5 deg resolution. Author (revised)

N94-11113 Atmospheric and Environmental Research, Inc., Cambridge, MA.

THE AIR FORCE INTERACTIVE METEOROLOGICAL SYSTEM: A RESEARCH TOOL FOR SATELLITE METEOROLOGY

Charles F. Ivaldi, Jr., Gary B. Gustafson, and Joseph Doherty 2 Dec.

1992 92 p Limited Reproducibility: More than 20% of this document may be affected by microfiche quality
(Contract F19628-91-C-0011)
(AD-A265957; PL-TR-92-2327; SR-2) Avail: Issuing Activity (Defense Technical Information Center (DTIC))

This report summarizes work that was performed under a research contract with the Satellite Meteorology Branch of the Phillips Laboratory (Geophysics Directorate) Atmospheric Sciences Division. The topic addressed is the use of the Air Force Interactive Meteorological System (AIMS) as a research tool for the acquisition, processing, display, and management of large sets of satellite data obtained from different platforms and sensors. Of particular importance is the foundation that AIMS provides for establishing an optimal satellite data processing system based on a systematic and integrated approach to data handling and manipulation. This foundation is composed of three functional areas: (1) access to meteorological data sources including--direct broadcast NOAA, DMSP, and GOES satellite data, global surface and upper air reports from the NWS Family of Services, and lightning data from the SUNY-Albany lightning detection network; (2) data visualization and processing that employs both 8-bit and 24-bit full color imaging workstations; and (3) interactive development, data analysis, and batch processing capabilities supported by mid-range performance minicomputers. This report includes a historical perspective of AIMS, its current configuration, a review of scientific applications supported by AIMS, ongoing work to provide an integrated approach to data management, analysis and processing, and a discussion of current short term needs and long range planning issues. DTIC

N94-11194# Colorado State Univ., Fort Collins. Dept. of Atmospheric Science.

UPDATED FORECAST OF ATLANTIC SEASONAL HURRICANE ACTIVITY FOR 1993

William M. Gray 5 Aug. 1993 16 p
Avail: CASI HC A03/MF A01

Details of the author's updated forecast of tropical cyclone activity for the Atlantic Ocean region including the Caribbean Sea and the Gulf of Mexico during 1993 are presented. This updated forecast utilizes meteorological data for June and July and is based on the author and his research colleagues ongoing research activities which relates the amount of seasonal Atlantic tropical cyclone activity to five factors: namely, (1) three measures of the Quasi-Biennial Oscillation of equatorial stratospheric zonal wind (QBO) at 50 mb (20 km) and 30 mb (23 km) and the absolute value of the shear between these levels; (2) the El Nino Southern Oscillation (ENSO) conditions as specified by the Equatorial East Pacific Sea Surface Temperature Anomaly (SSTA) and the value of the Tahiti minus Darwin surface pressure; (3) Caribbean basin Sea-Level Pressure Anomalies (SLPA) and upper tropospheric 200 mb Zonal Wind Anomalies (ZWA); (4) two measures of West African Rainfall (AR) anomalies, one of June-July in the Western Sahel region, and the other the previous year Aug. through Nov. precipitation in the Gulf of Guinea region; and (5) the surface west to east pressure and temperature gradients across the Western Sahel region of Africa during Feb. through May. Information received by the author through 4 Aug. 1993 indicates that the 1993 hurricane season should, overall be about an average season when compared with hurricane activity of the last 43 years. Our statistical analysis indicates that this season should have about 6 hurricanes, 10 named storms of at least tropical storm intensity, about 25 hurricane days, a total of 50 named storm days and a Hurricane Destruction Potential of 55. Because the Western Sahel is expected to again have below average rainfall this year, it is anticipated that there will be only two intense or major hurricanes of Saffir/Simpson intensity category 3, 4, or 5 this season. This updated forecast is for slightly calmer conditions than were suggested in the 24 Nov. 1992 and 4 Jun. 1993 forecasts for 1993. A verification of this forecast will be issued in late Nov. Author (revised)

N94-11598*# Alabama Univ., Huntsville. Earth System Science Lab.

[ACTIVITIES RELATING TO UNDERSTANDING THE INITIATION, ORGANIZATION AND STRUCTURE OF MOIST CONVECTION IN THE SOUTHEAST ENVIRONMENT] Final Report

Richard T. McNider 18 Jun. 1992 251 p
(Contract NAS8-36479)
(NASA-CR-193829; NAS 1.26:193829) Avail: CASI HC A12/MF A03

In the spring and summer of 1986, NASA/Marshall Space Flight Center (MSFC) will sponsor the Satellite Precipitation And Cloud Experiment (SPACE) to be conducted in the Central Tennessee, Northern Alabama, and Northeastern Mississippi area. The field program will incorporate high altitude flight experiments associated with meteorological remote sensor development for future space flight, and an investigation of precipitation processes associated with mesoscale and small convective systems. In addition to SPACE, the MIcroburst and Severe Thunderstorm (MIST) program, sponsored by the National Science Foundation (NSF), and the FAA-Lincoln Laboratory Operational Weather Study (FLOWS), sponsored by the Federal Aviation Administration (FAA), will take place concurrently within the SPACE experiment area. All three programs (under the joint acronym COHMEX (COoperative Huntsville Meteorological EXperiment)) will provide a data base for detailed analysis of mesoscale convective systems while providing ground truth comparisons for remote sensor evaluation. The purpose of this document is to outline the experiment design criteria for SPACE, and describe the special observing facilities and data sets that will be available under the COHMEX joint program. In addition to the planning of SPACE-COHMEX, this document covers three other parts of the program. The field program observations' main activity was the operation of an upper air rawinsonde network to provide ground truth for aircraft and spacecraft observations. Another part of the COHMEX program involved using boundary layer mesoscale models to study and simulate the initiation and organization of moist convection due to mesoscale thermal and mechanical circulations. The last part of the program was the collection, archival and distribution of the resulting COHMEX-SPACE data sets. Derived from text

N94-11614# Westinghouse Savannah River Co., Aiken, SC.

DEVELOPMENT OF A GRAPHICAL USER INTERFACE AND GRAPHICS DISPLAY FOR THE WIND SYSTEM

B. L. OSteen, J. D. Fast, and B. S. Suire 1992 13 p
(Contract DE-AC09-89SR-18035)
(DE93-011780; WSRC-RP-92-1425) Avail: CASI HC A03/MF A01

An advanced graphical user interface (GUI) and improved graphics for transport calculations have been developed for the Weather Information and Display System (WINDS). Two WINDS transport codes, Area Evac and 2DPUF, have been ported from their original VAX/VMS environment to a UNIX operating system and reconfigured to take advantage of the new graphics capability. A developmental prototype of this software is now available on a UNIX based IBM 340 workstation in the Dose Assessment Center (DAC). Automatic transfer of meteorological data from the WINDS VAX computers to the IBM workstation in the DAC has been implemented. This includes both regional National Weather Service (NWS) data and SRS tower data. The above developments fulfill a FY-93 DOE milestone. DOE

N94-11664# Westinghouse Savannah River Co., Aiken, SC.

WIND SYSTEM DOCUMENTATION

J. R. Froggatt and C. P. Tatum 15 Jan. 1993 61 p
(Contract DE-AC09-89SR-18035)
(DE93-010381; WSRC-RP-93-778) Avail: CASI HC A04/MF A01

Atmospheric transport and diffusion models have been developed by the Environmental Technology Section (ETS) of the Savannah River Technology Center to calculate the location and concentration of toxic or radioactive materials during an accidental release at the Savannah River Site (SRS). The output from these models has been used to support initial on-site and off-site emergency response activities such as protective action decision making and field monitoring coordination. These atmospheric transport and diffusion models have been incorporated into an automated computer-based system called the (Weather Information and Display) System and linked to real-time meteorological and radiological monitoring instruments to provide timely information for these emergency response activities. This report documents various aspects of the WIND system. DOE

N94-11685# Air Force Inst. of Tech., Wright-Patterson AFB, OH.

MODELING PRESENT AND FUTURE RIVER RUNOFF USING GLOBAL ATMOSPHERIC MODELS M.S. Thesis

Scott C. VanBlarcum Oct. 1992 120 p
(AD-A265274; AFIT/CI/CIA-92115) Avail: CASI HC A06/MF A02

A global atmospheric model is used to calculate the monthly river runoff for 30 of the world's major rivers for the present climate and for a doubled CO2 climate. The model has a horizontal resolution of 4 deg X 5 deg, but the runoff from each model box is quartered and added to the appropriate river drainage basin on a 2 deg X 2.5 deg resolution. A new routing scheme is used to allow runoff calculated for a particular grid box to flow to an adjacent downstream grid box and ultimately to the mouth of the river. The total instantaneous runoff leads runoff at the mouth by one to two months. The model generated runoff at the mouth is compared to observations for several different simulations. The runoff peaks of high-latitude rivers are due to spring snow melt and there is a time lag between when the snow melts and when the melt water reaches the mouth. The new routing scheme allows the calculation of runoff at any location in the river basin. Model-generated river runoff and precipitation for the Mississippi River and its tributaries are analyzed for the present climate, where annual precipitation is within 5% of the observed precipitation. However, model-generated monthly precipitation is too high in the spring and too low in the summer and fall. In a model simulation with doubled CO2, river runoff increases for 27 of the 30 rivers and in most cases coincides with increased precipitation. All high-latitude rivers show an increase in precipitation and runoff with a shift in the runoff maximum, approximately one month earlier, due to an earlier snow melt season. In a doubled CO2 climate, snow mass decreases for mid and high-latitude rivers in North America and northwestern Asia, but increases for rivers in northeastern Asia, where observed winter temperatures average -30 to -50 C. DTIC

N94-12408# Air Force Inst. of Tech., Wright-Patterson AFB, OH.
RAINFALL-RUNOFF ESTIMATION USING DIGITAL RADAR M.S. Thesis
Russell A. Kutzman 1992 119 p
(AD-A265390; AFIT/CI/CIA-92-114) Avail: CASI HC A06/MF A02

Storm runoff is a critical concern to meteorologists and hydrological forecasters. A runoff algorithm, part of a series of tropical weather algorithms developed for the NEXRAD (Next Generation Weather Radar) radar system, is presented. The algorithm is based on the relationship between the rainfall over the basin and the discharge response at the gauge station. The algorithm is designed to provide runoff as a function of time for a given input(s) of rainfall. With known overflow levels, flood potential can also be evaluated. The runoff algorithm examined outflow at five basins within the operating scope of the Pittsburgh National Weather Service (NES) radar. A comparison of the observed runoff was made with the algorithm generated discharge. In general, hydrograph accuracies improved with increasing rainfall excess. DTIC

N94-12539# Science and Technology Corp., Las Cruces, NM.
AN EXAMINATION OF THE EVOLUTION OF RADIATION AND ADVECTION FOGS Final Report
Montie M. Orgill Jan. 1993 71 p
(Contract DAAD07-89-C-0035)
(AD-A266127; ARL-CR-24) Avail: CASI HC A04/MF A01

A literature study was done on radiation and advection fog evolution. For radiation fog, six stages of fog evolution have been identified -- (1) precursor, (2) sunset, (3) conditioning, (4) mature, (5) sunrise, and (6) dissipation. The evolution of advection fog models has been in parallel with radiation fog models, but no identified stages in the evolution of advection fog have been proposed: (1) precursor, (2) initiation, (3) mature, and (4) dissipation. Radiation and advection fog models will require greater sophistication in order to study fog spatial and temporal variability. Physical aspects that require further study are discussed. DTIC

N94-12580*# Florida State Univ., Tallahassee. Dept. of Meteorology.
A STUDY OF THE MERRITT ISLAND, FLORIDA SEA BREEZE FLOW REGIMES AND THEIR EFFECT ON SURFACE HEAT AND MOISTURE FLUXES
M. T. Rubes, H. J. Cooper, and E. A. Smith Washington Jul. 1993 154 p
(Grant NAG8-916)
(NASA-CR-4537; M-727; NAS 1.26:4537) Avail: CASI HC A08/MF A02

Data collected during the Convective and Precipitation/Electrification Experiment were analyzed as part of an investigation of the sea breeze in the vicinity of Merritt Island, Florida. Analysis of near-surface divergence fields shows that the classical 24-hour oscillation in divergence over the island due to the direct sea breeze circulation is frequently disrupted and exhibits two distinct modes: the classical sea breeze pattern and deviations from that pattern. A comparison of clear day surface energy fluxes with fluxes on other days indicates that changes in magnitudes were dominated by the presence or absence of clouds. Non-classical sea breeze days tended to lose more available energy in the morning than classical sea breeze days due to earlier development of small cumulus over the island. A composite storm of surface winds, surface energy fluxes, rainfall, and satellite visible data was constructed. A spectral transmittance over the visible wavelengths for the cloud cover resulting from the composite storm was calculated. It is shown that pre-storm transmittances of 0.8 fall to values near 0.1 as the downdraft moves directly over the site. It is also found that under post-composite storm conditions of continuous clear sky days, 3.5 days are required to evaporate back into the atmosphere the latent heat energy lost to the surface by rainfall. Author (revised)

N94-12772*# Science Applications International Corp., Hampton, VA.
RADIOMETER OFFSETS AND COUNT CONVERSION COEFFICIENTS FOR THE EARTH RADIATION BUDGET EXPERIMENT (ERBE) SPACECRAFT FOR THE YEARS 1987, 1988, AND 1989 Final Report
Jack Paden, Dhirendra K. Pandey, Joseph C. Stassi, Robert Wilson, William Bolden, Susan Thomas, and M. Alan Gibson Washington Jul. 1993 213 p
(Contract NAS1-19570; RTOP 665-45-20-01)
(NASA-CR-191489; NAS 1.26:191489; SAIC(EARTH)-92/01) Avail: CASI HC A10/MF A03

This document contains a compendium of the ground and in-flight scanner and non-scanner offsets and count conversion (gain) coefficients used for the Earth Radiation Budget Experiment (ERBE) production processing of data from the ERBS satellite for the period from 1 January 1987 to 31 December 1989; for the NOAA-9 satellite, for the month of January 1987; and for the NOAA-10 satellite, for the period from 1 January 1987 to 31 May 1989. Author (revised)

N94-11082# Meteorological Satellite Center, Tokyo (Japan).
STATISTICAL STUDY ON THE REGIONAL AND SEASONAL DISTRIBUTION OF FOG IN THE FAR EAST REGION BY USING GMS IMAGERY
Motoi Matukawa *In its* Meteorological Satellite Center Mar. 1993 p 35-47 In JAPANESE (For primary document see N94-11079 01-42)
Avail: CASI HC A03/MF A01

N94-11962 Tokai Univ., Shizuoka (Japan). School of Marine Science and Technology.
AVAILABILITY OF WIND FIELD OVER THE NORTH PACIFIC DERIVED FROM DATA ON SHIPS-OF-OPPORTUNITY AND ANALYSIS OF LONG-TERM VARIABILITIES
Kunio Kutsuwada *In* Scientific Organizing Committee of PORSEC, Proceedings of the PORSEC 1992 in Okinawa: Conference for Pacific Ocean Environments and Probing, Volume 1 25 Aug. 1992 p 398-403 (For primary document see N94-11894 01-42)
Copyright Avail: Issuing Activity (Scientific Organizing Committee of PORSEC, P.O. Box 10, Shimizu, Shizuoka 424, Japan, HC)

N94-11963 Tokyo Univ. (Japan). Center for Climate System Research.
WIND FIELD ESTIMATE BY USING ONE HOUR GMS DATA
Akimasa Sumi and Tetsuo Nakazawa (Meteorological Research Inst., Tsukuba, Japan.) *In* Scientific Organizing Committee of PORSEC, Proceedings of the PORSEC 1992 in Okinawa: Conference for Pacific Ocean Environments and Probing, Volume 1 25 Aug. 1992 p 404-407 (For primary document see N94-11894 01-42)
Copyright Avail: Issuing Activity (Scientific Organizing Committee of PORSEC, P.O. Box 10, Shimizu, Shizuoka 424, Japan, HC)

N94-11964* Jet Propulsion Lab., California Inst. of Tech., Pasadena.
THE PACIFIC RESPONSES EXHIBITED BY AN OGCM TO VARIOUS WIND FIELDS
Wenqing Tang and W. Timothy Liu *In* Scientific Organizing Committee of PORSEC, Proceedings of the PORSEC 1992 in Okinawa: Conference for Pacific Ocean Environments and Probing, Volume 1 25 Aug. 1992 p 408-412 Sponsored by NASA, Washington (For primary document see N94-11894 01-42)
Copyright Avail: Issuing Activity (Scientific Organizing Committee of PORSEC, P.O. Box 10, Shimizu, Shizuoka 424, Japan, HC)

N94-12502# Meteorological Office, Bracknell (England).
USE OF ERS-1 WIND AND WAVE PRODUCTS IN OPERATIONAL METEOROLOGY
Stuart Bell and Martin Holt *In* ESA, Proceedings of 1st ERS-1 Symposium on Space at the Service of Our Environment, Volume 2 Mar. 1993 p 705-710 (For primary document see N94-12471 01-43)
Copyright Avail: CASI HC A02/MF A03; EPD, ESA, ESTEC, Noordwijk, Netherlands, HC

N94-12504# Atmospheric Environment Service, Toronto (Ontario).
USE OF ERS-1 SCATTEROMETER WINDS IN CANADIAN FORECAST CENTRES
Patrick King *In* ESA, Proceedings of 1st ERS-1 Symposium on Space at the Service of Our Environment, Volume 2 Mar. 1993 p 721-724 (For primary document see N94-12471 01-43)
Copyright Avail: CASI HC A01/MF A03; EPD, ESA, ESTEC, Noordwijk, Netherlands, HC

N94-12517# Oxford Univ. (England). Dept. of Atmospheric, Oceanic and Planetary Physics.
CLOUD STUDIES USING ATSR DATA
C. I. Rice and E. J. Williamson *In* ESA, Proceedings of 1st ERS-1 Symposium on Space at the Service of Our Environment, Volume 2 Mar. 1993 p 797-799 (For primary document see N94-12471 01-43)
Copyright Avail: CASI HC A01/MF A03; EPD, ESA, ESTEC, Noordwijk, Netherlands, HC

N94-12636 Tokai Univ., Shizuoka (Japan). School of Marine Science and Technology.
ANALYSIS OF GEOSAT WIND DATA
Masahisa Kubota *In* Scientific Organizing Committee of PORSEC, Proceedings of the PORSEC 1992 in Okinawa: Conference for Pacific Ocean Environments and Probing, Volume 2 25 Aug. 1992 p 555-561 (For primary document see N94-12635 01-42)
Copyright Avail: Issuing Activity (Scientific Organizing Committee of PORSEC, P.O. Box 10, Shimizu, Shizuoka 424, Japan, HC)

N94-12637* Jet Propulsion Lab., California Inst. of Tech., Pasadena. Earth and Space Sciences Div.
SSMI WIND SPEED VARIABILITY OVER THE PACIFIC OCEAN
David Halpern and William Knauss *In* Scientific Organizing Committee of PORSEC, Proceedings of the PORSEC 1992 in Okinawa: Conference for Pacific Ocean Environments and Probing, Volume 2 25 Aug. 1992 p 562-571 (For primary document see N94-12635 01-42)
(RTOP 578-22-26-40; RTOP 578-22-29-40)
Copyright Avail: Issuing Activity (Scientific Organizing Committee of PORSEC, P.O. Box 10, Shimizu, Shizuoka 424, Japan, HC)

N94-12663 Meteorological Research Inst., Tsukuba (Japan).
WORLDWIDE MAP OF RAINFALL AMOUNT OVER THE OCEAN DERIVED FROM PASSIVE MICROWAVE RADIOMETER
Akira Shibata *In* Scientific Organizing Committee of PORSEC, Proceedings of the PORSEC 1992 in Okinawa: Conference for Pacific Ocean Environments and Probing, Volume 2 25 Aug. 1992 p 709-714 (For primary document see N94-12635 01-42)
Copyright Avail: Issuing Activity (Scientific Organizing Committee of PORSEC, P.O. Box 10, Shimizu, Shizuoka 424, Japan, HC)

N94-12727 Marine Hydrophysical Inst., Sevastopol (USSR).
FIELD RESEARCH OF WIND WAVE SPECTRUM VARIABILITY
V. V. Efimov and A. V. Babanin *In* Scientific Organizing Committee of PORSEC, Proceedings of the PORSEC 1992 in Okinawa: Conference for Pacific Ocean Environments and Probing, Volume 2 25 Aug. 1992 p 1075-1078 (For primary document see N94-12635 01-42)
Copyright Avail: Issuing Activity (Scientific Organizing Committee of PORSEC, P.O. Box 10, Shimizu, Shizuoka 424, Japan, HC)

N94-12743 Academy of Sciences (USSR), Vladivostok. Pacific Oceanological Inst.
CLOUD LIQUID WATER CONTENT OVER THE PACIFIC OCEAN TROPICAL ZONE DERIVED FROM SHIP MICROWAVE RADIOMETRIC MEASUREMENT
L. M. Mitnik, M. L. Mitnik, and M. Yu. Shoom *In* Scientific Organizing Committee of PORSEC, Proceedings of the PORSEC 1992 in Okinawa: Conference for Pacific Ocean Environments and Probing, Volume 2 25 Aug. 1992 p 1160-1165 (For primary document see N94-12635 01-42)
Copyright Avail: Issuing Activity (Scientific Organizing Committee of PORSEC, P.O. Box 10, Shimizu, Shizuoka 424, Japan, HC)

N94-12766 Academy of Sciences (USSR), Moscow. Inst. of Computational Mathematics.
PROBLEM OF CLIMATE CHANGE PREDICTABILITY AND SATELLITE RADIATION BUDGET OBSERVATIONS
Vladimir V. Kozoderov *In* Scientific Organizing Committee of PORSEC, Proceedings of the PORSEC 1992 in Okinawa: Conference for Pacific Ocean Environments and Probing, Volume 2 25 Aug. 1992 p 1288-1292 (For primary document see N94-12635 01-42)
Copyright Avail: Issuing Activity (Scientific Organizing Committee of PORSEC, P.O. Box 10, Shimizu, Shizuoka 424, Japan, HC)

48 OCEANOGRAPHY

Includes biological, dynamic, and physical oceanography; and marine resources.

For related information see also *43 Earth Resources and Remote Sensing.*

N94-10153# Sandia National Labs., Albuquerque, NM.
SANDIA OCEAN MODELING SYSTEM PROGRAMMER'S GUIDE AND USER'S MANUAL
David Dietrich (Ecodynamics Research Associates, Inc., Albuquerque, NM.) Jan. 1993 141 p
(Contract DE-AC04-76DP-00789)
(DE93-007427; SAND-92-7286) Avail: CASI HC A07/MF A02

The Sandia Ocean Modeling System (SOMS) is not just one model but a modeling methodology to be applied in different modes (coarse or high resolution, boundary layers, with or without realistic topography, in a forecast or phenomenological mode, etc.) according to application requirements, hence its description as a modeling system. SOMS is applicable to a large range of geophysical flows from small lakes to large ocean basins. This document includes a description of governing equations and numerical methods and full details of the coding. Appendix A provides a complete listing of SOMS, including its movie-making modules. Appendix B presents the variables that appear in common blocks; this information is essential for a programmer intending to change the problem dimensions. Appendix C presents the results of a physical parameter sensitivity study. Appendix D presents results of a real ocean calculation. DOE

N94-10490# Naval Undersea Warfare Center, New London, CT.
PRELIMINARY RESULTS ON BACKSCATTERING STRENGTH FROM A WIND GENERATED BUBBLY OCEAN SURFACE
Edward Y. Kuo 25 Nov. 1992 34 p
(AD-A265006; NUWC-NL-TM-921240) Avail: CASI HC A03/MF A01

This report summarizes a preliminary result contained in an upcoming paper documenting continuing research effort in bubbly ocean surface scattering. As such, details will be referred to that paper. This report is written for a timely comparison with different sets of experimental data and is hoped to shed some light on a possible reason why there were apparent differences among experimental data sets. DTIC

N94-10517# Brookhaven National Lab., Upton, NY.
PRELIMINARY RESULTS OF THE COMPARISON OF ATSR MEASUREMENTS WITH IN SITU SEA TEMPERATURES
P. J. Minnett 17 Mar. 1993 42 p Presented at the Along Track Scanning Radiometer (ATSR) Science Team Meeting, Abingdon, England, 30 Mar. 1993
(Contract DE-AC02-76CH-00016)
(DE93-013399; BNL-48858; CONF-9303167-1) Avail: CASI HC A03/MF A01

During Oct. and Nov. 1991, the NATO Research Vessel Alliance sailed from Amsterdam into the western Mediterranean Sea, and measurements were made for the validation of ATSR data. This document reports the initial comparison between ATSR measurements and sea-surface temperatures (SST's) taken along the ship's track by an in situ thermometer at a depth of about 3m. DOE

N94-11200# Instituto de Pesquisas Espaciais, Sao Jose dos Campos (Brazil).
STUDY OF THE SURFACE CIRCULATION TO THE NORTH OF BRANSFIELD STRAIT, ANTARCTICA M.S. Thesis [ESTUDO DA CIRCULACAO SUPERFICIAL AO NORTE DO ESTREITO DE BRANSFIELD, ANTARTICA]
Ronald BussdeSouza Nov. 1992 183 p In PORTUGESE
(INPE-5472-TDI/503) Avail: CASI HC A09/MF A02

A study of the meso-scale circulation to the North of Bransfield Strait, Antarctica (61-62 degrees S, 52.5-58.5 degrees W), utilizing the displacement trajectory of a Brazilian drifting buoy, tracked by NOAA 10 and 11 satellites during 01/26-02/21/89, is presented. Buoy positional data, together with in situ oceanographic and meteorological data, were used to obtain a detailed description of the surface current. With a mean velocity of 7.5 cm/s, and a highly zonal direction (89 degrees), the current derived from the buoy trajectory was, in great part, forced by the winds, in agreement with the Ekman model. The Ekman currents were computed for 0 and 10 meter depths, obtaining 21 and 8. 5 cm/s toward 108 degrees and 25 degrees, respectively. The regional geostrophic circulation for the surface and 10 meter levels disagreed with the circulation pattern measured by the buoy. The mean geostrophic currents at those levels were about 2 cm/s to the North. Analyzing the Total, Mean, and the Eddy Kinetic Energies (EKT, EKM and EKE, respectively), it was found that time-variable fluctuations measured by EKE comprised 91.7 percent of the EKT. In 2 absolute values, EKM and EKE were equal to 28.1 sq cm/s(exp 2) and 357.4 sq cm/s(exp 2), respectively. With the use of auto-correlational analysis, it was determined that the displacement series of the buoy's trajectory contain dominant zonal and meridional component periods of 21.7 and 11.5 days, respectively. Using the Maximum Entropy Method (MEM) of spectral analysis, it was determined that 75.9 percent of total zonal energy was related to periods of 14.9 to 37.7 days. For the meridional component of the residual displacement series, 66.2 percent of the energy was related to periods between 11.5 and 21.2 days. The MEM analysis also shows that periods of 4-5 days and 1 day (tidal) were important in both displacement series. Comparison of the periods obtained from MEM for buoy and atmospheric pressure time series measured at the Brazilian Antarctic Station, showed that the atmospheric forcing was responsible for the 25.5, 11-12, and 5-6 days oscillations in the current. Cross-correlational analysis of buoy displacement and atmospheric pressure series shows that the currents follow the atmospheric forcing with a lag of 14 days. This period seems to be related to large-scale variation in the atmospheric system. Displacement loops present in the buoy's trajectory are shown to be caused by diurnal tides, the most important tidal component in the study region. The appearance of these loops in the buoy's trajectory was related to the presence of an oceanic front, localized in the western part of the study area. A second front to the East, formed by the justaposition of water influenced by the Bellingshausen Sea and the more cold and saline water from the Weddell Sea, resulted in a current that caused a strong southward deflection of the buoy. The utilization of the ARGOS compatible Brazilian drifting buoy is shown to be an efficient tool in meso-scale studies, offering the possibility of delineating oceanic fronts, fluxes of water masses with known characteristics, and atmospheric and tidal influences on the surface currents. Results of studies like this one can be used as support to more complex studies in the areas of air-sea interaction, climatology, and distribution of planctonic organisms of economic interest, for example. Author (revised)

N94-11287# Naval Research Lab., Bay Saint Louis, MS.
ATMOSPHERIC CORRECTION OF AVIRIS DATA IN OCEAN WATERS Final Report
Gregory Terrie and Robert Arnone Jun. 1992 5 p
(AD-A264931; NRLD-PR92-075-352) Avail: CASI HC A01/MF A01

Hyperspectral data offers unique capabilities for characterizing the ocean environment. The spectral characterization of the composition of ocean waters can be organized into biological and terrigenous components. Biological photosynthetic pigments in ocean waters have unique spectral ocean color signatures which can be associated with different biological species. Additionally, suspended sediment has different scattering coefficients which result in ocean color signatures. Measuring the spatial distributions of these components in the maritime environments provides important tools for understanding and monitoring the ocean environment. These tools have significant applications in pollution, carbon cycle, current and water mass detection, location of fronts and eddies, sewage discharge and fate etc. DTIC

N94-11299 Texas Univ., Austin.
ACOUSTICS OF BUBBLY SEDIMENTS Final Report
A. Bedford and J. A. Hawkins 1 Apr. 1993 118 p Limited Reproducibility: More than 20% of this document may be affected by microfiche quality
(Contract N00014-91-J-1809)
(AD-A263726) Avail: Issuing Activity: Defense Technical Information Center (DTIC))

The generation and detection of sound in the ocean is important in military applications, in biological research, and in the geoacoustic profiling of the ocean bottom and the underlying sediments. Although the free propagation of sound through seawater is an important area of underwater acoustics, the interaction of sound waves with the sea floor frequently must be accounted for. In particular, using remote acoustic measurements to obtain seismic profiles of the ocean bottom depend on a good understanding of the reflection of sound from the water-sediment interface and the sound absorption characteristics of the sediment below the interface. A simple model for the sediment is a compressible fluid. The reflection coefficient can then be calculated from the impedance of the fluid. This simple model can be improved by including viscosity in the model. DTIC

N94-11358*# National Aeronautics and Space Administration. Goddard Space Flight Center, Greenbelt, MD.
NORMAL MODES OF THE WORLD'S OCEANS: A NUMERICAL INVESTIGATION USING PROUDMAN FUNCTIONS
Braulio V. Sanchez and Dennis Morrow (Cray Research, Inc., Beltsville, MD.) May 1993 40 p
(RTOP 926-00-00)
(NASA-TM-104587; Rept-93B00078; NAS 1.15:104587) Avail: CASI HC A03/MF A01

The numerical modeling of the normal modes of the global oceans is addressed. The results of such modeling could be expected to serve as a guide in the analysis of observations and measurements intended to detect these modes. The numerical computation of normal modes of the global oceans is a field in which several investigations have obtained results during the past 15 years. The results seem to be model-dependent to an unsatisfactory extent. Some modeling areas, such as higher resolution of the bathymetry, inclusion of self-attraction and loading, the role of the Arctic Ocean, and systematic testing by means of diagnostic models are addressed. The results show that the present state of the art is such that a final solution to the normal mode problem still lies in the future. The numerical experiments show where some of the difficulties are and give some insight as to how to proceed in the future. Author (revised)

N94-11447 British Columbia Univ., Vancouver.
NEAR SURFACE OCEAN PROCESSES: ACOUSTICAL OBSERVATIONS, AMBIENT SOUND, AND LANGMUIR CIRCULATION Ph.D. Thesis
Len Zedel 1991 259 p
Avail: Univ. Microfilms Order No. DANN72696

A study of near surface ocean processes based on observations made with an instrument incorporating both active and passive acoustical systems is described. The topics addressed include the organization of bubble clouds by Langmuir circulation, the modulation of ambient sound levels by surface wave action, and the interactions of vortices associated with Langmuir circulation. Observations in a deep ocean environment reveal bubble clouds organized into plumes of 100 m length and widths of about 5 m aligned with the wind through the action of Langmuir circulation. The depth of these plumes varies somewhat with wind speed with the greatest depths of 12 m occurring at wind speeds of 13 m/s. Using acoustic Doppler techniques, downward vertical velocities of 0.06 m/s are observed at 8 m depth within the bubble plumes. Ambient sound observations at 8 kHz are used to search for possible relationships between wave breaking and Langmuir circulation: no systematic relationship is identified. This investigation does reveal the occurrence of modulations to ambient sound levels in phase with the long (approximately 150 m) surface waves passing over the instrumentation (positioned at 30 m depth). A model of sound generation at the ocean surface suggests that individual sources must have spacings of less than 6 m to reproduce the observations. Increased breaking activity (or greater source levels) are required at long wave crests to explain these modulations: it could be caused either by interactions between long and short waves, or variations in wind stress over the long waves. The observations of Langmuir circulation reveal many coexisting scales of spacing between the wind rows. A mechanism capable of generating small scale vorticity of the appropriate orientation through wave breaking and vortex stretching is developed. The consequences of interactions between this small scale, two dimensional vorticity is then explored using a Lagrangian vorticity model. This model demonstrates that continuous injection of small scale vorticity close to the ocean surface can lead to circulation similar to that expected for Langmuir circulation: a distribution of circulations cell sizes results, down welling speeds exceed upwelling speeds, and the cell spacing scales vary in proportion to the depth at which a bottom boundary is placed in the model. Dissert. Abstr.

N94-11853# Woods Hole Oceanographic Inst., MA.
THE SUBDUCTION EXPERIMENT. CRUISE REPORT, R/V OCEANUS, CRUISE NUMBER 250 LEGS 1 AND 2. SUBDUCTION 2 MOORING DEPLOYMENT AND RECOVERY CRUISE, 25 JANUARY-26 FEBRUARY 1992 Technical Report, 25 Jan. - 26 Feb. 1992
Richard P. Trask, Nancy J. Brink, Lloyd Regier, and Neil McPhee Mar. 1993 106 p
(Contract N00014-90-J-1490)
(AD-A264922; WHOI-93-13; UOP-TR-93-2) Avail: CASI HC A06/MF A02

Subduction is the mechanism by which water masses formed in the mixed layer and near the surface of the ocean find their way into the upper thermocline. The subduction process and its underlying mechanisms were studied through a combination of Eulerian and Langrangian measurements of velocity, measurements of tracer distributions and hydrographic properties, and modeling. An array of five surface moorings carrying meteorological and oceanographic instrumentation were deployed for a period of two years beginning in June 1991 as part of an Office of Naval Research (ONR) funded Subduction experiment. Three eight month deployments were planned. The initial deployment of five surface moorings took place during the third leg of R/V Oceanus cruise number 240. The moorings were deployed at 18 deg N 34 deg W, 18 deg N 22 deg W, 25.5 deg N 29 deg W, 33 deg N 22 deg W, and 33 deg N 34 deg W. A Vector Averaging Wind Recorder (VAWR) and an Improved Meteorological Recorder (IMET) collected wind speed and wind direction, sea surface temperature, air temperature, short wave radiation, barometric pressure, and relative humidity. The IMET also measured precipitation. The moorings were heavily instrumented below the surface with Vector Measuring Current Meters (VMCM) and single point temperature recorders. Expendable bathythermograph (XBT) data were collected and meteorological observations were made while transiting between mooring locations. This report describes the work that took place during R/V Oceanus cruise 250 which was the second scheduled Subduction mooring cruise. During this cruise the first setting of the moorings were recovered and redeployed for a second eight month period. DTIC

N94-11854# Woods Hole Oceanographic Inst., MA.
REAL-TIME TOMOGRAPHY MOORING
James Lynch, Daniel Frye, Kenneth Peal, Stephen Liberatore, and Sean Kery Jun. 1992 144 p
(Contract N00014-C-90-0098)
(AD-A264923; WHOI-92-29) Avail: CASI HC A07/MF A02

A real-time tomography system has been developed which combines ocean acoustic tomography with satellite-based time keeping and satellite telemetry. The basis of the system is the acoustic tomography transceiver and its associated acoustic navigation grid. To this basic system, a link to the surface has been added to provide a pathway for telemetry of the tomographic data to shore and a downlink for satellite-derived time which is used to correct the transceiver's clock. The surface buoy contains a GPS receiver, clock comparator, system controller, and multiple ID Argos transmitters. Processed tomography signals, transceiver location data, time, time drift, and surface buoy engineering data are transmitted to a satellite using a total of 32 data buffers transmitted every eight minutes. The report describes the real-time tomography system in detail, with particular emphasis on the modifications implemented to convert the standard tomography instrument to a real-time oceanographic tool. DTIC

N94-11868# Naval Postgraduate School, Monterey, CA.
AN INVESTIGATION USING EMPIRICAL ORTHOGONAL FUNCTIONS AND OBJECTIVE ANALYSIS TO ANALYSE THE VERTICAL TEMPERATURE STRUCTURE OF A GULF STREAM MEANDER M.S. Thesis
Martin J. Sauze Mar. 1993 157 p
(AD-A265116) Avail: CASI HC A08/MF A02

Expendable bathymetric temperature (XBT) data taken from an anticyclonic meander crest within the Gulf Stream is analyzed by looking at the empirical vertical structure. The ensemble averaged data is formed into a projection matrix that compares the value of the temperature at one depth with the temperature at a second depth. The data was smoothed with the correlation analysis being performed at ten metre intervals from five metres to a depth of 800 metres. The first four empirical orthogonal functions (EOF's) of the projection matrix were computed and the modal amplitudes for each XBT determined. Using objective analysis the modal amplitudes were interpolated onto a specified grid. Synthetic XBT's were then reconstructed at the grid positions using the interpolated grid modal amplitude values. A measure of the error at each grid point was determined. The objective analysis was subsequently repeated using successively fewer XBT's from the data set, until the resulting error in the interpolated XBT's at the grid points became unacceptable. DTIC

N94-12348# Scripps Institution of Oceanography, La Jolla, CA. Marine Physical Lab.
SHEAR, STRAIN AND THERMOHALINE VERTICAL FINE STRUCTURE IN THE UPPER OCEAN Ph.D. Thesis
Steve P. Anderson Jan. 1993 154 p
(Contract N00014-90-J-1099)
(AD-A265961; MPL-U-4/93; SIO-REF-93-3) Avail: CASI HC A08/MF A02

Observations of fine scale (1-100m) vertical shear, strain and thermohaline structure are interpreted in terms of internal wave and frontal zone dynamics. The date were collected with the Marine Physical Laboratory 161 kHz Doppler sonar and a pair of CTD's. The two systems were operated from R/P FLIP for 18 days during February-March, 1990, as part of the SWAPP (35 deg N, 127 deg W) experiment. These simultaneous measurements of velocity and density provide a unique opportunity to study the vertical advection of shear layers. The observed shear variance is dominated by near inertial waves, with 35 m vertical wavelengths. These inertial waves propagate down from the mixed layer and are vertically advected by higher frequency waves. Vertical wavenumber-frequency spectra of shear and strain are examined in Eulerian (fixed depth) and semi-Lagrangian (isopyncal following) coordinates. The semi-Lagrangian shear and strain variances are more consistent with variances modeled by a linear superposition of internal waves. The pdf's of buoyancy frequency and Froude number (buoyancy normalized shear) are determined using the kinematic strain model of Pinkel and Anderson. The Froude number distribution shows good agreement with data presented here and historical data. The advection of a frontal zone past the experiment site yielded detailed observations of frontal interleaving. Two vertical interleaving scales are observed. DTIC

N94-12349# Scripps Institution of Oceanography, La Jolla, CA. Marine Physical Lab.
PRELIMINARY ANALYSIS OF THE FLIP ARRAY DATA FROM THE NOBS EXPERIMENT
M. T. Hagerty, G. L. DSpain, and W. S. Hodgkiss May 1992 85 p
(Contract N00014-89-D-0142)
(AD-A265911; MPL-TM-429; MPL-U-42/92) Avail: CASI HC A05/MF A01

Preliminary analysis of the data collected by the array suspended below R/P FLIP (FLoating Instrument Platform) during the Noise Over Basalts and Sediments (NOBS) experiment are presented. This report gives a description of the FLIP array, a summary of the tape log kept aboard FLIP, a summary of the quality of the data collected, and the results of some initial data analysis. The initial examination of the data shows that a total of 36 vertical line array (VLA) hydrophones and all four channels of four ocean bottom seismometers (OBS) provided useable data. The quality of the recorded data is variable, but remains rather high for extended periods of time, especially for the 10 hours of data on tape 7. Analysis of tape 7's data indicates that the calibrated ambient noise spectra estimated from the VLA hydrophones data agree well with predicted noise levels in moderate to heavy shipping regions. At times, these spectra contain a peak centered at 18 Hz, which is probably indicative of the presence of whales. In addition, ship-generated signals are clearly visible in the spectra at those times when surface ship sightings were noted in the experiment log. Finally, large amplitude signals of unknown origin were observed in the root mean squared (RMS) time series plots for all functioning data channels. The coherence function estimates between the OBS hydrophones and between the VLA hydrophones for the large arrivals are consistent with a horizontally propagating acoustic wave. DTIC

N94-12350# Scripps Institution of Oceanography, La Jolla, CA. Marine Physical Lab.
MAPPING BATHYMETRIC SLOPES FROM BATHYMETRY DATA Final Report
Christian DeMoustier May 1993 4 p
(Contract N00014-89-J-3174)
(AD-A265923; MPL-U-26/93) Avail: CASI HC A01/MF A01

The objectives of this work were to develop slope calculation and mapping algorithms for use with Sea Beam bathymetry data. The ability to quantify and map in geographic coordinates apparent bottom slopes, as measured by the sonar in a given region, provides important clues for the level of acoustic bottom reverberation that can be expected from the region on purely geometric grounds DTIC

N94-10975*# Naval Undersea Warfare Center, West Palm Beach, FL.
UNDERWATER HYDROPHONE LOCATION SURVEY
Jack B. Cecil *In* NASA. Goddard Space Flight Center, The 24th Annual Precise Time and Time Interval (PTTI) Applications and Planning Meeting Jun. 1993 p 153-158 (For primary document see N94-10963 01-70)
Avail: CASI HC A01/MF A04

N94-11705# Technical Univ. of Denmark, Lyngby. Remote Sensing Unit.
SEA ICE: A CLIMATE COMPONENT
P. Gudmandsen *In* ESA, Proceedings of First ERS-1 Symposium on Space at the Service of Our Environment, Volume 1 Mar. 1993 p 9-13 (For primary document see N94-11704 01-43)
Copyright Avail: CASI HC A01/MF A04; EPD, ESA, ESTEC, Noordwijk, Netherlands, HC

N94-11708*# National Aeronautics and Space Administration. Wallops Flight Center, Wallops Island, VA.
THE GRAND BANKS ERS-1 SAR WAVE SPECTRA VALIDATION EXPERIMENT
P. W. Vachon (Canada Centre for Remote Sensing, Ottawa, Ontario.), F. W. Dobson (Bedford Inst. of Oceanography, Dartmouth, Nova Scotia.), S. D. Smith (Bedford Inst. of Oceanography, Dartmouth, Nova Scotia.), R. J. Anderson (Bedford Inst. of Oceanography, Dartmouth, Nova Scotia.), J. R. Buckley (Royal Roads Military Coll., Victoria, British Columbia.), M. Allingham (Royal Roads Military Coll., Victoria, British Columbia.), D. Vandemark, E. J. Walsh, M. Khandekar (Atmospheric Environment Service, Downsview, Ontario.), and R. Lalbeharry (Atmospheric Environment Service, Downsview, Ontario.) et al *In* ESA, Proceedings of First ERS-1 Symposium on Space at the Service of Our Environment, Volume 1 Mar. 1993 p 35-40 (For primary document see N94-11704 01-43)
Copyright Avail: CASI HC A02/MF A04; EPD, ESA, ESTEC, Noordwijk, Netherlands, HC

N94-11712# Institut Francais de Recherche pour l'Exploitation de la Mer, Brest. Dept. d'Oceanographie Spatiale.
ERS-1 STUDIES AT THE DEPARTMENT OF OCEANOGRAPHY FROM SPACE, IFREMER/BREST (FRANCE)
Kristina B. Katsaros, Abderrahim Bentamy, Alain Cavanie, Bertrand Chapron, Robert Ezraty, Patrick Farcy, Francis Gohin, Pierre Queffeulou, Yves Quilfen, and Jean Tournadre *In* ESA, Proceedings of First ERS-1 Symposium on Space at the Service of Our Environment, Volume 1 Mar. 1993 p 61-66 (For primary document see N94-11704 01-43)
Copyright Avail: CASI HC A02/MF A04; EPD, ESA, ESTEC, Noordwijk, Netherlands, HC

N94-11714# SACLANT ASW Research Center, La Spezia (Italy).
USE OF ERS-1 DATA AT SACLANT UNDERSEA RESEARCH CENTRE
H.-H. Essen *In* ESA, Proceedings of First ERS-1 Symposium on Space at the Service of Our Environment, Volume 1 Mar. 1993 p 75-77 (For primary document see N94-11704 01-43)
Copyright Avail: CASI HC A01/MF A04; EPD, ESA, ESTEC, Noordwijk, Netherlands, HC

N94-11717# Commonwealth Scientific and Industrial Research Organization, Hobart (Australia). Oceanography Div.
MAPPING OF THE EAST AUSTRALIAN CURRENT WITH THE ERS-1 SAR AND SHIPBORNE STUDIES
C. S. Nilsson, P. Tildesley, and J. Peterson *In* ESA, Proceedings of First ERS-1 Symposium on Space at the Service of Our Environment, Volume 1 Mar. 1993 p 95-100 (For primary document see N94-11704 01-43)
Copyright Avail: CASI HC A02/MF A04; EPD, ESA, ESTEC, Noordwijk, Netherlands, HC

N94-11719# Indian Space Research Organization, Ahmedabad. Space Applications Center.
PRELIMINARY ANALYSIS OF CIRCULATIONS OVER THE INDIAN OCEAN AND ADJOINING REGIONS USING ERS-1 SURFACE WINDS IN THE NCMRWF DATA ASSIMILATION SYSTEM
P. C. Joshi, B. Simon, M. S. Narayanan, S. R. H. Rizvi (National Centre for Medium Range Weather Forecasting, New Delhi, India.), and R. K. Bansal (National Centre for Medium Range Weather Forecasting, New Delhi, India.) *In* ESA, Proceedings of First ERS-1 Symposium on Space at the Service of Our Environment, Volume 1 Mar. 1993 p 107-111 (For primary document see N94-11704 01-43)
Copyright Avail: CASI HC A01/MF A04; EPD, ESA, ESTEC, Noordwijk, Netherlands, HC

N94-11720# Nansen Remote Sensing Center, Bergen (Norway).
COASTAL OCEAN STUDIES WITH ERS-1 SAR DURING NORCSEX 1991
J. A. Johannessen, R. A. Shuchman (Environmental Research Inst. of Michigan, Ann Arbor.), K. Davidson (Naval Postgraduate School, Monterey, CA.), O. Frette, G. Digranes, and O. M. Johannessen *In* ESA, Proceedings of First ERS-1 Symposium on Space at the Service of Our Environment, Volume 1 Mar. 1993 p 113-117 Sponsored by Norwegian Space Center; Bergen Univ.; ESA; Norwegian Navy; and NATO (For primary document see N94-11704 01-43)
Copyright Avail: CASI HC A01/MF A04; EPD, ESA, ESTEC, Noordwijk, Netherlands, HC

N94-11721# Southampton Univ. (England). Dept. of Oceanography.
SAR IMAGING OF DYNAMICAL FEATURES IN THE ENGLISH CHANNEL
Alison Scoon and Ian S. Robinson *In* ESA, Proceedings of First ERS-1 Symposium on Space at the Service of Our Environment, Volume 1 Mar. 1993 p 119-124 Sponsored in part by Natural Environmental Research Council (For primary document see N94-11704 01-43)
Copyright Avail: CASI HC A02/MF A04; EPD, ESA, ESTEC, Noordwijk, Netherlands, HC

N94-11722# Chilworth Research Centre, Southampton (England). Remote Sensing Applications Development Unit.
EFFECTS OF WAVE NONLINEARITY ON ERS-1 RADAR ALTIMETER RETURNS: A PRELIMINARY INVESTIGATION
M. A. Srokosz and G. D. Quartly *In* ESA, Proceedings of First ERS-1 Symposium on Space at the Service of Our Environment, Volume 1 Mar. 1993 p 125-130 (For primary document see N94-11704 01-43)
Copyright Avail: CASI HC A02/MF A04; EPD, ESA, ESTEC, Noordwijk, Netherlands, HC

N94-11723# Ocean Research and Engineering, Pasadena, CA.
SAR OCEAN IMAGING IN THE GULF OF ALASKA
O. H. Shemdin, D. W. Hayt, and D. P. Kasilingam *In* ESA, Proceedings

of First ERS-1 Symposium on Space at the Service of Our Environment, Volume 1 Mar. 1993 p 131-134 (For primary document see N94-11704 01-43)
Copyright Avail: CASI HC A01/MF A04; EPD, ESA, ESTEC, Noordwijk, Netherlands, HC

N94-11759# Bedford Inst. of Oceanography, Dartmouth (Nova Scotia). Physical and Chemical Sciences.
OCEAN CIRCULATION REVEALED BY ICE FLOE TRACKING
M. Ikeda and S. Prinsenberg *In* ESA, Proceedings of First ERS-1 Symposium on Space at the Service of Our Environment, Volume 1 Mar. 1993 p 351-353 (For primary document see N94-11704 01-43)
Copyright Avail: CASI HC A01/MF A04; EPD, ESA, ESTEC, Noordwijk, Netherlands, HC

N94-11769# Centre National d'Etudes Spatiales, Toulouse (France). Groupe de Recherche de Geodesie Spatiale.
SPACE AND TIME VARIABILITY OF THE GULF STREAM USING ERS-1 ALT-OPR02 DATA
J.-F. Minster, C. Brossier, M.-C. Gennero, S. Houry, and P. Vincent *In* ESA, Proceedings of First ERS-1 Symposium on Space at the Service of Our Environment, Volume 1 Mar. 1993 p 419-423 (For primary document see N94-11704 01-43)
Copyright Avail: CASI HC A01/MF A04; EPD, ESA, ESTEC, Noordwijk, Netherlands, HC

N94-11772# Technische Univ., Delft (Netherlands). Dept. of Aerospace Engineering.
ERS-1 RADAR ALTIMETRY OVER THE NORTH ATLANTIC
K. F. Wakker, E. Wisse, M. C. Naeije, R. Scharroo, P. N. A. M. Visser, and B. A. C. Ambrosius *In* ESA, Proceedings of First ERS-1 Symposium on Space at the Service of Our Environment, Volume 1 Mar. 1993 p 439-444 Sponsored by Space Research Organization Netherlands and Beleidscommissie Remote Sensing (For primary document see N94-11704 01-43)
Copyright Avail: CASI HC A02/MF A04; EPD, ESA, ESTEC, Noordwijk, Netherlands, HC

N94-11782# Chilworth Research Centre, Southampton (England). Center for Ocean Circulation.
SPATIAL SCALES OF WAVE HEIGHT
Peter G. Challenor *In* ESA, Proceedings of First ERS-1 Symposium on Space at the Service of Our Environment, Volume 1 Mar. 1993 p 493-498 Sponsored by Health and Safety Executive (For primary document see N94-11704 01-43)
Copyright Avail: CASI HC A02/MF A04; EPD, ESA, ESTEC, Noordwijk, Netherlands, HC

N94-11784# National Ocean Survey, Rockville, MD.
THE 1992 EL NINO VIEWED BY ERS-1 ALTIMETRY
Robert Cheney and John Lillibridge *In* ESA, Proceedings of First ERS-1 Symposium on Space at the Service of Our Environment, Volume 1 Mar. 1993 p 505-510 (For primary document see N94-11704 01-43)
Copyright Avail: CASI HC A02/MF A04; EPD, ESA, ESTEC, Noordwijk, Netherlands, HC

N94-11898 Fuyo Ocean Development and Engineering Co. Ltd., Tokyo (Japan).
EFFECTS OF WIND-ROUGHENED SEA SURFACE ON OCEAN COLOR REMOTE SENSING: NOISE DERIVED FROM REFLECTED LIGHT AND WHITECAPS
Susumu Kanno *In* Scientific Organizing Committee of PORSEC, Proceedings of the PORSEC 1992 in Okinawa: Conference for Pacific Ocean Environments and Probing, Volume 1 25 Aug. 1992 p 21-26 (For primary document see N94-11894 01-42)
Copyright Avail: Issuing Activity (Scientific Organizing Committee of PORSEC, P.O. Box 10, Shimizu, Shizuoka 424, Japan, HC)

N94-11899 Institute of Ocean Sciences, Sidney (British Columbia).
SATELLITE OBSERVATIONS OF RED TIDE EVENTS: PLANS FOR EESI
J. F. R. Gower *In* Scientific Organizing Committee of PORSEC, Proceedings of the PORSEC 1992 in Okinawa: Conference for Pacific Ocean Environments and Probing, Volume 1 25 Aug. 1992 p 27-33 (For primary document see N94-11894 01-42)
Copyright Avail: Issuing Activity (Scientific Organizing Committee of PORSEC, P.O. Box 10, Shimizu, Shizuoka 424, Japan, HC)

N94-11900 Commission of the European Communities, Ispra (Italy). Inst. for Remote Sensing Applications.
AN ALGORITHM FOR THE DETECTION OF MUCILAGE (GREEN SLIME) IN THE ADRIATIC SEA
Stelvio Tassan *In* Scientific Organizing Committee of PORSEC, Proceedings of the PORSEC 1992 in Okinawa: Conference for Pacific Ocean Environments and Probing, Volume 1 25 Aug. 1992 p 34-39 (For primary document see N94-11894 01-42)
Copyright Avail: Issuing Activity (Scientific Organizing Committee of PORSEC, P.O. Box 10, Shimizu, Shizuoka 424, Japan, HC)

N94-11901 Qingdao Inst. of Oceanology (China). Ocean Remote Sensing and Optics Lab.
REMOTE SENSING OF THE SUSPENDED MATTER DISTRIBUTION WITH HIGH CONCENTRATION IN CHINA SEA
Jun Ma, Xiao-Sheng Huang, Mao-Chong Shi, and Zhi-Shen Liu *In* Scientific Organizing Committee of PORSEC, Proceedings of the PORSEC 1992 in Okinawa: Conference for Pacific Ocean Environments and Probing, Volume 1 25 Aug. 1992 p 40-46 Sponsored by China National Foundation of Natural Science (For primary document see N94-11894 01-42)
Copyright Avail: Issuing Activity (Scientific Organizing Committee of PORSEC, P.O. Box 10, Shimizu, Shizuoka 424, Japan, HC)

N94-11903 Ministry of Posts and Telecommunications, Okinawa (Japan). Okinawa Radio Observatory.
MEASUREMENT OF WAVE PARAMETERS BY HF OCEAN RADAR
Yukiharu Hisaki and Masayuki Tokuda (Kokusai Kogyo Co. Ltd., Tokyo, Japan.) *In* Scientific Organizing Committee of PORSEC, Proceedings of the PORSEC 1992 in Okinawa: Conference for Pacific Ocean Environments and Probing, Volume 1 25 Aug. 1992 p 53-58 (For primary document see N94-11894 01-42)
Copyright Avail: Issuing Activity (Scientific Organizing Committee of PORSEC, P.O. Box 10, Shimizu, Shizuoka 424, Japan, HC)

N94-11904 Ministry of Posts and Telecommunications, Okinawa (Japan). Okinawa Radio Observatory.
KUROSHIO OBSERVATIONS BY THE HF OCEAN RADAR
Yuuichi Oono and Masayuki Tokuda (Kokusai Kogyo Co. Ltd., Tokyo, Japan.) *In* Scientific Organizing Committee of PORSEC, Proceedings of the PORSEC 1992 in Okinawa: Conference for Pacific Ocean Environments and Probing, Volume 1 25 Aug. 1992 p 59-64 (For primary document see N94-11894 01-42)
Copyright Avail: Issuing Activity (Scientific Organizing Committee of PORSEC, P.O. Box 10, Shimizu, Shizuoka 424, Japan, HC)

N94-11907 National Remote Sensing Agency, Hyderabad (India).
SATELLITE DERIVED SEA SURFACE TEMPERATURE APPLICATIONS FOR INDIAN OCEAN RESOURCES DEVELOPMENT
B. L. Deekshatulu, A. Narendra Nath, and M. V. Rao *In* Scientific Organizing Committee of PORSEC, Proceedings of the PORSEC 1992 in Okinawa: Conference for Pacific Ocean Environments and Probing, Volume 1 25 Aug. 1992 p 76-82 Sponsored by Dept. of Ocean Development (For primary document see N94-11894 01-42)
Copyright Avail: Issuing Activity (Scientific Organizing Committee of PORSEC, P.O. Box 10, Shimizu, Shizuoka 424, Japan, HC)

N94-11908 Tohoku Univ., Sendai (Japan). Disaster Control Research Center.
EXCHANGE OF BAY WATER WITH OCEAN CURRENT MONITORED BY THE NOAA SATELLITE
Masayuki Nagao, N. Hashimoto, F. Imamura, and N. Shutou *In* Scientific Organizing Committee of PORSEC, Proceedings of the PORSEC 1992 in Okinawa: Conference for Pacific Ocean Environments and Probing, Volume 1 25 Aug. 1992 p 83-88 Sponsored by Ministry of Education, Science and Culture and Shizugawa Town Office (For primary document see N94-11894 01-42)

Copyright Avail: Issuing Activity (Scientific Organizing Committee of PORSEC, P.O. Box 10, Shimizu, Shizuoka 424, Japan, HC)

N94-11911 Japan Marine Science and Technology Center, Tokyo.
CURRENT STRUCTURES IN THE WESTERN EQUATORIAL PACIFIC DURING JAPACS CRUISES
Yoshifumi Kuroda, Kentarou Andou, Kei Muneyama, and Michael J. McPhaden (National Oceanic and Atmospheric Administration, Seattle, WA.) *In* Scientific Organizing Committee of PORSEC, Proceedings of the PORSEC 1992 in Okinawa: Conference for Pacific Ocean Environments and Probing, Volume 1 25 Aug. 1992 p 100-105 Sponsored by Science and Technology Agency (For primary document see N94-11894 01-42)
Copyright Avail: Issuing Activity (Scientific Organizing Committee of PORSEC, P.O. Box 10, Shimizu, Shizuoka 424, Japan, HC)

N94-11912 National Inst. of Oceanography, Goa (India).
ACOUSTIC WAVEGUIDE CHARACTERISTICS OF THE INDIAN OCEAN NORTH OF EQUATOR
S. Prasanna Kumar, T. V. Ramana Murty, Y. K. Somayajulu, and C. S. Murty *In* Scientific Organizing Committee of PORSEC, Proceedings of the PORSEC 1992 in Okinawa: Conference for Pacific Ocean Environments and Probing, Volume 1 25 Aug. 1992 p 106-111 Sponsored by Dept. of Ocean Development (For primary document see N94-11894 01-42)
Copyright Avail: Issuing Activity (Scientific Organizing Committee of PORSEC, P.O. Box 10, Shimizu, Shizuoka 424, Japan, HC)

N94-11913 Hiroshima Univ. (Japan). Faculty of Engineering.
ONE-YEAR MOORING OF AN ADCP IN THE CENTRAL REGION OF THE KUROSHIO WEST OF OKINAWA
Hideo Nakajima, Arata Kaneko, Noriaki Gouda, Kazuo Kawatate (Kyushu Univ., Fukuoka, Japan.), and Shinjirou Mizuno (Kyushu Univ., Fukuoka, Japan.) *In* Scientific Organizing Committee of PORSEC, Proceedings of the PORSEC 1992 in Okinawa: Conference for Pacific Ocean Environments and Probing, Volume 1 25 Aug. 1992 p 112-115 (For primary document see N94-11894 01-42)
Copyright Avail: Issuing Activity (Scientific Organizing Committee of PORSEC, P.O. Box 10, Shimizu, Shizuoka 424, Japan, HC)

N94-11914 Hiroshima Univ. (Japan). Faculty of Engineering.
ACOUSTIC DOPPLER CURRENT PROFILING OF THE KUROSHIO OVER THE EAST CHINA SEA SHELF SLOPE
Noriaki Gouda, Arata Kaneko, Kazuo Kawatate (Kyushu Univ., Fukuoka, Japan.), and Shinjirou Mizuno (Kyushu Univ., Fukuoka, Japan.) *In* Scientific Organizing Committee of PORSEC, Proceedings of the PORSEC 1992 in Okinawa: Conference for Pacific Ocean Environments and Probing, Volume 1 25 Aug. 1992 p 116-119 (For primary document see N94-11894 01-42)
Copyright Avail: Issuing Activity (Scientific Organizing Committee of PORSEC, P.O. Box 10, Shimizu, Shizuoka 424, Japan, HC)

N94-11915 University of Electro-Communications, Chofu (Japan).
MEASUREMENT OF THE SURFACE LAYER CURRENT AVERAGED VERTICALLY USING MULTIPATHS INVERTED ECHOSOUNDER
Tomoyoshi Takeuchi and Keisuke Taira (Tokyo Univ., Japan.) *In* Scientific Organizing Committee of PORSEC, Proceedings of the PORSEC 1992 in Okinawa: Conference for Pacific Ocean Environments and Probing, Volume 1 25 Aug. 1992 p 120-125 (For primary document see N94-11894 01-42)
Copyright Avail: Issuing Activity (Scientific Organizing Committee of PORSEC, P.O. Box 10, Shimizu, Shizuoka 424, Japan, HC)

N94-11918 Florida State Univ., Tallahassee. Mesoscale Air-Sea Interaction Group.
VARIABILITY OF WIND STRESS, AND SENSIBLE AND LATENT HEAT FLUX IN THE NORTH ATLANTIC DURING SEASAT
David M. Legler and James J. OBrien *In* Scientific Organizing Committee of PORSEC, Proceedings of the PORSEC 1992 in Okinawa: Conference for Pacific Ocean Environments and Probing, Volume 1 25 Aug. 1992 p 138-143 (For primary document see N94-11894 01-42)
Copyright Avail: Issuing Activity (Scientific Organizing Committee of PORSEC, P.O. Box 10, Shimizu, Shizuoka 424, Japan, HC)

N94-11920 National Centre for Science Information Systems, Tokyo (Japan).
A NEW EXPRESSION FOR THE PRODUCTION RATE OF SEA WATER DROPLETS ON THE SEA SURFACE
Noriko Iida, Yoshiaki Toba (Tohoku Univ., Sendai, Japan.), and Masaaki Chaen (Kagoshima Univ., Japan.) *In* Scientific Organizing Committee of PORSEC, Proceedings of the PORSEC 1992 in Okinawa: Conference for Pacific Ocean Environments and Probing, Volume 1 25 Aug. 1992 p 150-155 (For primary document see N94-11894 01-42)
Copyright Avail: Issuing Activity (Scientific Organizing Committee of PORSEC, P.O. Box 10, Shimizu, Shizuoka 424, Japan, HC)

N94-11921 Tokyo Univ. (Japan). Center for Climate System Research.
EVALUATION OF ECMWF LATENT HEAT FLUX IN TOGA CD-ROM
Riko Yamane and Akimasa Sumi *In* Scientific Organizing Committee of PORSEC, Proceedings of the PORSEC 1992 in Okinawa: Conference for Pacific Ocean Environments and Probing, Volume 1 25 Aug. 1992 p 156-160 (For primary document see N94-11894 01-42)
Copyright Avail: Issuing Activity (Scientific Organizing Committee of PORSEC, P.O. Box 10, Shimizu, Shizuoka 424, Japan, HC)

N94-11923 Ryukyu Univ., Okinawa (Japan). Dept. of Marine Sciences.
SEA SURFACE HEAT FLUX IN THE BEGINNING OF THE KUROSHIO
Momoki Koga *In* Scientific Organizing Committee of PORSEC, Proceedings of the PORSEC 1992 in Okinawa: Conference for Pacific Ocean Environments and Probing, Volume 1 25 Aug. 1992 p 166-170 Sponsored by Ministry of Education, Science and Culture (For primary document see N94-11894 01-42)
Copyright Avail: Issuing Activity (Scientific Organizing Committee of PORSEC, P.O. Box 10, Shimizu, Shizuoka 424, Japan, HC)

N94-11924 Tokyo Univ. (Japan). Ocean Research Inst.
SEASONAL VARIATION OF THE SURFACE MIXED LAYER IN THE SUBTROPICAL RE-CIRCULATION AREA OF THE NORTH PACIFIC DURING OMLET
Hirotaka Otobe, Keisuke Taira, and Tomio Asai *In* Scientific Organizing Committee of PORSEC, Proceedings of the PORSEC 1992 in Okinawa: Conference for Pacific Ocean Environments and Probing, Volume 1 25 Aug. 1992 p 171-176 (For primary document see N94-11894 01-42)
Copyright Avail: Issuing Activity (Scientific Organizing Committee of PORSEC, P.O. Box 10, Shimizu, Shizuoka 424, Japan, HC)

N94-11925 Tokai Univ., Shizuoka (Japan). School of Marine Sciences and Technology.
MIXED LAYER HEAT BUDGET OF KUROSHIO-TANGO TRIANGLE USING SATELLITE AND SHIP OBSERVATIONS
Pankajakshan Thadathil (National Inst. of Oceanography, Goa, India.), Masatoshi Akiyama, Yasuhiro Sugimori, Jun Suwa, Y. Okada, and A. Siripong *In* Scientific Organizing Committee of PORSEC, Proceedings of the PORSEC 1992 in Okinawa: Conference for Pacific Ocean Environments and Probing, Volume 1 25 Aug. 1992 p 177-183 Sponsored by Ministry of Education, Science and Culture (For primary document see N94-11894 01-42)
Copyright Avail: Issuing Activity (Scientific Organizing Committee of PORSEC, P.O. Box 10, Shimizu, Shizuoka 424, Japan, HC)

N94-11927 National Aeronautics and Space Inst., Bandung (Indonesia).
THE USE OF REMOTE SENSING DATA FOR COASTAL ZONE MANAGEMENT AND ENVIRONMENT IN INDONESIA
Suharso Martadiwirya and Bidawi Hasyim *In* Scientific Organizing Committee of PORSEC, Proceedings of the PORSEC 1992 in Okinawa: Conference for Pacific Ocean Environments and Probing, Volume 1 25 Aug. 1992 p 189-192 (For primary document see N94-11894 01-42)
Copyright Avail: Issuing Activity (Scientific Organizing Committee of PORSEC, P.O. Box 10, Shimizu, Shizuoka 424, Japan, HC)

N94-11930 Qingdao Inst. of Oceanology (China). Ocean Remote Sensing and Ocean Optics Lab.
ANALYSIS OF THE CHARACTERISTIC AND MECHANISM OF SUSPENDED MATTER TRANSPORTATION IN HUANGHE DELTA SEA AREA USING REMOTE SENSING TECHNIQUES
Maochong Shi, Wei Huang, Ge Chen, and Mingxia He *In* Scientific

Organizing Committee of PORSEC, Proceedings of the PORSEC 1992 in Okinawa: Conference for Pacific Ocean Environments and Probing, Volume 1 25 Aug. 1992 p 205-210 (For primary document see N94-11894 01-42)
Copyright Avail: Issuing Activity (Scientific Organizing Committee of PORSEC, P.O. Box 10, Shimizu, Shizuoka 424, Japan, HC)

N94-11931 Nagasaki Univ., Bunkyo (Japan). Graduate School of Marine Science and Engineering.
THE EXTRACTION OF BOTTOM CHARACTERISTICS AND MAPPING IN KIN BAY, OKINAWA MAIN ISLAND, JAPAN, USING LANDSAT-5/TM AND SPOT-1/HRV DATA
Byungdug Jun, Keinosuke Gotou, Yoshihiko Tanabashi, and Sam Wouthuyzen *In* Scientific Organizing Committee of PORSEC, Proceedings of the PORSEC 1992 in Okinawa: Conference for Pacific Ocean Environments and Probing, Volume 1 25 Aug. 1992 p 211-216 (For primary document see N94-11894 01-42)
Copyright Avail: Issuing Activity (Scientific Organizing Committee of PORSEC, P.O. Box 10, Shimizu, Shizuoka 424, Japan, HC)

N94-11935* National Aeronautics and Space Administration. Goddard Space Flight Center, Greenbelt, MD.
OCEAN-ICE INTERACTION STUDY OF WAVES AND MESOSCALE FEATURES
Antony K. Liu and Chih Y. Peng (Science Systems and Applications, Inc., Lanham, MD.) *In* Scientific Organizing Committee of PORSEC, Proceedings of the PORSEC 1992 in Okinawa: Conference for Pacific Ocean Environments and Probing, Volume 1 25 Aug. 1992 p 237-242 (For primary document see N94-11894 01-42)
Copyright Avail: Issuing Activity (Scientific Organizing Committee of PORSEC, P.O. Box 10, Shimizu, Shizuoka 424, Japan, HC)

N94-11936 Kyoto Univ., Sakyoku (Japan). Dept. of Geophysics.
TIME EVOLUTION OF CROSS-STREAM EXCHANGE ASSOCIATED WITH THE VARIATIONS IN THE KUROSHIO
Toshiyuki Awaji, Kazunori Akimoto, and Norihisa Imasato *In* Scientific Organizing Committee of PORSEC, Proceedings of the PORSEC 1992 in Okinawa: Conference for Pacific Ocean Environments and Probing, Volume 1 25 Aug. 1992 p 243-248 (For primary document see N94-11894 01-42)
(Grant MOE-01646010)
Copyright Avail: Issuing Activity (Scientific Organizing Committee of PORSEC, P.O. Box 10, Shimizu, Shizuoka 424, Japan, HC)

N94-11937 Tokyo Univ. (Japan). Ocean Research Inst.
APPEARANCE, BEHAVIOR, AND OCEANIC STRUCTURES OF WARM STREAMERS IN THE KUROSHIO OYASHIO FRONTAL REGION
Takashige Sugimoto, Kenji Morinaga (Seikai Regional Fisheries Research Lab., Nagasaki, Japan.), and Yoshiharu Endou (Tohoku Univ., Sendai, Japan.) *In* Scientific Organizing Committee of PORSEC, Proceedings of the PORSEC 1992 in Okinawa: Conference for Pacific Ocean Environments and Probing, Volume 1 25 Aug. 1992 p 249-254 (For primary document see N94-11894 01-42)
Copyright Avail: Issuing Activity (Scientific Organizing Committee of PORSEC, P.O. Box 10, Shimizu, Shizuoka 424, Japan, HC)

N94-11938 Japan Fisheries Information Service Center, Tokyo.
WARM STREAMERS EXTENDED FROM WARM CORE RINGS (WCRS) AND THEIR ROLE ON FISH MIGRATION AND FISHING GROUND FORMATION
Hideo Tameishi and Takashige Sugimoto (Tokyo Univ., Japan.) *In* Scientific Organizing Committee of PORSEC, Proceedings of the PORSEC 1992 in Okinawa: Conference for Pacific Ocean Environments and Probing, Volume 1 25 Aug. 1992 p 255-260 (For primary document see N94-11894 01-42)
Copyright Avail: Issuing Activity (Scientific Organizing Committee of PORSEC, P.O. Box 10, Shimizu, Shizuoka 424, Japan, HC)

N94-11939 Ehime Univ., Matsuyama (Japan). Dept. of Civil and Ocean Engineering.
THE KYUCHO EVENTS IN SUKUMO BAY INDUCED BY KUROSHIO FRONT DISTURBANCES
Hideki Akiyama and Sei-Ichi Saitou (Japan Weather Association, Tokyo.) *In* Scientific Organizing Committee of PORSEC, Proceedings of the PORSEC 1992 in Okinawa: Conference for Pacific Ocean Environments and Probing, Volume 1 25 Aug. 1992 p 261-266 (For primary document see N94-11894 01-42)
Copyright Avail: Issuing Activity (Scientific Organizing Committee of PORSEC, P.O. Box 10, Shimizu, Shizuoka 424, Japan, HC)

N94-11940 Science Univ. of Tokyo, Chiba (Japan).
THE COHERENT STRUCTURE IN THE OCEANIC TURBULENCE AROUND JAPAN ISLANDS CHAIN FORCED BY AN AIR, SEA, AND SOLID EARTH INTERACTION
Tsukasa Nishimura, Soutarou Tanaka (Remote Sensing Technology Center, Tokyo, Japan.), Toshirou Sugimura (Remote Sensing Technology Center, Tokyo, Japan.), Yuuji Hatakeyama (Asia Air Survey Co. Ltd., Suita, Japan.), I. Hisano, and M. Tazuke *In* Scientific Organizing Committee of PORSEC, Proceedings of the PORSEC 1992 in Okinawa: Conference for Pacific Ocean Environments and Probing, Volume 1 25 Aug. 1992 p 267-272 (For primary document see N94-11894 01-42)
Copyright Avail: Issuing Activity (Scientific Organizing Committee of PORSEC, P.O. Box 10, Shimizu, Shizuoka 424, Japan, HC)

N94-11941 Kyushu Univ., Fukuoka (Japan). Research Inst. for Applied Mechanics.
WESTWARD PROPAGATION OF SEA SURFACE ANOMALIES IN THE WESTERN NORTH PACIFIC AS SEEN BY THE ALTIMETER AND RADIOMETER
Shigeru Aoki, Shirou Imawaki, and Kaoru Ichikawa (Kyoto Univ., Sakyoku, Japan.) *In* Scientific Organizing Committee of PORSEC, Proceedings of the PORSEC 1992 in Okinawa: Conference for Pacific Ocean Environments and Probing, Volume 1 25 Aug. 1992 p 273-278 (For primary document see N94-11894 01-42)
Copyright Avail: Issuing Activity (Scientific Organizing Committee of PORSEC, P.O. Box 10, Shimizu, Shizuoka 424, Japan, HC)

N94-11942 National Defense Medical Coll., Saitama (Japan). Dept. of Physics.
COASTAL PROCESSES DUE TO NEARSHORE CURRENT AROUND AN UPHEAVING ISLAND
Masahiro Hashima and Yasuhiro Sugimori (Tokai Univ., Shizuoka, Japan.) *In* Scientific Organizing Committee of PORSEC, Proceedings of the PORSEC 1992 in Okinawa: Conference for Pacific Ocean Environments and Probing, Volume 1 25 Aug. 1992 p 279-286 (For primary document see N94-11894 01-42)
Copyright Avail: Issuing Activity (Scientific Organizing Committee of PORSEC, P.O. Box 10, Shimizu, Shizuoka 424, Japan, HC)

N94-11945 Japan Marine Science and Technology Center, Tokyo.
AN APPLICATION OF REDUCED GRAVITY MODEL TO MESOSCALE EDDIES
T. Kawano, Kei Muneyama, and S. Nakamoto (Sanyo Techno Marine Co. Ltd., Tokyo, Japan.) *In* Scientific Organizing Committee of PORSEC, Proceedings of the PORSEC 1992 in Okinawa: Conference for Pacific Ocean Environments and Probing, Volume 1 25 Aug. 1992 p 299-303 (For primary document see N94-11894 01-42)
Copyright Avail: Issuing Activity (Scientific Organizing Committee of PORSEC, P.O. Box 10, Shimizu, Shizuoka 424, Japan, HC)

N94-11947 Tokai Univ., Shizuoka (Japan). School of Marine Science and Technology.
CZCS DERIVED CHLOROPHYLL DISTRIBUTION IN ANTARCTIC WATER DURING AUSTRAL SUMMER
Kedarnath Mahapatra, Yoshihiro Okada, and Yasuhiro Sugimori *In* Scientific Organizing Committee of PORSEC, Proceedings of the PORSEC 1992 in Okinawa: Conference for Pacific Ocean Environments and Probing, Volume 1 25 Aug. 1992 p 313-318 Sponsored in part by Matsumae International Foundation (For primary document see N94-11894 01-42)
Copyright Avail: Issuing Activity (Scientific Organizing Committee of PORSEC, P.O. Box 10, Shimizu, Shizuoka 424, Japan, HC)

N94-11948 National Inst. for Resources and Environment, Ibaraki (Japan).
SEASONAL CHANGES OF PHYTOPLANKTON DISTRIBUTIONS IN THE NORTHWEST PACIFIC DETECTED BY COASTAL ZONE COLOR SCANNER
J. Ishizaka and K. Nakata *In* Scientific Organizing Committee of PORSEC, Proceedings of the PORSEC 1992 in Okinawa: Conference for Pacific Ocean Environments and Probing, Volume 1 25 Aug. 1992 p 319-324 (For primary document see N94-11894 01-42)
Copyright Avail: Issuing Activity (Scientific Organizing Committee of PORSEC, P.O. Box 10, Shimizu, Shizuoka 424, Japan, HC)

N94-11950 Tokyo Univ. (Japan). Ocean Research Inst.
PARTICLE DYNAMICS IN THE WESTERN SUBARCTIC PACIFIC: IMPLICATIONS FROM CZCS IMAGERY
Toshirou Saino *In* Scientific Organizing Committee of PORSEC, Proceedings of the PORSEC 1992 in Okinawa: Conference for Pacific Ocean Environments and Probing, Volume 1 25 Aug. 1992 p 330-335 (For primary document see N94-11894 01-42)
Copyright Avail: Issuing Activity (Scientific Organizing Committee of PORSEC, P.O. Box 10, Shimizu, Shizuoka 424, Japan, HC)

N94-11972 Institute of Physical and Chemical Research, Saitama (Japan).
OPTICAL CHARACTERISTICS IN TOKYO BAY
Motoaki Kishino and Shigehiko Sugihara *In* Scientific Organizing Committee of PORSEC, Proceedings of the PORSEC 1992 in Okinawa: Conference for Pacific Ocean Environments and Probing, Volume 1 25 Aug. 1992 p 446-451 (For primary document see N94-11894 01-42)
Copyright Avail: Issuing Activity (Scientific Organizing Committee of PORSEC, P.O. Box 10, Shimizu, Shizuoka 424, Japan, HC)

N94-11974 Hokkaido Univ., Sapporo (Japan).
A DEVELOPMENT ON ESTIMATION METHOD OF UNDERSEA LIGHT
Masaaki Fukuda *In* Scientific Organizing Committee of PORSEC, Proceedings of the PORSEC 1992 in Okinawa: Conference for Pacific Ocean Environments and Probing, Volume 1 25 Aug. 1992 p 460-464 (For primary document see N94-11894 01-42)
Copyright Avail: Issuing Activity (Scientific Organizing Committee of PORSEC, P.O. Box 10, Shimizu, Shizuoka 424, Japan, HC)

N94-11985 Tokai Univ., Shizuoka (Japan). Faculty of Oceanography.
CIRCULATION OF NORTH PACIFIC INTERMEDIATE WATER
Masao Fukasawa, Naoki Hagiwara, and Yasuhiro Sugimori *In* Scientific Organizing Committee of PORSEC, Proceedings of the PORSEC 1992 in Okinawa: Conference for Pacific Ocean Environments and Probing, Volume 1 25 Aug. 1992 p 516-520 (For primary document see N94-11894 01-42)
Copyright Avail: Issuing Activity (Scientific Organizing Committee of PORSEC, P.O. Box 10, Shimizu, Shizuoka 424, Japan, HC)

N94-11986 Tokyo Univ. (Japan). Ocean Research Inst.
SOFAR FLOAT TRACKING IN THE SHIKOKU BASIN
Daigo Yanagimoto, Keisuke Taira, and Shouji Kitagawa *In* Scientific Organizing Committee of PORSEC, Proceedings of the PORSEC 1992 in Okinawa: Conference for Pacific Ocean Environments and Probing, Volume 1 25 Aug. 1992 p 521-526 (For primary document see N94-11894 01-42)
Copyright Avail: Issuing Activity (Scientific Organizing Committee of PORSEC, P.O. Box 10, Shimizu, Shizuoka 424, Japan, HC)

N94-11987 National Inst. of Oceanography, Goa (India).
ON AN UPWELLING FRONT, PROPAGATION OF UPWELLING AND VERTICAL VELOCITY IN THE EASTERN ARABIAN SEA DURING MONSOON, 1987
M. K. Antony and A. S. Unnikrishnan *In* Scientific Organizing Committee of PORSEC, Proceedings of the PORSEC 1992 in Okinawa: Conference for Pacific Ocean Environments and Probing, Volume 1 25 Aug. 1992 p 527-532 (For primary document see N94-11894 01-42)
Copyright Avail: Issuing Activity (Scientific Organizing Committee of PORSEC, P.O. Box 10, Shimizu, Shizuoka 424, Japan, HC)

N94-11988 National Inst. of Oceanography, Goa (India).
SEA SURFACE TEMPERATURE ANOMALIES IN THE ARABIAN SEA
M. R. Ramesh Kumar *In* Scientific Organizing Committee of PORSEC, Proceedings of the PORSEC 1992 in Okinawa: Conference for Pacific Ocean Environments and Probing, Volume 1 25 Aug. 1992 p 533-537 (For primary document see N94-11894 01-42)
Copyright Avail: Issuing Activity (Scientific Organizing Committee of PORSEC, P.O. Box 10, Shimizu, Shizuoka 424, Japan, HC)

N94-11990 Academia Sinica, Beijing (China). Inst. of Oceanology.
ROLES OF THE NEC AND MC IN THE FORMATION AND EVOLUTION OF THE EQUATORIAL PACIFIC WARM POOL
Ming Feng, Dunxin Hu, and Yongxiang Li *In* Scientific Organizing Committee of PORSEC, Proceedings of the PORSEC 1992 in Okinawa: Conference for Pacific Ocean Environments and Probing, Volume 1 25 Aug. 1992 p 550-554 (For primary document see N94-11894 01-42)
Copyright Avail: Issuing Activity (Scientific Organizing Committee of PORSEC, P.O. Box 10, Shimizu, Shizuoka 424, Japan, HC)

N94-12500# Norwegian Meteorological Inst., Blindern.
IMPACT OF ERS-1 WIND/WAVE/ICE DATA ON OPERATIONAL OCEAN FORECASTING
Johannes Guddal *In* ESA, Proceedings of 1st ERS-1 Symposium on Space at the Service of Our Environment, Volume 2 Mar. 1993 p 695-699 (For primary document see N94-12471 01-43)
Copyright Avail: CASI HC A01/MF A03; EPD, ESA, ESTEC, Noordwijk, Netherlands, HC

N94-12505# Johns Hopkins Univ., Laurel, MD. Applied Physics Lab.
ERS-1 AND ALMAZ SAR OCEAN WAVE IMAGING OVER THE GULF STREAM AND THE GRAND BANKS
David George Tilley and Robert Carl Beal *In* ESA, Proceedings of 1st ERS-1 Symposium on Space at the Service of Our Environment, Volume 2 Mar. 1993 p 729-734 (For primary document see N94-12471 01-43)
Copyright Avail: CASI HC A02/MF A03; EPD, ESA, ESTEC, Noordwijk, Netherlands, HC

N94-12506# Sydney Univ. (Australia). Ocean Technology Group.
REAL TIME PROCESSING WAVE SPECTRA FROM SATELLITE SAR
Ian S. F. Jones *In* ESA, Proceedings of 1st ERS-1 Symposium on Space at the Service of Our Environment, Volume 2 Mar. 1993 p 735-737 Sponsored by Esso-BHP (For primary document see N94-12471 01-43)
Copyright Avail: CASI HC A01/MF A03; EPD, ESA, ESTEC, Noordwijk, Netherlands, HC

N94-12507# Institut Francais de Recherche pour l'Exploitation de la Mer, Brest. Dept. d'Oceanographie Spatiale.
A STATISTICAL ANALYSIS OF SEA STATE SURFACE ERS-1 SAR-WAVE MODE IMAGETTES
B. Chapron, R. Garello (Ecole Nationale Superieure des Telecommunicatons, Brest, France.), and G. Engen (Forut, Tromsoe, Norway.) *In* ESA, Proceedings of 1st ERS-1 Symposium on Space at the Service of Our Environment, Volume 2 Mar. 1993 p 739-742 (For primary document see N94-12471 01-43)
Copyright Avail: CASI HC A01/MF A03; EPD, ESA, ESTEC, Noordwijk, Netherlands, HC

N94-12508# James Cook Univ. of North Queensland, Townsville (Australia). Dept. of Physics.
A NEW MODEL FOR SYNTHETIC APERTURE RADAR (SAR) IMAGES FROM OCEAN SCATTER
M. L. Heron and I. Amadou *In* ESA, Proceedings of 1st ERS-1 Symposium on Space at the Service of Our Environment, Volume 2 Mar. 1993 p 743-745 Sponsored by DSTO, Adelaide, Australia (For primary document see N94-12471 01-43)
Copyright Avail: CASI HC A01/MF A03; EPD, ESA, ESTEC, Noordwijk, Netherlands, HC

N94-12509# Hamburg Univ. (Germany). Inst. fuer Meereskunde.
ON THE EXTRACTION OF OCEAN WAVE SPECTRA FROM ERS-1 SAR WAVE MODE IMAGE SPECTRA

C. Bruening, S. Hasselmann (Max-Planck-Inst. fuer Meteorologie, Hamburg, Germany.), K. Hasselmann (Max-Planck-Inst. fuer Meteorologie, Hamburg, Germany.), S. Lehner (Max-Planck-Inst. fuer Meteorologie, Hamburg, Germany.), and T. Gerling (Johns Hopkins Univ., Laurel, MD.) *In* ESA, Proceedings of 1st ERS-1 Symposium on Space at the Service of Our Environment, Volume 2 Mar. 1993 p 747-752 (For primary document see N94-12471 01-43)
(Contract BMFT-01-QS-9014)
Copyright Avail: CASI HC A02/MF A03; EPD, ESA, ESTEC, Noordwijk, Netherlands, HC

N94-12510# Hamburg Univ. (Germany). Inst. fuer Meereskunde.
TIDE-GENERATED NONLINEAR INTERNAL WAVE PACKETS IN THE STRAIT OF GIBRALTAR OBSERVED BY THE SYNTHETIC APERTURE RADAR ABOARD THE ERS-1 SATELLITE
W. Alpers and P. E. LaViolette (Mississippi State Univ., Mississippi State.) *In* ESA, Proceedings of 1st ERS-1 Symposium on Space at the Service of Our Environment, Volume 2 Mar. 1993 p 753-758 (For primary document see N94-12471 01-43)
(Contract BMFT-01-QS-9014)
Copyright Avail: CASI HC A02/MF A03; EPD, ESA, ESTEC, Noordwijk, Netherlands, HC

N94-12514# Hamburg Univ. (Germany). Meteorologisches Inst.
ATSR CORRELATIVE SKIN MEASUREMENTS OF SEA SURFACE TEMPERATURE
Peter Schluessel and Jens Meywerk *In* ESA, Proceedings of 1st ERS-1 Symposium on Space at the Service of Our Environment, Volume 2 Mar. 1993 p 779-784 Sponsored by DFG, and BMFT (For primary document see N94-12471 01-43)
Copyright Avail: CASI HC A02/MF A03; EPD, ESA, ESTEC, Noordwijk, Netherlands, HC

N94-12518# British Antarctic Survey, Cambridge (England).
A COMPARISON OF ATSR AND SHIPBOARD RADIOMETER SST MEASUREMENTS ALONG TRANSECTS BETWEEN THE UK AND THE ANTARCTIC
J. P. Thomas, J. Turner, and C. J. Symon *In* ESA, Proceedings of 1st ERS-1 Symposium on Space at the Service of Our Environment, Volume 2 Mar. 1993 p 801-805 (For primary document see N94-12471 01-43)
Copyright Avail: CASI HC A01/MF A03; EPD, ESA, ESTEC, Noordwijk, Netherlands, HC

N94-12519# Chilworth Research Centre, Southampton (England). Center for Ocean Circulation.
PRELIMINARY VALIDATION OF ATSR SEA SURFACE TEMPERATURES NEAR THE FAEROES
T. N. Forrester, T. H. Guymer, and P. G. Challenor *In* ESA, Proceedings of 1st ERS-1 Symposium on Space at the Service of Our Environment, Volume 2 Mar. 1993 p 807-811 (For primary document see N94-12471 01-43)
Copyright Avail: CASI HC A01/MF A03; EPD, ESA, ESTEC, Noordwijk, Netherlands, HC

N94-12524# Liege Univ. (Belgium). Lab. de Geomorphologie et de Geologie du Quatenaire.
COASTAL MORPHODYNAMICS AND ENERGETIC CHARACTERISTICS OF SWELL STUDIED WITH ERS-1 SAR [MORPHODYNAMIQUE DES COTES ET CARACTERISTIQUES ENERGETIQUES DE LA HOULE ETUDIEE GRACE AU SAR DE ERS-1]
A. Ozer, Y. Cornet, and A. L. Comhaire *In* ESA, Proceedings of 1st ERS-1 Symposium on Space at the Service of Our Environment, Volume 2 Mar. 1993 p 851-855 In FRENCH (For primary document see N94-12471 01-43)
Copyright Avail: CASI HC A01/MF A03; EPD, ESA, ESTEC, Noordwijk, Netherlands, HC

N94-12525# Rijkswaterstaat, Rijswijk (Netherlands).
MAPPING OF SEA BOTTOM TOPOGRAPHY WITH ERS-1 C-BAND SAR
J. Vogelzang, G. J. Wensink (Delft Hydraulics Lab., Emmeloord, Netherlands.), M. W. A. vanderKooij (Physics and Electronics Lab. TNO, The Hague, Netherlands.), and G. vanderBurg (National Aerospace Lab., Emmeloord, Netherlands.) *In* ESA, Proceedings of 1st ERS-1 Symposium on Space at the Service of Our Environment, Volume 2 Mar. 1993 p 857-860 (For primary document see N94-12471 01-43)
Copyright Avail: CASI HC A01/MF A03; EPD, ESA, ESTEC, Noordwijk, Netherlands, HC

N94-12526# International Inst. for Aerospace Survey and Earth Sciences, Enschede (Netherlands).
ERS-1 IMAGING RADAR OVER THE WADDENSEA-NORTH NETHERLANDS
B. N. Koopmans and Wang Yiman (Academia Sinica, Beijing, China.) *In* ESA, Proceedings of 1st ERS-1 Symposium on Space at the Service of Our Environment, Volume 2 Mar. 1993 p 861-865 Sponsored by Beleidscommissie Remote Sensing Board, Delft, Netherlands (For primary document see N94-12471 01-43)
Copyright Avail: CASI HC A01/MF A03; EPD, ESA, ESTEC, Noordwijk, Netherlands, HC

N94-12527# City of London Polytechnic (England).
SAR IMAGING OF GEOLOGY AND BATHYMETRY: KENT COASTAL AREA - SOUTHERN NORTH SEA
B. DOlier (City of London Polytechnic, England.) and N. Lynn (Royal Naval Coll., Greenwich, London, England.) *In* ESA, Proceedings of 1st ERS-1 Symposium on Space at the Service of Our Environment, Volume 2 Mar. 1993 p 867-871 (For primary document see N94-12471 01-43)
Copyright Avail: CASI HC A01/MF A03; EPD, ESA, ESTEC, Noordwijk, Netherlands, HC

N94-12528# Army Cold Regions Research and Engineering Lab., Hanover, NH.
APPLICATIONS OF ERS-1 SAR DATA FOR ANALYZING RIVERINE AND COASTAL PROCESSES AND GEOMORPHOLOGY
L. W. Gatto, D. J. Calkins, E. F. Chacho, D. E. Lawson, and R. A. Melloh *In* ESA, Proceedings of 1st ERS-1 Symposium on Space at the Service of Our Environment, Volume 2 Mar. 1993 p 873-878 (For primary document see N94-12471 01-43)
Copyright Avail: CASI HC A02/MF A03; EPD, ESA, ESTEC, Noordwijk, Netherlands, HC

N94-12529# Consejo Superior de Investigaciones Cientificas, Barcelona (Spain). Inst. de Ciencies del Mar.
COMPARISON OF ERS-1 SAR IMAGES OF THE WESTERN MEDITERRANEAN TO IN SITU OCEANOGRAPHIC DATA: PRIM-1 CRUISE (MAY 1992)
J. Font, A. Martinez, E. G. Gorriz, E. Garcia (Universidad de Palma de Mallorca, Spain.), A. Castellon, A. Julia, M. Manriquez, A. Viudez (Universidad de Palma de Mallorca, Spain.), and M. R. Vitria *In* ESA, Proceedings of 1st ERS-1 Symposium on Space at the Service of Our Environment, Volume 2 Mar. 1993 p 883-887 Sponsored by Spanish National Program on Marine Resources and INISEL Espacio (For primary document see N94-12471 01-43)
Copyright Avail: CASI HC A01/MF A03; EPD, ESA, ESTEC, Noordwijk, Netherlands, HC

N94-12640 Japan Marine Science and Technology Center, Tokyo.
VARIABILITY OF SEA LEVEL AND SEA SURFACE TEMPERATURE ANOMALIES IN THE EQUATORIAL PACIFIC
K. Yoneyama, K. Andou, Ichirou Asanuma, and Kei Muneyama *In* Scientific Organizing Committee of PORSEC, Proceedings of the PORSEC 1992 in Okinawa: Conference for Pacific Ocean Environments and Probing, Volume 2 25 Aug. 1992 p 582-586 (For primary document see N94-12635 01-42)
Copyright Avail: Issuing Activity (Scientific Organizing Committee of PORSEC, P.O. Box 10, Shimizu, Shizuoka 424, Japan, HC)

N94-12646 Hamburg Univ. (Germany). Inst. fuer Meereskunde.
PRINCIPAL OSCILLATION PATTERN ANALYSIS OF SEA LEVEL VARIATIONS IN THE TROPICAL PACIFIC MEASURED BY THE GEOSAT ALTIMETER
Jiansheng Zou *In* Scientific Organizing Committee of PORSEC, Proceedings of the PORSEC 1992 in Okinawa: Conference for Pacific Ocean Environments and Probing, Volume 2 25 Aug. 1992 p 608-613 (For

primary document see N94-12635 01-42)
Copyright Avail: Issuing Activity (Scientific Organizing Committee of PORSEC, P.O. Box 10, Shimizu, Shizuoka 424, Japan, HC)

N94-12652 Kyoto Univ., Sakyoku (Japan). Dept. of Geophysics.
A NUMERICAL STUDY OF DEEP CONVECTION AT HIGH LATITUDES
Kazunori Akitomo, Toshiyuki Awaji, and Norihisa Imasato *In* Scientific Organizing Committee of PORSEC, Proceedings of the PORSEC 1992 in Okinawa: Conference for Pacific Ocean Environments and Probing, Volume 2 25 Aug. 1992 p 645-650 (For primary document see N94-12635 01-42)
Copyright Avail: Issuing Activity (Scientific Organizing Committee of PORSEC, P.O. Box 10, Shimizu, Shizuoka 424, Japan, HC)

N94-12657 Hokkaido Tokai Univ., Tokyo (Japan).
A SURFACE WATER MONITORING SYSTEM: A DEVICE FOR THE SEA-TRUTH OBSERVATIONS
Hiroshi Hattori, Atsuhiro Yanagisawa, and Mitsuo Fukuchi (National Inst. of Polar Research, Tokyo, Japan.) *In* Scientific Organizing Committee of PORSEC, Proceedings of the PORSEC 1992 in Okinawa: Conference for Pacific Ocean Environments and Probing, Volume 2 25 Aug. 1992 p 677-681 (For primary document see N94-12635 01-42)
Copyright Avail: Issuing Activity (Scientific Organizing Committee of PORSEC, P.O. Box 10, Shimizu, Shizuoka 424, Japan, HC)

N94-12658 National Research Inst. of Far Seas Fisheries, Shizuoka (Japan).
PRIMARY PRODUCTIVITY IN THE OYASHIO AREA IN THE SPRING AND SUMMER OF 1990
Akihiro Shiomoto, Katsuyuki Sasaki (National Research Inst. of Fisheries Science, Tokyo, Japan.), Satsuki Matsumura, and Tooru Shimoda (National Research Inst. of Fisheries Science, Tokyo, Japan.) *In* Scientific Organizing Committee of PORSEC, Proceedings of the PORSEC 1992 in Okinawa: Conference for Pacific Ocean Environments and Probing, Volume 2 25 Aug. 1992 p 682-687 (For primary document see N94-12635 01-42)
Copyright Avail: Issuing Activity (Scientific Organizing Committee of PORSEC, P.O. Box 10, Shimizu, Shizuoka 424, Japan, HC)

N94-12659 Tokai Univ., Shizuoka (Japan). School of Marine Science and Technology.
CHARACTERIZATION OF DISSOLVED ORGANIC MATTER IN THE OCEAN BY USING THE FLUORESCENCE EXCITATION-EMISSION MATRIX
Yasuhiro Senga and Naoya Tomii *In* Scientific Organizing Committee of PORSEC, Proceedings of the PORSEC 1992 in Okinawa: Conference for Pacific Ocean Environments and Probing, Volume 2 25 Aug. 1992 p 688-691 (For primary document see N94-12635 01-42)
Copyright Avail: Issuing Activity (Scientific Organizing Committee of PORSEC, P.O. Box 10, Shimizu, Shizuoka 424, Japan, HC)

N94-12673 Tokai Univ., Shizuoka (Japan). School of Marine Science and Technology.
EVALUATION OF THE METHOD OF GEOSTROPHIC FLOW USING NOAA-AVHRR DATA
Masatoshi Akiyama and Yasuhiro Sugimori *In* Scientific Organizing Committee of PORSEC, Proceedings of the PORSEC 1992 in Okinawa: Conference for Pacific Ocean Environments and Probing, Volume 2 25 Aug. 1992 p 768-773 (For primary document see N94-12635 01-42)
Copyright Avail: Issuing Activity (Scientific Organizing Committee of PORSEC, P.O. Box 10, Shimizu, Shizuoka 424, Japan, HC)

N94-12676 Remote Sensing Technology Center, Tokyo (Japan).
OBSERVATION OF WARM CURRENT AT THE BOUNDARY FROM NORTH EQUATORIAL CURRENT TO KUROSHIO BY NOAA/AVHRR
Toshirou Sugimura, Soutarou Tanaka, Tsukasa Nishimura (Tokyo Science Univ., Japan.), and Masataka Hishida (Maritime Safety Agency, Tokyo, Japan.) *In* Scientific Organizing Committee of PORSEC, Proceedings of the PORSEC 1992 in Okinawa: Conference for Pacific Ocean Environments and Probing, Volume 2 25 Aug. 1992 p 786-789 (For primary document see N94-12635 01-42)
Copyright Avail: Issuing Activity (Scientific Organizing Committee of PORSEC, P.O. Box 10, Shimizu, Shizuoka 424, Japan, HC)

N94-12679 Department of Scientific and Industrial Research, Lower Hutt (New Zealand). Image Processing Section.
ASPECTS OF APPLYING A RELAXATION METHOD TO COMPUTING SEA SURFACE VELOCITIES FROM SEA SURFACE TEMPERATURE IMAGES
Q. X. Wu, D. Pairman, and E. J. Barnes *In* Scientific Organizing Committee of PORSEC, Proceedings of the PORSEC 1992 in Okinawa: Conference for Pacific Ocean Environments and Probing, Volume 2 25 Aug. 1992 p 802-807 Sponsored by New Zealand Foundation for Research, Science and Technology, New Zealand (For primary document see N94-12635 01-42)
Copyright Avail: Issuing Activity (Scientific Organizing Committee of PORSEC, P.O. Box 10, Shimizu, Shizuoka 424, Japan, HC)

N94-12680 Kagoshima Univ. (Japan). Faculty of Fisheries.
SEA SURFACE TEMPERATURE DIFFERENCE BETWEEN NOAA/AVHRR AND IN-SITU OBSERVATION
Hiroshi Ichikawa, Katsutoshi Nishimura, and Masaaki Chaen *In* Scientific Organizing Committee of PORSEC, Proceedings of the PORSEC 1992 in Okinawa: Conference for Pacific Ocean Environments and Probing, Volume 2 25 Aug. 1992 p 808-813 (For primary document see N94-12635 01-42)
Copyright Avail: Issuing Activity (Scientific Organizing Committee of PORSEC, P.O. Box 10, Shimizu, Shizuoka 424, Japan, HC)

N94-12683 Yosu National Fisheries Coll. (Republic of Korea). Dept. of Oceanography.
INTRUSION OF KUROSHIO WARM WATER INTO SAGAMI BAY
Hyo Sang Choo, Takashige Sugimoto (Tokyo Univ., Japan.), and Hideo Tameishi (Japan Fisheries Information Service Center, Tokyo.) *In* Scientific Organizing Committee of PORSEC, Proceedings of the PORSEC 1992 in Okinawa: Conference for Pacific Ocean Environments and Probing, Volume 2 25 Aug. 1992 p 824-828 (For primary document see N94-12635 01-42)
Copyright Avail: Issuing Activity (Scientific Organizing Committee of PORSEC, P.O. Box 10, Shimizu, Shizuoka 424, Japan, HC)

N94-12685 Kyoto Univ., Sakyoku (Japan). Oceanographic Observatory.
SATELLITE THERMAL VARIATIONS OF KUROSHIO IN RELATION TO STORM FLOODS
Shigehisa Nakamura *In* Scientific Organizing Committee of PORSEC, Proceedings of the PORSEC 1992 in Okinawa: Conference for Pacific Ocean Environments and Probing, Volume 2 25 Aug. 1992 p 835-840 Sponsored by Ministry of Education, Science and Culture, Tokyo, Japan (For primary document see N94-12635 01-42)
Copyright Avail: Issuing Activity (Scientific Organizing Committee of PORSEC, P.O. Box 10, Shimizu, Shizuoka 424, Japan, HC)

N94-12686 First Inst. of Oceanography, Qingdao (China). First Inst. of Oceanography.
ADCP EVIDENCE FOR UPPER LAYER CIRCULATION IN NORTHEAST OF THE SOUTH CHINA SEA
Shuzhen Pu, Huiling Yu, and Songnian Jiang (National Marine Date and Information, Tianjin, China.) *In* Scientific Organizing Committee of PORSEC, Proceedings of the PORSEC 1992 in Okinawa: Conference for Pacific Ocean Environments and Probing, Volume 2 25 Aug. 1992 p 841-845 (For primary document see N94-12635 01-42)
Copyright Avail: Issuing Activity (Scientific Organizing Committee of PORSEC, P.O. Box 10, Shimizu, Shizuoka 424, Japan, HC)

N94-12687 Academy of Sciences (USSR), Moscow. Inst. of Oceanology.
FRONTAL ZONES IN PACIFIC OCEAN: SATELLITE AND SHIP DATA ANALYSIS
A. S. Kazmin *In* Scientific Organizing Committee of PORSEC, Proceedings of the PORSEC 1992 in Okinawa: Conference for Pacific Ocean Environments and Probing, Volume 2 25 Aug. 1992 p 846-850 (For primary document see N94-12635 01-42)
Copyright Avail: Issuing Activity (Scientific Organizing Committee of PORSEC, P.O. Box 10, Shimizu, Shizuoka 424, Japan, HC)

N94-12688 Universidad Catolica del Norte, Coquimbo (Chile). Facultad Ciencias del Mar.
SWORDFISH (XIPHIAS GLADIUS) CATCH DISTRIBUTIONS RELATIVE TO ENVIRONMENTAL FEATURES OBSERVED FROM SATELLITES OFF COQUIMBO, CHILE (30 DEG S)
Eduardo Uribe and Claudio Salazar (Pesquera Santa Lucia, Valparaiso, Chile.) *In* Scientific Organizing Committee of PORSEC, Proceedings of the PORSEC 1992 in Okinawa: Conference for Pacific Ocean Environments and Probing, Volume 2 25 Aug. 1992 p 851-857 (For primary document see N94-12635 01-42)
Copyright Avail: Issuing Activity (Scientific Organizing Committee of PORSEC, P.O. Box 10, Shimizu, Shizuoka 424, Japan, HC)

N94-12689 Korea Ocean Research and Development Inst., Seoul (Republic of Korea).
OBSERVATION OF COLD COASTAL WATER WITH HIGH TURBIDITY AROUND THE SOUTHWESTERN TIP OF KOREAN PENINSULA
Heung-Jae Lie, Hong-Rhyong Yoo, and Sang Sup Yuk *In* Scientific Organizing Committee of PORSEC, Proceedings of the PORSEC 1992 in Okinawa: Conference for Pacific Ocean Environments and Probing, Volume 2 25 Aug. 1992 p 858-863 (For primary document see N94-12635 01-42)
Copyright Avail: Issuing Activity (Scientific Organizing Committee of PORSEC, P.O. Box 10, Shimizu, Shizuoka 424, Japan, HC)

N94-12690 Iwate Univ., Morioka (Japan).
ON THE ERROR CHARACTERISTICS OF THE SEA SURFACE TEMPERATURE OBSERVED BY SATELLITE
Sumio Tanba, Takashi Souma, Yukifumi Iwakuma, Isao Yoshida, Takashi Watanabe, and Ryuuzou Yokoyama *In* Scientific Organizing Committee of PORSEC, Proceedings of the PORSEC 1992 in Okinawa: Conference for Pacific Ocean Environments and Probing, Volume 2 25 Aug. 1992 p 864-867 (For primary document see N94-12635 01-42)
Copyright Avail: Issuing Activity (Scientific Organizing Committee of PORSEC, P.O. Box 10, Shimizu, Shizuoka 424, Japan, HC)

N94-12691 Scripps Institution of Oceanography, La Jolla, CA.
THE WOCE/TOGA SURFACE VELOCITY PROGRAMME (SVP)
Pearn P. Niiler, Laurence Sombardier, and Andrew Sybrandy *In* Scientific Organizing Committee of PORSEC, Proceedings of the PORSEC 1992 in Okinawa: Conference for Pacific Ocean Environments and Probing, Volume 2 25 Aug. 1992 p 868-875 (For primary document see N94-12635 01-42)
Copyright Avail: Issuing Activity (Scientific Organizing Committee of PORSEC, P.O. Box 10, Shimizu, Shizuoka 424, Japan, HC)

N94-12692 Tokai Univ., Shizuoka (Japan). Graduate School of Marine Science and Technology.
DEVELOPMENT OF A SHUTTLE AUV FOR OCEANOGRAPHIC MEASUREMENT
Katsuyoshi Kawaguchi, Tamaki Ura, Yoshibumi Tomoda, and Heihachirou Kobayashi *In* Scientific Organizing Committee of PORSEC, Proceedings of the PORSEC 1992 in Okinawa: Conference for Pacific Ocean Environments and Probing, Volume 2 25 Aug. 1992 p 876-880 (For primary document see N94-12635 01-42)
Copyright Avail: Issuing Activity (Scientific Organizing Committee of PORSEC, P.O. Box 10, Shimizu, Shizuoka 424, Japan, HC)

N94-12693 Taisei Corp., Tokyo (Japan).
INTEGRATED MARINE SURVEY SYSTEM
Tadashi Kanzaki *In* Scientific Organizing Committee of PORSEC, Proceedings of the PORSEC 1992 in Okinawa: Conference for Pacific Ocean Environments and Probing, Volume 2 25 Aug. 1992 p 881-885 (For primary document see N94-12635 01-42)
Copyright Avail: Issuing Activity (Scientific Organizing Committee of PORSEC, P.O. Box 10, Shimizu, Shizuoka 424, Japan, HC)

N94-12694 Japan Weather Association, Tokyo.
DEVELOPMENT OF A BUOY SYSTEM FOR MONITORING MARINE WEATHER AND MARINE LIFE ABUNDANCE
Masafumi Ichikawa, Mamoru Shimanuki, Kouzou Okada, Harumi Yamada (Japan Marine Fishery Resources Research Center, Tokyo.), and Tadahiko Noda (Japan Meteorological Agency, Tokyo.) *In* Scientific Organizing Committee of PORSEC, Proceedings of the PORSEC 1992 in Okinawa: Conference for Pacific Ocean Environments and Probing, Volume 2 25 Aug. 1992 p 886-891 Original contains color illustrations (For primary document see N94-12635 01-42)
Copyright Avail: Issuing Activity (Scientific Organizing Committee of PORSEC, P.O. Box 10, Shimizu, Shizuoka 424, Japan, HC)

N94-12696 Taisei Corp., Narashino (Japan).
STUDY ON SEA WATER PURIFICATION USING A SUBSTRATUM OF MARINE ORGANISMS
Fumio Kaneko, Norio Katakura, and Tetsuo Yagura *In* Scientific Organizing Committee of PORSEC, Proceedings of the PORSEC 1992 in Okinawa: Conference for Pacific Ocean Environments and Probing, Volume 2 25 Aug. 1992 p 898-903 (For primary document see N94-12635 01-42)
Copyright Avail: Issuing Activity (Scientific Organizing Committee of PORSEC, P.O. Box 10, Shimizu, Shizuoka 424, Japan, HC)

N94-12698 Center for Oceanology Research and Development, Jakarta (Indonesia).
SEASONAL VARIABILITY OF SURFACE OCEAN COLOR IN THE OMURA BAY USING MULTITEMPORAL LANDSAT-5 TM DATA
Sam Wouthuyzen, Keinosuke Gotou (Nagasaki Univ., Japan.), and Shirou Uno (Seikai Regional Fisheries Research Lab., Nagasaki, Japan.) *In* Scientific Organizing Committee of PORSEC, Proceedings of the PORSEC 1992 in Okinawa: Conference for Pacific Ocean Environments and Probing, Volume 2 25 Aug. 1992 p 910-915 (For primary document see N94-12635 01-42)
Copyright Avail: Issuing Activity (Scientific Organizing Committee of PORSEC, P.O. Box 10, Shimizu, Shizuoka 424, Japan, HC)

N94-12702 National Defense Medical Coll., Saitama (Japan). Dept. of Physics.
STUDY OF GROWING PROCESSES OF A TOMBOLO USING AN AIR PHOTOGRAPH
Masahiro Hashima and Yasuhiro Sugimori (Tokai Univ., Shizuoka, Japan.) *In* Scientific Organizing Committee of PORSEC, Proceedings of the PORSEC 1992 in Okinawa: Conference for Pacific Ocean Environments and Probing, Volume 2 25 Aug. 1992 p 936-939 (For primary document see N94-12635 01-42)
Copyright Avail: Issuing Activity (Scientific Organizing Committee of PORSEC, P.O. Box 10, Shimizu, Shizuoka 424, Japan, HC)

N94-12707 National Taiwan Univ., Taipei. Inst. of Oceanography.
THE CIRCULATION NEAR LUZON
Cho-Teng Liu, Su-Cheng Pai, Gil Jacinto (University of the Philippines, Quezon City.), and Israel Bentillo (University of the Philippines, Quezon City.) *In* Scientific Organizing Committee of PORSEC, Proceedings of the PORSEC 1992 in Okinawa: Conference for Pacific Ocean Environments and Probing, Volume 2 25 Aug. 1992 p 964-968 (For primary document see N94-12635 01-42)
Copyright Avail: Issuing Activity (Scientific Organizing Committee of PORSEC, P.O. Box 10, Shimizu, Shizuoka 424, Japan, HC)

N94-12708 National Taiwan Univ., Taipei. Inst. of Oceanography.
CURRENT VARIABILITY ON THE SHELF BREAK NORTHEAST OF TAIWAN
T. Y. Tang, Y. J. Yang, and D. Lee *In* Scientific Organizing Committee of PORSEC, Proceedings of the PORSEC 1992 in Okinawa: Conference for Pacific Ocean Environments and Probing, Volume 2 25 Aug. 1992 p 969-974 (For primary document see N94-12635 01-42)
(Grant NCS-81-0209-M-002A-08)
Copyright Avail: Issuing Activity (Scientific Organizing Committee of PORSEC, P.O. Box 10, Shimizu, Shizuoka 424, Japan, HC)

N94-12709 National Sun Yat-Sen Univ., Kaohsiung (China). Inst. of Marine Geology.
SEDIMENTATION RATES AND PARTICULATE FLUXES IN THE SLOPE AND DEEP SEA AREAS OFF EASTERN TAIWAN
G. W. Hung and Y. Chung *In* Scientific Organizing Committee of PORSEC, Proceedings of the PORSEC 1992 in Okinawa: Conference for Pacific Ocean Environments and Probing, Volume 2 25 Aug. 1992

p 975-981 (For primary document see N94-12635 01-42)
Copyright Avail: Issuing Activity (Scientific Organizing Committee of PORSEC, P.O. Box 10, Shimizu, Shizuoka 424, Japan, HC)

N94-12711 Qingdao Inst. of Oceanology (China). Ocean Remote Sensing and Optics Lab.
INVESTIGATION OF MESO-SCALE FRONTS, EDDIES AND UPWELLINGS IN CHINA SEAS WITH AVHRR DATA
Ming Xia He, Ge Chen, and A. S. Kazmin *In* Scientific Organizing Committee of PORSEC, Proceedings of the PORSEC 1992 in Okinawa: Conference for Pacific Ocean Environments and Probing, Volume 2 25 Aug. 1992 p 989-998 (For primary document see N94-12635 01-42)
Copyright Avail: Issuing Activity (Scientific Organizing Committee of PORSEC, P.O. Box 10, Shimizu, Shizuoka 424, Japan, HC)

N94-12712 Joint Research Centre of the European Communities, Ispra (Italy). Inst. for Remote Sensing Applications.
COASTAL UPWELLING MONITORED BY SATELLITE DATA: METHODOLOGIES AND RESULTS
Leo Nykjaer, Lieve VanCamp, Trevor Barker, and Nick Jewell *In* Scientific Organizing Committee of PORSEC, Proceedings of the PORSEC 1992 in Okinawa: Conference for Pacific Ocean Environments and Probing, Volume 2 25 Aug. 1992 p 999-1003 (For primary document see N94-12635 01-42)
Copyright Avail: Issuing Activity (Scientific Organizing Committee of PORSEC, P.O. Box 10, Shimizu, Shizuoka 424, Japan, HC)

N94-12713 Nihon Univ., Funabashi (Japan). Coll. of Science and Technology.
THE WARM EDDY DETECTION FROM NOAA/AVHRR THERMAL IMAGES USING THE HOUGH TRANSFORMATION
Fumio Inoue, Akiyoshi Itou, Hiroshi Shinomiya (Nihon Univ., Tokyo, Japan.), Hideo Tameishi (Japan Fisheries Information Service Center, Tokyo.), Hiromichi Yamamoto (National Aerospace Lab., Tokyo, Japan.), and Masao Naka (National Aerospace Lab., Tokyo, Japan.) *In* Scientific Organizing Committee of PORSEC, Proceedings of the PORSEC 1992 in Okinawa: Conference for Pacific Ocean Environments and Probing, Volume 2 25 Aug. 1992 p 1004-1009 (For primary document see N94-12635 01-42)
Copyright Avail: Issuing Activity (Scientific Organizing Committee of PORSEC, P.O. Box 10, Shimizu, Shizuoka 424, Japan, HC)

N94-12716 Colorado Univ., Boulder.
THE RELATIONSHIP BETWEEN SKIN AND BULK SEA SURFACE TEMPERATURES
W. J. Emery, L. Kantha, G. A. Wick, and Peter Schluessel (Hamburg Univ., Germany.) *In* Scientific Organizing Committee of PORSEC, Proceedings of the PORSEC 1992 in Okinawa: Conference for Pacific Ocean Environments and Probing, Volume 2 25 Aug. 1992 p 1022-1027 (For primary document see N94-12635 01-42)
Copyright Avail: Issuing Activity (Scientific Organizing Committee of PORSEC, P.O. Box 10, Shimizu, Shizuoka 424, Japan, HC)

N94-12717 Institute of Disaster and Earth Sciences, Ibaraki (Japan).
VARIABILITY OF THE KUROSHIO OBSERVED FROM SATELLITE THERMAL IMAGERY
Takashi Toda, Atsushi Takeda, and Norihisa Imasato (Kyoto Univ., Japan.) *In* Scientific Organizing Committee of PORSEC, Proceedings of the PORSEC 1992 in Okinawa: Conference for Pacific Ocean Environments and Probing, Volume 2 25 Aug. 1992 p 1028-1033 (For primary document see N94-12635 01-42)
Copyright Avail: Issuing Activity (Scientific Organizing Committee of PORSEC, P.O. Box 10, Shimizu, Shizuoka 424, Japan, HC)

N94-12718 Delaware Univ., Newark. Coll. of Marine Studies.
VARIABILITY OF THE MIXED LAYER DEPTH IN THE NORTH PACIFIC OCEAN AS CALCULATED BY A 3-D SEMI-ANALYTICAL MIXED LAYER REMOTE SENSING MODEL
Xiao-Hai Yan and Akira Okubo (State Univ. of New York, Stony Brook.) *In* Scientific Organizing Committee of PORSEC, Proceedings of the PORSEC 1992 in Okinawa: Conference for Pacific Ocean Environments and Probing, Volume 2 25 Aug. 1992 p 1034-1039 Sponsored by NASA, Washington (For primary document see N94-12635 01-42)
(Contracts N00014-88-K-0207; N00014-91-J-1052; NSF OCE-91-16020)
Copyright Avail: Issuing Activity (Scientific Organizing Committee of PORSEC, P.O. Box 10, Shimizu, Shizuoka 424, Japan, HC)

N94-12719 Consiglio Nazionale delle Ricerche, Venice (Italy). Ist. per lo Studio della Dinamica delle Grandi Masse.
SST ASSIMILATION: EASTERN MEDITERRANEAN CASE STUDY
A. Bergamasco, W. Thacker, R. Long (National Oceanic and Atmospheric Administration, Miami, FL.), and P. Malanotte Rizzoli (Massachusetts Inst. of Tech., Cambridge.) *In* Scientific Organizing Committee of PORSEC, Proceedings of the PORSEC 1992 in Okinawa: Conference for Pacific Ocean Environments and Probing, Volume 2 25 Aug. 1992 p 1040-1043 (For primary document see N94-12635 01-42)
Copyright Avail: Issuing Activity (Scientific Organizing Committee of PORSEC, P.O. Box 10, Shimizu, Shizuoka 424, Japan, HC)

N94-12721 National Inst. of Oceanography, Goa (India).
ADVECTIVE SURFACE VELOCITY IN THE NORTH WEST PACIFIC DERIVED FROM NOAA AVHRR IMAGES
Pankajakshan Thadathil, Masatoshi Akiyama (Tokai Univ., Tokyo, Japan.), Y. Okada (Tokai Univ., Tokyo, Japan.), and Yasuhiro Sugimori (Tokai Univ., Tokyo, Japan.) *In* Scientific Organizing Committee of PORSEC, Proceedings of the PORSEC 1992 in Okinawa: Conference for Pacific Ocean Environments and Probing, Volume 2 25 Aug. 1992 p 1051-1057 (For primary document see N94-12635 01-42)
Copyright Avail: Issuing Activity (Scientific Organizing Committee of PORSEC, P.O. Box 10, Shimizu, Shizuoka 424, Japan, HC)

N94-12723 Academy of Sciences (USSR), Moscow. Inst. of Oceanology.
THE METHOD OF INVESTIGATION OF THE HORIZONTAL STRUCTURE OF THE THERMAL FRONTS
L. I. Koprova and Ju. A. Romanov *In* Scientific Organizing Committee of PORSEC, Proceedings of the PORSEC 1992 in Okinawa: Conference for Pacific Ocean Environments and Probing, Volume 2 25 Aug. 1992 p 1063-1065 (For primary document see N94-12635 01-42)
Copyright Avail: Issuing Activity (Scientific Organizing Committee of PORSEC, P.O. Box 10, Shimizu, Shizuoka 424, Japan, HC)

N94-12724 Academy of Sciences (USSR), Moscow. Inst. of Oceanology.
ON A NONSTATIONARY DYNAMICS OF THE NORTH-WEST PACIFIC OCEAN
A. I. Ginzburg *In* Scientific Organizing Committee of PORSEC, Proceedings of the PORSEC 1992 in Okinawa: Conference for Pacific Ocean Environments and Probing, Volume 2 25 Aug. 1992 p 1066-1069 (For primary document see N94-12635 01-42)
Copyright Avail: Issuing Activity (Scientific Organizing Committee of PORSEC, P.O. Box 10, Shimizu, Shizuoka 424, Japan, HC)

N94-12729 Academy of Sciences (USSR), Vladivostok. Pacific Oceanological Inst.
THE ACOUSTIC ARRANGEMENT FOR MEASURING VERTICAL STRUCTURE OF SEA CURRENT
V. Ya. Kogan, A. A. Voronin, Y. V. Petrova, and V. A. Bannov *In* Scientific Organizing Committee of PORSEC, Proceedings of the PORSEC 1992 in Okinawa: Conference for Pacific Ocean Environments and Probing, Volume 2 25 Aug. 1992 p 1085-1088 (For primary document see N94-12635 01-42)
Copyright Avail: Issuing Activity (Scientific Organizing Committee of PORSEC, P.O. Box 10, Shimizu, Shizuoka 424, Japan, HC)

N94-12730 Academy of Sciences (USSR), Moscow. Inst. of Oceanology.
TURBULENCE GENERATION IN THE PACIFIC UNDERCURRENT BY SHEAR
Konstantin A. Korotenko *In* Scientific Organizing Committee of PORSEC, Proceedings of the PORSEC 1992 in Okinawa: Conference for Pacific Ocean Environments and Probing, Volume 2 25 Aug. 1992 p 1089-1094 (For primary document see N94-12635 01-42)
Copyright Avail: Issuing Activity (Scientific Organizing Committee of PORSEC, P.O. Box 10, Shimizu, Shizuoka 424, Japan, HC)

N94-12731 Academy of Sciences (USSR), Vladivostok. Pacific Oceanological Inst.
THE PACIFIC SUBARCTIC FRONTAL ZONE: STRUCTURE AND DYNAMICS
T. R. Kilmatov and V. A. Kuzmin *In* Scientific Organizing Committee of PORSEC, Proceedings of the PORSEC 1992 in Okinawa: Conference for Pacific Ocean Environments and Probing, Volume 2 25 Aug. 1992 p 1095-1100 (For primary document see N94-12635 01-42)
Copyright Avail: Issuing Activity (Scientific Organizing Committee of PORSEC, P.O. Box 10, Shimizu, Shizuoka 424, Japan, HC)

N94-12733 Academy of Sciences (USSR), Moscow. Inst. of Oceanology.
A DETAILED INVESTIGATION OF THE BENTHIC REGIME IN THE CLARION-CLIPPERTON PROVINCE OF THE PACIFIC AND A FORECAST OF CONSEQUENCES OF MANGANESE NODULE MINING
Evgeny A. Kontar, Gleb N. Baturin, and Tatiana A. Demidova *In* Scientific Organizing Committee of PORSEC, Proceedings of the PORSEC 1992 in Okinawa: Conference for Pacific Ocean Environments and Probing, Volume 2 25 Aug. 1992 p 1107-1112 (For primary document see N94-12635 01-42)
Copyright Avail: Issuing Activity (Scientific Organizing Committee of PORSEC, P.O. Box 10, Shimizu, Shizuoka 424, Japan, HC)

N94-12734 Academy of Sciences (USSR), Moscow. Inst. of Oceanology.
BOTTOM CURRENTS AND POSSIBILITIES FOR NEAR BOTTOM LAYER ENVIRONMENTAL INVESTIGATIONS IN THE PACIFIC BY MEANS OF SELF CONTAINED BOTTOM STATIONS
Evgeny A. Kontar and Tatiana A. Demidova *In* Scientific Organizing Committee of PORSEC, Proceedings of the PORSEC 1992 in Okinawa: Conference for Pacific Ocean Environments and Probing, Volume 2 25 Aug. 1992 p 1113-1117 (For primary document see N94-12635 01-42)
Copyright Avail: Issuing Activity (Scientific Organizing Committee of PORSEC, P.O. Box 10, Shimizu, Shizuoka 424, Japan, HC)

N94-12735 Academy of Sciences (USSR), Moscow. Inst. of Oceanology.
AUTONOMOUS SELF CONTAINED BOTTOM POP-UP STATIONS FOR STUDY OF THE BENTHIC LAYER AND SEISMICITY OF THE OCEAN'S BOTTOM
Evgeny A. Kontar *In* Scientific Organizing Committee of PORSEC, Proceedings of the PORSEC 1992 in Okinawa: Conference for Pacific Ocean Environments and Probing, Volume 2 25 Aug. 1992 p 1118-1121 (For primary document see N94-12635 01-42)
Copyright Avail: Issuing Activity (Scientific Organizing Committee of PORSEC, P.O. Box 10, Shimizu, Shizuoka 424, Japan, HC)

N94-12737 Academy of Sciences (USSR), Vladivostok. Pacific Research Inst. of Fisheries and Oceanography.
INFLUENCE OF THE KUROSHIO WARM-CORE RINGS ON HYDROGRAPHIC AND FISHERY CONDITIONS OFF SOUTHERN KURIL ISLANDS
N. V. Bulatov and V. B. Lobanov *In* Scientific Organizing Committee of PORSEC, Proceedings of the PORSEC 1992 in Okinawa: Conference for Pacific Ocean Environments and Probing, Volume 2 25 Aug. 1992 p 1127-1131 (For primary document see N94-12635 01-42)
Copyright Avail: Issuing Activity (Scientific Organizing Committee of PORSEC, P.O. Box 10, Shimizu, Shizuoka 424, Japan, HC)

N94-12739 Academy of Sciences (USSR), Vladivostok. Pacific Inst. of Oceanology.
CONVECTIVE AND DYNAMIC INSTABILITY IN MERIDIONAL TRENCHES
L. F. Muratov *In* Scientific Organizing Committee of PORSEC, Proceedings of the PORSEC 1992 in Okinawa: Conference for Pacific Ocean Environments and Probing, Volume 2 25 Aug. 1992 p 1138-1144 (For primary document see N94-12635 01-42)
Copyright Avail: Issuing Activity (Scientific Organizing Committee of PORSEC, P.O. Box 10, Shimizu, Shizuoka 424, Japan, HC)

N94-12752 Academy of Sciences (USSR), Moscow. Inst. of Oceanology.
COUPLED NUMERICAL MODEL FOR ALTIMETRIC DATA ASSIMILATION AND VELOCITY FIELD ANALYSIS
A. L. Berestov and A. D. Marushkevich *In* Scientific Organizing Committee of PORSEC, Proceedings of the PORSEC 1992 in Okinawa: Conference for Pacific Ocean Environments and Probing, Volume 2 25 Aug. 1992 p 1205-1210 (For primary document see N94-12635 01-42)
Copyright Avail: Issuing Activity (Scientific Organizing Committee of PORSEC, P.O. Box 10, Shimizu, Shizuoka 424, Japan, HC)

N94-12754 Academy of Sciences (USSR), Vladivostok. Pacific Oceanological Inst.
MESOSCALE DYNAMIC STRUCTURES OF THE SUBARCTIC FRONTAL ZONE IN THE PACIFIC OCEAN
A. S. Vasiliev and V. P. Makashin *In* Scientific Organizing Committee of PORSEC, Proceedings of the PORSEC 1992 in Okinawa: Conference for Pacific Ocean Environments and Probing, Volume 2 25 Aug. 1992 p 1219-1224 (For primary document see N94-12635 01-42)
Copyright Avail: Issuing Activity (Scientific Organizing Committee of PORSEC, P.O. Box 10, Shimizu, Shizuoka 424, Japan, HC)

N94-12760 Academy of Sciences (USSR), Moscow. Inst. of Oceanology.
MIXING OF DRIFTER ENSEMBLE BY MESOSCALE CURRENTS
Tatyana G. Sazhina, Nikolay A. Maksimenko, and Natalya M. Mardashkina *In* Scientific Organizing Committee of PORSEC, Proceedings of the PORSEC 1992 in Okinawa: Conference for Pacific Ocean Environments and Probing, Volume 2 25 Aug. 1992 p 1251-1256 (For primary document see N94-12635 01-42)
Copyright Avail: Issuing Activity (Scientific Organizing Committee of PORSEC, P.O. Box 10, Shimizu, Shizuoka 424, Japan, HC)

N94-12763 Academy of Sciences (USSR), Vladivostok. Pacific Oceanological Inst.
GENERATION OF INTERNAL WAVES NEAR THE SHELF BOUNDARY
V. V. Navrotsky and S. V. Simonenko *In* Scientific Organizing Committee of PORSEC, Proceedings of the PORSEC 1992 in Okinawa: Conference for Pacific Ocean Environments and Probing, Volume 2 25 Aug. 1992 p 1269-1274 (For primary document see N94-12635 01-42)
Copyright Avail: Issuing Activity (Scientific Organizing Committee of PORSEC, P.O. Box 10, Shimizu, Shizuoka 424, Japan, HC)

N94-12764 Academy of Sciences (USSR), Vladivostok. Pacific Oceanological Inst.
EXPERIMENTAL AND THEORETICAL INVESTIGATION OF UNDULAR BORE FORMATION UPSTREAM THE BANK
S. V. Simonenko and V. Ya. Kogan *In* Scientific Organizing Committee of PORSEC, Proceedings of the PORSEC 1992 in Okinawa: Conference for Pacific Ocean Environments and Probing, Volume 2 25 Aug. 1992 p 1275-1280 (For primary document see N94-12635 01-42)
Copyright Avail: Issuing Activity (Scientific Organizing Committee of PORSEC, P.O. Box 10, Shimizu, Shizuoka 424, Japan, HC)

N94-12765 Academy of Sciences (USSR), Novosibirsk.
MODEL OF KUROSHIO REGION CIRCULATION
V. I. Kuzin, E. N. Golubeva, A. V. Martynov, and V. M. Moiseyev *In* Scientific Organizing Committee of PORSEC, Proceedings of the PORSEC 1992 in Okinawa: Conference for Pacific Ocean Environments and Probing, Volume 2 25 Aug. 1992 p 1281-1287 (For primary document see N94-12635 01-42)
Copyright Avail: Issuing Activity (Scientific Organizing Committee of PORSEC, P.O. Box 10, Shimizu, Shizuoka 424, Japan, HC)

51 LIFE SCIENCES (GENERAL)

N94-10360*# Sverdrup Technology, Inc., Huntsville, AL.
MICROBIOLOGICAL TEST RESULTS USING THREE URINE PRETREATMENT REGIMES WITH 316L STAINLESS STEEL

Timothy L. Huff Jul. 1993 19 p Original contains color illustrations
(Contract NAS8-37814)
(NASA-CR-192568; NAS 1.26:192568) Avail: CASI HC A03/MF A01; 2 functional color pages

Three urine pretreatments, (1) Oxone (Dupont) and sulfuric acid, (2) sodium hypochlorite and sulfuric acid, (3) and ozone, were studied for their ability to reduce microbial levels in urine and minimize surface attachment to 316L stainless steel coupons. Urine samples inoculated with Bacillus insolitus and a filamentous mold, organisms previously recovered from the vapor compression distillation subsystem of NASA Space Station Freedom water recovery test were tested in glass corrosion cells containing base or weld metal coupons. Microbial levels, changes in pH, color, turbidity, and odor of the fluid were monitored over the course of the 21-day test. Specimen surfaces were examined by scanning electron microscopy at completion of the test for microbial attachment. Ozonated urine samples were less turbid and had lower microbial levels than controls or samples receiving other pretreatments. Base metal coupons receiving pretreatment were relatively free of attached bacteria. However, well-developed biofilms were found in the heat-affected regions of welded coupons receiving Oxone and hypochlorite pretreatments. Few bacteria were observed in the same regions of the ozone pretreatment sample. Author (revised)

N94-10652# Cornell Univ., Ithaca, NY.
CONVERSION OF ACETIC ACID TO METHANE BY THERMOPHILES
S. H. Zinder 1993 13 p
(Contract DE-FG02-85ER-13370)
(DE93-014433; DOE/ER-13370/T2) Avail: CASI HC A03/MF A01

The primary goal of this project is to obtain a better understanding of thermophilic microorganisms which convert acetic acid to CH4. The previous funding period represents a departure from earlier research in this laboratory which was more physiological and ecological. The present work is centered on the biochemistry of the thermophile Methanothrix sp. strain CALS-1. This organism presents a unique opportunity, with its purity and relatively rapid growth, to do comparative biochemical studies with the other major acetotrophic genus Methanosarcina. We previously found that Methanothrix is capable of using acetate at concentrations 100 fold lower than Methanosarcina. This finding suggests that there are significant differences in the pathways of methanogenesis from acetate in the two genera. DOE

N94-10888 Kyoto Univ., Kumatori (Japan). Research Reactor Inst.
PROCEEDINGS OF THE SYMPOSIUM ON RADIATION RESEARCH IN LIFE SCIENCE
Takaji Ikushima, ed. May 1992 81 p Symposium held in Kumatori, Japan, 16-17 Jan. 1992 Limited Reproducibility: More than 20% of this document may be affected by microfiche quality
(DE93-754137; KURRI-TR-363; CONF-9201125) Avail: Issuing Activity (Department of Energy (DOE))

This issue is the collection of the papers presented at the Symposium on Radiation Research in Life Science. The 9 presented papers are indexed individually. DOE

N94-11020# Maryland Univ., College Park.
ALUMINUM AND MEMBRANE CHANNELS
M. Colombini 21 May 1993 8 p
(Contract N00014-90-J-1024)
(AD-A265241) Avail: CASI HC A02/MF A01

This publication is an invited chapter for a book dedicated to the actions of aluminum in biological systems. This contribution focuses on the effects of aluminum on voltage dependent anion-selective channels. This is a summary of results published in other journals by people in my laboratory. DTIC

N94-11045*# Pennsylvania State Univ., Hershey. Coll. of Medicine.
EFFECTS OF CSF HORMONES AND IONIC COMPOSITION ON SALT/WATER METABOLISM Final Technical Report, 1 Mar. 1981 - 31 Dec. 1992
Walter B. Severs 31 Dec. 1992 32 p
(Contract NCC2-127)
(NASA-CR-193232; NAS 1.26:193232) Avail: CASI HC A03/MF A01

The consequences of headward fluid shifts during manned spaceflight was studied. Such shifts were recognized early by both U.S. and Soviet scientists because of signs and symptoms referable to the head. Some of these include disturbed vision, puffiness in the face and periorbital areas, headache, vestibular dysfunction, and distended jugular veins. We posited that the fluid shift had an immediate effect on the brain and a long-term action requiring a neural interpretation of the flight environment. This would re-adjust both efferent neural as well as hormonal mechanisms to sustain cardiovascular and fluid/electrolyte balance consonent with survival in microgravity. Work along these lines is summarized. A synopsis of some of the main research is presented. The following topics were studied: (1) angiotensin and vasopressin action in the central nervous system; (2) intracranial pressure control; (3) research on subcommissural organ; and (4) research on the eye. Author (revised)

N94-11180*# Illinois Univ., Urbana-Champaign. Bioenvironmental Engineering Research Lab.
EFFECT OF DOUBLE DENSITY CAGING DURING SPACE SHUTTLE TRANSPORT OF LABORATORY RATS Final Report
G. L. Riskowski, H. W. Gonyou, P. C. Harrison, K. W. Kelley, and M. E. Tumbleson 22 Jun. 1993 100 p
(Grant NAG2-736)
(NASA-CR-193228; NAS 1.26:193228) Avail: CASI HC A05/MF A02; 1 functional color page

Male Sprague Dawley rats were housed in groups of four in polycarbonate cages at recommended density and thermal environmental conditions for 14 days prior to testing to ensure uniform acclimation to those conditions. Body weights averaged 286 +/- 7 g at the end of acclimation. Rat cages were assigned randomly to three treatments: (1) 4 rats/polycarbonate cage (877 sq cm, 20.3 cm high, 220 sq cm/rat), (2) 4 rats/mock AEM (MAEM) (620 sq cm, 155 sq cm/rat), and (3) 8 rats/MAEM (620 sq cm, 77.5 sq cm/rat). A comparison between the MAEM-DD and MAEM-SD treatments was done to determine if doubling rat density in AEM's stressed the rats. A comparison among MAEM treatments and the PC treatment was done to determine if any stress indications were due to the AEM. During this density challenge phase, all treatments were maintained at the same thermal environmental conditions (22.5 C and 50 percent RH) for 10 days. After the density challenge phase, half the rats from each group were sacrificed for body tissue and fluid analyses. The remaining half of the rats were housed at a density of 4 rats/cage in polycarbonate cages at normal thermal environmental conditions for an additional 10 days to determine if there were any differences in responses between treatments after a recovery period. The remaining rats were examined and sacrificed for body tissue and fluid analyses at the end of the recovery phase. Author (revised)

N94-11191*# National Aeronautics and Space Administration. Ames Research Center, Moffett Field, CA.
EXERCISE COUNTERMEASURES FOR BED-REST DECONDITIONING Final Report, 1986
John Greenleaf, ed. Jun. 1993 216 p
(RTOP 199-21-12-07)
(NASA-TM-103987; A-93008; NAS 1.15:103987) Avail: CASI HC A10/MF A03

The purpose for this 30-day bed rest study was to investigate the effects of short-term, high intensity isotonic and isokinetic exercise training on maintenance of working capacity (peak oxygen uptake), muscular strength and endurance, and on orthostatic tolerance, posture and gait. Other data were collected on muscle atrophy, bone mineralization and density, endocrine analyses concerning vasoactivity and fluid-electrolyte balance, muscle intermediary metabolism, and on performance and mood of the subjects. It was concluded that: The subjects maintained a relatively stable mood, high morale, and high esprit de corps throughout the study. Performance improved in nearly all tests in almost all the subjects. Isotonic training, as opposed to isokinetic exercise training, was associated more with decreasing levels of psychological tension, concentration, and motivation; and improvement in the quality of sleep. Working capacity (peak oxygen uptake) was maintained during bed rest with isotonic exercise training; it was not maintained with isokinetic or no exercise training. In general, there was no significant decrease in strength or endurance of arm or leg muscles during bed rest, in spite of some reduction in muscle size (atrophy) of some leg muscles. There was no effect of isotonic exercise training on orthostasis, since tilt-table tolerance was reduced similarly in all three groups following bed rest. Bed rest resulted in significant decreases of postural stability and self-selected step length, stride length, and walking velocity, which were not influenced by either exercise training regimen. Most pre-bed rest responses were restored by the fourth day of recovery. Author (revised)

N94-11201*# Sverdrup Technology, Inc., Huntsville, AL.
SPACELAB J AIR FILTER DEBRIS ANALYSIS Interim Report
Donald C. Obenhuber Jul. 1993 11 p
(Contract NAS8-37814)
(NASA-CR-192569; NAS 1.26:192569; STS-49-SLJ) Avail: CASI HC A03/MF A01

Filter debris from the Spacelab module SLJ of STS-49 was analyzed for microbial contamination. Debris for cabin and avionics filters was collected by Kennedy Space Center personnel on 1 Oct. 1992, approximately 5 days postflight. The concentration of microorganisms found was similar to previous Spacelab missions averaging 7.4E+4 CFU/mL for avionics filter debris and 4.5E+6 CFU/mL for the cabin filter debris. A similar diversity of bacterial types was found in the two filters. Of the 13 different bacterial types identified from the cabin and avionics samples, 6 were common to both filters. The overall analysis of these samples as compared to those of previous missions shows no significant differences. Author

N94-11583# Applimath Co., Brookline, MA.
RESEARCH ON ACOUSTIC COUPLING TO ELECTROMAGNETIC PULSES IN TISSUE Final Report, 1 Apr. 1988 - 31 Mar. 1993
Harry Moses 15 Apr. 1993 4 p
(Contract F49620-88-C-0070)
(AD-A264764; AFOSR-93-0334TR) Avail: CASI HC A01/MF A01

Over the course of the contract, Dr. Moses published 12 papers, and one is still pending. His work on novel electromagnetic wave propagation, together with insights regarding possible transmitters, is nothing short of terminal. Dr. Moses was the first to rigorously characterize the universal character of far field patterns produced by a source that operated over a finite time frame. Such patterns could be 'requested' and then the design/operating procedure of the source would be the fundamental unknown. Such possibilities were communicated to government lab researchers at AL (Brooks AFB), and subsequent work will be pursued by Dr. Moses, with their help. DTIC

N94-11648 Princeton Univ., NJ. Dept. of Physics.
PROBABILITY OF ALAMETHICIN CONDUCTANCE STATES VARIES WITH NONLAMELLAR TENDENCY OF BILAYER PHOSPHOLIPIDS
S. L. Keller, A. M. Bezrukov, S. M. Gruner, M. W. Tate, and I. Vodyanoy Feb. 1993 24 p Limited Reproducibility: More than 20% of this document may be affected by microfiche quality
(Contracts DE-FG02-87ER-60522; N00014-90-J-1702; N00014-91-F-0201; GM-32614)
(AD-A264957) Avail: CASI HC A03

With few exceptions, membrane lipids are usually regarded as a kind of filler or passive solvent for membrane proteins. Yet, cells exquisitely control membrane composition. Many phospholipids found in plasma membrane bilayers favor packing into inverted hexagonal bulk phases. It was suggested that the strain of forcing such lipids into a bilayer may affect membrane protein function, such as the operation of trans-membrane channels. To investigate this, we have inserted the peptide alamethicin into bilayer membranes composed of lipids of empirically determined inverted hexagonal phase 'spontaneous radii' Ro, which will have expectably different degrees of strain when forced into bilayer form. We observe a correlation between measured Ro and the relative probabilities of different conductance states. States of higher conductance are more probable in Dioleoyl Phosphatidyl Ethanolamine (DOPE), the lipid of highest curvature, 1/Ro, than in Dioleoyl Phosphatidyl Choline (DOPC), the lipid of lowest curvature. DTIC

N94-11667# Los Alamos National Lab., NM.
MOMENTUM INDUCED BY LASER-TISSUE INTERACTION
R. S. Dingus 1993 14 p Presented at the OE/LASE 1993: International Society for Optical Engineering (SPIE) Conference, Los Angeles, CA, 16-23 Jan. 1993
(Contract W-7405-eng-36)
(DE93-010737; LA-UR-93-1099; CONF-930159-22) Avail: CASI HC A03/MF A01

Impulsive momentum is imparted to residual tissue during pulsed-laser ablation because the mass ablated is generally ejected with a sizable velocity. Accurate measurements of the impulse are possible, which can provide an important monitor of the ablation process. Simple models can be used to predict the impulse under a variety of conditions; in some cases, complex radiation-hydrodynamic code calculations are required. In this paper, this modeling is discussed along with the dependence of momentum on the pulsed heating and target conditions. Momentum measurement techniques are discussed briefly. The behavior is explained in terms of dimensionless parameters and the impulse coupling coefficient as a function of incident fluence, which has a well defined threshold as well as a maximum. Complications in the mixed liquid-vapor phase are also addressed. DOE

N94-11861# Aerospace Medical Research Labs., Brooks AFB, TX.
EFFECT OF INTERMITTENT COLD EXPOSURE ON THE FIBER-TYPE COMPOSITION OF SELECTED SKELETAL MUSCLES IN RATS Final Technical Report, Mar. - Nov. 1990
Thomas J. Walters and Stefan H. Constable Apr. 1993 20 p
(AD-A265309; AL-TR-1992-0099) Avail: CASI HC A03/MF A01

The effect of long-term intermittent cold exposure (CE) on the fiber-type composition of the predominantly type I soleus and the predominantly type IIb extensor digitorum longus (EDL) muscles of the rats was examined. CE was accomplished by submerging the rats in shoulder-deep water, maintained at 20 +/- 0.5 C, for 1 h/d, 5 d/wk, for up to 19 weeks. Rats were randomly assigned to either a Control (CON) or Cold Exposure group. The efficacy of the treatment was tested by subjecting both groups to 20 C water for 45 minutes while measuring rectal temperature (T(sub re)) and VO2. The CE group displayed a 22% smaller reduction in T(sub re) (p less than 0.05) at the end of the exposure, and had a 23% greater VO2 (p less than 0.05) during the same period. Fiber-type composition was determined using routine histochemical methods for myosin-ATPase. The soleus muscle of the CE rats underwent a 156% increase in the number of type IIa fibers (p less than 0.05), with a 24% reduction in type I fibers (p less than 0.05). CE had no significant influence on the fiber-type composition of the EDL muscle. CE resulted in an increase in citrate synthase activity of 20% and 22% in the soleus and EDL muscles, respectively (p less than 0.05). It was demonstrated that intermittent CE induces a type I-to-type IIa transformation in the soleus muscle while having no influence on the EDL muscle. DTIC

N94-12278# Mitsubishi Heavy Industries Ltd., Tokyo (Japan).
COMPATIBILITY TESTS FOR BIOLOGICAL SPECIMENS TO ON-BOARD EXPERIMENTS IN THE SPACE SHUTTLE FLIGHT [SHATORU TOUSAI JIKKENYOU SEIBUTSU SHIRYOU NO TOUSAISEI KAKUNIN SHIKEN]
Tokyo, Japan National Space Development Agency 31 Mar. 1993 22 p In ENGLISH and JAPANESE
(NASDA-CNT-930003; JTN-93-80457) Avail: CASI HC A03/MF A01

A summary of the results of the verification test in accordance with the compatibility verification test requirements for biological specimen to onboard experiment is presented. Studies of the following items were conducted to optimize the electrophoresis conditions, sample concentrations, sample storage conditions, and electrophoresis chamber cleansing methods and to verify that the samples can be carried onboard as electrophoresis experiment samples: (1) keeping microorganism cells; (2) electrophoresis parameter test; (3) optical detection sensitivity of electrophoresis test samples; (4) recovery rate of post-electrophoresis samples; (5) electrophoresis chamber cleansing conditions; and (6) sample stability after electrophoresis. The electrophoresis of Salmonella typhimurium strains, detection of the electrophoresis of Salmonella typhimurium cells, absorbances of the collected fractions, effects of electrophoresis on the visibility of Salmonella typhimurium, efficiency of the bio-cleaning, etc. are shown. Author (NASDA)

N94-12417# Illinois Univ., Urbana. Dept. of Cell and Structural Biology.
THE ORGANIZATION OF THE SUPRACHIASMATIC CIRCADIAN PACEMAKER OF THE RAT AND ITS REGULATION BY NEUROTRANSMITTERS AND MODULATORS Annual Report, 1 Apr. 1990 - 31 Mar. 1993
Martha U. Gillette, Steven J. DeMarco, Jian M. Ding, Eve A. Gallman, and Lia E. Faiman 18 May 1993 18 p
(Grant AF-AFOSR-0205-90)
(AD-A266113; AFOSR-93-0423TR) Avail: CASI HC A03/MF A01

The long-term goal of these studies is to understand how cells of the suprachiasmatic nucleus (SCN) are organized to form a 24-h biological clock and what roles specific neurotransmitters and modulators play in timekeeping and resetting processes. We address these questions by assessing the pattern of spontaneous neuronal activity using extracellular and whole cell patch recording techniques in long-lived SCN brain slices from rats. We have observed that a robust pacemaker persists in the ventrolateral region of microdissected SCN and have begun to define the electrophysiological properties of neurons in this region. Further, we are investigating changing sensitivities of the SCN to resetting by exogenous neurotransmitters, such as glutamate, serotonin and neuropeptide Y, across the circadian cycle. Our findings emphasize the complexity of organization and control of mammalian circadian timing. DTIC

N94-12441# Hahnemann Medical Coll. and Hospital, Philadelphia, PA. Dept. of Mental Health Sciences.
LOCUS COERULEUS, VIGILANCE, AND STRESS: BRAIN MECHANISMS OF ADAPTIVE BEHAVIORAL RESPONSIVENESS Final Technical Report, 15 Dec. 1989 - 31 Dec. 1992
Gary A. Jones 13 May 1993 48 p
(Grant AF-AFOSR-0147-90)
(AD-A265657; AFOSR-93-0399TR) Avail: CASI HC A03/MF A01

We have developed techniques for recording stable unit activity from individual monkey locus coeruleus (LC) neurons using microwire electrodes (25 micrometers diameter). A combination of improved electrode design, new microadvancer, and methods to accurately localize the LC nucleus now permits stable recordings of high signal/noise (better than 3/1) from single neurons in the LC for several hours in the waking monkey performing a vigilance task. We have found that LC neurons vary activity phasically and tonically during vigilance performance. Phasic responses are selectively evoked by target cues, and follow new targets during acquisition of reversal in this task. Tonically, LC neurons vary activity levels in accordance with attentiveness to the task, as measured by the frequency of foveating a fix spot required to initiate each trial. Results indicate that the LC functions to regulate the lability of attention. In this view, performance on a task requiring focused attention varies with tonic LC activity in an inverted U relationship. Too little LC activity is associated with poor performance due to non-alertness, while high tonic LC activity corresponds to highly labile attention that prevents focusing attention for long time epochs. Together, these results indicate that optimal vigilance performance (e.g., radar monitoring activity) may require an intermediate level of LC activity and high phasic responsiveness of LC neurons. DTIC

N94-12559*# Wisconsin Univ., Madison. Dept. of Soil Science.
PLANT ARCHITECTURE, GROWTH AND RADIATIVE TRANSFER FOR TERRESTRIAL AND SPACE ENVIRONMENTS Final Report, 1 Feb. 1989 - 31 Jan. 1993
John M. Norman and Narendra S. Goel (State Univ. of New York, Binghamton.) 1993 9 p
(Grant NAGw-1575)
(NASA-CR-193476; NAS 1.26:193476) Avail: CASI HC A02/MF A01

The overall objective of this research was to develop a hardware implemented model that would incorporate realistic and dynamic descriptions of canopy architecture in physiologically based models of plant growth and functioning, with an emphasis on radiative transfer while accommodating other environmental constraints. The general approach has five parts: a realistic mathematical treatment of canopy architecture, a methodology for combining this general canopy architectural description with a general radiative transfer model, the inclusion of physiological and environmental aspects of plant growth, inclusion of plant phenology, and integration. Author (revised)

N94-10120*# Space Hardware Optimization Technology, Inc., Floyds Knobs, IN.
DESIGN OF MULTISAMPLE, MULTISTEP PHASE PARTITIONING APPARATUS FOR USE ON SPACE SHUTTLE SPACELAB, AND SPACELAB MISSIONS
Mark S. Deuser, James M. VanAlstine (Alabama Univ., Huntsville.), John C. Vellinger, Francis C. Wessling (Alabama Univ., Huntsville.), and Charles A. Lundquist (Alabama Univ., Huntsville.) *In* ESA, Proceedings of the 8th European Symposium on Materials and Fluid Sciences in Microgravity, Volume 1 Aug. 1992 p 337-341 (For primary document see N94-10070 01-29)
(Grants NAGw-812; NAGw-1196)
Copyright Avail: CASI HC A01/MF A04; ESA, EPD, ESTEC, Noordwijk, Netherlands, HC

N94-11548*# Hyperbaric Medicine, San Antonio, TX. Wound Care.
EVALUATION OF MEDICAL TREATMENTS TO INCREASE SURVIVAL OF EBULLISM IN GUINEA PIGS Abstract Only
Barbara J. Stegmann, Andrew A. Pilmanis (Aerospace Medical Research Labs., Brooks AFB, TX.), E. G. Wolf (Aerospace Medical Research Labs., Brooks AFB, TX.), Toniann Derion (Aerospace Medical Research Labs., Brooks AFB, TX.), J. W. Fanton (Aerospace Medical Research Labs., Brooks AFB, TX.), H. Davis (Aerospace Medical Research Labs., Brooks AFB, TX.), G. B. Kemper (Aerospace Medical Research Labs., Brooks AFB, TX.), and Terrell E. Scoggins (Aerospace Medical Research Labs., Brooks AFB, TX.) *In* NASA. Johnson Space Center, Sixth Annual Workshop on Space Operations Applications and Research (SOAR 1992), Volume 2 Feb. 1993 p 569 (For primary document see N94-11527 01-99)
Avail: CASI HC A01/MF A03

N94-11556*# National Aeronautics and Space Administration. Ames Research Center, Moffett Field, CA.
FIVE BIOMEDICAL EXPERIMENTS FLOWN IN AN EARTH ORBITING LABORATORY: LESSONS LEARNED FROM DEVELOPING THESE EXPERIMENTS ON THE FIRST INTERNATIONAL MICROGRAVITY MISSION FROM CONCEPT TO LANDING Abstract Only
C. M. Winget, J. J. Lashbrook, P. X. Callahan, and R. L. Schaefer (Lockheed Engineering and Sciences Co., Moffett Field, CA.) *In* NASA. Johnson Space Center, Sixth Annual Workshop on Space Operations Applications and Research (SOAR 1992), Volume 2 Feb. 1993 p 597 (For primary document see N94-11527 01-99)
Avail: CASI HC A01/MF A03

N94-11969 Electrotechnical Lab., Ibaraki (Japan). Life Electronics Research Center.
AUTOMATIC CLASSIFICATION SYSTEM FOR ZOOPLANKTON Abstract Only
H. Nakano and T. Sasaki *In* Scientific Organizing Committee of PORSEC, Proceedings of the PORSEC 1992 in Okinawa: Conference for Pacific Ocean Environments and Probing, Volume 1 25 Aug. 1992 p 436 (For primary document see N94-11894 01-42)
Copyright Avail: Issuing Activity (Scientific Organizing Committee of PORSEC, P.O. Box 10, Shimizu, Shizuoka 424, Japan, HC)

N94-12656 National Inst. for Resources and Environment, Ibaraki (Japan).
THE SEASONAL CHANGE OF PHYTOPLANKTON SIZE DISTRIBUTION USING OPTICAL FIBER SENSOR
Kisaburou Nakata, Fumio Horiguchi, and Tooru Nakane (Biological Research Inst., Ibaraki, Japan.) *In* Scientific Organizing Committee of PORSEC, Proceedings of the PORSEC 1992 in Okinawa: Conference for Pacific Ocean Environments and Probing, Volume 2 25 Aug. 1992 p 669-676 (For primary document see N94-12635 01-42)
Copyright Avail: Issuing Activity (Scientific Organizing Committee of PORSEC, P.O. Box 10, Shimizu, Shizuoka 424, Japan, HC)

N94-12660 Nagoya Univ. (Japan). Water Research Inst.
THE PHYTOPLANKTON BLOOM IN THE KINU-URA BAY, JAPAN IN THE RAINY SEASON
Junko Hama and Nobuhiko Handa *In* Scientific Organizing Committee of PORSEC, Proceedings of the PORSEC 1992 in Okinawa: Conference for Pacific Ocean Environments and Probing, Volume 2 25 Aug. 1992 p 692-697 (For primary document see N94-12635 01-42)
Copyright Avail: Issuing Activity (Scientific Organizing Committee of PORSEC, P.O. Box 10, Shimizu, Shizuoka 424, Japan, HC)

N94-12661 Nagoya Univ. (Japan). Water Research Inst.
VARIATION OF THE PHOTOSYNTHETIC PRODUCTS IN THE REGIONAL UPWELLING AREA AROUND THE IZU ISLANDS, JAPAN
Takeo Hama *In* Scientific Organizing Committee of PORSEC, Proceedings of the PORSEC 1992 in Okinawa: Conference for Pacific Ocean Environments and Probing, Volume 2 25 Aug. 1992 p 698-703 (For

primary document see N94-12635 01-42)
Copyright Avail: Issuing Activity (Scientific Organizing Committee of PORSEC, P.O. Box 10, Shimizu, Shizuoka 424, Japan, HC)

N94-12699 Tokyo Univ. (Japan). Ocean Research Inst.
ACOUSTIC ESTIMATION OF PLANKTON BIOMASS
Tadashi Inagaki, Ichirou Aoki, and Takeo Ishii *In* Scientific Organizing Committee of PORSEC, Proceedings of the PORSEC 1992 in Okinawa: Conference for Pacific Ocean Environments and Probing, Volume 2 25 Aug. 1992 p 916-921 (For primary document see N94-12635 01-42)
Copyright Avail: Issuing Activity (Scientific Organizing Committee of PORSEC, P.O. Box 10, Shimizu, Shizuoka 424, Japan, HC)

N94-12726 Academy of Sciences (USSR), Saint Petersburg. Inst. of Oceanology.
OPTIMUM SELECTION OF SPECTRAL CHANNELS IN THE PROBLEM OF REMOTE SENSING OF PHYTOPLANKTON CONCENTRATION IN OCEAN WATER
V. P. Kozlov, J. M. Levin, and L. V. Zolotukhin *In* Scientific Organizing Committee of PORSEC, Proceedings of the PORSEC 1992 in Okinawa: Conference for Pacific Ocean Environments and Probing, Volume 2 25 Aug. 1992 p 1073-1074 (For primary document see N94-12635 01-42)
Copyright Avail: Issuing Activity (Scientific Organizing Committee of PORSEC, P.O. Box 10, Shimizu, Shizuoka 424, Japan, HC)

N94-12758 Academy of Sciences (USSR), Vladivostok. Pacific Research Inst. of Fisheries and Oceanography.
HIGH BIOLOGICAL PRODUCTION OF THE TIDAL MIXING ZONES ON JAPAN SEA SHELF
Yury I. Zuenko *In* Scientific Organizing Committee of PORSEC, Proceedings of the PORSEC 1992 in Okinawa: Conference for Pacific Ocean Environments and Probing, Volume 2 25 Aug. 1992 p 1240-1244 (For primary document see N94-12635 01-42)
Copyright Avail: Issuing Activity (Scientific Organizing Committee of PORSEC, P.O. Box 10, Shimizu, Shizuoka 424, Japan, HC)

52 AEROSPACE MEDICINE

Includes physiological factors; biological effects of radiation; and effects of weightlessness on man and animals.

N94-10398* National Aeronautics and Space Administration, Washington, DC.
AEROSPACE MEDICINE AND BIOLOGY: A CONTINUING BIBLIOGRAPHY WITH INDEXES (SUPPLEMENT 375)
May 1993 83 p
(NASA-SP-7011(375); NAS 1.21:7011(375)) Avail: CASI HC A05

This bibliography lists 212 reports, articles, and other documents recently introduced into the NASA Scientific and Technical Information System database. Subject coverage includes the following: aerospace medicine and physiology, life support systems and man/system technology, protective clothing, exobiology and extraterrestrial life, planetary biology, and flight crew behavior and performance. Author (revised)

N94-10399* National Aeronautics and Space Administration, Washington, DC.
AEROSPACE MEDICINE AND BIOLOGY: A CONTINUING BIBLIOGRAPHY WITH INDEXES (SUPPLEMENT 376)
Jun. 1993 89 p
(NASA-SP-7011(376); NAS 1.21:7011(376)) Avail: CASI HC A05

This bibliography lists 265 reports, articles and other documents introduced into the NASA Scientific and Technical Information System during Jun. 1993. Subject coverage includes: aerospace medicine and physiology, life support systems and man/system technology, protective clothing, exobiology and extraterrestrial life, planetary biology, and flight crew behavior and performance. Author

N94-10813# Federal Aviation Agency, Oklahoma City, OK. Civil Aeromedical Inst.
AVIATION ACCIDENT RISK FOR AIRMEN WITH APHAKIA AND ARTIFICIAL LENS IMPLANTS Final Report
Van B. Nakagawara and Kathryn J. Wood Jul. 1993 15 p
(DOT/FAA/AM-93/11) Avail: CASI HC A03/MF A01

Airmen with aphakia and intraocular (IOL) implants who, on a case-by-case basis, may obtain a waiver for a medical certificate, have been previously associated with higher aviation accident rates when compared to the total civil airman population. This study analyzes the accident frequencies of these civil airmen for a 4-year period (1982-85). Medical records were evaluated for all certified airmen who carried FAA-specific pathology codes for aphakia and artificial lens implants during the study period. Aviation accident and active airman population frequencies were obtained from FAA databases. The entire population of aphakia and IOL airmen and those less than 50 years of age had significantly higher (p less than .50) accident rates than the corresponding non-aphakic airman population. Aeromedical certification considerations of the study findings are discussed. Further investigations into additional confounding factors between the aphakic and non-aphakic populations are recommended. Author

N94-10828 National Inst. of Health, Bethesda, MD.
NATIONAL INSTITUTE OF HEALTH ALMANAC, 1992 Annual Report
Nov. 1992 148 p Limited Reproducibility: More than 20% of this document may be affected by microfiche quality
(PB93-183556; NIH-PUB-92-5) Avail: Issuing Activity (National Technical Information Service (NTIS))

This report, which is published annually, presents pertinent facts about the National Institutes of Health--the Federal Government's principal biomedical research agency. It is designed as a ready reference source on the NIH's 13 research Institutes and 2 Divisions, the National Library of Medicine, the Clinical Center--a combined research hospital and laboratory complex--the National Center of Nursing Research, the National Center for Research Resources, and the John E. Fogarty International Center for Advanced Study in the Health Sciences. NTIS

N94-10872# Society for Research on Biological Rhythms, Charlottesville, VA.
THE 2ND ANNUAL MEETING OF THE SOCIETY FOR RESEARCH ON BIOLOGICAL RHYTHMS Final Report, 1 Mar. 1992 - 1 Mar. 1993
Fred W. Turek (Northwestern Univ., Evanston, IL.) 30 Apr. 1993 121 p
Meeting held in Jacksonville, FL, 9-13 May 1990
(Contract F49620-92-J-0181)
(AD-A264869; AFOSR-93-0345TR) Avail: CASI HC A06/MF A02

From 6-10 May 1992, the Society for Research on Biological Rhythms held its third meeting at Amelia Island Plantation, Florida. The Society was formed in 1987 to promote the advancement of basic and applied research in all aspects of biological rhythms, to disseminate important research results concerning biological rhythms to the general public, to develop and enhance the education and training of students and researchers in the field, and to foster interdisciplinary communication. This third meeting was successful in meeting the goals of the Society, particularly in the area of interdisciplinary communication. Researchers in the field of Biological Rhythms tend to be fragmented into many disciplines and are often divided along many different lines. One way of dividing the field is along frequency lines; while some workers study biological rhythms with a period of msec, others are interested in rhythms with periods in the range of minutes, hours (i.e. ultradian or pulsatile), a day (i.e. circadian), or a year (i.e. seasonal or circannual). The field is also divided along the lines of the major disciplines within biology since rhythms biologists can be either biochemists, molecular/cellular biologists, system physiologists, behaviorists, or ecologists. In addition, while many workers study the basic biological mechanisms involved in generating rhythmicity, others are interested in the clinical applications of a better understanding of biological rhythmicity. Even within the clinical field, researchers fall into many traditional categories including psychiatry, endocrinology, neurology, oncology, cardiology, and reproduction. DTIC

N94-11097# Naval Aerospace Medical Research Lab., Pensacola, FL.
MOTION AND SPATIAL DISORIENTATION SYSTEMS: SPECIAL RESEARCH CAPABILITIES Special Report
A. H. Rupert and R. E. Gadolin Apr. 1993 57 p
(AD-A265155; NAMRL-SR93-1) Avail: CASI HC A04/MF A01

The wide variety of unique devices together with the scientists and

technicians who operate them have enabled the Naval Aerospace Medical Research Laboratory (NAMRL) to develop an international reputation as a center of excellence in vestibular research and the dynamics of spatial orientation, and for training outstanding scientists who are engaged in basic research worldwide. This document contains a brief description of the man-rated acceleration research facilities of the United States Navy.
DTIC

N94-11224# Science Applications International Corp., Joppa, MD.
P2NBC2 HEAT STRAIN DECISION AID. USER'S GUIDE, VERSION 2.1
Apr. 1993 51 p
(Contract DAAL02-90-C-0071)
(AD-A266072) Avail: CASI HC A04/MF A01

This report describes the capabilities and proper use of the P2NBC2 Heat Strain Decision Aid Software System. The P2NBC2 HSDA is a stand alone analytical tool for evaluating the effects of heat stress on soldier performance limits. User inputs include clothing type/chemical protective posture, activity level based on military task type, soldier anthropometric characteristics and acclimatization status, and environmental conditions (air temperature, wind speed, humidity, and solar radiation). The P2NBC2 HSDA provides color graphics, tabular, and data file outputs for heat casualty risk, sustainable work/rest cycle limits, maximum safe work time, and associated drinking water requirements. DTIC

N94-11261# Brown Univ., Providence, RI.
THREE-DIMENSIONAL OBJECT RECOGNITION USING AN UNSUPERVISED BCM NETWORK: THE USEFULNESS OF DISTINGUISHING FEATURES
Nathan Intrator and Joshus I. Gold 17 May 1993 13 p
(Contract N00014-91-J-1316)
(AD-A264576; TR-65-ONR) Avail: CASI HC A03/MF A01

We propose an object recognition scheme based on a method for feature extraction from gray level images that corresponds to recent statistical theory, called projection pursuit, and is derived from a biological motivated feature extracting neuron. To evaluate the performance of this method we use a set of very detailed psychophysical 3D object recognition experiments. DTIC

N94-11449# Tristan Technologies, Inc., San Diego, CA.
LARGE ARRAY SQUID MAGNETOMETER FOR NDE Annual Report, 1 Apr. 1992 - 1993
Douglas N. Paulson 27 Apr. 1993 16 p
(Contract F49620-92-C-0026)
(AD-A264799; AFOSR-93-0348TR) Avail: CASI HC A03/MF A01

Tristan Technologies, Inc. is working to apply SQUID magnetometry to problems in nondestructive evaluation which are important to the Strategic Defense Initiative. We have designed and are nearing completion of an innovative Non Destructive Evaluation (NDE) instrument that, unlike most existing instruments, can be used for studying deep sources with applied fields. We will assess the effectiveness of this SQUID NDE system for a broad range of nondestructive evaluation problems related to high-performance aircraft bearings, nuclear reactor fuel tubes, titanium billets for aircraft turbine blades, high-temperature superconducting magnetic shields, and riveted joints in military and commercial aircraft. In various applications, SQUID magnetometers could facilitate the development of high-performance devices, reduce manufacturing costs, monitor performance and assure quality control in manufacturing, and help prevent catastrophic failures of aircraft, satellites, weapons and other military systems. During Phase 3 we will design and commercialize instruments specifically to meet the most promising NDE applications for SQUID magnetometers. DTIC

N94-11649 Tripler Army Medical Center, Honolulu, HI. Dept. of Clinical Investigation.
THE DEPARTMENT OF CLINICAL INVESTIGATION, REPORTS CONTROL SYMBOL MED-300(R-1) Annual Progress Report, Fiscal Year 1992
1 Oct. 1992 53 p Limited Reproducibility: More than 20% of this document may be affected by microfiche quality
(AD-A264969) Avail: CASI HC A04

The Tripler Department of Clinical Investigation had an exciting year in FY-92. Despite serious challenges to research in the form of personnel freezes, funding cuts, and increasing demands on health care professionals to provide clinical services, there was no significant fall in research productivity. More impressively, Dr. Cathy Yamauchi-Uyehara was awarded an American Heart Association grant after submitting the highest ranked proposal for the AHA district. This was made more significant in view of the AHA policy to not award grants to military investigators. The Joint Tripler AMC/Kapiolani Medical Center for Women and Children's Neonatal Fellowship Program, which conducts all non-human studies in Tripler's DCI, has continued to maintain its position at the forefront of neonatal pulmonary medicine. The contributions of Dr. John Claybaugh, Tripler's senior scientist, to both research and administration of DCI are undiminished. MAJ Thomas Mundie has provided inspiration to all phases of research at Tripler, and especially to the Joint Neonatal Fellowship Program. DTIC

N94-11681# Johns Hopkins Univ., Baltimore, MD. School of Medicine.
VISUAL PSYCHOPHYSICS OF EGOMOTION Interim Report, 1 Feb. 1992 - 31 Jan. 1993
Kathleen Turano 2 Mar. 1993 7 p
(Grant AF-AFOSR-0154-91)
(AD-A265253; AFOSR-93-0259TR) Avail: CASI HC A02/MF A01

One study investigated, under two viewing conditions, an observer's ability to determine whether she/he was moving forward along a straight or curved path using simulations of optic flow patterns. In one condition, the retinal image was stabilized against the effects of eye movements, in the other condition, eye movements were unrestricted. Stabilizing the retinal image decreased performance at slow speeds. A second study further explored the role of eye movements in the perception of motion. Speed-difference thresholds were measured under conditions of stabilized and free-viewing conditions. Despite the fact that eye movements can alter the direction and speed of the retinal-image motion relative to the stimulus motion, observers were able to judge speed differences in the free-viewing condition as well as in the stabilized-viewing condition, with the exception of the slowest speed. At the slowest speed, observers were able to detect smaller speed differences in the free-viewing condition. A third study determined the optimal stimulus for motion detection by searching the spatiotemporal stimulus whose direction was identified with least contrast energy. The best stimulus was determined to be at 3 cycles/deg, 1.67 deg/s with bandwidths of 7.06 Hz and 1-0.5 octaves. DTIC

N94-11689* National Aeronautics and Space Administration, Washington, DC.
AEROSPACE MEDICINE AND BIOLOGY: A CONTINUING BIBLIOGRAPHY WITH INDEXES (SUPPLEMENT 374)
Apr. 1993 77 p
(NASA-SP-7011(374); NAS 1.21:7011(374)) Avail: CASI HC A05

This bibliography lists 227 reports, articles and other documents introduced into the NASA Scientific and Technical Information System during Apr. 1993. Subject coverage includes: aerospace medicine and physiology, life support systems and man/system technology, protective clothing, exobiology and extraterrestrial life, planetary biology, and flight crew behavior and performance. Derived from text

N94-11787*# National Aeronautics and Space Administration, Washington, DC.
INTERNATIONAL TELEMEDICINE/DISASTER MEDICINE CONFERENCE: PAPERS AND PRESENTATIONS
1991 271 p Conference held in Bethesda, MD.; sponsored by Uniformed Services Univ. of the Health Sciences and AIAA
(NASA-NP-207; NAS 1.83:207) Avail: CASI HC A12/MF A03

The first International Telemedicine/Disaster Medicine Conference was held in Dec. 1991. The overall purpose was to convene an international, multidisciplinary gathering of experts to discuss the emerging field of telemedicine and assess its future directions; principally the application of space technology to disaster response and management, but also to clinical medicine, remote health care, public health, and other needs. This collection is intended to acquaint the reader with recent landmark efforts in telemedicine as applied to disaster management and remote health care, the technical requirements of telemedicine systems, the application of telemedicine and telehealth in the U.S. space program, and the social and humanitarian dimensions of this area of medicine. For individual titles, see N94-11788 through N94-11810.

N94-11788*# Utah Univ., Salt Lake City. School of Medicine.
MEDICAL INFORMATICS AND TELEMEDICINE: A VISION
Terry P. Clemmer *In* NASA, Washington, International Telemedicine/Disaster Medicine Conference: Papers and Presentations 1991 5 p (For primary document see N94-11787 01-52)
Avail: CASI HC A01/MF A03

The goal of medical informatics is to improve care. This requires the commitment and harmonious collaboration between the computer scientists and clinicians and an integrated database. The vision described is how medical information systems are going to impact the way medical care is delivered in the future. CASI

N94-11789*# Memorial Univ. of Newfoundland, Saint Johns. Faculty of Medicine.
THE CANADIAN EXPERIENCE: USING TELEMEDICINE FOR THE SUPPORT OF MEDICAL CARE AT REMOTE SITES
Maxwell House *In* NASA, Washington, International Telemedicine/Disaster Medicine Conference: Papers and Presentations 1991 8 p (For primary document see N94-11787 01-52)
Avail: CASI HC A02/MF A03

While the majority of Canadians live in a narrow strip about 200 miles wide just north of the 45th parallel, a significant proportion of the population lives in non-urban, remote and sometimes isolated areas. Given this widely dispersed population, the provision of health services has always been a challenge. A list of non-urban health needs include the following: consulting services; clinical laboratory resources; investigative techniques (e.g., EEG, radiology, ultrasound, nuclear medicine); continuing education for physicians, nurses and other health professionals; teaching and training programs for administrative and support staff (dietary, housekeeping, maintenance); community health education and improved general education for health workers and families. For nearly three decades physicians and other health care professionals in the United States and Canada have been exploring the application of telecommunications to health care in rural and remote areas. The terms telemedicine and telehealth are used interchangeably to describe this activity. The prefix 'tele' refers to distance and now includes all types of communication over distance that support health care and health educational programs. Actually, telemedicine is as old as the telephone, which is still the most widely used communications technology in health care. Author (revised)

N94-11790*# National Aeronautics and Space Administration, Washington, DC.
TELEMEDICINE AND INTERNATIONAL DISASTER RESPONSE: MEDICAL CONSULTATION TO ARMENIA AND RUSSIA VIA A TELEMEDICINE SPACEBRIDGE
Bruce A. Houtchens (Utah Univ., Salt Lake City.), Terry P. Clemmer (Utah Univ., Salt Lake City.), Harry C. Holloway (Uniformed Services Univ. of the Health Sciences, Bethesda, MD.), Alexander A. Kiselev (Nauchno-Proizvodstvennoe Obedinenie Soyuz Medinform, Moscow, Russia.), James S. Logan (Space Medical Services, Tulsa, OK.), Ronald C. Merrell (Texas Univ. Health Science Center, Houston.), Arnauld E. Nicogossian, Haik A. Nikogossian (Republic Diagnostic Center, Yerevan, Armenia.), Russell B. Rayman (Aerospace Medical Association, Alexandria, VA.), and Ashot E. Sarkisian (Republic Diagnostic Center, Yerevan, Armenia.) et al *In its* International Telemedicine/Disaster Medicine Conference: Papers and Presentations 1991 22 p Submitted for publication (For primary document see N94-11787 01-52)
Avail: CASI HC A03/MF A03

The Telemedicine Spacebridge, a satellite mediated audio-video-fax link between four U.S. and two Armenian and Russian medical centers, permitted remote American consultants to assist Armenian and Russian physicians in the management of medical problems following the December 1988 earthquake in Armenia and the June 1989 gas explosion near Ufa. During 12 weeks of operations, 247 Armenian and Russian and 175 American medical professionals participated in 34 half-day clinical conferences. 209 patients were discussed, requiring expertise in 20 specialty areas. Telemedicine consultations resulted in altered diagnoses for 54, new diagnostic studies for 70, altered diagnostic processes for 47, and modified treatment plans for 47 of 185 Armenian patients presented. Simultaneous participation of several U.S. medical centers was judged beneficial; quality of data transmission was judged excellent. These results suggest that interactive consultation by remote specialists can provide valuable assistance to onsite physicians and favorably influence clinical decisions in the aftermath of major disasters. Author (revised)

N94-11791*# National Aeronautics and Space Administration. Lyndon B. Johnson Space Center, Houston, TX.
USE OF TELESCIENCE FOR BIOMEDICAL RESEARCH DURING SPACE FLIGHT
Carolyn L. Huntoon, Howard J. Schneider, and Gayle M. Karamanos (General Electric Co., Houston, TX.) *In* NASA, Washington, International Telemedicine/Disaster Medicine Conference: Papers and Presentations 1991 5 p (For primary document see N94-11787 01-52)
Avail: CASI HC A01/MF A03

When the U.S. first embarked on a manned space flight program, NASA's use of medical telescience was focused on crew health monitoring. In recent years, medical telescience use has been expanded to include support of basic research in space medicine. It enables ground support personnel to assist on-board crews in the performance of experiments and improves the quality and quantity of data return. NASA is continuing to develop its telescience capabilities. Future plans include telemedicine that will enable physicians on Earth to support crewmembers during flight and telescience that will enable investigators at their home institutions to support and conduct in-flight medical research. NASA's use of telescience for crew safety and biomedical research from Project Mercury to the present is described and NASA's plans for the future are presented. Author (revised)

N94-11792*# Universite Catholique de Louvain (Belgium). School of Epidemiology and Public Health.
GLOBAL CONSIDERATIONS FOR IMPLEMENTATION OF TELEMEDICINE
M. F. Lechat *In* NASA, Washington, International Telemedicine/Disaster Medicine Conference: Papers and Presentations 1991 6 p (For primary document see N94-11787 01-52)
Avail: CASI HC A02/MF A03

In Dec. 1989, the United Nations proclaimed the Decade 1990-1999 as the International Decade for Natural Disasters Reduction (IDNDR). The Decade identified a number of research programs. IDNDR, provides a unique opportunity to explore the potential offered by the emerging technologies, and to promote, develop, and support those technologies deemed adequate to make the next century a safer one, especially in the poorest countries of the world. But all this improvement cannot be accomplished in a vacuum. We must begin now to eliminate pitfalls and illusions. A new attitude must emerge. In the scope of reducing human damages resulting from disasters, we must reconsider the cross-cultural understanding, and reach a real awareness which combines humility with a sense of relativeness. Promoting the right context is essential to the mandate of the Decade. Derived from text

N94-11793*# Uniformed Services Univ. of the Health Sciences, Bethesda, MD. Dept. of Preventative Medicine and Biometrics.
TROPICAL MEDICINE: TELECOMMUNICATIONS AND TECHNOLOGY TRANSFER
Llewellyn J. Legters *In* NASA, Washington, International Telemedicine/Disaster Medicine Conference: Papers and Presentations 1991 10 p (For primary document see N94-11787 01-52)
Avail: CASI HC A02/MF A03

The potential for global outbreaks of tropical infectious diseases, and our ability to identify and respond to such outbreaks is a major concern. Rapid, efficient telecommunications is viewed as part of the solution to this set of problems - the means to link a network of epidemiological field stations via satellite with U.S. academic institutions and government agencies, for purposes of research, training in tropical medicine, and observation of and response to epidemic emergencies. At a workshop, telecommunications and technology transfer were addressed and applications of telecommunications technology in long-distance consultation, teaching and disaster relief were demonstrated. Applications in teaching and consultation in tropical infectious diseases is discussed. Derived from text

N94-11794*# International Telecommunications Satellite Organization, Washington, DC. Service Assistance.

APPLICATIONS OF THE INTELSAT SYSTEM TO REMOTE HEALTH CARE

Andrea Maleter *In* NASA, Washington, International Telemedicine/Disaster Medicine Conference: Papers and Presentations 1991 9 p (For primary document see N94-11787 01-52)

Avail: CASI HC A02/MF A03

INTELSAT, the International Telecommunications Satellite Organization, is a not-for-profit commercial cooperate of 124 member nations, created on 20 August 1964. It owns and operates a global system of communications satellites that provides international telecommunications services to 180 countries, territories, and dependencies, and domestic telecommunications services to 40 nations. INTELSAT has actively encouraged the use of satellites for both telemedicine and disaster relief. Topics discussed include: INTELSAT domestic/regional services; use of transportable antennas; INTELNET; using the existing telecommunications infrastructure for remote health care applications: Project Access; INTELSAT's role in disaster telecommunications efforts; and how INTELSAT's existing infrastructure can be used for disaster telecommunications. Derived from text

N94-11795*# Texas Univ., Houston. Dept. of Surgery.

CLINICAL ASPECTS OF TELEMEDICINE

Ronald C. Merrell *In* NASA, Washington, International Telemedicine/Disaster Medicine Conference: Papers and Presentations 1991 3 p (For primary document see N94-11787 01-52)

Avail: CASI HC A01/MF A03

Communication among physicians is an essential in order to combine our experiences for the elucidation and application of new knowledge and for the accurate and uniform application of established medical practice. This communication requires an adequate understanding of the culture of the patient and the social context of disease and indeed the culture of the physician. Malnutrition in Bangladesh means caloric insufficiency, and a program to lower cholesterol would be impertinent, while a program to enhance the nutrition of patients in Texas by an international effort to import more grain would be ludicrous. In the same vein a public health effort to combat alcoholic cirrhosis in Mecca would be as silly as a program to increase fiber in the diet of the Bantu. Clinical communication must acknowledge the culture of the issue at hand and the differences in the experiential base of the physicians. Not only do geography and culture affect the potential differences in the experiential bases, but the world utilizes very different traditions of education and science in training physicians. We are influenced by the diseases we treat, and learn to look for the expected at least as much as we are attentive to the unexpected. A physician in Siberia would be much more likely to recognize frostbite than one from Buenos Aires, and the Argentine doctor would much more likely consider Chaga's Disease to explain abdominal pain than a colleague in Zurich. Beyond these obvious issues in communication among physicians we must deal with the many languages and idioms used in the world. An overview of using Telemedicine SpaceBridge after the earthquake in the Republic of Armenia in 1988 is presented. Author (revised)

N94-11796*# National Aeronautics and Space Administration. Lewis Research Center, Cleveland, OH.

NEW TECHNOLOGY APPLIED TO TELEMEDICINE

Edward F. Miller *In* NASA, Washington, International Telemedicine/Disaster Medicine Conference: Papers and Presentations 1991 19 p (For primary document see N94-11787 01-52)

Avail: CASI HC A03/MF A03

Satellite communications technology was used for establishing international telemedicine communications links in a number of instances, (e.g., Telemedicine SpaceBridge between Armenia and the United States in 1989, and the proposed linkages shown, for demonstration during this conference and during 1992 and 1993). In the current example, geostationary satellites are used to provide intercontinental communications links between the two countries and also for distribution within each country. Author

N94-11797*# Chicago Medical School, IL.

LINKING MEDICAL RECORDS TO AN EXPERT SYSTEM

Frank Naeymi-Rad, David Trace, and Fabio DeSouzaAlmeida (Kaiser Medical Center, Santa Clara, CA.) *In* NASA, Washington, International Telemedicine/Disaster Medicine Conference: Papers and Presentations 1991 15 p (For primary document see N94-11787 01-52)

Avail: CASI HC A03/MF A03

This presentation will be done using the IMR-Entry (Intelligent Medical Record Entry) system. IMR-Entry is a software program developed as a front-end to our diagnostic consultant software MEDAS (Medical Emergency Decision Assistance System). MEDAS (the Medical Emergency Diagnostic Assistance System) is a diagnostic consultant system using a multimembership Bayesian design for its inference engine and relational database technology for its knowledge base maintenance. Research on MEDAS began at the University of Southern California and the Institute of Critical Care in the mid 1970's with support from NASA and NSF. The MEDAS project moved to Chicago in 1982; its current progress is due to collaboration between Illinois Institute of Technology, The Chicago Medical School, Lake Forest College and NASA at KSC. Since the purpose of an expert system is to derive a hypothesis, its communication vocabulary is limited to features used by its knowledge base. The development of a comprehensive problem based medical record entry system which could handshake with an expert system while creating an electronic medical record at the same time was studied. IMR-E is a computer based patient record that serves as a front end to the expert system MEDAS. IMR-E is a graphically oriented comprehensive medical record. The programs major components are demonstrated. Author (revised)

N94-11798*# Telemedicine Systems Corp., Miami, FL.

COMMERCIAL APPLICATIONS OF TELEMEDICINE

Thomas A. Natiello *In* NASA, Washington, International Telemedicine/Disaster Medicine Conference: Papers and Presentations 1991 4 p (For primary document see N94-11787 01-52)

Avail: CASI HC A01/MF A03

Telemedicine Systems Corporation was established in 1976 and is a private commercial supplier of telemedicine systems. These systems are various combinations of communications and diagnostic technology, designed to allow the delivery of health care services to remote facilities. The technology and the health care services are paid for by the remote facilities, such as prisons. Author

N94-11799*# National Aeronautics and Space Administration. Lyndon B. Johnson Space Center, Houston, TX.

SPACE TECHNOLOGY IN REMOTE HEALTH CARE

Sam L. Pool *In* NASA, Washington, International Telemedicine/Disaster Medicine Conference: Papers and Presentations 1991 7 p (For primary document see N94-11787 01-52)

Avail: CASI HC A02/MF A03

Crews and passengers on future long-duration Earth orbital and interplanetary missions must be provided quality health services - to combat illnesses and accidental injuries, and for routine preventive care. People on Earth-orbital missions can be returned relatively easily to Earth, but those on interplanetary missions cannot. Accordingly, crews on long-duration missions will likely include at least one specially trained person, perhaps a physician's assistant, hospital corpsman, nurse, or physician who will be responsible for providing onboard health services. Specifically, we must determine the most effective way to administer health care to a remotely located population. NASA with the cooperation of the Department of Health, Education, and Welfare is pursuing a program for providing health services to remote locations on Earth as a necessary step to developing and verifying this capability on a spacecraft. The STARPAHC program is described. Author (revised)

N94-11800*# NYNEX Science and Technology, Inc., White Plains, NY.

THE USE OF COMMUNICATION TECHNOLOGY IN MEDICINE

Howard P. Reis *In* NASA, Washington, International Telemedicine/Disaster Medicine Conference: Papers and Presentations 1991 11 p (For primary document see N94-11787 01-52)

Avail: CASI HC A03/MF A03

NYNEX Science and Technology is engineering a multi-layered approach to multimedia communications by combining high-resolution images, video, voice, and text into a new fiber-optic service. The service, Media Broadband Service (MBS), is a network-based visual communications capability. It permits real time sharing of images in support of collaborative work among geographically dispersed locations. The health care industry was identified as a primary target market due to their need for high resolution images, the need to transport these images over great distances, and the need to achieve the transport in a short amount of time. The NYNEX Corporation, the current state of the MBS project, including the market needs driving the development of MBS, the overall design of the service, its current implementation and development status, and the progress of MBS projects underway for various customers participating in the initial service offering are described. Author (revised)

N94-11801*# Office of Emergency Preparedness, Rockville, MD.
THE NATIONAL DISASTER MEDICAL SYSTEM
Thomas P. Reutershan *In* NASA, Washington, International Telemedicine/Disaster Medicine Conference: Papers and Presentations 1991 8 p (For primary document see N94-11787 01-52)
Avail: CASI HC A02/MF A03

The Emergency Mobilization Preparedness Board developed plans for improved national preparedness in case of major catastrophic domestic disaster or the possibility of an overseas conventional conflict. Within the health and medical arena, the working group on health developed the concept and system design for the National Disaster Medical System (NDMS). A description of NDMS is presented including the purpose, key components, medical response, patient evacuation, definitive medical care, NDMS activation and operations, and summary and benefits. CASI

N94-11802*# Uniformed Services Univ. of the Health Sciences, Bethesda, MD. Dept. of Preventative Medicine and Biometrics.
SATELLITE, ENVIRONMENTAL, AND MEDICAL INFORMATION APPLIED TO EPIDEMIOLOGICAL MONITORING
Donald R. Roberts and Llewellyn J. Legters *In* NASA, Washington, International Telemedicine/Disaster Medicine Conference: Papers and Presentations 1991 7 p (For primary document see N94-11787 01-52)
Avail: CASI HC A02/MF A03

Improved communications and space-science technologies, such as remote sensing, offer hope of new, more holistic approaches to combating many arthropod-borne disease problems. The promise offered by these technologies has surfaced at a time when global and national efforts at disease control are in decline. Indeed, these programs seem to be losing ground against the arthropod-borne diseases just as rapidly as we seem to be moving forward in technological development. Given these circumstances, we can only hope that remote sensing and geographic information system (GIS) technologies can be pressed into service to help target the temporal and spatial application of control measures and to help in developing new control strategies. Author (revised)

N94-11803*# Interactive Telemedical Systems, Coral Gables, FL.
A TELEMEDICINE HEALTH CARE DELIVERY SYSTEM
Jay H. Sanders *In* NASA, Washington, International Telemedicine/Disaster Medicine Conference: Papers and Presentations 1991 4 p (For primary document see N94-11787 01-52)
Avail: CASI HC A01/MF A03

The Interactive Telemedicine Systems (ITS) system was specifically developed to address the ever widening gap between our medical care expertise and our medical care delivery system. The frustrating reality is that as our knowledge of how to diagnose and treat medical conditions has continued to advance, the system to deliver that care has remained in an embryonic stage. This has resulted in millions of people being denied their most basic health care needs. Telemedicine utilizes an interactive video system integrated with biomedical telemetry that allows a physician at a base station specialty medical complex or teaching hospital to examine and treat a patient at multiple satellite locations, such as rural hospitals, ambulatory health centers, correctional institutions, facilities caring for the elderly, community hospital emergency departments, or international health facilities. Based on the interactive nature of the system design, the consulting physician at the base station can do a complete history and physical examination, as if the patient at the satellite site was sitting in the physician's office. This system is described. Author (revised)

N94-11804*# Center for Public Service Communications, Arlington, VA.
COMMUNICATIONS INFRASTRUCTURE REQUIREMENTS FOR TELEMEDICINE/TELEHEALTH IN THE CONTEXT OF PLANNING FOR AND RESPONDING TO NATURAL DISASTERS: CONSIDERING THE NEED FOR SHARED REGIONAL NETWORKS
John Carver Scott *In* NASA, Washington, International Telemedicine/Disaster Medicine Conference: Papers and Presentations 1991 6 p (For primary document see N94-11787 01-52)
Avail: CASI HC A02/MF A03

During the course of recent years the frequency and magnitude of major disasters - of natural, technological, or ecological origin - have made the world community dramatically aware of the immense losses of human life and economic resources that are caused regularly by such calamities. Particularly hard hit are developing countries, for whom the magnitude of disasters frequently outstrips the ability of the society to cope with them. In many cases this situation can be prevented, and the recent trend in disaster management has been to emphasize the importance of preparedness and mitigation as a means of prevention. In cases of disaster, a system is needed to respond to relief requirements, particularly the delivery of medical care. There is no generic telecommunications infrastructure appropriate for the variety of applications in medical care and disaster management. The need to integrate telemedicine/telehealth into shared regional disaster management telecommunications networks is discussed. Focus is on the development of infrastructure designed to serve the needs of disaster prone regions of the developing world. Derived from text

N94-11805*# Uniformed Services Univ. of the Health Sciences, Tuscon, AZ. School of Medicine.
INTERNATIONAL DISASTER RESEARCH
Martin Elliot Silverstein *In* NASA, Washington, International Telemedicine/Disaster Medicine Conference: Papers and Presentations 1991 4 p (For primary document see N94-11787 01-52)
Avail: CASI HC A01/MF A03

No existing telecommunications system can be expected to provide strategy and tactics appropriate to the complex, many faceted problem of disaster. Despite the exciting capabilities of space, communications, remote sensing, and the miracles of modern medicine, complete turnkey transfers to the disaster problem do not make the fit, and cannot be expected to do so. In 1980, a Presidential team assigned the mission of exploring disaster response within the U.S. Federal Government encountered an unanticipated obstacle: disaster was essentially undefined. In the absence of a scientifically based paradigm of disaster, there can be no measure of cost effectiveness, optimum design of manpower structure, or precise application of any technology. These problems spawned a 10-year, multidisciplinary study designed to define the origins, anatomy, and necessary management techniques for catastrophes. The design of the study necessarily reflects interests and expertise in disaster medicine, emergency medicine, telecommunications, computer communications, and forencsic sciences. This study is described. Derived from text

N94-11806*# National Aeronautics and Space Administration, Washington, DC.
MEDICAL CARE DELIVERY IN THE US SPACE PROGRAM
Donald F. Stewart *In its* International Telemedicine/Disaster Medicine Conference: Papers and Presentations 1991 3 p (For primary document see N94-11787 01-52)
Avail: CASI HC A01/MF A03

The stated goal of this meeting is to examine the use of telemedicine in disaster management, public health, and remote health care. NASA has a vested interest in providing health care to crews in remote environments. NASA has unique requirements for telemedicine support, in that our flight crews conduct their job in the most remote of all work environments. Compounding the degree of remoteness are other environmental concerns, including confinement, lack of atmosphere, spaceflight physiological deconditioning, and radiation exposure, to name a few. In-flight medical care is a key component in the overall support for missions, which also includes extensive medical screening during selection, preventive medical programs for astronauts, and in-flight medical monitoring and consultation. This latter element constitutes the telemedicine aspect of crew health care. The level of in-flight resources dedicated to medical care is determined by the perceived risk of a given mission, which in turn is related to mission duration, planned crew activities, and length of time required for return to definitive medical care facilities. Derived from text

N94-11807*# Academy of Sciences (USSR), Moscow. Space Research Inst.

USE OF SATELLITE TELECOMMUNICATIONS FOR TELEMEDICINE

Gennady Tamkovich *In* NASA, Washington, International Telemedicine/Disaster Medicine Conference: Papers and Presentations 1991 5 p (For primary document see N94-11787 01-52)

Avail: CASI HC A01/MF A03

The use of space telecommunications facilities in the interests of medicine should establish a reliable and timely connection between the specialists involved and access for each of them to information sources the need. Since a certain global-scale program should be implemented for this goal to be achieved, one of the top-priority tasks is to determine appropriate orbital facilities for telecommunications as well as appropriate areas and countries for them, outlining the territories where portable data receive/transport records can be placed and stations that are cheap and simple enough to operate can be stored. Eventually the satellite telecommunications system should encourage health workers to unite in a world community on the basis of a regular and efficient information exchange with the goal of protecting the health of man and the peace of Earth. This goal could only be achieved by gradually removing differences in the domain of medical education and information in different regions over the globe, by providing a possibility of rapid and coordinated access to the information on medical problems of interest on the global scale, as well as by coordinating the discussion and solution of all problems associated with the development and progress of the satellite communications system.

Derived from text

N94-11808*# Nauchno-Proizvodstvennoe Obedinenie Precision Instruments, Moscow (Russia).

USE OF LOW ORBITAL SATELLITE COMMUNICATIONS SYSTEMS FOR HUMANITARIAN PROGRAMS

Vladimir N. Vlasov and Vladimir Gorkovoy *In* NASA, Washington, International Telemedicine/Disaster Medicine Conference: Papers and Presentations 1991 9 p (For primary document see N94-11787 01-52)

Avail: CASI HC A02/MF A03

Communication and information exchange play a decisive role in progress and social development. However, in many parts of the world the communication infrastructure is inadequate and the capacity for on-line exchange of information may not exist. This is true of underdeveloped countries, remote and relatively inaccessible regions, sites of natural disasters, and of all cases where the resources needed to create complex communication systems are limited. The creation of an inexpensive space communications system to service such areas is therefore a high priority task. In addition to a relatively low-cost space segment, an inexpensive space communications systems requires a large number of ground terminals, which must be relatively inexpensive, energy efficient (using power generated by storage batteries, or solar arrays, etc.), small in size, and must not require highly expert maintenance. The ground terminals must be portable, and readily deployable. Communications satellites in geostationary orbit at altitudes of about 36,000 km are very expensive and require complex and expensive ground stations and launch vehicles. Given current technology, it is categorically impossible to develop inexpensive satellite systems with portable ground terminals using such satellites. To solve the problem of developing an inexpensive satellite communications system that can operate with relatively small ground stations, including portable terminals, we propose to use a system with satellites in low Earth orbit, at an altitude of 900-1500 km. Because low orbital satellites are much closer to the Earth than geostationary ones and require vastly less energy expenditure by the satellite and ground terminals for transmission of messages, a system using them is relatively inexpensive. Such a system could use portable ground terminals no more complex than ordinary mobile police radios. Author (revised)

N94-11809*# National Aeronautics and Space Administration, Washington, DC.

US-USSR TELEMEDICINE CONSULTATION SPACEBRIDGE TO ARMENIA AND UFA Final Report

In its International Telemedicine/Disaster Medicine Conference: Papers and Presentations 1991 49 p Prepared in cooperation with Nauchno-Proizvodstvennoe Obedinenie Soyuz Medinform, Moscow, Russia (For primary document see N94-11787 01-52)

Avail: CASI HC A03/MF A03

The Final Report on the U.S.-U.S.S.R. Telemedicine Consultation Spacebride to Armenia and Ufa is presented. The goal of this activity was to provide expert medical consultation to the Armenian medical personnel in the areas of plastic and reconstructive surgery, physical and psychological rehabilitation, public health, and epidemiology following the devastating earthquake in Dec. 1988. The U.S. and U.S.S.R. implementation teams developed new standards for medical information transmittal as well as protocols and schedules on how to conduct medical consultations. The consultations were provided to the Republic Diagnostic Center in Yerevan, U.S.S.R. by four U.S. medical centers: University of Utah/LDS Hospital, University of Texas, Maryland Institute for Emergency Medical Service Systems, and Uniformed Services University of the Health Sciences.

Derived from text

N94-11810*# Committee on Government Operations (U.S. House).

THE REVITALIZATION OF HEALTH AND EDUCATION IN RURAL AMERICA ACT OF 1992

Glenn English *In* NASA, Washington, International Telemedicine/Disaster Medicine Conference: Papers and Presentations 1991 17 p (For primary document see N94-11787 01-52)

Avail: CASI HC A03/MF A03

During the preceding decade of the 1980's, rural communities witnessed an exodus of over 5 million residents to urban and suburban areas of the nation. It has become increasingly clear that rural parts of the country must adopt aggressive strategies to strengthen rural communities and enhance the quality of life for its citizens into the 21st century. Studies by the U.S. Department of Commerce, Office of Technology Assessment, and the Aspen Institute all identify advanced telecommunications systems as the linchpin for a vigorous future for rural America. The Revitalization of Health and Education in Rural America Act of 1992 incorporates these recommendations into viable strategies to improve health care and educational services for rural citizens. By linking up hospitals and schools through advanced telecommunications technology, vast geographic distances are instantly reduced. With the proper infrastructure in place, up-to-date telecommunications services will facilitate endless opportunities for improving the quality of life in remote areas. This comprehensive legislation is the critical first step in forging a partnership with urban communities to create an economically sound and technologically advanced America for generations to come. Improvement of health care and educational services in rural areas through the implementation of interactive telecommunications systems is addressed. A copy of the Act is included. Author (revised)

N94-11991*# Krug Life Sciences, Inc., Houston, TX.

PROCEEDINGS OF THE FIRST JOINT NASA CARDIOPULMONARY WORKSHOP

Suzanne M. Fortney, ed. (National Aeronautics and Space Administration. Lyndon B. Johnson Space Center, Houston, TX.) and Alan R. Hargens, ed. (National Aeronautics and Space Administration. Ames Research Center, Moffett Field, CA.) Apr. 1991 171 p Workshop held in Houston, TX, 5-7 Dec. 1990; sponsored by NASA. Washington and NASA. Johnson Space Center

(Contract NAS9-17720)

(NASA-CP-10068; NAS 1.55:10068) Avail: CASI HC A08/MF A02

The topics covered include the following: flight echocardiography, pulmonary function, central hemodynamics, glycerol hyperhydration, spectral analysis, lower body negative pressure countermeasures, orthostatic tolerance, autonomic function, cardiac deconditioning, fluid and renal responses to head-down tilt, local fluid regulation, endocrine regulation during bed rest, autogenic feedback, and chronic cardiovascular measurements. The program ended with a general discussion of weightlessness models and countermeasures. For individual titles, see N94-11992 through N94-12007.

N94-11992*# National Aeronautics and Space Administration. John F. Kennedy Space Center, Lompoc, CA.

CAROTID-CARDIAC BAROREFLEX: RELATION WITH ORTHOSTATIC HYPOTENSION FOLLOWING SIMULATED MICROGRAVITY AND IMPLICATIONS FOR DEVELOPMENT OF COUNTERMEASURES

Abstract Only

Victor A. Convertino *In* Krug Life Sciences, Inc., Proceedings of the First Joint NASA Cardiopulmonary Workshop Apr. 1991 p 3-5 (For

primary document see N94-11991 01-52)
Avail: CASI HC A01/MF A02

In a series of studies, we have examined the effects of exposure to simulated microgravity, varying states of vascular volume, and acute exercise on the function of the carotid-cardiac baroreflex in man. In the first study, exposure to simulated microgravity (6 degree headdown bedrest) reduced the sensitivity and buffer capacity of the vagal baroreceptor-cardiac reflex mechanisms and this impaired baroreflex function was associated with orthostatic hypotension. Since the reduction in plasma volume during BR was not correlated with impaired baroreflex function, a second study was conducted which demonstrated that the carotid-cardiac baroreflex response was not affected by either acute hypovolemia or hypervolemia. These results suggest that acute fluid replacement prior to reentry may not reverse impaired baroreflex function associated with postflight hypotension. In a third study, we demonstrated that one bout of maximal exercise increased baroreflex sensitivity and buffer capacity through 24 h post-exercise. These baroreflex changes were opposite to those observed following BR. Taken together, these data suggest that the contributions of reduced blood volume and impaired carotid-cardiac baroreflex function to orthostatic hypotension following exposure to microgravity are probably separate and additive; maximal exercise in addition to fluid replacement may provide an acute effective countermeasure against postflight hypotension. Author (revised)

N94-11993*# National Aeronautics and Space Administration. Lyndon B. Johnson Space Center, Houston, TX.
ECHOCARDIOGRAPHY IN THE FLIGHT PROGRAM
John B. Charles, Michael W. Bungo, and Sharon L. Mulvagh *In* Krug Life Sciences, Inc., Proceedings of the First Joint NASA Cardiopulmonary Workshop Apr. 1991 p 7-9 (For primary document see N94-11991 01-52)
Avail: CASI HC A01/MF A02

Observations on American and Soviet astronauts have documented the association of changes in cardiovascular function during orthostasis with space flight. A basic understanding of the cardiovascular changes occurring in astronauts requires the determination of cardiac output and total peripheral vascular resistance as a minimum. In 1982, we selected ultrasound echocardiography as our means of acquiring this information. Ultrasound offers a quick, non-invasive and accurate means of determining stroke volume which, when combined with the blood pressure and heart rate measurements of the stand test, allows calculation of changes in peripheral vascular resistance, the body's major response to orthostatic stress. The history of echocardiography in the Space Shuttle Program is discussed and the results are briefly presented. Derived from text

N94-11994*# California Univ., San Diego.
PULMONARY FUNCTION IN MICROGRAVITY: KC-135 EXPERIENCE
Abstract Only
Harold J. Guy and G. K. Prisk *In* Krug Life Sciences, Inc., Proceedings of the First Joint NASA Cardiopulmonary Workshop Apr. 1991 p 11 (For primary document see N94-11991 01-52)
Avail: CASI HC A01/MF A02

We have commenced a KC-135 program that parallels and proceeds our Spacelab (SLS-1) pulmonary function experiment. Our first task was to elucidate the affect of normal gravitation on the shape of the maximum expiratory flow volume (MEFV) curve. Nine normal subjects performed multiple MEFV maneuvers at 0-G, 1-G, and approximately 1.7-G. The MEFV curves for each subject were filtered, aligned at RV, and ensemble-averaged to produce an average MEFV curve for each state, allowing differences to be studied. Most subjects showed a decrease in the FVC at 0-G, which we attribute to an increased intrathoracic blood volume. In most of these subjects, the mean lung volume associated with a given flow was lower at 0-G, over about the upper half of the vital capacity. This is similar to the change previously reported during heat out immersion and is consistent with the known affect of engorgement of the lung with blood, on elastic recoil. There were also consistent but highly individual changes in the position and magnitude of detailed features of the curve, the individual patterns being similar to those previously reported on transition from the erect to the supine position. This supports the idea that the location and motion of choke points which determine the detailed individual configuration of MEFV curves, can be significantly influenced by gravitational forces, presumably via the effects of change in longitudinal tension on local airway pressure-diameter behavior and wave speed. We have developed a flight mass spectrometer and have commenced a study of single breath gradients in gas exchange, inert gas washouts, and rebreathing cardiac outputs and lung volumes at 0-G, 1-G, and 1.7-G. Comparison of our results with those from SLS-1 should identify the opportunities and limitations of the KC-135 as an accessible microgravity resource. Author (revised)

N94-11995*# Air Force Systems Command, Brooks AFB, TX.
CENTRAL CIRCULATORY HEMODYNAMICS AS A FUNCTION OF GRAVITATIONAL STRESS
Rick D. Latham, C. D. White, J. W. Fanton, R. W. Owens, J. F. Barber, B. E. Lewkowski, and O. T. Goff *In* Krug Life Sciences, Inc., Proceedings of the First Joint NASA Cardiopulmonary Workshop Apr. 1991 p 13-36 (For primary document see N94-11991 01-52)
Avail: CASI HC A03/MF A02

This study focuses on an evaluation of the central hemodynamics in a nonhuman primate model to variations in gravitational states. The baboon, phylogenectically close to man, was chosen as the human surrogate. The study environments selected are head-down and head-up tilt in the physiology laboratory, centrifugation to test hypergravic stress, and parabolic flights to test transient acute responses to microgravity. Derived from text

N94-11996*# New Mexico Univ., Albuquerque. Dept. of Biology.
GLYCEROL-INDUCED HYPERHYDRATION
Marvin L. Riedesel, Timothy P. Lyons, and M. Colleen McNamara *In* Krug Life Sciences, Inc., Proceedings of the First Joint NASA Cardiopulmonary Workshop Apr. 1991 p 37-49 (For primary document see N94-11991 01-52)
Avail: CASI HC A03/MF A02

Maintenance of euhydration is essential for maximum work performance. Environments which induce hypohydration reduce plasma volume and cardiovascular performance progressively declines as does work capacity. Hyperhydration prior to exposure to dehydrating environments appears to be a potential countermeasure to the debilitating effects of hypohydration. The extravascular fluid space, being the largest fluid compartment in the body, is the most logical space by which significant hyperhydration can be accomplished. Volume and osmotic receptors in the vascular space result in physiological responses which counteract hyperhydration. Our hypothesis is that glycerol-induced hyperhydration (GIH) can accomplish extravascular fluid expansion because of the high solubility of glycerol in lipid and aqueous media. A hypertonic solution of glycerol is rapidly absorbed from the gastrointestinal tract, results in mild increases in plasma osmolality and is distributed to 65 percent of the body mass. A large volume of water ingested within minutes after glycerol intake results in increased total body water because of the osmotic action and distribution of glycerol. The resulting expanded extravascular fluid space can act as a reservoir to maintain plasma volume during exposure to dehydrating environments. The fluid shifts associated with exposure to microgravity result in increased urine production and is another example of an environment which induces hypohydration. Our goal is to demonstrate that GIH will facilitate maintenance of euhydration and cardiovascular performance during space flight and upon return to a 1 g environment. Derived from text

N94-11997*# Kentucky Univ., Lexington. Center for Biomedical Engineering.
SPECTRAL ANALYSIS OF RESTING CARDIOVASCULAR VARIABLES AND RESPONSES TO OSCILLATORY LBNP BEFORE AND AFTER 6 DEGREE HEAD DOWM BEDREST
Charles F. Knapp, J. M. Evans, A. Patwardhan, D. Levenhagen, M. Wang, and John B. Charles *In* Krug Life Sciences, Inc., Proceedings of the First Joint NASA Cardiopulmonary Workshop Apr. 1991 p 51-60 (For primary document see N94-11991 01-52)
Avail: CASI HC A02/MF A02

A major focus of our research program is to develop noninvasive procedures for determining changes in cardiovascular function associated with the null gravity environment. We define changes in cardiovascular function to be (1) the result of the regulatory system operating at values different from 'normal' but with an overall control system basically unchanged by the null gravity exposure, or (2) the result of operating with a control system that has significantly different regulatory characteristics after an exposure. To this end, we have used a model of weightlessness that consisted of exposing humans to 2 hrs. in the launch position, followed by 20 hrs. of 6 deg head down bedrest. Our principal objective was to use

this model to measure cardiovascular responses to the 6 deg head down bedrest protocol and to develop the most sensitive 'systems identification' procedure for indicating change. A second objective, related to future experiments, is to use the procedure in combination with experiments designed to determine the degree to which a regulatory pathway has been altered and to determine the mechanisms responsible for the changes.
Derived from text

N94-11998*# National Aeronautics and Space Administration. Lyndon B. Johnson Space Center, Houston, TX.
EFFECT OF PROLONGED LBNP AND SALINE INGESTION ON PLASMA VOLUME AND ORTHOSTATIC RESPONSES DURING BED REST
Suzanne M. Fortney, Larry Dussack, Tracy Rehbein, Margie Wood, and Laura Steinmann *In* Krug Life Sciences, Inc., Proceedings of the First Joint NASA Cardiopulmonary Workshop Apr. 1991 p 61-70 (For primary document see N94-11991 01-52)
(RTOP 199-14-11-13)
Avail: CASI HC A02/MF A02

Orthostatic intolerance remains a significant problem following space flight despite frequent use of the saline fluid-loading countermeasure and volitional use of an anti-gravity suite during reentry and landing. The purpose of this project is to examine the plasma volume (PV), endocrine, and orthostatic responses of bedrested subjects following 2-hr and 4-hr treatments of lower body negative pressure (LBNP) and saline ingestion. Ten healthy men were randomly assigned into 2 groups. Group A underwent a 4-hr LBNP/saline treatment on best rest day 5 and the 2-hr treatment on day 11. Group B underwent the 2-hr treatment on day 6 and the 4-hr treatment on day 10. Blood volume was determined before and after bed rest using radiolabelling. Changes in PV between measurements were calculated from changes in hematocrit and estimated red cell volume. Urinary excretion of anti-diuretic hormone (ADH) and aldosterone (ALD) were measured each day during the study. Orthostatic responses were measured using a ramp LBNP protocol before bed rest, before each treatment, and 24 hours after each treatment. Both 2-hr and 4-hr treatments resulted in a restoration of PV to pre-bed rest levels which persisted at least 24 hours. This increase in PV was associated with significant increases in urinary excretion of ADH and ALD. Twenty-four hours after the 4-hr treatment, the heart rate and pulse pressure response to LBNP were significantly lower and stroke volumes during LBNP were increased. Twenty-four hours after the 2-hr treatment, there was no evidence of improvement in orthostatic responses. These results suggest that a countermeasure which simply restores PV during space flight may not be sufficient for restoring orthostatic responses. Author

N94-11999*# Texas Univ., Dallas. Div. of Cardiology.
FITNESS, AUTONOMIC REGULATION AND ORTHOSTATIC TOLERANCE
Jay C. Buckey *In* Krug Life Sciences, Inc., Proceedings of the First Joint NASA Cardiopulmonary Workshop Apr. 1991 p 71-78 (For primary document see N94-11991 01-52)
Avail: CASI HC A02/MF A02

Work on this grant has consisted of two major studies of cardiovascular regulation in athletes along with several smaller supporting studies. This summary will give a brief overview of two major studies, and then conclude with an analysis of what the findings from these studies mean practically, and how they can be applied to current problems with post-flight orthostatic intolerance. The first study addresses a cross-sectional analysis of orthostatic intolerance in highly aerobically trained individuals; the second addresses ventricular pressure/volume relationships in athletes. Author (revised)

N94-12000*# Medical Coll. of Virginia, Richmond. Depts. of Medicine and Physiology.
VALSALVA MANEUVER: INSIGHTS INTO BAROREFLEX MODULATION OF HUMAN SYMPATHETIC ACTIVITY
Michael L. Smith, Dwain L. Eckberg, Janice M. Fritsch, Larry A. Beightol, and Kenneth A. Ellenbogen *In* Krug Life Sciences, Inc., Proceedings of the First Joint NASA Cardiopulmonary Workshop Apr. 1991 p 79-87 (For primary document see N94-11991 01-52)
Avail: CASI HC A02/MF A02

Valsalva's maneuver, voluntary forced expiration against a closed glottis, is a well-characterized research tool, used to assess the integrity of human autonomic cardiovascular control. Valsalva straining provokes a stereotyped succession of alternating positive and negative arterial pressure and heart rate changes mediated in part by arterial baroreceptors. Arterial pressure changes result primarily from fluctuating levels of venous return to the heart and changes of sympathetic nerve activity. Muscle sympathetic activity was measured directly in nine volunteers to explore quantitatively the relation between arterial pressure and human sympathetic outflow during pressure transients provoked by controlled graded Valsalva maneuvers. Our results underscore several properties of sympathetic regulation during Valsalva straining. First, muscle sympathetic nerve activity changes as a mirror image of changes in arterial pressure. Second, the magnitude of sympathetic augmentation during Valsalva straining predicts phase 4 arterial pressure elevations. Third, post-Valsalva sympathetic inhibition persists beyond the return of arterial and right atrial pressures to baseline levels which reflects an alteration of the normal relation between arterial pressure and muscle sympathetic activity. Therefore, Valsalva straining may have some utility for investigating changes of reflex control of sympathetic activity after space flight; however, measurement of beat-to-beat arterial pressure is essential for this use. The utility of this technique in microgravity can not be determined from these data. Further investigations are necessary to determine whether these relations are affected by the expansion of intrathoracic blood volume associated with microgravity. Author (revised)

N94-12001*# Arizona Univ., Tucson. Dept. of Exercise and Sport Sciences.
MECHANISTIC STUDIES ON REDUCED EXERCISE PERFORMANCE AND CARDIAC DECONDITIONING WITH SIMULATED ZERO GRAVITY
Charles M. Tipton *In* Krug Life Sciences, Inc., Proceedings of the First Joint NASA Cardiopulmonary Workshop Apr. 1991 p 89-95 (For primary document see N94-11991 01-52)
(Grant NAG2-392)
Avail: CASI HC A02/MF A02

The primary purpose of this research is to study the physiological mechanisms associated with the exercise performance of rats subjected to conditions of simulated weightlessness. A secondary purpose is to study related physiological changes associated with other systems. To facilitate these goals, a rodent suspension model was developed (Overton-Tipton) and a VO2 max testing procedure was perfected. Three methodological developments occurred during this past year deserving of mention. The first was the refinement of the tail suspension model so that (1) the heat dissipation functions of the caudal artery can be better utilized, and (2) the blood flow distribution to the tail would have less external constriction. The second was the development on a one-leg weight bearing model for use in simulated weightlessness studies concerned with change in muscle mass, muscle enzyme activity, and hind limb blood flow. The chemical body composition of 30 rats was determined and used to develop a prediction equation for percent fat using underwater weighing procedures to measure carcass specific gravity and to calculate body density, body fat, and fat free mass. Author (revised)

N94-12002*# California Univ., San Diego, La Jolla. Dept. of Medicine.
FLUID COMPARTMENT AND RENAL FUNCTION ALTERATIONS IN THE RAT DURING 7 AND 14 DAY HEAD DOWN TILT
Bryan J. Tucker *In* Krug Life Sciences, Inc., Proceedings of the First Joint NASA Cardiopulmonary Workshop Apr. 1991 p 97-108 Sponsored by NASA. Ames Research Center (For primary document see N94-11991 01-52)
(Grant NAG2-659)
Avail: CASI HC A03/MF A02

Exposure to conditions of microgravity for any extended duration can modify the distribution of fluid within the vascular and interstitial spaces, and eventually intracellular volume. Whether the redistribution of fluid and resetting of volume homeostasis mechanisms is appropriate for the long term environmental requirements of the body in microgravity remains to be fully defined. The event that initiates the change in fluid volume homeostasis is the cephalad movement of fluid which potentially triggers volume sensors and stretch receptors (atrial stretch with the resulting release of atrial natriuretic peptide) and suppresses adrenergic activity via the carotid and aortic arch baroreceptors. All these events act in concert to reset blood and interstitial volume to new levels, which in turn modify the renin-angiotensin system. All these factors have an influence on the kidney, the end organ for fluid volume control. How the fluid compartment volume changes interrelate with alterations in renal functions under conditions of simulated microgravity is the focus of the present investigation which utilizes 25-30 deg head-down tilt in the rat. Author

N94-12003*# National Aeronautics and Space Administration. Ames Research Center, Moffett Field, CA.
LOCAL FLUID SHIFTS AND EDEMA IN HUMANS DURING SIMULATED MICROGRAVITY
Alan R. Hargens *In* Krug Life Sciences, Inc., Proceedings of the First Joint NASA Cardiopulmonary Workshop Apr. 1991 p 109-119 (For primary document see N94-11991 01-52)
(RTOP 199-14-12-04)
Avail: CASI HC A03/MF A02

Local fluid shifts and edema in humans during simulated microgravity is studied. Recent results and significance and future plans on the following research topics are discussed: mechanisms of headward edema formation during head-down tilt; postural responses of head and foot microcirculations and their sensitivity to bed rest; and transcapillary fluid transport associated with lower body negative pressure (LBNP) with and without saline ingestion. CASI

N94-12004*# National Aeronautics and Space Administration. Ames Research Center, Moffett Field, CA.
HORMONAL REGULATION OF FLUID AND ELECTROLYTE METABOLISM IN ZERO-G AND BEDREST
Joan Vernikos *In* Krug Life Sciences, Inc., Proceedings of the First Joint NASA Cardiopulmonary Workshop Apr. 1991 p 121-139 (For primary document see N94-11991 01-52)
(RTOP 199-14-12-03)
Avail: CASI HC A03/MF A02

The study of man in spaceflight has consistently indicated changes in fluid and electrolyte balance. Sodium (Na), Potassium (K), and Calcium (Ca) excretion are increased, accompanied by changes in the levels and responsiveness of adrenal hormones and the sympathetic nervous system (SNS). These hormones and neurohumors are critical to the regulation of blood pressure, blood flow, and blood volume. The primary objectives of the research conducted under this task have been to use -6 deg head down bedrest (BR) as the analog to spaceflight, to determine the long term changes in these systems, their relationship to orthostatic tolerance, and to develop and test suitable countermeasures. Author (revised)

N94-12005*# National Aeronautics and Space Administration. Ames Research Center, Moffett Field, CA.
HORMONAL REGULATION OF FLUID AND ELECTROLYTE METABOLISM DURING PERIODS OF HEADWARD FLUID SHIFTS
Lanny C. Keil, W. B. Severs (Pennsylvania State Univ., University Park.), T. Thrasher (California Univ., San Francisco.), and D. J. Ramsay (California Univ., San Francisco.) *In* Krug Life Sciences, Inc., Proceedings of the First Joint NASA Cardiopulmonary Workshop Apr. 1991 p 141-144 (For primary document see N94-11991 01-52)
Avail: CASI HC A01/MF A02

In the broadest sense, this project evaluates how spaceflight induced shifts of blood and interstitial fluids into the thorax affect regulation by the central nervous system (CNS) of fluid-electrolyte hormone secretion. Specifically, it focuses on the role of hormones related to salt/water balance and their potential function in the control of intracranial pressure and cerebrospinal fluid (CSF) composition. Fluid-electrolyte status during spaceflight gradually equilibrates, with a reduction in all body fluid compartments. Related to this is the cardiovascular deconditioning of spaceflight which is manifested upon return to earth as orthostatic intolerance. Author (revised)

N94-12006*# National Aeronautics and Space Administration. Ames Research Center, Moffett Field, CA.
AUTOGENIC-FEEDBACK TRAINING: A COUNTERMEASURE FOR ORTHOSTATIC INTOLERANCE
Patricia S. Cowings, William B. Toscano (California Univ., San Francisco.), Joe Kamiya (California Univ., San Francisco.), Neal E. Miller (Yale Univ., New Haven, CT.), and Thomas G. Pickering (Cornell Univ., New York, NY.) *In* Krug Life Sciences, Inc., Proceedings of the First Joint NASA Cardiopulmonary Workshop Apr. 1991 p 145-153 (For primary document see N94-11991 01-52)
Avail: CASI HC A02/MF A02

NASA has identified cardiovascular deconditioning as a serious biomedical problem associated with long-duration exposure to microgravity in space. High priority has been given to the development of countermeasures for this disorder and the resulting orthostatic intolerance experienced by crewmembers upon their return to the 1g norm of Earth. The present study was designed to examine the feasibility of training human subjects to control their own cardiovascular responses to gravitational stimulation (i.e., a tilt table). Using an operant conditioning procedure, Autogenic-Feedback Training (AFT), we would determine if subjects could learn to increase their own blood pressure voluntarily. Author (revised)

N94-12007*# Harvard Medical School, Boston, MA. Electrocardiography and Arrhythmia Labs.
CARDIOVASCULAR DYNAMICS DURING SPACE SICKNESS AND DECONDITIONING
Ary L. Goldberger and David R. Rigney *In* Krug Life Sciences, Inc., Proceedings of the First Joint NASA Cardiopulmonary Workshop Apr. 1991 p 155-163 Sponsored by NASA. Ames Research Center (For primary document see N94-11991 01-52)
(Grant NAG2-514)
Avail: CASI HC A02/MF A01

We are currently funded by NASA for the project, 'Cardiovascular Dynamics During Space Sickness and Deconditioning.' NASA has given priority to the investigation of two problems encountered in the long-term space flights currently being planned: (1) space motion sickness; and (2) cardiovascular deconditioning. We have proposed to use spectral and nonlinear dynamical analysis of heart rate data to quantify the presence of these problems and to evaluate countermeasures against them. Author (revised)

N94-12364# Army Medical Center, Aurora, CO.
PILOT TRIAL OF POTENTIATING NORMAL HEALING OF STRESS FRACTURES USING PULSING ELECTROMAGNETIC FIELDS Final Report, 15 Jan. 1991 - 14 Jan. 1993
Kent M. Karstetter, Richard A. Sherman, Howard May, and Paul Spezia 22 Feb. 1993 11 p Prepared for Army Medical Research and Development Command, Fort Detrick, MD
(Contract MIPR-91MM1519; DA Proj. 3M1-62787-A-874)
(AD-A264251) Avail: CASI HC A03/MF A01

Stress fractures usually take a long time to heal, and they prevent soldiers from participating in most physical activities. About half of the trainees at Ft. Sill diagnosed with stress fractures never return to active duty. This pilot program tests the feasibility of using pulsing electromagnetic fields, such as those used to potentiate the healing of non-unions, to speed healing of stress fractures. In the first trial, the field coil was embedded in the cast to produce a magnetic field around the fracture. The unit was supposed to be used for a minimum of six weeks but, due to change in treatment policies resulting from a turnover in staff with Desert Shield, the units were only used for a few weeks. Eighteen trainees used the units in their casts, ten just had casts (the standard treatment) during the treatment period and thirty-one just had the standard treatment before the treatment period. There was no difference between number of days it took those numbers of the groups able to return to duty to do so. However, only two of the treated soldiers had MEB's while twenty of the controls did. The pilot program will continue as an unfunded study at Ft. Sill. The proposed work and new investigators were identified in the annual report to MDRC for this project dated 6 Nov. 1992. DTIC

N94-12423# Army Aeromedical Research Lab., Fort Rucker, AL.
THE AGING MILITARY AVIATOR: A REVIEW AND ANNOTATED BIBLIOGRAPHY Final Report
Lewis W. Stone Jan. 1993 48 p
(DA Proj. 3M1-62787-A-879)
(AD-A265341; USAARL-93-11) Avail: CASI HC A03/MF A01

Studies suggest that aging is another factor which may affect performance of military pilots. Although these aviators generally are better-educated and healthier than their age peers in the general population, they, too, are subject to insidiously deteriorating physiological and sensory systems, a slowly increasing likelihood of acute pathologies, and a general slowing with age - all within the age range of military pilots. Reductions in some parameters might be offset to some degree by experience and maturity; however, age-related changes and the effects therefrom vary more between individuals in any age group than between the groups themselves. The real problem, though, is that we still do not know what effect, if any, age-related changes have on performance of military aviators. Neither is there a concerted effort to provide the aging pilot with a coping strategy for the approaching situation. DTIC

N94-10795# Boeing Co., Seattle, WA.
HEALTH AND SAFETY ISSUES FOR AEROSPACE WORKERS IN THE USE OF ADVANCED MATERIALS
James M. Peterson and Wilfrid L. Cameron (International Association of Machinists and Aerospace Workers, Washington, DC.) *In* FAA, Proceedings of the International Conference for the Promotion of Advanced Fire Resistant Aircraft Interior Materials Mar. 1993 p 339-344 (For primary document see N94-10766 01-03)
Avail: CASI HC A02/MF A03

N94-11542*# Space Biomedical Research Inst., Houston, TX. Environmental Physiology/Biophysics Section.
JOINT PAIN AND DOPPLER-DETECTABLE BUBBLES IN ALTITUDE (HYPOBARIC) DECOMPRESSION Abstract Only
Michael R. Powell *In* NASA. Johnson Space Center, Sixth Annual Workshop on Space Operations Applications and Research (SOAR 1992), Volume 2 Feb. 1993 p 546 (For primary document see N94-11527 01-99)
Avail: CASI HC A01/MF A03

N94-11543*# Aerospace Medical Research Labs., Brooks AFB, TX.
ARTERIAL GAS EMBOLI IN ALTITUDE-INDUCED DECOMPRESSION SICKNESS Abstract Only
Andrew A. Pilmanis and Robert M. Olson (Krug Life Sciences, Inc., San Antonio, TX.) *In* NASA. Johnson Space Center, Sixth Annual Workshop on Space Operations Applications and Research (SOAR 1992), Volume 2 Feb. 1993 p 547 (For primary document see N94-11527 01-99)
Avail: CASI HC A01/MF A03

N94-11544*# Space Biomedical Research Inst., Houston, TX.
TRANSCRANIAL DOPPLER ULTRASOUND AND THE ETIOLOGY OF NEUROLOGIC DECOMPRESSION SICKNESS DURING ALTITUDE DECOMPRESSION
W. T. Norfleet, M. R. Powell, K. Vasantha Kumar (Krug Life Sciences, Inc., Houston, TX.), and J. Waligora *In* NASA. Johnson Space Center, Sixth Annual Workshop on Space Operations Applications and Research (SOAR 1992), Volume 2 Feb. 1993 p 549-561 (For primary document see N94-11527 01-99)
Avail: CASI HC A03/MF A03

N94-11545*# Space Biomedical Research Inst., Houston, TX. Environmental Physiology/Biophysics Section.
A MECHANISM FOR THE REDUCTION IN RISK OF DECOMPRESSION SICKNESS IN MICROGRAVITY ENVIRONMENT Abstract Only
Michael R. Powell *In* NASA. Johnson Space Center, Sixth Annual Workshop on Space Operations Applications and Research (SOAR 1992), Volume 2 Feb. 1993 p 562 (For primary document see N94-11527 01-99)
Avail: CASI HC A01/MF A03

N94-11546*# National Aeronautics and Space Administration. Lyndon B. Johnson Space Center, Houston, TX.
RISK OF DECOMPRESSION SICKNESS IN THE PRESENCE OF CIRCULATING MICROBUBBLES
K. Vasantha Kumar (Krug Life Sciences, Inc., Houston, TX.) and Michael R. Powell *In its* Sixth Annual Workshop on Space Operations Applications and Research (SOAR 1992), Volume 2 Feb. 1993 p 563-567 (For primary document see N94-11527 01-99)
Avail: CASI HC A01/MF A03

N94-11547*# Space Biomedical Research Inst., Houston, TX. Environmental Physiology/Biophysics Section.
STRATEGIES AND METHODOLOGIES TO DEVELOP TECHNIQUES FOR COMPUTER-ASSISTED ANALYSIS OF GAS PHASE FORMATION DURING ALTITUDE DECOMPRESSION Abstract Only
Michael R. Powell and W. A. Hall (Krug Life Sciences, Inc., Houston, TX.) *In* NASA. Johnson Space Center, Sixth Annual Workshop on Space Operations Applications and Research (SOAR 1992), Volume 2 Feb. 1993 p 568 (For primary document see N94-11527 01-99)
Avail: CASI HC A01/MF A03

N94-11550*# National Aeronautics and Space Administration. Lyndon B. Johnson Space Center, Houston, TX.
PROMETHAZINE AND ITS USE AS A TREATMENT FOR SPACE MOTION SICKNESS Abstract Only
James P. Bagian and Bradley G. Beck *In its* Sixth Annual Workshop on Space Operations Applications and Research (SOAR 1992), Volume 2 Feb. 1993 p 574 (For primary document see N94-11527 01-99)
Avail: CASI HC A01/MF A03

N94-11551*# National Aeronautics and Space Administration. Lyndon B. Johnson Space Center, Houston, TX.
UPDATE ON THE INCIDENCE AND TREATMENT OF SPACE MOTION SICKNESS Abstract Only
Bradley G. Beck *In its* Sixth Annual Workshop on Space Operations Applications and Research (SOAR 1992), Volume 2 Feb. 1993 p 575 (For primary document see N94-11527 01-99)
Avail: CASI HC A01/MF A03

N94-11552*# National Aeronautics and Space Administration. Lyndon B. Johnson Space Center, Houston, TX.
BASELINE CHARACTERISTICS OF DIFFERENT STRATA OF ASTRONAUT CORPS Abstract Only
Peggy B. Hamm (Krug Life Sciences, Inc., Houston, TX.) and L. J. Pepper *In its* Sixth Annual Workshop on Space Operations Applications and Research (SOAR 1992), Volume 2 Feb. 1993 p 577 (For primary document see N94-11527 01-99)
Avail: CASI HC A01/MF A03

N94-11557*# Universities Space Research Association, Houston, TX.
PHYSIOLOGIC MECHANISMS OF CIRCULATORY AND BODY FLUID LOSSES IN WEIGHTLESSNESS IDENTIFIED BY MATHEMATICAL MODELING
K. E. Simanonok, R. S. Srinivasan (Krug Life Sciences, Inc., Houston, TX.), and J. B. Charles (Space Biomedical Research Inst., Houston, TX.) *In* NASA. Johnson Space Center, Sixth Annual Workshop on Space Operations Applications and Research (SOAR 1992), Volume 2 Feb. 1993 p 598-604 (For primary document see N94-11527 01-99)
Avail: CASI HC A02/MF A03

N94-11558*# National Aeronautics and Space Administration. Lyndon B. Johnson Space Center, Houston, TX.
POTENTIAL HEALTH EFFECTS OF SPACE RADIATION
Chui-Hsu Yang and Laurie M. Craise (California Univ., Berkeley. Lawrence Berkeley Lab.) *In its* Sixth Annual Workshop on Space Operations Applications and Research (SOAR 1992), Volume 2 Feb. 1993 p 605-610 (For primary document see N94-11527 01-99)
(NASA Order T-9297-R)
Avail: CASI HC A02/MF A03

N94-11560*# Kelsey Seybold Clinic, P.A., Houston, TX.
LONGITUDINAL STUDY OF ASTRONAUT HEALTH: MORTALITY IN THE YEARS 1959-1991 Abstract Only
Leif E. Peterson *In* NASA. Johnson Space Center, Sixth Annual Workshop on Space Operations Applications and Research (SOAR 1992), Volume 2 Feb. 1993 p 613 (For primary document see N94-11527 01-99)
Avail: CASI HC A01/MF A03

53 BEHAVIORAL SCIENCES

Includes psychological factors; individual and group behavior; crew training and evaluation; and psychiatric research.

N94-10251# Japan Atomic Energy Research Inst., Tokyo.
FUNCTIONAL REASONING, EXPLANATION, AND ANALYSIS
B. H. Far (Japan Atomic Energy Research Inst., Tokai.) Jan. 1992 104 p
(DE92-526832; JAERI-M-91-225) Avail: CASI HC A06/MF A02

Functional Reasoning (FR) enables people to derive the purpose of objects and explain their functions, JAERI's 'Human Acts Simulation Program (HASP)', started from 1987, has the goal of developing programs of the underlying technologies for intelligent robots by imitating the intelligent behavior of humans. FR is considered a useful reasoning method in HASP and applied to understand function of tools and objects in the Toolbox Project. First, the results of the diverse FR researches within a variety of disciplines are reviewed and the common core and basic problems are identified. Then the qualitative function formation (QFF) technique is introduced. Some points are: extending the common qualitative models to include interactions and timing of events by defining temporal and dependency constraints, and binding it with the conventional qualitative simulation. Function concepts are defined as interpretations of either a persistence or an order in the sequence of states, using the trace of the qualitative state vector derived by qualitative simulation on the extended qualitative model. This offers solutions to some of the FR problems and leads to a method for generalization and comparison of functions of different objects. DOE

N94-10731# National Aerospace Lab., Tokyo (Japan). Computational Sciences Div.
SUBROUTINE FUNCTIONS FOR GENERATING ANIMATION DATA [ANIMESHON YOU GAZOU DETA SEISEI SABURUCHIN KINOU NITSUITE]
Kazuyo Suematsu Apr. 1992 37 p In JAPANESE Original contains color illustrations
(DE93-767973; NAL-TR-1147; JTN-93-80430) Avail: CASI HC A03/MF A01

Several subroutine functions are reported which enable data generated by computer numerical simulations to be more efficiently animated and visualized. Included are functions to transform graphic data, a function to display overlapped surfaces, functions which create images little by little, and functions which add annotations. Author (NASDA)

N94-10909 North Carolina Univ., Chapel Hill. Dept. of Psychology.
VISUAL ENCODING OF SPATIAL RELATIONS Annual Report
Christina A. Burbeck 26 May 1993 40 p Limited Reproducibility: More than 20% of this document may be affected by microfiche quality
(Contract F49620-92-J-0114)
(AD-A266049; AFOSR-93-0420TR) Avail: CASI HC A03

Psychophysical studies of the processes underlying spatial localization and their relationship to both lower and higher level processing were conducted. The spatial extent of position integration areas was measured and found to be adequate to account for the increase in separation discrimination thresholds with separation. The influence of the spatial frequency of embedded targets was investigated and found to be insignificant, as it had previously been found to be for isolated targets. The relationship between separation discrimination and object formation was investigated and a model of the process of object formation developed. Studies on how area is encoded were conducted and related to the model of object formation. DTIC

N94-11098# Naval Aerospace Medical Research Lab., Pensacola, FL.
LANDING CRAFT AIR CUSHION (LCAC) CREW SELECTION SYSTEM MANUAL Final Report, 1988 - 1992
Kathleen T. Helton, Tatree Nontasak, and Daniel L. Dolgin Dec. 1992 73 p
(AD-A265158; NAMRL-SR-92-4) Avail: CASI HC A04/MF A01

The Naval Aerospace Medical Research Laboratory developed and validated a crew selection test battery for the Landing Craft Air Cushion (LCAC) vehicle. This battery, now called the Landing Craft Air Cushion Crew Selection System (LCSS), has been operationally implemented. This user's manual provides system information, test administration, and data management procedures. In addition, information on the development of the LCSS, its hardware configuration, and software components are included. DTIC

N94-11511*# Virginia Univ., Charlottesville. Dept. of Psychology.
PERCEPTUAL RESPONSE TO VISUAL NOISE AND DISPLAY MEDIA Final Report, 1 Jul. 1992 - 30 Jun. 1993
Frank H. Durgin and Dennis R. Proffitt 30 Jun. 1993 15 p
(Grant NAG2-814)
(NASA-CR-193406; NAS 1.26:193406) Avail: CASI HC A03/MF A01

The present project was designed to follow up an earlier investigation in which perceptual adaptation in response to the use of Night Vision Goggles, or image intensification (I squared) systems, such as those employed in the military were studied. Our chief concern in the earlier studies was with the dynamic visual noise that is a byproduct of the I(sup 2) technology: under low light conditions, there is a great deal of 'snow' or sporadic 'twinkling' of pixels in the I(sup 2) display which is more salient as the ambient light levels are lower. Because prolonged exposure to static visual noise produces strong adaptation responses, we reasoned that the dynamic visual noise of I(sup 2) displays might have a similar effect, which could have implications for their long term use. However, in the series of experiments reported last year, no evidence at all of such aftereffects following extended exposure to I(sup 2) displays were found. This finding surprised us, and led us to propose the following studies: (1) an investigation of dynamic visual noise and its capacity to produce after effects; and (2) an investigation of the perceptual consequences of characteristics of the display media. Author (revised)

N94-11701# Office of Naval Research European Office, FPO New York, NY.
THE 27TH INTERNATIONAL APPLIED MILITARY PSYCHOLOGY SYMPOSIUM: A FOCUS ON DECISION MAKING RESEARCH
Stanley C. Collyer 4 Aug. 1992 74 p
(AD-A265278; ONREUR-92-4-W) Avail: CASI HC A04/MF A01

The first International Applied Military Psychology Symposium (IAMPS) was held in 1963. Since then it has evolved into an important forum for information exchange among European and North American military psychologists. A wide array of topics are typically covered. These include personnel selection and classification, manpower planning, leadership, stress, training, simulation, and human factors. DTIC

N94-11867# Army War Coll., Carlisle Barracks, PA.
AVIATORS, AIR COMBAT, AND COMBAT STRESS: AN AIR F ORCE COMMANDER'S PRIMER Study Project
Mark K. Wells 22 Feb. 1993 47 p
(AD-A265083) Avail: CASI HC A03/MF A01

There is currently no interdisciplinary study which surveys the U.S. Air Force's philosophical and organizational responses to the problems of combat fatigue or psychological collapse during the history of air war. While stress and battle shock casualties are topics of concern inside the military medical community, the subjects receive little attention from contemporary aircrew, or, more importantly, among Air Force squadron and wing commanders. This study begins with a brief look at the human dimension of airpower, examines some of the characteristics of airmen, and reviews the risky nature of the air combat environment. It goes on to describe the impact of stress on airmen and covers the Air Force's historical responses to them. More than a simple survey, however, this monograph will make specific recommendations regarding the education and training of commanders, officers, and airmen so they will be equipped to deal realistically with the potential problem of stress related casualties. DTIC

N94-11890# Naval Command, Control and Ocean Surveillance Center, San Diego, CA.
NONLINEAR RESONANCE: NOISE-ASSISTED INFORMATION PROCESSING IN PHYSICAL AND NEUROPHYSIOLOGICAL SYSTEMS
Adi Bulsara, John K. Douglass, and Frank Moss Apr. 1993 8 p
(AD-A265161) Avail: CASI HC A02/MF A01

The distinctive hiss of radio 'noise' is familiar to all of us old enough to have listened to vintage A.M. radio shows and certainly to all those personnel who ever tried to 'pull in' a weak signal during a tour in military communications. Indeed, virtually since the birth of the telephone and radio and extending to today's sophisticated telecommunications designs, engineers have devoted prodigious efforts to eliminating or minimizing the effects of noise. In consequence, an entire discipline, known as linear filter theory, has evolved and is familiar to every electrical engineering and/or communications student, usually as one or a set of rather rigorous courses. By contrast, this paper is concerned with a nonlinear filtering process known as Stochastic Resonance (SR), research on which has been supported by the Physics Division of the Office of Naval Research (ONR) for several years and more recently by the Cognitive and Neural Sciences Division of the ONR. DTIC

N94-12276# Air Force Systems Command, Brooks AFB, TX. Armstrong Lab.

BASIC ATTRIBUTES TEST (BAT): OPERATIONAL PRE-IMPLEMENTATION ANALYSIS AND SCORE EQUATING Interim Report, Aug. 1991 - Apr. 1992

Thomas R. Carretta and Malcolm J. Ree May 1993 82 p
(AF Proj. 7719)
(AD-A265885; AL-TP-1993-0015) Avail: CASI HC A05/MF A01

The Air Force will implement a new pilot candidate selection system. Scores from a multiple aptitude test (Air Force Officer Qualifying Test or AFOQT), a computer-based test (Basic Attributes Test or BAT), and biographical information will be used to compute a pilot candidate selection composite score derived from an equation designed to indicate probability of success in undergraduate pilot training (UPT). The purpose of this study was to equate the experimental and operational tests. The pre-implementation equating was necessary for the following reasons: (1) to determine whether the tests measured the same psychological constructs, (2) to compare operational score distributions, and (3) to develop equating tables. Equating was required so that scores from operational tests could be used in proposed pilot candidate selection equations developed on the experimental tests of the BAT. Experimental and operational tests were administered to about 2,000 basic recruits. Analyses were performed at the test score and composite score level and several types of equatings were completed. Adjusted correlations between the experimental and operational BAT tests were acceptable and demonstrated measurement equivalence. Differences in the shapes of the distributions (i.e., skewness, kurtosis) were observed for several of the scores between the two forms. Several types of equatings (linear, equipercentile, smoothed equipercentile) were performed to develop conversion tables for use during implementation of operational tests. Scores will be renormed to the operational test metric and a new pilot candidate selection composite will be developed after a sufficient number of applicants have been tested and have completed UPT. DTIC

N94-11530*# National Aeronautics and Space Administration. Ames Research Center, Moffett Field, CA.

TRANSFER OF TRAINING FOR AEROSPACE OPERATIONS: HOW TO MEASURE, VALIDATE, AND IMPROVE IT

Malcolm M. Cohen *In* NASA. Johnson Space Center, Sixth Annual Workshop on Space Operations Applications and Research (SOAR 1992), Volume 2 Feb. 1993 p 482-487 (For primary document see N94-11527 01-99)
Avail: CASI HC A02/MF A03

N94-11531*# National Aeronautics and Space Administration. Lyndon B. Johnson Space Center, Houston, TX.

SIGNAL DETECTION THEORY AND METHODS FOR EVALUATING HUMAN PERFORMANCE IN DECISION TASKS

Kevin OBrien (Lockheed Engineering and Sciences Co., Houston, TX.) and Evan M. Feldman (Rice Univ., Houston, TX.) *In its* Sixth Annual Workshop on Space Operations Applications and Research (SOAR 1992), Volume 2 Feb. 1993 p 489-496 (For primary document see N94-11527 01-99)
Avail: CASI HC A02/MF A03

N94-11532*# National Aeronautics and Space Administration. Ames Research Center, Moffett Field, CA.

CRITERIA FOR ASSESSING PROBLEM SOLVING AND DECISION MAKING IN COMPLEX ENVIRONMENTS Abstract Only

Judith Orasanu *In* NASA. Johnson Space Center, Sixth Annual Workshop on Space Operations Applications and Research (SOAR 1992), Volume 2 Feb. 1993 p 497 (For primary document see N94-11527 01-99)
Avail: CASI HC A01/MF A03

N94-11533*# Krug Life Sciences, Inc., San Antonio, TX.

MONITORING COGNITIVE FUNCTION AND NEED WITH THE AUTOMATED NEUROPSYCHOLOGICAL ASSESSMENT METRICS IN DECOMPRESSION SICKNESS (DCS) RESEARCH Abstract Only

Thomas E. Nesthus and Sammuel G. Schiflett (Aerospace Medical Research Labs., Brooks AFB, TX.) *In* NASA. Johnson Space Center, Sixth Annual Workshop on Space Operations Applications and Research (SOAR 1992), Volume 2 Feb. 1993 p 498 (For primary document see N94-11527 01-99)
Avail: CASI HC A01/MF A03

N94-11534*# Jet Propulsion Lab., California Inst. of Tech., Pasadena.

ANALYZING HUMAN ERRORS IN FLIGHT MISSION OPERATIONS

Kristin J. Bruno, Linda L. Welz, G. Michael Barnes (California State Univ., Northridge.), and Josef Sherif *In* NASA. Johnson Space Center, Sixth Annual Workshop on Space Operations Applications and Research (SOAR 1992), Volume 2 Feb. 1993 p 499-505 Sponsored by NASA, Washington (For primary document see N94-11527 01-99)
Avail: CASI HC A02/MF A03

N94-11536*# National Aeronautics and Space Administration. John F. Kennedy Space Center, Cocoa Beach, FL.

VIGILANCE PROBLEMS IN ORBITER PROCESSING

William W. Swart (University of Central Florida, Orlando.), Robert R. Safford (University of Central Florida, Orlando.), David B. Kennedy (University of Central Florida, Orlando.), Bert A. Yadi (University of Central Florida, Orlando.), and Timothy S. Barth *In* NASA. Johnson Space Center, Sixth Annual Workshop on Space Operations Applications and Research (SOAR 1992), Volume 2 Feb. 1993 p 512-515 (For primary document see N94-11527 01-99)
Avail: CASI HC A01/MF A03

N94-11538*# National Aeronautics and Space Administration. Lyndon B. Johnson Space Center, Houston, TX.

NOISE LEVELS AND THEIR EFFECTS ON SHUTTLE CREWMEMBERS' PERFORMANCE: OPERATIONAL CONCERNS

Anton S. Koros (Lockheed Engineering and Sciences Co., Houston, TX.), Susan C. Adam, and Charles D. Wheelwright (Lockheed Engineering and Sciences Co., Houston, TX.) *In its* Sixth Annual Workshop on Space Operations Applications and Research (SOAR 1992), Volume 2 Feb. 1993 p 522-528 (For primary document see N94-11527 01-99)
(Contract NAS9-17900)
Avail: CASI HC A02/MF A03

N94-11539*# Aerospace Medical Research Labs., Wright-Patterson AFB, OH.

VISUAL EARTH OBSERVATION PERFORMANCE IN THE SPACE ENVIRONMENT. HUMAN PERFORMANCE MEASUREMENT 4: FLIGHT EXPERIMENTS

John F. Huth, James D. Whiteley, and John E. Hawker *In* NASA. Johnson Space Center, Sixth Annual Workshop on Space Operations Applications and Research (SOAR 1992), Volume 2 Feb. 1993 p 529-539 (For primary document see N94-11527 01-99)
Avail: CASI HC A03/MF A03

N94-11570*# SRI International Corp., Menlo Park, CA.

FORECASTING THE IMPACT OF VIRTUAL ENVIRONMENT TECHNOLOGY ON MAINTENANCE TRAINING

Mark S. Schlager, Duane Boman, Tom Piantanida, and Robert Stephenson (Aerospace Medical Research Labs., Brooks AFB, TX.) *In* NASA. Johnson Space Center, Sixth Annual Workshop on Space Operations Applications and Research (SOAR 1992), Volume 2 Feb. 1993 p 691-699 Sponsored in part by AF (For primary document see N94-11527 01-99)
Avail: CASI HC A02/MF A03

54 MAN/SYSTEM TECHNOLOGY AND LIFE SUPPORT

Includes human engineering; biotechnology; and space suits and protective clothing.

For related information see also *16 Space Transportation.*

N94-10296# Naval Air Warfare Center, Warminster, PA. Air Vehicle and Crew Systems Technology Dept.

MASS PROPERTIES TEST PROCEDURE FOR MANIKIN HEADFORMS AND HELMET SYSTEMS Final Report

Jeffrey M. Thornton and David J. Zaborowski (KR Systems, Inc., Warminster, PA.) Oct. 1992 47 p

(AD-A265654; NAWCADWAR-92092-60) Avail: CASI HC A03/MF A01

The mathematical modeling and comparison of manikin headforms and helmet systems requires that the mass properties be accurately determined. The specific properties that must be known are the weight, center of gravity location, magnitudes of the principal moments of inertia and orientation of the principal axes. This data is compared to the specifications of a specific program and also provides insight into issues such as helmet comfort/fit, fatigue and head accelerations/neck forces during ejection or emergency landings. The Mass Properties (M.P.) System and associated software, provide a relatively simple method for measuring these mass properties. This document is intended for use by persons responsible for operating the M.P. System. Included in this report are theoretical calculations, a description of materials required, and step-by-step procedures for system set-up, calibration and determination of weight, center of gravity, and magnitude and orientation of the principal mass moments of inertia. DTIC

N94-10806# Federal Aviation Administration, Oklahoma City, OK. Civil Aeromedical Inst.

HEAD AND FACE ANTHROPOMETRY OF ADULT US CIVILIANS Final Report

Joseph W. Young Jul. 1993 43 p

(DOT/FAA/AM-93/10) Avail: CASI HC A03/MF A01

A total of 17 traditional and 5 new head and facial dimensions from a random, composite U.S. female and male civilian population measured over a period of 30 years are presented. The 5 new measurements, identified to describe specific anatomical relationships of the face, can have a direct influence on equipment design concepts. The survey population includes 376 (195 females and 172 males) adult subjects in the age range of 17 through 69 years representing a predominantly high ratio of Caucasian subjects to other ethnic origin subjects. The data summary format is specifically intended for basic design concept use. These dimensions describe essential anatomical characteristics for use as basic design criteria in the development of protective equipment for the head and face. Because of the lack of standardization of anatomical and anthropometrical terminology, a thesaurus of selected anatomical and anthropometrical terms, specific to descriptive labels used, is provided as a cross reference for anthropometrical dimensions. Author (revised)

N94-11258*# Bionetics Corp., Cocoa Beach, FL.

STATISTICAL ANALYSIS OF ENVIRONMENTAL VARIABILITY WITHIN THE CELSS BREADBOARD PROJECT'S BIOMASS PRODUCTION CHAMBER

G. W. Stutte, P. V. Chetirkin, C. L. Mackowiak, and R. E. Fortson Feb. 1993 39 p

(Contract NAS10-11624)

(NASA-TM-109188; NAS 1.15:109188; REV-399) Avail: CASI HC A03/MF A01

Variability in the aerial and root environments of NASA's Breadboard Project's Biomass Production Chamber (BPC) was determined. Data from two lettuce and two potato growouts were utilized. One growout of each crop was conducted prior to separating the upper and lower chambers; the other was subsequent to separation. There were little or no differences in pH, EC, or solution temperature between the upper and lower chamber or within a chamber. Variation in the aerial environment within a chamber was two to three times greater than variation between chambers for air temperature, relative humidity, and PPF. High variability in air velocity, relative to tray position, was observed. Separating the BPC had no effect on PPF, air velocity, solution temperature, pH, or EC. Separation reduced the gradient in air temperature and relative humidity between the upper and lower chambers, but increased the variability within a chamber. Variation between upper and lower chambers was within 5 percent of environmental set-points and of little or no physiological significance. In contrast, the variability within a chamber limits the capability of the BPC to generate statistically reliable data from individual tray treatments at this time. Author (revised)

N94-11291# Army Aeromedical Research Lab., Fort Rucker, AL.

CORRELATION OF HGU-56/P AIRCREW HELMET FITTING WITH HEAD ANTHROPOMETRIC MEASUREMENTS Final Report

James E. Bruckart, Kevin T. Mason, Samuel G. Shannon, William E. McLean, and Steven P. Pacquette Feb. 1993 31 p

(DA Proj. 3M1-62787-A-879)

(AD-A264988; USAARL-93-14) Avail: CASI HC A03/MF A01

The U.S. Army is developing an Aircrew Integrated Helmet System to replace the current flight helmets. The HGU-56/P flight helmet is proposed in six sizes with a new fitting method based on a nonstandard measure of the aviator head length. Standard anthropometric head measurements and the Gentex Corporation fitting method for the HGU-56/P flight helmet are evaluated to determine the applicability of the fitting method and distribution of helmet sizes required to fit the U.S. Army aviator population. Two hundred forty-two volunteer aviators had standard anthropometric measurements of their heads. Each was fitted with an HGU-561P flight helmet in their recommended size) and a helmet one size larger and one size smaller than recommended. ANVIS compatibility with each helmet was tested for a subset of the subjects. DTIC

N94-11375*# National Aeronautics and Space Administration. Ames Research Center, Moffett Field, CA.

ALLOWABLE EXPOSURE LIMITS FOR CARBON DIOXIDE DURING EXTRAVEHICULAR ACTIVITY

Andrew J. Seter Apr. 1993 42 p

(RTOP 506-71-00)

(NASA-TM-103832; A-91045; NAS 1.15:103832) Avail: CASI HC A03/MF A01

The intent was to review the research pertaining to human exposure to carbon dioxide (CO2) and to recommend allowable exposure limits for extravehicular activity (EVA). Respiratory, renal, and gastrointestinal systems may be adversely affected by chronic low dose CO2 exposure. Ventilation was increased 15 percent with 1 percent CO2 and 50 percent with 2 percent CO2. Chronic exposure to less than 2 percent CO2 led to 20 day cycles of uncompensated and compensated respiratory acidosis. Acid-base changes were small. Histopathologic changes in guinea pig lungs have been noted with long term exposure to 1 percent CO2. No changes were seen with exposure to 0.5 percent CO2. Cycling of bone calcium stores with associated changes in blood and urinary calcium levels occurs with long term CO2 exposure. Histologic changes in bone have been noted in guinea pigs exposed to 1 percent CO2. Renal calcification has been noted in guinea pigs with exposure to as low as 0.5 percent CO2. An increase in gastric acidity was noted in subjects with long term exposure to 1 percent CO2. Cardiovascular and neurologic function were largely unaffected. A decrease in the incidence of respiratory, renal, and gastrointestinal disease was noted in submariners coincident with a decrease in ambient CO2 from 1.2 percent to 0.8-0.9 percent. Oxygen (O2) and CO2 stimulate respiration independently and cumulatively. The addition of CO2 to high dose O2 led to the faster onset of seizure activity in mice. Experiments evaluating the physiologic responses to intermittent, repetitive exposures to low dose CO2 and 100 percent O2 mixtures should be performed. A reduction in the current NASA standard for CO2 exposure during EVA of 1 percent (7.6 mmHg) for nominal and 2 percent (15.2 mmHg) for heavy exertion to 0.5 percent (3.8 mmHg) for nominal and 1 percent (7.6 mmHg) for heavy exertion may be prudent. At a minimum, the current NASA standard should not be liberalized. Author (revised)

N94-11627*# ECC International Corp., Orlando, FL.

TEACHING HIGH-PERFORMANCE SKILLS USING ABOVE-REAL-TIME TRAINING

Dutch Guckenberger, Kevin C. Uliano (University of Central Florida, Orlando.), and Norman E. Lane (University of Central Florida, Orlando.) Aug. 1993 60 p Sponsored by NASA. Dryden Flight Research Facility

(Grant NAG2-750; RTOP 505-68-00)
(NASA-CR-4528; H-1919; NAS 1.26:4528) Avail: CASI HC A04/MF A01

The above real-time training (ARTT) concept is an approach to teaching high-performance skills. ARTT refers to a training paradigm that places the operator in a simulated environment that functions at faster than normal time. It represents a departure from the intuitive, but not often supported, feeling that the best practice is determined by the training environment with the highest fidelity. This approach is hypothesized to provide greater 'transfer value' per simulation trial, by incorporating training techniques and instructional features into the simulator. Two related experiments are discussed. In the first, 25 naive male subjects performed three tank gunnery tasks on a simulator under varying levels of time acceleration (i.e., 1.0x, 1.6x, 2.0x, sequential, and mixed). They were then transferred to a standard (1.0x) condition for testing. Every accelerated condition or combination of conditions produced better training and transfer than the standard condition. Most effective was the presentation of trials at 1.0x, 1.6x, and 2.0x in a random order during training. Overall, the best ARTT group scored about 50 percent higher and trained in 25 percent less time compared to the real-time control group. In the second experiment, 24 mission-capable F-16 pilots performed three tasks on a part-task F-16A flight simulator under varying levels of time compression (i.e., 1.0x, 1.5x, 2.0x, and random). All subjects were then tested in a real-time environment. The emergency procedure (EP) task results showed increased accuracy for the ARTT groups. In testing (transfer), the ARTT groups not only performed the EP more accurately, but dealt with a simultaneous enemy significantly better than a real-time control group. Although the findings on an air combat maneuvering task and stern conversion task were mixed, most measures indicated that the ARTT groups performed better and faster than a real-time control group. Other implications for ARTT are discussed along with future research directions. Author (revised)

N94-11642# Aeronautical Systems Div., Wright-Patterson AFB, OH.
A COMPARISON OF HEAD-UP AND HEAD-DOWN DISPLAY FORMATS DURING INSTRUMENT FLYING TASKS Final Report, Mar. 1991 - Oct. 1992
Thomas C. Hughes, John A. Hassoun, and James M. Barnaba Nov. 1992 109 p
(AD-A266140; ASC-TR-93-5003) Avail: CASI HC A06/MF A02

In March 1989, the Chief of Staff of the Air Force issued a study regarding the status of instrument flying within the Air Force. In that report, specific recommendations were presented, first of which was the necessity to develop a standardized HUD format suitable for use as a primary flight reference. Since that time a HUD symbology set was proposed and adopted conditional upon final validation as a primary flight reference. The present report documents the simulation phase of the validation process in which a total of 38 pilots participated. The validation of the symbology set consisted of a comparison of pilot performance data during three instrument flight tasks (1) Unusual Attitude Recovery, (2) Precision Approach, and (3) Precision Instrument Maneuvering. Results indicated that pilot data were significantly improved while flying with the HUD during the Precision Approach and Instrument Maneuvering tasks. During the Unusual Attitude Recovery tasks, no significant differences were demonstrated; however, the HUD symbology showed a trend toward faster reaction times, particularly for the nose low recoveries. Based on these results, the CSEF recommended initiation of the follow-on flight test phase of the validation process. DTIC

N94-12346# Air Force Systems Command, Wright-Patterson AFB, OH. Armstrong Lab.
ACCURACY AND REPEATABILITY OF THE STANDARD AUTOMATED MASS PROPERTIES MEASUREMENT SYSTEM Interim Report, Dec. 1991 - Sep. 1992
Brian P. Self, Eric K. Spittle, Ints Kaleps, and Christopher Albery Sep. 1992 54 p
(AF Proj. 7231)
(AD-A265897; AL-TR-1992-0137) Avail: CASI HC A04/MF A01

The injury potential to pilots may be significantly affected by the inertial properties of helmet-mounted equipment. In order to accurately assess the effects of such equipment, reliable measurements of mass, center of mass, and mass moments of inertia must be obtained. The Manikin Testing Laboratory at the Armstrong Laboratory has developed the Standard Automated Mass Properties (STAMP) system to experimentally determine the inertial properties of various objects. It is necessary to quantitatively determine the accuracy and repeatability of measurements obtained by the STAMP system to confidently use these values in analytical models, in correlations between observed empirical response and the inertial properties of head-mounted equipment, and in determining compliance with inertial properties specifications of new helmet-mounted systems. DTIC

N94-12365*# Iowa State Univ. of Science and Technology, Ames. Inst. for Physical Research and Technology.
SPACE LIFE SUPPORT ENGINEERING PROGRAM Annual Progress Report, 1 Jul. 1992 - 30 Jun. 1993
Richard C. Seagrave 30 Jun. 1993 245 p
(Grant NAG2-722)
(NASA-CR-193474; NAS 1.26:193474) Avail: CASI HC A11/MF A03

This report covers the second year of research relating to the development of closed-loop long-term life support systems. Emphasis was directed toward concentrating on the development of dynamic simulation techniques and software and on performing a thermodynamic systems analysis in an effort to begin optimizing the system needed for water purification. Four appendices are attached. The first covers the ASPEN modeling of the closed loop Environmental Control Life Support System (ECLSS) and its thermodynamic analysis. The second is a report on the dynamic model development for water regulation in humans. The third regards the development of an interactive computer-based model for determining exercise limitations. The fourth attachment is an estimate of the second law thermodynamic efficiency of the various units comprising an ECLSS. For individual titles, see N94-12366 through N94-12369.

N94-12366*# Iowa State Univ. of Science and Technology, Ames.
[SYSTEMS ANALYSIS OF A CLOSED LOOP ECLSS USING THE ASPEN SIMULATION TOOL. THERMODYNAMIC EFFICIENCY ANALYSIS OF ECLSS COMPONENTS] M.S. Thesis
Sharmista Chatterjee *In its* Space Life Support Engineering Program 30 Jun. 1993 135 p (For primary document see N94-12365 01-54)
Avail: CASI HC A07/MF A03

Our first goal in this project was to perform a systems analysis of a closed loop Environmental Control Life Support System (ECLSS). This pertains to the development of a model of an existing real system from which to assess the state or performance of the existing system. Systems analysis is applied to conceptual models obtained from a system design effort. For our modelling purposes we used a simulator tool called ASPEN (Advanced System for Process Engineering). Our second goal was to evaluate the thermodynamic efficiency of the different components comprising an ECLSS. Use is made of the second law of thermodynamics to determine the amount of irreversibility of energy loss of each component. This will aid design scientists in selecting the components generating the least entropy, as our penultimate goal is to keep the entropy generation of the whole system at a minimum. Derived from text

N94-12367*# Iowa State Univ. of Science and Technology, Ames.
[PHYSIOLOGICAL WATER MODEL DEVELOPMENT]
Susan Doty *In its* Space Life Support Engineering Program 29 p(SEE N94-12365 01-54) 30 Jun. 1993 (For primary document see N94-12365 01-54)
Avail: CASI HC A03/MF A03

The water of the human body can be categorized as existing in two main compartments: intracellular water and extracellular water. The intracellular water consists of all the water within the cells and constitutes over half of the total body water. Since red blood cells are surrounded by plasma, and all other cells are surrounded by interstitial fluid, the intracellular compartment has been subdivided to represent these two cell types. The extracellular water, which includes all of the fluid outside of the cells, can be further subdivided into compartments which represent the interstitial fluid, circulating blood plasma, lymph, and transcellular water. The interstitial fluid surrounds cells outside of the vascular system whereas plasma is contained within the blood vessels. Avascular tissues such as dense connective tissue and cartilage contain interstitial water which slowly equilibrates with tracers used to determine extracellular fluid volume. For this reason, additional compartments are sometimes used to represent these avascular tissues. The average size of each compartment, in terms of percent body weight, has been determined for adult males and females. These compartments and the forces which cause flow between them are presented. The kidneys, a main compartment, receive about 25 percent of the cardiac output and filters out a fluid similar to plasma. The composition of this filtered fluid changes as it flows through the kidney tubules since compounds are continually being secreted and reabsorbed. Through this mechanism, the kidneys eliminate wastes while conserving body water, electrolytes, and metabolites. Since sodium accounts for over 90 percent of the cations in the extracellular fluid, and the number of cations is balanced by the number of anions, considering the renal handling sodium and water only should sufficiently describe the relationship between the plasma compartment and kidneys. A kidney function model is presented which has been adapted from a previous model of normal renal function in man. To test the validity of the proposed kidney model, results predicted by the model will be compared to actual data involving injected or ingested fluids and subsequent urine flow rates. Comparison of the model simulation to actual data following the ingestion of 1 liter of water is shown. The model simulation is also shown with actual data following the intravenous infusion of hypertonic saline. Derived from text

N94-12368*# Iowa State Univ. of Science and Technology, Ames. Dept. of Chemical Engineering.

MODIFICATIONS TO AN INTERACTIVE MODEL OF THE HUMAN BODY DURING EXERCISE: WITH SPECIAL EMPHASIS ON THERMOREGULATION M.S. Thesis

Megan Kay Scherb *In its* Space Life Support Engineering Program 64 p(SEE N94-12365 01-54) 30 Jun. 1993 (For primary document see N94-12365 01-54)

Avail: CASI HC A04/MF A03

Since 1988 an interactive computer model of the human body during exercise has been under development by a number of undergraduate students in the Department of Chemical Engineering at Iowa State University. The program, written under the direction of Dr. Richard C. Seagrave, uses physical characteristics of the user, environmental conditions and activity information to predict the onset of hypothermia, hyperthermia, dehydration, or exhaustion for various levels and durations of a specified exercise. The program however, was severely limited in predicting the onset of dehydration due to the lack of sophistication with which the program predicts sweat rate and its relationship to sensible water loss, degree of acclimatization, and level of physical training. Additionally, it was not known whether sweat rate also depended on age and gender. For these reasons, the goal of this creative component was to modify the program in the above mentioned areas by applying known information and empirical relationships from literature. Furthermore, a secondary goal was to improve the consistency with which the program was written by modifying user input statements and improving the efficiency and logic of the program calculations. Derived from text

N94-12369*# Iowa State Univ. of Science and Technology, Ames.

[AN ESTIMATE OF THE SECOND LAW THERMODYNAMIC EFFICIENCY OF THE VARIOUS UNITS COMPRISING AN ENVIRONMENTAL CONTROL AND LIFE SUPPORT SYSTEM (ECLSS)]

Sharmista Chatterjee and Richard C. Seagrave *In its* Space Life Support Engineering Program 12 p(SEE N94-12365 01-54) 30 Jun. 1993 Presented at the International Conference on Environmental Science, Jul. 1993 (For primary document see N94-12365 01-54)

Avail: CASI HC A03/MF A03

The objective of this paper is to present an estimate of the second law thermodynamic efficiency of the various units comprising an Environmental Control and Life Support System (ECLSS). The technique adopted here is based on an evaluation of the 'lost work' within each functional unit of the subsystem. Pertinent information for our analysis is obtained from a user interactive integrated model of an ECLSS. The model was developed using ASPEN. A potential benefit of this analysis is the identification of subsystems with high entropy generation as the most likely candidates for engineering improvements. This work has been motivated by the fact that the design objective for a long term mission should be the evaluation of existing ECLSS technologies not only the basis of the quantity of work needed for or obtained from each subsystem but also on the quality of work. In a previous study Brandhorst showed that the power consumption for partially closed and completely closed regenerable life support systems was estimated as 3.5 kw/individual and 10-12 kw/individual respectively. With the increasing cost and scarcity of energy resources, our attention is drawn to evaluate the existing ECLSS technologies on the basis of their energy efficiency. In general the first law efficiency of a system is usually greater than 50 percent. From literature, the second law efficiency is usually about 10 percent. The estimation of second law efficiency of the system indicates the percentage of energy degraded as irreversibilities within the process. This estimate offers more room for improvement in the design of equipment. From another perspective, our objective is to keep the total entropy production of a life support system as low as possible and still ensure a positive entropy gradient between the system and the surroundings. The reason for doing so is as the entropy production of the system increases, the entropy gradient between the system and the surroundings decreases, and the system will gradually approach equilibrium with the surroundings until it reaches the point where the entropy gradient is zero. At this point no work can be extracted from the system. This is called the 'dead state' of the system. Author

N94-11528*# Veterans Administration Hospital, Sepulveda, CA.

QUANTITATIVE EEG PATTERNS OF DIFFERENTIAL IN-FLIGHT WORKLOAD

M. B. Sterman, C. A. Mann, and D. A. Kaiser *In* NASA. Johnson Space Center, Sixth Annual Workshop on Space Operations Applications and Research (SOAR 1992), Volume 2 Feb. 1993 p 466-473 Prepared in cooperation with California Univ., Los Angeles (For primary document see N94-11527 01-99)

Avail: CASI HC A02/MF A03

N94-11529*# Aerospace Medical Research Labs., Wright-Patterson AFB, OH. Human Engineering Div.

PSYCHOPHYSIOLOGICAL MEASURES OF COGNITIVE WORKLOAD IN LABORATORY AND FLIGHT

Glenn F. Wilson and Albert Badeau *In* NASA. Johnson Space Center, Sixth Annual Workshop on Space Operations Applications and Research (SOAR 1992), Volume 2 Feb. 1993 p 474-481 (For primary document see N94-11527 01-99)

Avail: CASI HC A02/MF A03

N94-11537*# Lockheed Engineering and Sciences Co., Houston, TX.

MEASURING HUMAN PERFORMANCE ON NASA'S MICROGRAVITY AIRCRAFT

Randy B. Morris and Mihriban Whitmore *In* NASA. Johnson Space Center, Sixth Annual Workshop on Space Operations Applications and Research (SOAR 1992), Volume 2 Feb. 1993 p 516-521 (For primary document see N94-11527 01-99)

Avail: CASI HC A02/MF A03

N94-11540*# Krug Life Sciences, Inc., San Antonio, TX.

USE OF ULTRASOUND IN ALTITUDE DECOMPRESSION MODELING Abstract Only

Robert M. Olson and Andrew A. Pilmanis (Aerospace Medical Research Labs., Brooks AFB, TX.) *In* NASA. Johnson Space Center, Sixth Annual Workshop on Space Operations Applications and Research (SOAR 1992), Volume 2 Feb. 1993 p 543 (For primary document see N94-11527 01-99)

Avail: CASI HC A01/MF A03

N94-11541*# Krug Life Sciences, Inc., San Antonio, TX.

HYPOBARIC DECOMPRESSION PREBREATHE REQUIREMENTS AND BREATHING ENVIRONMENT Abstract Only

James T. Webb and Andrew A. Pilmanis (Aerospace Medical Research Labs., Brooks AFB, TX.) *In* NASA. Johnson Space Center, Sixth Annual Workshop on Space Operations Applications and Research (SOAR 1992), Volume 2 Feb. 1993 p 544 (For primary document see N94-11527 01-99)

Avail: CASI HC A01/MF A03

N94-11549*# Aerospace Medical Research Labs., Brooks AFB, TX. Sustained Operations Branch.

A PROTOTYPE URINE COLLECTION DEVICE FOR FEMALE AIRCREW

Roger U. Bisson and Karlyna L. Delger *In* NASA. Johnson Space Center, Sixth Annual Workshop on Space Operations Applications and Research (SOAR 1992), Volume 2 Feb. 1993 p 570-573 (For primary document see N94-11527 01-99)

Avail: CASI HC A01/MF A03

N94-11553*# National Aeronautics and Space Administration. Lyndon B. Johnson Space Center, Houston, TX.

COMPREHENSIVE ANALYSIS OF AIRBORNE CONTAMINANTS FROM RECENT SPACELAB MISSIONS

M. L. Matney (Krug Life Sciences, Inc., Houston, TX.), J. F. Boyd (Krug Life Sciences, Inc., Houston, TX.), P. A. Covington (Krug Life Sciences, Inc., Houston, TX.), H. J. Leano (Krug Life Sciences, Inc., Houston, TX.), D. L. Pierson, T. F. Limero (Krug Life Sciences, Inc., Houston, TX.), and J. T. James *In its* Sixth Annual Workshop on Space Operations Applications and Research (SOAR 1992), Volume 2 Feb. 1993 p 579-588 (For primary document see N94-11527 01-99)
Avail: CASI HC A02/MF A03

N94-11554*# National Aeronautics and Space Administration. Lyndon B. Johnson Space Center, Houston, TX.

TOXICITY STUDY OF DIMETHYLETHOXYSILANE (DMSES), THE WATERPROOFING AGENT FOR THE ORBITER HEAT PROTECTIVE SYSTEM Abstract Only

Chiu-Wing Lam (Krug Life Sciences, Inc., Houston, TX.), John T. James, Darol Dodd (ManTech Environmental Technology, Inc., Upton, NY.), Bruce Stuart (ManTech Environmental Technology, Inc., Upton, NY.), Simon Rothenberg (ManTech Environmental Technology, Inc., Upton, NY.), Mary Ann Kershaw (Brookhaven National Lab., Upton, NY.), and A. Thilagar (Sitek Research Labs., Rockville, MD.) *In its* Sixth Annual Workshop on Space Operations Applications and Research (SOAR 1992), Volume 2 Feb. 1993 p 589 (For primary document see N94-11527 01-99)
Avail: CASI HC A01/MF A03

N94-11555*# National Aeronautics and Space Administration. Lyndon B. Johnson Space Center, Houston, TX.

A COMBUSTION PRODUCTS ANALYZER FOR CONTINGENCY USE DURING THERMODEGRADATION EVENTS ON SPACECRAFT

Steve Wilson (Krug Life Sciences, Inc., Houston, TX.), Thomas F. Limero (Krug Life Sciences, Inc., Houston, TX.), Steve W. Beck (Krug Life Sciences, Inc., Houston, TX.), and John T. James *In its* Sixth Annual Workshop on Space Operations Applications and Research (SOAR 1992), Volume 2 Feb. 1993 p 590-596 (For primary document see N94-11527 01-99)
Avail: CASI HC A02/MF A03

N94-11561*# National Aeronautics and Space Administration. Lyndon B. Johnson Space Center, Houston, TX.

OPERATIONAL RADIOLOGICAL SUPPORT FOR THE US MANNED SPACE PROGRAM Abstract Only

Michael J. Golightly, Alva C. Hardy, William Atwell (Rockwell International Corp., Houston, TX.), Mark D. Weyland (Rockwell International Corp., Houston, TX.), John Kern (Rockwell International Corp., Houston, TX.), and Bernard L. Cash (Lockheed Engineering and Sciences Co., Houston, TX.) *In its* Sixth Annual Workshop on Space Operations Applications and Research (SOAR 1992), Volume 2 Feb. 1993 p 614 (For primary document see N94-11527 01-99)
Avail: CASI HC A01/MF A03

55 SPACE BIOLOGY

Includes exobiology; planetary biology; and extraterrestrial life.

N94-10865*# Cornell Univ., Ithaca, NY.

[PREPARING FOR THE INITIAL OBSERVATIONS OF THE TARGETED SEARCH AND THE SKY SURVEY SYSTEMS] Final Report

Michael M. Davis 20 Jan. 1993 2 p
(Grant NAG2-696)
(NASA-CR-193644; NAS 1.26:193644) Avail: CASI HC A01/MF A01

During this period, the SETI project prepared for the initial observations with both the Targeted Search and Sky Survey systems. I am nominally a member of the Targeted Search team, but participated actively in both parts of the project. My activities were concentrated primarily in three areas: coordination with Arecibo Observatory in preparation for the initial observations on October 12, 1992; development of a design concept for confirming observations; and participation (at JPL) in a design review of the rf system. Derived from text

59 MATHEMATICAL AND COMPUTER SCIENCES (GENERAL)

N94-10814*# National Aeronautics and Space Administration. Langley Research Center, Hampton, VA.

PROGRESS IN MULTIDISCIPLINARY DESIGN OPTIMIZATION AT NASA LANGLEY

Sharon L. Padula Jul. 1993 22 p Presented at the SIAM Annual Meeting, Philadelphia, PA, 12-16 Jul. 1993
(RTOP 505-63-36-06)
(NASA-TM-107754; NAS 1.15:107754) Avail: CASI HC A03/MF A01

Multidisciplinary Design Optimization refers to some combination of disciplinary analyses, sensitivity analysis, and optimization techniques used to design complex engineering systems. The ultimate objective of this research at NASA Langley Research Center is to help the US industry reduce the costs associated with development, manufacturing, and maintenance of aerospace vehicles while improving system performance. This report reviews progress towards this objective and highlights topics for future research. Aerospace design problems selected from the author's research illustrate strengths and weaknesses in existing multidisciplinary optimization techniques. The techniques discussed include multiobjective optimization, global sensitivity equations and sequential linear programming. Author

N94-11198*# Institute for Computer Applications in Science and Engineering, Hampton, VA.

[SUMMARY OF RESEARCH IN PROGRESS AT ICASE] Semiannual Report, 1 Oct. 1992 - 31 Mar. 1993

Jun. 1993 71 p
(Contract NAS1-19480; RTOP 505-90-52-01)
(NASA-CR-191481; NAS 1.26:191481) Avail: CASI HC A04/MF A01

This report summarizes research conducted at the Institute for Computer Applications in Science and Engineering in applied mathematics, fluid mechanics, and computer science during the period October 1, 1992 through March 31, 1993. Author

N94-11678 Army Research Office, Research Triangle Park, NC.

TRANSACTIONS OF THE 10TH ARMY CONFERENCE ON APPLIED MATHEMATICS AND COMPUTING

Mar. 1993 792 p Conference held in West Point, NY, 16-19 Jun. 1992
Limited Reproducibility: More than 20% of this document may be affected by microfiche quality
(AD-A265098) Avail: CASI HC A99

The Tenth Army Conference on Applied Mathematics and Computing was held at the U.S. Military Academy, West Point, on 16-19 June 1992. The 1992 conference was attend by more than 80 scientists and engineers representing various Army agencies and academia. The meeting featured seven invited speakers. These general talks covered several topics of current interest, including natural language processing, wavelet analysis, variational methods, small sample asymptotics, computational fluid dynamics, digital control programs, and parallel programming. The second part of the program consisted of special sessions on topics such as computational algebraic geometry, mathematical aspects of material sciences, scalability in high performance computing, and robust control and nonlinear systems. DTIC

N94-11817# Mathematical Association of America, Inc., Washington, DC.

CAREER INFORMATION IN THE MATHEMATICAL SCIENCES (CIMS) Annual Technical Progress Report

Andrew Sterrett May 1993 16 p Presented at the CBMS Council Meeting, Washington, DC, 1-2 May 1993
(Contract DE-FG02-93ER-75840)
(DE93-013780; DOE/ER-75840/1) Avail: CASI HC A03/MF A01

In Nov. 1992, a CBMS Steering Committee for Career Information was appointed by the CBMS Council. An informal meeting of those members in attendance at the Annual Meeting of the MAA and the AMS was held in Jan. 1993. The first meeting was held on 1-2 May in Washington, DC in conjunction with the CBMS Council meeting. Information on existing career materials was provided to the Council at that time and Council reactions were obtained. These reactions, along with reviews of material by students, faculty members, and counselors, were used by the Steering Committee to plan specific activities for the next 6-18 months. Three initiatives were given high priority: To produce and widely disseminate an annotated bibliography of career information relevant to the mathematical sciences; to remedy the lack of messages to junior high school students, parents, teachers and counselors on the importance of mathematics in finding good jobs in a technological society; and to encourage women and minorities to take all the mathematics that they can and to consider careers in which mathematics plays an important role. DOE

60 COMPUTER OPERATIONS AND HARDWARE

Includes hardware for computer graphics, firmware, and data processing.

For components see *33 Electronics and Electrical Engineering.*

N94-10146# Sandia National Labs., Albuquerque, NM.

RADIATION HARDENED NONVOLATILE MEMORY FOR SPACE AND STRATEGIC APPLICATIONS

M. Jacunski (Westinghouse Electric Corp., Linthicum Heights, MD.), D. Williams (Westinghouse Electric Corp., Linthicum Heights, MD.), D. Adams (Westinghouse Electric Corp., Linthicum Heights, MD.), R. Bishop (Westinghouse Electric Corp., Linthicum Heights, MD.), J. Murray, J. Jakubczak, and J. Rodriguez 1992 6 p Presented at the Government Microcircuit Applications Conference: Microelectronics in the New World Order, Las Vegas, NV, 9-12 Nov. 1992
(Contract DE-AC04-76DP-00789)
(DE93-000746; SAND-92-2043C; CONF-921188-1) Avail: CASI HC A02/MF A01 (US Sales Only)

As system complexity increases, so too do the nonvolatile memory needs for the storage of data and microcode. Electrically erasable programmatic read only memories (EEPROM's) are also the frequent choice for applications which in the past have been satisfied by read only memories (ROM's). For system engineers. the ability to electrically reprogram a system module on the fly is indispensable. Two different modes of operation must be considered when evaluating the radiation hardness of EEPROMS. For ROM applications, little if any programming occurs in the radiation environment, and only the read mode need be considered. The chip must (1) retain the information throughout the irradiation, and (2) maintain the functionality of the peripheral circuits necessary for reading the data. For nonvolatile SRAM type applications, the chip must also function in the write mode during the exposure. Unfortunately, commercial EEPROM's have not kept pace with the aggressive radiation specifications of many space and strategic systems. Several studies indicate that the most popular commercial floating gate (FG) technologies manufactured by Xicor, Atmel, and Seeq fail after total doses of just 4 to 18 Krad(Si) in the read mode and after less than 5 Krad(Si) in the write mode. In fact, the very nature of the commercial FG technology has been shown to be limited to a hardness of less than 100 Krad(Si). A 64K EEPROM designed by Sandia National Laboratories (SNL) and manufactured by Westinghouse Electric Corporation (WEC) is described. It is pin for pin compatible with commercial 64K EEPROMS. The nonvolatile memory clement is fabricated with a silicon/oxide/ nitride/oxide/semiconductor (SONOS) technology for which 1 Mrad(Si) hardness was demonstrated. In addition, the CMOS peripheral circuitry was hardened using techniques developed for Westinghouse's radiation hardened gate array products. DOE

N94-10268# Sandia National Labs., Albuquerque, NM.

AN ACCOUNT OF SANDIA'S RESEARCH BOOTH AT SUPERCOMPUTING 1992: A COLLABORATIVE EFFORT IN HIGH-PERFORMANCE COMPUTING AND NETWORKING

A. Breckenridge and M. O. Vahle Mar. 1993 15 p
(Contract DE-AC04-76DP-00789)
(DE93-012397; SAND-93-0224) Avail: CASI HC A03/MF A01

Supercomputing '92, a high-performance computing and communications conference was held during 16-20 Nov. 1992 in Minneapolis, Minnesota. This paper documents the applications and technologies that were showcased in Sandia's research booth at that conference. In particular the demonstrations in high-performance networking, audio-visual applications in engineering, virtual reality, and supercomputing applications are all described. DOE

N94-10278# Universiteit Twente, Enschede (Netherlands). Dept. of Computer Science.

FINITE STATE MACHINE MICROARCHITECTURE TRANSFORMATIONS DESCRIBED WITH RELATIONAL ALGEBRA

A. J. W. M. tenBerg Oct. 1992 43 p
(Memo-INF-92-63; ETN-93-94320) Copyright Avail: CASI HC A03/MF A01

A number of microarchitecture alternatives for the controlpath implementation of finite state machines by means of relational algebra are described. Relational algebra, developed for database design, can also be applied for hardware microarchitecture design. Relational algebra makes it easy to prove that the set of hardware functions in a decomposition perform a functional behavior equivalent to that of the canonical function. It describes operations on tables that represent the hardware functions. Such decompositions represent microarchitectures of the finite state machines in a direct way. Different finite state machine microarchitectures, formerly viewed as separate alternatives, are derived from each other by transformations described by short operation sequences. The traditionally algorithmically described Mealy to Moore machine transformation can be described in only a few operations with relational algebra. ESA

N94-10318# Argonne National Lab., IL. High Energy Physics Div.

A PROOF-OF-CONCEPT IMPLEMENTATION OF PERSISTENCE IN A HIERARCHICAL STORAGE SYSTEM

R. Grossman, Xiao Qin, and D. Lifka 1992 6 p Presented at the 12th IEEE Symposium on Mass Storage Systems, Monterey, CA, 25 Apr. 1993
(Contract W-31-109-eng-38)
(DE93-009959; ANL-HEP-CP-92-100; CONF-930461-2) Avail: CASI HC A02/MF A01

The concept of providing transparent access to a collection of files in a mass storage system is a familiar one. The goal of this project was to investigate the feasibility of providing similar access to a collection of persistent, complex objects. We describe an architecture for interfacing a persistent store of complex objects to a hierarchical storage system. Persistent object stores support the uniform creation, storage, and access of complex objects, regardless of their lifetimes. In other words, a mechanism is provided so that persistent objects outlive the processes which create them and can be accessed in a uniform manner by other processes. We validated this architecture by implementing a proof-of-concept system and testing the system on two stores of data. These tests indicate that this architecture supports the creation, storage and access of very large persistent object stores. DOE

N94-10724*# National Aeronautics and Space Administration. Lewis Research Center, Cleveland, OH.

DISTRIBUTED SIMULATION USING A REAL-TIME SHARED MEMORY NETWORK

Donald L. Simon, Duane L. Mattern (Sverdrup Technology, Inc., Bay Saint Louis, MS.), Edmond Wong, and Jeffrey L. Musgrave Jul. 1993 20 p
(DA Proj. 1L1-61102-AH-45; RTOP 505-62-50)
(NASA-TM-106239; E-7969; NAS 1.15:106239; AVSCOM-TR-92-C-020)
Avail: CASI HC A03/MF A01

The Advanced Control Technology Branch of the NASA Lewis Research Center performs research in the area of advanced digital controls for aeronautic and space propulsion systems. This work requires the real-time implementation of both control software and complex dynamical models of the propulsion system. We are implementing these systems in a distributed, multi-vendor computer environment. Therefore, a need exists for real-time communication and synchronization between the distributed multi-vendor computers. A shared memory network is a potential solution which offers several advantages over other real-time communication approaches. A candidate shared memory network was tested for basic performance. The shared memory network was then used to implement a distributed simulation of a ramjet engine. The accuracy and execution time of the distributed simulation was measured and compared to the performance of the non-partitioned simulation. The ease of partitioning the simulation, the minimal time required to develop for communication between the processors and the resulting execution time all indicate that the shared memory network is a real-time communication technique worthy of serious consideration.
Author (revised)

N94-11294# Rochester Univ., NY. Dept. of Computer Science.
ALLEVIATING MEMORY CONTENTION IN MATRIX COMPUTATIONS ON LARGE-SCALE SHARED-MEMORY MULTIPROCESSORS
Ricardo Bianchini, Mark E. Crovella, Leonidas I. Kontothanassis, and Thomas J. LeBlanc Apr. 1993 24 p
(Contract N00014-92-J-1801; NSF CDS-88-22724; ARPA Order 8930)
(AD-A265009; TR-449) Avail: CASI HC A03/MF A01

Memory contention can be a major source of overhead in large-scale shared-memory multiprocessors. There are many hardware solutions, but they are often complex and expensive, so software solutions are an attractive alternative. This paper evaluates one solution, block-column allocation, which is very effective at reducing memory contention for a large class of SPMD (Single-Program-Multiple-Data) programs, and can be implemented easily by the compiler. We first quantify the impact of memory contention on performance by simulating the execution of several application kernels on a large-scale multiprocessor. Our simulation results confirm that memory contention is widespread on large-scale machines; our applications suggest that contention is usually caused by synchronized access to a range of addresses (rather than to a single address). We show that block-column allocation can nearly eliminate this source of memory contention. As our main contribution, we compare block-column allocation to row-major allocation and logarithmic broadcasting. Our analysis demonstrates the clear superiority of block-column allocation over row-major allocation in the presence of memory contention. DTIC

N94-11875# Naval Postgraduate School, Monterey, CA.
GALLIUM ARSENIDE DYNAMIC RANDOM ACCESS MEMORY SUPPORT CIRCUITRY M.S. Thesis
Michael A. Morris Mar. 1993 528 p
(AD-A265176) Avail: CASI HC A23/MF A04

This thesis presents the design and layout of a Gallium Arsenide (GaAs) Dynamic Random Access Memory (DRAM) array of eight four-bit words including refresh circuitry. In the last several years, there has been significant research investigating the possibilities of producing fast, low power, and high density DRAM's using GaAs. Thus far, this research has yielded success on a limited basis using special materials and fabrication techniques. This design, tested and simulated using HSPICE, supports a memory access time of approximately three nanoseconds, faster than present commercial Static Random Access Memory (SRAM). The logic circuits are designed using GaAs enhancement-mode and depletion-mode (E/D) metal semiconductor field-effect transistors (MESFET's). Charge storage is facilitated by a single GaAs MESFET connected to a parallel plate capacitor and the required minimum time between refresh is approximately three milliseconds. Power consumption is acceptable and fabrication by Vitesse Semiconductor Corporation using the HGaAs3 process is in progress. The design techniques, power consumption, and timing are discussed and demonstrated for the basic logic circuits and the memory array read, write, and refresh cycles. A significant increase in DRAM memory bandwidth is gained narrowing the memory bandwidth differential between primary memory and the processor. DTIC

N94-12558*# Georgia Inst. of Tech., Atlanta. Center for Human-Machine Systems Research.
COGNITIVE ENGINEERING MODELS: A PREREQUISITE TO THE DESIGN OF HUMAN-COMPUTER INTERACTION IN COMPLEX DYNAMIC SYSTEMS Final Technical Report, 1 Jul. 1990 - 30 Nov. 1993
Christine M. Mitchell Jun. 1993 22 p
(Grant NAG9-422)
(NASA-CR-193472; NAS 1.26:193472) Avail: CASI HC A03/MF A01

This chapter examines a class of human-computer interaction applications, specifically the design of human-computer interaction for the operators of complex systems. Such systems include space systems (e.g., manned systems such as the Shuttle or space station, and unmanned systems such as NASA scientific satellites), aviation systems (e.g., the flight deck of 'glass cockpit' airplanes or air traffic control) and industrial systems (e.g., power plants, telephone networks, and sophisticated, e.g., 'lights out,' manufacturing facilities). The main body of human-computer interaction (HCI) research complements but does not directly address the primary issues involved in human-computer interaction design for operators of complex systems. Interfaces to complex systems are somewhat special. The 'user' in such systems - i.e., the human operator responsible for safe and effective system operation - is highly skilled, someone who in human-machine systems engineering is sometimes characterized as 'well trained, well motivated'. The 'job' or task context is paramount and, thus, human-computer interaction is subordinate to human job interaction. The design of human interaction with complex systems, i.e., the design of human job interaction, is sometimes called cognitive engineering. Author (revised)

61 COMPUTER PROGRAMMING AND SOFTWARE

Includes computer programs, routines, alogorithms, and specific applications, e.g., CAD/CAM.

N94-10164# Universiteit Twente, Enschede (Netherlands). Tele-Informatics and Open Systems Group.
BUNDLE EVENT STRUCTURES: A NON-INTERLEAVING SEMANTICS FOR LOTOS
Rom Langerak 11 Oct. 1992 20 p Sponsored in part by EEC
(Memo-INF-92-73; TIOS-92/30; ETN-93-94321) Copyright Avail: CASI HC A03/MF A01

The semantic model of bundle event structures, using a so called bundle set instead of a causality or flow relation, are defined. Several laws for set equivalence are presented. A representation called clean bundle event structures and an algorithm to turn any bundle event structure into a clean one are provided. Bundle event structures have an attractive graphical representation; the analysis is facilitated by providing several equivalence laws. Like in flow and stable event structures, events can be enabled in different ways. There are no self conflicting events like in flow event structures. Impossible events that can never happen but can always be removed are considered. A bundle event structure semantics is given for a Basic LOTOS subset containing all operators except disabling and process instantiation. This semantics is proven correct with respect to a simple event transition system. ESA

N94-10166# Universiteit Twente, Enschede (Netherlands). Dept. of Computer Science.
AN OBJECT-ORIENTED MODEL FOR EXTENSIBLE CONCURRENT SYSTEMS: THE COMPOSITION-FILTERS APPROACH
Lodewijk Bergmans, Mehmet Aksit, Ken Wakita, and Akinori Yonezawa (Tokyo Univ., Japan.) Dec. 1992 45 p
(Memo-INF-92-87; ETN-93-94325) Copyright Avail: CASI HC A03/MF A01

A new language model based on the concept of object composition filters is proposed. A composition filter is a modular extension to the conventional object model. It is able to express concurrency and synchronization mechanisms integrated with the concept of inheritance. The background and related work in the area of object oriented concurrent programming and synchronization are described. Inheritance anomalies and requirements of concurrent object oriented systems are studied. The mechanisms to support extensible concurrency and synchronization using composition filters are presented. Examples to demonstrate the capabilities of the proposed mechanisms to solve some well known synchronization problems are included. Examples in four different categories were chosen: process communication and coordination, implementation of functions, scheduling, and resource management. The composition filters model is evaluated with respect to the requirements. ESA

N94-10167# Universiteit Twente, Enschede (Netherlands). Dept. of Computer Science.
A CORRECT AND EFFICIENT INTERFACE FOR LOGICAL QUERY LANGUAGES WITH COMPLEX OBJECTS
Marcel Holsheimer, Rolf A. deBy, and Hassan Ait-Kaci Jan. 1993 14 p
(Memo-INF-93-01; ETN-93-94326) Copyright Avail: CASI HC A03/MF A01

A formal design for a logical query language using psi terms as data structures to interact effectively and efficiently with a relational database is described. The structure of psi terms provides an adequate representation for so called complex objects. They generalize conventional terms used in

logic programming: they are typed attributed structures, ordered thanks to a subtype ordering. Unification of psi terms is an effective means for integrating multiple inheritance and partial information into a deduction process. A compact database representation for psi terms, representing part of the subtyping relation in the database as well is defined. A retrieval algorithm based on an abstract interpretation of the psi term unification process is presented and its formal correctness is proven. This algorithm is efficient in that it incrementally retrieves only additional facts that are actually needed by a query, and never retrieves the same fact twice.
ESA

N94-10263# Lawrence Livermore National Lab., CA.
PANACEA USER'S MANUAL FOR PANACEA VERSION 2.0
S. A. Brown and D. Braddy Jan. 1993 99 p Revised
(Contract W-7405-eng-48)
(DE93-012502; LLNL-M-276-Rev-2) Avail: CASI HC A05/MF A02

A numerical simulation code is fundamentally a device to solve an initial value problem. Very often these programs are written starting with the routines that solve some system of equations. Unless care is taken to formulate these routines with regard to a host of issues (e.g., data flow), it can be very awkward to set up a problem or to look at the answers that the code returns. Furthermore, it can be nearly impossible to take advantage of some of the excellent work that various groups have done (e.g., equation solver packages) because the data flow and structuring issues have not been given sufficient attention in the program design stages. One way to avoid some of these difficulties is to write the data flow controls, the I/O mechanisms, and the database manager first. With these parts in place, there is a great deal of guidance for building the parts of a simulation code that deals with the specific set of equations to be solved; thus initial value data is input, and the solution is written out clearly and conveniently. Furthermore, this approach provides a basis for defining some conventions to allow the sharing of simulation modules. It also helps isolate the machine dependencies of a code in a very few places, which greatly enhances the portability of the code. PANACEA is a library of routines built to address these issues. In essence, PANACEA attempts to embody all of the functionality of a numerical simulation code, which is generic to all simulation codes. It accomplishes this by implementing a model of the simulation as a system of services (routines), which are bound together with the simulation specific routines provided by the code developer. One useful result of this approach is that it effectively imposes a discipline for the development of simulation codes that promote shareability, portability, and inter-operability.
DOE

N94-10265# Universiteit Twente, Enschede (Netherlands). Faculty of Applied Mathematics.
THE SUPER VECTORFIELD PACKAGE FOR REDUCE. VERSION 1.0
G. H. Marcel Roelofs Nov. 1992 21 p
(MEMO-1099; ETN-93-94312) Avail: CASI HC A03/MF A01

The super vectorfield package implements Z(sub 2) graded vectorfields and their action on Z(sub 2) graded functions in local coordinates in REDUCE. It can be used for the computation of symmetries and prolongation structures of (supersymmetric) systems of partial differential equations. The package is based on a former package developed by other investigators. A short description of the local picture of a graded manifold and vectorfields on these graded manifolds is given. An implementation of the vectorfields as algebraic operators is presented. Two procedures for extending the number of variables of a vectorfield are included. Simplified procedures to implement the action of a vectorfield and for multiplying two graded expressions are shown.
ESA

N94-10267# Lawrence Livermore National Lab., CA.
SURVEY TO DETERMINE THE VALUE OF DYNA
J. W. Walter and D. Bellshaw Jan. 1993 36 p
(Contract W-7405-eng-48)
(DE93-012390; UCRL-ID-112607) Avail: CASI HC A03/MF A01

This report presents the value of the DYNA software program to US Industry. The software conducts dynamic finite element analysis tailored specifically to simulating high energy impacts, such as car crashes or aircraft collisions with birds. DYNA is available at nearly zero cost to the public in two-dimensional (DYNA2D) and three-dimensional versions (DYNA3D). DYNA has had a major impact on US industry. Measuring this impact using conventional approaches, such as profitability or revenue size, does not apply to DYNA. A new approach is needed to estimate DYNA's value to US industry. Our challenge was two fold: (1) to develop a methodology for valuing technology transferred to the public domain; and (2) to apply this methodology to DYNA. We accomplished the evaluation task by using indirect measurements of value. These indicators encompassed three broad categories, answering three key questions: (1) Use of DYNA and 'DYNA-like' codes--Are companies, academic institutions, government agencies actually using DYNA and codes like it? (2) Savings generated from using these codes--Is the use of DYNA and codes like it creating a positive economic impact? and (3) Market size of all 'DYNA-like' codes--Has a commercial market developed for 'DYNA-like' codes? This study represents the results of interviews with people identified by Lawrence Livermore National Laboratory (LLNL) as users of DYNA. Some of the people surveyed for this study do not use DYNA. They rely upon other dynamic finite element analysis codes. We refer to these individuals as users of 'DYNA-like' codes or 'codes like DYNA.' Several of the 'DYNA-like' codes used DYNA as their core. These codes are descendants of DYNA.
DOE

N94-10291# Lawrence Livermore National Lab., CA.
VIRTUAL SOUND FOR VIRTUAL REALITY
Meera M. Blattner and Albert L. Papp, III Feb. 1993 7 p Presented at the 1993 Virtual Reality System, New York, NY, 15-17 Mar. 1993
(Contract W-7405-eng-48)
(DE93-010519; UCRL-JC-112806; CONF-9303127-1) Avail: CASI HC A02/MF A01

The computational limitations of real-time interactive computing do not meet our requirements for producing realistic images for virtual reality in a convincing manner. Regardless of the real-time restrictions on virtual reality interfaces, the representations can be no better than the graphics. Computer graphics is still limited in its ability to generate complex objects such as landscapes and humans. Nevertheless, useful and convincing visualizations are made through a variety of techniques. The central theme of this article is that a similar situation is true with sound for virtual reality. It is beyond our ability to create interactive soundscapes that create a faithful reproduction of real world sounds, however, by choosing one's application carefully and using sound to enhance a display rather than only mimic real-world scenes, a very effective use of sound can be made.
DOE

N94-10335# Planning Research Corp., Alexandria, VA.
SOFTWARE USABILITY ASSESSMENT GUIDE Final Report
Glade M. Bishop, Raymond J. Moffett, Rebecca Lickiss, and William Bourne 11 Apr. 1993 110 p Prepared in cooperation with American Systems Corp., Chantilly, VA
(Contract MDA903-88-D-0019)
(AD-A265017) Avail: CASI HC A06/MF A02

This guide shows independent operational evaluators and operational testers how to measure the usability (or User Friendliness) of computer software components that require human interaction. It shows how to measure the effectiveness and efficiency of human interactions with the software components of any weapon, equipment, computer, or information mission area system. The methodology in the guide can be applied during any phase of the Acquisition Process. It also addresses the inherent trainability of software components. It covers interfaces, preparation of questionnaires and other data collection instruments, data analysis, and the development of Usability Profiles to describe all the software interfaces of a system. It contains lists of questionnaire and checklist items, and examples of questionnaires, used to gather data on User Friendliness and human factors (or MANPRINT).
DTIC

N94-10343*# Nebraska Univ., Lincoln. Dept. of Electrical Engineering.
[STUDIES AND SIMULATIONS OF THE DigiCipher SYSTEM]
Semiannual Status Report, 15 Dec. 1992 - 15 Jun. 1993
K. Sayood, Y. C. Chen, and G. Kipp 1993 65 p
(Grant NAG5-1612)
(NASA-CR-193470; NAS 1.26:193470) Avail: CASI HC A04/MF A01

During this period the development of simulators for the various high definition television (HDTV) systems proposed to the FCC was continued. The FCC has indicated that it wants the various proposers to collaborate on a single system. Based on all available information this system will look very much like the advanced digital television (ADTV) system with major contributions only from the DigiCipher system. The results of our simulations of the DigiCipher system are described. This simulator was tested using test sequences from the MPEG committee. The results are extrapolated to HDTV video sequences. Once again, some caveats are in order. The sequences used for testing the simulator and generating the results are those used for testing the MPEG algorithm. The sequences are of much lower resolution than the HDTV sequences would be, and therefore the extrapolations are not totally accurate. One would expect to get significantly higher compression in terms of bits per pixel with sequences that are of higher resolution. However, the simulator itself is a valid one, and should HDTV sequences become available, they could be used directly with the simulator. A brief overview of the DigiCipher system is given. Some coding results obtained using the simulator are looked at. These results are compared to those obtained using the ADTV system. These results are evaluated in the context of the CCSDS specifications and make some suggestions as to how the DigiCipher system could be implemented in the NASA network. Simulations such as the ones reported can be biased depending on the particular source sequence used. In order to get more complete information about the system one needs to obtain a reasonable set of models which mirror the various kinds of sources encountered during video coding. A set of models which can be used to effectively model the various possible scenarios is provided. As this is somewhat tangential to the other work reported, the results are included as an appendix. Author (revised)

N94-10347# Lawrence Livermore National Lab., CA.
TECHNIQUES, PROCESSES, AND MEASURES FOR SOFTWARE SAFETY AND RELIABILITY
D. Sparkman 30 May 1992 55 p
(Contract W-7405-eng-48)
(DE93-012379; UCRL-ID-108725) Avail: CASI HC A04/MF A01

The purpose of this report is to provide a detailed survey of current recommended practices and measurement techniques for the development of reliable and safe software-based systems. This report is intended to assist the United States Nuclear Reaction Regulation (NRR) in determining the importance and maturity of the available techniques and in assessing the relevance of individual standards for application to instrumentation and control systems in nuclear power generating stations. Lawrence Livermore National Laboratory (LLNL) provides technical support for the Instrumentation and Control System Branch (ICSB) of NRR in advanced instrumentation and control systems, distributed digital systems, software reliability, and the application of verification and validation for the development of software. DOE

N94-10355# Technische Univ., Delft (Netherlands). Faculty of Technical Mathematics and Informatics.
A SIMPLICIAL APPROACH TO INTEGER PROGRAMMING
Chuangyin Dang and Hans vanMaaren 1993 28 p
(Rept-93-06; ETN-93-94301) Copyright Avail: CASI HC A03/MF A01

An algorithm to find an integral point in a polytope is proposed. It is based on an integer labelling rule and a triangulation of the space. It is proved that the algorithm determines an integral point in a polytope from a certain class. Numerical tests show the efficiency of the algorithm. The basic idea of the algorithm is to subdivide R(to the nth power) into simplices with integral vertices and assign an integer to each point in R(to the nth power). ESA

N94-10410 International Centre for Theoretical Physics, Trieste (Italy).
MODEL-BASED RECOGNITION OF 3-D OBJECTS BY GEOMETRIC HASHING TECHNIQUE
M. Severcan (Middle East Technical Univ., Ankara, Turkey.) and H. Uzunalioglu (Middle East Technical Univ., Ankara, Turkey.) Sep. 1992 14 p Limited Reproducibility: More than 20% of this document may be affected by microfiche quality
(DE93-612916; IC-92/295) Avail: Issuing Activity (Department of Energy (DOE)) (US Sales Only)

A model-based object recognition system is developed for recognition of polyhedral objects. The system consists of feature extraction, modeling, and matching stages. Linear features are used for object descriptions. Lines are obtained from edges using rotation transform. For modeling and recognition process, geometric hashing method is utilized. Each object is modeled using 2-D views taken from the viewpoints on the viewing sphere. A hidden line elimination algorithm is used to find these views from the wire frame model of the objects. The recognition experiments yielded satisfactory results. DOE

N94-10418# Universiteit Twente, Enschede (Netherlands). Faculty of Applied Mathematics.
THE INTEGRATOR PACKAGE FOR REDUCE, VERSION 1.0
G. H. Marcel Roelofs Nov. 1992 34 p
(MEMO-1100; ETN-93-94313) Avail: CASI HC A03/MF A01

The INTEGRATOR package for REDUCE can be used to solve overdetermined systems of partial differential equations. In particular those occurring in the computation of symmetries and prolongation structures of (supersymmetric) systems of partial differential equations. The package is based on a former package developed just for the determination of symmetry groups. The reasons for the implementation of this package is the need to have one combined integrator for both cases and the availability of improved versions of some of the procedures used in former packages. Additional tools for solving more equations at a time or for solving 'exceptional' equations are provided. ESA

N94-10419# Universiteit Twente, Enschede (Netherlands). Faculty of Applied Mathematics.
ALGORITHMS FOR THE MAXIMUM CLIQUE PROBLEM
J. P. vandenBerg Nov. 1992 12 p
(MEMO-1101; ETN-93-94314) Avail: CASI HC A03/MF A01

An arbitrary undirected graph G = (V,E) without multiple edges and loops is given, where V is the set of vertices and E is the set of edges. A clique is a subset of V in which all vertices are pairwise adjacent. A maximum clique is a clique with the highest cardinality in G. The algorithms presented to solve the maximum clique problem apply a branch and bound strategy. The structure of the branch and bound search tree is discussed. The branches of the branch and bound search tree which are the best to be proceeded are described. The performance of the algorithms is evaluated, using computer implementations on several random graphs with up to 3000 vertices and over one million edges. As benchmarks two algorithms are used that appeared to be the fastest algorithms known in the literature. The computational results suggest that the algorithms presented are faster than the algorithms in the literature. ESA

N94-10484# China Nuclear Information Centre, Beijing.
A FLEXIBLE MODELLING SOFTWARE FOR DATA ACQUISITION
Yantai Shu, Yanhui Chen, Songqi Yang, and Genchen Liu (Academia Sinica, Hefei, China.) Mar. 1992 15 p
(DE93-612915; CNIC-00599; ASIPP-0031) Avail: CASI HC A03/MF A01 (US Sales Only)

A flexible modeling software for data acquisition is based on an event-driven simulator. It can be used to simulate a wide variety of systems which can be modeled as open queuing networks. The main feature of the software is its flexibility to evaluate the performance of various data acquisition system, whether pulsed or not. The flexible features of this software are as follows: The user can choose the number of processors in the model and the route which every job takes to move the model. The service rate of a processor is automatically adapted. The simulator has a pipe-line mechanism. A job can be divided into several segments and a processor may be used as a compression component etc. Some modeling techniques and applications of this software in plasma physics laboratories are also presented. DOE

N94-10492# Southern Methodist Univ., Dallas, TX. Dept. of Computer Science and Engineering.
OPTIMIZATION ALGORITHMS FOR INTEGER NETWORKS WITH SIDE CONSTRAINTS FOR APPLICATION IN ROUTING AND SCHEDULING
Final Technical Report, 1 Jan. - 31 Dec. 1992
Jeffery L. Kennington 22 Feb. 1993 124 p
(Contract F49620-92-J-0032)
(AD-A265254; AFOSR-93-0295TR) Avail: CASI HC A06/MF A02

This document presents a new serial and parallel algorithms for the on-to-one shortest problem. This is the current best algorithms for this problem and we believe that our software implementation is the world's fastest code. Other algorithms for various network models, including the pure network problem, the generalized problem, and the multicommodity network problem with a piecewise linear convex cost function, are also presented. DTIC

N94-10494 Software Productivity Solutions, Inc., Indialantic, FL.
SYSTEM ENGINEERING CONCEPT DEMONSTRATION, TECHNOLOGY ASSESSMENTS, VOLUME 5 Final Report, Feb. 1990 - Jul. 1992
Guy Ivie and Sharon Rohde Dec. 1992 98 p Limited Reproducibility: More than 20% of this document may be affected by microfiche quality
(Contract F30602-90-C-0021)
(AD-A265471; RL-TR-92-345-Vol-5) Avail: CASI HC A05

The document is organized into six sections: (1) Integrated Workstations and Software Tools; (2) Peripherals; (3) Workplace Software; (4) Framework Software; (5) Tools; and (6) Conclusions. DTIC

N94-10495 Software Productivity Solutions, Inc., Indialantic, FL.
SYSTEM ENGINEERING CONCEPT DEMONSTRATION, TRADE STUDIES, VOLUME 6 Final Report, Feb. 1990 - Jul. 1992
Andres Rudmik, Edward Comer, and Sharon Rohde Dec. 1992 124 p Limited Reproducibility: More than 20% of this document may be affected by microfiche quality
(Contract F30602-90-C-0021)
(AD-A265472; RL-TR-92-345-Vol-6) Avail: CASI HC A06

The document is organized into five sections: (1) Environmental Studies; (2) SECD Environment and Rationale; (3) Technology Demonstrations; (4) Prototypes; and (5) Risk Evaluation. DTIC

N94-10639*# National Aeronautics and Space Administration. Lewis Research Center, Cleveland, OH.
SUBBAND/TRANSFORM FUNCTIONS FOR IMAGE PROCESSING
Daniel Glover Jun. 1993 37 p
(RTOP 144-10-10)
(NASA-TM-106183; E-7888; NAS 1.15:106183) Avail: CASI HC A03/MF A01

Functions for image data processing written for use with the MATLAB(TM) software package are presented. These functions provide the capability to transform image data with block transformations (such as the Walsh Hadamard) and to produce spatial frequency subbands of the transformed data. Block transforms are equivalent to simple subband systems. The transform coefficients are reordered using a simple permutation to give subbands. The low frequency subband is a low resolution version of the original image, while the higher frequency subbands contain edge information. The transform functions can be cascaded to provide further decomposition into more subbands. If the cascade is applied to all four of the first stage subbands (in the case of a four band decomposition), then a uniform structure of sixteen bands is obtained. If the cascade is applied only to the low frequency subband, an octave structure of seven bands results. Functions for the inverse transforms are also given. These functions can be used for image data compression systems. The transforms do not in themselves produce data compression, but prepare the data for quantization and compression. Sample quantization functions for subbands are also given. A typical compression approach is to subband the image data, quantize it, then use statistical coding (e.g., run-length coding followed by Huffman coding) for compression. Contour plots of image data and subbanded data are shown. Author (revised)

N94-10643*# Institute for Computer Applications in Science and Engineering, Hampton, VA.
LOW LATENCY MESSAGES ON DISTRIBUTED MEMORY MULTIPROCESSORS Final Report
Matthew Rosing and Joel Saltz (Maryland Univ., College Park.) Washington Jun. 1993 21 p Submitted for publication
(Contracts NAS1-19480; NAS1-18605; RTOP 505-90-52-01)
(NASA-CR-191479; NAS 1.26:191479; ICASE-93-30) Avail: CASI HC A03/MF A01

Many of the issues in developing an efficient interface for communication on distributed memory machines are described and a portable interface is proposed. Although the hardware component of message latency is less than one microsecond on many distributed memory machines, the software latency associated with sending and receiving typed messages is on the order of 50 microseconds. The reason for this imbalance is that the software interface does not match the hardware. By changing the interface to match the hardware more closely, applications with fine grained communication can be put on these machines. Based on several tests that were run on the iPSC/860, an interface that will better match current distributed memory machines is proposed. The model used in the proposed interface consists of a computation processor and a communication processor on each node. Communication between these processors and other nodes in the system is done through a buffered network. Information that is transmitted is either data or procedures to be executed on the remote processor. The dual processor system is better suited for efficiently handling asynchronous communications compared to a single processor system. The ability to send data or procedure is very flexible for minimizing message latency, based on the type of communication being performed. The test performed and the proposed interface are described. Author (revised)

N94-10711*# Texas Univ., Austin. Dept. of Computer Science.
SYSTEM MONITORING AND DIAGNOSIS WITH QUALITATIVE MODELS Final Report, 1 Mar. 1988 - 30 Sep. 1991
Benjamin Kuipers 30 Sep. 1991 17 p
(Grant NAG2-507)
(NASA-CR-193812; NAS 1.26:193812) Avail: CASI HC A03/MF A01

A substantial foundation of tools for model-based reasoning with incomplete knowledge was developed: QSIM (a qualitative simulation program) and its extensions for qualitative simulation; Q2, Q3 and their successors for quantitative reasoning on a qualitative framework; and the CC (component-connection) and QPC (Qualitative Process Theory) model compilers for building QSIM QDE (qualitative differential equation) models starting from different ontological assumptions. Other model-compilers for QDE's, e.g., using bond graphs or compartmental models, have been developed elsewhere. These model-building tools will support automatic construction of qualitative models from physical specifications, and further research into selection of appropriate modeling viewpoints. For monitoring and diagnosis, plausible hypotheses are unified against observations to strengthen or refute the predicted behaviors. In MIMIC (Model Integration via Mesh Interpolation Coefficients), multiple hypothesized models of the system are tracked in parallel in order to reduce the 'missing model' problem. Each model begins as a qualitative model, and is unified with a priori quantitative knowledge and with the stream of incoming observational data. When the model/data unification yields a contradiction, the model is refuted. When there is no contradiction, the predictions of the model are progressively strengthened, for use in procedure planning and differential diagnosis. Only under a qualitative level of description can a finite set of models guarantee the complete coverage necessary for this performance. The results of this research are presented in several publications. Abstracts of these published papers are presented along with abtracts of papers representing work that was synergistic with the NASA grant but funded otherwise. These 28 papers include but are not limited to: 'Combined qualitative and numerical simulation with Q3'; 'Comparative analysis and qualitative integral representations'; 'Model-based monitoring of dynamic systems'; 'Numerical behavior envelopes for qualitative models'; 'Higher-order derivative constraints in qualitative simulation'; and 'Non-intersection of trajectories in qualitative phase space: a global constraint for qualitative simulation.' Derived from text

N94-10862*# Texas Univ., Brownsville.
STABILITY BY LINEAR PROCESSES
1993 9 p
(Grant NAG5-2210)
(NASA-CR-194131; NAS 1.26:194131) Avail: CASI HC A02/MF A01

An algorithm is developed to find a quick way to determine the origin O in the complex plane C within the image of Q (a subset of the parameter space R(sup n)) under the multilinear function p(j omega, q) = f(q) + g(q)j for a fixed omega. Derived from text

N94-10878# Groningen Rijksuniv. (Netherlands). Computing Science Section.
WAIT-FREE LINEARIZATION WITH AN ASSERTIONAL PROOF
Wim H. Hesselink Dec. 1992 31 p
(CS-9208; WHH-139-0; ETN-93-94346) Copyright Avail: CASI HC A03/MF A01

A wait-free implementation of an arbitrary data object that requires memory of order n(exp 2) and that has a time complexity of order n is presented. Given a sequential implementation of an arbitrary data object, a wait-free, linearizable concurrent implementation is constructed with space complexity quadratic in the number of processes. The worst case time complexity is linear in the number of processes. The construction is based on a compare and swap register. The programming notations, the granularity of the commands, the data objects, and concurrent linearizable implementations of data objects are explained. An easier algorithm that uses an atomic action with a larger grain of atomicity than compare and swap registers is given. The actions on the main shared variables are shown, and the linearizability under assumption of seven invariants is demonstrated. The abstract algorithm is extended with private computations and with communication by means of other shared variables. The correctness of the program is proven by means of invariants and stability properties. ESA

N94-10893# Aircraft Research Association Ltd., Bedford (England).
GENERATION AND ANALYSIS OF HYBRID STRUCTURED/UNSTRUCTURED GRIDS
P. N. Childs and J. A. Shaw Apr. 1992 10 p Presented at the ICFD Conference on Numerical Methods for Fluid Dynamics, Reading, England, 7-10 Apr. 1992
(Contract SLS41B/2437)
(ARA-Memo-365) Avail: CASI HC A02/MF A01

The development of a hybrid structured/unstructured grid generation strategy is pursued. Automatic and flexible techniques are introduced for the generation of such meshes whereby local regions of unstructured grid are embedded within a global block-structured environment. Author

N94-10932*# Mississippi State Univ., Mississippi State. Dept. of Electrical and Computer Engineering.
AN INVESTIGATION OF ERROR CHARACTERISTICS AND CODING PERFORMANCE Annual Report, Jan. - Aug. 1993
William J. Ebel and Frank M. Ingels Aug. 1993 122 p
(Grant NAG5-2006)
(NASA-CR-193620; NAS 1.26:193620) Avail: CASI HC A06/MF A02

The first year's effort on NASA Grant NAG5-2006 was an investigation to characterize typical errors resulting from the EOS dorn link. The analysis methods developed for this effort were used on test data from a March 1992 White Sands Terminal Test. The effectiveness of a concatenated coding scheme of a Reed Solomon outer code and a convolutional inner code versus a Reed Solomon only code scheme has been investigated as well as the effectiveness of a Periodic Convolutional Interleaver in dispersing errors of certain types. The work effort consisted of development of software that allows simulation studies with the appropriate coding schemes plus either simulated data with errors or actual data with errors. The software program is entitled Communication Link Error Analysis (CLEAN) and models downlink errors, forward error correcting schemes, and interleavers. Derived from text

N94-10942*# Toledo Univ., OH. Dept. of Computer Science and Engineering.
EFFICIENT PARTITIONING AND ASSIGNMENT ON PROGRAMS FOR MULTIPROCESSOR EXECUTION Final Technical Report, 8 Feb. 1989 - 1 Oct. 1992
Hilda M. Standley 12 Jul. 1993 189 p
(Grant NAG3-975)
(NASA-CR-193458; NAS 1.26:193458) Avail: CASI HC A09/MF A02

The general problem studied is that of segmenting or partitioning programs for distribution across a multiprocessor system. Efficient partitioning and the assignment of program elements are of great importance since the time consumed in this overhead activity may easily dominate the computation, effectively eliminating any gains made by the use of the parallelism. In this study, the partitioning of sequentially structured programs (written in FORTRAN) is evaluated. Heuristics, developed for similar applications are examined. Finally, a model for queueing networks with finite queues is developed which may be used to analyze multiprocessor system architectures with a shared memory approach to the problem of partitioning. The properties of sequentially written programs form obstacles to large scale (at the procedure or subroutine level) parallelization. Data dependencies of even the minutest nature, reflecting the sequential development of the program, severely limit parallelism. The design of heuristic algorithms is tied to the experience gained in the parallel splitting. Parallelism obtained through the physical separation of data has seen some success, especially at the data element level. Data parallelism on a grander scale requires models that accurately reflect the effects of blocking caused by finite queues. A model for the approximation of the performance of finite queueing networks is developed. This model makes use of the decomposition approach combined with the efficiency of product form solutions. Author

N94-11031 Academy of Sciences of the Ukraine, Kiev. Inst. Yadernykh Issledovanij.
THE GRAPHICAL LIBRARY FOR TECHNOLOGICAL PROCESS AUTOMATIZATION [GRAFICHESKAYA BIBLIOTEKA DIYA AVTOMATIZATSII TEKHNOLOGICHESKIKH PROTSESSOV]
S. B. Kumshaev, E. V. Tkachenko, V. N. Gerasko, and A. P. Spektorovskij 1992 23 p In RUSSIAN Limited Reproducibility: More than 20% of this document may be affected by microfiche quality
(DE93-621316; KIYal-92-9) Avail: CASI HC A03 (US Sales Only)

The graphics library for computer-aided manufacturing and its subprograms are described. The developed algorithm for closed range stroking is realized. DOE

N94-11046*# Research Inst. for Advanced Computer Science, Moffett Field, CA.
THE 1987 RIACS ANNUAL REPORT
20 Jun. 1987 70 p
(Contract NCC2-387)
(NASA-CR-193220; NAS 1.26:193220) Avail: CASI HC A04/MF A01

The Research Institute for Advanced Computer Science (RIACS) was established at the NASA Ames Research Center in June of 1983. RIACS is privately operated by the Universities Space Research Association (USRA), a consortium of 64 universities with graduate programs in the aerospace sciences, under several Cooperative Agreements with NASA. RIACS's goal is to provide preeminent leadership in basic and applied computer science research as partners in support of NASA's goals and missions. In pursuit of this goal, RIACS contributes to several of the grand challenges in science and engineering facing NASA: flying an airplane inside a computer; determining the chemical properties of materials under hostile conditions in the atmospheres of earth and the planets; sending intelligent machines on unmanned space missions; creating a one-world network that makes all scientific resources, including those in space, accessible to all the world's scientists; providing intelligent computational support to all stages of the process of scientific investigation from problem formulation to results dissemination; and developing accurate global models for climatic behavior throughout the world. In working with these challenges, we seek novel architectures, and novel ways to use them, that exploit the potential of parallel and distributed computation and make possible new functions that are beyond the current reach of computing machines. The investigation includes pattern computers as well as the more familiar numeric and symbolic computers, and it includes networked systems of resources distributed around the world. We believe that successful computer science research is interdisciplinary: it is driven by (and drives) important problems in other disciplines. We believe that research should be guided by a clear long-term vision with planned milestones. And we believe that our environment must foster and exploit innovation. Our activities and accomplishments for the calendar year 1987 and our plans for 1988 are reported. Author (revised)

N94-11099# Naval Aerospace Medical Research Lab., Pensacola, FL.
COMPUTER SOFTWARE AND HARDWARE TO DETERMINE CONTRAST SENSITIVITY USING THREE METHODS: TRACKING, LIMITS, AND CONSTANT STIMULI Interim Report
Donald J. Hatcher, Terry L. DeVietti, and John A. DAndrea Dec. 1992 64 p
(AD-A265168; NAMRL-TM-92-4) Avail: CASI HC A04/MF A01

The software and hardware to obtain contrast sensitivity functions in a single session with monkeys are described. The versatility of the software allows the program to be used in a variety of sensory systems with minor programming modifications. It will permit absolute or difference threshold measurements with any one of three methods of threshold testing: (1) method of tracking; (2) method of limits; and (3) method of constant stimuli. DTIC

N94-11104 SRI International Corp., Menlo Park, CA.
A REAL-TIME SPOKEN-LANGUAGE SYSTEM FOR INTERACTIVE PROBLEM SOLVING Final Report
Patti J. Price and Robert C. Moore May 1993 177 p Limited Reproducibility: More than 20% of this document may be affected by

microfiche quality
(Contract N00014-90-C-0085)
(AD-A266046) Avail: CASI HC A09

SRI International (SRI) has carried out a three-year project to develop spoken-language understanding technology for interactive problem solving. The technology should have the following features: real-time performance, large vocabulary, high semantic accuracy, habitability, and robustness. This technology has been developed using an Air Travel Information System (ATIS) as a prototype application. We have developed technology that enables a user to retrieve airline schedules, fares, and related information by means of spoken natural-language queries. We have evaluated this technology in four ATIS benchmark evaluations, and we have incorporated it into a demonstration system, which we have also used for data collection. This final report consists of a summary of the research and other activities carried out under the project, followed by an Appendix containing 26 technical papers describing work performed on the project. The report covers work on speech recognition, natural-language understanding, speech and natural-language integration, data collection and analysis, performance evaluation, demonstration systems, and related activities. DTIC

N94-11109# Sandia National Labs., Albuquerque, NM.
USING A PRIVATE SMDS/ATM NETWORK TO PROVIDE LONG-HAUL SUPERCOMPUTING VISUALIZATION SERVICES
J. H. Naegle, N. Testi, C. Pavlakos, and H. Chen 1993 11 p Presented at the Gray Users Group Conference, Montreaux, Switzerland, 29 Mar. - 2 Apr. 1993
(Contract DE-AC04-76DP-00789)
(DE93-010692; SAND-93-0892C; CONF-9303131-1) Avail: CASI HC A03/MF A01

Sandia National Laboratories is prototyping a service for providing a distributed visualization capability between its Albuquerque, New Mexico and Livermore, California sites. The service will allow TCP/EP LAN users to process computationally intensive codes on the Cray Y-MP 8/864 and use the Application Visualization System, (AVS) running on a visualization server to display the results to desktops in Livermore (or Albuquerque). The long-haul environment presents several technical challenges such as high delays (up to 42 milliseconds), potential error rates, and security concerns which can affect the quality of the services. The network design requires low latency switch gear and high speed LAN connections (FDDI) to make the visualization/computational services useful to the customer. This paper will describe the network design used and will report performance characteristics of the applications utilizing this service. DOE

N94-11112# Lawrence Livermore National Lab., CA.
OBJECT ORIENTED IMPLEMENTATION OF ADAPTIVE MESH REFINEMENT ALGORITHMS
W. Y. Crutchfield and M. L. Welcome Apr. 1993 15 p Presented at the Object-Oriented Numerics Conference, Sunriver, OR, 25-27 Apr. 1993
(Contract W-7405-eng-48)
(DE93-011885; UCRL-JC-113502; CONF-9304114-1) Avail: CASI HC A03/MF A01

We describe C++ classes that simplify development of Adaptive Mesh Refinement (AMR) algorithms. The classes divide into two groups, generic classes that are broadly useful in adaptive algorithms, and application-specific classes that are the basis for our AMR algorithm. We employ two languages, with C++ responsible for the high-level data structures, and FORTRAN responsible for low-level numerics. The C++ implementation is as fast as the original FORTRAN implementation. Use of inheritance has allowed us to extend the original AMR algorithm to other problems with greatly reduced development time. DOE

N94-11123# Sandia National Labs., Albuquerque, NM.
ANIMATING ENGINEERING SCIENCE RESULTS USING AVS
J. F. Mareda 1993 2 p Presented at the Application Visualization System 1993 Users Group Meeting, Orlando, FL, 24-26 May 1993
(Contract DE-AC04-76DP-00789)
(DE93-011591; SAND-93-0921C; CONF-9305168-1) Avail: CASI HC A01/MF A01

This report discusses animating engineering science using an animation visualization system. DOE

N94-11139# General Atomic Co., San Diego, CA.
USER'S MANUAL FOR THE DAD-1 DATA ACQUISITION DAUGHTER BOARD FOR THE SUPERCARD-2
J. R. Ferron May 1993 45 p
(Contract DE-AC03-89ER-51114)
(DE93-012153; GA-A-21236) Avail: CASI HC A03/MF A01

A detailed description of how to use the DAD-1 data acquisition daughter board is given. The DAD-1 daughter board is used with the SuperCard-2, a VME format processor board manufactured by CSP Inc. that is based on the Intel i860 microprocessor. The daughter board provides high speed acquisition of digital data through a general purpose input port. Data are transferred through direct memory access operations to the memory on the SuperCard-2 board at a rate up to 40 million, 14 bit samples per second. A first-in, first-out memory is used to buffer the data during the transfer. Several different data acquisition operating modes are available that make a combination of a SuperCard-2 processor board and a DAD-1 daughter board suitable for a wide range of real time data analysis and feedback control functions. DOE

N94-11166# Instituto de Pesquisas Espaciais, Sao Jose dos Campos (Brazil).
VISUALIZATION AND SIMULATION OF A REAL PHYSICAL PROBLEM BASED ON PHYSICAL MODELING WITH THE USE OF COMPUTER ANIMATION Thesis [VISUALIZACAO E SIMULCAO DE UM PROBLEMA FISICO REAL BASEADAS EM MODELAGEM FISICO COM O USO DA ANIMACAO POR COMPUTADOR]
Claudia Alvares daSilvaVellosoFerreira Oct. 1992 83 p In PORTUGESE
(INPE-5492-TDI/509) Avail: CASI HC A05/MF A01

This work presents a computer animation application, its problems and necessities of the use of dynamics principles for motion simulation. One of the major problems in computer animation is the creation of a motion that appears as natural and realistic as possible. One solution is the use of dynamics for the motion control, in which the objects are treated as having mass and other physical properties, acting under the influence of external and internal forces and torques. One difficulty with this technique is to find the forces and torques required for each motion, thus it is necessary to apply the physical laws for the motion in question. Author (revised)

N94-11178# Instituto de Pesquisas Espaciais, Sao Jose dos Campos (Brazil).
A SURROGATE HEURISTIC FOR SET COVERING PROBLEMS
Luiz Antonio N. Lorena and Fabio Belo Lopes 1993 34 p Presented at Euro 12 TIMS 31 Joint International Conference, Helsinki, Finland, 29 Jun.-1 Jul. 1992
(INPE-5462-PRE/1770) Avail: CASI HC A03/MF A01

This paper presents a new heuristic for set covering problems, based upon continuous surrogate relaxation and subgradient optimization. We propose an adequate step size control that provides the surrogate bounds in few subgradient iterations, comparing to other relaxations. The algorithm also combines problem reduction tests and a technique to avoid the preliminary sorting to solve the continuous surrogate relaxation. Another feature is the definition of an efficient data structure in order to solve large set covering problems (up to 1,000 rows and 12,000 columns). Computational tests indicate better-quality results then algorithms based on Lagrangian relaxation in terms of final solutions and mainly in computer times. Author (revised)

N94-11181# Instituto de Pesquisas Espaciais, Sao Jose dos Campos (Brazil).
A TOOL FOR GENERATION OF EXPERT SYSTEM SHELLS M.S. Thesis [UMA FERRAMENTA PARA A GERACAO DE ARCABOUCOS DE SISTEMAS ESPECIALISTAS]
Mauricio Marengoni Dec. 1992 95 p In PORTUGESE
(INPE-5493-TDI/510) Avail: CASI HC A05/MF A01

A tool is proposed that integrates a modular graphical interface with an expert system shell generator. The use of the tool is divided in three phases. Initially, the user interactively specifies his needs according to the intended problem. In the second phase, these specifications are used by a shell generator system to select, from a program library, the modules containing the functions needed to build an expert system shell satisfying the specifications. These modules are integrated in a stand alone system, and this system is compiled. Finally, the compiled version of the specified shell is used to develop an expert system to solve the intended problem. The tool also provides graphical primitives and mechanisms for the integration of external algorithms needed for special image manipulations. The tool implementation has been motivated by the need to construct expert systems with different levels of complexity in the domain of image processing. A further motivation was the possibility of using such a tool as a teaching and research laboratory in knowledge representation and expert system architecture. This tool represents the artificial intelligence part of a larger project of developing an intelligent laboratory for image processing, where research and product development activities could be performed efficiently. The main contribution of this work is the specification and implementation of the inference engine generator module. This module is described in details and basic theoretical aspects about the components of the module are provided. Author (revised)

N94-11182# Polish Academy of Sciences, Warsaw. Inst. Podstawowych Problemow Techniki.

THE SOLVING OF EQUATIONS BY THE METHOD OF BOUNDARY ELEMENTS [ROZWIAZYWANIE ROWNAN METODY ELEMENTOW BRZEGOWYCH]

Jacek F. Maczynski 1991 40 p In POLISH
Avail: CASI HC A03/MF A01

PASCAL procedures related to algorithms for solving systems of linear algebraic equations which arise when implementing, among others, the Boundary Element Method are presented. By Higher Algebra the matrix of the linear system may be conceived to belong to a ring upon a ring of square real matrices. The PASCAL procedures perform the operations in such a ring together with other auxiliary operations related to factorization which is known to economize memory when creating a form which is close to an inverse in a formally operational sense. These procedures (19 in number) were tested with positive results. Author (revised)

N94-11188*# SRI International Corp., Menlo Park, CA.

A FORMALLY VERIFIED ALGORITHM FOR INTERACTIVE CONSISTENCY UNDER A HYBRID FAULT MODEL Final Report

Patrick Lincoln and John Rushby Washington Jul. 1993 72 p
(Contract NAS1-18969; RTOP 505-64-10-13)
(NASA-CR-4527; NAS 1.26:4527) Avail: CASI HC A04/MF A01

Consistent distribution of single-source data to replicated computing channels is a fundamental problem in fault-tolerant system design. The 'Oral Messages' (OM) algorithm solves this problem of Interactive Consistency (Byzantine Agreement) assuming that all faults are worst-cass. Thambidurai and Park introduced a 'hybrid' fault model that distinguished three fault modes: asymmetric (Byzantine), symmetric, and benign; they also exhibited, along with an informal 'proof of correctness', a modified version of OM. Unfortunately, their algorithm is flawed. The discipline of mechanically checked formal verification eventually enabled us to develop a correct algorithm for Interactive Consistency under the hybrid fault model. This algorithm withstands \$a\$ asymmetric, \$s\$ symmetric, and \$b\$ benign faults simultaneously, using \$m+1\$ rounds, provided \$n is greater than 2a + 2s + b + m\$, and \$mgeg a\$. We present this algorithm, discuss its subtle points, and describe its formal specification and verification in PVS. We argue that formal verification systems such as PVS are now sufficiently effective that their application to fault-tolerance algorithms should be considered routine. Author (revised)

N94-11196*# Institute for Computer Applications in Science and Engineering, Hampton, VA.

FLEXIBLE LANGUAGE CONSTRUCTS FOR LARGE PARALLEL PROGRAMS Final Report

Matthew Rosing and Robert Schnabel (Colorado Univ., Boulder.) Washington Jun. 1993 27 p Submitted for publication
(Contracts NAS1-18605; NAS1-19480; RTOP 505-90-52-01)
(NASA-CR-191478; NAS 1.26:191478; ICASE-93-29) Avail: CASI HC A03/MF A01

The goal of the research described is to develop flexible language constructs for writing large data parallel numerical programs for distributed memory (MIMD) multiprocessors. Previously, several models have been developed to support synchronization and communication. Models for global synchronization include SIMD (Single Instruction Multiple Data), SPMD (Single Program Multiple Data), and sequential programs annotated with data distribution statements. The two primary models for communication include implicit communication based on shared memory and explicit communication based on messages. None of these models by themselves seem sufficient to permit the natural and efficient expression of the variety of algorithms that occur in large scientific computations. An overview of a new language that combines many of these programming models in a clean manner is given. This is done in a modular fashion such that different models can be combined to support large programs. Within a module, the selection of a model depends on the algorithm and its efficiency requirements. An overview of the language and discussion of some of the critical implementation details is given. Author (revised)

N94-11197*# Georgia Inst. of Tech., Atlanta. Digital Signal Processing Lab.

NECESSARY CONDITIONS FOR THE OPTIMALITY OF VARIABLE RATE RESIDUAL VECTOR QUANTIZERS

Faouzi Kossentini, Mark J. T. Smith, and Christopher F. Barnes 15 Jun. 1993 38 p
(Grants NAG5-2187; NSF MIP-91-16113)
(NASA-CR-193730; NAS 1.26:193730) Avail: CASI HC A03/MF A01

Residual vector quantization (RVQ), or multistage VQ, as it is also called, has recently been shown to be a competitive technique for data compression. The competitive performance of RVQ reported in results from the joint optimization of variable rate encoding and RVQ direct-sum code books. In this paper, necessary conditions for the optimality of variable rate RVQ's are derived, and an iterative descent algorithm based on a Lagrangian formulation is introduced for designing RVQ's having minimum average distortion subject to an entropy constraint. Simulation results for these entropy-constrained RVQ's (EC-RVQ's) are presented for memory less Gaussian, Laplacian, and uniform sources. A Gauss-Markov source is also considered. The performance is superior to that of entropy-constrained scalar quantizers (EC-SQ's) and practical entropy-constrained vector quantizers (EC-VQ's), and is competitive with that of some of the best source coding techniques that have appeared in the literature. Author (revised)

N94-11220# Naval Command, Control and Ocean Surveillance Center, San Diego, CA. Research, Development, Test and Evaluation Div.

EFFECTIVE SOFTWARE REUSE IN AN EMBEDDED REALTIME SYSTEM Professional Paper

B. Barlin and J. M. Lawler (Mitre Corp., San Diego, CA.) Feb. 1993 9 p
(AD-A264993) Avail: CASI HC A02/MF A01

The Submarine Message Buffer (SMB) is a real time embedded message processing system developed at the Naval Command, Control and Ocean Surveillance Center, Research, Development, Test and Evaluation Division (NRaD). The SMB is sponsored by the Space and Naval Warfare Systems Command (SPAWAR) to support modernization of SSN (Los Angeles and Seawolf class submarines) radio rooms. The development strategy adopted for the SMB concentrated on the reuse of Ada software. This paper will focus on the design, processes and methodologies, which were used in the development of this system. Metrics will also be provided showing why this system has been identified as an Ada success story by the Ada Joint Program Office among others. DTIC

N94-11226# Sandia National Labs., Albuquerque, NM.

AN IMPROVED MATERIAL INTERFACE RECONSTRUCTION ALGORITHM FOR EULERIAN CODES

R. L. Bell (Amparo Corp., Albuquerque, NM.) and E. S. Hertel 1992 17 p Presented at the 1992 Nuclear Explosives Code Developers Conference, Sunnyvale, CA, 2-6 Nov. 1992
(Contract DE-AC04-76DP-00789)
(DE93-011679; SAND-92-1716C; CONF-9211128-7) Avail: CASI HC A03/MF A01 (US Sales Only)

In general, shock wave physics codes can be divided into two major categories: (1) Lagrangian codes and (2) Eulerian codes. (A third category, Arbitrary Lagrangian Eulerian (ALE) codes, allows the computational mesh to move with the material until some measure of mesh distortion is achieved, then the mesh is redefined and the materials are allowed to flow through the mesh, as in an Eulerian calculation.) With Lagrangian codes the cell boundaries also form the interface between different materials in a calculation. In an Eulerian calculation, the cell boundaries may initially form the interface between materials, but as the calculation proceeds and materials flow through the mesh, material interfaces will not lie on cell boundaries. Knowledge about the location of materials in a mixed material cell is necessary to determine the correct advection of materials from a mixed cell as an Eulerian (or ALE) code calculation progresses through time. Using a material interface reconstruction algorithm that is unable to accurately determine material interface locations is analogous to running a one material problem using a first order accurate differencing scheme. The material interface reconstruction method described here is an extension to the method developed by D.L. Youngs. Youngs' method uses volume fraction information from the donor cell and all surrounding cells to determine the orientation and location of planes dividing materials from one another in a mixed material cell. Many codes use the popular Simple Line. DOE

N94-11231*# National Aeronautics and Space Administration. Lewis Research Center, Cleveland, OH.
A DISTRIBUTED VERSION OF THE NASA ENGINE PERFORMANCE PROGRAM
Jeffrey T. Cours and Brian P. Curlett Jul. 1993 9 p
(RTOP 505-69-50)
(NASA-TM-106208; E-7918; NAS 1.15:106208) Avail: CASI HC A02/MF A01

Distributed NEPP, a version of the NASA Engine Performance Program, uses the original NEPP code but executes it in a distributed computer environment. Multiple workstations connected by a network increase the program's speed and, more importantly, the complexity of the cases it can handle in a reasonable time. Distributed NEPP uses the public domain software package, called Parallel Virtual Machine, allowing it to execute on clusters of machines containing many different architectures. It includes the capability to link with other computers, allowing them to process NEPP jobs in parallel. This paper discusses the design issues and granularity considerations that entered into programming Distributed NEPP and presents the results of timing runs. Author (revised)

N94-11232*# National Aeronautics and Space Administration. Lewis Research Center, Cleveland, OH.
PORTABLE PROGRAMMING ON PARALLEL/NETWORKED COMPUTERS USING THE APPLICATION PORTABLE PARALLEL LIBRARY (APPL)
Angela Quealy (Sverdrup Technology, Inc., Brook Park, OH.), Gary L. Cole, and Richard A. Blech Jul. 1993 25 p
(RTOP 505-62-52)
(NASA-TM-106238; E-7960; NAS 1.15:106238) Avail: CASI HC A03/MF A01

The Application Portable Parallel Library (APPL) is a subroutine-based library of communication primitives that is callable from applications written in FORTRAN or C. APPL provides a consistent programmer interface to a variety of distributed and shared-memory multiprocessor MIMD machines. The objective of APPL is to minimize the effort required to move parallel applications from one machine to another, or to a network of homogeneous machines. APPL encompasses many of the message-passing primitives that are currently available on commercial multiprocessor systems. This paper describes APPL (version 2.3.1) and its usage, reports the status of the APPL project, and indicates possible directions for the future. Several applications using APPL are discussed, as well as performance and overhead results. Author (revised)

N94-11240# Lawrence Livermore National Lab., CA.
RESOLUTION FOR LANCZOS AND PAIGE-SAUNDERS INVERSES IN TOMOGRAPHY
J. G. Berryman Mar. 1993 12 p Presented at the Stanford Exploration Project Program Review, Stanford, CA, 17-21 May 1993
(Contract W-7405-eng-48)
(DE93-012312; UCRL-JC-113380; CONF-9305169-1) Avail: CASI HC A03/MF A01

Methods have been developed for computing both the model and data resolution matrices for iterative inverses such as those produced by the Lanczos and Paige-Saunders (LSQR) schemes for constructing linear inverses. DOE

N94-11246# Westinghouse Savannah River Co., Aiken, SC.
GRISET CERTIFICATION PACKAGE
J. J. Taylor and G. R. Cefus Nov. 1992 4 p
(Contract DE-AC09-89SR-18035)
(DE93-011783; WSRC-TR-92-547) Avail: CASI HC A01/MF A01

The GRISET (GRIMHX setup) computer code is an input driver for the three dimensional GRIMHX computer code. GRISET provides a method for automating the creation of GRIMHX geometry and associated problem specific information such as the reactor maps and the cross section data references. GRISET provides methods which allow the user to model control rod positioning, safety rod insertion with any number failing, control rod withdrawal or insertion, and full or partial melting of control rods. GRISET also calculates the radial shape factor, tilt, roof-top-ratios, and the assembly power peaking. DOE

N94-11274*# National Aeronautics and Space Administration. Ames Research Center, Moffett Field, CA.
A SUMMARY OF IMAGE SEGMENTATION TECHNIQUES
Lilly Spirkovska Jun. 1993 14 p
(RTOP 506-59-31)
(NASA-TM-104022; A-93082; NAS 1.15:104022) Avail: CASI HC A03/MF A01

Machine vision systems are often considered to be composed of two subsystems: low-level vision and high-level vision. Low level vision consists primarily of image processing operations performed on the input image to produce another image with more favorable characteristics. These operations may yield images with reduced noise or cause certain features of the image to be emphasized (such as edges). High-level vision includes object recognition and, at the highest level, scene interpretation. The bridge between these two subsystems is the segmentation system. Through segmentation, the enhanced input image is mapped into a description involving regions with common features which can be used by the higher level vision tasks. There is no theory on image segmentation. Instead, image segmentation techniques are basically ad hoc and differ mostly in the way they emphasize one or more of the desired properties of an ideal segmenter and in the way they balance and compromise one desired property against another. These techniques can be categorized in a number of different groups including local vs. global, parallel vs. sequential, contextual vs. noncontextual, interactive vs. automatic. In this paper, we categorize the schemes into three main groups: pixel-based, edge-based, and region-based. Pixel-based segmentation schemes classify pixels based solely on their gray levels. Edge-based schemes first detect local discontinuities (edges) and then use that information to separate the image into regions. Finally, region-based schemes start with a seed pixel (or group of pixels) and then grow or split the seed until the original image is composed of only homogeneous regions. Because there are a number of survey papers available, we will not discuss all segmentation schemes. Rather than a survey, we take the approach of a detailed overview. We focus only on the more common approaches in order to give the reader a flavor for the variety of techniques available yet present enough details to facilitate implementation and experimentation. Author (revised)

N94-11279*# Virginia Polytechnic Inst. and State Univ., Blacksburg. Dept. of Engineering Science and Mechanics.
COMPUTATIONAL MECHANICS NEEDS STUDY Final Report
O. Hayden Griffin, Jr. Aug. 1993 9 p
(Grant NAG1-675)
(NASA-CR-193712; NAS 1.26:193712) Avail: CASI HC A02/MF A01

In order to assess the needs in computational mechanics over the next decade, we formulated a questionnaire and contacted computational mechanics researchers and users in industry, government, and academia. As expected, we found a wide variety of computational mechanics usage and research. This report outlines the activity discussed with those contacts, as well as that in our own organizations. It should be noted that most of the contacts were made before the recent decline of the defense industry. Therefore, areas which are strongly defense-oriented may decrease in relative importance. In order to facilitate updating of this study, names of a few key researchers in each area are included as starting points for future literature surveys. These lists of names are not intended to represent those persons doing the best research in that area, nor are they intended to be comprehensive. They are, as previously stated, offered as starting points for future literature searches. Overall, there is currently a broad activity in computational mechanics in this country, with the breadth and depth increasing as more sophisticated software and faster computers become more available. The needs and desires of the workers in this field are as diverse as their background and organizational products. There seems to be some degree of software development in any organization (although the level of activity is highly variable from one organization to another) which has any research component in its mission. It seems, however, that there is considerable use of commercial software in almost all organizations. In most industrial research organizations, it appears that very little actual software development is contracted out, but that most is done in-house, using a mixture of funding sources. Government agencies vary widely in the ratio of in-house to out-house ratio. There is a considerable amount of experimental verification in most, but not all, organizations. Generally, the amount of experimental verification is more than we expected. Of all the survey contacts, one or two believe that the resources they are allocated are sufficient, but most do not. Some believe they have only half the resources they need. Some see their resource deficits as short-term, while others see it as a trend which will continue or perhaps worsen. The pessimism is stronger in the defense and aerospace industry. When considering only the nonlinear development efforts, there appears to be an even mix of geometric and material nonlinearity. There is not much particular emphasis in linear analysis unless it is in extension of current analysis capabilities to larger problems. The primary exception is concern about modeling of composites, where proven methodologies have trailed element and computer hardware development. Most of the people we spoke to use finite element techniques, but there is some finite difference and boundary element work ongoing. There is also some interest in multiple methods. Coupling of finite elements and boundary elements appears to be of high interest, since the two analysis types are complementary.

Derived from text

N94-11295# California Inst. of Tech., Pasadena. Dept. of Computer Science.

SCALABLE CONCURRENT PROGRAMMING PROJECT Progress Report, 27 Apr. 1992 - 22 Mar. 1993

Stephen Taylor 22 Mar. 1993 80 p
(AD-A266097) Avail: CASI HC A05/MF A01

The Scalable Concurrent Programming Project is intended to provide significant advances in scalable, high-performance, concurrent programming technology. This is to be achieved through innovations in compiler technology and programming methods. The research builds on past successes in compiler design, program development tools, programming methods and applications expertise. Two exciting directions provide the central focus for future research: fine-grain multicomputing and irregular applications. A fine-grain multicomputer is an architecture that reduces the granularity of concurrent computation by integrating hardware support for processes and messages. DTIC

N94-11301 Materials Research Labs., Ascot Vale (Australia).

GRAFTED (GRAPHICAL FAULT TREE EDITOR): A FAULT TREE DESCRIPTION PROGRAM FOR TARGET VULNERABILITY/SURVIVABILITY ANALYSIS

Frank J. Tkalcevic and Norbert M. Burman Nov. 1992 63 p Limited Reproducibility: More than 20% of this document may be affected by microfiche quality
(AD-A264078; MRL-GD-0043; DODA-AR-006-911) Avail: Issuing Activity (Defense Technical Information Center (DTIC))

A computer program GRAFTED, 'GRAphical Fault Tree EDitor', has been written to simplify data entry and modification of component fault tree descriptions (FTD) used in military platform vulnerability/survivability analysis procedures. GRAFTED utilizes a unique, graphical, screen based data entry procedure to define and display both individual system component parameters and their hierarchical relationship in the overall system FTD. The generated component and system FTD output is in a format which is directly readable by the MRL version of the General Vulnerability Assessment Model (GVAM), computer programs. Although GRAFTED was specifically designed to generate FTD's for GVAM, it could be easily modified to accommodate data input formats and FTD output for assessment procedures which require user friendly data entry and graphical fault tree editing and visualisation. DTIC

N94-11422*# National Aeronautics and Space Administration. Goddard Space Flight Center, Greenbelt, MD.

PROCEEDINGS OF THE SEVENTEENTH ANNUAL SOFTWARE ENGINEERING WORKSHOP

Dec. 1992 423 p Workshop held in Greenbelt, MD, 2-3 Dec. 1992
(NASA-TM-109245; NAS 1.15:109245; SEL-92-004) Avail: CASI HC A18/MF A04

Proceedings of the Seventeenth Annual Software Engineering Workshop are presented. The software Engineering Laboratory (SEL) is an organization sponsored by NASA/Goddard Space Flight Center and created to investigate the effectiveness of software engineering technologies when applied to the development of applications software. Topics covered include: the Software Engineering Laboratory; process measurement; software reuse; software quality; lessons learned; and is Ada dying. For individual titles, see N94-11423 through N94-11437.

N94-11423*# National Aeronautics and Space Administration. Goddard Space Flight Center, Greenbelt, MD.

EXPERIMENTAL SOFTWARE ENGINEERING: SEVENTEEN YEARS OF LESSONS IN THE SEL

Frank E. McGarry *In its* Proceedings of the Seventeenth Annual Software Engineering Workshop Dec. 1992 14 p (For primary document see N94-11422 01-61)
Avail: CASI HC A03/MF A04

Seven key principles developed by the Software Engineering Laboratory (SEL) at the Goddard Space Flight Center (GSFC) of the National Aeronautics and Space Administration (NASA) are described. For the past 17 years, the SEL has been experimentally analyzing the development of production software as varying techniques and methodologies are applied in this one environment. The SEL has collected, archived, and studied detailed measures from more than 100 flight dynamics projects, thereby gaining significant insight into the effectiveness of numerous software techniques, as well as extensive experience in the overall effectiveness of 'Experimental Software Engineering'. This experience has helped formulate follow-on studies in the SEL, and it has helped other software organizations better understand just what can be accomplished and what cannot be accomplished through experimentation. Author (revised)

N94-11424*# Maryland Univ., College Park. Dept. of Computer Science.

THE EXPERIENCE FACTORY: CAN IT MAKE YOU A 5? OR WHAT IS ITS RELATIONSHIP TO OTHER QUALITY AND IMPROVEMENT CONCEPTS?

Victor R. Basili *In* NASA. Goddard Space Flight Center, Proceedings of the Seventeenth Annual Software Engineering Workshop Dec. 1992 19 p (For primary document see N94-11422 01-61)
Avail: CASI HC A03/MF A04

The concepts of quality improvements have permeated many businesses. It is clear that the nineties will be the quality era for software and there is a growing need to develop or adapt quality improvement approaches to the software business. Thus we must understand software as an artifact and software as a business. Since the business we are dealing with is software, we must understand the nature of software and software development. The software discipline is evolutionary and experimental; it is a laboratory science. Software is development not production. The technologies of the discipline are human based. There is a lack of models that allow us to reason about the process and the product. All software is not the same; process is a variable, goals are variable, etc. Packaged, reusable, experiences require additional resources in the form of organization, processes, people, etc. There have been a variety of organizational frameworks proposed to improve quality for various businesses. The ones discussed in this presentation include: Plan-Do-Check-Act, a quality improvement process based upon a feedback cycle for optimizing a single process model/production line; the Experience Factory/Quality Improvement Paradigm, continuous improvements through the experimentation, packaging, and reuse of experiences based upon a business's needs; Total Quality Management, a management approach to long term success through customer satisfaction based on the participation of all members of an organization; the SEI capability maturity model, a staged process improvement based upon assessment with regard to a set of key process areas until you reach a level 5 which represents a continuous process improvement; and Lean (software) Development, a principle supporting the concentration of the production on 'value added' activities and the elimination of reduction of 'not value added' activities. Author (revised)

N94-11425*# National Aeronautics and Space Administration. Goddard Space Flight Center, Greenbelt, MD.

IMPACTS OF OBJECT-ORIENTED TECHNOLOGIES: SEVEN YEARS OF SEL STUDIES

Michael Stark *In its* Proceedings of the Seventeenth Annual Software Engineering Workshop Dec. 1992 17 p (For primary document see N94-11422 01-61)

Avail: CASI HC A03/MF A04

The premise that object-oriented technology (OOT) is the most significant technology ever examined by the Software Engineering Laboratory is examined. The evolution of the use of OOT in the Software Engineering Laboratory (SEL) 'experience factory' is described in terms of the SEL's original expectations, focusing on how successive generations of projects have used OOT. General conclusions are drawn on how the usage of the technology has evolved in this environment. Author (revised)

N94-11426*# City Univ., London (England). School of Informatics.

THE MERMAID PROJECT

A. J. C. Cowderoy, John O. Jenkins, and A Poulymenakou *In* NASA. Goddard Space Flight Center, Proceedings of the Seventeenth Annual Software Engineering Workshop Dec. 1992 19 p (For primary document see N94-11422 01-61)

Avail: CASI HC A03/MF A04

The tendency for software development projects to be completed over schedule and over budget was documented extensively. Additionally many projects are completed within budgetary and schedule target only as a result of the customer agreeing to accept reduced functionality. In his classic book, The Mythical Man Month, Fred Brooks exposes the fallacy that effort and schedule are freely interchangeable. All current cost models are produced on the assumption that there is very limited scope for schedule compression unless there is a corresponding reduction in delivered functionality. The Metrication and Resources Modeling Aid (MERMAID) project, partially financed by the Commission of the European Communities (CEC) as Project 2046 began in Oct. 1988 and its goal were as follows: (1) improvement of understanding of the relationships between software development productivity and product and process metrics; (2) to facilitate the widespread technology transfer from the Consortium to the European Software Industry; and (3) to facilitate the widespread uptake of cost estimation techniques by the provision of prototype cost estimation tools. MERMAID developed a family of methods for cost estimation, many of which have had tools implemented in prototypes. These prototypes are best considered as toolkits or workbenches. Author (revised)

N94-11427*# AT and T Information Systems Labs., Denver, CO.

SOFTWARE PROCESS ASSESSMENTS

Sharon E. Miller, George T. Tucker, and Anthony J. Verducci, Jr. *In* NASA. Goddard Space Flight Center, Proceedings of the Seventeenth Annual Software Engineering Workshop Dec. 1992 17 p (For primary document see N94-11422 01-61)

Avail: CASI HC A03/MF A04

Software process assessments (SPA's) are part of an ongoing program of continuous quality improvements in AT&T. Their use was found to be very beneficial by software development organizations in identifying the issues facing the organization and the actions required to increase both quality and productivity in the organization. Author

N94-11428*# Paramax Systems Corp., Houston, TX.

THE ROLE OF METRICS AND MEASUREMENTS IN A SOFTWARE INTENSIVE TOTAL QUALITY MANAGEMENT ENVIRONMENT

Charles B. Daniels *In* NASA. Goddard Space Flight Center, Proceedings of the Seventeenth Annual Software Engineering Workshop Dec. 1992 29 p (For primary document see N94-11422 01-61)

Avail: CASI HC A03/MF A04

Paramax Space Systems began its mission as a member of the Rockwell Space Operations Company (RSOC) team which was the successful bidder on a massive operations consolidation contract for the Mission Operations Directorate (MOD) at JSC. The contract awarded to the team was the Space Transportation System Operations Contract (STSOC). Our initial challenge was to accept responsibility for a very large, highly complex and fragmented collection of software from eleven different contractors and transform it into a coherent, operational baseline. Concurrently, we had to integrate a diverse group of people from eleven different companies into a single, cohesive team. Paramax executives recognized the absolute necessity to develop a business culture based on the concept of employee involvement to execute and improve the complex process of our new environment. Our executives clearly understood that management needed to set the example and lead the way to quality improvement. The total quality management policy and the metrics used in this endeavor are presented. Derived from text

N94-11429*# Computer Sciences Corp., Lanham, MD.

MAXIMIZING REUSE: APPLYING COMMON SENSE AND DISCIPLINE

Sharon Waligora and James Langston *In* NASA. Goddard Space Flight Center, Proceedings of the Seventeenth Annual Software Engineering Workshop Dec. 1992 20 p (For primary document see N94-11422 01-61)

Avail: CASI HC A03/MF A04

Computer Sciences Corporation (CSC)/System Sciences Division (SSD) has maintained a long-term relationship with NASA/Goddard, providing satellite mission ground-support software and services for 23 years. As a partner in the Software Engineering Laboratory (SEL) since 1976, CSC has worked closely with NASA/Goddard to improve the software engineering process. This paper examines the evolution of reuse programs in this uniquely stable environment and formulates certain recommendations for developing reuse programs as a business strategy and as an integral part of production. It focuses on the management strategy and philosophy that have helped make reuse successful in this environment. Author

N94-11430*# Microelectronics and Computer Technology Corp., Austin, TX. EDS Research.

REUSE: A KNOWLEDGE-BASED APPROACH

Neil Iscoe, Zheng-Yang Liu, and Guohui Feng *In* NASA. Goddard Space Flight Center, Proceedings of the Seventeenth Annual Software Engineering Workshop Dec. 1992 23 p (For primary document see N94-11422 01-61)

Avail: CASI HC A03/MF A04

This paper describes our research in automating the reuse process through the use of application domain models. Application domain models are explicit formal representations of the application knowledge necessary to understand, specify, and generate application programs. Furthermore, they provide a unified repository for the operational structure, rules, policies, and constraints of a specific application area. In our approach, domain models are expressed in terms of a transaction-based meta-modeling language. This paper has described in detail the creation and maintenance of hierarchical structures. These structures are created through a process that includes reverse engineering of data models with supplementary enhancement from application experts. Source code is also reverse engineered but is not a major source of domain model instantiation at this time. In the second phase of the software synthesis process, program specifications are interactively synthesized from an instantiated domain model. These specifications are currently integrated into a manual programming process but will eventually be used to derive executable code with mechanically assisted transformations. This research is performed within the context of programming-in-the-large types of systems. Although our goals are ambitious, we are implementing the synthesis system in an incremental manner through which we can realize tangible results. The client/server architecture is capable of supporting 16 simultaneous X/Motif users and tens of thousands of attributes and classes. Domain models have been partially synthesized from five different application areas. As additional domain models are synthesized and additional knowledge is gathered, we will inevitably add to and modify our representation. However, our current experience indicates that it will scale and expand to meet our modeling needs. Author

N94-11431*# National Aeronautics and Space Administration. Goddard Space Flight Center, Greenbelt, MD.

LARGE PROJECT EXPERIENCES WITH OBJECT-ORIENTED METHODS AND REUSE

William Wessale (CAE Industries Ltd., Montreal, Quebec.), Donald J. Reifer (Reifer Consultants, Inc., Torrance, CA.), and David Weller (CAE Industries Ltd., Montreal, Quebec.) *In its* Proceedings of the Seventeenth Annual

Software Engineering Workshop Dec. 1992 22 p (For primary document see N94-11422 01-61)
Avail: CASI HC A03/MF A04

The SSVTF (Space Station Verification and Training Facility) project is completing the Preliminary Design Review of a large software development using object-oriented methods and systematic reuse. An incremental developmental lifecycle was tailored to provide early feedback and guidance on methods and products, with repeated attention to reuse. Object oriented methods were formally taught and supported by realistic examples. Reuse was readily accepted and planned by the developers. Schedule and budget issues were handled by agreements and work sharing arranged by the developers. Author

N94-11432*# Computer Sciences Corp., Lanham, MD.
DEVELOPMENT AND APPLICATION OF AN ACCEPTANCE TESTING MODEL
Rex D. Pendley, Caroline H. Noonan, and Kenneth R. Hall *In* NASA. Goddard Space Flight Center, Proceedings of the Seventeenth Annual Software Engineering Workshop Dec. 1992 27 p (For primary document see N94-11422 01-61)
Avail: CASI HC A03/MF A04

The process of acceptance testing large software systems for NASA has been analyzed, and an empirical planning model of the process constructed. This model gives managers accurate predictions of the staffing needed, the productivity of a test team, and the rate at which the system will pass. Applying the model to a new system shows a high level of agreement between the model and actual performance. The model also gives managers an objective measure of process improvement. Author

N94-11433*# IBM Federal Systems Div., Gaithersburg, MD.
A RECENT CLEANROOM SUCCESS STORY: THE REDWING PROJECT
c14
Philip A. Hausler *In* NASA. Goddard Space Flight Center, Proceedings of the Seventeenth Annual Software Engineering Workshop Dec. 1992 30 p (For primary document see N94-11422 01-61)
Avail: CASI HC A03/MF A04

Redwing is the largest completed Cleanroom software engineering project in IBM, both in terms of lines of code and project staffing. The product provides a decision-support facility that utilizes artificial intelligence (AI) technology for predicting and preventing complex operating problems in an MVS environment. The project used the Cleanroom process for development and realized a defect rate of 2.6 errors/KLOC, measured from first execution. This represents the total amount of errors that were found in testing and installation at three field test sites. Development productivity was 486 LOC/PM, which included all development labor expended in design specification through completion of incremental testing. In short, the Redwing team produced a complex systems software product with an extraordinarily low error rate, while maintaining high productivity. All of this was accomplished by a project team using Cleanroom for the first time. An 'introductory implementation' of Cleanroom was defined and used on Redwing. This paper describes the quality and productivity results, the Redwing project, and how Cleanroom was implemented.
Author (revised)

N94-11434*# Naval Postgraduate School, Monterey, CA. Information Sciences and Labs.
APPLYING RELIABILITY MODELS TO THE MAINTENANCE OF SPACE SHUTTLE SOFTWARE
Norman F. Schneidewind *In* NASA. Goddard Space Flight Center, Proceedings of the Seventeenth Annual Software Engineering Workshop Dec. 1992 18 p (For primary document see N94-11422 01-61)
Avail: CASI HC A03/MF A04

Software reliability models provide the software manager with a powerful tool for predicting, controlling, and assessing the reliability of software during maintenance. We show how a reliability model can be effectively employed for reliability prediction and the development of maintenance strategies using the Space Shuttle Primary Avionics Software Subsystem as an example. Author (revised)

N94-11435*# Syracuse Univ., NY. Center for Science and Technology.
INSIGHTS INTO SOFTWARE DEVELOPMENT IN JAPAN
Lorraine M. Duvall *In* NASA. Goddard Space Flight Center, Proceedings of the Seventeenth Annual Software Engineering Workshop Dec. 1992 19 p (For primary document see N94-11422 01-61)
Avail: CASI HC A03/MF A04

The interdependence of the U.S.-Japanese economies makes it imperative that we in the United States understand how business and technology developments take place in Japan. We can gain insight into these developments in software engineering by studying the context in which Japanese software is developed, the practices that are used, the problems encountered, the setting surrounding these problems, and the resolution of these problems. Context includes the technological and sociological characteristics of the software development environment, the software processes applied, personnel involved in the development process, and the corporate and social culture surrounding the development. Presented in this paper is a summary of results of a study that addresses these issues. Data for this study was collected during a three month visit to Japan where the author interviewed 20 software managers representing nine companies involved in developing software in Japan. These data are compared to similar data from the United States in which 12 managers from five companies were interviewed. Author

N94-11436*# Internal Revenue Service, Silver Spring, MD.
MYTHS AND REALITIES: DEFINING RE-ENGINEERING FOR A LARGE ORGANIZATION
Sandra Yin and Julia McCreary *In* NASA. Goddard Space Flight Center, Proceedings of the Seventeenth Annual Software Engineering Workshop Dec. 1992 40 p (For primary document see N94-11422 01-61)
Avail: CASI HC A03/MF A04

This paper describes the background and results of three studies concerning software reverse engineering, re-engineering, and reuse (R3) hosted by the Internal Revenue Service in 1991 and 1992. The situation at the Internal Revenue--aging, piecemeal computer systems and outdated technology maintained by a large staff--is familiar to many institutions, especially among management information systems. The IRS is distinctive for the sheer magnitude and diversity of its problems; the country's tax records are processed using assembly language and COBOL and spread across tape and network DBMS files. How do we proceed with replacing legacy systems? The three software re-engineering studies looked at methods, CASE tool support, and performed a prototype project using re-engineering methods and tools. During the course of these projects, we discovered critical issues broader than the mechanical definitions of methods and tool technology. Author (revised)

N94-11437*# General Electric Co., Philadelphia, PA. Management and Data Systems Engineering.
STGT PROGRAM: ADA CODING AND ARCHITECTURE LESSONS LEARNED
Paul Usavage and Don Nagurney *In* NASA. Goddard Space Flight Center, Proceedings of the Seventeenth Annual Software Engineering Workshop Dec. 1992 24 p (For primary document see N94-11422 01-61)
Avail: CASI HC A03/MF A04

STGT (Second TDRSS Ground Terminal) is currently halfway through the System Integration Test phase (Level 4 Testing). To date, many software architecture and Ada language issues have been encountered and solved. This paper, which is the transcript of a presentation at the 3 Dec. meeting, attempts to define these lessons plus others learned regarding software project management and risk management issues, training, performance, reuse, and reliability. Observations are included regarding the use of particular Ada coding constructs, software architecture trade-offs during the prototyping, development and testing stages of the project, and dangers inherent in parallel or concurrent systems, software, hardware, and operations engineering. Author (revised)

N94-11452# Department of Education, Washington, DC. Office of Information Resources Management Policy, Plans, and Oversight.
SOFTWARE MANAGEMENT GUIDE
Jun. 1992 37 p
(DE93-012034; DOE/AD-0028) Avail: CASI HC A03/MF A01

The Office of Information Resources Management Policy, Plans, and Oversight is responsible for ensuring that compliance with Department of Energy (DOE) 1330.1C is reached at each site. The purpose of a Departmental Software Management Guide is to assist the sites with developing a software management program. While the use of this guide is not mandatory, it does facilitate each site's compliance with the Order. Goals of DOE's Software Management Program are as follows: establish and maintain control of software integrity, and manage software acquisitions, developments, changes, maintenance, and disposition. DOE

N94-11522*# National Aeronautics and Space Administration. Langley Research Center, Hampton, VA.

DISCRETE KALMAN FILTERING EQUATIONS OF SECOND-ORDER FORM FOR CONTROL-STRUCTURE INTERACTION SIMULATIONS

K. C. Park (Colorado Univ., Boulder.), K. F. Alvin (Colorado Univ., Boulder.), and W. Keith Belvin 1991 24 p
(Grant NAG9-574)
(NASA-CR-193723; NAS 1.26:193723; AIAA Paper 90-3387) Avail: CASI HC A03/MF A01

A second-order form of discrete Kalman filtering equations is proposed as a candidate state estimator for efficient simulations of control-structure interactions in coupled physical coordinate configurations as opposed to decoupled modal coordinates. The resulting matrix equation of the present state estimator consists of the same symmetric, sparse N x N coupled matrices of the governing structural dynamics equations as opposed to unsymmetric 2N x 2N state space-based estimators. Thus, in addition to substantial computational efficiency improvement, the present estimator can be applied to control-structure design optimization for which the physical coordinates associated with the mass, damping and stiffness matrices of the structure are needed instead of modal coordinates. Author

N94-11611# Sandia National Labs., Albuquerque, NM.

BOUNDING THE VAPNIK-CHERVONENKIS DIMENSION OF CONCEPT CLASSES PARAMETERIZED BY REAL NUMBERS

P. Goldberg and M. Jerrum (Edinburgh Univ., Scotland.) 1993 11 p
Presented at the Conference on Learning Theory, Santa Cruz, CA, 26-28 Jul. 1993
(Contract DE-AC04-76DP-00789)
(DE93-011600; SAND-93-0483C; CONF-930772-1) Avail: CASI HC A03/MF A01

The Vapnik-Chervonenkis (V-C) dimension is an important combinatorial tool in the analysis of learning problems in the PAC framework. For polynomial learnability, we seek upper bounds on the V-C dimension that are polynomial in the syntactic complexity of concepts. Such upper bounds are automatic for discrete concept classes, but hitherto little has been known about what general conditions guarantee polynomial bounds on V-C dimension for classes in which concepts and examples are represented by tuples of real numbers. In this paper, we show that for two general kinds of concept class the V-C dimension is polynomially bounded as a function of the syntactic complexity of concepts. One is classes where the criterion for membership of an instance in a concept can be expressed as a formula with fixed quantification depth and exponentially-bounded length, whose atomic predicates are polynomial inequalities of exponentially-bounded degree. The other is classes where containment of an instance in a concept is testable in polynomial time, assuming we may compute standard arithmetic operations on reals exactly in constant time. Our results show that in the continuous case, as in the discrete, the real barrier to efficient learning in the Occam sense is complexity-theoretic and not information-theoretic. We present examples to show how these results apply to concept classes defined by geometrical figures and neural nets. Polynomial bounds on V-C dimension are derived for these classes, apparently for the first time. DOE

N94-11652 Massachusetts Inst. of Tech., Lexington. Lincoln Lab.

PARAMETRIC STUDY OF DIFFUSION-ENHANCEMENT NETWORKS FOR SPATIOTEMPORAL GROUPING IN REAL-TIME ARTIFICIAL VISION Final Technical Report

Robert K. Cunningham and Allen M. Waxman 6 Apr. 1993 70 p
Limited Reproducibility: More than 20% of this document may be affected by microfiche quality
(Contract F19628-90-C-0002)
(AD-A265065; ESC-TR-92-207) Avail: CASI HC A04

Spatiotemporal grouping phenomena are examined in the context of static and time-varying imagery. Dynamics that exhibit static feature grouping on multiple scales as a function of time and long-range apparent motion between time-varying inputs are developed for a biologically plausible diffusion-enhancement bilayer network. The architecture consists of a diffusion layer and a contrast-enhancement layer coupled by feedforward and feedback connections; time-varying input is provided by a separate feature extracting layer. The model is cast as an analog circuit that is realizable in very large scale integration, the parameters of which are selected to satisfy a psychophysical database of the following long-range apparent motion phenomena: gamma motion of a single light, smooth motion between two lights, reverse motion, split and merge among three lights, Ternus motion among multiple lights, and peripheral motion. The relation between motion on a uniform network (i.e, cortex) and inputs to a nonuniform sampling array (i.i, retina) are discussed in the context of a logarithmic scaling of space. A new interpretation of short- and long-range visual motion systems is introduced. DTIC

N94-11657# California Univ., Los Angeles.

RESEARCH IN COMPUTING AND APPLIED MATHEMATICS Final Report

Paul Roberts, Christopher Anderson, Bjorn Engquist, Charles Lange, and Stanley Osher 1992 11 p
(Contract N00014-86-K-0691)
(AD-A266137) Avail: CASI HC A03/MF A01

This contract was awarded for research into the development of numerical and analytic techniques useful in solving problems arising in continuum mechanics, especially fluid mechanics, and particularly in areas in which the PI and co-PIs have special expertise. Progress on projects that were pursued during tenure of the award is summarized. DTIC

N94-11679 General Dynamics/Convair, San Diego, CA.

RAMCAD (RELIABILITY, AVAILABILITY, AND MAINTAINABILITY IN COMPUTER-AIDED DESIGN) Final Report, Jul. 1987 - Jul. 1991

William J. Dawson, Peter J. Glor, Mary A. Klement, James C. McManus, and Sid E. Markowitz Nov. 1992 111 p Limited Reproducibility: More than 20% of this document may be affected by microfiche quality
(Contract F33615-87-C-0003)
(AD-A265143; GDC-RAMCAD-91-019; AL-TR-1992-0058) Avail: CASI HC A06

The Reliability, Availability and Maintainability in Computer-Aided Design (RAMCAD) Program was established by the Air Force Armstrong Laboratory (AL/HRGA) in 1987 as a direct result of the Computer-Aided Acquisition and Logistics Support (CALS) Initiatives. The purpose of RAMCAD was to solicit new and creative solutions to the problem of integrating Reliability, Maintainability, and Supportability into Computer-Aided Design. To provide a near-term RAMCAD capability, a principle task, funded by Armstrong Laboratory and the Army Armament, Munitions, and Chemical Command (AMCCOM) was contracted to General Dynamics to integrate stand-alone commercially available or public domain reliability, maintainability, and supportability analysis software with a computer-aided design workstation for electronic, mechanical, and structural design as a RAMCAD Prototype system. RAMCAD provides a common user interface and shared database for reliability, maintainability, and supportability of electronic, mechanical, and structural designs. Execution of analysis programs is transparent to the user through the common user interface. Additionally, RAMCAD provides a significant process improvement in the quality and robustness of reliability predictions for new designs. This is accomplished by analysis of the environmental stresses experienced by each component in the system, rather than relying on default values or average values for the unit under analysis. This report documents the development of the RAMCAD Prototype System and Lessons Learned. DTIC

N94-11680# Arkansas Univ., Fayetteville.

COMPUTATIONAL ALGORITHMS OR IDENTIFICATION OF DISTRIBUTED PARAMETER SYSTEMS Final Technical Report, 1 Sep. 1989 - 28 Feb. 1993

Dennis W. Brewer and Robert K. Powers 24 Apr. 1993 78 p
(Grant AF-AFOSR-0472-89)
(AD-A265252; AFOSR-93-0361TR) Avail: CASI HC A05/MF A01

This research established a general framework for the convergence of a parameter estimation algorithm based on quasi-linearization which applies to a class of distributed parameter systems described by linear dynamical systems. Conditions were established which guarantee local convergence of the identification algorithm. The algorithm was applied to delay and coefficient identification in systems of delay-differential equations. Such systems have been proposed as hereditary models of aeroelastic systems. A numerical identification algorithm was developed and tested for estimating parameters in a Volterra integral equation arising from a viscoelastic model of a flexible structure with Boltzmann damping. In particular, one of the parameters identified was the order of the derivative in Volterra integro-differential equations containing fractional derivatives, a form of viscoelastic damping. A Galerkin approximation in the space variable was used to approximate the partial differential equation with memory by a system of integro-differential equations. Numerical experiments were performed to test the ability of the algorithm to estimate unknown damping parameters in these systems. DTIC

N94-11688*# Computer Software Management and Information Center, Athens, GA.
COSMIC MONTHLY PROGRESS REPORT
Aug. 1993 43 p
(Contract NASw-4670)
(NASA-CR-194400; NAS 1.26:194400) Avail: CASI HC A03/MF A01

Activities of the Computer Software Management and Information Center (COSMIC) are summarized for the month of August, 1993. Tables showing the current inventory of programs available from COSMIC are presented and program processing and evaluation activities are discussed. Ten articles were prepared for publication in the NASA Tech Brief Journal. These articles (included in this report) describe the following software items: (1) MOM3D - A Method of Moments Code for Electromagnetic Scattering (UNIX Version); (2) EM-Animate - Computer Program for Displaying and Animating the Steady-State Time-Harmonic Electromagnetic Near Field and Surface-Current Solutions; (3) MOM3D - A Method of Moments Code for Electromagnetic Scattering (IBM PC Version); (4) M414 - MIL-STD-414 Variable Sampling Procedures Computer Program; (5) MEDOF - Minimum Euclidean Distance Optimal Filter; (6) CLIPS 6.0 - C Language Integrated Production System, Version 6.0 (Macintosh Version); (7) CLIPS 6.0 - C Language Integrated Production System, Version 6.0 (IBM PC Version); (8) CLIPS 6.0 - C Language Integrated Production System, Version 6.0 (UNIX Version); (9) CLIPS 6.0 - C Language Integrated Production System, Version 6.0 (DEC VAX VMS Version); and (10) TFSSRA - Thick Frequency Selective Surface with Rectangular Apertures. Activities in the areas of marketing, customer service, benefits identification, maintenance and support, and dissemination are also described along with a budget summary. CASI

N94-11695# Oak Ridge National Lab., TN.
AN INTRODUCTION TO CHORDAL GRAPHS AND CLIQUE TREES
J. R. S. Blair and B. W. Peyton Nov. 1992 44 p
(Contract DE-AC05-84OR-21400)
(DE93-012508; ORNL/TM-12203) Avail: CASI HC A03/MF A01

Clique trees and chordal graphs have carved out a niche for themselves in recent work on sparse matrix algorithms, due primarily to research questions associated with advanced computer architectures. This paper is a unified and elementary introduction to the standard characterizations of chordal graphs and clique trees. The pace is leisurely, and detailed proofs of all results are included. We also briefly discuss applications of chordal graphs and clique trees in sparse matrix computations. DOE

N94-11850# Institute for Defense Analyses, Alexandria, VA.
ANALYSIS AND GUIDELINES FOR REUSABLE Ada SOFTWARE Final Report
David A. Wheeler Aug. 1992 53 p
(Contract MDA903-89-C-0003)
(AD-A264918; IDA-P-2765; IDA/HQ-92-042441; AD-E501655) Avail: CASI HC A04/MF A01

SDIO is developing the Global Protection Against Limited Strikes (GPALS) system. Much of the software is to be developed in Ada, and software reuse will be considered in the software design and implementation phases. This document provides an analysis and candidate guidelines for developing reusable Ada software to supplement existing SDIO guidelines. The guidelines in this document are based on previous IDA work, IDA Paper P-2378, 'An Approach for Constructing Reusable Components in Ada' by Stephen Edwards. In addition, two other sources were examined: GPALS Software Standards by GE Aerospace, and Ada Quality and Style: Guidelines for Professional Programmers by the Software Productivity Consortium. The analysis shows that many of Edwards's guidelines are already included in Ada Quality and Style and thus will already be used by SDIO. Some of the guidelines require further research before inclusion in a candidate set of guidelines. The remaining guidelines are presented as candidate guidelines in a form similar to that of Ada Quality and Style. This document presents the candidate guidelines in a form which could be readily added to existing Ada development guidelines. DTIC

N94-11860# Air Force Inst. of Tech., Wright-Patterson AFB, OH.
DEVELOPMENT AND IMPLEMENTATION OF A GENERAL PURPOSE X-WINDOWS DISPLAY PROGRAM M.S. Thesis
Gregory D. Carson Dec. 1992 98 p
(AD-A265306; AFIT/CI/CIA-92-128) Avail: CASI HC A05/MF A02

The purpose of the work presented was to design and develop a portable, easy-to-use software package capable of displaying a gray scale image. The display of an image was in actuality only a part of the work. The program was also required to be both FORTRAN and C callable. Additionally, the program had to provide the user with the capability to draw on the image in color, and import tracings, or contours, and display them on the image. The final requirement was to engage recursive use of the program, to provide the ability to display multiple images simultaneously. This work is a presentation of the program developed to meet the above stated requirements. The program is called SEP. The first chapter contains a brief discussion of the reasoning behind the choice of the windowing system utilized. Also presented is an overview of the terminology and concepts involved in using that windowing system. The second chapter describes the internal operations of the program and how it meets the requirements. The third chapter is a description of the method used to interface the developed program to other computer programs. The fourth chapter then provides an explanation of how to use the developed program. The final chapter is a discussion of the testing and evaluation done to ensure the program meets its goal. DOE

N94-11874# Naval Postgraduate School, Monterey, CA.
THE RATIONAL BEHAVIOR MODEL: A MULTI-PARADIGM, TRI-LEVEL SOFTWARE ARCHITECTURE FOR THE CONTROL OF AUTONOMOUS VEHICLES Ph.D. Thesis
Ronald B. Byrnes, Jr. Mar. 1993 317 p
(AD-A265175) Avail: CASI HC A14/MF A03

There is currently a very strong interest among researchers in the fields of artificial intelligence and robotics in finding more effective means of linking high level symbolic computations relating to mission planning and control for autonomous vehicles to low level vehicle control software. The diversity exhibited by the many processes involved in such control has resulted in a number of proposals for a general software architecture intended to provide an efficient yet flexible framework for the organization and interaction of relevant software components. The Rational Behavior Model (RBM) has been developed with these requirements in mind and consists of three levels, called the Strategic, the Tactical, and the Execution levels, respectively. Each level reflects computations supporting the solution to the global control problem based on different abstraction mechanisms. The unique contribution of the RBM architecture is the idea of specifying different programming paradigms to realize each software level. Specifically, RBM uses rule-based programming for the Strategic level, thereby permitting field reconfiguration of missions by a mission specialist without reprogramming at lower levels. The Tactical level realizes vehicle behaviors as the methods of software objects programmed in an object-based language such as Ada. These behaviors are initiated by rule satisfaction at the Strategic level, thereby rationalizing their interaction. The Execution level is programmed in any imperative language capable of supporting efficient execution of real-time control of the underlying vehicle hardware. DTIC

N94-11878# Interface Foundation of North America, Inc., Fairfax Station, VA.
COMPUTING SCIENCE AND STATISTICS, VOLUME 24: GRAPHICS AND VISUALIZATION Final Report, 1 Mar. - 31 May 1992
N. J. Newton 20 Mar. 1993 658 p Presented at the 24th Symposium on the Interface, College Station, TX, 18-21 Mar. 1992
(Contract N00014-92-J-1459)
(AD-A265181) Avail: CASI HC A99/MF A06

The 24th Symposium on the Interface: Computing Science and Statistics was held 18-21 Mar. 1992 in College Station, Texas. The theme was Graphics and Visualization. Sixty invited papers were presented to more than 300 attendees. James Blinn gave the Keynote Address while Edward

Tufte gave the Plenary Address. There were 38 technical sessions, including a poster session. There was also a short course on Visualization. This report presents papers based on the presentations. Also included is a list of attendees. DTIC

N94-12008 Software Productivity Solutions, Inc., Indialantic, FL.
SYSTEM ENGINEERING CONCEPT DEMONSTRATION, PROCESS MODEL, VOLUME 3 Final Report, Feb. 1990 - Jul. 1992
Alberto Ortiz Dec. 1992 130 p Limited Reproducibility: More than 20% of this document may be affected by microfiche quality
(Contract F30602-90-C-0021)
(AD-A265469; RL-TR-92-345-Vol-3) Avail: CASI HC A07

This is the third volume of the Final Technical Report (FTR) for the System Engineering Concept Demonstration (SECD) which was sponsored and managed by the Air Force Rome Laboratory (RL). The SECD was an exploratory development effort which culminated in Catalyst, a fully researched and specified system concept which provides an automated environment of integrated, state-of-the-art software tools and methods. This document reports the results of the SECD Process Model Task. The SECD Process Model is a system acquisition and development model that emphasizes System Engineering activities over the entire system lifecycle. The Process model is a graphical representation of the System Engineering Lifecycle activities, agents, flows, feedbacks, and work products. This interactive Process Model provides a multi-dimensional view of government acquisition and contractor development activities. An integral part of the SECD program, the Process Model aided in developing the system's requirements which are documented in the System/Segment Specification (SSS). The model also demonstrated coverage and completeness of the System Engineering process. DTIC

N94-12332 Naval Postgraduate School, Monterey, CA.
THE INSTRUMENTATION OF THE MULTIMODEL AND MULTILINGUAL USER INTERFACE M.S. Thesis
Paul A. Bourgeois Mar. 1993 126 p Limited Reproducibility: More than 20% of this document may be affected by microfiche quality
(AD-A265444) Avail: CASI HC A07

The traditional approach to database management system (DBMS) designs focuses upon the implementation of a single data model and its corresponding data language in order to support applications for a given database task. Each of these monomodel and monolingual database systems represents a homogeneous database system, since only one data model-language can be supported on a single database system. The application diversity forces many organizations to operate several different homogeneous database systems to support its operations. A different approach to database-system design is the development of a DBMS which supports multiple data models and their data language. This approach is the focus of the multimodel and multilingual database system (MM and MLDS) as implemented on the Multibackend Database Supercomputer (MDBS). With the proliferation of new data model-languages in the database technology, the objective of MM&MLDS is to incorporate these new data model-languages onto the same MDBS. The goal is to develop procedures, methods, and tools for the incorporation of new data model-languages into MM&MLDS as new interfaces. Three areas of research are critical to achieving this goal: (1) the development of a MDBS user's manual for familiarization as well as instruction for system users; (2) the specifications of generic processing algorithms used as a foundation for each module of the new model-language interface; and (3) our software methodology considerations for new data model-language interface implementation. DTIC

N94-12358# Instituto de Pesquisas Espaciais, Sao Jose dos Campos (Brazil).
A NEW HEURISTIC FOR SET COVERING PROBLEMS Thesis [UMA NOVA HEURISTICA PARA PROBLEMAS DE COBERTURA DE CONJUNTOS]
Fabio Belo Lopes Oct. 1992 70 p In PORTUGESE
(INPE-5471-TDI/502) Avail: CASI HC A04/MF A01

This work presents a new heuristic for set covering problems, based upon Continuous Surrogate relaxation and subgradient optimization. We propose an adequate step size control that provides the Surrogate bounds in few subgradient iterations, compared to other relaxations. The algorithm also combines problem reduction tests and a technique to avoid the preliminary sorting to solve the Continuous Surrogate relaxation. Another feature is the definition of an efficient data structure in order to solve large set covering problems (up to 1,000 rows and 12,000 columns). Computational tests indicate better-quality results than algorithms based on Lagrangian relaxation in terms of final solutions and mainly in computer times. Author

N94-12383# European Space Agency. European Space Research and Technology Center, ESTEC, Noordwijk (Netherlands). Cost Analysis Div.
ESA COSTING SOFTWARE (ECOS) INTRODUCTION
Stefan Heerd, ed. 1992 6 p Limited Reproducibility: More than 20% of this document may be affected by color photographs Original contains color illustrations
(ESA-F-28) Copyright Avail: CASI HC A02/MF A01

The European Space Agency and its industrial partners have considerable experience of the demands placed on the management of technically complex, multi-national projects. It is not surprising therefore that to assist management, ESA developed a procedure for determining the allocation of tasks to industry during each phase of complex, multi-contractor projects. To minimize paperwork in this procedure, the Cost Analysis Division at ESTEC introduced the ESA Costing Software, ECOS. With ECOS, work can be divided down the industrial structure, and cost proposals can be generated and passes to higher levels of management. Data can be transferred to ESA either by telecommunications link or on diskettes. CASI

N94-12386# Department of the Navy, Washington, DC.
A HYBRID NEURAL NETWORK AND FEATURE EXTRACTION TECHNIQUE FOR TARGET RECOGNITION Patent Application
Ali Farsaie, inventor (to Navy) and Joseph J. Fuller, inventor (to Navy) 8 Mar. 1993 10 p
(AD-D015732; US-Patent-Appl-SN-028012; Navy-Case-74171) Avail: CASI HC A02/MF A01

An image scene sensed from different viewing angles for image data acquisition purposes in a target identifying system provides data from which target features are extracted, the extracted data being evaluated in an artificial neural network to identify a target at a location within the image scene from which the different viewing angles extend. DTIC

N94-12439# Carnegie-Mellon Univ., Pittsburgh, PA. Dept. of Computer Science.
AVOIDANCE AND SUPPRESSION OF COMPENSATION CODE IN A TRACE SCHEDULING COMPILER
S. M. Freudenberger, T. R. Gross, and P. G. Lowney Apr. 1993 50 p
(AD-A265612; CMU-CS-93-145) Avail: CASI HC A03/MF A01

Trace scheduling is an optimization technique that selects a sequence of basic blocks as a trace and schedules the operations from the trace. If an operation is moved across basic block boundaries, one or more compensation copies may be required in the off-trace code. This paper discusses the generation of compensation code in a trace scheduling compiler and presents techniques for limiting the amount of compensation code: avoidance (restricting code motion so that no compensation code is required) and suppression (analyzing the global flow of the program to detect when a copy is redundant). We evaluate the effectiveness of these techniques based on measurements for the SPEC89 suite and the Livermore Fortran Kernels, using our implementation of trace scheduling for a Multiflow Trace 7/300. The paper compares different compiler models, contrasting the performance of trace scheduling with the performance obtained from typical RISC compilation techniques. There are two key results of this study: First, the amount of compensation code generated is not large. For the SPEC89 suite, the average code size-increase due to trace scheduling is 6%. Avoidance is more important than suppression, although there are some kernels that benefit significantly from compensation code suppression. Since compensation code is not a major issue, a compiler can be more aggressive in code motion and loop unrolling. DTIC

N94-12448*# National Aeronautics and Space Administration. Goddard Space Flight Center, Greenbelt, MD.
TRANSPORTABLE APPLICATIONS ENVIRONMENT (TAE) TENTH USERS' CONFERENCE
Chris Rouff, ed., Elfrieda Harris, ed., and Arleen Yeager, ed. Jul. 1993

224 p Conference held in Greenbelt, MD, 14-17 Jun. 1993
(NASA-CP-3225; NAS 1.55:3225; Rept-93B00098) Avail: CASI HC A10/MF A03

Conference proceedings are represented in graphic visual-aid form. Presentation and panel discussion topics include user experiences with C++ and Ada; the design and interaction of the user interface; the history and goals of TAE; commercialization and testing of TAE Plus; Computer-Human Interaction Models (CHIMES); data driven objects; item-to-item connections and object dependencies; and integration with other software. There follows a list of conference attendees. CASI

N94-12591# Lawrence Livermore National Lab., CA.
OPTIMAL HEMICUBE SAMPLING
N. Max 17 Dec. 1992 14 p Presented at the Siggraph 1993 Conference, Anaheim, CA, 2-6 Aug. 1993
(Contract W-7405-eng-48)
(DE93-010499; UCRL-JC-112597; CONF-930881-1) Avail: CASI HC A03/MF A01

Radiosity algorithms for global illumination, either 'gathering' or 'shooting' versions, depend on the calculation of form factors. It is possible to calculate the form factors analytically, but this is difficult when occlusion is involved, so sampling methods are usually preferred. The necessary visibility information can be obtained by ray tracing in the sampled directions. However, area coherence makes it more efficient to project and scan-convert the scene onto a number of planes, for example, the faces of a hemicube. The hemicube faces have traditionally been divided into equal square pixels, but more general subdivisions are practical and can reduce the variance of the form factor estimates. The hemicube estimates of form factors are based on a finite set of sample directions. We obtain several optimal arrangements of sample directions, which minimize the variance of this estimate. Four approaches are changing the size of the pixels, the shape of the pixels, the shape of the hemicube, or using non-uniform pixel grids. The best approach reduces the variance by 43%. The variance calculation is based on the assumption that the errors in the estimate are caused by the projections of single edges of polygonal patches, and that the positions and orientations of these edges are random. DOE

N94-12593# Sandia National Labs., Albuquerque, NM.
FINDING A COVERING TRIANGULATION WHOSE MAXIMUM ANGLE IS PROVABLY SMALL
S. A. Mitchell and J. K. Park 3 Mar. 1993 13 p Presented at the Workshop on Algorithms and Data Structures, Montreal, Canada, 11-13 Aug. 1993
(Contract DE-AC04-76DP-00789)
(DE93-010691; SAND-93-0690C; CONF-930884-2) Avail: CASI HC A03/MF A01

Given a planar straight-line graph, we find a covering triangulation whose maximum angle is as small as possible. A covering triangulation is a triangulation whose vertex set contains the input vertex set and whose edge set contains the input edge set. Such a triangulation differs from the usual Steiner triangulation in that we may not add a Steiner vertex on any input edge. Covering triangulations provide a convenient method for triangulating multiple regions sharing a common boundary, as each region can be triangulated independently. As it is possible that no finite covering triangulation is optimal in terms of its maximum angle, we propose an approximation algorithm. Our algorithm produces a covering triangulation whose maximum angle gamma is probably close to gamma(sub opt), a lower bound on the maximum angle in any covering triangulation of the input graph. Note that we must have gamma less than or equal to 3(gamma)(sub opt), since we always have gamma(sub opt) greater than or equal to pi/3 and no triangulation can contain an angle of size greater than pi. We prove something significantly stronger. We show that pi - gamma greater than or equal to (pi - gamma(sub opt))/6, i.e., our gamma is not much closer to pi than is gamma(sub opt). This result represents the first nontrivial bound on a covering triangulation's maximum angle. We require a subroutine for the following problem: given a polygon with holes, find a Steiner triangulation whose maximum angle is bounded away from pi. No angle larger than 8(pi)/9 is sufficient for the bound on gamma claimed above. The number of Steiner vertices added by our algorithm and its running time are highly dependent on the corresponding bounds for the subroutine. Given an n-vertex planar straight-line graph, we require O(n + S(n)) Steiner vertices and O(n log n + T(n)) time, where S(n) is the number of Steiner vertices added by the subroutine and T(n) is its running time for an O(n)-vertex polygon with holes. DOE

N94-12606# Department of Energy, Washington, DC. Office of Scientific Computing.
THE DOE PROGRAM IN HIGH-PERFORMANCE COMPUTING AND COMMUNICATIONS (HPCC)
Mar. 1993 99 p
(DE93-013813; DOE/ER-0536) Avail: CASI HC A05/MF A02

This document is intended to serve two purposes. Its first purpose is to report to Congress, as mandated in the High-Performance Computing Act of 1991, the considerable progress that the Department of Energy has made in 1992 toward achieving the goals of the High-Performance Computing and Communications (HPCC) Program. Its second purpose is to provide a snapshot of and an introduction to the many programs administered by the Office of Scientific Computing under the auspices of the HPCC Program. DOE

N94-12608# Sandia National Labs., Albuquerque, NM.
IMPROVED MANY-ON-MANY ROUTE SOFTWARE DESCRIPTION
R. C. Ormesher Apr. 1993 42 p
(Contract DE-AC04-76DP-00789)
(DE93-013961; SAND-93-0858) Avail: CASI HC A03/MF A01 (US Sales Only)

This report describes the models and algorithms used in the Air Force Electronic Warfare Center's (AFEWC's) Improved Many-on-Many (IMOM) ROUTE simulation software. ROUTE simulates an attack aircraft as it penetrates enemy territory that is protected by ground-based search and tracking radars and ground-to-air defensive weapon systems. Self-protection and stand-off jamming are also modelled in the simulation. The overall algorithm for computing the effectiveness of several radars on a single aircraft is described. In particular, the algorithms and mathematical models for calculating the radar range equation, terrain effects using DMA mapping information, weapon system performance, and geometry are described. In addition, the mathematical models and algorithms for calculating the degradation of early-seaming, target-acquisition, fire-control, height-finding, and target-tracking radars due to stand-off and self-protection jammers are described. This document will be useful for analysts who use IMOM and for software developers who modify and extend IMOM's capabilities. Our analysis has examined and validated the theoretical bases for the IMOM ROUTE simulation and its implementation in the software. During the analysis, questions, comments, and concerns were communicated to AFEWC. DOE

N94-10068# CAE-FEM Engineering, Stuttgart (Germany).
SOLVING THE ESSENTIALS OF AN INNOVATIVE TENNIS RACKET PRODUCT: FUNCTIONALITY, SIMPLICITY, AND SUPER-LIGHTWEIGHT TECHNOLOGY
E. Schlenker *In* ESA, Advanced Materials for Lightweight Structures Oct. 1992 p 403-405 (For primary document see N94-10001 01-24)
Copyright Avail: CASI HC A01/MF A04

N94-10985*# Life Sciences Software, Camano Island, WA.
TIMESET: A COMPUTER PROGRAM THAT ACCESSES FIVE ATOMIC TIME SERVICES ON TWO CONTINENTS
P. L. Petrakis *In* NASA. Goddard Space Flight Center, The 24th Annual Precise Time and Time Interval (PTTI) Applications and Planning Meeting Jun. 1993 p 255-266 (For primary document see N94-10963 01-70)
Avail: CASI HC A03/MF A04

N94-10986*# Air System Technologies, Inc., Dallas, TX.
RIGHTIME: A REAL TIME CLOCK CORRECTING PROGRAM FOR MS-DOS-BASED COMPUTER SYSTEMS
G. Thomas Becker *In* NASA. Goddard Space Flight Center, The 24th Annual Precise Time and Time Interval (PTTI) Applications and Planning Meeting Jun. 1993 p 267-276 (For primary document see N94-10963 01-70)
Avail: CASI HC A02/MF A04

N94-10988*# Timing Solutions Corp., Boulder, CO.
ADVANCES IN TIME-SCALE ALGORITHMS

S. R. Stein *In* NASA. Goddard Space Flight Center, The 24th Annual Precise Time and Time Interval (PTTI) Applications and Planning Meeting Jun. 1993 p 289-302 (For primary document see N94-10963 01-70)
Avail: CASI HC A03/MF A04

N94-11338# Deutsche Forschungs- und Versuchsanstalt fuer Luft- und Raumfahrt, Munich (Germany). Inst. of Aeroelasticity.
ADAPTIVE ALGORITHMS FOR USE WITH DIGITAL FILTERS IN VIBRATION CONTROL
R. Wimmel *In* AGARD, Smart Structures for Aircraft and Spacecraft Apr. 1993 5 p (For primary document see N94-11317 01-24)
Copyright Avail: CASI HC A01/MF A04

N94-11564*# Air Force Human Resources Lab., Wright-Patterson AFB, OH. Logistics and Human Factors Div.
CREW CHIEF Abstract Only
Jill Easterly *In* NASA. Johnson Space Center, Sixth Annual Workshop on Space Operations Applications and Research (SOAR 1992), Volume 2 Feb. 1993 p 633 (For primary document see N94-11527 01-99)
Avail: CASI HC A01/MF A03

N94-11578*# Lockheed Engineering and Sciences Co., Houston, TX.
SPACE STATION MAINTENANCE STUDIES USING PLAID GRAPHICS Abstract Only
Mary E. Helm *In* NASA. Johnson Space Center, Sixth Annual Workshop on Space Operations Applications and Research (SOAR 1992), Volume 2 Feb. 1993 p 732 (For primary document see N94-11527 01-99)
Avail: CASI HC A01/MF A03

62 COMPUTER SYSTEMS

Includes computer networks and special application computer systems.

N94-10257# Sandia National Labs., Albuquerque, NM.
MASSIVELY PARALLEL MULTIFRONTAL METHODS FOR FINITE ELEMENT ANALYSIS ON MIMD COMPUTER SYSTEMS
R. E. Benner 1993 18 p Presented at the 8th International Conference on Vehicle Structural Mechanics and Computer-Aided Engineering, Traverse City, MI, 3-5 Jun. 1993
(Contract DE-AC04-76DP-00789)
(DE93-009838; SAND-91-2016C; CONF-9306145-1) Avail: CASI HC A03/MF A01

The development of highly parallel direct solvers for large, sparse linear systems of equations (e.g. for finite element or finite difference models) is lagging behind progress in parallel direct solvers for dense matrices and iterative methods for sparse matrices. We describe a massively parallel (MP) multifrontal solver for the direct solution of large sparse linear systems, such as those routinely encountered in finite element structural analysis, in an effort to address concerns about the viability of scalable, MP direct methods for sparse systems and enhance the software base for MP applications. Performance results are presented and future directions are outlined for research and development efforts in parallel multifrontal and related solvers. In particular, parallel efficiencies of 25% on 1024 NCUBE 2 nodes and 36% on 64 Intel iPSC860 nodes have been demonstrated, and parallel efficiencies of 60-85% are expected when a severe load imbalance is overcome by static mapping and dynamic load balance techniques previously developed for other parallel solvers and application codes. DOE

N94-10277# Universiteit Twente, Enschede (Netherlands). Dept. of Computer Science.
LAYERING TECHNIQUES FOR DEVELOPMENT OF PARALLEL SYSTEMS: AN ALGEBRAIC APPROACH
Mannes Poel and Job Zwiers Oct. 1992 24 p Sponsored in part by EEC
(Memo-INF-92-62; ETN-93-94319) Copyright Avail: CASI HC A03/MF A01

A language which makes clear the distinction between temporal order and causal order is presented. This allows for a transformational approach, in an algebraic way, to the specification and verification of concurrent systems. One of these is an algebraic formulation of the communication closed layers principle. These laws suffice to rewrite process terms that avoid specification of temporal ordering into a unique normal form. Other transformations allow for gradually imposing temporal ordering on an already functionally correct design. The combination of such laws enables a design strategy where architecture independent designs are transformed towards a form that matches a particular implementation architecture. This style of design is applied to various distributed algorithms, including the following: an algorithm for the 'point-in-polygon' problem transformed to a form suitable for pipeline execution on a tree network; the Floyd-Warshall algorithm for the all points shortest path transformed to a form suitable for execution on a Single Instruction Multiple Data stream (SIMD) architecture; and the CYK algorithm for parsing context free languages, on a Multiple Instruction Multiple Data stream (MIMD) architecture. ESA

N94-10324# Lawrence Livermore National Lab., CA.
PRACTICAL AUTHORIZATION IN LARGE HETEROGENEOUS DISTRIBUTED SYSTEMS
J. G. Fletcher and D. M. Nessett Nov. 1992 11 p Presented at the Privacy and Security Research Group Workshop on Network and Distributed Systems Security, San Diego, CA, 11-12 Feb. 1993
(Contract W-7405-eng-48)
(DE93-013192; UCRL-JC-112301; CONF-930245-1) Avail: CASI HC A03/MF A01

Requirements for access control, especially authorization, in practical computing environments are listed and discussed. These are used as the basis for a critique of existing access control mechanisms, which are found to present difficulties. A new mechanism, free of many of these difficulties, is then described and critiqued. DOE

N94-10340# Superconducting Super Collider Lab., Dallas, TX.
A PARALLEL IMPLEMENTATION OF PARTICLE TRACKING WITH SPACE CHARGE EFFECTS ON AN INTEL IPSC/860
L. C. Chang, G. Bourianoff, B. Cole, and S. Machida Apr. 1993 24 p Presented at the 5th Annual International Industrial Symposium on the Super Collider and Exhibition, San Francisco, CA, 6-8 May 1993 Revised
(Contract DE-AC35-89ER-40486)
(DE93-012307; SSCL-Preprint-149-Rev-1; CONF-930537-8-Rev-1) Avail: CASI HC A03/MF A01

Particle-tracking simulation is one of the scientific applications that is well-suited to parallel computations. At the Superconducting Super Collider, it has been theoretically and empirically demonstrated that particle tracking on a designed lattice can achieve very high parallel efficiency on a MIMD Intel iPSC/860 machine. The key to such success is the realization that the particles can be tracked independently without considering their interaction. The perfectly parallel nature of particle tracking is broken if the interaction effects between particles are included. The space charge introduces an electromagnetic force that will affect the motion of tracked particles in 3-D space. For accurate modeling of the beam dynamics with space charge effects, one needs to solve three-dimensional Maxwell field equations, usually by a particle-in-cell (PIC) algorithm. This will require each particle to communicate with its neighbor grids to compute the momentum changes at each time step. It is expected that the 3-D PIC method will degrade parallel efficiency of a particle-tracking implementation on any parallel computer. In this paper, we describe an efficient scheme for implementing particle tracking with space charge effects on an INTEL iPSC/860 machine. Experimental results show that a parallel efficiency of 75% can be obtained. DOE

N94-10368# National Aerospace Lab., Tokyo (Japan). Computational Sciences Div.
SIMULATION OF A PARALLEL COMPUTER [HEIRETSU KEISANKI NO KENSHOU MOGI]
Kouichi Harada, Masahiro Yoshida, and Kinuyo Nakamura May 1992 38 p In JAPANESE
(NAL-TR-1154; JTN-93-80439; DE93-793618) Avail: CASI HC A03/MF A01

Using the National Aerospace Laboratory (NAL) numerical simulater, a software program simulating a parallel computer configurated with 128 x 256 processing elements was run following the implementation of its associated assembly language. The software simulates a parallel computer's memory access and register operation at the clock level and generates an operational time diagram along with results, whereas the assembly language describe its execution procedures. The operation of this computer was evaluated by employing a basic function subroutine, with the instruction set and network between the memory and the processing elements, being subsequently examined, thereby enabling estimation of its maximum efficiency. In addition, efficiency was further evaluated by comparing the resultant parallel processing time using a two dimensional computational fluid dynamics program to the corresponding sequential processing time obtained with a processing element. Author (NASDA)

N94-10488# Naval Command, Control and Ocean Surveillance Center, San Diego, CA. Research, Development, Test and Evaluation Div.

APPLICATION OF PARALLEL PROCESSING TO A SURFACE PATCH/WIRE JUNCTION EFIE CODE

L. C. Russell and J. W. Rockway Mar. 1993 21 p
(AD-A264965) Avail: CASI HC A03/MF A01

A surface patch/wire junction EFIE method of moment algorithm, JUNCTION, developed by the University of Houston has been implemented in a transputer based parallel processing environment installed in a personal computer. This paper addresses transputer hardware and software options, the JUNCTION algorithm, techniques for parallelizing matrix analysis algorithms, and performance results. The transputer array was found to provide a flexible, low-cost, high performance desktop computing environment for method of moment analysis. DTIC

N94-10544 Academy of Sciences (USSR), Novosibirsk. Inst. Yadernoj Fiziki.

CONTROLLER OF SERIAL MULTIPLEX COMMUNICATION CHANNEL [KONTROLLER POSLEDOVATEL'NOGO KANALA SVYAZI]

A. N. Kvashnin, V. V. Konyukhov, and A. D. Khilchenko 1991 20 p In RUSSIAN Limited Reproducibility: More than 20% of this document may be affected by microfiche quality
(DE92-641157; IYaF-91-37) Avail: CASI HC A03 (US Sales Only)

Controller of serial multiplex communication channel is described. It is designed for the interface of node computers, based both on 'Q' and 'U' bus, with remote measurement and control units in distributed automated systems, including operation stations, based on microcomputers of 'Elektronika-60' type. The controller represents the main module of communication system, executing all exchange procedures, provided by 26765.52-87 standard. It operates with cable line of 1 km maximal length and services up to 30 attached units. DOE

N94-10738 Sandia National Labs., Albuquerque, NM.

BRINGING THEORY TO PRACTICE: THE REALITY OF INTERPROCESSOR COMMUNICATION

D. S. Greenberg and K. S. McCurley 1993 5 p Presented at the Workshop on Analyzing Scalibility of Parallel Algorithms, Newport Beach, CA, 13 Apr. 1993 Limited Reproducibility: More than 20% of this document may be affected by microfiche quality
(Contract DE-AC04-76DP-00789)
(DE93-012346; SAND-93-0955; CONF-9304140-1) Avail: CASI HC A01

Determining the best topology for the interconnection network of a scalable processor is not possible via theoretical models. However, we might hope that theoretical results would at least help researchers to make the most efficient use possible of existing machines. Unfortunately theoretical work often stops short of providing everything which the practitioner requires. In this paper two communication problems transpose and all-to-all broadcast, are used to illustrate the additional effort required to make the theoretical practical. DOE

N94-11027# Lawrence Livermore National Lab., CA.

THE ZIPCODE MESSAGE-PASSING SYSTEM

A. Skjellum, S. G. Smith, C. H. Still, A. P. Leung (Syracuse Univ., NY.), and M. Morari (California Inst. of Tech., Pasadena.) 12 Nov. 1992 18 p Presented at the 6th SIAM Conference on Parallel Processing for Scientific Computing, Norfolk, VA, 21-24 Mar. 1993
(Contract W-7405-eng-48)
(DE93-011958; UCRL-JC-112022; CONF-930331-9) Avail: CASI HC A03/MF A01

Zipcode is a message-passing system developed originally by the first author, beginning at Caltech and continuing to-date. Zipcode was created to address features and issues absent in then-existing message-passing systems. Currently, Zipcode continues to serve as a vehicle to demonstrate high-level message-passing research concepts and, more importantly, to provide the basis for supporting vendor-independent scalable concurrent libraries; notably, the Multicomputer Toolbox. The basic assertion of Zipcode is that carefully managed, expressive message-passing is an effective way to program multicomputers and distributed computers, while low-level message passing is admittedly both error-prone and difficult. The purpose of Zipcode is to manage the message-passing process within parallel codes in an open-ended way. This is done so that large-scale software can be constructed in a multicomputer application, with reduced likelihood that software so constructed will conflict in its dynamic resource use, thereby avoiding potentially hard-to-resolve, source-level conflicts. Furthermore, the message-passing-notations provided are to reflect the algorithms and data organizations of the concurrent algorithms, rather than predefined typing strategies. Typing, while generic and easy-to-understand, proves too low-level to support manageable application development well. Notational abstractions provide a means for the user to incorporate information through which the Zipcode library may make optimizations when a code runs on systems with specific hardware features. Abstraction is therefore seen as a means to higher performance, and notation is seen as a means towards more understandable, easier-to-develop and maintain concurrent software. Context registry provides a 'social contract' within which multiple libraries and codes can coexist reasonably. DOE

N94-11248# Lawrence Livermore National Lab., CA.

THE PVM SYSTEMS: AN IN-DEPTH ANALYSIS AND DOCUMENTING STUDY. CONCISE EDITION

B. K. Grant and A. Skjellum Nov. 1992 20 p Presented at the 9th International Conference on Systems Engineering 1993, Las Vegas, NV, 14-16 Jul. 1993
(Contract W-7405-eng-48)
(DE93-011959; UCRL-JC-112016; CONF-930773-1) Avail: CASI HC A03/MF A01

The Parallel Virtual Machine (PVM) is a basic message-passing system for heterogeneous collections of networked computers, developed at Oak Ridge National Laboratory, University of Tennessee, and Emory University. This report is our 'third-party' effort to answer most common questions about PVM and to dispel many misconceptions regarding its capabilities. We strive to present an accurate assessment of the system, while adding our own opinions regarding the system, and offering a few suggestions for the future of the system. PVM version 2.4.1, the latest version at the time of the writing of this report, is summarized within this document; our forthcoming full report includes significantly more detailed information. Information on how to get the full report is included. DOE

N94-11270# Sandia National Labs., Albuquerque, NM.

A HETEROGENEOUS GRAPHICS PROCEDURE FOR VISUALIZATION OF MASSIVELY PARALLEL SOLUTIONS

1993 6 p Presented at the American Society of Mechanical Engineers (ASME) Fluids Engineering Conference, Washington, DC, 20-24 Jun. 1993
(Contract DE-AC04-76DP-00789)
(DE93-009628; SAND-93-0227C; CONF-930621-3) Avail: CASI HC A02/MF A01

Scientific visualization is playing an increasingly important role in the analysis and interpretation of massively parallel CFD simulations due to the enormous volume of data that can be generated on these machines. In this paper we will describe the development of a visualization technique based on a parallel analogue to the Marching Cubes algorithm. The algorithm has been developed for Multiple-Instruction, Multiple-Data (MIMD) massively parallel computers and is designed to take advantage of the heterogeneous programming capabilities of the MIMD architecture. We examine several different configurations and conclude that for producing animations the best one, in terms of both frame generation time and disk usage, is to run the two applications heterogeneously and send the resulting geometry description directly to a workstation for rendering, thereby totally eliminating the use of files from the animation process. DOE

N94-11293# Naval Command, Control and Ocean Surveillance Center, San Diego, CA. Research, Development, Test and Evaluation Div.

HETEROGENEOUS SUPERCONCURRENT PARALLELISM (HeSCP) Professional Paper

R. F. Freund Mar. 1993 14 p
(AD-A265004) Avail: CASI HC A03/MF A01

HeSCP (Heterogeneous SuperConcurrent Parallelism, pronounced 'hee-skip') is the tuned use of diverse processors to solve distinct computational needs, in which codes or code portions are directed to the processor(s) best suited for their execution. Implicit in this definition is the idea that different tasks or different portions of these tasks indicate different architectural requirements or different balances of requirements. The processors themselves are generally parallel or other HPC machines. Typically the processors are used concurrently and it is often the case that tools and methodologies used for parallel and vector processing, e.g., code profiling, flow analysis, data dependencies, etc., can be extended to the larger, meta-parallel processor. The super in SuperConcurrent refers to the traditional supercomputing aims of HeSCP, as well as the heterogeneous concurrency superimposed on the various parallel processors, and finally the aim of superlinear performance from the tuned orchestration of the heterogeneous components. DTIC

N94-11308*# Institute for Computer Applications in Science and Engineering, Hampton, VA.
OPTIMAL CUBE-CONNECTED CUBE MULTIPROCESSORS Final Report
Xian-He Sun and Jie Wu Washington May 1993 17 p
(Contract NAS1-19480; RTOP 505-90-52-01)
(NASA-CR-191463; ICASE-93-23; NAS 1.26:191463) Avail: CASI HC A03/MF A01

Many CFD (computational fluid dynamics) and other scientific applications can be partitioned into subproblems. However, in general the partitioned subproblems are very large. They demand high performance computing power themselves, and the solutions of the subproblems have to be combined at each time step. The cube-connect cube (CCCube) architecture is studied. The CCCube architecture is an extended hypercube structure with each node represented as a cube. It requires fewer physical links between nodes than the hypercube, and provides the same communication support as the hypercube does on many applications. The reduced physical links can be used to enhance the bandwidth of the remaining links and, therefore, enhance the overall performance. The concept and the method to obtain optimal CCCubes, which are the CCCubes with a minimum number of links under a given total number of nodes, are proposed. The superiority of optimal CCCubes over standard hypercubes was also shown in terms of the link usage in the embedding of a binomial tree. A useful computation structure based on a semi-binomial tree for divide-and-conquer type of parallel algorithms was identified. It was shown that this structure can be implemented in optimal CCCubes without performance degradation compared with regular hypercubes. The result presented should provide a useful approach to design of scientific parallel computers. Author (revised)

N94-11475# Naval Research Lab., Washington, DC.
RELIABILITY ANALYSIS FOR FDDI DUAL HOMING NETWORKS
Gam D. Nguyen 7 May 1993 13 p
(AD-A266133; NRL/FR/5862-93-9552) Avail: CASI HC A03/MF A01

Fiber Distributed Data Interface (FDDI) is a high-speed, fiber-optic token network consisting of two counter-rotating rings. In addition to the fault tolerant level provided by the dual rings, the reliability of an FDDI network is enhanced by the use of station bypass switches or concentrators (CON's). A station equipped by a bypass switch is switched out of the ring when the station experiences a power failure. A CON facilitates the connection of stations to the ring and also switches out of the ring any faulty station connected to it. The use of reliable CON's to interconnect stations is the heart of the dual homing configuration. DTIC

N94-11650 Rochester Univ., NY. Dept. of Computer Science.
SCALABLE SPIN LOCKS FOR MULTIPROGRAMMED SYSTEMS
Robert W. Wisniewski, Leonidas I. Kontothanassis, and Michael L. Scott Apr. 1993 14 p Limited Reproducibility: More than 20% of this document may be affected by microfiche quality
(Contract N00014-92-J-1801; NSF CDA-88-227240; NSF CCR-90-05633; ARPA Order 8930)
(AD-A265007; TR-454) Avail: CASI HC A03

Synchronization primitives for large-scale multiprocessors need to provide low latency and low contention to achieve good performance. Queue-based locks (implemented in software with fetch and Phi instructions) can greatly reduce contention and improve overall performance by arranging for processors to spin only local locations. Unfortunately, queued locks exhibit poor behavior in the presence of multiprogramming: a process near the end of the queue, in addition to waiting for any process ahead of it in the queue. To solve this problem, we present two queue-based locks that recover from in queue preemption. The first employs the kernel interface of the NYU Symunix project. The second employs an extended interface that shares information in both directions across the user-kernel boundary. This results in simpler code and better performance. Experiments with these locks in both real and synthetic applications on SGI and KSR multiprocessors confirm the feasibility of high-performance software locks on systems that are both very large and multiprogrammed. DTIC

N94-11829# Bolt, Beranek, and Newman, Inc., Cambridge, MA. Systems and Technology Div.
HIGH-PERFORMANCE DISTRIBUTED SYSTEMS ARCHITECTURE Final Report, Aug. 1990 - Feb. 1992
Carl D. Howe, Kenneth J. Schroder, A. D. Owen, Richard Koolish, and Charles Lynn Mar. 1993 48 p
(Contract F30602-90-C-0036)
(AD-A265297; BBNI-7711; TR-93-1) Avail: CASI HC A03/MF A01

The objectives of the High Performance Distributed Systems Architecture (HPDSA) project are to integrate very high bandwidth networks with heterogeneous computer architectures (including parallel and specialized processors) and support multiple programming models with this system. The driving forces for this project are user demands for high-performance computing coupled with the availability of gigabit and high bandwidth networking. Command and control applications are increasingly requiring the capabilities of both specialized processors and supercomputer-class machines. These resources are often concentrated at computer centers while the data sources and users of these systems are geographically distributed. By linking users, data sources, and systems together with high-speed networks and distributed operating systems, the quality of command and control information can be substantially improved and that information can be provided to more people. A high-performance distributed operating system must satisfy a number of design goals to accomplish our architectural objectives. Foremost, it must be capable of accommodating a wide variety of computers, networks, and programming languages. DTIC

N94-11881# Carnegie-Mellon Univ., Pittsburgh, PA. Software Engineering Inst.
DISTRIBUTED REAL-TIME SYSTEM DESIGN: THEORETICAL CONCEPTS AND APPLICATIONS Final Report
Lui Sha and Shirish S. Sathaye Mar. 1993 39 p
(Contract F19628-90-C-0003)
(AD-A265199; CMU/SEI-93-TR-02; ESC-TR-93-179) Avail: CASI HC A03/MF A01

Distributed real-time system design raises new theoretical issues and application challenges that are beyond those found in centralized systems. Rate monotonic scheduling (RMS) theory has been successfully applied in the scheduling of centralized systems. RMS and its generalizations have been adopted by national high technology projects such as the Space Station and it has recently been supported by major open standards such as the IEEE Futurebus+ and POSIX.4. In this paper, we describe the use of generalized rate monotonic scheduling theory for the design and analysis of a distributed real-time system. We view the recent extensions of the theory to distributed system scheduling, examine the architectural requirements for use of the theory, and finally provide an application example. DTIC

N94-12540# Rome Lab., Griffiss AFB, NY.
PROBLEM SPECIFIC ENVIRONMENTS FOR PARALLEL SYSTEMS Technical Report, Apr. 1991 - Jan. 1992
Loretta S. Auvil Apr. 1993 84 p
(AF Proj. 5581)
(AD-A266129; RL-TR-93-43) Avail: CASI HC A05/MF A01

Parallelism is one of the key components of large scale, high performance computing. Extensive use of parallelism has yielded a tremendous increase in the raw processing speed of high performance systems, but parallel problem solving remains difficult. These difficulties are typically solved by building software tools, such as parallel programming environments. Existing parallel programming environments are general purpose, using a broad paradigm. This report illustrates that problem specific environments are more beneficial than general purpose environments by making a case study comparison of two classes of problems. The simple class consists of two classic graph problems, namely, all pairs shortest path and connected components. The complex class consists of an elliptic partial differential equations solved via domain decomposition. The general purpose tools BUILD and SCHEDULE are used to solve each class. A problem specific environment for solving each class is then described. Comparisons between special purpose environments and general purpose environments show that the special purpose environments allow the user to concentrate on the problem, while general purpose environments force the user to think about mapping the problem to the environment rather than solving the problem in parallel. DTIC

N94-12597# Lawrence Livermore National Lab., CA.
NETWORKS OF REAL-TIME PROCESSES
R. K. Yates Mar. 1993 17 p Presented at the 4th International Conference on Concurrency Theory, Hildesheim, Germany, 23-26 Aug. 1993
(Contract W-7405-eng-48)
(DE93-013049; UCRL-JC-113531; CONF-930898-1) Avail: CASI HC A03/MF A01

Networks of real-time processes prove that the input-output function computed by a network of asynchronous real-time processes is described by the unique fixed point of a network functional even though the components of the network may compute nonmonotonic functions. The techniques used are those of contractive functions on metric spaces rather than the usual Scott continuity on partial orders. Thus a well-known principle of Kahn is extended to an important model of parallel systems that has been resistant to the traditional approach using Scott continuity. DOE

63 CYBERNETICS

Includes feedback and control theory, artificial intelligence, robotics and expert systems.

For related information see also *54 Man/System Technology and Life Support.*

N94-10169# Technische Univ., Eindhoven (Netherlands). Dept. of Mathematics and Computing Science.
THE APPLICABILITY OF NEURAL NETS FOR DECISION SUPPORT
E. H. L. Aarts (Philips Gloeilampenfabrieken N.V., Eindhoven, Netherlands.), J. Wessels (International Inst. for Applied Systems Analysis, Laxenburg, Austria.), and P. J. Zwietering Nov. 1992 24 p
(MEMO-COSOR-92-49; ETN-93-94328) Copyright Avail: CASI HC A03/MF A01

The aim of the work is to discuss the possible role of neural nets for decision support. The discussion is conducted along two connected lines. The first line regards the possibilities to solve combinatorial optimization problems with multilayered perceptrons. Particular attention is given to the required complexity of such neural nets. The second line regards the use of neural nets as a kind of black box decision mechanism for decision problems for which the underlying processes are difficult or not well understood. For direct use of the results of the first line it would be essential to have cheap neuro-based computing aids available. Even without the availability of such aids, the results are useful for supporting the second line. The second line has its value independent of the availability of special neural computing aids. It provides an alternative paradigm for decision support, which can be simulated on traditional computing equipment. ESA

N94-10345*# North Carolina State Univ., Raleigh. Mars Mission Research Center.
TELEROBOTIC CONTROL OF A MOBILE COORDINATED ROBOTIC SERVER M.S. Thesis Annual Technical Report
Gordon Lee 10 Aug. 1993 75 p
(Grant NAG1-1283)
(NASA-CR-193465; NAS 1.26:193465) Avail: CASI HC A04/MF A01

The annual report on telerobotic control of a mobile coordinated robotic server is presented. The goal of this effort is to develop advanced control methods for flexible space manipulator systems. As such, an adaptive fuzzy logic controller was developed in which model structure as well as parameter constraints are not required for compensation. The work builds upon previous work on fuzzy logic controllers. Fuzzy logic controllers have been growing in importance in the field of automatic feedback control. Hardware controllers using fuzzy logic have become available as an alternative to the traditional PID controllers. Software has also been introduced to aid in the development of fuzzy logic rule-bases. The advantages of using fuzzy logic controllers include the ability to merge the experience and intuition of expert operators into the rule-base and that a model of the system is not required to construct the controller. A drawback of the classical fuzzy logic controller, however, is the many parameters needed to be turned off-line prior to application in the closed-loop. In this report, an adaptive fuzzy logic controller is developed requiring no system model or model structure. The rule-base is defined to approximate a state-feedback controller while a second fuzzy logic algorithm varies, on-line, parameters of the defining controller. Results indicate the approach is viable for on-line adaptive control of systems when the model is too complex or uncertain for application of other more classical control techniques. Author (revised)

N94-10487# Brown Univ., Providence, RI.
UNSUPERVISED SPLITTING RULES FOR NEURAL TREE CLASSIFIERS
Michael P. Perone and Nathan Intrator 17 May 1993 7 p
(Contract N00014-91-J-1316)
(AD-A264961) Avail: CASI HC A02/MF A01

This paper presents two unsupervised neural network splitting rules for use with CART-like neural tree algorithms in high dimensional data space. These splitting rules use an adaptive variance estimate to avoid some possible local minima which arise in unsupervised methods. We explain when the unsupervised splitting rules outperform supervised neural network splitting rules and when the unsupervised splitting rules outperform the standard node impurity splitting rules of CART. Using these unsupervised splitting rules lead to a nonparametric classifier for high dimensional space that extracts local features in an optimized way. DTIC

N94-10638*# Rensselaer Polytechnic Inst., Troy, NY. Center for Intelligent Robotic Systems for Space Exploration.
TASK PLANNING WITH UNCERTAINTY FOR ROBOTIC SYSTEMS Thesis
Tiehua Cao Mar. 1993 233 p
(Grant NAGw-1333)
(NASA-CR-193253; NAS 1.26:193253; CIRSSE-137) Copyright Avail: CASI HC A11/MF A03

In a practical robotic system, it is important to represent and plan sequences of operations and to be able to choose an efficient sequence from them for a specific task. During the generation and execution of task plans, different kinds of uncertainty may occur and erroneous states need to be handled to ensure the efficiency and reliability of the system. An approach to task representation, planning, and error recovery for robotic systems is demonstrated. Our approach to task planning is based on an AND/OR net representation, which is then mapped to a Petri net representation of all feasible geometric states and associated feasibility criteria for net transitions. Task decomposition of robotic assembly plans based on this representation is performed on the Petri net for robotic assembly tasks, and the inheritance of properties of liveness, safeness, and reversibility at all levels of decomposition are explored. This approach provides a framework for robust execution of tasks through the properties of traceability and viability. Uncertainty in robotic systems are modeled by local fuzzy variables, fuzzy marking variables, and global fuzzy variables which are incorporated in fuzzy Petri nets. Analysis of properties and reasoning about uncertainty are investigated using fuzzy reasoning structures built into the net. Two applications of fuzzy Petri nets, robot task sequence planning and sensor-based error recovery, are explored. In the first application, the search space for feasible and complete task sequences with correct precedence relationships is reduced via the use of global fuzzy variables in reasoning about subgoals. In the second application, sensory verification operations are modeled by mutually exclusive transitions to reason about local and global fuzzy variables on-line and automatically select a retry or an alternative error recovery sequence when errors occur. Task sequencing and task execution with error recovery capability for one and multiple soft components in robotic systems are investigated. Author

N94-10869# Technische Univ., Eindhoven (Netherlands). Dept. of Mathematics and Computing Science.
SAMPLE-DATA AND DISCRETE-TIME H2 OPTIMAL CONTROL
H. L. Trentelman (Groningen Rijksuniv., Netherlands.) and A. A. Stoorvogel
2 Dec. 1992 37 p
(MEMO-COSOR-92-53; ETN-93-94332) Copyright Avail: CASI HC A03/MF A01

The sampled data H(sub 2) optimal control problem is discussed. Given a linear time invariant continuous time system, the problem of minimizing the H(sub 2) performance over all sampled data controllers with a fixed sampling period can be reduced to a pure discrete time optimal control problem. This discrete time problem is always singular. The discrete time H(sub 2) optimal control problem in its full generality is studied. The results are applied to the singular discrete time H(sub 2) problem arising from the sampled data H(sub 2) problem. Conditions for the existence of optimal sampled data controllers are given. It is shown that the H(sub 2) performance of a continuous time controller can always be recovered asymptotically by choosing the sampling period sufficiently small. The optimal sampled data H(sub 2) performance is shown to converge to the continuous time optimal H(sub 2) performance as the sampling period converges to zero. ESA

N94-10898 Texas Univ., Austin.
THE DEVELOPMENT OF AN INTERACTIVE SYNTHESIS TOOL FOR INTELLIGENT CONTROLLERS OF MODULAR, RECONFIGURABLE ROBOTS Ph.D. Thesis
Catherine Glauber Ambrose 1992 318 p
Avail: Univ. Microfilms Order No. DA9309115

Intelligent controller design for modular, reconfigurable robot architectures was investigated. In robotic systems available today, the controller is the main limiting factor for enhanced performance. Numerous researchers are studying new controller architectures to allow for the implementation of advanced software, but few have targeted their research at reconfigurable designs. Focus was on the development of a modular controller architecture that can be reconfigured to meet the changing needs of new manipulators and new tasks. The dissertation work was divided into two parallel lines of research. First, a road map assessing the required technology for an intelligent controller was created. A complete model of robotic manipulators was developed which included the arm dynamics and the dynamics of the joint actuator systems. This model was used to determine the desired update rate for command signals from the robot controller. Second, a synthesis package was developed on a Silicon Graphics workstation to simulate controller architectures. This package allows the user to assemble computer components and select controller algorithms, and then evaluates the effectiveness of the design. Bottlenecks are easily identified and improved architectures can be rapidly created. This synthesis package was used to underscore the issues discussed in the road map. Author (revised)

N94-11049# Intelligent Reasoning Systems, Inc., Las Cruces, NM.
A HIGH-SPEED OBJECT RECOGNITION CHIP BASED ON BIOLOGICALLY-REALISTIC HYBRID TEMPORAL PROCESSING ELEMENT Progress Report No. 1, 1 Apr. - 31 May 1993
26 May 1993 22 p
(Contract N00014-93-C-0118)
(AD-A265490) Avail: CASI HC A03/MF A01

The technical objective of this Phase 1 effort is to evaluate the feasibility of a binocular object recognition system for the integrated active vision system (AVS) currently under development at IRSI. The AVS based on a custom very large scale integration (VLSI) Hybrid Temporal Processing Element (HTPE) developed by IRSI (patent pending). Active vision implies that the image collection and processing operations form a single, integrated, adaptive system in which high-level processes, such as object recognition, can augment lower-level processes through feedback connections and can itself be controlled by higher levels. For example, the object recognition process can instruct the oscillating saccadic perception system to enhance the image resolution by a particular amount to assist in the object recognition process. Higher level perception systems can guide the object recognition processes by using expectations of what objects might be present in the image. Therefore, the AVS behaves as single image collection and processing system with coupled low-and high-level capabilities. DTIC

N94-11289# Brown Univ., Providence, RI.
NEURAL NETWORK MODEL SELECTION USING ASYMPTOTIC JACKKNIFE ESTIMATOR AND CROSS-VALIDATION METHOD
Yong Liu 17 May 1993 9 p
(Contract N00014-91-J-1316)
(AD-A264960) Avail: CASI HC A02/MF A01

Two theorems and a lemma are presented about the use of jackknife estimator and the cross-validation method for model selection. Theorem 1 gives the asymptotic form for the jackknife estimator. Combined with the model selection criterion, this asymptotic form can be used to obtain the fit of a model. The model selection criterion we used is the negative of the average predictive likelihood, the choice of which is based on the idea of the cross-validation method. Lemma 1 provides a formula for further exploration of the asymptotics of the model selection criterion. Theorem 2 given an asymptotic form of the model selection criterion for the regression case, when the parameters optimization criterion has a penalty term. Theorem 2 also proves the asymptotic equivalence of Moody's model selection criterion (Moody, 1992) and the cross-validation method, when the distance measure between response y and regression function takes the form of a squared difference. DTIC

N94-11630 International Centre for Theoretical Physics, Trieste (Italy).
A REGIONAL INVERSE EIGENVALUE PROBLEM: SOLUTION WITH APPLICATION IN CONTROL THEORY
M. A. Shalaby Oct. 1992 11 p Limited Reproducibility: More than 20% of this document may be affected by microfiche quality
(DE93-619666; IC-92/323) Avail: CASI HC A03 (US Sales Only)

A new procedure for the solution of the regional inverse eigenvalue problem is suggested and applied to the pole assignment problem of control theory. Algebraic inequalities are derived, they set bounds on the real and imaginary parts of the closed-loop matrix eigenvalues. As a result, these eigenvalues are located inside a prescribed rectangular region in the complex plane, which is better in real applications to control the system performance by a controller matrix which is computed in a more simpler way. DOE

N94-11640 University of Southern Illinois, Carbondale.
MODEL REFERENCE ADAPTIVE CONTROL (MRAC) WITH APPLICATIONS TO ROBOTICS Ph.D. Thesis
Ricky Yin Jun Tam 1992 277 p
Avail. Univ. Microfilms Order No. DA9312081

Model reference adaptive control (MRAC) is investigated using a modified output error method (MOEM), a dual adaptive identifier/controller (DAIC), and a neuromorphic DAIC. It is shown that the adaptive law resulting from the error equation for MOEM does not require knowledge of the sign of the high frequency gain of the plant transfer function. Only a lower bound on the high frequency gain of the plant transfer function is necessary to assure the boundedness of all signals in the overall closed-loop system. No requirement of strictly positive realness is imposed on the reference model transfer function. A new dual adaptive identifier/controller is presented for model reference adaptive control. An inherent duality is shown to exist between adaptive identification and control in DAIC. An advantage of this duality in DAIC is that it enables the same adaptive algorithm to be used for both identification and control of an unknown plant. In the presence of an unbounded disturbance, an approach based on representing the unbounded disturbance functional in a series of bounded orthogonal functions is used for MRAC with a dual adaptive identifier/controller. A new method of extending the well known multilayered feed forward neural network with error back-propagation learning for the neuromorphic DAIC to perform on-line identification and control is also presented. It is demonstrated that the neuromorphic DAIC has a unique property, due to its duality: that an identical architecture of a modified multilayered feed forward neural network can be used for implementing both the neuromorphic identifier and the neuromorphic controller of DAIC. Parameter convergence and global stability of the overall closed-loop system resulting from the above three adaptive control methods are investigated. Proofs pertaining to the parameter convergence, global stability, and the derivation of the adaptive algorithms used for the adaptive control methods are included. Graphical results obtained from computer simulations of the adaptive control of a robotic manipulator system using the adaptive control methods studied are presented. Dissert. Abstr.

N94-11644# Argonne National Lab., IL. Reactor Analysis Div.
STATISTICAL AND OPTIMIZATION METHODS TO EXPEDITE NEURAL NETWORK TRAINING FOR TRANSIENT IDENTIFICATION
J. Reifman, E. J. Vitela, and J. C. Lee 1993 9 p Presented at the Meeting on Nuclear Plant Instrumentation, Control and Man-Machine Interface Technologies, Oak Ridge, TN, 18-21 Apr. 1993
(Contract W-31-109-eng-38)
(DE93-009985; ANL/RA/CP-77255; CONF-930401-12) Avail: CASI HC A02/MF A01

Two complementary methods, statistical feature selection and nonlinear optimization through conjugate gradients, are used to expedite feedforward neural network training. Statistical feature selection techniques in the form of linear correlation coefficients and information-theoretic entropy are used to eliminate redundant and non-informative plant parameters to reduce the size of the network. The method of conjugate gradients is used to accelerate the network training convergence and to systematically calculate the teaming and momentum constants at each iteration. The proposed techniques are compared with the backpropagation algorithm using the entire set of plant parameters in the training of neural networks to identify transients simulated with the Midland Nuclear Power Plant Unit 2 simulator. By using 25% of the plant parameters and the conjugate gradients, a 30-fold reduction in CPU time was obtained without degrading the diagnostic ability of the network. DOE

N94-11825 North Carolina State Univ., Raleigh.
AN ADAPTIVE AND ROBUST CONTROL FOR MOTION COORDINATION OF TWO-COOPERATING ROBOT MANIPULATORS Ph.D. Thesis
Hyeung-Sik Choi 1993 136 p
Avail: Univ. Microfilms Order No. DA9312374

In a two-arm system, the dynamics of the two robot arms are highly coupled to each other, and parameters of the robot arms and an object are often unknown. For this reason, a good motion coordination of a two-arm system cannot be achieved by conventional control schemes. By incorporating the dynamics of the object into a dynamics of one arm, the order of the two-arm dynamics is reduced. Based on the reduced order model, three different control schemes are devised to have a good motion coordination of the two-arm systems: the first, under no parametric uncertainties, a force/position control scheme is devised, which coordinates a leader arm while regulating the coupling forces; second, when system parameters are unknown, an adaptive control scheme on the top of the force/position control scheme is devised to estimate the unknown parameters such that the parametric uncertainties are reduced or eliminated. However, the devised control scheme requires the feedback of the second derivative of the interacting forces and the existence of the non-singular inertia matrix which is a function of parameter estimates; third, to avoid this feedback, a new adaptive control scheme is devised. Also, to compensate coupling forces between two arms and bounded input disturbances, a robust control scheme is devised. Stability robustness analyses of the control schemes are shown based on Lyapunov Second Method. Numerical examples are also shown to simulate the proposed control schemes. According to the numerical examples, the control schemes show a good trajectory following under significant parameter errors. Dissert. Abstr.

N94-12398# Advanced Resource Development Corp., Columbia, MD.
SIGNAL FEATURE ANALYSIS USING NEURAL NETWORKS AND PSYCHOACOUSTICS Final Report
May 1993 294 p
(Contract N00014-90-C-0228)
(AD-A266048) Avail: CASI HC A13/MF A03

The primary goal of this research was to compare the processing strategies used by human subjects and neural networks in classifying acoustic signals. Secondary goals were to compare subjects with and without sonar training and to investigate the effects on the neural networks of adding noise to the acoustic signals. DTIC

N94-12411# Lawrence Associates, Inc., Dayton, OH.
THERMAL ERROR COMPENSATION FEASIBILITY STUDY USING ARTIFICIAL INTELLIGENCE Final Report, 1 May 1991 - 20 Feb. 1993
D. J. Canfield, J. R. Pfeiffer, T. R. Sisson, and W. J. Zdeblick Feb. 1993 158 p
(Contract F33615-89-C-5708)
(AD-A266084; WL-TR-93-8020) Avail: CASI HC A08/MF A02

One of the major unresolved sources of machine tool errors is thermal effects. Neural networks potentially offer a means of predicting errors in machine tool positioning due to thermal effects. These can then be used for compensation resulting in more accurate machining. This study demonstrates the feasibility of using artificial neural networks to predict thermally induced positioning errors on a turning center. The potential for application to other types of machine tools and implementation issues leading to commercialization are also discussed. DTIC

N94-12428# Oak Ridge National Lab., TN.
PROCEEDINGS OF THE SEVENTH INTERNATIONAL SYMPOSIUM ON METHODOLOGIES FOR INTELLIGENT SYSTEMS (POSTER SESSION)
K. S. Harber, ed. May 1993 174 p Symposium held in Trondheim, Norway, 15-18 Jun. 1993
(Contract DE-AC05-84OR-21400)
(DE93-013470; ORNL/TM-12375; CONF-9306151) Avail: CASI HC A08/MF A02

This report contains the following papers: Implications in vivid logic; A self-learning Bayesian expert system; A natural language generation system for a heterogeneous distributed database system; 'Competence-switching' managed by intelligent systems; Strategy acquisition by an artificial neural network: Experiments in learning to play a stochastic game; Viewpoints and selective inheritance in object-oriented modeling; Multivariate discretization of continuous attributes for machine learning; Utilization of the case-based reasoning method to resolve dynamic problems; Formalization of an ontology of ceramic science in CLASSIC; Linguistic tools for intelligent systems; An application of rough sets in knowledge synthesis; and A relational model for imprecise queries. These papers have been indexed separately. DOE

N94-12537# Illinois Univ., Urbana. Dept. of Computer Science.
QUALITATIVE REASONING ABOUT THE PHYSICAL WORLD Final Report, Mar. 1985 - Dec. 1991
Kenneth D. Forbus Dec. 1992 7 p
(Contract N00014-85-K-0225)
(AD-A266117) Avail: CASI HC A02/MF A01

Qualitative physics is the subfield of artificial intelligence which investigates the kinds of representations and reasoning techniques which allow engineers, scientists, and just plain folks to understand and interact with the physical world. For example, Navy trainees learn to operate, maintain, and troubleshoot complex physical systems without needing advanced degrees in physics. Their common sense knowledge is augmented by their technical training and new skills, in order to carry out their tasks. To make computers that are capable of the same kind of flexible reasoning and learning regarding the physical world requires understanding common sense physics well enough to program it. DTIC

N94-12543# Oak Ridge National Lab., TN.
DERIVATION OF THREE CLOSED LOOP KINEMATIC VELOCITY MODELS USING NORMALIZED QUATERNION FEEDBACK FOR AN AUTONOMOUS REDUNDANT MANIPULATOR WITH APPLICATION TO INVERSE KINEMATICS
M. A. Unseren Apr. 1993 48 p
(Contract DE-AC05-84OR-21400)
(DE93-012823; ORNL/TM-12288) Avail: CASI HC A03/MF A01

The report discusses the orientation tracking control problem for a kinematically redundant, autonomous manipulator moving in a three dimensional workspace. The orientation error is derived using the normalized quaternion error method of Ickes, the Luh, Walker, and Paul error method, and a method suggested here utilizing the Rodrigues parameters, all of which are expressed in terms of normalized quaternions. The analytical time derivatives of the orientation errors are determined. The latter, along with the translational velocity error, form a closed loop kinematic velocity model of the manipulator using normalized quaternion and translational position feedback. An analysis of the singularities associated with expressing the models in a form suitable for solving the inverse kinematics problem is given. Two redundancy resolution algorithms originally developed using an open loop kinematic velocity model of the manipulator are extended to properly take into account the orientation tracking control problem. This report furnishes the necessary mathematical framework required prior to experimental implementation of the orientation tracking control schemes on the seven axis CESARm research manipulator or on the seven-axis Robotics Research K1207i dexterous manipulator, the latter of which is to be delivered to the Oak Ridge National Laboratory in 1993. DOE

N94-12598# Oak Ridge National Lab., TN.
EXPERIMENTS IN MOBILE ROBOT NAVIGATION AND RANGE IMAGING
J. P. Jones, O. H. Dorum (Norges Tekniske Hoegskole, Trondheim.), C. S. Andersen (Aalborg Univ., Denmark.), S. V. Jacobsen (Aalborg Univ., Denmark.), M. S. Jensen (Aalborg Univ., Denmark.), N. O. S. Kierkeby (Aalborg Univ., Denmark.), and S. Kristensen (Aalborg Univ., Denmark.) 1993 19 p Presented at the 8th Scandanavian Conference on Image Analysis, Tromso, Norway, 25-28 May 1993
(Contract DE-AC05-84OR-21400)
(DE93-013280; CONF-9305198-1) Avail: CASI HC A03/MF A01

This paper describes some experiments in sensor-based mobile robot navigation conducted at Oak Ridge National Laboratory over the past several years. Two implemented systems are described. One uses a laser range camera as the sole sensor. The other uses, in addition, an array of sonars and a stereo vision system. We discuss a communication system for heterogeneous LAN-connected multiprocessor systems, useful in reasonably large development projects such as these. We also describe some work on the estimation of curvature in range images which introduces a new variational principle motivated by minimization of the change of curvature. Application of this principle is shown to produce results which are more desirable in some respects than those obtained using standard quadratic variation. DOE

N94-11562*# Oceaneering Space Systems, Webster, TX.
DEVELOPMENT AND EVALUATION OF A PREDICTIVE ALGORITHM FOR TELEROBOTIC TASK COMPLEXITY
M. L. Gernhardt, R. C. Hunter, J. C. Hedgecock, and A. G. Stephenson *In* NASA. Johnson Space Center, Sixth Annual Workshop on Space Operations Applications and Research (SOAR 1992), Volume 2 Feb. 1993 p 616-625 (For primary document see N94-11527 01-99)
Avail: CASI HC A02/MF A03

64 NUMERICAL ANALYSIS

Includes iteration, difference equations, and numerical approximation.

N94-10163# Universiteit Twente, Enschede (Netherlands). Faculty of Applied Mathematics.
DEFORMATIONS AND RECURSION OPERATORS FOR EVOLUTION EQUATIONS
I. S. Krasilshchik and P. H. M. Kersten Dec. 1992 50 p
(MEMO-1104; ETN-93-94317) Avail: CASI HC A03/MF A01

In the differential geometric framework, an exposition of Richardson-Nijenhuis and Froelicher-Nijenhuis brackets is given. The theory of deformations is exposed and deformations of a number of classical integral equations are constructed leading to recursion operators for these equations. Recursion operators play an important role in the theory of differential equations possessing infinite series of symmetries. They are shown to be of cohomological nature. A series of computational examples is exposed. Deformations of Burgers' equation including a nonlocal variable, KdV equation, nonlinear Schroedinger equation, and classical Boussinesq equation, all in the setting of coverings, are discussed. For these examples recursion operators are obtained from the results in a straight forward way. The basic theories concerning the geometry of differential equations, Froelicher-Nijenhuis brackets, C cohomologies, and coverings are reviewed. ESA

N94-10168# Technische Univ., Eindhoven (Netherlands). Dept. of Mathematics and Computing Science.
A RELIABLE STABILITY TEST FOR EXPONENTIAL POLYNOMIALS
L. C. G. J. M. Habets Nov. 1992 21 p Sponsored by Netherlands Organization for Scientific Research
(MEMO-COSOR-92-48; ETN-93-94327) Copyright Avail: CASI HC A03/MF A01

An algorithm for determining the number of Right Half Plane (RHP) zeros of an exponential polynomial is proposed. A short introduction on the well known circle criterion with special emphasis on exponential polynomials is given. With this result it is possible to determine the exact number of RHP zeros of an exponential polynomial with a graphical test. It is shown that only a part of the image of the imaginary axis has to be considered to determine the number of RHP zeros. A reliable method is given to search the imaginary axis for the crucial information. Variable step length is the key word here. An example to illustrate the method derived is given. Although it is not really faster, the method is far more reliable than the algorithm that was commonly used for this problem up to now. ESA

N94-10259# Washington Univ., Seattle. Dept. of Physics.
DISCRETE SPACE-TIME SYMMETRIES
E. M. Henley 1992 12 p Presented at the Indian Summer School, Sazava, Czechoslovakia, 7-10 Sep. 1992
(Contract DE-FG06-88ER-40427)
(DE93-010199; DOE/ER-40427/32-N92; CONF-9209332-1) Avail: CASI HC A03/MF A01

Symmetries have always fascinated human beings; they are found in nature, art, and architecture. Physicists, like other scientists have often used symmetries as a basis of their understanding of nature. When the dynamics is unknown, symmetries serve to delineate and define it. When the dynamics is known, symmetries are used to study structure. These two lectures review the theory and present understanding and status of two discrete space-time symmetries, namely parity (P) and time reversal (T). DOE

N94-10273# Universiteit Twente, Enschede (Netherlands). Faculty of Applied Mathematics.
BALANCING OF THE NORMALIZED RIGHT COPRIME FACTORIZATION OF A NONLINEAR SYSTEM
J. M. A. Scherpen and A. J. vanderSchaft 27 Oct. 1992 15 p Sponsored by Dutch Systems and Control Theory Network, Netherlands
(MEMO-1096; ETN-93-94309) Avail: CASI HC A03/MF A01

A previously obtained method of balancing for stable nonlinear systems is extended to nonstable nonlinear systems in a similar way as this is done for linear systems. There exists a method of balancing for nonstable linear systems that makes use of the normalized right coprime factorization and the corresponding graph operator of the system. An extension of this method to nonstable nonlinear systems is proposed. The relation with balancing of the linearization is considered. Balancing of stable linear systems and balancing of the normal right coprime factorization of a linear system are reviewed. The concept of balancing for nonlinear systems and the linearization of this method of balancing are discussed. The results show that this matches with the linear theory. The normalized right coprime factorization of a nonlinear system and balancing based on this concept are considered. ESA

N94-10274# Universiteit Twente, Enschede (Netherlands). Faculty of Applied Mathematics.
CYCLES THROUGH PARTICULAR SUBGRAPHS OF CLAW-FREE GRAPHS
H. J. Broersma and M. Lu (Academia Sinica, Beijing, China.) 3 Nov. 1992 10 p
(MEMO-1097; ETN-93-94310) Avail: CASI HC A02/MF A01

Let G be a 2 connected claw free graph on n vertices, and let H be a subgraph of G. It is proven that G has a cycle containing all vertices of H whenever alpha(sub 3)(H) is less than or equal to kappa (G), where alpha(sub 3)(H) denotes the maximum number of vertices of H that are pairwise at distance at least three in G, and kappa(G) denotes the connectivity of G. This result extends a result of Fournier and Thomassen and generalizes the result of Zhang that G is Hamiltonian if the degree sum of any k(G) + 1 pairwise nonadjacent vertices is at least n - k(G). ESA

N94-10276# Universiteit Twente, Enschede (Netherlands). Faculty of Applied Mathematics.
ON OUTPUT LINEARIZATION OF OBSERVABLE DYNAMICS

Krzysztof Tchon (Technical Univ. of Wroclaw, Poland.) and Henk Nijmeijer Dec. 1992 41 p Sponsored by Univ. Twente, Enschede, Netherlands
(MEMO-1105; ETN-93-94318) Avail: CASI HC A03/MF A01

The problem of linearizing the observable dynamics by means of an output coordinate change is studied. The output linearization requires that the observability canonical form becomes linear after applying a suitable output diffeomorphism. The output linearization problem is completely solved. The problem of transforming a higher order differential equation in y variables to a linear form by means of a change of y coordinates is also solved. For both single-output and multi-output observed dynamics, necessary and sufficient conditions for the solvability of the above problems are derived. ESA

N94-10279# Universiteit Twente, Enschede (Netherlands). Dept. of Computer Science.
AN ALGEBRAIC APPROACH TO INCOMPARABLE FAMILIES OF FORMAL LANGUAGES
Peter R. J. Asveld Dec. 1992 26 p Repr. from Lindermayer Systems: Impacts on Theoretical Computer Science, Computer Graphics, and Developmental Biology (Heidelberg, Germany, Springer-Verlag), 1992, p 455-475
(Grant NWO-62-58)
(Memo-INF-92-82; ETN-93-94323) Copyright Avail: CASI HC A03/MF A01

A classic result in universal algebra says that the class of subalgebras Sa(A) of a given algebra A constitutes an algebraic or compactly generated lattice with set theoretical inclusion as partial order. In this context, the following problems are considered: the existence of a maximal or the largest proper subalgebra of A that includes a given proper subalgebra B; and the existence of a maximal or the largest subalgebra of A which is incomparable with a given subalgebra B in Sa(A), which possess a lattice theoretic character. Both problems are studied at the level of algebraic lattices and, particularly, for the algebraic lattice Sa(A). The results were applied to formal language theory, i.e., A equal to the family of all languages. Some results of Ginsburg and Spanier on incomparable full Abstract Families of Languages (AFL) are extended to similar structures like full hyper-AFL's, full hyper(1)-AFL's, and prequasoids. An approach based on universal algebra and lattice theory enables the establishment of Ginsburg and Spanier like theorems for several types of language families. Formal language theory provides language families that may serve as (counter)examples in algebra. ESA

N94-10283# Universidade do Estado do Rio de Janeiro (Brazil). Instituto de Engenharia Nuclear.
A SPECTRAL NODAL METHOD FOR DISCRETE ORDINATES PROBLEMS IN x,y GEOMETRY
R. C. deBarros and E. W. Larsen Jun. 1991 22 p In POLISH
(DE93-610128; IEN-23/91) Avail: CASI HC A03/MF A01 (US Sales Only)

A nodal method is proposed for the solution of S(sub N) problems in x,y-geometry. This method uses the Spectral Green's Function (SGF) scheme for solving the one-dimensional transverse-integrated nodal transport equations with no spatial truncation error. Thus, the only approximations in the x,y-geometry nodal method occur in the transverse leakage terms, as in diffusion theory. These leakage terms were approximated using a flat or constant approximation, and the resulting method is referred to as the SGF-Constant Nodal (SGF-CN) method. It is shown in numerical calculations that the SGF-CN method is much more accurate than other well-known transport nodal methods for coarse-mesh deep-penetration S(sub N) problems, even though the transverse leakage terms are approximated rather simply. DOE

N94-10325# International Centre for Theoretical Physics, Trieste (Italy).
CONVERGENCE OF EXPONENTIALLY CONVEX FUNCTIONS ON FOUNDATION SEMIGROUPS
A. S. OkbEl-Bab Oct. 1992 8 p
(DE93-619665; IC-92/296) Avail: CASI HC A02/MF A01 (US Sales Only)

Our main purpose in this thesis is to study the convergence of exponentially convex functions defined on foundation semigroups. In doing that it was realized that we can also weaken the conditions of continuity and boundedness imposed on these functions. Finally, we give an example. DOE

N94-10351# Center for Mathematics and Computer Science, Amsterdam (Netherlands). Dept. of Numerical Mathematics.
VECTORIZING MATRIX OPERATIONS ARISING FROM PDE DISCRETIZATION ON 9-POINT STENCILS
J. G. Blom and J. G. Verwer Nov. 1992 22 p
(Grant CRG-92.05)
(CWI-NM-R9221; ETN-93-94149) Copyright Avail: CASI HC A03/MF A01

When solving a system of Partial Differential Equations (PDE) discretized on 9-point stencils over a nonrectangular domain, the linear systems that arise will have matrices with an irregular block structure. For these type of matrices, the vectorization, of the matrix-vector multiply and of the Incomplete LU (ILU) factorization and backsolve are discussed. The implemented matrix-vector multiply uses a block diagonal storage with indirect addressing. The performance of this routine is 1 result per clock cycle. For the ILU factorization and backsolve concurrence is obtained by reordering the computations using a variant of the hyperplane method. The performance of the standard hyperplane method reaches its optimum only for large systems, because the resulting vector length is half the number of modes in the x-direction. The performance of the indirect addressing version has a Megaflop rate that is a factor 1.5 smaller. The results show that, even for the original, not explicitly reordered, version the gain in computational time compared with the general purpose routines of the Sparse Linear Algebra Package (SLAP) library is significant, especially for the factorization. ESA

N94-10352# Center for Mathematics and Computer Science, Amsterdam (Netherlands). Dept. of Operations Research, Statistics, and System Theory.
COMPLEX FUNCTIONS IN QUEUEING THEORY
J. W. Cohen Sep. 1992 22 p Sponsored in part by EEC
(CWI-BS-R9219; ETN-93-94150) Copyright Avail: CASI HC A03/MF A01

The background of an approach for solving the waiting time process problem for the GI/G/1 single server model is discussed. The Pollaczek's analysis of the GI/G/1 queueing model is reviewed. Techniques from the theory of complex functions constitute the core of his analysis. The advances in probability theory and in the theory of boundary value problems for analytic functions, which became known in the third quarter of our century have provided a wider context for the analysis of the GI/G/1 queueing model. For the time dependent as well as the stationary case this approach leads to the formulation of Riemann boundary value problems. The analysis of it for the stationary case is exposed and its solution is derived under slightly weaker conditions than originally considered by Pollaczek. ESA

N94-10362*# National Aeronautics and Space Administration. Lewis Research Center, Cleveland, OH.
LARGE TIME-STEP STABILITY OF EXPLICIT ONE-DIMENSIONAL ADVECTION SCHEMES
B. P. Leonard May 1993 30 p
(Contract NCC3-233; RTOP 505-90-5K)
(NASA-TM-106203; ICOMP-93-14; E-7867; NAS 1.15:106203) Avail: CASI HC A03/MF A01

There is a wide-spread belief that most explicit one-dimensional advection schemes need to satisfy the so-called 'CFL condition' - that the Courant number, c = udelta(t)/delta(x), must be less than or equal to one, for stability in the von Neumann sense. This puts severe limitations on the time-step in high-speed, fine-grid calculations and is an impetus for the development of implicit schemes, which often require less restrictive time-step conditions for stability, but are more expensive per time-step. However, it turns out that, at least in one dimension, if explicit schemes are formulated in a consistent flux-based conservative finite-volume form, von Neumann stability analysis does not place any restriction on the allowable Courant number. Any explicit scheme that is stable for c is less than 1, with a complex amplitude ratio, G(c), can be easily extended to arbitrarily large c. The complex amplitude ratio is then given by exp(-(Iota)(Nu)(Theta)) G(delta(c)), where N is the integer part of c, and delta(c) = c - N (less than 1); this is clearly stable. The CFL condition is, in fact, not a stability condition at all, but, rather, a 'range restriction' on the

'pieces' in a piece-wise polynomial interpolation. When a global view is taken of the interpolation, the need for a CFL condition evaporates. A number of well-known explicit advection schemes are considered and thus extended to large delta(t). The analysis also includes a simple interpretation of (large delta(t)) total-variation-diminishing (TVD) constraints.
Author (revised)

N94-10392 Tel-Aviv Univ. (Israel). Dept. of Solid Mechanics Materials and Structures.
BOUNDARY ELEMENT METHOD FOR EIGENVALUE PROBLEMS OF THIN PLATES M.S. Thesis
Ofer Weiss Aug. 1991 134 p In HEBREW
(ITN-93-85199) Copyright Avail: Issuing Activity (Tel-Aviv Univ., Exact Sciences Library, Ramat Aviv 69978, Israel)

The Boundary Element Method is a numerical method that can be used to solve elastodynamic problems by means of boundary integrals. In this work the method is implemented for calculating the natural frequencies of thin plates, taking into account the influence of internal forces. In addition, a method is developed for continuous plate analysis, in which the problem comprises several fields of different thickness, with the inclusion of internal supports. The solution is achieved by replacing the differential equation with an integral equation by means of the Rayleigh-Green second identity and the appropriate Green's functions. A dynamic Green's function is used, based on Henkel's first function of the zeroth order. The numerical procedure includes the discretization of the integral which leads to a matrix. The natural frequencies are obtained using a local minimum search of the determinant. Several examples are presented and the results are compared with analytical and with numerical solutions. The good agreement obtained illustrates the effectiveness of the method presented in this thesis.
Author (ISA)

N94-10531 International Centre for Theoretical Physics, Trieste (Italy).
CONVERGENCE THEOREMS FOR A CLASS OF NONLINEAR MAPS IN UNIFORMLY SMOOTH BANACH SPACES
C. E. Chidume and M. O. Osilike (Nigeria Univ., Nsukka.) May 1992 10 p Limited Reproducibility: More than 20% of this document may be affected by microfiche quality
(DE92-641347; IC-92/91) Avail: CASI HC A02 (US Sales Only)

Let K be a nonempty closed and convex subset of a real uniformly smooth Banach space, E, with modulus of smoothness of power type q greater than 1. Let T be a mapping of K into itself, T is an element of C (in the notion of Browder and Petryshyn; and Rhoades). It is proved that the Mann iteration process, under suitable conditions, converges strongly to the unique fixed point of T. If K is also bounded, then the Ishikawa iteration process converges to the fixed point of T. While our theorems generalize important known results, our method is also of independent interest. DOE

N94-10546# China Nuclear Information Centre, Beijing.
NUMERICAL METHOD OF SINGULAR PROBLEMS ON SINGULAR INTEGRALS
Huaiguo Zhao and Zongze Mou (Southwestern Inst. of Physics, Sichuan, China.) Feb. 1992 12 p
(DE93-613654; CNIC-00582; SIP-0047) Avail: CASI HC A03/MF A01 (US Sales Only)

As first part on the numerical research of singular problems, a numerical method is proposed for singular integrals. It is shown that the procedure is quite powerful for solving physics calculation with singularity such as the plasma dispersion function. Useful quadrature formulas for some class of the singular integrals are derived. In general, integrals with more complex singularities can be dealt by this method easily. DOE

N94-10642*# Institute for Computer Applications in Science and Engineering, Hampton, VA.
FINITE DIFFERENCE SCHEMES FOR LONG-TIME INTEGRATION Final Report
Zigo Haras (Weizmann Inst. of Science, Rehovoth, Israel.) and Shlomo Taasan (Weizmann Inst. of Science, Rehovoth, Israel.) Washington Jun. 1993 33 p Submitted for publication
(Contracts NAS1-19480; NAS1-18605; RTOP 505-90-52-01)
(NASA-CR-191471; NAS 1.26:191471; ICASE-93-25) Avail: CASI HC A03/MF A01

Finite difference schemes for the evaluation of first and second derivatives are presented. These second order compact schemes were designed for long-time integration of evolution equations by solving a quadratic constrained minimization problem. The quadratic cost function measures the global truncation error while taking into account the initial data. The resulting schemes are applicable for integration times fourfold, or more, longer than similar previously studied schemes. A similar approach was used to obtain improved integration schemes. Author

N94-10708# Sandia National Labs., Albuquerque, NM.
THE D-EDGE SHORTEST-PATH PROBLEM FOR A MONGE GRAPH
W. W. Bein (New Mexico Univ., Albuquerque.), L. L. Larmore (California Univ., Riverside.), and J. K. Park 14 Jul. 1992 10 p Presented at the Fourth Annaul ACM-SIAM Conference on Discrete Algorithms, Austin, TX, 25-27 Jan. 1993
(Contract DE-AC04-76DP-00789)
(DE93-009828; SAND-92-1724C; CONF-930194-1) Avail: CASI HC A02/MF A01

A complete edge-weighted directed graph on vertices 1,2,...,n that assigns cost c(i,j) to the edge (i,j) is called Monge if its edge costs form a Monge array, i.e., for all i less than k and j less than l, c(ij) + c(k,l) less than or = c(i,l) + c(k,j). One reason Monge graphs are interesting is that shortest paths can be computed quite quickly in such graphs. In particular, Wilber showed that the shortest path from vertex 1 to vertex n of a Monge graph can be computed in O(n) time, and Aggarwal, Klawe, Moran, Shor, and Wilber showed that the shortest d-edge 1-to-n path (i.e., the shortest path among all 1-to-n paths with exactly d edges) can be computed in O(dn) time. This paper's contribution is a new algorithm for the latter problem. Given certain assumptions, our algorithm runs in O(n(1 + 1g(U/L))) time. Thus, when d is much greater than 1 + 1g(U/L), our algorithm represents a significant improvement over Aggarwal et al.'s O(dn)-time algorithm. We also present several applications of our algorithm; they include length-limited Huffman coding, finding the maximum-perimeter d-gon inscribed in a given convex n-gon, and a digital signal compression problem. DOE

N94-10729# National Aerospace Lab., Tokyo (Japan). Aeroengine Div.
IMPROVEMENTS FOR OBTAINING ITERATIVE SOLUTIONS OF LARGE LINEAR SYSTEMS [TAGEN RENRITSU ICHIJI HOUTEISHIKI NI TAISURU HANPUKU KEISANHOU NO KAIRYOU NITSUITE]
Hideaki Nishimura Feb. 1992 25 p In JAPANESE
(DE93-767968; NAL-TR-1139; JTN-93-80425) Avail: CASI HC A03/MF A01

Improvements are presented for three iterative methods used for obtaining solutions of large sets of linear equations having symmetric, positive definite, yet sparse coefficient matrices. The investigated iterative methods are the incomplete approximate factorization procedure, conjugate gradient method, and Chebyshev semi-iterative method. Boundary-value problems of three dimensional descretized elliptic differential equations are solved with these methods, with the calculated results being subsequently compared using the resultant convergent rate. Author (NASDA)

N94-10825 National Inst. of Standards and Technology, Gaithersburg, MD.
BIBLIOGRAPHIC NOTES ON VORONOI DIAGRAMS
J. Bernal Apr. 1993 58 p Limited Reproducibility: More than 20% of this document may be affected by microfiche quality
(PB93-189298; NISTIR-5164) Avail: CASI HC A04

The paper presents a comprehensive annotated bibliography on various theoretical and algorithmic aspects of Voronoi diagrams and related diagrams. Bibliographic notes on the relationship between Voronoi diagrams and solutions to the Euclidean Traveling Salesman problem are also presented. NTIS

N94-10867# Technische Univ., Eindhoven (Netherlands). Dept. of Mathematics and Computing Science.
OPERATOR SUBSTITUTION
M. L. J. Hautus Dec. 1992 28 p
(MEMO-COSOR-92-51; ETN-93-94330) Copyright Avail: CASI HC A03/MF A01

The properties of operator substitution into an operator-valued analytic function are studied. The substitution operation described is a generalization of the more familiar operation of substituting an operator A into a scalar function f(z). A Bezout type theorem is used to derive a number of results. The tensor map, used to formulate solvability conditions for linear matrix equations, corresponding to a function F and an operator A is introduced. Some applications to system theory are given. ESA

N94-10881 Academy of Sciences of the Ukraine, Kiev. Inst. Teoreticheskoj Fiziki.
QUANTUM SOLITONS WITH CYLINDRICAL SYMMETRY
N. M. Chepilko, A. P. Kobushkin, and A. I. Syamtomov 1992 18 p Limited Reproducibility: More than 20% of this document may be affected by microfiche quality
(DE93-617659; ITP-92-28) Avail: CASI HC A03 (US Sales Only)

Soliton solutions with cylindrical symmetry are investigated within the nonlinear (sigma)-model disregarding the Skyrme-stabilized term. The solitons are stabilized by quantization of collective breathing mode and collapse in the h/2(pi) yields 0 limit. It is shown that for such stabilization mechanism the model, apart from solitons with integer topological number B, admits the solitons with half-odd B. The solitons with integer B have standard spin-isospin classification, but the B=1/2 solitons are shown to be characterized by spin, isospin and additional 'momentum'. DOE

N94-10905# Groningen Rijksuniv. (Netherlands). Dept. of Mathematics.
THE NEHARI PROBLEM FOR THE PRITCHARD-SALAMON CLASS OF INFINITE-DIMENSIONAL LINEAR SYSTEMS: A DIRECT APPROACH
R. F. Curtain and H. J. Zwart 1992 21 p
(CS-9216; ETN-93-94349) Copyright Avail: CASI HC A03/MF A01

An elementary derivation for the solution to the Nehari problem for the symbol G(s) = CB/(sI-A) is presented. The problem concerns a regular Pritchard-Salamon system (summation sign)(A,B,C) with A being the infinitesimal generator of an exponentially stable C(sub zero) semigroup on the separable Hilbert spaces V,W and Z. The approach is to solve an equivalent J spectral factorization problem. The Pritchard-Salamon class and several known properties are summarized. Some new properties on Lyapunov equations and Hankel operators are demonstrated. The Nehari problem is solved. ESA

N94-10906# Groningen Rijksuniv. (Netherlands). Dept. of Mathematics.
DETECTING NON-LINEARITIES IN STATIONARY TIME SERIES
F. Takens 1992 31 p
(W-9223; ETN-93-94350) Copyright Avail: CASI HC A03/MF A01

The results concerning the question of how to decide whether a given stationary time series is adequately described by a linear stochastic model or contains non linearities are surveyed . In particular, it is considered whether a given time series shows an indication that it is not adequately described by a linear model. Some concepts of (chaotic) dynamical systems and the time series which they can produce are reviewed. The evolutions of a dynamical, system with finite dimensional state space, are considered as deterministic evolutions. The spectral theory of linear stochastic systems, their optimal predictors and the relation of these predictors with time series from dynamical systems, are reviewed. The time series produced by such stochastic systems are considered as the prototype of random time series. In an numerical example, it is shown how the deterministic structure becomes less recognizable in the residues. ESA

N94-10907# Groningen Rijksuniv. (Netherlands). Dept. of Mathematics.
INTERMITTENCY FOLLOWING A HOPF BIFURCATION
H. M. Osinga 7 Dec. 1992 12 p
(W-9301; ETN-93-94351) Copyright Avail: CASI HC A03/MF A01

An intermittency of type 2, occurring in a bifurcation from periodic dynamics to intermittent chaotic dynamics through a subcritical Hopf bifurcation is studied. Intermittent chaotic dynamics means here that (almost) periodic behavior is interrupted by intervals where the dynamics is erratic. The aim is to clarify the discrepancy between theoretical analysis and numerical results reported in other investigations. A heuristic theoretical analysis of the behavior of the lengths of a laminar phase in a subcritical Hopf bifurcation is given. The results of a numerical simulation are presented and these two results are compared. The discrepancy between theoretical analysis and numerical results are discussed. ESA

N94-10908# Groningen Rijksuniv. (Netherlands). Dept. of Mathematics.
HOMOCLINIC INTERMITTENCY
Ale Jan Homburg 1993 10 p
(W-9302; ETN-93-94352) Copyright Avail: CASI HC A02/MF A01

A class of smooth vector fields on the R(exp 3) space is considered. They are vector fields with a hyperbolic singularity and a homoclinic orbit. Generalized homoclinic orbits are introduced and the study of bifurcations is carried out. A family of vector fields such that the center manifold is orientable is described. The nonorientable center manifold family of vector fields is studied. An explanation on how the homoclinic bifurcation gives rise to intermittency is provided. ESA

N94-10961# Sandia National Labs., Albuquerque, NM.
FINDING MINIMUM-QUOTIENT CUTS IN PLANAR GRAPHS
J. K. Park and C. A. Phillips 18 Nov. 1992 12 p Presented at the Association for Computing Machinery Symposium on the Theory of Computing, San Diego, CA, May 1993
(Contract DE-AC04-76DP-00789)
(DE93-011675; SAND-92-2585C; CONF-9305153-3) Avail: CASI HC A03/MF A01

Given a graph G = (V,E) where each vertex v element of V is assigned a weight w(v) and each edge e element of E is assigned a cost c(e), the quotient of a cut partitioning the vertices of V into sets S and (bar-S) is c(S,bar-S)/min(w(S),w(S)), where c(S,(bar-S)) is the sum of the costs of the edges crossing the cut and w(S) and w(bar-S) are the sum of the weights of the vertices in S and (bar-S), respectively. The problem of finding a cut whose quotient is minimum for a graph has in recent years attracted considerable attention. It has been shown that an algorithm (exact or approximation) for the minimum-quotient-cut problem can be used to obtain an approximation algorithm for the more famous minimum-b-balanced-cut problem, which requires finding a cut (S,bar-S) minimizing c(S,bar-S) subject to the constraint bW less than or equal to w(S) less than or equal to (1 - b)W, where W is the total vertex weight and b is some fixed balance in the range 0 less than bless than or equal to 1/2. Unfortunately, the minimum-quotient-cut problem is strongly NP-hard for general graphs, and the best polynomial-time approximation algorithm known for the general problem guarantees only a cut whose quotient is at most O(lg n) times optimal, where nis the size of the graph. However, for planar graphs, the minimum-quotient-cut problem appears more tractable, as Rao has developed several efficient approximation algorithms for the planar version of the problem capable of finding a cut whose quotient is at most some constant times optimal. In this paper, we improve Rao's algorithms, both in terms of accuracy and speed. As our first result, we present two pseudopolynomial-time exact algorithms for the planar minimum-quotient-cut problem. As Rao's most accurate approximation algorithm for the problem--also a pseudopolynomial-time algorithm--guarantees only a 1.5-times-optimal cut, our algorithms represent a significant advance. DOE

N94-11032 Joint Inst. for Nuclear Research, Dubna (USSR).
NON-EUCLIDEAN SPACE FOR LOCAL HIDDEN VARIABLES
M. Vinduska 1991 16 p Limited Reproducibility: More than 20% of this document may be affected by microfiche quality
(DE93-621341; JINR-E-5-91-534) Avail: CASI HC A03 (US Sales Only)

A model of the singlet state of photons is considered with local hidden variables (LHV) realized in Euclidean and pseudo-Euclidean spaces. It is shown that the metricity of the Euclidean space is transferred into the metric form of Bell, and of Braunstein and Caves inequalities, while the use of pseudo-Euclidean geometry leads to generalized inequalities which form is nonmetric. The use of the LHV in Minkowski space restores the quantum-mechanical results for correlations of photon linear polarizations. DOE

N94-11033 Gosudarstvennyi Komitet po Ispolzovaniyu Atomnoi Energii, Moscow (USSR).
A SYMMETRICAL FORM FOR EQUATIONS OF A NONLINEAR SPIRAL MAGNETIC [O SIMMETRICHNOJ FORME URAVNENIJ NELINEJNOGO SPIRL'NOGO MAGNETIKA]
E. A. Ivanchenko 1991 11 p In RUSSIAN Limited Reproducibility: More than 20% of this document may be affected by microfiche quality
(DE93-621350; KFTI-91-14) Avail: CASI HC A03 (US Sales Only)

A nonlinear evolution set of differential equations of a hydrodynamical type which describes an anisotropic spiral magnetic is reduced to the symmetrical t-hyperbolic set according to Fridrichs. For a three-dimensional case, shock waves (weak discontinuities) are predicted and propagation velocities of weak discontinuities are found. DOE

N94-11036 Academy of Sciences of the Ukraine, Kharkov. Fiziko-Teknicheskij Inst.
REGULAR TENSOR GREEN FUNCTIONS OF THE ROUND WAVEGUIDE [REGULYARNYE TENZORNYE FUNKTSII GRINA KRUGLOGO VOLNOVODA]
S. D. Prijmenko, V. G. Papkovich, and N. A. Khizhnyak 1991 16 p In RUSSIAN Limited Reproducibility: More than 20% of this document may be affected by microfiche quality
(DE93-621354; KFTI-91-42) Avail: CASI HC A03 (US Sales Only)

An exact mathematic solution of internal and external boundary problem for determination of tensor regular Green functions was found for electric and magnetic vector potential of a round waveguide. It was shown that for a synphase thread-like current source the Green function is described by simple series which in quasi static approximation can be represented by elementary expressions. A relation between the regular Green functions of point and thread-like current sources is established. The obtained results may be applied for design of UHF installations as well as for antenna and accelerating techniques using charged round waveguides. DOE

N94-11077 Joint Inst. for Nuclear Research, Dubna (USSR).
ON A p-ADIC METRICAL DIMENSION OF SPACE
N. Makhaldiani 1991 8 p Limited Reproducibility: More than 20% of this document may be affected by microfiche quality
(DE93-621374; JINR-E-2-91-573) Avail: CASI HC A02 (US Sales Only)

A metrical (fractal) dimension is defined by p-adic valuation of the number of covering elements. A usual fractal dimension is obtained as a sum of p-adic fractal dimensions. Metrical definitions of the dimension for quantum (fluctuating) geometry are considered. Useful inequality between the values of different definitions of dimension is proved. DOE

N94-11193# Instituto de Pesquisas Espaciais, Sao Jose dos Campos (Brazil).
BAYESIAN MODEL FOR PICTORIAL DATA FUSION OF SATELLITE IMAGE M.S. Thesis [USO DA TEORIA DE ESTIMACAO BAYESIANA NA FUSAO DE DADOS DE SATELITES]
Ana LuciaBezerraCandeias 1992 151 p In PORTUGESE
(INPE-5457-TDI/499) Avail: CASI HC A08/MF A02

Pictorial data fusion is the denomination of a set of techniques for generating synthetic images from the combination of primary images, by attempting to preserve the best characteristics from each primary image. In this dissertation, a Bayesian model for pictorial data fusion is proposed, based on the work of Brum (1989). As an example, such a model is applied to the image data fusion of SPOT satellite images. A comparison between the proposed technique with others that were presented in the literature is made. The Bayesian model has the advantage of offering the potential for adaptation to the local characteristics of the images in the synthesis process, besides its formal statistical formulation.
Author (revised)

N94-11217 Institute of Sound and Vibration Research, Southampton (England). Fluid Dynamics and Acoustics Group.
OPTIMISATION METHODS FOR SOLVING SEPARABLE NONLINEAR LEAST SQUARES PROBLEMS
M. Anciant, P. A. Nelson, and J. K. Hammond Apr. 1993 69 p
(ISVR-TR-219) Copyright Avail: Issuing Activity (Institute of Sound and Vibration Research, University of Southampton, Southampton SO9 5NH, England)

A comprehensive review of optimization methods for solving separable nonlinear Least Squares (LS) problems, which usually arise in array processing or interpolation problems, is proposed. The problem formulation is carried out for both single and multiple data vector processing. In addition to conventional optimization techniques (e.g. conjugate gradient, BFGS,...), the Gauss-Newton (GN) method, generally preferred for resolving LS problems, is introduced in case of separation scheme. Then, three different 'versions' of GN algorithm are derived. A series of numerical tests enables the illustration of the superiority of Kaufman's algorithm, in comparison with other GN algorithms or conventional optimization methods. Finally, alternative optimization methods such as, Alternating Projection Method or a nondeterministic method called Fast Simulated Annealing are presented, the main feature of the latest being to enable the escape from local minima and therefore possibly improve the global convergence of the search. Author

N94-11225# Sandia National Labs., Albuquerque, NM.
DEVELOPMENT OF GENERIC FIELD CLASSES FOR FINITE ELEMENT AND FINITE DIFFERENCE PROBLEMS
D. A. Verner, G. L. Heileman, K. G. Budge, and A. C. Robinson 1993 10 p Presented at the Object-Oriented Numerics Conference, Sunriver, OR, 25-27 Apr. 1993
(Contract DE-AC04-76DP-00789)
(DE93-011678; SAND-93-0767C; CONF-9304114-4) Avail: CASI HC A02/MF A01

This paper considers the development of a reusable object-oriented array library, as well as the use of this library in the construction of finite difference and finite element codes. The classes in this array library are also generic enough to be used to construct other classes specific to finite difference and finite element methods. The authors demonstrate the usefulness of this library by inserting it into two existing object-oriented scientific codes developed at Sandia National Laboratories. One of these codes is based on finite difference methods, while the other is based on finite element methods. Previously, these codes were separately maintained across a variety of sequential and parallel computing platforms. The use of object-oriented programming allows both codes to make use of common base classes. This offers a number of advantages related to optimization and portability. Optimization efforts, particularly important in large scientific codes, can be focused on a single library. Furthermore, by encapsulating machine dependencies within this library, the optimization of both codes on different architectures will only involve modification to a single library.
DOE

N94-11277*# Institute for Computer Applications in Science and Engineering, Hampton, VA.
LOOKING FOR O(N) NAVIER-STOKES SOLUTIONS ON NON-STRUCTURED MESHES Final Report
Eric Morano and Alain Dervieux (Institut National de Recherche d'Informatique et d'Automatique, Le Chesnay, France.) Jun. 1993 17 p Submitted for publication
(Contract NAS1-19480; RTOP 505-90-52-01)
(NASA-CR-191472; NAS 1.26:191472; ICASE-93-26) Avail: CASI HC A03/MF A01

Multigrid methods are good candidates for the resolution of the system arising in numerical fluid dynamics. However, the question is to know if those algorithms which are efficient for the Poisson equation on structured meshes will still apply well to the Euler and Navier-Stokes equations on unstructured meshes. The study of elliptic problems leads us to define the conditions where a full multigrid strategy has O(N) complexity. The aim of this paper is to build a comparison between the elliptic theory and practical CFD problems. First, as an introduction, we will recall some basic definitions and theorems applied to a model problem. The goal of this section is to point out the different properties that we need to produce an FMG algorithm with O(N) complexity. Then, we will show how we can apply this theory to the fluid dynamics equations such as Euler and Navier-Stokes equations. At last, we present some results which are 2nd-order accurate and some explanations about the behavior of the FMG process. Author (revised)

N94-11280*# Institute for Computer Applications in Science and Engineering, Hampton, VA.
ON CELL ENTROPY INEQUALITY FOR DISCONTINUOUS GALERKIN METHODS Final Report
Guangshan Jiang (Brown Univ., Providence, RI.) and Chi-Wang Shu (Brown Univ., Providence, RI.) Washington Jun. 1993 13 p Submitted for publication
(Contract NAG1-1145; DAAL03-91-G-0123; AF-AFOSR-0090-93; NSF DMS-92-11820; RTOP 505-90-52-01)
(NASA-CR-191493; NAS 1.26:191493; ICASE-93-37) Avail: CASI HC A03/MF A01

We prove a cell entropy inequality for a class of high order discontinuous Galerkin finite element methods approximating conservation laws, which implies convergence for the one dimensional scalar convex case. Author

N94-11348 International Centre for Theoretical Physics, Trieste (Italy).
THE LIP MICROBUNDLE REPRESENTATION THEOREM
Jing-Mei Guo Nov. 1992 19 p Limited Reproducibility: More than 20% of this document may be affected by microfiche quality
(DE93-619671; IC-92/386) Avail: CASI HC A03 (US Sales Only)

It is shown that a Lip n-microbundle contains a Lip n-bundle and that any two such are isomorphic. DOE

N94-11507# International Centre for Theoretical Physics, Trieste (Italy).
SPLINE APPROXIMATION FOR SYSTEM OF N-TH ORDER NONLINEAR ORDINARY DIFFERENTIAL EQUATIONS
M. N. AbouEl-Ela (Suez Canal Univ., Ismailia, Egypt.) and F. A. AbdEl-Salam (Zagazig Univ., Cairo, Egypt.) Sep. 1992 10 p
(DE93-608188; IC-92/259) Avail: CASI HC A02/MF A01 (US Sales Only)

A spline method for approximating the solution of a system of nonlinear ordinary differential equations is presented. Errors of the method are estimated and the stability of this method is proved. A method for approximating the solution of the Cauchy problem is introduced. DOE

N94-11608# Argonne National Lab., IL. Reactor Analysis Div.
DIRECT SOLUTION OF THE MATHEMATICAL ADJOINT EQUATIONS FOR AN INTERFACE CURRENT NODAL FORMULATION
T. A. Taiwo, W. S. Yang, and H. S. Khalil 1993 15 p Presented at the International Topical Meeting on Mathematical Methods and Supercomputing in Nuclear Applications (M&C+SNA '93), Karlsruhe (Germany), 19-23 Apr. 1993
(Contract W-31-109-eng-38)
(DE93-009961; ANL/RA/CP-76759; CONF-930404-10) Avail: CASI HC A03/MF A01

A numerical method for directly computing the mathematical adjoint flux moments and partial currents for the hexagonal-Z geometry interface current nodal formulation in the DIF3D code is described. The new scheme is developed as an alternative to an existing scheme that employs a similarity transformation of the physical adjoint solution to compute the mathematical adjoint. Whereas the existing scheme is rigorous only when the flat transverse-leakage approximation is employed, this new scheme is exact for all leakage approximations in the DIF3D nodal method. In the new scheme, adjoint nodal equations whose form is very similar to that of the forward nodal equations are derived by employing linear combinations of the adjoint partial currents as computational unknowns in the adjoint equations. This enables the use of the forward solution algorithm with only minor modifications for solving the mathematical adjoint equations. By using the new scheme as a reference method, it is shown numerically that while the results computed with the existing scheme are approximate, they are sufficiently accurate for calculations of global and local reactivity changes resulting from coolant voiding in a liquid metal reactor. DOE

N94-11631# International Centre for Theoretical Physics, Trieste (Italy).
THE COMPLETION HOMOMORPHISM IN EQUIVARIANT ELLIPTIC COHOMOLOGY
J. A. Devoto Nov. 1992 26 p
(DE93-619672; IC-92/388) Avail: CASI HC A03/MF A01 (US Sales Only)

We generalize the Atiyah-Segal completion theorem to the case of equivariant elliptic cohomology. The geometric aspect of the coefficient ring Ell*(sub G) and the analogies with the theory of representations of finite groups are also studied. DOE

N94-11632# International Centre for Theoretical Physics, Trieste (Italy).
ON CONVEXITY AND SCHOENBERG'S VARIATION DIMINISHING SPLINES
Yuyu Feng and J. Kozak (Ljubljana Univ., Yugoslavia.) Nov. 1992 12 p
(DE93-619673; IC-92/389) Avail: CASI HC A03/MF A01 (US Sales Only)

A convex function is characterized by the monotonicity of a particular variation diminishing spline sequence. The result extends the property known for the Bernstein polynomial sequence. DOE

N94-11663# Washington Univ., Seattle. Dept. of Physics.
QUENCHED CHIRAL LOGARITHMS
S. R. Sharpe Apr. 1992 44 p
(Contracts DE-FG06-91ER-40614; DE-AC05-84ER-40150)
(DE93-010195; DOE/ER-40614/25) Avail: CASI HC A03/MF A01

I develop a diagrammatic method for calculating chiral logarithms in the quenched approximation. While not rigorous, the method is based on physically reasonable assumptions which can be tested by numerical simulations. At the leading order in the chiral expansion, the reseults are as follows: (1) there are no chiral logarithms in quenched f(sub (pi)) m(sub u) = m(sub d); (2) the chiral logarithms in B(sub K) and related kaon B-parameters are, for m(sub d) = m(sub s) the same in the quenched approximation as in the full theory; and (3) for m(sub(pi)) and the condensate, there are extra chiral logarithms due to loops containing the eta('), which lead to a peculiar non-analytic dependence of these quantities on the bare quark mass. I discuss how there is a predictable finite volume dependence associated with each chiral logarithm. I compare the resulting predictions with numerical results; for most quantities the expected volume dependence is smaller than the errors, but for B(sub V) and B(sub A) there is an observed dependence which is consistent with the predictions. DOE

N94-11693 International Centre for Theoretical Physics, Trieste (Italy).
DIVERGENCES IN THE MODULI SPACE INTEGRAL AND ACCUMULATING HANDLES IN THE INFINITE-GENUS LIMIT
S. Davis Dec. 1992 24 p Limited Reproducibility: More than 20% of this document may be affected by microfiche quality
(DE93-619722; IC-92/431) Avail: CASI HC A03 (US Sales Only)

The symmetries associated with the bosonic string partition function integral are examined so that the integration region in Teichmuller space can be determined. The translation of the conditions on the period matrix defining the fundamental region can be translated to relations on the parameters of the uniformising Schottky group. The growth of the lower bound for the regularized partition function is derived through integration over a subset of the fundamental region. DOE

N94-11811 Weizmann Inst. of Science, Rehovoth (Israel). Dept. of Physics.
DUALITY TWISTED BOUNDARY CONDITIONS IN n-STA TE POTTS MODELS
G. Schuetz (Weizmann Inst. of Science, Rehovoth, Israel.) Nov. 1992 14 p Limited Reproducibility: More than 20% of this document may be affected by microfiche quality
(DE93-619724; WIS-PH-92-86) Avail: CASI HC A03 (US Sales Only)

We discuss a new class of toroidal boundary conditions for one-dimensional quantum Hamiltonian with S(sub n) symmetry which are related to two-dimensional n-state Potts models in the extreme anisotropic Hamiltonian limit. At their self-dual point (a point were a second-order phase transition occurs for n=2,3,4) the duality transformation is shown to be an additional symmetry giving rise to a new class of 'duality twisted' toroidal boundary conditions. This corresponding Hamiltonians are given in terms of generators of the periodic Temprely-Lieb algebra with an odd number of generators. We discuss as an example the critical Ising model. Here the complete spectrum for the new boundary conditions can be obtained from a projection mechanism in the spin-1/2 XXZ Heisenberg chain. DOE

N94-12776*# Research Inst. for Advanced Computer Science, Moffett Field, CA.
SUMMATION BY PARTS, PROJECTIONS, AND STABILITY
Pelle Olsson Jun. 1993 64 p Presented at the 1993 SIAM Annual Meeting, Philadelphia, PA, 12-16 Jul. 1993
(Contract NAS2-13721)
(NASA-CR-194290; NAS 1.26:194290; RIACS-TR-93-04) Avail: CASI HC A04/MF A01

We have derived stability results for high-order finite difference approximations of mixed hyperbolic-parabolic initial-boundary value problems (IBVP). The results are obtained using summation by parts and a new way of representing general linear boundary conditions as an orthogonal projection. By slightly rearranging the analytic equations, we can prove strict stability for hyperbolic-parabolic IBVP. Furthermore, we generalize our technique so as to yield strict stability on curvilinear non-smooth domains in two space dimensions. Finally, we show how to incorporate inhomogeneous boundary data while retaining strict stability. Using the same procedure one can prove strict stability in higher dimensions as well. Author (revised)

65 STATISTICS AND PROBABILITY

Includes data sampling and smoothing; Monte Carlo method; and stochastic processes.

N94-10353# Center for Mathematics and Computer Science, Amsterdam (Netherlands). Dept. of Operations Research, Statistics, and System Theory.
ON A CLASS OF TWO-DIMENSIONAL NEAREST NEIGHBORING RANDOM WALKS
J. W. Cohen Sep. 1992 30 p Sponsored in part by EEC
(CWI-BS-R9220; ETN-93-94151) Copyright Avail: CASI HC A03/MF A01

For positive recurrent nearest neighboring, semi-homogeneous random walks on the lattice (0,1,2,...,) x (0,1,2,...), the bivariate generating function of the stationary distribution is analyzed for the case where one-step transitions to the north, north-east and east at interior points of the state space all have zero probability. It is shown that this generating function can be represented by meromorphic functions. The construction of this representation is exposed for a variety of one-step transition vectors at the boundary points of the state space. The model of the nearest neighboring random walk is defined by its one-step transition vector at interior and at the boundary points of the state space. The poles are shown to be the only singularities of the analytic continuations. ESA

N94-10354# Center for Mathematics and Computer Science, Amsterdam (Netherlands). Dept. of Operations Research, Statistics, and System Theory.
APPLICATIONS OF CUT POLYHEDRA
Michel Deza (Ecole Normale Superieure, Paris, France.) and Monique Laurent (Ecole Normale Superieure, Paris, France.) Oct. 1992 77 p
(CWI-BS-R9221; ETN-93-94152) Copyright Avail: CASI HC A03/MF A01

The purpose of the work is to provide an extended bibliography on cut polyhedra and related areas. Many applications of the following polyhedra are presented: cut, boolean quadric, hypermetric and metric polyhedra. In particular, the following applications are considered: l(sub 1) and L(sub 1) metrics in functional analysis; the max-cut problem, the Boole problem and multicommodity flow problems in combinatorial optimization; lattice holes in geometry of numbers; density matrices of many fermions systems in quantum mechanics. Applications, in probability theory, statistical data analysis and design theory are included. ESA

N94-10757*# Alabama Univ., Huntsville. Dept. of Mathematical Sciences.
PARAMETRIC ANALYSIS OF ATMOSPHERIC PROCESSES Final Report
M. Elshamy Aug. 1993 45 p
(Contract NAS8-36955)
(NASA-CR-192523; NAS 1.26:192523) Avail: CASI HC A03/MF A01

The different phases of the space shuttle mission operations and system analyses are influenced by several dynamic atmospheric parameters. These parameters are random variables which are not independent. Probabilistic models incorporating dependence structure of the Markovian type are analyzed. The theory established could be used to predict a GO-NOGO decision in the different phases of a mission. Author

N94-10876# Technische Univ., Eindhoven (Netherlands). Dept. of Mathematics and Computing Science.
IMPRECISE HIGHEST DENSITY REGIONS RELATED TO INTERVALS OF MEASURES
Dec. 1992 17 p
(MEMO-COSOR-92-54; ETN-93-94333) Copyright Avail: CASI HC A03/MF A01

The theory of intervals of measures enables the use of a set of possible probability density functions for a random variable. The concept of highest density regions is generalized for situations where lack of perfect knowledge about the distribution of a random variable is represented by intervals of measures. An imprecise highest density region is defined together with a theorem that implies that such a region is equal to a highest density region for one particular probability density function. This result can be used within the theory of imprecise probabilities, as for sensitivity analysis with regard to the distribution of a random variable. In the Bayesian theory of statistics highest density regions play an important role. ESA

N94-11006# Los Alamos National Lab., NM.
INTRODUCTION TO BAYESIAN IMAGE ANALYSIS
K. M. Hanson 1993 16 p Presented at the SPIE Meeting on Medical Imaging, Newport Beach, CA, 14 Feb. 1993
(Contract W-7405-eng-36)
(DE93-012628; LA-UR-93-1179; CONF-9302108-1) Avail: CASI HC A03/MF A01

The basic concepts in the application of Bayesian methods to image analysis are introduced. The Bayesian approach has benefits in image analysis and interpretation because it permits the use of prior knowledge concerning the situation under study. The fundamental ideas are illustrated with a number of examples ranging from a problem in one and two dimensions to large problems in image reconstruction that make use of sophisticated prior information. DOE

N94-11882# Pennsylvania State Univ., University Park. Center for Multivariate Analysis.
APPLICATIONS OF MULTIVARIATE ANALYSIS Final Report, 1 May 1991 - 31 Jan. 1993
C. R. Rao 31 Jan. 1993 18 p
(Grant AF-AFOSR-0242-91)
(AD-A265250; AFOSR-93-0359TR) Avail: CASI HC A03/MF A01

Research was carried out in a number of areas of multivariate analysis. New methods have been proposed in the theory of M-estimation to safeguard against outliers. Asymptotic distributions have been derived under a minimal set of assumptions. Bootstrap techniques are extended to nonstandard situations. Theoretical and computational aspects of bootstrap are reviewed. Exact tests have been developed to test the significance of parent-offspring correlations. New methods have been devised for multitarget tracking. The new methods are found to be satisfactory as they depend on minimal assumptions and involve simpler computational algorithms. In the area of probability, Edgeworth expansions have been extended to cover the cases where some of the variables are not continuous, which is considered as a major advance from the point of view of practical applications. A new differential geometric structure of a statistical model is proposed which is more general and more informative than those considered earlier. The methods are applied to study properties of estimates of parameters. DTIC

N94-12390# Army Armament Research, Development and Engineering Center, Watervliet, NY. Benet Lab.
GENERALIZED MANDELBROT RULE FOR FRACTAL SECTIONS Final Report
L. V. Meisel Apr. 1993 14 p
(AD-A266010; ARCCB-TR-93016) Avail: CASI HC A03/MF A01

Mandelbrot's rule for sections is generalized to apply to the Hentschel and Procaccia fractal dimension at arbitrary q and on arbitrary sections. It is shown that for almost all (n-m)-dimensional sections, D(sup n)(q) = D(n-m)(q) + m, where the D(sup r)(q) are box-counting Hentschel and Procaccia generalized fractal dimensions of r-dimensional sections of homogeneous fractal point sets in Rn. The rule is shown to apply for finite 'thickness' sections as well as 'true' sections. A more general form of the rule applicable to inhomogeneous fractal sets is also presented. DTIC

N94-10607*# Negev Univ., Beersheva (Israel). Physics Dept.
WAVE AND PSEUDO-DIFFUSION EQUATIONS FROM SQUEEZED STATES
Jamil Daboul *In* NASA. Goddard Space Flight Center, The Second International Workshop on Squeezed States and Uncertainty Relations 1993 p 377-381 (For primary document see N94-10564 01-74)
Avail: CASI HC A01/MF A04

N94-12175*# Colorado Univ., Boulder. Lab. for Atmospheric and Space Physics.
POWER-LAW CONFUSION: YOU SAY INCREMENTAL, I SAY DIFFERENTIAL Abstract Only

Joshua E. Colwell *In* Lunar and Planetary Inst., Twenty-fourth Lunar and Planetary Science Conference. Part 1: A-F 1993 p 325-326 (For primary document see N94-12015 01-91)
Avail: CASI HC A01/MF A06

N94-12674 Qingdao Inst. of Oceanology (China). Ocean Remote Sensing and Ocean Optics Lab.
FURTHER STUDY OF THE NON-REGRESSION-COEFFICIENT SST RETRIEVAL METHOD
Ming Xia He, Yun Yue Yu, and Wei Huang *In* Scientific Organizing Committee of PORSEC, Proceedings of the PORSEC 1992 in Okinawa: Conference for Pacific Ocean Environments and Probing, Volume 2 25 Aug. 1992 p 774-779 Sponsored by NSF, Beijing, China (For primary document see N94-12635 01-42)
Copyright Avail: Issuing Activity (Scientific Organizing Committee of PORSEC, P.O. Box 10, Shimizu, Shizuoka 424, Japan, HC)

66 SYSTEMS ANALYSIS

Includes mathematical modeling; network analysis; and operations research.

N94-10162# Universiteit Twente, Enschede (Netherlands). Faculty of Applied Mathematics.
MARGINAL ALLOCATIONS IN THE CORE OF MINIMAL CHAIN-GAMES
Harry F. M. Aarts Nov. 1992 22 p
(MEMO-1103; ETN-93-94316) Avail: CASI HC A03/MF A01

A subclass of Minimum Cost Spanning Tree (MCST) games, called minimal chain games, are considered. For an arbitrary MCST game, one core element can be deduced directly from the underlying network, without first determining the data of the MCST game itself. This element is a marginal allocation corresponding to a specific ordering of the players. For minimal chain games, all marginal allocations can be deduced directly from the underlying network and a lot of marginal allocations turn out to be in the core. The main result gives necessary and sufficient conditions for an ordering of the players to guarantee that the corresponding marginal allocation in any minimal chain game is contained in the core of this game. ESA

N94-11568*# National Aeronautics and Space Administration. Langley Research Center, Hampton, VA.
IN-SPACE OPERATIONS FOR LUNAR AND MARS SPACE TRANSFER VEHICLES
James L. Raper, Sr. and Rick C. Vargo (McDonnell-Douglas Space Systems Co., Cocoa Beach, FL.) *In* NASA. Johnson Space Center, Sixth Annual Workshop on Space Operations Applications and Research (SOAR 1992), Volume 2 Feb. 1993 p 657-675 Repr. from AIAA/SAE/ASME/ASEE 28th Joint Propulsion Conference (Nashville, TN, AIAA), 1992 (For primary document see N94-11527 01-99)
(Contract NAS10-11400)
Avail: CASI HC A03/MF A03

N94-11569*# National Aeronautics and Space Administration. Langley Research Center, Hampton, VA.
IN-SPACE ASSEMBLY-SERVICING REQUIREMENTS
Charles E. Cockrell *In* NASA. Johnson Space Center, Sixth Annual Workshop on Space Operations Applications and Research (SOAR 1992), Volume 2 Feb. 1993 p 676-689 Repr. from AIAA/SAE/ASME/ASEE 28th Joint Propulsion Conference and Exhibit (Nashville, TN, AIAA), 1992 Previously announced in IAA as A92-38165 (For primary document see N94-11527 01-99)
Avail: CASI HC A03/MF A03

N94-11571*# Aerospace Corp., Sunnyvale, CA.
ON-ORBIT SERVICING FOR USAF SPACE MISSIONS: A PHASED DEVELOPMENT APPROACH Abstract Only
Bill Shanney *In* NASA. Johnson Space Center, Sixth Annual Workshop on Space Operations Applications and Research (SOAR 1992), Volume 2 Feb. 1993 p 700 (For primary document see N94-11527 01-99)
Avail: CASI HC A01/MF A03

N94-11572*# Dynamics Research Corp., Arlington, VA.
MORE SENSE FOR LESS CENTS: COST EFFECTIVE SERVICING OF REMOTE SENSING SATELLITES Abstract Only
Jeannie Lee, Tom Misencik, Bill Robertson, and Jack Sliney *In* NASA. Johnson Space Center, Sixth Annual Workshop on Space Operations Applications and Research (SOAR 1992), Volume 2 Feb. 1993 p 701 (For primary document see N94-11527 01-99)
Avail: CASI HC A01/MF A03

N94-11573*# Space Command, Peterson AFB, CO.
ASSURED MISSION SUPPORT SPACE ARCHITECTURE (AMSSA) STUDY Abstract Only
Rob Hamon *In* NASA. Johnson Space Center, Sixth Annual Workshop on Space Operations Applications and Research (SOAR 1992), Volume 2 Feb. 1993 p 702 (For primary document see N94-11527 01-99)
Avail: CASI HC A01/MF A03

N94-11574*# National Aeronautics and Space Administration. Lyndon B. Johnson Space Center, Houston, TX.
DEFINITION OF SPACECRAFT STANDARD INTERFACES BY THE NASA SPACE ASSEMBLY AND SERVICING WORKING GROUP (SASWG)
Robert Radtke (Tracor Applied Sciences, Inc., Kingwood, TX.), Charles Woolley, and Lana Arnold (Lockheed Engineering and Sciences Co., Houston, TX.) *In its* Sixth Annual Workshop on Space Operations Applications and Research (SOAR 1992), Volume 2 Feb. 1993 p 703-707 (For primary document see N94-11527 01-99)
Avail: CASI HC A01/MF A03

67 THEORETICAL MATHEMATICS

Includes topology and number theory.

N94-10272# Universiteit Twente, Enschede (Netherlands). Faculty of Applied Mathematics.
THE STRUCTURE OF HILBERT FLAG VARIETIES
G. F. Helminck and A. G. Helminck (North Carolina State Univ., Raleigh.) Oct. 1992 42 p
(MEMO-1095; ETN-93-94308) Avail: CASI HC A03/MF A01

A geometric realization of infinite dimensional analogs of the finite dimensional representations of the general linear group is presented. These representations are of importance in quantum field theory and in the framework of integrable systems. This requires a detailed analysis of the structure of the flag varieties involved and the line bundles over them. In general the action of the restricted linear group can not be lifted to the line bundles and thus leads to central extensions of this group. It is determined exactly when these extensions are nontrivial. As an application, it is shown how the flag varieties occur in the latter context. ESA

N94-10404 International Centre for Theoretical Physics, Trieste (Italy).
SINGULARITY SPECTRUM OF SELF-ORGANIZED CRITICALITY
E. Canessa Oct. 1992 20 p Limited Reproducibility: More than 20% of this document may be affected by microfiche quality
(DE93-613820; IC-92/334) Avail: Issuing Activity (Department of Energy (DOE)) (US Sales Only)

I introduce a simple continuous probability theory based on the Ginzburg-Landau equation that provides, for the first time, a common analytical basis to relate and describe the main features of two seemingly different phenomena of condensed-matter physics, namely self-organized criticality and multifractality. Numerical support is given by a comparison with reported simulation data. Within the theory, the origin of self-organized critical phenomena is analyzed in terms of a nonlinear singularity spectrum which is different from the typical convex shape due to multifractal measures. DOE

N94-10412# International Centre for Theoretical Physics, Trieste (Italy).
BOUNDARY OF FATOU SETS OF HYPERBOLIC RATIONAL MAPS OR DEGREE TWO
D. Ahmadi Oct. 1992 11 p
(DE93-613031; IC-92/322) Avail: CASI HC A03/MF A01 (US Sales Only)

If g(z) is a hyperbolic rational map of degree two which is not conjugate to z(sup 2) + c for some c is an element of C-bar and J(g), the Julia set of g, is connected, then we show that the boundary of the components of C-bar / J(g) are Jordan curves. DOE

N94-10547 Academy of Sciences of the Ukraine, Kiev. Inst. Teoreticheskoj Fiziki.

BOUND STATES OF THE N-DIMENSIONAL KLEIN-GORDON EQUATION WITH VECTOR AND SCALAR COULOMB POTENTIALS

R. S. Tutik 1992 10 p Limited Reproducibility: More than 20% of this document may be affected by microfiche quality
(DE93-617650; ITP-92-13) Avail: CASI HC A02 (US Sales Only)

The existence of bound states for the N-dimensional Klein-Gordon equation with vector and scalar Coulomb potentials is shown. The effects of the coupling strength on the bound states are discussed. The connection of the obtained energy eigenvalues with the spectrum of the Dirac equation is shown. DOE

N94-10548 Academy of Sciences of the Ukraine, Kiev. Inst. Teoreticheskoj Fiziki.

ON LOCAL FRAME FIELDS AND FERMION DYNAMICS IN SPACE WITH NONTRIVIAL TOPOLOGIES

P. I. Fomin and A. T. Zemlyakov 1991 23 p Limited Reproducibility: More than 20% of this document may be affected by microfiche quality
(DE93-617657; ITP-91-85) Avail: Issuing Activity (Department of Energy (DOE)) (US Sales Only)

The covariant operators of total angular momentum of fermion in spaces which possess Killing vector fields are defined. The classification of local frame fields in a closed world with S(sup 3) topology is performed. The vortex-type solution to Dirac equation in Minkowskii space is obtained by means of cylindrical local frame field. DOE

N94-10556 Academy of Sciences of the Ukraine, Kiev. Inst. Teoreticheskoj Fiziki.

COHERENCE INFLUENCE ON THE INTENSITY OF BOSE-EINSTEIN CORRELATIONS AND VISIBLE SIZE OF A SOURCE

Yu. M. Sinyukov and A. Yu. Tolstykh 1992 14 p Limited Reproducibility: More than 20% of this document may be affected by microfiche quality
(DE93-617697; ITP-92-5) Avail: Issuing Activity (Department of Energy (DOE)) (US Sales Only)

Two-particle correlations for both identical and unlike pion pairs are considered using the method of ensemble of sources with random phases. The dependence of the interferometric size of sources and coherence parameter on the source size and mean-squared momentum of the emitted pions is found. DOE

N94-10632 International Centre for Theoretical Physics, Trieste (Italy).

THE MODULAR GROUP AND SUPER-KMS FUNCTIONALS

O. Stoytchev Oct. 1992 10 p Limited Reproducibility: More than 20% of this document may be affected by microfiche quality
(DE93-613029; IC-92/307) Avail: CASI HC A02 (US Sales Only)

We show that with every normal, faithful, self-adjoint functional (omega) on a von Neumann algebra A there is associated a canonical one-parameter sigma-weakly continuous *-automorphism group sigma(sup omega) (the analogue of the modular group) and a canonical Z(sub 2) grading Gamma on A, commuting with sigma(sup omega). The functional omega satisfies the weak super-KMS property with respect to sigma(sup omega) and Gamma. Furthermore, sigma(sup omega) and Gamma are unique pair of a sigma-weakly continuous one-parameter *-automorphism group and a grading of the algebra, commuting with each other, with respect to which omega is weakly super-KMS. DOE

N94-10633# Instituto de Fisica Teorica, Sao Paulo (Brazil).

GENERATING FUNCTION FOR CLEBSCH-GORDAN COEFFICIENTS OF THE SU(SUB Q)(2) QUANTUM ALGEBRA

S. S. Avancini and D. P. Menezes (Sao Paulo Univ., Brazil.) May 1992 14 p
(DE93-613093; IFT-P-016/92) Avail: CASI HC A03/MF A01 (US Sales Only)

Some methods have been developed to calculate the SU(sub q)(2) Clebsch-Gordan coefficients (CGC). Here we develop a method based on the calculation of Clebsch-Gordan generating function through the use of quantum algebraic coherent states. Calculating the su(sub q)(2) CGC by means of this generating function is an easy and straight-forward task. DOE

N94-10636# Instituto de Engenharia Nuclear, Rio de Janeiro (Brazil).

A SPECTRAL NODAL METHOD FOR THE SOLUTION OF THE Sn EQUATIONS IN x, y GEOMETRY FOR HIGHLY ABSORBING DEEP PENETRATION PROBLEMS

R. C. deBarros Sep. 1991 27 p
(DE93-613520; IEN-24/91) Avail: CASI HC A03/MF A01 (US Sales Only)

Presented here is an attempt to improve the accuracy of transport nodal methods applied to deep penetration transport problems in x,y-geometry. The resulting nodal method uses the Spectral Green's Function (SGF) scheme for solving the one-dimensional transverse-integrated S(sub N) exponential nodal equations with no spatial truncation error. Based on the physics of deep penetration problems, we approximate the transverse leakage terms by approximate exponential shape functions. We show in numerical calculation that the SGF-Exponential Nodal (SGF-Exp N) method is much more accurate than other transport nodal methods for coarse-mesh deep penetration problems, specially in highly absorbing media. DOE

N94-10833 Academy of Sciences of the Ukraine, Kiev. Inst. Teoreticheskoj Fiziki.

A NEW APPROACH TO THE I/N-EXPANSION FOR THE DIRAC EQUATION

S. S. Stepanov and R. S. Tutik 1991 15 p Limited Reproducibility: More than 20% of this document may be affected by microfiche quality
(DE93-617647; ITP-91-94) Avail: Issuing Activity (Department of Energy (DOE)) (US Sales Only)

The difficulties associated with application of the I/N-expansion to the Dirac equation have been resolved by applying the method of (h/2(pi))-expansion. This technique does not involve converting the initial equation into the Schroedinger-like or Klein-Gordon-like form. Obtained recurrence formulae have a simple form and allow one to find the I/N-corrections of an arbitrary order in any of the I/N-expansion scheme. The method restores the exact results for the Coulomb potential. DOE

N94-10573*# Academy of Sciences (USSR), Moscow. Inst. od Physics and Technology.

AN EXACTLY SOLVABLE MODEL OF AN OSCILLATOR WITH NONLINEAR COUPLING AND ZEROS OF BESSEL FUNCTIONS

V. V. Dodonov and A. B. Klimov *In* NASA. Goddard Space Flight Center, The Second International Workshop on Squeezed States and Uncertainty Relations 1993 p 85-88 (For primary document see N94-10564 01-74)
Avail: CASI HC A01/MF A04

N94-10581*# Bulgarian Academy of Sciences, Sofia. Inst. for Nuclear Reseach and Nuclear Energy.

COMPLETENESS PROPERTIES OF THE MINIMUM UNCERTAINTY STATES

D. A. Trifonov *In* NASA. Goddard Space Flight Center, The Second International Workshop on Squeezed States and Uncertainty Relations 1993 p 157-162 (For primary document see N94-10564 01-74)
Avail: CASI HC A02/MF A04

N94-10583*# Johann-Wolfgang-Goethe-Univ., Frankfurt am Main (Germany).

ON A LAGRANGE-HAMILTON FORMALISM DESCRIBING POSITION AND MOMENTUM UNCERTAINTIES

Dieter Schuch *In* NASA. Goddard Space Flight Center, The Second International Workshop on Squeezed States and Uncertainty Relations 1993 p 177-182 Sponsored in part by Deutsche Forschungsgemeinschaft (For primary document see N94-10564 01-74)
Avail: CASI HC A02/MF A04

N94-10588*# Erlangen-Nuremberg Univ. (Germany). Inst. for Theoretical Physics III.

GEOMETRIC ASPECTS OF UNCERTAINTY AND CORRELATION

Sumiyoshi Abe *In* NASA. Goddard Space Flight Center, The Second

International Workshop on Squeezed States and Uncertainty Relations 1993 p 225-229 (For primary document see N94-10564 01-74)
Avail: CASI HC A01/MF A04

N94-10595*# Humboldt Univ., Berlin (German D.R.).
NONUNITARY AND UNITARY APPROACH TO EIGENVALUE PROBLEM OF BOSON OPERATORS AND SQUEEZED COHERENT STATES
A. Wunsche *In* NASA. Goddard Space Flight Center, The Second International Workshop on Squeezed States and Uncertainty Relations 1993 p 277-281 (For primary document see N94-10564 01-74)
Avail: CASI HC A01/MF A04

N94-10600*# Academy of Sciences of the Azerbaijan SSR, Baku. Institute of Physics.
EXACT AND QUASI-CLASSICAL DENSITY MATRIX AND WIGNER FUNCTIONS FOR A PARTICLE IN THE BOX AND HALF SPACE
E. A. Akhundova, V. V. Dodonov (Academy of Sciences, USSR, Moscow.), and V. I. Manko (Academy of Sciences, USSR, Moscow.) *In* NASA. Goddard Space Flight Center, The Second International Workshop on Squeezed States and Uncertainty Relations 1993 p 305-309 (For primary document see N94-10564 01-74)
Avail: CASI HC A01/MF A04

70 PHYSICS (GENERAL)

For precision time and time interval (PTTI) see *35 Instrumentation and Photography;* for geophysics, astrophysics or solar physics see *46 Geophysics, 90 Astrophysics,* or *92 Solar Physics.*

N94-10313# Centro Brasileiro de Pesquisas Fisicas, Rio de Janeiro.
MAGNETIZATION REVERSAL BY NUCLEATION
W. Baltensperger (Eidgenoessische Technische Hochschule, Zurich, Switzerland.), J. S. Broz (Eidgenoessische Technische Hochschule, Zurich, Switzerland.), and J. A. S. Helman 1991 9 p
(DE93-610313; CBPF-NF-033/91) Avail: CASI HC A02/MF A01 (US Sales Only)

The exact static solution of the Landau-Lifshitz equations for the magnetization, which were identified as describing nucleation centers for the magnetization reversal in ferromagnets, are compared with those of phenomenological models of spherical and cylindrical symmetry. It is found that the latter have higher critical fields. DOE

N94-10963*# National Aeronautics and Space Administration. Goddard Space Flight Center, Greenbelt, MD.
THE 24TH ANNUAL PRECISE TIME AND TIME INTERVAL (PTTI) APPLICATIONS AND PLANNING MEETING
Richard L. Sydnor (Jet Propulsion Lab., California Inst. of Tech., Pasadena.) Washington Jun. 1993 472 p Meeting held in McLean, VA, 1-3 Dec. 1992; sponsored by JPL, Naval Observatory, Space and Naval Warfare Systems Command, NRL, Army Electronics Technology and Devices Lab., Rome Lab., and AFOSR
(Contract NAS5-31000)
(NASA-CP-3218; Rept-93B00087; NAS 1.55:3218) Avail: CASI HC A20/MF A04

A compilation of technical papers presented at the 24th Precise Time and Time Interval (PTTI) Applications and Planning Meeting held in Dec. 1992 is presented. Papers are in the following categories: recent developments in rubidium, cesium, and hydrogen-based frequency standards, and in cryogenic and trapped-ion technology; international and transnational applications of PTTI technology with emphasis on satellite laser tracking networks, GLONASS timing, intercomparison of national time scales, and international telecommunications; applications of PTTI technology to the telecommunications, power distribution, and platform positioning, and geophysical survey industries; applications of PTTI technology to evolving military communications and navigation systems; and dissemination of precise time and frequency by means of GPS, GLONASS, MILSTAR, Loran, and synchronous communications satellites. For individual titles, see N94-10964 through N94-11003.

N94-10964*# ITT Aerospace/Communications Div., Clifton, NJ.
THE TIME KEEPING SYSTEM FOR GPS BLOCK IIR c04
H. C. Rawicz, M. A. Epstein, and J. A. Rajan *In* NASA. Goddard Space Flight Center, The 24th Annual Precise Time and Time Interval (PTTI) Applications and Planning Meeting Jun. 1993 p 5-16 (For primary document see N94-10963 01-70)
Avail: CASI HC A03/MF A04

The precision time keeping system (TKS) in the Global Positioning System (GPS), Block IIR satellites is designed to operate under severe natural and man made environmental conditions. The Block IIR TKS provides precise, autonomous time keeping for periods of up to seven months, without the intervention of the GPS Control Segment. The TKS is implemented using both linear and non-linear controls. The resulting TKS architecture uses a hybrid analog/digital phase locked loop (PLL). The paper provides details of the design and analysis of the TKS. The simulation techniques and the test bed activities used in performing the TKS design trade-offs are described. The effects of non-linear controls are analyzed using a TKS computer simulation of the PLL. The results from a hardware test bed are provided that verify desired TKS operation. The design criteria for the TKS computer simulation and the hardware test bed are indicated. The concepts for verification and testing of the TKS computer simulation and hardware test bed are presented. Author

N94-10965*# Bureau International des Poids et Mesures, Sevres (France).
PROGRESS ON GPS STANDARDIZATION c04
C. Thomas *In* NASA. Goddard Space Flight Center, The 24th Annual Precise Time and Time Interval (PTTI) Applications and Planning Meeting Jun. 1993 p 17-30 (For primary document see N94-10963 01-70)
Avail: CASI HC A03/MF A04

It has been clear for some time that a desirable and necessary step for improvement of the accuracy of GPS time comparisons is to establish GPS standards which may be adopted by receiver designers and users. For this reason, a formal body, the CCDS Group on GPS Time Transfer Standards (CGGTTS), was created in 1991. It operates under the auspices of the permanent CCDS Working Group on TAI, with the objective of recommending procedures and models for operational time transfer by the GPS common-view method. It works in close cooperation with the Subcommittee on Time of the Civil GPS Service Interface Committee. The members of the CGGTTS have met in December 1991 and in June 1992. Following these two formal meetings, a number of decisions were taken for unifying the treatment of GPS short-term data and for standardizing the format of GPS data files. A formal CGGTTS Recommendation is now being written concerning these points. This paper relates on the work carried out by the CGGTTS. Author (revised)

N94-10966*# Coast Guard, Washington, DC. GPS Information Center.
US COAST GUARD GPS INFORMATION CENTER (GPSIC) AND ITS FUNCTION WITHIN THE CIVIL GPS SERVICE (CGS) c04
In NASA. Goddard Space Flight Center, The 24th Annual Precise Time and Time Interval (PTTI) Applications and Planning Meeting Jun. 1993 p 31-46 (For primary document see N94-10963 01-70)
Avail: CASI HC A03/MF A04

In 1987, the U.S. Department of Defense (DOD) formally requested that the U.S. Department of Transportation (DOT) take responsibility for providing an office that would respond to nonmilitary user needs for GPS information, data, and assistance. DOT accepted this responsibility and in February 1989, named the Coast Guard as their lead agency for the project. Since that time, the U.S. Coast Guard has worked with the U.S. Space Command to develop requirements and implement a plan for providing the requested interface with the civil GPS community. The Civil GPS Service (CGS) consists of four main elements: GPS Information Center (GPSIC) - provides GPS status information to civilian users of the system: Civil GPS Service Interface Committee (CGSIC) - established to identify civil GPS user technical information needs in support of the CGS program; Differential GPS (DGPS) - Coast Guard Research and Development Project; and PPS Program Office (PPSPO) - (Under development) will administer the program allowing qualified civil users to have access to the PPS signal. Details about the services these organizations provide are described.
Author (revised)

N94-10967*# Bureau International des Poids et Mesures, Sevres (France).

COMPARISON OF GPS AND GLONASS COMMON-VIEW TIME TRANSFERS **c04**

W. Lewandowski, G. Petit, C. Thomas, G. T. Cherenkov (All-Union Research Inst. for Physical and Radiotechnical Measurements, Mendeleevo, USSR.), N. B. Koshelyaevsky (All-Union Research Inst. for Physical and Radiotechnical Measurements, Mendeleevo, USSR.), and S. B. Pushkin (All-Union Research Inst. for Physical and Radiotechnical Measurements, Mendeleevo, USSR.) *In* NASA. Goddard Space Flight Center, The 24th Annual Precise Time and Time Interval (PTTI) Applications and Planning Meeting Jun. 1993 p 47-58 (For primary document see N94-10963 01-70)

Avail: CASI HC A03/MF A04

It was already shown than even with a simple daily averaging of GLONASS data at each site, continental GLONASS time transfer can be achieved at a level of several tens of nanoseconds. A further step is to carry out observations of GLONASS satellites by the common-view method. A comparison of GPS and GLONASS common-view time transfers between Russia and Western Europe are reported. At each site, a GPS receiver and a GLONASS receiver are connected to the same atomic clock. Both GPS receivers are of NBS type and the GLONASS receivers are of type A-724. As GPS common-view time transfer between Sevres and Mendeleevo is accomplished at a level of a few nanoseconds in precision, it gives an excellent reference with which to evaluate the performance of GLONASS common-view time transfer. Author (revised)

N94-10968*# Ministry of Posts and Telecommunications, Kashima (Japan).

PULSAR ASTROMETRY BY USING VLBI (PSR0329 BETWEEN KASHIMA 26mPHI AND USUDA 64mPHI) **c89**

S. Hama, H. Kiuchi, Y. Hanado, Y. Takahashi, M. Imae, K. Fujisawa (Tokyo Univ., Japan.), H. Hirabayashi (Tokyo Univ., Japan.), and H. Kobayashi (Tokyo Univ., Japan.) *In* NASA. Goddard Space Flight Center, The 24th Annual Precise Time and Time Interval (PTTI) Applications and Planning Meeting Jun. 1993 p 65-72 (For primary document see N94-10963 01-70)

Avail: CASI HC A02/MF A04

Communications Research Laboratory (CRL) carried out a VLBI (Very Long Baseline Interferometer) experiment of the Pulsar 0329 plus 54 on November in 1992 between Kashima 26mPhi and Usuda 64mPhi. We got a correlation for it by using K-3 VLBI correlator which was developed by CRL. Though we observed a slow pulsar this time, we are going to make millisecond pulsar experiments by making good use of this result and by using K-4 correlator which is under developing in CRL. Its result will give us precise positions and proper motions of pulsars which are useful for obtaining precise pulsar timing. Author

N94-10969*# Bureau International des Poids et Mesures, Sevres (France).

AN ENSEMBLE PULSAR TIME **c90**

Gerard Petit, Claudine Thomas, and Patrizia Tavella (Instituto Elettrotecnico Nazionale, Galileo Ferraris, Turin, Italy.) *In* NASA. Goddard Space Flight Center, The 24th Annual Precise Time and Time Interval (PTTI) Applications and Planning Meeting Jun. 1993 p 73-86 (For primary document see N94-10963 01-70)

Avail: CASI HC A03/MF A04

Millisecond pulsars are galactic objects that exhibit a very stable spinning period. Several tens of these celestial clocks have now been discovered, which opens the possibility that an average time scale may be deduced through a long-term stability algorithm. Such an ensemble average makes it possible to reduce the level of the instabilities originating from the pulsars or from other sources of noise, which are unknown but independent. The basis for such an algorithm is presented and applied to real pulsar data. It is shown that pulsar time could shortly become more stable than the present atomic time, for averaging times of a few years. Pulsar time can also be used as a flywheel to maintain the accuracy of atomic time in case of temporary failure of the primary standards, or to transfer the improved accuracy of future standards back to the present. Author (revised)

N94-10970*# Maryland Univ., College Park. Dept. of Physics.

EXPERIMENTAL COMPARISON OF TIME SYNCHRONIZATION TECHNIQUES BY MEANS OF LIGHT SIGNALS AND CLOCK TRANSPORT ON THE ROTATING EARTH

R. A. Nelson, C. O. Alley, J. D. Rayner, Y. H. Shih, C. A. Steggerda, B. C. Wang, and B. W. Agnew *In* NASA. Goddard Space Flight Center, The 24th Annual Precise Time and Time Interval (PTTI) Applications and Planning Meeting Jun. 1993 p 87-104 (For primary document see N94-10963 01-70)

Avail: CASI HC A03/MF A04

An experiment was conducted to investigate the equivalence of two methods of time transfer in a noninertial reference frame: by means of an electromagnetic signal using laser light pulses and by means of the slow ground transport of a hydrogen maser atomic clock. The experiment may also be interpreted as an investigation of whether the one-way speeds of light in the east-west and west-east directions on the rotating earth are the same. The light pulses were sent from a laser coupled to a telescope at the NASA Goddard Optical Research Facility (GORF) in Greenbelt, Maryland to the U.S. Naval Observatory (USNO) in Washington, DC. The optical path was made possible by a 30-cm flat mirror on a water tower near GORF and a 25-cm flat mirror on top of the Washington National Cathedral near USNO. The path length was 26.0 km with an east-west component of 20.7 km. The pulses were reflected back over the same path by a portable array of corner cube reflectors. The transmission and return times were measured with a stationary Sigma Tau hydrogen maser and a University of Maryland event timer at GORF, while the times of reflection were measured with a similar maser and event timer combination carefully transported to USNO. Both timekeeping systems were housed in highly insulated enclosures and were maintained at constant temperatures to within +/- 0.1 C by microprocessor controllers. The portable system was also protected from shock and vibration by pneumatic supports. The difference delta(T) between the directly measured time of reflection according to the portable clock and the time of reflection calculated from the light pulse signal times measured by the stationary clock was determined. For a typical trip delta(T) is less than 100 ps and the corresponding limit on an anisotropy of the one-way speed of light is delta(c/c) is less than 1.5 x 10(exp -6). This the only experiment to date in which two atomic clocks were calibrated at one location, one was slowly transported to the other end of a path, and the times of transmission, reflection, and return of short light pulses sent in different directions along the path were registered. Author (revised)

N94-10971*# Maryland Univ., College Park. Dept. of Physics.

PLANS TO IMPROVE THE EXPERIMENTAL LIMIT IN THE COMPARISON OF THE EAST-WEST AND WEST-EAST ONE-WAY LIGHT PROPAGATION TIMES ON THE ROTATING EARTH **c74**

C. O. Alley, T. E. Kiess, R. A. Nelson, A. V. Sergienko, Y. H. Shih, B. C. Wang, and F. M. Yang *In* NASA. Goddard Space Flight Center, The 24th Annual Precise Time and Time Interval (PTTI) Applications and Planning Meeting Jun. 1993 p 105-112 (For primary document see N94-10963 01-70)

Avail: CASI HC A02/MF A04

The preceding paper describes the results so far (interrupted in the Spring of 1989 because of lack of funds) of an experiment comparing the one-way light propagation times on the surface of the rotating Earth. For the 20 Km path length component in the East-West direction the predicted difference between the opposite sense propagation times would be 160 ps, if the approximately 360 Km/s surface speed of the Earth gives effective light speeds of 3 x 10(exp 8) m/s +/- 360 m/s. This could lead to a prediction of the difference between the clock transport and the light pulse synchronization methods described in the preceding paper: delta(T) = 0.5 (160) = 80 ps. The current upper bound of approximately 100 ps for delta(T) is limited by poorly understood systematic errors. The most important seems to be intensity-dependent time delays in the remote light pulse avalanche photo-diode detector. This will be replaced by a continuously operating circular scan streak camera having single photon sensitivity and a time resolution of approximately 5 ps. (This camera has recently been developed by the Xian Institute of Optics and Precision Mechanics in the P.R.C.). Better isolation from shocks and vibration for the Sigma-Tau hydrogen maser during transport will be provided. It is hoped that delta(T) is less than 20 ps can be achieved. Author (revised)

N94-10972*# Centre d'Etudes et de Recherches Geodynamiques et Astronomiques, Grasse (France).

LASSO OBSERVATIONS AT MCDONALD AND OCA/CERGA: A PRELIMINARY ANALYSIS

Ch. Veillet, P. Fridelance, D. Feraudy, Y. Boudon, P. J. Shelus (McDonald Observatory, Fort Davis, TX.), R. L. Ricklefs (McDonald Observatory, Fort Davis, TX.), and J. R. Wiant (McDonald Observatory, Fort Davis, TX.) *In* NASA. Goddard Space Flight Center, The 24th Annual Precise Time and Time Interval (PTTI) Applications and Planning Meeting Jun. 1993 p 113-122 (For primary document see N94-10963 01-70)
Avail: CASI HC A02/MF A04

The Laser Synchronization from Synchronous Orbit (LASSO) observations between USA and Europe were made possible with the move of Meteosat 3/P2 toward 50 deg W. Two Lunar Laser Ranging stations participated into the observations: the MLRS at McDonald Observatory (Texas, USA) and OCA/CERGA (Grasse, France). Common sessions were performed since 30 Apr. 1992, and will be continued up to the next Meteosat 3/P2 move further West (planned for January 1993). The preliminary analysis made with the data already collected by the end of Nov. 1992 shows that the precision which can be obtained from LASSO is better than 100 ps, the accuracy depending on how well the stations maintain their time metrology, as well as on the quality of the calibration (still to be made.) For extracting such a precision from the data, the processing has been drastically changed compared to the initial LASSO data analysis. It takes into account all the measurements made, timings on board, and echoes at each station. This complete use of the data increased dramatically the confidence into the synchronization results. Author (revised)

N94-10973*# SFA, Inc., Landover, MD.

MIL-STDS AND PTTI: WHAT'S AVAILABLE AND WHAT NEEDS TO BE DONE

James A. Murray and Joseph D. White (Naval Research Lab., Washington, DC.) *In* NASA. Goddard Space Flight Center, The 24th Annual Precise Time and Time Interval (PTTI) Applications and Planning Meeting Jun. 1993 p 123-136 (For primary document see N94-10963 01-70)
Avail: CASI HC A03/MF A04

The systems developer who needs Precise Time and Time Interval (PTTI) capability has relatively little guidance in the form of military standards, particularly for systems using atomic clocks or other sources of very precise time and frequency. The existing standards, including MIL-STD-188-115, MIL-F-2991(EC), and DOD-STD-1399 are discussed. These documents were written several years ago and do not always reflect current practice or take advantage of more recent technology improvements. User needs have also changed over the years and some of those needs such as more detailed time codes are not being met. We will summarize what's available and what's good and bad about it. The second part will make suggestions about what should be done in the future to promote and facilitate good PTTI design practice. Topics will include clock performance parameters, environmental considerations, time codes, signal isolation, and time dissemination. Author (revised)

N94-10974*# Rockwell International Corp., Downey, CA. Space Systems Div.

PTTI-AIDED EPHEMERIS CALCULATION AND RAPID DATA LINK ACQUISITION FOR MANNED SPACE FLIGHT **c17**

Alfred Anderman *In* NASA. Goddard Space Flight Center, The 24th Annual Precise Time and Time Interval (PTTI) Applications and Planning Meeting Jun. 1993 p 137-152 (For primary document see N94-10963 01-70)
Avail: CASI HC A03/MF A04

Complexity of future manned space flight mission control can be significantly reduced by integrating GPS, the PTTI source, into telemetry, tracking, and command (TT&C). Future telecommunications, space tracking electronic intelligence, metrology, navigation, and data acquisition will thereby be served, including: on-board ephemeris determination, reduced synchronization time for time division multiple access (TDMA) links, and in-flight clock calibration, increasing on-board autonomy and reducing ground support costs. Manned space transportation through the first quarter of the 21st century will probably depend on a mix of vehicles, including the Advanced Manned Launch System (AMLS), the Personnel Launch System (PLS), and continued use of the Shuttle Fleet. Precise Ephemeris is important on-board for mission success, status monitoring, also for rendezvous and docking. Use of GPS can eliminate ground based tracking/processing, enhancing autonomy and reducing communications bandwidth. GPS time can simplify complicated functions used in bandwidth efficient time division multiple access (TDMA) communications, such as: precise and realtime synchronization of receive reference timing, transmit-timing and acquisition control, unique synchronization word (UW) detection, and elastic buffering. High clock accuracy provides increased signal-to-noise (S/N) ratio during acquisition, permitting narrower acquisition frequency and time windows. Spaceborne systems requirements to provide capabilities such as: refinement of the GEM-72 gravity model based on satellite tracking observations from ATS-6 to GEOS-3, relativistic clock experiments, NASA crustal dynamics program for developing space geodetic techniques to study the earth's crust, its gravity field, and earthquake mechanisms, and multi-disciplinary space geodetic tracking for studying global climatic changes are also reviewed. Author (revised)

N94-10975*# Naval Undersea Warfare Center, West Palm Beach, FL.

UNDERWATER HYDROPHONE LOCATION SURVEY **c48**

Jack B. Cecil *In* NASA. Goddard Space Flight Center, The 24th Annual Precise Time and Time Interval (PTTI) Applications and Planning Meeting Jun. 1993 p 153-158 (For primary document see N94-10963 01-70)
Avail: CASI HC A01/MF A04

The Atlantic Undersea Test and Evaluation Center (AUTEC) is a U.S. Navy test range located on Andros Island, Bahamas, and a Division of the Naval Undersea Warfare Center (NUWC), Newport, RI. The Headquarters of AUTEC is located at a facility in West Palm Beach, FL. AUTEC's primary mission is to provide the U.S. Navy with a deep-water test and evaluation facility for making underwater acoustic measurements, testing and calibrating sonars, and providing accurate underwater, surface, and in-air tracking data on surface ships, submarines, aircraft, and weapon systems. Many of these programs are in support of Antisubmarine Warfare (ASW), undersea research and development programs, and Fleet assessment and operational readiness trials. Most tests conducted at AUTEC require precise underwater tracking (plus or minus 3 yards) of multiple acoustic signals emitted with the correct waveshape and repetition criteria from either a surface craft or underwater vehicle. Author

N94-10976*# Stanford Univ., CA. Physics Dept.

A LASER-COOLED CESIUM FOUNTAIN FREQUENCY STANDARD AND A MEASUREMENT OF THE FREQUENCY SHIFT DUE TO ULTRA-COLD COLLISIONS Abstract Only

Kurt Gibble, Steven Kasapi, and Steven Chu *In* NASA. Goddard Space Flight Center, The 24th Annual Precise Time and Time Interval (PTTI) Applications and Planning Meeting Jun. 1993 p 159-162 (For primary document see N94-10963 01-70)
Avail: CASI HC A01/MF A04

A frequency standard based on an atomic fountain of cesium atoms may have an accuracy of 10(exp -16) due to longer interaction times and smaller anticipated systematic errors. All of the known systematic effects that now limit the accuracy of the Cs frequency standard increase either linearly or as some higher power of the atom's velocity. The one systematic frequency shift which is dramatically different is the frequency shift due to the collisions between the laser cooled atoms. At a temperature of a few micro-K, the de Broglie wavelength (lambda(sub deB) = h/p, where h is Planck's constant and p is the momentum of the atom) is much larger than the scale of the interatomic potential. Under these conditions the collision cross sections can be as large as (lambda(sub deB)(sup 2))/Pi and the frequency shift due to these collisions was recently calculated. In our Cs atomic fountain, we laser cooled and trapped 10(exp 10) Cs atoms in 0.4 s. By shifting the frequencies of the laser beams, the atoms were launched upwards at 2.5 m/s and a fraction of the atoms were optically pumped into the F=3 ground state. The unwanted atoms in the F=4 ground state were removed from the fountain with radiation pressure from a laser beam tuned to excite only those atoms. The Cs atoms in the F=3 state traveled ballistically upwards, were excited by the microwave cavity, and then returned back through the same cavity in the atomic fountain configuration. By varying the cold atom density, a density dependent shift of -12.9 +/- 0.7 mHz or -1.4 x 10-12 for an average fountain density of (2.7 +/- 1.5) 10(exp 9) atoms/cm(sup 3) was measured. Author (revised)

N94-10977*# TrueTime, Inc., Santa Rosa, CA.
DISCIPLINED RUBIDIUM OSCILLATOR WITH GPS SELECTIVE AVAILABILITY
Wayne P. Dewey *In* NASA. Goddard Space Flight Center, The 24th Annual Precise Time and Time Interval (PTTI) Applications and Planning Meeting Jun. 1993 p 163-172 (For primary document see N94-10963 01-70)
Avail: CASI HC A02/MF A04

A U.S. Department of Defense decision for continuous implementation of GPS Selective Availability (S/A) has made it necessary to modify Rubidium oscillator disciplining methods. One such method for reducing the effects of S/A on the oscillator disciplining process was developed which achieves results approaching pre-S/A GPS. The Satellite Hopping algorithm used in minimizing the effects of S/A on the oscillator disciplining process is described, and the results of using this process to those obtained prior to the implementation of S/A are compared. Test results are from a TrueTime Rubidium based Model GPS-DC timing receiver. Author (revised)

N94-10978*# TRAK Microwave Corp., Tampa, FL. TRAK Systems Div.
A PRECISE GPS-BASED TIME AND FREQUENCY SYSTEM
Jack McNabb and Earl Fossler *In* NASA. Goddard Space Flight Center, The 24th Annual Precise Time and Time Interval (PTTI) Applications and Planning Meeting Jun. 1993 p 173-184 (For primary document see N94-10963 01-70)
Avail: CASI HC A03/MF A04

An approach to implementing a compact, highly reliable and precise Master Time and Frequency subsystem usable in a variety of applications is described. These applications include, among others, Satellite Ground Terminals, Range Timing Stations, Communications Terminals, and Power Station Timing subsystems. All time and frequency output signals are locked to Universal Time via the GPS Satellite system. The system provides for continued output of precise signals in the event of GPS signal interruption from antenna or lead-in breakage or other causes. Cost/performance tradeoffs affecting system accuracy over the short, medium, and long term are discussed. A unique approach to redundant system design provides an architecture with the reliability advantage of triple-redundant majority voting and the cost advantages of dual-redundant elements. The system can be configured to output a variety of precise time and frequency signals and the design can be tailored to output as few, or as many, types and quantities of signals as are required by the application. Author (revised)

N94-10979*# Fiat Research Center, Orbassano, Turin (Italy).
POSSIBLE APPLICATIONS OF ATOMIC FREQUENCY STANDARDS WITH AN INTERNAL HIGH RESOLUTION DIGITAL SYNTHESIZER
E. Detoma and A. Stern (Time and Frequency Ltd., Holon, Israel.) *In* NASA. Goddard Space Flight Center, The 24th Annual Precise Time and Time Interval (PTTI) Applications and Planning Meeting Jun. 1993 p 185-198 (For primary document see N94-10963 01-70)
Avail: CASI HC A03/MF A04

The applications of Atomic Frequency Standards with an internal synthesizer (thereafter referred as 'Synthesized Frequency Standards or Oscillators') with a special emphasis on the Rb oscillator are reviewed. A fractional frequency synthesizer, developed by SEPA, was incorporated in the Frequency Locked Loop of a TFL Rubidium Frequency Standard. This combination allows a frequency settability in steps of 1.5 x 10(exp -12) (optional 1 x 10(exp -13) over a range of 6 x 10(exp -9) without having to resort to change the C-field to tune the output frequency of the device. This capability, coupled to the excellent short term stability of the Rb frequency standard, opens new possibilities for time and frequency users in the various fields (time metrology, navigation, communication, etc.) in which stable frequency standards find their application. Author (revised)

N94-10980*# KERNCO, Inc., Danvers, MA.
CAFS: A CESIUM ATOMIC FREQUENCY STANDARD FOR GPS BLOCK IIR
Jeffry A. Wisnia *In* NASA. Goddard Space Flight Center, The 24th Annual Precise Time and Time Interval (PTTI) Applications and Planning Meeting Jun. 1993 p 199-208 (For primary document see N94-10963 01-70)
Avail: CASI HC A02/MF A04

Kernco, Inc. was selected to design the Cesium Atomic Frequency Standards (CAFS) for the GPS Block IIR NAVSTAR satellites. These spacecraft are scheduled to be launched in the mid-1990's to replenish and upgrade the existing constellation of Global Positioning System satellites. The Block IIR CAFS output frequency is 13.4003378 MHz, the 686th submultiple of the cesium atomic resonance frequency. Using an integer submultiple simplifies the design of the atomic frequency standard's rf multiplier circuits, eliminating the secondary frequency synthesizer needed in previous designs. The GPS Block IIR CAFS design, particularly the improvements made on our earlier Block II design is described. Test results are included. Author (revised)

N94-10981*# Smithsonian Astrophysical Observatory, Cambridge, MA.
STATUS OF LOCAL OSCILLATORS FOR OPERATING ULTRA-HIGH RESOLUTION FREQUENCY DISCRIMINATORS AS FREQUENCY STANDARDS
R. F. C. Vessot, E. M. Mattison, M. W. Levine, and R. L. Walsworth *In* NASA. Goddard Space Flight Center, The 24th Annual Precise Time and Time Interval (PTTI) Applications and Planning Meeting Jun. 1993 p 209-220 (For primary document see N94-10963 01-70)
Avail: CASI HC A03/MF A04

The operation of new improved frequency standards based on new ultra-high-resolution frequency discriminators requires high stability local, or 'flywheel' oscillators. We review the spectral density of phase fluctuations of existing flywheel oscillators and the related time domain frequency stability of new and proposed cryogenically cooled oscillators suitable for this application. Presently used devices include the quartz crystal oscillator, the room-temperature actively oscillating atomic hydrogen (H) maser, and the superconducting maser oscillator. Future devices include the cryogenic H-maser and other cryogenic devices using resonators of superconducting metal or solid crystalline sapphire. The relation of the phase spectral density of these devices to the characteristics of present and proposed frequency discriminators based on trapped cooled ions and cold atoms is discussed in terms of their operation as frequency standards.
Author (revised)

N94-10982*# National Physical Lab., Teddington (England).
DEVELOPMENT OF A CRYOGENIC HYDROGEN MASER AT THE NPL
c36
R. Mossavati *In* NASA. Goddard Space Flight Center, The 24th Annual Precise Time and Time Interval (PTTI) Applications and Planning Meeting Jun. 1993 p 221-230 (For primary document see N94-10963 01-70)
Avail: CASI HC A02/MF A04

A prototype Cold Hydrogen Maser (CHM) was being developed for the past year. The features of this CHM, which is designed to operate initially at 4.2 K, are the use of low loss alumina, and later sapphire, in the fabrication of the microwave cavity; possible use of superconductors for shielding; use of a cryogenic amplifier; possible coating material; and a reliable RF discharge circuit for the dissociation of hydrogen. A numerical simulation was performed to find the dimensions of the microwave cavity for the TE011 mode and the model was confirmed experimentally. The system will be used to test various wall coatings adsorbed on top of a PTFE buffer underlayer. The CHM is expected to be used as a flywheel frequency standard at the NPL with medium-term stability of one part in 10(exp 14) or better. Author (revised)

N94-10983*# Naval Research Lab., Washington, DC.
TWO WAY TIME TRANSFER RESULTS AT NRL AND USNO
Ivan J. Galysh and G. Paul Landis *In* NASA. Goddard Space Flight Center, The 24th Annual Precise Time and Time Interval (PTTI) Applications and Planning Meeting Jun. 1993 p 231-242 (For primary document see N94-10963 01-70)
Avail: CASI HC A03/MF A04

The Naval Research Laboratory (NRL) has developed a two way time transfer modem system for the United States Naval Observatory (USNO). Two modems in conjunction with a pair of Very Small Aperture Terminal (VSAT) and a communication satellite can achieve sub nanosecond time transfer. This performance is demonstrated by the results of testing at and between NRL and USNO. The modems use Code Division Multiple Access (CDMA) methods to separate their signals through a single path in the satellite. Each modem transmitted a different Pseudo Random Noise (PRN) code and received the others PRN code. High precision time transfer is possible with two way methods because of reciprocity of many of the terms of the path and hardware delay between the two modems. The hardware description was given in a previous paper. Author (revised)

N94-10984*# Instituto Elettrotecnico Nazionale, Galileo Ferraris, Turin (Italy).

PERFORMANCES OF A DATE DISSEMINATION CODE ON TELEPHONE LINES USING COMMERCIAL MODEMS **c32**

F. Cordara, V. Pettiti, R. Quasso (Politecnico di Torino, Italy.), and E. Rubiola (Politecnico di Torino, Italy.) *In* NASA. Goddard Space Flight Center, The 24th Annual Precise Time and Time Interval (PTTI) Applications and Planning Meeting Jun. 1993 p 243-254 (For primary document see N94-10963 01-70)

Avail: CASI HC A03/MF A04

A coded time/date information dissemination system (CTD), based on telephone lines and commercial modems, is now in its experimental phase in Italy at IEN. This service, born from a cooperation with other metrological laboratories (TUG, Austria, SNT, Sweden, VSL, The Netherlands), represents an attempt towards an European standardization. Some results of an experimental analysis in which a few modems were tested, both in laboratory conditions and connected to the telephone network, in order to evaluate the timing capability of the system are given. When the system is used in a one-way mode, in many practical cases the modems delay turns out to be the main factor which limits the accuracy, even more than the telephone line delays. If the two-way mode is used, the modems asymmetry, i.e., the delay difference between transmission and reception, is almost always the most important source of uncertainty, provided the link is not including a space segment. Comparing the widely used V.22 modems to the old V.21 ones, the latters turn out to be better both in delay time (30-100 ms V.22, and 7-15 ms V.21) and asymmetry (10-50 micro-s V.22, and 10 ms V.22). Time transfer accuracies of 10 micron-s (same turn) to 100 micro-s (long distance calls) were obtained in two-way mode with commercial V.21 modems. Author

N94-10985*# Life Sciences Software, Camano Island, WA.

TIMESET: A COMPUTER PROGRAM THAT ACCESSES FIVE ATOMIC TIME SERVICES ON TWO CONTINENTS **c61**

P. L. Petrakis *In* NASA. Goddard Space Flight Center, The 24th Annual Precise Time and Time Interval (PTTI) Applications and Planning Meeting Jun. 1993 p 255-266 (For primary document see N94-10963 01-70)

Avail: CASI HC A03/MF A04

TimeSet is a shareware program for accessing digital time services by telephone. At its initial release, it was capable of capturing time signals only from the U.S. Naval Observatory to set a computer's clock. Later the ability to synchronize with the National Institute of Standards and Technology was added. Now, in Version 7.10, TimeSet is able to access three additional telephone time services in Europe - in Sweden, Austria, and Italy - making a total of five official services addressable by the program. A companion program, TimeGen, allows yet another source of telephone time data strings for callers equipped with TimeSet version 7.10. TimeGen synthesizes UTC time data strings in the Naval Observatory's format from an accurately set and maintained DOS computer clock, and transmits them to callers. This allows an unlimited number of 'freelance' time generating stations to be created. Timesetting from TimeGen is made feasible by the advent of Becker's RighTime, a shareware program that learns the drift characteristics of a computer's clock and continuously applies a correction to keep it accurate, and also brings .01 second resolution to the DOS clock. With clock regulation by RighTime and periodic update calls by the TimeGen station to an official time source via TimeSet, TimeGen offers the same degree of accuracy within the resolution of the computer clock as any official atomic time source. Author

N94-10986*# Air System Technologies, Inc., Dallas, TX.

RIGHTIME: A REAL TIME CLOCK CORRECTING PROGRAM FOR MS-DOS-BASED COMPUTER SYSTEMS **c61**

G. Thomas Becker *In* NASA. Goddard Space Flight Center, The 24th Annual Precise Time and Time Interval (PTTI) Applications and Planning Meeting Jun. 1993 p 267-276 (For primary document see N94-10963 01-70)

Avail: CASI HC A02/MF A04

A computer program is described which effectively eliminates the misgivings of the DOS system clock in PC/AT-class computers. RighTime is a small, sophisticated memory-resident program that automatically corrects both the DOS system clock and the hardware 'CMOS' real time clock (RTC) in real time. RighTime learns what corrections are required without operator interaction beyond the occasional accurate time set. Both warm (power on) and cool (power off) errors are corrected, usually yielding better than one part per million accuracy in the typical desktop computer with no additional hardware, and RighTime increases the system clock resolution from approximately 0.0549 second to 0.01 second. Program tools are also available which allow visualization of RighTime's actions, verification of its performance, display of its history log, and which provide data for graphing of the system clock behavior. The program has found application in a wide variety of industries, including astronomy, satellite tracking, communications, broadcasting, transportation, public utilities, manufacturing, medicine, and the military. Author (revised)

N94-10987*# National Inst. of Standards and Technology, Boulder, CO. Time and Frequency Div.

MEASUREMENT METHODS AND ALGORITHMS FOR COMPARISON OF LOCAL AND REMOTE CLOCKS

Judah Levine *In* NASA. Goddard Space Flight Center, The 24th Annual Precise Time and Time Interval (PTTI) Applications and Planning Meeting Jun. 1993 p 277-288 (For primary document see N94-10963 01-70)

Avail: CASI HC A03/MF A04

Several methods for characterizing the performance of clocks with special emphasis on using calibration information that is acquired via an unreliable or noisy channel is discussed. Time-domain variance estimators and frequency-domain techniques such as cross-spectral analysis are discussed. Each of these methods has advantages and limitations that will be illustrated using data obtained via GPS, ACTS, and other methods. No one technique will be optimum for all of these analyses, and some of these problems cannot be completely characterized by any of the techniques discussed. The inverse problem of communicating frequency and time corrections to a real-time steered clock are also discussed. Methods were developed to mitigate the disastrous problems of data corruption and loss of computer control. Author (revised)

N94-10988*# Timing Solutions Corp., Boulder, CO.

ADVANCES IN TIME-SCALE ALGORITHMS **c61**

S. R. Stein *In* NASA. Goddard Space Flight Center, The 24th Annual Precise Time and Time Interval (PTTI) Applications and Planning Meeting Jun. 1993 p 289-302 (For primary document see N94-10963 01-70)

Avail: CASI HC A03/MF A04

The term clock is usually used to refer to a device that counts a nearly periodic signal. A group of clocks, called an ensemble, is often used for time keeping in mission critical applications that cannot tolerate loss of time due to the failure of a single clock. The time generated by the ensemble of clocks is called a time scale. The question arises how to combine the times of the individual clocks to form the time scale. One might naively be tempted to suggest the expedient of averaging the times of the individual clocks, but a simple thought experiment demonstrates the inadequacy of this approach. Suppose a time scale is composed of two noiseless clocks having equal and opposite frequencies. The mean time scale has zero frequency. However if either clock fails, the time-scale frequency immediately changes to the frequency of the remaining clock. This performance is generally unacceptable and simple mean time scales are not used. First, previous time-scale developments are reviewed and then some new methods that result in enhanced performance are presented. The historical perspective is based upon several time scales: the AT1 and TA time scales of the National Institute of Standards and Technology (NIST), the A.1(MEAN) time scale of the US Naval observatory (USNO), the TAI time scale of the Bureau International des Poids et Measures (BIPM), and the KAS-1 time scale of the Naval Research laboratory (NRL). The new method was incorporated in the KAS-2 time scale recently developed by Timing Solutions Corporation. The goal is to present time-scale concepts in a nonmathematical form with as few equations as possible. Many other papers and texts discuss the details of the optimal estimation techniques that may be used to implement these concepts. Author (revised)

N94-10989*# Nippon Telegraph and Telephone Public Corp., Yokosuka (Japan). Transmission Systems Labs.

TIME SIGNAL DISTRIBUTION IN COMMUNICATION NETWORKS BASED ON SYNCHRONOUS DIGITAL HIERARCHY **c32**

Atsushi Imaoka and Masami Kihara *In* NASA. Goddard Space Flight Center, The 24th Annual Precise Time and Time Interval (PTTI) Applications and Planning Meeting Jun. 1993 p 303-312 (For primary document see N94-10963 01-70)
Avail: CASI HC A02/MF A04

A new method that uses round-trip paths to accurately measure transmission delay for time synchronization is proposed. The performance of the method in Synchronous Digital Hierarchy networks is discussed. The feature of this method is that it separately measures the initial round trip path delay and the variations in round-trip path delay. The delay generated in SDH equipment is determined by measuring the initial round-trip path delay. In an experiment with actual SDH equipment, the error of initial delay measurement was suppressed to 30ns. Author

N94-10990*# Telecom Solutions Ltd., San Jose, CA.
SYNOPSIS OF TIMING MEASUREMENT TECHNIQUES USED IN TELECOMMUNICATIONS **c32**
George Zampetti *In* NASA. Goddard Space Flight Center, The 24th Annual Precise Time and Time Interval (PTTI) Applications and Planning Meeting Jun. 1993 p 313-326 (For primary document see N94-10963 01-70)
Avail: CASI HC A03/MF A04

Historically, Maximum Time Interval Error (MTIE) and Maximum Relative Time Interval Error (MRTIE) have been the main measurement techniques used to characterize timing performance in telecommunications networks. Recently, a new measurement technique, Time Variance (TVAR) has gained acceptance in the North American (ANSI) standards body. TVAR was developed in concurrence with NIST to address certain inadequacies in the MTIE approach. The advantages and disadvantages of each of these approaches are described. Real measurement examples are presented to illustrate the critical issues in actual telecommunication applications. Finally, a new MTIE measurement is proposed (ZTIE) that complements TVAR. Together, TVAR and ZTIE provide a very good characterization of network timing. Author (revised)

N94-10991*# Bell Telephone Labs., Inc., Holmdel, NJ.
TIMING IN PRIVATE DIGITAL TELECOMMUNICATION NETWORKS **c32**
J. E. Abate, C. D. Near, and M. S. Russo *In* NASA. Goddard Space Flight Center, The 24th Annual Precise Time and Time Interval (PTTI) Applications and Planning Meeting Jun. 1993 p 327-336 (For primary document see N94-10963 01-70)
Avail: CASI HC A02/MF A04

For proper operation of today's large digital private networks, high quality synchronization must be achieved. A general telecommunication performance objective is to maintain long-term frequency accuracy of ten parts per trillion at all synchronous digital equipment in the network. Many times, however, this is not achieved in private networks. Low quality clocks, errored transmission facilities, and incorrectly designed synchronization plans are often cause for poor performance. It is shown that properly-designed private networks can operate with long term frequency averages between ten parts per trillion to ten parts per million. These performance levels can adversely impact customer applications. The most demanding applications are digital and voice band data, encrypted voice, facsimile, and video. In a typical private network operating at 0.01 parts per million, the user would experience reduced data throughput, dropped encrypted calls, unreadable facsimile pages, or interrupted video transmission dozens of times per day. The major contribution to poor private network synchronization performance is the interaction of Customer Premises Equipment (CPE) clocks and the network facilities used to distribute timing. The performance of typical CPE clocks and facilities, and their impact on customer applications, are discussed. CPE clock performance issues, along with private network architectural constraints, make synchronization planning extremely difficult. Planning is usually costly and requires specialized expertise. Author (revised)

N94-10992*# Alcatel Network Systems, Inc., Richardson, TX.
SONET SYNCHRONIZATION: WHAT'S HAPPENING **c74**
Robert W. Cubbage *In* NASA. Goddard Space Flight Center, The 24th Annual Precise Time and Time Interval (PTTI) Applications and Planning Meeting Jun. 1993 p 337-342 (For primary document see N94-10963 01-70)
Avail: CASI HC A02/MF A04

Almost everyone that has heard of SONET knows that the acronym stands for Synchronous Optical NETwork. There has been a host of magazine articles on SONET rings, SONET features, even SONET compatibility with digital radio. What has not been highly publicized is the critical relationship between SONET, network synchronization, and payload jitter. This topic is addressed. Author (revised)

N94-10993*# Johns Hopkins Univ., Laurel, MD. Applied Physics Lab.
PERFORMANCE OF LOW-COST COMMERCIAL FIBER-OPTIC TRANSCEIVERS FOR REFERENCE FREQUENCY DISTRIBUTION
Richard Dragonette and Joseph J. Suter *In* NASA. Goddard Space Flight Center, The 24th Annual Precise Time and Time Interval (PTTI) Applications and Planning Meeting Jun. 1993 p 343-356 (For primary document see N94-10963 01-70)
Avail: CASI HC A03/MF A04

Precision time and frequency reference signals were effectively disseminated using high-quality intricate fiber-optic distribution systems. The quality of signals distributed by such systems is excellent, but the cost of these systems makes them unavailable to many potential users. A study of signal quality maintained using inexpensive commercial transmitter/receiver pairs is undertaken. Seven different transmitter/receiver pairs obtained from four different manufacturers were thoroughly tested using a 5 MHz sinusoid derived from a precision, temperature controlled, crystal-controlled oscillator. The electrical signal output from each fiber-optic receiver was tested for spectral purity, single-sideband phase noise, and AM noise, and the results are tabulated and discussed without identification of the manufacturer or the equipment model number. Author (revised)

N94-10994*# Jet Propulsion Lab., California Inst. of Tech., Pasadena.
ULTRASTABLE REFERENCE FREQUENCY DISTRIBUTION UTILIZING A FIBER OPTIC LINK
Malcolm Calhoun and Paul Kuhnle *In* NASA. Goddard Space Flight Center, The 24th Annual Precise Time and Time Interval (PTTI) Applications and Planning Meeting Jun. 1993 p 357-364 (For primary document see N94-10963 01-70)
Avail: CASI HC A02/MF A04

The Frequency Standards Laboratory at the Jet Propulsion Laboratory (JPL) is responsible for the generation and distribution of ultra-stable reference frequency in NASA's Deep Space Network (DSN). Certain assemblies and components of the Radio Science and VLBI systems are located in the cones of tracking antennas hundreds of meters from the Frequency and Timing Subsystem's frequency standards. The very stringent requirements of these users challenge the performance of state-of-the-art frequency sources as well as the associated signal distribution system. The reference frequency distribution system described is designed around a low temperature coefficient of delay (TCD) optical fiber. On-site measurements of the fiber optic link alone indicate 100 MHz phase noise performance on the order of -120 dBc at 1 Hz from the carrier and Allan deviation on the order of parts in 10(exp 16) at 1000 seconds averaging time. The measured phase noise and stability of the link indicate that the performance characteristics of the hydrogen maser frequency standards are not degraded by the distribution system. Thus, optical fibers and electro-optic devices as distribution media appear to be a viable alternative to the classical coaxial cable distribution systems. Author (revised)

N94-10995*# Jet Propulsion Lab., California Inst. of Tech., Pasadena.
A WIDE-BAND FIBER OPTIC FREQUENCY DISTRIBUTION SYSTEM EMPLOYING THERMALLY CONTROLLED PHASE COMPENSATION
Dean Johnson (University of Western Michigan, Kalamazoo.), Malcolm Calhoun, Richard Sydnor, and George Lutes *In* NASA. Goddard Space Flight Center, The 24th Annual Precise Time and Time Interval (PTTI) Applications and Planning Meeting Jun. 1993 p 365-374 (For primary document see N94-10963 01-70)
Avail: CASI HC A02/MF A04

An active wide-band fiber optic frequency distribution system employing a thermally controlled phase compensator to stabilize phase variations induced by environmental temperature changes is described. The distribution system utilizes bidirectional dual wavelength transmission to provide optical feedback of induced phase variations of 100 MHz signals propagating along the distribution cable. The phase compensation considered differs from earlier narrow-band phase compensation designs in that it uses a thermally controlled fiber delay coil rather than a VCO or phase modulation to compensate for induced phase variations. Two advantages of the wide-band system over earlier designs are (1) that it provides phase compensation for all transmitted frequencies, and (2) the compensation is applied after the optical interface rather than electronically ahead of it as in earlier schemes. Experimental results on the first prototype shows that the thermal stabilizer reduces phase variations and Allan deviation by a factor of forty over an equivalent uncompensated fiber optic distribution system. Author

N94-10996*# Computer Sciences Corp., Patrick AFB, FL.
ANALYSIS OF THE EASTERN RANGE MULTIPLEXED FIBER OPTIC IRIG B120 DISTRIBUTION SYSTEM c32
Michael J. Duncan, John S. Martell, and James L. Wright *In* NASA. Goddard Space Flight Center, The 24th Annual Precise Time and Time Interval (PTTI) Applications and Planning Meeting Jun. 1993 p 375-384 (For primary document see N94-10963 01-70)
Avail: CASI HC A02/MF A04

A study was conducted to assess the effects of transmitting a precision clock synchronization signal over a commercial multiplexed fiber optic communication system. This study is an evaluation of the distortion and jitter introduced into the signal by this type of transmission system. An analysis comparing signal quality at the multiplexing and demultiplexing ends of the fiber optic communication system shows that the amplitude and phase distortion added to the clock synchronization signal by the transmission system is minimal. Author

N94-10997*# Trieste Univ. (Italy). Dip. di Elettrotecnica, Elettronica ed Informatica.
ESTIMATING THE INSTABILITIES OF N CLOCKS BY MEANS OF COMPARISON MEASUREMENTS
Amedeo Premoli and Patrizia Tavella (Instituto Elettrotecnico Nazionale, Galileo Ferraris, Turin, Italy.) *In* NASA. Goddard Space Flight Center, The 24th Annual Precise Time and Time Interval (PTTI) Applications and Planning Meeting Jun. 1993 p 385-398 (For primary document see N94-10963 01-70)
Avail: CASI HC A03/MF A04

The estimation of individual instabilities of N clocks, compared by measuring the differences of their readings, is considered without assuming a priori any hypotheses on their uncorrelation. Instabilities of the N clocks are described by a complete (non-diagonal) N x N covariance matrix R. Only differences of clock readings are available in order to estimate R. Statistical processing of these data allows one to calculate the (N-1)x(N-l) covariance matrix S of the differences relative to the N-th(reference) clock. By analyzing the relationships tying R and S, several pieces of information can be inferred and, in particular, the conditions for the validity of the uncorrelation hypothesis are established. The estimation of R from S is not unique: in any case R must be positive definite. A theorem states that R is positive definite if and only if its determinant is positive. Nevertheless infinitely many acceptable choices of R still fulfill the condition of positive definiteness. This paper shows that, by increasing the number N of compared clocks, the amount of arbitrariness in estimating R is reduced. The analysis of some experimental data illustrates the capability of the method. Author (revised)

N94-10998*# National Research Council of Canada, Ottawa (Ontario). Time and Frequency Standards Group.
TIME SCALE ALGORITHMS FOR AN INHOMOGENEOUS GROUP OF ATOMIC CLOCKS
C. Jacques, J.-S. Boulanger, R. J. Douglas, D. Morris, S. Cundy, and H. F. Lam *In* NASA. Goddard Space Flight Center, The 24th Annual Precise Time and Time Interval (PTTI) Applications and Planning Meeting Jun. 1993 p 399-412 (For primary document see N94-10963 01-70)
Avail: CASI HC A03/MF A04

Through the past 17 years, the time scale requirements at the National Research Council (NRC) have been met by the unsteered output of its primary laboratory cesium clocks, supplemented by hydrogen masers when short-term stability better than 2 x 10(exp -12)tau(sup -1/2) has been required. NRC now operates three primary laboratory cesium clocks, three hydrogen masers, and two commercial cesium clocks. NRC has been using ensemble averages for internal purposes for the past several years, and has a realtime algorithm operating on the outputs of its high-resolution (2 x 10(exp -13) s at 1 s) phase comparators. The slow frequency drift of the hydrogen masers has presented difficulties in incorporating their short-term stability into the ensemble average, while retaining the long-term stability of the laboratory cesium frequency standards. We report on this work on algorithms for an inhomogeneous ensemble of atomic clocks, and on our initial work on time scale algorithms that could incorporate frequency calibrations at NRC from the next generation of Zacharias fountain cesium frequency standards having frequency accuracies that might surpass 10(exp -15), or from single-trapped-ion frequency standards (Ba+, Sr+,...) with even higher potential accuracies. The requirements for redundancy in all the elements (including the algorithms) of an inhomogeneous ensemble that would give a robust real-time output of the algorithms are presented and discussed. Author (revised)

N94-10999*# Stanford Univ., CA. Experimental Physics Lab.
A MULTI-VARIANCE ANALYSIS IN THE TIME DOMAIN c33
Todd Walter *In* NASA. Goddard Space Flight Center, The 24th Annual Precise Time and Time Interval (PTTI) Applications and Planning Meeting Jun. 1993 p 413-426 (For primary document see N94-10963 01-70)
Avail: CASI HC A03/MF A04

Recently a new technique for characterizing the noise processes affecting oscillators was introduced. This technique minimizes the difference between the estimates of several different variances and their values as predicted by the standard power law model of noise. The method outlined makes two significant advancements: it uses exclusively time domain variances so that deterministic parameters such as linear frequency drift may be estimated, and it correctly fits the estimates using the chi-square distribution. These changes permit a more accurate fitting at long time intervals where there is the least information. This technique was applied to both simulated and real data with excellent results. Author (revised)

N94-11000*# Jet Propulsion Lab., California Inst. of Tech., Pasadena.
SPACECRAFT SIGNAL SOURCES PORTABLE TEST SYSTEM c32
Albert Kirk, Paul Kuhnle, Richard Sydnor, William Diener, and David Stowers *In* NASA. Goddard Space Flight Center, The 24th Annual Precise Time and Time Interval (PTTI) Applications and Planning Meeting Jun. 1993 p 427-438 (For primary document see N94-10963 01-70)
Avail: CASI HC A03/MF A04

There is a frequent need to measure the frequency stability and phase noise levels of very high performance signal sources that are required for certain spacecraft missions. These measurements need to be done at different locations as the spacecraft subsystems progress through the various stages of development, assembly, test, and integration. Allan Deviation and Phase Noise of high performance sources are generally measured by comparing the unit under test to a reference standard. Five basic requirements are associated with making these kind of measurements: (1) the reference standard performance needs to be equal or better than the unit under test; (2) the measurement system needs to accommodate odd, nonstandard measurement frequencies that can range from 4 MHz to 35 GHz; (3) warm-up frequency drift and aging can corrupt a measurement and must be dealt with; (4) test equipment generated noise must be understood and prevented from limiting the measurements; (5) test equipment noise performance must be verifiable in the field as needed. A portable measurement system that was built by JPL and used in the field is described. The methods of addressing the above requirements are outlined and some measurement noise floor values are given. This test set was recently used to measure state of the art crystal oscillator frequency standards on the TOPEX and MARS OBSERVER spacecraft during several stages of acceptance tests. Author (revised)

N94-11001*# Shaanxi Astronomical Observatory, Lintong (China).
THE LIMIT OF FREQUENCY ESTIMATION
Wei Guo *In* NASA. Goddard Space Flight Center, The 24th Annual Precise Time and Time Interval (PTTI) Applications and Planning Meeting Jun. 1993 p 439-444 (For primary document see N94-10963 01-70)
Avail: CASI HC A01/MF A04

In phase and frequency measurements, the measured phase and frequency are not the true phase and frequency but the ones which are disturbed by noises, due to the effects of the noise processes. The effects of three noise processes, i.e., White PM, White FM, and Random Walk FM, on the estimations of phase and frequency is discussed. It is indicated that the properties of these two estimations are very different. In phase estimation, the error can be reduced by properly selecting suitable smoothing length NT and smaple interval T. But in frequency estimation, the error cannot be reduced arbitrarily by means of improving estimator or measurement equipment. The precision of frequency is limited by the intrinsic noises in the clock. Author (revised)

N94-11002*# Xian Jiaotong Univ. (China). Dept. of Measurement and Instrumentation.
A NEW METHOD OF TIME DIFFERENCE MEASUREMENT: THE TIME DIFFERENCE METHOD BY DUAL PHASE COINCIDENCE POINTS DETECTION
Wei Zhou *In* NASA. Goddard Space Flight Center, The 24th Annual Precise Time and Time Interval (PTTI) Applications and Planning Meeting Jun. 1993 p 445-450 (For primary document see N94-10963 01-70)
Avail: CASI HC A02/MF A04

In the high accurate measurement of periodic signals, the greatest common factor frequency and its characteristics have special functions. A method of time difference measurement - the time difference method by dual 'phase coincidence points' detection is described. This method utilizes the characteristics of the greatest common factor frequency to measure time or phase difference between periodic signals. It can suit a very wide frequency range. Measurement precision and potential accuracy of several picoseconds were demonstrated with this new method. The instrument based on this method is very simple, and the demand for the common oscillator is low. This method and instrument can be used widely. Author (revised)

N94-11003*# National Inst. of Standards and Technology, Boulder, CO. Time and Frequency Div.
CONFIDENCE OF THE THREE-POINT ESTIMATOR OF FREQUENCY DRIFT
Marc A. Weiss and Christine Hackman *In* NASA. Goddard Space Flight Center, The 24th Annual Precise Time and Time Interval (PTTI) Applications and Planning Meeting Jun. 1993 p 451-460 (For primary document see N94-10963 01-70)
Avail: CASI HC A02/MF A04

It was shown that a three-point second difference estimator is nearly optimal for estimating frequency drift in many common atomic oscillators. A formula for the uncertainty of this estimate as a function of the integration time and of the Allan variance associated with this integration time is derived. Author (revised)

N94-11490# GEC Hirst Research Centre, Wembley (England). Long Range Research Lab.
CHAOTIC TIME SERIES ANALYSIS
Jaroslav Stark *In* AGARD, Stability in Aerospace Systems Feb. 1993 11 p (For primary document see N94-11489 01-08)
Copyright Avail: CASI HC A03/MF A03

N94-11495# Office National d'Etudes et de Recherches Aerospatiales, Paris (France). Directiondes Etudes de Synthese.
CHAOS, ENTROPY, AND REVERSIBILITY: A SIMPLE EXAMPLE
C. Marchal *In* AGARD, Stability in Aerospace Systems Feb. 1993 3 p (For primary document see N94-11489 01-08)
Copyright Avail: CASI HC A01/MF A03

71 ACOUSTICS

Includes sound generation, transmission and attenuation.
For noise pollution see *45 Environmental Pollution.*

N94-10358 Pennsylvania State Univ., University Park.
ESTIMATION OF THE DIRECT ACOUSTIC RADIATION FROM TURBULENT SPOTS USING BOUNDARY LAYER VELOCITY MEASUREMENTS Ph.D. Thesis
Michael H. Krane 1992 154 p
Avail: Univ. Microfilms Order No. DA9311669

To provide understanding of the acoustic source characteristics of the boundary layer transition region, unsteady velocity measurements of an isolated, artificially generated turbulent spot were made in a zero-pressure gradient laminar boundary layer. These measurements were performed in a water channel using a laser velocimeter and are used to describe the fluctuations of unsteady displacement thickness due to the passage of the turbulent spot. These fluctuations are related to the radiated noise through the Liepmann acoustic analogy. The velocity normal to the plate and the characteristic rise time, t(sub i), of the displacement thickness were calculated from the unsteady displacement thickness. Comparing the results at different streamwise stations shows that the rise time and displacement thickness fluctuation amplitude increase with distance from the generation point, while the peak amplitudes of the normal velocity increase early in the spot development, but level off. For all these parameters, the rate of spatial growth is highest in the stations closest to the turbulent spot generation point. Scaling analysis using the experimental results suggests that the sound radiated by the large-scale motion due to an isolated turbulent spot has a dipole character. Extrapolation to a natural transition zone indicates that the dipole source strength distribution peaks near the midpoint of the transition zone. Measurements of interacting turbulent spot pairs were carried out to test the limits of applicability of the isolated spot results to a natural transition zone. To the degree of interaction present in these experiments, the isolated spot growth was not significantly different from that found for the interacting spots. Dissert. Abstr.

N94-10408# International Centre for Theoretical Physics, Trieste (Italy).
PHOTOSTIMULATED ATTENUATION OF HYPERSOUND IN SUPERLATTICE
S. Y. Mensah, F. K. Allotey, and S. K. Adjepong Oct. 1992 9 p
(DE93-611231; IC-92/305) Avail: CASI HC A02/MF A01 (US Sales Only)

Photostimulated attenuation of hypersound in a semiconductor superlattice has been investigated. It is shown that the attenuation coefficient depends on the phonon wave vector q in an oscillatory manner and that from this oscillation the band width of superlattice can be found. DOE

N94-10752*# Virginia Polytechnic Inst. and State Univ., Blacksburg. Dept. of Aerospace and Ocean Engineering.
PERPENDICULAR BLADE VORTEX INTERACTION AND ITS IMPLICATIONS FOR HELICOPTER NOISE PREDICTION: WAVE-NUMBER FREQUENCY SPECTRA IN A TRAILING VORTEX FOR BWI NOISE PREDICTION Final Technical Report, period ending 15 Aug. 1993
William J. Devenport and Stewart A. L. Glegg (Florida Atlantic Univ., Boca Raton.) Aug. 1993 367 p Original contains color illustrations
(Grant NAG1-1119)
(NASA-CR-193623; NAS 1.26:193623) Avail: CASI HC A16/MF A03; 3 functional color pages

Perpendicular blade vortex interactions are a common occurrence in helicopter rotor flows. Under certain conditions they produce a substantial proportion of the acoustic noise. However, the mechanism of noise generation is not well understood. Specifically, turbulence associated with the trailing vortices shed from the blade tips appears insufficient to account for the noise generated. The hypothesis that the first perpendicular interaction experienced by a trailing vortex alters its turbulence structure in such a way as to increase the acoustic noise generated by subsequent interactions is examined. To investigate this hypothesis a two-part investigation was carried out. In the first part, experiments were performed to examine the behavior of a streamwise vortex as it passed over and downstream of a spanwise blade in incompressible flow. Blade vortex separations between +/- one eighth chord were studied for at a chord Reynolds number of 200,000. Three-component velocity and turbulence measurements were made in the flow from 4 chord lengths upstream to 15 chordlengths downstream of the blade using miniature 4-sensor hot wire probes. These measurements show that the interaction of the vortex with the blade and its wake causes the vortex core to loose circulation and diffuse much more rapidly than it otherwise would. Core radius increases and peak tangential velocity decreases with distance downstream of the blade. True turbulence levels within the core are much larger downstream than upstream of the blade. The net result is a much larger and more intense region of turbulent flow than that presented by the original vortex and thus, by implication, a greater potential for generating acoustic noise. In the second part, the turbulence measurements described above were used to derive the necessary inputs to a Blade Wake Interaction (BWI) noise prediction scheme. This resulted in significantly improved agreement between measurements and calculations of the BWI noise spectrum especially for the spectral peak at low frequencies, which previously was poorly predicted. Author (revised)

N94-11042 Japan Atomic Energy Research Inst., Tokyo.
BASIC EXPERIMENT ON AN ULTRASONIC METHOD OF LOCALIZATION
Yoshio Fujii, Shinji Inomata, Katsuo Suzuki, Tomoaki Suzudo, and Yoshikuni Shinohara Aug. 1992 70 p Limited Reproducibility: More than 20% of this document may be affected by microfiche quality
(DE93-754295; JAERI-M-92-112) Avail: Issuing Activity (Department of Energy (DOE))

The results of the basic experiment on ultrasonic method of localization of mobile robots working in very strong radiation environments in nuclear facilities or in a room filled with opaque medium such as dense smoke where video cameras cannot function are described. The basic characteristics of the ultrasonic sensors used, the outline of the system for sensor signal processing, and the parallel processing method for structured programs are also described. The results of the experiment show that it is possible to identify the location with sufficient accuracy by proper use of the ultrasonic sensors and of signal processing method. It is also shown that countermeasures must be taken to organize a precise and stable measurement system. The parallel processing method applied is effective when using synchronization for communication among multiple structured processes and can also be applied to other sensor signal processing systems. DOE

N94-11057 Notre Dame Univ., IN.
AN EXPERIMENTAL INVESTIGATION OF THE SOURCES OF PROPELLER NOISE DUE TO TURBULENCE INGESTION Ph.D. Thesis
Daniel Francis Scharpf 1993 287 p
Avail: Univ. Microfilms Order No. DA9311108

Experimental measurements were performed on a four-bladed, 10-inch diameter marine propeller operating in a new open-jet, anechoic wind tunnel. A significant portion of the work consisted of the design, construction, and calibration of the wind tunnel facility. The wind tunnel could be operated from 5-100 ft/s with open-jet lengths from 2-7 feet. When the wind tunnel was installed the majority of the chamber had a low-frequency cut-off of 150 Hz. The freestream velocity and propeller rotational speed were 33 ft/s and 3000 RPM, respectively. Turbulence was generated at the exit plane of the wind tunnel inlet by square-mesh grids composed of cylindrical rods which resulted in turbulence levels at the propeller location from 0.2-5.5 percent. Measurements included steady thrust and torque, detailed hot wire surveys of the incoming flow and propeller wake, and sound pressure levels detailing the acoustic spectra and directivity. Bicoherence measurements in the propeller wake showed high coherence between the blade passage harmonics and the broadband frequencies near the hub and tip regions of the blades which indicated that the wake interactions were primarily non-linear. Inflow turbulence reduced this coherence. The integrated broad-band sound pressure level increased by approximately 2 dB for every 1 percent increase in the turbulence. These increases were decomposed into smaller frequency bandwidths and related to the inflow turbulence spectrum. Dissert. Abstr.

N94-11176*# University of Southern California, Los Angeles. Dept. of Aerospace Engineering.
CONTROL OF JET NOISE Final Report, 1 Feb. 1992 - 30 Jun. 1993
Stefan Schreck 1993 45 p Submitted for publication
(Grant NAG1-1096)
(NASA-CR-193612; NAS 1.26:193612) Avail: CASI HC A03/MF A01

This reports describes experiments conducted at the High-Speed Jet Facility at the University of Southern California on supersonic jets. The goal of the study was to develop methods for controlling the noise emitted from supersonic jets by passive and/or active means. Work by Seiner et al (1991) indicates that eddy Mach wave radiation is the dominant noise source in a heated high speed jet. Eddy Mach radiation is caused by turbulent eddies traveling at supersonic speed in the shear layer of the jet. The convection velocity of the eddies decays with increasing distance from the nozzle exit due to the mixing of the jet stream with the ambient fluid. Once the convection speed reaches subsonic velocities, eddy Mach wave radiation ceases. To control noise, a rapid decay of the convection velocity is desired. This may be accomplished by enhanced mixing in the jet. In this study, small aspect ratio rectangular jet nozzles were tested. A flapping mode was noticed in the jets. By amplifying screech components of the jets and destabilizing the jet columns with a collar device, the flapping mode was excited. The result was a rapid decay of the jet velocity. A reduction in eddy Mach radiation in rectangular supersonic jets may be achieved with this device. Author

N94-11262# Pennsylvania State Univ., University Park.
MATERIALS FOR ADAPTIVE STRUCTURAL ACOUSTIC CONTROL, VOLUME 3 Annual Report, 1 Feb. 1992 - 31 Jan. 1993
L. E. Cross 6 Apr. 1993 70 p
(Contract N00014-92-J-1510)
(AD-A264621) Avail: CASI HC A04/MF A01

This report documents work carried out in the Materials Research Laboratory of the Pennsylvania State University over the first year of a new ONR sponsored University Research Initiative (URI) entitled Materials for Adaptive Structural Acoustic Control. For this report the activities have been grouped under the following topic headings: (1) General Summary Papers; (2) Materials Studies; (3) Composite Sensors; (4) Actuator Studies; (5) Integration Issues; (6) Processing Studies; and (7) Thin Film Ferroelectrics. In material studies important advances have been made in the understanding of the evaluation of relaxor behavior in the PLZT's and of the order-disorder behavior in lead scandium tantalate:lead titanate solid solutions and of the Morphotropic Phase Boundary in this system. For both composite sensors and actuators, we have continued to explore and exploit the remarkable versatility of the flextensional moonie type structure. Finite element (FEA) calculations have given a clear picture of the lower order resonant modes and permitted the evaluation of various end cap metals, cap geometries, and load conditions. In actuator studies multilayer structures have been combined with flextensional moonie endcaps to yield high displacement (50 micrometers) compact structures. Electrically controlled shape memory has been demonstrated in lead zirconate stannate titanate compositions, and used for controlling a simple latching relay. DTIC

N94-12615# Hiroshima Univ. (Japan). School of Engineering.
AERODYNAMIC SOUND DUE TO INTERACTION BETWEEN A TWO-DIMENSIONAL FREE SHEAR LAYER AND THE LEADING EDGE OF A PARALLEL FLAT PLATE [NIJIGEN SENDANSOU TO HEIBAN NO KANSHOU NIYORU HASSHIN TO KUURIKION]
Fujihiko Sakao *In* NAL, Proceedings of the 9th and 10th NAL Workshop on Investigation and Control of Boundary-Layer Transition Nov. 1992 p 15-22 In JAPANESE (For primary document see N94-12611 01-34)
Avail: CASI HC A02/MF A02

72 ATOMIC AND MOLECULAR PHYSICS

Includes atomic structure, electron properties, and molecular spectra.

N94-10154# Tennessee Univ., Knoxville. Dept. of Physics.
PHOTODETACHMENT STUDIES ON FEW-ELECTRON ATOMIC NEGATIVE IONS
D. J. Pegg 1992 3 p Presented at the Workshop on Atomic Physics, Ithaca, NY, Oct. 1992
(Contract DE-FG05-85ER-13456)
(DE93-008474; DOE/ER-13456/50; CONF-9210339-1) Avail: CASI HC A01/MF A01

A crossed laser-negative ion beams apparatus, situated at Oak Ridge National Laboratory, has been used for energy and angle-resolved photoelectron spectroscopic measurements following photodetachment. In the current grant period, measurements of the cross sections for photodetaching an electron from the Li(-) ion were finished. Measurements of the sigma(B(-))/sigma(Li(-)) ratio, with a goal of determining photodetachment cross section for B(-), were started. An investigation of the photodetachment of the metastable ion Be(-) also began. Preliminary data on the electron affinity, asymmetry parameter and cross section associated with the photodetachment of Be(-) at a photon energy of 2.076 eV is reported. DOE

N94-10254# Oak Ridge National Lab., TN.
HIGH SPIN PROPERTIES OF NUCLEI

C. Baktash 17 Nov. 1992 11 p
(Contract DE-AC05-84OR-21400)
(DE93-008788; ORNL/FTR-4469) Avail: CASI HC A03/MF A01 (US Sales Only)

The author presented an invited talk on 'Identical Bands in Odd-A-Nuclei' at the 21st INS International Symposium on Rapidly Rotating Nuclei 1992 and chaired one of the scientific sessions. The author also visited the Research Institute for Physical and Chemical Research (RIKEN) in Tokyo where he presented an invited talk entitled, 'Plans for Nuclear Structure Studies at the Oak Ridge RIB Facility' at the RIKEN Symposium. DOE

N94-10266 National Physical Lab., Teddington (England). Radiation Science and Acoustics Div.

AN INTERCOMPARISON OF THE RADIUM MASS STANDARDS OF THE UK AND THE USSR: 2

S. A. Woods, P. Cross, P Christmas, E. A. Kholnova (All-Union Scientific Research Inst., Saint Petersburg, Russia.), M. F. Yudin (All-Union Scientific Research Inst., Saint Petersburg, Russia.), and E. S. Gubkin (All-Union Scientific Research Inst., Saint Petersburg, Russia.) Oct. 1992 12 p
(NPL-RSA(EXT)-34; ETN-93-93747) Copyright Avail: Issuing Activity (National Physical Laboratory, Teddington, Middlesex, TW11 OLW, England)

A comparison of national radium standards of the UK and the USSR as part of bilateral cooperation in the field of activity measurements is presented. The measurement methods for calorimetric and ionometric comparisons are described. Tables show: observed counting rates in the 1764 keV photopeak together with calculated source transmissions; analysis of individual uncertainty components arising in the determination of the radium content of X5; and calculated mean energy components. The results of all measurements, decay corrected to a common reference time of 1 Jan. 1989, are tabulated, and show that good agreement between the various methods of measurement employed in the intercomparison was achieved. ESA

N94-10302# Brookhaven National Lab., Upton, NY.

TOP AND HIGGS MASSES IN A COMPOSITE BOSON MODEL

D. E. Kahana and S. H. Kahana Jan. 1993 5 p Presented at the Meeting of the Division of Particles and Fields of the American Physical Society, Batavia, IL, 10-14 Nov. 1992
(Contract DE-AC02-76CH-00016)
(DE93-010874; BNL-48605; CONF-921122-48) Avail: CASI HC A01/MF A01

Recently Nambu as well as Bardeen, Hill and Linden have suggested replacing the Higgs mechanism with a dynamical symmetry breaking generated by four fermion interactions of the top quark. In fact the model for replacing the scalar sector is that of Nambu and Jona-Lasinio (NJL) and one recovers the Higgs as a tt composite. Earlier authors have also treated vector mesons as composites within the NJL framework, with perhaps the earliest suggestion being that of Bjorken for a composite photon. Here we attempt to generate the entire electroweak interaction from a specific current-current, baryon number conserving form of the four fermion interaction. The W, Z and Higgs boson appear as coherent composites of all fermions, quarks and lepton, and not just of the top quark. The four fermion interaction is assumed to be valid at some high mass scale (mu), perhaps the low energy limit resulting by the elimination of non-fermionic degrees of freedom from a more basic theory. The cutoff (Lambda), necessary in the non-renormalizable NJL may be viewed then as the proper scale for this more basic theory. DOE

N94-10303# Brookhaven National Lab., Upton, NY.

PRODUCTION OF STRANGE CLUSTERS IN RELATIVISTIC HEAVY ION COLLISIONS

C. B. Dover, A. J. Baltz, Yang Pang, T. J. Schlagel, and S. H. Kahana Feb. 1993 17 p Presented at the HIPAGS Meeting, Cambridge, MA, 14-17 Jan. 1993
(Contract DE-AC02-76CH-00016)
(DE93-010876; BNL-48594; CONF-930173-5) Avail: CASI HC A03/MF A01

We address a number of issues related to the production of strangeness in high energy heavy ion collisions, including the possibility that stable states of multi-strange hypersonic or quark matter might exist, and the prospects that such objects may be created and detected in the laboratory. We make use of events generated by the cascade code ARC to estimate the rapidity distribution dN/dy of strange clusters produced in Si+Au and Au+Au collisions at AGS energies. These calculations are performed in a simple coalescence model, which yields a consistent description of the strange cluster (d, He-3, H-3, He-4) production at these energies. If a doubly strange, weakly bound (Lambda)(Lambda) dibaryon exists, we find that it is produced rather copiously in Au+Au collisions, with dN/dy (approximately)0.1 at mid-rapidity. If one adds another non-strange or strange baryon to a cluster, the production rate decreases by roughly one or two orders of magnitude, respectively. For instance, we predict that the hypernucleus (Lambda)(Lambda)He-6 should have dN/dy (approximately)5 x 10(sup -6) for Au+Au central collisions. It should be possible to measure the successive (Lambda) yields p(pi(-)) weak decays of this object. We comment on the possibility that conventional multi-strange hypernuclei may serve as 'doorway states' for the production of stable configurations of strange quark matter, if such states exist. DOE

N94-10304# Brookhaven National Lab., Upton, NY.

STRANGENESS PRODUCTION WITH PROTONS AND PIONS

C. B. Dover 1993 19 p Presented at the We-Heraeus Seminar: Hadronic Processes at Small Angles in Storage Rings, Bad Honnef, Germany, 1-3 Feb. 1993
(Contract DE-AC02-76CH-00016)
(DE93-010879; BNL-48595; CONF-930239-1) Avail: CASI HC A03/MF A01

We discuss the spectrum of physics questions related to strangeness which could be addressed with intense beams of protons and pions in the few GeV region. We focus on various aspects of strangeness production, including hyperon production in pp collisions, studies of hyperon-nucleon scattering, production of hypernuclei in proton and pion-nucleus collisions, and spin phenomena in hypernuclei. DOE

N94-10308# Brookhaven National Lab., Upton, NY.

SEARCHES FOR STRANGELETS AND OTHER EXOTICS AT THE AGS

P. H. Pile 1993 8 p Presented at the HIPAGS Meeting, Cambridge, MA, 14-17 Jan. 1993
(Contract DE-AC02-76CH-00016)
(DE93-013341; BNL-48736; CONF-930173-6) Avail: CASI HC A02/MF A01

This article describes some experiments either completed, in progress or planned at the Brookhaven National Laboratory AGS. In particular, the experiments described are searches for exotic forms of matter. The existence of such matter could provide a clear signature for the deconfinement or rearrangement of quarks outside the bounds of normal baryons. DOE

N94-10311# Flinders Univ., Adelaide (Australia). Electronic Structure of Materials Centre.

INTEGRATED CROSS SECTIONS FOR THE IONISATION OF ATOMIC HYDROGEN BY ELECTRON IMPACT

D. A. Konovalov and I. E. McCarthy May 1992 10 p
(DE93-610179; ESM-44) Avail: CASI HC A02/MF A01 (US Sales Only)

Distorted-wave Born approximation (DWBA) calculations are reported for singly-differential and total cross sections for the electron impact ionization for atomic hydrogen at 25, 40, 60, 100, 150, and 250 eV. The theory is compared with available experiments. At all the energies except 25 eV the theory predicts a lower singly-differential cross section for the low-energy side of the secondary-electron energies (less than 5 eV), compared to the only available absolute measurements of Shyn. The DWBA calculation is in good agreement with the experiment at 25 eV but only if e-e post-collision interaction is included in the theory in some way. DOE

N94-10312# Flinders Univ., Adelaide (Australia). Electronic Structure of Materials Centre.

CALCULATION OF THE TOTAL IONIZATION CROSS SECTION AND SPIN ASYMMETRY IN ELECTRON-HYDROGEN SCATTERING FROM THRESHOLD TO 500 eV

I. Bray and A. T. Stelbovics Jul. 1992 9 p
(DE93-610180; ESM-47) Avail: CASI HC A02/MF A01 (US Sales Only)

The total ionization cross section and spin asymmetry at projectile energies ranging from threshold to 500 eV for electron impact excitation of atomic hydrogen is presented. They are calculated using the convergent close-coupling formalism of Bray and Stelbovics. Both observables are found to be in complete quantitative agreement with measurements over almost the entire energy range. This is the only electron-atom scattering theory that is able to achieve this result to date. DOE

N94-10317# Osaka Univ., Ibaraki (Japan). Research Center for Nuclear Physics.

REPORT OF THE WORKSHOP ON LIGHT PARTICLE-INDUCED REACTIONS

1992 330 p Workshop held in Osaka, Japan, 5-7 Dec. 1991

(DE93-752300; RCNP-P-120; CONF-9112148) Avail: CASI HC A15/MF A03

The study meeting on light particle (mass number = 3 - 11) induced reaction was held for three days from 5-7 Dec. 1991 at the Research Center for Nuclear Physics, Osaka University. This book records the reports based on the lectures presented at the meeting. In the new facility of the RCNP, the experiment on the nuclear reaction using 400 MeV polarized protons and 200 MeV polarized deuterons is about to begin. When the acceleration of polarized He-3 beam which is being developed becomes feasible, by combining it with the high resolution spectrometer GRAND RAIDEN, it is expected that the unique, high accuracy research using the polarized He-3 having intermediate energy (540 MeV) becomes possible. At this time, by focusing attention to what new physics is developed by the nuclear reaction induced by the composite particles having the intermediate energy of mass number 3 - 11, this study meeting was planned and held. As the result, 29 lectures collected were to cover wide fields, and active discussion was carried out. DOE

N94-10327# Flinders Univ., Adelaide (Australia). Electronic Structure of Materials Centre.

SATELLITE STRUCTURE OF THE XENON VALENCE SHELL BY ELECTRON MOMENTUM SPECTROSCOPY

S. Braidwood, M. Brunger, and E. Weigold May 1992 25 p

(DE93-609993; ESM-43) Avail: CASI HC A03/MF A01 (US Sales Only)

Momentum distributions and spectroscopic factors are obtained in a high resolution electron momentum spectroscopy (EMS) study of xenon at 1000 eV. The shapes and relative magnitudes of the momentum profiles are in excellent agreement with distorted-wave impulse approximations using the target Dirac-Fock approximation. The DWDF approximation accurately describes the relative magnitudes of the 5p and 5s manifold cross sections as well as the shape of the 5s cross section. The use of nonrelativistic Hartree-Fock wavefunctions gives significantly poorer fits to the data. Spectroscopic factors for transitions belonging to the (sup 2)S(sup e)(sub 1/2),P(sup 0)(sub 1/2,3/2), and (sup 2)D(sup 3)(sub 3/2,5/2) manifolds are assigned up to a separation energy of 45 eV. The spectroscopic strength for the lowest 5s transition is 0.345 +/- 0.010 whereas that for the ground state 5p transition is 0.96 +/- 0.02. The 5s strength in the continuum above 33.1 eV is 0.115 +/- 0.025 and that for the 5p manifold is only 0.03 +/- 0.01. The first momentum profiles belong to excited (sup 2)P(sup 0) and (sup 2)D(sup e) manifolds are obtained. The latter, which must be entirely due to d-wave correlations in the xenon ground state, are in good agreement with DF 5d momentum profiles. Comparison is made with several many-body calculations and agreement with the latest relativistic calculation is very good. DOE

N94-10328# Flinders Univ., Adelaide (Australia). Electronic Structure of Materials Centre.

CONVERGENT CLOSE-COUPLING CALCULATIONS OF ELECTRON-HYDROGEN SCATTERING

Igor Bray and A. T. Stelbovics Apr. 1992 32 p

(DE93-610049; ESM-41) Avail: CASI HC A03/MF A01 (US Sales Only)

The convergence of the close-coupling formalism is studied by expanding the target states in an orthogonal L(sup 2) Laguerre basis. The theory is without approximation and convergence is established by simply increasing the basis size. The convergent elastic 2s and 2p differential cross sections, spin asymmetries, and angular correlation parameters for the 2p excitation at 35, 54.4, and 100 eV are calculated. Integrated and total cross sections as well as T-matrix elements for the first five partial waves are also given. DOE

N94-10329# Flinders Univ., Adelaide (Australia). Electronic Structure of Materials Centre.

CALCULATION OF SPIN-DEPENDENT OBSERVABLES IN ELECTRON-SODIUM SCATTERING USING THE COUPLED-CHANNEL OPTICAL METHOD

Igor Bray Apr. 1992 8 p

(DE93-610050; ESM-42) Avail: CASI HC A02/MF A01 (US Sales Only)

The calculations of the 3(sup 2)S and 3(sup 2)P spin asymmetries and the angular momentum for singlet and triplet scattering for projectile energies of 10 and 20 eV is presented. Together these observables give a most stringent test of any electron-atom scattering theory. An excellent agreement was found between the results of the coupled-channel optical method and experiment, which for the spin asymmetries can only be obtained by a good description of the couplings between the lower-lying target states and the target continuum. DOE

N94-10330# Flinders Univ., Adelaide (Australia). Electronic Structure of Materials Centre.

DISTORTED-WAVE CALCULATION OF He(e,2e) INCLUDING CORE-EXCHANGE

D. A. Konovalov and I. E. McCarthy Apr. 1992 14 p

(DE93-610072; ESM-40) Avail: CASI HC A03/MF A01 (US Sales Only)

Distorted-wave Born approximation (DWBA) calculations are reported for coplanar symmetric ionization of helium at energies of 100 and 200 eV. The best possible one-configuration incident distorted wave functions together with the capture scattering were used to produce a better agreement with absolute measurements at 100 eV compared with the previous DWBA calculations. However, the discrepancy between experiment and theory at 200 eV for large angles was not resolved by these modifications. Moreover capture scattering was found negligible at 28.6 to 200 eV. Similar DWBA calculations for hydrogen close to the threshold are also reported. Very good agreement with experiment was found at 17.6 eV. DOE

N94-10331# Flinders Univ., Adelaide (Australia). Electronic Structure of Materials Centre.

SPIN-DEPENDENT OBSERVABLES IN ELECTRON-SODIUM SCATTERING CALCULATED USING THE COUPLED-CHANNEL OPTICAL METHOD

I. Bray and I. E. McCarthy Jun. 1992 22 p

(DE93-610073; ESM-45) Avail: CASI HC A03/MF A01 (US Sales Only)

The calculations of 3(sup 2)S-3(sup 2)S and 3(sup 2)S-3(sup 2)P electron-sodium scattering at 1 to 40 eV is presented. An excellent agreement with measurements of the spin asymmetries and P'/P for both channels, and L the angular momentum for singlet, triplet, and summed spin states at all energies was found. This may only be achieved at energies above the ionization threshold by including the coupling of the low-lying target discrete states to the target continuum. DOE

N94-10332# Flinders Univ., Adelaide (Australia). Electronic Structure of Materials Centre.

ELECTRON MOMENTUM SPECTROSCOPY OF ATOMS, MOLECULES AND SOLIDS

E. Weigold Jan. 1992 16 p

(DE93-610148; ESM-38) Avail: CASI HC A03/MF A01 (US Sales Only)

Electron Momentum Spectroscopy (EMS) is the application of the (e,2e) technique to obtain detailed information on the dynamic structure of atoms, molecules, and condensed matter. The ability of EMS to provide wavefunction mapping, in terms of the independent particle representation of a many body system in momentum space, is discussed for valence electrons. The quantitative measurement of correlation effects in both the initial and final electron states is demonstrated. Correlations can significantly change the momentum density distribution, as well as giving rise to transitions forbidden in the independent particle approximation. The case of argon is discussed in some detail since both initial state correlations (d-wave correlations) and final state correlations (mainly in the 3s(sup -1) manifold) are present. The influence of relativistic effects in outer valence momentum densities is demonstrated for Xe and Pb. The importance of correlations in the outer valence orbitals of some molecules is discussed with particular reference to H2O. The first (e,2e) results on an excited target and also an oriented target are discussed, as are some recent high resolution measurements on amorphous carbon. DOE

N94-10333# Flinders Univ., Adelaide (Australia). Electronic Structure of Materials Centre.

RECENT ADVANCES IN ELECTRON MOMENTUM SPECTROSCOPY

E. Weigold Mar. 1992 36 p

(DE93-610149; ESM-39) Avail: CASI HC A03/MF A01 (US Sales Only)

The flexibility of the (e,2e) technique or electron momentum spectroscopy in obtaining information on the electronic structure of atoms, molecules, and solids is demonstrated. High resolution electron momentum spectroscopy measurements for argon including the first measurements of momentum profiles belonging to the (sup 2)p(sup 0) and (sup 2)D(sup e) manifolds are used to demonstrate the technique for atomic targets. The d-wave transitions in argon are entirely due to initial state correlations. The first (e,2e) measurements on an excited target and also on an oriented target are also discussed. Sodium atoms are pumped to the m(sub l) = +1 state of the excited 3p state by (sigma)(sup +) light from a laser. The (e,2e) measurements on this excited state are in excellent agreement with the momentum density given by the 3p (m(sub l) = 1) Hartree-Fock wavefunction. The recent measurements of the valence electron momentum distributions for ethane as well as some earlier results for water are used as an example of the application of EMS to the study of molecules. The application of the EMS technique to measure spectral momentum densities in condensed matter targets is demonstrated by some recent results on amorphous carbon. DOE

N94-10334# Lawrence Livermore National Lab., CA.

WORKSHOP ON NN BREMSSTRAHLUNG AND POLARIZATION OBSERVABLES

V. R. Brown 28 Jan. 1993 7 p Workshop held in Groningen, The Netherlands, 13-22 Nov. 1992

(Contract W-7405-eng-48)

(DE93-010181; DOE/FTR-93010181) Avail: CASI HC A02/MF A01 (US Sales Only)

The traveler participated in the discussions about the physics that can be learned in the experiments being planned, those presently running, or those recently completed by a growing number of major laboratories in Europe and the USA at the 'Workshop on NN Bremsstrahlung and Polarization Observables', where many representatives of these experimental programs were present. The traveler's research in this field is supported by a DOE Grant, and she has pioneered the early theoretical NN(lambda) treatments. In addition, she visited the Vrije University to collaborate with Professor Henk Blok on proton scattering from Zr-90 and neighboring nuclei. The traveler also visited NIKEF and discussed possible future experiments of mutual interest to be done at that laboratory. DOE

N94-10349# Los Alamos National Lab., NM.

THE EFFECT OF A SCALAR BOSON COUPLED TO NEUTRINOS ON THE BEHAVIOR OF THE TRITIUM BETA DECAY SPECTRUM NEAR THE END POINT

G. J. Stephenson, Jr. 1993 10 p Presented at the 13th Moriond Workshop on Perspectives in Neutrinos, Atomic Physics, and Gravitation, Villars-sur-Ollon, 30 Jan. - 6 Feb. 1993

(Contract W-7405-eng-36)

(DE93-012655; LA-UR-93-1243; CONF-930187-2) Avail: CASI HC A02/MF A01

Some consequences of a very light scalar boson coupled only to neutrinos are discussed. In particular, I argue that it is possible to sketch scenarios for the evolution of the Universe in which neutrinos cluster to a local density of approximately 10(exp 16) /cc, that such clusters would be attracted to matter gravitationally, and that the existence of such a neutrino density in the solar system provides an alternative to m(-)(sub ve)(sup 2) less than 0 in fitting tritium beta decay. DOE

N94-10414# International Centre for Theoretical Physics, Trieste (Italy).

ON PARITY CONSERVATION AND THE QUESTION OF THE MISSING, RIGHT-HANDED NEUTRINO

A. O. Barut and G. Ziino (Palermo Univ., Italy.) Sep. 1992 19 p

(DE93-613092; IC-92/279) Avail: CASI HC A03/MF A01 (US Sales Only)

The neutrino problem is set anew in the light of a reformulation of the Dirac field theory that provides a natural account for the effect commonly interpreted as 'P-violation', and restores P-mirror symmetry. A two-component (left-handed) neutrino field is automatically derived, whose P-mirror image does not correspond to a 'missing' particle but is the (right-handed) antineutrino field. DOE

N94-10502 International Centre for Theoretical Physics, Trieste (Italy).

MONTE CARLO SIMULATIONS OF A TWO-DIMENSIONAL HARD DIMER SYSTEM

K. W. Wojciechowski, A. C. Branka (Polish Academy of Sciences, Poznan.), and D. Frenkel (FOM-Inst. voor Atoom- en Molecuulfysica, Amsterdam, Netherlands.) Sep. 1992 37 p Limited Reproducibility: More than 20% of this document may be affected by microfiche quality

(DE93-613535; IC-92/278) Avail: CASI HC A03 (US Sales Only)

Monte Carlo simulations of a system of two-dimensional hard, homonuclear dimers are reported. The equation-of-state, structural and orientational properties, and the free energy were computed for the fluid phase and several crystalline and non-crystalline (non-periodic) solid structures. The differences in the Gibbs free energy between the various solid structures were found not to exceed 0.1k(sub B)T per particle. This is much less than the contribution to the entropy per particle due to degeneracy of the 'ground state' of the non-periodic solid which amounts to 0.857k(sub B)T. Hence, the thermodynamically stable solid structure of the system corresponds to a set of non-periodic arrangements of the molecular centers of mass and orientations. The coexistence pressure of the non-periodic solid and fluid is determined; it is located within the observed narrow hysteresis region. It is shown that structures of the crystalline solids are well approximated by a simple lattice model. DOE

N94-10503 International Centre for Theoretical Physics, Trieste (Italy).

STRUCTURE OF S - P BONDED METAL CLUSTERS WITH 8, 20 AND 40 VALENCE ELECTRONS

V. Kumar Oct. 1992 9 p Limited Reproducibility: More than 20% of this document may be affected by microfiche quality

(DE93-613643; IC-92/313) Avail: Issuing Activity (Department of Energy (DOE)) (US Sales Only)

From studies on some clusters of metals and semiconductors, there appear some similarities in the structure of clusters with a given number of atoms and having the number of valence electrons corresponding to a shell closing. Results of the atomic and electronic structure of a few other clusters with 20 and 40 valence electrons, namely Sb(sub 4), Sn(sub 5) and Sb(sub 8) using the density functional molecular dynamics method are presented. It is suggested that the similarities in the structure and deviation from them may help to understand bonding characteristics in clusters and its evolution to bulk behavior. Our results on Sb(sub 8) cluster are preliminary but indicate that above room temperature its structure is two weakly interacting tetrahedra which is in general agreement with the observation of predominently antimony tetramers at T greater than 300 K. DOE

N94-10532 Joint Inst. for Nuclear Research, Dubna (USSR). Lab. of Theoretical Physics.

INDICATION ON THE EXISTENCE OF THE BOUND STATE IN THE p ANTI p-SYSTEM [UKAZANIE NA SUSHCHESTVOVANIE SVYAZANNOGO SOSTOYANIYA V P ANTI P-SISTEME]

B. V. Bykovskij, V. A. Meshcheryakov, and D. V. Meshcheryakov (Moscow State Univ., Russia.) 1991 12 p In RUSSIAN Limited Reproducibility: More than 20% of this document may be affected by microfiche quality

(DE92-641575; JINR-R-2-90-311) Avail: Issuing Activity (Department of Energy (DOE)) (US Sales Only)

Two characteristics of proton-antiproton interaction rho(s) = ReF(sub proton-antiproton)/ImF(subpr oton-antiproton) and sigma(sub tot)(s) are considered. Theoretical consideration is based on the analytic properties of the forward scattering amplitude F(subproton-antiproton)(s). Experimental data on rho and sigma(sub tot) at P(sub l) less than 1 GeV/c have been analyzed, and satisfactory description of rho and sigma(sub tot) has been achieved only when a quasi-nuclear state is assumed to exist in the pp system with a mass close to 2m (m is the proton mass). DOE

N94-10549 Academy of Sciences of the Ukraine, Kiev. Inst. Teoreticheskoj Fiziki.

P-MATRIX DESCRIPTION OF THE TWO-PARTICLE INTERACTION

V. A. Babenko, N. M. Petrov, and A. G. Sitenko 1991 22 p Limited Reproducibility: More than 20% of this document may be affected by

microfiche quality
(DE93-617690; ITP-91-87) Avail: CASI HC A03 (US Sales Only)

The paper deals with the formalism of P-matrix description of the two-particle interaction within the framework of which the inverse scattering problem is considered. Separating explicitly the free motion contribution in the wave function yields a compact expression for the off-energy-shell scattering amplitude which immediately provides its separable expansion. DOE

N94-10550 Academy of Sciences of the Ukraine, Kiev. Inst. Teoreticheskoj Fiziki.
STUDIES OF P-MATRIX FORMALISM ON THE BASIS OF THE POTENTIAL DESCRIPTION OF TWO-PARTICLE INTERACTION
V. A. Babenko and N. M. Petrov 1991 22 p Limited Reproducibility: More than 20% of this document may be affected by microfiche quality
(DE93-617691; ITP-91-93) Avail: Issuing Activity (Department of Energy (DOE)) (US Sales Only)

A study is made of mathematical and physical aspects of the P-matrix approach within the framework of the potential description of two particle interaction when the dynamics is based on the nonrelativistic Schroedinger equation. A dispersion formula for the P-matrix is derived correctly; different ways of expansion that enable the development of approximate description methods of the quantities characterizing the two-particle interaction are suggested. DOE

N94-10551 Academy of Sciences of the Ukraine, Kiev. Inst. Teoreticheskoj Fiziki.
CROSSING-ODD SPIN EFFECTS IN THE DIPOLE MODEL OF HADRON SCATTERING
S. V. Akkelin and E. S. Martynov 1992 19 p Limited Reproducibility: More than 20% of this document may be affected by microfiche quality
(DE93-617692; ITP-92-11) Avail: CASI HC A03 (US Sales Only)

The spin amplitudes of the nucleon-nucleon and the meson-nucleon scattering at high energies and the bounded transferred momenta are calculated within the dipole pomeron model. In the case of non-degenerate input pomeron and odderon, the polarizations in proton-proton and proton-antiproton are shown to be opposite in sign and equal in value. In the meson-nucleon interactions, the polarization oscillates without changing its sign, the oscillation amplitude is then independent of energy in charge exchange process, and in the elastic scattering it gets decreased slowly. DOE

N94-10552 Academy of Sciences of the Ukraine, Kiev. Inst. Teoreticheskoj Fiziki.
MODEL FOR THE POMERON
L. L. Jenkovszky 1992 11 p Limited Reproducibility: More than 20% of this document may be affected by microfiche quality
(DE93-617693; ITP-92-29) Avail: CASI HC A03 (US Sales Only)

It is suggested that the bare pomeron is an infinite sum of Regge multipoles with unit intercepts alpha(0)=1 and decreasing weights C(sub n). Unitarity is restored by eikonalization. For phenomenological purposes, the bare pomeron with m=3 and a built-in dip mechanism (diffraction minimum) is feasible. DOE

N94-10553 Academy of Sciences of the Ukraine, Kiev. Inst. Teoreticheskoj Fiziki.
LOGARITHMICALLY RISING CROSS SECTION AND THE RATIO SIGMA(SUB el)/SIGMA(SUB t)
L. L. Jenkovszky and A. I. Lendel 1992 8 p Limited Reproducibility: More than 20% of this document may be affected by microfiche quality
(DE93-617694; ITP-92-3) Avail: CASI HC A02 (US Sales Only)

We refit the parameters of a dipole pomeron model for high energy elastic scattering and find that to accommodate for the observed rise of sigma(sub el)/sigma(sub t) one has to admit for - apart from an odderon contribution - a 'supercritical' pomeron intercept, alpha(sub p)(0) greater than 1. DOE

N94-10554 Academy of Sciences of the Ukraine, Kiev. Inst. Teoreticheskoj Fiziki.
DETECTING THE ODDERON
A. P. Contoguris, L. L. Jenkovszky, E. S. Martynov, and B. V. Stryminsky 1992 11 p Limited Reproducibility: More than 20% of this document may be affected by microfiche quality
(DE93-617695; ITP-92-31) Avail: Issuing Activity (Department of Energy (DOE)) (US Sales Only)

Using a proper combination of differential cross sections for pi(+/-)rho yields zeta(+-)rho and pi(-)rho yields rho(0)n or of inclusive cross sections for pi(+/-)rho yields rho X we propose certain tests which may conclusively verify of reject the odderon hypothesis throughout the range 0.05 approx. less than -t approx. less than 1 GeV(sup 2). DOE

N94-10555 Academy of Sciences of the Ukraine, Kiev. Inst. Teoreticheskoj Fiziki.
FINE STRUCTURE OF THE POMERON AND THE REAL PART OF THE ELASTIC SCATTERING AMPLITUDE
L. L. Jenkovszky, J. E. Kontros, and A. I. Lendel 1992 10 p Limited Reproducibility: More than 20% of this document may be affected by microfiche quality
(DE93-617696; ITP-92-41) Avail: Issuing Activity (Department of Energy (DOE)) (US Sales Only)

We investigate the role of the small-(t) structure in the elastic scattering amplitude in the determination of its real part in the Coulomb interference region. The presence of this structure follows from quite general analytic properties of the amplitude, but its detailed shape is model-dependent. DOE

N94-10557 Academy of Sciences of the Ukraine, Kiev. Inst. Teoreticheskoj Fiziki.
THE DETERMINATION OF NUCLEON-NUCLEON SCATTERING PHASES BY THE PHASE FUNCTIONS METHOD
I. S. Dotsenko, Yu. V. Sosov, and V. K. Tartakovskij 1992 16 p Limited Reproducibility: More than 20% of this document may be affected by microfiche quality
(DE93-617729; ITF-92-2) Avail: Issuing Activity (Department of Energy (DOE)) (US Sales Only)

The phases and mixing parameters of NN-scattering for Hamada-Johnston potential in the energy rangue (10-400 Mev) of incident nucleons and many values of the total angular momentum (0 less than or = j less than or = 20) pair been computed. The general character of their behavior is analyzed. It is shown, that the quasiclassical formula of phase shifting may be used for j greater than 12. DOE

N94-10634 Moscow State Univ. (Russia). Nauchno-Issledovatel'skij Inst. Yadernoj Fiziki.
PRINCIPLES OF GAUGE THEORY OF REAL HADRONS
L. M. Slad 1992 34 p Limited Reproducibility: More than 20% of this document may be affected by microfiche quality
(DE93-613094; INP-MSU-92-13-262; NIIYaF-MGU-92-13-262) Avail: CASI HC A03 (US Sales Only)

Complete classification of relativistically invariant equations of the Gelfand-Yaglom type, which are invariant in terms of gauge transformations, generated by vector representation of the Lorentz complete group, was made. DOE

N94-10649 Gosudarstvennyi Komitet po Ispolzovaniyu Atomnoi Energii, Moscow (USSR).
DIAGNOSTIC COMPLEX FOR THE SPACE-TIME ANALYSIS OF ENERGY AND CURRENT OF PULSED RELATIVISTIC PARTICLES [DIAGNOSTICHESKIJ KOMPLEKS DIYA PROSTRANSTVENNO-VREMENNOGO ANALIZA EHNERGII I TOKA IMPUL'SNYKH RELYATIVISTSKIKH PUCHKOV]
V. P. Zejdlits, Y. V. Tkach, V. G. Yarmak, S. P. Gubarev, G. A. Miroshnichenko, N. G. Pavlenko, and V. A. Tsurikov 1991 15 p In RUSSIAN Limited Reproducibility: More than 20% of this document may be affected by microfiche quality
(DE93-620980; KFTI-91-49) Avail: CASI HC A03 (US Sales Only)

A description and the technical characteristics of the designed and manufactured autonomic diagnostic complex for simultaneous measurement of current density distribution and a profile of energy radial distribution is given. The receiver of this complex permits us to investigate the energy distribution of 20 MeV electron beams and at the same time to register the flux density at its cross-sections from 1 to 100 sq mm with accuracy to 1%. DOE

N94-10661 Nagoya Univ. (Japan). Plasma Science Center.
ELECTRON RUNAWAY IN RF DISCHARGES
F. F. Chen Oct. 1992 26 p Limited Reproducibility: More than 20% of this document may be affected by microfiche quality
(DE93-771407; PSC-25) Avail: CASI HC A03

The critical electric field is computed as a function of pressure and starting energy for electrons to runaway to high energies in moderate pressure discharges. The runaway conditions depend critically on the shape of the elastic cross section vs. energy curve. Computations are made for H, H2, and He gases, and it is shown that runaway occurs much more readily in atomic hydrogen than in the other gases. The values of the runaway fields are larger than would normally occur in dc discharges, where large voltages would lead to arc formation. However, in rf discharges such electric fields can be sustained over times long compared to electron transit times but short compared to ion transit times. DOE

N94-10696 National Lab. for High Energy Physics, Ibaraki (Japan).
PROCEEDINGS OF THE THIRD WORKSHOP ON LIGHT QUARK MESON SPECTROSCOPY
Kunio Takamatsu, ed. and Tsuneaki Tsuru, ed. Sep. 1992 226 p Workshop held at Tsukuba, Japan, 28-29 Feb. 1992 Limited Reproducibility: More than 20% of this document may be affected by microfiche quality
(DE93-754138; KEK-PROC-92-8; CONF-9202147) Avail: Issuing Activity (Department of Energy (DOE))

The third workshop on the light quark meson spectroscopy was held on 28-29 Feb. 1992 at KEK. This issue is the collection of the papers presented at the meeting. The presented papers are indexed individually. DOE

N94-10720 Tokyo Univ., Tanashi (Japan). Inst. for Nuclear Study.
POSSIBILITY OF A CROSSED-BEAM EXPERIMENT INVOLVING SLOW-NEUTRON CAPTURE BY UNSTABLE NUCLEI RAPID-PROCESS-TRON
T. Yamazaki, I. Katayama, and Y. Uwamino Jul. 1992 14 p Limited Reproducibility: More than 20% of this document may be affected by microfiche quality
(DE93-754288; INS-940) Avail: Issuing Activity (Department of Energy (DOE))

The possibility of a crossed beam facility of slow neutrons crossed with unstable nuclei is examined in connection with the Japanese Hadron Project. With a pulsed proton beam of 50 Hz repetition with a 100 micro-Amp average beam current, one obtains a spallation neutron source of 2.4(10)(exp 8) thermal neutrons/cu cm/spill over a 60 cm length with a 3 msec average duration time by using a D2O moderator. By confining radioactive nuclei of 10(exp 9) ions in a beam circulation ring of 0.3 MHz revolution frequency, so that they pass through the neutron source, one obtains a collision luminosity of 3.9(10)(exp 24)/sq cm/s. A new research domain aimed at studying rapid processes in nuclear genetics will be created. DOE

N94-10722 Academy of Sciences of the Ukraine, Kiev. Inst. Teoreticheskoj Fiziki.
THREE-NUCLEON PROBLEM WITH PHASE EQUIVALENT POTENTIALS
O. M. Pushkash, D. V. Shapoval, and I. V. Simenog 1991 27 p Limited Reproducibility: More than 20% of this document may be affected by microfiche quality
(DE93-617731; ITP-91-49) Avail: Issuing Activity (Department of Energy (DOE)) (US Sales Only)

The effect of the t-matrix off-shell variations on the three-nucleon parameters is studied. The t-matrix off-shell variations have nonlocal phase equivalent N-N potentials. The variations, which lower or increase the tritium binding energy, are revealed. We show that under certain conditions, the three-nucleon low-energy observables are almost insensitive to the high energy behaviour of the negative parts of the scattering phase shifts. The inverse problem method is used to reconstruct simple S-wave potentials in order to provide a unified description of the two-nucleon and low-energy three-nucleon data. DOE

N94-10743 Los Alamos National Lab., NM.
RIETVELD REFINEMENT OF MAGNETIC STRUCTURES FROM PULSED-NEUTRON-SOURCE POWDER-DIFFRACTION DATA
R. A. Robinson, A. C. Lawson, A. C. Larson, R. B. VonDreele, and J. A. Goldstone 1993 12 p Presented at the 12th International Collaboration of Advanced Neutron Sources Meeting (ICANS), Abingdon, England, 24-28 May 1993 Limited Reproducibility: More than 20% of this document may be affected by microfiche quality
(Contract W-7405-eng-36)
(DE93-012740; LA-UR-93-1519; CONF-9305177-2) Avail: CASI HC A03

The General Structure Analysis System, GSAS, has recently been modified to include magnetic neutron-scattering cross-sections. Low-temperature diffraction data have been taken on the hexagonal noncollinear antiferromagnet UPdSn on both the HIPD and the NPD powder diffractometers at LANSCE. The low-resolution data reveal that the magnetic structure has orthorhombic symmetry (magnetic space group P(sub c)112(sub 1)) between 25K and 40K, and monoclinic symmetry (magnetic space group P(sub c)l12(sub 1)) below 25K. The high-resolution data reveal that there are structural distortions with corresponding symmetry changes in each of these phases, to give chemical space groups Cmc2(sub 1) and P2(sub 1) respectively, while the paramagnetic phase above 40K has space group P6(sub 3)mc. Using GSAS, we have refined data sets from both diffractometers simultaneously, including both magnetic and structural cross-sections. Magnetoelastic coefficients for the distortions have been extracted and we have determined the sip of the coupling between the structural monoclinicity and the magnetic monoclinicity. The magnetic results from Rietveld refinement are in good agreement with model fitting to the integrated intensities of seven independent magnetic reflections and these, in turn, agree with measurements made on the same sample using the constant-wavelength reactor technique. Our results therefore validate, to some level, both the technique of using spallation sources for complicated magnetic structures and the specifics of the GSAS Rietveld code. DOE

N94-10748# Stanford Linear Accelerator Center, CA.
STRANGE MESON SPECTROSCOPY IN K(OMEGA) AND K(PHI) AT 11 GeV/c AND CHERENKOV RING IMAGING AT SLD Ph.D. Thesis
Youngjoon Kwon Jan. 1993 286 p
(Contract DE-AC03-76SF-00515)
(DE93-013593; SU-SLAC-409) Avail: CASI HC A13/MF A03

This thesis consists of two independent parts: development of a Cherenkov Ring Imaging Detector (CRID) system; and analysis of high-statistics data of strange meson reactions from the LASS spectrometer. The CRID system is devoted to charged particle identification in the SLAC Large Detector (SLD) to study e(+)e(-) collisions at radical s = m(sub Z(exp 0)). By measuring the angles of emission of the Cherenkov photons inside liquid and gaseous radiators, pi/K/p separation will be achieved up to approximately 30 GeV/c. The signals from CRID are read in three coordinates, one of which is measured by charge-division technique. To obtain an approximately 1% spatial resolution in the charge-division, low-noise CRID preamplifier prototypes were developed and tested resulting in less than 1000 electrons noise for an average photoelectron signal with 2(10)(exp 5) gain. To help ensure the long-term stability of CRID operation at high efficiency, a comprehensive monitoring and control system was developed. Results from the partial wave analysis of strange meson final states in the reactions K(-)p yields K(-)(omega)p and K(-)p yields (K-bar)(exp 0)(phi)n are presented. The analyses are based on data from a 4.1 event/nb exposure of the LASS spectrometer in K(-)p interactions at 11 GeV/c. The data sample of K(-)(omega)p final state contains approximately 10(exp 5) events. From the partial wave analysis, resonance structures of J(exp P) = 2(-), 3(-), and 2(+) amplitudes are observed in the K(omega) system. The analysis of 2(-) amplitudes provides an evidence for two strange meson states in the mass region around 1.75 GeV/sq c. The appropriate branching fractions are calculated and compared with the SU(3) predictions. The partial wave analysis of (K-bar)(exp 0)(phi) system favors J(exp P) = 1(-) and 2(+) states in the 1.9-2.0 GeV/sq c region. DOE

N94-10750# Northwestern Univ., Evanston, IL. Dept. of Materials Science and Engineering.
ATOMIC STRUCTURES AND COMPOSITIONS OF INTERNAL INTERFACES
D. N. Seidman and K. L. Merkle (Argonne National Lab., IL.) 10 May 1993 10 p
(Contract DE-FG02-89ER-45403)
(DE93-014840; DOE/ER-45403/4) Avail: CASI HC A02/MF A01

This research program addresses fundamental questions concerning the relations between atomic structures and compositions of homophase and heterophase interfaces. Metal/ceramic heterophase interfaces are created via the process of internal oxidation of metallic alloys. The interfaces are studied via a combination of conventional transmission electron microscopy, high resolution electron microscopy, field-ion microscopy, and atom probe microscopy. The latter technique is employed to chemically sequence the interfacial region, and to show that the terminating (222) plane of MgO and CdO consists solely of oxygen atoms for the Cu/MgO (111) and Ag/CdO (111) heterophase interfaces, respectively; this is achieved with no deconvolution of the experimental data. The evolution of metal/ceramic heterophase interfaces is studied by following the process of internal oxidation on an atomic scale from its very earliest stages. It is demonstrated that, during the early stages of internal oxidation, metal atom clusters as well as hypo- and hyperstoichiometric metal-oxygen clusters are present. Solute-atom segregation to grain boundaries is studied in binary metal alloys employing the free energy simulations and the overlapping distribution Monte Carlo methodologies for dilute Pt(Au), Cu(Ni) and Pd(Ni) alloys for both twist and tilt boundaries. DOE

N94-10753 Lawrence Livermore National Lab., CA.
HIGH-ORDER HARMONIC CONVERSION EFFICIENCY IN HELIUM
J. K. Crane 23 Oct. 1992 24 p Limited Reproducibility: More than 20% of this document may be affected by microfiche quality
(Contract W-7405-eng-48)
(DE93-011714; UCRL-ID-112298) Avail: CASI HC A03

Calculated results are presented for the energy, number of photons, and conversion efficiency for high-order harmonic generation in helium. The results show the maximum values that we should expect to achieve experimentally with our current apparatus and the important parameters for scaling this source to higher output. In the desired operating regime where the coherence length, given by L(sub coh)=(pi)b/(q-1), is greater than the gas column length, l, the harmonic output can be summarized by a single equation: N(sub q)=((pi(sup z) n(sup 2) b(sup 3) tau(sub q)) (vert bar) d(sub q)(vert bar)(sup 2)) / 4h (left brace) p/q (2l/b)(sup 2)(r brace). N(sub q) - number of photons of q-th harmonic; n - atom density; b - laser confocal parameter; tau(sub q) - pulse width of harmonic radiation; q - harmonic order; p - effective order of nonlinearity. DOE

N94-10754 Massachusetts Univ., Amherst. Dept. of Physics and Astronomy.
A REVIEW OF TWO PHOTON PRODUCTION OF JETS AT PEP AND PETRA ENERGIES
R. R. Kofler 1992 8 p Presented at the 9th International Workshop on Photon-photon Collisions, San Diego, CA, 22-26 Mar. 1992 Limited Reproducibility: More than 20% of this document may be affected by microfiche quality
(Contract DE-AC02-85ER-40194)
(DE93-011742; CONF-9203159-9) Avail: CASI HC A02

Experimental results on the production of hadron jets in photon-photon interactions at PETRA and PEP are reviewed with special emphasis on the recent results from the TPC/2(gamma) experiment at PEP. All results have been compared with the predictions of Vector Dominance and Quark Parton Models and the experiments all find excess jet production at low Q(sup 2) and intermediate transverse momentum which cannot be explained on the basis of the simple VDM + QPM models. DOE

N94-10835 Academy of Sciences of the Ukraine, Kiev. Inst. Yadernykh Issledovanij.
THE MULTIPLICITY SPECTRA OF THE (169)Tm(n, GAMMA) REACTION [SPEKTRY MNOZHESTVENNOSTI REAKSII 169TM(N, GAMMA)]
Y. G. Shchepkin, E. A. Pavlenko, and T. A. Senchenko et al 1991 13 p In RUSSIAN Limited Reproducibility: More than 20% of this document may be affected by microfiche quality
(DE93-617733; KIYal-91-41) Avail: CASI HC A03 (US Sales Only)

The multiplicity spectra of the (169)Tm(n,gamma) reaction for neutron energy 2 keV with different thickness of shield from (169)Tm samples were researched. The multiplicity spectrum correlation with shield thickness was not discovered but the difference between spectra for neutron energy 2 keV and thermal neutrons is observed. This difference can be related with dependence of multiplicity spectra from the spin of compound nucleus. The multiplicity spectrometry method is proposed to use for the separation of capture average cross section on components with different spin. DOE

N94-10837 Academy of Sciences of the Ukraine, Kiev. Inst. Yadernykh Issledovanij.
MONTE CARLO ALGORITHMS IN SIMULATION OF 2BETA-DECAY AND PENETRATION OF ELECTRONS THROUGH MATTER [ALGORITMY MONTE-KARLO V ZADACHE MODELIROVANIYA 2BETA-RASPADA I PROKHOZHDENIYA EHLEKTRONOV CHEREZ VESHCHESTVO]
V. I. Tretyak 1992 14 p In RUSSIAN Limited Reproducibility: More than 20% of this document may be affected by microfiche quality
(DE93-617741; KIYal-92-8) Avail: CASI HC A03 (US Sales Only)

The algorithms are described what are used to sample the random variables with probability density functions which are connected with problems of simulation of 2(beta)-decay and electron penetration through matter (the initial spatial, angular, and energy distributions of electrons, angular deflections as the result of multiple scattering, energy losses, etc.). DOE

N94-10848 Academy of Sciences of the Ukraine, Kiev. Inst. Yadernykh Issledovanij.
SPIN CHARACTERISTICS OF ION BEAMS DURING THE MOTION OF ELECTROMAGNETIC ELEMENTS [SPINOVYE KHARAKTERISTIKI PUCHKA IONOV PRI PROKHOZHDENII EHLEKTROMAGNITNYKH POLEJ]
N. I. Zaika and M. I. Magal 1991 20 p In RUSSIAN Limited Reproducibility: More than 20% of this document may be affected by microfiche quality
(DE93-617448; KIYal-91-27) Avail: Issuing Activity (Department of Energy (DOE)) (US Sales Only)

The matrix method for description of the polarization components for ions moving through different electromagnetic systems: dipole magnets, cycle accelerators, quadrupole lenses, solenoids, wine filters, and electrostatic mirrors is developed in the paper. The expressions for elements of the transportation matrixes for the above-mentioned systems taking account of the projective trajectories are obtained. The program, TRANSPIN, for calculation of the beam polarization components after motion by ions of arbitrary number of electromagnetic elements along any possible trajectory is presented. The calculation results made for some of transportation lines for the isochronous cyclotron U-240 are discussed (trajectories for the ion motion were calculated by CERN-program TRANSPORT). The conditions for decrease of the polarization component dispersion because of difference between trajectories of the particles motion are also defined. DOE

N94-10875 Academy of Sciences of the Ukraine, Kharkov. Fiziko-Teckhnicheskij Inst.
THE INTRA-ATOMIC MOTION OF BOUND ELECTRONS AS A POSSIBLE SOURCE OF A SYSTEMATIC ERROR IN ELECTRON BEAM POLARIZATION MEASUREMENTS BY MEANS OF A MOELLER POLARIMETER
L. G. Levchuk 1992 12 p Limited Reproducibility: More than 20% of this document may be affected by microfiche quality
(DE93-620984; KFTI-92-32) Avail: CASI HC A03 (US Sales Only)

The role of the motion of electrons bound in target atoms in electron beam polarization measurements by means of a Moeller polarimeter is discussed. It is shown that this effect can result in an essential overestimate of the value being measured, which exceeds considerably the error of the target polarization determination, and therefore, it should be taken into account in the development of polarimeters. Some recommendations are given to eliminate this systematic error. DOE

N94-10889 National Lab. for High Energy Physics, Ibaraki (Japan).
PROCEEDINGS OF THE SECOND KEK TOPICAL CONFERENCE ON e(SUP +)e(SUP -) COLLISION PHYSICS
Takayuki Matsui, ed. Sep. 1992 513 p Conference held in Tsukuba, Japan, 26-29 Nov. 1991 Limited Reproducibility: More than 20% of this document may be affected by microfiche quality
(DE93-754139; KEK-PROC-92-9; CONF-9111189) Avail: CASI HC A22

This issue is the collection of the papers presented at the Second KEK Topical Conference on e(sup +)e(sup -) collision physics. Twenty-four of the presented papers are indexed individually. DOE

N94-10946*# Norfolk State Univ., VA.
WAVE GENERATION BY CONTAMINANT IONS Report, 1 Oct. 1992 - 30 Jun. 1993

N. Singh 1993 5 p
(Grant NAG3-1371)
(NASA-CR-193558; NAS 1.26:193558) Avail: CASI HC A01/MF A01

Investigations dealing with the generation of waves by contaminant ions are reported. The studies included the properties of the velocity distribution function of such ions. It was found that it takes about one ion-cyclotron period for the distribution function to transform from a beam to a ring distribution. A linear instability analysis was performed to examine the possibility of wave excitation by an ion beam streaming perpendicular to the ambient magnetic field in an ionospheric type of plasma. A simulation code was developed to study the nonlinear behavior of the waves excited by beam and ring types of ion distributions. The code treats both electrons and ions as particles kinetically to also factor in the possible involvement of lower-hybrid waves. CASI

N94-10952 Edgerton, Germeshausen and Grier, Inc., Idaho Falls, ID.
THE SEARCHLIGHT PROBLEM FOR NEUTRONS IN A SEMI-INFINITE MEDIUM
B. D. Ganapol (Arizona Univ., Tucson.), D. W. Nigg, S. N. Jahshan, and C. A. Wemple 1993 11 p Presented at the International Topical Meeting on Mathematical Methods and Supercomputing in Nuclear Applications (M/C+SNA 1993), Karlsruhe, Germany, 19-23 Apr. 1993 Limited Reproducibility: More than 20% of this document may be affected by microfiche quality
(Contract DE-AC07-76ID-01570)
(DE93-010796; EGG-M-92469; CONF-930404-14) Avail: CASI HC A03

The solution of the Search Light Problem for monoenergetic neutrons in a semi-infinite medium with isotropic scattering illuminated at the free surface is obtained by several methods at various planes within the medium. The sources considered are a normally-incident pencil beam and an isotropic point source. The analytic solution is effected by a recently developed numerical inversion technique applied to the Fourier-Bessel transform. This transform inversion results from the solution method of Rybicki, where the two-dimensional problem is solved by casting it as a variant of a one-dimensional problem. The numerical inversion process results in a highly accurate solution. Comparisons of the analytic solution with results from Monte Carlo (MCNP) and discrete ordinates transport (DORT) codes show excellent agreement. These comparisons, which are free of any associated data or cross section set dependencies, provide significant evidence of the proper operation of both the transport codes tested. DOE

N94-11010# Pennsylvania State Univ., University Park.
POLAR SOLVATION AND ELECTRON TRANSFER
13 Apr. 1993 5 p
(Contract DE-FG02-89ER-14020)
(DE93-013328; DOE/ER-14020/4) Avail: CASI HC A01/MF A01

The report is divided into the following sections: completion of previous studies on solvation dynamics, dipole lattice studies, inertial components of solvation response, simple models of solvation dynamics, rotational dynamics and dielectric friction, intramolecular electron transfer reactions, and intermolecular donor-acceptor complexes. DOE

N94-11011# Washington Univ., Saint Louis, MO. Dept. of Physics.
NON-EMPIRICAL INTERATOMIC POTENTIALS FOR TRANSITION METALS
1993 13 p
(Contract DE-FG02-84ER-45130)
(DE93-013705; DOE/ER-45130/8) Avail: CASI HC A03/MF A01

The report is divided into the following sections: potential-energy functions for d-band metals, potential-energy functions for aluminides and quasicrystals, electronic structure of complex structures and quasicrystals, potential-energy functions in transition-metal oxides, applications to defect structure and mechanical properties, and basic theory of interatomic potentials. DOE

N94-11029# Connecticut Univ., Storrs.
EXPERIMENTS IN ULTRACOLD COLLISIONS
P. L. Gould 1992 4 p
(Contract DE-FG02-92ER-14263)
(DE93-012110; DOE/ER-14263/1) Avail: CASI HC A01/MF A01

Conditions in an ultracold magneto-optical laser trap were studied; the trap is being used to investigate collisions of Rb-85 and Rb-87 atoms at temperatures below 1 mK. The ballistic time-of-flight method was used to determine the temperature. It was found that the temperature increases monotonically with laser intensity; this means that the temperature dependence of various collisional processes can probably be measured. The trap size was found to be independent of laser intensity, except at the lowest intensities. DOE

N94-11040 Tokyo Univ., Tanashi (Japan). Inst. for Nuclear Study.
DOUBLE-LAMBDA COMPOUND NUCLEUS AND THE FORMATION OF DOUBLE HYPERNUCLEI
Toshimitsu Yamazaki and Hirokazu Tamura Jul. 1992 12 p Limited Reproducibility: More than 20% of this document may be affected by microfiche quality
(DE93-754289; INS-941) Avail: Issuing Activity (Department of Energy (DOE))

The formation probabilities of single-Lambda and double-Lambda compound nuclei from Xi(-) following the (K(-), K(+)) reaction are calculated, showing that double-Lambda hypernuclei are formed with a fairly large probability through a hyperon compound process involving Xi(-) directly after the (K(-), K(+)) reaction. DOE

N94-11078 Joint Inst. for Nuclear Research, Dubna (USSR).
CREATION AND ANNIHILATION OF SOLITONS IN NONLINEAR INTEGRABLE SYSTEMS [ROZHDENIE I UNICHTOZHENIE SOLITONOV V NELINEJNYKH INTEGRIRUEMYKH SISTEMAKH]
V. K. Melnikov 1991 27 p In RUSSIAN Limited Reproducibility: More than 20% of this document may be affected by microfiche quality
(DE93-621379; JINR-R-2-91-473) Avail: Issuing Activity (Department of Energy (DOE)) (US Sales Only)

The conditions are found under which solitons can be created and annihilated in nonlinear integrable systems (modified Korteweg-de Vries equation with a self-consistent source, sine-Gordon equation with a self-consistent source, etc.). The eigenvalue of the discrete spectrum of the corresponding linear Dirac operator turns out to depend on time and disappearance of any of the eigenvalues and leads to annihilation of the corresponding soliton. On the contrary, appearance in the discrete spectrum of a new eigenvalue leads to creation of an additional soliton corresponding to this eigenvalue. DOE

N94-11089 Academy of Sciences (USSR), Leningrad. Inst. Yadernoj Fiziki.
FAST TRIGGER ALGORITHM FOR B-EVENTS SELECTION
G. A. Kolomenskij, G. Z. Obrant, and A. I. Smirnov 1991 22 p Limited Reproducibility: More than 20% of this document may be affected by microfiche quality
(DE93-621452; LIYaF-1699) Avail: CASI HC A03 (US Sales Only)

A fast trigger algorithm to select B-events with the use of a silicon strip vertex detector is proposed. This algorithm is based on the existence of secondary decay vertices and may be used in the case of a point or wire target. The estimated time of decision is shorter than 1 microsec. The trigger efficiency calculation results are presented both for secondary vertices trigger and for total transverse momentum trigger. The high efficiency and background rejection of the secondary vertices trigger is displayed. DOE

N94-11093# Pennsylvania State Univ., University Park. Dept. of Chemistry.
SITE DEPENDENCE OF THE APPARENT SHAPE OF A MOLECULE IN STM IMAGES: BENZENE ON Pt(111) Technical Report, 1 Jun. 1992 - 31 May 1993
P. S. Weiss and D. M. Eigler 1 Mar. 1993 12 p
(Contract N00014-91-J-1630)
(AD-A263488; TR-6) Avail: Issuing Activity (Defense Technical Information Center (DTIC))

We present scanning tunneling microscope images of benzene adsorbed on the Pt (111) surface. We find three distinct types of images for isolated benzene molecules, depending upon the benzene adsorption site. This site dependence is in agreement with recent theoretical calculations, and may limit the usefulness of the scanning tunneling microscope in elucidating the structures of adsorbed molecules. DTIC

N94-11100# California Univ., Santa Barbara. Dept. of Chemistry.
THE RESPONSE OF AN ELECTRON IN A BIASED DOUBLE WELL TO A STRONG LASER: DELOCALIZATION AND LOW FREQUENCY GENERATION Technical Report, 1 Jun. 1992 - 31 May 1993
Yuri Dakhnovskii, Raanan Bavli, and Horia Metiu 20 May 1993 17 p
(Contract N00014-90-J-1209)
(AD-A265169; TR-6-ONR) Avail: CASI HC A03/MF A01

We show that a strong laser acting on an electron in a quantum double well which is under the influence of a strong static field, will cause (for special values of the parameters) emission of intense low frequency radiation and can either completely delocalize or completely localize the electron. DTIC

N94-11147# Oregon Univ., Eugene.
RELATIVISTIC HEAVY-ION COLLISIONS
R. C. Hwa 1993 14 p
(Contract DE-FG06-91ER-40637)
(DE93-014844; DOE/ER-40637/6) Avail: CASI HC A03/MF A01

This report discusses the following topics: quark-hadron phase transition; hadron production without phase transition; fractal structure in multiparticle production; and j/psi suppression in pA collisions. DOE

N94-11172# Auburn Univ., AL. Dept. of Physics.
THEORETICAL ATOMIC PHYSICS FOR FUSION
M. S. Pindzola 1992 17 p
(Contract DE-FG05-86ER-53217)
(DE93-013872; DOE/ER-53217/T1) Avail: CASI HC A03/MF A01

The understanding of electron-ion collision processes in high temperature plasmas remains a key factor in the ultimate development of nuclear fusion as a viable energy source for the nation. Our 1990-1992 research proposal delineated three main areas of research in electron-ion scattering theory. Summaries our 1992 efforts in each of these research areas are presented. DOE

N94-11199*# Arizona Water Resources Research Center, Tucson. Dept. of Nuclear and Energy Engineering.
DEVELOPMENT OF DETERMINISTIC TRANSPORT METHODS FOR LOW ENERGY NEUTRONS FOR SHIELDING IN SPACE Final Report
Barry Ganapol 7 Sep. 1993 234 p
(Grant NAG1-1041)
(NASA-CR-194172; NAS 1.26:194172) Avail: CASI HC A11/MF A03

Transport of low energy neutrons associated with the galactic cosmic ray cascade is analyzed in this dissertation. A benchmark quality analytical algorithm is demonstrated for use with BRYNTRN, a computer program written by the High Energy Physics Division of NASA Langley Research Center, which is used to design and analyze shielding against the radiation created by the cascade. BRYNTRN uses numerical methods to solve the integral transport equations for baryons with the straight-ahead approximation, and numerical and empirical methods to generate the interaction probabilities. The straight-ahead approximation is adequate for charged particles, but not for neutrons. As NASA Langley improves BRYNTRN to include low energy neutrons, a benchmark quality solution is needed for comparison. The neutron transport algorithm demonstrated in this dissertation uses the closed-form Green's function solution to the galactic cosmic ray cascade transport equations to generate a source of neutrons. A basis function expansion for finite heterogeneous and semi-infinite homogeneous slabs with multiple energy groups and isotropic scattering is used to generate neutron fluxes resulting from the cascade. This method, called the FN method, is used to solve the neutral particle linear Boltzmann transport equation. As a demonstration of the algorithm coded in the programs MGSLAB and MGSEMI, neutron and ion fluxes are shown for a beam of fluorine ions at 1000 MeV per nucleon incident on semi-infinite and finite aluminum slabs. Also, to demonstrate that the shielding effectiveness against the radiation from the galactic cosmic ray cascade is not directly proportional to shield thickness, a graph of transmitted total neutron scalar flux versus slab thickness is shown. A simple model based on the nuclear liquid drop assumption is used to generate cross sections for the galactic cosmic ray cascade. The ENDF/B V database is used to generate the total and scattering cross sections for neutrons in aluminum. As an external verification, the results from MGSLAB and MGSEMI were compared to ANISN/PC, a routinely used neutron transport code, showing excellent agreement. In an application to an aluminum shield, the FN method seems to generate reasonable results. Author (revised)

N94-11284# Sandia National Labs., Albuquerque, NM.
A NEW DECOMPOSITION STRATEGY FOR PARALLEL BONDED MOLECULAR DYNAMICS
S. Plimpton, B. Hendrickson, and G. Heffelfinger 1992 11 p Presented at the 6th Society for Industrial and Applied Mathematics Conference on Parallel Processing for Scientific Computing, Norfolk, VA, 21-24 Mar. 1993
(Contract DE-AC04-76DP-00789)
(DE93-009839; SAND-92-0259C; CONF-930331-8) Avail: CASI HC A03/MF A01

A method is described for parallelizing molecular dynamics (MD) simulations by block-decomposing the matrix of bonded and non-bonded force computations. It is particularly useful for organic simulations (polymers, proteins) because unlike spatial-decomposition methods, it requires no geometric information about the simulation domain. Because its communication cost scales as N/(radical)P rather than N as in the all-to-all broadcast or ring-exchange techniques commonly used in this type of MD simulation, larger numbers of processors can be used effectively, yielding greater parallel speed-ups. DOE

N94-11349 Academy of Sciences of the Ukraine, Kiev. Inst. Teoreticheskoj Fiziki.
STRUCTURAL AND ELECTRONIC PROPERTIES OF ATOMIC CHAINS
O. I. Gerasimov, N. N. Hudyntzev, and A. G. Zagorodnij 1991 32 p Limited Reproducibility: More than 20% of this document may be affected by microfiche quality
(DE93-617758; ITP-91-95) Avail: Issuing Activity (Department of Energy (DOE)) (US Sales Only)

Structural and electronic properties of atomic chains are investigated in terms of transfer-matrix-technique within Landauer-model for electrical conductance. The role of structural defects (within deterministic and statistical models) in formation of resistivity and spectral properties is shown. A semi-phenomenological approach to elastic electron scattering on the adatomic complex is considered. DOE

N94-11360*# Oregon Univ., Eugene. Chemical Physics Inst.
ELECTRONIC EXCITATION OF GROUND STATE ATOMS BY COLLISION WITH HEAVY GAS PARTICLES Final Report, Jun. 1992 - Jun. 1993
C. Frederick Hansen Jun. 1993 20 p
(Grant NAG1-1427)
(NASA-CR-193364; NAS 1.26:193364) Avail: CASI HC A03/MF A01

Most of the important chemical reactions which occur in the very high temperature air produced around space vehicles as they enter the atmosphere were investigated both experimentally and theoretically, to some extent at least. One remaining reaction about which little is known, and which could be quite important at the extremely high temperatures that will be produced by the class of space vehicles now contemplated - such as the AOTV - is the excitation of bound electron states due to collisions between heavy gas particles. Rates of electronic excitation due to free electron collisions are known to be very rapid, but because these collisions quickly equilibrate the free and bound electron energy, the approach to full equilibrium with the heavy particle kinetic energy will depend primarily on the much slower process of bound electron excitation in heavy particle collisions and the subsequent rapid transfer to free electron energy. This may be the dominant mechanism leading to full equilibrium in the gas once the dissociation process has depleted the molecular states so the transfer between molecular vibrational energy and free electron energy is no longer available as a channel for equilibration of free electron and heavy particle kinetic energies. Two mechanisms seem probable in electronic excitation by heavy particle impact. One of these is the collision excitation and deexcitation of higher electronic states which are Rydberg like. A report, entitled 'Semi-Classical Theory of Electronic Excitation Rates', was submitted previously. This presented analytic expressions for the transition probabilities, assuming that the interaction potential is an exponential repulsion with a perturbation ripple due to the dipole-induced dipole effect in the case of neutral-neutral collisions, and to the ion-dipole interaction in the case of ion-neutral collisions. However the above may be, there is little doubt that excitation of ground state species by collision occurs at the point where the initial and final potentials cross, or at least come very close. Therefore, this mechanism would be applicable to the case where a gas is initially at very low temperature suddenly subjected to high energy heavy particle bombardment. This situation would model the measurement of excitation cross section by molecular beam techniques, for example. The purpose is to report values of cross sections and rate coefficients for collision excitation of ground state atoms estimated with the Landau-Zener transition theory and to compare results with measurement of excitation cross sections for a beam of Hydrogen atoms impacting Argon atom targets. Some very dubious approximations are used, and the comparison with measurement is found less than ideal, but results are at least consistent within order of magnitude. The same model is then applied to the case of N-N atom collisions, even though the approximations then become even more doubtful. Still the rate coefficients obtained are at least plausible in both magnitude and functional form, and as far as I am aware these are the only estimates available for such rate coefficients. Author (revised)

N94-11373# Wayne State Univ., Detroit, MI. Dept. of Physics and Astronomy.
RELATIVISTIC HEAVY ION RESEARCH
1992 72 p
(Contract DE-FG02-92ER-40713)
(DE93-013127; DOE/ER-40713/1) Avail: CASI HC A04/MF A01

Experimental work is reported on the following topics: transverse energy production in 10.7-GeV/c/u Au on Au collisions; first results on delta ray production and charged particle multiplicities with the Au beam at 10.7 GeV/c/A; preliminary studies on the feasibility of flow measurement with the E814 participant calorimeter; preliminary results from the E877 telescope; and low-p(sub t) baryon distribution in Si+Al, Pb collisions at the AGS. Then the status of the Hadronic Calorimeter project of AGS Experiment E864 ECOS (Exotic Composite Object Spectrometer) is reviewed. Next, the same is done for work of the STAR RHIC collaboration. The instrumentation section deals with the design and installation of a target rapidity telescope for BNL experiment 814/877 and a repair scheme for the E814/E877 participant calorimeter. Finally, the theory part addresses bosonic kinetics: thermalization of mesons and the pion p(sub perpendicular) spectrum in ultrarelativistic heavy-ion collisions and non-equilibrium properties of hadronic mixtures. DOE

N94-11455# Sandia National Labs., Albuquerque, NM.
PARALLEL MOLECULAR DYNAMICS WITH THE EMBEDDED ATOM METHOD
S. J. Plimpton and B. A. Hendrickson 1993 7 p Presented at the 16th Material Research Society International Symposium on the Scientific Basis for Nuclear Waste Management Fall Meeting, Boston, MA, 30 Nov. - 5 Dec. 1992
(Contract DE-AC04-76DP-00789)
(DE93-010683; SAND-93-0260C; CONF-921101-110) Avail: CASI HC A02/MF A01

Parallel computing offers new capabilities for using molecular dynamics (MD) to simulate larger numbers of atoms and longer time scales. In this paper we discuss two methods we have used to implement the embedded atom method (EAM) formalism for molecular dynamics on multiple-instruction/multiple-data (MIMD) parallel computers. The first method (atom-decomposition) is simple and suitable for small numbers of atoms. The second method (force-decomposition) is new and is particularly appropriate for the EAM because all the computations are between pairs of atoms. Both methods have the advantage of not requiring any geometric information about the physical domain being simulated. We present timing results for the two parallel methods on a benchmark EAM problem and briefly indicate how the methods can be used in other kinds of materials MD simulations. DOE

N94-11469# Stanford Linear Accelerator Center, CA.
TAU PHYSICS
M. L. Perl Mar. 1993 40 p Presented at the Stanford Linear Accelerator Center (SLAC) Summer Institute on Particle Accelerators: Third Family and the Physics of Flavor, Stanford, CA, 13-24 Jul. 1992
(Contract DE-AC03-76SF-00515)
(DE93-010956; SU-SLAC-Pub-6071; CONF-9207140-6) Avail: CASI HC A03/MF A01

This report discusses the following topics: (tau) production and related (tau) properties; general discussion of (tau) decays; leptonic decays; hadronic decays; the (tau) in atomic physics; and the (tau) neutrino--(nu)(sub (tau)). DOE

N94-11470# Washington Univ., Seattle. Dept. of Physics.
FEFF5: AN AB INITIO MULTIPLE SCATTERING XAFS CODE
J. J. Rehr and S. I. Zabinsky 1992 5 p
(Contract DE-FG06-90ER-45415)
(DE93-011000; DOE/ER-45415/7) Avail: CASI HC A01/MF A01

FEFF5 is an efficient automated code which calculates multiple scattering (MS) curved wave XAFS spectra for molecules and solids. The theoretical ingredients and approximations contained in the code are revised, with the aim of describing the how XAFS spectra are efficiently simulated. The FEFF5 code consists of 4 independent modules: a scattering potential and phase shift module, a path finder module, a scattering amplitude module, and an XAFS module. Multiple scattering Debye-Waller factors are built in using a correlated Debye model. DOE

N94-11509 Tokyo Univ., Tanashi (Japan). Inst. for Nuclear Study.
DEVELOPMENT OF MICROSTRIP GAS CHAMBERS WITH MULTI-CHIP TECHNOLOGY
T. Nagae, T. Tanimori, T. Kobayashi, and T. Miyagi Mar. 1992 15 p Limited Reproducibility: More than 20% of this document may be affected by microfiche quality
(DE93-753169; INS-919) Avail: CASI HC A03

The Microstrip Gas Chamber (MSGC) was developed by using Multi-Chip technology which supports high-density assembly of bare LSI chips on a silicon wafer. Our MSGC was operated steadily with approximately 10(exp 3) gain more than one week. An energy resolution of 15% for 5.9 keV X-ray of Fe-55 source was obtained. With a very thin polyimide substrate of 16 microns thickness, two interesting phenomena were observed; one was a strong dependence of gains on back plane potential, and the other was little time variation of gains. It was also found that a guard mask of a thin polyimide layer on the cathode edge reduced incidental electrical discharges between anode and cathode strips. DOE

N94-11510 National Lab. for High Energy Physics, Tsukuba (Japan).
CONCEPTUAL DESIGN REPORT FOR THE SDC BARREL AND INTERMEDIATE MUON DETECTORS BASED ON A JET-TYPE DRIFT CHAMBER
Y. Arai, Y. Funahashi, and Y. Higashi Apr. 1992 241 p Limited Reproducibility: More than 20% of this document may be affected by microfiche quality
(DE93-753173; KEK-92-1) Avail: CASI HC A11

A jet-type drift chamber for the barrel and intermediate muon detectors of SDC is proposed. The chamber system consists of large multiwire drift chambers having a simple box-type frame structure: 2.5 x 0.4 m(sup 2) in cross section and maximum 9 m in length. A chamber module consists of double layers of small jet cells. The drift cell is composed of a wire plane, including 3 sense wires, and cathode plates parallel to the wire plane. The two layers in a chamber are staggered to each other by half a cell width. The jet cell is tilted such that its principle axis points to the interaction point. Such an arrangement, together with a constant drift velocity of the jet cell, allows us to design a simple and powerful trigger system for high momentum muons utilizing a drift time sum between a pair of staggered cells. The multi-hit capability will be helpful to distinguish high momentum muon tracks from associated electromagnetic debris as was demonstrated by the Fermilab beam test T816. The maximum drift time fulfills the SDC requirement. A preliminary FEM analysis of the chamber module verified the excellent structural stiffness. It makes the support structure and the alignment system relatively simple. These features will reduce the total cost as well as ensure a good performance of the chamber system. DOE

N94-11580 National Inst. for Fusion Science, Nagoya (Japan).
COMPILATION OF EXCITATION CROSS SECTIONS FOR He ATOMS BY ELECTRON IMPACT
T. Kato, Y. Itikawa, and K. Sakimoto Mar. 1992 98 p Limited Reproducibility: More than 20% of this document may be affected by microfiche quality
(DE93-753246; NIFS-Data-15) Avail: CASI HC A05

Experimental and theoretical data are compiled on the cross section for the excitation of He atoms by electron impact. The available data are compared graphically. The survey of the literature was made through the end of 1991. DOE

N94-11581 International Centre for Theoretical Physics, Trieste (Italy).
FERMION-BOSON SCATTERING IN LADDER APPROXIMATION
R. G. Jafarov (Baku State Univ., Azerbaijan.) and S. A. Hadjiev (Baku State Univ., Azerbaijan.) Oct. 1992 10 p Limited Reproducibility: More than 20% of this document may be affected by microfiche quality
(DE93-613111; IC-92/326) Avail: CASI HC A02 (US Sales Only)

A method of calculation of forward scattering amplitude for fermions and scalar bosons with exchanging of scalar particle is suggested. The Bethe-Salpeter ladder equation for the imaginary part of the amplitude is constructed and a solution in Regge asymptotical form is found and the corrections to the amplitude due to the exit from mass shell are calculated. DOE

N94-11592 Japan Atomic Energy Research Inst., Tokyo.
A MOLECULAR DYNAMICS SIMULATION CODE ISIS
Shaw Kambayashi (Japan Atomic Energy Research Inst., Tokai.) Jun. 1992 51 p Limited Reproducibility: More than 20% of this document may be affected by microfiche quality
(DE93-753187; JAERI-M-92-080) Avail: CASI HC A04

Computer simulation based on the molecular dynamics (MD) method has become an important tool complementary to experiments and theoretical calculations in a wide range of scientific fields such as physics, chemistry, biology, and so on. In the MD method, the Newtonian equations of motion of classical particles are integrated numerically to reproduce a phase-space trajectory of the system. In the 1980's, several new techniques were developed for simulation at constant-temperature and/or constant-pressure to compare results of computer simulation with experimental results. The MD method for both microcanonical and canonical simulations is summarized. Then, an overview of a newly developed ISIS (Isokinetic Simulation of Soft-spheres) code and its performance on various computers including vector processors is presented. The ISIS code has a capability to make a MD simulation under constant-temperature condition by using the isokinetic constraint method. The equations of motion are integrated by a very accurate fifth-order finite differential algorithm. The bookkeeping method is also utilized to reduce the computational time. Furthermore, the ISIS code is well adopted for vector processing: speedup ratio ranged from 16 to 24 times is obtained on a VP2600/10 vector processor. DOE

N94-11613# Argonne National Lab., IL. High Energy Physics Div.
EXPERIMENTS TO MEASURE THE GLUON HELICITY DISTRIBUTION IN PROTONS
H. Spinka, M. E. Beddo, and D. G. Underwood 1993 6 p Presented at the Future Directions in Particle and Nuclear Physics at Multi-GeV Hadron Beam Facilities, Upton, NY, 4-6 Mar. 1993
(Contract W-31-109-eng-38)
(DE93-011756; ANL-HEP-CP-93-23; CONF-930389-2) Avail: CASI HC A02/MF A01

Several experiments are described that could obtain information about the gluon helicity distribution in protons. These experiments include inclusive direct-(gamma), direct-(gamma) + jet, jet, and jet + jet production with colliding beams of longitudinally-polarized protons. Some rates and kinematics are also discussed. DOE

N94-11620# Washington Univ., Seattle. Inst. for Nuclear Theory.
A GENERALIZED BETHE-WEIZSAECKER MASS FORMULA FOR STRANGE HADRONIC MATTER
C. B. Dover (Brookhaven National Lab., Upton, NY.) and A. Gal (Hebrew Univ., Jerusalem, Israel.) Dec. 1992 34 p
(Contracts DE-FG06-90ER-40561; DE-AC02-76CH-00016)
(DE93-011010; DOE/ER-40561/096) Avail: CASI HC A03/MF A01

The Bethe-Weizsaecker nuclear mass formula is extended to strange hadronic matter composed of nucleons, lambdas, and cascade hyperons. The generalized formula contains several volume and symmetry terms constrained by phenomenologically determined lambda-nuclear, xi-nuclear, and lambda(lambda) interaction parameters and by hyperon-hyperon (lambda(lambda), lambda(xi), xi(xi)) interaction parameters suggested by One-Boson-Exchange models. We find that hypernuclei are generally unstable to lambda(lambda) yields (xi)N conversion. For strange hadronic matter we determine, as a function of the baryon number A, the line of strong-interaction stability, along which a large strangeness fraction S/A approximately 0.5-1.1 and a low charge fraction q/A approximately less than 0.2 hold, and no fission occurs. The binding energy per baryon increases monotonically to its bulk limit, B/A yields 38 MeV, S/A yields 1.1 and q/A yields 0 for the parameters adopted here assuming that the hyperon species saturate at densities similar to those of protons and neutrons in nuclei. Even in the extreme limit of vanishingly small hyperon-hyperon interaction strengths, strange hadronic matter with B/A yields 15 MeV, S/A yields 0.7 and q/A yields 0 in the bulk limit should exist, the mass formula reproduces semi-quantitatively recent mean-field calculations which implicitly assumed weak hyperon-hyperon interactions. DOE

N94-11658# Purdue Univ., West Lafayette, IN. Dept. of Chemistry.
REAL-SPACE FORMATION AND DISSIPATION DYNAMICS OF HEXAGONAL RECONSTRUCTION ON Au(100) IN AQUEOUS MEDIA AS EXPLORED BY POTENTIODYNAMIC SCANNING TUNNELING MICROSCOPY
Xiaoping Gao, Gregory J. Edens, Antoinette Hamelin, and Michael J. Weaver Apr. 1993 48 p
(Contract N00014-91-J-1409)
(AD-A266138; TR-140) Avail: CASI HC A03/MF A01

The electrode potential-induced formation and dissipation dynamics of the hexagonal ('hex') reconstruction on ordered Au(100) in perchloric and sulfuric acid electrolytes has been studied by means of in-situ scanning tunneling microscopy (STM). The real-space/real-time evolution of surface structures associated with the potential-dependent hex reversable (1 x 1) phase transition was examined on timescales down to ca 1 s by acquiring STM images during appropriate potential sweeps and steps (dubbed here 'potentiodynamic STM'). Extensive hex domains can be formed by slow cooling following flame annealing and/or by holding the potential at values significantly below the potential of zero charge for the (1 x 1) surface. The sharp removal of the reconstruction seen voltammetrically, during positive-going potential sweeps, is accompanied by rapid (less than 1 s) formation of arrays of ordered (1 x 1) clusters, created from the release of the ca 24% additional gold atoms utilized in the (5 x 27) and related hex structures compared with the (1 x 1) substrate. These clusters are significantly, twofold, larger (ca 4-6 nm) when formed in sulfuric acid electrolyte, due probably to an enhanced surface mobility in the presence of adsorbed sulfate. DTIC

N94-11696# Oregon Univ., Eugene.
THEORY OF ELEMENTARY PARTICLES AND ACCELERATOR THEORY. TASK C: EXPERIMENTAL HIGH ENERGY PHYSICS
J. E. Brau 1992 70 p
(Contract DE-FG06-85ER-40224)
(DE93-013139; DOE/ER-40224/247) Avail: CASI HC A04/MF A01

The experimental high energy physics group at the University of Oregon broadened its effort during the past year. The SLD effort extends from maintaining and operating the SLD luminosity monitor which was built at Oregon, to significant responsibility in physics analysis, such as event selection and background analysis for the left-right asymmetry measurement. The OPAL work focussed on the luminosity monitor upgrade to a silicon-tungsten calorimeter. Building on the work done at Oregon for SLD, the tungsten for this upgrade was machined by the Oregon shops and shipped to CERN for assembly. The Oregon GEM effort now concentrates on tracking, specifically silicon tracking. Oregon also has developed a silicon strip preradiator prototype and tested it in a Brookhaven beam. DOE

N94-11813# Tennessee Technological Univ., Cookeville. Dept. of Physics.
NUCLEAR STRUCTURE MODELS: APPLICATIONS AND DEVELOPMENT
P. B. Semmes Apr. 1993 12 p
(Contract DE-FG05-92ER-40694)
(DE93-012934; DOE/ER-40694/2) Avail: CASI HC A03/MF A01

This report summarizes the progress made during the period 1 July 1992 to 30 Apr. 1993. The study of rotational structure at moderate spins in odd-odd nuclei has continued into the A approximately 80 region. Recent experimental data for the positive parity band in Y-82, including absolute BM1 and BE2 values, are rather well described with a 'prolatish' triaxial shape and a (pi)g(sub 9/2) (direct product) (nu)g(sub 9/2) configuration. Little effect from a proton-neutron interaction has been found so far. Current studies of odd mass nuclei are mainly focussing on low spin, low energy states in the A approximately 130 region as a probe to the evolving collectivity. These projects involve direct collaboration with experimental colleagues. Finally, a view of the microscopic foundation of particle-core coupling models approached from the equation of motion method is presented. DOE

N94-11815# Lawrence Livermore National Lab., CA.
SHORT PULSE LASERS FOR GENERATION OF FIELDS EXCEEDING 100 MG
J. H. Hammer, M. Glinsky, W. Kruer, M. Tabak, S. Wilks, and J. Woodworth Nov. 1992 10 p Presented at the 6th International Conference on Megagauss Magnetic Field Generation and Related Topics, Albuquerque, NM, 9-12 Nov. 1992
(Contract W-7405-eng-48)
(DE93-013346; UCRL-JC-111540; CONF-921133-19) Avail: CASI HC A02/MF A01

We consider the use of intense, short-pulse lasers for generation of ultra-high magnetic fields. Twenty MG-level fields were observed in CO2 laser-illuminated targets, however, the recent development of Nd glass lasers capable of delivering several Joules in approximately 1 ps at intensities great er than 10(exp 18) W/cm(exp 4) opens the possibility of much higher magnetic fields (B greater tha n 100 MG). Magnetic field generation is associated with the efficient production of energetic electrons at high values of intensity x wavelength(exp 2), I(lambda)(exp 2). I(lambda) is proportional to the square of the oscillating momentum of electrons in the laser EM field. For I(lambda)(exp 2) great er than 10(exp 17) W/cm(exp 2)-microns(exp 2), the electron motion becomes nonlinear and most of the absorbed energy appears as 'hot' electrons. The absorption of laser energy has been observed to be approximately 50% at 10(exp 18) W/cm(exp 2)-microns(exp 2) and is predicted to the same or higher at 10(exp 19) W/cm(exp 2)-microns(exp 2). The hot electron temperature is much greater than the background temperatures and approaches the oscillatory energy at high I(lambda)(exp 2). The new short pulse lasers reach high values of I(lambda)(exp 2) at much higher intensity and energy density than long wavelength CO2 lasers, which should lead to higher magnetic fields. DOE

N94-11826# Minnesota Univ., Minneapolis. Dept. of Chemistry.
CHROMATOGRAPHIC ASSESSMENT OF HYDROGEN-BOND DONATING ABILITY Technical Report, 1 Jun. 1992 - 31 May 1993
R. Wanke, M. C. Etter, and P. W. Carr 22 Apr. 1993 8 p
(Contract N00014-89-J-1301)
(AD-A265292; TR-21-ONR) Avail: CASI HC A02/MF A01

Generally, hydrogen bonding preferentially occurs between the best donors and best acceptors in the organic solid state. Knowledge of the relative hydrogen-bond acidity and basicity can, therefore, be used in molecular crystal engineering. A liquid chromatography method was developed to assess the hydrogen-bond acidity of potential hydrogen-bond donors used in cocrystallizations. Hydrogen-bond donor solutes are chromatographed on a poly(vinylpyridine - divinylbenzene) column under two different sets of mobile phase conditions. The relative retention is proportional to the hydrogen-bond acidity of the solute and therefore, provides an a priori measure of the hydrogen-bond acidity of a potential cocrystal component. DTIC

N94-12379# Materials Research Society, Pittsburg, PA.
ATOMIC-SCALE IMAGING OF SURFACES AND INTERFACES. MATERIALS RESEARCH SOCIETY SYMPOSIUM PROCEEDINGS, VOLUME 295
David K. Biegelsen, David J. Smith, and S. Y. Tong 1992 297 p Proceedings held in Boston, MA, 30 Nov. - 2 Dec. 1992
(Contract N00014-93-J-0023)
(AD-A265674) Avail: CASI HC A13/MF A03

The gap between imagining and imaging is getting ever smaller. The Atomic-Scale Imaging of Surfaces and Interfaces, Symposium W at the 1992 MRS Fall Meeting in Boston, Massachusetts, brought together researchers using state-of-the-art imaging techniques capable of resolving atomic features. Methods represented were scanning tunneling microscopy (STM), atomic force microscopy (AFM), low energy electron microscopy (LEEM), transmission (TEM) and reflection (REM) electron microscopy, scanning electron microscopy (SEM), atom probe field ion microscopy (APFIM or POSAP), high and low energy external source electron holographies, and internal source electron holographies. Some highlights from the STM papers included discussions of the limitations and future potential of STM as well as current findings. Several papers presented work with STM at elevated temperatures. Jene Golovchenko reviewed STM work showing cooperative diffusion events (Pb on Ge) involving many tens of substrate atoms. Don Eigler focused on atomic manipulation and some of its uses to enable fundamental studies of small atomic clusters. DTIC

N94-12395# Rensselaer Polytechnic Inst., Troy, NY.
BALLISTIC ELECTRON TRANSPORT STUDIES USING BEEM
Leo J. Schowalter 15 May 1993 5 p
(Contract N00014-92-J-1277)
(AD-A266029) Avail: CASI HC A01/MF A01

Most of the effort the first year of this program was devoted to the building of required instrumentation. The thin metal films required necessitated having a feed-back controller for the multihearth electron beam evaporator in the molecular beam epitaxy (MBE) system. Thus, one of our initial projects under this grant was the installation of a Inficon Sentinel controller in the MBE system. This project was successfully completed. The new electron beam evaporator, with its controller, will allow us to evaporate Pt and Au and Ge in the deposition chamber in addition to Si and Co which were already available. MBE growth of SiGe alloys was started and we expect to start ballistic electron emission microscopy (BEEM) studies of metal layers on SiGe alloys this summer. A key part is the ultra-high vacuum (UHV) BEEM studies of MBE grown material. After debating the alternatives, it was decided to install the UHV STM directly into the MBE chamber after testing it in air. DTIC

N94-12420# Purdue Univ., West Lafayette, IN. Dept. of Chemistry.
SOLVENT DYNAMICAL EFFECTS IN ELECTRON TRANSFER: MOLECULAR DYNAMICS SIMULATIONS OF REACTIONS IN METHANOL
Donald K. Phelps, Michael J. Weaver, and Branka M. Ladanyi Apr. 1993 41 p
(Contract N00014-91-J-1409)
(AD-A266061; TR-139) Avail: CASI HC A03/MF A01

Molecular-dynamics simulations of activated electron-transfer (ET) reactions in methanol have been undertaken in order to explore the physical nature of the solvent dynamics coupled to ET barrier crossing, and to probe some underlying reasons for the facile kinetics observed in this solvent. The reactant is modeled by a pair of Lennard-Jones (LJ) spheres in contact, of varying diameter (4 or 5 A), and containing a univalent charge (cation or anion) on one site so to probe possible effects of the ionic charge sign. Following equilibration, the collective solvent response to a sudden charge transfer between the spherical sites is followed, and described in terms of the response function C(t), describing the difference in the solvent-induced electrostatic potential between the initial and final solute states. In all cases, the C(t) curves exhibit a very rapid (50-100 fs) initial decay component associated with hydroxyl inertial motion, followed by components arising from hydrogen-bond librational and diffusive motions. DTIC

N94-12546# Pittsburgh Univ., PA. Dept. of Physics and Astronomy.
EXPERIMENTAL PARTICLE PHYSICS AT THE UNIVERSITY OF PITTSBURGH
W. E. Cleland, E. Engels, Jr., T. J. Humanic, U. Perera, P. F. Shepard, and J. A. Thompson Apr. 1993 215 p
(Contract DE-FG02-91ER-40646)
(DE93-013326; DOE/ER-40646/3) Avail: CASI HC A10/MF A03

During the past year, the HELIOS work drew to a close. In the first results from the electron-muon pair studies, no anomalous sources were seen. The final results and uncertainties are being set. First data from CMD2 will allow improvement of some phi branching ratios including some improved limits on forbidden decays. The engineering run for E865 is scheduled for June and July of 1993. The principal efforts of Task B, the Fermilab program, have been the completion of the analysis of the 1987-88 data with resulting publications, completion of the 1990-91 data run, and the beginning of the analysis of the 1990-91 data. In addition, the Task B group is taking a leadership role in developing a proposal to Fermilab for the upgrade of the CDF silicon vertex detector in preparation for the 1995 data run. Task C has recently submitted results of its fractionally charged particle searches. These results will place new upper limits on the abundance of naturally-occurring fractionally-charged particles in various materials. This group has recently been approved by the Brookhaven management for an exposure of their p-i-n diodes in a high intensity proton beam. This measurement, along with its subsequent analysis, will complete the program. Task D concerned itself with silicon drift chamber studies for the SSC. Task E was devoted to studies of electronics for the GEM Level 1 liquid Ar calorimeter trigger. DOE

N94-12609# Colorado Univ., Boulder. Dept. of Physics.
ELEMENTARY PARTICLE PHYSICS AND HIGH ENERGY PHENOMENA
A. R. Barker, J. P. Cumalat, S. P. DeAlwis, T. A. DeGrand, W. T. Ford, K. T. Mahanthappa, U. Nauenberg, P. Rankin, and J. G. Smith Jun. 1992 117 p
(Contract DE-FG02-91ER-40672)
(DE93-013971; Colo-HEP-314/2; DOE/ER-40672/2) Avail: CASI HC A06/MF A02

Experimental and theoretical high-energy physics programs at the University of Colorado are reported. Areas of concentration include the following: study of the properties of the Z(sup 0) with the SLD detector; fixed-target K-decay experiments; the R&D program for the muon system: the SDC detector; high-energy photoproduction of states containing heavy quarks; electron-positron physics with the CLEO II detector at CESR; lattice QCD; and spin models and dynamically triangulated random surfaces. DOE

N94-12781# Fermi National Accelerator Lab., Batavia, IL.
TOP QUARK SEARCH IN D(O) FROM THE LEPTON + JETS MODE
B. Klima Nov. 1992 5 p Presented at the Meeting of the Division of Particles and Fields of the American Physical Society, Batavia, IL, 10-14 Nov. 1992
(Contract DE-AC02-76CH-03000)
(DE93-014027; FNAL/C-93/051-E; CONF-921122-58) Avail: CASI HC A01/MF A01

The DO collaboration has searched for Top quark production at the square root of s = 1.8 TeV in p(bar-p) collisions at Fermilab using a data sample corresponding to an integrated luminosity of 1.1 pb(exp -1), collected during the 1992 Tevatron run. We report the preliminary results of a search for t(bar-t) production in which the Top quark decays to a W boson plus a b quark where one W decays leptonically and the other decays hadronically. Future prospects for extending the search for Top in the lepton plus jets channel are discussed. DOE

N94-12787# Superconducting Super Collider Lab., Dallas, TX.
QUARK AND LEPTON MASSES
S. Meshkov Apr. 1993 12 p Presented at the 5th Annual International Industrial Symposium on the Super Collider and Exhibition; Global Foundation International Conference on Unified Symmetry in the Small and in the Large, San Francisco, CA, Coral Gables, FL, 25-27 Jan. 1993 Submitted for publication
(Contract DE-AC35-89ER-40486)
(DE93-012308; SSCL-Preprint-241; CONF-930537-5; CONF-9301103-2)
Avail: CASI HC A03/MF A01

The BCS mechanism, augmented by an ad hoc, but reasonable symmetry breaking mechanism, describes both the quark and lepton masses and is consistent with the constraints imposed by the Cabbibo-Kobayashi-Maskawa mixing matrix. This mechanism may be incorporated into the study of various extensions of the Standard Model such as SUSY SU(5). The symmetry breaking at the unification scale is related to that at experimentally accessible scales by running the coefficients of the terms in the mass matrices characterized by their symmetries. DOE

N94-10579*# Korea Inst. of Tech., Tae-Jon (Republic of Korea). Physics Dept.
PHASING OPERATOR FOR TWO OSCILLATORS IN CLASSICAL FIELD
Jong-Jean Kim, Je-Hwan Koo, and Dong-Jae Bae (Pohang Inst. of Science and Technology, Republic of Korea.) *In* NASA. Goddard Space Flight Center, The Second International Workshop on Squeezed States and Uncertainty Relations 1993 p 143-148 (For primary document see N94-10564 01-74)
Avail: CASI HC A02/MF A04

N94-10582*# Maryland Univ. Baltimore County, Catonsville. Dept. of Physics.
STUDY OF EINSTEIN-PODOLSKY-ROSEN STATE FOR SPACE-TIME VARIABLES IN A TWO PHOTON INTERFERENCE EXPERIMENT
Y. H. Shih, A. V. Sergienko, and M. H. Rubin *In* NASA. Goddard Space Flight Center, The Second International Workshop on Squeezed States and Uncertainty Relations 1993 p 163-176 (For primary document see N94-10564 01-74)
Avail: CASI HC A03/MF A04

N94-10584*# Louisiana State Univ., Baton Rouge. Dept. of Physics.
DISSIPATION IN A SQUEEZED-STATE ENVIRONMENT
R. F. OConnell *In* NASA. Goddard Space Flight Center, The Second International Workshop on Squeezed States and Uncertainty Relations 1993 p 183-186 (For primary document see N94-10564 01-74)
(Contract N00014-90-J-1124)
Avail: CASI HC A01/MF A04

N94-10593*# Korean Air Force, Seoul (Republic of Korea). Dept. of Physics.
SQUEEZED STATES OF ELECTRONS AND TRANSITIONS OF THE DENSITY OF STATES
Seung Joo Lee and Chung In Um (Korea Univ., Seoul, Republic of Korea.) *In* NASA. Goddard Space Flight Center, The Second International Workshop on Squeezed States and Uncertainty Relations 1993 p 265-272 (For primary document see N94-10564 01-74)
Avail: CASI HC A02/MF A04

73 NUCLEAR AND HIGH-ENERGY PHYSICS

Includes elementary and nuclear particles; and reactor theory.
For space radiation see *93 Space Radiation.*

N94-10149# Sandia National Labs., Albuquerque, NM.
IN-REACTOR TESTING OF THE CLOSED CYCLE GAS CORE REACTOR: THE NUCLEAR LIGHT BULB CONCEPT
R. O. Gauntt, S. A. Slutz, G. A. Harms, T. S. Latham (United Technologies Research Center, East Hartford, CT.), W. C. Roman (United Technologies Research Center, East Hartford, CT.), and R. J. Rodgers (United Technologies Research Center, East Hartford, CT.) 16 Oct. 1992 11 p Presented at the 10th Symposium on Space Nuclear Power and Propulsion, Albuquerque, NM, 10-14 Jan. 1993
(Contract DE-AC04-76DP-00789)
(DE93-004053; SAND-92-1462C; CONF-930103-24) Avail: CASI HC A03/MF A01 (US Sales Only)

The Nuclear Light Bulb (NLB) concept is an advanced closed cycle space propulsion rocket engine design that offers unprecidented performance characteristics in terms of specific impulse (greater than 1800 s) and thrust (greater than 445 kN). The NLB is a gas-core nuclear reactor making use of thermal radiation from a high temperature U-plasma core to heat the hydrogen propellant to very high temperatures (greater than 4000 K). Analyses performed in support of the design of in-reactor tests that are planned to be performed in the Annular Core Research Reactor (ACRR) at Sandia National Laboratories in order to demonstrate the technical feasibility of this advanced concept are described. The tests will examine the stability of a hydrodynamically confined fissioning U-plasma under steady and transient conditions. Testing will also involve study of propellant heating by thermal radiation from the plasma and materials performance in the nuclear environment of the NLB. The analyses presented include neutronic performance studies and U-plasma radiation heat-transport studies of small vortex-confined fissioning U-plasma experiments that are irradiated in the ACRE. These analyses indicate that high U-plasma temperatures (4000 to 9000 K) can be sustained in the ACRE for periods of time on the order of 5 to 20 s. These testing conditions are well suited to examine the stability and performance requirements necessary to demonstrate the feasibility of this concept. DOE

N94-10156# California Univ., Berkeley. Lawrence Berkeley Lab.
EXPERIMENTAL EFFORTS AND RESULTS IN FINDING NEW HEAVY SCINTILLATORS
S. E. Derenzo and W. W. Moses Sep. 1992 11 p Presented at the Crystal 2000 International Workshop on Heavy Scintillators for Scientific and Industrial Applications, Chamonix, France, 22-26 Sep. 1992
(Contract DE-AC03-76SF-00098)
(DE93-010406; LBL-33295; CONF-9209253-4) Avail: CASI HC A03/MF A01

New heavy scintillators are being discovered with increasing frequency. In recent years NaI(TI) (with its high light output and energy resolution) has been joined by BCO (with its high stopping power), BaF2 (with its excellent timing resolution), and CeF3 (with its speed and short Moliere radius). More than 10 potentially useful scintillators have been under development in the past five years, such as PbSO4 and Lu2SiO5(Ce). We tabulate the characteristics of these and other scintillators, including wavelength, luminous efficiency, decay time, and initial intensity. We describe a search strategy and the prospects for finding the 'ideal' heavy scintillator, which would combine the light output of NAI(TI) and CsI(TI), the stopping power of BGO, and the speed of BaF2 and ZnO(Ga). DOE

N94-10260# Los Alamos National Lab., NM.
HIGH-ENERGY DENSITY PHYSICS AT LOS ALAMOS
P. Byrnes, ed. Mar. 1993 27 p
(Contract W-7405-eng-36)
(DE93-010271; LALP-93-17) Avail: CASI HC A03/MF A01

This brochure describes the facilities of the Above Ground Experiments 2 (AGEX 2) and the Inertial Confinement Fusion (ICF) programs at Los Alamo. Combined, these programs represent, an unparalleled capability to address important issues in high-energy density physics that are critical to the future defense, energy, and research needs of the United States. The mission of the AGEX 2 program at Los Alamos is to provide additional experimental opportunities for the nuclear weapons program. For this purpose we have assembled at Los Alamos the broadest array of high-energy density physics facilities of any laboratory in the world. Inertial confinement fusion seeks to achieve thermonuclear burn on a laboratory scale through the implosion of a small quantity of deuterium and tritium fuel to very high pressure and temperature. The Los Alamos ICF program is focused on target physics. With the largest scientific computing center in the world, We can perform calculations of unprecedented sophistication and precision. We field experiments at facilities worldwide--including our own Trident and Mercury lasers--to confirm our understanding and to provide the necessary data base to proceed toward the historic goal of controlled fusion in the laboratory. The ultrahigh magnetic fields produced in our high explosive pulsed-power generators can be used in a wide variety of solid state physics and temperature superconductor studies. The structure and dynamics of planetary atmospheres can be simulated through the compression of gas mixtures. DOE

N94-10316 Bhabha Atomic Research Centre, Bombay (India).
AN EXPERIMENTAL PROGRAM FOR COLLECTIVE ACCELERATION OF IONS USING INTENSE RELATIVISTIC ELECTRON BEAMS
T. Vijayan, P. Raychowdhury, and S. K. Iyengar (Bhabha Atomic Research Centre, Bombay, India.) 1992 68 p
(DE93-612205; BARC-1992/E/008) Avail: CASI HC A04/MF A01 (US Sales Only)

A program of collective ion acceleration using intense relativistic electron beam (IREB) of 0.25-1MeV, 6-80kA, 60ns on the Kilo Ampere Linear Injector (KALI) systems to accelerate light and heavy ions to high energies approaching GeV with currents over tens of amperes, is envisaged. The accelerator will make use of the intense space-charge field of electron beam in vacuum for accelerating ions which are injected into it. For ion injection, various alternatives, such as, localized gas puff, dielectric insert, laser plasma, etc. were considered as present and long-term objectives. Among the variety of diagnostic methods chosen for characterizing the accelerated ions include range-energy in foil, CR-39 track detector, nuclear activation technique and time-of-flight for energy and species determination; ion Faraday cup for current measurement; and Thomson parabola analyzer for determining the post-acceleration charge-state. In the proposed MAHAKALI collective accelerator, protons of energy over 10 MeV and higher charge state metal ions around a GeV are predicted using a REB of 1MeV, 30kA, 60ns from KALI-5000. In present experiments using KALI-200 with REB parameters of 250keV, 60kA, 80ns, protons over a MeV and carbon and fluorine ions respectively for 12MeV and 16MeV in significant currents were accelerated. DOE

N94-10409 China Nuclear Information Centre, Beijing.
NONLINEAR SPACE CHARGE EFFECT OF BUNCHED BEAM IN LINAC
Yinbao Chen (Institute of Atomic Energy, Beijing, China.) Feb. 1992 19 p Limited Reproducibility: More than 20% of this document may be affected by poor print
(DE93-612176; CNIC-00592; IAE-0100) Avail: Issuing Activity (Department of Energy (DOE)) (US Sales Only)

The nonlinear space charge effect due to the nonuniform particle density distribution in bunched beam of a linac is discussed. The formulae of nonlinear space charge effect and nonlinear focusing forces were derived for the bunched beam with Kapchinskij-Vladimirskij (K-V) distribution, waterbag (WB) distribution, parabolic (PA) distribution, and Gauss (GA) distribution in both of the space charge disk model and space charge cylinder model in the waveguide of a linac. DOE

N94-10529 Sandia National Labs., Albuquerque, NM.
A CRITICAL ASSEMBLY DESIGNED TO MEASURE NEUTRONIC BENCHMARKS IN SUPPORT OF THE SPACE NUCLEAR THERMAL PROPULSION PROGRAM
E. J. Parma, R. M. Ball (Babcock and Wilcox Co., Lynchburg, VA.), G. S. Hoovler (Babcock and Wilcox Co., Lynchburg, VA.), E. C. Selcow (Brookhaven National Lab., Upton, NY.), and R. J. Cerbone (Brookhaven National Lab., Upton, NY.) 1992 10 p Presented at the 10th Symposium on Space Nuclear Power and Propulsion, Albuquerque, NM, 10-14 Jan. 1993 Limited Reproducibility: More than 20% of this document may be affected by microfiche quality
(Contract DE-AC04-76DP-00789)
(DE92-040974; SAND-92-1407C; CONF-930103-12) Avail: CASI HC A02 (US Sales Only)

A reactor designed to perform criticality experiments in support of the Space Nuclear Thermal Propulsion program is currently in operation at the Sandia National Laboratories' reactor facility. The reactor is a small, water-moderated system that uses highly enriched uranium particle fuel in a 19-element configuration. Its purpose is to obtain neutronic measurements under a variety of experimental conditions that are subsequently used to benchmark reactor-design computer codes. Brookhaven National Laboratory, Babcock & Wilcox, and Sandia National Laboratories participated in determining the reactor's performance requirements, design, follow on experimentation, and in obtaining the licensing approvals. Brookhaven National Laboratory is primarily responsible for the analytical support, Babcock & Wilcox the hardware design, and Sandia National Laboratories the operational safety. All of the team members participate in determining the experimentation requirements, performance, and data reduction. Initial criticality was achieved in October 1989. An over-all description of the reactor is presented along with key design features and safety-related aspects. DOE

N94-10542 Academy of Sciences of the Ukraine, Kharkov. Fiziko-Teknicheskij Inst.
DYNAMICS OF ION ACCELERATION IN ELECTRON FLUX BY A VIRTUAL CATHODE POTENTIAL [INAMIKA USKORENIYA IONOV V POTOKE EHIEKTRONOV S VIRTUAL'NYM KATODOM]
V. V. Dolgopolov, Y. V. Kirichenko, S. S. Romanov, and Y. N. Tkach 1991 12 p In RUSSIAN Limited Reproducibility: More than 20% of this document may be affected by microfiche quality
(DE93-620978; KFTI-91-37) Avail: CASI HC A03 (US Sales Only)

Ion acceleration was investigated theoretically. Ions are described by the Vlasov equation. It was shown that the appearance of ions in a drift region may lead to an accelerated movement of the virtual cathode and following this, a potential hole slope without a considerable decrease of this slope change rate. This leads to an effective ion acceleration. DOE

N94-10719 Japan Atomic Energy Research Inst., Tokyo.
PROCEEDINGS OF THE SECOND TECHNICAL MEETING ON HIGH TEMPERATURE GAS-COOLED REACTORS
Jul. 1992 262 p Meeting held in Tokai, Japan, 11-12 Mar. 1992 Limited Reproducibility: More than 20% of this document may be affected

by microfiche quality
(DE93-754285; JAERI-M-92-090; CONF-9203213) Avail: CASI HC A12

The Second Technical Meeting on High Temperature Gas-cooled Reactors (HTGR's) was held on 11-12 Mar. 1992. The following topics were discussed: the present status and the results of Research and Development (R and D) of HTGR's; the items of R and D which should be promoted more positively in the future; and the strategy for development of high temperature engineering and examination in JAERI. This proceeding summarizes the papers that were presented. DOE

N94-10849 Academy of Sciences of the Ukraine, Kiev. Inst. Yadernykh Issledovanij.

MONOCHROMATOR SP-017. THE RESULTS OF THE FIRST EXPERIMENTS [MONOKHROMATOR SP-017. REZUL'TATY PERVYKH EHKSPERIMENTOV]

A. A. Shvedov, O. Y. Goryunov, and V. V. Ostashko et al 1992 15 p In RUSSIAN Limited Reproducibility: More than 20% of this document may be affected by microfiche quality
(DE93-617463; KIYal-92-7) Avail: CASI HC A03 (US Sales Only)

The results of the first experiments on parameter investigation of monochromator SP-017 as well as the energetic resolution of telescopes consisting of Si-detectors on beams of monochromated deuterons and alpha-particles are presented. The experiments showed that in the dispersion condition the monochromator SP-017 allows one to obtain the nonmonochromaticity 1.5 x 10(exp -3). It was established that the peak width of deuteron elastic scattering E(sub d) = 19.7 MeV in the Al-27 + alpha-reaction, caused by the intrinsic resolution of Ge-detector and beam nonmonochromaticity was 46 keV. The energetic telescope resolution of Si-detectors is delta-E(sub alpha) = 150 keV at E(sub alpha) = 39.5 MeV. DOE

N94-10890# Los Alamos National Lab., NM.

FULLY COUPLED NEUTRONIC AND HYDRODYNAMIC ANALYSIS OF SPACE NUCLEAR REACTOR REENTRY ACCIDENTS

J. J. Buksa, J. S. Elson, D. B. Kothe, J. M. McGhee, J. E. Morel, R. T. Perry, and W. J. Rider 1992 7 p Presented at the 1993 International Simulators Conference on High Performance Computing, Arlington, VA, 29 Mar. - 1 Apr. 1993
(Contract W-7405-eng-36)
(DE93-005459; LA-UR-92-4382; CONF-930372-2) Avail: CASI HC A02/MF A01 (US Sales Only)

A method is described for determining the fully coupled neutronic/hydrodynamic response of a space nuclear reactor upon reentry and impact. The code system NIKE-R/PAGOSA is used to accomplish this. This is in contrast to the typical methodology that computes these responses in a decoupled manner. The use of NIKE-R/PAGOSA will allow the seamless description of the phenomena without direct human intervention. This methodology is enabled by the use of modern supercomputers (CM-200). Two examples of this capability are presented: an impaction event modeled with hydrodynamics only (PAGOSA) with the neutron multiplication constant calculated at selected times, and a fully coupled simulation of a reactor immersed in water with its physical disassembly due to its supercritical configuration. DOE

N94-11043 Japan Atomic Energy Research Inst., Tokyo.

REPORT OF THE THIRD SEMINAR ON NUCLEAR PHYSICS AT THE ENERGY REGION OF THE JAERI TANDEM-BOOSTER ACCELERATOR

Akira Iwamoto, ed., Masumi Oshima, ed., Hiroshi Ikezoe, ed., Yuichiro Nagame, ed., and Nobuo Shinohara, ed. (Japan Atomic Energy Research Inst., Tokai.) Sep. 1992 121 p Seminar held in Tokai, Japan, 27-28 Feb. 1992 Limited Reproducibility: More than 20% of this document may be affected by microfiche quality
(DE93-754330; JAERI-M-92-138) Avail: Issuing Activity (Department of Energy (DOE))

A seminar on new experiments to be studied and new experimental apparatus suitable for the Japan Atomic Energy Research Institute (JAERI) tandem-booster accelerator under construction was held at Tokai Research Establishment of JAERI in the period from 27-28 Feb. 1992. Sixty eight participants from universities and from JAERI attended to discuss the following items: (1) physics at low temperature, (2) nuclear structure at high spin and at high excitation energy, (3) application of unstable beam and their spectroscopy, (4) nuclear reaction at intermediate energy, and (5) new facilities. DOE

N94-11124# Argonne National Lab., IL. Physics Div.

HEAVY ION FUSION AT SUB-BARRIER ENERGIES: PROGRESS AND QUESTIONS

R. R. Betts 1993 13 p Presented at the RIKEN International Workshop on Heavy-Ion Fusion Reactors with Neutron-Rich Beams, Saitama, Japan, 18-20 Feb. 1993
(Contract W-31-109-eng-38)
(DE93-011764; ANL/PHY/CP-79433; CONF-930275-2) Avail: CASI HC A03/MF A01

The current status of the experimental study of heavy-ion fusion at sub-barrier energies is reviewed. Emphasis is placed on areas of disagreement between experimental data and theoretical predictions. Suggestions for future experiments are discussed. DOE

N94-11245# National Lab. for High Energy Physics, Tsukuba (Japan).

LECTURE NOTE ON CIRCUIT TECHNOLOGY FOR HIGH ENERGY PHYSICS EXPERIMENT

Hirokazu Ikeda Jul. 1992 78 p
(DE93-771422; KEK-92-9) Avail: CASI HC A05/MF A01

This lecture discusses the basic ideas and practice of circuit technology in the context of a high energy physics experiment. The program of this lecture gives access to the integrated circuit technology to be applied for a high luminosity hadron collider experiment. DOE

N94-11296 Westinghouse Hanford Co., Richland, WA.

A FACILITY FOR TESTING 10- TO 100-kWe SPACE POWER REACTORS

W. F. Carlson and E. J. Bitten Jun. 1992 9 p Presented at the 10th Symposium on Space Nuclear Power and Propulsion, Albuquerque, NM, 10-14 Jan. 1993 Limited Reproducibility: More than 20% of this document may be affected by poor print and microfiche quality
(Contract DE-AC06-87RL-10930)
(DE92-040420; WHC-SA-1536; CONF-930103-9) Avail: Issuing Activity (Department of Energy (DOE)) (US Sales Only)

This paper describes an existing facility that could be used in a cost-effective manner to test space power reactors in the 10 to 100-kWe range before launch. The facility has been designed to conduct full power tests of 100-kWe SP-100 reactor systems and already has the structural feature that would be required for lower power testing. The paper describes a reasonable scenario starting with the acceptance at the test site of the unfueled reactor assembly and the separately shipped nuclear fuel. After fueling the reactor and installing it in the facility, cold critical tests are performed, and the reactor is then shipped to the launch site. The availability of this facility represents a cost-effective means of performing the required prelaunch test program. DOE

N94-11591 Japan Atomic Energy Research Inst., Tokyo.

DEVELOPMENT OF PLASTIC CAPSULE FOR RESEARCH REACTOR IRRADIATION

Kenji Arigane, Shigeo Shida, Heita Waragai, Isao Aoyama, Hidetake Takahashi, and Tadao Seguchi (Japan Atomic Energy Research Inst., Takasaki.) Jun. 1992 28 p Limited Reproducibility: More than 20% of this document may be affected by microfiche quality
(DE93-753186; JAERI-M-92-078) Avail: CASI HC A03

New irradiation capsule for the research reactor was developed using a radiation resistant polymer, Polyethylene-2,6-Naphthalate (PEN). This capsule has several merits such as low activity after irradiation, low price by mass production using injection moulding, and good irradiation performance for application to 12 hours irradiation in Japan Research Reactor No. 4 (JRR-4). Using this capsule, more efficient irradiation can be done because the sample can be taken off from the capsule immediately after irradiation, and this PEN capsule can be replaced with ordinary aluminum capsule for JRR-4 irradiation. The development of PEN capsule and the irradiation tests are described. DOE

N94-11595 Tokyo Univ. (Japan). Nuclear Engineering Research Lab.

RESEARCH RESULTS

1992 146 p Limited Reproducibility: More than 20% of this document

may be affected by microfiche quality
(DE93-753403; UTNL-R-0280) Avail: CASI HC A07

The results of the joint utilization of the nuclear reactor 'Yayoi' and the electron beam accelerator in the Nuclear Engineering Research Laboratory, University of Tokyo, in fiscal year 1991 are summarized. The Yayoi was operated smoothly throughout the year, and the number of research themes, for which the reactor Yayoi was jointly utilized, and the related themes reached 21 cases. After the linear accelerator was reconstructed as the twin linac, the joint utilization was resumed in October 1989, and the number of research themes was 15 cases. In addition to the utilization reports, the reports of 15 cases of Yayoi Study Meetings held in fiscal year 1991 are collected. DOE

N94-11618# Washington Univ., Seattle.
FUTURE HIGH PRECISION EXPERIMENTS AND NEW PHYSICS BEYOND STANDARD MODEL
Ming-Xing Luo 1993 33 p
(Contract DE-FG06-90ER-40561)
(DE93-011004; DOE/ER-40561/095) Avail: CASI HC A03/MF A01

High precision (less than 1%) electroweak experiments that have been done or are likely to be done in this decade are examined on the basis of Standard Model (SM) predictions of fourteen weak neutral current observables and fifteen W and Z properties to the one-loop level, the implications of the corresponding experimental measurements to various types of possible new physics that enter at the tree or loop level were investigated. Certain experiments appear to have special promise as probes of the new physics considered here. DOE

N94-11694# General Atomic Co., San Diego, CA.
TFE VERIFICATION PROGRAM
Jan. 1993 84 p
(Contract DE-AC03-86SF-16298)
(DE93-009609; GA-A-21210) Avail: CASI HC A05/MF A01 (US Sales Only)

The objective of the semiannual progress report is to summarize the technical results obtained during the latest reporting period. The information presented herein will include evaluated test data, design evaluations, the results of analyses and the significance of results. The program objective is to demonstrate the technology readiness of a TFE suitable for use as the basic element in a thermionic reactor with electric power output in the 0.5 to 5.0 MW(e) range, and a full-power life of 7 years. DOE

N94-11880# North Carolina Univ., Chapel Hill. Dept. of Chemistry.
APPLICATIONS OF IN-SITU ELLIPSOMETRY TO MICROWAVE ELECTRON CYCLOTRON RESONANCE PLASMA PROCESSES
Technical Report
Y. Z. Hu, J. Joseph, and E. A. Irene 4 May 1993 15 p
(Contract N00014-89-J-1178)
(AD-A265197; TR-57) Avail: CASI HC A03/MF A01

In-situ static spectroscopic ellipsometry (SE) is a powerful method for characterizing the optical properties and structure of multilayered thin films. However, the commonly used rotating element ellipsometry takes about 10 min for each spectral measurement. Using only a single wavelength gives less information, but each measurement time reduces to about 5 sec. It is shown that a combination of the techniques was adequate to investigate the plasma processes. Spectroscopic ellipsometry measurements for Si, Ge, InP, InSb, and GaAs showed that for properly selected photon energy ranges, the dependence of the dielectric functions on temperatures minimum while the sensitivity to surface modifications is high. The ECR plasma oxidation of Si is discussed first, since it is the simplest case, and then attention is given to more complex example of ECR plasma ion bombardment induced oxidation and damage in single crystal Ge. DTIC

N94-12435*# National Aeronautics and Space Administration. Langley Research Center, Hampton, VA.
FINAL STATE INTERACTIONS AND INCLUSIVE NUCLEAR COLLISIONS
Francis A. Cucinotta and Rajendra R. Dubey (Old Dominion Univ., Norfolk, VA.) Washington Aug. 1993 31 p
(RTOP 199-45-16-11)
(NASA-TP-3353; L-17240; NAS 1.60:3353) Avail: CASI HC A03/MF A01

A scattering formalism is developed in a multiple scattering model to describe inclusive momentum distributions for high-energy projectiles. The effects of final state interactions on response functions and momentum distributions are investigated. Calculations for high-energy protons that include shell model response functions are compared with experiments. Author

N94-12542# Wyoming Univ., Laramie.
EXPERIMENTS WITH ENERGETIC (MU)d AND (MU)t EMITTED FROM SOLID HYDROGEN
G. M. Marshall (Tri-Univ. Meson Facility, Vancouver, British Columbia.), J. L. Beveridge (Tri-Univ. Meson Facility, Vancouver, British Columbia.), J. M. Bailey (Liverpool Univ., England.), G. A. Beer (Victoria Univ., British Columbia.), P. E. Knowles (Victoria Univ., British Columbia.), G. R. Mason (Victoria Univ., British Columbia.), A. Olin (Victoria Univ., British Columbia.), J. H. Brewer (British Columbia Univ., Vancouver.), B. M. Forster (British Columbia Univ., Vancouver.), and T. M. Huber (Gustavus Adolphus Coll., Saint Peter, MN.) et al 1992 10 p Presented at the Muon 1992 Workshop, Uppsala, Sweden, 28 Jun. - 3 Jul. 1992
(Contract DE-FG02-87ER-40333)
(DE93-010252; DOE/ER-40333/136; CONF-9206276-5) Avail: CASI HC A02/MF A01

A set of experiments is reviewed which makes use of the emission of muonic deuterium from the surface of a layer of solid hydrogen. The behavior of muons in a solid target system has been studied via detection of muon decay electrons, muonic x-rays, and fusion products (neutrons and charged particles). The emission of muonic deuterium is understood to result from the Ramsauer-Townsend scattering minimum. The energy distribution of the emitted atoms ranges from tenths of eV to about 10eV, and can be controlled to some extent. A proposal is described to use muonic tritium emission to measure the energy dependence of muonic molecular formation. DOE

N94-12600# Purdue Univ., West Lafayette, IN.
EXPERIMENTAL AND THEORETICAL HIGH ENERGY PHYSICS PROGRAM
J. Finley, J. A. Gaidos, F. J. Loeffler, R. L. McIlwain, D. H. Miller, T. R. Palfrey, E. I. Shibata, and I. P. Shipsey Apr. 1993 123 p
(Contract DE-FG02-91ER-40681)
(DE93-013336; DOE/ER-40681/2) Avail: CASI HC A06/MF A02

Experimental and theoretical high-energy physics research at Purdue is summarized in a number of reports. Subjects treated include the following: the CLEO experiment for the study of heavy flavor physics; gas microstrip detectors; particle astrophysics; affine Kac-Moody algebra; nonperturbative mass bounds on scalar and fermion systems due to triviality and vacuum stability constraints; resonance neutrino oscillations; e(+)e(-) collisions at CERN; (bar p)-p collisions at FNAL; accelerator physics at Fermilab; development work for the SDC detector at SSC; TOPAZ; D-zero physics; physics beyond the standard model; and the Collider Detector at Fermilab. DOE

N94-12601# Brookhaven National Lab., Upton, NY.
SPECTRUM ANALYSIS IN BEAM DIAGNOSTICS
S. Y. Zhang and W. T. Weng 23 Apr. 1993 35 p
(Contract DE-AC02-76CH-00016)
(DE93-013401; BNL-48907) Avail: CASI HC A03/MF A01

In this article, we discuss fundamentals of the spectrum analysis in beam diagnostics, where several important particle motions in a circular accelerator are considered. The properties of the Fourier transform are presented. Then the coasting and the bunched beam motion in both longitudinal and transverse are studied. The discussions are separated for the signal particle, multiple particle, and the Schottky noise cases. To demonstrate the interesting properties of the beam motion spectrum, time domain functions are generated, and then the associated spectra are calculated and plotted. In order to show the whole picture in a single plot, some data have been scaled, therefore they may not be realistic in an accelerator. DOE

N94-12607# Texas A&M Univ., College Station. Cyclotron Inst.
PION CORRELATIONS AND CALORIMETER DESIGN FOR HIGH ENERGY HEAVY ION COLLISIONS

K. L. Wolf 1992 16 p
(Contract DE-FG05-88ER-40437)
(DE93-013861; DOE/ER-40437/4) Avail: CASI HC A03/MF A01

The 1992 research program is reported under the following topics: The EOS time projection chamber program; the NA44 experiment at CERN; sampling calorimeter construction. DOE

N94-12782# Brookhaven National Lab., Upton, NY.
ION SHAKING IN THE 200 MeV XLS-RING
E. Bozoki and S. L. Kramer 1992 4 p Presented at the 3rd European Particle Accelerator Conference (EPAC-3): Accelerators for Special Applications, Berlin, Germany, 24-28 Mar. 1992
(Contract DE-AC02-76CH-00016)
(DE93-014057; BNL-48679; CONF-920315-47) Avail: CASI HC A01/MF A01

It has been shown that ions, trapped inside the beam's potential, can be removed by the clearing electrodes when the amplitude of the ion oscillation is increased by vertically shaking the ions. We will report on a similar experiment in the 200 MeV XLS ring. The design of the ion clearing system for the ring and the first results obtained were already reported. In the present series of experiments, RF voltage was applied on a pair of vertical strip-lines. The frequency was scanned in the range of the ion (from H2 to CO2) bounce frequencies in the ring (1-10 MHz). The response of the beam size, vertical betatron tune, and lifetime was studied. DOE

N94-12785# Superconducting Super Collider Lab., Dallas, TX.
NONLINEAR EFFECTS IN FERRITE TUNED CAVITIES
Y. Goren, N. Mahale, L. Walling, T. Enegren, G. Hulsey, V. Yakoviev (Academy of Sciences, USSR, Novosibirsk.), and V. Petrov (Academy of Sciences, USSR, Novosibirsk.) May 1993 4 p Presented at the International Particle Accelerator Conference, Washington, DC, 17-20 May 1993 Submitted for publication
(Contract DE-AC35-89ER-40486)
(DE93-014136; SSCL-Preprint-355; CONF-930511-34) Avail: CASI HC A01/MF A01

The phenomenon of dependence of the resonance shape and frequency on the RF power level in perpendicular biased ferrite-tuned cavities has been observed in the SSC test cavity experiment. This paper presents a theoretical as well as numerical analysis of this phenomenon and compares the results with experimental data. The effect of this nonlinearity on the SSC low energy booster prototype cavity is discussed. DOE

N94-12786# Los Alamos National Lab., NM.
OPERATIONAL CHARACTERISTICS OF A 100-mA, 2-MeV RADIO-FREQUENCY QUADRUPOLE
K. F. Johnson, W. B. Cottingame, G. O. Bolme, C. M. Fortgang, W. B. Ingalls, J. Marquardt, D. P. Rusthoi, O. R. Sander, M. Smith, and G. T. Worth 1993 4 p Presented at the International Particle Accelerator Conference, Washington, DC, 17-20 May 1993
(Contract W-7405-eng-36)
(DE93-014474; LA-UR-93-1873; CONF-930511-47) Avail: CASI HC A01/MF A01

A 100-mA, 2.07-MeV Radio-Frequency Quadrupole (RFQ 3) has been commissioned and operated routinely on the Accelerator Test Stand (ATS) at Los Alamos National Laboratory. To characterize the RFQ output beam dynamics, measurements were made of the beam transmission and of the transverse and longitudinal phase-space distributions. Data were taken for different RFQ 3 operating conditions and compared to simulations. DOE

74 OPTICS

Includes light phenomena; and optical devices.
For lasers see *36 Lasers and Masers.*

N94-10339# Sandia National Labs., Albuquerque, NM.
PHYSICAL OPTICS MODELLING OF SOFT X RAY PROJECTION LITHOGRAPHY (SXPL) IMAGING EXPERIMENTS
Weng W. Chow, William C. Sweatt, George N. Lawrence (Applied Optics Research, Tucson, AZ.), and Tanya E. Jewell (Jewell, Tanya E., Boulder, CO.) 1993 4 p Presented at the Optical Society of America Topical Meeting on Soft X ray Projection Lithography, Monterey, CA, 10-12 May 1993
(Contract DE-AC04-76DP-00789)
(DE93-011556; SAND-93-0901C; CONF-9305159-2) Avail: CASI HC A01/MF A01

We report our progress on the physical optics modelling of Sandia/AT&T SXPL experiments. The code is benchmarked and the 10X Schwarzchild system is being studied. DOE

N94-10372# Department of the Navy, Washington, DC.
METHOD AND APPARATUS FOR POLARIZATION-MAINTAINING FIBER OPTICAL AMPLIFICATION WITH ORTHOGONAL POLARIZATION OUTPUT Patent Application
Irl N. Duling, inventor (to Navy) and Ronald D. Esman, inventor (to Navy) 15 Mar. 1993 38 p
(AD-D015756; US-Patent-Appl-SN-031251) Avail: CASI HC A03/MF A01

A single-polarization fiber optical amplifier and corresponding method is provided capable of amplifying an optical input signal by a fiber optic amplifier constructed of fiber which may be non-polarization-maintaining. The single-polarization fiber optical amplifier provides a direction-selective coupler which receives an optical input at a first port and outputs an optical output at a second port. A fiber optic amplifier is operatively connected to the direction-selective coupler at a bidirectional port for amplifying the optical input. A retro-reflecting orthogonal polarization converter is operatively connected to the fiber optic amplifier, reflecting the amplified optical input from the fiber optic amplifier in a return direction through the fiber optic amplifier and in an orthogonal polarization to the amplified optical input. The direction-selective coupler outputs the reflected amplified orthogonal optical input at the second port as the optical output of the direction-selective coupler. DTIC

N94-10373# Department of the Navy, Washington, DC.
TECHNIQUE TO PREPARE HIGH-REFLECTANCE OPTICAL FIBER BRAGG GRATINGS WITH SINGLE EXPOSURE IN-LINE ON FIBER DRAW TOWER Patent Application
Charles Askins, inventor (to Navy) and Edward Friebele, inventor (to Navy) 21 Jan. 1993 25 p
(AD-D015757; US-Patent-Appl-SN-006544) Avail: CASI HC A03/MF A01

A process for making an optical reflection grating in a glass fiber includes exposing an unjacketed optic fiber to a single writing pulse from a pair of interfering light beams that form an interference pattern in the fiber. A novel optical fiber has at least one optical grating with a preselected Bragg spacing in at least one region of the fiber, with a periodic modulation in its index of refraction, with high thermal stability and narrow linewidth. A process for making an array of optical reflection gratings in a glass fiber includes exposing a fiber to a plurality of writing pulse from a pair of interfering light beams that form an interference pattern in the fiber, where these pulses are applied sequentially as the fiber is drawn from a draw furnace. A novel optical fiber has a plurality of unspliced gratings with high thermal stability and narrow linewidth. Author (DTIC)

N94-10376# Department of the Navy, Washington, DC.
A FIBER OPTIC NETWORK SYSTEM WITH LOW CROSSTALK USING CODE-DIVISION MULTIPLEXING Patent Application
Alan D. Kersey, inventor (to Navy) and A. Dandridge, inventor (to Navy) 28 Jan. 1993 34 p
(AD-D015763; US-Patent-Appl-SN-010252) Avail: CASI HC A03/MF A01

Accordingly, one subject of the invention is to provide a fiber optic network system with low crosstalk between channels of the network by using spread spectrum and code-division multiplexing techniques. Another object of the invention is to provide a fiber optic ladder or star network system with low crosstalk between channels of the network by using spread spectrum and code-division multiplexing techniques. Another object of the invention is to provide an array of interferometric sensors using a fiber optic ladder or star configuration of interferometric fiber optic sensors and spread system and code-division multiplexing techniques to produce low crosstalk between sensors. A further object of the invention is to provide a fiber optic network system which utilizes spread spectrum and code-division multiplexing techniques to accomplish better suppression of unwanted signals with a shorter code sequence length. DTIC

N94-10486# Optical Society of America, Washington, DC.

NONLINEAR DYNAMICS IN OPTICAL SYSTEMS. POSTDEADLINE PAPERS PRESENTED AT THE OPTICAL SOCIETY OF AMERICA CONFERENCE

26 Jun. 1992 28 p Conference held in Alpbach, Austria, 22-26 Jun. 1992 Sponsored by AFOSR and ONR
(AD-A264958) Avail: CASI HC A03/MF A01

This document contains reports on the following: (1) Tracking unstable phenomena in chaotic laser experiments--Extending the region of stability in a multimode laser; (2) Two dimensional analysis on nonlinear interferometer and decay of spirals; and (3) Collapse of a transverse mode continuum in a photorefractive oscillator. DTIC

N94-10506*# Alabama Univ., Huntsville. Center for Applied Optics.

INTERFEROMETRIC AND OPTICAL TESTS OF WATER WINDOW IMAGING X RAY MICROSCOPES Final Report

R. Barry Johnson Jul. 1993 6 p
(NASA Order H-13030-D)
(NASA-CR-193369; NAS 1.26:193369; UAH-5-33018) Avail: CASI HC A02/MF A01

Interferometric tests of Schwarzchild X-ray Microscope are performed to evaluate the optical properties and alignment of the components. Photographic measurements of the spatial resolution, focal properties, and vignetting characteristics of the prototype Water Window Imaging X-ray Microscope are made and analyzed. Author

N94-10564*# National Aeronautics and Space Administration. Goddard Space Flight Center, Greenbelt, MD.

THE SECOND INTERNATIONAL WORKSHOP ON SQUEEZED STATES AND UNCERTAINTY RELATIONS

D. Han, ed., Y. S. Kim (Maryland Univ., College Park.), and V. I. Manko (Academy of Sciences, USSR, Moscow.) Washington 1993 415 p Workshop held in Moscow, Russia, 25-29 May 1992
(Contract NAS5-30376)
(NASA-CP-3219; Rept-93B00088; NAS 1.55:3219) Avail: CASI HC A18/MF A04

This conference publication contains the proceedings of the Second International Workshop on Squeezed States and Uncertainty Relations held in Moscow, Russia, on 25-29 May 1992. The purpose of this workshop was to study possible applications of squeezed states of light. The Workshop brought together many active researchers in squeezed states of light and those who may find the concept of squeezed states useful in their research, particularly in understanding the uncertainty relations. It was found at this workshop that the squeezed state has a much broader implication than the two-photon coherent states in quantum optics, since the squeeze transformation is one of the most fundamental transformations in physics. For individual titles, see N94-10565 through N94-10612.

N94-10565*# Texas A&M Univ., College Station. Dept. of Physics.

A PHASEONIUM MAGNETOMETER: A NEW OPTICAL MAGNETOMETER BASED ON INDEX ENHANCED MEDIA

Marlan O. Scully, Michael Fleischauer (Ludwig-Maximilians-Univ., Munich, Germany.), and Martin Graf (Ludwig-Maximilians-Univ., Munich, Germany.) *In* NASA. Goddard Space Flight Center, The Second International Workshop on Squeezed States and Uncertainty Relations 1993 p 5-15 (For primary document see N94-10564 01-74)
Avail: CASI HC A03/MF A04

An optical magnetometer based on quantum coherence and interference effects in atoms is proposed. The sensitivity of this device is potentially superior to the present state-of-the-art devices. Optimum operating conditions are derived, and a comparison to standard optical pumping magnetometers is made. Author (revised)

N94-10566*# Helsinki Univ. (Finland). Research Inst. for Theoretical Physics.

SMOOTHLY DEFORMED LIGHT

Stig Stenholm *In* NASA. Goddard Space Flight Center, The Second International Workshop on Squeezed States and Uncertainty Relations 1993 p 17-23 (For primary document see N94-10564 01-74)
Avail: CASI HC A02/MF A04

A single mode cavity is deformed smoothly to change its electromagnetic eigenfrequency. The system is modeled as a simple harmonic oscillator with a varying period. The Wigner function of the problem is obtained exactly by starting with a squeezed initial state. The result is evaluated for a linear change of the cavity length. The approach to the adiabatic limit is investigated. The maximum squeezing is found to occur for smooth change lasting only a fraction of the oscillational period. However, only a factor of two improvement over the adiabatic result proves to be possible. The sudden limit cannot be investigated meaningfully within the model. Author (revised)

N94-10567*# Moscow State Univ. (Russia). Dept. of Physics.

NONCLASSICAL STATES OF THE SECOND OPTICAL HARMONIC IN THE PRESENCE OF SELF-ACTION

A. S. Chirkin and N. V. Korolkova *In* NASA. Goddard Space Flight Center, The Second International Workshop on Squeezed States and Uncertainty Relations 1993 p 25-33 (For primary document see N94-10564 01-74)
Avail: CASI HC A02/MF A04

The quantum theory of coherent radiation frequency doubling in crystals with quadratic and cubic optical nonlinearities is developed. The possibility of producing the quadrature-squeezed state of the second harmonic (SH) field is shown. The nonclassical SH states arise due to self-action effect. Author (revised)

N94-10568*# Rochester Univ., NY. Dept. of Physics and Astronomy.

QUANTUM NOISE AND SQUEEZING IN OPTICAL PARAMETRIC OSCILLATOR WITH ARBITRARY OUTPUT COUPLING

Sudhakar Prasad (New Mexico Univ., Albuquerque.) *In* NASA. Goddard Space Flight Center, The Second International Workshop on Squeezed States and Uncertainty Relations 1993 p 35-48 (For primary document see N94-10564 01-74)
(Contract DE-FG02-90ER-14119)
Avail: CASI HC A03/MF A04

The redistribution of intrinsic quantum noise in the quadratures of the field generated in a sub-threshold degenerate optical parametric oscillator exhibits interesting dependences on the individual output mirror transmittances, when they are included exactly. We present a physical picture of this problem, based on mirror boundary conditions, which is valid for arbitrary transmittances. Hence, our picture applies uniformly to all values of the cavity Q factor representing, in the opposite extremes, both perfect oscillator and amplifier configurations. Beginning with a classical second-harmonic pump, we shall generalize our analysis to the finite amplitude and phase fluctuations of the pump. Author (revised)

N94-10569*# Technische Hogeschool, Eindhoven (Netherlands). Dept. of Theoretical Physics.

DISTURBANCE, THE UNCERTAINTY PRINCIPLE AND QUANTUM OPTICS

Hans Martens and Willem M. deMuynck *In* NASA. Goddard Space Flight Center, The Second International Workshop on Squeezed States and Uncertainty Relations 1993 p 49-54 (For primary document see N94-10564 01-74)
Avail: CASI HC A02/MF A04

It is shown how a disturbance-type uncertainty principle can be derived from an uncertainty principle for joint measurements. To achieve this, we first clarify the meaning of 'inaccuracy' and 'disturbance' in quantum mechanical measurements. The case of photon number and phase is treated as an example, and it is applied to a quantum non-demolition measurement using the optical Kerr effect. Author (revised)

N94-10570*# Budapest Science Univ. (Hungary). Research Lab. for Crystal Physics.

ONE DIMENSIONAL REPRESENTATIONS IN QUANTUM OPTICS

J. Janszky, P. Adam, I. Foldesi, and An. V. Vinogradov (Academy of Sciences, USSR, Moscow.) *In* NASA. Goddard Space Flight Center, The Second International Workshop on Squeezed States and Uncertainty Relations 1993 p 55-60 (For primary document see N94-10564 01-74)
(Contract NRFH-1444)
Avail: CASI HC A02/MF A04

The possibility of representing the quantum states of a harmonic oscillator not on the whole alpha-plane but on its one dimensional manifolds is considered. It is shown that a simple Gaussian distribution along a straight line describes a quadrature squeezed state while a similar Gaussian distribution along a circle leads to the amplitude squeezed state. The connection between the one dimensional representations and the usual Glauber representation is discussed. Author (revised)

N94-10571*# Academy of Sciences (USSR), Moscow. Institute of Physics and Technology.
HARMONIC OSCILLATOR INTERACTION WITH SQUEEZED RADIATION
V. V. Dodonov and D. E. Nikonov *In* NASA. Goddard Space Flight Center, The Second International Workshop on Squeezed States and Uncertainty Relations 1993 p 61-70 (For primary document see N94-10564 01-74)
Avail: CASI HC A02/MF A04

Although the problem of electromagnetic radiation by a quantum harmonic oscillator is considered in textbooks on quantum mechanics, some of its aspects have remained unclear until now. By this, we mean that usually the initial quantum states of both the oscillator and the field are assumed to be characterized by a definite energy level of the oscillator and definite occupation numbers of the field modes. In connection with growing interest in squeezed states, it would be interesting to analyze the general case when the initial states of both subsystems are arbitrary superpositions of energy eigenstates. This problem was considered in other work, where the power of the spontaneous emission was calculated in the case of an arbitrary oscillator's initial state, but the field was initially in a vacuum state. In the present article, we calculate the rate of the oscillator average energy, squeezing, and correlation parameter change under the influence of an arbitrary external radiation field. Some other problems relating to the interaction between quantum particles (atoms) or oscillators where the electromagnetic radiation is an arbitrary (in particular squeezed) state were investigated. Author (revised)

N94-10572*# Pavia Univ. (Italy).
PHOTON NUMBER AMPLIFICATION/DUPLICATION THROUGH PARAMETRIC CONVERSION
G. M. DAriano, C. Macchiavello, and M. Paris *In* NASA. Goddard Space Flight Center, The Second International Workshop on Squeezed States and Uncertainty Relations 1993 p 71-84 (For primary document see N94-10564 01-74)
Avail: CASI HC A03/MF A04

The performance of parametric conversion in achieving number amplification and duplication is analyzed. It is shown that the effective maximum gains G(sub *) remain well below their integer ideal values, even for large signals. Correspondingly, one has output Fano factors F(sub *) which are increasing functions of the input photon number. On the other hand, in the inverse (deamplifier/recombiner) operating mode quasi-ideal gains G(sub *) and small factors F(sub *) approximately equal to 10 percent are obtained. Output noise and non-ideal gains are ascribed to spontaneous parametric emission. Author (revised)

N94-10573*# Academy of Sciences (USSR), Moscow. Inst. od Physics and Technology.
AN EXACTLY SOLVABLE MODEL OF AN OSCILLATOR WITH NONLINEAR COUPLING AND ZEROS OF BESSEL FUNCTIONS **c67**
V. V. Dodonov and A. B. Klimov *In* NASA. Goddard Space Flight Center, The Second International Workshop on Squeezed States and Uncertainty Relations 1993 p 85-88 (For primary document see N94-10564 01-74)
Avail: CASI HC A01/MF A04

We consider an oscillator model with nonpolynomial interaction. The model admits exact solutions for two situations: for energy eigenvalues in terms of zeros of Bessel functions, that were considered as functions of the continuous index; and for the corresponding eigenstates in terms of Lommel polynomials. Author (revised)

N94-10574*# Rome Univ. (Italy).
NON CLASSICAL EFFECTS IN PLANAR WAVEGUIDES
M. Bertolotti, J. Jansky (Palacky Univ., Olomouc, Czechoslovakia.), J. Perina (Budapest Science Univ., Hungary.), V. Pernova (Budapest Science Univ., Hungary.), and C. Sibilia *In* NASA. Goddard Space Flight Center, The Second International Workshop on Squeezed States and Uncertainty Relations 1993 p 89-103 (For primary document see N94-10564 01-74)
Avail: CASI HC A03/MF A04

The quantum description of light propagation inside a planar waveguide is given. In particular, the description describes the behavior of the field inside a directions coupler. Nonclassical effects are presented and discussed. Author (revised)

N94-10575*# Academy of Sciences of the Moldavian SSR, Kishinev. Inst. of Applied Physics.
NONPERTURBATIVE METHODS IN THE PROBLEM OF MULTIPHOTON EXCITATION OF ATOM BY SQUEEZED LIGHT
A. V. Belousov and V. A. Kovarsky *In* NASA. Goddard Space Flight Center, The Second International Workshop on Squeezed States and Uncertainty Relations 1993 p 105-110 (For primary document see N94-10564 01-74)
Avail: CASI HC A02/MF A04

Multiphoton detectors for the strong squeezed light vacuum are considered. The result is compared with the perturbation theory. It is shown that as the degree of squeezing is increased the statistical factor decreases. Author (revised)

N94-10576*# Villanova Univ., PA. Dept. of Physics.
SQUEEZING IN PHASE-CONJUGATED RESONANCE FLUORESCENCE
Henk F. Arnoldus *In* NASA. Goddard Space Flight Center, The Second International Workshop on Squeezed States and Uncertainty Relations 1993 p 111-116 (For primary document see N94-10564 01-74)
Avail: CASI HC A02/MF A04

Emission of resonance fluorescence by an atom near the surface of a four-wave mixing phase conjugator is considered. The dipole radiation field, regarded as a Heisenberg-operator field, is decomposed into plane waves with the aid of Weyl's representation of the Green's function for the wave equation. Each plane-wave component which is incident on the surface of the nonlinear medium, is reflected as its phase-conjugate image. Summation of all reflected plane waves then yields the phase conjugate replica of the incident dipole radiation. This field adds to the radiation which is emitted by the atom into the direction away from the medium. The condition under which squeezing occurs in the emitted resonance fluorescence is investigated. Author

N94-10577*# Northwestern Univ., Evanston, IL.
THE LEGACY OF UNCERTAINTY **c77**
Laurie M. Brown *In* NASA. Goddard Space Flight Center, The Second International Workshop on Squeezed States and Uncertainty Relations 1993 p 119-132 (For primary document see N94-10564 01-74)
Avail: CASI HC A03/MF A04

An historical account is given of the circumstances whereby the uncertainty relations were introduced into physics by Heisenberg. The criticisms of QED on measurement-theoretical grounds by Landau and Peierls are then discussed, as well as the response to them by Bohr and Rosenfeld. Finally, some examples are given of how the new freedom to advance radical proposals, in part the result of the revolution brought about by 'uncertainty,' was implemented in dealing with the new phenomena encountered in elementary particle physics in the 1930's. Author (revised)

N94-10578*# Camerino Univ. (Italy).
QUANTUM NON DEMOLITION MEASUREMENT OF CYCLOTRON EXCITATIONS IN A PENNING TRAP **c77**
Irene Marzoli and Paolo Tombesi (Rome Univ., Italy.) *In* NASA. Goddard Space Flight Center, The Second International Workshop on Squeezed States and Uncertainty Relations 1993 p 133-142 Sponsored in part by Camerino Univ. (For primary document see N94-10564 01-74)
Avail: CASI HC A02/MF A04

The quantum non-demolition measurement of the cyclotron excitations of an electron confined in a Penning trap could be obtained by measuring the resonance frequency of the axial motion, which is coupled to the cyclotron motion through the relativistic shift of the electron mass. Author (revised)

N94-10579*# Korea Inst. of Tech., Tae-Jon (Republic of Korea). Physics Dept.
PHASING OPERATOR FOR TWO OSCILLATORS IN CLASSICAL FIELD **c72**

Jong-Jean Kim, Je-Hwan Koo, and Dong-Jae Bae (Pohang Inst. of Science and Technology, Republic of Korea.) *In* NASA. Goddard Space Flight Center, The Second International Workshop on Squeezed States and Uncertainty Relations 1993 p 143-148 (For primary document see N94-10564 01-74)
Avail: CASI HC A02/MF A04

The origin of Dicke cooperative states was studied by considering two harmonic oscillators driven by a common field of radiation. The origin is assumed for superradiance in a system of molecules where no mutual interactions exist, but all of the molecules encounter the same field of radiation. A phasing operator as Phi(sub Nu) equals D(alpha) + P(sub Nu)D(alpha), where D(alpha) is the displacing operator and P(sub Nu) the projection operator for constant energy Nu for two oscillators, was derived. The eigenstates of the phasing operator Phi are found to show a finite correlation as in the Dicke cooperative states. Author (revised)

N94-10580*# Liverpool Univ. (England).
GENERALISED SQUEEZING AND INFORMATION THEORY APPROACH TO QUANTUM ENTANGLEMENT c77
A. Vourdas *In* NASA. Goddard Space Flight Center, The Second International Workshop on Squeezed States and Uncertainty Relations 1993 p 149-156 (For primary document see N94-10564 01-74)
Avail: CASI HC A02/MF A04

It is shown that the usual one- and two-mode squeezing are based on reducible representations of the SU(1,1) group. Generalized squeezing is introduced with the use of different SU(1,1) rotations on each irreducible sector. Two-mode squeezing entangles the modes and information theory methods are used to study this entanglement. The entanglement of three modes is also studied with the use of the strong subadditivity property of the entropy. Author (revised)

N94-10581*# Bulgarian Academy of Sciences, Sofia. Inst. for Nuclear Reseach and Nuclear Energy.
COMPLETENESS PROPERTIES OF THE MINIMUM UNCERTAINTY STATES c67
D. A. Trifonov *In* NASA. Goddard Space Flight Center, The Second International Workshop on Squeezed States and Uncertainty Relations 1993 p 157-162 (For primary document see N94-10564 01-74)
Avail: CASI HC A02/MF A04

The completeness properties of the Schrodinger minimum uncertainty states (SMUS) and of some of their subsets are considered. The invariant measures and the resolution unity measures for the set of SMUS are constructed and the representation of squeezing and correlating operators and SMUS as superpositions of Glauber coherent states on the real line is elucidated. Author (revised)

N94-10582*# Maryland Univ. Baltimore County, Catonsville. Dept. of Physics.
STUDY OF EINSTEIN-PODOLSKY-ROSEN STATE FOR SPACE-TIME VARIABLES IN A TWO PHOTON INTERFERENCE EXPERIMENT c72
Y. H. Shih, A. V. Sergienko, and M. H. Rubin *In* NASA. Goddard Space Flight Center, The Second International Workshop on Squeezed States and Uncertainty Relations 1993 p 163-176 (For primary document see N94-10564 01-74)
Avail: CASI HC A03/MF A04

A pair of correlated photons generated from parametric down conversion was sent to two independent Michelson interferometers. Second order interference was studied by means of a coincidence measurement between the outputs of two interferometers. The reported experiment and analysis studied this second order interference phenomena from the point of view of Einstein-Podolsky-Rosen paradox. The experiment was done in two steps. The first step of the experiment used 50 psec and 3 nsec coincidence time windows simultaneously. The 50 psec window was able to distinguish a 1.5 cm optical path difference in the interferometers. The interference visibility was measured to be 38 percent and 21 percent for the 50 psec time window and 22 percent and 7 percent for the 3 nsec time window, when the optical path difference of the interferometers were 2 cm and 4 cm, respectively. By comparing the visibilities between these two windows, the experiment showed the non-classical effect which resulted from an E.P.R. state. The second step of the experiment used a 20 psec coincidence time window, which was able to distinguish a 6 mm optical path difference in the interferometers. The interference visibilities were measured to be 59 percent for an optical path difference of 7 mm. This is the first observation of visibility greater than 50 percent for a two interferometer E.P.R. experiment which demonstrates nonclassical correlation of space-time variables. Author (revised)

N94-10583*# Johann-Wolfgang-Goethe-Univ., Frankfurt am Main (Germany).
ON A LAGRANGE-HAMILTON FORMALISM DESCRIBING POSITION AND MOMENTUM UNCERTAINTIES c67
Dieter Schuch *In* NASA. Goddard Space Flight Center, The Second International Workshop on Squeezed States and Uncertainty Relations 1993 p 177-182 Sponsored in part by Deutsche Forschungsgemeinschaft (For primary document see N94-10564 01-74)
Avail: CASI HC A02/MF A04

According to Heisenberg's uncertainty relation, in quantum mechanics it is not possible to determine, simultaneously, exact values for the position and the momentum of a material system. Calculating the mean value of the Hamiltonian operator with the aid of exact analytic Gaussian wave packet solutions, these uncertainties cause an energy contribution additional to the classical energy of the system. For the harmonic oscillator, e.g., this nonclassical energy represents the ground state energy. It will be shown that this additional energy contribution can be considered as a Hamiltonian function, if it is written in appropriate variables. With the help of the usual Lagrange-Hamilton formalism known from classical particle mechanics, but now considering this new Hamiltonian function, it is possible to obtain the equations of motion for position and momentum uncertainties. Author (revised)

N94-10584*# Louisiana State Univ., Baton Rouge. Dept. of Physics.
DISSIPATION IN A SQUEEZED-STATE ENVIRONMENT c72
R. F. OConnell *In* NASA. Goddard Space Flight Center, The Second International Workshop on Squeezed States and Uncertainty Relations 1993 p 183-186 (For primary document see N94-10564 01-74)
(Contract N00014-90-J-1124)
Avail: CASI HC A01/MF A04

The problem of a quantum particle coupled to a quantum mechanical heat bath has a broad and general description in terms of a generalized quantum Langevin equation. Here we show how a squeezed state environment may be incorporated in this general framework. Author (revised)

N94-10585*# Nippon Telegraph and Telephone Public Corp., Tokyo (Japan). Basic Research Labs.
SQUEEZED SPIN STATES: SQUEEZING THE SPIN UNCERTAINTY RELATIONS c77
Masahiro Kitagawa and Masahito Ueda *In* NASA. Goddard Space Flight Center, The Second International Workshop on Squeezed States and Uncertainty Relations 1993 p 187-192 (For primary document see N94-10564 01-74)
Avail: CASI HC A02/MF A04

The notion of squeezing in spin systems is clarified, and the principle for spin squeezing is shown. Two twisting schemes are proposed as building blocks for spin squeezing and are shown to reduce the standard quantum noise, s/2, of the coherent S-spin state down to the order of S(sup 1/3) and 1/2. Applications to partition noise suppression are briefly discussed. Author (revised)

N94-10586*# Universidad Boliviana Mayor de San Simon, Cochabamba.
QUANTUM ENTROPY AND UNCERTAINTY FOR TWO-MODE SQUEEZED, COHERENT AND INTELLIGENT SPIN STATES c77
C. Aragone and D. Mundarain *In* NASA. Goddard Space Flight Center, The Second International Workshop on Squeezed States and Uncertainty Relations 1993 p 193-208 (For primary document see N94-10564 01-74)
Avail: CASI HC A03/MF A04

We compute the quantum entropy for monomode and two-mode systems set in squeezed states. Thereafter, the quantum entropy is also calculated for angular momentum algebra when the system is either in a coherent or in an intelligent spin state. These values are compared with the corresponding values of the respective uncertainties. In general, quantum entropies and uncertainties have the same minimum and maximum points. However, for coherent and intelligent spin states, it is found that some minima for the quantum entropy turn out to be uncertainty maxima. We feel that the quantum entropy we use provides the right answer, since it is given in an essentially unique way. Author (revised)

N94-10587*# Ferrara Univ. (Italy).
THE UNCERTAINTY PRINCIPLE IN RESONANT GRAVITATIONAL WAVE ANTENNAE AND QUANTUM NON-DEMOLITION MEASUREMENT SCHEMES **c77**
Pierluigi Fortini, Roberto Onofrio (Padua Univ., Italy.), and Alessandro Rioli (Bologna Univ., Italy.) *In* NASA. Goddard Space Flight Center, The Second International Workshop on Squeezed States and Uncertainty Relations 1993 p 209-224 (For primary document see N94-10564 01-74)
Avail: CASI HC A03/MF A04

A review of current efforts to approach and to surpass the fundamental limit in the sensitivity of the Weber type gravitational wave antennae is reported. Applications of quantum non-demolition techniques to the concrete example of an antenna resonant with the transducer are discussed in detail. Analogies and differences from the framework of the squeezed states in quantum optics are discussed. Author (revised)

N94-10588*# Erlangen-Nuremberg Univ. (Germany). Inst. for Theoretical Physics III.
GEOMETRIC ASPECTS OF UNCERTAINTY AND CORRELATION **c67**
Sumiyoshi Abe *In* NASA. Goddard Space Flight Center, The Second International Workshop on Squeezed States and Uncertainty Relations 1993 p 225-229 (For primary document see N94-10564 01-74)
Avail: CASI HC A01/MF A04

The fact that the metric induced on the quantum evolution submanifold of the protective Hilbert space describes the uncertainties and correlations of the operators generating the quantum-state evolution and exhibits the inherently-quantized geometry is discussed. Author (revised)

N94-10589*# Rutgers Univ., New Brunswick, NJ. Dept. of Mathematics.
OBSERVABLES, MEASUREMENTS AND PHASE OPERATORS FROM A BOHMIAN PERSPECTIVE **c77**
Martin Daumer and Sheldon Goldstein *In* NASA. Goddard Space Flight Center, The Second International Workshop on Squeezed States and Uncertainty Relations 1993 p 231-238 (For primary document see N94-10564 01-74)
(Grant NSF DMS-91-05661)
Avail: CASI HC A02/MF A04

Bohmian mechanics is a deterministic theory of point particles in motion. While avoiding all the paradoxes of nonrelativistic quantum mechanics, it yields the quantum formalism itself--especially the role of self-adjoint operators--as a macroscopic measurement formalism. As an 'application' it is shown that much of the confusion connected with the phase operator for the electromagnetic field arises from a misunderstanding of the role of operators in quantum theory. Author

N94-10590*# Texas Univ., Austin. Physics Dept.
UNCERTAINTY RELATIONS, ZERO POINT ENERGY AND THE LINEAR CANONICAL GROUP **c77**
E. C. G. Sudarshan *In* NASA. Goddard Space Flight Center, The Second International Workshop on Squeezed States and Uncertainty Relations 1993 p 241-250 (For primary document see N94-10564 01-74)
(Contract DE-FG05-85ER-40200)
Avail: CASI HC A02/MF A04

The close relationship between the zero point energy, the uncertainty relations, coherent states, squeezed states, and correlated states for one mode is investigated. This group-theoretic perspective enables the parametrization and identification of their multimode generalization. In particular the generalized Schroedinger-Robertson uncertainty relations are analyzed. An elementary method of determining the canonical structure of the generalized correlated states is presented. Author (revised)

N94-10591*# Los Alamos National Lab., NM. Theoretical Div.
SUPERSQUEEZED STATES FROM SQUEEZED STATES **c77**
Michael Martin Nieto *In* NASA. Goddard Space Flight Center, The Second International Workshop on Squeezed States and Uncertainty Relations 1993 p 251-258 (For primary document see N94-10564 01-74)
Avail: CASI HC A02/MF A04

Using super-Baker-Campbell-Hausdorff relations on the elements of the supergroup OSP(2/2), we derive the supersqueeze operator and the supersqueezed states, which are the supersymmetric generalization of the squeezed states of the harmonic oscillator. Author

N94-10592*# Imperial Coll. of Science and Technology, London (England). Blackett Lab.
INFORMATION ENTROPY VIA GLAUBER'S Q-REPRESENTATION **c77**
C. H. Keitel and K. Wodkiewicz (Warsaw Univ., Poland.) *In* NASA. Goddard Space Flight Center, The Second International Workshop on Squeezed States and Uncertainty Relations 1993 p 259-264 Sponsored in part by ONR (For primary document see N94-10564 01-74)
Avail: CASI HC A02/MF A04

We present a convenient way to evaluate the information entropy of a quantum mechanical state via the Glauber Q-representation. As an example we discuss the information entropy of a thermally relaxing squeezed state in terms of its Q-representation and show the validity of the corresponding entropic uncertainty- and Araki-Lieb inequalities. Author

N94-10593*# Korean Air Force, Seoul (Republic of Korea). Dept. of Physics.
SQUEEZED STATES OF ELECTRONS AND TRANSITIONS OF THE DENSITY OF STATES **c72**
Seung Joo Lee and Chung In Um (Korea Univ., Seoul, Republic of Korea.) *In* NASA. Goddard Space Flight Center, The Second International Workshop on Squeezed States and Uncertainty Relations 1993 p 265-272 (For primary document see N94-10564 01-74)
Avail: CASI HC A02/MF A04

Electron systems which have low dimensional properties have been constructed by squeezing the motion in zero, one, or two-directions. An isolated quantum dot is modeled by a potential box with delta-profiled, penetrable potential walls embedded in a large outer box with infinitely high potential walls which represent the world function with respect to vacuum. We show the smooth crossover of the density of states from the three-dimensional to the quasi-zero dimensional electron gas. Author (revised)

N94-10594*# Trakya Univ., Edirne (Turkey).
QUANTUM MECHANICAL EFFECTS OF TOPOLOGICAL ORIGIN **c77**
I. H. Duru (Marmara Research Inst., Gebze, Turkey.) *In* NASA. Goddard Space Flight Center, The Second International Workshop on Squeezed States and Uncertainty Relations 1993 p 273-275 (For primary document see N94-10564 01-74)
Avail: CASI HC A01/MF A04

Following a brief review of the original Casimir and Aharonov-Bohm effects, some other effects of similar natures are mentioned. A Casimir interaction between AB fluxes is presented. Possible realizations of the Casimir effects for massive charged fields in solid state structures and a new AB effect for photons are suggested. Author (revised)

N94-10595*# Humboldt Univ., Berlin (German D.R.).
NONUNITARY AND UNITARY APPROACH TO EIGENVALUE PROBLEM OF BOSON OPERATORS AND SQUEEZED COHERENT STATES **c67**
A. Wunsche *In* NASA. Goddard Space Flight Center, The Second International Workshop on Squeezed States and Uncertainty Relations 1993 p 277-281 (For primary document see N94-10564 01-74)
Avail: CASI HC A01/MF A04

The eigenvalue problem of the operator a + zeta(boson creation operator) is solved for arbitrarily complex zeta by applying a nonunitary operator to the vacuum state. This nonunitary approach is compared with the unitary approach leading for the absolute value of zeta less than 1 to squeezed coherent states. Author (revised)

N94-10596*# American Univ., Washington, DC. Dept. of Physics.
NON-GAUGE PHASE TRANSFORMATIONS IN QUANTUM TRANSITION AMPLITUDES **c77**
H. R. Reiss *In* NASA. Goddard Space Flight Center, The Second International Workshop on Squeezed States and Uncertainty Relations

1993 p 283-289 (For primary document see N94-10564 01-74)
(Grant PHYS-9113926)
Avail: CASI HC A02/MF A04

The prescription for introducing a gauge transformation into a quantum transition amplitude, nominally well known, contains an ambiguous feature. It is presumed by some authors that an appropriate transformation of the phase of a wave function will generate the associated gauge transformation. It is shown that this is a necessary but not sufficient step. Examples from the literature are cited to show the consequences of the failure of this procedure. One must distinguish between true gauge transformations and unitary transformations within a fixed gauge. Author

N94-10597*# Korea Inst. of Tech., Tae-Jon (Republic of Korea). Dept. of Physics.
COLLISION-INDUCED SQUEEZING IN A HARMONIC OSCILLATOR c77
Hai-Woong Lee *In* NASA. Goddard Space Flight Center, The Second International Workshop on Squeezed States and Uncertainty Relations 1993 p 291-293 Sponsored in part by Korea Science and Engineering Foundation (For primary document see N94-10564 01-74)
Avail: CASI HC A01/MF A04

The concept of squeezing has so far been applied mainly to light, as is evidenced by the number of research works on the subject of squeezed light. Since, in quantum mechanics, both light and the simple harmonic oscillator are described within the same mathematical framework, there is of course no difficulty in applying the concept to the simple harmonic oscillator as well. In fact, the theoretical development of squeezed states and squeezed light owes much to the physical insights that one obtains as the analogy between light and the harmonic oscillator is exploited. The example presented shows clearly that two states with different phases in general have different degrees of squeezing, even if they have the same state distribution. This means that, even if one considers collision processes that produce the same state distribution, the degree of squeezing obtained during and after the collisions can be quite different, depending on how the phases phi(sub n) of the probability amplitudes develop in time as the collisions proceed. It is therefore evident that, for a detailed study of collision-induced squeezing, further study on the time development of the phases in collisions and its relation to collision parameters such as potential energy surfaces and collision energy is needed. Derived from text

N94-10598*# Ghent Univ. (Belgium). Inst. for Theoretical Physics.
POSITIVE PHASE SPACE DISTRIBUTIONS AND UNCERTAINTY RELATIONS c77
Jan Kruger *In* NASA, Goddard Space Flight Center, The Second International Workshop on Squeezed States and Uncertainty Relations 1993 p 295-300 (For primary document see N94-10564 01-74)
Avail: CASI HC A02/MF A04

In contrast to a widespread belief, Wigner's theorem allows the construction of true joint probabilities in phase space for distributions describing the object system as well as for distributions depending on the measurement apparatus. The fundamental role of Heisenberg's uncertainty relations in Schroedinger form (including correlations) is pointed out for these two possible interpretations of joint probability distributions. Hence, in order that a multivariate normal probability distribution in phase space may correspond to a Wigner distribution of a pure or a mixed state, it is necessary and sufficient that Heisenberg's uncertainty relation in Schroedinger form should be satisfied. Author (revised)

N94-10599*# Akademiya Nauk BSSR, Minsk. Inst. of Physics.
SQUEEZED COLOUR STATES IN GLUON JET c77
S. Ya. Kilin, V. I. Kuvshinov, and S. A. Firago *In* NASA. Goddard Space Flight Center, The Second International Workshop on Squeezed States and Uncertainty Relations 1993 p 301-303 (For primary document see N94-10564 01-74)
Avail: CASI HC A01/MF A04

The possibility of the formation of squeezed states of gluon fields in quantum chromodynamics due to nonlinear nonperturbative self interaction during jet evolution in the process of e(+)e(-) annihilation into hadrons, which are analogous to the quantum photon squeezed states in quantum electrodynamics, is demonstrated. Additionally, the squeezing parameters are calculated. Author (revised)

N94-10600*# Academy of Sciences of the Azerbaijan SSR, Baku. Institute of Physics.
EXACT AND QUASI-CLASSICAL DENSITY MATRIX AND WIGNER FUNCTIONS FOR A PARTICLE IN THE BOX AND HALF SPACE c67
E. A. Akhundova, V. V. Dodonov (Academy of Sciences, USSR, Moscow.), and V. I. Manko (Academy of Sciences, USSR, Moscow.) *In* NASA. Goddard Space Flight Center, The Second International Workshop on Squeezed States and Uncertainty Relations 1993 p 305-309 (For primary document see N94-10564 01-74)
Avail: CASI HC A01/MF A04

The exact expressions for density matrix and Wigner functions of quantum systems are known only in special cases. Corresponding Hamiltonians are quadratic forms of Euclidean coordinates and momenta. In this paper we consider the problem of one-dimensional free particle movement in the bounded region 0 is less than x is less than a (including the case a = infinity). Author (revised)

N94-10601*# Universidad Boliviana Mayor de San Simon, Cochabamba.
NEW SQUEEZED LANDAU STATES c77
C. Aragone *In* NASA. Goddard Space Flight Center, The Second International Workshop on Squeezed States and Uncertainty Relations 1993 p 311-316 (For primary document see N94-10564 01-74)
Avail: CASI HC A02/MF A04

We introduce a new set of squeezed states through the coupled two-mode squeezed operator. It is shown that their behavior is simpler than the correlated coherent states introduced by Dodonov, Kurmyshev, and Man'ko in order to quantum mechanically describe the Landau system, i.e., a planar charged particle in a uniform magnetic field. We compare results for both sets of squeezed states. Author (revised)

N94-10602*# Academy of Sciences (USSR), Novosibirsk. Budker Inst. of Nuclear Physics.
THE UNCERTAINTY PRINCIPLE AND QUANTUM CHAOS c77
Boris V. Chirikov *In* NASA. Goddard Space Flight Center, The Second International Workshop on Squeezed States and Uncertainty Relations 1993 p 317-327 (For primary document see N94-10564 01-74)
Avail: CASI HC A03/MF A04

The conception of quantum chaos is described in some detail. The most striking feature of this novel phenomenon is that all the properties of classical dynamical chaos persist here but, typically, on the finite and different time scales only. The ultimate origin of such a universal quantum stability is in the fundamental uncertainty principle which makes discrete the phase space and, hence, the spectrum of bounded quantum motion. Reformulation of the ergodic theory, as a part of the general theory of dynamical systems, is briefly discussed. Author (revised)

N94-10603*# Hyderabad Univ. (India). School of Physics.
WIGNER FUNCTIONS FOR NONCLASSICAL STATES OF A COLLECTION OF TWO-LEVEL ATOMS c77
G. S. Agarwal (Max-Planck-Inst. fuer Quantenoptik, Munich, Germany.), Jonathan P. Dowling (Army Missile Research and Development Command, Redstone Arsenal, AL.), and Wolfgang P. Schleich (Ulm Univ., Germany.) *In* NASA. Goddard Space Flight Center, The Second International Workshop on Squeezed States and Uncertainty Relations 1993 p 329-339 Sponsored in part by the National Research Council (For primary document see N94-10564 01-74)
(Grant NSF INT-91-00685)
Avail: CASI HC A03/MF A04

The general theory of atomic angular momentum states is used to derive the Wigner distribution function for atomic angular momentum number states, coherent states, and squeezed states. These Wigner functions W(theta,phi) are represented as a pseudo-probability distribution in spherical coordinates theta and phi on the surface of a sphere of radius the square root of j(j +1) where j is the total angular momentum. Author (revised)

N94-10604*# National Aeronautics and Space Administration. Goddard Space Flight Center, Greenbelt, MD.
WAVELETS AND SPACETIME SQUEEZE
D. Han, Y. S. Kim (Maryland Univ., College Park.), and Marilyn E. Noz (New York Univ., New York.) *In its* The Second International Workshop on Squeezed States and Uncertainty Relations 1993 p 341-355 (For

primary document see N94-10564 01-74)
Avail: CASI HC A03/MF A04

It is shown that the wavelet is the natural language for the Lorentz covariant description of localized light waves. A model for covariant superposition is constructed for light waves with different frequencies. It is therefore possible to construct a wave function for light waves carrying a covariant probability interpretation. It is shown that the time-energy uncertainty relation (Delta(t))(Delta(w)) is approximately 1 for light waves is a Lorentz-invariant relation. The connection between photons and localized light waves is examined critically. Author (revised)

N94-10605*# State Meteorological Inst., Saint Petersburg (Russia).
NON-STATIONARY AND NON-LINEAR DISPERSIVE MEDIUM AS EXTERNAL FIELD WHICH GENERATES THE SQUEEZED STATES c77
A. A. Lobashov and V. M. Mostepanenko (Saint Petersburg Technical Univ., Russia.) *In* NASA. Goddard Space Flight Center, The Second International Workshop on Squeezed States and Uncertainty Relations 1993 p 359-362 (For primary document see N94-10564 01-74)
Avail: CASI HC A01/MF A04

The theory of quantum effects in nonlinear dielectric media is developed. The nonlinear dielectric media is influenced by an external pumping field. The diagonalization of the Hamiltonian of a quantized field is obtained by the canonical Bogoliubov transformations. The transformations allow us to obtain the general expressions for the number of created photons and for the degree of squeezing. In the case of a plane pumping wave, for example, the results are calculated by using the zero order of the secular perturbation theory, with small parameters characterizing the medium nonlinearity. The Heisenberg equations of motion are obtained for non-stationary case and a commonly used Hamiltonian is derived from the first principles of quantum electrodynamics. Author (revised)

N94-10606*# Korea Univ., Seoul (Republic of Korea). Dept. of Physics.
RELATION OF SQUEEZED STATES BETWEEN DAMPED HARMONIC AND SIMPLE HARMONIC OSCILLATORS c77
Chung-In Um, Kyu-Hwang Yeon (Chungbuk National Univ., Republic of Korea.), Thomas F. George (Washington State Univ., Pullman.), and Lakshmi N. Pandey (Washington State Univ., Pullman.) *In* NASA. Goddard Space Flight Center, The Second International Workshop on Squeezed States and Uncertainty Relations 1993 p 363-375 Sponsored in part by Center for Thermal and Statistical Physics, BSRI Program, and the Ministry of Education 1992 (For primary document see N94-10564 01-74)
(Grant NSF CHE-91-96214)
Avail: CASI HC A03/MF A04

The minimum uncertainty and other relations are evaluated in the framework of the coherent states of the damped harmonic oscillator. It is shown that the coherent states of the damped harmonic oscillator are the squeezed coherent states of the simple harmonic oscillator. The unitary operator is also constructed, and this connects coherent states with damped harmonic and simple harmonic oscillators. Author (revised)

N94-10607*# Negev Univ., Beersheva (Israel). Physics Dept.
WAVE AND PSEUDO-DIFFUSION EQUATIONS FROM SQUEEZED STATES c65
Jamil Daboul *In* NASA. Goddard Space Flight Center, The Second International Workshop on Squeezed States and Uncertainty Relations 1993 p 377-381 (For primary document see N94-10564 01-74)
Avail: CASI HC A01/MF A04

We show that the probability distributions P(sub n)(q,p;y) := the absolute value squared of (n(p,q;y), which are obtained from squeezed states, obey an interesting partial differential equation, to which we give two intuitive interpretations: as a wave equation in one space dimension; and as a pseudo-diffusion equation. We also study the corresponding Wehrl entropies S(sub n)(y), and we show that they have minima at zero squeezing, y = 0. Author (revised)

N94-10608*# California Univ., Berkeley. Lawrence Berkeley Lab. Physics Dept.
INFINITE-MODE SQUEEZED COHERENT STATES AND NON-EQUILIBRIUM STATISTICAL MECHANICS (PHASE-SPACE-PICTURE APPROACH) c77
Leehwa Yeh *In* NASA. Goddard Space Flight Center, The Second International Workshop on Squeezed States and Uncertainty Relations 1993 p 383-398 (For primary document see N94-10564 01-74)
(Contract DE-AC03-76SF-00098; NSF PHY-90-21139)
(LBL-32695; UCB-PTH-92/25) Avail: CASI HC A03/MF A04

The phase-space-picture approach to quantum non-equilibrium statistical mechanics via the characteristic function of infinite-mode squeezed coherent states is introduced. We use quantum Brownian motion as an example to show how this approach provides an interesting geometrical interpretation of quantum non-equilibrium phenomena. Author

N94-10609*# Academy of Sciences (USSR), Moscow. Inst. for Nuclear Research.
CORRELATED STATES OF A QUANTUM OSCILLATOR ACTED BY SHORT PULSES c77
O. V. Manko *In* NASA. Goddard Space Flight Center, The Second International Workshop on Squeezed States and Uncertainty Relations 1993 p 399-403 (For primary document see N94-10564 01-74)
Avail: CASI HC A01/MF A04

Correlated squeezed states for a quantum oscillator are constructed based on the method of quantum integrals of motion. The quantum oscillator is acted upon by short duration pulses. Three delta-kickings of frequency are used to model the pulses' dependence upon the time aspects of the frequency of the oscillator. Additionally, the correlation coefficient and quantum variances of operations of coordinates and momenta are written in explicit form. Author (revised)

N94-10610*# Academy of Sciences (USSR), Moscow. Lebedev Inst. of Physics.
FLOQUET OPERATOR AS INTEGRAL OF MOTION c77
V. I. Manko *In* NASA. Goddard Space Flight Center, The Second International Workshop on Squeezed States and Uncertainty Relations 1993 p 405-406 (For primary document see N94-10564 01-74)
Avail: CASI HC A01/MF A04

Nonstationary quantum systems have no energy levels. However, for time-dependent periodical quantum systems, the notion of quasi-energy levels has been introduced. The main point of the quasi-energy concept is to relate quasi-energies to eigenvalues of the Floquet operator or monodromy operators which is equal to the evolution operator of a quantum system taken at the moment coinciding with the period of the system. The purpose of this article is to relate the Floquet operator to integrals of the motion and to introduce a new operator which is the integral of motion and has the same quasi-energy spectrum that the Floquet operator has. We wish to discuss an explicit formula for this new integral of motion. Author (revised)

N94-10611*# Chungbuk National Univ. (Republic of Korea). Dept. of Physics.
COHERENT STATES AND UNCERTAINTY RELATIONS FOR THE DAMPED HARMONIC OSCILLATOR WITH TIME-DEPENDENT FREQUENCY c77
Kyu-Hwang Yeon, Chung-In Um (Korea Univ., Seoul, Republic of Korea.), Thomas F. George (Washington State Univ., Pullman.), and Lakshmi N. Pandey (Washington State Univ., Pullman.) *In* NASA. Goddard Space Flight Center, The Second International Workshop on Squeezed States and Uncertainty Relations 1993 p 407-414 (For primary document see N94-10564 01-74)
(Contract KSOEF-91-08-00-05; NSF CHE-91-96214)
Avail: CASI HC A02/MF A04

Starting with evaluations of propagator and wave function for the damped harmonic oscillator with time-dependent frequency, exact coherent states are constructed. These coherent states satisfy the properties which coherent states should generally have. Author

N94-10612*# Academy of Sciences (USSR), Moscow. Lebedev Physics Inst.
QUANTUM PROCESSES IN RESONATORS WITH MOVING WALLS c77
A. B. Klimov and V. V. Dodonov *In* NASA. Goddard Space Flight Center, The Second International Workshop on Squeezed States and Uncertainty Relations 1993 p 415-422 (For primary document see N94-10564 01-74)
Avail: CASI HC A02/MF A04

The behavior of an electromagnetic field in an ideal cavity with an oscillating boundary is considered in the resonance long-time limit. The rates of photon creation from the vacuum and thermal states are evaluated. The squeezing coefficients for the field modes are found, as well as the backward reaction of the field on the vibrating wall. Author (revised)

N94-10647 Allied-Signal Aerospace Co., Kansas City, MO.
FABRICATION AND ANALYSIS OF A SPECIAL OPTICAL CONNECTOR CONTAINING A 1/4-INCH-LONG OPTICAL FIBER FOR DOI TESTS
P. E. Klingsporn Apr. 1993 37 p Limited Reproducibility: More than 20% of this document may be affected by microfiche quality
(Contract DE-AC04-76DP-00613)
(DE93-013115; KCP-613-5039) Avail: CASI HC A03

A technique was developed for fabricating a special optical connector containing an optical fiber of approximately 1/4-inch length for positioning in one end of an adapter to mate with a standard SMA optical connector that terminates a much longer optical fiber. A special holding block was devised for lapping and polishing both ends of the short fibers in four connectors simultaneously. The very short connector was designed to use in experiments at Sandia National Laboratories (SNL) in coupling a high-energy laser beam through the short fiber into the long fiber cable. On the basis of geometrical optics, an analysis was made of the distribution of light energy arriving at the rear face of the short, straight optical fiber segment as a function of the half-angle of a cone of light incident on the front face of the fiber segment. DOE

N94-10651# Lawrence Livermore National Lab., CA.
WAVELENGTH CONSIDERATIONS IN SOFT X RAY PROJECTION LITHOGRAPHY
A. M. Hawryluk and N. M. Ceglio Aug. 1992 17 p Presented at the Soft X Ray Projection Lithography Topical Meeting, Monterey, CA, 6-8 Apr. 1992
(Contract W-7405-eng-48)
(DE93-014115; UCRL-JC-111712; CONF-9204120-8) Avail: CASI HC A03/MF A01

The choice of the operational wavelength for a SXPL system will affect a wide variety of system parameters such as optical design, sources, resists, and multilayer mirrors. Several system constraints limit the choice for the operational wavelength. In particular, optical imaging requirements place an upper limit and throughput issues place a lower limit on the wavelength selection. The authors have determined that there exist several discrete wavelength regions between 10 and 25 nm which satisfy the system imposed constraints of high resolution, large depth of focus, and high throughput. DOE

N94-10657* National Aeronautics and Space Administration. Pasadena Office, CA.
ALKALI METAL FOR ULTRAVIOLET BAND-PASS FILTER Patent
Nick Mardesich, inventor (to NASA) (Jet Propulsion Lab., California Inst. of Tech., Pasadena.), George A. Fraschetti, inventor (to NASA) (Jet Propulsion Lab., California Inst. of Tech., Pasadena.), Timothy A. McCann, inventor (to NASA) (Jet Propulsion Lab., California Inst. of Tech., Pasadena.), Sherwood D. Mayall, inventor (to NASA) (Jet Propulsion Lab., California Inst. of Tech., Pasadena.), Donald E. Dunn, inventor (to NASA) (Jet Propulsion Lab., California Inst. of Tech., Pasadena.), and John T. Trauger, inventor (to NASA) (Jet Propulsion Lab., California Inst. of Tech., Pasadena.) 17 Aug. 1993 7 p Filed 27 Aug. 1992 Supersedes N92-34241 (30 - 24, p 4257)
(NASA-Case-NPO-18433-1-CU; US-Patent-5,237,447; US-Patent-Appl-SN-936417; US-Patent-Class-359-359; US-Patent-Class-359-360; US-Patent-Class-359-582; US-Patent-Class-359-585; US-Patent-Class-359-892; Int-Patent-Class-G02B-1/10; Int-Patent-Class-G02B-5/20) Avail: US Patent and Trademark Office

An alkali metal filter having a layer of metallic bismuth deposited onto the alkali metal is provided. The metallic bismuth acts to stabilize the surface of the alkali metal to prevent substantial surface migration from occurring on the alkali metal, which may degrade optical characteristics of the filter. To this end, a layer of metallic bismuth is deposited by vapor deposition over the alkali metal to a depth of approximately 5 to 10 A. A complete alkali metal filter is described along with a method for fabricating the alkali metal filter.
Official Gazette of the U.S. Patent and Trademark Office

N94-10697 Syracuse Univ., NY.
DESIGN AND ANALYSIS OF AN OPTICAL INTERFACE MESSAGE PROCESSOR Final Report, May 1991 - Aug. 1992
Q. W. Song Mar. 1993 160 p Limited Reproducibility: More than 20% of this document may be affected by microfiche quality
(Contract F30602-91-C-0048)
(AD-A266079; RL-TR-93-19) Avail: CASI HC A08

Optical technology has become a significant part of communications networks. This effort will design, develop, and experimentally evaluate an optical interface message processor (OPTIMP) that exploits the high bandwidth, parallelism, and high storage density offered by optics. The most time consuming operations such as switching and routing in communications networks will be performed in the optical domain. Because of this, the OPTIMP will not suffer from the electrical - optical/optical - electrical conversion bottlenecks, and therefore, it will perform switching and routing in the gigabits/sec range. DTIC

N94-10735*# Johns Hopkins Univ., Laurel, MD. Applied Physics Lab.
CONTINUED DEVELOPMENT OF AN ULTRA-NARROW BANDPASS FILTER FOR SOLAR RESEARCH Final Technical Report
David M. Rust 9 Sep. 1993 17 p
(Grants NAGw-2416; AF-AFOSR-0077-87; AF-AFOSR-0102-90)
(NASA-CR-194169; NAS 1.26:194169) Avail: CASI HC A03/MF A01

The objective of work under this task was to develop ultranarrow optical bandpass filters and related technology necessary for construction of a compact solar telescope capable of operating unattended in space. The scientific problems to which such a telescope could be applied include solar seismology, solar activity monitoring, solar irradiance variations, solar magnetic field evolution, and the location of targets for narrow-field specialized telescopes. We have demonstrated a Y-cut lithium-niobate Fabry-Perot etalon. This filter will be used on the Flare Genesis Experiment. We also obtained solar images with a Z-cut etalon. The technical report on etalon filters is attached to this final report. We believe that work under this grant will lead to the commercial availability of a universal optical filter with approximately 0.1 A bandwidth. Progress was made toward making a suitable 1-2 A tunable blocker filter, but it now appears that the best approach is to make a double-cavity etalon that will not require such a narrow blocker. Broader band blockers are commercially available.
Derived from text

N94-11054*# National Aeronautics and Space Administration, Washington, DC.
ENHANCED DAMAGE-RESISTANT OPTICS FOR SPACEFLIGHT LASER SYSTEMS: WORKSHOP FINDINGS AND RECOMMENDATIONS
Norman Schulze, Marc Cimolino (Science and Technology Corp., Hampton, VA.), Arthur Guenther (Sandia National Labs., Albuquerque, NM.), Ted McMinn (McDonnell-Douglas Electronic Systems Co., Saint Louis, MO.), Frank Rainer (Lawrence Livermore National Lab., CA.), Ansgar Schmid (Rochester Univ., NY.), Steven C. Seitel (Montana Laser Optics, Inc., Bozeman.), M. J. Soileau (University of Central Florida, Orlando.), John S. Theon, and William Walz (Hughes Danbury Optical Systems, Inc., CT.) 1991 39 p Workshop held in Newport News, VA, 10-12 Sep. 1991
(NASA-TM-109243; NAS 1.15:109243) Avail: CASI HC A03/MF A01

NASA has defined a program to address critical laser-induced damage issues peculiar to its remote sensing systems. The Langley Research Center (LaRC), with input from the Goddard Space Flight Center (GSFC), has developed a program plan focusing on the certification of optical materials for spaceflight applications and the development of techniques to determine the reliability of such materials under extended laser exposures. This plan involves cooperative efforts between NASA and optics manufacturers to quantify the performance of optical materials for NASA systems and to ensure NASA's continued application of the highest quality optics possible for enhanced system reliability. A review panel was organized to assess NASA's optical damage concerns and to evaluate the effectiveness of the LaRC proposed program plan. This panel consisted of experts in the areas of laser-induced damage, optical coating manufacture, and the design and development of laser systems for space. The panel was presented information on NASA's current and planned laser remote sensing programs, laser-induced damage problems already encountered in NASA systems, and the proposed program plan to address these issues. Additionally, technical presentations were made on the state of the art in damage mechanisms, optical materials testing, and issues of coating manufacture germane to laser damage. Derived from text

N94-11242# Lawrence Livermore National Lab., CA.
NEEDS FOR SUPER-SMOOTH SURFACES
T. T. Saito May 1992 11 p Presented at the International Symposium on Optical Fabric Testing and Surface Evaluation, Tokyo, Japan, 6 Jun. 1992
(Contract W-7405-eng-48)
(DE93-012482; UCRL-JC-110274; CONF-9206297-2) Avail: CASI HC A03/MF A01

Understanding the needs for super smooth optics yields insights for optical fabricators tasked to produce them. These needs include substrates for metrology and a host of X-ray applications. In addition to some grazing angle of incidence optics, normal incidence optics with multilayer stacks have been recently produced. These optics have very demanding finish requirements. Lacquer and flow polishing have produced some interesting surfaces. DOE

N94-11286# California Univ., San Diego, La Jolla. Dept. of Electrical and Computer Engineering.
SMART SPATIAL LIGHT MODULATOR RESEARCH AND DEVELOPMENT Annual Report, 30 Sep. 1992 - 28 Feb. 1993
Sing H. Lee 28 Feb. 1993 30 p
(Contract F49620-92-J-0467)
(AD-A264928; AFOSR-93-0353TR) Avail: CASI HC A03/MF A01

The objective of our research is to demonstrate 'smart' spatial light modulators (S-SLM) where electronic logic circuits are combined with light modulators and detectors. Our previous studies, while providing valuable insights, indicated that shortcomings of certain approaches limit their applicability to combine Si-based driver and logic circuits with PLZT modulators. For example, PLZT substrate damage limited laser recrystallization approach. Lastly, voltage compatibility problem exists that imposes difficulties in the integration of the modulator driver circuit (requiring 30-50V) in the Si-waver containing logic circuits (operating at 5V). In order to resolve these limitations we explored (1) two methods of implementing thin films of Si-band driver circuits directly onto PLZT substrates and (2) flip-chip bonding of Si wafer containing detector and logic circuits onto the silicon bonded directly to bulk PLZT substrate for fabrication of S-SLM. DTIC

N94-11300 Rome Lab., Griffiss AFB, NY.
PRESORT PROCESSOR Final Report, Jan. 1989 - Dec. 1991
David Grucza Dec. 1992 22 p Limited Reproducibility: More than 20% of this document may be affected by microfiche quality
(AF Proj. 4600)
(AD-A263872; RL-TR-92-338) Avail: Issuing Activity (Defense Technical Information Center (DTIC))

Optical notch filtering is a technique utilizing acousto-optics and Fourier Transform Optics to excise bands of frequencies from a radio frequency spectrum. The purpose of the presort processor is to excise strong narrow band signals from a wideband radar return. The intent of this project was to upgrade a processor built for Rome Laboratory by Harris Corporation by upgrading certain components which have been improved in the years since the beginning of the Harris project. This upgrade has not been completed because of delays in the fabrication of new spatial light modulators, the component which actually performs the excision. Because of this delay and other factors outlined in the remainder of this report we have decided to design an entirely new system under a new project. Many of the program goals in this project have not been met, but have been transferred to JON 4600P112. DTIC

N94-11421# Environmental Research Inst. of Michigan, Ann Arbor.
SPATIAL LIGHT REBROADCASTER ARCHITECTURE STUDY Final Report, 1 Apr. 1990 - 30 Sep. 1992
J. Cederquist, D. Angell, A. Tai, S. Cartwright, and N. Subotic Dec. 1992 160 p
(Contract F33615-90-C-1437)
(AD-A266102; ERIM-226800-27-F; WL-TR-93-5004) Avail: CASI HC A08/MF A02

There is a need for a processor to perform real-time automatic target classification (ATC) that is compact and consumes little electrical power. Optical processors have the potential to provide the needed computational power in a small package. Substantial efforts have been expended in the development of spatial light modulators (SLMs) to meet the ATC requirements, but performance achieved thus far is still lacking. A new class of optical devices, spatial light rebroadcasters (SLRs) have been developed recently with potential performance far exceeding current SLMs. Instead of modulating the input light field, SLR absorbs the incident radiation and re-emits when triggered to do so. The triggering can be accomplished with an optical signal which also carries spatial information. The storage capability and the relationship between the intensities of the incident (input), triggering (readout) and emitted (output) radiations can be used to perform parallel processing of two-dimensional spatial data. In this report, several optical processing architectures were developed and five of the most promising were analyzed in detail. In addition, preliminary experiments were performed to evaluate the hardware required for two of the architectures. DTIC

N94-11653 Naval Postgraduate School, Monterey, CA.
IMPLEMENTATION AND USE OF A COMPUTATIONAL RAY-TRACING PROGRAM FOR THE DESIGN AND ANALYSIS OF COMPLEX OPTICAL SYSTEMS M.S. Thesis
James D. Atkinson, IV Mar. 1993 54 p Limited Reproducibility: More than 20% of this document may be affected by microfiche quality
(AD-A265075) Avail: CASI HC A04

A new ray-tracing computer program is presented as an analysis and design tool for the development of complex optical systems. The algorithms for the ray-tracing are presented for a wide variety of optical systems surface types. Unique methods for the prediction of two-beam interference patterns are implemented so that amplitude-splitting interferometers can be modeled. Modules for line shape analysis and data storage are also described. This program (DART) is validated using the previously established characteristics of the Middle Ultraviolet Spectral Analysis of Nitrogen Gasses (MUSTANG) instrument, which has a resolution of 10 A, an X-axis field-of-view of 1.2 milliradians, a Y-axis field-of-view of 37 milliradians, and 1600 A bandpass. DART is used to predict the optical characteristics of a new instrument, ISAAC, that is planned for satellite deployment in 1995. The full wavelength range of ISAAC is 1250 A, and the instantaneous band-pass is approximately 250 A. The full wavelength coverage is obtained by rotating a reflection grating in five discreet steps. Based on the DART calculations, the resolution of the ISAAC instrument will exceed 1.30 A for all bands, with resolutions as low as 1.06 A at the longer wavelengths. The predicted X-axis field-of-view is 0.5 milliradians and the Y-axis field-of-view is 36 milliradians. DTIC

N94-11656# Naval Research Lab., Washington, DC.
A COMPACT, FOUR-WAY IMAGE SPLITTER Interim Report
D. P. Murphy, T. A. Peyser, and R. E. Pechacek 26 May 1993 10 p
(AD-A266107; NRL/MR/6754-93-7322) Avail: CASI HC A02/MF A01

A compact, four-way, optical image splitter is described which maintains equal intensity and equal optical path length in each arm of the apparatus. The four output beams are colinear with the input light beam. DTIC

N94-11662# Lawrence Livermore National Lab., CA.
AIRBORNE OPTICAL TRACKING CONTROL SYSTEM DESIGN STUDY
11 Sep. 1992 52 p Prepared in cooperation with Kaman Aerospace Corp, Tucson, AZ
(Contract W-7405-eng-48)
(DE93-009515; UCRL-CR-113095) Avail: CASI HC A04/MF A01 (US Sales Only)

The Kestrel LOS Tracking Program involves the development of a computer and algorithms for use in passive tracking of airborne targets from a high altitude balloon platform. The computer receivers track error signals from a video tracker connected to one of the imaging sensors. In addition, an on-board IRU (gyro), accelerometers, a magnetometer, and a two-axis inclinometer provide inputs which are used for initial acquisitions and course and fine tracking. Signals received by the control processor from the video tracker, IRU, accelerometers, magnetometer, and inclinometer are utilized by the control processor to generate drive signals for the payload azimuth drive, the Gimballed Mirror System (GMS), and the Fast Steering Mirror (FSM). The hardware which will be procured under the LOS tracking activity is the Controls Processor (CP), the IRU, and the FSM. The performance specifications for the GMS and the payload canister azimuth driver are established by the LOS tracking design team in an effort to achieve a tracking jitter of less than 3 micro-rad, 1 sigma for one axis. DOE

N94-11676# Lawrence Livermore National Lab., CA.
NEW CHALLENGES IN OPTICAL MATERIALS DEVELOPMENT
W. F. Krupke Feb. 1993 9 p Presented at the Symposium on Optical Materials for High-Power Lasers, Boulder, CO, 28-30 Oct. 1992
(Contract W-7405-eng-48)
(DE93-011889; UCRL-JC-113188; CONF-921047-2) Avail: CASI HC A02/MF A01

The recent emergence of high performance semiconductor laser diodes and diode arrays emitting at wavelengths between 630 and 2300 nm has enabled the demonstration of several novel diode-pumped solid state laser materials. Narrowly, laser diode arrays may be viewed as simple replacements for conventional flash or arc lamp pumps in solid state lasers. The examples discussed in this paper illustrate that laser diode array pumps are considerably more versatile, enabling novel high performance lasers that are technically not feasible using conventional flashlamps. Additionally, several relatively new nonlinear optical materials, possessing high nonlinearities and excellent phase-matching properties, offer good prospects for the development of efficient, compact, wavelength-diverse all-solid-state laser sources. DOE

N94-11887# Aircraft Research Association Ltd., Bedford (England).
THE EVOLUTION OF WHOLE FIELD OPTICAL DIAGNOSTICS FOR EXTERNAL TRANSONIC TESTING
K. A. Fry and P. Bryanston-Cross (Warwick Univ., Coventry, England.) Sep. 1992 15 p Presented at the European Forum on Wind Tunnels and Wind Tunnel Testing Techniques, Southampton, England, 14-17 Sep. 1992
(ARA-Memo-379) Avail: CASI HC A03/MF A01

The diagnostic use of quantitative laser flow visualization techniques has increased rapidly over recent years. The limitations imposed by conventional single point techniques such as laser Doppler anemometry are addressed and how they have been overcome by the development of a new family of whole field measurement techniques is demonstrated. In particular near instantaneous whole field velocity data was obtained in a relatively hostile, industrial 2.74 m x 2.44 m transonic wind tunnel (TWT) at the Aircraft Research Association (ARA). The techniques were evaluated for their suitability for making quantitative measurements in the wing/pylon region of a model wing and engine combination. Three optical diagnostic techniques were successfully developed within the context of the ARA facility. The first technique, laser light sheet (LLS), combines the operation of a pulse laser and video capture system to provide a 'real time' visualization of the flow, whereas a second pulse laser technique, Particle Image Velocimetry (PIV) can be used to make specific quantitative whole field instantaneous velocity measurements. The third method, holography, was used to produce a stored three dimensional visualization of the unsteady and shock wave features of the transonic flow in the gully region. A description is made of their installation and operation, and examples are presented of current test results. Author (revised)

N94-12341# Aerospace Corp., El Segundo, CA. Technology Operations.
LIGHT SCATTERING FROM A SPHERICAL PARTICLE ON A CONDUCTING PLANE. PART 1: NORMAL INCIDENCE
B. R. Johnson 1 May 1993 52 p
(Contract F04701-88-C-0089)
(AD-A265920; TR-0091(6945-08)-Pt-1; SMC-TR-93-30-Pt-1) Avail: CASI HC A04/MF A01

A new procedure is developed for calculating light scattering from a spherical particle on a conducting plane. The discussion is limited to problems in which the incident light beam is perpendicular to the plane. A general proof is given for the method of images, which is used to convert the problem of a particle on a conducting plane to an equivalent two-particle problem. The scattering solution for the two-particle is then obtained by the multipole expansion method. Mirror symmetry is exploited to simplify the calculation. Formulas are developed for the extinction and absorption cross sections. Several example problems are calculated, and the exact solutions are compared to the results from two commonly used approximation procedures. DTIC

N94-12389# Rochester Univ., NY. Inst. of Optics.
LIMITATIONS TO THE QUALITY OF OPTICAL PHASE CONJUGATION BY STIMULATED BRILLOUIN SCATTERING Ph.D. Thesis
Thomas R. Moore 1993 138 p
(AD-A266006) Avail: CASI HC A07/MF A02

The process of optical phase conjugation by stimulated Brillouin scattering is studied both theoretically and experimentally, with emphasis on aspects that apply to phase-conjugate lasers. A theoretical formalism based on decomposing the optical field into a set of orthogonal modes is presented; this formalism is then used as the basis for numerical modeling. Many of the steady-state aspects of stimulated Brillouin scattering are investigated including the following: the distribution of energy in the interaction region, the spatial effects of distributed noise, phase pulling of the Strokes wave, and the affects of adding smooth aberrations to the pump beam. A new design for a robust, inexpensive, solid-state, phase-conjugate laser is also presented. DTIC

N94-12413# Naval Research Lab., Washington, DC.
ASYNCHRONOUS TRANSFER MODE (ATM) TECHNOLOGY: AN OVERVIEW Final Report
James R. Webster 4 Jun. 1993 23 p
(AD-A266087; NRL/MR/8143-93-7337) Avail: CASI HC A03/MF A01

This paper presents a brief overview of the emerging network protocol standard known as Asynchronous Transfer Mode or ATM. ATM was developed by the telecommunications industry as part of the long-term shift of communications services to the B-ISDN standard. By taking advantage of the highly reliable fiber optic networks available, ATM offers faster and more efficient data communications than existing protocols such as X.25. A rigorous, layered protocol exists that gives ATM the flexibility to carry many different types of traffic, including voice, imagery, and video, as well as data. DTIC

N94-12416# Rome Lab., Griffiss AFB, NY.
PRELIMINARY SURFACE-EMITTING LASER LOGIC DEVICE EVALUATION Final Report, Oct. 1991 - Sep. 1992
S. I. Libby, M. A. Parker, G. R. Olbright, and P. D. Swanson Mar. 1993 18 p
(AD-A266111; RL-TR-93-35) Avail: CASI HC A03/MF A01

This report discusses the evaluation of a monolithically integrated heterojunction phototransistor and vertical-cavity surface-emitting laser, designated the surface-Emitting Laser Logic device (CELL). Included is a discussion of the device structure and theory of operation, test procedures, results, and conclusions. Also presented is the CELL's opto-electronic input/output characteristics which includes spectral analysis, characteristic emitted light versus current and current versus voltage curves, input wavelength tolerance, output wavelength sensitivity to bias current, and insensitivity to input wavelength and power within a specified range. DTIC

N94-12444# Honeywell, Inc., Minneapolis, MN. Systems and Research Center.
OPTOELECTRONIC TECHNOLOGY CONSORTIUM Quarterly Technical Report No. 3, 1 Jan. - 1 Mar. 1993
Mary Hibbs-Brenner 12 May 1993 11 p
(Contract MDA972-92-C-0071)
(AD-A265691) Avail: CASI HC A03/MF A01

The Optoelectronic Technology Consortium has been established to position U.S. industry as the world leader in optical interconnect technology by developing, fabricating, integrating, and demonstrating the producibility of optoelectronic components for high-density/high-data-rate processors and accelerating the insertion of this technology into military and commercial applications. This objective will be accomplished by a program focused in three areas: (1) demonstrated performance--OETC will demonstrate an aggregate data transfer rate of 16 Gb/s between single transmitter and receiver packages, as well as the expandability of this technology by combining four links in parallel to achieve a 64 Gb/s link; (2) accelerated development--by collaborating during the precompetitive technology development stage, OETC will advance the development of optical components and produce links for a multiboard processor testbed demonstration; and (3) producibility--OETC's technology will achieve this performance by using components that are affordable, and reliable, with a line BER less than 10(exp -15) and MTTF greater than 10(exp 6). DTIC

N94-10047# Construcciones Aeronauticas S.A., Madrid (Spain). Space Div.
DEVELOPMENT TESTS FOR A HIGH STABILITY OPTICAL BENCH
E. Ozores, F. Arevalo, A. Ayuso, A. Bonet, S. Lareo, and A. Pradier (European Space Agency. European Space Research and Technology Center, ESTEC, Noordwijk, Netherlands.) *In* ESA, Advanced Materials for Lightweight Structures Oct. 1992 p 271-276 (For primary document see N94-10001 01-24)
Copyright Avail: CASI HC A02/MF A04

N94-10065# Southampton Univ. (England). Dept. of Electronics.
MULTIPLEXED AND DISTRIBUTED OPTICAL FIBRE SENSORS
J. P. Dakin *In* ESA, Advanced Materials for Lightweight Structures Oct. 1992 p 385-392 (For primary document see N94-10001 01-24)
Copyright Avail: CASI HC A02/MF A04

N94-10437# MetroLaser, Irvine, CA.
FLOW VISUALIZATION AND SPECTROSCOPY IN HYPERSONIC FLOWS: NEW TRENDS
James Trolinger, Georg Eitelberg (Deutsche Forschungsanstalt fuer Luft- und Raumfahrt, Goettingen, Germany.), and Marc Rapuc (Avions Marcel Dassault, Saint-Cloud, France.) *In* AGARD, Theoretical and Experimental Methods in Hypersonic Flows Apr. 1993 11 p (For primary document see N94-10421 01-02)
Copyright Avail: CASI HC A03/MF A04

N94-10971*# Maryland Univ., College Park. Dept. of Physics.
PLANS TO IMPROVE THE EXPERIMENTAL LIMIT IN THE COMPARISON OF THE EAST-WEST AND WEST-EAST ONE-WAY LIGHT PROPAGATION TIMES ON THE ROTATING EARTH
C. O. Alley, T. E. Kiess, R. A. Nelson, A. V. Sergienko, Y. H. Shih, B. C. Wang, and F. M. Yang *In* NASA. Goddard Space Flight Center, The 24th Annual Precise Time and Time Interval (PTTI) Applications and Planning Meeting Jun. 1993 p 105-112 (For primary document see N94-10963 01-70)
Avail: CASI HC A02/MF A04

N94-10992*# Alcatel Network Systems, Inc., Richardson, TX.
SONET SYNCHRONIZATION: WHAT'S HAPPENING
Robert W. Cubbage *In* NASA. Goddard Space Flight Center, The 24th Annual Precise Time and Time Interval (PTTI) Applications and Planning Meeting Jun. 1993 p 337-342 (For primary document see N94-10963 01-70)
Avail: CASI HC A02/MF A04

N94-11068# Academy of Sciences (USSR), Moscow. Physical Inst.
THE POSSIBILITY OF IMAGE RESTORATION UNDER OBSERVATION IN A REGIME OF STRONG SCATTERING
V. U. Zavorotny *In* National Astronomy and Ionosphere Center, Propagation Effects in Space VLBI 1993 p 79-85 (For primary document see N94-11060 01-32)
Avail: Issuing Activity

N94-11069# Academy of Sciences (USSR), Moscow.
THE SUPERRESOLUTION EFFECT OBSERVED THROUGH A RANDOM MEDIUM
M. I. Charnotskii, V. U. Zavorotny, and V. A. Myakinin *In* National Astronomy and Ionosphere Center, Propagation Effects in Space VLBI 1993 p 86-89 (For primary document see N94-11060 01-32)
Avail: Issuing Activity

N94-11967 Electrotechnical Lab., Ibaraki (Japan). Life Electronics Research Center.
THE DEVELOPMENT OF PHYTOPLANKTON SENSING SYSTEM WITH OPTICAL FIBER
T. Saitou, A. Nishimoto, Y. Kakui, R. Tsuda (Kinki Univ., Osaka, Japan.), M. Kumagai (Lake Biwa Research Inst., Shiga, Japan.), M. Ichihara (Mitsubishi Cable Industries Ltd., Amagasaki, Japan.), K. Yamazaki (Mitsubishi Cable Industries Ltd., Amagasaki, Japan.), M. Kimura (Mitsubishi Cable Industries Ltd., Amagasaki, Japan.), and K. Suzuki (Mitsubishi Cable Industries Ltd., Amagasaki, Japan.) *In* Scientific Organizing Committee of PORSEC, Proceedings of the PORSEC 1992 in Okinawa: Conference for Pacific Ocean Environments and Probing, Volume 1 25 Aug. 1992 p 425-429 (For primary document see N94-11894 01-42)
Copyright Avail: Issuing Activity (Scientific Organizing Committee of PORSEC, P.O. Box 10, Shimizu, Shizuoka 424, Japan, HC)

N94-12189*# POD Associates, Inc., Albuquerque, NM.
MODEL OF OPTICAL SCATTER FROM MICROIMPACTS ON THE HUBBLE TELESCOPE Abstract Only
L. B. Crowell *In* Lunar and Planetary Inst., Twenty-fourth Lunar and Planetary Science Conference. Part 1: A-F 1993 p 353-354 (For primary document see N94-12015 01-91)
Avail: CASI HC A01/MF A06

N94-12725 Academy of Sciences (USSR), Saint Petersburg. Inst. of Oceanology.
PROPAGATION OF LIGHT PULSES THROUGH A THREE-LAYER MEDIUM (CLOUD, PURE AIR, AND OCEAN WATER)
V. M. Greysukh and I. M. Levin *In* Scientific Organizing Committee of PORSEC, Proceedings of the PORSEC 1992 in Okinawa: Conference for Pacific Ocean Environments and Probing, Volume 2 25 Aug. 1992 p 1070-1072 (For primary document see N94-12635 01-42)
Copyright Avail: Issuing Activity (Scientific Organizing Committee of PORSEC, P.O. Box 10, Shimizu, Shizuoka 424, Japan, HC)

N94-12742 Academy of Sciences (USSR), Moscow. Inst. of Applied Mathematics.
OPTICAL TRANSFER OPERATOR OF THE ATMOSPHERE-OCEAN SYSTEM
T. A. Suchkevich *In* Scientific Organizing Committee of PORSEC, Proceedings of the PORSEC 1992 in Okinawa: Conference for Pacific Ocean Environments and Probing, Volume 2 25 Aug. 1992 p 1155-1159 (For primary document see N94-12635 01-42)
Copyright Avail: Issuing Activity (Scientific Organizing Committee of PORSEC, P.O. Box 10, Shimizu, Shizuoka 424, Japan, HC)

N94-12748 Moscow Physical-Engineering Inst. (Russia).
TRAJECTORY CURVING IN UNDERWATER PROPAGATION OF LIGHT
V. S. Remizovich, D. B. Rogozkin, and Sh. A. Shekhmametyev *In* Scientific Organizing Committee of PORSEC, Proceedings of the PORSEC 1992 in Okinawa: Conference for Pacific Ocean Environments and Probing, Volume 2 25 Aug. 1992 p 1184-1188 (For primary document see N94-12635 01-42)
Copyright Avail: Issuing Activity (Scientific Organizing Committee of PORSEC, P.O. Box 10, Shimizu, Shizuoka 424, Japan, HC)

75 PLASMA PHYSICS

Includes magnetohydrodynamics and plasma fusion.
For ionospheric plasmas see *46 Geophysics*. For space plasmas see *90 Astrophysics*.

N94-10157# Los Alamos National Lab., NM.
SOURCE TO DETECTOR SPECTRUM TRANSFORMATION AND ITS INVERSE FOR THE PEGASUS Z-PINCH
W. Matuska, Huan Lee, R. Hockaday, and D. Peterson 1993 9 p Presented at the 3rd International Conference on Dense Z-Pinches, London, England, 19-23 Apr. 1993
(Contract W-7405-eng-36)
(DE93-012674; LA-UR-93-1408; CONF-9304126-2) Avail: CASI HC A02/MF A01

We have developed a ray-tracing code which enables us to calculate the spectrum from a 2-D source simulation and compare it directly with experimental data. This code also allows us to study the various spectral components which can potentially be used to determine the source from measured data. DOE

N94-10158# Los Alamos National Lab., NM.
MHD SIMULATION OF DEUTERIUM-FIBER-INITIATED Z-PINCHES WITH TWO-FLUID EFFECTS
P. Sheehey (California Univ., Los Angeles.) and I. R. Lindemuth 1993 12 p Presented at the 3rd International Conference on Dense Z-Pinches,

London, 19-23 Apr. 1993
(Contract W-7405-eng-36)
(DE93-012682; LA-UR-93-1382; CONF-9304126-1) Avail: CASI HC A03/MF A01

Two-dimensional 'cold-start' resistive MHD computations of the formation and evolution of deuterium-fiber-initiated Z-pinches have been extended to include separate ion and electron energy equations and finite-Larmor-radius ordered terms. In the Ohm's Law (magnetic field evolution) equation, Hall and diamagnetic pressure terms have been added, and corresponding terms have been added to the energy equations. Comparison is made of the results of these computations with previous computations and with experiments. DOE

N94-10159# General Atomic Co., San Diego, CA.
EFFICIENCY OF FAST WAVE CURRENT DRIVE FOR A WEAKLY RELATIVISTIC PLASMA
S. C. Chiu, Y. R. Lin-Liu, and C. F. F. Karney (Princeton Univ., NJ.) Apr. 1993 4 p Presented at the 10th Topical Conference on Radio Frequency Power in Plasmas, Boston, MA, 1-3 Apr. 1993
(Contracts DE-AC03-89ER-51114; DE-AC02-76CH-03073)
(DE93-012775; GA-A-21254; CONF-9304112-4) Avail: CASI HC A01/MF A01

Current drive by fast waves (FWCD) is an important candidate for steady-state operation of tokamaks. Major experiments using this scheme are being carried out on D3-D. There has been considerable study of the theoretical efficiency of FWCD. In other research, the nonrelativistic efficiency of FWCD at arbitrary frequencies was studied. For D3-D parameters, the results can be considerably different from the Landau and Alfven limits. At the high temperatures of reactors and D3-D upgrade, relativistic effects become important. In this paper, the relativistic FWCD efficiency for arbitrary frequencies is studied. Assuming that the plasma is weakly relativistic, i.e., T(sub e)/Mc(exp 2) is small, an analytic expression for FWCD is obtained for high resonant energies (u(sub ph)/u(sub Te)(much greater than 1)). Comparisons with the results from a numerical code ADJ and the nonrelativistic results shall be made and analytical fits in the whole range of velocities shall be presented. DOE

N94-10253# Oak Ridge National Lab., TN.
HIGH HEAT FLUX COMPONENTS AND PLASMA SURFACE INTERACTIONS
L. L. Snead Dec. 1992 18 p
(Contract DE-AC05-84OR-21400)
(DE93-008786; ORNL/FTR-4495) Avail: CASI HC A03/MF A01 (US Sales Only)

The purpose of the US/Japan Workshop P-196 was to review the progress made in the area of plasma facing materials (PFM's). The emphasis of the workshop was on International Thermonuclear Experimental Reactor (ITER)-relevant materials, though more basic research was also presented. Of the 66 workshop participants, 48 were Japanese, 11 were from the United States, and 7 were observers from Europe. The addition of the European observers, whose areas of research were not limited to PFM's, had a very positive effect on the meeting. Also of interest is that a large number of Japanese industrial representatives attended. DOE

N94-10262# Lawrence Livermore National Lab., CA.
SIMULATIONS OF D3-D DIVERTOR BIASING WITH THE LEDGE CODE
M. E. Rensink, J. Milovich, and T. Rognlien Sep. 1992 15 p Presented at the IAEA Technical Committee Meeting on Tokamak Plasma Biasing, Montreal, Ottawa, 8-10 Sep. 1992
(Contract W-7405-eng-48)
(DE93-010500; UCRL-JC-110-843; CONF-9209181-7) Avail: CASI HC A03/MF A01

We use the LEDGE 2D fluid model to determine the effects of electrically biasing the outboard divertor plate in D3-D. The LEDGE code includes classical perpendicular and parallel current flows as well as E x B and diamagnetic drifts. Boundary conditions at the divertor plates allow the sheath parameters to vary with current flow across the sheath. Ohmic heating and convective heat flow associated with the current flow are included. Neutrals originating at the divertor plates due to recycling are represented by a fluid model. We explore the effect of cross-field drifts and variations in the bias voltage. The current-voltage characteristic, inboard/outboard heat flux asymmetry, and radial plasma profiles are computed. We show that cross-field drifts have a strong effect on the plasma profiles at the diverter plates. Differential biasing of the inboard and outboard divertor plates can significantly modify the naturally occurring outboard/inboard heat flux asymmetry, but it only weakly affects radial profiles at the outboard plate. DOE

N94-10284 Melbourne Univ., Parkville (Australia). School of Physics.
TWO FLUID PLASMAS IN THE VICINITY OF A SCHWARZSCHILD BLACK HOLE
V. Buzzi, K. C. Hines, and R. A. Treumann 1992 9 p
(DE93-610264; UM-P-92/19) Avail: CASI HC A02/MF A01 (US Sales Only)

The 3+1 split of general relativity was used to investigate the dispersion relation for certain plasma waves, together with the two stream instability, in the vicinity of a Schwarzschild black hole horizon. In contrast to the special relativistic results, the dispersion relations discussed contain additional terms involving the gravitational acceleration, a, and the lapse function (alpha). Some of these terms are imaginary and should correspond to gravitational damping effects. DOE

N94-10286# Lawrence Livermore National Lab., CA.
X RAY PRODUCTION (APPROXIMATELY)130 (ANGSTROM) FROM LASER-PRODUCED PLASMAS FOR PROJECTION X RAY LITHOGRAPHY APPLICATIONS
R. L. Kauffman, D. W. Phillion, and R. C. Spitzer 30 May 1992 14 p Presented at the Soft X Ray Projection Lithography Topical Meeting, Monterey, CA, 6-8 Apr. 1992
(Contract W-7405-eng-48)
(DE93-009256; UCRL-JC-110217; CONF-9204120-5) Avail: CASI HC A03/MF A01

X-ray production in the region around 130 A from laser-produced plasmas have been investigated as a source for projection x-ray lithography. The dependence of x-ray conversion efficiency on target material, intensity, and pulse length has been studied using a 0.53 micron laser with a maximum of 0.3 J. Conversion efficiency of 1% into a 3 A bandwidth has been demonstrated for Sn targets at intensities around 10(exp 11) W/sq cm using a 7.5 ns pulse. Intensity scaling suggests that laser spot size and two-dimensional expansion are important for optimizing x-ray production at these low irradiation intensities. DOE

N94-10289# Lawrence Livermore National Lab., CA.
PHYSICS AND MODELLING OF SCRAPE-OFF LAYER TRANSPORT
R. H. Cohen, S. L. Allen, J. A. Crotinger, T. B. Kaiser, J. L. Milovich, N. Mattor, W. M. Nevins, G. D. Porter, M. E. Rensink, and T. D. Rognlien et al 1992 9 p Presented at the 14th International Conference on Plasma Physics and Controlled Nuclear Fusion Research, Wurzburg, Germany, 30 Sep. - 7 Oct. 1992
(Contracts W-7405-eng-48; DE-FG05-80ET-53088; DE-FG03-88ER-53275; DE-AC04-76DP-00789; DE-AC03-89ER-51114)
(DE93-010510; UCRL-JC-110398; CONF-9209290-8) Avail: CASI HC A02/MF A01

We present studies of three schemes for reducing the peak heat flux on divertor plates: divertor biasing, impurity injection (radiative divertor), and neutral gas injection (gas target divertor). We report on theoretical analysis of a likely source of turbulent transport in the scrape-off layer (SOL) and incorporation of the resultant transport coefficients into self-consistent models. DOE

N94-10310# Oak Ridge National Lab., TN.
TRANSPORT MECHANISMS ACTING IN TOROIDAL DEVICES: A THEORETICIAN'S VIEW
B. A. Carreras Jan. 1993 26 p
(Contract DE-AC05-84OR-21400)
(DE93-013463; ORNL/TM-12209) Avail: CASI HC A03/MF A01

Understanding the basic mechanisms of transport in toroidal confinement devices remains one of the more challenging scientific issues in magnetic confinement. At the same time, it is a critical issue for the magnetic fusion program. Recent progress in understanding fluctuations and transport has been fostered by the development and use of new diagnostics, bringing new perspectives on these studies. This has stimulated new theoretical developments. A view of the most recent issues and progress in this area is given. The role of long wavelengths in core transport and the relation between shear flows and turbulence at the plasma edge are the primary topics considered. DOE

N94-10321# Texas Univ., Austin. Fusion Research Center.
TEXAS EXPERIMENTAL TOKAMAK
A. J. Wootton Apr. 1993 89 p
(Contract DE-FG05-88ER-53267)
(DE93-013377; DOE/ER-53267/6) Avail: CASI HC A05/MF A01

This progress report covers the period from November 1, 1990 to April 30, 1993. During that period, TEXT was operated as a circular tokamak with a material limiter. It was devoted to the study of basic plasma physics, in particular to the study of fluctuations, turbulence, and transport. The purpose is to operate and maintain TEXT Upgrade as a complete facility for applied tokamak physics, specifically to conduct a research program under the following main headings: (1) to elucidate the mechanisms of working gas, impurity, and thermal transport in tokamaks, in particular to understand the role of turbulence; (2) to study physics of the edge plasma, in particular the turbulence; (3) to study the physics or resonant magnetic fields (ergodic magnetic divertors, intra island pumping); and (4) to study the physics of electron cyclotron heating (ECRH). Results of studies in each of these areas are reported. DOE

N94-10346*# Colorado State Univ., Fort Collins. Dept. of Mechanical Engineering.
AN INVESTIGATION OF CONDUCTED AND RADIATED EMISSIONS FROM A HOLLOW-CATHODE PLASMA CONTACTOR Annual Report, 1 Jan. 1992 - 1 Jan. 1993
Brett W. Buchholtz and Paul J. Wilbur Jul. 1993 99 p
(Grant NAG3-776)
(NASA-CR-191172; NAS 1.26:191172) Avail: CASI HC A05/MF A02

An investigation conducted on the electrical interference induced by the operation of a hollow-cathode plasma contractor in a ground-based facility is described. The types of electrical interference, or noise, which are important to Space Station Freedom designers are classified as either conducted or radiated emissions. The procedures required to perform conducted and radiated emission measurements on a plasma contactor are examined. The experimental data obtained are typically examined in the frequency domain (i.e. amplitudes of the noise fluctuations versus frequency). Results presented indicate the conducted emissions, which are the current fluctuations from the contactor into the space station wiring, are affected by operating parameters such as expellant flow rate and discharge current. The radiated emissions, which are the electromagnetic waves induced and emitted by the contactor, appear to be influenced by the contactor emission current. Other experimental results suggest possible sources which are responsible for the observed noise. For example, the influence of the plasma environment downstream from the contactor on noise emission levels is described. In addition, a brief discussion is given on the correlation between conducted and radiated emissions and the mechanisms through which both are influenced by the plasma downstream of the contactor. Author

N94-10387 International Centre for Theoretical Physics, Trieste (Italy).
NONLINEAR SECOND HARMONIC GENERATION BY LIGHT WAVE-PLASMA INTERACTION IN OSCILLATING MAGNETIC FIELD
S. M. Khalil, B. F. Mohamed, and F. Sharaf Sep. 1992 7 p Limited Reproducibility: More than 20% of this document may be affected by microfiche quality
(DE93-613723; IC-92/290) Avail: CASI HC A02 (US Sales Only)

The nonlinear generation of second harmonic electromagnetic waves in a thin inhomogeneous (dense and rarefied) plasma layer (of length d) by obliquely and normally incident light waves is analyzed. We consider the effect of external time-dependent magnetic fields on the generation and amplification of waves. Two cases are considered: (1) the first case is when the magnetic field oscillates at a frequency equal to that of the incident wave; and (2) the second is when the magnetic field oscillates at a frequency that is double that of the incident wave. For normal incidence, waves are not radiated in the first case, while in the second case, the second harmonics are radiated equally from the plasma boundaries at $x = 0$ and $x = d$. For rarefied plasma, the second harmonics are radiated with equal amplitudes in both cases. DOE

N94-10395 Academy of Sciences of the Ukraine, Kiev. Inst. Teoreticheskoj Fiziki.
NONLINEAR MHD-WAVES IN A DISSIPATIVE PLASMA WITH HALL CURRENTS
S. V. Korsunskij 1991 28 p Limited Reproducibility: More than 20% of this document may be affected by microfiche quality
(DE93-617844; ITP-91-71) Avail: Issuing Activity (Department of Energy (DOE)) (US Sales Only)

We consider the propagation of nonlinear MHD-waves in a plasma of high but finite conductivity with Hall currents. Linear wave dispersion is investigated and the evolution equation for weak nonlinear waves is obtained. Exact quasi-periodic and stationary solutions for the complex Burgers-Schroedinger equations are found and analyzed. DOE

N94-10396 Academy of Sciences of the Ukraine, Kiev. Inst. Teoreticheskoj Fiziki.
GENERAL RENORMALIZED STATISTICAL APPROACH WITH FINITE CROSS-FIELD CORRELATIONS
M. O. Vakulenko 1992 11 p Limited Reproducibility: More than 20% of this document may be affected by microfiche quality
(DE93-617846; ITP-92-22) Avail: CASI HC A03 (US Sales Only)

The renormalized statistical approach is proposed. This approach will account for finite correlations of potential and magnetic fluctuations. It may be used for analysis of a wide class of nonlinear model equations describing the cross-correlated plasma states. The influence of a cross spectrum on stationary potential and magnetic ones is investigated. DOE

N94-10397 Academy of Sciences of the Ukraine, Kiev. Inst. Teoreticheskoj Fiziki.
STATIONARY SPECTRA IN A MAGNETIZED CURRENT-CARRYING PLASMA
M. O. Vakulenko 1992 15 p Limited Reproducibility: More than 20% of this document may be affected by microfiche quality
(DE93-617847; ITP-92-23) Avail: CASI HC A03 (US Sales Only)

The low-frequency (frequencies do not exceed the ion gyro-frequency) quasi-flute short-wave (wavelengths smaller than the ion gyroradius) potential, cross-field, and magnetic fluctuation spectra in a magnetized current-carrying plasma are calculated by using the canonical distribution, the general renormalized statisticalapproach with finite cross-field correlations, and the self-similar transformation method. DOE

N94-10523 Academy of Sciences of the Ukraine, Kiev. Inst. Teoreticheskoj Fiziki.
STATIONARY SPECTRA IN A PLASMA WITH A SHEAR (RENORMALIZED STATISTICAL APPROACH WITH NON-ZERO EIGENFREQUENCIES)
M. O. Vakulenko 1992 10 p Limited Reproducibility: More than 20% of this document may be affected by microfiche quality
(DE93-617851; ITP-92-27) Avail: CASI HC A02 (US Sales Only)

Short-wave low-frequency potential, magnetic and cross-field fluctuation spectra are found in an equilibrium state of a current-carrying plasma with a shear. A new renormalized approach according for shear frequencies is elaborated for statistical analysis on nonlinear plasma evolution. DOE

N94-10524 Academy of Sciences of the Ukraine, Kiev. Inst. Yadernykh Issledovanij.
OPTIMIZATION OF BREAK-DOWN CONDITIONS IN TOKAMAK TOTUS [OPTIMIZATSIYA USLOVIJ PROBOYA V TOKAMAKE TOTUS]
V. B. Vidzigovskij, A. A. Gurin, and V. I. Nedovba et al 1991 19 p In RUSSIAN Limited Reproducibility: More than 20% of this document may be affected by microfiche quality
(DE93-617863; KIYaI-91-15) Avail: CASI HC A03 (US Sales Only)

The results are given for first experiments on tokamak TOTUS, intended for research of problems of control by discharges and plasmas characteristics. The essential peculiarity of the device is the hybrid poloidal magnetic system, combining the functions of air inductor, control windings, and windings forming the plasma cross-section configuration. As the result of investigations the break-down conditions were established. It has created the multi-sectional programmed supply system of the poloidal winds for discharge plus start phase and its operating algorithm. The main parameters of device systems were optimized for break-down phase. DOE

N94-10538 Academy of Sciences of the Ukraine, Kiev. Inst. Teoreticheskoj Fiziki.

STATIONARY SPECTRA IN A FINITE-PRESSURE CURRENT-CARRYING PLASMA

M. O. Vakulenko 1992 12 p Limited Reproducibility: More than 20% of this document may be affected by microfiche quality
(DE93-617848; ITP-92-24) Avail: CASI HC A03 (US Sales Only)

The short-wave (wavelengths smaller than the ion gyroradius) low-frequency (frequencies less than the ion gyrofrequency) potential, cross, and magnetic stationary fluctuation spectra are found in a finite pressure current-carrying plasma on the basis of canonical distribution, a renormalized statistical approach with cross-field correlations, and a self-similar analysis. DOE

N94-10539 Academy of Sciences of the Ukraine, Kiev. Inst. Teoreticheskoj Fiziki.

STATIONARY SPECTRA IN A QUASI NEUTRAL CURRENT-CARRYING PLASMA

M. O. Vakulenko 1992 10 p Limited Reproducibility: More than 20% of this document may be affected by microfiche quality
(DE93-617849; ITP-92-25) Avail: CASI HC A02 (US Sales Only)

The low-frequency short-wave equilibrium spectra of electromagnetic fluctuations are obtained. In doing so, we account for the cross-field correlations. Statistical analysis shows that a longitudinal current in a dense quasi-neutral (alpha(sub e) = 4(pi)n(sub 0)m(sub e)c(exp 2)/beta(sub 0)(exp 2) is much greater than 1) plasma destroys the stationary of fluctuation spectra corresponding to zero fluxes of motion invariants, and it may also alter the anomalous electron heat conductivity. DOE

N94-10540 Academy of Sciences of the Ukraine, Kiev. Inst. Teoreticheskoj Fiziki.

STATIONARY SPECTRA IN A SHEARED PLASMA (LINEAR LIMIT)

M. O. Vakulenko 1992 10 p Limited Reproducibility: More than 20% of this document may be affected by microfiche quality
(DE93-617850; ITP-92-26) Avail: CASI HC A02 (US Sales Only)

The short-wave low-frequency stationary spectra of correlated electromagnetic fluctuations in a sheared current-currying plasma are obtained by a linear approximation. Even being weak, the shear may considerably alter the spectral characteristics of plasma perturbations. DOE

N94-10541 Academy of Sciences of the Ukraine, Kharkov. Fiziko-Tekhnicheskij Inst.

COLLECTIVE ACCELERATION OF IONS IN NEAR-ANODE PLASMA OF A STRONG-CURRENT RELATIVISTIC DIODE [KOLLEKTIVNOE USKORENIE IONOV V PRIANODNOJ PLAZME SIL'NOTOCHNOGO RELYATIVISTSKOGO DIODA]

N. I. Gaponenko and Y. V. Tkach 1991 20 p In RUSSIAN Limited Reproducibility: More than 20% of this document may be affected by microfiche quality
(DE93-620977; KFTI-91-33) Avail: CASI HC A03 (US Sales Only)

The results of experiments on collective acceleration of ions in the near-anode plasma of a strong-current relativistic diode with the short beam current pulse duration (10-20 ns) are given. The energy of accelerated ions that is dependent upon the change of plasma parameters, the length of the anode-cathode distance, and the value of the external magnetic field was measured. A description of the ion collective acceleration mechanism in plasma and the numerical modelling program of acceleration processes are given. DOE

N94-10558 Academy of Sciences of the Ukraine, Kharkov. Fiziko-Tekhnicheskij Inst.

SCATTERING OF MODULATED ULTRA-RELATIVISTIC ELECTRON BEAM (UREB) BY ATMOSPHERIC PLASMA [RASSEYANIE MODULIROVANNOGO UL'TRARELYATIVISTSKOGO EHLEKTRONNOGO PUCHKA (UREHP) ATMOSFERNYM PLAZMENNYM KANALOM]

V. I. Tkachenko, V. P. Zejdlits, O. Y. Naguchev, and A. V. Sinyugin 1992 20 p In RUSSIAN Limited Reproducibility: More than 20% of this document may be affected by microfiche quality
(DE93-620987; KFTI-92-5) Avail: CASI HC A03 (US Sales Only)

A physico-chemical model for analysis of the modulated ultra-relativistic electron beam (UREB) spreading in atmospheric plasma created by this beam is described. The mechanism of plasma channel formation in atmosphere is considered and a model of beam interaction with atmospheric plasma channel is calculated numerically. The dependence of instability increment on modulation-frequency, plasma and beam cross-sections, dissipation level and relativistic factor are determined. The proposed model may be applied for description of modulated UREB spreading in low-ionized collision plasma. DOE

N94-10641*# Alabama Univ., Huntsville. Dept. of Electrical and Computer Engineering and CSPAR.

COMPARISON OF HYDRODYNAMIC AND SEMI-KINETIC TREATMENTS FOR PLASMA FLOW ALONG CLOSED FIELD LINES

Nagendra Singh, G. R. Wilson, and J. L. Horwitz 2 Jul. 1993 47 p
(Grant NAGw-2128)
(NASA-CR-193589; NAS 1.26:193589) Avail: CASI HC A03/MF A01

Hydrodynamic and semi-kinetic treatments of plasma flow along closed geomagnetic field lines are compared. The hydrodynamic treatment is based on a simplified 16-moment set of transport equations as the equations for the heat flows are not solved; the heat flows are treated heuristically. The semi-kinetic treatment is based on a particle code. The comparison deals with the distributions of the plasma density, flow velocity, and parallel and perpendicular temperatures as obtained from the two treatments during the various stages of the flow. In the kinetic treatment, the appropriate boundary condition is the prescription of the velocity distribution functions for the particles entering the flux tubes at the ionospheric boundaries; those particles leaving the system are determined by the processes occurring in the flux tube. The prescribed distributions are half-Maxwellian with temperature T(sub 0) and density n(sub 0). In the hydrodynamic model, the prescribed boundary conditions are on density (n(sub 0)), flow velocity (V(sub 0)) and temperature (T(sub 0). It was found that results from the hydrodynamic treatment critically depend on V(sub 0); for early stages of the flow this treatment yields results in good agreement with those from the kinetic treatment, when V(sub 0) = square root of (kT(sub 0)/2 (pi)m), which is the average velocity of particles moving in a given direction for a Maxwellian distribution. During this early stage, the flows developing form the conjugate ionospheres show some distinct transitions. For the first hour or so, the flows are highly supersonic and penetrate deep into the opposite hemispheres, and both hydrodynamics and kinetic treatments yield almost similar features. It is found that during this period heatflow effects are negligibly small. When a flow penetrates deep into the opposite hemisphere, the kinetic treatment predicts reflection and setting up of counterstreaming. In contrast, the hydrodynamic treatment yields a shock in the flow. The reasons for this difference in the two treatments is discussed, showing that in view of the relatively warm ions, the coupling of ion beams and the consequent shock formation in the offequatorial region are not likely due to the enhancements in the beam temperatures. The counterstreaming in the kinetic treatment and the shock in the hydrodynamic treatment first advance upward to the equator and then downward to the ionospheric boundary from where the flow originated. The transit time for this advancement is found to be about 1 hour for the respective models. After 2 hours or so, both models predict that the flows from the ionospheric boundaries are generally subsonic with respect to the local ion-sound speed. At late stages of the flow, when a substantial fraction of ions entering the flux tube begin to return back in the kinetic treatment, the hydrodynamic treatment with the boundary condition V(sub 0) = square root of (kT(sub 0)/2(pi)m) yields an over-refilling, and the choice of V(sub 0) becomes uncertain. Author (revised)

N94-10662 National Inst. for Fusion Science, Nagoya (Japan).

ATOMIC AND MOLECULAR DATA FOR H2O, CO AND CO2 RELEVANT TO EDGE PLASMA IMPURITIES

Hiro Tawara Oct. 1992 78 p Limited Reproducibility: More than 20% of this document may be affected by microfiche quality
(DE93-771423; NIFS-DATA-19) Avail: CASI HC A05

The present status of atomic and molecular data under electron impact involving the most relevant plasma impurity species (H2O, CO, and CO2) has been surveyed and some data have been compiled and evaluated. The emphasis is the cross sections for ionization, dissociation, excitation, photon emission, and recombination processes. DOE

N94-10737 Lawrence Livermore National Lab., CA.

HIGH-FIELD CONDUCTOR TESTING AT THE FENIX FACILITY

S. S. Shen, M. R. Chaplin, B. Felker, W. V. Hassenzahl, K. I. Kishiyama, and J. M. Parker Apr. 1993 6 p Presented at the 8th United States-Japan Workshop on High-Field Superconductors Applied Superconducting Center, Madison, WI, 16-19 Mar. 1993 Limited Reproducibility: More than 20% of this document may be affected by microfiche quality
(Contract W-7405-eng-48)
(DE93-012318; UCRL-JC-113199; CONF-9303157-1) Avail: Issuing Activity (Department of Energy (DOE))

The Fusion Engineering International experiments (FENIX) Test Facility, which was commissioned at the end of 1991, is the first facility in the world capable of testing prototype conductors for the International Thermonuclear Experimental Reactor (ITER) superconducting magnets. The FENIX facility provides test conditions that simulate the ITER magnet operating environment; more importantly, it also accommodates specific experiments to determine the operational margins for the prototype conductors. The FENIX facility generates magnetic fields close to 14 T, and transport currents over 40 kA for testing the prototype conductors. This paper describes an experimental program that measures critical currents, current-sharing temperatures, forced-flow properties, and cyclic effects. DOE

N94-10744 Oak Ridge National Lab., TN.
LOOKING BEYOND ITER: TOROIDAL CONCEPT IMPROVEMENT
J. Sheffield 1993 6 p Presented at the Fusion Power Associates Annual Meeting, La Jolla, CA, 28-29 Jan. 1993 Limited Reproducibility: More than 20% of this document may be affected by microfiche quality
(Contract DE-AC05-84OR-21400)
(DE93-012762; CONF-9301106-1) Avail: CASI HC A02

The International Thermonuclear Experimental Reactor (ITER) will demonstrate ignition and undertake fusion reactor systems integration and testing. Its design will be based upon relatively conservative physics assumptions. More attractive reactor configurations than those based upon ITER physics and the ITER configuration appear possible. The Toroidal Physics Experiment (TPX) will study tokamak behavior under a variety of conditions which may allow operation of improved combinations of beta, transport, and recirculating power. However, TPX still retains a configuration similar to ITER. Two alternative approaches appear interesting, based upon recent experimental results: the very low aspect ratio tokamak, or spherical torus, and the stellarator. DOE

N94-10747# Wisconsin Univ., Madison. Plasma Physics Research.
REVERSED-FIELD PINCH STUDIES IN THE MADISON SYMMETRIC TORUS
S. Hokin, A. Almagri, M. Cekic, B. Chapman, N. Crocker, D. J. DenHartog, G. Fiksel, J. Henry, H. Ji, and S. Prager et al 3 Apr. 1993 18 p
(Contract DE-FG02-85ER-53198)
(DE93-013464; DOE/ER-53198/218) Avail: CASI HC A03/MF A01

Studies of large-size (R = 1.5 m, a = 0.5 m), moderate current (I less than 750 kA), reversed-field pinch (RFP) plasmas are carried out in the Madison Symmetric Torus in order to evaluate and improve RFP confinement, study general toroidal plasma MHD issues, determine the mechanism of the RFP dynamo, and measure fluctuation-induced transport and anomalous ion heating. MST confinement has been improved by reduction of magnetic field errors with correction coils in the primary circuit and reduction of impurities using boronization; high densities have been achieved with hydrogen pellet injection. MHD tearing modes with poloidal mode number m = 1 and toroidal mode numbers n = 5-7 are prevalent and nonlinearly couple to produce sudden relaxations akin to tokamak sawteeth. Edge fluctuation-induced transport has been measured with a variety of insertable probes. Ions exhibit anomalous heating, with increases of ion temperature occuring during strong MHD relaxation. The RFP dynamo has been studied with attention to various possible mechanisms, including motion-EMF drive, the Hall effect, and superthermal electrons. Initial profile control experiments have begun using insertable biased probes and plasma guns. The toroidal field capacity of MST will be upgraded during Summer, 1993 to allow low-current tokamak operation as well as improved RFP operation. DOE

N94-10807 National Inst. for Fusion Science, Nagoya (Japan).
KINETIC APPROACH TO LONG WAVE LENGTH MODES IN ROTATING PLASMAS
T. Yamagishi (Fukui Inst. of Tech., Japan.) Mar. 1992 42 p Limited Reproducibility: More than 20% of this document may be affected by microfiche quality
(DE93-771286; NIFS-138) Avail: CASI HC A03

Stability of low frequency, long wave length modes is studied by a kinetic approach in rotating Maxwellian plasmas. In the rigid rotator model, the centrifugal force due to the plasma rotation strongly destabilizes the ballooning modes, particularly when the Mach number is close to unity. The fluid flow shear weakly stabilizes the ballooning mode. Energetic particles effectively stabilize the ballooning mode, particularly in the high-(beta) region, even in rotating plasmas. The electric potential induced from the radial electric field increases the particle trapping rate for e(sub phi) greater than 0. For phi less than 0, as in tokamaks, the electron trapping rate increases. This destabilizes the dissipative trapped electron mode. DOE

N94-10839 Academy of Sciences of the Ukraine, Kiev. Inst. Teoreticheskoj Fiziki.
THE LANGEVIN'S APPROACH TO THE STATISTICAL THEORY OF BOUNDED PLASMA
A. G. Zagorodnij, A. S. Usenko, and I. P. Yakimenko 1991 15 p Limited Reproducibility: More than 20% of this document may be affected by microfiche quality
(DE93-617842; ITF-91-71) Avail: Issuing Activity (Department of Energy (DOE)) (US Sales Only)

The Langevin approach taking into account the own thermal radiation of the external medium is developed to create the correlation theory of semi-bounded non-equilibrium plasma. The equivalence of results obtained on the basis of the fluctuation-dissipation theorem and using the proposed Langevin approach with allowance for random sources in the whole space is shown. DOE

N94-10840 Academy of Sciences of the Ukraine, Kiev. Inst. Teoreticheskoj Fiziki.
STATIONARY SPECTRA OF SHORT-WAVE CONVECTIVE AND MAGNETOSTATIC FLUCTUATIONS IN A FINITE-PRESSURE PLASMA AND ANOMALOUS HEAT CONDUCTIVITY
M. O. Vakulenko 1992 14 p Limited Reproducibility: More than 20% of this document may be affected by microfiche quality
(DE93-617852; ITP-92-30) Avail: CASI HC A03 (US Sales Only)

Within the general renormalized statistical approach, the low-frequency short-wave stationary spectra of potential and magnetic perturbations in a finite-pressure plasma are obtained. Anomalous heat conductivity considerably enhances due to non-linear interaction between magnetic excitations. DOE

N94-10852# Wisconsin Univ., Madison. Plasma Physics Research.
MAGNETOHYDRODYNAMIC COMPUTATION OF FEEDBACK STABILIZATION OF RESISTIVE-SHELL INSTABILITIES IN THE REVERSED FIELD PINCH Ph.D. Thesis
E. J. Zita 1993 68 p
(Contract DE-FG02-85ER-53212)
(DE93-013466; DOE/ER-53212/212) Avail: CASI HC A04/MF A01

MHD computations demonstrate that feedback can sustain reversal and reduce loop voltage in resistive-shell reversed field pinch (RFP) plasmas. In the absence of a close-fitting conducting shell, feedback with conducting coils on approximately 2R/a tearing modes resonant near axis is found to restore plasma parameters to nearly their levels with a close-fitting conducting shell. When original dynamo modes are stabilized, neighboring tearing modes grow to maintain the RFP dynamo more efficiently. This suggests that experimentally observed limits on RFP pulselengths to the order of the shell time can be overcome by applying feedback to a few helical modes. Feedback with resistive coils yields information on requirements for more physically realistic feedback systems and on the potentiality of improvement of resistive-shell plasma parameters beyond the conducting-shell case. Plasma response to shell rotation is investigated, and issues relevant to mode locking and feedback rotation of individual modes are discussed. DOE

N94-10882 Academy of Sciences of the Ukraine, Kiev. Inst. Teoreticheskoj Fiziki.
FILAMENTATION INSTABILITY OF HOT QUARK-GLUON PLASMA WITH HARD JET

O. P. Pavlenko 1991 18 p Limited Reproducibility: More than 20% of this document may be affected by microfiche quality
(DE93-617679; ITP-91-103) Avail: CASI HC A03 (US Sales Only)

The filamentation instability of the quark-gluon plasma (QGP) caused by the hard jet of colored partons propagating through QGP is considered. The analysis is carried out with the successive account of plasma dispersion characteristics related to the expected high temperature of the quark-gluon matter in ultrarelativistic nuclear collisions. It is pointed to the opportunity for the diagnostics of the QGP initial temperature using hard jets on the basis of the filamentation effect. DOE

N94-10885 Academy of Sciences of the Ukraine, Kiev. Inst. Teoreticheskoj Fiziki.

SPATIAL HELICON-WAVE ECHO IN AN INHOMOGENEOUS MAGNETIZED PLASMA

E. A. Fedutenko, V. I. Lapshin, and A. G. Zagorodnij 1992 18 p Limited Reproducibility: More than 20% of this document may be affected by microfiche quality
(DE93-617845; ITP-92-1) Avail: CASI HC A03 (US Sales Only)

This paper investigates the possibility of the existence of the spatial helicon-wave echo in an inhomogeneous magnetized plasma. Values of generation coordinate and electro-magnetic fields of plasma responses on two and three wave external perturbations are obtained. The analysis shows the possibility of the using of this effect for plasma diagnostics. DOE

N94-10886 Academy of Sciences of the Ukraine, Kiev. Inst. Teoreticheskoj Fiziki.

DISTRIBUTION OF CHARGED PARTICLES NEAR THE PLASMA BOUNDARY IN THE PRESENCE OF EXTERNAL ELECTRIC FIELD

G. M. Korchinskij, I. P. Yakimenko, and A. G. Zagorodnij 1991 25 p Limited Reproducibility: More than 20% of this document may be affected by microfiche quality
(DE93-617862; ITP-91-58) Avail: Issuing Activity (Department of Energy (DOE)) (US Sales Only)

On the basis of the proposed numerical procedure the solution of the nonlinear Boltzmann-Poisson equation for bounded plasma in the presence of strong external electric field is obtained. The numerical analysis of the electric field, potential, and equilibrium profiles of charged particles distributions in the plasma half-space is performed in detail. DOE

N94-11074# Lawrence Livermore National Lab., CA.

ELECTRON TEMPERATURE MEASUREMENTS OF X RAY LASER PLASMAS

B. K. F. Young, A. L. Osterheld, R. L. Shepherd, G. M. Shimkaveg, C. J. Cerjan, W. H. Goldstein, M. D. Rosen, R. S. Walling, and R. E. Stewart Aug. 1992 4 p Presented at the 3rd International Colloquium on X Ray Lasers, Schliersee, Germany, 18-22 May 1992
(Contract W-7405-eng-48)
(DE93-011874; UCRL-JC-109804; CONF-920523-9) Avail: CASI HC A01/MF A01

We present results of recent experiments at the NOVA laser to measure the electron temperature of neon-like yttrium X-ray laser plasmas. Trace amounts of aluminum were introduced into yttrium exploding-foil targets. Time resolved electron temperatures were determined by comparing the measured aluminum K-shell spectra with detailed quasi-steady state calculations and are compared to 2D LASNEX hydrodynamics simulations. DOE

N94-11091 Academy of Sciences of the Ukraine, Kharkov. Fiziko-Tekhnicheskij Inst.

CALCULATION OF MERCIER STABILITY CRITERIUM IN STELLARATORS [RASCHETY KRITERIYA USTOJCHIVOSTI MERS'E V STELLARATORAKH]

V. V. Nemov 1991 19 p In RUSSIAN Limited Reproducibility: More than 20% of this document may be affected by microfiche quality
(DE93-621599; KFTI-91-44) Avail: CASI HC A03 (US Sales Only)

A method of Mercier stability criterium calculation in stellarators that takes into account the real distribution of their magnetic field is discussed. It is based on integration along magnetic force lines. This criterium was calculated for a slow pressure plasma with a finite local pressure gradient in the magnetic configuration of a torsatron with parameters close to those of 'Uragan-2M.' DOE

N94-11092 Gosudarstvennyi Komitet po Ispolzovaniyu Atomnoi Energii, Moscow (USSR).

POSSIBILITIES OF MAGNETIC DIAGNOSTICS IN STELLARATORS [VOZMOZHNOSTI MAGNITNOJ DIAGNOSTIKI V STELLARATORAKH]

V. K. Pashnev 1991 19 p In RUSSIAN Limited Reproducibility: More than 20% of this document may be affected by microfiche quality
(DE93-621608; KFTI-91-35) Avail: CASI HC A03 (US Sales Only)

Magnetic diagnostic methods can be used successfully in tokamaks, but a direct application of these methods in stellarators gives little effect. However, an additional measuring of magnetic fields in the helical plasma current allows us to obtain information about the limit parameters of magnetic configuration and additional integral relations compared with tokamaks. Measurements of plasma current magnetic fields outside of the plasma confinement volume in stellarators allow us to determine the profiles of important plasma parameters and the magnetic configuration. DOE

N94-11114# Lawrence Livermore National Lab., CA. Plasma Physics Research Inst.

THE ANGULAR STRUCTURE OF SECOND HARMONIC EMISSION FROM LASER-PRODUCED PLASMAS IRRADIATED AT MODERATE INTENSITY

R. P. Drake (California Univ., Davis.), B. S. Bauer, K. L. Baker (California Univ., Davis.), K. Mizuno (California Univ., Davis.), B. Sleaford (California Univ., Davis.), A. M. Rubenchik (California Univ., Davis.), K. Estabrook (California Univ., Davis.), C. Labaune (Ecole Polytechnique, Palaiseau, France.), S. Baton (Ecole Polytechnique, Palaiseau, France.), and T. Jalinaud (Ecole Polytechnique, Palaiseau, France.) et al Apr. 1993 6 p
(Contract W-7405-eng-48)
(DE93-013102; UCID-113435) Avail: CASI HC A02/MF A01

The authors have made the first simultaneous, multi-angle measurements of the time-resolved spectrum of second-harmonic emission from a laser-produced plasma. The experiments used from 1 to 80 J of 1.053 micron light to irradiate CH targets with 550 ps Gaussian pulses through a random phase plate. The intensities in the range of 10(exp 13) to 10(exp 14) W/sq cm were sufficient to drive the Ion Acoustic Decay Instability well above threshold, producing Stokes emission well-separated from the emission spike at the second harmonic of the laser frequency. The spectral structure of the Stokes emission was qualitatively similar for all intensities and angles of observation. DOE

N94-11118# Rice Univ., Houston, TX. Dept. of Space Physics and Astronomy.

RADIATIVE PROPERTIES OF STRONGLY MAGNETIZED PLASMAS

J. C. Weisheit Dec. 1992 4 p
(Contract DE-FG05-91ER-14213)
(DE93-014098; DOE/ER-14213/1) Avail: CASI HC A01/MF A01

The subject of atomic properties in the presence of very strong magnetic fields is experiencing a new wave of interest, especially insofar as non-hydrogenic systems are concerned, and we believe the research summarized here is on the crest of that wave. Only recently, the following articles have appeared: a major review of Thomas-Fermi theory; a new set of fundamental theorems pertaining to the Hamiltonian of a (Thomas-Fermi) atom in a strong field; and the first numerical, Hartree-Fock (HF) results for multi-electron atoms in strong B fields, but obtained under the restrictive assumption that the (rho)- and z-dependence of individual orbitals is completely separable. DOE

N94-11119 Gosudarstvennyi Komitet po Ispolzovaniyu Atomnoi Energii, Moscow (USSR).

CHARGED PARTICLE MOTION IN TORSATRONS, PART 1

M. S. Smirnova and A. A. Shishkin 1991 16 p Limited Reproducibility: More than 20% of this document may be affected by microfiche quality
(DE93-621639; KFTI-91-23-Pt-1) Avail: CASI HC A03 (US Sales Only)

The motion of collisionless particles and their confinement conditions in l = 2 torsatrons are analyzed. The considered devices were similar to real torsatron configurations such as Uragan-2M, ATF, and Heliotron E which differ in the number of helical field periods (M), ripple amplitude ratio (E(sub t)/E(sub l)), and in the spectrum of the helical magnetic field. The influence of the different compositions of the spectrum on the particle confinement was considered. DOE

N94-11120 Gosudarstvennyi Komitet po Ispolzovaniyu Atomnoi Energii, Moscow (USSR).
PARTICLE TRANSPORT ANALYSIS IN TORSATRON CONFIGURATIONS
M. S. Smirnova 1991 23 p Limited Reproducibility: More than 20% of this document may be affected by microfiche quality
(DE93-621640; KFTI-91-24) Avail: CASI HC A03 (US Sales Only)

The paper analyzes the transport and loss of particles in $l = 2$ torsatrons in the absence of the electric field. The parameters of the devices considered are similar to the real torsatron configurations of Uragan-2M and Heliotron E. The parameters differ in the number of helical field periods over the device length (M), in the ripple amplitude ratio (E(sub t)/E(sub l)), and the harmonic spectrum of the helical magnetic field. Numerical simulation of particle motion, taking the collisions into consideration, is performed by a Monte-Carlo method. The optimum criterion of the helical magnetic field harmonic spectrum from the point of view of particle confinement and transport in plasma is formulated. DOE

N94-11121 Academy of Sciences of the Ukraine, Kharkov. Fiziko-Tekhnicheskij.
PROBABILITY OF PARTICLE TRAPPING/DETRAPPING IN TORSATRONS
I. N. Sidorenko 1991 25 p Limited Reproducibility: More than 20% of this document may be affected by microfiche quality
(DE93-621641; KFTI-91-36) Avail: CASI HC A03 (US Sales Only)

By applying Kruskal's theorem, the analytical formulas of collisionless transition probability between classes of locally passing particles and helical trapped particles in magnetic configurations with complicated harmonic spectrum and radial electric field accounting have been obtained. Based on this analytical consideration, the conclusions were made about the fraction of trapped particles in the URAGAN-2M, ATF-1, HELIOTRON-E, and CHS configurations. The electric field potential at which this fraction is a minimum is also obtained. DOE

N94-11125# Lawrence Livermore National Lab., CA.
PHYSICS OF TOKAMAK SCRAPE-OFF LAYER CONFINEMENT
R. H. Cohen Mar. 1993 8 p Presented at the International Topical Conference on New Ideas in Tokamak Confinement, La Jolla, CA, 27-29 Jan. 1992
(Contract W-7405-eng-48)
(DE93-011949; UCRL-JC-109333; CONF-920142-4) Avail: CASI HC A02/MF A01

Confinement in the scrape-off layer (SOL) of a tokamak is believed to be governed by classical flows along magnetic field lines terminated by sheaths, and turbulent transport across field lines. In this paper, we review how these two effects conspire to establish the width of the SOL, and survey recent and ongoing work on mechanisms for turbulence in SOL's. The beneficial relationship between scrape-off layer turbulence in mitigating the heat flux density on divertors is noted, and tactics for actively altering SOL confinement so as to reduce the heat flux density are discussed. DOE

N94-11128# Nagoya Univ. (Japan). Plasma Science Center.
SIMULATION STUDY OF DYNAMO STRUCTURE IN REVERSED FIELD PINCH
A. Nagata (Osaka Inst. of Tech., Japan.), K. I. Sato, H. Ashida (Electrotechnical Lab., Ibaraki, Japan.), and T. Amano (National Inst. for Fusion Science, Nagoya, Japan.) Oct. 1992 23 p
(DE93-771406; PSC-24) Avail: CASI HC A03/MF A01

The dynamo structure in the reversed field pinch (RFP) is studied through the nonlinear dynamics of the single-helicity mode. Simulation is concentrated upon the physical structure of nonlinear interactions of the plasma flow and magnetic fluctuation. The result indicates that when the initial equilibrium profile is deformed by resistive diffusion, the radial flow is driven near the core of the plasma. As this flow forms a vortex structure and the magnetic fluctuation grows radially, the dynamo electric field is spirally induced just inside the reversal surface, and then, the toroidal flux is increased. This dynamo electric field correlates to nonlinear evolution of the kinetic energy of $m=1$ mode, and the increase of the toroidal flux is originated in the growth process of the magnetic energy of this mode. Consequently, the RFP configuration can be sustained by the single-helicity evolution of $m=1$ mode alone, and the electric field induced by the interactions of the toroidal velocity and the radial magnetic field is the most dominant source on the dynamo action. DOE

N94-11142# Texas Univ., Austin. Inst. for Fusion Studies.
GYROSHEATH NEAR THE TOKAMAK EDGE
R. D. Hazeltine, H. Xiao, and P. M. Valanju Mar. 1993 14 p
(Contract DE-FG05-80ET-53088)
(DE93-012191; DOE/ET-53088/599) Avail: CASI HC A03/MF A01

A new model for the structure of the radial electric field profile in the edge during the H-mode is proposed. Charge separation caused by the difference between electron and ion gyromotion, or more importantly in a tokamak, the banana motion (halo effect) can self-consistently produce an electric dipole moment that causes the sheared radial electric field. The calculated results based on the model are consistent with D-3D and TEXTOR experimental results. DOE

N94-11148# Technical Research Centre of Finland, Espoo.
STUDIES ON THE PARAMETRIC DECAY OF WAVES IN FUSION PLASMAS Ph.D. Thesis
T. Paettikangas Aug. 1992 166 p Prepared in cooperation with Helsinki Univ. of Technology, Otaniemi, Finland
(DE93-621659; VTT-PUB-110; ISBN-951-38-4228-2) Avail: CASI HC A08

Parametric instabilities of large-amplitude electromagnetic waves are investigated in fusion applications. In laser fusion, the electromagnetic wave reflected from the overdense plasma can act as a secondary pump wave and exite parametric instabilities. In double simulated Brilloun scattering (DSBS), both the incoming and the reflected pump wave scatter from a common ion sound wave. The stationary states and the dynamics of DSBS are investigated by using a simple envelope model. The ion sound wave that is exited in DSBS is shown to have soliton-like properties. The simulated Raman scattering (SRS) of free-electron-laser radiation can be applied to current drive in tokamaks. SRS generates fast longitudinal electron plasma waves which accelerate electrons to relativistic energies. Since the energetic current-carrying electrons are almost collisionless, the current decays very slowly. The feasibility of the Raman current drive in tokamaks is investigated theoretically. The current drive efficiency and the optimum free-electron-laser parameters are determined. The energy transfer to the fast electrons from the electrostatic wave is studied with relativistic Vlasov-Maxwell simulations. The parametric decay of a wave to half-harmonics is investigated. It is shown that the growth rate of the decay vanishes in the limit of a long wavelength of the pump wave even for general electromagnetic or electrostatic decay models. The results are applied to the decay of a fast magnetosonic waves in tokamak plasmas. DOE

N94-11149# Japan Atomic Energy Research Inst., Tokyo. Dept. of Fusion Plasma Research.
MOMENTUM AND HEAT FRICTIONS BETWEEN FAST IONS AND THERMAL PLASMA SPECIES
Jianping Wang, Masafumi Azumi, Keiji Tani, and J. D. Callen (Wisconsin Univ., Madison.) Jun. 1992 29 p
(DE93-771240; JAERI-M-92-087) Avail: CASI HC A03/MF A01

Momentum and heat friction forces between fast ions (isotropic to the lowest order) and thermal bulk plasma species (near Maxwellian) have been derived analytically for the first time using the linearized Fokker-Planck collision operator. Therefore effects of flow-type distortion of test particles and flow-type restoring from field particles are both retained self-consistently. w(sub (alpha)) (identical to) v-V(sub (alpha)) represents the random velocity measured in moving reference frame of test particles, and the superscript (alpha)/(beta) denotes test particles of (alpha) species colliding with field particles of (beta) species. The momentum and heat friction forces have been explicitly calculated for electron-fast ion collisions (F(sub K)(sup e/f)), fast ion-electron collisions (F(sub K)(sup f/e)), thermal ion-fast ion collisions (F(sub K)(sup i/f)) and fast ion-thermal ion collisions (F(sub K)(sup f/i)) wherein the subscripts k's correspond to the indices of Laguerre polynomials ($k = 0, 1$). The collisional moment matrix is shown asymmetric in the presence of fast ions because the approximate self-adjointness of the Coulomb collision operator is no longer a valid property. (author). DOE

N94-11170# Massachusetts Inst. of Tech., Cambridge. Plasma Fusion Center.
EXPERIMENTAL APPROACH TO THE PHYSICS OF THE HIGH DENSITY DIVERTOR
I. H. Hutchinson Mar. 1993 11 p
(Contract DE-AC02-78ET-51013)
(DE93-009149; DOE/FTR-93009149) Avail: CASI HC A03/MF A01 (US Sales Only)

The workshop was held from 25th to 27th February at the ITER co-center at Garching. The agenda is attached. Initial discussions focussed on the direction of the meeting. Parker expressed a hope that physics would emerge. Rebut outlined 3 elements of an approach to solving the divertor problem: (1) work on existing tokamaks; (2) code modelling; and (3) a simulator. Rebut wants to progress rapidly to identify a plan or agreement on work package(s) focused on ITER. Credit would be decided on a case-by-case basis. In answer to Parker's question whether a new specific divertor on an existing machine could receive credit, Rebut said, maybe. His view is that 20-30 million dollars is being spent on a coil testing facility and a roughly similar amount could be spent on divertor testing. It emerged later that Rebut's conception is that this would be a (single probably) facility designed to achieve dimensional equality (as far as possible) with ITER. DOE

N94-11171# Oak Ridge National Lab., TN.
INTENSE NEUTRON SOURCES FOR FUSION MATERIALS STUDIES
E. E. Bloom and M. J. Saltmarsh 26 Oct. 1992 17 p
(DE93-009782; ORNL/FTR-4444) Avail: CASI HC A03/MF A01 (US Sales Only)

The purpose of the trip was to participate in the International Energy Agency (IEA) Workshop on Intense Neutron Sources for Fusion Materials Studies; to discuss neutron source design issues with groups at Kernforschungszentrum Karlsruhe (KfK), Germany; the Culham and Joint European Torus (JET) Laboratories in the United Kingdom; and the Institut for Festkorperforschung, KFA Juelich, to discuss recent progress in fusion materials research and development. DOE

N94-11174 Academy of Sciences of the Ukraine, Kharkov. Fiziko-Tekhnicheskij Inst.
ANALYTICAL DESCRIPTION OF THE TORSATRON URAGAN-2M MAGNETIC CONFIGURATION WITH ACCOUNT OF PLASMA PRESSURE AND EXTERNAL CORRECTING MAGNETIC FIELD [ANALITICHESKOE OPISANIE MAGNITNOJ KONFIGURATSII TORSATRONA URAGAN-2M S UCHETOM DAVIENIYA PLAZMY I VNESHNEGO KORREKTIRUYUSHCHEGO MAGNITNOGO POLYA]
Y. K. Kuznetsov, I. B. Pinos, and V. I. Tyupa 1992 20 p In RUSSIAN Limited Reproducibility: More than 20% of this document may be affected by microfiche quality
(DE93-620983; KFTI-92-31) Avail: CASI HC A03 (US Sales Only)

Universal analytical expressions for determination of rotating transformation angles and an average magnetic hole stipulated by plasma pressure and external homogeneous transversal magnetic field are obtained with the help of averaging formulae. Analytical calculations of rotating transformation angles with account of an external transversal magnetic field for the torsatron 'Uragan-2M' are in a good agreement with numerical ones. DOE

N94-11207 Academy of Sciences of the Ukraine, Kharkov. Fiziko-Tekhnicheskij Inst.
KINETIC EFFECTS IN STOCHASTIC TOPOLOGICALLY NONTRIVIAL FIELD
A. V. Chechkin, A. V. Tur, and V. V. Yanovskij 1992 31 p Limited Reproducibility: More than 20% of this document may be affected by microfiche quality
(DE93-621642; KFTI-92-25) Avail: CASI HC A03 (US Sales Only)

The kinetic description of a particle system in an external, stochastic, helical field is examined. The kinetic equation is obtained, which contains an additional term proportional to the helicity. A solution that describes the evolution of the distribution function for arbitrary initial conditions is found. Particular examples of such an evolution and some new kinetic effects, connected with helicity, are discussed. It is shown that a particle beam with inhomogeneous velocity profile in an external stochastic helical field generates a new particle flow in the transverse direction. DOE

N94-11208 Academy of Sciences of the Ukraine, Kharkov. Fiziko-Teknicheskij Inst.
SIMPLE KINETIC MODEL FOR PLASMA IN STOCHASTIC HELICAL FIELD
A. V. Chechkin, A. V. Tur, and V. V. Yanovsky 1992 24 p Limited Reproducibility: More than 20% of this document may be affected by microfiche quality
(DE93-621643; KFTI-92-43) Avail: CASI HC A03 (US Sales Only)

The kinetic equation for a plasma in a stochastic electromagnetic helical field is constructed and examined. The kinetic equation contains an additional term, proportional to the helicity. The solution describing the evolution of the distribution function for arbitrary initial conditions is found, and the possible consequences of the presence of the helicity term are discussed. A model example is considered for when a single-momentum electron beam with inhomogeneous velocity profile creates a new particle flow in transverse direction, so that the resulting flow also possesses helicity. DOE

N94-11209 Academy of Sciences of the Ukraine, Kharkov. Fiziko-Tekhnicheskij Inst.
ELEMENTARY MECHANISM OF ELECTRON BEAM DISSIPATIVE INSTABILITY DEVELOPMENT [EHLEMENTARNYJ MECHANIZM RAZVITIYA DISSIPATIVNOJ NEUSTOJCHIVOSTI EHLEKTRONNOGO PUCHKA]
V. I. Miroshnichenko, A. E. Volkov, A. P. Tolstoluzhskij, and Y. B. Fajnberg 1991 7 p In RUSSIAN Limited Reproducibility: More than 20% of this document may be affected by microfiche quality
(DE93-621653; KFTI-91-38) Avail: CASI HC A02 (US Sales Only)

A mechanism of dissipative instability development was determined. Such factors as an electromagnetic field created by a single electron moving in a dissipative medium, the addition of electromagnetic fields resulting from superposition of separate electron fields and forming a modulated stream, and an inverse influence of the resulting field on electromagnetic stream modulation degree were considered. DOE

N94-11210 Academy of Sciences of the Ukraine, Kharkov. Fiziko-Tekhnicheskij Inst.
DISPERSION OF PLASMA WAVES IN A FINITE MAGNETIC FIELD (OMEGA(SUB H) GREATER THAN OMEGA(SUB p)) [DISPERSIYA PLAZMENNYKH VOIN V KONECHNOM MAGNITNOM POLE (OMEGA(H)>OMEGA(P))]
I. N. Onishchenko and G. V. Sotnikov 1991 23 p In RUSSIAN Limited Reproducibility: More than 20% of this document may be affected by microfiche quality
(DE93-621654; KFTI-91-41) Avail: CASI HC A03 (US Sales Only)

Dispersion plasma wave properties and their particularities for the case when the relation of electron to plasma gyrofrequencies has a finite value are investigated. Three models were used: an oblique wave in unlimited magnetoactive plasma; a cylindrical metal waveguide filled completely with magnetoactive plasma; and a tubular plasma waveguide. The results obtained in these models are compared. DOE

N94-11211 Academy of Sciences of the Ukraine, Kharkov. Fiziko-Tekhnicheskij Inst.
EXPERIMENTAL INVESTIGATION OF WAKE FIELD EXCITATION IN PLASMA BY A PERIODIC SUCCESSION OF RELATIVISTIC PARTICLE CLOTS [EHKSPERIMENTAL'NYE ISSLEDOVANIYA VOZBUZHDENIYA KIL'VATORNYKH POLEJ V PLAZME PERIODICHESKOJ POSLEDOVATEL'NOST'YU SGUSTKOV RELYATIVISTSKIKH CHASTITS]
A. K. Berezin, V. A. Kiselev, A. F. Linnik, I. N. Onishchenko, G. V. Sotnikov, V. V. Uskov, and Y. B. Fajnberg 1991 14 p In RUSSIAN Limited Reproducibility: More than 20% of this document may be affected by microfiche quality
(DE93-621655; KFTI-91-45) Avail: CASI HC A03 (US Sales Only)

Experimental results of wake field excitation in plasma and in gas by a periodic succession of short relativistic particle clots obtained with the help of a resonance linear accelerator are presented. Electron energy is 2 MeV, clot duration is 60 ps, and the number of particles in a clot is 2 x 10(exp 9). The density of plasma used in experiments provides a resonance between plasma frequency and clot succession frequency. In this case the modulated beam-plasma interaction is represented by a sum of wake fields depending on the number of clots and accompanied by interference and stochastic effects. DOE

N94-11212 Academy of Sciences of the Ukraine, Kharkov. Fiziko-Tekhnicheskij Inst.

NEGATIVE VISCOSITY AND GENERATION OF DISSIPATIVE SOLITONS AND ZONAL DISSIPATIVE STRUCTURES BY DRIFT WAVES

A. V. Chechkin, A. V. Tur, and V. V. Yanovskij 1991 35 p Limited Reproducibility: More than 20% of this document may be affected by microfiche quality

(DE93-621656; KFTI-91-50) Avail: Issuing Activity (Department of Energy (DOE)) (US Sales Only)

The stability of drift waves in a plasma with dissipation due to ion viscosity is examined. If the wave amplitude exceeds a threshold value, determined by ion-ion collisions, large-scale perturbations (i.e., with scales much greater than the drift wave length) grow. This effect is analogous to the negative viscosity effect in hydrodynamics. Maximum growth rate belongs to perturbations which are periodical along plasma inhomogeneity and constant in the transverse direction, i.e. azimuthal direction in cylindrical geometry (zonal dissipative structures). The analysis of the nonlinear stage of large-scale instability shows that the soliton-like large-scale structures of the electric field and vorticity are possible (dissipative solitons). DOE

N94-11213 Academy of Sciences of the Ukraine, Kharkov. Fiziko-Tekhnicheskij Inst.

SPREADING OF BIMODULATED ULTRA-RELATIVISTIC ELECTRON BEAM (BUEB) IN ATMOSPHERIC PLASMA CHANNEL (APCh) [RASPROSTRANENIE BIMODULIROVANNOGO UL'TRA RELYATIVISTSKOGO EHLEKTRONNOGO PUCHKA V ATMOSFERNOM PLAZMENNOM KANALE]

V. P. Zejdlits, V. I. Tkachenko, N. I. Ajzatskij, Y. V. Tkach, G. A. Miroshnichenko, and N. G. Pavlenko 1992 11 p In RUSSIAN Limited Reproducibility: More than 20% of this document may be affected by microfiche quality

(DE93-621658; KFTI-92-41) Avail: CASI HC A03 (US Sales Only)

The space-time structure of the bimodulated ultra-relativistic electron beam (BUEB) spreading in an atmospheric plasma channel (APCh) with a combined frequency was investigated experimentally. It was shown that such a beam spreads in APCh rather steadily on the distances defined by experimental conditions. A noticeable stabilization of its cross section was observed. An agreement with the earlier proposed theoretical model modified for a bimodulated beam was noted. A conclusion about the stabilizing influence of the low-frequency BUEB current modulation on its transportation in a high-dissipative plasma channel was made. DOE

N94-11214 Gosudarstvennyi Komitet po Ispolzovaniyu Atomnoi Energii, Moscow (USSR).

CHARACTERISTICS OF ICR-PRODUCED PERIPHERAL PLASMA IN THE URAGAN-3M TORSATRON

N. T. Besedin, V. V. Chechkin, and I. P. Fomin et al 1991 28 p Limited Reproducibility: More than 20% of this document may be affected by microfiche quality

(DE93-621666; KFTI-91-26) Avail: CASI HC A03 (US Sales Only)

Some plasma parameters outside the confinement volume near the last closed magnetic surface (LCMS) and in the divertor fluxes were studied by probe and microwave techniques during ICR production and heating of the plasma in the Uragan-3M torsatron. When moving around the LCMS, the steepness of the radial density, electron temperature, and potential profiles increase with distance away from the 'rib' of the LCMS. The quasi-steady radial electric field E(sub r) near the LCMS exceeds 100 V/cm and is directed outwards, opposite to the calculated ambipolar electric field inside the confinement volume. It is shown that the total flow of the diverted plasma in the spacing between two helical windings consists of a weakly mobile non-resonant component which is presumably formed at the periphery due to ionization, and a component whose value and poloidal location are sensitive to resonance conditions for RF power absorption, this flow being apparently formed by a plasma diffusing through the LCMS and/or generated near the LCMS, where the filed E(sub r) is localized. Based on plasma parameters measurements after the RF pulse is switched off, a qualitative model of peripheral plasma dynamics after the end of the RF heating is constructed. DOE

N94-11215 Academy of Sciences of the Ukraine, Kharkov. Fiziko-Tekhnicheskij Inst.

MAGNETIC ISLAND SUPPRESSION IN TORSATRON CONFIGURATIONS

A. V. Zolotukhin and A. A. Shishkin 1991 24 p Limited Reproducibility: More than 20% of this document may be affected by microfiche quality

(DE93-621681; KFTI-91-47) Avail: CASI HC A03 (US Sales Only)

An analytical approach is developed for the study of magnetic resonance structures in the vacuum magnetic configurations as well as with the plasma at low pressure (the low (beta)). The purpose of the paper is to find a feasible method for the magnetic island size control. It is realized, in particular, by the way of current redistribution in poloidal windings of the magnetic field. DOE

N94-11239# Nagoya Univ. (Japan). Plasma Science Center.

MACROSCOPIC BEHAVIOUR AND DISCRETE DYNAMO OF RFP PLASMA IN HIGH THETA DISCHARGE

H. Arimoto, K. I. Sato (Osaka Inst. of Tech., Japan.), A. Nakamura, A. Nagata (Osaka Inst. of Tech., Japan.), T. Ando, S. Kubota, S. Masamune (Kyoto Inst. of Tech., Japan.), M. Nagatsu, and T. Tsukishima Oct. 1992 20 p

(DE93-771408; PSC-26) Avail: CASI HC A03/MF A01

In this paper, the macroscopic MHD behavior of the RFP plasma produced by the high theta discharge is presented compared with that of the RFP plasma produced by the normal (ordinary) discharge, where theta is the ratio of the poloidal field at the wall to the averaged toroidal field. In the plasma generated by the high theta discharge, the mode coupling is frequently occurred due to its high magnetic shear configuration and the fluctuation is more turbulent. The discrete dynamo, which pulsively generates the toroidal flux in the high theta discharge plasma, is also examined. The results show that the discrete dynamo does not play an essential roll in the RFP dynamo. DOE

N94-11450 Massachusetts Univ., Lowell.

CHARACTERIZATION OF AN EXCIMER LASER-ABLATED PLASMA AND APPLICATIONS Ph.D. Thesis

Yong-Ill Lee 1992 205 p

Avail: Univ. Microfilms Order No. DA9311920

Laser ablation and the subsequent development of a high energy dense plasma are receiving increased attention for spectrochemical analysis of solid materials. Observation of the plasma using atomic emission spectroscopy is the most direct method for analysis and offers the possibility of simultaneous multielement analysis. The use of a powerful UV excimer laser for ablation is of growing interest because of the low reflectivity for most solid materials. The excimer laser improves energy coupling efficiency by offering the relatively short wavelength. The details for construction and operation of an excimer laser-ablated plasma with a wavelength of 193 nm are described. The characterization and evaluation of a new kind of excimer laser-ablated plasma and applications for direct spectrochemical analysis were investigated through time- and space-resolved spectroscopy. The characteristics of the plasma that were studied included the appearance, excitation temperature, emission spectra, ambient gas breakdown, ionization efficiency, and analytical performances. The shape, size, emission spectra, and excitation temperatures of the laser-ablated plasma are largely dependent on the atmospheric surroundings, the ambient gas composition, the pressure, and laser energy. Spatial discrimination may be desirable to increase the line-to-background (L/B) ratio in atomic emission spectroscopy. A reduced pressure (optimum pressure; 10 Torr) in argon atmosphere may be useful for laser-ablated atomic emission spectroscopy (LAAES) applications which give a high intensity and large L/B ratio for the analytical signal. Metal ion formation in the plasma varies with time as well as location in the plasma. Ion lines were emitted close to the target, while the atomic lines appeared in the further regions of the plasma. The ion concentration was dependent on the position in the plasma and reflected the local temperature in the plasma. Gas breakdown in the plasma influenced the plasma formation and the analytical emission intensity. Argon gas breakdown was observed in the plasma. The relationship between gas breakdown and the physical properties of different metal species was deduced and provided a confirmation of theoretical modeling of the laser-ablated plasma interactions. A direct spectrochemical analytical method for solid samples with good linearity was developed using the excimer laser-AES. The sensitivity of the analytical signal varied depending on the chemical matrix of the solid samples. A typical detection limit for potassium in a glass matrix was 0.13 micro-g/g and for chromium in a steel-alloy matrix was 18.7 micro-g/g. These applications demonstrate the potential of excimer laser-AES for direct spectrochemical analysis. Dissert. Abstr.

N94-11474# Naval Research Lab., Washington, DC.
ADVANCED CONCEPTS THEORY ANNUAL REPORT 1992 Final Report
26 May 1993 120 p
(AD-A266132; NRL/MR/6722-93-7301) Avail: CASI HC A06/MF A02

This report details the work of the Radiation Hydrodynamics Branch conducted in FY92 with respect to several critical problems concerning the design and analysis of z-pinch experiments, the electron dynamics of z-pinch implosions, and the optimization of their radiative output. Separate sections describe progress in: (1) the design of z-pinch wire and gas puff experiments, (2) the analysis and scaling of z-pinch experiments using phenomenological turbulence transport parameters, (3) the development of a non-Maxwellian electron distribution function analysis from which to calculate turbulence enhanced transport coefficients, (4) the development of L-shell atomic models, (5) the analysis of PRS argon experiments, and (6) the development of a POS transmission line model with which to study power flow in IES machines, POS/PRS interactions, and energy coupling to PRS loads. DTIC

N94-11477 Academy of Sciences of the Ukraine, Kiev. Inst. Teoreticheskoj Fiziki.
DECAY INTERACTION OF BULK AND SURFACE LANGMUIR WAVES
V. I. Zasenko 1991 19 p Limited Reproducibility: More than 20% of this document may be affected by microfiche quality
(DE93-617843; ITF-91-73) Avail: Issuing Activity (Department of Energy (DOE)) (US Sales Only)

Nonlinear stage of decay instability of surface waves in the field of bulk wave is considered. It is shown that amplitude of surface oscillations are saturated. DOE

N94-11512# Illinois Univ., Urbana. Fusion Studies Lab.
THE ROLE OF PLASMA ROTATION ON MHD INSTABILITIES IN TOKAMAKS
V. Varadarajan and G. H. Miley 1993 19 p Presented at the 6th Transport Task Force Workshop, Newport, RI, 21-25 Feb. 1993
(Contract DE-FG02-90ER-54092)
(DE93-013486; CONF-930281-7) Avail: CASI HC A03/MF A01

An improved analysis of the linear stage of the internal kink mode has been developed to include plasma rotation and finite aspect ratio effects. The linear instability growth rates are increased by the plasma rotation. A pseudo-variational, bilinear formalism is used to discretize the linear instability equations; Fourier decomposition is used in the periodic coordinate, and a mixed-finite element procedure is adopted in the radial direction. The numerical studies with the resulting PEST-like code can be used to predict the complex plasma eigenfrequencies. The finite aspect ratio results are similar to the large aspect ratio results for flow instability. The complex instability frequencies found in the 'fishbone' and TAE modes would be strong determined by the large plasma rotation velocities observed in present-day tokamak devices. These effects could be studied by using the computationally convenient bilinear form derived from the Frieman-Rotenberg equation. DOE

N94-11513# Illinois Univ., Urbana. Fusion Studies Lab.
HELIUM TRANSPORT SCALING LAW STUDIES
Junpeng Guo and G. H. Miley Nov. 1992 9 p Presented at the Meeting of the Division of Plasma Physics of the American Physical Society, Seattle, WA, 16-20 Nov. 1992
(Contract DE-FG02-90ER-54092)
(DE93-013487; CONF-921103-11-App-B) Avail: CASI HC A02/MF A01

Impurity behavior within the tokamak fusion plasma will be a main concern for the future tokamak operation such as ITER. Thermalized alpha particles, i.e., helium 'ashes' constitute a key impurity within the plasma core. The helium ash accumulation within the tokamak plasma not only dilutes the fusion fuel, but also enhances the radiation energy loss. Eventually, these effects can prevent the fusion ignition and degrade the fusion output power even after ignition. Great progress has been made in determining the transport coefficients D(r) and V(r) with helium puffing and simulation techniques. Obviously, those results are only valid for a specific machine under certain plasma conditions. The extrapolation to other devices still remains a problem. Physically, alpha particle transport is determined by the local plasma conditions. Therefore, the D and V should be a function of the plasma parameters. In our research, we assume that the helium transport scaling law has the form of power law. By using the experiment data from helium puffing in L-mode deuterium plasma on TFRR, the scaling laws of D and V are obtained with the least square analysis. Also, the significance of helium transport scaling law to the design is discussed. DOE

N94-11514# General Atomic Co., San Diego, CA.
RESULTS FROM THE D3-D ADVANCED DIVERTOR PROGRAM
M. J. Schaffer, N. H. Brooks, T. E. Evans, R. J. Groebner, F. L. Hinton, M. A. Hollerbach, A. W. Hyatt, G. L. Jackson, A. W. Leonard, and S. I. Lippmann et al Apr. 1993 7 p Presented at the 9th International Atomic Energy Agency (IAEA) Workshop on Stellarators, Garching, Germany, 10-14 May 1993
(Contracts DE-AC03-89ER-51114; W-7405-eng-48; DE-AC05-84OR-21400; DE-FG03-89ER-51121; DE-AC04-76DP-00789; DE-AC03-89ER-53277)
(DE93-015472; GA-A-21281; CONF-9305210-1) Avail: CASI HC A02/MF A01

This paper presents a summary of some recent DIII-D boundary and divertor experiments. The single-null poloidally diverted plasmas were studied in the standard DIII-D open divertor configuration and in interaction with the toroidally symmetric divertor biasing electrode and exhaust pump. Results are reported for: scrape-off layer (SOL) density and its effect on impurity influx; SOL density and divertor bias; divertor pumping; divertor bias and exhaust gas collection; divertor bias and H-mode threshold. Author

N94-11594 National Inst. for Fusion Science, Nagoya (Japan).
ATOMIC PROCESSES RELEVANT TO POLARIZATION PLASMA SPECTROSCOPY
T. Fujimoto, F. Koike, K. Sakimoto, R. Okasaka, K. Kawasaki, K. Takiyama, T. Oda, and T. Kato Apr. 1992 155 p Limited Reproducibility: More than 20% of this document may be affected by microfiche quality
(DE93-753240; NIFS-Data-16) Avail: Issuing Activity (Department of Energy (DOE))

When atoms (ions) are excited anisotropically, polarized excited atoms are produced and the radiation emitted by these atoms is polarized. From the standpoint of plasma spectroscopy research, the existing data for various atomic processes that are related to the polarization phenomena are reviewed. These processes are: electron impact excitation, excitation by atomic and ionic collisions, photoexcitation, radiative recombination, and bremsstrahlung. Collisional and radiative relaxation processes of atomic polarization follow. Other topics included are: electric-field measurement, self alignment, Lyman doublet intensity ratio, and magnetic-field measurement of the solar prominence. DOE

N94-11669# Texas Univ., Austin. Inst. for Fusion Studies.
DISCRETE VORTEX REPRESENTATION OF MAGNETOHYDRODYNAMICS
R. Kinney, T. Tajima, N. Petviashvili, and J. C. McWilliams (National Center for Atmospheric Research, Boulder, CO.) 25 Oct. 1992 16 p
(Contract DE-FG05-80ET-53088)
(DE93-012190; DOE/ET-53088/592; IFSR-592) Avail: CASI HC A03/MF A01

We present an alternative approach to statistical analysis of an intermittent ideal MHD fluid in two dimensions, based on the hydrodynamical discrete vortex model applied to the Elsasser variables. The model contains negative temperature states which predict the formation of magnetic islands, but it also includes a natural limit under which the equilibrium states revert to the familiar twin-vortex states predicted by hydrodynamical turbulence theories. Numerical dynamical calculations yield equilibrium spectra in agreement with the theoretical predictions. DOE

N94-11677# Lawrence Livermore National Lab., CA.
HIGH RESOLUTION TIME- AND 2-DIMENSIONAL SPACE-RESOLVED X RAY IMAGING OF PLASMAS AT NOVA
O. L. Landen 11 May 1992 12 p Presented at the 9th Topical Conference on High Temperature Plasma Diagnostics, Santa Fe, NM, 15-19 Mar. 1992
(Contract W-7405-eng-48)

(DE93-011892; UCRL-JC-109094; CONF-920362-46) Avail: CASI HC A03/MF A01

A streaked multiple pinhole camera technique, first used to record time- and 2-D space-resolved soft X-ray images of plasma pinches, has been implemented on laser plasmas at NOVA. The instrument is particularly useful for time-resolved imaging of small sources (less than 150 microns) such as implosions for which the necessary alignment accuracy is relaxed from less than 10 microns for a single pinhole, to 200 microns for a nine pinhole column. Results at 20 microns, 30 ps resolution are presented for greater than 2.5 keV imaging, complementing the existing 1-3 key streaked X-ray microscope capabilities at NOVA. DOE

N94-12370# Lawrence Livermore National Lab., CA.
INITIAL ASSESSMENT OF LOWER HYBRID CURRENT DRIVE IN D3-D
M. E. Fenstermacher and M. Porkolab Sep. 1992 32 p
(Contract W-7405-eng-48)
(DE93-013310; UCRL-ID-111838) Avail: CASI HC A03/MF A01

In this report we discuss the choice of rf frequency for LHCD in DIII-D, and its consequences for the operating regimes. We also discuss some Brambilla code results for particular launcher geometry, as well as edge density requirements for efficient coupling by the launcher. We present results of the ACCOME code modelling for selected frequency spectra. Finally, a summary is given, as well as suggestions for future studies. DOE

N94-12544# General Atomic Co., San Diego, CA.
AN EMERGING UNDERSTANDING OF H-MODE DISCHARGES IN TOKAMAKS
R. J. Groebner Dec. 1992 59 p Presented at the Meeting of the Division of Plasma Physics of the American Physical Society, Seattle, WA, 16-20 Nov. 1992
(Contract DE-AC03-89ER-51114)
(DE93-012829; GA-A-21128; CONF-921103-10) Avail: CASI HC A04/MF A01

A remarkable degree of consistency of experimental results from tokamaks throughout the world has developed with regard to the phenomenology of the transition from L-mode to H-mode confinement in tokamaks. The transition is initiated in a narrow layer at the plasma periphery where density fluctuations are suppressed and steep gradients of temperature and density form in a region with large first and second radial derivatives in the upsilon(sub E) = (E x B)/B(sup 2) flow velocity. These results are qualitatively consistent with theories which predict suppression of fluctuations by shear or curvature in (upsilon)E. The required (upsilon)E flow is generated very rapidly when the magnitude of the heating power or of an externally imposed radial current exceed threshold values and several theoretical models have been developed to explain the observed changes in the (upsilon)E flow. After the transition occurs, the altered boundary conditions enable the development of improved confinement in the plasma interior on a confinement time scale. The resulting H-mode discharge has typically twice the confinement of L-mode discharges and regimes of further improved confinement have been obtained in some H-mode scenarios. DOE

N94-12545# General Atomic Co., San Diego, CA.
STATISTICAL APPROACH TO LHCD MODELING USING THE WAVE KINETIC EQUATION
K. Kupfer, D. Moreau (Association Euratom-CEA, Saint Paul-les-Durance, France.), and X. Litaudon (Association Euratom-CEA, Saint Paul-les-Durance, France.) Apr. 1993 4 p Presented at the 10th Topical Conference on Radio Frequency Power in Plasmas, Boston, MA, 1-3 Apr. 1993
(Contract DE-AC03-89ER-51114)
(DE93-012831; GA-A-21258; CONF-9304112-5) Avail: CASI HC A01/MF A01

Recent work has shown that for parameter regimes typical of many present day current drive experiments, the orbits of the launched LH rays are chaotic (in the Hamiltonian sense), so that wave energy diffuses through the stochastic layer and fills the spectral gap. We have analyzed this problem using a statistical approach, by solving the wave kinetic equation for the coarse-grained spectral energy density. An interesting result is that the LH absorption profile is essentially independent of both the total injected power and the level of wave stochastic diffusion. DOE

N94-11066# Iowa Univ., Iowa City. Dept. of Physics.
VLBI AND THE DETECTION OF INTERSTELLAR MAGNETOHYDRODYNAMIC WAVES
Steven R. Spangler *In* National Astronomy and Ionosphere Center, Propagation Effects in Space VLBI 1993 p 57-67 (For primary document see N94-11060 01-32)
Avail: Issuing Activity

76 SOLID-STATE PHYSICS

Includes superconductivity.
For related information, see also *33 Electronics and Electrical Engineering* and *36 Lasers and Masers.*

N94-10281# International Centre for Theoretical Physics, Trieste (Italy).
INVARIANCE OF THE MOBILITY EDGE IN ANODIC TITANIUM OXIDES
N. Tit, J. W. Halley, and H. B. Shore May 1992 4 p
(DE92-642136; IC-92/85) Avail: CASI HC A01/MF A01 (US Sales Only)

A theoretical investigation to explain the electronic and optical properties of anodic rutile TiO2 thin films of different thicknesses (ranging from 5nm to 20nm) is described. There is experimental evidence that the observed gap state at 0.7eV below the edge of conduction-band is due to an oxygen vacancy. For this reason, oxygen vacancies are used as defects in our model. A comparison of the calculated bulk-photoconductivity to photospectroscopy experiment reveals that the films have bulk-like transport properties with a bandgap E(sub g) = 3.0 eV. On the other hand, a fit of the surface density of states to the scanning tunneling microscopy (STM) experiment on the (001) surfaces has suggested a surface defect density of 5% of oxygen vacancies. To resolve this discrepancy, the dc-conductivity where localization effects are included was calculated. Our results show an impurity band formation at about p(sub c) = 9% of oxygen vacancies. It was concluded that the studied films have defect densities below the threshold of impurity band formation. As a consequence the gap states seen in STM are localized (i.e. the oxygen vacancies are playing the role of trapping centers, deep levels) and the mobility edge is invariant. DOE

N94-10301# Brookhaven National Lab., Upton, NY.
SYMMETRY LOWERING IN CRYSTALLINE SOLID SOLUTIONS: A STUDY OF CINNAMAMIDE-THIENYLACRYLAMIDE BY X RAY AND NEUTRON DIFFRACTION AND SOLID-STATE PHOTOCHEMISTRY
L. J. W. Shimon, Y. Weissinger-Lewin, R. K. McMullan, M. Vaida, F. Frolow, M. Lahav, and L. Leiserowitz (Weizmann Inst. of Science, Rehovoth, Israel.) 1993 48 p Presented at the Faraday Division of Royal Society of Chemistry Conference on Crystal Growth, Glasgow, England, 14-16 Spr. 1993
(Contract DE-AC02-76CH-00016)
(DE93-010871; BNL-48645; CONF-9304113-1) Avail: CASI HC A03/MF A01

Principles are outlined for symmetry lowering of a mixed crystal. A survey is given of methods used to detect reduced symmetry: changes in crystal morphology, detection of enantiomeric segregation of chiral additives in 'centrosymmetric' crystals, generation of second harmonic optical signals, optical birefringence, asymmetric photoreactions in the crystalline state and X-ray and neutron diffraction. The last two methods are applied to mixed crystals of cinnamamide host and thienylacrylamide. Diffraction demonstrated that the mixed crystals are composed of six sectors of reduced symmetry, from monoclinic centrosymmetric P2(sub 1)/c to triclinic P1 in four sectors and possibly Pc in the remaining two. The X-ray diffraction data were not sufficiently accurate for assigning the absolute structures of the PI sectors of anomalous X-ray scattering. Thus, by this method one could not ascertain the absolute orientation of the guest molecules on the surface sites through which they were selectively occluded. This ambiguity was resolved by assignment of the absolute configuration of the chiral heterophotodimers, between host and guest, in enantiomeric excess in the PI sectors, after irradiation with UV light. This leads to the conclusion that the selective occlusion of thienylacrylamide arises from replacement of attractive C-H...pi(electron) interactions between host molecules by a repulsive sulfur (lone pair electron)...pi(electron) interactions between guest and host at the crystal surfaces. DOE

N94-10314# Centro Brasileiro de Pesquisas Fisicas, Rio de Janeiro.
EFFECT OF A DISTRIBUTION OF EXCHANGE PARAMETERS WITHIN A SIMPLE LOCALIZED-ITINERANT MODEL
L. Iannarella, A. P. Guimaraes, and X. A. daSilva 1991 16 p
(DE93-610314; CBPF-NF-034/91) Avail: CASI HC A03/MF A01 (US Sales Only)

The magnetic behavior at $T = 0$ K of a system consisting of conduction electrons coupled to localized electrons submitted to an axial crystal field is studied in the molecular field approximation. We assume that the exchange parameter J varies spatially with a Gaussian probability distribution. We define an average ionic magnetic moment and obtain the condition for spontaneous magnetic order, involving the crystal field parameter, the width and the mean value of the exchange parameter distribution. We also obtain graphs of the magnetic moment versus mean value of the exchange parameter distribution, for different distributions showing that the distribution of J's reduces the rate of increase of magnetization versus the mean J. DOE

N94-10386 International Centre for Theoretical Physics, Trieste (Italy).
ENHANCED STABILITY OF MAGIC CLUSTERS: A CASE STUDY OF ICOSAHEDRIC Al(SUB 12)X, X=B, Al, Ga, C, Si, Ge, Ti, As
X. G. Gong and V. Kumar Oct. 1992 12 p Limited Reproducibility: More than 20% of this document may be affected by microfiche quality
(DE93-613644; IC-92/314) Avail: CASI HC A03 (US Sales Only)

We present results of the electronic structure and stability of some 40 valence electron icosahedric Al12(X) (where X=B, Al, Ga, C, Si, Ge, Ti, and As) clusters within the local spin density functional theory. It is shown that the stability of the Al13 cluster can be substantially enhanced by proper doping. For neutral clusters, substitution of C at the center of the icosahedron leads to the largest gain in energy. However, Al12B(-) is the most bounded in this family. These results are in agreement with the recent experiments which also find Al12B(-) to be highly abundant. DOE

N94-10406# Melbourne Univ., Parkville (Australia). School of Physics.
HRTEM IN PROTEIN CRYSTALLOGRAPHY
P. W. Dyson, A. E. C. Spargo, P. A. Tulloch, and A. W. S. Johnson 1992 2 p
(DE93-610322; UM-P-92/15) Avail: CASI HC A01/MF A01 (US Sales Only)

Electron microscopy/diffraction (ED/D) using spot-scan and low-dose imaging has been successfully applied to investigate microcrystals of an alpha-helical coiled-coil protein extracted from ootheca of the praying mantis. Fourier transforms of the images show resolution out to 4 A and can be used to phase the corresponding ED data which shows reflections out to 2 A. DOE

N94-10411# International Centre for Theoretical Physics, Trieste (Italy).
A LATTICE GAS MODEL FOR ENZYME KINETICS WITH ALTERNATE INTERACTIONS
R. Mejdani Sep. 1992 19 p
(DE93-613027; IC-92/281) Avail: CASI HC A03/MF A01 (US Sales Only)

We have shown that by using three equivalent different techniques (the transfer matrix method, the correlated walks' theory, and the partition point technique) for a lattice gas model in one dimension with alternate nearest neighbor ferromagnetic interactions, we can find a new equation of the enzyme kinetics. This equation in the limit of no interaction between sites reduces to the classical Michaelis-Henri equation, while for the same interaction between sites reduces to another equation, which we have obtained before. This new equation can be useful for the experimental investigation. DOE

N94-10415 International Centre for Theoretical Physics, Trieste (Italy).
ORBITAL GLASS IN HTSC
F. V. Kusmartsev Oct. 1992 11 p Limited Reproducibility: More than 20% of this document may be affected by microfiche quality
(DE93-613988; IC-92/309) Avail: CASI HC A03 (US Sales Only)

The physical reasons why the orbital glass may exist in granular high-temperature superconductors and the existing experimental data that appeared recently are discussed. The orbital glass is characterized by the coexistence of the orbital paramagnetic state with the superconducting state and occurs at small magnetic fields H less than H(sub c0) much less than H(sub c1). The transition in orbital glass arises at the critical field H(sub c0) which is inversely proportional to the surface cross-area S of an average grain. In connection with theoretical predictions the possible experiments are proposed. DOE

N94-10416# Materials Research Society, Pittsburg, PA.
SOLID STATE IONICS 3. MATERIALS RESEARCH SOCIETY SYMPOSIUM PROCEEDINGS, VOLUME 293
Gholam A. Nazri, Jean M. Tarascon, and Michel Armand 1992 483 p
Proceedings held in Boston, MA, 30 Nov. - 4 Dec. 1992
(Contracts N00014-93-1-0215; DAAL03-92-G-0418)
(AD-A265675) Avail: CASI HC A21/MF A04

This proceedings volume includes most of the invited and contributed papers presented as Symposium U, Solid State Ionics, at the 1992 MRS Fall meeting in Boston, Massachusetts, U.S.A. The Symposium covered material aspects of solid state ionics, theory of ion transfer in solids, ionically and electronically conductive polymers and their application in solid state devices, and various in-situ and ex-situ techniques for materials characterization. The first part of this proceedings volume deals with physics and chemistry of insertion compounds and application of these in advanced solid state batteries. The optical and electrochemical properties of insertion compounds are also presented. The second part of the proceedings deals with ionic and electronic conductive polymers. A new class of rubbery phase polymer electrolytes and their structure-conductivity relationship are presented. Physical and chemical properties of polymer electrolytes and electrodes and their application in solid state devices are presented. DTIC

N94-10516# Lawrence Livermore National Lab., CA.
KINETICS OF HIGH CONCENTRATION ARSENIC DEACTIVATION AT MODERATE TO LOW TEMPERATURES
S. Luning (Stanford Univ., CA.), P. M. Rousseau (Stanford Univ., CA.), P. B. Griffin (Stanford Univ., CA.), J. D. Plummer (Stanford Univ., CA.), and P. G. Carey 14 Oct. 1992 5 p Presented at the International Electron Devices Meeting, San Francisco, CA, 6-9 Dec. 1992
(Contract W-7405-eng-48)
(DE93-013349; UCRL-JC-111945; CONF-921204-2) Avail: CASI HC A01/MF A01

This work investigates the kinetics of arsenic deactivation at temperatures from 500 to 800 C and for concentrations between 1 x 10(exp 20) and 1 x 10(exp 21)/cu cm. Using profiles created by repeated laser melt annealing, the authors determined mobility as a function of both active and inactive dopant concentration and then characterized the dynamics of carrier deactivation. Retrograde resistivity versus concentration was observed at high doses, which is explained by a mobility reduction due to the inactive arsenic and by retrograde electrical activity of the dopant itself. DOE

N94-10525 Academy of Sciences of the Ukraine, Kiev. Inst. Yadernykh Issledovanij.
THE PECULIARITIES OF THE SPIN GLASS STATE IN Fe(x)Mn(1-x)TiO3 [OSOBENNOSTI SOSTOYANIYA SPINOVOGO STEKLA V FE(X)MN(1-X)TIO3]
N. D. Marchuk and O. I. Guzhva 1992 25 p In RUSSIAN Limited Reproducibility: More than 20% of this document may be affected by microfiche quality
(DE93-617882; KIYaI-92-3) Avail: CASI HC A03 (US Sales Only)

It is shown that the exchange interactions of the ferrum and manganese sublattice in Fe(x)Mn(1-x)TiO3 cause the mixed phase that is the reentrant spin-glass phase. In addition, the results of neutron scattering presented confirm the existence of the frontier lines separating the ideal spin-glass phase and the reentrant spin-glass phase. DOE

N94-10537 International Centre for Theoretical Physics, Trieste (Italy).
A WINDOW LEAST SQUARES ALGORITHM FOR STATISTICAL NOISE SMOOTHING OF 2D-ACAR DATA
G. Adam and S. Adam (Institute of Physics and Technology of Radiation Devices, Bucharest, Romania.) Oct. 1992 16 p Limited Reproducibility: More than 20% of this document may be affected by microfiche quality
(DE93-613828; IC-92/303) Avail: Issuing Activity (Department of Energy (DOE)) (US Sales Only)

Taking into account a number of basic features of the histograms of two-dimensional angular correlation of the positron annihilation radiation (2D-ACAR), a window least squares technique for statistical noise smoothing is proposed. DOE

N94-10637 International Centre for Theoretical Physics, Trieste (Italy).
BOND DISTORTION AND ELECTRON TRAPPING IN CHARGED C60
X. Sun, R. T. Fu (Fudan Univ., Shanghai, China.), R. L. Fu (Academia Sinica, Shanghai, China.), and H. J. Ye (Academia Sinica, Shanghai, China.) Oct. 1992 19 p Limited Reproducibility: More than 20% of this document may be affected by microfiche quality
(DE93-613642; IC-92/310) Avail: CASI HC A03 (US Sales Only)

By considering both electron-electron and electron-lattice interactions, the effect of charge transfer on the bond structure and electronic states of doped C60 is studied without configuration limitation. The results show that the electron interaction does not eliminate the layer structure of the bond distortion and the self-trapping of transferred electrons. There still exist two localized electronic states, which possess laminar wave functions, and four nonequivalent groups of carbon atoms, which induce a fine-structure in the NMR spectrum line. DOE

N94-10645 Tokyo Univ., Tanashi (Japan). Inst. for Nuclear Study.
SPONTANEOUS SYMMETRY BREAKING IN QCD
Hirofumi Yamada Mar. 1992 25 p Limited Reproducibility: More than 20% of this document may be affected by microfiche quality
(DE93-753080; INS-918) Avail: CASI HC A03

We study dynamical chiral symmetry breaking in QCD by the use of the generalized Hartree-Fock method. The low energy quark mass is calculated to the second order of diagrammatic expansion around shifted perturbative vacuum where quarks are massive. We show that the low energy mass is finite and renormalization group invariant. We find that the finite mass gap emerges as the solutions of gap equation and stationarity condition, thereby breaking the chiral symmetry. We also discuss the possibility that the breaking solution may exist up to all orders. DOE

N94-10648 Notre Dame Univ., IN.
SINGLE-ELECTRON TUNNELING
S. T. Ruggiero 1993 7 p Limited Reproducibility: More than 20% of this document may be affected by microfiche quality
(Contract DE-FG02-88ER-45373)
(DE93-013337; DOE/ER-45373/5) Avail: CASI HC A02

Pictures were made of particles using the low-temperature microwave scanning tunneling microscope, and tunneling IV characteristics were determined. Strong, sometimes periodic negative differential resistance was observed in small-particle systems. Au and Ag droplets and particles were studied. DOE

N94-10705 Purdue Univ., West Lafayette, IN. Dept. of Chemistry.
SURFACE-ENHANCED RAMAN SPECTROSCOPY OF ELECTROACTIVE FILMS OF C60 AND AN Ir-C60 COMPLEX ON GOLD: SYMMETRY LOWERING, ELECTRON LOCALIZATION, AND COUNTERACTION EFFECTS Technical Report
Yun Zhang, Yuhua Du, John R. Shapley, and Michael J. Weaver Apr. 1993 19 p Limited Reproducibility: More than 20% of this document may be affected by microfiche quality
(Contract N00014-91-J-1409)
(AD-A265934; TR-136) Avail: CASI HC A03

Surface-enhanced Raman (SER) spectra are reported for thin films of C60 and (eta5-C9H7)Ir(CO)(eta2-C60) on gold electrodes in acetonitrile. The latter spectra display the hallmarks of vibrational symmetry lowering for C60 arising from metal coordination, involving splitting of the normally degenerate H(sub g) modes and the appearance of vibrationally forbidden bands. Only a milder selection rule relaxation is observed for SERS of uncoordinated C60. Electroreduction of both C60 and the Ir-C60 complex yielded similar frequency downshifts in the Ag pentagonal pinch mode. This indicates that electron addition to the latter is fullerene localized. These spectral shifts are sensitive to the nature of the countercation. DTIC

N94-10716 International Centre for Theoretical Physics, Trieste (Italy).
POWER LOSSES OF A TYPE 2 SUPERCONDUCTING SLAB OF ARBITRARY THICKNESS IN THE PRESENCE OF ALTERNATING CURRENT CONDUCTORS
A. G. Saif Oct. 1992 10 p Limited Reproducibility: More than 20% of this document may be affected by microfiche quality
(DE93-617892; IC-92/359) Avail: Issuing Activity (Department of Energy (DOE)) (US Sales Only)

Power loss and the associated constituent terms--due to dissipative and reactive energies--are developed for a system of a normal conducting wire (two wires) carrying a current parallel to a type 2 superconducting infinite slab of arbitrary thickness. The reactive term is found to be either capacitively or inductively reactive. When the thickness of the slab tends to infinity, it is found that the results are in a good agreement with the previous results. DOE

N94-10745 Sandia National Labs., Albuquerque, NM.
CRACK SUPPRESSION IN GaInSb BUFFER LAYERS INITIALLY UNDER TENSILE STRESS
T. J. Drummond and S. R. Lee 1992 22 p Presented at the Spring Meeting of the Materials Research Society, San Francisco, CA, 12-16 Apr. 1993 Limited Reproducibility: More than 20% of this document may be affected by microfiche quality
(Contract DE-AC04-76DP-00789)
(DE93-012839; SAND-92-2498C; CONF-930405-2) Avail: CASI HC A03

Epitaxial III-V compound semiconductor buffer layers typically relieve tensile stress by mixed crack and misfit dislocation formation. Crack suppression by p-doping GaInSb step graded buffers grown on InSb substrates by MBE is demonstrated. This complements a similar demonstration for InAsSb buffers grown by MOCVD. The depth dependence and reproducibility of the stress relaxation have been quantified using a novel k-map x-ray analysis. A model in which the p-doping enhances the nucleation and subsequent climb of dislocations has been formulated to explain the result. This model should also apply to other III-V buffer systems such as GaAsP/GaAs and InGaAs/InP. DOE

N94-10800 International Centre for Theoretical Physics, Trieste (Italy).
CONFINEMENT OF ACOUSTICAL MODES DUE TO THE ELECTRON-PHONON INTERACTION WITHIN 2D-ELECTRON GAS
V. A. Kochelap and O. Gulseren (Bilkent Univ., Ankara, Turkey.) Sep. 1992 18 p Limited Reproducibility: More than 20% of this document may be affected by microfiche quality
(DE93-613910; IC-92/282) Avail: Issuing Activity (Department of Energy (DOE)) (US Sales Only)

The confinement of acoustical modes within 2DEG due only to the electron-phonon interaction is studied. The confined modes split out from the bulk phonons even at uniform lattice parameters, when the 2DEG is created by means of modulation doping. The effect is more pronounced when the wave vector q of the modes increases and is maximum at q = 2k(sub F) (k(sub F) is the Fermi wave vector). In the case of several electron sheets the additional features of the confinement effect appear. In the limit of the strong electron-phonon coupling and high surface concentration of the electrons the considered system can suffer Peierls-type phase transition. In this case periodical deformation of the lattice and charge density wave are confined within the electron sheet. DOE

N94-10801 International Centre for Theoretical Physics, Trieste (Italy).
LIMITATION AND SUPPRESSION OF HOT ELECTRON FLUCTUATIONS IN SUBMICRON SEMICONDUCTOR STRUCTURES
V. A. Kochelap, N. A. Zahleniuk, and V. N. Sokolov (Academy of Sciences of the Ukraine, Kiev.) Sep. 1992 34 p Limited Reproducibility: More than 20% of this document may be affected by microfiche quality
(DE93-613911; IC-92/283) Avail: CASI HC A03 (US Sales Only)

Theoretical investigations of fluctuations of hot electrons in submicron active regions, where the dimensions 2d of the region is comparable to the electron energy relaxation length L(sub epsilon) are presented. The new physical phenomenon is reported; the fluctuations depend on the sample thickness, with 2d less than L(sub epsilon) a suppression of fluctuations arises in the range of fluctuation frequencies omega much less than tau(sup -1)(sub epsilon), tau(sub epsilon) is the electron energy relaxation time. DOE

N94-10809# Sandia National Labs., Albuquerque, NM.
RAPID THERMAL PROCESSING FOR STRAINED-LAYER SEMICONDUCTOR DEVICES
J. C. Zolper and D. R. Myers 1993 10 p Presented at the Spring

Meeting of the Materials Research Society, San Francisco, CA, 12-16 Apr. 1993
(Contract DE-AC04-76DP-00789)
(DE93-013754; SAND-93-1020C; CONF-930405-6) Avail: CASI HC A02/MF A01

Strained-layer semiconductors have revolutionized modern heterostructure devices by exploiting the modification of semiconductor band structure associated with the coherent strain of lattice-mismatched heteroepitaxy. The modified band structure improves transport of holes in heterostructures and enhances the operation of semiconductor lasers. Strained-layer epitaxy also can create materials whose band gaps match wavelengths (e.g. 1.06 and 1.32 microns) not attainable in ternary epitaxial systems lattice matched to binary substrates. Other benefits arise from metallurgical effects of modulated strain fields on dislocations. Lattice mismatched epitaxial layers that exceed the limits of equilibrium thermodynamics will degrade under sufficient thermal processing by converting the as-grown coherent epitaxy into a network of strain-relieving dislocations. After presenting the effects of strain on band structure, the authors describe the stability criterion for rapid-thermal processing of strained-layer structures and the effects of exceeding the thermodynamic limits. Finally, device results are reviewed for structures that benefit from high temperature processing of strained-layer superlattices. DOE

N94-10819*# Florida Inst. of Tech., Melbourne. Physics and Space Sciences Dept.
ELECTRONIC CHARACTERIZATION OF DEFECTS IN NARROW GAP SEMICONDUCTORS Semiannual Report, 25 Nov. 1992 - 25 Jun. 1993
James D. Patterson 25 Jun. 1993 59 p
(Grant NAG8-941)
(NASA-CR-193568; NAS 1.26:193568) Avail: CASI HC A04/MF A01

The study of point defects in semiconductors has a long and honorable history. In particular, the detailed understanding of shallow defects in common semiconductors traces back to the classic work of Kohn and Luttinger. However, the study of defects in narrow gap semiconductors represents a much less clear story. Here, both shallow defects (caused by long range potentials) and deep defects (from short range potentials) are far from being completely understood. In this study, all results are calculational and our focus is on the chemical trend of deep levels in narrow gap semiconductors. We study substitutional (including antisite), interstitial and ideal vacancy defects. For substitutional and interstitial impurities, the efects of relaxation are included. For materials like Hg(1-x)Cd(x)Te, we study how the deep levels vary with x, of particular interest is what substitutional and interstitial atoms yield energy levels in the gap i.e. actually produce deep ionized levels. Also, since the main technique utilized is Green's functions, we include some summary of that method. Derived from text

N94-10830 Atomic Energy Commission, Damascus (Syria). Dept. of Chemistry.
SZILARD-CHALMERS EFFECT IN SOLID HIO4.2H2O BY NEUTRON IRRADIATION
Salaheddin Takriti Sep. 1992 19 p In ARABIC Limited Reproducibility: More than 20% of this document may be affected by microfiche quality
(DE93-617173; AECS-C/FRSR-59) Avail: CASI HC A03 (US Sales Only)

The Szilard-Chalmers effect in solid was investigated. In order to study the initial distribution of (128)IO4 as a function of neutron flux, samples were irradiated utilizing both the manual vertical irradiation channel and the thermal column of the ET-RR-1 Research Reactor in Egypt. The initial retention was reached a maximum of 40% after 120 minutes at 5.5 x 10(sup 8) ns(exp -1)cm(exp -2). The data was analyzed using a first order reaction. As a result, the activation energy and the vibration constant were found to be E = 0.95 eV and K = 2.82 x 10(sup 11), respectively. Kinetics comparison of the dehydration and irradiation reactions for this solid shows disorder in the crystallographic form. Such disorder may be the result of dehydration or irradiation reaction, where the loss of water molecule will lead to formation of vacancies which, in turn, are responsible for the distribution process. DOE

N94-10843 Academy of Sciences of the Ukraine, Kiev. Inst. Yadernykh Issledovanij.
THE INFLUENCE OF IRRADIATION CONDITIONS, TYPE, AND CONCENTRATION OF IMPURITIES ON RADIATION DEFECTS CHARACTERISTICS IN INDIUM ANTIMONIDE UNDER ELECTRON IRRADIATION [VLIYANIE USLOVIJ OBLUCHENIYA TIPA I KONTSENTRATSII LEGIRUYUSHCHIKH PRIMSEEJ NA KHARAKTERISTIKI RADIASTSIONNYKH DEFEKTOV V ANTIMONIDE INDIYA PRI EHLEKTEONNOM OBLUCHENII]
G. A. Vikhlij, A. Y. Karpenko, P. G. Litovchenko, !. G. Megela, and L. I. Tarabrova 1991 41 p In RUSSIAN Limited Reproducibility: More than 20% of this document may be affected by microfiche quality
(DE93-617201; KIYal-91-24) Avail: CASI HC A03 (US Sales Only)

The data on influence of electron irradiation conditions (beam intensity - 1-10 mkA, irradiation temperature - 80-400 K, electron energy - 4-14 MeV, fluence) type and concentration of impurities on defects introduction rate in InSb, which are stable at room temperature, and the data on galvanomagnetic properties of InSb with such defects are presented. The results are explained by introduction, interaction, and annealing of point defects. Mechanisms of irradiation conditions influence on defect production are analyzed. DOE

N94-10845 Academy of Sciences of the Ukraine, Kiev. Inst. Yadernykh Issledovanij.
RADIATION DEFECT PRODUCTION IN InAs CRYSTALS UNDER ELECTRON IRRADIATION [RADIATSIONNOE DEFEKTOOBRAZOVANIE V KRISTALLAKH INAS PRI EHLEKTRONNOM OBLUCHENII]
E. Y. Brajlovskij, D. B. Goer, Y. I. Gutich, and I. G. Megela 1991 27 p In RUSSIAN Limited Reproducibility: More than 20% of this document may be affected by microfiche quality
(DE93-617202; KIYal-91-29) Avail: CASI HC A03 (US Sales Only)

The defect-production and annealing processes in InAs under 2.0/14.5 MeV electron irradiation up to a dose 7 x 10(exp 18) electrons/cm(exp 2) at 77 and 293 K have been investigated. It was shown that in undoped n-InAs crystals the n-value increase with irradiation dose at 293 K leads to the dependence (delta)n approximately = phi(exp 0.5) at all fluences. On the contrary, in the case of irradiation of n-InAs crystals doped with Sn and Te (n greater than 5 x 10(exp 17)) it was found that the n-value begins to increase after 'exhaustion' of the doping atoms only as a result of the RD-doping atom interaction. From optical free-carrier absorption measurements a decrease power index r in the dependence alpha approximately = omega(sup -r) is observed as a result of irradiation that was explained by the influence of local deformation fields in the vicinity of the RD on the scattering mechanisms. DOE

N94-10883 Academy of Sciences of the Ukraine, Kiev. Inst. Teoreticheskoj Fiziki.
GLUON GAS VISCOSITY IN NONPERTURBATIVE REGION
S. V. Ilin, O. A. Mogilevskij, S. A. Smolyanskij, and G. M. Zinovev 1992 13 p Limited Reproducibility: More than 20% of this document may be affected by microfiche quality
(DE93-617680; ITP-92-10) Avail: CASI HC A03 (US Sales Only)

Using the Green-Kubo-type formulae and the cutoff model motivated by Monte Carlo lattice gluodynamics simulations we find the temperature behaviour of shear viscosity of gluon gas in the region of deconfinement phase transition. DOE

N94-10884 Academy of Sciences of the Ukraine, Kiev. Inst. Teoreticheskoj Fiziki.
GAUGE INDEPENDENCE OF THE A(SUB 0)-CONDENSATE
V. V. Skalozub 1992 13 p Limited Reproducibility: More than 20% of this document may be affected by microfiche quality
(DE93-617681; ITP-92-12) Avail: CASI HC A03 (US Sales Only)

The problem of gauge dependence of the zero gauge field component condensate. A(sub 0)=const, in the framework of finite temperature SU(2) gluodynamics is investigated. In straight-forward calculations it is shown that the two-loop effective action W(A(sub 0),(zeta)) satisfies the generalized Nielsen identity. Thus, the gauge invariance of the A(sub 0)-condensation is proved. DOE

N94-10962# Argonne National Lab., IL. Materials Science Div.
SYNTHESIS AND PROPERTIES OF NANOPHASE MATERIALS

R. W. Siegel Mar. 1993 25 p Presented at the 3rd Joint Conference of European East-West Conference on Materials and Processes and European Materials Research Society Fall Meeting, Strasbourg, France, 3-6 Nov. 1992
(Contract W-31-109-eng-38)
(DE93-011757; ANL/MSD/CP-76872; CONF-921121-2) Avail: CASI HC A03/MF A01

Nanophase materials, with their grain sizes or phase dimensions in the nanometer size regime, are now being produced by a wide variety of synthesis and processing methods. The interest in these new ultrafine-grained materials results primarily from the special nature of their various physical, chemical, and mechanical properties and the possibilities to control these properties during the synthesis and subsequent processing procedures. Since it is now becoming increasingly apparent that their properties can be engineered effectively during synthesis and processing and that they can also be produced in quantity, nanophase materials should have considerable potential for technological development in a variety of applications. Some of the recent research on nanophase materials related to their synthesis and properties is briefly reviewed and the future potential of these new materials is considered. DOE

N94-11004# Argonne National Lab., IL. Materials and Components Technology Div.
MICROSTRUCTURE AND ASSOCIATED PROPERTIES OF YB2Cu3O(x) SUPERCONDUCTORS PREPARED BY MELT PROCESSING TECHNIQUES
U. Balachandran, W. Zhong, C. A. Youngdahl, and R. B. Poeppel Mar. 1993 19 p Presented at the Annual Meeting of The Metallurgical Society, Denver, CO, 21-25 Feb.1993
(Contract W-31-109-eng-38)
(DE93-010675; ANL/MCT/CP-76965; CONF-930202-6) Avail: CASI HC A03/MF A01

From the standpoint of applications, melt-processed bulk YBa2Cu3O(x) (YBCO) superconductors are of considerable interest. We have studied the microstructure and levitation force of melt-processed YBCO, YBCO plus Y2BaCuO5, and YBCO plus Pt samples. Large single crystalline samples, grown using a seeding technique, were also studied. The levitation force is highest in melt-processed samples made by the seeding technique. DOE

N94-11012# Massachusetts Inst. of Tech., Cambridge. Dept. of Materials Science and Engineering.
GRAIN BOUNDARIES IN COMPLEX OXIDES
Yet-Ming Chiang May 1993 4 p
(Contract DE-FG02-87ER-45307)
(DE93-013986; DOE/ER-45307/5) Avail: CASI HC A01/MF A01

A quantitative comparison was achieved between space charge theory and segregation at grain boundaries in the model system TiO2. The ionic space charge can be titrated from negative to positive potential. A space charge model was developed that includes the lattice defect chemistry. Defect formation energies in the Frenkel pair for TiO2 were studied. Grain boundary enthalpy was measured during coarsening. It was shown that it is the barium vacancy that forms near surfaces in donor-doped BaTiO3 electroceramics during oxidative-cooling. DOE

N94-11025 Academy of Sciences of the Ukraine, Kharkov. Fiziko-Tekhnicheskij Inst. Nizkikh Temperatur.
NONLINEAR EXCITATION IN QUASI-ONE-DIMENSIONAL PEIERLS DIELECTRICS WITH CHARGE DENSITY WAVES
Yu. S. Kivshar, A. V. Nedzwetskij, and A. S. Rozhavskij 1989 36 p Limited Reproducibility: More than 20% of this document may be affected by microfiche quality
(DE93-613827; FTINT-27-89) Avail: CASI HC A03 (US Sales Only)

A model is considered, which describes the interaction between a charge density wave and longitudinal ultrasound in a Peierls dielectrics (PD). It is shown that in such dielectrics besides solitons there may exist periodic nonlinear acoustic-electron waves. The dependence is of a threshold nature, which is due to appearance of soliton modes. DOE

N94-11073# Argonne National Lab., IL. Materials and Components Technology Div.
PROCESSING AND TRANSPORT PROPERTIES OF HIGH J(SUB c) SILVER CLAD BI-2223 TAPES AND COILS
P. Haldar (Intermagnetics General Corp., Guilderland, NY.), J. G. Hoehn, Jr. (Intermagnetics General Corp., Guilderland, NY.), U. Balachandran, and L. R. Motowidlo (IGC/Advanced Supercomputers, Inc., Waterbury, CT.) Feb. 1993 12 p Presented at the Annual Meeting of The Metallurgical Society, Denver, CO, 21-25 Feb. 1993
(Contract W-31-109-eng-38)
(DE93-010674; ANL/MCT/CP-79135; CONF-930202-7) Avail: CASI HC A03/MF A01

The powder-in-tube process has been used to fabricate long lengths of flexible, high J(sub c), silver clad Bi-2223 HTS conductors. By improving thermo-mechanical processing and precursor powder preparation we have succeeded in achieving J(sub c)'s exceeding 4 x 10(exp 4) A/sq cm at liquid nitrogen (77K) and greater than 10(exp 5) A/sq cm at liquid helium (4.2K) and liquid neon (27K) temperatures for short tape samples. Detailed measurements with high applied magnetic fields are reported. Several long tapes up to 10 meters in length have also been fabricated and co-wound into small superconducting pancake coils using the 'wind-and-react' approach. Transport measurements at 77K and 4.2K for these coils are also reported. DOE

N94-11090 Gosudarstvennyi Komitet po Ispolzovaniyu Atomnoi Energii, Moscow (USSR).
INTERATOMIC INTERACTIONS IN BCC AND FCC LATTICES OF TRANSITION METALS [MEZHATOMNYE VZAIMODEJSTVIYA V OTSK-GTSK PEREKHODNYKH METALLAKH]
V. V. Gann and V. I. Pokhodyashchij 1991 22 p In RUSSIAN Limited Reproducibility: More than 20% of this document may be affected by microfiche quality
(DE93-621541; KFTI-91-13) Avail: CASI HC A03 (US Sales Only)

A 3-parameter model for determining the coupling energy in transition metals with cubic lattices is proposed. The parameters of this model were adjusted to account for experimental data concerning the shear module, vacancy formation energy, and sublimation energy values. Elastic and dynamic properties of crystal lattices of some transition metals were calculated. It is concluded that the proposed model describes the properties of transition metals in a single manner and with a good degree of accuracy. DOE

N94-11115# Michigan State Univ., East Lansing. Dept. of Metallurgy, Mechanics and Material Science.
HIGH TEMPERATURE STABILITY, INTERFACE BONDING, AND MECHANICAL BEHAVIOR IN (BETA)-NIAI AND NI3AI MATRIX COMPOSITES WITH REINFORCEMENTS MODIFIED BY ION BEAM ENHANCED DEPOSITION
D. S. Grummon 21 Jan. 1993 7 p
(Contract DE-FG02-85ER-45205)
(DE93-013977; DOE/ER-45205/8) Avail: CASI HC A02/MF A01

Diffusion-bonded NiAl-Al2O3 and Ni3Al-Al2O3 couples were thermally fatigued at 900 C for 1500 and 3500 cycles. The fiber-matrix interface weakened after 3500 cycles for the Saphikon fibers, while the Altex, PRD-166, and FP fibers showed little, if any, degradation. Diffusion bonding of fibers to Nb matrix is being studied. Coating the fibers slightly increases the tensile strength and has a rule-of-mixtures effect on elastic modulus. Push-out tests on Sumitomo and FP fibers in Ni aluminide matrices were repeated. Al2O3 was evaporated directly from pure oxide rod onto acoustically levitated Si carbide particles, using a down-firing, rod-fed electron beam hearth; superior coatings were subsequently produced using concurrent irradiation with 200-eV argon ion-assist beam. The assist beam produced adherent films with reduced tensile stresses. In diffusion bonding in B-doped Ni3Al matrices subjected to compressive bonding at 40 MPa at 1100 C for 1 hr, the diffusion barriers failed to prevent catastrophic particle-matrix reaction, probably because of inadequate film quality. AlN coatings are currently being experimented with, produced by both reactive evaporation and by N(+)-ion enhanced deposition. A 3-kW rod-fed electron-beam-heated evaporation source has been brought into operation. DOE

N94-11117# Pittsburgh Univ., PA.
TIME-RESOLVED OPTICAL STUDIES OF CHARGE RELAXATION AND CHARGE TRANSFER AT ELECTRODE INTERFACES
1992 11 p
(Contract DE-FG02-89ER-14062)
(DE93-013985; DOE/ER-14062/3) Avail: CASI HC A03/MF A01

The following key components were identified in a quantitative model of carrier relaxation in semiconductor electrodes: nonlinear aspects of nonradiative and radiative recombination, effect of space charge field on carrier dynamics, self-absorption effects in direct gas semiconductors, and influence of surface state population kinetics on charge carrier recombination. For CdSe, the first three are operative (no direct proof of the last one). A realistic kinetic model for carrier recombination in the bulk of CdSe was used which includes important nonlinear effects, both radiative and nonradiative. The change in interfacial recombination velocity with the chemical nature of the interface was studied (n-CdSe/silane interfaces). Temperature effect (278 to 328 K) on fluorescence decay of n-CdSe in contact with 0.5 M KOH was found to be weak. An analytical solution was obtained for time-resolved fluorescence from electrodes under potential bias, and is being tested. Fluorescence work on a different material, CdS, indicate different recombination kinetics; this material was used to directly pump an optical transition of a surface state. DOE

N94-11243# Lawrence Livermore National Lab., CA.
INVESTIGATION OF OPTICALLY GENERATED ELECTRONIC DEFECTS AND PROTONIC TRANSPORT IN HYDROGEN-BONDED MOLECULAR SOLIDS: ISOMORPHS OF POTASSIUM DIHYDROGEN PHOSPHATE
J. E. Davis, R. S. Hughes, Jr., and H. W. H. Lee Oct. 1992 5 p
Presented at the Quantum Electronics and Laser Science Conference, Baltimore, MD, 2-7 May 1993
(Contract W-7405-eng-48)
(DE93-012498; UCRL-JC-112312; CONF-930586-5) Avail: CASI HC A01/MF A01

We present a coherent picture of a new class of defects that appear to affect hydrogen-bonded molecular solids represented in this study by isomorphs of KDP (DKDP, KDP, ADP). We also discuss the effects this defect has on two photon absorption measurements and the harmonic generation of UV pulses. DOE

N94-11263# Naval Command, Control and Ocean Surveillance Center, San Diego, CA. Research, Development, Technology and Evaluation Div.
FEMTOSECOND DYNAMICS, PHOTOEXCITATION, AND ESR SPECTRA OF MX CHAIN SOLIDS Professional Paper
J. T. Gammel, A. Saxena, L. Batistic, and A. R. Bishop Mar. 1993 10 p
(AD-A264689) Avail: CASI HC A02/MF A01

Nonlinear adiabatic dynamics and ESR spectra associated with nonlinear excitations in MX chain (M = Pt and X = CL,BrI) materials are numerically studied within a discrete, 3/4-filled, two-band, tight-binding extended Peierls-Hubbard model. Both Hartree-Fock (HF) adiabatic molecular relaxation and molecular dynamics techniques are employed to investigate the time evolution of solitons, polarons, bipolarons in charge-density-wave (CDW) ground state materials. The time evolution of excitons, defect pairs and/or breathers is studied subsequent to photoexcitation. The ESR spectra associated with the resulting spin carrying nonlinear excitations such as neutral solitons, triplet excitons as well as electron and hole polarons are then calculated within the above model. The superhyperfine structure in the ESR spectra is attributed to a small spin density present on the halogen sublattice. DTIC

N94-11268# Lawrence Livermore National Lab., CA.
DYNAMIC STUDIES OF CRYSTAL GROWTH USING THE AFM
A. J. Gratz, P. E. Hillner (California Univ., Santa Barbara.), S. Manne (California Univ., Santa Barbara.), and P. K. Hansma (California Univ., Santa Barbara.) 15 Apr. 1992 4 p Presented at the Society of Photo-Optical Instrumentation Engineers (SPIE) International Symposium on Laser Spectroscopy, Los Angeles, CA, 19-24 Jan. 1992
(Contract W-7405-eng-48)
(DE93-009549; UCRL-JC-110510; CONF-920124-29) Avail: CASI HC A01/MF A01

Recent advances in atomic force microscopy (AFM) technology allow direct observation of solution growth and dissolution (etching) processes, processes that are important in industry and nature, and direct tests of crystal growth models. We present results of studies of calcite and quartz including real-time, in situ observations. While both crystals experience layer growth/dissolution, calcite grows by direct addition of material to growth steps without an important contribution from surface diffusion; quartz surfaces are consistent with more traditional, BCF-type growth models. Dynamic AFM observations of growth processes may allow optimization of industrial systems. DOE

N94-11314 Illinois Inst. of Tech., Chicago.
TEXTURE ANALYSIS OF HIGH Tc SUPERCONDUCTORS Ph.D. Thesis
Anthony Charles Biondo 1992 172 p
Avail. Univ. Microfilms Order No. DA9311928

The effect of processing on the quantitative texture developed for the high T(sub c) superconductors Y1Ba2Cu3O(7-delta) and Bi2Sr2Ca1Cu2O8 was studied. Due to the anisotropic nature of the properties of these compounds, it is anticipated that this preferred orientation will effect the bulk properties of the processed samples. An effort to predict the properties using the quantitative texture data available in orientation distribution functions was made. Three methods of processing were studied: conventional processing of Y1Ba2Cu3O(7-delta), melt texture processing of Y1Ba2Cu3O(7-delta), and powder-in-tube processing of Bi2Sr2Ca1Cu2O8. The first two processing methods resulted in critical current densities which did not change with different preferred orientations. Thus, property prediction using the texture data was not possible. The third method did result in an increase of critical current density as the strength of the texture increased. Two models were used to predict the critical current density of these samples using the quantitative texture data. The first model used the J(sub c) anisotropy between the plane and the c-axis for the Bi2Sr2Ca1Cu2O8 compound as input; the anisotropy which best fit the data was 20:1. The second model checked the grain to grain misorientation using three different criteria for a strong link. The critical misorientation angle for a strong link was found to be 10 degrees. Dissert. Abstr.

N94-11439* North Carolina State Univ., Raleigh. Dept. of Materials Science and Engineering.
MEMORY EFFECTS IN THE ORGANOMETALLIC CHEMICAL BEAM EPITAXY OF COMPOUND SEMICONDUCTORS Final Report, 12 Jan. 1989 - 31 May 1993
Klaus J. Bachmann 1993 57 p
(Grant NAG1-1100)
(NASA-CR-193106; NAS 1.26:193106) Copyright Avail: Issuing Activity

The final report on memory effects in the organometallic chemical beam epitaxy of compound semiconductors is presented. The goal is the improvement of the control of the composition of heterostructures under the conditions of chemical beam epitaxy (CBE) and related low pressure chemical vapor deposition methods. The linkage to NASA's mission is the opportunity for containerless processing in space which is expected to significantly reduce memory effects in the fabrication of compound semiconductor heterostructures and heterostructures that integrate compound semiconductors with silicon technology. For individual titles, see N94-11440 through N94-11443.

N94-11440*# North Carolina State Univ., Raleigh. Dept. of Materials Science and Engineering.
REMOTE PLASMA ENHANCED CHEMICAL VAPOR DEPOSITION OF GaP WITH IN SITU GENERATION OF PHOSPHINE PRECURSORS
S. W. Choi, G. Lucovsky, and Klaus J. Bachmann *In its* Memory Effects in the Organometallic Chemical Beam Epitaxy of Compound Semiconductors 1993 4 p Repr. from J. Vac. Sci. Technol. B (American Vacuum Society), v. 10, no. 3, May/Jun. 1992 p 1070-1073 (For primary document see N94-11439 01-76)
Avail: Issuing Activity

Thin homoepitaxial films of gallium phosphide (GaP) were grown by remote plasma enhanced chemical vapor deposition utilizing in situ generated phosphine precursors. The GaP forming reaction is kinetically controlled with an activation energy of 0.65 eV. The increase of the growth rate with increasing radio frequency (rf) power between 20 and 100 W is due to the combined effects of increasingly complete excitation and the spatial extension of the glow discharge toward the substrate, however, the saturation of the growth rate at even higher rf power indicates the saturation of the generation rate of phosphine precursors at this condition. Slight interdiffusion of P into Si and Si into GaP is indicated from GaP/Si heterostructures grown under similar conditions as the GaP homojunctions.
Author (revised)

N94-11441*# North Carolina State Univ., Raleigh. Dept. of Materials Science and Engineering.

LATTICE-MATCHED HETEROEPITAXY OF WIDE GAP TERNARY COMPOUND SEMICONDUCTORS

Klaus J. Bachmann *In its* Memory Effects in the Organometallic Chemical Beam Epitaxy of Compound Semiconductors 1993 11 p Repr. from Materials Research Society Symposium Procedures, v. 242, 1992 p 707-717 (For primary document see N94-11439 01-76)
Avail: Issuing Activity

A variety of applications are identified for heteroepitaxial structures of wide gap I-III-VI(sub 2) and II-IV-V(sub 2) semiconductors, and are assessed in comparison with ternary III-V alloys and other wide gap materials. Non-linear optical applications of the I-III-VI(sub 2) and II-IV-V(sub 2) compound heterostructures are discussed, which require the growth of thick epitaxial layers imposing stringent requirements on the conditions of heteroepitaxy. In particular, recent results concerning the MOCVD growth of ZnSi(x)Ge(1-x)P2 alloys lattice matching Si or GaP substrates are reviewed. Also, heterostructures of Cu(z)Ag(1-z)GaS2 alloys that lattice-match Si, Ge, GaP, or GaAs substrates are considered in the context of optoelectronic devices operating in the blue wavelength regime. Since under the conditions of MOCVD, metastable alloys of the II-IV-V(sub 2) compounds and group IV elements are realized, II-IV-V(sub 2) alloys may also serve as interlayers in the integration of silicon and germanium with exactly lattice-matched tetrahedrally coordinated compound semiconductors, e.g. ZnSi(x)Ge(1-x)P2. Author (revised)

N94-11442*# North Carolina State Univ., Raleigh. Dept. of Materials Science and Engineering.

ORGANOMETALLIC CHEMICAL VAPOR DEPOSITION AND CHARACTERIZATION OF ZnGeP2/GaP MULTIPLE HETEROSTRUCTURES ON GaP SUBSTRATES

G. C. Xing and Klaus J. Bachmann *In its* Memory Effects in the Organometallic Chemical Beam Epitaxy of Compound Semiconductors 1993 13 p (For primary document see N94-11439 01-76)
(Grant NSF DMR-92-02210)
Avail: Issuing Activity

The growth of ZnGeP2/GaP double and multiple heterostructures on GaP substrates by organometallic chemical vapor deposition is reported. These epitaxial films were deposited at a temperature of 580 C using dimethylzinc, trimethylgallium, germane, and phosphine as source gases. With appropriate deposition conditions, mirror smooth epitaxial GaP/ZnGeP2 multiple heterostructures were obtained on (001) GaP substrates. Transmission electron microscopy (TEM) and secondary ion mass spectroscopy (SIMS) studies of the films showed that the interfaces are sharp and smooth. Etching study of the films showed dislocation density on the order of 5x10(exp 4)cm(sup -2). The growth rates of the GaP layers depend linearly on the flow rates of trimethylgallium. While the GaP layers crystallize in zinc-blende structure, the ZnGeP2 layers crystallize in the chalcopyrite structure as determined by (010) electron diffraction pattern. This is the first time that multiple heterostructures combining these two crystal structures were made. Author (revised)

N94-11443*# North Carolina State Univ., Raleigh. Dept. of Materials Science and Engineering.

ORGANOMETALLIC CHEMICAL VAPOR DEPOSITION AND CHARACTERIZATION OF ZnGe(1-x)Si(x)P2-Ge ALLOYS ON GaP SUBSTRATES

G. C. Xing, Klaus J. Bachmann, J. B. Posthill (Research Triangle Inst., Research Triangle Park, NC.), and M. L. Timmons (Research Triangle Inst., Research Triangle Park, NC.) *In its* Memory Effects in the Organometallic Chemical Beam Epitaxy of Compound Semiconductors 1993 7 p Repr. from Journal of Crystal Growth 113 (Netherlands, Elsevier Science Publishers B.V.), 1991 p 113-119 (For primary document see N94-11439 01-76)
Avail: Issuing Activity

The epitaxial growth of ZnGe(1-x)Si(x)P2-Ge alloys on GaP substrates by open tube organometallic chemical vapor deposition (OMCVD) is reported. The chemical composition of the alloys characterized by energy dispersive X-ray spectroscopy shows that alloys with x up to 0.13 can be deposited on (001) GaP. Epitaxial growth with mirror smooth surface morphology was achieved for x less than or equal to 0.05. Transmission electron microscopy (TEM) micrographs of these alloys show specular epitaxy and the absence of microstructural defects indicating a defect density of less than 10(exp 7) cm(sup -2). Selected area electron diffraction pattern of the alloy shows that the epitaxial layer crystallizes in the chalcopyrite structure with relatively weak superlattice reflections indicating certain degree of randomness in the cation sublattice. Hall measurements show that the alloys are p-type, like the unalloyed films; the carrier concentration, however, dropped about 10 times from 2 x 10(exp 18) to 2 x 10(exp 17) cm(sup -3). Absorption measurements indicate that the band tailing in the absorption spectra of the alloy was shifted about 0.04 eV towards shorter wavelength as compared to the unalloyed material. Diodes fabricated from the n(+)-GaP/p-ZnSiP2-ZnGeP2-Ge heterostructure at x = 0.05 have a reverse break-down voltage of -10.8 V and a reverse saturation current density of approximately 6 x 10(exp -8) A/sq cm. Author (revised)

N94-11457# Sandia National Labs., Albuquerque, NM.

FULLERENE SUPERCONDUCTORS: PHASE STABILITY AND ANOMALOUSLY LOW T(SUB c)'S IN SOME TERNARY COMPOUNDS

J. E. Schirber, D. L. Overmyer, W. R. Bayless, M. J. Rosseinsky (Bell Telephone Labs., Inc., Murray Hill, NJ.), O. Zhou (Bell Telephone Labs., Inc., Murray Hill, NJ.), D. W. Murphy (Bell Telephone Labs., Inc., Murray Hill, NJ.), Q. Zhu (Pennsylvania Univ., Philadelphia.), K. Kniaz (Pennsylvania Univ., Philadelphia.), and J. E. Fischer (Pennsylvania Univ., Philadelphia.) 1993 4 p Presented at the Spectroscopies in Novel Superconductors, Santa Fe, NM, 28 Jun. - 2 Jul. 1993
(Contracts DE-AC04-76DP-00789; DE-FG02-86ER-45254; DE-FG05-90ER-75596; DE-AC02-76CH-00016)
(DE93-010687; SAND-93-0744C; CONF-9306144-1) Avail: CASI HC A01/MF A01

AC impedance and x-ray diffraction measurements versus temperature and pressure for several ternary intercalation compounds are reported. Results support our previously established empirical correlation between superconducting onset temperature and 300K fcc lattice constant. Compounds which do not follow this correlation either phase separate or are otherwise unstable at low T and/or high P. DOE

N94-11458# Brookhaven National Lab., Upton, NY.

APICAL Cu-O BOND IN YBa2Cu3O(7-DELTA) SUPERCONDUCTORS BY XAFS

E. A. Stern (Washington Univ., Seattle.), M. Qian (Washington Univ., Seattle.), Y. Yacoby (Hebrew Univ., Jerusalem, Israel.), S. M. Heald, and H. Maeda (Okayama Univ., Japan.) 1993 5 p Presented at the 2nd Israeli International Conference on High Tc Superconductivity, Elat, Israel, 4-7 Jan. 1993
(Contracts DE-AC02-76CH-00016; DE-FG06-90ER-45425)
(DE93-010861; BNL-48568; CONF-930107-1) Avail: CASI HC A01/MF A01

Careful Cu K-edge X-ray absorption fine structure (XAFS) measurements on oriented powders of YBa2Cu3O(7 - delta) were made as a function of temperature, of delta, T(sub c), method of preparation, and grain size. The XAFS data were analyzed for the Cu(1) - O(4) apical bond distance distribution. All samples indicated evidence for a double-peak in the distribution with a splitting of 0.1 A, with the clearest case for the delta approximately equal to 0 samples occurring for the T(sub c) = 89K 20 microns grain samples and the least clear one for the 5 micron grain T(sub c) = 93K sample. There is no significant temperature dependence of the splitting. Because the XAFS evidence for the splitting depends on a small signal, it is prudent to verify its existence by other independent measurements. DOE

N94-11467# Brookhaven National Lab., Upton, NY.

X-RAY AND NEUTRON SCATTERING STUDIES OF MAGNETIC CRITICAL FLUCTUATIONS IN HOLMIUM

T. R. Thurston, G. Helgesen, D. Gibbs, G. Shirane, and J. P. Hill (Massachusetts Inst. of Tech., Cambridge.) 1993 11 p Presented at the Workshop on the Use of Neutrons and X Rays in the Study of Magnetism, Grenoble, France, 21-24 Jan. 1993
(Contract DE-AC02-76CH-00016)
(DE93-010873; BNL-48610; CONF-9301101-1) Avail: CASI HC A03/MF A01

We describe measurements of the magnetic critical fluctuations of holmium by x-ray scattering techniques. The x-ray results are compared to those obtained in neutron scattering experiments performed on the same sample. DOE

N94-11476# Sensors Unltd., Inc., Princeton, NJ.
AN INDIUM GALLIUM ARSENIDE CHARGE-COUPLED DEVICE (CCD) FOR 1-3 MICRON IMAGING Final Report, 1 Jul. 1992 - 15 Apr. 1993
Gregory H. Olsen and Marshall J. Cohen 28 May 1993 23 p
(Contract DAAL03-92-C-0039)
(AD-A266134; ARO-30480.1-EL-SBI) Avail: CASI HC A03/MF A01

The present program was the most ambitious and had as its primary objective the fabrication of an InGaAs resistive gate CCD with a long term goal of developing 1-3 micrometer InGaAs two dimensional imaging CCD's. The 1-3 micrometer band, at present, is ill-served for imaging. The existence of room temperature imager sensitive to this wavelength range is important for a wide variety of defense, scientific, and commercial applications. Operability at room temperature will allow the camera to be miniaturized, reduce its cost, and increase its ruggedness making it well suited for field applications. As a moderate-sensitivity thermal imager, cameras in this range will be able to detect on-coming vehicles and missiles as well as monitor manufacturing processes. The wavelength band also provides a better match to the natural illumination spectrum of the night sky providing enhance Night Vision capability. When combined with long wavelength (ca. 1.55 micrometer) illumination covert eye-safe surveillance is possible. Finally, one and two dimensional InGaAs arrays will span the gap between silicon based focal plane arrays and CCD's and middle infrared imagers and Fourier spectrometers for near infrared spectroscopic applications. DTIC

N94-11515 Materials Research Society, Pittsburg, PA.
WIDE BAND-GAP SEMICONDUCTORS. 1991 MATERIALS RESE ARCH SOCIETY SYMPOSIUM PROCEEDINGS Final Report, 15 Sep. 1991 - 14 Sep. 1992
John Ballance 14 Sep. 1992 810 p Symposium held in Boston, MA, 2-6 Dec. 1991 Limited Reproducibility: More than 20% of this document may be affected by poor print
(Grant AF-AFOSR-0411-91)
(AD-A263418; AFOSR-93-0180TR) Avail: Issuing Activity (Defense Technical Information Center (DTIC))

The following topics are discussed: theoretical studies of diamond surface chemistry and diamond-metal interfaces; growth technique for large area mosaic diamond films; chemical vapor deposition of diamond films using water:alcohol:organic-acid solutions; remote ECR plasma deposition of diamond thin films from water-methanol mixtures; deposition of flame grown diamond films in a controlled atmosphere; sequential growth of high quality diamond films from hydrocarbon and hydrogen gases; diamond growth from sputtered atomic carbon and hydrogen gas; the CVD diamond nucleation mechanism on Si overlaid with sp2 carbon; investigation into the use of a diffusion barrier in microwave plasma assisted chemical vapor deposition of diamond on iron based substrates; selective nucleation of diamond crystals on the apex of silicon pyramids; and effect of laser irradiation on carbon-implanted copper substrates. DTIC

N94-11518 Case Western Reserve Univ., Cleveland, OH. Dept. of Chemistry.
LOW ENERGY ELECTRON DIFFRACTION AND CYCLIC VOLTAMMETRY STUDIES OF FLAME-ANNEALED PLATINUM SINGLE CRYSTALS
F. H. Feddrix, E. B. Yeager, and B. D. Cahan 23 Apr. 1993 9 p Limited Reproducibility: More than 20% of this document may be affected by microfiche quality
(Contract N00014-90-J-1212)
(AD-A263566; TR-90-ONR) Avail: Issuing Activity (Defense Technical Information Center (DTIC))

Low energy electron diffraction (LEED) and cyclic voltammetry were used to examine the surface structure of flame-annealed platinum (100), (110), and (111) electrodes. Well-defined LEED patterns were obtained for these surfaces but only after heat treatment in vacuo at 400 C in order to remove surface contaminants. The cyclic voltammograms correspond to those expected for these low index platinum surface from prior studies. DTIC

N94-11605 Sandia National Labs., Albuquerque, NM.
GaAs PCSS: HIGH GAIN SWITCHING AND DEVICE RELIABILITY
F. J. Zutavern, G. M. Loubriel, D. L. McLaughlin, M. W. OMalley, W. D. Helgeson, and G. J. Denison 1992 5 p Presented at the OE/LASE 1993: International Society for Optical Engineering (SPIE) Conference, Los Angeles, CA, 16-23 Jan. 1993 Limited Reproducibility: More than 20% of this document may be affected by microfiche quality
(Contract DE-AC04-76DP-00789)
(DE93-009851; SAND-92-1636C; CONF-930159-23) Avail: Issuing Activity (Department of Energy (DOE)) (US Sales Only)

Characteristics of GaAs photoconductive semiconductor switches (PCSS) during the initiation and sustaining phases of high gain switching are studied in this paper. Infrared electro-photoluminescence data are presented which show current filaments during high gain switching mode. Triggering of these devices with multiple fiber optics is demonstrated and the implications for high average current density switching are discussed. Switch jitter with high field lateral PCSS has been tested and its impact on multi-switch systems is explored. Results from high repetition rate device lifetime testing are also reported. Lateral switches with several types of contacts (including: refractory metallizations, diffused and ion-implanted Ohmic layers) have been fabricated and tested. Switch characteristics and lifetime results are discussed for each of these fabrication schemes. DOE

N94-11610# Northwestern Univ., Evanston, IL. Dept. of Engineering Sciences and Applied Mathematics.
STABILITY AND DYNAMICS OF SPATIO-TEMPORAL STRUCTURES
H. Riecke Mar. 1993 7 p
(Contract DE-FG02-92ER-14303)
(DE93-011374; DOE/ER-14303/1) Avail: CASI HC A02/MF A01

The main goal of the project supported in this grant is to contribute to the understanding of localized spatial and spatio-temporal structures far from thermodynamic equilibrium. Here we report on our progress in the study of two classes of systems. We have started to investigate localized wave-pulses in binary-mixture convection. This work is based on our recently derived extension of the conventionally used complex Ginzburg-Landau equations. We are considering three regimes: dispersion-less supercritical waves; strongly dispersive subcritical waves; and localized waves as bound states of fronts between dispersionless subcritical waves and the motionless conductive state. We have completed our investigation of steady domain structures in which domains of structures with different wave numbers alternate, separated by domain walls. In particular, we have studied their regimes of existence and stability within the framework of a Ginzburg-Landau equation and have compared it to previous results. Those were based on a long-wavelength approximation, which misses certain aspects which turn out to be important for the stability of the domain structures in realistic situations. In addition, we give a description of our work on resonantly forced waves in two-dimensional anisotropic systems. DOE

N94-11646# Los Alamos National Lab., NM.
HIGHLY ANISOTROPIC BUT NODELESS GAP FROM A VALENCE-FLUCTUATION PAIRING MECHANISM
B. H. Brandow 1993 5 p Presented at the Conference on Spectroscopies in Novel Superconductors, Santa Fe, NM, 17-19 Mar. 1993
(Contract W-7405-eng-36)
(DE93-010738; LA-UR-93-1088; CONF-930367-1) Avail: CASI HC A01/MF A01

We have refined and quantitatively explored a valence-fluctuation pairing mechanism, the finite-U mechanism introduced by Newns. This can provide an s-like (nodeless) gap. We use an Anderson-lattice Hamiltonian, with realistic parameter values derived from photoemission and BIS data. The Landau-Luttinger quasiparticle spectrum and the pairing interaction are obtained from a many-body variational formalism. Adequate pairing attraction is obtained, together with band narrowing (mass enhancement) and an extremely short coherence length, in reasonable agreement with experiment. These fully self-consistent results were obtained with an isotropic approximation to the band structure of a single CuO2 plane. Now, using a simplified treatment for a more realistic band structure, we find that the gap has strong in-plane anisotropy, although, it should probably still remain nodeless. This conclusion is consistent with a variety of data. DOE

N94-11651 North Carolina Univ., Chapel Hill. Dept. of Chemistry.
AN ELLIPSOMETRY INVESTIGATION OF NUCLEATION AND GROWTH OF ELECTRON CYCLOTRON RESONANCE PLASMA DEPOSITED SILICON FILMS

M. Li, Y. Z. Hu, J. Wall, K. Conrad, and E. A. Irene 4 May 1993 17 p Limited Reproducibility: More than 20% of this document may be affected by microfiche quality
(Contract N00014-89-J-1178)
(AD-A265037; TR-58) Avail: CASI HC A03

The nucleation and initial growth of Si films is fundamental to the understanding and control of rapid thermal CVD, RTCVD, and plasma enhanced CVD, PECVD processes. Herein we report on the nucleation and growth of Si deposited on oxidized silicon wafers by ECR PECVD in 600-700 C temperature range, under low-pressures, and using both in situ spectroscopic ellipsometry (SE) and single wavelength real-time ellipsometry. An island growth and coalescence model is used to interpret the real-time ellipsometry data. Initial nuclei distance and growth-parameters are derived. Atomic Force Microscopy (AFM) was used to observe the early stage of nucleation. In situ spectroscopic ellipsometry is used to measure the final Si film thicknesses and optical properties. The structure of the deposited crystalline Si films were characterized by XTEM. DTIC

N94-11654# Minnesota Univ., Minneapolis. Dept. of Chemistry.
SOLID-STATE STRUCTURES OF GUANIDINIUM METHANE, ETHANE, AND TRIFLUOROMETHANESULFONATE Technical Report, 1 Jun. 1992 - 31 May 1993
V. A. Russell, M C. Etter, and M D. Ward 22 Apr. 1993 7 p
(Contract N00014-89-J-1301)
(AD-A265293; TR-20-ONR) Avail: CASI HC A02/MF A01

The solid-state structures of guanidinium sulfonates, C(NH2)3(+)RSO3(-), are being studied, and the role of hydrogen bonding in controlling molecular packing is being assessed. We have found that guanidinium sulfonates frequently self-assemble into two-dimensional sheets formed by hydrogen bonds between the six guanidinium protons and the six sulfonate oxygen lone electron pairs. X-ray structures of guanidinium methanesulfonate, guanidinium ethanesulfonate, and guanidinium triflate are reported here. Each of these salts crystallizes in a bilayer structure of hydrogen-bonded sheets. DTIC

N94-11659 International Centre for Theoretical Physics, Trieste (Italy).
THE ADDITIONAL CONTRIBUTION CAUSED BY COULOMB INTERACTION TO THE EXCITON DISPERSION IN MULTIPLE QUANTUM WELLS AND SUPERLATTICES FOR DIRECT BAND GAP CUBIC SEMICONDUCTORS
Nguyen Ai Viet (Institute of Theoretical Physics, Hanoi, Viet Nam.), Nguyen Thi Que Huong (Institute of Theoretical Physics, Hanoi, Viet Nam.), and Le Qui Thong (Hue Coll., Viet Nam.) Oct. 1992 7 p Limited Reproducibility: More than 20% of this document may be affected by microfiche quality
(DE93-613538; IC-92/318) Avail: Issuing Activity (Department of Energy (DOE)) (US Sales Only)

The exciton dispersion in multiple quantum wells and superlattices is studied for direct band gap cubic semiconductors in the three-band-model. The Coulomb interaction between the light and heavy exciton states in different wells is calculated. This leads to a direction dependence and split of the exciton dispersion. DOE

N94-11660 International Centre for Theoretical Physics, Trieste (Italy).
ON THE THEORY OF PHONORITON IN CUBIC SEMICONDUCTORS WITH A DEGENERATE VALENCE BAND
Nguyen Ai Viet (Institute of Theoretical Physics, Hanoi, Viet Nam.), Nguyen Thi Que Huong (Institute of Theoretical Physics, Hanoi, Viet Nam.), and Le Qui Thong (Hue Coll., Viet Nam.) Oct. 1992 13 p Limited Reproducibility: More than 20% of this document may be affected by microfiche quality
(DE93-613539; IC-92/320) Avail: Issuing Activity (Department of Energy (DOE)) (US Sales Only)

The 'phonoriton' is an elementary excitation constructed from an exciton polariton and phonon in semiconductors under intense excitation by an electromagnetic wave near the exciton resonance. A theory of phonoriton in direct band gap cubic semiconductor with a degenerate valence band using the simple model of J.L. Birman and B.S. Wang is developed. In addition to experimental proofs of the existence of phonoriton, an experiment to measure its flight time is proposed. DOE

N94-11682# Cornell Univ., Ithaca, NY. Dept. of Chemistry.
THE X RAY STANDING WAVES ON SURFACES
Hector D. Abruna 1993 20 p Sponsored in part by NSF and the Army Research Office
(AD-A265265) Avail: CASI HC A03/MF A01

The x-ray standing wave technique is a sensitive tool for determining the position of atoms within a crystal, adsorbed onto a surface or distributed within the crystal or at the interface. The technique is based on the x-ray standing wave field that arises as a result of the interference of coherently related incident and reflected plane waves and is described by the theory of dynamical diffraction of x-rays. When two coherently related traveling plane waves having the same wavelength pass through each other, their superposition results in a standing wave of period D = lambda/2 sin theta, where lambda is the wavelength of the traveling waves and 2 theta is the relative angle between them. The generation of a standing wave requires both an incident and a reflected wave, and the latter can be generated by either Bragg diffraction or total external reflection. DTIC

N94-11684# Wisconsin Univ., Madison. Dept. of Chemistry.
ADSORPTION AND DISSOCIATION OF DISILANE ON SI(001) STUDIED BY STM Interim Report, 1 Jun. 1992 - 31 May 1993
M. Bronikowski, Y. Wang, M. McEllistrem, D. Chen, and R. J. Hamers 18 May 1993 44 p
(Contract N00014-91-J-1629)
(AD-A265269) Avail: CASI HC A03/MF A01

The surface-adsorbed fragments resulting from the room-temperature adsorption and dissociation of disilane (Si2H6) on Si(001) are observed and identified using Scanning Tunneling Microscopy (STM). The predominant fragments are H and SiH2, which are identified by the symmetries of their binding sites on the surface. H atoms often bind near single or double dimer vacancy defects, while SiH2 tends to bind near C-type defects. We find that adsorbed H atoms induce buckling of the dimer rows on the Si(001) surface, while SiH2 groups do not. This difference is ascribed to differences in the electronic structure of the two surface-bound species. No systematic correlation between the positions of the H atom and SiH2 groups is evident, which indicates that the fragments of a single disilane molecule are not localized in a small region. This fact suggests that at least some of the molecular fragments from disilane dissociation are mobile on the Si(001) surface at room temperature. Further decomposition of the SiH2 fragments can be induced by annealing, which produces surface structures similar to those seen in molecular-beam epitaxial growth of silicon; small asymmetric islands form with low disilane coverages, whereas higher coverages give multilayer island growth. DTIC

N94-11700# Cornell Univ., Ithaca, NY. Dept. of Materials Science and Engineering.
EXPERIMENTAL STUDIES OF THE STRUCTURE OF GRAIN BOUNDARIES
S. L. Sass Apr. 1993 9 p
(Contract DE-FG02-85ER-45211)
(DE93-013979; DOE/ER-45211/22) Avail: CASI HC A02/MF A01

The goals of this project are as follows: to understand the factors affecting the structure of grain boundaries in intermetallic compounds; to understand how solute segregation affects grain boundary structure and causes embrittlement in Fe-base alloys; and to explore control of grain boundary properties. Fe and boron-doped Ni3Al and NiAl were studied. DOE

N94-11827# Minnesota Univ., Minneapolis. Dept. of Chemistry.
HYDROGEN-BOND POLYMORPHS OF GUANIDINIUM 4-BIPHENYLSULFONATE
V. A. Russell, M. C. Etter, and M. D. Ward 22 Apr. 1993 7 p
(Contract N00014-89-J-1301)
(AD-A265294; TR-23-0NR) Avail: CASI HC A02/MF A01

Hydrogen bonding is used to direct guanidinium sulfonates, C(NH2)3(+)RSO3(-), into specific molecular packing arrangements in the solid state. Guanidinium sulfonates frequently self-assemble into two-dimensional sheets formed by hydrogen bonds between the six guanidinium protons and the six sulfonate oxygen lone electron pairs. Guanidinium 4-biphenylsulfonate crystallizes hydrogen bonding patterns. Synthesis of these polymorphs and their characterization by FTIR spectroscopy and single crystal x-ray diffraction is reported. DTIC

N94-12010 Rice Univ., Houston, TX. Dept. of Chemistry.
PROGRESS TOWARD ATOMIC LAYER EPITAXY OF DIAMOND: DIAMOND FILMS GROWN ONE LAYER AT A TIME
Roy Gat, Terttu I. Hukka, Robin E. Rawles, and Mark P. DEvelyn May 1993 5 p Limited Reproducibility: More than 20% of this document may be affected by microfiche quality
(Contract N00014-91-J-1550)
(AD-A265530; TR-16-ONR) Avail: CASI HC A01

Diamond would be the ultimate coating for many applications; it is the hardest material known, it is chemically inert in most environments, it has a thermal conductivity five times that of copper, and it is optically transparent from ultraviolet through the mid- and far-infrared. However, conventional CVD methods for diamond have important limitations: many substrates of interest cannot withstand the 500-1000 C temperatures commonly employed, and the typically low nucleation density generates films with large crystal grains and rough morphologies. We are developing a novel low-pressure method for atomic layer epitaxy of diamond which should enable high-quality film growth at modest temperatures with very high nucleation densities. The method uses alternating fluxes of halocarbon radicals and atomic hydrogen, generated by reaction with atomic fluorine. Under suitable conditions, carbonatom additions to the growing film and subsequent rehydrogenation of the surface should each be self-limiting reactions resulting in deposition of one atomic layer of diamond per cycle. To date we have obtained evidence for diamond growth at rates up to 0.1 microns/hr from continuous flows of hydrogen and CHCL3, CH4, or C2H2 at reactor pressures between 10(exp -4) and 10(exp -2) Torr. DTIC

N94-12336 Utah Univ., Salt Lake City. Dept. of Physics.
HIGH FREQUENCY BEHAVIOR OF LONG AND SMALL JUNCTIONS Final Report, 1 Dec. 1988 - 30 Nov. 1992
Orest G. Symko 6 May 1993 19 p Limited Reproducibility: More than 20% of this document may be affected by microfiche quality
(Grant AF-AFOSR-0149-89)
(AD-A265670; AFOSR-93-0393TR) Avail: CASI HC A03

This research consisted of studies of the fundamentals and applications of long Josephson junctions and very small junctions, all fabricated out of NbN. We have developed technology for fabricating by reactive sputtering high quality long Josephson junctions with current densities of 100-1,000 A/sq cm. Such junctions were used for studies of giant steps on the 1-5 curve caused by fluxon pinning and of macroscopic quantum tunneling down to 15 mK. A new system, a long Josephson junction biased at Fiske steps, is presented for studies of Macroscopic Quantum Tunneling. Our results show applications of fluxons in long Josephson junctions for Fluxon Oscillator, Voltage Standard, and for observing Macroscopic Coherent Tunneling. We have also studied very small NbN junctions fabricated with a STM where single electron tunneling is observed. We were the first to present such tunneling at room temperature; this is important for several applications. Students and postdoctoral fellows were involved in this research. DTIC

N94-12339# Ibis Associates, Inc., Wellesley, MA.
ANALYSIS OF THE ECONOMICS OF DC ARC CVD DIAMOND Quarterly Report No. 1
1993 43 p
(Contract N00014-93-C-2044)
(AD-A265688) Avail: CASI HC A03/MF A01

From the research conducted to date, it appears that the cost today to produce 1,000 six-inch wafers, 1 mm thick, by DC arc deposition technology is $4,072/wafer. Of the six operations included in this analysis (substrate preparation, deposition, etching, polishing, metallizing, and inspection), the deposition step contributes the bulk of the cost (85%). The total cost of a finished substrate is dominated by the cost of equipment (30.6%) and materials (25%). High equipment costs are attributable to the low deposition rate and to the high capital investment for deposition equipment. High material costs are attributed to the lack of gas recycling and to the use of expensive high purity gases. DTIC

N94-12345# Naval Command, Control and Ocean Surveillance Center, San Diego, CA. Research, Development, Test and Evaluation.
POLARONIC CHARGE SEPARATION IN MIXED-HALIDE MX SOLIDS Professional Paper
A. Saxena, A. R. Bishop, X. Z. Huang, and J. T. Gammel Apr. 1993 58 p Limited Reproducibility: Document partially illegible
(AD-A266073) Avail: CASI HC A04/MF A01

We have obtained clear evidence for photoinduced electron hole pair separation in mixed-halide, halogen-bridged transition metal (MX) chain solids. Resonance Raman experiments on doped and photoexcited single crystals of mixed-halide (M = Pt; X=Cl, Br, and I) complexes indicate charge separation; electron polarons preferentially locate on the PtBr segment while hole polarons are trapped within PtCl segments. This polaron selectivity, which is potentially very useful for photovoltaic device applications, is demonstrated within theoretical calculations based on a discrete, 3/4-filled, two-band, tight-binding, extended Peierls-Hubbard model showing strong hybridization of PtCl and PtBr electronic bands as the driving force for separation. In contrast to PtCl(x)Br(1-x), the PtCl(x)I(1-x) system exhibits qualitatively different behavior such as 'self doping.' DTIC

N94-12363# Ames Lab., IA.
SYNTHESIS AND MAGNETIC PROPERTIES OF NOVEL La*2-x*M*x*CuO*4 EQUALS Y* COMPOSITIONS (La EQUALS La, Pr, Nd, Sm, Eu, Cd; M EQUALS Ca, Sr, Ba; O (LESS THAN OR EQUAL) x 0.2; -0.5 (LESS THAN OR EQUAL) y (LESS THAN OR EQUAL) 0.5)
Jin Hyung Cho 1 Mar. 1993 142 p
(Contract W-7405-eng-82)
(DE93-011359; IS-T-1536) Avail: CASI HC A07/MF A02

Ln2CuO4 undergo transitions to reduced Ln2CuO(4-d) (Ln = La, d = 1/3; Ln = Pr, Nd, Sm, Eu, Gd, d = 1/2). The Nd2CuO4-type (T'-phase) La2CuO(4+d) is observed after reoxidation of La2CuO(3.67) below 500 C. The magnetic properties of T/O (K2NiF4-type) La2CuO4 behaves differently compared with solid-state-reacted La2CuO4. The implications of these nonsuperconducting behaviors within superconducting carrier densities are discussed from a structural point of view. La(2-x)M(x)CuO(4+d) (M = Ca, Sr; x = 0.05, 0.15), synthesized by low temperature route, also contain excess O. La-139 NQR of nonsuperconducting La(1.85)Sr(0.15)CuO(4.04) show metallic properties. Tolerance factor, based on ionic radii, is to describe structures of K2NiF4 related cuprates. With anisotropic thermal motions of apical O in La2CuO4, we discuss the role of out-of-plane O for stabilization of cuprate structures. The magnetic phase diagram and phase separation of La(2-x)Sr(x)CuO(4+delta) system (0.000 less than or equal to x less than or equal to 0.030, 0.0 less than or equal to delta) are reported. From the decrease of T(sub c) by doping we infer localization and pair-breaking induced by doped holes. Phase separation is realized with antiferromagnetism. We also observe scaling properties of susceptibilities versus renormalized temperatures and infer the finite size effects by doped holes. La-139 NQR spin-lattice relaxation are presented for La(2-x)Sr(x)CuO(4), x = 0.02 to 0.08. The rate below approximately 2T(sub N)(x) shows a power-law critical behavior while above it, the rate is exponential with a small x-dependent spin-stiffness constant. The spin-lattice relaxation arises from fluctuations of staggered magnetization in locally ordered mesoscopic domains. Magnetically ordered state is not a conventional spin glass. DOE

N94-12371 Oregon Univ., Eugene. Dept. of Chemistry.
EXAMINATION OF THE SURFACE SECOND HARMONIC RESPONSE AT INFRARED WAVELENGTHS Technical Report, May 1992 - May 1993
E. K. Wong and G. L. Richmond 27 May 1993 28 p Limited Reproducibility: More than 20% of this document may be affected by microfiche quality
(Contract N00014-89-J-1261)
(AD-A265206; TR-1) Avail: CASI HC A03

Contributing factors to the second harmonic response from Ag(111) and Au(111) surfaces have been examined in the long wavelength limit where nonresonant conditions prevail. The rotational anisotropy in the nonlinear response is found to persist for both metals in the absence of surface resonances and to show convergent behavior in both the relative phase and intensity as the incident energy is lowered from resonant to nonresonant conditions. The phase difference between the in-plane and out-of-plane response in the long wavelength limit can be described by linear Fresnel theory. Whereas the tensor elements corresponding to the out-of-plane response are found to dominate, the in-plane contributions are found to be non-negligible. DTIC

N94-12375# Florida Univ., Gainesville. Dept. of Electrical Engineering.
DEVELOPMENT OF ULTRA-LOW NOISE, HIGH SENSITIVITY PLANAR METAL GRATING COUPLED 3 TO 5 MULTIQUANTUM WELL INFRARED DETECTORS FOR FOCAL PLANE ARRAY STARING IR SENSOR SYSTEMS Quarterly Progress Report No. 7
Shang S. Li 1 May 1993 72 p
(Contract N00014-91-J-1976)
(AD-A265599) Avail: CASI HC A04/MF A01

During this reporting period, we have continued to make progress towards the program goals. We have designed, fabricated, and characterized several new types of 2-D metal grating coupled n-type GaAs/AlGaAs, AlAS/AlGaAs, InAlAs/InGaAs, and InGaP/GaAs QWIPs for 2-14 microns focal plane arrays (FPAs) staring infrared sensor applications. In addition, a new normal incidence two-color p-type strained layer InGaAs/InAlAs QWIP has been developed for the first time with the highest detectivity and low dark current reported for a p-type QWIP. Specific tasks performed during this period include the following: (1) design, growth, and fabrication of a new normal incidence p-type strained InGaAs/InAlAs QWIP grown on InP substrate by MBE technique; (2) completed theoretical and experimental studies of four dual mod operation QWIPs fabricated from n-type GaAs/AlGaAs, InGaAs/InAlAs, and AlAs/AlGaAs material systems; (3) completed theoretical and experimental studies of a type-2 AlAs/AlGaAs QWIP; (4) developed a new 2-D square mesh metal grating coupled structure for an InAlAs/InGaAs BTM QWIP with significant improvement in detector's responsivity and detectivity; (5) performed noise characterization on the InGaAs/InAlAs QWIP and identified the noise sources in this QWIP; and (6) completed numerical simulations of coupling quantum efficiency versus grating periodicity and grating dimension for a 2-D square mesh metal grating coupler formed on both the standard and BTM QWIP's. DTIC

N94-12376# Cornell Univ., Ithaca, NY. Dept. of Chemistry.
THE EFFECTS OF ORGANIC ADSORBATES ON THE UNDERPOTENTIAL DEPOSITION OF SILVER ON Pt(111) ELECTRODES
D. L. Taylor and H. D. Abruna 1993 31 p
(AD-A265623) Avail: CASI HC A03/MF A01

Studies have been undertaken to determine the effects of competing organic adsorbates on the underpotential deposition of silver on Pt(111). The adsorbates studied are known to bind to Pt primarily through the hetero-atom (either nitrogen or sulfur) and include pyrazine, 2,2'-bipyridyl, 4,4'-bipyridyl, 4-phenylpyridine, 1,2-Bis(4-pyridyl)ethane, 2-mercaptopyridine, and 4-mercaptopyridine. The effects of the adsorbate layer on silver deposition are strongly dependent on the nature and structure of the co-adsorbed species. Adsorbates that bind primarily through a ring nitrogen atom were found to inhibit the deposition of the second, but not the first, silver monolayer. This may be explained by the formation of a Pt(111)/Ag/adsorbate structure in which the silver deposits underneath the adsorbate layer. These adsorbates also displayed a significant pH dependence likely due to protonation of the binding atom. In contrast, the sulfur-containing adsorbates inhibited all deposition processes at the electrode surface except that of bulk silver deposition. In this case there was a significant overpotential to bulk deposition. Moreover, a monolayer of electrodeposited silver could be displaced from the Pt surface upon exposure of the electrode to a solution of 2-mercaptopyridine. This behavior would indicate a higher bond strength between the sulfur atom and the Pt surface than that between the ring nitrogens and the Pt surface. These results are consistent with the expected strengths of adsorption. DTIC

N94-12388 Purdue Univ., West Lafayette, IN. Dept. of Chemistry.
ELECTRODE POTENTIAL-INDUCED RECONSTRUCTION OF Au(100): EFFECT OF CHEMISORPTION ON NANOSCALE DYNAMICS AS PROBED BY THE IN-SITU SCANNING TUNNELING MICROSCOPY
Xiaoping Gao and Michael J. Weaver Apr. 1993 21 p Limited Reproducibility: More than 20% of this document may be affected by microfiche quality
(Contract N00014-91-J-1409)
(AD-A265900) Avail: CASI HC A03

The effect of iodide chemisorption on the nanoscale real-space dynamics associated with the electrode potential-induced formation and removal of the hexagonal reconstruction on Au(100) in aqueous solution was examined by means of in-situ scanning tunneling microscopy under potentiodynamic conditions. Unlike in 'non-adsorbing' media such as perchloric acid where the (1 x 1) yields (hex) phase change is slow (T(sub 1/2) is approximately 10 min), requiring adatom diffusion from terrace edges, the potential-induced transition in iodide can be remarkably rapid (less than 0.2 s). The latter features facile large-scale (ca 10-20 nm) gold mass transport emanating from former (1 x 1) terraces as well as from terrace edges. The likely roles of chemisorption in inducing such remarkably rapid reconstruction are briefly discussed. Author (DTIC)

N94-12400# Department of the Navy, Washington, DC.
SPATIAL LIGHT MODULATOR HAVING PHOTOSENSITIVE AND FERROELECTRIC LAYERS Patent Application
Tak-Kin Chu, inventor (to Navy) 22 Jan. 1993 9 p
(AD-D015731; US-Patent-Appl-SN-007884; Navy-Case-74662) Avail: CASI HC A02/MF A01

A spatial light modulator is optically addressable by exposure of a vitreous selenium layer to illumination of a write beam through a transparent electrode film, thereby establishing an electrically conductive path from a voltage source to a ferroelectric liquid crystal layer in contact with conductive reflector elements arranged in a pixel pattern. Changes in polarization of the ferroelectric layer are detected by means of a read beam transmitted there through to the reflector elements for reflection and exit from another transparent electrode film through which the read beam is applied. DTIC

N94-12430*# National Aeronautics and Space Administration. Lewis Research Center, Cleveland, OH.
DIFFUSION LENGTH DAMAGE COEFFICIENT AND ANNEALING STUDIES IN PROTON-IRRADIATED InP
Roshanak Hakimzadeh (Sverdrup Technology, Inc., Brook Park, OH.), Carlos Vargas-Aburto (Kent State Univ., OH.), Sheila G. Bailey, and Wendell Williams (Case Western Reserve Univ., Cleveland, OH.) Jul. 1993 8 p Presented at the 5th International Conference on Indium Phosphide and Related Materials, Paris, France, 18-22 Apr. 1993; sponsored by the SEE, IEEE Lasers and Electro-Optics Society, and IEEE Electron Devices Society
(RTOP 506-41-11)
(NASA-TM-106262; E-7988; NAS 1.15:106262) Avail: CASI HC A02/MF A01

We report on the measurement of the diffusion length damage coefficient (K(sub L)) and the annealing characteristics of the minority carrier diffusion length (L(sub n)) in Czochralski-grown zinc-doped indium phosphide (InP), with a carrier concentration of 1 x 10(exp I8) cm(exp -3). In measuring K(sub L) irradiations were made with 0.5 MeV protons with fluences ranging from 1 x 10(exp 11) to 3 x 10(exp 13) cm(exp -2). Pre- and post-irradiation electron-beam induced current (EBIC) measurements allowed for the extraction of L(sub n) from which K(sub L) was determined. In studying the annealing characteristics of L(sub n) irradiations were made with 2 MeV protons with fluence of 5 x 10(exp 13) cm(exp -2). Post-irradiation studies of L(sub n) with time at room temperature, and with minority carrier photoinjection and forward-bias injection were carried out. The results showed that recovery under Air Mass Zero (AMO) photoinjection was complete. L(sub n) was also found to recover under forward-bias injection, where recovery was found to depend on the value of the injection current. However, no recovery of L(sub n) after proton irradiation was observed with time at room temperature, in contrast to the behavior of 1 MeV electron-irradiated InP solar cells reported previously. Author

N94-12438# Minnesota Univ., Minneapolis. Dept. of Chemistry.
ENGINEERING SOLID-STATE MATERIALS. STRATEGIES FOR MODELING AND PACKING CONTROL OF MOLECULAR ASSEMBLIES INTO 3-D NETWORKS Technical Report, 1 Jun. 1992 - 31 May 1993
V. Videnova-Adrabinska, M C. Etter, and M. D. Ward 22 Apr. 1993 16 p
(Contract N00014-89-J-1301)
(AD-A265291; TR-22-ONR) Avail: CASI HC A03/MF A01

The crystal structure and properties of a number of urea cocrystals are studied with regard to symmetry of the hydrogen-bonded molecular assemblies. The logical consequences of hydrogen bonding interactions are followed step-by-step. The problems of aggregate formation, nucleation, and crystal growth are also elucidated. Endeavor is made to envisage the 2-D and 3-D hydrogen bond network in a manageable way by exploiting graph set short hand. Strategies of how to control the symmetry of molecular packing are still to be elaborated. In our strategy, the programmed self-assembly has been based on the principle of molecular recognition of self- and hetero-complementary functional groups. However, the main focus for pre-organizational control has been put on the two-fold axis estimator of the urea molecule. DTIC

N94-12442# Microelectronics Center of North Carolina, Research Triangle Park.
MULTICOMPONENT AND MULTILAYERED THIN FILMS FOR ADVANCED MICROTECHNOLOGIES: TECHNIQUES, FUNDAMENTALS, AND DEVICES
Orlando Auciello 21 Mar. 1993 6 p
(Contract N00014-92-J-1015)
(AD-A265685) Avail: CASI HC A02/MF A01

The main objective of the Institute was to bring together scientists from different fields of research such as semiconductors, oxides, and metallic materials, as well as those working on the development of systems for thin film processing and characterization. The highly interdisciplinary nature of the Institute allowed participant scientists to interchange ideas in an environment rarely available in other international conferences. This has opened a window of opportunity for collaboration in research and development, which will continue to require interdisciplinary exchange of ideas. DTIC

N94-12563# Army Research Lab., Aberdeen Proving Ground, MD.
DEFORMATION MECHANISMS IN TUNGSTEN SINGLE CRYSTALS IN BALLISTIC IMPACT EXPERIMENTS Final Report, 1 Oct. 1991 - 30 Sep. 1992
W. J. Bruchey, Jr., R. N. Herring, P. W. Kingman, and E. J. Horwath May 1993 32 p
(DA Proj. 1L1-62618-AH-80)
(AD-A265701; ARL-TR-133) Avail: CASI HC A03/MF A01

The performance of tungsten single crystals in ballistic impact varies strongly as a function of crystallographic orientation. The deformation structure of recovered single crystal rods fired in ballistic environments has been characterized by optical microscopy, SEM and TEM, and x-ray diffraction. The observed microstructures are varied and provide substantial insights into the factors governing the penetration and flow behavior under ballistic conditions. Crystallographic orientation influences the potential for developing shear which enhances material flow, and this enhancement ultimately maximizes the energy available for target penetration. Microstructural analysis elucidates the various mechanisms occuring during the flow process for single crystals of high-symmetry orientations, and suggests possible analogies between the penetration behavior of the tungsten single crystals and other materials. DTIC

N94-12570*# Case Western Reserve Univ., Cleveland, OH. Dept. of Physics.
ELECTRONIC AND TOTAL ENERGY PROPERTIES OF TERNARY AND QUATERNARY SEMICONDUCTOR COMPOUNDS, ALLOYS AND SUPERLATTICES Final Technical Report, 1 Dec. 1988 - 10 Jan. 1992
Walter R. L. Lambrecht 28 Aug. 1992 6 p
(Grant NAG3-954)
(NASA-CR-192905; NAS 1.26:192905) Avail: CASI HC A02/MF A01

This proposal was mainly concerned with the theoretical study of semiconductor compounds, alloys, and superlattices of interest for photovoltaic applications. In the last year (1991) a study was devoted to metal/graphite bonding in relation to use of graphite fiber reinforcement of Cu for high thermal conductivity applications. The main research topics addressed during the full period of the grant are briefly described: studies of the In-Ga-As ternary system; band-offsets at common anion and InAs/GaSb/AlSb heterojunctions; alloy theory (cluster variation method); and Cu/graphite bonding. Most of the work was described more extensively in previous yearly reports and renewal applications and in publications. The last topic is described more fully in a separate report attached. A list of publications resulting directly from this grant or from other grants but related to this work and of conference presentations is given at the end. Author (revised)

N94-12586# State Univ. of New York, Buffalo. Dept. of Chemistry.
CORROSION AND PASSIVATION OF HIGH TEMPERATURE SUPERCONDUCTORS Final Report, 1 Jul. 1988 - 30 Sep. 1990
Stanley Bruckenstein 20 Dec. 1992 36 p
(Contract N00014-88-K-0621)
(AD-A265402) Avail: CASI HC A03/MF A01

Silver and copper were deposited by electroless deposition upon YBa2Cu3O7 (bulk pieces and fibers). The electrical properties of these coated materials were determined by the four-point resistivity method. Good electrical contact between electroless silver layers and the YBa2Cu3O7 substrate could be attained. Copper was electrodeposited on an electroless silver layer which provided excellent environment protection to the underlying YBa2Cu3O7. The stability of YBa2Cu3O(6.5+x) powder in various aqueous and nonaqueous environments was studied. The time dependence of sample weight and oxygen content, x, were determined for the samples exposed to atmospheres saturated with concentrated ammonium hydroxide, glacial acetic acid, acetone, hexane, toluene, ethanol, and methanol. Little evidence for reaction was found for the latter five organic vapors, while substantial reaction was found for the first two vapors. YBa2Cu3O(6.5+x) powder was also suspended in deionized water and aqueous 1 molar solutions of NaCl, KCl, KNO3, and NaBr. The results suggest that the reaction is minimal and probably involves only the surface of the powder. DTIC

N94-12587# Tennessee Univ., Knoxville. Dept. of Physics and Astronomy.
THEORETICAL INVESTIGATION OF SOME NOVEL PHENOMENAL IN ARTIFICIALLY STRUCTURED SEMICONDUCTORS Final Report
Xiaodong Zhu, Ximing Chen, Yun Zhu, and Xiaoguong Xia 31 Mar. 1993 8 p
(Contract N00014-90-J-1915)
(AD-A266142) Avail: CASI HC A02/MF A01

During the past three years my collaborators and I worked on problems in the following areas: Double quantum well systems; Impurity levels in quantum wells; Diagrammatic techniques for finite multilayer structures; Collective excitations at surfaces; and Magnetic polaron effects. DTIC

N94-12599# Ames Lab., IA.
LOW TEMPERATURE PATHWAYS TO CHEVREL PHASES VIA REDUCED MOLYBDENUM SULFIDE CLUSTER COMPLEXES Ph.D. Thesis
H. Shane 30 Mar. 1993 234 p
(Contract W-7405-eng-82)
(DE93-013282; IS-T-1609) Avail: CASI HC A11/MF A03

The initial cluster compound, Na(2y)Mo(6)S(8+y) py(sub x), was discovered by reacting Mo(6)Cl(12) with higher stoichiometries of sodium hydrosulfide and sodium butoxide in butanol/pyridine. This compound can subsequently undergo ligand exchange reactions to form a variety of cluster complexes. Single-crystal structure determinations are reported for the pyridine (py), piperidine (pip), and pyrrolidine (pyrr) complexes: triclinic Mo(6)S(8)(PY)(6) (center dot) 1.65py, cubic Mo(6)S(8)(py)(6) (center dot) 2py, Mo(6)S(8)(pip)(6) (center dot) 7pip, and Mo(6)S(8) (pyrr)(6) (center dot) 1pyrr. Delegation of the cluster complexes was explored. Direct heating under dynamic vacuum led to incomplete delegation. Reactions with tin and lead resulted in formation of corresponding Chevrel phase compounds along with MoS(2). Thermolysis reactions in the presence of flowing ammonia gas resulted in further delegation than was evidenced for reactions explored in vacuo. Solution reactions with strong acids were studied in an attempt to protonate the ligands and thus make them better leaving groups only limited success was achieved. A new preparative route was developed for ternary molybdenum sulfides. Cation exchange reactions with Na(2y)Mo(6)S(8+y)(MeOH)(x) were used to form the cobalt, tin, lead, and holmium compounds. Preliminary hydrodesulfurization studies on the sodium and cobalt compounds showed that they possess larger surface areas and thiophene conversion percentages than Chevrel phases, but a lower HDS rate. DOE

N94-10076# Aix-Marseilles Univ. (France). Inst. de Mecanique des Fluides.
INSTABILITY OF THERMOCAPILLARY CONVECTION IN FLOATING ZONES
G. Chen and Bernard Roux *In* ESA, Proceedings of the 8th European Symposium on Materials and Fluid Sciences in Microgravity, Volume 1 Aug. 1992 p 73-78 Sponsored by CNES (For primary document see N94-10070 01-29)
Copyright Avail: CASI HC A02/MF A04; ESA, EPD, ESTEC, Noordwijk, Netherlands, HC

N94-10080# Wisconsin Univ., Madison. Dept. of Materials Science and Engineering.
EFFECT OF ROTATION ON MICROGRAVITY FLOATING-ZONE CRYSTAL GROWTH
C. W. Lan, Sindo Kou, and B. C. Liao *In* ESA, Proceedings of the 8th European Symposium on Materials and Fluid Sciences in Microgravity, Volume 1 Aug. 1992 p 103-108 (For primary document see N94-10070 01-29)
(Grant NSF CTS-90-15217)
Copyright Avail: CASI HC A02/MF A04; ESA, EPD, ESTEC, Noordwijk, Netherlands, HC

N94-10081# Canadian Space Agency, Ottawa (Ontario).
MARANGONI AND BUOYANT CONVECTIONS IN ZONE MELTING OF GaAs WITH LIQUID ENCAPSULATION
Jing Li (Aix-Marseilles Univ., France.) and M. Ziad Saghir *In* ESA, Proceedings of the 8th European Symposium on Materials and Fluid Sciences in Microgravity, Volume 1 Aug. 1992 p 109-113 (For primary document see N94-10070 01-29)
Copyright Avail: CASI HC A01/MF A04; ESA, EPD, ESTEC, Noordwijk, Netherlands, HC

N94-10082# Perm State Univ. (Russia).
COUPLED THERMOVIBRATIONAL AND THERMOCAPILLARY CONVECTION IN LIQUID BRIDGE (FLOATING ZONE SYSTEM)
Grigory Z. Gershuni, Tatiana P. Lyubimova (Academy of Sciences, USSR, Perm.), D. V. Lyubimov (Academy of Sciences, USSR, Perm.), and Bernard Roux (Aix-Marseilles Univ., France.) *In* ESA, Proceedings of the 8th European Symposium on Materials and Fluid Sciences in Microgravity, Volume 1 Aug. 1992 p 117-122 Sponsored by Academy of Sciences, Perm, Russia, and CNES (For primary document see N94-10070 01-29)
Copyright Avail: CASI HC A02/MF A04; ESA, EPD, ESTEC, Noordwijk, Netherlands, HC

N94-10084# Splav Technical Center, Moscow (Russia).
ON SHAPE OF SINGLE CRYSTALS GROWN BY FZM IN MICROGRAVITY
Alexander S. Senchenkov and I. G. Smirnova *In* ESA, Proceedings of the 8th European Symposium on Materials and Fluid Sciences in Microgravity, Volume 1 Aug. 1992 p 131-134 (For primary document see N94-10070 01-29)
Copyright Avail: CASI HC A01/MF A04; ESA, EPD, ESTEC, Noordwijk, Netherlands, HC

N94-10111# Freiburg Univ. (Germany). Kristallographisches Inst.
CdTe CRYSTAL GROWTH IN THE SOVIET FACILITY ZONA 4
Manfred Salk, B. Lexow, K. W. Benz, D. G. Matioukhin (Scientific Research Inst. for Radioisotope Apparatus, Riga, Latvia.), Y. M. Gelfgat (Academy of Sciences of the Latvian SSR, Riga.), M. Z. Sorkin (Academy of Sciences of the Latvian SSR, Riga.), Alexander S. Senchenkov (Splav Technical Center, Moscow, Russia.), A. V. Egorov (Splav Technical Center, Moscow, Russia.), I. V. Barmin (Splav Technical Center, Moscow, Russia.), and Peter Sickinger (Kayser Threde G.m.b.H., Munich, Germany.) et al *In* ESA, Proceedings of the 8th European Symposium on Materials and Fluid Sciences in Microgravity, Volume 1 Aug. 1992 p 289-291 Sponsored by BMFT (For primary document see N94-10070 01-29)
Copyright Avail: CASI HC A01/MF A04; ESA, EPD, ESTEC, Noordwijk, Netherlands, HC

N94-10116# Splav Technical Center, Moscow (Russia).
CdTe CRYSTAL GROWTH BY THM WITH A ROTATING MAGNETIC FIELD
I. V. Barmin, A. V. Egorov, G. Filatov, Alexander S. Senchenkov, K. W. Benz (Freiburg Univ., Germany.), B. Lexow (Freiburg Univ., Germany.), Manfred Salk (Freiburg Univ., Germany.), Peter Hofmann (Kayser Threde G.m.b.H., Munich, Germany.), Peter Sickinger (Kayser Threde G.m.b.H., Munich, Germany.), and J. M. Gelfgat (Academy of Sciences of the Latvian SSR, Riga.) et al *In* ESA, Proceedings of the 8th European Symposium on Materials and Fluid Sciences in Microgravity, Volume 1 Aug. 1992 p 315-320 (For primary document see N94-10070 01-29)
Copyright Avail: CASI HC A02/MF A04; ESA, EPD, ESTEC, Noordwijk, Netherlands, HC

N94-10139# Kayser Threde G.m.b.H., Munich (Germany).
MISSION SUPPORT FOR CRYSTAL GROWTH EXPERIMENTS IN RUSSIAN UNMANNED CARRIERS
Peter Sickinger, Peter Hofmann, K. Kemmerle, E. Wulf, R. Klett, Alexander S. Senchenkov (Splav Technical Center, Moscow, Russia.), A. V. Egorov (Splav Technical Center, Moscow, Russia.), I. V. Barmin (Splav Technical Center, Moscow, Russia.), D. G. Matioukhin (Scientific Research Inst. for Radioisotope Apparatus, Riga, Latvia.), and Manfred Salk (Freiburg Univ., Germany.) et al *In* ESA, Proceedings of the 8th European Symposium on Materials and Fluid Sciences in Microgravity, Volume 1 Aug. 1992 p 433-434 (For primary document see N94-10070 01-29)
Copyright Avail: CASI HC A01/MF A04; ESA, EPD, ESTEC, Noordwijk, Netherlands, HC

N94-10173# Brussels Univ. (Belgium). Dept. of Chemical Physics.
ON THE ROLE OF SORET EFFECT IN CONCENTRATION DISTRIBUTION IN CRYSTALS GROWING FROM THE MELT
Stefan VanVaerenbergh, J. C. Legros, and Marcel Hennenberg *In* ESA, Proceedings of the 8th European Symposium on Materials and Fluid Sciences in Microgravity, Volume 2 Aug. 1992 p 469-474 (For primary document see N94-10171 01-29)
Copyright Avail: CASI HC A02/MF A04; ESA, EPD, ESTEC, Noordwijk, Netherlands, HC

N94-10177# Deutsche Forschungsanstalt fuer Luft- und Raumfahrt, Cologne (Germany). Space Simulation Inst.
MARANGONI MOTION DURING MELTING OF A HYPERMONOTECTIC ALLOY: NUMERICAL SIMULATIONS FOR THE D2 EXPERIMENT IHF04
L. Ratke, S. Diefenbach, B. Prinz (Metallgesellschaft A.G., Frankfurt am Main, Germany.), H. Ahlborn (Technische Univ., Hamburg, Germany.), and Berndt Feuerbacher *In* ESA, Proceedings of the 8th European Symposium on Materials and Fluid Sciences in Microgravity, Volume 2 Aug. 1992 p 495-501 (For primary document see N94-10171 01-29)
Copyright Avail: CASI HC A02/MF A04; ESA, EPD, ESTEC, Noordwijk, Netherlands, HC

N94-10179# Ishikawajima-Harima Heavy Industries Co. Ltd., Tokyo (Japan). Applied Science Dept.
NUMERICAL CALCULATION OF THE GROWTH OF InP BY THE TRAVELLING HEATER METHOD IN THE FIRST MISSION OF THE SPACE FLYER UNIT
K. Takahashi, Satoshi Adachi, M. Watanabe, Y. Ikegami, J. Ochiai, M. Kuribayashi, and H. Sakai (Institute for Unmanned Space Experiments Free Flyer, Tokyo, Japan.) *In* ESA, Proceedings of the 8th European Symposium on Materials and Fluid Sciences in Microgravity, Volume 2 Aug. 1992 p 507-511 Sponsored by New Energy and Industrial Technology Development Organization (For primary document see N94-10171 01-29)
Copyright Avail: CASI HC A01/MF A04; ESA, EPD, ESTEC, Noordwijk, Netherlands, HC

N94-10181# Aachener Centrum fuer Erstarrung unter Schwerelosigkeit e.V. (Germany).
VARIATIONS OF THE TEMPERATURE PROFILE IN THE GRADIENT FURNACE GFQ WITHIN A CYLINDRICAL SAMPLE USED FOR DIRECTIONAL SOLIDIFICATION
Martin Stehle and S. Rex *In* ESA, Proceedings of the 8th European Symposium on Materials and Fluid Sciences in Microgravity, Volume 2 Aug. 1992 p 521-526 (For primary document see N94-10171 01-29)
Copyright Avail: CASI HC A02/MF A04; ESA, EPD, ESTEC, Noordwijk, Netherlands, HC

N94-10183*# Aix-Marseilles Univ. (France). Inst. de Mecanique des Fluides.
FLOW TRANSITIONS IN A 2D DIRECTIONAL SOLIDIFICATION MODEL
Philippe Larroude, Jalil Ouazzani (Alabama Univ., Birmingham.), and J. Iwan D. Alexander (Alabama Univ., Birmingham.) *In* ESA, Proceedings of the 8th European Symposium on Materials and Fluid Sciences in Microgravity, Volume 2 Aug. 1992 p 533-538 Sponsored by NASA, Washington; Alabama Supercomputer Network; Alabama Univ.; CNES; and Inst. Mediterraneen de Technologie (For primary document see N94-10171

01-29)
Copyright Avail: CASI HC A02/MF A04; ESA, EPD, ESTEC, Noordwijk, Netherlands, HC

N94-10184# Deutsche Forschungsanstalt fuer Luft- und Raumfahrt, Cologne (Germany). Materials Research Inst.
TEXUS 28 EXPERIMENT: CONVECTIONS AND CRYSTAL GROWTH OF Ge:Ga. ANALYSIS OF TEMPERATURE MEASUREMENTS
Uwe Moeller, B. O. Hildmann, and G. Baehr *In* ESA, Proceedings of the 8th European Symposium on Materials and Fluid Sciences in Microgravity, Volume 2 Aug. 1992 p 539-543 (For primary document see N94-10171 01-29)
Copyright Avail: CASI HC A01/MF A04; ESA, EPD, ESTEC, Noordwijk, Netherlands, HC

N94-10185# Commissariat a l'Energie Atomique, Grenoble (France). Section d'Etudes de la Solification et de la Cristallogenese.
CONVECTION RELATED RADIAL SEGREGATION IN AN IDEALIZED HORIZONTAL BRIDGMAN CONFIGURATION
J. P. Garandet, Thierry Duffar, and Jean-Jacques Favier *In* ESA, Proceedings of the 8th European Symposium on Materials and Fluid Sciences in Microgravity, Volume 2 Aug. 1992 p 545-547 (For primary document see N94-10171 01-29)
Copyright Avail: CASI HC A01/MF A04; ESA, EPD, ESTEC, Noordwijk, Netherlands, HC

N94-10187# Academia Sinica, Beijing (China). Inst. of Physics.
IN SITU OBSERVATION OF TEMPERATURE DEPENDENCE OF CONCENTRATION FIELD DURING GROWTH OF KB5 CRYSTALS BY HOLOGRAPHIC INTERFEROMETRY
W. C. Chen, Y. X. Shen, and M. Y. Ma *In* ESA, Proceedings of the 8th European Symposium on Materials and Fluid Sciences in Microgravity, Volume 2 Aug. 1992 p 555-558 (For primary document see N94-10171 01-29)
Copyright Avail: CASI HC A01/MF A04; ESA, EPD, ESTEC, Noordwijk, Netherlands, HC

N94-10188*# National Inst. of Standards and Technology, Gaithersburg, MD.
PULSATILE INSTABILITY IN RAPID DIRECTIONAL SOLIDIFICATION: STRONGLY-NONLINEAR ANALYSIS
Richard J. Braun, G. J. Merchant (Stanford Univ., CA.), K. Brattkus (California Inst. of Tech., Pasadena.), and S. H. Davis (Northwestern Univ., Evanston, IL.) *In* ESA, Proceedings of the 8th European Symposium on Materials and Fluid Sciences in Microgravity, Volume 2 Aug. 1992 p 559-562 Sponsored by NASA, Washington (For primary document see N94-10171 01-29)
Copyright Avail: CASI HC A01/MF A04; ESA, EPD, ESTEC, Noordwijk, Netherlands, HC

N94-10189# Centre National de la Recherche Scientifique, Meudon-Bellevue (France). Lab. d'Aerothermique.
WETTING EFFECTS ON NYLON SPHERES ENGULFMENT IN ICE
M. Yemmou, M. A. Azouni, C. Allain (Paris-Sud Univ., Orsay, France.), and G. Petre (Brussels Univ., Belgium.) *In* ESA, Proceedings of the 8th European Symposium on Materials and Fluid Sciences in Microgravity, Volume 2 Aug. 1992 p 563-566 (For primary document see N94-10171 01-29)
Copyright Avail: CASI HC A01/MF A04; ESA, EPD, ESTEC, Noordwijk, Netherlands, HC

N94-10191# Parma Univ. (Italy). Dept. of Physics.
CRYSTAL GROWTH FROM LOW TEMPERATURE VAPOUR PHASE
Carlo Paorici (Consiglio Nazionale delle Ricerche, Parma, Italy.) *In* ESA, Proceedings of the 8th European Symposium on Materials and Fluid Sciences in Microgravity, Volume 2 Aug. 1992 p 577-583 Sponsored by Italian Space Agency and CNR (For primary document see N94-10171 01-29)
Copyright Avail: CASI HC A02/MF A04; ESA, EPD, ESTEC, Noordwijk, Netherlands, HC

N94-10192# Deutsche Forschungsanstalt fuer Luft- und Raumfahrt, Cologne (Germany).
NEW MECHANISM OF OSTWALD RIPENING IN LORENTZ-FORCE STABILIZED Cu-Pb DISPERSIONS
Dirk Uffelmann, L. Ratke, W. Bender, and Berndt Feuerbacher *In* ESA, Proceedings of the 8th European Symposium on Materials and Fluid Sciences in Microgravity, Volume 2 Aug. 1992 p 585-589 (For primary document see N94-10171 01-29)
Copyright Avail: CASI HC A01/MF A04; ESA, EPD, ESTEC, Noordwijk, Netherlands, HC

N94-10201# Aix-Marseilles Univ. (France). Inst. de Mecanique des Fluides.
CONDUCTIVE-RADIATIVE MODEL FOR PREDICTING THE SHAPE OF HgI2 CRYSTAL GROWN IN THE LTVG FURNACE
A. Roux, A. Fedoseyev (Institute of Biomedical Problems, Moscow, USSR.), and Bernard Roux *In* ESA, Proceedings of the 8th European Symposium on Materials and Fluid Sciences in Microgravity, Volume 2 Aug. 1992 p 641-644 Sponsored by Conseil Regional PACA (For primary document see N94-10171 01-29)
(Contract ESTEC-8431/89/F/BZ)
Copyright Avail: CASI HC A01/MF A04; ESA, EPD, ESTEC, Noordwijk, Netherlands, HC

N94-10203# Aix-Marseilles Univ. (France). Lab. de Physique Cristalline.
EFFECT OF EXPERIMENTAL PROCEDURE ON PATTERN FORMATION AND ARRAY DISORDER IN CELLULAR SOLIDIFICATION
Henri Nguyen Thi, Haik Jamgotchian, and B. Billia *In* ESA, Proceedings of the 8th European Symposium on Materials and Fluid Sciences in Microgravity, Volume 2 Aug. 1992 p 651-654 Sponsored by CNES and CNRS (For primary document see N94-10171 01-29)
Copyright Avail: CASI HC A01/MF A04; ESA, EPD, ESTEC, Noordwijk, Netherlands, HC

N94-10206# Ames Lab., IA.
COUPLED GROWTH OF CELLS AND BUBBLES IN DIRECTIONAL SOLIDIFICATION OF SUCCINONITRILE-ACETONE ALLOYS
Haik Jamgotchian (Iowa State Univ. of Science and Technology, Ames.), R. Trivedi (Iowa State Univ. of Science and Technology, Ames.), and B. Billia (Aix-Marseilles Univ., France.) *In* ESA, Proceedings of the 8th European Symposium on Materials and Fluid Sciences in Microgravity, Volume 2 Aug. 1992 p 669-672 Sponsored by CNRS-NSF and NATO (For primary document see N94-10171 01-29)
Copyright Avail: CASI HC A01/MF A04; ESA, EPD, ESTEC, Noordwijk, Netherlands, HC

N94-10209# Freiburg Univ. (Germany). Kristallographisches Inst.
THM-GROWTH OF III-V-SEMICONDUCTORS IN THE MAGNETIC FIELD
A. N. Danilewsky, P. Dold, and K. W. Benz *In* ESA, Proceedings of the 8th European Symposium on Materials and Fluid Sciences in Microgravity, Volume 2 Aug. 1992 p 685-689 Sponsored by BMFT (For primary document see N94-10171 01-29)
Copyright Avail: CASI HC A01/MF A04; ESA, EPD, ESTEC, Noordwijk, Netherlands, HC

N94-10213# Freiburg Univ. (Germany). Kristallographisches Inst.
CRYSTAL GROWTH IN THE ZONE MELTING FACILITY (ZMF)
Ralf Schwarz, A. N. Danilewsky, G. Bischopink, and K. W. Benz *In* ESA, Proceedings of the 8th European Symposium on Materials and Fluid Sciences in Microgravity, Volume 2 Aug. 1992 p 703-707 Sponsored by BMFT (For primary document see N94-10171 01-29)
Copyright Avail: CASI HC A01/MF A04; ESA, EPD, ESTEC, Noordwijk, Netherlands, HC

N94-10237# Politecnico di Torino (Italy). Dipt. di Scienza dei Materiali e Ingegneria Chimica.
INTERFACE REACTIONS OF (NI3AI) RIBBONS/AI-MMC IN GROUND PREPARATION AS PRELIMINARY TEST FOR MICROGRAVITY EXPERIMENTS
P. Appendino, C. Badini, M. Ferraris (Fiat Research Center, Orbassano, Turin, Italy.), and F. Marino (Trento Univ., Italy.) *In* ESA, Proceedings of the 8th European Symposium on Materials and Fluid Sciences in Microgravity,

Volume 2 Aug. 1992 p 845-847 (For primary document see N94-10171 01-29)
Copyright Avail: CASI HC A01/MF A04; ESA, EPD, ESTEC, Noordwijk, Netherlands, HC

N94-10245# Georgia Tech Research Inst., Atlanta. Zeolite Research Program.
SYNTHESIS OF MOLECULAR SIEVES FROM CLEAR SOLUTION
Rosemarie Szostak, Rosario Aiello (Calabria Univ., Arcavacta di Rende, Italy.), Flaviano Testa (Calabria Univ., Arcavacta di Rende, Italy.), and Alfonso Nasrto (Calabria Univ., Arcavacta di Rende, Italy.) *In* ESA, Proceedings of the 8th European Symposium on Materials and Fluid Sciences in Microgravity, Volume 2 Aug. 1992 p 891-893 Sponsored by Italian Space Agency (For primary document see N94-10171 01-29)
Copyright Avail: CASI HC A01/MF A04; ESA, EPD, ESTEC, Noordwijk, Netherlands, HC

N94-11385*# National Aeronautics and Space Administration. Lewis Research Center, Cleveland, OH.
ELECTROCHEMICAL CHARACTERIZATION OF p(+)n AND n(+)p DIFFUSED InP STRUCTURES
David M. Wilt, Maria Faur (Cleveland State Univ., OH.), Mircea Faur (Cleveland State Univ., OH.), M. Goradia (Cleveland State Univ., OH.), and Carlos Vargas-Aburto (Kent State Univ., OH.) *In its* Proceedings of the 12th Space Photovoltaic Research and Technology Conference (SPRAT 12) May 1993 p 33-42 (For primary document see N94-11380 01-20)
Avail: CASI HC A02/MF A03

N94-11386*# National Aeronautics and Space Administration. Lewis Research Center, Cleveland, OH.
ACTIVATION ENERGY AND CAPTURE CROSS SECTION OF MAJORITY CARRIER TRAPS IN Zn DOPED InP
George Rybicki and Wendell Williams (Case Western Reserve Univ., Cleveland, OH.) *In its* Proceedings of the 12th Space Photovoltaic Research and Technology Conference (SPRAT 12) May 1993 p 43-53 (For primary document see N94-11380 01-20)
Avail: CASI HC A03/MF A03

N94-11388*# National Aeronautics and Space Administration. Lewis Research Center, Cleveland, OH.
MEASUREMENT OF THE MINORITY CARRIER DIFFUSION LENGTH AND EDGE SURFACE-RECOMBINATION VELOCITY IN InP
Sheila G. Bailey and Roshanak Hakimzadeh (Sverdrup Technology, Inc., Brook Park, OH.) *In its* Proceedings of the 12th Space Photovoltaic Research and Technology Conference (SPRAT 12) May 1993 p 64-77 (For primary document see N94-11380 01-20)
Avail: CASI HC A03/MF A03

N94-11389*# National Aeronautics and Space Administration. Lewis Research Center, Cleveland, OH.
SURFACE PASSIVATION OF InP SOLAR CELLS WITH InAlAs LAYERS
Raj K. Jain, Dennis J. Flood, and Geoffrey A. Landis (Sverdrup Technology, Inc., Brook Park, OH.) *In its* Proceedings of the 12th Space Photovoltaic Research and Technology Conference (SPRAT 12) May 1993 p 78-87 (For primary document see N94-11380 01-20)
Avail: CASI HC A02/MF A03

N94-11404*# Naval Research Lab., Washington, DC.
RADIATION EFFECTS IN Ga(0.47)In(0.53)As SOLAR CELLS
R. J. Walters, G. J. Shaw, G. P. Summers, and S. R. Messenger (SFA, Inc., Landover, MD.) *In* NASA. Lewis Research Center, Proceedings of the 12th Space Photovoltaic Research and Technology Conference (SPRAT 12) May 1993 p 226-234 (For primary document see N94-11380 01-20)
Avail: CASI HC A02/MF A03

N94-11405*# Washington State Univ., Richland.
INVESTIGATION OF ZnSe-COATED SILICON SUBSTRATES FOR GaAs SOLAR CELLS
Daniel A. Huber, Larry C. Olsen, Glen Dunham, and F. William Addis *In* NASA. Lewis Research Center, Proceedings of the 12th Space Photovoltaic Research and Technology Conference (SPRAT 12) May 1993 p 235-248 Sponsored by USAF Phillips Lab. (For primary document see N94-11380 01-20)
Avail: CASI HC A03/MF A03

N94-11406*# English Electric Valve Co. Ltd., Chelmsford (England).
HETEROEPITAXIAL InP, AND ULTRATHIN, DIRECTLY GLASSED, GaAs 3-5 SOLAR CELLS
C. M. Hardingham and T. A. Cross *In* NASA. Lewis Research Center, Proceedings of the 12th Space Photovoltaic Research and Technology Conference (SPRAT 12) May 1993 p 249-255 (For primary document see N94-11380 01-20)
Avail: CASI HC A02/MF A03

N94-11414*# National Aeronautics and Space Administration. Lewis Research Center, Cleveland, OH.
WORKSHOP ON HETEROEPITAXIAL InP SOLAR CELLS
I. Weinberg and R. W. Walters (Naval Research Lab., Washington, DC.) *In its* Proceedings of the 12th Space Photovoltaic Research and Technology Conference (SPRAT 12) May 1993 p 326-328 (For primary document see N94-11380 01-20)
Avail: CASI HC A01/MF A03

N94-12174*# Washington Univ., Saint Louis, MO. Dept. of Earth and Planetary Sciences.
CRYSTAL-CHEMISTRY AND PARTITIONING OF REE IN WHITLOCKITE Abstract Only
R. O. Colson and B. L. Jolliff *In* Lunar and Planetary Inst., Twenty-fourth Lunar and Planetary Science Conference. Part 1: A-F 1993 p 323-324 (For primary document see N94-12015 01-91)
(Grant NAG9-56)
Avail: CASI HC A01/MF A06

77 THERMODYNAMICS AND STATISTICAL PHYSICS

Includes quantum mechanics; theoretical physics; and Bose and Fermi statistics.

For related information see also *25 Inorganic and Physical Chemistry* and *34 Fluid Mechanics and Heat Transfer.*

N94-10148# International Centre for Theoretical Physics, Trieste (Italy).
AHARONOV-BOHM EFFECT IN LUTTINGER LIQUID
F. V. Kusmartsev Oct. 1992 9 p
(DE93-613818; IC-92/311) Avail: CASI HC A02/MF A01 (US Sales Only)

We show that in the systems with the spin-charge separation the period of the Aharonov-Bohm oscillation becomes half of the flux quantum. The effect is related to the fact that for the creation of the holons (spinons) two electrons at least are needed. The effect is illustrated on the example of the Hubbard Hamiltonian with the aid of bosonization technique including topological numbers. The effect exists also in the Luttinger liquid on two chains. DOE

N94-10261# California Univ., Berkeley. Lawrence Berkeley Lab.
SOME NEW/OLD APPROACHES TO QCD
D. J. Gross Nov. 1992 20 p Presented at the STRINGS 1992, Rome, Italy, 2-8 Sep. 1992
(Contract DE-AC03-76SF-00098)
(DE93-010451; LBL-33232; CONF-9209333-1) Avail: CASI HC A03/MF A01

In this lecture I shall discuss recent attempts to revive some old ideas to address the problem of solving QCD. I believe that it is timely to return to this problem which has been woefully neglected for the last decade. QCD is a permanent part of the theoretical landscape and eventually we will have to develop analytic tools for dealing with the theory in the infrared. Lattice techniques are useful but they have not yet lived up to their promise. Even if one manages to derive the hadronic spectrum numerically, to an accuracy of 10% or even 1%, we will not be truly satisfied unless we have some analytic understanding of the results. Also, lattice Monte-Carlo methods can only be used to answer a small set of questions. Many issues of great conceptual and practical interest--in particular the calculation of scattering amplitudes--are thus far beyond lattice control. Any progress in controlling QCD in an explicit, analytic fashion would be of great conceptual value. It would also be of great practical aid to experimentalists, who must use rather ad-hoc and primitive models of QCD scattering amplitudes to estimate the backgrounds to interesting new physics. I will discuss an attempt to derive a string representation of QCD and a revival of the large N approach to QCD. Both of these ideas have a long history, many theorist-years have been devoted to their pursuit--so far with little success. I believe that it is time to try again. In part, this is because of the progress in the last few years in string theory. Our increased understanding of string theory should make the attempt to discover a stringy representation of QCD easier, and the methods explored in matrix models might be employed to study the large N limit of QCD. DOE

N94-10388 International Centre for Theoretical Physics, Trieste (Italy).
CANONICAL OPERATOR FORMULATION OF NONEQUILIBRIUM THERMODYNAMICS
M. Mehrafarin Sep. 1992 19 p Limited Reproducibility: More than 20% of this document may be affected by microfiche quality
(DE93-613028; IC-92/297) Avail: Issuing Activity (Department of Energy (DOE)) (US Sales Only)

A formulation of nonequilibrium thermodynamics is proposed which emphasizes the fundamental role played by the Boltzmann constant k in fluctuations. The equivalence of this and the stochastic formulation is demonstrated. The k approaches 0 limit of this theory yields the classical deterministic description of nonequilibrium thermodynamics. The new formulation possesses unique features which bear two important results namely the thermodynamic uncertainty principle and the quantization of entropy production rate. Such a theory becomes indispensable whenever fluctuations play a significant role. DOE

N94-10394 Academy of Sciences of the Ukraine, Kiev. Inst. Teoreticheskoj Fiziki.
ON THE RELATIVISTIC STRING SIZE AT FINITE TEMPERATURE
S. I. Lipskikh 1991 19 p Limited Reproducibility: More than 20% of this document may be affected by microfiche quality
(DE93-617658; ITP-91-98) Avail: Issuing Activity (Department of Energy (DOE)) (US Sales Only)

The spin dependence of the size of the spatial region occupied by the bosonic string at finite temperature is discussed. The expression for a free energy of the string with fixed spin and the distance between its ends is obtained. The sizes of bound states of light quarks in this model are analyzed. DOE

N94-10402 International Centre for Theoretical Physics, Trieste (Italy).
A GROUP-THEORETIC APPROACH TO THE STUDY OF SMALL OSCILLATIONS OF A DYNAMICAL SYSTEM WITH A KNOWN SYMMETRY
G. C. Chukwumah Sep. 1992 17 p Limited Reproducibility: More than 20% of this document may be affected by microfiche quality
(DE93-612971; IC-92/304) Avail: Issuing Activity (Department of Energy (DOE)) (US Sales Only)

By way of illustrating how group representations can be gainfully utilized in the study of oscillations of dynamical/mechanical systems with known symmetries, the oscillations of a simple dynamical system consisting of three identical masses with a triangular symmetry were studied. The particles are connected by light strings having the same stiffness constant. By use of irreducible representations of the symmetry group of the dynamical system, one obtains the frequencies of the normal modes of oscillation of the system without having to solve the characteristic equation of degree six in the eigenvalue of they system. This approach greatly simplifies the determination of the motion of the system and can easily be extended to other dynamical/mechanical problems with known symmetries. DOE

N94-10403 International Centre for Theoretical Physics, Trieste (Italy).
ON THERMODYNAMIC PROPERTIES OF HEAVY FERMION SYSTEMS IN MAGNETIC FIELD
Chen-Chung Lee, Chun Chen, and Xu Wang (Nankai Univ., Tiangjin, China.) Oct. 1992 25 p Limited Reproducibility: More than 20% of this document may be affected by microfiche quality
(DE93-613819; IC-92/329) Avail: Issuing Activity (Department of Energy (DOE)) (US Sales Only)

Using a two-conduction-band Anderson lattice model, the influence of magnetic fields on the thermodynamic properties of heavy fermion systems is studied by means of the slave boson mean-field theory. The depression of the heavy fermion state by magnetic fields is found. A theoretical explanation to the anomalous volume magneto-striction of heavy fermion systems is also given in this paper. DOE

N94-10405 Academy of Sciences of the Ukraine, Kiev. Inst. Teoreticheskoj Fiziki.
EFFECTIVE ACTION IN THE GAUGED NAMBU-JONA-LASINIO MODEL
V. P. Gusynin and V. A. Miranskij 1991 28 p In RUSSIAN Limited Reproducibility: More than 20% of this document may be affected by microfiche quality
(DE93-617654; ITF-91-50) Avail: CASI HC A03 (US Sales Only)

The gauged Nambu-Jona-Lasinio (NJL) model which underlies the modern mechanisms of dynamical electroweak symmetry breaking, without fundamental Higgs fields, is investigated. Using the approach based on the formalism of Green's functions of composite operators, the low energy effective action of the gauged NJL model is derived as a series in powers of the derivatives of composite fields. The explicit expression of the effective action in the case of weak (alpha much less than 1) gauge interaction is obtained. The structure of the effective action, with respect to scale transformation, is established in the whole region with alpha less than or equal to alpha(sub c) = pi/3. DOE

N94-10413# International Centre for Theoretical Physics, Trieste (Italy).
ON RENORMALIZATION GROUP FLOW IN MATRIX MODEL
H. B. Gao Oct. 1992 5 p
(DE93-613050; IC-92/302; ZIMP-92-18) Avail: CASI HC A01/MF A01 (US Sales Only)

The renormalization group flow recently found by Brezin and Zinn-Justin by integrating out redundant entries of the (N+1) x (N+1) Hermitian random matrix is studied. By introducing explicitly the RG flow parameter, and adding suitable counter terms to the matrix potential of the one matrix model, we deduce some interesting properties of the RG trajectories. In particular, the string equation for the general massive model interpolating between the UV and IR fixed points turns out to be a consequence of RG flow. An ambiguity in the UV region of the RG trajectory is remarked to be related to the large order behavior of the one matrix model. DOE

N94-10499 International Centre for Theoretical Physics, Trieste (Italy).
ON THE GENERALIZED JORDAN-BRANS-DICKE THEORY
YuanZhong Zhang (Academia Sinica, Beijing, China.) Oct. 1992 7 p Limited Reproducibility: More than 20% of this document may be affected by microfiche quality
(DE93-613051; IC-92/330) Avail: CASI HC A02 (US Sales Only)

Newtonian limit in the generalized Jordan-Brans-Dicke theory is discussed and some ambiguities are clarified. DOE

N94-10500 International Centre for Theoretical Physics, Trieste (Italy).
THE RING STRUCTURE OF CHIRAL OPERATORS FOR MINIMAL MODELS COUPLED TO 2D GRAVITY
M. H. Sarmadi Sep. 1992 8 p Limited Reproducibility: More than 20% of this document may be affected by microfiche quality
(DE93-613119; IC-92/301) Avail: Issuing Activity (Department of Energy (DOE)) (US Sales Only)

The BRST cohomology ring for (p,q) models coupled to gravity is discussed. In addition to the generators of the ghost number zero ring, the existence of a generator of ghost number -1 and its inverse is proved and used to construct the entire ring. Some comments are made regarding the algebra of the vector fields on the ring and the supersymmetric extension. DOE

N94-10501 Melbourne Univ., Parkville (Australia). School of Physics.
INTERFEROMETRY WITH PARTICLES OF NON-ZERO REST MASS
G. I. Opat 1992 12 p Limited Reproducibility: More than 20% of this document may be affected by microfiche quality
(DE93-613518; UM-P-92/57) Avail: CASI HC A03 (US Sales Only)

Interferometry as a space-time process is described. Starting from this viewpoint, a convenient formalism for the phase shifts which arise in particle interferometry is developed. This formalism is based on a covariant form of Hamilton's action principle and Lagrange's equations of motion. It is shown that this Lorentz invariant formalism yields a simple perturbation-theoretic expression for the general phase shift that arises in matter wave interferometry. The resulting formalism will be used to analyse the Sagnac effect, gravitational field measurements, and several Aharonov-Bohm-like topological phase shifts. DOE

N94-10528# Brookhaven National Lab., Upton, NY.
STANDARD MODEL STATUS (IN SEARCH OF NEW PHYSICS)
W. J. Marciano Mar. 1993 9 p Presented at the Future Directions in Particle and Nuclear Physics at Multi-GeV Hadron Beam Facilities, Upton, NY, 4-6 Mar. 1993
(Contract DE-AC02-76CH-00016)
(DE93-013288; BNL-48760; CONF-930389-3) Avail: CASI HC A02/MF A01

A perspective on the successes and shortcomings of the standard model is given. The complementarity between direct high energy probes of new physics and lower energy searches via precision measurements and rare reactions is described. Several illustrative examples are discussed. DOE

N94-10535 Moscow State Univ. (Russia). Nauchno-Issledovatel'skij Inst. Yadernoj Fiziki.
FROM THE WEYL THEORY TO A THEORY OF LOCALLY ANISOTROPIC SPACE-TIME
G. Y. Bogoslovsky 1991 14 p Limited Reproducibility: More than 20% of this document may be affected by microfiche quality
(DE92-644734; INP-MSU-91-15-219; NIIYaF-MGU-91-15-219) Avail: Issuing Activity (Department of Energy (DOE)) (US Sales Only)

It is shown that Weyl ideas, pertaining to local conformal invariance, find natural embodiment within the framework of a relativistic theory based on a viable Finslerian model of space-time. This is associated with the peculiar property of the conformal invariant Finslerian metric which describes a locally anisotropic space of events. The local conformal transformations of the Riemannian metric tensor leave invariant rest masses as well as all observables and thus, appear as local gauge transformations. The corresponding Finslerian theory of gravitation turns out, as a result, to be an Abelian gauge theory. It satisfies the principle of correspondence with Einstein theory and predicts a number of nontrivial physical effects accessible for experimental test under laboratory conditions. DOE

N94-10536# International Centre for Theoretical Physics, Trieste (Italy).
THE EFFECT OF PRESSURE AND QUADRUPOLAR INTERACTIONS ON THE NEMATIC-ISOTROPIC TRANSITION PROPERTIES: NUMERICAL RESULTS FOR A SYSTEM OF PROLATE ELLIPSOIDS INCLUDING SECOND AND FOURTH RANK ORIENTATIONAL ORDER PARAMETERS
K. Singh Oct. 1992 8 p
(DE93-613540; IC-92/321) Avail: CASI HC A02/MF A01 (US Sales Only)

The theory of isotropic-nematic transition described in earlier papers is applied to investigate the influence of quadrupolar interactions and pressure on the stability, ordering, and thermodynamic transition properties retaining second and fourth rank orientational order parameters in the calculation for a system of hard ellipsoids of revolution characterized by its length-to-width ratio (x(sub 0) = 2a/2b). Results are in accordance with experimental observations. DOE

N94-10545# International Centre for Theoretical Physics, Trieste (Italy).
PLANCK SCALE EFFECTS ON THE MAJORON
E. Kh. Akhmedov, Z. G. Berezhiani (Muenster Univ., Germany.), R. N. Mohapatra (Maryland Univ., College Park.), and G. Senjanovic Oct. 1992 11 p
(DE93-613120; IC-92/328; UMDHEP-93-020; LMU-12/92; SISSA-149/92/EP) Avail: CASI HC A03/MF A01 (US Sales Only)

The hypothesis that non-perturbative gravitational effects lead to explicit breaking of global symmetries is considered in the context of Majoron models. We find that the nonvanishing Majoron mass generated by these effects can overclose the universe unless the massive Majoron is unstable. The cosmological mass density constraints can then be satisfied only if V(sub BL) less than 10 TeV, where V(sub BL) is the scale of B - L symmetry breaking. DOE

N94-10631# International Centre for Theoretical Physics, Trieste (Italy).
A LATTICE GAS MODEL FOR ENZYME KINETICS WITH NEXT-NEAREST NEIGHBOR INTERACTIONS
R. Mejdani, A. Gashi (Tirana Univ., Albania.), and M. Ifti (Tirana Univ., Albania.) Sep. 1992 12 p
(DE93-613026; IC-92/280) Avail: CASI HC A03/MF A01 (US Sales Only)

It is shown that, by using a one-dimensional lattice gas model with the next-nearest neighbor interactions and calculating the thermodynamic potential of the system by means of the transfer matrix method, we can find numerically for enzyme kinetics some new diagrams of saturation curve. These diagrams in the limit of no interactions between sites reduce to the classical Michaelis-Henri diagrams and in the limit of the nearest neighbor interactions to some other diagrams which we have obtained before by using a correlated walks theory. These new diagrams of saturation curve can be useful for the experimental investigation. DOE

N94-10635 International Centre for Theoretical Physics, Trieste (Italy).
S(SUP 1) X S(SUP 2) AS A BAG MEMBRANE AND ITS EINSTEIN-WEYL GEOMETRY
H. Rosu Oct. 1992 10 p Limited Reproducibility: More than 20% of this document may be affected by microfiche quality
(DE93-613149; IC-92/316) Avail: Issuing Activity (Department of Energy (DOE)) (US Sales Only)

In the hybrid skyrmion in which an anti-de Sitter bag is embedded into the skyrmion configuration a S(sup 1) x S(sup 2) membrane is lying on the compactified spatial infinity of the bag. The connection between the quark degrees of freedom and the mesonic ones is made through the membrane. This 3-dimensional manifold is at the same time Weyl-Einstein space. We present what is known until the present time to people working in the differential geometry of these spaces. DOE

N94-10718 Tokyo Univ., Tanashi (Japan). Inst. for Nuclear Study.
DIMENSIONAL TRANSITION OF THE SPACE-TIME AT THE MINIMUM ACTION NEAR THE PLANCK SCALE
Hidezumi Terazawa May 1992 13 p Limited Reproducibility: More than 20% of this document may be affected by microfiche quality
(DE93-754192; INS-932) Avail: Issuing Activity (Department of Energy (DOE))

In a model of the extended n-dimensional Einstein-Hilbert action integral for space-time and matter, it is suggested that space-time (or the universe), when contracted, may transit into a new dimension, either higher or lower, at the minimum action near the Planck scale. DOE

N94-10721 Academy of Sciences of the Ukraine, Kiev. Inst. Teoreticheskoj Fiziki.
QUASI-RELATIVISTIC EFFECTS IN BARRIER-PENETRATION PROCESSES
D. V. Anchishkin 1991 23 p Limited Reproducibility: More than 20% of this document may be affected by microfiche quality
(DE93-617730; ITP-91-18) Avail: Issuing Activity (Department of Energy (DOE)) (US Sales Only)

The problem of a particle tunneling through a potential barrier is solved within the quasi-relativistic Schroedinger equation. It is shown that the relativistic effects of the subcarrier add significantly tothe penetration coefficient when some relations between the parameters of the barrier and the mass of a tunneling particle are satisfied. An account of these effects for the penetration of low energy pi(+)-mesons through the Coulomb barrier of a U-298 nuclei yields an increase in penetration coefficient of 30 percent as compared to the nonrelativistic one. Also, we give the criteria in which the contribution of the 'under-barrier relativism' to the penetration coefficient becomes essential. DOE

N94-10802 International Centre for Theoretical Physics, Trieste (Italy).
GENERALIZED SPIN SYSTEMS AND SIGMA-MODELS
S. RandjbarDaemi, A. Salam, and J. Strathdee Sep. 1992 35 p Limited Reproducibility: More than 20% of this document may be affected by

microfiche quality
(DE93-613981; IC-92/294) Avail: Issuing Activity (Department of Energy (DOE)) (US Sales Only)

A generalization of the SU(2)-spin systems on a lattice and their continuum limit to an arbitrary compact group G is discussed. The continuum limits are, in general, non-relativistic (sigma)-model type field theories targeted on a homogeneous space G/H, where H contains the maximal torus of G. In the ferromagnetic case the equations of motion derived from our continuum Lagrangian generalize the Landau-Lifshitz equations with quadratic dispersion relation for small wave vectors. In the antiferromagnetic case the dispersion law is always linear in the long wavelength limit. The models become relativistic only when G/H is a symmetric space. Also discussed are a generalization of the Holstein-Primakoff representation of the SU(N) algebra, the topological term, and the existence of the instanton type solutions in the continuum limit of the antiferromagnetic systems. DOE

N94-10831 Academy of Sciences of the Ukraine, Kiev. Inst. Teoreticheskoj Fiziki.
ON THE POSSIBLE UNOBSERVABILITY OF THE WU-YANG PHASE FACTOR IN CURVED SPACE [OVOZMOZHNOJ NENABLYUDAEMOSTI FAZOVOGO FAKTORA VU-YANGA V ISKRIVLENNOM PROSTRANSTVE]
Y. A. Sitenko 1992 23 p In RUSSIAN Limited Reproducibility: More than 20% of this document may be affected by microfiche quality
(DE93-617645; ITF-92-6) Avail: Issuing Activity (Department of Energy (DOE)) (US Sales Only)

The Aharonov-Bohm effect is shown to vanish in the case of a strong enough static gravitational source. This is due to the impossibility of formulating the scattering problem for some classes of noncompact surfaces with the topology pi(sub 1) = Z. DOE

N94-10832 Academy of Sciences of the Ukraine, Kiev. Inst. Teoreticheskoj Fiziki.
EXACT SOLUTIONS OF A MANY-ANYON PROBLEM
S. V. Mashkevich 1991 30 p Limited Reproducibility: More than 20% of this document may be affected by microfiche quality
(DE93-617646; ITP-91-106) Avail: Issuing Activity (Department of Energy (DOE)) (US Sales Only)

A scheme of obtaining exact analytic solutions of the problem of an arbitrary number of anyons in a harmonic well is developed. Its essence consists in establishing a set of wavefunctions with the demanded interchange properties followed by finding stationary state functions within this set by the method of successive approximations. The energy of the corresponding states depends linearly on the statistical parameter. DOE

N94-10834 Academy of Sciences of the Ukraine, Kiev. Inst. Teoreticheskoj Fiziki.
EXACT SOLUTION OF THE N-DIMENSIONAL GENERALIZED DIRAC-COULOMB EQUATION
R. S. Tutik 1992 11 p Limited Reproducibility: More than 20% of this document may be affected by microfiche quality
(DE93-617649; ITP-91-107) Avail: CASI HC A03 (US Sales Only)

An exact solution to the bound state problem for the N-dimensional generalized Dirac-Coulomb equation, whose potential contains both the Lorentz-vector and Lorentz-scalar terms of the Coulomb form, is obtained. DOE

N94-10853# National Inst. of Standards and Technology, Gaithersburg, MD.
THEORETICAL EVALUATION OF R22 AND R502 ALTERNATIVES
P. A. Domanski and D. A. Didion Jan. 1993 26 p Prepared for Air-Conditioning and Refrigeration Technology Inst., Inc., Arlington, VA
(Contract DE-FG02-91CE-23810)
(DE93-014767; DOE/CE-23810/7) Avail: CASI HC A03/MF A01

The study was conducted using a semi-theoretical model, CYCLE-11, with a pure cross-flow representation of heat transfer in the evaporator and condenser. The Carnahan-Starling-DeSantis equation of state was used for calculating thermodynamic properties. Transport properties were not involved in the simulations. Simulations were conducted for 'drop-in' performance, for performance in a modified system to assess the fluids' potentials, and for performance in a modified system equipped with a liquid-line/suction-line heat exchanger. The results--presented on a relative basis to R22 and R502 performance--include the volumetric capacity, coefficient of performance, pressure increase across the compressor, and compressor discharge pressure and temperature. DOE

N94-10874 California Univ., Berkeley. Dept. of Chemistry.
QUANTUM DYNAMICS OF HELIUM CLUSTERS Final Report, Mar. 1989 - Mar. 1993
K. B. Whaley Mar. 1993 44 p Limited Reproducibility: More than 20% of this document may be affected by microfiche quality
(Contract N00014-89-J-1755)
(AD-A266060) Avail: CASI HC A03

Our study of helium clusters was motivated by the desire to understand the scaling of the unusual properties of bulk He-4, a quantum liquid, in finite size systems as one goes from the macroscopic regime to the regime of molecular dimensions. This is fully in the spirit of general cluster research, namely to develop our understanding of how the transition from molecular to bulk systems (or vice versa) is reflected in the internal structure and dynamics of finite size aggregates. The unique feature of helium is its dominant quantum behavior, resulting from a low mass and weak interatomic binding energy. Clusters of helium are therefore very weakly bound van der Waals species, whose properties were expected to be dominated by zero point delocalization effects. During this grant period, we devoted our attention exclusively to clusters of He-4, which are bose systems. These are more strongly bound than the fermionic species He-3(sub N), and are also easier and cheaper to study experimentally. Furthermore, analogy with the bulk behavior suggests that any superfluid effects if present will occur at considerably higher and therefore experimentally more readily accessible temperatures for the He-4 species. In addition to the helium clusters, we also applied our Monte Carlo techniques to clusters of molecular hydrogen, which for J = 0 are also Bose clusters. These are more strongly bound than clusters of helium, yet are still very delocalized by chemical standards and offer an intriguing possibility for a new superfluid. DTIC

N94-10880 Academy of Sciences of the Ukraine, Kiev. Inst. Teoreticheskoj Fiziki.
ALL POSSIBLE ELECTROWEAK MODELS FROM Z ORBIFOLD
H. Sato, H. Kataoka, H. Munakata, and S. Tanaka 1991 18 p Limited Reproducibility: More than 20% of this document may be affected by microfiche quality
(DE93-617656; ITP-91-78) Avail: Issuing Activity (Department of Energy (DOE)) (US Sales Only)

Considering all possible combinations of two Wilson lines it is shown that only three independent electroweak models with three generations are obtained from Z orbifold compactification. We obtain this result by analyzing particle spectra of both untwisted and twisted sectors explicitly. DOE

N94-10887 Tokyo Univ., Tanashi (Japan). Inst. for Nuclear Study.
PROCEEDINGS OF THE WORKSHOP ON NEW ASPECTS OF QUANTUM FIELD THEORIES
Shin-ichi Nojiri, ed. Sep. 1992 200 p Workshop held in Tanashi, Japan, 17-19 Feb. 1992 Limited Reproducibility: More than 20% of this document may be affected by microfiche quality
(DE93-754136; INS-T-513; CONF-9202146) Avail: Issuing Activity (Department of Energy (DOE))

This issue is the collection of the papers presented at the Workshop on New Aspects of Quantum Field Theories. The 4 presented papers are indexed individually. DOE

N94-10956# Stanford Linear Accelerator Center, CA.
QUANTIZED CONIC SECTIONS; QUANTUM GRAVITY
H. P. Noyes 15 Mar. 1993 15 p Presented at the ANPA WEST 9 Conference, Stanford, CA, 13-15 Feb. 1993
(Contract DE-AC03-76SF-00515)
(DE93-010950; SU-SLAC-PUB-6057; CONF-9302102-1) Avail: CASI HC A03/MF A01

Starting from free relativistic particles whose position and velocity can only be measured to a precision less than Delta(r)Delta(v) greater than equivalent to (+/-)k/2 sq m/s, we use the relativistic conservation laws to define the relative motion of the coordinate r = r(sub 1) - r(sub 2) of two particles of mass m(sub 1), m(sub 2), and relative velocity v = Beta(c) = k(sub 1) - k(sub 2)/k(sub 1) + k(sub 2) in terms of conic section equation v(exp 2) = Gamma(2/r +/- 1/a) where '+' corresponds to hyperbolic

and '-' to elliptical trajectories. The equation is quantized by expressing Kepler's Second Law as conservation of angular momentum per unit mass in units of k. In a sense, we obtain 'spin' from this quantization. Since (Gamma)/a cannot reach c(exp 2) without predicting either circular or asymptotic velocities equal to the limiting velocity for particulate motion, we can also quantize velocities in terms of the principle quantum number.
DOE

N94-11039 Academy of Sciences of the Ukraine, Kharkov. Fiziko-Tekhnicheskij Inst.
DISSIPATIVE PHASE TRANSITIONS IN FIELD THEORY MODELS WITH SPONTANEOUS SYMMETRY VIOLATION [DISSIPATIVNYE FAZOVYE PEREKHODY V MODELYAKH TEORII POLYA SO SPONTANNYM NARUSHENIEM SIMMETRII]
I. V. Krive and S. M. Latinskij 1992 12 p In RUSSIAN Limited Reproducibility: More than 20% of this document may be affected by microfiche quality
(DE93-621382; KFTI-92-7) Avail: CASI HC A03 (US Sales Only)

Influence of dissipation on the dynamic symmetry violation mechanism at an example of low-dimension CP(sup N-1) model was investigated. Its influence on the critical temperature of spontaneously violated symmetry restoration in zeta (sup 4) model frames and the kink energy in sinus-Gordon model were considered.
DOE

N94-11047# International Centre for Theoretical Physics, Trieste (Italy).
COSMOLOGICAL RESTRICTIONS ON CONFORMALLY-INVARIANT SU(5) GUT MODELS
G. Esposito, G. Miele (Istituto Nazionale di Fisica Nucleare, Naples, Italy.), and L. Rosa (Istituto Nazionale di Fisica Nucleare, Naples, Italy.) Nov. 1992 26 p
(DE93-619770; IC-92/387) Avail: CASI HC A03/MF A01 (US Sales Only)

Dirac's theory of constrained Hamiltonian systems is applied to the minimal conformally-invariant SU(5) grand-unified model studied at 1-loop level in a de Sitter universe. For this model, which represents a simple and interesting example of GUT theory and at the same time is a step towards theories with large gauge group like SO(10), second-class constraints in the Euclidean-time regime exist. In particular, they enable one to prove that, to be consistent with the experimentally established electroweak standard model and with inflationary cosmology, the residual gauge-symmetry group of the early universe, during the whole de Sitter era, is bound to be SU(3)xSU(2)xU(1). Moreover, the numerical solution of the field equations subject to second-class constraints is obtained. This confirms the existence of a sufficiently long de Sitter phase of the early universe, in agreement with the initial assumptions.
DOE

N94-11086 Academy of Sciences of the Ukraine, Kharkov. Fiziko-Tekhnicheskij Inst.
NON-BARRIER TUNNELING IN PRESENCE OF DISSIPATIONS [TUNNELIROVANIE BEZ BA'ERA PRI DISSIPATSII]
S. M. Latinskij 1992 12 p In RUSSIAN Limited Reproducibility: More than 20% of this document may be affected by microfiche quality
(DE93-621381; KFTI-92-6) Avail: CASI HC A03 (US Sales Only)

The influence of dissipation on the interaction between classical and tunneling mechanisms removing a system from metastable state was investigated. It was shown that, depending upon the potential parameters, such a removal in the presence of dissipation may be suppressed either on classical or on tunneling trajectories. In its turn, a strong dissipation always suppresses the tunneling mechanism.
DOE

N94-11087 Gosudarstvennyi Komitet po Ispolzovaniyu Atomnoi Energii, Moscow (USSR).
SUPERFIELD DESCRIPTION OF N = 2 EXTENDED ONE-DIMENSIONAL SUPERSYMMETRIC QUANTUM MECHANICS
V. P. Berezovoj and A. I. Pashnev 1991 10 p Limited Reproducibility: More than 20% of this document may be affected by microfiche quality
(DE93-621420; KFTI-91-20) Avail: CASI HC A02 (US Sales Only)

A description of $N = 2$ superfields is used to construct the action for the one-dimensional $N = 2$ extended supersymmetric quantum mechanics.
DOE

N94-11088 Academy of Sciences of the Ukraine, Kharkov. Fiziko-Tekhnicheskij Inst.
GREEN-SCHWARZ SUPERSTRINGS IN THE GENERALIZED HARMONICAL NEWMANN-PENROSE FORMALISM
I. A. Bandos and A. A. Zheltukhin 1991 12 p Limited Reproducibility: More than 20% of this document may be affected by microfiche quality
(DE93-621422; KFTI-91-46) Avail: CASI HC A03 (US Sales Only)

Green-Schwarz superstring theory in $D = 4$ and 10 is formulated in an extended space including additional spinor coordinates of the Cartesian moving frame. These spinor coordinates, which are realized in the form of the Lorentz harmonics, are used for the construction of covariant irreducible generators of fermionic H-symmetry. The generalizations of this Lorentz harmonical superstring formulation to the case of super-p-branes with p greater than 1 (including supermembranes $p = 2$) are discussed shortly.
DOE

N94-11162# Los Alamos National Lab., NM.
SIMILARITY OF THE LEADING CONTRIBUTIONS TO THE SELF-ENERGY AND THE THERMODYNAMICS IN TWO- AND THREE-DIMENSIONAL FERMI LIQUIDS
D. Coffey and K. S. Bedell 1993 5 p Presented at the Conference on Spectroscopies in Novel Superconductors, Santa Fe, NM, 17-19 Mar. 1993
(Contract W-7405-eng-36)
(DE93-012673; LA-UR-93-1414; CONF-930367-4) Avail: CASI HC A01/MF A01

We compare the self-energy and entropy of a two- and three-dimensional Fermi Liquids (FL's) using a model with a contact interaction between fermions. For a two-dimensional (2D) FL we find that there are T(exp 2) contributions to the entropy from interactions separate from those due to the collective modes. These T(sup 2) contributions arise from nonanalytic corrections to the real part of the self-energy and are analogous to T(exp 3)lnT contributions present in the entropy of a three-dimensional (3D) FL. The difference between the 2D and 3D results arises solely from the different phase space factors.
DOE

N94-11163# International Centre for Theoretical Physics, Trieste (Italy).
A VERSION OF SUPERSTRING WITH FOUR SPACE-TIME DIMENSIONS
Dao Vong Duc (Academy of Science of Vietnam, Hanoi.), Nguyen Hong Ha, and Nguyen Lan Oanh Aug. 1992 5 p
(DE93-608196; IC-92/220) Avail: CASI HC A01/MF A01 (US Sales Only)

We consider a version of reducing the critical dimension of space-time for superstrings based on the internal symmetry group O(p,q). The new additional oscillators used are antisymmetric second rank tensors associated with this group. The model admits the solution without extra spatial dimension.
DOE

N94-11164 Gosudarstvennyi Komitet po Ispolzovaniyu Atomnoi Energii, Moscow (USSR).
THREE-DIMENSIONAL N = 4 EXTENDED SUPERSYMMETRICAL QUANTUM MECHANICS
V. P. Berezovoj and A. I. Pashnev 1991 12 p Limited Reproducibility: More than 20% of this document may be affected by microfiche quality
(DE93-621421; KFTI-91-21) Avail: CASI HC A03 (US Sales Only)

A description of 3-dimensional $N = 4$ extended supersymmetrical quantum mechanics is proposed. The description is based upon the superfield construction of the action. The main feature of the approach is the unification of the 3-dimensional bosonic coordinate vector and the fermionic spinor of 0(3) in one irreducible representation of $N = 4$ supersymmetry algebra.
DOE

N94-11523*# Fluidtherm Engineering, Boulder, CO.
SWIRL AS A MEANS OF LIQUID MANAGEMENT IN LOW GRAVITY
W. Gene Steward Aug. 1993 22 p
(NASA Order A-41524-C)
(NASA-CR-4545; A-93116; NAS 1.26:4545) Avail: CASI HC A03/MF A01

Swirling of a liquid in a container may prove to be a more desirable method of managing liquids in low gravity (space) environments than by rotating the entire container. By injecting a relatively high velocity liquid tangentially into the body of the fluid, swirl can best be started rapidly, however an estimate of the quantity and velocity of jetflow, or mechanical power of a pump impeller required to maintain a given radial acceleration (G force) is needed to assess the feasibility of such a method. While the key aspect of the problem is determining the rate of rotational energy dissipation by wall friction in the container, there are other considerations, and the present study investigates the possible additional effects of axial variation of tangential velocity and secondary (radial and axial) flow components within the rotating fluid. Author (revised)

N94-11821 Waterloo Univ. (Ontario).
NEW TESTS OF THE EQUIVALENCE PRINCIPLE USING NON-METRIC COUPLINGS OF ELECTROMAGNETISM AND GRAVITATION Ph.D. Thesis
Jody Hupton Palmer 1992 141 p
Avail: Univ. Microfilms Order No. DANN72425

Calculations are performed for the physical predictions made by theories of gravity that introduce non-metric couplings of gravitation to electromagnetism. These results are then compared with existing observations in order to place limits on the viability of describing the solar gravitational field by theories that employ an Algebraically Extended (AE) metric in the gravitational field equations. The prototypical AE theory used in these calculations is Moffat's Nonsymmetric Gravitation Theory (NGT). It is shown that a class of AE theories of gravity, which includes NGT, using a particular general form of coupling, predicts a polarization dependent speed of light. This leads directly to polarization dependent bending of light (gravitationally induced birefringence) and radar echo time delay. It also leads to an orientation dependence of the energy of certain atomic transitions. Finally, the theory predicts an observed depolarization of solar spectral lines near the limb of the Sun. The theoretical maximum of observable circular polarization is compared with observations of Stokes V for certain spectral lines. This comparison is used to place limits on the NGT contributions to gravitational physics in the solar system. The limits are weakly dependent on a parameter involved in modeling of the solar atmosphere. A highly conservative model gives limits approximately 70 times stronger than previous limits. A model using the best available estimate of the solar modeling parameter gives a limit that is three orders of magnitude tighter than previous limits. Dissert. Abstr.

N94-11822 Toronto Univ. (Ontario).
EXPLORATIONS IN QUANTUM GRAVITY: FROM ONE LOOP EFFECTIVE ACTIONS TO TWO-DIMENSIONAL THEORIES Ph.D. Thesis
Lev Tarasoff 1992 154 p
Avail: Univ. Microfilms Order No. DANN73737

Issues and approaches relating to the quantization of gravity are explored. The one-loop effective action of quantum gravity coupled to scalar fields in n dimensions is recalculated using a unique regulating scheme, operator regularization, that avoids all divergences. For the above case as well as for Chi(sup N)(sub 4) theory and quantum scalars on a curved background, non-renormalizability is shown to manifest itself in the presence of scale-dependent terms not present in the original Lagrangian. Thus non-renormalizability of quantum gravity need not be interpreted as uncontrollable divergences in the perturbative expansions. In this case, non-renormalizability indicates fundamental indeterminancies in the theory. Using the simple brick wall model of 't Hooft, the black hole horizon is seen to have a cutoff effect on quantum states of surrounding fields that is independent of the black hole charge and mass for all space time dimensions greater than 3. The issues around the breakdown of this result for 2 dimensions are also discussed. Two-dimensional (2D) modeling of gravity and quantum gravity is explored. First, black hole solutions of a 2D version of the Einstein field equations are discussed. Then, based on an action that allows couplings to matter fields, a fully covariant Hamiltonian analysis of the 2D gravity theory is carried out. An exact solution to the quantum constraints is obtained for the case of gravity coupled to electromagnetism. The results of the above studies support the thesis that non-renormalizability of quantum gravity is indicative of the inconsistency of applying perturbative quantum field theoretic methods to gravitational theory (i.e. general relativity). The brick wall model traces part of this incompatibility to the major role that the causal structure of spacetime plays in the dynamics of quantum fields. Current approaches to Quantum Field Theory generally rely on a fixed causal structure and therefore violate the integrity of general relativity. The 2D gravity theory is then shown to be a useful model for exploring the quantization of gravity. The calculational simplicity of the model and its similarity to (3 + 1) dimensional general relativity suggests that it will be useful in developing approaches to quantum gravity that do not require a fixed background structure. Dissert. Abstr.

N94-11877# California Univ., Santa Barbara. Dept. of Chemistry.
ABSORPTION SPECTRUM CALCULATIONS USING MIXED QUANTUM-GAUSSIAN WAVE PACKET DYNAMICS Technical Report, 1 Jun. 1992 - 31 May 1993
K. Haug and H. Metiu 20 May 1993 44 p
(Contract N00014-90-J-1209)
(AD-A265179) Avail: CASI HC A03/MF A01

We calculate the absorption spectrum of a cluster using a computational method in which classical-like degrees of freedom for the nuclei are described by Gaussian wave packets while the valence electrons are treated quantum mechanically. We examine the spectral features in comparison to an even simpler mixed quantum-classical model in which the nuclear motion is treated by purely classical mechanics. Anomalous features (such as negative absorption) in the absorption spectrum which can arise from mixed quantum-classical methods are examined and the Gaussian wave packet nuclear dynamics is found to substantially reduce these anomalous features. This method is applied to a two-coordinate model problem in which exact numerical results can be obtained, and we find that the method works fairly well. We also apply the method to the valence electronic absorption spectrum for a KXe6 cluster. The method does not suffer from the dramatic failure seen when Xe motion is treated classically. The method is used to calculate the vibrational width and the vibrational structure of the electronic absorption spectrum. DTIC

N94-12343*# Massachusetts Inst. of Tech., Cambridge. Dept. of Mechanical Engineering.
ESTABLISHING BASELINE DATA FOR AN EXPERIMENTAL APPRATUS THAT MEASURES HEAT TRANSFER UNDER CONDITIONS OF OSCILLATING PRESSURE AND FLOW M.S. Thesis
Charles E. Dean May 1993 148 p Sponsored in part by Martin Marietta Energy Systems, Inc.
(Grant NAG3-1076)
(NASA-CR-193772; NAS 1.26:193772; AD-A265925) Avail: CASI HC A07/MF A02

Mathematical correlations for predicting heat transfer under conditions of oscillating pressure and flow are in their developmental infancy. Such heat transfer is commonly found in reciprocating machinery such as internal combustion engines, gas springs, and Stirling cycle engines. In order to understand and improve the thermodynamic performance of reciprocal engines, it is necessary that mathematical correlations be developed that accurately predict heat loss through the walls of the components within these systems. A heat transfer apparatus has been built that models the oscillating flow of a gas in a pipe as found in the regenerator of a Stirling engine. The apparatus is capable of measuring stream temperature and velocity at any point across the diameter of the pipe, the wall temperature, gas pressure, and gas to wall heat flux. This work addresses the collection of baseline heat transfer data for this apparatus under conditions of oscillating flow and pressure by (1) explaining the addition of a laser Doppler velocimeter to measure stream velocities, (2) investigating velocity profiles within the test section as the flow oscillates, and (3) recording and analyzing baseline heat transfer data. Results show a close correlation between the phase angle between the two compressors mounted at each end of the test section and the complex-valued Nusselt number that has been derived. DTIC

N94-12535# Arnold Engineering Development Center, Arnold AFS, TN.
BOILING HEAT-TRANSFER PROCESSES AND THEIR APPLICATION IN THE COOLING OF HIGH HEAT FLUX DEVICES Final Report, Oct. 1990 - Oct. 1992
G. R. Beitel Jun. 1993 148 p
(AD-A266086; AEDC-TR-93-3) Avail: CASI HC A07/MF A02

Water cooling is used extensively at AEDC to prevent the failure of high-enthalpy arc heater components at elevated heat loads where cooling by radiation, conduction, and natural convection from air circulation are ineffective. Other cooling techniques such as the use of liquid metals, transpiration, or film cooling pose their own disadvantages or limitations and are certainly possibilities for providing cooling at much more severe heating conditions where water cooling alone may be inadequate. The current interest is in exploiting backside water cooling to the limit of its capability, especially for arc heater nozzles. Such an application requires an understanding of the parameters that affect the cooling processes and the determination of the limiting point where the surface fails due to inadequate cooling. This report reviews the different processes encountered in backside water cooling and identifies those processes that are desirable for effective cooling of high-enthalpy facility components; identifies those parameters which affect the cooling processes of interest and the trend of cooling performance when the parameters are individually varied; and presents a summary of applicable theoretical, analytical, and experimental work in surface cooling performed in the past 50 years. DTIC

N94-10230# Paris VIII Univ., Villetaneuse (France). Inst. Galilee.
TRANSPORT OF HEAT AND MASS IN NEAR-CRITICAL FLUIDS
Yves Garrabos, B. LeNeindre, P. Guenoun (Commissariat a l'Energie Atomique, Gif-sur-Yvette, France.), F. Perrot (Commissariat a l'Energie Atomique, Gif-sur-Yvette, France.), and Daniel Beysens (Commissariat a l'Energie Atomique, Gif-sur-Yvette, France.) *In* ESA, Proceedings of the 8th European Symposium on Materials and Fluid Sciences in Microgravity, Volume 2 Aug. 1992 p 807-813 Sponsored by CNES and ESA (For primary document see N94-10171 01-29)
Copyright Avail: CASI HC A02/MF A04; ESA, EPD, ESTEC, Noordwijk, Netherlands, HC

N94-10448# European Space Agency. European Space Research and Technology Center, ESTEC, Noordwijk (Netherlands). Propulsion and Aerothermodynamics Div.
THERMODYNAMIC MODEL OF AIR IN CHEMICAL EQUILIBRIUM
D. Giordano and L. Marraffa *In* AGARD, Theoretical and Experimental Methods in Hypersonic Flows Apr. 1993 15 p (For primary document see N94-10421 01-02)
Copyright Avail: CASI HC A03/MF A04

N94-10577*# Northwestern Univ., Evanston, IL.
THE LEGACY OF UNCERTAINTY
Laurie M. Brown *In* NASA. Goddard Space Flight Center, The Second International Workshop on Squeezed States and Uncertainty Relations 1993 p 119-132 (For primary document see N94-10564 01-74)
Avail: CASI HC A03/MF A04

N94-10578*# Camerino Univ. (Italy).
QUANTUM NON DEMOLITION MEASUREMENT OF CYCLOTRON EXCITATIONS IN A PENNING TRAP
Irene Marzoli and Paolo Tombesi (Rome Univ., Italy.) *In* NASA. Goddard Space Flight Center, The Second International Workshop on Squeezed States and Uncertainty Relations 1993 p 133-142 Sponsored in part by Camerino Univ. (For primary document see N94-10564 01-74)
Avail: CASI HC A02/MF A04

N94-10580*# Liverpool Univ. (England).
GENERALISED SQUEEZING AND INFORMATION THEORY APPROACH TO QUANTUM ENTANGLEMENT
A. Vourdas *In* NASA. Goddard Space Flight Center, The Second International Workshop on Squeezed States and Uncertainty Relations 1993 p 149-156 (For primary document see N94-10564 01-74)
Avail: CASI HC A02/MF A04

N94-10585*# Nippon Telegraph and Telephone Public Corp., Tokyo (Japan). Basic Research Labs.
SQUEEZED SPIN STATES: SQUEEZING THE SPIN UNCERTAINTY RELATIONS
Masahiro Kitagawa and Masahito Ueda *In* NASA. Goddard Space Flight Center, The Second International Workshop on Squeezed States and Uncertainty Relations 1993 p 187-192 (For primary document see N94-10564 01-74)
Avail: CASI HC A02/MF A04

N94-10586*# Universidad Boliviana Mayor de San Simon, Cochabamba.
QUANTUM ENTROPY AND UNCERTAINTY FOR TWO-MODE SQUEEZED, COHERENT AND INTELLIGENT SPIN STATES
C. Aragone and D. Mundarain *In* NASA. Goddard Space Flight Center, The Second International Workshop on Squeezed States and Uncertainty Relations 1993 p 193-208 (For primary document see N94-10564 01-74)
Avail: CASI HC A03/MF A04

N94-10587*# Ferrara Univ. (Italy).
THE UNCERTAINTY PRINCIPLE IN RESONANT GRAVITATIONAL WAVE ANTENNAE AND QUANTUM NON-DEMOLITION MEASUREMENT SCHEMES
Pierluigi Fortini, Roberto Onofrio (Padua Univ., Italy.), and Alessandro Rioli (Bologna Univ., Italy.) *In* NASA. Goddard Space Flight Center, The Second International Workshop on Squeezed States and Uncertainty Relations 1993 p 209-224 (For primary document see N94-10564 01-74)
Avail: CASI HC A03/MF A04

N94-10589*# Rutgers Univ., New Brunswick, NJ. Dept. of Mathematics.
OBSERVABLES, MEASUREMENTS AND PHASE OPERATORS FROM A BOHMIAN PERSPECTIVE
Martin Daumer and Sheldon Goldstein *In* NASA. Goddard Space Flight Center, The Second International Workshop on Squeezed States and Uncertainty Relations 1993 p 231-238 (For primary document see N94-10564 01-74)
(Grant NSF DMS-91-05661)
Avail: CASI HC A02/MF A04

N94-10590*# Texas Univ., Austin. Physics Dept.
UNCERTAINTY RELATIONS, ZERO POINT ENERGY AND THE LINEAR CANONICAL GROUP
E. C. G. Sudarshan *In* NASA. Goddard Space Flight Center, The Second International Workshop on Squeezed States and Uncertainty Relations 1993 p 241-250 (For primary document see N94-10564 01-74)
(Contract DE-FG05-85ER-40200)
Avail: CASI HC A02/MF A04

N94-10591*# Los Alamos National Lab., NM. Theoretical Div.
SUPERSQUEEZED STATES FROM SQUEEZED STATES
Michael Martin Nieto *In* NASA. Goddard Space Flight Center, The Second International Workshop on Squeezed States and Uncertainty Relations 1993 p 251-258 (For primary document see N94-10564 01-74)
Avail: CASI HC A02/MF A04

N94-10592*# Imperial Coll. of Science and Technology, London (England). Blackett Lab.
INFORMATION ENTROPHY VIA GLAUBER'S Q-REPRESENTATION
C. H. Keitel and K. Wodkiewicz (Warsaw Univ., Poland.) *In* NASA. Goddard Space Flight Center, The Second International Workshop on Squeezed States and Uncertainty Relations 1993 p 259-264 Sponsored in part by ONR (For primary document see N94-10564 01-74)
Avail: CASI HC A02/MF A04

N94-10594*# Trakya Univ., Edirne (Turkey).
QUANTUM MECHANICAL EFFECTS OF TOPOLOGICAL ORIGIN
I. H. Duru (Marmara Research Inst., Gebze, Turkey.) *In* NASA. Goddard Space Flight Center, The Second International Workshop on Squeezed States and Uncertainty Relations 1993 p 273-275 (For primary document see N94-10564 01-74)
Avail: CASI HC A01/MF A04

N94-10596*# American Univ., Washington, DC. Dept. of Physics.
NON-GAUGE PHASE TRANSFORMATIONS IN QUANTUM TRANSITION AMPLITUDES
H. R. Reiss *In* NASA. Goddard Space Flight Center, The Second International Workshop on Squeezed States and Uncertainty Relations 1993 p 283-289 (For primary document see N94-10564 01-74)
(Grant PHYS-9113926)
Avail: CASI HC A02/MF A04

N94-10597*# Korea Inst. of Tech., Tae-Jon (Republic of Korea). Dept. of Physics.
COLLISION-INDUCED SQUEEZING IN A HARMONIC OSCILLATOR

Hai-Woong Lee *In* NASA. Goddard Space Flight Center, The Second International Workshop on Squeezed States and Uncertainty Relations 1993 p 291-293 Sponsored in part by Korea Science and Engineering Foundation (For primary document see N94-10564 01-74)
Avail: CASI HC A01/MF A04

N94-10598*# Ghent Univ. (Belgium). Inst. for Theoretical Physics.
POSITIVE PHASE SPACE DISTRIBUTIONS AND UNCERTAINTY RELATIONS
Jan Kruger *In* NASA, Goddard Space Flight Center, The Second International Workshop on Squeezed States and Uncertainty Relations 1993 p 295-300 (For primary document see N94-10564 01-74)
Avail: CASI HC A02/MF A04

N94-10599*# Akademiya Nauk BSSR, Minsk. Inst. of Physics.
SQUEEZED COLOUR STATES IN GLUON JET
S. Ya. Kilin, V. I. Kuvshinov, and S. A. Firago *In* NASA. Goddard Space Flight Center, The Second International Workshop on Squeezed States and Uncertainty Relations 1993 p 301-303 (For primary document see N94-10564 01-74)
Avail: CASI HC A01/MF A04

N94-10601*# Universidad Boliviana Mayor de San Simon, Cochabamba.
NEW SQUEEZED LANDAU STATES
C. Aragone *In* NASA. Goddard Space Flight Center, The Second International Workshop on Squeezed States and Uncertainty Relations 1993 p 311-316 (For primary document see N94-10564 01-74)
Avail: CASI HC A02/MF A04

N94-10602*# Academy of Sciences (USSR), Novosibirsk. Budker Inst. of Nuclear Physics.
THE UNCERTAINTY PRINCIPLE AND QUANTUM CHAOS
Boris V. Chirikov *In* NASA. Goddard Space Flight Center, The Second International Workshop on Squeezed States and Uncertainty Relations 1993 p 317-327 (For primary document see N94-10564 01-74)
Avail: CASI HC A03/MF A04

N94-10603*# Hyderabad Univ. (India). School of Physics.
WIGNER FUNCTIONS FOR NONCLASSICAL STATES OF A COLLECTION OF TWO-LEVEL ATOMS
G. S. Agarwal (Max-Planck-Inst. fuer Quantenoptik, Munich, Germany.), Jonathan P. Dowling (Army Missile Research and Development Command, Redstone Arsenal, AL.), and Wolfgang P. Schleich (Ulm Univ., Germany.) *In* NASA. Goddard Space Flight Center, The Second International Workshop on Squeezed States and Uncertainty Relations 1993 p 329-339 Sponsored in part by the National Research Council (For primary document see N94-10564 01-74)
(Grant NSF INT-91-00685)
Avail: CASI HC A03/MF A04

N94-10605*# State Meteorological Inst., Saint Petersburg (Russia).
NON-STATIONARY AND NON-LINEAR DISPERSIVE MEDIUM AS EXTERNAL FIELD WHICH GENERATES THE SQUEEZED STATES
A. A. Lobashov and V. M. Mostepanenko (Saint Petersburg Technical Univ., Russia.) *In* NASA. Goddard Space Flight Center, The Second International Workshop on Squeezed States and Uncertainty Relations 1993 p 359-362 (For primary document see N94-10564 01-74)
Avail: CASI HC A01/MF A04

N94-10606*# Korea Univ., Seoul (Republic of Korea). Dept. of Physics.
RELATION OF SQUEEZED STATES BETWEEN DAMPED HARMONIC AND SIMPLE HARMONIC OSCILLATORS
Chung-In Um, Kyu-Hwang Yeon (Chungbuk National Univ., Republic of Korea.), Thomas F. George (Washington State Univ., Pullman.), and Lakshmi N. Pandey (Washington State Univ., Pullman.) *In* NASA. Goddard Space Flight Center, The Second International Workshop on Squeezed States and Uncertainty Relations 1993 p 363-375 Sponsored in part by Center for Thermal and Statistical Physics, BSRI Program, and the Ministry of Education 1992 (For primary document see N94-10564 01-74)
(Grant NSF CHE-91-96214)
Avail: CASI HC A03/MF A04

N94-10608*# California Univ., Berkeley. Lawrence Berkeley Lab. Physics Dept.
INFINITE-MODE SQUEEZED COHERENT STATES AND NON-EQUILIBRIUM STATISTICAL MECHANICS (PHASE-SPACE-PICTURE APPROACH)
Leehwa Yeh *In* NASA. Goddard Space Flight Center, The Second International Workshop on Squeezed States and Uncertainty Relations 1993 p 383-398 (For primary document see N94-10564 01-74)
(Contract DE-AC03-76SF-00098; NSF PHY-90-21139)
(LBL-32695; UCB-PTH-92/25) Avail: CASI HC A03/MF A04

N94-10609*# Academy of Sciences (USSR), Moscow. Inst. for Nuclear Research.
CORRELATED STATES OF A QUANTUM OSCILLATOR ACTED BY SHORT PULSES
O. V. Manko *In* NASA. Goddard Space Flight Center, The Second International Workshop on Squeezed States and Uncertainty Relations 1993 p 399-403 (For primary document see N94-10564 01-74)
Avail: CASI HC A01/MF A04

N94-10610*# Academy of Sciences (USSR), Moscow. Lebedev Inst. of Physics.
FLOQUET OPERATOR AS INTEGRAL OF MOTION
V. I. Manko *In* NASA. Goddard Space Flight Center, The Second International Workshop on Squeezed States and Uncertainty Relations 1993 p 405-406 (For primary document see N94-10564 01-74)
Avail: CASI HC A01/MF A04

N94-10611*# Chungbuk National Univ. (Republic of Korea). Dept. of Physics.
COHERENT STATES AND UNCERTAINTY RELATIONS FOR THE DAMPED HARMONIC OSCILLATOR WITH TIME-DEPENDENT FREQUENCY
Kyu-Hwang Yeon, Chung-In Um (Korea Univ., Seoul, Republic of Korea.), Thomas F. George (Washington State Univ., Pullman.), and Lakshmi N. Pandey (Washington State Univ., Pullman.) *In* NASA. Goddard Space Flight Center, The Second International Workshop on Squeezed States and Uncertainty Relations 1993 p 407-414 (For primary document see N94-10564 01-74)
(Contract KSOEF-91-08-00-05; NSF CHE-91-96214)
Avail: CASI HC A02/MF A04

N94-10612*# Academy of Sciences (USSR), Moscow. Lebedev Physics Inst.
QUANTUM PROCESSES IN RESONATORS WITH MOVING WALLS
A. B. Klimov and V. V. Dodonov *In* NASA. Goddard Space Flight Center, The Second International Workshop on Squeezed States and Uncertainty Relations 1993 p 415-422 (For primary document see N94-10564 01-74)
Avail: CASI HC A02/MF A04

N94-12028*# Bechtel Corp., San Francisco, CA.
THERMODYNAMICS OF LUNAR ILMENITE REDUCTION Abstract Only
B. H. Altenberg, H. A. Franklin, and C. H. Jones *In* Lunar and Planetary Inst., Twenty-fourth Lunar and Planetary Science Conference. Part 1: A-F 1993 p 27-28 (For primary document see N94-12015 01-91)
Avail: CASI HC A01/MF A06

80 SOCIAL SCIENCES (GENERAL)

Includes educational matters.

N94-11517 District of Columbia Univ., Washington, DC.
A SUMMER PROGRAM IN MATHEMATICS AND COMPUTER SCIENCE FOR ACADEMICALLY ORIENTED STUDENT Report, Jun. 11 - Jul. 1992
Bernis Barnes 24 Jul. 1992 164 p Sponsored by ONR Limited Reproducibility: More than 20% of this document may be affected by microfiche quality
(AD-A263467) Avail: Issuing Activity (Defense Technical Information Center (DTIC))

The 1992 UDC-Navy summer intervention program in mathematics and computer science for academically oriented students, as did the 1991 program, ranks among the most successful programs. The five-week intensive and rigorous academic program for the thirty-six mainly ninth and tenth grade students had a good mix of students from the public, private, and parochial schools of the D.C. area. As in the past ten years, the under-representation of minorities, especially Blacks and Hispanics, in engineering, natural science, and other mathematics-based fields was given a high priority. The students, most of whom are from the under-representative groups, had an opportunity to strengthen their background in mathematics and were encourage to pursue careers in mathematics-based fields. They also had an opportunity to increase their awareness of the many career opportunities that are available in mathematics-based fields and of the preparation that is necessary to pursue careers in these areas. The program faculty, which has had several years of experience in teaching local minority students, provided encouragement and motivation, as well as, a caring and supportive environment. DTIC

N94-11599*# Fayetteville State Univ., NC.
PROJECT TIMS (TEACHING INTEGRATED MATH/SCIENCE) Annual Report
Leo Edwards, Jr. 11 Jun. 1993 143 p
(Grant NAGw-3083)
(NASA-CR-194288; NAS 1.26:194288) Avail: CASI HC A07/MF A02

The goal of this project is to increase the scientific knowledge and appreciation bases and skills of pre-service and in-service middle school teachers, so as to impact positively on teaching, learning, and student retention. This report lists the objectives and summarizes the progress thus far. Included is the working draft of the TIMS (Teaching Integrated Math/Science) curriculum outline. Seven of the eight instructional subject-oriented modules are also included. The modules include informative materials and corresponding questions and educational activities in a textbook format. The subjects included here are the universe and stars; the sun and its place in the universe; our solar system; astronomical instruments and scientific measurements; the moon and eclipses; the earth's atmosphere: its nature and composition; and the earth: directions, time, and seasons. The module not included regards winds and circulation. CASI

81 ADMINISTRATION AND MANAGEMENT

Includes management planning and research.

N94-10145# General Technology Systems Ltd., Uxbridge (England).
ANALYSIS OF THE COST EVALUATION OF ESA PROGRAMMES AND COMPARABLE NATIONAL AND INTERNATIONAL PROGRAMMES Final Report
L. P. White, S. R. Dauncey, and R. T. Gibson Jun. 1992 141 p
(Contract ESA-9915/92/F/EM)
(GTS-92063) Copyright Avail: CASI HC A07/MF A02

The objective of the study is to investigate cost and cost trends of ESA programs and comparable national and international programs for the purpose of identifying cost over-runs and the reasons for these. As well as satellite programs, these include a selection of civil and military aircraft programs. The emphasis is on the main development phase in each case, though for the non-ESA programs the costs for these are usually less readily separable than is the case with ESA records. Derived from text

N94-10296# Defense Personnel Security Research Centre, Monterey, CA.
A COMPARISON OF HIGH AND LOW-IMPACT REPORTS OF INVESTIGATION ON ADJUDICATORS' DECISION MAKING: A PILOT STUDY
James E. Suchan Jan. 1993 58 p
(AD-A265747; PERS-93-002) Avail: CASI HC A04/MF A01

This report examines the effect of style of written communication on personnel security determinations. Forty senior adjudicators from four sites reviewed two cases containing significant derogatory information. The results indicate that format of the ROI did not affect the overall adjudication determination, but site-specific processes in reaching the decision were evident. A discussion is presented of outside-the-document factors that may affect readers' processing of written communications. DTIC

N94-10868# Technische Univ., Eindhoven (Netherlands). Dept. of Mathematics and Computing Science.
AN ADVISOR MODULE FOR TACTICAL AND STRATEGIC STATE-ORIENTED PLANNING SYSTEMS WITH AN APPLICATION IN MANPOWER PLANNING
H. Boers, W. Z. Venema, and J. Wessels (International Inst. for Applied Systems Analysis, Laxenburg, Austria.) Dec. 1992 30 p
(MEMO-COSOR-92-57; ETN-93-94331) Copyright Avail: CASI HC A03/MF A01

A user-controlled breath-first search method is discussed. The method is developed for generating qualitative and quantitative advice in tactical and strategic state oriented planning situations that are modeled with a network structure. A practical application in the field of manpower planning is demonstrated. The results show that the method can be implemented with little risk of combinatorial explosion. It is demonstrated that for some situations it is sensible to combine rule based with algorithmic approaches. ESA

N94-10910# General Accounting Office, Washington, DC. National Security and Internal Affairs Div.
NATIONAL AERO-SPACE PLANE: A NEED FOR PROGRAM DIRECTION AND FUNDING DECISIONS
Louis J. Rodrigues Jun. 1993 13 p
(GAO/NSIAD-93-207; B-235387) Avail: CASI HC A03/MF A01; GAO, PO Box 6015, Gaithersburg, MD 20877 HC

This report discusses the status of efforts to resolve the National Aero-Space Plane (NASP) Program's cost, schedule, and technical problems. The Program is a joint endeavor of the Department of Defense (DOD) and National Aeronautics and Space Administration (NASA) aimed at developing basic technology for future launch and hypersonic flight vehicles. The Program is currently in the second of three phases. Phase 1 evaluated the feasibility and technical concept for the aerospace plane. Phase 2, which ends in March 1994, is the technology development and maturation phase. Phase 3 involves designing, building, and testing the X-30. Funding constraints and technical concerns have caused DOD and NASA to reconsider the planned schedule. Additionally they have not achieved concensus on funding needs. The General Accounting Office recommends better management of the Program. In particular, GAO suggests that the Secretary of Defense and the NASA Administrator provide specific direction on the Program's long-term technical objectives and goals and that the Director, Office of Science and Technology Policy provide clear direction and guidance for the NASP Program. CASI

N94-10941# General Accounting Office, Washington, DC. National Security and International Affairs Div.
NASA PROCUREMENT: PROPOSED CHANGES TO THE JET PROPULSION LABORATORY CONTRACT. REPORT TO CONGRESSIONAL REQUESTERS
Jul. 1993 22 p
(GAO/NSIAD-93-178; B-253238) Avail: CASI HC A03/MF A01, GAO, PO Box 6015, Gaithersburg, MD 20877 HC

Selected provisions of the current contract for managing and performing research and development at the Jet Propulsion Laboratory (JPL) are discussed. JPL, a federally funded research and development center (FFRDC), is operated by the California Institute of Technology, and their next contract with the National Aeronautics and Space Administration (NASA) is being negotiated. In accordance with federal regulations, FFRDC's are operated by universities, other nonprofit organizations, or autonomous units of industrial firms. They are funded to meet specific long-term needs that cannot be met in any other way. The current contract's deviations from the Federal Acquisition Regulations (FAR) are mentioned; 27 were approved, but the new contract will likely have fewer. The Government Accounting Office recommends that JPL's scope of work be highly specific, be carefully reviewed, and that the contract state clearly that 'working meals' are an unallowable cost. NASA is advised to determine to what extent they should pay for college tuition for dependents of JPL employees. Advice on NASA fee-paying policies is also provided. CASI

N94-11473# M and R Associates, Rockville, MD.
FEDERAL CONTRACTORS IN APPALACHIA
R. F. Fullenbaum and M. A. McNeil Mar. 1993 92 p Sponsored by

Appalachian Regional Commission, Washington, DC
(Contract ARC-91-132-CO-10783-91-I-302-0)
(PB93-188779) Avail: CASI HC A05/MF A01

The research provides information on the characteristics of Appalachian small firms that have been successful in obtaining federal contract awards and suggests state policy initiatives that would likely be the most productive in stimulating the acquisition of federal contracts. The three groups studied for 1984, 1986, and 1988 are all small Appalachian federal contractors, women-owned small business contractors, and minority-owned small business contractors. Federal contractors in the United States are more likely to be divisions of larger sized firms; located in metropolitan areas; and focused on products and services such as nonresidential construction, some aspects of manufacturing, wholesale machinery and equipment, and miscellaneous business services. By comparison, the profile of the typical small Appalachian business is a single establishment with one to nine or 10 to 49 employees; only marginally more likely to be located in a metropolitan area; and more focused on retail trade, residential construction, and services such as hotel, motel, and auto repair. NTIS

N94-11600# Virginia Polytechnic Inst. and State Univ., Blacksburg.
RESEARCH AND DEVELOPMENT OF POST-CLASSICAL MANAGEMENT TOOLS FOR GOVERNMENT PROGRAM OFFICES, VOLUME 2
H. A. Kurstedt and D. S. Sink Feb. 1993 309 p
(Contract DE-FG02-91NP-00119)
(DE93-010236; DOE/NP-00119/3-Vol-2) Avail: CASI HC A14/MF A03 (US Sales Only)

A critical link in the GSS model is documenting, experience - lessons teamed from cases of similar past and contemporary organizations, and the ongoing experience of the target organization. The primary purpose of this research area is to support the development of a process by which managers of large complex programs can access information from research literature, from past cases, and especially from organizational experience to adapt planned strategy to meet future demands and goals. This process is a means of implementing the Grand Strategy System. It provides a framework for an integrated systems perspective and the need for an organizational learning process. A systems perspective is approached here on two levels: (1) the formal and informal methods and procedures (systems) that operate in order to get things done (from purchasing to political accommodation) in an organization (e.g., Waterman, et. al., 1980), and (2) a systems thinking approach to planning, problem solving and decision making which incorporates interrelationships among systems as primary elements of the manager's conceptual representation (mental model) of the organization (e.g., Hicks, 1991). Organizational Teaming can be characterized as a process through which management teams coordinate and modify their mental models of the organization, its goals, its environment, and the information, strategies, systems, and actions required to achieve continuous improvement (e.g., Senge, 1990; De Geus, 1988). The activities of this research area focus on documenting and organizing past strategies to augment systems thinking and organizational learning. DOE

N94-11661# Virginia Polytechnic Inst. and State Univ., Blacksburg. Dept. of Industrial and Systems Engineering.
DESIGN, DEVELOPMENT, AND TESTING OF AN AUTOMATED KNOWLEDGE-ACQUISITION TOOL TO AID PROBLEM SOLVING, DECISION MAKING, AND PLANNING Ph.D. Thesis
T. G. Kotnour 14 Sep. 1992 239 p
(Contract DE-FG02-91NP-00119)
(DE93-010239; DOE/NP-00119/T4) Avail: CASI HC A11/MF A03 (US Sales Only)

This research studies the process of acquiring knowledge from experts. Forty subjects used a machine-aided knowledge-acquisition tool to model a word processing task. With this tool, the subjects developed models that were 72.8% accurate with baseline model and 88.5% consistent. Thirty-one knowledge-acquisition methods were evaluated and one chosen and automated in the form of a machine-aided knowledge-acquisition tool (choice is made using 5 criteria including information processing model of problem solving). Performance of this tool is evaluated in terms of accuracy and consistency of the knowledge bases generated. A baseline is derived to which other knowledge-acquisition tools' performance can be compared. Four groups of changes are suggested for the user interface and operation modes. DOE

N94-11844 Faucett (Jack) Associates, Inc., Bethesda, MD.
PATTERN OF FEDERAL PROCUREMENT FROM MINORITY AND WOMEN-OWNED SMALL BUSINESS Final Report
J. Skolnik and H. J. Chmelynski 22 Jul. 1992 121 p Limited Reproducibility: More than 20% of this document may be affected by microfiche quality
(Contract SBA-5645-OA-90)
(PB93-189355; JackFau-92-414) Avail: Issuing Activity (National Technical Information Service (NTIS))

In 1988, 3.0 percent of the $195 billion spent by the federal government in procuring goods and services went to minority-owned firms. Although minority- and women-owned firm procurement seems quite low, this does not necessarily mean that an inequitable situation exists. It has been suggested, for example, that federal government procurement may be concentrated in industries that are dominated by large businesses. By comparing the pattern of federal procurement from minority- and women-owned firms with statistics on the prevalence of minority- and women-owned businesses in the economy as a whole, the study measures that extent to which miniority- and women-owned businesseS receive a proportionate share of federal procurement. The study also identifies the sectors where minority- and women-owned businesses have been successful or unsuccessful in obtaining federal business. NTIS

N94-11856# Logistics Management Inst., Bethesda, MD.
ASSESSING THE ADEQUACY OF THE INDUSTRIAL BASE Final Report
David P. Garner, Salvatore J. Culosi, William W. Bothwell, Maurice E. Edlund, Michael G. Jackson, James S. Thomason, Peter S. Brooks, Richard Cheslow, Janet Nauta, and John F. Starns et al May 1992 426 p
Prepared in cooperation with Army Logistics Evaluation Agency, Cumberland, PA; Inst. for Defense Analysis, Alexandria, VA; and Analytic Sciences Corp., and Analytic Sciences Corp., Alexandria, VA
(Contract MDA903-90-C-0006)
(AD-A264954) Avail: CASI HC A19/MF A04

In the wake of Operations Desert Shield/Desert Storm and as a means of preparing to meet the challenges confronting it over the next 10 years, the Army chartered the Integrated Army Mobilization Study (IAMS) in Jan. 1991 to identify the major impediments to mobilizing U.S. Forces to meet future contingencies. Facing declining procurement budgets, termination of production runs, and possible loss of critical subtier vendors, the Army was especially concerned with the adequacy of the industrial base to satisfy future warfighting materiel requirements. Accordingly, as part of the total IAMS effort, the Assistant Secretary of the Army for Installations, Logistics, and Environment asked the Deputy Chief of Staff for Logistics to sponsor a study to assess the adequacy of the industrial base to support Operation Desert Storm and similar contingencies in FY-99. As the study evolved, the Army defined its desired taskings more clearly and assigned tasks to separate organizations. In all, four contracts were authorized to address distinct segments of the issue. DTIC

N94-12360# Phillips Lab., Hanscom AFB, MA.
GUIDELINES FOR THE ESTABLISHMENT AND OPERATION OF AN RFP (REQUEST FOR PROPOSAL) LIBRARY Interim Report
Bill Reid and Jean Chisholm 29 Mar. 1993 37 p
(AF Proj. 9993)
(AD-A265894; AD-E201466; PL-TR-93-2090; SR-272; XC-PL/HANSCOM) Avail: CASI HC A03/MF A01

This report describes guidelines for the establishment and operation of a Request for Proposal (RFP) Library. An RFP Library is a set of documents, often ranging in level of classification and limitation, that is viewed by potential government contractors. The report is divided into three sections. The first part contains the information necessary to set up an unlimited, unclassified RFP Library. The second section of the report outlines the security measures that must be taken with limited and classified documents. The final part of the report contains information on how to sign potential contractors into and out of the RFP Library. DTIC

N94-12410# Office of the Secretary of Defense, Washington, DC.
NATIONAL SBIR PHASE 3 COMMERCIALIZATION CONFERENCE Final Report, 10-11 Jun. 1993
Jun. 1993 159 p Conference held in Orlando, FL, 10-11 Jun. 1993
(AD-A266083) Avail: CASI HC A08/MF A02

The Small Business Innovation Research Phase III Conference, 10-11

June 1993, was organized to foster partnerships between the most successful SBIR firms and other small businesses, major corporations, venture capitalists, and technical representatives of Federal organizations. This document, provided to participants, describes the capabilities and goals of over 160 of the companies that were represented at the conference. Participating small companies all have been successful in developing technically innovative products and processes under the Federal SBIR program. Goals of the SBIR program include stimulating technological innovation, strengthening the role of small business in meeting Federal R&D needs, encouraging participation by minority and disadvantaged firms, and increasing the commercial application of Federally-supported research and development results. Conference attendees included: 75 major corporations, 233 small businesses, and 17 venture capitalists. DTIC

N94-12443# General Accounting Office, Washington, DC. Accounting and Financial Management Div.
FINANCIAL MANAGEMENT: NASA'S FINANCIAL REPORTS ARE BASED ON UNRELIABLE DATA
Oct. 1992 77 p
(AD-A265690; GAO/AFMD-93-3) Avail: CASI HC A05/MF A01

This report presents the results of GAO's review of the National Aeronautics and Space Administration's (NASA) financial management operations. It discusses a number of systems and internal control weaknesses which have resulted in unreliable data for managing and reporting on NASA's operations, as well as the status of related improvement efforts. GAO undertook this review at NASA's four largest Centers and its headquarters offices to evaluate NASA's high-risk areas that are vulnerable to waste, abuse, and mismanagement. The Office of Management and Budget (OMB) has designated NASA's financial management systems to be at risk, and OMB and GAO have designated NASA's contract administration as high risk because of previously identified weakness and NASA's increased reliance on its contractors for data. DTIC

82 DOCUMENTATION AND INFORMATION SCIENCE

Includes information management; information storage and retrieval technology; technical writing; graphic arts; and micrography.

For computer documentation see *61 Computer Programming and Software.*

N94-10374# Department of the Navy, Washington, DC.
VARIABLE RATE TRANSFER OF OPTICAL INFORMATION Patent Application
Sonlink N. Phuvan, inventor (to Navy) 24 Mar. 1993 18 p
(AD-D015758; US-Patent-Appl-SN-046254) Avail: CASI HC A03/MF A01

In accordance with the present invention, a variable optical delay module is introduced within an optical ring to provide control of the data transfer rate and optical unity gain. Two optically addressed spatial light modulators of the ferroelectric liquid crystal based type, according to one embodiment, are utilized in the optical delay module to avoid corruption of the data within the optical ring. The data is stored in one of the spatial light modulators during data transfer to the other spatial light modulator so that neither modulator would be reading from itself to overwrite and corrupt its data. An image input impinges on one spatial light modulator producing a charge distribution within the spatial modulators which matches the local intensity of the image input. This charge distribution switches the orientation of the ferroelectric liquid if it exceeds a selected threshold charge magnitude. DTIC

N94-10485# International Centre for Theoretical Physics, Trieste (Italy).
SYMBOLIC DYNAMICS AND DESCRIPTION OF COMPLEXITY
Bailin Hao Oct. 1992 21 p
(DE93-613030; IC-92/308) Avail: CASI HC A03/MF A01 (US Sales Only)

Symbolic dynamics provides a general framework to describe complexity of dynamical behavior. After a discussion of the state of the filed special emphasis will be made on the role of transfer matrix (the Stefan matrix) both in deriving the grammar from known symbolic dynamics and in extracting the rules from experimental data. The block structure of the Stefan matrix may serve as another indicator of complexity of the associated dynamics. DOE

N94-10491# Army Aeromedical Research Lab., Fort Rucker, AL.
AUTOMATICITY OF PROCESSING LOCATION VERSUS IDENTITY INFORMATION IN BRIEF VISUAL DISPLAYS Final Report
Robert L. Stephens and Jacquelyn Y. Pearson Mar. 1993 23 p
(DA Proj. 3M2-63002-D-995)
(AD-A265013; USAARL-93-17) Avail: CASI HC A03/MF A01

Differential levels of automaticity for processing information from tachistoscopic displays were studied using three variations of the partial report procedure. Processing of both spatial and identity information in letter displays was assessed simultaneously and then independently. Analyses indicated feature extraction is a highly automated process while spatial information extraction is a controlled process. Implications for separate processing pathways in the visual system are discussed. DTIC

N94-10515*# Teleos Research, Palo Alto, CA.
ACTING TO GAIN INFORMATION Final Technical Report
Stanley J. Rosenchein, J. Brian Burns, David Chapman, Leslie P. Kaelbling, Philip Kahn, H. Keith Nishihara, and Matthew Turk 30 Jul. 1993 68 p
Original contains color illustrations
(Contract NAS2-13326)
(NASA-CR-193399; NAS 1.26:193399; TR-93-03) Avail: CASI HC A04/MF A01; 2 functional color pages

This report is concerned with agents that act to gain information. In previous work, we developed agent models combining qualitative modeling with real-time control. That work, however, focused primarily on actions that affect physical states of the environment. The current study extends that work by explicitly considering problems of active information-gathering and by exploring specialized aspects of information-gathering in computational perception, learning, and language. In our theoretical investigations, we analyzed agents into their perceptual and action components and identified these with elements of a state-machine model of control. The mathematical properties of each was developed in isolation and interactions were then studied. We considered the complexity dimension and the uncertainty dimension and related these to intelligent-agent design issues. We also explored active information gathering in visual processing. Working within the active vision paradigm, we developed a concept of 'minimal meaningful measurements' suitable for demand-driven vision. We then developed and tested an architecture for ongoing recognition and interpretation of visual information. In the area of information gathering through learning, we explored techniques for coping with combinatorial complexity. We also explored information gathering through explicit linguistic action by considering the nature of conversational rules, coordination, and situated communication behavior. Author (revised)

N94-10559 Japan Broadcasting Corp., Tokyo. Science and Technical Research Lab.
PROCESSING PROPER NOUNS IN MACHINE TRANSLATION FOR ENGLISH NEWS
Naoto Katoh, Noriyoshi Uratani, and Teruaki Aizawa Apr. 1993 11 p
(NHK-Serial-414) Copyright Avail: Issuing Activity (NHK Science and Technical Research Laboratories, 1-10-11, Kinuta, Setagaya, Tokyo, 157 Japan)

NHK has been developing an English-to-Japanese machine translation system to translate a large volume of wire-service news texts delivered by foreign news agencies. One bottleneck of machine translations is that it is difficult to translate proper nouns, which appear frequently in news texts. This paper describes a method of processing proper nouns in machine translation. Author

N94-10646 Westinghouse Savannah River Co., Aiken, SC.
REPORT ON SUBGROUP ON DATA BANKS FOR RISK ASSESSMENT
W. S. Durant 1993 13 p Presented at the Energy Facility Contractors Group Safety Analysis Meeting, Denver, CO, 16-18 Jun. 1993 Limited Reproducibility: More than 20% of this document may be affected by microfiche quality
(Contract DE-AC09-89SR-18035)
(DE93-012150; WSRC-MS-93-146; CONF-9306143-1) Avail: CASI HC A03

As a result of recent discussions the Safety Analysis Working Group Steering Committee agreed to sponsor the formation of a subgroup on data banks for risk assessment. The newly created Safety Analysis Working Group Subgroup on Data Banks for Risk Assessment met 2-3 Feb. 1993 in Augusta, Georgia. This report highlights the topics of this meeting.
DOE

N94-10723*# National Aeronautics and Space Administration. Marshall Space Flight Center, Huntsville, AL.
A BROWSE FACILITY FOR EARTH SCIENCE REMOTE SENSING DATA: CENTER DIRECTOR'S DISCRETIONARY FUND FINAL REPORT
P. J. Meyer May 1993 16 p
(Proj. 91-09)
(NASA-TM-108413; NAS 1.15:108413) Avail: CASI HC A03/MF A01

An image data visual browse facility is developed for a UNIX platform using the X Windows 11 system. It allows one to visually examine reduced resolution image data to determine which data are applicable for further research. Links with a relational data base manager then allow one to extract not only the full resolution image data, but any other ancillary data related to the case study. Various techniques are examined for compression of the image data in order to reduce data storage requirements and time necessary to transmit the data on the internet. Data used were from the WetNet project. Author (revised)

N94-10829 National Inst. of Standards and Technology, Gaithersburg, MD. Advanced Systems Div.
THE FIRST TEXT RETRIEVAL CONFERENCE (TREC-1)
Donna K. Harman, ed. Mar. 1993 517 p Conference held in Gaithersburg, MD, 4-6 Nov. 1992; sponsored by NIST and DARPA Limited Reproducibility: More than 20% of this document may be affected by microfiche quality
(PB93-191641; NIST/SP-500/207) Avail: Issuing Activity (National Technical Information Service (NTIS))

The first Text REtrieval Conference (TREC-1) was held in early November 1992 and was attended by about 100 people involved in the 25 participating groups. The goal of the conference was to bring research groups together to discuss their work on a new large test collection. There was a large variation of retrieval techniques reported on, including methods using automatic thesauri, sophisticated term weighting, natural language techniques, relevance feedback, and advanced pattern matching. As results had been run through a common evaluation package, groups were able to compare the effectiveness of different techniques and discuss how differences among the systems affected performance. NTIS

N94-10903# Groningen Rijksuniv. (Netherlands). Computing Science Section.
AUTOMATIC WORD CATEGORIZATION: AN INFORMATION-THEORETIC APPROACH
Marc M. Lankhorst and Rudy Moddemeijer 18 Dec. 1992 18 p
(CS-9209; ETN-93-94347) Copyright Avail: CASI HC A03/MF A01

A novel approach to the automatic categorization of words from raw data is presented. Occurrences of word pairs in text are counted. A hierarchical clustering technique on this frequency data is used to obtain a classification of words into linguistic categories. As a distance criterion in the clustering process, the loss of mutual information caused by combining two clusters into a single new cluster is used. The main advantage of such a method is the ability to construct linguistic categories that combine both syntactic and semantic/pragmatic factors. Results of the application of this method on letter data and on a word corpus are shown. Words are not only classified on the basis of their syntactic categories, but also with respect to aspects that are related to their meanings. The method can form the basis of a system that uses a much finer categorization of words than is feasible using traditional grammar based approaches. Plans to use it in a layered system of artificial neural networks that are trained to recognize higher level constituents are considered. ESA

N94-11105# Argonne National Lab., IL.
DATABASE COMPUTING IN HEP
C. T. Day, S. Loken, J. F. MacFarlane (California Univ., Berkeley. Lawrence Berkeley Lab.), E. May, D. Lifka, E. Lusk, L. E. Price, and A. Baden 1992 5 p
(Contract W-31-109-eng-38)
(DE93-011765; ANL-HEP-TR-92-129) Avail: CASI HC A01/MF A01

The major Superconducting SuperCollider (SSC) experiments are expected to produce up to 1 Petabyte of data per year each. Once the primary reconstruction is completed by farms of inexpensive processors, I/O becomes a major factor in further analysis of the data. We believe that the application of database techniques can significantly reduce the I/O performed in these analyses. We present examples of such I/O reductions in a prototype based on relational and object-oriented databases of Collider Detector and Fermilab (CDF) data samples. DOE

N94-11137# EG and G Energy Measurements, Inc., Albuquerque, NM.
AN ALTERNATIVE TO SNEAKERNET
S. Orrell and S. Ralstin 1993 14 p Presented at the 15th Computer Security Group Training Conference: Mission Possible-Connected and Protected, Albuquerque, NM, 3-6 May 1993
(Contract DE-AC08-88NV-10617)
(DE93-012130; EGG-10617-6097; CONF-9305151-1) Avail: CASI HC A03/MF A01

Security plans for classified computer systems often specify that only a small percentage of the data processed will be classified. Thus, the bulk of the data on such secure systems is unclassified. This situation requires that some mechanism be provided for moving files to or from the open environment. For many years, this has been accomplished by writing selected files to a magnetic medium, and carrying it to another system where the files are retrieved. These procedures, in many cases, have been developed informally and ad hoc to a specific transfer requirement. This media transport process, referred to as sneakernet, often is manually logged, if at all, and controlled only by administrative procedures. While sneakernets may isolate secure systems from direct attack, other security concerns remain. There has been little guidance available for handling such transfers in a secure manner. Comprehensive criteria for the security evaluation of the procedures used for these transfers have yet to be published. This paper examines the security concerns associated with transfers of unclassified files between security environments and develops a set of criteria which can be used in evaluating the security of any system or procedure for that purpose. Methods for bidirectional unclassified file transfer between secure and open environments could range from completely manual to fully automated. The criteria developed, however, are intended to be generic and to apply to any system for the purpose, existing or proposed. DOE

N94-11288# CSA Engineering, Inc., Palo Alto, CA.
FLIGHT DYNAMICS DIRECTORATE (FDD) HISTORICALLY BLACK COLLEGES AND UNIVERSITIES (HBCU'S) DATABASE MANAGMENT SYSTEM: A USER'S GUIDE Final Report, May 1991 - Sep. 1992
James R. Johnson Nov. 1992 18 p
(Contract F33615-90-C-3211)
(AD-A264947; ASIAC-TR-92-10; WL-TR-92-3109) Avail: CASI HC A03/MF A01

Structural Research Capability Database of HBCU's was developed which can be used to recall data about HBCU faculty capabilities and research interests, and university research facilities. The records are focused toward Flight Dynamics Directorate research and technology needs and should facilitate and increase faculty and student participation in the Flight Dynamics Directorate research programs by familiarizing Flight Dynamics Directorate in-house researchers with those at the cited HBCU's. Additional records may be appended to the database. More data were obtained than was contemplated, some universities provided brochures and other additional published data. This report serves as a user's guide for the database program. DTIC

N94-11352*# National Aeronautics and Space Administration. Langley Research Center, Hampton, VA.
NASA/DOD AEROSPACE KNOWLEDGE DIFFUSION RESEARCH PROJECT. REPORT 17: A COMPARISON OF THE TECHNICAL COMMUNICATION PRACTICES OF DUTCH AND US AEROSPACE ENGINEERS AND SCIENTISTS
Rebecca O. Barclay (Rensselaer Polytechnic Inst., Troy, NY.), Thomas E. Pinelli, and John M. Kennedy (Indiana Univ., Bloomington.) Washington Jul. 1993 70 p
(RTOP 505-90-00)
(NASA-TM-108987; NAS 1.15:108987) Avail: CASI HC A04/MF A01

As part of Phase 4 of the NASA/DoD Aerospace Knowledge Diffusion Research Project, two studies were conducted that investigated the technical communications practices of Dutch and U.S. aerospace engineers and scientists. Both studies have the same seven objectives: first, to solicit the opinions of aerospace engineers and scientists regarding the importance of technical communications to their profession; second, to determine the use and production of technical communications by aerospace engineers and scientists; third, to seek their views about the appropriate content of an undergraduate course in technical communications; fourth, to determine aerospace engineers' and scientists' use of libraries, technical information centers, and on-line data bases; fifth, to determine the use and importance of computer and information technology to them; sixth, to determine their use of electronic networks; and seventh, to determine their use of foreign and domestically produced technical reports. A self-administered questionnaire was distributed to aerospace engineers and scientists at the National Aerospace Laboratory (NLR), and NASA Ames Research Center, and the NASA Langley Research Center. The completion rates for the Dutch and U.S. surveys were 55 and 61 percent, respectively. Responses of the Dutch and U.S. participants to selected questions are presented. Author (revised)

N94-11369# Oak Ridge National Lab., TN.
ABBREVIATIONS, ACRONYMS, AND INITIALISMS FREQUENTLY USED BY MARTIN MARIETTA ENERGY SYSTEMS, INCORPORATED
J. T. Miller Apr. 1993 179 p
(Contract DE-AC05-84OR-21400)
(DE93-012509; DOE/OR-21400/T474; ES/IRA-1) Avail: CASI HC A09/MF A02

Guidelines are given for using abbreviations, acronyms, and initialisms (AAI's) in documents prepared by US Department of Energy facilities managed by Martin Marietta Energy Systems, Inc., in Oak Ridge, Tennessee. The more than 8000 AAI's listed represent only a small portion of those found in recent documents prepared by contributing editors of the Publications Division of Oak Ridge National Laboratory, the Oak Ridge K-25 Site, and the Oak Ridge Y-12 Plant. This document expands on AAI's listed in the Document Preparation Guide and is intended as a companion document. DOE

N94-11520 Maryland Univ., College Park. Dept. of Computer Science.
DESIGN ISSUES FOR HIGH PERFORMANCE ENGINEERING INFORMATION SYSTEMS Final Report, 1 Mar. 1989 - 30 Apr. 1992
Nick Roussopoulos, Timos Sellis, Leo Mark, and Christos Faloutsos 20 Apr. 1992 21 p Limited Reproducibility: More than 20% of this document may be affected by microfiche quality
(Grant AF-AFOSR-0303-89)
(AD-A264839; AFOSR-93-0210TR) Avail: Issuing Activity (Defense Technical Information Center (DTIC))

It is increasingly being recognized that an Engineering Information System will be the fundamental component of any design and manufacturing system in the future and that all components in such a system have to be engineered around the management and control of information. Commercially available database systems do not meet the information and processing needs of design and manufacturing environments. Consequently, extensions to database systems are necessary to realize Engineering Information Systems. These systems will support multimedia databases of significant size and complexity, and, therefore, one of the most important issues is performance. The computational and architectural aspects of EIS and rule management techniques for maintaining consistency were addressed in this project. The studies produced promising models and solutions. DTIC

N94-11588# Department of Energy, Washington, DC. Office of Information Resources Management.
INFORMATION RESOURCES MANAGEMENT LONG-RANGE PLAN, FY1994
Apr. 1993 145 p
(DE93-013898; DOE/AD-0043) Avail: CASI HC A07/MF A02

This document describes IRM activities and the information technology resources and capabilities of the Department, the future requirements, and the strategies and plans to satisfy the identified requirements. The long-range planning process provides the systematic means to meet this objective and assists the Department in assuring that information technology (IT) support is provided in an efficient, effective, and timely manner so that its programmatic missions can be accomplished. Another important objective of the Plan is to promote better understanding, both within and external to the Department, of its IT environment, requirements, issues, and recommended solutions. This DOE IRM Plan takes into consideration the IRM requirements of approximately 50 different sites. The annual long-range planning cycle for supporting this Plan was initiated by a Call in August 1991 for site plans to be submitted in February 1992 by those Departmental components and contractors with major IRM requirements. DOE

N94-11589*# National Aeronautics and Space Administration, Washington, DC.
CORRESPONDENCE STANDARDS
Jan. 1992 154 p Revised
(NHB-1450.10B; NAS 1.18:1450.10B) Avail: CASI HC A08/MF A02

This revised handbook covers the drafting, preparation, and review of NASA letters, memorandums, informal communications, electronic communications, envelopes and mailing, and classified correspondence. The appendices address specific guidelines for administrator's correspondence, White House and Congressional correspondance, Privacy Act correspondence, and foreign correspondence. Also incorporated as appendices are quick references for forms of address, compound words, and capitalization of words frequently used at NASA. CASI

N94-11818# International Atomic Energy Agency, Vienna (Austria).
DIRECTORY OF IAEA DATABASES
Dec. 1992 126 p
(DE93-622837; INIS-mf-13507) Avail: CASI HC A07/MF A02 (US Sales Only)

This second edition of the Directory of IAEA Databases has been prepared within the Division of Scientific and Technical Information (NESI). Its main objective is to describe the computerized information sources available to staff members. This directory contains all databases produced at the IAEA, including databases stored on the mainframe, LAN's and PC's. All IAEA Division Directors have been requested to register the existence of their databases with NESI. For the second edition database owners were requested to review the existing entries for their databases and answer four additional questions. The four additional questions concerned the type of database (e.g. Bibliographic, Text, Statistical etc.), the category of database (e.g. Administrative, Nuclear Data etc.), the available documentation and the type of media used for distribution. In the individual entries on the following pages the answers to the first two questions (type and category) is always listed, but the answers to the second two questions (documentation and media) is only listed when information has been made available. DOE

N94-11846# Naval Postgraduate School, Monterey, CA.
THE RELATIONAL-TO-OBJECT-ORIENTED CROSS-MODEL ACCESSING CAPABILITY IN A MULTI-MODEL AND MULTI-LINGUAL DATABASE SYSTEM M.S. Thesis
Richard K. Johnston Mar. 1993 89 p
(AD-A264911) Avail: CASI HC A05/MF A01

Conventional database management systems (DBMS) are stand-alone, each supporting a single data model and corresponding data language (ML). One organization might operate several stand-alone DBMS's independently, each of which requires the knowledge of a different ML to operate. The multi-model and multi-lingual database system offers a different approach. This system supports multiple ML's in a single database system. Thus, a relational database user of the multi-model and multi-lingual database system can create and manipulate a database according to the relational model and the SQL data language. On the same system, a hierarchical user can create and manipulate a database according to the hierarchical model and DL/I data language. Besides supporting many different models and languages on a single system, the multi-model and multi-lingual database system also allows the user to access a database created according to one ML as if it were created according to another. Thus, a relational user could manipulate a hierarchical database as if it is relational, i.e., the user would use a relational schema and SQL commands to manipulate a hierarchical database. The Cross-model accessing capability, Database design, Database implementation, Database management systems, base-model, and base-language (i.e., hierarchical and DL/1) are invisible to the user. This additional capability is termed the cross-model accessing capability. At this time the multi-model and multi-lingual database system supports the following ML's: relational and SQL, hierarchical and DL/I, network and CODASYL-DML, and object-oriented and the object-oriented data language. The system also supports a relational-to-hierarchical cross-model accessing capability. DTIC

N94-12014# Office of Management and Budget, Washington, DC. Office of Information and Regulatory Affairs.
INFORMATION RESOURCES MANAGEMENT PLAN OF THE FEDERAL GOVERNMENT
Nov. 1992 298 p Prepared in cooperation with General Services Administration, Washington, DC, and Commerce Dept., Washington, DC
(ISBN-0-16-037895-8) Avail: CASI HC A13/MF A03; SOD HC

Bulletin 92-05, 'Information Resources Management (IRM) Plans', issued 6 Mar. 1992, encourages Federal agencies to establish an integrated approach to information resources management. Moreover, the Bulletin required agencies to describe their commitments and accomplishments toward establishing a comprehensive strategy for managing agency information resources throughout the 'information life cycle,' including information creation, collection, processing, dissemination and management. The purposes of this publication are the following: to reflect Federal agencies' focus on program priorities by identifying how plans for major information collections and information technology will support those priorities; to provide an accounting of actual reductions in the burden of Federal information collection and recordkeeping accomplished by Federal agencies during Fiscal Year (FY) 1991 and of the reductions planned by these agencies for FY 1992 and FY 1993; to promote program-based planning for the use of information resources that will make Government service delivery more effective, efficient, and responsive; to support the activities of Congress and other oversight agencies; to provide information to Federal agencies on trends and directions in information resources management; and to inform the public of the current state of Federal IRM activities so that they can more meaningfully participate in those activities. Author (revised)

N94-12385# Federal Coordinating Council for Science, Engineering and Technology, Washington, DC. Committee on Industry and Technology.
MACHINE TRANSLATION TECHNOLOGY: A POTENTIAL KEY TO THE INFORMATION AGE
Jan. 1993 59 p See also AD-225965 and PB92-861731
(PB93-134336) Avail: CASI HC A04/MF A01

Today nearly half of the world's scientific and technological literature is written in languages other than English. Currently, machine translation (MT) can produce comprehensible translated text in a few languages, but human editing is often required to produce a truly polished translation. The United States is strong in basic research on natural language processing, and leads the world in the diversity of language pairs under development. The challenge is in converting its formidable research potential and know-how into commercial operating systems. The single most challenging competitor-nation in MT is Japan. Japan is ahead of the United States in development of MT systems--in terms of the number of systems, variety of applications, and development of knowledge sources--but not in basic research. Japan also leads the U.S. in commercial use and general acceptance of MT, and in integration of MT into the office environment. Author

N94-12445# General Accounting Office, Washington, DC. Information Management and Technology Div.
DEFENSE: HEALTH CARE
3 Jun. 1993 8 p Sponsored by DOD
(AD-A265914; GAO/IMTEC-93-29R) Avail: CASI HC A02/MF A01

In Oct. 1989 the Department of Defense introduced its Corporate Information Management (CIM) initiative to reengineer its business practices and make better use of information technology. In May 1990, a Medical Functional Group was established within the Office of the Assistant Secretary of Defense for Health Affairs to institutionalize the CIM process within the Military Health Services System. This letter addresses our review of CIN's implementation in military health services--one of the eight functional areas selected for initial CIM implementation. At a time when health care costs are rising dramatically, CIM offers opportunities to reduce not only health care information technology expenses but, more important, the overall costs of providing care. DTIC

N94-12579# Maryland Univ., College Park.
ANALYSIS OF THE ARMY'S INSTALLATION SUPPORT MODULES WITH THE PRIVATE SECTOR'S OPEN INFORMATION SYSTEMS Final Report
Paul G. Andrews 9 Apr. 1993 76 p
(AD-A265667) Avail: CASI HC A05/MF A01

Installation management within the U.S. Army is comprised of a myriad of basic management functions such as real property acquisition and personnel accountability. These functions are performed by installation organizations which are responsible for managing the manpower, funds, and equipment assigned to the installation during peace and wartime conditions. Each installation organization uses an information system tailored to its specific mission to perform daily tasks. However, this network configuration is characterized by the lack of data sharing capability, and it does not promote qualitative management of military resources. In order to incorporate data sharing among the installation organizations and enhance installation management, the Army has developed a new information system called Installation Support Modules (ISM). The ISM is a computer hardware, software, and communications-infrastructure designed to provide installation organizations with the capability of horizontal and vertical data sharing. The Army's acquisition strategy for the ISM is to develop the system with the latest computer and information technology, Open Systems Environment (OSE). DTIC

N94-10793# Maryland Univ., College Park. Dept. of Fire Protection Engineering.
DEVELOPMENT OF A HYPERMEDIA KNOWLEDGE BASE OF AIRCRAFT FIRE SAFETY REGULATIONS
Samuel A. Denny and Frederick W. Mowrer *In* FAA, Proceedings of the International Conference for the Promotion of Advanced Fire Resistant Aircraft Interior Materials Mar. 1993 p 321-331 (For primary document see N94-10766 01-03)
Avail: CASI HC A03/MF A03

N94-11575*# Environmental Research Inst. of Michigan, Ann Arbor.
THE GUIDE TO DESIGN FOR ON-ORBIT SPACECRAFT SERVICING (DFOSS) MANUAL: PRODUCING A CONSENSUS DOCUMENT
Janice Nyman *In* NASA. Johnson Space Center, Sixth Annual Workshop on Space Operations Applications and Research (SOAR 1992), Volume 2 Feb. 1993 p 708-715 (For primary document see N94-11527 01-99)
Avail: CASI HC A02/MF A03

N94-12662 National Oceanic and Atmospheric Administration, Camp Springs, MD. Ocean Products Center.
AN INTEGRATED APPROACH TO TOTAL END-TO-END QUALITY CONTROL OF OCEAN DATA IN THE REAL-TIME ENVIRONMENT
Walton B. Campbell and Marshall P. Waters *In* Scientific Organizing Committee of PORSEC, Proceedings of the PORSEC 1992 in Okinawa: Conference for Pacific Ocean Environments and Probing, Volume 2 25 Aug. 1992 p 704-708 (For primary document see N94-12635 01-42)
Copyright Avail: Issuing Activity (Scientific Organizing Committee of PORSEC, P.O. Box 10, Shimizu, Shizuoka 424, Japan, HC)

N94-12669 Qingdao Inst. of Oceanology (China).
SIMPLE AND LOW COST IMAGE PROCESSING SYSTEM FOR SATELLITE REMOTE SENSING DATA
Ting-Lu Zhang, Zhi-Sheng Liu, and Huang-Tao et al *In* Scientific Organizing Committee of PORSEC, Proceedings of the PORSEC 1992 in Okinawa: Conference for Pacific Ocean Environments and Probing, Volume 2 25 Aug. 1992 p 748-750 (For primary document see N94-12635 01-42)
Copyright Avail: Issuing Activity (Scientific Organizing Committee of PORSEC, P.O. Box 10, Shimizu, Shizuoka 424, Japan, HC)

N94-12749 Academy of Sciences (USSR), Vladivostok. Inst. for Automation and Control Processes.
DISTERM: A SHIPBOARD DATA SYSTEM FOR SATELLITE MONITORING OF OCEAN AND ATMOSPHERE
E. E. Gherbek, Ju. G. Proshyants, Ju. V. Naumkin, and I. I. Gorin *In* Scientific Organizing Committee of PORSEC, Proceedings of the PORSEC 1992 in Okinawa: Conference for Pacific Ocean Environments and Probing, Volume 2 25 Aug. 1992 p 1189-1193 (For primary document see

N94-12635 01-42)
Copyright Avail: Issuing Activity (Scientific Organizing Committee of PORSEC, P.O. Box 10, Shimizu, Shizuoka 424, Japan, HC)

N94-12751 Academy of Sciences (USSR), Vladivostok. Pacific Oceanological Inst.
THE STRUCTURE OF HYDROPHYSICAL MEASURING SYSTEMS OF VERTICAL SOUNDING AND SELF-CONTAINED STATIONS
G. V. Smirnov, V. V. Gorbachev, A. G. Starikov, and N. A. Shmyrov *In* Scientific Organizing Committee of PORSEC, Proceedings of the PORSEC 1992 in Okinawa: Conference for Pacific Ocean Environments and Probing, Volume 2 25 Aug. 1992 p 1200-1204 (For primary document see N94-12635 01-42)
Copyright Avail: Issuing Activity (Scientific Organizing Committee of PORSEC, P.O. Box 10, Shimizu, Shizuoka 424, Japan, HC)

83 ECONOMICS AND COST ANALYSIS

Includes cost effectiveness studies.

N94-11186# National Science Foundation, Washington, DC.
NATIONAL PATTERNS OF R AND D RESOURCES, 1992
John E. Jankowski, Jr. Oct. 1992 85 p
(NSF-92-330) Avail: CASI HC A05/MF A01

The National Science Foundation (NSF) sponsors a series of surveys to collect information on the financial and human resources devoted to research and development (R&D). In this report, such NSF survey data on the various sectors of the U.S. economy - industry, government, academia and selected nonprofit organizations - are aggregated so that the components of the overall R&D effort are placed in a national context. Information presented in National Patterns includes: the level of R&D expenditures; the sources of such funds; the sector or organization performing the R&D; the character of work undertaken (i.e., whether it is basic research, applied research, or development); the number of scientists and engineers employed in R&D; and international comparisons with the U.S. effort. The national totals reported here incorporate data available from the several Division of Science Resources Studies (SRS) surveys as of May 14, 1992. These notes provide a brief introduction to the concepts used in the report. Important changes and revisions from previous National Patterns reports also are highlighted. Complete definitions, descriptions of projection methodologies, and references to the underlying survey reports are included in an appendix. Derived from text

84 LAW, POLITICAL SCIENCE AND SPACE POLICY

Includes NASA appropriation hearings; aviation law; space law and policy; international law; international cooperation; and patent policy.

N94-11351# Executive Office of the President, Washington, DC. National Performance Review.
FROM RED TAPE TO RESULTS: CREATING A GOVERNMENT THAT WORKS BETTER AND COSTS LESS
Albert Gore, Jr. et al 7 Sep. 1993 170 p Revised Original contains color illustrations
Avail: CASI HC A08/MF A02; SOD HC

This report represents the beginning of what will be--what must be--an ongoing commitment to change. It includes actions that will be taken now, by directive of the President; actions that will be taken by the cabinet secretaries and agency heads; and recommendations for congressional action. The National Performance Review focused primarily on how government should work, not on what it should do. Our job was to improve performance in areas where policymakers had already decided government should play a role. We examined every cabinet department and 10 agencies. Derived from text

N94-11353# Executive Office of the President, Washington, DC. National Performance Review.
FROM RED TAPE TO RESULTS: CREATING A GOVERNMENT THAT WORKS BETTER AND COSTS LESS. EXECUTIVE SUMMARY
Albert Gore, Jr. et al 7 Sep. 1993 24 p Original contains color illustrations
Avail: CASI HC A03/MF A01; SOD HC

The National Performance Review is about change--historic change--in the way the government works. It's time we had a new customer service contract with the American people, a new guarantee of effective, efficient, and responsive government that puts our customers first and demonstrates to the American people that their tax dollars will be treated with respect for the hard work that earned them. The National Performance Review is about moving from red tape to results to create a government that works better and costs less. This is a summary of the first product of our efforts. In it, we make hundreds of recommendations saving $108 billion over five years. Derived from text

N94-10678# National Space Development Agency, Tokyo (Japan). SAFISY Program Office.
CONSIDERATIONS FOR FUTURE REGIONAL SPACE COOPERATION Abstract Only
Tasuku Tanaka and Akiko Suzuki *In* Science and Technology Agency, Space Activities in the Asia Pacific Region 16 Nov. 1992 p 14 (For primary document see N94-10676 01-12)
Avail: CASI HC A01/MF A01

N94-10680# State Science and Technology Commission, Beijing (China). Dept. of Fundamental Research and High Technology.
INTERNATIONAL SPACE YEAR IN CHINA
Quan Lin *In* Science and Technology Agency, Space Activities in the Asia Pacific Region 16 Nov. 1992 p 24-26 Original language document was announced as N93-21272 (For primary document see N94-10676 01-12)
Avail: CASI HC A01/MF A01

N94-10695# Ministry of Posts and Telecommunications, Tokyo (Japan). Communications Policy Bureau.
PARTNERS
Kiyoshi Ooida *In* Science and Technology Agency, Space Activities in the Asia Pacific Region 16 Nov. 1992 p 83-84 Original language document was announced as N93-21287 (For primary document see N94-10676 01-12)
Avail: CASI HC A01/MF A01

85 URBAN TECHNOLOGY AND TRANSPORTATION

Includes applications of space technology to urban problems; technology transfer; technology assessment; and surface and mass transportation.

For related information see also *03 Air Transportation and Safety, 16 Space Transportation,* and *44 Energy Production and Conversion.*

N94-10736 ENSCO, Inc., Springfield, VA. Applied Technology and Engineering Div.
SAFETY OF HIGH SPEED GROUND TRANSPORTATION SYSTEMS: X2000 US DEMONSTRATION VEHICLE DYNAMICS TRIALS, PRELIMINARY TEST REPORT, OCTOBER 1992 - JANUARY 1993
B. T. Whitten and J. K. Kesler Jan. 1993 100 p See also PB91-129668 Sponsored by Federal Railroad Administration, Washington, DC Limited Reproducibility: More than 20% of this document may be affected by microfiche quality
(Contract DTFR53-90-C-00025)
(PB93-194645; ENSCO-ATE-93-02; DOT/FRA/ORD-93/13) Avail: CASI HC A05

The report documents the procedures, events, and results of vehicle dynamic tests carried out on the ASEA-Brown Boveri (ABB) X2000 tilt body trainset in the U.S. between Oct. 1992 and Jan. 1993. These tests, sponsored by Amtrak and supported by the FRA, were conducted to assess the suitability of the X2000 trainset for safe operation at elevated cant deficiencies and speeds in Amtrak's Northeast Corridor under existing track conditions in a revenue service demonstration. The report describes the safety criteria against which the performance of the X2000 test train was examined, the instrumentation used, the test locations, and the track conditions. Preliminary results are presented from tests conducted on Amtrak lines between Philadelphia and Harrisburg, PA, and between Washington DC and New York NY, in which cant deficiencies of 12.5 inches and speeds of 154 mph were reached in a safe and controlled manner. The significance of the results is discussed, and preliminary conclusions and recommendations are presented. NTIS

N94-11059# California Univ., Berkeley. Lawrence Berkeley Lab.
TECHNOLOGY TRANSFER AT LAWRENCE BERKELEY LABORATORY
D. Johnson, ed. Sep. 1992 25 p
(Contract DE-AC03-76SF-00098)
(DE93-010460; LBL-PUB-671) Avail: CASI HC A03/MF A01

Lawrence Berkeley Laboratory (LBL) is dedicated to commercializing new technology in such fields as advanced materials, biotechnology, and electronics. Technology transfer between national laboratories and the industrial community is important in maintaining America's competitive edge. This document examines opportunities to establish working relationships with LBL. Streamlined methods for technology transfer are available with the aid of the Technology Transfer Department and the Patent Department at LBL. Research activities at LBL are concentrated in three major program areas: Energy Sciences, General Sciences, and Biosciences. Each program area consists of three research divisions. LBL welcomes both requests for information and proposals to conduct research. DOE

88 SPACE SCIENCES (GENERAL)

N94-11183*# National Aeronautics and Space Administration. Hugh L. Dryden Flight Research Facility, Edwards, CA.
TECHNICAL UPDATE: JOHNSON SPACE CENTER SYSTEM USING A SOLID ELECTROLYTIC CELL IN A REMOTE LOCATION TO MEASURE OXYGEN FUGACITIES IN CO/CO2 CONTROLLED-ATMOSPHERE FURNACES Interim Report
A. J. G. Jurewicz (Lockheed Engineering and Sciences Co., Houston, TX.), R. J. Williams, L. Le (Lockheed Engineering and Sciences Co., Houston, TX.), J. Wagstaff (Lockheed Engineering and Sciences Co., Houston, TX.), G. Lofgren, A. Lanier (Lockheed Engineering and Sciences Co., Houston, TX.), W. Carter (Lockheed Engineering and Sciences Co., Houston, TX.), and A. Roshko (National Inst. of Standards and Technology, Boulder, CO.) Sep. 1993 39 p
(Contract NAS9-11410)
(NASA-TM-104774; S-727; NAS 1.15:104774) Avail: CASI HC A03/MF A01

Details are given for the design and application of a (one atmosphere) redox-control system. This system differs from that given in NASA Technical Memorandum 58234 in that it uses a single solid-electrolytic cell in a remote location to measure the oxygen fugacities of multiple CO/CO2 controlled-atmosphere furnaces. This remote measurement extends the range of sample-furnace conditions that can be measured using a solid-electrolytic cell, and cuts costs by extending the life of the sensors and by minimizing the number of sensors in use. The system consists of a reference furnace and an exhaust-gas manifold. The reference furnace is designed according to the redox control system of NASA Technical Memorandum 58234, and any number of CO/CO2 controlled-atmosphere furnaces can be attached to the exhaust-gas manifold. Using the manifold, the exhaust gas from individual CO/CO2 controlled atmosphere furnaces can be diverted through the reference furnace, where a solid-electrolyte cell is used to read the ambient oxygen fugacity. The oxygen fugacity measured in the reference furnace can then be used to calculate the oxygen fugacity in the individual CO/CO2 controlled-atmosphere furnace. A BASIC computer program was developed to expedite this calculation. Author (revised)

N94-11229*# TRW Space Technology Labs., Redondo Beach, CA.
GAS-GRAIN SIMULATION FACILITY (GGSF). VOLUME 2: CONCEPTUAL DESIGN DEFINITION
James M. Zamel Aug. 1993 99 p
(Contract NAS2-13408)
(NASA-CR-177613; A-93101-Vol-2; NAS 1.26:177613) Avail: CASI HC A05/MF A02

This document is Volume 2 of the Final Report for the Phase A Study of the Gas-Grain Simulation Facility (GGSF), and presents the GGSF Conceptual Design. It is a follow-on to the Volume 1 Facility Definition Study, NASA report CR 177606. The development of a conceptual design for a Space Station Freedom (SSF) facility that will be used for investigating particle interactions in varying environments, including various gas mixtures, pressures, and temperatures is delineated. It's not possible to study these experiments on earth due to the long reaction times associated with this type of phenomena, hence the need for extended periods of microgravity. The particle types will vary in composition (solids and liquids), sizes (from submicrons to centimeters), and concentrations (from single particles to 10(exp 10) per cubic centimeter). The results of the experiments pursued in the GGSF will benefit a variety of scientific inquiries. These investigations span such diverse topics as the formation of planets and planetary rings, cloud and haze processes in planetary atmospheres, the composition and structure of astrophysical objects, and the viability of airborne microbes (e.g., in a manned spacecraft). Author (revised)

89 ASTRONOMY

Includes radio, gamma-ray, and infrared astronomy, and astrometry.

N94-10866*# National Aeronautics and Space Administration. Marshall Space Flight Center, Huntsville, AL.
NASA MARSHALL SPACE FLIGHT CENTER SOLAR OBSERVATORY REPORT, JANUARY - JUNE 1993
J. E. Smith Jul. 1993 56 p
(NASA-TM-108417; NAS 1.15:108417) Avail: CASI HC A04/MF A01

This report provides a description of the NASA Marshall Space Flight Center's Solar Vector Magnetograph Facility and gives a summary of its observations and data reduction during January-June 1993. The systems that make up the facility are a magnetograph telescope, an H-alpha telescope, a Questar telescope, and a computer code. Author

N94-11305*# Radiophysics, Inc., Boulder, CO.
DETECTION OF DUST IMPACTS BY THE VOYAGER PLANETARY RADIO ASTRONOMY EXPERIMENT Final Report, 14 May 1991 - 20 Apr. 1993
David R. Evans 13 Jul. 1993 59 p
(Contract NASw-4617)
(NASA-CR-193281; NAS 1.26:193281) Avail: CASI HC A04/MF A01

The Planetary Radio Astronomy (PRA) instrument detected large numbers of dust particles during the Voyager 2 encounter with Neptune. The signatures of these impacts are analyzed in some detail. The major conclusions are described. PRA detects impacts from all over the spacecraft body, not just the PRA antennas. The signatures of individual impacts last substantially longer than was expected from complementary Plasma Wave Subsystem (PWS) data acquired by another Voyager experiment. The signatures of individual impacts demonstrate very rapid fluctuations in signal strength, so fast that the data are limited by the speed of response of the instrument. The PRA detects events at a rate consistently lower than does the Plasma Wave subsystem. Even so, the impact rate is so great near the inbound crossing of the ring plane that no reliable estimate of impact rate can be made for this period. The data are consistent with the presence of electrons accelerated by ions within an expanding plasma cloud from the point of impact. An ancillary conclusion is that the anomalous appearance of data acquired at 900 kHz appears to be due to an error in processing the PRA data prior to their delivery rather than due to overload of the PRA instrument. Author (revised)

N94-11306*# National Aeronautics and Space Administration. Goddard Space Flight Center, Greenbelt, MD.
DETECTION OF ACCRETING CIRCUMSTELLAR GAS AROUND WEAK EMISSION-LINE HERBIG Ae/Be STARS
C. A. Grady (Applied Research Corp., Landover, MD.), M. R. Perez, and P. S. The (Amsterdam Univ., Netherlands.) 1993 5 p
(NASA-TM-108256; NAS 1.15:108256) Avail: CASI HC A01/MF A01

Archival and recent International Ultraviolet Explorer (IUE) high dispersion spectra of late B stars which reveal the presence of accreting gas with velocities as high as 350 km/s, collisional ionization of the accreting gas to temperatures above the stellar T(sub eff), and column densities intermediate between those observed toward classical Herbig Ae/Be stars and the nearby proto-planetary system beta Pictoris are presented. One of the stars HD 176386, while lacking obvious optical signatures of youth, is a member of the R CrA star formation region, and with an inferred age of 2.8 Myr has not yet arrived on the zero-age main sequence (ZAMS). The other object, an isolated, field B star with pronounced IR excess due to warm, circumstellar dust, 51 Oph, exhibits only modest H(alpha) emission. The combination of high velocity, accreting gas in systems with IR excesses due to circumstellar dust suggests that not only are these objects candidate proto-planetary systems, but that they may represent an extension to higher stellar masses of the weak-emission pre-main sequence (PMS) stars.
Author (revised)

N94-11356*# System Studies and Simulation, Inc., Huntsville, AL.
LUNAR-ULTRAVIOLET TELESCOPE EXPERIMENT (LUTE) INTEGRATED PROGRAM PLAN Final Report
Janice F. Smith, comp. and Larry Forrest (Cockerham, John M. and Associates, Inc., Huntsville, AL.) 13 Jul. 1993 20 p
(NASA Order H-20750-D)
(NASA-CR-193267; NAS 1.26:193267; Rept-5307-00-9307-F) Avail: CASI HC A03/MF A01

A detailed Lunar Ultraviolet Telescope Experiment (LUTE) program plan representing major decisions and tasks leading to those decisions for program execution are presented. The purpose of this task was to develop an integrated plan of project activities for the LUTE project, and to display the plan as an integrated network that shows the project activities, all critical interfaces, and schedules. The integrated network will provide the project manager with a frame work for strategic planning and risk management throughout the life of the project. Author (revised)

N94-12573*# Citadel Coll., Charleston, SC. Dept. of Physics.
THE ABUNDANCES OF THE ELEMENTS IN SHARP-LINED EARLY TYPE STARS Final Report, 1 May - 31 Jul. 1992
Saul J. Adelman 3 Aug. 1992 8 p
(Grant NAG5-1402)
(NASA-CR-194055; NAS 1.26:194055) Avail: CASI HC A02/MF A01

An International Ultraviolet Explorer (IUE) observing strategy that has yielded co-added spectra with enhanced S/N ratios for several A and B stars was established. New observations by Roby and Adelman using the same technique were added two new Hg-Mn stars into this sample. A long-term study of elemental abundances in this uniform, high-quality set of IUE spectra for 13 stars was begun. The first stages of this project are reported: abundances for N, Cr, Mn, Fe, Co, and Ni. The study of the Fe-peak elements show that our data set can provide accurate abundances and that abundances obtained from UV and optical spectra often are in good agreement. The groundwork for selfconsistent abundance analyses of more exotic elements in our long term project was provided.
Author (revised)

N94-12574*# Pennsylvania State Univ., University Park. Dept. of Astronomy and Astrophysics.
[HEAO-1 ANALYSIS OF LOW ENERGY DETECTORS (LED)] Final Report, Oct. 1990 - Dec. 1991
John A. Nousek 3 Mar. 1992 3 p
(Grant NAG5-941)
(NASA-CR-194087; NAS 1.26:194087) Avail: CASI HC A01/MF A01

The activities at Penn State University are described. During the period Oct. 1990 to Dec. 1991 work on HEAO-1 analysis of the Low Energy Detectors (LED) concentrated on using the improved detector spectral simulation model and fitting diffuse x-ray background spectral data. Spectral fitting results, x-ray point sources, and diffuse x-ray sources are described.
Author (revised)

N94-12768*# Arizona Univ., Tucson. Dept. of Planetary Sciences.
PLANETARY ASTRONOMY OF MARS. MARS DATA REDUCTION Final Technical Report, 1 Oct. 1988 - 30 Sep. 1990
Robert B. Singer 30 Sep. 1990 8 p
(Grants NAGw-1408; NAGw-1913)
(NASA-CR-193515; NAS 1.26:193515) Avail: CASI HC A02/MF A01

Grant #NAGW-1408 was specifically awarded to obtain telescopic visible and near-IR spectral imaging of Mars during the 1988 apparition (9/28/88). The observing program was highly successful producing approximately 2 Gbytes of data, but was only funded for one year and virtually all of the funds were spent in data acquisition. The follow-up grant was funded the following year for reduction of these data into a scientifically productive form, which because of the size and nature of our observations, was a non-trivial task. A more detailed scientific analysis of these data (fully reduced) is in progress now and will take a number of years. Extended geologic analyses of the astronomical data are being funded by the NASA Planetary Geology and Geophysics program. The objective was to produce detailed reflectance spectra for contiguous, spatially resolved surface elements covering most of the planet (about +50 degrees to -90 degrees latitude, all longitudes). A total of 6 observing runs, of 3-4 days duration each, were conducted on the University of Arizona's 1.5m telescope on Mt. Bigelow. We present a sketch map showing the approximate total extent of our spectral image coverage. Nearly all of Mars south of 40 degrees N was observed at least once. About half of the area shown was observed multiple times. South of 65 degrees S, including the south polar cap, our coverage is heavily redundant. The first run was conducted June 29 - July 1, 1988 (all dates are UT) to serve as a baseline prior to possible dust storm activity on Mars. The other observing runs were closer to opposition: Sept. 3-6, 13-15, 24-26, and Oct. 5-7 and 16-18. The September and October observations were scheduled to provide maximum longitudinal coverage. This was also intended to provide a balance between surface observations and observations of predicted dust storm activity. No global dust storm developed in 1988, so we have a large volume of data for the surface of Mars. Derived from text

N94-10968*# Ministry of Posts and Telecommunications, Kashima (Japan).
PULSAR ASTROMETRY BY USING VLBI (PSR0329 BETWEEN KASHIMA 26mPHI AND USUDA 64mPHI)
S. Hama, H. Kiuchi, Y. Hanado, Y. Takahashi, M. Imae, K. Fujisawa (Tokyo Univ., Japan.), H. Hirabayashi (Tokyo Univ., Japan.), and H. Kobayashi (Tokyo Univ., Japan.) *In* NASA. Goddard Space Flight Center, The 24th Annual Precise Time and Time Interval (PTTI) Applications and Planning Meeting Jun. 1993 p 65-72 (For primary document see N94-10963 01-70)
Avail: CASI HC A02/MF A04

N94-11836# Nagoya Univ. (Japan). School of Science.
REFRIGERATOR UTILIZATION IN INFRARED ASTRONOMY [SEKIGAISEN TENMONGAKU NI OKERU REITOUKI NO RIYOU]
Toshio Matsumoto *In* NASDA, The Second Workshop on Refrigerating System Utilization Onboard the JEM 31 Mar. 1993 p 104-114 In JAPANESE (For primary document see N94-11831 01-31)
Avail: CASI HC A03/MF A02

N94-12053*# National Aeronautics and Space Administration. Ames Research Center, Moffett Field, CA.
A COMPARISON OF TELESCOPIC AND PHOBOS-2 ISM SPECTRA OF MARS IN THE SHORT-WAVE NEAR-INFRARED (0.76-1.02 MICRONS) Abstract Only
James F. Bell, III and John F. Mustard (Brown Univ., Providence, RI.) *In* Lunar and Planetary Inst., Twenty-fourth Lunar and Planetary Science Conference. Part 1: A-F 1993 p 81-82 Sponsored by NASA. Washington (For primary document see N94-12015 01-91)
Avail: CASI HC A01/MF A06

N94-12140*# Jet Propulsion Lab., California Inst. of Tech., Pasadena.
PRELIMINARY REPORT OF LUNAR OBSERVATIONS BY THE NEAR-INFRARED MAPPING SPECTROMETER (NIMS) DURING THE SECOND GALILEO EARTH-MOON ENCOUNTER Abstract Only
R. W. Carlson, H. H. Kieffer (Geological Survey, Flagstaff, AZ.), K. H. Baines, K. J. Becker (Geological Survey, Flagstaff, AZ.), G. E. Danielson (California Inst. of Tech., Pasadena.), K. Edwards (Geological Survey, Flagstaff, AZ.), F. P. Fanale (Hawaii Univ., Honolulu.), J. Forsythe (SETS Technology, Inc., Mililani, HI.), L. R. Gaddis (Geological Survey, Flagstaff, AZ.), and J. C. Granahan (Hawaii Univ., Honolulu.) et al *In* Lunar and Planetary Inst., Twenty-fourth Lunar and Planetary Science Conference. Part 1: A-F 1993 p 255-256 (For primary document see N94-12015 01-91)
Avail: CASI HC A01/MF A06

90 ASTROPHYSICS

Includes cosmology; celestial mechanics; space plasmas; and interstellar and interplanetary gases and dust.
For related information see also *75 Plasma Physics.*

N94-10292# Washington Univ., Seattle.
NUCLEAR ASTROPHYSICS
W. C. Haxton 1992 6 p Presented at the 2nd International Nuclear Physics Conference, Wiesbaden, Germany, 26 Jul. - 1 Aug. 1992
(Contract DE-FG06-90ER-40561)
(DE93-010569; DOE/ER-40561/080; CONF-920708-7) Avail: CASI HC A02/MF A01

The problem of core-collapse supernovae is used to illustrate the many connections between nuclear astrophysics and the problems nuclear physicists study in terrestrial laboratories. Efforts to better understand the collapse and mantle ejection are also motivated by a variety of interdisciplinary issues in nuclear, particle, and astrophysics, including galactic chemical evolution, neutrino masses and mixing, and stellar cooling by the emission of new particles. The current status of theory and observations is summarized. DOE

N94-10511*# North Carolina State Univ., Raleigh. Dept. of Physics.
ACCELERATION OF POSITRONS IN SUPERNOVA SHOCKS Final Technical Report, 15 Apr. 1989 - 15 Apr. 1992
Donald C. Ellison 15 Apr. 1992 4 p
(Grant NAG5-1131)
(NASA-CR-193713; NAS 1.26:193713) Avail: CASI HC A01/MF A01

During this project we investigated the acceleration of leptons (electrons and positrons) in collisionless shock waves. In particular, we were interested in how leptons are accelerated in the blast waves existing in the remnants of supernova explosions. Supernova remnants (SNRs) have long been considered as the most likely source of galactic cosmic rays but no definite connection between SNRs and the cosmic rays seen at earth can be made. Only by understanding lepton acceleration in shocks can the rich SNR data base be properly used to understand cosmic ray origins. Our project was directed at the neglected aspects of lepton acceleration. We showed that the efficiency of lepton acceleration depended critically on the lepton injection energy. We showed that, even when infection effects are not important, that proton and lepton distribution functions produced by shocks are quite different in the critical energy range for producing the observed synchrotron emission. We also showed that transrelativistic effects produced proton spectra that were not in agreement with standard results from radio observations, but that the lepton spectra were, in fact, consistent with observations. We performed simulations of relativistic shocks (shocks where the flow speed is a sizable fraction of the speed of light) and discovered some interesting effects. We first demonstrated the power of the Monte Carlo technique by determining the shock jump conditions in relativistic shocks. We then proceeded to determine how relativistic shocks accelerate particles. We found that nonlinear relativistic shocks treat protons and leptons even more differently than nonrelativistic shocks. The transrelativistic effects on the shock structure from the heavy ion component reduces the lepton acceleration to a tiny fraction of the ion acceleration. This effect is dramatic even if high energy leptons (many times thermal energy) are injected, and was totally unexpected. Our results have important consequences for astrophysical environments expected to harbor relativistic flows such as extra-galactic radio sources and accretion onto compact objects. Derived from text

N94-10943*# Pennsylvania State Univ., University Park. Dept. of Astronomy and Astrophysics.
ADVANCED STATISTICAL METHODS FOR IMPROVED DATA ANALYSIS OF NASA ASTROPHYSICS MISSIONS Final Technical Report, 1 Feb. 1990 - 31 Jan. 1992
Eric D. Feigelson 1992 14 p
(Grant NAGw-1917)
(NASA-CR-193514; NAS 1.26:193514) Avail: CASI HC A03/MF A01

The investigators under this grant studied ways to improve the statistical analysis of astronomical data. They looked at existing techniques, the development of new techniques, and the production and distribution of specialized software to the astronomical community. Abstracts of nine papers that were produced are included, as well as brief descriptions of four software packages. The articles that are abstracted discuss analytical and Monte Carlo comparisons of six different linear least squares fits, a (second) paper on linear regression in astronomy, two reviews of public domain software for the astronomer, subsample and half-sample methods for estimating sampling distributions, a nonparametric estimation of survival functions under dependent competing risks, censoring in astronomical data due to nondetections, an astronomy survival analysis computer package called ASURV, and improving the statistical methodology of astronomical data analysis. CASI

N94-11136# International Centre for Theoretical Physics, Trieste (Italy).
A THEORETICAL KINEMATICAL STUDY OF THE GRADIENT OF ANY COSMIC SCALAR FIELD
M. Melek Jun. 1992 5 p
(DE92-644731; IC-92/95) Avail: CASI HC A01/MF A01 (US Sales Only)

Attention is called to a simple theoretical kinematical study of the gradient of any cosmic scalar field in the universe which might be used for an alternative interpretation for the very recent results obtained by COBE, regarding the matter density gradient and in turn the temperature gradient in the universe. DOE

N94-11152# International Centre for Theoretical Physics, Trieste (Italy).
ONE-LOOP QUANTUM GRAVITY ON DE SITTER SPACE
D. V. Vassilevich Jun. 1992 19 p
(DE92-641349; IC-92/99) Avail: CASI HC A03/MF A01 (US Sales Only)

We demonstrate that being formulated properly, all the approaches to de Sitter quantum gravity give the same one-loop path integral as was obtained by Taylor and Veneziano in a framework of the gauge fixed procedure. DOE

N94-11153*# Fermi National Accelerator Lab., Batavia, IL. NASA/Fermilab Astrophysics Center.
THE THREE-POINT FUNCTION AS A PROBE OF MODELS FOR LARGE-SCALE STRUCTURE
Joshua A. Frieman and Enrique Gaztanaga (Oxford Univ., England.) 19 Jun. 1993 28 p
(Grant NAGw-2381)
(NASA-CR-193249; NAS 1.26:193249; FERMILAB-Pub-93/140-A) Avail: CASI HC A03/MF A01

The consequences of models of structure formation for higher-order (n-point) galaxy correlation functions in the mildly non-linear regime are analyzed. Several variations of the standard Omega = 1 cold dark matter model with scale-invariant primordial perturbations were recently introduced to obtain more power on large scales, R(sub p) is approximately 20 h(sup -1) Mpc, e.g., low-matter-density (non-zero cosmological constant) models, 'tilted' primordial spectra, and scenarios with a mixture of cold and hot dark matter. They also include models with an effective scale-dependent bias, such as the cooperative galaxy formation scenario of Bower, etal. It is shown that higher-order (n-point) galaxy correlation functions can provide a useful test of such models and can discriminate between models with true large-scale power in the density field and those where the galaxy power arises from scale-dependent bias: a bias with rapid scale-dependence leads to a dramatic decrease of the hierarchical amplitudes Q(sub J) at large scales, r is approximately greater than R(sub p). Current observational constraints on the three-point amplitudes Q(sub 3) and S(sub 3) can place limits on the bias parameter(s) and appear to disfavor, but not yet rule out, the hypothesis that scale-dependent bias is responsible for the extra power observed on large scales. Author (revised)

N94-11187 California Univ., Santa Cruz.
THE CONTROLLING PARAMETERS OF THE INTEGRATED FLUX OF A STELLAR POPULATION Ph.D. Thesis
Guy Worthey 1992 325 p
Avail: Univ. Microfilms Order No. DA9312446

Stellar evolutionary isochrones are coupled with mostly theoretical flux distributions of stars in order to predict the flux distributions and colors of stellar populations as a function of population age and metallicity. Twenty one empirical indices of absorption feature strengths are measured for ensembles of stars of differing ages, temperatures, and metallicities. These indices are expressed as polynomials in stellar temperature, surface gravity, and metallicity, and are applied to the population models to predict index strengths as a function of population age and metallicity. Checks are made against stellar observations. The model predictions are compared to measured indices of elliptical galaxies. The logarithmic ratio (Mg/Fe) (which is zero for a scaled solar ratio) is shown to be greater than that of the most metal-rich stars in the solar neighborhood in giant elliptical galaxies. Since (Mg/Fe) is probably near zero for metal-rich stars, (Mg/Fe) appears to be greater than zero in giant ellipticals, but not in smaller, M32-class, ellipticals. This behavior is probably mirrored in Na and CN indices, suggesting that all light elements are relatively enhanced in giant ellipticals, on average. The nucleosynthetic history of giant ellipticals must differ from that of smaller ellipticals. Surface brightness fluctuation magnitudes are predicted. Models agree with the empirical I-band calibration, giving extragalactic distances which may be good to 10 percent for galaxies well-measured in two passbands. Qualitative agreement is also reached in fluctuation color-color diagrams and color-index diagrams. A fluctuation magnitude which is independent of color probably exists between Cousins I and Johnson J. The model results are tabulated. The sensitivity of all model predictions with age and metallicity are explored. H(Beta) and the G band provide the best age sensitivity of any color or index yet studied; Fe features are the most metallicity sensitive in the absence of abundance ratio differences. A factor of three change in age produces the same change in most colors and indices as a factor of two in Z. The effects of Z, age, and abundance ratio differences most profoundly affect the integrated light of stellar population. Other parameters have effects comparable to the model uncertainties. Dissert. Abstr.

N94-11582 Northwestern Univ., Evanston, IL.
THE EXCITATION OF CYANOGEN AND IONIZED CARBON IN INTERSTELLAR AND EXTRAGALACTIC GAS CLOUDS Ph.D. Thesis
Katherine Carol Roth 1992 223 p
Avail: Univ. Microfilms Order No. DA9309445

The goal of this dissertation is to precisely determine the temperature of the cosmic microwave background (CMB) and explore the behavior of this radiation in the past through observations of interstellar CN and C II in QSO absorption-line systems. We have measured the CN excitation in the diffuse clouds toward zeta Ophiuchi, zeta Persei, HD 27778, HD 21483 and HD 154368. We find J = 0 to 1 rotational excitation temperatures of T(sub ex) = 2.737 +/- 0.025, 2.774(+0.086, -0.091), 2.769(+0.093, -0.099), 2.771(+0.057, -0.060) and 2.68(+0.22, -0.33) K respectively. The fact that these values are all consistent with each other strongly suggests that local processes contribute little to the CN rotational excitation. After small corrections for these effects, we find a weighted average temperature of T(sub CMB) = 2.733(+0.023, -0.031) K for the CMB at 2.64 mm. This value agrees very well with the preliminary COBE temperature of T(sub CMB) = 2.735 +/- 0.06 K found from direct measurements of the short-wavelength CMB spectrum. The agreement in these two measurements resulting from completely different methods attests to the accuracy of each approach and reaffirms the global nature of the CMB radiation. We have obtained spectra of the C II lines in several damped Lyman alpha QSO absorbers in an effort to measure the temperature of the CMB in the past. The implied fine-structure population ratio toward the QSO 0347-383 (z(sub em) = 3.228) yields an upper limit of T(sub CMB) less than or = 14K at a red shift Z(sub abs) = 3.024. Since the observed excitation is most likely dominated by local collisional processes, we find respective upper limits on the electron and hydrogen atom densities of 0.02 and 10 cm(exp -3) in this system. The weak Zn II lines serve as an indicator of the system metallicity, which we have determined to be approximately = 10 percent solar for this absorber. In addition, the measured dust depletions determined from Cr II and Ni II absorption imply that both the 0347-383 and O551-366 (Z(sub abs) = 1.961) systems have dust-to-gas ratio about 10 percent of the Milky Way disk value. These results are consistent with previous work by Meyer and Roth (1990b) on damped Lyman-alpha absorbers at a red shift of Z(sub abs) is approximately = 2. Author

N94-11590*# Alabama Univ., Tuscaloosa.
THE IR PROPERTIES OF RINGED GALAXIES AND THE IRAS DATABASE Final Technical Report, 1 Jul. 1991 - 30 Jun. 1993
Ronald J. Buta and Deborah A. Crocker Jun. 1993 4 p
(Grant NAG5-1643)
(NASA-CR-194286; NAS 1.26:194286) Avail: CASI HC A01/MF A01

Our study of the Infrared Astronomy Satellite (IRAS) properties of ringed galaxies has been largely successful. We have identified what we think is the probable cause of the differences in the IRAS properties among non-interacting barred galaxies as the pattern speed of the bar. The key to identifying this parameter has been our focusing the study on outer-ringed galaxies where we know precisely what is present in the central regions (from available BVI CCD images in our library of images). The theory is that outer rings, through their morphology and other characteristics, can be identified with the outer Lindblad resonance, one of the major resonances in galaxy structure. Using a library of n-body simulations for comparison, we can reliably infer both low and high pattern speed galaxies from the appearance of outer rings and the existence of other ring features. It is clear that in some barred galaxies, the bar pattern speed is high enough to avoid an inner Lindblad resonance, hence such objects do not contain nuclear or circumnuclear star formation. The IRAS observations are most sensitive to nuclear star formation in early-type barred galaxies, and will thus select those barred galaxies where the pattern speed is low enough to allow an inner Lindblad resonance to exist. High pattern speed barred galaxies therefore weaken the correlation between bars and infrared excess. This finding helps to reconcile the inconsistent results found between different studies on the correlation between bars and far-IR emission. Derived from text

N94-11596 Texas Univ., Austin.
ON THE DEPLETION IN THE OUTER ASTEROID BELT AND THE STRUCTURE OF THE 4 TO 3 MEAN MOTION RESONANCE Ph.D. Thesis
Judit Gyoergyey Ries 1992 133 p
Avail: Univ. Microfilms Order No. DA9309264

The orbits of about 3000 fictitious asteroids, representing a possible distribution of bodies in the early Solar System, were investigated by numerical integration spanning approximately 38000 years in an effort to reproduce the observed distribution of outer belt asteroids. The equations of the elliptic restricted three body problem were regularized in order to handle close encounters with Jupiter. The estimate of the largest Lyapunov characteristic number and the slope of these estimates were calculated, and their usefulness as indicators of escape orbits was tested. The semimajor axis distribution for orbits that were bounded after 38000 years showed an excess of bodies compared to the observed distribution. The excess is associated with mean motion resonances and high eccentricity orbits. The structure of the 4:3 resonance was investigated by the same method with finer spatial resolution and longer integration time. Based on the estimate of the largest Lyapunov characteristic exponent, the resonance seems to be mostly chaotic. However, longer integration of individual orbits indicated that large Lyapunov characteristic numbers are not reliable predictors of unbounded motion in the elliptic restricted three body problem. They proved to be the most unreliable at mean motion resonances. The observed distribution of the outer belt asteroids could not be fully explained within the framework of the elliptic restricted three body problem only. A study to understand the behavior of orbits at mean motion resonances in the presence of additional perturbations is suggested. Author

N94-11597 Hawaii Univ., Honolulu.
THE MORPHOLOGIES OF DISTANT RADIO GALAXIES Ph.D. Thesis
Michael Anthony Rigler 1992 162 p
Avail: Univ. Microfilms Order No. DA9312216

Multicolor line and continuum images of a complete sample of 13 3C radio galaxies at 0.8 less than z less than 1.3, spanning the range 2500 A to 1 micrometer in the rest frame, are presented and analyzed. Quantitative analysis of these images shows that the infrared images are less elongated than those at optical wavelengths and show only a much weaker 'alignment effect' with the radio source axis. The quadrupole moment$ show a progressive reduction from short to long wavelengths, as expected if a symmetric component dominates at infrared wavelengths. A spectral decomposition based on these moments suggests that the aligned component probably has a roughly flat spectral energy distribution (f(sub v) approximately equals 0 to -1) while the symmetric red component that dominates in the infrared probably has a spectral energy distribution similar to that of a gE galaxy. In typical 3C galaxies at z = 1, the active aligned component contributes 10 percent of the infrared light. While more active objects have a larger contamination, these generally modest components are insufficient to perturb significantly either the scatter in, or the continuity of, the observed K-z relation. A model surface fitting analysis of the reddest member of the sample, 3C 65, and of another red galaxy, 3C 437 (z = 1.480), shows that the infrared surface brightness profiles are well fit by a deVaucouleurs r(exp 1/4) law characteristic of giant ellipticals, with characteristic photometric parameters comparable to those of brightest cluster members and low-redshift radio galaxies for standard cosmologies. Several of these radio galaxies are accompanied by small red companion galaxies that are prominent on our infrared images at random position angles relative to the radio axis. These are interpreted as representing a conventional trigger for the radio sources. There is a preference for these companions to be associated with the bluest, most aligned, and generally most active objects. Author

N94-11628*# Southwest Research Inst., San Antonio, TX. Instrumentation and Space Research Div.

ORIGINS OF SOLAR SYSTEMS WORKSHOP: THE ORIGIN, EVOLUTION, AND DETECTABILITY OF SHORT PERIOD COMETS Final Report

S. Alan Stern 30 Jun. 1993 44 p Workshop held in San Antonio, TX, 30 Jun. 1993
(SwRI Proj. 15-5296)
(NASA-CR-194255; NAS 1.26:194255) Avail: CASI HC A03/MF A01

The origin of the short period comets (SPC) (periods less than 200 years), the dynamical formation of their present reservoir(s), the cause and rate of their transport to the inner planetary region where they can be detected, and the magnitude of selection effects in their discovery are important research questions directly coupled to the goals of understanding the origin and evolution of the Solar System. To address these questions in an intensive way, an interdisciplinary, five month long Workshop from Jan. to May 1993 at Southwest Research Institute (SwRI) in San Antonio was convened. The goal of this Workshop was to advance the state of understanding about the origins, dynamical evolution, and present location of short period comets and their reservoir(s). For individual titles, see N94-11629 through N94-11629.

N94-11629*# Southwest Research Inst., San Antonio, TX. Space Sciences Dept.

THE LONG-TERM DYNAMICAL BEHAVIOR OF SHORT-PERIOD COMETS

Harold F. Levison and Martin J. Duncan (Queens Univ., Kingston, Ontario.) *In its* Origins of Solar Systems Workshop: The Origin, Evolution, and Detectability of Short Period Comets 30 Jun. 1993 p 1-36 (For primary document see N94-11628 01-90)
Avail: CASI HC A03/MF A01

The orbits of the known short-period comets under the influence of the Sun and all the planets except Mercury and Pluto are numerically integrated. The calculation was undertaken in order to determine the dynamical lifetimes for these objects as well as explaining the current orbital element distribution. It is found that a comet can move between Jupiter-family and Halley-family comets several times in its dynamical lifetime. The median lifetime of the known short-period comets from the time they are first injected into a short-period comet orbit to ultimate ejection is approximately 50,000 years. The very flat inclination distribution of Jupiter-family comets is observed to become more distended as it ages. The only possible explanation for the observed flat distribution is that the comets become extinct before their inclination distribution can change significantly. It is shown that the anomalous concentration of the argument of perihelion of Jupiter-family comets near 0 and 180 deg is a direct result of their aphelion distance being close to 5.2AU and the comet being recently perturbed onto a Jupiter-family orbit. Also the concentration of their aphelion near Jupiter's orbit is a result of the conservation of the Tisserand invariant during the capture process. Author (revised)

N94-11692# International Centre for Theoretical Physics, Trieste (Italy).

THE SOLUTIONS OF COSMIC STRING LOOP EQUATION IN EXPANDING UNIVERSE

Xinzhou Li and Jianzu Zhang (Shanghai Normal Univ., China.) Sep. 1992 9 p
(DE93-619717; IC-92/285) Avail: CASI HC A02/MF A01 (US Sales Only)

The cosmic string loop equation is studied analytically during the radiation-dominated era in the Robertson-Walker universe. If the loops expand with Hubble flow at the time of formation of loops, the cosmic string loops occur always collapsing. We also discuss the initial radii R(sub s)(t*) dependence of the lifetime tau(sub s) without considering the oscillations, as a first approximation, where t* denotes the time of formation of loops. We find that the lifetime factor gamma = c tau(sub s)/R(sub s)(t*) is (pi)/2 in the little initial radius limit. DOE

N94-11812 International Centre for Theoretical Physics, Trieste (Italy).

THE MAGNETIC FIELD OF ROTATING BODIES

F. I. Mikhail (Ain Shams Univ., Cairo, Egypt.), M. I. Wanas (Cairo Univ., Giza, Egypt.), and A. M. Eid Sep. 1991 18 p Limited Reproducibility: More than 20% of this document may be affected by microfiche quality
(DE93-619769; IC-91/253) Avail: CASI HC A03 (US Sales Only)

The paper discusses the possibility of interpreting the magnetic fields of astronomical bodies in the framework of a unified field theory. Using one of the solutions of the generalized field theory, a direct relation between the polar magnetic field, the angular velocity and the gravitational potential of the body considered, is obtained. The model used for applications has spherical symmetry. The predictions of the theoretical formula, obtained from the model, are compared with available observational data, and with the empirical relation of Blackett. The theoretical formula gives a possible interpretation of a seed magnetic field which will develop and produce the largescale magnetic field observed for celestial objects. The formula shows that the field may be generated as a result of the rotation of the massive object. DOE

N94-12557*# Wellesley Coll., MA.

SUBMISSION OF EARTH-BASED RING OCCULTATION OBSERVATIONS TO THE NASA PLANETARY DATA SYSTEM RINGS DISCIPLINE NODE Technical Report, 1 Jul. 1992 - 30 Jun. 1993

Richard G. French 2 Aug. 1993 40 p
(Grant NAG2-814)
(NASA-CR-193469; NAS 1.26:193469) Avail: CASI HC A03/MF A01

This is a technical report summarizing our progress in our program of contributing high quality Earth-based occultation observations to NASA's Planetary Data System (PDS) Rings Node. During our first year of funding, we selected five data sets for eventual inclusion in the PDS Rings Node. These were Uranus occultation observations obtained by the PI and co-workers from the IRTF of event stars U34 (26 April 1986), U1052 (5 May 1988), U65 (21 June 1990), U7872 (25 June 1991), and U7808 (28 June 1991). In our original proposal, we described four tasks: data sets to a common format; documentation of the occultation observations and associated calibrations; calculation of the occultation geometry for each event; establish prototype PDS templates. As discussed in our renewal proposal, submitted 8 June 1993, we have completed the first three tasks, and are working on the fourth. As an indication of our progress to date, we provide information about each of the data sets, their formats, the documentation, and the method used for reconstructing the occultation geometry. Author (revised)

N94-12566*# Minnesota Univ., Minneapolis. Physics Lab.

COORDINATED RADIO, ELECTRON, AND WAVES EXPERIMENT (CREWE) FOR THE NASA COMET RENDEZVOUS AND ASTEROID FLYBY (CRAF) INSTRUMENT Final Technical Report

Jack D. Scudder 1992 80 p

(Grant NAG5-983)
(NASA-CR-194376; NAS 1.26:194376) Avail: CASI HC A05/MF A01

The Coordinated Radio, Electron, and Waves Experiment (CREWE) was designed to determine density, bulk velocity and temperature of the electrons for the NASA Comet Rendezvous and Asteroid Flyby Spacecraft, to define the MHD-SW IMF flow configuration; to clarify the role of impact ionization processes, to comment on the importance of anomalous ionization phenomena (via wave particle processes), to quantify the importance of wave turbulence in the cometary interaction, to establish the importance of photoionization via the presence of characteristic lines in a structured energy spectrum, to infer the presence and grain size of significant ambient dust column density, to search for the theoretically suggested 'impenetrable' contact surface, and to quantify the flow of heat (in the likelihood that no surface exists) that will penetrate very deep into the atmosphere supplying a good deal of heat via impact and charge exchange ionization. This final report provides an instrument description, instrument test plans, list of deliverables/schedule, flight and support equipment and software schedule, CREWE accommodation issues, resource requirements, status of major contracts, an explanation of the non-NASA funded efforts, status of EIP and IM plan, descope options, and Brinton questions. CASI

N94-12595*# Applied Research Corp., Landover, MD.
ADP STUDY OF THE STRUCTURE OF THE IUE HALO Final Report, 2 Mar. 1990 - 1 Mar. 1992
Derck Massa 1992 8 p
(Contract NAS5-30788)
(NASA-CR-194374; NAS 1.26:194374) Avail: CASI HC A02/MF A01

Results of a two year ADP study of gas in the Galactic halo are presented. This is partly a summary of 2 papers which were published in referred journals and partly a discussion of work currently underway. Author

N94-12767*# Texas Univ., Austin.
ANALYSIS OF INTERSTELLAR FRAGMENTATION STRUCTURE BASED ON IRAS IMAGES Final Report, 1 Jun. 1987 - 31 May 1989
John M. Scalo 31 May 1989 6 p
(Contract JPL-958003)
(NASA-CR-193518; NAS 1.26:193518) Avail: CASI HC A02/MF A01

The goal of this project was to develop new tools for the analysis of the structure of densely sampled maps of interstellar star-forming regions. A particular emphasis was on the recognition and characterization of nested hierarchical structure and fractal irregularity, and their relation to the level of star formation activity. The panoramic IRAS images provided data with the required range in spatial scale, greater than a factor of 100, and in column density, greater than a factor of 50. In order to construct a densely sampled column density map of a cloud complex which is both self-gravitating and not (yet?) stirred up much by star formation, a column density image of the Taurus region has been constructed from IRAS data. The primary drawback to using the IRAS data for this purpose is that it contains no velocity information, and the possible importance of projection effects must be kept in mind. Derived from text

N94-12770*# California Univ., Berkeley. Space Sciences Lab.
GIOTTO DATA ANALYSIS: ELECTRON PLASMA AND HEAVY ION COMPOSITION MEASUREMENTS AT COMET HALLEY Final Report, 1 May 1988 - 31 Aug. 1991
Robert P. Lin 18 Mar. 1992 5 p
(Grant NAGw-1298)
(NASA-CR-193587; NAS 1.26:193587) Avail: CASI HC A01/MF A01

This investigation involved the analysis of electron plasma and heavy ion composition measurements made by the COPERNIC (COmplete Positive ion, Electron, and Ram Negative Ion measurements near Comet Halley) plasma experiment during the close fly-by of Halley by the European Space Agency's Giotto spacecraft. The experiment provided measurements of the full 3-dimensional distribution of 10 eV-30 keV electrons, and mass analysis of cold cometary ions from 10-210 amu. The analysis of the COPERNIC data has yielded some remarkable results, including: The discovery of negatively charged ions in the inner coma; the discovery of far heavier (mass is greater than 50 amu) ions than predicted, dominated by complex molecular ions made up of C, H, O, and N; the discovery of an adiabatic heating effect on electrons from the compression of the solar wind plasma; the identification of several organic and sulfur bearing ions; and the discovery of a new 'mystery region' where electrons are accelerated to high energies. These discoveries were in addition to the detailed analysis of 'expected' features at Comet Halley. Although this grant has expired, analysis continues on the data at a low (unfunded) level, and it is expected that more significant results will be obtained. A bibliography of the papers resulting from this research is attached, and a copy of each paper is included. Derived from text

N94-10969*# Bureau International des Poids et Mesures, Sevres (France).
AN ENSEMBLE PULSAR TIME
Gerard Petit, Claudine Thomas, and Patrizia Tavella (Instituto Elettrotecnico Nazionale, Galileo Ferraris, Turin, Italy.) *In* NASA. Goddard Space Flight Center, The 24th Annual Precise Time and Time Interval (PTTI) Applications and Planning Meeting Jun. 1993 p 73-86 (For primary document see N94-10963 01-70)
Avail: CASI HC A03/MF A04

N94-12016*# Niels Bohr Inst., Copenhagen (Denmark).
MOESSBAUER SPECTROSCOPY OF THE SNC METEORITE ZAGAMI Abstract Only
D. P. Agerkvist and L. Vistisen *In* Lunar and Planetary Inst., Twenty-fourth Lunar and Planetary Science Conference. Part 1: A-F 1993 p 1-2 (For primary document see N94-12015 01-91)
Avail: CASI HC A01/MF A06

N94-12020*# Academy of Sciences (USSR), Moscow. Inst. of Geochemistry and Analytic Chemistry.
DISPERSION OF THE RATIOS OF COSMOGENIC ISOTOPES OF NOBLE GASES IN CHONDRITES OF DIFFERENT COSMIC-RAY EXPOSURE AGES Abstract Only
V. A. Alexeev *In* Lunar and Planetary Inst., Twenty-fourth Lunar and Planetary Science Conference. Part 1: A-F 1993 p 9-10 (For primary document see N94-12015 01-91)
Avail: CASI HC A01/MF A06

N94-12021*# Academy of Sciences (USSR), Moscow. Inst. of Geochemistry and Analytic Chemistry.
PECULIARITIES OF DISTRIBUTIONS OF THE COSMIC-RAY EXPOSURE AGES OF H CHONDRITE FALLS AND FINDS Abstract Only
V. A. Alexeev *In* Lunar and Planetary Inst., Twenty-fourth Lunar and Planetary Science Conference. Part 1: A-F 1993 p 11-12 (For primary document see N94-12015 01-91)
Avail: CASI HC A01/MF A06

N94-12022*# Academy of Sciences (USSR), Moscow. Inst. of Geochemistry and Analytical Chemistry.
SEARCH FOR EFFECTS OF A SUPERNOVA EXPLOSION 30 TO 40 THOUSAND YEARS AGO IN CHONDRITES Abstract Only
V. A. Alexeev and G. K. Ustinova *In* Lunar and Planetary Inst., Twenty-fourth Lunar and Planetary Science Conference. Part 1: A-F 1993 p 13-14 (For primary document see N94-12015 01-91)
Avail: CASI HC A01/MF A06

N94-12025*# Lockheed Engineering and Sciences Co., Houston, TX.
CALORIMETRIC THERMOMETRY OF METEORITIC TROILITE: A FEASIBILITY STUDY Abstract Only
J. H. Allton and J. L. Gooding (National Aeronautics and Space Administration. Lyndon B. Johnson Space Center, Houston, TX.) *In* Lunar and Planetary Inst., Twenty-fourth Lunar and Planetary Science Conference. Part 1: A-F 1993 p 21-22 (For primary document see N94-12015 01-91)
Avail: CASI HC A01/MF A06

N94-12035*# Manchester Univ. (England). Dept. of Geology
CARBON IN WEATHERED ORDINARY CHONDRITES FROM ROOSEVELT COUNTY Abstract Only
R. D. Ash and C. T. Pillinger (Open Univ., Milton, England.) *In* Lunar and Planetary Inst., Twenty-fourth Lunar and Planetary Science Conference. Part 1: A-F 1993 p 43-44 (For primary document see N94-12015 01-91)
Avail: CASI HC A01/MF A06

N94-12036*# Arizona Univ., Tucson.
EJECTING BASALTIC ACHONDRITES FROM VESTA: HYDRODYNAMICAL IMPACT MODELS Abstract Only
E. Asphaug, H. J. Melosh, and E. Ryan (Planetary Science Inst., Tucson, AZ.) *In* Lunar and Planetary Inst., Twenty-fourth Lunar and Planetary Science Conference. Part 1: A-F 1993 p 45-46 (For primary document see N94-12015 01-91)
Avail: CASI HC A01/MF A06

N94-12057*# Washington Univ., Saint Louis, MO. Dept. of Earth and Planetary Sciences and Center for the Space Sciences.
ORBITAL SIMULATIONS OF SATELLITE ESCAPE/CAPTURE AND THE ORIGIN OF SATELLITES SUCH AS TRITON Abstract Only
Lance A. M. Benner and William B. McKinnon *In* Lunar and Planetary Inst., Twenty-fourth Lunar and Planetary Science Conference. Part 1: A-F 1993 p 89-90 (For primary document see N94-12015 01-91)
Avail: CASI HC A01/MF A06

N94-12058*# Arkansas Univ., Fayetteville. Cosmochemistry Group.
THE GREAT 8 MA EVENT AND THE STRUCTURE OF THE H-CHONDRITE PARENT BODY Abstract Only
P. H. Benoit and D. W. G. Sears *In* Lunar and Planetary Inst., Twenty-fourth Lunar and Planetary Science Conference. Part 1: A-F 1993 p 91-92 (For primary document see N94-12015 01-91)
(Grant NAG9-81)
Avail: CASI HC A01/MF A06

N94-12059*# Arkansas Univ., Fayetteville. Cosmochemistry Group.
METEORITES FROM RECENT AMOR-TYPE ORBITS Abstract Only
P. H. Benoit and D. W. G. Sears *In* Lunar and Planetary Inst., Twenty-fourth Lunar and Planetary Science Conference. Part 1: A-F 1993 p 93-94 (For primary document see N94-12015 01-91)
(Grant NAG9-81)
Avail: CASI HC A01/MF A06

N94-12061*# Tennessee Univ., Knoxville. Dept. of Geological Sciences.
METALLOGRAPHIC COOLING RATES OF L-GROUP ORDINARY CHONDRITES Abstract Only
Marvin E. Bennett and Harry Y. McSween, Jr. *In* Lunar and Planetary Inst., Twenty-fourth Lunar and Planetary Science Conference. Part 1: A-F 1993 p 97-98 (For primary document see N94-12015 01-91)
Avail: CASI HC A01/MF A06

N94-12062*# Arizona Univ., Tucson. Observatory and Lunar Planetary Lab.
EXPLICIT 3D CONTINUUM FRACTURE MODELING WITH SMOOTH PARTICLE HYDRODYNAMICS Abstract Only
W. Benz and E. Asphaug *In* Lunar and Planetary Inst., Twenty-fourth Lunar and Planetary Science Conference. Part 1: A-F 1993 p 99-100 (For primary document see N94-12015 01-91)
Avail: CASI HC A01/MF A06

N94-12063*# Lockheed Engineering and Sciences Co., Houston, TX.
COMPOSITION AND MODAL FREQUENCIES OF HYPERVELOCITY PARTICLES LESS THAN 1 MILLIMETER IN DIAMETER IN LOW-EARTH ORBIT Abstract Only
R. P. Bernhard, T. H. See, and F. Hoerz (National Aeronautics and Space Administration. Lyndon B. Johnson Space Center, Houston, TX.) *In* Lunar and Planetary Inst., Twenty-fourth Lunar and Planetary Science Conference. Part 1: A-F 1993 p 101-102 (For primary document see N94-12015 01-91)
Avail: CASI HC A01/MF A06

N94-12068*# Massachusetts Inst. of Tech., Cambridge. Dept. of Earth, Atmospheric, and Planetary Sciences.
THE ASTEROID-METEORITE CONNECTION: FORGING A NEW LINK TO VESTA AS THE PARENT BODY OF BASALTIC ACHONDRITE (HED) METEORITES Abstract Only
R. P. Binzel *In* Lunar and Planetary Inst., Twenty-fourth Lunar and Planetary Science Conference. Part 1: A-F 1993 p 111 (For primary document see N94-12015 01-91)
Avail: CASI HC A01/MF A06

N94-12069*# Muenster Univ. (Germany). Inst. for Planetologie.
ALKALI-GRANITOIDS AS FRAGMENTS WITHIN THE ORDINARY CHONDRITE ADZHI-BOGDO: EVIDENCE FOR HIGHLY FRACTIONATED, ALKALI-GRANITIC LIQUIDS ON ASTEROIDS Abstract Only
A. Bischoff *In* Lunar and Planetary Inst., Twenty-fourth Lunar and Planetary Science Conference. Part 1: A-F 1993 p 113-114 (For primary document see N94-12015 01-91)
Avail: CASI HC A01/MF A06

N94-12078*# Houston Univ., Clear Lake, TX.
USING SOLAR FLARE TRACK DENSITIES TO DETERMINE THE ORIGIN OF INTERPLANETARY DUST PARTICLES Abstract Only
George E. Blanford *In* Lunar and Planetary Inst., Twenty-fourth Lunar and Planetary Science Conference. Part 1: A-F 1993 p 131-132 (For primary document see N94-12015 01-91)
Avail: CASI HC A01/MF A06

N94-12092*# Arizona Univ., Tucson. Lunar and Planetary Lab.
COLLISION LIFETIMES AND IMPACT STATISTICS OF NEAR-EARTH ASTEROIDS
W. F. Bottke, Jr., M. C. Nolan, and R. Greenberg *In* Lunar and Planetary Inst., Twenty-fourth Lunar and Planetary Science Conference. Part 1: A-F 1993 p 159-160 (For primary document see N94-12015 01-91)
Avail: CASI HC A01/MF A06

N94-12094*# California Univ., Berkeley. Dept. of Geology.
MINOR AND TRACE ELEMENT COMPOSITION AND AGE OF YUKON PROBABLE-MICROTEKTITES Abstract Only
S. Q. Boundy-Sanders and R. L. Hervig (Arizona State Univ., Tempe.) *In* Lunar and Planetary Inst., Twenty-fourth Lunar and Planetary Science Conference. Part 1: A-F 1993 p 163-164 (For primary document see N94-12015 01-91)
Avail: CASI HC A01/MF A06

N94-12098*# MVA, Inc., Norcross, GA.
UNEQUILIBRATED, EQUILIBRATED, AND REDUCED AGGREGATES IN ANHYDROUS INTERPLANETARY DUST PARTICLES Abstract Only
J. P. Bradley *In* Lunar and Planetary Inst., Twenty-fourth Lunar and Planetary Science Conference. Part 1: A-F 1993 p 171-172 (For primary document see N94-12015 01-91)
Avail: CASI HC A01/MF A06

N94-12101*# Naturhistorisches Museum, Vienna (Austria).
MINERALOGY VERSUS BULK COMPOSITION OF THE CARBONACEOUS CHONDRITE CLAST KAIDUN 2 Abstract Only
F. Brandstaetter, G. Kurat, A. V. Ivanov (Academy of Sciences, USSR, Moscow.), H. Palme (Max-Planck-Inst. fuer Chemie, Mainz, Germany.), and B. Spettel (Max-Planck-Inst. fuer Chemie, Mainz, Germany.) *In* Lunar and Planetary Inst., Twenty-fourth Lunar and Planetary Science Conference. Part 1: A-F 1993 p 177-178 (For primary document see N94-12015 01-91)
Avail: CASI HC A01/MF A06

N94-12105*# New Mexico Univ., Albuquerque. Dept. of Earth and Planetary Sciences.
CHONDRITE THERMAL HISTORIES FROM LOW-CA PYROXENE MICROSTRUCTURES: AUTOMETAMORPHISM VERSUS PROGRADE METAMORPHISM REVISITED Abstract Only
Adrian J. Brearley, Rhian H. Jones, and J. J. Papike *In* Lunar and Planetary Inst., Twenty-fourth Lunar and Planetary Science Conference. Part 1: A-F 1993 p 185-186 (For primary document see N94-12015 01-91)
(Grant NAG9-497)
Avail: CASI HC A01/MF A06

N94-12106*# New Mexico Univ., Albuquerque. Dept. of Earth and Planetary Sciences.
SXRF DETERMINATION OF TRACE ELEMENTS IN CHONDRULE RIMS IN THE UNEQUILIBRATED CO3 CHONDRITE, ALH A77307 Abstract Only
Adrian J. Brearley, Sasa Bajt (Brookhaven National Lab., Upton, NY.), Steve R. Sutton (Brookhaven National Lab., Upton, NY.), and J. J. Papike

In Lunar and Planetary Inst., Twenty-fourth Lunar and Planetary Science Conference. Part 1: A-F 1993 p 187-188 (For primary document see N94-12015 01-91)
(Grants NAG9-437; NAG9-106)
Avail: CASI HC A01/MF A06

__N94-12107*#__ Geological Survey, Menlo Park, CA.
__MARTIAN PARTICLE SIZE BASED ON THERMAL INERTIA CORRECTED FOR ELEVATION-DEPENDENT ATMOSPHERIC PROPERTIES Abstract Only__
N. T. Bridges *In* Lunar and Planetary Inst., Twenty-fourth Lunar and Planetary Science Conference. Part 1: A-F 1993 p 189-190 (For primary document see N94-12015 01-91)
Avail: CASI HC A01/MF A06

__N94-12111*#__ Arizona Univ., Tucson. Lunar and Planetary Lab.
__THE 1.2 TO 3.5 MICRONS OBSERVATIONS OF ASTEROID 4179 TOUTATIS Abstract Only__
D. T. Britt, E. S. Howell, J. F. Bell (Hawaii Univ., Honolulu.), and L. A. Lebofsky *In* Lunar and Planetary Inst., Twenty-fourth Lunar and Planetary Science Conference. Part 1: A-F 1993 p 197 (For primary document see N94-12015 01-91)
Avail: CASI HC A01/MF A06

__N94-12114*#__ Tennessee Univ., Knoxville. Dept. of Geological Sciences.
__DETERMINING THE RELATIVE EXTENT OF ALTERATION IN CM CHONDRITES Abstract Only__
Lauren B. Browning, Harry Y. McSween, Jr., and Michael Zolensky (National Aeronautics and Space Administration. Lyndon B. Johnson Space Center, Houston, TX.) *In* Lunar and Planetary Inst., Twenty-fourth Lunar and Planetary Science Conference. Part 1: A-F 1993 p 203-204 (For primary document see N94-12015 01-91)
Avail: CASI HC A01/MF A06

__N94-12115*#__ Washington Univ., Seattle. Dept. of Astronomy.
__IDENTIFICATION OF COMETARY AND ASTEROIDAL PARTICLES IN STRATOSPHERIC IDP COLLECTIONS Abstract Only__
D. E. Brownlee, D. J. Joswiak, S. G. Love, A. O. Nier (Minnesota Univ., Minneapolis.), D. J. Schlutter (Minnesota Univ., Minneapolis.), and J. P. Bradley (MVA, Inc., Norcross, GA.) *In* Lunar and Planetary Inst., Twenty-fourth Lunar and Planetary Science Conference. Part 1: A-F 1993 p 205-206 (For primary document see N94-12015 01-91)
Avail: CASI HC A01/MF A06

__N94-12124*#__ Smithsonian Astrophysical Observatory, Cambridge, MA.
__HOW DIVERSE IS THE ASTEROID BELT? Abstract Only__
Thomas H. Burbine and Jeffrey F. Bell (Hawaii Univ., Honolulu.) *In* Lunar and Planetary Inst., Twenty-fourth Lunar and Planetary Science Conference. Part 1: A-F 1993 p 223-224 (For primary document see N94-12015 01-91)
Avail: CASI HC A01/MF A06

__N94-12125*#__ Arizona Univ., Tucson. Lunar and Planetary Lab.
__STUDIES OF THE RELEASE OF RADIOGENIC Xe-129 FROM BJURBOELE: EVIDENCE AGAINST SIMPLE DIFFUSION MODELS Abstract Only__
M. K. Burkland, T. D. Swindle, and S. L. Baldwin *In* Lunar and Planetary Inst., Twenty-fourth Lunar and Planetary Science Conference. Part 1: A-F 1993 p 225-226 (For primary document see N94-12015 01-91)
Avail: CASI HC A01/MF A06

__N94-12132*#__ Arkansas Coll., Batesville. Dept. of Chemistry.
__VOLATILES IN FOURTEEN INTERPLANETARY DUST PARTICLES: A COMPARISON WITH CI AND CM CHONDRITES Abstract Only__
R. Bustin, E. K. Gibson, Jr. (National Aeronautics and Space Administration. Lyndon B. Johnson Space Center, Houston, TX.), and S. J. Wentworth (National Aeronautics and Space Administration. Lyndon B. Johnson Space Center, Houston, TX.) *In* Lunar and Planetary Inst., Twenty-fourth Lunar and Planetary Science Conference. Part 1: A-F 1993 p 239-240 (For primary document see N94-12015 01-91)
Avail: CASI HC A01/MF A06

__N94-12135*#__ Massachusetts Inst. of Tech., Cambridge. Center for Astrophysics.
__THE GIANT IMPACT PRODUCED A PRECIPITATED MOON Abstract Only__
A. G. W. Cameron *In* Lunar and Planetary Inst., Twenty-fourth Lunar and Planetary Science Conference. Part 1: A-F 1993 p 245-246 (For primary document see N94-12015 01-91)
Avail: CASI HC A01/MF A06

__N94-12142*#__ Field Museum of Natural History, Chicago, IL. Dept. of Geology.
__METAL-RICH METEORITES FROM THE AUBRITE PARENT BODY Abstract Only__
I. Casanova, T. J. McCoy (Hawaii Univ., Hilo.), and K. Keil (Hawaii Univ., Hilo.) *In* Lunar and Planetary Inst., Twenty-fourth Lunar and Planetary Science Conference. Part 1: A-F 1993 p 259-260 (For primary document see N94-12015 01-91)
Avail: CASI HC A01/MF A06

__N94-12146*#__ Dartmouth Coll., Hanover, NH. Dept. of Earth Sciences.
__OXYGEN ISOTOPES AS TRACERS OF TEKTITE SOURCE ROCKS: AN EXAMPLE FROM THE IVORY COAST TEKTITES AND LAKE BOSUMTWI CRATER Abstract Only__
Joel D. Blum, Christian Koeberl (Wien Univ., Austria.), and C. Page Chamberlain *In* Lunar and Planetary Inst., Twenty-fourth Lunar and Planetary Science Conference. Part 1: A-F 1993 p 267-268 (For primary document see N94-12015 01-91)
Avail: CASI HC A01/MF A06

__N94-12150*#__ California Inst. of Tech., Pasadena. Div. of Geological and Planetary Sciences.
__LEW88516 AND SNC METEORITES Abstract Only__
J. H. Chen and G. J. Wasserburg *In* Lunar and Planetary Inst., Twenty-fourth Lunar and Planetary Science Conference. Part 1: A-F 1993 p 275-276 (For primary document see N94-12015 01-91)
Avail: CASI HC A01/MF A06

__N94-12151*#__ California Inst. of Tech., Pasadena. Div. of Geological and Planetary Sciences.
__THE Th AND U ABUNDANCES IN CHONDRITIC METEORITES Abstract Only__
J. H. Chen, G. J. Wasserburg, and D. A. Papanastassiou *In* Lunar and Planetary Inst., Twenty-fourth Lunar and Planetary Science Conference. Part 1: A-F 1993 p 277-278 (For primary document see N94-12015 01-91)
Avail: CASI HC A01/MF A06

__N94-12157*#__ National Aeronautics and Space Administration. Goddard Space Flight Center, Greenbelt, MD.
__COLLISIONS OF SMALL SPACEWATCH ASTEROIDS WITH THE EARTH Abstract Only__
C. F. Chyba *In* Lunar and Planetary Inst., Twenty-fourth Lunar and Planetary Science Conference. Part 1: A-F 1993 p 289-290 (For primary document see N94-12015 01-91)
Avail: CASI HC A01/MF A06

__N94-12162*#__ Hawaii Univ., Honolulu. Planetary Geosciences.
__FIRST RESULTS OF THE SEVEN-COLOR ASTEROID SURVEY Abstract Only__
Beth E. Clark, Jeffrey F. Bell, Fraser P. Fanale, and Paul G. Lucey *In* Lunar and Planetary Inst., Twenty-fourth Lunar and Planetary Science Conference. Part 1: A-F 1993 p 299-300 (For primary document see N94-12015 01-91)
Avail: CASI HC A01/MF A06

__N94-12163*#__ Hawaii Univ., Honolulu. Planetary Geosciences.
__SIMULATION OF POSSIBLE REGOLITH OPTICAL ALTERATION EFFECTS ON CARBONACEOUS CHONDRITE METEORITES Abstract Only__
Beth E. Clark, Fraser P. Fanale, and Mark S. Robinson *In* Lunar and Planetary Inst., Twenty-fourth Lunar and Planetary Science Conference.

Part 1: A-F 1993 p 301-302 (For primary document see N94-12015 01-91)
Avail: CASI HC A01/MF A06

N94-12164*# Hawaii Univ., Honolulu. Planetary Geosciences.
SPECTRAL MIXING MODELS OF S-TYPE ASTEROIDS Abstract Only
Beth E. Clark, Paul G. Lucey, Jeffrey F. Bell, and Fraser P. Fanale *In* Lunar and Planetary Inst., Twenty-fourth Lunar and Planetary Science Conference. Part 1: A-F 1993 p 303-304 (For primary document see N94-12015 01-91)
Avail: CASI HC A01/MF A06

N94-12166*# Clemson Univ., SC. Dept. of Physics and Astronomy.
CARBON AND NITROGEN IN TYPE 2 SUPERNOVA DIAMONDS Abstract Only
Donald D. Clayton, Mounib ElEid, and Lawrence E. Brown *In* Lunar and Planetary Inst., Twenty-fourth Lunar and Planetary Science Conference. Part 1: A-F 1993 p 307-308 (For primary document see N94-12015 01-91)
Avail: CASI HC A01/MF A06

N94-12167*# Stanford Univ., CA. Dept. of Chemistry.
MEASUREMENT OF POLYCYCLIC AROMATIC HYDROCARBON (PAHs) IN INTERPLANETARY DUST PARTICLES Abstract Only
S. J. Clemett, C. R. Maechling, R. N. Zare, P. D. Swan (Washington Univ., Saint Louis, MO.), and R. M. Walker (Washington Univ., Saint Louis, MO.) *In* Lunar and Planetary Inst., Twenty-fourth Lunar and Planetary Science Conference. Part 1: A-F 1993 p 309-310 (For primary document see N94-12015 01-91)
Avail: CASI HC A01/MF A06

N94-12171*# Alberta Univ., Calgary.
OLIVINE-RICH ASTEROIDS, PALLASITIC OLIVINE AND OLIVINE-METAL MIXTURES: COMPARISONS OF REFLECTANCE SPECTRA Abstract Only
E. A. Cloutis *In* Lunar and Planetary Inst., Twenty-fourth Lunar and Planetary Science Conference. Part 1: A-F 1993 p 317-318 (For primary document see N94-12015 01-91)
Avail: CASI HC A01/MF A06

N94-12172*# Newcastle-upon-Tyne Univ. (England). Dept. of Physics.
REMANENT MAGNETISM OF HED METEORITES: IMPLICATIONS FOR THEIR EVOLUTION AND ANCIENT MAGNETIC FIELDS Abstract Only
D. W. Collinson and S. J. Morden *In* Lunar and Planetary Inst., Twenty-fourth Lunar and Planetary Science Conference. Part 1: A-F 1993 p 319-320 (For primary document see N94-12015 01-91)
Avail: CASI HC A01/MF A06

N94-12176*# Rutgers Univ., New Brunswick, NJ. Dept. of Geological Science.
THE EXPERIMENTAL PRODUCTION OF MATRIX LUMPS WITHIN CHONDRULES: EVIDENCE OF POST-FORMATIONAL PROCESSES Abstract Only
Harold C. Connolly, Jr. and Roger H. Hewins *In* Lunar and Planetary Inst., Twenty-fourth Lunar and Planetary Science Conference. Part 1: A-F 1993 p 327-328 (For primary document see N94-12015 01-91)
(Grant NGT-50836)
Avail: CASI HC A01/MF A06

N94-12177*# Rutgers Univ., New Brunswick, NJ. Dept. of Geological Sciences.
FLASH MELTING OF CHONDRULE PRECURSORS IN EXCESS OF 1600 C. SERIES 1: TYPE 2 (B1) CHONDRULE COMPOSITION EXPERIMENTS Abstract Only
Harold C. Connolly, Jr., Roger H. Hewins, and Gary E. Lofgren (National Aeronautics and Space Administration. Lyndon B. Johnson Space Center, Houston, TX.) *In* Lunar and Planetary Inst., Twenty-fourth Lunar and Planetary Science Conference. Part 1: A-F 1993 p 329-330 (For primary document see N94-12015 01-91)
(Grant NGT-50836)
Avail: CASI HC A01/MF A06

N94-12181*# Brown Univ., Providence, RI. Dept. of Geological Sciences.
MACROSCOPIC ELECTRIC CHARGE SEPARATION DURING HYPERVELOCITY IMPACTS: POTENTIAL IMPLICATIONS FOR PLANETARY PALEOMAGNETISM Abstract Only
D. A. Crawford and P. H. Schultz *In* Lunar and Planetary Inst., Twenty-fourth Lunar and Planetary Science Conference. Part 1: A-F 1993 p 337-338 (For primary document see N94-12015 01-91)
Avail: CASI HC A01/MF A06

N94-12182*# University of Southern California, Pasadena. Div. of Geological and Planetary Sciences.
RHENIUM-OSMIUM ISOTOPE SYSTEMATICS OF GROUP 2A AND GROUP 4A IRON METEORITES Abstract Only
R. A. Creaser (Alberta Univ., Edmonton.), D. A. Papanastassiou, and G. J. Wasserburg *In* Lunar and Planetary Inst., Twenty-fourth Lunar and Planetary Science Conference. Part 1: A-F 1993 p 339-340 (For primary document see N94-12015 01-91)
(Grant NAG9-43)
Avail: CASI HC A01/MF A06

N94-12183*# Toronto Univ. (Ontario). Iso Trace Lab.
SEPARATION OF SPALLATION AND TERRESTRIAL C-14 IN CHONDRITES Abstract Only
R. G. Cresswell, R. P. Beukens, and J. C. Rucklidge *In* Lunar and Planetary Inst., Twenty-fourth Lunar and Planetary Science Conference. Part 1: A-F 1993 p 341-342 (For primary document see N94-12015 01-91)
Avail: CASI HC A01/MF A06

N94-12186*# Arizona Univ., Tucson. Lunar and Planetary Lab.
POROSITY AND THE ECOLOGY OF ICY SATELLITES Abstract Only
Steven K. Croft *In* Lunar and Planetary Inst., Twenty-fourth Lunar and Planetary Science Conference. Part 1: A-F 1993 p 347-348 (For primary document see N94-12015 01-91)
Avail: CASI HC A01/MF A06

N94-12191*# Washington Univ., Saint Louis, MO. Dept. of Earth and Planetary Sciences.
ANOMALOUS REE PATTERNS IN UNEQUILIBRATED ENSTATITE CHONDRITES: EVIDENCE AND IMPLICATIONS Abstract Only
Ghislaine Crozaz and Weibiao Hsu *In* Lunar and Planetary Inst., Twenty-fourth Lunar and Planetary Science Conference. Part 1: A-F 1993 p 357-358 (For primary document see N94-12015 01-91)
Avail: CASI HC A01/MF A06

N94-12200*# Chicago Univ., IL.
TRACE ELEMENT DISTRIBUTIONS IN PRIMITIVE ACHONDRITES Abstract Only
Andrew M. Davis, Martin Prinz (American Museum of Natural History, New York, NY.), and Michael K. Weisberg (American Museum of Natural History, New York, NY.) *In* Lunar and Planetary Inst., Twenty-fourth Lunar and Planetary Science Conference. Part 1: A-F 1993 p 375-376 (For primary document see N94-12015 01-91)
Avail: CASI HC A01/MF A06

N94-12201*# Planetary Science Inst., Tucson, AZ.
DEVIATIONS FROM THE STRAIGHT LINE: BUMPS (AND GRINDS) IN THE COLLISIONALLY EVOLVED SIZE DISTRIBUTION OF ASTEROIDS Abstract Only
D. R. Davis, P. Farinella (Pisa Univ., Italy.), P. Paolicchi (Pisa Univ., Italy.), A. C. Bagatin (Pisa Univ., Italy.), A. Cellino (Osservatorio Astronomico, Turin, Italy.), and E. Zappala (Osservatorio Astronomico, Turin, Italy.) *In* Lunar and Planetary Inst., Twenty-fourth Lunar and Planetary Science Conference. Part 1: A-F 1993 p 377-378 (For primary document see N94-12015 01-91)
Avail: CASI HC A01/MF A06

N94-12205*# European Space Research Organization, Noordwikj (Netherlands). Space Science Dept.
A METHOD TO DETERMINE ASTEROID POLES Abstract Only
G. DeAngelis *In* Lunar and Planetary Inst., Twenty-fourth Lunar and

Planetary Science Conference. Part 1: A-F 1993 p 385-386 (For primary document see N94-12015 01-91)
Avail: CASI HC A01/MF A06

N94-12206*# Arkansas Univ., Fayetteville. Core Labs.
CATHODOLUMINESCENCE PROPERTIES OF COMPONENTS IN ENSTATITE CHONDRITES Abstract Only
John M. DeHart and Gary E. Lofgren (National Aeronautics and Space Administration. Lyndon B. Johnson Space Center, Houston, TX.) *In* Lunar and Planetary Inst., Twenty-fourth Lunar and Planetary Science Conference. Part 1: A-F 1993 p 387-388 (For primary document see N94-12015 01-91)
Avail: CASI HC A01/MF A06

N94-12208*# Rutgers Univ., New Brunswick, NJ. Dept. of Geological Sciences.
THE Fe/Mn CONSTRAINT ON PRECURSORS OF BASALTIC ACHONDRITES Abstract Only
Jeremy S. Delaney and Joseph S. Boesenberg *In* Lunar and Planetary Inst., Twenty-fourth Lunar and Planetary Science Conference. Part 1: A-F 1993 p 391-392 (For primary document see N94-12015 01-91)
Avail: CASI HC A01/MF A06

N94-12211*# State Univ. of New York, Albany. Dept. of Geological Sciences.
SORET DIFFUSION: A POSSIBLE CAUSE OF COMPOSITIONAL HETEROGENEITY WITHIN TEKTITES Abstract Only
J. W. Delano, Y.-G. Liu (Oregon State Univ., Corvallis.), and R. A. Schmitt (Oregon State Univ., Corvallis.) *In* Lunar and Planetary Inst., Twenty-fourth Lunar and Planetary Science Conference. Part 1: A-F 1993 p 397-398 (For primary document see N94-12015 01-91)
Avail: CASI HC A01/MF A06

N94-12215*# State Univ. of New York, Stony Brook. Dept. of Earth and Space Sciences.
A CM CHONDRITE CLUSTER AND CM STREAMS Abstract Only
R. T. Dodd and M. E. Lipschutz (Purdue Univ., West Lafayette, IN.) *In* Lunar and Planetary Inst., Twenty-fourth Lunar and Planetary Science Conference. Part 1: A-F 1993 p 405-406 (For primary document see N94-12015 01-91)
Avail: CASI HC A01/MF A06

N94-12224*# California Univ., San Diego, La Jolla. Dept. of Chemistry.
DEVELOPMENT OF A MOLECULAR BEAM TECHNIQUE TO STUDY EARLY SOLAR SYSTEM SILICON REACTIONS Abstract Only
Q. W. Dong and M. H. Thiemens *In* Lunar and Planetary Inst., Twenty-fourth Lunar and Planetary Science Conference. Part 1: A-F 1993 p 423-424 (For primary document see N94-12015 01-91)
Avail: CASI HC A01/MF A06

N94-12225*# Academy of Sciences (USSR), Moscow. Inst. of Geochemistry.
ON HIGH-TEMPERATURE FORMATION OF IRON-RICH OLIVINE IN THE EARLY SOLAR SYSTEM Abstract Only
V. A. Dorofeyeva, A. B. Makalkin, and A. V. Vityazev *In* Lunar and Planetary Inst., Twenty-fourth Lunar and Planetary Science Conference. Part 1: A-F 1993 p 425-426 (For primary document see N94-12015 01-91)
Avail: CASI HC A01/MF A06

N94-12226*# Academy of Sciences (USSR), Moscow. Inst. of Geochemistry.
RECONDENSATION OF CHONDRITIC MATERIAL IN THE EARLY SOLAR SYSTEM: RESULTS OF THERMODYNAMIC SIMULATION Abstract Only
V. A. Dorofeyeva, A. B. Makalkin, M. V. Mironenko, and A. V. Vityazev *In* Lunar and Planetary Inst., Twenty-fourth Lunar and Planetary Science Conference. Part 1: A-F 1993 p 427-428 (For primary document see N94-12015 01-91)
Avail: CASI HC A01/MF A06

N94-12230*# Arizona State Univ., Tempe. Dept. of Geology and Chemistry.
PRIMORDIAL LIGHTNING: EVIDENCE PRESERVED IN CHONDRITES Abstract Only
D. Eisenhour and P. R. Buseck *In* Lunar and Planetary Inst., Twenty-fourth Lunar and Planetary Science Conference. Part 1: A-F 1993 p 435-436 (For primary document see N94-12015 01-91)
Avail: CASI HC A01/MF A06

N94-12231*# Arizona State Univ., Tempe. Dept. of Geology and Chemistry.
MICRO-ZONING IN MINERALS OF A LANDES SILICATE INCLUSION Abstract Only
D. D. Eisenhour, P. R. Buseck, H. Palme (Max-Planck-Inst. fuer Chemie, Mainz, Germany.), and J. Zipfel (Max-Planck-Inst. fuer Chemie, Mainz, Germany.) *In* Lunar and Planetary Inst., Twenty-fourth Lunar and Planetary Science Conference. Part 1: A-F 1993 p 437-438 (For primary document see N94-12015 01-91)
Avail: CASI HC A01/MF A06

N94-12233*# Centre de Spectrometrie Nucleaire et de Spectrometrie de Masse du CNRS, Orsay (France).
A NEW CARBON-RICH PHASE (COPS) IN ANTARCTIC MICROMETEORITES Abstract Only
C. Engrand, M. Maurette, G. Kurat (Naturhistorisches Museum, Vienna, Austria.), F. Brandstatter (Naturhistorisches Museum, Vienna, Austria.), and M. Perreau (Office National d'Etudes et de Recherches Aeronautiques, Paris, France.) *In* Lunar and Planetary Inst., Twenty-fourth Lunar and Planetary Science Conference. Part 1: A-F 1993 p 441-442 (For primary document see N94-12015 01-91)
Avail: CASI HC A01/MF A06

N94-12234*# Viale Univ., Rome (Italy).
AUTOMATIC DEFINITION OF SPECTRAL UNITS IN THE EQUATORIAL REGIONS OF MARS Abstract Only
Stephane Erard, Priscilla Cerroni, and Angioletta Coradini *In* Lunar and Planetary Inst., Twenty-fourth Lunar and Planetary Science Conference. Part 1: A-F 1993 p 443-444 (For primary document see N94-12015 01-91)
Avail: CASI HC A01/MF A06

N94-12237*# Australian National Univ., Canberra. Research School of Earth Sciences.
Re-Os DATING OF 3AB IRON METEORITES Abstract Only
Tezer M. Esat and Victoria Bennett *In* Lunar and Planetary Inst., Twenty-fourth Lunar and Planetary Science Conference. Part 1: A-F 1993 p 449-450 (For primary document see N94-12015 01-91)
Avail: CASI HC A01/MF A06

N94-12238*# Universidad Nacional Autonoma de Mexico, Mexico City. Inst. de Geofisica.
MODELLING OF DISPERSAL AND DEPOSITION OF IMPACT GLASS SPHERULES FROM THE CRETACEOUS-TERTIARY BOUNDARY DEPOSIT Abstract Only
J. M. Espindola, S. Carey (Rhode Island Univ., Narragansett.), and H. Sigurdsson (Rhode Island Univ., Narragansett.) *In* Lunar and Planetary Inst., Twenty-fourth Lunar and Planetary Science Conference. Part 1: A-F 1993 p 451-452 (For primary document see N94-12015 01-91)
Avail: CASI HC A01/MF A06

N94-12239*# Bern Univ. (Switzerland). Physikalisches Inst.
THE Xe-Q IN LODRANITES AND A HINT FOR Xe-L. FRO90011 ANOTHER LODRANITE? Abstract Only
O. Eugster and A. Weigel *In* Lunar and Planetary Inst., Twenty-fourth Lunar and Planetary Science Conference. Part 1: A-F 1993 p 453-454 (For primary document see N94-12015 01-91)
Avail: CASI HC A01/MF A06

N94-12241*# California Inst. of Tech., Pasadena. Lab. of Experimental Geophysics.
PROJECTILE-TARGET MIXING IN MELTED EJECTA FORMED DURING A HYPERVELOCITY IMPACT CRATERING EVENT Abstract Only

Noreen Joyce Evans, Thomas J. Ahrens, M. Shahinpoor, and W. W. Anderson *In* Lunar and Planetary Inst., Twenty-fourth Lunar and Planetary Science Conference. Part 1: A-F 1993 p 457-458 (For primary document see N94-12015 01-91)
Avail: CASI HC A01/MF A06

N94-12244*# Hawaii Univ., Manoa. Planetary Geosciences.
CHONDRITES, S ASTEROIDS, AND SPACE WEATHERING: THUMPING NOISES FROM THE COFFIN? Abstract Only
F. P. Fanale and B. E. Clark *In* Lunar and Planetary Inst., Twenty-fourth Lunar and Planetary Science Conference. Part 1: A-F 1993 p 463-464 (For primary document see N94-12015 01-91)
Avail: CASI HC A01/MF A06

N94-12252*# Academy of Sciences (USSR), Moscow. Inst. of Geochemistry and Analytical Chemistry.
DIAMOND THERMOLUMINESCENCE PROPERTIES OF DIFFERENT CHONDRITES Abstract Only
A. V. Fisenko, L. L. Kashkarov, L. F. Semjonova, and C. T. Pillinger (Open Univ., Milton, England.) *In* Lunar and Planetary Inst., Twenty-fourth Lunar and Planetary Science Conference. Part 1: A-F 1993 p 479-480 (For primary document see N94-12015 01-91)
Avail: CASI HC A01/MF A06

N94-12253*# Academy of Sciences (USSR), Moscow. Inst. of Geochemistry and Analytical Chemistry.
THE UNUSUAL METALLIC PARTICLES IN KRYMKA LL3.0 CHONDRITE Abstract Only
A. V. Fisenko, A. Yu. Ljul, L. F. Semjonova, and K. I. Ignatenko *In* Lunar and Planetary Inst., Twenty-fourth Lunar and Planetary Science Conference. Part 1: A-F 1993 p 481-482 (For primary document see N94-12015 01-91)
Avail: CASI HC A01/MF A06

N94-12254*# Academy of Sciences (USSR), Moscow. Inst. of Geochemistry and Analytical Chemistry.
ON POSSIBILITY OF DIAMOND FORMATIONS IN RADIATION PROCESS Abstract Only
A. V. Fisenko, L. F. Semjonova, L. N. Bolsheva, T. V. Grachjova, A. B. Verchovsky, and Yu. A. Shukolyukov *In* Lunar and Planetary Inst., Twenty-fourth Lunar and Planetary Science Conference. Part 1: A-F 1993 p 483-484 (For primary document see N94-12015 01-91)
Avail: CASI HC A01/MF A06

N94-12255*# Academy of Sciences (USSR), Moscow. Inst. of Geochemistry and Analytical Chemistry.
THE CARBON ISOTOPIC COMPOSITION OF NOVO UREI DIAMONDS Abstract Only
A. V. Fisenko, L. F. Semjenova, A. B. Verchovsky, S. S. Russell, and C. T. Pillinger (Open Univ., Milton, England.) *In* Lunar and Planetary Inst., Twenty-fourth Lunar and Planetary Science Conference. Part 1: A-F 1993 p 485-486 (For primary document see N94-12015 01-91)
Avail: CASI HC A01/MF A06

N94-12257*# Massachusetts Inst. of Tech., Cambridge. Dept. of Earth, Atmospheric and Planetary Sciences.
CRONSTEDTITE AND IRON SULFIDE MINERALOGY OF CM-TYPE CARBONACEOUS CHONDRITES FROM CRYOGENIC MOESSBAUER SPECTRA Abstract Only
Duncan S. Fisher and Roger G. Burns *In* Lunar and Planetary Inst., Twenty-fourth Lunar and Planetary Science Conference. Part 1: A-F 1993 p 489-490 (For primary document see N94-12015 01-91)
(Grants NAGw-2049; NAGw-2220)
Avail: CASI HC A01/MF A06

N94-12260*# State Univ. of New York, Plattsburgh. Dept. of Physics.
TRACE ELEMENT CONTENT OF CHONDRITIC COSMIC DUST: VOLATILE ENRICHMENTS, THERMAL ALTERATIONS, AND THE POSSIBILITY OF CONTAMINATION Abstract Only
G. J. Flynn, S. R. Sutton (Chicago Univ., IL.), and S. Bajt (Chicago Univ., IL.) *In* Lunar and Planetary Inst., Twenty-fourth Lunar and Planetary Science Conference. Part 1: A-F 1993 p 495-496 (For primary document see N94-12015 01-91)
Avail: CASI HC A01/MF A06

N94-12261*# State Univ. of New York, Plattsburgh. Dept. of Physics.
DEPLETIONS OF SULFUR AND/OR ZINC IN IDPs: ARE THEY RELIABLE INDICATORS OF ATMOSPHERIC ENTRY HEATING? Abstract Only
G. J. Flynn, S. R. Sutton (Chicago Univ., IL.), S. Bajt (Chicago Univ., IL.), W. Kloeck (Westfaelische Wilhelms Univ., Muenster, Germany.), K. L. Thomas (Lockheed Corp., Houston, TX.), and L. P. Keller (National Aeronautics and Space Administration. Lyndon B. Johnson Space Center, Houston, TX.) *In* Lunar and Planetary Inst., Twenty-fourth Lunar and Planetary Science Conference. Part 1: A-F 1993 p 497-498 (For primary document see N94-12015 01-91)
Avail: CASI HC A01/MF A06

N94-12262*# State Univ. of New York, Plattsburgh. Dept. of Physics.
NEW LOW-NI (IGNEOUS?) PARTICLES AMONG THE C AND C? TYPES OF COSMIC DUST Abstract Only
G. J. Flynn, S. R. Sutton (Chicago Univ., IL.), S. Bajt (Chicago Univ., IL.), and W. Kloeck (Westfaelische Wilhelms Univ., Muenster, Germany.) *In* Lunar and Planetary Inst., Twenty-fourth Lunar and Planetary Science Conference. Part 1: A-F 1993 p 499-500 (For primary document see N94-12015 01-91)
Avail: CASI HC A01/MF A06

N94-12263*# California Univ., San Diego, La Jolla.
MASS AND SPATIAL DISTRIBUTION OF CARBONACEOUS COMPONENT IN COMET HALLEY Abstract Only
M. Fomenkova and S. Chang *In* Lunar and Planetary Inst., Twenty-fourth Lunar and Planetary Science Conference. Part 1: A-F 1993 p 501-502 (For primary document see N94-12015 01-91)
Avail: CASI HC A01/MF A06

N94-12264*# Brown Univ., Providence, RI. Dept. of Geological Sciences.
PRIMITIVE SNC PARENT MAGMAS AND CRYSTALLIZATION: LOW PH2O EXPERIMENTS Abstract Only
D. J. Ford and M. J. Rutherford *In* Lunar and Planetary Inst., Twenty-fourth Lunar and Planetary Science Conference. Part 1: A-F 1993 p 503-504 (For primary document see N94-12015 01-91)
Avail: CASI HC A01/MF A06

N94-12265*# Paris XI Univ., Orsay (France).
PHASE TRANSITIONS AND 2D SPHERICAL CONVECTION IN A LARGE ICY SATELLITE Abstract Only
O. Forni, C. Federico (Perugia Univ., Italy.), and A. Coradini (Consiglio Nazionale delle Ricerche, Rome, Italy.) *In* Lunar and Planetary Inst., Twenty-fourth Lunar and Planetary Science Conference. Part 1: A-F 1993 p 505-506 (For primary document see N94-12015 01-91)
Avail: CASI HC A01/MF A06

91 LUNAR AND PLANETARY EXPLORATION

Includes planetology; and manned and unmanned flights.
For spacecraft design or space stations see *18 Spacecraft Design, Testing and Performance.*

N94-10144*# Boeing Defense and Space Group, Huntsville, AL.
LUNAR CAMPSITE CONCEPT: SPACE TRANSFER CONCEPTS AND ANALYSIS FOR EXPLORATION MISSIONS
May 1991 59 p
(Contract NAS8-37857)
(NASA-CR-192602; NAS 1.26:192602) Avail: CASI HC A04/MF A01

The lunar Campsite concept responds to a perceived need to identify early manned science and exploration missions that require minimal initial funding. The Campsite concept defers the build-up of many infrastructure components without escalating total program costs. The lunar Campsite has been sized nominally for four crew for 42 days (1 lunar night and 2 lunar days), but can be modified to span two lunar nights up to 60 days.

Total mission fulfillment requires five Earth-to-LEO launches, four (100 mt class launch vehicle) for the two vehicle assemblies and one (PLS or NSTS) for the crew. The lunar Campsite mission mode is tandem direct using a booster stage and a lander stage. The booster is separated from the lander after the TLI burn and is expended into the Earth's atmosphere. In the Campsite mode, the lander lands on the surface not to be returned. In the crew delivery mode, the lander is guided to a precision landing about 500 m from the Campsite, and with enough propellant to return the crew to Earth. The Campsite consists of a habitat and airlock, body mounted radiators with a surface shield, sun tracking solar arrays, and an Earth-tracking high-gain antenna. The CV is very similar to the campsite delivery vehicle. The CV does not, however, have radiators or solar arrays. The vehicle stacks are essentially common in that they utilize the same structure system and engines, the same propellant tanks, the same 'cut-out' in which the CRV and payloads are incorporated, and the same RCS locations. The booster and lander stage propellant tank propellant capacities are identical and have margins which would allow additional fueling for propulsive capture of the boost stage into Earth orbit. This contractual study was performed to identify Campsite and vehicle interfaces and vehicle requirements, and to surface issues related to the integration of the Campsite and LTV's. Derived from text

N94-10817*# Cornell Univ., Ithaca, NY. Center for Radiophysics and Space Research.
PHYSICAL STUDIES OF PLANETARY AND SATELLITE SURFACES Final Technical Report, 1 Jul. 1975 - 31 Mar. 1991
Joseph Veverka Nov. 1991 9 p
(Grant NsG-7156)
(NASA-CR-193545; NAS 1.26:193545) Avail: CASI HC A02/MF A01

The publications and doctoral dissertations generated by this NASA grant are presented in bibliographic form. The topics include but are not limited to the photometric properties and surface morphology of planets and their satellites. CASI

N94-10823*# Harvard Univ., Cambridge, MA. Center for Earth and Planetary Physics.
PHOTOCHEMICAL MODELLING OF VENUS CLOUDS USING PIONEER VENUS DATA Final Report
Michael B. McElroy 24 Apr. 1985 22 p
(Grant NAG2-264)
(NASA-CR-194108; NAS 1.26:194108) Avail: CASI HC A03/MF A01

In order to understand the evolution of water on Venus, we must know the hydrogen escape flux as a function of the tropospheric water abundance. We have studied the connection between total stratospheric hydrogen and exobase hydrogen available to non-thermal escape processes and examined the details of the photochemical trap for water at the Venus cloud tops. Our immediate goal is to calculate the stratospheric water abundance as a function of the tropospheric water abundance. Photochemical production of H2SO4 acts as a sink for both water and sulfur and is capable of keeping stratospheric abundances low if a proper balance exists between the tropospheric abundances. If production of H2SO4 were the only sink for H2O and SO2, the excess in tropospheric abundance of one over the other would reach the stratosphere, and the functional dependence of stratospheric H2O on tropospheric H2O would be linear near the present state. On Venus, however, sulfuric acid condenses at cloud top temperatures and the resulting aerosols can absorb additional water of hydration. This complicates the water budget, increasing the efficiency of sulfur as a sink for water. We have investigated the balance between tropospheric H2O and SO2 and how delicate the balance is. Our major conclusions from this work are the following: (1) H2O and SO2 are mutually limiting if proper tropospheric balance is maintained; (2) changes in tropospheric abundances on the order of 5 ppm are significant; and (3) changes in mixing rates near the cloud tops can cause dramatic changes in SO2 without causing dramatic changes in H2O. Derived from text

N94-11184 Arizona State Univ., Tempe.
EVOLUTION OF STEEP MARTIAN SLOPES Ph.D. Thesis
Robert John Sullivan, Jr. 1992 204 p
Avail: Univ. Microfilms Order No. DA9307143

The physical properties and evolution of steep slopes on the planet Mars are examined. Where martian slopes are steepest and of greatest relief, the slope morphology is distinctive and characterized by regular, alternating spurs and gullies. Previous workers identified these martian gullies as dry debris avalanche chutes, partially because a nonspecific 'dry mass-wasting' explanation seemed compatible, initially, with current surface conditions. An evacuated avalanche chute provides the opportunity to back analyze the stability of the mobile layer of the chute at the time of its failure. For the martian slope problem a new stability back-analysis technique was developed which incorporates the third dimension (chute width) into the back-analysis calculation, allowing unambiguous determination of the average cohesion and angle of internal friction of the mobile layer. A series of trials was performed to investigate the effects of gravitational acceleration, average slope angle, and average mobile layer density, cohesion, and angle of internal friction on the size and shape of the transverse chute cross-section. Results indicate that: (1) variations in density, gravitational acceleration, and cohesion affect the overall size of the cross-section but not its width:depth ratio, and (2) the contrast between average slope angle and angle of internal friction is most influential on the width:depth ratio of the cross-section. The difference between these two parameters is inversely proportional to the width:depth ratio. Application of the three-dimensional back-analysis technique to proposed martian avalanche chutes yields values of cohesion and angle of internal friction of the mobile layers that are similar mechanically (without genetic implications) to those of terrestrial glacial till, a poorly sorted material with moderate inter-grain cohesion, or lunar soils under normal stresses representative of (lunar) depths of between ten and twenty meters. Material of these strengths is not capable of supporting long, steep martian slopes visible on Viking Orbiter images. These results imply that weathering and weakening of initially stronger martian slope materials penetrated to depths of tens of meters before downslope failure of weathered material occurred (creating the observed avalanche chutes). Dissert. Abstr.

N94-11185 California Univ., Los Angeles.
WAVE STRUCTURE IN PLANETARY RINGS Ph.D. Thesis
Linda Joyce Horn 1992 276 p
Avail: Univ. Microfilms Order No. DA9310920

Planetary rings contain a wealth of wavelike structure that is driven by gravitational resonance interactions with nearby satellites. Wave behavior is a powerful tool for estimating physical ring parameters that are key to our understanding of ring origin and evolution. A new technique, utilizing the Burg autoregressive power spectral algorithm, was developed for probing the physical characteristics of rings and for detecting waves that are not otherwise visible. Data from the Voyager photopolarimeter (PPS) stellar occultations by the rings of Saturn, Uranus, and Neptune and the Voyager radio science (RSS) occultation by Saturn's rings were used. Local surface mass density estimates are obtained from the dispersion of 40 spiral density waves in Saturn's A ring, including 10 weaker waves not previously analyzed. Surface mass densities vary from 20 to 60 gm sq cm. Increasing optical depth is not correlated with increasing surface mass density, especially after the Keeler gap, suggesting that ring particle size and composition are not uniform throughout the A ring. Saturn's A ring mass is reestimated using the surface mass densities and is 5.2 +/- 1.3 x 10(exp 21) gm. The wakes of Saturn's satellite Pan are not short timescale phenomena because the effects of Pan's gravitational perturbations persist for more than one Pan encounter. Four additional Pan wakes were discovered at longitudes greater than 360 deg. Collective effects such as collisions modify the wake dispersion more extensively at greater longitudes. Pan is the dominant mass in the Encke gap. A spiral density wave was detected inside the Uranian delta ring. Upper and lower bounds were estimated for the surface mass density of the delta ring 5 less than or equal to sigma less than or equal to 10 gm/sq cm, the viscosity 10 less than or equal to nu less than or equal to 40 sq cm/sec, and the local ring height 7 less than or equal to h less than or equal to 20 m. These values are comparable to the corresponding values at Saturn. An Adams ring arc and the Leverrier ring were detected in the PPS data. The Adams arc is 43 km wide with an equivalent depth of 0.77 +/- 0.13 km. The Leverrier ring is 113 km in wide with an equivalent depth of 0.7 +/- 0.2 km. Values for the Adams ring arc are consistent with Voyager ultraviolet spectrometer and ground-based numbers while the Leverrier ring was not detected in these data sets. Dissert. Abstr.

N94-11361*# Stanford Univ., CA. Center for Radar Astronomy.
THEORETICAL STUDIES OF THE RADAR PROPERTIES OF THE ICY GALILEAN MOONS OF JUPITER Final Report

Von R. Eshleman Jul. 1993 57 p
(Grant NAGw-1964)
(NASA-CR-193407; NAS 1.26:193407) Avail: CASI HC A04/MF A01

The icy Galilean satellites of Jupiter - Europa, Ganymede, and Callisto - have unusual radar scattering properties compared with those of the terrestrial planets or Earth's Moon. There are three main features of the data that distinguish these targets: (1) the radar cross-section normalized by the geometrical cross-section is an order of magnitude larger than that of any terrestrial planet; (2) the reflected power is almost evenly distributed between two orthogonal polarizations with more power being returned in the same circular polarization as was transmitted whereas virtually all of the power returned from the terrestrial planets is contained in the opposite circular polarization to the one that was transmitted; and (3) the echo power spectra have a broad shape indicating a nearly uniformly radar-bright surface in contrast to the spectra from the terrestrial planets that contain a strong quasi-specular component from the vicinity of the sub-radar point and very little reflected power from the rest of the surface. The normalized radar cross-sections decrease as the areal water ice coverage decreases from Europa to Ganymede to Callisto. Recently, radar echoes from the polar caps of Mars and Mercury, and from Saturn's satellite Titan imply similarly strong cross-sections and have classically unexpected polarization properties and it is also thought that this is due to the presence of ice on the surface. A model called the radar glory model is analyzed and it is shown that the main features of the radar echoes calculated from this model agree well with the observations from all three icy Galilean satellites. This model involves long radar paths in the ice below the surface and special structures in which the refractive index decreases abruptly at a hemispherical boundary. It is not known whether such structures exist or how they could be created, but possible scenarios can be imagined such as the formation of an impact crater followed by deposition of a frost layer followed by a resurfacing event in which a layer of solid ice is placed above the layer of frost. Regardless of the exact geophysical processes required to create such structures, the superior ability of this model to account for all of the important observations with very few adjustable parameters and with no ad hoc assumptions is a compelling argument in support of at least the electromagnetic model. The key features of the electromagnetic model are multiple subsurface scattering events, total internal reflection, and a low degree of randomness imposed on a deterministic geometry that strongly favors backscattering.

Author (revised)

N94-12015*# Lunar and Planetary Inst., Houston, TX.

TWENTY-FOURTH LUNAR AND PLANETARY SCIENCE CONFERENCE. PART 1: A-F Abstracts Only

1993 597 p Conference held in Houston, TX, 15-19 Mar. 1993
(Contract NASw-4574)
(NASA-CR-193095; NAS 1.26:193095) Avail: CASI HC A25/MF A06

The topics covered include the following: petrology, petrography, meteoritic composition, planetary geology, atmospheric composition, astronomical spectroscopy, lunar geology, Mars (planet), Mars composition, Mars surface, volcanology, Mars volcanoes, Mars craters, lunar craters, mineralogy, mineral deposits, lithology, asteroids, impact melts, planetary composition, planetary atmospheres, planetary mapping, cosmic dust, photogeology, stratigraphy, lunar craters, lunar exploration, space exploration, geochronology, tectonics, atmospheric chemistry, astronomical models, and geochemistry. For individual titles, see N94-12016 through N94-12268.

N94-12016*# Niels Bohr Inst., Copenhagen (Denmark).

MOESSBAUER SPECTROSCOPY OF THE SNC METEORITE ZAGAMI Abstract Only c90

D. P. Agerkvist and L. Vistisen *In* Lunar and Planetary Inst., Twenty-fourth Lunar and Planetary Science Conference. Part 1: A-F 1993 p 1-2 (For primary document see N94-12015 01-91)
Avail: CASI HC A01/MF A06

We have performed Mossbauer spectroscopy on two different pieces of the meteorite Zagami belonging to the group of SNC meteorites. In one of the samples we found a substantial amount of olivine inter grown with one kind of pyroxene, and also another kind of pyroxene very similar to the pyroxene in the other sample we examined. Both samples showed less than 1 percent of Fe(3+) in the silicate phase. The group of SNC meteorites called shergottites, to which Zagami belongs, are achondrites whose texture, mineralogy and composition resembles those of terrestrial diabases. The results from the investigation are presented.

Derived from text

N94-12017*# Lunar Industries, Inc., Houston, TX.

PRODUCTION OF ELECTRONIC GRADE LUNAR SILICON BY DISPROPORTIONATION OF SILICON DIFLUORIDE Abstract Only

William N. Agosto *In* Lunar and Planetary Inst., Twenty-fourth Lunar and Planetary Science Conference. Part 1: A-F 1993 p 3-4 (For primary document see N94-12015 01-91)
Avail: CASI HC A01/MF A06

Waldron has proposed to extract lunar silicon by sodium reduction of sodium fluorosilicate derived from reacting sodium fluoride with lunar silicon tetrafluoride. Silicon tetrafluoride is obtained by the action of hydrofluoric acid on lunar silicates. While these reactions are well understood, the resulting lunar silicon is not likely to meet electronic specifications of 5 nines purity. Dale and Margrave have shown that silicon difluoride can be obtained by the action of silicon tetrafluoride on elemental silicon at elevated temperatures (1100-1200 C) and low pressures (1-2 torr). The resulting silicon difluoride will then spontaneously disproportionate into hyperpure silicon and silicon tetrafluoride in vacuum at approximately 400 C. On its own merits, silicon difluoride polymerizes into a tough waxy solid in the temperature range from liquid nitrogen to about 100 C. It is the silicon analog of teflon. Silicon difluoride ignites in moist air but is stable under lunar surface conditions and may prove to be a valuable industrial material that is largely lunar derived for lunar surface applications. The most effective driver for lunar industrialization may be the prospects for industrial space solar power systems in orbit or on the moon that are built with lunar materials. Such systems would require large quantities of electronic grade silicon or compound semiconductors for photovoltaics and electronic controls. Since silicon is the most abundant semimetal in the silicate portion of any solar system rock (approximately 20 wt percent), lunar silicon production is bound to be an important process in such a solar power project. The lunar silicon extraction process is discussed.

Derived from text

N94-12018*# Centre National de la Recherche Scientifique, Meudon-Bellevue (France). Laboratoire d'Aerothermique.

RATES OF FLUVIO-THERMAL EROSION ON MARS Abstract Only

J. Aguirre-Puente, Francois M. Costard (Centre National de la Recherche Scientifique, Caen, France.), and R. Posado-Cano *In* Lunar and Planetary Inst., Twenty-fourth Lunar and Planetary Science Conference. Part 1: A-F 1993 p 5-6 (For primary document see N94-12015 01-91)
Avail: CASI HC A01/MF A06

In order to get some ideas about the order of magnitude of fluvio-thermal recession rate, a mathematical thermal model for Martian outflow channels is proposed. This model corresponds to a system undergoing a permanent thermal regime where the surface temperature is constant and equal to the phase change temperature (due to the immediate removal of melted materials). This is an ablation model. For its application, estimations of the heat transfer coefficient h and thermal flux q are necessary. Determination of these coefficients needs the calculation of dimensionless numbers (Reynolds, Prandtl, and Nusselt), and the consideration of turbulent regime of the flow.

Derived from text

N94-12019*# California Inst. of Tech., Pasadena. Lab. of Experimental Geophysics.

GIANT IMPACT-INDUCED ATMOSPHERIC BLOW-OFF Abstract Only

Thomas J. Ahrens *In* Lunar and Planetary Inst., Twenty-fourth Lunar and Planetary Science Conference. Part 1: A-F 1993 p 7-8 (For primary document see N94-12015 01-91)
Avail: CASI HC A01/MF A06

The relationship between the present atmospheres of the Earth, Venus, and Mars and the earliest (primordial) atmospheres which surrounded these planets is discussed. The termination of the co-accretion of an atmosphere results from at least three different mechanisms, and these mechanisms are presented. To calculate the energy, and hence, approximate planetesimal size, such that upon impact the entire planetary atmosphere is blown off, a different approach than previous efforts is employed, and a shock wave that is entirely propagated within a terrestrial planet is considered.

Derived from text

N94-12020*# Academy of Sciences (USSR), Moscow. Inst. of Geochemistry and Analytic Chemistry.
DISPERSION OF THE RATIOS OF COSMOGENIC ISOTOPES OF NOBLE GASES IN CHONDRITES OF DIFFERENT COSMIC-RAY EXPOSURE AGES Abstract Only **c90**
V. A. Alexeev *In* Lunar and Planetary Inst., Twenty-fourth Lunar and Planetary Science Conference. Part 1: A-F 1993 p 9-10 (For primary document see N94-12015 01-91)
Avail: CASI HC A01/MF A06

The dispersion of ratios of (He-3/Ne-21)c and (Ne-22/Ne-21)c depending on the cosmic-ray exposure ages of meteorites is analyzed. The dispersion is increased as age decreases. This effect may be stipulated by presence of a more significant portion of meteorites of small preatmospheric sizes among meteorites of small radiation ages in comparison to meteorites of higher exposure age. Derived from text

N94-12021*# Academy of Sciences (USSR), Moscow. Inst. of Geochemistry and Analytic Chemistry.
PECULIARITIES OF DISTRIBUTIONS OF THE COSMIC-RAY EXPOSURE AGES OF H CHONDRITE FALLS AND FINDS Abstract Only **c90**
V. A. Alexeev *In* Lunar and Planetary Inst., Twenty-fourth Lunar and Planetary Science Conference. Part 1: A-F 1993 p 11-12 (For primary document see N94-12015 01-91)
Avail: CASI HC A01/MF A06

Well known peak in the distribution of the cosmic-ray exposure ages of H chondrites at 6-7 My can be employed as mark in comparison of different populations of H chondrites. It is found the age corresponding to maximum of peak for non-Antarctic falls is higher by (15+/-5) percent of this for non-Antarctic finds. Antarctic H chondrites occupy intermediate position. This effect is probably due to process of weathering. Derived from text

N94-12022*# Academy of Sciences (USSR), Moscow. Inst. of Geochemistry and Analytical Chemistry.
SEARCH FOR EFFECTS OF A SUPERNOVA EXPLOSION 30 TO 40 THOUSAND YEARS AGO IN CHONDRITES Abstract Only **c90**
V. A. Alexeev and G. K. Ustinova *In* Lunar and Planetary Inst., Twenty-fourth Lunar and Planetary Science Conference. Part 1: A-F 1993 p 13-14 (For primary document see N94-12015 01-91)
Avail: CASI HC A01/MF A06

The relative increases in Al-26 and Mn-53 equilibrium radioactivity of chondrites with different cosmic-ray exposure and terrestrial ages due to a possible supernova explosion 30-40 thousand years ago have been calculated. The results are discussed. Derived from text

N94-12023*# Washington Univ., Saint Louis, MO. Dept. of Earth and Planetary Sciences and Center for the Space Sciences.
MORPHOLOGY OF LARGE IMPACT CRATERS AND BASINS ON VENUS: IMPLICATIONS FOR RING FORMATION Abstract Only
Jim S. Alexopoulos and William B. McKinnon *In* Lunar and Planetary Inst., Twenty-fourth Lunar and Planetary Science Conference. Part 1: A-F 1993 p 15-16 (For primary document see N94-12015 01-91)
Avail: CASI HC A01/MF A06

A nearly complete examination of the Magellan radar data for the Venusian surface reveals 72 unequivocal peak-ring craters and 4 larger structures that we interpret to be multiringed. This report updates our earlier studies and that of the Magellan team. The general morphology of peak-ring craters, decreasing ring diameter ratio trends with increasing crater diameter, and the general size-morphology progression from complex central-peak crater to peak-ring crater on Venus and the terrestrial planets suggest similar processes of peak-ring formation. Observations are consistent with a model of dynamic collapse, downward and outward, of an unstable central peak to form a ring. We interpret the four larger ringed structures (Klenova, Lise Meitner, Mead, and Isabella) to be morphologically similar to the Orientale Basin on the Moon, and thus, true multiringed basins. Derived from text

N94-12024*# Lockheed Engineering and Sciences Co., Houston, TX.
EFFECTS OF MICROSCOPIC IRON METAL ON THE REFLECTANCE SPECTRA OF GLASS AND MINERALS Abstract Only
C. C. Allen, R. V. Morris (National Aeronautics and Space Administration. Lyndon B. Johnson Space Center, Houston, TX.), H. V. Lauer, Jr., and D. S. McKay (National Aeronautics and Space Administration. Lyndon B. Johnson Space Center, Houston, TX.) *In* Lunar and Planetary Inst., Twenty-fourth Lunar and Planetary Science Conference. Part 1: A-F 1993 p 17-18 (For primary document see N94-12015 01-91)
Avail: CASI HC A01/MF A06

Maturity, which is a measure of the time lunar soils have been in the upper approximately 1 mm of the surface, is correlated with changes in the soils' optical properties. Mature soil is darker and somewhat redder than immature soil of the same composition, and features in the reflectance spectrum become more subdued with increasing maturity. The maturation process also involves accumulation of agglutinitic glass and submicroscopic metallic iron particles. We have produced submicrometer iron metal blebs on the surface and within glass and mineral grains by the method of high-temperature reduction. This technique has permitted the determination of optical changes in samples much simpler than lunar soil, and offers a useful tool with which to investigate the maturation process. Derived from text

N94-12025*# Lockheed Engineering and Sciences Co., Houston, TX.
CALORIMETRIC THERMOMETRY OF METEORITIC TROILITE: A FEASIBILITY STUDY Abstract Only **c90**
J. H. Allton and J. L. Gooding (National Aeronautics and Space Administration. Lyndon B. Johnson Space Center, Houston, TX.) *In* Lunar and Planetary Inst., Twenty-fourth Lunar and Planetary Science Conference. Part 1: A-F 1993 p 21-22 (For primary document see N94-12015 01-91)
Avail: CASI HC A01/MF A06

Two solid-state phase transitions in troilite (FeS) can be readily measured by differential scanning calorimetry (DSC) on samples of only a few milligrams. Troilite from the Mundrabilla iron meteorite displays a DSC fingerprint which is distinct from that of terrestrial troilite from Del Norte Co., California; their response to subsequent heating also differ significantly. Further work may establish whether troilite thermometry of meteorites is possible using DSC. Derived from text

N94-12026*# National Aeronautics and Space Administration. Lyndon B. Johnson Space Center, Houston, TX.
COLD PRESS SINTERING OF SIMULATED LUNAR BASALT Abstract Only **c31**
D. A. Altemir *In* Lunar and Planetary Inst., Twenty-fourth Lunar and Planetary Science Conference. Part 1: A-F 1993 p 23-24 Sponsored by NASA. Washington (For primary document see N94-12015 01-91)
Avail: CASI HC A01/MF A06

In order to predict the conditions for which the lunar regolith may be adequately sintered, experiments were conducted in which samples of simulated lunar basalt (MLS-1) were pressed at high pressures and then heated in an electric furnace. This sintering process may be referred to as cold press sintering since the material is pressed at room temperature. Although test articles were produced which possessed compressive strengths comparable to that of terrestrial concrete, the cold press sintering process requires very high press pressures and sintering temperatures in order to achieve that strength. Additionally, the prospect of poor internal heat transfer adversely affecting the quality of sintered lunar material is a major concern. Therefore, it is concluded that cold press sintering will most likely be undesirable for the production of lunar construction materials. Derived from text

N94-12027*# National Aeronautics and Space Administration. Lyndon B. Johnson Space Center, Houston, TX.
GENERAL OVERVIEW OF AN INTEGRATED LUNAR OXYGEN PRODUCTION/BRICKMAKING SYSTEM Abstract Only **c31**
D. A. Altemir *In* Lunar and Planetary Inst., Twenty-fourth Lunar and Planetary Science Conference. Part 1: A-F 1993 p 25-26 Sponsored by NASA. Washington (For primary document see N94-12015 01-91)
Avail: CASI HC A01/MF A06

On the moon, various processing systems would compete for the same resources, most notably power, raw materials, and perhaps human attention. Therefore, it may be advantageous for two or more processes to be combined such that the integrated system would require fewer resources than separate systems working independently. The synergistic marriage of two such processes--lunar oxygen production and the manufacture of bricks from sintered lunar regolith--is considered. Derived from text

N94-12028*# Bechtel Corp., San Francisco, CA.
THERMODYNAMICS OF LUNAR ILMENITE REDUCTION Abstract Only c77
B. H. Altenberg, H. A. Franklin, and C. H. Jones *In* Lunar and Planetary Inst., Twenty-fourth Lunar and Planetary Science Conference. Part 1: A-F 1993 p 27-28 (For primary document see N94-12015 01-91)
Avail: CASI HC A01/MF A06

With the prospect of returning to the moon, the development of a lunar occupation would fulfill one of the goals of the Space Exploration Initiative (SEI) of the late 1980's. Processing lunar resources into useful products, such as liquid oxygen for fuel and life support, would be one of many aspects of an active lunar base. ilmenite ($FeTiO_3$) is found on the lunar surface and can be used as a feed stock to produce oxygen. Understanding the various ilmenite-reduction reactions elucidates many processing options. Defining the thermodynamic chemical behavior at equilibrium under various conditions of temperature and pressures can be helpful in specifying optimal operating conditions. Differences between a previous theoretical analysis and experimentally determined results has sparked interest in trying to understand the effect of operating pressure on the hydrogen-reduction-of-ilmenite reaction. Various aspects of this reduction reaction are discussed. Derived from text

N94-12029*# Washington Univ., Saint Louis, MO. Center for the Space Sciences and the Physics Dept.
INTERSTELLAR GRAPHITE IN MURCHISON: CONTINUED SEARCH FOR ISOTOPICALLY DISTINCT COMPONENTS Abstract Only c27
Sachiko Amari, Ernst Zinner, and Roy S. Lewis (Chicago Univ., IL.) *In* Lunar and Planetary Inst., Twenty-fourth Lunar and Planetary Science Conference. Part 1: A-F 1993 p 29-30 (For primary document see N94-12015 01-91)
Avail: CASI HC A01/MF A06

We have measured C-, N-, and O-isotopic ratios of individual graphite grains from the Murchison density fractions KFB1 (2.1-2.15 g/cc) and KFC1 (2.15 -2.20 g/cc). According to the C-isotopic composition, KFC1 consists of two populations: one has light C while the other has heavy C. In addition to these two populations, KFB1 also contains grains whose C-isotopic ratios are approximately normal. In view of these isotopic distributions, it is difficult to understand why the Kr-isotopic compositions of these two separates are so different. In contrast to the lighter density fractions KE1 (1.6-2.05 g/cc) and KFA1 (2.05-2.10 g/cc), the separates KFB1 and KFC1 do not seem to contain many grains with significant O-18 excess. Derived from text

N94-12030*# Arizona State Univ., Tempe. Dept. of Geology.
FOURIER DOMAIN TARGET TRANSFORMATION ANALYSIS IN THE THERMAL INFRARED Abstract Only c43
D. L. Anderson *In* Lunar and Planetary Inst., Twenty-fourth Lunar and Planetary Science Conference. Part 1: A-F 1993 p 31-32 (For primary document see N94-12015 01-91)
Avail: CASI HC A01/MF A06

Remote sensing uses of principal component analysis (PCA) of multispectral images include band selection and optimal color selection for display of information content. PCA has also been used for quantitative determination of mineral types and abundances given end member spectra. The preliminary results of the investigation of target transformation PCA (TTPCA) in the fourier domain to both identify end member spectra in an unknown spectrum, and to then calculate the relative concentrations of these selected end members are presented. Identification of endmember spectra in an unknown sample has previously been performed through bandmatching, expert systems, and binary classifiers. Both bandmatching and expert system techniques require the analyst to select bands or combinations of bands unique to each endmember. Thermal infrared mineral spectra have broad spectral features which vary subtly with composition. This makes identification of unique features difficult. Alternatively, whole spectra can be used in the classification process, in which case there is not need for an expert to identify unique spectra. Use of binary classifiers on whole spectra to identify endmember components has met with some success. These techniques can be used, along with a least squares fit approach on the endmembers identified, to derive compositional information. An alternative to the approach outlined above usese target transformation in conjunction with PCA to both identify and quantify the composition of unknown spectra. Preprocessing of the library and unknown spectra into the fourier domain, and using only a specific number of the components, allows for significant data volume reduction while maintaining a linear relationship in a Beer's Law sense. The approach taken here is to iteratively calculate concentrations, reducing the number of endmember components until only non-negative concentrations remain. Derived from text

N94-12031*# Pittsburgh Univ., PA.
LINEAMENT ANALYSIS AND TECTONIC INTERPRETATION FOR THE THARSIS REGION Abstract Only
Robert Anderson *In* Lunar and Planetary Inst., Twenty-fourth Lunar and Planetary Science Conference. Part 1: A-F 1993 p 33 (For primary document see N94-12015 01-91)
Avail: CASI HC A01/MF A06

The Tharsis region of Mars is critical to any study of Martian tectonics. This region (65 N and 65 S latitude; 45 W to 157.5 W longitude) is characterized by an asymmetrical dome-shaped topographic high approximately 8000 km across. Affecting over 25 percent of the surface area, this region has been the center of most of the major tectonic and volcanic activity that has taken place on the Martian surface. Lineament studies are the primary tool available for studying tectonic processes on terrestrial planets such as Mars. At least three major lineament systems can be delineated in the Tharsis region; north-south and east-west trending lineament systems are superimposed on an older northwest trending lineament system. Four centers of uplift have been identified based on the occurrence of radial fracture patterns. Preliminary results indicate that the formation of the Tharsis Dome may not have resulted from a single uplift event, but may instead have resulted from as many as four uplift events. The northwest trending fracture may represent a pre-existing zone of weakness which contributed to the early formation of the Tharsis Dome. The 1:2,000,000 scale photo mosaic maps of Mars were examined and lineaments were identified. The end points of each lineament were measured and recorded in an X-Y reference coordinate frame. Derived from text

N94-12032*# Iowa Geological Survey, Iowa City.
DESCRIPTIONS AND PRELIMINARY INTERPRETATIONS OF CORES RECOVERED FROM THE MANSON IMPACT STRUCTURE (IOWA) Abstract Only c46
R. R. Anderson, B. J. Witzke, J. B. Hartung, E. M. Shoemaker (Geological Survey, Flagstaff, AZ.), and D. J. Roddy (Geological Survey, Flagstaff, AZ.) *In* Lunar and Planetary Inst., Twenty-fourth Lunar and Planetary Science Conference. Part 1: A-F 1993 p 35-36 (For primary document see N94-12015 01-91)
Avail: CASI HC A01/MF A06

A core drilling program initiated by the Iowa Geological Survey Bureau and U.S. Geological Survey in 1991 and 1992 collected 12 cores totalling over 1200 m from the Manson Impact Structure, a probable K-T boundary structure located in north-central Iowa. Cores were recovered from each of the major structural terranes, with 2 cores (M-3 and M-4) from the Terrace Terrane, 4 cores (M-2, M-2A, M-6, and M-9) from the Crater Moat, and 6 cores (M-1, M-5, M-7, M-8, M-10, and M-11) from the Central Peak. These supplemented 2 central peak cores (1-A and 2-A) drilled in 1953. The cores penetrated five major impact lithologies: (1) sedimentary clast breccia; (2) impact ejecta; (3) central peak crystallite rocks; (4) crystalline clast breccia with sandy matrix; and (5) crystallite clast breccia with a melt matrix. Descriptions and preliminary interpretations of these cores are presented. Derived from text

N94-12033*# California Univ., San Diego, La Jolla. Dept. of Chemistry.
MEASUREMENTS OF COSMOGENIC NUCLIDES IN LUNAR ROCK 64455 Abstract Only
J. R. Arnold, C. P. Kohl, K. Nishiizumi (California Univ., Berkeley.), M. W. Caffee (Lawrence Livermore National Lab., CA.), R. C. Finkel (Lawrence Livermore National Lab., CA.), and J. R. Southon (Lawrence Livermore National Lab., CA.) *In* Lunar and Planetary Inst., Twenty-fourth Lunar and Planetary Science Conference. Part 1: A-F 1993 p 39-40 (For primary document see N94-12015 01-91)
Avail: CASI HC A01/MF A06

Eleven samples were ground from the glass coated surface of lunar rock 64455,82 with an average depth resolution of 50 microns and were measured for Be-10, Al-26, and Cl-36 using AMS (accelerator mass spectrometry). Results show no evidence of SCR (solar cosmic ray) effects. The flat cosmogenic nuclide profiles and activity levels are consistent with a 2 My exposure history for the rock and a sample location on the bottom of the rock. These AMS measurements are some of the most precise ever obtained for these three nuclides. This precision and the demonstrated fine depth resolution will enable us to conduct a number of detailed studies of depth effects in lunar and meteoritic samples, including investigating SCR effects in the surface exposed top of the glass coating of 64455 and possibly in the underlying rock. Derived from text

N94-12034*# Washington Univ., Saint Louis, MO. Center for Space Sciences, Earth and Planetary Sciences.
MARSLINK Abstract Only
R. E. Arvidson, Louis D. Friedman (Planetary Society, Pasadena, CA.), and C. J. Stadum (Planetary Society, Pasadena, CA.) *In* Lunar and Planetary Inst., Twenty-fourth Lunar and Planetary Science Conference. Part 1: A-F 1993 p 41-42 (For primary document see N94-12015 01-91)
Avail: CASI HC A01/MF A06

The Marslink Project focuses on the development, dissemination, and evaluation of instructional materials about the composition, structure, and dynamics of the Martian atmosphere, surface, and interior. A multi-year effort is underway so that middle and high school students can follow a full Martian year of seasonal changes using data from NASA's Mars Observer spacecraft, and the Mars Observer Project has time to process and release the appropriate data sets. Monthly activity packets for students, teacher enhancement sessions, a teacher resource center, an on-call Mars data specialist, daily SPACELINK electronic bulletin board updates, and semi-annual NASA Select TV broadcasts will constitute the basis of the Marslink Project. Various aspects of the Marslink Project are briefly discussed. Derived from text

N94-12035*# Manchester Univ. (England). Dept. of Geology
CARBON IN WEATHERED ORDINARY CHONDRITES FROM ROOSEVELT COUNTY Abstract Only c90
R. D. Ash and C. T. Pillinger (Open Univ., Milton, England.) *In* Lunar and Planetary Inst., Twenty-fourth Lunar and Planetary Science Conference. Part 1: A-F 1993 p 43-44 (For primary document see N94-12015 01-91)
Avail: CASI HC A01/MF A06

A suite of Roosevelt County ordinary chondrites of known terrestrial age have been analyzed for carbon content and isotopic composition. Initial results indicate that significant carbon contamination is evident only in samples with a terrestrial age greater than 40 ka. These samples are of weathering grade D and E and contain three times more carbon than the less weathered samples. The soil in which they were preserved has a carbon content of ca. 1.5 percent. Over 200 meteorites have been recovered from a series of soil depleted areas of New Mexico and West Texas. Most have been recovered from blowouts near Clovis in Roosevelt County (RC) on the high plains of New Mexico. The mineralogical and petrologic Al effects of weathering upon these samples have been studied previously and show that the degree of weathering is largely depend ant upon the terrestrial residence time. The study was undertaken to determine the effects of prolonged exposure to the soil and climate of Roosevelt County upon ordinary chondrites in the hope that this will enable a better understanding of the problems associated with the collection of meteoritic falls. A suite of ten grade 4 to 6 H, L, and LL ordinary chondrites were analyzed for carbon content and isotopic composition. Derived from text

N94-12036*# Arizona Univ., Tucson.
EJECTING BASALTIC ACHONDRITES FROM VESTA: HYDRODYNAMICAL IMPACT MODELS Abstract Only c90
E. Asphaug, H. J. Melosh, and E. Ryan (Planetary Science Inst., Tucson, AZ.) *In* Lunar and Planetary Inst., Twenty-fourth Lunar and Planetary Science Conference. Part 1: A-F 1993 p 45-46 (For primary document see N94-12015 01-91)
Avail: CASI HC A01/MF A06

Vesta is a large asteroid whose crust is mostly basaltic. Spectral heterogeneity suggests a sizable olivine feature which may be explained as impact excavation. The spectral data probably show a localized feature approximately 200 km in diameter or a diffuse feature approximately 400 km in diameter. Lightcurve irregularities suggest heterogeneity on a similar scale. This heterogeneity may represent the crater bowl, the extent of its ejecta deposit, or indeed something unrelated to cratering. In any case, drawing direct inferences about the state of Vesta's surface on the basis of these observations involves substantial speculation. We are still far from understanding the boundary between cratering and catastrophic disruption, particularly on targets for which strength and self-gravity both matter. But we are now able to model the underlying physical process -- dynamic fragmentation -- accurately with fragmentation hydrocodes such as SALE 2D and SPH3D. We present several impact scenarios for Vesta; our study is similar to a previous impact model for the formation of Stickney crater on Phobos. We illustrate the effects of impactors of different sizes and velocities, and the effect of gravity and structural inhomogeneity. Derived from text

N94-12037*# Brown Univ., Providence, RI. Dept. of Geological Sciences.
VENUS SMALL VOLCANO CLASSIFICATION AND DESCRIPTION Abstract Only
J. C. Aubele *In* Lunar and Planetary Inst., Twenty-fourth Lunar and Planetary Science Conference. Part 1: A-F 1993 p 47-48 (For primary document see N94-12015 01-91)
Avail: CASI HC A01/MF A06

The high resolution and global coverage of the Magellan radar image data set allows detailed study of the smallest volcanoes on the planet. A modified classification scheme for volcanoes less than 20 km in diameter is shown and described. It is based on observations of all members of the 556 significant clusters or fields of small volcanoes located and described by this author during data collection for the Magellan Volcanic and Magmatic Feature Catalog. This global study of approximately 10 exp 4 volcanoes provides new information for refining small volcano classification based on individual characteristics. Total number of these volcanoes was estimated to be 10 exp 5 to 10 exp 6 planetwide based on pre-Magellan analysis of Venera 15/16, and during preparation of the global catalog, small volcanoes were identified individually or in clusters in every C1-MIDR mosaic of the Magellan data set. Basal diameter (based on 1000 measured edifices) generally ranges from 2 to 12 km with a mode of 34 km, and follows an exponential distribution similar to the size frequency distribution of seamounts as measured from GLORIA sonar images. This is a typical distribution for most size-limited natural phenomena unlike impact craters which follow a power law distribution and continue to infinitely increase in number with decreasing size. Using an exponential distribution calculated from measured small volcanoes selected globally at random, we can calculate total number possible given a minimum size. The paucity of edifice diameters less than 2 km may be due to inability to identify very small volcanic edifices in this data set; however, summit pits are recognizable at smaller diameters, and 2 km may represent a significant minimum diameter related to style of volcanic eruption. Guest, et al, discussed four general types of small volcanic edifices on Venus: (1) small lava shields; (2) small volcanic cones; (3) small volcanic domes; and (4) scalloped margin domes ('ticks'). Steep-sided domes or 'pancake domes', larger than 20 km in diameter, were included with the small volcanic domes. For the purposes of this study, only volcanic edifices less than 20 km in diameter are discussed. This forms a convenient cutoff since most of the steep-sided domes ('pancake domes') and scalloped margin domes ('ticks') are 20 to 100 km in diameter, are much less numerous globally than are the smaller diameter volcanic edifices (2 to 3 orders of magnitude lower in total global number), and do not commonly occur in large clusters or fields of large numbers of edifices. Derived from text

N94-12038*# Los Alamos National Lab., NM. Space Science and Technology Div.
THE LOS ALAMOS NEUTRON SPECTROMETER FOR THE LUNAR SCOUT-1 MISSION Abstract Only c35
George Auchampaugh, Bruce Barraclough, Roger Byrd, Darrell Drake, William Feldman, Calvin Moss, and Robert Reedy *In* Lunar and Planetary Inst., Twenty-fourth Lunar and Planetary Science Conference. Part 1: A-F 1993 p 49-50 (For primary document see N94-12015 01-91)
Avail: CASI HC A01/MF A06

We review the current status of the Los Alamos program to develop a neutron spectrometer for the Lunar Scout-1 mission, which is the first of two such missions to obtain global compositional, gravity, topography, and image maps of the lunar surface during nominal one-year missions. The neutron spectrometer will measure fast and slow (epithermal and thermal) neutrons in the ranges of 0.5 MeV to 25 MeV and 0.01 eV to more than 1 keV, respectively. The neutron spectrometer will consist of two independent instruments, a fast-neutron one, and a thermal and epithermal one. The measured neutron fluxes are very sensitive to hydrogen in the top meter of the lunar surface and provide additional information about lunar composition. Derived from text

N94-12039*# Academy of Sciences (USSR), Moscow. Inst. of Geochemistry and Analytical Chemistry.

VAPORIZATION BY SHOCK LOADING OF ALBITE, JADEITE, AND PYREX GLASS: EXPERIMENTAL STUDY Abstract Only c27

D. D. Badjukov and T. L. Petrova (Institute of Lithosphere, Moscow, Russia.) *In* Lunar and Planetary Inst., Twenty-fourth Lunar and Planetary Science Conference. Part 1: A-F 1993 p 51-52 (For primary document see N94-12015 01-91)

Avail: CASI HC A01/MF A06

Produced by shock experiments impact melts of albite, jadeite, and Pyrex glass demonstrate a loss of both Na and Al relative to Si, which can be due to selective vaporization. It is suggested that the high volatility of Al is related to volatility of a Na-Al compound of proposed $NaAlO_2$ composition. The similar loss of Al and Na seems to be possible during tektite-forming processes. A degree of selective vaporization and modification of a melt chemical composition during impact processes is still poorly understood. The selective vaporization of some elements has been shown by shock experiments. The vaporization and condensation processes can take place in the lunar regolith. On this basis, there are hypotheses explaining differentiation of planetary bodies through the impact vaporization. On the other hand, studies of tektites, impact glasses, and lunar soils show that bulk compositions of impact melts are not modified significantly. In order to estimate degree of the vaporization during shock fusion, chemical compositions of experimentally produced impact melts were studied. We chose Al-containing compositions, because a high volatilization of Al during unequlibrated evaporization had been demonstrated. Derived from text

N94-12040*# Academy of Sciences (USSR), Moscow. Inst. of Geochemistry and Analytical Chemistry.

SHOCK TRANSFORMATIONS IN QUARTZITE Abstract Only c27

D. D. Badjukov, E. A. Koslov (Institute of Technical Physics, Chelyabinsk, Russia.), Yu. N. Zhugin (Institute of Technical Physics, Chelyabinsk, Russia.), and E. V. Abakshin (Institute of Technical Physics, Chelyabinsk, Russia.) *In* Lunar and Planetary Inst., Twenty-fourth Lunar and Planetary Science Conference. Part 1: A-F 1993 p 53-54 (For primary document see N94-12015 01-91)

Avail: CASI HC A01/MF A06

We report results of studies of experimental shock metamorphism in a quartzite sample. Shock pressure increases in the experiment from a rim to a center of the bowl-shaped sample due to a design of a recovery assembly. The section along an equatorial plane shows a progressive development of shock metamorphism. On the basis of observations, it is proposed that diaplectic glass can be a product of quenching a melt. Derived from text

N94-12041*# National Aeronautics and Space Administration, Washington, DC.

RECONSTRUCTION OF THE DYNAMICS OF THE 1800-1801 HUALALAI ERUPTION: IMPLICATIONS FOR PLANETARY LAVA FLOWS Abstract Only c46

Stephen Baloga and Paul Spudis (Lunar and Planetary Inst., Houston, TX.) *In* Lunar and Planetary Inst., Twenty-fourth Lunar and Planetary Science Conference. Part 1: A-F 1993 p 55-56 (For primary document see N94-12015 01-91)

Avail: CASI HC A01/MF A06

The 1800-1801 eruption of alkalic basalt from the Hualalai volcano, Hawaii provides a unique opportunity for investigating the dynamics of lava flow emplacement with eruption rates and compositions comparable to those that have been suggested for planetary eruptions. Field observations suggest new considerations must be used to reconstruct the emplacement of these lava flows. These observations are: (1) the flow traversed the 15 km from the vent to the sea so rapidly that no significant crust formed and an observation of the eruption reported that the flow reach the sea from the vent in approximately 1 hour; (2) the drainage of beds of xenolith nodules indicates a highly fluid, low viscosity lava; (3) overspills and other morphologic evidence for a very low viscosity host fluid; (4) no significant longitudinal increase in flow thickness that might be associated with an increase in the rheological properties of the lava; and (5) the relatively large size of channels associated with the flow, up to 80 meters across and several km long. Models for many geologic mass movements and fast moving fluids with various loadings and suspensions are discussed. Derived from text

N94-12042*# Jet Propulsion Lab., California Inst. of Tech., Pasadena.

HORIZONTAL STRESSES INDUCED BY VERTICAL PROCESSES IN PLANETARY LITHOSPHERES Abstract Only c46

W. B. Banerdt *In* Lunar and Planetary Inst., Twenty-fourth Lunar and Planetary Science Conference. Part 1: A-F 1993 p 57-58 (For primary document see N94-12015 01-91)

Avail: CASI HC A01/MF A06

Understanding the state of stress in the elastic lithosphere is of fundamental importance for planetary geophysics, as it is the link between the observed geologic structures on the surface and the processes which form and modify these structures. As such, it can provide valuable constraints for the difficult problem of determining interior structure and processes. On the Earth, most large scale, organized deformation can be related to lateral tectonics associated with plate dynamics; however, the tectonics on many extraterrestrial bodies (such as the Moon, Mars, and most of the outer-planet satellites) appears to be primarily vertical in nature, and the horizontal stresses induced by vertical motions and loads are expected to dominate the deformation of their lithospheres. The largest stress contributions from vertical loading come from the flexure of the lithosphere, which induces both bending moments and membrane stresses. We are concerned here only with nonflexural changes in the state of stress induced by processes such as sedimentary and volcanic deposition, erosional denudation, and changes in the thermal gradient that induce uplift or subsidence. This analysis is important both for evaluating stresses for specific regions in which the vertical stress history can be estimated, as well as for applying the proper loading conditions to global stress models. It is also of interest for providing a reference state of stress for interpreting stress measurements in the crust of the Earth. Derived from text

N94-12043*# Lunar and Planetary Inst., Houston, TX.

INCREASED DEPTH-DIAMETER RATIOS IN THE MEDUSAE FOSSAE FORMATION DEPOSITS OF MARS Abstract Only

N. G. Barlow *In its* Twenty-fourth Lunar and Planetary Science Conference. Part 1: A-F 1993 p 61-62 (For primary document see N94-12015 01-91)

Avail: CASI HC A01/MF A06

Depth to diameter ratios for fresh impact craters on Mars are commonly cited as approximately 0.2 for simple craters and 0.1 for complex craters. Recent computation of depth-diameter ratios in the Amazonis-Memnonia region of Mars indicates that craters within the Medusae Fossae Formation deposits found in this region display greater depth-diameter ratios than expected for both simple and complex craters. Photoclinometric and shadow length techniques have been used to obtain depths of craters within the Amazonis-Memnonia region. The 37 craters in the 2 to 29 km diameter range and displaying fresh impact morphologies were identified in the area of study. This region includes the Amazonian aged upper and middle members of the Medusae Fossae Formation and Noachian aged cratered and hilly units. The Medusae Fossae Formation is characterized by extensive, flat to gently undulating deposits of controversial origin. These deposits appear to vary from friable to indurated. Early analysis of crater degradation in the Medusae Fossae region suggested that simple craters excavated to greater depths than expected based on the general depth-diameter relationships derived for Mars. However, too few craters were available in the initial analysis to estimate the actual depth-diameter ratios within this region. Although the analysis is continuing, we are now beginning to see a convergence towards specific values for the depth-diameter ratio depending on geologic unit. Derived from text

N94-12044*# Brown Univ., Providence, RI. Dept. of Geological Sciences.

BEHAVIOR OF VORTICES GENERATED BY AN ADVANCING EJECTA CURTAIN IN THEORY, IN THE LABORATORY, AND ON MARS Abstract Only c34

O. S. Barnouin and P. H. Schultz *In* Lunar and Planetary Inst., Twenty-fourth Lunar and Planetary Science Conference. Part 1: A-F 1993 p 63-64

(For primary document see N94-12015 01-91)
Avail: CASI HC A01/MF A06

Several papers assess the interaction between an atmosphere and advancing ejecta to assess possible atmospheric processes affecting ejecta emplacement. Ejecta travel through an atmosphere in two modes: larger ejecta blocks follow ballistic trajectories unhindered by the atmosphere; finer ejecta are entrained in a turbulent basal cloud, which develops as the advancing ejecta curtain generates strong atmospheric winds. Laboratory experiments reveal that this cloud of fine ejecta produce ramparts, flow lobes, or radial scouring that superposes larger ballistic ejecta emplaced earlier. Martian, Venusian, and terrestrial ejecta facies can be interpreted in terms of processes observed in the laboratory with appropriate first-order corrections for scaling. A continuum model of the atmospheric flow around an advancing inclined plate simulated and reproduced some of the complex flow patterns observed in front and at the top of the curtain. Here we consider improvements to the model to compare quantitatively the approximate position of ejecta deposition (i.e., run-out distance) with laboratory experiments and Martian ejecta facies. Derived from text

N94-12045*# Lockheed Engineering and Sciences Co., Houston, TX.
MINERALOGY OF CHONDRITIC INTERPLANETARY DUST PARTICLE IMPACT RESIDUES FROM LDEF Abstract Only **c25**
R. A. Barrett, M. E. Zolensky (National Aeronautics and Space Administration. Lyndon B. Johnson Space Center, Houston, TX.), and R. Bernhard *In* Lunar and Planetary Inst., Twenty-fourth Lunar and Planetary Science Conference. Part 1: A-F 1993 p 65-66 (For primary document see N94-12015 01-91)
Avail: CASI HC A01/MF A06

A detailed structural and compositional analysis of several impactor residues was performed utilizing transmission electron microscopy, energy dispersive spectroscopy, and electron diffraction. Residues from the interior of several craters in gold surfaces were removed with a tungsten needle, mounted in EMBED-812 epoxy, and ultramicrotomed. The presence in these residues of equilibrated ferromagnesian minerals, recrystallization textures, glass, and melted metal and sulfide bodies decorating grain boundaries is indicative of varying degrees of shock metamorphism in all impact residues we have characterized. Derived from text

N94-12046*# Brown Univ., Providence, RI. Dept. of Geological Sciences.
ESTIMATION OF AGE OF DALI-GANIS RIFTING AND ASSOCIATED VOLCANIC ACTIVITY, VENUS Abstract Only
A. T. Basilevsky (Academy of Sciences, USSR, Moscow.) *In* Lunar and Planetary Inst., Twenty-fourth Lunar and Planetary Science Conference. Part 1: A-F 1993 p 67-68 (For primary document see N94-12015 01-91)
Avail: CASI HC A01/MF A06

This paper deals with the estimation of age for the Dali and Ganis Chasma rift zones and their associated volcanism based on photogeologic analysis of stratigraphic relations of rift-associated features with impact craters which have associated features indicative of their age. The features are radar-dark and parabolic, and they are believed to be mantles of debris derived from fallout of the craters' ejecta. They are thought to be among the youngest features on the Venusian surface, so their 'parent' craters must also be very young, evidently among the youngest 10 percent of Venus' crater population. Dali Chasma and Ganis Chasma are a part of a system of rift zones contained within eastern Aphrodite and Atla Regio which is a significant component of Venus tectonics. The rifts of this system are fracture belts which dissect typical Venusian plains with rare islands of tessera terrain. The rift zone system consists of several segments following each other (Diane, Dali, Ganis) and forming the major rift zone line, about 10,000 km long, which has junctions with several other rift zones, including Parga Chasma Rift. The junctions are usually locations of rift-associated volcanism in the form of volcanic edifices (Maat and Ozza Montes) or plain-forming flows flooding some areas within the rift zones and the adjacent plains. Derived from text

N94-12047*# Brown Univ., Providence, RI. Dept. of Geological Sciences.
REGIONAL GEOLOGY OF THE VEGA LANDING SITES: TENTATIVE RESULTS OF PHOTOGEOLOGIC MAPPING Abstract Only
A. T. Basilevsky (Academy of Sciences, USSR, Moscow.) and C. M. Weitz (Jet Propulsion Lab., California Inst. of Tech., Pasadena.) *In* Lunar and Planetary Inst., Twenty-fourth Lunar and Planetary Science Conference. Part 1: A-F 1993 p 69-70 (For primary document see N94-12015 01-91)
Avail: CASI HC A01/MF A06

The regional geology of the two Vega landing sites, where geochemical measurements on the Venusian surface were made, was studied using Magellan CI-MIDRP imagery and MIT-processed altimetry for the large region which we will call the Vega region (22.90 deg. N to 22.90 deg. S and 154.12 deg. W to 211.12 deg. E). The results of the analysis were compiled in the form of a synoptic geologic map of about 1:10 m scale. Derived from text

N94-12048*# Brown Univ., Providence, RI. Dept. of Geological Science.
REGIONAL GEOLOGY OF THE VENERA LANDING SITES: TENTATIVE RESULTS OF PHOTOGEOLOGIC MAPPING Abstract Only
A. T. Basilevsky (Academy of Sciences, USSR, Moscow.) and C. M. Weitz (Jet Propulsion Lab., California Inst. of Tech., Pasadena.) *In* Lunar and Planetary Inst., Twenty-fourth Lunar and Planetary Science Conference. Part 1: A-F 1993 p 71-72 (For primary document see N94-12015 01-91)
Avail: CASI HC A01/MF A06

The regional geology of the five Venera landing sites, where geochemical measurements and TV observations on the Venusian surface were made, was studied based on the photogeologic analysis of the Magellan C1-MIDRP imagery for the large area that we will call the Venera region (38 deg. N to 22.6 deg. S and 268 to 344 deg. E). The results of the analysis were compiled in the form of a synoptical geologic map at about 1:10 M scale. MIT-processed Magellan altimetry was also used for the analysis. Derived from text

N94-12049*# Nebraska Univ., Lincoln. Dept. of Electrical Engineering.
INTERPRETATION OF LUNAR AND PLANETARY ELECTROMAGNETIC SCATTERING USING THE FULL WAVE SOLUTIONS Abstract Only
E. Bahar and M. Haugland *In* Lunar and Planetary Inst., Twenty-fourth Lunar and Planetary Science Conference. Part 1: A-F 1993 p 73-74 (For primary document see N94-12015 01-91)
Avail: CASI HC A01/MF A06

Bistatic radar experiments carried out during the Apollo 14, 15, and 16 missions provide a very useful data set with which to compare theoretical models and experimental data. Vesecky, et al. report that their model for near grazing angles compares favorably with experimental data. However, for angles of incidence around 80 degrees, all the analytical models considered by Vesecky, et al. predict values for the quasi-specular cross sections that are about half the corresponding values taken from the Apollo 16 data. In this work, questions raised by this discrepancy between the reported analytical and experimental results are addressed. The unified full wave solutions are shown to be in good agreement with the bistatic radar taken during Apollo 14 and 16 missions. Using the full wave approach, the quasi-specular contributions to the scattered field from the large scale surface roughness as well as the diffuse Bragg-like scattering from the small scale surface roughness are accounted for in a unified self-consistent manner. Since the full wave computer codes for the scattering cross sections contain ground truth data only, it is shown how it can be reliably used to predict the rough surface parameters of planets based on the measured data. Derived from text

N94-12050*# Indiana Univ., Bloomington. Dept. of Geological Sciences.
APOLLO 16 CORE 60013/14 AS A PRODUCT OF PATH 1 AND PATH 2 REGOLITH EVOLUTION PROCESSES Abstract Only
A. Basu, K. McBride (Lockheed Engineering and Sciences Co., Houston, TX.), S. J. Wentworth (Lockheed Engineering and Sciences Co., Houston, TX.), and D. S. McKay (National Aeronautics and Space Administration. Lyndon B. Johnson Space Center, Houston, TX.) *In* Lunar and Planetary Inst., Twenty-fourth Lunar and Planetary Science Conference. Part 1: A-F 1993 p 75-76 (For primary document see N94-12015 01-91)
Avail: CASI HC A01/MF A06

We have made a petrographic study of 12 samples along the 62 cm profile of Apollo 16 core 60013/14 taken at Station 10 near the lunar module. The basic core description and maturity variations have been discussed earlier. This core is important because it enables a stratigraphic comparison with nearby cores 60001-7 and 60009/10. These cores form a triangle with sides 35-40 m. FMR data show a maturity-match between 60009/10 and 60013/14. Unfortunately, segments of the core 60001-7 are too disturbed for any cm scale comparison. We present new data on the grain size distribution and the modal petrography for six samples from six levels of 60013 using the same approach and rationale used for 60014. We have combined the new data with our previous data on 60014 to plot the variations of grain size distributions and grain type abundances, in the 500-1000 m and 90-150 micrometers size fractions, with depth. Agglutinate abundances match the I sub s/FeO profile and both show a significant break at a depth of about 45 cm, with lower maturity material below that point. Grain size distributions show that for all analyzed samples, the mean grain size is below 90 micrometers. The two lowest samples are somewhat more coarse-grained than the rest of the core. The break at about 45 cm is the most prominent feature of the core and was described during the initial dissection as a pronounced change in color from dark to light. It now seems clear that this break is primarily one of maturity rather than of bulk chemical composition. Derived from text

N94-12051*# Minnesota Univ., Minneapolis. School of Physics and Astronomy.
NITROGEN AND NOBLE GASES IN A GLASS SAMPLE FROM LEW88516 Abstract Only c25
R. H. Becker and R. O. Pepin *In* Lunar and Planetary Inst., Twenty-fourth Lunar and Planetary Science Conference. Part 1: A-F 1993 p 77-78
(For primary document see N94-12015 01-91)
Avail: CASI HC A01/MF A06

The Antarctic meteorite LEW88516 has been classified as a member of the SNC group of meteorites, specifically a shergottite. It is reported to be remarkably similar in mineralogy, petrogenesis and chemistry to the previously known ALH77005 shergottite, with both being compositionally distinct from other shergottites. LEW88516 shows pervasive shock features and has been found to contain glass veins attributable to a shock origin. In an effort to determine whether the glass in LEW88516 contains any of the isotopically-heavy trapped nitrogen component observed in EETA 79001 glass, as well as the related high-Ar-40/Ar-36 and high-Xe-129/Xe-132 components, we undertook an analysis of an 11.9 mg glass sample (LEW88516,4) provided to us by H. Y. McSween, Jr. as part of a consortium study of this meteorite. Nitrogen and noble gases were extracted from LEW88516,4 in a series of combustion steps at increasing temperatures followed by a final pyrolysis. Initial steps at 550 C were intended to remove any surface-sited nitrogen-containing contaminants, while the 700 C step was expected to show the onset of release of a trapped argon component, based on our previous data for EETA 79001. It was hoped that the bulk of any trapped gas release would be concentrated in one of two steps at 1100 C and approximately 1400 C, maximizing our analytical sensitivity. Results of the analysis are shown. Except for He and Ne, data obtained for the 550 C steps will be omitted from further consideration on the assumption that they represent terrestrial contamination. Derived from text

N94-12052*# California Inst. of Tech., Pasadena. Div. of Geological and Planetary Sciences.
THE STABILITY OF HIBONITE AND OTHER ALUMINOUS PHASES IN SILICATE MELTS: IMPLICATIONS FOR THE ORIGIN OF HIBONITE-BEARING INCLUSIONS Abstract Only c25
J. R. Beckett and E. Stolper *In* Lunar and Planetary Inst., Twenty-fourth Lunar and Planetary Science Conference. Part 1: A-F 1993 p 79-80
(For primary document see N94-12015 01-91)
Avail: CASI HC A01/MF A06

Phase fields in which hibonite (Hib) and silicate melt coexist with spinel (Sp), CaAl4O7 (CA2), gehlenitic melilite (Mel), anorthite (An), or corundum (Cor) in the system CaO-MgO-Al2O3-SiO2-TiO2 (CMAST) were determined and activity models developed for Mel and Hib solid solutions. Experimentally determined partition coefficients for Ti between Hib and coexisting melt, D sub t, vary from 0.8 to 2.1 and generally decrease with increasing TiO2 content in the liquid (L). Based on Ti partioning between Hib and melt, bulk inclusion compositions and Hib-saturated liquid use phase diagrams, the Hib in Fluffy Type A inclusions (FTA's) from Allende and at least some of the Hib from Hib-rich inclusions is relict; much of the Hib from Hib-glass spherules probably crystallized from a melt under nonequilibrium conditions. Bulk compositions for all of these Ca-Al-rich inclusions (CAI's) are consistent with an origin as Mel + Hib + Sp + perovskite (Pv) proto-inclusions in which Mel was partially altered. In some cases, the proto-inclusion was partially or completely melted with vaporization occurring over a period of time sufficient to remove any Na introduced by the alteration process but frequently insufficient to dissolve all of the original hibonite. If equilibration temperatures based on Hib-bearing CAI's reflect condensation in a cooling gas of solar composition, then Hib + Cor condensed at approximately 1260 C (referenced to 10 exp -3 atm) and Hib + Sp + Mel at approximately 1215 +/- 10 C. Simple thermochemical models for the substitution of trace elements into the Ca-site of meteoritic Hib suggest that virtually all Eu is divalent in early condensate Hibs but that Eu(2+)/Eu(3+) decreases by a factor of 20 or more during the course of condensation, primarily because the ratio is proportional to the partial pressure of Al, which decreases dramatically as aluminous phases condense. The relative sizes of Eu and Yb anomalies in meteoritic Hibs and CAI's may be influenced by this effect. Derived from text

N94-12053*# National Aeronautics and Space Administration. Ames Research Center, Moffett Field, CA.
A COMPARISON OF TELESCOPIC AND PHOBOS-2 ISM SPECTRA OF MARS IN THE SHORT-WAVE NEAR-INFRARED (0.76-1.02 MICRONS) Abstract Only c89
James F. Bell, III and John F. Mustard (Brown Univ., Providence, RI.) *In* Lunar and Planetary Inst., Twenty-fourth Lunar and Planetary Science Conference. Part 1: A-F 1993 p 81-82 Sponsored by NASA. Washington (For primary document see N94-12015 01-91)
Avail: CASI HC A01/MF A06

Recent analyses of near-IR (0.76-3.16 microns) Mars surface reflectance spectra obtained by the Phobos-2 ISM instrument during early 1989 have revealed the presence of substantial variability in surface spectral properties. Strong absorption features seen in the 0.85-1.05 micron region are up to 10-15 percent deep relative to the local continuum and have been interpreted as evidence of Fe(2+) and Fe(3+) bearing minerals (pyroxenes and iron oxides, respectively). Though these observed band depths are comparable to those seen in laboratory reflectance spectra, they are up to three times larger than most previously reported band depths for Mars spectra at these wavelengths. Six regions of variable albedo and geologic setting were identified where ISM and 1988 opposition telescopic coverage either overlapped physically or sampled the same surface geologic unit. The areal sizes and positions of the regions measured telescopically were compiled by Bell et al. ISM pixels falling within these spots were averaged to produce a spatially convolved spectrum that simulates what would have been seen telescopically. To facilitate comparisons of absorption band positions and relative strengths, the convolved ISM data and the 1988 telescopic spectra were scaled to unity at 0.81 microns and are presented. The data have also been convolved to equivalent band pass normalized reflectances in the region of spectral overlap. A scatter diagram of telescopic vs. ISM reflectances is shown. The results from the investigation are discussed. Derived from text

N94-12054*# National Aeronautics and Space Administration. Ames Research Center, Moffett Field, CA.
AN OBSERVATIONAL SEARCH FOR CO2 ICE CLOUDS ON MARS Abstract Only
James F. Bell, III, Wendy M. Calvin (Geological Survey, Flagstaff, AZ.), James B. Pollack, and David Crisp (Jet Propulsion Lab., California Inst. of Tech., Pasadena.) *In* Lunar and Planetary Inst., Twenty-fourth Lunar and Planetary Science Conference. Part 1: A-F 1993 p 83-84 (For primary document see N94-12015 01-91)
Avail: CASI HC A01/MF A06

CO2 ice clouds were first directly identified on Mars by the Mariner 6 and 7 infrared spectrometer limb scans. These observations provided support for early theoretical modeling efforts of CO2 condensation. Mariner 9 IRIS temperature profiles of north polar hood clouds were interpreted as indicating that these clouds were composed of H2O ice at lower latitudes and CO2 ice at higher latitudes. The role of CO2 condensation on Mars has recently received increased attention because (1) Kasting's model results indicated that CO2 cloud condensation limits the magnitude of the proposed early Mars CO2/H2O greenhouse, and (2) Pollack el al.'s GCM results indicated that the formation of CO2 ice clouds is favorable at all polar latitudes during the fall and winter seasons. These latter authors have shown that CO2 clouds play an important role in the polar energy balance, as the amount of CO2 contained in the polar caps is constrained by a balance between latent heat release, heat advected from lower latitudes, and thermal emission to space. The polar hood clouds reduce the amount of CO2 condensation on the polar caps because they reduce the net emission to space. There have been many extensive laboratory spectroscopic studies of H2O and CO2 ices and frosts. In this study, we use results from these and other sources to search for the occurrence of diagnostic CO2 (and H2O) ice and/or frost absorption features in ground based near-infrared imaging spectroscopic data of Mars. Our primary goals are (1) to try to confirm the previous direct observations of CO2 clouds on Mars; (2) to determine the spatial extent, temporal variability, and composition (H2O/CO2 ratio) of any clouds detected; and (3) through radiative transfer modeling, to try to determine the mean particle size and optical depth of polar hood clouds, thus, assessing their role in the polar heat budget.

Derived from text

N94-12055*# National Aeronautics and Space Administration. Ames Research Center, Moffett Field, CA.

CHANGES IN HAWAIIAN PALAGONITE FE MINERALOGY ASSOCIATED WITH THERMAL ALTERATION: IMPLICATIONS FOR MARS Abstract Only **c46**

James F. Bell, III, Richard V. Morris (National Aeronautics and Space Administration. Lyndon B. Johnson Space Center, Houston, TX.), and John B. Adams (Washington Univ., Seattle.) *In* Lunar and Planetary Inst., Twenty-fourth Lunar and Planetary Science Conference. Part 1: A-F 1993 p 85-86 Sponsored by NASA. Washington (For primary document see N94-12015 01-91)

Avail: CASI HC A01/MF A06

We have studied six Hawaiian palagonitic tephra samples (PH-1 through PH-6) from a site where a Mauna Loa lava flow has partially embayed a Mauna Kea cinder cone Tephra samples that were not affected by the lava flow (PH-5, PH-6) consist of partially palagonitized coarse-grained glassy Hawaiitic particles whose iron mineralogy is dominated by nanophase ferric oxide (np-Ox) and olivine. Samples closest to the lava flow (PH-1 through PH-4) have been strongly altered and their iron mineralogy is dominated by np-Ox, magnetite, and hematite. This suite of samples has many spectral similarities to Martian bright regions; thus, this localized thermal alteration event may be an analog to similar processes on Mars that lead to the production of small amounts of crystalline ferric oxides within a poorly-crystalline or amorphous palagonitic matrix.

Derived from text

N94-12056*# Iowa Univ., Iowa City. Dept. of Geology.

PETROGRAPHY AND PRELIMINARY INTERPRETATIONS OF THE CRYSTALLINE BRECCIAS FROM THE MANSON M-1 CORE Abstract Only **c46**

M. S. Bell, M. K. Reagan, R. R. Anderson, and C. T. Foster, Jr. *In* Lunar and Planetary Inst., Twenty-fourth Lunar and Planetary Science Conference. Part 1: A-F 1993 p 87-88 (For primary document see N94-12015 01-91)

Avail: CASI HC A01/MF A06

The M-1 core was drilled on the eastern edge of the central uplift within the Manson Impact Structure in Iowa. The lower 107.9 m of the core consists of crystalline breccias. Twelve intervals of thin sections from this core have been studied for preliminary discussion. The breccias are divided into three units by matrix size and abundance. Unit 1 is characterized by a high volume fraction of matrix, and a decreasing proportion of matrix with depth. This matrix is nearly isotropic and consists of grains less than 0.005 to less than 0.02 mm in length. The matrix between 112 and 146 meters depth consists of a crystalline intergrowth of felsic and opaque minerals with or without chlorite. This was the hottest section of the core after impact, and may have undergone high temperature metamorphic recrystallization. Unit 2 is transitional between units 1 and 3, and is delineated by a rapid increase in grain size to .01-.04 mm and a decrease in matrix abundance to 10 percent. Unit 3 has a coarse, often porous matrix, whose abundance changes from about 10 percent at the top to about 2 percent at the base. Grain sizes range from 0.01-0.1 mm over this interval and coarsen with depth. Changes in the character of the matrix as well as the changes in clast lithology and abundance outlined below suggest that unit 3 is in-situ brecciated basement with injected melt and shale fragments; unit 1 is a crater veneer deposit consisting of transported basement materials and unit 2 is a mixed zone between units 1 and 3. Derived from text

N94-12057*# Washington Univ., Saint Louis, MO. Dept. of Earth and Planetary Sciences and Center for the Space Sciences.

ORBITAL SIMULATIONS OF SATELLITE ESCAPE/CAPTURE AND THE ORIGIN OF SATELLITES SUCH AS TRITON Abstract Only **c90**

Lance A. M. Benner and William B. McKinnon *In* Lunar and Planetary Inst., Twenty-fourth Lunar and Planetary Science Conference. Part 1: A-F 1993 p 89-90 (For primary document see N94-12015 01-91)

Avail: CASI HC A01/MF A06

We investigate satellite escape/capture in the context of the restricted, circular three body problem as applied to the Sun, Neptune, and Triton. We have computed a large number of coplanar prograde and retrograde orbital simulations over a range of initial distances and velocities. The satellite starts at superior conjunction within approximately 2 Hill radii of Neptune and has a velocity orthogonal to the Sun-planet line. Orbits with these initial conditions can be reflected with respect to time, so an escape is simply the reverse of a capture. We numerically integrate the equations of motion to compute the satellite's position until it escapes, collides with Neptune, or after 100 planetary years fails to escape, when computations cease. The initial distance x and velocity v in the restricted problem uniquely define the Jacobi constant C, a conserved energy-like quantity. Plots of the simulation outcomes in the prograde and retrograde C, x phase spaces reveal distinct zones in which temporary satellites approach the planet closely enough that permanent capture can be effected by gas drag with a protoplanetary nebula or by collision with a pre-existing satellite. Single and double close-flybys constitute the most common possible capture orbits. Long term multiple flyby orbits occur near the stability limits between bound and unbound orbits, and are more common among retrograde captures. Derived from text

N94-12058*# Arkansas Univ., Fayetteville. Cosmochemistry Group.

THE GREAT 8 MA EVENT AND THE STRUCTURE OF THE H-CHONDRITE PARENT BODY Abstract Only **c90**

P. H. Benoit and D. W. G. Sears *In* Lunar and Planetary Inst., Twenty-fourth Lunar and Planetary Science Conference. Part 1: A-F 1993 p 91-92 (For primary document see N94-12015 01-91)
(Grant NAG9-81)

Avail: CASI HC A01/MF A06

The H-chondrites have been the subject of several recent controversies, including the question of whether Antarctic and non-Antarctic meteorites are or are not the same and whether there or is not evidence for stratigraphic layering in the original parent body. We have identified two distinct groups of H5 chondrites in the Antarctic collection. One group has induced thermoluminescence (TL) peak temperatures less than 190 C and metallographic cooling rates between S to 50 K/Myr, similar to modern falls. It also has a variety of cosmic ray exposure ages, many being greater than 107 years. The other group has TL peak temperatures greater than 190 C, metallographic cooling rates of 100 K/Myr and cosmic ray exposure ages of 8 Ma. The members of this group were generals smaller than those of the greater than 190 C group (including the mode falls) during cosmic ray exposure. Detailed study of the cosmogenic nuclide concentrations of these groups indicates that they are not solely the result of pairing of a few unusual meteorites. It is likely that the greater than 190 C group was an important part of the H-chondrite flux about 1 million years ago, but has since decreased in importance relative to the less than 190 C group. In a previous work, we discussed several possible origins for the greater than 190 C group, including multiple H-chondrite parent bodies, unusual parent body structure, and creation during the 8 Ma event. In this paper, we present new data for H4 chondrites in light of these ideas.

Derived from text

N94-12059*# Arkansas Univ., Fayetteville. Cosmochemistry Group.

METEORITES FROM RECENT AMOR-TYPE ORBITS Abstract Only **c90**

P. H. Benoit and D. W. G. Sears *In* Lunar and Planetary Inst., Twenty-fourth Lunar and Planetary Science Conference. Part 1: A-F 1993 p 93-94 (For primary document see N94-12015 01-91)
(Grant NAG9-81)

Avail: CASI HC A01/MF A06

We report here the discovery of a recent meteorite shower in Antarctica, the members of which have very high natural thermoluminescence levels. It is apparent from these data that the shower has been on Earth only a short time (approximately 1000 years) and the meteorite probably came to

Earth through rapid (less than 10 exp 5 years) evolution from an orbit with perihelion greater than 1.1 AU, similar to Amor asteroids. Only a very small number of meteorites, including a few modern falls, appear to have had similar orbital histories. Derived from text

N94-12060*# Arkansas Univ., Fayetteville. Cosmochemistry Group.
NATURAL THERMOLUMINESCENCE PROFILES IN LUNAR CORES AND IMPLICATIONS FOR METEORITES Abstract Only
P. H. Benoit and D. W. G. Sears *In* Lunar and Planetary Inst., Twenty-fourth Lunar and Planetary Science Conference. Part 1: A-F 1993 p 95-96
(For primary document see N94-12015 01-91)
(Grants NAG9-81; NSF DPP-91-15521)
Avail: CASI HC A01/MF A06

Meteorites and lunar samples have been irradiated by high energy cosmic rays, typically for millions of years. In addition to producing isotopic changes, the irradiation creates ionization which may be recorded in the form of stored thermoluminescence (TL) in certain minerals, the most important of which is feldspar. One aspect of interpreting the TL of these samples is the effect of 'shielding' or depth control, which is particularly important for meteorites, since they have lost an unknown amount of mass during atmospheric entry. Here we report theoretical calculations which we compare with samples from lunar cores for which we have excellent stratigraphic control. We then discuss the implications for these results for the TL of meteorites, which have a different irradiation geometry. We find that, in general, calculated profiles are similar to those observed in lunar samples and meteorites. Additional effects, such as orbital (thermal) history and terrestrial age must also be considered in the case of meteorites. Author

N94-12061*# Tennessee Univ., Knoxville. Dept. of Geological Sciences.
METALLOGRAPHIC COOLING RATES OF L-GROUP ORDINARY CHONDRITES Abstract Only c90
Marvin E. Bennett and Harry Y. McSween, Jr. *In* Lunar and Planetary Inst., Twenty-fourth Lunar and Planetary Science Conference. Part 1: A-F 1993 p 97-98 (For primary document see N94-12015 01-91)
Avail: CASI HC A01/MF A06

Shock metamorphism appears to be a ubiquitous feature in L-group ordinary chondrites. Brecciation and heterogeneous melting obscure much of the early history of this meteorite group and have caused confusion as to whether L chondrites have undergone thermal metamorphism within onion-shell or rubble-pile parent bodies. Employing the most recent shock criteria, we have examined 55 Antarctic and 24 non-Antarctic L chondrites in order to identify those which have been least affected by post-accretional shock. Six low-shock samples (those with shock grade less than S4) of petrographic types L3-L5 were selected from both populations and metallographic cooling rates were obtained following the technique of Willis and Goldstein. All non-Antarctic L6 chondrites inspected were too heavily shocked to be included in this group. However, 4 shocked L6 chondrites were analyzed in order to determine what effects shock may impose on metallographic cooling rates. Metallographic cooling rates were derived by analyzing the cores of taenite grains and then measuring the distance to the nearest grain edge. Taenites were identified using backscatter imaging on a Cameca SX-50 electron microprobe. Using backscatter we were able to locate homogeneous, rust-free, nearly spherical grains. M-shaped profiles taken from grain traverses were also used to help locate the central portions of selected grains. All points which contained phosphorus above detection limits were discarded. Plots of cooling-rate data are summarized and data from the high-shock samples are presented. The lack of coherency of cooling rates for individual samples is indicative of heterogeneous cooling following shock. The data confirms the statement expressed by numerous workers that extreme care must be taken when selecting samples of L chondrites for cooling-rate studies. Data for the 6 non-Antarctic low-shock samples are also presented. The samples display a general trend in cooling rates. The lowest metamorphic grade yielded the slowest cooling rates and an increase in grade follows an increase in cooling rate. This is the opposite relationship to that predicted by the onion-shell model. Derived from text

N94-12062*# Arizona Univ., Tucson. Observatory and Lunar Planetary Lab.
EXPLICIT 3D CONTINUUM FRACTURE MODELING WITH SMOOTH PARTICLE HYDRODYNAMICS Abstract Only c90
W. Benz and E. Asphaug *In* Lunar and Planetary Inst., Twenty-fourth Lunar and Planetary Science Conference. Part 1: A-F 1993 p 99-100
(For primary document see N94-12015 01-91)
Avail: CASI HC A01/MF A06

Impact phenomena shaped our solar system. As usual for most solar system processes, the scales are far different than we can address directly in the laboratory. Impact velocities are often much higher than we can achieve, sizes are often vastly larger, and most impacts take place in an environment where the only gravitational force is the mutual pull of the impactors. The Smooth Particle Hydrodynamics (SPH) technique has been applied in the past to the simulations of giant impacts. In these simulations, the colliding objects were so massive (at least a sizeable fraction of the Earth's mass) that material strength was negligible compared to gravity. This assumption can no longer be made when the bodies are much smaller. To this end, we have developed a 3D SPH code that includes a strength model to which we have added a von Mises yielding relation for stresses beyond the Hugoniot Elastic Limit. At the lower stresses associated with brittle failure, we use a rate-dependent strength based on the nucleation of incipient flaws whose number density is given by a Weibull distribution. Following Grady and Kipp and Melosh et al., we introduce a state variable D ('damage'), 0 less than D less than 1, which expresses the local reduction in strength due to crack growth under tensile loading. Unfortunately for the hydrodynamics, Grady and Kipp's model predicts which fragments are the most probable ones and not the ones that are really formed. This means, for example, that if a given laboratory experiment is modeled, the fragment distribution obtained from the Grady-Kipp theory would be equivalent to a ensemble average over many realizations of the experiment. On the other hand, the hydrodynamics itself is explicit and evolves not an ensemble average but very specific fragments. Hence, there is a clear incompatibility with the deterministic nature of the hydrodynamics equations and the statistical approach of the Grady-Kipp dynamical fracture model. We remedy these shortcomings by making the incipient flaw distribution explicit, i.e., particles carry activation strains which are distributed at random with a probability of occurrence given by the Weibull distribution. If the local principal axis strain exceeds this limit, damage starts to grow. By growing explicit cracks together with statistical cracks (damage) at the sub-particle scale, we ensure that material strength and fragmentation is independent of model resolution. We tested our scheme by simulating laboratory impact experiments on basalt spheres. Derived from text

N94-12063*# Lockheed Engineering and Sciences Co., Houston, TX.
COMPOSITION AND MODAL FREQUENCIES OF HYPERVELOCITY PARTICLES LESS THAN 1 MILLIMETER IN DIAMETER IN LOW-EARTH ORBIT Abstract Only c90
R. P. Bernhard, T. H. See, and F. Hoerz (National Aeronautics and Space Administration. Lyndon B. Johnson Space Center, Houston, TX.) *In* Lunar and Planetary Inst., Twenty-fourth Lunar and Planetary Science Conference. Part 1: A-F 1993 p 101-102 (For primary document see N94-12015 01-91)
Avail: CASI HC A01/MF A06

We have continued to systematically analyze the projectile residues associated with hypervelocity impact features on the surfaces of the 'Chemistry of Micrometeoroid Experiment' (CME) that was in low-Earth orbit (LEO) for 5.7 years aboard the Long Duration Exposure Facility (LDEF). Last year we reported on the systematic analysis, via SEM-EDX methods, of all craters greater than 20 microns in diameter on the collectors from LDEF's trailing edge and approximately 200 craters greater than 75 microns in diameter from the aluminum 1100 substrates from the forward-facing surfaces. This latter group represents less than 20 percent of all craters on the A11 collectors, because the particle flux is substantially higher for the forward-facing orientations relative to the trailing-edge surfaces. To date, we have analyzed some 600 craters on the A11 aluminum collectors, yet this report summarizes only 400 features, because not all of the results have been completely reduced and entered into our database. Derived from text

N94-12064*# California Inst. of Tech., Pasadena.
THERMAL STUDIES OF MARTIAN CHANNELS AND VALLEYS USING TERMOSKAN DATA Abstract Only
B. H. Betts and B. C. Murray *In* Lunar and Planetary Inst., Twenty-fourth Lunar and Planetary Science Conference. Part 1: A-F 1993 p 103-104

(For primary document see N94-12015 01-91)
Avail: CASI HC A01/MF A06

The Termoskan instrument on board the Phobos '88 spacecraft acquired the highest spatial resolution thermal data ever obtained for Mars. Included in the thermal images are 2 km per pixel observations of 4 major channel and valley systems: Shalbatana Vallis; Simud Vallis, Hydraotes Chaos, and the associated outflow channel connecting it with the eastern end of Vallis Marineris; Al-Qahira Vallis; and Ma'adim Vallis. Simultaneous broad band visible channel data were obtained for all but Ma'adim Vallis. We find that all 4 valley systems have higher inertias than their surroundings, consistent with previous thermal studies of Martian channels. We conclude that the higher inertia is likely due to some intrinsic difference associated with the channel floors, rather than due only to dark aeolian deposits as suggested by some previous studies. Our conclusion is based largely upon the localized nature of the dark deposits in contrast with the thermal homogeneity of the channel floors. Thus, these channels and valleys show an uncommon (for Mars) connection between morphology and inertia. Derived from text

N94-12065*# National Aeronautics and Space Administration. Goddard Space Flight Center, Greenbelt, MD.

SPECTRAL ANALYSIS OF THE GRAVITY AND TOPOGRAPHY OF MARS Abstract Only

Bruce G. Bills, Herbert V. Frey, Walter S. Kiefer, R. Steven Nerem, and Maria T. Zuber (Johns Hopkins Univ., Baltimore, MD.) *In* Lunar and Planetary Inst., Twenty-fourth Lunar and Planetary Science Conference. Part 1: A-F 1993 p 105-106 (For primary document see N94-12015 01-91)
Avail: CASI HC A01/MF A06

New spherical harmonic models of the gravity and topography of Mars place important constraints on the structure and dynamics of the interior. The gravity and topography models are significantly phase coherent for harmonic degrees n less than 30 (wavelengths greater than 700 km). Loss of coherence below that wavelength is presumably due to inadequacies of the models, rather than a change in behavior of the planet. The gravity/topography admittance reveals two very different spectral domains: for n greater than 4, a simple Airy compensation model, with mean depth of 100 km, faithfully represents the observed pattern; for degrees 2 and 3, the effective compensation depths are 1400 and 550 km, respectively, strongly arguing for dynamic compensation at those wavelengths. The gravity model has been derived from a reanalysis of the tracking data for Mariner 9 and the Viking Orbiters, The topography model was derived by harmonic analysis of the USGS digital elevation model of Mars. Before comparing gravity and topography for internal structure inferences, we must ensure that both are consistently referenced to a hydrostatic datum. For the gravity, this involves removal of hydrostatic components of the even degree zonal coefficients. For the topography, it involves adding the degree 4 equipotential reference surface, to get spherically referenced values, and then subtracting the full degree 50 equipotential. Variance spectra and phase coherence of orthometric heights and gravity anomalies are addressed. Derived from text

N94-12066*# Princeton Univ., NJ. Dept. of Geological and Geophysical Sciences.

GLOBAL ORGANIZATION OF TECTONIC DEFORMATION ON VENUS Abstract Only

Frank Bilotti, Chris Connors, and John Suppe *In* Lunar and Planetary Inst., Twenty-fourth Lunar and Planetary Science Conference. Part 1: A-F 1993 p 107-108 (For primary document see N94-12015 01-91)
Avail: CASI HC A01/MF A06

The geographic organization of surface deformation on Venus as on Earth is a key to understanding the global tectonic system. To date we have mapped the distribution of three unambiguous tectonic land forms on Venus: (1) linear foldbelts analogous to those at plate margins of the Earth; (2) linear rift zones, analogous to continental rifts on the Earth; and (3) distributed plains deformation in the form of wrinkle ridges and extensional faults and fractures. The linear foldbelts are the dominant structural style in the Northern Hemisphere; ninety percent of the planet's foldbelts lie above the equator. In contrast, compressive deformation in the Southern Hemisphere is dominated by two large, sweeping patterns of wrinkle ridges. The two hemispheres are divided by an equatorial region that is largely covered by rift zones and several large tessera blocks. A tectonic model of generally poleward convergence of the Northern Hemisphere explains the distribution of foldbelts and rift zones. In our model, a northern hemispherical plate (or system of plates) moves poleward and deforms along discrete, predominately longitudinal bands. We recognize four types of foldbelts based on their relationships to other large-scale tectonic features on Venus. There are foldbelts that lie within the low plains, foldbelts associated with coronae, novae and chasmata, foldbelts that lie at the margins of poly-deformed tessera plateaus, and the folded mountain belts around Lakshmi Planum. We see a geometric increase in the area of fold belts when normalized to percent area at a given latitude. This increase is consistent with our model of poleward convergence. Also, the orientations of most foldbelts are either approximately north-south or parallel to lines of latitude in the northern hemisphere. This observation is also consistent with the model in that the longitudinal bands are the result of the decreasing area of the sphere as the plate moves poleward and the latitudinal belts are the direct result of poleward compression. The trends of wrinkle ridges have been mapped over the planet and several large, sweeping patterns evidently reflect long-wavelength topography. Using wrinkle ridges as paleostress indicators, we have developed local and regional stress trajectory maps. Derived from text

N94-12067*# California Univ., Los Angeles. Dept. of Earth and Space Sciences.

VENUS' CENTER OF MASS - CENTER OF FIGURE DISPLACEMENT AND IMPLICATIONS Abstract Only

D. L. Bindschadler and G. Schubert *In* Lunar and Planetary Inst., Twenty-fourth Lunar and Planetary Science Conference. Part 1: A-F 1993 p 109-110 (For primary document see N94-12015 01-91)
Avail: CASI HC A01/MF A06

Earth, Moon, Mars, and Venus all have centers of mass (C.M.) that are displaced from their centers of figure (C.F.) by amounts which range from 340 meters (Venus) to 2.5 km (Mars). These offsets have all been calculated from the first degree terms in spherical harmonic expansions of topography. We describe an alternate method for calculating C.M. - C.F. offsets directly from a global topographic data set and apply it to Venus. Using Magellan altimetry, we find that Venus' C.F. is displaced approximately 280 meters from its C.M. in the direction of Western Aphrodite Terra (4.4 deg S, 135.8 deg E). We investigate several simple models for this offset and find that it is most consistent with thickened crust in Ovda and Thetis Regiones (which constitute most of W. Aphrodite). The location of the C.F. offset also places constraints on the degree of crustal thickening in Western Ishtar Terra and/or this highland's mode of origin. We favor a model in which offset due to thick crust in Western Ishtar Terra is balanced by an opposing offset due to cold, downwelling mantle material beneath the highland. Derived from text

N94-12068*# Massachusetts Inst. of Tech., Cambridge. Dept. of Earth, Atmospheric, and Planetary Sciences.

THE ASTEROID-METEORITE CONNECTION: FORGING A NEW LINK TO VESTA AS THE PARENT BODY OF BASALTIC ACHONDRITE (HED) METEORITES Abstract Only c90

R. P. Binzel *In* Lunar and Planetary Inst., Twenty-fourth Lunar and Planetary Science Conference. Part 1: A-F 1993 p 111 (For primary document see N94-12015 01-91)
Avail: CASI HC A01/MF A06

Asteroid 4 Vesta has been at the center of the debate over the identity of the howardite eucrite diogenite (HED) parent body since the early 1970s. Despite its unique (among the 500 largest asteroids) compositional match to HED meteorites, substantial dynamical difficulties in delivering fragments from Vesta to the Earth have precluded any conclusive HED parent body link. These dynamical difficulties arise because Vesta's orbital location is far from known resonances. Consequently, it has been argued as dynamically improbable that meteoroid-sized (1 km) fragments could be excavated from Vesta with sufficient velocities to reach the resonances. Through new astronomical observations, numerous small (4-7 km) asteroids between Vesta and the 3:1 resonance have been discovered to have eucrite and diogenite compositions. Based on similar orbital elements to Vesta, all of these new asteroids are likely large impact fragments excavated from Vesta. Their current orbits imply ejection velocities in excess of 700 m/sec. Smaller (1 km) fragments can therefore be expected to have been ejected with velocities greater than 1 km/sec, sufficient to reach the 3:1 and v6 resonances. Thus it now appears to be dynamically viable for Vesta to be linked as the HED parent body. Author (revised)

N94-12069*# Muenster Univ. (Germany). Inst. for Planetologie.
ALKALI-GRANITOIDS AS FRAGMENTS WITHIN THE ORDINARY CHONDRITE ADZHI-BOGDO: EVIDENCE FOR HIGHLY FRACTIONATED, ALKALI-GRANITIC LIQUIDS ON ASTEROIDS Abstract Only **c90**
A. Bischoff *In* Lunar and Planetary Inst., Twenty-fourth Lunar and Planetary Science Conference. Part 1: A-F 1993 p 113-114 (For primary document see N94-12015 01-91)
Avail: CASI HC A01/MF A06

Adzhi-Bogdo is an ordinary chondrite regolith breccia (LL3-6) that fell October 30, 1949 in Gobi Altay, Mongolia. The rock consists of submm- to cm-sized fragments embedded in a fine-grained elastic matrix. The breccia contains various types of clasts, some of which must be of foreign heritage. Based on chemical compositions of olivine some components have to be classified as L-type. Components of the breccia include chondrules, impact melts (some are K-rich, similar to those found in other LL-chondrites, highly recrystalized rock fragments ('granulites'), pyroxene-rich fragments with achondritic textures, and alkali-granitoidal fragments that mainly consist of K-feldspar and quartz or tridymite. Probably, this is the first report on granitoids from asteroids. It can be ruled out that these fragments represent huge rock assemblages of the parent body like granites do on Earth. Therefore, to avoid misunderstandings, these rocks will be designated as granitoids. In one thin section four granitoids were observed. The main phases within these clasts are K-feldspar and SiO2-phases. Minor phases include albite, Cl-apatite, whitlockite, ilmenite, zircon, Ca-poor pyroxene, and an unidentified Na,Ti-bearing silicate. Based on chemical composition and on optical properties quartz appears to be the SiO2-phase in two fragments, whereas tridymite seems to occur in the other two. The calculated formula of the unknown Na,Ti-rich silicate is very close to (Na,Ca)2.7(Fe,Mg)6(Ti)1.3(Si)7(O)24. Quartz and K-feldspar can reach sizes of up to 700 microns. Thus, the fragments can be described as coarse-grained (by chondritic standards). This is especially the case considering that quartz and K-feldspar are very rare minerals in ordinary chondrites. Representative analyses of minerals from some granitoidal clasts are given. Based on the mineral compositions and the modal abundances the bulk compositions were calculated. Besides these granitoidal rocks, pyroxene-rich fragments occur that show exsolution textures that are similar to those found in eucrites. Derived from text

N94-12070*# Brown Univ., Providence, RI.
REFLECTANCE SPECTRA OF SULFATE-AND CARBONATE-BEARING Fe(3+)-DOPED MONTMORILLONITES AS MARS SOIL ANALOGS Abstract Only
Janice L. Bishop, Carle M. Pieters, and Roger G. Burns (Massachusetts Inst. of Tech., Cambridge.) *In* Lunar and Planetary Inst., Twenty-fourth Lunar and Planetary Science Conference. Part 1: A-F 1993 p 115-116 (For primary document see N94-12015 01-91)
(Grants NAGw-28; NAGw-2220; NAGw-748)
Avail: CASI HC A01/MF A06

Ferric smectites and ferrihydrite may be common alteration products of igneous lithologies on Mars, and experiments involving montmorillonite enriched with Fe(3+) support the likelihood of ferric smectites on Mars. Mossbauer spectroscopy has been used to identify ferrihydrite (Fe4(O,OH,H2O)12) as the primary ferric material in Fe(3+)-doped montmorillonite. Ferrihydrite is especially interesting due to its role as a precursor in the formation of hematite and goethite. Reflectance spectroscopy in the visible and infrared regions are coupled with Mossbauer spectroscopy in this study to characterize the ferric material in montmorillonites containing Fe(3+), as well as carbonates or sulfates, in the interlayer region. Derived from text

N94-12071*# Brown Univ., Providence, RI.
THE EFFECTS OF ATMOSPHERIC PRESSURE ON INFRARED REFLECTANCE SPECTRA OF MARTIAN ANALOGS Abstract Only
Janice L. Bishop, Carle M. Pieters, Stephen F. Pratt, and William Patterson *In* Lunar and Planetary Inst., Twenty-fourth Lunar and Planetary Science Conference. Part 1: A-F 1993 p 117-118 (For primary document see N94-12015 01-91)
(Grants NAGw-28; NAGw-748)
Avail: CASI HC A01/MF A06

The use of terrestrial samples as analogs of Mars soils are complicated by the Martian atmosphere. Spectral features due to the Martian atmosphere can be removed from telescopic spectra of Mars and ISM spectra of Mars, but this does not account for any spectral differences resulting from atmospheric pressure or any interactions between the atmosphere and the surface. We are examining the effects of atmospheric pressure on reflectance spectra of powdered samples in the laboratory. Contrary to a previous experiment with granite, no significant changes in albedo or the Christiansen feature were observed from 1 bar pressure down to a pressure of 8 micrometers Hg. However, reducing the atmospheric pressure does have a pronounced affect on the hydration features, even for samples retained in a dry environment for years. Derived from text

N94-12072*# Lancaster Univ. (England). Environmental Science Div.
STABLE ISOTOPE ANALYSES OF THE PERALKALINE VOLCANICS GREGORY RIFT VALLEY, KENYA Abstract Only **c46**
S. Black, R. Macdonald, A. E. Fallick (Scottish Research Reactor Centre, East Kilbride.), and M. Kelly *In* Lunar and Planetary Inst., Twenty-fourth Lunar and Planetary Science Conference. Part 1: A-F 1993 p 119-120 (For primary document see N94-12015 01-91)
Avail: CASI HC A01/MF A06

Delta O-18 analyses of the Naivasha rhyolites, basalts, Menengai trachytes and the Yatta phonolite are presented together with D/H analyses of the Naivasha rhyolites. Delta O-18 results vary from 5.7 to 8.9 per mill which is within the reported range of delta O-18 analyses for continental volcanics. Closure temperatures calulated from the basalts and rhyolites show equilibration to be at magmatic temperatures. D/H values range from -40 to -148 per mill indicating that the rhyolites have undergone large scale degasssing. Derived from text

N94-12073*# Lancaster Univ. (England). Environmental Science Div.
TH-230 - U-238 SERIES DISEQUILIBRIUM OF THE OLKARIA BASALTS GREGORY RIFT VALLEY, KENYA Abstract Only **c46**
S. Black, R. Macdonald, and M. Kelly *In* Lunar and Planetary Inst., Twenty-fourth Lunar and Planetary Science Conference. Part 1: A-F 1993 p 121-122 (For primary document see N94-12015 01-91)
Avail: CASI HC A01/MF A06

U-Th disequilibrium analyses of the Naivasha basalts show a very small (U-238/Th-230) ratios which are lower than any previously analyzed basalts. The broadly positive internal isochron trend from one sample indicates that the basalts may have source heterogeneities, this is supported by earlier work. The Naivasha complex comprises a bimodal suite of basalts and rhyolites. The basalts are divided into two stratigraphic groups each of a transitional nature. The early basalt series (EBS) which were erupted prior to the Group 1 comendites and, the late basalt series (LBS) which erupted temporally between the Broad Acres and the Ololbutot centers. The basalts represent a very small percentage of the overall eruptive volume of material at Naivasha (less than 2 percent). The analyzed samples come from four stratigraphic units in close proximity around Ndabibi, Hell's Gate and Akira areas. The earliest units occur as vesicular flows from the Ndabibi plain. These basalts are olivine-plagioclase phyric with the associated hawaiites being sparsely plagioclase phyric. An absolute age of 0.5Ma was estimated for these basalts. The next youngest basalts flows occur as younger tuft cones in the Ndabibi area and are mainly olivine-plagioclase-clinopyroxcene phyric with one purely plagioclase phyric sample. The final phase of activity at Ndabibi resulted in much younger tuft cones consisting of air fall ashes and lapilli tufts. Many of these contain resorbed plagioclase phenocrysts with sample number 120c also being clinopyroxene phyric. The isotopic evidence for the basalt formation is summarized. Derived from text

N94-12074*# Lancaster Univ. (England). Environmental Science Div.
TH-230 - U-238 SERIES DISEQUILIBRIUM OF THE OLKARIA BASALTS GREGORY RIFT VALLEY, KENYA: PETROGENESIS Abstract Only **c46**
S. Black, R. Macdonald, and M. Kelly *In* Lunar and Planetary Inst., Twenty-fourth Lunar and Planetary Science Conference. Part 1: A-F 1993 p 123-124 (For primary document see N94-12015 01-91)
Avail: CASI HC A01/MF A06

Strong mixing trends on a (Th-230/Th-232) versus Th diagram show that the basalts are mixed magmas which have undergone interaction with the crust. Instantaneous Th/U ratios are less than time integrated ones but these exceed the Th/U ratios in the MORB and OIB sources. This indicates that the mantle may have undergone some metasomatic fluxing, crustal contamination of the basalts will also enhance these ratios. Early activity on the Akira plain is represented by early basalts and hawaiites.

The early basalt samples are known to predate the earliest comendites. The most recent phase of activity is represented by another cinder cone 40-50 m high being feldspar and clinopyroxene phyric. Inclusions which occur in the comendites vary in size and distribution. The largest and most porphyritic are the trachytes (up to 40 cm) with alkali feldspar phases up to 6 mm and small pyroxenes in the ground mass. The second set of inclusions are smaller (up to 10 cm) and are largely aphyric. The distribution of the inclusions are not uniform, the Broad Acres (C5) lavas contain 2-5 percent. The size of the inclusions decrease from south to north, as does the abundance of the trachytic inclusions. The major element variations in the Naivasha basalts, hawaiites and magmatic inclusions are discussed.
Derived from text

N94-12075*# Lancaster Univ. (England). Environmental Science Div.
TH-230 - U-238 SERIES DISEQUILIBRIUM OF THE OLKARIA RHYOLITES GREGORY RIFT VALLEY, KENYA: PETROGENESIS Abstract Only **c46**
S. Black, R. Macdonald, and M. Kelly *In* Lunar and Planetary Inst., Twenty-fourth Lunar and Planetary Science Conference. Part 1: A-F 1993 p 125-126 (For primary document see N94-12015 01-91)
Avail: CASI HC A01/MF A06

Positive correlations of (U-238/Th-230) versus Th show the rhyolites to be products of partial melting. Positive correlations of U and Cl and U and F show that the U enrichment in the rhyolites is associated with the halogen contents which may be related to the minor phenocryst phase fractionation. Instantaneous Th/U ratios exceed time integrated Th/U ratios providing further evidence of the hydrous nature of the Olkaria rhyolite source. Excess (U-238/Th-230) in the subduction related rocks has been associated to the preferential incorporation of uranium in slab derived fluids, but no evaluation of the size of this flux has been made. The majority of the Naivasha samples show a (U-238/Th-230) less than 1 and plot close to the subduction related samples indicating the Naivasha rhyolites may also have been influenced by fluids during their formation. In general samples with high (U-238/Th-230) ratios reflecting recent enrichment of uranium relative to thorium have high thorium contents, thereby the high (U-238/Th-230) ratios are restricted to the most incompatible element enriched magmas and, hence, are a good indication that the rhyolites were formed by partial melting. If a fluid phase had some influence on the formation of the rhyolites then the uranium and thorium may have some correlation with F and Cl contents which can be mirrored by the peralkalinity. Plots of uranium against F and Cl contents are shown. The positive correlation indicates that the uranium enrichments are associated with the halogen contents. There seems to be a greater correlation for U against Cl than F indicating that the U may be transported preferentially as Cl complexes. Derived from text

N94-12076*# Lancaster Univ. (England). Environmental Science Div.
TH-230 - U-238 SERIES DISEQUILIBRIUM OF THE OLKARIA RHYOLITES GREGORY RIFT VALLEY, KENYA: RESIDENCE TIMES Abstract Only **c46**
S. Black, R. Macdonald, and M. Kelly *In* Lunar and Planetary Inst., Twenty-fourth Lunar and Planetary Science Conference. Part 1: A-F 1993 p 127-128 (For primary document see N94-12015 01-91)
Avail: CASI HC A01/MF A06

U-series disequilibrium analyses have been conducted on samples from Olkaria rhyolite centers with ages being available for all but one center using both internal and whole rock isochrons. 67 percent of the rhyolites analyzed show U-Th disequilibrium, ranging from 27 percent excess thorium to 36 percent excess uranium. Internal and whole rock isochrons give crystallization/formation ages between 65 ka and 9 ka, in every case these are substantially older than the eruptive dates. The residence times of the rhyolites (U-Th age minus the eruption date) have decreased almost linearly with time, from 45 ka to 7 Ka suggesting a possible increase of activity within the system related to increased basaltic input. The long residence times are mirrored by large Rn-222 fluxes from the centers which cannot be explained by larger U contents. Derived from text

N94-12077*# Jet Propulsion Lab., California Inst. of Tech., Pasadena.
USING HIGH SPECTRAL RESOLUTION SPECTROPHOTOMETRY TO STUDY BROAD MINERAL ABSORPTION FEATURES ON MARS Abstract Only
D. L. Blaney and D. Crisp *In* Lunar and Planetary Inst., Twenty-fourth Lunar and Planetary Science Conference. Part 1: A-F 1993 p 129-130 (For primary document see N94-12015 01-91)
Avail: CASI HC A01/MF A06

Traditionally telescopic measurements of mineralogic absorption features have been made using relatively low to moderate (R=30-300) spectral resolution. Mineralogic absorption features tend to be broad so high resolution spectroscopy (R greater than 10,000) does not provide significant additional compositional information. Low to moderate resolution spectroscopy allows an observer to obtain data over a wide wavelength range (hundreds to thousands of wavenumbers) compared to the several wavenumber intervals that are collected using high resolution spectrometers. However, spectrophotometry at high resolution has major advantages over lower resolution spectroscopy in situations that are applicable to studies of the Martian surface, i.e., at wavelengths where relatively weak surface absorption features and atmospheric gas absorption features both occur.
Derived from text

N94-12078*# Houston Univ., Clear Lake, TX.
USING SOLAR FLARE TRACK DENSITIES TO DETERMINE THE ORIGIN OF INTERPLANETARY DUST PARTICLES Abstract Only **c90**
George E. Blanford *In* Lunar and Planetary Inst., Twenty-fourth Lunar and Planetary Science Conference. Part 1: A-F 1993 p 131-132 (For primary document see N94-12015 01-91)
Avail: CASI HC A01/MF A06

Sandford theoretically explored the use of solar flare track densities in interplanetary dust particles (IDP's) to distinguish whether they were of cometary or asteroidal origin. He determined that there were differences in the characteristic distributions of track densities that would occur from these two possible sources. Flynn examined the heating of IDP's on atmospheric entry and concluded that IDP's must be predominantly from asteroidal sources because these asteroidal particles would have sufficiently low velocities to survive atmospheric heating with little or no modification whereas cometary particles would ordinarily have velocities that are much higher. This paper looks at what we can learn by combining the approaches of Sandford and Flynn. Derived from text

N94-12079*# Hawaii Univ., Honolulu. Planetary Geosciences.
SPECTRAL AND MULTISPECTRAL IMAGING STUDIES OF LUNAR MANTLED MARE DEPOSITS Abstract Only
D. T. Blewett, B. R. Hawke, P. G. Lucey, J. F. Bell, III (National Aeronautics and Space Administration. Ames Research Center, Moffett Field, CA.), R. Jaumann (Deutsche Versuchsanstalt fuer Luft- und Raumfahrt, Oberpfaffenhofen, Germany.), H. Hiesinger (Deutsche Versuchsanstalt fuer Luft- und Raumfahrt, Oberpfaffenhofen, Germany.), G. Neukum (Deutsche Versuchsanstalt fuer Luft- und Raumfahrt, Oberpfaffenhofen, Germany.), and P. D. Spudis (Lunar and Planetary Inst., Houston, TX.) *In* Lunar and Planetary Inst., Twenty-fourth Lunar and Planetary Science Conference. Part 1: A-F 1993 p 133-134 (For primary document see N94-12015 01-91)
Avail: CASI HC A01/MF A06

Near-IR reflectance spectra (0.6-2.5 microns) and CCD images in the extended visible range (0.4-1.0 microns) obtained with Earth-based telescopes have been used to investigate the composition and origin of formations in the Schiller-Schickard region of the Moon. Of particular interest are the Schickard light plains, which represent an area of mantled mare basalt, or cryptomare. Here local pre-existing mare basalts were eroded and incorporated into a highlands-rich deposit by eject a from the Orientale Basin. Spectra observations of mature and immature highland and mare surfaces, as well as dark-halo crater materials provide information on the mafic mineralogy of features in the area. Analyses of the '1 micron' absorption band and spectral mixing models indicate that selected spots in the light plains contain on the order of 50 percent mare basalt. CCD image cubes can be used to map the amount of basalt in the light plains and evaluate changes with radial distance from Orientale.
Derived from text

N94-12080*# Dartmouth Coll., Hanover, NH. Dept. of Earth Sciences.
STRONTIUM AND OXYGEN ISOTOPE STUDY OF M-1, M-3 AND M-4 DRILL CORE SAMPLES FROM THE MANSON IMPACT STRUCTURE, IOWA: COMPARISON WITH HAITIAN K-T IMPACT GLASSES Abstract Only **c46**
Joel D. Blum, C. Page Chamberlain, Michael P. Hingston, and Christian

Koeberl (Wien Univ., Austria.) *In* Lunar and Planetary Inst., Twenty-fourth Lunar and Planetary Science Conference. Part 1: A-F 1993 p 135-136 (For primary document see N94-12015 01-91)
Avail: CASI HC A01/MF A06

Strontium and oxygen isotope analyses were performed on 8 samples from the M-1, M-3, and M-4 cores recently drilled at the Manson impact structure. The samples were three elastic sedimentary rocks (of probable Cretaceous age) which occurred as clasts within the sedimentary clast breccia, two samples of crystalline rock breccia matrix, and three samples of dolomite and limestone. The Sr-87/Sr-86 (corrected to 65 Ma) ratios were much higher than those in impact glasses from the Haitian Cretaceous-Tertiary (K-T) boundary. Isotope mixing calculations demonstrate that neither the silicate or carbonate rocks analyzed from the Manson crater, or mixtures of these rocks are appropriate source materials for the Haitian impact glasses. However, the Sr-87/Sr-86 (65Ma) ratio and delta O-18 value of the Ca-rich Haitian glasses are well reproduced by mixtures of Si-rich Haitian glass with platform carbonate of K-T age.
Derived from text

N94-12081*# Rutgers Univ., New Brunswick, NJ. Dept. of Geological Sciences.
PRELIMINARY RESULTS OF Mn PARTITIONING EXPERIMENTS ON MURCHISON ANALOGUES Abstract Only **c46**
Joseph S. Boesenberg and Jeremy S. Delaney *In* Lunar and Planetary Inst., Twenty-fourth Lunar and Planetary Science Conference. Part 1: A-F 1993 p 137-138 (For primary document see N94-12015 01-91)
Avail: CASI HC A01/MF A06

Eucrites, howardites, and diogenites have Fe/Mn ratios between 30 and 45, while carbonaceous chondrites have much higher values between 90 and 150. Stolper (1977) first showed that basaltic achondrites could evolve from a precursor chondritic material through simple partial melting. These experiments indicated that chondritic material heated to temperatures near 1180 C with a fugacity of one log unit below the iron-wustite buffer curve, produced a eucritic mineralogy that contained olivine, pigeonite, plagioclase, spinel, glass, and metal. The partial melting experiments of Jurewicz et al. (1992) on an hydrous Murchison and Allende also showed that HED compositions were produceable at temperatures between 1130 C and 1325 C with fugacities below and above the iron-wustite buffer curve. However, the MnO abundances of Jurewicz were too low to produce suitable Fe/Mn ratios for HED's. We present below our results of partial melting experiments on Murchison analogues that involved temperatures between 1180 C and 1580 C and fugacities below the iron-wustite buffer curve. Our experiments resulted in MnO abundances nearly twice that of Jurewicz and indicate that the production of basaltic achondrite-like Fe/Mn ratios from precursor chondritic material are possible. Derived from text

N94-12082*# National Aeronautics and Space Administration. Lyndon B. Johnson Space Center, Houston, TX.
NOBLE GASES IN LEW88516 SHERGOTTITE: EVIDENCE FOR EXPOSURE AGE PAIRING WITH ALH77005 Abstract Only **c25**
D. D. Bogard and D. H. Garrison *In* Lunar and Planetary Inst., Twenty-fourth Lunar and Planetary Science Conference. Part 1: A-F 1993 p 139-140 (For primary document see N94-12015 01-91)
Avail: CASI HC A01/MF A06

LEW88516 contains excess amounts of radiogenic Ar-40 and Xe-129 that are slightly greater than those observed in ALH77005, but in the same relative proportion as much larger excesses observed in EET79001. Cosmogenic He-3 and Ne-21 abundances in LEW88516 are very similar to those for ALH77005 and are consistent with a common initiation of cosmic ray exposure -2.8 Myr ago for four of the five shergottites. Exposure of these four shergottites could have been under different shielding in a common meteoroid, or in several objects. Author (revised)

N94-12083*# National Aeronautics and Space Administration. Lyndon B. Johnson Space Center, Houston, TX.
Ar-39 - Ar-40 AGES OF ACAPULCOITES AND LODRANITES: EVIDENCE FOR EARLY PARENT BODY HEATING Abstract Only **c46**
D. D. Bogard, D. H. Garrison, T. J. McCoy (Hawaii Univ., Honolulu.), and K. Keil (Hawaii Univ., Honolulu.) *In* Lunar and Planetary Inst., Twenty-fourth Lunar and Planetary Science Conference. Part 1: A-F 1993 p 141-142 (For primary document see N94-12015 01-91)
Avail: CASI HC A01/MF A06

New age dating of acapulcoites (Acapulco, Monument Draw) and lodranites (Gibson) allow us to reconstruct the history of their parent body in a chronological framework. These meteorites originated on a common parent body -4.55 Ga ago. Non-collisional heating caused partial melting, with lodranites having been heated slightly higher than acapulcoites. This parent body cooled to the Ar closure temperature at -4.51 Ga for acapulcoites and -4.48 Ga for lodranites. The difference in ages is consistent with the higher temperature and longer cooling time for lodranites. Cooling probably occurred at a few to tens of deg C/Ma, with slower cooling rates at lower temperatures. Author (revised)

N94-12084*# Geological Survey, Denver, CO.
ARROYO EL MIMBRAL, MEXICO, K/T UNIT: ORIGIN AS DEBRIS FLOW/TURBIDITE, NOT A TSUNAMI DEPOSIT Abstract Only **c46**
Bruce F. Bohor and William J. Betterton *In* Lunar and Planetary Inst., Twenty-fourth Lunar and Planetary Science Conference. Part 1: A-F 1993 p 143-144 (For primary document see N94-12015 01-91)
Avail: CASI HC A01/MF A06

Coarse, spherule-bearing, elastic units have been discovered at 10 marine sites that span the K/T boundary in northeastern Mexico. We examined one of the best exposed sites in Arroyo el Mimbral, northwest of Tampico. The Mimbral outcrop displays a layered elastic unit up to 3 m thick enclosed by marly limestones of the Mendez (Latest Maastrichian) and Velasco (Earliest Danian) Formations. At its thickest point, this channelized elastic unit is comprised of 3 subunits: (1) a basal, poorly-sorted, ungraded calcareous spherule bed 1 m thick containing relict impact glass and shocked mineral grains, (2) a massive set of laminated calcite-cemented sandstones up to 2 m thick with plant debris at its base, (3) capped by a thin (up to 20 cm) set of rippled sandstone layers separated by silty mudstone drapes containing a small (921 pg/g) iridium anomaly. This tripartite elastic unit is conformably overlain by marls of the Velasco Formation. We also visited the La Lajilla site east of Ciudad Victoria; its stratigraphy is similar to Mimbral's, but its elastic beds are thinner and less extensive laterally. The Mimbral elastic unit has been interpreted previously as being deposited by a megawave or tsunami produced by an asteroid impact on nearby Yucatan (Chicxulub crater). However, a presumed 400-m paleodepth of water at the Mimbral site, channeling of the spherule subunit into the underlying Mendez Formation marls, and the overtopping of the basal, spherule-bearing subunit by the laminated sandstone subunit, all suggest a combined debris flow/turbidite origin for this elastic unit similar to that proposed for Upper Pleistocene sand/silt beds occurring elsewhere in the Gulf of Mexico. In this latter model, the sediment source region for the elastic unit is the lower continental shelf and slope escarpment. For the K/T unit at Mimbral, we propose that thick ejecta blanket deposits composed mostly of spherules were rapidly loaded onto the lower shelf and slope from an impact-generated ejecta curtain. Derived from text

N94-12085*# Geological Survey, Denver, CO.
K/T SPHERULES FROM HAITI AND WYOMING: ORIGIN, DIAGENESIS, AND SIMILARITY TO SOME MICROTEKTITES Abstract Only **c46**
B. F. Bohor, B. P. Glass (Delaware Univ., Newark.), and W. J. Betterton *In* Lunar and Planetary Inst., Twenty-fourth Lunar and Planetary Science Conference. Part 1: A-F 1993 p 145-146 (For primary document see N94-12015 01-91)
Avail: CASI HC A01/MF A06

Spherules with relict glass cores in the K/T boundary bed of Haiti allow for a comparison of these bodies with hollow goyazite shells in the K/T boundary claystone of Wyoming and with younger microtektites of the Ivory Coast strewn field. Samples of the Haitian beds from undisturbed sections at Beloc, as determined by Jehanno et al., contain both hollow shells and relict glass cores rimmed by palagonite that has been partially converted to smectite. These palagonite rims developed from hydration zones formed when hot, splash-form droplets of andesitic impact glass were deposited into water. Mutual collisions between these droplets in the ejecta curtain may have formed point-source stresses on their surfaces. Initiation of hydration would be facilitated at these surface stress points and propagated radially into the glass. The inner surface of these merged hemispherical fronts appears mammillary, which is reflected as scalloping in Haitian relict glass cores. Derived from text

N94-12086*# Max-Planck-Inst. fuer Chemie, Mainz (Germany).
THE SOLUBILITY OF GOLD IN SILICATE MELTS: FIRST RESULTS Abstract Only c26
A. Borisov, H. Palme, and B. Spettel *In* Lunar and Planetary Inst., Twenty-fourth Lunar and Planetary Science Conference. Part 1: A-F 1993 p 147-148 (For primary document see N94-12015 01-91)
Avail: CASI HC A01/MF A06

The effects of oxygen fugacity and temperature on the solubility of Au in silicate melts were determined. Pd-Au alloys were equilibrated with silicate of anorthite-diopside eutectic composition at different T-fO2 conditions. The behavior of Au was found to be similar to that of Pd reported recently. Au solubilities for alloys with 30 to 40 at. percent Au decrease at 1400 C from 12 ppm in air to 160 ppb at a log fO2 = -8.7. The slope of the log(Me-solubility) vs. log(fO2) curve is close to 1/4 for Au and the simultaneously determined Pd suggesting a formal valence of Au and Pd of 1+. Near the IW buffer Pd and Au solubilities become even less dependent on fO2 perhaps reflecting the presence of some metallic Au and Pd. Author (revised)

N94-12087*# Sandia National Labs., Albuquerque, NM.
SI-29 NMR SPECTROSCOPY OF NATURALLY-SHOCKED QUARTZ FROM METEOR CRATER, ARIZONA: CORRELATION TO KIEFFER'S CLASSIFICATION SCHEME Abstract Only c25
M. B. Boslough, R. T. Cygan, and R. J. Kirkpatrick (Illinois Univ., Urbana.) *In* Lunar and Planetary Inst., Twenty-fourth Lunar and Planetary Science Conference. Part 1: A-F 1993 p 149-150 (For primary document see N94-12015 01-91)
Avail: CASI HC A01/MF A06

We have applied solid state Si-29 nuclear magnetic resonance (NMR) spectroscopy to five naturally-shocked Coconino Sandstone samples from Meteor Crater, Arizona, with the goal of examining possible correlations between NMR spectral characteristics and shock level. This work follows our observation of a strong correlation between the width of a Si-29 resonance and peak shock pressure for experimentally shocked quartz powders. The peak width increase is due to the shock-induced formation of amorphous silica, which increases as a function of shock pressure over the range that we studied (7.5 to 22 GPa). The Coconino Sandstone spectra are in excellent agreement with the classification scheme of Kieffer in terms of presence and approximate abundances of quartz, coesite, stishovite, and glass. We also observe a new resonance in two moderately shocked samples that we have tentatively identified with silicon in tetrahedra with one hydroxyl group in a densified form of amorphous silica. Derived from text

N94-12088*# Carnegie Institution of Washington, DC.
MIDPLANE TEMPERATURES IN THE SOLAR NEBULA Abstract Only c92
A. P. Boss *In* Lunar and Planetary Inst., Twenty-fourth Lunar and Planetary Science Conference. Part 1: A-F 1993 p 151-152 (For primary document see N94-12015 01-91)
Avail: CASI HC A01/MF A06

Cosmochemical analyses of meteorites imply that maximum temperatures in the inner solar nebula were on the order of 1300 K, yet standard viscous accretion disk models predict much lower midplane temperatures (approx. 300 K at 2 AU to 3 AU) in a minimum mass nebula. A second-order accurate radiative hydrodynamics code has been used to construct models of the late-phase solar nebula appropriate for low-mass star formation (M is approximately 10(exp -6) to 10(exp -5) solar-M yr(exp -1). For a minimum mass (0.02 solar-M) nebula and a solar-mass protostar, the new models show that compressional heating due to mass accretion onto the nebula and subsequent vertical contraction of the nebula are sufficient to lead to midplane temperatures T(sub m) greater than 1400 K at 1 AU and T(sub m) greater than 1000 K at 2.5 AU. Author (revised)

N94-12089*# Carnegie Institution of Washington, DC.
CHONDRULE FORMATION BY CLUMPY ACCRETION ONTO THE SOLAR NEBULA Abstract Only c92
A. P. Boss and J. A. Graham *In* Lunar and Planetary Inst., Twenty-fourth Lunar and Planetary Science Conference. Part 1: A-F 1993 p 153-154 (For primary document see N94-12015 01-91)
Avail: CASI HC A01/MF A06

Chondrule textures and compositions appear to require rapid heating of precursor grain aggregates to temperatures in the range 1500 K to 2100 K, cooling times on the order of hours, and episodic and variable intensity events in order to produce chondrule rims and chemically distinct groups. Nebula shock waves have been proposed by Hood and Horanyi as a physical mechanism that may be capable of meeting the meteoritical constraints. Motivated by astronomical observations of the close environments of young stars, we suggest that the source of the nebula shock waves may be clumpy accretion onto the solar nebula - that is, episodic impacts onto the nebula by discrete cloud clumps with masses of at least 10(exp 22) g. If the cloud clumps are massive enough (10(exp 26) g), the resulting shockwave may be able to propagate to the midplane and process precursor aggregates residing in a dust sub-disk. Author (revised)

N94-12090*# Carnegie Institution of Washington, DC.
INITIATING SOLAR SYSTEM FORMATION THROUGH STELLAR SHOCK WAVES c92
A. P. Boss and E. A. Myhill *In* Lunar and Planetary Inst., Twenty-fourth Lunar and Planetary Science Conference. Part 1: A-F 1993 p 155-156 (For primary document see N94-12015 01-91)
Avail: CASI HC A01/MF A06

Isotopic anomalies in presolar grains and other meteoritical components require nucleosynthesis in stellar interiors, condensation into dust grains in stellar envelopes, transport of the grains through the interstellar medium by stellar outflows, and finally injection of the grains into the presolar nebula. The proximity of the presolar cloud to these energetic stellar events suggests that a shock wave from a stellar outflow might have initiated the collapse of an otherwise stable presolar cloud. We have begun to study the interactions of stellar shock waves with thermally supported, dense molecular cloud cores, using a three spatial dimension (3D) radiative hydrodynamics code. Supernova shock waves have been shown by others to destroy quiescent clouds, so we are trying to determine if the much smaller shock speeds found in, e.g., asymptotic giant branch (AGB) star winds, are strong enough to initiate collapse in an otherwise stable, rotating, solar-mass cloud core, without leading to destruction of the cloud. Author (revised)

N94-12091*# California Univ., Los Angeles. Inst. of Geophysics and Planetary Physics.
IMPACT MINERALOGY AND CHEMISTRY OF THE CRETACEOUS-TERTIARY BOUNDARY AT DSDP SITE 576 Abstract Only c46
Jennifer A. Bostwick and Frank T. Kyte *In* Lunar and Planetary Inst., Twenty-fourth Lunar and Planetary Science Conference. Part 1: A-F 1993 p 157-158 (For primary document see N94-12015 01-91)
Avail: CASI HC A01/MF A06

We have identified the K/T boundary in pelagic clay sediments from cores at DSDP Site 576 in the western North Pacific. Detailed geochemical and trace mineralogical analyses of this boundary section are in progress and initial results indicate similarities and differences relative to the only other clay core investigated in detail; DSDP Site 596, a locality in the western South Pacific. Peak Ir concentrations of 13 ng/g in DSDP Hole 576B are virtually identical with those observed in the South Pacific, but in the North Pacific this peak is much narrower and the integrated Ir fluence of 85 ng cm(exp -2) is 4 times lower (320 in Hole 596). Of the 34 elements measured, only Ir and Cr were found to have anomalous concentrations in K/T boundary samples. Trace mineral residues were obtained by washing away clays and sequential chemical leaches (including HF) to remove typical hydrogenous and biogenous sediment components (e.g., zeolites and radiolarian opal). We attempted to quantitatively recover the entire trace mineral assemblage for grains greater than 30 micrometers in diameter. Our mineral residues were dominated by two phases: quartz and magnesioferrite spinel. Other non-opaque mineral grains we have positively identified were trace K-feldspar, plagioclase, corundum, and muscovite. Of these only K-feldspar exhibited planar deformation features (PDF). We have not found abundant plagioclase, as in the South Pacific suggesting that this phase was either not preserved in the North Pacific, or that in the south, it has a non-impact (i.e., volcanic) source. PDF in quartz were commonly obscured by secondary overgrowths on the surfaces of quartz grains, presumably from diagenetic reprecipitation of silica dissolved from opaline radiolarian tests that are common in these sediments. However, careful examination revealed that most grains had multiple sets of PDF. Of the 133 quartz grains greater than 30 micrometers analyzed, 62 percent showed evidence of shock. The largest shocked grain recovered to date had a maximum diameter of 160 micrometers, consistent with other sites in the Pacific. Derived from text

N94-12092*# Arizona Univ., Tucson. Lunar and Planetary Lab.

COLLISION LIFETIMES AND IMPACT STATISTICS OF NEAR-EARTH ASTEROIDS c90

W. F. Bottke, Jr., M. C. Nolan, and R. Greenberg *In* Lunar and Planetary Inst., Twenty-fourth Lunar and Planetary Science Conference. Part 1: A-F 1993 p 159-160 (For primary document see N94-12015 01-91)

Avail: CASI HC A01/MF A06

We have examined the lifetimes of Near-Earth asteroids (NEA's) by directly computing the collision probabilities with other asteroids and with the terrestrial planets. We compare these to the dynamical lifetimes, and to collisional lifetimes assumed by other workers. We discuss the implications of the differences. The lifetimes of NEA's are important because, along with the statistics of craters on the Earth and Moon, they help us to compute the number of NEA's and the rate at which new NEA's are brought to the vicinity of the Earth. Assuming that the NEA population is in steady-state, the lifetimes determine the flux of new bodies needed to replenish the population. Earlier estimates of the lifetimes ignored (or incompletely accounted for) the differences in the velocities of asteroids as they move in their orbits, so our results differ from (for example) Greenberg and Chapman (1983, Icarus 55, 455) and Wetherill (1988, Icarus 76, 1) by factors of 2 to 10. We have computed the collision rates and relative velocities of NEA's with each other, the main-belt asteroids, and the terrestrial planets, using the corrected method described by Bottke et. al. (1992, GRL, in press). We find that NEA's typically have shorter collisional lifetimes than do main-belt asteroids of the same size, due to their high eccentricities, which typically give them aphelia in the main belt. Consequently, they spend a great deal of time in the main belt, and are moving much slower than the bodies around them, making them 'sitting ducks' for impacts with other asteroids. They cross the paths of many objects, and their typical collision velocities are much higher (10-15 km/s) than the collision velocities (5 km/s) among objects within the main belt. These factors combine to give them substantially shorter lifetimes than had been previously estimated. Derived from text

N94-12093*# Toronto Univ. (Ontario).

AGE OF POPIGAI IMPACT EVENT USING THE Ar-40 - Ar-39 METHOD Abstract Only c46

R. J. Bottomley and R. A. F. Grieve (Geological Survey of Canada, Ottawa, Ontario.) *In* Lunar and Planetary Inst., Twenty-fourth Lunar and Planetary Science Conference. Part 1: A-F 1993 p 161-162 (For primary document see N94-12015 01-91)

Avail: CASI HC A01/MF A06

The Popigai impact structure of central Siberia is the largest known impact crater in the Commonwealth of Independent States with an original diameter of some 100 km. The age of the crater is constrained by the existing stratigraphy to a period between 5-65 Ma. Attempts to date the impact event using conventional K-Ar on whole rock samples and fission track dating on glasses yield a spread of ages between 30 and 45 Ma. Argon step-heating analyses of several whole-rock samples performed with the Argon Laserprobe at the University of Toronto indicated an age of impact of about 36 Ma. However, a more recently reported Ar-40 - Ar-49 result on glass separated from a suevite sample gave a 65 Ma age and raised the possibility that Popigai was involved with the K/T boundary event. We have pursued further analyses at the University of Toronto on a broader spectrum of Popigai samples. These results confirm an age of about 36 Ma for the formation of this crater, and indicate that Popigai was not associated with the K/T boundary event. Derived from text

N94-12094*# California Univ., Berkeley. Dept. of Geology.

MINOR AND TRACE ELEMENT COMPOSITION AND AGE OF YUKON PROBABLE-MICROTEKTITES Abstract Only c90

S. Q. Boundy-Sanders and R. L. Hervig (Arizona State Univ., Tempe.) *In* Lunar and Planetary Inst., Twenty-fourth Lunar and Planetary Science Conference. Part 1: A-F 1993 p 163-164 (For primary document see N94-12015 01-91)

Avail: CASI HC A01/MF A06

Major, minor, and trace element composition of the candidate microtektites from Yukon Territory suggest a possible impact site of hydrothermally altered limestone and sand or chert, or possibly a carbonatite. Their REE/chondrite curve is similar in character to, but higher than, shale composites of North America, Australia, and Europe. Relative to these same composites, the Yukon droplets are enriched in Y, F, S, Sr, P, Mn, Mg, and Ca. They are depleted in Rb, Li, Th, Nb, Ti, K, Na, Fe, Si, and Al. Biostratigraphic constraints on the droplets indicate they are Middle to Late Devonian, more likely Middle Devonian, in age. Derived from text

N94-12095*# National Aeronautics and Space Administration, Washington, DC.

A STRUCTURAL ORIGIN FOR THE CANTALOUPE TERRAIN OF TRITON Abstract Only

Joseph M. Boyce *In* Lunar and Planetary Inst., Twenty-fourth Lunar and Planetary Science Conference. Part 1: A-F 1993 p 165-166 (For primary document see N94-12015 01-91)

Avail: CASI HC A01/MF A06

Cantaloupe terrain is unique to Triton. It is Triton's oldest terrain and includes about 250,000 km sq. region displaying sparsely cratered, closely spaced, nearly circular dimples about 30-40 km across. This terrain is found on no other planet because, only on Triton the final major global thermal pulse (1) caused completed (or nearly) interior melting resulting in a cooling history where large thermal stresses shattered and contorted a thin, weak lithosphere, and (2) occurred after heavy bombardment so that the surface features were preserved. The cantaloupe terrain is composed of intersecting sets of structures (folds and/or faults) that have developed as a result of global compression generated by volumetric changes associated with cooling of Triton's interior. Further, it is proposed that these structures developed after the period of heavy bombardment, and resulted from the last major global thermal epoch in Triton's unique history (either caused by tidal or radio metric heating). Initially, as the body cooled and the structures formed, their surface topography was most likely modified by thermal relaxation of the warm surface ices. In other bodies like Mercury, thermal stresses generated from global cooling and contraction have resulted in widely spaced thrust faults, whereas on Triton, thermal stresses produced more closely-spaced folds and faults sets. This difference in structural style is probably due to differences in lithospheric properties (thickness, strength, etc.), the magnitude of stress (directly dependent on the thermal history), and when the structures formed, relative to the period of heavy bombardment. Derived from text

N94-12096*# Arizona Univ., Tucson. Lunar and Planetary Lab.

TRACE-ELEMENT ABUNDANCES IN SEVERAL NEW UREILITES Abstract Only c25

William V. Boynton and Dolores H. Hill *In* Lunar and Planetary Inst., Twenty-fourth Lunar and Planetary Science Conference. Part 1: A-F 1993 p 167-168 (For primary document see N94-12015 01-91)

Avail: CASI HC A01/MF A06

Four new ureilites are analyzed for trace-element abundances. Frontier Mountain (FRO) 90054 is an augite-rich ureilite and has high rare earth element (REE) abundances with a pattern expected of augite. FRO 90036 and Acfer 277 have REE patterns similar to the V-shape pattern of other ureilites. Nuevo Mercurio (b) has very high REE abundances, but they look like they are due to terrestrial alteration. The siderophile-element pattern of these ureilites are similar to those of known ureilites. Derived from text

N94-12097*# Washington Univ., Saint Louis, MO. Dept. of Earth and Planetary Sciences.

COMPOSITIONAL AND TEXTURAL INFORMATION FROM THE DUAL INVERSION OF VISIBLE, NEAR AND THERMAL INFRARED REMOTELY SENSED DATA Abstract Only c43

Robert A. Brackett and Raymond E. Arvidson *In* Lunar and Planetary Inst., Twenty-fourth Lunar and Planetary Science Conference. Part 1: A-F 1993 p 169-170 (For primary document see N94-12015 01-91)

Avail: CASI HC A01/MF A06

A technique is presented that allows extraction of compositional and textural information from visible, near and thermal infrared remotely sensed data. Using a library of both emissivity and reflectance spectra, endmember abundances and endmember thermal inertias are extracted from AVIRIS (Airborne Visible and Infrared Imaging Spectrometer) and TIMS (Thermal Infrared Mapping Spectrometer) data over Lunar Crater Volcanic Field, Nevada, using a dual inversion. The inversion technique is motivated by upcoming Mars Observer data and the need for separation of composition and texture parameters from sub pixel mixtures of bedrock and dust. The model employed offers the opportunity to extract compositional and textural information for a variety of endmembers within a given pixel. Geologic inferences concerning grain size, abundance, and source of endmembers can be made directly from the inverted data. These parameters are of direct relevance to Mars exploration, both for Mars Observer and for follow-on missions. Derived from text

N94-12098*# MVA, Inc., Norcross, GA.
UNEQUILIBRATED, EQUILIBRATED, AND REDUCED AGGREGATES IN ANHYDROUS INTERPLANETARY DUST PARTICLES Abstract Only **c90**
J. P. Bradley *In* Lunar and Planetary Inst., Twenty-fourth Lunar and Planetary Science Conference. Part 1: A-F 1993 p 171-172 (For primary document see N94-12015 01-91)
Avail: CASI HC A01/MF A06

Track-rich anhydrous IDP's are probably the most primitive IDP's because they have escaped significant post-accretional alteration; they exhibit evidence of (nebular) gas phase reactions; their mineralogy is similar to comet Halley's dust; and some of them exhibit comet-like IR spectral characteristics. However, basic questions about the mineralogy and petrography of anhydrous IDP's remain unanswered, because they contain aggregated components that can be heterogeneous on a scale of nanometers. In some IDP's, aggregates account for greater than 75 percent of the volume of the particle. The aggregates have been systematically examined using an analytical electron microscope (AEM), which provides probe-forming optics and (x-ray and electron) spectrometers necessary to analyze individual nanometer-sized grains. The AEM results reveal at least three mineralogically distinct classes of aggregates in an hydrous IDP's, with mineralogies reflecting significantly different formation/aggregation environments. Derived from text

N94-12099*# MVA, Inc., Norcross, GA.
CARBON ANALYSES OF IDP'S SECTIONED IN SULFUR AND SUPPORTED ON BERYLLIUM FILMS Abstract Only **c25**
J. P. Bradley, L. Keller (National Aeronautics and Space Administration. Lyndon B. Johnson Space Center, Houston, TX.), K. L. Thomas (Lockheed Corp., Houston, TX.), T. B. VanderWood, and D. E. Brownlee (Washington Univ., Seattle.) *In* Lunar and Planetary Inst., Twenty-fourth Lunar and Planetary Science Conference. Part 1: A-F 1993 p 173-174 (For primary document see N94-12015 01-91)
Avail: CASI HC A01/MF A06

Carbon is the only major element in interplanetary dust whose abundance, distribution and chemical state are not well understood. Information about carbon could clarify the relationship between the various classes of IDP's, conventional meteorites, and sources (e.g., comets vs. asteroids). To date, the most reliable estimates of C abundance in Interplanetary Dust Particles (IDP's) have been obtained by analyzing particles on thick-flat Be substrates using thin-window energy-dispersive spectroscopy in the SEM. These estimates of C abundance are valid only if C is homogeneously distributed, because detected C x-rays originate from the outer 0.1 micrometers of the particle. An alternative and potentially more accurate method of measuring C abundances is to analyze multiple thin sections (each less than 0.1 less than 0.1 micrometers thick) of IDP's. These efforts however, have been stymied because of a lack of a suitable non-carbonaceous embedding medium and the availability of C-free conductive substrates. We have embedded and thin-sectioned IDP's in glassy sulfur, and transferred the thin sections to Be support films approximately 25 nm thick. The sections were then analyzed in a 200 KeV analytical TEM. S sublimes rapidly under vacuum in the TEM, leaving non-embedded sections supported on Be. Apart from quantitative C (and O) analyses, S sectioning dramatically expands the range of analytical measurements that can be performed on a single IDP. Derived from text

N94-12100*# Dartmouth Coll., Hanover, NH. Surficial Processes Lab.
MODERN SHELF ICE, EQUATORIAL AEOLIS QUADRANGLE, MARS Abstract Only
G. R. Brakenridge *In* Lunar and Planetary Inst., Twenty-fourth Lunar and Planetary Science Conference. Part 1: A-F 1993 p 175-176 (For primary document see N94-12015 01-91)
Avail: CASI HC A01/MF A06

As part of a detailed study of the geological and geomorphological evolution of Aeolis Quadrangle, I have encountered evidence suggesting that near surface ice exists at low latitudes and was formed by partial or complete freezing of an inland sea. The area of interest is centered at approximately -2 deg, 196 deg. As seen in a suite of Viking Orbiter frames obtained at a range of approximately 600 km, the plains surface at this location is very lightly cratered or uncratered, and it is thus of late Amazonian age. Extant topographic data indicate that the Amazonian plains at this location occupy a trough whose surface lies at least 1000 m below the Mars datum. A reasonable hypothesis is that quite recent surface water releases, perhaps associated with final evolution of large 'outflow chasms' to the south, but possibly from other source areas, filled this trough, that ice floes formed almost immediately, and that either grounded ice or an ice-covered sea still persists. A reasonable hypothesis is that quite recent surface water releases, perhaps associated with final evolution of large 'outflow chasms' to the south, but possibly from other source areas, filled this trough, that ice floes formed almost immediately, and that either grounded ice or an ice-covered sea still persists. In either case, the thin (a few meters at most) high albedo, low thermal inertia cover of aeolian materials was instrumental in allowing ice preservation, and at least the lower portions of this dust cover may be cemented by water ice. Detailed mapping using Viking stereopairs and quantitative comparisons to terrestrial shelf ice geometries are underway. Derived from text

N94-12101*# Naturhistorisches Museum, Vienna (Austria).
MINERALOGY VERSUS BULK COMPOSITION OF THE CARBONACEOUS CHONDRITE CLAST KAIDUN 2 Abstract Only **c90**
F. Brandstaetter, G. Kurat, A. V. Ivanov (Academy of Sciences, USSR, Moscow.), H. Palme (Max-Planck-Inst. fuer Chemie, Mainz, Germany.), and B. Spettel (Max-Planck-Inst. fuer Chemie, Mainz, Germany.) *In* Lunar and Planetary Inst., Twenty-fourth Lunar and Planetary Science Conference. Part 1: A-F 1993 p 177-178 (For primary document see N94-12015 01-91)
Avail: CASI HC A01/MF A06

Kaidun is an unusual chondritic meteorite. Its main mass is of CR-type (Kaidun I) and contains CI-like (Kaidun II), EL, and EH clasts. The classification of Kaidun II based on mineralogy and bulk chemical criteria does not allow an unambigious assignment to CI. Here we report on the bulk chemical composition and the mineralogy of the Kaidun II clasts. The results of our investigation show that Kaidun II has some characteristics of both CI and CM chondrites. A possible relationship to the texture and composition of micrometeorites is indicated. The Kaidun II clast shows some conflicting mineralogical and chemical characteristics that do not allow an unambigious assignment to the well established carbonaceous chondrite classes. The overall texture of the matrix-rich clast and morphology of opaques are typical for CI's. Bulk matrix and bulk sample compositions reveal similarities with CM's. In addition, the presence of low-Fe Mn-enriched olivines and the relatively high abundance of enstatite resembles some micrometeorites. Derived from text

N94-12102*# Witwatersrand Univ., Johannesburg (South Africa). Dept. of Geology.
A STRUCTURAL AND PETROGRAPHIC INVESTIGATION OF THE PRETORIA SALTPAN IMPACT STRUCTURE Abstract Only **c46**
D. Brandt and W. U. Reimold *In* Lunar and Planetary Inst., Twenty-fourth Lunar and Planetary Science Conference. Part 1: A-F 1993 p 179-180 Sponsored in part by the Barringer Crater Co. (For primary document see N94-12015 01-91)
Avail: CASI HC A01/MF A06

The Pretoria Saltpan crater is located in the southern portion of the Bushveld Igneous Complex some 40 km NNW of Pretoria, South Africa, at 25 deg 24 min 30 sec S/28 deg 4 min 59 sec E. The near-circular structure of 1.13 km diameter exhibits a well-preserved, uptilted granite rim. Granitic breccia overlies Karroo sediment in places, indicating a post-Karroo age for the cratering event. The coincidence of the spacial occurrence of the crater with respect to various alkaline and ultramafic intrusives has been the main argument put for yard against an impact origin for the structure. Detailed mapping of the crater rim exposures and the crater environs was carried out and revealed many occurrences of intrusives in the whole region. Structural analysis along the rim revealed the presence of typical impact crater related structures. Comparative petrographic and chemical studies of crater-related and non-related intrusives showed close similarities between these sample suites. Derived from text

N94-12103*# Witwatersrand Univ., Johannesburg (South Africa). Dept. of Geology.

GEOPHYSICAL SIGNATURE OF THE PRETORIA SALTPAN IMPACT STRUCTURE AND A POSSIBLE SATELLITE CRATER Abstract Only c46

D. Brandt, R. J. Durrheim, and W. U. Reimold *In* Lunar and Planetary Inst., Twenty-fourth Lunar and Planetary Science Conference. Part 1: A-F 1993 p 181-182 Sponsored in part by the Barringer Crater Co. (For primary document see N94-12015 01-91)

Avail: CASI HC A01/MF A06

The Pretoria Saltpan Crater is located in the southern portion of the Bushveld Igneous Complex, some 40 km NNW of Pretoria, South Africa, at 25 deg 24 min 30 sec S/28 deg 4 min 59 sec E. An origin by impact for this crater structure was recently confirmed. The results of the only gravity reconnaissance carried out over the crater to date failed to support an impact origin. With the aid of recent results obtained from a central drill-core, it was necessary to carry out more geophysical work which would include a gravity profile of higher resolution. A second, smaller, circular depression (about 400 m in diameter) to the SW of the crater is suggestive of a twin crater. This site had never been investigated, and thus various geophysical surveys were conducted. Derived from text

N94-12104*# New Mexico Univ., Albuquerque. Dept. of Earth and Planetary Sciences.

CARBONACEOUS CHONDRITE CLASTS IN THE KAPOETA HOWARDITE Abstract Only c46

Adrian J. Brearley and J. J. Papike *In* Lunar and Planetary Inst., Twenty-fourth Lunar and Planetary Science Conference. Part 1: A-F 1993 p 183-184 (For primary document see N94-12015 01-91)

(Grant NAG9-497)

Avail: CASI HC A01/MF A06

A petrographic and mineralogical study of a number of carbonaceous chondrite clasts in the Kapoeta howardite has been carried out. Most of the clasts have mineralogical and chemical properties which link them to the CM carbonaceous chondrites. Some clasts contain chondrules which often have well-developed fine-grained rims, but many have been extensively brecciated. PCP-rich objects are common and pentlandite and pyrrhotite also occur. Calcite has also been found. The remainder of the clasts are extremely fine-grained and appear to be closely related to CI carbonaceous chondrites. In these clasts magnetite framboids are common and finegrained sulfides and magnetite occur disseminated throughout the matrix. Derived from text

N94-12105*# New Mexico Univ., Albuquerque. Dept. of Earth and Planetary Sciences.

CHONDRITE THERMAL HISTORIES FROM LOW-CA PYROXENE MICROSTRUCTURES: AUTOMETAMORPHISM VERSUS PROGRADE METAMORPHISM REVISITED Abstract Only c90

Adrian J. Brearley, Rhian H. Jones, and J. J. Papike *In* Lunar and Planetary Inst., Twenty-fourth Lunar and Planetary Science Conference. Part 1: A-F 1993 p 185-186 (For primary document see N94-12015 01-91)

(Grant NAG9-497)

Avail: CASI HC A01/MF A06

In order to constrain the thermal histories of chondritic meteorites, a detailed study of the microstructures of low-Ca pyroxenes produced experimentally and in types 4 and 5 ordinary chondrites was carried out. Cooling experiments on synthetic MgSiO3 at cooling rates between 2 and 10000 C/hr from the protopyroxene stability field into that of orthopyroxene (OPX) were performed and the products of these experiments were annealed for a variety of annealing times. There are clear microstructural differences between samples which were cooled and those which were subsequently annealed. A comparison of the microstructures observed in the experimental samples with those in H4-5 ordinary chondrites shows that they cannot have experienced a single stage cooling history, as proposed for the autometamorphism model. Author (revised)

N94-12106*# New Mexico Univ., Albuquerque. Dept. of Earth and Planetary Sciences.

SXRF DETERMINATION OF TRACE ELEMENTS IN CHONDRULE RIMS IN THE UNEQUILIBRATED CO3 CHONDRITE, ALH A77307 Abstract Only c90

Adrian J. Brearley, Sasa Bajt (Brookhaven National Lab., Upton, NY.), Steve R. Sutton (Brookhaven National Lab., Upton, NY.), and J. J. Papike *In* Lunar and Planetary Inst., Twenty-fourth Lunar and Planetary Science Conference. Part 1: A-F 1993 p 187-188 (For primary document see N94-12015 01-91)

(Grants NAG9-437; NAG9-106)

Avail: CASI HC A01/MF A06

The concentrations of Ni, Cu, Zn, Ga, Ge, and Se in five chondrule rims in the CO3 chondrite ALH A77307 (3.0) using the synchrotron x-ray fluorescence (SXRF) microprobe at Brookhaven National Laboratory were determined. The data show that the trace element chemistry of rims on different chondrules is remarkably similar, consistent with data obtained for the major elements by electron microprobe. These results support the idea that rims are not genetically related to individual chondrules, but all sampled the same reservoir of homogeneously mixed dust. Of the trace elements analyzed Zn and Ga show depletions relative to CI chondrite values, but in comparison with bulk CO chondrites all the elements are enriched by approximately 1.5 to 3.5 x CO. The high concentrations of the highly volatile elements Se and Ga and moderately volatile Zn (1.5 to 2 x CO) in rims show that matrix is the major reservoir of volatile elements in ALH A77307. Author (revised)

N94-12107*# Geological Survey, Menlo Park, CA.

MARTIAN PARTICLE SIZE BASED ON THERMAL INERTIA CORRECTED FOR ELEVATION-DEPENDENT ATMOSPHERIC PROPERTIES Abstract Only c90

N. T. Bridges *In* Lunar and Planetary Inst., Twenty-fourth Lunar and Planetary Science Conference. Part 1: A-F 1993 p 189-190 (For primary document see N94-12015 01-91)

Avail: CASI HC A01/MF A06

Thermal inertia is commonly used to derive physical properties of the Martian surface. If the surface is composed of loosely consolidated grains, then the thermal conductivity derived from the inertia can theoretically be used to compute the particle size. However, one persistent difficulty associated with the interpretation of thermal inertia and the derivation of particle size from it has been the degree to which atmospheric properties affect both the radiation balance at the surface and the gas conductivity. These factors vary with atmospheric pressure so that derived thermal inertias and particle sizes are a function of elevation. By utilizing currently available thermal models and laboratory information, a fine component thermal inertia map was convolved with digital topography to produce particle size maps of the Martian surface corrected for these elevation-dependent effects. Such an approach is especially applicable for the highest elevations on Mars, where atmospheric back radiation and gas conductivity are low. Author (revised)

N94-12108*# Open Univ., Milton (England). Planetary Sciences Unit.

MULTIPLE NITROGEN COMPONENTS IN LUNAR SOIL SAMPLE 12023 Abstract Only

D. R. Brilliant, I. A. Franchi, and C. T. Pillinger *In* Lunar and Planetary Inst., Twenty-fourth Lunar and Planetary Science Conference. Part 1: A-F 1993 p 191-192 (For primary document see N94-12015 01-91)

Avail: CASI HC A01/MF A06

Nitrogen is one of the enigmatic elements in lunar soils and breccias. The large range in (delta)N-15 values found within lunar soils was initially attributed to a secular increase in the N-15/N-14 ratio of 50 percent within the solar corona, and hence in the implanted nitrogen within the lunar regolith. However, more recent explanations have proposed a two (or many) component mixing model of solar wind nitrogen with some hypothetical non-solar components. Such components could include indigenous lunar nitrogen, nitrogen contained in interstellar grains in primitive meteorites, and magnetospheric nitrogen from the terrestrial atmosphere. To understand the makeup of multi-component mixtures it is advantageous to have carbon and noble gas data measured simultaneously, particularly in the case of lunar soils, where the solar wind is a likely fundamental contributor of nitrogen. To this end, a new nitrogen instrument was adapted to give some of the desired data in parallel. Conjoint measurements of N abundance and (delta)N-15 together with N/Ar-36 and Ar-36/Ar-38 ratios obtained during a stepped combustion of lunar soil 12023. The results are preliminary to a much more comprehensive investigation of well characterized fractions of the sample which we still have available from a previous study. Stepped combustion of a sample of 12023,7 yielded 94 ppm nitrogen with a (delta)N-15 = +22.2 percent, as well as the characteristic heavy-light-heavy pattern observed for lunar samples. The low temperature maximum was +75.1 percent at 550 C, the minimum at 800 C with (delta)N-15 = -16.7 percent and the high temperature (delta)N-15 peak is +90.6 percent at 1250 C. The major releases of nitrogen occurred between 650 C - 800 C in the form of a double peak; a third, substantial release occurred at 1150 C yielding 14.2 ppm of nitrogen coinciding with a small but recognizable drop in (delta)N-15 against a regularly increasing trend. Author (revised)

N94-12109*# Scripps Institution of Oceanography, La Jolla, CA.
A REEXAMINATION OF AMINO ACIDS IN LUNAR SOIL Abstract Only
K. L. F. Brinton, J. L. Bada, and J. R. Arnold (California Univ., San Diego, La Jolla.) *In* Lunar and Planetary Inst., Twenty-fourth Lunar and Planetary Science Conference. Part 1: A-F 1993 p 193-194 (For primary document see N94-12015 01-91)
Avail: CASI HC A01/MF A06

Amino acids in lunar soils provide an important indicator of the level of prebiotic organic compounds on the moon. The results provide insight into the chemistry of amino acid precursors, and furthermore, given the flux of carbonaceous material to the moon, we can evaluate the survival of organics upon impact. The amino acid contents of both hydrolyzed and unhydrolyzed hot-water extracts of Apollo 17 lunar soil were determined using ophthaldialdehyde/N-acetyl cysteine (OPA/NAC) derivatization followed by HPLC analysis. Previous studies of lunar amino acids were inconclusive, as the technique used (derivatization with ninhydrin followed by HPLC analysis) was unable to discriminate between cosmogenic amino acids and terrestrial contaminants. Cosmogenic amino acids are racemic, and many of the amino acids found in carbonaceous meteorites such as Murchison, i.e., alpha-amino-i-butyric acid (aib), are extremely rare on Earth. The ninhydrin method does not distinguish amino acid enantiomers, nor does it detect alpha-alkyl amino acids such as aib, whereas the OPA/NAC technique does both. Author (revised)

N94-12110*# Arizona Univ., Tucson. Lunar and Planetary Lab.
THE SPECTRAL EFFECTS OF SUBSOLIDUS REDUCTION OF OLIVINE AND PYROXENE Abstract Only **c25**
D. T. Britt *In* Lunar and Planetary Inst., Twenty-fourth Lunar and Planetary Science Conference. Part 1: A-F 1993 p 195-196 (For primary document see N94-12015 01-91)
Avail: CASI HC A01/MF A06

The surfaces of atmosphereless bodies are subjected to a variety of chemical, thermal, accretionary, and shock processes related to their regolith environment. These processes are responsible for a number of alterations that occur in regoliths. Alterations include particle size commutation, implantation of solar wind gases, formation of agglutinates, spectral darkening, and, in the lunar case, the development of the very strong red continuum slope in the visible and near infrared spectra. A great deal of work has pointed to the role of agglutinates as the principal agent for darkening and reddening the lunar soil. The measures of regolith maturity are strongly linked to the accumulation of agglutinates. Recent work has suggested that the finest fractions of agglutinitic glass are major source of the spectral red slope. In particular, the red slope is most strongly associated with the agglutinitic glasses that are rich in blebs of sub-micron sized metal particles. It is thought that these metal particles, because of their size and scattering efficiently relative to the wavelength of light, are responsible for the red continuum slope. This fine fraction of metal particles is produced primarily by reduction of Fe(+2) from silicates. One mechanism for the reduction process is the reaction of solar implanted wind protons with the regolith soil during impact events. In this case the presence of hydrogen creates a reducing environment and the thermal pulse from the impact greatly speeds the reaction kinetics. To explore other reducing and thermal environments a series of experiments were done using samples in evacuated capsules buffered by Tantalum and heated to subsolidus temperatures. Author (revised)

N94-12111*# Arizona Univ., Tucson. Lunar and Planetary Lab.
THE 1.2 TO 3.5 MICRONS OBSERVATIONS OF ASTEROID 4179 TOUTATIS Abstract Only **c90**
D. T. Britt, E. S. Howell, J. F. Bell (Hawaii Univ., Honolulu.), and L. A. Lebofsky *In* Lunar and Planetary Inst., Twenty-fourth Lunar and Planetary Science Conference. Part 1: A-F 1993 p 197 (For primary document see N94-12015 01-91)
Avail: CASI HC A01/MF A06

The close Earth approach of the Apollo asteroid 4179 Toutatis during the winter of 1992-1993 provided a unique opportunity for detailed ground-based observations of a near earth asteroid (NEA). Because of their relatively small size NEA's are usually far too faint to be observable by most ground-based instruments. This opposition by Toutatis was, however, exceptionally favorable. Toutatis approached within 0.03 AU of Earth and was as bright as 11th visual magnitude. This made the object observable in a wide variety of wavelengths including radar, thermal IR, near IR, and visual. Author (revised)

N94-12112*# Arizona State Univ., Tempe. Dept. of Geology.
FLEXURE AND THE ROLE OF INPLANE FORCE AROUND CORONAE ON VENUS Abstract Only
C. David Brown and Robert E. Grimm *In* Lunar and Planetary Inst., Twenty-fourth Lunar and Planetary Science Conference. Part 1: A-F 1993 p 199-200 (For primary document see N94-12015 01-91)
Avail: CASI HC A01/MF A06

Large coronae on Venus, such as Artemis and Latona, are rimmed by conspicuous trenches and associated outer rises. Sandwell and Schubert have observed that these systems resemble terrestrial subduction zones in planform and have succeeded in fitting an elastic plate bending equation to the inferred flexural topography. However, the first zero crossing bending moments required are -2.5 x 10(exp 17) N for Artemis and -5.0 x 10(exp 16) N for Latona. Since these moments are similar in magnitude to those of subducting slabs on Earth, a rollback subduction mechanism was proposed to explain the flexure around the largest coronae, although a differential thermal subsidence model is sufficient to account for the topography around some coronae. The purpose is to investigate the effect of inplane force as a possible alternative to large applied moments in producing flexure at Artemis and Latona. The close correlation of gravity to topography on Venus implies the absence of a low viscosity zone and the strong coupling of the lithosphere to mantle convection. If coronae are the surface manifestations of mantle plumes, they may be the sites of active convective stress coupling. As the upwelling reaches the lithosphere, it spreads radially outward, inducing shear tractions on the base of the plate. In addition, the hot, expanding corona may load the surrounding plate horizonally. Both the basal shear stresses and radial loading can be treated as an equivalent compressive inplane force in the mechanical lithosphere, which contributes to the bending of the outlying plate. Using a model that relates inplane force to the measured gravity anomalies, a rough value of the inplane force at Artemis was calculated. Recent Pioneer Venus spherical harmonic gravity models indicate a geoid anomaly of about 75 m over Artemis, which corresponds to an estimated inplane force on the order of -1x10(exp 13) N/m. The gravity model is unable to resolve Latona, but an inplane force of similar dimensions is assumed. The maximum possible inplane force based on the expected rheology can be constrained by using the approximate 5 K/km thermal gradient inferred from the best fit 30 km elastic plate at Artemis and Latona. For a dry olivine flow law in the upper mantle, the compressional load limit of the 60 km thick mechanical lithosphere is -4 x 10(exp 13) N/m. This value is equivalent to a load of -8 x 10(exp 13) N/m on a 30 km thick elastic plate. Author (revised)

N94-12113*# Arizona State Univ., Tempe. Dept. of Geology.
VISCOUS RELAXATION OF THE MOHO UNDER LARGE LUNAR BASINS Abstract Only
C. David Brown and Robert E. Grimm *In* Lunar and Planetary Inst., Twenty-fourth Lunar and Planetary Science Conference. Part 1: A-F 1993 p 201-202 (For primary document see N94-12015 01-91)
Avail: CASI HC A01/MF A06

Viscously relaxed topography on the Moon is evidence of a period in lunar history of higher internal temperatures and greater surface activity. Previous work has demonstrated the viscous relaxation of the Tranquilitatis basin surface. Profiles of the lunar Moho under nine basins were constructed from an inversion of lunar gravity data. These profiles show a pattern of increasingly subdued relief with age, for which two explanations have been proposed. First, ancient basins may have initially had extreme Moho relief like that of younger basins like Orientale, but, due to higher internal temperatures in early lunar history, this relief viscously relaxed to that observed today. Second, ductile flow in the crust immediately after basin formation resulted in an initially shallow basin and subdued mantle uplift. The intent is to test the first hypothesis. Author (revised)

N94-12114*# Tennessee Univ., Knoxville. Dept. of Geological Sciences.
DETERMINING THE RELATIVE EXTENT OF ALTERATION IN CM CHONDRITES Abstract Only c90
Lauren B. Browning, Harry Y. McSween, Jr., and Michael Zolensky (National Aeronautics and Space Administration. Lyndon B. Johnson Space Center, Houston, TX.) *In* Lunar and Planetary Inst., Twenty-fourth Lunar and Planetary Science Conference. Part 1: A-F 1993 p 203-204 (For primary document see N94-12015 01-91)
Avail: CASI HC A01/MF A06

The aqueous alteration of CM chondrites provides a record of the processes attending the earliest stages of parent body evolution. However, resolving the alteration pathways of chondritic evolution requires a means for distinguishing the relative extent of alteration that individual samples have experienced. Three new indices for gauging the relative degree of alteration in CM chondrites based on modal and compositional analyses of 7 CM falls were proposed. The proposed alteration parameters are consistent with the basic tenets of several previous models and correlate with additional indices to produce an integrated method for determining the relative extent of alteration. The model predicts the following order of progressive alteration: Murchison (MC) is less than or equal to Bells (BL) is less than Murray (MY) is less than Cochabamba (CC) is less than Mighei (MI) is less than Nogoya (NG) is less than or equal to Cold Bokkeveld (CB). The broad range of CM phyllosilicate compositions observed within individual meteorites is fundamental to the characterization of the aqueous alteration process. Chemical analyses of CM phyllosilicates suggest that these phases became systematically enriched in Mg and depleted in Fe with increasing alteration. Author (revised)

N94-12115*# Washington Univ., Seattle. Dept. of Astronomy.
IDENTIFICATION OF COMETARY AND ASTEROIDAL PARTICLES IN STRATOSPHERIC IDP COLLECTIONS Abstract Only c90
D. E. Brownlee, D. J. Joswiak, S. G. Love, A. O. Nier (Minnesota Univ., Minneapolis.), D. J. Schlutter (Minnesota Univ., Minneapolis.), and J. P. Bradley (MVA, Inc., Norcross, GA.) *In* Lunar and Planetary Inst., Twenty-fourth Lunar and Planetary Science Conference. Part 1: A-F 1993 p 205-206 (For primary document see N94-12015 01-91)
Avail: CASI HC A01/MF A06

He release temperature curves were determined for a specially processed set of 5 microns to 15 microns stratospheric IDP's whose masses, densities, and compositions were accurately measured. The He release temperature in combination with atmospheric entry calculations yields a most probable entry velocity for each particle and association with either an asteroidal (low velocity) or cometary (high velocity) origin. It was found that over half of the 5-15 microns IDP's have entry velocities consistent with asteroidal origin and that at least 20 percent have cometary origins. A few of the asteroidal particles are porous aggregates and it appears that there may be close material similarities among some primitive asteroids and comets. In the processing of individual 5 microns IDP's and determination of entry velocities, a few dozen microtome slices that can be used for a variety of detailed TEM, IR, and ion probe studies were preserved. These procedures provide laboratory samples that can be generically associated with asteroids and comets and are in a sense a limited sample return mission from these primitive bodies. Author (revised)

N94-12116*# Hawaii Univ., Honolulu. Dept. of Geology and Geophysics.
QUANTIFYING THE EFFECT OF RHEOLOGY ON PLAN-VIEW SHAPES OF LAVA FLOWS Abstract Only c46
B. C. Bruno, G. J. Taylor, and R. M. C. Lopes-Gautier (Jet Propulsion Lab., California Inst. of Tech., Pasadena.) *In* Lunar and Planetary Inst., Twenty-fourth Lunar and Planetary Science Conference. Part 1: A-F 1993 p 207-208 (For primary document see N94-12015 01-91)
Avail: CASI HC A01/MF A06

This study aims at quantifying the effect of rheology on the plan-view shapes of lava flows. Plan-view shapes of lava flows are important because they reflect the processes governing flow emplacement and may provide insight into lava flow rheology and dynamics. In our earlier investigation, it was reported that plan-view shapes of tholeite basalts are fractal, having a characteristic shape regardless of scale. It was also found one could use the fractal dimension (a parameter which quantifies flow margin convolution) to distinguish between the two major types of basalts: a'a and pahoehoe. Encouraged by these earlier results, a similar method for use on silicic flows are being developed and our preliminary work is presented. Author (revised)

N94-12117*# Houston Univ., TX. Dept. of Geosciences.
THE EET87513 CLAST N: A CM2 FRAGMENT IN AN HED POLYMICT BRECCIA Abstract Only
P. C. Buchanan, M. E. Zolensky (National Aeronautics and Space Administration. Lyndon B. Johnson Space Center, Houston, TX.), A. M. Reid, and R. A. Barrett (Lockheed Engineering and Sciences Co., Houston, TX.) *In* Lunar and Planetary Inst., Twenty-fourth Lunar and Planetary Science Conference. Part 1: A-F 1993 p 209-210 (For primary document see N94-12015 01-91)
Avail: CASI HC A01/MF A06

Xenoliths of material resembling carbonaceous chondrites have been found in several HED polymict breccias. Most workers concluded that these clasts are related to CM2 meteorites on the basis of texture, bulk composition, and mineralogy. Data on clast N, a carbonaceous chondrite fragment from the howardite EET87513 large enough (approximately 4x5mm on the surface of the slab from which it was separated) to extract bulk samples for INAA and oxygen isotope analysis and to provide a thin section for electron microprobe, SEM, and TEM analysis is reported. Preliminary data for this clast were previously reported. INAA was performed at Oregon State University and bulk oxygen isotopic composition was determined at the University of Chicago. These data confirm that EET87513 clast N is a fragment of CM2 material. Author (revised)

N94-12118*# Columbia Univ., Palisades, NY. Dept. of Geological Sciences.
CAN WEAK CRUST EXPLAIN THE CORRELATION OF GEOID AND TOPOGRAPHY ON VENUS? Abstract Only
W. Roger Buck (Iceland Univ., Reykjavik.) *In* Lunar and Planetary Inst., Twenty-fourth Lunar and Planetary Science Conference. Part 1: A-F 1993 p 211-212 (For primary document see N94-12015 01-91)
Avail: CASI HC A01/MF A06

The effect on geoid and topography of low viscosity crust overlying a steady-state convecting mantle is estimated under the assumption that the shear between crust and mantle does not alter the mantle flow. The weak crustal layer can change the sign of the geoid to topography ratio (admittance). The positive long wavelength admittance for Venus is consistent with a weak crust overlying a mantle with a viscosity that increases strongly with depth. The accepted interpretation of the strong positive correlation of geoid and topography on Venus, is that the convecting mantle of Venus has a constant viscosity with depth. Topography results from vertical normal stresses caused by mantle convection and highlands occur where mantle upwells. For topography to be supported by normal stress, the time scale for crustal flow must be long compared to the time scale for changes in the pattern of mantle flow. Because the high surface temperature of Venus may cause the crust to have a low viscosity, this assumption may be false. Topography should then be dominated by shear coupling between the crust and mantle. In the absence of a crustal layer, convection in a constant viscosity layer gives rise to a geoid anomaly that correlates positively with surface topography. When the viscosity in the layer increases with depth by several orders of magnitude, the surface topography and geoid anomaly become anti-correlated. Author (revised)

N94-12119*# Colorado Univ., Boulder. Lab. for Atmospheric and Space Physics.
VENUS RESURFACING RATES: CONSTRAINTS PROVIDED BY 3-D MONTE CARLO SIMULATIONS Abstract Only
M. A. Bullock, D. H. Grinspoon, and J. W. Head (Brown Univ., Providence, RI.) *In* Lunar and Planetary Inst., Twenty-fourth Lunar and Planetary Science Conference. Part 1: A-F 1993 p 213-214 (For primary document see N94-12015 01-91)
Avail: CASI HC A01/MF A06

A 3-D Monte Carlo model that simulates the evolving surface of Venus under the influence of a flux of impacting objects and a variety of styles of volcanic resurfacing was implemented. For given rates of impact events and resurfacing, the model predicts the size-frequency and areal distributions of surviving impact craters as a function of time. The number of craters partially modified by volcanic events is also calculated as the surface evolves. It was found that a constant, global resurfacing rate of approximately 0.4 km(sup 3)/yr is required to explain the observed distributions of both the entire crater population, and the population of craters partially modified by volcanic processes. Author (revised)

N94-12120*# London Univ. Observatory (England).
SCALLOPED MARGIN DOMES: WHAT ARE THE PROCESSES RESPONSIBLE AND HOW DO THEY OPERATE?
M. H. Bulmer, J. E. Guest, G. Michaels (Jet Propulsion Lab., California Inst. of Tech., Pasadena.), and S. Saunders (Jet Propulsion Lab., California Inst. of Tech., Pasadena.) *In* Lunar and Planetary Inst., Twenty-fourth Lunar and Planetary Science Conference. Part 1: A-F 1993 p 215-216 (For primary document see N94-12015 01-91)
Avail: CASI HC A01/MF A06

Studies of scalloped margin domes (SMD) indicate the scallops are the result of slope failure. SMD's have similar but smaller average diameters (26.5 km) to unmodified domes (29.8 km), and the majority plot at altitudes ranging from 0.5-4.7 km, relative to the mean planetary diameter. A range of morphological types exist from those least modified to those that show heavy modification. Of the 200 SMD's examined, 33 have clearly discernible debris aprons. Examination and comparison of debris aprons with mass movement features on the Moon, Mars, and in sub-aerial and submarine environments on Earth using H/L against area (km(sup 2)), suggests there are three main types of failure; debris avalanche, slumps, and debris flow. The five examples representing the morphological range within the SMD's, show the different modified forms and the different types of slope failures that have occurred. Author (revised)

N94-12121*# Academy of Sciences (USSR), Moscow.
YANA RING STRUCTURE, NORTH-EASTERN SIBERIA: A POSSIBLE COUNTERPART OF CORONAE ON VENUS Abstert Only **c46**
G. A. Burba *In* Lunar and Planetary Inst., Twenty-fourth Lunar and Planetary Science Conference. Part 1: A-F 1993 p 217-218 (For primary document see N94-12015 01-91)
Avail: CASI HC A01/MF A06

An arch of Verkhoyansky Range in NE Siberia, Russia is considered as W and S parts of the rim of the large ring structure, referred hereafter as Yana Ring Structure (YRS). It has general appearance similar to coronae on Venus and could be considered as the terrestrial counter part of coronae. The structure is located between 63 and 70 deg N, 125 and 140 deg E. The outer diameter of YRS (between the rim feet) is 680-700 km. The rim crest diameter is 500-520 km. The inner diameters (between the inner feet of the rim) is 320-350 km. The rim of YRS consist of the following topographic features: W segment is Orulgan Range (N part of Verkhoyansky Range), SW and S segments consist of S part of Verkhoyansky Range, SE segment is Elginskoye Ploskogorye (Tableland), E segment is Chersky Range (its part W of Indigirka River), NE segment is Selennyakhsky Range, and NW segment is Kular Range. Inside this ring of mountains Yanskoye Ploskogorye (Tableland) is located. The circular outlines of YRS are marked with the large river valleys located outside: Lena River (lower of Aldan River mouth) is located W from YRS, Aldan River (lower of Amga River mouth) is from S, Indigirka River (between 64 and 67 deg N lat) is from E, and Selennyakh River (the part running N to S) is from NE. The ring patterns inside the mountaineous rim of YRS are marked with the tributaries of Yana River. The largest ring here, 300 km in diameter, consists of Bytangay (with Bellyakh) River at W, Nelgese and Derbeke Rivers at S/SE, and Tuostakh River at E. The typical altitudes of YRS mountain rim are 1000-2000 m. The maximal ones are: 2400 m in W part of the rim, 2300 m in S, 1600 m in SE, 2200-2500 m in E, and 1300-1500 m in N. The central part of YRS have typical altitudes of 400-600 m. There are lowlands with altitudes 50-200 m to the S, W, N, and NW outside YRS Oymyakonskoye Nagorye (Highland) is located SE of YRS at 500-1500 m altitudes. It should be recognized from this description YRS have a general appearance of circular highland with its central plateau located 1000-2000 m lower than surrounding mountain rim, but 300-400 m higher than plains of lowlands located outside the rim. Such topographic patterns are typical for coronae on Venus. The diameter of YRS is equal to the largest coronae on Venus. There are only 3 or 4 structures of such or larger size on the whole Venus. This calls to compare morphology and geologic evolution of YRS with morphology and models of coronae evolutions especially the largest ones, to search the similarities and/or differences in geologic histories of the structures on the Earth and Venus. Author (revised)

N94-12122*# Academy of Sciences (USSR), Moscow.
RUSSIA'S CONTRIBUTION TO REGIONAL GEOLOGIC MAPPING OF VENUS Progress Report, 1992 Abstract Only
G. A. Burba, N. N. Bobina, and V. P. Shashkina *In* Lunar and Planetary Inst., Twenty-fourth Lunar and Planetary Science Conference. Part 1: A-F 1993 p 219-220 (For primary document see N94-12015 01-91)
Avail: CASI HC A01/MF A06

Geologic maps in Magellan C1-format were produced by six geologists and three cartographer in Russia during 1992. More sheets are in progress. The work is coordinated by Vernadsky Institute. The Magellan SRR images in form of C1-format photomaps were used as a base for geologic-geomorphic regional mapping of Venus at approximately 1:8,000,000 scale. This work took place in Russia at Vernadsky Institute and at the Department of Geology, Lomonosov Moscow University. The aim is to produce a preliminary geologic survey of Venus with the new high resolution images obtained by Magellan. It took place at the cartographic division, Laboratory of Comparative Planetology and Meteoritics, Vernadsky Institute, Russsia's Academy of Sciences. Author (revised)

N94-12123*# Academy of Sciences (USSR), Moscow. Geographical Dept.
LANDSCAPE AND GEOMORPHIC SURVEY OF ZHAMANSHIN AREA, NORTHERN KAZAKHSTAN: PRELIMINARY REPORT ON 1992 FIELD TRIP DATA **c46**
G. G. Burba, Jr. and V. A. Meshcherskaya *In* Lunar and Planetary Inst., Twenty-fourth Lunar and Planetary Science Conference. Part 1: A-F 1993 p 221-222 (For primary document see N94-12015 01-91)
Avail: CASI HC A01/MF A06

The June 1992 geographical expedition to Zhamanshin crater area made a landscape and geomorphic survey of this impact structure. Observational points in the area of 300 sq km give new data on the geographical processes in the impact crater. The data obtained could be applied to search for unknown impact structures anywhere through the traces of such features in landscapes. Author (revised)

N94-12124*# Smithsonian Astrophysical Observatory, Cambridge, MA.
HOW DIVERSE IS THE ASTEROID BELT? Abstract Only **c90**
Thomas H. Burbine and Jeffrey F. Bell (Hawaii Univ., Honolulu.) *In* Lunar and Planetary Inst., Twenty-fourth Lunar and Planetary Science Conference. Part 1: A-F 1993 p 223-224 (For primary document see N94-12015 01-91)
Avail: CASI HC A01/MF A06

For approximately twenty years, many different asteroid taxonomies, which used many different observational data sets, have been developed to try to group asteroids into classes that contain members with similar spectral characteristics. However, to understand the structure of the asteroid belt, the resulting classes are only useful if they are grouping together asteroids with somewhat similar mineralogies and thermal histories. Until recently, these taxonomies have focused on spectral reflectance data from 0.3 to 1.1 microns and visual albedo. But in the last five years, observational data sets (e.g., 0.8 to 2.5 microns spectra, CCD spectra, 3 microns spectra, and radar albedos) for a small number of asteroids were compiled that can give a better mineralogical interpretation, but whose use in asteroid taxonomy was relatively limited. Analyses of these 'supplementary' data sets show that most asteroid classes contain members with different compositions and/or thermal histories. To understand the diversity of the asteroid belt, the number of objects with these observations must be expanded and used in the next generation of taxonomies. Author (revised)

N94-12125*# Arizona Univ., Tucson. Lunar and Planetary Lab.
STUDIES OF THE RELEASE OF RADIOGENIC Xe-129 FROM BJURBOELE: EVIDENCE AGAINST SIMPLE DIFFUSION MODELS Abstract Only **c90**
M. K. Burkland, T. D. Swindle, and S. L. Baldwin *In* Lunar and Planetary

Inst., Twenty-fourth Lunar and Planetary Science Conference. Part 1: A-F 1993 p 225-226 (For primary document see N94-12015 01-91)
Avail: CASI HC A01/MF A06

The I-Xe system, based on the decay of 15.7 Ma I-129, is a potentially precise chronometer of early solar system events. However, it is not known how the system responded to thermal events during the post-formation histories of ordinary chondrites, severely limiting the usefulness of this system. Isothermal experiments on Bjurbole for different heating durations suggest that at least three domains are responsible for the thermal release of radiogenic Xe-129 (Xe*-129) and that the system may be less susceptible to thermal resetting than some calculations indicated. Two scenarios for the release of Xe*-129 were proposed. In one, the mobility of Xe*-129 is governed by diffusion in mineral grains. This leads to predicted closure temperatures comparable to, or less than, metamorphic temperatures. In the second, mineral grains that solidified at specific temperatures trapped I-129 within them, and the resulting Xe*-129 is only released when those minerals melt, such that isotopic closure occurs at the temperature of solidification. Author (revised)

N94-12126*# Jet Propulsion Lab., California Inst. of Tech., Pasadena.
A PATTERN RECOGNITION SYSTEM FOR LOCATING SMALL VOLVANOES IN MAGELLAN SAR IMAGES OF VENUS Abstract Only
M. C. Burl, U. M. Fayyad, P. Smyth, J. C. Aubele (Brown Univ., Providence, RI.), and L. S. Crumpler (Brown Univ., Providence, RI.) *In* Lunar and Planetary Inst., Twenty-fourth Lunar and Planetary Science Conference. Part 1: A-F 1993 p 227-228 (For primary document see N94-12015 01-91)
Avail: CASI HC A01/MF A06

The Magellan data set constitutes an example of the large volumes of data that today's instruments can collect, providing more detail of Venus than was previously available from Pioneer Venus, Venera 15/16, or ground-based radar observations put together. However, data analysis technology has not kept pace with data collection and storage technology. Due to the sheer size of the data, complete and comprehensive scientific analysis of such large volumes of image data is no longer feasible without the use of computational aids. Our progress towards developing a pattern recognition system for aiding in the detection and cataloging of small-scale natural features in large collections of images is reported. Combining classical image processing, machine learning, and a graphical user interface, the detection of the 'small-shield' volcanoes (less than 15km in diameter) that constitute the most abundant visible geologic feature in the more that 30,000 synthetic aperture radar (SAR) images of the surface of Venus are initially targeted. Our eventual goal is to provide a general, trainable tool for locating small-scale features where scientists specify what to look for simply by providing examples and attributes of interest to measure. This contrasts with the traditional approach of developing problem specific programs for detecting Specific patterns. The approach and initial results in the specific context of locating small volcanoes is reported. It is estimated, based on extrapolating from previous studies and knowledge of the underlying geologic processes, that there should be on the order of 10(exp 5) to 10(exp 6) of these volcanoes visible in the Magellan data. Identifying and studying these volcanoes is fundamental to a proper understanding of the geologic evolution of Venus. However, locating and parameterizing them in a manual manner is forbiddingly time-consuming. Hence, the development of techniques to partially automate this task were undertaken. The primary constraints for this particular problem are that the method must be reasonably robust and fast. Unlike most geological features, the small volcanoes of Venus can be ascribed to a basic process that produces features with a short list of readily defined characteristics differing significantly from other surface features on Venus. For pattern recognition purposes the relevant criteria include (1) a circular planimetric outline, (2) known diameter frequency distribution from preliminary studies, (3) a limited number of basic morphological shapes, and (4) the common occurrence of a single, circular summit pit at the center of the edifice. Author (revised)

N94-12127*# University of Southern California, Pasadena. Geological and Planetary Sciences.
SOURCES OF Na FOR THE Io ATMOSPHERE Abstract Only
D. S. Burnett, Susan B. Ellis, A. Rice, and S. Epstein *In* Lunar and Planetary Inst., Twenty-fourth Lunar and Planetary Science Conference. Part 1: A-F 1993 p 229-230 (For primary document see N94-12015 01-91)
Avail: CASI HC A01/MF A06

The physics and geology of Io have been extensively studied, but there has been little discussion of the chemistry. Relatively little is known about Io chemistry, but there are constraints. Further, it will be a long time before improvements will result from direct observation, given the severe difficulties with the Galileo mission. Via laboratory simulation experiments, plausible thermochemical and photochemical processes which determine the nature and amounts of surface constituents of Io are explored. The well-known density of Io shows that the planet overall is rocky. Because the orbit of Io is well within the magnetosphere of Jupiter and because Io only has a thin, transient SO2 atmosphere, the surface is continually sputtered with magnetospheric ions. Complex processes ionize and accelerate the Io surface atoms to keV and MeV energies. Remarkably, only S, O, and Na ions were found by Voyager. Sputtering also produces an atomic cloud of Na and S (O not observable) with a trace of K. Both gaseous and solid SO2 are known from spectroscopic studies. A trace of H2S and possibly CO2 are present. Geologic features are interpreted in terms of elemental S, but there is no direct evidence for this constituent. We thus have a rocky planet which does not have rocks on the surface. Our general goal is to understand the cycling of Na, S, and O through the crust and atmosphere on present-day Io and to understand how Io evolved to this state. A specific objective was to determine the phases on the surface which are the source of the Na in the atmosphere of Io.
Author (revised)

N94-12128*# Massachusetts Inst. of Tech., Cambridge. Dept. of Earth, Atmospheric and Planetary Sciences.
CHEMICAL WEATHERING ON MARS: RATE OF OXIDATION OF IRON DISSOLVED IN BRINES Abstract Only
Roger G. Burns *In* Lunar and Planetary Inst., Twenty-fourth Lunar and Planetary Science Conference. Part 1: A-F 1993 p 231-232 (For primary document see N94-12015 01-91)
Avail: CASI HC A01/MF A06

Salts believed to occur in Martian regolith imply that brines occur on Mars, which may have facilitated the oxidation of dissolved Fe(2+) ions after they were released during chemical weathering of basaltic ferromagnesian silicate and iron sulfide minerals. Calculations show that the rate of oxidation of Fe(2+) ions at -35 C in a 6M chloride-sulfate brine that might exist on Mars is about 10(exp 6) times slower that the oxidation rate of iron in ice-cold terrestrial seawater. Author (revised)

N94-12129*# Massachusetts Inst. of Tech., Cambridge. Dept. of Earth, Atmospheric and Planetary Sciences.
VENUS MOUNTAIN-TOP MINERALOGY: MISCONCEPTIONS ABOUT PYRITE AS THE HIGH RADAR-REFLECTING PHASE Abstract Only
Roger G. Burns and DArcy W. Straub *In* Lunar and Planetary Inst., Twenty-fourth Lunar and Planetary Science Conference. Part 1: A-F 1993 p 233-234 (For primary document see N94-12015 01-91)
Avail: CASI HC A01/MF A06

Altitude-dependent, high radar-reflectivity surfaces on Venus are observed on most mountainous volcanic terranes above a planetary radius of about 6054 km. However, high radar-reflectivity areas also occur at lower altitudes in some impact craters and plain terranes. Pyrite (FeS2) is commonly believed to be responsible for the high radar reflectivities at high elevations on Venus, on account of large dielectric constants measured for sulfide-bearing rocks that were erroneously attributed to pyrite instead of pyrrhotite. Pentlandite-pyrrhotite assemblages may be responsible for high reflectivities associated with impact craters on the Venusian surface, by analogy with Fe-Ni sulfide deposits occurring in terrestrial astroblemes. Mixed-valence Fe(2+)-Fe(3+) silicates, including oxyhornblende, oxybiotite, and ilvaite, may contribute to high radar reflecting surfaces on mountain-tops of Venus. Author (revised)

N94-12130*# Brown Univ., Providence, RI. Dept. of Geological Sciences.
BUOYANT SUBDUCTION ON VENUS: IMPLICATIONS FOR SUBDUCTION AROUND CORONAE Abstract Only
J. D. Burt and J. W. Head *In* Lunar and Planetary Inst., Twenty-fourth Lunar and Planetary Science Conference. Part 1: A-F 1993 p 235-236 (For primary document see N94-12015 01-91)
Avail: CASI HC A01/MF A06

Potentially low lithospheric densities, caused by high Venus surface and perhaps mantle temperatures, could inhibit the development of negative buoyancy-driven subduction and a global system of plate tectonics/crustal recycling on that planet. No evidence for a global plate tectonic system was found so far, however, specific features strongly resembling terrestrial subduction zones in planform and topographic cross-section were described, including trenches around large coronae and chasmata in eastern Aphrodite Terra. The cause for the absence, or an altered expression, of plate tectonics on Venus remains to be found. Slab buoyancy may play a role in this difference, with higher lithospheric temperatures and a tendency toward positive buoyancy acting to oppose the descent of slabs and favoring under thrusting instead. The effect of slab buoyancy on subduction was explored and the conditions which would lead to under thrusting versus those allowing the formation of trenches and self-perpetuating subduction were defined. Applying a finite element code to assess the effects of buoyant forces on slabs subducting into a viscous mantle, it was found that mantle flow induced by horizontal motion of the convergent lithosphere greatly influences subduction angle, while buoyancy forces produce a lesser effect. Induced mantle flow tends to decrease subduction angle to near an under thrusting position when the subducting lithosphere converges on a stationary overriding lithosphere. When the overriding lithosphere is in motion, as in the case of an expanding corona, subduction angles are expected to increase. An initial stage involved estimating the changes in slab buoyancy due to slab healing and pressurization over the course of subduction. Modeling a slab, descending at a fixed angle and heated by conduction, radioactivity, and the heat released in phase changes, slab material density changes due to changing temperature, phase, and pressure were derived.
Author (revised)

N94-12131*# London Univ. Observatory (England).
THE ORIGIN OF VENUSIAN CHANNELS: MODELLING OF THERMAL EROSION BY LAVA Abstract Only
D. B. J. Bussey, S-A. Sorensen, and J. E. Guest *In* Lunar and Planetary Inst., Twenty-fourth Lunar and Planetary Science Conference. Part 1: A-F 1993 p 237-238 (For primary document see N94-12015 01-91)
Avail: CASI HC A01/MF A06

Magellan imagery has revealed that channels, apparently volcanic in origin, are abundant on the surface of Venus. There has been much debate about the origin of these channels. Are they the result of erosional (either thermal or mechanical) or constructional processes? A common characteristic of the simple sinuous channels is that they show evidence of erosion near their source and then become purely constructional, forming levees and in some cases roofing over completely. One method of showing that thermal erosion is capable of producing the type of channels seen is to use computer modeling incorporating the physical conditions on Venus and the physical characteristics of the different types of lava that may have been erupted. It is possible to calculate, relatively easily, two channel parameters. The first is the erosion rate, which combined with eruption duration, gives depth. The second is for how long after leaving the source the erupted lava will continue to be capable of thermal erosion before constructional processes dominate. Making assumptions about the rheology of the lava (e.g., assume it behaves as a Bingham plastic) along with the slope angle yields a flow velocity and therefore a distance over which thermal erosion will take place. Due to the resolution (both vertical and horizontal) of the Magellan altimetric data, the distance from the source that the channel is erosional can be much more accurately measured than the depth of the channel. This will remain the case until stereo imagery becomes available for large areas of the planet. Author (revised)

N94-12132*# Arkansas Coll., Batesville. Dept. of Chemistry.
VOLATILES IN FOURTEEN INTERPLANETARY DUST PARTICLES: A COMPARISON WITH CI AND CM CHONDRITES Abstract Only c90
R. Bustin, E. K. Gibson, Jr. (National Aeronautics and Space Administration. Lyndon B. Johnson Space Center, Houston, TX.), and S. J. Wentworth (National Aeronautics and Space Administration. Lyndon B. Johnson Space Center, Houston, TX.) *In* Lunar and Planetary Inst., Twenty-fourth Lunar and Planetary Science Conference. Part 1: A-F 1993 p 239-240 (For primary document see N94-12015 01-91)
Avail: CASI HC A01/MF A06

In an attempt to classify the nature of volatiles within interplanetary dust particles (IDP's), 14 IDP's using a laser microprobe/mass spectrometer (LM/MS) technique were studied. Volatile abundances and distributions found for the IDP's are compared with those measured for carbonaceous chondrites in order to determine if the IDP's are related to the parent bodies of these primitive meteorites. Author (revised)

N94-12133*# Observatoire de Paris-Meudon (France).
AN ANCIENT INNER LAKE IN MAADIM VALLIS Abstract Only
N. A. Cabrol, E. A. Grin, A. Dollfus, and G. Dawidowicz (Paris Univ., France.) *In* Lunar and Planetary Inst., Twenty-fourth Lunar and Planetary Science Conference. Part 1: A-F 1993 p 241-242 (For primary document see N94-12015 01-91)
Avail: CASI HC A01/MF A06

The survey of Ma'adim Vallis and crater Gusev area by the new topographic Aeolis southeast map allows to document the hydrodynamics processes which occurred in the valley. The inner Ma'adim Vallis hypsometric and volume deposits analyses point out that Gusev impact was subsequent to the first incision of Ma'adim Vallis in the craterized upland. The study of the deposit distributions as revealed by the topography leads to reconstruct the chronology of three major events in the Aeolis Region : Ma'adim incision, Gusev impact, and Apollinaris Patera/flow interactions.
Author (revised)

N94-12134*# Geological Survey, Flagstaff, AZ.
SPATIAL VARIATION IN THE SEASONAL SOUTH POLAR CAP OF MARS AS OBSERVED BY MARINER 7 Abstract Only
Wendy M. Calvin, Terry Z. Martin (Jet Propulsion Lab., California Inst. of Tech., Pasadena.), and Gary B. Hansen (Washington Univ., Seattle.) *In* Lunar and Planetary Inst., Twenty-fourth Lunar and Planetary Science Conference. Part 1: A-F 1993 p 243-244 (For primary document see N94-12015 01-91)
Avail: CASI HC A01/MF A06

Spatial variations in infrared spectra of the seasonal south polar cap of Mars were noted by the original Mariner 7 IRS instrument team as well as in subsequent examinations of the Mariner 7 data set. Up to now, however, there has been little effort to synthesize this information to understand variations in the south seasonal cap as a function of position or latitude. An attempt to quantify the spectra is made by providing estimates of CO2 grain sizes as well as upper limits on the amount of water frost contained in the polar collar. The variation in brightness at two wavelengths as well as the band depth of a weak CO2-ice feature at 2.28 microns as a function of spectrum number or subsequent location on the cap is presented. The full spectra, corrected only for the solar incidence angle, of three of the most significant areas are compared. Author (revised)

N94-12135*# Massachusetts Inst. of Tech., Cambridge. Center for Astrophysics.
THE GIANT IMPACT PRODUCED A PRECIPITATED MOON Abstract Only c90
A. G. W. Cameron *In* Lunar and Planetary Inst., Twenty-fourth Lunar and Planetary Science Conference. Part 1: A-F 1993 p 245-246 (For primary document see N94-12015 01-91)
Avail: CASI HC A01/MF A06

The author's current simulations of Giant Impacts on the protoearth show the development of large hot rock vapor atmospheres. The Balbus-Hawley mechanism will pump mass and angular momentum outwards in the equatorial plane; upon cooling and expansion the rock vapor will condense refractory material beyond the Roche distance, where it is available for lunar formation. During the last seven years, the author together with several colleagues has carried out a series of numerical investigations of the Giant Impact theory for the origin of the Moon. These involved three-dimensional simulations of the impact and its aftermath using Smooth Particle Hydrodynamics (SPH), in which the matter in the system is divided into discrete particles whose motions and internal energies are determined as a result of the imposed initial conditions. Densities and pressures are determined from the combined overlaps of the particles, which have a bell-shaped density distribution characterized by a smoothing length. In the original series of runs all particle masses and smoothing lengths had the same values; the matter in the colliding bodies consisted of initial iron cores and rock (dunite) mantles. Each of 41 runs used 3,008 particles, took several weeks of continuous computation, and gave fairly good representations of the ultimate state of the post-collision body or bodies but at best crude and qualitative information about individual particles in orbit. During the last two years an improved SPH program was used in which the masses and smoothing lengths of the particles are variable, and the intent of the current series of computations is to investigate the behavior of the matter exterior to the main parts of the body or bodies subsequent to the collisions. These runs are taking times comparable to a year of continuous computation in each case; they use 10,000 particles with 5,000 particles in the target and 5,000 in the impactor, and the particles thus have variable masses and smoothing lengths (the latter are dynamically adjusted so that a particle typically overlaps a few tens of its neighbors). Since the matter in the impactor provides the majority of the mass left in orbit after the collision, and since the masses of the particles that originated in the impactor are smaller than those in the target, the mass resolution in the exterior parts of the problem is greatly improved and the exterior particles properly simulate atmospheres in hydrostatic equilibrium.

Author (revised)

N94-12136*# National Air and Space Museum, Washington, DC. Center for Earth and Planetary Studies.

GEOLOGY AND SURFACE CHARACTERISTICS OF BELL REGIO, VENUS Abstract Only

Bruce A. Campbell and Patricia G. Rogers (National Aeronautics and Space Administration, Washington, DC.) *In* Lunar and Planetary Inst., Twenty-fourth Lunar and Planetary Science Conference. Part 1: A-F 1993 p 247-248 (For primary document see N94-12015 01-91)

Avail: CASI HC A01/MF A06

Bell Regio is a broad topographic rise located at approximately 30 deg N, 45 deg E which extends approximately 1500 km in the N-S direction and is characterized by extensive volcanism. The geology and surface characteristics of Bell Regio are examined in order to understand the geologic evolution of the region and the surface characteristics of the major volcanic units. Relationships between Magellan SAR backscatter values and altimeter-derived ring slope data are analyzed, and terrestrial SAR data are used to suggest possible surface morphologies.

Author (revised)

N94-12137*# National Air and Space Museum, Washington, DC. Center for Earth and Planetary Studies.

LAVA FLOWS ON VENUS: ANALYSIS OF MOTION AND COOLING Abstract Only

Bruce A. Campbell and James R. Zimbelman *In* Lunar and Planetary Inst., Twenty-fourth Lunar and Planetary Science Conference. Part 1: A-F 1993 p 249-250 (For primary document see N94-12015 01-91)

Avail: CASI HC A01/MF A06

Effusive volcanism is a major mechanism for resurfacing on Venus. The large edifice complexes are marked by lava flow fields which extend hundreds of kilometers from their apparent source vents. Earlier work on the emplacement of lava predicted few major differences in flow length between Venus and the Earth (for similar magmas) based primarily on assessment of the relative rates of heat loss to their respective atmospheres. This analysis, combined with the obvious presence of very long lava flows on Venus, has led to suggestions that basalt magmas on Venus may be of generally lower viscosity or that magma effusion rates exceed terrestrial norms. If correct, these hypotheses might imply systematically different chemical and dynamic characteristics for volcanic processes on Venus, and a somewhat catastrophic history for many of the large edifices and flow fields. The mechanics of magma motion and cooling are re-examined, and some of the issues involved in analyzing flows on Venus are discussed.

Author (revised)

N94-12138*# Rhode Island Univ., Narragansett. Graduate School of Oceanography.

STRATIGRAPHY AND SEDIMENTOLOGY OF THE K/T BOUNDARY DEPOSIT IN HAITI Abstract Only c46

S. Carey, H. Sigurdsson, S. DHondt, and J. M. Espindola (Universidad Nacional Autonoma de Mexico, Mexico City.) *In* Lunar and Planetary Inst., Twenty-fourth Lunar and Planetary Science Conference. Part 1: A-F 1993 p 251-252 (For primary document see N94-12015 01-91)

Avail: CASI HC A01/MF A06

The K/T boundary sequence is exposed in uplifted carbonate sediments of the southwest peninsula of Haiti. It is found at 15 localities within the Beloc formation, a sequence of limestone and marls interpreted as a monoclinal nappe structure thrust to the north. This tectonic deformation has affected the K/T boundary deposit to varying degrees. In some cases the less competent K/T deposit has acted as a slip plane leading to extensive shearing of the boundary layer, as well as duplication of the section. The presence of glassy tektites, shocked quartz, and an Ir anomaly directly link the deposit to a bolide impact. Stratigraphic and sedimentological features of the tripartite sequence indicate that it was formed by deposition from ballistic fallout of coarse tektites, emplacement of particle gravity flows and fine grained fallout of widely dispersed impact ejecta.

Author (revised)

N94-12139*# Jet Propulsion Lab., California Inst. of Tech., Pasadena.

GALILEO/NIMS NEAR-INFRARED THERMAL IMAGERY OF THE SURFACE OF VENUS Abstract Only

R. W. Carlson, K. H. Baines, M. Girard, L. W. Kamp, P. Drossart (Observatoire de Paris-Meudon, France.), T. Encrenaz (Observatoire de Paris-Meudon, France.), and F. W. Taylor (Oxford Univ., England.) *In* Lunar and Planetary Inst., Twenty-fourth Lunar and Planetary Science Conference. Part 1: A-F 1993 p 253 (For primary document see N94-12015 01-91)

Avail: CASI HC A01/MF A06

Numerous highland and lowland features on the surface of Venus are observed in multispectral imagery acquired at approximately 50 km spatial resolution by the Near-Infrared Mapping Spectrometer (NIMS) on board the Galileo spacecraft in Feb. 1990. Specifically, such features are observed at 1.18 microns, a wavelength particularly sensitive to thermal emission from the hot, lower atmosphere (less than 10 km) and surface, and show up particularly well when this image is 'de-clouded' using a simultaneously-acquired 2.3-microns image of the upper, cloudy atmosphere. Due to the steep atmospheric temperature gradient (approximately 8 degrees per kilometer), hot lowland areas appear relatively bright, while cooler, highland areas appear dark (due to the steep atmospheric temperature gradient - approximately 8 degrees per kilometer - surface temperatures span approximately 100 K over the 13 kilometer range of surface altitudes observed in this image). Prominent highland features include Maxwell Montes (approximately 12 km altitude), Alpha Regio (2.5 km), Eistla Regio (approximately 2.0 km), Bell Regio (2-3 km), and the western edge of Aphrodite Terra (2-2.5 km). Low-lying regions include Sedna Planitia (-1.0 km), Tinatin Planitia (-0.5 km), and the Bereghinya Planitia (0 km). From correlations with radar altimetry maps, such imagery may place useful constraints on surface emissivity and temperature variations, as well as on the nature of continuum opacity of CO2 in the 1-micron region.

Author (revised)

N94-12140*# Jet Propulsion Lab., California Inst. of Tech., Pasadena.

PRELIMINARY REPORT OF LUNAR OBSERVATIONS BY THE NEAR-INFRARED MAPPING SPECTROMETER (NIMS) DURING THE SECOND GALILEO EARTH-MOON ENCOUNTER Abstract Only c89

R. W. Carlson, H. H. Kieffer (Geological Survey, Flagstaff, AZ.), K. H. Baines, K. J. Becker (Geological Survey, Flagstaff, AZ.), G. E. Danielson (California Inst. of Tech., Pasadena.), K. Edwards (Geological Survey, Flagstaff, AZ.), F. P. Fanale (Hawaii Univ., Honolulu.), J. Forsythe (SETS Technology, Inc., Mililani, HI.), L. R. Gaddis (Geological Survey, Flagstaff, AZ.), and J. C. Granahan (Hawaii Univ., Honolulu.) et al *In* Lunar and Planetary Inst., Twenty-fourth Lunar and Planetary Science Conference. Part 1: A-F 1993 p 255-256 (For primary document see N94-12015 01-91)

Avail: CASI HC A01/MF A06

The Galileo encounter with the Earth-Moon system on 8 Dec. 1992, provided a unique opportunity to observe the Moon. Galileo's closest approach to the Moon was at an altitude of about 110,000 km above an area at about latitude 60N, longitude 60E. During the 12 hours surrounding the time of lunar closest approach, 12 observational sequences were executed by the near-infrared mapping spectrometer (NIMS), many in coordination with other Galileo instruments. These NIMS observations provided nearly complete coverage of the illuminated crescent from phase angles of 123 deg to 14 deg. This phase-angle coverage with nearly constant illumination is not possible from Earth; it is expected to provide substantial new information on the nature of the lunar photometric function over wavelength. As of Jan. 1993, most of the analysis has focused on the highest resolution data (55 km/pixel).

Author (revised)

N94-12141*# Field Museum of Natural History, Chicago, IL. Dept. of Geology.

DISTRIBUTION OF VANADIUM AND MELTING OF OPAQUE ASSEMBLAGES IN EFREMOVKA CAI'S Abstract Only c46

I. Casanova and L. Grossman (Chicago Univ., IL.) *In* Lunar and Planetary Inst., Twenty-fourth Lunar and Planetary Science Conference. Part 1: A-F 1993 p 257-258 (For primary document see N94-12015 01-91)

Avail: CASI HC A01/MF A06

A petrographic and chemical study of compact Type A CAI's from the Efremovka CV3 chondrite strongly suggests that the opaque assemblages (OA's) that they contain were molten at temperatures below the CAI silicate solidus, and that the V-rich magnetite presently observed in association with OA's formed by in situ oxidation of their FeNi. Author

N94-12142*# Field Museum of Natural History, Chicago, IL. Dept. of Geology.

METAL-RICH METEORITES FROM THE AUBRITE PARENT BODY Abstract Only c90

I. Casanova, T. J. McCoy (Hawaii Univ., Hilo.), and K. Keil (Hawaii Univ., Hilo.) *In* Lunar and Planetary Inst., Twenty-fourth Lunar and Planetary Science Conference. Part 1: A-F 1993 p 259-260 (For primary document see N94-12015 01-91)

Avail: CASI HC A01/MF A06

Three metal-rich meteorites - Mt. Egerton, Horse Creek, and LEW 88055 - were studied and it is suggested that they formed in the aubrite parent body. LEW 85369 and 88631 may also have a common origin, but these rocks have not yet been studied in detail. This body was probably heated to about 1600 C by a very strong heat source. While molten, metal agglomerated into sizeable nodules which never segregated efficiently to form a core, but were trapped in the silicate mantle. Different clasts and lithologies in aubrites solidified and cooled under local equilibrium conditions of oxygen fugacity, and with different thermal histories. Impacts mixed clasts from throughout the parent body, creating the typical aubrite breccias. Author (revised)

N94-12143*# National Aeronautics and Space Administration. Ames Research Center, Moffett Field, CA.

WHY CONVECTIVE HEAT TRANSPORT IN THE SOLAR NEBULA WAS INEFFICIENT Abstract Only c92

P. Cassen *In* Lunar and Planetary Inst., Twenty-fourth Lunar and Planetary Science Conference. Part 1: A-F 1993 p 261-262 (For primary document see N94-12015 01-91)

Avail: CASI HC A01/MF A06

The radial distributions of the effective temperatures of circumstellar disks associated with pre-main sequence (T Tauri) stars are relatively well-constrained by ground-based and spacecraft infrared photometry and radio continuum observations. If the mechanisms by which energy is transported vertically in the disks are understood, these data can be used to constrain models of the thermal structure and evolution of solar nebula. Several studies of the evolution of the solar nebula have included the calculation of the vertical transport of heat by convection. Such calculations rely on a mixing length theory of transport and some assumption regarding the vertical distribution of internal dissipation. In all cases, the results of these calculations indicate that transport by radiation dominates that by convection, even when the nebula is convectively unstable. A simple argument that demonstrates the generality (and limits) of this result, regardless of the details of mixing length theory or the precise distribution of internal heating is presented. It is based on the idea that the radiative gradient in an optically thick nebula generally does not greatly exceed the adiabatic gradient. Author (revised)

N94-12144*# Geological Survey, Flagstaff, AZ.

FAULT GEOMETRIES AND EXTENSION IN THE VALLES MARINERIS, MARS Abstract Only

D. J. Chadwick and B. K. Lucchitta *In* Lunar and Planetary Inst., Twenty-fourth Lunar and Planetary Science Conference. Part 1: A-F 1993 p 263-264 (For primary document see N94-12015 01-91)

Avail: CASI HC A01/MF A06

The central troughs of the Valles Marineris system on Mars are generally regarded to be of tectonic origin because they are linear and bounded by faults. Their radial orientation to the Tharsis rise suggests that at least their incipient formation was influenced by the formation of the rise, but the exact role of Tharsis is not yet well understood. Collapse and erosion may have significantly modified the original tectonic troughs. To better understand the magnitude and mechanism of crustal extension across the Valles Marineris, the attitudes of trough-wall faults that parallel the long axes of the troughs were studied. Our results will help to determine if the extension is related to the Tharsis rise, to a local arch along which the troughs lie, or to other mechanisms. Fault-plane attitudes were obtained by performing a photogrammetric study of fault traces in the walls of Candor and Melas Chasmata. If the exposed wall faults are not major trough-bounding faults, it is assumed that these major faults are buried at the base of the walls and have similar geometries to the exposed faults. Three dimensional coordinates of several points along each fault trace were obtained and three-point solutions to their geometries were constructed. As expected, the results show that the faults dip toward the interior of the troughs, suggesting that they are indeed normal faults associated with trough formation. Author (revised)

N94-12145*# Geological Survey, Flagstaff, AZ.

A TWO-STAGE (TURBULENT-DRAINAGE) MECHANISM FOR THE EMPLACEMENT OF IMPACT CRATER OUTFLOWS ON VENUS Abstract Only

D. J. Chadwick and G. G. Schaber *In* Lunar and Planetary Inst., Twenty-fourth Lunar and Planetary Science Conference. Part 1: A-F 1993 p 265-266 (For primary document see N94-12015 01-91)

Avail: CASI HC A01/MF A06

Several emplacement mechanisms were proposed for the unique flow features associated with 402 of the 912 impact craters found on Venus to date. Studies based on rheological models and laboratory results have suggested two separate depositional flow mechanisms: a turbulent emplacement and a lava like emplacement. Schultz proposed a progressive transition from the turbulent to the lava like mechanism during deceleration of some turbulent flows. He suggested that these composite flows were emplaced prior to the deposition of the normal ejecta. After an examination of the geomorphologic, stratigraphic, and topographic relations of the flows associated with the 402 craters, it is suggested that most of the outflows result from a two-stage emplacement process. In the first stage, a turbulent, proximal part is usually emplaced downrange of the impact site after the other ejecta materials. In the second stage, a distal part, composed of low-viscosity melt, slowly drains via dendritic channels from the proximal deposit and flows like lava. A few flows were identified that appear to have been emplaced prior to the ejecta; these flows likely result from a different mechanism. Author (revised)

N94-12146*# Dartmouth Coll., Hanover, NH. Dept. of Earth Sciences.

OXYGEN ISOTOPES AS TRACERS OF TEKTITE SOURCE ROCKS: AN EXAMPLE FROM THE IVORY COAST TEKTITES AND LAKE BOSUMTWI CRATER Abstract Only c90

Joel D. Blum, Christian Koeberl (Wien Univ., Austria.), and C. Page Chamberlain *In* Lunar and Planetary Inst., Twenty-fourth Lunar and Planetary Science Conference. Part 1: A-F 1993 p 267-268 (For primary document see N94-12015 01-91)

Avail: CASI HC A01/MF A06

Oxygen isotope studies of tektites and impact glasses provide an important tool to help in identifying the target lithologies for terrestrial impacts, including the K-T boundary impact. However, such studies may be complicated by modification of the original oxygen isotope values of some source rocks during the tektite formation process either by vapor fractionation or incorporation of meteoric water. To further investigate the relationship between the oxygen isotopic composition of tektites and their source rocks, Ivory Coast tektites and samples of impact glasses and bedrock lithologies from the Bosumtwi Crater in Ghana--which is widely believed to be the source crater for the Ivory Coast tektites--were studied. Our preliminary results suggest that the phyllites and metagraywackes from the Bosumtwi Crater were the predominant source materials for the impact glasses and tektites and that no significant oxygen isotope modification (less than 1 percent delta(O-18)) took place during impact melting. This contrasts with previous studies of moldavites and Australasian tektites and their sedimentary source materials which suggests a 4 to 5 percent lowering of delta(O-18) due to meteoric water incorporation during impact melting. Author (revised)

N94-12147*# Lunar and Planetary Inst., Houston, TX.
CRATERING ON GASPRA Abstract Only
Clark R. Chapman, Gerhard Neukum (Deutsche Forschungsanstalt fuer Luft- und Raumfahrt, Oberpfaffenhofen, Germany.), Joseph Veverka (Cornell Univ., Ithaca, NY.), and Michael Belton (Kitt Peak National Observatory, Tucson, AZ.) *In its* Twenty-fourth Lunar and Planetary Science Conference. Part 1: A-F 1993 p 269-270 (For primary document see N94-12015 01-91)
Avail: CASI HC A01/MF A06

The October 1991 Galileo flyby of Gaspra shows that its crater population is dominated by fresh craters several hundred meters in diameter and smaller. They appear to represent a production population because the spatial density is relatively low (few overlaps) and because fresh craters are very abundant; equilibrium could be attained at diameters near to or below the resolution limit of the best image. These craters are the first direct record of the population of main-belt asteroids some tens of meters in diameter. Craters primarily from the highest resolution, 'high phase' image, on which over 600 craters are visible in 90 sq. km were counted, measured, and classified; earlier counts were made on the lower resolution four-color images, which show an order of magnitude fewer craters because of the resolution limit. The population index (exponent of the differential power law approximately describing the crater sizes) has a very high negative value (-4.3 +/- 0.3, meaning that the log-log slope is 'steep'), appreciably steeper than the value of -3.5 thought to reflect collisional equilibrium according to theory. Author (revised)

N94-12148*# Geological Survey, Flagstaff, AZ.
BASAL SCARP, PALEOGLACIER, AND FISSURE FLOWS OF ELYSIUM MONS, MARS Abstract Only
Mary G. Chapman *In* Lunar and Planetary Inst., Twenty-fourth Lunar and Planetary Science Conference. Part 1: A-F 1993 p 271-272 (For primary document see N94-12015 01-91)
Avail: CASI HC A01/MF A06

Geological mapping at 1:500,000 scale of the Granicus Valles area west of Elysium Mons (MTM quadrangles 30227, 30222, and 25227) indicates that (1) the oldest deposits in the area are Upper Hesperian lavas of the Elysium shield; (2) a basal scarp formed by Early Amazonian faulting around the northwest flank of Elysium Mons triggered growth of Elysium Fossae; (3) a glacier or an ice sheet west and north of the scarp was of long duration; (4) water and lava flows from Elysium Fossae became dominant during and after glacial recession; and (5) the last volcanic-fissure-related flows resulted in linear chains of small domes on the Elysium shield. Author (revised)

N94-12149*# California Inst. of Tech., Pasadena. Lab. of Experimental Geophysics.
SHOCK INDUCED REACTION IN CHICXULUB TARGET MATERIALS (CaSO4 AND SIO2) AND THEIR RELATION TO EXTINCTIONS Abstract Only **c46**
Guangqing Chen and Thomas J. Ahrens *In* Lunar and Planetary Inst., Twenty-fourth Lunar and Planetary Science Conference. Part 1: A-F 1993 p 273-274 (For primary document see N94-12015 01-91)
Avail: CASI HC A01/MF A06

The global platinum element rich layer, the presence of shocked quartz grains (in some cases with stishovite), and the observation of a tektite-rich layer, precisely at the K-T boundary, are the three major arguments for the extinction bolide impact hypothesis of Alvarez et al. Tektites (spherules) from Beloc in Haiti and Mimbral in Mexico received particular interest because of their geological proximity to the Chicxulub impact structure, which is a leading candidate for at least one of the K-T impact craters. Although in most localities the original glass has weathered to clay minerals, some shock-induced glass is found in outcrops and drill cores which is used for Ar-38/Ar-39 dating. The glassy tektites were found to be chemically similar and coeval at 65.0 Ma with Chicxulub melt rock. Two kinds of K-T spherules were discovered: (1) a silic black glass; and (2) a yellow glass, enriched in Ca, Mg, and S. The high sulfur content of the glass and the abundance of anhydrite (CaSO4) in the carbonate-evaporite sequence observed in Drill Holes Y-1 and Y-2 at Chicxulub prompted studies of calcium sulfate devolatization. Further discussion of our experiments is presented. Author (revised)

N94-12150*# California Inst. of Tech., Pasadena. Div. of Geological and Planetary Sciences.
LEW88516 AND SNC METEORITES Abstract Only **c90**
J. H. Chen and G. J. Wasserburg *In* Lunar and Planetary Inst., Twenty-fourth Lunar and Planetary Science Conference. Part 1: A-F 1993 p 275-276 (For primary document see N94-12015 01-91)
Avail: CASI HC A01/MF A06

We report on the isotopic composition of Pb and the concentration of Pb, U, and Th in a sample of LEW88516 (LEW). LEW was a 13-g stone recovered from Antarctica and was classified as a new member of the Shergottite group. This work was undertaken with the hope that LEW might yield new information to elucidate further the origin and evolution of Shergottites and other SNC meteorites. We have previously studied U-Th-Pb in other Shergottites, namely Shergotty, Zagami, EETA79001, and ALHA77005, as well as Nakhla. The results indicate that the initial leads of these Shergottites were well defined, were distinct from each other, and have high Pb-204/Pb-206 (from 0.0652 to 0.0739). These leads evolved in different reservoirs over most of solar system history in a low U-238/Pb-204(micro) is approximately equal to 5 environment. The U-Th-Pb isotopic systems are quite regular, which unambiguously indicates an event of U-Th-Pb fractionation at approximately 200 m.y. The details of the data arrays are complex. The young age is in general agreement with some of the ages obtained by other methods, but precise concordance between the different methods is not established. The new results on LEW are remarkably similar to those of ALHA77005 and support the other observations based on the mineralogy, petrology, and bulk composition. The clear distinction between the Shergottites and Nakhla is confirmed. We consider that the Shergottites and possibly all the SNC's were derived from an impact on the regolith of a differentiated terrestrial type planetary body (Mars?) with a high content of volatiles as compared to the earth. Author (revised)

N94-12151*# California Inst. of Tech., Pasadena. Div. of Geological and Planetary Sciences.
THE Th AND U ABUNDANCES IN CHONDRITIC METEORITES Abstract Only **c90**
J. H. Chen, G. J. Wasserburg, and D. A. Papanastassiou *In* Lunar and Planetary Inst., Twenty-fourth Lunar and Planetary Science Conference. Part 1: A-F 1993 p 277-278 (For primary document see N94-12015 01-91)
Avail: CASI HC A01/MF A06

We present new analyses of Th-232/U-238 in CI and CM meteorites. The relative abundance of these nuclides is important in estimates of the age of r-process elements. The cosmochronology based upon the Th-232/U-238 ratio (kappa) depends on the precise determinations of these two different elements in meteorites and on the production ratios. Both parameters are subject to substantial errors. Recent recalculations of this chronology have used selected values from compilations but do not adequately address the errors in terms of a reliable data base. Morgan and Lovering provided extensive neutron activation analyses for ordinary chondrites which yield an average kappa of 3.6 +/- 0.4. Their work on carbonaceous chondrites showed a wide range in kappa from 2 to 6. More recent investigations by isotopic dilution have established the following: (1) highly variable kappa from 2.7 to 11 in Allende Ca-Al-rich inclusions and a value of 3.6 in the Orgueil CI1 chondrite; (2) a range from 2.71 to 6.63 for 7 L-type chondrites and a range from 2.7 to 4.4 for 6 L, H, and LL chondrites. A further investigation of this subject matter is presented. Author (revised)

N94-12152*# Johns Hopkins Univ., Laurel, MD. Applied Physics Lab.
LUNAR SCOUT TWO SPACECRAFT GRAVITY EXPERIMENT Abstract Only
Andrew F. Cheng *In* Lunar and Planetary Inst., Twenty-fourth Lunar and Planetary Science Conference. Part 1: A-F 1993 p 279 (For primary document see N94-12015 01-91)
Avail: CASI HC A01/MF A06

Measurement of the gravity field of the Moon has a high science priority because of its implications for the internal structure and thermal history of the Moon, and it has a high priority for future exploration activities because of the influence of lunar gravity on spacecraft navigation and orbit maintenance. The current state of knowledge in the lunar gravity field (and the uncertainty in the knowledge) is based primarily on data accumulated from the Lunar Orbiter and Apollo programs. Data are sparse and emphasize the equatorial band (+/- 30 deg) on the near side of the Moon. There are no tracking data on the far side and only the Lunar Orbiter 5 provides a small amount of high inclination data. A host of gravity models developed from different combinations of tracking data have large discrepancies in their predictions of spacecraft motion and orbit lifetimes. There are also large disagreements in the Mercator projections of the gravity acceleration from each model, especially on the far side, where the contours tend to have no obvious relationship with the local topography. The science and engineering requirements for global gravity field mapping will be satisfied with continuous radio metric tracking of Lunar Scout 1 in a low polar orbit using the Deep Space Network and Lunar Scout 2 in a high elliptical orbit. The gravity field of the Moon will be mapped during the Scout Program using a two spacecraft concept. In the two spacecraft concept, one spacecraft is placed in a high altitude eccentric orbit while the second spacecraft is in a low altitude polar orbit. The gravity experiment requires a radio frequency that will permit two-way Doppler tracking between the spacecraft and the Deep Space Network (DSN). Both spacecraft carry NASA standard transponder systems for data transmission to Earth as well as for tracking and orbit determination. Data sufficient to produce a gravity field map could be acquired within one month with this system. Author (revised)

N94-12153*# European Space Research Lab., Noordwijk (Netherlands). Space Research and Technology Center.
MISSION TO THE MOON: AN ESA STUDY ON FUTURE EXPLORATION Abstract Only
A. F. Chicarro *In* Lunar and Planetary Inst., Twenty-fourth Lunar and Planetary Science Conference. Part 1: A-F 1993 p 281-282 (For primary document see N94-12015 01-91)
Avail: CASI HC A01/MF A06

The increasing worldwide interest in the continuation of lunar exploration has convinced ESA to carry out an investigation of the motivations to return to the Moon to establish a permanent or a semi-permanent manned lunar base. This study also considers the possible role Europe could play in the future exploration and possible utilization of the Moon. The study concentrated in this first phase mainly on scientific questions, leaving technological issues such as transportation, the role of humans, infrastructure, and policy matters to a later phase. It only partially considered questions relating to the exploitation of lunar resources and the impact of human activities on science. Author (revised)

N94-12154*# Hawaii Univ., Honolulu. Dept. of Geology and Geophysics.
FRACTAL DIMENSIONS OF RAMPART IMPACT CRATERS ON MARS Abstract Only
Delwyn Ching, G. Jeffrey Taylor, Peter Mouginis-Mark, and Barbara C. Bruno *In* Lunar and Planetary Inst., Twenty-fourth Lunar and Planetary Science Conference. Part 1: A-F 1993 p 283-284 (For primary document see N94-12015 01-91)
Avail: CASI HC A01/MF A06

Ejecta blanket morphologies of Martian rampart craters may yield important clues to the atmospheric densities during impact, and the nature of target materials (e.g., hard rock, fine-grained sediments, presence of volatiles). In general, the morphologies of such craters suggest emplacement by a fluidized, ground hugging flow instead of ballistic emplacement by dry ejecta. We have quantitatively characterized the shape of the margins of the ejecta blankets of 15 rampart craters using fractal geometry. Our preliminary results suggest that the craters are fractals and are self-similar over scales of approximately 0.1 km to 30 km. Fractal dimensions (a measure of the extent to which a line fills a plane) range from 1.06 to 1.31. No correlations of fractal dimension with target type, elevation, or crater size were observed, though the data base is small. The range in fractal dimension and lack of correlation may be due to a complex interplay of target properties (grain size, volatile content), atmospheric pressure, and crater size. The mere fact that the ejecta margins are fractals, however, indicates that viscosity and yield strength of the ejecta were at least as low as those of basalts, because silicic lava flows are not generally fractals. Author (revised)

N94-12155*# Arizona State Univ., Tempe. Dept. of Geology.
A SIMPLE MODEL OF CLASTIC SEDIMENTS ON MARS Abstract Only
Philip R. Christensen and Michael C. Malin (Malin Space Science Systems, San Diego, CA.) *In* Lunar and Planetary Inst., Twenty-fourth Lunar and Planetary Science Conference. Part 1: A-F 1993 p 285-286 (For primary document see N94-12015 01-91)
Avail: CASI HC A01/MF A06

In preparation for the start of Mars Observer operations at Mars later this year, Viking Infrared Thermal Mapper (IRTM) observations were synthesized into a simple but geologically coherent conceptual model for use in establishing targets for coordinated Thermal Emission Spectrometer (TES) and Mars Observer Camera (MOC) observations. The model is based on three assumptions that are, at best, only partly true: that albedo is a measure of the presence or absence of dust; that thermal inertia is a measure of the weighted average particle size; and that rock abundance is a measure of the statistical thickness of fine sediment (i.e., that the observed areal abundance of rock reflects the whole or partial burial of rocks). Using this model, it is possible to show that, on the scale of 30 km, mantles of wind-transportable sediment (dust and sand) are at most about 1 m thick, and that on a global average such mantles are about 35 cm thick. It is shown that 3.8 x 10(exp 19) cu cm of such sediment covers Mars equatorward of +/- 60 deg latitude. Using the model, interpretation of digital maps of IRTM data focus attention not only on areas where dust is the primary sediment (e.g., Arabia Terra), but also on areas where sand is the primary sediment (e.g., eastern Valles Marineris) and where rocks and other coarse materials are abundant (e.g., eastern Kasei Vallis). Three IRTM data sets are used in the analysis: Viking 1 and 2 pre-dawn observations mosaiced into a global map of single-point thermal inertias at 0.5 deg/bin resolution; Pleskot and Miner's global albedo map using the best available, clear-period IRTM observations (1x/bin); and Christensen's 1 deg/bin rock abundance map. Uncertainty analyses indicate these data sets to be accurate to 5 percent, 2 percent, and 20 percent, respectively. Author (revised)

N94-12156*# Arizona State Univ., Tempe. AX646679
THERMAL-INFRARED EMISSION SPECTROSCOPY OF NATURAL SURFACES: APPLICATION TO COATED SURFACES Abstract Only
c25
Philip R. Christensen, Stephanie T. Harrison (National Aeronautics and Space Administration. Goddard Space Flight Center, Greenbelt, MD.), Paul Barbera, and Steve Ruff *In* Lunar and Planetary Inst., Twenty-fourth Lunar and Planetary Science Conference. Part 1: A-F 1993 p 287-288 (For primary document see N94-12015 01-91)
Avail: CASI HC A01/MF A06

Thermal-infrared vibrational spectroscopy has great potential for remotely determining the composition of planetary surface materials by taking advantage of fundamental molecular vibrational modes that produce spectral features in the range from approximately 3 to greater than 50 microns. Much of the current interest in the thermal infrared wavelength region stems from the deployment of multispectral scanners, such as the Thermal Infrared Multispectral Scanner (TIMS) and the Mars Observer Thermal Emission Spectrometer (TES). In order to support these missions, it is necessary to develop an appropriate library of laboratory measurements. The purpose of this work was to develop a technique which, with a very limited set of assumptions, can be used to determine the emissivity of natural surfaces directly by using emitted energy. Author (revised)

N94-12157*# National Aeronautics and Space Administration. Goddard Space Flight Center, Greenbelt, MD.
COLLISIONS OF SMALL SPACEWATCH ASTEROIDS WITH THE EARTH Abstract Only **c90**
C. F. Chyba *In* Lunar and Planetary Inst., Twenty-fourth Lunar and Planetary Science Conference. Part 1: A-F 1993 p 289-290 (For primary document see N94-12015 01-91)
Avail: CASI HC A01/MF A06

The discovery, with the Spacewatch Telescope, of 8 Earth-approaching objects smaller than 100 m in diameter has been reported. I have calculated the probability and velocity of collision with Earth for each of these objects. Using a code we have successfully employed to model the Tunguska and Revelstoke atmospheric explosions, I have simulated the entry of these objects into Earth's atmosphere, assuming iron, stony, carbonaceous, and cometary compositions. The smallest of these objects, with tens to hundreds of kilotons of kinetic energy, pose a substantial threat at the surface only if they are iron objects. An object is taken to 'pose a substantial threat' if it either craters the ground, or explodes in the atmosphere with sufficient energy at low enough altitude to create an overpressure at the surface capable of felling trees or destroying buildings. Larger objects, with energies greater than about a megaton, devastate the surface regardless of whether they are of iron, stony, or carbonaceous composition. Iron objects crater the ground, whereas stony and carbonaceous objects explode in the atmosphere low enough to fell trees and damage buildings over thousands of square kilometers. Spacewatch objects, if presumed to be of carbonaceous composition, are as dangerous as their stony counterparts, as the former objects' lower yield strengths (and hence, higher explosion altitudes) are roughly compensated by their larger masses (as derived from their lower albedos for a given observed magnitude). Although comets are intrinsically less dangerous than asteroids, the 90 m diameter Spacewatch objects would devastate hundreds of square kilometers at the surface, even if cometary. Author (revised)

N94-12158*# National Aeronautics and Space Administration. Lyndon B. Johnson Space Center, Houston, TX.
DIFFERENTIAL SCALING: IMPLICATIONS FOR CENTRAL STRUCTURES IN LARGE LUNAR CRATERS Abstract Only
M. J. Cintala and R. A. F. Grieve (Geological Survey of Canada, Ottawa, Ontario.) *In* Lunar and Planetary Inst., Twenty-fourth Lunar and Planetary Science Conference. Part 1: A-F 1993 p 291-292 (For primary document see N94-12015 01-91)
Avail: CASI HC A01/MF A06

The change in morphology of central structures with crater size on the terrestrial planets has been studied by many investigators. While the progression of morphological change essentially follows the same basic pattern, the appearance of central peaks, and the transitions from single to multiple peaks and peaks to peak rings occur at crater diameters that appear to be dependent on parameters associated with the target planet. Statistical data, morphological information, and model results exist for central structures in large craters, but the amount of 'ground truth' is comparatively meager. What, for instance, is the amount of stratigraphic uplift in craters? Answers to questions such as this will provide useful constraints on models of origin for central structures and would help in interpretation of remote-sensing data. This contribution uses terrestrial information and model calculations to estimate the amount of stratigraphic uplift for central-peak craters on the Moon--the only planet other than Earth for which sufficient topographic data are available. Author (revised)

N94-12159*# National Aeronautics and Space Administration. Lyndon B. Johnson Space Center, Houston, TX.
IMPACT COMMINUTION OF GLASSES: IMPLICATIONS FOR LUNAR REGOLITH EVOLUTION Abstract Only
Mark J. Cintala, Sheila Smith (Baylor Univ., Waco, TX.), and Friedrich Hoerz *In* Lunar and Planetary Inst., Twenty-fourth Lunar and Planetary Science Conference. Part 1: A-F 1993 p 293-294 (For primary document see N94-12015 01-91)
Avail: CASI HC A01/MF A06

Glasses are important parts of every lunar regolith sample, whether in the form of indigenous melts such as mesostasis or pyroclastics, or as quenched impact melts. The modal proportions of agglutinitic impact melts alone can exceed 50 percent for some mature regoliths, and glasses are commonly the most dominant single component of lunar soils. They therefore participate in and possibly affect all evolutionary processes to which regoliths are subjected, such as comminution and attendant chemical fractionation as a function of grain size, the retention of solar-wind products, the production of superparamagnetic iron, and others. Because they are such an integral part of lunar regoliths, a more complete understanding of regolith evolution must include the role played by these vitreous components. This contribution examines the comminution behavior of a variety of glasses and a fine-grained basalt under conditions of repetitive impact, and compares this behavior to those of crystalline components, such as lithic fragments and major rock-forming minerals. Author (revised)

N94-12160*# California Univ., Davis. Dept. of Geology.
MICROTEKTITE-LIKE GLASS SPHERULES IN LATE DEVONIAN (367 MA) SHALES Abstract Only
Philippe Claeys and Jean-Georges Casier (Institut Royal des Sciences Naturelles de Belgique, Brussels.) *In* Lunar and Planetary Inst., Twenty-fourth Lunar and Planetary Science Conference. Part 1: A-F 1993 p 295-296 (For primary document see N94-12015 01-91)
Avail: CASI HC A01/MF A06

Glass spherules are found closely associated with the Frasnian-Famennain (FF) boundary in two sections, Senzeille and Hony, located in the Dinant basin in the South of Belgium. These spherules are interpreted, based on their chemistry and low water content, as impact produced microtektite-like glass. Craters of Late Devonian ages include the Siljan Ring (Sweden), Charlevoix (Quebec), and Taihu Lake (China). The occurrence of microtektite-like glass closely associated with the FF mass extinction is intriguing. The relationships between the impact and the extinction event deserve further study. Author (revised)

N94-12161*# California Univ., Davis. Dept. of Geology.
KT BOUNDARY IMPACT GLASSES FROM THE GULF OF MEXICO REGION Abstract Only **c46**
Philippe Claeys, Walter Alvarez (California Univ., Berkeley.), Jan Smit (Vrije Univ., Amsterdam, Netherlands.), A. R. Hildebrand (Geological Survey of Canada, Ottawa, Ontario.), and Alessandro Montanari (Osservatorio Geologico di Coldigioco, Aprio, Italy.) *In* Lunar and Planetary Inst., Twenty-fourth Lunar and Planetary Science Conference. Part 1: A-F 1993 p 297-298 (For primary document see N94-12015 01-91)
Avail: CASI HC A01/MF A06

Cretaceous-Tertiary boundary (KTB) tektite glasses occur at several sites around the Gulf of Mexico. Contrary to rumor among KTB workers, glass fragments have been found by several researchers in the base of the spherule bed at Arroyo el Mimbral in NE Mexico. The presence of green, red, and transparent glass fragments at Mimbral only, demonstrates that the Mimbral glass is not a laboratory contamination by Beloc glass. The chemistry and ages of the glass are consistent with an origin from the Chixculub impact crater in Yucatan. No evidence supports a volcanic origin for the KTB glasses. A discussion of tektite glass from the KT boundary is presented. Author (revised)

N94-12162*# Hawaii Univ., Honolulu. Planetary Geosciences.
FIRST RESULTS OF THE SEVEN-COLOR ASTEROID SURVEY Abstract Only **c90**
Beth E. Clark, Jeffrey F. Bell, Fraser P. Fanale, and Paul G. Lucey *In* Lunar and Planetary Inst., Twenty-fourth Lunar and Planetary Science Conference. Part 1: A-F 1993 p 299-300 (For primary document see N94-12015 01-91)
Avail: CASI HC A01/MF A06

The new Seven-Color infrared filter system (SCAS), designed specifically to capture the essential mineralogical information present in asteroid spectra, is composed of seven broad-band filters which allow for IR observations of objects as faint as 17th magnitude. The first test of the SCAS system occurred in Jul. 1992. In four nights at the IRTF on Mauna Kea, Hawaii, over 67 objects were observed. Five of the observations were to test the new system for accuracy relative to previous observations with the high-resolution 52 Color Infrared Survey and with the Eight-Color Asteroid Survey (ECAS). In three cases, the match with previous data was good. In two cases, the match to previous observations was not as good. In addition, sixty S-Type asteroids were measured with the SCAS system. Forty of those asteroids were also observed with the ECAS system. Among the new observations is infrared data of 371 Bohemia, a main belt asteroid which was classified 'QSV' according to its UBV colors in the taxonomic system of D.J. Tholen. There are no corresponding ECAS data for 371. Q-type asteroids are of special interest as they are proposed to be the elusive parent bodies of the ordinary chondrite meteorites. Most Q-types are Earth-crossing asteroids and have not yet been observed in the infrared (except, perhaps, 371). Positive identification of a large main belt Q-type would be of major importance in the scheme of the geological structure of the asteroid belt. Without visible wavelength data, however, the classification of 371 Bohemia remains ambiguous. An attempt to conjoin Bohemia SCAS data with ECAS data of both a typical Q-Type asteroid and an average S-Type asteroid is shown. This figure thus illustrates the importance of visible wavelength data to the SCAS system. In other words, without ECAS data of 371 Bohemia we cannot use its spectral characteristics to identify it as a possible parent body of ordinary chondrite meteorites. Author (revised)

N94-12163*# Hawaii Univ., Honolulu. Planetary Geosciences.
SIMULATION OF POSSIBLE REGOLITH OPTICAL ALTERATION EFFECTS ON CARBONACEOUS CHONDRITE METEORITES Abstract Only c90
Beth E. Clark, Fraser P. Fanale, and Mark S. Robinson *In* Lunar and Planetary Inst., Twenty-fourth Lunar and Planetary Science Conference. Part 1: A-F 1993 p 301-302 (For primary document see N94-12015 01-91)
Avail: CASI HC A01/MF A06

As the spectral reflectance search continues for links between meteorites and their parent body asteroids, the effects of optical surface alteration processes need to be considered. We present the results of an experimental simulation of the melting and recrystallization that occurs to a carbonaceous chondrite meteorite regolith powder upon heating. As done for the ordinary chondrite meteorites, we show the effects of possible parent-body regolith alteration processes on reflectance spectra of carbonaceous chondrites (CC's). For this study, six CC's of different mineralogical classes were obtained from the Antarctic Meteorite Collection: two CM meteorites, two CO meteorites, one CK, and one CV. Each sample was ground with a ceramic mortar and pestle to powders with maximum grain sizes of 180 and 90 microns. The reflectance spectra of these powders were measured at RELAB (Brown University) from 0.3 to 2.5 microns. Following comminution, the 90 micron grain size was melted in a nitrogen controlled-atmosphere fusion furnace at an approximate temperature of 1700 C. The fused sample was immediately held above a flow of nitrogen at 0 C for quenching. Following melting and recrystallization, the samples were reground to powders, and the reflectance spectra were remeasured. The effects on spectral reflectance for a sample of the CM carbonaceous chondrite called Murchison are shown. Author (revised)

N94-12164*# Hawaii Univ., Honolulu. Planetary Geosciences.
SPECTRAL MIXING MODELS OF S-TYPE ASTEROIDS Abstract Only c90
Beth E. Clark, Paul G. Lucey, Jeffrey F. Bell, and Fraser P. Fanale *In* Lunar and Planetary Inst., Twenty-fourth Lunar and Planetary Science Conference. Part 1: A-F 1993 p 303-304 (For primary document see N94-12015 01-91)
Avail: CASI HC A01/MF A06

This paper presents the results of an attempt to determine S-Type asteroid mineralogies with the use of Hapke theory spectral mixing modelling. Previous attempts to understand the spectral variations present in this single class of asteroids have concentrated on spectral parameters such as absorption band center wavelengths, band area ratios, and geometric albedos. The procedure taken here is to utilize the Hapke spectral reflectance model to calculate single scatter albedo as a function of wavelength for a suite of candidate end-member materials. These materials are then mixed linearly in single scatter albedo space, and the mixture is converted, assuming intimate particle mixing, back to reflectance for the spectrum matching routine. A total of 39 S-Type asteroids selected from the Bell et al. survey have been matched with mixture model spectra. Author (revised)

N94-12165*# Albright Coll., Reading, Pa.
REMOTE SENSING X RAY FLUORESCENCE SPECTROMETRY FOR FUTURE LUNAR EXPLORATION MISSIONS Abstract Only
Pamela E. Clark, Larry G. Evans (Computer Sciences Corp., Calverton, MD.), and Jacob I. Trombka (National Aeronautics and Space Administration. Goddard Space Flight Center, Greenbelt, MD.) *In* Lunar and Planetary Inst., Twenty-fourth Lunar and Planetary Science Conference. Part 1: A-F 1993 p 305-306 (For primary document see N94-12015 01-91)
Avail: CASI HC A01/MF A06

Measurement of discrete line X-ray emission from space can be used to obtain both qualitative and quantitative elemental surface composition information. Remote orbital X-ray elemental analysis is the measurement of characteristic X-rays following the interaction of solar X-rays with the surface of a given solid body. Thus, X-ray emission from a surface is strongly dependent on the incident solar spectrum as well as on the chemical composition of the surface. In this paper, the relationship between the solar flux and the major lunar element fluorescence and scattered X-ray flux is characterized. A model was developed to calculate lunar surface X-ray fluorescence emission spectra under a variety of solar conditions and, in particular, conditions that might be expected for a Lunar Scout mission proposed for 1995 or 1996. This time period should be during solar minimum. Author (revised)

N94-12166*# Clemson Univ., SC. Dept. of Physics and Astronomy.
CARBON AND NITROGEN IN TYPE 2 SUPERNOVA DIAMONDS Abstract Only c90
Donald D. Clayton, Mounib ElEid, and Lawrence E. Brown *In* Lunar and Planetary Inst., Twenty-fourth Lunar and Planetary Science Conference. Part 1: A-F 1993 p 307-308 (For primary document see N94-12015 01-91)
Avail: CASI HC A01/MF A06

Abundant diamonds found in meteorites seem either to have condensed within supernova interiors during their expansions and coolings or to have been present around those explosions. Either alternative allows implantation of Xe-HL prior to interstellar mixing. A puzzling feature is the near normalcy of the carbon isotopes, considering that the only C-rich matter, the He-burning shell, is pure C-12 in that region. That last fact has caused many to associate supernova carbon with C-12 carbon, so that its SUNOCONS have been anticipated as very C-12-rich. We show that this expectation is misleading because the C-13-rich regions of Type 2's have been largely overlooked in this thinking. We here follow the idea that the diamonds nucleated in the C-12-rich He shell, the only C-rich site for nucleation, but then attached C-13-rich carbon during turbulent encounters with overlying C-13-rich matter. That is, the initial diamonds continued to grow during the same collisional encounters that cause the Xe-HL implantation. Instead of interacting with the small carbon mass having $13/12 = 0.2$ in the upper He zone, however, we have calculated the remnants of the initial H-burning core, which left behind C-13-rich matter as it receded during core hydrogen burning. Howard et al. described why the velocity mixing would be essential to understanding the implantation of both the Xe-H and Xe-L components. Velocity mixing is now known to occur from the X-ray and gamma-ray light curves of supernova 1987A. Using the stellar evolution code developed at Goettingen, we calculated at Clemson the evolution of a grid of massive stars up to the beginning of core He burning. We paid attention to all H-burning reactions throughout the star, to the treatment of both convection and semiconvection, and to the recession of the outer boundary of the convective H-burning core as the star expands toward a larger redder state. This program was to generate a careful map of the CNO isotope distribution as He burning begins. Our result for the 30 solar mass star is shown. Author (revised)

N94-12167*# Stanford Univ., CA. Dept. of Chemistry.
MEASUREMENT OF POLYCYCLIC AROMATIC HYDROCARBON (PAHs) IN INTERPLANETARY DUST PARTICLES Abstract Only c90
S. J. Clemett, C. R. Maechling, R. N. Zare, P. D. Swan (Washington Univ., Saint Louis, MO.), and R. M. Walker (Washington Univ., Saint Louis, MO.) *In* Lunar and Planetary Inst., Twenty-fourth Lunar and Planetary Science Conference. Part 1: A-F 1993 p 309-310 (For primary document see N94-12015 01-91)
Avail: CASI HC A01/MF A06

We report here the first definitive measurements of specific organic molecules (polycyclic aromatic hydrocarbons (PAH's)) in interplanetary dust particles (IDP's). An improved version of the microbeam-two-step laser mass spectrometer was used for the analysis. Two IDP's gave similar mass spectra showing an abundance of PAH's. Control samples, including particles of probable terrestrial origin from the same stratospheric collector, gave either null results or quite different spectra. We conclude that the PAH's are probably indigenous to the IDP's and are not terrestrial contaminants. The instrument used to study the particles is a two-step laser mass spectrometer. Constituent neutral molecules of the sample are first desorbed with a pulsed infrared laser beam focussed to 40 micrometers. In the second step, PAH's in the desorbed plume are preferentially ionized by a pulsed UV laser beam. Resulting ions produced by resonant absorption are extracted into a reflectron time-of-flight mass spectrometer. This instrument has high spatial resolution, high ion transmission, unlimited mass range, and multichannel detection of all ion masses from a single laser shot. Author (revised)

N94-12168*# Lunar and Planetary Inst., Houston, TX.
MARS: THE INITIAL EMPLACEMENT OF GROUND ICE IN RESPONSE TO THE THERMAL EVOLUTION OF ITS EARLY CRUST Abstract Only
Stephen M. Clifford *In its* Twenty-fourth Lunar and Planetary Science

Conference. Part 1: A-F 1993 p 311-312 (For primary document see N94-12015 01-91)
Avail: CASI HC A01/MF A06

Given the geomorphic evidence for the widespread occurrence of water and ice in the early martian crust, and the difficulty involved in accounting for this distribution given the present climate, it has been suggested that the planet's early climate was originally more Earth-like, permitting the global emplacement of crustal H2O by direct precipitation as snow or rain. The resemblance of the martian valley networks to terrestrial runoff channels, and their almost exclusive occurrence in the planet's ancient (approximately 4 billion year old) heavily cratered terrain, is often cited as evidence of just such a period. An alternative school of thought suggests that the early climate did not differ substantially from that of today. Advocates of this view find no compelling reason to invoke a warmer, wetter period to explain the origin of the valley networks. Rather, they cite evidence that the primary mechanism of valley formation was ground water sapping, a process that does not require that surface water exist in equilibrium with the atmosphere. However, while sapping may successfully explain the origin of the small valleys, it fails to address how the crust was initially charged with ice as the climate evolved towards its present state. Therefore, given the uncertainty regarding the environmental conditions that prevailed on early Mars, the initial emplacement of ground ice is considered from two perspectives: (1) that the early climate started warm and wet, but gradually cooled with time; and (2) that it never differed substantially from that of today. Author (revised)

N94-12169*# Lunar and Planetary Inst., Houston, TX.
THE ROLE OF THE GEOTHERMAL GRADIENT IN THE EMPLACEMENT AND REPLENISHMENT OF GROUND ICE ON MARS Abstract Only
Stephen M. Clifford *In its* Twenty-fourth Lunar and Planetary Science Conference. Part 1: A-F 1993 p 313-314 (For primary document see N94-12015 01-91)
Avail: CASI HC A01/MF A06

Knowledge of the mechanisms by which ground ice is emplaced, removed, and potentially replenished, are critical to understanding the climatic and hydrologic behavior of water on Mars, as well as the morphologic evolution of its surface. Because of the strong temperature dependence of the saturated vapor pressure of H2O, the atmospheric emplacement or replenishment of ground ice is prohibited below the depth at which crustal temperatures begin to monotonically increase due to geothermal heating. In contrast, the emplacement and replenishment of ground ice from reservoirs of H2O residing deep within the crust can occur by at least three different thermally-driven processes, involving all three phases of water. In this regard, Clifford has discussed how the presence of a geothermal gradient as small as 15 K/km can give rise to a corresponding vapor pressure gradient sufficient to drive the vertical transport of 1 km of water from a reservoir of ground water at depth to the base of the cryosphere every 10(exp 6) - 10(exp 7) years. This abstract expands on this earlier treatment by considering the influence of thermal gradients on the transport of H2O at temperatures below the freezing point. Author (revised)

N94-12170*# Lunar and Planetary Inst., Houston, TX.
THE THERMODYNAMIC CASE FOR A WATER-RICH MARS Abstract Only
Stephen M. Clifford *In its* Twenty-fourth Lunar and Planetary Science Conference. Part 1: A-F 1993 p 315-316 (For primary document see N94-12015 01-91)
Avail: CASI HC A01/MF A06

The geologic evidence for a water-rich Mars has been reviewed, and it has been concluded that it is consistent with an outgassed inventory of H2O equivalent to global ocean 0.5-1 km deep. The most persuasive support for this conclusion comes from the martian outflow channels, whose distribution, size, and range of ages, suggests that a significant body of ground water was present on Mars throughout much of its geologic history. In this abstract, the thermodynamic implications of the outflow channels are considered. The results of this analysis suggest that if the outflow channels were carved by the discharge of ground water in diffusive and thermodynamic equilibrium with the overlying frozen crust, it implies a minimum planetary inventory of water in excess of 300 m. However, if the global inventory of ground water on Mars at the time of outflow channel formation was as high as the 500 m estimate of other researchers, then the total inventory of water on Mars could well exceed 750 m.
Author (revised)

N94-12171*# Alberta Univ., Calgary.
OLIVINE-RICH ASTEROIDS, PALLASITIC OLIVINE AND OLIVINE-METAL MIXTURES: COMPARISONS OF REFLECTANCE SPECTRA Abstract Only c90
E. A. Cloutis *In* Lunar and Planetary Inst., Twenty-fourth Lunar and Planetary Science Conference. Part 1: A-F 1993 p 317-318 (For primary document see N94-12015 01-91)
Avail: CASI HC A01/MF A06

The recent acquisition of high resolution 0.3 - 2.6 micron reflectance spectra for a number of olivine-rich asteroids permits the analysis of their surface compositions to be made on the basis of new and existing laboratory spectral data for pallasitic olivines and olivine-metal mixtures. Analysis of the spectral data for the latter has revealed a number of spectral parameters which can be used to constrain olivine and metal abundances, grain sizes, and olivine compositions. The following topics are discussed in greater detail: pallasite olivine spectra, olivine-metal mixture spectra, and olivine-rich asteroid spectra. Author (revised)

N94-12172*# Newcastle-upon-Tyne Univ. (England). Dept. of Physics.
REMANENT MAGNETISM OF HED METEORITES: IMPLICATIONS FOR THEIR EVOLUTION AND ANCIENT MAGNETIC FIELDS Abstract Only c90
D. W. Collinson and S. J. Morden *In* Lunar and Planetary Inst., Twenty-fourth Lunar and Planetary Science Conference. Part 1: A-F 1993 p 319-320 (For primary document see N94-12015 01-91)
Avail: CASI HC A01/MF A06

The magnetic properties of extraterrestrial materials, in particular natural remanent magnetization (NRM), is a potentially useful study for detecting ancient Solar System magnetic fields and for elucidating meteorite evolutionary processes. Results are presented for the following: howardites--Kapoeta, Petersburg, Le Teilleul, and EET 87503; eucrites--Sioux County and Millbillillie; and diogenites--Shalka and Johnstown. Significant features of their magnetism are within-sample in homogeneity of NRM directions in several of the meteorites and within-sample uniformity of axes of an isotropy of magnetic susceptibility. Both these phenomena bear on the meteorites' evolution and the timing of the magnetization process.
Author (revised)

N94-12173*# Washington Univ., Saint Louis, MO. Dept. of Earth and Planetary Sciences.
GRAPHITE SOLUBILITY AND CO-VESICULATION IN BASALT-LIKE MELTS AT ONE-ATM Abstract Only
R. O. Colson *In* Lunar and Planetary Inst., Twenty-fourth Lunar and Planetary Science Conference. Part 1: A-F 1993 p 321-322 (For primary document see N94-12015 01-91)
Avail: CASI HC A01/MF A06

The identity and source of the vapor phase that caused lunar lava-fountaining and vesiculation in lunar basalts continues to be of interest because of its implications for the composition and state of the lunar interior and because of its implications for lunar resources. In light of the apparent near-absence of H2O on the Moon, it has been suggested that the vapor phase may be CO2-CO. This premise is supported by the presence of carbon on the surface of volcanic glass beads. However, although the rapid exsolution of CO2 from a melt during decompression may be consistent with firefountaining, it fails to provide a satisfying explanation for vesiculation in mare basalt where exsolution of the gas phase would more reasonably be related to cooling/crystallization at low pressure rather than decompression from high pressure. Also, geochemical trends in lunar volcanic glasses suggest that their source has an oxygen fugacity more reducing than the iron-wustite buffer, an oxygen fugacity that is inconsistent with presence of dissolved CO2-CO at depth. The results of experiments in which a vesicular 'basalt' is produced from a melt equilibrated with graphite and pure CO gas at one atmosphere pressure are reported. The vesiculation is apparently related to exsolution of CO or a CO species during cooling of the melt or growth of quench crystals. Additionally, particulate carbon dispersed through the quenched sample suggests that elemental carbon is either in solution in the melt prior to quenching or tends to go into suspension perhaps as colloid-like particles. These two observations may provide insight into the nature of fire-fountaining and vesiculation on the Moon. Author (revised)

N94-12174*# Washington Univ., Saint Louis, MO. Dept. of Earth and Planetary Sciences.
CRYSTAL-CHEMISTRY AND PARTITIONING OF REE IN WHITLOCKITE Abstract Only **c76**
R. O. Colson and B. L. Jolliff *In* Lunar and Planetary Inst., Twenty-fourth Lunar and Planetary Science Conference. Part 1: A-F 1993 p 323-324 (For primary document see N94-12015 01-91)
(Grant NAG9-56)
Avail: CASI HC A01/MF A06

Partitioning of Rare Earth Elements (REE) in whitlockite is complicated by the fact that two or more charge-balancing substitutions are involved and by the fact that concentrations of REE in natural whitlockites are sufficiently high such that simple partition coefficients are not expected to be constant even if mixing in the system is completely ideal. The present study combines preexisting REE partitioning data in whitlockites with new experiments in the same compositional system and at the same temperature (approximately 1030 C) to place additional constraints on the complex variations of REE partition coefficients and to test theoretical models for how REE partitioning should vary with REE concentration and other compositional variables. With this data set, and by combining crystallographic and thermochemical constraints with a SAS simultaneous-equation best-fitting routine, it is possible to infer answers to the following questions: what is the speciation on the individual sites Ca(B), Mg, and Ca(IIA) (where the ideal structural formula is Ca(B)18 Mg2Ca(IIA)2P14O56); how are REE's charge-balanced in the crystal; and is mixing of REE in whitlockite ideal or non-ideal. This understanding is necessary in order to extrapolate derived partition coefficients to other compositional systems and provides a broadened understanding of the crystal chemistry of whitlockite. Author (revised)

N94-12175*# Colorado Univ., Boulder. Lab. for Atmospheric and Space Physics.
POWER-LAW CONFUSION: YOU SAY INCREMENTAL, I SAY DIFFERENTIAL Abstract Only **c65**
Joshua E. Colwell *In* Lunar and Planetary Inst., Twenty-fourth Lunar and Planetary Science Conference. Part 1: A-F 1993 p 325-326 (For primary document see N94-12015 01-91)
Avail: CASI HC A01/MF A06

Power-law distributions are commonly used to describe the frequency of occurrences of crater diameters, stellar masses, ring particle sizes, planetesimal sizes, and meteoroid masses to name a few. The distributions are simple, and this simplicity has led to a number of misstatements in the literature about the kind of power-law that is being used: differential, cumulative, or incremental. Although differential and cumulative power-laws are mathematically trivial, it is a hybrid incremental distribution that is often used and the relationship between the incremental distribution and the differential or cumulative distributions is not trivial. In many cases the slope of an incremental power-law will be nearly identical to the slope of the cumulative power-law of the same distribution, not the differential slope. The discussion that follows argues for a consistent usage of these terms and against the oft-made implicit claim that incremental and differential distributions are indistinguishable. Author (revised)

N94-12176*# Rutgers Univ., New Brunswick, NJ. Dept. of Geological Science.
THE EXPERIMENTAL PRODUCTION OF MATRIX LUMPS WITHIN CHONDRULES: EVIDENCE OF POST-FORMATIONAL PROCESSES Abstract Only **c90**
Harold C. Connolly, Jr. and Roger H. Hewins *In* Lunar and Planetary Inst., Twenty-fourth Lunar and Planetary Science Conference. Part 1: A-F 1993 p 327-328 (For primary document see N94-12015 01-91)
(Grant NGT-50836)
Avail: CASI HC A01/MF A06

The processes that acted upon chondrules after their formation are as important clues to the nature of the early solar nebula as are the exact processes that formed the chondrules. Recent experiments have studied the rim forming processes and the effects the processes have on chondrules. We present below information on how matrix inclusions found within chondrules may have been formed and the potential usefulness of this information. Author (revised)

N94-12177*# Rutgers Univ., New Brunswick, NJ. Dept. of Geological Sciences.
FLASH MELTING OF CHONDRULE PRECURSORS IN EXCESS OF 1600 C. SERIES 1: TYPE 2 (B1) CHONDRULE COMPOSITION EXPERIMENTS Abstract Only **c90**
Harold C. Connolly, Jr., Roger H. Hewins, and Gary E. Lofgren (National Aeronautics and Space Administration. Lyndon B. Johnson Space Center, Houston, TX.) *In* Lunar and Planetary Inst., Twenty-fourth Lunar and Planetary Science Conference. Part 1: A-F 1993 p 329-330 (For primary document see N94-12015 01-91)
(Grant NGT-50836)
Avail: CASI HC A01/MF A06

Several questions in chondrule production remain an enigma despite years of experiments. What were the melting temperatures experienced by chondrules? What were the physical characteristics of chondrule precursors? How and why did volatile elements (i.e. Na) found within chondrules survive the formation process? We present the initial results of a series of experiments designed to investigate the above questions by using flash melting to duplicate the melting stage of chondrule formation. Author

N94-12178*# POD Associates, Inc., Albuquerque, NM.
MODELLING HYPERVELOCITY IMPACTS INTO ALUMINUM STRUCTURES BASED ON LDEF DATA Abstract Only **c39**
C. R. Coombs, D. R. Atkinson, A. J. Watts, J. R. Wagner, M. K. Allbrooks, and C. J. Hennessy *In* Lunar and Planetary Inst., Twenty-fourth Lunar and Planetary Science Conference. Part 1: A-F 1993 p 331-332 (For primary document see N94-12015 01-91)
Avail: CASI HC A01/MF A06

Realizing and understanding the effects of the near-Earth space environment on a spacecraft during its mission lifetime is becoming more important with the regeneration of America's space program. Included among these potential effects are the following: erosion and surface degradation due to atomic oxygen impingement; ultraviolet exposure embrittlement; and delamination, pitting, cratering, and ring formation due to micrometeoroid and debris impacts. These effects may occur synergistically and may alter the spacecraft materials enough to modify the resultant crater, star crack, and/or perforation. This study concentrates on modelling the effects of micrometeoroid and debris hypervelocity impacts into aluminum materials (6061-T6). Space debris exists in all sizes, and has the possibility of growing into a potentially catastrophic problem, particularly since self-collisions between particles can rapidly escalate the number of small impactors. We have examined the morphologies of the Long Duration Exposure Facility (LDEF) impact craters and the relationship between the observed impact damage on LDEF versus the existing models for both the natural (micrometeoroid) and manmade (debris) environments in order to better define these environments. Author (revised)

N94-12179*# Lunar and Planetary Inst., Houston, TX.
USING LUNAR SOUNDER IMAGERY TO DISTINGUISH SURFACE FROM SUBSURFACE REFLECTORS IN LUNAR HIGHLANDS AREAS Abstract Only
Bonnie L. Cooper and James L. Carter (Texas Univ., Dallas.) *In its* Twenty-fourth Lunar and Planetary Science Conference. Part 1: A-F 1993 p 333-334 (For primary document see N94-12015 01-91)
Avail: CASI HC A01/MF A06

We have developed a method using the Apollo 17 Lunar Sounder imagery data which appears capable of filtering out off-nadir surface noise from highland area profiles, so that subsurface features may now be detected in highland areas as well as mare areas. Previously, this had been impossible because the rough topography in the highland areas created noise in the profiles which could not be distinguished from subsurface echoes. The new method is an image processing procedure involving the computerized selection of pixels which represent intermediate echo intensity values, then manually removing those pixels from the profile. Using this technique, a subsurface feature with a horizontal extent of about 150 km, at a calculated depth of approximately 3 km, has been detected beneath the crater Riccioli in the highlands near Oceanus Procellarum. This result shows that the ALSE data contain much useful information that remains to be extracted and used. Author (revised)

N94-12180*# National Air and Space Museum, Washington, DC. Center for Earth and Planetary Studies.

GEOLOGIC HISTORY OF CENTRAL CHRYSE PLANITIA AND THE VIKING 1 LANDING SITE, MARS Abstract Only

Robert A. Craddock, L. S. Crumpler (Brown Univ., Providence, RI.), and Jayne C. Aubele (Brown Univ., Providence, RI.) *In* Lunar and Planetary Inst., Twenty-fourth Lunar and Planetary Science Conference. Part 1: A-F 1993 p 335-336 (For primary document see N94-12015 01-91)

Avail: CASI HC A01/MF A06

A 1:500,000 scale geologic mapping was undertaken to synthesize the broad-scale geology of Chryse Planitia with the local geology of the Viking 1 landing site. The geology of Mars Transverse Mercators (MTM's) 20047 and 25047 has been presented previously. As part of the goals for the Mars Geologic Mapping program, the rational and scientific objectives for a return mission to Chryse Planitia and the Viking 1 Lander have also been presented. However, in mapping central Chryse Planitia our principle objective was to determine the depositional and erosional history of the Chryse Planitia basin. These results are presented. Author (revised)

N94-12181*# Brown Univ., Providence, RI. Dept. of Geological Sciences.

MACROSCOPIC ELECTRIC CHARGE SEPARATION DURING HYPERVELOCITY IMPACTS: POTENTIAL IMPLICATIONS FOR PLANETARY PALEOMAGNETISM Abstract Only c90

D. A. Crawford and P. H. Schultz *In* Lunar and Planetary Inst., Twenty-fourth Lunar and Planetary Science Conference. Part 1: A-F 1993 p 337-338 (For primary document see N94-12015 01-91)

Avail: CASI HC A01/MF A06

The production of transient magnetic fields by hypervelocity meteoroid impact has been proposed to possibly explain the presence of paleomagnetic fields in certain lunar samples as well as across broader areas of the lunar surface. In an effort to understand the lunar magnetic record, continued experiments at the NASA Ames Vertical Gun Range allow characterizing magnetic fields produced by the 5 km/s impacts of 0.32-0.64 cm projectiles over a broad range of impact angles and projectile/target compositions. From such studies, another phenomenon has emerged, macroscopic electric charge separation, that may have importance for the magnetic state of solid-body surfaces. This phenomenon was observed during explosive cratering experiments, but the magnetic consequences of macroscopic electric charge separation (as opposed to plasma production) during explosion and impact cratering have not, to our knowledge, been explored before now. It is straightforward to show that magnetic field production due to this process may scale as a weakly increasing function of impactor kinetic energy, although more work is needed to precisely assess the scaling dependence. The original intent of our experiments was to assess the character of purely electrostatic signals for comparison with inferred electrostatic noise signals acquired by shielded magnetic sensors buried within particulate dolomite targets. The results demonstrated that electrostatic noise does affect the magnetic sensors but only at relatively short distances (less than 4 cm) from the impact point (our magnetic studies are generally performed at distances greater than approximately 5.5 cm). However, to assess models for magnetic field generation during impact, measurements are needed of the magnetic field as close to the impact point as possible; hence, work with an improved magnetic sensor design is in progress. In this paper, we focus on electric charge separation during hypervelocity impacts as a potential transient magnetic field production mechanism in its own right. Author (revised)

N94-12182*# University of Southern California, Pasadena. Div. of Geological and Planetary Sciences.

RHENIUM-OSMIUM ISOTOPE SYSTEMATICS OF GROUP 2A AND GROUP 4A IRON METEORITES Abstract Only c90

R. A. Creaser (Alberta Univ., Edmonton.), D. A. Papanastassiou, and G. J. Wasserburg *In* Lunar and Planetary Inst., Twenty-fourth Lunar and Planetary Science Conference. Part 1: A-F 1993 p 339-340 (For primary document see N94-12015 01-91)

(Grant NAG9-43)

Avail: CASI HC A01/MF A06

We are investigating the Re-Os isotope systematics of two groups of magmatic iron meteorites (2A, 4A) in an attempt to establish precise 'total rock' isochrons by the Re-Os system. The Re-187/Os-187 isotope system is recognized as a method by which the ages of iron meteorites can be directly determined and that can provide information on the timing of FeNi segregation and core formation in planetesimals. The Re-Os isotope system permits the direct absolute dating of the metal phase in iron meteorites. Indirect dating of iron meteorites has been achieved in the past through the Rb-Sr, K-Ar, and most recently, Sm-Nd for silicate inclusions, where present. Relative dating has been obtained directly by extensive studies of the short-lived system Pd-107/Ag-107 for the metal and sulfide phases and indirectly using I-129/Xe-129 in silicate and sulfide inclusions. Author (revised)

N94-12183*# Toronto Univ. (Ontario). Iso Trace Lab.

SEPARATION OF SPALLATION AND TERRESTRIAL C-14 IN CHONDRITES Abstract Only c90

R. G. Cresswell, R. P. Beukens, and J. C. Rucklidge *In* Lunar and Planetary Inst., Twenty-fourth Lunar and Planetary Science Conference. Part 1: A-F 1993 p 341-342 (For primary document see N94-12015 01-91)

Avail: CASI HC A01/MF A06

Weathering products and contamination severely hamper our ability to accurately measure the C-14 spallation component in meteorites, but can give insights into a sample's terrestrial history. A procedure was developed to measure the C-14 in these components using CO and CO2 separations from temperature extractions from 200-500 mg of material. The Bruderheim (L6) chondrite was chosen as a standard following the practice of previous researchers, crosschecked against Peace River (L6), Abee (EH4), and Juvinas (EUC). Low temperature fractions (less than 900 C) give C-14 signatures consistent with a modern terrestrial C-14 source; melt fractions show elevated levels attesting to a spallogenic origin. Higher yields of CO in the melt fraction are less affected by the low levels of experimental contamination than the CO2. This fraction gave a mean CO:CO2 ratio in Bruderheim of 81.6 +/- 7.7; the ratio of the spallation component is 79.8 +/- 8.1. These values suggest equilibrium release of gases on the olivine-silica-pyroxene-iron buffer. This is corroborated by approximately equal release of the two components at 900 C. The chondrites gave an average saturation level of 54.3 +/- 2.9 dpm/kg; the achondrite gave 49.6 +/- 2.0 dpm/kg. No clear correlation with oxygen content is apparent, though shielding effects have yet to be evaluated. A further evaluation of this subject matter is given. Author (revised)

N94-12184*# Jet Propulsion Lab., California Inst. of Tech., Pasadena.

NEAR-INFRARED SPECTRA OF THE MARTIAN SURFACE: READING BETWEEN THE LINES Abstract Only

D. Crisp and J. F. Bell, III (National Aeronautics and Space Administration. Ames Research Center, Moffett Field, CA.) *In* Lunar and Planetary Inst., Twenty-fourth Lunar and Planetary Science Conference. Part 1: A-F 1993 p 343-344 (For primary document see N94-12015 01-91)

Avail: CASI HC A01/MF A06

Moderate-resolution near-infrared (NIR) spectra of Mars have been widely used in studies of the Martian surface because many candidate surface materials have distinctive absorption features at these wavelengths. Recent advances in NIR detector technology and instrumentation have also encouraged studies in this spectral region. The use of moderate spectral resolution has often been justified for NIR surface observations because the spectral features produced by most surface materials are relatively broad, and easily discriminated at this resolution. In spite of this, NIR spectra of Mars are usually very difficult to interpret quantitatively. One problem is that NIR surface absorption features are often only a few percent deep, requiring observations with great signal-to-noise ratios. A more significant problem is that gases in the Martian atmosphere contribute numerous absorption features at these wavelengths. Ground-based observers must also contend with variable absorption by several gases in the Earth's atmosphere (H2O, CO2, O3, N2O, CH4, O2). The strong CO2 bands near 1.4, 1.6, 2.0, 2.7, 4.3, and 4.8 micrometers largely preclude the analysis of surface spectral features at these wavelengths. Martian atmospheric water vapor also contributes significant absorption near 1.33, 1.88, and 2.7 micrometers, but water vapor in the Earth's atmosphere poses a much larger problem to ground-based studies of these spectral regions. The third most important NIR absorber in the Martian atmosphere is CO. This gas absorbs most strongly in the relatively-transparent spectral windows near 4.6 and 2.3 micrometers. It also produces 1-10 percent absorption in the solar spectrum at these NIR wavelengths. This solar CO absorption cannot be adequately removed by dividing the Martian spectrum by that of a star, as is commonly done to calibrate ground-based spectroscopic observations, because most stars do not have identical amounts of CO absorption in their spectra. Here, we describe tow effective methods for eliminating contamination of Martian surface spectra by absorption in the solar, terrestrial, and Martian atmospheres. Both methods involve the use of very-high-resolution spectra that completely resolve the narrow atmospheric absorption lines. Author (revised)

N94-12185*# Arizona Univ., Tucson. Lunar and Planetary Lab.
GEOMORPHOLOGY OF TRITON'S POLAR MATERIALS Abstract Only
Steven K. Croft *In* Lunar and Planetary Inst., Twenty-fourth Lunar and Planetary Science Conference. Part 1: A-F 1993 p 345-346 (For primary document see N94-12015 01-91)
Avail: CASI HC A01/MF A06

One of Triton's most debated puzzles is the nature, distribution, and transport of its atmospheric volatiles. The full potential of constraints provided by detailed observations of the morphology and distribution of the polar deposits has not been realized. The objective of this study is characterization of the morphology, distribution, stratigraphy, and geologic setting of Triton's polar materials. Author

N94-12186*# Arizona Univ., Tucson. Lunar and Planetary Lab.
POROSITY AND THE ECOLOGY OF ICY SATELLITES Abstract Only **c90**
Steven K. Croft *In* Lunar and Planetary Inst., Twenty-fourth Lunar and Planetary Science Conference. Part 1: A-F 1993 p 347-348 (For primary document see N94-12015 01-91)
Avail: CASI HC A01/MF A06

The case for a significant role for porosity in the structure and evolution of icy bodies in the Solar System has been difficult to establish. We present a relevant new data set and a series of structure models including a mechanical compression, not thermal creep, model for porosity that accounts satisfactorily for observed densities, moments of inertia, geologic activity, and sizes of tectonic features on icy satellites. Several types of observational data sets have been used to infer significant porosity, but until recently, alternative explanations have been preferred. Our first area of concern is the occurrence of cryovolcanism as a function of satellite radius; simple radiogenic heating models of icy satellites suggest minimum radii for melting and surface cryovolcanism to be 400 to 500 km, yet inferred melt deposits are seen on satellites half that size. One possible explanation is a deep, low conductivity regolith which lowers conductivity and raises internal temperatures, but other possibilities include tidal heating or crustal compositions of low conductivity. Our second area of concern is the occurrence and magnitude of tectonic strain; tectonic structures have been seen on icy satellites as small as Mimas and Proteus. The structures are almost exclusively extensional, with only a few possible compression Al features, and inferred global strains are on the order of 1 percent expansion. Expansions of this order in small bodies like Mimas and prevention of late compressional tectonics due to formation of ice mantles in larger bodies like Rhea are attained only in structure models including low-conductivity, and thus possibly high porosity, crusts. Thirdly, inferred moments of inertia less than 0.4 in Mimas and Tethys can be explained by high-porosity crusts, but also by differentiation of a high density core. Finally, the relatively low densities of smaller satellites like Mimas and Miranda relative to larger neighbors can be explained by deep porosity, but also by bulk compositional differences. Recent work has strengthened the case for significant porosity. Halley's nucleus was found to have a density near 0.6 g/cu cm, Janus and Epimethus were proposed to have densities near 0.7 g/cu cm, densities almost certainly due to high porosity. The irregular-spherical shape transition of icy satellites was quantitatively explained by low conductivity regoliths. A creative structure/thermal history model for Mimas simultaneously accounts quantitatively for Mimas' low density and moment of inertia by invoking initial high-porosity and subsequent compaction in the deep interior by thermal creep. The main problem with this promising model is that approximately 7 percent predicts a reduction in Mimas' radius, implying significant compressional failure and prevention of extensional tectonics, in contradiction to the observed extensional features and inferred 1 percent expansion in radius. Author (revised)

N94-12187*# Arizona Univ., Tucson. Lunar and Planetary Lab.
TECTONICS ON TRITON Abstract Only
Steven K. Croft *In* Lunar and Planetary Inst., Twenty-fourth Lunar and Planetary Science Conference. Part 1: A-F 1993 p 349-350 (For primary document see N94-12015 01-91)
Avail: CASI HC A01/MF A06

Tectonic features on Triton have been mapped as part of a larger study of the geology of Triton. Few purely tectonic structures are found on Triton: some grabens and possibly some compressive ridges. However, most of the other structures seen (primarily cryovolcanic in origin) exhibit tectonic control. A regional tectonic network has the following dominant orientations: N-S, E-W, NE-SW, and NW-SE. Most of the orientations are consistent with tidal deformations related to Triton's decreasing orbital radius. Localized quasi-concentric patterns may be due to interior processes such as mantle plumes. Author (revised)

N94-12188*# New Mexico Univ., Albuquerque. Dept. of Earth and Planetary Sciences.
POST-IMPACT ALTERATION OF THE MANSON IMPACT STRUCTURE Abstract Only **c46**
L. J. Crossey and P. McCarville *In* Lunar and Planetary Inst., Twenty-fourth Lunar and Planetary Science Conference. Part 1: A-F 1993 p 351-352 (For primary document see N94-12015 01-91)
Avail: CASI HC A01/MF A06

Core materials from the Manson impact site (Manson, Iowa) are examined in order to evaluate post-impact alteration processes. Diagenetic interpretation of post-impact events is based on petrologic, mineralogic, and geochemical investigation of core materials including the following: target strata, disturbed and disrupted strata, ejecta, breccias, microbreccias, and impact melt. The diagenetic study utilizes research cores obtained by the continental scientific drilling project (CSDP) at the Manson structure, as well as core and cuttings of related materials. Samples include impactites (breccias, microbreccias, and melt material), crater fill material (sedimentary clast breccias), disturbed and disrupted target rocks, and reference target material (Amoco Eisheid No. 1 materials). The study of multiple cores will permit development of a regional picture of post-impact thermal history. The specific objectives are as follows: (1) provide a detailed description of authigenic and alteration mineralogy from diverse lithologies encountered in research drill cores at the Manson impact structure, and (2) identify and relate significant post-impact mineral alteration to post-impact thermal regime (extent and duration). Results will provide mineralogical and geochemical constraints on models for post-impact processes including the following: infilling of the crater depression; cooling and hydrothermal alteration of melt rocks; and subsequent long-term, low-temperature alteration of target rocks, breccias, and melt rocks. Preliminary petrologic and x-ray diffraction examination of fracture linings and void fillings from research core M1 indicate the presence of quartz, chlorite, mixed-layer clays, gypsum/anhydrite, calcite, and minor pyrite. Author (revised)

N94-12189*# POD Associates, Inc., Albuquerque, NM.
MODEL OF OPTICAL SCATTER FROM MICROIMPACTS ON THE HUBBLE TELESCOPE Abstract Only **c74**
L. B. Crowell *In* Lunar and Planetary Inst., Twenty-fourth Lunar and Planetary Science Conference. Part 1: A-F 1993 p 353-354 (For primary document see N94-12015 01-91)
Avail: CASI HC A01/MF A06

The investigation and modelling of optical scatter from damaged or contaminated mirrors is of interest to those who wish to estimate the working life cycle of an optical system. A space born telescope faces a threat to its survival from naturally occurring micrometeoroids and man-made debris. High velocity, in the range of 4 to 14 km/s, impacts of small particles, in the range of 1 to 100 microns, will produce small craters on the impacted surface. These microcraters will typically have a size range of 3 to 300 microns for debris impacts and 6 to 600 microns for micrometeoroid impacts. If the microcraters accumulate on a telescope mirror, there will be an increase in optical scatter and a loss of image resolution. The micrometeoroid model of Cour-Palais and the orbital debris model of Kessler have been encoded in a computer program (SPENV) by the author. The output from this program has been matched with previous calculations and compared with impact data on the LDEF satellite. Subsequent work has been done to marry this computer program with an algorithm to compute optical scatter. The optical scatter algorithm employs Mie theory of scatter from small particles. Author (revised)

N94-12190*# Jet Propulsion Lab., California Inst. of Tech., Pasadena.
VOLCANISM IN SOUTHERN GUINEVERE PLANITIA, VENUS: REGIONAL VOLCANIC HISTORY AND MORPHOLOGY OF VOLCANIC DOMES Abstract Only
David A. Crown, Ellen R. Stofan, and Jeffrey J. Plaut *In* Lunar and Planetary Inst., Twenty-fourth Lunar and Planetary Science Conference. Part 1: A-F 1993 p 355-356 (For primary document see N94-12015 01-91)
Avail: CASI HC A01/MF A06

Guinevere Planitia is a low-lying region located between the highlands of Beta Regio and Eistla Regio. Analyses of Pioneer Venus, Goldstone, and Arecibo radar data suggested that the surface of Guinevere Planitia is dominated by volcanism, primarily in the form of bright, dark, and mottled plains units. Also identified in this region was the Beta-Eistla Deformation Zone, composed of ovoids and discontinuous segments of lineament belts that have been embayed by the surrounding plains. The resolution of Magellan SAR images allows detailed investigations of the volcanic deposits found in the area in order to determine the types of eruptive activity which have occurred and to constrain the regional volcanic history. Analyses of an area of southern Guinevere Planitia between 0-25 deg N and 300-330 deg indicate the presence of a wide variety of volcanic land forms, including large shield volcanoes, widespread plains, lava flow fields, and small domes, cones, and shields as well as coronae and other circular structures that have associated volcanic deposits. Author (revised)

N94-12191*# Washington Univ., Saint Louis, MO. Dept. of Earth and Planetary Sciences.
ANOMALOUS REE PATTERNS IN UNEQUILIBRATED ENSTATITE CHONDRITES: EVIDENCE AND IMPLICATIONS Abstract Only c90
Ghislaine Crozaz and Weibiao Hsu *In* Lunar and Planetary Inst., Twenty-fourth Lunar and Planetary Science Conference. Part 1: A-F 1993 p 357-358 (For primary document see N94-12015 01-91)
Avail: CASI HC A01/MF A06

We present here a study of Rare Earth Element (REE) microdistributions in unequilibrated enstatite chondrites (EOC's). Although the whole rock REE contents are similar in both unequilibrated and equilibrated chondrites, the host minerals of these refractory elements are different. In the least equilibrated ordinary chondrites (UOC's), the REE reside mainly in glass whereas, in their more equilibrated counterparts, the bulk of the REE is in calcium phosphate, a metamorphic mineral that formed by oxidation of phosphorous originally contained in metal. In the smaller group of enstatite (E) chondrites, calcium phosphate is absent and the phase that contains the highest REE concentrations is a minor mineral, CaS (oldhamite), which contains approximately 50 percent of the total Ca present. In E chondrites, elements typically considered to be lithophiles (such as Ca and Mn) occur in sulfides rather than silicates. This indicates formation under extremely reducing conditions, thus in a region of the solar nebula distinct from those that supplied the more abundant ordinary and carbonaceous chondrites. Previously, we observed a variety of REE patterns in the oldhamite of UEC's; they range from almost flat to some with pronounced positive Eu and Yb anomalies. Here, we searched for complementary REE patterns in other minerals from E chondrites and found them in the major mineral, enstatite. Whenever Eu and Yb anomalies are present in this mineral, they are always negative. Author (revised)

N94-12192*# Brown Univ., Providence, RI. Dept. of Geological Sciences.
COMPARISON OF THE DISTRIBUTION OF LARGE MAGMATIC CENTERS ON EARTH, VENUS, AND MARS Abstract Only
L. S. Crumpler *In* Lunar and Planetary Inst., Twenty-fourth Lunar and Planetary Science Conference. Part 1: A-F 1993 p 359-360 (For primary document see N94-12015 01-91)
Avail: CASI HC A01/MF A06

Volcanism is widely distributed over the surfaces of the major terrestrial planets: Venus, Earth, and Mars. Anomalous centers of magmatic activity occur on each planet and are characterized by evidence for unusual concentrations of volcanic centers, long-lived activity, unusual rates of effusion, extreme size of volcanic complexes, compositionally unusual magmatism, and evidence for complex geological development. The purpose of this study is to compare the characteristics and distribution of these magmatic anomalies on Earth, Venus, and Mars in order to assess these characteristics as they may relate to global characteristics and evolution of the terrestrial planets. Author (revised)

N94-12193*# Brown Univ., Providence, RI. Dept. of Geological Sciences.
THE MAGELLAN VOLCANIC AND MAGMATIC FEATURE CATALOG Abstract Only
L. S. Crumpler, Jayne C. Aubele, and J. W. Head *In* Lunar and Planetary Inst., Twenty-fourth Lunar and Planetary Science Conference. Part 1: A-F 1993 p 361-362 (For primary document see N94-12015 01-91)
Avail: CASI HC A01/MF A06

A catalog summarizing the location and characteristics of 1663 volcanic and magmatic centers identified in Magellan radar images of the surface of Venus is in final preparation to be submitted as a Geological Society of America Special Paper. The following is a brief summary preview of the contents and methods used in assembling the final data set, the organization of the catalog, and other notes of interest to potential users. Author (revised)

N94-12194*# Brown Univ., Providence, RI. Dept. of Geological Sciences.
SYNTHESIS OF GLOBAL THEMATIC MAPPING, VENUS: GEOLOGIC CORRELATIONS/QUESTIONS FOR THE MAGELLAN GRAVITY MISSION Abstract Only
L. S. Crumpler, J. C. Aubele, and J. W. Head *In* Lunar and Planetary Inst., Twenty-fourth Lunar and Planetary Science Conference. Part 1: A-F 1993 p 363-364 (For primary document see N94-12015 01-91)
Avail: CASI HC A01/MF A06

An important characteristic of the Magellan mission and the resulting data is that it is both global in coverage as well as extremely high in resolution. As a result, global questions may be addressed based on the constraints of extremely detailed geological evidence. An important first step in the task of interpreting the global geological record will be a synthesis of the primary geological characteristics and their relationship to significant questions. The following is a brief synthesis based on a comparison of mapped distributions, initial interpretations, and some questions that these results raise. Author (revised)

N94-12195*# Brown Univ., Providence, RI. Dept. of Geological Sciences.
LARGE VOLCANOES ON VENUS: EXAMPLES OF GEOLOGIC AND STRUCTURAL CHARACTERISTICS FROM DIFFERENT CLASSES Abstract Only
L. S. Crumpler, J. W. Head, and J. C. Aubele *In* Lunar and Planetary Inst., Twenty-fourth Lunar and Planetary Science Conference. Part 1: A-F 1993 p 365-366 (For primary document see N94-12015 01-91)
Avail: CASI HC A01/MF A06

Large volcanoes characterized by radial lava flows and similar evidence for a topographic edifice are widely distributed over the surface of Venus and geologically diverse. Based on the global identification of more than 165 examples and preliminary geologic mapping, large volcanoes range from those characterized geologically as simple lava edifices to those bearing evidence of complexly developed volcanic and structural histories. Many large volcanoes exhibit characteristics transitional to other large magnetic center types such as coronae and novae. In this study, we examine the geology and structure of several type examples of large volcanoes not addressed in previous studies which are representative of several of the morphological classes. Derived from text

N94-12196*# Brown Univ., Providence, RI. Dept. of Geological Sciences.
REGIONAL MANTLE UPWELLING ON VENUS: THE BETA-ATLA-THEMIS ANOMALY AND CORRELATION WITH GLOBAL TECTONIC PATTERNS Abstract Only
L. S. Crumpler, J. W. Head, and Jayne C. Aubele *In* Lunar and Planetary Inst., Twenty-fourth Lunar and Planetary Science Conference. Part 1: A-F 1993 p 367-368 (For primary document see N94-12015 01-91)
Avail: CASI HC A01/MF A06

The morphology and global distribution of volcanic centers and their association with other geological characteristics offers significant insight into the global patterns of geology, tectonic style, thermal state, and interior dynamics of Venus. Magellan data permit the detailed geological interpretation necessary to address questions about interior dynamics of Venus particularly as they reflect relatively physical, chemical, and thermal conditions of the interior. This paper focuses on the distribution of anomalous concentrations of volcanic centers on Venus and regional patterns of tectonic deformation as it may relate to the identification of global internal anomalies, including mantle dynamic, petrological, or thermal patterns.

Derived from text

N94-12197*# Hawaii Univ., Honolulu. Dept. of Geology and Geophysics.

THE GRANULITE SUITE: IMPACT MELTS AND METAMORPHIC BRECCIAS OF THE EARLY LUNAR CRUST Abstract Only **c46**

J. A. Cushing, G. J. Taylor, M. D. Norman, and K. Keil *In* Lunar and Planetary Inst., Twenty-fourth Lunar and Planetary Science Conference. Part 1: A-F 1993 p 369-370 (For primary document see N94-12015 01-91)

Avail: CASI HC A01/MF A06

The granulite suite consists of two major types of rocks. One is coarse-grained and poikilitic with many euhedral crystals of olivine and plagioclase. These characteristics indicate crystallization from a melt; the poikilitic granulites are impact melt breccias. The other group is finer-grained and granoblastic, with numerous triple junctions; the granoblastic granulites are metamorphic rocks. Compositional groups identified by Lindstrom and Lindstrom contain both textural types. Two pyroxene thermometry indicates that both groups equilibrated at 1000 to 1150 C. Calculations suggest that the granoblastic group, which has an average grain size of about 80 microns, was annealed for less than 6 x 10 exp 4 y at 1000 C, and for less than 2500 y at 1150 C. Similar equilibration temperatures suggest that both groups were physically associated after impact events produced the poikilitic melts. Granulitic impactites hold important information about the pre-Nectarian bombardment history of the Moon, and the composition and thermal evolution of the early lunar crust. Granulitic impactites are widely considered to be an important rock type in the lunar crust, but how they formed is poorly understood. Metal compositions and elevated concentrations of meteoritic siderophile elements suggest that most lunar granulites are impact breccias. Their occurrence as clasts in approximately 3.9 Ga breccias, and Ar-(40-39) ages greater than or = 4.2 Ga for some granulites show that they represent a component of the lunar crust which formed prior to the Nectarian cataclysm. Petrographic characteristics of lunar granulites indicate at least two endmember textural variants which apparently formed in fundamentally different ways. One type has granoblastic textures consisting of equant, polygonal to rounded grains, and abundant triple junctions with small dispersions around 120 degrees indicating a close approach to textural equilibrium. As suggested by many authors, granoblastic granulites probably formed by subsolidus annealing and recrystallization of fragmental or glassy protoliths. Examples of this type include 15418, 78155, and 79215. The other textural type consists of poikilitic to poikiloblastic rocks with euhedral to subhedral plagioclase and olivine enclosed by interstitial pyroxene. In some cases, the texture resembles that of an orthocumulate. Examples of this type include 60035, 67955, and 77017. Rounding of grain edges is common in poikilitic granulites, but the regular crystal shapes and widely dispersed dihedral angles show they are far from textural equilibrium. The textures of poikilitic granulites are more consistent with the formation of these rocks by crystallization from a melt than by subsolidus metamorphism. A few samples have been recognized with textural characteristics transitional between those of the granoblastic and poikiloblastic endmembers (e.g., 72559, 78527). Pyroxene compositions taken from the literature and determined for this study by electron microprobe were used to calculate equilibration temperatures. The Kretz Ca transfer (solvus) thermometer and the Lindsley and Anderson graphical method both give similar temperatures, which range from approximately 1000 to 1150 C. There is no apparent temperature difference between granoblastic and poikilitic varieties, but there is a hint in these data that the more ferroan varieties equilibrated to lower temperatures. Additional studies are in progress to test this possibility.

Derived from text

N94-12198*# Arizona State Univ., Tempe.

GALILEO EM-2 CONTRIBUTIONS TO THE LUNAR CONTROL NETWORK Abstract Only

M. E. Davies, T. R. Colvin (RAND Corp., Santa Monica, CA.), M. J. S. Belton (Kitt Peak National Observatory, Tucson, AZ.), and R. Greeley *In* Lunar and Planetary Inst., Twenty-fourth Lunar and Planetary Science Conference. Part 1: A-F 1993 p 371 (For primary document see N94-12015 01-91)

Avail: CASI HC A01/MF A06

A local control network is being developed using Galileo images that cover the region north of the Apollo area and lie between 10 and 100 degrees east longitude. This network is tied to the Apollo control network and will have a positional accuracy of approximately 500-1500 m. This region has been photographed by Earth-based telescopes and the Mariner 10 and Lunar Orbiter spacecraft, but the Gallileo images are preferred for control because of their superior viewing angles, resolution, and Galileo's geometrically stable sensor. Based on Davies et al., 1987, the potential accuracy of the near-side Apollo network is estimated to be between 50 and 300 m. The laser ranging retroreflector locations at the Apollo 11, 14, and 15 sites and the Lunikhod 2 site have been determined with an accuracy of about 10 m. The locations of the ALSEP transmitters relative to the retroreflectors have also been measured. These known coordinates are used to estimate errors in the Apollo network. The telescopic control is approximately bounded by 75 degrees north and south latitude and 75 degrees east and west longitudes. The accuracy of the telescopic network is thought to be about one to two km. Thus, the Galileo network might improve coordinates in the telescopic area as well as north and east of it.

Derived from text

N94-12199*# Chicago Univ., IL.

IRON AND NICKEL ISOTOPIC MASS FRACTIONATION IN DEEP-SEA SPHERULES Abstract Only **c46**

Andrew M. Davis and Donald E. Brownlee (Washington Univ., Seattle.) *In* Lunar and Planetary Inst., Twenty-fourth Lunar and Planetary Science Conference. Part 1: A-F 1993 p 373-374 (For primary document see N94-12015 01-91)

Avail: CASI HC A01/MF A06

Magnetite-wuestite spherules collected from deep-sea sediments are thought to have originally been Fe-Ni metal particles at the top of the atmosphere that were oxidized and melted during entry into the earth's atmosphere. Some likely sources for the metal particles are Fe-Ni interplanetary dust particles (IDP's) and metal or sulfide from stony IDP's that separated after melting. Davis et al. reported that four of these spherules are enriched in the heavy isotopes of iron, with enrichments of 8-23%/amu. We have developed a technique for analysis of both iron and nickel isotopes on the same ion microprobe spot and have applied this technique to a number of deep-sea spherules in order to better understand the processes leading to isotopic mass fractionation. Eight spherules show iron and nickel isotopic mass fractionation, with iron and nickel enriched in the heavy isotopes by 10-19%/amu and 4-32%/amu, respectively. If the mass fractionations are due to Rayleigh fractionation during evaporation, these spherules lost 76-94% of their original mass. We have analyzed the four magnetite-wuestite spherules for which iron isotopic data were reported by Davis et al. as well as four new spherules.

Derived from text

N94-12200*# Chicago Univ., IL.

TRACE ELEMENT DISTRIBUTIONS IN PRIMITIVE ACHONDRITES Abstract Only **c90**

Andrew M. Davis, Martin Prinz (American Museum of Natural History, New York, NY.), and Michael K. Weisberg (American Museum of Natural History, New York, NY.) *In* Lunar and Planetary Inst., Twenty-fourth Lunar and Planetary Science Conference. Part 1: A-F 1993 p 375-376 (For primary document see N94-12015 01-91)

Avail: CASI HC A01/MF A06

The primitive achondrites have approximately chondritic bulk chemical composition but achondritic textures. Clayton et al. show that nine of these meteorites, the acapulcoites and the lodranites, have similar oxygen isotopic compositions. The acapulcoites appear to be highly metamorphosed, but undifferentiated meteorites of chondritic composition; whereas, the lodranites appear to have lost a feldspathic partial melt. In order to learn more about metamorphic processes and partial melt removal, we have measured the trace element compositions of constituent phases of a number of primitive achondrites by ion microprobe. We have analyzed two acapulcoites, Acapulco and ALH81261 (paired with ALH77081), and three londranites, Lodran, LEW88280, and MAC88177. In addition, we analyzed LEW88663, which has the bulk composition, mineral chemistry, and oxygen isotopic composition of L-chondrites, but is metal-free and has an achondrite texture; and Divnoe, a plagioclase-poor, olivine-rich primitive achondrite with an oxygen isotopic composition similar to that of the group IAB iron meteorites. These meteorites show a variety of REE patterns in their constituent phases, and there are consistent differences between acapulcoites and lodranites that are consistent with removal of a LREE- and Eu-enriched melt that is apparently responsible for the low plagioclase content of lodranites. Derived from text

N94-12201*# Planetary Science Inst., Tucson, AZ.

DEVIATIONS FROM THE STRAIGHT LINE: BUMPS (AND GRINDS) IN THE COLLISIONALLY EVOLVED SIZE DISTRIBUTION OF ASTEROIDS Abstract Only c90

D. R. Davis, P. Farinella (Pisa Univ., Italy.), P. Paolicchi (Pisa Univ., Italy.), A. C. Bagatin (Pisa Univ., Italy.), A. Cellino (Osservatorio Astronomico, Turin, Italy.), and E. Zappala (Osservatorio Astronomico, Turin, Italy.) *In* Lunar and Planetary Inst., Twenty-fourth Lunar and Planetary Science Conference. Part 1: A-F 1993 p 377-378 (For primary document see N94-12015 01-91)

Avail: CASI HC A01/MF A06

Dohnanyi established that the size distribution of a collisionally relaxed population is a power-law with a -3.5 slope (incremental diameter), provided that: (1) collisional parameters are independent of size and (2) there is no lower limit on the population size for shattering impacts. In the course of studying collisional effects over a wide range of asteroid sizes (cm up to hundreds of km range), we have investigated the consequences of relaxing the second condition, while maintaining the first one. Derived from text

N94-12202*# Geological Survey, Flagstaff, AZ.

SMALL VOLCANOES IN TEMPE TERRA, MARS: THEIR DETAILED MORPHOMETRY AND INFERRED GEOLOGIC SIGNIFICANCE Abstract Only

P. A. Davis and K. L. Tanaka *In* Lunar and Planetary Inst., Twenty-fourth Lunar and Planetary Science Conference. Part 1: A-F 1993 p 379-380 (For primary document see N94-12015 01-91)

Avail: CASI HC A01/MF A06

The Tempe Terra province contains a variety of volcanic landforms that range in size from small vents (less than 10 km in diameter) to moderately sized volcanoes (150 km in diameter). The volcanoes are aligned along the dominant northerly and northeasterly trends of the faults in this region, and many of the volcanoes occur on grabens. Some workers have speculated on the nature of some of the volcanoes on the basis of their general morphology, shadow measurement height, lateral dimension, and geologic setting. As part of a larger study, we have obtained detailed photoclinometric profiles across five of the more conspicuous small volcanoes in the Tempe Terra region. For these data, we extracted for each volcano its flank width and edifice height and the width and depth of its summit crater. We statistically compared these dimensions for each volcano with a set of average dimensions for each type of terrestrial volcanic feature listed in Pike and Clow (1981). These comparisons indicate that the morphometries of the Martian volcanoes 1, 2, and 3 most closely match Earth's cratered basaltic lava shields, and the morphometries of volcanoes 4 and 5 are similar to those of terrestrial basaltic tuff rings. Derived from text

N94-12203*# Geological Survey, Flagstaff, AZ.

SHALLOW CRUSTAL DISCONTINUITIES AND GRABEN AND SCARP FORMATION IN THE THARSIS REGION OF MARS Abstract Only

P. A. Davis, K. L. Tanaka, and M. P. Golombek (Jet Propulsion Lab., California Inst. of Tech., Pasadena.) *In* Lunar and Planetary Inst., Twenty-fourth Lunar and Planetary Science Conference. Part 1: A-F 1993 p 381-382 (For primary document see N94-12015 01-91)

Avail: CASI HC A01/MF A06

We recently obtained photoclinometric profiles across all simple grabens and erosional landforms (e.g., troughs, pits, wall-valley heads, and scarps that are bounded above and below by flat surfaces) that occur within Tempe Terra. These data, together with similar data that we obtained for Syria, Sinai, and Lunae Plana and the Alba Patera region, allow regional examination of shallow crust Al discontinuities between latitude 30 deg. S and 50 deg. N and longitude 50 deg. W and 112 deg. W. The profile for each simple graben was used with an appropriate structural model to estimate the depth to the base of the faulted layer. The depths of erosional wall scarps may also indicate the depths of mechanical discontinuities such as a local lithologic or cryospheric boundary. Examination of these data indicates a surprisingly consistent set of shallow crust Al discontinuities for the Tharsis region at depths of 0.4-0.6 km, 1.0-1.4 km, and 2 km; the maximum depth of the features in most study areas appears to be about 4 km. The concentration of values between 0.4 and 0.6 km in most scarp and some faulted-layer depth data is similar to the range in estimated thicknesses of individual exposed Noachian and Hesperian plains units in the Tharsis region. The regional depth data also show two modes near 1 and 2 km in some study areas and a maximum depth near 4 km in most study areas; the faulted-layer depths in excess of 4 km at Alba Patera occur near the summit of the caldera and could be attributed to volcanic loading. Our detailed examination of these depth data includes the following observations: (1) The mode at 1.0-1.4 km depth transcends age and geologic setting in this broad study area; (2) The 2-km mode is most obvious at Alba Patera and moderately well developed at Syria and Sinai Plana, but it is muted at Tempe Terra, which is in the same latitude range as Alba Patera but older; and (3) The 2-km-depth mode is not present in all areas that have features of Amazonian age. We suggest two possible explanations for our observations in the Tharsis region. Derived from text

N94-12204*# Brown Univ., Providence, RI. Dept. of Geological Sciences.

CHARACTERISTICS OF ARACHNOIDS FROM MAGELLAN DATA Abstract Only

C. B. Dawson and L. S. Crumpler *In* Lunar and Planetary Inst., Twenty-fourth Lunar and Planetary Science Conference. Part 1: A-F 1993 p 383-384 (For primary document see N94-12015 01-91)

Avail: CASI HC A01/MF A06

Current high resolution Magellan data enables more detailed geological study of arachnoids, first identified by Barsukov et al. as features characterized by a combination of radar-bright, concentric rings and radiating lineations, named 'arachnoids' on the basis of their spider and web-like appearance. Identification of arachnoids in Magellan data has been based on SAR images, in keeping with the original definition. However, there is some overlap by other workers in identification of arachnoids, corona (predominantly bright rings), and novae (predominantly radiating lineations), as all of these features share some common characteristics. Features used in this survey were chosen based on their classification as arachnoids in Head et al.'s catalog and on SAR characteristics matching Barsukov et al.'s original definition. The 259 arachnoids have been currently identified on Venus, all of which were considered in this study. Fifteen arachnoids from different regions, chosen for their 'type' characteristics and lack of deformation by other regional processes, were studied in depth, using SAR and altimetric data to map and profile these arachnoids in an attempt to better determine their geologic and altimetric characteristics and possible formation sequences. Derived from text

N94-12205*# European Space Research Organization, Noordwikj (Netherlands). Space Science Dept.

A METHOD TO DETERMINE ASTEROID POLES Abstract Only c90

G. DeAngelis *In* Lunar and Planetary Inst., Twenty-fourth Lunar and Planetary Science Conference. Part 1: A-F 1993 p 385-386 (For primary document see N94-12015 01-91)

Avail: CASI HC A01/MF A06

The determination of spin axis and shape is well known to be of fundamental importance for studies about the rotational and physical properties of asteroids. In particular, knowledge that the pole coordinate distribution is random or not could indicate the probable non-Maxwellian distribution of asteroid spin axes, while the distribution in terms of size and shape could place important constraints on the theories about the collisional history of some individual asteroids, of asteroid families, and of the asteroid population as a whole. Many kinds of methods have been developed to determine pole coordinates. An EA method is presented, from which it is possible to obtain the solution with no trial poles, but with a simultaneous least square fit on both the E and A part. Results for rotational and shape parameters were obtained for 18 asteroids: the values of the obtained parameters are generally in close agreement with those of others. Derived from text

N94-12206*# Arkansas Univ., Fayetteville. Core Labs.

CATHODOLUMINESCENCE PROPERTIES OF COMPONENTS IN ENSTATITE CHONDRITES Abstract Only c90

John M. DeHart and Gary E. Lofgren (National Aeronautics and Space Administration. Lyndon B. Johnson Space Center, Houston, TX.) *In* Lunar and Planetary Inst., Twenty-fourth Lunar and Planetary Science Conference. Part 1: A-F 1993 p 387-388 (For primary document see N94-12015 01-91)
Avail: CASI HC A01/MF A06

As a group, the enstatite chondrites are notable by the extremely low FeO content of most of their silicates. This property predisposes many of these materials to emit Cathodoluminescence (CL). Since examination of the CL properties of meteoritic components in ordinary and carbonaceous chondrites have proven to be a useful technique, we have initiated a survey of the enstatite chondrites in order to better characterize the chemical and physical properties of their luminescing phases. Because of the diversity encountered in this study, it is first necessary to describe the number and types of materials observed to emit CL in these meteorites. Two CL techniques were used. First, the initial survey work was conducted at low magnification using a Nuclide (now MAAS) Luminoscope mounted to a Wild MP binocular microscope equipped for photomicroscopy. The beam conditions used were 14 +/- KeV and 7 +/- 1 milliamps, with the beam focussed to the diameter of the field of view of the microscope at 20x (appox. 1.25 cm). Photomosaics were produced for each section using Ecktar 1000 film and an exposure time of 15 to 30 seconds. Second, high magnification (400x) photos were obtained of individual components of interest by mounting a 35mm camera to the optical system of the Cameca Camebax microprobe located at the Johnson Space Center. Beam conditions used were 15 KeV and 600 nA. Ecktar 1000 film was also used, but exposure times of 6 minutes were necessary to produce a useful image. The components in E chondrites that produce CL can be divided into four broad categories. These are clasts and aggregates, chondrules, matrix components, and refractory objects. Components in each category are discussed. Derived from text

N94-12207*# Northeast Louisiana State Coll., Monroe. Dept. of Geosciences.

CLASSIFICATION OF MARTIAN DELTAS Abstract Only

R. A. DeHon *In* Lunar and Planetary Inst., Twenty-fourth Lunar and Planetary Science Conference. Part 1: A-F 1993 p 389-390 (For primary document see N94-12015 01-91)
Avail: CASI HC A01/MF A06

Water-borne sediments in streams are deposited, upon eventual cessation of flow, either as deltas or as alluvial fans or plains. Deltas and alluvial fans share a common characteristic; both may be described as deposition Al plains at the mouth of a river or stream. A delta is formed where a stream or river deposits its sedimentary load into a standing body of water such as an ocean or lake. An alluvial fan is produced where a stream loses capacity by a greatly decreased gradient. A delta has subaerial and subaqueous components, but an alluvial fan is entirely subaerial. In terrestrial conditions, deltas and alluvial fans are reasonably distinct landforms. The juxtaposition of concomitant features composition and internal structure are sufficiently explicit as to avoid any confusion regarding their proper identification on Mars, the recognition of deltas and their distinction from alluvial fans is made difficult by low resolution imaging. Further, although it may be demonstrated that standing bodies of water existed on the surface of Mars, many of these bodies may have existed for extremely short periods of time (a few days to months); hence, distinctive shoreline features were not developed. Thus, in an attempt to derive a Martian classification of deltas, the inclusion of wholly subaerial deposits may be unavoidable. A simple, broad, morphological classification of Martian deltas, primarily on planimetric shape, includes digitate deltas, fan-shaped deltas, and re-entrant deltas. A fourth, somewhat problematical class includes featureless plains at the end of many valley systems. Derived from text

N94-12208*# Rutgers Univ., New Brunswick, NJ. Dept. of Geological Sciences.

THE Fe/Mn CONSTRAINT ON PRECURSORS OF BASALTIC ACHONDRITES Abstract Only **c90**

Jeremy S. Delaney and Joseph S. Boesenberg *In* Lunar and Planetary Inst., Twenty-fourth Lunar and Planetary Science Conference. Part 1: A-F 1993 p 391-392 (For primary document see N94-12015 01-91)
Avail: CASI HC A01/MF A06

Most achondritic meteorites have Fe/Mn ratios that are lower than those of carbonaceous chondrites and of course are lower than the solar system abundance ratio of these elements. Models of the origin of achondritic assemblages must, therefore, account for these ratios. Fe/Mn ratios are suggested to be distinctive for samples from each achondrite parent body and for the Earth and Moon, but the correspondence between the Fe/Mn systematics of achondrites and chondritic precursors is unclear. Most models of achondrite genesis involve magmatic differentiation of chondritic precursors. The Fe/Mn difference between achondrites and chondrites is particularly significant since Fe and Mn are geochemically similar elements with similar partitioning behavior in familiar magmatic systems and are generally coupled during crystal-liquid fractionation. In contrast, however, Mn is more volatile than Fe in a nebular setting. Variation of Fe/Mn ratios based on the relative volatility of these elements in the early nebula provides a constraint for models by which the basaltic achondrites (with Fe/Mn ratios approximately = 25-50) are derived from mixtures of nebular components that were enriched in volatile components such as Mn. However, such volatile enriched components have not been identified in chondrites. When the abundance in achondrites of elements of similar volatility is examined, anomalies appear. For example, Na is massively depleted in basaltic achondrites when compared to Mn. These anomalies might be explained using current models but the alternative hypothesis, that Fe/Mn ratio is controlled not by nebular volatility constraints, but by planetary differentiation should be explored. Derived from text

N94-12209*# State Univ. of New York, Albany. Dept. of Geological Sciences.

COMPOSITIONAL HETEROGENEITY WITHIN A DUMBBELL-SHAPED APOLLO 15 GREEN GLASS: EVIDENCE FOR SIMULTANEOUS ERUPTION OF DIFFERENT MAGMAS Abstract Only

J. W. Delano *In* Lunar and Planetary Inst., Twenty-fourth Lunar and Planetary Science Conference. Part 1: A-F 1993 p 393-394 (For primary document see N94-12015 01-91)
Avail: CASI HC A01/MF A06

The Apollo 15 green glasses that occur most prominently in 15425, 15426, and 15427 consist of compositionally distinct groups. The six groups that have thus far been defined are thought to represent different batches of magma that were erupted as fire-fountains, probably at different times in lunar history; although isotopic analyses of representative glasses within some of these groups have not yet found any differences in age at the +/- 100 Ma precision. While the petrogenesis of these picritic magmas has been contentious, the discovery of a compositionally heterogeneous, dumbbell-shaped green glass raises additional questions and problems about their origin. Derived from text

N94-12210*# State Univ. of New York, Albany. Dept. of Geological Sciences.

OXIDATION STATE OF THE EARTH'S UPPER MANTLE DURING THE LAST 3800 MILLION YEARS: IMPLICATIONS FOR THE ORIGIN OF LIFE Abstract Only **c46**

J. W. Delano *In* Lunar and Planetary Inst., Twenty-fourth Lunar and Planetary Science Conference. Part 1: A-F 1993 p 395-396 (For primary document see N94-12015 01-91)
Avail: CASI HC A01/MF A06

A popular, as well as scientifically rigorous, scenario for the origin of life on Earth involves the production of organic molecules by interaction of lightning (or other forms of energy) with a chemically reducing atmosphere in the early history of Earth. Experiments since the 1950's have convincingly demonstrated that the yield of organic molecules is high when the atmosphere contains molecular hydrogen, methane, ammonia, and water vapor. Additional work has also shown that such a highly reducing atmosphere might not, however, have been sufficiently long-lived in the presence of intense solar ultraviolet radiation for life to have formed from it. One way of maintaining such an atmosphere would be to have a continual replenishment of the reduced gases by prolonged volcanic outgassing from a reducing of Earth's interior. The length of time that this replenishment might need to continue is in part constrained by the flux of asteroids onto the Earth's surface containing sufficient energy to destroy most, if not all, life that had developed up to that point in time. If a reducing atmosphere is a key ingredient for the origin of life on Earth, the time of the last environmental sterilization due to large impacts would be an important constraint. In a deep marine setting (e.g., hydrothermal vent), the last global sterilization might have occurred at 4200-4000 Ma. On the Earth's surface, the last global sterilization event might have occurred at

4000-3700 Ma. If these are meaningful constraints, how likely is it that a reducing atmosphere could have survived on the Earth until about 3800 Ma ago? Due to the importance of replenishing this atmosphere with reducing components by volcanic outgassing from the mantle, geochemical information on the history of the mantle's oxidation state would be useful for addressing this question. Geochemical and experimental data discussed in this abstract suggest that extrusive mafic volcanics derived from the upper mantle have had oxidation states near the fayalite-magnetite quartz buffer throughout the last 3800 Ma. At magmatic temperatures, the gases released from volcanoes having this oxidation state would have been, as they are today, composed dominantly of carbon dioxide and water vapor, and would not contain the ingredients for maintaining a reducing atmosphere. Consequently, geochemical data do not favor the survival of a reducing atmosphere until about 3800 Ma. Alternative venues and pathways for the origin of life need to be investigated (e.g., hydrothermal vents along oceanic ridges). Derived from text

N94-12211*# State Univ. of New York, Albany. Dept. of Geological Sciences.

SORET DIFFUSION: A POSSIBLE CAUSE OF COMPOSITIONAL HETEROGENEITY WITHIN TEKTITES Abstract Only c90

J. W. Delano, Y.-G. Liu (Oregon State Univ., Corvallis.), and R. A. Schmitt (Oregon State Univ., Corvallis.) *In* Lunar and Planetary Inst., Twenty-fourth Lunar and Planetary Science Conference. Part 1: A-F 1993 p 397-398 (For primary document see N94-12015 01-91)

Avail: CASI HC A01/MF A06

Although a terrestrial origin for tektites is well-established on geochemical evidence, the physical processes involved in tektite formation have been largely ignored by geochemists and petrologists. For example, two observations that potentially bear on the physics of their origin are the following: (1) The flange of an australite is often more heterogeneous than its core; and (2) microtektites are compositionally more diverse than tektites. The first observation contradicts the traditional view of flange formation since a second heating to super-liquidus temperatures during atmospheric re-entry should, by chemical diffusion and mixing, have tended to homogenize the melt as it flowed off the leading edge of the core to form the flange. Analyses of an australite flange have been performed by electron microprobe. The results of those analyses emphasize the magnitude of the heterogeneity, as well as the well-defined elemental correlations that may constrain the process responsible for it. The second observation that the bulk compositions of microtektites are more divers than the tektites within the same strewnfield is a well-known characteristic, for which no quantitative explanation has been offered. The current investigation has involved the analysis of 43 Australasian microtektites from the Wharton Basin by electron microprobe, as well as trace-element abundances on fifteen of these microtecktites by INAA. Derived from text

N94-12212*# University of Southern California, Pasadena. Div. of Geology Planetary Sciences.

ISOTOPIC AND TRACE ELEMENT CHARACTERISTICS OF AN UNUSUAL REFRACTORY INCLUSION FROM ESSEBI Abstract Only c92

E. Deloule, A. K. Kennedy, I. D. Hutcheon, and A. ElGoresy (Max-Planck-Inst. fuer Kernphysik, Heidelberg, Germany.) *In* Lunar and Planetary Inst., Twenty-fourth Lunar and Planetary Science Conference. Part 1: A-F 1993 p 399-400 (For primary document see N94-12015 01-91)

Avail: CASI HC A01/MF A06

The isotopic and chemical properties of Ca-Al-rich inclusions (CAI) provide important clues to the early solar nebula environment. While the abundances of refractory major and trace elements are similar to those expected for high temperature condensates, the variety of textural, chemical, and isotopic signatures indicate most CAI experienced complex, multi-stage histories involving repeated episodes of condensation, evaporation, and metamorphism. Evidence of multiple processes is especially apparent in an unusual refractory inclusion from Essebi (URIE) described by El Goresy et al. The melilite (mel)-rich core of URIE contains polygonal framboids of spinel (sp) and hibonite (hb) or sp and fassaite (fas) and is surrounded by a rim sequence consisting of five layers. In contrast to rims on Allende, the mineralogy of the URIE rim layers becomes increasingly refractory from the core outwards, ending in a layer of spinel-Al2O3 solid solution + Sc-rich fassaite. The chemical and mineralogical features of URIE are inconsistent with crystallization from a homogeneous melt, and El Goresy et al. proposed a multi-step history involving condensation of sp + hb and aggregation into framboids, capture of framboids by a refractory silicate melt droplet, condensation of rim layers, and alteration of mel to calcite and feldspathoid. The PANURGE ion probe was used to investigate the isotopic and trace element characteristics of URIE to develop a more complete picture of the multiple processes leading to formation and metamorphism. Derived from text

N94-12213*# Deutsche Forschungsanstalt fuer Luft- und Raumfahrt, Berlin (Germany). Inst. for Planetary Exploration.

DISK-RESOLVED SPECTRAL CHARACTERISTICS OF SATURN'S MEDIUM-SIZED SATELLITES Abstract Only

Tilmann Denk, Ralf Jaumann, and Gerhard Neukum *In* Lunar and Planetary Inst., Twenty-fourth Lunar and Planetary Science Conference. Part 1: A-F 1993 p 401-402 (For primary document see N94-12015 01-91)

Avail: CASI HC A01/MF A06

Voyager-1 and -2 images of six Saturnian satellites were investigated in the orange, green and violet spectral range. The objective of this study is to examine and compare spectral differences of surface features in order to obtain information about compositional trends. Author (revised)

N94-12214*# Academy of Sciences (USSR), Moscow.

THE CORRELATION OF ALKALIS AND ALUMINUM DURING HIGH-TEMPERATURE VOLATILIZATION OF ALBITE AND NEPHELINE Abstract Only c25

Yu. P. Dikov, M. V. Gerasimov, O. I. Yakovlev, and F. Wlotzka (Max-Planck-Inst. fuer Chemie, Mainz, Germany.) *In* Lunar and Planetary Inst., Twenty-fourth Lunar and Planetary Science Conference. Part 1: A-F 1993 p 403-404 (For primary document see N94-12015 01-91)

Avail: CASI HC A01/MF A06

Our previous study of high-temperature evaporation of mafic targets has shown a systematic enrichment of newly-formed condensates in silicon and alkalis and depletion in refractory elements (Al, Ca, Ti). This effect, which is consistent with the volatility of the elements, was also tested for several experiments with acidic targets. In one case it was the impact evaporation of granite targets using a light-gas gun facility. Analyses of the condensate which was collected during the impact show that it was enriched in Al and Na so that the composition of the condensate became close to nepheline. In the work of Nagahara, an incongruent evaporation of alkali feldspars under stationary conditions has been also proposed. These discoveries required a more detailed study of high-temperaure evaporation of monomineralic Al-silicate targets. In these experiments, we have used samples of oligoclase and of nepheline. Vaporization of samples was performed in a hermetic cell filled with helium at normal temperature and pressure using a powerful Nd-laser focused on the sample. Laser pulses had the following parameters: luminous energy approximately 600 J, duration approximately 10(exp -3) s, density of luminosity was approximately 5 x 10(exp 6) W/sq cm, the temperature of vaporization is about 3000-4000 K. About 4 cm from the sample, a nickel foil was placed on which the condensate was collected. Films of condensate were analyzed using X-Ray Photo-Electron spectrometer ES-2401. The measurement of internal chemical composition and of the charging state of elements through the whole depth of the condensed films was made layer by layer with argon-ion etching of 200 A of the film per step. Results of this study are given. The bottom layers of condensed film correspond to the front parts of the evaporated cloud or to condensation at the beginning of the evaporative process and surface layers to condensation at the end of the process. Author (revised)

N94-12215*# State Univ. of New York, Stony Brook. Dept. of Earth and Space Sciences.

A CM CHONDRITE CLUSTER AND CM STREAMS Abstract Only c90

R. T. Dodd and M. E. Lipschutz (Purdue Univ., West Lafayette, IN.) *In* Lunar and Planetary Inst., Twenty-fourth Lunar and Planetary Science Conference. Part 1: A-F 1993 p 405-406 (For primary document see N94-12015 01-91)

Avail: CASI HC A01/MF A06

An elongate year-day concentration of CM meteoroid falls between 1921 and 1969 is inconsistent with a random flux of CM meteoroids and suggests that most or all such meteorites, and perhaps the Kaidun C-E chondrite breccia, resulted from streams of meteoroids in nearly circular, Earth-like orbits. To establish whether the post-1920 cluster might have arisen from random sampling, we determined the year-day distribution of 14 falls between 1879 and 1969 by treating each as the corner of a cell of specified dimensions (e.g. 30 years x 30 days) and calculated how many falls occurred in that cell. We then compared the CM cell distribution with random distributions over the same range of years. The results show that for 30 x 30 and 45 x 45 cells, fewer than 5 percent of random sets match the CM distribution with respect to maximum cell content and number of one-fall cells. Author (revised)

N94-12216*# Geological Survey, Flagstaff, AZ.
RELATION BETWEEN AGES AND ELEVATIONS OF MARTIAN CHANNELS Abstract Only
James M. Dohm and David H. Scott *In* Lunar and Planetary Inst., Twenty-fourth Lunar and Planetary Science Conference. Part 1: A-F 1993 p 407-408 (For primary document see N94-12015 01-91)
Avail: CASI HC A01/MF A06

Mapping highland and lowland channels and reassessing their time-stratigraphic positions shows that many channels in the cratered highlands are younger than Noachian, that all channels in the lowland plains are Hesperian or younger, and that although Martian channels formed throughout the planet's history, the rate of their formation appears to have declined with time. This detailed examination of the age relation between Martian terrains and the channels that transect them was made possible by the completion of the global geologic maps of Mars and the availability of other geologic maps at scales of 1:5,000,000, 1:2,000,000, and 1:500,000. The present study focuses on the sources (heads) of the channels of the initial study to see if there is a relation between channel age and elevation. Author (revised)

N94-12217*# Lunar and Planetary Inst., Houston, TX.
DOES THE THERMAL WIND EXIST NEAR THE EARTH'S CORE BOUNDARY? Abstract Only **c46**
A. Z. Dolginov *In its* Twenty-fourth Lunar and Planetary Science Conference. Part 1: A-F 1993 p 409-410 (For primary document see N94-12015 01-91)
Avail: CASI HC A01/MF A06

Temperature distribution in the Earth core determines many important processes such as the following: convective motion, magnetic field generation, matter exchange between the core and the mantle, and the thermal flux. This distribution depends on conditions in the core-mantle boundary and on the distribution of the thermal conductivity in the mantle. Seismic tomography shows that large horizontal temperature and compositional gradients exists at the core-mantle boundary. The simple assumption that these inhomogeneities are extended into the top of the core contradicts the common opinion that the horizontal temperature gradient (the thermal wind) wipes them out in a short time. However, this conclusion has been obtained without taking into account that the core volume is closed and the motion, if it is started, can lead to a small redistribution of composition that stops this motion. Author (revised)

N94-12218*# Lunar and Planetary Inst., Houston, TX.
MAGNETIC FIELDS AND NONUNIFORM STRUCTURES OF THE MOON Abstract Only
A. Z. Dolginov *In its* Twenty-fourth Lunar and Planetary Science Conference. Part 1: A-F 1993 p 411-412 (For primary document see N94-12015 01-91)
Avail: CASI HC A01/MF A06

Direct magnetic measurements performed by space probes demonstrated the existence of small-scale, stationary surface magnetic fields on the Moon. The magnetic field averaged over a region of approximately 600 km was found to be no larger than approximately 10(exp -5) G, that of the regions approximately 100-200 km is approximately 10(exp -5) to 10(exp -4) G, and that of approximately 10-100 km reaches approximately 10(exp -3) G. Investigations of certain lunar rocks reveal stable residual magnetization, which could have been acquired during the crystallization of the rocks in the presence of the outer magnetic field, provided such a field existed at the initial stage of lunar evolution. Estimates show that 4 x 10(exp 9) yr ago the field was small, then it rose to approximately 1.3 G at the beginning of 3.9 x 10(exp 9) yr with a subsequent exponential decrease during the period of 3.9 x 10(exp 9) yr to 3.2 x 10(exp 9) yr ago. Small-scale fields have been explained by some authors as due to mechanical impacts produced by meteors. The theory of this effect is not elaborated in detail. This can in no way explain the paleomagnetic data. These data are commonly explained as a result of the dynamo action in the liquid lunar core. Author (revised)

N94-12219*# Lunar and Planetary Inst., Houston, TX.
POLARITY REVERSALS AND TILT OF THE EARTH'S MAGNETIC DIPOLE Abstract Only **c46**
A. Z. Dolginov *In its* Twenty-fourth Lunar and Planetary Science Conference. Part 1: A-F 1993 p 413-414 (For primary document see N94-12015 01-91)
Avail: CASI HC A01/MF A06

There is evidence that the terrestrial magnetic field is connected with the Earth's mantle: (1) there are magnetic anomalies that do not take part in the westward drift of the main field, but are fixed with respect to the mantle; (2) the geomagnetic pole position flips in a particular way by preferred meridional paths during a reversal; and (3) magnetic polarity reversals are correlated with the activations of geological processes. These facts may be explained if we take into account that a significant horizontal temperature gradient can exist in the top levels of the liquid core because of the different thermoconductivity of the different areas of the core-mantle boundary. These temperature inhomogeneities can penetrate the core because fluxes along the core boundary (the thermal wind) can be strongly suppressed by a small redistribution of the chemical composition in the top of the core. The nonparallel gradients of the temperature, density, and composition on the top of the core create a curled electric field that produces a current and a magnetic field. This seed-field can be amplified by motions in the core. The resulting field does not forget the seed-field distribution and in this way the field on the Earth surface (that can be created only in regions with high conductivity, i.e. in the core) is connected with the core-mantle boundary. Contrary to the usual approach to the dynamo problem, we will take into account that the seed field of thermoelectric origin is acting not only at some initial moment of time but permanently. Author (revised)

N94-12220*# Lunar and Planetary Inst., Houston, TX.
ARE COSMIC RAYS EFFECTIVE FOR IONIZATION OF THE SOLAR NEBULA? Abstract Only **c92**
A. Z. Dolginov and T. F. Stepinski *In its* Twenty-fourth Lunar and Planetary Science Conference. Part 1: A-F 1993 p 415-416 (For primary document see N94-12015 01-91)
Avail: CASI HC A01/MF A06

In this paper, we argue that the effectiveness of cosmic rays to ionize the bulk of the nebular gas may be further impaired by the influence of the magnetic field on the propagation of cosmic rays. When cosmic rays enter the nebular disk they ionize the gas and make the dynamo generation of magnetic fields possible. However, once magnetic fields are embedded in the nebular gas, the upcoming cosmic rays can no longer penetrate directly into the nebular disk because they start to interact with the magnetic field and lose their energy before propagating significantly toward the midplane. That, in turn, undercuts the ionization source within the bulk of the gas stopping the dynamo action. Nebular dynamo models ignored this back reaction of magnetic fields on cosmic rays. We calculate this back reaction effect, but for the sake of mathematical simplicity, we ignore the effect of magnetic field weakening due to diminishing ionization by cosmic rays. Author (revised)

N94-12221*# Academy of Sciences (USSR), Moscow.
ON THE UNIQUE STRUCTURE OF THE MAGNETIC FIELDS OF URANUS AND NEPTUNE Abstract Only
Sh. Sh. Dolginov *In* Lunar and Planetary Inst., Twenty-fourth Lunar and Planetary Science Conference. Part 1: A-F 1993 p 417-418 (For primary document see N94-12015 01-91)
Avail: CASI HC A01/MF A06

The magnetic fields of Uranus and Neptune, which have comparable dipole, quadrupole, and octupole harmonics, are unique in the present-day solar system, but they resemble the geomagnetic field at the epochs of excursions and reversals known from paleomagnetic data. The precession dynamo model, in which the dominant role in the generation of the planetary magnetic fields is played by external gravitational forces, allows us to propose two scenarios for the formation of the unique topology of the magnetic fields of Uranus and Neptune. In the first case, tidal flows in the 'oceans' of these two planets extend down to the depths where the matter has a noticeable electric conductivity and velocity. A hydromagnetic interaction of the moving conducting fluid with the planetary magnetic field outside the generation region results in the deformation of the field and the deceleration of the motion under the action of the radial magnetic field. In the second case, the deformation of the field facilitates drastic changes in cyclonic cells within the generation region causing instabilities that result in a multi-polar field structure, excursions, and inversions. This paper considers this problem in greater detail by using the Neptune-Triton system as an example. Author (revised)

N94-12222*# Academy of Sciences (USSR), Moscow.
PRECESSION OF URANUS AND NEPTUNE AND THEIR MAGNETIC FIELD Abstract Only
Sh. Sh. Dolginov *In* Lunar and Planetary Inst., Twenty-fourth Lunar and Planetary Science Conference. Part 1: A-F 1993 p 419-420 (For primary document see N94-12015 01-91)
Avail: CASI HC A01/MF A06

The strength of the dipole magnetic field of a planet, H(sub p), can be estimated relative to that of the Earth at the epoch of the observation. The generation of magnetic fields in Uranus and Neptune occurs at very different depths for different values of sigma. This assertion is confirmed by the estimation of the Reynolds number (R(sub m)) and agrees with the difference of the contributions of the Joule heat losses into the observed heat fluxes of Uranus and Neptune. Author (revised)

N94-12223*# Observatoire de Paris-Meudon (France).
DUST IN THE MARTIAN ATMOSPHERE: POLARIMETRIC SENSING Abstract Only
A. Dollfus and S. Ebisawa (Tokyo Astronomical Observatory, Japan.) *In* Lunar and Planetary Inst., Twenty-fourth Lunar and Planetary Science Conference. Part 1: A-F 1993 p 421-422 (For primary document see N94-12015 01-91)
Avail: CASI HC A01/MF A06

Telescopic optical polarimetry over the planet Mars enables us to detect and localize scatterers in the Martian atmosphere. Polarization discriminates between crystal clouds and dust particles. For dust grains, sizes can be derived. There is an increase in size from very small grains forming the permanent dust haze to sub-micrometer size grains for the local dust veils and the several micrometer size pieces found in the dust storm clouds. From all these polarimetric results, an overview emerges about the behavior of dust particles in the Martian atmosphere. Author (revised)

N94-12224*# California Univ., San Diego, La Jolla. Dept. of Chemistry.
DEVELOPMENT OF A MOLECULAR BEAM TECHNIQUE TO STUDY EARLY SOLAR SYSTEM SILICON REACTIONS Abstract Only **c90**
Q. W. Dong and M. H. Thiemens *In* Lunar and Planetary Inst., Twenty-fourth Lunar and Planetary Science Conference. Part 1: A-F 1993 p 423-424 (For primary document see N94-12015 01-91)
Avail: CASI HC A01/MF A06

Silicon monoxide is one of the major gas phase silicon bearing components observed in astronomical environments. Silicon oxide serves as the major rock forming material for terrestrial and meteoritic bodies. It is known that several gas phase reactions produce mass independent isotopic fractionations which possess the same delta(O-17)/delta(O-18) ratio observed in Allende inclusions. The general symmetry dependence of the chemically produced mass independent isotopic fractionation process suggests that there are several plausible reactions which could occur in the early solar system which may lead to production of the observed meteoritic oxygen isotopic anomalies. An important component in exploring the role of such processes is the need to experimentally determine the isotopic fractionations for specific reactions of relevance to the early solar system. It has already been demonstrated that atomic oxygen reaction with CO, a major nebular oxygen bearing species, produces a large (approximately 90 percent), mass independent isotopic fractionation. The next hurdle regarding assessing the involvement of symmetry dependent isotopic fractionation processes in the pre-solar nebula is to determine isotopic fractionation factors associated with gas phase reactions of metallic oxides. In particular, a reaction such as O + SiO yields SiO2 is a plausible nebular reaction which could produce a delta(O-17) is approximately delta(O-18) fractionation based upon molecular symmetry considerations. While the isotopic fractionations during silicate evaporation and condensation have been determined, there are no isotopic studies of controlled, gas phase nucleation processes. In order to carefully control the reaction kinetics, a molecular beam apparatus has been constructed. This system produces a supersonic, collimated beam of SiO molecules which is reacted with a second beam of oxygen atoms. An important feature of molecular beams is that they operate at sufficiently low pressures and high temperatures in the jet that avalanche nucleation and clustering processes may be avoided. Author (revised)

N94-12225*# Academy of Sciences (USSR), Moscow. Inst. of Geochemistry.
ON HIGH-TEMPERATURE FORMATION OF IRON-RICH OLIVINE IN THE EARLY SOLAR SYSTEM Abstract Only **c90**
V. A. Dorofeyeva, A. B. Makalkin, and A. V. Vityazev *In* Lunar and Planetary Inst., Twenty-fourth Lunar and Planetary Science Conference. Part 1: A-F 1993 p 425-426 (For primary document see N94-12015 01-91)
Avail: CASI HC A01/MF A06

A kinetic restriction on the formation of fayalite-rich olivine in equilibrium with the cooling solar-composition gas appears to exist at the low temperature of approximately 500 K. We offer a high-temperature formation mechanism (different from simple condensation) which operates at high hydrogen depletion (up to 300 times) relative to solar abundance. We show how the necessary depletion rate decreases with temperature (thermodynamical equilibrium is suggested). The consequences for planet formation are considered. Author (revised)

N94-12226*# Academy of Sciences (USSR), Moscow. Inst. of Geochemistry.
RECONDENSATION OF CHONDRITIC MATERIAL IN THE EARLY SOLAR SYSTEM: RESULTS OF THERMODYNAMIC SIMULATION Abstract Only **c90**
V. A. Dorofeyeva, A. B. Makalkin, M. V. Mironenko, and A. V. Vityazev *In* Lunar and Planetary Inst., Twenty-fourth Lunar and Planetary Science Conference. Part 1: A-F 1993 p 427-428 (For primary document see N94-12015 01-91)
Avail: CASI HC A01/MF A06

We have performed a thermodynamic simulation of the recondensation of evaporated meteoritic material. We suggest that evaporation and recondensation occurred in impact events during the intercollision of planetesimals during the early evolution of the solar system. The source materials adopted for our model are the chondrites CI Orgueil and H5 Richardton. These chondrites are representative examples of the two extremes regarding volatile content and oxidation state. We calculated equilibrium mineral compositions of the closed systems of the Orgueil's and Richardton's elemental composition at the P-T conditions characteristic of the explosion cloud formed at a planetesimal collision. The P-T conditions are as follows: 10(exp -4) bar, and 1500 and 2000 K. The results are presented. Author (revised)

N94-12227*# Los Alamos National Lab., NM. Space Science and Technology Div.
ANALYTIC EXPRESSION FOR EPITHERMAL NEUTRON SPECTRA AMPLITUDES AS A FUNCTION OF WATER CONTENT Abstract Only
Darrell Drake *In* Lunar and Planetary Inst., Twenty-fourth Lunar and Planetary Science Conference. Part 1: A-F 1993 p 429-430 (For primary document see N94-12015 01-91)
Avail: CASI HC A01/MF A06

The epithermal portion of an equilibrium neutron spectrum in a planetary body is a function of the water content of its material. The neutrons are produced at high energies but are moderated by elastic and inelastic scattering until they either are captured by surrounding nuclei or escape. We have derived an expression that explicitly shows the dependance of epithermal neutron spectra on water content. Additionally, we compared its predictions to calculations done by Boltzman transport code for infinite media for silicon, oxygen, and a possible lunar composition, and we have obtained very good agreement. Author (revised)

N94-12228*# Arizona Univ., Tucson. Lunar and Planetary Lab.
NOBLE GAS EVIDENCE OF AN AQUEOUS RESERVOIR NEAR THE SURFACE OF MARS MORE RECENTLY THAN 1.3 Ga Abstract Only

Michael J. Drake, Toby Owen (Hawaii Univ., Manoa.), Timothy Swindle, and Donald Musselwhite *In* Lunar and Planetary Inst., Twenty-fourth Lunar and Planetary Science Conference. Part 1: A-F 1993 p 431-432 (For primary document see N94-12015 01-91)
Avail: CASI HC A01/MF A06

Considerable evidence points to a Martian origin of the SNC meteorites. One of these meteorites, Nakhla, contains a leachable component which has an elevated Xe-129/Xe-132 ratio relative to its Kr-84/Xe-132 ratio when compared to the approximately linear array defined by Chassigny, most shergottites, and lithology C of EETA 79001. This array is thought to be a mixing line between Martian mantle and Martian atmosphere. The leachable component probably consists in part of iddingsite, an alteration product produced by interaction of olivine with aqueous fluid at temperatures lower than 150 C. The radiogenic Xe component may represent a distinct reservoir in the Martian crust or mantle. More plausibly, it is Martian atmosphere, fractionated by solution in liquid water and by interaction with sediment. The crystallization age of Nakhla is 1.3 Ga. Its low shock state suggests that it was ejected from near the surface of Mars. Liquid water is required for the formation of iddingsite. These observations provide further evidence for the near surface existence of aqueous fluids more recently than 1.3 Ga. Author (revised)

N94-12229*# National Aeronautics and Space Administration. Lyndon B. Johnson Space Center, Houston, TX.
EXPLORATION PLANNING IN THE CONTEXT OF HUMAN EXPLORATION AND DEVELOPMENT OF THE MOON Abstract Only
Michael B. Duke and Donald A. Morrison *In* Lunar and Planetary Inst., Twenty-fourth Lunar and Planetary Science Conference. Part 1: A-F 1993 p 433 (For primary document see N94-12015 01-91)
Avail: CASI HC A01/MF A06

It is widely believed that the next step beyond low Earth orbit in attaining the United States' stated goal of 'Expanding human presence beyond the Earth' should be to reestablish a lunar capability, building on the Apollo program, and preparing the way for eventual human missions to Mars. The Moon offers important questions in planetary and Earth science, can provide a unique platform for making astronomical observations of high resolution and sensitivity, and can be in the development path for unlocking resources of the inner solar system to support space activities and return benefits to Earth. NASA's Office of Exploration has undertaken the planning of future lunar exploration missions with the assistance of the Solar System Exploration Division in matters dealing with the quality of scientific data and the manner in which it will be made available to the scientific community. The initial elements of the proposed program include the Lunar Scout missions, which consist of two small identical spacecraft in polar orbit around the Moon, which can accomplish most of the objectives associated with previous proposals for Lunar Polar Orbiters. These missions would be followed by 'Artemis' landers, capable of emplacing up to 200 kg payloads anywhere on the Moon. In addition, the exploration program must incorporate data obtained from other missions, including the Galileo lunar flybys, the Clementine high orbital observations, and Japanese penetrator missions. In the past year, a rather detailed plan for a 'First Lunar Outpost (FLO)' which would place 4 astronauts on the lunar surface for 45 days has been developed as a possible initial step of a renewed human exploration program. In the coming year, the FLO concept will be reviewed and evolved to become more highly integrated with planning for the initial human exploration of Mars, which could come perhaps 5 years after the reestablishment of lunar capability. Both programs could benefit from the common development of systems and subsystems, where that is sensible from a performance perspective. Author (revised)

N94-12230*# Arizona State Univ., Tempe. Dept. of Geology and Chemistry.
PRIMORDIAL LIGHTNING: EVIDENCE PRESERVED IN CHONDRITES Abstract Only **c90**
D. Eisenhour and P. R. Buseck *In* Lunar and Planetary Inst., Twenty-fourth Lunar and Planetary Science Conference. Part 1: A-F 1993 p 435-436 (For primary document see N94-12015 01-91)
Avail: CASI HC A01/MF A06

An increasing body of evidence suggests that transient heating events were important in forming or modifying many constituents of chondritic meteorites. For example, chondrule compositions and textures imply high cooling rates (approximately 5 to greater than 2000 C/hr) with only limited exposure to elevated temperatures (greater than 1200 C). Similarly, experimental studies of CAI's exhibiting igneous textures suggest cooling rates from 0.5 to 1000 C/hr, and thermal pulses as short as milliseconds may be responsible for CAI rim formation. Additionally, the spectrum of organic compounds observed in chondrites suggests that transient heating may also have played an important role in their formation. The exact nature of these transient events is less clear. A variety of mechanisms have been proposed (e.g., shock melting, drag heating, volcanism, electric discharges, and magnetic reconnection). However, a consensus is lacking as to which or what combination of these mechanisms was responsible for the range of features we observe in chondrites today. Much of the difficulty lies in the inability to identify features unique to any given process. Here we discuss electric discharges ('lightning') as a transient heat source and describe its unique signature preserved in chondrites.
Author (revised)

N94-12231*# Arizona State Univ., Tempe. Dept. of Geology and Chemistry.
MICRO-ZONING IN MINERALS OF A LANDES SILICATE INCLUSION Abstract Only **c90**
D. D. Eisenhour, P. R. Buseck, H. Palme (Max-Planck-Inst. fuer Chemie, Mainz, Germany.), and J. Zipfel (Max-Planck-Inst. fuer Chemie, Mainz, Germany.) *In* Lunar and Planetary Inst., Twenty-fourth Lunar and Planetary Science Conference. Part 1: A-F 1993 p 437-438 (For primary document see N94-12015 01-91)
Avail: CASI HC A01/MF A06

There is an increasing number of meteorites with chondritic bulk composition but completely different textures than the conventional chondrite groups. Winonaites, Acapulcoites and silicate inclusions in IAB-iron meteorites have in common coarse grain size, highly equilibrated mineralogy with frequent 120 deg triple junctions and they record a significantly lower degree of oxidation than ordinary chondrites. They all have equilibration temperatures, based on Ca-exchange among pyroxenes, of around 900 to 1100 deg C. However, on cooling disequilibrium features may develop: (1) Olivine in IAB-inclusions has lower Fa-content than equilibrium Fs-content of pyroxenes requires; (2) CaO-zoning in olivine was established at temperatures of around 500 deg C, several hundred degrees below pyroxene equilibration temperatures. Obviously, olivine responded faster to changes in fO2 (Fa in olivine) and temperature (Ca-zoning) than pyroxenes. Differences in diffusion coefficients can readily explain the observed trends. Here we report on much more subtle zoning features in pyroxenes. TEM-observations reveal large compositional gradients in Ca, Na, Cr, Ti and Fe within the first micrometer of cpx and opx crystals. In summary, the data reflect the complicated subsolidus history of a chondritic mineral assemblage that was in thermodynamic equilibrium at about 900 deg C and cooled slowly from this temperature whereby oxidation reactions and different closure temperatures for various minerals and elements played an important role. The oxidation of P dissolved in metal and formation of phosphate, which is thermodynamically stable at low temperatures, is suggested to be responsible for most of the observed zoning.
Derived from text

N94-12232*# Los Alamos National Lab., NM. Space Plasma Physics, Geology and Geophysics Group.
SOLAR WIND-INDUCED SECONDARY IONS AND THEIR RELATION TO LUNAR SURFACE COMPOSITION Abstract Only **c92**
R. C. Elphic, H. O Funsten, III, and R. L. Hervig (Arizona State Univ., Tempe.) *In* Lunar and Planetary Inst., Twenty-fourth Lunar and Planetary Science Conference. Part 1: A-F 1993 p 439 (For primary document see N94-12015 01-91)
Avail: CASI HC A01/MF A06

Based on previous laboratory experiments simulating solar wind sputtering of lunar surface materials, it appears that solar wind ions sputter secondary ions in sufficient numbers to be measured from low-altitude lunar orbit. Solar wind protons are hundreds of times less efficient than those used in standard secondary ion mass spectrometry; nevertheless secondary ions of Na, Mg, Al, Si, K, Ca, Mn, Ti and Fe were observed sputtered from sample simulants of mare and highland soils. These secondary ion fluxes depend both on concentration in the soil and on probability of ionization; yields of easily ionized elements such as K and Na are relatively much greater than those for the more electronegative elements and compounds. The principal geochemical indicator elements

Na, Mg, Al, Si, K, Ca, Ti, Mn and Fe are nevertheless detectable. However, it has not been shown that the observed secondary ions vary strictly one-to-one with their concentrations in the geochemically distinct soil simulants used here. While we have a first order understanding of secondary ion sputtering, it is not clear that the observed ion yields can be linked with great accuracy to the simulant's composition. The simulants were analyzed by electron microprobe to establish their detailed composition. The observed secondary ion fluxes can then be compared with the microprobe results. For example Ti(+) fluxes from the three simulants correspond to the true composition with accuracies of better than 10 percent for the high-Ti basalt, and about 20 percent for the low-Ti simulant. The highlands simulant produced a statistically insignificant Ti(+) count rate. Here we discuss the results of further SIMS experiments using the ASU/Center for Solid State Science facility. With careful isolation and preparation of samples, we avoid the problems of the previous experiments. In particular, we will make use of ground-up sample to mimic the sputtering behavior of regolith, and will avoid charging by placing the soil on a conducting indium substrate. We report the results of a blind test of the SIMS technique using a sample of unknown composition. Author (revised)

N94-12233*# Centre de Spectrometrie Nucleaire et de Spectrometrie de Masse du CNRS, Orsay (France).

A NEW CARBON-RICH PHASE (COPS) IN ANTARCTIC MICROMETEORITES Abstract Only **c90**

C. Engrand, M. Maurette, G. Kurat (Naturhistorisches Museum, Vienna, Austria.), F. Brandstatter (Naturhistorisches Museum, Vienna, Austria.), and M. Perreau (Office National d'Etudes et de Recherches Aeronautiques, Paris, France.) *In* Lunar and Planetary Inst., Twenty-fourth Lunar and Planetary Science Conference. Part 1: A-F 1993 p 441-442 (For primary document see N94-12015 01-91)

Avail: CASI HC A01/MF A06

The contemporary flux of micrometeorites with sizes greater than 50 microns reaching the Earth's surface each year (about 20,000 tons/a) is much greater than the value of approximately 100 tons/a reported for conventional meteorites up to masses of approximately 10,000 tons. Moreover, on the average, Antarctic micrometeorites contain at least as much carbon as does Orgueil, the most C-rich meteorite. Micrometeorites are thus responsible for most of the carbon accreted by the Earth. In this paper we report SEM observations of a new C-rich 'dirty magnetite' phase observed as tiny inclusions in both melted and unmelted micrometeorites. This phase, which is enriched in C, O, P, S, Fe, frequently shows Ni contents in excess of 0.2 percent, strongly suggestive of an 'extraterrestrial' origin. We also discovered this 'COPS' phase in the fusion crust of Murchison. It appears likely that COPS is a product of meteoroid reprocessing during frictional heating in the Earth's atmosphere and/or its fast 'weathering' in the upper atmosphere. Upon 'catalyzed' hydrolysis this phase might have facilitated the functioning of micrometeorites as 'micro-chondritic-reactors' for the synthesis of prebiotic molecules on the early Earth. Derived from text

N94-12234*# Viale Univ., Rome (Italy).

AUTOMATIC DEFINITION OF SPECTRAL UNITS IN THE EQUATORIAL REGIONS OF MARS Abstract Only **c90**

Stephane Erard, Priscilla Cerroni, and Angioletta Coradini *In* Lunar and Planetary Inst., Twenty-fourth Lunar and Planetary Science Conference. Part 1: A-F 1993 p 443-444 (For primary document see N94-12015 01-91)

Avail: CASI HC A01/MF A06

ISM was the first instrument that acquired spectra of small areas (25x25 sq km) on a planetary surface. The data set consists mainly in images made up of about 3000 such pixels, each one corresponding to a near-infrared spectrum (0.76 to 3.15 microns in 128 spectral channels) with high signal-to-noise ratio. These data were used to define spectral units and to constrain the mineralogy of surface materials in the equatorial regions of the planet. Future spaceborne imaging spectrometers (e.g. OMEGA on board the Mars-94 Russian spacecraft) are expected to provide several hundred times as much data as ISM, so there's a strong need for fast and reliable processing methods. The present work is an attempt to define spectral units in the region of Syrtis Major-Isidis Planitia by means of G-mode analysis. The method allows to cluster the spectra according to their similarities; different levels of classification can be achieved by tuning a threshold of confidence. Derived from text

N94-12235*# Viale Univ., Rome (Italy).

COMPOSITION OF THE MARTIAN AEROSOLS THROUGH NEAR-IR SPECTROSCOPY Abstract Only

Stephane Erard, Priscilla Cerroni, and Angioletta Coradini *In* Lunar and Planetary Inst., Twenty-fourth Lunar and Planetary Science Conference. Part 1: A-F 1993 p 445-446 (For primary document see N94-12015 01-91)

Avail: CASI HC A01/MF A06

Near-infrared spectroscopy is a powerful technique to study the composition of planetary surfaces, as the main minerals exhibit absorption bands in this spectral range. It gave important information on the mineralogy and petrology of Mars in the past twenty years although in this case it is well known that a large fraction of light is scattered by the airborne particles before reaching the surface. The measured signal is thus the sum of two different contributions that should be studied separately: One from the surface and one from the aerosols that depends on their density, size distribution and composition. Data from the ISM imaging spectrometer are used here to derive the aerosols spectrum. They consist in sets of spectra (from 0.76 to 3.16 microns) of approximately 3000 pixels approximately 25x25 sq km in size. The resulting spectrum exhibits both water-ice and clay mineral features superimposed on a scattering continuum. Derived from text

N94-12236*# Ottawa Univ. (Ontario). Dept. of Geology.

GIANT RADIATING DYKE SWARMS ON EARTH AND VENUS Abstract Only **c46**

Richard E. Ernst, James W. Head (Brown Univ., Providence, RI.), Elisabeth Parfitt (Brown Univ., Providence, RI.), Lionel Wilson (Brown Univ., Providence, RI.), and Eric Grosfils (Brown Univ., Providence, RI.) *In* Lunar and Planetary Inst., Twenty-fourth Lunar and Planetary Science Conference. Part 1: A-F 1993 p 447-448 (For primary document see N94-12015 01-91)

Avail: CASI HC A01/MF A06

On Earth, giant radiating dyke swarms are usually preserved as fan-shaped fragments which have been dismembered from their original configuration by subsequent plate tectonic rifting events. Analysis of the largest fragments and consideration of their original configuration has led to the idea that many swarms are plume related, and that dyke swarms radiate away from plume centers. Magellan radar data reveal abundant intact giant radiating swarms on Venus which are similar in scale and pattern to those on Earth. The absence of intense weathering and plate tectonic processes on Venus accounts for the preservation of the primary radiating patterns. It is characteristic of both Earth and Venus that giant radiating dikes are emplaced laterally for distances of at least 2000 km away from plume centers. At distances beyond the influence of the plume on both Earth and Venus, the radiating dyke pattern is often swept into a linear pattern aligned with the regional stress field. There is tremendous potential synergism between the characterization and analysis of terrestrial dyke swarms (where significant erosion has revealed their structure and emplacement directions at depth) and the giant swarms of Venus (where the complete circumferential structure is preserved, and the surface fracture systems above near surface dikes and the nature of the central source regions are revealed). In this study, we report on the characteristics of radial dyke swarms on Earth and Venus and draw some preliminary comparisons from the two perspectives. In summary, on both planets there is evidence for plume-related magmatic centers associated with vertical and lateral injection of magma over considerable distances (up to at least 2000 km). The abundance of very broadly radiating swarms on Venus supports the notion that the swarms on Earth were radiating over broad sectors at the time of intrusion but were dissected by later events. The Venus data show that a swarm can change from radiating (proximal) to regional (distal) subparallel orientations. An implication for Earth is that many regional linear swarms which do not have a radiating pattern may be due to fragmentation of the swarm during later plate tectonic rifting. Completion of the global classification and census of Venus features, comparison to the terrestrial synthesis, and documentation of the mode of emplacement of dikes in these environments (buffered and unbuffered conditions) should lead to additional general insight into mechanisms of formation and evolution and their relation to plumes. Derived from text

N94-12237*# Australian National Univ., Canberra. Research School of Earth Sciences.

Re-Os DATING OF 3AB IRON METEORITES Abstract Only **c90**

Tezer M. Esat and Victoria Bennett *In* Lunar and Planetary Inst., Twenty-fourth Lunar and Planetary Science Conference. Part 1: A-F 1993 p 449-450 (For primary document see N94-12015 01-91)

Avail: CASI HC A01/MF A06

Recently, Creaser et al., and Volkening and Heumann, have demonstrated the efficient production of large (approximately 10 exp -11 A) ion beams by negative thermal ionization mass spectrometry (NTIMS) using standard laboratory solutions of Os compounds. Horan et al., have applied NTIMS to a group of 7 IIA iron meteorites and obtained a Re-Os closure age of 4596 +/- 152 million years. The initial Os-187/Os-186 ratio was 0.8007 plus or minus 0.0029. In addition they analyzed 3 IIIA meteorite samples which indicated an age of 4554 +/- 180 million years and Os initial of 0.8120 +/- 0.0075 which does not overlap with the initial for the IIA irons. We have been independently pursuing a similar program with the direct aim of determining possible variations in the initial (Os-187)/(Os-186) ratio or Re-Os closure age of different classes of iron meteorite. We have applied NTIMS to Os extracted from the most common group of iron meteorites the IIIAB. These meteorites are believed to be of magmatic origin, formed by fractional crystallization of molten cores of asteroidal bodies. The present results point to a significantly lower initial (Os-187)/(Os-186) ratio of 0.7731 plus or minus 0.0050 than previously determined. Author

N94-12238*# Universidad Nacional Autonoma de Mexico, Mexico City. Inst. de Geofisica.

MODELLING OF DISPERSAL AND DEPOSITION OF IMPACT GLASS SPHERULES FROM THE CRETACEOUS-TERTIARY BOUNDARY DEPOSIT Abstract Only **c90**

J. M. Espindola, S. Carey (Rhode Island Univ., Narragansett.), and H. Sigurdsson (Rhode Island Univ., Narragansett.) *In* Lunar and Planetary Inst., Twenty-fourth Lunar and Planetary Science Conference. Part 1: A-F 1993 p 451-452 (For primary document see N94-12015 01-91)

Avail: CASI HC A01/MF A06

The dispersal of glass spherules or tektites from a bolide impact with the Earth is modelled as ballistic trajectories in standard atmosphere. Ballistic dispersal of Cretaceous-Tertiary boundary impact glass spherules found in Haiti and Mimbral, Mexico requires a fireball radius in excess of 50 km but less than 100 km to account for the observed distribution. Glass spherules from 1 and up to 8 mm in diameter have been found at the KT boundary at Beloc in Haiti, at Mimbral, Mexico, and at DSDP Sites 536 and 540 in the Gulf of Mexico corresponding to paleodistances of 600 to 1000 km from the Chicxulub crater. In Haiti the basal and major glass-bearing unit at the KT boundary is attributed to fallout on basis of sedimentologic features. When compared with theoretical and observed dispersal of volcanic ejecta, the grain size versus distance relationship of the KT boundary tektite fallout is extreme, and rules out a volcanic fallout origin. At a comparable distance from source, the KT impact glass spherules are more than an order of mangitude coarser than ejecta of the largest known volcanic events. We model the dispersal of KT boundary impact glass spherules as ballistic ejecta from a fireball generated by the impact of a 10 km diameter bolide. Mass of ejecta in the fireball is taken as twice the bolide mass. Melt droplets are accelerated by gas flow in the fireball cloud, and leave the fireball on ballistic trajectories within the atmosphere, subject to drag, depending on angle of ejection and altitude. The model for ballistic dispersal is based on equations of motion, drag and ablation for silicate spheres in standard atmosphere. Author

N94-12239*# Bern Univ. (Switzerland). Physikalisches Inst.

THE Xe-Q IN LODRANITES AND A HINT FOR Xe-L. FRO90011 ANOTHER LODRANITE? Abstract Only **c90**

O. Eugster and A. Weigel *In* Lunar and Planetary Inst., Twenty-fourth Lunar and Planetary Science Conference. Part 1: A-F 1993 p 453-454 (For primary document see N94-12015 01-91)

Avail: CASI HC A01/MF A06

The Lodran achondrite contains about one-quarter metallic Fe/Ni, two-thirds olivine and pyroxene, some troilite, plus minor phases. In a previous study we demonstrated that Lodran and three other lodranites - LEW88280, Yamato-791491, and MAC88177 - yield the same cosmic-ray exposure age of a few million years, suggesting that they originate from the same parent body. In the present work we show that the mineral phases of Lodran contain large concentrations of planetary-type but no solar-type trapped noble gases. Surprisingly, the highest concentrations were observed in the Fe/Ni-phase (e.g. 1520 x 10(exp -12) cc STP per g (132)Xe). A large fraction of the trapped gas is released between 1200 C and 1400 C. The Xe isotopic pattern is similar to that of Xe-Q. The 1400 C fraction of the Fe/Ni-phase shows excesses of (124)Xe, (126)Xe, and (128)Xe similar to Xe-L (pre-solar Xe enriched in the light isotopes) that has, until now, only been observed in combination with Xe-H (pre-solar Xe enriched in the heavy isotopes). Author

N94-12240*# Bern Univ. (Switzerland). Physikalisches Inst.

ON THE ORIGIN OF (4)He AND (40)Ar IN NATURAL GOLD Abstract Only **c26**

O. Eugster, B. Hofmann, S. Niedermann, and Ch. Thalmann *In* Lunar and Planetary Inst., Twenty-fourth Lunar and Planetary Science Conference. Part 1: A-F 455-456 (SEE N94-12015 01-91) 1993 (For primary document see N94-12015 01-91)

Avail: CASI HC A01/MF A06

In a first report on our investigations of noble gases in native gold we demonstrated that placer gold contains an excess of radiogenic (4)He and (40)Ar relative to the concentrations expected from in situ decay of U, Th, and K, respectively, during the geologic age of about 30 Ma of the samples. We also showed that the U/Th-(4)He age of 36 Ma of vein-type gold from the Southern Alps agrees with its K-Ar formation age derived from associated muscovite and biotite. We now studied the question of the origin of the (4)He and (40)Ar excesses of placer gold. We conclude that gold contains two components of noble gases, a low-temperature component from fluid inclusions or phases which release noble gases at less than 800 C and a high-temperature component released when gold melts (1064 C). In some samples extremely high U and K concentrations or an unreasonably high formation age would be required to explain the observed (4)He abundances. Thus, trapped (4)He and (40)Ar must be present in gold. Author

N94-12241*# California Inst. of Tech., Pasadena. Lab. of Experimental Geophysics.

PROJECTILE-TARGET MIXING IN MELTED EJECTA FORMED DURING A HYPERVELOCITY IMPACT CRATERING EVENT Abstract Only **c90**

Noreen Joyce Evans, Thomas J. Ahrens, M. Shahinpoor, and W. W. Anderson *In* Lunar and Planetary Inst., Twenty-fourth Lunar and Planetary Science Conference. Part 1: A-F 1993 p 457-458 (For primary document see N94-12015 01-91)

Avail: CASI HC A01/MF A06

Tektites contain little to no projectile contamination while, in contrast, some distal ejecta deposits can be relatively projectile-rich (e.g. the Cretaceous-Tertiary (K-T) boundary clay). This compositional difference motivated an experimental study of hypervelocity target-projectile mixing processes. We hope to scale up the results from these experiments and apply them to terrestrial impact structures like the Chicxulub Crater, Yucutan, Mexico, the leading contender as the site for the impact that caused the mass extinction that marks the K-T boundary. Shock decomposition of the approximately 500m thickness of anhydrite, or greater thickness of limestone, in the target rocks at Chicxulub may have been a critical mechanism for either global cooling via SO3, and subsequently H2SO4, formation, or possibly, global warming via increased CO2 formation. Understanding target-projectile mixing processes during hypervelocity impact may permit more accurate estimates of the amount of potentially toxic, target-derived material reaching stratospheric heights. Author

N94-12242*# Academy of Sciences (USSR), Moscow. Space Research Inst.

MOESSBAUER SPECTROMETER FOR MINERALOGICAL ANALYSIS OF THE MARS SURFACE: MOESSBAUER SOURCE CONSIDERATIONS Abstract Only

E. N. Evlanov, V. A. Frolov, O. F. Prilutskii, G. V. Veselova, A. M. Rodin (Moscow Physical-Engineering Inst., Russia.), and G. Klingelhoefer (Technische Univ., Darmstadt, Germany.) *In* Lunar and Planetary Inst., Twenty-fourth Lunar and Planetary Science Conference. Part 1: A-F 1993 p 459-460 (For primary document see N94-12015 01-91)

Avail: CASI HC A01/MF A06

Development of space rocketry and cosmic instrument making has made it possible to create interplanetary stations to be sent to the solar system bodies. In the last decade of the century the planet Mars will be in the focus of planetary science problems. Russia, USA (the NASA) and Europe (the ESA) plan to do a new step in the study of the planetary system by spacecraft missions to Mars. One part of the programs of these missions is Martian surface measurements of iron, which is a dominant element in both the Martian soil and rocks (about 13 percent by weight). The chemistry of iron in space is strongly coupled to the chemistry of abundant elements (to begin with hydrogen, carbon, oxygen) and it is this coupling of chemical cycles of abundant elements that gives us the possibility of understanding some features of the chemical evolution of matter. In this connection of extremely great importance for the understanding of the evolution of the solar system are the oxidation state of the iron and its mineral composition of the Mars surface. Being highly successful, the Viking landers had no instrumentation to answer these questions. Such instrumentation has to be specifically sensitive to mineralogy. For this purpose the back scattering Moessbauer spectrometer (MS-96) was proposed to be installed on a rover to be launched on board the Russian spacecraft Mars-96 mission to Mars. Due to power and mass restrictions three systems of the device MS-96 (velocity transducer, detector and electronic components) have been extremely miniaturized in comparison to a standard system. In this paper we intend to place for consideration a radioactive source to find out what characteristics it should have to be suitable for purposes of the experiment. Author (trans.)

N94-12243*# Lancaster Univ. (England). Environmental Science Div.
VULCANIAN EXPLOSIVE ERUPTIONS: A MECHANISM FOR LOCALISED PYROCLAST DISPERSAL ON VENUS Abstract Only
S. A. Fagents and L. Wilson *In* Lunar and Planetary Inst., Twenty-fourth Lunar and Planetary Science Conference. Part 1: A-F 1993 p 461-462 (For primary document see N94-12015 01-91)
Avail: CASI HC A01/MF A06

A model of the mechanisms involved in transient (vulcanian-type) explosive eruptions has enabled us to place constraints on the velocities of blocks ejected during such events on Earth as well as on the excess pressure and concentration of gas in the vent prior to the onset of the explosion. This model, suitably modified, can predict the results of similar eruptions occurring under the differing Venusian environmental conditions. It is found that the much higher atmospheric pressure (approximately 100 bars at the mean planetary radius) dominates the form of the resulting deposit in two main ways: (1) by inhibiting the expansion out of the vent of overpressured gas, hence reducing ejecta velocity; and (2) by retarding the flight of ejected blocks via drag effects. Thus, it is expected that such deposits will typically extend to approximately 200 m on Venus as compared to several km for documented terrestrial deposits. Author

N94-12244*# Hawaii Univ., Manoa. Planetary Geosciences.
CHONDRITES, S ASTEROIDS, AND SPACE WEATHERING: THUMPING NOISES FROM THE COFFIN? Abstract Only **c90**
F. P. Fanale and B. E. Clark *In* Lunar and Planetary Inst., Twenty-fourth Lunar and Planetary Science Conference. Part 1: A-F 1993 p 463-464 (For primary document see N94-12015 01-91)
Avail: CASI HC A01/MF A06

Most of the spectral characteristics of ordinary chondrites and S-asteroids in the visible and infrared can be reduced to three numerical values. These values represent the depth of the absorption band resulting from octahedrally coordinated Fe(sup 2+), the reflectance at 0.56 microns and the slope of the continuum (as measured according to convention). By plotting these three characteristics, it is possible to immediately compare the spectral characteristics of large numbers of ordinary chondrites and S-asteroids. Commonality of spectral characteristics between these populations can thus be evaluated on the basis of overlap in position on three two-coordinate systems: albedo vs. band depth, band depth vs. slope, and slope vs. albedo. In order to establish identity, members of the two populations must overlap on all three of these independent parameter spaces. In this coordinate system, spectra of 23 ordinary chondrites (representing all metamorphic grades), and 39 S-asteroids were compared. It was found that there was no overlap between the two populations in terms of the slope vs. band depth parameters, nor were most chondrites identical to the S-asteroids with respect to the other criteria. However, the controversial question remains: Where are the parent bodies of the chondrites? Perhaps an even more critical question is: Where are our samples of the S-asteroids? Considering the geography of the asteroid belt and the theory that early solar-system electromagnetic induction heating differentiated protoasteroids in the inner portion of the main belt, it was suggested that although S-asteroids and ordinary chondrites have very similar mineralogy, the S-asteroids are mixtures of metallic nickel iron and silicates which resulted from magmatism induced by electromagnetic heating whereas chondrites were only slightly metamorphosed nebular condensates. In this scenario chondrites would have been derived from a population of bodies with thermal lag times so short that they were not subjected to melting during the phase of the electromagnetic induction heating event but only to various degrees of pervasive metamorphism. Furthermore, these objects would then have been too small to be observed and systematically included in the library of asteroidal spectra. It was also suggested that the parametric distribution of S-asteroid spectra could be reproduced by mixing various proportions of NiFe meteorite and achondritic materials. This has also been demonstrated in the laboratory. Author

N94-12245*# Science Applications International Corp., Falls Church, VA.
A COMPARISON OF THE VISIBLE AND NEAR INFRARED REFLECTANCE OF HYDROVOLCANIC PALAGONITE TUFFS AND MARTIAN WEATHERED SOILS Abstract Only
W. H. Farrand and R. B. Singer (Arizona Univ., Tucson.) *In* Lunar and Planetary Inst., Twenty-fourth Lunar and Planetary Science Conference. Part 1: A-F 1993 p 465-466 (For primary document see N94-12015 01-91)
Avail: CASI HC A01/MF A06

The visible and near infrared reflectance of Martian weathered soils, abundant in the bright regions, have been shown to resemble certain examples of the X-ray amorphous mineraloid palagonite. To date, most comparisons between terrestrial palagonites and Martian telescopic spectra have been done using palagonites that were formed under ambient semi-arid weathering conditions on Hawaiian volcanoes such as Mauna Kea. Here we examine palagonites associated with the tephra deposits that make up tuff rings and tuff cones. Tuff rings and tuff cones result from hydrovolcanic activity, defined as the interaction of magmas (in this instance, of basaltic composition) with surface or near-surface water. Tuff rings and tuff cones can contain variable amounts of country rock and juvenile crystals, but their primary constituent is fine grained sideromelane (basaltic glass). Sideromelane alters to palagonite. Unlike the aforementioned Hawaiian palagonites, the alteration of sideromelane to palagonite seems to occur relatively rapidly in tuff cones, on the order of days to months. In comparing the spectra of hydrovolcanically produced palagonites with telescopic spectra of Mars, one is struck by their similarity in the VNIR and dissimilarity in the SWIR. Author

N94-12246*# Washington Univ., Saint Louis, MO. Dept. of Earth and Planetary Sciences.
THE RATE OF CHEMICAL WEATHERING OF PYRITE ON THE SURFACE OF VENUS Abstract Only
B. Fegley, Jr. and K. Lodders *In* Lunar and Planetary Inst., Twenty-fourth Lunar and Planetary Science Conference. Part 1: A-F 1993 p 467-468 (For primary document see N94-12015 01-91)
Avail: CASI HC A01/MF A06

This abstract reports results of an experimental study of the chemical weathering of pyrite (FeS2) under Venus-like conditions. This work, which extends the earlier study by Fegley and Treiman, is part of a long range research program to experimentally measure the rates of thermochemical gas-solid reactions important in the atmospheric-lithospheric sulfur cycle on Venus. The objectives of this research are (1) to measure the kinetics of thermochemical gas-solid reactions responsible for both the production (e.g., anhydrite formation) and destruction (e.g., pyrrhotite oxidation) of sulfur-bearing minerals on the surface of Venus and (2) to incorporate these and other constraints into holistic models of the chemical interactions between the atmosphere and surface of Venus. Experiments were done with single crystal cubes of natural pyrite (Navajun, Logrono, Spain) that were cut and polished into slices of known weight and surface area. The slices were isothermally heated at atmospheric pressure in 99.99 percent CO2 (Coleman Instrument Grade) at either 412 C (685 K) or 465 C (738 K) for time periods up to 10 days. These two isotherms correspond to temperatures at about 6 km and 0 km altitude, respectively, on Venus. The reaction rate was determined by measuring the weight loss of the reacted slices after removal from the furnace. The reaction products were characterized by X-ray diffraction, scanning electron microscopy, and energy dispersive spectroscopy on the SEM. Author

N94-12247*# Bechtel Corp., San Francisco, CA.

TERRESTRIAL CASE STUDIES OF ILMENITE EXPLORATION AND LUNAR IMPLICATIONS Abstract Only

S. C. Feldman and H. A. Franklin *In* Lunar and Planetary Inst., Twenty-fourth Lunar and Planetary Science Conference. Part 1: A-F 1993 p 469-470 (For primary document see N94-12015 01-91)

Avail: CASI HC A01/MF A06

The Space Exploration Initiative (SEI) includes space resource utilization as one of the four architectures to achieve U.S. goals in space. Space resource utilization will make use of lunar resources to support long term activities on the lunar surface. Lunar ilmenite and regolith are two of the materials that can be mined and processed for lunar oxygen production. During this investigation, several sources were reviewed to assess terrestrial exploration methods used for locating ilmenite resources. These sources included published reports on terrestrial ilmenite exploration methods, analytical methods, case histories, chemical and physical properties, and associations with other minerals. Using a terrestrial analog and considering the differences between terrestrial and lunar environmental conditions, rocks, and minerals, exploration methods and analytical instruments can be recommended for a lunar orbiter and lander for assessing lunar resources. Twelve terrestrial case histories were reviewed to gain insight into ilmenite exploration on the Moon. All exploration case histories follow the same pattern. They begin with a model, use remote geophysical techniques, define regional sampling sites from the model and geophysics, narrow down the area of exploration based on the preceding work, collect more samples and cores, and perform laboratory analyses of samples. An important part of this process is the collection of samples to determine the correctness of the model. Surface and core samples are collected in areas expected to contain both high and low concentration of the commodity to test the model. After samples are analyzed and the area of mineralization is defined, reserves are calculated to determine the cost/benefit ratio, the necessary capacity of the processing plant, and the life of the mine. The exploration methods used for locating terrestrial ilmenite resources are reviewed with respect to the petrology, chemistry, and mineral associations of the terrestrial and lunar environments. Author

N94-12248*# Arizona Univ., Tucson. Dept. of Geosciences.

MORPHOTECTONICS OF VENUS Abstract Only

V. J. Finn, V. R. Baker, and A. Z. Dolginov (Lunar and Planetary Inst., Houston, TX.) *In* Lunar and Planetary Inst., Twenty-fourth Lunar and Planetary Science Conference. Part 1: A-F 1993 p 471-472 (For primary document see N94-12015 01-91)

Avail: CASI HC A01/MF A06

Venus topography can be mapped morphostructurally to reveal nested hierarchical patterns of quasi-circular upland/lowland complexes. These patterns are interpreted as surficial effects of hierarchically structured, long-acting mantle convection. Beta Regio, Alpha Regio, and Artemis illustrate this process of dynamical interaction between the deforming lithosphere and the convecting mantle. Author

N94-12249*# Arizona Univ., Tucson. Dept. of Geosciences.

TRANSMANTLE FLUX TECTONICS Abstract Only **c46**

V. J. Finn, A. Z. Dolginov (Lunar and Planetary Inst., Houston, TX.), and V. R. Baker *In* Lunar and Planetary Inst., Twenty-fourth Lunar and Planetary Science Conference. Part 1: A-F 1993 p 473-474 (For primary document see N94-12015 01-91)

Avail: CASI HC A01/MF A06

Venus, Earth, and Mars have surfaces that display topographic domes and depressions with quasi-circular planimetric shapes, relief of 0 to several km, and large spatial scales (10(exp 2) to 10(exp 4) km). Our morphostructural mapping reveals hierarchical arrangements of these features. They are explained by a model of long-acting mantle convection, as a particular case of convection in a stratified and random inhomogeneous medium, which develops the form of a hierarchy of different convective pattern scales, each arising from different levels in the mantle. The hypothesis of transmantle flux tectonics parsimoniously explains a diversity of seemingly unrelated terrestrial planetary phenomena, including Earth megaplumes, global resurfacing epochs on Venus, and cyclic ocean formation and global climate change for Mars. All these phenomenon are hypothesized to be parsimoniously explained by a process of transmantle flux tectonics in which long-acting mantle convection generates stresses in blocks of planetary lithosphere to produce distinctive quasi-circular global-hierarchical morphostructure (QGM) patterns. Transmantle flux tectonics differs from plume tectonics in that individual plumes are not considered in isolation. Rather, a wholly interactive process is envisioned in which various spatial and temporal scales of convection operate contemporaneously and hierarchically within other scales. This process of continual change by hierarchical convective cells affects the surface at varying temporal and spatial scales, and its effects are discernable through their relic geological manifestations, the QGM patterns. Author (revised)

N94-12250*# Brown Univ., Providence, RI. Dept. of Geological Sciences.

ASSIMILATION IN LUNAR BASALTS AND VOLCANIC GLASSES: IMPLICATIONS FOR A HETEROGENOUS MANTLE SOURCE REGION Abstract Only

A. B. Finnila, P. C. Hess, and M. J. Rutherford *In* Lunar and Planetary Inst., Twenty-fourth Lunar and Planetary Science Conference. Part 1: A-F 1993 p 475-476 (For primary document see N94-12015 01-91)

Avail: CASI HC A01/MF A06

Several scientists have called on assimilation of anorthositic crustal material or KREEP compositions to explain various lunar lithologies. In order to address the practicality of such processes, some techniques for calculating how much assimilation is possible in magma chambers and dikes based on thermal energy balances and simple fluid mechanical constraints are outlined. In a previous effort, it was demonstrated that dissolution of plagioclase in an iron-free basalt was too slow to contaminate magmas, and that the energy cost of melting plagioclase-rich crustal material was prohibitive both in magma chambers and in dike conduits. This analysis was extended to include dissolution rates in an orange glass composition and to quantitatively predict the maximum contamination possible due to assimilation of both lunar crustal material and KREEP. Author (revised)

N94-12251*# Brown Univ., Providence, RI. Dept. of Geological Sciences.

MEASURING AND DISTINGUISHING COMPOSITIONAL AND MATURITY PROPERTIES OF LUNAR SOILS BY REMOTE VIS-NIR SPECTROSCOPY Abstract Only

Erich M. Fischer and Carle M. Pieters *In* Lunar and Planetary Inst., Twenty-fourth Lunar and Planetary Science Conference. Part 1: A-F 477-478 (SEE N94-12015 01-91) 1993 (For primary document see N94-12015 01-91)

(Grant NAGw-28)

Avail: CASI HC A01/MF A06

Space weathering on the lunar surface affects the spectra/optical character of an exposed lunar soil in three ways: the reflectance is reduced, absorption band depths are reduced, and a red-sloped continuum is created and increased with exposure. As a result, the spectrum of a lunar soil is dependent upon both the degree of exposure at the lunar surface and the original composition. It is critical to the remote analysis of lunar soils to differentiate between the optical effects of maturity and the effects of composition. In the laboratory, it is possible to determine and consequently distinguish the degree of exposure, or soil maturity, as measured by parameters such as I(sub s)/FeO (e.g., 1; mature defined as I(sub s)/FeO greater than or equal to 60), and the composition, as measured by various chemical and petrographical techniques. Lunar soils returned by the Apollo missions provide important ground truth for developing methods for remotely measuring the maturity and the concentration of Fe-bearing minerals in lunar soil. The ground truth spectral data analyzed are from the John Adams lunar soil spectra collection. Soils collected from or near highland terrains are emphasized in the discussion. The mineralogical makeup of mare soils results in behavior somewhat different from highland soils. Author (revised)

N94-12252*# Academy of Sciences (USSR), Moscow. Inst. of Geochemistry and Analytical Chemistry.

DIAMOND THERMOLUMINESCENCE PROPERTIES OF DIFFERENT CHONDRITES Abstract Only **c90**

A. V. Fisenko, L. L. Kashkarov, L. F. Semjonova, and C. T. Pillinger (Open Univ., Milton, England.) *In* Lunar and Planetary Inst., Twenty-fourth

Lunar and Planetary Science Conference. Part 1: A-F 1993 p 479-480 (For primary document see N94-12015 01-91)
Avail: CASI HC A01/MF A06

It was found that thermoluminescence (TL) glows of diamonds depend on the origin of diamonds and the chondrite metamorphism degree. The investigation of TL of diamonds was continued and the results for diamonds from Murchison CM2, Krymka LL3.0, Kainsaz CO3, and Abee E4 were considered. The diamonds synthesized by CVD-process (samples 133, 159) and by detonation from soot (DDS-B14-89) were also analyzed for comparison. Before the TL measuring samples were annealed at approximately 350 C for a few seconds and then irradiated by gamma-rays of Cs-137 up to dose approximately 200 krad. TL-measurements were performed in the air atmosphere on the standard equipment. TL data for samples are shown. TL glow for some diamonds are also presented. Author (revised)

N94-12253*# Academy of Sciences (USSR), Moscow. Inst. of Geochemistry and Analytical Chemistry.

THE UNUSUAL METALLIC PARTICLES IN KRYMKA LL3.0 CHONDRITE Abstract Only c90

A. V. Fisenko, A. Yu. Ljul, L. F. Semjonova, and K. I. Ignatenko *In* Lunar and Planetary Inst., Twenty-fourth Lunar and Planetary Science Conference. Part 1: A-F 1993 p 481-482 (For primary document see N94-12015 01-91)
Avail: CASI HC A01/MF A06

The composition, structure peculiarities, and possible scenario of formation of unusual metallic particles in Krymka LL3.0 are shown. In metal released from gentle crushed after removal of chondrules of Krymka LL3.0 chondrite matter, two types of unusual metallic particles were detected. The first type of particle mainly consists of coarse-grained (greater than or equal to 50 microns) kamacite and fine-grained (less than or equal to 10 microns) Ni-high (approximately 53 wt. percent) taenite. These particles have well-defined zonal structure: kamacite is in central part of particles whereas taenite is in outside and the grains of taenite form the mantle around kamacite. In the second type of particle Fe,Ni-phase contains only fine-grained Ni-rich taenite. In both particle types there are also fine-grained phosphate, troilite, and silicate. Both particle types have mostly rounded to subrounded form. Author (revised)

N94-12254*# Academy of Sciences (USSR), Moscow. Inst. of Geochemistry and Analytical Chemistry.

ON POSSIBILITY OF DIAMOND FORMATIONS IN RADIATION PROCESS Abstract Only c90

A. V. Fisenko, L. F. Semjonova, L. N. Bolsheva, T. V. Grachjova, A. B. Verchovsky, and Yu. A. Shukolyukov *In* Lunar and Planetary Inst., Twenty-fourth Lunar and Planetary Science Conference. Part 1: A-F 1993 p 483-484 (For primary document see N94-12015 01-91)
Avail: CASI HC A01/MF A06

The possibility of diamond formation in radiation processes was checked by studying diamond contents in carburanium sample. The diamonds were not found and this result is discussed. At present one possible process of formation of nanometer-size diamond crystals in some meteorites and Earth's diamonds (carbonado), the radiation mechanism, is suggested: the formation of diamonds from carbonaceous matter in tracks of U fragment fissions and heavy fragmentation due to the action of energetic particles of cosmic rays. Bjakov et. al. have carried out the calculations and shown that the volume of formed diamonds in carbonaceous chondrites by radiation processes corresponds to discovery of diamond volume in chondrites. The discovery by Ozima et. al. of the unsupported fission of Xe and Kr in carbonado supports the supposition that carbonado could be formed by radiation processes. The possibility of diamond formation in radiation processes leads to the study of diamond contents in Earth's samples enriched by uranium and carbon. The attempt to release the diamonds from carburanium was undertaken. Author (revised)

N94-12255*# Academy of Sciences (USSR), Moscow. Inst. of Geochemistry and Analytical Chemistry.

THE CARBON ISOTOPIC COMPOSITION OF NOVO UREI DIAMONDS Abstract Only c90

A. V. Fisenko, L. F. Semjenova, A. B. Verchovsky, S. S. Russell, and C. T. Pillinger (Open Univ., Milton, England.) *In* Lunar and Planetary Inst., Twenty-fourth Lunar and Planetary Science Conference. Part 1: A-F 1993 p 485-486 (For primary document see N94-12015 01-91)
Avail: CASI HC A01/MF A06

The carbon isotopic composition of diamond grains isolated from the Novo Urei meteorite are discussed. A diamond separate was obtained from 2g of whole rock using the chemical treatments described aimed at obtaining very pure diamond. X ray diffraction of the residue, which represented 5000 ppm of the parent mass, indicated only the presence of the desired mineral. The diamond crystals were 1-30 microns in diameter, and some grains had a yellow color. The chemical treatments were followed by a size separation to give a 1-10 microns and a 5-30 microns fraction, which were named DNU-1 and DNU-2, respectively. Author (revised)

N94-12256*# Academy of Sciences (USSR), Moscow. Inst. of Geochemistry and Analytical Chemistry.

THE FRACTIONATION OF NOBLE GASES IN DIAMONDS OF CV3 EFREMOVKA CHONDRITE Abstract Only c25

A. V. Fisenko, A. B. Verchovsky, L. F. Semjonova, and Yu. A. Shukolyukov *In* Lunar and Planetary Inst., Twenty-fourth Lunar and Planetary Science Conference. Part 1: A-F 1993 p 487-488 (For primary document see N94-12015 01-91)
Avail: CASI HC A01/MF A06

It was shown that in diamonds of Efremovka CV3 the noble gases with normal isotopic compositions are fractionated in different degree while the correlation of isotopic anomalous components is nearly constant. Some data for noble gases in DE-4 sample of Efremovka chondrite are considered. In contrast to DE-2 sample the DE-4 was treated except conc. $HClO_4$, 220 C in addition with mixture of conc. $H_2SO_4+H_3PO_4$ (1:1), 220 C, twice. Noble gases analysis were performed in Germany at Max Plank Institute fur Chemie. Noble gases were released by oxidation of samples at stepped heating from 420 C to 810 C and by pyrolysis at 580, 590, and 680 C. Author (revised)

N94-12257*# Massachusetts Inst. of Tech., Cambridge. Dept. of Earth, Atmospheric and Planetary Sciences.

CRONSTEDTITE AND IRON SULFIDE MINERALOGY OF CM-TYPE CARBONACEOUS CHONDRITES FROM CRYOGENIC MOESSBAUER SPECTRA Abstract Only c90

Duncan S. Fisher and Roger G. Burns *In* Lunar and Planetary Inst., Twenty-fourth Lunar and Planetary Science Conference. Part 1: A-F 1993 p 489-490 (For primary document see N94-12015 01-91)
(Grants NAGw-2049; NAGw-2220)
Avail: CASI HC A01/MF A06

Determinations of oxidation states and the crystal chemistry of iron-bearing minerals in CM meteorites by Moessbauer spectroscopy are complicated by thermally-induced electron hopping in cronstedtite and by ill-defined contributions from the hydrous iron sulphide phase believed to be tochilinite. Moessbauer spectral measurements at 30 K of several cronstedtite and tochilinite specimens have enabled modal proportions of these minerals, as well as Fe(3+)/Fe(2+) ratios, to be determined quantitatively for a suite of CM-type carbonaceous chondrites that included Murchison, Murray, Cold Bokkeveld, ALH 83100, and LEW 90500. Author (revised)

N94-12258*# Stanford Univ., CA. Dept. of Geology.

NMR SPECTROSCOPY OF EXPERIMENTALLY SHOCKED SINGLE CRYSTAL QUARTZ: A REEXAMINATION OF THE NMR SHOCK BAROMETER Abstract Only c25

P. S. Fiske, A. J. Gratz (Lawrence Livermore National Lab., CA.), and W. J. Nellis (Lawrence Livermore National Lab., CA.) *In* Lunar and Planetary Inst., Twenty-fourth Lunar and Planetary Science Conference. Part 1: A-F 1993 p 491-492 (For primary document see N94-12015 01-91)
Avail: CASI HC A01/MF A06

Cygan and others report a broadening of the Si-29 nuclear magnetic resonance (NMR) peak for synthetic quartz powders with increasing shock pressure which they propose as a shock wave barometer for natural systems. These results are expanded by studying single crystal quartz shocked to 12 and 33 GPa using the 6.5 m two-stage light-gas gun at Lawrence Livermore National Laboratories. Our NMR results differ substantially from those of Cygan and others and suggest that the proposed shock wave barometer may require refinement. The difference in results between this study and that of Cygan and others is most likely caused by different starting materials (single crystal vs. powder) and different shock loading histories. NMR results from single crystal studies may be more applicable to natural systems. Author (revised)

N94-12259*# State Univ. of New York, Plattsburgh. Dept. of Physics.
ORGANIC MATTER ON THE EARLY SURFACE OF MARS: AN ASSESSMENT OF THE CONTRIBUTION BY INTERPLANETARY DUST Abstract Only
G. J. Flynn *In* Lunar and Planetary Inst., Twenty-fourth Lunar and Planetary Science Conference. Part 1: A-F 1993 p 493-494 (For primary document see N94-12015 01-91)
Avail: CASI HC A01/MF A06

Calculations by Anders and Chyba et al. have recently revived interest in the suggestion that organic compounds important to the development of life were delivered to the primitive surface of the Earth by comets, asteroids or the interplanetary dust derived from these two sources. Anders has shown that the major post-accretion contribution of extraterrestrial organic matter to the surface of the Earth is from interplanetary dust. Since Mars is a much more favorable site for the gentle deceleration of interplanetary dust particles than is Earth, model calculations show that biologically important organic compounds are likely to have been delivered to the early surface of Mars by the interplanetary dust in an order-of-magnitude higher surface density than onto the early Earth. Using the method described by Flynn and McKay, the size frequency distribution, and the atmospheric entry velocity distribution of IDP's at Mars were calculated. The entry velocity distribution, coupled with the atmospheric entry heating model developed by Whipple and extended by Fraundorf was used to calculate the fraction of the particles in each mass decade which survives atmospheric entry without melting (i.e., those not heated above 1600K). The incident mass and surviving mass in each mass decade are shown for both Earth and Mars. Author (revised)

N94-12260*# State Univ. of New York, Plattsburgh. Dept. of Physics.
TRACE ELEMENT CONTENT OF CHONDRITIC COSMIC DUST: VOLATILE ENRICHMENTS, THERMAL ALTERATIONS, AND THE POSSIBILITY OF CONTAMINATION Abstract Only c90
G. J. Flynn, S. R. Sutton (Chicago Univ., IL.), and S. Bajt (Chicago Univ., IL.) *In* Lunar and Planetary Inst., Twenty-fourth Lunar and Planetary Science Conference. Part 1: A-F 1993 p 495-496 (For primary document see N94-12015 01-91)
Avail: CASI HC A01/MF A06

Trace element abundances in 51 chondritic Interplanetary Dust Particles (IDP's) were measured by Synchrotron X-Ray Fluorescence (SXRF). The data allow us to determine an average composition of chondritic IDP's and to examine the questions of volatile loss during the heating pulse experienced on atmospheric entry and possible element addition due to contamination during atmospheric entry, stratospheric residence, and curation. Author (revised)

N94-12261*# State Univ. of New York, Plattsburgh. Dept. of Physics.
DEPLETIONS OF SULFUR AND/OR ZINC IN IDPs: ARE THEY RELIABLE INDICATORS OF ATMOSPHERIC ENTRY HEATING? Abstract Only c90
G. J. Flynn, S. R. Sutton (Chicago Univ., IL.), S. Bajt (Chicago Univ., IL.), W. Kloeck (Westfaelische Wilhelms Univ., Muenster, Germany.), K. L. Thomas (Lockheed Corp., Houston, TX.), and L. P. Keller (National Aeronautics and Space Administration. Lyndon B. Johnson Space Center, Houston, TX.) *In* Lunar and Planetary Inst., Twenty-fourth Lunar and Planetary Science Conference. Part 1: A-F 1993 p 497-498 (For primary document see N94-12015 01-91)
Avail: CASI HC A01/MF A06

The degree of heating of interplanetary dust particles (IDP's) on Earth atmospheric entry is important in distinguishing cometary particles from main-belt asteroidal particles. Depletions in the volatile elements S and Zn were proposed as chemical indicators of significant entry heating. The S and Zn contents of cosmic dust particles were correlated with physical indicators of atmospheric entry heating, such as the production of magnetite and the loss of solar wind implanted He. The results indicate that the Zn content of IDP's is a useful indicator of entry heating, but the S content seems to be less useful. Author (revised)

N94-12262*# State Univ. of New York, Plattsburgh. Dept. of Physics.
NEW LOW-NI (IGNEOUS?) PARTICLES AMONG THE C AND C? TYPES OF COSMIC DUST Abstract Only c90
G. J. Flynn, S. R. Sutton (Chicago Univ., IL.), S. Bajt (Chicago Univ., IL.), and W. Kloeck (Westfaelische Wilhelms Univ., Muenster, Germany.) *In* Lunar and Planetary Inst., Twenty-fourth Lunar and Planetary Science Conference. Part 1: A-F 1993 p 499-500 (For primary document see N94-12015 01-91)
Avail: CASI HC A01/MF A06

Low-Ni particles with major element abundances, optical properties, and morphologies sufficiently similar to chondritic interplanetery dust particles (IDP's) to receive JSC Cosmic Dust Catalog classifications of C or C?-types were shown to have trace element contents and mineralogies similar to igneous material. Examination of the JSC Catalog EDX spectra by Cooke et al. has shown that 13 percent of the C-type and 38 percent of the C?-type particles are potentially low-Ni particles. Two new low-Ni particles were identified, and it was shown that an additional fragment from the L2002*C cluster has an igneous composition. A newly analyzed fragment of the W7066*A cluster has a chondritic composition. The W7066*A cluster is important because it has yielded a fragment of igneous composition and another fragment having high concentrations of He and Ne suggesting an extraterrestrial origin. Author (revised)

N94-12263*# California Univ., San Diego, La Jolla.
MASS AND SPATIAL DISTRIBUTION OF CARBONACEOUS COMPONENT IN COMET HALLEY Abstract Only c90
M. Fomenkova and S. Chang *In* Lunar and Planetary Inst., Twenty-fourth Lunar and Planetary Science Conference. Part 1: A-F 1993 p 501-502 (For primary document see N94-12015 01-91)
Avail: CASI HC A01/MF A06

Cometary grains containing large amounts of carbon and/or organic matter were discovered by in situ measurements of cometary dust composition during VEGA and GIOTTO fly-by missions. In accordance with the classification for the data of PUMA-1 and PUMA-2 mass-spectrometers on board the VEGA spacecraft, particles with a ratio of C to any rock-forming element (Mg, Si, Fe, Ca etc.) greater than 10, were categorized as CHON. There are 464 such particles in PUMA-1 data and 51 in PUMA-2 data. Application of cluster analysis to these grains revealed several distinct compositional classes, namely: (H,C,N,O), (H,C,N), (H,C), (H,C,O), (C,N), (C,O), (C,N,O), and (C). Similar classes were identified among particles analyzed by PIA. Also, about a third of all particles fell into groups (H) and (O) characterized by abundances of these elements beyond chemically reasonable limits. Author (revised)

N94-12264*# Brown Univ., Providence, RI. Dept. of Geological Sciences.
PRIMITIVE SNC PARENT MAGMAS AND CRYSTALLIZATION: LOW PH2O EXPERIMENTS Abstract Only c90
D. J. Ford and M. J. Rutherford *In* Lunar and Planetary Inst., Twenty-fourth Lunar and Planetary Science Conference. Part 1: A-F 1993 p 503-504 (For primary document see N94-12015 01-91)
Avail: CASI HC A01/MF A06

SNC meteorites are generally believed to present one of the best opportunities to study the composition and petrogenesis of Mars magmas. The crystallization ages, noble gas content, oxygen isotopic composition, and shocked minerals of the meteorites are consistent with a Martian origin. The samples range from dunite to clinopyroxenite to microgabbro. Efforts by researchers to determine parental magmas for the more primitive SNC meteorites have been complicated by crystal accumulation and possible melt segregation and removal. This has resulted in a range of parent magma estimates, although all appear to be Fe-rich and Al-poor. One major objective is to refine the Chassigny parent magma estimate by forcing olivine + clinopyroxene saturation upon the proposed melt composition. EETA 79001 magma compositions are also being investigated to determine the parent magma and the origin of the coarse-grained olivine and orthopyroxene megacrysts. Low pressure experiments with small but finite P(sub H2O) are being utilized to facilitate equilibrium, and to simulate the H2O indicated for these magmas. The presence of small (0.5-1.0 wt percent) amounts of H2O in SNC magmas appears to be required by the occurrence of hydrous minerals and textures in melts trapped by growing phenocrysts. This evidence for hydrous melts occurs in all SNC's except EETA 79001 and ALHA 77005, where the inclusion textures were obscured

by shock effects. The lack of hydrous minerals or low temperature melts in the intercumulus regions of these rocks suggests that final emplacement was sufficiently close to the surface to allow degassing as the magma equilibrated with the low P atmosphere. Any H2O left in intercumulus phases would also tend to be lost during impact heating. Thus, although the bulk H2O of SNC's is very low, it is believed that this is explained by the near Mars surface emplacement of SNC magmas and by shock effects. Magmatic processes involving H2O need to be examined in order to characterize SNC magmas immediately prior to their final emplacement.
Author (revised)

N94-12265*# Paris XI Univ., Orsay (France).
PHASE TRANSITIONS AND 2D SPHERICAL CONVECTION IN A LARGE ICY SATELLITE Abstract Only **c90**
O. Forni, C. Federico (Perugia Univ., Italy.), and A. Coradini (Consiglio Nazionale delle Ricerche, Rome, Italy.) *In* Lunar and Planetary Inst., Twenty-fourth Lunar and Planetary Science Conference. Part 1: A-F 1993 p 505-506 (For primary document see N94-12015 01-91)
Avail: CASI HC A01/MF A06

Three ice phase transitions, based on experimental and theoretical results, were incorporated into a 2D spherical convection model. These phase transitions are the exothermic Ice 1-2, the endothermic Ice 2-6, and the exothermic Ice 6-8 phase transitions. The fluid is assumed isoviscous and the anelastic liquid formulation was used. The object is an icy satellite whose physical characteristics resemble those of Ganymede or Callisto. Structural models, similar to those of Mueller and McKinnon, with different core sizes, i.e. with different degree of differentiation were studied. The shells, i.e. the mantle of the satellite, is heated both internally and from below to account for the decaying radiogenic heating and the heat flow from the solid core. The lower boundary of the mantle is rigid and isothermal, the upper boundary is isothermal. Calculations with rigid and shear stress free upper boundary are carried out in order to assess the role of the different boundary conditions. Two different Rayleigh numbers, depending on the assumed value of the viscosity, were used in the calculations and the thermal evolution of the satellite was studied. The suit of calculations presented demonstrates that phase transition cannot be ignored when the thermal evolution of a large icy satellite has to be studied. The importance of the construction of the realistic phase diagram for ice was also documented. On the other hand the degree of differentiation, simulated with the structures with different core's radius does not seem to drastically influence the overall behavior of the convective activity. Within the limits of our simulations, the post-accretional evolution seems to be independent on the degree of primordial differentiation. Author (revised)

N94-12266*# National Aeronautics and Space Administration. Goddard Space Flight Center, Albuquerque, NM.
DO LARGE IMPACT BASINS IN THE SOUTHERN HEMISPHERE OF MARS CONTROL THE DISTRIBUTION OF POLAR STRUCTURES AND DEPOSITS? Abstract Only
Herbert Frey and Anne-Marie Reidy (Maryland Univ., College Park.) *In* Lunar and Planetary Inst., Twenty-fourth Lunar and Planetary Science Conference. Part 1: A-F 1993 p 509-510 (For primary document see N94-12015 01-91)
Avail: CASI HC A01/MF A06

Among the outstanding problems in Martian geology are the cause of the off-axis and asymmetric distribution of the southern polar layered terrain and residual ice deposits and the cause of the orientation of scarps, valleys, and re-entrant canyons which occur there. A perhaps related problem region is the apparently small number of large (D greater than 500 km) impact basins seen in the relatively well-preserved cratered terrain of the south polar region. Previously only the 850 km wide South Polar Basin was easily recognized. The south polar region was mapped in detail, searching for evidence of ancient, highly degraded impact basins that may have escaped earlier notice, for two reasons: (1) to determine whether the apparent absence of large impact basins is due to incomplete mapping and recognition or a fundamental characteristic of the Martian crust related to the origin of the Martian crustal dichotomy, and (2) to determine whether ancient impact basins, if they exist, exert some control on the distribution of volcanic and polar deposits in the southern hemisphere and on the topography on which these deposits lie. Several promising candidates, including a large pre-Hellas basin in the Malea Planum region and an older but comparably sized basin overlapping South Polar, were previously described. Concentration is on the possible influence of the candidate basins in localizing the asymmetric distribution of polar deposits and in controlling the orientation of structures found within these deposits.
Author (revised)

N94-12267*# National Aeronautics and Space Administration. Goddard Space Flight Center, Greenbelt, MD.
FREE-AIR AND BOUGUER GRAVITY ANOMALIES AND THE MARTIAN CRUSTAL DICHOTOMY Abstract Only
Herbert Frey, Bruce G. Bills, Walter S. Kiefer, R. Steven Nerem, James H. Roark, and Maria T. Zuber *In* Lunar and Planetary Inst., Twenty-fourth Lunar and Planetary Science Conference. Part 1: A-F 1993 p 511-512 (For primary document see N94-12015 01-91)
Avail: CASI HC A01/MF A06

Free-air and Bouguer gravity anomalies from a 50x50 field, derived from re-analysis of Viking Orbiter and Mariner 9 tracking data and using a 50x50 expansion of the current Mars topography and the GSFC degree 50 geoid as the equipotential reference surface, with the Martian crustal dichotomy are compared. The spherical harmonic topography used has zero mean elevation, and differs from the USGS maps by about 2 km. In this field the dichotomy boundary in eastern Mars lies mostly at -1 to -2 km elevation. Bouguer gravity anomalies are shown on a map of Noachian, Hesperian, and Amazonian age terrains, simplified from current geologic maps. The map is centered at 300 deg W to show the continuity of the dichotomy boundary. Contour interval is 100 mgals. Gravity and topography were compared along approximately 40 profiles oriented parallel to the dichotomy boundary topographic gradient, to determine how the geophysical character of the boundary changes along its length and what this implies for its origin and development. Author (revised)

N94-12268*# National Aeronautics and Space Administration. Goddard Space Flight Center, Greenbelt, MD.
NEW MARS FREE-AIR AND BOUGUER GRAVITY: CORRELATION WITH TOPOGRAPHY, GEOLOGY AND LARGE IMPACT BASINS Abstract Only
Herbert Frey, Bruce G. Bills, Walter S. Kiefer, R. Steven Nerem, James H. Roark, and Maria T. Zuber *In* Lunar and Planetary Inst., Twenty-fourth Lunar and Planetary Science Conference. Part 1: A-F 1993 p 513-514 (For primary document see N94-12015 01-91)
Avail: CASI HC A01/MF A06

Free-air and Bouguer gravity anomalies from a 50x50 field (MGM635), derived at the Goddard Space Flight Center, with global topography, geology, and the distribution of large impact basins was compared. The free-air gravity anomalies were derived from re-analysis of Viking Orbiter and Mariner 9 tracking data and have a spatial resolution of 250-300 km. Bouguer anomalies were calculated using a 50x50 expansion of the current Mars topography and the GSFC degree 50 geoid as the equipotential reference surface. Rotational flattening was removed using a moment of inertia of 0.365 and the corrections from Table B2 of Sleep and Phillips. Crustal density and mean density were assumed to be 2.9 and 3.93 gm/cm(sup 3). The spherical harmonic topography used has zero mean elevation, and differs from the USGS maps by about 2 km. Comparisons with global geology use a simplified map with about 1/3 the number of units on the current maps. For correlation with impact basins, the recent compilation by Schultz and Frey was used. Author (revised)

N94-12323# National Space Development Agency, Ibaraki (Japan). Launch Vehicle and Satellite System Lab.
CONCEPTUAL STUDIES REPORT ON LUNAR AND PLANETARY EXPLORATION Report No. 2 [TSUKI WAKUSEI TANSA MISSHON GAINEN KENKYUU SEIKA HOUKOKUSHO]
Aug. 1992 129 p In JAPANESE Original contains color illustrations
(NASDA-TK-SS0438; JTN-93-80451) Avail: CASI HC A07/MF A02

The following topics were discussed: Japanese spacecraft, space missions, mission planning, spacecraft design, lunar exploration, Mars exploration, lunar site, lunar probes, lunar roving satellite, lunar roving vehicle, mars probes, spacecraft components, spacecraft equipment, spacecraft instruments, remote sensors, spacecraft orbits, spacecraft control, propulsion system, spacecraft power supplies, thermal control, spacecraft configurations, telecommunication, life support system, automatic control, space transportation system, and Mars surface samples. For individual titles, see N94-12324 through N94-12328.

N94-12324# National Space Development Agency, Ibaraki (Japan). Launch Vehicle and Satellite System Lab.
SIGNIFICANCE AND SCENARIOS OF LUNAR AND PLANETARY EXPLORATION MISSIONS [TSUKI WAKUSEI TANSA MISSHON NO IGI OYOBI SINARIO]
Tsutomu Iwata and Kazuo Oota *In its* Conceptual Studies Report on Lunar and Planetary Exploration Mission Aug. 1992 p 1-7 In JAPANESE (For primary document see N94-12323 01-91)
Avail: CASI HC A02/MF A02

Significance of moon and planet exploitation and their utilization are described. Topics discussed include: search for the truth concerning the universe; broadening the sphere of human activity; solving energy; resource; environmental problems; scenarios for lunar and Mars missions; and interrelationship between moon and planet exploitation technologies. This report is represented in viewgraphs only. Author (NASDA)

N94-12325# National Space Development Agency, Ibaraki (Japan). Launch Vehicle and Satellite System Lab.
UNMANNED LUNAR EXPLORATION MISSION [MUJIN TSUKI TANSA MISSHON]
Takeshi Kawazoe, Kazuo Oota, and Yutaka Kaneko *In its* Conceptual Studies Report on Lunar and Planetary Exploration Mission Aug. 1992 p 9-59 In JAPANESE (For primary document see N94-12323 01-91)
Avail: CASI HC A03/MF A02

Mission objectives, such as detail mapping and resource exploration of the lunar surface and lunar soft landing experiment (optional), mission examples, prerequisites, and models are outlined. Outlines and their characteristics of lunar revolving satellite, lunar roving vehicle, lunar landing module, lunar hopper, and sample return system such as lunar revolving altitude variations, weight and electric power allocations, system diagram, system configurations, subsystem characteristics, solar paddle types, and development schedule are also presented. This report is represented in viewgraphs only. Author (NASDA)

N94-12326# National Space Development Agency, Ibaraki (Japan). Launch Vehicle and Satellite System Lab.
MANNED LUNAR EXPLORATION MISSIONS [YUUJIN TSUKI TANSA MISSHON]
Yutaka Takano *In its* Conceptual Studies Report on Lunar and Planetary Exploration Mission Aug. 1992 p 67-90 In JAPANESE (For primary document see N94-12323 01-91)
Avail: CASI HC A03/MF A02

The objectives, major missions, outlines of the systems, system structures, system configurations of the manned lunar surface site, and manned lunar transportation system are presented. Environmental Control and Life Support System (ECLSS), pressurized environment conditions, and operation schedule of manned lunar surface site are also outlined. This report is represented in viewgraphs only. Author (NASDA)

N94-12327# National Space Development Agency, Ibaraki (Japan). Launch Vehicle and Satellite System Lab.
MARS EXPLORATION MISSIONS [KASEI TANSA MISSHON]
Kazuo Oota and Toshihide Maeda *In its* Conceptual Studies Report on Lunar and Planetary Exploration Mission Aug. 1992 p 91-139 In JAPANESE (For primary document see N94-12323 01-91)
Avail: CASI HC A03/MF A02

Outlines of Mars exploration missions and Mars explorer systems such as Explorer of Martian Environment Research (EMER), Mars Landing Explorer (MALE), mars mobile explorer, and Mars Moon Sample Return (MMSR) are explained. Mission objectives, onboard equipments, system configurations, system outlines, orbits, power and weight, and communication subsystems of the explorers are also mentioned. This report is represented in viewgraphs only. Author (NASDA)

N94-12328# National Space Development Agency, Ibaraki (Japan). Launch Vehicle and Satellite System Lab.
TECHNICAL PROBLEMS ON LUNAR AN PLANETARY EXPLORATION MISSION [TSUKI WAKUSEI TANSA MISSHON NO GIJUTSU KADAI]
Tsutomu Iwata, Kazuo Oota, Takeshi Kawazoe, Yutaka Kaneko, Yutaka Takano, and Korehiro Maeda *In its* Conceptual Studies Report on Lunar and Planetary Exploration Mission Aug. 1992 p 141-145 In JAPANESE (For primary document see N94-12323 01-91)
Avail: CASI HC A01/MF A02

Technical problems on unmanned lunar mission, manned lunar mission, and unmanned Mars exploration missions are outlined. Topics discussed include: attitude and orbit control profile for transient orbit injection; attitude control at lunar revolving orbit injection; problems on lunar revolving observation satellite; lunar landing vehicle; lunar surface rover; manned lunar transport system; manned lunar surface site; lunar surface operation robot; high-accuracy orbit and attitude establishment; high accuracy navigation sensors; problems on Mars revolving observation satellite; Mars landing and exploring vehicle; Mars surface rover; and Phobos and Deimos sample return. This report is represented in viewgraphs only. Author (NASDA)

N94-12429*# Washington Univ., Saint Louis, MO.
AN INTERFEROMETRIC SPECTRAL MAPPER FOR THE CASSINI MISSION TO SATURN AND TITAN Final Report
William Hayden Smith 31 Oct. 1991 5 p
(Grant NAGw-1801)
(NASA-CR-193805; NAS 1.26:193805) Avail: CASI HC A01/MF A01

The research reported resulted in a detailed proposal for the Cassini Mission that addressed fundamental atmospheric structure and composition questions for both Saturn and Titan. Due to the brief time available between the initiation of the research and the proposal date, it was necessary to develop the science goals in close synchronicity with the instrument design. A major goal of the program was to acquire, implement, and test SWIR and MWIR arrays suitable for use with the DIGITAL ARRAY SCANNED INTERFEROMETERS, (DASI's), for the extended goal of developing DASI's for a range of spectral mapping research in solar system exploration. These goals were all reached or exceeded in the course of this work. Author (revised)

N94-12446*# Brown Univ., Providence, RI. Dept. of Geological Sciences.
INTERDISCIPLINARY SCIENTIST PARTICIPATION IN THE PHOBOS MISSION Final Report, 15 Sep. 1989 - 14 Jun. 1992
14 Jun. 1992 5 p
(Grant NAGw-1868)
(NASA-CR-193715; NAS 1.26:193715) Avail: CASI HC A01/MF A01

Data was acquired from VSK (2 wide-angle visible-NIR TV cameras at 0.4 to 0.6 micrometers and 0.8 to 1.1 micrometers, and a narrow-angle TV camera), KRFM (10-band UV-visible spectrometer at 0.3 to 0.6 micrometers and a 6-band radiometer at 5-50 micrometers), and ISM (a 128-channel NIR imaging spectrometer at 0.8 to 3 micrometers). These data provided improved mapping coverage of Phobos; improved mass, shape, and volume determinations, with the density shown to be lower than that of all known meteorites, suggesting a porous interior; evidence for a physically, spectrally and possibly compositionally heterogeneous surface; and proof that the spectral properties do not closely resemble those of unaltered carbonaceous chondrites, but show more resemblance to the spectra of altered mafic material. For Mars, the data show that the underlying rock type can be distinguished through the global dust cover; that the spectral properties and possibly composition vary laterally between and within the geologic provinces; that the surface physical properties vary laterally, and in many cases, the boundaries coincide with those of the geologic units; and the acquired data also demonstrate the value of reflectance spectroscopy and radiometry to the study of Martian geology. CASI

92 SOLAR PHYSICS

Includes solar activity, solar flares, solar radiation and sunspots. For related information see *93 Space Radiation.*

N94-10741 Los Alamos National Lab., NM.
SOLAR WIND CHANNELS FOR MeV PARTICLES
D. E. Page (Jet Propulsion Lab., California Inst. of Tech., Pasadena.), B. G. Goldstein (Jet Propulsion Lab., California Inst. of Tech., Pasadena.), and S. J. Bame 1993 5 p Presented at the International Cosmic Ray Conference, Calgary, Alberta, 19-20 Jul. 1993 Limited Reproducibility: More than 20% of this document may be affected by microfiche quality

(Contract W-7405-eng-36)
(DE93-012648; LA-UR-93-1286; CONF-930779-8) Avail: CASI HC A01

Plasma, magnetic field and charged particle data from the Ulysses spacecraft is used to demonstrate that MeV particles follow channels defined by solar wind flow regimes. DOE

N94-10949*# Cornell Univ., Ithaca, NY.
ANALYSIS OF IRAS SOLAR SYSTEM DUST DATA Final Technical Report, 1 Jun. 1989 - 31 Dec. 1991
S. F. Dermott and P. D. Nicholson 1991 5 p
(Grant NAG5-1261)
(NASA-CR-193704; NAS 1.26:193704) Avail: CASI HC A01/MF A01

Data in the Infrared Astronomical Satellite (IRAS) Zodiacal History File were analyzed to extract dust band locations and peak brightness measurements from approximately 1,000 individual IRAS scans. The study had three goals. One was to show that the prominent solar system dust bands are associated with Hirayama asteroid families and thus that collisions between asteroids account for a significant fraction of the particles in the zodiacal cloud. Recent work suggests that while the Hirayama families are a major source of the dust in the bands, there may also be contributions from two or three smaller, more recently recognized asteroid families. A second goal was to show that there is evidence in the IRAS dust data for the transport of particles from asteroid belt to the Earth by Poynting-Robertson light drag and thus account for the fact that asteroid particles are collected in the Earth's stratosphere. Results of the study will confirm the location of the dust bands within the inner asteroid belt, and show conclusively that the material seen by IRAS is now spread over a wide range of distances from the sun. The third goal was to construct a model of the background zodiacal cloud that satisfies the proper dynamical constraints. Figures are provided to show the scans processed to remove zodiacal background and Galactic signals, and the resulting polynomial fits to the 25 micron scan. The latter provided objective estimates of band widths, peak locations, and peak fluxes. Modelling and analysis of the resulting band data has been presented at several conferences and is the subject of a number of forthcoming papers. CASI

N94-11048*# Lockheed Missiles and Space Co., Palo Alto, CA. Solar and Astrophysics Lab.
SMM X RAY POLYCHROMATOR Final Report, Jun. 1988 - Jul. 1993
J. L. R. Saba 7 Jul. 1993 52 p
(Contract NAS5-30431)
(NASA-CR-193282; NAS 1.26:193282) Avail: CASI HC A04/MF A01

The objective of the X-ray Polychromator (XRP) experiment was to study the physical properties of solar flare plasma and its relation to the parent active region to understand better the flare mechanism and related solar activity. Observations were made to determine the temperature, density, and dynamic structure of the pre-flare and flare plasma as a function of wavelength, space and time, the extent to which the flare plasma departs from thermal equilibrium, and the variation of this departure with time. The experiment also determines the temperature and density structure of active regions and flare-induced changes in the regions. Author (revised)

N94-11619# Washington Univ., Seattle. Inst. for Nuclear Theory.
SOLAR NEUTRINOS WITH THREE FLAVOR MIXINGS
D. Harley, J. Pantaleone, and T. K. Kuo (Purdue Univ., West Lafayette, IN.) 1992 10 p
(Contract DE-FG06-90ER-40561)
(DE93-011006; DOE/ER-40561/077) Avail: CASI HC A02/MF A01

The recent Ga-71 solar neutrino observation is combined with the Cl-37 and Kamiokande-2 observations in an analysis for neutrino masses and mixings. The allowed parameter region is found for matter enhanced mixings among all three neutrino flavors. Distortions of the solar neutrino spectrum unique to three flavors are possible and may be observed in continuing and next generation experiments. DOE

N94-12414# Naval Research Lab., Washington, DC.
YOHKOH BRAGG CRYSTAL SPECTROMETER LIGHT CURVES FOR CA XIX (3.1631-3.1912A): 1 OCTOBER 1991 - 30 SEPTEMBER 1992
John T. Mariska, R. D. Bentley, and C. D. Pike 4 Apr. 1993 195 p
(AD-A266090; NRL/MR/7673-93-7313) Avail: CASI HC A09/MF A03

This Memo Report summarizes the data produced during the first year of operation by the Bragg Crystal Spectrometer (BCS) on the Yohkoh spacecraft. Each page shows the total count rate in the Ca XIX channel of the BCS for a single day. This channel nominally observes the Sun in the wavelength range from 3.1631 to 3.1912 A. These plots are useful for identifying flare data for further analysis and for determining the data file name and tape name that contain the data. DTIC

N94-12427*# Alabama Univ., Huntsville. Dept. of Physics.
DATA ANALYSIS TASKS: BATSE Final Report, 30 Sep. 1991 - 27 Feb. 1993
William S. Paciesas May 1993 44 p
(Contract NAS8-38609)
(NASA-CR-192598; NAS 1.26:192598) Avail: CASI HC A03/MF A01

Miscellaneous tasks related to the operation of, and analysis of data from, the Burst and Transient Experiment (BATSE) on the Compton Gamma Ray Observatory (CGRO) were performed. The results are summarized and relevant references are included. Author

N94-12088*# Carnegie Institution of Washington, DC.
MIDPLANE TEMPERATURES IN THE SOLAR NEBULA Abstract Only
A. P. Boss *In* Lunar and Planetary Inst., Twenty-fourth Lunar and Planetary Science Conference. Part 1: A-F 1993 p 151-152 (For primary document see N94-12015 01-91)
Avail: CASI HC A01/MF A06

N94-12089*# Carnegie Institution of Washington, DC.
CHONDRULE FORMATION BY CLUMPY ACCRETION ONTO THE SOLAR NEBULA Abstract Only
A. P. Boss and J. A. Graham *In* Lunar and Planetary Inst., Twenty-fourth Lunar and Planetary Science Conference. Part 1: A-F 1993 p 153-154 (For primary document see N94-12015 01-91)
Avail: CASI HC A01/MF A06

N94-12090*# Carnegie Institution of Washington, DC.
INITIATING SOLAR SYSTEM FORMATION THROUGH STELLAR SHOCK WAVES
A. P. Boss and E. A. Myhill *In* Lunar and Planetary Inst., Twenty-fourth Lunar and Planetary Science Conference. Part 1: A-F 1993 p 155-156 (For primary document see N94-12015 01-91)
Avail: CASI HC A01/MF A06

N94-12143*# National Aeronautics and Space Administration. Ames Research Center, Moffett Field, CA.
WHY CONVECTIVE HEAT TRANSPORT IN THE SOLAR NEBULA WAS INEFFICIENT Abstract Only
P. Cassen *In* Lunar and Planetary Inst., Twenty-fourth Lunar and Planetary Science Conference. Part 1: A-F 1993 p 261-262 (For primary document see N94-12015 01-91)
Avail: CASI HC A01/MF A06

N94-12212*# University of Southern California, Pasadena. Div. of Geology Planetary Sciences.
ISOTOPIC AND TRACE ELEMENT CHARACTERISTICS OF AN UNUSUAL REFRACTORY INCLUSION FROM ESSEBI Abstract Only
E. Deloule, A. K. Kennedy, I. D. Hutcheon, and A. ElGoresy (Max-Planck-Inst. fuer Kernphysik, Heidelberg, Germany.) *In* Lunar and Planetary Inst., Twenty-fourth Lunar and Planetary Science Conference. Part 1: A-F 1993 p 399-400 (For primary document see N94-12015 01-91)
Avail: CASI HC A01/MF A06

N94-12220*# Lunar and Planetary Inst., Houston, TX.
ARE COSMIC RAYS EFFECTIVE FOR IONIZATION OF THE SOLAR NEBULA? Abstract Only
A. Z. Dolginov and T. F. Stepinski *In its* Twenty-fourth Lunar and Planetary Science Conference. Part 1: A-F 1993 p 415-416 (For primary document see N94-12015 01-91)
Avail: CASI HC A01/MF A06

N94-12232*# Los Alamos National Lab., NM. Space Plasma Physics, Geology and Geophysics Group.
SOLAR WIND-INDUCED SECONDARY IONS AND THEIR RELATION TO LUNAR SURFACE COMPOSITION Abstract Only
R. C. Elphic, H. O Funsten, III, and R. L. Hervig (Arizona State Univ.,

Tempe.) *In* Lunar and Planetary Inst., Twenty-fourth Lunar and Planetary Science Conference. Part 1: A-F 1993 p 439 (For primary document see N94-12015 01-91)
Avail: CASI HC A01/MF A06

93 SPACE RADIATION

Includes cosmic radiation; and inner and outer earth's radiation belts.

For biological effects of radiation see *52 Aerospace Medicine*. For theory see *73 Nuclear and High-Energy Physics*.

N94-10507*# Alabama Univ., Huntsville.
[COSMOLOGICAL GAMMA-RAY BURST MODEL] Final Report
J. J. Brainerd 1993 7 p
(Grant NAG5-2056)
(NASA-CR-193368; NAS 1.26:193368) Avail: CASI HC A02/MF A01

A cosmological gamma-ray burst model that reproduces the observed gamma-ray spectra was developed. This model, which is an outgrowth of work on synchrotron emission from cosmological sources, creates the observed spectra from a power law spectrum through Compton attenuation in dense molecular clouds. It restricts the burst source to the centers of galaxies, and it is easily tested through comparisons with time dependent burst spectra. Dr. Brainerd continued development of a Monte Carlo code that tracks the random walk of a gamma-ray through a plasma in a strong magnetic field and used this code to show that a two temperature plasma in a strong magnetic field can suppress soft x-ray emission. Author

N94-10534 Joint Inst. for Nuclear Research, Dubna (USSR). Lab. of Nuclear Reactions.
INVESTIGATION OF SOFT ERRORS IN MOS RAM UNDER INFLUENCE OF HEAVY IONS [ISSLEDOVANIE SBOEV V BIS OZU POD DEJSTVIEM TYAZHELYKH LONOV]
N. G. Goleminov (Moscow Physical-Engineering Inst., Russia.), D. V. Akinshin, A. Y. Didyk, and V. A. Skuratov 1991 8 p In RUSSIAN Limited Reproducibility: More than 20% of this document may be affected by microfiche quality
(DE92-644554; JINR-R-13-91-201) Avail: Issuing Activity (Department of Energy (DOE)) (US Sales Only)

The data about deposition of electromagnetic and nuclear processes of galactic cosmic ray interaction with CMOS constructive materials are presented. The experimental results of the investigations of CMOS RAM response on of about 1 MeV/a.m.u. heavy ion influence are given. In particular, the energetic dependence of memory element sensitivity and temporary dependence of soft error accumulation are described. DOE

N94-10759*# National Aeronautics and Space Administration. Langley Research Center, Hampton, VA.
NONPERTURBATIVE METHODS IN HZE ION TRANSPORT
John W. Wilson, Francis F. Badavi (Christopher Newport Coll., Newport News, VA.), Robert C. Costen, and Judy L. Shinn Washington Aug. 1993 27 p
(RTOP 199-45-16-11)
(NASA-TP-3363; L-17241; NAS 1.60:3363) Avail: CASI HC A03/MF A01

A nonperturbative analytic solution of the high charge and energy (HZE) Green's function is used to implement a computer code for laboratory ion beam transport. The code is established to operate on the Langley Research Center nuclear fragmentation model used in engineering applications. Computational procedures are established to generate linear energy transfer (LET) distributions for a specified ion beam and target for comparison with experimental measurements. The code is highly efficient and compares well with the perturbation approximations. Author

N94-11278*# National Aeronautics and Space Administration. Langley Research Center, Hampton, VA.
A PROPOSED PERFORMANCE INDEX FOR GALACTIC COSMIC RAY SHIELDING MATERIALS
John W. Wilson, J. S. Wood, Judy L. Shinn, Francis A. Cucinotta, and John E. Nealy Washington Aug. 1993 10 p
(RTOP 592-43-21-01)
(NASA-TM-4444; L-17199; NAS 1.15:4444) Avail: CASI HC A02/MF A01

In past studies, the reductions in absorbed dose and dose equivalent due to choice of material composition have been used to indicate shield effectiveness against exposure to galactic cosmic rays. However, these quantities are highly inaccurate in assessing shield effectiveness for protection against the biological effects of long-term exposure to the galactic heavy ions. A new quantity for shield performance is defined that correlates well with cell killing and cell transformation behind various shield thicknesses and materials. In addition, a relative performance index is identified that is inversely related to biological injury for different materials at a fixed shield mass and is directly related to the ratio of the fourth- and the second-order linear energy transfer (LET) moments. Author (revised)

N94-11312*# Radiophysics, Inc., Boulder, CO.
MODELS OF NEPTUNE'S SMOOTH RECURRENT RADIO EMISSION Final Report, 4 June 1992 - 9 Jul. 1993
Constance Sawyer 9 Jul. 1993 14 p
(Contract NASw-4697)
(NASA-CR-193283; NAS 1.26:193283) Avail: CASI HC A03/MF A01

The quantitative response of the Planetary Radio Astronomy (PRA) instrument to a wave with polarization ellipse of arbitrary shape and orientation, arriving at the antennas from any direction, can be determined. This capability is used to model the time variation of intensity and circular polarization over a range of radio frequencies for proposed radio-source locations and emission characteristics at Neptune. At frequencies below 400 kHz the observed variation of intensity, polarization, and phase are closely simulated in an offset tilted dipole magnetic field by conjugate sources at midlatitude with filled emission cones. The phase of emission at higher frequencies is reproduced by sources at lower latitude. Modeled wide-cone emission does not reach the spacecraft at the observed phase nor have the polarization sense observed before closest approach. Source-surface maps of apparent polarization for the period before closest approach when instrumental response is especially sensitive to source location is presented. The method is capable of extension to more realistic models of the magnetic field. Author (revised)

N94-11486*# California Inst. of Tech., Pasadena.
POST-LAUNCH ANALYSIS OF DATA FROM THE HIGH ENERGY ASTROPHYSICAL OBSERVATORY HEAVY NUCLEI EXPERIMENT (HEAO-C3) Final Report, period ending 31 Mar. 1992
E. C. Stone 1992 4 p
(Grants NAGw-1930; NAGw-1934; NAGw-1954)
(NASA-CR-193513; NAS 1.26:193513) Avail: CASI HC A01/MF A01

The Final Report on the continuing analysis of data from the Heavy Nuclei Experiment (HNE), flown on the HEAO-3 mission, is presented. The HNE was designed to measure the elemental abundances of relativistic cosmic ray nuclei covering the charge range 17 is less than or equal to Z is less than or equal to 130. The result of these measurements is significant to the study of nucleosynthesis, the origin, acceleration, and propagation of cosmic ray nuclei, and the properties of the interstellar medium. Author (revised)

N94-12357# Instituto de Pesquisas Espaciais, Sao Jose dos Campos (Brazil).
SEARCH FOR STRUCTURES IN THE COSMIC MICROWAVE BACKGROUND RADIATION M.S. Thesis, 1992 [APLICACAO DE UM METODO PARA DETECCAO DE FLUTUACOES NA RADIACAO COSMICA DE FUNDO]
Angelica deOliveiraCosta Jan. 1993 90 p In PORTUGESE
(INPE-5491-TDI/508) Avail: CASI HC A05/MF A01

We applied a method to search for fluctuations in the cosmic microwave background radiation based on the assumption that such fluctuations can be described by a random Gaussian field. We used two maps, one at 3.3 mm and another obtained combining the 3.3 mm and 12 mm maps, both experiments had beam size of 7 degrees (FWHM). Although two regions, one hot and another cold, have been detected in the 3.3 mm data set at 2 sigma (or 95.45% of C.L.), they cannot be considered as Hot or Cold Spots because both structures were smaller than the region covered by the beam size. Author

N94-12434*# National Aeronautics and Space Administration. Langley Research Center, Hampton, VA.

COULOMB EFFECTS IN LOW-ENERGY NUCLEAR FRAGMENTATION

John W. Wilson, Sang Y. Chun (Old Dominion Univ., Norfolk, VA.), Francis F. Badavi (Christopher Newport Coll., Newport News, VA.), and Sarah John (Vigyan Research Associates, Inc., Hampton, VA.) Washington Aug. 1993 12 p
(RTOP 199-45-16-11)
(NASA-TP-3352; L-17226; NAS 1.60:3352) Avail: CASI HC A03/MF A01

Early versions of the Langley nuclear fragmentation code NUCFRAG (and a publicly released version called HZEFRG1) assumed straight-line trajectories throughout the interaction. As a consequence, NUCFRAG and HZEFRG1 give unrealistic cross sections for large mass removal from the projectile and target at low energies. A correction for the distortion of the trajectory by the nuclear Coulomb fields is used to derive fragmentation cross sections. A simple energy-loss term is applied to estimate the energy downshifts that greatly alter the Coulomb trajectory at low energy. The results, which are far more realistic than prior versions of the code, should provide the data base for future transport calculations. The systematic behavior of charge-removal cross sections compares favorably with results from low-energy experiments. Author (revised)

N94-12589*# Massachusetts Inst. of Tech., Lexington.

OBSERVATIONS OF OPTICAL COUNTERPARTS OF GAMMA-RAY BURSTS Final Technical Report, Dec. 1987 - Mar. 1989

Frederick K. Knight 3 Sep. 1992 4 p
(Grant NAGw-1168)
(NASA-CR-193573; NAS 1.26:193573) Avail: CASI HC A01/MF A01

This is a final report for a contract begun in Dec. 1987 and ended in Mar. 1989 to use the existing Lincoln Laboratory Experimental Test Site in Socorro, NM to search for optical counterparts to gamma-ray bursts. The objective was to develop an autonomous staring system to search for stationary, transient optical flashes. The search was to use an existing 31-inch telescope equipped with a sensitive video detector. The approach for the search was to develop real-time processing software to monitor the video signal from the detector and to record any transient, point-like flashes that occurred in the field of view. The system would have been able to detect fainter flashes (B is approximately 15(sup m) in 1/30 s, delta(m(sub v)) = 0.25(sup m)) than other systems but lacked a large field of view (only 1.2 deg diameter) necessary to give a high probability of detecting a random flash on the sky. As such, the plan was to monitor known gamma-ray burst error boxes and wait for a repetition of an earlier event. The high payoff of good sensitivity with high angular resolution (1 pixel = 10sec) and good time resolution (30 s) to allow post-burst searches warranted funding if the cost was not prohibitive. The contract began in the middle of the three-year cycle for High Energy Astrophysics Gamma-Ray Astronomy Research and Analysis Program. This final report briefly describes the portion of the plan completed under the original contract. Author (revised)

N94-12771*# Chicago Univ., IL.

ANALYSIS AND INTERPRETATION OF HIGH ENERGY COSMIC RAYS MEASURED ON SPACELAB-2 Final Technical Report, 1 Jan. 1988 - 31 Dec. 1990

Dietrich Mueller, Peter Meyer, Jacques LHeureux, and Simon Swordy Dec. 1991 5 p
(Grant NAGw-1311)
(NASA-CR-193586; NAS 1.26:193586) Avail: CASI HC A01/MF A01

Under the contract with NASA's Marshall Space Flight Center (NAS8-32828) the University of Chicago designed, built and delivered the CRN instrument for flight in the Spacelab-2 configuration. The instrument was flown from July 29 to August 5, 1985 on the Space Shuttle Challenger. The performance of our experiment was entirely successful and we reached our scientific goals. The contract included funds for the first year of data analysis. Further data analysis was carried out under the grant NAGW-1311 which ran from January 1, 1988 through December 31, 1990, and on which we report. The final products of this grant are the published scientific papers with the results from the experiment. We attach copies of the papers that have been published to date, and which we consider the most important part of this report. However, in order to put them into context we give a brief account of the project as a whole for which the grant covered the final phase. Derived from text

N94-11065# Cornell Univ., Ithaca, NY. Dept. of Astronomy.

INTERSTELLAR SCATTERING AND THE PULSAR STUDIES WITH SPACE VLBI

James M. Cordes *In* National Astronomy and Ionosphere Center, Propagation Effects in Space VLBI 1993 p 45-56 Sponsored by National Astronomy and Ionosphere Center (For primary document see N94-11060 01-32)
Avail: Issuing Activity

99 GENERAL

N94-10356*# National Aeronautics and Space Administration. Lewis Research Center, Cleveland, OH.

THE NASA LEWIS RESEARCH CENTER SBIR PROGRAM: AN ASSESSMENT

Hubert H. Grimes (Omni Corp., Brook Park, OH.), Marie E. Metzger (Omni Corp., Brook Park, OH.), and Walter S. Kim Jun. 1993 30 p
(RTOP 324-89-00)
(NASA-TM-106205; E-7914; NAS 1.15:106205) Avail: CASI HC A03/MF A01

An assessment was made of the NASA Lewis Small Business Innovation Research (SBIR) Program for the years 1983 to 1989. The assessment was based on the study of 99 Phase 1 contracts and 39 Phase 2 contracts. The overall impact of SBIR was found to be very positive, contributing strongly to many NASA programs. In addition, many successful efforts were commercialized benefiting the small business, federal agencies, and the aerospace industry. The program was evaluated in terms of contract quality, innovativeness, comparison to the state-of-the-art, achievement of goals, difficulty, and impact. Program difficulties were also identified, which could suggest possible program improvements. Much of the information gained in this assessment provided a basis for a SBIR data base which will be updated every year. This data base is computerized and will provide an excellent source of information about past SBIR efforts and company capabilities. Author (revised)

N94-10850 National Inst. of Standards and Technology, Gaithersburg, MD.

JOURNAL OF RESEARCH OF THE NATIONAL INSTITUTE OF STANDARDS AND TECHNOLOGY, VOLUME 98, NUMBER 2, MARCH - APRIL 1993

1993 135 p See also PB93-195236 through PB93-196293 and PB93-166817. Also available from Supt. of Docs. as SN703-027-00051-2 Limited Reproducibility: More than 20% of this document may be affected by microfiche quality
(PB93-196228) Avail: CASI HC A07

The following topics are discussed: absolute spatially- and temporally-resolved optical emission measurement of rf glow discharges in Argon; optimizing complex kinetics experiments using Least-Squares Methods; measuring low frequency tilts; optical fiber geometry--accurate measurement of cladding diameter; drift eliminating designs for non-simultaneous comparison calibrations; a three-ratio scheme for the measurement of isotopic ratios of silicon; 'Wolf Shifts' and their physical interpretation under laboratory conditions. NTIS

N94-11379# European Space Agency. European Space Research and Technology Center, ESTEC, Noordwijk (Netherlands). Publications Div.

ESA/ESOC: 25 YEARS

Jocelyne Landeau-Constantin, comp., Oscar Bischof, comp., Pauline Bolle-Mead, comp., Siegmar Pallaschke, comp., Inge Schlicker, comp., Yves Trehin, comp., and Norman Longdon, ed. 1992 36 p Limited Reproducibility: More than 20% of this document may be affected by color photographs Original contains color illustrations
(ESA-BR-90; ISBN-92-9092-139-0) Avail: CASI HC A03/MF A01

Activities of the European Space Agency's European Space Operations Center are described. A history of the organization is included. A description of various satellites and programs over the last 25 years is given. CASI

N94-11527*# National Aeronautics and Space Administration. Lyndon B. Johnson Space Center, Houston, TX.

SIXTH ANNUAL WORKSHOP ON SPACE OPERATIONS APPLICATIONS AND RESEARCH (SOAR 1992), VOLUME 2

Kumar Krishen, ed. Feb. 1993 294 p Workshop held in Houston, TX, 4-6 Aug. 1992; sponsored by NASA, Washington, AF, and Houston Univ.
(NASA-CP-3187-Vol-2; S-706-Vol-2; NAS 1.55:3187-Vol-2) Avail: CASI HC A13/MF A03

This document contains papers presented at the Space Operations, Applications, and Research Symposium (SOAR) hosted by the U.S. Air Force (USAF) on 4-6 Aug. 1992. The symposium was cosponsored by the Air Force Material Command and by NASA/JSC. Key technical areas covered during the symposium were robotics and telepresence, automation and intelligent systems, human factors, life sciences, and space maintenance and servicing. The SOAR differed from most other conferences in that it was concerned with Government-sponsored research and development relevant to aerospace operations. Symposium proceedings include papers covering various disciplines presented by experts from NASA, the USAF, universities, and industry. For individual titles, see N94-11528 through N94-11579.

N94-11528*# Veterans Administration Hospital, Sepulveda, CA.

QUANTITATIVE EEG PATTERNS OF DIFFERENTIAL IN-FLIGHT WORKLOAD **c54**

M. B. Sterman, C. A. Mann, and D. A. Kaiser *In* NASA. Johnson Space Center, Sixth Annual Workshop on Space Operations Applications and Research (SOAR 1992), Volume 2 Feb. 1993 p 466-473 Prepared in cooperation with California Univ., Los Angeles (For primary document see N94-11527 01-99)
Avail: CASI HC A02/MF A03

Four test pilots were instrumented for in-flight EEG recordings using a custom portable recording system. Each flew six, two minute tracking tasks in the Calspan NT-33 experimental trainer at Edwards AFB. With the canopy blacked out, pilots used a HUD display to chase a simulated aircraft through a random flight course. Three configurations of flight controls altered the flight characteristics to achieve low, moderate, and high workload, as determined by normative Cooper-Harper ratings. The test protocol was administered by a command pilot in the back seat. Corresponding EEG and tracking data were compared off-line. Tracking performance was measured as deviation from the target aircraft and combined with control difficulty to achieve an estimate of 'cognitive workload'. Trended patterns of parietal EEG activity at 8-12 Hz were sorted according to this classification. In all cases, high workload produced a significantly greater suppression of 8-12 Hz activity than low workload. Further, a clear differentiation of EEG trend patterns was obtained in 80 percent of the cases. High workload produced a sustained suppression of 8-12 Hz activity, while moderate workload resulted in an initial suppression followed by a gradual increment. Low workload was associated with a modulated pattern lacking any periods of marked or sustained suppression. These findings suggest that quantitative analysis of appropriate EEG measures may provide an objective and reliable in-flight index of cognitive effort that could facilitate workload assessment.
Author (revised)

N94-11529*# Aerospace Medical Research Labs., Wright-Patterson AFB, OH. Human Engineering Div.

PSYCHOPHYSIOLOGICAL MEASURES OF COGNITIVE WORKLOAD IN LABORATORY AND FLIGHT **c54**

Glenn F. Wilson and Albert Badeau *In* NASA. Johnson Space Center, Sixth Annual Workshop on Space Operations Applications and Research (SOAR 1992), Volume 2 Feb. 1993 p 474-481 (For primary document see N94-11527 01-99)
Avail: CASI HC A02/MF A03

Psychophysiological data have been recorded during different levels of cognitive workload in laboratory and flight settings. Cardiac, eye blink, and brain data have shown meaningful changes as a function of the levels of mental workload. Increased cognitive workload is generally associated with increased heart rates, decreased blink rates and eye closures, and decreased evoked potential amplitudes. However, comparisons of laboratory and flight data show that direct transference of laboratory findings to the flight environment is not possible in many cases. While the laboratory data are valuable, a data base from flight is required so that 'real world' data can be properly interpreted.
Author (revised)

N94-11530*# National Aeronautics and Space Administration. Ames Research Center, Moffett Field, CA.

TRANSFER OF TRAINING FOR AEROSPACE OPERATIONS: HOW TO MEASURE, VALIDATE, AND IMPROVE IT **c53**

Malcolm M. Cohen *In* NASA. Johnson Space Center, Sixth Annual Workshop on Space Operations Applications and Research (SOAR 1992), Volume 2 Feb. 1993 p 482-487 (For primary document see N94-11527 01-99)
Avail: CASI HC A02/MF A03

It has been a commonly accepted practice to train pilots and astronauts in expensive, extremely sophisticated, high fidelity simulators, with as much of the real-world feel and response as possible. High fidelity and high validity have often been assumed to be inextricably interwoven, although this assumption may not be warranted. The Project Mercury rate-damping task on the Naval Air Warfare Center's Human Centrifuge Dynamic Flight Simulator, the shuttle landing task on the NASA-ARC Vertical Motion Simulator, and the almost complete acceptance by the airline industry of full-up Boeing 767 flight simulators, are just a few examples of this approach. For obvious reasons, the classical models of transfer of training have never been adequately evaluated in aerospace operations, and there have been few, if any, scientifically valid replacements for the classical models. This paper reviews some of the earlier work involving transfer of training in aerospace operations, and discusses some of the methods by which appropriate criteria for assessing the validity of training may be established.
Author (revised)

N94-11531*# National Aeronautics and Space Administration. Lyndon B. Johnson Space Center, Houston, TX.

SIGNAL DETECTION THEORY AND METHODS FOR EVALUATING HUMAN PERFORMANCE IN DECISION TASKS **c53**

Kevin OBrien (Lockheed Engineering and Sciences Co., Houston, TX.) and Evan M. Feldman (Rice Univ., Houston, TX.) *In its* Sixth Annual Workshop on Space Operations Applications and Research (SOAR 1992), Volume 2 Feb. 1993 p 489-496 (For primary document see N94-11527 01-99)
Avail: CASI HC A02/MF A03

Signal Detection Theory (SDT) can be used to assess decision making performance in tasks that are not commonly thought of as perceptual. SDT takes into account both the sensitivity and biases in responding when explaining the detection of external events. In the standard SDT tasks, stimuli are selected in order to reveal the sensory capabilities of the observer. SDT can also be used to describe performance when decisions must be made as to the classification of easily and reliably sensed stimuli. Numbers are stimuli that are minimally affected by sensory processing and can belong to meaningful categories that overlap. Multiple studies have shown that the task of categorizing numbers from overlapping normal distributions produces performance predictable by SDT. These findings are particularly interesting in view of the similarity between the task of the categorizing numbers and that of determining the status of a mechanical system based on numerical values that represent sensor readings. Examples of the use of SDT to evaluate performance in decision tasks are reviewed. The methods and assumptions of SDT are shown to be effective in the measurement, evaluation, and prediction of human performance in such tasks.
Author

N94-11532*# National Aeronautics and Space Administration. Ames Research Center, Moffett Field, CA.

CRITERIA FOR ASSESSING PROBLEM SOLVING AND DECISION MAKING IN COMPLEX ENVIRONMENTS Abstract Only **c53**

Judith Orasanu *In* NASA. Johnson Space Center, Sixth Annual Workshop on Space Operations Applications and Research (SOAR 1992), Volume 2 Feb. 1993 p 497 (For primary document see N94-11527 01-99)
Avail: CASI HC A01/MF A03

Training crews to cope with unanticipated problems in high-risk, high-stress environments requires models of effective problem solving and decision making. Existing decision theories use the criteria of logical consistency and mathematical optimality to evaluate decision quality. While these approaches are useful under some circumstances, the assumptions underlying these models frequently are not met in dynamic time-pressured operational environments. Also, applying formal decision models is both labor and time intensive, a luxury often lacking in operational environments. Alternate approaches and criteria are needed. Given that operational problem solving and decision making are embedded in ongoing tasks, evaluation criteria must address the relation between those activities and satisfaction of broader task goals. Effectiveness and efficiency become relevant for judging reasoning performance in operational environments. New questions must be addressed: What is the relation between the quality of decisions and overall performance by crews engaged in critical high risk tasks? Are different strategies most effective for different types of decisions? How can various decision types be characterized? A preliminary model of decision types found in air transport environments will be described along with a preliminary performance model based on an analysis of 30 flight crews. The performance analysis examined behaviors that distinguish more and less effective crews (based on performance errors). Implications for training and system design will be discussed. Author (revised)

N94-11533*# Krug Life Sciences, Inc., San Antonio, TX.
MONITORING COGNITIVE FUNCTION AND NEED WITH THE AUTOMATED NEUROPSYCHOLOGICAL ASSESSMENT METRICS IN DECOMPRESSION SICKNESS (DCS) RESEARCH Abstract Only c53
Thomas E. Nesthus and Sammuel G. Schiflett (Aerospace Medical Research Labs., Brooks AFB, TX.) *In* NASA. Johnson Space Center, Sixth Annual Workshop on Space Operations Applications and Research (SOAR 1992), Volume 2 Feb. 1993 p 498 (For primary document see N94-11527 01-99)
Avail: CASI HC A01/MF A03

Hypobaric decompression sickness (DCS) research presents the medical monitor with the difficult task of assessing the onset and progression of DCS largely on the basis of subjective symptoms. Even with the introduction of precordial Doppler ultrasound techniques for the detection of venous gas emboli (VGE), correct prediction of DCS can be made only about 65 percent of the time according to data from the Armstrong Laboratory's (AL's) hypobaric DCS database. An AL research protocol concerned with exercise and its effects on denitrogenation efficiency includes implementation of a performance assessment test battery to evaluate cognitive functioning during a 4-h simulated 30,000 ft (9144 m) exposure. Information gained from such a test battery may assist the medical monitor in identifying early signs of DCS and subtle neurologic dysfunction related to cases of asymptomatic, but advanced, DCS. This presentation concerns the selection and integration of a test battery and the timely graphic display of subject test results for the principal investigator and medical monitor. A subset of the Automated Neuropsychological Assessment Metrics (ANAM) developed through the Office of Military Performance Assessment Technology (OMPAT) was selected. The ANAM software provides a library of simple tests designed for precise measurement of processing efficiency in a variety of cognitive domains. For our application and time constraints, two tests requiring high levels of cognitive processing and memory were chosen along with one test requiring fine psychomotor performance. Accuracy, speed, and processing throughout variables as well as RMS error were collected. An automated mood survey provided 'state' information on six scales including anger, happiness, fear, depression, activity, and fatigue. An integrated and interactive LOTUS 1-2-3 macro was developed to import and display past and present task performance and mood-change information.
Author (revised)

N94-11534*# Jet Propulsion Lab., California Inst. of Tech., Pasadena.
ANALYZING HUMAN ERRORS IN FLIGHT MISSION OPERATIONS c53
Kristin J. Bruno, Linda L. Welz, G. Michael Barnes (California State Univ., Northridge.), and Josef Sherif *In* NASA. Johnson Space Center, Sixth Annual Workshop on Space Operations Applications and Research (SOAR 1992), Volume 2 Feb. 1993 p 499-505 Sponsored by NASA, Washington (For primary document see N94-11527 01-99)
Avail: CASI HC A02/MF A03

A long-term program is in progress at JPL to reduce cost and risk of flight mission operations through a defect prevention/error management program. The main thrust of this program is to create an environment in which the performance of the total system, both the human operator and the computer system, is optimized. To this end, 1580 Incident Surprise Anomaly reports (ISA's) from 1977-1991 were analyzed from the Voyager and Magellan projects. A Pareto analysis revealed that 38 percent of the errors were classified as human errors. A preliminary cluster analysis based on the Magellan human errors (204 ISA's) is presented here. The resulting clusters described the underlying relationships among the ISA's. Initial models of human error in flight mission operations are presented. Next, the Voyager ISA's will be scored and included in the analysis. Eventually, these relationships will be used to derive a theoretically motivated and empirically validated model of human error in flight mission operations. Ultimately, this analysis will be used to make continuous process improvements continuous process improvements to end-user applications and training requirements. This Total Quality Management approach will enable the management and prevention of errors in the future. Author (revised)

N94-11535*# National Aeronautics and Space Administration. Ames Research Center, Moffett Field, CA.
MEASURES FOR SIMULATOR EVALUATION OF A HELICOPTER OBSTACLE AVOIDANCE SYSTEM c09
Joe DeMaio (Army Aviation Systems Command, Moffett Field, CA.), Thomas J. Sharkey (Monterey Technologies, Inc., Carmel, CA.), David Kennedy (Monterey Technologies, Inc., Carmel, CA.), Micheal Hughes (CAE Electronics Ltd., Saint Laurent, Quebec.), and Perry Meade (CAE Electronics Ltd., Saint Laurent, Quebec.) *In* NASA. Johnson Space Center, Sixth Annual Workshop on Space Operations Applications and Research (SOAR 1992), Volume 2 Feb. 1993 p 507-511 (For primary document see N94-11527 01-99)
Avail: CASI HC A01/MF A03

The U.S. Army Aeroflightdynamics Directorate (AFDD) has developed a high-fidelity, full-mission simulation facility for the demonstration and evaluation of advanced helicopter mission equipment. The Crew Station Research and Development Facility (CSRDF) provides the capability to conduct one- or two-crew full-mission simulations in a state-of-the-art helicopter simulator. The CSRDF provides a realistic, full field-of-regard visual environment with simulation of state-of-the-art weapons, sensors, and flight control systems. We are using the CSRDF to evaluate the ability of an obstacle avoidance system (OASYS) to support low altitude flight in cluttered terrain using night vision goggles (NVG). The OASYS uses a laser radar to locate obstacles to safe flight in the aircraft's flight path. A major concern is the detection of wires, which can be difficult to see with NVG, but other obstacles--such as trees, poles or the ground--are also a concern. The OASYS symbology is presented to the pilot on a head-up display mounted on the NVG (NVG-HUD). The NVG-HUD presents head-stabilized symbology to the pilot while allowing him to view the image intensified, out-the-window scene through the HUD. Since interference with viewing through the display is a major concern, OASYS symbology must be designed to present usable obstacle clearance information with a minimum of clutter. Author (revised)

N94-11536*# National Aeronautics and Space Administration. John F. Kennedy Space Center, Cocoa Beach, FL.
VIGILANCE PROBLEMS IN ORBITER PROCESSING c53
William W. Swart (University of Central Florida, Orlando.), Robert R. Safford (University of Central Florida, Orlando.), David B. Kennedy (University of Central Florida, Orlando.), Bert A. Yadi (University of Central Florida, Orlando.), and Timothy S. Barth *In* NASA. Johnson Space Center, Sixth Annual Workshop on Space Operations Applications and Research (SOAR 1992), Volume 2 Feb. 1993 p 512-515 (For primary document see N94-11527 01-99)
Avail: CASI HC A01/MF A03

A pilot experiment was done to determine what factors influence potential performance errors related to vigilance in Orbiter processing activities. The selected activities include post flight inspection for burned gap filler material and pre-rollout inspection for tile processing shim material. It was determined that the primary factors related to performance decrement were the color of the target and the difficulty of the target presentation. Author (revised)

N94-11537*# Lockheed Engineering and Sciences Co., Houston, TX.
MEASURING HUMAN PERFORMANCE ON NASA'S MICROGRAVITY AIRCRAFT c54
Randy B. Morris and Mihriban Whitmore *In* NASA. Johnson Space Center, Sixth Annual Workshop on Space Operations Applications and Research (SOAR 1992), Volume 2 Feb. 1993 p 516-521 (For primary document see N94-11527 01-99)
Avail: CASI HC A02/MF A03

Measuring human performance in a microgravity environment will aid in identifying the design requirements, human capabilities, safety, and productivity of future astronauts. The preliminary understanding of the microgravity effects on human performance can be achieved through evaluations conducted onboard NASA's KC-135 aircraft. These evaluations can be performed in relation to hardware performance, human-hardware interface, and hardware integration. Measuring human performance in the KC-135 simulated environment will contribute to the efforts of optimizing the human-machine interfaces for future and existing space vehicles. However, there are limitations, such as limited number of qualified subjects, unexpected hardware problems, and miscellaneous plane movements which must be taken into consideration. Examples for these evaluations, the results, and their implications are discussed in the paper. Author (revised)

N94-11538*# National Aeronautics and Space Administration. Lyndon B. Johnson Space Center, Houston, TX.

NOISE LEVELS AND THEIR EFFECTS ON SHUTTLE CREWMEMBERS' PERFORMANCE: OPERATIONAL CONCERNS **c53**

Anton S. Koros (Lockheed Engineering and Sciences Co., Houston, TX.), Susan C. Adam, and Charles D. Wheelwright (Lockheed Engineering and Sciences Co., Houston, TX.) *In its* Sixth Annual Workshop on Space Operations Applications and Research (SOAR 1992), Volume 2 Feb. 1993 p 522-528 (For primary document see N94-11527 01-99)
(Contract NAS9-17900)
Avail: CASI HC A02/MF A03

When excessive, noise can result in sleep interference, fatigue, interference with verbal communication, and hearing damage. Shuttle crewmembers are exposed to noise throughout their mission. The contribution of noise to decrements in crew performance over these extended exposure durations was the focus of this study. On the STS-40/SLS-1, mission noise levels were evaluated through the use of a sound level meter and a crew questionnaire. Crewmembers noted that sleep, concentration, and relaxation were negatively impacted by high noise levels. Speech Interference Levels (SIL's), calculated from the sound level measurements, suggested that crewmembers were required to raise their voice in order to be heard. No difficulty detecting caution and warning alarms was noted. The higher than desirable noise levels in Spacelab were attributed to flight specific payloads for which acoustic waivers were granted. It is recommended that current noise levels be reduced in Spacelab and the Orbiter Middeck especially as longer missions are planned for the buildup of Space Station Freedom. Levels of NC 50 are recommended in areas where speech communication is required and NC 40 in sleep areas. These levels are in accordance with the NASA Man-Systems Integration Standards. Measurements proposed for subsequent orbiter missions are discussed. Author (revised)

N94-11539*# Aerospace Medical Research Labs., Wright-Patterson AFB, OH.

VISUAL EARTH OBSERVATION PERFORMANCE IN THE SPACE ENVIRONMENT. HUMAN PERFORMANCE MEASUREMENT 4: FLIGHT EXPERIMENTS **c53**

John F. Huth, James D. Whiteley, and John E. Hawker *In* NASA. Johnson Space Center, Sixth Annual Workshop on Space Operations Applications and Research (SOAR 1992), Volume 2 Feb. 1993 p 529-539 (For primary document see N94-11527 01-99)
Avail: CASI HC A03/MF A03

A wide variety of secondary payloads have flown on the Space Transportation System (STS) since its first flight in the 1980's. These experiments have typically addressed specific issues unique to the zero-gravity environment. Additionally, the experiments use the experience and skills of the mission and payload specialist crew members to facilitate data collection and ensure successful completion. This paper presents the results of the Terra Scout experiment, which flew aboard STS-44 in November 1991. This unique Earth Observation experiment specifically required a career imagery analyst to operate the Spaceborne Direct-View Optical System (SpaDVOS), a folded optical path telescope system designed to mount inside the shuttle on the overhead aft flight deck windows. Binoculars and a small telescope were used as backup optics. Using his imagery background, coupled with extensive target and equipment training, the payload specialist was tasked with documenting the following: (1) the utility of the equipment; (2) his ability to acquire and track ground targets; (3) the level of detail he could discern; (4) the atmospheric conditions; and (5) other in-situ elements which contributed to or detracted from his ability to analyze targets. Special emphasis was placed on the utility of a manned platform for research and development of future spaceborne sensors. The results and lessons learned from Terra Scout will be addressed including human performance and equipment design issues.
Author (revised)

N94-11540*# Krug Life Sciences, Inc., San Antonio, TX.

USE OF ULTRASOUND IN ALTITUDE DECOMPRESSION MODELING Abstract Only **c54**

Robert M. Olson and Andrew A. Pilmanis (Aerospace Medical Research Labs., Brooks AFB, TX.) *In* NASA. Johnson Space Center, Sixth Annual Workshop on Space Operations Applications and Research (SOAR 1992), Volume 2 Feb. 1993 p 543 (For primary document see N94-11527 01-99)
Avail: CASI HC A01/MF A03

A model that predicts the probability of developing decompression sickness (DCS) with various denitrogenation schedules is being developed by the Armstrong Laboratory, using human data from previous exposures. It was noted that refinements are needed to improve the accuracy and scope of the model. A commercially developed ultrasonic echo imaging system is being used in this model development. Using this technique, bubbles images from a subject at altitude can be seen in the gall bladder, hepatic veins, vena cava, and chambers of the heart. As judged by their motion and appearance in the vena cava, venous bubbles near the heart range in size from 30 to 300 M. The larger bubbles skim along the top, whereas the smaller ones appear as faint images near the bottom of the vessel. Images from growing bubbles in a model altitude chamber indicate that they grow rapidly, going from 20 to 100 M in 3 sec near 30,000 ft altitude. Information such as this is valuable in verifying those aspects of the DCS model dealing with bubble size, their growth rate, and their site of origin. Author (revised)

N94-11541*# Krug Life Sciences, Inc., San Antonio, TX.

HYPOBARIC DECOMPRESSION PREBREATHE REQUIREMENTS AND BREATHING ENVIRONMENT Abstract Only **c54**

James T. Webb and Andrew A. Pilmanis (Aerospace Medical Research Labs., Brooks AFB, TX.) *In* NASA. Johnson Space Center, Sixth Annual Workshop on Space Operations Applications and Research (SOAR 1992), Volume 2 Feb. 1993 p 544 (For primary document see N94-11527 01-99)
Avail: CASI HC A01/MF A03

To reduce incidence of decompression sickness (DCS), prebreathing 100 percent oxygen to denitrogenate is required prior to hypobaric decompressions from a sea level pressure breathing environment to pressures lower than 350 mm Hg (20,000 ft; 6.8 psia). The tissue ratio (TR) of such exposures equals or exceeds 1.7; TR being the tissue nitrogen pressure prior to decompression divided by the total pressure after decompression (((0.781)(14.697))/6.758). Designing pressure suits capable of greater pressure differentials, lower TR's, and procedures which limit the potential for DCS occurrence would enhance operational efficiency. The current 10.2 psia stage decompression prior to extravehicular activity (EVA) from the Shuttle in the 100 percent oxygen, 4.3 psia suit, results in a TR of 1.65 and has proven to be relatively free of DCS. Our recent study of zero-prebreathe decompressions to 6.8 psia breathing 100 percent oxygen (TR = 1.66) also resulted in no DCS (N = 10). The level of severe, Spencer Grades 3 or 4, venous gas emboli (VGE) increased from 0 percent at 9.5 psia to 40 percent at 6.8 psia yielding a Probit curve of VGE risk for the 51 male subjects who participated in these recent studies. Earlier, analogous decompressions using a 50 percent oxygen, 50 percent nitrogen breathing mixture resulted in one case of DCS and significantly higher levels of severe VGE, e.g., at 7.8 psia, the mixed gas breathing environment resulted in a 56 percent incidence of severe VGE versus 10 percent with use of 100 percent oxygen. The report of this study recommended use of 100 percent oxygen during zero-prebreathe exposure to 6.8 psia if such a suit could be developed. For future, long-term missions, we suggest study of the effects of decompression over several days to a breathing environment of 150 mmHg O2 and approximately 52 mmHg He as a means of eliminating DCS and VGE hazards during subsequent excursions. Once physiologically adapted to a 4 psia vehicle, base, or space station segment, crew members could use greatly simplified EVA suits with greater mobility and no prebreathe requirement.
Author (revised)

N94-11542*# Space Biomedical Research Inst., Houston, TX. Environmental Physiology/Biophysics Section.

JOINT PAIN AND DOPPLER-DETECTABLE BUBBLES IN ALTITUDE (HYPOBARIC) DECOMPRESSION Abstract Only c52

Michael R. Powell *In* NASA. Johnson Space Center, Sixth Annual Workshop on Space Operations Applications and Research (SOAR 1992), Volume 2 Feb. 1993 p 546 (For primary document see N94-11527 01-99)

Avail: CASI HC A01/MF A03

The observation that altitude decompression sickness (DCS) is associated with pain in the lower extremities is not new, although it is not a consistent finding. DCS in divers is generally in the upper body, an effect often attributed to non-loading of the body while immersed. In caisson workers, DCS is reported more in the lower extremities. Surprisingly, many researchers do not mention the location of DCS joint pain, apparently considering it to be random. This is not the case for the tissue ratios encountered in studying decompression associated with simulated EVA. In NASA/JSC tests, altitude DCS generally presented first in either the ankle, knee, or hip (83 percent = 73/88). There was a definite statistical relation between the maximum Spencer precordial Doppler Grade and the incidence of DCS in the extremity, although this is not meant to imply a casual relation between circulating gas bubbles and joint pain. The risk of DCS with Grade 4 was considerably higher than that of Grades 0 to 3. The DCS risk was independent of the 'tissue ratio.' There was a predominance of lower extremity DCS even when exercise was performed with the upper body. The reason for these locations we hypothesize to be attributed to the formation of tissue gas micronuclei from kinetic and tensile forces (stress-assisted nucleation) and are the result of the individuals ambulating in a 1g environment. Additionally, since these showers of Doppler bubbles can persist for hours, it is difficult to imagine that they are emanating solely from tendons and ligaments, the supposed site of joint pain. This follows from Henry's law linking the volume of joint tissue (the solvent) and the solubility coefficient of inert gas; there is volumetrically insufficient connective tissue to produce the prolonged release of gas bubbles. If gas bubbles are spawned and released from connective tissue, their volume is increased by those from muscle tissue. Therefore, the nexus between Doppler-detectable gas bubbles and joint-pain decompression sickness is essentially a statistical, rather than a direct, one. Author (revised)

N94-11543*# Aerospace Medical Research Labs., Brooks AFB, TX.

ARTERIAL GAS EMBOLI IN ALTITUDE-INDUCED DECOMPRESSION SICKNESS Abstract Only c52

Andrew A. Pilmanis and Robert M. Olson (Krug Life Sciences, Inc., San Antonio, TX.) *In* NASA. Johnson Space Center, Sixth Annual Workshop on Space Operations Applications and Research (SOAR 1992), Volume 2 Feb. 1993 p 547 (For primary document see N94-11527 01-99)

Avail: CASI HC A01/MF A03

Exposure to high altitudes can result in the evolved-gas condition referred to as decompression sickness (DCS). Ultrasonic monitoring techniques have clearly demonstrated the presence of venous gas emboli (VGE) during decompression. Although important to DCS research and our understanding of the physiological mechanisms of this condition, Venus gas emboli have not been considered clinically hazardous, unless in extreme numbers. Arterial gas emboli (AGE), on the other hand, are generally viewed with great concern. Arterial gas emboli can enter the cerebral arterial circulation and arrest blood flow resulting in potentially serious injury. Left ventricular gas emboli were observed with echo imaging in five volunteer subjects during exposure to simulated altitude. These serendipitous findings occurred during altitude exposure under 3 separate research protocols involving 79 subject exposures. The voluntary, fully informed consent of the subjects used in this research was obtained as required by AFR 169-3. A Hewlett-Packard SONOS 1000 Echo Imaging System was used to monitor for precordial gas emboli. The improved resolution of the SONOS 1000 appears to account for these new findings. Four subjects had high incidence DCS and VGE during previous research flights. One subject only had one flight. The altitudes and AGE onset times for the five cases were: (1) 25,500 ft/2:23, (2) 29,000 ft/0:27, (3) 19,500 ft/3:49, (4) 29,500 ft/3:15, and (5) 29,500 ft/1:31. In all five cases, at the time of AGE onset, the VGE scores were high from all monitored locations. Four of the cases were symptomatic at the time of AGE onset (pain and skin mottling). No cerebral manifestations were observed. All subjects were immediately recompressed to ground level and successfully treated with 2 hours of post-breathing or with hyperbaric oxygen therapy. In conclusion, previously undetected AGE were demonstrated--with and without DCS symptoms--during exposure to altitude. It appears that this gas transferred from the venous side to the arterial side via either intracardiac defects or the pulmonary circulation. The clinical and operational implications of this finding are yet to be determined. Author (revised)

N94-11544*# Space Biomedical Research Inst., Houston, TX.

TRANSCRANIAL DOPPLER ULTRASOUND AND THE ETIOLOGY OF NEUROLOGIC DECOMPRESSION SICKNESS DURING ALTITUDE DECOMPRESSION c52

W. T. Norfleet, M. R. Powell, K. Vasantha Kumar (Krug Life Sciences, Inc., Houston, TX.), and J. Waligora *In* NASA. Johnson Space Center, Sixth Annual Workshop on Space Operations Applications and Research (SOAR 1992), Volume 2 Feb. 1993 p 549-561 (For primary document see N94-11527 01-99)

Avail: CASI HC A03/MF A03

The presence of gas bubbles in the arterial circulation can occur from iatrogenic mishaps, cardiopulmonary bypass devices, or following decompression, e.g., in deep-sea or SCUBA diving or in astronauts during extravehicular activities (EVA). We have examined the pathophysiology of neurological decompression sickness in human subjects who developed a large number of small gas bubbles in the right side of the heart as a result of hypobaric exposures. In one case, gas bubbles were detected in the middle cerebral artery (MCA) and the subject developed neurological symptoms; a 'resting' patent foramen ovalae (PFO) was found upon saline contrast echocardiography. A PFO was also detected in another individual who developed Spencer Grade 4 precordial Doppler ultrasound bubbles, but no evidence was seen of arterialization of bubbles upon insonation of either the MCA or common carotid artery. The reason for this difference in the behavior of intracardiac bubbles in these two individuals is not known. To date, we have not found evidence of right-to-left shunting of bubbles through pulmonary vasculature. The volume of gas bubbles present following decompression is examined and compared with the number arising from saline contrast injection. The estimates are comparable. Author (revised)

N94-11545*# Space Biomedical Research Inst., Houston, TX. Environmental Physiology/Biophysics Section.

A MECHANISM FOR THE REDUCTION IN RISK OF DECOMPRESSION SICKNESS IN MICROGRAVITY ENVIRONMENT Abstract Only c52

Michael R. Powell *In* NASA. Johnson Space Center, Sixth Annual Workshop on Space Operations Applications and Research (SOAR 1992), Volume 2 Feb. 1993 p 562 (For primary document see N94-11527 01-99)

Avail: CASI HC A01/MF A03

There is an apparent reduction in the incidence of decompression sickness reported by astronauts (from both the USA and the USSR) during extravehicular activity (EVA). The expected incidence, based on studies conducted under unit gravity conditions in Earth-based laboratories, is greater than that encountered during EVA. A biophysical explanation has been proposed for this difference based upon the mechanism of stress-assisted nucleation. Since the partial pressure ratio at which this gas phase forms is considerably smaller in living systems that in quiescent in vitro models, it was proposed that mechanical forces are involved. In that the lower extremities of astronautics are not gravitationally loaded in microgravity, it is possible that tissue gas micronuclei are but minimally regenerated. Most likely, gas micronuclei formed on Earth (by ambulation under 1 g conditions) would be eventually depleted. In a crossover study, 20 individuals were decompressed--from 1 ATA to 0.43 ATA for 3 hours--following either being fully ambulatory at unit gravity or following being hypokinetic and adynamic (simulated microgravity of 3-day bed rest). The subjects were monitored for gas phase formation by means of precordial Doppler monitoring. The results indicate a reduction in whole body gas phase formation in individuals who were bed rested as compared with themselves when fully ambulatory ($p = 0.02$). In hypokinetic individuals, the protection conferred was equivalent to an extra 175 minutes of oxygen prebreathe. These results are compatible with a hypothesis relating stress-assisted nucleation to the continual formation of tissue gas micronuclei and their gradual depletion with hypokinesia. Author (revised)

N94-11546*# National Aeronautics and Space Administration. Lyndon B. Johnson Space Center, Houston, TX.

RISK OF DECOMPRESSION SICKNESS IN THE PRESENCE OF CIRCULATING MICROBUBBLES **c52**

K. Vasantha Kumar (Krug Life Sciences, Inc., Houston, TX.) and Michael R. Powell *In its* Sixth Annual Workshop on Space Operations Applications and Research (SOAR 1992), Volume 2 Feb. 1993 p 563-567 (For primary document see N94-11527 01-99)

Avail: CASI HC A01/MF A03

In this study, we examined the association between microbubbles formed in the circulation from a free gas phase and symptoms of altitude decompression sickness (DCS). In a subgroup of 59 males of mean (S.D) age 31.2 (5.8) years who developed microbubbles during exposure to 26.59 kPa (4.3 psi) under simulated extravehicular activities (EVA), symptoms of DCS occurred in 24 (41 percent) individuals. Spencer grade 1 microbubbles occurred in 4 (7 percent), grade 2 in 9 (15 percent), grade 3 in 15 (25 percent), and grade 4 in 31 (53 percent) of subjects. Survival analysis using Cox proportional hazards regression showed that individuals with less than grade 3 CMB showed 2.46 times (95 percent confidence interval = 1.26 to 5.34) higher risk of symptoms. This information is crucial for defining the risk of DCS for inflight Doppler monitoring under space EVA. Altitude decompression sickness (DCS) occurs when there is acute reduction in ambient pressure. The symptoms of DCS are due to the formation of a free gas phase (in the form of gas microbubbles) in tissues during decompression. Musculo-skeletal pain of bends is the commonest form of DCS in altitude exposures. In the space flight environment, there is a risk of DCS when astronauts decompress from the normobaric shuttle pressure into the hypobaric space suit pressure (currently about 29.65 kPa (4.3 psi) for extra-vehicular activities (EVA). This risk is counterbalanced by a judicious combination of prior denitrogenation and staged decompression. Studies of DCS are limited by the duration of the test at reduced pressure. Since only a proportion of subjects tested develop symptoms, the information on DCS is generally incomplete or 'censored'. Many studies employ Doppler ultrasound monitoring of the precordial area for detecting circulating microbubbles (CMB). Although the association between CMB and bends pain is not causal, CMB are frequently monitored during decompression. In this paper, we examine the association between CMB and symptoms of DCS under simulated EVA profiles. Author (revised)

N94-11547*# Space Biomedical Research Inst., Houston, TX. Environmental Physiology/Biophysics Section.

STRATEGIES AND METHODOLOGIES TO DEVELOP TECHNIQUES FOR COMPUTER-ASSISTED ANALYSIS OF GAS PHASE FORMATION DURING ALTITUDE DECOMPRESSION Abstract Only **c52**

Michael R. Powell and W. A. Hall (Krug Life Sciences, Inc., Houston, TX.) *In* NASA. Johnson Space Center, Sixth Annual Workshop on Space Operations Applications and Research (SOAR 1992), Volume 2 Feb. 1993 p 568 (For primary document see N94-11527 01-99)

Avail: CASI HC A01/MF A03

It would be of operational significance if one possessed a device that would indicate the presence of gas phase formation in the body during hypobaric decompression. Automated analysis of Doppler gas bubble signals has been attempted for 2 decades but with generally unfavorable results, except with surgically implanted transducers. Recently, efforts have intensified with the introduction of low-cost computer programs. Current NASA work is directed towards the development of a computer-assisted method specifically targeted to EVA, and we are most interested in Spencer Grade 4. We note that Spencer Doppler Grades 1 to 3 have increased in the FFT sonogram and spectrogram in the amplitude domain, and the frequency domain is sometimes increased over that created by the normal blood flow envelope. The amplitude perturbations are of very short duration, in both systole and diastole and at random temporal positions. Grade 4 is characteristic in the amplitude domain but with modest increases in the FFT sonogram and spectral frequency power from 2K to 4K over all of the cardiac cycle. Heart valve motion appears to characteristic display signals: (1) the demodulated Doppler signal amplitude is considerably above the Doppler-shifted blow flow signal (even Grade 4); and (2) demodulated Doppler frequency shifts are considerably greater (often several kHz) than the upper edge of the blood flow envelope. Knowledge of these facts will aid in the construction of a real-time, computer-assisted discriminator to eliminate cardiac motion artifacts. There could also exist perturbations in the following: (1) modifications of the pattern of blood flow in accordance with Poiseuille's Law, (2) flow changes with a change in the Reynolds number, (3) an increase in the pulsatility index, and/or (4) diminished diastolic flow or 'runoff.' Doppler ultrasound devices have been constructed with a three-transducer array and a pulsed frequency generator.

Author (revised)

N94-11548*# Hyperbaric Medicine, San Antonio, TX. Wound Care.

EVALUATION OF MEDICAL TREATMENTS TO INCREASE SURVIVAL OF EBULLISM IN GUINEA PIGS Abstract Only **c51**

Barbara J. Stegmann, Andrew A. Pilmanis (Aerospace Medical Research Labs., Brooks AFB, TX.), E. G. Wolf (Aerospace Medical Research Labs., Brooks AFB, TX.), Toniann Derion (Aerospace Medical Research Labs., Brooks AFB, TX.), J. W. Fanton (Aerospace Medical Research Labs., Brooks AFB, TX.), H. Davis (Aerospace Medical Research Labs., Brooks AFB, TX.), G. B. Kemper (Aerospace Medical Research Labs., Brooks AFB, TX.), and Terrell E. Scoggins (Aerospace Medical Research Labs., Brooks AFB, TX.) *In* NASA. Johnson Space Center, Sixth Annual Workshop on Space Operations Applications and Research (SOAR 1992), Volume 2 Feb. 1993 p 569 (For primary document see N94-11527 01-99)

Avail: CASI HC A01/MF A03

Spaceflight carriers run a constant risk of exposure to vacuum. Above 63,000 ft (47 mmHg), the ambient pressure falls below the vapor pressure of water at 37 C, and tissue vaporization (ebullism) begins. Little is know about appropriate resuscitative protocols after such an ebullism exposure. This study identified injury patterns and mortality rates associated with ebullism while verifying effectiveness of traditional pulmonary resuscitative techniques. Male Hartley guinea pigs were exposed to 87,000 ft for periods of 40 to 115 sec. After descent, those animals that did not breathe spontaneously were given artificial ventilation by bag and mask for up to 15 minutes. Those animals surviving were randomly assigned to one of three treatment groups--hyperbaric oxygen (HBO), ground-level oxygen (GLO2), and ground-level air (GLAIR). The HBO group was treated on a standard treatment table 6A while the GLO2 animals received O2 for an equivalent length of time. Those animals in the GLAIR group were observed only. All surviving animals were humanely sacrificed at 48 hours. Inflation of the animal's lungs after the exposure was found to be difficult and, at times, impossible. This may be due to surfactant disruption at the alveolar lining. Electron microscopy identified a disruption of the surfactant layer in animals that did not survive initial exposure. Mortality was found to increase with exposure time: 40 sec--0 percent; 60 sec--6 percent; 70 sec--40 percent; 80 sec--13 percent; 100 sec--38 percent; 110 sec--40 percent; and 115 sec--100 percent. There was no difference in the delayed mortality among the treatment groups (HBO--15 percent, GLO2--11 percent, GLAIR--11 percent). However, since resuscitation was ineffective, the effectiveness of any post-exposure treatment was severely limited. Preliminary results indicate that reuscitation of guinea pigs following ebullism exposure is difficult, and that current techniques (such as traditional CPR) may not be appropriate. Author (revised)

N94-11549*# Aerospace Medical Research Labs., Brooks AFB, TX. Sustained Operations Branch.

A PROTOTYPE URINE COLLECTION DEVICE FOR FEMALE AIRCREW **c54**

Roger U. Bisson and Karlyna L. Delger *In* NASA. Johnson Space Center, Sixth Annual Workshop on Space Operations Applications and Research (SOAR 1992), Volume 2 Feb. 1993 p 570-573 (For primary document see N94-11527 01-99)

Avail: CASI HC A01/MF A03

Women are gaining increased access to small military cockpits. This shift has stimulated the search for practical urine containment and disposal methods for female aircrew. There are no external urine collection devices (UCD) for women that are comfortable, convenient, and leak free. We describe a prototype UCD that begins to meet this need. Materials used to make custom aviator masks were adapted to mold a perineal mask. First, a perineal cast (negative) was used to make a mold (positive). Next, a perineal mask made of wax was formed to fit the positive mold. Finally, a soft, pliable perineal mask was fabricated using the wax model as a guide. The prototype was tested for comfort, fit, and leakage. In the sitting position, less than 5 cc of urine leakage occurred with each 600 cc of urine collected. Comfort was mostly satisfactory, but ambulation was limited and the outlet design could lead to kinking and obstruction. We concluded that a perineal mask may serve as a comfortable and functional external UCD acceptable for use by females in confined environments. Changes are needed to improve comfort, fit, and urine drainage. Integration into cockpits, pressure suits, chemical defense gear, and environments where access to relief facilities is restricted is planned. Author (revised)

N94-11550*# National Aeronautics and Space Administration. Lyndon B. Johnson Space Center, Houston, TX.

PROMETHAZINE AND ITS USE AS A TREATMENT FOR SPACE MOTION SICKNESS Abstract Only c52

James P. Bagian and Bradley G. Beck *In its* Sixth Annual Workshop on Space Operations Applications and Research (SOAR 1992), Volume 2 Feb. 1993 p 574 (For primary document see N94-11527 01-99)
Avail: CASI HC A01/MF A03

Until Mar. 1989, no effective treatment--either prophylactic or symptomatic--for space motion sickness (SMS) had been discovered. Since Mar. 1989, intramuscular (IM) promethazine (PMZ) has been used in the treatment of SMS with extremely favorably results reported by the crew. A retrospective study was undertaken to quantify the efficacy of IM PMZ since its institution and the incidence of its major anticipated side-effect drowsiness and sedation. The results from a standardized crew medical debriefing conducted immediately after landing and follow-up interviews with the crews were used in establishing the efficacy and incidence of side effects from treatment. Only crews from the first 44 Shuttle flights on their first mission were considered. For a total of 132 crewmembers, 96 exhibited symptoms of SMS; and, of these, 20 were treated with IM PMZ. Ninety percent of those receiving IM PMZ 25-50mg received nearly immediate (less than 2 hours) relief of symptoms and 75 percent required no further treatment through the first 2 days of spaceflight. Those not receiving this treatment did not have any near-term resolution of their symptoms, and 50 percent were still ill through the second day of flight. This represents a significant difference at the $p = 0.46$ level. In stark contrast to the 60 percent to 73 percent incidence of sedation or drowsiness reported in individuals treated with PMZ in terrestrial environment at the doses used here, less than 5 percent reported these symptoms during spaceflight. IM PMZ is an effective therapy for SMS and is associated with minimal incidence of sedation or drowsiness. This combination of efficacy that is absent of significant side effects represents a substantial improvement in the operational situation of crewmembers afflicted with SMS. Studies to understand the mechanisms underlying these observations will be undertaken in the future. Author (revised)

N94-11551*# National Aeronautics and Space Administration. Lyndon B. Johnson Space Center, Houston, TX.

UPDATE ON THE INCIDENCE AND TREATMENT OF SPACE MOTION SICKNESS Abstract Only c52

Bradley G. Beck *In its* Sixth Annual Workshop on Space Operations Applications and Research (SOAR 1992), Volume 2 Feb. 1993 p 575 (For primary document see N94-11527 01-99)
Avail: CASI HC A01/MF A03

Flight surgeons routinely monitor crew symptoms and treatment of space motion sickness (SMS), not only during flight, but also to obtain information postflight from each crewmember. Recent statistics indicate that the incidence of SMS has not changed since STS-26 in Sep. 1988. The percentages of mild, moderate, and severe cases has only changed slightly. However, the treatment of SMS has significantly changed since STS-26. Scopolamine/dexedrine is no longer used as a prophylaxis for SMS symptoms because of evidence of delay in symptoms. Intramuscular promethazine has been used in more than 30 individuals with a reported decrease in symptoms greater than 90 percent. A delay in symptoms has not been reported, and the duration of certain SMS symptoms has decreased due to use of intramuscular promethazine. Case studies will be discussed and several therapeutic options and doses will be demonstrated. Further treatment possibilities will be examined. Author (revised)

N94-11552*# National Aeronautics and Space Administration. Lyndon B. Johnson Space Center, Houston, TX.

BASELINE CHARACTERISTICS OF DIFFERENT STRATA OF ASTRONAUT CORPS Abstract Only c52

Peggy B. Hamm (Krug Life Sciences, Inc., Houston, TX.) and L. J. Pepper *In its* Sixth Annual Workshop on Space Operations Applications and Research (SOAR 1992), Volume 2 Feb. 1993 p 577 (For primary document see N94-11527 01-99)
Avail: CASI HC A01/MF A03

The Longitudinal Study of Astronaut Health (LSAH) is an epidemiological study designed to study the effects of the occupational exposures incurred by astronauts in health outcomes and changes in physiological variables. Between 1959 and 1991, 195 individuals were selected for the program. The medical standards for selection have remained essentially unchanged since the Mercury Program, but the range and stringency of these criteria have been modified. Demographic and physiological variables identified during the selection year are examined for various strata of the Astronaut Corps. Specifically, age, sex, race, education, usual occupation, military affiliation, medical history, family medical history, visual and hearing measurements, physical exam variables, and specific laboratory values are investigated. Differences are examined in astronauts for the following criteria: (1) were selected prior to 1970 ($n = 73$) versus those selected after 1970 ($n = 122$); (2) have flown multiple missions versus those who have flown less than two missions; (3) have walked in space versus all others; (4) have more than 500 hours of mission time versus all others; and (5) have gone to the Moon versus all others. Length of time served in the Astronaut Corps is examined for each of these strata. Author (revised)

N94-11553*# National Aeronautics and Space Administration. Lyndon B. Johnson Space Center, Houston, TX.

COMPREHENSIVE ANALYSIS OF AIRBORNE CONTAMINANTS FROM RECENT SPACELAB MISSIONS c54

M. L. Matney (Krug Life Sciences, Inc., Houston, TX.), J. F. Boyd (Krug Life Sciences, Inc., Houston, TX.), P. A. Covington (Krug Life Sciences, Inc., Houston, TX.), H. J. Leano (Krug Life Sciences, Inc., Houston, TX.), D. L. Pierson, T. F. Limero (Krug Life Sciences, Inc., Houston, TX.), and J. T. James *In its* Sixth Annual Workshop on Space Operations Applications and Research (SOAR 1992), Volume 2 Feb. 1993 p 579-588 (For primary document see N94-11527 01-99)
Avail: CASI HC A02/MF A03

The Shuttle experiences unique air contamination problems because of microgravity and the closed environment. Contaminant build-up in the closed atmosphere and the lack of a gravitational settling mechanism have produced some concern in previous missions about the amount of solid and volatile airborne contaminants in the Orbiter and Spacelab. Degradation of air quality in the Orbiter/Spacelab environment, through processes such as chemical contamination, high solid-particulate levels, and high microbial levels, may affect crew performance and health. A comprehensive assessment of the Shuttle air quality was undertaken during STS-40 and STS-42 missions, in which a variety of air sampling and monitoring techniques were employed to determine the contaminant load by characterizing and quantitating airborne contaminants. Data were collected on the airborne concentrations of volatile organic compounds, microorganisms, and particulate matter collected on Orbiter/Spacelab air filters. The results showed that STS-40/42 Orbiter/Spacelab air was toxicologically safe to breathe, except during STS-40 when the Orbiter Refrigerator/Freezer unit was releasing noxious gases in the middeck. On STS-40, the levels of airborne bacteria appeared to increase as the mission progressed; however, this trend was not observed for the STS-42 mission. Particulate matter in the Orbiter/Spacelab air filters was chemically analyzed in order to determine the source of particles. Only small amounts of rat hair and food bar (STS-40) and traces of soiless medium (STS-42) were detected in the Spacelab air filters, indicating that containment for Spacelab experiments was effective. Author (revised)

N94-11554*# National Aeronautics and Space Administration. Lyndon B. Johnson Space Center, Houston, TX.

TOXICITY STUDY OF DIMETHYLETHOXYSILANE (DMSES), THE WATERPROOFING AGENT FOR THE ORBITER HEAT PROTECTIVE SYSTEM Abstract Only c54

Chiu-Wing Lam (Krug Life Sciences, Inc., Houston, TX.), John T. James, Darol Dodd (ManTech Environmental Technology, Inc., Upton, NY.), Bruce Stuart (ManTech Environmental Technology, Inc., Upton, NY.), Simon Rothenberg (ManTech Environmental Technology, Inc., Upton, NY.), Mary Ann Kershaw (Brookhaven National Lab., Upton, NY.), and A. Thilagar (Sitek Research Labs., Rockville, MD.) *In its* Sixth Annual Workshop on Space Operations Applications and Research (SOAR 1992), Volume 2

Feb. 1993 p 589 (For primary document see N94-11527 01-99)
Avail: CASI HC A01/MF A03

DMES, a volatile liquid, is used by NASA to waterproof the Orbiter thermal protective system. During waterproofing operations at the Orbiter Processing Facility at KSC, workers could be exposed to DMES vapor. To assess the toxicity of DMES, acute and subchronic (2-week and 13-week) inhalation studies were conducted with rats. Studies were also conducted to assess the potential of DMES. Inhalation exposure concentrations ranged from 40 ppm to 4000 ppm. No mortality was observed during the studies. Exposures to 2100 ppm produced narcosis and ataxia. Post-exposure recovery from these CNS effects was rapid (less than 1 hr). These effects were concentration-dependent and relatively independent of exposure length. Exposure to 3000 ppm for 2 weeks (5 h/d, 5 d/wk) produced testicular toxicity. The 13-week study yielded similar results. Results from the genotoxicity assays (in vivo/in vitro unscheduled DNA synthesis in rat primary heptaocytes, chromosomal aberrations in rat bone marrow cells; reverse gene mutation in Salmonella typhimurium; and forward mutation in Chinese hamster culture cells) were negative. These studies indicated that DMES is mildly to moderately toxic but not a multagen. Author (revised)

N94-11555*# National Aeronautics and Space Administration. Lyndon B. Johnson Space Center, Houston, TX.

A COMBUSTION PRODUCTS ANALYZER FOR CONTINGENCY USE DURING THERMODEGRADATION EVENTS ON SPACECRAFT **c54**

Steve Wilson (Krug Life Sciences, Inc., Houston, TX.), Thomas F. Limero (Krug Life Sciences, Inc., Houston, TX.), Steve W. Beck (Krug Life Sciences, Inc., Houston, TX.), and John T. James *In its* Sixth Annual Workshop on Space Operations Applications and Research (SOAR 1992), Volume 2 Feb. 1993 p 590-596 (For primary document see N94-11527 01-99)
Avail: CASI HC A02/MF A03

The Toxicology Laboratory at JSC and Exidyne Instrumentation Technologies (EIT) have developed a prototype Combustion Products Analyzer (CPA) to monitor, in real time, combustion products from a thermodegradation event on board spacecraft. The CPA monitors the four gases that are the most hazardous compounds (based on the toxicity potential and quantity produced) likely to be released during thermodegradation of synthetic materials: hydrogen fluoride (HF), hydrogen chloride (HCl), hydrogen cyanide (HCN), and carbon monoxide (CO). The levels of these compounds serve as markers to assist toxicologists in determining when the cabin atmosphere is safe for the crew to breathe following the contingency event. The CPA is a hand-held, battery-operated instrument containing four electrochemical sensors, one for each target gas, and a pump for drawing air across the sensors. The sensors are unique in their small size and zero-g compatibility. The immobilized electrolytes in each sensor permit the instrument to function in space and eliminate the possibility of electrolye leaks. The sample inlet system is equipped with a particulate filter that prevents clogging from airborne particulate matter. The CPA has a large digital display for gas concentrations and warming signals for low flow and low battery conditions. The CPA has flown on 13 missions beginning with STS 41 in Oct. 1990. Current efforts include the development of a microprocessor, an improved carbon monoxide sensor, and a ground-based test program to evaluate the CPA during actual thermodegradation of selected materials. Author (revised)

N94-11556*# National Aeronautics and Space Administration. Ames Research Center, Moffett Field, CA.

FIVE BIOMEDICAL EXPERIMENTS FLOWN IN AN EARTH ORBITING LABORATORY: LESSONS LEARNED FROM DEVELOPING THESE EXPERIMENTS ON THE FIRST INTERNATIONAL MICROGRAVITY MISSION FROM CONCEPT TO LANDING Abstract Only **c51**

C. M. Winget, J. J. Lashbrook, P. X. Callahan, and R. L. Schaefer (Lockheed Engineering and Sciences Co., Moffett Field, CA.) *In* NASA. Johnson Space Center, Sixth Annual Workshop on Space Operations Applications and Research (SOAR 1992), Volume 2 Feb. 1993 p 597 (For primary document see N94-11527 01-99)
Avail: CASI HC A01/MF A03

There are numerous problems associated with accommodating complex biological systems in microgravity in the flexible laboratory systems installed in the Orbiter cargo bay. This presentation will focus upon some of the lessons learned along the way from the University laboratory to the IML-1 Microgravity Laboratory. The First International Microgravity Laboratory (IML-1) mission contained a large number of specimens, including: 72 million nematodes, US-1; 3 billion yeast cells, US-2; 32 million mouse limb-bud cells, US-3; and 540 oat seeds (96 planted), FOTRAN. All five of the experiments had to undergo significant redevelopment effort in order to allow the investigator's ideas and objectives to be accommodated within the constraints of the IML-1 mission. Each of these experiments were proposed as unique entities rather than part of the mission, and many procedures had to be modified from the laboratory practice to meet IML-1 constraints. After a proposal is accepted by NASA for definition, an interactive process is begun between the Principal Investigator and the developer to ensure a maximum science return. The success of the five SLSPO-managed experiments was the result of successful completion of all preflight biological testing and hardware verification finalized at the KSC Life Sciences Support Facility housed in Hangar L. The ESTEC Biorack facility housed three U.S. experiments (US-1, US-2, and US-3). The U.S. Gravitational Plant Physiology Facility housed GTHRES and FOTRAN. The IML-1 mission (launched from KSC on 22 Jan. 1992, and landed at Dryden Flight Research Facility on 30 Jan. 1992) was an outstanding success--close to 100 percent of the prelaunch anticipated science return was achieved and, in some cases, greater than 100 percent was achieved (because of an extra mission day). Author (revised)

N94-11557*# Universities Space Research Association, Houston, TX.

PHYSIOLOGIC MECHANISMS OF CIRCULATORY AND BODY FLUID LOSSES IN WEIGHTLESSNESS IDENTIFIED BY MATHEMATICAL MODELING **c52**

K. E. Simanonok, R. S. Srinivasan (Krug Life Sciences, Inc., Houston, TX.), and J. B. Charles (Space Biomedical Research Inst., Houston, TX.) *In* NASA. Johnson Space Center, Sixth Annual Workshop on Space Operations Applications and Research (SOAR 1992), Volume 2 Feb. 1993 p 598-604 (For primary document see N94-11527 01-99)
Avail: CASI HC A02/MF A03

Central volume expansion due to fluid shifts in weightlessness is believed to activate adaptive reflexes which ultimately result in a reduction of the total circulating blood volume. However, the flight data suggests that a central volume overdistention does not persist, in which case some other factor or factors must be responsible for body fluid losses. We used a computer simulation to test the hypothesis that factors other than central volume overdistention are involved in the loss of blood volume and other body fluid volumes observed in weightlessness and in weightless simulations. Additionally, the simulation was used to identify these factors. The results predict that atrial volumes and pressures return to their prebedrest baseline values within the first day of exposure to head down tilt (HDT) as the blood volume is reduced by an elevated urine formation. They indicate that the mechanisms for large and prolonged body fluid losses in weightlessness is red cell hemoconcentration that elevates blood viscosity and peripheral resistance, thereby lowering capillary pressure. This causes a prolonged alteration of the balance of Starling forces, depressing the extracellular fluid volume until the hematocrit is returned to normal through a reduction of the red cell mass, which also allows some restoration of the plasma volume. We conclude that the red cell mass becomes the physiologic driver for a large 'undershoot' of the body fluid volumes after the normalization of atrial volumes and pressures. Author

N94-11558*# National Aeronautics and Space Administration. Lyndon B. Johnson Space Center, Houston, TX.

POTENTIAL HEALTH EFFECTS OF SPACE RADIATION **c52**

Chui-Hsu Yang and Laurie M. Craise (California Univ., Berkeley. Lawrence Berkeley Lab.) *In its* Sixth Annual Workshop on Space Operations Applications and Research (SOAR 1992), Volume 2 Feb. 1993 p 605-610 (For primary document see N94-11527 01-99)
(NASA Order T-9297-R)
Avail: CASI HC A02/MF A03

Crewmembers on missions to the Moon or Mars will be exposed to radiation belts, galactic cosmic rays, and possibly solar particle events. The potential health hazards due to these space radiations must be considered carefully to ensure the success of space exploration. Because there is no human radioepidemiological data for acute and late effects of high-LET (Linear-Energy-Transfer) radiation, the biological risks of energetic charged particles have to be estimated from experimental results on animals and cultured cells. Experimental data obtained to date indicate that charged particle radiation can be much more effective than photons in causing chromosome aberrations, cell killing, mutation, and tumor induction. The relative biological effectiveness (RBE) varies with biological endpoints and depends on the LET of heavy ions. Most lesions induced by low-LET radiation can be repaired in mammalian cells. Energetic heavy ions, however, can produce large complex DNA damages, which may lead to large deletions and are irreparable. For high-LET radiation, therefore, there are less or no dose rate effects. Physical shielding may not be effective in minimizing the biological effects on energetic heavy ions, since fragments of the primary particles can be effective in causing biological effects. At present the uncertainty of biological effects of heavy particles is still very large. With further understanding of the biological effects of space radiation, the career doses can be kept at acceptable levels so that the space radiation environment need not be a barrier to the exploitation of the promise of space. Author (revised)

N94-11559*# National Aeronautics and Space Administration. Lyndon B. Johnson Space Center, Houston, TX.

RADIATION CONSIDERATIONS FOR INTERPLANETARY MISSIONS Abstract Only **c18**

Gautam D. Badwar, Patrick M. ONeill (National Aeronautics and Space Administration. Langley Research Center, Hampton, VA.), and Francis A. Cucinotta (National Aeronautics and Space Administration. Langley Research Center, Hampton, VA.) *In its* Sixth Annual Workshop on Space Operations Applications and Research (SOAR 1992), Volume 2 Feb. 1993 p 611 (For primary document see N94-11527 01-99)

Avail: CASI HC A01/MF A03

Galactic cosmic radiation (GCR) poses a serious radiation hazard for long-duration missions. In designing a lunar habitat or Mars transfer vehicle, the worst-case radiation exposure determines shielding thickness and, hence, the weight of spacecraft. Using the spherically symmetric diffusion theory of the solar modulation of GCR, it was possible to use data on the differential energy spectra of hydrogen, helium, oxygen, and iron from 1954 to 1989 to show that the flux at 1 A.U. is determined by the diffusion parameter, K, which is a function of the time in the solar cycle. This analysis also showed that the solar minimum of 1976 to 1977 was the deepest minimum in the last 37 years. Using this theory, we have obtained the GCR spectra for all the nuclei and calculated the depth-dose as a function of aluminum shield thickness. Using the ICRP-26 definition of the quality factor, it is shown that the shielding required to stay below the LEO recommended annual limit of 50 cSv is 17.5 (+8, -3), g/sq cm of aluminum; if the limit is raised to 60 cSv, the required shielding is 9 (5, -1.5) g/sq cm. We also discuss the issues and shielding needs for protection against solar particle events. Author (revised)

N94-11560*# Kelsey Seybold Clinic, P.A., Houston, TX.

LONGITUDINAL STUDY OF ASTRONAUT HEALTH: MORTALITY IN THE YEARS 1959-1991 Abstract Only **c52**

Leif E. Peterson *In* NASA. Johnson Space Center, Sixth Annual Workshop on Space Operations Applications and Research (SOAR 1992), Volume 2 Feb. 1993 p 613 (For primary document see N94-11527 01-99)

Avail: CASI HC A01/MF A03

We conducted a historical cohort study of mortality among 195 astronauts who were exposed to space and medical sources of radiation between 1959 and 1991. Cumulative occupational and medical radiation exposures were obtained from the astronaut radiation exposure history data base. Causes of death were obtained from obligatory death certificates and autopsy reports that were on file in the medical records. A total of 18 deaths occurred during the 32-year follow-up period for which the all-cause standardized mortality ratio (SMR) was 142 (95 percent confidence interval 84 225). There was one cancer death in the buccal cavity and pharynegeal ICD-9 rubric whose occurrence was significantly beyond expectation. Mortality for coronary disease was 59 percent lower than expected (2 deaths; SMR = 41; 95 percent confidence limit 5 147). The crude death rate for 10 occupationally related accidents was 400 deaths per 100,000 person-years, which is an order of magnitude greater than accidental death rates in mining industries. The SMR of 1027 for fatal accidents was significantly beyond expectation (14 deaths; 95 percent confidence limit 561 1723) and was similar to SMRs for accidents among aerial pesticide applications. The 10-year cumulative risk of occupational fatalities based on the exponential, Weibull, Gompertz, and linear-exponential distributions was 10 percent. Mortality from motor vehicle accidents was slightly higher than expected but was not significant (1 death; SMR = 145; 95 percent confidence limit 2 808). Radiation exposures from medical procedures accounted for a majority of cumulative dose when compared with space radiation exposures. The results of the study do not confirm the impression that astronauts are at increased risk of cancer, but this does not obviate the need for further study. Overall, it was found that astronauts are at a health disadvantage as a result of catastrophic accidents. Author (revised)

N94-11561*# National Aeronautics and Space Administration. Lyndon B. Johnson Space Center, Houston, TX.

OPERATIONAL RADIOLOGICAL SUPPORT FOR THE US MANNED SPACE PROGRAM Abstract Only **c54**

Michael J. Golightly, Alva C. Hardy, William Atwell (Rockwell International Corp., Houston, TX.), Mark D. Weyland (Rockwell International Corp., Houston, TX.), John Kern (Rockwell International Corp., Houston, TX.), and Bernard L. Cash (Lockheed Engineering and Sciences Co., Houston, TX.) *In its* Sixth Annual Workshop on Space Operations Applications and Research (SOAR 1992), Volume 2 Feb. 1993 p 614 (For primary document see N94-11527 01-99)

Avail: CASI HC A01/MF A03

Radiological support for the manned space program is provided by the Space Radiation Analysis Group at NASA/JSC. This support ensures crew safety through mission design analysis, real-time space environment monitoring, and crew exposure measurements. Preflight crew exposure calculations using mission design information are used to ensure that crew exposures will remain within established limits. During missions, space environment conditions are continuously monitored from within the Mission Control Center. In the event of a radiation environment enhancement, the impact to crew exposure is assessed and recommendations are provided to flight management. Radiation dosimeters are placed throughout the spacecraft and provided to each crewmember. During a radiation contingency, the crew could be requested to provide dosimeter readings. This information would be used for projecting crew dose enhancements. New instrumentation and computer technology are being developed to improve the support. Improved instruments include tissue equivalent proportional counter (TEPC)-based dosimeters and charged particle telescopes. Data from these instruments will be telemetered and will provide flight controllers with unprecedented information regarding the radiation environment in and around the spacecraft. New software is being acquired and developed to provide 'smart' space environmental data displays for use by flight controllers. Author (revised)

N94-11562*# Oceaneering Space Systems, Webster, TX.

DEVELOPMENT AND EVALUATION OF A PREDICTIVE ALGORITHM FOR TELEROBOTIC TASK COMPLEXITY **c63**

M. L. Gernhardt, R. C. Hunter, J. C. Hedgecock, and A. G. Stephenson *In* NASA. Johnson Space Center, Sixth Annual Workshop on Space Operations Applications and Research (SOAR 1992), Volume 2 Feb. 1993 p 616-625 (For primary document see N94-11527 01-99)

Avail: CASI HC A02/MF A03

There is a wide range of complexity in the various telerobotic servicing tasks performed in subsea, space, and hazardous material handling environments. Experience with telerobotic servicing has evolved into a knowledge base used to design tasks to be 'telerobot friendly.' This knowledge base generally resides in a small group of people. Written documentation and requirements are limited in conveying this knowledge base to serviceable equipment designers and are subject to misinterpretation. A mathematical model of task complexity based on measurable task parameters and telerobot performance characteristics would be a valuable tool to designers and operational planners. Oceaneering Space Systems and TRW have performed an independent research and development project to develop such a tool for telerobotic orbital replacement unit (ORU) exchange. This algorithm was developed to predict an ORU exchange degree of difficulty rating (based on the Cooper-Harper rating used to assess piloted operations). It is based on measurable parameters of the ORU, attachment receptacle and quantifiable telerobotic performance characteristics (e.g., link length, joint ranges, positional accuracy, tool lengths, number of cameras, and locations). The resulting algorithm can be used to predict task complexity as the ORU parameters, receptacle parameters, and telerobotic characteristics are varied. Author (revised)

N94-11563*# Aeronautical Radio, Inc., Annapolis, MD. Advanced Research and Development Group.

DESIGN FOR TESTABILITY AND DIAGNOSIS AT THE SYSTEM-LEVEL **c38**

William R. Simpson and John W. Sheppard *In* NASA. Johnson Space Center, Sixth Annual Workshop on Space Operations Applications and Research (SOAR 1992), Volume 2 Feb. 1993 p 627-632 (For primary document see N94-11527 01-99)

Avail: CASI HC A02/MF A03

The growing complexity of full-scale systems has surpassed the capabilities of most simulation software to provide detailed models or gate-level failure analyses. The process of system-level diagnosis approaches the fault-isolation problem in a manner that differs significantly from the traditional and exhaustive failure mode search. System-level diagnosis is based on a functional representation of the system. For example, one can exercise one portion of a radar algorithm (the Fast Fourier Transform (FFT) function) by injecting several standard input patterns and comparing the results to standardized output results. An anomalous output would point to one of several items (including the FFT circuit) without specifying the gate or failure mode. For system-level repair, identifying an anomalous chip is sufficient. We describe here an information theoretic and dependency modeling approach that discards much of the detailed physical knowledge about the system and analyzes its information flow and functional interrelationships. The approach relies on group and flow associations and, as such, is hierarchical. Its hierarchical nature allows the approach to be applicable to any level of complexity and to any repair level. This approach has been incorporated in a product called STAMP (System Testability and Maintenance Program) which was developed and refined through more than 10 years of field-level applications to complex system diagnosis. The results have been outstanding, even spectacular in some cases. In this paper we describe system-level testability, system-level diagnoses, and the STAMP analysis approach, as well as a few STAMP applications. Author (revised)

N94-11564*# Air Force Human Resources Lab., Wright-Patterson AFB, OH. Logistics and Human Factors Div.

CREW CHIEF Abstract Only **c61**

Jill Easterly *In* NASA. Johnson Space Center, Sixth Annual Workshop on Space Operations Applications and Research (SOAR 1992), Volume 2 Feb. 1993 p 633 (For primary document see N94-11527 01-99)

Avail: CASI HC A01/MF A03

This software package does ergonomic human modeling for maintenance tasks. Technician capabilities can be directed to represent actual situations of work environment, strengths and capabilities of the individual, particular limitations (such as constraining characteristics of a particular space suit), tools required, and procedures or tasks to be performed. Author (revised)

N94-11565*# Air Force Human Resources Lab., Wright-Patterson AFB, OH.

ON-ORBIT REFUELING Abstract Only **c12**

Pospisil *In* NASA. Johnson Space Center, Sixth Annual Workshop on Space Operations Applications and Research (SOAR 1992), Volume 2 Feb. 1993 p 635 (For primary document see N94-11527 01-99)

Avail: CASI HC A01/MF A03

The goal of this program is to increase operational availability of space assets by refueling with an expendable launch vehicle (not the Shuttle) in LEO or GEO. Information is drawn from the on-orbit refueling model, COSEMS model, COMA study, and information provided from the San Antonio Air Logistics Center. Author (revised)

N94-11566*# National Aeronautics and Space Administration. Lyndon B. Johnson Space Center, Houston, TX.

ON-ORBIT REFUELING Abstract Only **c12**

James S. Moore and Shelby L. Owens (Hernandez Engineering, Inc., Houston, TX.) *In its* Sixth Annual Workshop on Space Operations Applications and Research (SOAR 1992), Volume 2 Feb. 1993 p 636 (For primary document see N94-11527 01-99)

Avail: CASI HC A01/MF A03

During the past decade, both NASA and the DOD have conducted numerous space servicing studies. These studies have shown that fluid resupply of on-orbit spacecraft is feasible and would allow for extended spacecraft utilization. In order to prove that the studies have validity, an on-orbit flight demonstration of automatic fluid resupply is required. To embark on this flight demonstration, the system concepts, operational procedures, and conceptual service and target vehicles must be identified. Hernandez Engineering, Inc. (HEI), under the direction of the Space Servicing System Project Office of the NASA/JSC New Initiatives Office, has conducted a systems engineering and integration study. The study objective was to develop preliminary concepts for a flight demonstration of automatic rendezvous, proximity operations, capture, and fluid transfer utilizing servicer and target vehicles. The results show that a servicer vehicle/target kit can be launched to orbit with an ELV and automatically rendezvous and dock with the explorer platform (EP). The servicer vehicle can then separate from the EP/kit, perform proximity maneuvers, redock with the EP/kit, and perform fluid transfer operations. After the on-orbit flight demonstration is completed, the servicer/kit can be separated from the EP and be deorbited into the Earth's atmosphere. Author (revised)

N94-11567*# Air Force Logistics Command, Kelly AFB, TX.

PRELIMINARY ANALYSIS OF THE BENEFITS DERIVED TO US AIR FORCE SPACECRAFT FROM ON-ORBIT REFUELING **c12**

Scott Smith *In* NASA. Johnson Space Center, Sixth Annual Workshop on Space Operations Applications and Research (SOAR 1992), Volume 2 Feb. 1993 p 637-655 (For primary document see N94-11527 01-99)

Avail: CASI HC A03/MF A03

This analysis was undertaken during FY-91 as a preliminary step to identify potential benefits from refueling Air Force satellites on orbit. Both economic and operational benefits were included. Operational benefits were related in economic terms to allow evaluation. All economic comparisons were made using FY-91 costs. An additional purpose of the effort was to identify the preferred mission parameters, for an on-orbit refueling system. A companion study was being concurrently conducted by SSD/XRP and NASA/JPL to develop a hardware concept for an on-orbit refueling system. The mass estimates for refueling missions obtained from the companion study were used in conducting the economic analyses of this benefits study. For this study, on-orbit refueling was based on the concept developed in the companion JPL study. The concept involves launching an S/C carrying fuel that would be transferred to another 'target' S/C which is already in orbit. The two S/C would then rendezvous, dock, and transfer fuel. Another fluid, such as a cryogenic, might be included if needed by the target S/C. The hardware concept for refueling was intended to minimize costs. The re-fueler S/C was designated to be expendable and would contain only the minimal capabilities. It would be launched into the orbit plane and altitude of the target S/C(s). The re-fueler S/C would rendezvous and dock with the target S/C and the fluid transfer would occur. When the refueling mission was completed, the re-fueler S/C would be ejected from the orbit. In order to optimize launch costs, some missions involved launching two re-fueler S/C on the LV. In this case the second re-fueler S/C would be placed in a storage orbit until needed. Author (revised)

N94-11568*# National Aeronautics and Space Administration. Langley Research Center, Hampton, VA.

IN-SPACE OPERATIONS FOR LUNAR AND MARS SPACE TRANSFER VEHICLES **c66**

James L. Raper, Sr. and Rick C. Vargo (McDonnell-Douglas Space Systems Co., Cocoa Beach, FL.) *In* NASA. Johnson Space Center, Sixth Annual Workshop on Space Operations Applications and Research (SOAR 1992), Volume 2 Feb. 1993 p 657-675 Repr. from AIAA/SAE/ASME/ASEE 28th Joint Propulsion Conference (Nashville, TN, AIAA), 1992 (For primary document see N94-11527 01-99)

(Contract NAS10-11400)

Avail: CASI HC A03/MF A03

The objective of this paper is to discuss the in-space operations required to process the lunar and Mars mission vehicles envisioned for the Space Exploration Initiative (SEI). Recent studies, which have examined the degree to which on-orbit operations change as a function of the Earth-to-orbit (ETO) launch vehicle size, identified a common set of on-orbit vehicle processing tasks, and generated functional requirements for in-space processing nodes are summarized in this paper. Timelines for on-orbit processing of two different lunar transfer vehicles (LTV's) were developed to compare a 'current practice,' labor-intensive EVA approach to ones utilizing telerobotics and advanced automation. LTV aerobrake concepts ranging from simple deployment to considerable assembly are compared. Similar timelines for the on-orbit processing of a nuclear Mars transfer vehicle (MTV) are also presented. Aerobrakes can be processed in a timely manner and should not be ruled out for SEI missions. The 'tall pole' time interval for on-orbit vehicle initial processing is the delivery of elements to orbit, not the processing tasks. Author (revised)

N94-11569*# National Aeronautics and Space Administration. Langley Research Center, Hampton, VA.

IN-SPACE ASSEMBLY-SERVICING REQUIREMENTS c66

Charles E. Cockrell *In* NASA. Johnson Space Center, Sixth Annual Workshop on Space Operations Applications and Research (SOAR 1992), Volume 2 Feb. 1993 p 676-689 Repr. from AIAA/SAE/ASME/ASEE 28th Joint Propulsion Conference and Exhibit (Nashville, TN, AIAA), 1992 Previously announced in IAA as A92-38165 (For primary document see N94-11527 01-99)

Avail: CASI HC A03/MF A03

A method for developing the requirements for in-space assembly, servicing, and checkout of the proposed Mars space transfer vehicles is discussed. Required in-space operations and functions are identified in relation to various Earth to Orbit (ETO) vehicles by looking at the manifesting options of baseline Mars Space Transfer Vehicles (STV). Each operation is then reduced to a minimum complexity state resulting in a set of operational primitive functions. These primitive functions are used to assess the tradeoffs between robotic, telerobotic, and EVA operations. The study demonstrates that the complexity of the in-space operations remains stable with ETO vehicle size, and therefore the functions, and ultimately the infrastructure required to support proposed missions, are relatively unaffected by varying the ETO vehicle size within the range considered for this study. Author (revised)

N94-11570*# SRI International Corp., Menlo Park, CA.

FORECASTING THE IMPACT OF VIRTUAL ENVIRONMENT TECHNOLOGY ON MAINTENANCE TRAINING c53

Mark S. Schlager, Duane Boman, Tom Piantanida, and Robert Stephenson (Aerospace Medical Research Labs., Brooks AFB, TX.) *In* NASA. Johnson Space Center, Sixth Annual Workshop on Space Operations Applications and Research (SOAR 1992), Volume 2 Feb. 1993 p 691-699 Sponsored in part by AF (For primary document see N94-11527 01-99)

Avail: CASI HC A02/MF A03

To assist NASA and the Air Force in determining how and when to invest in virtual environment (VE) technology for maintenance training, we identified possible roles for VE technology in such training, assessed its cost-effectiveness relative to existing technologies, and formulated recommendations for a research agenda that would address instructional and system development issues involved in fielding a VE training system. In the first phase of the study, we surveyed VE developers to forecast capabilities, maturity, and estimated costs for VE component technologies. We then identified maintenance tasks and their training costs through interviews with maintenance technicians, instructors, and training developers. Ten candidate tasks were selected from two classes of maintenance tasks (seven aircraft maintenance and three space maintenance) using five criteria developed to identify types of tasks most likely to benefit from VE training. Three tasks were used as specific cases for cost-benefit analysis. In formulating research recommendations, we considered three aspects of feasibility: technological considerations, cost-effectiveness, and anticipated R&D efforts. In this paper, we describe the major findings in each of these areas and suggest research efforts that we believe will help achieve the goal of a cost-effective VE maintenance training system by the next decade. Author

N94-11571*# Aerospace Corp., Sunnyvale, CA.

ON-ORBIT SERVICING FOR USAF SPACE MISSIONS: A PHASED DEVELOPMENT APPROACH Abstract Only c66

Bill Shanney *In* NASA. Johnson Space Center, Sixth Annual Workshop on Space Operations Applications and Research (SOAR 1992), Volume 2 Feb. 1993 p 700 (For primary document see N94-11527 01-99)

Avail: CASI HC A01/MF A03

On-orbit servicing has been studied for years by the U.S. Air Force Space Systems Division--which recently cosponsored the Space Assembly, Maintenance, and Servicing Study with NASA and SDIO; but an Air force servicing program has yet to emerge. The Air Force has a limited set of servicing requirements, and the practices of 'pipelining' (incremental improvements to a space vehicle series) and orbital sparing provide many similar benefits. It is postulated that an Air Force Program will be initiated in response to a new critical mission requirement that calls for a spacecraft with the operational character of a Servicer, which will evolve into a servicing program. Such a requirement may be emerging. The Air Force organizations charged with on-orbit test safety for the Department of Defense are concerned with the hazard from uncontrolled reentry of low Earth orbit test spacecraft, which are increasing in number. Analysis and observations of actual reentries show that debris reaches the Earth's surface. A phased development of a system to remove these spacecraft from orbit can evolve into a servicing program. Author (revised)

N94-11572*# Dynamics Research Corp., Arlington, VA.

MORE SENSE FOR LESS CENTS: COST EFFECTIVE SERVICING OF REMOTE SENSING SATELLITES Abstract Only c66

Jeannie Lee, Tom Misencik, Bill Robertson, and Jack Sliney *In* NASA. Johnson Space Center, Sixth Annual Workshop on Space Operations Applications and Research (SOAR 1992), Volume 2 Feb. 1993 p 701 (For primary document see N94-11527 01-99)

Avail: CASI HC A01/MF A03

This paper addresses the design considerations for Earth observation spacecraft bus and payload subsystems such that cost-effective spacecraft maintainability is enhanced through optimized reliability and the application of robotic on-orbit support. In the past, for most satellites, maintainability has been associated with the clever application of telemetry reconfiguration and the use of redundant systems as necessary over the life cycle of the spacecraft. This presentation addresses the opportunities and challenges of leveraging the extensive work already accomplished in the development of on-orbit servicing technologies. Author (revised)

N94-11573*# Space Command, Peterson AFB, CO.

ASSURED MISSION SUPPORT SPACE ARCHITECTURE (AMSSA) STUDY Abstract Only c66

Rob Hamon *In* NASA. Johnson Space Center, Sixth Annual Workshop on Space Operations Applications and Research (SOAR 1992), Volume 2 Feb. 1993 p 702 (For primary document see N94-11527 01-99)

Avail: CASI HC A01/MF A03

The assured mission support space architecture (AMSSA) study was conducted with the overall goal of developing a long-term requirements-driven integrated space architecture to provide responsive and sustained space support to the combatant commands. Although derivation of an architecture was the focus of the study, there are three significant products from the effort. The first is a philosophy that defines the necessary attributes for the development and operation of space systems to ensure an integrated, interoperable architecture that, by design, provides a high degree of combat utility. The second is the architecture itself; based on an interoperable system-of-systems strategy, it reflects a long-range goal for space that will evolve as user requirements adapt to a changing world environment. The third product is the framework of a process that, when fully developed, will provide essential information to key decision makers for space systems acquisition in order to achieve the AMSSA goal. It is a categorical imperative that military space planners develop space systems that will act as true force multipliers. AMSSA provides the philosophy, process, and architecture that, when integrated with the DOD requirements and acquisition procedures, can yield an assured mission support capability from space to the combatant commanders. An important feature of the AMSSA initiative is the participation by every organization that has a role or interest in space systems development and operation. With continued community involvement, the concept of the AMSSA will become a reality. In summary, AMSSA offers a better way to think about space (philosophy) that can lead to the effective utilization of limited resources (process) with an infrastructure designed to meet the future space needs (architecture) of our combat forces. Author

N94-11574*# National Aeronautics and Space Administration. Lyndon B. Johnson Space Center, Houston, TX.

DEFINITION OF SPACECRAFT STANDARD INTERFACES BY THE NASA SPACE ASSEMBLY AND SERVICING WORKING GROUP (SASWG) c66

Robert Radtke (Tracor Applied Sciences, Inc., Kingwood, TX.), Charles Woolley, and Lana Arnold (Lockheed Engineering and Sciences Co., Houston, TX.) *In its* Sixth Annual Workshop on Space Operations Applications and Research (SOAR 1992), Volume 2 Feb. 1993

p 703-707 (For primary document see N94-11527 01-99)
Avail: CASI HC A01/MF A03

The purpose of the NASA Space Assembly and Servicing Working Group (SASWG) is to study enabling technologies for on-orbit spacecraft maintenance and servicing. One key technology required for effective space logistics activity is the development of standard spacecraft interfaces, including the 'Basic Set' defined by NASA, the U.S. Space Command, and industry panelists to be the following: (1) navigation aids; (2) grasping, berthing, and docking; and (3) utility connections for power, data, and fluids. Draft standards have been prepared and referred to professional standards organizations, including the AIAA, EIA, and SAE space standards committee. The objective of the SASWG is to support these committees with the technical expertise required to prepare standards, guidelines, and recommended practices which will be accepted by the ANSI and international standards organizations, including the ISO, IEC, and PASC. Author (revised)

N94-11575*# Environmental Research Inst. of Michigan, Ann Arbor.
THE GUIDE TO DESIGN FOR ON-ORBIT SPACECRAFT SERVICING (DFOSS) MANUAL: PRODUCING A CONSENSUS DOCUMENT c82
Janice Nyman *In* NASA. Johnson Space Center, Sixth Annual Workshop on Space Operations Applications and Research (SOAR 1992), Volume 2 Feb. 1993 p 708-715 (For primary document see N94-11527 01-99)
Avail: CASI HC A02/MF A03

Increasing interaction and changing economies at the national and international levels have accelerated the call for standardization in space systems design. The benefits of standardization--compatibility, interchangeability, and lower costs--are maximized when achieved through consensus. Reaching consensus in standardization means giving everyone who will be affected by a standard an opportunity to have input into creating that standard. The DFOSS manual was initiated with the goal of developing standards through consensus. The present Proposed Guide derives from work begun by the Space Automation and Robotics Center (SpARC), a NASA Center for the Commercial Development of Space, and has continued as a standards project through the American Institute of Aeronautics and Astronautics (AIAA). The Proposed Guide was released by AIAA in Jan. 1992 for sale during a one-year, trial-use period. DFOSS is a response to the need for one document that contains all the guidelines required by on-orbit spacecraft servicing designers for astronaut extravehicular activity and/or telerobotic servicing. The manual's content is driven by spacecraft design considerations, and its composition has been achieved by interaction and cooperation among government, industry, and research organizations. While much work lies ahead to maximize the potential of DFOSS, the Proposed Guide represents evidence of the benefits of industry-wide consensus, points the way for broader application, and provides an example for similar projects. Author (revised)

N94-11576*# Air Force Systems Command, Norton AFB, CA. National Launch System Joint Program Office.
THE NATIONAL LAUNCH SYSTEM ADVANCED DEVELOPMENT PROGRAM: A BRIEF OVERVIEW c15
J. A. Battenburg *In* NASA. Johnson Space Center, Sixth Annual Workshop on Space Operations Applications and Research (SOAR 1992), Volume 2 Feb. 1993 p 716-717 (For primary document see N94-11527 01-99)
Avail: CASI HC A01/MF A03

A broad-based Advanced Development Program is being conducted to modernize the technological base and support the systems design of the National Launch System. While the principal concentration of efforts has been in propulsion, significant work is being accomplished in all of the disciplinary areas associated with space launch. Tasks are selected that offer reduced costs, increased reliability, and enhanced operability with anticipated task completion times which are consistent with NLS development. Author (revised)

N94-11577*# Jet Propulsion Lab., California Inst. of Tech., Pasadena.
SUPERVISED AUTONOMOUS CONTROL, SHARED CONTROL, AND TELEOPERATION FOR SPACE SERVICING c37
Paul G. Backes *In* NASA. Johnson Space Center, Sixth Annual Workshop on Space Operations Applications and Research (SOAR 1992), Volume 2 Feb. 1993 p 720-731 Sponsored by NASA, Washington (For primary document see N94-11527 01-99)
Avail: CASI HC A03/MF A03

A local-remote telerobot system for single- and dual-arm supervised autonomy, shared control, and teleoperation has been demonstrated. The system is composed of two distinct parts: the local site, where the operator resides; and the remote site, where the robots reside. The system could be further separated into dual local sites communicating with a common remote site. This is valuable for potential space missions where a space based robotic system may be controlled either by a space based operator or by a ground based operator. Also, multiple modes of control integrated into a common system are valuable for satisfying different servicing scenarios. The remote site single arm control system is described, and its parameterization for different supervised autonomous control, shared control, and teleoperation tasks are given. Experimental results are also given for selected tasks. The tasks include compliant grasping, orbital replacement unit changeout, bolt seating and turning, electronics card removal and insertion, and door opening. Author (revised)

N94-11578*# Lockheed Engineering and Sciences Co., Houston, TX.
SPACE STATION MAINTENANCE STUDIES USING PLAID GRAPHICS Abstract Only c61
Mary E. Helm *In* NASA. Johnson Space Center, Sixth Annual Workshop on Space Operations Applications and Research (SOAR 1992), Volume 2 Feb. 1993 p 732 (For primary document see N94-11527 01-99)
Avail: CASI HC A01/MF A03

The Graphics Analysis Facility (GRAF) has been used frequently to study extravehicular activity (EVA) maintenance scenarios on Space Station Freedom. The ability to use 3-dimensional visualization gives one a more accurate estimate of the Space Station environment. Moreover, human EVA and robotic kinematics can be accurately simulated for volumetric reach and collision detection analysis. An animation of this kind was developed for a research group at JSC to study and discover problem areas involved with doing external Space Station maintenance tasks. On the EVA side, it was discovered that items such as handholds and temporary restraint mechanisms should more effectively facilitate EVA movement about the Space Station structure for the suited personnel. Issues concerning CETA cart configuration, PWP storage locations, and locations of EVA storage areas were also identified by use of the animation. In the area of EVA versus robotics, it was found that there is a strong desire to make EVA and robotics interfaces compatible on items such as replacement units and unpressurized logistics carriers. The animation also showed that the use of robotics within an EVA task increases the difficulty and duration of the task setup, leaving less time available for the maintenance task itself. Graphics animation provides a mechanism to simultaneously analyze several mission parameters (i.e., EVA reach, volumetric analysis, and task timelines), and thus, it has proven to be an effective method for mission evaluation. Author (revised)

N94-11579*# National Aeronautics and Space Administration. Goddard Space Flight Center, Greenbelt, MD.
ROBOTIC SERVICING ON EARTH ORBITING SATELLITES Abstract Only c18
Stanford Ollendorf *In* NASA. Johnson Space Center, Sixth Annual Workshop on Space Operations Applications and Research (SOAR 1992), Volume 2 Feb. 1993 p 733 (For primary document see N94-11527 01-99)
Avail: CASI HC A01/MF A03

An articulated calibration experiment (ACE) concept study was conducted by GSFC to prove the feasibility of instrument calibration by a resident robot on the EOS spacecraft. This study provided a basis for determining the most suitable robot design and operations concepts required to perform accurate instrument calibration on the EOS platform. During the study, the first-order dynamics of robot walking and docking motions as it moves about were evaluated to determine the accelerations and torques imparted into the spacecraft. The major perturbation to the spacecraft was the effect of robot motion and impact on the EOS platform attitude control system. If not carefully controlled, these levels could exceed the maximum allowable levels. As a result of the EOS/ACE feasibility study, a GSFC robotic ground development effort was established. This effort, as described on the paper, will identify the technology required to resolve issues associated with robot in-space servicing dynamics and its impact on spacecraft and designs. Of primary concern are those relating to robot contact loads, docking of robotic systems on space platforms, and basic motion and mobility. Author (revised)

N94-11820# Advisory Group for Aerospace Research and Development, Neuilly-Sur-Seine (France).

AGARD HIGHLIGHTS 92/2, SEPTEMBER 1992

Sep. 1992 36 p

(AGARD-Highlights-92/2) Avail: CASI HC A03/MF A01

Highlights of the activities of the Advisory Group for Aerospace Research & Development (AGARD) are presented. Articles addressing the award of the von Karman Medal and the Scientific Achievement Award for 1992 are included along with a review of the 'Open Skies' negotiations in Vienna, the role of the Independent European Programme Group (IEPG), and EUCLID (European Cooperation for the Long Term in Defense). CASI

N94-12334 Naval Research Lab., Washington, DC.

NRL REVIEW FOR 1993

1993 286 p Limited Reproducibility: More than 20% of this document may be affected by microfiche quality

(AD-A265666; NRL/PU/5230-92-235) Avail: CASI HC A13

Recent research projects at NRL are presented: opioid peptides--X-ray characterization of two potent enkephalin analogs; ultrathin magnetic film research at NRL; communicating with chaos; trans-oceanic acoustic propagation and global warming; acoustics--electroacoustic transducer transient suppression--BiKR-A range-dependent, normal-mode reverberation model for bistatic geometries; predicting acoustic signal distortion in shallow water; chemical/biochemical research--development of polyurethane/epoxy based interpenetrating polymer networks for damping applications; ultrafast photochemical processes; chemical adhesion across composite interfaces; nanocapillarity in fullerine tubules; and neuronal patterning. DTIC

SUBJECT INDEX

Typical Subject Index Listing

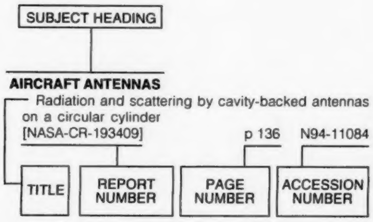

The subject heading is a key to the subject content of the document. Titles, report numbers, and accession numbers of pertinent documents are provided under each subject heading. When the title is insufficiently descriptive of the document content, a title extension is added, separated from the title by three hyphens. The report number helps to indicate the type of document cited (e.g., NASA report, NASA translation, NASA contractor report). The accession number is the number by which the document abstracts are arranged in this journal and by which the document is sold or requested. The page number helps you locate the citation in the abstract section. The titles, with title extensions if present, are arranged under each subject heading in ascending accession number order. The subject headings have been selected from the latest revision of the *NASA Thesaurus*.

A

A STARS
The abundances of the elements in sharp-lined early type stars [NASA-CR-194055] p 424 N94-12573

ABLATION
Arcjet exploratory tests of ARC optical window design for the AFE vehicle [NASA-CR-192655] p 34 N94-10930
Rates of fluvio-thermal erosion on Mars p 435 N94-12018

ABLATIVE MATERIALS
Design concepts for load-carrying hot structures for reentry bodies p 57 N94-10012
Level 3 material characterization of NARC HRPF, HRHU, HRHF, and HRPU [NASA-CR-192579] p 65 N94-10812
The laser ablation of gold films at the electrode surface of a quartz crystal microbalance [AD-A265535] p 175 N94-12012

ABRASION RESISTANCE
Weld overlay coatings for erosion control [DE93-013592] p 84 N94-11816

ABSORBENTS
Synthesis of molecular sieves from clear solution p 124 N94-10245

ABSORBERS (EQUIPMENT)
A theory of membrane absorbers [ISVR-TR-217] p 76 N94-11216

ABSORPTION CROSS SECTIONS
Activation energy and capture cross section of majority carrier traps in Zn doped InP p 49 N94-11386

ABSORPTION SPECTRA
Radiation defect production in InAs crystals under electron irradiation [DE93-617202] p 397 N94-10845
Organometallic chemical vapor deposition and characterization of ZnGe(1-x)Si(x)P2-Ge alloys on GaP substrates p 400 N94-11443
FEFF5: An ab initio multiple scattering XAFS code [DE93-011000] p 367 N94-11470
The excitation of cyanogen and ionized carbon in interstellar and extragalactic gas clouds p 426 N94-11582
Absorption spectrum calculations using mixed quantum-gaussian wave packet dynamics [AD-A265179] p 413 N94-11877
A comparison of telescopic and Phobos-2 ISM spectra of Mars in the short-wave near-infrared (0.76-1.02 microns) p 424 N94-12053
Spectral mixing models of S-Type asteroids p 431 N94-12164
Chondrites, S asteroids, and space weathering: Thumping noises from the coffin? p 433 N94-12244
ADP study of the structure of the IUE halo [NASA-CR-194374] p 428 N94-12595

ABSORPTION SPECTROSCOPY
Radiation defect production in InAs crystals under electron irradiation [DE93-617202] p 397 N94-10845
X ray absorption spectroscopy of electrochemically generated species [AD-A264749] p 77 N94-11265
Apical Cu-O bond in YBa2Cu3O(7-delta) superconductors by XAFS [DE93-010861] p 400 N94-11458
In situ XANES studies of the passive film on Fe and Fe-26Cr [DE93-010869] p 84 N94-11459

ABSORPTIVITY
Optical characteristics in Tokyo Bay p 204 N94-11972

ABSTRACTS
Advanced statistical methods for improved data analysis of NASA astrophysics missions [NASA-CR-193514] p 425 N94-10943

ABUNDANCE
Post-launch analysis of data from the High Energy Astrophysical Observatory Heavy Nuclei Experiment (HEAO-C3) [NASA-CR-193513] p 484 N94-11486
Trace-element abundances in several new ureilites p 80 N94-12096
Volatiles in fourteen interplanetary dust particles: A comparison with CI and CM chondrites p 430 N94-12132
The Th and U abundances in chondritic meteorites p 430 N94-12151
New low-Ni (igneous?) particles among the C and C? types of cosmic dust p 433 N94-12262
The abundances of the elements in sharp-lined early type stars [NASA-CR-194055] p 424 N94-12573

ACCELERATED LIFE TESTS
TAB interconnects for space concentrator solar cell arrays p 51 N94-11400

ACCELERATION TOLERANCE
Motion and spatial disorientation systems: Special research capabilities [AD-A265155] p 303 N94-11097

ACCELEROMETERS
Calibration of accelerometers on drop tower Bremen p 108 N94-10121
An experimental investigation of high-speed water-entry for full-size and scale-model pointed nose vehicles [DE93-008491] p 147 N94-10252
Sine and random vibration program evaluation on vibration control systems [DE93-011974] p 188 N94-11460

ACCEPTOR MATERIALS
Polar solvation and electron transfer [DE93-013328] p 365 N94-11010
Chromatographic assessment of hydrogen-bond donating ability [AD-A265292] p 369 N94-11826

ACCESS CONTROL
An efficient medium access control strategy for high speed WDM multiaccess networks [MEMO-INF-92-74] p 131 N94-10165
An object-oriented model for extensible concurrent systems: The composition-filters approach [MEMO-INF-92-87] p 320 N94-10166
Formal specification of the plain UCN layer in LOTOS [MEMO-INF-92-83] p 131 N94-10280
Practical authorization in large heterogeneous distributed systems [DE93-013192] p 335 N94-10324

ACCIDENT PRONENESS
Aviation accident risk for airmen with aphakia and artificial lens implants [DOT/FAA/AM-93/11] p 303 N94-10813

ACCIDENTS
Toxic chemical release inventory reporting Form R and instructions. Revised 1992 version. Section 313 of the Emergency Planning and Community Right-to-Know Act [PB93-194140] p 264 N94-10836
Fully coupled neutronic and hydrodynamic analysis of space nuclear reactor reentry accidents [DE93-005459] p 372 N94-10890
Wind system documentation [DE93-010381] p 285 N94-11664

ACCLIMATIZATION
Effect of double density caging during Space Shuttle transport of laboratory rats [NASA-CR-193228] p 300 N94-11180

ACCRETION DISKS
Accretion disk viscosity and internal waves in disks p 153 N94-11615
Midplane temperatures in the solar nebula p 448 N94-12088

ACCUMULATORS
Experimental and theoretical investigations of Cs-Ba vapor tacitron inverter for power conditioning in space power systems [DE93-012971] p 48 N94-11372

ACCURACY
Helicopter approach capability using the differential Global Positioning System [NASA-CR-177618] p 24 N94-12355

ACETATES
Conversion of acetic acid to methane by thermophiles [DE93-014433] p 300 N94-10652
Acetate concentrations and oxidation in salt marsh sediments p 269 N94-12459
Elevated acetate concentrations in the rhizosphere of Spartina alterniflora and potential influences on sulfate reduction p 271 N94-12468

ACETIC ACID
Conversion of acetic acid to methane by thermophiles [DE93-014433] p 300 N94-10652

ACETONE
Coupled growth of cells and bubbles in directional solidification of succinonitrile-acetone alloys p 118 N94-10206

ACETONITRILE
Surface-enhanced raman spectroscopy of electroactive films of C60 and an Ir-C60 complex on gold: Symmetry lowering, electron localization, and counteraction effects [AD-A265934] p 396 N94-10705

ACHONDRITES
Moessbauer spectroscopy of the SNC meteorite Zagami p 428 N94-12016
Ejecting basaltic achondrites from Vesta: Hydrodynamical impact models p 429 N94-12036
Nitrogen and noble gases in a glass sample from LEW88516 p 80 N94-12051
The asteroid-meteorite connection: Forging a new link to Vesta as the parent body of basaltic achondrite (HED) meteorites p 429 N94-12068
Preliminary results of Mn partitioning experiments on Murchison analogues p 281 N94-12081
Ar-39 - Ar-40 ages of acapulcoites and lodranites: Evidence for early parent body heating p 281 N94-12083
Metal-rich meteorites from the aubrite parent body p 430 N94-12142

Separation of spallation and terrestrial C-14 in chondrites p 431 N94-12183
Trace element distributions in primitive achondrites p 431 N94-12200
The Fe/Mn constraint on precursors of basaltic achondrites p 432 N94-12208
The Xe-Q in lodranites and a hint for Xe-L. FRO90011 another lodranite? p 432 N94-12239

ACID RAIN
The effects of acid deposition on sulfate reduction and methane production in peatlands p 270 N94-12465
DMS emissions from Sphagnum-dominated wetlands p 271 N94-12466

ACOUSTIC ATTENUATION
A new FR water resistant acoustic insulation material for aircraft p 18 N94-10773
Acoustics of bubbly sediments [AD-A263726] p 288 N94-11299

ACOUSTIC COUPLING
Research on acoustic coupling to electromagnetic pulses in tissue [AD-A264764] p 301 N94-11583

ACOUSTIC EMISSION
Fiber-optic sensor systems for measuring strain and the detection of acoustic emissions in smart structures p 71 N94-11337

ACOUSTIC FATIGUE
Development of a fatigue analysis approach for CFRP structures under acoustic loading p 58 N94-10018

ACOUSTIC LEVITATION
Protein, glass, aerosol research, containerless processing and diagnostics technology for microgravity application p 106 N94-10112
Determination of the viscous acoustic field for liquid drop positioning/forcing in an acoustic levitation chamber in microgravity p 110 N94-10131

ACOUSTIC MEASUREMENT
Underwater hydrophone location survey p 290 N94-10975
Noise levels and their effects on Shuttle crewmembers' performance: Operational concerns p 314 N94-11538
Ultrasonic wave interaction with advanced complex materials for nondestructive evaluation applications [AD-A265704] p 74 N94-12401

ACOUSTIC PROPAGATION
Acoustics of bubbly sediments [AD-A263726] p 288 N94-11299
Acoustic waveguide characteristics of the Indian Ocean north of equator p 193 N94-11912
Measurement of the surface layer current averaged vertically using Multipaths Inverted Echosounder p 194 N94-11915
Study on color video pictures transmission by digital acoustic signal p 139 N94-11917
NRL review for 1993 [AD-A265666] p 497 N94-12334

ACOUSTIC PROPERTIES
Low power digital recorder development [AD-A265921] p 170 N94-10704
Materials for adaptive structural acoustic control, volume 3 [AD-A264621] p 358 N94-11262
Acoustic characteristics of side scan sonar and sub-bottom profiler for 10,000 m class ROV p 172 N94-11916

ACOUSTIC SCATTERING
Preliminary results on backscattering strength from a wind generated bubbly ocean surface [AD-A265006] p 287 N94-10490

ACOUSTIC SOUNDING
Acoustic estimation of plankton biomass p 218 N94-12699
The acoustic arrangement for measuring vertical structure of sea current p 223 N94-12729

ACOUSTIC VELOCITY
Sensing glass transitions in thin polymer films on acoustic wave microsensors [DE93-010805] p 87 N94-10295
Preliminary results on backscattering strength from a wind generated bubbly ocean surface [AD-A265006] p 287 N94-10490
Elastic deformations and sound in anisotrope superconductors near critical temperature [DE93-620636] p 188 N94-11364
Acoustic waveguide characteristics of the Indian Ocean north of equator p 193 N94-11912

ACOUSTICS
Real-time tomography mooring [AD-A264923] p 289 N94-11854
Distributed combustion in solid propellants [AD-A265727] p 99 N94-12564

ACOUSTO-OPTICS
Application of normalized gray-scale correlation [DE93-013765] p 141 N94-10521
Presort processor — optical filtering [AD-A263872] p 382 N94-11300

ACRYLATES
Photoinitiated radical polymerization of liquid monomers in microgravity p 124 N94-10246

ACTIVATION ANALYSIS
Report of the IAEA Consultants' Meeting on Real-Time Nondestructive Monitoring of Wear and Corrosion Using the Thin Layer Activation Technique [DE93-617422] p 183 N94-10847

ACTIVATION ENERGY
Szilard-Chalmers effect in solid HIO4.2H2O by neutron irradiation [DE93-617173] p 397 N94-10830
Advanced diagnostics for in situ measurement of particle formation and deposition in thermally stressed jet fuels [DE93-009798] p 98 N94-11366
Activation energy and capture cross section of majority carrier traps in Zn doped InP p 49 N94-11386
Distributed combustion in solid propellants [AD-A265727] p 99 N94-12564

ACTIVE CONTROL
Smart materials for helicopter rotor active control p 27 N94-11321
The impact of active controls technology on the structural integrity of aeronautical vehicles p 27 N94-11341
Aircraft smart structures research in the USAF Wright Laboratory p 72 N94-11343
Active landing gear control for improved ride quality during ground roll p 27 N94-11345
Active damping augmentation of elastomechanical systems using piezoelectric sensors and actuators p 72 N94-11346
Multidimensional intelligent control for superlight air vehicles p 27 N94-11347
Active vibration control of adaptive flexible structures using piezoelectric smart sensors and actuators p 189 N94-11823
A determination of the external forces required to move the benchmark active controls testing model in pure plunge and pure pitch [NASA-TM-107743] p 16 N94-12421

ACTIVITY CYCLES (BIOLOGY)
The 2nd Annual Meeting of the Society for Research on Biological Rhythms [AD-A264869] p 303 N94-10872

ACTUATORS
Telerobot control system [NASA-CASE-NPO-18116-1-CU] p 179 N94-10670
Momentum management in redundant manipulators for vibration suppression [NASA-CR-194112] p 180 N94-10821
Materials for adaptive structural acoustic control, volume 3 [AD-A264621] p 358 N94-11262
Adaptive structure design employing shape memory actuators p 70 N94-11331
Ceramic actuators for smart materials [AD-A265664] p 93 N94-12331
A determination of the external forces required to move the benchmark active controls testing model in pure plunge and pure pitch [NASA-TM-107743] p 16 N94-12421

ADA (PROGRAMMING LANGUAGE)
Effective software reuse in an embedded realtime system [AD-A264993] p 326 N94-11220
STGT program: Ada coding and architecture lessons learned p 330 N94-11437
Analysis and guidelines for reusable Ada software [AD-A264918] p 332 N94-11850

ADAPTATION
Perceptual response to visual noise and display media [NASA-CR-193406] p 313 N94-11511

ADAPTIVE CONTROL
Nonlinear stability and control study of highly maneuverable high performance aircraft [NASA-CR-193480] p 25 N94-10344
Telerobotic control of a mobile coordinated robotic server [NASA-CR-193465] p 338 N94-10345
Materials for adaptive structural acoustic control, volume 3 [AD-A264621] p 358 N94-11262
Adaptive structures for spacecraft: A USAF perspective p 45 N94-11319
On the stability of shape memory materials and their properties in static and dynamic applications p 69 N94-11329
Adaptive structure design employing shape memory actuators p 70 N94-11331
Adaptive algorithms for use with digital filters in vibration control p 71 N94-11338
Advances in adaptive structures at Jet Propulsion Laboratory p 72 N94-11344
Adaptive reconfigurable flight controls for high angle of attack aircraft agility p 32 N94-11502
Active vibration control of adaptive flexible structures using piezoelectric smart sensors and actuators p 189 N94-11823
An adaptive and robust control for motion coordination of two-cooperating robot manipulators p 340 N94-11825

ADAPTIVE FILTERS
Continuous-time adaptive learning circuit [AD-D015773] p 140 N94-10384

ADAPTIVE OPTICS
Generalization of Dyson criterion for the amplitude-phase fluctuations case and for the system of interferometers p 135 N94-11067
Laser system design for the generation of a sodium-layer laser guide star [DE93-014127] p 176 N94-12784

ADDITIVES
Radiation defect production in InAs crystals under electron irradiation [DE93-617202] p 397 N94-10845

ADHESION
Development of bioelastic materials for the prevention of adhesions: Polypenta- and polytetrapeptides [AD-A264851] p 88 N94-10863

ADHESION TESTS
Effect of surface cleanliness of bearing steel on adhesive strength and tribological properties of sputter-deposited gold films [DE93-767974] p 82 N94-10732

ADHESIVE BONDING
Advanced methods of permanently joining carbon materials p 63 N94-10057
Uralane (tm) 5774-A/B: Ciba-Geigy's advanced urethane adhesive for the aircraft industry p 18 N94-10777

ADHESIVES
Advanced methods of permanently joining carbon materials p 63 N94-10057
New thermoplastic laminating adhesives for the aircraft industry with low heat release and low smoke emission p 17 N94-10767
Uralane (tm) 5774-A/B: Ciba-Geigy's advanced urethane adhesive for the aircraft industry p 18 N94-10777
TAB interconnects for space concentrator solar cell arrays p 51 N94-11400

ADIABATIC FLOW
Examination of wall functions for a parabolized Navier-Stokes code for supersonic flow [DE93-011590] p 14 N94-11111

ADJOINTS
Direct solution of the mathematical adjoint equations for an interface current nodal formulation [DE93-009961] p 346 N94-11608

ADMIXTURES
Study of the admixture diffusion in the sea using remote techniques p 228 N94-12759

ADRIATIC SEA
An algorithm for the detection of mucilage (green slime) in the Adriatic Sea p 191 N94-11900

ADSORPTION
Surface tension and adsorption kinetics in immiscible liquid systems at microgravity p 121 N94-10225
Studies of critical point phenomena of fluids: Bulk fluids, fluids in pores, and at interfaces p 80 N94-10228
Site dependence of the apparent shape of a molecule in STM images: Benzene on Pt(111) [AD-A263488] p 365 N94-11093
Adsorption and dissociation of disilane on Si(001) studied by STM [AD-A265269] p 402 N94-11684
A vibrational spectroscopic study of the structure of electroactive self-assembled monolayers of viologen derivatives [AD-A265705] p 78 N94-12273
The effects of organic adsorbates on the underpotential deposition of silver on Pt(111) electrodes [AD-A265623] p 404 N94-12376
The adsorption and surface reaction of SiCl4 on Si(100)-(2x1) [AD-A266124] p 79 N94-12538

ADVANCED VERY HIGH RESOLUTION RADIOMETER
Retrieval of radiation budgets in the Arctic from satellite measurements p 229 N94-10714
Surface roughness variations across the Iceland-Faroes frontal region observed by the GEOSAT altimeter and NOAA AVHRR p 201 N94-11958

ADVECTION
Large time-step stability of explicit one-dimensional advection schemes [NASA-TM-106203] p 342 N94-10362
Shear, strain and thermohaline vertical fine structure in the upper ocean [AD-A265961] p 289 N94-12348

An examination of the evolution of radiation and advection fogs
[AD-A266127] p 286 N94-12539

Advective surface velocity in the north west Pacific derived from NOAA AVHRR images
p 222 N94-12721

AERIAL PHOTOGRAPHY

The optical/computer hybrid processing of extracting ocean wave directional spectrum by airborne photograph
p 197 N94-11934

Study of growing processes of a tombolo using an air photograph p 218 N94-12702

Wind-wave and foam dynamics from optical and radar airborne observations p 226 N94-12745

AEROACOUSTICS

Control of jet noise
[NASA-CR-193612] p 358 N94-11176

Direct numerical simulation of hot jets
p 156 N94-12295

AEROASSIST

Arcjet exploratory tests of ARC optical window design for the AFE vehicle
[NASA-CR-192655] p 34 N94-10930

AERODYNAMIC CHARACTERISTICS

Aerodynamic and aerothermal challenges for the design of the Hermes spaceplane p 3 N94-10423

Experimental results in aerodynamic stability and control of a TSTO configuration p 3 N94-10424

In-flight evaluation of aerodynamic predictions of an air-launched space booster p 3 N94-10427

Planetary entry vehicle design for planned and potential ESA missions to Titan, Mars, and Earth return (FGE TN 51/92) p 4 N94-10428

Proceedings of the 10th NAL Symposium on Aircraft Computational Aerodynamics: CFD Workshop on GK Airfoil and ONERA M5 Geometry
[NAL-SP-20] p 10 N94-10466

Description of 2D problem: Aerodynamic analysis of Garabedian-Korn 75-06-12 airfoil p 10 N94-10467

Aerodynamic characteristics analysis of Garabedian-Korn 75-06-12 airfoil
[PAPER-2D-2] p 10 N94-10468

Aerodynamic characteristics analysis of Garabedian-Korn 75-06-12 airfoil
[PAPER-2D-3] p 10 N94-10469

Aerodynamic characteristics analysis of Garabedian-Korn 75-06-12 airfoil: Computation using q-omega 2 equation turbulence model
[PAPER-2D-4] p 10 N94-10470

Aerodynamic characteristics analysis of Garabedian-Korn 75-06-12 airfoils: Computation using Baldwin-Lomax turbulence model
[PAPER-2D-5] p 11 N94-10471

Aerodynamic characteristics analysis of Garabedian-Korn 75-06-12 aircraft
[PAPER-2D-7] p 11 N94-10472

Aerodynamic characteristics analysis of Garabedian-Korn 75-06-12 airfoil
[PAPER-2D-8] p 11 N94-10473

Aerodynamic characteristics analysis of Garabedian-Korn 75-06-12 airfoil
[PAPER-2D-9] p 11 N94-10474

Aerodynamic characteristics analysis of Garabedian-Korn 75-06-12 airfoil: Compendium of results p 11 N94-10475

Description of 3D problem: Flow analysis around ONERA model M5 configuration p 11 N94-10476

Flow analysis around ONERA model M5 configuration
[PAPER-3D-1] p 11 N94-10477

Flow analysis around ONERA model M5 configuration
[PAPER-3D-2] p 12 N94-10478

Flow analysis around ONERA model M5 configuration
[PAPER-3D-3] p 12 N94-10479

Flow analysis around ONERA model M5 configuration
[PAPER-3D-4] p 12 N94-10480

Flow analysis around ONERA model M5 configuration
[PAPER-3D-5] p 12 N94-10481

Flow analysis around ONERA model M5 configuration: Compendium of results p 12 N94-10482

Space Shuttle hypersonic aerodynamic and aerothermodynamic flight research and the comparison to ground test results
[NASA-TM-4499] p 13 N94-10820

New aerodynamic information obtained from the solution of the inverse problem for aerofoils
[NAL-TR-1172] p 14 N94-10860

Nonlinear and dynamic analysis of flight
p 32 N94-11496

AERODYNAMIC DRAG

Method of reducing drag in aerodynamic systems
[NASA-CASE-LEW-14791-1] p 12 N94-10672

Simulated and experimental aerodynamic characteristics of tapered annular wings
[NAL-TR-1157] p 13 N94-10856

AERODYNAMIC HEAT TRANSFER

Design and production of insulated wind tunnel models of the Hermes shuttle for heat transfer measurements at hypersonic speeds p 4 N94-10431

AERODYNAMIC HEATING

Space Shuttle hypersonic aerodynamic and aerothermodynamic flight research and the comparison to ground test results
[NASA-TM-4499] p 13 N94-10820

Arcjet exploratory tests of ARC optical window design for the AFE vehicle
[NASA-CR-192655] p 34 N94-10930

Depletions of sulfur and/or zinc in IDPs: Are they reliable indicators of atmospheric entry heating?
p 433 N94-12261

AERODYNAMIC INTERFERENCE

Wall interference correction based on interface measurements in subsonic wind tunnel testing
p 15 N94-11154

Aerodynamic sound due to interaction between a two-dimensional free shear layer and the leading edge of a parallel flat plate p 163 N94-12615

AERODYNAMIC LOADS

Nonlinear aspects of transonic aeroelasticity
p 2 N94-10357

NASTRAN modeling of flight test components for UH-60A airloads program test configuration
[NASA-CR-193614] p 186 N94-10937

Fatigue life prediction for wind turbines: A case study on loading spectra and parameter sensitivity
[DE93-011597] p 263 N94-11173

Modeling nonlinear aerodynamic loads for aircraft stability and control analysis p 32 N94-11499

Nonlinear aspects of transonic aeroelasticity
[UTIAS-RN-345] p 15 N94-11857

General aviation aircraft-normal acceleration data analysis and collection project
[AD-A265055] p 26 N94-11858

AERODYNAMIC NOISE

Direct numerical simulation of hot jets
p 156 N94-12295

AERODYNAMIC STABILITY

Experimental results in aerodynamic stability and control of a TSTO configuration p 3 N94-10424

Extraction of stability and control derivatives from orbiter flight data
[NASA-TM-4500] p 13 N94-10707

Physics of forebody flow control
[NASA-CR-193626] p 15 N94-11195

Stability in Aerospace Systems
[AGARD-R-789] p 31 N94-11489

Stability analysis and aerospace vehicle dynamics
p 31 N94-11491

On non-linear longitudinal stability of an aircraft in a dive in the presence of atmospheric disturbances
p 31 N94-11492

X-29: Longitudinal instability at high angle-of-attack
p 33 N94-11504

AERODYNAMIC STALLING

Unsteady flow past a NACA 0012 airfoil pitching at constant rates
[AD-A265159] p 16 N94-11889

AERODYNAMICS

Aeronautical engineering: A continuing bibliography with indexes (supplement 293)
[NASA-SP-7037(293)] p 1 N94-10420

Summary of research in progress at ICASE
[NASA-CR-191481] p 318 N94-11198

Flight Dynamics Directorate (FDD) Historically Black Colleges and Universities (HBCU's) database managment system: A user's guide
[AD-A264947] p 419 N94-11288

Experimental software engineering: Seventeen years of lessons in the SEL p 328 N94-11423

Nonlinear and dynamic analysis of flight
p 32 N94-11496

Stability model of the atmosphere p 32 N94-11500

Aeronautical engineering: A continuing bibliography with indexes (supplement 289)
[NASA-SP-7037(289)] p 1 N94-11687

Aeronautical engineering: A continuing bibliography with indexes (supplement 291)
[NASA-SP-7037(291)] p 1 N94-11690

Aeronautical engineering: A continuing bibliography with indexes (supplement 290)
[NASA-SP-7037(290)] p 1 N94-11691

Computational methods for problems in aerodynamics using parallel and vector architectures
[AD-A265626] p 16 N94-12377

AEROELASTICITY

Nonlinear aspects of transonic aeroelasticity
p 2 N94-10357

Determining XV-15 aeroelastic modes from flight data with frequency-domain methods
[NASA-TP-3330] p 25 N94-10935

Ground vibration and flight flutter tests of the single-seat F-16XL aircraft with a modified wing
[NASA-TM-104269] p 26 N94-11233

Computational algorithms or identification of distributed parameter systems
[AD-A265252] p 331 N94-11680

Nonlinear aspects of transonic aeroelasticity
[UTIAS-RN-345] p 15 N94-11857

AEROEMBOLISM

Hypobaric decompression prebreathe requirements and breathing environment p 317 N94-11541

Arterial gas emboli in altitude-induced decompression sickness p 312 N94-11543

AEROGELS

Effects of aqueous solution compositions on Aerocapacitor energy density
[DE93-013431] p 140 N94-10309

AERONAUTICAL ENGINEERING

Analysis of the cost evaluation of ESA programmes and comparable national and international programmes
[GTS-92063] p 416 N94-10145

Aeronautical engineering: A continuing bibliography with indexes (supplement 293)
[NASA-SP-7037(293)] p 1 N94-10420

Aeronautical engineering: A continuing bibliography with indexes (supplement 289)
[NASA-SP-7037(289)] p 1 N94-11687

Aeronautical engineering: A continuing bibliography with indexes (supplement 291)
[NASA-SP-7037(291)] p 1 N94-11690

Aeronautical engineering: A continuing bibliography with indexes (supplement 290)
[NASA-SP-7037(290)] p 1 N94-11691

AERONAUTICS

AGARD highlights 92/2, September 1992
[AGARD-HIGHLIGHTS-92/2] p 497 N94-11820

AEROSERVOELASTICITY

Ground vibration and flight flutter tests of the single-seat F-16XL aircraft with a modified wing
[NASA-TM-104269] p 26 N94-11233

AEROSOLS

Aerosol sampling models survey
[AD-A265903] p 75 N94-10337

User's manual for the plume visibility model PLUVUE 2 (revised)
[PB93-188233] p 265 N94-11016

Characterization of gas-aerosol interaction kinetics using morphology dependent stimulated Raman scattering
[DE93-012324] p 77 N94-11359

Study of the atmospheric chemistry of radon progeny in laboratory and real indoor atmospheres
[DE93-012236] p 266 N94-11671

A statistical method to determine aerosol path radiance and its application to atmospheric correction for CZCS imagery p 191 N94-11897

Distribution of mineral aerosols over the North Pacific
p 204 N94-11976

Study of climatic effects of cloud-aerosol interaction
p 204 N94-11977

Implications of aerosol retrieval and atmospheric correction in remote sensing p 205 N94-11978

Composition of the Martian aerosols through near-IR spectroscopy p 475 N94-12235

AEROSPACE ENGINEERING

Space Storable Rocket Technology program (SSRT). Option 1 program
[NASA-CR-191171] p 46 N94-10938

Theoretical investigation of 3-D shock wave turbulent boundary layer interactions
[AD-A265275] p 150 N94-11014

NASA/DOD Aerospace Knowledge Diffusion Research Project. Report 17: A comparison of the technical communication practices of Dutch and US aerospace engineers and scientists
[NASA-TM-108987] p 419 N94-11352

AGARD highlights 92/2, September 1992
[AGARD-HIGHLIGHTS-92/2] p 497 N94-11820

NRL review for 1993
[AD-A265666] p 497 N94-12334

AEROSPACE ENVIRONMENTS

Preliminary system design of a Three Arm Capture Mechanism (TACM) flight demonstration article
[NASA-CR-192573] p 177 N94-10341

Fractography handbook of spaceflight metals
[NASA-RP-1291] p 81 N94-10504

The properties of perfluoropolyethers used for space applications
[NASA-TM-106275] p 88 N94-10864

Vacuum stability requirements of polymeric material for spacecraft application
[NASA-TM-109216] p 91 N94-11350

Effects of solar cell environment on contact integrity
p 49 N94-11387

Investigation of the radiation resistance of triple-junction a-Si:H alloy solar cells irradiated with 1.00 MeV protons
p 50 N94-11391

Risk of decompression sickness in the presence of circulating microbubbles p 312 N94-11546
An investigation of the near Earth space environments
[AD-A265295] p 278 N94-11828
Modelling hypervelocity impacts into aluminum structures based on LDEF data p 190 N94-12178
Lessons learned from the Long Duration Exposure Facility
[AD-A266026] p 44 N94-12394
The Third Workshop on Two Phase Fluid Experiment in the Space Environment
[NASDA-CON-930002] p 161 N94-12547
Developmental research of thermal control system in space environment p 162 N94-12551
Two phase flow and isopycnic liquid-liquid two phase fluid in reduced gravity field p 162 N94-12552
Devices related for thermal control systems used in microgravity p 162 N94-12553
Research and development of cold plate for two phase fluid loop thermal control system p 162 N94-12555

AEROSPACE INDUSTRY
Analysis of the cost evaluation of ESA programmes and comparable national and international programmes
[GTS-92063] p 416 N94-10145
The NASA Lewis Research Center SBIR program: An assessment
[NASA-TM-106205] p 485 N94-10356
Health and safety issues for aerospace workers in the use of advanced materials p 21 N94-10795

AEROSPACE MEDICINE
Aerospace medicine and biology: A continuing bibliography with indexes (supplement 375)
[NASA-SP-7011(375)] p 303 N94-10398
Aerospace medicine and biology: A continuing bibliography with indexes (supplement 376)
[NASA-SP-7011(376)] p 303 N94-10399
Motion and spatial disorientation systems: Special research capabilities
[AD-A265155] p 303 N94-11097
Exercise countermeasures for bed-rest deconditioning
[NASA-TM-103987] p 300 N94-11191
Project ARGO: Gas phase formation in simulated microgravity
[NASA-TM-104762] p 125 N94-11235
Promethazine and its use as a treatment for space motion sickness p 312 N94-11550
Update on the incidence and treatment of space motion sickness p 312 N94-11551
Operational radiological support for the US manned space program p 318 N94-11561
Aerospace medicine and biology: A continuing bibliography with indexes (supplement 374)
[NASA-SP-7011(374)] p 304 N94-11689
Use of telescience for biomedical research during space flight p 305 N94-11791
Medical care delivery in the US space program p 307 N94-11806
Proceedings of the First Joint NASA Cardiopulmonary Workshop
[NASA-CP-10068] p 308 N94-11991
Carotid-cardiac baroreflex: Relation with orthostatic hypotension following simulated microgravity and implications for development of countermeasures p 308 N94-11992
Pulmonary function in microgravity: KC-135 experience p 309 N94-11994
Central circulatory hemodynamics as a function of gravitational stress p 309 N94-11995
Glycerol-induced hyperhydration p 309 N94-11996
Spectral analysis of resting cardiovascular variables and responses to oscillatory LBNP before and after 6 degree head dowm bedrest p 309 N94-11997
Effect of prolonged LBNP and saline ingestion on plasma volume and orthostatic responses during bed rest p 310 N94-11998
Fitness, autonomic regulation and orthostatic tolerance p 310 N94-11999
Hormonal regulation of fluid and electrolyte metabolism in zero-g and bedrest p 311 N94-12004
Cardiovascular dynamics during space sickness and deconditioning p 311 N94-12007

AEROSPACE PLANES
High temperature materials for hypersonic transport p 56 N94-10003
Aerodynamic and aerothermal challenges for the design of the Hermes spaceplane p 3 N94-10423
National Aero-Space Plane: A need for program direction and funding decisions
[GAO/NSIAD-93-207] p 416 N94-10910

AEROSPACE SAFETY
Achievements and challenges of Space Station Freedom's safety review process
[NASA-TM-106199] p 40 N94-10640
Extraction of stability and control derivatives from orbiter flight data
[NASA-TM-4500] p 13 N94-10707

AEROSPACE SYSTEMS
An analysis of the modes and states for generic avionics
[NASA-CR-188253] p 27 N94-10664
The magnitude of impact damage on LDEF materials
[NASA-CR-188258] p 43 N94-10666
On possible applications of smart structures to control of space systems p 45 N94-11342
Vacuum stability requirements of polymeric material for spacecraft application
[NASA-TM-109216] p 91 N94-11350
Stability in Aerospace Systems
[AGARD-R-789] p 31 N94-11489
Sixth Annual Workshop on Space Operations Applications and Research (SOAR 1992), volume 2
[NASA-CP-3187-VOL-2] p 486 N94-11527
Transfer of training for aerospace operations: How to measure, validate, and improve it p 314 N94-11530
On-orbit servicing for USAF space missions: A phased development approach p 348 N94-11571
Assured Mission Support Space Architecture (AMSSA) study p 348 N94-11573
The guide to Design For On-orbit Spacecraft Servicing (DFOSS) manual: Producing a consensus document p 421 N94-11575

AEROSPACE TECHNOLOGY TRANSFER
Solving the essentials of an innovative tennis racket product: Functionality, simplicity, and super-lightweight technology p 65 N94-10068
Considerations for future regional space cooperation p 35 N94-10678

AEROSPACE VEHICLES
A CFD validation roadmap for hypersonic flows p 5 N94-10439
Stability analysis and aerospace vehicle dynamics p 31 N94-11491

AEROTHERMOCHEMISTRY
Issues and approach to develop validated analysis tools for hypersonic flows: One perspective p 7 N94-10446

AEROTHERMODYNAMICS
Planetary entry vehicle design for planned and potential ESA missions to Titan, Mars, and Earth return (FGE TN 51/92) p 4 N94-10428
Issues and approach to develop validated analysis tools for hypersonic flows: One perspective p 7 N94-10446
Thermodynamic model of air in chemical equilibrium p 7 N94-10448
Three-dimensional hypersonic rarefied flow calculations using direct simulation Monte Carlo method p 7 N94-10449
Numerical methods for aerothermodynamic design of hypersonic space transport vehicles p 9 N94-10459
Local aerothermal problems during Hermes re-entry p 10 N94-10464
Exergy decrease in shock waves and boundary layers of space launch vehicles
[AD-A265272] p 42 N94-10493
Space Shuttle hypersonic aerodynamic and aerothermodynamic flight research and the comparison to ground test results
[NASA-TM-4499] p 13 N94-10820
Arcjet exploratory tests of ARC optical window design for the AFE vehicle
[NASA-CR-192655] p 34 N94-10930
Computation of hypersonic nosetip heat transfer rates for an M829-like projectile
[AD-A263226] p 16 N94-11870

AFRICAN RIFT SYSTEM
Stable isotope analyses of the peralkaline volcanics Gregory Rift Valley, Kenya p 281 N94-12072
Th-230 - U-238 series disequilibrium of the Olkaria basalts Gregory Rift Valley, Kenya p 281 N94-12073
Th-230 - U-238 series disequilibrium of the Olkaria basalts Gregory Rift Valley, Kenya: Petrogenesis p 281 N94-12074
Th-230 - U-238 series disequilibrium of the Olkaria rhyolites Gregory Rift Valley, Kenya: Petrogenesis p 281 N94-12075
Th-230 - U-238 series disequilibrium of the Olkaria rhyolites Gregory Rift Valley, Kenya: Residence times p 281 N94-12076

AGE FACTOR
Aviation accident risk for airmen with aphakia and artificial lens implants
[DOT/FAA/AM-93/11] p 303 N94-10813

AGGLOMERATION
Columbus proto-planetesimal dust aggregation experiment p 123 N94-10236

AGGLUTINATION
The spectral effects of subsolidus reduction of olivine and pyroxene p 81 N94-12110

AGGREGATES
Unequilibrated, equilibrated, and reduced aggregates in anhydrous interplanetary dust particles p 429 N94-12098

AGING
Ar-39 - Ar-40 ages of acapulcoites and lodranites: Evidence for early parent body heating p 281 N94-12083

AGING (BIOLOGY)
The aging military aviator: A review and annotated bibliography
[AD-A265341] p 311 N94-12423

AGING (MATERIALS)
DBTT measurement by use of Small Punch (SP) test
[DE93-753188] p 183 N94-11168

AGING (METALLURGY)
Welding tritium aged stainless steel
[DE93-011782] p 181 N94-11228

AGRICULTURE
The use of ERS-1 SAR data to study surface states p 247 N94-12480
Preliminary ERS-1 assessment for Canadian agriculture and forestry applications p 248 N94-12486
Integration of ERS-1 data into the European project of agriculture statistics p 248 N94-12490

AIR
Influence of neutral particles concentration on flame propagation in methane-air mixtures at zero and normal gravity conditions p 121 N94-10224

AIR BREATHING ENGINES
A CFD validation roadmap for hypersonic flows p 5 N94-10439
An environmental study of the National Aerospace Plane
[AD-A266071] p 25 N94-10945
Advanced control for airbreathing engines, volume 1: Pratt and Whitney
[NASA-CR-189203] p 29 N94-12270
Advanced control for airbreathing engines, volume 2: General Electric aircraft engines
[NASA-CR-189204] p 29 N94-12271
Advanced controls for airbreathing engines, volume 3: Allison gas turbine
[NASA-CR-189205] p 29 N94-12272

AIR CUSHION LANDING SYSTEMS
Landing Craft Air Cushion (LCAC) crew selection system manual
[AD-A265158] p 313 N94-11098

AIR FILTERS
Spacelab J air filter debris analysis
[NASA-CR-192569] p 301 N94-11201
Comprehensive analysis of airborne contaminants from recent Spacelab missions p 318 N94-11553

AIR FLOW
A four-dimensional, mesoscale, non-gaussian multispectral smoke model. Phase 1: Feasibility study
[AD-A264805] p 152 N94-11519
Fluctuations of longitudinal vortices along a concave wall p 16 N94-12616

AIR JETS
Atomization characteristics of a prefilming airblast atomizer
[NAL-TM-644] p 148 N94-10727

AIR LAND INTERACTIONS
The coherent structure in the oceanic turbulence around Japan Islands Chain forced by an air, sea, and solid Earth interaction p 198 N94-11940

AIR NAVIGATION
National Airspace System operational concept
[DOT/FAA/SE-93/1] p 23 N94-10933

AIR POLLUTION
User's manual for the plume visibility model PLUVUE 2 (revised)
[PB93-188233] p 265 N94-11016
Control of jet noise
[NASA-CR-193612] p 358 N94-11176
Application of jet-shear-layer mixing and effervescent atomization to the development of a low-NO(x) combustor
[NASA-TM-105888] p 28 N94-11234
Methodologies for estimating air emissions from three non-traditional source categories: Oil spills, petroleum vessel loading and unloading, and cooling towers
[PB93-181592] p 266 N94-11471
Renewable energy sources 1991, part 3
[DE93-605594] p 263 N94-11505
A four-dimensional, mesoscale, non-gaussian multispectral smoke model. Phase 1: Feasibility study
[AD-A264805] p 152 N94-11519
A combustion products analyzer for contingency use during thermodegradation events on spacecraft p 318 N94-11555
Novel mass spectrometric instrument for gaseous and particulate characterization and monitoring
[DE93-014093] p 272 N94-12783

AIR QUALITY
Comprehensive analysis of airborne contaminants from recent Spacelab missions p 318 N94-11553

AIR SAMPLING
Aerosol sampling models survey [AD-A265903] p 75 N94-10337
Methodologies for estimating air emissions from three non-traditional source categories: Oil spills, petroleum vessel loading and unloading, and cooling towers [PB93-181592] p 266 N94-11471
Comprehensive analysis of airborne contaminants from recent Spacelab missions p 318 N94-11553

AIR SEA ICE INTERACTIONS
Sea ice: A climate component p 232 N94-11705
Air-sea-ice interactions in the Weddell Sea p 239 N94-11753
Waves and mesoscale features in the marginal ice zone p 240 N94-11757
The seasonal Sea Ice Monitoring and Modelling Site (SIMMS): Using ERS-1 in climate research p 240 N94-11758
Ocean-ice interaction study of waves and mesoscale features p 197 N94-11935

AIR TRAFFIC
FAA air traffic activity [AD-A266043] p 22 N94-12397

AIR TRAFFIC CONTROL
National Airspace System operational concept [DOT/FAA/SE-93/1] p 23 N94-10933
Impact of shutting down en route primary radars within CONUS interior [DOT-VNTSC-FAA-93-1] p 23 N94-11626
Evaluation of the capacity and delay benefits of terminal air traffic control automation [AD-A265323] p 24 N94-11863
FAA air traffic activity [AD-A266043] p 22 N94-12397
SATORI: Situation Assessment Through the Re-creation of Incidents [DOT/FAA/AM-93/12] p 38 N94-12567

AIR TRANSPORTATION
A real-time spoken-language system for interactive problem solving [AD-A266046] p 324 N94-11104
Federal Aviation Administration aviation forecasts [AD-A265611] p 2 N94-12578

AIR WATER INTERACTIONS
Preliminary results on backscattering strength from a wind generated bubbly ocean surface [AD-A265006] p 287 N94-10490
ERS-1 studies at the Department of Oceanography from Space, IFREMER/Brest (France) p 233 N94-11712
Latent and sensible heat flux estimated from ERS-1 data p 244 N94-11783
Proceedings of the PORSEC 1992 in Okinawa: Conference for Pacific Ocean Environments and Probing, volume 1 [JTN-93-80418] p 191 N94-11894
Remote sensing and the air-sea boundary layers p 191 N94-11896
Variability of wind stress, and sensible and latent heat flux in the North Atlantic during SEASAT p 194 N94-11918
Evaporation and thermal/hydrologic balance in the Pacific p 195 N94-11919
A new expression for the production rate of sea water droplets on the sea surface p 195 N94-11920
Evaluation of ECMWF latent heat flux in TOGA CD-ROM p 195 N94-11921
Air-sea fluxes and universal constants in weak-turbulence theory of surface gravity waves p 195 N94-11922
Sea surface heat flux in the beginning of the Kuroshio p 195 N94-11923
Seasonal variation of the surface mixed layer in the subtropical re-circulation area of the North Pacific during OMLET p 195 N94-11924
Mixed layer heat budget of Kuroshio-Tango triangle using satellite and ship observations p 196 N94-11925
The coherent structure in the oceanic turbulence around Japan Islands Chain forced by an air, sea, and solid Earth interaction p 198 N94-11940
Air-sea interaction: Fluxes, a review p 201 N94-11955
The Pacific responses exhibited by an OGCM to various wind fields p 202 N94-11964
On the error characteristics of the sea surface temperature observed by satellite p 216 N94-12690
Study on air-sea interactions in the OMLET (Ocean Mixed Layer Experiment) area using satellite remote sensing p 220 N94-12710
Variability of the mixed layer depth in the North Pacific Ocean as calculated by a 3-D semi-analytical mixed layer remote sensing model p 221 N94-12718
Optical transfer operator of the atmosphere-ocean system p 225 N94-12742
Wind-wave and foam dynamics from optical and radar airborne observations p 226 N94-12745

AIRBORNE EQUIPMENT
Global monitoring of atmospheric properties by the EOS MODIS [NASA-TM-109237] p 231 N94-11485
The ERS-1/CV 580 SAR cross-calibration experiment: Sault Ste Marie, October 26 - November 2, 1991 p 236 N94-11729
Calibration results for the ERS-1, AIRSAR, and PHARS p 236 N94-11731

AIRBORNE/SPACEBORNE COMPUTERS
Data processing units for eight magnetospheric particle and field sensors [AD-A264403] p 276 N94-11463

AIRCRAFT ACCIDENT INVESTIGATION
Aircraft Accident/Incident Summary Report: Loss of control. Business Express, Inc., Beechcraft 1900C N811BE near Block Island, Rhode Island, December 28, 1991 [PB93-910405] p 22 N94-11044

AIRCRAFT ACCIDENTS
Development and analysis of insulation constructions for aerospace wiring applications p 21 N94-10791
Aviation accident risk for airmen with aphakia and artificial lens implants [DOT/FAA/AM-93/11] p 303 N94-10813
Aircraft Accident/Incident Summary Report: Loss of control. Business Express, Inc., Beechcraft 1900C N811BE near Block Island, Rhode Island, December 28, 1991 [PB93-910405] p 22 N94-11044

AIRCRAFT ANTENNAS
Radiation and scattering by cavity-backed antennas on a circular cylinder [NASA-CR-193409] p 136 N94-11084

AIRCRAFT COMPARTMENTS
Applications of continuous fiber reinforced thermoplastics in aircraft interiors p 18 N94-10775
Future material development trends for commercial airplane interiors p 21 N94-10792
Future needs in the development of materials for aircraft interiors and equipment p 21 N94-10794
Analytical method for water vapor collection and analysis in aircraft cabin fires [DOT/FAA/CT-TN93/33] p 22 N94-12575

AIRCRAFT CONFIGURATIONS
Proceedings of the 10th NAL Symposium on Aircraft Computational Aerodynamics: CFD Workshop on GK Airfoil and ONERA M5 Geometry [NAL-SP-20] p 10 N94-10466
Description of 3D problem: Flow analysis around ONERA model M5 configuration p 11 N94-10476
Flow analysis around ONERA model M5 configuration [PAPER-3D-1] p 11 N94-10477
Flow analysis around ONERA model M5 configuration [PAPER-3D-2] p 12 N94-10478
Flow analysis around ONERA model M5 configuration [PAPER-3D-3] p 12 N94-10479
Flow analysis around ONERA model M5 configuration [PAPER-3D-5] p 12 N94-10481
Flow analysis around ONERA model M5 configuration: Compendium of results p 12 N94-10482
NASTRAN modeling of flight test components for UH-60A airloads program test configuration [NASA-CR-193614] p 186 N94-10937
SAUNA: A system for grid generation and flow simulation using hybrid structured/unstructured grids [ARA-MEMO-370] p 154 N94-11859
Evaluation of the C/EC/KC-135 ground collision avoidance system (GCAS), Study 2 [AD-A265193] p 24 N94-11879
The modelling of aerodynamic flows by solution of the Euler equations on mixed polyhedral grids [ARA-84] p 16 N94-11888

AIRCRAFT CONSTRUCTION MATERIALS
Application of composite materials for production nacelle structures p 56 N94-10006
The application of advanced materials to aircraft nacelle structures p 57 N94-10011
Investigations on aluminium-lithium alloys for damage tolerant application p 59 N94-10023
Cost effectiveness of structural applications of fibre reinforced thermoplastics p 60 N94-10032
Structural material, manufacture, and design requirements for high-temperature fasteners for space plane technologies p 63 N94-10055
Proceedings of the International Conference for the Promotion of Advanced Fire Resistant Aircraft Interior Materials [DOT/FAA/CT-93/3] p 17 N94-10766
New thermoplastic laminating adhesives for the aircraft industry with low heat release and low smoke emission p 17 N94-10767
A new low smoke, low heat release structural foam p 17 N94-10768
Polyimide foam insulation systems: A major weight reduction and improvement in fire resistance of sidewall systems p 17 N94-10769
A polyimide foam for advanced fire resistant aircraft applications p 17 N94-10770
A repair patching system for aircraft cargo liners p 17 N94-10771
Primaset (tm): A safer material for aircraft interior applications p 18 N94-10772
A new FR water resistant acoustic insulation material for aircraft p 18 N94-10773
New technology for effective control of flammability in polyolefin fiber/textiles p 18 N94-10774
Advanced phenolic systems for aircraft interiors p 18 N94-10776
The fire properties of insulation bags, as installed and after aircraft operations p 19 N94-10778
Computer-aided molecular design of fire resistant aircraft materials p 19 N94-10779
A non-halogenated, flame retarded polycarbonate p 19 N94-10781
An investigation into aircraft fuselage fire hardening p 19 N94-10782
The OSU heat release rate test using the oxygen consumption principle p 20 N94-10784
Fire resistance and mechanical properties for phenolic prepregs p 20 N94-10786
Developments needed to expand the role of fire modeling in material fire hazard assessment p 20 N94-10787
Flammability parameters of materials: Ignition, combustion, and flame spread p 20 N94-10788
Factors that affect OSU thermal performance of aircraft interior materials p 20 N94-10789
Aircraft material fire testing and the creation of an international working group p 21 N94-10790
Future material development trends for commercial airplane interiors p 21 N94-10792
Future needs in the development of materials for aircraft interiors and equipment p 21 N94-10794
Health and safety issues for aerospace workers in the use of advanced materials p 21 N94-10795
Advanced aircraft materials research and development plan p 22 N94-10796
Thermal stability of sealants for military aircraft: Modification of polysulfide prepolymers with ether and thioether monomers [AD-A264079] p 89 N94-11107
Proceedings of the International Conference for the Promotion of Advanced Fire Resistant Aircraft Interior Materials [AD-A266057] p 22 N94-12384
Fatigue in single crystal nickel superalloys [AD-A266116] p 85 N94-12418

AIRCRAFT CONTROL
In-flight simulation of backside operating models using direct lift controller [NAL-TR-1152] p 30 N94-10734
Specification and testing for power by wire aircraft [NASA-TM-106232] p 46 N94-10765
Criteria for design of integrated flight/propulsion control systems for STOVL fighter aircraft [NASA-TP-3356] p 30 N94-11134
Physics of forebody flow control [NASA-CR-193626] p 15 N94-11195
Application of controller partitioning optimization procedure to integrated flight/propulsion control design for a STOVL aircraft [NASA-TM-106265] p 30 N94-11251
Stability in Aerospace Systems [AGARD-R-789] p 31 N94-11489
Stability analysis and aerospace vehicle dynamics p 31 N94-11491
On non-linear longitudinal stability of an aircraft in a dive in the presence of atmospheric disturbances p 31 N94-11492
Nonlinear and dynamic analysis of flight p 32 N94-11496
Decoupling of aircraft responses p 32 N94-11497
Modeling nonlinear aerodynamic loads for aircraft stability and control analysis p 32 N94-11499
Utilizing quantitative feedback theory design technique for flight control system p 32 N94-11501
Adaptive reconfigurable flight controls for high angle of attack aircraft agility p 32 N94-11502
Toward intelligent flight control p 33 N94-11503
X-29: Longitudinal instability at high angle-of-attack p 33 N94-11504
Further studies using matched filter theory and stochastic simulation for gust loads prediction [NASA-TM-109010] p 26 N94-11587

AIRCRAFT DESIGN
High temperature materials for hypersonic transport p 56 N94-10003
Investigations on aluminium-lithium alloys for damage tolerant application p 59 N94-10023
Structural material, manufacture, and design requirements for high-temperature fasteners for space plane technologies p 63 N94-10055

Applications of continuous fiber reinforced thermoplastics in aircraft interiors p 18 N94-10775

Progress in multidisciplinary design optimization at NASA Langley [NASA-TM-107754] p 318 N94-10814

Criteria for design of integrated flight/propulsion control systems for STOVL fighter aircraft [NASA-TP-3356] p 30 N94-11134

Supersonic airplane study and design [NASA-CR-193219] p 25 N94-11150

Smart structures: A technology for next generation aircraft p 27 N94-11318

The impact of active controls technology on the structural integrity of aeronautical vehicles p 27 N94-11341

Performance of traffic-alert collision avoidance (TCAS) antennas in the presence of scatterers [NASA-CR-193569] p 23 N94-11525

Idea of underground airplane p 27 N94-12630

AIRCRAFT DETECTION

Improved Many-On-Many ROUTE software description [DE93-013961] p 334 N94-12608

AIRCRAFT ENGINES

A Recommended Methodology for Quantifying NDE/NDI Based on Aircraft Engine Experience [AGARD-LS-190] p 28 N94-11022

Application of controller partitioning optimization procedure to integrated flight/propulsion control design for a STOVL aircraft [NASA-TM-106265] p 30 N94-11251

Advanced control for airbreathing engines, volume 1: Pratt and Whitney [NASA-CR-189203] p 29 N94-12270

Advanced control for airbreathing engines, volume 2: General Electric aircraft engines [NASA-CR-189204] p 29 N94-12271

Advanced controls for airbreathing engines, volume 3: Allison gas turbine [NASA-CR-189205] p 29 N94-12272

AIRCRAFT EQUIPMENT

The radar eye blinded: The USAF and electronic warfare, 1945-1955 [AD-A265494] p 132 N94-10497

Method of reducing drag in aerodynamic systems [NASA-CASE-LEW-14791-1] p 12 N94-10672

AIRCRAFT FUELS

Advanced diagnostics for in situ measurement of particle formation and deposition in thermally stressed jet fuels [DE93-009798] p 98 N94-11366

A novel test method for fuel thermal stability [AD-A265853] p 99 N94-12275

Advanced thermally stable coal-derived jet fuels: Compositional factors affecting thermal degradation of jet fuels [AD-A265842] p 99 N94-12282

AIRCRAFT GUIDANCE

Toward intelligent flight control p 33 N94-11503

AIRCRAFT HAZARDS

Lee waves: Benign and malignant [NASA-CR-186024] p 283 N94-10725

Practical hazard assessment: An approach to the fire safety p 20 N94-10785

Developments needed to expand the role of fire modeling in material fire hazard assessment p 20 N94-10787

Analytical method for water vapor collection and analysis in aircraft cabin fires [DOT/FAA/CT-TN93/33] p 22 N94-12575

AIRCRAFT ICING

A preliminary study on ice shape tracing with a laser light sheet [NASA-TM-105964] p 174 N94-11132

AIRCRAFT INSTRUMENTS

A C-band wind scatterometer model derived from the data obtained during the ERS-1 calibration/validation campaign p 233 N94-11711

AIRCRAFT LANDING

The Memphis Precision Runway Monitor Program Instrument Landing System final approach study [AD-A266035] p 23 N94-11103

Active landing gear control for improved ride quality during ground roll p 27 N94-11345

AIRCRAFT MAINTENANCE

Environmentally Safe and Effective Processes for Paint Removal [AGARD-R-791] p 126 N94-10613

Paint removal activities in the US Navy p 126 N94-10614

Paint removal activities in Canada p 126 N94-10615

Procedures without danger to the environment and efficiency (PSDEE) for the removal of paint. Point on the French activities concerning the removal of paint p 126 N94-10616

Paint removal activities in Germany p 126 N94-10617

The development of alternative paint removal techniques in the RAF p 126 N94-10618

Operational aspects of F.16 plastic media blasting, as carried out by Fokker Aircraft Services p 126 N94-10619

Use of robots for aircraft dry stripping via plastic media blasting p 127 N94-10620

German Air Forces experiences with plastic media blasting and future requirements p 127 N94-10621

Plastic media blasting activities at Hill Air Force Base p 127 N94-10622

Large Aircraft Robotic Paint Stripping (LARPS) system and the high pressure water process p 127 N94-10623

Automated Laser Paint Stripping (ALPS) update p 127 N94-10624

Aquastrip (tm): An innovative paint removal technology p 127 N94-10625

Paint removal and surface cleaning using ice particles p 128 N94-10626

Paint removal using wheat starch blast media p 128 N94-10627

IATA taskforce: Paintstripping p 128 N94-10628

Selectively strippable paint schemes p 128 N94-10629

A repair patching system for aircraft cargo liners p 17 N94-10771

A Recommended Methodology for Quantifying NDE/NDI Based on Aircraft Engine Experience [AGARD-LS-190] p 28 N94-11022

Smart structures: A technology for next generation aircraft p 27 N94-11318

In-flight aircraft structure health monitoring based on smart structures technology p 22 N94-11333

AIRCRAFT MANEUVERS

Physics of forebody flow control [NASA-CR-193626] p 15 N94-11195

Adaptive reconfigurable flight controls for high angle of attack aircraft agility p 32 N94-11502

A comparison of head-up and head-down display formats during instrument flying tasks [AD-A266140] p 316 N94-11642

AIRCRAFT MODELS

NASTRAN modeling of flight test components for UH-60A airloads program test configuration [NASA-CR-193614] p 186 N94-10937

On non-linear longitudinal stability of an aircraft in a dive in the presence of atmospheric disturbances p 31 N94-11492

Nonlinear and dynamic analysis of flight p 32 N94-11496

Adaptive reconfigurable flight controls for high angle of attack aircraft agility p 32 N94-11502

Lift enhancement of a wing/strake using pneumatic blowing [AD-A265074] p 26 N94-11872

AIRCRAFT NOISE

Perpendicular blade vortex interaction and its implications for helicopter noise prediction: Wave-number frequency spectra in a trailing vortex for BWI noise prediction [NASA-CR-193623] p 357 N94-10752

AIRCRAFT PERFORMANCE

Nonlinear stability and control study of highly maneuverable high performance aircraft [NASA-CR-193480] p 25 N94-10344

Progress in multidisciplinary design optimization at NASA Langley [NASA-TM-107754] p 318 N94-10814

The Memphis Precision Runway Monitor Program Instrument Landing System final approach study [AD-A266035] p 23 N94-11103

Preliminary supersonic flight test evaluation of performance seeking control [NASA-TM-4494] p 28 N94-11205

Comparing aircraft agility using mahalanobis distances [PB93-175446] p 26 N94-11464

Decoupling of aircraft responses p 32 N94-11497

Stability model of the atmosphere p 32 N94-11500

AIRCRAFT PILOTS

Aviation accident risk for airmen with aphakia and artificial lens implants [DOT/FAA/AM-93/11] p 303 N94-10813

Correlation of HGU-56/P aircrew helmet fitting with head anthropometric measurements [AD-A264988] p 315 N94-11291

A prototype urine collection device for female aircrew p 317 N94-11549

Aviators, air combat, and combat stress: An Air F orce commander's primer [AD-A265083] p 313 N94-11867

US civil airmen statistics for calendar year 1991 [AD-A266085] p 2 N94-12412

The aging military aviator: A review and annotated bibliography [AD-A265341] p 311 N94-12423

AIRCRAFT SAFETY

Proceedings of the International Conference for the Promotion of Advanced Fire Resistant Aircraft Interior Materials [DOT/FAA/CT-93/3] p 17 N94-10766

An investigation into aircraft fuselage fire hardening p 19 N94-10782

Practical hazard assessment: An approach to the fire safety p 20 N94-10785

Aircraft material fire testing and the creation of an international working group p 21 N94-10790

Development of a hypermedia knowledge base of aircraft fire safety regulations p 21 N94-10793

Advanced aircraft materials research and development plan p 22 N94-10796

The future of aircraft cabin fire safety p 22 N94-10797

Aircraft Accident/Incident Summary Report: Loss of control. Business Express, Inc., Beechcraft 1900C N811BE near Block Island, Rhode Island, December 28, 1991 [PB93-910405] p 22 N94-11044

Impact of shutting down en route primary radars within CONUS interior [DOT-VNTSC-FAA-93-1] p 23 N94-11626

Proceedings of the International Conference for the Promotion of Advanced Fire Resistant Aircraft Interior Materials [AD-A266057] p 22 N94-12384

Analytical method for water vapor collection and analysis in aircraft cabin fires [DOT/FAA/CT-TN93/33] p 22 N94-12575

AIRCRAFT STABILITY

Nonlinear stability and control study of highly maneuverable high performance aircraft [NASA-CR-193480] p 25 N94-10344

Aerodynamic model identification of quiet STOL experimental aircraft ASKA from dynamic flight test data [DE93-767967] p 25 N94-10728

Physics of forebody flow control [NASA-CR-193626] p 15 N94-11195

Stability in Aerospace Systems [AGARD-R-789] p 31 N94-11489

Stability analysis and aerospace vehicle dynamics p 31 N94-11491

On non-linear longitudinal stability of an aircraft in a dive in the presence of atmospheric disturbances p 31 N94-11492

Decoupling of aircraft responses p 32 N94-11497

Modeling nonlinear aerodynamic loads for aircraft stability and control analysis p 32 N94-11499

Stability model of the atmosphere p 32 N94-11500

X-29: Longitudinal instability at high angle-of-attack p 33 N94-11504

AIRCRAFT STRUCTURES

The application of advanced materials to aircraft nacelle structures p 57 N94-10011

Investigations on aluminium-lithium alloys for damage tolerant application p 59 N94-10023

Smart Structures for Aircraft and Spacecraft [AGARD-CP-531] p 68 N94-11317

Smart structures: A technology for next generation aircraft p 27 N94-11318

In-flight aircraft structure health monitoring based on smart structures technology p 22 N94-11333

Structural health monitoring using embedded fibre optic sensors p 22 N94-11334

Fiber-optic sensor systems for measuring strain and the detection of acoustic emissions in smart structures p 71 N94-11337

Aircraft smart structures research in the USAF Wright Laboratory p 72 N94-11343

AIRCRAFT WAKES

Simulated wake characteristics of tapered annular wings by a discrete vortex method [NAL-TR-1156] p 13 N94-10855

AIRFOILS

Nonlinear aspects of transonic aeroelasticity p 2 N94-10357

Proceedings of the 10th NAL Symposium on Aircraft Computational Aerodynamics: CFD Workshop on GK Airfoil and ONERA M5 Geometry [NAL-SP-20] p 10 N94-10466

Description of 2D problem: Aerodynamic analysis of Garabedian-Korn 75-06-12 airfoil p 10 N94-10467

Aerodynamic characteristics analysis of Garabedian-Korn 75-06-12 airfoil [PAPER-2D-2] p 10 N94-10468

Aerodynamic characteristics analysis of Garabedian-Korn 75-06-12 airfoil [PAPER-2D-3] p 10 N94-10469

Aerodynamic characteristics analysis of Garabedian-Korn 75-06-12 airfoil: Computation using q-omega 2 equation turbulence model [PAPER-2D-4] p 10 N94-10470

Aerodynamic characteristics analysis of Garabedian-Korn 75-06-12 airfoils: Computation using Baldwin-Lomax turbulence model [PAPER-2D-5] p 11 N94-10471
Aerodynamic characteristics analysis of Garabedian-Korn 75-06-12 aircraft [PAPER-2D-7] p 11 N94-10472
Aerodynamic characteristics analysis of Garabedian-Korn 75-06-12 airfoil [PAPER-2D-8] p 11 N94-10473
Aerodynamic characteristics analysis of Garabedian-Korn 75-06-12 airfoil [PAPER-2D-9] p 11 N94-10474
Aerodynamic characteristics analysis of Garabedian-Korn 75-06-12 airfoil: Compendium of results p 11 N94-10475
Description of 3D problem: Flow analysis around ONERA model M5 configuration p 11 N94-10476
New aerodynamic information obtained from the solution of the inverse problem for aerofoils [NAL-TR-1172] p 14 N94-10860
Nonlinear aspects of transonic aeroelasticity [UTIAS-RN-345] p 15 N94-11857
Unsteady flow past a NACA 0012 airfoil pitching at constant rates [AD-A265159] p 16 N94-11889

AIRLINE OPERATIONS
A real-time spoken-language system for interactive problem solving [AD-A266046] p 324 N94-11104
Federal Aviation Administration aviation forecasts [AD-A265611] p 2 N94-12578

AIRPORTS
The Memphis Precision Runway Monitor Program Instrument Landing System final approach study [AD-A266035] p 23 N94-11103
Federal Aviation Administration aviation forecasts [AD-A265611] p 2 N94-12578

ALASKA
Applications of ERS-1 SAR data for analyzing riverine and coastal processes and geomorphology p 254 N94-12528

ALBEDO
Studies of the net surface radiative flux from satellite radiances during FIFE [NASA-CR-193150] p 230 N94-10953
A simple model of clastic sediments on Mars p 460 N94-12155
Spectral mixing models of S-Type asteroids p 431 N94-12164
Chondrites, S asteroids, and space weathering: Thumping noises from the coffin? p 433 N94-12244

ALCOHOLS
Synthesis and thermal evolution of structure in alkoxide-derived niobium pentoxide gels [NASA-TM-106259] p 90 N94-11257

ALERTNESS
Locus coeruleus, vigilance, and stress: Brain mechanisms of adaptive behavioral responsiveness [AD-A265657] p 302 N94-12441

ALGAE
An algorithm for the detection of mucilage (green slime) in the Adriatic Sea p 191 N94-11900
Information capability of NOAA-AVHRR data for monitoring oceanographic and atmospheric pollution p 214 N94-12677
Mapping of high density area of benthic diatom in Ariake Sea p 222 N94-12720

ALGEBRA
Finite state machine microarchitecture transformations described with relational algebra [MEMO-INF-92-63] p 319 N94-10278
An algebraic approach to incomparable families of formal languages [MEMO-INF-92-82] p 342 N94-10279
Generating function for Clebsch-Gordan coefficients of the SU(sub q)(2) quantum algebra [DE93-613093] p 349 N94-10633
Three-dimensional N = 4 extended supersymmetrical quantum mechanics [DE93-621421] p 412 N94-11164

ALGORITHMS
A reliable stability test for exponential polynomials [MEMO-COSOR-92-48] p 341 N94-10168
Numerical simulation of multi-droplet hydrodynamic interactions in liquid dispersions p 114 N94-10182
A simplicial approach to integer programming [REPT-93-06] p 322 N94-10355
Object recognition in industrial environment by means of tactile sensor [ITN-93-85200] p 178 N94-10393
Algorithms for the maximum clique problem [MEMO-1101] p 322 N94-10419
Unsupervised splitting rules for neural tree classifiers [AD-A264961] p 338 N94-10487
Optimization algorithms for integer networks with side constraints for application in routing and scheduling [AD-A265254] p 322 N94-10492
A window least squares algorithm for statistical noise smoothing of 2D-ACAR data [DE93-613828] p 395 N94-10537
A new HMM learning algorithm for continuous speech recognition [NHK-SERIAL-413] p 132 N94-10560
Sensor abstractions to support many-robot systems [AD-A265907] p 180 N94-10803
Monte Carlo algorithms in simulation of 2beta-decay and penetration of electrons through matter [DE93-617741] p 364 N94-10837
Stability by linear processes [NASA-CR-194131] p 323 N94-10862
Finding minimum-quotient cuts in planar graphs [DE93-011675] p 344 N94-10961
Time scale algorithms for an inhomogeneous group of atomic clocks p 356 N94-10998
Fast trigger algorithm for B-events selection [DE93-621452] p 365 N94-11089
Object oriented implementation of adaptive mesh refinement algorithms [DE93-011885] p 325 N94-11112
Node assignment in heterogeneous computing [NASA-CR-4534] p 142 N94-11131
A formally verified algorithm for interactive consistency under a hybrid fault model [NASA-CR-4527] p 326 N94-11188
Necessary conditions for the optimality of variable rate residual vector quantizers [NASA-CR-193730] p 326 N94-11197
Optimisation methods for solving separable nonlinear least squares problems [ISVR-TR-219] p 345 N94-11217
Fuzzification of ASAT's rule based aimpoint selection [AD-A266068] p 43 N94-11223
An improved material interface reconstruction algorithm for Eulerian codes [DE93-011679] p 326 N94-11226
Resolution for Lanczos and Paige-Saunders inverses in tomography [DE93-012312] p 327 N94-11240
Adaptive algorithms for use with digital filters in vibration control p 71 N94-11338
Development and evaluation of a predictive algorithm for telerobotic task complexity p 341 N94-11562
Computational algorithms or identification of distributed parameter systems [AD-A265252] p 331 N94-11680
Evaluation of two January - June 1992 ERS-1 AMI wind vector data sets p 235 N94-11724
An algorithm for the detection of mucilage (green slime) in the Adriatic Sea p 191 N94-11900
Remote sensing for numerical modelling of radiative transfer processes in ocean environment p 204 N94-11973
Atmospheric correction plans for SeaWiFS p 204 N94-11975
Implications of aerosol retrieval and atmospheric correction in remote sensing p 205 N94-11978
The upwelling radiation at the top of the atmosphere in coastal region p 205 N94-11981
A new heuristic for set covering problems [INPE-5471-TDI/502] p 333 N94-12358
An optoelectronic graphics display processor [AD-A266011] p 171 N94-12391
Worldwide map of rainfall amount over the ocean derived from passive microwave radiometer p 211 N94-12663
Delineation of mesoscale features of ocean on satellite IR image p 214 N94-12675
The warm eddy detection from NOAA/AVHRR thermal images using the Hough transformation p 220 N94-12713
Optimum selection of spectral channels in the problem of remote sensing of phytoplankton concentration in ocean water p 223 N94-12726
Coupled numerical model for altimetric data assimilation and velocity field analysis p 227 N94-12752
The algorithm of primary production determination p 228 N94-12761
Non-image visible polarization remote sensing of the ocean p 229 N94-12762

ALIGNMENT
Analysis of the alignment of a Schlieren system for tele-operation p 111 N94-10140

ALKALI METALS
Alkali metal for ultraviolet band-pass filter [NASA-CASE-NPO-18433-1-CU] p 381 N94-10657

ALKALIES
The correlation of alkalis and aluminum during high-temperature volatilization of albite and nepheline p 81 N94-12214

ALKALINE BATTERIES
Aluminum based alkaline battery [AD-D015775] p 140 N94-10390

ALKYLATION
Studies in bioorganic chemistry [AD-A265532] p 55 N94-12011

ALLOYING
The effect of processing on the microstructure and tensile properties of a (gamma)-TiAl based alloy [DE93-013221] p 84 N94-11488

ALLOYS
Solidification in immiscible systems: The influence of processing conditions on resulting microstructures p 112 N94-10174
Coupled growth of cells and bubbles in directional solidification of succinonitrile-acetone alloys p 118 N94-10206

ALLUVIUM
Classification of Martian deltas p 470 N94-12207

ALPHA DECAY
Study of the atmospheric chemistry of radon progeny in laboratory and real indoor atmospheres [DE93-012236] p 266 N94-11671

ALPHA PARTICLES
Helium transport scaling law studies [DE93-013487] p 393 N94-11513

ALTERNATING CURRENT
Power losses of a type 2 superconducting slab of arbitrary thickness in the presence of alternating current conductors [DE93-617892] p 396 N94-10716
Large amplitude shape oscillations in a mercury drop using a drop tower [DE93-767972] p 125 N94-10730

ALTERNATING DIRECTION IMPLICIT METHODS
Aerodynamic characteristics analysis of Garabedian-Korn 75-06-12 airfoil [PAPER-2D-9] p 11 N94-10474
Flow analysis around ONERA model M5 configuration [PAPER-3D-1] p 11 N94-10477
Flow analysis around ONERA model M5 configuration [PAPER-3D-5] p 12 N94-10481

ALTIMETERS
Using transponders with the ERS-1 altimeter to measure orbit altitude to +/- 3 cm p 244 N94-11785
Use of ERS-1 wind and wave products in operational meteorology p 250 N94-12502

ALTIMETRY
Removal of orbital error and the local geoid effects from ERS-1 altimeter data p 242 N94-11770
ERS-1 precise orbits and altimetry analysis p 242 N94-11771
Characteristics of arachnoids from Magellan data p 469 N94-12204

ALTITUDE
A method for calculating exact geodetic latitude and altitude [AD-A265783] p 229 N94-10417
Arterial gas emboli in altitude-induced decompression sickness p 312 N94-11543

ALTITUDE SIMULATION
Use of ultrasound in altitude decompression modeling p 317 N94-11540
Arterial gas emboli in altitude-induced decompression sickness p 312 N94-11543

ALUMINIDES
The microstructure and mechanical properties of hot worked FeAl intermetallic alloys p 58 N94-10020
Interface reactions of (Ni3Al) ribbons/Al-MMC in ground preparation as preliminary test for microgravity experiments p 123 N94-10237
Hydrogen partitioning and transport in titanium aluminides [NASA-CR-194117] p 76 N94-10713
Production of reactive sintered nickel aluminide [DE93-014434] p 83 N94-11127
Processing, properties, and wear resistance of aluminides [DE93-012186] p 83 N94-11141

ALUMINUM
Interface reactions of (Ni3Al) ribbons/Al-MMC in ground preparation as preliminary test for microgravity experiments p 123 N94-10237
Enhanced stability of magic clusters: A case study of icosahedric Al(sub 12)X, X=B, Al, Ga, C, Si, Ge, Ti, As [DE93-613644] p 395 N94-10386
Aluminum based alkaline battery [AD-D015775] p 140 N94-10390
Dimensional scaling for impact cratering and perforation [NASA-CR-188259] p 42 N94-10665
Advanced zinc phosphate conversion and pre-ceramic polymetallosiloxane coatings for corrosion protection of steel and aluminum, and characteristics of polyphenyletheretherketone-based materials [DE93-008717] p 88 N94-10891

Aluminum and membrane channels
[AD-A265241] p 300 N94-11020

Development of deterministic transport methods for low energy neutrons for shielding in space
[NASA-CR-194172] p 366 N94-11199

Aluminum-phosphorus chemistry: Preparation and structural characterization of (Et2AlP(SiMe3)2)2, Et(Cl)2Al(dot)P(SiMe3)3, and i-Bu2(Cl)Al(dot)P(SiMe3)3
[AD-A265268] p 78 N94-11683

Modelling hypervelocity impacts into aluminum structures based on LDEF data p 190 N94-12178

ALUMINUM ALLOYS

Spinforming characteristics of a net shape forming process p 56 N94-10004

Comparison of Al-Fe alloys produced by PFC and USGA techniques p 58 N94-10019

Aluminium-lithium forgings: Properties and potential satellite applications p 58 N94-10021

Mechanical and fatigue properties of fibre reinforced aluminium-lithium alloy and aluminium-lithium MMC based laminates p 58 N94-10022

Investigations on aluminium-lithium alloys for damage tolerant application p 59 N94-10023

SPF/DB: A manufacturing technique for lightweight structures p 59 N94-10026

Aluminum-beryllium alloys for aerospace applications
p 60 N94-10029

Design of inspection and acceptance test methodology for TIG welded aluminum-alloy bracket for camera housings for IRS-1A space craft and executing it
p 61 N94-10037

Spin-rolling, welding, and heat treatment of aluminium 2219 for Ariane 5 GAM high pressure vessel liners
p 62 N94-10045

Stress relaxation forming of Ariane 5 front skirt outer skin panels p 62 N94-10046

Structure and properties of an RS Al-Si-Ni-Mn-Zr alloy for high temperature applications p 64 N94-10063

TEM study of a space processed Al-Al2O3 metallic composite p 75 N94-10186

EUSO-D2-experiment: Unidirectional solidification with quenching of an AlSi11 alloy p 86 N94-10199

On problem about nature of Portevin-Le Chatelier effect in irradiated aluminium alloys
[DE93-617200] p 82 N94-10842

High temperature stability, interface bonding, and mechanical behavior in (beta)-NiAl and Ni3Al matrix composites with reinforcements modified by ion beam enhanced deposition
[DE93-013977] p 398 N94-11115

NiAl alloys for structural uses
[NASA-CR-194113] p 85 N94-12447

ALUMINUM CARBIDES

The reaction between titanium carbide and aluminium carbide in liquid aluminium; a microgravity study
p 123 N94-10238

ALUMINUM COATINGS

Space environmental effects on the integrity of chromic acid anodized coatings
[NASA-CR-191468] p 55 N94-10947

ALUMINUM COMPOUNDS

Aluminum and membrane channels
[AD-A265241] p 300 N94-11020

ALUMINUM ISOTOPES

Measurements of cosmogenic nuclides in lunar rock 64455 p 437 N94-12033

Isotopic and trace element characteristics of an unusual refractory inclusion from Essebi p 471 N94-12212

ALUMINUM NITRIDES

High temperature stability, interface bonding, and mechanical behavior in (beta)-NiAl and Ni3Al matrix composites with reinforcements modified by ion beam enhanced deposition
[DE93-013977] p 398 N94-11115

ALUMINUM OXIDES

New processes for lightweight ceramic matrix composites p 61 N94-10043

Particle attraction effects on the centrifugal casting and extrusion of alumina
[DE93-011559] p 82 N94-10957

The stability of hibonite and other aluminous phases in silicate melts: Implications for the origin of hibonite-bearing inclusions p 80 N94-12052

Prediction of alumina penetration
[DE93-014017] p 95 N94-12610

ALUMINUM SILICATES

Vaporization by shock loading of albite, jadeite, and pyrex glass: Experimental study p 97 N94-12039

In-situ crystallization of silicate glass films deposited on alpha- Al2O3
[DE93-012969] p 95 N94-12596

ALUMINUM 26

Search for effects of a supernova explosion 30 to 40 thousand years ago in chondrites p 428 N94-12022

ALUMINUM 27

Monochromator SP-017. The results of the first experiments
[DE93-617463] p 372 N94-10849

ALVEOLI

Evaluation of medical treatments to increase survival of ebullism in guinea pigs p 302 N94-11548

AMBIENCE

Preliminary analysis of the FLIP array data from the NOBS experiment
[AD-A265911] p 289 N94-12349

AMINES

Resist materials design: Base-catalyzed chemical amplification
[AD-A265286] p 145 N94-11819

AMINO ACIDS

A reexamination of amino acids in lunar soil
p 452 N94-12109

AMORPHOUS MATERIALS

An ultralight carbon-carbon composite with amorphous matrix p 61 N94-10042

Radiation-induced aperiodicity in irradiated ceramics
[DE93-013335] p 91 N94-11698

Changes in Hawaiian palagonite FE mineralogy associated with thermal alteration: Implications for Mars
p 281 N94-12055

Properties of interfacial tribo-films
[AD-A265591] p 182 N94-12374

The 13C and 15N solid-state NMR of copolymers of nylon 6 and 7: Observation of a stable pseudohexagonal phase
[AD-A265799] p 94 N94-12381

AMORPHOUS SILICON

Thermal-optical switching of a silicon based interference filter
[AD-A265152] p 174 N94-11095

Polyimide based amorphous silicon solar modules
p 49 N94-11390

Measurement and modeling of the stability of hydrogenated amorphous silicon solar cells and films after intense illumination p 263 N94-11638

AMPLIFICATION

Method and apparatus for polarization-maintaining fiber optical amplification with orthogonal polarization output
[AD-D015756] p 374 N94-10372

Photon number amplification/duplication through parametric conversion p 376 N94-10572

Multiple laser beam combining and phasing using closed-loop control
[DE93-009830] p 175 N94-11283

Development of microstrip gas chambers with multi-chip technology
[DE93-753169] p 367 N94-11509

Resist materials design: Base-catalyzed chemical amplification
[AD-A265286] p 145 N94-11819

AMPLIFIER DESIGN

Wide band 140 GHz TWTA p 132 N94-10514

AMPLITUDE DISTRIBUTION ANALYSIS

Performance of traffic-alert collision avoidance (TCAS) antennas in the presence of scatterers
[NASA-CR-193569] p 23 N94-11525

AMPLITUDES

Decay interaction of bulk and surface Langmuir waves
[DE93-617843] p 393 N94-11477

AMPOULES

Concept and design of ampoule for melt growth of gallium arsenide in first mission of space flyer unit
p 107 N94-10115

ANALOG CIRCUITS

Parametric study of diffusion-enhancement networks for spatiotemporal grouping in real-time artificial vision
[AD-A265065] p 331 N94-11652

Superconducting SQUID amplifiers for IR detectors and other applications, phase 2
[AD-A265447] p 145 N94-12333

ANALOG TO DIGITAL CONVERTERS

GaAs sigma-delta modulator modeling for Analog to Digital Converters (ADC's)
[AD-A263419] p 144 N94-11516

ANALOGIES

Similarity of the leading contributions to the self-energy and the thermodynamics in two- and three-dimensional Fermi Liquids
[DE93-012673] p 412 N94-11162

ANALYTIC FUNCTIONS

The structure of Hilbert flag varieties
[MEMO-1095] p 348 N94-10272

Operator substitution
[MEMO-COSOR-92-51] p 343 N94-10867

ANALYTICAL CHEMISTRY

Quality assurance for environmental chemistry: 1991, volume 2
[DE93-011792] p 272 N94-12780

ANEMOMETERS

Calibration of anemometers at low speed by means of towing carriage p 164 N94-12619

ANGLE OF ATTACK

Aerodynamic characteristics analysis of Garabedian-Korn 75-06-12 airfoil
[PAPER-2D-8] p 11 N94-10473

Physics of forebody flow control
[NASA-CR-193626] p 15 N94-11195

Modeling nonlinear aerodynamic loads for aircraft stability and control analysis p 32 N94-11499

Adaptive reconfigurable flight controls for high angle of attack aircraft agility p 32 N94-11502

X-29: Longitudinal instability at high angle-of-attack
p 33 N94-11504

Lift enhancement of a wing/strake using pneumatic blowing
[AD-A265074] p 26 N94-11872

ANGLES (GEOMETRY)

Needs for super-smooth surfaces
[DE93-012482] p 382 N94-11242

Fundamental studies of radar scattering from water surfaces: The Lake Washington experiment
[NASA-CR-194030] p 139 N94-12778

ANGULAR ACCELERATION

SWIRL as a means of liquid management in low gravity
[NASA-CR-4545] p 412 N94-11523

ANGULAR CORRELATION

Convergent close-coupling calculations of electron-hydrogen scattering
[DE93-610049] p 360 N94-10328

A window least squares algorithm for statistical noise smoothing of 2D-ACAR data
[DE93-613828] p 395 N94-10537

ANGULAR DISTRIBUTION

Monte Carlo algorithms in simulation of 2beta-decay and penetration of electrons through matter
[DE93-617741] p 364 N94-10837

ANGULAR MOMENTUM

Calculation of spin-dependent observables in electron-sodium scattering using the coupled-channel optical method
[DE93-610050] p 360 N94-10329

Spin-dependent observables in electron-sodium scattering calculated using the coupled-channel optical method
[DE93-610073] p 360 N94-10331

On local frame fields and fermion dynamics in space with nontrivial topologies
[DE93-617657] p 349 N94-10548

Quantum entropy and uncertainty for two-mode squeezed, coherent and intelligent spin states
p 377 N94-10586

Wigner functions for nonclassical states of a collection of two-level atoms p 379 N94-10603

Accretion disk viscosity and internal waves in disks
p 153 N94-11615

ANGULAR RESOLUTION

The superresolution effect observed through a random medium p 136 N94-11069

ANGULAR VELOCITY

Monte Carlo algorithms in simulation of 2beta-decay and penetration of electrons through matter
[DE93-617741] p 364 N94-10837

Instantaneous engine frictional torque: Its components and piston assembly friction
[DE93-011639] p 182 N94-11625

Precession of Uranus and Neptune and their magnetic field p 473 N94-12222

Laboratory studies on the velocity of fragments from impact disruptions p 189 N94-12359

ANHYDRIDES

Unequilibrated, equilibrated, and reduced aggregates in anhydrous interplanetary dust particles
p 429 N94-12098

ANISOTROPIC PLATES

Ultrasonic wave interaction with advanced complex materials for nondestructive evaluation applications
[AD-A265704] p 74 N94-12401

ANISOTROPY

From the Weyl theory to a theory of locally anisotropic space-time
[DE92-644734] p 410 N94-10535

Texture analysis of high Tc superconductors
p 399 N94-11314

Elastic deformations and sound in anisotrope superconductors near critical temperature
[DE93-620636] p 188 N94-11364

Stability and dynamics of spatio-temporal structures
[DE93-011374] p 401 N94-11610

Highly anisotropic but nodeless gap from a valence-fluctuation pairing mechanism
[DE93-010738] p 401 N94-11646

The physics of pattern formation of liquid interfaces
[DE93-013333] p 154 N94-11814

Synthesis and magnetic properties of novel La*2-x*M*x*CuO*4 equals y* compositions (La equals La, Pr, Nd, Sm, Eu, Cd; M equals Ca, Sr, Ba; O (less than or equal) x 0.2; -0.5 (less than or equal) y (less than or equal) 0.5) [DE93-011359] p 403 N94-12363

Examination of the surface second harmonic response at infrared wavelengths [AD-A265206] p 403 N94-12371

Polar mesospheric waves and structure [AD-A265360] p 279 N94-12561

ANNEALING

Kinetics of high concentration arsenic deactivation at moderate to low temperatures [DE93-013349] p 395 N94-10516

The influence of irradiation conditions, type, and concentration of impurities on radiation defects characteristics in indium antimonide under electron irradiation [DE93-617201] p 397 N94-10843

Radiation defect production in InAs crystals under electron irradiation [DE93-617202] p 397 N94-10845

A detailed study of the photo-injection annealing of thermally diffused InP solar cells p 48 N94-11381

High temperature annealing of minority carrier traps in irradiated MOCVD n(+)p InP solar cell junctions p 48 N94-11382

Results of some initial space qualification testing on triple junction a-Si and CuInSe2 thin film solar cells p 50 N94-11392

Chondrite thermal histories from Low-CA pyroxene microstructures: Autometamorphism versus prograde metamorphism revisited p 429 N94-12105

Diffusion length damage coefficient and annealing studies in proton-irradiated InP [NASA-TM-106262] p 404 N94-12430

ANNIHILATION REACTIONS

A window least squares algorithm for statistical noise smoothing of 2D-ACAR data [DE93-613828] p 395 N94-10537

Squeezed colour states in gluon jet p 379 N94-10599

Creation and annihilation of solitons in nonlinear integrable systems [DE93-621379] p 365 N94-11078

ANNUAL VARIATIONS

Statistical study on the regional and seasonal distribution of fog in the far east region by using GMS imagery p 190 N94-11082

Greenland Sea observations p 239 N94-11752

Sea ice radar signatures from ERS-1 SAR during late Summer and Fall in the Beaufort and Chukchi Seas p 240 N94-11756

The seasonal Sea Ice Monitoring and Modelling Site (SIMMS): Using ERS-1 in climate research p 240 N94-11758

One-year mooring of an ADCP in the central region of the Kuroshio west of Okinawa p 194 N94-11913

Seasonal changes of phytoplankton distributions in the Northwest Pacific detected by Coastal Zone Color Scanner p 200 N94-11948

Particle dynamics in the western subarctic Pacific: Implications from CZCS imagery p 200 N94-11950

Availability of wind field over the North Pacific derived from data on ships-of-opportunity and analysis of long-term variabilities p 202 N94-11962

Roles of the NEC and MC in the formation and evolution of the Equatorial Pacific Warm Pool p 206 N94-11990

SSMI wind speed variability over the Pacific Ocean p 207 N94-12637

Principal oscillation pattern analysis of sea level variations in the tropical Pacific measured by the GEOSAT altimeter p 209 N94-12646

Pacific rim sea ice as observed with the NIMBUS-7 SMMR p 210 N94-12651

The seasonal change of phytoplankton size distribution using optical fiber sensor p 210 N94-12656

Primary productivity in the Oyashio area in the spring and summer of 1990 p 211 N94-12658

The phytoplankton bloom in the Kinu-ura Bay, Japan in the rainy season p 211 N94-12660

A study of front dynamics off northeastern Taiwan based on the NOAA-AVHRR satellite remote sensing data p 215 N94-12684

Satellite thermal variations of Kuroshio in relation to storm floods p 215 N94-12685

Observation of cold coastal water with high turbidity around the southwestern tip of Korean Peninsula p 216 N94-12689

Seasonal variability of surface ocean color in the Omura Bay using multitemporal LANDSAT-5 TM data p 218 N94-12698

Estimation of areal evapotranspiration using LANDSAT TM data: Kitami City, Hokkaido, Japan p 219 N94-12703

Coastal upwelling monitored by satellite data: Methodologies and results p 220 N94-12712

High biological production of the tidal mixing zones on Japan Sea shelf p 228 N94-12758

Model of Kuroshio region circulation p 229 N94-12765

ANNULAR FLOW

Laser anemometer measurements and computations for transonic flow conditions in an annular cascade of high turning core turbine vanes [NASA-TP-3383] p 15 N94-11133

ANODES

Aluminum based alkaline battery [AD-D015775] p 140 N94-10390

ANODIZING

Space environmental effects on the integrity of chromic acid anodized coatings [NASA-CR-191468] p 55 N94-10947

ANOMALIES

On the importance of mesoscale potential vorticity anomalies and topographic forcing during cyclone redevelopment across the Appalachians: A GALE case study p 284 N94-10822

Special investigation report: Commercial space launch incident, launch procedure anomaly orbital sciences corporation PEGASUS/SCD-1, 80 nautical miles east of Cape Canaveral, Florida, February 9, 1993 [PB93-917003] p 40 N94-11893

Westward propagation of sea surface anomalies in the western North Pacific as seen by the altimeter and radiometer p 198 N94-11941

Sea surface temperature anomalies in the Arabian Sea p 206 N94-11988

Variability of sea level and sea surface temperature anomalies in the equatorial Pacific p 208 N94-12640

Measurement of eddy structure and movement in the north-east Pacific with the GEOSAT altimeter p 209 N94-12647

ANOMALOUS TEMPERATURE ZONES

Sea surface temperature anomalies in the Arabian Sea p 206 N94-11988

ANTARCTIC OCEAN

Comparisons of ERS-1 altimeter height data and the Fine Resolution Antarctic Model (FRAM) p 235 N94-11725

ANTARCTIC REGIONS

Study of the surface circulation to the North of Bransfield Strait, Antarctica [INPE-5472-TDI/503] p 288 N94-11200

Signatures of Antarctic firn by means of ERS-1 AMI and by field measurements p 237 N94-11737

Analysis of ERS-1 altimeter data over the polar ice sheets p 237 N94-11738

Some results of the derivation of ice sheet elevations in Antarctica from ERS-1 altimeter data p 237 N94-11739

Utilisation of ERS-1 data for mapping of Antarctica p 237 N94-11740

Preliminary evaluation of ERS-1 altimetry over Filchner-Ronne Ice Shelf, Antarctica p 238 N94-11742

Validating the UK-PAF land ice product surface elevation p 244 N94-11780

A new carbon-rich phase (COPS) in Antarctic micrometeorites p 432 N94-12233

Facts about the US Antarctic program [NSF-92-134] p 279 N94-12568

ANTENNA ARRAYS

An approach to high precision antenna structures by a CFRP core sandwich concept p 57 N94-10008

Multiple Antenna Implementation System (MAntIS) [DE93-012515] p 131 N94-10270

Wideband beamforming for a sparse nonuniform spaced sensor array [AD-A265909] p 133 N94-10660

Radiation and scattering by cavity-backed antennas on a circular cylinder [NASA-CR-193409] p 136 N94-11084

Sampling and position effects in the Electronically Steered Thinned Array Radiometer (ESTAR) [NASA-TM-108998] p 245 N94-12432

ANTENNA COMPONENTS

An approach to high precision antenna structures by a CFRP core sandwich concept p 57 N94-10008

Multiple Antenna Implementation System (MAntIS) [DE93-012515] p 131 N94-10270

ANTENNA DESIGN

Multiple Antenna Implementation System (MAntIS) [DE93-012515] p 131 N94-10270

The uncertainty principle in resonant gravitational wave antennae and quantum non-demolition measurement schemes p 378 N94-10587

Design of a matching network for dipole antennas [AD-A265115] p 136 N94-11158

Magnetic Earth Ionosphere Resonant Frequencies (MEIRF) project [NASA-CR-193182] p 276 N94-11355

Conversion of the four-strap array in D3-D to a tunable traveling wave antenna [DE93-012085] p 137 N94-11453

PO/PTD diffraction synthesis of array-fed reflector antennas for satellite and radar applications p 137 N94-11636

Coordinated Radio, Electron, and Waves Experiment (CREWE) for the NASA Comet Rendezvous and Asteroid Flyby (CRAF) instrument [NASA-CR-194376] p 427 N94-12566

ANTENNA RADIATION PATTERNS

Performance of traffic-alert collision avoidance (TCAS) antennas in the presence of scatterers [NASA-CR-193569] p 23 N94-11525

ERS-1 preliminary antenna elevation pattern measured by ground-receivers p 235 N94-11727

Design of a continuous resistively loaded monopole antenna [AD-A265852] p 138 N94-12281

ANTENNAS

An approach to high precision antenna structures by a CFRP core sandwich concept p 57 N94-10008

Universal adjustable mould for antenna reflectors p 59 N94-10027

Linear antenna of an arbitrary orientation and position in cylindric screen [DE93-621353] p 134 N94-11035

Pre-operation analysis of ERS-1 tracking and operation, part 2-F [NASDA-CNT-930002-PT-2-F] p 230 N94-11130

ANTHROPOMETRY

Head and face anthropometry of adult US civilians [DOT/FAA/AM-93/10] p 315 N94-10806

Correlation of HGU-56/P aircrew helmet fitting with head anthropometric measurements [AD-A264988] p 315 N94-11291

ANTIFERROMAGNETISM

The peculiarities of the spin glass state in Fe(x)Mn(1-x)TiO3 [DE93-617882] p 395 N94-10525

ANTIMISSILE MISSILES

Fuzzification of ASAT's rule based aimpoint selection [AD-A266068] p 43 N94-11223

ANTINEUTRINOS

On parity conservation and the question of the missing, right-handed neutrino [DE93-613092] p 361 N94-10414

ANTIPROTONS

Indication on the existence of the bound state in the p anti p-system [DE92-641575] p 361 N94-10532

ANTIREFLECTION COATINGS

UV testing of solar cells: Effects of antireflective coating, prior irradiation, and UV source p 53 N94-11408

Preparation of stable photopatternable polymeric materials for non-linear optics [AD-A265359] p 95 N94-12577

APEXES

Finding minimum-quotient cuts in planar graphs [DE93-011675] p 344 N94-10961

Finding a covering triangulation whose maximum angle is provably small [DE93-010691] p 334 N94-12593

APOLLO ASTEROIDS

The 1.2 to 3.5 microns observations of asteroid 4179 Toutatis p 430 N94-12111

APOLLO 17 FLIGHT

Using lunar sounder imagery to distinguish surface from subsurface reflectors in lunar highlands areas p 464 N94-12179

APPALACHIAN MOUNTAINS (NORTH AMERICA)

On the importance of mesoscale potential vorticity anomalies and topographic forcing during cyclone redevelopment across the Appalachians: A GALE case study p 284 N94-10822

APPLICATION SPECIFIC INTEGRATED CIRCUITS

Flexible high-speed CODEC [NASA-CR-191169] p 146 N94-12433

APPLICATIONS PROGRAMS (COMPUTERS)

Massively parallel multifrontal methods for finite element analysis on MIMD computer systems [DE93-009838] p 335 N94-10257

CRESLAF. Version 4.0: A Fortran program for modeling laminar, chemically reacting, boundary-layer flow in cylindrical or planar channels [DE93-012835] p 152 N94-11371

Reuse: A knowledge-based approach p 329 N94-11430

The role of plasma rotation on MHD instabilities in tokamaks [DE93-013486] p 393 N94-11512

Crew chief p 335 N94-11564

Disturbance Impact Assessment System (DIAS), version 2.0. System design document
[AD-A265251] p 138 N94-11883

Transportable Applications Environment (TAE) Tenth Users' Conference
[NASA-CP-3225] p 333 N94-12448

Three-dimensional finite element analysis of explosive safety facilities: A technology assessment
[AD-A265700] p 35 N94-12562

The 1991 version of the plume impingement computer program. Volume 2: User's input guide
[NASA-CR-194191] p 166 N94-12774

The 1991 version of the plume impingement computer program. Volume 1: Description
[NASA-CR-194192] p 166 N94-12775

VIB3D: Method for calculating 3-D unsteady flow through turbomachinery blades
[CUED/A-TURBO/TR.128] p 166 N94-12777

VIB2D: Quasi 3-D unsteady viscous flow method for blade flutter calculation
[CUED/A-TURBO/TR.129] p 166 N94-12779

APPROACH CONTROL

Helicopter approach capability using the differential Global Positioning System
[NASA-CR-177618] p 24 N94-12355

APPROPRIATIONS

National Aero-Space Plane: A need for program direction and funding decisions
[GAO/NSIAD-93-207] p 416 N94-10910

APPROXIMATION

A method for calculating exact geodetic latitude and altitude
[AD-A265783] p 229 N94-10417

The Nehari problem for the Pritchard-Salamon class of infinite-dimensional linear systems: A direct approach
[CS-9216] p 344 N94-10905

Finding a covering triangulation whose maximum angle is provably small
[DE93-010691] p 334 N94-12593

Summation by parts, projections, and stability
[NASA-CR-194290] p 346 N94-12776

APTITUDE

Basic attributes test (BAT): Operational pre-implementation analysis and score equating
[AD-A265885] p 314 N94-12276

AQUATIC PLANTS

High-reflectance water mass in Off-Sanriku area observed by CZCS p 200 N94-11951

AQUEOUS SOLUTIONS

Effects of aqueous solution compositions on Aerocapacitor energy density
[DE93-013431] p 140 N94-10309

Studies in bioorganic chemistry
[AD-A265532] p 55 N94-12011

Electrode potential-induced reconstruction of Au(100): Effect of chemisorption on nanoscale dynamics as probed by the in-situ scanning tunneling microscopy
[AD-A265900] p 404 N94-12388

Corrosion and passivation of high temperature superconductors
[AD-A265402] p 405 N94-12586

AQUICULTURE

Role of remote sensing and its cost effectiveness in site selection for coastal aquaculture
p 217 N94-12697

ARABIAN SEA

Sea surface temperature anomalies in the Arabian Sea p 206 N94-11988

ARAMID FIBERS

Factors that affect OSU thermal performance of aircraft interior materials p 20 N94-10789

ARC HEATING

The upgrading of the arc heated wind tunnel of the DLR (LBK) with respect to its effects on the material testing
p 4 N94-10432

ARC JET ENGINES

Arcjet space thrusters
[NASA-CR-193191] p 46 N94-10700

A soft-start circuit for arcjet ignition
[NASA-TM-106287] p 180 N94-10760

Arcjet exploratory tests of ARC optical window design for the AFE vehicle
[NASA-CR-192655] p 34 N94-10930

A study of DC-DC converters with MCTs for arcjet power supplies
[NASA-CR-193457] p 142 N94-10931

Development of a high specific 1.5 to 5 kW thermal arcjet
[NASA-CR-193133] p 47 N94-11354

ARC WELDING

Welding tritium aged stainless steel
[DE93-011782] p 181 N94-11228

ARCHITECTURE

Technical Conference on Tropical Urban Climates: Extended Abstracts
[WMO/TD-538] p 283 N94-10561

ARCHITECTURE (COMPUTERS)

Layering techniques for development of parallel systems: An algebraic approach
[MEMO-INF-92-62] p 335 N94-10277

Finite state machine microarchitecture transformations described with relational algebra
[MEMO-INF-92-63] p 319 N94-10278

Optimization algorithms for integer networks with side constraints for application in routing and scheduling
[AD-A265254] p 322 N94-10492

Bringing theory to practice: The reality of interprocessor communication
[DE93-012346] p 336 N94-10738

Efficient partitioning and assignment on programs for multiprocessor execution
[NASA-CR-193458] p 324 N94-10942

Node assignment in heterogeneous computing
[NASA-CR-4534] p 142 N94-11131

Summary of research in progress at ICASE
[NASA-CR-191481] p 318 N94-11198

Neural network model selection using asymptotic jackknife estimator and cross-validation method
[AD-A264960] p 339 N94-11289

Scalable concurrent programming project
[AD-A266097] p 328 N94-11295

Spatial light rebroadcaster architecture study
[AD-A266102] p 382 N94-11421

An introduction to chordal graphs and clique trees
[DE93-012508] p 332 N94-11695

High-performance distributed systems architecture
[AD-A265297] p 337 N94-11829

The rational behavior model: A multi-paradigm, tri-level software architecture for the control of autonomous vehicles
[AD-A265175] p 332 N94-11874

Distributed real-time system design: Theoretical concepts and applications
[AD-A265199] p 337 N94-11881

An optoelectronic graphics display processor
[AD-A266011] p 171 N94-12391

ARCTIC OCEAN

Arctic coastal polynya observations with ERS-1 SAR and DMSP SSM/I p 239 N94-11748

ARCTIC REGIONS

Retrieval of radiation budgets in the Arctic from satellite measurements p 229 N94-10714

Energy flow in an Arctic aquatic ecosystem
[DE93-013178] p 267 N94-11697

Investigations of Arctic ice-sheets and glaciers using ERS-1 SAR p 238 N94-11743

Summer Arctic ice concentrations and characteristics from SAR and SSM/I data p 241 N94-11762

Arctic geodynamics: Continental shelf and deep ocean geophysics. ERS-1 satellite altimetry: A first look
p 243 N94-11776

ARGON

Journal of Research of the National Institute of Standards and Technology, volume 98, number 2, March - April 1993
[PB93-196228] p 485 N94-10850

ARGON ISOTOPES

Radiogenic age and isotopic studies
[DE93-610548] p 274 N94-10407

Peculiarities of distributions of the cosmic-ray exposure ages of H chondrite falls and finds p 428 N94-12021

Nitrogen and noble gases in a glass sample from LEW88516 p 80 N94-12051

Noble gases in LEW88516 shergottite: Evidence for exposure age pairing with ALH77005 p 80 N94-12082

Ar-39 - Ar-40 ages of acapulcoites and lodranites: Evidence for early parent body heating
p 281 N94-12083

Age of Popigai impact event using the Ar-40 - Ar-39 method p 282 N94-12093

On the origin of (4)He and (40)Ar in natural gold
p 87 N94-12240

ARGON PLASMA

Journal of Research of the National Institute of Standards and Technology, volume 98, number 2, March - April 1993
[PB93-196228] p 485 N94-10850

ARIANE LAUNCH VEHICLE

Stress relaxation forming of Ariane 5 front skirt outer skin panels p 62 N94-10046

ARMED FORCES (UNITED STATES)

The radar eye blinded: The USAF and electronic warfare, 1945-1955
[AD-A265494] p 132 N94-10497

Assured Mission Support Space Architecture (AMSSA) study p 348 N94-11573

ARROYOS

Arroyo el Mimbral, Mexico, K/T unit: Origin as debris flow/turbidite, not a tsunami deposit
p 281 N94-12084

ARSENIC

Kinetics of high concentration arsenic deactivation at moderate to low temperatures
[DE93-013349] p 395 N94-10516

ARTERIES

Arterial gas emboli in altitude-induced decompression sickness p 312 N94-11543

Transcranial Doppler ultrasound and the etiology of neurologic decompression sickness during altitude decompression p 312 N94-11544

ARTIFICIAL INTELLIGENCE

Functional reasoning, explanation, and analysis
[DE92-526832] p 313 N94-10251

System monitoring and diagnosis with qualitative models
[NASA-CR-193812] p 323 N94-10711

Enhancements to the Engine Data Interpretation System (EDIS)
[NASA-CR-192593] p 180 N94-10815

The development of an interactive synthesis tool for intelligent controllers of modular, reconfigurable robots
p 339 N94-10898

Functional approximation using artificial neural networks in structural mechanics
[NASA-TM-105820] p 188 N94-11254

A recent Cleanroom success story: The Redwing project p 39 N94-11433

Toward intelligent flight control p 33 N94-11503

The rational behavior model: A multi-paradigm, tri-level software architecture for the control of autonomous vehicles
[AD-A265175] p 332 N94-11874

Thermal error compensation feasibility study using artificial intelligence
[AD-A266084] p 340 N94-12411

Proceedings of the Seventh International Symposium on Methodologies for Intelligent Systems (poster session)
[DE93-013470] p 340 N94-12428

Qualitative reasoning about the physical world
[AD-A266117] p 340 N94-12537

ARTIFICIAL SATELLITES

Aluminium-lithium forgings: Properties and potential satellite applications p 58 N94-10021

Satellite situation report, volume 32, no. 1
[NASA-TM-109233] p 42 N94-10562

Satellite situation report, volume 32, no. 2
[NASA-TM-109234] p 42 N94-10563

Satellite situation report, volume 31, no. 4
[NASA-TM-109232] p 39 N94-10659

Maximizing reuse: Applying common sense and discipline p 329 N94-11429

ASCENT

Aerodynamic and aerothermal challenges for the design of the Hermes spaceplane p 3 N94-10423

ASHES

Overwater atmospheric dispersion of volcanic smokes from Mt. Sakurajima observed in NOAA-AVHRR data
p 205 N94-11979

ASIA

Space Activities in the Asia Pacific Region
[JTN-93-80421] p 35 N94-10676

Current status of space activities in Asia Pacific region
p 35 N94-10677

Considerations for future regional space cooperation
p 35 N94-10678

Panel discussion: Role of space program in the Asia Pacific Region p 37 N94-10694

ASPECT RATIO

Marangoni flows in open cavities with differentially heated end walls p 104 N94-10097

ASSEMBLY LANGUAGE

Simulation of a parallel computer
[NAL-TR-1154] p 335 N94-10368

ASSESSMENTS

Report on Subgroup on Data Banks for Risk Assessment
[DE93-012150] p 418 N94-10646

Computer models used to support cleanup decision-making at hazardous and radioactive waste sites
[PB93-183333] p 274 N94-10698

ASSIMILATION

Assimilation in lunar basalts and volcanic glasses: Implications for a heterogenous mantle source region
p 478 N94-12250

Preliminary results from a satellite altimetric data assimilation using a Kalman filter and smoother
p 209 N94-12648

ASTEROID BELTS

On the depletion in the outer asteroid belt and the structure of the 4 to 3 mean motion resonance
p 426 N94-11596

Collision lifetimes and impact statistics of near-Earth asteroids p 429 N94-12092

How diverse is the asteroid belt? p 430 N94-12124

Cratering on Gaspra p 459 N94-12147
First results of the seven-color asteroid survey p 430 N94-12162
ASTEROIDS
On the depletion in the outer asteroid belt and the structure of the 4 to 3 mean motion resonance p 426 N94-11596
Collision lifetimes and impact statistics of near-Earth asteroids p 429 N94-12092
Identification of cometary and asteroidal particles in stratospheric IDP collections p 430 N94-12115
How diverse is the asteroid belt? p 430 N94-12124
Collisions of small Spacewatch asteroids with the Earth p 430 N94-12157
First results of the seven-color asteroid survey p 430 N94-12162
Simulation of possible regolith optical alteration effects on carbonaceous chondrite meteorites p 430 N94-12163
Spectral mixing models of S-Type asteroids p 431 N94-12164
Olivine-rich asteroids, pallasitic olivine and olivine-metal mixtures: Comparisons of reflectance spectra p 431 N94-12171
Deviations from the straight line: Bumps (and grinds) in the collisionally evolved size distribution of asteroids p 431 N94-12201
A method to determine asteroid poles p 431 N94-12205
Chondrites, S asteroids, and space weathering: Thumping noises from the coffin? p 433 N94-12244
ASTRIONICS
An analysis of the modes and states for generic avionics
[NASA-CR-188253] p 27 N94-10664
ASTROMETRY
Statistical description of tectonic motions
[NASA-CR-193701] p 275 N94-10950
Pulsar astrometry by using VLBI (PSR0329 between Kashima 26mPhi and Usuda 64mPhi) p 351 N94-10968
Tropospheric and ionospheric effects on differential astrometry with a ground-space based VLBI array p 136 N94-11070
ASTRONAUT PERFORMANCE
Visual Earth observation performance in the space environment. Human performance measurement 4: Flight experiments p 314 N94-11539
ASTRONAUT TRAINING
Transfer of training for aerospace operations: How to measure, validate, and improve it p 314 N94-11530
ASTRONAUTS
Measuring human performance on NASA's microgravity aircraft p 317 N94-11537
A mechanism for the reduction in risk of decompression sickness in microgravity environment p 312 N94-11545
Baseline characteristics of different strata of astronaut corps p 312 N94-11552
Longitudinal study of astronaut health: Mortality in the years 1959-1991 p 312 N94-11560
ASTRONOMICAL INTERFEROMETRY
Propagation Effects in Space VLBI p 134 N94-11060
Generalization of Dyson criterion for the amplitude-phase fluctuations case and for the system of interferometers p 135 N94-11067
The possibility of image restoration under observation in a regime of strong scattering p 136 N94-11068
An interferometric spectral mapper for the Cassini mission to Saturn and Titan
[NASA-CR-193805] p 482 N94-12429
ASTRONOMICAL MODELS
Cosmological gamma-ray burst model
[NASA-CR-193368] p 484 N94-10507
Planck scale effects on the Majoron
[DE93-613120] p 410 N94-10545
On the depletion in the outer asteroid belt and the structure of the 4 to 3 mean motion resonance p 426 N94-11596
Deviations from the straight line: Bumps (and grinds) in the collisionally evolved size distribution of asteroids p 431 N94-12201
A method to determine asteroid poles p 431 N94-12205
ASTRONOMICAL PHOTOMETRY
Physical studies of planetary and satellite surfaces
[NASA-CR-193545] p 434 N94-10817
A method to determine asteroid poles p 431 N94-12205
Disk-resolved spectral characteristics of Saturn's medium-sized satellites p 471 N94-12213
ASTRONOMICAL POLARIMETRY
Dust in the Martian atmosphere: Polarimetric sensing p 473 N94-12223
ASTRONOMICAL SPECTROSCOPY
A comparison of telescopic and Phobos-2 ISM spectra of Mars in the short-wave near-infrared (0.76-1.02 microns) p 424 N94-12053
Chondrites, S asteroids, and space weathering: Thumping noises from the coffin? p 433 N94-12244
ASTRONOMY
Advanced statistical methods for improved data analysis of NASA astrophysics missions
[NASA-CR-193514] p 425 N94-10943
Project TIMS (Teaching Integrated Math/Science)
[NASA-CR-194288] p 416 N94-11599
ASTROPHYSICS
Advanced statistical methods for improved data analysis of NASA astrophysics missions
[NASA-CR-193514] p 425 N94-10943
VLBI and the detection of interstellar magnetohydrodynamic waves p 135 N94-11066
ASYMPTOTIC METHODS
Asymptotic expressions for regular Green functions of a round cylindrical screen
[DE93-621356] p 134 N94-11038
ASYMPTOTIC SERIES
On the possible unobservability of the Wu-Yang phase factor in curved space
[DE93-617645] p 411 N94-10831
Applications of multivariate analysis
[AD-A265250] p 347 N94-11882
ATLANTIC OCEAN
ERS-1 radar altimetry over the North Atlantic p 242 N94-11772
Variability of wind stress, and sensible and latent heat flux in the North Atlantic during SEASAT p 194 N94-11918
ATMOSPHERIC ATTENUATION
Propagation of light pulses through a three-layer medium (cloud, pure air, and ocean water) p 222 N94-12725
Atmospheric correction for determination of average SST fields based on AVHRR data p 227 N94-12750
ATMOSPHERIC BOUNDARY LAYER
Development of a balloon-borne stabilized platform for measuring radiative flux profiles in the atmospheric boundary layer
[DE93-013186] p 274 N94-10323
A self-consistent model of non-linear parameterization of turbulent diffusion in atmospheric boundary layer
[DE93-011950] p 275 N94-11052
Large eddy simulations of the atmospheric boundary layer east of the Colorado Rockies p 277 N94-11465
The impact of vegetation on the atmospheric boundary layer and convective storms p 277 N94-11480
Activities relating to understanding the initiation, organization and structure of moist convection in the Southeast environment
[NASA-CR-193829] p 285 N94-11598
An atmospheric boundary layer stability estimator for urban areas
[AD-A265189] p 279 N94-12422
Estimations of the surface fluxes from satellite observations of boundary layer and the surface p 252 N94-12513
ATMOSPHERIC CHEMISTRY
Review of SHARC 2.0 O3 kinetics and spectroscopy
[AD-A265481] p 274 N94-10496
Environmental Sciences Division
[DE93-013865] p 264 N94-10650
User's manual for the plume visibility model PLUVUE 2 (revised)
[PB93-188233] p 265 N94-11016
The Air Force Interactive Meteorological System: A research tool for satellite meteorology
[AD-A265957] p 284 N94-11113
Characterization of gas-aerosol interaction kinetics using morphology dependent stimulated Raman scattering
[DE93-012324] p 77 N94-11359
Global monitoring of atmospheric properties by the EOS MODIS
[NASA-TM-109237] p 231 N94-11485
Study of the atmospheric chemistry of radon progeny in laboratory and real indoor atmospheres
[DE93-012236] p 266 N94-11671
Oxidation state of the Earth's upper mantle during the last 3800 million years: Implications for the origin of life p 283 N94-12210
The rate of chemical weathering of pyrite on the surface of Venus p 477 N94-12246
DMS emissions from Sphagnum-dominated wetlands p 271 N94-12466
Emissions of biogenic sulfur gases from northern bogs and fens p 271 N94-12467
Sulfur gas exchange in Sphagnum-dominated wetlands p 271 N94-12470
Stratospheric aircraft exhaust plume and wake chemistry
[NASA-CR-191495] p 279 N94-12572
ATMOSPHERIC CIRCULATION
Preliminary validation of the low frequency variability of tropospheric temperature and circulation simulated for the AMIP by the ECMWF model
[DE93-012382] p 284 N94-10739
A self-consistent model of non-linear parameterization of turbulent diffusion in atmospheric boundary layer
[DE93-011950] p 275 N94-11052
A toolkit for building Earth system models
[DE93-012147] p 276 N94-11138
The impact of vegetation on the atmospheric boundary layer and convective storms p 277 N94-11480
Stability model of the atmosphere p 32 N94-11500
An overview of intertropical convergence and intertropical discontinuity
[DE93-619229] p 277 N94-11603
Wind system documentation
[DE93-010381] p 285 N94-11664
Behavior of vortices generated by an advancing ejecta curtain in theory, in the laboratory, and on Mars p 169 N94-12044
A study of the Merritt Island, Florida sea breeze flow regimes and their effect on surface heat and moisture fluxes
[NASA-CR-4537] p 286 N94-12580
ATMOSPHERIC COMPOSITION
In situ detection of tropospheric OH, HO2, NO2, and NO by laser-induced fluorescence in detection chambers at reduced pressures
[NASA-CR-193189] p 274 N94-10701
Satellite observation of atmospheric tracer components: JEM/POP p 130 N94-11836
Study of climatic effects of cloud-aerosol interaction p 204 N94-11977
An observational search for CO2 ice clouds on Mars p 441 N94-12054
Geomorphology of Triton's polar materials p 466 N94-12185
Oxidation state of the Earth's upper mantle during the last 3800 million years: Implications for the origin of life p 283 N94-12210
Studies of dynamical processes affecting the distribution of stratospheric ozone
[NASA-CR-193477] p 279 N94-12560
ATMOSPHERIC CORRECTION
Atmospheric correction of AVIRIS data in ocean waters
[AD-A264931] p 288 N94-11287
A statistical method to determine aerosol path radiance and its application to atmospheric correction for CZCS imagery p 191 N94-11897
Effects of wind-roughened sea surface on ocean color remote sensing: Noise derived from reflected light and whitecaps p 191 N94-11898
Atmospheric correction plans for SeaWiFS p 204 N94-11975
Implications of aerosol retrieval and atmospheric correction in remote sensing p 205 N94-11978
The upwelling radiation at the top of the atmosphere in coastal region p 205 N94-11981
Validation of the ATSR/M microwave radiometer data p 252 N94-12511
ATSR correlative skin measurements of sea surface temperature p 252 N94-12514
A basic consideration for remote sensing using microwave radars on a satellite p 212 N94-12665
Atmospheric correction for determination of average SST fields based on AVHRR data p 227 N94-12750
ATMOSPHERIC DIFFUSION
User's manual for the plume visibility model PLUVUE 2 (revised)
[PB93-188233] p 265 N94-11016
ATMOSPHERIC EFFECTS
Scattering of modulated Ultra-Relativistic Electron Beam (UREB) by atmospheric plasma
[DE93-620987] p 387 N94-10558
Tropospheric and ionospheric effects on differential astrometry with a ground-space based VLBI array p 136 N94-11070
Elimination of the influence of the atmosphere on the accuracy of solutions to astrometric problems by means of a ground-space VLBI network p 136 N94-11071
Pre-operation analysis of ERS-1 tracking and operation, part 2-F
[NASDA-CNT-930002-PT-2-F] p 230 N94-11130
Variability of wind stress, and sensible and latent heat flux in the North Atlantic during SEASAT p 194 N94-11918
Distribution of mineral aerosols over the North Pacific p 204 N94-11976
ATMOSPHERIC ENTRY
Planetary entry vehicle design for planned and potential ESA missions to Titan, Mars, and Earth return (FGE TN 51/92) p 4 N94-10428
Identification of cometary and asteroidal particles in stratospheric IDP collections p 430 N94-12115

Organic matter on the early surface of Mars: An assessment of the contribution by interplanetary dust
p 480 N94-12259
Trace element content of chondritic cosmic dust: Volatile enrichments, thermal alterations, and the possibility of contamination p 433 N94-12260
Depletions of sulfur and/or zinc in IDPs: Are they reliable indicators of atmospheric entry heating?
p 433 N94-12261

ATMOSPHERIC GENERAL CIRCULATION EXPERIMENT
Design of a global soil moisture initialization procedure for the simple biosphere model
[NASA-TM-104590] p 284 N94-10940

ATMOSPHERIC GENERAL CIRCULATION MODELS
Sandia ocean modeling system programmer's guide and user's manual
[DE93-007427] p 287 N94-10153
The impact of horizontal resolution on moist processes in the ECMWF model
[DE93-011718] p 276 N94-11227
A modeling perspective on cloud radiative forcing
[DE93-012383] p 276 N94-11241
Large eddy simulations of the atmospheric boundary layer east of the Colorado Rockies p 277 N94-11465
An observational search for CO2 ice clouds on Mars
p 441 N94-12054

ATMOSPHERIC HEATING
Trace element content of chondritic cosmic dust: Volatile enrichments, thermal alterations, and the possibility of contamination p 433 N94-12260

ATMOSPHERIC IONIZATION
Results from a year-long auroral-E measurement campaign
[AD-A265059] p 278 N94-11871

ATMOSPHERIC LASERS
Laser system design for the generation of a sodium-layer laser guide star
[DE93-014127] p 176 N94-12784

ATMOSPHERIC MODELS
AMIP: The Atmospheric Model Intercomparison Project
[DE93-007400] p 273 N94-10151
AMIP: The Atmospheric Model Intercomparison Project
[DE93-007413] p 273 N94-10152
The cloud radiative feedback of a midlatitude squall line system and implication for climate study
[DE93-010511] p 283 N94-10290
Preliminary validation of the low frequency variability of tropospheric temperature and circulation simulated for the AMIP by the ECMWF model
[DE93-012382] p 284 N94-10739
Photochemical modelling of Venus clouds using Pioneer Venus data
[NASA-CR-194108] p 434 N94-10823
User's manual for the plume visibility model PLUVUE 2 (revised)
[PB93-188233] p 265 N94-11016
A toolkit for building Earth system models
[DE93-012147] p 276 N94-11138
Numerical simulations on the redistribution of atmospheric trace chemicals through cloud processes
p 265 N94-11189
A modeling perspective on cloud radiative forcing
[DE93-012383] p 276 N94-11241
Characterization of gas-aerosol interaction kinetics using morphology dependent stimulated Raman scattering
[DE93-012324] p 77 N94-11359
On non-linear longitudinal stability of an aircraft in a dive in the presence of atmospheric disturbances
p 31 N94-11492
Stability model of the atmosphere p 32 N94-11500
Development of a graphical user interface and graphics display for the WIND system
[DE93-011780] p 285 N94-11614
Wind system documentation
[DE93-010381] p 285 N94-11664
Modeling present and future river runoff using global atmospheric models
[AD-A265274] p 285 N94-11685
Validation of ERS-1 wind and wave data by use of operational forecast models p 233 N94-11710
Evaluation of ECMWF latent heat flux in TOGA CD-ROM p 195 N94-11921
Behavior of vortices generated by an advancing ejecta curtain in theory, in the laboratory, and on Mars
p 169 N94-12044
A new data collection system for ionospheric modelling and related topics
[AD-A265893] p 278 N94-12277
An atmospheric boundary layer stability estimator for urban areas
[AD-A265189] p 279 N94-12422
Comments on possible causes of recent global warming
[DE93-010501] p 272 N94-12592
Verification of the atmosphere-ocean radiative transfer parametric models p 225 N94-12738
Atmospheric correction for determination of average SST fields based on AVHRR data p 227 N94-12750

ATMOSPHERIC MOISTURE
Investigation of passive atmospheric sounding using millimeter and submillimeter wavelength channels
[NASA-CR-193627] p 274 N94-10726
Photochemical modelling of Venus clouds using Pioneer Venus data
[NASA-CR-194108] p 434 N94-10823
Studies of the net surface radiative flux from satellite radiances during FIFE
[NASA-CR-193150] p 230 N94-10953
The impact of horizontal resolution on moist processes in the ECMWF model
[DE93-011718] p 276 N94-11227
Activities relating to understanding the initiation, organization and structure of moist convection in the Southeast environment
[NASA-CR-193829] p 285 N94-11598
Effects of satellite spectral resolution and atmospheric water vapor on retrieval of near-ground temperatures
[AD-A264920] p 245 N94-11851
Evaporation and thermal/hydrologic balance in the Pacific p 195 N94-11919
Near-infrared spectra of the Martian surface: Reading between the lines p 465 N94-12184
An examination of the evolution of radiation and advection fogs
[AD-A266127] p 286 N94-12539
Worldwide map of rainfall amount over the ocean derived from passive microwave radiometer p 211 N94-12663
Cloud liquid water content over the Pacific Ocean tropical zone derived from ship microwave radiometric measurement p 225 N94-12743

ATMOSPHERIC PHYSICS
Environmental Sciences Division
[DE93-013865] p 264 N94-10650
The Air Force Interactive Meteorological System: A research tool for satellite meteorology
[AD-A265957] p 284 N94-11113

ATMOSPHERIC PRESSURE
The effects of atmospheric pressure on infrared reflectance spectra of Martian analogs
p 445 N94-12071
Martian particle size based on thermal inertia corrected for elevation-dependent atmospheric properties
p 430 N94-12107

ATMOSPHERIC RADIATION
Development of a balloon-borne stabilized platform for measuring radiative flux profiles in the atmospheric boundary layer
[DE93-013186] p 274 N94-10323
Retrieval of radiation budgets in the Arctic from satellite measurements p 229 N94-10714

ATMOSPHERIC SCATTERING
A statistical method to determine aerosol path radiance and its application to atmospheric correction for CZCS imagery p 191 N94-11897
Implications of aerosol retrieval and atmospheric correction in remote sensing p 205 N94-11978

ATMOSPHERIC SOUNDING
In situ detection of tropospheric OH, HO2, NO2, and NO by laser-induced fluorescence in detection chambers at reduced pressures
[NASA-CR-193189] p 274 N94-10701
Investigation of passive atmospheric sounding using millimeter and submillimeter wavelength channels
[NASA-CR-193627] p 274 N94-10726
Effects of energetic particle events on VLF/LF propagation parameters/1989
[AD-A265266] p 275 N94-11013
TOVS soundings: Impact on the synoptic analysis over the south and southeast regions of Brazil from March 18 to March 19, 1991
[INPE-5497-TDI/512] p 230 N94-11179
Activities relating to understanding the initiation, organization and structure of moist convection in the Southeast environment
[NASA-CR-193829] p 285 N94-11598
Satellite observation of atmospheric tracer components: JEM/POP p 130 N94-11836
Submillimeter wave observation experiment of Earth atmosphere with SIS mixer p 130 N94-11837
Effects of satellite spectral resolution and atmospheric water vapor on retrieval of near-ground temperatures
[AD-A264920] p 245 N94-11851
Estimations of the surface fluxes from satellite observations of boundary layer and the surface
p 252 N94-12513
Cloud liquid water content over the Pacific Ocean tropical zone derived from ship microwave radiometric measurement p 225 N94-12743

ATMOSPHERIC TEMPERATURE
Preliminary validation of the low frequency variability of tropospheric temperature and circulation simulated for the AMIP by the ECMWF model
[DE93-012382] p 284 N94-10739
On the importance of mesoscale potential vorticity anomalies and topographic forcing during cyclone redevelopment across the Appalachians: A GALE case study p 284 N94-10822
Modeling present and future river runoff using global atmospheric models
[AD-A265274] p 285 N94-11685
An investigation using empirical orthogonal functions and objective analysis to analyse the vertical temperature structure of a gulf stream meander
[AD-A265116] p 289 N94-11868
Study of climatic effects of cloud-aerosol interaction
p 204 N94-11977
Sea surface temperature anomalies in the Arabian Sea p 206 N94-11988
Galileo/NIMS near-infrared thermal imagery of the surface of Venus p 457 N94-12139
Estimations of the surface fluxes from satellite observations of boundary layer and the surface
p 252 N94-12513

ATMOSPHERIC TURBULENCE
Lee waves: Benign and malignant
[NASA-CR-186024] p 283 N94-10725
Characteristic scales and vortex features of mesoscale vortices observed by the satellites during the winter
p 199 N94-11943
Behavior of vortices generated by an advancing ejecta curtain in theory, in the laboratory, and on Mars
p 169 N94-12044
Turbulence modeling and compressibility
p 163 N94-12614

ATMOSPHERICS
Telescience capability for the Sondre Stromfjord, Greenland, incoherent-scatter radar facility
[NASA-CR-193683] p 136 N94-11206

ATOMIC CLOCKS
Comparison of GPS and GLONASS common-view time transfers p 24 N94-10967
An ensemble pulsar time p 351 N94-10969
Experimental comparison of time synchronization techniques by means of light signals and clock transport on the rotating earth p 351 N94-10970
Possible applications of atomic frequency standards with an internal high resolution digital synthesizer
p 353 N94-10979
CAFS: A Cesium Atomic Frequency Standard for GPS block IIR p 353 N94-10980
Time scale algorithms for an inhomogeneous group of atomic clocks p 356 N94-10998

ATOMIC COLLISIONS
Laser cooling and trapping of atoms in microgravity: Ultracold atoms collisions p 124 N94-10241
Calculation of the total ionization cross section and spin asymmetry in electron-hydrogen scattering from threshold to 500 eV
[DE93-610180] p 359 N94-10312
Calculation of spin-dependent observables in electron-sodium scattering using the coupled-channel optical method
[DE93-610050] p 360 N94-10329
Spin-dependent observables in electron-sodium scattering calculated using the coupled-channel optical method
[DE93-610073] p 360 N94-10331
Collision-induced squeezing in a harmonic oscillator
p 379 N94-10597
Filamentation instability of hot quark-gluon plasma with hard jet
[DE93-617679] p 388 N94-10882
Structural and electronic properties of atomic chains
[DE93-617758] p 366 N94-11349
Compilation of excitation cross sections for He atoms by electron impact
[DE93-753246] p 367 N94-11580
Final state interactions and inclusive nuclear collisions
[NASA-TP-3353] p 373 N94-12435

ATOMIC ENERGY LEVELS
Spin-dependent observables in electron-sodium scattering calculated using the coupled-channel optical method
[DE93-610073] p 360 N94-10331
A phaseonium magnetometer: A new optical magnetometer based on index enhanced media
p 375 N94-10565
Wigner functions for nonclassical states of a collection of two-level atoms p 379 N94-10603
Dynamics of charge-transfer excited states relevant to photochemical energy conversion
[DE93-013981] p 263 N94-11116

Femtosecond dynamics, photoexcitation, and ESR spectra of MX chain solids
[AD-A264689] p 399 N94-11263

ATOMIC EXCITATIONS
Application of spin-sensitive electron spectroscopies to investigations of electronic and magnetic properties of solid surfaces and epitaxial systems
[DE93-015079] p 76 N94-10854
Dynamics of charge-transfer excited states relevant to photochemical energy conversion
[DE93-013981] p 263 N94-11116
Theoretical atomic physics for fusion
[DE93-013872] p 366 N94-11172
Electronic excitation of ground state atoms by collision with heavy gas particles
[NASA-CR-193364] p 366 N94-11360
Compilation of excitation cross sections for He atoms by electron impact
[DE93-753246] p 367 N94-11580
Atomic processes relevant to polarization plasma spectroscopy
[DE93-753240] p 393 N94-11594

ATOMIC INTERACTIONS
Interatomic interactions in BCC and FCC lattices of transition metals
[DE93-621541] p 398 N94-11090

ATOMIC PHYSICS
Laser cooling and trapping of atoms in microgravity: Ultracold atoms collisions p 124 N94-10241
Radiative properties of strongly magnetized plasmas
[DE93-014098] p 389 N94-11118
Wide Band-Gap Semiconductors. 1991 Materials Research Society Symposium proceedings
[AD-A263418] p 401 N94-11515
Atomic processes relevant to polarization plasma spectroscopy
[DE93-753240] p 393 N94-11594

ATOMIC STRUCTURE
Satellite structure of the xenon valence shell by electron momentum spectroscopy
[DE93-609993] p 360 N94-10327
Calculation of spin-dependent observables in electron-sodium scattering using the coupled-channel optical method
[DE93-610050] p 360 N94-10329
Electron momentum spectroscopy of atoms, molecules and solids
[DE93-610148] p 360 N94-10332
Recent advances in electron momentum spectroscopy
[DE93-610149] p 361 N94-10333
Enhanced stability of magic clusters: A case study of icosahedric Al(sub 12)X, X=B, Al, Ga, C, Si, Ge, Ti, As
[DE93-613644] p 395 N94-10386
Structure of s - p bonded metal clusters with 8, 20 and 40 valence electrons
[DE93-613643] p 361 N94-10503
Bond distortion and electron trapping in charged C60
[DE93-613642] p 396 N94-10637
Atomic structures and compositions of internal interfaces
[DE93-014840] p 363 N94-10750
Adsorption and dissociation of disilane on Si(001) studied by STM
[AD-A265269] p 402 N94-11684
Publications/Patents/Presentations/Honors/Student eport
[AD-A265136] p 78 N94-11873
Progress toward atomic layer epitaxy of diamond: Diamond films grown one layer at a time
[AD-A265530] p 403 N94-12010
Atomic-scale imaging of surfaces and interfaces. Materials Research Society Symposium Proceedings, volume 295
[AD-A265674] p 369 N94-12379
Electrode potential-induced reconstruction of Au(100): Effect of chemisorption on nanoscale dynamics as probed by the in-situ scanning tunneling microscopy
[AD-A265900] p 404 N94-12388
Corrosion control by vitreous films on aluminum and high T(sub c) superconductors
[AD-A266016] p 85 N94-12393
Nonlinear optical spectroscopy of Ag(111) in electrolyte and in vacuum
[AD-A265622] p 79 N94-12534

ATOMIZERS
Atomization characteristics of a prefilming airblast atomizer
[NAL-TM-644] p 148 N94-10727
Application of jet-shear-layer mixing and effervescent atomization to the development of a low-NO(x) combustor
[NASA-TM-105888] p 28 N94-11234

ATOMIZING
Shear coaxial injector atomization phenomena for combusting and non-combusting conditions
[NASA-CR-193339] p 152 N94-11526

ATOMS
Laser cooling and trapping of atoms in microgravity: Ultracold atoms collisions p 124 N94-10241
Atomic and molecular data for H2O, CO and CO2 relevant to edge plasma impurities
[DE93-771423] p 387 N94-10662

ATTACK AIRCRAFT
Adaptive reconfigurable flight controls for high angle of attack aircraft agility p 32 N94-11502

ATTENTION
Vigilance problems in orbiter processing
p 314 N94-11536

ATTENUATION COEFFICIENTS
Photostimulated attenuation of hypersound in superlattice
[DE93-611231] p 357 N94-10408
Remote sensing of subsurface water temperature profile and backscattering coefficient in the China Sea by Ocean Lidar (OLIDAR) p 203 N94-11970

ATTENUATORS
Underwing compression vortex attenuation device
[NASA-CASE-LAR-14744-1] p 12 N94-10673

ATTITUDE (INCLINATION)
Estimation of the attitude motion of the small satellite ORIZURU
[NAL-TR-1145] p 42 N94-10366
Safety of high speed ground transportation systems: X2000 US demonstration vehicle dynamics trials, preliminary test report, October 1992 - January 1993
[PB93-194645] p 422 N94-10736

AUDIO EQUIPMENT
Sensing glass transitions in thin polymer films on acoustic wave microsensors
[DE93-010805] p 87 N94-10295

AUDIO SIGNALS
Underwater hydrophone location survey
p 290 N94-10975

AUGER SPECTROSCOPY
Hydrogen partitioning and transport in titanium aluminides
[NASA-CR-194117] p 76 N94-10713

AURORAS
Analysis of geophysical measurements and spacecraft interactions
[AD-A266064] p 43 N94-10944
Studies of electrostatic waves and VLF-wave particle interaction in the ionosphere
[AD-A266013] p 278 N94-12392

AUSTRALIA
Mapping of the East Australian current with the ERS-1 SAR and shipborne studies p 234 N94-11717

AUSTRALIAN SPACE PROGRAM
National space program in Australia
p 37 N94-10691

AUSTRALITES
Soret diffusion: A possible cause of compositional heterogeneity within tektites p 432 N94-12211

AUTOCATALYSIS
Chemical pattern formation under microgravity
p 121 N94-10227

AUTOCORRELATION
Study of the surface circulation to the North of Bransfield Strait, Antarctica
[INPE-5472-TDI/503] p 288 N94-11200

AUTOIONIZATION
Progress in zirconium resonance ionization spectroscopy
[DE93-011881] p 76 N94-11075

AUTOMATA THEORY
Lattice gas hydrodynamics: Theory and simulations
[DE93-013297] p 147 N94-10320
Acting to gain information
[NASA-CR-193399] p 418 N94-10515
Evaluation of the capacity and delay benefits of terminal air traffic control automation
[AD-A265323] p 24 N94-11863

AUTOMATIC CONTROL
AGF (Automatic Gradient Furnace): A proposed microgravity facility p 112 N94-10141
Stability analysis and aerospace vehicle dynamics
p 31 N94-11491
Supervised autonomous control, shared control, and teleoperation for space servicing p 183 N94-11577
The rational behavior model: A multi-paradigm, tri-level software architecture for the control of autonomous vehicles
[AD-A265175] p 332 N94-11874

AUTOMATIC FLIGHT CONTROL
Flight simulator experiment of the cockpit advisory system
[NAL-TR-1151] p 33 N94-10733

AUTOMATIC PILOTS
The Memphis Precision Runway Monitor Program Instrument Landing System final approach study
[AD-A266035] p 23 N94-11103

AUTOMATIC WEATHER STATIONS
Development of a buoy system for monitoring marine weather and marine life abundance p 217 N94-12694

AUTOMATION
Use of robots for aircraft dry stripping via plastic media blasting p 127 N94-10620
Large Aircraft Robotic Paint Stripping (LARPS) system and the high pressure water process
p 127 N94-10623
Reuse: A knowledge-based approach
p 329 N94-11430

AUTOMOBILE FUELS
Business fleet refueling assessment
[PB93-189892] p 98 N94-11017

AUTOMOBILES
Business fleet refueling assessment
[PB93-189892] p 98 N94-11017
Life-cycle cost analysis of conventional and fuel cell/battery powered urban passenger vehicles
[DE93-010770] p 182 N94-11438
Electric and hybrid vehicle site operators program: Thinking of the future
[DE93-011231] p 144 N94-11609
Polymer electrolyte fuel cells: Potential transportation and stationary applications
[DE93-010734] p 264 N94-11666

AUTOMORPHISMS
The modular group and super-KMS functionals
[DE93-613029] p 349 N94-10632

AUTONOMIC NERVOUS SYSTEM
Proceedings of the First Joint NASA Cardiopulmonary Workshop
[NASA-CP-10068] p 308 N94-11991

AUTONOMOUS NAVIGATION
Sensor abstractions to support many-robot systems
[AD-A265907] p 180 N94-10803

AUTONOMY
The rational behavior model: A multi-paradigm, tri-level software architecture for the control of autonomous vehicles
[AD-A265175] p 332 N94-11874

AUXILIARY POWER SOURCES
Investigation of alternate power source for Space Shuttle Orbiter hydraulic system
[NASA-CR-193229] p 46 N94-10911

AVALANCHES
Evolution of steep Martian slopes p 434 N94-11184
Scalloped margin domes: What are the processes responsible and how do they operate?
p 454 N94-12120

AVIATION METEOROLOGY
Stability model of the atmosphere p 32 N94-11500

AVIONICS
An analysis of the modes and states for generic avionics
[NASA-CR-188253] p 27 N94-10664

AXIAL FLOW
Laboratory study on the natural modes of a rotating two-phase fluid system subject to axial excitation
p 106 N94-10106
Development of passive superconducting bearings. Phase 3
[AD-A266050] p 180 N94-10706

AXIAL LOADS
Numerical simulation and experimental results of filament wound CFRP tubes tested under biaxial load
p 58 N94-10015
Analytical prediction and test verification of the multiaxial behaviour of high-strength steel for lightweight structures
p 58 N94-10016
Effects of axial and centrifugal forces on the stability of liquid bridges p 102 N94-10083
Design and development of a miniature column-based interface (MCBI) stress gage
[AD-A266054] p 170 N94-10873
Nonlinear response of a clamped-clamped beam with internal resonance under sinusoidal excitation
p 186 N94-10897

AXISYMMETRIC FLOW
Stability of hypersonic boundary-layer flows with chemistry p 7 N94-10451

AZIDES (INORGANIC)
Polymers for microelectronics
[AD-A266036] p 94 N94-12396

AZIDES (ORGANIC)
A novel photosensitive polyimide resist consisting of a soluble polyimide and a bis(perfluorophenyl azide) as a cross-linker
[AD-A265998] p 93 N94-12353
Polymers for microelectronics
[AD-A266036] p 94 N94-12396

AZO COMPOUNDS
A relaxation study of poled nonlinear optical polymers by infrared reflection-absorption spectroscopy
[AD-A265797] p 93 N94-12380

NMR characterization of polymers formed in diazotizing mixtures of luminol and 3-amino-L-tyrosine [AD-A266093] p 94 N94-12536

B

B STARS

The abundances of the elements in sharp-lined early type stars [NASA-CR-194055] p 424 N94-12573

B-52 AIRCRAFT

The radar eye blinded: The USAF and electronic warfare, 1945-1955 [AD-A265494] p 132 N94-10497

Special investigation report: Commercial space launch incident, launch procedure anomaly orbital sciences corporation PEGASUS/SCD-1, 80 nautical miles east of Cape Canaveral, Florida, February 9, 1993 [PB93-917003] p 40 N94-11893

BABOONS

Central circulatory hemodynamics as a function of gravitational stress p 309 N94-11995

BACILLUS

Microbiological test results using three urine pretreatment regimes with 316L stainless steel [NASA-CR-192568] p 299 N94-10360

BACKGROUND NOISE

A multi-variance analysis in the time domain p 146 N94-10999

BACKGROUND RADIATION

The excitation of cyanogen and ionized carbon in interstellar and extragalactic gas clouds p 426 N94-11582

Search for structures in the cosmic microwave background radiation [INPE-5491-TDI/508] p 484 N94-12357

HEAO-1 analysis of Low Energy Detectors (LED) [NASA-CR-194087] p 424 N94-12574

BACKSCATTERING

Preliminary results on backscattering strength from a wind generated bubbly ocean surface [AD-A265006] p 287 N94-10490

Application of spin-sensitive electron spectroscopies to investigations of electronic and magnetic properties of solid surfaces and epitaxial systems [DE93-015079] p 76 N94-10854

Enhancement effects in polarimetric radar returns: Phase difference statistics [NASA-CR-193408] p 231 N94-11309

A C-band wind scatterometer model derived from the data obtained during the ERS-1 calibration/validation campaign p 233 N94-11711

The activity of the ERS-1 Venice (Italy) group on scatterometry p 233 N94-11713

A preliminary C-band scatterometer model function for the ERS-1 AMI instrument p 233 N94-11715

Signatures of Antarctic firn by means of ERS-1 AMI and by field measurements p 237 N94-11737

Spatial patterns in backscatter strength across the Greenland Ice Sheet p 238 N94-11744

C-band SAR backscatter from ice on shallow tundra lakes: Observations and modelling p 240 N94-11755

The effect of rain on ERS-1 altimeter data p 243 N94-11773

Effect of species structure and dielectric constant on C-band forest backscatter [NASA-TM-109219] p 245 N94-11885

Ocean wave detection by SAR p 197 N94-11932

On the determination of the SAR ocean surface scattering patch size p 197 N94-11933

Physical processes of microwave backscattering from laboratory wind-wave surfaces p 200 N94-11952

Experiment and results of the Italian activity in the field of ocean microwave backscattering p 200 N94-11953

The microwave backscattering from wind waves p 201 N94-11959

Remote sensing of subsurface water temperature profile and backscattering coefficient in the China Sea by Ocean Lidar (OLIDAR) p 203 N94-11970

Geology and surface characteristics of Bell Regio, Venus p 457 N94-12136

Application of a dynamic subgrid-scale model to turbulent recirculating flows p 156 N94-12290

Snow and glacier investigations by ERS-1 SAR: First results p 247 N94-12481

Extraction of plant and soil parameters from multitemporal ERS-1 SLC data of the Freiburg test site p 248 N94-12491

Observations of ERS-1 SAR sensitivities to changes in aboveground biomass in young loblolly pine forests p 249 N94-12494

Polarisation of backscattering radiation at remote sensing of ocean with impulse laser beam p 177 N94-12722

Fundamental studies of radar scattering from water surfaces: The Lake Washington experiment [NASA-CR-194030] p 139 N94-12778

BACKWARD FACING STEPS

Direct numerical simulation of turbulent flow over a backward-facing step p 156 N94-12296

BACKWARD WAVE TUBES

On the stability of stationary regimes in a distributed autovibration system with external feedback [DE93-620979] p 141 N94-10543

To the theory of irregular auto modulation in electron beam-backward electromagnetic wave dynamic system [DE93-620982] p 133 N94-11030

Non-linear dynamics of automodulation processes in coupled distributed autovibration systems with delay [DE93-620976] p 143 N94-11365

BACTERIA

Conversion of acetic acid to methane by thermophiles [DE93-014433] p 300 N94-10652

Biogeochemical factors which regulate the formation and fate of sulfide in wetlands p 270 N94-12464

The effects of acid deposition on sulfate reduction and methane production in peatlands p 270 N94-12465

BAFFLES

Flow visualization of shock propagation in baffle systems [DE93-013312] p 147 N94-10307

A theory of membrane absorbers [ISVR-TR-217] p 76 N94-11216

BALL BEARINGS

Application of powder metallurgy techniques to produce improved bearing elements for liquid rocket engines [NASA-CR-193731] p 82 N94-10804

BALLISTIC MISSILES

Estimation with multisensor/multiscan detection fusion [AD-A265673] p 138 N94-12338

BALLISTIC TRAJECTORIES

Behavior of vortices generated by an advancing ejecta curtain in theory, in the laboratory, and on Mars p 169 N94-12044

BALLISTICS

Deformation mechanisms in tungsten single crystals in ballistic impact experiments [AD-A265701] p 405 N94-12563

BALLOON-BORNE INSTRUMENTS

Development of a balloon-borne stabilized platform for measuring radiative flux profiles in the atmospheric boundary layer [DE93-013186] p 274 N94-10323

BALLOONING MODES

Kinetic approach to long wave length modes in rotating plasmas [DE93-771286] p 388 N94-10807

BALTIC SEA

Finnish ERS-1 Baltic Sea ice experiment in Winter 1992 p 239 N94-11750

BANACH SPACE

Convergence theorems for a class of nonlinear maps in uniformly smooth Banach spaces [DE92-641347] p 343 N94-10531

BANDPASS FILTERS

Alkali metal for ultraviolet band-pass filter [NASA-CASE-NPO-18433-1-CU] p 381 N94-10657

Continued development of an ultra-narrow bandpass filter for solar research [NASA-CR-194169] p 381 N94-10735

BANDWIDTH

Limited bandwidth microwave filter [AD-D015744] p 145 N94-12322

BARENTS SEA

Ice studies in the Barents Sea by ERS-1 SAR during SIZEX 92 p 238 N94-11745

Ice studies in the Barents Sea by ERS-1 during SIZEX 1992 p 210 N94-12653

BARIUM COMPOUNDS

Grain boundaries in complex oxides [DE93-013986] p 398 N94-11012

BARIUM OXIDES

Grain boundaries in complex oxides [DE93-013986] p 398 N94-11012

BARORECEPTORS

Carotid-cardiac baroreflex: Relation with orthostatic hypotension following simulated microgravity and implications for development of countermeasures p 308 N94-11992

BARRED GALAXIES

The IR properties of ringed galaxies and the IRAS database [NASA-CR-194286] p 426 N94-11590

BARS (LANDFORMS)

Coastal processes due to nearshore current around an upheaving island p 199 N94-11942

Study of growing processes of a tombolo using an air photograph p 218 N94-12702

BARYONS

Development of deterministic transport methods for low energy neutrons for shielding in space [NASA-CR-194172] p 366 N94-11199

A generalized Bethe-Weizsaecker mass formula for strange hadronic matter [DE93-011010] p 368 N94-11620

BASALT

The Lathrop Wells Volcanic Center: Status of field and geochronology studies [DE93-008917] p 273 N94-10285

Radiogenic age and isotopic studies [DE93-610548] p 274 N94-10407

In situ secondary ion mass spectrometry analysis [DE93-012185] p 76 N94-11140

Cold press sintering of simulated lunar basalt p 131 N94-12026

Ejecting basaltic achondrites from Vesta: Hydrodynamical impact models p 429 N94-12036

Stable isotope analyses of the peralkaline volcanics Gregory Rift Valley, Kenya p 281 N94-12072

Th-230 - U-238 series disequilibrium of the Olkaria basalts Gregory Rift Valley, Kenya p 281 N94-12073

Th-230 - U-238 series disequilibrium of the Olkaria basalts Gregory Rift Valley, Kenya: Petrogenesis p 281 N94-12074

Th-230 - U-238 series disequilibrium of the Olkaria rhyolites Gregory Rift Valley, Kenya: Residence times p 281 N94-12076

Spectral and multispectral imaging studies of lunar mantled mare deposits p 446 N94-12079

Graphite solubility and co-vesiculation in basalt-like melts at one-ATM p 463 N94-12173

The Fe/Mn constraint on precursors of basaltic achondrites p 432 N94-12208

Assimilation in lunar basalts and volcanic glasses: Implications for a heterogeneous mantle source region p 478 N94-12250

BASE PRESSURE

An experimental investigation of high-speed water-entry for full-size and scale-model pointed nose vehicles [DE93-008491] p 147 N94-10252

BATHYMETERS

An investigation using empirical orthogonal functions and objective analysis to analyse the vertical temperature structure of a gulf stream meander [AD-A265116] p 289 N94-11868

Mapping bathymetric slopes from bathymetry data [AD-A265923] p 290 N94-12350

SAR imaging of geology and bathymetry: Kent coastal area - southern North Sea p 254 N94-12527

BATHYTHERMOGRAPHS

The subduction experiment. Cruise report, R/V Oceanus, cruise number 250 legs 1 and 2. Subduction 2 mooring deployment and recovery cruise, 25 January-26 February 1992 [AD-A264922] p 289 N94-11853

An investigation using empirical orthogonal functions and objective analysis to analyse the vertical temperature structure of a gulf stream meander [AD-A265116] p 289 N94-11868

BAYES THEOREM

Bayesian reliability analysis with imprecise prior probabilities [MEMO-COSOR-92-50] p 183 N94-10170

The theory for, and demonstration of, information theory applied to radar target identification [DE93-006393] p 132 N94-10315

Imprecise highest density regions related to intervals of measures [MEMO-COSOR-92-54] p 347 N94-10876

Introduction to Bayesian image analysis [DE93-012628] p 347 N94-11006

Bayesian model for pictorial data fusion of satellite image [INPE-5457-TDI/499] p 345 N94-11193

Per-field filtering and classification of multitemporal ERS-1 SAR imagery p 247 N94-12485

BAYS (STRUCTURAL UNITS)

Analysis of the characteristic and mechanism of suspended matter transportation in Huanghe delta sea area using remote sensing techniques p 197 N94-11930

BAYS (TOPOGRAPHIC FEATURES)

Data management strategy for the Tampa Bay National Estuary Program: Recommendations and implementation plan [PB93-191633] p 267 N94-11864

Exchange of bay water with ocean current monitored by the NOAA satellite p 193 N94-11908

The extraction of bottom characteristics and mapping in Kin Bay, Okinawa Main Island, Japan, using LANDSAT-5/TM and SPOT-1/HRV data p 197 N94-11931

The Kyucho events in Sukumo Bay induced by Kuroshio front disturbances p 198 N94-11939

Optical characteristics in Tokyo Bay p 204 N94-11972
Validation test system for sea surface temperature detected by satellites in Mutsu Bay p 213 N94-12670
Intrusion of Kuroshio warm water into Sagami Bay p 215 N94-12683

BCH CODES
Flexible high-speed CODEC
[NASA-CR-191169] p 146 N94-12433

BEAM CURRENTS
Collective acceleration of ions in near-anode plasma of a strong-current relativistic diode
[DE93-620977] p 387 N94-10541
Diagnostic complex for the space-time analysis of energy and current of pulsed relativistic particles
[DE93-620980] p 362 N94-10649
Possibility of a crossed-beam experiment involving slow-neutron capture by unstable nuclei rapid-process-tron
[DE93-754288] p 363 N94-10720

BEAM INJECTION
An experimental program for collective acceleration of ions using intense relativistic electron beams
[DE93-612205] p 371 N94-10316
Experimental investigation of wake field excitation in plasma by a periodic succession of relativistic particle clots
[DE93-621655] p 391 N94-11211

BEAM INTERACTIONS
Scattering of modulated Ultra-Relativistic Electron Beam (UREB) by atmospheric plasma
[DE93-620987] p 387 N94-10558

BEAM SPLITTERS
A compact, four-way image splitter
[AD-A266107] p 382 N94-11656

BEAMFORMING
Wideband beamforming for a sparse nonuniform spaced sensor array
[AD-A265909] p 133 N94-10660

BEAMS (SUPPORTS)
Payload sensitivity in coupled bending and torsional vibrations in flexible beams
[MEMO-1102] p 184 N94-10161
Nonlinear response of a clamped-clamped beam with internal resonance under sinusoidal excitation p 186 N94-10897

BEARING ALLOYS
Application of powder metallurgy techniques to produce improved bearing elements for liquid rocket engines
[NASA-CR-193731] p 82 N94-10804

BEARINGS
Dynamic tester for rotor seals and bearings
[NASA-CASE-MFS-28493-1] p 33 N94-10669
Effect of surface cleanliness of bearing steel on adhesive strength and tribological properties of sputter-deposited gold films
[DE93-767974] p 82 N94-10732

BEAUFORT SEA (NORTH AMERICA)
Sea ice deformation observed with ERS-1 SAR p 239 N94-11749

BED REST
Exercise countermeasures for bed-rest deconditioning
[NASA-TM-103987] p 300 N94-11191
Glycerol-induced hyperhydration p 309 N94-11996
Spectral analysis of resting cardiovascular variables and responses to oscillatory LBNP before and after 6 degree head dowm bedrest p 309 N94-11997
Effect of prolonged LBNP and saline ingestion on plasma volume and orthostatic responses during bed rest p 310 N94-11998
Hormonal regulation of fluid and electrolyte metabolism in zero-g and bedrest p 311 N94-12004

BEHAVIOR
Effect of double density caging during Space Shuttle transport of laboratory rats
[NASA-CR-193228] p 300 N94-11180

BENARD CELLS
Experimental analysis of Benard-convection by the combined application of liquid crystals and PIV p 106 N94-10109

BEND TESTS
Evaluation of test specimen shape effects on the flexural fatigue of CFRP laminates
[NAL-TR-1159] p 65 N94-10857
Understanding cracking failures of coatings: A fracture mechanics approach p 187 N94-11218

BENDING
Payload sensitivity in coupled bending and torsional vibrations in flexible beams
[MEMO-1102] p 184 N94-10161
Test specifications, specimen design and instrumentation test data interpretation
[DE93-012338] p 188 N94-11367

BENDING FATIGUE
Evaluation of test specimen shape effects on the flexural fatigue of CFRP laminates
[NAL-TR-1159] p 65 N94-10857
Fracture mechanics and full scale pipe break testing for the Department of Environment's New Production Reactor-Heavy Water Reactor
[DE93-005428] p 187 N94-11169
Failure prediction of thin beryllium sheets used in spacecraft structures
[NASA-CR-194164] p 187 N94-11190

BENDING MOMENTS
Imperfection sensitivity of the Brazier effect for orthotropic cylindrical shells
[LR-687] p 186 N94-10879

BENDING THEORY
Flexure and the role of inplane force around coronae on Venus p 452 N94-12112

BENZENE
Site dependence of the apparent shape of a molecule in STM images: Benzene on Pt(111)
[AD-A263488] p 365 N94-11093

BERYLLIUM
Failure prediction of thin beryllium sheets used in spacecraft structures
[NASA-CR-194164] p 187 N94-11190
Carbon analyses of IDP's sectioned in sulfur and supported on beryllium films p 81 N94-12099

BERYLLIUM ALLOYS
Aluminum-beryllium alloys for aerospace applications p 60 N94-10029

BERYLLIUM ISOTOPES
Measurements of cosmogenic nuclides in lunar rock 64455 p 437 N94-12033

BESSEL FUNCTIONS
An exactly solvable model of an oscillator with nonlinear coupling and zeros of Bessel functions p 349 N94-10573

BETA PARTICLES
The effect of a scalar boson coupled to neutrinos on the behavior of the tritium beta decay spectrum near the end point
[DE93-012655] p 361 N94-10349
On parity conservation and the question of the missing, right-handed neutrino
[DE93-613092] p 361 N94-10414
Monte Carlo algorithms in simulation of 2beta-decay and penetration of electrons through matter
[DE93-617741] p 364 N94-10837
Review of betavoltaic energy conversion p 53 N94-11407

BETATRONS
Ion shaking in the 200 MeV XLS-ring
[DE93-014057] p 374 N94-12782

BETHE-SALPETER EQUATION
Fermion-boson scattering in ladder approximation
[DE93-613111] p 368 N94-11581

BIAS
The three-point function as a probe of models for large-scale structure
[NASA-CR-193249] p 425 N94-11153
Effects of wave nonlinearity on ERS-1 radar altimeter returns: A preliminary investigation p 235 N94-11722
Estimation with multisensor/multiscan detection fusion
[AD-A265673] p 138 N94-12338

BIBLIOGRAPHIES
Bibliography on Hot Isostatic Pressing (HIP) technology
[AD-A265668] p 81 N94-10297
Aeronautical engineering: A continuing bibliography with indexes (supplement 293)
[NASA-SP-7037(293)] p 1 N94-10420
Bibliographic notes on Voronoi diagrams
[PB93-189298] p 343 N94-10825
Biscayne bay: A bibliography of the marine environment
[PB93-184802] p 266 N94-11451
Aeronautical engineering: A continuing bibliography with indexes (supplement 289)
[NASA-SP-7037(289)] p 1 N94-11687
Aeronautical engineering: A continuing bibliography with indexes (supplement 291)
[NASA-SP-7037(291)] p 1 N94-11690
Aeronautical engineering: A continuing bibliography with indexes (supplement 290)
[NASA-SP-7037(290)] p 1 N94-11691

BIDIRECTIONAL REFLECTANCE
Global monitoring of atmospheric properties by the EOS MODIS
[NASA-TM-109237] p 231 N94-11485
Bi-directional reflectance by oceanic waters studied via Monte-Carlo simulations p 203 N94-11971

BINARY ALLOYS
Ground results of the Mephisto program: Benefits and space experiments orientation p 86 N94-10197
Ripening of immiscible liquid droplets in microgravity with constrained Marangoni drift p 117 N94-10200
A study of the quasibinary Al-W-Mo system. Part 1: Preliminary investigations and preparation for microgravity experiments p 119 N94-10211
A study of the quasibinary Al-Mo-W system. Part 2: A physico-mechanical investigation of the system fabricated under the gravitylessness conditions p 119 N94-10212
Atomic structures and compositions of internal interfaces
[DE93-014840] p 363 N94-10750

BINARY MIXTURES
Stability and dynamics of spatio-temporal structures
[DE93-011374] p 401 N94-11610

BINARY SYSTEMS (MATERIALS)
Laboratory study on the natural modes of a rotating two-phase fluid system subject to axial excitation p 106 N94-10106

BINOCULAR VISION
A high-speed object recognition chip based on biologically-realistic hybrid temporal processing element
[AD-A265490] p 339 N94-11049

BIOASSAY
Five biomedical experiments flown in an Earth orbiting laboratory: Lessons learned from developing these experiments on the first international microgravity mission from concept to landing p 302 N94-11556
Quality assurance for environmental chemistry: 1991, volume 2
[DE93-011792] p 272 N94-12780

BIOASTRONAUTICS
Echocardiography in the flight program p 309 N94-11993
Pulmonary function in microgravity: KC-135 experience p 309 N94-11994

BIOCHEMISTRY
Conversion of acetic acid to methane by thermophiles
[DE93-014433] p 300 N94-10652
Aluminum and membrane channels
[AD-A265241] p 300 N94-11020
Studies in bioorganic chemistry
[AD-A265532] p 55 N94-12011
The role of certain infauna and vascular plants in the mediation of redox reactions in marine sediments p 268 N94-12454
Emissions of biogenic sulfur gases from Alaskan tundra p 268 N94-12455
Acetate concentrations and oxidation in salt marsh sediments p 269 N94-12459

BIOCOMPATIBILITY
Compatibility tests for biological specimens to on-board experiments in the Space Shuttle flight
[NASDA-CNT-930003] p 301 N94-12278

BIOCONVERSION
Coprocessing of fossil fuels and biomass for CO2 emission reduction in the transportation sector
[PB93-194165] p 267 N94-11845
The effects of acid deposition on sulfate reduction and methane production in peatlands p 270 N94-12465

BIODEGRADATION
Primary productivity in the Oyashio area in the spring and summer of 1990 p 211 N94-12658
Characterization of dissolved organic matter in the ocean by using the fluorescence excitation-emission matrix p 211 N94-12659

BIOELECTRICITY
Aluminum and membrane channels
[AD-A265241] p 300 N94-11020
Role of spatially distributed ion channels in single neuron computation
[AD-A265972] p 79 N94-12351

BIOGEOCHEMISTRY
Terminal Decomposition and Gaseous Sulfur Release from Tidal Wetlands
[NASA-CR-193466] p 267 N94-12451
Sulfate reduction and other sedimentary biogeochemistry in a northern New England salt marsh p 268 N94-12453
Biogeochemical factors which regulate the formation and fate of sulfide in wetlands p 270 N94-12464
The effects of acid deposition on sulfate reduction and methane production in peatlands p 270 N94-12465
DMS emissions from Sphagnum-dominated wetlands p 271 N94-12466
Emissions of biogenic sulfur gases from northern bogs and fens p 271 N94-12467
Elevated acetate concentrations in the rhizosphere of Spartina alterniflora and potential influences on sulfate reduction p 271 N94-12468
Factors controlling sulfur gas exchange in Sphagnum-dominated wetlands p 271 N94-12469
Sulfur gas exchange in Sphagnum-dominated wetlands p 271 N94-12470

BIOGRAPHY
Basic attributes test (BAT): Operational pre-implementation analysis and score equating [AD-A265885] p 314 N94-12276
BIOINSTRUMENTATION
Amperometric biosensors based on 3-dimensional hydrogel-forming epoxy networks [AD-A265528] p 87 N94-10510
BIOLOGICAL EFFECTS
Aerospace medicine and biology: A continuing bibliography with indexes (supplement 375) [NASA-SP-7011(375)] p 303 N94-10398
Aerospace medicine and biology: A continuing bibliography with indexes (supplement 376) [NASA-SP-7011(376)] p 303 N94-10399
Proceedings of the Symposium on Radiation Research in Life Science [DE93-754137] p 300 N94-10888
A proposed performance index for galactic cosmic ray shielding materials [NASA-TM-4444] p 484 N94-11278
Aerospace medicine and biology: A continuing bibliography with indexes (supplement 374) [NASA-SP-7011(374)] p 304 N94-11689
BIOLOGICAL EVOLUTION
Oxidation state of the Earth's upper mantle during the last 3800 million years: Implications for the origin of life p 283 N94-12210
BIOLOGICAL MODELS (MATHEMATICS)
Plant architecture, growth and radiative transfer for terrestrial and space environments [NASA-CR-193476] p 302 N94-12559
BIOMASS
Statistical analysis of environmental variability within the CELSS breadboard project's biomass production chamber [NASA-TM-109188] p 315 N94-11258
Coprocessing of fossil fuels and biomass for CO2 emission reduction in the transportation sector [PB93-194165] p 267 N94-11845
Automatic classification system for zooplankton p 203 N94-11969
Extraction of plant and soil parameters from multitemporal ERS-1 SLC data of the Freiburg test site p 248 N94-12491
Observations of ERS-1 SAR sensitivities to changes in aboveground biomass in young loblolly pine forests p 249 N94-12494
The phytoplankton bloom in the Kinu-ura Bay, Japan in the rainy season p 211 N94-12660
Variation of the photosynthetic products in the regional upwelling area around the Izu Islands, Japan p 211 N94-12661
Study on sea water purification using a substratum of marine organisms p 217 N94-12696
Acoustic estimation of plankton biomass p 218 N94-12699
The algorithm of primary production determination p 228 N94-12761
BIOMASS ENERGY PRODUCTION
Coprocessing of fossil fuels and biomass for CO2 emission reduction in the transportation sector [PB93-194165] p 267 N94-11845
BIOPHYSICS
Extended ecosystem signatures with application to Eos synergism requirements [NASA-CR-193398] p 266 N94-11374
BIOPOLYMERS
Development of bioelastic materials for the prevention of adhesions: Polypenta- and polytetrapeptides [AD-A264851] p 88 N94-10863
BIOPROCESSING
Design of multisample, multistep phase partitioning apparatus for use on Space Shuttle Spacelab, and Spacelab missions p 108 N94-10120
Compatibility tests for biological specimens to on-board experiments in the Space Shuttle flight [NASDA-CNT-930003] p 301 N94-12278
BIOSPHERE
Design of a global soil moisture initialization procedure for the simple biosphere model [NASA-TM-104590] p 284 N94-10940
BIOTECHNOLOGY
Design of multisample, multistep phase partitioning apparatus for use on Space Shuttle Spacelab, and Spacelab missions p 108 N94-10120
Environmental Sciences Division [DE93-013865] p 264 N94-10650
BISMALEIMIDE
An analysis of fiber-matrix interface failure stresses for a range of ply stress states [NASA-TM-108999] p 67 N94-11276
BISMUTH
Alkali metal for ultraviolet band-pass filter [NASA-CASE-NPO-18433-1-CU] p 381 N94-10657
BISMUTH ALLOYS
Containerless processing of equiatomic Mn50Bi50 in a drop tube p 118 N94-10205
BISMUTH OXIDES
Processing and transport properties of high J(sub c) silver clad Bi-2223 tapes and coils [DE93-010674] p 398 N94-11073
BISPHENOLS
New aromatic activated dihalides and bisphenol monomers for the preparation of novel poly(arylene ethers) [NASA-CR-193190] p 55 N94-10513
BIT ERROR RATE
An optoelectronic graphics display processor [AD-A266011] p 171 N94-12391
BLACK HOLES (ASTRONOMY)
Two fluid plasmas in the vicinity of a Schwarzschild black hole [DE93-610264] p 385 N94-10284
BLADE-VORTEX INTERACTION
Perpendicular blade vortex interaction and its implications for helicopter noise prediction: Wave-number frequency spectra in a trailing vortex for BWI noise prediction [NASA-CR-193623] p 357 N94-10752
Simulated wake characteristics of tapered annular wings by a discrete vortex method [NAL-TR-1156] p 13 N94-10855
Lift enhancement of a wing/strake using pneumatic blowing [AD-A265074] p 26 N94-11872
BLAST LOADS
Design and development of a miniature column-based interface (MCBI) stress gage [AD-A266054] p 170 N94-10873
BLOCK COPOLYMERS
Interfacial modification through end group complexation in polymer blends [AD-A265887] p 93 N94-12340
BLOOD
Hormonal regulation of fluid and electrolyte metabolism during periods of headward fluid shifts p 311 N94-12005
BLOOD CIRCULATION
Risk of decompression sickness in the presence of circulating microbubbles p 312 N94-11546
Central circulatory hemodynamics as a function of gravitational stress p 309 N94-11995
Physiological water model development p 316 N94-12367
BLOOD FLOW
Arterial gas emboli in altitude-induced decompression sickness p 312 N94-11543
Strategies and methodologies to develop techniques for computer-assisted analysis of gas phase formation during altitude decompression p 312 N94-11547
Mechanistic studies on reduced exercise performance and cardiac deconditioning with simulated zero gravity p 310 N94-12001
Hormonal regulation of fluid and electrolyte metabolism during periods of headward fluid shifts p 311 N94-12005
BLOOD PLASMA
Effect of prolonged LBNP and saline ingestion on plasma volume and orthostatic responses during bed rest p 310 N94-11998
BLOOD PRESSURE
Echocardiography in the flight program p 309 N94-11993
Valsalva maneuver: Insights into baroreflex modulation of human sympathetic activity p 310 N94-12000
Autogenic-feedback training: A countermeasure for orthostatic intolerance p 311 N94-12006
BLOOD VOLUME
Physiologic mechanisms of circulatory and body fluid losses in weightlessness identified by mathematical modeling p 312 N94-11557
Carotid-cardiac baroreflex: Relation with orthostatic hypotension following simulated microgravity and implications for development of countermeasures p 308 N94-11992
Pulmonary function in microgravity: KC-135 experience p 309 N94-11994
Effect of prolonged LBNP and saline ingestion on plasma volume and orthostatic responses during bed rest p 310 N94-11998
Hormonal regulation of fluid and electrolyte metabolism during periods of headward fluid shifts p 311 N94-12005
BLOWING
Lift enhancement of a wing/strake using pneumatic blowing [AD-A265074] p 26 N94-11872
DNS on control of laminar-turbulent transition in channel flow with suction and blowing p 163 N94-12613
BLUNT BODIES
Comparison of computation and experiment for a high enthalpy, heated-driver, shock-tube environment p 7 N94-10447
Stability of hypersonic flow over a blunt body p 7 N94-10450
Studies of hypersonic viscous flows p 8 N94-10454
BODY CENTERED CUBIC LATTICES
Monte Carlo simulations of phase transformations in Fe-Cr alloys [DE93-013847] p 81 N94-10522
Interatomic interactions in BCC and FCC lattices of transition metals [DE93-621541] p 398 N94-11090
BODY FLUIDS
Physiologic mechanisms of circulatory and body fluid losses in weightlessness identified by mathematical modeling p 312 N94-11557
Glycerol-induced hyperhydration p 309 N94-11996
Effect of prolonged LBNP and saline ingestion on plasma volume and orthostatic responses during bed rest p 310 N94-11998
Fluid compartment and renal function alterations in the rat during 7 and 14 day head down tilt p 310 N94-12002
Local fluid shifts and edema in humans during simulated microgravity p 311 N94-12003
Hormonal regulation of fluid and electrolyte metabolism in zero-g and bedrest p 311 N94-12004
Physiological water model development p 316 N94-12367
BODY KINEMATICS
Position and force control of a vehicle with two or more steerable drive wheels [DE93-012512] p 177 N94-10269
BODY TEMPERATURE
Effect of intermittent cold exposure on the fiber-type composition of selected skeletal muscles in rats [AD-A265309] p 301 N94-11861
BODY-WING CONFIGURATIONS
In-flight evaluation of aerodynamic predictions of an air-launched space booster p 3 N94-10427
BOILING
Two-phase flow heat transfer and hydrodynamics in an electric field p 103 N94-10093
Single bubble experiments in pool boiling: Results from TEXUS 26 p 124 N94-10243
Boiling heat-transfer processes and their application in the cooling of high heat flux devices [AD-A266086] p 413 N94-12535
Compilation of proposals for boiling and evaporation experiments in space environments and proposals concerning experiment projects p 161 N94-12549
BOLIDES
Shock induced reaction in Chicxulub target materials (CaSO4 and SiO2) and their relation to extinctions p 282 N94-12149
BOLTZMANN TRANSPORT EQUATION
Development of deterministic transport methods for low energy neutrons for shielding in space [NASA-CR-194172] p 366 N94-11199
Chaos, entropy, and reversibility: A simple example p 31 N94-11495
BONDED JOINTS
A study of strength evaluations of EDNi/EDCu/NARloy-Z bonded joints [NASA-TM-108418] p 188 N94-11275
BONDING
Joints between dissimilar metallic and ceramic materials p 63 N94-10052
Processing and properties of coated HPZ fiber reinforced glass-ceramic matrix composites [AD-A265177] p 92 N94-11876
BONES
Pilot trial of potentiating normal healing of stress fractures using pulsing electromagnetic fields [AD-A264251] p 311 N94-12364
BOOMS (EQUIPMENT)
In-orbit performance tests and tele-command systems of the umbrella test satellite (DEBUT) [NAL-TR-1165] p 43 N94-10859
BORN APPROXIMATION
Integrated cross sections for the ionisation of atomic hydrogen by electron impact [DE93-610179] p 359 N94-10311
Distorted-wave calculation of He(e,2e) including core-exchange [DE93-610072] p 360 N94-10330
BOROSILICATE GLASS
Vaporization by shock loading of albite, jadeite, and pyrex glass: Experimental study p 97 N94-12039
BOSONS
Aharonov-Bohm effect in Luttinger liquid [DE93-613818] p 408 N94-10148
Top and Higgs masses in a composite boson model [DE93-010874] p 359 N94-10302

The effect of a scalar boson coupled to neutrinos on the behavior of the tritium beta decay spectrum near the end point [DE93-012655] p 361 N94-10349

On thermodynamic properties of heavy fermion systems in magnetic field [DE93-613819] p 409 N94-10403

Nonunitary and unitary approach to Eigenvalue problem of Boson operators and squeezed coherent states p 350 N94-10595

Exact solutions of a many-anyon problem [DE93-617646] p 411 N94-10832

Fermion-boson scattering in ladder approximation [DE93-613111] p 368 N94-11581

Future high precision experiments and new physics beyond Standard Model [DE93-011004] p 373 N94-11618

Top quark search in D(O) from the lepton + jets mode [DE93-014027] p 370 N94-12781

BOUNDARIES

Does the thermal wind exist near the Earth's core boundary? p 283 N94-12217

Finding a covering triangulation whose maximum angle is provably small [DE93-010691] p 334 N94-12593

BOUNDARY CONDITIONS

Studies of P-matrix formalism on the basis of the potential description of two-particle interaction [DE93-617691] p 362 N94-10550

Quantum processes in resonators with moving walls p 380 N94-10612

Quasi-relativistic effects in barrier-penetration processes [DE93-617730] p 410 N94-10721

On the possible unobservability of the Wu-Yang phase factor in curved space [DE93-617645] p 411 N94-10831

Distribution of charged particles near the plasma boundary in the presence of external electric field [DE93-617862] p 389 N94-10886

The searchlight problem for neutrons in a semi-infinite medium [DE93-010796] p 365 N94-10952

High order accurate solutions of viscous problems [NASA-TM-106267] p 151 N94-11253

On temperature distribution in non-participating medium with radiation boundary condition [DE93-619375] p 153 N94-11604

Duality twisted boundary conditions in n-sta te Potts models [DE93-619724] p 346 N94-11811

Summation by parts, projections, and stability [NASA-CR-194290] p 346 N94-12776

BOUNDARY ELEMENT METHOD

Boundary element method for eigenvalue problems of thin plates [ITN-93-85199] p 343 N94-10392

The solving of equations by the method of boundary elements p 326 N94-11182

BOUNDARY INTEGRAL METHOD

Ultrasonic inspection, material noise and surface roughness [DE93-011560] p 183 N94-11110

Boundary integral solution to the electromagnetic scattering from coated surfaces containing edges, gaps, and periodic gratings p 137 N94-11639

BOUNDARY LAYER CONTROL

Method of reducing drag in aerodynamic systems [NASA-CASE-LEW-14791-1] p 12 N94-10672

Receptivity in parallel flows: An adjoint approach p 157 N94-12301

Proceedings of the 9th and 10th NAL Workshop on Investigation and Control of Boundary-Layer Transition [NAL-SP-18] p 163 N94-12611

DNS on control of laminar-turbulent transition in channel flow with suction and blowing p 163 N94-12613

Turbulent drag reduction of a d-type rough wall boundary layer with longitudinal ribs placed within the grooves p 165 N94-12627

BOUNDARY LAYER FLOW

Experimental, analytical, and computational methods applied to hypersonic compression ramp flows p 6 N94-10444

Stability of hypersonic boundary-layer flows with chemistry p 7 N94-10451

On the instability of hypersonic flow past a pointed cone: Comparison of theoretical and experimental results at Mach 8 p 8 N94-10453

Exergy decrease in shock waves and boundary layers of space launch vehicles [AD-A265272] p 42 N94-10493

The effects of successive distortions on a turbulent boundary layer in a supersonic flow p 14 N94-11058

High order accurate solutions of viscous problems [NASA-TM-106267] p 151 N94-11253

CRESLAF. Version 4.0: A Fortran program for modeling laminar, chemically reacting, boundary-layer flow in cylindrical or planar channels [DE93-012835] p 152 N94-11371

BOUNDARY LAYER PLASMAS

Results from the D3-D advanced divertor program [DE93-015472] p 393 N94-11514

BOUNDARY LAYER SEPARATION

Unsteady flow past a NACA 0012 airfoil pitching at constant rates [AD-A265159] p 16 N94-11889

BOUNDARY LAYER STABILITY

An atmospheric boundary layer stability estimator for urban areas [AD-A265189] p 279 N94-12422

Proceedings of the 9th and 10th NAL Workshop on Investigation and Control of Boundary-Layer Transition [NAL-SP-18] p 163 N94-12611

Nonlinear stability calculations of pipe flow p 163 N94-12612

DNS on control of laminar-turbulent transition in channel flow with suction and blowing p 163 N94-12613

Turbulence modeling and compressibility p 163 N94-12614

Aerodynamic sound due to interaction between a two-dimensional free shear layer and the leading edge of a parallel flat plate p 163 N94-12615

Experiment on a high Reynolds number turbulent boundary layer p 164 N94-12617

On the wake behind a high speed train p 164 N94-12618

Calibration of anemometers at low speed by means of towing carriage p 164 N94-12619

Criteria for onset of boundary-layer transition on spinning bodies p 164 N94-12620

On the formation process of Karman vortex street p 16 N94-12621

Nonlinear instability of a laminar flow in a rectangular duct and generation of the turbulent secondary flow p 164 N94-12622

Curvature effects in three-dimensional boundary layers p 164 N94-12623

Simultaneous 3D turbulent large-scale structures in a flood flow by multi-channels measuring system p 165 N94-12624

A numerical experiment of boundary layer transition at subcritical Reynolds numbers p 165 N94-12625

Turbulent boundary layer interacting with spanwise periodic longitudinal vortex arrays p 165 N94-12626

Turbulent drag reduction of a d-type rough wall boundary layer with longitudinal ribs placed within the grooves p 165 N94-12627

Coherent structure in near wall turbulence with riblets p 165 N94-12628

Instability around an isolated roughness element p 165 N94-12629

Idea of underground airplane p 27 N94-12630

Growth and breakdown of Taylor-Goertler vortices in rotating Blasius boundary layer p 165 N94-12631

Traveling disturbances appearing in yawed cylinder boundary layer transition p 166 N94-12632

Visual structure of Karman vortex streets in a route to chaotic states excited by oscillation of a circular cylinder p 17 N94-12633

Boundary conditions and bifurcations in plane Poiseuille flow p 166 N94-12634

BOUNDARY LAYER TRANSITION

Estimation of the direct acoustic radiation from turbulent spots using boundary layer velocity measurements p 357 N94-10358

Theoretical and Experimental Methods in Hypersonic Flows [AGARD-CP-514] p 2 N94-10421

Control effectiveness at hypersonic speeds p 3 N94-10426

Design and production of insulated wind tunnel models of the Hermes shuttle for heat transfer measurements at hypersonic speeds p 4 N94-10431

On the instability of hypersonic flow past a pointed cone: Comparison of theoretical and experimental results at Mach 8 p 8 N94-10453

Space Shuttle hypersonic aerodynamic and aerothermodynamic flight research and the comparison to ground test results [NASA-TM-4499] p 13 N94-10820

A research program for improving heat transfer prediction for the laminar to turbulent transition region of turbine vanes/blades [NASA-TM-106278] p 151 N94-11256

Boundary layer transition: Prediction and wind tunnel simulation p 32 N94-11498

Topics in pattern formation and chaotic systems [AD-A265922] p 161 N94-12342

Proceedings of the 9th and 10th NAL Workshop on Investigation and Control of Boundary-Layer Transition [NAL-SP-18] p 163 N94-12611

Nonlinear stability calculations of pipe flow p 163 N94-12612

DNS on control of laminar-turbulent transition in channel flow with suction and blowing p 163 N94-12613

Turbulence modeling and compressibility p 163 N94-12614

Aerodynamic sound due to interaction between a two-dimensional free shear layer and the leading edge of a parallel flat plate p 163 N94-12615

Experiment on a high Reynolds number turbulent boundary layer p 164 N94-12617

On the wake behind a high speed train p 164 N94-12618

Calibration of anemometers at low speed by means of towing carriage p 164 N94-12619

Criteria for onset of boundary-layer transition on spinning bodies p 164 N94-12620

On the formation process of Karman vortex street p 16 N94-12621

Nonlinear instability of a laminar flow in a rectangular duct and generation of the turbulent secondary flow p 164 N94-12622

Curvature effects in three-dimensional boundary layers p 164 N94-12623

Simultaneous 3D turbulent large-scale structures in a flood flow by multi-channels measuring system p 165 N94-12624

A numerical experiment of boundary layer transition at subcritical Reynolds numbers p 165 N94-12625

Turbulent boundary layer interacting with spanwise periodic longitudinal vortex arrays p 165 N94-12626

Turbulent drag reduction of a d-type rough wall boundary layer with longitudinal ribs placed within the grooves p 165 N94-12627

Coherent structure in near wall turbulence with riblets p 165 N94-12628

Instability around an isolated roughness element p 165 N94-12629

Idea of underground airplane p 27 N94-12630

Growth and breakdown of Taylor-Goertler vortices in rotating Blasius boundary layer p 165 N94-12631

Traveling disturbances appearing in yawed cylinder boundary layer transition p 166 N94-12632

Visual structure of Karman vortex streets in a route to chaotic states excited by oscillation of a circular cylinder p 17 N94-12633

Boundary conditions and bifurcations in plane Poiseuille flow p 166 N94-12634

BOUNDARY LAYERS

Thermocapillary migration of bubbles: A semi-analytical solution for large Marangoni numbers p 104 N94-10095

Coupled thermogravitational and thermocapillary convection in a two-layer fluid system p 105 N94-10101

Sandia ocean modeling system programmer's guide and user's manual [DE93-007427] p 287 N94-10153

On the role of Soret effect in concentration distribution in crystals growing from the melt p 112 N94-10173

Instability of thermocapillary convection in multiple superposed immiscible liquid layers p 120 N94-10218

Exergy decrease in shock waves and boundary layers of space launch vehicles [AD-A265272] p 42 N94-10493

Theoretical investigation of 3-D shock wave turbulent boundary layer interactions [AD-A265275] p 150 N94-11014

Examination of wall functions for a parabolized Navier-Stokes code for supersonic flow [DE93-011590] p 14 N94-11111

CRESLAF. Version 4.0: A Fortran program for modeling laminar, chemically reacting, boundary-layer flow in cylindrical or planar channels [DE93-012835] p 152 N94-11371

Integral equation methods for mixed boundary problem of fracture mechanics p 188 N94-11617

Direct simulation of compressible wall-bounded turbulence p 156 N94-12294

Reynolds stress closure modeling in wall-bounded flows p 157 N94-12298

Receptivity in parallel flows: An adjoint approach p 157 N94-12301

Generation of internal waves near the shelf boundary p 229 N94-12763

BOUNDARY LUBRICATION

Durability of a carbon segmented circumferential seal for a liquid oxygen turbopump [NAL-TR-1155] p 178 N94-10369

BOUNDARY VALUE PROBLEMS

PANACEA user's manual for PANACEA version 2.0 [DE93-012502] p 321 N94-10263

Complex functions in queueing theory [CWI-BS-R9219] p 342 N94-10352

Boundary of Fatou sets of hyperbolic rational maps or degree two [DE93-613031] p 348 N94-10412
Numerical method of singular problems on singular integrals [DE93-613654] p 343 N94-10546
Improvements for obtaining iterative solutions of large linear systems [DE93-767968] p 343 N94-10729
Regular tensor Green functions of the round waveguide [DE93-621354] p 345 N94-11036
Integral equation methods for mixed boundary problem of fracture mechanics p 188 N94-11617
Summation by parts, projections, and stability [NASA-CR-194290] p 346 N94-12776

BOUSSINESQ APPROXIMATION
Model of convective motion under low gravity p 103 N94-10088
Uni-directional waves over slowly varying bottom. Part 1: Derivation of a KdV-type of equation [MEMO-1098] p 147 N94-10275

BOW WAVES
Exergy decrease in shock waves and boundary layers of space launch vehicles [AD-A265272] p 42 N94-10493

BOXES (CONTAINERS)
Surface-tension driven convection in finite-size containers p 103 N94-10090

BRACKETS
Design of inspection and acceptance test methodology for TIG welded aluminum-alloy bracket for camera housings for IRS-1A space craft and executing it p 61 N94-10037

BRAIN
Psychophysiological measures of cognitive workload in laboratory and flight p 317 N94-11529
Locus coeruleus, vigilance, and stress: Brain mechanisms of adaptive behavioral responsiveness [AD-A265657] p 302 N94-12441

BRAIN CIRCULATION
Physiologic mechanisms of circulatory and body fluid losses in weightlessness identified by mathematical modeling p 312 N94-11557

BRANCHING (MATHEMATICS)
Intermittency following a Hopf bifurcation [W-9301] p 344 N94-10907

BRANCHING (PHYSICS)
Boundary conditions and bifurcations in plane Poiseuille flow p 166 N94-12634

BRASSES
Damping measurements for ultra-high carbon steel/brass laminates [DE93-011886] p 82 N94-11076

BRAZIL
TOVS soundings: Impact on the synoptic analysis over the south and southeast regions of Brazil from March 18 to March 19, 1991 [INPE-5497-TDI/512] p 230 N94-11179

BRAZING
Ceramic technology project database [DE93-012432] p 91 N94-11673

BREADBOARD MODELS
Continued development of an ultra-narrow bandpass filter for solar research [NASA-CR-194169] p 381 N94-10735
Dry in-line thermoplastic matrix impregnation, phase 1 [AD-A265016] p 67 N94-11221

BREAKING
The formation and breakage of liquid bridges under microgravity p 100 N94-10071

BREAKWATERS
Coastal processes due to nearshore current around an upheaving island p 199 N94-11942
Study on sea water purification using a substratum of marine organisms p 217 N94-12696

BREATHING
Transcranial Doppler ultrasound and the etiology of neurologic decompression sickness during altitude decompression p 312 N94-11544

BRECCIA
Descriptions and preliminary interpretations of cores recovered from the Manson Impact Structure (Iowa) p 281 N94-12032
Petrography and preliminary interpretations of the crystalline breccias from the Manson M-1 core p 281 N94-12056
Carbonaceous chondrite clasts in the Kapoeta howardite p 282 N94-12104
The EET87513 clast N: A CM2 fragment in an HED polymict breccia p 453 N94-12117
Post-impact alteration of the Manson impact structure p 282 N94-12188
The granulite suite: Impact melts and metamorphic breccias of the early lunar crust p 282 N94-12197

BREMSSTRAHLUNG
Workshop on NN Bremsstrahlung and Polarization Observables [DE93-010181] p 361 N94-10334
Atomic processes relevant to polarization plasma spectroscopy [DE93-753240] p 393 N94-11594

BREWSTER ANGLE
An analytic model for calculating pump-induced wavefront distortions in laser slabs [DE93-011953] p 174 N94-11126

BRICKS
General overview of an integrated lunar oxygen production/brickmaking system p 131 N94-12027

BRIDGMAN METHOD
The effect of gravitational modulation on convection in vertical Bridgman growth p 113 N94-10178
Flow transitions in a 2D directional solidification model p 114 N94-10183
TEXUS 28 experiment: Convections and crystal growth of Ge:Ga. Analysis of temperature measurements p 114 N94-10184
Convection related radial segregation in an idealized horizontal Bridgman configuration p 115 N94-10185
Effect of experimental procedure on pattern formation and array disorder in cellular solidification p 117 N94-10203

BRIGHTNESS TEMPERATURE
Dependence of oceanic microwave emission on wind direction p 201 N94-11957
Validation of ATSR-1 using aircraft radiometer measurements over the South Atlantic p 252 N94-12515
On the error characteristics of the sea surface temperature observed by satellite p 216 N94-12690

BRILLOUIN EFFECT
Limitations to the quality of optical phase conjugation by stimulated Brillouin scattering [AD-A266006] p 383 N94-12389

BRINES
Hygroscopic absorption to falling films: The effects of the concentration level [ITN-93-85198] p 148 N94-10391
Chemical weathering on Mars: Rate of oxidation of iron dissolved in brines p 455 N94-12128

BRITTLENESS
Particle attraction effects on the centrifugal casting and extrusion of alumina [DE93-011559] p 82 N94-10957
Production of reactive sintered nickel aluminide [DE93-014434] p 83 N94-11127
DBTT measurement by use of Small Punch (SP) test [DE93-753188] p 183 N94-11168

BROADBAND
Wideband beamforming for a sparse nonuniform spaced sensor array [AD-A265909] p 133 N94-10660

BROADCASTING
Building penetration loss measurements for DAB signals at 211 MHz [BBC-RD-1992/14] p 133 N94-11024

BROKEN SYMMETRY
Effective action in the gauged Nambu-Jona-Lasinio model [DE93-617654] p 409 N94-10405
Standard model status (in search of new physics) [DE93-013288] p 410 N94-10528
Planck scale effects on the Majoron [DE93-613120] p 410 N94-10545
Spontaneous symmetry breaking in QCD [DE93-753080] p 396 N94-10645
Proceedings of the Workshop on New Aspects of Quantum Field Theories [DE93-754136] p 411 N94-10887
Dissipative phase transitions in field theory models with spontaneous symmetry violation [DE93-621382] p 412 N94-11039
Cosmological restrictions on conformally-invariant SU(5) GUT models [DE93-619770] p 412 N94-11047
Quark and lepton masses [DE93-012308] p 370 N94-12787

BROWNIAN MOVEMENTS
Infinite-mode squeezed coherent states and non-equilibrium statistical mechanics (phase-space-picture approach) [LBL-32695] p 380 N94-10608
Chaos, entropy, and reversibility: A simple example p 31 N94-11495

BRUDERHEIM METEORITE
Separation of spallation and terrestrial C-14 in chondrites p 431 N94-12183

BSCCO SUPERCONDUCTORS
Development of commercially viable high-T(sub c) Bi-2223 superconductor tapes [DE93-009966] p 142 N94-10951
Texture analysis of high Tc superconductors p 399 N94-11314

BUBBLES
Thermocapillary migration of bubbles: A semi-analytical solution for large Marangoni numbers p 104 N94-10095
Bubbles and drops behaviour under low-gravity: A space experiment for the IML-2 mission p 104 N94-10098
Thermocapillary slug flow in a capillary tube p 105 N94-10104
Numerical simulation of Marangoni convection around gas bubbles in a liquid matrix p 106 N94-10107
Coupled growth of cells and bubbles in directional solidification of succinonitrile-acetone alloys p 118 N94-10206
Study of vapor bubble growth in a supersaturated liquid p 122 N94-10232
Single bubble experiments in pool boiling: Results from TEXUS 26 p 124 N94-10243
VLBI and the detection of interstellar magnetohydrodynamic waves p 135 N94-11066
Acoustics of bubbly sediments [AD-A263726] p 288 N94-11299
Use of ultrasound in altitude decompression modeling p 317 N94-11540
Joint pain and Doppler-detectable bubbles in altitude (Hypobaric) decompression p 312 N94-11542
Transcranial Doppler ultrasound and the etiology of neurologic decompression sickness during altitude decompression p 312 N94-11544
Risk of decompression sickness in the presence of circulating microbubbles p 312 N94-11546
Strategies and methodologies to develop techniques for computer-assisted analysis of gas phase formation during altitude decompression p 312 N94-11547

BUCKLING
Design evaluation of GLARE laminate lay-ups p 63 N94-10051
Perforated plates for thin-walled structures p 63 N94-10056
Hydrostatic testing of thick laminated composite cylinders for performance model validation [DE93-012728] p 184 N94-10264
Imperfection sensitivity of the Brazier effect for orthotropic cylindrical shells [LR-687] p 186 N94-10879

BUILDINGS
Building penetration loss measurements for DAB signals at 211 MHz [BBC-RD-1992/14] p 133 N94-11024
Study of the atmospheric chemistry of radon progeny in laboratory and real indoor atmospheres [DE93-012236] p 266 N94-11671

BUOYANCY
Marangoni and buoyant convections in zone melting of GaAs with liquid encapsulation p 101 N94-10081
Calculation of the effects of magnetic field damping in fluid flow: Comparison of magnetohydrodynamic models of different complexity p 103 N94-10089
Heat and mass transfer mechanisms of the polymerization under terrestrial and microgravity conditions p 103 N94-10092
Boundary layers along horizontal free surfaces due to combined effects of temperature and concentration gradients p 106 N94-10108
Appearance of convective instabilities caused by liquid-liquid phase separation under small buoyancy forces p 120 N94-10221
The kinematics of buoyancy induced mixing p 123 N94-10239
Buoyant subduction on Venus: Implications for subduction around coronae p 455 N94-12130
Large eddy simulations of time-dependent and buoyancy-driven channel flows p 155 N94-12287

BUOYS
Study of the surface circulation to the North of Bransfield Strait, Antarctica [INPE-5472-TDI/503] p 288 N94-11200
Development of a buoy system for monitoring marine weather and marine life abundance p 217 N94-12694

BURGER EQUATION
Application of incremental unknowns to the Burgers equation p 156 N94-12293

BURNERS
Distributed combustion in solid propellants [AD-A265727] p 99 N94-12564

BURNING RATE
Methanol pan fires in an enclosed space: Effect of pressure and oxygen concentration [AD-A266108] p 79 N94-12415

BURNTHROUGH (FAILURE)
Polyimide foam insulation systems: A major weight reduction and improvement in fire resistance of sidewall systems p 17 N94-10769
A new FR water resistant acoustic insulation material for aircraft p 18 N94-10773

An investigation into aircraft fuselage fire hardening p 19 N94-10782

BY-PRODUCTS
Feature association without a motion estimate [AD-A265162] p 138 N94-11891

C

C BAND
A C-band wind scatterometer model derived from the data obtained during the ERS-1 calibration/validation campaign p 233 N94-11711
A preliminary C-band scatterometer model function for the ERS-1 AMI instrument p 233 N94-11715
Preliminary analysis of circulations over the Indian Ocean and adjoining regions using ERS-1 surface winds in the NCMRWF data assimilation system p 234 N94-11719
Assessment of ERS-1 SAR data for soil moisture estimation p 249 N94-12492
Mapping of sea bottom topography with ERS-1 C-band SAR p 254 N94-12525

C++ (PROGRAMMING LANGUAGE)
Object oriented implementation of adaptive mesh refinement algorithms [DE93-011885] p 325 N94-11112

CABIN ATMOSPHERES
A combustion products analyzer for contingency use during thermodegradation events on spacecraft p 318 N94-11555

CADMIUM SELENIDES
Synthesis and electronic properties of nanophase semiconductor materials [AD-A265287] p 146 N94-12584

CADMIUM TELLURIDES
CdTe crystal growth in the Soviet facility zona 4 p 106 N94-10111
CdTe crystal growth by THM with a rotating magnetic field p 107 N94-10116
Mission support for crystal growth experiments in Russian unmanned carriers p 111 N94-10139
Flexible polycrystalline thin-film photovoltaics for space applications p 50 N94-11393

CALCITE
Dynamic studies of crystal growth using the AFM [DE93-009549] p 399 N94-11268

CALCIUM
Isotopic and trace element characteristics of an unusual refractory inclusion from Essebi p 471 N94-12212

CALCIUM SILICATES
In-situ crystallization of silicate glass films deposited on alpha- Al2O3 [DE93-012969] p 95 N94-12596

CALCULUS
Delineation of mesoscale features of ocean on satellite IR image p 214 N94-12675
The algorithm of primary production determination p 228 N94-12761

CALDERAS
Giant radiating dyke swarms on Earth and Venus p 283 N94-12236

CALIBRATING
Calibration of accelerometers on drop tower Bremen p 108 N94-10121
Particle image velocimetry technique: Calibration tests p 111 N94-10137
An overview of the Defence Research Agency photovoltaic programme p 53 N94-11412
Robotic servicing on Earth orbiting satellites p 45 N94-11579
Calibration and validation of the ERS-1 wind scatterometer p 232 N94-11706
Validation of directional wave spectra from the ERS-1 during the ESA CAL/VAL campaign p 232 N94-11707
The Grand Banks ERS-1 SAR wave spectra validation experiment p 232 N94-11708
Validation of ERS-1 wind and wave data by use of operational forecast models p 233 N94-11710
ERS-1 studies at the Department of Oceanography from Space, IFREMER/Brest (France) p 233 N94-11712
Calibration of ERS-1 altimetry over the North Sea p 234 N94-11716
ERS-1 SAR calibration strategy p 235 N94-11726
ERS-1 preliminary antenna elevation pattern measured by ground-receivers p 235 N94-11727
Preliminary results of the experiment I-7 p 235 N94-11728
The ERS-1/CV 580 SAR cross-calibration experiment: Sault Ste Marie, October 26 - November 2, 1991 p 236 N94-11729
Calibration of the ERS-1 SAR fast-delivery images p 236 N94-11730
Calibration results for the ERS-1, AIRSAR, and PHARS p 236 N94-11731
The use of active devices in the ERS-1 radiometric calibration p 236 N94-11732
An experiment for the radiometric calibration of the ERS-1 SAR p 236 N94-11733
The height calibration of the ERS-1 radar altimeter p 241 N94-11764
Validating the UK-PAF land ice product surface elevation p 244 N94-11780
Global wave height climatologies from ERS-1 altimeter data, and comparisons with those from GEOSAT p 244 N94-11781
A determination of the external forces required to move the benchmark active controls testing model in pure plunge and pure pitch [NASA-TM-107743] p 16 N94-12421
Validation of the ATSR/M microwave radiometer data p 252 N94-12511
Calibration of anemometers at low speed by means of towing carriage p 164 N94-12619

CALLISTO
Theoretical studies of the radar properties of the icy Galilean moons of Jupiter [NASA-CR-193407] p 434 N94-11361

CALORIMETERS
A new method for hysteresis measurements developed for C(sub v) measurements at the critical point during the D2-mission p 107 N94-10114
Experimental approach to non-contact calorimetry in space p 112 N94-10143
Relativistic heavy ion research [DE93-013127] p 367 N94-11373
Theory of elementary particles and accelerator theory. Task C: Experimental high energy physics [DE93-013139] p 368 N94-11696
Calorimetric thermometry of meteoritic troilite: A feasibility study p 428 N94-12025
Experimental particle physics at the University of Pittsburgh [DE93-013326] p 369 N94-12546
Hot-gas-side heat transfer characteristics of subscale, plug-nozzle rocket calorimeter chamber [NASA-TP-3380] p 55 N94-12569
Upgraded D(O) calorimeter electronics for short Tevatron bunch space and the effect of pile-up on the W mass measurement [DE93-013566] p 146 N94-12603
Pion correlations and calorimeter design for high energy heavy ion collisions [DE93-013861] p 373 N94-12607

CAMERAS
Design of CCD camera system for use inside electron beam furnace [DE93-009525] p 170 N94-11267
An indium gallium arsenide charge-coupled device (CCD) for 1-3 micron imaging [AD-A266134] p 401 N94-11476
Ultraviolet plume instrument description and plume data reduction methodology [AD-A266141] p 54 N94-11643

CANADA
Radiogenic age and isotopic studies [DE93-610548] p 274 N94-10407
Paint removal activities in Canada p 126 N94-10615
Wind and surface features in SAR images: The Canadian program p 234 N94-11718

CANADIAN SPACE PROGRAM
Canada's longterm space plan and ISY activities p 37 N94-10692

CANADIAN SPACECRAFT
Satellite observations of red tide events: Plans for EESI p 191 N94-11899

CANARD CONFIGURATIONS
X-29: Longitudinal instability at high angle-of-attack p 33 N94-11504

CANCER
Longitudinal study of astronaut health: Mortality in the years 1959-1991 p 312 N94-11560

CANONICAL FORMS
On output linearization of observable dynamics [MEMO-1105] p 341 N94-10276

CANOPIES (VEGETATION)
Plant architecture, growth and radiative transfer for terrestrial and space environments [NASA-CR-193476] p 302 N94-12559

CAPACITANCE
New experimental techniques for solar cells p 52 N94-11403

CAPACITORS
Effects of aqueous solution compositions on Aerocapacitor energy density [DE93-013431] p 140 N94-10309
Lightweight linear alternators with and without capacitive tuning [NASA-CR-185273] p 140 N94-10505

CAPILLARY FLOW
Thermocapillary convection instability in microgravity crystal growth p 112 N94-10172
Vibrational-thermocapillary parallel flows and stability p 120 N94-10220

CAPILLARY TUBES
Thermocapillary slug flow in a capillary tube p 105 N94-10104

CAPILLARY WAVES
Wind-wave and foam dynamics from optical and radar airborne observations p 226 N94-12745
Observations of surface signatures in the north-west Pacific Ocean with the spaceborne SAR p 226 N94-12746
Radar observation of internal waves field in the north-west Pacific p 226 N94-12747

CAPTURE EFFECT
Orbital simulations of satellite escape/capture and the origin of satellites such as Triton p 429 N94-12057

CARBOHYDRATES
Characterization of dissolved organic matter in the ocean by using the fluorescence excitation-emission matrix p 211 N94-12659
The phytoplankton bloom in the Kinu-ura Bay, Japan in the rainy season p 211 N94-12660

CARBON
An experimental program for collective acceleration of ions using intense relativistic electron beams [DE93-612205] p 371 N94-10316
Electrochemical process and product therefrom [AD-D015767] p 75 N94-10380
Preparation of carbon monoliths having tailored pore structure from porous polymer precursors [DE93-011576] p 89 N94-10958
Ionization potentials of small carbon clusters [AD-A264379] p 67 N94-11260
The excitation of cyanogen and ionized carbon in interstellar and extragalactic gas clouds p 426 N94-11582
Energy flow in an Arctic aquatic ecosystem [DE93-013178] p 267 N94-11697
Carbon in weathered ordinary chondrites from Roosevelt County p 428 N94-12035
Carbon analyses of IDP's sectioned in sulfur and supported on beryllium films p 81 N94-12099

CARBON CYCLE
Energy flow in an Arctic aquatic ecosystem [DE93-013178] p 267 N94-11697

CARBON DIOXIDE
Transport of heat and mass in near-critical fluids p 122 N94-10230
Atomic and molecular data for H2O, CO and CO2 relevant to edge plasma impurities [DE93-771423] p 387 N94-10662
Allowable exposure limits for carbon dioxide during extravehicular activity [NASA-TM-103832] p 315 N94-11375
Coprocessing of fossil fuels and biomass for CO2 emission reduction in the transportation sector [PB93-194165] p 267 N94-11845
An observational search for CO2 ice clouds on Mars p 441 N94-12054
Spatial variation in the seasonal south polar cap of Mars as observed by Mariner 7 p 456 N94-12134
Graphite solubility and co-vesiculation in basalt-like melts at one-ATM p 463 N94-12173

CARBON DIOXIDE CONCENTRATION
Modeling present and future river runoff using global atmospheric models [AD-A265274] p 285 N94-11685

CARBON DIOXIDE LASERS
Optimization of a CO2 laser Thomson scattering alpha particle diagnostic [DE93-012782] p 173 N94-10160
Controlling chaotic behavior in CO2 and other lasers [AD-A264811] p 174 N94-10870
Controlling chaotic behavior in a CO2 and other lasers [AD-A265458] p 176 N94-12372

CARBON FIBER REINFORCED PLASTICS
Lightweight CFRP frame structures for a Rotex-derived manipulator system p 56 N94-10005
Design and development of a CFRP central cylinder for satellites p 56 N94-10007
An approach to high precision antenna structures by a CFRP core sandwich concept p 57 N94-10008
Low cost and thermally stable sandwich design for FIRST p 57 N94-10009
Design and manufacturing of filament wound thrust cylinder p 57 N94-10010
Numerical simulation and experimental results of filament wound CFRP tubes tested under biaxial load p 58 N94-10015
Development of a fatigue analysis approach for CFRP structures under acoustic loading p 58 N94-10018
Design and manufacturing of CFRP rings by RTM p 59 N94-10025
Cost effectiveness of structural applications of fibre reinforced thermoplastics p 60 N94-10032

Development tests for a high stability optical bench p 62 N94-10047
Fibre optic strain and temperature measurement in composite materials: A review of the OSTIC programme p 65 N94-10066
Evaluation of test specimen shape effects on the flexural fatigue of CFRP laminates [NAL-TR-1159] p 65 N94-10857
Fibre reinforced polymer matrix composites: Microstructure and mechanical properties [DLR-FB-92-28] p 66 N94-11085

CARBON FIBERS
Design concepts for load-carrying hot structures for reentry bodies p 57 N94-10012
Distortions and stresses in thin shells due to anisotropic thermal expansion p 57 N94-10014
Numerical simulation and experimental results of filament wound CFRP tubes tested under biaxial load p 58 N94-10015
Mechanical properties of magnesium/carbon composites developed by hot pressing under medium pressure p 59 N94-10024
Hydrostatic testing of thick laminated composite cylinders for performance model validation [DE93-012728] p 184 N94-10264
Strain measurement of carbon/epoxy composite with fibre optics white light quasi distributed polarimetric sensor p 69 N94-11328

CARBON ISOTOPES
Interstellar graphite in Murchison: Continued search for isotopically distinct components p 97 N94-12029
The carbon isotopic composition of Novo Urei diamonds p 433 N94-12255

CARBON MONOXIDE
Atomic and molecular data for H2O, CO and CO2 relevant to edge plasma impurities [DE93-771423] p 387 N94-10662

CARBON STEELS
Damping measurements for ultra-high carbon steel/brass laminates [DE93-011886] p 82 N94-11076

CARBON 12
Carbon and nitrogen in Type 2 supernova diamonds p 431 N94-12166

CARBON 13
The 13C and 15N solid-state NMR of copolymers of nylon 6 and 7: Observation of a stable pseudohexagonal phase [AD-A265799] p 94 N94-12381
Primary productivity in the Oyashio area in the spring and summer of 1990 p 211 N94-12658

CARBON 14
Separation of spallation and terrestrial C-14 in chondrites p 431 N94-12183

CARBON-CARBON COMPOSITES
Design concepts for load-carrying hot structures for reentry bodies p 57 N94-10012
Distortions and stresses in thin shells due to anisotropic thermal expansion p 57 N94-10014
An ultralight carbon-carbon composite with amorphous matrix p 61 N94-10042
Advanced methods of permanently joining carbon materials p 63 N94-10057
High temperature composites in Aerospatiale activities p 64 N94-10062
The possibility of using carbon-graphite materials for microwave plasma diagnostics in large fusion devices [DE93-621609] p 66 N94-11143

CARBON-PHENOLIC COMPOSITES
An ultralight carbon-carbon composite with amorphous matrix p 61 N94-10042
Level 3 material characterization of NARC HRPF, HRHU, HRHF, and HRPU [NASA-CR-192579] p 65 N94-10812

CARBONACEOUS CHONDRITES
Mineralogy versus bulk composition of the carbonaceous chondrite clast Kaidun 2 p 429 N94-12101
Carbonaceous chondrite clasts in the Kapoeta howardite p 282 N94-12104
SXRF determination of trace elements in chondrule rims in the unequilibrated CO3 chondrite, ALH A77307 p 429 N94-12106
The EET87513 clast N: A CM2 fragment in an HED polymict breccia p 453 N94-12117
Volatiles in fourteen interplanetary dust particles: A comparison with CI and CM chondrites p 430 N94-12132
Distribution of vanadium and melting of opaque assemblages in Efremovka CAI's p 282 N94-12141
The Th and U abundances in chondritic meteorites p 430 N94-12151
Simulation of possible regolith optical alteration effects on carbonaceous chondrite meteorites p 430 N94-12163
Separation of spallation and terrestrial C-14 in chondrites p 431 N94-12183
Anomalous REE patterns in unequilibrated enstatite chondrites: Evidence and implications p 431 N94-12191
Cathodoluminescence properties of components in enstatite chondrites p 432 N94-12206
The Fe/Mn constraint on precursors of basaltic achondrites p 432 N94-12208
A new carbon-rich phase (COPS) in Antarctic micrometeorites p 432 N94-12233
On possibility of diamond formations in radiation process p 433 N94-12254
The fractionation of noble gases in diamonds of CV3 Efremovka chondrite p 81 N94-12256
Cronstedtite and iron sulfide mineralogy of CM-type carbonaceous chondrites from cryogenic Moessbauer spectra p 433 N94-12257

CARBONACEOUS MATERIALS
A reexamination of amino acids in lunar soil p 452 N94-12109
Mass and spatial distribution of carbonaceous component in Comet Halley p 433 N94-12263

CARBONACEOUS METEORITES
A new carbon-rich phase (COPS) in Antarctic micrometeorites p 432 N94-12233

CARDIAC OUTPUT
Echocardiography in the flight program p 309 N94-11993
Pulmonary function in microgravity: KC-135 experience p 309 N94-11994

CARDIOLOGY
Pulmonary function in microgravity: KC-135 experience p 309 N94-11994

CARDIOVASCULAR SYSTEM
Proceedings of the First Joint NASA Cardiopulmonary Workshop [NASA-CP-10068] p 308 N94-11991
Carotid-cardiac baroreflex: Relation with orthostatic hypotension following simulated microgravity and implications for development of countermeasures p 308 N94-11992
Echocardiography in the flight program p 309 N94-11993
Pulmonary function in microgravity: KC-135 experience p 309 N94-11994
Central circulatory hemodynamics as a function of gravitational stress p 309 N94-11995
Glycerol-induced hyperhydration p 309 N94-11996
Spectral analysis of resting cardiovascular variables and responses to oscillatory LBNP before and after 6 degree head dowm bedrest p 309 N94-11997
Fitness, autonomic regulation and orthostatic tolerance p 310 N94-11999
Valsalva maneuver: Insights into baroreflex modulation of human sympathetic activity p 310 N94-12000
Hormonal regulation of fluid and electrolyte metabolism during periods of headward fluid shifts p 311 N94-12005
Autogenic-feedback training: A countermeasure for orthostatic intolerance p 311 N94-12006
Cardiovascular dynamics during space sickness and deconditioning p 311 N94-12007

CARRIAGES
Calibration of anemometers at low speed by means of towing carriage p 164 N94-12619

CARRIER DENSITY (SOLID STATE)
Organometallic chemical vapor deposition and characterization of ZnGe(1-x)Si(x)P2-Ge alloys on GaP substrates p 400 N94-11443

CARRIER LIFETIME
Response of silicon solar cell to pulsed laser illumination p 51 N94-11396

CARRIER MOBILITY
Kinetics of high concentration arsenic deactivation at moderate to low temperatures [DE93-013349] p 395 N94-10516

CARTESIAN COORDINATES
A spectral nodal method for discrete ordinates problems in x,y geometry [DE93-610128] p 342 N94-10283

CASCADE FLOW
Solving the inverse problem for incompressible potential flow through two-dimensional cascades [NAL-TR-1162] p 147 N94-10365
Laser anemometer measurements and computations for transonic flow conditions in an annular cascade of high turning core turbine vanes [NASA-TP-3383] p 15 N94-11133

CASSINI MISSION
An interferometric spectral mapper for the Cassini mission to Saturn and Titan [NASA-CR-193805] p 482 N94-12429

CASTING
Comparison of Al-Fe alloys produced by PFC and USGA techniques p 58 N94-10019
Marangoni motion during melting of a hypermonotectic alloy: Numerical simulations for the D2 experiment IHF04 p 113 N94-10177
Bibliography on Hot Isostatic Pressing (HIP) technology [AD-A265668] p 81 N94-10297
Physical properties of injection molded liquid crystal polymers and high temperature engineering polymers [AD-A264912] p 87 N94-10508

CASUALTIES
Aviators, air combat, and combat stress: An Air F orce commander's primer [AD-A265083] p 313 N94-11867

CATALOGS (PUBLICATIONS)
Satellite situation report, volume 32, no. 1 [NASA-TM-109233] p 42 N94-10562
Satellite situation report, volume 32, no. 2 [NASA-TM-109234] p 42 N94-10563
Satellite situation report, volume 31, no. 4 [NASA-TM-109232] p 39 N94-10659
Venus small volcano classification and description p 438 N94-12037
The Magellan volcanic and magmatic feature catalog p 467 N94-12193

CATALYSIS
A model of elementary chemistry and fluid mechanics in the combustion of hydrogen on platinum surfaces [DE93-012767] p 77 N94-11370
Catalytic oxidation of organics in vapor streams at remediation sites [PB93-182962] p 266 N94-11472

CATALYSTS
Charge distribution analysis of catalysts under simulated reaction conditions [DE93-013604] p 78 N94-11699
Resist materials design: Base-catalyzed chemical amplification [AD-A265286] p 145 N94-11819
Low temperature pathways to Chevrel phases via reduced molybdenum sulfide cluster complexes [DE93-013282] p 405 N94-12599

CATALYTIC ACTIVITY
A model of elementary chemistry and fluid mechanics in the combustion of hydrogen on platinum surfaces [DE93-012767] p 77 N94-11370

CATARACTS
Aviation accident risk for airmen with aphakia and artificial lens implants [DOT/FAA/AM-93/11] p 303 N94-10813

CATHODES
Dynamics of ion acceleration in electron flux by a virtual cathode potential [DE93-620978] p 371 N94-10542

CATHODOLUMINESCENCE
Cathodoluminescence properties of components in enstatite chondrites p 432 N94-12206

CAUCHY PROBLEM
Spline approximation for system of n-th order nonlinear ordinary differential equations [DE93-608188] p 346 N94-11507

CAVITIES
On the Sobolev systems with ellipsoid cavities [DE92-641290] p 148 N94-10530
Smoothly deformed light p 375 N94-10566
Quantum processes in resonators with moving walls p 380 N94-10612
Controlling chaotic behavior in CO2 and other lasers [AD-A264811] p 174 N94-10870
On the coupling of electromagnetic radiation into cavities [DE93-011406] p 137 N94-11621
Nonlinear analysis of a magnicon output cavity [AD-A265342] p 145 N94-12424

CAVITY FLOW
Application of a dynamic subgrid-scale model to turbulent recirculating flows p 156 N94-12290

CAVITY RESONATORS
Semiconductor ring lasers [DE93-012386] p 174 N94-11005
Performance characteristics of the INS 25.5-MHz split coaxial RFQ [DE93-753168] p 144 N94-11508
On the coupling of electromagnetic radiation into cavities [DE93-011406] p 137 N94-11621
Three-cavity circuit studies of the Maryland gyroklystron [DE93-010173] p 145 N94-11645

CD-ROM
Evaluation of ECMWF latent heat flux in TOGA CD-ROM p 195 N94-11921

CELESTIAL BODIES
The magnetic field of rotating bodies [DE93-619769] p 427 N94-11812

CELESTIAL MECHANICS

Orbital simulations of satellite escape/capture and the origin of satellites such as Triton p 429 N94-12057

CELLS (BIOLOGY)

Aluminum and membrane channels
[AD-A265241] p 300 N94-11020

CEMENTS

Mechanical interaction between synthetic fiber and cement base matrix in FRC composites
[AD-A265310] p 73 N94-11686

CENTER OF GRAVITY

Accuracy and repeatability of the standard automated mass properties measurement system
[AD-A265897] p 316 N94-12346

CENTER OF MASS

Venus' center of mass - center of figure displacement and implications p 444 N94-12067

Accuracy and repeatability of the standard automated mass properties measurement system
[AD-A265897] p 316 N94-12346

CENTRAL NERVOUS SYSTEM

Toxicity study of dimethylethoxysilane (DMSES), the waterproofing agent for the Orbiter heat protective system p 318 N94-11554

Hormonal regulation of fluid and electrolyte metabolism during periods of headward fluid shifts
p 311 N94-12005

Autogenic-feedback training: A countermeasure for orthostatic intolerance p 311 N94-12006

CENTRIFUGAL CASTING

Particle attraction effects on the centrifugal casting and extrusion of alumina
[DE93-011559] p 82 N94-10957

CENTRIFUGAL FORCE

Effects of axial and centrifugal forces on the stability of liquid bridges p 102 N94-10083

Kinetic approach to long wave length modes in rotating plasmas
[DE93-771286] p 388 N94-10807

CERAMIC COATINGS

Design and production of insulated wind tunnel models of the Hermes shuttle for heat transfer measurements at hypersonic speeds p 4 N94-10431

Advanced zinc phosphate conversion and pre-ceramic polymetallosiloxane coatings for corrosion protection of steel and aluminum, and characteristics of polyphenyletheretherketone-based materials
[DE93-008717] p 88 N94-10891

CERAMIC FIBERS

High temperature composites in Aerospatiale activities
p 64 N94-10062

Damping mechanisms in chemically vapor deposited SiC fibers
[NASA-TM-106334] p 66 N94-11135

Processing and properties of coated HPZ fiber reinforced glass-ceramic matrix composites
[AD-A265177] p 92 N94-11876

CERAMIC MATRIX COMPOSITES

High temperature materials for hypersonic transport
p 56 N94-10003

Design concepts for load-carrying hot structures for reentry bodies p 57 N94-10012

Fibre-reinforced ceramic components by filament winding for intermediate temperature applications
p 61 N94-10041

New processes for lightweight ceramic matrix composites p 61 N94-10043

Ceramic matrix composites: High performance materials for space application p 62 N94-10044

Joints between dissimilar metallic and ceramic materials p 63 N94-10052

Micromechanisms of fatigue crack growth and fracture toughness in metal matrix composites
[AD-A265153] p 187 N94-11096

Assessment of damage in ceramics and ceramic matrix composites using ultrasonic techniques
[NASA-TM-106121] p 67 N94-11237

Creep deformation and mechanical properties of sintered glass and polycrystalline matrix composites
p 67 N94-11315

High-temperature corrosion of ceramic-ceramic composites in a waste incinerator environment
[DE93-012430] p 72 N94-11368

The effects of an aggressive environment on the subcritical crack growth of a continuous-fiber ceramic composite
[DE93-011690] p 73 N94-11612

Processing and properties of coated HPZ fiber reinforced glass-ceramic matrix composites
[AD-A265177] p 92 N94-11876

CERAMICS

Study of the tribological behavior of SiC and Si3N4 ceramic couples in terms of temperature: The reality
p 64 N94-10061

Zerodur polishing process for high surface quality and high efficiency
[DE93-012596] p 87 N94-10271

Fracture behavior of surface-modified ceramics
[DE93-013707] p 88 N94-10710

Development and testing of a superconducting link for an IR detector
[NASA-CR-193674] p 170 N94-10948

Micromechanisms of fatigue crack growth and fracture toughness in metal matrix composites
[AD-A265153] p 187 N94-11096

Low-expansion ceramics initiative
[DE93-011860] p 89 N94-11106

Assessment of damage in ceramics and ceramic matrix composites using ultrasonic techniques
[NASA-TM-106121] p 67 N94-11237

A study of strength evaluations of EDNi/EDCu/NARloy-Z bonded joints
[NASA-TM-108418] p 188 N94-11275

Structural development in ceramic precursor sols and gels
[AD-A264354] p 90 N94-11281

Heat flux measurements on ceramics with thin film thermocouples
[NASA-TM-106305] p 170 N94-11310

High-temperature corrosion of ceramic-ceramic composites in a waste incinerator environment
[DE93-012430] p 72 N94-11368

The effects of an aggressive environment on the subcritical crack growth of a continuous-fiber ceramic composite
[DE93-011690] p 73 N94-11612

Ceramics technology project database
[DE93-012431] p 91 N94-11672

Ceramic technology project database
[DE93-012432] p 91 N94-11673

Radiation-induced aperiodicity in irradiated ceramics
[DE93-013335] p 91 N94-11698

Chemical Vapor Deposition of Refractory Metals and Ceramics 2. Materials Research Society Symposium proceedings
[AD-A265072] p 92 N94-11866

Ceramics formed by pyrolysis of either linear or thermosetting carborane (siloxane or silane) acetylene based precursor polymers
[AD-D015747] p 93 N94-12330

Prediction of alumina penetration
[DE93-014017] p 95 N94-12610

CEREBRAL CORTEX

Locus coeruleus, vigilance, and stress: Brain mechanisms of adaptive behavioral responsiveness
[AD-A265657] p 302 N94-12441

CEREBROSPINAL FLUID

Effects of CSF hormones and ionic composition on salt/water metabolism
[NASA-CR-193232] p 300 N94-11045

CERENKOV COUNTERS

Post-launch analysis of data from the High Energy Astrophysical Observatory Heavy Nuclei Experiment (HEAO-C3)
[NASA-CR-193513] p 484 N94-11486

CERTIFICATION

GRISET certification package
[DE93-011783] p 327 N94-11246

CESIUM

A laser-cooled cesium fountain frequency standard and a measurement of the frequency shift due to ultra-cold collisions p 352 N94-10976

CAFS: A Cesium Atomic Frequency Standard for GPS block IIR p 353 N94-10980

Time scale algorithms for an inhomogeneous group of atomic clocks p 356 N94-10998

CHALCOGENIDES

Low temperature pathways to Chevrel phases via reduced molybdenum sulfide cluster complexes
[DE93-013282] p 405 N94-12599

CHANGE DETECTION

Techniques and applications of SAR interferometry for ERS-1: Topographic mapping, change detection, and slope measurement p 236 N94-11734

Shoreline change detection using remote sensing and GIS in Vietnam p 196 N94-11928

Segmentation and change detection in ERS-1 images over East Anglia p 248 N94-12487

Observations of ERS-1 SAR sensitivities to changes in aboveground biomass in young loblolly pine forests
p 249 N94-12494

Study of growing processes of a tombolo using an air photograph p 218 N94-12702

CHANNEL FLOW

An ancient inner lake in Maadim Vallis
p 456 N94-12133

Large eddy simulations of time-dependent and buoyancy-driven channel flows p 155 N94-12287

A normal stress subgrid-scale eddy viscosity model in large eddy simulation p 155 N94-12288

Large-eddy simulation of turbulent flow with a surface-mounted two-dimensional obstacle
p 156 N94-12291

Reynolds stress closure modeling in wall-bounded flows p 157 N94-12298

DNS on control of laminar-turbulent transition in channel flow with suction and blowing p 163 N94-12613

Fluctuations of longitudinal vortices along a concave wall p 16 N94-12616

Simultaneous 3D turbulent large-scale structures in a flood flow by multi-channels measuring system
p 165 N94-12624

CHANNELS

Rates of fluvio-thermal erosion on Mars
p 435 N94-12018

Thermal studies of Martian channels and valleys using Termoskan data p 443 N94-12064

CHANNELS (DATA TRANSMISSION)

Formal specification of the plain UCN layer in LOTOS
[MEMO-INF-92-83] p 131 N94-10280

Microwave multiplexer with channels of varying fractional bandwidths
[AD-D015754] p 140 N94-10389

Controller of serial multiplex communication channel
[DE92-641157] p 336 N94-10544

Preliminary analysis of the FLIP array data from the NOBS experiment
[AD-A265911] p 289 N94-12349

CHAOS

The kinematics of buoyancy induced mixing
p 123 N94-10239

The uncertainty principle and quantum chaos
p 379 N94-10602

Controlling chaotic behavior in CO2 and other lasers
[AD-A264811] p 174 N94-10870

Intermittency following a Hopf bifurcation
[W-9301] p 344 N94-10907

Stability in Aerospace Systems
[AGARD-R-789] p 31 N94-11489

Chaotic time series analysis p 31 N94-11490

Chaos, entropy, and reversibility: A simple example
p 31 N94-11495

NRL review for 1993
[AD-A265666] p 497 N94-12334

Topics in pattern formation and chaotic systems
[AD-A265922] p 161 N94-12342

Controlling chaotic behavior in a CO2 and other lasers
[AD-A265458] p 176 N94-12372

Visual structure of Karman vortex streets in a route to chaotic states excited by oscillation of a circular cylinder
p 17 N94-12633

CHARACTERIZATION

Material characterization and modeling with shearography
[NASA-CR-192576] p 185 N94-10342

Characterization of an excimer laser-ablated plasma and applications p 392 N94-11450

CHARGE CARRIERS

Time-resolved optical studies of charge relaxation and charge transfer at electrode interfaces
[DE93-013985] p 398 N94-11117

Charge distribution analysis of catalysts under simulated reaction conditions
[DE93-013604] p 78 N94-11699

CHARGE COUPLED DEVICES

Design of CCD camera system for use inside electron beam furnace
[DE93-009525] p 170 N94-11267

An indium gallium arsenide charge-coupled device (CCD) for 1-3 micron imaging
[AD-A266134] p 401 N94-11476

CHARGE DISTRIBUTION

Charge distribution analysis of catalysts under simulated reaction conditions
[DE93-013604] p 78 N94-11699

CHARGE TRANSFER

Bond distortion and electron trapping in charged C60
[DE93-613642] p 396 N94-10637

Dynamics of charge-transfer excited states relevant to photochemical energy conversion
[DE93-013981] p 263 N94-11116

Time-resolved optical studies of charge relaxation and charge transfer at electrode interfaces
[DE93-013985] p 398 N94-11117

Ionization potentials of small carbon clusters
[AD-A264379] p 67 N94-11260

CHARGED PARTICLES

Aharonov-Bohm effect in Luttinger liquid
[DE93-613818] p 408 N94-10148

New squeezed landau states p 379 N94-10601

Solar wind channels for MeV particles
[DE93-012648] p 482 N94-10741

Strange meson spectroscopy in K(omega) and K(phi) at 11 GeV/c and Cherenkov ring imaging at SLD
[DE93-013593] p 363 N94-10748

The heat transfer by radiation between two media
[DE93-617820] p 149 N94-10838
Distribution of charged particles near the plasma boundary in the presence of external electric field
[DE93-617862] p 389 N94-10886
Fast trigger algorithm for B-events selection
[DE93-621452] p 365 N94-11089
Charged particle motion in torsatrons, part 1
[DE93-621639] p 389 N94-11119
Particle transport analysis in torsatron configurations
[DE93-621640] p 390 N94-11120
Relativistic heavy ion research
[DE93-013127] p 367 N94-11373
Experimental particle physics at the University of Pittsburgh
[DE93-013326] p 369 N94-12546

CHEBYSHEV APPROXIMATION
Improvements for obtaining iterative solutions of large linear systems
[DE93-767968] p 343 N94-10729

CHEMICAL ANALYSIS
Synthesis, characterization, and modification of poly(organophosphazenes), that bear both 2,2,2-trifluoroethoxy and phenoxy groups
[AD-A264913] p 92 N94-11847
Dispersion of the ratios of cosmogenic isotopes of noble gases in chondrites of different cosmic-ray exposure ages p 428 N94-12020
Carbon analyses of IDP's sectioned in sulfur and supported on beryllium films p 81 N94-12099
Carbonaceous chondrite clasts in the Kapoeta howardite p 282 N94-12104
Determining the relative extent of alteration in CM chondrites p 430 N94-12114
Distribution of vanadium and melting of opaque assemblages in Efremovka CAI's p 282 N94-12141
The Xe-Q in lodranites and a hint for Xe-L. FRO90011 another lodranite? p 432 N94-12239
On the origin of (4)He and (40)Ar in natural gold
p 87 N94-12240
Quality assurance for environmental chemistry: 1991, volume 2
[DE93-011792] p 272 N94-12780
Novel mass spectrometric instrument for gaseous and particulate characterization and monitoring
[DE93-014093] p 272 N94-12783

CHEMICAL BONDS
Investigation of optically generated electronic defects and protonic transport in hydrogen-bonded molecular solids: Isomorphs of potassium dihydrogen phosphate
[DE93-012498] p 399 N94-11243
A new decomposition strategy for parallel bonded molecular dynamics
[DE93-009839] p 366 N94-11284
TAB interconnects for space concentrator solar cell arrays p 51 N94-11400
The effects of organic adsorbates on the underpotential deposition of silver on Pt(111) electrodes
[AD-A265623] p 404 N94-12376

CHEMICAL CLEANING
Ellipsometry studies of semiconductors surface cleaning
[AD-A265150] p 142 N94-11094

CHEMICAL CLOUDS
Numerical simulations on the redistribution of atmospheric trace chemicals through cloud processes
p 265 N94-11189

CHEMICAL COMPOSITION
Thermodynamic model of air in chemical equilibrium
p 7 N94-10448
Improving reservoir conformance using gelled polymer systems
[DE93-014532] p 88 N94-10749
Numerical simulations on the redistribution of atmospheric trace chemicals through cloud processes
p 265 N94-11189
Organometallic chemical vapor deposition and characterization of ZnGe(1-x)Si(x)P2-Ge alloys on GaP substrates p 400 N94-11443
Weld overlay coatings for erosion control
[DE93-013592] p 84 N94-11816
Mechanistic studies on reduced exercise performance and cardiac deconditioning with simulated zero gravity
p 310 N94-12001
Carbon in weathered ordinary chondrites from Roosevelt County p 428 N94-12035
Apollo 16 core 60013/14 as a product of path 1 and path 2 regolith evolution processes p 440 N94-12050
Sources of Na for the Io atmosphere
p 455 N94-12127
Remote sensing x ray fluorescence spectrometry for future lunar exploration missions p 462 N94-12165
Trace element distributions in primitive achondrites
p 431 N94-12200
Compositional heterogeneity within a dumbbell-shaped Apollo 15 green glass: Evidence for simultaneous eruption of different magmas p 470 N94-12209
Trace element content of chondritic cosmic dust: Volatile enrichments, thermal alterations, and the possibility of contamination p 433 N94-12260
Depletions of sulfur and/or zinc in IDPs: Are they reliable indicators of atmospheric entry heating?
p 433 N94-12261
New low-Ni (igneous?) particles among the C and C? types of cosmic dust p 433 N94-12262
Quality assurance for environmental chemistry: 1991, volume 2
[DE93-011792] p 272 N94-12780

CHEMICAL EFFECTS
Szilard-Chalmers effect in solid HIO4.2H2O by neutron irradiation
[DE93-617173] p 397 N94-10830

CHEMICAL ENGINEERING
Engineering solid-state materials. Strategies for modeling and packing control of molecular assemblies into 3-D networks
[AD-A265291] p 404 N94-12438

CHEMICAL EQUILIBRIUM
The upgrading of the arc heated wind tunnel of the DLR (LBK) with respect to its effects on the material testing
p 4 N94-10432
Thermodynamic model of air in chemical equilibrium
p 7 N94-10448
Combustion chamber analysis code
[NASA-CR-192585] p 46 N94-10934

CHEMICAL EVOLUTION
Nuclear astrophysics
[DE93-010569] p 425 N94-10292
Oxidation state of the Earth's upper mantle during the last 3800 million years: Implications for the origin of life
p 283 N94-12210

CHEMICAL FRACTIONATION
Impact comminution of glasses: Implications for lunar regolith evolution p 461 N94-12159
The fractionation of noble gases in diamonds of CV3 Efremovka chondrite p 81 N94-12256

CHEMICAL INDICATORS
Depletions of sulfur and/or zinc in IDPs: Are they reliable indicators of atmospheric entry heating?
p 433 N94-12261

CHEMICAL PROPERTIES
Solid state ionics 3. Materials Research Society Symposium Proceedings, volume 293
[AD-A265675] p 395 N94-10416
Isotopic and trace element characteristics of an unusual refractory inclusion from Essebi p 471 N94-12212

CHEMICAL REACTIONS
Numerical simulation of the flow through a scramjet engine p 3 N94-10425
Thermodynamic model of air in chemical equilibrium
p 7 N94-10448
Three-dimensional hypersonic rarefied flow calculations using direct simulation Monte Carlo method
p 7 N94-10449
User's manual for the plume visibility model PLUVUE 2 (revised)
[PB93-188233] p 265 N94-11016
KIVA-3: A KIVA program with block-structured mesh for complex geometries
[DE93-011986] p 77 N94-11249
Size dependence of chemical reactivity of gaseous metal clusters: A new mechanistic probe
[AD-A264690] p 77 N94-11264
Characterization of gas-aerosol interaction kinetics using morphology dependent stimulated Raman scattering
[DE93-012324] p 77 N94-11359
Aluminum-phosphorus chemistry: Preparation and structural characterization of (Et2AlP(SiMe3)2)2, Et(Cl)2Al(dot)P(SiMe3)3, and i-Bu2(Cl)Al(dot)P(SiMe3)3
[AD-A265268] p 78 N94-11683
Progress toward atomic layer epitaxy of diamond: Diamond films grown one layer at a time
[AD-A265530] p 403 N94-12010
The rate of chemical weathering of pyrite on the surface of Venus p 477 N94-12246
Theories of turbulent combustion in high speed flows
[AD-A265735] p 79 N94-12403
Mid-latitude ionospheric response to active experiments
[NASA-CR-193549] p 280 N94-12583

CHEMICAL REACTORS
Design of a CVD reactor for the deposition of diamond in a microgravity environment p 109 N94-10127

CHEMICAL VAPOR INFILTRATION
New processes for lightweight ceramic matrix composites p 61 N94-10043

CHEMICAL WARFARE
Tandem mass spectrometric analysis of phosphate esters
[AD-A265483] p 78 N94-12009

CHEMILUMINESCENCE
NMR characterization of polymers formed in diazotizing mixtures of luminol and 3-amino-L-tyrosine
[AD-A266093] p 94 N94-12536

CHEMISORPTION
Electrode potential-induced reconstruction of Au(100): Effect of chemisorption on nanoscale dynamics as probed by the in-situ scanning tunneling microscopy
[AD-A265900] p 404 N94-12388

CHINA
International Space Year in China p 36 N94-10680

CHIPS (ELECTRONICS)
RF vacuum microelectronics
[AD-A266066] p 142 N94-10818
Development of microstrip gas chamber and application to imaging gamma-ray detector
[DE93-754294] p 34 N94-11041
A high-speed object recognition chip based on biologically-realistic hybrid temporal processing element
[AD-A265490] p 339 N94-11049
Programmable logic devices
[DE93-013117] p 144 N94-11479
Development of microstrip gas chambers with multi-chip technology
[DE93-753169] p 367 N94-11509
Low cost high efficiency GaAs monolithic RF module for SARSAT distress beacons
[NASA-CR-194235] p 146 N94-12773

CHIRAL DYNAMICS
Quenched chiral logarithms
[DE93-010195] p 346 N94-11663

CHLORINE
Measurements of cosmogenic nuclides in lunar rock 64455 p 437 N94-12033

CHLOROPHYLLS
The use of CZCS for primary production estimate in the Pacific p 199 N94-11946
CZCS derived chlorophyll distribution in Antarctic water during austral summer p 199 N94-11947
The development of phytoplankton sensing system with optical fiber p 203 N94-11967
Bi-directional reflectance by oceanic waters studied via Monte-Carlo simulations p 203 N94-11971
The phytoplankton bloom in the Kinu-ura Bay, Japan in the rainy season p 211 N94-12660
Variation of the photosynthetic products in the regional upwelling area around the Izu Islands, Japan
p 211 N94-12661
The algorithm of primary production determination
p 228 N94-12761
Non-image visible polarization remote sensing of the ocean p 229 N94-12762

CHLOROSILANES
The adsorption and surface reaction of SiCl4 on Si(100)-(2x1)
[AD-A266124] p 79 N94-12538

CHONDRITES
Dispersion of the ratios of cosmogenic isotopes of noble gases in chondrites of different cosmic-ray exposure ages p 428 N94-12020
Peculiarities of distributions of the cosmic-ray exposure ages of H chondrite falls and finds p 428 N94-12021
Search for effects of a supernova explosion 30 to 40 thousand years ago in chondrites p 428 N94-12022
Carbon in weathered ordinary chondrites from Roosevelt County p 428 N94-12035
Mineralogy of chondritic interplanetary dust particle impact residues from LDEF p 80 N94-12045
The great 8 MA event and the structure of the H-chondrite parent body p 429 N94-12058
Metallographic cooling rates of L-group ordinary chondrites p 429 N94-12061
Alkali-granitoids as fragments within the ordinary chondrite Adzhi-Bogdo: Evidence for highly fractionated, alkali-granitic liquids on asteroids p 429 N94-12069
Preliminary results of Mn partitioning experiments on Murchison analogues p 281 N94-12081
Ar-39 - Ar-40 ages of acapulcoites and lodranites: Evidence for early parent body heating
p 281 N94-12083
Chondrite thermal histories from Low-CA pyroxene microstructures: Autometamorphism versus prograde metamorphism revisited p 429 N94-12105
Cathodoluminescence properties of components in enstatite chondrites p 432 N94-12206
The Fe/Mn constraint on precursors of basaltic achondrites p 432 N94-12208
A CM chondrite cluster and CM streams
p 432 N94-12215
On high-temperature formation of iron-rich olivine in the early solar system p 432 N94-12225
Recondensation of chondritic material in the early solar system: Results of thermodynamic simulation
p 432 N94-12226
Primordial lightning: Evidence preserved in chondrites
p 432 N94-12230

Micro-zoning in minerals of a Landes silicate inclusion p 432 N94-12231
Chondrites, S asteroids, and space weathering: Thumping noises from the coffin? p 433 N94-12244
Diamond thermoluminescence properties of different chondrites p 433 N94-12252
The unusual metallic particles in Krymka LL3.0 chondrite p 433 N94-12253

CHONDRULE
Chondrule formation by clumpy accretion onto the solar nebula p 448 N94-12089
SXRF determination of trace elements in chondrule rims in the unequilibrated CO3 chondrite, ALH A77307 p 429 N94-12106
The experimental production of matrix lumps within chondrules: Evidence of post-formational processes p 431 N94-12176
Flash melting of chondrule precursors in excess of 1600 C. Series 1: Type 2 (B1) chondrule composition experiments p 431 N94-12177
Primordial lightning: Evidence preserved in chondrites p 432 N94-12230
The unusual metallic particles in Krymka LL3.0 chondrite p 433 N94-12253

CHROMATES
Monochromator SP-017. The results of the first experiments
[DE93-617463] p 372 N94-10849

CHROMIC ACID
Space environmental effects on the integrity of chromic acid anodized coatings
[NASA-CR-191468] p 55 N94-10947

CHROMIUM ALLOYS
Solidification and metastable phase formation of highly undercooled Fe-Cr-Ni alloy melts p 87 N94-10204
Monte Carlo simulations of phase transformations in Fe-Cr alloys
[DE93-013847] p 81 N94-10522
In situ XANES studies of the passive film on Fe and Fe-26Cr
[DE93-010869] p 84 N94-11459

CHROMIUM STEELS
DBTT measurement by use of Small Punch (SP) test
[DE93-753188] p 183 N94-11168

CHRONOLOGY
The Lathrop Wells Volcanic Center: Status of field and geochronology studies
[DE93-008917] p 273 N94-10285
The Th and U abundances in chondritic meteorites p 430 N94-12151

CHRONOMETERS
Studies of the release of radiogenic Xe-129 from Bjurboele: Evidence against simple diffusion models p 430 N94-12125

CHUTES
Evolution of steep Martian slopes p 434 N94-11184

CIRCADIAN RHYTHMS
The organization of the suprachiasmatic circadian pacemaker of the rat and its regulation by neurotransmitters and modulators
[AD-A266113] p 301 N94-12417

CIRCUIT DIAGRAMS
Direct current transducer
[DE92-644548] p 141 N94-10533

CIRCUITS
Continuous-time adaptive learning circuit
[AD-D015773] p 140 N94-10384
A soft-start circuit for arcjet ignition
[NASA-TM-106287] p 180 N94-10760
Tin whiskers in electronic circuits
[AD-A265917] p 146 N94-12565

CIRCULAR CYLINDERS
Radiation and scattering by cavity-backed antennas on a circular cylinder
[NASA-CR-193409] p 136 N94-11084
Vortex-induced forces on oscillating bluff cylinders
[AD-A265056] p 154 N94-11865

CIRCULAR PLATES
Failure prediction of thin beryllium sheets used in spacecraft structures
[NASA-CR-194164] p 187 N94-11190

CIRCULAR POLARIZATION
Models of Neptune's smooth recurrent radio emission
[NASA-CR-193283] p 484 N94-11312

CIRCULATION CONTROL AIRFOILS
Navier-Stokes flowfield computation of wing/rotor interaction for a tilt rotor aircraft in hover
[NASA-CR-4532] p 13 N94-10758

CIRCULATION DISTRIBUTION
Circulation of North Pacific Intermediate Water p 206 N94-11985
SOFAR float tracking in the Shikoku basin p 206 N94-11986

CIRRUS CLOUDS
Characteristic scales and vortex features of mesoscale vortices observed by the satellites during the winter p 199 N94-11943

CITIES
Technical Conference on Tropical Urban Climates: Extended Abstracts
[WMO/TD-538] p 283 N94-10561

CIVIL AVIATION
FAA air traffic activity
[AD-A266043] p 22 N94-12397
US civil airmen statistics for calendar year 1991
[AD-A266085] p 2 N94-12412
Federal Aviation Administration aviation forecasts
[AD-A265611] p 2 N94-12578

CLADDING
Short wavelength crystal fiber devices
[AD-A265716] p 176 N94-12402

CLASSICAL MECHANICS
Exact and quasi-classical density matrix and Wigner functions for a particle in the box and half space p 350 N94-10600
Non-barrier tunneling in presence of dissipations
[DE93-621381] p 412 N94-11086
Absorption spectrum calculations using mixed quantum-gaussian wave packet dynamics
[AD-A265179] p 413 N94-11877

CLASSIFICATIONS
Unsupervised splitting rules for neural tree classifiers
[AD-A264961] p 338 N94-10487
Automatic classification system for zooplankton p 203 N94-11969
How diverse is the asteroid belt? p 430 N94-12124
First results of the seven-color asteroid survey p 430 N94-12162
Classification of Martian deltas p 470 N94-12207
Guidelines for the establishment and operation of an RFP (Request for proposal) library
[AD-A265894] p 417 N94-12360
Radarmap of Germany: First mosaic and classification p 246 N94-12477
Per-field filtering and classification of multitemporal ERS-1 SAR imagery p 247 N94-12485
Land use/land cover mapping of central water shed of Iran area based on satellite data interpretation p 219 N94-12704
A method to minimize reference data in classifying satellite remote sensing data into land cover classes p 219 N94-12705

CLASSIFIERS
Unsupervised splitting rules for neural tree classifiers
[AD-A264961] p 338 N94-10487

CLAYS
Reflectance spectra of sulfate-and carbonate-bearing Fe(3+)-doped montmorillonites as Mars soil analogs p 445 N94-12070
Impact mineralogy and chemistry of the cretaceous-tertiary boundary at DSDP site 576 p 282 N94-12091

CLEANING
Operational aspects of F.16 plastic media blasting, as carried out by Fokker Aircraft Services p 126 N94-10619
Use of robots for aircraft dry stripping via plastic media blasting p 127 N94-10620
German Air Forces experiences with plastic media blasting and future requirements p 127 N94-10621
Plastic media blasting activities at Hill Air Force Base p 127 N94-10622
Paint removal and surface cleaning using ice particles p 128 N94-10626

CLEANLINESS
Effect of surface cleanliness of bearing steel on adhesive strength and tribological properties of sputter-deposited gold films
[DE93-767974] p 82 N94-10732

CLEBSCH-GORDAN COEFFICIENTS
Generating function for Clebsch-Gordan coefficients of the SU(sub q)(2) quantum algebra
[DE93-613093] p 349 N94-10633

CLIMATE
AMIP: The Atmospheric Model Intercomparison Project
[DE93-007400] p 273 N94-10151
AMIP: The Atmospheric Model Intercomparison Project
[DE93-007413] p 273 N94-10152
The cloud radiative feedback of a midlatitude squall line system and implication for climate study
[DE93-010511] p 283 N94-10290
Topex/Poseidon: A United States/France mission. Oceanography from space: The oceans and climate
[NASA-TM-108253] p 43 N94-10699
Preliminary validation of the low frequency variability of tropospheric temperature and circulation simulated for the AMIP by the ECMWF model
[DE93-012382] p 284 N94-10739
A toolkit for building Earth system models
[DE93-012147] p 276 N94-11138
Development of a graphical user interface and graphics display for the WIND system
[DE93-011780] p 285 N94-11614
Central Equatorial Pacific Experiment (CEPEX)
[DE93-011656] p 190 N94-11674
Modeling present and future river runoff using global atmospheric models
[AD-A265274] p 285 N94-11685
Sea ice: A climate component p 232 N94-11705
Mars: The initial emplacement of ground ice in response to the thermal evolution of its early crust p 462 N94-12168
Comments on possible causes of recent global warming
[DE93-010501] p 272 N94-12592
Problem of climate change predictability and satellite radiation budget observations p 229 N94-12766

CLIMATE CHANGE
Space program in Indonesia p 36 N94-10681
Topex/Poseidon: A United States/France mission. Oceanography from space: The oceans and climate
[NASA-TM-108253] p 43 N94-10699
Global monitoring of atmospheric properties by the EOS MODIS
[NASA-TM-109237] p 231 N94-11485
Central Equatorial Pacific Experiment (CEPEX)
[DE93-011656] p 190 N94-11674
The seasonal Sea Ice Monitoring and Modelling Site (SIMMS): Using ERS-1 in climate research p 240 N94-11758
Study of climatic effects of cloud-aerosol interaction p 204 N94-11977
Problem of climate change predictability and satellite radiation budget observations p 229 N94-12766

CLIMATOLOGY
AMIP: The Atmospheric Model Intercomparison Project
[DE93-007400] p 273 N94-10151
AMIP: The Atmospheric Model Intercomparison Project
[DE93-007413] p 273 N94-10152
Database blending for the climatology of cloud statistics program
[AD-A265034] p 283 N94-10336
Technical Conference on Tropical Urban Climates: Extended Abstracts
[WMO/TD-538] p 283 N94-10561
Topex/Poseidon: A United States/France mission. Oceanography from space: The oceans and climate
[NASA-TM-108253] p 43 N94-10699
Estimating Photosynthetically Available Radiation (PAR) at the Earth's surface from satellite observations p 230 N94-10955
A toolkit for building Earth system models
[DE93-012147] p 276 N94-11138
Central Equatorial Pacific Experiment (CEPEX)
[DE93-011656] p 190 N94-11674
Study of climatic effects of cloud-aerosol interaction p 204 N94-11977
Problem of climate change predictability and satellite radiation budget observations p 229 N94-12766

CLINICAL MEDICINE
National Institute of Health Almanac, 1992
[PB93-183556] p 303 N94-10828
The Department of Clinical Investigation, reports control symbol MED-300(R-1)
[AD-A264969] p 304 N94-11649
International Telemedicine/Disaster Medicine Conference: Papers and Presentations
[NASA-NP-207] p 304 N94-11787
Medical informatics and telemedicine: A vision p 305 N94-11788
Telemedicine and international disaster response: Medical consultation to Armenia and Russia via a telemedicine spacebridge p 305 N94-11790
Clinical aspects of telemedicine p 306 N94-11795
New technology applied to telemedicine p 306 N94-11796
Linking medical records to an expert system p 306 N94-11797
Commercial applications of telemedicine p 306 N94-11798
The use of communication technology in medicine p 306 N94-11800

CLOCKS
Disciplined rubidium oscillator with GPS selective availability p 353 N94-10977
TimeSet: A computer program that accesses five atomic time services on two continents p 334 N94-10985

RighTime: A real time clock correcting program for MS-DOS-based computer systems p 334 N94-10986
Measurement methods and algorithms for comparison of local and remote clocks p 354 N94-10987
Advances in time-scale algorithms p 334 N94-10988
The limit of frequency estimation p 356 N94-11001

CLOSED ECOLOGICAL SYSTEMS
Statistical analysis of environmental variability within the CELSS breadboard project's biomass production chamber [NASA-TM-109188] p 315 N94-11258
Comprehensive analysis of airborne contaminants from recent Spacelab missions p 318 N94-11553
Space Life Support Engineering Program [NASA-CR-193474] p 316 N94-12365
Systems analysis of a closed loop ECLSS using the ASPEN simulation tool. Thermodynamic efficiency analysis of ECLSS components p 316 N94-12366
An estimate of the second law thermodynamic efficiency of the various units comprising an Environmental Control and Life Support System (ECLSS) p 317 N94-12369

CLOUD COVER
Database blending for the climatology of cloud statistics program [AD-A265034] p 283 N94-10336
A modeling perspective on cloud radiative forcing [DE93-012383] p 276 N94-11241
Estimation of solar radiation at the sea surface with geostationary meteorological satellite data p 196 N94-11926
Study of climatic effects of cloud-aerosol interaction p 204 N94-11977
Incident shortwave and longwave radiations over the western North Pacific and the Sea of Okhotsk derived from GMS-WEFAX images p 205 N94-11982
Propagation of light pulses through a three-layer medium (cloud, pure air, and ocean water) p 222 N94-12725

CLOUD PHYSICS
Numerical simulations on the redistribution of atmospheric trace chemicals through cloud processes p 265 N94-11189
Global monitoring of atmospheric properties by the EOS MODIS [NASA-TM-109237] p 231 N94-11485
Central Equatorial Pacific Experiment (CEPEX) [DE93-011656] p 190 N94-11674

CLOUDS (METEOROLOGY)
The impact of horizontal resolution on moist processes in the ECMWF model [DE93-011718] p 276 N94-11227
Estimation of solar radiation at the sea surface with geostationary meteorological satellite data p 196 N94-11926
Study of climatic effects of cloud-aerosol interaction p 204 N94-11977
Incident shortwave and longwave radiations over the western North Pacific and the Sea of Okhotsk derived from GMS-WEFAX images p 205 N94-11982
Cloud studies using ATSR data p 253 N94-12517
Propagation of light pulses through a three-layer medium (cloud, pure air, and ocean water) p 222 N94-12725

CLUSTER ANALYSIS
Analyzing human errors in flight mission operations p 314 N94-11534
Mass and spatial distribution of carbonaceous component in Comet Halley p 433 N94-12263

CLUSTERS
Enhanced stability of magic clusters: A case study of icosahedric Al(sub 12)X, X=B, Al, Ga, C, Si, Ge, Ti, As [DE93-613644] p 395 N94-10386
Structure of s - p bonded metal clusters with 8, 20 and 40 valence electrons [DE93-613643] p 361 N94-10503
Atomic structures and compositions of internal interfaces [DE93-014840] p 363 N94-10750
Ionization potentials of small carbon clusters [AD-A264379] p 67 N94-11260
Size dependence of chemical reactivity of gaseous metal clusters: A new mechanistic probe [AD-A264690] p 77 N94-11264

CMOS
Radiation hardened nonvolatile memory for space and strategic applications [DE93-000746] p 319 N94-10146
Investigation of soft errors in MOS RAM under influence of heavy ions [DE92-644554] p 484 N94-10534
Relationship between IBICC imaging and SEU in CMOS ICs [DE93-009854] p 143 N94-11285

COAL DERIVED LIQUIDS
Advanced thermally stable coal-derived jet fuels: Compositional factors affecting thermal degradation of jet fuels [AD-A265842] p 99 N94-12282

COALESCING
A method of influence regions in the theory of vacancy swelling of metals [DE93-620579] p 83 N94-11363

COASTAL CURRENTS
Coastal ocean studies with ERS-1 SAR during NORCSEX 1991 p 234 N94-11720
SAR imaging of dynamical features in the English Channel p 234 N94-11721
Kuroshio observations by the HF ocean radar p 192 N94-11904
Statistical study of HF ocean radar echo p 139 N94-11905
Groundwave HF ocean surface radar p 139 N94-11906
One-year mooring of an ADCP in the central region of the Kuroshio west of Okinawa p 194 N94-11913
Acoustic Doppler current profiling of the Kuroshio over the East China Sea shelf slope p 194 N94-11914
Sea surface heat flux in the beginning of the Kuroshio p 195 N94-11923
Seasonal variation of the surface mixed layer in the subtropical re-circulation area of the North Pacific during OMLET p 195 N94-11924
Mixed layer heat budget of Kuroshio-Tango triangle using satellite and ship observations p 196 N94-11925
Analysis of the characteristic and mechanism of suspended matter transportation in Huanghe delta sea area using remote sensing techniques p 197 N94-11930
Time evolution of cross-stream exchange associated with the variations in the Kuroshio p 197 N94-11936
Appearance, behavior, and oceanic structures of warm streamers in the Kuroshio Oyashio frontal region p 198 N94-11937
Warm streamers extended from Warm Core Rings (WCRs) and their role on fish migration and fishing ground formation p 198 N94-11938
The Kyucho events in Sukumo Bay induced by Kuroshio front disturbances p 198 N94-11939
Coastal processes due to nearshore current around an upheaving island p 199 N94-11942
SOFAR float tracking in the Shikoku basin p 206 N94-11986
On an upwelling front, propagation of upwelling and vertical velocity in the eastern Arabian Sea during monsoon, 1987 p 206 N94-11987
Observations of eddy fields in the Northwest Pacific by GEOSAT altimetry p 207 N94-12639
Fluctuations of the Kuroshio extension detected by the GEOSAT altimetry data p 209 N94-12649
Mean flow and variability in the Kuroshio extension from GEOSAT altimetry data p 209 N94-12650
Primary productivity in the Oyashio area in the spring and summer of 1990 p 211 N94-12658
Evaluation of the method of geostrophic flow using NOAA-AVHRR data p 213 N94-12673
Satellite observations of the northeast monsoon coastal current p 214 N94-12678
Aspects of applying a relaxation method to computing sea surface velocities from sea surface temperature images p 214 N94-12679
Statistical features of mesoscale eddies at the Kuroshio front p 215 N94-12682
Intrusion of Kuroshio warm water into Sagami Bay p 215 N94-12683
A study of front dynamics off northeastern Taiwan based on the NOAA-AVHRR satellite remote sensing data p 215 N94-12684
Satellite thermal variations of Kuroshio in relation to storm floods p 215 N94-12685
ADCP evidence for upper layer circulation in northeast of the South China Sea p 215 N94-12686
Frontal zones in Pacific Ocean: Satellite and ship data analysis p 216 N94-12687
The circulation near Luzon p 219 N94-12707
Current variability on the shelf break northeast of Taiwan p 219 N94-12708
Sedimentation rates and particulate fluxes in the slope and deep sea areas off eastern Taiwan p 220 N94-12709
Investigation of meso-scale fronts, eddies and upwellings in China Seas with AVHRR data p 220 N94-12711
The warm eddy detection from NOAA/AVHRR thermal images using the Hough transformation p 220 N94-12713
Satellite and moored buoy observations of polar frontal system over the Yamato Rise in the Japan Sea p 221 N94-12715
Variability of the Kuroshio observed from satellite thermal imagery p 221 N94-12717
Advective surface velocity in the north west Pacific derived from NOAA AVHRR images p 222 N94-12721
On a nonstationary dynamics of the north-west Pacific Ocean p 222 N94-12724
Influence of the Kuroshio warm-core rings on hydrographic and fishery conditions off southern Kuril Islands p 224 N94-12737
Coupled numerical model for altimetric data assimilation and velocity field analysis p 227 N94-12752
Mesoscale dynamic structures of the Subarctic Frontal Zone in the Pacific Ocean p 227 N94-12754
Model of Kuroshio region circulation p 229 N94-12765

COASTAL ECOLOGY
Arctic coastal polynya observations with ERS-1 SAR and DMSP SSM/I p 239 N94-11748
Automatic classification system for zooplankton p 203 N94-11969

COASTAL PLAINS
Energy flow in an Arctic aquatic ecosystem [DE93-013178] p 267 N94-11697

COASTAL WATER
Remote sensing of subsurface water temperature profile and backscattering coefficient in the China Sea by Ocean Lidar (OLIDAR) p 203 N94-11970
Pilot project PPF12. Coastal and fluvial environment in French Guiana: First results of ERS-1 SAR data analysis p 254 N94-12523
ERS-1 imaging radar over the Waddensea-North Netherlands p 254 N94-12526
Observation of wave crests by satellite remote sensed data p 207 N94-12638
Study on diffusion phenomena of river effluents issued into sea around Japan with satellite remote sensing data p 212 N94-12664
Remote sensing of polluting focal points and coastal disturbances in the Gulf of Arauco and adjacent bays, central Chile p 217 N94-12695
Study on sea water purification using a substratum of marine organisms p 217 N94-12696
Role of remote sensing and its cost effectiveness in site selection for coastal aquaculture p 217 N94-12697
Application of remote sensing for coastal management in the north coast of Java p 218 N94-12701
Sedimentation rates and particulate fluxes in the slope and deep sea areas off eastern Taiwan p 220 N94-12709
Applicability of satellite infrared data for the monitoring of coastal environments p 220 N94-12714
Variability of spectral reflectance in coastal waters near the river plumes p 226 N94-12744
A possibility to define the location of epipelagic fish concentrations with assistance of satellite sensing p 228 N94-12757
High biological production of the tidal mixing zones on Japan Sea shelf p 228 N94-12758
Study of the admixture diffusion in the sea using remote techniques p 228 N94-12759

COASTAL ZONE COLOR SCANNER
A statistical method to determine aerosol path radiance and its application to atmospheric correction for CZCS imagery p 191 N94-11897
The use of CZCS for primary production estimate in the Pacific p 199 N94-11946
CZCS derived chlorophyll distribution in Antarctic water during austral summer p 199 N94-11947
Seasonal changes of phytoplankton distributions in the Northwest Pacific detected by Coastal Zone Color Scanner p 200 N94-11948
Satellite-derived oceanic features p 200 N94-11949
Particle dynamics in the western subarctic Pacific: Implications from CZCS imagery p 200 N94-11950
High-reflectance water mass in Off-Sanriku area observed by CZCS p 200 N94-11951
Atmospheric correction plans for SeaWiFS p 204 N94-11975
Distribution of mineral aerosols over the North Pacific p 204 N94-11976
Implications of aerosol retrieval and atmospheric correction in remote sensing p 205 N94-11978

COASTS
Summary of implementation and demonstration projects in bays and estuaries [PB93-194637] p 265 N94-10846
Biscayne bay: A bibliography of the marine environment [PB93-184802] p 266 N94-11451
Energy flow in an Arctic aquatic ecosystem [DE93-013178] p 267 N94-11697
Coastal morphodynamics and energetic characteristics of swell studied with ERS-1 SAR p 254 N94-12524

Applications of ERS-1 SAR data for analyzing riverine and coastal processes and geomorphology
p 254 N94-12528
Study of growing processes of a tombolo using an air photograph p 218 N94-12702
Model of Kuroshio region circulation
p 229 N94-12765

COATING
Damage threshold study of ion beam sputtered coatings for a visible high-repetition laser at LLNL
[DE93-013430] p 95 N94-12602
Performance aspects of de Laval spray-forming nozzles
[DE93-013671] p 163 N94-12604

COATINGS
Formulating infrared coatings for defence applications
[MRL-RR-1-93] p 90 N94-11302
Boundary integral solution to the electromagnetic scattering from coated surfaces containing edges, gaps, and periodic gratings p 137 N94-11639
Damage threshold study of ion beam sputtered coatings for a visible high-repetition laser at LLNL
[DE93-013430] p 95 N94-12602

COAXIAL FLOW
Shear coaxial injector atomization phenomena for combusting and non-combusting conditions
[NASA-CR-193339] p 152 N94-11526

COBALT ALLOYS
Ostwald ripening of solid cobalt particles in liquid copper p 87 N94-10202

COBALT OXIDES
Microanalysis of directionally solidified cobalt oxide-zirconia eutectic
[DE93-013207] p 88 N94-10527

COBALT 60
Demonstration prototype gamma-ray hodoscope alternative to CARGOSCAN for rocket stage monitoring
[DE93-006908] p 169 N94-10326

COCKPIT SIMULATORS
Flight simulator experiment of the cockpit advisory system
[NAL-TR-1151] p 33 N94-10733
Measures for simulator evaluation of a helicopter obstacle avoidance system p 35 N94-11535

CODE DIVISION MULTIPLE ACCESS
Two way time transfer results at NRL and USNO
p 353 N94-10983

CODE DIVISION MULTIPLEXING
A fiber optic network system with low crosstalk using code-division multiplexing
[AD-D015763] p 374 N94-10376

CODERS
Flexible high-speed CODEC
[NASA-CR-191169] p 146 N94-12433

CODING
STGT program: Ada coding and architecture lessons learned p 330 N94-11437

COEFFICIENT OF FRICTION
Turbulent drag reduction of a d-type rough wall boundary layer with longitudinal ribs placed within the grooves
p 165 N94-12627

COEFFICIENTS
Low cost and thermally stable sandwich design for FIRST p 57 N94-10009

COGNITION
Qualitative reasoning about the physical world
[AD-A266117] p 340 N94-12537

COGNITIVE PSYCHOLOGY
Vigilance problems in orbiter processing
p 314 N94-11536
Cognitive engineering models: A prerequisite to the design of human-computer interaction in complex dynamic systems
[NASA-CR-193472] p 320 N94-12558

COHERENT LIGHT
Smoothly deformed light p 375 N94-10566
LCLS optics: Selected technological issues and scientific opportunities
[DE93-010953] p 175 N94-11468

COHERENT RADIATION
Coherence effects in radiometry and in spectroscopy
[DE93-013437] p 75 N94-10519
Nonclassical states of the second optical harmonic in the presence of self-action p 375 N94-10567
Spatial coherence of soft x ray lasers
[DE93-012497] p 176 N94-12590

COLD ACCLIMATIZATION
Effect of intermittent cold exposure on the fiber-type composition of selected skeletal muscles in rats
[AD-A265309] p 301 N94-11861

COLD BOKKEVELD METEORITE
Determining the relative extent of alteration in CM chondrites p 430 N94-12114

COLD FLOW TESTS
Space nuclear thermal propulsion nuclear element tests at Sandia National Laboratories
[DE93-002301] p 45 N94-10282

COLD FRONTS
On the importance of mesoscale potential vorticity anomalies and topographic forcing during cyclone redevelopment across the Appalachians: A GALE case study p 284 N94-10822

COLD PRESSING
Cold press sintering of simulated lunar basalt
p 131 N94-12026

COLLAPSE
Finite element simulation of the 2D collapse of a polyelectrolyte gel disk
[DE93-010693] p 91 N94-11665

COLLIMATION
Monochromator SP-017. The results of the first experiments
[DE93-617463] p 372 N94-10849

COLLISION AVOIDANCE
Preliminary system design of a Three Arm Capture Mechanism (TACM) flight demonstration article
[NASA-CR-192573] p 177 N94-10341
Performance of traffic-alert collision avoidance (TCAS) antennas in the presence of scatterers
[NASA-CR-193569] p 23 N94-11525
Evaluation of the C/EC/KC-135 ground collision avoidance system (GCAS), Study 2
[AD-A265193] p 24 N94-11879

COLLISION PARAMETERS
Collision-induced squeezing in a harmonic oscillator
p 379 N94-10597
Collision lifetimes and impact statistics of near-Earth asteroids p 429 N94-12092
Deviations from the straight line: Bumps (and grinds) in the collisionally evolved size distribution of asteroids
p 431 N94-12201

COLLISION RATES
Collision lifetimes and impact statistics of near-Earth asteroids p 429 N94-12092

COLLISIONAL PLASMAS
Scattering of modulated Ultra-Relativistic Electron Beam (UREB) by atmospheric plasma
[DE93-620987] p 387 N94-10558
Kinetic effects in stochastic topologically nontrivial field
[DE93-621642] p 391 N94-11207
Simple kinetic model for plasma in stochastic helical field
[DE93-621643] p 391 N94-11208
Experimental investigation of wake field excitation in plasma by a periodic succession of relativistic particle clots
[DE93-621655] p 391 N94-11211

COLLISIONLESS PLASMAS
Charged particle motion in torsatrons, part 1
[DE93-621639] p 389 N94-11119

COLLOIDS
Synthesis and thermal evolution of structure in alkoxide-derived niobium pentoxide gels
[NASA-TM-106259] p 90 N94-11257
The physics of pattern formation of liquid interfaces
[DE93-013333] p 154 N94-11814

COLOR
Squeezed colour states in gluon jet
p 379 N94-10599

COLOR TELEVISION
Study on color video pictures transmission by digital acoustic signal p 139 N94-11917

COLOR-COLOR DIAGRAM
The controlling parameters of the integrated flux of a stellar population p 426 N94-11187

COLUMBUS SPACE STATION
Columbus proto-planetesimal dust aggregation experiment p 123 N94-10236

COMBAT
Assured Mission Support Space Architecture (AMSSA) study p 348 N94-11573
Aviators, air combat, and combat stress: An Air F orce commander's primer
[AD-A265083] p 313 N94-11867

COMBINATORIAL ANALYSIS
Algorithms for the maximum clique problem
[MEMO-1101] p 322 N94-10419
Bounding the Vapnik-Chervonenkis dimension of concept classes parameterized by real numbers
[DE93-011600] p 331 N94-11611

COMBUSTIBLE FLOW
The evolution equation for the flame surface density in turbulent premixed combustion p 81 N94-12316
Study and modeling of finite rate chemistry effects in turbulent non-premixed flames p 81 N94-12317
Generation of two-dimensional vortices in a cross-flow
p 160 N94-12318

COMBUSTION
Some aspects of combustion modelling by low and normal gravity p 124 N94-10244
Microgravity combustion of dust suspension in a spherical chamber p 80 N94-10248
Flammability parameters of materials: Ignition, combustion, and flame spread p 20 N94-10788
Preprints of the 13th Hydrogen Energy System Symposium
[DE93-781115] p 99 N94-11444

COMBUSTION CHAMBERS
External combustion engine having a combustion expansion chamber
[AD-D015761] p 178 N94-10375
Heat regenerative external combustion engine
[AD-D015765] p 178 N94-10378
Axisymmetric single shear element combustion instability experiment
[NASA-TM-106327] p 46 N94-10763
Combustion chamber analysis code
[NASA-CR-192585] p 46 N94-10934
Application of jet-shear-layer mixing and effervescent atomization to the development of a low-NO(x) combustor
[NASA-TM-105888] p 28 N94-11234
On the combustion of a laminar spray
[NASA-TM-106210] p 28 N94-11238
A study of strength evaluations of EDNi/EDCu/NARloy-Z bonded joints
[NASA-TM-108418] p 188 N94-11275
Preprints of the 13th Hydrogen Energy System Symposium
[DE93-781115] p 99 N94-11444

COMBUSTION CHEMISTRY
The intensity of knock in an internal combustion engine: An experimental and modeling study
[DE93-013089] p 177 N94-10322
Study and modeling of finite rate chemistry effects in turbulent non-premixed flames p 81 N94-12317
Distributed combustion in solid propellants
[AD-A265727] p 99 N94-12564

COMBUSTION CONTROL
Shear flow control of gas jets in liquids
[AD-A264673] p 152 N94-11448

COMBUSTION EFFICIENCY
Application of jet-shear-layer mixing and effervescent atomization to the development of a low-NO(x) combustor
[NASA-TM-105888] p 28 N94-11234

COMBUSTION PHYSICS
Some aspects of combustion modelling by low and normal gravity p 124 N94-10244
Microgravity combustion of dust suspension in a spherical chamber p 80 N94-10248
Summary of research in progress at ICASE
[NASA-CR-191481] p 318 N94-11198
KIVA-3: A KIVA program with block-structured mesh for complex geometries
[DE93-011986] p 77 N94-11249
Mapping closures for turbulent combustion
[AD-A265671] p 79 N94-12378
Distributed combustion in solid propellants
[AD-A265727] p 99 N94-12564

COMBUSTION PRODUCTS
Application of jet-shear-layer mixing and effervescent atomization to the development of a low-NO(x) combustor
[NASA-TM-105888] p 28 N94-11234
Pulsed plasma processing for control of diesel engine emissions
[DE93-011884] p 181 N94-11247
High-temperature corrosion of ceramic-ceramic composites in a waste incinerator environment
[DE93-012430] p 72 N94-11368
A model of elementary chemistry and fluid mechanics in the combustion of hydrogen on platinum surfaces
[DE93-012767] p 77 N94-11370
A combustion products analyzer for contingency use during thermodegradation events on spacecraft
p 318 N94-11555
Analytical method for water vapor collection and analysis in aircraft cabin fires
[DOT/FAA/CT-TN93/33] p 22 N94-12575
Information capability of NOAA-AVHRR data for monitoring oceanographic and atmospheric pollution
p 214 N94-12677

COMBUSTION STABILITY
Axisymmetric single shear element combustion instability experiment
[NASA-TM-106327] p 46 N94-10763

COMBUSTION TEMPERATURE
The pyrene laser induced fluorescence technique as a diagnostic tool for combustion thermometry in microgravity p 107 N94-10113

COMET RENDEZVOUS ASTEROID FLYBY MISSION

Coordinated Radio, Electron, and Waves Experiment (CREWE) for the NASA Comet Rendezvous and Asteroid Flyby (CRAF) instrument [NASA-CR-194376] p 427 N94-12566

COMETS

Origins of Solar Systems Workshop: The Origin, Evolution, and Detectability of Short Period Comets [NASA-CR-194255] p 427 N94-11628

The long-term dynamical behavior of short-period comets p 427 N94-11629

Identification of cometary and asteroidal particles in stratospheric IDP collections p 430 N94-12115

COMMAND AND CONTROL

In-orbit performance tests and tele-command systems of the umbrella test satellite (DEBUT) [NAL-TR-1165] p 43 N94-10859

High-performance distributed systems architecture [AD-A265297] p 337 N94-11829

Special investigation report: Commercial space launch incident, launch procedure anomaly orbital sciences corporation PEGASUS/SCD-1, 80 nautical miles east of Cape Canaveral, Florida, February 9, 1993 [PB93-917003] p 40 N94-11893

COMMERCE

Business fleet refueling assessment [PB93-189892] p 98 N94-11017

Pattern of federal procurement from minority and women-owned small business [PB93-189355] p 417 N94-11844

COMMINUTION

Impact comminution of glasses: Implications for lunar regolith evolution p 461 N94-12159

COMMITTEE ON SPACE RESEARCH

Pakistan Space and Upper Atmosphere Research Commission p 37 N94-10693

COMMUNICATION

Correspondence standards [NHB-1450.10B] p 420 N94-11589

COMMUNICATION NETWORKS

Potential markets for advanced satellite communications [NASA-CR-191145] p 41 N94-10512

PARTNERS p 38 N94-10695

Design and analysis of an optical interface message processor [AD-A266079] p 381 N94-10697

An investigation of error characteristics and coding performance [NASA-CR-193620] p 324 N94-10932

Time signal distribution in communication networks based on synchronous digital hierarchy p 139 N94-10989

Telescience capability for the Sondre Stromfjord, Greenland, incoherent-scatter radar facility [NASA-CR-193683] p 136 N94-11206

Use of telescience for biomedical research during space flight p 305 N94-11791

Asynchronous Transfer Mode (ATM) technology: An overview [AD-A266087] p 383 N94-12413

The DOE Program in High-Performance Computing and Communications (HPCC) [DE93-013813] p 334 N94-12606

COMMUNICATION SATELLITES

Preliminary system design of a Three Arm Capture Mechanism (TACM) flight demonstration article [NASA-CR-192573] p 177 N94-10341

COMMUNICATIONS TECHNOLOGY SATELLITE

Overview of KITSAT p 36 N94-10683

PARTNERS p 38 N94-10695

COMMUTER AIRCRAFT

Aircraft Accident/Incident Summary Report: Loss of control. Business Express, Inc., Beechcraft 1900C N811BE near Block Island, Rhode Island, December 28, 1991 [PB93-910405] p 22 N94-11044

COMPACTING

Dynamic high-pressure shock compaction of diamond powders [AD-A266004] p 93 N94-12354

COMPARISON

An intercomparison of the radium mass standards of the UK and the USSR: 2 [NPL-RSA(EXT)-34] p 359 N94-10266

COMPATIBILITY

The guide to Design For On-orbit Spacecraft Servicing (DFOSS) manual: Producing a consensus document p 421 N94-11575

COMPENSATORS

A wide-band fiber optic frequency distribution system employing thermally controlled phase compensation p 355 N94-10995

Project of an attitude control system (three axis) of a satellite using the LQG/LTR methodology [INPE-5473-TDI/504] p 44 N94-12356

COMPILERS

Scalable concurrent programming project [AD-A266097] p 328 N94-11295

Avoidance and suppression of compensation code in a trace scheduling compiler [AD-A265612] p 333 N94-12439

COMPLEX SYSTEMS

Symbolic dynamics and description of complexity [DE93-613030] p 418 N94-10485

Five biomedical experiments flown in an Earth orbiting laboratory: Lessons learned from developing these experiments on the first international microgravity mission from concept to landing p 302 N94-11556

Design for testability and diagnosis at the system-level p 184 N94-11563

Implementation and use of a computational ray-tracing program for the design and analysis of complex optical systems [AD-A265075] p 382 N94-11653

Cognitive engineering models: A prerequisite to the design of human-computer interaction in complex dynamic systems [NASA-CR-193472] p 320 N94-12558

COMPLEXITY

Symbolic dynamics and description of complexity [DE93-613030] p 418 N94-10485

COMPONENT RELIABILITY

Tin whiskers in electronic circuits [AD-A265917] p 146 N94-12565

COMPOSITE MATERIALS

The EUREKA project portfolio in new materials p 56 N94-10002

Application of composite materials for production nacelle structures p 56 N94-10006

Numerical simulation and experimental results of filament wound CFRP tubes tested under biaxial load p 58 N94-10015

Special problems of 3-D ultrasonic QNDI techniques and applications to composites aerospace structures p 61 N94-10036

Material advances for lightweight TPS p 62 N94-10049

Joints between dissimilar metallic and ceramic materials p 63 N94-10052

A new and efficient way to join composite pipes p 63 N94-10054

High temperature composites in Aerospatiale activities p 64 N94-10062

Fibre optic strain and temperature measurement in composite materials: A review of the OSTIC programme p 65 N94-10066

The Satellite Attack Warning and Assessment Flight Experiment (SAWAFE) p 45 N94-11323

Optical fibre techniques for structural monitoring in composites p 69 N94-11324

Smart processing of composite materials for enhanced performance and properties p 69 N94-11325

On the stability of shape memory materials and their properties in static and dynamic applications p 69 N94-11329

Crystallinity and dielectric properties of PEEK, a thermoplastic poly(ether ether ketone) [AD-A266027] p 91 N94-11487

Analytical models for describing the mechanical behavior of fiber reinforced composites [AD-A265906] p 74 N94-12347

Ultrasonic wave interaction with advanced complex materials for nondestructive evaluation applications [AD-A265704] p 74 N94-12401

COMPOSITE PROPELLANTS

Time-temperature shift factors for gun propellants [AD-A264979] p 97 N94-10489

COMPOSITE STRUCTURES

Application of composite materials for production nacelle structures p 56 N94-10006

The application of advanced materials to aircraft nacelle structures p 57 N94-10011

Development of a fatigue analysis approach for CFRP structures under acoustic loading p 58 N94-10018

Quantifying disbond area p 61 N94-10038

A new and efficient way to join composite pipes p 63 N94-10054

Fibre reinforced structures with glass matrix p 64 N94-10064

LAMINV: A computer code for creating laminates having prescribed properties p 65 N94-10069

Use of robots for aircraft dry stripping via plastic media blasting p 127 N94-10620

Computational simulation of hot composite structures [NASA-TM-106200] p 186 N94-10762

Fiber optic sensing for composite smart structures p 69 N94-11327

Adaptive structure design employing shape memory actuators p 70 N94-11331

Analytical models for describing the mechanical behavior of fiber reinforced composites [AD-A265906] p 74 N94-12347

COMPOSITION (PROPERTY)

Compositional and textural information from the dual inversion of visible, near and thermal infrared remotely sensed data p 258 N94-12097

COMPRESSED AIR

An investigation on the effectiveness of the piping interference removal system for STOL aircraft wind tunnel tests [NAL-TM-647] p 2 N94-10350

COMPRESSED GAS

Vehicular fleet operation on natural gas and propane: An overview [PB93-194603] p 98 N94-10844

A picosecond high pressure gas switch [DE93-011897] p 142 N94-11050

COMPRESSIBILITY

Inverting ultrasonic data on solid/fluid mixtures for Biot-Gassmann parameters [DE93-011952] p 150 N94-11026

Cold press sintering of simulated lunar basalt p 131 N94-12026

Theories of turbulent combustion in high speed flows [AD-A265735] p 79 N94-12403

COMPRESSIBILITY EFFECTS

Turbulence modeling and compressibility p 163 N94-12614

COMPRESSIBLE FLOW

Aerodynamic characteristics analysis of Garabedian-Korn 75-06-12 aircraft [PAPER-2D-7] p 11 N94-10472

Large eddy simulation of shock turbulence interaction p 155 N94-12289

Direct simulation of compressible wall-bounded turbulence p 156 N94-12294

Turbulence modeling and compressibility p 163 N94-12614

COMPRESSIBLE FLUIDS

Acoustics of bubbly sediments [AD-A263726] p 288 N94-11299

COMPRESSING

Quantum noise and squeezing in optical parametric oscillator with arbitrary output coupling p 375 N94-10568

Squeezing in phase-conjugated resonance fluorescence p 376 N94-10576

Generalised squeezing and information theory approach to quantum entanglement p 377 N94-10580

Completeness properties of the minimum uncertainty states p 349 N94-10581

Squeezed spin states: Squeezing the spin uncertainty relations p 377 N94-10585

Squeezed states of electrons and transitions of the density of states p 370 N94-10593

Collision-induced squeezing in a harmonic oscillator p 379 N94-10597

Non-stationary and non-linear dispersive medium as external field which generates the squeezed states p 380 N94-10605

Wave and pseudo-diffusion equations from squeezed states p 347 N94-10607

Quantum processes in resonators with moving walls p 380 N94-10612

COMPRESSION TESTS

Level 3 material characterization of NARC HRPF, HRHU, HRHF, and HRPU [NASA-CR-192579] p 65 N94-10812

COMPRESSORS

Method of reducing drag in aerodynamic systems [NASA-CASE-LEW-14791-1] p 12 N94-10672

Cooled spool piston compressor [NASA-CASE-MSC-22020-1] p 179 N94-10674

Theoretical evaluation of R22 and R502 alternatives [DE93-014767] p 411 N94-10853

Accelerated screening methods for predicting lubricant performance in refrigerant compressors [DE93-014773] p 89 N94-11146

COMPULSATORS

Investigation of multiphase railgun systems p 40 N94-11637

COMPUTATION

Numerical calculation of the growth of InP by the travelling heater method in the first mission of the Space Flyer Unit p 114 N94-10179

Heterogeneous SuperConcurrent Parallelism (HeSCP) [AD-A265004] p 336 N94-11293

Alleviating memory contention in matrix computations on large-scale shared-memory multiprocessors [AD-A265009] p 320 N94-11294

COMPUTATIONAL ASTROPHYSICS

Acceleration of positrons in supernova shocks [NASA-CR-193713] p 425 N94-10511

COMPUTATIONAL CHEMISTRY

Comparison of computation and experiment for a high enthalpy, heated-driver, shock-tube environment p 7 N94-10447

A new decomposition strategy for parallel bonded molecular dynamics [DE93-009839] p 366 N94-11284

COMPUTATIONAL FLUID DYNAMICS

Large time-step stability of explicit one-dimensional advection schemes [NASA-TM-106203] p 342 N94-10362

Simulation of a parallel computer [NAL-TR-1154] p 335 N94-10368

Theoretical and Experimental Methods in Hypersonic Flows [AGARD-CP-514] p 2 N94-10421

CFD analysis of hypersonic, chemically reacting flow fields p 2 N94-10422

Numerical simulation of the flow through a scramjet engine p 3 N94-10425

In-flight evaluation of aerodynamic predictions of an air-launched space booster p 3 N94-10427

A CFD validation roadmap for hypersonic flows p 5 N94-10439

Synthesis of the Workshop on Hypersonic Flows for ReEntry Problems p 5 N94-10440

Problems in the validation of CFD codes through comparison with experiment p 6 N94-10441

Experimental and computational comparisons of Mach 6 high Reynolds number heat transfer and skin friction p 6 N94-10443

Joint computational and experimental aerodynamic research on a hypersonic vehicle p 6 N94-10445

Issues and approach to develop validated analysis tools for hypersonic flows: One perspective p 7 N94-10446

Comparison of computation and experiment for a high enthalpy, heated-driver, shock-tube environment p 7 N94-10447

On the instability of hypersonic flow past a pointed cone: Comparison of theoretical and experimental results at Mach 8 p 8 N94-10453

Studies of hypersonic viscous flows p 8 N94-10454

Calculations of viscous nonequilibrium flows in nozzles p 8 N94-10455

Nonequilibrium hypersonic flow in a wind-tunnel nozzle p 8 N94-10456

Some experimental study and numerical simulation in wind tunnel flow p 8 N94-10457

A CFD-based aerodynamic design procedure for hypersonic wind-tunnel nozzles p 9 N94-10458

Numerical methods for aerothermodynamic design of hypersonic space transport vehicles p 9 N94-10459

Hypersonic flow computations around re-entry vehicles p 9 N94-10461

On the accuracy and efficiency of CFD methods in real gas hypersonics p 9 N94-10462

A comparison of high resolution upwind solvers on 3-D inviscid hypersonic flows p 10 N94-10463

Local aerothermal problems during Hermes re-entry p 10 N94-10464

Thermal and chemical non equilibrium hypersonic flow computations p 10 N94-10465

Proceedings of the 10th NAL Symposium on Aircraft Computational Aerodynamics: CFD Workshop on GK Airfoil and ONERA M5 Geometry [NAL-SP-20] p 10 N94-10466

Description of 2D problem: Aerodynamic analysis of Garabedian-Korn 75-06-12 airfoil p 10 N94-10467

Aerodynamic characteristics analysis of Garabedian-Korn 75-06-12 airfoil [PAPER-2D-2] p 10 N94-10468

Aerodynamic characteristics analysis of Garabedian-Korn 75-06-12 airfoil [PAPER-2D-3] p 10 N94-10469

Aerodynamic characteristics analysis of Garabedian-Korn 75-06-12 airfoil: Computation using q-omega 2 equation turbulence model [PAPER-2D-4] p 10 N94-10470

Aerodynamic characteristics analysis of Garabedian-Korn 75-06-12 airfoils: Computation using Baldwin-Lomax turbulence model [PAPER-2D-5] p 11 N94-10471

Aerodynamic characteristics analysis of Garabedian-Korn 75-06-12 aircraft [PAPER-2D-7] p 11 N94-10472

Aerodynamic characteristics analysis of Garabedian-Korn 75-06-12 airfoil [PAPER-2D-8] p 11 N94-10473

Aerodynamic characteristics analysis of Garabedian-Korn 75-06-12 airfoil [PAPER-2D-9] p 11 N94-10474

Aerodynamic characteristics analysis of Garabedian-Korn 75-06-12 airfoil: Compendium of results p 11 N94-10475

Description of 3D problem: Flow analysis around ONERA model M5 configuration p 11 N94-10476

Flow analysis around ONERA model M5 configuration [PAPER-3D-1] p 11 N94-10477

Flow analysis around ONERA model M5 configuration [PAPER-3D-2] p 12 N94-10478

Flow analysis around ONERA model M5 configuration [PAPER-3D-3] p 12 N94-10479

Flow analysis around ONERA model M5 configuration [PAPER-3D-4] p 12 N94-10480

Flow analysis around ONERA model M5 configuration [PAPER-3D-5] p 12 N94-10481

Flow analysis around ONERA model M5 configuration: Compendium of results p 12 N94-10482

Navier-Stokes flowfield computation of wing/rotor interaction for a tilt rotor aircraft in hover [NASA-CR-4532] p 13 N94-10758

A comparative study of full Navier-Stokes and Reduced Navier-Stokes analyses for separating flows within a diffusing inlet S-duct [NASA-TM-106250] p 39 N94-10764

Development of an unstructured solution adaptive method for the quasi-three-dimensional Euler and Navier-Stokes equations [NASA-CR-191161] p 28 N94-10816

Development of a Delaunay-based adaption scheme with applications to complex three-dimensional rotational flows p 149 N94-10824

New aerodynamic information obtained from the solution of the inverse problem for aerofoils [NAL-TR-1172] p 14 N94-10860

Numerical wind tunnel project and computational fluid dynamics at National Aerospace Laboratory, Japan [NAL-TM-648T] p 149 N94-10861

Generation and analysis of hybrid structured/unstructured grids [ARA-MEMO-365] p 324 N94-10893

Combustion chamber analysis code [NASA-CR-192585] p 46 N94-10934

New developments in the method of space-time conservation element and solution element: Applications to the Euler and Navier-Stokes equations [NASA-TM-106226] p 150 N94-10939

FORCE2: A state-of-the-art two-phase code for hydrodynamic calculations [DE93-010661] p 150 N94-11072

Turbulent wall jet in blast wave precursor [DE93-011955] p 151 N94-11144

Supersonic airplane study and design [NASA-CR-193219] p 25 N94-11150

Summary of research in progress at ICASE [NASA-CR-191481] p 318 N94-11198

Looking for O(N) Navier-Stokes solutions on non-structured meshes [NASA-CR-191472] p 345 N94-11277

Viscous analysis of three-dimensional rotor flows using a multigrid method [NASA-TM-106266] p 152 N94-11481

Massively parallel hydrodynamics on unstructured grids [DE93-007325] p 153 N94-11601

Modelling quasi-two-dimensional turbulent shear flow p 153 N94-11616

Turbulence modeling for thrust reverser flow field prediction methods [AD-A266139] p 154 N94-11641

Transactions of the 10th Army Conference on Applied Mathematics and Computing [AD-A265098] p 318 N94-11678

SAUNA: A system for grid generation and flow simulation using hybrid structured/unstructured grids [ARA-MEMO-370] p 154 N94-11859

Computation of hypersonic nosetip heat transfer rates for an M829-like projectile [AD-A263226] p 16 N94-11870

The modelling of aerodynamic flows by solution of the Euler equations on mixed polyhedral grids [ARA-84] p 16 N94-11888

Annual Research Briefs, 1992 [NASA-CR-194389] p 155 N94-12284

A local dynamic model for large eddy simulation p 155 N94-12285

Parameterization of subgrid-scale stress by the velocity gradient tensor p 155 N94-12286

Direct simulation of compressible wall-bounded turbulence p 156 N94-12294

Regeneration of near-wall turbulence structures p 158 N94-12308

The three-dimensional evolution of a plane wake p 159 N94-12310

Mixing in a stratified shear flow: Energetics and sampling p 159 N94-12311

Tensoral: A system for post-processing turbulence simulation data p 75 N94-12320

Computational methods for problems in aerodynamics using parallel and vector architectures [AD-A265626] p 16 N94-12377

A determination of the external forces required to move the benchmark active controls testing model in pure plunge and pure pitch [NASA-TM-107743] p 16 N94-12421

Towards a cell-vertex Navier-Stokes algorithm for three-dimensional structured/unstructured meshes [ARA-MEMO-366] p 161 N94-12437

Hypersonic, nonequilibrium flow over a cylindrically blunted 6 deg wedge [NASA-TM-108994] p 162 N94-12571

Modeling void growth and movement with phase change in thermal energy storage canisters [NASA-TM-106288] p 163 N94-12576

Proceedings of the 9th and 10th NAL Workshop on Investigation and Control of Boundary-Layer Transition [NAL-SP-18] p 163 N94-12611

VIB3D: Method for calculating 3-D unsteady flow through turbomachinery blades [CUED/A-TURBO/TR.128] p 166 N94-12777

COMPUTATIONAL GEOMETRY

Bibliographic notes on Voronoi diagrams [PB93-189298] p 343 N94-10825

Transactions of the 10th Army Conference on Applied Mathematics and Computing [AD-A265098] p 318 N94-11678

COMPUTATIONAL GRIDS

A grid generation method to calculate the flow field in a three-dimensional cascade of blades [NAL-TR-1158] p 147 N94-10364

CFD analysis of hypersonic, chemically reacting flow fields p 2 N94-10422

Hypersonic flow computations around re-entry vehicles p 9 N94-10461

Viscous flow simulation using an upwind method for hexahedral based adaptive meshes [AD-A265901] p 148 N94-10703

Development of an unstructured solution adaptive method for the quasi-three-dimensional Euler and Navier-Stokes equations [NASA-CR-191161] p 28 N94-10816

Generation and analysis of hybrid structured/unstructured grids [ARA-MEMO-365] p 324 N94-10893

A dynamically adaptive mesh method for internal flows p 149 N94-10896

New developments in the method of space-time conservation element and solution element: Applications to the Euler and Navier-Stokes equations [NASA-TM-106226] p 150 N94-10939

DILUTE: A code for studying beam evolution under RF noise [DE93-011605] p 133 N94-10960

Object oriented implementation of adaptive mesh refinement algorithms [DE93-011885] p 325 N94-11112

An improved material interface reconstruction algorithm for Eulerian codes [DE93-011679] p 326 N94-11226

Quality factors and local adaption (with applications in Eulerian hydrodynamics) [DE93-010502] p 151 N94-11272

Viscous analysis of three-dimensional rotor flows using a multigrid method [NASA-TM-106266] p 152 N94-11481

Grid optimization and multigrid techniques for fluid flow and transport problems p 154 N94-11824

SAUNA: A system for grid generation and flow simulation using hybrid structured/unstructured grids [ARA-MEMO-370] p 154 N94-11859

The modelling of aerodynamic flows by solution of the Euler equations on mixed polyhedral grids [ARA-84] p 16 N94-11888

A local dynamic model for large eddy simulation p 155 N94-12285

Parameterization of subgrid-scale stress by the velocity gradient tensor p 155 N94-12286

Large eddy simulations of time-dependent and buoyancy-driven channel flows p 155 N94-12287

A normal stress subgrid-scale eddy viscosity model in large eddy simulation p 155 N94-12288

Large eddy simulation of shock turbulence interaction p 155 N94-12289

Application of a dynamic subgrid-scale model to turbulent recirculating flows p 156 N94-12290

Hypersonic, nonequilibrium flow over a cylindrically blunted 6 deg wedge [NASA-TM-108994] p 162 N94-12571

COMPUTER AIDED DESIGN

Numerical methods for aerothermodynamic design of hypersonic space transport vehicles p 9 N94-10459

Computer-aided molecular design of fire resistant aircraft materials p 19 N94-10779

Multilevel computer-aided optimum design of structural systems using multiple basis vectors p 187 N94-11055

Blading models for TURBAN and CSPAN turbomachine design codes
[NASA-CR-191164] p 15 N94-11203
Large project experiences with object-oriented methods and reuse p 329 N94-11431
Utilizing quantitative feedback theory design technique for flight control system p 32 N94-11501
RAMCAD (reliability, availability, and maintainability in computer-aided design)
[AD-A265143] p 331 N94-11679

COMPUTER AIDED MANUFACTURING
The graphical library for technological process automatization
[DE93-621316] p 324 N94-11031

COMPUTER AIDED MAPPING
Analysis of IRAS solar system dust data
[NASA-CR-193704] p 483 N94-10949

COMPUTER AIDED TOMOGRAPHY
Resolution for Lanczos and Paige-Saunders inverses in tomography
[DE93-012312] p 327 N94-11240
Potential techniques for non-destructive evaluation of cable materials
[DE93-008350] p 183 N94-11586

COMPUTER ANIMATION
Subroutine functions for generating animation data
[DE93-767973] p 313 N94-10731
Animating engineering science results using AVS
[DE93-011591] p 325 N94-11123
Visualization and simulation of a real physical problem based on physical modeling with the use of computer animation
[INPE-5492-TDI/509] p 325 N94-11166

COMPUTER DESIGN
Optimal cube-connected cube multiprocessors
[NASA-CR-191463] p 337 N94-11308

COMPUTER GRAPHICS
Virtual sound for virtual reality
[DE93-010519] p 321 N94-10291
The graphical library for technological process automatization
[DE93-621316] p 324 N94-11031
Using a private SMDS/ATM network to provide long-haul supercomputing visualization services
[DE93-010692] p 325 N94-11109
Animating engineering science results using AVS
[DE93-011591] p 325 N94-11123
Visualization and simulation of a real physical problem based on physical modeling with the use of computer animation
[INPE-5492-TDI/509] p 325 N94-11166
A heterogeneous graphics procedure for visualization of massively parallel solutions
[DE93-009628] p 336 N94-11270
Space Station maintenance studies using plaid graphics p 335 N94-11578
Development of a graphical user interface and graphics display for the WIND system
[DE93-011760] p 285 N94-11614
Development and implementation of a general purpose x-windows display program
[AD-A265306] p 332 N94-11860
The 1991 version of the plume impingement computer program. Volume 1: Description
[NASA-CR-194192] p 166 N94-12775

COMPUTER INFORMATION SECURITY
Using a private SMDS/ATM network to provide long-haul supercomputing visualization services
[DE93-010692] p 325 N94-11109
An alternative to sneakernet
[DE93-012130] p 419 N94-11137

COMPUTER NETWORKS
Practical authorization in large heterogeneous distributed systems
[DE93-013192] p 335 N94-10324
A flexible modelling software for data acquisition
[DE93-612915] p 322 N94-10484
Optimization algorithms for integer networks with side constraints for application in routing and scheduling
[AD-A265254] p 322 N94-10492
Optimal routing of IP packets to multi-homed servers
[DE93-010949] p 133 N94-10709
Distributed simulation using a real-time shared memory network
[NASA-TM-106239] p 319 N94-10724
Timing in private digital telecommunication networks
p 139 N94-10991
SONET synchronization: What's happening
p 355 N94-10992
A distributed version of the NASA Engine Performance Program
[NASA-TM-106208] p 327 N94-11231
Portable programming on parallel/networked computers using the Application Portable Parallel Library (APPL)
[NASA-TM-106238] p 327 N94-11232
High-performance distributed systems architecture
[AD-A265297] p 337 N94-11829
Distributed real-time system design: Theoretical concepts and applications
[AD-A265199] p 337 N94-11881
Analysis of the Army's installation support modules with the private sector's open information systems
[AD-A265667] p 421 N94-12579
Networks of real-time processes
[DE93-013049] p 338 N94-12597

COMPUTER PROGRAMMING
Sandia ocean modeling system programmer's guide and user's manual
[DE93-007427] p 287 N94-10153
System engineering concept demonstration, trade studies, volume 6
[AD-A265472] p 323 N94-10495
An investigation of error characteristics and coding performance
[NASA-CR-193620] p 324 N94-10932
The 1987 RIACS annual report
[NASA-CR-193220] p 324 N94-11046
Portable programming on parallel/networked computers using the Application Portable Parallel Library (APPL)
[NASA-TM-106238] p 327 N94-11232
Proceedings of the Seventeenth Annual Software Engineering Workshop
[NASA-TM-109245] p 328 N94-11422
Experimental software engineering: Seventeen years of lessons in the SEL p 328 N94-11423
The experience factory: Can it make you a 5? or what is its relationship to other quality and improvement concepts? p 328 N94-11424
Impacts of object-oriented technologies: Seven years of SEL studies p 329 N94-11425
Maximizing reuse: Applying common sense and discipline p 329 N94-11429
Analysis and guidelines for reusable Ada software
[AD-A264918] p 332 N94-11850
Development and implementation of a general purpose x-windows display program
[AD-A265306] p 332 N94-11860
System engineering concept demonstration, process model, volume 3
[AD-A265469] p 333 N94-12008
Tensoral: A system for post-processing turbulence simulation data p 75 N94-12320
Avoidance and suppression of compensation code in a trace scheduling compiler
[AD-A265612] p 333 N94-12439

COMPUTER PROGRAMS
LAMINV: A computer code for creating laminates having prescribed properties p 65 N94-10069
Computational procedures for determining parameters in Ramberg-Osgood elastoplastic model based on modulus and damping versus strain
[DE93-013309] p 185 N94-10306
Software usability assessment guide
[AD-A265017] p 321 N94-10335
Techniques, processes, and measures for software safety and reliability
[DE93-012379] p 322 N94-10347
Numerical simulation of sidebands in free electron laser oscillators
[DE93-612675] p 173 N94-10483
Application of parallel processing to a surface patch/wire junction EFIE code
[AD-A264965] p 336 N94-10488
Computer models used to support cleanup decision-making at hazardous and radioactive waste sites
[PB93-183333] p 274 N94-10698
NASA Marshall Space Flight Center solar observatory report, January - June 1993
[NASA-TM-108417] p 423 N94-10866
An investigation of error characteristics and coding performance
[NASA-CR-193620] p 324 N94-10932
Efficient partitioning and assignment on programs for multiprocessor execution
[NASA-CR-193458] p 324 N94-10942
RighTime: A real time clock correcting program for MS-DOS-based computer systems p 334 N94-10986
The graphical library for technological process automatization
[DE93-621316] p 324 N94-11031
FORCE2: A state-of-the-art two-phase code for hydrodynamic calculations
[DE93-010661] p 150 N94-11072
Landing Craft Air Cushion (LCAC) crew selection system manual
[AD-A265158] p 313 N94-11098
Computer software and hardware to determine contrast sensitivity using three methods: Tracking, limits, and constant stimuli
[AD-A265168] p 324 N94-11099
An alternative to sneakernet
[DE93-012130] p 419 N94-11137
A toolkit for building Earth system models
[DE93-012147] p 276 N94-11138
ACARA user's manual
[NASA-TM-106277] p 183 N94-11167
Development of deterministic transport methods for low energy neutrons for shielding in space
[NASA-CR-194172] p 366 N94-11199
P2NBC2 Heat Strain Decision Aid. User's guide, version 2.1
[AD-A266072] p 304 N94-11224
Development of generic field classes for finite element and finite difference problems
[DE93-011678] p 345 N94-11225
A distributed version of the NASA Engine Performance Program
[NASA-TM-106208] p 327 N94-11231
GRISET certification package
[DE93-011783] p 327 N94-11246
Computational mechanics needs study
[NASA-CR-193712] p 327 N94-11279
GRAFTED (GRAphical Fault Tree EDitor): A fault tree description program for target vulnerability/survivability analysis
[AD-A264078] p 328 N94-11301
The role of metrics and measurements in a software intensive total quality management environment
p 329 N94-11428
Maximizing reuse: Applying common sense and discipline p 329 N94-11429
Development and application of an acceptance testing model p 330 N94-11432
STGT program: Ada coding and architecture lessons learned p 330 N94-11437
Software management guide
[DE93-012034] p 330 N94-11452
Implementation and use of a computational ray-tracing program for the design and analysis of complex optical systems
[AD-A265075] p 382 N94-11653
Wind system documentation
[DE93-010381] p 285 N94-11664
COSMIC monthly progress report
[NASA-CR-194400] p 332 N94-11688
NASCAP programmer's reference manual
[NASA-CR-191044] p 278 N94-11702
Linking medical records to an expert system
p 306 N94-11797
Analysis and guidelines for reusable Ada software
[AD-A264918] p 332 N94-11850
FFTSCAN: A program for spectral smoothing using Fourier transforms
[AD-A264921] p 278 N94-11852
The rational behavior model: A multi-paradigm, tri-level software architecture for the control of autonomous vehicles
[AD-A265175] p 332 N94-11874
Avoidance and suppression of compensation code in a trace scheduling compiler
[AD-A265612] p 333 N94-12439
Transportable Applications Environment (TAE) Tenth Users' Conference
[NASA-CP-3225] p 333 N94-12448
TREES project: A suite of tools for information extraction from ERS-1 SAR data p 250 N94-12498
Prediction of alumina penetration
[DE93-014017] p 95 N94-12610
Migration of operational ice analysis and forecasting to a workstation platform at the Joint Ice Center
p 212 N94-12666
Simple and low cost image processing system for satellite remote sensing data p 212 N94-12669

COMPUTER STORAGE DEVICES
Holographic multiplexing for 3D optical memory
[AD-A266099] p 171 N94-11420

COMPUTER SYSTEMS DESIGN
Finite state machine microarchitecture transformations described with relational algebra
[MEMO-INF-92-63] p 319 N94-10278
Distributed real-time system design: Theoretical concepts and applications
[AD-A265199] p 337 N94-11881
The instrumentation of the multimodel and multilingual user interface
[AD-A265444] p 333 N94-12332
Transportable Applications Environment (TAE) Tenth Users' Conference
[NASA-CP-3225] p 333 N94-12448
Analysis of the Army's installation support modules with the private sector's open information systems
[AD-A265667] p 421 N94-12579
Simple and low cost image processing system for satellite remote sensing data p 212 N94-12669

COMPUTER SYSTEMS PERFORMANCE
Massively parallel multifrontal methods for finite element analysis on MIMD computer systems
[DE93-009838] p 335 N94-10257
A formally verified algorithm for interactive consistency under a hybrid fault model
[NASA-CR-4527] p 326 N94-11188
Reliability analysis for FDDI dual homing networks
[AD-A266133] p 337 N94-11475
COMPUTER SYSTEMS PROGRAMS
Massively parallel multifrontal methods for finite element analysis on MIMD computer systems
[DE93-009838] p 335 N94-10257
The super vectorfield package for REDUCE. Version 1.0
[MEMO-1099] p 321 N94-10265
Wait-free linearization with an assertional proof
[CS-9208] p 323 N94-10878
A recent Cleanroom success story: The Redwing project p 39 N94-11433
Applying reliability models to the maintenance of Space Shuttle software p 330 N94-11434
The rational behavior model: A multi-paradigm, tri-level software architecture for the control of autonomous vehicles
[AD-A265175] p 332 N94-11874
COMPUTER SYSTEMS SIMULATION
Node assignment in heterogeneous computing
[NASA-CR-4534] p 142 N94-11131
COMPUTER TECHNIQUES
The 2nd Annual Meeting of the Society for Research on Biological Rhythms
[AD-A264869] p 303 N94-10872
The 1987 RIACS annual report
[NASA-CR-193220] p 324 N94-11046
Summary of research in progress at ICASE
[NASA-CR-191481] p 318 N94-11198
Computational mechanics needs study
[NASA-CR-193712] p 327 N94-11279
Experimental software engineering: Seventeen years of lessons in the SEL p 328 N94-11423
Strategies and methodologies to develop techniques for computer-assisted analysis of gas phase formation during altitude decompression p 312 N94-11547
COMPUTER VISION
Model-based recognition of 3-D objects by geometric hashing technique
[DE93-612916] p 322 N94-10410
A high-speed object recognition chip based on biologically-realistic hybrid temporal processing element
[AD-A265490] p 339 N94-11049
A summary of image segmentation techniques
[NASA-TM-104022] p 327 N94-11274
Parametric study of diffusion-enhancement networks for spatiotemporal grouping in real-time artificial vision
[AD-A265065] p 331 N94-11652
Experiments in mobile robot navigation and range imaging
[DE93-013280] p 341 N94-12598
COMPUTERIZED SIMULATION
Deformation mechanisms of continuous fibre-reinforced thermoplastic composites during manufacturing: A probabilistic approach p 60 N94-10030
Solving the essentials of an innovative tennis racket product: Functionality, simplicity, and super-lightweight technology p 65 N94-10068
Effect of rotation on microgravity floating-zone crystal growth p 101 N94-10080
Towards real time numerical stimulation of Marangoni convection: A help for telescience microgravity experiments p 102 N94-10087
Numerical simulation of Marangoni convection around gas bubbles in a liquid matrix p 106 N94-10107
TOLS (Telescience On-Line Simulator): An essential instrument for micro-gravity interactive experiment
p 39 N94-10134
Marangoni motion during melting of a hypermonotectic alloy: Numerical simulations for the D2 experiment IHF04 p 113 N94-10177
Numerical simulation of multi-droplet hydrodynamic interactions in liquid dispersions p 114 N94-10182
Conductive-radiative model for predicting the shape of Hgl2 crystal grown in the LTVG furnace
p 117 N94-10201
Simulations of D3-D divertor biasing with the LEDGE code
[DE93-010500] p 385 N94-10262
Survey to determine the value of DYNA
[DE93-012390] p 321 N94-10267
A spectral nodal method for discrete ordinates problems in x,y geometry
[DE93-610128] p 342 N94-10283
A study of the magnetic field annihilation process in the magnetosphere and some geotechnical applications
[DE93-013248] p 273 N94-10319
A parallel implementation of particle tracking with space charge effects on an Intel iPSC/860
[DE93-012307] p 335 N94-10340
Studies and simulations of the DigiCipher system
[NASA-CR-193470] p 321 N94-10343
Theoretical and Experimental Methods in Hypersonic Flows
[AGARD-CP-514] p 2 N94-10421
Synthesis of the Workshop on Hypersonic Flows for ReEntry Problems p 5 N94-10440
Joint computational and experimental aerodynamic research on a hypersonic vehicle p 6 N94-10445
Three-dimensional hypersonic rarefied flow calculations using direct simulation Monte Carlo method
p 7 N94-10449
Hypersonic multi block flow simulations around space vehicles including non-equilibrium chemistry
p 9 N94-10460
Numerical simulation of sidebands in free electron laser oscillators
[DE93-612675] p 173 N94-10483
A flexible modelling software for data acquisition
[DE93-612915] p 322 N94-10484
Acceleration of positrons in supernova shocks
[NASA-CR-193713] p 425 N94-10511
Computer models used to support cleanup decision-making at hazardous and radioactive waste sites
[PB93-183333] p 274 N94-10698
Arcjet space thrusters
[NASA-CR-193191] p 46 N94-10700
Viscous flow simulation using an upwind method for hexahedral based adaptive meshes
[AD-A265901] p 148 N94-10703
System monitoring and diagnosis with qualitative models
[NASA-CR-193812] p 323 N94-10711
Distributed simulation using a real-time shared memory network
[NASA-TM-106239] p 319 N94-10724
Computational simulation of hot composite structures
[NASA-TM-106200] p 186 N94-10762
Computer-aided molecular design of fire resistant aircraft materials p 19 N94-10779
Fully coupled neutronic and hydrodynamic analysis of space nuclear reactor reentry accidents
[DE93-005459] p 372 N94-10890
Advanced statistical methods for improved data analysis of NASA astrophysics missions
[NASA-CR-193514] p 425 N94-10943
The time keeping system for GPS block IIR
p 24 N94-10964
Development of a cryogenic hydrogen maser at the NPL p 176 N94-10982
FORCE2: A state-of-the-art two-phase code for hydrodynamic calculations
[DE93-010661] p 150 N94-11072
Animating engineering science results using AVS
[DE93-011591] p 325 N94-11123
Visualization and simulation of a real physical problem based on physical modeling with the use of computer animation
[INPE-5492-TDI/509] p 325 N94-11166
Fatigue life prediction for wind turbines: A case study on loading spectra and parameter sensitivity
[DE93-011597] p 263 N94-11173
Numerical simulations on the redistribution of atmospheric trace chemicals through cloud processes
p 265 N94-11189
Summary of research in progress at ICASE
[NASA-CR-191481] p 318 N94-11198
A comparison between numerically modelled and experimentally measured loss mechanisms in wave rotors
[NASA-TM-106279] p 29 N94-11255
Computational mechanics needs study
[NASA-CR-193712] p 327 N94-11279
A new decomposition strategy for parallel bonded molecular dynamics
[DE93-009839] p 366 N94-11284
Approaches to solar cell design for pulsed laser power receivers p 51 N94-11397
Further studies using matched filter theory and stochastic simulation for gust loads prediction
[NASA-TM-109010] p 26 N94-11587
A molecular dynamics simulation code ISIS
[DE93-753187] p 368 N94-11592
Model reference adaptive control (MRAC) with applications to robotics p 339 N94-11640
Grid optimization and multigrid techniques for fluid flow and transport problems p 154 N94-11824
The flow structure around a cylindrical pier for the flow of transcritical Reynolds number p 169 N94-11944
An application of reduced gravity model to mesoscale eddies p 199 N94-11945
Bi-directional reflectance by oceanic waters studied via Monte-Carlo simulations p 203 N94-11971
Remote sensing for numerical modelling of radiative transfer processes in ocean environment
p 204 N94-11973
The evaluation of radiative process in the atmosphere-ground system by Monte Carlo method
p 205 N94-11980
The upwelling radiation at the top of the atmosphere in coastal region p 205 N94-11981
The origin of Venusian channels: Modelling of thermal erosion by lava p 456 N94-12131
The giant impact produced a precipitated Moon
p 430 N94-12135
A local dynamic model for large eddy simulation
p 155 N94-12285
Parameterization of subgrid-scale stress by the velocity gradient tensor p 155 N94-12286
Large eddy simulations of time-dependent and buoyancy-driven channel flows p 155 N94-12287
A normal stress subgrid-scale eddy viscosity model in large eddy simulation p 155 N94-12288
Large eddy simulation of shock turbulence interaction
p 155 N94-12289
Application of a dynamic subgrid-scale model to turbulent recirculating flows p 156 N94-12290
Large-eddy simulation of turbulent flow with a surface-mounted two-dimensional obstacle
p 156 N94-12291
Similarity states of homogeneous stably-stratified turbulence at infinite Froude number
p 156 N94-12292
Regeneration of near-wall turbulence structures
p 158 N94-12308
Mixing in a stratified shear flow: Energetics and sampling p 159 N94-12311
Tensoral: A system for post-processing turbulence simulation data p 75 N94-12320
Space Life Support Engineering Program
[NASA-CR-193474] p 316 N94-12365
Systems analysis of a closed loop ECLSS using the ASPEN simulation tool. Thermodynamic efficiency analysis of ECLSS components p 316 N94-12366
Modifications to an interactive model of the human body during exercise: With special emphasis on thermoregulation p 317 N94-12368
An estimate of the second law thermodynamic efficiency of the various units comprising an Environmental Control and Life Support System (ECLSS) p 317 N94-12369
The DOE Program in High-Performance Computing and Communications (HPCC)
[DE93-013813] p 334 N94-12606
Improved Many-On-Many ROUTE software description
[DE93-013961] p 334 N94-12608
A basic consideration for remote sensing using microwave radars on a satellite p 212 N94-12665
Generation of internal waves near the shelf boundary
p 229 N94-12763
Model of Kuroshio region circulation
p 229 N94-12765
COMPUTERS
System engineering concept demonstration, technology assessments, volume 5
[AD-A265471] p 323 N94-10494
System engineering concept demonstration, trade studies, volume 6
[AD-A265472] p 323 N94-10495
The 1987 RIACS annual report
[NASA-CR-193220] p 324 N94-11046
CONCATENATED CODES
An investigation of error characteristics and coding performance
[NASA-CR-193620] p 324 N94-10932
CONCENTRATION (COMPOSITION)
Boundary layers along horizontal free surfaces due to combined effects of temperature and concentration gradients p 106 N94-10108
On the role of Soret effect in concentration distribution in crystals growing from the melt p 112 N94-10173
TEXUS 28 experiment: Convections and crystal growth of Ge:Ga. Analysis of temperature measurements
p 114 N94-10184
In situ observation of temperature dependence of concentration field during growth of KB5 crystals by holographic interferometry p 115 N94-10187
Hygroscopic absorption to falling films: The effects of the concentration level
[ITN-93-85198] p 148 N94-10391
Determination of concentration profiles at interfaces and surfaces of partially miscible polymer blends
[DE93-013140] p 89 N94-11007
A combustion products analyzer for contingency use during thermodegradation events on spacecraft
p 318 N94-11555

CONCENTRATORS
Recent developments in refractive concentrators for space photovoltaic power systems p 52 N94-11402

CONCRETE STRUCTURES
Study on sea water purification using a substratum of marine organisms p 217 N94-12696

CONCRETES
Cold press sintering of simulated lunar basalt
p 131 N94-12026
Three-dimensional finite element analysis of explosive safety facilities: A technology assessment
[AD-A265700] p 35 N94-12562

CONCURRENT PROCESSING
An object-oriented model for extensible concurrent systems: The composition-filters approach
[MEMO-INF-92-87] p 320 N94-10166
Heterogeneous SuperConcurrent Parallelism (HeSCP)
[AD-A265004] p 336 N94-11293
Scalable concurrent programming project
[AD-A266097] p 328 N94-11295
Networks of real-time processes
[DE93-013049] p 338 N94-12597

CONDENSATION
New aromatic activated dihalides and bisphenol monomers for the preparation of novel poly(arylene ethers)
[NASA-CR-193190] p 55 N94-10513
Recondensation of chondritic material in the early solar system: Results of thermodynamic simulation
p 432 N94-12226

CONDENSED MATTER PHYSICS
STARDUST: A simulation experiment of cosmic dust analogues production in microgravity conditions
p 113 N94-10175
Electron momentum spectroscopy of atoms, molecules and solids
[DE93-610148] p 360 N94-10332
Recent advances in electron momentum spectroscopy
[DE93-610149] p 361 N94-10333
Singularity spectrum of self-organized criticality
[DE93-613820] p 348 N94-10404

CONDENSING
Two-phase flow heat transfer and hydrodynamics in an electric field p 103 N94-10093

CONDITIONING (LEARNING)
Computer software and hardware to determine contrast sensitivity using three methods: Tracking, limits, and constant stimuli
[AD-A265168] p 324 N94-11099

CONDUCTING FLUIDS
The effect of a uniform magnetic field on the onset of steady Marangoni convection in a layer of conducting fluid p 120 N94-10222
On the unique structure of the magnetic fields of Uranus and Neptune p 472 N94-12221

CONDUCTING POLYMERS
X ray absorption spectroscopy of electrochemically generated species
[AD-A264749] p 77 N94-11265
Smart polymeric system for electromechanical transduction p 70 N94-11330

CONDUCTION BANDS
Electronic characterization of defects in narrow gap semiconductors
[NASA-CR-193568] p 397 N94-10819

CONDUCTION ELECTRONS
Effect of a distribution of exchange parameters within a simple localized-itinerant model
[DE93-610314] p 395 N94-10314

CONDUCTIVE HEAT TRANSFER
Heat analysis of thermoplastic components during the initial stages of manufacturing: A probabilistic approach
p 60 N94-10031
Conductive-radiative model for predicting the shape of HgI2 crystal grown in the LTVG furnace
p 117 N94-10201
Stationary spectra of short-wave convective and magnetostatic fluctuations in a finite-pressure plasma and anomalous heat conductivity
[DE93-617852] p 388 N94-10840

CONES (VOLCANOES)
Venus small volcano classification and description
p 438 N94-12037
Volcanism in southern Guinevere Planitia, Venus: Regional volcanic history and morphology of volcanic domes p 467 N94-12190

CONFERENCES
Advanced Materials for Lightweight Structures
[ESA-SP-336] p 56 N94-10001
Proceedings of the 8th European Symposium on Materials and Fluid Sciences in Microgravity, volume 1
[ESA-SP-333-VOL-1] p 99 N94-10070
Proceedings of the 8th European Symposium on Materials and Fluid Sciences in Microgravity, volume 2
[ESA-SP-333-VOL-2] p 112 N94-10171
An account of Sandia's research booth at Supercomputing 1992: A collaborative effort in high-performance computing and networking
[DE93-012397] p 319 N94-10268
Solid state ionics 3. Materials Research Society Symposium Proceedings, volume 293
[AD-A265675] p 395 N94-10416
Proceedings of the 10th NAL Symposium on Aircraft Computational Aerodynamics: CFD Workshop on GK Airfoil and ONERA M5 Geometry
[NAL-SP-20] p 10 N94-10466
Nonlinear Dynamics in Optical Systems. Postdeadline papers presented at the Optical Society of America Conference
[AD-A264958] p 375 N94-10486
Technical Conference on Tropical Urban Climates: Extended Abstracts
[WMO/TD-538] p 283 N94-10561
The Second International Workshop on Squeezed States and Uncertainty Relations
[NASA-CP-3219] p 375 N94-10564
Environmentally Safe and Effective Processes for Paint Removal
[AGARD-R-791] p 126 N94-10613
Space Activities in the Asia Pacific Region
[JTN-93-80421] p 35 N94-10676
Panel discussion: Role of space program in the Asia Pacific Region p 37 N94-10694
Proceedings of the Second Technical Meeting on High Temperature Gas-Cooled Reactors
[DE93-754285] p 371 N94-10719
The First Text Retrieval Conference (TREC-1)
[PB93-191641] p 419 N94-10829
Proceedings of the Workshop on New Aspects of Quantum Field Theories
[DE93-754136] p 411 N94-10887
Preprints of the 13th Hydrogen Energy System Symposium
[DE93-781115] p 99 N94-11444
Sixth Annual Workshop on Space Operations Applications and Research (SOAR 1992), volume 2
[NASA-CP-3187-VOL-2] p 486 N94-11527
Transactions of the 10th Army Conference on Applied Mathematics and Computing
[AD-A265098] p 318 N94-11678
The 27th International Applied Military Psychology Symposium: A Focus on Decision Making Research
[AD-A265278] p 313 N94-11701
Proceedings of First ERS-1 Symposium on Space at the Service of Our Environment, volume 1
[ESA-SP-359-VOL-1] p 232 N94-11704
Chemical Vapor Deposition of Refractory Metals and Ceramics 2. Materials Research Society Symposium proceedings
[AD-A265072] p 92 N94-11866
Computing science and statistics, Volume 24: Graphics and visualization
[AD-A265181] p 332 N94-11878
Proceedings of the PORSEC 1992 in Okinawa: Conference for Pacific Ocean Environments and Probing, volume 1
[JTN-93-80418] p 191 N94-11894
Proceedings of the First Joint NASA Cardiopulmonary Workshop
[NASA-CP-10068] p 308 N94-11991
Twenty-fourth Lunar and Planetary Science Conference. Part 1: A-F
[NASA-CR-193095] p 435 N94-12015
Atomic-scale imaging of surfaces and interfaces. Materials Research Society Symposium Proceedings, volume 295
[AD-A265674] p 369 N94-12379
Proceedings of the International Conference for the Promotion of Advanced Fire Resistant Aircraft Interior Materials
[AD-A266057] p 22 N94-12384
National SBIR Phase 3 Commercialization Conference
[AD-A266083] p 417 N94-12410
Proceedings of the Seventh International Symposium on Methodologies for Intelligent Systems (poster session)
[DE93-013470] p 340 N94-12428
Multicomponent and multilayered thin films for advanced microtechnologies: Techniques, fundamentals, and devices
[AD-A265685] p 405 N94-12442
Transportable Applications Environment (TAE) Tenth Users' Conference
[NASA-CP-3225] p 333 N94-12448
Proceedings of 1st ERS-1 Symposium on Space at the Service of Our Environment, Volume 2
[ESA-SP-359-VOL-2] p 245 N94-12471
Organization and management policy for two phase fluid experiment in space environment p 162 N94-12556
Proceedings of the PORSEC 1992 in Okinawa: Conference for Pacific Ocean Environments and Probing, volume 2
[JTN-93-80419] p 207 N94-12635

CONFIDENCE LIMITS
Longitudinal study of astronaut health: Mortality in the years 1959-1991 p 312 N94-11560

CONFINEMENT
Temperature effects on failure thickness and deflagration-to-detonation transition in PBX 9502 and TATB
[DE93-010742] p 97 N94-10294
Quantum non demolition measurement of cyclotron excitations in a Penning trap p 376 N94-10578
Reversed-field pinch studies in the Madison Symmetric Torus
[DE93-013464] p 388 N94-10747
Confinement of acoustical modes due to the electron-phonon interaction within 2D-electron gas
[DE93-613910] p 396 N94-10800
Charged particle motion in torsatrons, part 1
[DE93-621639] p 389 N94-11119

CONFORMAL MAPPING
From the Weyl theory to a theory of locally anisotropic space-time
[DE92-644734] p 410 N94-10535

CONGRESSIONAL REPORTS
National Aero-Space Plane: A need for program direction and funding decisions
[GAO/NSIAD-93-207] p 416 N94-10910
NASA procurement: Proposed changes to the Jet Propulsion Laboratory contract. Report to Congressional Requesters
[GAO/NSIAD-93-178] p 416 N94-10941
From red tape to results: Creating a government that works better and costs less p 422 N94-11351
From red tape to results: Creating a government that works better and costs less. Executive summary
p 422 N94-11353
The DOE Program in High-Performance Computing and Communications (HPCC)
[DE93-013813] p 334 N94-12606

CONICAL BODIES
On the instability of hypersonic flow past a pointed cone: Comparison of theoretical and experimental results at Mach 8 p 8 N94-10453

CONICS
Quantized conic sections; quantum gravity
[DE93-010950] p 411 N94-10956

CONIFERS
Observations of ERS-1 SAR sensitivities to changes in aboveground biomass in young loblolly pine forests
p 249 N94-12494

CONJUGATE GRADIENT METHOD
Improvements for obtaining iterative solutions of large linear systems
[DE93-767968] p 343 N94-10729
Statistical and optimization methods to expedite neural network training for transient identification
[DE93-009985] p 340 N94-11644

CONJUGATES
Squeezing in phase-conjugated resonance fluorescence p 376 N94-10576

CONNECTIVE TISSUE
Joint pain and Doppler-detectable bubbles in altitude (Hypobaric) decompression p 312 N94-11542

CONNECTORS
Fabrication and analysis of a special optical connector containing a 1/4-inch-long optical fiber for DOI tests
[DE93-013115] p 381 N94-10647

CONSERVATION EQUATIONS
Arcjet space thrusters
[NASA-CR-193191] p 46 N94-10700

CONSERVATION LAWS
New developments in the method of space-time conservation element and solution element: Applications to the Euler and Navier-Stokes equations
[NASA-TM-106226] p 150 N94-10939
On cell entropy inequality for discontinuous Galerkin methods
[NASA-CR-191493] p 345 N94-11280

CONSISTENCY
A formally verified algorithm for interactive consistency under a hybrid fault model
[NASA-CR-4527] p 326 N94-11188

CONSOLIDATION
Dynamic high-pressure shock compaction of diamond powders
[AD-A266004] p 93 N94-12354

CONSTITUTIVE EQUATIONS
A modeling investigation of thermal and strain induced recovery and nonlinear hardening in potential based viscoplasticity
[NASA-TM-106122] p 188 N94-11482

CONSTRAINTS
Multilevel computer-aided optimum design of structural systems using multiple basis vectors p 187 N94-11055
CONSTRUCTION
Department of Energy fundamentals handbook: Engineering symbology, prints, and drawings [DE93-012220] p 129 N94-11670
CONSULTING
Telemedicine and international disaster response: Medical consultation to Armenia and Russia via a telemedicine spacebridge p 305 N94-11790
Tropical medicine: Telecommunications and technology transfer p 305 N94-11793
US-USSR telemedicine consultation spacebridge to Armenia and Ufa p 308 N94-11809
CONTACTORS
An investigation of conducted and radiated emissions from a hollow-cathode plasma contactor [NASA-CR-191172] p 386 N94-10346
CONTAINERLESS MELTS
Protein, glass, aerosol research, containerless processing and diagnostics technology for microgravity application p 106 N94-10112
Gas film levitator for containerless processing of glasses in microgravity conditions: Early concept and technology demonstration p 108 N94-10122
TEMPUS: An electromagnetic levitation facility for containerless processing under micro-g in Spacelab p 109 N94-10125
Force and power efficiency of micro-g electromagnetic levitation coils p 110 N94-10129
Determination of the viscous acoustic field for liquid drop positioning/forcing in an acoustic levitation chamber in microgravity p 110 N94-10131
Solidification in immiscible systems: The influence of processing conditions on resulting microstructures p 112 N94-10174
Thermophysical properties of undercooled liquid metals p 86 N94-10190
Non-equilibrium solidification in undercooled Ni-B alloys p 86 N94-10196
Solidification and metastable phase formation of highly undercooled Fe-Cr-Ni alloy melts p 87 N94-10204
Containerless processing of equiatomic Mn50Bi50 in a drop tube p 118 N94-10205
Memory effects in the organometallic chemical beam epitaxy of compound semiconductors [NASA-CR-193106] p 399 N94-11439
CONTAINMENT
A prototype urine collection device for female aircrew p 317 N94-11549
CONTAMINANTS
Wave generation by contaminant ions [NASA-CR-193558] p 364 N94-10946
A self-consistent model of non-linear parameterization of turbulent diffusion in atmospheric boundary layer [DE93-011950] p 275 N94-11052
Methodologies for estimating air emissions from three non-traditional source categories: Oil spills, petroleum vessel loading and unloading, and cooling towers [PB93-181592] p 266 N94-11471
Comprehensive analysis of airborne contaminants from recent Spacelab missions p 318 N94-11553
Study of the admixture diffusion in the sea using remote techniques p 228 N94-12759
Novel mass spectrometric instrument for gaseous and particulate characterization and monitoring [DE93-014093] p 272 N94-12783
CONTAMINATION
Presentations to the Mexican Physics Society on Environmental Contamination [DE93-009565] p 264 N94-10256
Effect of surface cleanliness of bearing steel on adhesive strength and tribological properties of sputter-deposited gold films [DE93-767974] p 82 N94-10732
Immediate response to free product discovery [PB93-182970] p 265 N94-11015
Catalytic oxidation of organics in vapor streams at remediation sites [PB93-182962] p 266 N94-11472
Property changes induced by the space environment in composite materials on LDEF: Solar array materials passive LDEF experiment A0171 (SAMPLE) [NASA-CR-192572] p 73 N94-11484
Comprehensive analysis of airborne contaminants from recent Spacelab missions p 318 N94-11553
KT boundary impact glasses from the Gulf of Mexico region p 282 N94-12161
The 1991 version of the plume impingement computer program. Volume 2: User's input guide [NASA-CR-194191] p 166 N94-12774
CONTINENTAL SHELVES
Coastal ocean studies with ERS-1 SAR during NORCSEX 1991 p 234 N94-11720
Acoustic Doppler current profiling of the Kuroshio over the East China Sea shelf slope p 194 N94-11914
Sedimentation rates and particulate fluxes in the slope and deep sea areas off eastern Taiwan p 220 N94-12709
High biological production of the tidal mixing zones on Japan Sea shelf p 228 N94-12758
Generation of internal waves near the shelf boundary p 229 N94-12763
CONTINUOUS RADIATION
Semiconductor ring lasers [DE93-012386] p 174 N94-11005
CONTINUOUS SPECTRA
Disk-resolved spectral characteristics of Saturn's medium-sized satellites p 471 N94-12213
CONTINUOUS WAVE RADAR
HF ocean radar system at Okinawa Radio Observatory p 139 N94-11902
Measurement of wave parameters by HF ocean radar p 192 N94-11903
Kuroshio observations by the HF ocean radar p 192 N94-11904
Statistical study of HF ocean radar echo p 139 N94-11905
CONTINUUM MECHANICS
Research in computing and applied mathematics [AD-A266137] p 331 N94-11657
CONTINUUM MODELING
Behavior of vortices generated by an advancing ejecta curtain in theory, in the laboratory, and on Mars p 169 N94-12044
Explicit 3D continuum fracture modeling with smooth particle hydrodynamics p 429 N94-12062
CONTINUUMS
Generalized spin systems and sigma-models [DE93-613981] p 410 N94-10802
CONTRACT MANAGEMENT
Federal contractors in appalachia [PB93-188779] p 416 N94-11473
Guidelines for the establishment and operation of an RFP (Request for proposal) library [AD-A265894] p 417 N94-12360
Financial management: NASA's financial reports are based on unreliable data [AD-A265690] p 418 N94-12443
CONTRACT NEGOTIATION
NASA procurement: Proposed changes to the Jet Propulsion Laboratory contract. Report to Congressional Requesters [GAO/NSIAD-93-178] p 416 N94-10941
CONTRACTION
Finite element simulation of the 2D collapse of a polyelectrolyte gel disk [DE93-010693] p 91 N94-11665
CONTRACTORS
The NASA Lewis Research Center SBIR program: An assessment [NASA-TM-106205] p 485 N94-10356
Abbreviations, acronyms, and initialisms frequently used by Martin Marietta Energy Systems, Incorporated [DE93-012509] p 420 N94-11369
Department of Energy fundamentals handbook: Engineering symbology, prints, and drawings [DE93-012181] p 129 N94-11456
Federal contractors in appalachia [PB93-188779] p 416 N94-11473
Department of Energy fundamentals handbook: Engineering symbology, prints, and drawings [DE93-012220] p 129 N94-11670
Guidelines for the establishment and operation of an RFP (Request for proposal) library [AD-A265894] p 417 N94-12360
National SBIR Phase 3 Commercialization Conference [AD-A266083] p 417 N94-12410
Financial management: NASA's financial reports are based on unreliable data [AD-A265690] p 418 N94-12443
CONTRACTS
Landsat as a commercial enterprise [INPE-5477-TAE/019] p 232 N94-11524
Guidelines for the establishment and operation of an RFP (Request for proposal) library [AD-A265894] p 417 N94-12360
CONTRAILS
Stratospheric aircraft exhaust plume and wake chemistry [NASA-CR-191495] p 279 N94-12572
CONTRAST
Computer software and hardware to determine contrast sensitivity using three methods: Tracking, limits, and constant stimuli [AD-A265168] p 324 N94-11099
CONTROL EQUIPMENT
A portable controller for unmanned ground vehicles [AD-A264963] p 181 N94-11290
Decoupling of aircraft responses p 32 N94-11497
Utilizing quantitative feedback theory design technique for flight control system p 32 N94-11501
An optoelectronic graphics display processor [AD-A266011] p 171 N94-12391
CONTROL RODS
GRISET certification package [DE93-011783] p 327 N94-11246
CONTROL SIMULATION
Mechanical analysis of parallel manipulators with simulation, design, and control applications [ISBN-0-315-72013-1] p 181 N94-11156
CONTROL STABILITY
Physics of forebody flow control [NASA-CR-193626] p 15 N94-11195
Stability in Aerospace Systems [AGARD-R-789] p 31 N94-11489
Stability analysis and aerospace vehicle dynamics p 31 N94-11491
On non-linear longitudinal stability of an aircraft in a dive in the presence of atmospheric disturbances p 31 N94-11492
CONTROL SURFACES
Underwing compression vortex attenuation device [NASA-CASE-LAR-14744-1] p 12 N94-10673
Ground vibration and flight flutter tests of the single-seat F-16XL aircraft with a modified wing [NASA-TM-104269] p 26 N94-11233
CONTROL SYSTEMS DESIGN
Position and force control of a vehicle with two or more steerable drive wheels [DE93-012512] p 177 N94-10269
Telerobotic control of a mobile coordinated robotic server [NASA-CR-193465] p 338 N94-10345
Telerobot control system [NASA-CASE-NPO-18116-1-CU] p 179 N94-10670
Momentum management in redundant manipulators for vibration suppression [NASA-CR-194112] p 180 N94-10821
AD100/ADSIM, ACSL, and MATLAB output comparisons using frequency-response analysis [DE93-009640] p 47 N94-11122
Criteria for design of integrated flight/propulsion control systems for STOVL fighter aircraft [NASA-TP-3356] p 30 N94-11134
Physics of forebody flow control [NASA-CR-193626] p 15 N94-11195
Application of controller partitioning optimization procedure to integrated flight/propulsion control design for a STOVL aircraft [NASA-TM-106265] p 30 N94-11251
Adaptive structures for spacecraft: A USAF perspective p 45 N94-11319
Dynamic tests on the NASA Langley CSI evolutionary model p 45 N94-11320
Adaptive structure design employing shape memory actuators p 70 N94-11331
Multidimensional intelligent control for superlight air vehicles p 27 N94-11347
Shear flow control of gas jets in liquids [AD-A264673] p 152 N94-11448
Stability in Aerospace Systems [AGARD-R-789] p 31 N94-11489
Stability analysis and aerospace vehicle dynamics p 31 N94-11491
Utilizing quantitative feedback theory design technique for flight control system p 32 N94-11501
Adaptive reconfigurable flight controls for high angle of attack aircraft agility p 32 N94-11502
Toward intelligent flight control p 33 N94-11503
X-29: Longitudinal instability at high angle-of-attack p 33 N94-11504
Discrete Kalman filtering equations of second-order form for control-structure interaction simulations [NASA-CR-193723] p 331 N94-11522
Airborne optical tracking control system design study [DE93-009515] p 382 N94-11662
Microgravity vibration isolation technology: Development to demonstration [NASA-TM-106320] p 1 N94-11703
Galileo EM-2 contributions to the lunar control network p 468 N94-12198
Advanced control for airbreathing engines, volume 1: Pratt and Whitney [NASA-CR-189203] p 29 N94-12270
Advanced control for airbreathing engines, volume 2: General Electric aircraft engines [NASA-CR-189204] p 29 N94-12271
Project of an attitude control system (three axis) of a satellite using the LQG/LTR methodology [INPE-5473-TDI/504] p 44 N94-12356
CONTROL THEORY
Acting to gain information [NASA-CR-193399] p 418 N94-10515
Intelligent structures: A technology overview and assessment p 68 N94-11322

On possible applications of smart structures to control of space systems p 45 N94-11342

A regional inverse eigenvalue problem: Solution with application in control theory [DE93-619666] p 339 N94-11630

Receptivity in parallel flows: An adjoint approach p 157 N94-12301

Control of large space structures with varying configuration [AD-A265764] p 44 N94-12387

CONTROL VALVES

Dual valve plate two-way pressure relief valve [AD-D015766] p 178 N94-10379

CONTROLLED ATMOSPHERES

Wide Band-Gap Semiconductors. 1991 Materials Research Society Symposium proceedings [AD-A263418] p 401 N94-11515

CONTROLLED FUSION

High-energy density physics at Los Alamos [DE93-010271] p 371 N94-10260

Multiple Antenna Implementation System (MAntIS) [DE93-012515] p 131 N94-10270

CONTROLLERS

Telerobotic control of a mobile coordinated robotic server [NASA-CR-193465] p 338 N94-10345

Controller of serial multiplex communication channel [DE92-641157] p 336 N94-10544

Telerobot control system [NASA-CASE-NPO-18116-1-CU] p 179 N94-10670

In-flight simulation of backside operating models using direct lift controller [NAL-TR-1152] p 30 N94-10734

Sample-data and discrete-time H2 optimal control [MEMO-COSOR-92-53] p 339 N94-10869

The development of an interactive synthesis tool for intelligent controllers of modular, reconfigurable robots p 339 N94-10898

Application of controller partitioning optimization procedure to integrated flight/propulsion control design for a STOVL aircraft [NASA-TM-106265] p 30 N94-11251

A portable controller for unmanned ground vehicles [AD-A264963] p 181 N94-11290

Sine and random vibration program evaluation on vibration control systems [DE93-011974] p 188 N94-11460

Ballistic electron transport studies using BEEM [AD-A266029] p 369 N94-12395

CONVECTION

Marangoni and buoyant convections in zone melting of GaAs with liquid encapsulation p 101 N94-10081

Space and temporal behavior and control of the residual convection in microgravity p 104 N94-10099

The effect of gravity modulation on thermosolutal convection p 105 N94-10103

Chemical pattern formation under microgravity p 121 N94-10227

Some aspects of combustion modelling by low and normal gravity p 124 N94-10244

Stationary spectra of short-wave convective and magnetostatic fluctuations in a finite-pressure plasma and anomalous heat conductivity [DE93-617852] p 388 N94-10840

Transmantle flux tectonics p 283 N94-12249

Phase transitions and 2D spherical convection in a large icy satellite p 433 N94-12265

Topics in pattern formation and chaotic systems [AD-A265922] p 161 N94-12342

Observing and modelling F-region ionospheric dynamics using the (O2) 7320A emission [AD-A265407] p 279 N94-12419

A numerical study of deep convection at high latitudes p 210 N94-12652

CONVECTION CELLS

Marangoni instability in a liquid layer with two free surfaces [NASA-TM-106166] p 152 N94-11376

CONVECTION CLOUDS

Activities relating to understanding the initiation, organization and structure of moist convection in the Southeast environment [NASA-CR-193829] p 285 N94-11598

CONVECTION CURRENTS

Large eddy simulations of the atmospheric boundary layer east of the Colorado Rockies p 277 N94-11465

An investigation of the near Earth space environments [AD-A265295] p 278 N94-11628

CONVECTION-DIFFUSION EQUATION

Concept and design of ampoule for melt growth of gallium arsenide in first mission of space flyer unit p 107 N94-10115

New developments in the method of space-time conservation element and solution element: Applications to the Euler and Navier-Stokes equations [NASA-TM-106226] p 150 N94-10939

CONVECTIVE FLOW

Model of convective motion under low gravity p 103 N94-10088

Coupled thermogravitational and thermocapillary convection in a two-layer fluid system p 105 N94-10101

Flow transitions in a 2D directional solidification model p 114 N94-10183

TEXUS 28 experiment: Convections and crystal growth of Ge:Ga. Analysis of temperature measurements p 114 N94-10184

The kinematics of buoyancy induced mixing p 123 N94-10239

Large eddy simulations of time-dependent and buoyancy-driven channel flows p 155 N94-12287

A numerical study of deep convection at high latitudes p 210 N94-12652

CONVECTIVE HEAT TRANSFER

Numerical simulation of Marangoni convection around gas bubbles in a liquid matrix p 106 N94-10107

Simulations of D3-D divertor biasing with the LEDGE code [DE93-010500] p 385 N94-10262

On temperature distribution in non-participating medium with radiation boundary condition [DE93-619375] p 153 N94-11604

Why convective heat transport in the solar nebula was inefficient p 458 N94-12143

Does the thermal wind exist near the Earth's core boundary? p 283 N94-12217

Phase transitions and 2D spherical convection in a large icy satellite p 433 N94-12265

Hypersonic, nonequilibrium flow over a cylindrically blunted 6 deg wedge [NASA-TM-108994] p 162 N94-12571

CONVERGENCE

Convergence of exponentially convex functions on foundation semigroups [DE93-619665] p 342 N94-10325

Convergence theorems for a class of nonlinear maps in uniformly smooth Banach spaces [DE92-641347] p 343 N94-10531

Computational algorithms or identification of distributed parameter systems [AD-A265252] p 331 N94-11680

CONVERGENT NOZZLES

Evaluation of dual flow thrust vectored nozzles with exhaust stream impingement [NASA-CR-193292] p 150 N94-10912

CONVERGENT-DIVERGENT NOZZLES

Nonequilibrium hypersonic flow in a wind-tunnel nozzle p 8 N94-10456

CONVEXITY

Bibliographic notes on Voronoi diagrams [PB93-189298] p 343 N94-10825

COOLERS

The Second Workshop on Refrigerating System Utilization Onboard the JEM [NASDA-CON-930001] p 129 N94-11831

Development of space refrigerator p 129 N94-11833

Studies on refrigerator sensors and cooling section interface p 129 N94-11834

Trend of miniature refrigerator utilization in earth observation area p 130 N94-11835

Submillimeter wave observation experiment of Earth atmosphere with SIS mixer p 130 N94-11837

Refrigerator utilization in infrared astronomy p 130 N94-11838

Study on various cryogenic refrigeration cycles using all purpose refrigerators p 130 N94-11839

Development test on 2 K cooling systems p 130 N94-11840

Generation of superfluid He by G-M cycle cryogenic refrigerator p 130 N94-11841

Development of 4 K refrigerator using highly efficient heat accumulating reservoir p 130 N94-11842

Utilization of superconductivity in the area of space p 131 N94-11843

COOLING

Measurements of heat capacity in undercooled metals p 87 N94-10231

Laser cooling and trapping of atoms in microgravity: Ultracold atoms collisions p 124 N94-10241

Titanium alloys milling assistance by high pressure lubricoolant jet [DE93-013302] p 82 N94-11008

Metallographic cooling rates of L-group ordinary chondrites p 429 N94-12061

Chondrite thermal histories from Low-CA pyroxene microstructures: Autometamorphism versus prograde metamorphism revisited p 429 N94-12105

COOLING SYSTEMS

Experiments in ultracold collisions [DE93-012110] p 365 N94-11029

The Second Workshop on Refrigerating System Utilization Onboard the JEM [NASDA-CON-930001] p 129 N94-11831

Summary of the pre-AO of the JEM onboard scientific and engineering experiments for refrigerator utilization p 129 N94-11832

Development of space refrigerator p 129 N94-11833

Studies on refrigerator sensors and cooling section interface p 129 N94-11834

Trend of miniature refrigerator utilization in earth observation area p 130 N94-11835

Satellite observation of atmospheric tracer components: JEM/POP p 130 N94-11836

Submillimeter wave observation experiment of Earth atmosphere with SIS mixer p 130 N94-11837

Refrigerator utilization in infrared astronomy p 130 N94-11838

Study on various cryogenic refrigeration cycles using all purpose refrigerators p 130 N94-11839

Development test on 2 K cooling systems p 130 N94-11840

Generation of superfluid He by G-M cycle cryogenic refrigerator p 130 N94-11841

Development of 4 K refrigerator using highly efficient heat accumulating reservoir p 130 N94-11842

Utilization of superconductivity in the area of space p 131 N94-11843

A unique facility to support cryogenic wind tunnel operations [ARA-MEMO-377] p 34 N94-12436

COOPERATION

National Aero-Space Plane: A need for program direction and funding decisions [GAO/NSIAD-93-207] p 416 N94-10910

COORDINATE TRANSFORMATIONS

On output linearization of observable dynamics [MEMO-1105] p 341 N94-10276

Subroutine functions for generating animation data [DE93-767973] p 313 N94-10731

COORDINATES

Exact and quasi-classical density matrix and Wigner functions for a particle in the box and half space p 350 N94-10600

COPOLYMERS

The 13C and 15N solid-state NMR of copolymers of nylon 6 and 7: Observation of a stable pseudohexagonal phase [AD-A265799] p 94 N94-12381

COPPER

Grain boundary creep in copper [DE93-610974] p 84 N94-12361

Corrosion behavior of metal matrix composites [AD-A265352] p 85 N94-12404

COPPER ALLOYS

New mechanism of Ostwald ripening in Lorentz-force stabilized Cu-Pb dispersions p 116 N94-10192

Ostwald ripening of solid cobalt particles in liquid copper p 87 N94-10202

A study of strength evaluations of EDNi/EDCu/NARloy-Z bonded joints [NASA-TM-108418] p 188 N94-11275

CORAL REEFS

Evaluating the spread of red soil with LANDSAT TM data in coral reefs of Okinawa main island, southwestern Japan p 212 N94-12668

CORE FLOW

Appearance, behavior, and oceanic structures of warm streamers in the Kuroshio Oyashio frontal region p 198 N94-11937

Satellite observations of the northeast monsoon coastal current p 214 N94-12678

Intrusion of Kuroshio warm water into Sagami Bay p 215 N94-12683

Influence of the Kuroshio warm-core rings on hydrographic and fishery conditions off southern Kuril Islands p 224 N94-12737

CORE SAMPLING

Descriptions and preliminary interpretations of cores recovered from the Manson Impact Structure (Iowa) p 281 N94-12032

Apollo 16 core 60013/14 as a product of path 1 and path 2 regolith evolution processes p 440 N94-12050

Petrography and preliminary interpretations of the crystalline breccias from the Manson M-1 core p 281 N94-12056

Strontium and oxygen isotope study of M-1, M-3 and M-4 drill core samples from the Manson impact structure, Iowa: Comparison with Haitian K-T impact glasses p 281 N94-12080

Post-impact alteration of the Manson impact structure p 282 N94-12188

CORES

Apollo 16 core 60013/14 as a product of path 1 and path 2 regolith evolution processes p 440 N94-12050

CORIOLIS EFFECT

Growth and breakdown of Taylor-Goertler vortices in rotating Blasius boundary layer p 165 N94-12631

CORNER FLOW

Corner vortex suppressor [AD-D015772] p 147 N94-10383

The effects of successive distortions on a turbulent boundary layer in a supersonic flow p 14 N94-11058

CORNERS

Applications of a model to predict flame spread over interior finish materials in a compartment p 19 N94-10783

CORONAS

Flexure and the role of inplane force around coronae on Venus p 452 N94-12112

CORRECTION

Sea surface temperature difference between NOAA/AVHRR and in-situ observation p 215 N94-12680

CORRELATION

Stationary spectra in a finite-pressure current-carrying plasma [DE93-617848] p 387 N94-10538

Completeness properties of the minimum uncertainty states p 349 N94-10581

Geometric aspects of uncertainty and correlation p 349 N94-10588

Space Shuttle hypersonic aerodynamic and aerothermodynamic flight research and the comparison to ground test results [NASA-TM-4499] p 13 N94-10820

The heat transfer by radiation between two media [DE93-617820] p 149 N94-10838

The Langevin's approach to the statistical theory of bounded plasma [DE93-617842] p 388 N94-10839

Sea surface temperature anomalies in the Arabian Sea p 206 N94-11988

Fractal dimensions of rampart impact craters on Mars p 460 N94-12154

Basic attributes test (BAT): Operational pre-implementation analysis and score equating [AD-A265885] p 314 N94-12276

CORRELATION COEFFICIENTS

Correlated states of a quantum oscillator acted by short pulses p 380 N94-10609

Comparison of GEOSAT sea surface height and model-simulated surface dynamic height p 208 N94-12644

CORROSION

Heavy-section steel technology program [DE93-009222] p 184 N94-10155

Report of the IAEA Consultants' Meeting on Real-Time Nondestructive Monitoring of Wear and Corrosion Using the Thin Layer Activation Technique [DE93-617422] p 183 N94-10847

A survey of techniques for corrosion monitoring [DE93-012131] p 83 N94-11250

High-temperature corrosion of ceramic-ceramic composites in a waste incinerator environment [DE93-012430] p 72 N94-11368

Corrosion and passivation of high temperature superconductors [AD-A265402] p 405 N94-12586

CORROSION PREVENTION

Advanced zinc phosphate conversion and pre-ceramic polymetallosiloxane coatings for corrosion protection of steel and aluminum, and characteristics of polyphenyletheretherketone-based materials [DE93-008717] p 88 N94-10891

Experimental proof of the new IR-induced mechanism of crevice corrosion and its consequences regarding protection schemes p 83 N94-11316

Corrosion control by vitreous films on aluminum and high T(sub c) superconductors [AD-A266016] p 85 N94-12393

Corrosion behavior of metal matrix composites [AD-A265352] p 85 N94-12404

CORROSION RESISTANCE

Low-expansion ceramics initiative [DE93-011860] p 89 N94-11106

Field evaluation of six protective coatings applied to T-56 turbine blades after 2500 hours of engine use [ARL-TR-27] p 90 N94-11311

Weld overlay coatings for erosion control [DE93-013592] p 84 N94-11816

Corrosion behavior of metal matrix composites [AD-A265352] p 85 N94-12404

CORROSION TESTS

Report of the IAEA Consultants' Meeting on Real-Time Nondestructive Monitoring of Wear and Corrosion Using the Thin Layer Activation Technique [DE93-617422] p 183 N94-10847

Facility for stress corrosion cracking test of irradiated material in high temperature water [DE93-753189] p 84 N94-11593

COSMIC BACKGROUND EXPLORER SATELLITE

A theoretical kinematical study of the gradient of any cosmic scalar field [DE92-644731] p 425 N94-11136

COSMIC DUST

STARDUST: A simulation experiment of cosmic dust analogues production in microgravity conditions p 113 N94-10175

Columbus proto-planetesimal dust aggregation experiment p 123 N94-10236

COSMIC RAYS

Post-launch analysis of data from the High Energy Astrophysical Observatory Heavy Nuclei Experiment (HEAO-C3) [NASA-CR-193513] p 484 N94-11486

Dispersion of the ratios of cosmogenic isotopes of noble gases in chondrites of different cosmic-ray exposure ages p 428 N94-12020

Peculiarities of distributions of the cosmic-ray exposure ages of H chondrite falls and finds p 428 N94-12021

Search for effects of a supernova explosion 30 to 40 thousand years ago in chondrites p 428 N94-12022

Natural thermoluminescence profiles in lunar cores and implications for meteorites p 443 N94-12060

Are cosmic rays effective for ionization of the solar nebula? p 472 N94-12220

Search for structures in the cosmic microwave background radiation [INPE-5491-TDI/508] p 484 N94-12357

Analysis and interpretation of high energy cosmic rays measured on Spacelab-2 [NASA-CR-193586] p 485 N94-12771

COSMOCHEMISTRY

Midplane temperatures in the solar nebula p 448 N94-12088

COSMOLOGY

The effect of a scalar boson coupled to neutrinos on the behavior of the tritium beta decay spectrum near the end point [DE93-012655] p 361 N94-10349

Cosmological gamma-ray burst model [NASA-CR-193368] p 484 N94-10507

Planck scale effects on the Majoron [DE93-613120] p 410 N94-10545

Cosmological restrictions on conformally-invariant SU(5) GUT models [DE93-619770] p 412 N94-11047

The solutions of cosmic string loop equation in expanding universe [DE93-619717] p 427 N94-11692

Measurements of cosmogenic nuclides in lunar rock 64455 p 437 N94-12033

COST ANALYSIS

Analysis of the cost evaluation of ESA programmes and comparable national and international programmes [GTS-92063] p 416 N94-10145

Space Station Redesign Team: Final report to the Advisory Committee on the Redesign of the Space Station [NASA-TM-109241] p 42 N94-10663

Vehicular fleet operation on natural gas and propane: An overview [PB93-194603] p 98 N94-10844

ACARA user's manual [NASA-TM-106277] p 183 N94-11167

Life-cycle cost analysis of conventional and fuel cell/battery powered urban passenger vehicles [DE93-010770] p 182 N94-11438

Information resources management long-range plan, FY1994 [DE93-013898] p 420 N94-11588

Analysis of the economics of DC arc CVD diamond [AD-A265688] p 403 N94-12339

ESA Costing Software (ECOS) introduction [ESA-F-28] p 333 N94-12383

COST EFFECTIVENESS

Advanced Materials for Lightweight Structures [ESA-SP-336] p 56 N94-10001

Department of Energy solar process heat program: FY 1991 solar process heat prefeasibility studies activity [DE93-010010] p 262 N94-10258

Vehicular fleet operation on natural gas and propane: An overview [PB93-194603] p 98 N94-10844

Engineering performance metrics [DE93-012084] p 128 N94-11028

From red tape to results: Creating a government that works better and costs less p 422 N94-11351

From red tape to results: Creating a government that works better and costs less. Executive summary p 422 N94-11353

Forecasting the impact of virtual environment technology on maintenance training p 314 N94-11570

More sense for less cents: Cost effective servicing of remote sensing satellites p 348 N94-11572

Polymer electrolyte fuel cells: Potential transportation and stationary applications [DE93-010734] p 264 N94-11666

COST ESTIMATES

The MERMAID project p 329 N94-11426

Evaluation of the capacity and delay benefits of terminal air traffic control automation [AD-A265323] p 24 N94-11863

COST REDUCTION

Space Station redesign option A: Modular buildup concept [NASA-TM-108415] p 43 N94-10808

From red tape to results: Creating a government that works better and costs less p 422 N94-11351

The guide to Design For On-orbit Spacecraft Servicing (DFOSS) manual: Producing a consensus document p 421 N94-11575

Evaluation of the capacity and delay benefits of terminal air traffic control automation [AD-A265323] p 24 N94-11863

COSTS

NASA procurement: Proposed changes to the Jet Propulsion Laboratory contract. Report to Congressional Requesters [GAO/NSIAD-93-178] p 416 N94-10941

Fracture behavior of ionomers and ionomeric blends [AD-A265379] p 94 N94-12407

Defense: Health care [AD-A265914] p 421 N94-12445

Coordinated Radio, Electron, and Waves Experiment (CREWE) for the NASA Comet Rendezvous and Asteroid Flyby (CRAF) instrument [NASA-CR-194376] p 427 N94-12566

COUETTE FLOW

Direct simulation of compressible wall-bounded turbulence p 156 N94-12294

COULOMB COLLISIONS

Particle transport analysis in torsatron configurations [DE93-621640] p 390 N94-11120

Momentum and heat frictions between fast ions and thermal plasma species [DE93-771240] p 390 N94-11149

Coulomb effects in low-energy nuclear fragmentation [NASA-TP-3352] p 485 N94-12434

COULOMB POTENTIAL

Bound states of the N-dimensional Klein-Gordon equation with vector and scalar Coulomb potentials [DE93-617650] p 349 N94-10547

Exact solution of the N-dimensional generalized Dirac-Coulomb equation [DE93-617649] p 411 N94-10834

COUNTER ROTATION

AGBT advanced counter-rotating gearbox detailed design report [NASA-CR-180883] p 179 N94-10400

COUNTERMEASURES

Exercise countermeasures for bed-rest deconditioning [NASA-TM-103987] p 300 N94-11191

Dynamic loading in manufacturing and service: Australia's shock testing capability p 128 N94-11304

COUNTERS

An optoelectronic graphics display processor [AD-A266011] p 171 N94-12391

COUPLED MODES

Macroscopic behaviour and discrete dynamo of RFP plasma in high theta discharge [DE93-771408] p 392 N94-11239

Decoupling of aircraft responses p 32 N94-11497

COUPLING

Coupled thermogravitational and thermocapillary convection in a two-layer fluid system p 105 N94-10101

Transient effects in the Benard instabilities: Coupling between capillary and gravity effects p 119 N94-10216

COUPLING COEFFICIENTS

Receptivity in parallel flows: An adjoint approach p 157 N94-12301

COVALENT BONDS

A relaxation study of poled nonlinear optical polymers by infrared reflection-absorption spectroscopy [AD-A265797] p 93 N94-12380

Fracture behavior of ionomers and ionomeric blends [AD-A265379] p 94 N94-12407

Glucose electrodes based on cross-linked (Os(bpy)2Ci)(sup +/2+) complexed poly(1-vinylimidazole) films [AD-A265404] p 94 N94-12425

COVARIANCE

Application of normalized gray-scale correlation [DE93-013765] p 141 N94-10521

On local frame fields and fermion dynamics in space with nontrivial topologies [DE93-617657] p 349 N94-10548

Estimating the instabilities of N clocks by means of comparison measurements p 356 N94-10997

Optimal hemicube sampling [DE93-010499] p 334 N94-12591

CRACK ARREST

Crack suppression in GaInSb buffer layers initially under tensile stress [DE93-012839] p 396 N94-10745

CRACK GEOMETRY

Elastic plastic fracture mechanics methodology for surface cracks [NASA-CR-194129] p 185 N94-10712

CRACK INITIATION

Fatigue-life behavior and matrix fatigue crack spacing in unnotched SCS-6/Timetal 21S metal matrix composites [NASA-CR-191467] p 185 N94-10715

Microstructure-based fatigue life prediction methods for naval steel structures [AD-A265429] p 85 N94-12426

Proposed framework for thermomechanical life modeling of metal matrix composites [NASA-TP-3320] p 74 N94-12449

Isothermal fatigue mechanisms in Ti-based metal matrix composites [NASA-CR-191181] p 74 N94-12594

CRACK PROPAGATION

Potential change in flaw geometry during pressurized-thermal-shock transients [DE93-009709] p 184 N94-10288

Fracture behavior of surface-modified ceramics [DE93-013707] p 88 N94-10710

Elastic plastic fracture mechanics methodology for surface cracks [NASA-CR-194129] p 185 N94-10712

Combustion-induced crack propagation process in a solid-propellant crack cavity p 98 N94-10901

Micromechanisms of fatigue crack growth and fracture toughness in metal matrix composites [AD-A265153] p 187 N94-11096

Fracture mechanics and full scale pipe break testing for the Department of Environment's New Production Reactor-Heavy Water Reactor [DE93-005428] p 187 N94-11169

Fatigue life prediction for wind turbines: A case study on loading spectra and parameter sensitivity [DE93-011597] p 263 N94-11173

Understanding cracking failures of coatings: A fracture mechanics approach p 187 N94-11218

The effects of an aggressive environment on the subcritical crack growth of a continuous-fiber ceramic composite [DE93-011690] p 73 N94-11612

Microstructure-based fatigue life prediction methods for naval steel structures [AD-A265429] p 85 N94-12426

CRACKS

Heavy-section steel technology program [DE93-009222] p 184 N94-10155

Extensions of some guidelines for the mechanical design of coaxial compression pin seals [DE93-012385] p 177 N94-10348

Test specifications, specimen design and instrumentation test data interpretation [DE93-012338] p 188 N94-11367

The effects of an aggressive environment on the subcritical crack growth of a continuous-fiber ceramic composite [DE93-011690] p 73 N94-11612

Processing and properties of coated HPZ fiber reinforced glass-ceramic matrix composites [AD-A265177] p 92 N94-11876

CRASHES

Aircraft Accident/Incident Summary Report: Loss of control. Business Express, Inc., Beechcraft 1900C N811BE near Block Island, Rhode Island, December 28, 1991 [PB93-910405] p 22 N94-11044

CRATERING

Dimensional scaling for impact cratering and perforation [NASA-CR-188259] p 42 N94-10665

Ejecting basaltic achondrites from Vesta: Hydrodynamical impact models p 429 N94-12036

Cratering on Gaspra p 459 N94-12147

Macroscopic electric charge separation during hypervelocity impacts: Potential implications for planetary paleomagnetism p 431 N94-12181

CRATERS

Dimensional scaling for impact cratering and perforation [NASA-CR-188259] p 42 N94-10665

Mineralogy of chondritic interplanetary dust particle impact residues from LDEF p 80 N94-12045

Composition and modal frequencies of hypervelocity particles less than 1 millimeter in diameter in low-Earth orbit p 429 N94-12063

Spectral and multispectral imaging studies of lunar mantled mare deposits p 446 N94-12079

A structural origin for the cantaloupe terrain of Triton p 449 N94-12095

A structural and petrographic investigation of the pretoria saltpan impact structure p 282 N94-12102

Geophysical signature of the Pretoria saltpan impact structure and a possible satellite crater p 282 N94-12103

CRAY COMPUTERS

Using a private SMDS/ATM network to provide long-haul supercomputing visualization services [DE93-010692] p 325 N94-11109

CREEP PROPERTIES

Constitutive laws for describing the service relevant creep behaviour of metallic materials p 64 N94-10060

Particle attraction effects on the centrifugal casting and extrusion of alumina [DE93-011559] p 82 N94-10957

Creep deformation and mechanical properties of sintered glass and polycrystalline matrix composites p 67 N94-11315

A modeling investigation of thermal and strain induced recovery and nonlinear hardening in potential based viscoplasticity [NASA-TM-106122] p 188 N94-11482

Porosity and the ecology of icy satellites p 431 N94-12186

Grain boundary creep in copper [DE93-610974] p 84 N94-12361

CREEP STRENGTH

Interface considerations in Al2O3/NiAl composite [NASA-CR-191167] p 66 N94-11202

Effect of powder processing on slip casting parameters and sintering of Si3N4-Y2O3-SiO2 [AD-A264474] p 83 N94-11445

NiAl alloys for structural uses [NASA-CR-194113] p 85 N94-12447

CREEP TESTS

Grain boundary creep in copper [DE93-610974] p 84 N94-12361

CRETACEOUS-TERTIARY BOUNDARY

Descriptions and preliminary interpretations of cores recovered from the Manson Impact Structure (Iowa) p 281 N94-12032

Arroyo el Mimbral, Mexico, K/T unit: Origin as debris flow/turbidite, not a tsunami deposit p 281 N94-12084

K/T spherules from Haiti and Wyoming: Origin, diagenesis, and similarity to some microtektites p 281 N94-12085

Impact mineralogy and chemistry of the cretaceous-tertiary boundary at DSDP site 576 p 282 N94-12091

Age of Popigai impact event using the Ar-40 - Ar-39 method p 282 N94-12093

Stratigraphy and sedimentology of the K/T boundary deposit in Haiti p 282 N94-12138

Oxygen isotopes as tracers of tektite source rocks: An example from the Ivory Coast tektites and Lake Bosumtwi Crater p 430 N94-12146

Shock induced reaction in Chicxulub target materials (CaSO4 and SiO2) and their relation to extinctions p 282 N94-12149

KT boundary impact glasses from the Gulf of Mexico region p 282 N94-12161

Modelling of dispersal and deposition of impact glass spherules from the Cretaceous-Tertiary boundary deposit p 432 N94-12238

CREW PROCEDURES (INFLIGHT)

Flight simulator experiment of the cockpit advisory system [NAL-TR-1151] p 33 N94-10733

CRITERIA

Calculation of Mercier stability criterium in stellarators [DE93-621599] p 389 N94-11091

Criteria for onset of boundary-layer transition on spinning bodies p 164 N94-12620

CRITICAL POINT

A new method for hysteresis measurements developed for C(sub v) measurements at the critical point during the D2-mission p 107 N94-10114

Studies of critical point phenomena of fluids: Bulk fluids, fluids in pores, and at interfaces p 80 N94-10228

Transport of heat and mass in near-critical fluids p 122 N94-10230

Phase separation at gas-liquid critical points p 122 N94-10233

The critical facility on IML-1 p 44 N94-10250

CRITICAL TEMPERATURE

Elastic deformations and sound in anisotrope superconductors near critical temperature [DE93-620636] p 188 N94-11364

CRITICAL VELOCITY

Analysis of geophysical measurements and spacecraft interactions [AD-A266064] p 43 N94-10944

CROP GROWTH

Land cover monitoring with multi-temporal ERS-1 SAR observations in the Netherlands p 246 N94-12473

Per-field filtering and classification of multitemporal ERS-1 SAR imagery p 247 N94-12485

ERS-1 SAR crop monitoring experiment in East Anglia, UK p 248 N94-12488

CROP IDENTIFICATION

Land cover monitoring with multi-temporal ERS-1 SAR observations in the Netherlands p 246 N94-12473

Preliminary ERS-1 assessment for Canadian agriculture and forestry applications p 248 N94-12486

CROSS CORRELATION

General renormalized statistical approach with finite cross-field correlations [DE93-617846] p 386 N94-10396

Measurement of eddy structure and movement in the north-east Pacific with the GEOSAT altimeter p 209 N94-12647

Advective surface velocity in the north west Pacific derived from NOAA AVHRR images p 222 N94-12721

CROSS FLOW

Theoretical evaluation of R22 and R502 alternatives [DE93-014767] p 411 N94-10853

On nonlinear Tollmien-Schlichting/vortex interaction in three-dimensional boundary layers [NASA-TM-106184] p 152 N94-11377

Generation of two-dimensional vortices in a cross-flow p 160 N94-12318

CROSS POLARIZATION

Enhancement effects in polarimetric radar returns: Phase difference statistics [NASA-CR-193408] p 231 N94-11309

CROSSED FIELDS

Simulations of D3-D divertor biasing with the LEDGE code [DE93-010500] p 385 N94-10262

General renormalized statistical approach with finite cross-field correlations [DE93-617846] p 386 N94-10396

Stationary spectra in a magnetized current-carrying plasma [DE93-617847] p 386 N94-10397

Stationary spectra in a plasma with a shear (renormalized statistical approach with non-zero eigenfrequencies) [DE93-617851] p 386 N94-10523

Stationary spectra in a finite-pressure current-carrying plasma [DE93-617848] p 387 N94-10538

Stationary spectra in a quasi neutral current-carrying plasma [DE93-617849] p 387 N94-10539

CROSSLINKING

Improving reservoir conformance using gelled polymer systems [DE93-014532] p 88 N94-10749

Development of bioelastic materials for the prevention of adhesions: Polypenta- and polytetrapeptides [AD-A264851] p 88 N94-10863

X ray absorption spectroscopy of electrochemically generated species [AD-A264749] p 77 N94-11265

The synthesis of photocrosslinkable chalcone-bearing polyphosphazenes [AD-A264915] p 92 N94-11849

Ceramics formed by pyrolysis of either linear or thermosetting carborane (siloxane or silane) acetylene based precursor polymers [AD-D015747] p 93 N94-12330

A novel photosensitive polyimide resist consisting of a soluble polyimide and a bis(perfluorophenyl azide) as a cross-linker [AD-A265998] p 93 N94-12353

A relaxation study of poled nonlinear optical polymers by infrared reflection-absorption spectroscopy [AD-A265797] p 93 N94-12380

Glucose electrodes based on cross-linked (Os(bpy)2Cl)(sup +/2+) complexed poly(1-vinylimidazole) films [AD-A265404] p 94 N94-12425

CROSSTALK

A fiber optic network system with low crosstalk using code-division multiplexing [AD-D015763] p 374 N94-10376

CRRES (SATELLITE)

Chemical release and radiation effects (CRRES) data directory [NASA-CR-192551] p 279 N94-12581

CRUDE OIL

Improving reservoir conformance using gelled polymer systems [DE93-014532] 88 N94-10749

Gulf of Mexico sales 147 and 150: Central and western planning areas. Draft environmental impact statement. Volume 1: Sections 1 through 4.C
[PB93-190304] p 265 N94-11018

Gulf of Mexico sales 147 and 150: Central and western planning areas. Draft environmental impact statement. Volume 2: Sections 4.D through 9
[PB93-190312] p 265 N94-11019

Methodologies for estimating air emissions from three non-traditional source categories: Oil spills, petroleum vessel loading and unloading, and cooling towers
[PB93-181592] p 266 N94-11471

Information capability of NOAA-AVHRR data for monitoring oceanographic and atmospheric pollution
p 214 N94-12677

CRUSTAL FRACTURES

Statistical description of tectonic motions
[NASA-CR-193701] p 275 N94-10950

CRYOGENIC COOLING

The superfluid Stirling refrigerator, a new method for cooling below 0.5 K
[DE93-012672] p 128 N94-11161

The Second Workshop on Refrigerating System Utilization Onboard the JEM
[NASDA-CON-930001] p 129 N94-11831

Summary of the pre-AO of the JEM onboard scientific and engineering experiments for refrigerator utilization
p 129 N94-11832

Trend of miniature refrigerator utilization in earth observation area p 130 N94-11835

Study on various cryogenic refrigeration cycles using all purpose refrigerators p 130 N94-11839

Development test on 2 K cooling systems
p 130 N94-11840

Generation of superfluid He by G-M cycle cryogenic refrigerator p 130 N94-11841

Development of 4 K refrigerator using highly efficient heat accumulating reservoir p 130 N94-11842

Utilization of superconductivity in the area of space
p 131 N94-11843

CRYOGENIC EQUIPMENT

The superfluid Stirling refrigerator, a new method for cooling below 0.5 K
[DE93-012672] p 128 N94-11161

The Second Workshop on Refrigerating System Utilization Onboard the JEM
[NASDA-CON-930001] p 129 N94-11831

Development of space refrigerator
p 129 N94-11833

Trend of miniature refrigerator utilization in earth observation area p 130 N94-11835

Study on various cryogenic refrigeration cycles using all purpose refrigerators p 130 N94-11839

Generation of superfluid He by G-M cycle cryogenic refrigerator p 130 N94-11841

Development of 4 K refrigerator using highly efficient heat accumulating reservoir p 130 N94-11842

CRYOGENIC FLUIDS

SWIRL as a means of liquid management in low gravity
[NASA-CR-4545] p 412 N94-11523

CRYOGENIC WIND TUNNELS

A unique facility to support cryogenic wind tunnel operations
[ARA-MEMO-377] p 34 N94-12436

CRYOGENICS

Preliminary analysis of the benefits derived to US Air Force spacecraft from on-orbit refueling
p 38 N94-11567

CRYSTAL DEFECTS

Electronic characterization of defects in narrow gap semiconductors
[NASA-CR-193568] p 397 N94-10819

Radiation defect production in InAs crystals under electron irradiation
[DE93-617202] p 397 N94-10845

Investigation of optically generated electronic defects and protonic transport in hydrogen-bonded molecular solids: Isomorphs of potassium dihydrogen phosphate
[DE93-012498] p 399 N94-11243

CRYSTAL DISLOCATIONS

Workshop on Heteroepitaxial InP Solar Cells
p 54 N94-11414

CRYSTAL FIELD THEORY

Effect of a distribution of exchange parameters within a simple localized-itinerant model
[DE93-610314] p 395 N94-10314

CRYSTAL GROWTH

Instability of thermocapillary convection in floating zones p 101 N94-10076

CdTe crystal growth in the Soviet facility zona 4
p 106 N94-10111

Laser beam deflection: A diagnostic tool for vapour growth experiments in microgravity p 111 N94-10135

Mission support for crystal growth experiments in Russian unmanned carriers p 111 N94-10139

Microgravity experiments using TR-1A rocket
p 112 N94-10142

Thermocapillary convection instability in microgravity crystal growth p 112 N94-10172

On the role of Soret effect in concentration distribution in crystals growing from the melt p 112 N94-10173

Flow transitions in a 2D directional solidification model
p 114 N94-10183

Convection related radial segregation in an idealized horizontal Bridgman configuration p 115 N94-10185

In situ observation of temperature dependence of concentration field during growth of KB5 crystals by holographic interferometry p 115 N94-10187

Wetting effects on nylon spheres engulfment in ice
p 115 N94-10189

Crystal growth from low temperature vapour phase
p 115 N94-10191

Conductive-radiative model for predicting the shape of Hgl2 crystal grown in the LTVG furnace
p 117 N94-10201

Effect of gravity on the dissolution and liquid phase epitaxial growth processes in a horizontal sandwich system p 118 N94-10208

THM-growth of III-V-semiconductors in the magnetic field p 118 N94-10209

Crystallization of zeolites in the microgravity environment of space p 119 N94-10210

Crystal growth in the Zone Melting Facility (ZMF)
p 119 N94-10213

The International Microgravity Laboratory, a Spacelab for materials and life sciences p 125 N94-10249

Dynamic studies of crystal growth using the AFM
[DE93-009549] p 399 N94-11268

An ellipsometry investigation of nucleation and growth of electron cyclotron resonance plasma deposited silicon films
[AD-A265037] p 401 N94-11651

The experimental production of matrix lumps within chondrules: Evidence of post-formational processes
p 431 N94-12176

Flash melting of chondrule precursors in excess of 1600 C. Series 1: Type 2 (B1) chondrule composition experiments p 431 N94-12177

Short wavelength crystal fiber devices
[AD-A265716] p 176 N94-12402

Tin whiskers in electronic circuits
[AD-A265917] p 146 N94-12565

Process modelling for materials preparation experiments
[NASA-CR-193556] p 56 N94-12588

CRYSTAL LATTICES

A lattice gas model for enzyme kinetics with alternate interactions
[DE93-613027] p 395 N94-10411

The peculiarities of the spin glass state in Fe(x)Mn(1-x)TiO3
[DE93-617882] p 395 N94-10525

A lattice gas model for enzyme kinetics with next-nearest neighbor interactions
[DE93-613026] p 410 N94-10631

Electronic characterization of defects in narrow gap semiconductors
[NASA-CR-193568] p 397 N94-10819

Polar solvation and electron transfer
[DE93-013328] p 365 N94-11010

Structural and electronic properties of atomic chains
[DE93-617758] p 366 N94-11349

Lattice-matched heteroepitaxy of wide gap ternary compound semiconductors p 400 N94-11441

CRYSTAL OPTICS

Squeezing in phase-conjugated resonance fluorescence p 376 N94-10576

CRYSTAL OSCILLATORS

Performance of low-cost commercial fiber-optic transceivers for reference frequency distribution
p 355 N94-10993

CRYSTAL STRUCTURE

Scientific specifications for an automated facility for growing large semiconducting crystals from the melt in space p 114 N94-10180

Conductive-radiative model for predicting the shape of Hgl2 crystal grown in the LTVG furnace
p 117 N94-10201

Organometallic chemical vapor deposition and characterization of ZnGeP2/GaP multiple heterostructures on GaP substrates p 400 N94-11442

The x ray standing waves on surfaces
[AD-A265265] p 402 N94-11682

Micro-zoning in minerals of a Landes silicate inclusion
p 432 N94-12231

Engineering solid-state materials. Strategies for modeling and packing control of molecular assemblies into 3-D networks
[AD-A265291] p 404 N94-12438

CRYSTAL SURFACES

Low energy electron diffraction and cyclic voltammetry studies of flame-annealed platinum single crystals
[AD-A263566] p 401 N94-11518

The x ray standing waves on surfaces
[AD-A265265] p 402 N94-11682

CRYSTALLINITY

Symmetry lowering in crystalline solid solutions: A study of cinnamamide-thienylacrylamide by x ray and neutron diffraction and solid-state photochemistry
[DE93-010871] p 394 N94-10301

Monte Carlo simulations of a two-dimensional hard dimer system
[DE93-613535] p 361 N94-10502

Crystallinity and dielectric properties of PEEK, a thermoplastic poly(ether ether ketone)
[AD-A266027] p 91 N94-11487

The 13C and 15N solid-state NMR of copolymers of nylon 6 and 7: Observation of a stable pseudohexagonal phase
[AD-A265799] p 94 N94-12381

CRYSTALLITES

Preparation of carbon monoliths having tailored pore structure from porous polymer precursors
[DE93-011576] p 89 N94-10958

CRYSTALLIZATION

Advanced protein, crystallization facility and associated new developments p 39 N94-10119

Proceedings of the 8th European Symposium on Materials and Fluid Sciences in Microgravity, volume 2
[ESA-SP-333-VOL-2] p 112 N94-10171

New mechanism of Ostwald ripening in Lorentz-force stabilized Cu-Pb dispersions p 116 N94-10192

Effects of a microgravity environment on the crystallization of biological macromolecules
p 117 N94-10198

Ripening of immiscible liquid droplets in microgravity with constrained Marangoni drift p 117 N94-10200

Ostwald ripening of solid cobalt particles in liquid copper p 87 N94-10202

Solidification and metastable phase formation of highly undercooled Fe-Cr-Ni alloy melts p 87 N94-10204

Crystallization of zeolites in the microgravity environment of space p 119 N94-10210

Synthesis of molecular sieves from clear solution
p 124 N94-10245

Synthesis and thermal evolution of structure in alkoxide-derived niobium pentoxide gels
[NASA-TM-106259] p 90 N94-11257

Structural development in ceramic precursor sols and gels
[AD-A264354] p 90 N94-11281

Aluminum-phosphorus chemistry: Preparation and structural characterization of (Et2AIP(SiMe3)2)2, Et(Cl)2Al(dot)P(SiMe3)3, and i-Bu2(Cl)Al(dot)P(SiMe3)3
[AD-A265268] p 78 N94-11683

Chromatographic assessment of hydrogen-bond donating ability
[AD-A265292] p 369 N94-11826

In-situ crystallization of silicate glass films deposited on alpha- Al2O3
[DE93-012969] p 95 N94-12596

CRYSTALLOGRAPHY

HRTEM in protein crystallography
[DE93-610322] p 395 N94-10406

Unequilibrated, equilibrated, and reduced aggregates in anhydrous interplanetary dust particles
p 429 N94-12098

Crystal-chemistry and partitioning of REE in whitlockite
p 408 N94-12174

The granulite suite: Impact melts and metamorphic breccias of the early lunar crust p 282 N94-12197

Deformation mechanisms in tungsten single crystals in ballistic impact experiments
[AD-A265701] p 405 N94-12563

CRYSTALS

Experimental efforts and results in finding new heavy scintillators
[DE93-010406] p 371 N94-10156

Nonclassical states of the second optical harmonic in the presence of self-action p 375 N94-10567

Second and third order nonlinear optical properties of crystalline inorganic/organic complexes
[DE93-011883] p 173 N94-10755

Nonlinear excitation in quasi-one-dimensional Peierls dielectrics with charge density waves
[DE93-613827] p 398 N94-11025

Dynamic studies of crystal growth using the AFM
[DE93-009549] p 399 N94-11268

Energy transfer dynamics and impact sensitivity
[DE93-009551] p 98 N94-11269

Crystal-chemistry and partitioning of REE in whitlockite
p 408 N94-12174

A 1.94 micron laser apparatus, system, and method using a thulium-doped yttrium-lithium-fluoride laser crystal pumped with a diode laser
[AD-D015740] p 176 N94-12321

Short wavelength crystal fiber devices
[AD-A265716] p 176 N94-12402

CURING

Application of the infrared photoacoustic spectroscopy to the study of the cure mechanisms of structural epoxy adhesives p 61 N94-10040

Smart processing of composite materials for enhanced performance and properties p 69 N94-11325

CURRENT DENSITY

Stationary spectra in a sheared plasma (linear limit)
[DE93-617850] p 387 N94-10540

Diagnostic complex for the space-time analysis of energy and current of pulsed relativistic particles
[DE93-620980] p 362 N94-10649

Development of commercially viable high-T(sub c) Bi-2223 superconductor tapes
[DE93-009966] p 142 N94-10951

Elementary mechanism of electron beam dissipative instability development
[DE93-621653] p 391 N94-11209

Experimental and theoretical investigations of Cs-Ba vapor tacitron inverter for power conditioning in space power systems
[DE93-012971] p 48 N94-11372

Assessment of the impact of HTSC's on superconducting fault-current limiters
[DE93-009986] p 143 N94-11454

High frequency behavior of long and small junctions
[AD-A265670] p 403 N94-12336

CURVATURE

Curvature effects in three-dimensional boundary layers
p 164 N94-12623

CURVE FITTING

General aviation aircraft-normal acceleration data analysis and collection project
[AD-A265055] p 26 N94-11858

CURVES (GEOMETRY)

Homoclinic intermittency
[W-9302] p 344 N94-10908

CUTTING

Performance characteristics of the INS 25.5-MHz split coaxial RFQ
[DE93-753168] p 144 N94-11508

CYANOGEN

The excitation of cyanogen and ionized carbon in interstellar and extragalactic gas clouds
p 426 N94-11582

CYCLES

Cycles through particular subgraphs of claw-free graphs
[MEMO-1097] p 341 N94-10274

CYCLIC HYDROCARBONS

Measurement of polycyclic aromatic hydrocarbon (PAHs) in interplanetary dust particles
p 431 N94-12167

CYCLOGENESIS

On the importance of mesoscale potential vorticity anomalies and topographic forcing during cyclone redevelopment across the Appalachians: A GALE case study p 284 N94-10822

CYCLONES

On the importance of mesoscale potential vorticity anomalies and topographic forcing during cyclone redevelopment across the Appalachians: A GALE case study p 284 N94-10822

Updated forecast of Atlantic seasonal hurricane activity for 1993 p 285 N94-11194

CYCLOPROPANE

Vibrational overtone activation of methylcyclopropene
[AD-A265588] p 79 N94-12373

CYCLOTRON FREQUENCY

Dispersion of plasma waves in a finite magnetic field (omega(sub H) greater than omega(sub p))
[DE93-621654] p 391 N94-11210

CYCLOTRON RADIATION

Applications of in-situ ellipsometry to microwave electron cyclotron resonance plasma processes
[AD-A265197] p 373 N94-11880

CYCLOTRON RESONANCE

Gyrosheath near the tokamak edge
[DE93-012191] p 390 N94-11142

Ionization potentials of small carbon clusters
[AD-A264379] p 67 N94-11260

Conversion of the four-strap array in D3-D to a tunable traveling wave antenna
[DE93-012085] p 137 N94-11453

Wide Band-Gap Semiconductors. 1991 Materials Research Society Symposium proceedings
[AD-A263418] p 401 N94-11515

An ellipsometry investigation of nucleation and growth of electron cyclotron resonance plasma deposited silicon films
[AD-A265037] p 401 N94-11651

Applications of in-situ ellipsometry to microwave electron cyclotron resonance plasma processes
[AD-A265197] p 373 N94-11880

CYCLOTRON RESONANCE DEVICES

Characterization of high-power RF structures using time-domain field codes
[DE93-013416] p 132 N94-10518

CYCLOTRONS

Quantum non demolition measurement of cyclotron excitations in a Penning trap p 376 N94-10578

Spin characteristics of ion beams during the motion of electromagnetic elements
[DE93-617448] p 364 N94-10848

CYLINDRICAL BODIES

Variations of the temperature profile in the gradient furnace GFQ within a cylindrical sample used for directional solidification p 114 N94-10181

Vortex-induced forces on oscillating bluff cylinders
[AD-A265056] p 154 N94-11865

The flow structure around a cylindrical pier for the flow of transcritical Reynolds number p 169 N94-11944

Traveling disturbances appearing in yawed cylinder boundary layer transition p 166 N94-12632

CYLINDRICAL SHELLS

Hydrostatic testing of thick laminated composite cylinders for performance model validation
[DE93-012728] p 184 N94-10264

D

DAMAGE ASSESSMENT

Dimensional scaling for impact cratering and perforation
[NASA-CR-188259] p 42 N94-10665

The magnitude of impact damage on LDEF materials
[NASA-CR-188258] p 43 N94-10666

Fatigue life prediction for wind turbines: A case study on loading spectra and parameter sensitivity
[DE93-011597] p 263 N94-11173

Assessment of damage in ceramics and ceramic matrix composites using ultrasonic techniques
[NASA-TM-106121] p 67 N94-11237

Disturbance Impact Assessment System (DIAS), version 2.0. System design document
[AD-A265251] p 138 N94-11883

DAMPING

The use of magnetic fields for damping unsteady Marangoni convection in GaAs floating zones under microgravity p 100 N94-10073

Calculation of the effects of magnetic field damping in fluid flow: Comparison of magnetohydrodynamic models of different complexity p 103 N94-10089

Check valve with poppet damping mechanism
[NASA-CASE-MSC-21903-1] p 179 N94-10655

Damping measurements for ultra-high carbon steel/brass laminates
[DE93-011886] p 82 N94-11076

Damping mechanisms in chemically vapor deposited SiC fibers
[NASA-TM-106334] p 66 N94-11135

Elastic deformations and sound in anisotrope superconductors near critical temperature
[DE93-620636] p 188 N94-11364

Improvement of method for experimental determination of flutter speed by parameter identification
[NASA-CR-193555] p 33 N94-12769

DARK MATTER

The three-point function as a probe of models for large-scale structure
[NASA-CR-193249] p 425 N94-11153

DATA ACQUISITION

A flexible modelling software for data acquisition
[DE93-612915] p 322 N94-10484

The 2nd Annual Meeting of the Society for Research on Biological Rhythms
[AD-A264869] p 303 N94-10872

A real-time spoken-language system for interactive problem solving
[AD-A266046] p 324 N94-11104

User's manual for the DAD-1 data acquisition daughter board for the SuperCard-2
[DE93-012153] p 325 N94-11139

Visual Earth observation performance in the space environment. Human performance measurement 4: Flight experiments p 314 N94-11539

The effect of rain on ERS-1 altimeter data
p 243 N94-11773

Groundwave HF ocean surface radar
p 139 N94-11906

Venus small volcano classification and description
p 438 N94-12037

A new data collection system for ionospheric modelling and related topics
[AD-A265893] p 278 N94-12277

A hybrid neural network and feature extraction technique for target recognition
[AD-D015732] p 333 N94-12386

Use of SAR-wave, altimeter, and wind-scatterometer data in an operational swell forecasting system
p 250 N94-12503

Experimental particle physics at the University of Pittsburgh
[DE93-013326] p 369 N94-12546

A surface water monitoring system: A device for the sea-truth observations p 210 N94-12657

The structure of hydrophysical measuring systems of vertical sounding and self-contained stations
p 227 N94-12751

DATA BASE MANAGEMENT SYSTEMS

PANACEA user's manual for PANACEA version 2.0
[DE93-012502] p 321 N94-10263

Report on Subgroup on Data Banks for Risk Assessment
[DE93-012150] p 418 N94-10646

Environmental Sciences Division
[DE93-013865] p 264 N94-10650

Database computing in HEP
[DE93-011765] p 419 N94-11105

Flight Dynamics Directorate (FDD) Historically Black Colleges and Universities (HBCU's) database managment system: A user's guide
[AD-A264947] p 419 N94-11288

The relational-to-object-oriented cross-model accessing capability in a multi-model and multi-lingual database system
[AD-A264911] p 420 N94-11846

Data management strategy for the Tampa Bay National Estuary Program: Recommendations and implementation plan
[PB93-191633] p 267 N94-11864

The instrumentation of the multimodel and multilingual user interface
[AD-A265444] p 333 N94-12332

Proceedings of the Seventh International Symposium on Methodologies for Intelligent Systems (poster session)
[DE93-013470] p 340 N94-12428

DATA BASES

Database blending for the climatology of cloud statistics program
[AD-A265034] p 283 N94-10336

Review of SHARC 2.0 O3 kinetics and spectroscopy
[AD-A265481] p 274 N94-10496

Report on Subgroup on Data Banks for Risk Assessment
[DE93-012150] p 418 N94-10646

The First Text Retrieval Conference (TREC-1)
[PB93-191641] p 419 N94-10829

Database computing in HEP
[DE93-011765] p 419 N94-11105

Pre-operation analysis of ERS-1 tracking and operation, part 2-A
[NASDA-CNT-930001-PT-2-A] p 230 N94-11129

Flight Dynamics Directorate (FDD) Historically Black Colleges and Universities (HBCU's) database managment system: A user's guide
[AD-A264947] p 419 N94-11288

Biscayne bay: A bibliography of the marine environment
[PB93-184802] p 266 N94-11451

Design issues for high performance engineering information systems
[AD-A264839] p 420 N94-11520

Ceramics technology project database
[DE93-012431] p 91 N94-11672

Ceramic technology project database
[DE93-012432] p 91 N94-11673

RAMCAD (reliability, availability, and maintainability in computer-aided design)
[AD-A265143] p 331 N94-11679

Medical informatics and telemedicine: A vision
p 305 N94-11788

Directory of IAEA databases
[DE93-622837] p 420 N94-11818

The relational-to-object-oriented cross-model accessing capability in a multi-model and multi-lingual database system
[AD-A264911] p 420 N94-11846

General aviation aircraft-normal acceleration data analysis and collection project
[AD-A265055] p 26 N94-11858

Shoreline change detection using remote sensing and GIS in Vietnam p 196 N94-11928

Proceedings of the Seventh International Symposium on Methodologies for Intelligent Systems (poster session)
[DE93-013470] p 340 N94-12428

DATA COMPRESSION
Subband/transform functions for image processing [NASA-TM-106183] p 323 N94-10639

DATA FLOW ANALYSIS
PANACEA user's manual for PANACEA version 2.0 [DE93-012502] p 321 N94-10263
Node assignment in heterogeneous computing [NASA-CR-4534] p 142 N94-11131

DATA INTEGRATION
Bayesian model for pictorial data fusion of satellite image [INPE-5457-TDI/499] p 345 N94-11193
Integration of ERS-1 data into the European project of agriculture statistics p 248 N94-12490

DATA LINKS
Development of a hypermedia knowledge base of aircraft fire safety regulations p 21 N94-10793
PTTI-aided ephemeris calculation and rapid data link acquisition for manned space flight p 42 N94-10974

DATA MANAGEMENT
A proof-of-concept implementation of persistence in a hierarchical storage system [DE93-009959] p 319 N94-10318
A browse facility for Earth science remote sensing data: Center director's discretionary fund final report [NASA-TM-108413] p 419 N94-10723
The Air Force Interactive Meteorological System: A research tool for satellite meteorology [AD-A265957] p 284 N94-11113
Analysis and guidelines for reusable Ada software [AD-A264918] p 332 N94-11850
Data management strategy for the Tampa Bay National Estuary Program: Recommendations and implementation plan [PB93-191633] p 267 N94-11864
An integrated approach to total end-to-end quality control of ocean data in the real-time environment p 211 N94-12662
Simple and low cost image processing system for satellite remote sensing data p 212 N94-12669

DATA PROCESSING
A correct and efficient interface for logical query languages with complex objects [MEMO-INF-93-01] p 320 N94-10167
Virtual sound for virtual reality [DE93-010519] p 321 N94-10291
Database blending for the climatology of cloud statistics program [AD-A265034] p 283 N94-10336
A flexible modelling software for data acquisition [DE93-612915] p 322 N94-10484
Processing proper nouns in machine translation for English news [NHK-SERIAL-414] p 418 N94-10559
Subband/transform functions for image processing [NASA-TM-106183] p 323 N94-10639
Advanced statistical methods for improved data analysis of NASA astrophysics missions [NASA-CR-193514] p 425 N94-10943
Analysis of IRAS solar system dust data [NASA-CR-193704] p 483 N94-10949
Overview of training seminar for the use of Japanese Earth Resources Satellite-1 (JERS-1) data p 190 N94-11083
The Air Force Interactive Meteorological System: A research tool for satellite meteorology [AD-A265957] p 284 N94-11113
Optimisation methods for solving separable nonlinear least squares problems [ISVR-TR-219] p 345 N94-11217
Proceedings of First ERS-1 Symposium on Space at the Service of Our Environment, volume 1 [ESA-SP-359-VOL-1] p 232 N94-11704
Effects of wave nonlinearity on ERS-1 radar altimeter returns: A preliminary investigation p 235 N94-11722
Preliminary geophysical investigation with ERS-1 35-day altimeter data p 243 N94-11775
Nonlinear resonance: Noise-assisted information processing in physical and neurophysiological systems [AD-A265161] p 313 N94-11890
Tensoral: A system for post-processing turbulence simulation data p 75 N94-12320
TREES project: A suite of tools for information extraction from ERS-1 SAR data p 250 N94-12498
The 1991 version of the plume impingement computer program. Volume 1: Description [NASA-CR-194192] p 166 N94-12775

DATA PROCESSING EQUIPMENT
The Air Force Interactive Meteorological System: A research tool for satellite meteorology [AD-A265957] p 284 N94-11113
Data processing units for eight magnetospheric particle and field sensors [AD-A264403] p 276 N94-11463
A user appraisal of ATSR near-real-time products p 252 N94-12516

DATA RECORDING
Low power digital recorder development [AD-A265921] p 170 N94-10704
Some results with the new digital ionosonde in San Diego [AD-A265178] p 275 N94-11101

DATA REDUCTION
A browse facility for Earth science remote sensing data: Center director's discretionary fund final report [NASA-TM-108413] p 419 N94-10723
NASA Marshall Space Flight Center solar observatory report, January - June 1993 [NASA-TM-108417] p 423 N94-10866
Advanced statistical methods for improved data analysis of NASA astrophysics missions [NASA-CR-193514] p 425 N94-10943
Overview of training seminar for the use of Japanese Earth Resources Satellite-1 (JERS-1) data p 190 N94-11083
Test specifications, specimen design and instrumentation test data interpretation [DE93-012338] p 188 N94-11367
Ultraviolet plume instrument description and plume data reduction methodology [AD-A266141] p 54 N94-11643
A consideration on principal component analysis of satellite IR data p 193 N94-11909
The optical/computer hybrid processing of extracting ocean wave directional spectrum by airborne photograph p 197 N94-11934
Remote sensing for numerical modelling of radiative transfer processes in ocean environment p 204 N94-11973
Atmospheric correction plans for SeaWiFS p 204 N94-11975
DISTERM: A shipboard data system for satellite monitoring of ocean and atmosphere p 226 N94-12749
The structure of hydrophysical measuring systems of vertical sounding and self-contained stations p 227 N94-12751
The algorithm of primary production determination p 228 N94-12761
Non-image visible polarization remote sensing of the ocean p 229 N94-12762

DATA RETRIEVAL
A correct and efficient interface for logical query languages with complex objects [MEMO-INF-93-01] p 320 N94-10167

DATA SAMPLING
Sample-data and discrete-time H2 optimal control [MEMO-COSOR-92-53] p 339 N94-10869

DATA STORAGE
A proof-of-concept implementation of persistence in a hierarchical storage system [DE93-009959] p 319 N94-10318
Holographic multiplexing for 3D optical memory [AD-A266099] p 171 N94-11420

DATA STRUCTURES
Wait-free linearization with an assertional proof [CS-9208] p 323 N94-10878
Object oriented implementation of adaptive mesh refinement algorithms [DE93-011885] p 325 N94-11112

DATA SYSTEMS
An analysis of the modes and states for generic avionics [NASA-CR-188253] p 27 N94-10664
Enhancements to the Engine Data Interpretation System (EDIS) [NASA-CR-192593] p 180 N94-10815
Pre-operation analysis of ERS-1 tracking and operation, part 2-A [NASDA-CNT-930001-PT-2-A] p 230 N94-11129
Simple and low cost image processing system for satellite remote sensing data p 212 N94-12669
DISTERM: A shipboard data system for satellite monitoring of ocean and atmosphere p 226 N94-12749

DATA TRANSFER (COMPUTERS)
Variable rate transfer of optical information [AD-D015758] p 418 N94-10374

DATA TRANSMISSION
Formal specification of the plain UCN layer in LOTOS [MEMO-INF-92-83] p 131 N94-10280
Controller of serial multiplex communication channel [DE92-641157] p 336 N94-10544
The Zipcode message-passing system [DE93-011958] p 336 N94-11027
An alternative to sneakernet [DE93-012130] p 419 N94-11137
The PVM systems: An in-depth analysis and documenting study. Concise edition [DE93-011959] p 336 N94-11248
Use of telescience for biomedical research during space flight p 305 N94-11791
Study on color video pictures transmission by digital acoustic signal p 139 N94-11917
Asynchronous Transfer Mode (ATM) technology: An overview [AD-A266087] p 383 N94-12413

DEACTIVATION
Kinetics of high concentration arsenic deactivation at moderate to low temperatures [DE93-013349] p 395 N94-10516

DEATH
Longitudinal study of astronaut health: Mortality in the years 1959-1991 p 312 N94-11560

DEBONDING (MATERIALS)
Quantifying disbond area p 61 N94-10038
Isothermal fatigue mechanisms in Ti-based metal matrix composites [NASA-CR-191181] p 74 N94-12594

DEBRIS
Spacelab J air filter debris analysis [NASA-CR-192569] p 301 N94-11201
Arroyo el Mimbral, Mexico, K/T unit: Origin as debris flow/turbidite, not a tsunami deposit p 281 N94-12084
Scalloped margin domes: What are the processes responsible and how do they operate? p 454 N94-12120

DECARBOXYLATION
Resist materials design: Base-catalyzed chemical amplification [AD-A265286] p 145 N94-11819
Photogenerated base in polymer imaging. Synthesis and photopatterning of poly(2-cyano-2-(p-vinylphenyl) butanoic acid) [AD-A265288] p 95 N94-12585

DECISION MAKING
The applicability of neural nets for decision support [MEMO-COSOR-92-49] p 338 N94-10169
A comparison of high and low-impact reports of investigation on adjudicators' decision making: A pilot study [AD-A265747] p 416 N94-10298
Computer models used to support cleanup decision-making at hazardous and radioactive waste sites [PB93-183333] p 274 N94-10698
An advisor module for tactical and strategic state-oriented planning systems with an application in manpower planning [MEMO-COSOR-92-57] p 416 N94-10868
P2NBC2 Heat Strain Decision Aid. User's guide, version 2.1 [AD-A266072] p 304 N94-11224
Signal detection theory and methods for evaluating human performance in decision tasks p 314 N94-11531
Criteria for assessing problem solving and decision making in complex environments p 314 N94-11532
Intergovernmental decisionmaking for environmental protection and public works [PB93-176824] p 266 N94-11584
The 27th International Applied Military Psychology Symposium: A Focus on Decision Making Research [AD-A265278] p 313 N94-11701

DECISION THEORY
The applicability of neural nets for decision support [MEMO-COSOR-92-49] p 338 N94-10169
Neural network model selection using asymptotic jackknife estimator and cross-validation method [AD-A264960] p 339 N94-11289
Signal detection theory and methods for evaluating human performance in decision tasks p 314 N94-11531

DECODERS
Flexible high-speed CODEC [NASA-CR-191169] p 146 N94-12433

DECOMPOSITION
A new decomposition strategy for parallel bonded molecular dynamics [DE93-009839] p 366 N94-11284
Advanced thermally stable coal-derived jet fuels: Compositional factors affecting thermal degradation of jet fuels [AD-A265842] p 99 N94-12282
The helical decomposition and the instability assumption p 158 N94-12306
Terminal Decomposition and Gaseous Sulfur Release from Tidal Wetlands [NASA-CR-193466] p 267 N94-12451

DECOMPRESSION SICKNESS
Project ARGO: Gas phase formation in simulated microgravity [NASA-TM-104762] p 125 N94-11235
Monitoring cognitive function and need with the automated neuropsychological assessment metrics in Decompression Sickness (DCS) research p 314 N94-11533

Use of ultrasound in altitude decompression modeling p 317 N94-11540
Hypobaric decompression prebreathe requirements and breathing environment p 317 N94-11541
Joint pain and Doppler-detectable bubbles in altitude (Hypobaric) decompression p 312 N94-11542
Arterial gas emboli in altitude-induced decompression sickness p 312 N94-11543
Transcranial Doppler ultrasound and the etiology of neurologic decompression sickness during altitude decompression p 312 N94-11544
A mechanism for the reduction in risk of decompression sickness in microgravity environment p 312 N94-11545
Risk of decompression sickness in the presence of circulating microbubbles p 312 N94-11546

DECONDITIONING
Exercise countermeasures for bed-rest deconditioning [NASA-TM-103987] p 300 N94-11191
Mechanistic studies on reduced exercise performance and cardiac deconditioning with simulated zero gravity p 310 N94-12001
Autogenic-feedback training: A countermeasure for orthostatic intolerance p 311 N94-12006
Cardiovascular dynamics during space sickness and deconditioning p 311 N94-12007

DECOUPLING
Decoupling of aircraft responses p 32 N94-11497

DEEP SPACE NETWORK
Ultrastable reference frequency distribution utilizing a fiber optic link p 355 N94-10994

DEEP WATER
SOFAR float tracking in the Shikoku basin p 206 N94-11986
On an upwelling front, propagation of upwelling and vertical velocity in the eastern Arabian Sea during monsoon, 1987 p 206 N94-11987
A detailed investigation of the benthic regime in the Clarion-Clipperton province of the Pacific and a forecast of consequences of manganese nodule mining p 224 N94-12733
Bottom currents and possibilities for near bottom layer environmental investigations in the Pacific by means of self contained bottom stations p 224 N94-12734
Autonomous self contained bottom pop-up stations for study of the benthic layer and seismicity of the ocean's bottom p 224 N94-12735
Convective and dynamic instability in meridional trenches p 225 N94-12739
Observations of surface signatures in the north-west Pacific Ocean with the spaceborne SAR p 226 N94-12746
Radar observation of internal waves field in the north-west Pacific p 226 N94-12747

DEFECTS
Imperfection sensitivity of the Brazier effect for orthotropic cylindrical shells [LR-687] p 186 N94-10879
Fibre reinforced polymer matrix composites: Microstructure and mechanical properties [DLR-FB-92-28] p 66 N94-11085
Fracture mechanics and full scale pipe break testing for the Department of Environment's New Production Reactor-Heavy Water Reactor [DE93-005428] p 187 N94-11169
Investigation of optically generated electronic defects and protonic transport in hydrogen-bonded molecular solids: Isomorphs of potassium dihydrogen phosphate [DE93-012498] p 399 N94-11243
Femtosecond dynamics, photoexcitation, and ESR spectra of MX chain solids [AD-A264689] p 399 N94-11263
Effect of switched-bias bakes on the postirradiation electrical response of MOS devices [DE93-009629] p 143 N94-11271

DEFENSE PROGRAM
Assured Mission Support Space Architecture (AMSSA) study p 348 N94-11573
Assessing the adequacy of the industrial base [AD-A264954] p 417 N94-11856
Defense: Health care [AD-A265914] p 421 N94-12445

DEFLECTION
Laser beam deflection: A diagnostic tool for vapour growth experiments in microgravity p 111 N94-10135

DEFORESTATION
International Space Year in China p 36 N94-10680

DEFORMATION
Low cost and thermally stable sandwich design for FIRST p 57 N94-10009
Experimental study of axisymmetric thermocapillary flows p 100 N94-10072
Smoothly deformed light p 375 N94-10566
Global organization of tectonic deformation on Venus p 444 N94-12066
Tectonics on Triton p 466 N94-12187
Regional mantle upwelling on Venus: The Beta-Atla-Themis anomaly and correlation with global tectonic patterns p 467 N94-12196
NiAl alloys for structural uses [NASA-CR-194113] p 85 N94-12447
Deformation mechanisms in tungsten single crystals in ballistic impact experiments [AD-A265701] p 405 N94-12563

DEGRADATION
DBTT measurement by use of Small Punch (SP) test [DE93-753188] p 183 N94-11168
UV testing of solar cells: Effects of antireflective coating, prior irradiation, and UV source p 53 N94-11408
The UoSAT-5 solar cell experiment: First year in orbit p 53 N94-11409
Results of thermal vacuum tests for the PASP+ flight modules p 53 N94-11410
Potential techniques for non-destructive evaluation of cable materials [DE93-008350] p 183 N94-11586
Advanced thermally stable coal-derived jet fuels: Compositional factors affecting thermal degradation of jet fuels [AD-A265842] p 99 N94-12282

DEHYDRATION
Glycerol-induced hyperhydration p 309 N94-11996
Modifications to an interactive model of the human body during exercise: With special emphasis on thermoregulation p 317 N94-12368

DELAY LINES
Variable rate transfer of optical information [AD-D015758] p 418 N94-10374

DELINEATION
Methodological considerations for use of ERS-1 imagery for the delineation of river networks in tropical forest areas p 247 N94-12484

DELTA MODULATION
GaAs sigma-delta modulator modeling for Analog to Digital Converters (ADC's) [AD-A263419] p 144 N94-11516

DELTA WINGS
Estimation of critical values and vibration characteristics on supersonic delta wings. Part 1: On-line time series analysis of stationary random response [NAL-TR-1153] p 2 N94-10363
Control effectiveness at hypersonic speeds p 3 N94-10426
A comparison of high resolution upwind solvers on 3-D inviscid hypersonic flows p 10 N94-10463
Modeling nonlinear aerodynamic loads for aircraft stability and control analysis p 32 N94-11499

DELTAS
Classification of Martian deltas p 470 N94-12207

DEMOGRAPHY
Baseline characteristics of different strata of astronaut corps p 312 N94-11552

DEMULTIPLEXING
An efficient medium access control strategy for high speed WDM multiaccess networks [MEMO-INF-92-74] p 131 N94-10165
Analysis of the eastern range multiplexed fiber optic IRIG B120 distribution system p 139 N94-10996
Holographic multiplexing for 3D optical memory [AD-A266099] p 171 N94-11420

DENDRITIC CRYSTALS
Solidification of undercooled Ni-32.5 wt percent Sn eutectic alloy p 86 N94-10194
Non-equilibrium solidification in undercooled Ni-B alloys p 86 N94-10196

DENITROGENATION
Monitoring cognitive function and need with the automated neuropsychological assessment metrics in Decompression Sickness (DCS) research p 314 N94-11533
Use of ultrasound in altitude decompression modeling p 317 N94-11540

DENSE PLASMAS
Nonlinear second harmonic generation by light wave-plasma interaction in oscillating magnetic field [DE93-613723] p 386 N94-10387
Characterization of an excimer laser-ablated plasma and applications p 392 N94-11450

DENSIFICATION
Processing, properties, and wear resistance of aluminides [DE93-012186] p 83 N94-11141

DENSITY (MASS/VOLUME)
Measurement of viscosity, density and gas solubility of refrigerant blends [DE93-014772] p 89 N94-11145
Wave structure in planetary rings p 434 N94-11185
The Pacific Subarctic Frontal Zone: Structure and dynamics p 223 N94-12731

DENSITY DISTRIBUTION
Laser beam deflection: A diagnostic tool for vapour growth experiments in microgravity p 111 N94-10135
Nonlinear space charge effect of bunched beam in linac [DE93-612176] p 371 N94-10409
Diagnostic complex for the space-time analysis of energy and current of pulsed relativistic particles [DE93-620980] p 362 N94-10649
Imprecise highest density regions related to intervals of measures [MEMO-COSOR-92-54] p 347 N94-10876
Determination of concentration profiles at interfaces and surfaces of partially miscible polymer blends [DE93-013140] p 89 N94-11007
Analysis of interstellar fragmentation structure based on IRAS images [NASA-CR-193518] p 428 N94-12767

DEOXYRIBONUCLEIC ACID
Studies in bioorganic chemistry [AD-A265532] p 55 N94-12011

DEPLETION
On the depletion in the outer asteroid belt and the structure of the 4 to 3 mean motion resonance p 426 N94-11596
Depletions of sulfur and/or zinc in IDPs: Are they reliable indicators of atmospheric entry heating? p 433 N94-12261

DEPOSITION
The surface plasmon spectroscopy as diagnostic technique in microgravity experiments p 110 N94-10133
Advanced diagnostics for in situ measurement of particle formation and deposition in thermally stressed jet fuels [DE93-009798] p 98 N94-11366
Modelling of dispersal and deposition of impact glass spherules from the Cretaceous-Tertiary boundary deposit p 432 N94-12238
The effects of organic adsorbates on the underpotential deposition of silver on Pt(111) electrodes [AD-A265623] p 404 N94-12376
Performance aspects of de Laval spray-forming nozzles [DE93-013671] p 163 N94-12604
Sedimentation rates and particulate fluxes in the slope and deep sea areas off eastern Taiwan p 220 N94-12709

DEPOSITS
Spectral and multispectral imaging studies of lunar mantled mare deposits p 446 N94-12079
Arroyo el Mimbral, Mexico, K/T unit: Origin as debris flow/turbidite, not a tsunami deposit p 281 N94-12084
Geomorphology of Triton's polar materials p 466 N94-12185
A novel test method for fuel thermal stability [AD-A265853] p 99 N94-12275

DEPTH MEASUREMENT
The extraction of bottom characteristics and mapping in Kin Bay, Okinawa Main Island, Japan, using LANDSAT-5/TM and SPOT-1/HRV data p 197 N94-11931

DERIVATION
ISAR motion compensation using the burst derivative measure as a focal quality indicator [AD-A265647] p 138 N94-12440

DESERTS
International Space Year in China p 36 N94-10680

DESIGN ANALYSIS
Design and development of a CFRP central cylinder for satellites p 56 N94-10007
Introducing SMaSE: An aide memoire on structural materials and space engineering p 63 N94-10053
Structural material, manufacture, and design requirements for high-temperature fasteners for space plane technologies p 63 N94-10055
In-flight evaluation of aerodynamic predictions of an air-launched space booster p 3 N94-10427
Conceptual design report for the SDC barrel and intermediate muon detectors based on a jet-type drift chamber [DE93-753173] p 367 N94-11510

DESORPTION
Measurement of polycyclic aromatic hydrocarbon (PAHs) in interplanetary dust particles p 431 N94-12167

DESTRUCTIVE TESTS
DBTT measurement by use of Small Punch (SP) test [DE93-753188] p 183 N94-11168

DESULFURIZING
Low temperature pathways to Chevrel phases via reduced molybdenum sulfide cluster complexes [DE93-013282] p 405 N94-12599

DETECTION
Sensing glass transitions in thin polymer films on acoustic wave microsensors [DE93-010805] p 87 N94-10295

DETONABLE GAS MIXTURES

A model of elementary chemistry and fluid mechanics in the combustion of hydrogen on platinum surfaces
[DE93-012767] p 77 N94-11370

DETONATION WAVES

Turbulent wall jet in blast wave precursor
[DE93-011955] p 151 N94-11144

Computational methods for problems in aerodynamics using parallel and vector architectures
[AD-A265626] p 16 N94-12377

DEUTERIUM

MHD simulation of deuterium-fiber-initiated Z-pinches with two-fluid effects
[DE93-012682] p 384 N94-10158

High-energy density physics at Los Alamos
[DE93-010271] p 371 N94-10260

Dynamics of dissociation versus ionization in strong laser fields
[DE93-009261] p 173 N94-10287

DEUTERIUM COMPOUNDS

Dynamics of dissociation versus ionization in strong laser fields
[DE93-009261] p 173 N94-10287

DEUTERONS

Monochromator SP-017. The results of the first experiments
[DE93-617463] p 372 N94-10849

DEVELOPING NATIONS

Communications infrastructure requirements for telemedicine/telehealth in the context of planning for and responding to natural disasters: Considering the need for shared regional networks p 307 N94-11804

DIAMAGNETISM

MHD simulation of deuterium-fiber-initiated Z-pinches with two-fluid effects
[DE93-012682] p 384 N94-10158

DIAMOND FILMS

Design of a CVD reactor for the deposition of diamond in a microgravity environment p 109 N94-10127

Wide Band-Gap Semiconductors. 1991 Materials Rese arch Society Symposium proceedings
[AD-A263418] p 401 N94-11515

Progress toward atomic layer epitaxy of diamond: Diamond films grown one layer at a time
[AD-A265530] p 403 N94-12010

DIAMONDS

Progress toward atomic layer epitaxy of diamond: Diamond films grown one layer at a time
[AD-A265530] p 403 N94-12010

Carbon and nitrogen in Type 2 supernova diamonds
p 431 N94-12166

Diamond thermoluminescence properties of different chondrites p 433 N94-12252

Analysis of the economics of DC arc CVD diamond
[AD-A265688] p 403 N94-12339

Dynamic high-pressure shock compaction of diamond powders
[AD-A266004] p 93 N94-12354

DIASTOLE

Strategies and methodologies to develop techniques for computer-assisted analysis of gas phase formation during altitude decompression p 312 N94-11547

DIATOMIC MOLECULES

Dynamics of dissociation versus ionization in strong laser fields
[DE93-009261] p 173 N94-10287

DICARBOXYLIC ACIDS

Engineering solid-state materials. Strategies for modeling and packing control of molecular assemblies into 3-D networks
[AD-A265291] p 404 N94-12438

DICTIONARIES

Abbreviations, acronyms, and initialisms frequently used by Martin Marietta Energy Systems, Incorporated
[DE93-012509] p 420 N94-11369

DIELECTRIC POLARIZATION

Charge distribution analysis of catalysts under simulated reaction conditions
[DE93-013604] p 78 N94-11699

DIELECTRIC PROPERTIES

Crystallinity and dielectric properties of PEEK, a thermoplastic poly(ether ether ketone)
[AD-A266027] p 91 N94-11487

Applications of in-situ ellipsometry to microwave electron cyclotron resonance plasma processes
[AD-A265197] p 373 N94-11880

DIELECTRICS

Dielectric liquid bridge stabilization in microgravity by means of electric fields p 100 N94-10075

Non-stationary and non-linear dispersive medium as external field which generates the squeezed states
p 380 N94-10605

Dielectric resonator
[US-PATENT-4,580,116] p 141 N94-10668

Polar solvation and electron transfer
[DE93-013328] p 365 N94-11010

Nonlinear excitation in quasi-one-dimensional Peierls dielectrics with charge density waves
[DE93-613827] p 398 N94-11025

Characterization of the Si/SiO2 interfere morphology from quantum oscillations in Fowler-Nordheim tunneling currents
[AD-A265149] p 143 N94-11160

Charge distribution analysis of catalysts under simulated reaction conditions
[DE93-013604] p 78 N94-11699

Dielectric breakdown and its influence on ignition
[AD-A264925] p 78 N94-11855

Effect of species structure and dielectric constant on C-band forest backscatter
[NASA-TM-109219] p 245 N94-11885

DIESEL ENGINES

Low-expansion ceramics initiative
[DE93-011860] p 89 N94-11106

Pulsed plasma processing for control of diesel engine emissions
[DE93-011884] p 181 N94-11247

Instantaneous engine frictional torque: Its components and piston assembly friction
[DE93-011639] p 182 N94-11625

DIETHYL ETHER

Thermal stability of sealants for military aircraft: Modification of polysulfide prepolymers with ether and thioether monomers
[AD-A264079] p 89 N94-11107

DIFFERENTIAL EQUATIONS

Deformations and recursion operators for evolution equations
[MEMO-1104] p 341 N94-10163

System monitoring and diagnosis with qualitative models
[NASA-CR-193812] p 323 N94-10711

The nonlinear evolution of modes on unstable stratified shear layers
[NASA-CR-191492] p 149 N94-10810

A symmetrical form for equations of a nonlinear spiral magnetic
[DE93-621350] p 344 N94-11033

Dynamics and control of coherent structures in the turbulent wall layer: An overview p 31 N94-11494

Nonlinear and dynamic analysis of flight
p 32 N94-11496

Spline approximation for system of n-th order nonlinear ordinary differential equations
[DE93-608188] p 346 N94-11507

DIFFERENTIAL GEOMETRY

S(sup 1) x S(sup 2) as a bag membrane and its Einstein-Weyl geometry
[DE93-613149] p 410 N94-10635

Non-Euclidean space for local hidden variables
[DE93-621341] p 344 N94-11032

Computational gearing mechanics
[NASA-CR-193666] p 181 N94-11157

DIFFRACTION PATTERNS

Surface and near-surface atom imaging with photoelectron holography
[DE93-013197] p 169 N94-10526

Study of Einstein-Podolsky-Rosen state for space-time variables in a two photon interference experiment
p 370 N94-10582

Organometallic chemical vapor deposition and characterization of ZnGeP2/GaP multiple heterostructures on GaP substrates p 400 N94-11442

DIFFRACTOMETERS

Rietveld refinement of magnetic structures from pulsed-neutron-source powder-diffraction data
[DE93-012740] p 363 N94-10743

DIFFUSE RADIATION

Interpretation of lunar and planetary electromagnetic scattering using the full wave solutions
p 440 N94-12049

DIFFUSION

On the role of Soret effect in concentration distribution in crystals growing from the melt p 112 N94-10173

Chemical pattern formation under microgravity
p 121 N94-10227

Hygroscopic absorption to falling films: The effects of the concentration level
[ITN-93-85198] p 148 N94-10391

DILUTE: A code for studying beam evolution under RF noise
[DE93-011605] p 133 N94-10960

Wind system documentation
[DE93-010381] p 285 N94-11664

Overwater atmospheric dispersion of volcanic smokes from Mt. Sakurajima observed in NOAA-AVHRR data
p 205 N94-11979

Soret diffusion: A possible cause of compositional heterogeneity within tektites p 432 N94-12211

Study of the admixture diffusion in the sea using remote techniques p 228 N94-12759

Mixing of drifter ensemble by mesoscale currents
p 228 N94-12760

DIFFUSION COEFFICIENT

DILUTE: A code for studying beam evolution under RF noise
[DE93-011605] p 133 N94-10960

Glucose electrodes based on cross-linked (Os(bpy)2Cl)(sup +/2+) complexed poly(1-vinylimidazole) films
[AD-A265404] p 94 N94-12425

DIFFUSION FLAMES

Influence of gravity and ambient pressure variations on the behavior of buoyant laminar diffusion flames
p 123 N94-10240

Theories of turbulent combustion in high speed flows
[AD-A265735] p 79 N94-12403

DIFFUSION LENGTH

Measurement of the minority carrier diffusion length and edge surface-recombination velocity in InP
p 49 N94-11388

Diffusion length damage coefficient and annealing studies in proton-irradiated InP
[NASA-TM-106262] p 404 N94-12430

DIFFUSION WELDING

SPF/DB: A manufacturing technique for lightweight structures p 59 N94-10026

High temperature stability, interface bonding, and mechanical behavior in (beta)-NiAl and Ni3Al matrix composites with reinforcements modified by ion beam enhanced deposition
[DE93-013977] p 398 N94-11115

DIFFUSIVITY

Why does preferential diffusion strongly affect premixed turbulent combustion? p 81 N94-12319

DIFLUORIDES

Production of electronic grade lunar silicon by disproportionation of silicon difluoride
p 435 N94-12017

DIGITAL DATA

User's manual for the DAD-1 data acquisition daughter board for the SuperCard-2
[DE93-012153] p 325 N94-11139

DIGITAL FILTERS

Adaptive algorithms for use with digital filters in vibration control p 71 N94-11338

DIGITAL RADAR SYSTEMS

Rainfall-runoff estimation using digital radar
[AD-A265390] p 286 N94-12408

DIGITAL SIMULATION

Solving the inverse problem for incompressible potential flow through two-dimensional cascades
[NAL-TR-1162] p 147 N94-10365

Numerical calculation of scramjet inlet flow
[NAL-TR-1174T] p 27 N94-10370

Aerodynamic model identification of quiet STOL experimental aircraft ASKA from dynamic flight test data
[DE93-767967] p 25 N94-10728

Proceedings of the 9th and 10th NAL Workshop on Investigation and Control of Boundary-Layer Transition
[NAL-SP-18] p 163 N94-12611

Nonlinear stability calculations of pipe flow
p 163 N94-12612

DNS on control of laminar-turbulent transition in channel flow with suction and blowing p 163 N94-12613

Turbulence modeling and compressibility
p 163 N94-12614

Aerodynamic sound due to interaction between a two-dimensional free shear layer and the leading edge of a parallel flat plate p 163 N94-12615

Experiment on a high Reynolds number turbulent boundary layer p 164 N94-12617

On the wake behind a high speed train
p 164 N94-12618

Calibration of anemometers at low speed by means of towing carriage p 164 N94-12619

Criteria for onset of boundary-layer transition on spinning bodies p 164 N94-12620

On the formation process of Karman vortex street
p 16 N94-12621

Nonlinear instability of a laminar flow in a rectangular duct and generation of the turbulent secondary flow
p 164 N94-12622

Curvature effects in three-dimensional boundary layers
p 164 N94-12623

Simultaneous 3D turbulent large-scale structures in a flood flow by multi-channels measuring system
p 165 N94-12624

A numerical experiment of boundary layer transition at subcritical Reynolds numbers p 165 N94-12625

Turbulent boundary layer interacting with spanwise periodic longitudinal vortex arrays p 165 N94-12626

Turbulent drag reduction of a d-type rough wall boundary layer with longitudinal ribs placed within the grooves
p 165 N94-12627

Coherent structure in near wall turbulence with riblets
p 165 N94-12628

Instability around an isolated roughness element p 165 N94-12629
Idea of underground airplane p 27 N94-12630
Growth and breakdown of Taylor-Goertler vortices in rotating Blasius boundary layer p 165 N94-12631
Traveling disturbances appearing in yawed cylinder boundary layer transition p 166 N94-12632
Visual structure of Karman vortex streets in a route to chaotic states excited by oscillation of a circular cylinder p 17 N94-12633
Boundary conditions and bifurcations in plane Poiseuille flow p 166 N94-12634

DIGITAL SYSTEMS
Some results with the new digital ionosonde in San Diego
[AD-A265178] p 275 N94-11101
Preliminary supersonic flight test evaluation of performance seeking control
[NASA-TM-4494] p 28 N94-11205
Transactions of the 10th Army Conference on Applied Mathematics and Computing
[AD-A265098] p 318 N94-11678

DIGITAL TELEVISION
Studies and simulations of the DigiCipher system
[NASA-CR-193470] p 321 N94-10343

DIMENSIONAL ANALYSIS
Dimensional scaling for impact cratering and perforation
[NASA-CR-188259] p 42 N94-10665
A version of superstring with four space-time dimensions
[DE93-608196] p 412 N94-11163

DIMENSIONAL MEASUREMENT
A preliminary study on ice shape tracing with a laser light sheet
[NASA-TM-105964] p 174 N94-11132

DIMENSIONS
Generalized Mandelbrot rule for fractal sections
[AD-A266010] p 347 N94-12390

DIMERS
Monte Carlo simulations of a two-dimensional hard dimer system
[DE93-613535] p 361 N94-10502
Szilard-Chalmers effect in solid HIO4.2H2O by neutron irradiation
[DE93-617173] p 397 N94-10830
Adsorption and dissociation of disilane on Si(001) studied by STM
[AD-A265269] p 402 N94-11684

DIMETHYL COMPOUNDS
Application of static and dynamic enclosures in determining DMS and OCS fluxes in Sphagnum peatlands p 269 N94-12460
Environmental factors controlling fluxes of dimethyl sulfide in a New Hampshire fen p 270 N94-12462
DMS emissions from Sphagnum-dominated wetlands p 271 N94-12466
Factors controlling sulfur gas exchange in Sphagnum-dominated wetlands p 271 N94-12469

DIPOLE ANTENNAS
Design of a matching network for dipole antennas
[AD-A265115] p 136 N94-11158
Coordinated Radio, Electron, and Waves Experiment (CREWE) for the NASA Comet Rendezvous and Asteroid Flyby (CRAF) instrument
[NASA-CR-194376] p 427 N94-12566

DIPOLE MOMENTS
Crossing-odd spin effects in the dipole model of hadron scattering
[DE93-617692] p 362 N94-10551

DIPOLES
Polar solvation and electron transfer
[DE93-013328] p 365 N94-11010

DIRAC EQUATION
On parity conservation and the question of the missing, right-handed neutrino
[DE93-613092] p 361 N94-10414
Bound states of the N-dimensional Klein-Gordon equation with vector and scalar Coulomb potentials
[DE93-617650] p 349 N94-10547
On local frame fields and fermion dynamics in space with nontrivial topologies
[DE93-617657] p 349 N94-10548
A new approach to the I/N-expansion for the Dirac equation
[DE93-617647] p 349 N94-10833
Exact solution of the N-dimensional generalized Dirac-Coulomb equation
[DE93-617649] p 411 N94-10834

DIRECT BROADCAST SATELLITES
Potential markets for advanced satellite communications
[NASA-CR-191145] p 41 N94-10512

DIRECT CURRENT
Direct current transducer
[DE92-644548] p 141 N94-10533

DIRECTIONAL SOLIDIFICATION (CRYSTALS)
The effect of gravity modulation on thermosolutal convection p 105 N94-10103
AGF (Automatic Gradient Furnace): A proposed microgravity facility p 112 N94-10141
Solidification in immiscible systems: The influence of processing conditions on resulting microstructures p 112 N94-10174
Solidification from supercooled melt under microgravity p 113 N94-10176
The effect of gravitational modulation on convection in vertical Bridgman growth p 113 N94-10178
Variations of the temperature profile in the gradient furnace GFQ within a cylindrical sample used for directional solidification p 114 N94-10181
Flow transitions in a 2D directional solidification model p 114 N94-10183
TEXUS 28 experiment: Convections and crystal growth of Ge:Ga. Analysis of temperature measurements p 114 N94-10184
Pulsatile instability in rapid directional solidification: Strongly-nonlinear analysis p 115 N94-10188
EUSO-D2-experiment: Unidirectional solidification with quenching of an AlSi11 alloy p 86 N94-10199
Effect of experimental procedure on pattern formation and array disorder in cellular solidification p 117 N94-10203
Coupled growth of cells and bubbles in directional solidification of succinonitrile-acetone alloys p 118 N94-10206

DIRECTORIES
Directory of IAEA databases
[DE93-622837] p 420 N94-11818

DISASTERS
Telemedicine and international disaster response: Medical consultation to Armenia and Russia via a telemedicine spacebridge p 305 N94-11790
Global considerations for implementation of telemedicine p 305 N94-11792
Tropical medicine: Telecommunications and technology transfer p 305 N94-11793
Applications of the INTELSAT system to remote health care p 306 N94-11794
The National Disaster Medical System p 307 N94-11801
Communications infrastructure requirements for telemedicine/telehealth in the context of planning for and responding to natural disasters: Considering the need for shared regional networks p 307 N94-11804
International disaster research p 307 N94-11805
Flood monitoring in northern part of Central Java by remote sensing technique. Case study: The flooding of Semarang in January, 1990 p 206 N94-11989

DISCOLORATION
User's manual for the plume visibility model PLUVUE 2 (revised)
[PB93-188233] p 265 N94-11016

DISCONTINUITY
Shallow crustal discontinuities and graben and scarp formation in the Tharsis region of Mars p 469 N94-12203

DISCRETE FUNCTIONS
Vectorizing matrix operations arising from PDE discretization on 9-point stencils
[CWI-NM-R9221] p 342 N94-10351

DISORDERS
Effect of experimental procedure on pattern formation and array disorder in cellular solidification p 117 N94-10203

DISORIENTATION
Motion and spatial disorientation systems: Special research capabilities
[AD-A265155] p 303 N94-11097

DISPERSING
Non-stationary and non-linear dispersive medium as external field which generates the squeezed states p 380 N94-10605
A self-consistent model of non-linear parameterization of turbulent diffusion in atmospheric boundary layer
[DE93-011950] p 275 N94-11052
Modelling of dispersal and deposition of impact glass spherules from the Cretaceous-Tertiary boundary deposit p 432 N94-12238
Vulcanian explosive eruptions: A mechanism for localised pyroclast dispersal on Venus p 477 N94-12243

DISPERSIONS
Numerical simulation of multi-droplet hydrodynamic interactions in liquid dispersions p 114 N94-10182
New mechanism of Ostwald ripening in Lorentz-force stabilized Cu-Pb dispersions p 116 N94-10192
Ostwald ripening of solid cobalt particles in liquid copper p 87 N94-10202
Overwater atmospheric dispersion of volcanic smokes from Mt. Sakurajima observed in NOAA-AVHRR data p 205 N94-11979

DISPLACEMENT
Improving reservoir conformance using gelled polymer systems
[DE93-014532] p 88 N94-10749
Venus' center of mass - center of figure displacement and implications p 444 N94-12067

DISPLACEMENT MEASUREMENT
An electro-optical system for the measurement of strains p 186 N94-10900
Sea ice deformation observed with ERS-1 SAR p 239 N94-11749
Physical processes of microwave backscattering from laboratory wind-wave surfaces p 200 N94-11952

DISPLAY DEVICES
Automaticity of processing location versus identity information in brief visual displays
[AD-A265013] p 418 N94-10491
Measurement of display transfer characteristics using test pictures
[BBC-RD-1992/13] p 133 N94-11023
Computer software and hardware to determine contrast sensitivity using three methods: Tracking, limits, and constant stimuli
[AD-A265168] p 324 N94-11099
Perceptual response to visual noise and display media
[NASA-CR-193406] p 313 N94-11511
Development of a graphical user interface and graphics display for the WIND system
[DE93-011780] p 285 N94-11614
Wind system documentation
[DE93-010381] p 285 N94-11664
Development and implementation of a general purpose x-windows display program
[AD-A265306] p 332 N94-11860

DISRUPTING
Aircraft windscreens enhance visual search disruption produced by laser glare
[AD-A265167] p 26 N94-11892

DISSIPATION
Nonlinear MHD-waves in a dissipative plasma with hall currents
[DE93-617844] p 386 N94-10395
Dissipation in a squeezed-state environment p 370 N94-10584
Negative viscosity and generation of dissipative solitons and zonal dissipative structures by drift waves
[DE93-621656] p 392 N94-11212
Turbulence generation in the Pacific undercurrent by shear p 223 N94-12730

DISSOCIATION
Adsorption and dissociation of disilane on Si(001) studied by STM
[AD-A265269] p 402 N94-11684

DISSOLVING
Effect of gravity on the dissolution and liquid phase epitaxial growth processes in a horizontal sandwich system p 118 N94-10208
Dynamic studies of crystal growth using the AFM
[DE93-009549] p 399 N94-11268

DISTORTION
An analytic model for calculating pump-induced wavefront distortions in laser slabs
[DE93-011953] p 174 N94-11126

DISTRIBUTED PARAMETER SYSTEMS
Computational algorithms or identification of distributed parameter systems
[AD-A265252] p 331 N94-11680
Control of large space structures with varying configuration
[AD-A265764] p 44 N94-12387

DISTRIBUTED PROCESSING
Practical authorization in large heterogeneous distributed systems
[DE93-013192] p 335 N94-10324
Low latency messages on distributed memory multiprocessors
[NASA-CR-191479] p 323 N94-10643
Distributed simulation using a real-time shared memory network
[NASA-TM-106239] p 319 N94-10724
The Zipcode message-passing system
[DE93-011958] p 336 N94-11027
A formally verified algorithm for interactive consistency under a hybrid fault model
[NASA-CR-4527] p 326 N94-11188
Flexible language constructs for large parallel programs
[NASA-CR-191478] p 326 N94-11196
A distributed version of the NASA Engine Performance Program
[NASA-TM-106208] p 327 N94-11231
Portable programming on parallel/networked computers using the Application Portable Parallel Library (APPL)
[NASA-TM-106238] p 327 N94-11232
High-performance distributed systems architecture
[AD-A265297] p 337 N94-11829

Distributed real-time system design: Theoretical concepts and applications
[AD-A265199] p 337 N94-11881

DISTRIBUTION (PROPERTY)
Effect of experimental procedure on pattern formation and array disorder in cellular solidification
p 117 N94-10203

DISTRIBUTION FUNCTIONS
On a class of two-dimensional nearest neighboring random walks
[CWI-BS-R9220] p 347 N94-10353
The heat transfer by radiation between two media
[DE93-617820] p 149 N94-10838
The Langevin's approach to the statistical theory of bounded plasma
[DE93-617842] p 388 N94-10839
Wave generation by contaminant ions
[NASA-CR-193558] p 364 N94-10946
Kinetic effects in stochastic topologically nontrivial field
[DE93-621642] p 391 N94-11207
Simple kinetic model for plasma in stochastic helical field
[DE93-621643] p 391 N94-11208
Power-law confusion: You say incremental, I say differential p 347 N94-12175

DIURNAL VARIATIONS
Selected upper-air wind speed distributions
[AD-A264822] p 284 N94-10871
One-year mooring of an ADCP in the central region of the Kuroshio west of Okinawa p 194 N94-11913
Current variability on the shelf break northeast of Taiwan p 219 N94-12708

DIVERTERS
Simulations of D3-D divertor biasing with the LEDGE code
[DE93-010500] p 385 N94-10262
Physics and modelling of scrape-off layer transport
[DE93-010510] p 385 N94-10289
Physics of tokamak scrape-off layer confinement
[DE93-011949] p 390 N94-11125
Experimental approach to the physics of the high density divertor
[DE93-009149] p 391 N94-11170
Characteristics of ICR-produced peripheral plasma in the Uragan-3M torsatron
[DE93-621666] p 392 N94-11214
Magnetic island suppression in torsatron configurations
[DE93-621681] p 392 N94-11215
Results from the D3-D advanced divertor program
[DE93-015472] p 393 N94-11514

DMSP SATELLITES
Preliminary analysis of the benefits derived to US Air Force spacecraft from on-orbit refueling
p 38 N94-11567

DOCUMENTS
Correspondence standards
[NHB-1450.10B] p 420 N94-11589

DOMES (GEOLOGY)
Scalloped margin domes: What are the processes responsible and how do they operate?
p 454 N94-12120

DOMES (STRUCTURAL FORMS)
Lineament analysis and tectonic interpretation for the Tharsis region p 437 N94-12031

DONOR MATERIALS
Polar solvation and electron transfer
[DE93-013328] p 365 N94-11010
Chromatographic assessment of hydrogen-bond donating ability
[AD-A265292] p 369 N94-11826

DOPED CRYSTALS
Results of crystal growth experiments by FZM on Zona facilities in microgravity p 116 N94-10193
The influence of irradiation conditions, type, and concentration of impurities on radiation defects characteristics in indium antimonide under electron irradiation
[DE93-617201] p 397 N94-10843
Radiation defect production in InAs crystals under electron irradiation
[DE93-617202] p 397 N94-10845
Grain boundaries in complex oxides
[DE93-013986] p 398 N94-11012
Activation energy and capture cross section of majority carrier traps in Zn doped InP p 49 N94-11386
Measurement of the minority carrier diffusion length and edge surface-recombination velocity in InP
p 49 N94-11388
Experimental studies of the structure of grain boundaries
[DE93-013979] p 402 N94-11700
Polaronic charge separation in mixed-halide MX solids
[AD-A266073] p 403 N94-12345
Synthesis and magnetic properties of novel La*2-x*M*x*CuO*4 equals y* compositions (La equals La, Pr, Nd, Sm, Eu, Cd; M equals Ca, Sr, Ba; O (less than or equal) x 0.2; -0.5 (less than or equal) y (less than or equal) 0.5)
[DE93-011359] p 403 N94-12363
A relaxation study of poled nonlinear optical polymers by infrared reflection-absorption spectroscopy
[AD-A265797] p 93 N94-12380
Diffusion length damage coefficient and annealing studies in proton-irradiated InP
[NASA-TM-106262] p 404 N94-12430

DOPPLER RADAR
Groundwave HF ocean surface radar
p 139 N94-11906

DOWNLINKING
An investigation of error characteristics and coding performance
[NASA-CR-193620] p 324 N94-10932
Real-time tomography mooring
[AD-A264923] p 289 N94-11854

DOWNWASH
Navier-Stokes flowfield computation of wing/rotor interaction for a tilt rotor aircraft in hover
[NASA-CR-4532] p 13 N94-10758

DRAG REDUCTION
Method of reducing drag in aerodynamic systems
[NASA-CASE-LEW-14791-1] p 12 N94-10672
Supersonic airplane study and design
[NASA-CR-193219] p 25 N94-11150
Turbulent drag reduction of a d-type rough wall boundary layer with longitudinal ribs placed within the grooves
p 165 N94-12627

DRAINAGE
Design of a global soil moisture initialization procedure for the simple biosphere model
[NASA-TM-104590] p 284 N94-10940
Modeling present and future river runoff using global atmospheric models
[AD-A265274] p 285 N94-11685
Rainfall-runoff estimation using digital radar
[AD-A265390] p 286 N94-12408

DRILLING
Gulf of Mexico sales 147 and 150: Central and western planning areas. Draft environmental impact statement. Volume 1: Sections 1 through 4.C
[PB93-190304] p 265 N94-11018
Gulf of Mexico sales 147 and 150: Central and western planning areas. Draft environmental impact statement. Volume 2: Sections 4.D through 9
[PB93-190312] p 265 N94-11019
Descriptions and preliminary interpretations of cores recovered from the Manson Impact Structure (Iowa)
p 281 N94-12032

DROP SIZE
Shear coaxial injector atomization phenomena for combusting and non-combusting conditions
[NASA-CR-193339] p 152 N94-11526

DROP TESTS
Gas-liquid jets under reduced gravity conditions
p 103 N94-10091
Measurement of the thermal conductivity of molten InSb in a drop shaft p 105 N94-10102
Containerless processing of equiatomic Mn50Bi50 in a drop tube p 118 N94-10205

DROP TOWERS
Calibration of accelerometers on drop tower Bremen
p 108 N94-10121
Undercooled W-Re and Mo-Re drops in an ultra high vacuum drop tube p 86 N94-10195
Large amplitude shape oscillations in a mercury drop using a drop tower
[DE93-767972] p 125 N94-10730

DROPS (LIQUIDS)
Marangoni instability induced convection in an evaporating liquid droplet p 104 N94-10094
Bubbles and drops behaviour under low-gravity: A space experiment for the IML-2 mission p 104 N94-10098
Thermocapillary slug flow in a capillary tube
p 105 N94-10104
Determination of the viscous acoustic field for liquid drop positioning/forcing in an acoustic levitation chamber in microgravity p 110 N94-10131
Numerical simulation of multi-droplet hydrodynamic interactions in liquid dispersions p 114 N94-10182
Single-electron tunneling
[DE93-013337] p 396 N94-10648
Large amplitude shape oscillations in a mercury drop using a drop tower
[DE93-767972] p 125 N94-10730
Experimental study of multiple droplet evaporative cooling
[PB93-198463] p 149 N94-10851
A new expression for the production rate of sea water droplets on the sea surface p 195 N94-11920
Minor and trace element composition and age of Yukon probable-microtektites p 429 N94-12094
Worldwide map of rainfall amount over the ocean derived from passive microwave radiometer p 211 N94-12663

DROUGHT
International Space Year in China p 36 N94-10680

DRY FRICTION
Study of the tribological behavior of SiC and Si3N4 ceramic couples in terms of temperature: The reality
p 64 N94-10061

DUAL THRUST NOZZLES
Evaluation of dual flow thrust vectored nozzles with exhaust stream impingement
[NASA-CR-193292] p 150 N94-10912

DUCTED FLOW
A comparative study of full Navier-Stokes and Reduced Navier-Stokes analyses for separating flows within a diffusing inlet S-duct
[NASA-TM-106250] p 39 N94-10764
Nonlinear instability of a laminar flow in a rectangular duct and generation of the turbulent secondary flow
p 164 N94-12622

DUCTILITY
Design with high strength steel: A case of failure and its implications p 58 N94-10017
Material removal processes: Engineering mechanics consideration
[DE93-010733] p 126 N94-10293
Extensions of some guidelines for the mechanical design of coaxial compression pin seals
[DE93-012385] p 177 N94-10348
Particle attraction effects on the centrifugal casting and extrusion of alumina
[DE93-011559] p 82 N94-10957
Production of reactive sintered nickel aluminide
[DE93-014434] p 83 N94-11127
DBTT measurement by use of Small Punch (SP) test
[DE93-753188] p 183 N94-11168
NiAl alloys for structural uses
[NASA-CR-194113] p 85 N94-12447

DUMMIES
Mass properties test procedure for manikin headforms and helmet systems
[AD-A265654] p 315 N94-10296

DUST
Microgravity combustion of dust suspension in a spherical chamber p 80 N94-10248
Turbulent wall jet in blast wave precursor
[DE93-011955] p 151 N94-11144
Distribution of mineral aerosols over the North Pacific
p 204 N94-11976
A simple model of clastic sediments on Mars
p 460 N94-12155
Dust in the Martian atmosphere: Polarimetric sensing
p 473 N94-12223
Composition of the Martian aerosols through near-IR spectroscopy p 475 N94-12235

DUST STORMS
Dust in the Martian atmosphere: Polarimetric sensing
p 473 N94-12223

DYE LASERS
Progress in zirconium resonance ionization spectroscopy
[DE93-011881] p 76 N94-11075
Thermal-optical switching of a silicon based interference filter
[AD-A265152] p 174 N94-11095

DYNAMIC CHARACTERISTICS
Comprehensive dynamic analysis of a bladed disk-turborotor-bearing system
[ISBN-0-315-73646-1] p 180 N94-11155
Air-sea fluxes and universal constants in weak-turbulence theory of surface gravity waves
p 195 N94-11922
Lava flows on Venus: Analysis of motion and cooling
p 457 N94-12137

DYNAMIC CONTROL
Mechanical analysis of parallel manipulators with simulation, design, and control applications
[ISBN-0-315-72013-1] p 181 N94-11156
Dynamics and control of coherent structures in the turbulent wall layer: An overview p 31 N94-11494

DYNAMIC LOADS
Design and development of a miniature column-based interface (MCBI) stress gage
[AD-A266054] p 170 N94-10873
Response of composite laminates to dynamic surface loads p 66 N94-10902

DYNAMIC MODELS
Topex orbit determination using GPS tracking system
p 38 N94-10359
Estimation of the attitude motion of the small satellite ORIZURU
[NAL-TR-1145] p 42 N94-10366

Mechanical analysis of parallel manipulators with simulation, design, and control applications [ISBN-0-315-72013-1] p 181 N94-11156

Visualization and simulation of a real physical problem based on physical modeling with the use of computer animation [INPE-5492-TDI/509] p 325 N94-11166

Trajectory pattern inverse dynamics and control of nonlinear dynamics systems with application to flexible structures p 181 N94-11219

A local dynamic model for large eddy simulation p 155 N94-12285

Large eddy simulations of time-dependent and buoyancy-driven channel flows p 155 N94-12287

A normal stress subgrid-scale eddy viscosity model in large eddy simulation p 155 N94-12288

Application of a dynamic subgrid-scale model to turbulent recirculating flows p 156 N94-12290

Large-eddy simulation of turbulent flow with a surface-mounted two-dimensional obstacle p 156 N94-12291

Physiological water model development p 316 N94-12367

Problem of climate change predictability and satellite radiation budget observations p 229 N94-12766

DYNAMIC PRESSURE

Dynamic tester for rotor seals and bearings [NASA-CASE-MFS-28493-1] p 33 N94-10669

Improvement of method for experimental determination of flutter speed by parameter identification [NASA-CR-193555] p 33 N94-12769

DYNAMIC RESPONSE

Dynamic tests on the NASA Langley CSI evolutionary model p 45 N94-11320

Project of an attitude control system (three axis) of a satellite using the LQG/LTR methodology [INPE-5473-TDI/504] p 44 N94-12356

Ultrasonic wave interaction with advanced complex materials for nondestructive evaluation applications [AD-A265704] p 74 N94-12401

Space truss zero gravity dynamics [AD-A266130] p 44 N94-12541

Three-dimensional finite element analysis of explosive safety facilities: A technology assessment [AD-A265700] p 35 N94-12562

DYNAMIC STABILITY

Convective and dynamic instability in meridional trenches p 225 N94-12739

DYNAMIC STRUCTURAL ANALYSIS

Comprehensive dynamic analysis of a bladed disk-turborotor-bearing system [ISBN-0-315-73646-1] p 180 N94-11155

The impact of active controls technology on the structural integrity of aeronautical vehicles p 27 N94-11341

Discrete Kalman filtering equations of second-order form for control-structure interaction simulations [NASA-CR-193723] p 331 N94-11522

Space truss zero gravity dynamics [AD-A266130] p 44 N94-12541

Three-dimensional finite element analysis of explosive safety facilities: A technology assessment [AD-A265700] p 35 N94-12562

DYNAMIC TESTS

Dynamic tester for rotor seals and bearings [NASA-CASE-MFS-28493-1] p 33 N94-10669

Safety of high speed ground transportation systems: X2000 US demonstration vehicle dynamics trials, preliminary test report, October 1992 - January 1993 [PB93-194645] p 422 N94-10736

Dynamic tests on the NASA Langley CSI evolutionary model p 45 N94-11320

Reduced gravity multibody dynamics testing [NASA-CR-192589] p 125 N94-11483

Three-dimensional finite element analysis of explosive safety facilities: A technology assessment [AD-A265700] p 35 N94-12562

DYNAMICAL SYSTEMS

On output linearization of observable dynamics [MEMO-1105] p 341 N94-10276

A group-theoretic approach to the study of small oscillations of a dynamical system with a known symmetry [DE93-612971] p 409 N94-10402

Symbolic dynamics and description of complexity [DE93-613030] p 418 N94-10485

The uncertainty principle and quantum chaos p 379 N94-10602

Intermittency following a Hopf bifurcation [W-9301] p 344 N94-10907

To the complexity of dynamic system problem [DE93-621355] p 134 N94-11037

Stability analysis and aerospace vehicle dynamics p 31 N94-11491

DYNAMO THEORY

Polarity reversals and tilt of the Earth's magnetic dipole p 283 N94-12219

Are cosmic rays effective for ionization of the solar nebula? p 472 N94-12220

Precession of Uranus and Neptune and their magnetic field p 473 N94-12222

E

EARTH ATMOSPHERE

A self-consistent model of non-linear parameterization of turbulent diffusion in atmospheric boundary layer [DE93-011950] p 275 N94-11052

A modeling perspective on cloud radiative forcing [DE93-012383] p 276 N94-11241

FFTSCAN: A program for spectral smoothing using Fourier transforms [AD-A264921] p 278 N94-11852

Collisions of small Spacewatch asteroids with the Earth p 430 N94-12157

EARTH CORE

Does the thermal wind exist near the Earth's core boundary? p 283 N94-12217

EARTH CRUST

Wave propagation characteristics of short-period crustal phases near ARCESS and NORESS [AD-A265959] p 275 N94-11102

EARTH ENVIRONMENT

Space Activities in the Asia Pacific Region [JTN-93-80421] p 35 N94-10676

Russian space system for the Earth remote sensing p 37 N94-10688

Sun-synchronous and geo-synchronous satellite data utilization for environmental studies p 37 N94-10689

Remote sensing and global environment p 191 N94-11895

EARTH GRAVITATION

The Earth's gravity model for the ERS-1 commissioning phase p 243 N94-11778

EARTH IONOSPHERE

Magnetic Earth Ionosphere Resonant Frequencies (MEIRF) project [NASA-CR-193182] p 276 N94-11355

Construction and testing of a space ready rectenna [NASA-CR-193310] p 137 N94-11357

One-dimensional calculation of high-power microwave pulse compression by the earth's ionosphere [DE93-009517] p 137 N94-11466

An investigation of the near Earth space environments [AD-A265295] p 278 N94-11828

A new data collection system for ionospheric modelling and related topics [AD-A265893] p 278 N94-12277

Mid-latitude ionospheric response to active experiments [NASA-CR-193549] p 280 N94-12583

EARTH MAGNETOSPHERE

A study of the magnetic field annihilation process in the magnetosphere and some geotechnical applications [DE93-013249] p 273 N94-10305

A study of the magnetic field annihilation process in the magnetosphere and some geotechnical applications [DE93-013248] p 273 N94-10319

Imaging of magnetospheric dynamics using low energy neutral atom detection [DE93-012656] p 275 N94-10742

A study on the magnetospheric activity using the AE, ap, and Dst geomagnetic indices [INPE-5470-TDI/501] p 276 N94-11165

An investigation of the near Earth space environments [AD-A265295] p 278 N94-11828

EARTH MANTLE

Wave propagation characteristics of short-period crustal phases near ARCESS and NORESS [AD-A265959] p 275 N94-11102

A model for the subduction mechanics of flexible lithosphere and its viscous coupling to the mantle using power-law rheologies p 277 N94-11585

Oxidation state of the Earth's upper mantle during the last 3800 million years: Implications for the origin of life p 283 N94-12210

Does the thermal wind exist near the Earth's core boundary? p 283 N94-12217

Polarity reversals and tilt of the Earth's magnetic dipole p 283 N94-12219

EARTH MOVEMENTS

Analysis of gravity, magnetic, and seismic reflection data from Tibet and neighboring regions of China [NASA-CR-193405] p 278 N94-11886

EARTH OBSERVATIONS (FROM SPACE)

Landsat as a commercial enterprise [INPE-5477-TAE/019] p 232 N94-11524

Visual Earth observation performance in the space environment. Human performance measurement 4: Flight experiments p 314 N94-11539

More sense for less cents: Cost effective servicing of remote sensing satellites p 348 N94-11572

EARTH ORBITAL ENVIRONMENTS

The magnitude of impact damage on LDEF materials [NASA-CR-188258] p 43 N94-10666

Space environmental effects on the integrity of chromic acid anodized coatings [NASA-CR-191468] p 55 N94-10947

Property changes induced by the space environment in composite materials on LDEF: Solar array materials passive LDEF experiment A0171 (SAMPLE) [NASA-CR-192572] p 73 N94-11484

Visual Earth observation performance in the space environment. Human performance measurement 4: Flight experiments p 314 N94-11539

Operational radiological support for the US manned space program p 318 N94-11561

On-orbit refueling p 38 N94-11565

On-orbit refueling p 38 N94-11566

Use of low orbital satellite communications systems for humanitarian programs p 308 N94-11808

Molecular properties of polymeric materials for space applications [NASA-CR-194370] p 94 N94-12450

EARTH ORBITS

Satellite situation report, volume 32, no. 1 [NASA-TM-109233] p 42 N94-10562

Satellite situation report, volume 32, no. 2 [NASA-TM-109234] p 42 N94-10563

Satellite situation report, volume 31, no. 4 [NASA-TM-109232] p 39 N94-10659

EOL performance comparison of GaAs/Ge and Si BSF/R solar arrays p 51 N94-11398

Five biomedical experiments flown in an Earth orbiting laboratory: Lessons learned from developing these experiments on the first international microgravity mission from concept to landing p 302 N94-11556

Robotic servicing on Earth orbiting satellites p 45 N94-11579

EARTH PLANETARY STRUCTURE

Landscape and geomorphic survey of Zhamanshin area, Northern Kazakhstan: Preliminary report on 1992 field trip data p 282 N94-12123

Stratigraphy and sedimentology of the K/T boundary deposit in Haiti p 282 N94-12138

EARTH RADIATION BUDGET

Retrieval of radiation budgets in the Arctic from satellite measurements p 229 N94-10714

Problem of climate change predictability and satellite radiation budget observations p 229 N94-12766

EARTH RADIATION BUDGET EXPERIMENT

Retrieval of radiation budgets in the Arctic from satellite measurements p 229 N94-10714

Radiometer offsets and count conversion coefficients for the Earth Radiation Budget Experiment (ERBE) spacecraft for the years 1987, 1988, and 1989 [NASA-CR-191489] p 286 N94-12772

EARTH RESOURCES

Space Activities in the Asia Pacific Region [JTN-93-80421] p 35 N94-10676

Status of remote sensing and Geographic Information System (GIS) applications in the Environment and Natural Resources (ENR) sector p 36 N94-10687

Panel discussion: Role of space program in the Asia Pacific Region p 37 N94-10694

The use of remote sensing data for coastal zone management and environment in Indonesia p 196 N94-11927

Shoreline change detection using remote sensing and GIS in Vietnam p 196 N94-11928

EARTH ROTATION

Statistical description of tectonic motions [NASA-CR-193701] p 275 N94-10950

Plans to improve the experimental limit in the comparison of the east-west and west-east one-way light propagation times on the rotating earth p 351 N94-10971

EARTH SCIENCES

Environmental Sciences Division [DE93-013865] p 264 N94-10650

A browse facility for Earth science remote sensing data: Center director's discretionary fund final report [NASA-TM-108413] p 419 N94-10723

Facts about the US Antarctic program [NSF-92-134] p 279 N94-12568

EARTH SURFACE

Satellite-derived photosynthetically available and total solar irradiance at the surface during FIFE's intensive field campaigns p 230 N94-10954

Estimating Photosynthetically Available Radiation (PAR) at the Earth's surface from satellite observations p 230 N94-10955

Comparison of the distribution of large magmatic centers on Earth, Venus, and Mars p 467 N94-12192

Giant radiating dyke swarms on Earth and Venus p 283 N94-12236
A comparison of the visible and near infrared reflectance of hydrovolcanic palagonite tuffs and Martian weathered soils p 477 N94-12245

EARTH TIDES
High biological production of the tidal mixing zones on Japan Sea shelf p 228 N94-12758

EARTH-MOON SYSTEM
The giant impact produced a precipitated Moon p 430 N94-12135
Preliminary report of lunar observations by the Near-Infrared Mapping Spectrometer (NIMS) during the second Galileo Earth-Moon encounter p 425 N94-12140

EARTHQUAKES
Autonomous self contained bottom pop-up stations for study of the benthic layer and seismicity of the ocean's bottom p 224 N94-12735

ECHO SOUNDING
Measurement of the surface layer current averaged vertically using Multipaths Inverted Echosounder p 194 N94-11915
Acoustic characteristics of side scan sonar and sub-bottom profiler for 10,000 m class ROV p 172 N94-11916
Acoustic estimation of plankton biomass p 218 N94-12699

ECHOCARDIOGRAPHY
Proceedings of the First Joint NASA Cardiopulmonary Workshop [NASA-CP-10068] p 308 N94-11991
Echocardiography in the flight program p 309 N94-11993

ECOLOGY
Porosity and the ecology of icy satellites p 431 N94-12186

ECONOMIC ANALYSIS
Department of Energy solar process heat program: FY 1991 solar process heat prefeasibility studies activity [DE93-010010] p 262 N94-10258
Survey to determine the value of DYNA [DE93-012390] p 321 N94-10267
Life-cycle cost analysis of conventional and fuel cell/battery powered urban passenger vehicles [DE93-010770] p 182 N94-11438
Analysis of the economics of DC arc CVD diamond [AD-A265688] p 403 N94-12339
Role of remote sensing and its cost effectiveness in site selection for coastal aquaculture p 217 N94-12697

ECONOMIC FACTORS
Gulf of Mexico sales 147 and 150: Central and western planning areas. Draft environmental impact statement. Volume 1: Sections 1 through 4.C [PB93-190304] p 265 N94-11018
Gulf of Mexico sales 147 and 150: Central and western planning areas. Draft environmental impact statement. Volume 2: Sections 4.D through 9 [PB93-190312] p 265 N94-11019
Landsat as a commercial enterprise [INPE-5477-TAE/019] p 232 N94-11524
Role of remote sensing and its cost effectiveness in site selection for coastal aquaculture p 217 N94-12697

ECONOMIC IMPACT
Renewable energy sources 1991, part 3 [DE93-605594] p 263 N94-11505
Renewable energy sources 1991, part 2 [DE93-605634] p 263 N94-11506
Evaluation of the capacity and delay benefits of terminal air traffic control automation [AD-A265323] p 24 N94-11863

ECONOMICS
Vehicular fleet operation on natural gas and propane: An overview [PB93-194603] p 98 N94-10844

ECOSYSTEMS
Environmental Sciences Division [DE93-013865] p 264 N94-10650
Extended ecosystem signatures with application to Eos synergism requirements [NASA-CR-193398] p 266 N94-11374
Energy flow in an Arctic aquatic ecosystem [DE93-013178] p 267 N94-11697
TREES project: A case study on the use of multi-temporal ERS-1 SAR data and SPOT data for monitoring tropical ecosystems p 249 N94-12497
TREES project: Overview and status of the ERS-1 SAR contribution p 250 N94-12499

EDDY CURRENTS
Quantifying disbond area p 61 N94-10038

EDDY VISCOSITY
A Galilean and tensorial invariant k-epsilon model for near wall turbulence [NASA-TM-106263] p 151 N94-11192
A local dynamic model for large eddy simulation p 155 N94-12285
A normal stress subgrid-scale eddy viscosity model in large eddy simulation p 155 N94-12288
The helical decomposition and the instability assumption p 158 N94-12306

EDEMA
Local fluid shifts and edema in humans during simulated microgravity p 311 N94-12003

EDGE DETECTION
Delineation of mesoscale features of ocean on satellite IR image p 214 N94-12675
Observation of warm current at the boundary from north equatorial current to Kuroshio by NOAA/AVHRR p 214 N94-12676
Frontal zones in Pacific Ocean: Satellite and ship data analysis p 216 N94-12687
Observation of cold coastal water with high turbidity around the southwestern tip of Korean Peninsula p 216 N94-12689
Variability of the Kuroshio observed from satellite thermal imagery p 221 N94-12717
The method of investigation of the horizontal structure of the thermal fronts p 222 N94-12723
On a nonstationary dynamics of the north-west Pacific Ocean p 222 N94-12724
The Pacific Subarctic Frontal Zone: Structure and dynamics p 223 N94-12731
Influence of the Kuroshio warm-core rings on hydrographic and fishery conditions off southern Kuril Islands p 224 N94-12737
Variability of spectral reflectance in coastal waters near the river plumes p 226 N94-12744

EDGE DISLOCATIONS
A method of influence regions in the theory of vacancy swelling of metals [DE93-620579] p 83 N94-11363

EDGES
Boundary integral solution to the electromagnetic scattering from coated surfaces containing edges, gaps, and periodic gratings p 137 N94-11639

EDUCATION
Space program in Indonesia p 36 N94-10681
Overview of training seminar for the use of Japanese Earth Resources Satellite-1 (JERS-1) data p 190 N94-11083
Large project experiences with object-oriented methods and reuse p 329 N94-11431
Department of Energy fundamentals handbook: Engineering symbology, prints, and drawings [DE93-012181] p 129 N94-11456
A summer program in mathematics and computer science for academically oriented student [AD-A263467] p 415 N94-11517
Project TIMS (Teaching Integrated Math/Science) [NASA-CR-194288] p 416 N94-11599
Tropical medicine: Telecommunications and technology transfer p 305 N94-11793
The revitalization of health and education in Rural America Act of 1992 p 308 N94-11810
Career Information in the Mathematical Sciences (CIMS) [DE93-013780] p 318 N94-11817
The requirement for global training programmes to meet the new remote sensing technology p 196 N94-11929
Marslink p 438 N94-12034

EFFICIENCY
Force and power efficiency of micro-g electromagnetic levitation coils p 110 N94-10129

EFFLUENTS
Study on diffusion phenomena of river effluents issued into sea around Japan with satellite remote sensing data p 212 N94-12664

EFFUSIVES
Vulcanian explosive eruptions: A mechanism for localised pyroclast dispersal on Venus p 477 N94-12243

EIGENVALUES
Boundary element method for eigenvalue problems of thin plates [ITN-93-85199] p 343 N94-10392
Bound states of the N-dimensional Klein-Gordon equation with vector and scalar Coulomb potentials [DE93-617650] p 349 N94-10547
An exactly solvable model of an oscillator with nonlinear coupling and zeros of Bessel functions p 349 N94-10573
Nonunitary and unitary approach to Eigenvalue problem of Boson operators and squeezed coherent states p 350 N94-10595
Floquet operator as integral of motion p 380 N94-10610
Creation and annihilation of solitons in nonlinear integrable systems [DE93-621379] p 365 N94-11078
A regional inverse eigenvalue problem: Solution with application in control theory [DE93-619666] p 339 N94-11630

EIGENVECTORS
Disturbance, the uncertainty principle and quantum optics p 375 N94-10569
Harmonic oscillator interaction with squeezed radiation p 376 N94-10571
An exactly solvable model of an oscillator with nonlinear coupling and zeros of Bessel functions p 349 N94-10573
Geometric aspects of uncertainty and correlation p 349 N94-10588
Nonunitary and unitary approach to Eigenvalue problem of Boson operators and squeezed coherent states p 350 N94-10595

EINSTEIN EQUATIONS
Dimensional transition of the space-time at the minimum action near the planck scale [DE93-754192] p 410 N94-10718
Explorations in quantum gravity: From one loop effective actions to two-dimensional theories p 413 N94-11822

EJECTA
Descriptions and preliminary interpretations of cores recovered from the Manson Impact Structure (Iowa) p 281 N94-12032
Ejecting basaltic achondrites from Vesta: Hydrodynamical impact models p 429 N94-12036
Behavior of vortices generated by an advancing ejecta curtain in theory, in the laboratory, and on Mars p 169 N94-12044
Estimation of age of Dali-Ganis rifting and associated volcanic activity, Venus p 440 N94-12046
Arroyo el Mimbral, Mexico, K/T unit: Origin as debris flow/turbidite, not a tsunami deposit p 281 N94-12084
K/T spherules from Haiti and Wyoming: Origin, diagenesis, and similarity to some microtektites p 281 N94-12085
A two-stage (turbulent-drainage) mechanism for the emplacement of impact crater outflows on Venus p 458 N94-12145
Fractal dimensions of rampart impact craters on Mars p 460 N94-12154
Post-impact alteration of the Manson impact structure p 282 N94-12188
Projectile-target mixing in melted ejecta formed during a hypervelocity impact cratering event p 432 N94-12241
Laboratory studies on the velocity of fragments from impact disruptions p 189 N94-12359

EJECTION
Vulcanian explosive eruptions: A mechanism for localised pyroclast dispersal on Venus p 477 N94-12243

EL NINO
The 1992 El Nino viewed by ERS-1 altimetry p 244 N94-11784
Current structures in the western equatorial Pacific during JAPACS cruises p 193 N94-11911
Principal oscillation pattern analysis of sea level variations in the tropical Pacific measured by the GEOSAT altimeter p 209 N94-12646

ELASTIC DEFORMATION
Elastic deformations and sound in anisotrope superconductors near critical temperature [DE93-620636] p 188 N94-11364

ELASTIC PROPERTIES
Potential change in flaw geometry during pressurized-thermal-shock transients [DE93-009709] p 184 N94-10288
Development of bioelastic materials for the prevention of adhesions: Polypenta- and polytetrapeptides [AD-A264851] p 88 N94-10863
Low-expansion ceramics initiative [DE93-011860] p 89 N94-11106
Elastic deformations and sound in anisotrope superconductors near critical temperature [DE93-620636] p 188 N94-11364
Ceramic technology project database [DE93-012432] p 91 N94-11673
Ceramic actuators for smart materials [AD-A265664] p 93 N94-12331
Analytical models for describing the mechanical behavior of fiber reinforced composites [AD-A265906] p 74 N94-12347

ELASTIC SCATTERING
Workshop on NN Bremsstrahlung and Polarization Observables [DE93-010181] p 361 N94-10334
Indication on the existence of the bound state in the p anti p-system [DE92-641575] p 361 N94-10532
Studies of P-matrix formalism on the basis of the potential description of two-particle interaction [DE93-617691] p 362 N94-10550

Crossing-odd spin effects in the dipole model of hadron scattering
[DE93-617692] p 362 N94-10551
Logarithmically rising cross section and the ratio sigma(sub el)/sigma(sub t)
[DE93-617694] p 362 N94-10553
Detecting the odderon
[DE93-617695] p 362 N94-10554
Fine structure of the Pomeron and the real part of the elastic scattering amplitude
[DE93-617696] p 362 N94-10555
The determination of nucleon-nucleon scattering phases by the phase functions method
[DE93-617729] p 362 N94-10557
Phasing operator for two oscillators in classical field
p 370 N94-10579
Structural and electronic properties of atomic chains
[DE93-617758] p 366 N94-11349

ELASTIC WAVES
Evaluation of dual flow thrust vectored nozzles with exhaust stream impingement
[NASA-CR-193292] p 150 N94-10912

ELASTODYNAMICS
Boundary element method for eigenvalue problems of thin plates
[ITN-93-85199] p 343 N94-10392
Response of composite laminates to dynamic surface loads p 66 N94-10902

ELASTOMERS
Development of bioelastic materials for the prevention of adhesions: Polypenta- and polytetrapeptides
[AD-A264851] p 88 N94-10863
Radiation-induced modifications of allylamino-substituted polyphosphazenes
[AD-A264914] p 92 N94-11848

ELASTOPLASTICITY
Computational procedures for determining parameters in Ramberg-Osgood elastoplastic model based on modulus and damping versus strain
[DE93-013309] p 185 N94-10306
Elastic plastic fracture mechanics methodology for surface cracks
[NASA-CR-194129] p 185 N94-10712

ELECTRIC BATTERIES
Solid state ionics 3. Materials Research Society Symposium Proceedings, volume 293
[AD-A265675] p 395 N94-10416
Electromechanical batteries and the electric locomotive
[DE93-013311] p 142 N94-11009
Life-cycle cost analysis of conventional and fuel cell/battery powered urban passenger vehicles
[DE93-010770] p 182 N94-11438
Research development and demonstration of a fuel cell/battery powered bus system
[DE93-013778] p 182 N94-12605
Low cost high efficiency GaAs monolithic RF module for SARSAT distress beacons
[NASA-CR-194235] p 146 N94-12773

ELECTRIC CHARGE
Macroscopic electric charge separation during hypervelocity impacts: Potential implications for planetary paleomagnetism p 431 N94-12181

ELECTRIC CONDUCTORS
High-field conductor testing at the FENIX facility
[DE93-012318] p 387 N94-10737

ELECTRIC CONNECTORS
Optoelectronic technology consortium
[AD-A265691] p 383 N94-12444

ELECTRIC CURRENT
Nonlinear MHD-waves in a dissipative plasma with hall currents
[DE93-617844] p 386 N94-10395
Stationary spectra in a magnetized current-carrying plasma
[DE93-617847] p 386 N94-10397
Stationary spectra in a finite-pressure current-carrying plasma
[DE93-617848] p 387 N94-10538
Stationary spectra in a quasi neutral current-carrying plasma
[DE93-617849] p 387 N94-10539
A thermal ionization model for the sustaining phase of lock-on in GaAs
[DE93-011558] p 144 N94-11624

ELECTRIC DISCHARGES
Analysis of geophysical measurements and spacecraft interactions
[AD-A266064] p 43 N94-10944

ELECTRIC FIELDS
Dielectric liquid bridge stabilization in microgravity by means of electric fields p 100 N94-10075
Two-phase flow heat transfer and hydrodynamics in an electric field p 103 N94-10093
Gravity and electric field effects on pool boiling heat transfer p 121 N94-10226
Electron runaway in RF discharges
[DE93-771407] p 363 N94-10661
Power losses of a type 2 superconducting slab of arbitrary thickness in the presence of alternating current conductors
[DE93-617892] p 396 N94-10716
Large amplitude shape oscillations in a mercury drop using a drop tower
[DE93-767972] p 125 N94-10730
Distribution of charged particles near the plasma boundary in the presence of external electric field
[DE93-617862] p 389 N94-10886
Nonlinear excitation in quasi-one-dimensional Peierls dielectrics with charge density waves
[DE93-613827] p 398 N94-11025
Linear antenna of an arbitrary orientation and position in cylindric screen
[DE93-621353] p 134 N94-11035
A picosecond high pressure gas switch
[DE93-011897] p 142 N94-11050
Particle transport analysis in torsatron configurations
[DE93-621640] p 390 N94-11120
Gyrosheath near the tokamak edge
[DE93-012191] p 390 N94-11142
Performance characteristics of the INS 25.5-MHz split coaxial RFQ
[DE93-753168] p 144 N94-11508

ELECTRIC GENERATORS
Lightweight linear alternators with and without capacitive tuning
[NASA-CR-185273] p 140 N94-10505

ELECTRIC HYBRID VEHICLES
Research development and demonstration of a fuel cell/battery powered bus system
[DE93-013778] p 182 N94-12605

ELECTRIC MOTOR VEHICLES
Electromechanical batteries and the electric locomotive
[DE93-013311] p 142 N94-11009
Electric and hybrid vehicle site operators program: Thinking of the future
[DE93-011231] p 144 N94-11609
Polymer electrolyte fuel cells: Potential transportation and stationary applications
[DE93-010734] p 264 N94-11666
Research development and demonstration of a fuel cell/battery powered bus system
[DE93-013778] p 182 N94-12605

ELECTRIC NETWORKS
ENSAFE fireset flex circuit analysis
[DE93-013106] p 144 N94-11478

ELECTRIC POTENTIAL
Effect of effective mass differences on the tunneling current-voltage behaviour of a resonant diode in the presence of space charge build-up
[DE93-613817] p 142 N94-10799
A picosecond high pressure gas switch
[DE93-011897] p 142 N94-11050
Pulsed plasma processing for control of diesel engine emissions
[DE93-011884] p 181 N94-11247
Experimental proof of the new IR-induced mechanism of crevice corrosion and its consequences regarding protection schemes p 83 N94-11316
New experimental techniques for solar cells
p 52 N94-11403
High frequency behavior of long and small junctions
[AD-A265670] p 403 N94-12336
Spatial light modulator having photosensitive and ferroelectric layers
[AD-D015731] p 404 N94-12400
Ion shaking in the 200 MeV XLS-ring
[DE93-014057] p 374 N94-12782

ELECTRIC POWER PLANTS
Applicability of satellite infrared data for the monitoring of coastal environments p 220 N94-12714

ELECTRIC PROPULSION
A soft-start circuit for arcjet ignition
[NASA-TM-106287] p 180 N94-10760

ELECTRIC PULSES
Characterization of the pulse transformer
[AD-A263414] p 143 N94-11298

ELECTRIC SPARKS
Inexpensive capillary discharge x-ray laser driver
[AD-A265932] p 176 N94-12382

ELECTRIC WELDING
Welding tritium aged stainless steel
[DE93-011782] p 181 N94-11228

ELECTRIC WIRE
Specification and testing for power by wire aircraft
[NASA-TM-106232] p 46 N94-10765

ELECTRICAL FAULTS
Assessment of the impact of HTSC's on superconducting fault-current limiters
[DE93-009986] p 143 N94-11454
Crystallinity and dielectric properties of PEEK, a thermoplastic poly(ether ether ketone)
[AD-A266027] p 91 N94-11487
Dielectric breakdown and its influence on ignition
[AD-A264925] p 78 N94-11855

ELECTRICAL IMPEDANCE
Design of a matching network for dipole antennas
[AD-A265115] p 136 N94-11158
Polar mesospheric waves and structure
[AD-A265360] p 279 N94-12561

ELECTRICAL INSULATION
Development and analysis of insulation constructions for aerospace wiring applications p 21 N94-10791
Crystallinity and dielectric properties of PEEK, a thermoplastic poly(ether ether ketone)
[AD-A266027] p 91 N94-11487
Potential techniques for non-destructive evaluation of cable materials
[DE93-008350] p 183 N94-11586

ELECTRICAL MEASUREMENT
Amperometric biosensors based on 3-dimensional hydrogel-forming epoxy networks
[AD-A265528] p 87 N94-10510
Experimental proof of the new IR-induced mechanism of crevice corrosion and its consequences regarding protection schemes p 83 N94-11316

ELECTRICAL PROPERTIES
Experimental measurement of the plasma conductivity of Z93 and Z93P thermal control paint
[NASA-TM-106284] p 43 N94-10756
Crystallinity and dielectric properties of PEEK, a thermoplastic poly(ether ether ketone)
[AD-A266027] p 91 N94-11487
Synthesis and electronic properties of nanophase semiconductor materials
[AD-A265287] p 146 N94-12584

ELECTRICAL RESISTIVITY
Kinetics of high concentration arsenic deactivation at moderate to low temperatures
[DE93-013349] p 395 N94-10516
A survey of techniques for corrosion monitoring
[DE93-012131] p 83 N94-11250
Corrosion and passivation of high temperature superconductors
[AD-A265402] p 405 N94-12586
Resistivity and radar void detectors for tunneling machines p 140 N94-12706

ELECTRICITY
US areal wind resource assessment
[DE93-011905] p 262 N94-11051

ELECTRO-OPTICS
Controlling chaotic behavior in CO2 and other lasers
[AD-A264811] p 174 N94-10870
An electro-optical system for the measurement of strains p 186 N94-10900
Some results with the new digital ionosonde in San Diego
[AD-A265178] p 275 N94-11101
An optoelectronic graphics display processor
[AD-A266011] p 171 N94-12391
Optoelectronic technology consortium
[AD-A265691] p 383 N94-12444
Preparation of stable photopatternable polymeric materials for non-linear optics
[AD-A265359] p 95 N94-12577

ELECTROACOUSTIC TRANSDUCERS
NRL review for 1993
[AD-A265666] p 497 N94-12334

ELECTROCHEMICAL CELLS
Effects of aqueous solution compositions on Aerocapacitor energy density
[DE93-013431] p 140 N94-10309

ELECTROCHEMICAL CORROSION
Experimental proof of the new IR-induced mechanism of crevice corrosion and its consequences regarding protection schemes p 83 N94-11316
Corrosion behavior of metal matrix composites
[AD-A265352] p 85 N94-12404

ELECTROCHEMISTRY
Electrochemical process and product therefrom
[AD-D015767] p 75 N94-10380
Aluminum and membrane channels
[AD-A265241] p 300 N94-11020
A survey of techniques for corrosion monitoring
[DE93-012131] p 83 N94-11250
X ray absorption spectroscopy of electrochemically generated species
[AD-A264749] p 77 N94-11265
Electrochemical characterization of p(+)n and n(+)p diffused InP structures p 49 N94-11385
Real-space formation and dissipation dynamics of hexagonal reconstruction on Au(100) in aqueous media as explored by potentiodynamic scanning tunneling microscopy
[AD-A266138] p 368 N94-11658

Publications/Patents/Presentations/Honors/Student eport
[AD-A265136] p 78 N94-11873

ELECTRODE MATERIALS
Aluminum based alkaline battery
[AD-D015775] p 140 N94-10390
Thin film preparation and interfacial reaction study of solid oxide fuel cell materials p 263 N94-11313

ELECTRODEPOSITION
Plating under reduced pressure
[DE93-011896] p 84 N94-11668
The effects of organic adsorbates on the underpotential deposition of silver on Pt(111) electrodes
[AD-A265623] p 404 N94-12376
Synthesis and electronic properties of nanophase semiconductor materials
[AD-A265287] p 146 N94-12584
Corrosion and passivation of high temperature superconductors
[AD-A265402] p 405 N94-12586

ELECTRODES
Time-resolved optical studies of charge relaxation and charge transfer at electrode interfaces
[DE93-013985] p 398 N94-11117
Low energy electron diffraction and cyclic voltammetry studies of flame-annealed platinum single crystals
[AD-A263566] p 401 N94-11518
The laser ablation of gold films at the electrode surface of a quartz crystal microbalance
[AD-A265535] p 175 N94-12012
A vibrational spectroscopic study of the structure of electroactive self-assembled monolayers of viologen derivatives
[AD-A265705] p 78 N94-12273
Ceramic actuators for smart materials
[AD-A265664] p 93 N94-12331
Examination of the surface second harmonic response at infrared wavelengths
[AD-A265206] p 403 N94-12371
The effects of organic adsorbates on the underpotential deposition of silver on Pt(111) electrodes
[AD-A265623] p 404 N94-12376
Glucose electrodes based on cross-linked (Os(bpy)2Cl)(sup +/2+) complexed poly(1-vinylimidazole) films
[AD-A265404] p 94 N94-12425
Ion shaking in the 200 MeV XLS-ring
[DE93-014057] p 374 N94-12782

ELECTROENCEPHALOGRAPHY
Quantitative EEG patterns of differential in-flight workload p 317 N94-11528

ELECTROHYDRODYNAMICS
Dielectric liquid bridge stabilization in microgravity by means of electric fields p 100 N94-10075
Electrohydrodynamic effects in continuous flow electrophoresis observations on Earth and in microgravity p 122 N94-10234

ELECTROLESS DEPOSITION
Plating under reduced pressure
[DE93-011896] p 84 N94-11668
Corrosion and passivation of high temperature superconductors
[AD-A265402] p 405 N94-12586

ELECTROLYTE METABOLISM
Hormonal regulation of fluid and electrolyte metabolism in zero-g and bedrest p 311 N94-12004
Hormonal regulation of fluid and electrolyte metabolism during periods of headward fluid shifts
p 311 N94-12005

ELECTROLYTES
Solid state ionics 3. Materials Research Society Symposium Proceedings, volume 293
[AD-A265675] p 395 N94-10416
Particle attraction effects on the centrifugal casting and extrusion of alumina
[DE93-011559] p 82 N94-10957
A combustion products analyzer for contingency use during thermodegradation events on spacecraft
p 318 N94-11555
Finite element simulation of the 2D collapse of a polyelectrolyte gel disk
[DE93-010693] p 91 N94-11665
Hormonal regulation of fluid and electrolyte metabolism in zero-g and bedrest p 311 N94-12004
Nonlinear optical spectroscopy of Ag(111) in electrolyte and in vacuum
[AD-A265622] p 79 N94-12534

ELECTROLYTIC CELLS
Technical Update: Johnson Space Center system using a solid electrolytic cell in a remote location to measure oxygen fugacities in CO/CO2 controlled-atmosphere furnaces
[NASA-TM-104774] p 423 N94-11183
Polymer electrolyte fuel cells: Potential transportation and stationary applications
[DE93-010734] p 264 N94-11666

ELECTROMAGNETIC ABSORPTION
Radiation defect production in InAs crystals under electron irradiation
[DE93-617202] p 397 N94-10845
Thermographic properties of eight blue-emitting phosphors
[DE93-011459] p 78 N94-11622

ELECTROMAGNETIC COMPATIBILITY
An investigation of conducted and radiated emissions from a hollow-cathode plasma contactor
[NASA-CR-191172] p 386 N94-10346

ELECTROMAGNETIC COUPLING
On the coupling of electromagnetic radiation into cavities
[DE93-011406] p 137 N94-11621
Initial assessment of lower hybrid current drive in D3-D
[DE93-013310] p 394 N94-12370

ELECTROMAGNETIC FIELDS
Force and power efficiency of micro-g electromagnetic levitation coils p 110 N94-10129
Multiple Antenna Implementation System (MAntIS)
[DE93-012515] p 131 N94-10270
Wave function collapse: An unnecessary condition for the dynamical description of the Zeno and partial Zeno effect
[DE93-612970] p 132 N94-10401
Smoothly deformed light p 375 N94-10566
Non classical effects in planar waveguides
p 376 N94-10574
Nonperturbative methods in the problem of multiphoton excitation of atom by squeezed light
p 376 N94-10575
Phasing operator for two oscillators in classical field
p 370 N94-10579
Wigner functions for nonclassical states of a collection of two-level atoms p 379 N94-10603
Quantum processes in resonators with moving walls
p 380 N94-10612
Kinetic approach to long wave length modes in rotating plasmas
[DE93-771286] p 388 N94-10807
The heat transfer by radiation between two media
[DE93-617820] p 149 N94-10838
The Langevin's approach to the statistical theory of bounded plasma
[DE93-617842] p 388 N94-10839
Kinetic effects in stochastic topologically nontrivial field
[DE93-621642] p 391 N94-11207
Simple kinetic model for plasma in stochastic helical field
[DE93-621643] p 391 N94-11208
Elementary mechanism of electron beam dissipative instability development
[DE93-621653] p 391 N94-11209
On the coupling of electromagnetic radiation into cavities
[DE93-011406] p 137 N94-11621
Pilot trial of potentiating normal healing of stress fractures using pulsing electromagnetic fields
[AD-A264251] p 311 N94-12364

ELECTROMAGNETIC INTERACTIONS
Effective action in the gauged Nambu-Jona-Lasinio model
[DE93-617654] p 409 N94-10405
Future high precision experiments and new physics beyond Standard Model
[DE93-011004] p 373 N94-11618

ELECTROMAGNETIC INTERFERENCE
An investigation of conducted and radiated emissions from a hollow-cathode plasma contactor
[NASA-CR-191172] p 386 N94-10346
Specification and testing for power by wire aircraft
[NASA-TM-106232] p 46 N94-10765
Performance of traffic-alert collision avoidance (TCAS) antennas in the presence of scatterers
[NASA-CR-193569] p 23 N94-11525

ELECTROMAGNETIC NOISE
Nonlinear resonance: Noise-assisted information processing in physical and neurophysiological systems
[AD-A265161] p 313 N94-11890

ELECTROMAGNETIC PROPULSION
Investigation of multiphase railgun systems
p 40 N94-11637

ELECTROMAGNETIC PULSES
One-dimensional calculation of high-power microwave pulse compression by the earth's ionosphere
[DE93-009517] p 137 N94-11466
Research on acoustic coupling to electromagnetic pulses in tissue
[AD-A264764] p 301 N94-11583

ELECTROMAGNETIC RADIATION
Nonlinear second harmonic generation by light wave-plasma interaction in oscillating magnetic field
[DE93-613723] p 386 N94-10387
General renormalized statistical approach with finite cross-field correlations
[DE93-617846] p 386 N94-10396
Characterization of high-power RF structures using time-domain field codes
[DE93-013416] p 132 N94-10518
Harmonic oscillator interaction with squeezed radiation
p 376 N94-10571
Phasing operator for two oscillators in classical field
p 370 N94-10579
The Langevin's approach to the statistical theory of bounded plasma
[DE93-617842] p 388 N94-10839
Non-linear dynamics of automodulation processes in coupled distributed autovibration systems with delay
[DE93-620976] p 143 N94-11365
On the coupling of electromagnetic radiation into cavities
[DE93-011406] p 137 N94-11621
On the theory of phonoriton in cubic semiconductors with a degenerate valence band
[DE93-613539] p 402 N94-11660

ELECTROMAGNETIC SCATTERING
Investigation of passive atmospheric sounding using millimeter and submillimeter wavelength channels
[NASA-CR-193627] p 274 N94-10726
Performance of traffic-alert collision avoidance (TCAS) antennas in the presence of scatterers
[NASA-CR-193569] p 23 N94-11525
Boundary integral solution to the electromagnetic scattering from coated surfaces containing edges, gaps, and periodic gratings p 137 N94-11639
Interpretation of lunar and planetary electromagnetic scattering using the full wave solutions
p 440 N94-12049

ELECTROMAGNETIC SPECTRA
Stationary spectra in a plasma with a shear (renormalized statistical approach with non-zero eigenfrequencies)
[DE93-617851] p 386 N94-10523

ELECTROMAGNETIC WAVE TRANSMISSION
Some results with the new digital ionosonde in San Diego
[AD-A265178] p 275 N94-11101
Research on acoustic coupling to electromagnetic pulses in tissue
[AD-A264764] p 301 N94-11583

ELECTROMAGNETISM
New tests of the equivalence principle using non-metric couplings of electromagnetism and gravitation
p 413 N94-11821
Explorations in quantum gravity: From one loop effective actions to two-dimensional theories p 413 N94-11822

ELECTROMAGNETS
Application of parallel processing to a surface patch/wire junction EFIE code
[AD-A264965] p 336 N94-10488

ELECTROMECHANICS
Electromechanical batteries and the electric locomotive
[DE93-013311] p 142 N94-11009
Smart polymeric system for electromechanical transduction p 70 N94-11330
Recent developments in piezoelectric and electrostrictive sensors and actuators for smart structures p 70 N94-11332

ELECTRON ACCELERATORS
Research results
[DE93-753403] p 372 N94-11595

ELECTRON AFFINITY
Photodetachment studies on few-electron atomic negative ions
[DE93-008474] p 358 N94-10154

ELECTRON BEAMS
The electron beam furnace: A new facility for materials science research p 109 N94-10126
Nonlinear space charge effect of bunched beam in linac
[DE93-612176] p 371 N94-10409
Collective acceleration of ions in near-anode plasma of a strong-current relativistic diode
[DE93-620977] p 387 N94-10541
Dynamics of ion acceleration in electron flux by a virtual cathode potential
[DE93-620978] p 371 N94-10542
On the stability of stationary regimes in a distributed autovibration system with external feedback
[DE93-620979] p 141 N94-10543
Diagnostic complex for the space-time analysis of energy and current of pulsed relativistic particles
[DE93-620980] p 362 N94-10649
The intra-atomic motion of bound electrons as a possible source of a systematic error in electron beam polarization measurements by means of a Moeller polarimeter
[DE93-620984] p 364 N94-10875

DILUTE: A code for studying beam evolution under RF noise
[DE93-011605] p 133 N94-10960
Simple kinetic model for plasma in stochastic helical field
[DE93-621643] p 391 N94-11208
Elementary mechanism of electron beam dissipative instability development
[DE93-621653] p 391 N94-11209
Experimental investigation of wake field excitation in plasma by a periodic succession of relativistic particle clots
[DE93-621655] p 391 N94-11211
Spreading of Bimodulated Ultra-relativistic Electron Beam (BUEB) in Atmospheric Plasma Channel (APCh)
[DE93-621658] p 392 N94-11213
Design of CCD camera system for use inside electron beam furnace
[DE93-009525] p 170 N94-11267
Non-linear dynamics of automodulation processes in coupled distributed autovibration systems with delay
[DE93-620976] p 143 N94-11365
LCLS optics: Selected technological issues and scientific opportunities
[DE93-010953] p 175 N94-11468
Research results
[DE93-753403] p 372 N94-11595
Low voltage electron beam lithography
[AD-A265358] p 145 N94-12405
Operational characteristics of a 100-mA, 2-MeV radio-frequency quadrupole
[DE93-014474] p 374 N94-12786

ELECTRON CAPTURE
Distorted-wave calculation of He(e,2e) including core-exchange
[DE93-610072] p 360 N94-10330
Bond distortion and electron trapping in charged C60
[DE93-613642] p 396 N94-10637

ELECTRON CYCLOTRON HEATING
Characterization of high-power RF structures using time-domain field codes
[DE93-013416] p 132 N94-10518

ELECTRON DENSITY (CONCENTRATION)
Radiowaves propagation through inhomogeneous interstellar plasma p 134 N94-11061
Interstellar scattering and the pulsar studies with space VLBI p 135 N94-11065
Some results with the new digital ionosonde in San Diego
[AD-A265178] p 275 N94-11101
Experimental investigation of wake field excitation in plasma by a periodic succession of relativistic particle clots
[DE93-621655] p 391 N94-11211
Demonstration designs for optical-field-ionized plasma x-ray lasers
[DE93-009227] p 175 N94-11266
Polar mesospheric waves and structure
[AD-A265360] p 279 N94-12561

ELECTRON DIFFRACTION
HRTEM in protein crystallography
[DE93-610322] p 395 N94-10406
Surface and near-surface atom imaging with photoelectron holography
[DE93-013197] p 169 N94-10526
Low energy electron diffraction and cyclic voltammetry studies of flame-annealed platinum single crystals
[AD-A263566] p 401 N94-11518
Mineralogy of chondritic interplanetary dust particle impact residues from LDEF p 80 N94-12045

ELECTRON DIFFUSION
Measurement of the minority carrier diffusion length and edge surface-recombination velocity in InP
p 49 N94-11388
Grain boundary creep in copper
[DE93-610974] p 84 N94-12361
Glucose electrodes based on cross-linked (Os(bpy)2Cl)(sup +/2+) complexed poly(1-vinylimidazole) films
[AD-A265404] p 94 N94-12425

ELECTRON DISTRIBUTION
Giotto data analysis: Electron plasma and heavy ion composition measurements at Comet Halley
[NASA-CR-193587] p 428 N94-12770

ELECTRON EMISSION
Submicrosecond, synchronizable x ray source
[AD-D015745] p 176 N94-12337

ELECTRON ENERGY
MHD simulation of deuterium-fiber-initiated Z-pinches with two-fluid effects
[DE93-012682] p 384 N94-10158
Limitation and suppression of hot electron fluctuations in submicron semiconductor structures
[DE93-613911] p 396 N94-10801
The influence of irradiation conditions, type, and concentration of impurities on radiation defects characteristics in indium antimonide under electron irradiation
[DE93-617201] p 397 N94-10843
Application of spin-sensitive electron spectroscopies to investigations of electronic and magnetic properties of solid surfaces and epitaxial systems
[DE93-015079] p 76 N94-10854
Electron temperature measurements of x ray laser plasmas
[DE93-011874] p 389 N94-11074
Experimental investigation of wake field excitation in plasma by a periodic succession of relativistic particle clots
[DE93-621655] p 391 N94-11211
Characteristics of ICR-produced peripheral plasma in the Uragan-3M torsatron
[DE93-621666] p 392 N94-11214
Short pulse lasers for generation of fields exceeding 100 MG
[DE93-013346] p 369 N94-11815

ELECTRON IMPACT
Integrated cross sections for the ionisation of atomic hydrogen by electron impact
[DE93-610179] p 359 N94-10311
Calculation of the total ionization cross section and spin asymmetry in electron-hydrogen scattering from threshold to 500 eV
[DE93-610180] p 359 N94-10312
Atomic and molecular data for H2O, CO and CO2 relevant to edge plasma impurities
[DE93-771423] p 387 N94-10662
Theoretical atomic physics for fusion
[DE93-013872] p 366 N94-11172
Compilation of excitation cross sections for He atoms by electron impact
[DE93-753246] p 367 N94-11580
Tandem mass spectrometric analysis of phosphate esters
[AD-A265483] p 78 N94-12009

ELECTRON IRRADIATION
The influence of irradiation conditions, type, and concentration of impurities on radiation defects characteristics in indium antimonide under electron irradiation
[DE93-617201] p 397 N94-10843
Radiation defect production in InAs crystals under electron irradiation
[DE93-617202] p 397 N94-10845
Radiation effects in Ga(0.47)In(0.53)As solar cells
p 52 N94-11404
UV testing of solar cells: Effects of antireflective coating, prior irradiation, and UV source p 53 N94-11408

ELECTRON MASS
Quantum non demolition measurement of cyclotron excitations in a Penning trap p 376 N94-10578

ELECTRON MICROSCOPES
Single-electron tunneling
[DE93-013337] p 396 N94-10648
Atomic-scale imaging of surfaces and interfaces. Materials Research Society Symposium Proceedings, volume 295
[AD-A265674] p 369 N94-12379

ELECTRON MICROSCOPY
TEM study of a space processed Al-Al2O3 metallic composite p 75 N94-10186
Microanalysis of directionally solidified cobalt oxide-zirconia eutectic
[DE93-013207] p 88 N94-10527
Single-electron tunneling
[DE93-013337] p 396 N94-10648

ELECTRON MOBILITY
Short pulse lasers for generation of fields exceeding 100 MG
[DE93-013346] p 369 N94-11815

ELECTRON PHONON INTERACTIONS
Confinement of acoustical modes due to the electron-phonon interaction within 2D-electron gas
[DE93-613910] p 396 N94-10800

ELECTRON PLASMA
Dispersion of plasma waves in a finite magnetic field (omega(sub H) greater than omega(sub p))
[DE93-621654] p 391 N94-11210
Giotto data analysis: Electron plasma and heavy ion composition measurements at Comet Halley
[NASA-CR-193587] p 428 N94-12770

ELECTRON PRECIPITATION
A new data collection system for ionospheric modelling and related topics
[AD-A265893] p 278 N94-12277

ELECTRON RADIATION
Molecular properties of polymeric materials for space applications
[NASA-CR-194370] p 94 N94-12450

ELECTRON SCATTERING
Calculation of the total ionization cross section and spin asymmetry in electron-hydrogen scattering from threshold to 500 eV
[DE93-610180] p 359 N94-10312
Convergent close-coupling calculations of electron-hydrogen scattering
[DE93-610049] p 360 N94-10328
Calculation of spin-dependent observables in electron-sodium scattering using the coupled-channel optical method
[DE93-610050] p 360 N94-10329
Distorted-wave calculation of He(e,2e) including core-exchange
[DE93-610072] p 360 N94-10330
Spin-dependent observables in electron-sodium scattering calculated using the coupled-channel optical method
[DE93-610073] p 360 N94-10331
Monte Carlo algorithms in simulation of 2beta-decay and penetration of electrons through matter
[DE93-617741] p 364 N94-10837
Interstellar scattering and the pulsar studies with space VLBI p 135 N94-11065
Theoretical atomic physics for fusion
[DE93-013872] p 366 N94-11172
Structural and electronic properties of atomic chains
[DE93-617758] p 366 N94-11349

ELECTRON SOURCES
Thin-film edge field emitter device and method of manufacture therefore
[AD-D015764] p 140 N94-10377
Atomic-scale imaging of surfaces and interfaces. Materials Research Society Symposium Proceedings, volume 295
[AD-A265674] p 369 N94-12379

ELECTRON SPECTROSCOPY
Satellite structure of the xenon valence shell by electron momentum spectroscopy
[DE93-609993] p 360 N94-10327
Electron momentum spectroscopy of atoms, molecules and solids
[DE93-610148] p 360 N94-10332
Recent advances in electron momentum spectroscopy
[DE93-610149] p 361 N94-10333
Microanalysis of directionally solidified cobalt oxide-zirconia eutectic
[DE93-013207] p 88 N94-10527
Application of spin-sensitive electron spectroscopies to investigations of electronic and magnetic properties of solid surfaces and epitaxial systems
[DE93-015079] p 76 N94-10854
Corrosion control by vitreous films on aluminum and high T(sub c) superconductors
[AD-A266016] p 85 N94-12393
Coordinated Radio, Electron, and Waves Experiment (CREWE) for the NASA Comet Rendezvous and Asteroid Flyby (CRAF) instrument
[NASA-CR-194376] p 427 N94-12566

ELECTRON SPIN
Calculation of the total ionization cross section and spin asymmetry in electron-hydrogen scattering from threshold to 500 eV
[DE93-610180] p 359 N94-10312
Calculation of spin-dependent observables in electron-sodium scattering using the coupled-channel optical method
[DE93-610050] p 360 N94-10329
Spin-dependent observables in electron-sodium scattering calculated using the coupled-channel optical method
[DE93-610073] p 360 N94-10331

ELECTRON STATES
Electron momentum spectroscopy of atoms, molecules and solids
[DE93-610148] p 360 N94-10332
Bond distortion and electron trapping in charged C60
[DE93-613642] p 396 N94-10637
Electronic excitation of ground state atoms by collision with heavy gas particles
[NASA-CR-193364] p 366 N94-11360

ELECTRON TRANSFER
Bond distortion and electron trapping in charged C60
[DE93-613642] p 396 N94-10637
Polar solvation and electron transfer
[DE93-013328] p 365 N94-11010
Ballistic electron transport studies using BEEM
[AD-A266029] p 369 N94-12395
Solvent dynamical effects in electron transfer: Molecular dynamics simulations of reactions in methanol
[AD-A266061] p 369 N94-12420

ELECTRON TRANSITIONS
Squeezed states of electrons and transitions of the density of states p 370 N94-10593

ELECTRON TUNNELING
Single-electron tunneling
[DE93-013337] p 396 N94-10648
Characterization of the Si/SiO2 interfere morphology from quantum oscillations in Fowler-Nordheim tunneling currents
[AD-A265149] p 143 N94-11160
High frequency behavior of long and small junctions
[AD-A265670] p 403 N94-12336
ELECTRON-POSITRON PAIRS
Proceedings of the Second KEK Topical Conference on e(sup +)e(sup -) collision physics
[DE93-754139] p 364 N94-10889
ELECTRONIC COUNTERMEASURES
The radar eye blinded: The USAF and electronic warfare, 1945-1955
[AD-A265494] p 132 N94-10497
ELECTRONIC EQUIPMENT
Extensions of some guidelines for the mechanical design of coaxial compression pin seals
[DE93-012385] p 177 N94-10348
The radar eye blinded: The USAF and electronic warfare, 1945-1955
[AD-A265494] p 132 N94-10497
Proton transport methods for satellite shield modeling
[DE93-013602] p 42 N94-10520
Application of normalized gray-scale correlation
[DE93-013765] p 141 N94-10521
Liquid Cooled Heat Sink with through Vias (LCHS)
[AD-A266008] p 73 N94-12344
ELECTRONIC MODULES
Low cost high efficiency GaAs monolithic RF module for SARSAT distress beacons
[NASA-CR-194235] p 146 N94-12773
ELECTRONIC PACKAGING
RF vacuum microelectronics
[AD-A266066] p 142 N94-10818
ELECTRONIC WARFARE
The radar eye blinded: The USAF and electronic warfare, 1945-1955
[AD-A265494] p 132 N94-10497
ELECTRONS
Dynamics of ion acceleration in electron flux by a virtual cathode potential
[DE93-620978] p 371 N94-10542
Electron runaway in RF discharges
[DE93-771407] p 363 N94-10661
Application of spin-sensitive electron spectroscopies to investigations of electronic and magnetic properties of solid surfaces and epitaxial systems
[DE93-015079] p 76 N94-10854
The intra-atomic motion of bound electrons as a possible source of a systematic error in electron beam polarization measurements by means of a Moeller polarimeter
[DE93-620984] p 364 N94-10875
The response of an electron in a biased double well to a strong laser: Delocalization and low frequency generation
[AD-A265169] p 366 N94-11100
Absorption spectrum calculations using mixed quantum-gaussian wave packet dynamics
[AD-A265179] p 413 N94-11877
ELECTROPHORESIS
Electrohydrodynamic effects in continuous flow electrophoresis observations on Earth and in microgravity p 122 N94-10234
Compatibility tests for biological specimens to on-board experiments in the Space Shuttle flight
[NASDA-CNT-930003] p 301 N94-12278
ELECTROPHYSIOLOGY
Role of spatially distributed ion channels in single neuron computation
[AD-A265972] p 79 N94-12351
The organization of the suprachiasmatic circadian pacemaker of the rat and its regulation by neurotransmitters and modulators
[AD-A266113] p 301 N94-12417
ELECTROPLATING
Tin whiskers in electronic circuits
[AD-A265917] p 146 N94-12565
ELECTROSTATIC WAVES
Studies on the parametric decay of waves in fusion plasmas
[DE93-621659] p 390 N94-11148
Studies of electrostatic waves and VLF-wave particle interaction in the ionosphere
[AD-A266013] p 278 N94-12392
ELECTROSTATICS
NASCAP programmer's reference manual
[NASA-CR-191044] p 278 N94-11702
Dielectric breakdown and its influence on ignition
[AD-A264925] p 78 N94-11855
ELECTROSTRICTION
Ceramic actuators for smart materials
[AD-A265664] p 93 N94-12331
ELEMENTARY EXCITATIONS
Highly anisotropic but nodeless gap from a valence-fluctuation pairing mechanism
[DE93-010738] p 401 N94-11646
On the theory of phonoriton in cubic semiconductors with a degenerate valence band
[DE93-613539] p 402 N94-11660
ELEMENTARY PARTICLE INTERACTIONS
Development of deterministic transport methods for low energy neutrons for shielding in space
[NASA-CR-194172] p 366 N94-11199
ELEMENTARY PARTICLES
Searches for strangelets and other exotics at the AGS
[DE93-013341] p 359 N94-10308
Quasi-relativistic effects in barrier-penetration processes
[DE93-617730] p 410 N94-10721
Theory of elementary particles and accelerator theory. Task C: Experimental high energy physics
[DE93-013139] p 368 N94-11696
Elementary particle physics and high energy phenomena
[DE93-013971] p 370 N94-12609
ELEVATION
Relation between ages and elevations of Martian channels p 472 N94-12216
ELEVATION ANGLE
ERS-1 preliminary antenna elevation pattern measured by ground-receivers p 235 N94-11727
ELLIPSOIDS
On the Sobolev systems with ellipsoid cavities
[DE92-641290] p 148 N94-10530
The effect of pressure and quadrupolar interactions on the nematic-isotropic transition properties: Numerical results for a system of prolate ellipsoids including second and fourth rank orientational order parameters
[DE93-613540] p 410 N94-10536
ELLIPSOMETERS
Ellipsometry studies of semiconductors surface cleaning
[AD-A265150] p 142 N94-11094
ELLIPSOMETRY
Ellipsometry studies of semiconductors surface cleaning
[AD-A265150] p 142 N94-11094
Applications of spectroscopic ellipsometry to microelectronics
[AD-A265148] p 143 N94-11159
An ellipsometry investigation of nucleation and growth of electron cyclotron resonance plasma deposited silicon films
[AD-A265037] p 401 N94-11651
Applications of in-situ ellipsometry to microwave electron cyclotron resonance plasma processes
[AD-A265197] p 373 N94-11880
ELLIPTICAL GALAXIES
The controlling parameters of the integrated flux of a stellar population p 426 N94-11187
ELONGATION
A method for determination of the elongational viscosity of viscoelastic fluids without body forces
p 124 N94-10247
EMBEDDING
Factors affecting the embedding of optical fibre sensors in advanced composite structures p 70 N94-11336
Carbon analyses of IDP's sectioned in sulfur and supported on beryllium films p 81 N94-12099
Pilot trial of potentiating normal healing of stress fractures using pulsing electromagnetic fields
[AD-A264251] p 311 N94-12364
EMBRITTLEMENT
Heavy-section steel technology program
[DE93-009222] p 184 N94-10155
Experimental studies of the structure of grain boundaries
[DE93-013979] p 402 N94-11700
EMERGENCIES
The National Disaster Medical System
p 307 N94-11801
International disaster research p 307 N94-11805
US-USSR telemedicine consultation spacebridge to Armenia and Ufa p 308 N94-11809
EMISSION
Methodologies for estimating air emissions from three non-traditional source categories: Oil spills, petroleum vessel loading and unloading, and cooling towers
[PB93-181592] p 266 N94-11471
Emissions of sulfur gases from wetlands
p 269 N94-12458
EMISSION SPECTRA
FFTSCAN: A program for spectral smoothing using Fourier transforms
[AD-A264921] p 278 N94-11852
Thermal-infrared emission spectroscopy of natural surfaces: Application to coated surfaces
p 81 N94-12156
Olivine-rich asteroids, pallasitic olivine and olivine-metal mixtures: Comparisons of reflectance spectra
p 431 N94-12171
Molecular properties of polymeric materials for space applications
[NASA-CR-194370] p 94 N94-12450
Emissions of sulfur gases from marine and freshwater wetlands of the Florida Everglades: Rates and extrapolation using remote sensing p 269 N94-12457
HEAO-1 analysis of Low Energy Detectors (LED)
[NASA-CR-194087] p 424 N94-12574
EMISSIVITY
Formulating infrared coatings for defence applications
[MRL-RR-1-93] p 90 N94-11302
Measurement of the sea surface emissivity
p 213 N94-12672
EMITTANCE
A new matrix for the ageless 21.6-keV Eu-151 nuclear gamma ray Moessbauer source
[DE93-009795] p 75 N94-10338
Experiments with energetic (mu)d and (mu)t emitted from solid hydrogen
[DE93-010252] p 373 N94-12542
EMITTERS
Thin-film edge field emitter device and method of manufacture therefore
[AD-D015764] p 140 N94-10377
High efficiency direct thermal to electric energy conversion from radioisotope decay using selective emitters and spectrally tuned solar cells
[NASA-TM-106227] p 47 N94-11307
ENAMELS
Ceramics technology project database
[DE93-012431] p 91 N94-11672
ENCAPSULATING
Marangoni and buoyant convections in zone melting of GaAs with liquid encapsulation p 101 N94-10081
ENCLOSURES
Effect of double density caging during Space Shuttle transport of laboratory rats
[NASA-CR-193228] p 300 N94-11180
END-TO-END DATA SYSTEMS
An integrated approach to total end-to-end quality control of ocean data in the real-time environment
p 211 N94-12662
ENERGETIC PARTICLES
Nonperturbative methods in HZE ion transport
[NASA-TP-3363] p 484 N94-10759
Effects of energetic particle events on VLF/LF propagation parameters/1989
[AD-A265266] p 275 N94-11013
Potential health effects of space radiation
p 312 N94-11558
Experiments with energetic (mu)d and (mu)t emitted from solid hydrogen
[DE93-010252] p 373 N94-12542
ENERGY ABSORPTION FILMS
PM technology and mechanical properties of metallic foams p 64 N94-10059
ENERGY BUDGETS
Energy flow in an Arctic aquatic ecosystem
[DE93-013178] p 267 N94-11697
An observational search for CO2 ice clouds on Mars
p 441 N94-12054
Proceedings of the PORSEC 1992 in Okinawa: Conference for Pacific Ocean Environments and Probing, volume 2
[JTN-93-80419] p 207 N94-12635
Surface eddy fluxes from the GEOSAT satellite altimeter p 208 N94-12643
The thermodynamics of the nonlinear shear flows
p 169 N94-12728
Turbulence generation in the Pacific undercurrent by shear p 223 N94-12730
ENERGY CONSERVATION
Exergy decrease in shock waves and boundary layers of space launch vehicles
[AD-A265272] p 42 N94-10493
Demonstration designs for optical-field-ionized plasma x-ray lasers
[DE93-009227] p 175 N94-11266
An estimate of the second law thermodynamic efficiency of the various units comprising an Environmental Control and Life Support System (ECLSS) p 317 N94-12369
ENERGY CONSUMPTION
The physics of pattern formation of liquid interfaces
[DE93-013333] p 154 N94-11814
Gallium arsenide dynamic random access memory support circuitry
[AD-A265176] p 320 N94-11875
ENERGY CONVERSION
Review of betavoltaic energy conversion
p 53 N94-11407
ENERGY CONVERSION EFFICIENCY
Polyimide based amorphous silicon solar modules
p 49 N94-11390

InGaAs concentrator cells for laser power converters and tandem cells p 50 N94-11394
The efficiency of photovoltaic cells exposed to pulsed laser light p 50 N94-11395
Response of silicon solar cell to pulsed laser illumination p 51 N94-11396
Approaches to solar cell design for pulsed laser power receivers p 51 N94-11397
Review of betavoltaic energy conversion p 53 N94-11407
Computation of photovoltaic parameters under lunar temperature variation p 53 N94-11411
NASDA activities in space solar power system research, development and applications p 54 N94-11413
Workshop summary: New silicon cells p 54 N94-11417
Measurement and modeling of the stability of hydrogenated amorphous silicon solar cells and films after intense illumination p 263 N94-11638

ENERGY DISSIPATION
Monte Carlo algorithms in simulation of 2beta-decay and penetration of electrons through matter [DE93-617741] p 364 N94-10837
Application of spin-sensitive electron spectroscopies to investigations of electronic and magnetic properties of solid surfaces and epitaxial systems [DE93-015079] p 76 N94-10854
Pulsed plasma processing for control of diesel engine emissions [DE93-011884] p 181 N94-11247
Probability density distribution of velocity differences at high Reynolds numbers p 158 N94-12304

ENERGY DISTRIBUTION
Monte Carlo algorithms in simulation of 2beta-decay and penetration of electrons through matter [DE93-617741] p 364 N94-10837

ENERGY GAPS (SOLID STATE)
Invariance of the mobility edge in anodic titanium oxides [DE92-642136] p 394 N94-10281
Review of betavoltaic energy conversion p 53 N94-11407
Computation of photovoltaic parameters under lunar temperature variation p 53 N94-11411
Multi-band gap and new solar cell options workshop p 54 N94-11418
Wide Band-Gap Semiconductors. 1991 Materials Rese arch Society Symposium proceedings [AD-A263418] p 401 N94-11515

ENERGY LEVELS
Harmonic oscillator interaction with squeezed radiation p 376 N94-10571
Floquet operator as integral of motion p 380 N94-10610
The intra-atomic motion of bound electrons as a possible source of a systematic error in electron beam polarization measurements by means of a Moeller polarimeter [DE93-620984] p 364 N94-10875
Interatomic interactions in BCC and FCC lattices of transition metals [DE93-621541] p 398 N94-11090
Nuclear structure models: Applications and development [DE93-012934] p 368 N94-11813

ENERGY METHODS
Summation by parts, projections, and stability [NASA-CR-194290] p 346 N94-12776

ENERGY OF FORMATION
Interatomic interactions in BCC and FCC lattices of transition metals [DE93-621541] p 398 N94-11090

ENERGY POLICY
Vehicular fleet operation on natural gas and propane: An overview [PB93-194603] p 98 N94-10844

ENERGY SOURCES
Renewable energy sources 1991, part 3 [DE93-605594] p 263 N94-11505

ENERGY SPECTRA
Optimization of a CO2 laser Thomson scattering alpha particle diagnostic [DE93-012782] p 173 N94-10160
Diagnostic complex for the space-time analysis of energy and current of pulsed relativistic particles [DE93-620980] p 362 N94-10649
Monochromator SP-017. The results of the first experiments [DE93-617463] p 372 N94-10849
Radiation considerations for interplanetary missions p 45 N94-11559
Analysis and interpretation of high energy cosmic rays measured on Spacelab-2 [NASA-CR-193586] p 485 N94-12771

ENERGY STORAGE
Effects of aqueous solution compositions on Aerocapacitor energy density [DE93-013431] p 140 N94-10309
A picosecond high pressure gas switch [DE93-011897] p 142 N94-11050
Computation of photovoltaic parameters under lunar temperature variation p 53 N94-11411

ENERGY TECHNOLOGY
High-energy density physics at Los Alamos [DE93-010271] p 371 N94-10260
Japan's Sunshine Project [DE93-767980] p 262 N94-10498
Technology transfer at Lawrence Berkeley Laboratory [DE93-010460] p 423 N94-11059
Low-expansion ceramics initiative [DE93-011860] p 89 N94-11106
Renewable energy sources 1991, part 3 [DE93-605594] p 263 N94-11505
Renewable energy sources 1991, part 2 [DE93-605634] p 263 N94-11506

ENERGY TRANSFER
Review of SHARC 2.0 O3 kinetics and spectroscopy [AD-A265481] p 274 N94-10496
Development of deterministic transport methods for low energy neutrons for shielding in space [NASA-CR-194172] p 366 N94-11199
Energy transfer dynamics and impact sensitivity [DE93-009551] p 98 N94-11269
Non-linear dynamics of automodulation processes in coupled distributed autovibration systems with delay [DE93-620976] p 143 N94-11365
The ideal Kolmogorov inertial range and constant p 158 N94-12305
The helical decomposition and the instability assumption p 158 N94-12306

ENGINE AIRFRAME INTEGRATION
A comparative study of full Navier-Stokes and Reduced Navier-Stokes analyses for separating flows within a diffusing inlet S-duct [NASA-TM-106250] p 39 N94-10764

ENGINE CONTROL
Preliminary supersonic flight test evaluation of performance seeking control [NASA-TM-4494] p 28 N94-11205
Application of controller partitioning optimization procedure to integrated flight/propulsion control design for a STOVL aircraft [NASA-TM-106265] p 30 N94-11251
Advanced control for airbreathing engines, volume 1: Pratt and Whitney [NASA-CR-189203] p 29 N94-12270
Advanced control for airbreathing engines, volume 2: General Electric aircraft engines [NASA-CR-189204] p 29 N94-12271
Advanced controls for airbreathing engines, volume 3: Allison gas turbine [NASA-CR-189205] p 29 N94-12272

ENGINE DESIGN
External combustion engine having a combustion expansion chamber [AD-D015761] p 178 N94-10375
Heat regenerative external combustion engine [AD-D015765] p 178 N94-10378
Arcjet space thrusters [NASA-CR-193191] p 46 N94-10700
Vehicular fleet operation on natural gas and propane: An overview [PB93-194603] p 98 N94-10844
A distributed version of the NASA Engine Performance Program [NASA-TM-106208] p 327 N94-11231
Advanced control for airbreathing engines, volume 2: General Electric aircraft engines [NASA-CR-189204] p 29 N94-12271
Advanced controls for airbreathing engines, volume 3: Allison gas turbine [NASA-CR-189205] p 29 N94-12272
Hot-gas-side heat transfer characteristics of subscale, plug-nozzle rocket calorimeter chamber [NASA-TP-3380] p 55 N94-12569

ENGINE INLETS
Numerical calculation of scramjet inlet flow [NAL-TR-1174T] p 27 N94-10370

ENGINE MONITORING INSTRUMENTS
Enhancements to the Engine Data Interpretation System (EDIS) [NASA-CR-192593] p 180 N94-10815

ENGINE PARTS
Probabilistic evaluation of uncertainties and risks in aerospace components [NASA-TM-105603] p 185 N94-10361
Instantaneous engine frictional torque: Its components and piston assembly friction [DE93-011639] p 182 N94-11625

ENGINE STARTERS
A soft-start circuit for arcjet ignition [NASA-TM-106287] p 180 N94-10760

ENGINE TESTS
Characterization of in-flight performance of ion propulsion systems [NASA-TM-106283] p 46 N94-10761
Preprints of the 13th Hydrogen Energy System Symposium [DE93-781115] p 99 N94-11444

ENGINEERING
Technology transfer at Lawrence Berkeley Laboratory [DE93-010460] p 423 N94-11059
Qualitative reasoning about the physical world [AD-A266117] p 340 N94-12537

ENGINEERING DRAWINGS
Department of Energy fundamentals handbook: Engineering symbology, prints, and drawings [DE93-012181] p 129 N94-11456
Department of Energy fundamentals handbook: Engineering symbology, prints, and drawings [DE93-012220] p 129 N94-11670

ENGINEERING MANAGEMENT
National Airspace System operational concept [DOT/FAA/SE-93/1] p 23 N94-10933
Engineering performance metrics [DE93-012084] p 128 N94-11028

ENGINEERS
NASA/DOD Aerospace Knowledge Diffusion Research Project. Report 17: A comparison of the technical communication practices of Dutch and US aerospace engineers and scientists [NASA-TM-108987] p 419 N94-11352

ENGLISH CHANNEL
SAR imaging of dynamical features in the English Channel p 234 N94-11721

ENGLISH LANGUAGE
Processing proper nouns in machine translation for English news [NHK-SERIAL-414] p 418 N94-10559

ENSTATITE
Anomalous REE patterns in unequilibrated enstatite chondrites: Evidence and implications p 431 N94-12191
Cathodoluminescence properties of components in enstatite chondrites p 432 N94-12206

ENTHALPY
The high enthalpy facilities HEG and TH 2 in Germany p 4 N94-10430
The upgrading of the arc heated wind tunnel of the DLR (LBK) with respect to its effects on the material testing p 4 N94-10432

ENTRAINMENT
Shear flow control of gas jets in liquids [AD-A264673] p 152 N94-11448

ENTROPY
Canonical operator formulation of nonequilibrium thermodynamics [DE93-613028] p 409 N94-10388
Exergy decrease in shock waves and boundary layers of space launch vehicles [AD-A265272] p 42 N94-10493
Quantum entropy and uncertainty for two-mode squeezed, coherent and intelligent spin states p 377 N94-10586
Information entrophy via Glauber's Q-representation p 378 N94-10592
Similarity of the leading contributions to the self-energy and the thermodynamics in two- and three-dimensional Fermi Liquids [DE93-012673] p 412 N94-11162
Necessary conditions for the optimality of variable rate residual vector quantizers [NASA-CR-193730] p 326 N94-11197
On cell entropy inequality for discontinuous Galerkin methods [NASA-CR-191493] p 345 N94-11280
Chaos, entropy, and reversibility: A simple example p 31 N94-11495
An estimate of the second law thermodynamic efficiency of the various units comprising an Environmental Control and Life Support System (ECLSS) p 317 N94-12369
ISAR motion compensation using the burst derivative measure as a focal quality indicator [AD-A265647] p 138 N94-12440
The thermodynamics of the nonlinear shear flows p 169 N94-12728

ENVIRONMENT EFFECTS
Environmental Protection Agency's life cycle methodology: Guidelines for use in development of packaging [PB93-194199] p 265 N94-10841
Gulf of Mexico sales 147 and 150: Central and western planning areas. Draft environmental impact statement. Volume 1: Sections 1 through 4.C [PB93-190304] p 265 N94-11018

Gulf of Mexico sales 147 and 150: Central and western planning areas. Draft environmental impact statement. Volume 2: Sections 4.D through 9 [PB93-190312] p 265 N94-11019

Renewable energy sources 1991, part 2 [DE93-605634] p 263 N94-11506

The use of remote sensing data for coastal zone management and environment in Indonesia p 196 N94-11927

Study of climatic effects of cloud-aerosol interaction p 204 N94-11977

Factors controlling fluxes of volatile sulfur compounds in Sphagnum peatlands p 268 N94-12456

Comments on possible causes of recent global warming [DE93-010501] p 272 N94-12592

ENVIRONMENT MANAGEMENT

International Space Year in China p 36 N94-10680

Intergovernmental decisionmaking for environmental protection and public works [PB93-176824] p 266 N94-11584

Remote sensing and global environment p 191 N94-11895

The requirement for global training programmes to meet the new remote sensing technology p 196 N94-11929

ENVIRONMENT MODELS

Design of a global soil moisture initialization procedure for the simple biosphere model [NASA-TM-104590] p 284 N94-10940

Extended ecosystem signatures with application to Eos synergism requirements [NASA-CR-193398] p 266 N94-11374

ENVIRONMENT POLLUTION

Presentations to the Mexican Physics Society on Environmental Contamination [DE93-009565] p 264 N94-10256

International Space Year in China p 36 N94-10680

Immediate response to free product discovery [PB93-182970] p 265 N94-11015

Evaluating the spread of red soil with LANDSAT TM data in coral reefs of Okinawa main island, southwestern Japan p 212 N94-12668

Information capability of NOAA-AVHRR data for monitoring oceanographic and atmospheric pollution p 214 N94-12677

ENVIRONMENT PROTECTION

Environmentally Safe and Effective Processes for Paint Removal [AGARD-R-791] p 126 N94-10613

Paint removal activities in the US Navy p 126 N94-10614

Procedures without danger to the environment and efficiency (PSDEE) for the removal of paint. Point on the French activities concerning the removal of paint p 126 N94-10616

Paint removal activities in Germany p 126 N94-10617

The development of alternative paint removal techniques in the RAF p 126 N94-10618

Health and safety issues for aerospace workers in the use of advanced materials p 21 N94-10795

Environmental Protection Agency's life cycle methodology: Guidelines for use in development of packaging [PB93-194199] p 265 N94-10841

Summary of implementation and demonstration projects in bays and estuaries [PB93-194637] p 265 N94-10846

Some environmental aspects of the application of fibre reinforced plastics in structures [LM-998] p 88 N94-10877

Immediate response to free product discovery [PB93-182970] p 265 N94-11015

Gulf of Mexico sales 147 and 150: Central and western planning areas. Draft environmental impact statement. Volume 1: Sections 1 through 4.C [PB93-190304] p 265 N94-11018

Gulf of Mexico sales 147 and 150: Central and western planning areas. Draft environmental impact statement. Volume 2: Sections 4.D through 9 [PB93-190312] p 265 N94-11019

Intergovernmental decisionmaking for environmental protection and public works [PB93-176824] p 266 N94-11584

ENVIRONMENT SIMULATION

Molecular properties of polymeric materials for space applications [NASA-CR-194370] p 94 N94-12450

ENVIRONMENTAL CHEMISTRY

Environmental factors controlling fluxes of dimethyl sulfide in a New Hampshire fen p 270 N94-12462

Sulfur transformations in the sediments of a New Hampshire salt marsh p 270 N94-12463

Quality assurance for environmental chemistry: 1991, volume 2 [DE93-011792] p 272 N94-12780

ENVIRONMENTAL CONTROL

Systems analysis of a closed loop ECLSS using the ASPEN simulation tool. Thermodynamic efficiency analysis of ECLSS components p 316 N94-12366

An estimate of the second law thermodynamic efficiency of the various units comprising an Environmental Control and Life Support System (ECLSS) p 317 N94-12369

ENVIRONMENTAL ENGINEERING

Technical Conference on Tropical Urban Climates: Extended Abstracts [WMO/TD-538] p 283 N94-10561

ENVIRONMENTAL MONITORING

Presentations to the Mexican Physics Society on Environmental Contamination [DE93-009565] p 264 N94-10256

Space Activities in the Asia Pacific Region [JTN-93-80421] p 35 N94-10676

Current status of space activities in Asia Pacific region p 35 N94-10677

Space research and remote sensing programmes in Bangladesh p 35 N94-10679

International Space Year in China p 36 N94-10680

National space programmes and application of the remote sensing data in Mongolia p 36 N94-10686

Status of remote sensing and Geographic Information System (GIS) applications in the Environment and Natural Resources (ENR) sector p 36 N94-10687

Russian space system for the Earth remote sensing p 37 N94-10688

Sun-synchronous and geo-synchronous satellite data utilization for environmental studies p 37 N94-10689

Thailand ISY activities p 37 N94-10690

Panel discussion: Role of space program in the Asia Pacific Region p 37 N94-10694

An environmental study of the National Aerospace Plane [AD-A266071] p 25 N94-10945

Statistical analysis of environmental variability within the CELSS breadboard project's biomass production chamber [NASA-TM-109188] p 315 N94-11258

Remote surface water monitoring radio based telemetry system [DE93-009643] p 41 N94-11282

Biscayne bay: A bibliography of the marine environment [PB93-184802] p 266 N94-11451

Operational radiological support for the US manned space program p 318 N94-11561

Satellite, environmental, and medical information applied to epidemiological monitoring p 307 N94-11802

Data management strategy for the Tampa Bay National Estuary Program: Recommendations and implementation plan [PB93-191633] p 267 N94-11864

Remote sensing and global environment p 191 N94-11895

An algorithm for the detection of mucilage (green slime) in the Adriatic Sea p 191 N94-11900

Remote sensing of the suspended matter distribution with high concentration in China Sea p 192 N94-11901

The requirement for global training programmes to meet the new remote sensing technology p 196 N94-11929

A study of pollution courses of spilled oil floatation in the outer ocean p 205 N94-11983

Terminal Decomposition and Gaseous Sulfur Release from Tidal Wetlands [NASA-CR-193466] p 267 N94-12451

Proceedings of 1st ERS-1 Symposium on Space at the Service of Our Environment, Volume 2 [ESA-SP-359-VOL-2] p 245 N94-12471

Monitoring of snowcover in high mountain terrain with ERS-1 SAR p 247 N94-12482

Geoecological monitoring of an agricultural area p 248 N94-12489

The TREES project: Pre-processing and generation of terrain data for inclusion in an ERS-1 SAR classification scheme p 249 N94-12496

TREES project: A case study on the use of multi-temporal ERS-1 SAR data and SPOT data for monitoring tropical ecosystems p 249 N94-12497

TREES project: A suite of tools for information extraction from ERS-1 SAR data p 250 N94-12498

TREES project: Overview and status of the ERS-1 SAR contribution p 250 N94-12499

A user appraisal of ATSR near-real-time products p 252 N94-12516

ERS-1 imaging radar over the Waddensea-North Netherlands p 254 N94-12526

Applications of ERS-1 SAR data for analyzing riverine and coastal processes and geomorphology p 254 N94-12528

Evaluating the spread of red soil with LANDSAT TM data in coral reefs of Okinawa main island, southwestern Japan p 212 N94-12668

Information capability of NOAA-AVHRR data for monitoring oceanographic and atmospheric pollution p 214 N94-12677

Development of a buoy system for monitoring marine weather and marine life abundance p 217 N94-12694

Remote sensing of polluting focal points and coastal disturbances in the Gulf of Arauco and adjacent bays, central Chile p 217 N94-12695

Applicability of satellite infrared data for the monitoring of coastal environments p 220 N94-12714

DISTERM: A shipboard data system for satellite monitoring of ocean and atmosphere p 226 N94-12749

Laser fluorescent monitoring of dissolved organic matter in natural water p 177 N94-12755

Ecological application of Surface Enhanced Raman Spectroscopy p 227 N94-12756

ENVIRONMENTAL SURVEYS

An environmental study of the National Aerospace Plane [AD-A266071] p 25 N94-10945

Gulf of Mexico sales 147 and 150: Central and western planning areas. Draft environmental impact statement. Volume 1: Sections 1 through 4.C [PB93-190304] p 265 N94-11018

Gulf of Mexico sales 147 and 150: Central and western planning areas. Draft environmental impact statement. Volume 2: Sections 4.D through 9 [PB93-190312] p 265 N94-11019

ENVIRONMENTAL TESTS

Investigation of the radiation resistance of triple-junction a-Si:H alloy solar cells irradiated with 1.00 MeV protons p 50 N94-11391

Results of some initial space qualification testing on triple junction a-Si and CuInSe2 thin film solar cells p 50 N94-11392

An overview of the Defence Research Agency photovoltaic programme p 53 N94-11412

Factors controlling fluxes of volatile sulfur compounds in Sphagnum peatlands p 268 N94-12456

ENZYMES

A lattice gas model for enzyme kinetics with alternate interactions [DE93-613027] p 395 N94-10411

Amperometric biosensors based on 3-dimensional hydrogel-forming epoxy networks [AD-A265528] p 87 N94-10510

A lattice gas model for enzyme kinetics with next-nearest neighbor interactions [DE93-613026] p 410 N94-10631

Studies in bioorganic chemistry [AD-A265532] p 55 N94-12011

Glucose electrodes based on cross-linked (Os(bpy)2Cl)(sup +/2+) complexed poly(1-vinylimidazole) films [AD-A265404] p 94 N94-12425

EPHEMERIDES

Analysis of geophysical measurements and spacecraft interactions [AD-A266064] p 43 N94-10944

Precision GPS ephemerides and baselines [NASA-CR-194171] p 23 N94-11177

EPHEMERIS TIME

PTTI-aided ephemeris calculation and rapid data link acquisition for manned space flight p 42 N94-10974

EPIDEMIOLOGY

Baseline characteristics of different strata of astronaut corps p 312 N94-11552

Satellite, environmental, and medical information applied to epidemiological monitoring p 307 N94-11802

EPITAXY

Heteroepitaxial InP, and ultrathin, directly glassed, GaAs 3-5 solar cells p 52 N94-11406

Workshop on Heteroepitaxial InP Solar Cells p 54 N94-11414

Lattice-matched heteroepitaxy of wide gap ternary compound semiconductors p 400 N94-11441

Progress toward atomic layer epitaxy of diamond: Diamond films grown one layer at a time [AD-A265530] p 403 N94-12010

EPOXY COMPOUNDS

Amperometric biosensors based on 3-dimensional hydrogel-forming epoxy networks [AD-A265528] p 87 N94-10510

EPOXY MATRIX COMPOSITES

Application of the infrared photoacoustic spectroscopy to the study of the cure mechanisms of structural epoxy adhesives p 61 N94-10040

Strain measurement of carbon/epoxy composite with fibre optics white light quasi distributed polarimetric sensor p 69 N94-11328

Strain concentration assessment of laminates subjected to low velocity impact [AD-A264497] p 73 N94-11446

Property changes induced by the space environment in composite materials on LDEF: Solar array materials passive LDEF experiment A0171 (SAMPLE)
[NASA-CR-192572] p 73 N94-11484

EPOXY RESINS

Application of the infrared photoacoustic spectroscopy to the study of the cure mechanisms of structural epoxy adhesives p 61 N94-10040

Amperometric biosensors based on 3-dimensional hydrogel-forming epoxy networks
[AD-A265528] p 87 N94-10510

EQUATIONS OF MOTION

Stationary spectra in a quasi neutral current-carrying plasma
[DE93-617849] p 387 N94-10539

Floquet operator as integral of motion
p 380 N94-10610

Generalized spin systems and sigma-models
[DE93-613981] p 410 N94-10802

Trajectory pattern inverse dynamics and control of nonlinear dynamics systems with application to flexible structures p 181 N94-11219

On possible applications of smart structures to control of space systems p 45 N94-11342

A molecular dynamics simulation code ISIS
[DE93-753187] p 368 N94-11592

Nonlinear analysis of a magnicon output cavity
[AD-A265342] p 145 N94-12424

Improvement of method for experimental determination of flutter speed by parameter identification
[NASA-CR-193555] p 33 N94-12769

EQUATIONS OF STATE

Monte Carlo simulations of a two-dimensional hard dimer system
[DE93-613535] p 361 N94-10502

Polymer-polymer interactions
[AD-A265304] p 91 N94-11830

EQUATORIAL REGIONS

Current structures in the western equatorial Pacific during JAPACS cruises p 193 N94-11911

Roles of the NEC and MC in the formation and evolution of the Equatorial Pacific Warm Pool p 206 N94-11990

Automatic definition of spectral units in the equatorial regions of Mars p 432 N94-12234

EQUIPMENT SPECIFICATIONS

Scientific specifications for an automated facility for growing large semiconducting crystals from the melt in space p 114 N94-10180

Head and face anthropometry of adult US civilians
[DOT/FAA/AM-93/10] p 315 N94-10806

An interferometric spectral mapper for the Cassini mission to Saturn and Titan
[NASA-CR-193805] p 482 N94-12429

Coordinated Radio, Electron, and Waves Experiment (CREWE) for the NASA Comet Rendezvous and Asteroid Flyby (CRAF) instrument
[NASA-CR-194376] p 427 N94-12566

EROSION

Weld overlay coatings for erosion control
[DE93-013592] p 84 N94-11816

Rates of fluvio-thermal erosion on Mars
p 435 N94-12018

Horizontal stresses induced by vertical processes in planetary lithospheres p 281 N94-12042

The origin of Venusian channels: Modelling of thermal erosion by lava p 456 N94-12131

ERROR ANALYSIS

Particle image velocimetry technique: Calibration tests
p 111 N94-10137

Topex orbit determination using GPS tracking system
p 38 N94-10359

Investigation of soft errors in MOS RAM under influence of heavy ions
[DE92-644554] p 484 N94-10534

An investigation of error characteristics and coding performance
[NASA-CR-193620] p 324 N94-10932

Pre-operation analysis of ERS-1 tracking and operation, part 2-F
[NASDA-CNT-930002-PT-2-F] p 230 N94-11130

Model reference adaptive control (MRAC) with applications to robotics p 339 N94-11640

Theory and oceanographic applications of satellite altimeter measurements p 208 N94-12641

Analysis of collinear passes of satellite altimeter data
p 208 N94-12642

Preliminary results from a satellite altimetric data assimilation using a Kalman filter and smoother
p 209 N94-12648

On the error characteristics of the sea surface temperature observed by satellite p 216 N94-12690

ERROR CORRECTING CODES

Task planning with uncertainty for robotic systems
[NASA-CR-193253] p 338 N94-10638

Development of a Delaunay-based adaption scheme with applications to complex three-dimensional rotational flows p 149 N94-10624

Measurement methods and algorithms for comparison of local and remote clocks p 354 N94-10987

ERROR CORRECTING DEVICES

Flexible high-speed CODEC
[NASA-CR-191169] p 146 N94-12433

ERROR SIGNALS

Airborne optical tracking control system design study
[DE93-009515] p 382 N94-11662

ERRORS

AMIP: The Atmospheric Model Intercomparison Project
[DE93-007400] p 273 N94-10151

AMIP: The Atmospheric Model Intercomparison Project
[DE93-007413] p 273 N94-10152

The intra-atomic motion of bound electrons as a possible source of a systematic error in electron beam polarization measurements by means of a Moeller polarimeter
[DE93-620984] p 364 N94-10875

A recent Cleanroom success story: The Redwing project p 39 N94-11433

Analyzing human errors in flight mission operations
p 314 N94-11534

Vigilance problems in orbiter processing
p 314 N94-11536

Removal of orbital error and the local geoid effects from ERS-1 altimeter data p 242 N94-11770

Theory and oceanographic applications of satellite altimeter measurements p 208 N94-12641

Analysis of collinear passes of satellite altimeter data
p 208 N94-12642

ERS-1 (ESA SATELLITE)

Proceedings of First ERS-1 Symposium on Space at the Service of Our Environment, volume 1
[ESA-SP-359-VOL-1] p 232 N94-11704

Sea ice: A climate component p 232 N94-11705

Calibration and validation of the ERS-1 wind scatterometer p 232 N94-11706

Validation of directional wave spectra from the ERS-1 during the ESA CAL/VAL campaign p 232 N94-11707

The Grand Banks ERS-1 SAR wave spectra validation experiment p 232 N94-11708

ERS-1 scatterometer data characteristics and wind retrieval skill p 233 N94-11709

Validation of ERS-1 wind and wave data by use of operational forecast models p 233 N94-11710

A C-band wind scatterometer model derived from the data obtained during the ERS-1 calibration/validation campaign p 233 N94-11711

ERS-1 studies at the Department of Oceanography from Space, IFREMER/Brest (France) p 233 N94-11712

The activity of the ERS-1 Venice (Italy) group on scatterometry p 233 N94-11713

Use of ERS-1 data at Saclant Undersea Research Centre p 233 N94-11714

A preliminary C-band scatterometer model function for the ERS-1 AMI instrument p 233 N94-11715

Calibration of ERS-1 altimetry over the North Sea
p 234 N94-11716

Mapping of the East Australian current with the ERS-1 SAR and shipborne studies p 234 N94-11717

Wind and surface features in SAR images: The Canadian program p 234 N94-11718

Preliminary analysis of circulations over the Indian Ocean and adjoining regions using ERS-1 surface winds in the NCMRWF data assimilation system p 234 N94-11719

Coastal ocean studies with ERS-1 SAR during NORCSEX 1991 p 234 N94-11720

SAR imaging of dynamical features in the English Channel p 234 N94-11721

Effects of wave nonlinearity on ERS-1 radar altimeter returns: A preliminary investigation p 235 N94-11722

SAR ocean imaging in the Gulf of Alaska
p 235 N94-11723

Evaluation of two January - June 1992 ERS-1 AMI wind vector data sets p 235 N94-11724

Comparisons of ERS-1 altimeter height data and the Fine Resolution Antarctic Model (FRAM)
p 235 N94-11725

ERS-1 SAR calibration strategy p 235 N94-11726

ERS-1 preliminary antenna elevation pattern measured by ground-receivers p 235 N94-11727

Preliminary results of the experiment I-7
p 235 N94-11728

The ERS-1/CV 580 SAR cross-calibration experiment: Sault Ste Marie, October 26 - November 2, 1991
p 236 N94-11729

Calibration of the ERS-1 SAR fast-delivery images
p 236 N94-11730

Calibration results for the ERS-1, AIRSAR, and PHARS p 236 N94-11731

The use of active devices in the ERS-1 radiometric calibration p 236 N94-11732

An experiment for the radiometric calibration of the ERS-1 SAR p 236 N94-11733

Techniques and applications of SAR interferometry for ERS-1: Topographic mapping, change detection, and slope measurement p 236 N94-11734

SAR interferometry experiments with ERS-1
p 237 N94-11735

SAR-interferometry applying ERS-1: Some preliminary test results p 237 N94-11736

Signatures of Antarctic firn by means of ERS-1 AMI and by field measurements p 237 N94-11737

Analysis of ERS-1 altimeter data over the polar ice sheets p 237 N94-11738

Some results of the derivation of ice sheet elevations in Antarctica from ERS-1 altimeter data
p 237 N94-11739

Utilisation of ERS-1 data for mapping of Antarctica
p 237 N94-11740

Monitoring of the Greenland Ice Sheet using ERS-1 synthetic aperture radar imagery p 237 N94-11741

Preliminary evaluation of ERS-1 altimetry over Filchner-Ronne Ice Shelf, Antarctica
p 238 N94-11742

Investigations of Arctic ice-sheets and glaciers using ERS-1 SAR p 238 N94-11743

Spatial patterns in backscatter strength across the Greenland Ice Sheet p 238 N94-11744

Ice studies in the Barents Sea by ERS-1 SAR during SIZEX 92 p 238 N94-11745

Experiences from the Swedish sea ice programme during BEERS-1992 p 239 N94-11751

Greenland Sea observations p 239 N94-11752

C-band SAR backscatter from ice on shallow tundra lakes: Observations and modelling p 240 N94-11755

The height calibration of the ERS-1 radar altimeter
p 241 N94-11764

Separation of geoid and sea surface topography in shallow water regions: A first ERS-1 radar altimeter data evaluation p 242 N94-11766

An analysis of the gravity field in the Norwegian Sea and mapping of the ice cap of Greenland using ERS-1 altimeter measurements p 242 N94-11768

Removal of orbital error and the local geoid effects from ERS-1 altimeter data p 242 N94-11770

ERS-1 precise orbits and altimetry analysis
p 242 N94-11771

ERS-1 radar altimetry over the North Atlantic
p 242 N94-11772

The effect of rain on ERS-1 altimeter data
p 243 N94-11773

Operational ERS-1 orbit determination at D-PAF
p 243 N94-11774

Preliminary geophysical investigation with ERS-1 35-day altimeter data p 243 N94-11775

Arctic geodynamics: Continental shelf and deep ocean geophysics. ERS-1 satellite altimetry: A first look
p 243 N94-11776

Quick-look monitoring of the sea surface with ERS-1 fast delivery altimeter data p 243 N94-11777

The Earth's gravity model for the ERS-1 commissioning phase p 243 N94-11778

ERS-1 precise orbit determination
p 244 N94-11779

Global wave height climatologies from ERS-1 altimeter data, and comparisons with those from GEOSAT
p 244 N94-11781

Latent and sensible heat flux estimated from ERS-1 data p 244 N94-11783

The 1992 El Nino viewed by ERS-1 altimetry
p 244 N94-11784

Using transponders with the ERS-1 altimeter to measure orbit altitude to +/- 3 cm p 244 N94-11785

Ocean circulation revealed by altimeter data
p 245 N94-11786

Proceedings of 1st ERS-1 Symposium on Space at the Service of Our Environment, Volume 2
[ESA-SP-359-VOL-2] p 245 N94-12471

Segmented land use classification of multitemporal ERS-1 SAR data using a majority filter
p 245 N94-12472

Land cover monitoring with multi-temporal ERS-1 SAR observations in the Netherlands p 246 N94-12473

Mapping a dynamic playa surface using multitemporal ERS-1 SAR data: First results p 246 N94-12474

ERS-1 altimetry of inland water and land
p 246 N94-12475

Preliminary studies on the application of ERS-1 data to topographic mapping p 246 N94-12476

Radarmap of Germany: First mosaic and classification
p 246 N94-12477

Combined analysis of ERS-1 SAR and visible/infrared remote sensing data for land cover/land use mapping in a tropical zone: A case study in Guinea
p 246 N94-12478

Example of SPOT/ERS-1 complementarity
p 247 N94-12479

The use of ERS-1 SAR data to study surface states p 247 N94-12480
Snow and glacier investigations by ERS-1 SAR: First results p 247 N94-12481
Monitoring of snowcover in high mountain terrain with ERS-1 SAR p 247 N94-12482
Application of ERS-1 SAR data to snow mapping p 247 N94-12483
Methodological considerations for use of ERS-1 imagery for the delineation of river networks in tropical forest areas p 247 N94-12484
Preliminary ERS-1 assessment for Canadian agriculture and forestry applications p 248 N94-12486
Segmentation and change detection in ERS-1 images over East Anglia p 248 N94-12487
ERS-1 SAR crop monitoring experiment in East Anglia, UK p 248 N94-12488
Geoecological monitoring of an agricultural area p 248 N94-12489
Integration of ERS-1 data into the European project of agriculture statistics p 248 N94-12490
Extraction of plant and soil parameters from multitemporal ERS-1 SLC data of the Freiburg test site p 248 N94-12491
Assessment of ERS-1 SAR data for soil moisture estimation p 249 N94-12492
Temporal monitoring of soil moisture using ERS-1 SAR data p 249 N94-12493
Observations of ERS-1 SAR sensitivities to changes in aboveground biomass in young loblolly pine forests p 249 N94-12494
Seeing the Black Forest by ERS-1 and AIRSAR: A comparison p 249 N94-12495
The TREES project: Pre-processing and generation of terrain data for inclusion in an ERS-1 SAR classification scheme p 249 N94-12496
TREES project: A case study on the use of multi-temporal ERS-1 SAR data and SPOT data for monitoring tropical ecosystems p 249 N94-12497
TREES project: A suite of tools for information extraction from ERS-1 SAR data p 250 N94-12498
TREES project: Overview and status of the ERS-1 SAR contribution p 250 N94-12499
Impact of ERS-1 wind/wave/ice data on operational ocean forecasting p 250 N94-12500
Use of ERS-1 wind and wave products in operational meteorology p 250 N94-12502
Validation of ATSR-1 using aircraft radiometer measurements over the South Atlantic p 252 N94-12515
A user appraisal of ATSR near-real-time products p 252 N94-12516
Cloud studies using ATSR data p 253 N94-12517
Preliminary validation of ATSR sea surface temperatures near the Faeroes p 253 N94-12519
Artificial oil pollution detection and wave observation in the sea adjacent to Japan by ERS-1 SAR p 253 N94-12520
Ship traffic monitoring using the ERS-1 SAR p 253 N94-12521
Pilot project PPF12. Coastal and fluvial environment in French Guiana: First results of ERS-1 SAR data analysis p 254 N94-12523
Coastal morphodynamics and energetic characteristics of swell studied with ERS-1 SAR p 254 N94-12524
Mapping of sea bottom topography with ERS-1 C-band SAR p 254 N94-12525
ERS-1 imaging radar over the Waddensea-North Netherlands p 254 N94-12526
Applications of ERS-1 SAR data for analyzing riverine and coastal processes and geomorphology p 254 N94-12528
Comparison of ERS-1 SAR images of the Western Mediterranean to in situ oceanographic data: PRIM-1 Cruise (May 1992) p 255 N94-12529
Regional orbit precision in the Mediterranean area p 39 N94-12530
Topography of the Western Mediterranean from the ERS-1 altimeter p 255 N94-12531

ESA SATELLITES
ESA/ESOC: 25 years
[ESA-BR-90] p 485 N94-11379

ESA SPACECRAFT
ESA/ESOC: 25 years
[ESA-BR-90] p 485 N94-11379

ESCARPMENTS
Shallow crustal discontinuities and graben and scarp formation in the Tharsis region of Mars p 469 N94-12203

ESSENTIALLY NON-OSCILLATORY SCHEMES
Large eddy simulation of shock turbulence interaction p 155 N94-12289
Computational methods for problems in aerodynamics using parallel and vector architectures
[AD-A265626] p 16 N94-12377

ESTERS
Tandem mass spectrometric analysis of phosphate esters
[AD-A265483] p 78 N94-12009

ESTIMATES
US areal wind resource assessment
[DE93-011905] p 262 N94-11051
Feature association without a motion estimate
[AD-A265162] p 138 N94-11891

ESTIMATING
Advances in time-scale algorithms p 334 N94-10988
Confidence of the three-point estimator of frequency drift p 357 N94-11003
Neural network model selection using asymptotic jackknife estimator and cross-validation method
[AD-A264960] p 339 N94-11289
Discrete Kalman filtering equations of second-order form for control-structure interaction simulations
[NASA-CR-193723] p 331 N94-11522
Estimation of solar radiation at the sea surface with geostationary meteorological satellite data p 196 N94-11926

ESTUARIES
Summary of implementation and demonstration projects in bays and estuaries
[PB93-194637] p 265 N94-10846
Biscayne bay: A bibliography of the marine environment
[PB93-184802] p 266 N94-11451
Data management strategy for the Tampa Bay National Estuary Program: Recommendations and implementation plan
[PB93-191633] p 267 N94-11864

ETALONS
Continued development of an ultra-narrow bandpass filter for solar research
[NASA-CR-194169] p 381 N94-10735

ETCHING
Electrochemical process and product therefrom
[AD-D015767] p 75 N94-10380
Dynamic studies of crystal growth using the AFM
[DE93-009549] p 399 N94-11268
Radiation-induced modifications of allylamino-substituted polyphosphazenes
[AD-A264914] p 92 N94-11848
Low voltage electron beam lithography
[AD-A265358] p 145 N94-12405

ETHERS
New aromatic activated dihalides and bisphenol monomers for the preparation of novel poly(arylene ethers)
[NASA-CR-193190] p 55 N94-10513
The properties of perfluoropolyethers used for space applications
[NASA-TM-106275] p 88 N94-10864
Thermal stability of sealants for military aircraft: Modification of polysulfide prepolymers with ether and thioether monomers
[AD-A264079] p 89 N94-11107

ETHYL COMPOUNDS
Thermal stability of sealants for military aircraft: Modification of polysulfide prepolymers with ether and thioether monomers
[AD-A264079] p 89 N94-11107

ETHYLENEDIAMINETETRAACETIC ACIDS
In situ secondary ion mass spectrometry analysis
[DE93-012185] p 76 N94-11140

ETIOLOGY
Transcranial Doppler ultrasound and the etiology of neurologic decompression sickness during altitude decompression p 312 N94-11544

EULER BUCKLING
Nonlinear response of a clamped-clamped beam with internal resonance under sinusoidal excitation p 186 N94-10897

EULER EQUATIONS OF MOTION
Hypersonic flow computations around re-entry vehicles p 9 N94-10461
A comparison of high resolution upwind solvers on 3-D inviscid hypersonic flows p 10 N94-10463
Development of an unstructured solution adaptive method for the quasi-three-dimensional Euler and Navier-Stokes equations
[NASA-CR-191161] p 28 N94-10816
An improved material interface reconstruction algorithm for Eulerian codes
[DE93-011679] p 326 N94-11226
Looking for O(N) Navier-Stokes solutions on non-structured meshes
[NASA-CR-191472] p 345 N94-11277
The modelling of aerodynamic flows by solution of the Euler equations on mixed polyhedral grids
[ARA-84] p 16 N94-11888

EULER-LAGRANGE EQUATION
Time evolution of cross-stream exchange associated with the variations in the Kuroshio p 197 N94-11936

EURECA (ESA)
Results of mission preparation support to microgravity experiments on board of Eureca 1 p 111 N94-10138

EUROPA
Theoretical studies of the radar properties of the icy Galilean moons of Jupiter
[NASA-CR-193407] p 434 N94-11361

EUROPE
Integration of ERS-1 data into the European project of agriculture statistics p 248 N94-12490

EUROPEAN AIRBUS
Future needs in the development of materials for aircraft interiors and equipment p 21 N94-10794

EUROPEAN SPACE AGENCY
Analysis of the cost evaluation of ESA programmes and comparable national and international programmes
[GTS-92063] p 416 N94-10145
ESA/ESOC: 25 years
[ESA-BR-90] p 485 N94-11379
Spain: Success story in space
[ESA-BR-81] p 38 N94-11461
ESRO's first scientific satellite programme, 1961 - 1966
[ESA-HSR-2] p 44 N94-11462
Mission to the Moon: An ESA study on future exploration p 460 N94-12153
ESA Costing Software (ECOS) introduction
[ESA-F-28] p 333 N94-12383

EUROPEAN SPACE PROGRAMS
ESA/ESOC: 25 years
[ESA-BR-90] p 485 N94-11379

EUROPIUM COMPOUNDS
A new matrix for the ageless 21.6-keV Eu-151 nuclear gamma ray Moessbauer source
[DE93-009795] p 75 N94-10338

EUTECTIC ALLOYS
Solidification of undercooled Ni-32.5 wt percent Sn eutectic alloy p 86 N94-10194
EUSO-D2-experiment: Unidirectional solidification with quenching of an AlSi11 alloy p 86 N94-10199

EUTECTICS
Microanalysis of directionally solidified cobalt oxide-zirconia eutectic
[DE93-013207] p 88 N94-10527

EUTROPHICATION
Characterization of dissolved organic matter in the ocean by using the fluorescence excitation-emission matrix p 211 N94-12659

EVALUATION
A surface water monitoring system: A device for the sea-truth observations p 210 N94-12657

EVAPORATION
Evaporation under microgravity conditions p 102 N94-10086
Single bubble experiments in pool boiling: Results from TEXUS 26 p 124 N94-10243
Evaporation and thermal/hydrologic balance in the Pacific p 195 N94-11919
Evaluation of ECMWF latent heat flux in TOGA CD-ROM p 195 N94-11921
Recondensation of chondritic material in the early solar system: Results of thermodynamic simulation p 432 N94-12226
Compilation of proposals for boiling and evaporation experiments in space environments and proposals concerning experiment projects p 161 N94-12549

EVAPORATION RATE
Marangoni instability induced convection in an evaporating liquid droplet p 104 N94-10094

EVAPORATIVE COOLING
Experimental study of multiple droplet evaporative cooling
[PB93-198463] p 149 N94-10851

EVAPORATORS
Theoretical evaluation of R22 and R502 alternatives
[DE93-014767] p 411 N94-10853
Ballistic electron transport studies using BEEM
[AD-A266029] p 369 N94-12395

EVAPOTRANSPIRATION
Design of a global soil moisture initialization procedure for the simple biosphere model
[NASA-TM-104590] p 284 N94-10940
Estimation of areal evapotranspiration using LANDSAT TM data: Kitami City, Hokkaido, Japan p 219 N94-12703

EVERGLADES (FL)
Emissions of sulfur gases from marine and freshwater wetlands of the Florida Everglades: Rates and extrapolation using remote sensing p 269 N94-12457

EXCIMER LASERS
Characterization of an excimer laser-ablated plasma and applications p 392 N94-11450

EXCIMERS
Dynamics of charge-transfer excited states relevant to photochemical energy conversion [DE93-013981] p 263 N94-11116
EXCITATION
Nonperturbative methods in the problem of multiphoton excitation of atom by squeezed light p 376 N94-10575
Quantum non demolition measurement of cyclotron excitations in a Penning trap p 376 N94-10578
Nonlinear excitation in quasi-one-dimensional Peierls dielectrics with charge density waves [DE93-613827] p 398 N94-11025
About excitation of round waveguide by a point current source [DE93-621352] p 133 N94-11034
Characterization of gas-aerosol interaction kinetics using morphology dependent stimulated Raman scattering [DE93-012324] p 77 N94-11359
Non-linear dynamics of automodulation processes in coupled distributed autovibration systems with delay [DE93-620976] p 143 N94-11365
EXCITONS
Dynamics of charge-transfer excited states relevant to photochemical energy conversion [DE93-013981] p 263 N94-11116
Femtosecond dynamics, photoexcitation, and ESR spectra of MX chain solids [AD-A264689] p 399 N94-11263
The additional contribution caused by Coulomb interaction to the exciton dispersion in multiple quantum wells and superlattices for direct band gap cubic semiconductors [DE93-613538] p 402 N94-11659
EXERCISE PHYSIOLOGY
Mechanistic studies on reduced exercise performance and cardiac deconditioning with simulated zero gravity p 310 N94-12001
Modifications to an interactive model of the human body during exercise: With special emphasis on thermoregulation p 317 N94-12368
EXHAUST EMISSION
Pulsed plasma processing for control of diesel engine emissions [DE93-011884] p 181 N94-11247
EXHAUST GASES
Evaluation of dual flow thrust vectored nozzles with exhaust stream impingement [NASA-CR-193292] p 150 N94-10912
Pulsed plasma processing for control of diesel engine emissions [DE93-011884] p 181 N94-11247
Results from the D3-D advanced divertor program [DE93-015472] p 393 N94-11514
Ultraviolet plume instrument description and plume data reduction methodology [AD-A266141] p 54 N94-11643
Stratospheric aircraft exhaust plume and wake chemistry [NASA-CR-191495] p 279 N94-12572
The 1991 version of the plume impingement computer program. Volume 2: User's input guide [NASA-CR-194191] p 166 N94-12774
EXOBIOLOGY
Aerospace medicine and biology: A continuing bibliography with indexes (supplement 375) [NASA-SP-7011(375)] p 303 N94-10398
Aerospace medicine and biology: A continuing bibliography with indexes (supplement 376) [NASA-SP-7011(376)] p 303 N94-10399
Aerospace medicine and biology: A continuing bibliography with indexes (supplement 374) [NASA-SP-7011(374)] p 304 N94-11689
Proceedings of the First Joint NASA Cardiopulmonary Workshop [NASA-CP-10068] p 308 N94-11991
EXPERIMENT DESIGN
Bubbles and drops behaviour under low-gravity: A space experiment for the IML-2 mission p 104 N94-10098
CdTe crystal growth by THM with a rotating magnetic field p 107 N94-10116
Microgravity Applications Furnace Facility (MAFF) for parabolic flights p 109 N94-10128
Microgravity experiments using TR-1A rocket p 112 N94-10142
Theoretical and Experimental Methods in Hypersonic Flows [AGARD-CP-514] p 2 N94-10421
A Recommended Methodology for Quantifying NDE/NDI Based on Aircraft Engine Experience [AGARD-LS-190] p 28 N94-11022
Gas-Grain Simulation Facility (GGSF). Volume 2: Conceptual design definition [NASA-CR-177613] p 423 N94-11229
Activities relating to understanding the initiation, organization and structure of moist convection in the Southeast environment [NASA-CR-193829] p 285 N94-11598
EXPERT SYSTEMS
Enhancements to the Engine Data Interpretation System (EDIS) [NASA-CR-192593] p 180 N94-10815
A tool for generation of expert system shells [INPE-5493-TDI/510] p 325 N94-11181
An expert system shell for inferring vegetation characteristics: Prototype help system (Task 1) [NASA-CR-193411] p 231 N94-11236
Toward intelligent flight control p 33 N94-11503
Design, development, and testing of an automated knowledge-acquisition tool to aid problem solving, decision making, and planning [DE93-010239] p 417 N94-11661
Linking medical records to an expert system p 306 N94-11797
Proceedings of the Seventh International Symposium on Methodologies for Intelligent Systems (poster session) [DE93-013470] p 340 N94-12428
EXPLOSIONS
Turbulent wall jet in blast wave precursor [DE93-011955] p 151 N94-11144
Vulcanian explosive eruptions: A mechanism for localised pyroclast dispersal on Venus p 477 N94-12243
Three-dimensional finite element analysis of explosive safety facilities: A technology assessment [AD-A265700] p 35 N94-12562
EXPLOSIVES
The solubility of epsilon-CL-20 in selected materials [DE93-009304] p 77 N94-11602
EXPONENTIAL FUNCTIONS
Convergence of exponentially convex functions on foundation semigroups [DE93-619665] p 342 N94-10325
EXPOSURE
Arterial gas emboli in altitude-induced decompression sickness p 312 N94-11543
Evaluation of medical treatments to increase survival of ebullism in guinea pigs p 302 N94-11548
Toxicity study of dimethylethoxysilane (DMSES), the waterproofing agent for the Orbiter heat protective system p 318 N94-11554
EXTERNAL COMBUSTION ENGINES
External combustion engine having a combustion expansion chamber [AD-D015761] p 178 N94-10375
Heat regenerative external combustion engine [AD-D015765] p 178 N94-10378
EXTERNAL TANKS
Debris/ice/TPS assessment and integrated photographic analysis for Shuttle Mission STS-57 [NASA-TM-107562] p 40 N94-10805
EXTINCTION
Shock induced reaction in Chicxulub target materials (CaSO4 and SiO2) and their relation to extinctions p 282 N94-12149
EXTRACTION
Production of electronic grade lunar silicon by disproportionation of silicon difluoride p 435 N94-12017
EXTRAGALACTIC RADIO SOURCES
Intraday variability and the compactness of extragalactic radio sources p 135 N94-11064
Interstellar scattering and the pulsar studies with space VLBI p 135 N94-11065
EXTRATERRESTRIAL ENVIRONMENTS
Vulcanian explosive eruptions: A mechanism for localised pyroclast dispersal on Venus p 477 N94-12243
EXTRATERRESTRIAL RADIATION
Longitudinal study of astronaut health: Mortality in the years 1959-1991 p 312 N94-11560
Operational radiological support for the US manned space program p 318 N94-11561
Coulomb effects in low-energy nuclear fragmentation [NASA-TP-3352] p 485 N94-12434
EXTRAVEHICULAR ACTIVITY
Allowable exposure limits for carbon dioxide during extravehicular activity [NASA-TM-103832] p 315 N94-11375
A mechanism for the reduction in risk of decompression sickness in microgravity environment p 312 N94-11545
Risk of decompression sickness in the presence of circulating microbubbles p 312 N94-11546
In-space assembly-servicing requirements p 348 N94-11569
Space Station maintenance studies using plaid graphics p 335 N94-11578
EXTREMELY HIGH FREQUENCIES
Fundamental studies of radar scattering from water surfaces: The Lake Washington experiment [NASA-CR-194030] p 139 N94-12778
EXTRUDING
Particle attraction effects on the centrifugal casting and extrusion of alumina [DE93-011559] p 82 N94-10957
EYE (ANATOMY)
Aviation accident risk for airmen with aphakia and artificial lens implants [DOT/FAA/AM-93/11] p 303 N94-10813
Psychophysiological measures of cognitive workload in laboratory and flight p 317 N94-11529
Aircraft windscreens enhance visual search disruption produced by laser glare [AD-A265167] p 26 N94-11892
EYE MOVEMENTS
Visual psychophysics of egomotion [AD-A265253] p 304 N94-11681

F

F REGION
Some results with the new digital ionosonde in San Diego [AD-A265178] p 275 N94-11101
Observing and modelling F-region ionospheric dynamics using the (O2) 7320A emission [AD-A265407] p 279 N94-12419
F-15 AIRCRAFT
Decoupling of aircraft responses p 32 N94-11497
F-16 AIRCRAFT
Ground vibration and flight flutter tests of the single-seat F-16XL aircraft with a modified wing [NASA-TM-104269] p 26 N94-11233
Decoupling of aircraft responses p 32 N94-11497
FABRICATION
Fibre reinforced structures with glass matrix p 64 N94-10064
Technique to prepare high-reflectance optical fiber bragg gratings with single exposure in-line on fiber draw tower [AD-D015757] p 374 N94-10373
Thin-film edge field emitter device and method of manufacture therefore [AD-D015764] p 140 N94-10377
Fabrication and analysis of a special optical connector containing a 1/4-inch-long optical fiber for DOI tests [DE93-013115] p 381 N94-10647
Method for producing a hybridization of detector array and integrated circuit for readout [NASA-CASE-NPO-18062-1-CU] p 141 N94-10656
Alkali metal for ultraviolet band-pass filter [NASA-CASE-NPO-18433-1-CU] p 381 N94-10657
Sensor abstractions to support many-robot systems [AD-A265907] p 180 N94-10803
Application of powder metallurgy techniques to produce improved bearing elements for liquid rocket engines [NASA-CR-193731] p 82 N94-10804
Development of commercially viable high-T(sub c) Bi-2223 superconductor tapes [DE93-009966] p 142 N94-10951
Processing and transport properties of high J(sub c) silver clad Bi-2223 tapes and coils [DE93-010674] p 398 N94-11073
A history of tungsten- and molybdenum-base alloys [DE93-010283] p 82 N94-11108
Dry in-line thermoplastic matrix impregnation, phase 1 [AD-A265016] p 67 N94-11221
A prototype urine collection device for female aircrew p 317 N94-11549
The physics of pattern formation of liquid interfaces [DE93-013333] p 154 N94-11814
High frequency behavior of long and small junctions [AD-A265670] p 403 N94-12336
Liquid Cooled Heat Sink with through Vias (LCHS) [AD-A266008] p 73 N94-12344
Dynamic high-pressure shock compaction of diamond powders [AD-A266004] p 93 N94-12354
Development of ultra-low noise, high sensitivity planar metal grating coupled 3 to 5 multiquantum well infrared detectors for focal plane array staring IR sensor systems [AD-A265599] p 404 N94-12375
Performance aspects of de Laval spray-forming nozzles [DE93-013671] p 163 N94-12604
FABRICS
On the mechanical development of the Flexible External Insulation (FEI) for Hermes spaceplane p 62 N94-10048
FABRY-PEROT INTERFEROMETERS
Continued development of an ultra-narrow bandpass filter for solar research [NASA-CR-194169] p 381 N94-10735

Localized and distributed fiber-optic strain sensors embedded in composite materials [UTIAS-346] p 73 N94-12013

FACE CENTERED CUBIC LATTICES

Interatomic interactions in BCC and FCC lattices of transition metals [DE93-621541] p 398 N94-11090

Fullerene superconductors: Phase stability and anomalously low T(sub c)'s in some ternary compounds [DE93-010687] p 400 N94-11457

FACTORIZATION

Balancing of the normalized right coprime factorization of a nonlinear system [MEMO-1096] p 341 N94-10273

Vectorizing matrix operations arising from PDE discretization on 9-point stencils [CWI-NM-R9221] p 342 N94-10351

Improvements for obtaining iterative solutions of large linear systems [DE93-767968] p 343 N94-10729

FAILURE

Hydrostatic testing of thick laminated composite cylinders for performance model validation [DE93-012728] p 184 N94-10264

Temperature effects on failure thickness and deflagration-to-detonation transition in PBX 9502 and TATB [DE93-010742] p 97 N94-10294

Fatigue life prediction for wind turbines: A case study on loading spectra and parameter sensitivity [DE93-011597] p 263 N94-11173

Scalloped margin domes: What are the processes responsible and how do they operate? p 454 N94-12120

FAILURE ANALYSIS

Probabilistic evaluation of uncertainties and risks in aerospace components [NASA-TM-105603] p 185 N94-10361

Fractography handbook of spaceflight metals [NASA-RP-1291] p 81 N94-10504

ACARA user's manual [NASA-TM-106277] p 183 N94-11167

Failure prediction of thin beryllium sheets used in spacecraft structures [NASA-CR-194164] p 187 N94-11190

An analysis of fiber-matrix interface failure stresses for a range of ply stress states [NASA-TM-108999] p 67 N94-11276

ENSAFE fireset flex circuit analysis [DE93-013106] p 144 N94-11478

Design for testability and diagnosis at the system-level p 184 N94-11563

Isothermal fatigue mechanisms in Ti-based metal matrix composites [NASA-CR-191181] p 74 N94-12594

FAILURE MODES

Design for testability and diagnosis at the system-level p 184 N94-11563

FAR FIELDS

Research on acoustic coupling to electromagnetic pulses in tissue [AD-A264764] p 301 N94-11583

Plane mixing layer vortical structure kinematics p 159 N94-12313

FAR INFRARED RADIATION

Atmospheric and spectroscopic research in the far infrared [NASA-CR-193551] p 280 N94-12582

FARM CROPS

Statistical analysis of environmental variability within the CELSS breadboard project's biomass production chamber [NASA-TM-109188] p 315 N94-11258

ERS-1 SAR crop monitoring experiment in East Anglia, UK p 248 N94-12488

Integration of ERS-1 data into the European project of agriculture statistics p 248 N94-12490

FAST FOURIER TRANSFORMATIONS

FFT-based methods for nonlinear image restoration in confocal microscopy [CS-9301] p 174 N94-10904

Design for testability and diagnosis at the system-level p 184 N94-11563

FASTENERS

Structural material, manufacture, and design requirements for high-temperature fasteners for space plane technologies p 63 N94-10055

Self locking set screw [AD-D015774] p 178 N94-10385

FATIGUE (MATERIALS)

Mechanical and fatigue properties of fibre reinforced aluminium-lithium alloy and aluminium-lithium MMC based laminates p 58 N94-10022

Micromechanisms of fatigue crack growth and fracture toughness in metal matrix composites [AD-A265153] p 187 N94-11096

FATIGUE LIFE

Fatigue-life behavior and matrix fatigue crack spacing in unnotched SCS-6/Timetal 21S metal matrix composites [NASA-CR-191467] p 185 N94-10715

Computational simulation of hot composite structures [NASA-TM-106200] p 186 N94-10762

Structural health monitoring using embedded fibre optic sensors p 22 N94-11334

The impact of active controls technology on the structural integrity of aeronautical vehicles p 27 N94-11341

Microstructure-based fatigue life prediction methods for naval steel structures [AD-A265429] p 85 N94-12426

Proposed framework for thermomechanical life modeling of metal matrix composites [NASA-TP-3320] p 74 N94-12449

Isothermal fatigue mechanisms in Ti-based metal matrix composites [NASA-CR-191181] p 74 N94-12594

FATIGUE TESTS

Fatigue-life behavior and matrix fatigue crack spacing in unnotched SCS-6/Timetal 21S metal matrix composites [NASA-CR-191467] p 185 N94-10715

Evaluation of test specimen shape effects on the flexural fatigue of CFRP laminates [NAL-TR-1159] p 65 N94-10857

Fiber-optic sensor systems for measuring strain and the detection of acoustic emissions in smart structures p 71 N94-11337

General aviation aircraft-normal acceleration data analysis and collection project [AD-A265055] p 26 N94-11858

FAULT DETECTION

Fault location in structures using neural networks p 70 N94-11335

FAULT TOLERANCE

A formally verified algorithm for interactive consistency under a hybrid fault model [NASA-CR-4527] p 326 N94-11188

FAULT TREES

Techniques, processes, and measures for software safety and reliability [DE93-012379] p 322 N94-10347

GRAFTED (GRAphical Fault Tree EDitor): A fault tree description program for target vulnerability/survivability analysis [AD-A264078] p 328 N94-11301

FAYALITE

On high-temperature formation of iron-rich olivine in the early solar system p 432 N94-12225

FEASIBILITY

Department of Energy solar process heat program: FY 1991 solar process heat prefeasibility studies activity [DE93-010010] p 262 N94-10258

FEASIBILITY ANALYSIS

A proof-of-concept implementation of persistence in a hierarchical storage system [DE93-009959] p 319 N94-10318

A feasibility study regarding the addition of a fifth control to a rotorcraft in-flight simulator [NASA-CR-193240] p 30 N94-10895

Investigation of alternate power source for Space Shuttle Orbiter hydraulic system [NASA-CR-193229] p 46 N94-10911

Thermal error compensation feasibility study using artificial intelligence [AD-A266084] p 340 N94-12411

FEDERAL BUDGETS

From red tape to results: Creating a government that works better and costs less p 422 N94-11351

From red tape to results: Creating a government that works better and costs less. Executive summary p 422 N94-11353

Assessing the adequacy of the industrial base [AD-A264954] p 417 N94-11856

Financial management: NASA's financial reports are based on unreliable data [AD-A265690] p 418 N94-12443

FEEDBACK

The cloud radiative feedback of a midlatitude squall line system and implication for climate study [DE93-010511] p 283 N94-10290

On the stability of stationary regimes in a distributed autovibration system with external feedback [DE93-620979] p 141 N94-10543

Magnetohydrodynamic computation of feedback stabilization of resistive-shell instabilities in the reversed field pinch [DE93-013466] p 388 N94-10852

Non-linear dynamics of automodulation processes in coupled distributed autovibration systems with delay [DE93-620976] p 143 N94-11365

FEEDBACK CONTROL

In-flight simulation of backside operating models using direct lift controller [NAL-TR-1152] p 30 N94-10734

Application of controller partitioning optimization procedure to integrated flight/propulsion control design for a STOVL aircraft [NASA-TM-106265] p 30 N94-11251

Multiple laser beam combining and phasing using closed-loop control [DE93-009830] p 175 N94-11283

Decoupling of aircraft responses p 32 N94-11497

Utilizing quantitative feedback theory design technique for flight control system p 32 N94-11501

A regional inverse eigenvalue problem: Solution with application in control theory [DE93-619666] p 339 N94-11630

Model reference adaptive control (MRAC) with applications to robotics p 339 N94-11640

An adaptive and robust control for motion coordination of two-cooperating robot manipulators p 340 N94-11825

Derivation of three closed loop kinematic velocity models using normalized quaternion feedback for an autonomous redundant manipulator with application to inverse kinematics [DE93-012823] p 340 N94-12543

FEEDFORWARD CONTROL

In-flight simulation of backside operating models using direct lift controller [NAL-TR-1152] p 30 N94-10734

FELDSPARS

Vaporization by shock loading of albite, jadeite, and pyrex glass: Experimental study p 97 N94-12039

The stability of hibonite and other aluminous phases in silicate melts: Implications for the origin of hibonite-bearing inclusions p 80 N94-12052

The correlation of alkalis and aluminum during high-temperature volatilization of albite and nepheline p 81 N94-12214

FEMALES

A prototype urine collection device for female aircrew p 317 N94-11549

Pattern of federal procurement from minority and women-owned small business [PB93-189355] p 417 N94-11844

FERMI LIQUIDS

Similarity of the leading contributions to the self-energy and the thermodynamics in two- and three-dimensional Fermi Liquids [DE93-012673] p 412 N94-11162

FERMIONS

Top and Higgs masses in a composite boson model [DE93-010874] p 359 N94-10302

On thermodynamic properties of heavy fermion systems in magnetic field [DE93-613819] p 409 N94-10403

On local frame fields and fermion dynamics in space with nontrivial topologies [DE93-617657] p 349 N94-10548

Exact solutions of a many-anyon problem [DE93-617646] p 411 N94-10832

Similarity of the leading contributions to the self-energy and the thermodynamics in two- and three-dimensional Fermi Liquids [DE93-012673] p 412 N94-11162

Fermion-boson scattering in ladder approximation [DE93-613111] p 368 N94-11581

FERRITES

Nonlinear effects in ferrite tuned cavities [DE93-014136] p 374 N94-12785

FERROELECTRICITY

Materials for adaptive structural acoustic control, volume 3 [AD-A264621] p 358 N94-11262

Spatial light modulator having photosensitive and ferroelectric layers [AD-D015731] p 404 N94-12400

FERROMAGNETIC MATERIALS

Effect of a distribution of exchange parameters within a simple localized-itinerant model [DE93-610314] p 395 N94-10314

A lattice gas model for enzyme kinetics with alternate interactions [DE93-613027] p 395 N94-10411

FERROMAGNETISM

Magnetization reversal by nucleation [DE93-610313] p 350 N94-10313

FIBER COMPOSITES

The application of advanced materials to aircraft nacelle structures p 57 N94-10011

Hybrid materials for use at elevated temperatures p 57 N94-10013

Distortions and stresses in thin shells due to anisotropic thermal expansion p 57 N94-10014

Mechanical properties of magnesium/carbon composites developed by hot pressing under medium pressure p 59 N94-10024
Deformation mechanisms of continuous fibre-reinforced thermoplastic composites during manufacturing: A probabilistic approach p 60 N94-10030
Cost effectiveness of structural applications of fibre reinforced thermoplastics p 60 N94-10032
Application of advanced thermoplastics p 60 N94-10033
Low cost thermoplastic composites for structural applications: Design concepts using new materials and processes p 60 N94-10034
New x ray scanning topographic approaches to nondestructive evaluation of composites p 61 N94-10039
Fibre-reinforced ceramic components by filament winding for intermediate temperature applications p 61 N94-10041
New processes for lightweight ceramic matrix composites p 61 N94-10043
Introducing SMaSE: An aide memoire on structural materials and space engineering p 63 N94-10053
Fibre reinforced structures with glass matrix p 64 N94-10064
Silicon-based elementary particle tracking system: Materials science and mechanical engineering design [DE93-012630] p 65 N94-10740
Interface considerations in Al2O3/NiAl composite [NASA-CR-191167] p 66 N94-11202
Dry in-line thermoplastic matrix impregnation, phase 1 [AD-A265016] p 67 N94-11221
An analysis of fiber-matrix interface failure stresses for a range of ply stress states [NASA-TM-108999] p 67 N94-11276
Factors affecting the embedding of optical fibre sensors in advanced composite structures p 70 N94-11336
The effects of an aggressive environment on the subcritical crack growth of a continuous-fiber ceramic composite [DE93-011690] p 73 N94-11612
Mechanical interaction between synthetic fiber and cement base matrix in FRC composites [AD-A265310] p 73 N94-11686
Processing and properties of coated HPZ fiber reinforced glass-ceramic matrix composites [AD-A265177] p 92 N94-11876
Localized and distributed fiber-optic strain sensors embedded in composite materials [UTIAS-346] p 73 N94-12013
Analytical models for describing the mechanical behavior of fiber reinforced composites [AD-A265906] p 74 N94-12347
Proposed framework for thermomechanical life modeling of metal matrix composites [NASA-TP-3320] p 74 N94-12449

FIBER OPTICS
Multiplexed and distributed optical fibre sensors p 64 N94-10065
Fibre optic strain and temperature measurement in composite materials: A review of the OSTIC programme p 65 N94-10066
Method and apparatus for polarization-maintaining fiber optical amplification with orthogonal polarization output [AD-D015756] p 374 N94-10372
A fiber optic network system with low crosstalk using code-division multiplexing [AD-D015763] p 374 N94-10376
NASA's first in-space optical gyroscope: A technology experiment on the X ray Timing Explorer spacecraft [NASA-TM-109242] p 170 N94-10667
Design and analysis of an optical interface message processor [AD-A266079] p 381 N94-10697
Performance of low-cost commercial fiber-optic transceivers for reference frequency distribution p 355 N94-10993
Ultrastable reference frequency distribution utilizing a fiber optic link p 355 N94-10994
A wide-band fiber optic frequency distribution system employing thermally controlled phase compensation p 355 N94-10995
Analysis of the eastern range multiplexed fiber optic IRIG B120 distribution system p 139 N94-10996
Optical fibre techniques for structural monitoring in composites p 69 N94-11324
Fiber optic sensing for composite smart structures p 69 N94-11327
Fiber-optic sensor systems for measuring strain and the detection of acoustic emissions in smart structures p 71 N94-11337
Fiber-optic interferometric strain gauge for smart structures applications: First flight tests p 71 N94-11340
Reliability analysis for FDDI dual homing networks [AD-A266133] p 337 N94-11475
Localized and distributed fiber-optic strain sensors embedded in composite materials [UTIAS-346] p 73 N94-12013
Improved super luminescent light source specification [AD-D015746] p 176 N94-12329
Short wavelength crystal fiber devices [AD-A265716] p 176 N94-12402

FIELD COILS
Pilot trial of potentiating normal healing of stress fractures using pulsing electromagnetic fields [AD-A264251] p 311 N94-12364

FIELD EFFECT TRANSISTORS
A study of DC-DC converters with MCTs for arcjet power supplies [NASA-CR-193457] p 142 N94-10931
Characterization of the Si/SiO2 interfere morphology from quantum oscillations in Fowler-Nordheim tunneling currents [AD-A265149] p 143 N94-11160
GaAs sigma-delta modulator modeling for Analog to Digital Converters (ADC's) [AD-A263419] p 144 N94-11516
Gallium arsenide dynamic random access memory support circuitry [AD-A265176] p 320 N94-11875

FIELD EMISSION
Thin-film edge field emitter device and method of manufacture therefore [AD-D015764] p 140 N94-10377

FIELD OF VIEW
Implementation and use of a computational ray-tracing program for the design and analysis of complex optical systems [AD-A265075] p 382 N94-11653

FIELD THEORY (PHYSICS)
From the Weyl theory to a theory of locally anisotropic space-time [DE92-644734] p 410 N94-10535
Supersqueezed states from squeezed states p 378 N94-10591
All possible electroweak models from Z orbifold [DE93-617656] p 411 N94-10880
Dissipative phase transitions in field theory models with spontaneous symmetry violation [DE93-621382] p 412 N94-11039
A theoretical kinematical study of the gradient of any cosmic scalar field [DE92-644731] p 425 N94-11136
One-loop quantum gravity on de Sitter space [DE92-641349] p 425 N94-11152
Duality twisted boundary conditions in n-sta te Potts models [DE93-619724] p 346 N94-11811

FIGHTER AIRCRAFT
Criteria for design of integrated flight/propulsion control systems for STOVL fighter aircraft [NASA-TP-3356] p 30 N94-11134

FIGURE OF MERIT
Advanced control for airbreathing engines, volume 2: General Electric aircraft engines [NASA-CR-189204] p 29 N94-12271
Advanced controls for airbreathing engines, volume 3: Allison gas turbine [NASA-CR-189205] p 29 N94-12272

FILAMENT WINDING
Lightweight CFRP frame structures for a Rotex-derived manipulator system p 56 N94-10005
Design and manufacturing of filament wound thrust cylinder p 57 N94-10010
Tape winding of thermoplastic composites p 60 N94-10035
Fibre-reinforced ceramic components by filament winding for intermediate temperature applications p 61 N94-10041

FILM COOLING
A laboratory model of a hydrogen/oxygen engine for combustion and nozzle studies [NASA-TM-106281] p 47 N94-11252

FILM THICKNESS
The surface plasmon spectroscopy as diagnostic technique in microgravity experiments p 110 N94-10133
Polymers for microelectronics [AD-A266036] p 94 N94-12396

FILMS
Carbon analyses of IDP's sectioned in sulfur and supported on beryllium films p 81 N94-12099

FINANCIAL MANAGEMENT
Analysis of the cost evaluation of ESA programmes and comparable national and international programmes [GTS-92063] p 416 N94-10145
National patterns of R and D resources, 1992 [NSF-92-330] p 422 N94-11186
Financial management: NASA's financial reports are based on unreliable data [AD-A265690] p 418 N94-12443

FINE STRUCTURE
Fine structure of the Pomeron and the real part of the elastic scattering amplitude [DE93-617696] p 362 N94-10555
X ray and gamma ray spectroscopy of solids under pressure [DE93-014847] p 76 N94-10653
X ray absorption spectroscopy of electrochemically generated species [AD-A264749] p 77 N94-11265
Apical Cu-O bond in YBa2Cu3O(7-delta) superconductors by XAFS [DE93-010861] p 400 N94-11458

FINITE DIFFERENCE THEORY
Finite difference schemes for long-time integration [NASA-CR-191471] p 343 N94-10642
Viscous flow simulation using an upwind method for hexahedral based adaptive meshes [AD-A265901] p 148 N94-10703
Combustion chamber analysis code [NASA-CR-192585] p 46 N94-10934
New developments in the method of space-time conservation element and solution element: Applications to the Euler and Navier-Stokes equations [NASA-TM-106226] p 150 N94-10939
Development of generic field classes for finite element and finite difference problems [DE93-011678] p 345 N94-11225
Application of incremental unknowns to the Burgers equation p 156 N94-12293
Direct numerical simulation of turbulent flow over a backward-facing step p 156 N94-12296
Numerical simulation using vorticity-vector potential formulation p 157 N94-12297
Summation by parts, projections, and stability [NASA-CR-194290] p 346 N94-12776

FINITE ELEMENT METHOD
Lightweight CFRP frame structures for a Rotex-derived manipulator system p 56 N94-10005
Numerical simulation and experimental results of filament wound CFRP tubes tested under biaxial load p 58 N94-10015
Development of a fatigue analysis approach for CFRP structures under acoustic loading p 58 N94-10018
Solving the essentials of an innovative tennis racket product: Functionality, simplicity, and super-lightweight technology p 65 N94-10068
Massively parallel multifrontal methods for finite element analysis on MIMD computer systems [DE93-009838] p 335 N94-10257
Survey to determine the value of DYNA [DE93-012390] p 321 N94-10267
NASTRAN modeling of flight test components for UH-60A airloads program test configuration [NASA-CR-193614] p 186 N94-10937
New developments in the method of space-time conservation element and solution element: Applications to the Euler and Navier-Stokes equations [NASA-TM-106226] p 150 N94-10939
Failure prediction of thin beryllium sheets used in spacecraft structures [NASA-CR-194164] p 187 N94-11190
Development of generic field classes for finite element and finite difference problems [DE93-011678] p 345 N94-11225
A study of strength evaluations of EDNi/EDCu/NARloy-Z bonded joints [NASA-TM-108418] p 188 N94-11275
Computational mechanics needs study [NASA-CR-193712] p 327 N94-11279
On cell entropy inequality for discontinuous Galerkin methods [NASA-CR-191493] p 345 N94-11280
Fault location in structures using neural networks p 70 N94-11335
Structural analysis and optimization of adaptive structures by use of the finite element method p 71 N94-11339
ENSAFE fireset flex circuit analysis [DE93-013106] p 144 N94-11478
Stability of viscoelastic flow: Physical and numerical considerations p 31 N94-11493
Massively parallel hydrodynamics on unstructured grids [DE93-007325] p 153 N94-11601
Finite element simulation of the 2D collapse of a polyelectrolyte gel disk [DE93-010693] p 91 N94-11665
Numerical simulation using vorticity-vector potential formulation p 157 N94-12297
Three-dimensional finite element analysis of explosive safety facilities: A technology assessment [AD-A265700] p 35 N94-12562
Model of Kuroshio region circulation p 229 N94-12765

FINITE VOLUME METHOD
Calculations of viscous nonequilibrium flows in nozzles p 8 N94-10455
Hypersonic multi block flow simulations around space vehicles including non-equilibrium chemistry p 9 N94-10460
Flow analysis around ONERA model M5 configuration [PAPER-3D-2] p 12 N94-10478
Flow analysis around ONERA model M5 configuration [PAPER-3D-4] p 12 N94-10480
A dynamically adaptive mesh method for internal flows p 149 N94-10896
Massively parallel hydrodynamics on unstructured grids [DE93-007325] p 153 N94-11601
Modeling void growth and movement with phase change in thermal energy storage canisters [NASA-TM-106288] p 163 N94-12576
FINS
Theoretical investigation of 3-D shock wave turbulent boundary layer interactions [AD-A265275] p 150 N94-11014
FIRE DAMAGE
Applications of a model to predict flame spread over interior finish materials in a compartment p 19 N94-10783
FIRE PREVENTION
Applications of continuous fiber reinforced thermoplastics in aircraft interiors p 18 N94-10775
An investigation into aircraft fuselage fire hardening p 19 N94-10782
Practical hazard assessment: An approach to the fire safety p 20 N94-10785
Developments needed to expand the role of fire modeling in material fire hazard assessment p 20 N94-10787
Aircraft material fire testing and the creation of an international working group p 21 N94-10790
Future needs in the development of materials for aircraft interiors and equipment p 21 N94-10794
Advanced aircraft materials research and development plan p 22 N94-10796
The future of aircraft cabin fire safety p 22 N94-10797
FIRES
Developments needed to expand the role of fire modeling in material fire hazard assessment p 20 N94-10787
Development of a hypermedia knowledge base of aircraft fire safety regulations p 21 N94-10793
Methanol pan fires in an enclosed space: Effect of pressure and oxygen concentration [AD-A266108] p 79 N94-12415
Analytical method for water vapor collection and analysis in aircraft cabin fires [DOT/FAA/CT-TN93/33] p 22 N94-12575
FISHERIES
Application of the airborne ocean color imager for commercial fishing [NASA-TM-103986] p 231 N94-11378
Satellite derived sea surface temperature applications for Indian Ocean resources development p 193 N94-11907
The use of remote sensing data for coastal zone management and environment in Indonesia p 196 N94-11927
Warm streamers extended from Warm Core Rings (WCRs) and their role on fish migration and fishing ground formation p 198 N94-11938
Application of NOAA AVHRR data to fisheries p 215 N94-12681
Swordfish (Xiphias gladius) catch distributions relative to environmental features observed from satellites off Coquimbo, Chile (30 deg S) p 216 N94-12688
Role of remote sensing and its cost effectiveness in site selection for coastal aquaculture p 217 N94-12697
FISHES
Satellite derived sea surface temperature applications for Indian Ocean resources development p 193 N94-11907
Warm streamers extended from Warm Core Rings (WCRs) and their role on fish migration and fishing ground formation p 198 N94-11938
Application of NOAA AVHRR data to fisheries p 215 N94-12681
Swordfish (Xiphias gladius) catch distributions relative to environmental features observed from satellites off Coquimbo, Chile (30 deg S) p 216 N94-12688
A possibility to define the location of epipelagic fish concentrations with assistance of satellite sensing p 228 N94-12757
FISHING
Application of NOAA AVHRR data to fisheries p 215 N94-12681
Swordfish (Xiphias gladius) catch distributions relative to environmental features observed from satellites off Coquimbo, Chile (30 deg S) p 216 N94-12688
FITTING
Correlation of HGU-56/P aircrew helmet fitting with head anthropometric measurements [AD-A264988] p 315 N94-11291
FLAME CALORIMETERS
Computer-aided molecular design of fire resistant aircraft materials p 19 N94-10779
FLAME PROPAGATION
Influence of neutral particles concentration on flame propagation in methane-air mixtures at zero and normal gravity conditions p 121 N94-10224
Some aspects of combustion modelling by low and normal gravity p 124 N94-10244
Applications of a model to predict flame spread over interior finish materials in a compartment p 19 N94-10783
Flammability parameters of materials: Ignition, combustion, and flame spread p 20 N94-10788
On the combustion of a laminar spray [NASA-TM-106210] p 28 N94-11238
Why does preferential diffusion strongly affect premixed turbulent combustion? p 81 N94-12319
FLAME RETARDANTS
Proceedings of the International Conference for the Promotion of Advanced Fire Resistant Aircraft Interior Materials [DOT/FAA/CT-93/3] p 17 N94-10766
A polyimide foam for advanced fire resistant aircraft applications p 17 N94-10770
New technology for effective control of flammability in polyolefin fiber/textiles p 18 N94-10774
Uralane (tm) 5774-A/B: Ciba-Geigy's advanced urethane adhesive for the aircraft industry p 18 N94-10777
The fire properties of insulation bags, as installed and after aircraft operations p 19 N94-10778
Fire-resistant hydrolytically stable poly(arylene phosphine oxide) material systems p 19 N94-10780
A non-halogenated, flame retarded polycarbonate p 19 N94-10781
Advanced aircraft materials research and development plan p 22 N94-10796
FLAMES
The pyrene laser induced fluorescence technique as a diagnostic tool for combustion thermometry in microgravity p 107 N94-10113
On the combustion of a laminar spray [NASA-TM-106210] p 28 N94-11238
Study and modeling of finite rate chemistry effects in turbulent non-premixed flames p 81 N94-12317
Distributed combustion in solid propellants [AD-A265727] p 99 N94-12564
FLAMMABILITY
Proceedings of the International Conference for the Promotion of Advanced Fire Resistant Aircraft Interior Materials [DOT/FAA/CT-93/3] p 17 N94-10766
New thermoplastic laminating adhesives for the aircraft industry with low heat release and low smoke emission p 17 N94-10767
A new low smoke, low heat release structural foam p 17 N94-10768
Polyimide foam insulation systems: A major weight reduction and improvement in fire resistance of sidewall systems p 17 N94-10769
A polyimide foam for advanced fire resistant aircraft applications p 17 N94-10770
A repair patching system for aircraft cargo liners p 17 N94-10771
Primaset (tm): A safer material for aircraft interior applications p 18 N94-10772
New technology for effective control of flammability in polyolefin fiber/textiles p 18 N94-10774
Uralane (tm) 5774-A/B: Ciba-Geigy's advanced urethane adhesive for the aircraft industry p 18 N94-10777
The fire properties of insulation bags, as installed and after aircraft operations p 19 N94-10778
Fire-resistant hydrolytically stable poly(arylene phosphine oxide) material systems p 19 N94-10780
A non-halogenated, flame retarded polycarbonate p 19 N94-10781
The OSU heat release rate test using the oxygen consumption principle p 20 N94-10784
Practical hazard assessment: An approach to the fire safety p 20 N94-10785
Fire resistance and mechanical properties for phenolic prepregs p 20 N94-10786
Developments needed to expand the role of fire modeling in material fire hazard assessment p 20 N94-10787
Flammability parameters of materials: Ignition, combustion, and flame spread p 20 N94-10788
Factors that affect OSU thermal performance of aircraft interior materials p 20 N94-10789
Development and analysis of insulation constructions for aerospace wiring applications p 21 N94-10791
Proceedings of the International Conference for the Promotion of Advanced Fire Resistant Aircraft Interior Materials [AD-A266057] p 22 N94-12384
FLAPERONS
Determining XV-15 aeroelastic modes from flight data with frequency-domain methods [NASA-TP-3330] p 25 N94-10935
FLAT PLATES
Theoretical investigation of 3-D shock wave turbulent boundary layer interactions [AD-A265275] p 150 N94-11014
Aerodynamic sound due to interaction between a two-dimensional free shear layer and the leading edge of a parallel flat plate p 163 N94-12615
FLATNESS
New aerodynamic information obtained from the solution of the inverse problem for aerofoils [NAL-TR-1172] p 14 N94-10860
FLAVOR (PARTICLE PHYSICS)
Solar neutrinos with three flavor mixings [DE93-011006] p 483 N94-11619
FLEXIBLE BODIES
Payload sensitivity in coupled bending and torsional vibrations in flexible beams [MEMO-1102] p 184 N94-10161
Trajectory pattern inverse dynamics and control of nonlinear dynamics systems with application to flexible structures p 181 N94-11219
Reduced gravity multibody dynamics testing [NASA-CR-192589] p 125 N94-11483
Computational algorithms or identification of distributed parameter systems [AD-A265252] p 331 N94-11680
Control of large space structures with varying configuration [AD-A265764] p 44 N94-12387
FLEXIBLE WINGS
Multidimensional intelligent control for superlight air vehicles p 27 N94-11347
FLEXING
Evaluation of test specimen shape effects on the flexural fatigue of CFRP laminates [NAL-TR-1159] p 65 N94-10857
Flexure and the role of inplane force around coronae on Venus p 452 N94-12112
FLIGHT CHARACTERISTICS
Criteria for design of integrated flight/propulsion control systems for STOVL fighter aircraft [NASA-TP-3356] p 30 N94-11134
Application of controller partitioning optimization procedure to integrated flight/propulsion control design for a STOVL aircraft [NASA-TM-106265] p 30 N94-11251
Moving-base simulation evaluation of thrust margins for vertical landing for the NASA YAV-8B Harrier aircraft [NASA-TM-104008] p 30 N94-11259
Comparing aircraft agility using mahalanobis distances [PB93-175446] p 26 N94-11464
Decoupling of aircraft responses p 32 N94-11497
FLIGHT CLOTHING
Correlation of HGU-56/P aircrew helmet fitting with head anthropometric measurements [AD-A264988] p 315 N94-11291
FLIGHT CONDITIONS
Studies on scramjet nozzles. Part 1: Performance of two dimensional nozzles [NAL-TR-1149] p 27 N94-10367
Parametric analysis of atmospheric processes [NASA-CR-192523] p 347 N94-10757
Fiber-optic interferometric strain gauge for smart structures applications: First flight tests p 71 N94-11340
FLIGHT CONTROL
Experimental results in aerodynamic stability and control of a TSTO configuration p 3 N94-10424
Extraction of stability and control derivatives from orbiter flight data [NASA-TM-4500] p 13 N94-10707
Space Shuttle hypersonic aerodynamic and aerothermodynamic flight research and the comparison to ground test results [NASA-TM-4499] p 13 N94-10820
A feasibility study regarding the addition of a fifth control to a rotorcraft in-flight simulator [NASA-CR-193240] p 30 N94-10895
Criteria for design of integrated flight/propulsion control systems for STOVL fighter aircraft [NASA-TP-3356] p 30 N94-11134
Preliminary supersonic flight test evaluation of performance seeking control [NASA-TM-4494] p 28 N94-11205

Application of controller partitioning optimization procedure to integrated flight/propulsion control design for a STOVL aircraft [NASA-TM-106265] p 30 N94-11251
Stability in Aerospace Systems [AGARD-R-789] p 31 N94-11489
Stability analysis and aerospace vehicle dynamics p 31 N94-11491
On non-linear longitudinal stability of an aircraft in a dive in the presence of atmospheric disturbances p 31 N94-11492
Nonlinear and dynamic analysis of flight p 32 N94-11496
Decoupling of aircraft responses p 32 N94-11497
Modeling nonlinear aerodynamic loads for aircraft stability and control analysis p 32 N94-11499
Utilizing quantitative feedback theory design technique for flight control system p 32 N94-11501
Adaptive reconfigurable flight controls for high angle of attack aircraft agility p 32 N94-11502
Toward intelligent flight control p 33 N94-11503
X-29: Longitudinal instability at high angle-of-attack p 33 N94-11504
Measures for simulator evaluation of a helicopter obstacle avoidance system p 35 N94-11535

FLIGHT CREWS
Correlation of HGU-56/P aircrew helmet fitting with head anthropometric measurements [AD-A264988] p 315 N94-11291
Criteria for assessing problem solving and decision making in complex environments p 314 N94-11532
In-space assembly-servicing requirements p 348 N94-11569
Aviators, air combat, and combat stress: An Air F orce commander's primer [AD-A265083] p 313 N94-11867

FLIGHT ENVELOPES
Extraction of stability and control derivatives from orbiter flight data [NASA-TM-4500] p 13 N94-10707

FLIGHT OPERATIONS
Analyzing human errors in flight mission operations p 314 N94-11534

FLIGHT PATHS
Measures for simulator evaluation of a helicopter obstacle avoidance system p 35 N94-11535

FLIGHT SAFETY
Aviation accident risk for airmen with aphakia and artificial lens implants [DOT/FAA/AM-93/11] p 303 N94-10813

FLIGHT SIMULATION
Nonlinear stability and control study of highly maneuverable high performance aircraft [NASA-CR-193480] p 25 N94-10344
Aerodynamic model identification of quiet STOL experimental aircraft ASKA from dynamic flight test data [DE93-767967] p 25 N94-10728
Flight simulator experiment of the cockpit advisory system [NAL-TR-1151] p 33 N94-10733
In-flight simulation of backside operating models using direct lift controller [NAL-TR-1152] p 30 N94-10734
Advanced rotorcraft flight simulation: Model development, validation and parallel implementation p 25 N94-11056
Boundary layer transition: Prediction and wind tunnel simulation p 32 N94-11498
Measures for simulator evaluation of a helicopter obstacle avoidance system p 35 N94-11535

FLIGHT SIMULATORS
A feasibility study regarding the addition of a fifth control to a rotorcraft in-flight simulator [NASA-CR-193240] p 30 N94-10895

FLIGHT TESTS
Characterization of in-flight performance of ion propulsion systems [NASA-TM-106283] p 46 N94-10761
Space Shuttle hypersonic aerodynamic and aerothermodynamic flight research and the comparison to ground test results [NASA-TM-4499] p 13 N94-10820
Determining XV-15 aeroelastic modes from flight data with frequency-domain methods [NASA-TP-3330] p 25 N94-10935
Performance and rotor loads measurements of the Lynx XZ170 helicopter with rectangular blades [NASA-TM-104000] p 1 N94-10936
NASTRAN modeling of flight test components for UH-60A airloads program test configuration [NASA-CR-193614] p 186 N94-10937
An environmental study of the National Aerospace Plane [AD-A266071] p 25 N94-10945
Preliminary supersonic flight test evaluation of performance seeking control [NASA-TM-4494] p 28 N94-11205
Ground vibration and flight flutter tests of the single-seat F-16XL aircraft with a modified wing [NASA-TM-104269] p 26 N94-11233
Fiber-optic interferometric strain gauge for smart structures applications: First flight tests p 71 N94-11340
Workshop on Solar Electric Propulsion p 54 N94-11416
Reduced gravity multibody dynamics testing [NASA-CR-192589] p 125 N94-11483
On non-linear longitudinal stability of an aircraft in a dive in the presence of atmospheric disturbances p 31 N94-11492
X-29: Longitudinal instability at high angle-of-attack p 33 N94-11504
On-orbit refueling p 38 N94-11566
Helicopter approach capability using the differential Global Positioning System [NASA-CR-177618] p 24 N94-12355
Improvement of method for experimental determination of flutter speed by parameter identification [NASA-CR-193555] p 33 N94-12769

FLOAT ZONES
Experimental study of axisymmetric thermocapillary flows p 100 N94-10072
The use of magnetic fields for damping unsteady Marangoni convection in GaAs floating zones under microgravity p 100 N94-10073
Instability of thermocapillary convection in floating zones p 101 N94-10076
Effect of rotation on microgravity floating-zone crystal growth p 101 N94-10080
Coupled thermovibrational and thermocapillary convection in liquid bridge (floating zone system) p 101 N94-10082
On shape of single crystals grown by FZM in microgravity p 102 N94-10084
Liquid bridges and floating zones p 102 N94-10085
Towards real time numerical stimulation of Marangoni convection: A help for telescience microgravity experiments p 102 N94-10087
Marangoni motion during melting of a hypermonotectic alloy: Numerical simulations for the D2 experiment IHF04 p 113 N94-10177
Results of crystal growth experiments by FZM on Zona facilities in microgravity p 116 N94-10193

FLOATS
Mixing of drifter ensemble by mesoscale currents p 228 N94-12760

FLOCCULATING
Particle attraction effects on the centrifugal casting and extrusion of alumina [DE93-011559] p 82 N94-10957

FLOOD DAMAGE
Flood monitoring in northern part of Central Java by remote sensing technique. Case study: The flooding of Semarang in January, 1990 p 206 N94-11989

FLOOD PREDICTIONS
Flood monitoring in northern part of Central Java by remote sensing technique. Case study: The flooding of Semarang in January, 1990 p 206 N94-11989

FLOODS
International Space Year in China p 36 N94-10680
Simultaneous 3D turbulent large-scale structures in a flood flow by multi-channels measuring system p 165 N94-12624

FLOQUET THEOREM
The effect of gravity modulation on thermosolutal convection p 105 N94-10103
The effect of gravitational modulation on convection in vertical Bridgman growth p 113 N94-10178
Floquet operator as integral of motion p 380 N94-10610

FLOW CHARACTERISTICS
Experimental and computational comparisons of Mach 6 high Reynolds number heat transfer and skin friction p 6 N94-10443
Proceedings of the 10th NAL Symposium on Aircraft Computational Aerodynamics: CFD Workshop on GK Airfoil and ONERA M5 Geometry [NAL-SP-20] p 10 N94-10466
Description of 2D problem: Aerodynamic analysis of Garabedian-Korn 75-06-12 airfoil p 10 N94-10467
Aerodynamic characteristics analysis of Garabedian-Korn 75-06-12 airfoil: Compendium of results p 11 N94-10475
Description of 3D problem: Flow analysis around ONERA model M5 configuration p 11 N94-10476
Flow analysis around ONERA model M5 configuration [PAPER-3D-1] p 11 N94-10477
Flow analysis around ONERA model M5 configuration [PAPER-3D-2] p 12 N94-10478
Flow analysis around ONERA model M5 configuration [PAPER-3D-3] p 12 N94-10479
Flow analysis around ONERA model M5 configuration [PAPER-3D-4] p 12 N94-10480
Flow analysis around ONERA model M5 configuration [PAPER-3D-5] p 12 N94-10481
Flow analysis around ONERA model M5 configuration: Compendium of results p 12 N94-10482
Viscous flow simulation using an upwind method for hexahedral based adaptive meshes [AD-A265901] p 148 N94-10703
Improvement of the flow quality in the ARA transonic tunnel by means of a long cell honeycomb [ARA-MEMO-375] p 34 N94-10894
Laser anemometer measurements and computations for transonic flow conditions in an annular cascade of high turning core turbine vanes [NASA-TP-3383] p 15 N94-11133
The coherent structure in the oceanic turbulence around Japan Islands Chain forced by an air, sea, and solid Earth interaction p 198 N94-11940
Superfluid turbulence p 158 N94-12307

FLOW DISTORTION
A comparative study of full Navier-Stokes and Reduced Navier-Stokes analyses for separating flows within a diffusing inlet S-duct [NASA-TM-106250] p 39 N94-10764
The effects of successive distortions on a turbulent boundary layer in a supersonic flow p 14 N94-11058

FLOW DISTRIBUTION
Transient three-dimensional numerical simulation of Marangoni flow in a liquid column under microgravity p 101 N94-10079
Marangoni flows in open cavities with differentially heated end walls p 104 N94-10097
The kinematics of buoyancy induced mixing p 123 N94-10239
A grid generation method to calculate the flow field in a three-dimensional cascade of blades [NAL-TR-1158] p 147 N94-10364
Numerical calculation of scramjet inlet flow [NAL-TR-1174T] p 27 N94-10370
CFD analysis of hypersonic, chemically reacting flow fields p 2 N94-10422
The upgrading of the arc heated wind tunnel of the DLR (LBK) with respect to its effects on the material testing p 4 N94-10432
Flow development in a circular pipe in the UTIAS/RPI M = 8.3 gun tunnel p 6 N94-10442
Issues and approach to develop validated analysis tools for hypersonic flows: One perspective p 7 N94-10446
Stability of hypersonic flow over a blunt body p 7 N94-10450
Nonequilibrium hypersonic flow in a wind-tunnel nozzle p 8 N94-10456
A CFD-based aerodynamic design procedure for hypersonic wind-tunnel nozzles p 9 N94-10458
On the accuracy and efficiency of CFD methods in real gas hypersonics p 9 N94-10462
Aerodynamic characteristics analysis of Garabedian-Korn 75-06-12 airfoil [PAPER-2D-3] p 10 N94-10469
Lee waves: Benign and malignant [NASA-CR-186024] p 283 N94-10725
Navier-Stokes flowfield computation of wing/rotor interaction for a tilt rotor aircraft in hover [NASA-CR-4532] p 13 N94-10758
Development of an unstructured solution adaptive method for the quasi-three-dimensional Euler and Navier-Stokes equations [NASA-CR-191161] p 28 N94-10816
New aerodynamic information obtained from the solution of the inverse problem for aerofoils [NAL-TR-1172] p 14 N94-10860
Laser velocimeter measurements of the flow field generated by a forward-swept propfan during flutter [NASA-TM-106195] p 14 N94-10892
A dynamically adaptive mesh method for internal flows p 149 N94-10896
Flowfield structure of swept shock wave/turbulent boundary-layer interactions p 149 N94-10899
Wall interference correction based on interface measurements in subsonic wind tunnel testing p 15 N94-11154
A Galilean and tensorial invariant k-epsilon model for near wall turbulence [NASA-TM-106263] p 151 N94-11192
Physics of forebody flow control [NASA-CR-193626] p 15 N94-11195
A laboratory model of a hydrogen/oxygen engine for combustion and nozzle studies [NASA-TM-106281] p 47 N94-11252
Shear coaxial injector atomization phenomena for combusting and non-combusting conditions [NASA-CR-193339] p 152 N94-11526

Turbulence modeling for thrust reverser flow field prediction methods [AD-A266139] p 154 N94-11641
Time evolution of cross-stream exchange associated with the variations in the Kuroshio p 197 N94-11936
Appearance, behavior, and oceanic structures of warm streamers in the Kuroshio Oyashio frontal region p 198 N94-11937
Warm streamers extended from Warm Core Rings (WCRs) and their role on fish migration and fishing ground formation p 198 N94-11938
The flow structure around a cylindrical pier for the flow of transcritical Reynolds number p 169 N94-11944
Lava flows on Venus: Analysis of motion and cooling p 457 N94-12137
Suppression of the near wall burst process of a fully developed turbulent pipe flow [AD-A265995] p 161 N94-12352
Fluctuations of longitudinal vortices along a concave wall p 16 N94-12616
On the wake behind a high speed train p 164 N94-12618
Simultaneous 3D turbulent large-scale structures in a flood flow by multi-channels measuring system p 165 N94-12624
Study on diffusion phenomena of river effluents issued into sea around Japan with satellite remote sensing data p 212 N94-12664
Evaluation of the method of geostrophic flow using NOAA-AVHRR data p 213 N94-12673
Observation of warm current at the boundary from north equatorial current to Kuroshio by NOAA/AVHRR p 214 N94-12676
Satellite thermal variations of Kuroshio in relation to storm floods p 215 N94-12685
ADCP evidence for upper layer circulation in northeast of the South China Sea p 215 N94-12686
The WOCE/TOGA Surface Velocity Programme (SVP) p 216 N94-12691
The circulation near Luzon p 219 N94-12707
Current variability on the shelf break northeast of Taiwan p 219 N94-12708
Investigation of meso-scale fronts, eddies and upwellings in China Seas with AVHRR data p 220 N94-12711
Variability of the Kuroshio observed from satellite thermal imagery p 221 N94-12717
On a nonstationary dynamics of the north-west Pacific Ocean p 222 N94-12724
The acoustic arrangement for measuring vertical structure of sea current p 223 N94-12729
A detailed investigation of the benthic regime in the Clarion-Clipperton province of the Pacific and a forecast of consequences of manganese nodule mining p 224 N94-12733
Bottom currents and possibilities for near bottom layer environmental investigations in the Pacific by means of self contained bottom stations p 224 N94-12734
Autonomous self contained bottom pop-up stations for study of the benthic layer and seismicity of the ocean's bottom p 224 N94-12735
Coupled numerical model for altimetric data assimilation and velocity field analysis p 227 N94-12752
Mesoscale dynamic structures of the Subarctic Frontal Zone in the Pacific Ocean p 227 N94-12754
Mixing of drifter ensemble by mesoscale currents p 228 N94-12760
Model of Kuroshio region circulation p 229 N94-12765
The 1991 version of the plume impingement computer program. Volume 2: User's input guide [NASA-CR-194191] p 166 N94-12774
The 1991 version of the plume impingement computer program. Volume 1: Description [NASA-CR-194192] p 166 N94-12775

FLOW EQUATIONS
Tensoral: A system for post-processing turbulence simulation data p 75 N94-12320

FLOW MEASUREMENT
Pressure and force measurements on models set in hypersonic flows: A review p 5 N94-10435
Problems in the validation of CFD codes through comparison with experiment p 6 N94-10441
Experimental, analytical, and computational methods applied to hypersonic compression ramp flows p 6 N94-10444
Studies of hypersonic viscous flows p 8 N94-10454
Perpendicular blade vortex interaction and its implications for helicopter noise prediction: Wave-number frequency spectra in a trailing vortex for BWI noise prediction [NASA-CR-193623] p 357 N94-10752
An experimental investigation of the sources of propeller noise due to turbulence ingestion p 358 N94-11057
Relativistic heavy ion research [DE93-013127] p 367 N94-11373
Overview of the 1989 Wind Tunnel Calibration Workshop [NASA-TP-3393] p 34 N94-11869
One-year mooring of an ADCP in the central region of the Kuroshio west of Okinawa p 194 N94-11913
Acoustic Doppler current profiling of the Kuroshio over the East China Sea shelf slope p 194 N94-11914
Measurement of the surface layer current averaged vertically using Multipaths Inverted Echosounder p 194 N94-11915
Quantifying the effect of rheology on plan-view shapes of lava flows p 282 N94-12116
An overview of the capabilities of ARA for the measurement of nozzle discharge and thrust [ARA-MEMO-378] p 55 N94-12283
Experiments on near-wall structure of three-dimensional boundary layers p 159 N94-12309
Development of the one-component diode-array velocimeter [AD-A265552] p 171 N94-12533
Simultaneous 3D turbulent large-scale structures in a flood flow by multi-channels measuring system p 165 N94-12624
The acoustic arrangement for measuring vertical structure of sea current p 223 N94-12729

FLOW RESISTANCE
SWIRL as a means of liquid management in low gravity [NASA-CR-4545] p 412 N94-11523

FLOW STABILITY
Dielectric liquid bridge stabilization in microgravity by means of electric fields p 100 N94-10075
Instability of thermocapillary convection in floating zones p 101 N94-10076
Thermocapillary instabilities in cylindrical liquid bridges: Mechanisms and transition boundaries p 101 N94-10077
Stability of liquid bridges between parallel plates p 101 N94-10078
Effects of axial and centrifugal forces on the stability of liquid bridges p 102 N94-10083
Liquid bridges and floating zones p 102 N94-10085
The effect of gravity modulation on thermosolutal convection p 105 N94-10103
Proceedings of the 8th European Symposium on Materials and Fluid Sciences in Microgravity, volume 2 [ESA-SP-333-VOL-2] p 112 N94-10171
Thermocapillary convection instability in microgravity crystal growth p 112 N94-10172
Pulsatile instability in rapid directional solidification: Strongly-nonlinear analysis p 115 N94-10188
Ground results of the Mephisto program: Benefits and space experiments orientation p 86 N94-10197
Transient effects in the Benard instabilities: Coupling between capillary and gravity effects p 119 N94-10216
Numerical investigations on Marangoni-Benard instability in multi layer systems p 120 N94-10217
Instability of thermocapillary convection in multiple superposed immiscible liquid layers p 120 N94-10218
Vibrational-thermocapillary parallel flows and stability p 120 N94-10220
Appearance of convective instabilities caused by liquid-liquid phase separation under small buoyancy forces p 120 N94-10221
The combined influence of anticonvective and thermocapillary mechanisms on the stability of systems with interface p 121 N94-10223
Large time-step stability of explicit one-dimensional advection schemes [NASA-TM-106203] p 342 N94-10362
Stability of hypersonic flow over a blunt body p 7 N94-10450
Stability of hypersonic boundary-layer flows with chemistry p 7 N94-10451
On the instability of hypersonic flow past a pointed cone: Comparison of theoretical and experimental results at Mach 8 p 8 N94-10453
Examination of wall functions for a parabolized Navier-Stokes code for supersonic flow [DE93-011590] p 14 N94-11111
Stability in Aerospace Systems [AGARD-R-789] p 31 N94-11489
Stability of viscoelastic flow: Physical and numerical considerations p 31 N94-11493
Boundary layer transition: Prediction and wind tunnel simulation p 32 N94-11498
Stability model of the atmosphere p 32 N94-11500
The role of plasma rotation on MHD instabilities in tokamaks [DE93-013486] p 393 N94-11512
A simple model of melt fracture [AD-A265311] p 92 N94-11862
Similarity states of homogeneous stably-stratified turbulence at infinite Froude number p 156 N94-12292
Direct numerical simulation of hot jets p 156 N94-12295
Receptivity in parallel flows: An adjoint approach p 157 N94-12301
Numerical simulation of the non-Newtonian mixing layer p 159 N94-12314
The Third Workshop on Two Phase Fluid Experiment in the Space Environment [NASDA-CON-930002] p 161 N94-12547
Developmental research of thermal control system in space environment p 162 N94-12551
Two phase flow and isopycnic liquid-liquid two phase fluid in reduced gravity field p 162 N94-12552
Research on two phase flow in microgravity p 162 N94-12554
Nonlinear stability calculations of pipe flow p 163 N94-12612
Nonlinear instability of a laminar flow in a rectangular duct and generation of the turbulent secondary flow p 164 N94-12622
On a nonstationary dynamics of the north-west Pacific Ocean p 222 N94-12724

FLOW VELOCITY
Comparison of hydrodynamic and semi-kinetic treatments for plasma flow along closed field lines [NASA-CR-193589] p 387 N94-10641
Laser anemometer measurements and computations for transonic flow conditions in an annular cascade of high turning core turbine vanes [NASA-TP-3383] p 15 N94-11133
Shear coaxial injector atomization phenomena for combusting and non-combusting conditions [NASA-CR-193339] p 152 N94-11526
Kuroshio observations by the HF ocean radar p 192 N94-11904
Groundwave HF ocean surface radar p 139 N94-11906
Current structures in the western equatorial Pacific during JAPACS cruises p 193 N94-11911
One-year mooring of an ADCP in the central region of the Kuroshio west of Okinawa p 194 N94-11913
Acoustic Doppler current profiling of the Kuroshio over the East China Sea shelf slope p 194 N94-11914
Measurement of the surface layer current averaged vertically using Multipaths Inverted Echosounder p 194 N94-11915
Suppression of the near wall burst process of a fully developed turbulent pipe flow [AD-A265995] p 161 N94-12352
Rainfall-runoff estimation using digital radar [AD-A265390] p 286 N94-12408
Fluctuations of longitudinal vortices along a concave wall p 16 N94-12616
Evaluation of the method of geostrophic flow using NOAA-AVHRR data p 213 N94-12673
The circulation near Luzon p 219 N94-12707
Current variability on the shelf break northeast of Taiwan p 219 N94-12708
Advective surface velocity in the north west Pacific derived from NOAA AVHRR images p 222 N94-12721
The acoustic arrangement for measuring vertical structure of sea current p 223 N94-12729
Coupled numerical model for altimetric data assimilation and velocity field analysis p 227 N94-12752
Mixing of drifter ensemble by mesoscale currents p 228 N94-12760

FLOW VISUALIZATION
Experimental study of axisymmetric thermocapillary flows p 100 N94-10072
Experimental analysis of Benard-convection by the combined application of liquid crystals and PIV p 106 N94-10109
Flow visualization of shock propagation in baffle systems [DE93-013312] p 147 N94-10307
Control effectiveness at hypersonic speeds p 3 N94-10426
Flow visualization and spectroscopy in hypersonic flows: New trends p 5 N94-10437
Joint computational and experimental aerodynamic research on a hypersonic vehicle p 6 N94-10445
Schlieren photographs and internal pressure distributions for three-dimensional sidewall-compression scramjet inlets at a Mach number of 6 in CF4 [NASA-TM-4479] p 148 N94-10644
Evaluation of dual flow thrust vectored nozzles with exhaust stream impingement [NASA-CR-193292] p 150 N94-10912
SAUNA: A system for grid generation and flow simulation using hybrid structured/unstructured grids [ARA-MEMO-370] p 154 N94-11859
The evolution of whole field optical diagnostics for external transonic testing [ARA-MEMO-379] p 383 N94-11887

Experiments on near-wall structure of three-dimensional boundary layers p 159 N94-12309
Proceedings of the 9th and 10th NAL Workshop on Investigation and Control of Boundary-Layer Transition [NAL-SP-18] p 163 N94-12611
Visual structure of Karman vortex streets in a route to chaotic states excited by oscillation of a circular cylinder p 17 N94-12633

FLUE GASES
High-temperature corrosion of ceramic-ceramic composites in a waste incinerator environment [DE93-012430] p 72 N94-11368

FLUENCE
Proton transport methods for satellite shield modeling [DE93-013602] p 42 N94-10520
The influence of irradiation conditions, type, and concentration of impurities on radiation defects characteristics in indium antimonide under electron irradiation [DE93-617201] p 397 N94-10843
Momentum induced by laser-tissue interaction [DE93-010737] p 301 N94-11667

FLUID BOUNDARIES
The combined influence of anticonvective and thermocapillary mechanisms on the stability of systems with interface p 121 N94-10223

FLUID DYNAMICS
Non-linear liquid bridge dynamics p 100 N94-10074
Transient three-dimensional numerical simulation of Marangoni flow in a liquid column under microgravity p 101 N94-10079
Towards real time numerical stimulation of Marangoni convection: A help for telescience microgravity experiments p 102 N94-10087
Protein, glass, aerosol research, containerless processing and diagnostics technology for microgravity application p 106 N94-10112
Description of the liquid structure facility architecture and experimental demonstration of the diagnostic capabilities p 39 N94-10118
The advanced fluid physics module: How to achieve scientific goals for Spacelab D2 p 39 N94-10136
The kinematics of buoyancy induced mixing p 123 N94-10239
Dynamics and control of coherent structures in the turbulent wall layer: An overview p 31 N94-11494
Stability model of the atmosphere p 32 N94-11500
Reconstruction of the dynamics of the 1800-1801 Hualalai eruption: Implications for planetary lava flows p 281 N94-12041

FLUID FILMS
Fluid-fluid interfacial instabilities induced by gravity p 121 N94-10229
Hygroscopic absorption to falling films: The effects of the concentration level [ITN-93-85198] p 148 N94-10391
Determination of concentration profiles at interfaces and surfaces of partially miscible polymer blends [DE93-013140] p 89 N94-11007

FLUID FLOW
Effect of rotation on microgravity floating-zone crystal growth p 101 N94-10080
Thermocapillary slug flow in a capillary tube p 105 N94-10104
Numerical simulation of Marangoni convection around gas bubbles in a liquid matrix p 106 N94-10107
Vibrational-thermocapillary parallel flows and stability p 120 N94-10220
Grid optimization and multigrid techniques for fluid flow and transport problems p 154 N94-11824
A study of pollution courses of spilled oil floatation in the outer ocean p 205 N94-11983
Reconstruction of the dynamics of the 1800-1801 Hualalai eruption: Implications for planetary lava flows p 281 N94-12041
Quantifying the effect of rheology on plan-view shapes of lava flows p 282 N94-12116
Large volcanoes on Venus: Examples of geologic and structural characteristics from different classes p 467 N94-12195

FLUID MANAGEMENT
SWIRL as a means of liquid management in low gravity [NASA-CR-4545] p 412 N94-11523

FLUID MECHANICS
The International Microgravity Laboratory, a Spacelab for materials and life sciences p 125 N94-10249
On the Sobolev systems with ellipsoid cavities [DE92-641290] p 148 N94-10530
Summary of research in progress at ICASE [NASA-CR-191481] p 318 N94-11198
A model of elementary chemistry and fluid mechanics in the combustion of hydrogen on platinum surfaces [DE93-012767] p 77 N94-11370
Research in computing and applied mathematics [AD-A266137] p 331 N94-11657

FLUIDIZED BED PROCESSORS
Granular instability in fluidized beds: A small-over-large instability p 122 N94-10235

FLUORESCENCE
Dynamics of charge-transfer excited states relevant to photochemical energy conversion [DE93-013981] p 263 N94-11116
The development of phytoplankton sensing system with optical fiber p 203 N94-11967
Characterization of dissolved organic matter in the ocean by using the fluorescence excitation-emission matrix p 211 N94-12659

FLUORINE
An experimental program for collective acceleration of ions using intense relativistic electron beams [DE93-612205] p 371 N94-10316
Minor and trace element composition and age of Yukon probable-microtektites p 429 N94-12094

FLUOROSILICATES
Production of electronic grade lunar silicon by disproportionation of silicon difluoride p 435 N94-12017

FLUTTER
Estimation of critical values and vibration characteristics on supersonic delta wings. Part 1: On-line time series analysis of stationary random response [NAL-TR-1153] p 2 N94-10363
Ground vibration and flight flutter tests of the single-seat F-16XL aircraft with a modified wing [NASA-TM-104269] p 26 N94-11233

FLUTTER ANALYSIS
Nonlinear aspects of transonic aeroelasticity p 2 N94-10357
Estimation of critical values and vibration characteristics on supersonic delta wings. Part 1: On-line time series analysis of stationary random response [NAL-TR-1153] p 2 N94-10363
Laser velocimeter measurements of the flow field generated by a forward-swept propfan during flutter [NASA-TM-106195] p 14 N94-10892
Ground vibration and flight flutter tests of the single-seat F-16XL aircraft with a modified wing [NASA-TM-104269] p 26 N94-11233
Nonlinear aspects of transonic aeroelasticity [UTIAS-RN-345] p 15 N94-11857
Improvement of method for experimental determination of flutter speed by parameter identification [NASA-CR-193555] p 33 N94-12769
VIB2D: Quasi 3-D unsteady viscous flow method for blade flutter calculation [CUED/A-TURBO/TR.129] p 166 N94-12779

FLUX (RATE)
Dynamics of ion acceleration in electron flux by a virtual cathode potential [DE93-620978] p 371 N94-10542
Photochemical modelling of Venus clouds using Pioneer Venus data [NASA-CR-194108] p 434 N94-10823
Szilard-Chalmers effect in solid HIO4.2H2O by neutron irradiation [DE93-617173] p 397 N94-10830
Air-sea fluxes and universal constants in weak-turbulence theory of surface gravity waves p 195 N94-11922
Surface eddy fluxes from the GEOSAT satellite altimeter p 208 N94-12643

FLUX DENSITY
Dynamics of ion acceleration in electron flux by a virtual cathode potential [DE93-620978] p 371 N94-10542
Diagnostic complex for the space-time analysis of energy and current of pulsed relativistic particles [DE93-620980] p 362 N94-10649
Intraday variability and the compactness of extragalactic radio sources p 135 N94-11064
Short pulse lasers for generation of fields exceeding 100 MG [DE93-013346] p 369 N94-11815
Probability density distribution of velocity differences at high Reynolds numbers p 158 N94-12304
The ideal Kolmogorov inertial range and constant p 158 N94-12305

FLUX VECTOR SPLITTING
On the accuracy and efficiency of CFD methods in real gas hypersonics p 9 N94-10462

FLUXES
Advanced soldering processes [DE93-009856] p 129 N94-11606

FLY BY WIRE CONTROL
Specification and testing for power by wire aircraft [NASA-TM-106232] p 46 N94-10765

FOAMS
A new low smoke, low heat release structural foam p 17 N94-10768
Polyimide foam insulation systems: A major weight reduction and improvement in fire resistance of sidewall systems p 17 N94-10769
A polyimide foam for advanced fire resistant aircraft applications p 17 N94-10770

FOCAL PLANE DEVICES
Superconducting SQUID amplifiers for IR detectors and other applications, phase 2 [AD-A265447] p 145 N94-12333
Development of ultra-low noise, high sensitivity planar metal grating coupled 3 to 5 multiquantum well infrared detectors for focal plane array staring IR sensor systems [AD-A265599] p 404 N94-12375

FOG
Statistical study on the regional and seasonal distribution of fog in the far east region by using GMS imagery p 190 N94-11082
An examination of the evolution of radiation and advection fogs [AD-A266127] p 286 N94-12539

FOKKER-PLANCK EQUATION
Momentum and heat frictions between fast ions and thermal plasma species [DE93-771240] p 390 N94-11149

FOLDS (GEOLOGY)
Global organization of tectonic deformation on Venus p 444 N94-12066

FORBIDDEN BANDS
Surface-enhanced raman spectroscopy of electroactive films of C60 and an Ir-C60 complex on gold: Symmetry lowering, electron localization, and counteraction effects [AD-A265934] p 396 N94-10705

FORCED VIBRATION
Vortex-induced forces on oscillating bluff cylinders [AD-A265056] p 154 N94-11865

FOREBODIES
Physics of forebody flow control [NASA-CR-193626] p 15 N94-11195

FORECASTING
Forecasting the impact of virtual environment technology on maintenance training p 314 N94-11570
HF-OTH radar performance results [AD-A266106] p 138 N94-11655
Disturbance Impact Assessment System (DIAS), version 2.0. System design document [AD-A265251] p 138 N94-11883
Impact of ERS-1 wind/wave/ice data on operational ocean forecasting p 250 N94-12500
Federal Aviation Administration aviation forecasts [AD-A265611] p 2 N94-12578

FOREST FIRE DETECTION
A method to minimize reference data in classifying satellite remote sensing data into land cover classes p 219 N94-12705

FOREST MANAGEMENT
International Space Year in China p 36 N94-10680
Satellite inventory of Minnesota forest resources [NASA-CR-193565] p 231 N94-11521
The use of remote sensing data for coastal zone management and environment in Indonesia p 196 N94-11927
Preliminary ERS-1 assessment for Canadian agriculture and forestry applications p 248 N94-12486

FORESTS
Effect of species structure and dielectric constant on C-band forest backscatter [NASA-TM-109219] p 245 N94-11885
Methodological considerations for use of ERS-1 imagery for the delineation of river networks in tropical forest areas p 247 N94-12484
Observations of ERS-1 SAR sensitivities to changes in aboveground biomass in young loblolly pine forests p 249 N94-12494
Seeing the Black Forest by ERS-1 and AIRSAR: A comparison p 249 N94-12495
Properties of spectral reflectance of crown and crown structure of mangrove species in Okinawa p 218 N94-12700

FORM FACTORS
Optimal hemicube sampling [DE93-010499] p 334 N94-12591

FORMALISM
An algebraic approach to incomparable families of formal languages [MEMO-INF-92-82] p 342 N94-10279
On a Lagrange-Hamilton formalism describing position and momentum uncertainties p 349 N94-10583
Observables, measurements and phase operators from a Bohmian perspective p 378 N94-10589
Green-Schwarz superstrings in the generalized harmonical Newmann-Penrose formalism [DE93-621422] p 412 N94-11088

FORMAT
Correspondence standards [NHB-1450.10B] p 420 N94-11589

FORMING TECHNIQUES
SPF/DB: A manufacturing technique for lightweight structures p 59 N94-10026
Application of advanced thermoplastics p 60 N94-10033

FORTRAN
CRESLAF. Version 4.0: A Fortran program for modeling laminar, chemically reacting, boundary-layer flow in cylindrical or planar channels [DE93-012835] p 152 N94-11371
Avoidance and suppression of compensation code in a trace scheduling compiler [AD-A265612] p 333 N94-12439

FORWARD SCATTERING
Indication on the existence of the bound state in the p anti p-system [DE92-641575] p 361 N94-10532
Fermion-boson scattering in ladder approximation [DE93-613111] p 368 N94-11581
Light scattering from a spherical particle on a conducting plane. Part 1: Normal incidence [AD-A265920] p 383 N94-12341

FOSSIL FUELS
Coprocessing of fossil fuels and biomass for CO2 emission reduction in the transportation sector [PB93-194165] p 267 N94-11845

FOUR-WAVE MIXING
Nonclassical states of the second optical harmonic in the presence of self-action p 375 N94-10567
Squeezing in phase-conjugated resonance fluorescence p 376 N94-10576

FOURIER ANALYSIS
Finite difference schemes for long-time integration [NASA-CR-191471] p 343 N94-10642
The role of plasma rotation on MHD instabilities in tokamaks [DE93-013486] p 393 N94-11512
Spectrum analysis in beam diagnostics [DE93-013401] p 373 N94-12601

FOURIER TRANSFORMATION
Ionization potentials of small carbon clusters [AD-A264379] p 67 N94-11260
Presort processor — optical filtering [AD-A263872] p 382 N94-11300
FFTSCAN: A program for spectral smoothing using Fourier transforms [AD-A264921] p 278 N94-11852
Fourier domain target transformation analysis in the thermal infrared p 258 N94-12030
A novel test method for fuel thermal stability [AD-A265853] p 99 N94-12275

FOURIER-BESSEL TRANSFORMATIONS
The searchlight problem for neutrons in a semi-infinite medium [DE93-010796] p 365 N94-10952

FRACTALS
Singularity spectrum of self-organized criticality [DE93-613820] p 348 N94-10404
To the complexity of dynamic system problem [DE93-621355] p 134 N94-11037
On a p-adic metrical dimension of space [DE93-621374] p 345 N94-11077
Observations of the fractal properties of the Japan sea surface temperature patterns p 205 N94-11984
Fractal dimensions of rampart impact craters on Mars p 460 N94-12154
Generalized Mandelbrot rule for fractal sections [AD-A266010] p 347 N94-12390

FRACTIONATION
LEW88516 and SNC meteorites p 430 N94-12150
Iron and nickel isotopic mass fractionation in deep-sea spherules p 282 N94-12199
The Fe/Mn constraint on precursors of basaltic achondrites p 432 N94-12208
Development of a molecular beam technique to study early solar system silicon reactions p 432 N94-12224

FRACTOGRAPHY
Fractography handbook of spaceflight metals [NASA-RP-1291] p 81 N94-10504

FRACTURE MECHANICS
Design with high strength steel: A case of failure and its implications p 58 N94-10017
Heavy-section steel technology program [DE93-009222] p 184 N94-10155
Potential change in flaw geometry during pressurized-thermal-shock transients [DE93-009709] p 184 N94-10288
Fracture behavior of surface-modified ceramics [DE93-013707] p 88 N94-10710
Elastic plastic fracture mechanics methodology for surface cracks [NASA-CR-194129] p 185 N94-10712
Micromechanisms of fatigue crack growth and fracture toughness in metal matrix composites [AD-A265153] p 187 N94-11096
DBTT measurement by use of Small Punch (SP) test [DE93-753188] p 183 N94-11168
Fracture mechanics and full scale pipe break testing for the Department of Environment's New Production Reactor-Heavy Water Reactor [DE93-005428] p 187 N94-11169
Understanding cracking failures of coatings: A fracture mechanics approach p 187 N94-11218
Integral equation methods for mixed boundary problem of fracture mechanics p 188 N94-11617
Explicit 3D continuum fracture modeling with smooth particle hydrodynamics p 429 N94-12062
Fracture behavior of ionomers and ionomeric blends [AD-A265379] p 94 N94-12407
Fatigue in single crystal nickel superalloys [AD-A266116] p 85 N94-12418

FRACTURE STRENGTH
Extensions of some guidelines for the mechanical design of coaxial compression pin seals [DE93-012385] p 177 N94-10348
Elastic plastic fracture mechanics methodology for surface cracks [NASA-CR-194129] p 185 N94-10712
Micromechanisms of fatigue crack growth and fracture toughness in metal matrix composites [AD-A265153] p 187 N94-11096
Interface considerations in Al2O3/NiAl composite [NASA-CR-191167] p 66 N94-11202
NiAl alloys for structural uses [NASA-CR-194113] p 85 N94-12447

FRACTURES (MATERIALS)
Damage thresholds of fluoride multilayers at 355 nm [DE93-009523] p 90 N94-11230
Pilot trial of potentiating normal healing of stress fractures using pulsing electromagnetic fields [AD-A264251] p 311 N94-12364

FRACTURING
Fracture behavior of surface-modified ceramics [DE93-013707] p 88 N94-10710
Test specifications, specimen design and instrumentation test data interpretation [DE93-012338] p 188 N94-11367
The effect of processing on the microstructure and tensile properties of a (gamma)-TiAl based alloy [DE93-013221] p 84 N94-11488
Ceramic technology project database [DE93-012432] p 91 N94-11673
Pilot trial of potentiating normal healing of stress fractures using pulsing electromagnetic fields [AD-A264251] p 311 N94-12364
Fracture behavior of ionomers and ionomeric blends [AD-A265379] p 94 N94-12407

FRAGMENTATION
Ejecting basaltic achondrites from Vesta: Hydrodynamical impact models p 429 N94-12036
Analysis of interstellar fragmentation structure based on IRAS images [NASA-CR-193518] p 428 N94-12767

FRAGMENTS
Laboratory studies on the velocity of fragments from impact disruptions p 189 N94-12359

FRAMES (DATA PROCESSING)
Formal specification of the plain UCN layer in LOTOS [MEMO-INF-92-83] p 131 N94-10280

FREE ATMOSPHERE
Free-air and Bouguer gravity anomalies and the Martian crustal dichotomy p 481 N94-12267
New Mars free-air and Bouguer gravity: Correlation with topography, geology and large impact basins p 481 N94-12268

FREE BOUNDARIES
Marangoni flows in open cavities with differentially heated end walls p 104 N94-10097
Boundary layers along horizontal free surfaces due to combined effects of temperature and concentration gradients p 106 N94-10108
Numerical calculation of the growth of InP by the travelling heater method in the first mission of the Space Flyer Unit p 114 N94-10179
Convective motion in a multi-layered system with a free surface p 120 N94-10219

FREE CONVECTION
Solidification from supercooled melt under microgravity p 113 N94-10176
The effect of gravitational modulation on convection in vertical Bridgman growth p 113 N94-10178
Convection related radial segregation in an idealized horizontal Bridgman configuration p 115 N94-10185
Effect of gravity on the dissolution and liquid phase epitaxial growth processes in a horizontal sandwich system p 118 N94-10208
Marangoni instability in a liquid layer with two free surfaces [NASA-TM-106166] p 152 N94-11376
Numerical simulations of thermal convection in rapidly rotating spherical fluid shells p 153 N94-11635

FREE ELECTRON LASERS
Numerical simulation of sidebands in free electron laser oscillators [DE93-612675] p 173 N94-10483
The efficiency of photovoltaic cells exposed to pulsed laser light p 50 N94-11395
LCLS optics: Selected technological issues and scientific opportunities [DE93-010953] p 175 N94-11468

FREE ENERGY
Atomic structures and compositions of internal interfaces [DE93-014840] p 363 N94-10750

FREE FLIGHT
Boundary layer transition: Prediction and wind tunnel simulation p 32 N94-11498

FREE FLOW
Boundary layer transition: Prediction and wind tunnel simulation p 32 N94-11498
Fluctuations of longitudinal vortices along a concave wall p 16 N94-12616

FRENKEL DEFECTS
Grain boundaries in complex oxides [DE93-013986] p 398 N94-11012

FREQUENCIES
Coherent states and uncertainty relations for the damped harmonic oscillator with time-dependent frequency p 380 N94-10611
The 2nd Annual Meeting of the Society for Research on Biological Rhythms [AD-A264869] p 303 N94-10872

FREQUENCY CONVERTERS
A study of DC-DC converters with MCTs for arcjet power supplies [NASA-CR-193457] p 142 N94-10931

FREQUENCY DISCRIMINATORS
Status of local oscillators for operating ultra-high resolution frequency discriminators as frequency standards p 353 N94-10981

FREQUENCY DISTRIBUTION
Performance of low-cost commercial fiber-optic transceivers for reference frequency distribution p 355 N94-10993
Ultrastable reference frequency distribution utilizing a fiber optic link p 355 N94-10994
A wide-band fiber optic frequency distribution system employing thermally controlled phase compensation p 355 N94-10995
Venus small volcano classification and description p 438 N94-12037

FREQUENCY MEASUREMENT
Journal of Research of the National Institute of Standards and Technology, volume 98, number 2, March - April 1993 [PB93-196228] p 485 N94-10850
A laser-cooled cesium fountain frequency standard and a measurement of the frequency shift due to ultra-cold collisions p 352 N94-10976
Measurement methods and algorithms for comparison of local and remote clocks p 354 N94-10987
Spacecraft signal sources portable test system p 139 N94-11000
The limit of frequency estimation p 356 N94-11001
A new method of time difference measurement: The time difference method by dual phase coincidence points detection p 357 N94-11002

FREQUENCY MODULATION
Spreading of Bimodulated Ultra-relativistic Electron Beam (BUEB) in Atmospheric Plasma Channel (APCh) [DE93-621658] p 392 N94-11213

FREQUENCY RANGES
Design of a matching network for dipole antennas [AD-A265115] p 136 N94-11158
Improvement of method for experimental determination of flutter speed by parameter identification [NASA-CR-193555] p 33 N94-12769

FREQUENCY RESPONSE
AD100/ADSIM, ACSL, and MATLAB output comparisons using frequency-response analysis [DE93-009640] p 47 N94-11122

FREQUENCY SHIFT
A laser-cooled cesium fountain frequency standard and a measurement of the frequency shift due to ultra-cold collisions p 352 N94-10976
Confidence of the three-point estimator of frequency drift p 357 N94-11003

FREQUENCY STABILITY
Possible applications of atomic frequency standards with an internal high resolution digital synthesizer p 353 N94-10979
Status of local oscillators for operating ultra-high resolution frequency discriminators as frequency standards p 353 N94-10981
Estimating the instabilities of N clocks by means of comparison measurements p 356 N94-10997

A multi-variance analysis in the time domain
p 146 N94-10999
Spacecraft signal sources portable test system
p 139 N94-11000
The limit of frequency estimation p 356 N94-11001

FREQUENCY STANDARDS
The 24th Annual Precise Time and Time Interval (PTTI) Applications and Planning Meeting
[NASA-CP-3218] p 350 N94-10963
A laser-cooled cesium fountain frequency standard and a measurement of the frequency shift due to ultra-cold collisions p 352 N94-10976
A precise GPS-based time and frequency system
p 353 N94-10978
Possible applications of atomic frequency standards with an internal high resolution digital synthesizer
p 353 N94-10979
CAFS: A Cesium Atomic Frequency Standard for GPS block IIR p 353 N94-10980
Status of local oscillators for operating ultra-high resolution frequency discriminators as frequency standards p 353 N94-10981
Development of a cryogenic hydrogen maser at the NPL p 176 N94-10982
Performance of low-cost commercial fiber-optic transceivers for reference frequency distribution
p 355 N94-10993
Ultrastable reference frequency distribution utilizing a fiber optic link p 355 N94-10994
Estimating the instabilities of N clocks by means of comparison measurements p 356 N94-10997
Time scale algorithms for an inhomogeneous group of atomic clocks p 356 N94-10998
Spacecraft signal sources portable test system
p 139 N94-11000

FREQUENCY SYNTHESIZERS
Possible applications of atomic frequency standards with an internal high resolution digital synthesizer
p 353 N94-10979

FRESNEL LENSES
Recent developments in refractive concentrators for space photovoltaic power systems p 52 N94-11402

FRICTION
Titanium alloys milling assistance by high pressure lubricoolant jet
[DE93-013302] p 82 N94-11008
Polar solvation and electron transfer
[DE93-013328] p 365 N94-11010
Momentum and heat frictions between fast ions and thermal plasma species
[DE93-771240] p 390 N94-11149
Instantaneous engine frictional torque: Its components and piston assembly friction
[DE93-011639] p 182 N94-11625
Ceramics technology project database
[DE93-012431] p 91 N94-11672
Progress in modeling hypersonic turbulent boundary layers p 157 N94-12300
Properties of interfacial tribo-films
[AD-A265591] p 182 N94-12374

FRICTION FACTOR
Instantaneous engine frictional torque: Its components and piston assembly friction
[DE93-011639] p 182 N94-11625

FRICTION MEASUREMENT
Durability of a carbon segmented circumferential seal for a liquid oxygen turbopump
[NAL-TR-1155] p 178 N94-10369
Tribological characteristics of hot-pressed self-lubricating composites
[NAL-TR-1160] p 66 N94-10858

FRONTAL WAVES
Coastal ocean studies with ERS-1 SAR during NORCSEX 1991 p 234 N94-11720

FROST
Spatial variation in the seasonal south polar cap of Mars as observed by Mariner 7 p 456 N94-12134

FROUDE NUMBER
Similarity states of homogeneous stably-stratified turbulence at infinite Froude number
p 156 N94-12292

FUEL CELL POWER PLANTS
Polymer electrolyte fuel cells: Potential transportation and stationary applications
[DE93-010734] p 264 N94-11666

FUEL CELLS
Thin film preparation and interfacial reaction study of solid oxide fuel cell materials p 263 N94-11313
Life-cycle cost analysis of conventional and fuel cell/battery powered urban passenger vehicles
[DE93-010770] p 182 N94-11438
Polymer electrolyte fuel cells: Potential transportation and stationary applications
[DE93-010734] p 264 N94-11666
Research development and demonstration of a fuel cell/battery powered bus system
[DE93-013778] p 182 N94-12605

FUEL COMBUSTION
Application of jet-shear-layer mixing and effervescent atomization to the development of a low-NO(x) combustor
[NASA-TM-105888] p 28 N94-11234
On the combustion of a laminar spray
[NASA-TM-106210] p 28 N94-11238
A laboratory model of a hydrogen/oxygen engine for combustion and nozzle studies
[NASA-TM-106281] p 47 N94-11252
Life-cycle cost analysis of conventional and fuel cell/battery powered urban passenger vehicles
[DE93-010770] p 182 N94-11438

FUEL INJECTION
Space Storable Rocket Technology program (SSRT). Option 1 program
[NASA-CR-191171] p 46 N94-10938
Application of jet-shear-layer mixing and effervescent atomization to the development of a low-NO(x) combustor
[NASA-TM-105888] p 28 N94-11234
A laboratory model of a hydrogen/oxygen engine for combustion and nozzle studies
[NASA-TM-106281] p 47 N94-11252
Shear flow control of gas jets in liquids
[AD-A264673] p 152 N94-11448

FUEL PRODUCTION
Thermodynamics of lunar ilmenite reduction
p 415 N94-12028

FUEL SPRAYS
Atomization characteristics of a prefilming airblast atomizer
[NAL-TM-644] p 148 N94-10727
On the combustion of a laminar spray
[NASA-TM-106210] p 28 N94-11238

FUEL TANKS
Propellant management in surface tension tanks
p 106 N94-10110

FUEL TESTS
A novel test method for fuel thermal stability
[AD-A265853] p 99 N94-12275

FULL SCALE TESTS
An experimental investigation of high-speed water-entry for full-size and scale-model pointed nose vehicles
[DE93-008491] p 147 N94-10252

FULLERENES
Bond distortion and electron trapping in charged C60
[DE93-613642] p 396 N94-10637
Surface-enhanced raman spectroscopy of electroactive films of C60 and an Ir-C60 complex on gold: Symmetry lowering, electron localization, and counteraction effects
[AD-A265934] p 396 N94-10705
Fullerene superconductors: Phase stability and anomalously low T(sub c)'s in some ternary compounds
[DE93-010687] p 400 N94-11457

FUNCTION SPACE
One-loop quantum gravity on de Sitter space
[DE92-641349] p 425 N94-11152
Divergences in the moduli space integral and accumulating handles in the infinite-genus limit
[DE93-619722] p 346 N94-11693

FUNCTIONAL ANALYSIS
Functional reasoning, explanation, and analysis
[DE92-526832] p 313 N94-10251
Applications of cut polyhedra
[CWI-BS-R9221] p 347 N94-10354
Functional approximation using artificial neural networks in structural mechanics
[NASA-TM-105820] p 188 N94-11254
Comparison of multiresolution techniques for digital signal processing
[AD-A265364] p 138 N94-12406

FUNCTIONALS
The modular group and super-KMS functionals
[DE93-613029] p 349 N94-10632

FUNCTIONS (MATHEMATICS)
Complex functions in queueing theory
[CWI-BS-R9219] p 342 N94-10352

FURNACES
The electron beam furnace: A new facility for materials science research p 109 N94-10126
Microgravity Applications Furnace Facility (MAFF) for parabolic flights p 109 N94-10128
MUZO: The programmable multi zone furnace for gas payloads and sounding rockets p 110 N94-10132
AGF (Automatic Gradient Furnace): A proposed microgravity facility p 112 N94-10141
Variations of the temperature profile in the gradient furnace GFQ within a cylindrical sample used for directional solidification p 114 N94-10181
Design of CCD camera system for use inside electron beam furnace
[DE93-009525] p 170 N94-11267

FUSELAGES
An investigation into aircraft fuselage fire hardening
p 19 N94-10782

FUSION REACTORS
Looking beyond ITER: Toroidal concept improvement
[DE93-012762] p 388 N94-10744
Applying design principles to fusion reactor configurations for propulsion in space
[NASA-TM-106247] p 47 N94-11053
The possibility of using carbon-graphite materials for microwave plasma diagnostics in large fusion devices
[DE93-621609] p 66 N94-11143
Experimental approach to the physics of the high density divertor
[DE93-009149] p 391 N94-11170
Intense neutron sources for fusion materials studies
[DE93-009782] p 391 N94-11171
Damage thresholds of fluoride multilayers at 355 nm
[DE93-009523] p 90 N94-11230

FUZZY SYSTEMS
Telerobotic control of a mobile coordinated robotic server
[NASA-CR-193465] p 338 N94-10345
Task planning with uncertainty for robotic systems
[NASA-CR-193253] p 338 N94-10638
Fuzzification of ASAT's rule based aimpoint selection
[AD-A266068] p 43 N94-11223

G

GALACTIC CLUSTERS
The three-point function as a probe of models for large-scale structure
[NASA-CR-193249] p 425 N94-11153

GALACTIC COSMIC RAYS
Acceleration of positrons in supernova shocks
[NASA-CR-193713] p 425 N94-10511
Development of deterministic transport methods for low energy neutrons for shielding in space
[NASA-CR-194172] p 366 N94-11199
A proposed performance index for galactic cosmic ray shielding materials
[NASA-TM-4444] p 484 N94-11278
Potential health effects of space radiation
p 312 N94-11558
Radiation considerations for interplanetary missions
p 45 N94-11559
Final state interactions and inclusive nuclear collisions
[NASA-TP-3353] p 373 N94-12435

GALACTIC EVOLUTION
Nuclear astrophysics
[DE93-010569] p 425 N94-10292
The three-point function as a probe of models for large-scale structure
[NASA-CR-193249] p 425 N94-11153

GALACTIC HALOS
ADP study of the structure of the IUE halo
[NASA-CR-194374] p 428 N94-12595

GALACTIC ROTATION
ADP study of the structure of the IUE halo
[NASA-CR-194374] p 428 N94-12595

GALACTIC STRUCTURE
The three-point function as a probe of models for large-scale structure
[NASA-CR-193249] p 425 N94-11153
The morphologies of distant radio galaxies
p 426 N94-11597

GALAXIES
Cosmological gamma-ray burst model
[NASA-CR-193368] p 484 N94-10507

GALERKIN METHOD
On cell entropy inequality for discontinuous Galerkin methods
[NASA-CR-191493] p 345 N94-11280
Dynamics and control of coherent structures in the turbulent wall layer: An overview p 31 N94-11494

GALILEO PROJECT
Galileo EM-2 contributions to the lunar control network p 468 N94-12198

GALLIUM ANTIMONIDES
Crack suppression in GaInSb buffer layers initially under tensile stress
[DE93-012839] p 396 N94-10745

GALLIUM ARSENIDES
The use of magnetic fields for damping unsteady Marangoni convection in GaAs floating zones under microgravity p 100 N94-10073
Marangoni and buoyant convections in zone melting of GaAs with liquid encapsulation p 101 N94-10081
Concept and design of ampoule for melt growth of gallium arsenide in first mission of space flyer unit
p 107 N94-10115
Method for producing a hybridization of detector array and integrated circuit for readout
[NASA-CASE-NPO-18062-1-CU] p 141 N94-10656

Investigation of ZnSe-coated silicon substrates for GaAs solar cells p 52 N94-11405

GaAs sigma-delta modulator modeling for Analog to Digital Converters (ADC's) [AD-A263419] p 144 N94-11516

GaAs PCSS: High gain switching and device reliability [DE93-009851] p 401 N94-11605

A thermal ionization model for the sustaining phase of lock-on in GaAs [DE93-011558] p 144 N94-11624

Gallium arsenide dynamic random access memory support circuitry [AD-A265176] p 320 N94-11875

Low cost high efficiency GaAs monolithic RF module for SARSAT distress beacons [NASA-CR-194235] p 146 N94-12773

GALLIUM PHOSPHIDES

Remote plasma enhanced chemical vapor deposition of GaP with in situ generation of phosphine precursors p 399 N94-11440

GALVANOMAGNETIC EFFECTS

The influence of irradiation conditions, type, and concentration of impurities on radiation defects characteristics in indium antimonide under electron irradiation [DE93-617201] p 397 N94-10843

GAME THEORY

Marginal allocations in the core of minimal chain-games [MEMO-1103] p 348 N94-10162

GAMMA RAY ASTRONOMY

Data analysis tasks: BATSE [NASA-CR-192598] p 483 N94-12427

Observations of optical counterparts of Gamma-Ray bursts [NASA-CR-193573] p 485 N94-12589

GAMMA RAY BURSTS

Cosmological gamma-ray burst model [NASA-CR-193368] p 484 N94-10507

Data analysis tasks: BATSE [NASA-CR-192598] p 483 N94-12427

Observations of optical counterparts of Gamma-Ray bursts [NASA-CR-193573] p 485 N94-12589

GAMMA RAY OBSERVATORY

Data analysis tasks: BATSE [NASA-CR-192598] p 483 N94-12427

GAMMA RAY SPECTRA

Cosmological gamma-ray burst model [NASA-CR-193368] p 484 N94-10507

The multiplicity spectra of the (169)Tm(n, gamma) reaction [DE93-617733] p 364 N94-10835

GAMMA RAY TELESCOPES

Observations of optical counterparts of Gamma-Ray bursts [NASA-CR-193573] p 485 N94-12589

GAMMA RAYS

Demonstration prototype gamma-ray hodoscope alternative to CARGOSCAN for rocket stage monitoring [DE93-006908] p 169 N94-10326

A new matrix for the ageless 21.6-keV Eu-151 nuclear gamma ray Moessbauer source [DE93-009795] p 75 N94-10338

On problem about nature of Portevin-Le Chatelier effect in irradiated aluminium alloys [DE93-617200] p 82 N94-10842

Development of microstrip gas chamber and application to imaging gamma-ray detector [DE93-754294] p 34 N94-11041

GANYMEDE

Theoretical studies of the radar properties of the icy Galilean moons of Jupiter [NASA-CR-193407] p 434 N94-11361

GAPS

Boundary integral solution to the electromagnetic scattering from coated surfaces containing edges, gaps, and periodic gratings p 137 N94-11639

GAS ANALYSIS

Separation of spallation and terrestrial C-14 in chondrites p 431 N94-12183

Geomorphology of Triton's polar materials p 466 N94-12185

The fractionation of noble gases in diamonds of CV3 Efremovka chondrite p 81 N94-12256

A preliminary study of the variability and magnitude of the flux of biogenic sulfur gases from a New Hampshire salt marsh p 267 N94-12452

Analytical method for water vapor collection and analysis in aircraft cabin fires [DOT/FAA/CT-TN93/33] p 22 N94-12575

The 1991 version of the plume impingement computer program. Volume 2: User's input guide [NASA-CR-194191] p 166 N94-12774

GAS ATOMIZATION

Comparison of Al-Fe alloys produced by PFC and USGA techniques p 58 N94-10019

GAS COMPOSITION

A combustion products analyzer for contingency use during thermodegradation events on spacecraft p 318 N94-11555

GAS DETECTORS

Development of microstrip gas chambers with multi-chip technology [DE93-753169] p 367 N94-11509

GAS DISSOCIATION

Dynamics of dissociation versus ionization in strong laser fields [DE93-009261] p 173 N94-10287

The high enthalpy facilities HEG and TH 2 in Germany p 4 N94-10430

Comparison of computation and experiment for a high enthalpy, heated-driver, shock-tube environment p 7 N94-10447

Electronic excitation of ground state atoms by collision with heavy gas particles [NASA-CR-193364] p 366 N94-11360

GAS DYNAMICS

Lattice gas hydrodynamics: Theory and simulations [DE93-013297] p 147 N94-10320

Issues and approach to develop validated analysis tools for hypersonic flows: One perspective p 7 N94-10446

GAS EXCHANGE

Emissions of biogenic sulfur gases from northern bogs and fens p 271 N94-12467

Factors controlling sulfur gas exchange in Sphagnum-dominated wetlands p 271 N94-12469

Sulfur gas exchange in Sphagnum-dominated wetlands p 271 N94-12470

GAS FLOW

The 1991 version of the plume impingement computer program. Volume 2: User's input guide [NASA-CR-194191] p 166 N94-12774

GAS HEATING

Pulsed plasma processing for control of diesel engine emissions [DE93-011884] p 181 N94-11247

GAS IONIZATION

Detection of accreting circumstellar gas around weak emission-line Herbig Ae/Be stars [NASA-TM-108256] p 424 N94-11306

Are cosmic rays effective for ionization of the solar nebula? p 472 N94-12220

GAS JETS

Gas-liquid jets under reduced gravity conditions p 103 N94-10091

Preprints of the 13th Hydrogen Energy System Symposium [DE93-781115] p 99 N94-11444

Shear flow control of gas jets in liquids [AD-A264673] p 152 N94-11448

GAS MIXTURES

Influence of neutral particles concentration on flame propagation in methane-air mixtures at zero and normal gravity conditions p 121 N94-10224

Thermodynamic model of air in chemical equilibrium p 7 N94-10448

Gas-Grain Simulation Facility (GGSF). Volume 2: Conceptual design definition [NASA-CR-177613] p 423 N94-11229

GAS PRESSURE

Effect of powder processing on slip casting parameters and sintering of Si3N4-Y2O3-SiO2 [AD-A264474] p 83 N94-11445

Hypobaric decompression prebreathe requirements and breathing environment p 317 N94-11541

Instantaneous engine frictional torque: Its components and piston assembly friction [DE93-011639] p 182 N94-11625

Vulcanian explosive eruptions: A mechanism for localised pyroclast dispersal on Venus p 477 N94-12243

GAS STREAMS

Evaluation of dual flow thrust vectored nozzles with exhaust stream impingement [NASA-CR-193292] p 150 N94-10912

GAS TUNGSTEN ARC WELDING

Design of inspection and acceptance test methodology for TIG welded aluminum-alloy bracket for camera housings for IRS-1A space craft and executing it p 61 N94-10037

GAS TURBINE ENGINES

Low-expansion ceramics initiative [DE93-011860] p 89 N94-11106

Icing of turbine intake louvers [AD-A265714] p 29 N94-12274

GAS TURBINES

Proceedings of the Second Technical Meeting on High Temperature Gas-Cooled Reactors [DE93-754285] p 371 N94-10719

Preprints of the 13th Hydrogen Energy System Symposium [DE93-781115] p 99 N94-11444

Advanced controls for airbreathing engines, volume 3: Allison gas turbine [NASA-CR-189205] p 29 N94-12272

GAS VISCOSITY

Gluon gas viscosity in nonperturbative region [DE93-617680] p 397 N94-10883

GAS-LIQUID INTERACTIONS

Gas-liquid jets under reduced gravity conditions p 103 N94-10091

Marangoni Benard instabilities in liquid mixtures with Soret effect p 119 N94-10215

Instability of thermocapillary convection in multiple superposed immiscible liquid layers p 120 N94-10218

Studies of critical point phenomena of fluids: Bulk fluids, fluids in pores, and at interfaces p 80 N94-10228

Transport of heat and mass in near-critical fluids p 122 N94-10230

Phase separation at gas-liquid critical points p 122 N94-10233

Granular instability in fluidized beds: A small-over-large instability p 122 N94-10235

Hygroscopic absorption to falling films: The effects of the concentration level [ITN-93-85198] p 148 N94-10391

GAS-SOLID INTERACTIONS

The rate of chemical weathering of pyrite on the surface of Venus p 477 N94-12246

GASEOUS ROCKET PROPELLANTS

Shear coaxial injector atomization phenomena for combusting and non-combusting conditions [NASA-CR-193339] p 152 N94-11526

GAUGE INVARIANCE

Discrete space-time symmetries [DE93-010199] p 341 N94-10259

Effective action in the gauged Nambu-Jona-Lasinio model [DE93-617654] p 409 N94-10405

Standard model status (in search of new physics) [DE93-013288] p 410 N94-10528

From the Weyl theory to a theory of locally anisotropic space-time [DE92-644734] p 410 N94-10535

Non-gauge phase transformations in quantum transition amplitudes p 378 N94-10596

Principles of gauge theory of real hadrons [DE93-613094] p 362 N94-10634

All possible electroweak models from Z orbifold [DE93-617656] p 411 N94-10880

Gauge independence of the A(sub 0)-condensate [DE93-617681] p 397 N94-10884

Cosmological restrictions on conformally-invariant SU(5) GUT models [DE93-619770] p 412 N94-11047

Green-Schwarz superstrings in the generalized harmonical Newmann-Penrose formalism [DE93-621422] p 412 N94-11088

One-loop quantum gravity on de Sitter space [DE92-641349] p 425 N94-11152

GAUGE THEORY

Principles of gauge theory of real hadrons [DE93-613094] p 362 N94-10634

Gauge independence of the A(sub 0)-condensate [DE93-617681] p 397 N94-10884

GAUSS EQUATION

Optimisation methods for solving separable nonlinear least squares problems [ISVR-TR-219] p 345 N94-11217

GEAR TEETH

Computational gearing mechanics [NASA-CR-193666] p 181 N94-11157

GEARS

AGBT advanced counter-rotating gearbox detailed design report [NASA-CR-180883] p 179 N94-10400

Computational gearing mechanics [NASA-CR-193666] p 181 N94-11157

GELATION

Improving reservoir conformance using gelled polymer systems [DE93-014532] p 88 N94-10749

GELS

Amperometric biosensors based on 3-dimensional hydrogel-forming epoxy networks [AD-A265528] p 87 N94-10510

Improving reservoir conformance using gelled polymer systems [DE93-014532] p 88 N94-10749

Low temperature synthesis of monolithic transparent Ta2O5 gels from hydrolysis of metal alkoxide [NASA-TM-106246] p 89 N94-11204

Synthesis and thermal evolution of structure in alkoxide-derived niobium pentoxide gels [NASA-TM-106259] p 90 N94-11257

Structural development in ceramic precursor sols and gels
[AD-A264354] p 90 N94-11281
Smart polymeric system for electromechanical transduction p 70 N94-11330
Finite element simulation of the 2D collapse of a polyelectrolyte gel disk
[DE93-010693] p 91 N94-11665

GENE EXPRESSION
Studies in bioorganic chemistry
[AD-A265532] p 55 N94-12011

GENERAL AVIATION AIRCRAFT
General aviation aircraft-normal acceleration data analysis and collection project
[AD-A265055] p 26 N94-11858
Federal Aviation Administration aviation forecasts
[AD-A265611] p 2 N94-12578

GEOCHEMISTRY
Environmental Sciences Division
[DE93-013865] p 264 N94-10650
Regional geology of the Vega landing sites: Tentative results of photogeologic mapping p 440 N94-12047
Impact mineralogy and chemistry of the cretaceous-tertiary boundary at DSDP site 576 p 282 N94-12091
Mineralogy versus bulk composition of the carbonaceous chondrite clast Kaidun 2 p 429 N94-12101
Graphite solubility and co-vesiculation in basalt-like melts at one-ATM p 463 N94-12173
Post-impact alteration of the Manson impact structure p 282 N94-12188
Oxidation state of the Earth's upper mantle during the last 3800 million years: Implications for the origin of life p 283 N94-12210
Soret diffusion: A possible cause of compositional heterogeneity within tektites p 432 N94-12211
Solar wind-induced secondary ions and their relation to lunar surface composition p 474 N94-12232

GEOCHRONOLOGY
The Lathrop Wells Volcanic Center: Status of field and geochronology studies
[DE93-008917] p 273 N94-10285
Radiogenic age and isotopic studies
[DE93-610548] p 274 N94-10407
Central Equatorial Pacific Experiment (CEPEX)
[DE93-011656] p 190 N94-11674
Twenty-fourth Lunar and Planetary Science Conference. Part 1: A-F
[NASA-CR-193095] p 435 N94-12015
Age of Popigai impact event using the Ar-40 - Ar-39 method p 282 N94-12093
Minor and trace element composition and age of Yukon probable-microtektites p 429 N94-12094
Modern shelf ice, equatorial Aeolis Quadrangle, Mars p 450 N94-12100
A structural and petrographic investigation of the pretoria saltpan impact structure p 282 N94-12102
Rhenium-osmium isotope systematics of Group 2A and Group 4A iron meteorites p 431 N94-12182
Relation between ages and elevations of Martian channels p 472 N94-12216
Re-Os dating of 3AB iron meteorites p 432 N94-12237

GEODESY
A method for calculating exact geodetic latitude and altitude
[AD-A265783] p 229 N94-10417
Toward 10(exp 9) GPS geodesy: Vector baselines, Earth rotation and reference frames
[NASA-CR-193184] p 229 N94-10702
Removal of orbital error and the local geoid effects from ERS-1 altimeter data p 242 N94-11770

GEODETIC ACCURACY
Statistical description of tectonic motions
[NASA-CR-193701] p 275 N94-10950
Removal of orbital error and the local geoid effects from ERS-1 altimeter data p 242 N94-11770

GEODETIC SURVEYS
A method for calculating exact geodetic latitude and altitude
[AD-A265783] p 229 N94-10417

GEODYNAMICS
Toward 10(exp 9) GPS geodesy: Vector baselines, Earth rotation and reference frames
[NASA-CR-193184] p 229 N94-10702
Precision GPS ephemerides and baselines
[NASA-CR-194171] p 23 N94-11177
Arctic geodynamics: Continental shelf and deep ocean geophysics. ERS-1 satellite altimetry: A first look p 243 N94-11776

GEOGRAPHIC INFORMATION SYSTEMS
Status of remote sensing and Geographic Information System (GIS) applications in the Environment and Natural Resources (ENR) sector p 36 N94-10687

GEOIDS
First results for the simultaneous estimation of the geoid and the sea surface topography by ERS-1 altimeter data p 241 N94-11765
Separation of geoid and sea surface topography in shallow water regions: A first ERS-1 radar altimeter data evaluation p 242 N94-11766
Removal of orbital error and the local geoid effects from ERS-1 altimeter data p 242 N94-11770
Preliminary geophysical investigation with ERS-1 35-day altimeter data p 243 N94-11775
Can weak crust explain the correlation of geoid and topography on Venus? p 453 N94-12118

GEOLOGICAL FAULTS
Estimation of age of Dali-Ganis rifting and associated volcanic activity, Venus p 440 N94-12046
Global organization of tectonic deformation on Venus p 444 N94-12066
Fault geometries and extension in the Valles Marineris, Mars p 458 N94-12144
Tectonics on Triton p 466 N94-12187
Shallow crustal discontinuities and graben and scarp formation in the Tharsis region of Mars p 469 N94-12203

GEOLOGICAL SURVEYS
Radiogenic age and isotopic studies
[DE93-610548] p 274 N94-10407
Descriptions and preliminary interpretations of cores recovered from the Manson Impact Structure (Iowa) p 281 N94-12032
Russia's contribution to regional geologic mapping of Venus p 454 N94-12122
Landscape and geomorphic survey of Zhamanshin area, Northern Kazakhstan: Preliminary report on 1992 field trip data p 282 N94-12123
An ancient inner lake in Maadim Vallis p 456 N94-12133
Geologic history of central Chryse Planitia and the Viking 1 landing site, Mars p 465 N94-12180
Large volcanoes on Venus: Examples of geologic and structural characteristics from different classes p 467 N94-12195

GEOLOGY
The Lathrop Wells Volcanic Center: Status of field and geochronology studies
[DE93-008917] p 273 N94-10285
Tectonics on Triton p 466 N94-12187
Synthesis of global thematic mapping, Venus: Geologic correlations/questions for the Magellan gravity mission p 467 N94-12194
Pilot project PPF12. Coastal and fluvial environment in French Guiana: First results of ERS-1 SAR data analysis p 254 N94-12523
SAR imaging of geology and bathymetry: Kent coastal area - southern North Sea p 254 N94-12527

GEOMAGNETISM
Analysis of geophysical measurements and spacecraft interactions
[AD-A266064] p 43 N94-10944
A study on the magnetospheric activity using the AE, ap, and Dst geomagnetic indices
[INPE-5470-TDI/501] p 276 N94-11165
Polarity reversals and tilt of the Earth's magnetic dipole p 283 N94-12219
On the unique structure of the magnetic fields of Uranus and Neptune p 472 N94-12221

GEOMETRICAL THEORY OF DIFFRACTION
PO/PTD diffraction synthesis of array-fed reflector antennas for satellite and radar applications p 137 N94-11636

GEOMETRY
Geometric aspects of uncertainty and correlation p 349 N94-10588
On a p-adic metrical dimension of space
[DE93-621374] p 345 N94-11077
The completion homomorphism in equivariant elliptic cohomology
[DE93-619672] p 346 N94-11631

GEOMORPHOLOGY
Morphology of large impact craters and basins on Venus: Implications for ring formation p 436 N94-12023
Mars: The initial emplacement of ground ice in response to the thermal evolution of its early crust p 462 N94-12168
Geomorphology of Triton's polar materials p 466 N94-12185
Volcanism in southern Guinevere Planitia, Venus: Regional volcanic history and morphology of volcanic domes p 467 N94-12190
Classification of Martian deltas p 470 N94-12207
Compositional heterogeneity within a dumbbell-shaped Apollo 15 green glass: Evidence for simultaneous eruption of different magmas p 470 N94-12209
Relation between ages and elevations of Martian channels p 472 N94-12216
Morphotectonics of Venus p 478 N94-12248
Pilot project PPF12. Coastal and fluvial environment in French Guiana: First results of ERS-1 SAR data analysis p 254 N94-12523
Applications of ERS-1 SAR data for analyzing riverine and coastal processes and geomorphology p 254 N94-12528

GEOPHYSICS
Sandia ocean modeling system programmer's guide and user's manual
[DE93-007427] p 287 N94-10153
Radiogenic age and isotopic studies
[DE93-610548] p 274 N94-10407
Analysis of geophysical measurements and spacecraft interactions
[AD-A266064] p 43 N94-10944
The Air Force Interactive Meteorological System: A research tool for satellite meteorology
[AD-A265957] p 284 N94-11113
Theoretical studies of the radar properties of the icy Galilean moons of Jupiter
[NASA-CR-193407] p 434 N94-11361
Finnish ERS-1 Baltic Sea ice experiment in Winter 1992 p 239 N94-11750
Arctic sea ice microwave signature and geophysical processes study p 240 N94-11754
Preliminary geophysical investigation with ERS-1 35-day altimeter data p 243 N94-11775
Horizontal stresses induced by vertical processes in planetary lithospheres p 281 N94-12042
Geophysical signature of the Pretoria saltpan impact structure and a possible satellite crater p 282 N94-12103
Fundamental studies of radar scattering from water surfaces: The Lake Washington experiment
[NASA-CR-194030] p 139 N94-12778

GEOSAT SATELLITES
Global wave height climatologies from ERS-1 altimeter data, and comparisons with those from GEOSAT p 244 N94-11781

GERMANY
Radarmap of Germany: First mosaic and classification p 246 N94-12477

GIBBS FREE ENERGY
Monte Carlo simulations of a two-dimensional hard dimer system
[DE93-613535] p 361 N94-10502

GIOTTO MISSION
Giotto data analysis: Electron plasma and heavy ion composition measurements at Comet Halley
[NASA-CR-193587] p 428 N94-12770

GLACIERS
Investigations of Arctic ice-sheets and glaciers using ERS-1 SAR p 238 N94-11743
Snow and glacier investigations by ERS-1 SAR: First results p 247 N94-12481
Disintegrating ice front of Shirase Glacier, East Antarctica p 210 N94-12654

GLARE
Aircraft windscreens enhance visual search disruption produced by laser glare
[AD-A265167] p 26 N94-11892

GLASS
Gas film levitator for containerless processing of glasses in microgravity conditions: Early concept and technology demonstration p 108 N94-10122
Sensing glass transitions in thin polymer films on acoustic wave microsensors
[DE93-010805] p 87 N94-10295
Extensions of some guidelines for the mechanical design of coaxial compression pin seals
[DE93-012385] p 177 N94-10348
Orbital glass in HTSC
[DE93-613988] p 395 N94-10415
Radiation-induced aperiodicity in irradiated ceramics
[DE93-013335] p 91 N94-11698
Processing and properties of coated HPZ fiber reinforced glass-ceramic matrix composites
[AD-A265177] p 92 N94-11876
Effects of microscopic iron metal on the reflectance spectra of glass and minerals p 436 N94-12024
Shock transformations in quartzite p 97 N94-12040
Nitrogen and noble gases in a glass sample from LEW88516 p 80 N94-12051
Changes in Hawaiian palagonite FE mineralogy associated with thermal alteration: Implications for Mars p 281 N94-12055
Strontium and oxygen isotope study of M-1, M-3 and M-4 drill core samples from the Manson impact structure, Iowa: Comparison with Haitian K-T impact glasses p 281 N94-12080
K/T spherules from Haiti and Wyoming: Origin, diagenesis, and similarity to some microtektites p 281 N94-12085
Unequilibrated, equilibrated, and reduced aggregates in anhydrous interplanetary dust particles p 429 N94-12098

Impact comminution of glasses: Implications for lunar regolith evolution p 461 N94-12159
Microtektite-like glass spherules in Late Devonian (367 MA) shales p 461 N94-12160
KT boundary impact glasses from the Gulf of Mexico region p 282 N94-12161
Anomalous REE patterns in unequilibrated enstatite chondrites: Evidence and implications p 431 N94-12191
Compositional heterogeneity within a dumbbell-shaped Apollo 15 green glass: Evidence for simultaneous eruption of different magmas p 470 N94-12209
Modelling of dispersal and deposition of impact glass spherules from the Cretaceous-Tertiary boundary deposit p 432 N94-12238
In-situ crystallization of silicate glass films deposited on alpha- Al2O3
[DE93-012969] p 95 N94-12596

GLASS FIBER REINFORCED PLASTICS
Vectra insulative support structures within spacecraft p 62 N94-10050
Fibre reinforced structures with glass matrix p 64 N94-10064
Fibre optic strain and temperature measurement in composite materials: A review of the OSTIC programme p 65 N94-10066
Some environmental aspects of the application of fibre reinforced plastics in structures
[LM-998] p 88 N94-10877
Strain concentration assessment of laminates subjected to low velocity impact
[AD-A264497] p 73 N94-11446

GLASS FIBERS
Material advances for lightweight TPS p 62 N94-10049
Technique to prepare high-reflectance optical fiber bragg gratings with single exposure in-line on fiber draw tower
[AD-D015757] p 374 N94-10373

GLASS LASERS
Short pulse lasers for generation of fields exceeding 100 MG
[DE93-013346] p 369 N94-11815

GLASS TRANSITION TEMPERATURE
Sensing glass transitions in thin polymer films on acoustic wave microsensors
[DE93-010805] p 87 N94-10295

GLAUBER THEORY
Information entropy via Glauber's Q-representation p 378 N94-10592

GLIDE PATHS
On non-linear longitudinal stability of an aircraft in a dive in the presence of atmospheric disturbances p 31 N94-11492
Helicopter approach capability using the differential Global Positioning System
[NASA-CR-177618] p 24 N94-12355

GLOBAL POSITIONING SYSTEM
Topex orbit determination using GPS tracking system p 38 N94-10359
Toward 10(exp 9) GPS geodesy: Vector baselines, Earth rotation and reference frames
[NASA-CR-193184] p 229 N94-10702
Statistical description of tectonic motions
[NASA-CR-193701] p 275 N94-10950
The time keeping system for GPS block IIR p 24 N94-10964
Progress on GPS standardization p 24 N94-10965
US Coast Guard GPS Information Center (GPSIC) and its function within the Civil GPS Service (CGS) p 24 N94-10966
Comparison of GPS and GLONASS common-view time transfers p 24 N94-10967
PTTI-aided ephemeris calculation and rapid data link acquisition for manned space flight p 42 N94-10974
Disciplined rubidium oscillator with GPS selective availability p 353 N94-10977
A precise GPS-based time and frequency system p 353 N94-10978
CAFS: A Cesium Atomic Frequency Standard for GPS block IIR p 353 N94-10980
Precision GPS ephemerides and baselines
[NASA-CR-194171] p 23 N94-11177
Real-time tomography mooring
[AD-A264923] p 289 N94-11854
Helicopter approach capability using the differential Global Positioning System
[NASA-CR-177618] p 24 N94-12355

GLOBAL WARMING
NRL review for 1993
[AD-A265666] p 497 N94-12334
Comments on possible causes of recent global warming
[DE93-010501] p 272 N94-12592

GLOW DISCHARGES
Journal of Research of the National Institute of Standards and Technology, volume 98, number 2, March - April 1993
[PB93-196228] p 485 N94-10850
Damage thresholds of fluoride multilayers at 355 nm
[DE93-009523] p 90 N94-11230

GLUCOSE
Glucose electrodes based on cross-linked (Os(bpy)2Cl)(sup +/2+) complexed poly(1-vinylimidazole) films
[AD-A265404] p 94 N94-12425

GLUONS
Searches for strangelets and other exotics at the AGS
[DE93-013341] p 359 N94-10308
Squeezed colour states in gluon jet p 379 N94-10599
Filamentation instability of hot quark-gluon plasma with hard jet
[DE93-617679] p 388 N94-10882
Gluon gas viscosity in nonperturbative region
[DE93-617680] p 397 N94-10883
Gauge independence of the A(sub 0)-condensate
[DE93-617681] p 397 N94-10884
Experiments to measure the gluon helicity distribution in protons
[DE93-011756] p 368 N94-11613

GOERTLER INSTABILITY
LIF measurements of scalar mixing in turbulent shear layers p 159 N94-12312
Fluctuations of longitudinal vortices along a concave wall p 16 N94-12616
Criteria for onset of boundary-layer transition on spinning bodies p 164 N94-12620
Growth and breakdown of Taylor-Goertler vortices in rotating Blasius boundary layer p 165 N94-12631

GOLD
Surface-enhanced raman spectroscopy of electroactive films of C60 and an Ir-C60 complex on gold: Symmetry lowering, electron localization, and counteraction effects
[AD-A265934] p 396 N94-10705
Real-space formation and dissipation dynamics of hexagonal reconstruction on Au(100) in aqueous media as explored by potentiodynamic scanning tunneling microscopy
[AD-A266138] p 368 N94-11658
The laser ablation of gold films at the electrode surface of a quartz crystal microbalance
[AD-A265535] p 175 N94-12012
The solubility of gold in silicate melts: First results p 87 N94-12086
Electrode potential-induced reconstruction of Au(100): Effect of chemisorption on nanoscale dynamics as probed by the in-situ scanning tunneling microscopy
[AD-A265900] p 404 N94-12388

GOLD ISOTOPES
On the origin of (4)He and (40)Ar in natural gold p 87 N94-12240

GOVERNMENT PROCUREMENT
NASA procurement: Proposed changes to the Jet Propulsion Laboratory contract. Report to Congressional Requesters
[GAO/NSIAD-93-178] p 416 N94-10941
Federal contractors in appalachia
[PB93-188779] p 416 N94-11473
Pattern of federal procurement from minority and women-owned small business
[PB93-189355] p 417 N94-11844
Assessing the adequacy of the industrial base
[AD-A264954] p 417 N94-11856
National SBIR Phase 3 Commercialization Conference
[AD-A266083] p 417 N94-12410

GOVERNMENT/INDUSTRY RELATIONS
Landsat as a commercial enterprise
[INPE-5477-TAE/019] p 232 N94-11524

GOVERNMENTS
National Institute of Health Almanac, 1992
[PB93-183556] p 303 N94-10828
From red tape to results: Creating a government that works better and costs less p 422 N94-11351
From red tape to results: Creating a government that works better and costs less. Executive summary p 422 N94-11353

GRAIN BOUNDARIES
Atomic structures and compositions of internal interfaces
[DE93-014840] p 363 N94-10750
Grain boundaries in complex oxides
[DE93-013986] p 398 N94-11012
Experimental studies of the structure of grain boundaries
[DE93-013979] p 402 N94-11700
Grain boundary creep in copper
[DE93-610974] p 84 N94-12361

GRAIN SIZE
Synthesis and properties of nanophase materials
[DE93-011757] p 397 N94-10962
Processing, properties, and wear resistance of aluminides
[DE93-012186] p 83 N94-11141
Apical Cu-O bond in YBa2Cu3O(7-delta) superconductors by XAFS
[DE93-010861] p 400 N94-11458
Unequilibrated, equilibrated, and reduced aggregates in anhydrous interplanetary dust particles p 429 N94-12098
Impact comminution of glasses: Implications for lunar regolith evolution p 461 N94-12159

GRAMMARS
An algebraic approach to incomparable families of formal languages
[MEMO-INF-92-82] p 342 N94-10279
Symbolic dynamics and description of complexity
[DE93-613030] p 418 N94-10485

GRAND UNIFIED THEORY
Supersqueezed states from squeezed states p 378 N94-10591
Cosmological restrictions on conformally-invariant SU(5) GUT models
[DE93-619770] p 412 N94-11047

GRANITE
The correlation of alkalis and aluminum during high-temperature volatilization of albite and nepheline p 81 N94-12214

GRAPH THEORY
Cycles through particular subgraphs of claw-free graphs
[MEMO-1097] p 341 N94-10274
Algorithms for the maximum clique problem
[MEMO-1101] p 322 N94-10419
The d-edge shortest-path problem for a Monge graph
[DE93-009828] p 343 N94-10708
Finding minimum-quotient cuts in planar graphs
[DE93-011675] p 344 N94-10961
An introduction to chordal graphs and clique trees
[DE93-012508] p 332 N94-11695
Finding a covering triangulation whose maximum angle is provably small
[DE93-010691] p 334 N94-12593

GRAPHICAL USER INTERFACE
A tool for generation of expert system shells
[INPE-5493-TDI/510] p 325 N94-11181
GRAFTED (GRAphical Fault Tree EDitor): A fault tree description program for target vulnerability/survivability analysis
[AD-A264078] p 328 N94-11301
A pattern recognition system for locating small volvanoes in Magellan SAR images of Venus p 455 N94-12126

GRAPHITE
Proceedings of the Second Technical Meeting on High Temperature Gas-Cooled Reactors
[DE93-754285] p 371 N94-10719
The possibility of using carbon-graphite materials for microwave plasma diagnostics in large fusion devices
[DE93-621609] p 66 N94-11143
Interstellar graphite in Murchison: Continued search for isotopically distinct components p 97 N94-12029
Graphite solubility and co-vesiculation in basalt-like melts at one-ATM p 463 N94-12173

GRAPHITE-EPOXY COMPOSITES
Response of composite laminates to dynamic surface loads p 66 N94-10902

GRAPHS (CHARTS)
An introduction to chordal graphs and clique trees
[DE93-012508] p 332 N94-11695

GRATINGS (SPECTRA)
Technique to prepare high-reflectance optical fiber bragg gratings with single exposure in-line on fiber draw tower
[AD-D015757] p 374 N94-10373
Boundary integral solution to the electromagnetic scattering from coated surfaces containing edges, gaps, and periodic gratings p 137 N94-11639
Development of ultra-low noise, high sensitivity planar metal grating coupled 3 to 5 multiquantum well infrared detectors for focal plane array staring IR sensor systems
[AD-A265599] p 404 N94-12375

GRAVITATION
Dimensional transition of the space-time at the minimum action near the planck scale
[DE93-754192] p 410 N94-10718
Classical gravity coupled to Liouville theory
[DE93-613049] p 275 N94-10798
Quantized conic sections; quantum gravity
[DE93-010950] p 411 N94-10956
Explorations in quantum gravity: From one loop effective actions to two-dimensional theories p 413 N94-11822

GRAVITATION THEORY
On the generalized Jordan-Brans-Dicke theory
[DE93-613051] p 409 N94-10499

From the Weyl theory to a theory of locally anisotropic space-time
[DE92-644734] p 410 N94-10535
Planck scale effects on the Majoron
[DE93-613120] p 410 N94-10545
One-loop quantum gravity on de Sitter space
[DE92-641349] p 425 N94-11152
New tests of the equivalence principle using non-metric couplings of electromagnetism and gravitation
p 413 N94-11821

GRAVITATIONAL EFFECTS
Evaporation under microgravity conditions
p 102 N94-10086
Heat and mass transfer mechanisms of the polymerization under terrestrial and microgravity conditions p 103 N94-10092
Coupled thermogravitational and thermocapillary convection in a two-layer fluid system
p 105 N94-10101
The effect of gravity modulation on thermosolutal convection p 105 N94-10103
Separation of gravitational effects on the flow of suspension in tubes by measurements in weightlessness
p 105 N94-10105
Numerical simulation of Marangoni convection around gas bubbles in a liquid matrix p 106 N94-10107
CdTe crystal growth in the Soviet facility zona 4
p 106 N94-10111
The effect of gravitational modulation on convection in vertical Bridgman growth p 113 N94-10178
TEXUS 28 experiment: Convections and crystal growth of Ge:Ga. Analysis of temperature measurements
p 114 N94-10184
TEM study of a space processed Al-Al2O3 metallic composite p 75 N94-10186
Effect of gravity on the dissolution and liquid phase epitaxial growth processes in a horizontal sandwich system p 118 N94-10208
Transient effects in the Benard instabilities: Coupling between capillary and gravity effects
p 119 N94-10216
Influence of neutral particles concentration on flame propagation in methane-air mixtures at zero and normal gravity conditions p 121 N94-10224
Influence of gravity and ambient pressure variations on the behavior of buoyant laminar diffusion flames
p 123 N94-10240
Planck scale effects on the Majoron
[DE93-613120] p 410 N94-10545
Wave structure in planetary rings p 434 N94-11185
SWIRL as a means of liquid management in low gravity
[NASA-CR-4545] p 412 N94-11523
Ejecting basaltic achondrites from Vesta: Hydrodynamical impact models p 429 N94-12036
Orbital simulations of satellite escape/capture and the origin of satellites such as Triton p 429 N94-12057
Lunar Scout Two spacecraft gravity experiment
p 459 N94-12152

GRAVITATIONAL FIELDS
Gravity and electric field effects on pool boiling heat transfer p 121 N94-10226
Fluid-fluid interfacial instabilities induced by gravity
p 121 N94-10229
Interferometry with particles of non-zero rest mass
[DE93-613518] p 409 N94-10501
On the possible unobservability of the Wu-Yang phase factor in curved space
[DE93-617645] p 411 N94-10831
An analysis of the gravity field in the Norwegian Sea and mapping of the ice cap of Greenland using ERS-1 altimeter measurements p 242 N94-11768
Arctic geodynamics: Continental shelf and deep ocean geophysics. ERS-1 satellite altimetry: A first look
p 243 N94-11776
Lunar Scout Two spacecraft gravity experiment
p 459 N94-12152

GRAVITATIONAL PHYSIOLOGY
Project ARGO: Gas phase formation in simulated microgravity
[NASA-TM-104762] p 125 N94-11235
A mechanism for the reduction in risk of decompression sickness in microgravity environment
p 312 N94-11545
Five biomedical experiments flown in an Earth orbiting laboratory: Lessons learned from developing these experiments on the first international microgravity mission from concept to landing p 302 N94-11556
Physiologic mechanisms of circulatory and body fluid losses in weightlessness identified by mathematical modeling p 312 N94-11557
Proceedings of the First Joint NASA Cardiopulmonary Workshop
[NASA-CP-10068] p 308 N94-11991
Carotid-cardiac baroreflex: Relation with orthostatic hypotension following simulated microgravity and implications for development of countermeasures
p 308 N94-11992
Echocardiography in the flight program
p 309 N94-11993
Pulmonary function in microgravity: KC-135 experience
p 309 N94-11994
Central circulatory hemodynamics as a function of gravitational stress p 309 N94-11995
Cardiovascular dynamics during space sickness and deconditioning p 311 N94-12007

GRAVITATIONAL WAVE ANTENNAS
The uncertainty principle in resonant gravitational wave antennae and quantum non-demolition measurement schemes p 378 N94-10587

GRAVITATIONAL WAVES
The uncertainty principle in resonant gravitational wave antennae and quantum non-demolition measurement schemes p 378 N94-10587

GRAVITONS
On the generalized Jordan-Brans-Dicke theory
[DE93-613051] p 409 N94-10499

GRAVITY ANOMALIES
Geophysical signature of the Pretoria saltpan impact structure and a possible satellite crater
p 282 N94-12103
Flexure and the role of inplane force around coronae on Venus p 452 N94-12112
Free-air and Bouguer gravity anomalies and the Martian crustal dichotomy p 481 N94-12267
New Mars free-air and Bouguer gravity: Correlation with topography, geology and large impact basins
p 481 N94-12268
Pseudo magnetic anomaly derived from satellite altimetry and its application to the tectonics in the North Fuji Basin p 208 N94-12645

GRAVITY WAVES
Lee waves: Benign and malignant
[NASA-CR-186024] p 283 N94-10725
Air-sea fluxes and universal constants in weak-turbulence theory of surface gravity waves
p 195 N94-11922
Polar mesospheric waves and structure
[AD-A265360] p 279 N94-12561

GRAY SCALE
Application of normalized gray-scale correlation
[DE93-013765] p 141 N94-10521
Development and implementation of a general purpose x-windows display program
[AD-A265306] p 332 N94-11860

GRAZING INCIDENCE
Needs for super-smooth surfaces
[DE93-012482] p 382 N94-11242
Interpretation of lunar and planetary electromagnetic scattering using the full wave solutions
p 440 N94-12049
Fundamental studies of radar scattering from water surfaces: The Lake Washington experiment
[NASA-CR-194030] p 139 N94-12778

GREEN'S FUNCTIONS
A spectral nodal method for discrete ordinates problems in x,y geometry
[DE93-610128] p 342 N94-10283
A spectral nodal method for the solution of the Sn equations in x, y geometry for highly absorbing deep penetration problems
[DE93-613520] p 349 N94-10636
Nonperturbative methods in HZE ion transport
[NASA-TP-3363] p 484 N94-10759
Electronic characterization of defects in narrow gap semiconductors
[NASA-CR-193568] p 397 N94-10819
Regular tensor Green functions of the round waveguide
[DE93-621354] p 345 N94-11036
Asymptotic expressions for regular Green functions of a round cylindrical screen
[DE93-621356] p 134 N94-11038
Radiation and scattering by cavity-backed antennas on a circular cylinder
[NASA-CR-193409] p 136 N94-11084

GREENHOUSE EFFECT
An observational search for CO2 ice clouds on Mars
p 441 N94-12054

GREENLAND
Analysis of ERS-1 altimeter data over the polar ice sheets p 237 N94-11738
Monitoring of the Greenland Ice Sheet using ERS-1 synthetic aperture radar imagery p 237 N94-11741
Spatial patterns in backscatter strength across the Greenland Ice Sheet p 238 N94-11744
Use of ERS-1 SAR to measure ice flux in the East Greenland current p 238 N94-11746
An analysis of the gravity field in the Norwegian Sea and mapping of the ice cap of Greenland using ERS-1 altimeter measurements p 242 N94-11768

GRID GENERATION (MATHEMATICS)
A grid generation method to calculate the flow field in a three-dimensional cascade of blades
[NAL-TR-1158] p 147 N94-10364
Numerical methods for aerothermodynamic design of hypersonic space transport vehicles p 9 N94-10459
Development of a Delaunay-based adaption scheme with applications to complex three-dimensional rotational flows p 149 N94-10824
Generation and analysis of hybrid structured/unstructured grids
[ARA-MEMO-365] p 324 N94-10893
A dynamically adaptive mesh method for internal flows
p 149 N94-10896
Object oriented implementation of adaptive mesh refinement algorithms
[DE93-011885] p 325 N94-11112
KIVA-3: A KIVA program with block-structured mesh for complex geometries
[DE93-011986] p 77 N94-11249
Quality factors and local adaption (with applications in Eulerian hydrodynamics)
[DE93-010502] p 151 N94-11272
SAUNA: A system for grid generation and flow simulation using hybrid structured/unstructured grids
[ARA-MEMO-370] p 154 N94-11859
Direct numerical simulation of turbulent flow over a backward-facing step p 156 N94-12296
Towards a cell-vertex Navier-Stokes algorithm for three-dimensional structured/unstructured meshes
[ARA-MEMO-366] p 161 N94-12437

GROUND BASED CONTROL
TOLS (Telescience On-Line Simulator): An essential instrument for micro-gravity interactive experiment
p 39 N94-10134
Helicopter approach capability using the differential Global Positioning System
[NASA-CR-177618] p 24 N94-12355

GROUND EFFECT (AERODYNAMICS)
Moving-base simulation evaluation of thrust margins for vertical landing for the NASA YAV-8B Harrier aircraft
[NASA-TM-104008] p 30 N94-11259
Turbulence modeling for thrust reverser flow field prediction methods
[AD-A266139] p 154 N94-11641

GROUND SUPPORT EQUIPMENT
Results of mission preparation support to microgravity experiments on board of Eureca 1 p 111 N94-10138
Pre-operation analysis of ERS-1 tracking and operation, part 2-F
[NASDA-CNT-930002-PT-2-F] p 230 N94-11130
Using transponders with the ERS-1 altimeter to measure orbit altitude to +/- 3 cm p 244 N94-11785

GROUND SUPPORT SYSTEMS
Mission support for crystal growth experiments in Russian unmanned carriers p 111 N94-10139
Pre-operation analysis of ERS-1 tracking and operation, part 2-A
[NASDA-CNT-930001-PT-2-A] p 230 N94-11129
Pre-operation analysis of ERS-1 tracking and operation, part 2-F
[NASDA-CNT-930002-PT-2-F] p 230 N94-11130
Maximizing reuse: Applying common sense and discipline p 329 N94-11429

GROUND TESTS
Experimental approach to non-contact calorimetry in space p 112 N94-10143
Interface reactions of (Ni3Al) ribbons/Al-MMC in ground preparation as preliminary test for microgravity experiments p 123 N94-10237
An investigation of conducted and radiated emissions from a hollow-cathode plasma contactor
[NASA-CR-191172] p 386 N94-10346
Characterization of in-flight performance of ion propulsion systems
[NASA-TM-106283] p 46 N94-10761
Space Shuttle hypersonic aerodynamic and aerothermodynamic flight research and the comparison to ground test results
[NASA-TM-4499] p 13 N94-10820
Ground vibration and flight flutter tests of the single-seat F-16XL aircraft with a modified wing
[NASA-TM-104269] p 26 N94-11233

GROUND TRUTH
Ice studies in the Barents Sea by ERS-1 SAR during SIZEX 92 p 238 N94-11745
ERS-1 SAR crop monitoring experiment in East Anglia, UK p 248 N94-12488
Extraction of plant and soil parameters from multitemporal ERS-1 SLC data of the Freiburg test site
p 248 N94-12491
Coastal morphodynamics and energetic characteristics of swell studied with ERS-1 SAR p 254 N94-12524

Applications of ERS-1 SAR data for analyzing riverine and coastal processes and geomorphology
p 254 N94-12528

GROUND WATER
Immediate response to free product discovery
[PB93-182970] p 265 N94-11015
Catalytic oxidation of organics in vapor streams at remediation sites
[PB93-182962] p 266 N94-11472
The role of the geothermal gradient in the emplacement and replenishment of ground ice on Mars
p 463 N94-12169
The thermodynamic case for a water-rich Mars
p 463 N94-12170

GROUP THEORY
The structure of Hilbert flag varieties
[MEMO-1095] p 348 N94-10272
Convergence of exponentially convex functions on foundation semigroups
[DE93-619665] p 342 N94-10325
A group-theoretic approach to the study of small oscillations of a dynamical system with a known symmetry
[DE93-612971] p 409 N94-10402
Uncertainty relations, zero point energy and the linear canonical group p 378 N94-10590
The modular group and super-KMS functionals
[DE93-613029] p 349 N94-10632

GUANIDINES
Solid-state structures of guanidinium methane, ethane, and trifluoromethanesulfonate
[AD-A265293] p 402 N94-11654

GUINEA PIGS
Evaluation of medical treatments to increase survival of ebullism in guinea pigs p 302 N94-11548

GULF OF ALASKA
SAR ocean imaging in the Gulf of Alaska
p 235 N94-11723

GULF OF MEXICO
Gulf of Mexico sales 147 and 150: Central and western planning areas. Draft environmental impact statement. Volume 1: Sections 1 through 4.C
[PB93-190304] p 265 N94-11018
Gulf of Mexico sales 147 and 150: Central and western planning areas. Draft environmental impact statement. Volume 2: Sections 4.D through 9
[PB93-190312] p 265 N94-11019
KT boundary impact glasses from the Gulf of Mexico region p 282 N94-12161

GULF STREAM
Space and time variability of the Gulf Stream using ERS-1 ALT-OPR02 data p 242 N94-11769
Ocean circulation revealed by altimeter data
p 245 N94-11786
An investigation using empirical orthogonal functions and objective analysis to analyse the vertical temperature structure of a gulf stream meander
[AD-A265116] p 289 N94-11868
Measurement of the surface layer current averaged vertically using Multipaths Inverted Echosounder
p 194 N94-11915
ERS-1 and Almaz SAR ocean wave imaging over the Gulf Stream and the Grand Banks p 251 N94-12505

GUN PROPELLANTS
Time-temperature shift factors for gun propellants
[AD-A264979] p 97 N94-10489

GUST LOADS
Further studies using matched filter theory and stochastic simulation for gust loads prediction
[NASA-TM-109010] p 26 N94-11587

GYROFREQUENCY
Stationary spectra in a finite-pressure current-carrying plasma
[DE93-617848] p 387 N94-10538
Dispersion of plasma waves in a finite magnetic field (omega(sub H) greater than omega(sub p))
[DE93-621654] p 391 N94-11210
Studies of electrostatic waves and VLF-wave particle interaction in the ionosphere
[AD-A266013] p 278 N94-12392

GYROSCOPIC STABILITY
Estimation of the attitude motion of the small satellite ORIZURU
[NAL-TR-1145] p 42 N94-10366

H

H-60 HELICOPTER
NASTRAN modeling of flight test components for UH-60A airloads program test configuration
[NASA-CR-193614] p 186 N94-10937

HABITATS
Terminal Decomposition and Gaseous Sulfur Release from Tidal Wetlands
[NASA-CR-193466] p 267 N94-12451
Emissions of biogenic sulfur gases from Alaskan tundra p 268 N94-12455

HADRONS
Some new/old approaches to QCD
[DE93-010451] p 408 N94-10261
Crossing-odd spin effects in the dipole model of hadron scattering
[DE93-617692] p 362 N94-10551
Squeezed colour states in gluon jet
p 379 N94-10599
Principles of gauge theory of real hadrons
[DE93-613094] p 362 N94-10634
Possibility of a crossed-beam experiment involving slow-neutron capture by unstable nuclei rapid-process-tron
[DE93-754288] p 363 N94-10720
A review of two photon production of jets at PEP and PETRA energies
[DE93-011742] p 364 N94-10754
Relativistic heavy-ion collisions
[DE93-014844] p 366 N94-11147
Lecture note on circuit technology for high energy physics experiment
[DE93-771422] p 372 N94-11245

HALF LIFE
A new matrix for the ageless 21.6-keV Eu-151 nuclear gamma ray Moessbauer source
[DE93-009795] p 75 N94-10338

HALF SPACES
Exact and quasi-classical density matrix and Wigner functions for a particle in the box and half space
p 350 N94-10600

HALL EFFECT
The influence of irradiation conditions, type, and concentration of impurities on radiation defects characteristics in indium antimonide under electron irradiation
[DE93-617201] p 397 N94-10843

HALLEY'S COMET
Mass and spatial distribution of carbonaceous component in Comet Halley p 433 N94-12263
Giotto data analysis: Electron plasma and heavy ion composition measurements at Comet Halley
[NASA-CR-193587] p 428 N94-12770

HAMILTONIAN FUNCTIONS
Aharonov-Bohm effect in Luttinger liquid
[DE93-613818] p 408 N94-10148
Cycles through particular subgraphs of claw-free graphs
[MEMO-1097] p 341 N94-10274
Uni-directional waves over slowly varying bottom. Part 1: Derivation of a KdV-type of equation
[MEMO-1098] p 147 N94-10275
Effect of a distribution of exchange parameters within a simple localized-itinerant model
[DE93-610314] p 395 N94-10314
Wave function collapse: An unnecessary condition for the dynamical description of the Zeno and partial Zeno effect
[DE93-612970] p 132 N94-10401
On a Lagrange-Hamilton formalism describing position and momentum uncertainties p 349 N94-10583
Exact and quasi-classical density matrix and Wigner functions for a particle in the box and half space
p 350 N94-10600
Non-stationary and non-linear dispersive medium as external field which generates the squeezed states
p 380 N94-10605
On the possible unobservability of the Wu-Yang phase factor in curved space
[DE93-617645] p 411 N94-10831
Cosmological restrictions on conformally-invariant SU(5) GUT models
[DE93-619770] p 412 N94-11047
Superfield description of N = 2 extended one-dimensional supersymmetric quantum mechanics
[DE93-621420] p 412 N94-11087
Radiative properties of strongly magnetized plasmas
[DE93-014098] p 389 N94-11118
Three-dimensional N = 4 extended supersymmetrical quantum mechanics
[DE93-621421] p 412 N94-11164
Duality twisted boundary conditions in n-sta te Potts models
[DE93-619724] p 346 N94-11811

HAND (ANATOMY)
Head and face anthropometry of adult US civilians
[DOT/FAA/AM-93/10] p 315 N94-10806

HANDBOOKS
Department of Energy fundamentals handbook: Engineering symbology, prints, and drawings
[DE93-012181] p 129 N94-11456
Correspondence standards
[NHB-1450.10B] p 420 N94-11589
Department of Energy fundamentals handbook: Engineering symbology, prints, and drawings
[DE93-012220] p 129 N94-11670

HANKEL FUNCTIONS
Balancing of the normalized right coprime factorization of a nonlinear system
[MEMO-1096] p 341 N94-10273
The Nehari problem for the Pritchard-Salamon class of infinite-dimensional linear systems: A direct approach
[CS-9216] p 344 N94-10905

HARDENING (MATERIALS)
DBTT measurement by use of Small Punch (SP) test
[DE93-753188] p 183 N94-11168

HARDNESS
Radiation hardness of Mo/Si multilayers designed for use in a soft x ray projection lithography system
[DE93-011879] p 143 N94-11273
Ceramic technology project database
[DE93-012432] p 91 N94-11673

HARDNESS TESTS
DBTT measurement by use of Small Punch (SP) test
[DE93-753188] p 183 N94-11168

HARMONIC ANALYSIS
Spectral analysis of the gravity and topography of Mars p 444 N94-12065

HARMONIC EXCITATION
Nonlinear response of a clamped-clamped beam with internal resonance under sinusoidal excitation
p 186 N94-10897
Examination of the surface second harmonic response at infrared wavelengths
[AD-A265206] p 403 N94-12371

HARMONIC GENERATIONS
Nonlinear second harmonic generation by light wave-plasma interaction in oscillating magnetic field
[DE93-613723] p 386 N94-10387
High-order harmonic conversion efficiency in helium
[DE93-011714] p 364 N94-10753
The angular structure of second harmonic emission from laser-produced plasmas irradiated at moderate intensity
[DE93-013102] p 389 N94-11114
Elementary mechanism of electron beam dissipative instability development
[DE93-621653] p 391 N94-11209
Investigation of optically generated electronic defects and protonic transport in hydrogen-bonded molecular solids: Isomorphs of potassium dihydrogen phosphate
[DE93-012498] p 399 N94-11243
Examination of the surface second harmonic response at infrared wavelengths
[AD-A265206] p 403 N94-12371
Controlling chaotic behavior in a CO2 and other lasers
[AD-A265458] p 176 N94-12372
Nonlinear optical spectroscopy of Ag(111) in electrolyte and in vacuum
[AD-A265622] p 79 N94-12534
Preparation of stable photopatternable polymeric materials for non-linear optics
[AD-A265359] p 95 N94-12577

HARMONIC OSCILLATORS
Smoothly deformed light p 375 N94-10566
One dimensional representations in quantum optics
p 375 N94-10570
Harmonic oscillator interaction with squeezed radiation
p 376 N94-10571
Phasing operator for two oscillators in classical field
p 370 N94-10579
On a Lagrange-Hamilton formalism describing position and momentum uncertainties p 349 N94-10583
Supersqueezed states from squeezed states
p 378 N94-10591
Collision-induced squeezing in a harmonic oscillator
p 379 N94-10597
Relation of squeezed states between damped harmonic and simple harmonic oscillators p 380 N94-10606
Wave and pseudo-diffusion equations from squeezed states p 347 N94-10607
Correlated states of a quantum oscillator acted by short pulses p 380 N94-10609
Coherent states and uncertainty relations for the damped harmonic oscillator with time-dependent frequency
p 380 N94-10611
Quantum processes in resonators with moving walls
p 380 N94-10612
Exact solutions of a many-anyon problem
[DE93-617646] p 411 N94-10832

HARMONIC RADIATION
High-order harmonic conversion efficiency in helium
[DE93-011714] p 364 N94-10753

HARRIER AIRCRAFT
Moving-base simulation evaluation of thrust margins for vertical landing for the NASA YAV-8B Harrier aircraft
[NASA-TM-104008] p 30 N94-11259

HARTREE APPROXIMATION

Satellite structure of the xenon valence shell by electron momentum spectroscopy [DE93-609993] p 360 N94-10327

Recent advances in electron momentum spectroscopy [DE93-610149] p 361 N94-10333

Spontaneous symmetry breaking in QCD [DE93-753060] p 396 N94-10645

Radiative properties of strongly magnetized plasmas [DE93-014098] p 389 N94-11118

Femtosecond dynamics, photoexcitation, and ESR spectra of MX chain solids [AD-A264689] p 399 N94-11263

HAWAII

Reconstruction of the dynamics of the 1800-1801 Hualalai eruption: Implications for planetary lava flows p 281 N94-12041

Changes in Hawaiian palagonite FE mineralogy associated with thermal alteration: Implications for Mars p 281 N94-12055

HAZARDS

Achievements and challenges of Space Station Freedom's safety review process [NASA-TM-106199] p 40 N94-10640

HAZE

Dust in the Martian atmosphere: Polarimetric sensing p 473 N94-12223

HEAD (ANATOMY)

Mass properties test procedure for manikin headforms and helmet systems [AD-A265654] p 315 N94-10296

HEAD DOWN TILT

Physiologic mechanisms of circulatory and body fluid losses in weightlessness identified by mathematical modeling p 312 N94-11557

Carotid-cardiac baroreflex: Relation with orthostatic hypotension following simulated microgravity and implications for development of countermeasures p 308 N94-11992

Spectral analysis of resting cardiovascular variables and responses to oscillatory LBNP before and after 6 degree head dowm bedrest p 309 N94-11997

Fluid compartment and renal function alterations in the rat during 7 and 14 day head down tilt p 310 N94-12002

Local fluid shifts and edema in humans during simulated microgravity p 311 N94-12003

Hormonal regulation of fluid and electrolyte metabolism in zero-g and bedrest p 311 N94-12004

HEAD-UP DISPLAYS

Measures for simulator evaluation of a helicopter obstacle avoidance system p 35 N94-11535

A comparison of head-up and head-down display formats during instrument flying tasks [AD-A266140] p 316 N94-11642

HEALING

Development of bioelastic materials for the prevention of adhesions: Polypenta- and polytetrapeptides [AD-A264851] p 88 N94-10863

Pilot trial of potentiating normal healing of stress fractures using pulsing electromagnetic fields [AD-A264251] p 311 N94-12364

HEALTH

National Institute of Health Almanac, 1992 [PB93-183556] p 303 N94-10828

Baseline characteristics of different strata of astronaut corps p 312 N94-11552

The Department of Clinical Investigation, reports control symbol MED-300(R-1) [AD-A264969] p 304 N94-11649

Medical care delivery in the US space program p 307 N94-11806

HEALTH PHYSICS

Potential health effects of space radiation p 312 N94-11558

HEAO 1

HEAO-1 analysis of Low Energy Detectors (LED) [NASA-CR-194087] p 424 N94-12574

HEARING

Noise levels and their effects on Shuttle crewmembers' performance: Operational concerns p 314 N94-11538

HEART FUNCTION

Transcranial Doppler ultrasound and the etiology of neurologic decompression sickness during altitude decompression p 312 N94-11544

Proceedings of the First Joint NASA Cardiopulmonary Workshop [NASA-CP-10068] p 308 N94-11991

Spectral analysis of resting cardiovascular variables and responses to oscillatory LBNP before and after 6 degree head dowm bedrest p 309 N94-11997

Fitness, autonomic regulation and orthostatic tolerance p 310 N94-11999

Autogenic-feedback training: A countermeasure for orthostatic intolerance p 311 N94-12006

HEART RATE

Psychophysiological measures of cognitive workload in laboratory and flight p 317 N94-11529

Echocardiography in the flight program p 309 N94-11993

Valsalva maneuver: Insights into baroreflex modulation of human sympathetic activity p 310 N94-12000

Cardiovascular dynamics during space sickness and deconditioning p 311 N94-12007

HEART VALVES

Strategies and methodologies to develop techniques for computer-assisted analysis of gas phase formation during altitude decompression p 312 N94-11547

HEAT ACCLIMATIZATION

P2NBC2 Heat Strain Decision Aid. User's guide, version 2.1 [AD-A266072] p 304 N94-11224

Modifications to an interactive model of the human body during exercise: With special emphasis on thermoregulation p 317 N94-12368

HEAT BALANCE

Evaporation and thermal/hydrologic balance in the Pacific p 195 N94-11919

Seasonal variation of the surface mixed layer in the subtropical re-circulation area of the North Pacific during OMLET p 195 N94-11924

Mixed layer heat budget of Kuroshio-Tango triangle using satellite and ship observations p 196 N94-11925

Estimation of solar radiation at the sea surface with geostationary meteorological satellite data p 196 N94-11926

HEAT BUDGET

Proceedings of the PORSEC 1992 in Okinawa: Conference for Pacific Ocean Environments and Probing, volume 1 [JTN-93-80418] p 191 N94-11894

Seasonal variation of the surface mixed layer in the subtropical re-circulation area of the North Pacific during OMLET p 195 N94-11924

Mixed layer heat budget of Kuroshio-Tango triangle using satellite and ship observations p 196 N94-11925

Estimation of solar radiation at the sea surface with geostationary meteorological satellite data p 196 N94-11926

Study on air-sea interactions in the OMLET (Ocean Mixed Layer Experiment) area using satellite remote sensing p 220 N94-12710

Variability of the mixed layer depth in the North Pacific Ocean as calculated by a 3-D semi-analytical mixed layer remote sensing model p 221 N94-12718

HEAT ENGINES

Heat regenerative external combustion engine [AD-D015765] p 178 N94-10378

HEAT EXCHANGERS

Proceedings of the Second Technical Meeting on High Temperature Gas-Cooled Reactors [DE93-754285] p 371 N94-10719

Theoretical evaluation of R22 and R502 alternatives [DE93-014767] p 411 N94-10853

HEAT FLUX

Transient effects in the Benard instabilities: Coupling between capillary and gravity effects p 119 N94-10216

High heat flux components and plasma surface interactions [DE93-008786] p 385 N94-10253

Physics and modelling of scrape-off layer transport [DE93-010510] p 385 N94-10289

Thermal flux measurements in hypersonic flows: A review p 5 N94-10438

The OSU heat release rate test using the oxygen consumption principle p 20 N94-10784

Design of CCD camera system for use inside electron beam furnace [DE93-009525] p 170 N94-11267

Heat flux measurements on ceramics with thin film thermocouples [NASA-TM-106305] p 170 N94-11310

Latent and sensible heat flux estimated from ERS-1 data p 244 N94-11783

Variability of wind stress, and sensible and latent heat flux in the North Atlantic during SEASAT p 194 N94-11918

Evaporation and thermal/hydrologic balance in the Pacific p 195 N94-11919

Evaluation of ECMWF latent heat flux in TOGA CD-ROM p 195 N94-11921

Sea surface heat flux in the beginning of the Kuroshio p 195 N94-11923

Seasonal variation of the surface mixed layer in the subtropical re-circulation area of the North Pacific during OMLET p 195 N94-11924

Mixed layer heat budget of Kuroshio-Tango triangle using satellite and ship observations p 196 N94-11925

Sea surface temperature anomalies in the Arabian Sea p 206 N94-11988

Roles of the NEC and MC in the formation and evolution of the Equatorial Pacific Warm Pool p 206 N94-11990

Does the thermal wind exist near the Earth's core boundary? p 283 N94-12217

Estimations of the surface fluxes from satellite observations of boundary layer and the surface p 252 N94-12513

Study on air-sea interactions in the OMLET (Ocean Mixed Layer Experiment) area using satellite remote sensing p 220 N94-12710

HEAT MEASUREMENT

Experimental approach to non-contact calorimetry in space p 112 N94-10143

The OSU heat release rate test using the oxygen consumption principle p 20 N94-10784

Flammability parameters of materials: Ignition, combustion, and flame spread p 20 N94-10788

Heat flux measurements on ceramics with thin film thermocouples [NASA-TM-106305] p 170 N94-11310

HEAT OF DISSOCIATION

Tandem mass spectrometric analysis of phosphate esters [AD-A265483] p 78 N94-12009

HEAT PUMPS

Theoretical evaluation of R22 and R502 alternatives [DE93-014767] p 411 N94-10853

HEAT RADIATORS

The Third Workshop on Two Phase Fluid Experiment in the Space Environment [NASDA-CON-930002] p 161 N94-12547

Summary of studies on JEM utilization experiment projects p 161 N94-12548

Two phase flow and isopycnic liquid-liquid two phase fluid in reduced gravity field p 162 N94-12552

Devices related for thermal control systems used in microgravity p 162 N94-12553

Research and development of cold plate for two phase fluid loop thermal control system p 162 N94-12555

HEAT RESISTANT ALLOYS

Weld overlay coatings for erosion control [DE93-013592] p 84 N94-11816

Fatigue in single crystal nickel superalloys [AD-A266116] p 85 N94-12418

NiAl alloys for structural uses [NASA-CR-194113] p 85 N94-12447

HEAT SHIELDING

Design concepts for load-carrying hot structures for reentry bodies p 57 N94-10012

HEAT SINKS

Liquid Cooled Heat Sink with through Vias (LCHS) [AD-A266008] p 73 N94-12344

Research and development of cold plate for two phase fluid loop thermal control system p 162 N94-12555

HEAT STORAGE

Modeling void growth and movement with phase change in thermal energy storage canisters [NASA-TM-106288] p 163 N94-12576

HEAT TOLERANCE

P2NBC2 Heat Strain Decision Aid. User's guide, version 2.1 [AD-A266072] p 304 N94-11224

HEAT TRANSFER

Transient three-dimensional numerical simulation of Marangoni flow in a liquid column under microgravity p 101 N94-10079

Effect of rotation on microgravity floating-zone crystal growth p 101 N94-10080

Heat and mass transfer mechanisms of the polymerization under terrestrial and microgravity conditions p 103 N94-10092

Two-phase flow heat transfer and hydrodynamics in an electric field p 103 N94-10093

Gravity and electric field effects on pool boiling heat transfer p 121 N94-10226

Transport of heat and mass in near-critical fluids p 122 N94-10230

Single bubble experiments in pool boiling: Results from TEXUS 26 p 124 N94-10243

Control effectiveness at hypersonic speeds p 3 N94-10426

Experimental and computational comparisons of Mach 6 high Reynolds number heat transfer and skin friction p 6 N94-10443

Real gas and surface transpiration effects upon swept leading edge high speed flow including transition p 8 N94-10452

Studies of hypersonic viscous flows p 8 N94-10454

New thermoplastic laminating adhesives for the aircraft industry with low heat release and low smoke emission p 17 N94-10767

A new low smoke, low heat release structural foam p 17 N94-10768

The OSU heat release rate test using the oxygen consumption principle p 20 N94-10784

Experimental study of multiple droplet evaporative cooling
[PB93-198463] p 149 N94-10851
Theoretical evaluation of R22 and R502 alternatives
[DE93-014767] p 411 N94-10853
A research program for improving heat transfer prediction for the laminar to turbulent transition region of turbine vanes/blades
[NASA-TM-106278] p 151 N94-11256
Establishing baseline data for an experimental appratus that measures heat transfer under conditions of oscillating pressure and flow
[NASA-CR-193772] p 413 N94-12343
Modifications to an interactive model of the human body during exercise: With special emphasis on thermoregulation p 317 N94-12368
Boiling heat-transfer processes and their application in the cooling of high heat flux devices
[AD-A266086] p 413 N94-12535
Hot-gas-side heat transfer characteristics of subscale, plug-nozzle rocket calorimeter chamber
[NASA-TP-3380] p 55 N94-12569

HEAT TRANSFER COEFFICIENTS
Developmental research of thermal control system in space environment p 162 N94-12551
Research on two phase flow in microgravity p 162 N94-12554

HEAT TRANSMISSION
Estimation of solar radiation at the sea surface with geostationary meteorological satellite data p 196 N94-11926
Liquid Cooled Heat Sink with through Vias (LCHS)
[AD-A266008] p 73 N94-12344
The Third Workshop on Two Phase Fluid Experiment in the Space Environment
[NASDA-CON-930002] p 161 N94-12547
Compilation of proposals for boiling and evaporation experiments in space environments and proposals concerning experiment projects p 161 N94-12549
Condensation phenomena p 162 N94-12550
Developmental research of thermal control system in space environment p 162 N94-12551
Two phase flow and isopycnic liquid-liquid two phase fluid in reduced gravity field p 162 N94-12552
Devices related for thermal control systems used in microgravity p 162 N94-12553
Research on two phase flow in microgravity p 162 N94-12554
Research and development of cold plate for two phase fluid loop thermal control system p 162 N94-12555
Organization and management policy for two phase fluid experiment in space environment p 162 N94-12556

HEAT TREATMENT
Heat analysis of thermoplastic components during the initial stages of manufacturing: A probabilistic approach p 60 N94-10031
Spin-rolling, welding, and heat treatment of aluminium 2219 for Ariane 5 GAM high pressure vessel liners p 62 N94-10045
Thermal stability of sealants for military aircraft: Modification of polysulfide prepolymers with ether and thioether monomers
[AD-A264079] p 89 N94-11107
Cold press sintering of simulated lunar basalt p 131 N94-12026

HEATING
Ar-39 - Ar-40 ages of acapulcoites and lodranites: Evidence for early parent body heating p 281 N94-12083
Simulation of possible regolith optical alteration effects on carbonaceous chondrite meteorites p 430 N94-12163
The 1991 version of the plume impingement computer program. Volume 2: User's input guide
[NASA-CR-194191] p 166 N94-12774

HEATING EQUIPMENT
Boiling heat-transfer processes and their application in the cooling of high heat flux devices
[AD-A266086] p 413 N94-12535

HEAVY IONS
Production of strange clusters in relativistic heavy ion collisions
[DE93-010876] p 359 N94-10303
Investigation of soft errors in MOS RAM under influence of heavy ions
[DE92-644554] p 484 N94-10534
Heavy ion fusion at sub-barrier energies: Progress and questions
[DE93-011764] p 372 N94-11124
Relativistic heavy-ion collisions
[DE93-014844] p 366 N94-11147
Relativistic heavy ion research
[DE93-013127] p 367 N94-11373
Potential health effects of space radiation p 312 N94-11558
Pion correlations and calorimeter design for high energy heavy ion collisions
[DE93-013861] p 373 N94-12607
Giotto data analysis: Electron plasma and heavy ion composition measurements at Comet Halley
[NASA-CR-193587] p 428 N94-12770

HEAVY NUCLEI
Post-launch analysis of data from the High Energy Astrophysical Observatory Heavy Nuclei Experiment (HEAO-C3)
[NASA-CR-193513] p 484 N94-11486
Analysis and interpretation of high energy cosmic rays measured on Spacelab-2
[NASA-CR-193586] p 485 N94-12771

HEAVY WATER REACTORS
Fracture mechanics and full scale pipe break testing for the Department of Environment's New Production Reactor-Heavy Water Reactor
[DE93-005428] p 187 N94-11169

HEIGHT
Spatial scales of wave height p 244 N94-11782

HEISENBERG THEORY
The Second International Workshop on Squeezed States and Uncertainty Relations
[NASA-CP-3219] p 375 N94-10564
Disturbance, the uncertainty principle and quantum optics p 375 N94-10569
Squeezing in phase-conjugated resonance fluorescence p 376 N94-10576
The legacy of uncertainty p 376 N94-10577
Completeness properties of the minimum uncertainty states p 349 N94-10581
The uncertainty principle in resonant gravitational wave antennae and quantum non-demolition measurement schemes p 378 N94-10587
Geometric aspects of uncertainty and correlation p 349 N94-10588
Information entropy via Glauber's Q-representation p 378 N94-10592
Positive phase space distributions and uncertainty relations p 379 N94-10598
The uncertainty principle and quantum chaos p 379 N94-10602
Relation of squeezed states between damped harmonic and simple harmonic oscillators p 380 N94-10606

HELICAL FLOW
Simple kinetic model for plasma in stochastic helical field
[DE93-621643] p 391 N94-11208

HELICAL WINDINGS
Characteristics of ICR-produced peripheral plasma in the Uragan-3M torsatron
[DE93-621666] p 392 N94-11214

HELICOPTER CONTROL
A feasibility study regarding the addition of a fifth control to a rotorcraft in-flight simulator
[NASA-CR-193240] p 30 N94-10895

HELICOPTER DESIGN
NASTRAN modeling of flight test components for UH-60A airloads program test configuration
[NASA-CR-193614] p 186 N94-10937

HELICOPTER PERFORMANCE
Performance and rotor loads measurements of the Lynx XZ170 helicopter with rectangular blades
[NASA-TM-104000] p 1 N94-10936

HELICOPTER WAKES
Perpendicular blade vortex interaction and its implications for helicopter noise prediction: Wave-number frequency spectra in a trailing vortex for BWI noise prediction
[NASA-CR-193623] p 357 N94-10752

HELICOPTERS
Performance and rotor loads measurements of the Lynx XZ170 helicopter with rectangular blades
[NASA-TM-104000] p 1 N94-10936
Measures for simulator evaluation of a helicopter obstacle avoidance system p 35 N94-11535

HELIOS A
Experimental particle physics at the University of Pittsburgh
[DE93-013326] p 369 N94-12546

HELIOTRONS
Charged particle motion in torsatrons, part 1
[DE93-621639] p 389 N94-11119
Particle transport analysis in torsatron configurations
[DE93-621640] p 390 N94-11120
Probability of particle trapping/detrapping in torsatrons
[DE93-621641] p 390 N94-11121

HELIUM
High-order harmonic conversion efficiency in helium
[DE93-011714] p 364 N94-10753
Helium transport scaling law studies
[DE93-013487] p 393 N94-11513
Compilation of excitation cross sections for He atoms by electron impact
[DE93-753246] p 367 N94-11580

HELIUM ISOTOPES
Dispersion of the ratios of cosmogenic isotopes of noble gases in chondrites of different cosmic-ray exposure ages p 428 N94-12020
Noble gases in LEW88516 shergottite: Evidence for exposure age pairing with ALH77005 p 80 N94-12082
On the origin of (4)He and (40)Ar in natural gold p 87 N94-12240

HELMET MOUNTED DISPLAYS
Accuracy and repeatability of the standard automated mass properties measurement system
[AD-A265897] p 316 N94-12346

HELMETS
Mass properties test procedure for manikin headforms and helmet systems
[AD-A265654] p 315 N94-10296
Correlation of HGU-56/P aircrew helmet fitting with head anthropometric measurements
[AD-A264988] p 315 N94-11291
Accuracy and repeatability of the standard automated mass properties measurement system
[AD-A265897] p 316 N94-12346

HELMHOLTZ RESONATORS
A theory of membrane absorbers
[ISVR-TR-217] p 76 N94-11216

HEMATITE
Changes in Hawaiian palagonite FE mineralogy associated with thermal alteration: Implications for Mars p 281 N94-12055

HEMATOCRIT
Physiologic mechanisms of circulatory and body fluid losses in weightlessness identified by mathematical modeling p 312 N94-11557

HEMODYNAMICS
Proceedings of the First Joint NASA Cardiopulmonary Workshop
[NASA-CP-10068] p 308 N94-11991
Central circulatory hemodynamics as a function of gravitational stress p 309 N94-11995

HERMES MANNED SPACEPLANE
On the mechanical development of the Flexible External Insulation (FEI) for Hermes spaceplane p 62 N94-10048
Material advances for lightweight TPS p 62 N94-10049
Structural material, manufacture, and design requirements for high-temperature fasteners for space plane technologies p 63 N94-10055

HERMITIAN POLYNOMIAL
On renormalization group flow in matrix model
[DE93-613050] p 409 N94-10413

HETEROCYCLIC COMPOUNDS
Ring-opening polymerization of phosphazenes
[AD-A265000] p 90 N94-11292

HETERODYNING
Laser photoheterodyne interferometers for oceanographic investigations p 177 N94-12732

HETEROGENEITY
A heterogeneous graphics procedure for visualization of massively parallel solutions
[DE93-009628] p 336 N94-11270
Compositional heterogeneity within a dumbbell-shaped Apollo 15 green glass: Evidence for simultaneous eruption of different magmas p 470 N94-12209
Soret diffusion: A possible cause of compositional heterogeneity within tektites p 432 N94-12211

HETEROJUNCTIONS
Confinement of acoustical modes due to the electron-phonon interaction within 2D-electron gas
[DE93-613910] p 396 N94-10800
Memory effects in the organometallic chemical beam epitaxy of compound semiconductors
[NASA-CR-193106] p 399 N94-11439
Organometallic chemical vapor deposition and characterization of ZnGeP2/GaP multiple heterostructures on GaP substrates p 400 N94-11442
Preliminary surface-emitting laser logic device evaluation
[AD-A266111] p 383 N94-12416
Electronic and total energy properties of ternary and quaternary semiconductor compounds, alloys and superlattices
[NASA-CR-192905] p 405 N94-12570

HEURISTIC METHODS
Enhancements to the Engine Data Interpretation System (EDIS)
[NASA-CR-192593] p 180 N94-10815
Efficient partitioning and assignment on programs for multiprocessor execution
[NASA-CR-193458] p 324 N94-10942
A surrogate heuristic for set covering problems
[INPE-5462-PRE/1770] p 325 N94-11178
A new heuristic for set covering problems
[INPE-5471-TDI/502] p 333 N94-12358

HIGH DEFINITION TELEVISION

Studies and simulations of the DigiCipher system [NASA-CR-193470] p 321 N94-10343

HIGH ENERGY INTERACTIONS

Report of the Workshop on Light Particle-Induced Reactions [DE93-752300] p 360 N94-10317

Development of deterministic transport methods for low energy neutrons for shielding in space [NASA-CR-194172] p 366 N94-11199

Lecture note on circuit technology for high energy physics experiment [DE93-771422] p 372 N94-11245

Conceptual design report for the SDC barrel and intermediate muon detectors based on a jet-type drift chamber [DE93-753173] p 367 N94-11510

Future high precision experiments and new physics beyond Standard Model [DE93-011004] p 373 N94-11618

Theory of elementary particles and accelerator theory. Task C: Experimental high energy physics [DE93-013139] p 368 N94-11696

Final state interactions and inclusive nuclear collisions [NASA-TP-3353] p 373 N94-12435

Experimental particle physics at the University of Pittsburgh [DE93-013326] p 369 N94-12546

Experimental and theoretical high energy physics program [DE93-013336] p 373 N94-12600

Elementary particle physics and high energy phenomena [DE93-013971] p 370 N94-12609

HIGH FREQUENCIES

HF ocean radar system at Okinawa Radio Observatory p 139 N94-11902

Measurement of wave parameters by HF ocean radar p 192 N94-11903

Kuroshio observations by the HF ocean radar p 192 N94-11904

Statistical study of HF ocean radar echo p 139 N94-11905

Groundwave HF ocean surface radar p 139 N94-11906

High frequency behavior of long and small junctions [AD-A265670] p 403 N94-12336

HIGH GAIN

Force reflection with compliance control [NASA-CASE-NPO-18668-1-CU] p 179 N94-10654

Development of microstrip gas chamber and application to imaging gamma-ray detector [DE93-754294] p 34 N94-11041

Demonstration designs for optical-field-ionized plasma x-ray lasers [DE93-009227] p 175 N94-11266

GaAs PCSS: High gain switching and device reliability [DE93-009851] p 401 N94-11605

HIGH LEVEL LANGUAGES

Tensoral: A system for post-processing turbulence simulation data p 75 N94-12320

HIGH POLYMERS

Ring-opening polymerization of phosphazenes [AD-A265000] p 90 N94-11292

The synthesis of photocrosslinkable chalcone-bearing polyphosphazenes [AD-A264915] p 92 N94-11849

Molecular properties of polymeric materials for space applications [NASA-CR-194370] p 94 N94-12450

HIGH POWER LASERS

Start-up imprinting and shock dynamics in laser-target interaction [DE93-008051] p 172 N94-10150

Multiple laser beam combining and phasing using closed-loop control [DE93-009830] p 175 N94-11283

HIGH PRESSURE

High-energy density physics at Los Alamos [DE93-010271] p 371 N94-10260

X ray and gamma ray spectroscopy of solids under pressure [DE93-014847] p 76 N94-10653

Titanium alloys milling assistance by high pressure lubricoolant jet [DE93-013302] p 82 N94-11008

A picosecond high pressure gas switch [DE93-011897] p 142 N94-11050

HIGH RESOLUTION

Status of local oscillators for operating ultra-high resolution frequency discriminators as frequency standards p 353 N94-10981

High resolution time- and 2-dimensional space-resolved x ray imaging of plasmas at NOVA [DE93-011892] p 393 N94-11677

HIGH REYNOLDS NUMBER

Experimental and computational comparisons of Mach 6 high Reynolds number heat transfer and skin friction p 6 N94-10443

Similarity states of homogeneous stably-stratified turbulence at infinite Froude number p 156 N94-12292

Local isotropy in high Reynolds number turbulent shear flows p 157 N94-12302

An investigation of small scales of turbulence in a boundary layer at high Reynolds numbers p 157 N94-12303

Probability density distribution of velocity differences at high Reynolds numbers p 158 N94-12304

Superfluid turbulence p 158 N94-12307

Experiment on a high Reynolds number turbulent boundary layer p 164 N94-12617

HIGH SPEED

Flexible high-speed CODEC [NASA-CR-191169] p 146 N94-12433

Turbulence modeling and compressibility p 163 N94-12614

On the wake behind a high speed train p 164 N94-12618

HIGH STRENGTH ALLOYS

A study of strength evaluations of EDNi/EDCu/NARloy-Z bonded joints [NASA-TM-108418] p 188 N94-11275

Advances in low carbon, high strength ferrous alloys [AD-A265264] p 85 N94-12532

HIGH STRENGTH STEELS

Analytical prediction and test verification of the multiaxial behaviour of high-strength steel for lightweight structures p 58 N94-10016

Design with high strength steel: A case of failure and its implications p 58 N94-10017

Microstructure-based fatigue life prediction methods for naval steel structures [AD-A265429] p 85 N94-12426

Advances in low carbon, high strength ferrous alloys [AD-A265264] p 85 N94-12532

HIGH TEMPERATURE

Microgravity Applications Furnace Facility (MAFF) for parabolic flights p 109 N94-10128

High temperature processing and diagnostic technologies for microgravity applications p 110 N94-10130

MUZO: The programmable multi zone furnace for gas payloads and sounding rockets p 110 N94-10132

High temperature stability, interface bonding, and mechanical behavior in (beta)-NiAl and Ni3Al matrix composites with reinforcements modified by ion beam enhanced deposition [DE93-013977] p 398 N94-11115

The correlation of alkalis and aluminum during high-temperature volatilization of albite and nepheline p 81 N94-12214

On high-temperature formation of iron-rich olivine in the early solar system p 432 N94-12225

HIGH TEMPERATURE AIR

Electronic excitation of ground state atoms by collision with heavy gas particles [NASA-CR-193364] p 366 N94-11360

HIGH TEMPERATURE ENVIRONMENTS

High-temperature corrosion of ceramic-ceramic composites in a waste incinerator environment [DE93-012430] p 72 N94-11368

Potential techniques for non-destructive evaluation of cable materials [DE93-008350] p 183 N94-11586

Advanced thermally stable coal-derived jet fuels: Compositional factors affecting thermal degradation of jet fuels [AD-A265842] p 99 N94-12282

HIGH TEMPERATURE GAS COOLED REACTORS

Proceedings of the Second Technical Meeting on High Temperature Gas-Cooled Reactors [DE93-754285] p 371 N94-10719

HIGH TEMPERATURE LUBRICANTS

Tribological characteristics of sputtered Au/Cr films on alumina substrates at elevated temperatures [NASA-TM-106078] p 55 N94-11362

HIGH TEMPERATURE PLASMAS

Nonlinear MHD-waves in a dissipative plasma with hall currents [DE93-617844] p 386 N94-10395

Filamentation instability of hot quark-gluon plasma with hard jet [DE93-617679] p 388 N94-10882

Submicrosecond, synchronizable x ray source [AD-D015745] p 176 N94-12337

Inexpensive capillary discharge x-ray laser driver [AD-A265932] p 176 N94-12382

HIGH TEMPERATURE SUPERCONDUCTORS

Orbital glass in HTSC [DE93-613988] p 395 N94-10415

A window least squares algorithm for statistical noise smoothing of 2D-ACAR data [DE93-613828] p 395 N94-10537

Development and testing of a superconducting link for an IR detector [NASA-CR-193674] p 170 N94-10948

Processing and transport properties of high J(sub c) silver clad Bi-2223 tapes and coils [DE93-010674] p 398 N94-11073

Elastic deformations and sound in anisotrope superconductors near critical temperature [DE93-620636] p 188 N94-11364

Large array SQUID magnetometer for NDE [AD-A264799] p 304 N94-11449

Assessment of the impact of HTSC's on superconducting fault-current limiters [DE93-009986] p 143 N94-11454

Improvement of azimuthal homogeneity in permanent-magnet bearing rotors [DE93-009954] p 144 N94-11607

Highly anisotropic but nodeless gap from a valence-fluctuation pairing mechanism [DE93-010738] p 401 N94-11646

Corrosion control by vitreous films on aluminum and high T(sub c) superconductors [AD-A266016] p 85 N94-12393

HIGH TEMPERATURE TESTS

Comparison of computation and experiment for a high enthalpy, heated-driver, shock-tube environment p 7 N94-10447

Proceedings of the Second Technical Meeting on High Temperature Gas-Cooled Reactors [DE93-754285] p 371 N94-10719

Development and analysis of insulation constructions for aerospace wiring applications p 21 N94-10791

Field evaluation of six protective coatings applied to T-56 turbine blades after 2500 hours of engine use [ARL-TR-27] p 90 N94-11311

Tribological characteristics of sputtered Au/Cr films on alumina substrates at elevated temperatures [NASA-TM-106078] p 55 N94-11362

HIGH VACUUM

Design of CCD camera system for use inside electron beam furnace [DE93-009525] p 170 N94-11267

HIGH VOLTAGES

A study of DC-DC converters with MCTs for arcjet power supplies [NASA-CR-193457] p 142 N94-10931

HIGHLANDS

Using lunar sounder imagery to distinguish surface from subsurface reflectors in lunar highlands areas p 464 N94-12179

HIGHLY MANEUVERABLE AIRCRAFT

Nonlinear stability and control study of highly maneuverable high performance aircraft [NASA-CR-193480] p 25 N94-10344

HILBERT SPACE

The structure of Hilbert flag varieties [MEMO-1095] p 348 N94-10272

Geometric aspects of uncertainty and correlation p 349 N94-10588

HISTOCHEMICAL ANALYSIS

Effect of intermittent cold exposure on the fiber-type composition of selected skeletal muscles in rats [AD-A265309] p 301 N94-11861

HISTOGRAMS

A window least squares algorithm for statistical noise smoothing of 2D-ACAR data [DE93-613828] p 395 N94-10537

HISTORIES

The legacy of uncertainty p 376 N94-10577

A history of tungsten- and molybdenum-base alloys [DE93-010283] p 82 N94-11108

ESRO's first scientific satellite programme, 1961 - 1966 [ESA-HSR-2] p 44 N94-11462

Longitudinal study of astronaut health: Mortality in the years 1959-1991 p 312 N94-11560

HODOSCOPES

Demonstration prototype gamma-ray hodoscope alternative to CARGOSCAN for rocket stage monitoring [DE93-006908] p 169 N94-10326

HOLE MOBILITY

Invariance of the mobility edge in anodic titanium oxides [DE92-642136] p 394 N94-10281

HOLES (ELECTRON DEFICIENCIES)

Polaronic charge separation in mixed-halide MX solids [AD-A266073] p 403 N94-12345

HOLMIUM

X-ray and neutron scattering studies of magnetic critical fluctuations in holmium [DE93-010873] p 400 N94-11467

HOLOGRAPHIC INTERFEROMETRY

The sensitivity of an optical fiber holographic interferometer p 107 N94-10117

Holographic interferometry for microgravity applications p 108 N94-10123

In situ observation of temperature dependence of concentration field during growth of KB5 crystals by holographic interferometry p 115 N94-10187

HOLOGRAPHY

Surface and near-surface atom imaging with photoelectron holography [DE93-013197] p 169 N94-10526

Holographic multiplexing for 3D optical memory [AD-A266099] p 171 N94-11420

The evolution of whole field optical diagnostics for external transonic testing [ARA-MEMO-379] p 383 N94-11887

HOMEOSTASIS

Fluid compartment and renal function alterations in the rat during 7 and 14 day head down tilt p 310 N94-12002

HOMOGENEITY

Analytical details of the instability threshold of the laser-Lorenz model [DE93-619707] p 175 N94-11634

Remanent magnetism of HED meteorites: Implications for their evolution and ancient magnetic fields p 431 N94-12172

HOMOGENEOUS TURBULENCE

Similarity states of homogeneous stably-stratified turbulence at infinite Froude number p 156 N94-12292

HOMOJUNCTIONS

Progress in p(+)n InP solar cells fabricated by thermal diffusion p 48 N94-11384

Heteroepitaxial InP, and ultrathin, directly glassed, GaAs 3-5 solar cells p 52 N94-11406

HOMOLOGY

Deformations and recursion operators for evolution equations [MEMO-1104] p 341 N94-10163

The completion homomorphism in equivariant elliptic cohomology [DE93-619672] p 346 N94-11631

HOMOMORPHISMS

The completion homomorphism in equivariant elliptic cohomology [DE93-619672] p 346 N94-11631

HONEYCOMB STRUCTURES

Computer-aided molecular design of fire resistant aircraft materials p 19 N94-10779

Improvement of the flow quality in the ARA transonic tunnel by means of a long cell honeycomb [ARA-MEMO-375] p 34 N94-10894

HORIZONTAL FLIGHT

Advanced rotorcraft flight simulation: Model development, validation and parallel implementation p 25 N94-11056

HORIZONTAL TAIL SURFACES

A feasibility study regarding the addition of a fifth control to a rotorcraft in-flight simulator [NASA-CR-193240] p 30 N94-10895

HOSES

An investigation on the effectiveness of the piping interference removal system for STOL aircraft wind tunnel tests [NAL-TM-647] p 2 N94-10350

HOSPITALS

National Institute of Health Almanac, 1992 [PB93-183556] p 303 N94-10828

HOT ELECTRONS

Limitation and suppression of hot electron fluctuations in submicron semiconductor structures [DE93-613911] p 396 N94-10801

Short pulse lasers for generation of fields exceeding 100 MG [DE93-013346] p 369 N94-11815

HOT ISOSTATIC PRESSING

Bibliography on Hot Isostatic Pressing (HIP) technology [AD-A265668] p 81 N94-10297

Processing, properties, and wear resistance of aluminides [DE93-012186] p 83 N94-11141

Processing and properties of coated HPZ fiber reinforced glass-ceramic matrix composites [AD-A265177] p 92 N94-11876

HOT PRESSING

Mechanical properties of magnesium/carbon composites developed by hot pressing under medium pressure p 59 N94-10024

HOT WORKING

The microstructure and mechanical properties of hot worked FeAl intermetallic alloys p 58 N94-10020

HOT-FILM ANEMOMETERS

Visual structure of Karman vortex streets in a route to chaotic states excited by oscillation of a circular cylinder p 17 N94-12633

HOT-WIRE ANEMOMETERS

On the wake behind a high speed train p 164 N94-12618

Traveling disturbances appearing in yawed cylinder boundary layer transition p 166 N94-12632

HOVERING

Navier-Stokes flowfield computation of wing/rotor interaction for a tilt rotor aircraft in hover [NASA-CR-4532] p 13 N94-10758

HUBBLE SPACE TELESCOPE

Model of optical scatter from microimpacts on the Hubble Telescope p 384 N94-12189

HUBS

A grid generation method to calculate the flow field in a three-dimensional cascade of blades [NAL-TR-1158] p 147 N94-10364

HUDSON BAY (CANADA)

Wind and surface features in SAR images: The Canadian program p 234 N94-11718

HUMAN BEINGS

Transcranial Doppler ultrasound and the etiology of neurologic decompression sickness during altitude decompression p 312 N94-11544

HUMAN BODY

Physiological water model development p 316 N94-12367

Modifications to an interactive model of the human body during exercise: With special emphasis on thermoregulation p 317 N94-12368

HUMAN FACTORS ENGINEERING

Mass properties test procedure for manikin headforms and helmet systems [AD-A265654] p 315 N94-10296

Software usability assessment guide [AD-A265017] p 321 N94-10335

Head and face anthropometry of adult US civilians [DOT/FAA/AM-93/10] p 315 N94-10806

Allowable exposure limits for carbon dioxide during extravehicular activity [NASA-TM-103832] p 315 N94-11375

Sixth Annual Workshop on Space Operations Applications and Research (SOAR 1992), volume 2 [NASA-CP-3187-VOL-2] p 486 N94-11527

Vigilance problems in orbiter processing p 314 N94-11536

A comparison of head-up and head-down display formats during instrument flying tasks [AD-A266140] p 316 N94-11642

The 27th International Applied Military Psychology Symposium: A Focus on Decision Making Research [AD-A265278] p 313 N94-11701

Cognitive engineering models: A prerequisite to the design of human-computer interaction in complex dynamic systems [NASA-CR-193472] p 320 N94-12558

HUMAN PERFORMANCE

P2NBC2 Heat Strain Decision Aid. User's guide, version 2.1 [AD-A266072] p 304 N94-11224

Signal detection theory and methods for evaluating human performance in decision tasks p 314 N94-11531

Criteria for assessing problem solving and decision making in complex environments p 314 N94-11532

Monitoring cognitive function and need with the automated neuropsychological assessment metrics in Decompression Sickness (DCS) research p 314 N94-11533

Noise levels and their effects on Shuttle crewmembers' performance: Operational concerns p 314 N94-11538

Crew chief p 335 N94-11564

Locus coeruleus, vigilance, and stress: Brain mechanisms of adaptive behavioral responsiveness [AD-A265657] p 302 N94-12441

HUMAN REACTIONS

Effects of CSF hormones and ionic composition on salt/water metabolism [NASA-CR-193232] p 300 N94-11045

Evaluation of the C/EC/KC-135 ground collision avoidance system (GCAS), Study 2 [AD-A265193] p 24 N94-11879

Valsalva maneuver: Insights into baroreflex modulation of human sympathetic activity p 310 N94-12000

HUMAN RESOURCES

National patterns of R and D resources, 1992 [NSF-92-330] p 422 N94-11186

HUMAN TOLERANCES

Allowable exposure limits for carbon dioxide during extravehicular activity [NASA-TM-103832] p 315 N94-11375

HUMIDITY

The impact of horizontal resolution on moist processes in the ECMWF model [DE93-011718] p 276 N94-11227

Effects of solar cell environment on contact integrity p 49 N94-11387

Estimations of the surface fluxes from satellite observations of boundary layer and the surface p 252 N94-12513

HURRICANES

The effect of rain on ERS-1 altimeter data p 243 N94-11773

HYBRID CIRCUITS

Statistical process control in the hybrid microelectronics manufacturing industry: A Navy view point [AD-A265164] p 145 N94-11884

HYDRATION

Glycerol-induced hyperhydration p 309 N94-11996

HYDRAULIC EQUIPMENT

Investigation of alternate power source for Space Shuttle Orbiter hydraulic system [NASA-CR-193229] p 46 N94-10911

HYDRAULIC JETS

Large Aircraft Robotic Paint Stripping (LARPS) system and the high pressure water process p 127 N94-10623

Aquastrip (tm): An innovative paint removal technology p 127 N94-10625

Titanium alloys milling assistance by high pressure lubricoolant jet [DE93-013302] p 82 N94-11008

HYDRAZINE ENGINES

Studies on scramjet nozzles. Part 1: Performance of two dimensional nozzles [NAL-TR-1149] p 27 N94-10367

HYDROBALLISTICS

An experimental investigation of high-speed water-entry for full-size and scale-model pointed nose vehicles [DE93-008491] p 147 N94-10252

HYDROCARBON FUELS

The pyrene laser induced fluorescence technique as a diagnostic tool for combustion thermometry in microgravity p 107 N94-10113

Catalytic oxidation of organics in vapor streams at remediation sites [PB93-182962] p 266 N94-11472

HYDROCARBONS

Advanced thermally stable coal-derived jet fuels: Compositional factors affecting thermal degradation of jet fuels [AD-A265842] p 99 N94-12282

HYDRODYNAMICS

Evaporation under microgravity conditions p 102 N94-10086

Numerical simulation of multi-droplet hydrodynamic interactions in liquid dispersions p 114 N94-10182

Lattice gas hydrodynamics: Theory and simulations [DE93-013297] p 147 N94-10320

Comparison of hydrodynamic and semi-kinetic treatments for plasma flow along closed field lines [NASA-CR-193589] p 387 N94-10641

On the doubling of hydrodynamic theorems in relativistic theory of superfluidity [DE93-617895] p 148 N94-10717

Gluon gas viscosity in nonperturbative region [DE93-617680] p 397 N94-10883

Fully coupled neutronic and hydrodynamic analysis of space nuclear reactor reentry accidents [DE93-005459] p 372 N94-10890

FORCE2: A state-of-the-art two-phase code for hydrodynamic calculations [DE93-010661] p 150 N94-11072

Electron temperature measurements of x ray laser plasmas [DE93-011874] p 389 N94-11074

An improved material interface reconstruction algorithm for Eulerian codes [DE93-011679] p 326 N94-11226

Quality factors and local adaption (with applications in Eulerian hydrodynamics) [DE93-010502] p 151 N94-11272

Massively parallel hydrodynamics on unstructured grids [DE93-007325] p 153 N94-11601

Ejecting basaltic achondrites from Vesta: Hydrodynamical impact models p 429 N94-12036

Explicit 3D continuum fracture modeling with smooth particle hydrodynamics p 429 N94-12062

Initiating solar system formation through stellar shock waves p 448 N94-12090

An ancient inner lake in Maadim Vallis p 456 N94-12133

The giant impact produced a precipitated Moon p 430 N94-12135

Modeling void growth and movement with phase change in thermal energy storage canisters
[NASA-TM-106288] p 163 N94-12576

HYDROELECTRICITY
Renewable energy sources 1991, part 2
[DE93-605634] p 263 N94-11506

HYDROGEN
Hydrogen partitioning and transport in titanium aluminides
[NASA-CR-194117] p 76 N94-10713
A model of elementary chemistry and fluid mechanics in the combustion of hydrogen on platinum surfaces
[DE93-012767] p 77 N94-11370
Shear coaxial injector atomization phenomena for combusting and non-combusting conditions
[NASA-CR-193339] p 152 N94-11526
Experiments with energetic (mu)d and (mu)t emitted from solid hydrogen
[DE93-010252] p 373 N94-12542

HYDROGEN BONDS
Solid-state structures of guanidinium methane, ethane, and trifluoromethanesulfonate
[AD-A265293] p 402 N94-11654
Chromatographic assessment of hydrogen-bond donating ability
[AD-A265292] p 369 N94-11826
Hydrogen-bond polymorphs of guanidinium 4-biphenylsulfonate
[AD-A265294] p 402 N94-11827
Polymer-polymer interactions
[AD-A265304] p 91 N94-11830
Engineering solid-state materials. Strategies for modeling and packing control of molecular assemblies into 3-D networks
[AD-A265291] p 404 N94-12438

HYDROGEN EMBRITTLEMENT
Hydrogen partitioning and transport in titanium aluminides
[NASA-CR-194117] p 76 N94-10713

HYDROGEN ENGINES
Preprints of the 13th Hydrogen Energy System Symposium
[DE93-781115] p 99 N94-11444

HYDROGEN FUELS
An environmental study of the National Aerospace Plane
[AD-A266071] p 25 N94-10945
Preprints of the 13th Hydrogen Energy System Symposium
[DE93-781115] p 99 N94-11444

HYDROGEN IONS
Dynamics of dissociation versus ionization in strong laser fields
[DE93-009261] p 173 N94-10287
Size dependence of chemical reactivity of gaseous metal clusters: A new mechanistic probe
[AD-A264690] p 77 N94-11264

HYDROGEN MASERS
The 24th Annual Precise Time and Time Interval (PTTI) Applications and Planning Meeting
[NASA-CP-3218] p 350 N94-10963
Experimental comparison of time synchronization techniques by means of light signals and clock transport on the rotating earth p 351 N94-10970
Development of a cryogenic hydrogen maser at the NPL p 176 N94-10982
Ultrastable reference frequency distribution utilizing a fiber optic link p 355 N94-10994
Time scale algorithms for an inhomogeneous group of atomic clocks p 356 N94-10998

HYDROGEN OXYGEN ENGINES
Axisymmetric single shear element combustion instability experiment
[NASA-TM-106327] p 46 N94-10763
A laboratory model of a hydrogen/oxygen engine for combustion and nozzle studies
[NASA-TM-106281] p 47 N94-11252

HYDROGRAPHY
The subduction experiment. Cruise report, R/V Oceanus, cruise number 250 legs 1 and 2. Subduction 2 mooring deployment and recovery cruise, 25 January-26 February 1992
[AD-A264922] p 289 N94-11853

HYDROLOGICAL CYCLE
Evaporation and thermal/hydrologic balance in the Pacific p 195 N94-11919

HYDROLOGY
Rainfall-runoff estimation using digital radar
[AD-A265390] p 286 N94-12408
The use of ERS-1 SAR data to study surface states p 247 N94-12480
Pilot project PPF12. Coastal and fluvial environment in French Guiana: First results of ERS-1 SAR data analysis p 254 N94-12523

HYDROLYSIS
Low temperature synthesis of monolithic transparent Ta2O5 gels from hydrolysis of metal alkoxide
[NASA-TM-106246] p 89 N94-11204
Structural development in ceramic precursor sols and gels
[AD-A264354] p 90 N94-11281

HYDROPHONES
Underwater hydrophone location survey p 290 N94-10975
Preliminary analysis of the FLIP array data from the NOBS experiment
[AD-A265911] p 289 N94-12349

HYDROSTATICS
Hydrostatic testing of thick laminated composite cylinders for performance model validation
[DE93-012728] p 184 N94-10264

HYDROXYL RADICALS
In situ detection of tropospheric OH, HO2, NO2, and NO by laser-induced fluorescence in detection chambers at reduced pressures
[NASA-CR-193189] p 274 N94-10701

HYGROSCOPICITY
Hygroscopic absorption to falling films: The effects of the concentration level
[ITN-93-85198] p 148 N94-10391
Study of the atmospheric chemistry of radon progeny in laboratory and real indoor atmospheres
[DE93-012236] p 266 N94-11671

HYPERBOLIC DIFFERENTIAL EQUATIONS
Summation by parts, projections, and stability
[NASA-CR-194290] p 346 N94-12776

HYPERBOLIC FUNCTIONS
Boundary of Fatou sets of hyperbolic rational maps or degree two
[DE93-613031] p 348 N94-10412

HYPERCUBE MULTIPROCESSORS
A heterogeneous graphics procedure for visualization of massively parallel solutions
[DE93-009628] p 336 N94-11270
Optimal cube-connected cube multiprocessors
[NASA-CR-191463] p 337 N94-11308

HYPERNUCLEI
Double-lambda compound nucleus and the formation of double hypernuclei
[DE93-754289] p 365 N94-11040
A generalized Bethe-Weizsaecker mass formula for strange hadronic matter
[DE93-011010] p 368 N94-11620

HYPERONS
Production of strange clusters in relativistic heavy ion collisions
[DE93-010876] p 359 N94-10303
Strangeness production with protons and pions
[DE93-010879] p 359 N94-10304

HYPERPLANES
Vectorizing matrix operations arising from PDE discretization on 9-point stencils
[CWI-NM-R9221] p 342 N94-10351

HYPERSONIC BOUNDARY LAYER
Stability of hypersonic boundary-layer flows with chemistry p 7 N94-10451
Progress in modeling hypersonic turbulent boundary layers p 157 N94-12300

HYPERSONIC FLIGHT
In-flight evaluation of aerodynamic predictions of an air-launched space booster p 3 N94-10427
Extraction of stability and control derivatives from orbiter flight data
[NASA-TM-4500] p 13 N94-10707
Direct simulation of compressible wall-bounded turbulence p 156 N94-12294

HYPERSONIC FLOW
Theoretical and Experimental Methods in Hypersonic Flows
[AGARD-CP-514] p 2 N94-10421
CFD analysis of hypersonic, chemically reacting flow fields p 2 N94-10422
Numerical simulation of the flow through a scramjet engine p 3 N94-10425
New hypersonic test methods developed at ONERA: The R5 and F4 wind tunnels p 4 N94-10429
The high enthalpy facilities HEG and TH 2 in Germany p 4 N94-10430
Local measurement of temperatures and concentrations: A review for hypersonic flows p 4 N94-10434
Velocity measurements in hypersonic flows: A review p 5 N94-10436
Flow visualization and spectroscopy in hypersonic flows: New trends p 5 N94-10437
Thermal flux measurements in hypersonic flows: A review p 5 N94-10438
A CFD validation roadmap for hypersonic flows p 5 N94-10439
Synthesis of the Workshop on Hypersonic Flows for ReEntry Problems p 5 N94-10440
Problems in the validation of CFD codes through comparison with experiment p 6 N94-10441
Flow development in a circular pipe in the UTIAS/RPI M = 8.3 gun tunnel p 6 N94-10442
Experimental and computational comparisons of Mach 6 high Reynolds number heat transfer and skin friction p 6 N94-10443
Experimental, analytical, and computational methods applied to hypersonic compression ramp flows p 6 N94-10444
Issues and approach to develop validated analysis tools for hypersonic flows: One perspective p 7 N94-10446
Three-dimensional hypersonic rarefied flow calculations using direct simulation Monte Carlo method p 7 N94-10449
Stability of hypersonic flow over a blunt body p 7 N94-10450
On the instability of hypersonic flow past a pointed cone: Comparison of theoretical and experimental results at Mach 8 p 8 N94-10453
Studies of hypersonic viscous flows p 8 N94-10454
Nonequilibrium hypersonic flow in a wind-tunnel nozzle p 8 N94-10456
Some experimental study and numerical simulation in wind tunnel flow p 8 N94-10457
Hypersonic multi block flow simulations around space vehicles including non-equilibrium chemistry p 9 N94-10460
Hypersonic flow computations around re-entry vehicles p 9 N94-10461
On the accuracy and efficiency of CFD methods in real gas hypersonics p 9 N94-10462
A comparison of high resolution upwind solvers on 3-D inviscid hypersonic flows p 10 N94-10463
Thermal and chemical non equilibrium hypersonic flow computations p 10 N94-10465
Theoretical investigation of 3-D shock wave turbulent boundary layer interactions
[AD-A265275] p 150 N94-11014
Hypersonic, nonequilibrium flow over a cylindrically blunted 6 deg wedge
[NASA-TM-108994] p 162 N94-12571

HYPERSONIC HEAT TRANSFER
Computation of hypersonic nosetip heat transfer rates for an M829-like projectile
[AD-A263226] p 16 N94-11870

HYPERSONIC NOZZLES
Theoretical and Experimental Methods in Hypersonic Flows
[AGARD-CP-514] p 2 N94-10421
A CFD-based aerodynamic design procedure for hypersonic wind-tunnel nozzles p 9 N94-10458

HYPERSONIC REENTRY
Synthesis of the Workshop on Hypersonic Flows for ReEntry Problems p 5 N94-10440
Local aerothermal problems during Hermes re-entry p 10 N94-10464

HYPERSONIC SPEED
Experimental results in aerodynamic stability and control of a TSTO configuration p 3 N94-10424
Control effectiveness at hypersonic speeds p 3 N94-10426
Schlieren photographs and internal pressure distributions for three-dimensional sidewall-compression scramjet inlets at a Mach number of 6 in CF4
[NASA-TM-4479] p 148 N94-10644
Space Shuttle hypersonic aerodynamic and aerothermodynamic flight research and the comparison to ground test results
[NASA-TM-4499] p 13 N94-10820
Progress in modeling hypersonic turbulent boundary layers p 157 N94-12300

HYPERSONIC TEST APPARATUS
Recommendations for future research in hypersonic instrumentation p 4 N94-10433
Velocity measurements in hypersonic flows: A review p 5 N94-10436
Flow visualization and spectroscopy in hypersonic flows: New trends p 5 N94-10437

HYPERSONIC VEHICLES
High temperature materials for hypersonic transport p 56 N94-10003
Problems in the validation of CFD codes through comparison with experiment p 6 N94-10441
Joint computational and experimental aerodynamic research on a hypersonic vehicle p 6 N94-10445
Numerical methods for aerothermodynamic design of hypersonic space transport vehicles p 9 N94-10459

HYPERSONIC WIND TUNNELS
Experimental results in aerodynamic stability and control of a TSTO configuration p 3 N94-10424
New hypersonic test methods developed at ONERA: The R5 and F4 wind tunnels p 4 N94-10429

Pressure and force measurements on models set in hypersonic flows: A review p 5 N94-10435

Calculations of viscous nonequilibrium flows in nozzles p 8 N94-10455

Some experimental study and numerical simulation in wind tunnel flow p 8 N94-10457

HYPERSONICS

Recommendations for future research in hypersonic instrumentation p 4 N94-10433

Space Shuttle hypersonic aerodynamic and aerothermodynamic flight research and the comparison to ground test results
[NASA-TM-4499] p 13 N94-10820

An environmental study of the National Aerospace Plane
[AD-A266071] p 25 N94-10945

HYPERVELOCITY FLOW

Real gas and surface transpiration effects upon swept leading edge high speed flow including transition p 8 N94-10452

HYPERVELOCITY IMPACT

Dimensional scaling for impact cratering and perforation
[NASA-CR-188259] p 42 N94-10665

The magnitude of impact damage on LDEF materials
[NASA-CR-188258] p 43 N94-10666

Explicit 3D continuum fracture modeling with smooth particle hydrodynamics p 429 N94-12062

Composition and modal frequencies of hypervelocity particles less than 1 millimeter in diameter in low-Earth orbit p 429 N94-12063

Macroscopic electric charge separation during hypervelocity impacts: Potential implications for planetary paleomagnetism p 431 N94-12181

Projectile-target mixing in melted ejecta formed during a hypervelocity impact cratering event p 432 N94-12241

HYPERVELOCITY PROJECTILES

Composition and modal frequencies of hypervelocity particles less than 1 millimeter in diameter in low-Earth orbit p 429 N94-12063

HYPERVOLEMIA

Carotid-cardiac baroreflex: Relation with orthostatic hypotension following simulated microgravity and implications for development of countermeasures p 308 N94-11992

HYPOKINESIA

Project ARGO: Gas phase formation in simulated microgravity
[NASA-TM-104762] p 125 N94-11235

HYPOTENSION

Carotid-cardiac baroreflex: Relation with orthostatic hypotension following simulated microgravity and implications for development of countermeasures p 308 N94-11992

HYPOTHERMIA

Effect of intermittent cold exposure on the fiber-type composition of selected skeletal muscles in rats
[AD-A265309] p 301 N94-11861

HYPOVOLEMIA

Carotid-cardiac baroreflex: Relation with orthostatic hypotension following simulated microgravity and implications for development of countermeasures p 308 N94-11992

HYSTERESIS

A new method for hysteresis measurements developed for C(sub v) measurements at the critical point during the D2-mission p 107 N94-10114

The High Precision Thermostat HPT-HYDRA p 109 N94-10124

I

ICE

Wetting effects on nylon spheres engulfment in ice p 115 N94-10189

Paint removal and surface cleaning using ice particles p 128 N94-10626

A preliminary study on ice shape tracing with a laser light sheet
[NASA-TM-105964] p 174 N94-11132

Phase equilibria and volumetric properties for the system NaCl-CaCl2-H2O
[DE93-013590] p 76 N94-11244

Analysis of ERS-1 altimeter data over the polar ice sheets p 237 N94-11738

Some results of the derivation of ice sheet elevations in Antarctica from ERS-1 altimeter data p 237 N94-11739

An observational search for CO2 ice clouds on Mars p 441 N94-12054

Mars: The initial emplacement of ground ice in response to the thermal evolution of its early crust p 462 N94-12168

The role of the geothermal gradient in the emplacement and replenishment of ground ice on Mars p 463 N94-12169

Porosity and the ecology of icy satellites p 431 N94-12186

ICE CLOUDS

An observational search for CO2 ice clouds on Mars p 441 N94-12054

ICE ENVIRONMENTS

Facts about the US Antarctic program
[NSF-92-134] p 279 N94-12568

ICE FLOES

Use of ERS-1 SAR to measure ice flux in the East Greenland current p 238 N94-11746

Ocean circulation revealed by ice floe tracking p 240 N94-11759

Modern shelf ice, equatorial Aeolis Quadrangle, Mars p 450 N94-12100

Ice studies in the Barents Sea by ERS-1 during SIZEX 1992 p 210 N94-12653

Disintegrating ice front of Shirase Glacier, East Antarctica p 210 N94-12654

ICE FORMATION

Icing of turbine intake louvers
[AD-A265714] p 29 N94-12274

ICE MAPPING

Utilisation of ERS-1 data for mapping of Antarctica p 237 N94-11740

Finnish ERS-1 Baltic Sea ice experiment in Winter 1992 p 239 N94-11750

Applications of ERS-1 SAR data for analyzing riverine and coastal processes and geomorphology p 254 N94-12528

Pacific rim sea ice as observed with the NIMBUS-7 SMMR p 210 N94-12651

Ice studies in the Barents Sea by ERS-1 during SIZEX 1992 p 210 N94-12653

Disintegrating ice front of Shirase Glacier, East Antarctica p 210 N94-12654

Migration of operational ice analysis and forecasting to a workstation platform at the Joint Ice Center p 212 N94-12666

ICE PREVENTION

Icing of turbine intake louvers
[AD-A265714] p 29 N94-12274

ICE REPORTING

Analysis of ERS-1 altimeter data over the polar ice sheets p 237 N94-11738

Preliminary evaluation of ERS-1 altimetry over Filchner-Ronne Ice Shelf, Antarctica p 238 N94-11742

Use of ERS-1 SAR to measure ice flux in the East Greenland current p 238 N94-11746

Greenland Sea observations p 239 N94-11752

Arctic sea ice microwave signature and geophysical processes study p 240 N94-11754

C-band SAR backscatter from ice on shallow tundra lakes: Observations and modelling p 240 N94-11755

Sea ice radar signatures from ERS-1 SAR during late Summer and Fall in the Beaufort and Chukchi Seas p 240 N94-11756

The seasonal Sea Ice Monitoring and Modelling Site (SIMMS): Using ERS-1 in climate research p 240 N94-11758

Ocean circulation revealed by ice floe tracking p 240 N94-11759

Preliminary evaluation of ERS-1 SAR data for operational use in the Canadian sea ice monitoring program p 241 N94-11760

Sea ice feature and type identification in merged ERS-1 SAR and LANDSAT Thematic Mapper imagery p 241 N94-11761

Summer Arctic ice concentrations and characteristics from SAR and SSM/I data p 241 N94-11762

Evaluating ERS-1 ice motion and classification products p 241 N94-11763

Pacific rim sea ice as observed with the NIMBUS-7 SMMR p 210 N94-12651

Ice studies in the Barents Sea by ERS-1 during SIZEX 1992 p 210 N94-12653

Migration of operational ice analysis and forecasting to a workstation platform at the Joint Ice Center p 212 N94-12666

ICOSAHEDRONS

Enhanced stability of magic clusters: A case study of icosahedric Al(sub 12)X, X=B, Al, Ga, C, Si, Ge, Ti, As
[DE93-613644] p 395 N94-10386

ICY SATELLITES

Porosity and the ecology of icy satellites p 431 N94-12186

Phase transitions and 2D spherical convection in a large icy satellite p 433 N94-12265

IDEAL FLUIDS

On the Sobolev systems with ellipsoid cavities
[DE92-641290] p 148 N94-10530

Discrete vortex representation of magnetohydrodynamics
[DE93-012190] p 393 N94-11669

The thermodynamics of the nonlinear shear flows p 169 N94-12728

IDENTIFYING

A hybrid neural network and feature extraction technique for target recognition
[AD-D015732] p 333 N94-12386

IGNEOUS ROCKS

Noble gas evidence of an aqueous reservoir near the surface of Mars more recently than 1.3 Ga p 473 N94-12228

Primitive SNC parent magmas and crystallization: Low PH2O experiments p 433 N94-12264

IGNITION

The intensity of knock in an internal combustion engine: An experimental and modeling study
[DE93-013089] p 177 N94-10322

A soft-start circuit for arcjet ignition
[NASA-TM-106287] p 180 N94-10760

Flammability parameters of materials: Ignition, combustion, and flame spread p 20 N94-10788

A study of DC-DC converters with MCTs for arcjet power supplies
[NASA-CR-193457] p 142 N94-10931

Dielectric breakdown and its influence on ignition
[AD-A264925] p 78 N94-11855

IGNITION SYSTEMS

A soft-start circuit for arcjet ignition
[NASA-TM-106287] p 180 N94-10760

ILLUMINATING

Measurement and modeling of the stability of hydrogenated amorphous silicon solar cells and films after intense illumination p 263 N94-11638

Spatial light modulator having photosensitive and ferroelectric layers
[AD-D015731] p 404 N94-12400

ILMENITE

Thermodynamics of lunar ilmenite reduction p 415 N94-12028

Alkali-granitoids as fragments within the ordinary chondrite Adzhi-Bogdo: Evidence for highly fractionated, alkali-granitic liquids on asteroids p 429 N94-12069

Terrestrial case studies of ilmenite exploration and lunar implications p 478 N94-12247

IMAGE ANALYSIS

Particle image velocimetry technique: Calibration tests p 111 N94-10137

Introduction to Bayesian image analysis
[DE93-012628] p 347 N94-11006

Visual Earth observation performance in the space environment. Human performance measurement 4: Flight experiments p 314 N94-11539

Arctic coastal polynya observations with ERS-1 SAR and DMSP SSM/I p 239 N94-11748

Experiences from the Swedish sea ice programme during BEERS-1992 p 239 N94-11751

Preliminary evaluation of ERS-1 SAR data for operational use in the Canadian sea ice monitoring program p 241 N94-11760

Evaluating ERS-1 ice motion and classification products p 241 N94-11763

A consideration on principal component analysis of satellite IR data p 193 N94-11909

The optical/computer hybrid processing of extracting ocean wave directional spectrum by airborne photograph p 197 N94-11934

Automatic classification system for zooplankton p 203 N94-11969

Regional geology of the Venera landing sites: Tentative results of photogeologic mapping p 440 N94-12048

Compositional and textural information from the dual inversion of visible, near and thermal infrared remotely sensed data p 258 N94-12097

Automatic definition of spectral units in the equatorial regions of Mars p 432 N94-12234

Interdisciplinary scientist participation in the Phobos mission
[NASA-CR-193715] p 482 N94-12446

Preliminary studies on the application of ERS-1 data to topographic mapping p 246 N94-12476

Segmentation and change detection in ERS-1 images over East Anglia p 248 N94-12487

Further study of the Non-Regression-Coefficient SST retrieval method p 213 N94-12674

Delineation of mesoscale features of ocean on satellite IR image p 214 N94-12675

Aspects of applying a relaxation method to computing sea surface velocities from sea surface temperature images p 214 N94-12679

Application of NOAA AVHRR data to fisheries p 215 N94-12681

Remote sensing of polluting focal points and coastal disturbances in the Gulf of Arauco and adjacent bays, central Chile p 217 N94-12695

Role of remote sensing and its cost effectiveness in site selection for coastal aquaculture p 217 N94-12697

The warm eddy detection from NOAA/AVHRR thermal images using the Hough transformation p 220 N94-12713

Applicability of satellite infrared data for the monitoring of coastal environments p 220 N94-12714

Wind-wave and foam dynamics from optical and radar airborne observations p 226 N94-12745

Observations of surface signatures in the north-west Pacific Ocean with the spaceborne SAR p 226 N94-12746

Radar observation of internal waves field in the north-west Pacific p 226 N94-12747

Analysis of interstellar fragmentation structure based on IRAS images [NASA-CR-193518] p 428 N94-12767

IMAGE CLASSIFICATION

Satellite inventory of Minnesota forest resources [NASA-CR-193565] p 231 N94-11521

Sea ice feature and type identification in merged ERS-1 SAR and LANDSAT Thematic Mapper imagery p 241 N94-11761

IMAGE CONTRAST

Measurement of display transfer characteristics using test pictures [BBC-RD-1992/13] p 133 N94-11023

IMAGE ENHANCEMENT

Oil spill detection using satellite-based SAR: Experience from a field experiment p 253 N94-12522

IMAGE FILTERS

Segmented land use classification of multitemporal ERS-1 SAR data using a majority filter p 245 N94-12472

IMAGE INTENSIFIERS

Characterization of a scannerless LADAR system [DE93-011582] p 174 N94-10959

Perceptual response to visual noise and display media [NASA-CR-193406] p 313 N94-11511

IMAGE MOTION COMPENSATION

ISAR motion compensation using the burst derivative measure as a focal quality indicator [AD-A265647] p 138 N94-12440

IMAGE PROCESSING

Physical optics modelling of Soft X ray Projection Lithography (SXPL) imaging experiments [DE93-011556] p 374 N94-10339

Model-based recognition of 3-D objects by geometric hashing technique [DE93-612916] p 322 N94-10410

Surface and near-surface atom imaging with photoelectron holography [DE93-013197] p 169 N94-10526

Test of a method for phase retrieval in HRTEM [DE93-612641] p 170 N94-10630

Subband/transform functions for image processing [NASA-TM-106183] p 323 N94-10639

A browse facility for Earth science remote sensing data: Center director's discretionary fund final report [NASA-TM-108413] p 419 N94-10723

Subroutine functions for generating animation data [DE93-767973] p 313 N94-10731

FFT-based methods for nonlinear image restoration in confocal microscopy [CS-9301] p 174 N94-10904

Introduction to Bayesian image analysis [DE93-012628] p 347 N94-11006

A high-speed object recognition chip based on biologically-realistic hybrid temporal processing element [AD-A265490] p 339 N94-11049

Meteorological Satellite Center [MSC-TN-26] p 190 N94-11079

Fine tuning of stretched-VISSR image mapping p 190 N94-11080

A tool for generation of expert system shells [INPE-5493-TDI/510] p 325 N94-11181

Bayesian model for pictorial data fusion of satellite image [INPE-5457-TDI/499] p 345 N94-11193

Necessary conditions for the optimality of variable rate residual vector quantizers [NASA-CR-193730] p 326 N94-11197

A summary of image segmentation techniques [NASA-TM-104022] p 327 N94-11274

Atmospheric correction of AVIRIS data in ocean waters [AD-A264931] p 288 N94-11287

Spaceborne SAR study: LDRD 1992 [DE93-011485] p 232 N94-11623

Visual psychophysics of egomotion [AD-A265253] p 304 N94-11681

Sea ice feature and type identification in merged ERS-1 SAR and LANDSAT Thematic Mapper imagery p 241 N94-11761

A consideration on principal component analysis of satellite IR data p 193 N94-11909

Study on color video pictures transmission by digital acoustic signal p 139 N94-11917

The optical/computer hybrid processing of extracting ocean wave directional spectrum by airborne photograph p 197 N94-11934

Automatic classification system for zooplankton p 203 N94-11969

Atmospheric correction plans for SeaWiFS p 204 N94-11975

Fourier domain target transformation analysis in the thermal infrared p 258 N94-12030

A pattern recognition system for locating small volvanoes in Magellan SAR images of Venus p 455 N94-12126

A hybrid neural network and feature extraction technique for target recognition [AD-D015732] p 333 N94-12386

TREES project: A suite of tools for information extraction from ERS-1 SAR data p 250 N94-12498

Simple and low cost image processing system for satellite remote sensing data p 212 N94-12669

Delineation of mesoscale features of ocean on satellite IR image p 214 N94-12675

Aspects of applying a relaxation method to computing sea surface velocities from sea surface temperature images p 214 N94-12679

Application of NOAA AVHRR data to fisheries p 215 N94-12681

Remote sensing of polluting focal points and coastal disturbances in the Gulf of Arauco and adjacent bays, central Chile p 217 N94-12695

Role of remote sensing and its cost effectiveness in site selection for coastal aquaculture p 217 N94-12697

The warm eddy detection from NOAA/AVHRR thermal images using the Hough transformation p 220 N94-12713

Applicability of satellite infrared data for the monitoring of coastal environments p 220 N94-12714

Verification of the atmosphere-ocean radiative transfer parametric models p 225 N94-12738

Wind-wave and foam dynamics from optical and radar airborne observations p 226 N94-12745

Observations of surface signatures in the north-west Pacific Ocean with the spaceborne SAR p 226 N94-12746

Complex (hydrodynamic, satellite) monitoring of dynamic structures in the western Pacific with the aim of forecasting the marine ecosystems behaviour p 227 N94-12753

IMAGE RECONSTRUCTION

FFT-based methods for nonlinear image restoration in confocal microscopy [CS-9301] p 174 N94-10904

Introduction to Bayesian image analysis [DE93-012628] p 347 N94-11006

The possibility of image restoration under observation in a regime of strong scattering p 136 N94-11068

Complex (hydrodynamic, satellite) monitoring of dynamic structures in the western Pacific with the aim of forecasting the marine ecosystems behaviour p 227 N94-12753

IMAGE RESOLUTION

Characterization of a scannerless LADAR system [DE93-011582] p 174 N94-10959

A high-speed object recognition chip based on biologically-realistic hybrid temporal processing element [AD-A265490] p 339 N94-11049

On resolution of underwater stereo photogrammetry p 172 N94-11966

Model of optical scatter from microimpacts on the Hubble Telescope p 384 N94-12189

Comparison of multiresolution techniques for digital signal processing [AD-A265364] p 138 N94-12406

IMAGERY

Integrating the services' imagery architectures [AD-A265487] p 171 N94-12335

IMAGES

Site dependence of the apparent shape of a molecule in STM images: Benzene on Pt(111) [AD-A263488] p 365 N94-11093

IMAGING SPECTROMETERS

SMM x ray polychromator [NASA-CR-193282] p 483 N94-11048

Compositional and textural information from the dual inversion of visible, near and thermal infrared remotely sensed data p 258 N94-12097

Galileo/NIMS near-infrared thermal imagery of the surface of Venus p 457 N94-12139

Automatic definition of spectral units in the equatorial regions of Mars p 432 N94-12234

Composition of the Martian aerosols through near-IR spectroscopy p 475 N94-12235

IMAGING TECHNIQUES

Particle image velocimetry technique: Calibration tests p 111 N94-10137

Physical optics modelling of Soft X ray Projection Lithography (SXPL) imaging experiments [DE93-011556] p 374 N94-10339

HRTEM in protein crystallography [DE93-610322] p 395 N94-10406

Interferometric and optical tests of water window imaging x ray microscopes [NASA-CR-193369] p 375 N94-10506

Wavelength considerations in soft x ray projection lithography [DE93-014115] p 381 N94-10651

Subroutine functions for generating animation data [DE93-767973] p 313 N94-10731

Imaging of magnetospheric dynamics using low energy neutral atom detection [DE93-012656] p 275 N94-10742

An electro-optical system for the measurement of strains p 186 N94-10900

Development of microstrip gas chamber and application to imaging gamma-ray detector [DE93-754294] p 34 N94-11041

Basic experiment on an ultrasonic method of localization [DE93-754295] p 358 N94-11042

A high-speed object recognition chip based on biologically-realistic hybrid temporal processing element [AD-A265490] p 339 N94-11049

The superresolution effect observed through a random medium p 136 N94-11069

Design of CCD camera system for use inside electron beam furnace [DE93-009525] p 170 N94-11267

Radiation hardness of Mo/Si multilayers designed for use in a soft x ray projection lithography system [DE93-011879] p 143 N94-11273

A summary of image segmentation techniques [NASA-TM-104022] p 327 N94-11274

Relationship between IBICC imaging and SEU in CMOS ICs [DE93-009854] p 143 N94-11285

Use of ultrasound in altitude decompression modeling p 317 N94-11540

Arterial gas emboli in altitude-induced decompression sickness p 312 N94-11543

A compact, four-way image splitter [AD-A266107] p 382 N94-11656

High resolution time- and 2-dimensional space-resolved x ray imaging of plasmas at NOVA [DE93-011892] p 393 N94-11677

Feature association without a motion estimate [AD-A265162] p 138 N94-11891

Atomic-scale imaging of surfaces and interfaces. Materials Research Society Symposium Proceedings, volume 295 [AD-A265674] p 369 N94-12379

ISAR motion compensation using the burst derivative measure as a focal quality indicator [AD-A265647] p 138 N94-12440

Development of the one-component diode-array velocimeter [AD-A265552] p 171 N94-12533

Photogenerated base in polymer imaging. Synthesis and photopatterning of poly(2-cyano-2-(p-vinylphenyl) butanoic acid) [AD-A265288] p 95 N94-12585

The warm eddy detection from NOAA/AVHRR thermal images using the Hough transformation p 220 N94-12713

IMPACT DAMAGE

Dimensional scaling for impact cratering and perforation [NASA-CR-188259] p 42 N94-10665

The magnitude of impact damage on LDEF materials [NASA-CR-188258] p 43 N94-10666

Strain concentration assessment of laminates subjected to low velocity impact [AD-A264497] p 73 N94-11446

Giant impact-induced atmospheric blow-off p 435 N94-12019

A structural and petrographic investigation of the pretoria saltpan impact structure p 282 N94-12102

Geophysical signature of the Pretoria saltpan impact structure and a possible satellite crater p 282 N94-12103

Collisions of small Spacewatch asteroids with the Earth p 430 N94-12157

Modelling hypervelocity impacts into aluminum structures based on LDEF data p 190 N94-12178

Laboratory studies on the velocity of fragments from impact disruptions p 189 N94-12359

Deformation mechanisms in tungsten single crystals in ballistic impact experiments [AD-A265701] p 405 N94-12563

Prediction of alumina penetration
[DE93-014017] p 95 N94-12610

IMPACT LOADS
The 1991 version of the plume impingement computer program. Volume 2: User's input guide
[NASA-CR-194191] p 166 N94-12774

IMPACT MELTS
Measurements of cosmogenic nuclides in lunar rock 64455 p 437 N94-12033
Vaporization by shock loading of albite, jadeite, and pyrex glass: Experimental study p 97 N94-12039
Strontium and oxygen isotope study of M-1, M-3 and M-4 drill core samples from the Manson impact structure, Iowa: Comparison with Haitian K-T impact glasses p 281 N94-12080
Impact mineralogy and chemistry of the cretaceous-tertiary boundary at DSDP site 576 p 282 N94-12091
Impact comminution of glasses: Implications for lunar regolith evolution p 461 N94-12159
Post-impact alteration of the Manson impact structure p 282 N94-12188
The granulite suite: Impact melts and metamorphic breccias of the early lunar crust p 282 N94-12197

IMPACT PREDICTION
Prediction of alumina penetration
[DE93-014017] p 95 N94-12610

IMPACT RESISTANCE
Energy transfer dynamics and impact sensitivity
[DE93-009551] p 98 N94-11269
Prediction of alumina penetration
[DE93-014017] p 95 N94-12610

IMPACT TESTS
An experimental investigation of high-speed water-entry for full-size and scale-model pointed nose vehicles
[DE93-008491] p 147 N94-10252
Understanding cracking failures of coatings: A fracture mechanics approach p 187 N94-11218

IMPACTORS
Modelling hypervelocity impacts into aluminum structures based on LDEF data p 190 N94-12178

IMPEDANCE MATCHING
Design of a matching network for dipole antennas
[AD-A265115] p 136 N94-11158

IMPEDANCE MEASUREMENT
Fullerene superconductors: Phase stability and anomalously low T(sub c)'s in some ternary compounds
[DE93-010687] p 400 N94-11457

IMPINGEMENT
Evaluation of dual flow thrust vectored nozzles with exhaust stream impingement
[NASA-CR-193292] p 150 N94-10912
Modelling hypervelocity impacts into aluminum structures based on LDEF data p 190 N94-12178
The 1991 version of the plume impingement computer program. Volume 2: User's input guide
[NASA-CR-194191] p 166 N94-12774
The 1991 version of the plume impingement computer program. Volume 1: Description
[NASA-CR-194192] p 166 N94-12775

IMPLOSIONS
Start-up imprinting and shock dynamics in laser-target interaction
[DE93-008051] p 172 N94-10150
Source to detector spectrum transformation and its inverse for the Pegasus Z-pinch
[DE93-012674] p 384 N94-10157
High-energy density physics at Los Alamos
[DE93-010271] p 371 N94-10260
Advanced concepts theory annual report 1992
[AD-A266132] p 393 N94-11474

IMPREGNATING
Dry in-line thermoplastic matrix impregnation, phase 1
[AD-A265016] p 67 N94-11221

IMPULSES
Momentum induced by laser-tissue interaction
[DE93-010737] p 301 N94-11667

IMPURITIES
Unsupervised splitting rules for neural tree classifiers
[AD-A264961] p 338 N94-10487
Atomic and molecular data for H2O, CO and CO2 relevant to edge plasma impurities
[DE93-771423] p 387 N94-10662
Electronic characterization of defects in narrow gap semiconductors
[NASA-CR-193568] p 397 N94-10819
The influence of irradiation conditions, type, and concentration of impurities on radiation defects characteristics in indium antimonide under electron irradiation
[DE93-617201] p 397 N94-10843
Helium transport scaling law studies
[DE93-013487] p 393 N94-11513

IN SITU MEASUREMENT
In situ detection of tropospheric OH, HO2, NO2, and NO by laser-induced fluorescence in detection chambers at reduced pressures
[NASA-CR-193189] p 274 N94-10701
Localized and distributed fiber-optic strain sensors embedded in composite materials
[UTIAS-346] p 73 N94-12013

IN-FLIGHT MONITORING
In-flight evaluation of aerodynamic predictions of an air-launched space booster p 3 N94-10427
Smart structures: A technology for next generation aircraft p 27 N94-11318
Smart materials for helicopter rotor active control p 27 N94-11321
The Satellite Attack Warning and Assessment Flight Experiment (SAWAFE) p 45 N94-11323
In-flight aircraft structure health monitoring based on smart structures technology p 22 N94-11333
Structural health monitoring using embedded fibre optic sensors p 22 N94-11334
Factors affecting the embedding of optical fibre sensors in advanced composite structures p 70 N94-11336
Aircraft smart structures research in the USAF Wright Laboratory p 72 N94-11343
Use of telescience for biomedical research during space flight p 305 N94-11791

INCIDENT RADIATION
Squeezing in phase-conjugated resonance fluorescence p 376 N94-10576

INCINERATORS
High-temperature corrosion of ceramic-ceramic composites in a waste incinerator environment
[DE93-012430] p 72 N94-11368

INCLUSIONS
Creep deformation and mechanical properties of sintered glass and polycrystalline matrix composites p 67 N94-11315
The stability of hibonite and other aluminous phases in silicate melts: Implications for the origin of hibonite-bearing inclusions p 80 N94-12052
Distribution of vanadium and melting of opaque assemblages in Efremovka CAI's p 282 N94-12141
The experimental production of matrix lumps within chondrules: Evidence of post-formational processes p 431 N94-12176
Rhenium-osmium isotope systematics of Group 2A and Group 4A iron meteorites p 431 N94-12182
Isotopic and trace element characteristics of an unusual refractory inclusion from Essebi p 471 N94-12212
Development of a molecular beam technique to study early solar system silicon reactions p 432 N94-12224
Micro-zoning in minerals of a Landes silicate inclusion p 432 N94-12231

INCOHERENT SCATTER RADAR
Telescience capability for the Sondre Stromfjord, Greenland, incoherent-scatter radar facility
[NASA-CR-193683] p 136 N94-11206

INCOHERENT SCATTERING
The possibility of image restoration under observation in a regime of strong scattering p 136 N94-11068

INCOMPRESSIBLE BOUNDARY LAYER
On nonlinear Tollmien-Schlichting/vortex interaction in three-dimensional boundary layers
[NASA-TM-106184] p 152 N94-11377

INCOMPRESSIBLE FLOW
Solving the inverse problem for incompressible potential flow through two-dimensional cascades
[NAL-TR-1162] p 147 N94-10365
The three-dimensional evolution of a plane wake p 159 N94-12310

INCOMPRESSIBLE FLUIDS
Deformation mechanisms of continuous fibre-reinforced thermoplastic composites during manufacturing: A probabilistic approach p 60 N94-10030
Uni-directional waves over slowly varying bottom. Part 1: Derivation of a KdV-type of equation
[MEMO-1098] p 147 N94-10275
Lee waves: Benign and malignant
[NASA-CR-186024] p 283 N94-10725

INDEXES (DOCUMENTATION)
Aeronautical engineering: A continuing bibliography with indexes (supplement 293)
[NASA-SP-7037(293)] p 1 N94-10420
Aeronautical engineering: A continuing bibliography with indexes (supplement 289)
[NASA-SP-7037(289)] p 1 N94-11687
Aeronautical engineering: A continuing bibliography with indexes (supplement 291)
[NASA-SP-7037(291)] p 1 N94-11690
Aeronautical engineering: A continuing bibliography with indexes (supplement 290)
[NASA-SP-7037(290)] p 1 N94-11691
Directory of IAEA databases
[DE93-622837] p 420 N94-11818

INDIAN OCEAN
Preliminary analysis of circulations over the Indian Ocean and adjoining regions using ERS-1 surface winds in the NCMRWF data assimilation system p 234 N94-11719
Satellite derived sea surface temperature applications for Indian Ocean resources development p 193 N94-11907
Acoustic waveguide characteristics of the Indian Ocean north of equator p 193 N94-11912

INDIUM ANTIMONIDES
Measurement of the thermal conductivity of molten InSb in a drop shaft p 105 N94-10102
Crack suppression in GaInSb buffer layers initially under tensile stress
[DE93-012839] p 396 N94-10745
The influence of irradiation conditions, type, and concentration of impurities on radiation defects characteristics in indium antimonide under electron irradiation
[DE93-617201] p 397 N94-10843

INDIUM ARSENIDES
Crack suppression in GaInSb buffer layers initially under tensile stress
[DE93-012839] p 396 N94-10745
Radiation defect production in InAs crystals under electron irradiation
[DE93-617202] p 397 N94-10845

INDIUM GALLIUM ARSENIDES
Crack suppression in GaInSb buffer layers initially under tensile stress
[DE93-012839] p 396 N94-10745
InGaAs concentrator cells for laser power converters and tandem cells p 50 N94-11394
An indium gallium arsenide charge-coupled device (CCD) for 1-3 micron imaging
[AD-A266134] p 401 N94-11476

INDIUM PHOSPHIDES
Radiation effects in heteroepitaxial InP solar cells p 48 N94-11383
Progress in p(+)n InP solar cells fabricated by thermal diffusion p 48 N94-11384
Electrochemical characterization of p(+)n and n(+)p diffused InP structures p 49 N94-11385
Surface passivation of InP solar cells with InAlAs layers p 49 N94-11389
Heteroepitaxial InP, and ultrathin, directly glassed, GaAs 3-5 solar cells p 52 N94-11406
The UoSAT-5 solar cell experiment: First year in orbit p 53 N94-11409
Workshop on Heteroepitaxial InP Solar Cells p 54 N94-11414
Diffusion length damage coefficient and annealing studies in proton-irradiated InP
[NASA-TM-106262] p 404 N94-12430

INDONESIA
The use of remote sensing data for coastal zone management and environment in Indonesia p 196 N94-11927
Flood monitoring in northern part of Central Java by remote sensing technique. Case study: The flooding of Semarang in January, 1990 p 206 N94-11989

INDONESIAN SPACE PROGRAM
Space program in Indonesia p 36 N94-10681

INDUCTANCE
Assessment of the impact of HTSC's on superconducting fault-current limiters
[DE93-009986] p 143 N94-11454

INDUSTRIAL MANAGEMENT
Integrating the services' imagery architectures
[AD-A265487] p 171 N94-12335

INDUSTRIAL PLANTS
Toxic chemical release inventory reporting Form R and instructions. Revised 1992 version. Section 313 of the Emergency Planning and Community Right-to-Know Act
[PB93-194140] p 264 N94-10836
Statistical process control in the hybrid microelectronics manufacturing industry: A Navy view point
[AD-A265164] p 145 N94-11884

INDUSTRIAL SAFETY
Health and safety issues for aerospace workers in the use of advanced materials p 21 N94-10795

INDUSTRIAL WASTES
Toxic chemical release inventory reporting Form R and instructions. Revised 1992 version. Section 313 of the Emergency Planning and Community Right-to-Know Act
[PB93-194140] p 264 N94-10836

INDUSTRIES
Survey to determine the value of DYNA
[DE93-012390] p 321 N94-10267
Pattern of federal procurement from minority and women-owned small business
[PB93-189355] p 417 N94-11844
Optoelectronic technology consortium
[AD-A265691] p 383 N94-12444

INEQUALITIES
On cell entropy inequality for discontinuous Galerkin methods
[NASA-CR-191493] p 345 N94-11280
Bounding the Vapnik-Chervonenkis dimension of concept classes parameterized by real numbers
[DE93-011600] p 331 N94-11611

INERTIA
Martian particle size based on thermal inertia corrected for elevation-dependent atmospheric properties
p 430 N94-12107

INERTIAL CONFINEMENT FUSION
High-energy density physics at Los Alamos
[DE93-010271] p 371 N94-10260

INFECTIOUS DISEASES
Tropical medicine: Telecommunications and technology transfer p 305 N94-11793

INFORMATION DISSEMINATION
Performances of a date dissemination code on telephone lines using commercial modems
p 139 N94-10984
NASA/DOD Aerospace Knowledge Diffusion Research Project. Report 17: A comparison of the technical communication practices of Dutch and US aerospace engineers and scientists
[NASA-TM-108987] p 419 N94-11352
Marslink p 438 N94-12034
An integrated approach to total end-to-end quality control of ocean data in the real-time environment
p 211 N94-12662

INFORMATION FLOW
PANACEA user's manual for PANACEA version 2.0
[DE93-012502] p 321 N94-10263
Design for testability and diagnosis at the system-level
p 184 N94-11563

INFORMATION MANAGEMENT
Software management guide
[DE93-012034] p 330 N94-11452
Information resources management long-range plan, FY1994
[DE93-013898] p 420 N94-11588
COSMIC monthly progress report
[NASA-CR-194400] p 332 N94-11688
Information resources management plan of the Federal Government
[ISBN-0-16-037895-8] p 421 N94-12014
Defense: Health care
[AD-A265914] p 421 N94-12445
An integrated approach to total end-to-end quality control of ocean data in the real-time environment
p 211 N94-12662
Quality assurance for environmental chemistry: 1991, volume 2
[DE93-011792] p 272 N94-12780

INFORMATION PROCESSING (BIOLOGY)
Functional reasoning, explanation, and analysis
[DE92-526832] p 313 N94-10251
Automaticity of processing location versus identity information in brief visual displays
[AD-A265013] p 418 N94-10491

INFORMATION RETRIEVAL
The First Text Retrieval Conference (TREC-1)
[PB93-191641] p 419 N94-10829

INFORMATION SYSTEMS
Software usability assessment guide
[AD-A265017] p 321 N94-10335
Acting to gain information
[NASA-CR-193399] p 418 N94-10515
US Coast Guard GPS Information Center (GPSIC) and its function within the Civil GPS Service (CGS)
p 24 N94-10966
A real-time spoken-language system for interactive problem solving
[AD-A266046] p 324 N94-11104
Design issues for high performance engineering information systems
[AD-A264839] p 420 N94-11520
Information resources management long-range plan, FY1994
[DE93-013898] p 420 N94-11588
COSMIC monthly progress report
[NASA-CR-194400] p 332 N94-11688
Medical informatics and telemedicine: A vision
p 305 N94-11788
Use of satellite telecommunications for telemedicine
p 308 N94-11807
Directory of IAEA databases
[DE93-622837] p 420 N94-11818
Shoreline change detection using remote sensing and GIS in Vietnam p 196 N94-11928
Information resources management plan of the Federal Government
[ISBN-0-16-037895-8] p 421 N94-12014
Marslink p 438 N94-12034
Defense: Health care
[AD-A265914] p 421 N94-12445

INFORMATION THEORY
The theory for, and demonstration of, information theory applied to radar target identification
[DE93-006393] p 132 N94-10315
Symbolic dynamics and description of complexity
[DE93-613030] p 418 N94-10485
Acting to gain information
[NASA-CR-193399] p 418 N94-10515
Generalised squeezing and information theory approach to quantum entanglement p 377 N94-10580
Information entrophy via Glauber's Q-representation
p 378 N94-10592
Automatic word categorization: An information-theoretic approach
[CS-9209] p 419 N94-10903
Design for testability and diagnosis at the system-level
p 184 N94-11563
Bounding the Vapnik-Chervonenkis dimension of concept classes parameterized by real numbers
[DE93-011600] p 331 N94-11611

INFORMATION TRANSFER
NASA/DOD Aerospace Knowledge Diffusion Research Project. Report 17: A comparison of the technical communication practices of Dutch and US aerospace engineers and scientists
[NASA-TM-108987] p 419 N94-11352

INFRARED ASTRONOMY
Refrigerator utilization in infrared astronomy
p 130 N94-11838
First results of the seven-color asteroid survey
p 430 N94-12162
Analysis of interstellar fragmentation structure based on IRAS images
[NASA-CR-193518] p 428 N94-12767
Planetary astronomy of Mars. Mars data reduction
[NASA-CR-193515] p 424 N94-12768

INFRARED ASTRONOMY SATELLITE
Analysis of IRAS solar system dust data
[NASA-CR-193704] p 483 N94-10949
Analysis of interstellar fragmentation structure based on IRAS images
[NASA-CR-193518] p 428 N94-12767

INFRARED DETECTORS
Development and testing of a superconducting link for an IR detector
[NASA-CR-193674] p 170 N94-10948
Trouble areas in the IRT measurement of the Earth surface temperature p 193 N94-11910
Superconducting SQUID amplifiers for IR detectors and other applications, phase 2
[AD-A265447] p 145 N94-12333
Development of ultra-low noise, high sensitivity planar metal grating coupled 3 to 5 multiquantum well infrared detectors for focal plane array staring IR sensor systems
[AD-A265599] p 404 N94-12375
An interferometric spectral mapper for the Cassini mission to Saturn and Titan
[NASA-CR-193805] p 482 N94-12429

INFRARED IMAGERY
Fine tuning of stretched-VISSR image mapping
p 190 N94-11080
Simulation of images of water vapor channel and infrared split channel p 190 N94-11081
Atmospheric correction of AVIRIS data in ocean waters
[AD-A264931] p 288 N94-11287
An indium gallium arsenide charge-coupled device (CCD) for 1-3 micron imaging
[AD-A266134] p 401 N94-11476
The morphologies of distant radio galaxies
p 426 N94-11597
A consideration on principal component analysis of satellite IR data p 193 N94-11909
Thermal studies of Martian channels and valleys using Termoskan data p 443 N94-12064
Compositional and textural information from the dual inversion of visible, near and thermal infrared remotely sensed data p 258 N94-12097
Galileo/NIMS near-infrared thermal imagery of the surface of Venus p 457 N94-12139
The relationship between skin and bulk sea surface temperatures p 221 N94-12716
Mapping of high density area of benthic diatom in Ariake Sea p 222 N94-12720
Analysis of interstellar fragmentation structure based on IRAS images
[NASA-CR-193518] p 428 N94-12767
Planetary astronomy of Mars. Mars data reduction
[NASA-CR-193515] p 424 N94-12768

INFRARED INSTRUMENTS
An indium gallium arsenide charge-coupled device (CCD) for 1-3 micron imaging
[AD-A266134] p 401 N94-11476

INFRARED RADIATION
The morphologies of distant radio galaxies
p 426 N94-11597
A consideration on principal component analysis of satellite IR data p 193 N94-11909

INFRARED RADIOMETERS
Proceedings of 1st ERS-1 Symposium on Space at the Service of Our Environment, Volume 2
[ESA-SP-359-VOL-2] p 245 N94-12471
ATSR correlative skin measurements of sea surface temperature p 252 N94-12514
Validation of ATSR-1 using aircraft radiometer measurements over the South Atlantic
p 252 N94-12515
A user appraisal of ATSR near-real-time products
p 252 N94-12516
Cloud studies using ATSR data p 253 N94-12517
A comparison of ATSR and shipboard radiometer SST measurements along transects between the UK and the Antarctic p 253 N94-12518
Preliminary validation of ATSR sea surface temperatures near the Faeroes p 253 N94-12519
Statistical features of mesoscale eddies at the Kuroshio front p 215 N94-12682

INFRARED REFLECTION
A vibrational spectroscopic study of the structure of electroactive self-assembled monolayers of viologen derivatives
[AD-A265705] p 78 N94-12273

INFRARED SCANNERS
METEOSAT second generation programme SEVIRI: An enhanced visible and IR radiometer for meteorology
p 212 N94-12667

INFRARED SPECTRA
On renormalization group flow in matrix model
[DE93-613050] p 409 N94-10413
The IR properties of ringed galaxies and the IRAS database
[NASA-CR-194286] p 426 N94-11590
Fourier domain target transformation analysis in the thermal infrared p 258 N94-12030
A comparison of telescopic and Phobos-2 ISM spectra of Mars in the short-wave near-infrared (0.76-1.02 microns) p 424 N94-12053
The effects of atmospheric pressure on infrared reflectance spectra of Martian analogs
p 445 N94-12071
Spatial variation in the seasonal south polar cap of Mars as observed by Mariner 7 p 456 N94-12134
Automatic definition of spectral units in the equatorial regions of Mars p 432 N94-12234
A comparison of the visible and near infrared reflectance of hydrovolcanic palagonite tuffs and Martian weathered soils p 477 N94-12245
A vibrational spectroscopic study of the structure of electroactive self-assembled monolayers of viologen derivatives
[AD-A265705] p 78 N94-12273
Examination of the surface second harmonic response at infrared wavelengths
[AD-A265206] p 403 N94-12371
A relaxation study of poled nonlinear optical polymers by infrared reflection-absorption spectroscopy
[AD-A265797] p 93 N94-12380
Atmospheric and spectroscopic research in the far infrared
[NASA-CR-193551] p 280 N94-12582

INFRARED SPECTROMETERS
Automatic definition of spectral units in the equatorial regions of Mars p 432 N94-12234

INFRARED SPECTROSCOPY
Thermal-infrared emission spectroscopy of natural surfaces: Application to coated surfaces
p 81 N94-12156
Near-infrared spectra of the Martian surface: Reading between the lines p 465 N94-12184
Composition of the Martian aerosols through near-IR spectroscopy p 475 N94-12235
A novel test method for fuel thermal stability
[AD-A265853] p 99 N94-12275
Atmospheric and spectroscopic research in the far infrared
[NASA-CR-193551] p 280 N94-12582
Ecological application of Surface Enhanced Raman Spectroscopy p 227 N94-12756

INFRARED TELESCOPES
An approach to high precision antenna structures by a CFRP core sandwich concept p 57 N94-10008
Refrigerator utilization in infrared astronomy
p 130 N94-11838

INJECTION
Titanium alloys milling assistance by high pressure lubricoolant jet
[DE93-013302] p 82 N94-11008

INJECTION MOLDING
Physical properties of injection molded liquid crystal polymers and high temperature engineering polymers
[AD-A264912] p 87 N94-10508

INJECTORS
Space Storable Rocket Technology program (SSRT). Option 1 program
[NASA-CR-191171] p 46 N94-10938
Shear coaxial injector atomization phenomena for combusting and non-combusting conditions
[NASA-CR-193339] p 152 N94-11526
INLAND WATERS
ERS-1 altimetry of inland water and land
p 246 N94-12475
Variability of spectral reflectance in coastal waters near the river plumes p 226 N94-12744
INLET FLOW
A comparative study of full Navier-Stokes and Reduced Navier-Stokes analyses for separating flows within a diffusing inlet S-duct
[NASA-TM-106250] p 39 N94-10764
INORGANIC CHEMISTRY
Publications/Patents/Presentations/Honors/Student eport
[AD-A265136] p 78 N94-11873
INSECTS
HRTEM in protein crystallography
[DE93-610322] p 395 N94-10406
INSOLATION
Satellite-derived photosynthetically available and total solar irradiance at the surface during FIFE's intensive field campaigns p 230 N94-10954
INSPECTION
Special problems of 3-D ultrasonic QNDI techniques and applications to composites aerospace structures
p 61 N94-10036
Design of inspection and acceptance test methodology for TIG welded aluminum-alloy bracket for camera housings for IRS-1A space craft and executing it
p 61 N94-10037
A Recommended Methodology for Quantifying NDE/NDI Based on Aircraft Engine Experience
[AGARD-LS-190] p 28 N94-11022
Vigilance problems in orbiter processing
p 314 N94-11536
INSTANTONS
Generalized spin systems and sigma-models
[DE93-613981] p 410 N94-10802
INSTRUCTORS
Career Information in the Mathematical Sciences (CIMS)
[DE93-013780] p 318 N94-11817
INSTRUMENT APPROACH
The Memphis Precision Runway Monitor Program Instrument Landing System final approach study
[AD-A266035] p 23 N94-11103
A comparison of head-up and head-down display formats during instrument flying tasks
[AD-A266140] p 316 N94-11642
FAA air traffic activity
[AD-A266043] p 22 N94-12397
INSTRUMENT ERRORS
Particle image velocimetry technique: Calibration tests
p 111 N94-10137
INSTRUMENT FLIGHT RULES
A comparison of head-up and head-down display formats during instrument flying tasks
[AD-A266140] p 316 N94-11642
INSTRUMENT LANDING SYSTEMS
The Memphis Precision Runway Monitor Program Instrument Landing System final approach study
[AD-A266035] p 23 N94-11103
Evaluation of the C/EC/KC-135 ground collision avoidance system (GCAS), Study 2
[AD-A265193] p 24 N94-11879
INSULATION
On the mechanical development of the Flexible External Insulation (FEI) for Hermes spaceplane
p 62 N94-10048
Design and production of insulated wind tunnel models of the Hermes shuttle for heat transfer measurements at hypersonic speeds p 4 N94-10431
The fire properties of insulation bags, as installed and after aircraft operations p 19 N94-10778
INTAKE SYSTEMS
Theoretical investigation of 3-D shock wave turbulent boundary layer interactions
[AD-A265275] p 150 N94-11014
INTEGRAL EQUATIONS
Numerical method of singular problems on singular integrals
[DE93-613654] p 343 N94-10546
The nonlinear evolution of modes on unstable stratified shear layers
[NASA-CR-191492] p 149 N94-10810
Design of a continuous resistively loaded monopole antenna
[AD-A265852] p 138 N94-12281
INTEGRALS
Floquet operator as integral of motion
p 380 N94-10610
Divergences in the moduli space integral and accumulating handles in the infinite-genus limit
[DE93-619722] p 346 N94-11693
INTEGRATED CIRCUITS
Continuous-time adaptive learning circuit
[AD-D015773] p 140 N94-10384
Method for producing a hybridization of detector array and integrated circuit for readout
[NASA-CASE-NPO-18062-1-CU] p 141 N94-10656
Semiconductor ring lasers
[DE93-012386] p 174 N94-11005
Lecture note on circuit technology for high energy physics experiment
[DE93-771422] p 372 N94-11245
Relationship between IBICC imaging and SEU in CMOS ICs
[DE93-009854] p 143 N94-11285
ENSAFE fireset flex circuit analysis
[DE93-013106] p 144 N94-11478
Programmable logic devices
[DE93-013117] p 144 N94-11479
An ellipsometry investigation of nucleation and growth of electron cyclotron resonance plasma deposited silicon films
[AD-A265037] p 401 N94-11651
Resist materials design: Base-catalyzed chemical amplification
[AD-A265286] p 145 N94-11819
Gallium arsenide dynamic random access memory support circuitry
[AD-A265176] p 320 N94-11875
Statistical process control in the hybrid microelectronics manufacturing industry: A Navy view point
[AD-A265164] p 145 N94-11884
Limited bandwidth microwave filter
[AD-D015744] p 145 N94-12322
An optoelectronic graphics display processor
[AD-A266011] p 171 N94-12391
Optoelectronic technology consortium
[AD-A265691] p 383 N94-12444
Low cost high efficiency GaAs monolithic RF module for SARSAT distress beacons
[NASA-CR-194235] p 146 N94-12773
INTEGRATED OPTICS
Spatial light rebroadcaster architecture study
[AD-A266102] p 382 N94-11421
INTEGRATORS
Continuous-time adaptive learning circuit
[AD-D015773] p 140 N94-10384
INTELLIGENCE
Integrating the services' imagery architectures
[AD-A265487] p 171 N94-12335
INTELSAT SATELLITES
Applications of the INTELSAT system to remote health care p 306 N94-11794
INTERACTIONAL AERODYNAMICS
Navier-Stokes flowfield computation of wing/rotor interaction for a tilt rotor aircraft in hover
[NASA-CR-4532] p 13 N94-10758
Turbulent boundary layer interacting with spanwise periodic longitudinal vortex arrays p 165 N94-12626
VIB2D: Quasi 3-D unsteady viscous flow method for blade flutter calculation
[CUED/A-TURBO/TR.129] p 166 N94-12779
INTERATOMIC FORCES
Non-empirical interatomic potentials for transition metals
[DE93-013705] p 365 N94-11011
Interatomic interactions in BCC and FCC lattices of transition metals
[DE93-621541] p 398 N94-11090
A new decomposition strategy for parallel bonded molecular dynamics
[DE93-009839] p 366 N94-11284
INTERCALATION
Fullerene superconductors: Phase stability and anomalously low T(sub c)'s in some ternary compounds
[DE93-010687] p 400 N94-11457
INTERFACE STABILITY
Fluid-fluid interfacial instabilities induced by gravity
p 121 N94-10229
INTERFACES
The combined influence of anticonvective and thermocapillary mechanisms on the stability of systems with interface p 121 N94-10223
INTERFACIAL TENSION
Proceedings of the 8th European Symposium on Materials and Fluid Sciences in Microgravity, volume 1
[ESA-SP-333-VOL-1] p 99 N94-10070
The formation and breakage of liquid bridges under microgravity p 100 N94-10071
Non-linear liquid bridge dynamics p 100 N94-10074
Dielectric liquid bridge stabilization in microgravity by means of electric fields p 100 N94-10075
Thermocapillary instabilities in cylindrical liquid bridges: Mechanisms and transition boundaries
p 101 N94-10077
Transient three-dimensional numerical simulation of Marangoni flow in a liquid column under microgravity
p 101 N94-10079
Coupled thermovibrational and thermocapillary convection in liquid bridge (floating zone system)
p 101 N94-10082
Effects of axial and centrifugal forces on the stability of liquid bridges p 102 N94-10083
Liquid bridges and floating zones p 102 N94-10085
Surface-tension driven convection in finite-size containers p 103 N94-10090
Gas-liquid jets under reduced gravity conditions
p 103 N94-10091
Coupled thermogravitational and thermocapillary convection in a two-layer fluid system
p 105 N94-10101
Boundary layers along horizontal free surfaces due to combined effects of temperature and concentration gradients p 106 N94-10108
Solidification in immiscible systems: The influence of processing conditions on resulting microstructures
p 112 N94-10174
Thermophysical properties of undercooled liquid metals p 86 N94-10190
Marangoni-driven solitary waves p 119 N94-10214
Surface tension and adsorption kinetics in immiscible liquid systems at microgravity p 121 N94-10225
Marangoni instability in a liquid layer with two free surfaces
[NASA-TM-106166] p 152 N94-11376
Interfacial modification through end group complexation in polymer blends
[AD-A265887] p 93 N94-12340
INTERFERENCE
Interference photocathode
[AD-D015770] p 132 N94-10382
INTERFERENCE GRATING
Analysis of the alignment of a Schlieren system for tele-operation p 111 N94-10140
INTERFEROMETERS
A fiber optic network system with low crosstalk using code-division multiplexing
[AD-D015763] p 374 N94-10376
Nonlinear Dynamics in Optical Systems. Postdeadline papers presented at the Optical Society of America Conference
[AD-A264958] p 375 N94-10486
Implementation and use of a computational ray-tracing program for the design and analysis of complex optical systems
[AD-A265075] p 382 N94-11653
Effects of satellite spectral resolution and atmospheric water vapor on retrieval of near-ground temperatures
[AD-A264920] p 245 N94-11851
An interferometric spectral mapper for the Cassini mission to Saturn and Titan
[NASA-CR-193805] p 482 N94-12429
Laser photoheterodyne interferometers for oceanographic investigations p 177 N94-12732
INTERFEROMETRY
Interferometry with particles of non-zero rest mass
[DE93-613518] p 409 N94-10501
Interferometric and optical tests of water window imaging x ray microscopes
[NASA-CR-193369] p 375 N94-10506
An electro-optical system for the measurement of strains p 186 N94-10900
Fiber-optic interferometric strain gauge for smart structures applications: First flight tests
p 71 N94-11340
Techniques and applications of SAR interferometry for ERS-1: Topographic mapping, change detection, and slope measurement p 236 N94-11734
SAR interferometry experiments with ERS-1
p 237 N94-11735
SAR-interferometry applying ERS-1: Some preliminary test results p 237 N94-11736
The TREES project: Pre-processing and generation of terrain data for inclusion in an ERS-1 SAR classification scheme p 249 N94-12496
INTERMETALLICS
The microstructure and mechanical properties of hot worked FeAl intermetallic alloys p 58 N94-10020
Containerless processing of equiatomic Mn50Bi50 in a drop tube p 118 N94-10205
Bibliography on Hot Isostatic Pressing (HIP) technology
[AD-A265668] p 81 N94-10297
Hydrogen partitioning and transport in titanium aluminides
[NASA-CR-194117] p 76 N94-10713

Production of reactive sintered nickel aluminide
[DE93-014434] p 83 N94-11127
Interface considerations in Al2O3/NiAl composite
[NASA-CR-191167] p 66 N94-11202
X ray absorption spectroscopy of electrochemically generated species
[AD-A264749] p 77 N94-11265
Experimental studies of the structure of grain boundaries
[DE93-013979] p 402 N94-11700
NiAl alloys for structural uses
[NASA-CR-194113] p 85 N94-12447

INTERMITTENCY
Homoclinic intermittency
[W-9302] p 344 N94-10908

INTERMOLECULAR FORCES
Polar solvation and electron transfer
[DE93-013328] p 365 N94-11010

INTERNAL COMBUSTION ENGINES
The intensity of knock in an internal combustion engine: An experimental and modeling study
[DE93-013089] p 177 N94-10322
Life-cycle cost analysis of conventional and fuel cell/battery powered urban passenger vehicles
[DE93-010770] p 182 N94-11438
Ceramics technology project database
[DE93-012431] p 91 N94-11672
Direct simulation of compressible wall-bounded turbulence p 156 N94-12294

INTERNAL PRESSURE
Schlieren photographs and internal pressure distributions for three-dimensional sidewall-compression scramjet inlets at a Mach number of 6 in CF4
[NASA-TM-4479] p 148 N94-10644

INTERNAL WAVES
Submarine internal waves
[MRL-GD-0049] p 98 N94-11303
Accretion disk viscosity and internal waves in disks
p 153 N94-11615
Shear, strain and thermohaline vertical fine structure in the upper ocean
[AD-A265961] p 289 N94-12348
Radar observation of internal waves field in the north-west Pacific p 226 N94-12747
Generation of internal waves near the shelf boundary
p 229 N94-12763
Experimental and theoretical investigation of undular bore formation upstream the bank p 229 N94-12764

INTERNATIONAL COOPERATION
Considerations for future regional space cooperation
p 35 N94-10678
International Space Year in China p 36 N94-10680
PARTNERS p 38 N94-10695
International disaster research p 307 N94-11805
AGARD highlights 92/2, September 1992
[AGARD-HIGHLIGHTS-92/2] p 497 N94-11820
ESA Costing Software (ECOS) introduction
[ESA-F-28] p 333 N94-12383

INTERNATIONAL RELATIONS
Landsat as a commercial enterprise
[INPE-5477-TAE/019] p 232 N94-11524

INTERNATIONAL SPACE YEAR
Space Activities in the Asia Pacific Region
[JTN-93-80421] p 35 N94-10676
Current status of space activities in Asia Pacific region
p 35 N94-10677
Considerations for future regional space cooperation
p 35 N94-10678
Space research and remote sensing programmes in Bangladesh p 35 N94-10679
International Space Year in China p 36 N94-10680
Space program in Indonesia p 36 N94-10681
Japanese space activities p 36 N94-10682
Thailand ISY activities p 37 N94-10690
National space program in Australia
p 37 N94-10691
Canada's longterm space plan and ISY activities
p 37 N94-10692
Pakistan Space and Upper Atmosphere Research Commission p 37 N94-10693
PARTNERS p 38 N94-10695

INTERPLANETARY DUST
Analysis of IRAS solar system dust data
[NASA-CR-193704] p 483 N94-10949
Detection of dust impacts by the Voyager planetary radio astronomy experiment
[NASA-CR-193281] p 423 N94-11305
Mineralogy of chondritic interplanetary dust particle impact residues from LDEF p 80 N94-12045
Using solar flare track densities to determine the origin of interplanetary dust particles p 429 N94-12078
Unequilibrated, equilibrated, and reduced aggregates in anhydrous interplanetary dust particles
p 429 N94-12098
Carbon analyses of IDP's sectioned in sulfur and supported on beryllium films p 81 N94-12099
Volatiles in fourteen interplanetary dust particles: A comparison with CI and CM chondrites
p 430 N94-12132
Measurement of polycyclic aromatic hydrocarbon (PAHs) in interplanetary dust particles
p 431 N94-12167
Iron and nickel isotopic mass fractionation in deep-sea spherules p 282 N94-12199
Organic matter on the early surface of Mars: An assessment of the contribution by interplanetary dust
p 480 N94-12259
Trace element content of chondritic cosmic dust: Volatile enrichments, thermal alterations, and the possibility of contamination p 433 N94-12260
Depletions of sulfur and/or zinc in IDPs: Are they reliable indicators of atmospheric entry heating?
p 433 N94-12261
New low-Ni (igneous?) particles among the C and C? types of cosmic dust p 433 N94-12262

INTERPLANETARY MEDIUM
The influence of the propagation medium on the sensitivity and resolution of meter wavelength aperture synthesis systems p 134 N94-11062
The possibility of image restoration under observation in a regime of strong scattering p 136 N94-11068

INTERPOLATION
A four-dimensional, mesoscale, non-gaussian multispectral smoke model. Phase 1: Feasibility study
[AD-A264805] p 152 N94-11519

INTERPROCESSOR COMMUNICATION
Bringing theory to practice: The reality of interprocessor communication
[DE93-012346] p 336 N94-10738
Portable programming on parallel/networked computers using the Application Portable Parallel Library (APPL)
[NASA-TM-106238] p 327 N94-11232

INTERSTELLAR GAS
Radiowaves propagation through inhomogeneous interstellar plasma p 134 N94-11061
Interstellar scattering and the selection of extragalactic radiosources with highly compact components
p 134 N94-11063
The excitation of cyanogen and ionized carbon in interstellar and extragalactic gas clouds
p 426 N94-11582
ADP study of the structure of the IUE halo
[NASA-CR-194374] p 428 N94-12595

INTERSTELLAR MAGNETIC FIELDS
Are cosmic rays effective for ionization of the solar nebula? p 472 N94-12220

INTERSTELLAR MATTER
Intraday variability and the compactness of extragalactic radio sources p 135 N94-11064
Interstellar scattering and the pulsar studies with space VLBI p 135 N94-11065
VLBI and the detection of interstellar magnetohydrodynamic waves p 135 N94-11066
Interstellar graphite in Murchison: Continued search for isotopically distinct components p 97 N94-12029
Identification of cometary and asteroidal particles in stratospheric IDP collections p 430 N94-12115

INTERSTITIALS
Electronic characterization of defects in narrow gap semiconductors
[NASA-CR-193568] p 397 N94-10819

INVARIANCE
On parity conservation and the question of the missing, right-handed neutrino
[DE93-613092] p 361 N94-10414

INVENTORIES
Satellite inventory of Minnesota forest resources
[NASA-CR-193565] p 231 N94-11521

INVERSE KINEMATICS
Derivation of three closed loop kinematic velocity models using normalized quaternion feedback for an autonomous redundant manipulator with application to inverse kinematics
[DE93-012823] p 340 N94-12543

INVERSE SCATTERING
P-matrix description of the two-particle interaction
[DE93-617690] p 361 N94-10549

INVERTERS
Experimental and theoretical investigations of Cs-Ba vapor tacitron inverter for power conditioning in space power systems
[DE93-012971] p 48 N94-11372

INVISCID FLOW
Numerical simulation of the flow through a scramjet engine p 3 N94-10425
On the accuracy and efficiency of CFD methods in real gas hypersonics p 9 N94-10462
A comparison of high resolution upwind solvers on 3-D inviscid hypersonic flows p 10 N94-10463
High order accurate solutions of viscous problems
[NASA-TM-106267] p 151 N94-11253
Numerical simulation of the non-Newtonian mixing layer p 159 N94-12314
Computational methods for problems in aerodynamics using parallel and vector architectures
[AD-A265626] p 16 N94-12377

IO
Sources of Na for the Io atmosphere
p 455 N94-12127

IODIDES
Conductive-radiative model for predicting the shape of HgI2 crystal grown in the LTVG furnace
p 117 N94-10201

IODINE COMPOUNDS
Szilard-Chalmers effect in solid HIO4.2H2O by neutron irradiation
[DE93-617173] p 397 N94-10830

IODINE ISOTOPES
Szilard-Chalmers effect in solid HIO4.2H2O by neutron irradiation
[DE93-617173] p 397 N94-10830
Studies of the release of radiogenic Xe-129 from Bjurboele: Evidence against simple diffusion models
p 430 N94-12125

ION ACCELERATORS
An experimental program for collective acceleration of ions using intense relativistic electron beams
[DE93-612205] p 371 N94-10316
Report of the third Seminar on Nuclear Physics at the Energy Region of the JAERI Tandem-Booster Accelerator
[DE93-754330] p 372 N94-11043
Performance characteristics of the INS 25.5-MHz split coaxial RFQ
[DE93-753168] p 144 N94-11508

ION BEAMS
Photodetachment studies on few-electron atomic negative ions
[DE93-008474] p 358 N94-10154
An experimental program for collective acceleration of ions using intense relativistic electron beams
[DE93-612205] p 371 N94-10316
Collective acceleration of ions in near-anode plasma of a strong-current relativistic diode
[DE93-620977] p 387 N94-10541
Dynamics of ion acceleration in electron flux by a virtual cathode potential
[DE93-620978] p 371 N94-10542
Comparison of hydrodynamic and semi-kinetic treatments for plasma flow along closed field lines
[NASA-CR-193589] p 387 N94-10641
Nonperturbative methods in HZE ion transport
[NASA-TP-3363] p 484 N94-10759
Spin characteristics of ion beams during the motion of electromagnetic elements
[DE93-617448] p 364 N94-10848
Monochromator SP-017. The results of the first experiments
[DE93-617463] p 372 N94-10849
Wave generation by contaminant ions
[NASA-CR-193558] p 364 N94-10946
Short wavelength crystal fiber devices
[AD-A265716] p 176 N94-12402
Damage threshold study of ion beam sputtered coatings for a visible high-repetition laser at LLNL
[DE93-013430] p 95 N94-12602
Ion shaking in the 200 MeV XLS-ring
[DE93-014057] p 374 N94-12782

ION CONCENTRATION
Size dependence of chemical reactivity of gaseous metal clusters: A new mechanistic probe
[AD-A264690] p 77 N94-11264

ION CYCLOTRON RADIATION
Ionization potentials of small carbon clusters
[AD-A264379] p 67 N94-11260
Conversion of the four-strap array in D3-D to a tunable traveling wave antenna
[DE93-012085] p 137 N94-11453

ION DENSITY (CONCENTRATION)
Solar wind-induced secondary ions and their relation to lunar surface composition p 474 N94-12232

ION ENGINES
Characterization of in-flight performance of ion propulsion systems
[NASA-TM-106283] p 46 N94-10761

ION EXCHANGING
Aluminum and membrane channels
[AD-A265241] p 300 N94-11020

ION MICROSCOPES
Atomic-scale imaging of surfaces and interfaces. Materials Research Society Symposium Proceedings, volume 295
[AD-A265674] p 369 N94-12379

ION MOTION
Spin characteristics of ion beams during the motion of electromagnetic elements
[DE93-617448] p 364 N94-10848

ION PROPULSION
Characterization of in-flight performance of ion propulsion systems
[NASA-TM-106283] p 46 N94-10761
ION SCATTERING
Theoretical atomic physics for fusion
[DE93-013872] p 366 N94-11172
Solar wind-induced secondary ions and their relation to lunar surface composition p 474 N94-12232
IONIC COLLISIONS
Photodetachment studies on few-electron atomic negative ions
[DE93-008474] p 358 N94-10154
Production of strange clusters in relativistic heavy ion collisions
[DE93-010876] p 359 N94-10303
Relativistic heavy-ion collisions
[DE93-014844] p 366 N94-11147
Momentum and heat frictions between fast ions and thermal plasma species
[DE93-771240] p 390 N94-11149
Theoretical atomic physics for fusion
[DE93-013872] p 366 N94-11172
Relativistic heavy ion research
[DE93-013127] p 367 N94-11373
Pion correlations and calorimeter design for high energy heavy ion collisions
[DE93-013861] p 373 N94-12607
IONIZATION
Integrated cross sections for the ionisation of atomic hydrogen by electron impact
[DE93-610179] p 359 N94-10311
Theoretical atomic physics for fusion
[DE93-013872] p 366 N94-11172
Demonstration designs for optical-field-ionized plasma x-ray lasers
[DE93-009227] p 175 N94-11266
A thermal ionization model for the sustaining phase of lock-on in GaAs
[DE93-011558] p 144 N94-11624
IONIZATION CHAMBERS
Post-launch analysis of data from the High Energy Astrophysical Observatory Heavy Nuclei Experiment (HEAO-C3)
[NASA-CR-193513] p 484 N94-11486
IONIZATION CROSS SECTIONS
Integrated cross sections for the ionisation of atomic hydrogen by electron impact
[DE93-610179] p 359 N94-10311
Calculation of the total ionization cross section and spin asymmetry in electron-hydrogen scattering from threshold to 500 eV
[DE93-610180] p 359 N94-10312
Atomic and molecular data for H2O, CO and CO2 relevant to edge plasma impurities
[DE93-771423] p 387 N94-10662
Progress in zirconium resonance ionization spectroscopy
[DE93-011881] p 76 N94-11075
Electronic excitation of ground state atoms by collision with heavy gas particles
[NASA-CR-193364] p 366 N94-11360
IONIZATION POTENTIALS
Ionization potentials of small carbon clusters
[AD-A264379] p 67 N94-11260
Demonstration designs for optical-field-ionized plasma x-ray lasers
[DE93-009227] p 175 N94-11266
IONIZING RADIATION
Nonperturbative methods in HZE ion transport
[NASA-TP-3363] p 484 N94-10759
IONOGRAMS
Some results with the new digital ionosonde in San Diego
[AD-A265178] p 275 N94-11101
IONOSONDES
Some results with the new digital ionosonde in San Diego
[AD-A265178] p 275 N94-11101
IONOSPHERIC CURRENTS
Observing and modelling F-region ionospheric dynamics using the (O2) 7320A emission
[AD-A265407] p 279 N94-12419
IONOSPHERIC DISTURBANCES
Effects of energetic particle events on VLF/LF propagation parameters/1989
[AD-A265266] p 275 N94-11013
Some results with the new digital ionosonde in San Diego
[AD-A265178] p 275 N94-11101
IONOSPHERIC ION DENSITY
Observing and modelling F-region ionospheric dynamics using the (O2) 7320A emission
[AD-A265407] p 279 N94-12419
IONOSPHERIC PROPAGATION
Some results with the new digital ionosonde in San Diego
[AD-A265178] p 275 N94-11101
One-dimensional calculation of high-power microwave pulse compression by the earth's ionosphere
[DE93-009517] p 137 N94-11466
IONS
Collective acceleration of ions in near-anode plasma of a strong-current relativistic diode
[DE93-620977] p 387 N94-10541
Dynamics of ion acceleration in electron flux by a virtual cathode potential
[DE93-620978] p 371 N94-10542
Wave generation by contaminant ions
[NASA-CR-193558] p 364 N94-10946
Tandem mass spectrometric analysis of phosphate esters
[AD-A265483] p 78 N94-12009
Role of spatially distributed ion channels in single neuron computation
[AD-A265972] p 79 N94-12351
Ion shaking in the 200 MeV XLS-ring
[DE93-014057] p 374 N94-12782
IOWA
Petrography and preliminary interpretations of the crystalline breccias from the Manson M-1 core
p 281 N94-12056
IRAN
Land use/land cover mapping of central water shed of Iran area based on satellite data interpretation
p 219 N94-12704
IRIDIUM
Surface-enhanced raman spectroscopy of electroactive films of C60 and an Ir-C60 complex on gold: Symmetry lowering, electron localization, and counteraction effects
[AD-A265934] p 396 N94-10705
IRON
Effects of microscopic iron metal on the reflectance spectra of glass and minerals p 436 N94-12024
Chemical weathering on Mars: Rate of oxidation of iron dissolved in brines p 455 N94-12128
Moessbauer spectrometer for mineralogical analysis of the Mars surface: Moessbauer source considerations
p 476 N94-12242
IRON ALLOYS
Comparison of Al-Fe alloys produced by PFC and USGA techniques p 58 N94-10019
The microstructure and mechanical properties of hot worked FeAl intermetallic alloys p 58 N94-10020
Solidification and metastable phase formation of highly undercooled Fe-Cr-Ni alloy melts p 87 N94-10204
Monte Carlo simulations of phase transformations in Fe-Cr alloys
[DE93-013847] p 81 N94-10522
DBTT measurement by use of Small Punch (SP) test
[DE93-753188] p 183 N94-11168
In situ XANES studies of the passive film on Fe and Fe-26Cr
[DE93-010869] p 84 N94-11459
NiAl alloys for structural uses
[NASA-CR-194113] p 85 N94-12447
IRON COMPOUNDS
Measuring and distinguishing compositional and maturity properties of lunar soils by remote VIS-NIR spectroscopy p 478 N94-12251
IRON ISOTOPES
Iron and nickel isotopic mass fractionation in deep-sea spherules p 282 N94-12199
IRON METEORITES
Calorimetric thermometry of meteoritic troilite: A feasibility study p 428 N94-12025
Rhenium-osmium isotope systematics of Group 2A and Group 4A iron meteorites p 431 N94-12182
Trace element distributions in primitive achondrites
p 431 N94-12200
Re-Os dating of 3AB iron meteorites
p 432 N94-12237
Cronstedtite and iron sulfide mineralogy of CM-type carbonaceous chondrites from cryogenic Moessbauer spectra p 433 N94-12257
IRON OXIDES
Changes in Hawaiian palagonite FE mineralogy associated with thermal alteration: Implications for Mars
p 281 N94-12055
Cathodoluminescence properties of components in enstatite chondrites p 432 N94-12206
IRRADIANCE
Studies of the net surface radiative flux from satellite radiances during FIFE
[NASA-CR-193150] p 230 N94-10953
Satellite-derived photosynthetically available and total solar irradiance at the surface during FIFE's intensive field campaigns p 230 N94-10954
Optical characteristics in Tokyo Bay
p 204 N94-11972
IRRADIATION
On problem about nature of Portevin-Le Chatelier effect in irradiated aluminium alloys
[DE93-617200] p 82 N94-10842
The angular structure of second harmonic emission from laser-produced plasmas irradiated at moderate intensity
[DE93-013102] p 389 N94-11114
Effect of switched-bias bakes on the postirradiation electrical response of MOS devices
[DE93-009629] p 143 N94-11271
Radiation hardness of Mo/Si multilayers designed for use in a soft x ray projection lithography system
[DE93-011879] p 143 N94-11273
A detailed study of the photo-injection annealing of thermally diffused InP solar cells p 48 N94-11381
High temperature annealing of minority carrier traps in irradiated MOCVD n(+)p InP solar cell junctions
p 48 N94-11382
Radiation effects in heteroepitaxial InP solar cells
p 48 N94-11383
Development of plastic capsule for research reactor irradiation
[DE93-753186] p 372 N94-11591
Radiation-induced aperiodicity in irradiated ceramics
[DE93-013335] p 91 N94-11698
Natural thermoluminescence profiles in lunar cores and implications for meteorites p 443 N94-12060
NMR characterization of polymers formed in diazotizing mixtures of luminol and 3-amino-L-tyrosine
[AD-A266093] p 94 N94-12536
ISING MODEL
The peculiarities of the spin glass state in Fe(x)Mn(1-x)TiO3
[DE93-617882] p 395 N94-10525
ISLANDS
Coastal processes due to nearshore current around an upheaving island p 199 N94-11942
A new data collection system for ionospheric modelling and related topics
[AD-A265893] p 278 N94-12277
ISOCHORIC PROCESSES
A new method for hysteresis measurements developed for C(sub v) measurements at the critical point during the D2-mission p 107 N94-10114
ISOMERIZATION
Preparation of stable photopatternable polymeric materials for non-linear optics
[AD-A265359] p 95 N94-12577
ISOTHERMS
Observations of the fractal properties of the Japan sea surface temperature patterns p 205 N94-11984
ISOTONICITY
Exercise countermeasures for bed-rest deconditioning
[NASA-TM-103987] p 300 N94-11191
ISOTOPES
A new matrix for the ageless 21.6-keV Eu-151 nuclear gamma ray Moessbauer source
[DE93-009795] p 75 N94-10338
Journal of Research of the National Institute of Standards and Technology, volume 98, number 2, March - April 1993
[PB93-196228] p 485 N94-10850
Carbon in weathered ordinary chondrites from Roosevelt County p 428 N94-12035
Stable isotope analyses of the peralkaline volcanics Gregory Rift Valley, Kenya p 281 N94-12072
Th-230 - U-238 series disequilibrium of the Olkaria basalts Gregory Rift Valley, Kenya p 281 N94-12073
Th-230 - U-238 series disequilibrium of the Olkaria basalts Gregory Rift Valley, Kenya: Petrogenesis
p 281 N94-12074
Th-230 - U-238 series disequilibrium of the Olkaria rhyolites Gregory Rift Valley, Kenya: Petrogenesis
p 281 N94-12075
Th-230 - U-238 series disequilibrium of the Olkaria rhyolites Gregory Rift Valley, Kenya: Residence times
p 281 N94-12076
Isotopic and trace element characteristics of an unusual refractory inclusion from Essebi p 471 N94-12212
ISOTROPY
Advanced Materials for Lightweight Structures
[ESA-SP-336] p 56 N94-10001
The searchlight problem for neutrons in a semi-infinite medium
[DE93-010796] p 365 N94-10952
Highly anisotropic but nodeless gap from a valence-fluctuation pairing mechanism
[DE93-010738] p 401 N94-11646
Remanent magnetism of HED meteorites: Implications for their evolution and ancient magnetic fields
p 431 N94-12172
Local isotropy in high Reynolds number turbulent shear flows p 157 N94-12302

ITERATIVE SOLUTION
Massively parallel multifrontal methods for finite element analysis on MIMD computer systems
[DE93-009838] p 335 N94-10257
Convergence theorems for a class of nonlinear maps in uniformly smooth Banach spaces
[DE92-641347] p 343 N94-10531
Improvements for obtaining iterative solutions of large linear systems
[DE93-767968] p 343 N94-10729
Stability by linear processes
[NASA-CR-194131] p 323 N94-10862
FFT-based methods for nonlinear image restoration in confocal microscopy
[CS-9301] p 174 N94-10904
Necessary conditions for the optimality of variable rate residual vector quantizers
[NASA-CR-193730] p 326 N94-11197
Resolution for Lanczos and Paige-Saunders inverses in tomography
[DE93-012312] p 327 N94-11240
Parallel molecular dynamics with the embedded atom method
[DE93-010683] p 367 N94-11455
Fourier domain target transformation analysis in the thermal infrared p 258 N94-12030

IUE
The abundances of the elements in sharp-lined early type stars
[NASA-CR-194055] p 424 N94-12573
ADP study of the structure of the IUE halo
[NASA-CR-194374] p 428 N94-12595

J

JAMMING
Improved Many-On-Many ROUTE software description
[DE93-013961] p 334 N94-12608

JAPAN
Processing proper nouns in machine translation for English news
[NHK-SERIAL-414] p 418 N94-10559
Insights into software development in Japan
p 330 N94-11435
The Kyucho events in Sukumo Bay induced by Kuroshio front disturbances p 198 N94-11939

JAPANESE SPACE PROGRAM
Japanese space activities p 36 N94-10682

JAPANESE SPACECRAFT
Japanese space activities p 36 N94-10682
Flight data analysis of Japanese Earth Resources Satellite-1 (JERS-1)
[NASDA-CNT-930004] p 245 N94-12279
Conceptual studies report on lunar and planetary exploration
[NASDA-TK-SS0438] p 481 N94-12323
Significance and scenarios of lunar and planetary exploration missions p 482 N94-12324
Unmanned lunar exploration mission
p 482 N94-12325
Manned lunar exploration missions
p 482 N94-12326
Mars exploration missions p 482 N94-12327
Technical problems on lunar an planetary exploration mission p 482 N94-12328
The Third Workshop on Two Phase Fluid Experiment in the Space Environment
[NASDA-CON-930002] p 161 N94-12547
Summary of studies on JEM utilization experiment projects p 161 N94-12548

JET AIRCRAFT NOISE
Control of jet noise
[NASA-CR-193612] p 358 N94-11176

JET CONTROL
Space Shuttle hypersonic aerodynamic and aerothermodynamic flight research and the comparison to ground test results
[NASA-TM-4499] p 13 N94-10820

JET ENGINE FUELS
Advanced diagnostics for in situ measurement of particle formation and deposition in thermally stressed jet fuels
[DE93-009798] p 98 N94-11366
A novel test method for fuel thermal stability
[AD-A265853] p 99 N94-12275
Advanced thermally stable coal-derived jet fuels: Compositional factors affecting thermal degradation of jet fuels
[AD-A265842] p 99 N94-12282

JET EXHAUST
Application of jet-shear-layer mixing and effervescent atomization to the development of a low-NO(x) combustor
[NASA-TM-105888] p 28 N94-11234

JET FLOW
Gas-liquid jets under reduced gravity conditions
p 103 N94-10091
Direct numerical simulation of hot jets
p 156 N94-12295

JET IMPINGEMENT
Turbulence modeling for thrust reverser flow field prediction methods
[AD-A266139] p 154 N94-11641

JFET
Lecture note on circuit technology for high energy physics experiment
[DE93-771422] p 372 N94-11245

JOINTS (JUNCTIONS)
Joints between dissimilar metallic and ceramic materials p 63 N94-10052
Advanced methods of permanently joining carbon materials p 63 N94-10057
Project ARGO: Gas phase formation in simulated microgravity
[NASA-TM-104762] p 125 N94-11235
Apical Cu-O bond in YBa2Cu3O(7-delta) superconductors by XAFS
[DE93-010861] p 400 N94-11458

JOSEPHSON JUNCTIONS
High frequency behavior of long and small junctions
[AD-A265670] p 403 N94-12336

JUDGMENTS
A comparison of high and low-impact reports of investigation on adjudicators' decision making: A pilot study
[AD-A265747] p 416 N94-10298

JUNCTION DIODES
Effect of effective mass differences on the tunneling current-voltage behaviour of a resonant diode in the presence of space charge build-up
[DE93-613817] p 142 N94-10799

K

K-EPSILON TURBULENCE MODEL
A Galilean and tensorial invariant k-epsilon model for near wall turbulence
[NASA-TM-106263] p 151 N94-11192
Turbulence modeling for thrust reverser flow field prediction methods
[AD-A266139] p 154 N94-11641

KALMAN FILTERS
Discrete Kalman filtering equations of second-order form for control-structure interaction simulations
[NASA-CR-193723] p 331 N94-11522
First results for the simultaneous estimation of the geoid and the sea surface topography by ERS-1 altimeter data
p 241 N94-11765
Estimation with multisensor/multiscan detection fusion
[AD-A265673] p 138 N94-12338
Preliminary results from a satellite altimetric data assimilation using a Kalman filter and smoother
p 209 N94-12648

KAONS
Strange meson spectroscopy in K(omega) and K(phi) at 11 GeV/c and Cherenkov ring imaging at SLD
[DE93-013593] p 363 N94-10748

KAPOETA ACHONDRITE
Carbonaceous chondrite clasts in the Kapoeta howardite p 282 N94-12104
Remanent magnetism of HED meteorites: Implications for their evolution and ancient magnetic fields
p 431 N94-12172

KARMAN VORTEX STREET
On the formation process of Karman vortex street
p 16 N94-12621
Visual structure of Karman vortex streets in a route to chaotic states excited by oscillation of a circular cylinder
p 17 N94-12633

KELVIN-HELMHOLTZ INSTABILITY
LIF measurements of scalar mixing in turbulent shear layers p 159 N94-12312

KENYA
Stable isotope analyses of the peralkaline volcanics Gregory Rift Valley, Kenya p 281 N94-12072
Th-230 - U-238 series disequilibrium of the Olkaria basalts Gregory Rift Valley, Kenya p 281 N94-12073
Th-230 - U-238 series disequilibrium of the Olkaria basalts Gregory Rift Valley, Kenya: Petrogenesis
p 281 N94-12074
Th-230 - U-238 series disequilibrium of the Olkaria rhyolites Gregory Rift Valley, Kenya: Petrogenesis
p 281 N94-12075
Th-230 - U-238 series disequilibrium of the Olkaria rhyolites Gregory Rift Valley, Kenya: Residence times
p 281 N94-12076

KERNEL FUNCTIONS
Scalable spin locks for multiprogrammed systems
[AD-A265007] p 337 N94-11650

KETONES
New aromatic activated dihalides and bisphenol monomers for the preparation of novel poly(arylene ethers)
[NASA-CR-193190] p 55 N94-10513

KIDNEYS
Physiological water model development
p 316 N94-12367

KINEMATICS
The kinematics of buoyancy induced mixing
p 123 N94-10239
A theoretical kinematical study of the gradient of any cosmic scalar field
[DE92-644731] p 425 N94-11136
Plane mixing layer vortical structure kinematics
p 159 N94-12313

KINETIC ENERGY
Collisions of small Spacewatch asteroids with the Earth p 430 N94-12157
Reynolds stress closure modeling in wall-bounded flows p 157 N94-12298
An investigation of small scales of turbulence in a boundary layer at high Reynolds numbers
p 157 N94-12303
Surface eddy fluxes from the GEOSAT satellite altimeter p 208 N94-12643
The thermodynamics of the nonlinear shear flows
p 169 N94-12728
Turbulence generation in the Pacific undercurrent by shear p 223 N94-12730

KINETIC EQUATIONS
Kinetic effects in stochastic topologically nontrivial field
[DE93-621642] p 391 N94-11207
Simple kinetic model for plasma in stochastic helical field
[DE93-621643] p 391 N94-11208
Statistical approach to LHCD modeling using the wave kinetic equation
[DE93-012831] p 394 N94-12545

KINETIC HEATING
Studies of hypersonic viscous flows p 8 N94-10454

KINETICS
Surface tension and adsorption kinetics in immiscible liquid systems at microgravity p 121 N94-10225

KLEIN-GORDON EQUATION
Bound states of the N-dimensional Klein-Gordon equation with vector and scalar Coulomb potentials
[DE93-617650] p 349 N94-10547

KLYSTRONS
Three-cavity circuit studies of the Maryland gyroklystron
[DE93-010173] p 145 N94-11645

KNOWLEDGE BASED SYSTEMS
Reuse: A knowledge-based approach
p 329 N94-11430
Design, development, and testing of an automated knowledge-acquisition tool to aid problem solving, decision making, and planning
[DE93-010239] p 417 N94-11661
Linking medical records to an expert system
p 306 N94-11797

KNOWLEDGE BASES (ARTIFICIAL INTELLIGENCE)
Development of a hypermedia knowledge base of aircraft fire safety regulations p 21 N94-10793
Design, development, and testing of an automated knowledge-acquisition tool to aid problem solving, decision making, and planning
[DE93-010239] p 417 N94-11661

KOLMOGOROV THEORY
An investigation of small scales of turbulence in a boundary layer at high Reynolds numbers
p 157 N94-12303
The ideal Kolmogorov inertial range and constant
p 158 N94-12305

KORTEWEG-DEVRIES EQUATION
Marangoni-driven solitary waves p 119 N94-10214
Uni-directional waves over slowly varying bottom. Part 1: Derivation of a KdV-type of equation
[MEMO-1098] p 147 N94-10275
Generation of internal waves near the shelf boundary
p 229 N94-12763

KREEP
Assimilation in lunar basalts and volcanic glasses: Implications for a heterogenous mantle source region
p 478 N94-12250

L

LABORATORIES
Technology transfer at Lawrence Berkeley Laboratory
[DE93-010460] p 423 N94-11059

LABORATORY EQUIPMENT
Five biomedical experiments flown in an Earth orbiting laboratory: Lessons learned from developing these experiments on the first international microgravity mission from concept to landing p 302 N94-11556
LAGRANGIAN FUNCTION
Necessary conditions for the optimality of variable rate residual vector quantizers [NASA-CR-193730] p 326 N94-11197
Quality factors and local adaption (with applications in Eulerian hydrodynamics) [DE93-010502] p 151 N94-11272
LAGUERRE FUNCTIONS
Convergent close-coupling calculations of electron-hydrogen scattering [DE93-610049] p 360 N94-10328
LAKE ICE
C-band SAR backscatter from ice on shallow tundra lakes: Observations and modelling p 240 N94-11755
LAKES
Sandia ocean modeling system programmer's guide and user's manual [DE93-007427] p 287 N94-10153
LAMINAR BOUNDARY LAYER
Estimation of the direct acoustic radiation from turbulent spots using boundary layer velocity measurements p 357 N94-10358
Joint computational and experimental aerodynamic research on a hypersonic vehicle p 6 N94-10445
Method of reducing drag in aerodynamic systems [NASA-CASE-LEW-14791-1] p 12 N94-10672
CRESLAF. Version 4.0: A Fortran program for modeling laminar, chemically reacting, boundary-layer flow in cylindrical or planar channels [DE93-012835] p 152 N94-11371
LAMINAR FLOW
Influence of gravity and ambient pressure variations on the behavior of buoyant laminar diffusion flames p 123 N94-10240
Studies on scramjet nozzles. Part 1: Performance of two dimensional nozzles [NAL-TR-1149] p 27 N94-10367
On the combustion of a laminar spray [NASA-TM-106210] p 28 N94-11238
A research program for improving heat transfer prediction for the laminar to turbulent transition region of turbine vanes/blades [NASA-TM-106278] p 151 N94-11256
On temperature distribution in non-participating medium with radiation boundary condition [DE93-619375] p 153 N94-11604
Numerical simulation using vorticity-vector potential formulation p 157 N94-12297
DNS on control of laminar-turbulent transition in channel flow with suction and blowing p 163 N94-12613
Fluctuations of longitudinal vortices along a concave wall p 16 N94-12616
LAMINATES
Hybrid materials for use at elevated temperatures p 57 N94-10013
Mechanical and fatigue properties of fibre reinforced aluminium-lithium alloy and aluminium-lithium MMC based laminates p 58 N94-10022
Special problems of 3-D ultrasonic QNDI techniques and applications to composites aerospace structures p 61 N94-10036
Design evaluation of GLARE laminate lay-ups p 63 N94-10051
LAMINV: A computer code for creating laminates having prescribed properties p 65 N94-10069
Hydrostatic testing of thick laminated composite cylinders for performance model validation [DE93-012728] p 184 N94-10264
New thermoplastic laminating adhesives for the aircraft industry with low heat release and low smoke emission p 17 N94-10767
A new low smoke, low heat release structural foam p 17 N94-10768
Advanced phenolic systems for aircraft interiors p 18 N94-10776
Response of composite laminates to dynamic surface loads p 66 N94-10902
Damping measurements for ultra-high carbon steel/brass laminates [DE93-011886] p 82 N94-11076
Materials for adaptive structural acoustic control, volume 3 [AD-A264621] p 358 N94-11262
An analysis of fiber-matrix interface failure stresses for a range of ply stress states [NASA-TM-108999] p 67 N94-11276
Strain concentration assessment of laminates subjected to low velocity impact [AD-A264497] p 73 N94-11446
Localized and distributed fiber-optic strain sensors embedded in composite materials [UTIAS-346] p 73 N94-12013
LAND
ERS-1 altimetry of inland water and land p 246 N94-12475
Land use/land cover mapping of central water shed of Iran area based on satellite data interpretation p 219 N94-12704
A method to minimize reference data in classifying satellite remote sensing data into land cover classes p 219 N94-12705
LAND ICE
Signatures of Antarctic firn by means of ERS-1 AMI and by field measurements p 237 N94-11737
Utilisation of ERS-1 data for mapping of Antarctica p 237 N94-11740
Preliminary evaluation of ERS-1 altimetry over Filchner-Ronne Ice Shelf, Antarctica p 238 N94-11742
Validating the UK-PAF land ice product surface elevation p 244 N94-11780
Modern shelf ice, equatorial Aeolis Quadrangle, Mars p 450 N94-12100
Microwave radiometry of ice cover in polar regions p 210 N94-12655
LAND MANAGEMENT
Space Activities in the Asia Pacific Region [JTN-93-80421] p 35 N94-10676
Space research and remote sensing programmes in Bangladesh p 35 N94-10679
Status of remote sensing and Geographic Information System (GIS) applications in the Environment and Natural Resources (ENR) sector p 36 N94-10687
Shoreline change detection using remote sensing and GIS in Vietnam p 196 N94-11928
Land use/land cover mapping of central water shed of Iran area based on satellite data interpretation p 219 N94-12704
A method to minimize reference data in classifying satellite remote sensing data into land cover classes p 219 N94-12705
LAND USE
Summary of implementation and demonstration projects in bays and estuaries [PB93-194637] p 265 N94-10846
Segmented land use classification of multitemporal ERS-1 SAR data using a majority filter p 245 N94-12472
Land cover monitoring with multi-temporal ERS-1 SAR observations in the Netherlands p 246 N94-12473
Combined analysis of ERS-1 SAR and visible/infrared remote sensing data for land cover/land use mapping in a tropical zone: A case study in Guinea p 246 N94-12478
Per-field filtering and classification of multitemporal ERS-1 SAR imagery p 247 N94-12485
Geoecological monitoring of an agricultural area p 248 N94-12489
Land use/land cover mapping of central water shed of Iran area based on satellite data interpretation p 219 N94-12704
LANDAU FACTOR
New squeezed landau states p 379 N94-10601
LANDAU-GINZBURG EQUATIONS
Stability and dynamics of spatio-temporal structures [DE93-011374] p 401 N94-11610
LANDFORMS
Global organization of tectonic deformation on Venus p 444 N94-12066
Modern shelf ice, equatorial Aeolis Quadrangle, Mars p 450 N94-12100
Shallow crustal discontinuities and graben and scarp formation in the Tharsis region of Mars p 469 N94-12203
Giant radiating dyke swarms on Earth and Venus p 283 N94-12236
LANDING GEAR
Active landing gear control for improved ride quality during ground roll p 27 N94-11345
LANDING SIMULATION
In-flight simulation of backside operating models using direct lift controller [NAL-TR-1152] p 30 N94-10734
LANDING SITES
Regional geology of the Vega landing sites: Tentative results of photogeologic mapping p 440 N94-12047
Regional geology of the Venera landing sites: Tentative results of photogeologic mapping p 440 N94-12048
LANDSAT SATELLITES
Landsat as a commercial enterprise [INPE-5477-TAE/019] p 232 N94-11524
LANGEVIN FORMULA
Dissipation in a squeezed-state environment p 370 N94-10584
The heat transfer by radiation between two media [DE93-617820] p 149 N94-10838
The Langevin's approach to the statistical theory of bounded plasma [DE93-617842] p 388 N94-10839
LANGUAGE PROGRAMMING
Layering techniques for development of parallel systems: An algebraic approach [MEMO-INF-92-62] p 335 N94-10277
An algebraic approach to incomparable families of formal languages [MEMO-INF-92-82] p 342 N94-10279
LANGUAGES
Processing proper nouns in machine translation for English news [NHK-SERIAL-414] p 418 N94-10559
LANTHANUM COMPOUNDS
Smart spatial light modulator research and development [AD-A264928] p 382 N94-11286
LARGE SCALE INTEGRATION
Development of microstrip gas chambers with multi-chip technology [DE93-753169] p 367 N94-11509
LARGE SPACE STRUCTURES
Progress in multidisciplinary design optimization at NASA Langley [NASA-TM-107754] p 318 N94-10814
Adaptive structures for spacecraft: A USAF perspective p 45 N94-11319
Dynamic tests on the NASA Langley CSI evolutionary model p 45 N94-11320
Smart structures at Aastra Corporation p 69 N94-11326
Active damping augmentation of elastomechanical systems using piezoelectric sensors and actuators p 72 N94-11346
Control of large space structures with varying configuration [AD-A265764] p 44 N94-12387
Space truss zero gravity dynamics [AD-A266130] p 44 N94-12541
LASER ABLATION
Characterization of an excimer laser-ablated plasma and applications p 392 N94-11450
Momentum induced by laser-tissue interaction [DE93-010737] p 301 N94-11667
The laser ablation of gold films at the electrode surface of a quartz crystal microbalance [AD-A265535] p 175 N94-12012
LASER ANEMOMETERS
Laser anemometer measurements and computations for transonic flow conditions in an annular cascade of high turning core turbine vanes [NASA-TP-3383] p 15 N94-11133
LASER APPLICATIONS
Laser beam deflection: A diagnostic tool for vapour growth experiments in microgravity p 111 N94-10135
Laser cooling and trapping of atoms in microgravity: Ultracold atoms collisions p 124 N94-10241
Material characterization and modeling with shearography [NASA-CR-192576] p 185 N94-10342
Laser Synchrotron Source (LSS) [AD-D015755] p 173 N94-10371
Paint removal activities in the US Navy p 126 N94-10614
Paint removal activities in Canada p 126 N94-10615
Automated Laser Paint Stripping (ALPS) update p 127 N94-10624
Atomization characteristics of a prefilming airblast atomizer [NAL-TM-644] p 148 N94-10727
The response of an electron in a biased double well to a strong laser: Delocalization and low frequency generation [AD-A265169] p 366 N94-11100
A preliminary study on ice shape tracing with a laser light sheet [NASA-TM-105964] p 174 N94-11132
Aircraft windscreens enhance visual search disruption produced by laser glare [AD-A265167] p 26 N94-11892
The development of phytoplankton sensing system with optical fiber p 203 N94-11967
Ocean measuring experiments using optical fiber distributed temperature sensor p 172 N94-11968
Laser photoheterodyne interferometers for oceanographic investigations p 177 N94-12732
LASER BEAMS
Laser beam deflection: A diagnostic tool for vapour growth experiments in microgravity p 111 N94-10135
Start-up imprinting and shock dynamics in laser-target interaction [DE93-008051] p 172 N94-10150

Fabrication and analysis of a special optical connector containing a 1/4-inch-long optical fiber for DOI tests
[DE93-013115] p 381 N94-10647
Multiple laser beam combining and phasing using closed-loop control
[DE93-009830] p 175 N94-11283
Aircraft windscreens enhance visual search disruption produced by laser glare
[AD-A265167] p 26 N94-11892
Short wavelength crystal fiber devices
[AD-A265716] p 176 N94-12402

LASER CAVITIES
The laser second threshold: Its exact analytical dependence on detuning and relaxation rates
[DE93-619706] p 175 N94-11633

LASER DAMAGE
Enhanced Damage-Resistant Optics for Spaceflight Laser Systems: Workshop findings and recommendations
[NASA-TM-109243] p 381 N94-11054
Damage thresholds of fluoride multilayers at 355 nm
[DE93-009523] p 90 N94-11230
Aircraft windscreens enhance visual search disruption produced by laser glare
[AD-A265167] p 26 N94-11892
Damage threshold study of ion beam sputtered coatings for a visible high-repetition laser at LLNL
[DE93-013430] p 95 N94-12602

LASER DOPPLER VELOCIMETERS
Experimental analysis of Benard-convection by the combined application of liquid crystals and PIV
p 106 N94-10109
Particle image velocimetry technique: Calibration tests
p 111 N94-10137
Laser velocimeter measurements of the flow field generated by a forward-swept propfan during flutter
[NASA-TM-106195] p 14 N94-10892

LASER FUSION
Start-up imprinting and shock dynamics in laser-target interaction
[DE93-008051] p 172 N94-10150
Studies on the parametric decay of waves in fusion plasmas
[DE93-621659] p 390 N94-11148
Damage thresholds of fluoride multilayers at 355 nm
[DE93-009523] p 90 N94-11230

LASER GUIDANCE
Laser system design for the generation of a sodium-layer laser guide star
[DE93-014127] p 176 N94-12784

LASER HEATING
An analytic model for calculating pump-induced wavefront distortions in laser slabs
[DE93-011953] p 174 N94-11126

LASER INDUCED FLUORESCENCE
The pyrene laser induced fluorescence technique as a diagnostic tool for combustion thermometry in microgravity p 107 N94-10113
In situ detection of tropospheric OH, HO2, NO2, and NO by laser-induced fluorescence in detection chambers at reduced pressures
[NASA-CR-193189] p 274 N94-10701
Development of shipboard ocean lidar
p 140 N94-11965
LIF measurements of scalar mixing in turbulent shear layers p 159 N94-12312
Laser fluorescent monitoring of dissolved organic matter in natural water p 177 N94-12755

LASER INTERFEROMETRY
Semiconductor ring lasers
[DE93-012386] p 174 N94-11005

LASER MATERIALS
New challenges in optical materials development
[DE93-011889] p 383 N94-11676

LASER MICROSCOPY
FFT-based methods for nonlinear image restoration in confocal microscopy
[CS-9301] p 174 N94-10904

LASER OUTPUTS
Optimization of a CO2 laser Thomson scattering alpha particle diagnostic
[DE93-012782] p 173 N94-10160
Dynamics of dissociation versus ionization in strong laser fields
[DE93-009261] p 173 N94-10287
High-order harmonic conversion efficiency in helium
[DE93-011714] p 364 N94-10753
Multiple laser beam combining and phasing using closed-loop control
[DE93-009830] p 175 N94-11283
A 1.94 micron laser apparatus, system, and method using a thulium-doped yttrium-lithium-fluoride laser crystal pumped with a diode laser
[AD-D015740] p 176 N94-12321
Spatial coherence of soft x ray lasers
[DE93-012497] p 176 N94-12590

LASER PLASMA INTERACTIONS
Optimization of a CO2 laser Thomson scattering alpha particle diagnostic
[DE93-012782] p 173 N94-10160
High-energy density physics at Los Alamos
[DE93-010271] p 371 N94-10260
X ray production (approximately)130 (Angstrom) from laser-produced plasmas for projection x ray lithography applications
[DE93-009256] p 385 N94-10286
Controlling chaotic behavior in CO2 and other lasers
[AD-A264811] p 174 N94-10870
Electron temperature measurements of x ray laser plasmas
[DE93-011874] p 389 N94-11074
The angular structure of second harmonic emission from laser-produced plasmas irradiated at moderate intensity
[DE93-013102] p 389 N94-11114
Inexpensive capillary discharge x-ray laser driver
[AD-A265932] p 176 N94-12382

LASER PLASMAS
Controlling chaotic behavior in CO2 and other lasers
[AD-A264811] p 174 N94-10870
Electron temperature measurements of x ray laser plasmas
[DE93-011874] p 389 N94-11074
Demonstration designs for optical-field-ionized plasma x-ray lasers
[DE93-009227] p 175 N94-11266
High resolution time- and 2-dimensional space-resolved x ray imaging of plasmas at NOVA
[DE93-011892] p 393 N94-11677

LASER POWER BEAMING
Fabrication and analysis of a special optical connector containing a 1/4-inch-long optical fiber for DOI tests
[DE93-013115] p 381 N94-10647
InGaAs concentrator cells for laser power converters and tandem cells p 50 N94-11394
The efficiency of photovoltaic cells exposed to pulsed laser light p 50 N94-11395
Response of silicon solar cell to pulsed laser illumination p 51 N94-11396
Approaches to solar cell design for pulsed laser power receivers p 51 N94-11397
Workshop summary: Receivers for laser power beaming p 54 N94-11419

LASER PUMPING
High power z pinches as x ray laser photopumps
[DE93-012842] p 173 N94-10746
An analytic model for calculating pump-induced wavefront distortions in laser slabs
[DE93-011953] p 174 N94-11126
New challenges in optical materials development
[DE93-011889] p 383 N94-11676
A 1.94 micron laser apparatus, system, and method using a thulium-doped yttrium-lithium-fluoride laser crystal pumped with a diode laser
[AD-D015740] p 176 N94-12321
Inexpensive capillary discharge x-ray laser driver
[AD-A265932] p 176 N94-12382

LASER RANGE FINDERS
LASSO observations at McDonald and OCA/CERGA: A preliminary analysis p 352 N94-10972

LASER RANGER/TRACKER
LASSO observations at McDonald and OCA/CERGA: A preliminary analysis p 352 N94-10972
ERS-1 precise orbits and altimetry analysis
p 242 N94-11771
Operational ERS-1 orbit determination at D-PAF
p 243 N94-11774

LASER SPECTROMETERS
Measurement of polycyclic aromatic hydrocarbon (PAHs) in interplanetary dust particles
p 431 N94-12167

LASER SPECTROSCOPY
Laser spectroscopy
[DE93-009403] p 173 N94-10255
Atomic processes relevant to polarization plasma spectroscopy
[DE93-753240] p 393 N94-11594
Laser fluorescent monitoring of dissolved organic matter in natural water p 177 N94-12755

LASER TARGET INTERACTIONS
Start-up imprinting and shock dynamics in laser-target interaction
[DE93-008051] p 172 N94-10150
Momentum induced by laser-tissue interaction
[DE93-010737] p 301 N94-11667

LASER TARGETS
Short pulse lasers for generation of fields exceeding 100 MG
[DE93-013346] p 369 N94-11815
Submicrosecond, synchronizable x ray source
[AD-D015745] p 176 N94-12337

LASERS
X ray production (approximately)130 (Angstrom) from laser-produced plasmas for projection x ray lithography applications
[DE93-009256] p 385 N94-10286
The laser second threshold: Its exact analytical dependence on detuning and relaxation rates
[DE93-619706] p 175 N94-11633
Analytical details of the instability threshold of the laser-Lorenz model
[DE93-619707] p 175 N94-11634

LASING
High power z pinches as x ray laser photopumps
[DE93-012842] p 173 N94-10746
High-order harmonic conversion efficiency in helium
[DE93-011714] p 364 N94-10753
A 1.94 micron laser apparatus, system, and method using a thulium-doped yttrium-lithium-fluoride laser crystal pumped with a diode laser
[AD-D015740] p 176 N94-12321

LATENT HEAT
Latent and sensible heat flux estimated from ERS-1 data p 244 N94-11783
Variability of wind stress, and sensible and latent heat flux in the North Atlantic during SEASAT
p 194 N94-11918
Evaluation of ECMWF latent heat flux in TOGA CD-ROM p 195 N94-11921
Sea surface temperature anomalies in the Arabian Sea p 206 N94-11988

LATITUDE
A method for calculating exact geodetic latitude and altitude
[AD-A265783] p 229 N94-10417
A simple model of clastic sediments on Mars
p 460 N94-12155

LATTICE PARAMETERS
Confinement of acoustical modes due to the electron-phonon interaction within 2D-electron gas
[DE93-613910] p 396 N94-10800
Fullerene superconductors: Phase stability and anomalously low T(sub c)'s in some ternary compounds
[DE93-010687] p 400 N94-11457

LATTICE VIBRATIONS
Energy transfer dynamics and impact sensitivity
[DE93-009551] p 98 N94-11269

LATTICES (MATHEMATICS)
An algebraic approach to incomparable families of formal languages
[MEMO-INF-92-82] p 342 N94-10279
Generalized spin systems and sigma-models
[DE93-613981] p 410 N94-10802

LAUNCH VEHICLES
Exergy decrease in shock waves and boundary layers of space launch vehicles
[AD-A265272] p 42 N94-10493
Space transportation alternatives for large space programs: The International Space University Summer Session, 1992
[NASA-TM-106271] p 40 N94-10811
On-orbit refueling p 38 N94-11565
In-space operations for lunar and Mars space transfer vehicles p 348 N94-11568
The National Launch System Advanced Development Program: A brief overview p 40 N94-11576

LAUNCHERS
Initial assessment of lower hybrid current drive in D3-D
[DE93-013310] p 394 N94-12370

LAVA
The Lathrop Wells Volcanic Center: Status of field and geochronology studies
[DE93-008917] p 273 N94-10285
Reconstruction of the dynamics of the 1800-1801 Hualalai eruption: Implications for planetary lava flows
p 281 N94-12041
Changes in Hawaiian palagonite FE mineralogy associated with thermal alteration: Implications for Mars
p 281 N94-12055
Quantifying the effect of rheology on plan-view shapes of lava flows p 282 N94-12116
Lava flows on Venus: Analysis of motion and cooling
p 457 N94-12137
Large volcanoes on Venus: Examples of geologic and structural characteristics from different classes
p 467 N94-12195

LEAD ALLOYS
New mechanism of Ostwald ripening in Lorentz-force stabilized Cu-Pb dispersions p 116 N94-10192
Effect of experimental procedure on pattern formation and array disorder in cellular solidification
p 117 N94-10203

LEAD ISOTOPES
Radiogenic age and isotopic studies
[DE93-610548] p 274 N94-10407
LEW88516 and SNC meteorites p 430 N94-12150

LEAD ZIRCONATE TITANATES
Smart spatial light modulator research and development [AD-A264928] p 382 N94-11286
Recent developments in piezoelectric and electrostrictive sensors and actuators for smart structures p 70 N94-11332

LEADING EDGE FLAPS
A determination of the external forces required to move the benchmark active controls testing model in pure plunge and pure pitch [NASA-TM-107743] p 16 N94-12421

LEADING EDGE SWEEP
Real gas and surface transpiration effects upon swept leading edge high speed flow including transition p 8 N94-10452
Schlieren photographs and internal pressure distributions for three-dimensional sidewall-compression scramjet inlets at a Mach number of 6 in CF4 [NASA-TM-4479] p 148 N94-10644

LEADING EDGES
Aerodynamic sound due to interaction between a two-dimensional free shear layer and the leading edge of a parallel flat plate p 163 N94-12615
A numerical experiment of boundary layer transition at subcritical Reynolds numbers p 165 N94-12625

LEAF AREA INDEX
Extraction of plant and soil parameters from multitemporal ERS-1 SLC data of the Freiburg test site p 248 N94-12491

LEAKAGE
Catalytic oxidation of organics in vapor streams at remediation sites [PB93-182962] p 266 N94-11472
A prototype urine collection device for female aircrew p 317 N94-11549
A combustion products analyzer for contingency use during thermodegradation events on spacecraft p 318 N94-11555

LEARNING THEORY
Acting to gain information [NASA-CR-193399] p 418 N94-10515

LEAST SQUARES METHOD
A window least squares algorithm for statistical noise smoothing of 2D-ACAR data [DE93-613828] p 395 N94-10537
Optimisation methods for solving separable nonlinear least squares problems [ISVR-TR-219] p 345 N94-11217
Fourier domain target transformation analysis in the thermal infrared p 258 N94-12030
Analysis of collinear passes of satellite altimeter data p 208 N94-12642

LECTURES
Laser spectroscopy [DE93-009403] p 173 N94-10255
Discrete space-time symmetries [DE93-010199] p 341 N94-10259
Some new/old approaches to QCD [DE93-010451] p 408 N94-10261
Lecture note on circuit technology for high energy physics experiment [DE93-771422] p 372 N94-11245

LEE WAVES
Lee waves: Benign and malignant [NASA-CR-186024] p 283 N94-10725

LENSES
Aviation accident risk for airmen with aphakia and artificial lens implants [DOT/FAA/AM-93/11] p 303 N94-10813

LEPTONS
Acceleration of positrons in supernova shocks [NASA-CR-193713] p 425 N94-10511
Top quark search in D(O) from the lepton + jets mode [DE93-014027] p 370 N94-12781
Quark and lepton masses [DE93-012308] p 370 N94-12787

LEVITATION
Gas film levitator for containerless processing of glasses in microgravity conditions: Early concept and technology demonstration p 108 N94-10122
TEMPUS: An electromagnetic levitation facility for containerless processing under micro-g in Spacelab p 109 N94-10125
Force and power efficiency of micro-g electromagnetic levitation coils p 110 N94-10129
Development of passive superconducting bearings. Phase 3 [AD-A266050] p 180 N94-10706
Improvement of azimuthal homogeneity in permanent-magnet bearing rotors [DE93-009954] p 144 N94-11607

LEVITATION MELTING
Force and power efficiency of micro-g electromagnetic levitation coils p 110 N94-10129
Microstructure and associated properties of YB2Cu3O(x) superconductors prepared by melt processing techniques [DE93-010675] p 398 N94-11004

LIBRARIES
Portable programming on parallel/networked computers using the Application Portable Parallel Library (APPL) [NASA-TM-106238] p 327 N94-11232
Guidelines for the establishment and operation of an RFP (Request for proposal) library [AD-A265894] p 417 N94-12360

LICENSING
Intergovernmental decisionmaking for environmental protection and public works [PB93-176824] p 266 N94-11584

LIE GROUPS
One-loop quantum gravity on de Sitter space [DE92-641349] p 425 N94-11152

LIFE (DURABILITY)
Environmental Protection Agency's life cycle methodology: Guidelines for use in development of packaging [PB93-194199] p 265 N94-10841
Model of optical scatter from microimpacts on the Hubble Telescope p 384 N94-12189

LIFE CYCLE COSTS
ACARA user's manual [NASA-TM-106277] p 183 N94-11167
In-flight aircraft structure health monitoring based on smart structures technology p 22 N94-11333
Life-cycle cost analysis of conventional and fuel cell/battery powered urban passenger vehicles [DE93-010770] p 182 N94-11438

LIFE SCIENCES
The International Microgravity Laboratory, a Spacelab for materials and life sciences p 125 N94-10249
Aerospace medicine and biology: A continuing bibliography with indexes (supplement 375) [NASA-SP-7011(375)] p 303 N94-10398
Aerospace medicine and biology: A continuing bibliography with indexes (supplement 376) [NASA-SP-7011(376)] p 303 N94-10399
Proceedings of the Symposium on Radiation Research in Life Science [DE93-754137] p 300 N94-10888
Five biomedical experiments flown in an Earth orbiting laboratory: Lessons learned from developing these experiments on the first international microgravity mission from concept to landing p 302 N94-11556
Aerospace medicine and biology: A continuing bibliography with indexes (supplement 374) [NASA-SP-7011(374)] p 304 N94-11689

LIFE SUPPORT SYSTEMS
Aerospace medicine and biology: A continuing bibliography with indexes (supplement 375) [NASA-SP-7011(375)] p 303 N94-10398
Aerospace medicine and biology: A continuing bibliography with indexes (supplement 376) [NASA-SP-7011(376)] p 303 N94-10399
Aerospace medicine and biology: A continuing bibliography with indexes (supplement 374) [NASA-SP-7011(374)] p 304 N94-11689
Space Life Support Engineering Program [NASA-CR-193474] p 316 N94-12365
Systems analysis of a closed loop ECLSS using the ASPEN simulation tool. Thermodynamic efficiency analysis of ECLSS components p 316 N94-12366
Modifications to an interactive model of the human body during exercise: With special emphasis on thermoregulation p 317 N94-12368
An estimate of the second law thermodynamic efficiency of the various units comprising an Environmental Control and Life Support System (ECLSS) p 317 N94-12369

LIFT
In-flight simulation of backside operating models using direct lift controller [NAL-TR-1152] p 30 N94-10734

LIGANDS
Publications/Patents/Presentations/Honors/Student eport [AD-A265136] p 78 N94-11873

LIGHT (VISIBLE RADIATION)
Optical transfer operator of the atmosphere-ocean system p 225 N94-12742

LIGHT AMPLIFIERS
Method and apparatus for polarization-maintaining fiber optical amplification with orthogonal polarization output [AD-D015756] p 374 N94-10372

LIGHT BEAMS
A compact, four-way image splitter [AD-A266107] p 382 N94-11656
Development of the one-component diode-array velocimeter [AD-A265552] p 171 N94-12533

LIGHT CURVE
A method to determine asteroid poles p 431 N94-12205
Yohkoh Bragg Crystal Spectrometer light curves for Ca XIX (3.1631-3.1912A): 1 October 1991 - 30 September 1992 [AD-A266090] p 483 N94-12414

LIGHT EMISSION
Journal of Research of the National Institute of Standards and Technology, volume 98, number 2, March - April 1993 [PB93-196228] p 485 N94-10850
Thermographic properties of eight blue-emitting phosphors [DE93-011459] p 78 N94-11622
Observations of optical counterparts of Gamma-Ray bursts [NASA-CR-193573] p 485 N94-12589

LIGHT EMITTING DIODES
Improved super luminescent light source specification [AD-D015746] p 176 N94-12329

LIGHT MODULATION
Smart spatial light modulator research and development [AD-A264928] p 382 N94-11286
Spatial light modulator having photosensitive and ferroelectric layers [AD-D015731] p 404 N94-12400

LIGHT SCATTERING
Optimization of a CO2 laser Thomson scattering alpha particle diagnostic [DE93-012782] p 173 N94-10160
Phasing operator for two oscillators in classical field p 370 N94-10579
Flowfield structure of swept shock wave/turbulent boundary-layer interactions p 149 N94-10899
Advanced diagnostics for in situ measurement of particle formation and deposition in thermally stressed jet fuels [DE93-009798] p 98 N94-11366
Bi-directional reflectance by oceanic waters studied via Monte-Carlo simulations p 203 N94-11971
Dust in the Martian atmosphere: Polarimetric sensing p 473 N94-12223
Light scattering from a spherical particle on a conducting plane. Part 1: Normal incidence [AD-A265920] p 383 N94-12341
Limitations to the quality of optical phase conjugation by stimulated Brillouin scattering [AD-A266006] p 383 N94-12389
Remote sensing of light scattering coefficient of sea water vertical distribution by the means of airborne lidar p 224 N94-12736

LIGHT SOURCES
LCLS optics: Selected technological issues and scientific opportunities [DE93-010953] p 175 N94-11468
Improved super luminescent light source specification [AD-D015746] p 176 N94-12329

LIGHT TRANSMISSION
Smoothly deformed light p 375 N94-10566
Non classical effects in planar waveguides p 376 N94-10574
Nonperturbative methods in the problem of multiphoton excitation of atom by squeezed light p 376 N94-10575
Wigner functions for nonclassical states of a collection of two-level atoms p 379 N94-10603
Radiation defect production in InAs crystals under electron irradiation [DE93-617202] p 397 N94-10845
Plans to improve the experimental limit in the comparison of the east-west and west-east one-way light propagation times on the rotating earth p 351 N94-10971
A development on estimation method of undersea light p 204 N94-11974
Propagation of light pulses through a three-layer medium (cloud, pure air, and ocean water) p 222 N94-12725
Trajectory curving in underwater propagation of light p 226 N94-12748

LIGHTNING
Oxidation state of the Earth's upper mantle during the last 3800 million years: Implications for the origin of life p 283 N94-12210
Primordial lightning: Evidence preserved in chondrites p 432 N94-12230

LIMITER CIRCUITS
Assessment of the impact of HTSC's on superconducting fault-current limiters [DE93-009986] p 143 N94-11454

LINE SHAPE
Implementation and use of a computational ray-tracing program for the design and analysis of complex optical systems [AD-A265075] p 382 N94-11653

LINE SPECTRA

NMR spectroscopy of experimentally shocked single crystal quartz: A reexamination of the NMR shock barometer p 81 N94-12258

LINEAR ACCELERATORS

Nonlinear space charge effect of bunched beam in linac [DE93-612176] p 371 N94-10409

DILUTE: A code for studying beam evolution under RF noise [DE93-011605] p 133 N94-10960

Experimental investigation of wake field excitation in plasma by a periodic succession of relativistic particle clots [DE93-621655] p 391 N94-11211

LCLS optics: Selected technological issues and scientific opportunities [DE93-010953] p 175 N94-11468

Operational characteristics of a 100-mA, 2-MeV radio-frequency quadrupole [DE93-014474] p 374 N94-12786

LINEAR ALTERNATORS

Lightweight linear alternators with and without capacitive tuning [NASA-CR-185273] p 140 N94-10505

LINEAR ENERGY TRANSFER (LET)

Nonperturbative methods in HZE ion transport [NASA-TP-3363] p 484 N94-10759

LINEAR EQUATIONS

The solving of equations by the method of boundary elements p 326 N94-11182

LINEAR EVOLUTION EQUATIONS

Curvature effects in three-dimensional boundary layers p 164 N94-12623

LINEAR PROGRAMMING

A simplicial approach to integer programming [REPT-93-06] p 322 N94-10355

Progress in multidisciplinary design optimization at NASA Langley [NASA-TM-107754] p 318 N94-10814

LINEAR QUADRATIC GAUSSIAN CONTROL

Project of an attitude control system (three axis) of a satellite using the LQG/LTR methodology [INPE-5473-TDI/504] p 44 N94-12356

LINEAR SYSTEMS

Sample-data and discrete-time H2 optimal control [MEMO-COSOR-92-53] p 339 N94-10869

The Nehari problem for the Pritchard-Salamon class of infinite-dimensional linear systems: A direct approach [CS-9216] p 344 N94-10905

Discrete Kalman filtering equations of second-order form for control-structure interaction simulations [NASA-CR-193723] p 331 N94-11522

Computational algorithms or identification of distributed parameter systems [AD-A265252] p 331 N94-11680

LINEAR TRANSFORMATIONS

Stability by linear processes [NASA-CR-194131] p 323 N94-10862

LINEARIZATION

On output linearization of observable dynamics [MEMO-1105] p 341 N94-10276

Wait-free linearization with an assertional proof [CS-9208] p 323 N94-10878

Computational algorithms or identification of distributed parameter systems [AD-A265252] p 331 N94-11680

LINGUISTICS

Automatic word categorization: An information-theoretic approach [CS-9209] p 419 N94-10903

Proceedings of the Seventh International Symposium on Methodologies for Intelligent Systems (poster session) [DE93-013470] p 340 N94-12428

LININGS

Spin-rolling, welding, and heat treatment of aluminium 2219 for Ariane 5 GAM high pressure vessel liners p 62 N94-10045

A repair patching system for aircraft cargo liners p 17 N94-10771

Ceramics technology project database [DE93-012431] p 91 N94-11672

LIOUVILLE THEOREM

Classical gravity coupled to Liouville theory [DE93-613049] p 275 N94-10798

LIPIDS

Probability of alamethicin conductance states varies with nonlamellar tendency of bilayer phospholipids [AD-A264957] p 301 N94-11648

LIQUEFACTION

Condensation phenomena p 162 N94-12550

LIQUID CHROMATOGRAPHY

Chromatographic assessment of hydrogen-bond donating ability [AD-A265292] p 369 N94-11826

Characterization of dissolved organic matter in the ocean by using the fluorescence excitation-emission matrix p 211 N94-12659

LIQUID COOLING

Liquid Cooled Heat Sink with through Vias (LCHS) [AD-A266008] p 73 N94-12344

Boiling heat-transfer processes and their application in the cooling of high heat flux devices [AD-A266086] p 413 N94-12535

Hot-gas-side heat transfer characteristics of subscale, plug-nozzle rocket calorimeter chamber [NASA-TP-3380] p 55 N94-12569

LIQUID CRYSTALS

Vectra insulative support structures within spacecraft p 62 N94-10050

Solidification from supercooled melt under microgravity p 113 N94-10176

Physical properties of injection molded liquid crystal polymers and high temperature engineering polymers [AD-A264912] p 87 N94-10508

Stability and dynamics of spatio-temporal structures [DE93-011374] p 401 N94-11610

Spatial light modulator having photosensitive and ferroelectric layers [AD-D015731] p 404 N94-12400

LIQUID HELIUM

Quantum dynamics of helium clusters [AD-A266060] p 411 N94-10874

Development of commercially viable high-T(sub c) Bi-2223 superconductor tapes [DE93-009966] p 142 N94-10951

Superfluid turbulence p 158 N94-12307

LIQUID HYDROGEN

An environmental study of the National Aerospace Plane [AD-A266071] p 25 N94-10945

Preprints of the 13th Hydrogen Energy System Symposium [DE93-781115] p 99 N94-11444

LIQUID INJECTION

Atomization characteristics of a prefilming airblast atomizer [NAL-TM-644] p 148 N94-10727

LIQUID METALS

Measurement of the thermal conductivity of molten InSb in a drop shaft p 105 N94-10102

Experimental approach to non-contact calorimetry in space p 112 N94-10143

Thermophysical properties of undercooled liquid metals p 86 N94-10190

Ostwald ripening of solid cobalt particles in liquid copper p 87 N94-10202

Measurements of heat capacity in undercooled metals p 87 N94-10231

The reaction between titanium carbide and aluminium carbide in liquid aluminium; a microgravity study p 123 N94-10238

Shear flow control of gas jets in liquids [AD-A264673] p 152 N94-11448

Performance aspects of de Laval spray-forming nozzles [DE93-013671] p 163 N94-12604

LIQUID NITROGEN

Development of commercially viable high-T(sub c) Bi-2223 superconductor tapes [DE93-009966] p 142 N94-10951

LIQUID OXYGEN

Shear coaxial injector atomization phenomena for combusting and non-combusting conditions [NASA-CR-193339] p 152 N94-11526

Thermodynamics of lunar ilmenite reduction p 415 N94-12028

LIQUID PHASE EPITAXY

Effect of gravity on the dissolution and liquid phase epitaxial growth processes in a horizontal sandwich system p 118 N94-10208

LIQUID PHASE SINTERING

Liquid phase sintering of tungsten composites under microgravity. Effect of matrix composition p 118 N94-10207

LIQUID PHASES

The stability of hibonite and other aluminous phases in silicate melts: Implications for the origin of hibonite-bearing inclusions p 80 N94-12052

LIQUID PROPELLANT ROCKET ENGINES

Axisymmetric single shear element combustion instability experiment [NASA-TM-106327] p 46 N94-10763

Combustion chamber analysis code [NASA-CR-192585] p 46 N94-10934

LIQUID ROCKET PROPELLANTS

Development of a high specific 1.5 to 5 kW thermal arcjet [NASA-CR-193133] p 47 N94-11354

Shear coaxial injector atomization phenomena for combusting and non-combusting conditions [NASA-CR-193339] p 152 N94-11526

LIQUID SURFACES

Thermocapillary instabilities in cylindrical liquid bridges: Mechanisms and transition boundaries p 101 N94-10077

Evaporation under microgravity conditions p 102 N94-10086

Boundary layers along horizontal free surfaces due to combined effects of temperature and concentration gradients p 106 N94-10108

Description of the liquid structure facility architecture and experimental demonstration of the diagnostic capabilities p 39 N94-10118

Instability of thermocapillary convection in multiple superposed immiscible liquid layers p 120 N94-10218

Convective motion in a multi-layered system with a free surface p 120 N94-10219

LIQUID-LIQUID INTERFACES

Proceedings of the 8th European Symposium on Materials and Fluid Sciences in Microgravity, volume 1 [ESA-SP-333-VOL-1] p 99 N94-10070

The formation and breakage of liquid bridges under microgravity p 100 N94-10071

Non-linear liquid bridge dynamics p 100 N94-10074

Dielectric liquid bridge stabilization in microgravity by means of electric fields p 100 N94-10075

Thermocapillary instabilities in cylindrical liquid bridges: Mechanisms and transition boundaries p 101 N94-10077

Stability of liquid bridges between parallel plates p 101 N94-10078

Transient three-dimensional numerical simulation of Marangoni flow in a liquid column under microgravity p 101 N94-10079

Coupled thermovibrational and thermocapillary convection in liquid bridge (floating zone system) p 101 N94-10082

Effects of axial and centrifugal forces on the stability of liquid bridges p 102 N94-10083

High Prandtl number fluids in a multilayered system under 1-g or micro-g environment p 104 N94-10096

Benard and Marangoni convection in multiple liquid layers p 105 N94-10100

Coupled thermogravitational and thermocapillary convection in a two-layer fluid system p 105 N94-10101

Thermocapillary slug flow in a capillary tube p 105 N94-10104

Proceedings of the 8th European Symposium on Materials and Fluid Sciences in Microgravity, volume 2 [ESA-SP-333-VOL-2] p 112 N94-10171

Transient effects in the Benard instabilities: Coupling between capillary and gravity effects p 119 N94-10216

Numerical investigations on Marangoni-Benard instability in multi layer systems p 120 N94-10217

Instability of thermocapillary convection in multiple superposed immiscible liquid layers p 120 N94-10218

Convective motion in a multi-layered system with a free surface p 120 N94-10219

Appearance of convective instabilities caused by liquid-liquid phase separation under small buoyancy forces p 120 N94-10221

Surface tension and adsorption kinetics in immiscible liquid systems at microgravity p 121 N94-10225

Fluid-fluid interfacial instabilities induced by gravity p 121 N94-10229

Use of inert immiscible liquid for crystal separation out of its feeding solution in weightlessness p 124 N94-10242

LIQUID-SOLID INTERFACES

Proceedings of the 8th European Symposium on Materials and Fluid Sciences in Microgravity, volume 1 [ESA-SP-333-VOL-1] p 99 N94-10070

The formation and breakage of liquid bridges under microgravity p 100 N94-10071

Experimental study of axisymmetric thermocapillary flows p 100 N94-10072

Non-linear liquid bridge dynamics p 100 N94-10074

Dielectric liquid bridge stabilization in microgravity by means of electric fields p 100 N94-10075

Thermocapillary instabilities in cylindrical liquid bridges: Mechanisms and transition boundaries p 101 N94-10077

Stability of liquid bridges between parallel plates p 101 N94-10078

Effects of axial and centrifugal forces on the stability of liquid bridges p 102 N94-10083

Liquid bridges and floating zones p 102 N94-10085

Separation of gravitational effects on the flow of suspension in tubes by measurements in weightlessness p 105 N94-10105

On the role of Soret effect in concentration distribution in crystals growing from the melt p 112 N94-10173

TEXUS 28 experiment: Convections and crystal growth of Ge:Ga. Analysis of temperature measurements
p 114 N94-10184
Convection related radial segregation in an idealized horizontal Bridgman configuration p 115 N94-10185
Ground results of the Mephisto program: Benefits and space experiments orientation p 86 N94-10197
Transient effects in the Benard instabilities: Coupling between capillary and gravity effects
p 119 N94-10216
The physics of pattern formation of liquid interfaces
[DE93-013333] p 154 N94-11814

LIQUIDS
Marangoni Benard instabilities in liquid mixtures with Soret effect p 119 N94-10215

LIQUIDUS
Phase equilibria and volumetric properties for the system NaCl-CaCl2-H2O
[DE93-013590] p 76 N94-11244

LITHIUM ALLOYS
Aluminium-lithium forgings: Properties and potential satellite applications p 58 N94-10021
Mechanical and fatigue properties of fibre reinforced aluminium-lithium alloy and aluminium-lithium MMC based laminates p 58 N94-10022
Investigations on aluminium-lithium alloys for damage tolerant application p 59 N94-10023

LITHIUM CHLORIDES
Aluminum-phosphorus chemistry: Preparation and structural characterization of (Et2AlP(SiMe3)2)2, Et(Cl)2Al(dot)P(SiMe3)3, and i-Bu2(Cl)Al(dot)P(SiMe3)3
[AD-A265268] p 78 N94-11683

LITHIUM FLUORIDES
Modeling void growth and movement with phase change in thermal energy storage canisters
[NASA-TM-106288] p 163 N94-12576

LITHIUM NIOBATES
Structural development in ceramic precursor sols and gels
[AD-A264354] p 90 N94-11281

LITHOGRAPHY
X ray production (approximately)130 (Angstrom) from laser-produced plasmas for projection x ray lithography applications
[DE93-009256] p 385 N94-10286
Physical optics modelling of Soft X ray Projection Lithography (SXPL) imaging experiments
[DE93-011556] p 374 N94-10339
Wavelength considerations in soft x ray projection lithography
[DE93-014115] p 381 N94-10651
Radiation hardness of Mo/Si multilayers designed for use in a soft x ray projection lithography system
[DE93-011879] p 143 N94-11273
A novel photosensitive polyimide resist consisting of a soluble polyimide and a bis(perfluorophenyl azide) as a cross-linker
[AD-A265998] p 93 N94-12353
Low voltage electron beam lithography
[AD-A265358] p 145 N94-12405
Photogenerated base in polymer imaging. Synthesis and photopatterning of poly(2-cyano-2-(p-vinylphenyl) butanoic acid)
[AD-A265288] p 95 N94-12585

LITHOLOGY
Descriptions and preliminary interpretations of cores recovered from the Manson Impact Structure (Iowa)
p 281 N94-12032
Petrography and preliminary interpretations of the crystalline breccias from the Manson M-1 core
p 281 N94-12056
Oxygen isotopes as tracers of tektite source rocks: An example from the Ivory Coast tektites and Lake Bosumtwi Crater p 430 N94-12146
Post-impact alteration of the Manson impact structure
p 282 N94-12188
Noble gas evidence of an aqueous reservoir near the surface of Mars more recently than 1.3 Ga
p 473 N94-12228
Assimilation in lunar basalts and volcanic glasses: Implications for a heterogenous mantle source region
p 478 N94-12250

LITHOSPHERE
A model for the subduction mechanics of flexible lithosphere and its viscous coupling to the mantle using power-law rheologies p 277 N94-11585
Horizontal stresses induced by vertical processes in planetary lithospheres p 281 N94-12042
Buoyant subduction on Venus: Implications for subduction around coronae p 455 N94-12130
Transmantle flux tectonics p 283 N94-12249

LITTORAL DRIFT
Coastal processes due to nearshore current around an upheaving island p 199 N94-11942

LITTORAL TRANSPORT
Coastal processes due to nearshore current around an upheaving island p 199 N94-11942

LOAD DISTRIBUTION (FORCES)
Method of recertifying a loaded bearing member using a phase point
[NASA-CASE-LAR-14741-1] p 185 N94-10671

LOAD TESTS
Numerical simulation and experimental results of filament wound CFRP tubes tested under biaxial load
p 58 N94-10015
Analytical prediction and test verification of the multiaxial behaviour of high-strength steel for lightweight structures
p 58 N94-10016

LOADS (FORCES)
Perforated plates for thin-walled structures
p 63 N94-10056
Method of recertifying a loaded bearing member using a phase point
[NASA-CASE-LAR-14741-1] p 185 N94-10671
Materials for adaptive structural acoustic control, volume 3
[AD-A264621] p 358 N94-11262
A model for the subduction mechanics of flexible lithosphere and its viscous coupling to the mantle using power-law rheologies p 277 N94-11585
Mechanical interaction between synthetic fiber and cement base matrix in FRC composites
[AD-A265310] p 73 N94-11686

LOCAL AREA NETWORKS
Formal specification of the plain UCN layer in LOTOS
[MEMO-INF-92-83] p 131 N94-10280
Using a private SMDS/ATM network to provide long-haul supercomputing visualization services
[DE93-010692] p 325 N94-11109
Reliability analysis for FDDI dual homing networks
[AD-A266133] p 337 N94-11475

LOCKING
Self locking set screw
[AD-D015774] p 178 N94-10385

LOCOMOTIVES
Electromechanical batteries and the electric locomotive
[DE93-013311] p 142 N94-11009

LOGARITHMS
Quenched chiral logarithms
[DE93-010195] p 346 N94-11663

LOGIC CIRCUITS
Smart spatial light modulator research and development
[AD-A264928] p 382 N94-11286
Programmable logic devices
[DE93-013117] p 144 N94-11479

LOGIC PROGRAMMING
A correct and efficient interface for logical query languages with complex objects
[MEMO-INF-93-01] p 320 N94-10167

LOGISTICS
Assessing the adequacy of the industrial base
[AD-A264954] p 417 N94-11856

LOGISTICS MANAGEMENT
On-orbit refueling p 38 N94-11565
Analysis of the Army's installation support modules with the private sector's open information systems
[AD-A265667] p 421 N94-12579

LONG DURATION EXPOSURE FACILITY
The magnitude of impact damage on LDEF materials
[NASA-CR-188258] p 43 N94-10666
Space environmental effects on the integrity of chromic acid anodized coatings
[NASA-CR-191468] p 55 N94-10947
Property changes induced by the space environment in composite materials on LDEF: Solar array materials passive LDEF experiment A0171 (SAMPLE)
[NASA-CR-192572] p 73 N94-11484
Mineralogy of chondritic interplanetary dust particle impact residues from LDEF p 80 N94-12045
Composition and modal frequencies of hypervelocity particles less than 1 millimeter in diameter in low-Earth orbit p 429 N94-12063
Modelling hypervelocity impacts into aluminum structures based on LDEF data p 190 N94-12178
Lessons learned from the Long Duration Exposure Facility
[AD-A266026] p 44 N94-12394

LONG DURATION SPACE FLIGHT
Hormonal regulation of fluid and electrolyte metabolism in zero-g and bedrest p 311 N94-12004
Hormonal regulation of fluid and electrolyte metabolism during periods of headward fluid shifts
p 311 N94-12005

LONG TERM EFFECTS
Property changes induced by the space environment in composite materials on LDEF: Solar array materials passive LDEF experiment A0171 (SAMPLE)
[NASA-CR-192572] p 73 N94-11484
Lessons learned from the Long Duration Exposure Facility
[AD-A266026] p 44 N94-12394

LONG WAVE RADIATION
Stationary spectra of short-wave convective and magnetostatic fluctuations in a finite-pressure plasma and anomalous heat conductivity
[DE93-617852] p 388 N94-10840
Studies of the net surface radiative flux from satellite radiances during FIFE
[NASA-CR-193150] p 230 N94-10953

LONGITUDINAL STABILITY
On non-linear longitudinal stability of an aircraft in a dive in the presence of atmospheric disturbances
p 31 N94-11492

LONGITUDINAL WAVES
Turbulent boundary layer interacting with spanwise periodic longitudinal vortex arrays p 165 N94-12626

LOOP ANTENNAS
Multiple Antenna Implementation System (MAntIS)
[DE93-012515] p 131 N94-10270

LORENTZ FORCE
Force and power efficiency of micro-g electromagnetic levitation coils p 110 N94-10129
New mechanism of Ostwald ripening in Lorentz-force stabilized Cu-Pb dispersions p 116 N94-10192

LOSSES
Power losses of a type 2 superconducting slab of arbitrary thickness in the presence of alternating current conductors
[DE93-617892] p 396 N94-10716

LOUDSPEAKERS
On the formation process of Karman vortex street
p 16 N94-12621

LOUVERS
Icing of turbine intake louvers
[AD-A265714] p 29 N94-12274

LOW CONCENTRATIONS
Study of the atmospheric chemistry of radon progeny in laboratory and real indoor atmospheres
[DE93-012236] p 266 N94-11671

LOW CONDUCTIVITY
Experimental study of multiple droplet evaporative cooling
[PB93-198463] p 149 N94-10851

LOW COST
Processing, properties, and wear resistance of aluminides
[DE93-012186] p 83 N94-11141
Inexpensive capillary discharge x-ray laser driver
[AD-A265932] p 176 N94-12382
Limitations to the quality of optical phase conjugation by stimulated Brillouin scattering
[AD-A266006] p 383 N94-12389

LOW CURRENTS
Development of ultra-low noise, high sensitivity planar metal grating coupled 3 to 5 multiquantum well infrared detectors for focal plane array staring IR sensor systems
[AD-A265599] p 404 N94-12375

LOW DENSITY MATERIALS
An ultralight carbon-carbon composite with amorphous matrix p 61 N94-10042

LOW FREQUENCIES
Stationary spectra in a magnetized current-carrying plasma
[DE93-617847] p 386 N94-10397
Stationary spectra in a plasma with a shear (renormalized statistical approach with non-zero eigenfrequencies)
[DE93-617851] p 386 N94-10523
Stationary spectra in a finite-pressure current-carrying plasma
[DE93-617848] p 387 N94-10538
Stationary spectra in a quasi neutral current-carrying plasma
[DE93-617849] p 387 N94-10539
Stationary spectra in a sheared plasma (linear limit)
[DE93-617850] p 387 N94-10540
Low power digital recorder development
[AD-A265921] p 170 N94-10704
Effects of energetic particle events on VLF/LF propagation parameters/1989
[AD-A265266] p 275 N94-11013
The response of an electron in a biased double well to a strong laser: Delocalization and low frequency generation
[AD-A265169] p 366 N94-11100
Energy transfer dynamics and impact sensitivity
[DE93-009551] p 98 N94-11269

LOW GRAVITY MANUFACTURING
Solidification in immiscible systems: The influence of processing conditions on resulting microstructures
p 112 N94-10174
Ripening of immiscible liquid droplets in microgravity with constrained Marangoni drift p 117 N94-10200

A study of the quasibinary Al-W-Mo system. Part 1: Preliminary investigations and preparation for microgravity experiments p 119 N94-10211
A study of the quasibinary Al-Mo-W system. Part 2: A physico-mechanical investigation of the system fabricated under the gravitylessness conditions
p 119 N94-10212

LOW PASS FILTERS
Force reflection with compliance control
[NASA-CASE-NPO-18668-1-CU] p 179 N94-10654

LOW PRESSURE
Plating under reduced pressure
[DE93-011896] p 84 N94-11668

LOW SPEED
Strain concentration assessment of laminates subjected to low velocity impact
[AD-A264497] p 73 N94-11446
Calibration of anemometers at low speed by means of towing carriage p 164 N94-12619

LOW TEMPERATURE
Crystal growth from low temperature vapour phase
p 115 N94-10191
Experiments in ultracold collisions
[DE93-012110] p 365 N94-11029
Phase equilibria and volumetric properties for the system NaCl-CaCl2-H2O
[DE93-013590] p 76 N94-11244
Synthesis and magnetic properties of novel La*2-x*M*x*CuO*4 equals y* compositions (La equals La, Pr, Nd, Sm, Eu, Cd; M equals Ca, Sr, Ba; O (less than or equal) x 0.2; -0.5 (less than or equal) y (less than or equal) 0.5)
[DE93-011359] p 403 N94-12363

LOW TEMPERATURE ENVIRONMENTS
Icing of turbine intake louvers
[AD-A265714] p 29 N94-12274

LOW THRUST
A laboratory model of a hydrogen/oxygen engine for combustion and nozzle studies
[NASA-TM-106281] p 47 N94-11252

LOW VOLTAGE
Low voltage electron beam lithography
[AD-A265358] p 145 N94-12405

LOWER BODY NEGATIVE PRESSURE
Glycerol-induced hyperhydration p 309 N94-11996
Spectral analysis of resting cardiovascular variables and responses to oscillatory LBNP before and after 6 degree head dowm bedrest p 309 N94-11997
Effect of prolonged LBNP and saline ingestion on plasma volume and orthostatic responses during bed rest
p 310 N94-11998

LUBRICANTS
The properties of perfluoropolyethers used for space applications
[NASA-TM-106275] p 88 N94-10864
Measurement of viscosity, density and gas solubility of refrigerant blends
[DE93-014772] p 89 N94-11145
Accelerated screening methods for predicting lubricant performance in refrigerant compressors
[DE93-014773] p 89 N94-11146
Ceramics technology project database
[DE93-012431] p 91 N94-11672

LUBRICATION
Accelerated screening methods for predicting lubricant performance in refrigerant compressors
[DE93-014773] p 89 N94-11146
Advanced model of gradual wear of viscoelastic surface film
[AD-A265130] p 90 N94-11222
Tribological characteristics of sputtered Au/Cr films on alumina substrates at elevated temperatures
[NASA-TM-106078] p 55 N94-11362
Properties of interfacial tribo-films
[AD-A265591] p 182 N94-12374

LUBRICATION SYSTEMS
AGBT advanced counter-rotating gearbox detailed design report
[NASA-CR-180883] p 179 N94-10400

LUMINAIRES
Parametric study of diffusion-enhancement networks for spatiotemporal grouping in real-time artificial vision
[AD-A265065] p 331 N94-11652

LUMINESCENCE
Improved super luminescent light source specification
[AD-D015746] p 176 N94-12329

LUMINOSITY
Experimental efforts and results in finding new heavy scintillators
[DE93-010406] p 371 N94-10156
Upgraded D(O) calorimeter electronics for short Tevatron bunch space and the effect of pile-up on the W mass measurement
[DE93-013566] p 146 N94-12603

LUNAR BASED EQUIPMENT
General overview of an integrated lunar oxygen production/brickmaking system p 131 N94-12027
Galileo EM-2 contributions to the lunar control network p 468 N94-12198

LUNAR BASES
Lunar campsite concept: Space transfer concepts and analysis for exploration missions
[NASA-CR-192602] p 433 N94-10144
Radiation considerations for interplanetary missions
p 45 N94-11559
Cold press sintering of simulated lunar basalt
p 131 N94-12026
General overview of an integrated lunar oxygen production/brickmaking system p 131 N94-12027
Thermodynamics of lunar ilmenite reduction
p 415 N94-12028
Mission to the Moon: An ESA study on future exploration p 460 N94-12153
Exploration planning in the context of human exploration and development of the Moon p 474 N94-12229
Conceptual studies report on lunar and planetary exploration
[NASDA-TK-SS0438] p 481 N94-12323
Manned lunar exploration missions
p 482 N94-12326

LUNAR COMPOSITION
Multiple nitrogen components in lunar soil sample 12023 p 451 N94-12108
Solar wind-induced secondary ions and their relation to lunar surface composition p 474 N94-12232
Measuring and distinguishing compositional and maturity properties of lunar soils by remote VIS-NIR spectroscopy p 478 N94-12251

LUNAR CONSTRUCTION EQUIPMENT
Cold press sintering of simulated lunar basalt
p 131 N94-12026

LUNAR CRATERS
Differential scaling: Implications for central structures in large lunar craters p 461 N94-12158

LUNAR CRUST
The granulite suite: Impact melts and metamorphic breccias of the early lunar crust p 282 N94-12197
Assimilation in lunar basalts and volcanic glasses: Implications for a heterogenous mantle source region
p 478 N94-12250

LUNAR DUST
Solar wind-induced secondary ions and their relation to lunar surface composition p 474 N94-12232

LUNAR EVOLUTION
Magnetic fields and nonuniform structures of the Moon p 472 N94-12218

LUNAR EXPLORATION
Lunar campsite concept: Space transfer concepts and analysis for exploration missions
[NASA-CR-192602] p 433 N94-10144
The Los Alamos neutron spectrometer for the Lunar Scout-1 mission p 172 N94-12038
Mission to the Moon: An ESA study on future exploration p 460 N94-12153
Remote sensing x ray fluorescence spectrometry for future lunar exploration missions p 462 N94-12165
Exploration planning in the context of human exploration and development of the Moon p 474 N94-12229
Terrestrial case studies of ilmenite exploration and lunar implications p 478 N94-12247
Significance and scenarios of lunar and planetary exploration missions p 482 N94-12324
Unmanned lunar exploration mission
p 482 N94-12325
Manned lunar exploration missions
p 482 N94-12326

LUNAR GEOLOGY
Twenty-fourth Lunar and Planetary Science Conference. Part 1: A-F
[NASA-CR-193095] p 435 N94-12015
Measurements of cosmogenic nuclides in lunar rock 64455 p 437 N94-12033
Apollo 16 core 60013/14 as a product of path 1 and path 2 regolith evolution processes p 440 N94-12050
Spectral and multispectral imaging studies of lunar mantled mare deposits p 446 N94-12079
Multiple nitrogen components in lunar soil sample 12023 p 451 N94-12108
Viscous relaxation of the Moho under large lunar basins p 452 N94-12113
Mission to the Moon: An ESA study on future exploration p 460 N94-12153
Differential scaling: Implications for central structures in large lunar craters p 461 N94-12158
Macroscopic electric charge separation during hypervelocity impacts: Potential implications for planetary paleomagnetism p 431 N94-12181
The granulite suite: Impact melts and metamorphic breccias of the early lunar crust p 282 N94-12197
Magnetic fields and nonuniform structures of the Moon p 472 N94-12218
Solar wind-induced secondary ions and their relation to lunar surface composition p 474 N94-12232
Assimilation in lunar basalts and volcanic glasses: Implications for a heterogenous mantle source region
p 478 N94-12250

LUNAR GRAVITATION
Lunar Scout Two spacecraft gravity experiment
p 459 N94-12152
Magnetic fields and nonuniform structures of the Moon p 472 N94-12218

LUNAR LANDING MODULES
Unmanned lunar exploration mission
p 482 N94-12325

LUNAR LOGISTICS
Lunar campsite concept: Space transfer concepts and analysis for exploration missions
[NASA-CR-192602] p 433 N94-10144

LUNAR MAGNETIC FIELDS
Macroscopic electric charge separation during hypervelocity impacts: Potential implications for planetary paleomagnetism p 431 N94-12181
Magnetic fields and nonuniform structures of the Moon p 472 N94-12218

LUNAR MANTLE
Assimilation in lunar basalts and volcanic glasses: Implications for a heterogenous mantle source region
p 478 N94-12250

LUNAR MARIA
Spectral and multispectral imaging studies of lunar mantled mare deposits p 446 N94-12079
Graphite solubility and co-vesiculation in basalt-like melts at one-ATM p 463 N94-12173
Using lunar sounder imagery to distinguish surface from subsurface reflectors in lunar highlands areas
p 464 N94-12179

LUNAR MINING
Terrestrial case studies of ilmenite exploration and lunar implications p 478 N94-12247

LUNAR PROBES
Conceptual studies report on lunar and planetary exploration
[NASDA-TK-SS0438] p 481 N94-12323
Unmanned lunar exploration mission
p 482 N94-12325

LUNAR RADAR ECHOES
Interpretation of lunar and planetary electromagnetic scattering using the full wave solutions
p 440 N94-12049

LUNAR RESOURCES
Terrestrial case studies of ilmenite exploration and lunar implications p 478 N94-12247

LUNAR ROCKS
Production of electronic grade lunar silicon by disproportionation of silicon difluoride
p 435 N94-12017
Cold press sintering of simulated lunar basalt
p 131 N94-12026
General overview of an integrated lunar oxygen production/brickmaking system p 131 N94-12027
Thermodynamics of lunar ilmenite reduction
p 415 N94-12028
Measurements of cosmogenic nuclides in lunar rock 64455 p 437 N94-12033
Vaporization by shock loading of albite, jadeite, and pyrex glass: Experimental study p 97 N94-12039
Apollo 16 core 60013/14 as a product of path 1 and path 2 regolith evolution processes p 440 N94-12050
Natural thermoluminescence profiles in lunar cores and implications for meteorites p 443 N94-12060
Impact comminution of glasses: Implications for lunar regolith evolution p 461 N94-12159
Macroscopic electric charge separation during hypervelocity impacts: Potential implications for planetary paleomagnetism p 431 N94-12181
The granulite suite: Impact melts and metamorphic breccias of the early lunar crust p 282 N94-12197
The Fe/Mn constraint on precursors of basaltic achondrites p 432 N94-12208
Compositional heterogeneity within a dumbbell-shaped Apollo 15 green glass: Evidence for simultaneous eruption of different magmas p 470 N94-12209
Magnetic fields and nonuniform structures of the Moon p 472 N94-12218

LUNAR ROVING VEHICLES
Unmanned lunar exploration mission
p 482 N94-12325

LUNAR SATELLITES
Conceptual studies report on lunar and planetary exploration
[NASDA-TK-SS0438] p 481 N94-12323
Unmanned lunar exploration mission
p 482 N94-12325

LUNAR SHELTERS
Lunar campsite concept: Space transfer concepts and analysis for exploration missions
[NASA-CR-192602] p 433 N94-10144
LUNAR SOIL
Production of electronic grade lunar silicon by disproportionation of silicon difluoride
p 435 N94-12017
Effects of microscopic iron metal on the reflectance spectra of glass and minerals p 436 N94-12024
Thermodynamics of lunar ilmenite reduction
p 415 N94-12028
Measurements of cosmogenic nuclides in lunar rock 64455 p 437 N94-12033
Vaporization by shock loading of albite, jadeite, and pyrex glass: Experimental study p 97 N94-12039
Apollo 16 core 60013/14 as a product of path 1 and path 2 regolith evolution processes p 440 N94-12050
Multiple nitrogen components in lunar soil sample 12023 p 451 N94-12108
A reexamination of amino acids in lunar soil
p 452 N94-12109
Impact comminution of glasses: Implications for lunar regolith evolution p 461 N94-12159
Macroscopic electric charge separation during hypervelocity impacts: Potential implications for planetary paleomagnetism p 431 N94-12181
Solar wind-induced secondary ions and their relation to lunar surface composition p 474 N94-12232
Measuring and distinguishing compositional and maturity properties of lunar soils by remote VIS-NIR spectroscopy p 478 N94-12251
LUNAR SPACECRAFT
Lunar campsite concept: Space transfer concepts and analysis for exploration missions
[NASA-CR-192602] p 433 N94-10144
The Los Alamos neutron spectrometer for the Lunar Scout-1 mission p 172 N94-12038
Lunar Scout Two spacecraft gravity experiment
p 459 N94-12152
LUNAR SURFACE
Spectral and multispectral imaging studies of lunar mantled mare deposits p 446 N94-12079
Preliminary report of lunar observations by the Near-Infrared Mapping Spectrometer (NIMS) during the second Galileo Earth-Moon encounter
p 425 N94-12140
Using lunar sounder imagery to distinguish surface from subsurface reflectors in lunar highlands areas
p 464 N94-12179
Macroscopic electric charge separation during hypervelocity impacts: Potential implications for planetary paleomagnetism p 431 N94-12181
Solar wind-induced secondary ions and their relation to lunar surface composition p 474 N94-12232
Measuring and distinguishing compositional and maturity properties of lunar soils by remote VIS-NIR spectroscopy p 478 N94-12251
LUNAR TOPOGRAPHY
Viscous relaxation of the Moho under large lunar basins p 452 N94-12113
LUNGS
Evaluation of medical treatments to increase survival of ebullism in guinea pigs p 302 N94-11548
Pulmonary function in microgravity: KC-135 experience
p 309 N94-11994

M

MACH NUMBER
Numerical calculation of scramjet inlet flow
[NAL-TR-1174T] p 27 N94-10370
Exergy decrease in shock waves and boundary layers of space launch vehicles
[AD-A265272] p 42 N94-10493
Kinetic approach to long wave length modes in rotating plasmas
[DE93-771286] p 388 N94-10807
Progress in modeling hypersonic turbulent boundary layers p 157 N94-12300
MACHINE LEARNING
A new HMM learning algorithm for continuous speech recognition
[NHK-SERIAL-413] p 132 N94-10560
Toward intelligent flight control p 33 N94-11503
Statistical and optimization methods to expedite neural network training for transient identification
[DE93-009985] p 340 N94-11644
A pattern recognition system for locating small volvanoes in Magellan SAR images of Venus
p 455 N94-12126
MACHINE TOOLS
Material removal processes: Engineering mechanics consideration
[DE93-010733] p 126 N94-10293
Thermal error compensation feasibility study using artificial intelligence
[AD-A266084] p 340 N94-12411
MACHINE TRANSLATION
Processing proper nouns in machine translation for English news
[NHK-SERIAL-414] p 418 N94-10559
Machine translation technology: A potential key to the information age
[PB93-134336] p 421 N94-12385
MACHINING
Material removal processes: Engineering mechanics consideration
[DE93-010733] p 126 N94-10293
Thermal error compensation feasibility study using artificial intelligence
[AD-A266084] p 340 N94-12411
MACROMOLECULES
Effects of a microgravity environment on the crystallization of biological macromolecules
p 117 N94-10198
MAGELLAN PROJECT (NASA)
Russia's contribution to regional geologic mapping of Venus p 454 N94-12122
Synthesis of global thematic mapping, Venus: Geologic correlations/questions for the Magellan gravity mission
p 467 N94-12194
Characteristics of arachnoids from Magellan data
p 469 N94-12204
MAGELLAN SPACECRAFT (NASA)
The origin of Venusian channels: Modelling of thermal erosion by lava p 456 N94-12131
MAGMA
Th-230 - U-238 series disequilibrium of the Olkaria basalts Gregory Rift Valley, Kenya: Petrogenesis
p 281 N94-12074
Lava flows on Venus: Analysis of motion and cooling
p 457 N94-12137
Comparison of the distributinn of large magmatic centers on Earth, Venus, and Mars p 467 N94-12192
The Magellan volcanic and magmatic feature catalog
p 467 N94-12193
Compositional heterogeneity within a dumbbell-shaped Apollo 15 green glass: Evidence for simultaneous eruption of different magmas p 470 N94-12209
Vulcanian explosive eruptions: A mechanism for localised pyroclast dispersal on Venus
p 477 N94-12243
Primitive SNC parent magmas and crystallization: Low PH2O experiments p 433 N94-12264
MAGNESIUM ALLOYS
Mechanical properties of magnesium/carbon composites developed by hot pressing under medium pressure p 59 N94-10024
MAGNESIUM ISOTOPES
Isotopic and trace element characteristics of an unusual refractory inclusion from Essebi p 471 N94-12212
MAGNET COILS
High-field conductor testing at the FENIX facility
[DE93-012318] p 387 N94-10737
Magnetic island suppression in torsatron configurations
[DE93-621681] p 392 N94-11215
MAGNETIC ANOMALIES
A study on the magnetospheric activity using the AE, ap, and Dst geomagnetic indices
[INPE-5470-TDI/501] p 276 N94-11165
Polarity reversals and tilt of the Earth's magnetic dipole p 283 N94-12219
Pseudo magnetic anomaly derived from satellite altimetry and its application to the tectonics in the North Fuji Basin p 208 N94-12645
MAGNETIC BEARINGS
Development of passive superconducting bearings. Phase 3
[AD-A266050] p 180 N94-10706
Improvement of azimuthal homogeneity in permanent-magnet bearing rotors
[DE93-009954] p 144 N94-11607
MAGNETIC CIRCUITS
Direct current transducer
[DE92-644548] p 141 N94-10533
MAGNETIC COILS
Processing and transport properties of high J(sub c) silver clad Bi-2223 tapes and coils
[DE93-010674] p 398 N94-11073
MAGNETIC COMPRESSION
MHD simulation of deuterium-fiber-initiated Z-pinches with two-fluid effects
[DE93-012682] p 384 N94-10158
MAGNETIC CONTROL
Magnetic island suppression in torsatron configurations
[DE93-621681] p 392 N94-11215
MAGNETIC DIPOLES
Polarity reversals and tilt of the Earth's magnetic dipole p 283 N94-12219
MAGNETIC EFFECTS
The effect of a uniform magnetic field on the onset of steady Marangoni convection in a layer of conducting fluid p 120 N94-10222
On thermodynamic properties of heavy fermion systems in magnetic field
[DE93-613819] p 409 N94-10403
Analytical description of the torsatron Uragan-2M magnetic configuration with account of plasma pressure and external correcting magnetic field
[DE93-620983] p 391 N94-11174
Are cosmic rays effective for ionization of the solar nebula? p 472 N94-12220
MAGNETIC FIELD CONFIGURATIONS
Optimization of break-down conditions in tokamak TOTUS
[DE93-617863] p 386 N94-10524
Calculation of Mercier stability criterium in stellarators
[DE93-621599] p 389 N94-11091
Charged particle motion in torsatrons, part 1
[DE93-621639] p 389 N94-11119
Particle transport analysis in torsatron configurations
[DE93-621640] p 390 N94-11120
Analytical description of the torsatron Uragan-2M magnetic configuration with account of plasma pressure and external correcting magnetic field
[DE93-620983] p 391 N94-11174
Simple kinetic model for plasma in stochastic helical field
[DE93-621643] p 391 N94-11208
Magnetic island suppression in torsatron configurations
[DE93-621681] p 392 N94-11215
Short pulse lasers for generation of fields exceeding 100 MG
[DE93-013346] p 369 N94-11815
Nonlinear analysis of a magnicon output cavity
[AD-A265342] p 145 N94-12424
MAGNETIC FIELD INVERSIONS
Polarity reversals and tilt of the Earth's magnetic dipole p 283 N94-12219
MAGNETIC FIELD RECONNECTION
A study of the magnetic field annihilation process in the magnetosphere and some geotechnical applications
[DE93-013249] p 273 N94-10305
A study of the magnetic field annihilation process in the magnetosphere and some geotechnical applications
[DE93-013248] p 273 N94-10319
Simulation study of dynamo structure in reversed field pinch
[DE93-771406] p 390 N94-11128
Macroscopic behaviour and discrete dynamo of RFP plasma in high theta discharge
[DE93-771408] p 392 N94-11239
MAGNETIC FIELDS
The use of magnetic fields for damping unsteady Marangoni convection in GaAs floating zones under microgravity p 100 N94-10073
Calculation of the effects of magnetic field damping in fluid flow: Comparison of magnetohydrodynamic models of different complexity p 103 N94-10089
CdTe crystal growth in the Soviet facility zona 4
p 106 N94-10111
CdTe crystal growth by THM with a rotating magnetic field p 107 N94-10116
New mechanism of Ostwald ripening in Lorentz-force stabilized Cu-Pb dispersions p 116 N94-10192
Results of crystal growth experiments by FZM on Zona facilities in microgravity p 116 N94-10193
THM-growth of III-V-semiconductors in the magnetic field p 118 N94-10209
The effect of a uniform magnetic field on the onset of steady Marangoni convection in a layer of conducting fluid p 120 N94-10222
Nonlinear second harmonic generation by light wave-plasma interaction in oscillating magnetic field
[DE93-613723] p 386 N94-10387
Stationary spectra in a magnetized current-carrying plasma
[DE93-617847] p 386 N94-10397
On thermodynamic properties of heavy fermion systems in magnetic field
[DE93-613819] p 409 N94-10403
Stationary spectra in a finite-pressure current-carrying plasma
[DE93-617848] p 387 N94-10538
Stationary spectra in a sheared plasma (linear limit)
[DE93-617850] p 387 N94-10540
Quantum mechanical effects of topological origin
p 378 N94-10594
New squeezed landau states p 379 N94-10601

Power losses of a type 2 superconducting slab of arbitrary thickness in the presence of alternating current conductors
[DE93-617892] p 396 N94-10716
Reversed-field pinch studies in the Madison Symmetric Torus
[DE93-013464] p 388 N94-10747
Stationary spectra of short-wave convective and magnetostatic fluctuations in a finite-pressure plasma and anomalous heat conductivity
[DE93-617852] p 388 N94-10840
Calculation of Mercier stability criterium in stellarators
[DE93-621599] p 389 N94-11091
Possibilities of magnetic diagnostics in stellarators
[DE93-621608] p 389 N94-11092
Radiative properties of strongly magnetized plasmas
[DE93-014098] p 389 N94-11118
Magnetic Earth Ionosphere Resonant Frequencies (MEIRF) project
[NASA-CR-193182] p 276 N94-11355
Accretion disk viscosity and internal waves in disks
p 153 N94-11615
The magnetic field of rotating bodies
[DE93-619769] p 427 N94-11812
Polarity reversals and tilt of the Earth's magnetic dipole p 283 N94-12219
On the unique structure of the magnetic fields of Uranus and Neptune p 472 N94-12221
Pilot trial of potentiating normal healing of stress fractures using pulsing electromagnetic fields
[AD-A264251] p 311 N94-12364

MAGNETIC FILMS
NRL review for 1993
[AD-A265666] p 497 N94-12334

MAGNETIC FLUX
Quantum mechanical effects of topological origin
p 378 N94-10594
On the possible unobservability of the Wu-Yang phase factor in curved space
[DE93-617645] p 411 N94-10831

MAGNETIC LENSES
Spin characteristics of ion beams during the motion of electromagnetic elements
[DE93-617448] p 364 N94-10848

MAGNETIC MEASUREMENT
Large array SQUID magnetometer for NDE
[AD-A264799] p 304 N94-11449
Magnetic fields and nonuniform structures of the Moon p 472 N94-12218

MAGNETIC MOMENTS
Effect of a distribution of exchange parameters within a simple localized-itinerant model
[DE93-610314] p 395 N94-10314

MAGNETIC PERMEABILITY
Remanent magnetism of HED meteorites: Implications for their evolution and ancient magnetic fields
p 431 N94-12172

MAGNETIC POLES
A method to determine asteroid poles
p 431 N94-12205
Polarity reversals and tilt of the Earth's magnetic dipole p 283 N94-12219

MAGNETIC PROPERTIES
Effect of a distribution of exchange parameters within a simple localized-itinerant model
[DE93-610314] p 395 N94-10314
Rietveld refinement of magnetic structures from pulsed-neutron-source powder-diffraction data
[DE93-012740] p 363 N94-10743
Application of spin-sensitive electron spectroscopies to investigations of electronic and magnetic properties of solid surfaces and epitaxial systems
[DE93-015079] p 76 N94-10854
Remanent magnetism of HED meteorites: Implications for their evolution and ancient magnetic fields
p 431 N94-12172
Synthesis and magnetic properties of novel La*2-x*M*x*CuO*4 equals y* compositions (La equals La, Pr, Nd, Sm, Eu, Cd; M equals Ca, Sr, Ba; O (less than or equal) x 0.2; -0.5 (less than or equal) y (less than or equal) 0.5)
[DE93-011359] p 403 N94-12363

MAGNETIC RESONANCE
Magnetic island suppression in torsatron configurations
[DE93-621681] p 392 N94-11215

MAGNETIC SPECTROSCOPY
NMR spectroscopy of experimentally shocked single crystal quartz: A reexamination of the NMR shock barometer p 81 N94-12258

MAGNETIC SURVEYS
Pseudo magnetic anomaly derived from satellite altimetry and its application to the tectonics in the North Fuji Basin p 208 N94-12645

MAGNETIC SUSPENSION
Electromechanical batteries and the electric locomotive
[DE93-013311] p 142 N94-11009
Improvement of azimuthal homogeneity in permanent-magnet bearing rotors
[DE93-009954] p 144 N94-11607

MAGNETITE
Changes in Hawaiian palagonite FE mineralogy associated with thermal alteration: Implications for Mars
p 281 N94-12055
Iron and nickel isotopic mass fractionation in deep-sea spherules p 282 N94-12199

MAGNETIZATION
Magnetization reversal by nucleation
[DE93-610313] p 350 N94-10313

MAGNETO-OPTICS
Experiments in ultracold collisions
[DE93-012110] p 365 N94-11029

MAGNETOHYDRODYNAMIC FLOW
Comparison of hydrodynamic and semi-kinetic treatments for plasma flow along closed field lines
[NASA-CR-193589] p 387 N94-10641
Physics of tokamak scrape-off layer confinement
[DE93-011949] p 390 N94-11125
Simulation study of dynamo structure in reversed field pinch
[DE93-771406] p 390 N94-11128

MAGNETOHYDRODYNAMIC STABILITY
Kinetic approach to long wave length modes in rotating plasmas
[DE93-771286] p 388 N94-10807
Magnetohydrodynamic computation of feedback stabilization of resistive-shell instabilities in the reversed field pinch
[DE93-013466] p 388 N94-10852
Calculation of Mercier stability criterium in stellarators
[DE93-621599] p 389 N94-11091
The angular structure of second harmonic emission from laser-produced plasmas irradiated at moderate intensity
[DE93-013102] p 389 N94-11114
Gyrosheath near the tokamak edge
[DE93-012191] p 390 N94-11142
Studies on the parametric decay of waves in fusion plasmas
[DE93-621659] p 390 N94-11148
Elementary mechanism of electron beam dissipative instability development
[DE93-621653] p 391 N94-11209
Experimental investigation of wake field excitation in plasma by a periodic succession of relativistic particle clots
[DE93-621655] p 391 N94-11211
Negative viscosity and generation of dissipative solitons and zonal dissipative structures by drift waves
[DE93-621656] p 392 N94-11212
Spreading of Bimodulated Ultra-relativistic Electron Beam (BUEB) in Atmcspheric Plasma Channel (APCh)
[DE93-621658] p 392 N94-11213
The role of plasma rotation on MHD instabilities in tokamaks
[DE93-013486] p 393 N94-11512
Initial assessment of lower hybrid current drive in D3-D
[DE93-013310] p 394 N94-12370

MAGNETOHYDRODYNAMIC WAVES
Efficiency of fast wave current drive for a weakly relativistic plasma
[DE93-012775] p 385 N94-10159
Nonlinear MHD-waves in a dissipative plasma with hall currents
[DE93-617844] p 386 N94-10395

MAGNETOHYDRODYNAMICS
Calculation of the effects of magnetic field damping in fluid flow: Comparison of magnetohydrodynamic models of different complexity p 103 N94-10089
Source to detector spectrum transformation and its inverse for the Pegasus Z-pinch
[DE93-012674] p 384 N94-10157
MHD simulation of deuterium-fiber-initiated Z-pinches with two-fluid effects
[DE93-012682] p 384 N94-10158
Reversed-field pinch studies in the Madison Symmetric Torus
[DE93-013464] p 388 N94-10747
Magnetohydrodynamic computation of feedback stabilization of resistive-shell instabilities in the reversed field pinch
[DE93-013466] p 388 N94-10852
Discrete vortex representation of magnetohydrodynamics
[DE93-012190] p 393 N94-11669
On the unique structure of the magnetic fields of Uranus and Neptune p 472 N94-12221

MAGNETOMETERS
A phaseonium magnetometer: A new optical magnetometer based on index enhanced media
p 375 N94-10565
NASA Marshall Space Flight Center solar observatory report, January - June 1993
[NASA-TM-108417] p 423 N94-10866
Large array SQUID magnetometer for NDE
[AD-A264799] p 304 N94-11449

MAGNETOPAUSE
A study of the magnetic field annihilation process in the magnetosphere and some geotechnical applications
[DE93-013249] p 273 N94-10305
A study of the magnetic field annihilation process in the magnetosphere and some geotechnical applications
[DE93-013248] p 273 N94-10319

MAGNETOSTATICS
Stationary spectra of short-wave convective and magnetostatic fluctuations in a finite-pressure plasma and anomalous heat conductivity
[DE93-617852] p 388 N94-10840

MAGNETOSTRICTION
On thermodynamic properties of heavy fermion systems in magnetic field
[DE93-613819] p 409 N94-10403

MAGNETS
Spin characteristics of ion beams during the motion of electromagnetic elements
[DE93-617448] p 364 N94-10848
Operational characteristics of a 100-mA, 2-MeV radio-frequency quadrupole
[DE93-014474] p 374 N94-12786

MAGNONS
The peculiarities of the spin glass state in Fe(x)Mn(1-x)TiO3
[DE93-617882] p 395 N94-10525
Generalized spin systems and sigma-models
[DE93-613981] p 410 N94-10802
A symmetrical form for equations of a nonlinear spiral magnetic
[DE93-621350] p 344 N94-11033

MAIN SEQUENCE STARS
The abundances of the elements in sharp-lined early type stars
[NASA-CR-194055] p 424 N94-12573

MAINTAINABILITY
More sense for less cents: Cost effective servicing of remote sensing satellites p 348 N94-11572
RAMCAD (reliability, availability, and maintainability in computer-aided design)
[AD-A265143] p 331 N94-11679

MAINTENANCE
Applying reliability models to the maintenance of Space Shuttle software p 330 N94-11434
Department of Energy fundamentals handbook: Engineering symbology, prints, and drawings
[DE93-012181] p 129 N94-11456
Department of Energy fundamentals handbook: Engineering symbology, prints, and drawings
[DE93-012220] p 129 N94-11670

MAINTENANCE TRAINING
Exercise countermeasures for bed-rest deconditioning
[NASA-TM-103987] p 300 N94-11191
Forecasting the impact of virtual environment technology on maintenance training p 314 N94-11570

MAJORITY CARRIERS
Electrochemical characterization of p(+)n and n(+)p diffused InP structures p 49 N94-11385
Activation energy and capture cross section of majority carrier traps in Zn doped InP p 49 N94-11386

MAMMALS
The organization of the suprachiasmatic circadian pacemaker of the rat and its regulation by neurotransmitters and modulators
[AD-A266113] p 301 N94-12417

MAN MACHINE SYSTEMS
Virtual sound for virtual reality
[DE93-010519] p 321 N94-10291
Aerospace medicine and biology: A continuing bibliography with indexes (supplement 375)
[NASA-SP-7011(375)] p 303 N94-10398
Aerospace medicine and biology: A continuing bibliography with indexes (supplement 376)
[NASA-SP-7011(376)] p 303 N94-10399
A new HMM learning algorithm for continuous speech recognition
[NHK-SERIAL-413] p 132 N94-10560
Sixth Annual Workshop on Space Operations Applications and Research (SOAR 1992), volume 2
[NASA-CP-3187-VOL-2] p 486 N94-11527
Noise levels and their effects on Shuttle crewmembers' performance: Operational concerns p 314 N94-11538
Aerospace medicine and biology: A continuing bibliography with indexes (supplement 374)
[NASA-SP-7011(374)] p 304 N94-11689

MAN-COMPUTER INTERFACE
Software usability assessment guide
[AD-A265017] p 321 N94-10335
Low latency messages on distributed memory multiprocessors
[NASA-CR-191479] p 323 N94-10643
Flight simulator experiment of the cockpit advisory system
[NAL-TR-1151] p 33 N94-10733
Measuring human performance on NASA's microgravity aircraft p 317 N94-11537
Computing science and statistics, Volume 24: Graphics and visualization
[AD-A265181] p 332 N94-11878
The instrumentation of the multimodel and multilingual user interface
[AD-A265444] p 333 N94-12332
Transportable Applications Environment (TAE) Tenth Users' Conference
[NASA-CP-3225] p 333 N94-12448
Cognitive engineering models: A prerequisite to the design of human-computer interaction in complex dynamic systems
[NASA-CR-193472] p 320 N94-12558

MANAGEMENT INFORMATION SYSTEMS
Myths and realities: Defining re-engineering for a large organization p 330 N94-11436
Design issues for high performance engineering information systems
[AD-A264839] p 420 N94-11520
Data management strategy for the Tampa Bay National Estuary Program: Recommendations and implementation plan
[PB93-191633] p 267 N94-11864
Analysis of the Army's installation support modules with the private sector's open information systems
[AD-A265667] p 421 N94-12579

MANAGEMENT METHODS
Space Station Redesign Team: Final report to the Advisory Committee on the Redesign of the Space Station
[NASA-TM-109241] p 42 N94-10663
Engineering performance metrics
[DE93-012084] p 128 N94-11028
From red tape to results: Creating a government that works better and costs less p 422 N94-11351
From red tape to results: Creating a government that works better and costs less. Executive summary
p 422 N94-11353
Maximizing reuse: Applying common sense and discipline p 329 N94-11429
Insights into software development in Japan
p 330 N94-11435
Research and development of post-classical management tools for government program offices, volume 2
[DE93-010236] p 417 N94-11600
International disaster research p 307 N94-11805

MANAGEMENT PLANNING
An advisor module for tactical and strategic state-oriented planning systems with an application in manpower planning
[MEMO-COSOR-92-57] p 416 N94-10868
US Coast Guard GPS Information Center (GPSIC) and its function within the Civil GPS Service (CGS)
p 24 N94-10966
Lunar-Ultraviolet Telescope Experiment (LUTE) integrated program plan
[NASA-CR-193267] p 424 N94-11356
Software management guide
[DE93-012034] p 330 N94-11452
Intergovernmental decisionmaking for environmental protection and public works
[PB93-176824] p 266 N94-11584
Information resources management long-range plan, FY1994
[DE93-013898] p 420 N94-11588
ESA Costing Software (ECOS) introduction
[ESA-F-28] p 333 N94-12383
Defense: Health care
[AD-A265914] p 421 N94-12445

MANAGEMENT SYSTEMS
Financial management: NASA's financial reports are based on unreliable data
[AD-A265690] p 418 N94-12443
Quality assurance for environmental chemistry: 1991, volume 2
[DE93-011792] p 272 N94-12780

MANEUVERABILITY
Physics of forebody flow control
[NASA-CR-193626] p 15 N94-11195
Comparing aircraft agility using mahalanobis distances
[PB93-175446] p 26 N94-11464
Adaptive reconfigurable flight controls for high angle of attack aircraft agility p 32 N94-11502

MANGANESE
A detailed investigation of the benthic regime in the Clarion-Clipperton province of the Pacific and a forecast of consequences of manganese nodule mining
p 224 N94-12733

MANGANESE ALLOYS
Structure and properties of an RS Al-Si-Ni-Mn-Zr alloy for high temperature applications p 64 N94-10063
Containerless processing of equiatomic Mn50Bi50 in a drop tube p 118 N94-10205

MANGANESE ISOTOPES
Search for effects of a supernova explosion 30 to 40 thousand years ago in chondrites p 428 N94-12022

MANIFOLDS (MATHEMATICS)
The structure of Hilbert flag varieties
[MEMO-1095] p 348 N94-10272
One dimensional representations in quantum optics
p 375 N94-10570
S(sup 1) x S(sup 2) as a bag membrane and its Einstein-Weyl geometry
[DE93-613149] p 410 N94-10635
Homoclinic intermittency
[W-9302] p 344 N94-10908
The Lip microbundle representation theorem
[DE93-619671] p 346 N94-11348

MANIPULATORS
Lightweight CFRP frame structures for a Rotex-derived manipulator system p 56 N94-10005
Force reflection with compliance control
[NASA-CASE-NPO-18668-1-CU] p 179 N94-10654
Telerobot control system
[NASA-CASE-NPO-18116-1-CU] p 179 N94-10670
Momentum management in redundant manipulators for vibration suppression
[NASA-CR-194112] p 180 N94-10821
Mechanical analysis of parallel manipulators with simulation, design, and control applications
[ISBN-0-315-72013-1] p 181 N94-11156
Model reference adaptive control (MRAC) with applications to robotics p 339 N94-11640
Derivation of three closed loop kinematic velocity models using normalized quaternion feedback for an autonomous redundant manipulator with application to inverse kinematics
[DE93-012823] p 340 N94-12543

MANNED MARS MISSIONS
In-space assembly-servicing requirements
p 348 N94-11569

MANNED SPACE FLIGHT
Lunar campsite concept: Space transfer concepts and analysis for exploration missions
[NASA-CR-192602] p 433 N94-10144
PTTI-aided ephemeris calculation and rapid data link acquisition for manned space flight p 42 N94-10974
Effects of CSF hormones and ionic composition on salt/water metabolism
[NASA-CR-193232] p 300 N94-11045

MANPOWER
An advisor module for tactical and strategic state-oriented planning systems with an application in manpower planning
[MEMO-COSOR-92-57] p 416 N94-10868

MANUALS
The guide to Design For On-orbit Spacecraft Servicing (DFOSS) manual: Producing a consensus document
p 421 N94-11575

MANUFACTURING
Lightweight CFRP frame structures for a Rotex-derived manipulator system p 56 N94-10005
Cost effectiveness of structural applications of fibre reinforced thermoplastics p 60 N94-10032
Spin-rolling, welding, and heat treatment of aluminium 2219 for Ariane 5 GAM high pressure vessel liners
p 62 N94-10045
PM technology and mechanical properties of metallic foams p 64 N94-10059
Dry in-line thermoplastic matrix impregnation, phase 1
[AD-A265016] p 67 N94-11221
Large array SQUID magnetometer for NDE
[AD-A264799] p 304 N94-11449
The effect of processing on the microstructure and tensile properties of a (gamma)-TiAl based alloy
[DE93-013221] p 84 N94-11488
Design issues for high performance engineering information systems
[AD-A264839] p 420 N94-11520
Space Solar Power Program
[DE93-011750] p 55 N94-11675
Statistical process control in the hybrid microelectronics manufacturing industry: A Navy view point
[AD-A265164] p 145 N94-11884

MANY BODY PROBLEM
Satellite structure of the xenon valence shell by electron momentum spectroscopy
[DE93-609993] p 360 N94-10327
Reduced gravity multibody dynamics testing
[NASA-CR-192589] p 125 N94-11483
Highly anisotropic but nodeless gap from a valence-fluctuation pairing mechanism
[DE93-010738] p 401 N94-11646

MAPPING
Mapping of the East Australian current with the ERS-1 SAR and shipborne studies p 234 N94-11717
Techniques and applications of SAR interferometry for ERS-1: Topographic mapping, change detection, and slope measurement p 236 N94-11734
The extraction of bottom characteristics and mapping in Kin Bay, Okinawa Main Island, Japan, using LANDSAT-5/TM and SPOT-1/HRV data
p 197 N94-11931
Mapping bathymetric slopes from bathymetry data
[AD-A265923] p 290 N94-12350
Land cover monitoring with multi-temporal ERS-1 SAR observations in the Netherlands p 246 N94-12473
Mapping a dynamic playa surface using multitemporal ERS-1 SAR data: First results p 246 N94-12474
Preliminary studies on the application of ERS-1 data to topographic mapping p 246 N94-12476
Combined analysis of ERS-1 SAR and visible/infrared remote sensing data for land cover/land use mapping in a tropical zone: A case study in Guinea
p 246 N94-12478
Example of SPOT/ERS-1 complementarity
p 247 N94-12479
Application of ERS-1 SAR data to snow mapping
p 247 N94-12483
Methodological considerations for use of ERS-1 imagery for the delineation of river networks in tropical forest areas p 247 N94-12484
The TREES project: Pre-processing and generation of terrain data for inclusion in an ERS-1 SAR classification scheme p 249 N94-12496
Mapping of sea bottom topography with ERS-1 C-band SAR p 254 N94-12525
ERS-1 imaging radar over the Waddensea-North Netherlands p 254 N94-12526
SAR imaging of geology and bathymetry: Kent coastal area - southern North Sea p 254 N94-12527
Application of remote sensing for coastal management in the north coast of Java p 218 N94-12701
Estimation of areal evapotranspiration using LANDSAT TM data: Kitami City, Hokkaido, Japan
p 219 N94-12703
Land use/land cover mapping of central water shed of Iran area based on satellite data interpretation
p 219 N94-12704
A method to minimize reference data in classifying satellite remote sensing data into land cover classes
p 219 N94-12705

MAPS
Boundary of Fatou sets of hyperbolic rational maps or degree two
[DE93-613031] p 348 N94-10412
Convergence theorems for a class of nonlinear maps in uniformly smooth Banach spaces
[DE92-641347] p 343 N94-10531
Worldwide map of rainfall amount over the ocean derived from passive microwave radiometer p 211 N94-12663

MARAGING STEELS
Weldability of maraging steels p 59 N94-10028

MARANGONI CONVECTION
Experimental study of axisymmetric thermocapillary flows p 100 N94-10072
The use of magnetic fields for damping unsteady Marangoni convection in GaAs floating zones under microgravity p 100 N94-10073
Instability of thermocapillary convection in floating zones p 101 N94-10076
Thermocapillary instabilities in cylindrical liquid bridges: Mechanisms and transition boundaries
p 101 N94-10077
Transient three-dimensional numerical simulation of Marangoni flow in a liquid column under microgravity
p 101 N94-10079
Marangoni and buoyant convections in zone melting of GaAs with liquid encapsulation p 101 N94-10081
Coupled thermovibrational and thermocapillary convection in liquid bridge (floating zone system)
p 101 N94-10082
Towards real time numerical stimulation of Marangoni convection: A help for telescience microgravity experiments p 102 N94-10087
Surface-tension driven convection in finite-size containers p 103 N94-10090
Marangoni instability induced convection in an evaporating liquid droplet p 104 N94-10094
Thermocapillary migration of bubbles: A semi-analytical solution for large Marangoni numbers
p 104 N94-10095
High Prandtl number fluids in a multilayered system under 1-g or micro-g environment p 104 N94-10096

Marangoni flows in open cavities with differentially heated end walls p 104 N94-10097

Benard and Marangoni convection in multiple liquid layers p 105 N94-10100

Coupled thermogravitational and thermocapillary convection in a two-layer fluid system p 105 N94-10101

Thermocapillary slug flow in a capillary tube p 105 N94-10104

Numerical simulation of Marangoni convection around gas bubbles in a liquid matrix p 106 N94-10107

Microgravity experiments using TR-1A rocket p 112 N94-10142

Thermocapillary convection instability in microgravity crystal growth p 112 N94-10172

Marangoni motion during melting of a hypermonotectic alloy: Numerical simulations for the D2 experiment IHF04 p 113 N94-10177

Numerical calculation of the growth of InP by the travelling heater method in the first mission of the Space Flyer Unit p 114 N94-10179

Ripening of immiscible liquid droplets in microgravity with constrained Marangoni drift p 117 N94-10200

Marangoni-driven solitary waves p 119 N94-10214

Marangoni Benard instabilities in liquid mixtures with Soret effect p 119 N94-10215

Numerical investigations on Marangoni-Benard instability in multi layer systems p 120 N94-10217

Instability of thermocapillary convection in multiple superposed immiscible liquid layers p 120 N94-10218

Convective motion in a multi-layered system with a free surface p 120 N94-10219

Vibrational-thermocapillary parallel flows and stability p 120 N94-10220

Appearance of convective instabilities caused by liquid-liquid phase separation under small buoyancy forces p 120 N94-10221

The effect of a uniform magnetic field on the onset of steady Marangoni convection in a layer of conducting fluid p 120 N94-10222

The combined influence of anticonvective and thermocapillary mechanisms on the stability of systems with interface p 121 N94-10223

Single bubble experiments in pool boiling: Results from TEXUS 26 p 124 N94-10243

Marangoni instability in a liquid layer with two free surfaces
[NASA-TM-106166] p 152 N94-11376

MARINE ENVIRONMENTS

Near surface ocean processes: Acoustical observations, ambient sound, and Langmuir circulation p 288 N94-11447

Biscayne bay: A bibliography of the marine environment
[PB93-184802] p 266 N94-11451

Automatic classification system for zooplankton p 203 N94-11969

Study on sea water purification using a substratum of marine organisms p 217 N94-12696

DISTERM: A shipboard data system for satellite monitoring of ocean and atmosphere p 226 N94-12749

MARINE METEOROLOGY

Development of a buoy system for monitoring marine weather and marine life abundance p 217 N94-12694

MARINE PROPULSION

Icing of turbine intake louvers
[AD-A265714] p 29 N94-12274

MARINE RESOURCES

Space research and remote sensing programmes in Bangladesh p 35 N94-10679

Biscayne bay: A bibliography of the marine environment
[PB93-184802] p 266 N94-11451

The requirement for global training programmes to meet the new remote sensing technology p 196 N94-11929

Primary productivity in the Oyashio area in the spring and summer of 1990 p 211 N94-12658

Characterization of dissolved organic matter in the ocean by using the fluorescence excitation-emission matrix p 211 N94-12659

Development of a buoy system for monitoring marine weather and marine life abundance p 217 N94-12694

Acoustic estimation of plankton biomass p 218 N94-12699

MARKET RESEARCH

Potential markets for advanced satellite communications
[NASA-CR-191145] p 41 N94-10512

Business fleet refueling assessment
[PB93-189892] p 98 N94-11017

Space Solar Power Program
[DE93-011750] p 55 N94-11675

MARKOV CHAINS

Parametric analysis of atmospheric processes
[NASA-CR-192523] p 347 N94-10757

MARKOV PROCESSES

A new HMM learning algorithm for continuous speech recognition
[NHK-SERIAL-413] p 132 N94-10560

MARS

Significance and scenarios of lunar and planetary exploration missions p 482 N94-12324

Mars exploration missions p 482 N94-12327

Technical problems on lunar an planetary exploration mission p 482 N94-12328

MARS (PLANET)

Evolution of steep Martian slopes p 434 N94-11184

Giant impact-induced atmospheric blow-off p 435 N94-12019

Marslink p 438 N94-12034

Mars: The initial emplacement of ground ice in response to the thermal evolution of its early crust p 462 N94-12168

Small volcanoes in Tempe Terra, Mars: Their detailed morphometry and inferred geologic significance p 469 N94-12202

Shallow crustal discontinuities and graben and scarp formation in the Tharsis region of Mars p 469 N94-12203

Classification of Martian deltas p 470 N94-12207

A comparison of the visible and near infrared reflectance of hydrovolcanic palagonite tuffs and Martian weathered soils p 477 N94-12245

Planetary astronomy of Mars. Mars data reduction
[NASA-CR-193515] p 424 N94-12768

MARS ATMOSPHERE

Marslink p 438 N94-12034

Behavior of vortices generated by an advancing ejecta curtain in theory, in the laboratory, and on Mars p 169 N94-12044

An observational search for CO2 ice clouds on Mars p 441 N94-12054

The effects of atmospheric pressure on infrared reflectance spectra of Martian analogs p 445 N94-12071

Near-infrared spectra of the Martian surface: Reading between the lines p 465 N94-12184

Dust in the Martian atmosphere: Polarimetric sensing p 473 N94-12223

Noble gas evidence of an aqueous reservoir near the surface of Mars more recently than 1.3 Ga p 473 N94-12228

Composition of the Martian aerosols through near-IR spectroscopy p 475 N94-12235

Organic matter on the early surface of Mars: An assessment of the contribution by interplanetary dust p 480 N94-12259

MARS CRATERS

Increased depth-diameter ratios in the Medusae Fossae Formation deposits of Mars p 439 N94-12043

Behavior of vortices generated by an advancing ejecta curtain in theory, in the laboratory, and on Mars p 169 N94-12044

Modern shelf ice, equatorial Aeolis Quadrangle, Mars p 450 N94-12100

Fractal dimensions of rampart impact craters on Mars p 460 N94-12154

MARS ENVIRONMENT

Dust in the Martian atmosphere: Polarimetric sensing p 473 N94-12223

MARS OBSERVER

A simple model of clastic sediments on Mars p 460 N94-12155

MARS PHOTOGRAPHS

Geologic history of central Chryse Planitia and the Viking 1 landing site, Mars p 465 N94-12180

MARS PROBES

A comparison of telescopic and Phobos-2 ISM spectra of Mars in the short-wave near-infrared (0.76-1.02 microns) p 424 N94-12053

Conceptual studies report on lunar and planetary exploration
[NASDA-TK-SS0438] p 481 N94-12323

Mars exploration missions p 482 N94-12327

MARS SURFACE

Twenty-fourth Lunar and Planetary Science Conference. Part 1: A-F
[NASA-CR-193095] p 435 N94-12015

Rates of fluvio-thermal erosion on Mars p 435 N94-12018

Lineament analysis and tectonic interpretation for the Tharsis region p 437 N94-12031

Increased depth-diameter ratios in the Medusae Fossae Formation deposits of Mars p 439 N94-12043

Behavior of vortices generated by an advancing ejecta curtain in theory, in the laboratory, and on Mars p 169 N94-12044

A comparison of telescopic and Phobos-2 ISM spectra of Mars in the short-wave near-infrared (0.76-1.02 microns) p 424 N94-12053

Changes in Hawaiian palagonite FE mineralogy associated with thermal alteration: Implications for Mars p 281 N94-12055

Thermal studies of Martian channels and valleys using Termoskan data p 443 N94-12064

Spectral analysis of the gravity and topography of Mars p 444 N94-12065

Reflectance spectra of sulfate-and carbonate-bearing Fe(3+)-doped montmorillonites as Mars soil analogs p 445 N94-12070

The effects of atmospheric pressure on infrared reflectance spectra of Martian analogs p 445 N94-12071

Using high spectral resolution spectrophotometry to study broad mineral absorption features on Mars p 446 N94-12077

Modern shelf ice, equatorial Aeolis Quadrangle, Mars p 450 N94-12100

Martian particle size based on thermal inertia corrected for elevation-dependent atmospheric properties p 430 N94-12107

Chemical weathering on Mars: Rate of oxidation of iron dissolved in brines p 455 N94-12128

An ancient inner lake in Maadim Vallis p 456 N94-12133

Spatial variation in the seasonal south polar cap of Mars as observed by Mariner 7 p 456 N94-12134

Fault geometries and extension in the Valles Marineris, Mars p 458 N94-12144

Basal scarp, paleoglacier, and fissure flows of Elysium Mons, Mars p 459 N94-12148

Fractal dimensions of rampart impact craters on Mars p 460 N94-12154

A simple model of clastic sediments on Mars p 460 N94-12155

Mars: The initial emplacement of ground ice in response to the thermal evolution of its early crust p 462 N94-12168

The role of the geothermal gradient in the emplacement and replenishment of ground ice on Mars p 463 N94-12169

The thermodynamic case for a water-rich Mars p 463 N94-12170

Geologic history of central Chryse Planitia and the Viking 1 landing site, Mars p 465 N94-12180

Near-infrared spectra of the Martian surface: Reading between the lines p 465 N94-12184

Comparison of the distribution of large magmatic centers on Earth, Venus, and Mars p 467 N94-12192

Small volcanoes in Tempe Terra, Mars: Their detailed morphometry and inferred geologic significance p 469 N94-12202

Shallow crustal discontinuities and graben and scarp formation in the Tharsis region of Mars p 469 N94-12203

Classification of Martian deltas p 470 N94-12207

Relation between ages and elevations of Martian channels p 472 N94-12216

Noble gas evidence of an aqueous reservoir near the surface of Mars more recently than 1.3 Ga p 473 N94-12228

Automatic definition of spectral units in the equatorial regions of Mars p 432 N94-12234

Moessbauer spectrometer for mineralogical analysis of the Mars surface: Moessbauer source considerations p 476 N94-12242

A comparison of the visible and near infrared reflectance of hydrovolcanic palagonite tuffs and Martian weathered soils p 477 N94-12245

Organic matter on the early surface of Mars: An assessment of the contribution by interplanetary dust p 480 N94-12259

Primitive SNC parent magmas and crystallization: Low PH2O experiments p 433 N94-12264

Do large impact basins in the southern hemisphere of Mars control the distribution of polar structures and deposits? p 481 N94-12266

Free-air and Bouguer gravity anomalies and the Martian crustal dichotomy p 481 N94-12267

New Mars free-air and Bouguer gravity: Correlation with topography, geology and large impact basins p 481 N94-12268

Interdisciplinary scientist participation in the Phobos mission
[NASA-CR-193715] p 482 N94-12446

Planetary astronomy of Mars. Mars data reduction
[NASA-CR-193515] p 424 N94-12768

MARS VOLCANOES

Twenty-fourth Lunar and Planetary Science Conference. Part 1: A-F
[NASA-CR-193095] p 435 N94-12015

Lineament analysis and tectonic interpretation for the Tharsis region p 437 N94-12031

Basal scarp, paleoglacier, and fissure flows of Elysium Mons, Mars p 459 N94-12148

Small volcanoes in Tempe Terra, Mars: Their detailed morphometry and inferred geologic significance p 469 N94-12202
Shallow crustal discontinuities and graben and scarp formation in the Tharsis region of Mars p 469 N94-12203

MARSHLANDS
A preliminary study of the variability and magnitude of the flux of biogenic sulfur gases from a New Hampshire salt marsh p 267 N94-12452
Sulfate reduction and other sedimentary biogeochemistry in a northern New England salt marsh p 268 N94-12453
Emissions of sulfur gases from wetlands p 269 N94-12458
Acetate concentrations and oxidation in salt marsh sediments p 269 N94-12459
Sulfur transformations in the sediments of a New Hampshire salt marsh p 270 N94-12463
Emissions of biogenic sulfur gases from northern bogs and fens p 271 N94-12467
Elevated acetate concentrations in the rhizosphere of Spartina alterniflora and potential influences on sulfate reduction p 271 N94-12468

MARTENSITIC STAINLESS STEELS
Weldability of maraging steels p 59 N94-10028

MASKING
A novel photosensitive polyimide resist consisting of a soluble polyimide and a bis(perfluorophenyl azide) as a cross-linker
[AD-A265998] p 93 N94-12353

MASKS
RF vacuum microelectronics
[AD-A266066] p 142 N94-10818
A prototype urine collection device for female aircrew p 317 N94-11549

MASS
Quark and lepton masses
[DE93-012308] p 370 N94-12787

MASS DISTRIBUTION
Power-law confusion: You say incremental, I say differential p 347 N94-12175
Mass and spatial distribution of carbonaceous component in Comet Halley p 433 N94-12263
Accuracy and repeatability of the standard automated mass properties measurement system
[AD-A265897] p 316 N94-12346

MASS FLOW
An overview of the capabilities of ARA for the measurement of nozzle discharge and thrust
[ARA-MEMO-378] p 55 N94-12283
Sedimentation rates and particulate fluxes in the slope and deep sea areas off eastern Taiwan p 220 N94-12709

MASS FLOW RATE
Development of a high specific 1.5 to 5 kW thermal arcjet
[NASA-CR-193133] p 47 N94-11354

MASS SPECTRA
Measurement of polycyclic aromatic hydrocarbon (PAHs) in interplanetary dust particles p 431 N94-12167

MASS SPECTROMETERS
Ionization potentials of small carbon clusters
[AD-A264379] p 67 N94-11260
Measurement of polycyclic aromatic hydrocarbon (PAHs) in interplanetary dust particles p 431 N94-12167

MASS SPECTROSCOPY
Progress in zirconium resonance ionization spectroscopy
[DE93-011881] p 76 N94-11075
Tandem mass spectrometric analysis of phosphate esters
[AD-A265483] p 78 N94-12009
Novel mass spectrometric instrument for gaseous and particulate characterization and monitoring
[DE93-014093] p 272 N94-12783

MASS TRANSFER
Heat and mass transfer mechanisms of the polymerization under terrestrial and microgravity conditions p 103 N94-10092
Transport of heat and mass in near-critical fluids p 122 N94-10230
Experimental study of multiple droplet evaporative cooling
[PB93-198463] p 149 N94-10851

MASSIVELY PARALLEL PROCESSORS
Massively parallel multifrontal methods for finite element analysis on MIMD computer systems
[DE93-009838] p 335 N94-10257
A heterogeneous graphics procedure for visualization of massively parallel solutions
[DE93-009628] p 336 N94-11270
Massively parallel hydrodynamics on unstructured grids
[DE93-007325] p 153 N94-11601

MATCHED FILTERS
Further studies using matched filter theory and stochastic simulation for gust loads prediction
[NASA-TM-109010] p 26 N94-11587

MATERIAL ABSORPTION
Hygroscopic absorption to falling films: The effects of the concentration level
[ITN-93-85198] p 148 N94-10391

MATERIAL BALANCE
Disintegrating ice front of Shirase Glacier, East Antarctica p 210 N94-12654

MATERIALS TESTS
Polyimide foam insulation systems: A major weight reduction and improvement in fire resistance of sidewall systems p 17 N94-10769
A polyimide foam for advanced fire resistant aircraft applications p 17 N94-10770
Development and testing of a superconducting link for an IR detector
[NASA-CR-193674] p 170 N94-10948
Lessons learned from the Long Duration Exposure Facility
[AD-A266026] p 44 N94-12394

MATHEMATICAL LOGIC
Finite state machine microarchitecture transformations described with relational algebra
[MEMO-INF-92-63] p 319 N94-10278

MATHEMATICAL MODELS
Constitutive laws for describing the service relevant creep behaviour of metallic materials p 64 N94-10060
Effects of axial and centrifugal forces on the stability of liquid bridges p 102 N94-10083
Liquid bridges and floating zones p 102 N94-10085
Model of convective motion under low gravity p 103 N94-10088
Space and temporal behavior and control of the residual convection in microgravity p 104 N94-10099
Concept and design of ampoule for melt growth of gallium arsenide in first mission of space flyer unit p 107 N94-10115
CdTe crystal growth by THM with a rotating magnetic field p 107 N94-10116
Computational procedures for determining parameters in Ramberg-Osgood elastoplastic model based on modulus and damping versus strain
[DE93-013309] p 185 N94-10306
Topex orbit determination using GPS tracking system p 38 N94-10359
A lattice gas model for enzyme kinetics with alternate interactions
[DE93-613027] p 395 N94-10411
A flexible modelling software for data acquisition
[DE93-612915] p 322 N94-10484
A lattice gas model for enzyme kinetics with next-nearest neighbor interactions
[DE93-613026] p 410 N94-10631
Arcjet space thrusters
[NASA-CR-193191] p 46 N94-10700
System monitoring and diagnosis with qualitative models
[NASA-CR-193812] p 323 N94-10711
Dimensional transition of the space-time at the minimum action near the planck scale
[DE93-754192] p 410 N94-10718
Bringing theory to practice: The reality of interprocessor communication
[DE93-012346] p 336 N94-10738
Applications of a model to predict flame spread over interior finish materials in a compartment p 19 N94-10783
Practical hazard assessment: An approach to the fire safety p 20 N94-10785
Developments needed to expand the role of fire modeling in material fire hazard assessment p 20 N94-10787
Classical gravity coupled to Liouville theory
[DE93-613049] p 275 N94-10798
The Langevin's approach to the statistical theory of bounded plasma
[DE93-617842] p 388 N94-10839
Combustion-induced crack propagation process in a solid-propellant crack cavity p 98 N94-10901
Evaluation of dual flow thrust vectored nozzles with exhaust stream impingement
[NASA-CR-193292] p 150 N94-10912
Studies of the net surface radiative flux from satellite radiances during FIFE
[NASA-CR-193150] p 230 N94-10953
Advances in time-scale algorithms p 334 N94-10988
Synopsis of timing measurement techniques used in telecommunications p 139 N94-10990
An analytic model for calculating pump-induced wavefront distortions in laser slabs
[DE93-011953] p 174 N94-11126
The three-point function as a probe of models for large-scale structure
[NASA-CR-193249] p 425 N94-11153
Comprehensive dynamic analysis of a bladed disk-turborotor-bearing system
[ISBN-0-315-73646-1] p 180 N94-11155
Similarity of the leading contributions to the self-energy and the thermodynamics in two- and three-dimensional Fermi Liquids
[DE93-012673] p 412 N94-11162
A version of superstring with four space-time dimensions
[DE93-608196] p 412 N94-11163
The controlling parameters of the integrated flux of a stellar population p 426 N94-11187
Blading models for TURBAN and CSPAN turbomachine design codes
[NASA-CR-191164] p 15 N94-11203
A comparison between numerically modelled and experimentally measured loss mechanisms in wave rotors
[NASA-TM-106279] p 29 N94-11255
Computational mechanics needs study
[NASA-CR-193712] p 327 N94-11279
Submarine internal waves
[MRL-GD-0049] p 98 N94-11303
Normal modes of the world's oceans: A numerical investigation using Proudman functions
[NASA-TM-104587] p 288 N94-11358
Extended ecosystem signatures with application to Eos synergism requirements
[NASA-CR-193398] p 266 N94-11374
Surface passivation of InP solar cells with InAlAs layers p 49 N94-11389
The impact of vegetation on the atmospheric boundary layer and convective storms p 277 N94-11480
A modeling investigation of thermal and strain induced recovery and nonlinear hardening in potential based viscoplasticity
[NASA-TM-106122] p 188 N94-11482
On non-linear longitudinal stability of an aircraft in a dive in the presence of atmospheric disturbances p 31 N94-11492
Modeling nonlinear aerodynamic loads for aircraft stability and control analysis p 32 N94-11499
Accretion disk viscosity and internal waves in disks p 153 N94-11615
Integral equation methods for mixed boundary problem of fracture mechanics p 188 N94-11617
A C-band wind scatterometer model derived from the data obtained during the ERS-1 calibration/validation campaign p 233 N94-11711
New tests of the equivalence principle using non-metric couplings of electromagnetism and gravitation p 413 N94-11821
A simple model of melt fracture
[AD-A265311] p 92 N94-11862
Effect of species structure and dielectric constant on C-band forest backscatter
[NASA-TM-109219] p 245 N94-11885
The modelling of aerodynamic flows by solution of the Euler equations on mixed polyhedral grids
[ARA-84] p 16 N94-11888
Evaluation of ECMWF latent heat flux in TOGA CD-ROM p 195 N94-11921
Air-sea fluxes and universal constants in weak-turbulence theory of surface gravity waves p 195 N94-11922
The extraction of bottom characteristics and mapping in Kin Bay, Okinawa Main Island, Japan, using LANDSAT-5/TM and SPOT-1/HRV data p 197 N94-11931
The Pacific responses exhibited by an OGCM to various wind fields p 202 N94-11964
Remote sensing for numerical modelling of radiative transfer processes in ocean environment p 204 N94-11973
Rates of fluvio-thermal erosion on Mars p 435 N94-12018
Ejecting basaltic achondrites from Vesta: Hydrodynamical impact models p 429 N94-12036
Power-law confusion: You say incremental, I say differential p 347 N94-12175
Deviations from the straight line: Bumps (and grinds) in the collisionally evolved size distribution of asteroids p 431 N94-12201
Modelling of dispersal and deposition of impact glass spherules from the Cretaceous-Tertiary boundary deposit p 432 N94-12238
Phase transitions and 2D spherical convection in a large icy satellite p 433 N94-12265
A local dynamic model for large eddy simulation p 155 N94-12285

Parameterization of subgrid-scale stress by the velocity gradient tensor p 155 N94-12286

Experiments on near-wall structure of three-dimensional boundary layers p 159 N94-12309

The evolution equation for the flame surface density in turbulent premixed combustion p 81 N94-12316

Study and modeling of finite rate chemistry effects in turbulent non-premixed flames p 81 N94-12317

Why does preferential diffusion strongly affect premixed turbulent combustion? p 81 N94-12319

Analytical models for describing the mechanical behavior of fiber reinforced composites [AD-A265906] p 74 N94-12347

Project of an attitude control system (three axis) of a satellite using the LQG/LTR methodology [INPE-5473-TDI/504] p 44 N94-12356

Ultrasonic wave interaction with advanced complex materials for nondestructive evaluation applications [AD-A265704] p 74 N94-12401

Sampling and position effects in the Electronically Steered Thinned Array Radiometer (ESTAR) [NASA-TM-108998] p 245 N94-12432

Modeling void growth and movement with phase change in thermal energy storage canisters [NASA-TM-106288] p 163 N94-12576

Process modelling for materials preparation experiments [NASA-CR-193556] p 56 N94-12588

Proceedings of the PORSEC 1992 in Okinawa: Conference for Pacific Ocean Environments and Probing, volume 2 [JTN-93-80419] p 207 N94-12635

A numerical study of deep convection at high latitudes p 210 N94-12652

A basic consideration for remote sensing using microwave radars on a satellite p 212 N94-12665

Variability of the mixed layer depth in the North Pacific Ocean as calculated by a 3-D semi-analytical mixed layer remote sensing model p 221 N94-12718

SST assimilation: Eastern Mediterranean case study p 221 N94-12719

Optimum selection of spectral channels in the problem of remote sensing of phytoplankton concentration in ocean water p 223 N94-12726

The thermodynamics of the nonlinear shear flows p 169 N94-12728

Turbulence generation in the Pacific undercurrent by shear p 223 N94-12730

Verification of the atmosphere-ocean radiative transfer parametric models p 225 N94-12738

Convective and dynamic instability in meridional trenches p 225 N94-12739

Optical transfer operator of the atmosphere-ocean system p 225 N94-12742

Trajectory curving in underwater propagation of light p 226 N94-12748

Atmospheric correction for determination of average SST fields based on AVHRR data p 227 N94-12750

Coupled numerical model for altimetric data assimilation and velocity field analysis p 227 N94-12752

Complex (hydrodynamic, satellite) monitoring of dynamic structures in the western Pacific with the aim of forecasting the marine ecosystems behaviour p 227 N94-12753

Mesoscale dynamic structures of the Subarctic Frontal Zone in the Pacific Ocean p 227 N94-12754

Mixing of drifter ensemble by mesoscale currents p 228 N94-12760

Non-image visible polarization remote sensing of the ocean p 229 N94-12762

The 1991 version of the plume impingement computer program. Volume 1: Description [NASA-CR-194192] p 166 N94-12775

VIB2D: Quasi 3-D unsteady viscous flow method for blade flutter calculation [CUED/A-TURBO/TR.129] p 166 N94-12779

MATHEMATICAL PROGRAMMING

A surrogate heuristic for set covering problems [INPE-5462-PRE/1770] p 325 N94-11178

MATHEMATICS

Project TIMS (Teaching Integrated Math/Science) [NASA-CR-194288] p 416 N94-11599

Career Information in the Mathematical Sciences (CIMS) [DE93-013780] p 318 N94-11817

MATRICES (MATHEMATICS)

Vectorizing matrix operations arising from PDE discretization on 9-point stencils [CWI-NM-R9221] p 342 N94-10351

On renormalization group flow in matrix model [DE93-613050] p 409 N94-10413

Symbolic dynamics and description of complexity [DE93-613030] p 418 N94-10485

Operator substitution [MEMO-COSOR-92-51] p 343 N94-10867

Alleviating memory contention in matrix computations on large-scale shared-memory multiprocessors [AD-A265009] p 320 N94-11294

Discrete Kalman filtering equations of second-order form for control-structure interaction simulations [NASA-CR-193723] p 331 N94-11522

Direct solution of the mathematical adjoint equations for an interface current nodal formulation [DE93-009961] p 346 N94-11608

MATRIX MATERIALS

Fatigue-life behavior and matrix fatigue crack spacing in unnotched SCS-6/Timetal 21S metal matrix composites [NASA-CR-191467] p 185 N94-10715

Interface considerations in Al2O3/NiAl composite [NASA-CR-191167] p 66 N94-11202

An analysis of fiber-matrix interface failure stresses for a range of ply stress states [NASA-TM-108999] p 67 N94-11276

Moessbauer spectrometer for mineralogical analysis of the Mars surface: Moessbauer source considerations p 476 N94-12242

Proposed framework for thermomechanical life modeling of metal matrix composites [NASA-TP-3320] p 74 N94-12449

MATRIX METHODS

A lattice gas model for enzyme kinetics with alternate interactions [DE93-613027] p 395 N94-10411

Spin characteristics of ion beams during the motion of electromagnetic elements [DE93-617448] p 364 N94-10848

MATTER (PHYSICS)

A theoretical kinematical study of the gradient of any cosmic scalar field [DE92-644731] p 425 N94-11136

MAXIMUM ENTROPY METHOD

Study of the surface circulation to the North of Bransfield Strait, Antarctica [INPE-5472-TDI/503] p 288 N94-11200

MAXIMUM LIKELIHOOD ESTIMATES

Segmented land use classification of multitemporal ERS-1 SAR data using a majority filter p 245 N94-12472

Per-field filtering and classification of multitemporal ERS-1 SAR imagery p 247 N94-12485

MAXWELL EQUATION

A parallel implementation of particle tracking with space charge effects on an Intel iPSC/860 [DE93-012307] p 335 N94-10340

Stationary spectra in a magnetized current-carrying plasma [DE93-617847] p 386 N94-10397

The heat transfer by radiation between two media [DE93-617820] p 149 N94-10838

MAXWELL FLUIDS

Kinetic approach to long wave length modes in rotating plasmas [DE93-771286] p 388 N94-10807

Stability of viscoelastic flow: Physical and numerical considerations p 31 N94-11493

MEAN FREE PATH

Electron runaway in RF discharges [DE93-771407] p 363 N94-10661

MEASURE AND INTEGRATION

Finite difference schemes for long-time integration [NASA-CR-191471] p 343 N94-10642

MEASURING INSTRUMENTS

Recommendations for future research in hypersonic instrumentation p 4 N94-10433

Pressure and force measurements on models set in hypersonic flows: A review p 5 N94-10435

Velocity measurements in hypersonic flows: A review p 5 N94-10436

Thermal flux measurements in hypersonic flows: A review p 5 N94-10438

Overview of the 1989 Wind Tunnel Calibration Workshop [NASA-TP-3393] p 34 N94-11869

MECHANICAL ENGINEERING

Material removal processes: Engineering mechanics consideration [DE93-010733] p 126 N94-10293

RAMCAD (reliability, availability, and maintainability in computer-aided design) [AD-A265143] p 331 N94-11679

MECHANICAL PROPERTIES

The microstructure and mechanical properties of hot worked FeAl intermetallic alloys p 58 N94-10020

Aluminium-lithium forgings: Properties and potential satellite applications p 58 N94-10021

Weldability of maraging steels p 59 N94-10028

Aluminum-beryllium alloys for aerospace applications p 60 N94-10029

Ceramic matrix composites: High performance materials for space application p 62 N94-10044

LAMINV: A computer code for creating laminates having prescribed properties p 65 N94-10069

Physical properties of injection molded liquid crystal polymers and high temperature engineering polymers [AD-A264912] p 87 N94-10508

Computational simulation of hot composite structures [NASA-TM-106200] p 186 N94-10762

Primaset (tm): A safer material for aircraft interior applications p 18 N94-10772

Fire resistance and mechanical properties for phenolic prepregs p 20 N94-10786

Level 3 material characterization of NARC HRPF, HRHU, HRHF, and HRPU [NASA-CR-192579] p 65 N94-10812

Synthesis and properties of nanophase materials [DE93-011757] p 397 N94-10962

Fibre reinforced polymer matrix composites: Microstructure and mechanical properties [DLR-FB-92-28] p 66 N94-11085

Mechanical interaction between synthetic fiber and cement base matrix in FRC composites [AD-A265310] p 73 N94-11686

Experimental studies of the structure of grain boundaries [DE93-013979] p 402 N94-11700

Fracture behavior of ionomers and ionomeric blends [AD-A265379] p 94 N94-12407

Molecular properties of polymeric materials for space applications [NASA-CR-194370] p 94 N94-12450

MEDICAL PERSONNEL

US-USSR telemedicine consultation spacebridge to Armenia and Ufa p 308 N94-11809

MEDICAL SCIENCE

National Institute of Health Almanac, 1992 [PB93-183556] p 303 N94-10828

Development of bioelastic materials for the prevention of adhesions: Polypenta- and polytetrapeptides [AD-A264851] p 88 N94-10863

The Department of Clinical Investigation, reports control symbol MED-300(R-1) [AD-A264969] p 304 N94-11649

Global considerations for implementation of telemedicine p 305 N94-11792

A telemedicine health care delivery system p 307 N94-11803

MEDICAL SERVICES

International Telemedicine/Disaster Medicine Conference: Papers and Presentations [NASA-NP-207] p 304 N94-11787

Medical informatics and telemedicine: A vision p 305 N94-11788

The Canadian experience: Using telemedicine for the support of medical care at remote sites p 305 N94-11789

Telemedicine and international disaster response: Medical consultation to Armenia and Russia via a telemedicine spacebridge p 305 N94-11790

Use of telescience for biomedical research during space flight p 305 N94-11791

Global considerations for implementation of telemedicine p 305 N94-11792

Tropical medicine: Telecommunications and technology transfer p 305 N94-11793

Clinical aspects of telemedicine p 306 N94-11795

Commercial applications of telemedicine p 306 N94-11798

Space technology in remote health care p 306 N94-11799

The use of communication technology in medicine p 306 N94-11800

The National Disaster Medical System p 307 N94-11801

A telemedicine health care delivery system p 307 N94-11803

Communications infrastructure requirements for telemedicine/telehealth in the context of planning for and responding to natural disasters: Considering the need for shared regional networks p 307 N94-11804

Use of satellite telecommunications for telemedicine p 308 N94-11807

US-USSR telemedicine consultation spacebridge to Armenia and Ufa p 308 N94-11809

The revitalization of health and education in Rural America Act of 1992 p 308 N94-11810

Defense: Health care [AD-A265914] p 421 N94-12445

MEDITERRANEAN SEA

Preliminary results of the comparison of ATSR measurements with in situ sea temperatures [DE93-013399] p 287 N94-10517

The activity of the ERS-1 Venice (Italy) group on scatterometry p 233 N94-11713

SST assimilation: Eastern Mediterranean case study p 221 N94-12719

MELT SPINNING

Comparison of Al-Fe alloys produced by PFC and USGA techniques p 58 N94-10019

MELTING

Marangoni motion during melting of a hypermonotectic alloy: Numerical simulations for the D2 experiment IHF04 p 113 N94-10177

Preliminary results of Mn partitioning experiments on Murchison analogues p 281 N94-12081

Simulation of possible regolith optical alteration effects on carbonaceous chondrite meteorites p 430 N94-12163

Flash melting of chondrule precursors in excess of 1600 C. Series 1: Type 2 (B1) chondrule composition experiments p 431 N94-12177

Primordial lightning: Evidence preserved in chondrites p 432 N94-12230

MELTS (CRYSTAL GROWTH)

Effect of rotation on microgravity floating-zone crystal growth p 101 N94-10080

Coupled thermovibrational and thermocapillary convection in liquid bridge (floating zone system) p 101 N94-10082

On shape of single crystals grown by FZM in microgravity p 102 N94-10084

Liquid bridges and floating zones p 102 N94-10085

Space and temporal behavior and control of the residual convection in microgravity p 104 N94-10099

CdTe crystal growth in the Soviet facility zona 4 p 106 N94-10111

Concept and design of ampoule for melt growth of gallium arsenide in first mission of space flyer unit p 107 N94-10115

CdTe crystal growth by THM with a rotating magnetic field p 107 N94-10116

Proceedings of the 8th European Symposium on Materials and Fluid Sciences in Microgravity, volume 2 [ESA-SP-333-VOL-2] p 112 N94-10171

On the role of Soret effect in concentration distribution in crystals growing from the melt p 112 N94-10173

Solidification from supercooled melt under microgravity p 113 N94-10176

Numerical calculation of the growth of InP by the travelling heater method in the first mission of the Space Flyer Unit p 114 N94-10179

Scientific specifications for an automated facility for growing large semiconducting crystals from the melt in space p 114 N94-10180

TEXUS 28 experiment: Convections and crystal growth of Ge:Ga. Analysis of temperature measurements p 114 N94-10184

Results of crystal growth experiments by FZM on Zona facilities in microgravity p 116 N94-10193

Non-equilibrium solidification in undercooled Ni-B alloys p 86 N94-10196

Conductive-radiative model for predicting the shape of HgI2 crystal grown in the LTVG furnace p 117 N94-10201

THM-growth of III-V-semiconductors in the magnetic field p 118 N94-10209

Crystal growth in the Zone Melting Facility (ZMF) p 119 N94-10213

The stability of hibonite and other aluminous phases in silicate melts: Implications for the origin of hibonite-bearing inclusions p 80 N94-12052

The solubility of gold in silicate melts: First results p 87 N94-12086

Graphite solubility and co-vesiculation in basalt-like melts at one-ATM p 463 N94-12173

Flash melting of chondrule precursors in excess of 1600 C. Series 1: Type 2 (B1) chondrule composition experiments p 431 N94-12177

Process modelling for materials preparation experiments [NASA-CR-193556] p 56 N94-12588

MEMBRANES

Aluminum and membrane channels [AD-A265241] p 300 N94-11020

A theory of membrane absorbers [ISVR-TR-217] p 76 N94-11216

Probability of alamethicin conductance states varies with nonlamellar tendency of bilayer phospholipids [AD-A264957] p 301 N94-11648

MEMORY (COMPUTERS)

Radiation hardened nonvolatile memory for space and strategic applications [DE93-000746] p 319 N94-10146

A proof-of-concept implementation of persistence in a hierarchical storage system [DE93-009959] p 319 N94-10318

Simulation of a parallel computer [NAL-TR-1154] p 335 N94-10368

Low latency messages on distributed memory multiprocessors [NASA-CR-191479] p 323 N94-10643

Flexible language constructs for large parallel programs [NASA-CR-191478] p 326 N94-11196

Alleviating memory contention in matrix computations on large-scale shared-memory multiprocessors [AD-A265009] p 320 N94-11294

Data processing units for eight magnetospheric particle and field sensors [AD-A264403] p 276 N94-11463

Gallium arsenide dynamic random access memory support circuitry [AD-A265176] p 320 N94-11875

MENTAL PERFORMANCE

Psychophysiological measures of cognitive workload in laboratory and flight p 317 N94-11529

Analyzing human errors in flight mission operations p 314 N94-11534

MERCURY CADMIUM TELLURIDES

Process modelling for materials preparation experiments [NASA-CR-193556] p 56 N94-12588

MERCURY COMPOUNDS

Conductive-radiative model for predicting the shape of HgI2 crystal grown in the LTVG furnace p 117 N94-10201

MERIDIONAL FLOW

Numerical simulations of thermal convection in rapidly rotating spherical fluid shells p 153 N94-11635

MEROMORPHIC FUNCTIONS

On a class of two-dimensional nearest neighboring random walks [CWI-BS-R9220] p 347 N94-10353

MERRITT ISLAND (FL)

A study of the Merritt Island, Florida sea breeze flow regimes and their effect on surface heat and moisture fluxes [NASA-CR-4537] p 286 N94-12580

MESON-NUCLEON INTERACTIONS

Strangeness production with protons and pions [DE93-010879] p 359 N94-10304

Crossing-odd spin effects in the dipole model of hadron scattering [DE93-617692] p 362 N94-10551

MESONS

Proceedings of the third workshop on light quark meson spectroscopy [DE93-754138] p 363 N94-10696

Strange meson spectroscopy in K(omega) and K(phi) at 11 GeV/c and Cherenkov ring imaging at SLD [DE93-013593] p 363 N94-10748

MESOSCALE PHENOMENA

On the importance of mesoscale potential vorticity anomalies and topographic forcing during cyclone redevelopment across the Appalachians: A GALE case study p 284 N94-10822

Study of the surface circulation to the North of Bransfield Strait, Antarctica [INPE-5472-TDI/503] p 288 N94-11200

A four-dimensional, mesoscale, non-gaussian multispectral smoke model. Phase 1: Feasibility study [AD-A264805] p 152 N94-11519

Activities relating to understanding the initiation, organization and structure of moist convection in the Southeast environment [NASA-CR-193829] p 285 N94-11598

Ocean circulation revealed by altimeter data p 245 N94-11786

Ocean-ice interaction study of waves and mesoscale features p 197 N94-11935

Comparison of ERS-1 SAR images of the Western Mediterranean to in situ oceanographic data: PRIM-1 Cruise (May 1992) p 255 N94-12529

On a nonstationary dynamics of the north-west Pacific Ocean p 222 N94-12724

Mesoscale dynamic structures of the Subarctic Frontal Zone in the Pacific Ocean p 227 N94-12754

MESOSPHERE

Polar mesospheric waves and structure [AD-A265360] p 279 N94-12561

MESSAGE PROCESSING

Low latency messages on distributed memory multiprocessors [NASA-CR-191479] p 323 N94-10643

Design and analysis of an optical interface message processor [AD-A266079] p 381 N94-10697

The Zipcode message-passing system [DE93-011958] p 336 N94-11027

A formally verified algorithm for interactive consistency under a hybrid fault model [NASA-CR-4527] p 326 N94-11188

Effective software reuse in an embedded realtime system [AD-A264993] p 326 N94-11220

Portable programming on parallel/networked computers using the Application Portable Parallel Library (APPL) [NASA-TM-106238] p 327 N94-11232

The PVM systems: An in-depth analysis and documenting study. Concise edition [DE93-011959] p 336 N94-11248

METABOLISM

Effect of intermittent cold exposure on the fiber-type composition of selected skeletal muscles in rats [AD-A265309] p 301 N94-11861

METAL BONDING

High temperature stability, interface bonding, and mechanical behavior in (beta)-NiAl and Ni3Al matrix composites with reinforcements modified by ion beam enhanced deposition [DE93-013977] p 398 N94-11115

Electronic and total energy properties of ternary and quaternary semiconductor compounds, alloys and superlattices [NASA-CR-192905] p 405 N94-12570

METAL COMBUSTION

Shear flow control of gas jets in liquids [AD-A264673] p 152 N94-11448

Distributed combustion in solid propellants [AD-A265727] p 99 N94-12564

METAL CRYSTALS

Deformation mechanisms in tungsten single crystals in ballistic impact experiments [AD-A265701] p 405 N94-12563

METAL FATIGUE

Fatigue in single crystal nickel superalloys [AD-A266116] p 85 N94-12418

Isothermal fatigue mechanisms in Ti-based metal matrix composites [NASA-CR-191181] p 74 N94-12594

METAL FILMS

Tribological characteristics of sputtered Au/Cr films on alumina substrates at elevated temperatures [NASA-TM-106078] p 55 N94-11362

In situ XANES studies of the passive film on Fe and Fe-26Cr [DE93-010869] p 84 N94-11459

The laser ablation of gold films at the electrode surface of a quartz crystal microbalance [AD-A265535] p 175 N94-12012

METAL FOAMS

PM technology and mechanical properties of metallic foams p 64 N94-10059

METAL FUELS

Shear flow control of gas jets in liquids [AD-A264673] p 152 N94-11448

METAL HALIDES

Chemical Vapor Deposition of Refractory Metals and Ceramics 2. Materials Research Society Symposium proceedings [AD-A265072] p 92 N94-11866

METAL HYDRIDES

X ray and gamma ray spectroscopy of solids under pressure [DE93-014847] p 76 N94-10653

METAL IONS

Photodetachment studies on few-electron atomic negative ions [DE93-008474] p 358 N94-10154

X ray absorption spectroscopy of electrochemically generated species [AD-A264749] p 77 N94-11265

METAL MATRIX COMPOSITES

Hybrid materials for use at elevated temperatures p 57 N94-10013

Mechanical and fatigue properties of fibre reinforced aluminium-lithium alloy and aluminium-lithium MMC based laminates p 58 N94-10022

Mechanical properties of magnesium/carbon composites developed by hot pressing under medium pressure p 59 N94-10024

Design evaluation of GLARE laminate lay-ups p 63 N94-10051

Joints between dissimilar metallic and ceramic materials p 63 N94-10052

Introducing SMaSE: An aide memoire on structural materials and space engineering p 63 N94-10053

Constitutive laws for describing the service relevant creep behaviour of metallic materials p 64 N94-10060

Liquid phase sintering of tungsten composites under microgravity. Effect of matrix composition p 118 N94-10207

A study of the quasibinary Al-W-Mo system. Part 1: Preliminary investigations and preparation for microgravity experiments p 119 N94-10211

A study of the quasibinary Al-Mo-W system. Part 2: A physico-mechanical investigation of the system fabricated under the gravitylessness conditions p 119 N94-10212

Interface reactions of (Ni3Al) ribbons/Al-MMC in ground preparation as preliminary test for microgravity experiments p 123 N94-10237

Fatigue-life behavior and matrix fatigue crack spacing in unnotched SCS-6/Timetal 21S metal matrix composites
[NASA-CR-191467] p 185 N94-10715

Computational simulation of hot composite structures
[NASA-TM-106200] p 186 N94-10762

Tribological characteristics of hot-pressed self-lubricating composites
[NAL-TR-1160] p 66 N94-10858

Micromechanisms of fatigue crack growth and fracture toughness in metal matrix composites
[AD-A265153] p 187 N94-11096

Corrosion behavior of metal matrix composites
[AD-A265352] p 85 N94-12404

Proposed framework for thermomechanical life modeling of metal matrix composites
[NASA-TP-3320] p 74 N94-12449

Isothermal fatigue mechanisms in Ti-based metal matrix composites
[NASA-CR-191181] p 74 N94-12594

METAL OXIDE SEMICONDUCTORS

A study of DC-DC converters with MCTs for arcjet power supplies
[NASA-CR-193457] p 142 N94-10931

METAL PARTICLES

Processing, properties, and wear resistance of aluminides
[DE93-012186] p 83 N94-11141

Effects of microscopic iron metal on the reflectance spectra of glass and minerals p 436 N94-12024

The spectral effects of subsolidus reduction of olivine and pyroxene p 81 N94-12110

Iron and nickel isotopic mass fractionation in deep-sea spherules p 282 N94-12199

The unusual metallic particles in Krymka LL3.0 chondrite p 433 N94-12253

Distributed combustion in solid propellants
[AD-A265727] p 99 N94-12564

METAL PLATES

Advances in low carbon, high strength ferrous alloys
[AD-A265264] p 85 N94-12532

METAL POWDER

The effect of processing on the microstructure and tensile properties of a (gamma)-TiAl based alloy
[DE93-013221] p 84 N94-11488

METAL PROPELLANTS

Shear flow control of gas jets in liquids
[AD-A264673] p 152 N94-11448

METAL SHEETS

Hybrid materials for use at elevated temperatures
p 57 N94-10013

Failure prediction of thin beryllium sheets used in spacecraft structures
[NASA-CR-194164] p 187 N94-11190

METAL SPINNING

Spinforming characteristics of a net shape forming process p 56 N94-10004

Spin-rolling, welding, and heat treatment of aluminium 2219 for Ariane 5 GAM high pressure vessel liners
p 62 N94-10045

METAL SPRAYING

Performance aspects of de Laval spray-forming nozzles
[DE93-013671] p 163 N94-12604

METAL SURFACES

Hydrogen partitioning and transport in titanium aluminides
[NASA-CR-194117] p 76 N94-10713

Application of spin-sensitive electron spectroscopies to investigations of electronic and magnetic properties of solid surfaces and epitaxial systems
[DE93-015079] p 76 N94-10854

Real-space formation and dissipation dynamics of hexagonal reconstruction on Au(100) in aqueous media as explored by potentiodynamic scanning tunneling microscopy
[AD-A266138] p 368 N94-11658

Nonlinear optical spectroscopy of Ag(111) in electrolyte and in vacuum
[AD-A265622] p 79 N94-12534

METAL VAPORS

Design of CCD camera system for use inside electron beam furnace
[DE93-009525] p 170 N94-11267

METAL-GAS SYSTEMS

Atomic structures and compositions of internal interfaces
[DE93-014840] p 363 N94-10750

METALLIC STARS

The controlling parameters of the integrated flux of a stellar population p 426 N94-11187

METALLIZING

Method for producing a hybridization of detector array and integrated circuit for readout
[NASA-CASE-NPO-18062-1-CU] p 141 N94-10656

Effects of solar cell environment on contact integrity
p 49 N94-11387

Chemical Vapor Deposition of Refractory Metals and Ceramics 2. Materials Research Society Symposium proceedings
[AD-A265072] p 92 N94-11866

METALLOGRAPHY

Metallographic cooling rates of L-group ordinary chondrites p 429 N94-12061

METALORGANIC CHEMICAL VAPOR DEPOSITION

High temperature annealing of minority carrier traps in irradiated MOCVD n(+)p InP solar cell junctions
p 48 N94-11382

Investigation of ZnSe-coated silicon substrates for GaAs solar cells p 52 N94-11405

Heteroepitaxial InP, and ultrathin, directly glassed, GaAs 3-5 solar cells p 52 N94-11406

Remote plasma enhanced chemical vapor deposition of GaP with in situ generation of phosphine precursors
p 399 N94-11440

Organometallic chemical vapor deposition and characterization of ZnGeP2/GaP multiple heterostructures on GaP substrates p 400 N94-11442

Organometallic chemical vapor deposition and characterization of ZnGe(1-x)Si(x)P2-Ge alloys on GaP substrates p 400 N94-11443

METALS

Structure of s - p bonded metal clusters with 8, 20 and 40 valence electrons
[DE93-613643] p 361 N94-10503

Monte Carlo simulations of phase transformations in Fe-Cr alloys
[DE93-013847] p 81 N94-10522

A method of influence regions in the theory of vacancy swelling of metals
[DE93-620579] p 83 N94-11363

METAMORPHISM (GEOLOGY)

Shock transformations in quartzite p 97 N94-12040

Mineralogy of chondritic interplanetary dust particle impact residues from LDEF p 80 N94-12045

Petrography and preliminary interpretations of the crystalline breccias from the Manson M-1 core
p 281 N94-12056

Metallographic cooling rates of L-group ordinary chondrites p 429 N94-12061

Chondrite thermal histories from Low-CA pyroxene microstructures: Autometamorphism versus prograde metamorphism revisited p 429 N94-12105

Anomalous REE patterns in unequilibrated enstatite chondrites: Evidence and implications
p 431 N94-12191

The granulite suite: Impact melts and metamorphic breccias of the early lunar crust p 282 N94-12197

Trace element distributions in primitive achondrites
p 431 N94-12200

Isotopic and trace element characteristics of an unusual refractory inclusion from Essebi p 471 N94-12212

METASTABLE STATE

Photodetachment studies on few-electron atomic negative ions
[DE93-008474] p 358 N94-10154

Application of spin-sensitive electron spectroscopies to investigations of electronic and magnetic properties of solid surfaces and epitaxial systems
[DE93-015079] p 76 N94-10854

Non-barrier tunneling in presence of dissipations
[DE93-621381] p 412 N94-11086

Polymeric nitrogen
[DE93-012600] p 89 N94-11151

METEORITE COLLISIONS

Explicit 3D continuum fracture modeling with smooth particle hydrodynamics p 429 N94-12062

Collisions of small Spacewatch asteroids with the Earth p 430 N94-12157

Macroscopic electric charge separation during hypervelocity impacts: Potential implications for planetary paleomagnetism p 431 N94-12181

Modelling of dispersal and deposition of impact glass spherules from the Cretaceous-Tertiary boundary deposit p 432 N94-12238

METEORITE CRATERS

Morphology of large impact craters and basins on Venus: Implications for ring formation p 436 N94-12023

Descriptions and preliminary interpretations of cores recovered from the Manson Impact Structure (Iowa)
p 281 N94-12032

Increased depth-diameter ratios in the Medusae Fossae Formation deposits of Mars p 439 N94-12043

Behavior of vortices generated by an advancing ejecta curtain in theory, in the laboratory, and on Mars
p 169 N94-12044

Strontium and oxygen isotope study of M-1, M-3 and M-4 drill core samples from the Manson impact structure, Iowa: Comparison with Haitian K-T impact glasses
p 281 N94-12080

Si-29 NMR spectroscopy of naturally-shocked quartz from Meteor Crater, Arizona: Correlation to Kieffer's classification scheme p 80 N94-12087

Age of Popigai impact event using the Ar-40 - Ar-39 method p 282 N94-12093

Shock induced reaction in Chicxulub target materials (CaSO4 and SiO2) and their relation to extinctions
p 282 N94-12149

Collisions of small Spacewatch asteroids with the Earth p 430 N94-12157

Microtektite-like glass spherules in Late Devonian (367 MA) shales p 461 N94-12160

KT boundary impact glasses from the Gulf of Mexico region p 282 N94-12161

Post-impact alteration of the Manson impact structure
p 282 N94-12188

Model of optical scatter from microimpacts on the Hubble Telescope p 384 N94-12189

Laboratory studies on the velocity of fragments from impact disruptions p 189 N94-12359

METEORITES

Meteorites from recent amor-type orbits
p 429 N94-12059

Natural thermoluminescence profiles in lunar cores and implications for meteorites p 443 N94-12060

Arroyo el Mimbral, Mexico, K/T unit: Origin as debris flow/turbidite, not a tsunami deposit
p 281 N94-12084

Chondrule formation by clumpy accretion onto the solar nebula p 448 N94-12089

METEORITIC COMPOSITION

Twenty-fourth Lunar and Planetary Science Conference. Part 1: A-F
[NASA-CR-193095] p 435 N94-12015

Moessbauer spectroscopy of the SNC meteorite Zagami p 428 N94-12016

Dispersion of the ratios of cosmogenic isotopes of noble gases in chondrites of different cosmic-ray exposure ages p 428 N94-12020

Peculiarities of distributions of the cosmic-ray exposure ages of H chondrite falls and finds p 428 N94-12021

Search for effects of a supernova explosion 30 to 40 thousand years ago in chondrites p 428 N94-12022

Calorimetric thermometry of meteoritic troilite: A feasibility study p 428 N94-12025

Interstellar graphite in Murchison: Continued search for isotopically distinct components p 97 N94-12029

Fourier domain target transformation analysis in the thermal infrared p 258 N94-12030

Carbon in weathered ordinary chondrites from Roosevelt County p 428 N94-12035

Nitrogen and noble gases in a glass sample from LEW88516 p 80 N94-12051

The stability of hibonite and other aluminous phases in silicate melts: Implications for the origin of hibonite-bearing inclusions p 80 N94-12052

The great 8 MA event and the structure of the H-chondrite parent body p 429 N94-12058

Natural thermoluminescence profiles in lunar cores and implications for meteorites p 443 N94-12060

Composition and modal frequencies of hypervelocity particles less than 1 millimeter in diameter in low-Earth orbit p 429 N94-12063

The asteroid-meteorite connection: Forging a new link to Vesta as the parent body of basaltic achondrite (HED) meteorites p 429 N94-12068

Alkali-granitoids as fragments within the ordinary chondrite Adzhi-Bogdo: Evidence for highly fractionated, alkali-granitic liquids on asteroids p 429 N94-12069

Preliminary results of Mn partitioning experiments on Murchison analogues p 281 N94-12081

Noble gases in LEW88516 shergottite: Evidence for exposure age pairing with ALH77005 p 80 N94-12082

Ar-39 - Ar-40 ages of acapulcoites and lodranites: Evidence for early parent body heating
p 281 N94-12083

Midplane temperatures in the solar nebula
p 448 N94-12088

Chondrule formation by clumpy accretion onto the solar nebula p 448 N94-12089

Minor and trace element composition and age of Yukon probable-microtektites p 429 N94-12094

Trace-element abundances in several new ureilites
p 80 N94-12096

Mineralogy versus bulk composition of the carbonaceous chondrite clast Kaidun 2
p 429 N94-12101

Carbonaceous chondrite clasts in the Kapoeta howardite p 282 N94-12104

SXRF determination of trace elements in chondrule rims in the unequilibrated CO3 chondrite, ALH A77307
p 429 N94-12106

Determining the relative extent of alteration in CM chondrites p 430 N94-12114

The EET87513 clast N: A CM2 fragment in an HED polymict breccia p 453 N94-12117

Volatiles in fourteen interplanetary dust particles: A comparison with CI and CM chondrites p 430 N94-12132

Distribution of vanadium and melting of opaque assemblages in Efremovka CAI's p 282 N94-12141

Metal-rich meteorites from the aubrite parent body p 430 N94-12142

Oxygen isotopes as tracers of tektite source rocks: An example from the Ivory Coast tektites and Lake Bosumtwi Crater p 430 N94-12146

LEW88516 and SNC meteorites p 430 N94-12150

The Th and U abundances in chondritic meteorites p 430 N94-12151

Microtektite-like glass spherules in Late Devonian (367 MA) shales p 461 N94-12160

KT boundary impact glasses from the Gulf of Mexico region p 282 N94-12161

Simulation of possible regolith optical alteration effects on carbonaceous chondrite meteorites p 430 N94-12163

Spectral mixing models of S-Type asteroids p 431 N94-12164

Olivine-rich asteroids, pallasitic olivine and olivine-metal mixtures: Comparisons of reflectance spectra p 431 N94-12171

Remanent magnetism of HED meteorites: Implications for their evolution and ancient magnetic fields p 431 N94-12172

The experimental production of matrix lumps within chondrules: Evidence of post-formational processes p 431 N94-12176

Flash melting of chondrule precursors in excess of 1600 C. Series 1: Type 2 (B1) chondrule composition experiments p 431 N94-12177

Trace element distributions in primitive achondrites p 431 N94-12200

Cathodoluminescence properties of components in enstatite chondrites p 432 N94-12206

The Fe/Mn constraint on precursors of basaltic achondrites p 432 N94-12208

Soret diffusion: A possible cause of compositional heterogeneity within tektites p 432 N94-12211

Isotopic and trace element characteristics of an unusual refractory inclusion from Essebi p 471 N94-12212

On high-temperature formation of iron-rich olivine in the early solar system p 432 N94-12225

Recondensation of chondritic material in the early solar system: Results of thermodynamic simulation p 432 N94-12226

Primordial lightning: Evidence preserved in chondrites p 432 N94-12230

Micro-zoning in minerals of a Landes silicate inclusion p 432 N94-12231

A new carbon-rich phase (COPS) in Antarctic micrometeorites p 432 N94-12233

The Xe-Q in lodranites and a hint for Xe-L. FRO90011 another lodranite? p 432 N94-12239

Projectile-target mixing in melted ejecta formed during a hypervelocity impact cratering event p 432 N94-12241

The unusual metallic particles in Krymka LL3.0 chondrite p 433 N94-12253

On possibility of diamond formations in radiation process p 433 N94-12254

The carbon isotopic composition of Novo Urei diamonds p 433 N94-12255

The fractionation of noble gases in diamonds of CV3 Efremovka chondrite p 81 N94-12256

Cronstedtite and iron sulfide mineralogy of CM-type carbonaceous chondrites from cryogenic Moessbauer spectra p 433 N94-12257

Primitive SNC parent magmas and crystallization: Low PH2O experiments p 433 N94-12264

METEORITIC DAMAGE

Post-impact alteration of the Manson impact structure p 282 N94-12188

Laboratory studies on the velocity of fragments from impact disruptions p 189 N94-12359

METEORITIC DIAMONDS

On possibility of diamond formations in radiation process p 433 N94-12254

The carbon isotopic composition of Novo Urei diamonds p 433 N94-12255

The fractionation of noble gases in diamonds of CV3 Efremovka chondrite p 81 N94-12256

METEORITIC MICROSTRUCTURES

Metallographic cooling rates of L-group ordinary chondrites p 429 N94-12061

Microtektite-like glass spherules in Late Devonian (367 MA) shales p 461 N94-12160

METEOROID CONCENTRATION

A CM chondrite cluster and CM streams p 432 N94-12215

METEOROID SHOWERS

Meteorites from recent amor-type orbits p 429 N94-12059

METEOROIDS

The magnitude of impact damage on LDEF materials [NASA-CR-188258] p 43 N94-10666

Meteorites from recent amor-type orbits p 429 N94-12059

A CM chondrite cluster and CM streams p 432 N94-12215

METEOROLOGICAL CHARTS

Use of ERS-1 scatterometer winds in Canadian forecast centres p 250 N94-12504

METEOROLOGICAL INSTRUMENTS

The subduction experiment. Cruise report, R/V Oceanus, cruise number 250 legs 1 and 2. Subduction 2 mooring deployment and recovery cruise, 25 January-26 February 1992 [AD-A264922] p 289 N94-11853

METEOROLOGICAL PARAMETERS

Database blending for the climatology of cloud statistics program [AD-A265034] p 283 N94-10336

Parametric analysis of atmospheric processes [NASA-CR-192523] p 347 N94-10757

The Air Force Interactive Meteorological System: A research tool for satellite meteorology [AD-A265957] p 284 N94-11113

TOVS soundings: Impact on the synoptic analysis over the south and southeast regions of Brazil from March 18 to March 19, 1991 [INPE-5497-TDI/512] p 230 N94-11179

Global monitoring of atmospheric properties by the EOS MODIS [NASA-TM-109237] p 231 N94-11485

Development of a graphical user interface and graphics display for the WIND system [DE93-011780] p 285 N94-11614

Characteristic scales and vortex features of mesoscale vortices observed by the satellites during the winter p 199 N94-11943

Scatterometer observations: Review p 201 N94-11956

An atmospheric boundary layer stability estimator for urban areas [AD-A265189] p 279 N94-12422

A study of the Merritt Island, Florida sea breeze flow regimes and their effect on surface heat and moisture fluxes [NASA-CR-4537] p 286 N94-12580

An integrated approach to total end-to-end quality control of ocean data in the real-time environment p 211 N94-12662

Worldwide map of rainfall amount over the ocean derived from passive microwave radiometer p 211 N94-12663

METEOROLOGICAL RADAR

Impact of shutting down en route primary radars within CONUS interior [DOT-VNTSC-FAA-93-1] p 23 N94-11626

Rainfall-runoff estimation using digital radar [AD-A265390] p 286 N94-12408

METEOROLOGICAL SATELLITES

Database blending for the climatology of cloud statistics program [AD-A265034] p 283 N94-10336

Meteorological Satellite Center [MSC-TN-26] p 190 N94-11079

Simulation of images of water vapor channel and infrared split channel p 190 N94-11081

Statistical study on the regional and seasonal distribution of fog in the far east region by using GMS imagery p 190 N94-11082

Overview of training seminar for the use of Japanese Earth Resources Satellite-1 (JERS-1) data p 190 N94-11083

METEOROLOGICAL SERVICES

Development of a graphical user interface and graphics display for the WIND system [DE93-011780] p 285 N94-11614

METEOROLOGICAL SOLENOIDS

Characteristic scales and vortex features of mesoscale vortices observed by the satellites during the winter p 199 N94-11943

METEOROLOGY

Preliminary results of the comparison of ATSR measurements with in situ sea temperatures [DE93-013399] p 287 N94-10517

Environmental Sciences Division [DE93-013865] p 264 N94-10650

The Air Force Interactive Meteorological System: A research tool for satellite meteorology [AD-A265957] p 284 N94-11113

An overview of intertropical convergence and intertropical discontinuity [DE93-619229] p 277 N94-11603

Development of a graphical user interface and graphics display for the WIND system [DE93-011780] p 285 N94-11614

Effects of satellite spectral resolution and atmospheric water vapor on retrieval of near-ground temperatures [AD-A264920] p 245 N94-11851

The subduction experiment. Cruise report, R/V Oceanus, cruise number 250 legs 1 and 2. Subduction 2 mooring deployment and recovery cruise, 25 January-26 February 1992 [AD-A264922] p 289 N94-11853

METHANE

Influence of neutral particles concentration on flame propagation in methane-air mixtures at zero and normal gravity conditions p 121 N94-10224

Conversion of acetic acid to methane by thermophiles [DE93-014433] p 300 N94-10652

Solid-state structures of guanidinium methane, ethane, and trifluoromethanesulfonate [AD-A265293] p 402 N94-11654

METHOD OF MOMENTS

Design of a continuous resistively loaded monopole antenna [AD-A265852] p 138 N94-12281

METHYL ALCOHOL

Methanol pan fires in an enclosed space: Effect of pressure and oxygen concentration [AD-A266108] p 79 N94-12415

Solvent dynamical effects in electron transfer: Molecular dynamics simulations of reactions in methanol [AD-A266061] p 369 N94-12420

METHYL COMPOUNDS

Vibrational overtone activation of methylcyclopropene [AD-A265588] p 79 N94-12373

METHYLATION

Studies in bioorganic chemistry [AD-A265532] p 55 N94-12011

METHYLENE

Vibrational overtone activation of methylcyclopropene [AD-A265588] p 79 N94-12373

METRIC SPACE

S(sup 1) x S(sup 2) as a bag membrane and its Einstein-Weyl geometry [DE93-613149] p 410 N94-10635

New tests of the equivalence principle using non-metric couplings of electromagnetism and gravitation p 413 N94-11821

METRICATION

The MERMAID project p 329 N94-11426

METROLOGY

Needs for super-smooth surfaces [DE93-012482] p 382 N94-11242

MICHELSON INTERFEROMETERS

Study of Einstein-Podolsky-Rosen state for space-time variables in a two photon interference experiment p 370 N94-10582

Localized and distributed fiber-optic strain sensors embedded in composite materials [UTIAS-346] p 73 N94-12013

MICROANALYSIS

Microanalysis of directionally solidified cobalt oxide-zirconia eutectic [DE93-013207] p 88 N94-10527

MICROBALANCES

The laser ablation of gold films at the electrode surface of a quartz crystal microbalance [AD-A265535] p 175 N94-12012

A novel test method for fuel thermal stability [AD-A265853] p 99 N94-12275

MICROCHANNELS

Liquid Cooled Heat Sink with through Vias (LCHS) [AD-A266008] p 73 N94-12344

MICROCOMPUTERS

Controller of serial multiplex communication channel [DE92-641157] p 336 N94-10544

MICROCRACKS

Micromechanisms of fatigue crack growth and fracture toughness in metal matrix composites [AD-A265153] p 187 N94-11096

Fatigue in single crystal nickel superalloys [AD-A266116] p 85 N94-12418

MICROCRYSTALS

HRTEM in protein crystallography [DE93-610322] p 395 N94-10406

MICROELECTRONICS

RF vacuum microelectronics [AD-A266066] p 142 N94-10818

Applications of spectroscopic ellipsometry to microelectronics [AD-A265148] p 143 N94-11159

Resist materials design: Base-catalyzed chemical amplification [AD-A265286] p 145 N94-11819

Statistical process control in the hybrid microelectronics manufacturing industry: A Navy view point
[AD-A265164] p 145 N94-11884

Polymers for microelectronics
[AD-A266036] p 94 N94-12396

Multicomponent and multilayered thin films for advanced microtechnologies: Techniques, fundamentals, and devices
[AD-A265685] p 405 N94-12442

MICROGRAVITY

Project ARGO: Gas phase formation in simulated microgravity
[NASA-TM-104762] p 125 N94-11235

Reduced gravity multibody dynamics testing
[NASA-CR-192589] p 125 N94-11483

SWIRL as a means of liquid management in low gravity
[NASA-CR-4545] p 412 N94-11523

Five biomedical experiments flown in an Earth orbiting laboratory: Lessons learned from developing these experiments on the first international microgravity mission from concept to landing p 302 N94-11556

Microgravity vibration isolation technology: Development to demonstration
[NASA-TM-106320] p 1 N94-11703

An application of reduced gravity model to mesoscale eddies p 199 N94-11945

Echocardiography in the flight program
p 309 N94-11993

Space truss zero gravity dynamics
[AD-A266130] p 44 N94-12541

The Third Workshop on Two Phase Fluid Experiment in the Space Environment
[NASDA-CON-930002] p 161 N94-12547

Research on two phase flow in microgravity
p 162 N94-12554

Modeling void growth and movement with phase change in thermal energy storage canisters
[NASA-TM-106288] p 163 N94-12576

MICROGRAVITY APPLICATIONS

Protein, glass, aerosol research, containerless processing and diagnostics technology for microgravity application p 106 N94-10112

Design of a CVD reactor for the deposition of diamond in a microgravity environment p 109 N94-10127

Force and power efficiency of micro-g electromagnetic levitation coils p 110 N94-10129

Determination of the viscous acoustic field for liquid drop positioning/forcing in an acoustic levitation chamber in microgravity p 110 N94-10131

The surface plasmon spectroscopy as diagnostic technique in microgravity experiments
p 110 N94-10133

Microgravity experiments using TR-1A rocket
p 112 N94-10142

Thermocapillary convection instability in microgravity crystal growth p 112 N94-10172

Solidification in immiscible systems: The influence of processing conditions on resulting microstructures
p 112 N94-10174

Scientific specifications for an automated facility for growing large semiconducting crystals from the melt in space p 114 N94-10180

Crystal growth from low temperature vapour phase
p 115 N94-10191

MICROHARDNESS

DBTT measurement by use of Small Punch (SP) test
[DE93-753188] p 183 N94-11168

MICROMECHANICS

Sensor abstractions to support many-robot systems
[AD-A265907] p 180 N94-10803

Micromechanisms of fatigue crack growth and fracture toughness in metal matrix composites
[AD-A265153] p 187 N94-11096

An analysis of fiber-matrix interface failure stresses for a range of ply stress states
[NASA-TM-106999] p 67 N94-11276

Mechanical interaction between synthetic fiber and cement base matrix in FRC composites
[AD-A265310] p 73 N94-11686

Analytical models for describing the mechanical behavior of fiber reinforced composites
[AD-A265906] p 74 N94-12347

Properties of interfacial tribo-films
[AD-A265591] p 182 N94-12374

MICROMETEORITES

K/T spherules from Haiti and Wyoming: Origin, diagenesis, and similarity to some microtektites
p 281 N94-12065

A new carbon-rich phase (COPS) in Antarctic micrometeorites p 432 N94-12233

MICROMETEOROIDS

Dimensional scaling for impact cratering and perforation
[NASA-CR-188259] p 42 N94-10665

Composition and modal frequencies of hypervelocity particles less than 1 millimeter in diameter in low-Earth orbit p 429 N94-12063

Modelling hypervelocity impacts into aluminum structures based on LDEF data p 190 N94-12178

Model of optical scatter from microimpacts on the Hubble Telescope p 384 N94-12189

MICROORGANISMS

Spacelab J air filter debris analysis
[NASA-CR-192569] p 301 N94-11201

The role of certain infauna and vascular plants in the mediation of redox reactions in marine sediments
p 268 N94-12454

MICROPROCESSORS

User's manual for the DAD-1 data acquisition daughter board for the SuperCard-2
[DE93-012153] p 325 N94-11139

Data processing units for eight magnetospheric particle and field sensors
[AD-A264403] p 276 N94-11463

MICROSCOPES

Interferometric and optical tests of water window imaging x ray microscopes
[NASA-CR-193369] p 375 N94-10506

MICROSCOPY

Ballistic electron transport studies using BEEM
[AD-A266029] p 369 N94-12395

MICROSTRIP DEVICES

Development of microstrip gas chamber and application to imaging gamma-ray detector
[DE93-754294] p 34 N94-11041

MICROSTRUCTURE

The microstructure and mechanical properties of hot worked FeAl intermetallic alloys p 58 N94-10020

Structure and properties of an RS Al-Si-Ni-Mn-Zr alloy for high temperature applications p 64 N94-10063

Solidification in immiscible systems: The influence of processing conditions on resulting microstructures
p 112 N94-10174

TEM study of a space processed Al-Al2O3 metallic composite p 75 N94-10186

Pulsatile instability in rapid directional solidification: Strongly-nonlinear analysis p 115 N94-10188

Solidification of undercooled Ni-32.5 wt percent Sn eutectic alloy p 86 N94-10194

Undercooled W-Re and Mo-Re drops in an ultra high vacuum drop tube p 86 N94-10195

Microanalysis of directionally solidified cobalt oxide-zirconia eutectic
[DE93-013207] p 88 N94-10527

Preparation of carbon monoliths having tailored pore structure from porous polymer precursors
[DE93-011576] p 89 N94-10958

Synthesis and properties of nanophase materials
[DE93-011757] p 397 N94-10962

Microstructure and associated properties of YB2Cu3O(x) superconductors prepared by melt processing techniques
[DE93-010675] p 398 N94-11004

Damping measurements for ultra-high carbon steel/brass laminates
[DE93-011886] p 82 N94-11076

Fibre reinforced polymer matrix composites: Microstructure and mechanical properties
[DLR-FB-92-28] p 66 N94-11085

Damping mechanisms in chemically vapor deposited SiC fibers
[NASA-TM-106334] p 66 N94-11135

Structural development in ceramic precursor sols and gels
[AD-A264354] p 90 N94-11281

High-temperature corrosion of ceramic-ceramic composites in a waste incinerator environment
[DE93-012430] p 72 N94-11368

Organometallic chemical vapor deposition and characterization of ZnGe(1-x)Si(x)P2-Ge alloys on GaP substrates p 400 N94-11443

The effect of processing on the microstructure and tensile properties of a (gamma)-TiAl based alloy
[DE93-013221] p 84 N94-11488

Mechanical interaction between synthetic fiber and cement base matrix in FRC composites
[AD-A265310] p 73 N94-11686

Processing and properties of coated HPZ fiber reinforced glass-ceramic matrix composites
[AD-A265177] p 92 N94-11876

Chondrite thermal histories from Low-CA pyroxene microstructures: Autometamorphism versus prograde metamorphism revisited p 429 N94-12105

Fracture behavior of ionomers and ionomeric blends
[AD-A265379] p 94 N94-12407

Microstructure-based fatigue life prediction methods for naval steel structures
[AD-A265429] p 85 N94-12426

Multicomponent and multilayered thin films for advanced microtechnologies: Techniques, fundamentals, and devices
[AD-A265685] p 405 N94-12442

Deformation mechanisms in tungsten single crystals in ballistic impact experiments
[AD-A265701] p 405 N94-12563

MICROWAVE AMPLIFIERS

Wide band 140 GHz TWTA p 132 N94-10514

Nonlinear analysis of a magnicon output cavity
[AD-A265342] p 145 N94-12424

MICROWAVE ATTENUATION

A basic consideration for remote sensing using microwave radars on a satellite p 212 N94-12665

MICROWAVE CIRCUITS

Three-cavity circuit studies of the Maryland gyroklystron
[DE93-010173] p 145 N94-11645

Limited bandwidth microwave filter
[AD-D015744] p 145 N94-12322

Low cost high efficiency GaAs monolithic RF module for SARSAT distress beacons
[NASA-CR-194235] p 146 N94-12773

MICROWAVE EQUIPMENT

Microwave multiplexer with channels of varying fractional bandwidths
[AD-D015754] p 140 N94-10389

MICROWAVE FILTERS

Limited bandwidth microwave filter
[AD-D015744] p 145 N94-12322

MICROWAVE IMAGERY

Summer Arctic ice concentrations and characteristics from SAR and SSM/I data p 241 N94-11762

Ocean wave detection by SAR p 197 N94-11932

On the determination of the SAR ocean surface scattering patch size p 197 N94-11933

Measurements of ocean cross-section with a side-looking airborne radar p 201 N94-11954

SSMI wind speed variability over the Pacific Ocean
p 207 N94-12637

Microwave radiometry of ice cover in polar regions
p 210 N94-12655

MICROWAVE OSCILLATORS

Dielectric resonator
[US-PATENT-4,580,116] p 141 N94-10668

MICROWAVE POWER BEAMING

Construction and testing of a space ready rectenna
[NASA-CR-193310] p 137 N94-11357

MICROWAVE RADIOMETERS

Investigation of passive atmospheric sounding using millimeter and submillimeter wavelength channels
[NASA-CR-193627] p 274 N94-10726

Physical processes of microwave backscattering from laboratory wind-wave surfaces p 200 N94-11952

Dependence of oceanic microwave emission on wind direction p 201 N94-11957

On the variability of wind speeds in the North Western Pacific observed by altimeter/GEOSAT and SSM/I/DMSP p 201 N94-11960

Sampling and position effects in the Electronically Steered Thinned Array Radiometer (ESTAR)
[NASA-TM-108998] p 245 N94-12432

Validation of the ATSR/M microwave radiometer data
p 252 N94-12511

SSMI wind speed variability over the Pacific Ocean
p 207 N94-12637

Microwave radiometry of ice cover in polar regions
p 210 N94-12655

Worldwide map of rainfall amount over the ocean derived from passive microwave radiometer p 211 N94-12663

MICROWAVE RESONANCE

Applications of in-situ ellipsometry to microwave electron cyclotron resonance plasma processes
[AD-A265197] p 373 N94-11880

MICROWAVE SCATTERING

ERS-1 studies at the Department of Oceanography from Space, IFREMER/Brest (France) p 233 N94-11712

The activity of the ERS-1 Venice (Italy) group on scatterometry p 233 N94-11713

A preliminary C-band scatterometer model function for the ERS-1 AMI instrument p 233 N94-11715

On the determination of the SAR ocean surface scattering patch size p 197 N94-11933

Experiment and results of the Italian activity in the field of ocean microwave backscattering p 200 N94-11953

Scatterometer observations: Review
p 201 N94-11956

The microwave backscattering from wind waves
p 201 N94-11959

A basic consideration for remote sensing using microwave radars on a satellite p 212 N94-12665

MICROWAVE SIGNATURES

Arctic sea ice microwave signature and geophysical processes study p 240 N94-11754

MICROWAVE SOUNDING
Submillimeter wave observation experiment of Earth atmosphere with SIS mixer p 130 N94-11837
MICROWAVE SPECTRA
Validation of directional wave spectra from the ERS-1 during the ESA CAL/VAL campaign p 232 N94-11707
The Grand Banks ERS-1 SAR wave spectra validation experiment p 232 N94-11708
MICROWAVE TRANSMISSION
Construction and testing of a space ready rectenna [NASA-CR-193310] p 137 N94-11357
One-dimensional calculation of high-power microwave pulse compression by the earth's ionosphere [DE93-009517] p 137 N94-11466
MICROWAVES
Single-electron tunneling [DE93-013337] p 396 N94-10648
The possibility of using carbon-graphite materials for microwave plasma diagnostics in large fusion devices [DE93-621609] p 66 N94-11143
Characteristics of ICR-produced peripheral plasma in the Uragan-3M torsatron [DE93-621666] p 392 N94-11214
The excitation of cyanogen and ionized carbon in interstellar and extragalactic gas clouds p 426 N94-11582
Search for structures in the cosmic microwave background radiation [INPE-5491-TDI/508] p 484 N94-12357
MIE SCATTERING
Model of optical scatter from microimpacts on the Hubble Telescope p 384 N94-12189
Light scattering from a spherical particle on a conducting plane. Part 1: Normal incidence [AD-A265920] p 383 N94-12341
MIGRATION
Warm streamers extended from Warm Core Rings (WCRs) and their role on fish migration and fishing ground formation p 198 N94-11938
MILITARY AIRCRAFT
Thermal stability of sealants for military aircraft: Modification of polysulfide prepolymers with ether and thioether monomers [AD-A264079] p 89 N94-11107
MILITARY OPERATIONS
Assessing the adequacy of the industrial base [AD-A264954] p 417 N94-11856
Improved Many-On-Many ROUTE software description [DE93-013961] p 334 N94-12608
MILITARY PSYCHOLOGY
The 27th International Applied Military Psychology Symposium: A Focus on Decision Making Research [AD-A265278] p 313 N94-11701
MILITARY SPACECRAFT
Fuzzification of ASAT's rule based aimpoint selection [AD-A266068] p 43 N94-11223
MILITARY TECHNOLOGY
Assured Mission Support Space Architecture (AMSSA) study p 348 N94-11573
MILLIMETER WAVES
Investigation of passive atmospheric sounding using millimeter and submillimeter wavelength channels [NASA-CR-193627] p 274 N94-10726
MILLING
Titanium alloys milling assistance by high pressure lubricoolant jet [DE93-013302] p 82 N94-11008
MIMD (COMPUTERS)
Massively parallel multifrontal methods for finite element analysis on MIMD computer systems [DE93-009838] p 335 N94-10257
Layering techniques for development of parallel systems: An algebraic approach [MEMO-INF-92-62] p 335 N94-10277
A parallel implementation of particle tracking with space charge effects on an Intel iPSC/860 [DE93-012307] p 335 N94-10340
Flexible language constructs for large parallel programs [NASA-CR-191478] p 326 N94-11196
Portable programming on parallel/networked computers using the Application Portable Parallel Library (APPL) [NASA-TM-106238] p 327 N94-11232
A heterogeneous graphics procedure for visualization of massively parallel solutions [DE93-009628] p 336 N94-11270
Parallel molecular dynamics with the embedded atom method [DE93-010683] p 367 N94-11455
MIMO (CONTROL SYSTEMS)
Utilizing quantitative feedback theory design technique for flight control system p 32 N94-11501
MINERAL DEPOSITS
Twenty-fourth Lunar and Planetary Science Conference. Part 1: A-F [NASA-CR-193095] p 435 N94-12015
Increased depth-diameter ratios in the Medusae Fossae Formation deposits of Mars p 439 N94-12043
Petrography and preliminary interpretations of the crystalline breccias from the Manson M-1 core p 281 N94-12056
MINERAL EXPLORATION
Terrestrial case studies of ilmenite exploration and lunar implications p 478 N94-12247
MINERALOGY
Twenty-fourth Lunar and Planetary Science Conference. Part 1: A-F [NASA-CR-193095] p 435 N94-12015
Moessbauer spectroscopy of the SNC meteorite Zagami p 428 N94-12016
Carbon in weathered ordinary chondrites from Roosevelt County p 428 N94-12035
Mineralogy of chondritic interplanetary dust particle impact residues from LDEF p 80 N94-12045
Nitrogen and noble gases in a glass sample from LEW88516 p 80 N94-12051
Changes in Hawaiian palagonite FE mineralogy associated with thermal alteration: Implications for Mars p 281 N94-12055
Alkali-granitoids as fragments within the ordinary chondrite Adzhi-Bogdo: Evidence for highly fractionated, alkali-granitic liquids on asteroids p 429 N94-12069
Spectral and multispectral imaging studies of lunar mantled mare deposits p 446 N94-12079
Impact mineralogy and chemistry of the cretaceous-tertiary boundary at DSDP site 576 p 282 N94-12091
Mineralogy versus bulk composition of the carbonaceous chondrite clast Kaidun 2 p 429 N94-12101
Carbonaceous chondrite clasts in the Kapoeta howardite p 282 N94-12104
The EET87513 clast N: A CM2 fragment in an HED polymict breccia p 453 N94-12117
Venus mountain-top mineralogy: Misconceptions about pyrite as the high radar-reflecting phase p 455 N94-12129
LEW88516 and SNC meteorites p 430 N94-12150
First results of the seven-color asteroid survey p 430 N94-12162
Simulation of possible regolith optical alteration effects on carbonaceous chondrite meteorites p 430 N94-12163
Crystal-chemistry and partitioning of REE in whitlockite p 408 N94-12174
Post-impact alteration of the Manson impact structure p 282 N94-12188
The correlation of alkalis and aluminum during high-temperature volatilization of albite and nepheline p 81 N94-12214
Micro-zoning in minerals of a Landes silicate inclusion p 432 N94-12231
The Xe-Q in Iodranites and a hint for Xe-L. FRO90011 another Iodranite? p 432 N94-12239
Moessbauer spectrometer for mineralogical analysis of the Mars surface: Moessbauer source considerations p 476 N94-12242
Measuring and distinguishing compositional and maturity properties of lunar soils by remote VIS-NIR spectroscopy p 478 N94-12251
Cronstedtite and iron sulfide mineralogy of CM-type carbonaceous chondrites from cryogenic Moessbauer spectra p 433 N94-12257
MINERALS
Distribution of mineral aerosols over the North Pacific p 204 N94-11976
Effects of microscopic iron metal on the reflectance spectra of glass and minerals p 436 N94-12024
Fourier domain target transformation analysis in the thermal infrared p 258 N94-12030
Petrography and preliminary interpretations of the crystalline breccias from the Manson M-1 core p 281 N94-12056
Using high spectral resolution spectrophotometry to study broad mineral absorption features on Mars p 446 N94-12077
Near-infrared spectra of the Martian surface: Reading between the lines p 465 N94-12184
Trace element distributions in primitive achondrites p 431 N94-12200
Primitive SNC parent magmas and crystallization: Low PH2O experiments p 433 N94-12264
MINIATURIZATION
Design and development of a miniature column-based interface (MCBI) stress gage [AD-A266054] p 170 N94-10873
MINKOWSKI SPACE
On local frame fields and fermion dynamics in space with nontrivial topologies [DE93-617657] p 349 N94-10548
Non-Euclidean space for local hidden variables [DE93-621341] p 344 N94-11032
Green-Schwarz superstrings in the generalized harmonical Newmann-Penrose formalism [DE93-621422] p 412 N94-11088
MINNESOTA
Satellite inventory of Minnesota forest resources [NASA-CR-193565] p 231 N94-11521
MINORITIES
Flight Dynamics Directorate (FDD) Historically Black Colleges and Universities (HBCU's) database managment system: A user's guide [AD-A264947] p 419 N94-11288
A summer program in mathematics and computer science for academically oriented student [AD-A263467] p 415 N94-11517
Pattern of federal procurement from minority and women-owned small business [PB93-189355] p 417 N94-11844
MINORITY CARRIERS
High temperature annealing of minority carrier traps in irradiated MOCVD n(+)p InP solar cell junctions p 48 N94-11382
Measurement of the minority carrier diffusion length and edge surface-recombination velocity in InP p 49 N94-11388
Surface passivation of InP solar cells with InAlAs layers p 49 N94-11389
Investigation of ZnSe-coated silicon substrates for GaAs solar cells p 52 N94-11405
MIRROR FUSION
Applying design principles to fusion reactor configurations for propulsion in space [NASA-TM-108247] p 47 N94-11053
MIRRORS
Zerodur polishing process for high surface quality and high efficiency [DE93-012596] p 87 N94-10271
Spin characteristics of ion beams during the motion of electromagnetic elements [DE93-617448] p 364 N94-10848
Damage thresholds of fluoride multilayers at 355 nm [DE93-009523] p 90 N94-11230
Needs for super-smooth surfaces [DE93-012482] p 382 N94-11242
Model of optical scatter from microimpacts on the Hubble Telescope p 384 N94-12189
Light scattering from a spherical particle on a conducting plane. Part 1: Normal incidence [AD-A265920] p 383 N94-12341
Comparison of multiresolution techniques for digital signal processing [AD-A265364] p 138 N94-12406
MIS (SEMICONDUCTORS)
Squeezed states of electrons and transitions of the density of states p 370 N94-10593
MISSILE DETECTION
Estimation with multisensor/multiscan detection fusion [AD-A265673] p 138 N94-12338
MISSILE TRACKING
Ultraviolet plume instrument description and plume data reduction methodology [AD-A266141] p 54 N94-11643
MISSION PLANNING
Results of mission preparation support to microgravity experiments on board of Eureca 1 p 111 N94-10138
Mission support for crystal growth experiments in Russian unmanned carriers p 111 N94-10139
Numerical calculation of the growth of InP by the travelling heater method in the first mission of the Space Flyer Unit p 114 N94-10179
Aerodynamic and aerothermal challenges for the design of the Hermes spaceplane p 3 N94-10423
An analysis of the modes and states for generic avionics [NASA-CR-188253] p 27 N94-10664
Parametric analysis of atmospheric processes [NASA-CR-192523] p 347 N94-10757
Lunar-Ultraviolet Telescope Experiment (LUTE) integrated program plan [NASA-CR-193267] p 424 N94-11356
Five biomedical experiments flown in an Earth orbiting laboratory: Lessons learned from developing these experiments on the first international microgravity mission from concept to landing p 302 N94-11556
Operational radiological support for the US manned space program p 318 N94-11561
On-orbit refueling p 38 N94-11565
The rational behavior model: A multi-paradigm, tri-level software architecture for the control of autonomous vehicles [AD-A265175] p 332 N94-11874
The requirement for global training programmes to meet the new remote sensing technology p 196 N94-11929
Conceptual studies report on lunar and planetary exploration [NASDA-TK-SS0438] p 481 N94-12323

Significance and scenarios of lunar and planetary exploration missions p 482 N94-12324
Unmanned lunar exploration mission
p 482 N94-12325
Manned lunar exploration missions
p 482 N94-12326
Mars exploration missions p 482 N94-12327
The Third Workshop on Two Phase Fluid Experiment in the Space Environment
[NASDA-CON-930002] p 161 N94-12547
Summary of studies on JEM utilization experiment projects p 161 N94-12548
METEOSAT second generation programme SEVIRI: An enhanced visible and IR radiometer for meteorology
p 212 N94-12667

MISSISSIPPI RIVER (US)
Modeling present and future river runoff using global atmospheric models
[AD-A265274] p 285 N94-11685

MITOCHONDRIA
Effect of intermittent cold exposure on the fiber-type composition of selected skeletal muscles in rats
[AD-A265309] p 301 N94-11861

MIXED CRYSTALS
Symmetry lowering in crystalline solid solutions: A study of cinnamamide-thienylacrylamide by x ray and neutron diffraction and solid-state photochemistry
[DE93-010871] p 394 N94-10301

MIXED OXIDES
Grain boundaries in complex oxides
[DE93-013986] p 398 N94-11012

MIXING
Projectile-target mixing in melted ejecta formed during a hypervelocity impact cratering event
p 432 N94-12241

MIXING LAYERS (FLUIDS)
The kinematics of buoyancy induced mixing
p 123 N94-10239
Seasonal variation of the surface mixed layer in the subtropical re-circulation area of the North Pacific during OMLET p 195 N94-11924
Mixed layer heat budget of Kuroshio-Tango triangle using satellite and ship observations p 196 N94-11925
A normal stress subgrid-scale eddy viscosity model in large eddy simulation p 155 N94-12288
LIF measurements of scalar mixing in turbulent shear layers p 159 N94-12312
Plane mixing layer vortical structure kinematics
p 159 N94-12313
Numerical simulation of the non-Newtonian mixing layer p 159 N94-12314

MIXING LENGTH FLOW THEORY
Why convective heat transport in the solar nebula was inefficient p 458 N94-12143
Mixing in a stratified shear flow: Energetics and sampling p 159 N94-12311

MIXTURES
Marangoni Benard instabilities in liquid mixtures with Soret effect p 119 N94-10215
Measurement of viscosity, density and gas solubility of refrigerant blends
[DE93-014772] p 89 N94-11145

MODAL RESPONSE
Nonlinear response of a clamped-clamped beam with internal resonance under sinusoidal excitation
p 186 N94-10897
Dynamic tests on the NASA Langley CSI evolutionary model p 45 N94-11320

MODEL REFERENCE ADAPTIVE CONTROL
Model reference adaptive control (MRAC) with applications to robotics p 339 N94-11640

MODELS
Neural network model selection using asymptotic jackknife estimator and cross-validation method
[AD-A264960] p 339 N94-11289

MODEMS
Two way time transfer results at NRL and USNO
p 353 N94-10983
Performances of a date dissemination code on telephone lines using commercial modems
p 139 N94-10984

MODULATION
Controlling chaotic behavior in CO2 and other lasers
[AD-A264811] p 174 N94-10870
To the theory of irregular auto modulation in electron beam-backward electromagnetic wave dynamic system
[DE93-620982] p 133 N94-11030
Telemetering and telecommunications research
[NASA-CR-193235] p 42 N94-11297
Experimental and theoretical investigations of Cs-Ba vapor tacitron inverter for power conditioning in space power systems
[DE93-012971] p 48 N94-11372

MODULATION TRANSFER FUNCTION
Fundamental studies of radar scattering from water surfaces: The Lake Washington experiment
[NASA-CR-194030] p 139 N94-12778

MODULATORS
Variable rate transfer of optical information
[AD-D015758] p 418 N94-10374
Controlling chaotic behavior in CO2 and other lasers
[AD-A264811] p 174 N94-10870
Smart spatial light modulator research and development
[AD-A264928] p 382 N94-11286
GaAs sigma-delta modulator modeling for Analog to Digital Converters (ADC's)
[AD-A263419] p 144 N94-11516

MODULES
A tool for generation of expert system shells
[INPE-5493-TDI/510] p 325 N94-11181

MODULUS OF ELASTICITY
High temperature stability, interface bonding, and mechanical behavior in (beta)-NiAl and Ni3Al matrix composites with reinforcements modified by ion beam enhanced deposition
[DE93-013977] p 398 N94-11115

MOISTURE CONTENT
Photochemical modelling of Venus clouds using Pioneer Venus data
[NASA-CR-194108] p 434 N94-10823
Microtektite-like glass spherules in Late Devonian (367 MA) shales p 461 N94-12160
Analytic expression for epithermal neutron spectra amplitudes as a function of water content
p 473 N94-12227
Cloud liquid water content over the Pacific Ocean tropical zone derived from ship microwave radiometric measurement p 225 N94-12743

MOLDING MATERIALS
Universal adjustable mould for antenna reflectors
p 59 N94-10027

MOLDS
Universal adjustable mould for antenna reflectors
p 59 N94-10027

MOLECULAR BEAM EPITAXY
Crack suppression in GaInSb buffer layers initially under tensile stress
[DE93-012839] p 396 N94-10745
Rapid thermal processing for strained-layer semiconductor devices
[DE93-013754] p 396 N94-10809
Memory effects in the organometallic chemical beam epitaxy of compound semiconductors
[NASA-CR-193106] p 399 N94-11439
Ballistic electron transport studies using BEEM
[AD-A266029] p 369 N94-12395

MOLECULAR BEAMS
In situ secondary ion mass spectrometry analysis
[DE93-012185] p 76 N94-11140
Development of a molecular beam technique to study early solar system silicon reactions p 432 N94-12224

MOLECULAR CHAINS
Structural and electronic properties of atomic chains
[DE93-617758] p 366 N94-11349

MOLECULAR CLOUDS
Cosmological gamma-ray burst model
[NASA-CR-193368] p 484 N94-10507
The excitation of cyanogen and ionized carbon in interstellar and extragalactic gas clouds
p 426 N94-11582
Initiating solar system formation through stellar shock waves p 448 N94-12090

MOLECULAR COLLISIONS
Collision-induced squeezing in a harmonic oscillator
p 379 N94-10597

MOLECULAR DIFFUSION
Why does preferential diffusion strongly affect premixed turbulent combustion? p 81 N94-12319
Mapping closures for turbulent combustion
[AD-A265671] p 79 N94-12378

MOLECULAR ENERGY LEVELS
Dynamics of charge-transfer excited states relevant to photochemical energy conversion
[DE93-013981] p 263 N94-11116

MOLECULAR EXCITATION
Dynamics of dissociation versus ionization in strong laser fields
[DE93-009261] p 173 N94-10287
Review of SHARC 2.0 O3 kinetics and spectroscopy
[AD-A265481] p 274 N94-10496
Phasing operator for two oscillators in classical field
p 370 N94-10579
The excitation of cyanogen and ionized carbon in interstellar and extragalactic gas clouds
p 426 N94-11582
Thermal-infrared emission spectroscopy of natural surfaces: Application to coated surfaces
p 81 N94-12156

MOLECULAR GASES
Dynamics of dissociation versus ionization in strong laser fields
[DE93-009261] p 173 N94-10287
Quantum dynamics of helium clusters
[AD-A266060] p 411 N94-10874

MOLECULAR INTERACTIONS
Engineering solid-state materials. Strategies for modeling and packing control of molecular assemblies into 3-D networks
[AD-A265291] p 404 N94-12438

MOLECULAR PHYSICS
Polar solvation and electron transfer
[DE93-013328] p 365 N94-11010
Parallel molecular dynamics with the embedded atom method
[DE93-010683] p 367 N94-11455
Chaos, entropy, and reversibility: A simple example
p 31 N94-11495
A molecular dynamics simulation code ISIS
[DE93-753187] p 368 N94-11592

MOLECULAR RELAXATION
Femtosecond dynamics, photoexcitation, and ESR spectra of MX chain solids
[AD-A264689] p 399 N94-11263

MOLECULAR ROTATION
The excitation of cyanogen and ionized carbon in interstellar and extragalactic gas clouds
p 426 N94-11582

MOLECULAR STRUCTURE
Chemical pattern formation under microgravity
p 121 N94-10227
Electron momentum spectroscopy of atoms, molecules and solids
[DE93-610148] p 360 N94-10332
Recent advances in electron momentum spectroscopy
[DE93-610149] p 361 N94-10333
Site dependence of the apparent shape of a molecule in STM images: Benzene on Pt(111)
[AD-A263488] p 365 N94-11093
Femtosecond dynamics, photoexcitation, and ESR spectra of MX chain solids
[AD-A264689] p 399 N94-11263
Adsorption and dissociation of disilane on Si(001) studied by STM
[AD-A265269] p 402 N94-11684
The global potential energy surfaces of the lowest two 1A' states of the ozone molecule: Theoretical determination and analysis p 267 N94-12269
Fracture behavior of ionomers and ionomeric blends
[AD-A265379] p 94 N94-12407
Engineering solid-state materials. Strategies for modeling and packing control of molecular assemblies into 3-D networks
[AD-A265291] p 404 N94-12438

MOLECULAR WEIGHT
Synthesis, characterization, and modification of poly(organophosphazenes), that bear both 2,2,2-trifluoroethoxy and phenoxy groups
[AD-A264913] p 92 N94-11847
Radiation-induced modifications of allylamino-substituted polyphosphazenes
[AD-A264914] p 92 N94-11848
Glucose electrodes based on cross-linked (Os(bpy)2Cl)(sup +/2+) complexed poly(1-vinylimidazole) films
[AD-A265404] p 94 N94-12425

MOLECULES
Pulsed plasma processing for control of diesel engine emissions
[DE93-011884] p 181 N94-11247
A new decomposition strategy for parallel bonded molecular dynamics
[DE93-009839] p 366 N94-11284
FEFF5: An ab initio multiple scattering XAFS code
[DE93-011000] p 367 N94-11470

MOLYBDENUM
Radiation hardness of Mo/Si multilayers designed for use in a soft x ray projection lithography system
[DE93-011879] p 143 N94-11273

MOLYBDENUM ALLOYS
A history of tungsten- and molybdenum-base alloys
[DE93-010283] p 82 N94-11108

MOLYBDENUM SULFIDES
Low temperature pathways to Chevrel phases via reduced molybdenum sulfide cluster complexes
[DE93-013282] p 405 N94-12599

MOMENTS OF INERTIA
Porosity and the ecology of icy satellites
p 431 N94-12186
Accuracy and repeatability of the standard automated mass properties measurement system
[AD-A265897] p 316 N94-12346

MOMENTUM
On a Lagrange-Hamilton formalism describing position and momentum uncertainties p 349 N94-10583

Momentum and heat frictions between fast ions and thermal plasma species
[DE93-771240] p 390 N94-11149
Momentum induced by laser-tissue interaction
[DE93-010737] p 301 N94-11667
Surface eddy fluxes from the GEOSAT satellite altimeter p 208 N94-12643

MOMENTUM TRANSFER
Crossing-odd spin effects in the dipole model of hadron scattering
[DE93-617692] p 362 N94-10551
Momentum management in redundant manipulators for vibration suppression
[NASA-CR-194112] p 180 N94-10821
Accretion disk viscosity and internal waves in disks
p 153 N94-11615
Air-sea fluxes and universal constants in weak-turbulence theory of surface gravity waves
p 195 N94-11922
Mixed layer heat budget of Kuroshio-Tango triangle using satellite and ship observations p 196 N94-11925

MONGOLIA
National space programmes and application of the remote sensing data in Mongolia p 36 N94-10686

MONITORS
Measurement of display transfer characteristics using test pictures
[BBC-RD-1992/13] p 133 N94-11023

MONKEYS
Computer software and hardware to determine contrast sensitivity using three methods: Tracking, limits, and constant stimuli
[AD-A265168] p 324 N94-11099
Locus coeruleus, vigilance, and stress: Brain mechanisms of adaptive behavioral responsiveness
[AD-A265657] p 302 N94-12441

MONOCHROMATORS
Moncchromator SP-017. The results of the first experiments
[DE93-617463] p 372 N94-10849

MONOMERS
Photoinitiated radical polymerization of liquid monomers in microgravity p 124 N94-10246
New aromatic activated dihalides and bisphenol monomers for the preparation of novel poly(arylene ethers)
[NASA-CR-193190] p 55 N94-10513
Thermal stability of sealants for military aircraft: Modification of polysulfide prepolymers with ether and thioether monomers
[AD-A264079] p 89 N94-11107
The 13C and 15N solid-state NMR of copolymers of nylon 6 and 7: Observation of a stable pseudohexagonal phase
[AD-A265799] p 94 N94-12381
Synthesis and polymerization of oligomeric multiple aromatic ether-containing phthalonitriles
[AD-D015729] p 94 N94-12399

MONOPOLE ANTENNAS
Design of a matching network for dipole antennas
[AD-A265115] p 136 N94-11158
Design of a continuous resistively loaded monopole antenna
[AD-A265852] p 138 N94-12281

MONOPOLES
Design of a continuous resistively loaded monopole antenna
[AD-A265852] p 138 N94-12281

MONOTECTIC ALLOYS
Marangoni motion during melting of a hypermonotectic alloy: Numerical simulations for the D2 experiment IHF04 p 113 N94-10177

MONTE CARLO METHOD
Deformation mechanisms of continuous fibre-reinforced thermoplastic composites during manufacturing: A probabilistic approach p 60 N94-10030
Heat analysis of thermoplastic components during the initial stages of manufacturing: A probabilistic approach
p 60 N94-10031
Techniques, processes, and measures for software safety and reliability
[DE93-012379] p 322 N94-10347
Three-dimensional hypersonic rarefied flow calculations using direct simulation Monte Carlo method
p 7 N94-10449
Monte Carlo simulations of a two-dimensional hard dimer system
[DE93-613535] p 361 N94-10502
Cosmological gamma-ray burst model
[NASA-CR-193368] p 484 N94-10507
Acceleration of positrons in supernova shocks
[NASA-CR-193713] p 425 N94-10511
Monte Carlo simulations of phase transformations in Fe-Cr alloys
[DE93-013847] p 81 N94-10522
Monte Carlo algorithms in simulation of 2beta-decay and penetration of electrons through matter
[DE93-617741] p 364 N94-10837
ACARA user's manual
[NASA-TM-106277] p 183 N94-11167
Bi-directional reflectance by oceanic waters studied via Monte-Carlo simulations p 203 N94-11971
The evaluation of radiative process in the atmosphere-ground system by Monte Carlo method
p 205 N94-11980
Venus resurfacing rates: Constraints provided by 3-D Monte Carlo simulations p 453 N94-12119
PDF approach for turbulent scalar field: Some recent developments p 160 N94-12315
Propagation of light pulses through a three-layer medium (cloud, pure air, and ocean water) p 222 N94-12725

MONTMORILLONITE
Reflectance spectra of sulfate-and carbonate-bearing Fe(3+)-doped montmorillonites as Mars soil analogs
p 445 N94-12070

MOON
Lunar Scout Two spacecraft gravity experiment
p 459 N94-12152
Mission to the Moon: An ESA study on future exploration p 460 N94-12153
Exploration planning in the context of human exploration and development of the Moon p 474 N94-12229
Significance and scenarios of lunar and planetary exploration missions p 482 N94-12324
Technical problems on lunar an planetary exploration mission p 482 N94-12328

MOORING
Real-time tomography mooring
[AD-A264923] p 289 N94-11854

MORPHOLOGY
Ground results of the Mephisto program: Benefits and space experiments orientation p 86 N94-10197
Physical studies of planetary and satellite surfaces
[NASA-CR-193545] p 434 N94-10817
Characterization of the Si/SiO2 interfere morphology from quantum oscillations in Fowler-Nordheim tunneling currents
[AD-A265149] p 143 N94-11160
Characterization of gas-aerosol interaction kinetics using morphology dependent stimulated Raman scattering
[DE93-012324] p 77 N94-11359
The morphologies of distant radio galaxies
p 426 N94-11597
Yana ring structure, North-Eastern Siberia: A possible counterpart of coronae on Venus p 282 N94-12121
Differential scaling: Implications for central structures in large lunar craters p 461 N94-12158
Small volcanoes in Tempe Terra, Mars: Their detailed morphometry and inferred geologic significance
p 469 N94-12202

MORTALITY
Evaluation of medical treatments to increase survival of ebullism in guinea pigs p 302 N94-11548
Longitudinal study of astronaut health: Mortality in the years 1959-1991 p 312 N94-11560

MOSAICS
Radarmap of Germany: First mosaic and classification
p 246 N94-12477

MOSSBAUER EFFECT
A new matrix for the ageless 21.6-keV Eu-151 nuclear gamma ray Moessbauer source
[DE93-009795] p 75 N94-10338
The peculiarities of the spin glass state in Fe(x)Mn(1-x)TiO3
[DE93-617882] p 395 N94-10525
X ray and gamma ray spectroscopy of solids under pressure
[DE93-014847] p 76 N94-10653
Moessbauer spectroscopy of the SNC meteorite Zagami p 428 N94-12016
Moessbauer spectrometer for mineralogical analysis of the Mars surface: Moessbauer source considerations
p 476 N94-12242
Cronstedtite and iron sulfide mineralogy of CM-type carbonaceous chondrites from cryogenic Moessbauer spectra p 433 N94-12257

MOTION PERCEPTION
Visual psychophysics of egomotion
[AD-A265253] p 304 N94-11681

MOTION SICKNESS
Motion and spatial disorientation systems: Special research capabilities
[AD-A265155] p 303 N94-11097
Promethazine and its use as a treatment for space motion sickness p 312 N94-11550
Update on the incidence and treatment of space motion sickness p 312 N94-11551
Cardiovascular dynamics during space sickness and deconditioning p 311 N94-12007

MOTION SIMULATION
Mechanical analysis of parallel manipulators with simulation, design, and control applications
[ISBN-0-315-72013-1] p 181 N94-11156

MOTOR VEHICLES
Coprocessing of fossil fuels and biomass for CO2 emission reduction in the transportation sector
[PB93-194165] p 267 N94-11845

MOUNTAINS
The Lathrop Wells Volcanic Center: Status of field and geochronology studies
[DE93-008917] p 273 N94-10285
The evaluation of radiative process in the atmosphere-ground system by Monte Carlo method
p 205 N94-11980
Monitoring of snowcover in high mountain terrain with ERS-1 SAR p 247 N94-12482

MSM (SEMICONDUCTORS)
Effects of solar cell environment on contact integrity
p 49 N94-11387

MULTICHANNEL COMMUNICATION
An efficient medium access control strategy for high speed WDM multiaccess networks
[MEMO-INF-92-74] p 131 N94-10165

MULTIGRID METHODS
Hypersonic flow computations around re-entry vehicles p 9 N94-10461
Looking for O(N) Navier-Stokes solutions on non-structured meshes
[NASA-CR-191472] p 345 N94-11277
Viscous analysis of three-dimensional rotor flows using a multigrid method
[NASA-TM-106266] p 152 N94-11481
Grid optimization and multigrid techniques for fluid flow and transport problems p 154 N94-11824
Application of incremental unknowns to the Burgers equation p 156 N94-12293
Towards a cell-vertex Navier-Stokes algorithm for three-dimensional structured/unstructured meshes
[ARA-MEMO-366] p 161 N94-12437

MULTIMEDIA
Development of a hypermedia knowledge base of aircraft fire safety regulations p 21 N94-10793
Design issues for high performance engineering information systems
[AD-A264839] p 420 N94-11520
The use of communication technology in medicine
p 306 N94-11800

MULTIPHASE FLOW
Nonlinear aspects of transonic aeroelasticity
p 2 N94-10357
Nonlinear aspects of transonic aeroelasticity
[UTIAS-RN-345] p 15 N94-11857

MULTIPHOTON ABSORPTION
Nonperturbative methods in the problem of multiphoton excitation of atom by squeezed light
p 376 N94-10575

MULTIPLE ACCESS
An efficient medium access control strategy for high speed WDM multiaccess networks
[MEMO-INF-92-74] p 131 N94-10165
Optimal routing of IP packets to multi-homed servers
[DE93-010949] p 133 N94-10709

MULTIPLEXING
Multiplexed and distributed optical fibre sensors
p 64 N94-10065
A fiber optic network system with low crosstalk using code-division multiplexing
[AD-D015763] p 374 N94-10376
Microwave multiplexer with channels of varying fractional bandwidths
[AD-D015754] p 140 N94-10389
Controller of serial multiplex communication channel
[DE92-641157] p 336 N94-10544
SONET synchronization: What's happening
p 355 N94-10992
Analysis of the eastern range multiplexed fiber optic IRIG B120 distribution system p 139 N94-10996
Holographic multiplexing for 3D optical memory
[AD-A266099] p 171 N94-11420
Superconducting SQUID amplifiers for IR detectors and other applications, phase 2
[AD-A265447] p 145 N94-12333

MULTIPOLAR FIELDS
On the unique structure of the magnetic fields of Uranus and Neptune p 472 N94-12221

MULTIPOLES
Model for the pomeron
[DE93-617693] p 362 N94-10552

MULTIPROCESSING (COMPUTERS)
Efficient partitioning and assignment on programs for multiprocessor execution
[NASA-CR-193458] p 324 N94-10942
The Zipcode message-passing system
[DE93-011958] p 336 N94-11027

Node assignment in heterogeneous computing
[NASA-CR-4534] p 142 N94-11131
Portable programming on parallel/networked computers using the Application Portable Parallel Library (APPL)
[NASA-TM-106238] p 327 N94-11232
Alleviating memory contention in matrix computations on large-scale shared-memory multiprocessors
[AD-A265009] p 320 N94-11294
Scalable concurrent programming project
[AD-A266097] p 328 N94-11295
Scalable spin locks for multiprogrammed systems
[AD-A265007] p 337 N94-11650

MULTIPROGRAMMING
Scalable concurrent programming project
[AD-A266097] p 328 N94-11295
Scalable spin locks for multiprogrammed systems
[AD-A265007] p 337 N94-11650

MULTISENSOR APPLICATIONS
Estimation with multisensor/multiscan detection fusion
[AD-A265673] p 138 N94-12338

MULTISPECTRAL BAND SCANNERS
Thermal-infrared emission spectroscopy of natural surfaces: Application to coated surfaces
p 81 N94-12156

MULTISTATIC RADAR
Interpretation of lunar and planetary electromagnetic scattering using the full wave solutions
p 440 N94-12049

MULTIVARIATE STATISTICAL ANALYSIS
A multi-variance analysis in the time domain
p 146 N94-10999
Applications of multivariate analysis
[AD-A265250] p 347 N94-11882

MUONS
Conceptual design report for the SDC barrel and intermediate muon detectors based on a jet-type drift chamber
[DE93-753173] p 367 N94-11510
Experiments with energetic (mu)d and (mu)t emitted from solid hydrogen
[DE93-010252] p 373 N94-12542

MURCHISON METEORITE
Interstellar graphite in Murchison: Continued search for isotopically distinct components p 97 N94-12029
Determining the relative extent of alteration in CM chondrites p 430 N94-12114
A new carbon-rich phase (COPS) in Antarctic micrometeorites p 432 N94-12233

MUSCULAR FUNCTION
Effect of intermittent cold exposure on the fiber-type composition of selected skeletal muscles in rats
[AD-A265309] p 301 N94-11861

MUSCULAR STRENGTH
Exercise countermeasures for bed-rest deconditioning
[NASA-TM-103987] p 300 N94-11191

MUSCULOSKELETAL SYSTEM
Risk of decompression sickness in the presence of circulating microbubbles p 312 N94-11546

MUTATIONS
Proceedings of the Symposium on Radiation Research in Life Science
[DE93-754137] p 300 N94-10888

MYLAR (TRADEMARK)
Thermal testing of aluminized Mylar
[NASA-TM-108414] p 89 N94-11175

N

NACELLES
Application of composite materials for production nacelle structures p 56 N94-10006
The application of advanced materials to aircraft nacelle structures p 57 N94-10011

NARROWBAND
Continued development of an ultra-narrow bandpass filter for solar research
[NASA-CR-194169] p 381 N94-10735
Non-linear dynamics of automodulation processes in coupled distributed autovibration systems with delay
[DE93-620976] p 143 N94-11365

NASA PROGRAMS
The NASA Lewis Research Center SBIR program: An assessment
[NASA-TM-106205] p 485 N94-10356
NASA Marshall Space Flight Center solar observatory report, January - June 1993
[NASA-TM-108417] p 423 N94-10866
National Aero-Space Plane: A need for program direction and funding decisions
[GAO/NSIAD-93-207] p 416 N94-10910
NASA procurement: Proposed changes to the Jet Propulsion Laboratory contract. Report to Congressional Requesters
[GAO/NSIAD-93-178] p 416 N94-10941
Advanced statistical methods for improved data analysis of NASA astrophysics missions
[NASA-CR-193514] p 425 N94-10943
The 1987 RIACS annual report
[NASA-CR-193220] p 324 N94-11046
The role of metrics and measurements in a software intensive total quality management environment
p 329 N94-11428
Development and application of an acceptance testing model p 330 N94-11432
Financial management: NASA's financial reports are based on unreliable data
[AD-A265690] p 418 N94-12443

NASA SPACE PROGRAMS
Transportation systems analyses: Volume 1: Executive Summary
[NASA-CR-192583] p 41 N94-10826
Transportation systems analyses. Volume 2: Technical/programmatics
[NASA-CR-192582] p 41 N94-10827

NASTRAN
NASTRAN modeling of flight test components for UH-60A airloads program test configuration
[NASA-CR-193614] p 186 N94-10937

NATIONAL AEROSPACE PLANE PROGRAM
CFD analysis of hypersonic, chemically reacting flow fields p 2 N94-10422
National Aero-Space Plane: A need for program direction and funding decisions
[GAO/NSIAD-93-207] p 416 N94-10910
An environmental study of the National Aerospace Plane
[AD-A266071] p 25 N94-10945

NATIONAL AIRSPACE SYSTEM
National Airspace System operational concept
[DOT/FAA/SE-93/1] p 23 N94-10933
FAA air traffic activity
[AD-A266043] p 22 N94-12397

NATIONAL LAUNCH VEHICLE PROGRAM
The National Launch System Advanced Development Program: A brief overview p 40 N94-11576

NATURAL GAS
Vehicular fleet operation on natural gas and propane: An overview
[PB93-194603] p 98 N94-10844
Business fleet refueling assessment
[PB93-189892] p 98 N94-11017

NATURAL LANGUAGE (COMPUTERS)
A real-time spoken-language system for interactive problem solving
[AD-A266046] p 324 N94-11104
Transactions of the 10th Army Conference on Applied Mathematics and Computing
[AD-A265098] p 318 N94-11678
Machine translation technology: A potential key to the information age
[PB93-134336] p 421 N94-12385
Proceedings of the Seventh International Symposium on Methodologies for Intelligent Systems (poster session)
[DE93-013470] p 340 N94-12428

NATURAL LANGUAGE PROCESSING
Automatic word categorization: An information-theoretic approach
[CS-9209] p 419 N94-10903

NATURAL SATELLITES
Physical studies of planetary and satellite surfaces
[NASA-CR-193545] p 434 N94-10817
Orbital simulations of satellite escape/capture and the origin of satellites such as Triton p 429 N94-12057

NAVIER-STOKES EQUATION
Numerical calculation of scramjet inlet flow
[NAL-TR-1174T] p 27 N94-10370
Experimental, analytical, and computational methods applied to hypersonic compression ramp flows
p 6 N94-10444
A CFD-based aerodynamic design procedure for hypersonic wind-tunnel nozzles p 9 N94-10458
Hypersonic multi block flow simulations around space vehicles including non-equilibrium chemistry
p 9 N94-10460
Aerodynamic characteristics analysis of Garabedian-Korn 75-06-12 airfoil
[PAPER-2D-2] p 10 N94-10468
Aerodynamic characteristics analysis of Garabedian-Korn 75-06-12 airfoil
[PAPER-2D-3] p 10 N94-10469
Aerodynamic characteristics analysis of Garabedian-Korn 75-06-12 airfoil: Computation using q-omega 2 equation turbulence model
[PAPER-2D-4] p 10 N94-10470
Aerodynamic characteristics analysis of Garabedian-Korn 75-06-12 airfoils: Computation using Baldwin-Lomax turbulence model
[PAPER-2D-5] p 11 N94-10471
Aerodynamic characteristics analysis of Garabedian-Korn 75-06-12 aircraft
[PAPER-2D-7] p 11 N94-10472
Aerodynamic characteristics analysis of Garabedian-Korn 75-06-12 airfoil
[PAPER-2D-9] p 11 N94-10474
Flow analysis around ONERA model M5 configuration
[PAPER-3D-1] p 11 N94-10477
Flow analysis around ONERA model M5 configuration
[PAPER-3D-2] p 12 N94-10478
Flow analysis around ONERA model M5 configuration
[PAPER-3D-4] p 12 N94-10480
Flow analysis around ONERA model M5 configuration
[PAPER-3D-5] p 12 N94-10481
Navier-Stokes flowfield computation of wing/rotor interaction for a tilt rotor aircraft in hover
[NASA-CR-4532] p 13 N94-10758
A comparative study of full Navier-Stokes and Reduced Navier-Stokes analyses for separating flows within a diffusing inlet S-duct
[NASA-TM-106250] p 39 N94-10764
Development of an unstructured solution adaptive method for the quasi-three-dimensional Euler and Navier-Stokes equations
[NASA-CR-191161] p 28 N94-10816
A dynamically adaptive mesh method for internal flows
p 149 N94-10896
Combustion chamber analysis code
[NASA-CR-192585] p 46 N94-10934
New developments in the method of space-time conservation element and solution element: Applications to the Euler and Navier-Stokes equations
[NASA-TM-106226] p 150 N94-10939
Theoretical investigation of 3-D shock wave turbulent boundary layer interactions
[AD-A265275] p 150 N94-11014
Examination of wall functions for a parabolized Navier-Stokes code for supersonic flow
[DE93-011590] p 14 N94-11111
High order accurate solutions of viscous problems
[NASA-TM-106267] p 151 N94-11253
Looking for O(N) Navier-Stokes solutions on non-structured meshes
[NASA-CR-191472] p 345 N94-11277
Computation of hypersonic nosetip heat transfer rates for an M829-like projectile
[AD-A263226] p 16 N94-11870
A local dynamic model for large eddy simulation
p 155 N94-12285
Application of incremental unknowns to the Burgers equation p 156 N94-12293
Direct numerical simulation of turbulent flow over a backward-facing step p 156 N94-12296
Towards a cell-vertex Navier-Stokes algorithm for three-dimensional structured/unstructured meshes
[ARA-MEMO-366] p 161 N94-12437
Proceedings of the 9th and 10th NAL Workshop on Investigation and Control of Boundary-Layer Transition
[NAL-SP-18] p 163 N94-12611

NAVIGATION
Helicopter approach capability using the differential Global Positioning System
[NASA-CR-177618] p 24 N94-12355
Experiments in mobile robot navigation and range imaging
[DE93-013280] p 341 N94-12598

NAVIGATION AIDS
National Airspace System operational concept
[DOT/FAA/SE-93/1] p 23 N94-10933
Toward intelligent flight control p 33 N94-11503
Definition of spacecraft standard interfaces by the NASA Space Assembly and Servicing Working Group (SASWG) p 348 N94-11574

NAVIGATION SATELLITES
The time keeping system for GPS block IIR
p 24 N94-10964

NAVY
Statistical process control in the hybrid microelectronics manufacturing industry: A Navy view point
[AD-A265164] p 145 N94-11884

NEAR INFRARED RADIATION
Formulating infrared coatings for defence applications
[MRL-RR-1-93] p 90 N94-11302
A comparison of telescopic and Phobos-2 ISM spectra of Mars in the short-wave near-infrared (0.76-1.02 microns) p 424 N94-12053
Compositional and textural information from the dual inversion of visible, near and thermal infrared remotely sensed data p 258 N94-12097
A comparison of the visible and near infrared reflectance of hydrovolcanic palagonite tuffs and Martian weathered soils p 477 N94-12245
Planetary astronomy of Mars. Mars data reduction
[NASA-CR-193515] p 424 N94-12768

NEBULAE

Midplane temperatures in the solar nebula p 448 N94-12088

Initiating solar system formation through stellar shock waves p 448 N94-12090

NECK (ANATOMY)

Mass properties test procedure for manikin headforms and helmet systems [AD-A265654] p 315 N94-10296

NEGATIVE IONS

Photodetachment studies on few-electron atomic negative ions [DE93-008474] p 358 N94-10154

NEODYMIUM ISOTOPES

Radiogenic age and isotopic studies [DE93-610548] p 274 N94-10407

NEODYMIUM LASERS

Thermal-optical switching of a silicon based interference filter [AD-A265152] p 174 N94-11095

An analytic model for calculating pump-induced wavefront distortions in laser slabs [DE93-011953] p 174 N94-11126

Short pulse lasers for generation of fields exceeding 100 MG [DE93-013346] p 369 N94-11815

NEON ISOTOPES

Dispersion of the ratios of cosmogenic isotopes of noble gases in chondrites of different cosmic-ray exposure ages p 428 N94-12020

Peculiarities of distributions of the cosmic-ray exposure ages of H chondrite falls and finds p 428 N94-12021

Noble gases in LEW88516 shergottite: Evidence for exposure age pairing with ALH77005 p 80 N94-12082

NEPHELINE

The correlation of alkalis and aluminum during high-temperature volatilization of albite and nepheline p 81 N94-12214

NEPTUNE (PLANET)

Detection of dust impacts by the Voyager planetary radio astronomy experiment [NASA-CR-193281] p 423 N94-11305

Models of Neptune's smooth recurrent radio emission [NASA-CR-193283] p 484 N94-11312

Orbital simulations of satellite escape/capture and the origin of satellites such as Triton p 429 N94-12057

On the unique structure of the magnetic fields of Uranus and Neptune p 472 N94-12221

Precession of Uranus and Neptune and their magnetic field p 473 N94-12222

NETWORK ANALYSIS

Networks of real-time processes [DE93-013049] p 338 N94-12597

NETWORK CONTROL

Galileo EM-2 contributions to the lunar control network p 468 N94-12198

NETWORKS

Design of a matching network for dipole antennas [AD-A265115] p 136 N94-11158

Galileo EM-2 contributions to the lunar control network p 468 N94-12198

NEURAL NETS

The applicability of neural nets for decision support [MEMO-COSOR-92-49] p 338 N94-10169

Nonlinear stability and control study of highly maneuverable high performance aircraft [NASA-CR-193480] p 25 N94-10344

Unsupervised splitting rules for neural tree classifiers [AD-A264961] p 338 N94-10487

Functional approximation using artificial neural networks in structural mechanics [NASA-TM-105820] p 188 N94-11254

Three-dimensional object recognition using an unsupervised BCM network: The usefulness of distinguishing features [AD-A264576] p 304 N94-11261

Neural network model selection using asymptotic jackknife estimator and cross-validation method [AD-A264960] p 339 N94-11289

Fault location in structures using neural networks p 70 N94-11335

Spatial light rebroadcaster architecture study [AD-A266102] p 382 N94-11421

Adaptive reconfigurable flight controls for high angle of attack aircraft agility p 32 N94-11502

Toward intelligent flight control p 33 N94-11503

Bounding the Vapnik-Chervonenkis dimension of concept classes parameterized by real numbers [DE93-011600] p 331 N94-11611

Model reference adaptive control (MRAC) with applications to robotics p 339 N94-11640

Statistical and optimization methods to expedite neural network training for transient identification [DE93-009985] p 340 N94-11644

Parametric study of diffusion-enhancement networks for spatiotemporal grouping in real-time artificial vision [AD-A265065] p 331 N94-11652

A hybrid neural network and feature extraction technique for target recognition [AD-D015732] p 333 N94-12386

Signal feature analysis using neural networks and psychoacoustics [AD-A266048] p 340 N94-12398

Thermal error compensation feasibility study using artificial intelligence [AD-A266084] p 340 N94-12411

Proceedings of the Seventh International Symposium on Methodologies for Intelligent Systems (poster session) [DE93-013470] p 340 N94-12428

NEUROLOGY

Transcranial Doppler ultrasound and the etiology of neurologic decompression sickness during altitude decompression p 312 N94-11544

NEURONS

Three-dimensional object recognition using an unsupervised BCM network: The usefulness of distinguishing features [AD-A264576] p 304 N94-11261

Role of spatially distributed ion channels in single neuron computation [AD-A265972] p 79 N94-12351

Locus coeruleus, vigilance, and stress: Brain mechanisms of adaptive behavioral responsiveness [AD-A265657] p 302 N94-12441

NEUROPHYSIOLOGY

Monitoring cognitive function and need with the automated neuropsychological assessment metrics in Decompression Sickness (DCS) research p 314 N94-11533

Nonlinear resonance: Noise-assisted information processing in physical and neurophysiological systems [AD-A265161] p 313 N94-11890

NRL review for 1993 [AD-A265666] p 497 N94-12334

The organization of the suprachiasmatic circadian pacemaker of the rat and its regulation by neurotransmitters and modulators [AD-A266113] p 301 N94-12417

NEUROTRANSMITTERS

The organization of the suprachiasmatic circadian pacemaker of the rat and its regulation by neurotransmitters and modulators [AD-A266113] p 301 N94-12417

NEUTRAL ATOMS

Imaging of magnetospheric dynamics using low energy neutral atom detection [DE93-012656] p 275 N94-10742

NEUTRAL BUOYANCY SIMULATION

Propellant management in surface tension tanks p 106 N94-10110

NEUTRAL CURRENTS

Future high precision experiments and new physics beyond Standard Model [DE93-011004] p 373 N94-11618

NEUTRAL PARTICLES

Influence of neutral particles concentration on flame propagation in methane-air mixtures at zero and normal gravity conditions p 121 N94-10224

NEUTRINOS

The effect of a scalar boson coupled to neutrinos on the behavior of the tritium beta decay spectrum near the end point [DE93-012655] p 361 N94-10349

On parity conservation and the question of the missing, right-handed neutrino [DE93-613092] p 361 N94-10414

Planck scale effects on the Majoron [DE93-613120] p 410 N94-10545

Tau physics [DE93-010956] p 367 N94-11469

NEUTRON BEAMS

Possibility of a crossed-beam experiment involving slow-neutron capture by unstable nuclei rapid-process-tron [DE93-754288] p 363 N94-10720

NEUTRON DIFFRACTION

Symmetry lowering in crystalline solid solutions: A study of cinnamamide-thienylacrylamide by x ray and neutron diffraction and solid-state photochemistry [DE93-010871] p 394 N94-10301

Rietveld refinement of magnetic structures from pulsed-neutron-source powder-diffraction data [DE93-012740] p 363 N94-10743

NEUTRON IRRADIATION

Szilard-Chalmers effect in solid HIO4.2H2O by neutron irradiation [DE93-617173] p 397 N94-10830

Facility for stress corrosion cracking test of irradiated material in high temperature water [DE93-753189] p 84 N94-11593

NEUTRON SCATTERING

Rietveld refinement of magnetic structures from pulsed-neutron-source powder-diffraction data [DE93-012740] p 363 N94-10743

The searchlight problem for neutrons in a semi-infinite medium [DE93-010796] p 365 N94-10952

Energy transfer dynamics and impact sensitivity [DE93-009551] p 98 N94-11269

X-ray and neutron scattering studies of magnetic critical fluctuations in holmium [DE93-010873] p 400 N94-11467

NEUTRON SOURCES

Intense neutron sources for fusion materials studies [DE93-009782] p 391 N94-11171

NEUTRON SPECTRA

Analytic expression for epithermal neutron spectra amplitudes as a function of water content p 473 N94-12227

NEUTRON SPECTROMETERS

The Los Alamos neutron spectrometer for the Lunar Scout-1 mission p 172 N94-12038

NEUTRONS

A spectral nodal method for the solution of the Sn equations in x, y geometry for highly absorbing deep penetration problems [DE93-613520] p 349 N94-10636

The searchlight problem for neutrons in a semi-infinite medium [DE93-010796] p 365 N94-10952

Development of deterministic transport methods for low energy neutrons for shielding in space [NASA-CR-194172] p 366 N94-11199

NICKEL

Plating under reduced pressure [DE93-011896] p 84 N94-11668

NICKEL ALLOYS

Structure and properties of an RS Al-Si-Ni-Mn-Zr alloy for high temperature applications p 64 N94-10063

Solidification and metastable phase formation of highly undercooled Fe-Cr-Ni alloy melts p 87 N94-10204

Interface reactions of (Ni3Al) ribbons/Al-MMC in ground preparation as preliminary test for microgravity experiments p 123 N94-10237

Production of reactive sintered nickel aluminide [DE93-014434] p 83 N94-11127

Fatigue in single crystal nickel superalloys [AD-A266116] p 85 N94-12418

NiAl alloys for structural uses [NASA-CR-194113] p 85 N94-12447

NICKEL HYDROGEN BATTERIES

Space Station Freedom advanced photovoltaics and battery technology development planning p 52 N94-11401

NICKEL ISOTOPES

Iron and nickel isotopic mass fractionation in deep-sea spherules p 282 N94-12199

NIGHT VISION

Perceptual response to visual noise and display media [NASA-CR-193406] p 313 N94-11511

NIOBIUM

Experimental approach to non-contact calorimetry in space p 112 N94-10143

Space Storable Rocket Technology program (SSRT). Option 1 program [NASA-CR-191171] p 46 N94-10938

NIOBIUM COMPOUNDS

High frequency behavior of long and small junctions [AD-A265670] p 403 N94-12336

NIOBIUM OXIDES

Synthesis and thermal evolution of structure in alkoxide-derived niobium pentoxide gels [NASA-TM-106259] p 90 N94-11257

NITRAMINE PROPELLANTS

Time-temperature shift factors for gun propellants [AD-A264979] p 97 N94-10489

NITRATES

The phytoplankton bloom in the Kinu-ura Bay, Japan in the rainy season p 211 N94-12660

Variation of the photosynthetic products in the regional upwelling area around the Izu Islands, Japan p 211 N94-12661

NITRIC OXIDE

In situ detection of tropospheric OH, HO2, NO2, and NO by laser-induced fluorescence in detection chambers at reduced pressures [NASA-CR-193189] p 274 N94-10701

NITRILES

Coupled growth of cells and bubbles in directional solidification of succinonitrile-acetone alloys p 118 N94-10206

NITROGEN
Polymeric nitrogen
[DE93-012600] p 89 N94-11151
Nitrogen and noble gases in a glass sample from LEW88516 p 80 N94-12051
Multiple nitrogen components in lunar soil sample 12023 p 451 N94-12108
Carbon and nitrogen in Type 2 supernova diamonds
p 431 N94-12166
NITROGEN DIOXIDE
In situ detection of tropospheric OH, HO2, NO2, and NO by laser-induced fluorescence in detection chambers at reduced pressures
[NASA-CR-193189] p 274 N94-10701
NITROGEN ISOTOPES
Interstellar graphite in Murchison: Continued search for isotopically distinct components p 97 N94-12029
NITROGEN OXIDES
User's manual for the plume visibility model PLUVUE 2 (revised)
[PB93-188233] p 265 N94-11016
Application of jet-shear-layer mixing and effervescent atomization to the development of a low-NO(x) combustor
[NASA-TM-105888] p 28 N94-11234
NITROGEN 15
The 13C and 15N solid-state NMR of copolymers of nylon 6 and 7: Observation of a stable pseudohexagonal phase
[AD-A265799] p 94 N94-12381
NOAA SATELLITES
Radiometer offsets and count conversion coefficients for the Earth Radiation Budget Experiment (ERBE) spacecraft for the years 1987, 1988, and 1989
[NASA-CR-191489] p 286 N94-12772
NOAA 10 SATELLITE
Radiometer offsets and count conversion coefficients for the Earth Radiation Budget Experiment (ERBE) spacecraft for the years 1987, 1988, and 1989
[NASA-CR-191489] p 286 N94-12772
NOAA 9 SATELLITE
Radiometer offsets and count conversion coefficients for the Earth Radiation Budget Experiment (ERBE) spacecraft for the years 1987, 1988, and 1989
[NASA-CR-191489] p 286 N94-12772
NOBLE METALS
Field evaluation of six protective coatings applied to T-56 turbine blades after 2500 hours of engine use
[ARL-TR-27] p 90 N94-11311
Examination of the surface second harmonic response at infrared wavelengths
[AD-A265206] p 403 N94-12371
NODULES
A detailed investigation of the benthic regime in the Clarion-Clipperton province of the Pacific and a forecast of consequences of manganese nodule mining
p 224 N94-12733
NOISE
A window least squares algorithm for statistical noise smoothing of 2D-ACAR data
[DE93-613828] p 395 N94-10537
NOISE GENERATORS
Control of jet noise
[NASA-CR-193612] p 358 N94-11176
NOISE INTENSITY
Spacecraft signal sources portable test system
p 139 N94-11000
Noise levels and their effects on Shuttle crewmembers' performance: Operational concerns p 314 N94-11538
Preliminary analysis of the FLIP array data from the NOBS experiment
[AD-A265911] p 289 N94-12349
NOISE REDUCTION
Control of jet noise
[NASA-CR-193612] p 358 N94-11176
A theory of membrane absorbers
[ISVR-TR-217] p 76 N94-11216
Using lunar sounder imagery to distinguish surface from subsurface reflectors in lunar highlands areas
p 464 N94-12179
NOISE SPECTRA
Preliminary analysis of the FLIP array data from the NOBS experiment
[AD-A265911] p 289 N94-12349
NOMENCLATURES
Effect of switched-bias bakes on the postirradiation electrical response of MOS devices
[DE93-009629] p 143 N94-11271
NONDESTRUCTIVE TESTS
Special problems of 3-D ultrasonic QNDI techniques and applications to composites aerospace structures
p 61 N94-10036
Design of inspection and acceptance test methodology for TIG welded aluminum-alloy bracket for camera housings for IRS-1A space craft and executing it
p 61 N94-10037
Quantifying disbond area p 61 N94-10038
New x ray scanning topographic approaches to nondestructive evaluation of composites
p 61 N94-10039
Material characterization and modeling with shearography
[NASA-CR-192576] p 185 N94-10342
Report of the IAEA Consultants' Meeting on Real-Time Nondestructive Monitoring of Wear and Corrosion Using the Thin Layer Activation Technique
[DE93-617422] p 183 N94-10847
Response of composite laminates to dynamic surface loads p 66 N94-10902
A Recommended Methodology for Quantifying NDE/NDI Based on Aircraft Engine Experience
[AGARD-LS-190] p 28 N94-11022
Fibre reinforced polymer matrix composites: Microstructure and mechanical properties
[DLR-FB-92-28] p 66 N94-11085
Ultrasonic inspection, material noise and surface roughness
[DE93-011560] p 183 N94-11110
A survey of techniques for corrosion monitoring
[DE93-012131] p 83 N94-11250
Large array SQUID magnetometer for NDE
[AD-A264799] p 304 N94-11449
Potential techniques for non-destructive evaluation of cable materials
[DE93-008350] p 183 N94-11586
Ultrasonic wave interaction with advanced complex materials for nondestructive evaluation applications
[AD-A265704] p 74 N94-12401
NONEQUILIBRIUM CONDITIONS
The High Precision Thermostat HPT-HYDRA
p 109 N94-10124
Non-equilibrium solidification in undercooled Ni-B alloys p 86 N94-10196
NONEQUILIBRIUM FLOW
Studies on scramjet nozzles. Part 1: Performance of two dimensional nozzles
[NAL-TR-1149] p 27 N94-10367
Calculations of viscous nonequilibrium flows in nozzles
p 8 N94-10455
Nonequilibrium hypersonic flow in a wind-tunnel nozzle
p 8 N94-10456
Hypersonic, nonequilibrium flow over a cylindrically blunted 6 deg wedge
[NASA-TM-108994] p 162 N94-12571
NONEQUILIBRIUM THERMODYNAMICS
Canonical operator formulation of nonequilibrium thermodynamics
[DE93-613028] p 409 N94-10388
Nonequilibrium hypersonic flow in a wind-tunnel nozzle
p 8 N94-10456
Hypersonic multi block flow simulations around space vehicles including non-equilibrium chemistry
p 9 N94-10460
Thermal and chemical non equilibrium hypersonic flow computations p 10 N94-10465
Arcjet space thrusters
[NASA-CR-193191] p 46 N94-10700
NONFLAMMABLE MATERIALS
Proceedings of the International Conference for the Promotion of Advanced Fire Resistant Aircraft Interior Materials
[DOT/FAA/CT-93/3] p 17 N94-10766
Fire-resistant hydrolytically stable poly(arylene phosphine oxide) material systems p 19 N94-10780
A non-halogenated, flame retarded polycarbonate
p 19 N94-10781
Flammability parameters of materials: Ignition, combustion, and flame spread p 20 N94-10788
Future material development trends for commercial airplane interiors p 21 N94-10792
Future needs in the development of materials for aircraft interiors and equipment p 21 N94-10794
Proceedings of the International Conference for the Promotion of Advanced Fire Resistant Aircraft Interior Materials
[AD-A266057] p 22 N94-12384
NONINTRUSIVE MEASUREMENT
Local measurement of temperatures and concentrations: A review for hypersonic flows
p 4 N94-10434
NONLINEAR EQUATIONS
Non-linear liquid bridge dynamics p 100 N94-10074
General renormalized statistical approach with finite cross-field correlations
[DE93-617846] p 386 N94-10396
A symmetrical form for equations of a nonlinear spiral magnetic
[DE93-621350] p 344 N94-11033
Dynamics and control of coherent structures in the turbulent wall layer: An overview p 31 N94-11494
Nonlinear and dynamic analysis of flight
p 32 N94-11496
Spline approximation for system of n-th order nonlinear ordinary differential equations
[DE93-608188] p 346 N94-11507
NONLINEAR FILTERS
Nonlinear resonance: Noise-assisted information processing in physical and neurophysiological systems
[AD-A265161] p 313 N94-11890
NONLINEAR OPTICS
Nonlinear Dynamics in Optical Systems. Postdeadline papers presented at the Optical Society of America Conference
[AD-A264958] p 375 N94-10486
Nonclassical states of the second optical harmonic in the presence of self-action p 375 N94-10567
Disturbance, the uncertainty principle and quantum optics p 375 N94-10569
Photon number amplification/duplication through parametric conversion p 376 N94-10572
Non classical effects in planar waveguides
p 376 N94-10574
Squeezing in phase-conjugated resonance fluorescence p 376 N94-10576
Second and third order nonlinear optical properties of crystalline inorganic/organic complexes
[DE93-011883] p 173 N94-10755
Lattice-matched heteroepitaxy of wide gap ternary compound semiconductors p 400 N94-11441
The laser second threshold: Its exact analytical dependence on detuning and relaxation rates
[DE93-619706] p 175 N94-11633
A relaxation study of poled nonlinear optical polymers by infrared reflection-absorption spectroscopy
[AD-A265797] p 93 N94-12380
Limitations to the quality of optical phase conjugation by stimulated Brillouin scattering
[AD-A266006] p 383 N94-12389
Engineering solid-state materials. Strategies for modeling and packing control of molecular assemblies into 3-D networks
[AD-A265291] p 404 N94-12438
Nonlinear optical spectroscopy of Ag(111) in electrolyte and in vacuum
[AD-A265622] p 79 N94-12534
Preparation of stable photopatternable polymeric materials for non-linear optics
[AD-A265359] p 95 N94-12577
NONLINEAR SYSTEMS
Chemical pattern formation under microgravity
p 121 N94-10227
Balancing of the normalized right coprime factorization of a nonlinear system
[MEMO-1096] p 341 N94-10273
On output linearization of observable dynamics
[MEMO-1105] p 341 N94-10276
Nonlinear Dynamics in Optical Systems. Postdeadline papers presented at the Optical Society of America Conference
[AD-A264958] p 375 N94-10486
On the Sobolev systems with ellipsoid cavities
[DE92-641290] p 148 N94-10530
Convergence theorems for a class of nonlinear maps in uniformly smooth Banach spaces
[DE92-641347] p 343 N94-10531
Classical gravity coupled to Liouville theory
[DE93-613049] p 275 N94-10798
Detecting non-linearities in stationary time series
[W-9223] p 344 N94-10906
Creation and annihilation of solitons in nonlinear integrable systems
[DE93-621379] p 365 N94-11078
Optimisation methods for solving separable nonlinear least squares problems
[ISVR-TR-219] p 345 N94-11217
Trajectory pattern inverse dynamics and control of nonlinear dynamics systems with application to flexible structures p 181 N94-11219
Stability in Aerospace Systems
[AGARD-R-789] p 31 N94-11489
Chaotic time series analysis p 31 N94-11490
On non-linear longitudinal stability of an aircraft in a dive in the presence of atmospheric disturbances
p 31 N94-11492
Modeling nonlinear aerodynamic loads for aircraft stability and control analysis p 32 N94-11499
Transactions of the 10th Army Conference on Applied Mathematics and Computing
[AD-A265098] p 318 N94-11678
Nonlinear stability calculations of pipe flow
p 163 N94-12612
Nonlinear instability of a laminar flow in a rectangular duct and generation of the turbulent secondary flow
p 164 N94-12622
The thermodynamics of the nonlinear shear flows
p 169 N94-12728

NONLINEARITY

Effects of axial and centrifugal forces on the stability of liquid bridges p 102 N94-10083

Nonlinear second harmonic generation by light wave-plasma interaction in oscillating magnetic field
[DE93-613723] p 386 N94-10387

Nonlinear MHD-waves in a dissipative plasma with hall currents
[DE93-617844] p 386 N94-10395

Singularity spectrum of self-organized criticality
[DE93-613820] p 348 N94-10404

On the Sobolev systems with ellipsoid cavities
[DE92-641290] p 148 N94-10530

On the stability of stationary regimes in a distributed autovibration system with external feedback
[DE93-620979] p 141 N94-10543

An exactly solvable model of an oscillator with nonlinear coupling and zeros of Bessel functions
p 349 N94-10573

Non-stationary and non-linear dispersive medium as external field which generates the squeezed states
p 380 N94-10605

The nonlinear evolution of modes on unstable stratified shear layers
[NASA-CR-191492] p 149 N94-10810

A self-consistent model of non-linear parameterization of turbulent diffusion in atmospheric boundary layer
[DE93-011950] p 275 N94-11052

Time-resolved optical studies of charge relaxation and charge transfer at electrode interfaces
[DE93-013985] p 398 N94-11117

Simulation study of dynamo structure in reversed field pinch
[DE93-771406] p 390 N94-11128

Negative viscosity and generation of dissipative solitons and zonal dissipative structures by drift waves
[DE93-621656] p 392 N94-11212

Non-linear dynamics of automodulation processes in coupled distributed autovibration systems with delay
[DE93-620976] p 143 N94-11365

Effects of wave nonlinearity on ERS-1 radar altimeter returns: A preliminary investigation p 235 N94-11722

Nonlinear aspects of transonic aeroelasticity
[UTIAS-RN-345] p 15 N94-11857

Nonlinear resonance: Noise-assisted information processing in physical and neurophysiological systems
[AD-A265161] p 313 N94-11890

Cardiovascular dynamics during space sickness and deconditioning p 311 N94-12007

Estimation with multisensor/multiscan detection fusion
[AD-A265673] p 138 N94-12338

A relaxation study of poled nonlinear optical polymers by infrared reflection-absorption spectroscopy
[AD-A265797] p 93 N94-12380

Nonlinear optical spectroscopy of Ag(111) in electrolyte and in vacuum
[AD-A265622] p 79 N94-12534

Three-dimensional finite element analysis of explosive safety facilities: A technology assessment
[AD-A265700] p 35 N94-12562

Preparation of stable photopatternable polymeric materials for non-linear optics
[AD-A265359] p 95 N94-12577

Nonlinear effects in ferrite tuned cavities
[DE93-014136] p 374 N94-12785

NONNEWTONIAN FLOW

Numerical simulation of the non-Newtonian mixing layer p 159 N94-12314

NONRELATIVISTIC MECHANICS

Observables, measurements and phase operators from a Bohmian perspective p 378 N94-10589

Non-gauge phase transformations in quantum transition amplitudes p 378 N94-10596

NONUNIFORMITY

DILUTE: A code for studying beam evolution under RF noise
[DE93-011605] p 133 N94-10960

NORMAL DENSITY FUNCTIONS

Positive phase space distributions and uncertainty relations p 379 N94-10598

NORMALITY

Balancing of the normalized right coprime factorization of a nonlinear system
[MEMO-1096] p 341 N94-10273

NORMALIZING (STATISTICS)

ERS-1 scatterometer data characteristics and wind retrieval skill p 233 N94-11709

NORTH ATLANTIC TREATY ORGANIZATION (NATO)

AGARD highlights 92/2, September 1992
[AGARD-HIGHLIGHTS-92/2] p 497 N94-11820

NORTH SEA

Calibration of ERS-1 altimetry over the North Sea
p 234 N94-11716

NORWAY

Coastal ocean studies with ERS-1 SAR during NORCSEX 1991 p 234 N94-11720

NOSE TIPS

Computation of hypersonic nosetip heat transfer rates for an M829-like projectile
[AD-A263226] p 16 N94-11870

NOZZLE DESIGN

Gas-liquid jets under reduced gravity conditions
p 103 N94-10091

A CFD-based aerodynamic design procedure for hypersonic wind-tunnel nozzles p 9 N94-10458

Control of jet noise
[NASA-CR-193612] p 358 N94-11176

NOZZLE FLOW

Numerical simulation of the flow through a scramjet engine p 3 N94-10425

Calculations of viscous nonequilibrium flows in nozzles
p 8 N94-10455

Static internal performance of a single expansion ramp nozzle with multiaxis thrust vectoring capability
[NASA-TM-4450] p 12 N94-10675

Control of jet noise
[NASA-CR-193612] p 358 N94-11176

An overview of the capabilities of ARA for the measurement of nozzle discharge and thrust
[ARA-MEMO-378] p 55 N94-12283

NOZZLE GEOMETRY

Studies on scramjet nozzles. Part 1: Performance of two dimensional nozzles
[NAL-TR-1149] p 27 N94-10367

NUCLEAR ASTROPHYSICS

Nuclear astrophysics
[DE93-010569] p 425 N94-10292

Planck scale effects on the Majoron
[DE93-613120] p 410 N94-10545

Experimental and theoretical high energy physics program
[DE93-013336] p 373 N94-12600

NUCLEAR BINDING ENERGY

Recent advances in electron momentum spectroscopy
[DE93-610149] p 361 N94-10333

Three-nucleon problem with phase equivalent potentials
[DE93-617731] p 363 N94-10722

Quantum dynamics of helium clusters
[AD-A266060] p 411 N94-10874

Interatomic interactions in BCC and FCC lattices of transition metals
[DE93-621541] p 398 N94-11090

A generalized Bethe-Weizsaecker mass formula for strange hadronic matter
[DE93-011010] p 368 N94-11620

NUCLEAR ENERGY

Directory of IAEA databases
[DE93-622837] p 420 N94-11818

NUCLEAR EXPLOSIONS

Sensitivities of calculated residual stress to separation distances of two simultaneous events
[DE92-019571] p 98 N94-10751

NUCLEAR FUEL ELEMENTS

Space nuclear thermal propulsion nuclear element tests at Sandia National Laboratories
[DE93-002301] p 45 N94-10282

A critical assembly designed to measure neutronic benchmarks in support of the Space Nuclear Thermal Propulsion program
[DE92-040974] p 371 N94-10529

TFE verification program
[DE93-009609] p 373 N94-11694

NUCLEAR FUSION

Heavy ion fusion at sub-barrier energies: Progress and questions
[DE93-011764] p 372 N94-11124

Experiments with energetic (mu)d and (mu)t emitted from solid hydrogen
[DE93-010252] p 373 N94-12542

NUCLEAR LIGHTBULB ENGINES

In-reactor testing of the closed cycle gas core reactor: The Nuclear Light Bulb concept
[DE93-004053] p 370 N94-10149

NUCLEAR MAGNETIC RESONANCE

Si-29 NMR spectroscopy of naturally-shocked quartz from Meteor Crater, Arizona: Correlation to Kieffer's classification scheme p 80 N94-12087

NMR spectroscopy of experimentally shocked single crystal quartz: A reexamination of the NMR shock barometer p 81 N94-12258

The 13C and 15N solid-state NMR of copolymers of nylon 6 and 7: Observation of a stable pseudohexagonal phase
[AD-A265799] p 94 N94-12381

NMR characterization of polymers formed in diazotizing mixtures of luminol and 3-amino-L-tyrosine
[AD-A266093] p 94 N94-12536

NUCLEAR MODELS

Coulomb effects in low-energy nuclear fragmentation
[NASA-TP-3352] p 485 N94-12434

NUCLEAR PHYSICS

Report of the Workshop on Light Particle-Induced Reactions
[DE93-752300] p 360 N94-10317

The legacy of uncertainty p 376 N94-10577

Report of the third Seminar on Nuclear Physics at the Energy Region of the JAERI Tandem-Booster Accelerator
[DE93-754330] p 372 N94-11043

Directory of IAEA databases
[DE93-622837] p 420 N94-11818

NUCLEAR POTENTIAL

Quasi-relativistic effects in barrier-penetration processes
[DE93-617730] p 410 N94-10721

NUCLEAR POWER PLANTS

Techniques, processes, and measures for software safety and reliability
[DE93-012379] p 322 N94-10347

Renewable energy sources 1991, part 3
[DE93-605594] p 263 N94-11505

Statistical and optimization methods to expedite neural network training for transient identification
[DE93-009985] p 340 N94-11644

Department of Energy fundamentals handbook: Engineering symbology, prints, and drawings
[DE93-012220] p 129 N94-11670

NUCLEAR PROPULSION

Space nuclear thermal propulsion nuclear element tests at Sandia National Laboratories
[DE93-002301] p 45 N94-10282

Space nuclear technology
[DE93-010184] p 45 N94-10299

A critical assembly designed to measure neutronic benchmarks in support of the Space Nuclear Thermal Propulsion program
[DE92-040974] p 371 N94-10529

Applying design principles to fusion reactor configurations for propulsion in space
[NASA-TM-108247] p 47 N94-11053

NUCLEAR RADIATION SPECTROSCOPY

Proceedings of the third workshop on light quark meson spectroscopy
[DE93-754138] p 363 N94-10696

NUCLEAR REACTIONS

Report of the Workshop on Light Particle-Induced Reactions
[DE93-752300] p 360 N94-10317

The multiplicity spectra of the (169)Tm(n, gamma) reaction
[DE93-617733] p 364 N94-10835

Monochromator SP-017. The results of the first experiments
[DE93-617463] p 372 N94-10849

Double-lambda compound nucleus and the formation of double hypernuclei
[DE93-754289] p 365 N94-11040

Report of the third Seminar on Nuclear Physics at the Energy Region of the JAERI Tandem-Booster Accelerator
[DE93-754330] p 372 N94-11043

Coulomb effects in low-energy nuclear fragmentation
[NASA-TP-3352] p 485 N94-12434

Final state interactions and inclusive nuclear collisions
[NASA-TP-3353] p 373 N94-12435

NUCLEAR REACTOR CONTROL

GRISET certification package
[DE93-011783] p 327 N94-11246

NUCLEAR REACTORS

GRISET certification package
[DE93-011783] p 327 N94-11246

Research results
[DE93-753403] p 372 N94-11595

NUCLEAR RESEARCH

Directory of IAEA databases
[DE93-622837] p 420 N94-11818

NUCLEAR RESEARCH AND TEST REACTORS

In-reactor testing of the closed cycle gas core reactor: The Nuclear Light Bulb concept
[DE93-004053] p 370 N94-10149

Space nuclear technology
[DE93-010184] p 45 N94-10299

A critical assembly designed to measure neutronic benchmarks in support of the Space Nuclear Thermal Propulsion program
[DE92-040974] p 371 N94-10529

Development of plastic capsule for research reactor irradiation
[DE93-753186] p 372 N94-11591

NUCLEAR ROCKET ENGINES

Space nuclear technology
[DE93-010184] p 45 N94-10299

Applying design principles to fusion reactor configurations for propulsion in space
[NASA-TM-108247] p 47 N94-11053

NUCLEAR SPIN

High spin properties of nuclei [DE93-008788] p 358 N94-10254

The multiplicity spectra of the (169)Tm(n, gamma) reaction [DE93-617733] p 364 N94-10835

NUCLEAR STRUCTURE

High spin properties of nuclei [DE93-006788] p 358 N94-10254

Nuclear structure models: Applications and development [DE93-012934] p 368 N94-11813

NUCLEATE BOILING

Gravity and electric field effects on pool boiling heat transfer p 121 N94-10226

NUCLEATION

STARDUST: A simulation experiment of cosmic dust analogues production in microgravity conditions p 113 N94-10175

Coupled growth of cells and bubbles in directional solidification of succinonitrile-acetone alloys p 118 N94-10206

Study of vapor bubble growth in a supersaturated liquid p 122 N94-10232

Magnetization reversal by nucleation [DE93-610313] p 350 N94-10313

Structural development in ceramic precursor sols and gels [AD-A264354] p 90 N94-11281

Joint pain and Doppler-detectable bubbles in altitude (Hypobaric) decompression p 312 N94-11542

A mechanism for the reduction in risk of decompression sickness in microgravity environment p 312 N94-11545

An ellipsometry investigation of nucleation and growth of electron cyclotron resonance plasma deposited silicon films [AD-A265037] p 401 N94-11651

Carbon and nitrogen in Type 2 supernova diamonds p 431 N94-12166

Development of a molecular beam technique to study early solar system silicon reactions p 432 N94-12224

NUCLEI (NUCLEAR PHYSICS)

Report of the third Seminar on Nuclear Physics at the Energy Region of the JAERI Tandem-Booster Accelerator [DE93-754330] p 372 N94-11043

NUCLEON-NUCLEON INTERACTIONS

Workshop on NN Bremsstrahlung and Polarization Observables [DE93-010181] p 361 N94-10334

P-matrix description of the two-particle interaction [DE93-617690] p 361 N94-10549

Studies of P-matrix formalism on the basis of the potential description of two-particle interaction [DE93-617691] p 362 N94-10550

The determination of nucleon-nucleon scattering phases by the phase functions method [DE93-617729] p 362 N94-10557

Three-nucleon problem with phase equivalent potentials [DE93-617731] p 363 N94-10722

NUCLEON-NUCLEON SCATTERING

Crossing-odd spin effects in the dipole model of hadron scattering [DE93-617692] p 362 N94-10551

The determination of nucleon-nucleon scattering phases by the phase functions method [DE93-617729] p 362 N94-10557

NUCLEONS

Crossing-odd spin effects in the dipole model of hadron scattering [DE93-617692] p 362 N94-10551

A generalized Bethe-Weizsaecker mass formula for strange hadronic matter [DE93-011010] p 368 N94-11620

NUCLEOPHILES

Synthesis, characterization, and modification of poly(organophosphazenes), that bear both 2,2,2-trifluoroethoxy and phenoxy groups [AD-A264913] p 92 N94-11847

NUCLIDES

Measurements of cosmogenic nuclides in lunar rock 64455 p 437 N94-12033

NUMERICAL ANALYSIS

Aerosol sampling models survey [AD-A265903] p 75 N94-10337

Summary of research in progress at ICASE [NASA-CR-191481] p 318 N94-11198

Normal modes of the world's oceans: A numerical investigation using Proudman functions [NASA-TM-104587] p 288 N94-11358

Numerical simulations of thermal convection in rapidly rotating spherical fluid shells p 153 N94-11635

Research in computing and applied mathematics [AD-A266137] p 331 N94-11657

Measurement of wave parameters by HF ocean radar p 192 N94-11903

Time evolution of cross-stream exchange associated with the variations in the Kuroshio p 197 N94-11936

An application of reduced gravity model to mesoscale eddies p 199 N94-11945

Remote sensing for numerical modelling of radiative transfer processes in ocean environment p 204 N94-11973

A development on estimation method of undersea light p 204 N94-11974

Atmospheric correction plans for SeaWiFS p 204 N94-11975

Implications of aerosol retrieval and atmospheric correction in remote sensing p 205 N94-11978

The upwelling radiation at the top of the atmosphere in coastal region p 205 N94-11981

Incident shortwave and longwave radiations over the western North Pacific and the Sea of Okhotsk derived from GMS-WEFAX images p 205 N94-11982

Studies of dynamical processes affecting the distribution of stratospheric ozone [NASA-CR-193477] p 279 N94-12560

Observations of eddy fields in the Northwest Pacific by GEOSAT altimetry p 207 N94-12639

Theory and oceanographic applications of satellite altimeter measurements p 208 N94-12641

A numerical study of deep convection at high latitudes p 210 N94-12652

Microwave radiometry of ice cover in polar regions p 210 N94-12655

Study on diffusion phenomena of river effluents issued into sea around Japan with satellite remote sensing data p 212 N94-12664

Delineation of mesoscale features of ocean on satellite IR image p 214 N94-12675

The warm eddy detection from NOAA/AVHRR thermal images using the Hough transformation p 220 N94-12713

Variability of the mixed layer depth in the North Pacific Ocean as calculated by a 3-D semi-analytical mixed layer remote sensing model p 221 N94-12718

Coupled numerical model for altimetric data assimilation and velocity field analysis p 227 N94-12752

NUMERICAL CONTROL

Position and force control of a vehicle with two or more steerable drive wheels [DE93-012512] p 177 N94-10269

AD100/ADSIM, ACSL, and MATLAB output comparisons using frequency-response analysis [DE93-009640] p 47 N94-11122

Airborne optical tracking control system design study [DE93-009515] p 382 N94-11662

NUMERICAL FLOW VISUALIZATION

Study on diffusion phenomena of river effluents issued into sea around Japan with satellite remote sensing data p 212 N94-12664

Aspects of applying a relaxation method to computing sea surface velocities from sea surface temperature images p 214 N94-12679

NUMERICAL INTEGRATION

On the depletion in the outer asteroid belt and the structure of the 4 to 3 mean motion resonance p 426 N94-11596

NUMERICAL STABILITY

A reliable stability test for exponential polynomials [MEMO-COSOR-92-48] p 341 N94-10168

Numerical simulations of thermal convection in rapidly rotating spherical fluid shells p 153 N94-11635

Summation by parts, projections, and stability [NASA-CR-194290] p 346 N94-12776

NUMERICAL WEATHER FORECASTING

Simulation of images of water vapor channel and infrared split channel p 190 N94-11081

Validation of ERS-1 wind and wave data by use of operational forecast models p 233 N94-11710

A preliminary C-band scatterometer model function for the ERS-1 AMI instrument p 233 N94-11715

NUSSELT NUMBER

On temperature distribution in non-participating medium with radiation boundary condition [DE93-619375] p 153 N94-11604

NYLON (TRADEMARK)

Wetting effects on nylon spheres engulfment in ice p 115 N94-10189

The 13C and 15N solid-state NMR of copolymers of nylon 6 and 7: Observation of a stable pseudohexagonal phase [AD-A265799] p 94 N94-12381

O

O RING SEALS

Durability of a carbon segmented circumferential seal for a liquid oxygen turbopump [NAL-TR-1155] p 178 N94-10369

Check valve with poppet dashpot/frictional damping mechanism [NASA-CASE-MSC-21950-1] p 179 N94-10658

OBJECT-ORIENTED PROGRAMMING

An object-oriented model for extensible concurrent systems: The composition-filters approach [MEMO-INF-92-87] p 320 N94-10166

Database computing in HEP [DE93-011765] p 419 N94-11105

Object oriented implementation of adaptive mesh refinement algorithms [DE93-011885] p 325 N94-11112

Development of generic field classes for finite element and finite difference problems [DE93-011678] p 345 N94-11225

Impacts of object-oriented technologies: Seven years of SEL studies p 329 N94-11425

The MERMAID project p 329 N94-11426

Reuse: A knowledge-based approach p 329 N94-11430

Large project experiences with object-oriented methods and reuse p 329 N94-11431

The relational-to-object-oriented cross-model accessing capability in a multi-model and multi-lingual database system [AD-A264911] p 420 N94-11846

OBLIQUE SHOCK WAVES

Numerical calculation of scramjet inlet flow [NAL-TR-1174T] p 27 N94-10370

Flow development in a circular pipe in the UTIAS/RPI M = 8.3 gun tunnel p 6 N94-10442

Development of a Delaunay-based adaption scheme with applications to complex three-dimensional rotational flows p 149 N94-10824

Evaluation of dual flow thrust vectored nozzles with exhaust stream impingement [NASA-CR-193292] p 150 N94-10912

OBSERVABILITY (SYSTEMS)

On output linearization of observable dynamics [MEMO-1105] p 341 N94-10276

OBSTACLE AVOIDANCE

Measures for simulator evaluation of a helicopter obstacle avoidance system p 35 N94-11535

OCCLUSION

Optimal hemicube sampling [DE93-010499] p 334 N94-12591

OCCUPATION

A summer program in mathematics and computer science for academically oriented student [AD-A263467] p 415 N94-11517

Career Information in the Mathematical Sciences (CIMS) [DE93-013780] p 318 N94-11817

OCEAN BOTTOM

Low power digital recorder development [AD-A265921] p 170 N94-10704

Acoustics of bubbly sediments [AD-A263726] p 288 N94-11299

A model for the subduction mechanics of flexible lithosphere and its viscous coupling to the mantle using power-law rheologies p 277 N94-11585

Acoustic characteristics of side scan sonar and sub-bottom profiler for 10,000 m class ROV p 172 N94-11916

The extraction of bottom characteristics and mapping in Kin Bay, Okinawa Main Island, Japan, using LANDSAT-5/TM and SPOT-1/HRV data p 197 N94-11931

On resolution of underwater stereo photogrammetry p 172 N94-11966

Impact mineralogy and chemistry of the cretaceous-tertiary boundary at DSDP site 576 p 282 N94-12091

Iron and nickel isotopic mass fractionation in deep-sea spherules p 282 N94-12199

Preliminary analysis of the FLIP array data from the NOBS experiment [AD-A265911] p 289 N94-12349

Mapping bathymetric slopes from bathymetry data [AD-A265923] p 290 N94-12350

Mapping of sea bottom topography with ERS-1 C-band SAR p 254 N94-12525

Integrated marine survey system p 217 N94-12693

A detailed investigation of the benthic regime in the Clarion-Clipperton province of the Pacific and a forecast of consequences of manganese nodule mining p 224 N94-12733

Bottom currents and possibilities for near bottom layer environmental investigations in the Pacific by means of self contained bottom stations p 224 N94-12734

Autonomous self contained bottom pop-up stations for study of the benthic layer and seismicity of the ocean's bottom p 224 N94-12735

Convective and dynamic instability in meridional trenches p 225 N94-12739

Model of Kuroshio region circulation p 229 N94-12765

OCEAN COLOR SCANNER

Application of the airborne ocean color imager for commercial fishing [NASA-TM-103986] p 231 N94-11378

OCEAN CURRENTS

Topex/Poseidon: A United States/France mission. Oceanography from space: The oceans and climate [NASA-TM-108253] p 43 N94-10699

Study of the surface circulation to the North of Bransfield Strait, Antarctica [INPE-5472-TDI/503] p 288 N94-11200

Near surface ocean processes: Acoustical observations, ambient sound, and Langmuir circulation p 288 N94-11447

Mapping of the East Australian current with the ERS-1 SAR and shipborne studies p 234 N94-11717

Preliminary analysis of circulations over the Indian Ocean and adjoining regions using ERS-1 surface winds in the NCMRWF data assimilation system p 234 N94-11719

Ocean circulation revealed by ice floe tracking p 240 N94-11759

ERS-1 radar altimetry over the North Atlantic p 242 N94-11772

An investigation using empirical orthogonal functions and objective analysis to analyse the vertical temperature structure of a gulf stream meander [AD-A265116] p 289 N94-11868

Proceedings of the PORSEC 1992 in Okinawa: Conference for Pacific Ocean Environments and Probing, volume 1 [JTN-93-80418] p 191 N94-11894

HF ocean radar system at Okinawa Radio Observatory p 139 N94-11902

Exchange of bay water with ocean current monitored by the NOAA satellite p 193 N94-11908

Current structures in the western equatorial Pacific during JAPACS cruises p 193 N94-11911

Ocean-ice interaction study of waves and mesoscale features p 197 N94-11935

The coherent structure in the oceanic turbulence around Japan Islands Chain forced by an air, sea, and solid Earth interaction p 198 N94-11940

An application of reduced gravity model to mesoscale eddies p 199 N94-11945

A study of pollution courses of spilled oil floatation in the outer ocean p 205 N94-11983

Circulation of North Pacific Intermediate Water p 206 N94-11985

Roles of the NEC and MC in the formation and evolution of the Equatorial Pacific Warm Pool p 206 N94-11990

Proceedings of the PORSEC 1992 in Okinawa: Conference for Pacific Ocean Environments and Probing, volume 2 [JTN-93-80419] p 207 N94-12635

Surface eddy fluxes from the GEOSAT satellite altimeter p 208 N94-12643

Measurement of eddy structure and movement in the north-east Pacific with the GEOSAT altimeter p 209 N94-12647

Observation of warm current at the boundary from north equatorial current to Kuroshio by NOAA/AVHRR p 214 N94-12676

The WOCE/TOGA Surface Velocity Programme (SVP) p 216 N94-12691

The acoustic arrangement for measuring vertical structure of sea current p 223 N94-12729

Turbulence generation in the Pacific undercurrent by shear p 223 N94-12730

A detailed investigation of the benthic regime in the Clarion-Clipperton province of the Pacific and a forecast of consequences of manganese nodule mining p 224 N94-12733

Bottom currents and possibilities for near bottom layer environmental investigations in the Pacific by means of self contained bottom stations p 224 N94-12734

Autonomous self contained bottom pop-up stations for study of the benthic layer and seismicity of the ocean's bottom p 224 N94-12735

Complex (hydrodynamic, satellite) monitoring of dynamic structures in the western Pacific with the aim of forecasting the marine ecosystems behaviour p 227 N94-12753

Study of the admixture diffusion in the sea using remote techniques p 228 N94-12759

Mixing of drifter ensemble by mesoscale currents p 228 N94-12760

Experimental and theoretical investigation of undular bore formation upstream the bank p 229 N94-12764

OCEAN DATA ACQUISITIONS SYSTEMS

One-year mooring of an ADCP in the central region of the Kuroshio west of Okinawa p 194 N94-11913

Acoustic Doppler current profiling of the Kuroshio over the East China Sea shelf slope p 194 N94-11914

Measurement of the surface layer current averaged vertically using Multipaths Inverted Echosounder p 194 N94-11915

Acoustic characteristics of side scan sonar and sub-bottom profiler for 10,000 m class ROV p 172 N94-11916

The development of phytoplankton sensing system with optical fiber p 203 N94-11967

Ocean measuring experiments using optical fiber distributed temperature sensor p 172 N94-11968

ERS-1 and Almaz SAR ocean wave imaging over the Gulf Stream and the Grand Banks p 251 N94-12505

Proceedings of the PORSEC 1992 in Okinawa: Conference for Pacific Ocean Environments and Probing, volume 2 [JTN-93-80419] p 207 N94-12635

A surface water monitoring system: A device for the sea-truth observations p 210 N94-12657

ADCP evidence for upper layer circulation in northeast of the South China Sea p 215 N94-12686

Development of a shuttle AUV for oceanographic measurement p 217 N94-12692

Integrated marine survey system p 217 N94-12693

Development of a buoy system for monitoring marine weather and marine life abundance p 217 N94-12694

Laser photoheterodyne interferometers for oceanographic investigations p 177 N94-12732

Autonomous self contained bottom pop-up stations for study of the benthic layer and seismicity of the ocean's bottom p 224 N94-12735

DISTERM: A shipboard data system for satellite monitoring of ocean and atmosphere p 226 N94-12749

The structure of hydrophysical measuring systems of vertical sounding and self-contained stations p 227 N94-12751

OCEAN DYNAMICS

Normal modes of the world's oceans: A numerical investigation using Proudman functions [NASA-TM-104587] p 288 N94-11358

Use of ERS-1 data at Saclant Undersea Research Centre p 233 N94-11714

Mapping of the East Australian current with the ERS-1 SAR and shipborne studies p 234 N94-11717

SAR imaging of dynamical features in the English Channel p 234 N94-11721

SAR ocean imaging in the Gulf of Alaska p 235 N94-11723

Comparisons of ERS-1 altimeter height data and the Fine Resolution Antarctic Model (FRAM) p 235 N94-11725

Air-sea-ice interactions in the Weddell Sea p 239 N94-11753

Space and time variability of the Gulf Stream using ERS-1 ALT-OPR02 data p 242 N94-11769

Circulation of North Pacific Intermediate Water p 206 N94-11985

Shear, strain and thermohaline vertical fine structure in the upper ocean [AD-A265961] p 289 N94-12348

ERS-1 and Almaz SAR ocean wave imaging over the Gulf Stream and the Grand Banks p 251 N94-12505

A new model for Synthetic Aperture Radar (SAR) images from ocean scatter p 251 N94-12508

On the extraction of ocean wave spectra from ERS-1 SAR wave mode image spectra p 251 N94-12509

Coastal morphodynamics and energetic characteristics of swell studied with ERS-1 SAR p 254 N94-12524

ERS-1 imaging radar over the Waddensea-North Netherlands p 254 N94-12526

Comparison of GEOSAT sea surface height and model-simulated surface dynamic height p 208 N94-12644

Wind-wave and foam dynamics from optical and radar airborne observations p 226 N94-12745

OCEAN MODELS

Validation of ERS-1 wind and wave data by use of operational forecast models p 233 N94-11710

Use of ERS-1 data at Saclant Undersea Research Centre p 233 N94-11714

Evaluation of two January - June 1992 ERS-1 AMI wind vector data sets p 235 N94-11724

Comparisons of ERS-1 altimeter height data and the Fine Resolution Antarctic Model (FRAM) p 235 N94-11725

Air-sea-ice interactions in the Weddell Sea p 239 N94-11753

Remote sensing and the air-sea boundary layers p 191 N94-11896

Evaluation of ECMWF latent heat flux in TOGA CD-ROM p 195 N94-11921

Circulation of North Pacific Intermediate Water p 206 N94-11985

A new model for Synthetic Aperture Radar (SAR) images from ocean scatter p 251 N94-12508

Proceedings of the PORSEC 1992 in Okinawa: Conference for Pacific Ocean Environments and Probing, volume 2 [JTN-93-80419] p 207 N94-12635

Comparison of GEOSAT sea surface height and model-simulated surface dynamic height p 208 N94-12644

Measurement of eddy structure and movement in the north-east Pacific with the GEOSAT altimeter p 209 N94-12647

Preliminary results from a satellite altimetric data assimilation using a Kalman filter and smoother p 209 N94-12648

Fluctuations of the Kuroshio extension detected by the GEOSAT altimetry data p 209 N94-12649

Mean flow and variability in the Kuroshio extension from GEOSAT altimetry data p 209 N94-12650

A numerical study of deep convection at high latitudes p 210 N94-12652

Verification of the atmosphere-ocean radiative transfer parametric models p 225 N94-12738

Convective and dynamic instability in meridional trenches p 225 N94-12739

Atmospheric correction for determination of average SST fields based on AVHRR data p 227 N94-12750

Coupled numerical model for altimetric data assimilation and velocity field analysis p 227 N94-12752

Complex (hydrodynamic, satellite) monitoring of dynamic structures in the western Pacific with the aim of forecasting the marine ecosystems behaviour p 227 N94-12753

Mesoscale dynamic structures of the Subarctic Frontal Zone in the Pacific Ocean p 227 N94-12754

Generation of internal waves near the shelf boundary p 229 N94-12763

Experimental and theoretical investigation of undular bore formation upstream the bank p 229 N94-12764

Model of Kuroshio region circulation p 229 N94-12765

Problem of climate change predictability and satellite radiation budget observations p 229 N94-12766

OCEAN SURFACE

Preliminary results on backscattering strength from a wind generated bubbly ocean surface [AD-A265006] p 287 N94-10490

Topex/Poseidon: A United States/France mission. Oceanography from space: The oceans and climate [NASA-TM-108253] p 43 N94-10699

Study of the surface circulation to the North of Bransfield Strait, Antarctica [INPE-5472-TDI/503] p 288 N94-11200

Near surface ocean processes: Acoustical observations, ambient sound, and Langmuir circulation p 288 N94-11447

A C-band wind scatterometer model derived from the data obtained during the ERS-1 calibration/validation campaign p 233 N94-11711

Calibration of ERS-1 altimetry over the North Sea p 234 N94-11716

Preliminary analysis of circulations over the Indian Ocean and adjoining regions using ERS-1 surface winds in the NCMRWF data assimilation system p 234 N94-11719

First results for the simultaneous estimation of the geoid and the sea surface topography by ERS-1 altimeter data p 241 N94-11765

Separation of geoid and sea surface topography in shallow water regions: A first ERS-1 radar altimeter data evaluation p 242 N94-11766

A stochastic-deterministic approach as an alternative to classical cross-over techniques in small ocean basins p 242 N94-11767

ERS-1 radar altimetry over the North Atlantic p 242 N94-11772

Preliminary geophysical investigation with ERS-1 35-day altimeter data p 243 N94-11775

Quick-look monitoring of the sea surface with ERS-1 fast delivery altimeter data p 243 N94-11777

Spatial scales of wave height p 244 N94-11782

Proceedings of the PORSEC 1992 in Okinawa: Conference for Pacific Ocean Environments and Probing, volume 1 [JTN-93-80418] p 191 N94-11894

Remote sensing and the air-sea boundary layers p 191 N94-11896

Effects of wind-roughened sea surface on ocean color remote sensing: Noise derived from reflected light and whitecaps p 191 N94-11898

An algorithm for the detection of mucilage (green slime) in the Adriatic Sea p 191 N94-11900

Remote sensing of the suspended matter distribution with high concentration in China Sea p 192 N94-11901

Statistical study of HF ocean radar echo p 139 N94-11905

Exchange of bay water with ocean current monitored by the NOAA satellite p 193 N94-11908

Variability of wind stress, and sensible and latent heat flux in the North Atlantic during SEASAT p 194 N94-11918

Evaporation and thermal/hydrologic balance in the Pacific p 195 N94-11919

A new expression for the production rate of sea water droplets on the sea surface p 195 N94-11920

Evaluation of ECMWF latent heat flux in TOGA CD-ROM p 195 N94-11921

Air-sea fluxes and universal constants in weak-turbulence theory of surface gravity waves p 195 N94-11922

Sea surface heat flux in the beginning of the Kuroshio p 195 N94-11923

Seasonal variation of the surface mixed layer in the subtropical re-circulation area of the North Pacific during OMLET p 195 N94-11924

Mixed layer heat budget of Kuroshio-Tango triangle using satellite and ship observations p 196 N94-11925

Estimation of solar radiation at the sea surface with geostationary meteorological satellite data p 196 N94-11926

Ocean wave detection by SAR p 197 N94-11932

On the determination of the SAR ocean surface scattering patch size p 197 N94-11933

The optical/computer hybrid processing of extracting ocean wave directional spectrum by airborne photograph p 197 N94-11934

Ocean-ice interaction study of waves and mesoscale features p 197 N94-11935

Time evolution of cross-stream exchange associated with the variations in the Kuroshio p 197 N94-11936

Warm streamers extended from Warm Core Rings (WCRs) and their role on fish migration and fishing ground formation p 198 N94-11938

The Kyucho events in Sukumo Bay induced by Kuroshio front disturbances p 198 N94-11939

The coherent structure in the oceanic turbulence around Japan Islands Chain forced by an air, sea, and solid Earth interaction p 198 N94-11940

Westward propagation of sea surface anomalies in the western North Pacific as seen by the altimeter and radiometer p 198 N94-11941

An application of reduced gravity model to mesoscale eddies p 199 N94-11945

The use of CZCS for primary production estimate in the Pacific p 199 N94-11946

CZCS derived chlorophyll distribution in Antarctic water during austral summer p 199 N94-11947

Seasonal changes of phytoplankton distributions in the Northwest Pacific detected by Coastal Zone Color Scanner p 200 N94-11948

Satellite-derived oceanic features p 200 N94-11949

Particle dynamics in the western subarctic Pacific: Implications from CZCS imagery p 200 N94-11950

High-reflectance water mass in Off-Sanriku area observed by CZCS p 200 N94-11951

Physical processes of microwave backscattering from laboratory wind-wave surfaces p 200 N94-11952

Experiment and results of the Italian activity in the field of ocean microwave backscattering p 200 N94-11953

Measurements of ocean cross-section with a side-looking airborne radar p 201 N94-11954

Dependence of oceanic microwave emission on wind direction p 201 N94-11957

Surface roughness variations across the Iceland-Faroes frontal region observed by the GEOSAT altimeter and NOAA AVHRR p 201 N94-11958

On the variability of wind speeds in the North Western Pacific observed by altimeter/GEOSAT and SSM/I/DMSP p 201 N94-11960

Observation of wind and waves by GEOSAT altimeter p 202 N94-11961

Availability of wind field over the North Pacific derived from data on ships-of-opportunity and analysis of long-term variabilities p 202 N94-11962

Wind field estimate by using one hour GMS data p 202 N94-11963

The Pacific responses exhibited by an OGCM to various wind fields p 202 N94-11964

Development of shipboard ocean lidar p 140 N94-11965

Bi-directional reflectance by oceanic waters studied via Monte-Carlo simulations p 203 N94-11971

Optical characteristics in Tokyo Bay p 204 N94-11972

Remote sensing for numerical modelling of radiative transfer processes in ocean environment p 204 N94-11973

Observations of the fractal properties of the Japan sea surface temperature patterns p 205 N94-11984

Sea surface temperature anomalies in the Arabian Sea p 206 N94-11988

Preliminary analysis of the FLIP array data from the NOBS experiment
[AD-A265911] p 289 N94-12349

A statistical analysis of sea state surface ERS-1 SAR-wave mode imagettes p 251 N94-12507

Ship traffic monitoring using the ERS-1 SAR p 253 N94-12521

Topography of the Western Mediterranean from the ERS-1 altimeter p 255 N94-12531

Proceedings of the PORSEC 1992 in Okinawa: Conference for Pacific Ocean Environments and Probing, volume 2
[JTN-93-80419] p 207 N94-12635

Analysis of GEOSAT wind data p 207 N94-12636

SSMI wind speed variability over the Pacific Ocean p 207 N94-12637

Observation of wave crests by satellite remote sensed data p 207 N94-12638

Observations of eddy fields in the Northwest Pacific by GEOSAT altimetry p 207 N94-12639

Variability of sea level and sea surface temperature anomalies in the equatorial Pacific p 208 N94-12640

Theory and oceanographic applications of satellite altimeter measurements p 208 N94-12641

Analysis of collinear passes of satellite altimeter data p 208 N94-12642

Surface eddy fluxes from the GEOSAT satellite altimeter p 208 N94-12643

Comparison of GEOSAT sea surface height and model-simulated surface dynamic height p 208 N94-12644

Principal oscillation pattern analysis of sea level variations in the tropical Pacific measured by the GEOSAT altimeter p 209 N94-12646

Measurement of eddy structure and movement in the north-east Pacific with the GEOSAT altimeter p 209 N94-12647

Preliminary results from a satellite altimetric data assimilation using a Kalman filter and smoother p 209 N94-12648

Fluctuations of the Kuroshio extension detected by the GEOSAT altimetry data p 209 N94-12649

Mean flow and variability in the Kuroshio extension from GEOSAT altimetry data p 209 N94-12650

Pacific rim sea ice as observed with the NIMBUS-7 SMMR p 210 N94-12651

The seasonal change of phytoplankton size distribution using optical fiber sensor p 210 N94-12656

A surface water monitoring system: A device for the sea-truth observations p 210 N94-12657

The phytoplankton bloom in the Kinu-ura Bay, Japan in the rainy season p 211 N94-12660

Evaluating the spread of red soil with LANDSAT TM data in coral reefs of Okinawa main island, southwestern Japan p 212 N94-12668

Measurement of the sea surface emissivity p 213 N94-12672

Evaluation of the method of geostrophic flow using NOAA-AVHRR data p 213 N94-12673

Satellite observations of the northeast monsoon coastal current p 214 N94-12678

Aspects of applying a relaxation method to computing sea surface velocities from sea surface temperature images p 214 N94-12679

Sea surface temperature difference between NOAA/AVHRR and in-situ observation p 215 N94-12680

Statistical features of mesoscale eddies at the Kuroshio front p 215 N94-12682

Intrusion of Kuroshio warm water into Sagami Bay p 215 N94-12683

A study of front dynamics off northeastern Taiwan based on the NOAA-AVHRR satellite remote sensing data p 215 N94-12684

Satellite thermal variations of Kuroshio in relation to storm floods p 215 N94-12685

Frontal zones in Pacific Ocean: Satellite and ship data analysis p 216 N94-12687

Swordfish (Xiphias gladius) catch distributions relative to environmental features observed from satellites off Coquimbo, Chile (30 deg S) p 216 N94-12688

Observation of cold coastal water with high turbidity around the southwestern tip of Korean Peninsula p 216 N94-12689

On the error characteristics of the sea surface temperature observed by satellite p 216 N94-12690

Seasonal variability of surface ocean color in the Omura Bay using multitemporal LANDSAT-5 TM data p 218 N94-12698

Study on air-sea interactions in the OMLET (Ocean Mixed Layer Experiment) area using satellite remote sensing p 220 N94-12710

The warm eddy detection from NOAA/AVHRR thermal images using the Hough transformation p 220 N94-12713

Applicability of satellite infrared data for the monitoring of coastal environments p 220 N94-12714

Satellite and moored buoy observations of polar frontal system over the Yamato Rise in the Japan Sea p 221 N94-12715

The relationship between skin and bulk sea surface temperatures p 221 N94-12716

Variability of the Kuroshio observed from satellite thermal imagery p 221 N94-12717

Variability of the mixed layer depth in the North Pacific Ocean as calculated by a 3-D semi-analytical mixed layer remote sensing model p 221 N94-12718

SST assimilation: Eastern Mediterranean case study p 221 N94-12719

Mapping of high density area of benthic diatom in Ariake Sea p 222 N94-12720

Advective surface velocity in the north west Pacific derived from NOAA AVHRR images p 222 N94-12721

Polarisation of backscattering radiation at remote sensing of ocean with impulse laser beam p 177 N94-12722

The method of investigation of the horizontal structure of the thermal fronts p 222 N94-12723

On a nonstationary dynamics of the north-west Pacific Ocean p 222 N94-12724

Optimum selection of spectral channels in the problem of remote sensing of phytoplankton concentration in ocean water p 223 N94-12726

Field research of wind wave spectrum variability p 223 N94-12727

Influence of the Kuroshio warm-core rings on hydrographic and fishery conditions off southern Kuril Islands p 224 N94-12737

Spatial variability of the ocean underwater dynamic noise from satellite radar sensing data p 225 N94-12740

Observations of film slicks and internal waves with Ka-band scatterometer p 225 N94-12741

Optical transfer operator of the atmosphere-ocean system p 225 N94-12742

Variability of spectral reflectance in coastal waters near the river plumes p 226 N94-12744

Wind-wave and foam dynamics from optical and radar airborne observations p 226 N94-12745

Observations of surface signatures in the north-west Pacific Ocean with the spaceborne SAR p 226 N94-12746

Radar observation of internal waves field in the north-west Pacific p 226 N94-12747

Atmospheric correction for determination of average SST fields based on AVHRR data p 227 N94-12750

Coupled numerical model for altimetric data assimilation and velocity field analysis p 227 N94-12752

Complex (hydrodynamic, satellite) monitoring of dynamic structures in the western Pacific with the aim of forecasting the marine ecosystems behaviour p 227 N94-12753

Mesoscale dynamic structures of the Subarctic Frontal Zone in the Pacific Ocean p 227 N94-12754

A possibility to define the location of epipelagic fish concentrations with assistance of satellite sensing p 228 N94-12757

High biological production of the tidal mixing zones on Japan Sea shelf p 228 N94-12758

Study of the admixture diffusion in the sea using remote techniques p 228 N94-12759

The algorithm of primary production determination p 228 N94-12761

Non-image visible polarization remote sensing of the ocean p 229 N94-12762

Generation of internal waves near the shelf boundary p 229 N94-12763

Experimental and theoretical investigation of undular bore formation upstream the bank p 229 N94-12764

Model of Kuroshio region circulation p 229 N94-12765

OCEAN TEMPERATURE

Preliminary results of the comparison of ATSR measurements with in situ sea temperatures
[DE93-013399] p 287 N94-10517

Proceedings of the PORSEC 1992 in Okinawa: Conference for Pacific Ocean Environments and Probing, volume 1
[JTN-93-80418] p 191 N94-11894

Ocean measuring experiments using optical fiber distributed temperature sensor p 172 N94-11968

Remote sensing of subsurface water temperature profile and backscattering coefficient in the China Sea by Ocean Lidar (OLIDAR) p 203 N94-11970

On an upwelling front, propagation of upwelling and vertical velocity in the eastern Arabian Sea during monsoon, 1987 p 206 N94-11987

Roles of the NEC and MC in the formation and evolution of the Equatorial Pacific Warm Pool p 206 N94-11990

Shear, strain and thermohaline vertical fine structure in the upper ocean
[AD-A265961] p 289 N94-12348
Proceedings of the PORSEC 1992 in Okinawa: Conference for Pacific Ocean Environments and Probing, volume 2
[JTN-93-80419] p 207 N94-12635
A possibility to define the location of epipelagic fish concentrations with assistance of satellite sensing
p 228 N94-12757
Generation of internal waves near the shelf boundary
p 229 N94-12763

OCEANOGRAPHIC PARAMETERS
Remote sensing and the air-sea boundary layers
p 191 N94-11896
Satellite observations of red tide events: Plans for EESI p 191 N94-11899
An algorithm for the detection of mucilage (green slime) in the Adriatic Sea p 191 N94-11900
Remote sensing of the suspended matter distribution with high concentration in China Sea
p 192 N94-11901
Measurement of wave parameters by HF ocean radar
p 192 N94-11903
Kuroshio observations by the HF ocean radar
p 192 N94-11904
Groundwave HF ocean surface radar
p 139 N94-11906
Air-sea interaction: Fluxes, a review
p 201 N94-11955
Impact of ERS-1 wind/wave/ice data on operational ocean forecasting p 250 N94-12500
A surface water monitoring system: A device for the sea-truth observations p 210 N94-12657
An integrated approach to total end-to-end quality control of ocean data in the real-time environment
p 211 N94-12662

OCEANOGRAPHY
Preliminary results of the comparison of ATSR measurements with in situ sea temperatures
[DE93-013399] p 287 N94-10517
Topex/Poseidon: A United States/France mission. Oceanography from space: The oceans and climate
[NASA-TM-108253] p 43 N94-10699
Study of the surface circulation to the North of Bransfield Strait, Antarctica
[INPE-5472-TDI/503] p 288 N94-11200
Validation of directional wave spectra from the ERS-1 during the ESA CAL/VAL campaign p 232 N94-11707
ERS-1 studies at the Department of Oceanography from Space, IFREMER/Brest (France) p 233 N94-11712
Use of ERS-1 data at Saclant Undersea Research Centre p 233 N94-11714
Arctic sea ice microwave signature and geophysical processes study p 240 N94-11754
Spatial scales of wave height p 244 N94-11782
The subduction experiment. Cruise report, R/V Oceanus, cruise number 250 legs 1 and 2. Subduction 2 mooring deployment and recovery cruise, 25 January-26 February 1992
[AD-A264922] p 289 N94-11853
Real-time tomography mooring
[AD-A264923] p 289 N94-11854
The requirement for global training programmes to meet the new remote sensing technology p 196 N94-11929
Remote sensing for numerical modelling of radiative transfer processes in ocean environment
p 204 N94-11973
Use of SAR-wave, altimeter, and wind-scatterometer data in an operational swell forecasting system
p 250 N94-12503
Real time processing wave spectra from satellite SAR
p 251 N94-12506
DISTERM: A shipboard data system for satellite monitoring of ocean and atmosphere
p 226 N94-12749

OCEANS
Sandia ocean modeling system programmer's guide and user's manual
[DE93-007427] p 287 N94-10153
Normal modes of the world's oceans: A numerical investigation using Proudman functions
[NASA-TM-104587] p 288 N94-11358
Real-time tomography mooring
[AD-A264923] p 289 N94-11854
The thermodynamic case for a water-rich Mars
p 463 N94-12170
Study on diffusion phenomena of river effluents issued into sea around Japan with satellite remote sensing data
p 212 N94-12664
Trajectory curving in underwater propagation of light
p 226 N94-12748
DISTERM: A shipboard data system for satellite monitoring of ocean and atmosphere
p 226 N94-12749

ODD-EVEN NUCLEI
High spin properties of nuclei
[DE93-008788] p 358 N94-10254

ODD-ODD NUCLEI
Nuclear structure models: Applications and development
[DE93-012934] p 368 N94-11813

OH-6 HELICOPTER
Advanced rotorcraft flight simulation: Model development, validation and parallel implementation
p 25 N94-11056

OHMIC DISSIPATION
Non-barrier tunneling in presence of dissipations
[DE93-621381] p 412 N94-11086
Elementary mechanism of electron beam dissipative instability development
[DE93-621653] p 391 N94-11209
Spreading of Bimodulated Ultra-relativistic Electron Beam (BUEB) in Atmospheric Plasma Channel (APCh)
[DE93-621658] p 392 N94-11213

OIL EXPLORATION
Gulf of Mexico sales 147 and 150: Central and western planning areas. Draft environmental impact statement. Volume 1: Sections 1 through 4.C
[PB93-190304] p 265 N94-11018
Gulf of Mexico sales 147 and 150: Central and western planning areas. Draft environmental impact statement. Volume 2: Sections 4.D through 9
[PB93-190312] p 265 N94-11019

OIL FIELDS
Information capability of NOAA-AVHRR data for monitoring oceanographic and atmospheric pollution
p 214 N94-12677

OIL POLLUTION
A study of pollution courses of spilled oil floatation in the outer ocean p 205 N94-11983

OIL SLICKS
Gulf of Mexico sales 147 and 150: Central and western planning areas. Draft environmental impact statement. Volume 1: Sections 1 through 4.C
[PB93-190304] p 265 N94-11018
Gulf of Mexico sales 147 and 150: Central and western planning areas. Draft environmental impact statement. Volume 2: Sections 4.D through 9
[PB93-190312] p 265 N94-11019
Methodologies for estimating air emissions from three non-traditional source categories: Oil spills, petroleum vessel loading and unloading, and cooling towers
[PB93-181592] p 266 N94-11471
A study of pollution courses of spilled oil floatation in the outer ocean p 205 N94-11983
Artificial oil pollution detection and wave observation in the sea adjacent to Japan by ERS-1 SAR
p 253 N94-12520
Ship traffic monitoring using the ERS-1 SAR
p 253 N94-12521
Oil spill detection using satellite-based SAR: Experience from a field experiment p 253 N94-12522
Observations of film slicks and internal waves with Ka-band scatterometer p 225 N94-12741

OLIGOMERS
Synthesis and polymerization of oligomeric multiple aromatic ether-containing phthalonitriles
[AD-D015729] p 94 N94-12399

OLIVINE
Changes in Hawaiian palagonite FE mineralogy associated with thermal alteration: Implications for Mars
p 281 N94-12055
Olivine-rich asteroids, pallasitic olivine and olivine-metal mixtures: Comparisons of reflectance spectra
p 431 N94-12171
On high-temperature formation of iron-rich olivine in the early solar system p 432 N94-12225
Micro-zoning in minerals of a Landes silicate inclusion
p 432 N94-12231

ON-LINE SYSTEMS
TOLS (Telescience On-Line Simulator): An essential instrument for micro-gravity interactive experiment
p 39 N94-10134
Estimation of critical values and vibration characteristics on supersonic delta wings. Part 1: On-line time series analysis of stationary random response
[NAL-TR-1153] p 2 N94-10363
The First Text Retrieval Conference (TREC-1)
[PB93-191641] p 419 N94-10829
A survey of techniques for corrosion monitoring
[DE93-012131] p 83 N94-11250

ONBOARD DATA PROCESSING
Data processing units for eight magnetospheric particle and field sensors
[AD-A264403] p 276 N94-11463
DISTERM: A shipboard data system for satellite monitoring of ocean and atmosphere
p 226 N94-12749

ONBOARD EQUIPMENT
Integrated marine survey system p 217 N94-12693
DISTERM: A shipboard data system for satellite monitoring of ocean and atmosphere
p 226 N94-12749

ONE DIMENSIONAL FLOW
A comparison between numerically modelled and experimentally measured loss mechanisms in wave rotors
[NASA-TM-106279] p 29 N94-11255

OPERATING COSTS
Space transportation alternatives for large space programs: The International Space University Summer Session, 1992
[NASA-TM-106271] p 40 N94-10811
Transportation systems analyses. Volume 2: Technical/programmatics
[NASA-CR-192582] p 41 N94-10827
Pulsed plasma processing for control of diesel engine emissions
[DE93-011884] p 181 N94-11247
Life-cycle cost analysis of conventional and fuel cell/battery powered urban passenger vehicles
[DE93-010770] p 182 N94-11438
Forecasting the impact of virtual environment technology on maintenance training p 314 N94-11570

OPERATING SYSTEMS (COMPUTERS)
Transportable Applications Environment (TAE) Tenth Users' Conference
[NASA-CP-3225] p 333 N94-12448

OPERATING TEMPERATURE
Thin film preparation and interfacial reaction study of solid oxide fuel cell materials p 263 N94-11313

OPERATIONAL PROBLEMS
Criteria for assessing problem solving and decision making in complex environments p 314 N94-11532

OPERATIONS RESEARCH
An advisor module for tactical and strategic state-oriented planning systems with an application in manpower planning
[MEMO-COSOR-92-57] p 416 N94-10868

OPERATOR PERFORMANCE
Analyzing human errors in flight mission operations
p 314 N94-11534
Vigilance problems in orbiter processing
p 314 N94-11536
Measuring human performance on NASA's microgravity aircraft p 317 N94-11537
Visual Earth observation performance in the space environment. Human performance measurement 4: Flight experiments p 314 N94-11539
SATORI: Situation Assessment Through the Re-creation of Incidents
[DOT/FAA/AM-93/12] p 38 N94-12567

OPERATORS (MATHEMATICS)
Deformations and recursion operators for evolution equations
[MEMO-1104] p 341 N94-10163
The super vectorfield package for REDUCE. Version 1.0
[MEMO-1099] p 321 N94-10265
Balancing of the normalized right coprime factorization of a nonlinear system
[MEMO-1096] p 341 N94-10273
The ring structure of chiral operators for minimal models coupled to 2D gravity
[DE93-613119] p 409 N94-10500
On local frame fields and fermion dynamics in space with nontrivial topologies
[DE93-617657] p 349 N94-10548
Observables, measurements and phase operators from a Bohmian perspective p 378 N94-10589
Nonunitary and unitary approach to Eigenvalue problem of Boson operators and squeezed coherent states
p 350 N94-10595
Wave and pseudo-diffusion equations from squeezed states p 347 N94-10607
Operator substitution
[MEMO-COSOR-92-51] p 343 N94-10867
The Nehari problem for the Pritchard-Salamon class of infinite-dimensional linear systems: A direct approach
[CS-9216] p 344 N94-10905
Optical transfer operator of the atmosphere-ocean system p 225 N94-12742

OPERATORS (PERSONNEL)
Department of Energy fundamentals handbook: Engineering symbology, prints, and drawings
[DE93-012181] p 129 N94-11456
Department of Energy fundamentals handbook: Engineering symbology, prints, and drawings
[DE93-012220] p 129 N94-11670

OPTICAL COMMUNICATION
Design and analysis of an optical interface message processor
[AD-A266079] p 381 N94-10697
Experimental comparison of time synchronization techniques by means of light signals and clock transport on the rotating earth p 351 N94-10970

OPTICAL COMPUTERS
Design and analysis of an optical interface message processor
[AD-A266079] p 381 N94-10697
Spatial light rebroadcaster architecture study
[AD-A266102] p 382 N94-11421
OPTICAL CORRECTION PROCEDURE
Optical transfer operator of the atmosphere-ocean system p 225 N94-12742
OPTICAL CORRELATORS
Application of normalized gray-scale correlation
[DE93-013765] p 141 N94-10521
OPTICAL DATA PROCESSING
Variable rate transfer of optical information
[AD-D015758] p 418 N94-10374
Design and analysis of an optical interface message processor
[AD-A266079] p 381 N94-10697
The optical/computer hybrid processing of extracting ocean wave directional spectrum by airborne photograph
p 197 N94-11934
OPTICAL EQUIPMENT
Development tests for a high stability optical bench
p 62 N94-10047
Technique to prepare high-reflectance optical fiber bragg gratings with single exposure in-line on fiber draw tower
[AD-D015757] p 374 N94-10373
Wavelength considerations in soft x ray projection lithography
[DE93-014115] p 381 N94-10651
Optoelectronic technology consortium
[AD-A265691] p 383 N94-12444
OPTICAL FIBERS
Multiplexed and distributed optical fibre sensors
p 64 N94-10065
Fibre optic strain and temperature measurement in composite materials: A review of the OSTIC programme
p 65 N94-10066
The sensitivity of an optical fiber holographic interferometer p 107 N94-10117
Method and apparatus for polarization-maintaining fiber optical amplification with orthogonal polarization output
[AD-D015756] p 374 N94-10372
Technique to prepare high-reflectance optical fiber bragg gratings with single exposure in-line on fiber draw tower
[AD-D015757] p 374 N94-10373
Fabrication and analysis of a special optical connector containing a 1/4-inch-long optical fiber for DOI tests
[DE93-013115] p 381 N94-10647
Journal of Research of the National Institute of Standards and Technology, volume 98, number 2, March - April 1993
[PB93-196228] p 485 N94-10850
Factors affecting the embedding of optical fibre sensors in advanced composite structures p 70 N94-11336
Ocean measuring experiments using optical fiber distributed temperature sensor p 172 N94-11968
Localized and distributed fiber-optic strain sensors embedded in composite materials
[UTIAS-346] p 73 N94-12013
OPTICAL FILTERS
Continued development of an ultra-narrow bandpass filter for solar research
[NASA-CR-194169] p 381 N94-10735
Thermal-optical switching of a silicon based interference filter
[AD-A265152] p 174 N94-11095
Design of CCD camera system for use inside electron beam furnace
[DE93-009525] p 170 N94-11267
Presort processor --- optical filtering
[AD-A263872] p 382 N94-11300
Comparison of multiresolution techniques for digital signal processing
[AD-A265364] p 138 N94-12406
OPTICAL GYROSCOPES
NASA's first in-space optical gyroscope: A technology experiment on the X ray Timing Explorer spacecraft
[NASA-TM-109242] p 170 N94-10667
OPTICAL MATERIALS
Second and third order nonlinear optical properties of crystalline inorganic/organic complexes
[DE93-011883] p 173 N94-10755
Arcjet exploratory tests of ARC optical window design for the AFE vehicle
[NASA-CR-192655] p 34 N94-10930
Enhanced Damage-Resistant Optics for Spaceflight Laser Systems: Workshop findings and recommendations
[NASA-TM-109243] p 381 N94-11054
Damage thresholds of fluoride multilayers at 355 nm
[DE93-009523] p 90 N94-11230
Vacuum stability requirements of polymeric material for spacecraft application
[NASA-TM-109216] p 91 N94-11350
New challenges in optical materials development
[DE93-011889] p 383 N94-11676
OPTICAL MEASUREMENT
Holographic interferometry for microgravity applications p 108 N94-10123
Pressure and force measurements on models set in hypersonic flows: A review p 5 N94-10435
Flow visualization and spectroscopy in hypersonic flows: New trends p 5 N94-10437
A preliminary study on ice shape tracing with a laser light sheet
[NASA-TM-105964] p 174 N94-11132
The evolution of whole field optical diagnostics for external transonic testing
[ARA-MEMO-379] p 383 N94-11887
OPTICAL MEASURING INSTRUMENTS
Local measurement of temperatures and concentrations: A review for hypersonic flows
p 4 N94-10434
Possibility of a crossed-beam experiment involving slow-neutron capture by unstable nuclei rapid-process-tron
[DE93-754288] p 363 N94-10720
Optical fibre techniques for structural monitoring in composites p 69 N94-11324
Strain measurement of carbon/epoxy composite with fibre optics white light quasi distributed polarimetric sensor p 69 N94-11328
The development of phytoplankton sensing system with optical fiber p 203 N94-11967
The seasonal change of phytoplankton size distribution using optical fiber sensor p 210 N94-12656
OPTICAL MEMORY (DATA STORAGE)
Holographic multiplexing for 3D optical memory
[AD-A266099] p 171 N94-11420
OPTICAL PATHS
Study of Einstein-Podolsky-Rosen state for space-time variables in a two photon interference experiment
p 370 N94-10582
OPTICAL PROPERTIES
Invariance of the mobility edge in anodic titanium oxides
[DE92-642136] p 394 N94-10281
Solid state ionics 3. Materials Research Society Symposium Proceedings, volume 293
[AD-A265675] p 395 N94-10416
Interferometric and optical tests of water window imaging x ray microscopes
[NASA-CR-193369] p 375 N94-10506
Fabrication and analysis of a special optical connector containing a 1/4-inch-long optical fiber for DOI tests
[DE93-013115] p 381 N94-10647
Space environmental effects on the integrity of chromic acid anodized coatings
[NASA-CR-191468] p 55 N94-10947
Investigation of optically generated electronic defects and protonic transport in hydrogen-bonded molecular solids: Isomorphs of potassium dihydrogen phosphate
[DE93-012498] p 399 N94-11243
Implementation and use of a computational ray-tracing program for the design and analysis of complex optical systems
[AD-A265075] p 382 N94-11653
Applications of in-situ ellipsometry to microwave electron cyclotron resonance plasma processes
[AD-A265197] p 373 N94-11880
Optical characteristics in Tokyo Bay
p 204 N94-11972
Progress toward atomic layer epitaxy of diamond: Diamond films grown one layer at a time
[AD-A265530] p 403 N94-12010
Effects of microscopic iron metal on the reflectance spectra of glass and minerals p 436 N94-12024
Simulation of possible regolith optical alteration effects on carbonaceous chondrite meteorites
p 430 N94-12163
OPTICAL PUMPING
A phaseonium magnetometer: A new optical magnetometer based on index enhanced media
p 375 N94-10565
High power z pinches as x ray laser photopumps
[DE93-012842] p 173 N94-10746
New challenges in optical materials development
[DE93-011889] p 383 N94-11676
OPTICAL RADAR
Characterization of a scannerless LADAR system
[DE93-011582] p 174 N94-10959
Measures for simulator evaluation of a helicopter obstacle avoidance system p 35 N94-11535
Development of shipboard ocean lidar
p 140 N94-11965
Remote sensing of subsurface water temperature profile and backscattering coefficient in the China Sea by Ocean Lidar (OLIDAR) p 203 N94-11970
Polarisation of backscattering radiation at remote sensing of ocean with impulse laser beam
p 177 N94-12722
Remote sensing of light scattering coefficient of sea water vertical distribution by the means of airborne lidar
p 224 N94-12736
OPTICAL REFLECTION
An expert system shell for inferring vegetation characteristics: Prototype help system (Task 1)
[NASA-CR-193411] p 231 N94-11236
Effects of wind-roughened sea surface on ocean color remote sensing: Noise derived from reflected light and whitecaps p 191 N94-11898
The upwelling radiation at the top of the atmosphere in coastal region p 205 N94-11981
OPTICAL SWITCHING
Design and analysis of an optical interface message processor
[AD-A266079] p 381 N94-10697
Thermal-optical switching of a silicon based interference filter
[AD-A265152] p 174 N94-11095
A thermal ionization model for the sustaining phase of lock-on in GaAs
[DE93-011558] p 144 N94-11624
Preliminary surface-emitting laser logic device evaluation
[AD-A266111] p 383 N94-12416
OPTICAL THICKNESS
Implications of aerosol retrieval and atmospheric correction in remote sensing p 205 N94-11978
OPTICAL TRACKING
The 24th Annual Precise Time and Time Interval (PTTI) Applications and Planning Meeting
[NASA-CP-3218] p 350 N94-10963
Airborne optical tracking control system design study
[DE93-009515] p 382 N94-11662
OPTICAL TRANSFER FUNCTION
Optical transfer operator of the atmosphere-ocean system p 225 N94-12742
OPTICAL WAVEGUIDES
Semiconductor ring lasers
[DE93-012386] p 174 N94-11005
OPTIMAL CONTROL
Nonlinear stability and control study of highly maneuverable high performance aircraft
[NASA-CR-193480] p 25 N94-10344
Sample-data and discrete-time H2 optimal control
[MEMO-COSOR-92-53] p 339 N94-10869
Application of controller partitioning optimization procedure to integrated flight/propulsion control design for a STOVL aircraft
[NASA-TM-106265] p 30 N94-11251
OPTIMIZATION
Perforated plates for thin-walled structures
p 63 N94-10056
LAMINV: A computer code for creating laminates having prescribed properties p 65 N94-10069
Marginal allocations in the core of minimal chain-games
[MEMO-1103] p 348 N94-10162
Applications of cut polyhedra
[CWI-BS-R9221] p 347 N94-10354
Optimization algorithms for integer networks with side constraints for application in routing and scheduling
[AD-A265254] p 322 N94-10492
The d-edge shortest-path problem for a Monge graph
[DE93-009828] p 343 N94-10708
Progress in multidisciplinary design optimization at NASA Langley
[NASA-TM-107754] p 318 N94-10814
Multilevel computer-aided optimum design of structural systems using multiple basis vectors
p 187 N94-11055
Optimisation methods for solving separable nonlinear least squares problems
[ISVR-TR-219] p 345 N94-11217
Grid optimization and multigrid techniques for fluid flow and transport problems p 154 N94-11824
A new heuristic for set covering problems
[INPE-5471-TDI/502] p 333 N94-12358
OPTOELECTRONIC DEVICES
Multiplexed and distributed optical fibre sensors
p 64 N94-10065
Ultrastable reference frequency distribution utilizing a fiber optic link p 355 N94-10994
Lattice-matched heteroepitaxy of wide gap ternary compound semiconductors p 400 N94-11441
ORBIT CALCULATION
Topex orbit determination using GPS tracking system
p 38 N94-10359
Precision GPS ephemerides and baselines
[NASA-CR-194171] p 23 N94-11177
Removal of orbital error and the local geoid effects from ERS-1 altimeter data p 242 N94-11770

ERS-1 precise orbits and altimetry analysis p 242 N94-11771
Operational ERS-1 orbit determination at D-PAF p 243 N94-11774
The Earth's gravity model for the ERS-1 commissioning phase p 243 N94-11778
ERS-1 precise orbit determination p 244 N94-11779
Lunar Scout Two spacecraft gravity experiment p 459 N94-12152

ORBIT TRANSFER VEHICLES
Workshop on Solar Electric Propulsion p 54 N94-11416

ORBITAL ASSEMBLY
In-space operations for lunar and Mars space transfer vehicles p 348 N94-11568
On-orbit servicing for USAF space missions: A phased development approach p 348 N94-11571
Definition of spacecraft standard interfaces by the NASA Space Assembly and Servicing Working Group (SASWG) p 348 N94-11574

ORBITAL ELEMENTS
The long-term dynamical behavior of short-period comets p 427 N94-11629

ORBITAL MECHANICS
Orbital simulations of satellite escape/capture and the origin of satellites such as Triton p 429 N94-12057

ORBITAL POSITION ESTIMATION
Pre-operation analysis of ERS-1 tracking and operation, part 2-F [NASDA-CNT-930002-PT-2-F] p 230 N94-11130
Regional orbit precision in the Mediterranean area p 39 N94-12530

ORBITAL RESONANCES (CELESTIAL MECHANICS)
The IR properties of ringed galaxies and the IRAS database [NASA-CR-194286] p 426 N94-11590
On the depletion in the outer asteroid belt and the structure of the 4 to 3 mean motion resonance p 426 N94-11596

ORBITAL SERVICING
On-orbit refueling p 38 N94-11565
On-orbit refueling p 38 N94-11566
Preliminary analysis of the benefits derived to US Air Force spacecraft from on-orbit refueling p 38 N94-11567
In-space operations for lunar and Mars space transfer vehicles p 348 N94-11568
In-space assembly-servicing requirements p 348 N94-11569
Definition of spacecraft standard interfaces by the NASA Space Assembly and Servicing Working Group (SASWG) p 348 N94-11574
Supervised autonomous control, shared control, and teleoperation for space servicing p 183 N94-11577

ORBITS
The long-term dynamical behavior of short-period comets p 427 N94-11629

ORDER-DISORDER TRANSFORMATIONS
X-ray and neutron scattering studies of magnetic critical fluctuations in holmium [DE93-010873] p 400 N94-11467

ORGANELLES
Probability of alamethicin conductance states varies with nonlamellar tendency of bilayer phospholipids [AD-A264957] p 301 N94-11648

ORGANIC CHEMISTRY
Studies in bioorganic chemistry [AD-A265532] p 55 N94-12011

ORGANIC COMPOUNDS
Second and third order nonlinear optical properties of crystalline inorganic/organic complexes [DE93-011883] p 173 N94-10755
Comprehensive analysis of airborne contaminants from recent Spacelab missions p 318 N94-11553
Synthesis, characterization, and modification of poly(organophosphazenes), that bear both 2,2,2-trifluoroethoxy and phenoxy groups [AD-A264913] p 92 N94-11847
Tandem mass spectrometric analysis of phosphate esters [AD-A265483] p 78 N94-12009
A reexamination of amino acids in lunar soil p 452 N94-12109
Oxidation state of the Earth's upper mantle during the last 3800 million years: Implications for the origin of life p 283 N94-12210

ORGANIC MATERIALS
Organic matter on the early surface of Mars: An assessment of the contribution by interplanetary dust p 480 N94-12259
Mass and spatial distribution of carbonaceous component in Comet Halley p 433 N94-12263
The effects of organic adsorbates on the underpotential deposition of silver on Pt(111) electrodes [AD-A265623] p 404 N94-12376
Primary productivity in the Oyashio area in the spring and summer of 1990 p 211 N94-12658
Characterization of dissolved organic matter in the ocean by using the fluorescence excitation-emission matrix p 211 N94-12659
Variation of the photosynthetic products in the regional upwelling area around the Izu Islands, Japan p 211 N94-12661
Non-image visible polarization remote sensing of the ocean p 229 N94-12762

ORGANIC SOLIDS
Laser fluorescent monitoring of dissolved organic matter in natural water p 177 N94-12755
Ecological application of Surface Enhanced Raman Spectroscopy p 227 N94-12756

ORGANISMS
Compatibility tests for biological specimens to on-board experiments in the Space Shuttle flight [NASDA-CNT-930003] p 301 N94-12278
Study on sea water purification using a substratum of marine organisms p 217 N94-12696
Application of remote sensing for coastal management in the north coast of Java p 218 N94-12701
The algorithm of primary production determination p 228 N94-12761
Non-image visible polarization remote sensing of the ocean p 229 N94-12762

ORGANIZATIONS
Engineering performance metrics [DE93-012084] p 128 N94-11028
Insights into software development in Japan p 330 N94-11435
Myths and realities: Defining re-engineering for a large organization p 330 N94-11436
Research and development of post-classical management tools for government program offices, volume 2 [DE93-010236] p 417 N94-11600
Electric and hybrid vehicle site operators program: Thinking of the future [DE93-011231] p 144 N94-11609
AGARD highlights 92/2, September 1992 [AGARD-HIGHLIGHTS-92/2] p 497 N94-11820

ORGANOMETALLIC COMPOUNDS
Aluminum-phosphorus chemistry: Preparation and structural characterization of (Et2AlP(SiMe3)2)2, Et(Cl)2Al(dot)P(SiMe3)3, and i-Bu2(Cl)Al(dot)P(SiMe3)3 [AD-A265268] p 78 N94-11683

ORIGINS
Using solar flare track densities to determine the origin of interplanetary dust particles p 429 N94-12078

ORTHOGONAL FUNCTIONS
An investigation using empirical orthogonal functions and objective analysis to analyse the vertical temperature structure of a gulf stream meander [AD-A265116] p 289 N94-11868

ORTHOSTATIC TOLERANCE
Exercise countermeasures for bed-rest deconditioning [NASA-TM-103987] p 300 N94-11191
Proceedings of the First Joint NASA Cardiopulmonary Workshop [NASA-CP-10068] p 308 N94-11991
Carotid-cardiac baroreflex: Relation with orthostatic hypotension following simulated microgravity and implications for development of countermeasures p 308 N94-11992
Echocardiography in the flight program p 309 N94-11993
Effect of prolonged LBNP and saline ingestion on plasma volume and orthostatic responses during bed rest p 310 N94-11998
Fitness, autonomic regulation and orthostatic tolerance p 310 N94-11999
Hormonal regulation of fluid and electrolyte metabolism in zero-g and bedrest p 311 N94-12004
Autogenic-feedback training: A countermeasure for orthostatic intolerance p 311 N94-12006

ORTHOTROPIC CYLINDERS
Imperfection sensitivity of the Brazier effect for orthotropic cylindrical shells [LR-687] p 186 N94-10879

OSCILLATING CYLINDERS
Vortex-induced forces on oscillating bluff cylinders [AD-A265056] p 154 N94-11865

OSCILLATING FLOW
On the combustion of a laminar spray [NASA-TM-106210] p 28 N94-11238
High order accurate solutions of viscous problems [NASA-TM-106267] p 151 N94-11253
A simple model of melt fracture [AD-A265311] p 92 N94-11862
Establishing baseline data for an experimental appratus that measures heat transfer under conditions of oscillating pressure and flow [NASA-CR-193772] p 413 N94-12343

OSCILLATIONS
Aharonov-Bohm effect in Luttinger liquid [DE93-613818] p 408 N94-10148
Pulsatile instability in rapid directional solidification: Strongly-nonlinear analysis p 115 N94-10188
A group-theoretic approach to the study of small oscillations of a dynamical system with a known symmetry [DE93-612971] p 409 N94-10402
Characterization of the Si/SiO2 interfere morphology from quantum oscillations in Fowler-Nordheim tunneling currents [AD-A265149] p 143 N94-11160
Sine and random vibration program evaluation on vibration control systems [DE93-011974] p 188 N94-11460
Decay interaction of bulk and surface Langmuir waves [DE93-617843] p 393 N94-11477
On the coupling of electromagnetic radiation into cavities [DE93-011406] p 137 N94-11621

OSCILLATORS
Numerical simulation of sidebands in free electron laser oscillators [DE93-612675] p 173 N94-10483
Nonlinear Dynamics in Optical Systems. Postdeadline papers presented at the Optical Society of America Conference [AD-A264958] p 375 N94-10486
Review of SHARC 2.0 O3 kinetics and spectroscopy [AD-A265481] p 274 N94-10496
Quantum noise and squeezing in optical parametric oscillator with arbitrary output coupling p 375 N94-10568
An exactly solvable model of an oscillator with nonlinear coupling and zeros of Bessel functions p 349 N94-10573
Dissipation in a squeezed-state environment p 370 N94-10584
Disciplined rubidium oscillator with GPS selective availability p 353 N94-10977
A multi-variance analysis in the time domain p 146 N94-10999
A new method of time difference measurement: The time difference method by dual phase coincidence points detection p 357 N94-11002
Confidence of the three-point estimator of frequency drift p 357 N94-11003

OSMIUM
Glucose electrodes based on cross-linked (Os(bpy)2Cl)(sup +/2+) complexed poly(1-vinylimidazole) films [AD-A265404] p 94 N94-12425

OSMIUM ISOTOPES
Rhenium-osmium isotope systematics of Group 2A and Group 4A iron meteorites p 431 N94-12182
Re-Os dating of 3AB iron meteorites p 432 N94-12237

OSMOSIS
Physiological water model development p 316 N94-12367

OUTCROPS
Arroyo el Mimbral, Mexico, K/T unit: Origin as debris flow/turbidite, not a tsunami deposit p 281 N94-12084

OUTGASSING
Vacuum stability requirements of polymeric material for spacecraft application [NASA-TM-109216] p 91 N94-11350
Oxidation state of the Earth's upper mantle during the last 3800 million years: Implications for the origin of life p 283 N94-12210

OVER-THE-HORIZON RADAR
HF-OTH radar performance results [AD-A266106] p 138 N94-11655

OXIDATION
Atomic structures and compositions of internal interfaces [DE93-014840] p 363 N94-10750
Assessment of damage in ceramics and ceramic matrix composites using ultrasonic techniques [NASA-TM-106121] p 67 N94-11237
Catalytic oxidation of organics in vapor streams at remediation sites [PB93-182962] p 268 N94-11472
Potential techniques for non-destructive evaluation of cable materials [DE93-008350] p 183 N94-11586
Chemical weathering on Mars: Rate of oxidation of iron dissolved in brines p 455 N94-12128
Oxidation state of the Earth's upper mantle during the last 3800 million years: Implications for the origin of life p 283 N94-12210

OXIDATION RESISTANCE

Protective coatings for high-temperature polymer matrix composites
[NASA-TM-106276] p 74 N94-12431

OXIDATION-REDUCTION REACTIONS

Technical Update: Johnson Space Center system using a solid electrolytic cell in a remote location to measure oxygen fugacities in CO/CO2 controlled-atmosphere furnaces
[NASA-TM-104774] p 423 N94-11183

X ray absorption spectroscopy of electrochemically generated species
[AD-A264749] p 77 N94-11265

Publications/Patents/Presentations/Honors/Student eport
[AD-A265136] p 78 N94-11873

The Fe/Mn constraint on precursors of basaltic achondrites p 432 N94-12208

Glucose electrodes based on cross-linked (Os(bpy)2Cl)(sup +/2+) complexed poly(1-vinylimidazole) films
[AD-A265404] p 94 N94-12425

Sulfate reduction and other sedimentary biogeochemistry in a northern New England salt marsh p 268 N94-12453

The role of certain infauna and vascular plants in the mediation of redox reactions in marine sediments p 268 N94-12454

Acetate concentrations and oxidation in salt marsh sediments p 269 N94-12459

The effects of acid deposition on sulfate reduction and methane production in peatlands p 270 N94-12465

Elevated acetate concentrations in the rhizosphere of Spartina alterniflora and potential influences on sulfate reduction p 271 N94-12468

OXIDE FILMS

Damage threshold study of ion beam sputtered coatings for a visible high-repetition laser at LLNL
[DE93-013430] p 95 N94-12602

OXIDES

Multicomponent and multilayered thin films for advanced microtechnologies: Techniques, fundamentals, and devices
[AD-A265685] p 405 N94-12442

OXYGEN

Hypobaric decompression prebreathe requirements and breathing environment p 317 N94-11541

Methanol pan fires in an enclosed space: Effect of pressure and oxygen concentration
[AD-A266108] p 79 N94-12415

OXYGEN ATOMS

Atomic structures and compositions of internal interfaces
[DE93-014840] p 363 N94-10750

OXYGEN BREATHING

Hypobaric decompression prebreathe requirements and breathing environment p 317 N94-11541

OXYGEN CONSUMPTION

The OSU heat release rate test using the oxygen consumption principle p 20 N94-10784

OXYGEN ISOTOPES

Interstellar graphite in Murchison: Continued search for isotopically distinct components p 97 N94-12029

The EET87513 clast N: A CM2 fragment in an HED polymict breccia p 453 N94-12117

Oxygen isotopes as tracers of tektite source rocks: An example from the Ivory Coast tektites and Lake Bosumtwi Crater p 430 N94-12146

Trace element distributions in primitive achondrites p 431 N94-12200

OXYGEN METABOLISM

Exercise countermeasures for bed-rest deconditioning
[NASA-TM-103987] p 300 N94-11191

OXYGEN PRODUCTION

General overview of an integrated lunar oxygen production/brickmaking system p 131 N94-12027

Thermodynamics of lunar ilmenite reduction p 415 N94-12028

OXYGEN SUPPLY EQUIPMENT

General overview of an integrated lunar oxygen production/brickmaking system p 131 N94-12027

OXYGEN 17

Development of a molecular beam technique to study early solar system silicon reactions p 432 N94-12224

OXYGEN 18

Strontium and oxygen isotope study of M-1, M-3 and M-4 drill core samples from the Manson impact structure, Iowa: Comparison with Haitian K-T impact glasses p 281 N94-12080

Development of a molecular beam technique to study early solar system silicon reactions p 432 N94-12224

OZONE

Review of SHARC 2.0 O3 kinetics and spectroscopy
[AD-A265481] p 274 N94-10496

The global potential energy surfaces of the lowest two 1A' states of the ozone molecule: Theoretical determination and analysis p 267 N94-12269

Studies of dynamical processes affecting the distribution of stratospheric ozone
[NASA-CR-193477] p 279 N94-12560

OZONE DEPLETION

Mid-latitude ionospheric response to active experiments
[NASA-CR-193549] p 280 N94-12583

OZONOSPHERE

Atmospheric and spectroscopic research in the far infrared
[NASA-CR-193551] p 280 N94-12582

P

P-I-N JUNCTIONS

Radiation effects in Ga(0.47)In(0.53)As solar cells p 52 N94-11404

Measurement and modeling of the stability of hydrogenated amorphous silicon solar cells and films after intense illumination p 263 N94-11638

P-N JUNCTIONS

Electrochemical characterization of p(+)n and n(+)p diffused InP structures p 49 N94-11385

New experimental techniques for solar cells p 52 N94-11403

P-TYPE SEMICONDUCTORS

Organometallic chemical vapor deposition and characterization of ZnGe(1-x)Si(x)P2-Ge alloys on GaP substrates p 400 N94-11443

PACIFIC OCEAN

Central Equatorial Pacific Experiment (CEPEX)
[DE93-011656] p 190 N94-11674

Proceedings of the PORSEC 1992 in Okinawa: Conference for Pacific Ocean Environments and Probing, volume 1
[JTN-93-80418] p 191 N94-11894

Acoustic Doppler current profiling of the Kuroshio over the East China Sea shelf slope p 194 N94-11914

Seasonal variation of the surface mixed layer in the subtropical re-circulation area of the North Pacific during OMLET p 195 N94-11924

The Kyucho events in Sukumo Bay induced by Kuroshio front disturbances p 198 N94-11939

Westward propagation of sea surface anomalies in the western North Pacific as seen by the altimeter and radiometer p 198 N94-11941

Coastal processes due to nearshore current around an upheaving island p 199 N94-11942

Availability of wind field over the North Pacific derived from data on ships-of-opportunity and analysis of long-term variabilities p 202 N94-11962

Circulation of North Pacific Intermediate Water p 206 N94-11985

Roles of the NEC and MC in the formation and evolution of the Equatorial Pacific Warm Pool p 206 N94-11990

SSMI wind speed variability over the Pacific Ocean p 207 N94-12637

Observations of eddy fields in the Northwest Pacific by GEOSAT altimetry p 207 N94-12639

Variability of sea level and sea surface temperature anomalies in the equatorial Pacific p 208 N94-12640

Pseudo magnetic anomaly derived from satellite altimetry and its application to the tectonics in the North Fuji Basin p 208 N94-12645

Principal oscillation pattern analysis of sea level variations in the tropical Pacific measured by the GEOSAT altimeter p 209 N94-12646

Measurement of eddy structure and movement in the north-east Pacific with the GEOSAT altimeter p 209 N94-12647

Preliminary results from a satellite altimetric data assimilation using a Kalman filter and smoother p 209 N94-12648

Mean flow and variability in the Kuroshio extension from GEOSAT altimetry data p 209 N94-12650

Pacific rim sea ice as observed with the NIMBUS-7 SMMR p 210 N94-12651

Variation of the photosynthetic products in the regional upwelling area around the Izu Islands, Japan p 211 N94-12661

Sea surface temperature images of Geostationary Meteorological Satellite (GMS) and sea truth data from ferry boats p 213 N94-12671

Intrusion of Kuroshio warm water into Sagami Bay p 215 N94-12683

On a nonstationary dynamics of the north-west Pacific Ocean p 222 N94-12724

PACKAGING

Environmental Protection Agency's life cycle methodology: Guidelines for use in development of packaging
[PB93-194199] p 265 N94-10841

PACKING DENSITY

Dynamic high-pressure shock compaction of diamond powders
[AD-A266004] p 93 N94-12354

PAIN

Project ARGO: Gas phase formation in simulated microgravity
[NASA-TM-104762] p 125 N94-11235

Joint pain and Doppler-detectable bubbles in altitude (Hypobaric) decompression p 312 N94-11542

PAINTS

Environmentally Safe and Effective Processes for Paint Removal
[AGARD-R-791] p 126 N94-10613

Paint removal activities in the US Navy p 126 N94-10614

Paint removal activities in Canada p 126 N94-10615

Procedures without danger to the environment and efficiency (PSDEE) for the removal of paint. Point on the French activities concerning the removal of paint p 126 N94-10616

Paint removal activities in Germany p 126 N94-10617

The development of alternative paint removal techniques in the RAF p 126 N94-10618

Operational aspects of F.16 plastic media blasting, as carried out by Fokker Aircraft Services p 126 N94-10619

Use of robots for aircraft dry stripping via plastic media blasting p 127 N94-10620

German Air Forces experiences with plastic media blasting and future requirements p 127 N94-10621

Plastic media blasting activities at Hill Air Force Base p 127 N94-10622

Large Aircraft Robotic Paint Stripping (LARPS) system and the high pressure water process p 127 N94-10623

Automated Laser Paint Stripping (ALPS) update p 127 N94-10624

Aquastrip (tm): An innovative paint removal technology p 127 N94-10625

Paint removal and surface cleaning using ice particles p 128 N94-10626

Paint removal using wheat starch blast media p 128 N94-10627

IATA taskforce: Paintstripping p 128 N94-10628

Selectively strippable paint schemes p 128 N94-10629

Experimental measurement of the plasma conductivity of Z93 and Z93P thermal control paint
[NASA-TM-106284] p 43 N94-10756

Understanding cracking failures of coatings: A fracture mechanics approach p 187 N94-11218

Formulating infrared coatings for defence applications
[MRL-RR-1-93] p 90 N94-11302

PAIR PRODUCTION

Coherence influence on the intensity of Bose-Einstein correlations and visible size of a source
[DE93-617697] p 349 N94-10556

Top quark search in D(O) from the lepton + jets mode
[DE93-014027] p 370 N94-12781

PAKISTAN SPACE PROGRAM

Pakistan Space and Upper Atmosphere Research Commission p 37 N94-10693

PALEOMAGNETISM

Macroscopic electric charge separation during hypervelocity impacts: Potential implications for planetary paleomagnetism p 431 N94-12181

Magnetic fields and nonuniform structures of the Moon p 472 N94-12218

PANELS

Stress relaxation forming of Ariane 5 front skirt outer skin panels p 62 N94-10046

PARABOLIC DIFFERENTIAL EQUATIONS

Summation by parts, projections, and stability
[NASA-CR-194290] p 346 N94-12776

PARABOLIC FLIGHT

The formation and breakage of liquid bridges under microgravity p 100 N94-10071

Microgravity Applications Furnace Facility (MAFF) for parabolic flights p 109 N94-10128

PARACHUTES

Parachute having improved vent line stacking
[NASA-CASE-MFS-28508-1] p 14 N94-11021

PARADOXES

Study of Einstein-Podolsky-Rosen state for space-time variables in a two photon interference experiment p 370 N94-10582

Observables, measurements and phase operators from a Bohmian perspective p 378 N94-10589

PARALLEL COMPUTERS

Simulation of a parallel computer
[NAL-TR-1154] p 335 N94-10368

Low latency messages on distributed memory multiprocessors
[NASA-CR-191479] p 323 N94-10643
The PVM systems: An in-depth analysis and documenting study. Concise edition
[DE93-011959] p 336 N94-11248
A heterogeneous graphics procedure for visualization of massively parallel solutions
[DE93-009628] p 336 N94-11270
Optimal cube-connected cube multiprocessors
[NASA-CR-191463] p 337 N94-11308

PARALLEL FLOW
Vibrational-thermocapillary parallel flows and stability
p 120 N94-10220
Receptivity in parallel flows: An adjoint approach
p 157 N94-12301

PARALLEL PLATES
Stability of liquid bridges between parallel plates
p 101 N94-10078

PARALLEL PROCESSING (COMPUTERS)
Massively parallel multifrontal methods for finite element analysis on MIMD computer systems
[DE93-009838] p 335 N94-10257
Layering techniques for development of parallel systems: An algebraic approach
[MEMO-INF-92-62] p 335 N94-10277
A parallel implementation of particle tracking with space charge effects on an Intel iPSC/860
[DE93-012307] p 335 N94-10340
CFD analysis of hypersonic, chemically reacting flow fields p 2 N94-10422
Application of parallel processing to a surface patch/wire junction EFIE code
[AD-A264965] p 336 N94-10488
Optimization algorithms for integer networks with side constraints for application in routing and scheduling
[AD-A265254] p 322 N94-10492
Bringing theory to practice: The reality of interprocessor communication
[DE93-012346] p 336 N94-10738
Efficient partitioning and assignment on programs for multiprocessor execution
[NASA-CR-193458] p 324 N94-10942
The Zipcode message-passing system
[DE93-011958] p 336 N94-11027
Basic experiment on an ultrasonic method of localization
[DE93-754295] p 358 N94-11042
Advanced rotorcraft flight simulation: Model development, validation and parallel implementation
p 25 N94-11056
Summary of research in progress at ICASE
[NASA-CR-191481] p 318 N94-11198
A distributed version of the NASA Engine Performance Program
[NASA-TM-106208] p 327 N94-11231
Portable programming on parallel/networked computers using the Application Portable Parallel Library (APPL)
[NASA-TM-106238] p 327 N94-11232
The PVM systems: An in-depth analysis and documenting study. Concise edition
[DE93-011959] p 336 N94-11248
A heterogeneous graphics procedure for visualization of massively parallel solutions
[DE93-009628] p 336 N94-11270
Heterogeneous SuperConcurrent Parallelism (HeSCP)
[AD-A265004] p 336 N94-11293
Optimal cube-connected cube multiprocessors
[NASA-CR-191463] p 337 N94-11308
Parallel molecular dynamics with the embedded atom method
[DE93-010683] p 367 N94-11455
Massively parallel hydrodynamics on unstructured grids
[DE93-007325] p 153 N94-11601
High-performance distributed systems architecture
[AD-A265297] p 337 N94-11829
Problem specific environments for parallel systems
[AD-A266129] p 337 N94-12540
Networks of real-time processes
[DE93-013049] p 338 N94-12597
The DOE Program in High-Performance Computing and Communications (HPCC)
[DE93-013813] p 334 N94-12606

PARALLEL PROGRAMMING
Advanced rotorcraft flight simulation: Model development, validation and parallel implementation
p 25 N94-11056
Flexible language constructs for large parallel programs
[NASA-CR-191478] p 326 N94-11196
Scalable spin locks for multiprogrammed systems
[AD-A265007] p 337 N94-11650
Transactions of the 10th Army Conference on Applied Mathematics and Computing
[AD-A265098] p 318 N94-11678
An introduction to chordal graphs and clique trees
[DE93-012508] p 332 N94-11695
Problem specific environments for parallel systems
[AD-A266129] p 337 N94-12540

PARAMAGNETISM
Orbital glass in HTSC
[DE93-613988] p 395 N94-10415

PARAMETER IDENTIFICATION
Microwave radiometry of ice cover in polar regions
p 210 N94-12655
Trajectory curving in underwater propagation of light
p 226 N94-12748
Mixing of drifter ensemble by mesoscale currents
p 228 N94-12760
Improvement of method for experimental determination of flutter speed by parameter identification
[NASA-CR-193555] p 33 N94-12769

PARAMETERIZATION
A self-consistent model of non-linear parameterization of turbulent diffusion in atmospheric boundary layer
[DE93-011950] p 275 N94-11052
Supervised autonomous control, shared control, and teleoperation for space servicing p 183 N94-11577
Parameterization of subgrid-scale stress by the velocity gradient tensor p 155 N94-12286

PARAMETRIC AMPLIFIERS
Quantum noise and squeezing in optical parametric oscillator with arbitrary output coupling
p 375 N94-10568
Photon number amplification/duplication through parametric conversion p 376 N94-10572

PARASITIC DISEASES
Satellite, environmental, and medical information applied to epidemiological monitoring p 307 N94-11802

PARITY
Discrete space-time symmetries
[DE93-010199] p 341 N94-10259
On parity conservation and the question of the missing, right-handed neutrino
[DE93-613092] p 361 N94-10414
Nuclear structure models: Applications and development
[DE93-012934] p 368 N94-11813

PARSING ALGORITHMS
Layering techniques for development of parallel systems: An algebraic approach
[MEMO-INF-92-62] p 335 N94-10277

PARTIAL DIFFERENTIAL EQUATIONS
Vectorizing matrix operations arising from PDE discretization on 9-point stencils
[CWI-NM-R9221] p 342 N94-10351
The INTEGRATOR package for REDUCE, version 1.0
[MEMO-1100] p 322 N94-10418
Wave and pseudo-diffusion equations from squeezed states p 347 N94-10607
DILUTE: A code for studying beam evolution under RF noise
[DE93-011605] p 133 N94-10960
Quality factors and local adaption (with applications in Eulerian hydrodynamics)
[DE93-010502] p 151 N94-11272
Control of large space structures with varying configuration
[AD-A265764] p 44 N94-12387

PARTIAL PRESSURE
A mechanism for the reduction in risk of decompression sickness in microgravity environment
p 312 N94-11545

PARTICLE ACCELERATION
Acceleration of positrons in supernova shocks
[NASA-CR-193713] p 425 N94-10511

PARTICLE ACCELERATOR TARGETS
Fast trigger algorithm for B-events selection
[DE93-621452] p 365 N94-11089
Experiments to measure the gluon helicity distribution in protons
[DE93-011756] p 368 N94-11613

PARTICLE ACCELERATORS
Proceedings of the Second KEK Topical Conference on e(sup +)e(sup -) collision physics
[DE93-754139] p 364 N94-10889

PARTICLE BEAMS
Kinetic effects in stochastic topologically nontrivial field
[DE93-621642] p 391 N94-11207
Spectrum analysis in beam diagnostics
[DE93-013401] p 373 N94-12601

PARTICLE COLLISIONS
Strangeness production with protons and pions
[DE93-010879] p 359 N94-10304
Possibility of a crossed-beam experiment involving slow-neutron capture by unstable nuclei rapid-process-tron
[DE93-754288] p 363 N94-10720
Strange meson spectroscopy in K(omega) and K(phi) at 11 GeV/c and Cherenkov ring imaging at SLD
[DE93-013593] p 363 N94-10748
The intra-atomic motion of bound electrons as a possible source of a systematic error in electron beam polarization measurements by means of a Moeller polarimeter
[DE93-620984] p 364 N94-10875
Proceedings of the Second KEK Topical Conference on e(sup +)e(sup -) collision physics
[DE93-754139] p 364 N94-10889
Experiments in ultracold collisions
[DE93-012110] p 365 N94-11029
Electronic excitation of ground state atoms by collision with heavy gas particles
[NASA-CR-193364] p 366 N94-11360
Experiments to measure the gluon helicity distribution in protons
[DE93-011756] p 368 N94-11613
Top quark search in D(O) from the lepton + jets mode
[DE93-014027] p 370 N94-12781

PARTICLE DENSITY (CONCENTRATION)
Nonlinear space charge effect of bunched beam in linac
[DE93-612176] p 371 N94-10409

PARTICLE EMISSION
NASCAP programmer's reference manual
[NASA-CR-191044] p 278 N94-11702

PARTICLE IMAGE VELOCIMETRY
The evolution of whole field optical diagnostics for external transonic testing
[ARA-MEMO-379] p 383 N94-11887
Unsteady flow past a NACA 0012 airfoil pitching at constant rates
[AD-A265159] p 16 N94-11889

PARTICLE INTERACTIONS
Indication on the existence of the bound state in the p anti p-system
[DE92-641575] p 361 N94-10532
Studies of P-matrix formalism on the basis of the potential description of two-particle interaction
[DE93-617691] p 362 N94-10550
Gas-Grain Simulation Facility (GGSF). Volume 2: Conceptual design definition
[NASA-CR-177613] p 423 N94-11229
Studies of electrostatic waves and VLF-wave particle interaction in the ionosphere
[AD-A266013] p 278 N94-12392

PARTICLE MASS
Top and Higgs masses in a composite boson model
[DE93-010874] p 359 N94-10302
Report of the Workshop on Light Particle-Induced Reactions
[DE93-752300] p 360 N94-10317

PARTICLE MOTION
Exact and quasi-classical density matrix and Wigner functions for a particle in the box and half space
p 350 N94-10600
New squeezed landau states p 379 N94-10601
Charged particle motion in torsatrons, part 1
[DE93-621639] p 389 N94-11119
Particle transport analysis in torsatron configurations
[DE93-621640] p 390 N94-11120
Development of deterministic transport methods for low energy neutrons for shielding in space
[NASA-CR-194172] p 366 N94-11199
Helium transport scaling law studies
[DE93-013487] p 393 N94-11513
Short pulse lasers for generation of fields exceeding 100 MG
[DE93-013346] p 369 N94-11815
Spectrum analysis in beam diagnostics
[DE93-013401] p 373 N94-12601

PARTICLE PRECIPITATION
Processing, properties, and wear resistance of aluminides
[DE93-012186] p 83 N94-11141

PARTICLE PRODUCTION
Production of strange clusters in relativistic heavy ion collisions
[DE93-010876] p 359 N94-10303
Strangeness production with protons and pions
[DE93-010879] p 359 N94-10304
Fast trigger algorithm for B-events selection
[DE93-621452] p 365 N94-11089
Relativistic heavy-ion collisions
[DE93-014844] p 366 N94-11147
Tau physics
[DE93-010956] p 367 N94-11469
Experiments to measure the gluon helicity distribution in protons
[DE93-011756] p 368 N94-11613

PARTICLE SIZE DISTRIBUTION
Ostwald ripening of solid cobalt particles in liquid copper p 87 N94-10202

Granular instability in fluidized beds: A small-over-large instability p 122 N94-10235
Martian particle size based on thermal inertia corrected for elevation-dependent atmospheric properties p 430 N94-12107
Organic matter on the early surface of Mars: An assessment of the contribution by interplanetary dust p 480 N94-12259
Dynamic high-pressure shock compaction of diamond powders [AD-A266004] p 93 N94-12354

PARTICLE SPIN
Aharonov-Bohm effect in Luttinger liquid [DE93-613818] p 408 N94-10148

PARTICLE THEORY
Top and Higgs masses in a composite boson model [DE93-010874] p 359 N94-10302
The legacy of uncertainty p 376 N94-10577
S(sup 1) x S(sup 2) as a bag membrane and its Einstein-Weyl geometry [DE93-613149] p 410 N94-10635
All possible electroweak models from Z orbifold [DE93-617656] p 411 N94-10880
Elementary particle physics and high energy phenomena [DE93-013971] p 370 N94-12609

PARTICLE TRACKS
Conceptual design report for the SDC barrel and intermediate muon detectors based on a jet-type drift chamber [DE93-753173] p 367 N94-11510
Theory of elementary particles and accelerator theory. Task C: Experimental high energy physics [DE93-013139] p 368 N94-11696

PARTICLE TRAJECTORIES
Spin characteristics of ion beams during the motion of electromagnetic elements [DE93-617448] p 364 N94-10848
Quantized conic sections; quantum gravity [DE93-010950] p 411 N94-10956
Non-barrier tunneling in presence of dissipations [DE93-621381] p 412 N94-11086
Probability of particle trapping/detrapping in torsatrons [DE93-621641] p 390 N94-11121
A four-dimensional, mesoscale, non-gaussian multispectral smoke model. Phase 1: Feasibility study [AD-A264805] p 152 N94-11519
Coulomb effects in low-energy nuclear fragmentation [NASA-TP-3352] p 485 N94-12434

PARTICLES
Light scattering from a spherical particle on a conducting plane. Part 1: Normal incidence [AD-A265920] p 383 N94-12341

PARTICULATES
Advanced diagnostics for in situ measurement of particle formation and deposition in thermally stressed jet fuels [DE93-009798] p 98 N94-11366
Novel mass spectrometric instrument for gaseous and particulate characterization and monitoring [DE93-014093] p 272 N94-12783

PARTITIONS (MATHEMATICS)
A lattice gas model for enzyme kinetics with alternate interactions [DE93-613027] p 395 N94-10411

PASCAL (PROGRAMMING LANGUAGE)
The solving of equations by the method of boundary elements p 326 N94-11182

PASSENGERS
Federal Aviation Administration aviation forecasts [AD-A265611] p 2 N94-12578

PASSIVITY
Surface passivation of InP solar cells with InAlAs layers p 49 N94-11389
In situ XANES studies of the passive film on Fe and Fe-26Cr [DE93-010869] p 84 N94-11459
Corrosion and passivation of high temperature superconductors [AD-A265402] p 405 N94-12586

PATTERN RECOGNITION
Object recognition in industrial environment by means of tactile sensor [ITN-93-85200] p 178 N94-10393
Model-based recognition of 3-D objects by geometric hashing technique [DE93-612916] p 322 N94-10410
Unsupervised splitting rules for neural tree classifiers [AD-A264961] p 338 N94-10487
Automaticity of processing location versus identity information in brief visual displays [AD-A265013] p 418 N94-10491
Application of normalized gray-scale correlation [DE93-013765] p 141 N94-10521
Introduction to Bayesian image analysis [DE93-012628] p 347 N94-11006
A high-speed object recognition chip based on biologically-realistic hybrid temporal processing element [AD-A265490] p 339 N94-11049
Three-dimensional object recognition using an unuspervised BCM network: The usefulness of distinguishing features [AD-A264576] p 304 N94-11261
A summary of image segmentation techniques [NASA-TM-104022] p 327 N94-11274
Remote sensing of the suspended matter distribution with high concentration in China Sea p 192 N94-11901
A pattern recognition system for locating small volvanoes in Magellan SAR images of Venus p 455 N94-12126

PAYLOAD INTEGRATION
The advanced fluid physics module: How to achieve scientific goals for Spacelab D2 p 39 N94-10136

PAYLOADS
Description of the liquid structure facility architecture and experimental demonstration of the diagnostic capabilities p 39 N94-10118

PEAT
Application of static and dynamic enclosures in determining DMS and OCS fluxes in Sphagnum peatlands p 269 N94-12460
Effects of inorganic sulfur addition on fluxes of volatile sulfur compounds in Sphagnum peatlands p 270 N94-12461
Environmental factors controlling fluxes of dimethyl sulfide in a New Hampshire fen p 270 N94-12462

PEEK
Advanced zinc phosphate conversion and pre-ceramic polymetallosiloxane coatings for corrosion protection of steel and aluminum, and characteristics of polyphenyletheretherketone-based materials [DE93-008717] p 88 N94-10891
Crystallinity and dielectric properties of PEEK, a thermoplastic poly(ether ether ketone) [AD-A266027] p 91 N94-11487

PEGASUS AIR-LAUNCHED BOOSTER
In-flight evaluation of aerodynamic predictions of an air-launched space booster p 3 N94-10427
Special investigation report: Commercial space launch incident, launch procedure anomaly orbital sciences corporation PEGASUS/SCD-1, 80 nautical miles east of Cape Canaveral, Florida, February 9, 1993 [PB93-917003] p 40 N94-11893

PELLETS
Dielectric breakdown and its influence on ignition [AD-A264925] p 78 N94-11855

PENETRATION
A spectral nodal method for the solution of the Sn equations in x, y geometry for highly absorbing deep penetration problems [DE93-613520] p 349 N94-10636
Monte Carlo algorithms in simulation of 2beta-decay and penetration of electrons through matter [DE93-617741] p 364 N94-10837
Deformation mechanisms in tungsten single crystals in ballistic impact experiments [AD-A265701] p 405 N94-12563
Prediction of alumina penetration [DE93-014017] p 95 N94-12610

PENNING EFFECT
Quantum non demolition measurement of cyclotron excitations in a Penning trap p 376 N94-10578

PEPTIDES
Development of bioelastic materials for the prevention of adhesions: Polypenta- and polytetrapeptides [AD-A264851] p 88 N94-10863
Probability of alamethicin conductance states varies with nonlamellar tendency of bilayer phospholipids [AD-A264957] p 301 N94-11648

PERFLUORO COMPOUNDS
The properties of perfluoropolyethers used for space applications [NASA-TM-106275] p 88 N94-10864

PERFORATED PLATES
Perforated plates for thin-walled structures p 63 N94-10056

PERFORMANCE
From red tape to results: Creating a government that works better and costs less p 422 N94-11351
From red tape to results: Creating a government that works better and costs less. Executive summary p 422 N94-11353

PERFORMANCE PREDICTION
Hydrostatic testing of thick laminated composite cylinders for performance model validation [DE93-012728] p 184 N94-10264
Characterization of a scannerless LADAR system [DE93-011582] p 174 N94-10959
Accelerated screening methods for predicting lubricant performance in refrigerant compressors [DE93-014773] p 89 N94-11146
A comparison between numerically modelled and experimentally measured loss mechanisms in wave rotors [NASA-TM-106279] p 29 N94-11255
Applying reliability models to the maintenance of Space Shuttle software p 330 N94-11434
Criteria for assessing problem solving and decision making in complex environments p 314 N94-11532
HF-OTH radar performance results [AD-A266106] p 138 N94-11655

PERFORMANCE TESTS
An approach to high precision antenna structures by a CFRP core sandwich concept p 57 N94-10008
The electron beam furnace: A new facility for materials science research p 109 N94-10126
Particle image velocimetry technique: Calibration tests p 111 N94-10137
Hydrostatic testing of thick laminated composite cylinders for performance model validation [DE93-012728] p 184 N94-10264
Space nuclear thermal propulsion nuclear element tests at Sandia National Laboratories [DE93-002301] p 45 N94-10282
Demonstration prototype gamma-ray hodoscope alternative to CARGOSCAN for rocket stage monitoring [DE93-006908] p 169 N94-10326
AGBT advanced counter-rotating gearbox detailed design report [NASA-CR-180883] p 179 N94-10400
Static internal performance of a single expansion ramp nozzle with multiaxis thrust vectoring capability [NASA-TM-4450] p 12 N94-10675
Characterization of in-flight performance of ion propulsion systems [NASA-TM-106283] p 46 N94-10761
Vehicular fleet operation on natural gas and propane: An overview [PB93-194603] p 98 N94-10844
In-orbit performance tests and tele-command systems of the umbrella test satellite (DEBUT) [NAL-TR-1165] p 43 N94-10859
Performance and rotor loads measurements of the Lynx XZ170 helicopter with rectangular blades [NASA-TM-104000] p 1 N94-10936
Landing Craft Air Cushion (LCAC) crew selection system manual [AD-A265158] p 313 N94-11098
Pre-operation analysis of ERS-1 tracking and operation, part 2-F [NASDA-CNT-930002-PT-2-F] p 230 N94-11130
Accelerated screening methods for predicting lubricant performance in refrigerant compressors [DE93-014773] p 89 N94-11146
Development and application of an acceptance testing model p 330 N94-11432
Monitoring cognitive function and need with the automated neuropsychological assessment metrics in Decompression Sickness (DCS) research p 314 N94-11533
Electric and hybrid vehicle site operators program: Thinking of the future [DE93-011231] p 144 N94-11609
Theory of elementary particles and accelerator theory. Task C: Experimental high energy physics [DE93-013139] p 368 N94-11696
Basic attributes test (BAT): Operational pre-implementation analysis and score equating [AD-A265885] p 314 N94-12276
FR/GE/US radar receiver pulse compression ratio [AD-A265391] p 138 N94-12409

PERIOD DOUBLING
To the theory of irregular auto modulation in electron beam-backward electromagnetic wave dynamic system [DE93-620982] p 133 N94-11030

PERIODIC VARIATIONS
A grid generation method to calculate the flow field in a three-dimensional cascade of blades [NAL-TR-1158] p 147 N94-10364
Large amplitude shape oscillations in a mercury drop using a drop tower [DE93-767972] p 125 N94-10730
Space and time variability of the Gulf Stream using ERS-1 ALT-OPR02 data p 242 N94-11769
Proceedings of the PORSEC 1992 in Okinawa: Conference for Pacific Ocean Environments and Probing, volume 1 [JTN-93-80418] p 191 N94-11894
Acoustic Doppler current profiling of the Kuroshio over the East China Sea shelf slope p 194 N94-11914
Sea surface heat flux in the beginning of the Kuroshio p 195 N94-11923
Seasonal variation of the surface mixed layer in the subtropical re-circulation area of the North Pacific during OMLET p 195 N94-11924
The Kyucho events in Sukumo Bay induced by Kuroshio front disturbances p 198 N94-11939

Current variability on the shelf break northeast of Taiwan p 219 N94-12708

PERMANENT MAGNETS
Lightweight linear alternators with and without capacitive tuning [NASA-CR-185273] p 140 N94-10505
Improvement of azimuthal homogeneity in permanent-magnet bearing rotors [DE93-009954] p 144 N94-11607

PEROVSKITES
The stability of hibonite and other aluminous phases in silicate melts: Implications for the origin of hibonite-bearing inclusions p 80 N94-12052

PERSONAL COMPUTERS
Estimation of critical values and vibration characteristics on supersonic delta wings. Part 1: On-line time series analysis of stationary random response [NAL-TR-1153] p 2 N94-10363
Application of parallel processing to a surface patch/wire junction EFIE code [AD-A264965] p 336 N94-10488

PERSONALITY TESTS
Basic attributes test (BAT): Operational pre-implementation analysis and score equating [AD-A265885] p 314 N94-12276

PERSONNEL
Department of Energy fundamentals handbook: Engineering symbology, prints, and drawings [DE93-012181] p 129 N94-11456
The 27th International Applied Military Psychology Symposium: A Focus on Decision Making Research [AD-A265278] p 313 N94-11701

PERSONNEL SELECTION
A comparison of high and low-impact reports of investigation on adjudicators' decision making: A pilot study [AD-A265747] p 416 N94-10298
Landing Craft Air Cushion (LCAC) crew selection system manual [AD-A265158] p 313 N94-11098
The 27th International Applied Military Psychology Symposium: A Focus on Decision Making Research [AD-A265278] p 313 N94-11701
Basic attributes test (BAT): Operational pre-implementation analysis and score equating [AD-A265885] p 314 N94-12276

PERTURBATION THEORY
Nonperturbative methods in the problem of multiphoton excitation of atom by squeezed light p 376 N94-10575
Direct solution of the mathematical adjoint equations for an interface current nodal formulation [DE93-009961] p 346 N94-11608

PETRI NETS
Task planning with uncertainty for robotic systems [NASA-CR-193253] p 338 N94-10638

PETROGRAPHY
Apollo 16 core 60013/14 as a product of path 1 and path 2 regolith evolution processes p 440 N94-12050
Petrography and preliminary interpretations of the crystalline breccias from the Manson M-1 core p 281 N94-12056
The great 8 MA event and the structure of the H-chondrite parent body p 429 N94-12058
Trace-element abundances in several new ureilites p 80 N94-12096
Distribution of vanadium and melting of opaque assemblages in Efremovka CAI's p 282 N94-12141

PETROLEUM PRODUCTS
Immediate response to free product discovery [PB93-182970] p 265 N94-11015
Methodologies for estimating air emissions from three non-traditional source categories: Oil spills, petroleum vessel loading and unloading, and cooling towers [PB93-181592] p 266 N94-11471

PETROLOGY
Twenty-fourth Lunar and Planetary Science Conference. Part 1: A-F [NASA-CR-193095] p 435 N94-12015
Carbon in weathered ordinary chondrites from Roosevelt County p 428 N94-12035
Nitrogen and noble gases in a glass sample from LEW88516 p 80 N94-12051
The great 8 MA event and the structure of the H-chondrite parent body p 429 N94-12058
Th-230 - U-238 series disequilibrium of the Olkaria basalts Gregory Rift Valley, Kenya: Petrogenesis p 281 N94-12074
Th-230 - U-238 series disequilibrium of the Olkaria rhyolites Gregory Rift Valley, Kenya: Petrogenesis p 281 N94-12075
Mineralogy versus bulk composition of the carbonaceous chondrite clast Kaidun 2 p 429 N94-12101
A structural and petrographic investigation of the pretoria saltpan impact structure p 282 N94-12102
Carbonaceous chondrite clasts in the Kapoeta howardite p 282 N94-12104
LEW88516 and SNC meteorites p 430 N94-12150
Flash melting of chondrule precursors in excess of 1600 C. Series 1: Type 2 (B1) chondrule composition experiments p 431 N94-12177
Rhenium-osmium isotope systematics of Group 2A and Group 4A iron meteorites p 431 N94-12182
Regional mantle upwelling on Venus: The Beta-Atla-Themis anomaly and correlation with global tectonic patterns p 467 N94-12196
The granulite suite: Impact melts and metamorphic breccias of the early lunar crust p 282 N94-12197
Compositional heterogeneity within a dumbbell-shaped Apollo 15 green glass: Evidence for simultaneous eruption of different magmas p 470 N94-12209
Soret diffusion: A possible cause of compositional heterogeneity within tektites p 432 N94-12211

PH
A survey of techniques for corrosion monitoring [DE93-012131] p 83 N94-11250

PH FACTOR
Size dependence of chemical reactivity of gaseous metal clusters: A new mechanistic probe [AD-A264690] p 77 N94-11264

PHASE CHANGE MATERIALS
Modeling void growth and movement with phase change in thermal energy storage canisters [NASA-TM-106288] p 163 N94-12576

PHASE COHERENCE
Coherent structure in near wall turbulence with riblets p 165 N94-12628

PHASE CONJUGATION
Limitations to the quality of optical phase conjugation by stimulated Brillouin scattering [AD-A266006] p 383 N94-12389

PHASE DEMODULATORS
Localized and distributed fiber-optic strain sensors embedded in composite materials [UTIAS-346] p 73 N94-12013

PHASE DIAGRAMS
Phase equilibria and volumetric properties for the system NaCl-CaCl2-H2O [DE93-013590] p 76 N94-11244
Synthesis and magnetic properties of novel La*2-x*M*x*CuO*4 equals y* compositions (La equals La, Pr, Nd, Sm, Eu, Cd; M equals Ca, Sr, Ba; O (less than or equal) x 0.2; -0.5 (less than or equal) y (less than or equal) 0.5) [DE93-011359] p 403 N94-12363

PHASE ERROR
The limit of frequency estimation p 356 N94-11001

PHASE LOCKED SYSTEMS
Method of recertifying a loaded bearing member using a phase point [NASA-CASE-LAR-14741-1] p 185 N94-10671

PHASE MATCHING
New challenges in optical materials development [DE93-011889] p 383 N94-11676

PHASE SEPARATION (MATERIALS)
Design of multisample, multistep phase partitioning apparatus for use on Space Shuttle Spacelab, and Spacelab missions p 108 N94-10120
Appearance of convective instabilities caused by liquid-liquid phase separation under small buoyancy forces p 120 N94-10221
Phase separation at gas-liquid critical points p 122 N94-10233
Use of inert immiscible liquid for crystal separation out of its feeding solution in weightlessness p 124 N94-10242

PHASE SHIFT
Interferometry with particles of non-zero rest mass [DE93-613518] p 409 N94-10501
Three-nucleon problem with phase equivalent potentials [DE93-617731] p 363 N94-10722
Characterization of a scannerless LADAR system [DE93-011582] p 174 N94-10959
FEFF5: An ab initio multiple scattering XAFS code [DE93-011000] p 367 N94-11470

PHASE SHIFT KEYING
Telemetering and telecommunications research [NASA-CR-193235] p 42 N94-11297
Flexible high-speed CODEC [NASA-CR-191169] p 146 N94-12433

PHASE STABILITY (MATERIALS)
Fluid-fluid interfacial instabilities induced by gravity p 121 N94-10229

PHASE TRANSFORMATIONS
Studies of critical point phenomena of fluids: Bulk fluids, fluids in pores, and at interfaces p 80 N94-10228
Singularity spectrum of self-organized criticality [DE93-613820] p 348 N94-10404
Monte Carlo simulations of phase transformations in Fe-Cr alloys [DE93-013847] p 81 N94-10522
Non-gauge phase transformations in quantum transition amplitudes p 378 N94-10596
Confinement of acoustical modes due to the electron-phonon interaction within 2D-electron gas [DE93-613910] p 396 N94-10800
Non-barrier tunneling in presence of dissipations [DE93-621381] p 412 N94-11086
Low temperature synthesis of monolithic transparent Ta2O5 gels from hydrolysis of metal alkoxide [NASA-TM-106246] p 89 N94-11204
Real-space formation and dissipation dynamics of hexagonal reconstruction on Au(100) in aqueous media as explored by potentiodynamic scanning tunneling microscopy [AD-A266138] p 368 N94-11658
Shock transformations in quartzite p 97 N94-12040
Phase transitions and 2D spherical convection in a large icy satellite p 433 N94-12265
Electrode potential-induced reconstruction of Au(100): Effect of chemisorption on nanoscale dynamics as probed by the in-situ scanning tunneling microscopy [AD-A265900] p 404 N94-12388

PHASE VELOCITY
Wave propagation characteristics of short-period crustal phases near ARCESS and NORESS [AD-A265959] p 275 N94-11102

PHASE-SPACE INTEGRAL
Correlated states of a quantum oscillator acted by short pulses p 380 N94-10609

PHENOL FORMALDEHYDE
Primaset (tm): A safer material for aircraft interior applications p 18 N94-10772
Advanced phenolic systems for aircraft interiors p 18 N94-10776
Fire resistance and mechanical properties for phenolic prepregs p 20 N94-10786

PHENOLIC RESINS
Primaset (tm): A safer material for aircraft interior applications p 18 N94-10772
Advanced phenolic systems for aircraft interiors p 18 N94-10776

PHENYLS
The synthesis of photocrosslinkable chalcone-bearing polyphosphazenes [AD-A264915] p 92 N94-11849

PHILIPPINES
Status of remote sensing and Geographic Information System (GIS) applications in the Environment and Natural Resources (ENR) sector p 36 N94-10687

PHOBOS
Interdisciplinary scientist participation in the Phobos mission [NASA-CR-193715] p 482 N94-12446

PHONONS
Energy transfer dynamics and impact sensitivity [DE93-009551] p 98 N94-11269
On the theory of phonoriton in cubic semiconductors with a degenerate valence band [DE93-613539] p 402 N94-11680

PHOSPHATES
Advanced zinc phosphate conversion and pre-ceramic polymetallosiloxane coatings for corrosion protection of steel and aluminum, and characteristics of polyphenyletheretherketone-based materials [DE93-008717] p 88 N94-10891
In situ secondary ion mass spectrometry analysis [DE93-012185] p 76 N94-11140
Radiation-induced aperiodicity in irradiated ceramics [DE93-013335] p 91 N94-11698
Tandem mass spectrometric analysis of phosphate esters [AD-A265483] p 78 N94-12009

PHOSPHAZENE
Ring-opening polymerization of phosphazenes [AD-A265000] p 90 N94-11292
Synthesis, characterization, and modification of poly(organophosphazenes), that bear both 2,2,2-trifluoroethoxy and phenoxy groups [AD-A264913] p 92 N94-11847
Radiation-induced modifications of allylamino-substituted polyphosphazenes [AD-A264914] p 92 N94-11848
The synthesis of photocrosslinkable chalcone-bearing polyphosphazenes [AD-A264915] p 92 N94-11849

PHOSPHINES
Remote plasma enhanced chemical vapor deposition of GaP with in situ generation of phosphine precursors p 399 N94-11440

PHOSPHORESCENCE
Thermographic properties of eight blue-emitting phosphors [DE93-011459] p 78 N94-11622

PHOSPHORS
Thermographic properties of eight blue-emitting phosphors [DE93-011459] p 78 N94-11622
PHOSPHORUS COMPOUNDS
Aluminum-phosphorus chemistry: Preparation and structural characterization of (Et2AlP(SiMe3)2)2, Et(Cl)2Al(dot)P(SiMe3)3, and i-Bu2(Cl)Al(dot)P(SiMe3)3 [AD-A265268] p 78 N94-11683
PHOSPHORUS POLYMERS
Fire-resistant hydrolytically stable poly(arylene phosphine oxide) material systems p 19 N94-10780
PHOTOACOUSTIC SPECTROSCOPY
Application of the infrared photoacoustic spectroscopy to the study of the cure mechanisms of structural epoxy adhesives p 61 N94-10040
PHOTOCATHODES
Interference photocathode [AD-D015770] p 132 N94-10382
PHOTOCHEMICAL REACTIONS
Photoinitiated radical polymerization of liquid monomers in microgravity p 124 N94-10246
Symmetry lowering in crystalline solid solutions: A study of cinnamamide-thienylacrylamide by x ray and neutron diffraction and solid-state photochemistry [DE93-010871] p 394 N94-10301
Photochemical modelling of Venus clouds using Pioneer Venus data [NASA-CR-194108] p 434 N94-10823
Dynamics of charge-transfer excited states relevant to photochemical energy conversion [DE93-013981] p 263 N94-11116
The synthesis of photocrosslinkable chalcone-bearing polyphosphazenes [AD-A264915] p 92 N94-11849
NRL review for 1993 [AD-A265666] p 497 N94-12334
A novel photosensitive polyimide resist consisting of a soluble polyimide and a bis(perfluorophenyl azide) as a cross-linker [AD-A265998] p 93 N94-12353
Photogenerated base in polymer imaging. Synthesis and photopatterning of poly(2-cyano-2-(p-vinylphenyl) butanoic acid) [AD-A265288] p 95 N94-12585
PHOTOCONDUCTIVITY
A thermal ionization model for the sustaining phase of lock-on in GaAs [DE93-011558] p 144 N94-11624
PHOTOCONDUCTORS
GaAs PCSS: High gain switching and device reliability [DE93-009851] p 401 N94-11605
PHOTODETACHMENT
Photodetachment studies on few-electron atomic negative ions [DE93-008474] p 358 N94-10154
PHOTODIODES
New challenges in optical materials development [DE93-011889] p 383 N94-11676
Development of the one-component diode-array velocimeter [AD-A265552] p 171 N94-12533
PHOTOELECTRIC EMISSION
Highly anisotropic but nodeless gap from a valence-fluctuation pairing mechanism [DE93-010738] p 401 N94-11646
PHOTOELECTRON SPECTROSCOPY
Surface and near-surface atom imaging with photoelectron holography [DE93-013197] p 169 N94-10526
Effect of surface cleanliness of bearing steel on adhesive strength and tribological properties of sputter-deposited gold films [DE93-767974] p 82 N94-10732
Tribological characteristics of hot-pressed self-lubricating composites [NAL-TR-1160] p 66 N94-10858
PHOTOELECTRONS
Photodetachment studies on few-electron atomic negative ions [DE93-008474] p 358 N94-10154
Surface and near-surface atom imaging with photoelectron holography [DE93-013197] p 169 N94-10526
Strange meson spectroscopy in K(omega) and K(phi) at 11 GeV/c and Cherenkov ring imaging at SLD [DE93-013593] p 363 N94-10748
PHOTOEXCITATION
Femtosecond dynamics, photoexcitation, and ESR spectra of MX chain solids [AD-A264689] p 399 N94-11263
Atomic processes relevant to polarization plasma spectroscopy [DE93-753240] p 393 N94-11594
Polaronic charge separation in mixed-halide MX solids [AD-A266073] p 403 N94-12345
PHOTOGEOLOGY
Estimation of age of Dali-Ganis rifting and associated volcanic activity, Venus p 440 N94-12046
Regional geology of the Vega landing sites: Tentative results of photogeologic mapping p 440 N94-12047
Regional geology of the Venera landing sites: Tentative results of photogeologic mapping p 440 N94-12048
PHOTOGRAMMETRY
On resolution of underwater stereo photogrammetry p 172 N94-11966
PHOTOGRAPHIC MEASUREMENT
Interferometric and optical tests of water window imaging x ray microscopes [NASA-CR-193369] p 375 N94-10506
PHOTOINTERPRETATION
Satellite inventory of Minnesota forest resources [NASA-CR-193565] p 231 N94-11521
PHOTOIONIZATION
Dynamics of dissociation versus ionization in strong laser fields [DE93-009261] p 173 N94-10287
High power z pinches as x ray laser photopumps [DE93-012842] p 173 N94-10746
PHOTOLITHOGRAPHY
Radiation-induced modifications of allylamino-substituted polyphosphazenes [AD-A264914] p 92 N94-11848
PHOTOLUMINESCENCE
GaAs PCSS: High gain switching and device reliability [DE93-009851] p 401 N94-11605
Thermographic properties of eight blue-emitting phosphors [DE93-011459] p 78 N94-11622
PHOTOLYSIS
Vibrational overtone activation of methylcyclopropene [AD-A265588] p 79 N94-12373
PHOTOMAPPING
Regional geology of the Vega landing sites: Tentative results of photogeologic mapping p 440 N94-12047
Regional geology of the Venera landing sites: Tentative results of photogeologic mapping p 440 N94-12048
PHOTOMASKS
A novel photosensitive polyimide resist consisting of a soluble polyimide and a bis(perfluorophenyl azide) as a cross-linker [AD-A265998] p 93 N94-12353
PHOTONICS
Semiconductor ring lasers [DE93-012386] p 174 N94-11005
Preliminary surface-emitting laser logic device evaluation [AD-A266111] p 383 N94-12416
PHOTONS
Disturbance, the uncertainty principle and quantum optics p 375 N94-10569
Photon number amplification/duplication through parametric conversion p 376 N94-10572
Non classical effects in planar waveguides p 376 N94-10574
Nonperturbative methods in the problem of multiphoton excitation of atom by squeezed light p 376 N94-10575
Study of Einstein-Podolsky-Rosen state for space-time variables in a two photon interference experiment p 370 N94-10582
Squeezed colour states in gluon jet p 379 N94-10599
Wavelets and spacetime squeeze p 379 N94-10604
Strange meson spectroscopy in K(omega) and K(phi) at 11 GeV/c and Cherenkov ring imaging at SLD [DE93-013593] p 363 N94-10748
A review of two photon production of jets at PEP and PETRA energies [DE93-011742] p 364 N94-10754
Non-Euclidean space for local hidden variables [DE93-621341] p 344 N94-11032
Investigation of optically generated electronic defects and protonic transport in hydrogen-bonded molecular solids: Isomorphs of potassium dihydrogen phosphate [DE93-012498] p 399 N94-11243
LCLS optics: Selected technological issues and scientific opportunities [DE93-010953] p 175 N94-11468
Applications of in-situ ellipsometry to microwave electron cyclotron resonance plasma processes [AD-A265197] p 373 N94-11880
PHOTOPRODUCTION
A review of two photon production of jets at PEP and PETRA energies [DE93-011742] p 364 N94-10754
PHOTOSYNTHESIS
Estimating Photosynthetically Available Radiation (PAR) at the Earth's surface from satellite observations p 230 N94-10955
Coprocessing of fossil fuels and biomass for CO2 emission reduction in the transportation sector [PB93-194165] p 267 N94-11845
Variation of the photosynthetic products in the regional upwelling area around the Izu Islands, Japan p 211 N94-12661
PHOTOTRANSISTORS
Preliminary surface-emitting laser logic device evaluation [AD-A266111] p 383 N94-12416
PHOTOVOLTAGES
Adsorption and dissociation of disilane on Si(001) studied by STM [AD-A265269] p 402 N94-11684
PHOTOVOLTAIC CELLS
Flexible polycrystalline thin-film photovoltaics for space applications p 50 N94-11393
Space Station Freedom advanced photovoltaics and battery technology development planning p 52 N94-11401
Computation of photovoltaic parameters under lunar temperature variation p 53 N94-11411
PHOTOVOLTAIC CONVERSION
Japan's Sunshine Project [DE93-767980] p 262 N94-10498
High efficiency direct thermal to electric energy conversion from radioisotope decay using selective emitters and spectrally tuned solar cells [NASA-TM-106227] p 47 N94-11307
Proceedings of the 12th Space Photovoltaic Research and Technology Conference (SPRAT 12) [NASA-CP-3210] p 48 N94-11380
Flexible polycrystalline thin-film photovoltaics for space applications p 50 N94-11393
Space Station Freedom advanced photovoltaics and battery technology development planning p 52 N94-11401
Workshop summary: Receivers for laser power beaming p 54 N94-11419
PHOTOVOLTAIC EFFECT
An overview of the Defence Research Agency photovoltaic programme p 53 N94-11412
NASDA activities in space solar power system research, development and applications p 54 N94-11413
Thin film solar cell workshop p 54 N94-11415
Polaronic charge separation in mixed-halide MX solids [AD-A266073] p 403 N94-12345
PHYSICAL CHEMISTRY
Proceedings of the 8th European Symposium on Materials and Fluid Sciences in Microgravity, volume 2 [ESA-SP-333-VOL-2] p 112 N94-10171
Crystal-chemistry and partitioning of REE in whitlockite p 408 N94-12174
PHYSICAL EXERCISE
Exercise countermeasures for bed-rest deconditioning [NASA-TM-103987] p 300 N94-11191
Monitoring cognitive function and need with the automated neuropsychological assessment metrics in Decompression Sickness (DCS) research p 314 N94-11533
Carotid-cardiac baroreflex: Relation with orthostatic hypotension following simulated microgravity and implications for development of countermeasures p 308 N94-11992
Mechanistic studies on reduced exercise performance and cardiac deconditioning with simulated zero gravity p 310 N94-12001
Modifications to an interactive model of the human body during exercise: With special emphasis on thermoregulation p 317 N94-12368
PHYSICAL OPTICS
Physical optics modelling of Soft X ray Projection Lithography (SXPL) imaging experiments [DE93-011556] p 374 N94-10339
PO/PTD diffraction synthesis of array-fed reflector antennas for satellite and radar applications p 137 N94-11636
PHYSICAL SCIENCES
Project TIMS (Teaching Integrated Math/Science) [NASA-CR-194288] p 416 N94-11599
PHYSICIANS
Clinical aspects of telemedicine p 306 N94-11795
PHYSIOLOGICAL EFFECTS
Effects of CSF hormones and ionic composition on salt/water metabolism [NASA-CR-193232] p 300 N94-11045
Exercise countermeasures for bed-rest deconditioning [NASA-TM-103987] p 300 N94-11191
PHYSIOLOGICAL RESPONSES
Unsupervised splitting rules for neural tree classifiers [AD-A264961] p 338 N94-10487
Effect of double density caging during Space Shuttle transport of laboratory rats [NASA-CR-193228] p 300 N94-11180

Allowable exposure limits for carbon dioxide during extravehicular activity
[NASA-TM-103832] p 315 N94-11375
A mechanism for the reduction in risk of decompression sickness in microgravity environment
p 312 N94-11545
Proceedings of the First Joint NASA Cardiopulmonary Workshop
[NASA-CP-10068] p 308 N94-11991
Central circulatory hemodynamics as a function of gravitational stress p 309 N94-11995
Glycerol-induced hyperhydration p 309 N94-11996
Spectral analysis of resting cardiovascular variables and responses to oscillatory LBNP before and after 6 degree head dowm bedrest p 309 N94-11997
Effect of prolonged LBNP and saline ingestion on plasma volume and orthostatic responses during bed rest
p 310 N94-11998
Fitness, autonomic regulation and orthostatic tolerance p 310 N94-11999
Local fluid shifts and edema in humans during simulated microgravity p 311 N94-12003
Autogenic-feedback training: A countermeasure for orthostatic intolerance p 311 N94-12006

PHYSIOLOGY
Conversion of acetic acid to methane by thermophiles
[DE93-014433] p 300 N94-10652
Motion and spatial disorientation systems: Special research capabilities
[AD-A265155] p 303 N94-11097
Arterial gas emboli in altitude-induced decompression sickness p 312 N94-11543
Physiological water model development
p 316 N94-12367

PHYTOPLANKTON
Seasonal changes of phytoplankton distributions in the Northwest Pacific detected by Coastal Zone Color Scanner p 200 N94-11948
Particle dynamics in the western subarctic Pacific: Implications from CZCS imagery p 200 N94-11950
Development of shipboard ocean lidar
p 140 N94-11965
The development of phytoplankton sensing system with optical fiber p 203 N94-11967
The seasonal change of phytoplankton size distribution using optical fiber sensor p 210 N94-12656
The phytoplankton bloom in the Kinu-ura Bay, Japan in the rainy season p 211 N94-12660
Variation of the photosynthetic products in the regional upwelling area around the Izu Islands, Japan
p 211 N94-12661
Optimum selection of spectral channels in the problem of remote sensing of phytoplankton concentration in ocean water p 223 N94-12726
High biological production of the tidal mixing zones on Japan Sea shelf p 228 N94-12758

PHYTOTRONS
Statistical analysis of environmental variability within the CELSS breadboard project's biomass production chamber
[NASA-TM-109188] p 315 N94-11258

PIEZOELECTRIC CERAMICS
Smart structures at Aastra Corporation
p 69 N94-11326
Recent developments in piezoelectric and electrostrictive sensors and actuators for smart structures p 70 N94-11332
Ceramic actuators for smart materials
[AD-A265664] p 93 N94-12331

PIEZOELECTRIC TRANSDUCERS
Active vibration control of adaptive flexible structures using piezoelectric smart sensors and actuators
p 189 N94-11823

PIEZOELECTRICITY
Recent developments in piezoelectric and electrostrictive sensors and actuators for smart structures p 70 N94-11332
Structural analysis and optimization of adaptive structures by use of the finite element method
p 71 N94-11339
Active damping augmentation of elastomechanical systems using piezoelectric sensors and actuators
p 72 N94-11346
Ceramic actuators for smart materials
[AD-A265664] p 93 N94-12331

PIGMENTS
Formulating infrared coatings for defence applications
[MRL-RR-1-93] p 90 N94-11302

PILOT PERFORMANCE
Aviation accident risk for airmen with aphakia and artificial lens implants
[DOT/FAA/AM-93/11] p 303 N94-10813
Quantitative EEG patterns of differential in-flight workload p 317 N94-11528
Psychophysiological measures of cognitive workload in laboratory and flight p 317 N94-11529
Criteria for assessing problem solving and decision making in complex environments p 314 N94-11532
A comparison of head-up and head-down display formats during instrument flying tasks
[AD-A266140] p 316 N94-11642
The aging military aviator: A review and annotated bibliography
[AD-A265341] p 311 N94-12423

PILOT SELECTION
Basic attributes test (BAT): Operational pre-implementation analysis and score equating
[AD-A265885] p 314 N94-12276

PILOT TRAINING
Flight simulator experiment of the cockpit advisory system
[NAL-TR-1151] p 33 N94-10733
Transfer of training for aerospace operations: How to measure, validate, and improve it p 314 N94-11530
Criteria for assessing problem solving and decision making in complex environments p 314 N94-11532
Basic attributes test (BAT): Operational pre-implementation analysis and score equating
[AD-A265885] p 314 N94-12276

PINHOLE CAMERAS
High resolution time- and 2-dimensional space-resolved x ray imaging of plasmas at NOVA
[DE93-011892] p 393 N94-11677

PINNING
High frequency behavior of long and small junctions
[AD-A265670] p 403 N94-12336

PINS
Extensions of some guidelines for the mechanical design of coaxial compression pin seals
[DE93-012385] p 177 N94-10348

PINTLES
Atomization characteristics of a prefilming airblast atomizer
[NAL-TM-644] p 148 N94-10727

PION BEAMS
Relativistic heavy ion research
[DE93-013127] p 367 N94-11373

PIONS
Strangeness production with protons and pions
[DE93-010879] p 359 N94-10304
Crossing-odd spin effects in the dipole model of hadron scattering
[DE93-617692] p 362 N94-10551
Coherence influence on the intensity of Bose-Einstein correlations and visible size of a source
[DE93-617697] p 349 N94-10556
Pion correlations and calorimeter design for high energy heavy ion collisions
[DE93-013861] p 373 N94-12607

PIPE FLOW
Flow development in a circular pipe in the UTIAS/RPI M = 8.3 gun tunnel p 6 N94-10442
Suppression of the near wall burst process of a fully developed turbulent pipe flow
[AD-A265995] p 161 N94-12352
Nonlinear stability calculations of pipe flow
p 163 N94-12612

PIPES (TUBES)
A new and efficient way to join composite pipes
p 63 N94-10054
Separation of gravitational effects on the flow of suspension in tubes by measurements in weightlessness
p 105 N94-10105
An investigation on the effectiveness of the piping interference removal system for STOL aircraft wind tunnel tests
[NAL-TM-647] p 2 N94-10350
Fracture mechanics and full scale pipe break testing for the Department of Environment's New Production Reactor-Heavy Water Reactor
[DE93-005428] p 187 N94-11169

PISTONS
Cooled spool piston compressor
[NASA-CASE-MSC-22020-1] p 179 N94-10674
Instantaneous engine frictional torque: Its components and piston assembly friction
[DE93-011639] p 182 N94-11625
Ceramics technology project database
[DE93-012431] p 91 N94-11672

PITCH
On non-linear longitudinal stability of an aircraft in a dive in the presence of atmospheric disturbances
p 31 N94-11492

PITCHING MOMENTS
Unsteady flow past a NACA 0012 airfoil pitching at constant rates
[AD-A265159] p 16 N94-11889

PITTING
Plating under reduced pressure
[DE93-011896] p 84 N94-11668

PIXELS
Optimal hemicube sampling
[DE93-010499] p 334 N94-12591

PLAINS
Modern shelf ice, equatorial Aeolis Quadrangle, Mars
p 450 N94-12100
Shallow crustal discontinuities and graben and scarp formation in the Tharsis region of Mars
p 469 N94-12203

PLANE WAVES
Squeezing in phase-conjugated resonance fluorescence p 376 N94-10576
Effects of energetic particle events on VLF/LF propagation parameters/1989
[AD-A265266] p 275 N94-11013

PLANETARY ATMOSPHERES
Twenty-fourth Lunar and Planetary Science Conference. Part 1: A-F
[NASA-CR-193095] p 435 N94-12015
Giant impact-induced atmospheric blow-off
p 435 N94-12019
An interferometric spectral mapper for the Cassini mission to Saturn and Titan
[NASA-CR-193805] p 482 N94-12429

PLANETARY COMPOSITION
Marslink p 438 N94-12034
Venus mountain-top mineralogy: Misconceptions about pyrite as the high radar-reflecting phase
p 455 N94-12129
Automatic definition of spectral units in the equatorial regions of Mars p 432 N94-12234
Composition of the Martian aerosols through near-IR spectroscopy p 475 N94-12235
Primitive SNC parent magmas and crystallization: Low PH2O experiments p 433 N94-12264

PLANETARY CRATERS
Twenty-fourth Lunar and Planetary Science Conference. Part 1: A-F
[NASA-CR-193095] p 435 N94-12015
Estimation of age of Dali-Ganis rifting and associated volcanic activity, Venus p 440 N94-12046
Regional geology of the Vega landing sites: Tentative results of photogeologic mapping p 440 N94-12047
Landscape and geomorphic survey of Zhamanshin area, Northern Kazakhstan: Preliminary report on 1992 field trip data p 282 N94-12123
A two-stage (turbulent-drainage) mechanism for the emplacement of impact crater outflows on Venus
p 458 N94-12145
Cratering on Gaspra p 459 N94-12147

PLANETARY CRUSTS
Venus' center of mass - center of figure displacement and implications p 444 N94-12067
Can weak crust explain the correlation of geoid and topography on Venus? p 453 N94-12118
Fault geometries and extension in the Valles Marineris, Mars p 458 N94-12144
Mars: The initial emplacement of ground ice in response to the thermal evolution of its early crust
p 462 N94-12168
The role of the geothermal gradient in the emplacement and replenishment of ground ice on Mars
p 463 N94-12169
The thermodynamic case for a water-rich Mars
p 463 N94-12170
Porosity and the ecology of icy satellites
p 431 N94-12186
Noble gas evidence of an aqueous reservoir near the surface of Mars more recently than 1.3 Ga
p 473 N94-12228
Do large impact basins in the southern hemisphere of Mars control the distribution of polar structures and deposits? p 481 N94-12266
Free-air and Bouguer gravity anomalies and the Martian crustal dichotomy p 481 N94-12267
New Mars free-air and Bouguer gravity: Correlation with topography, geology and large impact basins
p 481 N94-12268

PLANETARY EVOLUTION
Columbus proto-planetesimal dust aggregation experiment p 123 N94-10236
Giant impact-induced atmospheric blow-off
p 435 N94-12019
Metal-rich meteorites from the aubrite parent body
p 430 N94-12142
On high-temperature formation of iron-rich olivine in the early solar system p 432 N94-12225
Recondensation of chondritic material in the early solar system: Results of thermodynamic simulation
p 432 N94-12226
Laboratory studies on the velocity of fragments from impact disruptions p 189 N94-12359

PLANETARY GEOLOGY
Radiogenic age and isotopic studies
[DE93-610548] p 274 N94-10407

Physical studies of planetary and satellite surfaces
[NASA-CR-193545] p 434 N94-10817
Evolution of steep Martian slopes p 434 N94-11184
Analysis of gravity, magnetic, and seismic reflection data from Tibet and neighboring regions of China
[NASA-CR-193405] p 278 N94-11886
Twenty-fourth Lunar and Planetary Science Conference. Part 1: A-F
[NASA-CR-193095] p 435 N94-12015
Rates of fluvio-thermal erosion on Mars
p 435 N94-12018
Morphology of large impact craters and basins on Venus: Implications for ring formation p 436 N94-12023
Lineament analysis and tectonic interpretation for the Tharsis region p 437 N94-12031
Reconstruction of the dynamics of the 1800-1801 Hualalai eruption: Implications for planetary lava flows
p 281 N94-12041
Horizontal stresses induced by vertical processes in planetary lithospheres p 281 N94-12042
Increased depth-diameter ratios in the Medusae Fossae Formation deposits of Mars p 439 N94-12043
Estimation of age of Dali-Ganis rifting and associated volcanic activity, Venus p 440 N94-12046
Regional geology of the Vega landing sites: Tentative results of photogeologic mapping p 440 N94-12047
Regional geology of the Venera landing sites: Tentative results of photogeologic mapping p 440 N94-12048
Changes in Hawaiian palagonite FE mineralogy associated with thermal alteration: Implications for Mars
p 281 N94-12055
Petrography and preliminary interpretations of the crystalline breccias from the Manson M-1 core
p 281 N94-12056
Thermal studies of Martian channels and valleys using Termoskan data p 443 N94-12064
Spectral analysis of the gravity and topography of Mars p 444 N94-12065
Global organization of tectonic deformation on Venus
p 444 N94-12066
Venus' center of mass - center of figure displacement and implications p 444 N94-12067
Using high spectral resolution spectrophotometry to study broad mineral absorption features on Mars
p 446 N94-12077
Venus resurfacing rates: Constraints provided by 3-D Monte Carlo simulations p 453 N94-12119
Scalloped margin domes: What are the processes responsible and how do they operate?
p 454 N94-12120
Yana ring structure, North-Eastern Siberia: A possible counterpart of coronae on Venus p 282 N94-12121
Russia's contribution to regional geologic mapping of Venus p 454 N94-12122
Chemical weathering on Mars: Rate of oxidation of iron dissolved in brines p 455 N94-12128
Geology and surface characteristics of Bell Regio, Venus p 457 N94-12136
Fault geometries and extension in the Valles Marineris, Mars p 458 N94-12144
A two-stage (turbulent-drainage) mechanism for the emplacement of impact crater outflows on Venus
p 458 N94-12145
Mars: The initial emplacement of ground ice in response to the thermal evolution of its early crust
p 462 N94-12168
The thermodynamic case for a water-rich Mars
p 463 N94-12170
Geologic history of central Chryse Planitia and the Viking 1 landing site, Mars p 465 N94-12180
Large volcanoes on Venus: Examples of geologic and structural characteristics from different classes
p 467 N94-12195
Regional mantle upwelling on Venus: The Beta-Atla-Themis anomaly and correlation with global tectonic patterns p 467 N94-12196
Small volcanoes in Tempe Terra, Mars: Their detailed morphometry and inferred geologic significance
p 469 N94-12202
Shallow crustal discontinuities and graben and scarp formation in the Tharsis region of Mars
p 469 N94-12203
Characteristics of arachnoids from Magellan data
p 469 N94-12204
Soret diffusion: A possible cause of compositional heterogeneity within tektites p 432 N94-12211
Isotopic and trace element characteristics of an unusual refractory inclusion from Essebi p 471 N94-12212
Relation between ages and elevations of Martian channels p 472 N94-12216
Automatic definition of spectral units in the equatorial regions of Mars p 432 N94-12234
Giant radiating dyke swarms on Earth and Venus
p 283 N94-12236
Terrestrial case studies of ilmenite exploration and lunar implications p 478 N94-12247
Transmantle flux tectonics p 283 N94-12249
Do large impact basins in the southern hemisphere of Mars control the distribution of polar structures and deposits? p 481 N94-12266
New Mars free-air and Bouguer gravity: Correlation with topography, geology and large impact basins
p 481 N94-12268
Interdisciplinary scientist participation in the Phobos mission
[NASA-CR-193715] p 482 N94-12446
Planetary astronomy of Mars. Mars data reduction
[NASA-CR-193515] p 424 N94-12768

PLANETARY GRAVITATION
Spectral analysis of the gravity and topography of Mars p 444 N94-12065

PLANETARY MAGNETIC FIELDS
Interpretation of lunar and planetary electromagnetic scattering using the full wave solutions
p 440 N94-12049
On the unique structure of the magnetic fields of Uranus and Neptune p 472 N94-12221
Precession of Uranus and Neptune and their magnetic field p 473 N94-12222

PLANETARY MAGNETOTAILS
An investigation of the near Earth space environments
[AD-A265295] p 278 N94-11828

PLANETARY MANTLES
Can weak crust explain the correlation of geoid and topography on Venus? p 453 N94-12118
Buoyant subduction on Venus: Implications for subduction around coronae p 455 N94-12130
Regional mantle upwelling on Venus: The Beta-Atla-Themis anomaly and correlation with global tectonic patterns p 467 N94-12196
Noble gas evidence of an aqueous reservoir near the surface of Mars more recently than 1.3 Ga
p 473 N94-12228
Morphotectonics of Venus p 478 N94-12248
Transmantle flux tectonics p 283 N94-12249

PLANETARY MAPPING
Meteorological Satellite Center
[MSC-TN-26] p 190 N94-11079
Fine tuning of stretched-VISSR image mapping
p 190 N94-11080
Russia's contribution to regional geologic mapping of Venus p 454 N94-12122
Geologic history of central Chryse Planitia and the Viking 1 landing site, Mars p 465 N94-12180
Synthesis of global thematic mapping, Venus: Geologic correlations/questions for the Magellan gravity mission
p 467 N94-12194
Relation between ages and elevations of Martian channels p 472 N94-12216
Free-air and Bouguer gravity anomalies and the Martian crustal dichotomy p 481 N94-12267
Interdisciplinary scientist participation in the Phobos mission
[NASA-CR-193715] p 482 N94-12446

PLANETARY NEBULAE
Midplane temperatures in the solar nebula
p 448 N94-12088
Chondrule formation by clumpy accretion onto the solar nebula p 448 N94-12089
The experimental production of matrix lumps within chondrules: Evidence of post-formational processes
p 431 N94-12176
Anomalous REE patterns in unequilibrated enstatite chondrites: Evidence and implications
p 431 N94-12191

PLANETARY RINGS
Wave structure in planetary rings p 434 N94-11185
Submission of Earth-based ring occultation observations to the NASA planetary data system rings discipline node
[NASA-CR-193469] p 427 N94-12557

PLANETARY ROTATION
A method to determine asteroid poles
p 431 N94-12205

PLANETARY STRUCTURE
Marslink p 438 N94-12034
Noble gas evidence of an aqueous reservoir near the surface of Mars more recently than 1.3 Ga
p 473 N94-12228

PLANETARY SURFACES
Physical studies of planetary and satellite surfaces
[NASA-CR-193545] p 434 N94-10817
Yana ring structure, North-Eastern Siberia: A possible counterpart of coronae on Venus p 282 N94-12121
Cratering on Gaspra p 459 N94-12147
Thermal-infrared emission spectroscopy of natural surfaces: Application to coated surfaces
p 81 N94-12156
Transmantle flux tectonics p 283 N94-12249

PLANETOLOGY
Planetary astronomy of Mars. Mars data reduction
[NASA-CR-193515] p 424 N94-12768

PLANKTON
Acoustic estimation of plankton biomass
p 218 N94-12699
A possibility to define the location of epipelagic fish concentrations with assistance of satellite sensing
p 228 N94-12757

PLANNING
Information resources management long-range plan, FY1994
[DE93-013898] p 420 N94-11588

PLANT ROOTS
Acetate concentrations and oxidation in salt marsh sediments p 269 N94-12459

PLANTS (BOTANY)
Plant architecture, growth and radiative transfer for terrestrial and space environments
[NASA-CR-193587] p 302 N94-12559

PLASMA ACCELERATION
Dispersion of plasma waves in a finite magnetic field (omega(sub H) greater than omega(sub p))
[DE93-621654] p 391 N94-11210

PLASMA COMPOSITION
Physics and modelling of scrape-off layer transport
[DE93-010510] p 385 N94-10289
Atomic and molecular data for H2O, CO and CO2 relevant to edge plasma impurities
[DE93-771423] p 387 N94-10662
Electron temperature measurements of x ray laser plasmas
[DE93-011874] p 389 N94-11074
Helium transport scaling law studies
[DE93-013487] p 393 N94-11513
Giotto data analysis: Electron plasma and heavy ion composition measurements at Comet Halley
[NASA-CR-193587] p 428 N94-12770

PLASMA CONDUCTIVITY
Experimental measurement of the plasma conductivity of Z93 and Z93P thermal control paint
[NASA-TM-106284] p 43 N94-10756
Stationary spectra of short-wave convective and magnetostatic fluctuations in a finite-pressure plasma and anomalous heat conductivity
[DE93-617852] p 388 N94-10840

PLASMA CONTROL
Transport mechanisms acting in toroidal devices: A theoretician's view
[DE93-013463] p 385 N94-10310
Optimization of break-down conditions in tokamak TOTUS
[DE93-617863] p 386 N94-10524
Reversed-field pinch studies in the Madison Symmetric Torus
[DE93-013464] p 388 N94-10747
Calculation of Mercier stability criterium in stellarators
[DE93-621599] p 389 N94-11091
Possibilities of magnetic diagnostics in stellarators
[DE93-621608] p 389 N94-11092
Particle transport analysis in torsatron configurations
[DE93-621640] p 390 N94-11120
Physics of tokamak scrape-off layer confinement
[DE93-011949] p 390 N94-11125
Simulation study of dynamo structure in reversed field pinch
[DE93-771406] p 390 N94-11128
Analytical description of the torsatron Uragan-2M magnetic configuration with account of plasma pressure and external correcting magnetic field
[DE93-620983] p 391 N94-11174
Characteristics of ICR-produced peripheral plasma in the Uragan-3M torsatron
[DE93-621666] p 392 N94-11214
The role of plasma rotation on MHD instabilities in tokamaks
[DE93-013486] p 393 N94-11512
Results from the D3-D advanced divertor program
[DE93-015472] p 393 N94-11514
Initial assessment of lower hybrid current drive in D3-D
[DE93-013310] p 394 N94-12370
An emerging understanding of H-mode discharges in tokamaks
[DE93-012829] p 394 N94-12544

PLASMA CURRENTS
Efficiency of fast wave current drive for a weakly relativistic plasma
[DE93-012775] p 385 N94-10159
Possibilities of magnetic diagnostics in stellarators
[DE93-621608] p 389 N94-11092
Initial assessment of lower hybrid current drive in D3-D
[DE93-013310] p 394 N94-12370

PLASMA DENSITY
Comparison of hydrodynamic and semi-kinetic treatments for plasma flow along closed field lines
[NASA-CR-193589] p 387 N94-10641

Dispersion of plasma waves in a finite magnetic field (omega(sub H) greater than omega(sub p))
[DE93-621654] p 391 N94-11210
Spreading of Bimodulated Ultra-relativistic Electron Beam (BUEB) in Atmospheric Plasma Channel (APCh)
[DE93-621658] p 392 N94-11213
Initial assessment of lower hybrid current drive in D3-D
[DE93-013310] p 394 N94-12370

PLASMA DIAGNOSTICS
Optimization of a CO2 laser Thomson scattering alpha particle diagnostic
[DE93-012782] p 173 N94-10160
Electron temperature measurements of x ray laser plasmas
[DE93-011874] p 389 N94-11074
Possibilities of magnetic diagnostics in stellarators
[DE93-621608] p 389 N94-11092
The possibility of using carbon-graphite materials for microwave plasma diagnostics in large fusion devices
[DE93-621609] p 66 N94-11143
High resolution time- and 2-dimensional space-resolved x ray imaging of plasmas at NOVA
[DE93-011892] p 393 N94-11677
Inexpensive capillary discharge x-ray laser driver
[AD-A265932] p 176 N94-12382
Spectrum analysis in beam diagnostics
[DE93-013401] p 373 N94-12601

PLASMA DIFFUSION
Numerical method of singular problems on singular integrals
[DE93-613654] p 343 N94-10546

PLASMA DRIFT
Observing and modelling F-region ionospheric dynamics using the (O2) 7320A emission
[AD-A265407] p 279 N94-12419

PLASMA DYNAMICS
Characteristics of ICR-produced peripheral plasma in the Uragan-3M torsatron
[DE93-621666] p 392 N94-11214

PLASMA EQUILIBRIUM
Stationary spectra in a quasi neutral current-carrying plasma
[DE93-617849] p 387 N94-10539

PLASMA ETCHING
Resist materials design: Base-catalyzed chemical amplification
[AD-A265286] p 145 N94-11819

PLASMA FREQUENCIES
Stationary spectra in a magnetized current-carrying plasma
[DE93-617847] p 386 N94-10397
Spreading of Bimodulated Ultra-relativistic Electron Beam (BUEB) in Atmospheric Plasma Channel (APCh)
[DE93-621658] p 392 N94-11213
Decay interaction of bulk and surface Langmuir waves
[DE93-617843] p 393 N94-11477

PLASMA GUNS
Experimental investigation of wake field excitation in plasma by a periodic succession of relativistic particle clots
[DE93-621655] p 391 N94-11211

PLASMA HEATING
Efficiency of fast wave current drive for a weakly relativistic plasma
[DE93-012775] p 385 N94-10159
Simulations of D3-D divertor biasing with the LEDGE code
[DE93-010500] p 385 N94-10262
Multiple Antenna Implementation System (MAntIS)
[DE93-012515] p 131 N94-10270
Characterization of high-power RF structures using time-domain field codes
[DE93-013416] p 132 N94-10518
Reversed-field pinch studies in the Madison Symmetric Torus
[DE93-013464] p 388 N94-10747
Kinetic effects in stochastic topologically nontrivial field
[DE93-621642] p 391 N94-11207
Characteristics of ICR-produced peripheral plasma in the Uragan-3M torsatron
[DE93-621666] p 392 N94-11214
Conversion of the four-strap array in D3-D to a tunable traveling wave antenna
[DE93-012085] p 137 N94-11453
Statistical approach to LHCD modeling using the wave kinetic equation
[DE93-012831] p 394 N94-12545

PLASMA INTERACTIONS
High heat flux components and plasma surface interactions
[DE93-008786] p 385 N94-10253
Results from the D3-D advanced divertor program
[DE93-015472] p 393 N94-11514
Applications of in-situ ellipsometry to microwave electron cyclotron resonance plasma processes
[AD-A265197] p 373 N94-11880
Giotto data analysis: Electron plasma and heavy ion composition measurements at Comet Halley
[NASA-CR-193587] p 428 N94-12770

PLASMA JETS
Macroscopic behaviour and discrete dynamo of RFP plasma in high theta discharge
[DE93-771408] p 392 N94-11239

PLASMA LAYERS
Simulations of D3-D divertor biasing with the LEDGE code
[DE93-010500] p 385 N94-10262
Physics and modelling of scrape-off layer transport
[DE93-010510] p 385 N94-10289
Nonlinear second harmonic generation by light wave-plasma interaction in oscillating magnetic field
[DE93-613723] p 386 N94-10387
Physics of tokamak scrape-off layer confinement
[DE93-011949] p 390 N94-11125
Results from the D3-D advanced divertor program
[DE93-015472] p 393 N94-11514

PLASMA OSCILLATIONS
Spatial helicon-wave echo in an inhomogeneous magnetized plasma
[DE93-617845] p 389 N94-10885
Ion shaking in the 200 MeV XLS-ring
[DE93-014057] p 374 N94-12782

PLASMA PHYSICS
Two fluid plasmas in the vicinity of a Schwarzschild black hole
[DE93-610264] p 385 N94-10284
Texas experimental tokamak
[DE93-013377] p 386 N94-10321
A flexible modelling software for data acquisition
[DE93-612915] p 322 N94-10484
Cosmological gamma-ray burst model
[NASA-CR-193368] p 484 N94-10507
Numerical method of singular problems on singular integrals
[DE93-613654] p 343 N94-10546
Distribution of charged particles near the plasma boundary in the presence of external electric field
[DE93-617862] p 389 N94-10886
To the complexity of dynamic system problem
[DE93-621355] p 134 N94-11037
VLBI and the detection of interstellar magnetohydrodynamic waves p 135 N94-11066

PLASMA PINCH
High resolution time- and 2-dimensional space-resolved x ray imaging of plasmas at NOVA
[DE93-011892] p 393 N94-11677

PLASMA POTENTIALS
Electron runaway in RF discharges
[DE93-771407] p 363 N94-10661
NASCAP programmer's reference manual
[NASA-CR-191044] p 278 N94-11702

PLASMA PRESSURE
Analytical description of the torsatron Uragan-2M magnetic configuration with account of plasma pressure and external correcting magnetic field
[DE93-620983] p 391 N94-11174
Magnetic island suppression in torsatron configurations
[DE93-621681] p 392 N94-11215

PLASMA PROPULSION
Arcjet space thrusters
[NASA-CR-193191] p 46 N94-10700

PLASMA RADIATION
Advanced concepts theory annual report 1992
[AD-A266132] p 393 N94-11474

PLASMA SHEATHS
Simulations of D3-D divertor biasing with the LEDGE code
[DE93-010500] p 385 N94-10262
Physics of tokamak scrape-off layer confinement
[DE93-011949] p 390 N94-11125
Gyrosheath near the tokamak edge
[DE93-012191] p 390 N94-11142

PLASMA SPECTRA
Stationary spectra of short-wave convective and magnetostatic fluctuations in a finite-pressure plasma and anomalous heat conductivity
[DE93-617852] p 388 N94-10840

PLASMA TURBULENCE
Transport mechanisms acting in toroidal devices: A theoretician's view
[DE93-013463] p 385 N94-10310
Texas experimental tokamak
[DE93-013377] p 386 N94-10321
Stationary spectra in a quasi neutral current-carrying plasma
[DE93-617849] p 387 N94-10539
Stationary spectra in a sheared plasma (linear limit)
[DE93-617850] p 387 N94-10540
VLBI and the detection of interstellar magnetohydrodynamic waves p 135 N94-11066
Physics of tokamak scrape-off layer confinement
[DE93-011949] p 390 N94-11125
Discrete vortex representation of magnetohydrodynamics
[DE93-012190] p 393 N94-11669

PLASMA WAVES
Two fluid plasmas in the vicinity of a Schwarzschild black hole
[DE93-610264] p 385 N94-10284
General renormalized statistical approach with finite cross-field correlations
[DE93-617846] p 386 N94-10396
Stationary spectra in a magnetized current-carrying plasma
[DE93-617847] p 386 N94-10397
Stationary spectra in a finite-pressure current-carrying plasma
[DE93-617848] p 387 N94-10538
Spatial helicon-wave echo in an inhomogeneous magnetized plasma
[DE93-617845] p 389 N94-10885
The angular structure of second harmonic emission from laser-produced plasmas irradiated at moderate intensity
[DE93-013102] p 389 N94-11114
Studies on the parametric decay of waves in fusion plasmas
[DE93-621659] p 390 N94-11148
Dispersion of plasma waves in a finite magnetic field (omega(sub H) greater than omega(sub p))
[DE93-621654] p 391 N94-11210
Experimental investigation of wake field excitation in plasma by a periodic succession of relativistic particle clots
[DE93-621655] p 391 N94-11211
Negative viscosity and generation of dissipative solitons and zonal dissipative structures by drift waves
[DE93-621656] p 392 N94-11212
Studies of electrostatic waves and VLF-wave particle interaction in the ionosphere
[AD-A266013] p 278 N94-12392

PLASMA-ELECTROMAGNETIC INTERACTION
The Langevin's approach to the statistical theory of bounded plasma
[DE93-617842] p 388 N94-10839
Distribution of charged particles near the plasma boundary in the presence of external electric field
[DE93-617862] p 389 N94-10886
Studies on the parametric decay of waves in fusion plasmas
[DE93-621659] p 390 N94-11148

PLASMA-PARTICLE INTERACTIONS
Momentum and heat frictions between fast ions and thermal plasma species
[DE93-771240] p 390 N94-11149

PLASMAS (PHYSICS)
MHD simulation of deuterium-fiber-initiated Z-pinches with two-fluid effects
[DE93-012682] p 384 N94-10158
Simulations of D3-D divertor biasing with the LEDGE code
[DE93-010500] p 385 N94-10262
X ray production (approximately)130 (Angstrom) from laser-produced plasmas for projection x ray lithography applications
[DE93-009256] p 385 N94-10286
An investigation of conducted and radiated emissions from a hollow-cathode plasma contactor
[NASA-CR-191172] p 386 N94-10346
Stationary spectra in a magnetized current-carrying plasma
[DE93-617847] p 386 N94-10397
Stationary spectra in a plasma with a shear (renormalized statistical approach with non-zero eigenfrequencies)
[DE93-617851] p 386 N94-10523
Stationary spectra in a finite-pressure current-carrying plasma
[DE93-617848] p 387 N94-10538
Stationary spectra in a quasi neutral current-carrying plasma
[DE93-617849] p 387 N94-10539
Stationary spectra in a sheared plasma (linear limit)
[DE93-617850] p 387 N94-10540
Atomic and molecular data for H2O, CO and CO2 relevant to edge plasma impurities
[DE93-771423] p 387 N94-10662
The heat transfer by radiation between two media
[DE93-617820] p 149 N94-10838
The Langevin's approach to the statistical theory of bounded plasma
[DE93-617842] p 388 N94-10839
Magnetohydrodynamic computation of feedback stabilization of resistive-shell instabilities in the reversed field pinch
[DE93-013466] p 388 N94-10852

Wave generation by contaminant ions [NASA-CR-193558] p 364 N94-10946

Calculation of Mercier stability criterium in stellarators [DE93-621599] p 389 N94-11091

Possibilities of magnetic diagnostics in stellarators [DE93-621608] p 389 N94-11092

The angular structure of second harmonic emission from laser-produced plasmas irradiated at moderate intensity [DE93-013102] p 389 N94-11114

Radiative properties of strongly magnetized plasmas [DE93-014098] p 389 N94-11118

Particle transport analysis in torsatron configurations [DE93-621640] p 390 N94-11120

Simulation study of dynamo structure in reversed field pinch [DE93-771406] p 390 N94-11128

Negative viscosity and generation of dissipative solitons and zonal dissipative structures by drift waves [DE93-621656] p 392 N94-11212

Spreading of Bimodulated Ultra-relativistic Electron Beam (BUEB) in Atmospheric Plasma Channel (APCh) [DE93-621658] p 392 N94-11213

Characteristics of ICR-produced peripheral plasma in the Uragan-3M torsatron [DE93-621666] p 392 N94-11214

Discrete vortex representation of magnetohydrodynamics [DE93-012190] p 393 N94-11669

An investigation of the near Earth space environments [AD-A265295] p 278 N94-11828

PLASMONS

The surface plasmon spectroscopy as diagnostic technique in microgravity experiments p 110 N94-10133

PLASTIC DEFORMATION

A simple model of melt fracture [AD-A265311] p 92 N94-11862

PLASTIC FLOW

A simple model of melt fracture [AD-A265311] p 92 N94-11862

PLASTIC PROPERTIES

Design evaluation of GLARE laminate lay-ups p 63 N94-10051

PLATE THEORY

Boundary element method for eigenvalue problems of thin plates [ITN-93-85199] p 343 N94-10392

PLATES (STRUCTURAL MEMBERS)

Development tests for a high stability optical bench p 62 N94-10047

PLATES (TECTONICS)

A model for the subduction mechanics of flexible lithosphere and its viscous coupling to the mantle using power-law rheologies p 277 N94-11585

Horizontal stresses induced by vertical processes in planetary lithospheres p 281 N94-12042

Buoyant subduction on Venus: Implications for subduction around coronae p 455 N94-12130

Morphotectonics of Venus p 478 N94-12248

PLATING

Plating under reduced pressure [DE93-011896] p 84 N94-11668

PLATINUM

Site dependence of the apparent shape of a molecule in STM images: Benzene on Pt(111) [AD-A263488] p 365 N94-11093

A model of elementary chemistry and fluid mechanics in the combustion of hydrogen on platinum surfaces [DE93-012767] p 77 N94-11370

Low energy electron diffraction and cyclic voltammetry studies of flame-annealed platinum single crystals [AD-A263566] p 401 N94-11518

Shock induced reaction in Chicxulub target materials (CaSO4 and SiO2) and their relation to extinctions p 282 N94-12149

The effects of organic adsorbates on the underpotential deposition of silver on Pt(111) electrodes [AD-A265623] p 404 N94-12376

PLAYAS

Mapping a dynamic playa surface using multitemporal ERS-1 SAR data: First results p 246 N94-12474

PLUG NOZZLES

Hot-gas-side heat transfer characteristics of subscale, plug-nozzle rocket calorimeter chamber [NASA-TP-3380] p 55 N94-12569

PLUMES

User's manual for the plume visibility model PLUVUE 2 (revised) [PB93-188233] p 265 N94-11016

Ultraviolet plume instrument description and plume data reduction methodology [AD-A266141] p 54 N94-11643

Tectonics on Triton p 466 N94-12187

The 1991 version of the plume impingement computer program. Volume 2: User's input guide [NASA-CR-194191] p 166 N94-12774

The 1991 version of the plume impingement computer program. Volume 1: Description [NASA-CR-194192] p 166 N94-12775

PLUNGERS

Check valve with poppet dashpot/frictional damping mechanism [NASA-CASE-MSC-21950-1] p 179 N94-10658

PNEUMATICS

Lift enhancement of a wing/strake using pneumatic blowing [AD-A265074] p 26 N94-11872

POINCARE PROBLEM

Chaos, entropy, and reversibility: A simple example p 31 N94-11495

POINT DEFECTS

Electronic characterization of defects in narrow gap semiconductors [NASA-CR-193568] p 397 N94-10819

The influence of irradiation conditions, type, and concentration of impurities on radiation defects characteristics in indium antimonide under electron irradiation [DE93-617201] p 397 N94-10843

A method of influence regions in the theory of vacancy swelling of metals [DE93-620579] p 83 N94-11363

POINT IMPACT

Detection of dust impacts by the Voyager planetary radio astronomy experiment [NASA-CR-193281] p 423 N94-11305

POINT SOURCES

The searchlight problem for neutrons in a semi-infinite medium [DE93-010796] p 365 N94-10952

About excitation of round waveguide by a point current source [DE93-621352] p 133 N94-11034

POISSON EQUATION

Looking for O(N) Navier-Stokes solutions on non-structured meshes [NASA-CR-191472] p 345 N94-11277

POLAR CAPS

Spatial variation in the seasonal south polar cap of Mars as observed by Mariner 7 p 456 N94-12134

A new data collection system for ionospheric modelling and related topics [AD-A265893] p 278 N94-12277

POLAR METEOROLOGY

Studies of dynamical processes affecting the distribution of stratospheric ozone [NASA-CR-193477] p 279 N94-12560

POLAR ORBITS

Exploration planning in the context of human exploration and development of the Moon p 474 N94-12229

POLAR REGIONS

Sea ice: A climate component p 232 N94-11705

Analysis of ERS-1 altimeter data over the polar ice sheets p 237 N94-11738

Geomorphology of Triton's polar materials p 466 N94-12185

A first assessment of the value of ERS-1 scatterometer winds for meteorological studies in the polar regions p 250 N94-12501

Polar mesospheric waves and structure [AD-A265360] p 279 N94-12561

POLARIMETERS

The intra-atomic motion of bound electrons as a possible source of a systematic error in electron beam polarization measurements by means of a Moeller polarimeter [DE93-620984] p 364 N94-10875

Localized and distributed fiber-optic strain sensors embedded in composite materials [UTIAS-346] p 73 N94-12013

Seeing the Black Forest by ERS-1 and AIRSAR: A comparison p 249 N94-12495

POLARIMETRY

Enhancement effects in polarimetric radar returns: Phase difference statistics [NASA-CR-193408] p 231 N94-11309

POLARITONS

On the theory of phonoriton in cubic semiconductors with a degenerate valence band [DE93-613539] p 402 N94-11660

POLARITY

Polarity reversals and tilt of the Earth's magnetic dipole p 283 N94-12219

POLARIZATION (CHARGE SEPARATION)

Gyrosheath near the tokamak edge [DE93-012191] p 390 N94-11142

Macroscopic electric charge separation during hypervelocity impacts: Potential implications for planetary paleomagnetism p 431 N94-12181

Polaronic charge separation in mixed-halide MX solids [AD-A266073] p 403 N94-12345

POLARIZATION (WAVES)

Method and apparatus for polarization-maintaining fiber optical amplification with orthogonal polarization output [AD-D015756] p 374 N94-10372

Polarisation of backscattering radiation at remote sensing of ocean with impulse laser beam p 177 N94-12722

Non-image visible polarization remote sensing of the ocean p 229 N94-12762

POLARIZATION CHARACTERISTICS

Polarisation of backscattering radiation at remote sensing of ocean with impulse laser beam p 177 N94-12722

POLARIZED LIGHT

New tests of the equivalence principle using non-metric couplings of electromagnetism and gravitation p 413 N94-11821

Non-image visible polarization remote sensing of the ocean p 229 N94-12762

POLARIZED RADIATION

Atomic processes relevant to polarization plasma spectroscopy [DE93-753240] p 393 N94-11594

POLARONS

Femtosecond dynamics, photoexcitation, and ESR spectra of MX chain solids [AD-A264689] p 399 N94-11263

Polaronic charge separation in mixed-halide MX solids [AD-A266073] p 403 N94-12345

POLICIES

National Aero-Space Plane: A need for program direction and funding decisions [GAO/NSIAD-93-207] p 416 N94-10910

NASA procurement: Proposed changes to the Jet Propulsion Laboratory contract. Report to Congressional Requesters [GAO/NSIAD-93-178] p 416 N94-10941

The Department of Clinical Investigation, reports control symbol MED-300(R-1) [AD-A264969] p 304 N94-11649

POLISHING

Zerodur polishing process for high surface quality and high efficiency [DE93-012596] p 87 N94-10271

POLLUTION CONTROL

Environmental Protection Agency's life cycle methodology: Guidelines for use in development of packaging [PB93-194199] p 265 N94-10841

Summary of implementation and demonstration projects in bays and estuaries [PB93-194637] p 265 N94-10846

Immediate response to free product discovery [PB93-182970] p 265 N94-11015

Gulf of Mexico sales 147 and 150: Central and western planning areas. Draft environmental impact statement. Volume 1: Sections 1 through 4.C [PB93-190304] p 265 N94-11018

Control of jet noise [NASA-CR-193612] p 358 N94-11176

Application of jet-shear-layer mixing and effervescent atomization to the development of a low-NO(x) combustor [NASA-TM-105888] p 28 N94-11234

Catalytic oxidation of organics in vapor streams at remediation sites [PB93-182962] p 266 N94-11472

POLLUTION MONITORING

International Space Year in China p 36 N94-10680

Remote surface water monitoring radio based telemetry system [DE93-009643] p 41 N94-11282

Methodologies for estimating air emissions from three non-traditional source categories: Oil spills, petroleum vessel loading and unloading, and cooling towers [PB93-181592] p 266 N94-11471

Satellite observations of red tide events: Plans for EESI p 191 N94-11899

An algorithm for the detection of mucilage (green slime) in the Adriatic Sea p 191 N94-11900

A study of pollution courses of spilled oil floatation in the outer ocean p 205 N94-11983

Information capability of NOAA-AVHRR data for monitoring oceanographic and atmospheric pollution p 214 N94-12677

Novel mass spectrometric instrument for gaseous and particulate characterization and monitoring [DE93-014093] p 272 N94-12783

POLLUTION TRANSPORT

A study of pollution courses of spilled oil floatation in the outer ocean p 205 N94-11983

POLONIUM ISOTOPES

Study of the atmospheric chemistry of radon progeny in laboratory and real indoor atmospheres [DE93-012236] p 266 N94-11671

POLYACRYLONITRILE

A new FR water resistant acoustic insulation material for aircraft p 18 N94-10773

Preparation of carbon monoliths having tailored pore structure from porous polymer precursors
[DE93-011576] p 89 N94-10958

POLYBUTADIENE

Investigation of the reason for the softening behaviour of filled polymers p 63 N94-10058

Interfacial modification through end group complexation in polymer blends
[AD-A265887] p 93 N94-12340

POLYCARBONATES

A non-halogenated, flame retarded polycarbonate p 19 N94-10781

POLYCRYSTALS

Flexible polycrystalline thin-film photovoltaics for space applications p 50 N94-11393

Grain boundary creep in copper
[DE93-610974] p 84 N94-12361

POLYETHYLENES

Determination of concentration profiles at interfaces and surfaces of partially miscible polymer blends
[DE93-013140] p 89 N94-11007

Development of plastic capsule for research reactor irradiation
[DE93-753186] p 372 N94-11591

POLYGONS

Finding a covering triangulation whose maximum angle is provably small
[DE93-010691] p 334 N94-12593

POLYHEDRONS

Applications of cut polyhedra
[CWI-BS-R9221] p 347 N94-10354

Model-based recognition of 3-D objects by geometric hashing technique
[DE93-612916] p 322 N94-10410

POLYIMIDES

Polyimide foam insulation systems: A major weight reduction and improvement in fire resistance of sidewall systems p 17 N94-10769

A polyimide foam for advanced fire resistant aircraft applications p 17 N94-10770

Semiconductor ring lasers
[DE93-012386] p 174 N94-11005

A novel photosensitive polyimide resist consisting of a soluble polyimide and a bis(perfluorophenyl azide) as a cross-linker
[AD-A265998] p 93 N94-12353

Protective coatings for high-temperature polymer matrix composites
[NASA-TM-106276] p 74 N94-12431

POLYMER BLENDS

Determination of concentration profiles at interfaces and surfaces of partially miscible polymer blends
[DE93-013140] p 89 N94-11007

Interfacial modification through end group complexation in polymer blends
[AD-A265887] p 93 N94-12340

POLYMER CHEMISTRY

New aromatic activated dihalides and bisphenol monomers for the preparation of novel poly(arylene ethers)
[NASA-CR-193190] p 55 N94-10513

Ring-opening polymerization of phosphazenes
[AD-A265000] p 90 N94-11292

Polymer-polymer interactions
[AD-A265304] p 91 N94-11830

Molecular properties of polymeric materials for space applications
[NASA-CR-194370] p 94 N94-12450

Photogenerated base in polymer imaging. Synthesis and photopatterning of poly(2-cyano-2-(p-vinylphenyl) butanoic acid)
[AD-A265288] p 95 N94-12585

POLYMER MATRIX COMPOSITES

Vectra insulative support structures within spacecraft p 62 N94-10050

The Netherlands innovation oriented research programme on polymer composites and special polymers 1985-1993 p 65 N94-10067

Fibre reinforced polymer matrix composites: Microstructure and mechanical properties
[DLR-FB-92-28] p 66 N94-11085

Protective coatings for high-temperature polymer matrix composites
[NASA-TM-106276] p 74 N94-12431

POLYMER PHYSICS

A simple model of melt fracture
[AD-A265311] p 92 N94-11862

POLYMERIC FILMS

Sensing glass transitions in thin polymer films on acoustic wave microsensors
[DE93-010805] p 87 N94-10295

The fire properties of insulation bags, as installed and after aircraft operations p 19 N94-10778

Glucose electrodes based on cross-linked (Os(bpy)2Cl)(sup +/2+) complexed poly(1-vinylimidazole) films
[AD-A265404] p 94 N94-12425

Preparation of stable photopatternable polymeric materials for non-linear optics
[AD-A265359] p 95 N94-12577

Performance aspects of de Laval spray-forming nozzles
[DE93-013671] p 163 N94-12604

POLYMERIZATION

Heat and mass transfer mechanisms of the polymerization under terrestrial and microgravity conditions p 103 N94-10092

Photoinitiated radical polymerization of liquid monomers in microgravity p 124 N94-10246

Fire-resistant hydrolytically stable poly(arylene phosphine oxide) material systems p 19 N94-10780

Polymeric nitrogen
[DE93-012600] p 89 N94-11151

Ring-opening polymerization of phosphazenes
[AD-A265000] p 90 N94-11292

Radiation-induced modifications of allylamino-substituted polyphosphazenes
[AD-A264914] p 92 N94-11848

Synthesis and polymerization of oligomeric multiple aromatic ether-containing phthalonitriles
[AD-D015729] p 94 N94-12399

NMR characterization of polymers formed in diazotizing mixtures of luminol and 3-amino-L-tyrosine
[AD-A266093] p 94 N94-12536

POLYMERS

The Netherlands innovation oriented research programme on polymer composites and special polymers 1985-1993 p 65 N94-10067

Physical properties of injection molded liquid crystal polymers and high temperature engineering polymers
[AD-A264912] p 87 N94-10508

Preparation of carbon monoliths having tailored pore structure from porous polymer precursors
[DE93-011576] p 89 N94-10958

Polymeric nitrogen
[DE93-012600] p 89 N94-11151

A new decomposition strategy for parallel bonded molecular dynamics
[DE93-009839] p 366 N94-11284

Vacuum stability requirements of polymeric material for spacecraft application
[NASA-TM-109216] p 91 N94-11350

Fracture behavior of ionomers and ionomeric blends
[AD-A265379] p 94 N94-12407

NMR characterization of polymers formed in diazotizing mixtures of luminol and 3-amino-L-tyrosine
[AD-A266093] p 94 N94-12536

Photogenerated base in polymer imaging. Synthesis and photopatterning of poly(2-cyano-2-(p-vinylphenyl) butanoic acid)
[AD-A265288] p 95 N94-12585

POLYMETHYL METHACRYLATE

A relaxation study of poled nonlinear optical polymers by infrared reflection-absorption spectroscopy
[AD-A265797] p 93 N94-12380

POLYMORPHISM

Hydrogen-bond polymorphs of guanidinium 4-biphenylsulfonate
[AD-A265294] p 402 N94-11827

POLYNOMIALS

A reliable stability test for exponential polynomials
[MEMO-COSOR-92-48] p 341 N94-10168

An exactly solvable model of an oscillator with nonlinear coupling and zeros of Bessel functions p 349 N94-10573

On convexity and Schoenberg's variation diminishing splines
[DE93-619673] p 346 N94-11632

POLYPROPYLENE

New technology for effective control of flammability in polyolefin fiber/textiles p 18 N94-10774

POLYSACCHARIDES

Improving reservoir conformance using gelled polymer systems
[DE93-014532] p 88 N94-10749

POLYSTYRENE

Polymer-polymer interactions
[AD-A265304] p 91 N94-11830

Polymers for microelectronics
[AD-A266036] p 94 N94-12396

POLYSULFIDES

Thermal stability of sealants for military aircraft: Modification of polysulfide prepolymers with ether and thioether monomers
[AD-A264079] p 89 N94-11107

POLYTOPES

Applications of cut polyhedra
[CWI-BS-R9221] p 347 N94-10354

A simplicial approach to integer programming
[REPT-93-06] p 322 N94-10355

POMERONS

Crossing-odd spin effects in the dipole model of hadron scattering
[DE93-617692] p 362 N94-10551

Model for the pomeron
[DE93-617693] p 362 N94-10552

Logarithmically rising cross section and the ratio sigma(sub el)/sigma(sub t)
[DE93-617694] p 362 N94-10553

Detecting the odderon
[DE93-617695] p 362 N94-10554

Fine structure of the Pomeron and the real part of the elastic scattering amplitude
[DE93-617696] p 362 N94-10555

PONDS

Application of remote sensing for coastal management in the north coast of Java p 218 N94-12701

POPULATIONS

Automatic classification system for zooplankton p 203 N94-11969

POROSITY

Improving reservoir conformance using gelled polymer systems
[DE93-014532] p 88 N94-10749

Inverting ultrasonic data on solid/fluid mixtures for Biot-Gassmann parameters
[DE93-011952] p 150 N94-11026

Plating under reduced pressure
[DE93-011896] p 84 N94-11668

Porosity and the ecology of icy satellites p 431 N94-12186

POROUS MATERIALS

Preparation of carbon monoliths having tailored pore structure from porous polymer precursors
[DE93-011576] p 89 N94-10958

PORTABLE EQUIPMENT

A portable controller for unmanned ground vehicles
[AD-A264963] p 181 N94-11290

DISTERM: A shipboard data system for satellite monitoring of ocean and atmosphere p 226 N94-12749

POSEIDON SATELLITE

Topex/Poseidon: A United States/France mission. Oceanography from space: The oceans and climate
[NASA-TM-108253] p 43 N94-10699

POSITION (LOCATION)

Visual encoding of spatial relations
[AD-A266049] p 313 N94-10909

Analysis of IRAS solar system dust data
[NASA-CR-193704] p 483 N94-10949

Joint pain and Doppler-detectable bubbles in altitude (Hypobaric) decompression p 312 N94-11542

The Magellan volcanic and magmatic feature catalog p 467 N94-12193

POSITION ERRORS

Force reflection with compliance control
[NASA-CASE-NPO-18668-1-CU] p 179 N94-10654

Thermal error compensation feasibility study using artificial intelligence
[AD-A266084] p 340 N94-12411

POSITIONING

Determination of the viscous acoustic field for liquid drop positioning/forcing in an acoustic levitation chamber in microgravity p 110 N94-10131

Thermal error compensation feasibility study using artificial intelligence
[AD-A266084] p 340 N94-12411

POSITRON ANNIHILATION

A window least squares algorithm for statistical noise smoothing of 2D-ACAR data
[DE93-613828] p 395 N94-10537

POSITRONS

Acceleration of positrons in supernova shocks
[NASA-CR-193713] p 425 N94-10511

POSTFLIGHT ANALYSIS

Debris/ice/TPS assessment and integrated photographic analysis for Shuttle Mission STS-57
[NASA-TM-107562] p 40 N94-10805

Promethazine and its use as a treatment for space motion sickness p 312 N94-11550

POSTLAUNCH REPORTS

Flight data analysis of Japanese Earth Resources Satellite-1 (JERS-1)
[NASDA-CNT-930004] p 245 N94-12279

POSTMISSION ANALYSIS (SPACECRAFT)

Debris/ice/TPS assessment and integrated photographic analysis for Shuttle Mission STS-57
[NASA-TM-107562] p 40 N94-10805

POTASSIUM ISOTOPES

Radiogenic age and isotopic studies
[DE93-610548] p 274 N94-10407

POTENTIAL ENERGY
Non-empirical interatomic potentials for transition metals
[DE93-013705] p 365 N94-11011
Demonstration designs for optical-field-ionized plasma x-ray lasers
[DE93-009227] p 175 N94-11266
The global potential energy surfaces of the lowest two 1A' states of the ozone molecule: Theoretical determination and analysis p 267 N94-12269

POTENTIAL FLOW
Solving the inverse problem for incompressible potential flow through two-dimensional cascades
[NAL-TR-1162] p 147 N94-10365

POWDER (PARTICLES)
Development of commercially viable high-T(sub c) Bi-2223 superconductor tapes
[DE93-009966] p 142 N94-10951
Production of reactive sintered nickel aluminide
[DE93-014434] p 83 N94-11127
Processing, properties, and wear resistance of aluminides
[DE93-012186] p 83 N94-11141
Effect of powder processing on slip casting parameters and sintering of Si3N4-Y2O3-SiO2
[AD-A264474] p 83 N94-11445
Apical Cu-O bond in YBa2Cu3O(7-delta) superconductors by XAFS
[DE93-010861] p 400 N94-11458
Simulation of possible regolith optical alteration effects on carbonaceous chondrite meteorites
p 430 N94-12163
Dynamic high-pressure shock compaction of diamond powders
[AD-A266004] p 93 N94-12354

POWDER METALLURGY
Bibliography on Hot Isostatic Pressing (HIP) technology
[AD-A265668] p 81 N94-10297
Application of powder metallurgy techniques to produce improved bearing elements for liquid rocket engines
[NASA-CR-193731] p 82 N94-10804
A history of tungsten- and molybdenum-base alloys
[DE93-010283] p 82 N94-11108
Production of reactive sintered nickel aluminide
[DE93-014434] p 83 N94-11127
Effect of powder processing on slip casting parameters and sintering of Si3N4-Y2O3-SiO2
[AD-A264474] p 83 N94-11445
The effect of processing on the microstructure and tensile properties of a (gamma)-TiAl based alloy
[DE93-013221] p 84 N94-11488

POWDERED ALUMINUM
PM technology and mechanical properties of metallic foams p 64 N94-10059

POWER AMPLIFIERS
Low cost high efficiency GaAs monolithic RF module for SARSAT distress beacons
[NASA-CR-194235] p 146 N94-12773

POWER CONDITIONING
Experimental and theoretical investigations of Cs-Ba vapor tacitron inverter for power conditioning in space power systems
[DE93-012971] p 48 N94-11372

POWER EFFICIENCY
InGaAs concentrator cells for laser power converters and tandem cells p 50 N94-11394
A high specific power solar array for low to mid-power spacecraft p 51 N94-11399

POWER GAIN
Design of a matching network for dipole antennas
[AD-A265115] p 136 N94-11158

POWER LINES
Potential techniques for non-destructive evaluation of cable materials
[DE93-008350] p 183 N94-11586

POWER SERIES
Deviations from the straight line: Bumps (and grinds) in the collisionally evolved size distribution of asteroids
p 431 N94-12201

POWER SPECTRA
Polar mesospheric waves and structure
[AD-A265380] p 279 N94-12561

POWER SUPPLY CIRCUITS
A soft-start circuit for arcjet ignition
[NASA-TM-106287] p 180 N94-10760

PRANDTL NUMBER
Instability of thermocapillary convection in floating zones p 101 N94-10076
High Prandtl number fluids in a multilayered system under 1-g or micro-g environment p 104 N94-10096

PRE-MAIN SEQUENCE STARS
Detection of accreting circumstellar gas around weak emission-line Herbig Ae/Be stars
[NASA-TM-108256] p 424 N94-11306

PRECESSION
Precession of Uranus and Neptune and their magnetic field p 473 N94-12222

PRECIPITATION (METEOROLOGY)
Design of a global soil moisture initialization procedure for the simple biosphere model
[NASA-TM-104590] p 284 N94-10940
The impact of horizontal resolution on moist processes in the ECMWF model
[DE93-011718] p 276 N94-11227
Activities relating to understanding the initiation, organization and structure of moist convection in the Southeast environment
[NASA-CR-193829] p 285 N94-11598
Modeling present and future river runoff using global atmospheric models
[AD-A265274] p 285 N94-11685
Evaporation and thermal/hydrologic balance in the Pacific p 195 N94-11919
Measurements of ocean cross-section with a side-looking airborne radar p 201 N94-11954
A basic consideration for remote sensing using microwave radars on a satellite p 212 N94-12665

PRECIPITATION HARDENING
On problem about nature of Portevin-Le Chatelier effect in irradiated aluminium alloys
[DE93-617200] p 82 N94-10842
Corrosion behavior of metal matrix composites
[AD-A265352] p 85 N94-12404

PREDICTION ANALYSIS TECHNIQUES
Parametric analysis of atmospheric processes
[NASA-CR-192523] p 347 N94-10757
Failure prediction of thin beryllium sheets used in spacecraft structures
[NASA-CR-194164] p 187 N94-11190
A comparison between numerically modelled and experimentally measured loss mechanisms in wave rotors
[NASA-TM-106279] p 29 N94-11255
A research program for improving heat transfer prediction for the laminar to turbulent transition region of turbine vanes/blades
[NASA-TM-106278] p 151 N94-11256
Computational mechanics needs study
[NASA-CR-193712] p 327 N94-11279
Chaotic time series analysis p 31 N94-11490
Boundary layer transition: Prediction and wind tunnel simulation p 32 N94-11498
Further studies using matched filter theory and stochastic simulation for gust loads prediction
[NASA-TM-109010] p 26 N94-11587
Problem of climate change predictability and satellite radiation budget observations p 229 N94-12766

PREFORMS
Design and manufacturing of CFRP rings by RTM
p 59 N94-10025

PRELAUNCH TESTS
A facility for testing 10- to 100-kWe space power reactors
[DE92-040420] p 372 N94-11296

PREMIXED FLAMES
Influence of gravity and ambient pressure variations on the behavior of buoyant laminar diffusion flames
p 123 N94-10240
The evolution equation for the flame surface density in turbulent premixed combustion p 81 N94-12316
Generation of two-dimensional vortices in a cross-flow
p 160 N94-12318
Why does preferential diffusion strongly affect premixed turbulent combustion? p 81 N94-12319

PREMIXING
Application of jet-shear-layer mixing and effervescent atomization to the development of a low-NO(x) combustor
[NASA-TM-105888] p 28 N94-11234

PREPOLYMERS
Thermal stability of sealants for military aircraft: Modification of polysulfide prepolymers with ether and thioether monomers
[AD-A264079] p 89 N94-11107

PREPREGS
Hybrid materials for use at elevated temperatures
p 57 N94-10013
Advanced phenolic systems for aircraft interiors
p 18 N94-10776
Fire resistance and mechanical properties for phenolic prepregs p 20 N94-10786

PREPROCESSING
The TREES project: Pre-processing and generation of terrain data for inclusion in an ERS-1 SAR classification scheme p 249 N94-12496
The 1991 version of the plume impingement computer program. Volume 1: Description
[NASA-CR-194192] p 166 N94-12775

PRESIDENTIAL REPORTS
From red tape to results: Creating a government that works better and costs less p 422 N94-11351
From red tape to results: Creating a government that works better and costs less. Executive summary
p 422 N94-11353

PRESSING (FORMING)
Cost effectiveness of structural applications of fibre reinforced thermoplastics p 60 N94-10032

PRESSURE BREATHING
Hypobaric decompression prebreathe requirements and breathing environment p 317 N94-11541

PRESSURE DEPENDENCE
The effect of pressure and quadrupolar interactions on the nematic-isotropic transition properties: Numerical results for a system of prolate ellipsoids including second and fourth rank orientational order parameters
[DE93-613540] p 410 N94-10536
Phase equilibria and volumetric properties for the system NaCl-CaCl2-H2O
[DE93-013590] p 76 N94-11244

PRESSURE DISTRIBUTION
Schlieren photographs and internal pressure distributions for three-dimensional sidewall-compression scramjet inlets at a Mach number of 6 in CF4
[NASA-TM-4479] p 148 N94-10644

PRESSURE EFFECTS
Influence of gravity and ambient pressure variations on the behavior of buoyant laminar diffusion flames
p 123 N94-10240
The effect of pressure and quadrupolar interactions on the nematic-isotropic transition properties: Numerical results for a system of prolate ellipsoids including second and fourth rank orientational order parameters
[DE93-613540] p 410 N94-10536
Phase equilibria and volumetric properties for the system NaCl-CaCl2-H2O
[DE93-013590] p 76 N94-11244
Thermodynamics of lunar ilmenite reduction
p 415 N94-12028
Shock transformations in quartzite p 97 N94-12040
The effects of atmospheric pressure on infrared reflectance spectra of Martian analogs
p 445 N94-12071
Methanol pan fires in an enclosed space: Effect of pressure and oxygen concentration
[AD-A266108] p 79 N94-12415

PRESSURE GAGES
Analysis of Hopkinson bar pressure gage
[AD-A262366] p 171 N94-12362

PRESSURE GRADIENTS
Underwing compression vortex attenuation device
[NASA-CASE-LAR-14744-1] p 12 N94-10673
A Galilean and tensorial invariant k-epsilon model for near wall turbulence
[NASA-TM-106263] p 151 N94-11192
The role of the geothermal gradient in the emplacement and replenishment of ground ice on Mars
p 463 N94-12169
Large eddy simulations of time-dependent and buoyancy-driven channel flows p 155 N94-12287
Progress in modeling hypersonic turbulent boundary layers p 157 N94-12300
Fluctuations of the Kuroshio extension detected by the GEOSAT altimetry data p 209 N94-12649

PRESSURE MEASUREMENT
Microgravity combustion of dust suspension in a spherical chamber p 80 N94-10248
An experimental investigation of high-speed water-entry for full-size and scale-model pointed nose vehicles
[DE93-008491] p 147 N94-10252
Pressure and force measurements on models set in hypersonic flows: A review p 5 N94-10435
Flow development in a circular pipe in the UTIAS/RPI M = 8.3 gun tunnel p 6 N94-10442
Experimental and computational comparisons of Mach 6 high Reynolds number heat transfer and skin friction
p 6 N94-10443
Some experimental study and numerical simulation in wind tunnel flow p 8 N94-10457
Wall interference correction based on interface measurements in subsonic wind tunnel testing
p 15 N94-11154
A laboratory model of a hydrogen/oxygen engine for combustion and nozzle studies
[NASA-TM-106281] p 47 N94-11252
Overview of the 1989 Wind Tunnel Calibration Workshop
[NASA-TP-3393] p 34 N94-11869
Analysis of Hopkinson bar pressure gage
[AD-A262366] p 171 N94-12362

PRESSURE OSCILLATIONS
Establishing baseline data for an experimental appratus that measures heat transfer under conditions of oscillating pressure and flow
[NASA-CR-193772] p 413 N94-12343

PRESSURE REDUCTION

Hypobaric decompression prebreathe requirements and breathing environment p 317 N94-11541

Joint pain and Doppler-detectable bubbles in altitude (Hypobaric) decompression p 312 N94-11542

Arterial gas emboli in altitude-induced decompression sickness p 312 N94-11543

Transcranial Doppler ultrasound and the etiology of neurologic decompression sickness during altitude decompression p 312 N94-11544

Risk of decompression sickness in the presence of circulating microbubbles p 312 N94-11546

Strategies and methodologies to develop techniques for computer-assisted analysis of gas phase formation during altitude decompression p 312 N94-11547

PRESSURE REGULATORS

Dual valve plate two-way pressure relief valve [AD-D015766] p 178 N94-10379

A comparison between numerically modelled and experimentally measured loss mechanisms in wave rotors [NASA-TM-106279] p 29 N94-11255

PRESSURE SENSORS

Combustion-induced crack propagation process in a solid-propellant crack cavity p 98 N94-10901

A laboratory model of a hydrogen/oxygen engine for combustion and nozzle studies [NASA-TM-106281] p 47 N94-11252

PRESSURE SUITS

Motion and spatial disorientation systems: Special research capabilities [AD-A265155] p 303 N94-11097

Hypobaric decompression prebreathe requirements and breathing environment p 317 N94-11541

PRESSURE VESSEL DESIGN

A new and efficient way to join composite pipes p 63 N94-10054

PRESSURE VESSELS

Design with high strength steel: A case of failure and its implications p 58 N94-10017

Spin-rolling, welding, and heat treatment of aluminium 2219 for Ariane 5 GAM high pressure vessel liners p 62 N94-10045

Heavy-section steel technology program [DE93-009222] p 184 N94-10155

Potential change in flaw geometry during pressurized-thermal-shock transients [DE93-009709] p 184 N94-10288

PRESSURIZED WATER REACTORS

Potential change in flaw geometry during pressurized-thermal-shock transients [DE93-009709] p 184 N94-10288

PRETREATMENT

Microbiological test results using three urine pretreatment regimes with 316L stainless steel [NASA-CR-192568] p 299 N94-10360

PRINCIPAL COMPONENTS ANALYSIS

A consideration on principal component analysis of satellite IR data p 193 N94-11909

Fourier domain target transformation analysis in the thermal infrared p 258 N94-12030

PRINTED CIRCUITS

Radiation hardness of Mo/Si multilayers designed for use in a soft x ray projection lithography system [DE93-011879] p 143 N94-11273

PROBABILITY DENSITY FUNCTIONS

Probabilistic evaluation of uncertainties and risks in aerospace components [NASA-TM-105603] p 185 N94-10361

Probability density distribution of velocity differences at high Reynolds numbers p 158 N94-12304

PDF approach for turbulent scalar field: Some recent developments p 160 N94-12315

PROBABILITY DISTRIBUTION FUNCTIONS

Bayesian reliability analysis with imprecise prior probabilities [MEMO-COSOR-92-50] p 183 N94-10170

Probabilistic evaluation of uncertainties and risks in aerospace components [NASA-TM-105603] p 185 N94-10361

Imprecise highest density regions related to intervals of measures [MEMO-COSOR-92-54] p 347 N94-10876

PROBABILITY THEORY

Applications of cut polyhedra [CWI-BS-R9221] p 347 N94-10354

Singularity spectrum of self-organized criticality [DE93-613820] p 348 N94-10404

Positive phase space distributions and uncertainty relations p 379 N94-10598

Wavelets and spacetime squeeze p 379 N94-10604

Wave and pseudo-diffusion equations from squeezed states p 347 N94-10607

Probability of particle trapping/detrapping in torsatrons [DE93-621641] p 390 N94-11121

Probability of alamethicin conductance states varies with nonlamellar tendency of bilayer phospholipids [AD-A264957] p 301 N94-11648

Applications of multivariate analysis [AD-A265250] p 347 N94-11882

Collisions of small Spacewatch asteroids with the Earth p 430 N94-12157

PROBLEM SOLVING

A real-time spoken-language system for interactive problem solving [AD-A266046] p 324 N94-11104

Criteria for assessing problem solving and decision making in complex environments p 314 N94-11532

Design, development, and testing of an automated knowledge-acquisition tool to aid problem solving, decision making, and planning [DE93-010239] p 417 N94-11661

Problem specific environments for parallel systems [AD-A266129] p 337 N94-12540

PROCEDURES

Insights into software development in Japan p 330 N94-11435

PROCESS HEAT

Department of Energy solar process heat program: FY 1991 solar process heat prefeasibility studies activity [DE93-010010] p 262 N94-10258

PRODUCT DEVELOPMENT

Solving the essentials of an innovative tennis racket product: Functionality, simplicity, and super-lightweight technology p 65 N94-10068

Future material development trends for commercial airplane interiors p 21 N94-10792

PRODUCTION COSTS

Space transportation alternatives for large space programs: The International Space University Summer Session, 1992 [NASA-TM-106271] p 40 N94-10811

Space Solar Power Program [DE93-011750] p 55 N94-11675

Analysis of the economics of DC arc CVD diamond [AD-A265688] p 403 N94-12339

PRODUCTION ENGINEERING

Object recognition in industrial environment by means of tactile sensor [ITN-93-85200] p 178 N94-10393

PRODUCTIVITY

Measuring human performance on NASA's microgravity aircraft p 317 N94-11537

High biological production of the tidal mixing zones on Japan Sea shelf p 228 N94-12758

PROGRAM VERIFICATION (COMPUTERS)

A formally verified algorithm for interactive consistency under a hybrid fault model [NASA-CR-4527] p 326 N94-11188

Development and application of an acceptance testing model p 330 N94-11432

A recent Cleanroom success story: The Redwing project p 39 N94-11433

The 1991 version of the plume impingement computer program. Volume 1: Description [NASA-CR-194192] p 166 N94-12775

PROGRAMMABLE LOGIC DEVICES

Programmable logic devices [DE93-013117] p 144 N94-11479

PROGRAMMERS

Insights into software development in Japan p 330 N94-11435

Analysis and guidelines for reusable Ada software [AD-A264918] p 332 N94-11850

PROGRAMMING ENVIRONMENTS

Reuse: A knowledge-based approach p 329 N94-11430

A recent Cleanroom success story: The Redwing project p 39 N94-11433

Problem specific environments for parallel systems [AD-A266129] p 337 N94-12540

PROGRAMMING LANGUAGES

Bundle event structures: A non-interleaving semantics for LOTOS [MEMO-INF-92-73] p 320 N94-10164

An object-oriented model for extensible concurrent systems: The composition-filters approach [MEMO-INF-92-87] p 320 N94-10166

Techniques, processes, and measures for software safety and reliability [DE93-012379] p 322 N94-10347

Flexible language constructs for large parallel programs [NASA-CR-191478] p 326 N94-11196

The instrumentation of the multimodel and multilingual user interface [AD-A265444] p 333 N94-12332

PROJECT MANAGEMENT

Analysis of the cost evaluation of ESA programmes and comparable national and international programmes [GTS-92063] p 416 N94-10145

The 40 kWe S-PRIME Thermionic Design and Technology Demonstration Program [DE93-004738] p 40 N94-10147

Summary of implementation and demonstration projects in bays and estuaries [PB93-194637] p 265 N94-10846

Engineering performance metrics [DE93-012084] p 128 N94-11028

Development and application of an acceptance testing model p 330 N94-11432

STGT program: Ada coding and architecture lessons learned p 330 N94-11437

Software management guide [DE93-012034] p 330 N94-11452

Research and development of post-classical management tools for government program offices, volume 2 [DE93-010236] p 417 N94-11600

Quality assurance in basic research and R/D [DE93-010825] p 183 N94-11647

The Department of Clinical Investigation, reports control symbol MED-300(R-1) [AD-A264969] p 304 N94-11649

The requirement for global training programmes to meet the new remote sensing technology p 196 N94-11929

PROJECT PLANNING

Canada's longterm space plan and ISY activities p 37 N94-10692

National Aero-Space Plane: A need for program direction and funding decisions [GAO/NSIAD-93-207] p 416 N94-10910

Lunar-Ultraviolet Telescope Experiment (LUTE) integrated program plan [NASA-CR-193267] p 424 N94-11356

The requirement for global training programmes to meet the new remote sensing technology p 196 N94-11929

Devices related for thermal control systems used in microgravity p 162 N94-12553

Organization and management policy for two phase fluid experiment in space environment p 162 N94-12556

METEOSAT second generation programme SEVIRI: An enhanced visible and IR radiometer for meteorology p 212 N94-12667

PROJECT SETI

Preparing for the initial observations of the Targeted Search and the Sky Survey systems [NASA-CR-193644] p 318 N94-10865

PROJECTILE CRATERING

A two-stage (turbulent-drainage) mechanism for the emplacement of impact crater outflows on Venus p 458 N94-12145

Projectile-target mixing in melted ejecta formed during a hypervelocity impact cratering event p 432 N94-12241

PROLATENESS

The effect of pressure and quadrupolar interactions on the nematic-isotropic transition properties: Numerical results for a system of prolate ellipsoids including second and fourth rank orientational order parameters [DE93-613540] p 410 N94-10536

PROMETHAZINE

Promethazine and its use as a treatment for space motion sickness p 312 N94-11550

Update on the incidence and treatment of space motion sickness p 312 N94-11551

PROP-FAN TECHNOLOGY

AGBT advanced counter-rotating gearbox detailed design report [NASA-CR-180883] p 179 N94-10400

Laser velocimeter measurements of the flow field generated by a forward-swept propfan during flutter [NASA-TM-106195] p 14 N94-10892

PROPANE

Vehicular fleet operation on natural gas and propane: An overview [PB93-194603] p 98 N94-10844

PROPELLANT GRAINS

Combustion-induced crack propagation process in a solid-propellant crack cavity p 98 N94-10901

PROPELLANT TANKS

Spinforming characteristics of a net shape forming process p 56 N94-10004

PROPELLANT TESTS

On the combustion of a laminar spray [NASA-TM-106210] p 28 N94-11238

PROPELLANT TRANSFER

Propellant management in surface tension tanks p 106 N94-10110

On-orbit refueling p 38 N94-11566

PROPELLER NOISE

An experimental investigation of the sources of propeller noise due to turbulence ingestion p 358 N94-11057

PROPELLER SLIPSTREAMS

An experimental investigation of the sources of propeller noise due to turbulence ingestion p 358 N94-11057

PROPHYLAXIS
Update on the incidence and treatment of space motion sickness p 312 N94-11551
PROPORTIONAL COUNTERS
Analysis and interpretation of high energy cosmic rays measured on Spacelab-2 [NASA-CR-193586] p 485 N94-12771
PROPULSION SYSTEM CONFIGURATIONS
Distributed simulation using a real-time shared memory network [NASA-TM-106239] p 319 N94-10724
PROPULSION SYSTEM PERFORMANCE
Space nuclear thermal propulsion nuclear element tests at Sandia National Laboratories [DE93-002301] p 45 N94-10282
Arcjet space thrusters [NASA-CR-193191] p 46 N94-10700
Characterization of in-flight performance of ion propulsion systems [NASA-TM-106283] p 46 N94-10761
Space Storable Rocket Technology program (SSRT). Option 1 program [NASA-CR-191171] p 46 N94-10938
A distributed version of the NASA Engine Performance Program [NASA-TM-106208] p 327 N94-11231
PROPYLENE
Determination of concentration profiles at interfaces and surfaces of partially miscible polymer blends [DE93-013140] p 89 N94-11007
PROTECTIVE CLOTHING
Aerospace medicine and biology: A continuing bibliography with indexes (supplement 375) [NASA-SP-7011(375)] p 303 N94-10398
Aerospace medicine and biology: A continuing bibliography with indexes (supplement 376) [NASA-SP-7011(376)] p 303 N94-10399
Aerospace medicine and biology: A continuing bibliography with indexes (supplement 374) [NASA-SP-7011(374)] p 304 N94-11689
PROTECTIVE COATINGS
Selectively strippable paint schemes p 128 N94-10629
Advanced zinc phosphate conversion and pre-ceramic polymetallosiloxane coatings for corrosion protection of steel and aluminum, and characteristics of polyphenyletheretherketone-based materials [DE93-008717] p 88 N94-10891
Understanding cracking failures of coatings: A fracture mechanics approach p 187 N94-11218
Field evaluation of six protective coatings applied to T-56 turbine blades after 2500 hours of engine use [ARL-TR-27] p 90 N94-11311
High-temperature corrosion of ceramic-ceramic composites in a waste incinerator environment [DE93-012430] p 72 N94-11368
Weld overlay coatings for erosion control [DE93-013592] p 84 N94-11816
Protective coatings for high-temperature polymer matrix composites [NASA-TM-106276] p 74 N94-12431
Corrosion and passivation of high temperature superconductors [AD-A265402] p 405 N94-12586
PROTEIN CRYSTAL GROWTH
Advanced protein, crystallization facility and associated new developments p 39 N94-10119
Effects of a microgravity environment on the crystallization of biological macromolecules p 117 N94-10198
PROTEINS
Electrohydrodynamic effects in continuous flow electrophoresis observations on Earth and in microgravity p 122 N94-10234
HRTEM in protein crystallography [DE93-610322] p 395 N94-10406
Amperometric biosensors based on 3-dimensional hydrogel-forming epoxy networks [AD-A265528] p 87 N94-10510
Aluminum and membrane channels [AD-A265241] p 300 N94-11020
A new decomposition strategy for parallel bonded molecular dynamics [DE93-009839] p 366 N94-11284
Probability of alamethicin conductance states varies with nonlamellar tendency of bilayer phospholipids [AD-A264957] p 301 N94-11648
The phytoplankton bloom in the Kinu-ura Bay, Japan in the rainy season p 211 N94-12660
PROTOCOL (COMPUTERS)
An efficient medium access control strategy for high speed WDM multiaccess networks [MEMO-INF-92-74] p 131 N94-10165
Asynchronous Transfer Mode (ATM) technology: An overview [AD-A266087] p 383 N94-12413
PROTON BEAMS
Possibility of a crossed-beam experiment involving slow-neutron capture by unstable nuclei rapid-process-tron [DE93-754288] p 363 N94-10720
Experimental particle physics at the University of Pittsburgh [DE93-013326] p 369 N94-12546
PROTON IRRADIATION
Investigation of the radiation resistance of triple-junction a-Si:H alloy solar cells irradiated with 1.00 MeV protons p 50 N94-11391
Diffusion length damage coefficient and annealing studies in proton-irradiated InP [NASA-TM-106262] p 404 N94-12430
PROTON SCATTERING
Indication on the existence of the bound state in the p anti p-system [DE92-641575] p 361 N94-10532
PROTON-PROTON REACTIONS
Strangeness production with protons and pions [DE93-010879] p 359 N94-10304
PROTONS
Indication on the existence of the bound state in the p anti p-system [DE92-641575] p 361 N94-10532
Experiments to measure the gluon helicity distribution in protons [DE93-011756] p 368 N94-11613
Solid-state structures of guanidinium methane, ethane, and trifluoromethanesulfonate [AD-A265293] p 402 N94-11654
PROTOPLANETS
Columbus proto-planetesimal dust aggregation experiment p 123 N94-10236
Giant impact-induced atmospheric blow-off p 435 N94-12019
Recondensation of chondritic material in the early solar system: Results of thermodynamic simulation p 432 N94-12226
PROTOSTARS
Initiating solar system formation through stellar shock waves p 448 N94-12090
PROTOTYPES
Characterization of a scannerless LADAR system [DE93-011582] p 174 N94-10959
A prototype urine collection device for female aircrew p 317 N94-11549
PROVING
Validation of directional wave spectra from the ERS-1 during the ESA CAL/VAL campaign p 232 N94-11707
The Grand Banks ERS-1 SAR wave spectra validation experiment p 232 N94-11708
Validation of ERS-1 wind and wave data by use of operational forecast models p 233 N94-11710
Validation test system for sea surface temperature detected by satellites in Mutsu Bay p 213 N94-12670
Evaluation of the method of geostrophic flow using NOAA-AVHRR data p 213 N94-12673
Further study of the Non-Regression-Coefficient SST retrieval method p 213 N94-12674
PSYCHOACOUSTICS
Signal feature analysis using neural networks and psychoacoustics [AD-A266048] p 340 N94-12398
PSYCHOLOGICAL TESTS
Basic attributes test (BAT): Operational pre-implementation analysis and score equating [AD-A265885] p 314 N94-12276
PSYCHOMOTOR PERFORMANCE
Landing Craft Air Cushion (LCAC) crew selection system manual [AD-A265158] p 313 N94-11098
Measuring human performance on NASA's microgravity aircraft p 317 N94-11537
PSYCHOPHYSICS
Visual encoding of spatial relations [AD-A266049] p 313 N94-10909
Visual psychophysics of egomotion [AD-A265253] p 304 N94-11681
PSYCHOPHYSIOLOGY
Psychophysiological measures of cognitive workload in laboratory and flight p 317 N94-11529
PUBLIC HEALTH
Technical Conference on Tropical Urban Climates: Extended Abstracts [WMO/TD-538] p 283 N94-10561
International Telemedicine/Disaster Medicine Conference: Papers and Presentations [NASA-NP-207] p 304 N94-11787
The Canadian experience: Using telemedicine for the support of medical care at remote sites p 305 N94-11789
Applications of the INTELSAT system to remote health care p 306 N94-11794
Clinical aspects of telemedicine p 306 N94-11795
Commercial applications of telemedicine p 306 N94-11798
Space technology in remote health care p 306 N94-11799
The National Disaster Medical System p 307 N94-11801
Satellite, environmental, and medical information applied to epidemiological monitoring p 307 N94-11802
A telemedicine health care delivery system p 307 N94-11803
Use of satellite telecommunications for telemedicine p 308 N94-11807
US-USSR telemedicine consultation spacebridge to Armenia and Ufa p 308 N94-11809
The revitalization of health and education in Rural America Act of 1992 p 308 N94-11810
PULMONARY FUNCTIONS
Project ARGO: Gas phase formation in simulated microgravity [NASA-TM-104762] p 125 N94-11235
Proceedings of the First Joint NASA Cardiopulmonary Workshop [NASA-CP-10068] p 308 N94-11991
Pulmonary function in microgravity: KC-135 experience p 309 N94-11994
PULSAR MAGNETOSPHERES
Interstellar scattering and the pulsar studies with space VLBI p 135 N94-11065
PULSARS
Pulsar astrometry by using VLBI (PSR0329 between Kashima 26mPhi and Usuda 64mPhi) p 351 N94-10968
An ensemble pulsar time p 351 N94-10969
PULSE COMMUNICATION
Study on color video pictures transmission by digital acoustic signal p 139 N94-11917
PULSE COMPRESSION
One-dimensional calculation of high-power microwave pulse compression by the earth's ionosphere [DE93-009517] p 137 N94-11466
FR/GE/US radar receiver pulse compression ratio [AD-A265391] p 138 N94-12409
PULSE DURATION
Response of silicon solar cell to pulsed laser illumination p 51 N94-11396
PULSE DURATION MODULATION
A study of DC-DC converters with MCTs for arcjet power supplies [NASA-CR-193457] p 142 N94-10931
PULSE GENERATORS
Characterization of the pulse transformer [AD-A263414] p 143 N94-11298
Advanced concepts theory annual report 1992 [AD-A266132] p 393 N94-11474
PULSED LASER DEPOSITION
In-situ crystallization of silicate glass films deposited on alpha- Al2O3 [DE93-012969] p 95 N94-12596
PULSED LASERS
Progress in zirconium resonance ionization spectroscopy [DE93-011881] p 76 N94-11075
Thermal-optical switching of a silicon based interference filter [AD-A265152] p 174 N94-11095
The efficiency of photovoltaic cells exposed to pulsed laser light p 50 N94-11395
Response of silicon solar cell to pulsed laser illumination p 51 N94-11396
Approaches to solar cell design for pulsed laser power receivers p 51 N94-11397
Short pulse lasers for generation of fields exceeding 100 MG [DE93-013346] p 369 N94-11815
Submicrosecond, synchronizable x ray source [AD-D015745] p 176 N94-12337
Damage threshold study of ion beam sputtered coatings for a visible high-repetition laser at LLNL [DE93-013430] p 95 N94-12602
PULSED RADIATION
Laser Synchrotron Source (LSS) [AD-D015755] p 173 N94-10371
Propagation of light pulses through a three-layer medium (cloud, pure air, and ocean water) p 222 N94-12725
PULSES
Propagation of light pulses through a three-layer medium (cloud, pure air, and ocean water) p 222 N94-12725
PURIFICATION
Electrohydrodynamic effects in continuous flow electrophoresis observations on Earth and in microgravity p 122 N94-10234
PURITY
Production of electronic grade lunar silicon by disproportionation of silicon difluoride p 435 N94-12017

PYRITES
The rate of chemical weathering of pyrite on the surface of Venus p 477 N94-12246
PYROLYSIS
Fibre-reinforced ceramic components by filament winding for intermediate temperature applications
p 61 N94-10041
Applications of a model to predict flame spread over interior finish materials in a compartment
p 19 N94-10783
Preparation of carbon monoliths having tailored pore structure from porous polymer precursors
[DE93-011576] p 89 N94-10958
Nitrogen and noble gases in a glass sample from LEW88516 p 80 N94-12051
Separation of spallation and terrestrial C-14 in chondrites p 431 N94-12183

Q

Q FACTORS
Quality factors and local adaption (with applications in Eulerian hydrodynamics)
[DE93-010502] p 151 N94-11272
QUADRATURES
Numerical method of singular problems on singular integrals
[DE93-613654] p 343 N94-10546
Quantum noise and squeezing in optical parametric oscillator with arbitrary output coupling
p 375 N94-10568
One dimensional representations in quantum optics
p 375 N94-10570
Comparison of multiresolution techniques for digital signal processing
[AD-A265364] p 138 N94-12406
QUADRUPOLES
Fabrication and test of a superconducting RFQ
[DE93-010860] p 140 N94-10300
The effect of pressure and quadrupolar interactions on the nematic-isotropic transition properties: Numerical results for a system of prolate ellipsoids including second and fourth rank orientational order parameters
[DE93-613540] p 410 N94-10536
Performance characteristics of the INS 25.5-MHz split coaxial RFQ
[DE93-753168] p 144 N94-11508
On the unique structure of the magnetic fields of Uranus and Neptune p 472 N94-12221
Operational characteristics of a 100-mA, 2-MeV radio-frequency quadrupole
[DE93-014474] p 374 N94-12786
QUALITATIVE ANALYSIS
Field evaluation of six protective coatings applied to T-56 turbine blades after 2500 hours of engine use
[ARL-TR-27] p 90 N94-11311
QUALITY
The experience factory: Can it make you a 5? or what is its relationship to other quality and improvement concepts? p 328 N94-11424
QUALITY CONTROL
Software process assessments p 329 N94-11427
Large array SQUID magnetometer for NDE
[AD-A264799] p 304 N94-11449
Quality assurance in basic research and R/D
[DE93-010825] p 183 N94-11647
An integrated approach to total end-to-end quality control of ocean data in the real-time environment
p 211 N94-12662
Quality assurance for environmental chemistry: 1991, volume 2
[DE93-011792] p 272 N94-12780
QUANTITATIVE ANALYSIS
Quantitative EEG patterns of differential in-flight workload p 317 N94-11528
Novel mass spectrometric instrument for gaseous and particulate characterization and monitoring
[DE93-014093] p 272 N94-12783
QUANTUM AMPLIFIERS
Photon number amplification/duplication through parametric conversion p 376 N94-10572
QUANTUM CHROMODYNAMICS
Some new/old approaches to QCD
[DE93-010451] p 408 N94-10261
Squeezed colour states in gluon jet
p 379 N94-10599
Spontaneous symmetry breaking in QCD
[DE93-753080] p 396 N94-10645
Experiments to measure the gluon helicity distribution in protons
[DE93-011756] p 368 N94-11613
Quenched chiral logarithms
[DE93-010195] p 346 N94-11663
Top quark search in D(O) from the lepton + jets mode
[DE93-014027] p 370 N94-12781
Quark and lepton masses
[DE93-012308] p 370 N94-12787
QUANTUM EFFICIENCY
Development of ultra-low noise, high sensitivity planar metal grating coupled 3 to 5 multiquantum well infrared detectors for focal plane array staring IR sensor systems
[AD-A265599] p 404 N94-12375
QUANTUM ELECTRODYNAMICS
The legacy of uncertainty p 376 N94-10577
Non-gauge phase transformations in quantum transition amplitudes p 378 N94-10596
Squeezed colour states in gluon jet
p 379 N94-10599
Non-stationary and non-linear dispersive medium as external field which generates the squeezed states
p 380 N94-10605
Quantized conic sections; quantum gravity
[DE93-010950] p 411 N94-10956
QUANTUM ELECTRONICS
The response of an electron in a biased double well to a strong laser: Delocalization and low frequency generation
[AD-A265169] p 366 N94-11100
High frequency behavior of long and small junctions
[AD-A265670] p 403 N94-12336
QUANTUM MECHANICS
Some new/old approaches to QCD
[DE93-010451] p 408 N94-10261
Wave function collapse: An unnecessary condition for the dynamical description of the Zeno and partial Zeno effect
[DE93-612970] p 132 N94-10401
A group-theoretic approach to the study of small oscillations of a dynamical system with a known symmetry
[DE93-612971] p 409 N94-10402
Standard model status (in search of new physics)
[DE93-013288] p 410 N94-10528
Bound states of the N-dimensional Klein-Gordon equation with vector and scalar Coulomb potentials
[DE93-617650] p 349 N94-10547
The Second International Workshop on Squeezed States and Uncertainty Relations
[NASA-CP-3219] p 375 N94-10564
One dimensional representations in quantum optics
p 375 N94-10570
Harmonic oscillator interaction with squeezed radiation
p 376 N94-10571
Non classical effects in planar waveguides
p 376 N94-10574
Phasing operator for two oscillators in classical field
p 370 N94-10579
On a Lagrange-Hamilton formalism describing position and momentum uncertainties p 349 N94-10583
Dissipation in a squeezed-state environment
p 370 N94-10584
Squeezed spin states: Squeezing the spin uncertainty relations p 377 N94-10585
Observables, measurements and phase operators from a Bohmian perspective p 378 N94-10589
Uncertainty relations, zero point energy and the linear canonical group p 378 N94-10590
Information entrophy via Glauber's Q-representation
p 378 N94-10592
Squeezed states of electrons and transitions of the density of states p 370 N94-10593
Quantum mechanical effects of topological origin
p 378 N94-10594
Collision-induced squeezing in a harmonic oscillator
p 379 N94-10597
Positive phase space distributions and uncertainty relations p 379 N94-10598
The uncertainty principle and quantum chaos
p 379 N94-10602
Relation of squeezed states between damped harmonic and simple harmonic oscillators p 380 N94-10606
Infinite-mode squeezed coherent states and non-equilibrium statistical mechanics (phase-space-picture approach)
[LBL-32695] p 380 N94-10608
Correlated states of a quantum oscillator acted by short pulses p 380 N94-10609
Floquet operator as integral of motion
p 380 N94-10610
Exact solutions of a many-anyon problem
[DE93-617646] p 411 N94-10832
Quantum dynamics of helium clusters
[AD-A266060] p 411 N94-10874
Superfield description of N = 2 extended one-dimensional supersymmetric quantum mechanics
[DE93-621420] p 412 N94-11087
Three-dimensional N = 4 extended supersymmetrical quantum mechanics
[DE93-621421] p 412 N94-11164
Absorption spectrum calculations using mixed quantum-gaussian wave packet dynamics
[AD-A265179] p 413 N94-11877
QUANTUM NUMBERS
Quantized conic sections; quantum gravity
[DE93-010950] p 411 N94-10956
QUANTUM OPTICS
The Second International Workshop on Squeezed States and Uncertainty Relations
[NASA-CP-3219] p 375 N94-10564
A phaseonium magnetometer: A new optical magnetometer based on index enhanced media
p 375 N94-10565
Smoothly deformed light p 375 N94-10566
Nonclassical states of the second optical harmonic in the presence of self-action p 375 N94-10567
Quantum noise and squeezing in optical parametric oscillator with arbitrary output coupling
p 375 N94-10568
Disturbance, the uncertainty principle and quantum optics p 375 N94-10569
One dimensional representations in quantum optics
p 375 N94-10570
Photon number amplification/duplication through parametric conversion p 376 N94-10572
Non classical effects in planar waveguides
p 376 N94-10574
Completeness properties of the minimum uncertainty states p 349 N94-10581
Uncertainty relations, zero point energy and the linear canonical group p 378 N94-10590
Information entrophy via Glauber's Q-representation
p 378 N94-10592
Positive phase space distributions and uncertainty relations p 379 N94-10598
Wavelets and spacetime squeeze
p 379 N94-10604
QUANTUM STATISTICS
Coherence influence on the intensity of Bose-Einstein correlations and visible size of a source
[DE93-617697] p 349 N94-10556
Relation of squeezed states between damped harmonic and simple harmonic oscillators p 380 N94-10606
Infinite-mode squeezed coherent states and non-equilibrium statistical mechanics (phase-space-picture approach)
[LBL-32695] p 380 N94-10608
QUANTUM THEORY
Discrete space-time symmetries
[DE93-010199] p 341 N94-10259
The structure of Hilbert flag varieties
[MEMO-1095] p 348 N94-10272
Standard model status (in search of new physics)
[DE93-013288] p 410 N94-10528
From the Weyl theory to a theory of locally anisotropic space-time
[DE92-644734] p 410 N94-10535
The Second International Workshop on Squeezed States and Uncertainty Relations
[NASA-CP-3219] p 375 N94-10564
A phaseonium magnetometer: A new optical magnetometer based on index enhanced media
p 375 N94-10565
Nonclassical states of the second optical harmonic in the presence of self-action p 375 N94-10567
Disturbance, the uncertainty principle and quantum optics p 375 N94-10569
Generalised squeezing and information theory approach to quantum entanglement p 377 N94-10580
Study of Einstein-Podolsky-Rosen state for space-time variables in a two photon interference experiment
p 370 N94-10582
Dissipation in a squeezed-state environment
p 370 N94-10584
Squeezed spin states: Squeezing the spin uncertainty relations p 377 N94-10585
Quantum entropy and uncertainty for two-mode squeezed, coherent and intelligent spin states
p 377 N94-10586
Geometric aspects of uncertainty and correlation
p 349 N94-10588
Nonunitary and unitary approach to Eigenvalue problem of Boson operators and squeezed coherent states
p 350 N94-10595
Non-gauge phase transformations in quantum transition amplitudes p 378 N94-10596
Exact and quasi-classical density matrix and Wigner functions for a particle in the box and half space
p 350 N94-10600
New squeezed landau states p 379 N94-10601
The uncertainty principle and quantum chaos
p 379 N94-10602

Wigner functions for nonclassical states of a collection of two-level atoms p 379 N94-10603

Infinite-mode squeezed coherent states and non-equilibrium statistical mechanics (phase-space-picture approach) [LBL-32695] p 380 N94-10608

Quantum processes in resonators with moving walls p 380 N94-10612

Limitation and suppression of hot electron fluctuations in submicron semiconductor structures [DE93-613911] p 396 N94-10801

Quantum solitons with cylindrical symmetry [DE93-617659] p 344 N94-10881

Proceedings of the Workshop on New Aspects of Quantum Field Theories [DE93-754136] p 411 N94-10887

Dissipative phase transitions in field theory models with spontaneous symmetry violation [DE93-621382] p 412 N94-11039

Creation and annihilation of solitons in nonlinear integrable systems [DE93-621379] p 365 N94-11078

Non-barrier tunneling in presence of dissipations [DE93-621381] p 412 N94-11086

Green-Schwarz superstrings in the generalized harmonical Newmann-Penrose formalism [DE93-621422] p 412 N94-11088

A theoretical kinematical study of the gradient of any cosmic scalar field [DE92-644731] p 425 N94-11136

One-loop quantum gravity on de Sitter space [DE92-641349] p 425 N94-11152

Characterization of the Si/SiO2 interfere morphology from quantum oscillations in Fowler-Nordheim tunneling currents [AD-A265149] p 143 N94-11160

Divergences in the moduli space integral and accumulating handles in the infinite-genus limit [DE93-619722] p 346 N94-11693

Duality twisted boundary conditions in n-sta te Potts models [DE93-619724] p 346 N94-11811

Explorations in quantum gravity: From one loop effective actions to two-dimensional theories p 413 N94-11822

Superfluid turbulence p 158 N94-12307

QUANTUM WELLS

Non-gauge phase transformations in quantum transition amplitudes p 378 N94-10596

Effect of effective mass differences on the tunneling current-voltage behaviour of a resonant diode in the presence of space charge build-up [DE93-613817] p 142 N94-10799

The response of an electron in a biased double well to a strong laser: Delocalization and low frequency generation [AD-A265169] p 366 N94-11100

The additional contribution caused by Coulomb interaction to the exciton dispersion in multiple quantum wells and superlattices for direct band gap cubic semiconductors [DE93-613538] p 402 N94-11659

Development of ultra-low noise, high sensitivity planar metal grating coupled 3 to 5 multiquantum well infrared detectors for focal plane array staring IR sensor systems [AD-A265599] p 404 N94-12375

Theoretical investigation of some novel phenomenal in artificially structured semiconductors [AD-A266142] p 405 N94-12587

QUARK MODELS

Quenched chiral logarithms [DE93-010195] p 346 N94-11663

QUARKS

Top and Higgs masses in a composite boson model [DE93-010874] p 359 N94-10302

Production of strange clusters in relativistic heavy ion collisions [DE93-010876] p 359 N94-10303

Searches for strangelets and other exotics at the AGS [DE93-013341] p 359 N94-10308

On the relativistic string size at finite temperature [DE93-617658] p 409 N94-10394

S(sup 1) x S(sup 2) as a bag membrane and its Einstein-Weyl geometry [DE93-613149] p 410 N94-10635

Proceedings of the third workshop on light quark meson spectroscopy [DE93-754138] p 363 N94-10696

Filamentation instability of hot quark-gluon plasma with hard jet [DE93-617679] p 388 N94-10882

Gluon gas viscosity in nonperturbative region [DE93-617680] p 397 N94-10883

Relativistic heavy-ion collisions [DE93-014844] p 366 N94-11147

Experiments to measure the gluon helicity distribution in protons [DE93-011756] p 368 N94-11613

Quenched chiral logarithms [DE93-010195] p 346 N94-11663

Top quark search in D(O) from the lepton + jets mode [DE93-014027] p 370 N94-12781

Quark and lepton masses [DE93-012308] p 370 N94-12787

QUARTZ

Dynamic studies of crystal growth using the AFM [DE93-009549] p 399 N94-11268

Si-29 NMR spectroscopy of naturally-shocked quartz from Meteor Crater, Arizona: Correlation to Kieffer's classification scheme p 80 N94-12087

QUARTZ CRYSTALS

The laser ablation of gold films at the electrode surface of a quartz crystal microbalance [AD-A265535] p 175 N94-12012

NMR spectroscopy of experimentally shocked single crystal quartz: A reexamination of the NMR shock barometer p 81 N94-12258

A novel test method for fuel thermal stability [AD-A265853] p 99 N94-12275

QUARTZITE

Shock transformations in quartzite p 97 N94-12040

QUATERNARY ALLOYS

Electronic and total energy properties of ternary and quaternary semiconductor compounds, alloys and superlattices [NASA-CR-192905] p 405 N94-12570

QUATERNIONS

Derivation of three closed loop kinematic velocity models using normalized quaternion feedback for an autonomous redundant manipulator with application to inverse kinematics [DE93-012823] p 340 N94-12543

QUENCHING (COOLING)

AGF (Automatic Gradient Furnace): A proposed microgravity facility p 112 N94-10141

EUSO-D2-experiment: Unidirectional solidification with quenching of an AlSi11 alloy p 86 N94-10199

QUERY LANGUAGES

A correct and efficient interface for logical query languages with complex objects [MEMO-INF-93-01] p 320 N94-10167

The relational-to-object-oriented cross-model accessing capability in a multi-model and multi-lingual database system [AD-A264911] p 420 N94-11846

QUESTOL AIRCRAFT

An investigation on the effectiveness of the piping interference removal system for STOL aircraft wind tunnel tests [NAL-TM-647] p 2 N94-10350

Aerodynamic model identification of quiet STOL experimental aircraft ASKA from dynamic flight test data [DE93-767967] p 25 N94-10728

Flight simulator experiment of the cockpit advisory system [NAL-TR-1151] p 33 N94-10733

QUEUEING THEORY

Complex functions in queueing theory [CWI-BS-R9219] p 342 N94-10352

Scalable spin locks for multiprogrammed systems [AD-A265007] p 337 N94-11650

QUOTIENTS

Finding minimum-quotient cuts in planar graphs [DE93-011675] p 344 N94-10961

R

RADAR APPROACH CONTROL

SATORI: Situation Assessment Through the Re-creation of Incidents [DOT/FAA/AM-93/12] p 38 N94-12567

RADAR CORNER REFLECTORS

An experiment for the radiometric calibration of the ERS-1 SAR p 236 N94-11733

RADAR CROSS SECTIONS

Theoretical studies of the radar properties of the icy Galilean moons of Jupiter [NASA-CR-193407] p 434 N94-11361

ERS-1 scatterometer data characteristics and wind retrieval skill p 233 N94-11709

A preliminary C-band scatterometer model function for the ERS-1 AMI instrument p 233 N94-11715

Ocean wave detection by SAR p 197 N94-11932

Measurements of ocean cross-section with a side-looking airborne radar p 201 N94-11954

Fundamental studies of radar scattering from water surfaces: The Lake Washington experiment [NASA-CR-194030] p 139 N94-12778

RADAR DATA

Groundwave HF ocean surface radar p 139 N94-11906

Volcanism in southern Guinevere Planitia, Venus: Regional volcanic history and morphology of volcanic domes p 467 N94-12190

Synthesis of global thematic mapping, Venus: Geologic correlations/questions for the Magellan gravity mission p 467 N94-12194

SATORI: Situation Assessment Through the Re-creation of Incidents [DOT/FAA/AM-93/12] p 38 N94-12567

Fundamental studies of radar scattering from water surfaces: The Lake Washington experiment [NASA-CR-194030] p 139 N94-12778

RADAR DETECTION

Improved Many-On-Many ROUTE software description [DE93-013961] p 334 N94-12608

RADAR ECHOES

Statistical study of HF ocean radar echo p 139 N94-11905

Measurements of ocean cross-section with a side-looking airborne radar p 201 N94-11954

Development of shipboard ocean lidar p 140 N94-11965

Fundamental studies of radar scattering from water surfaces: The Lake Washington experiment [NASA-CR-194030] p 139 N94-12778

RADAR EQUIPMENT

The radar eye blinded: The USAF and electronic warfare, 1945-1955 [AD-A265494] p 132 N94-10497

HF ocean radar system at Okinawa Radio Observatory p 139 N94-11902

Resistivity and radar void detectors for tunneling machines p 140 N94-12706

RADAR IMAGERY

Validation of directional wave spectra from the ERS-1 during the ESA CAL/VAL campaign p 232 N94-11707

Wind and surface features in SAR images: The Canadian program p 234 N94-11718

Coastal ocean studies with ERS-1 SAR during NORCSEX 1991 p 234 N94-11720

SAR imaging of dynamical features in the English Channel p 234 N94-11721

SAR ocean imaging in the Gulf of Alaska p 235 N94-11723

Preliminary results of the experiment I-7 p 235 N94-11728

Calibration of the ERS-1 SAR fast-delivery images p 236 N94-11730

The use of active devices in the ERS-1 radiometric calibration p 236 N94-11732

Techniques and applications of SAR interferometry for ERS-1: Topographic mapping, change detection, and slope measurement p 236 N94-11734

SAR interferometry experiments with ERS-1 p 237 N94-11735

SAR-interferometry applying ERS-1: Some preliminary test results p 237 N94-11736

Monitoring of the Greenland Ice Sheet using ERS-1 synthetic aperture radar imagery p 237 N94-11741

Use of ERS-1 SAR to measure ice flux in the East Greenland current p 238 N94-11746

Validation of ERS-1 SAR measurements of sea ice during ARCTIC-1991 p 238 N94-11747

Ocean circulation revealed by ice floe tracking p 240 N94-11759

Evaluating ERS-1 ice motion and classification products p 241 N94-11763

A stochastic-deterministic approach as an alternative to classical cross-over techniques in small ocean basins p 242 N94-11767

An analysis of the gravity field in the Norwegian Sea and mapping of the ice cap of Greenland using ERS-1 altimeter measurements p 242 N94-11768

Proceedings of the PORSEC 1992 in Okinawa: Conference for Pacific Ocean Environments and Probing, volume 1 [JTN-93-80418] p 191 N94-11894

Ocean-ice interaction study of waves and mesoscale features p 197 N94-11935

The microwave backscattering from wind waves p 201 N94-11959

Venus small volcano classification and description p 438 N94-12037

A pattern recognition system for locating small volvanoes in Magellan SAR images of Venus p 455 N94-12126

Using lunar sounder imagery to distinguish surface from subsurface reflectors in lunar highlands areas p 464 N94-12179

Volcanism in southern Guinevere Planitia, Venus: Regional volcanic history and morphology of volcanic domes p 467 N94-12190

The Magellan volcanic and magmatic feature catalog p 467 N94-12193

Characteristics of arachnoids from Magellan data p 469 N94-12204

ISAR motion compensation using the burst derivative measure as a focal quality indicator [AD-A265647] p 138 N94-12440

Methodological considerations for use of ERS-1 imagery for the delineation of river networks in tropical forest areas p 247 N94-12484

Per-field filtering and classification of multitemporal ERS-1 SAR imagery p 247 N94-12485

Extraction of plant and soil parameters from multitemporal ERS-1 SLC data of the Freiburg test site p 248 N94-12491

The TREES project: Pre-processing and generation of terrain data for inclusion in an ERS-1 SAR classification scheme p 249 N94-12496

TREES project: A suite of tools for information extraction from ERS-1 SAR data p 250 N94-12498

ERS-1 and Almaz SAR ocean wave imaging over the Gulf Stream and the Grand Banks p 251 N94-12505

Real time processing wave spectra from satellite SAR p 251 N94-12506

A statistical analysis of sea state surface ERS-1 SAR-wave mode imagettes p 251 N94-12507

A new model for Synthetic Aperture Radar (SAR) images from ocean scatter p 251 N94-12508

On the extraction of ocean wave spectra from ERS-1 SAR wave mode image spectra p 251 N94-12509

Tide-generated nonlinear internal wave packets in the Strait of Gibraltar observed by the synthetic aperture radar aboard the ERS-1 satellite p 252 N94-12510

Cloud studies using ATSR data p 253 N94-12517

Artificial oil pollution detection and wave observation in the sea adjacent to Japan by ERS-1 SAR p 253 N94-12520

Ship traffic monitoring using the ERS-1 SAR p 253 N94-12521

Pilot project PPF12. Coastal and fluvial environment in French Guiana: First results of ERS-1 SAR data analysis p 254 N94-12523

Coastal morphodynamics and energetic characteristics of swell studied with ERS-1 SAR p 254 N94-12524

Mapping of sea bottom topography with ERS-1 C-band SAR p 254 N94-12525

ERS-1 imaging radar over the Waddensea-North Netherlands p 254 N94-12526

SAR imaging of geology and bathymetry: Kent coastal area - southern North Sea p 254 N94-12527

Comparison of ERS-1 SAR images of the Western Mediterranean to in situ oceanographic data: PRIM-1 Cruise (May 1992) p 255 N94-12529

Ice studies in the Barents Sea by ERS-1 during SIZEX 1992 p 210 N94-12653

A basic consideration for remote sensing using microwave radars on a satellite p 212 N94-12665

Remote sensing of light scattering coefficient of sea water vertical distribution by the means of airborne lidar p 224 N94-12736

Spatial variability of the ocean underwater dynamic noise from satellite radar sensing data p 225 N94-12740

Wind-wave and foam dynamics from optical and radar airborne observations p 226 N94-12745

Observations of surface signatures in the north-west Pacific Ocean with the spaceborne SAR p 226 N94-12746

Radar observation of internal waves field in the north-west Pacific p 226 N94-12747

RADAR MAPS

Mapping of the East Australian current with the ERS-1 SAR and shipborne studies p 234 N94-11717

Radarmap of Germany: First mosaic and classification p 246 N94-12477

Combined analysis of ERS-1 SAR and visible/infrared remote sensing data for land cover/land use mapping in a tropical zone: A case study in Guinea p 246 N94-12478

Example of SPOT/ERS-1 complementarity p 247 N94-12479

The use of ERS-1 SAR data to study surface states p 247 N94-12480

Application of ERS-1 SAR data to snow mapping p 247 N94-12483

RADAR MEASUREMENT

Using transponders with the ERS-1 altimeter to measure orbit altitude to +/- 3 cm p 244 N94-11785

Measurement of wave parameters by HF ocean radar p 192 N94-11903

Kuroshio observations by the HF ocean radar p 192 N94-11904

Experiment and results of the Italian activity in the field of ocean microwave backscattering p 200 N94-11953

Air-sea interaction: Fluxes, a review p 201 N94-11955

Polar mesospheric waves and structure [AD-A265360] p 279 N94-12561

Remote sensing of light scattering coefficient of sea water vertical distribution by the means of airborne lidar p 224 N94-12736

RADAR RANGE

Improved Many-On-Many ROUTE software description [DE93-013961] p 334 N94-12608

RADAR RECEIVERS

FR/GE/US radar receiver pulse compression ratio [AD-A265391] p 138 N94-12409

RADAR SCANNING

Multichannel dual angle approach for sea surface temperature retrieval in context of ERS-1 scenario p 252 N94-12512

Validation of ATSR-1 using aircraft radiometer measurements over the South Atlantic p 252 N94-12515

Cloud studies using ATSR data p 253 N94-12517

A comparison of ATSR and shipboard radiometer SST measurements along transects between the UK and the Antarctic p 253 N94-12518

Preliminary validation of ATSR sea surface temperatures near the Faeroes p 253 N94-12519

RADAR SCATTERING

Theoretical studies of the radar properties of the icy Galilean moons of Jupiter [NASA-CR-193407] p 434 N94-11361

Development of shipboard ocean lidar p 140 N94-11965

Remote sensing of subsurface water temperature profile and backscattering coefficient in the China Sea by Ocean Lidar (OLIDAR) p 203 N94-11970

Polarisation of backscattering radiation at remote sensing of ocean with impulse laser beam p 177 N94-12722

Fundamental studies of radar scattering from water surfaces: The Lake Washington experiment [NASA-CR-194030] p 139 N94-12778

RADAR SIGNATURES

The theory for, and demonstration of, information theory applied to radar target identification [DE93-006393] p 132 N94-10315

Signatures of Antarctic firn by means of ERS-1 AMI and by field measurements p 237 N94-11737

Experiences from the Swedish sea ice programme during BEERS-1992 p 239 N94-11751

Air-sea-ice interactions in the Weddell Sea p 239 N94-11753

Arctic sea ice microwave signature and geophysical processes study p 240 N94-11754

C-band SAR backscatter from ice on shallow tundra lakes: Observations and modelling p 240 N94-11755

Sea ice radar signatures from ERS-1 SAR during late Summer and Fall in the Beaufort and Chukchi Seas p 240 N94-11756

RADAR TARGETS

The theory for, and demonstration of, information theory applied to radar target identification [DE93-006393] p 132 N94-10315

ISAR motion compensation using the burst derivative measure as a focal quality indicator [AD-A265647] p 138 N94-12440

RADAR TRACKING

Mid-latitude ionospheric response to active experiments [NASA-CR-193549] p 280 N94-12583

Improved Many-On-Many ROUTE software description [DE93-013961] p 334 N94-12608

RADAR TRANSMISSION

HF-OTH radar performance results [AD-A266106] p 138 N94-11655

RADIAL FLOW

Development of passive superconducting bearings. Phase 3 [AD-A266050] p 180 N94-10706

Simulation study of dynamo structure in reversed field pinch [DE93-771406] p 390 N94-11128

Large volcanoes on Venus: Examples of geologic and structural characteristics from different classes p 467 N94-12195

RADIANCE

A statistical method to determine aerosol path radiance and its application to atmospheric correction for CZCS imagery p 191 N94-11897

Distribution of mineral aerosols over the North Pacific p 204 N94-11976

The evaluation of radiative process in the atmosphere-ground system by Monte Carlo method p 205 N94-11980

Seasonal variability of surface ocean color in the Omura Bay using multitemporal LANDSAT-5 TM data p 218 N94-12698

Optimum selection of spectral channels in the problem of remote sensing of phytoplankton concentration in ocean water p 223 N94-12726

Trajectory curving in underwater propagation of light p 226 N94-12748

RADIANT FLUX DENSITY

Retrieval of radiation budgets in the Arctic from satellite measurements p 229 N94-10714

Radiation hardness of Mo/Si multilayers designed for use in a soft x ray projection lithography system [DE93-011879] p 143 N94-11273

EOL performance comparison of GaAs/Ge and Si BSF/R solar arrays p 51 N94-11398

RADIATION BELTS

Proton transport methods for satellite shield modeling [DE93-013602] p 42 N94-10520

Analysis of geophysical measurements and spacecraft interactions [AD-A266064] p 43 N94-10944

Potential health effects of space radiation p 312 N94-11558

RADIATION COUNTERS

Silicon-based elementary particle tracking system: Materials science and mechanical engineering design [DE93-012630] p 65 N94-10740

Effects of energetic particle events on VLF/LF propagation parameters/1989 [AD-A265266] p 275 N94-11013

Conceptual design report for the SDC barrel and intermediate muon detectors based on a jet-type drift chamber [DE93-753173] p 367 N94-11510

Experimental particle physics at the University of Pittsburgh [DE93-013326] p 369 N94-12546

RADIATION DAMAGE

Proton transport methods for satellite shield modeling [DE93-013602] p 42 N94-10520

EOL performance comparison of GaAs/Ge and Si BSF/R solar arrays p 51 N94-11398

Results of thermal vacuum tests for the PASP+ flight modules p 53 N94-11410

Multi-band gap and new solar cell options workshop p 54 N94-11418

Potential health effects of space radiation p 312 N94-11558

Diffusion length damage coefficient and annealing studies in proton-irradiated InP [NASA-TM-106262] p 404 N94-12430

RADIATION DETECTORS

Analysis and interpretation of high energy cosmic rays measured on Spacelab-2 [NASA-CR-193586] p 485 N94-12771

RADIATION DISTRIBUTION

A modeling perspective on cloud radiative forcing [DE93-012383] p 276 N94-11241

On possibility of diamond formations in radiation process p 433 N94-12254

RADIATION DOSAGE

Proton transport methods for satellite shield modeling [DE93-013602] p 42 N94-10520

A window least squares algorithm for statistical noise smoothing of 2D-ACAR data [DE93-613828] p 395 N94-10537

On problem about nature of Portevin-Le Chatelier effect in irradiated aluminium alloys [DE93-617200] p 82 N94-10842

Radiation defect production in InAs crystals under electron irradiation [DE93-617202] p 397 N94-10845

A proposed performance index for galactic cosmic ray shielding materials [NASA-TM-4444] p 484 N94-11278

Activation energy and capture cross section of majority carrier traps in Zn doped InP p 49 N94-11386

Potential health effects of space radiation p 312 N94-11558

Radiation considerations for interplanetary missions p 45 N94-11559

Longitudinal study of astronaut health: Mortality in the years 1959-1991 p 312 N94-11560

Operational radiological support for the US manned space program p 318 N94-11561

Lessons learned from the Long Duration Exposure Facility [AD-A266026] p 44 N94-12394

Experimental particle physics at the University of Pittsburgh [DE93-013326] p 369 N94-12546

RADIATION EFFECTS

Radiation hardened nonvolatile memory for space and strategic applications [DE93-000746] p 319 N94-10146

High heat flux components and plasma surface interactions [DE93-008786] p 385 N94-10253

Workshop on NN Bremsstrahlung and Polarization Observables
[DE93-010181] p 361 N94-10334
Investigation of soft errors in MOS RAM under influence of heavy ions
[DE92-644554] p 484 N94-10534
Szilard-Chalmers effect in solid HIO4.2H2O by neutron irradiation
[DE93-617173] p 397 N94-10830
On problem about nature of Portevin-Le Chatelier effect in irradiated aluminium alloys
[DE93-617200] p 82 N94-10842
The influence of irradiation conditions, type, and concentration of impurities on radiation defects characteristics in indium antimonide under electron irradiation
[DE93-617201] p 397 N94-10843
Radiation defect production in InAs crystals under electron irradiation
[DE93-617202] p 397 N94-10845
Proceedings of the Symposium on Radiation Research in Life Science
[DE93-754137] p 300 N94-10888
Combustion chamber analysis code
[NASA-CR-192585] p 46 N94-10934
Welding tritium aged stainless steel
[DE93-011782] p 181 N94-11228
Effect of switched-bias bakes on the postirradiation electrical response of MOS devices
[DE93-009629] p 143 N94-11271
Proceedings of the 12th Space Photovoltaic Research and Technology Conference (SPRAT 12)
[NASA-CP-3210] p 48 N94-11380
Radiation effects in heteroepitaxial InP solar cells
p 48 N94-11383
Results of some initial space qualification testing on triple junction a-Si and CuInSe2 thin film solar cells
p 50 N94-11392
Radiation effects in Ga(0.47)In(0.53)As solar cells
p 52 N94-11404
The UoSAT-5 solar cell experiment: First year in orbit
p 53 N94-11409
Potential health effects of space radiation
p 312 N94-11558
Potential techniques for non-destructive evaluation of cable materials
[DE93-008350] p 183 N94-11586
Radiation-induced aperiodicity in irradiated ceramics
[DE93-013335] p 91 N94-11698
The upwelling radiation at the top of the atmosphere in coastal region p 205 N94-11981
On possibility of diamond formations in radiation process p 433 N94-12254
Chemical release and radiation effects (CRRES) data directory
[NASA-CR-192551] p 279 N94-12581

RADIATION HARDENING
Radiation hardened nonvolatile memory for space and strategic applications
[DE93-000746] p 319 N94-10146
Specification and testing for power by wire aircraft
[NASA-TM-106232] p 46 N94-10765
Effect of switched-bias bakes on the postirradiation electrical response of MOS devices
[DE93-009629] p 143 N94-11271

RADIATION HAZARDS
Fully coupled neutronic and hydrodynamic analysis of space nuclear reactor reentry accidents
[DE93-005459] p 372 N94-10890
Radiation considerations for interplanetary missions
p 45 N94-11559

RADIATION MEASUREMENT
An intercomparison of the radium mass standards of the UK and the USSR: 2
[NPL-RSA(EXT)-34] p 359 N94-10266
Demonstration prototype gamma-ray hodoscope alternative to CARGOSCAN for rocket stage monitoring
[DE93-006908] p 169 N94-10326

RADIATION PRESSURE
Using solar flare track densities to determine the origin of interplanetary dust particles p 429 N94-12078

RADIATION PROTECTION
Report on Subgroup on Data Banks for Risk Assessment
[DE93-012150] p 418 N94-10646
A proposed performance index for galactic cosmic ray shielding materials
[NASA-TM-4444] p 484 N94-11278

RADIATION SHIELDING
Proton transport methods for satellite shield modeling
[DE93-013602] p 42 N94-10520
Development of deterministic transport methods for low energy neutrons for shielding in space
[NASA-CR-194172] p 366 N94-11199
A proposed performance index for galactic cosmic ray shielding materials
[NASA-TM-4444] p 484 N94-11278
Radiation considerations for interplanetary missions
p 45 N94-11559

RADIATION SOURCES
Intense neutron sources for fusion materials studies
[DE93-009782] p 391 N94-11171
Advanced concepts theory annual report 1992
[AD-A266132] p 393 N94-11474

RADIATION TOLERANCE
A detailed study of the photo-injection annealing of thermally diffused InP solar cells p 48 N94-11381
High temperature annealing of minority carrier traps in irradiated MOCVD n(+)p InP solar cell junctions
p 48 N94-11382
Radiation effects in heteroepitaxial InP solar cells
p 48 N94-11383
Progress in p(+)n InP solar cells fabricated by thermal diffusion p 48 N94-11384
Electrochemical characterization of p(+)n and n(+)p diffused InP structures p 49 N94-11385
Investigation of the radiation resistance of triple-junction a-Si:H alloy solar cells irradiated with 1.00 MeV protons
p 50 N94-11391
Results of some initial space qualification testing on triple junction a-Si and CuInSe2 thin film solar cells
p 50 N94-11392
Radiation effects in Ga(0.47)In(0.53)As solar cells
p 52 N94-11404
The UoSAT-5 solar cell experiment: First year in orbit
p 53 N94-11409
An overview of the Defence Research Agency photovoltaic programme p 53 N94-11412
Workshop on Heteroepitaxial InP Solar Cells
p 54 N94-11414
Development of plastic capsule for research reactor irradiation
[DE93-753186] p 372 N94-11591

RADIATIVE HEAT TRANSFER
The cloud radiative feedback of a midlatitude squall line system and implication for climate study
[DE93-010511] p 283 N94-10290
The heat transfer by radiation between two media
[DE93-617820] p 149 N94-10838
Meteorological Satellite Center
[MSC-TN-26] p 190 N94-11079
Why convective heat transport in the solar nebula was inefficient p 458 N94-12143

RADIATIVE RECOMBINATION
Time-resolved optical studies of charge relaxation and charge transfer at electrode interfaces
[DE93-013985] p 398 N94-11117
Atomic processes relevant to polarization plasma spectroscopy
[DE93-753240] p 393 N94-11594

RADIATIVE TRANSFER
Conductive-radiative model for predicting the shape of HgI2 crystal grown in the LTVG furnace
p 117 N94-10201
Retrieval of radiation budgets in the Arctic from satellite measurements p 229 N94-10714
Studies of the net surface radiative flux from satellite radiances during FIFE
[NASA-CR-193150] p 230 N94-10953
Simulation of images of water vapor channel and infrared split channel p 190 N94-11081
Effects of satellite spectral resolution and atmospheric water vapor on retrieval of near-ground temperatures
[AD-A264920] p 245 N94-11851
Remote sensing for numerical modelling of radiative transfer processes in ocean environment
p 204 N94-11973
The evaluation of radiative process in the atmosphere-ground system by Monte Carlo method
p 205 N94-11980
An observational search for CO2 ice clouds on Mars
p 441 N94-12054
Multichannel dual angle approach for sea surface temperature retrieval in context of ERS-1 scenario
p 252 N94-12512
Optimal hemicube sampling
[DE93-010499] p 334 N94-12591
Verification of the atmosphere-ocean radiative transfer parametric models p 225 N94-12738

RADIO ALTIMETERS
Topex/Poseidon: A United States/France mission. Oceanography from space: The oceans and climate
[NASA-TM-108253] p 43 N94-10699
Proceedings of First ERS-1 Symposium on Space at the Service of Our Environment, volume 1
[ESA-SP-359-VOL-1] p 232 N94-11704
Effects of wave nonlinearity on ERS-1 radar altimeter returns: A preliminary investigation p 235 N94-11722
The height calibration of the ERS-1 radar altimeter
p 241 N94-11764
Separation of geoid and sea surface topography in shallow water regions: A first ERS-1 radar altimeter data evaluation p 242 N94-11766
Operational ERS-1 orbit determination at D-PAF
p 243 N94-11774
Validating the UK-PAF land ice product surface elevation p 244 N94-11780
Surface roughness variations across the Iceland-Faroes frontal region observed by the GEOSAT altimeter and NOAA AVHRR p 201 N94-11958
On the variability of wind speeds in the North Western Pacific observed by altimeter/GEOSAT and SSM/I/DMSP p 201 N94-11960
Observation of wind and waves by GEOSAT altimeter
p 202 N94-11961
Topography of the Western Mediterranean from the ERS-1 altimeter p 255 N94-12531

RADIO ANTENNAS
Multiple Antenna Implementation System (MAntIS)
[DE93-012515] p 131 N94-10270

RADIO ASTRONOMY
Interstellar scattering and the selection of extragalactic radiosources with highly compact components
p 134 N94-11063
Interstellar scattering and the pulsar studies with space VLBI p 135 N94-11065
The possibility of image restoration under observation in a regime of strong scattering p 136 N94-11068
Detection of dust impacts by the Voyager planetary radio astronomy experiment
[NASA-CR-193281] p 423 N94-11305
Models of Neptune's smooth recurrent radio emission
[NASA-CR-193283] p 484 N94-11312

RADIO BEACONS
Low cost high efficiency GaAs monolithic RF module for SARSAT distress beacons
[NASA-CR-194235] p 146 N94-12773

RADIO COMMUNICATION
Disturbance Impact Assessment System (DIAS), version 2.0. System design document
[AD-A265251] p 138 N94-11883

RADIO EMISSION
Models of Neptune's smooth recurrent radio emission
[NASA-CR-193283] p 484 N94-11312

RADIO EQUIPMENT
Preparing for the initial observations of the Targeted Search and the Sky Survey systems
[NASA-CR-193644] p 318 N94-10865

RADIO FREQUENCIES
Multiple Antenna Implementation System (MAntIS)
[DE93-012515] p 131 N94-10270
Characterization of high-power RF structures using time-domain field codes
[DE93-013416] p 132 N94-10518
Electron runaway in RF discharges
[DE93-771407] p 363 N94-10661
RF vacuum microelectronics
[AD-A266066] p 142 N94-10818
Journal of Research of the National Institute of Standards and Technology, volume 98, number 2, March - April 1993
[PB93-196228] p 485 N94-10850
DILUTE: A code for studying beam evolution under RF noise
[DE93-011605] p 133 N94-10960
Initial assessment of lower hybrid current drive in D3-D
[DE93-013310] p 394 N94-12370
Operational characteristics of a 100-mA, 2-MeV radio-frequency quadrupole
[DE93-014474] p 374 N94-12786

RADIO FREQUENCY HEATING
Conversion of the four-strap array in D3-D to a tunable traveling wave antenna
[DE93-012085] p 137 N94-11453

RADIO GALAXIES
The morphologies of distant radio galaxies
p 426 N94-11597

RADIO INTERFEROMETERS
The influence of the propagation medium on the sensitivity and resolution of meter wavelength aperture synthesis systems p 134 N94-11062
Elimination of the influence of the atmosphere on the accuracy of solutions to astrometric problems by means of a ground-space VLBI network p 136 N94-11071

RADIO OBSERVATION
HF ocean radar system at Okinawa Radio Observatory p 139 N94-11902

RADIO RECEIVERS
Coordinated Radio, Electron, and Waves Experiment (CREWE) for the NASA Comet Rendezvous and Asteroid Flyby (CRAF) instrument
[NASA-CR-194376] p 427 N94-12566

RADIO SIGNALS
Elimination of the influence of the atmosphere on the accuracy of solutions to astrometric problems by means of a ground-space VLBI network p 136 N94-11071
RADIO SOURCES (ASTRONOMY)
Tropospheric and ionospheric effects on differential astrometry with a ground-space based VLBI array
p 136 N94-11070
Models of Neptune's smooth recurrent radio emission
[NASA-CR-193283] p 484 N94-11312
RADIO TELEMETRY
The 17th Transducer Workshop
[AD-A265526] p 141 N94-10509
Remote surface water monitoring radio based telemetry system
[DE93-009643] p 41 N94-11282
RADIO TRANSMISSION
Building penetration loss measurements for DAB signals at 211 MHz
[BBC-RD-1992/14] p 133 N94-11024
Propagation Effects in Space VLBI
p 134 N94-11060
Radiowaves propagation through inhomogeneous interstellar plasma p 134 N94-11061
Interstellar scattering and the selection of extragalactic radiosources with highly compact components
p 134 N94-11063
Intraday variability and the compactness of extragalactic radio sources p 135 N94-11064
RADIO TRANSMITTERS
In-orbit performance tests and tele-command systems of the umbrella test satellite (DEBUT)
[NAL-TR-1165] p 43 N94-10859
Low cost high efficiency GaAs monolithic RF module for SARSAT distress beacons
[NASA-CR-194235] p 146 N94-12773
RADIOACTIVE AGE DETERMINATION
Radiogenic age and isotopic studies
[DE93-610548] p 274 N94-10407
Dispersion of the ratios of cosmogenic isotopes of noble gases in chondrites of different cosmic-ray exposure ages p 428 N94-12020
Peculiarities of distributions of the cosmic-ray exposure ages of H chondrite falls and finds p 428 N94-12021
Search for effects of a supernova explosion 30 to 40 thousand years ago in chondrites p 428 N94-12022
Re-Os dating of 3AB iron meteorites
p 432 N94-12237
The Xe-Q in lodranites and a hint for Xe-L. FRO90011 another lodranite? p 432 N94-12239
On the origin of (4)He and (40)Ar in natural gold
p 87 N94-12240
RADIOACTIVE DECAY
Nuclear astrophysics
[DE93-010569] p 425 N94-10292
The effect of a scalar boson coupled to neutrinos on the behavior of the tritium beta decay spectrum near the end point
[DE93-012655] p 361 N94-10349
On parity conservation and the question of the missing, right-handed neutrino
[DE93-613092] p 361 N94-10414
High efficiency direct thermal to electric energy conversion from radioisotope decay using selective emitters and spectrally tuned solar cells
[NASA-TM-106227] p 47 N94-11307
Tau physics
[DE93-010956] p 367 N94-11469
RADIOACTIVE ISOTOPES
Spin characteristics of ion beams during the motion of electromagnetic elements
[DE93-617448] p 364 N94-10848
RADIOACTIVE MATERIALS
Wind system documentation
[DE93-010381] p 285 N94-11664
Moessbauer spectrometer for mineralogical analysis of the Mars surface: Moessbauer source considerations
p 476 N94-12242
RADIOACTIVE WASTES
Computer models used to support cleanup decision-making at hazardous and radioactive waste sites
[PB93-183333] p 274 N94-10698
RADIOGENIC MATERIALS
The Lathrop Wells Volcanic Center: Status of field and geochronology studies
[DE93-008917] p 273 N94-10285
Radiogenic age and isotopic studies
[DE93-610548] p 274 N94-10407
Noble gases in LEW88516 shergottite: Evidence for exposure age pairing with ALH77005 p 80 N94-12082
Studies of the release of radiogenic Xe-129 from Bjurboele: Evidence against simple diffusion models
p 430 N94-12125
RADIOGRAPHY
Design of inspection and acceptance test methodology for TIG welded aluminum-alloy bracket for camera housings for IRS-1A space craft and executing it
p 61 N94-10037
New x ray scanning topographic approaches to nondestructive evaluation of composites
p 61 N94-10039
RADIOLOGY
Operational radiological support for the US manned space program p 318 N94-11561
RADIOMETERS
Development of a balloon-borne stabilized platform for measuring radiative flux profiles in the atmospheric boundary layer
[DE93-013186] p 274 N94-10323
Coherence effects in radiometry and in spectroscopy
[DE93-013437] p 75 N94-10519
Progress in multidisciplinary design optimization at NASA Langley
[NASA-TM-107754] p 318 N94-10814
Atmospheric correction plans for SeaWiFS
p 204 N94-11975
Radiometer offsets and count conversion coefficients for the Earth Radiation Budget Experiment (ERBE) spacecraft for the years 1987, 1988, and 1989
[NASA-CR-191489] p 286 N94-12772
RADIOMETRIC RESOLUTION
Preliminary results of the experiment I-7
p 235 N94-11728
Calibration of the ERS-1 SAR fast-delivery images
p 236 N94-11730
The use of active devices in the ERS-1 radiometric calibration p 236 N94-11732
An experiment for the radiometric calibration of the ERS-1 SAR p 236 N94-11733
RADIOSONDES
Cloud liquid water content over the Pacific Ocean tropical zone derived from ship microwave radiometric measurement p 225 N94-12743
RADIUM ISOTOPES
An intercomparison of the radium mass standards of the UK and the USSR: 2
[NPL-RSA(EXT)-34] p 359 N94-10266
RADON
Study of the atmospheric chemistry of radon progeny in laboratory and real indoor atmospheres
[DE93-012236] p 266 N94-11671
RAIL TRANSPORTATION
Safety of high speed ground transportation systems: X2000 US demonstration vehicle dynamics trials, preliminary test report, October 1992 - January 1993
[PB93-194645] p 422 N94-10736
Experiment on a high Reynolds number turbulent boundary layer p 164 N94-12617
On the wake behind a high speed train
p 164 N94-12618
RAILGUN ACCELERATORS
Investigation of multiphase railgun systems
p 40 N94-11637
RAIN
The effect of rain on ERS-1 altimeter data
p 243 N94-11773
Flood monitoring in northern part of Central Java by remote sensing technique. Case study: The flooding of Semarang in January, 1990 p 206 N94-11989
Rainfall-runoff estimation using digital radar
[AD-A265390] p 286 N94-12408
The phytoplankton bloom in the Kinu-ura Bay, Japan in the rainy season p 211 N94-12660
Worldwide map of rainfall amount over the ocean derived from passive microwave radiometer p 211 N94-12663
RAIN EROSION
Evaluating the spread of red soil with LANDSAT TM data in coral reefs of Okinawa main island, southwestern Japan p 212 N94-12668
RAIN FORESTS
TREES project: A suite of tools for information extraction from ERS-1 SAR data p 250 N94-12498
RAMAN SPECTRA
Surface-enhanced raman spectroscopy of electroactive films of C60 and an Ir-C60 complex on gold: Symmetry lowering, electron localization, and counteraction effects
[AD-A265934] p 396 N94-10705
Characterization of gas-aerosol interaction kinetics using morphology dependent stimulated Raman scattering
[DE93-012324] p 77 N94-11359
Ecological application of Surface Enhanced Raman Spectroscopy p 227 N94-12756
RAMAN SPECTROSCOPY
Surface-enhanced raman spectroscopy of electroactive films of C60 and an Ir-C60 complex on gold: Symmetry lowering, electron localization, and counteraction effects
[AD-A265934] p 396 N94-10705
RANDOM ACCESS MEMORY
Investigation of soft errors in MOS RAM under influence of heavy ions
[DE92-644554] p 484 N94-10534
Gallium arsenide dynamic random access memory support circuitry
[AD-A265176] p 320 N94-11875
RANDOM PROCESSES
Intermittency following a Hopf bifurcation
[W-9301] p 344 N94-10907
Search for structures in the cosmic microwave background radiation
[INPE-5491-TDI/508] p 484 N94-12357
RANDOM SAMPLING
A CM chondrite cluster and CM streams
p 432 N94-12215
RANDOM VARIABLES
Parametric analysis of atmospheric processes
[NASA-CR-192523] p 347 N94-10757
Monte Carlo algorithms in simulation of 2beta-decay and penetration of electrons through matter
[DE93-617741] p 364 N94-10837
RANDOM VIBRATION
Development of a fatigue analysis approach for CFRP structures under acoustic loading p 58 N94-10018
Sine and random vibration program evaluation on vibration control systems
[DE93-011974] p 188 N94-11460
RANDOM WALK
On a class of two-dimensional nearest neighboring random walks
[CWI-BS-R9220] p 347 N94-10353
Cosmological gamma-ray burst model
[NASA-CR-193368] p 484 N94-10507
The limit of frequency estimation p 356 N94-11001
RAPID QUENCHING (METALLURGY)
Structure and properties of an RS Al-Si-Ni-Mn-Zr alloy for high temperature applications p 64 N94-10063
RAPID TRANSIT SYSTEMS
Safety of high speed ground transportation systems: X2000 US demonstration vehicle dynamics trials, preliminary test report, October 1992 - January 1993
[PB93-194645] p 422 N94-10736
RARE EARTH ELEMENTS
Minor and trace element composition and age of Yukon probable-microtektites p 429 N94-12094
Crystal-chemistry and partitioning of REE in whitlockite
p 408 N94-12174
Anomalous REE patterns in unequilibrated enstatite chondrites: Evidence and implications
p 431 N94-12191
RARE GASES
Joint pain and Doppler-detectable bubbles in altitude (Hypobaric) decompression p 312 N94-11542
Nitrogen and noble gases in a glass sample from LEW88516 p 80 N94-12051
Noble gases in LEW88516 shergottite: Evidence for exposure age pairing with ALH77005 p 80 N94-12082
Noble gas evidence of an aqueous reservoir near the surface of Mars more recently than 1.3 Ga
p 473 N94-12228
The fractionation of noble gases in diamonds of CV3 Efremovka chondrite p 81 N94-12256
RAREFIED GAS DYNAMICS
Three-dimensional hypersonic rarefied flow calculations using direct simulation Monte Carlo method
p 7 N94-10449
RAREFIED PLASMAS
Nonlinear second harmonic generation by light wave-plasma interaction in oscillating magnetic field
[DE93-613723] p 386 N94-10387
RATES (PER TIME)
Rates of fluvio-thermal erosion on Mars
p 435 N94-12018
RATIOS
Damping measurements for ultra-high carbon steel/brass laminates
[DE93-011886] p 82 N94-11076
RATS
Toxicity study of dimethylethoxysilane (DMSES), the waterproofing agent for the Orbiter heat protective system p 318 N94-11554
Mechanistic studies on reduced exercise performance and cardiac deconditioning with simulated zero gravity
p 310 N94-12001
Fluid compartment and renal function alterations in the rat during 7 and 14 day head down tilt
p 310 N94-12002
The organization of the suprachiasmatic circadian pacemaker of the rat and its regulation by neurotransmitters and modulators
[AD-A266113] p 301 N94-12417
RAY TRACING
Source to detector spectrum transformation and its inverse for the Pegasus Z-pinch
[DE93-012674] p 384 N94-10157

Implementation and use of a computational ray-tracing program for the design and analysis of complex optical systems
[AD-A265075] p 382 N94-11653
Optimal hemicube sampling
[DE93-010499] p 334 N94-12591

RAYLEIGH-BENARD CONVECTION
Evaporation under microgravity conditions
p 102 N94-10086
Benard and Marangoni convection in multiple liquid layers p 105 N94-10100
Marangoni-driven solitary waves p 119 N94-10214
Transient effects in the Benard instabilities: Coupling between capillary and gravity effects
p 119 N94-10216
Numerical investigations on Marangoni-Benard instability in multi layer systems p 120 N94-10217
Appearance of convective instabilities caused by liquid-liquid phase separation under small buoyancy forces p 120 N94-10221
Large eddy simulations of time-dependent and buoyancy-driven channel flows p 155 N94-12287
Convective and dynamic instability in meridional trenches p 225 N94-12739

REACTING FLOW
CFD analysis of hypersonic, chemically reacting flow fields p 2 N94-10422
Stability of hypersonic boundary-layer flows with chemistry p 7 N94-10451
Nonequilibrium hypersonic flow in a wind-tunnel nozzle
p 8 N94-10456
Some experimental study and numerical simulation in wind tunnel flow p 8 N94-10457
Hypersonic multi block flow simulations around space vehicles including non-equilibrium chemistry
p 9 N94-10460
Thermal and chemical non equilibrium hypersonic flow computations p 10 N94-10465
Combustion chamber analysis code
[NASA-CR-192585] p 46 N94-10934
CRESLAF. Version 4.0: A Fortran program for modeling laminar, chemically reacting, boundary-layer flow in cylindrical or planar channels
[DE93-012835] p 152 N94-11371
PDF approach for turbulent scalar field: Some recent developments p 160 N94-12315
Theories of turbulent combustion in high speed flows
[AD-A265735] p 79 N94-12403

REACTION BONDING
High-temperature corrosion of ceramic-ceramic composites in a waste incinerator environment
[DE93-012430] p 72 N94-11368

REACTION KINETICS
Chemical pattern formation under microgravity
p 121 N94-10227
The reaction between titanium carbide and aluminium carbide in liquid aluminium; a microgravity study
p 123 N94-10238
Report of the Workshop on Light Particle-Induced Reactions
[DE93-752300] p 360 N94-10317
The intensity of knock in an internal combustion engine: An experimental and modeling study
[DE93-013089] p 177 N94-10322
Comparison of computation and experiment for a high enthalpy, heated-driver, shock-tube environment
p 7 N94-10447
Review of SHARC 2.0 O3 kinetics and spectroscopy
[AD-A265481] p 274 N94-10496
Kinetics of high concentration arsenic deactivation at moderate to low temperatures
[DE93-013349] p 395 N94-10516
A lattice gas model for enzyme kinetics with next-nearest neighbor interactions
[DE93-613026] p 410 N94-10631
Szilard-Chalmers effect in solid HIO4.2H2O by neutron irradiation
[DE93-617173] p 397 N94-10830
Journal of Research of the National Institute of Standards and Technology, volume 98, number 2, March - April 1993
[PB93-196228] p 485 N94-10850
KIVA-3: A KIVA program with block-structured mesh for complex geometries
[DE93-011986] p 77 N94-11249
Synthesis and thermal evolution of structure in alkoxide-derived niobium pentoxide gels
[NASA-TM-106259] p 90 N94-11257
Characterization of gas-aerosol interaction kinetics using morphology dependent stimulated Raman scattering
[DE93-012324] p 77 N94-11359
A model of elementary chemistry and fluid mechanics in the combustion of hydrogen on platinum surfaces
[DE93-012767] p 77 N94-11370
CRESLAF. Version 4.0: A Fortran program for modeling laminar, chemically reacting, boundary-layer flow in cylindrical or planar channels
[DE93-012835] p 152 N94-11371
The evolution equation for the flame surface density in turbulent premixed combustion p 81 N94-12316
Study and modeling of finite rate chemistry effects in turbulent non-premixed flames p 81 N94-12317
Solvent dynamical effects in electron transfer: Molecular dynamics simulations of reactions in methanol
[AD-A266061] p 369 N94-12420

REACTION TIME
Evaluation of the C/EC/KC-135 ground collision avoidance system (GCAS), Study 2
[AD-A265193] p 24 N94-11879

REACTOR CORES
Facility for stress corrosion cracking test of irradiated material in high temperature water
[DE93-753189] p 84 N94-11593

REACTOR DESIGN
A critical assembly designed to measure neutronic benchmarks in support of the Space Nuclear Thermal Propulsion program
[DE92-040974] p 371 N94-10529
Looking beyond ITER: Toroidal concept improvement
[DE93-012762] p 388 N94-10744
Applying design principles to fusion reactor configurations for propulsion in space
[NASA-TM-108247] p 47 N94-11053
Experimental approach to the physics of the high density divertor
[DE93-009149] p 391 N94-11170

REACTOR MATERIALS
High heat flux components and plasma surface interactions
[DE93-008786] p 385 N94-10253
The possibility of using carbon-graphite materials for microwave plasma diagnostics in large fusion devices
[DE93-621609] p 66 N94-11143
Intense neutron sources for fusion materials studies
[DE93-009782] p 391 N94-11171

REACTOR PHYSICS
A critical assembly designed to measure neutronic benchmarks in support of the Space Nuclear Thermal Propulsion program
[DE92-040974] p 371 N94-10529

REACTOR SAFETY
Techniques, processes, and measures for software safety and reliability
[DE93-012379] p 322 N94-10347
Proceedings of the Second Technical Meeting on High Temperature Gas-Cooled Reactors
[DE93-754285] p 371 N94-10719
Fracture mechanics and full scale pipe break testing for the Department of Environment's New Production Reactor-Heavy Water Reactor
[DE93-005428] p 187 N94-11169
GRISET certification package
[DE93-011783] p 327 N94-11246

REACTOR TECHNOLOGY
A critical assembly designed to measure neutronic benchmarks in support of the Space Nuclear Thermal Propulsion program
[DE92-040974] p 371 N94-10529
Intense neutron sources for fusion materials studies
[DE93-009782] p 391 N94-11171
Development of plastic capsule for research reactor irradiation
[DE93-753186] p 372 N94-11591
Research results
[DE93-753403] p 372 N94-11595

READ-ONLY MEMORY DEVICES
Radiation hardened nonvolatile memory for space and strategic applications
[DE93-000746] p 319 N94-10146

READOUT
Method for producing a hybridization of detector array and integrated circuit for readout
[NASA-CASE-NPO-18062-1-CU] p 141 N94-10656

REAL GASES
Issues and approach to develop validated analysis tools for hypersonic flows: One perspective p 7 N94-10446
Real gas and surface transpiration effects upon swept leading edge high speed flow including transition
p 8 N94-10452
On the accuracy and efficiency of CFD methods in real gas hypersonics p 9 N94-10462

REAL NUMBERS
Bounding the Vapnik-Chervonenkis dimension of concept classes parameterized by real numbers
[DE93-011600] p 331 N94-11611

REAL TIME OPERATION
Towards real time numerical stimulation of Marangoni convection: A help for telescience microgravity experiments p 102 N94-10087
Virtual sound for virtual reality
[DE93-010519] p 321 N94-10291
A flexible modelling software for data acquisition
[DE93-612915] p 322 N94-10484
Application of normalized gray-scale correlation
[DE93-013765] p 141 N94-10521
Distributed simulation using a real-time shared memory network
[NASA-TM-106239] p 319 N94-10724
Report of the IAEA Consultants' Meeting on Real-Time Nondestructive Monitoring of Wear and Corrosion Using the Thin Layer Activation Technique
[DE93-617422] p 183 N94-10847
RighTime: A real time clock correcting program for MS-DOS-based computer systems p 334 N94-10986
A real-time spoken-language system for interactive problem solving
[AD-A266046] p 324 N94-11104
Effective software reuse in an embedded realtime system
[AD-A264993] p 326 N94-11220
Application of the airborne ocean color imager for commercial fishing
[NASA-TM-103986] p 231 N94-11378
Spatial light rebroadcaster architecture study
[AD-A266102] p 382 N94-11421
A combustion products analyzer for contingency use during thermodegradation events on spacecraft
p 318 N94-11555
Teaching high-performance skills using above-real-time training
[NASA-CR-4528] p 315 N94-11627
Parametric study of diffusion-enhancement networks for spatiotemporal grouping in real-time artificial vision
[AD-A265065] p 331 N94-11652
Real-time tomography mooring
[AD-A264923] p 289 N94-11854
Distributed real-time system design: Theoretical concepts and applications
[AD-A265199] p 337 N94-11881
ISAR motion compensation using the burst derivative measure as a focal quality indicator
[AD-A265647] p 138 N94-12440
Real time processing wave spectra from satellite SAR
p 251 N94-12506
A user appraisal of ATSR near-real-time products
p 252 N94-12516
Networks of real-time processes
[DE93-013049] p 338 N94-12597
An integrated approach to total end-to-end quality control of ocean data in the real-time environment
p 211 N94-12662
Novel mass spectrometric instrument for gaseous and particulate characterization and monitoring
[DE93-014093] p 272 N94-12783

RECEIVERS
Diagnostic complex for the space-time analysis of energy and current of pulsed relativistic particles
[DE93-620980] p 362 N94-10649
Progress on GPS standardization p 24 N94-10965
Workshop summary: Receivers for laser power beaming p 54 N94-11419
Airborne optical tracking control system design study
[DE93-009515] p 382 N94-11662
Studies of electrostatic waves and VLF-wave particle interaction in the ionosphere
[AD-A266013] p 278 N94-12392

RECEPTORS (PHYSIOLOGY)
Probability of alamethicin conductance states varies with nonlamellar tendency of bilayer phospholipids
[AD-A264957] p 301 N94-11648

RECESSION
Rates of fluvio-thermal erosion on Mars
p 435 N94-12018

RECOMBINATION REACTIONS
Surface passivation of InP solar cells with InAlAs layers p 49 N94-11389

RECONNAISSANCE
Integrating the services' imagery architectures
[AD-A265487] p 171 N94-12335

RECRYSTALLIZATION
Petrography and preliminary interpretations of the crystalline breccias from the Manson M-1 core
p 281 N94-12056
Simulation of possible regolith optical alteration effects on carbonaceous chondrite meteorites
p 430 N94-12163

RECTANGULAR WAVEGUIDES
Nonlinear instability of a laminar flow in a rectangular duct and generation of the turbulent secondary flow
p 164 N94-12622

RECTENNAS
Construction and testing of a space ready rectenna
[NASA-CR-193310] p 137 N94-11357

RECURSIVE FUNCTIONS
Deformations and recursion operators for evolution equations
[MEMO-1104] p 341 N94-10163
RECYCLING
Environmental Protection Agency's life cycle methodology: Guidelines for use in development of packaging
[PB93-194199] p 265 N94-10841
Some environmental aspects of the application of fibre reinforced plastics in structures
[LM-998] p 88 N94-10877
RED TIDE
Satellite observations of red tide events: Plans for EESI p 191 N94-11899
REDOX CELLS
Technical Update: Johnson Space Center system using a solid electrolytic cell in a remote location to measure oxygen fugacities in CO/CO2 controlled-atmosphere furnaces
[NASA-TM-104774] p 423 N94-11183
REDUCED GRAVITY
Proceedings of the 8th European Symposium on Materials and Fluid Sciences in Microgravity, volume 1
[ESA-SP-333-VOL-1] p 99 N94-10070
Experimental study of axisymmetric thermocapillary flows p 100 N94-10072
The use of magnetic fields for damping unsteady Marangoni convection in GaAs floating zones under microgravity p 100 N94-10073
Transient three-dimensional numerical simulation of Marangoni flow in a liquid column under microgravity p 101 N94-10079
Effect of rotation on microgravity floating-zone crystal growth p 101 N94-10080
On shape of single crystals grown by FZM in microgravity p 102 N94-10084
Liquid bridges and floating zones p 102 N94-10085
Model of convective motion under low gravity p 103 N94-10088
Gas-liquid jets under reduced gravity conditions p 103 N94-10091
Heat and mass transfer mechanisms of the polymerization under terrestrial and microgravity conditions p 103 N94-10092
High Prandtl number fluids in a multilayered system under 1-g or micro-g environment p 104 N94-10096
Bubbles and drops behaviour under low-gravity: A space experiment for the IML-2 mission p 104 N94-10098
Space and temporal behavior and control of the residual convection in microgravity p 104 N94-10099
Measurement of the thermal conductivity of molten InSb in a drop shaft p 105 N94-10102
The effect of gravity modulation on thermosolutal convection p 105 N94-10103
Separation of gravitational effects on the flow of suspension in tubes by measurements in weightlessness p 105 N94-10105
Numerical simulation of Marangoni convection around gas bubbles in a liquid matrix p 106 N94-10107
Propellant management in surface tension tanks p 106 N94-10110
CdTe crystal growth in the Soviet facility zona 4 p 106 N94-10111
The pyrene laser induced fluorescence technique as a diagnostic tool for combustion thermometry in microgravity p 107 N94-10113
A new method for hysteresis measurements developed for C(sub v) measurements at the critical point during the D2-mission p 107 N94-10114
CdTe crystal growth by THM with a rotating magnetic field p 107 N94-10116
Advanced protein, crystallization facility and associated new developments p 39 N94-10119
Design of multisample, multistep phase partitioning apparatus for use on Space Shuttle Spacelab, and Spacelab missions p 108 N94-10120
Calibration of accelerometers on drop tower Bremen p 108 N94-10121
Gas film levitator for containerless processing of glasses in microgravity conditions: Early concept and technology demonstration p 108 N94-10122
Holographic interferometry for microgravity applications p 108 N94-10123
The High Precision Thermostat HPT-HYDRA p 109 N94-10124
TEMPUS: An electromagnetic levitation facility for containerless processing under micro-g in Spacelab p 109 N94-10125
The electron beam furnace: A new facility for materials science research p 109 N94-10126
Design of a CVD reactor for the deposition of diamond in a microgravity environment p 109 N94-10127
Microgravity Applications Furnace Facility (MAFF) for parabolic flights p 109 N94-10128
Force and power efficiency of micro-g electromagnetic levitation coils p 110 N94-10129
High temperature processing and diagnostic technologies for microgravity applications p 110 N94-10130
Determination of the viscous acoustic field for liquid drop positioning/forcing in an acoustic levitation chamber in microgravity p 110 N94-10131
MUZO: The programmable multi zone furnace for gas payloads and sounding rockets p 110 N94-10132
The surface plasmon spectroscopy as diagnostic technique in microgravity experiments p 110 N94-10133
TOLS (Telescience On-Line Simulator): An essential instrument for micro-gravity interactive experiment p 39 N94-10134
Laser beam deflection: A diagnostic tool for vapour growth experiments in microgravity p 111 N94-10135
The advanced fluid physics module: How to achieve scientific goals for Spacelab D2 p 39 N94-10136
Results of mission preparation support to microgravity experiments on board of Eureca 1 p 111 N94-10138
AGF (Automatic Gradient Furnace): A proposed microgravity facility p 112 N94-10141
Microgravity experiments using TR-1A rocket p 112 N94-10142
Proceedings of the 8th European Symposium on Materials and Fluid Sciences in Microgravity, volume 2
[ESA-SP-333-VOL-2] p 112 N94-10171
Thermocapillary convection instability in microgravity crystal growth p 112 N94-10172
STARDUST: A simulation experiment of cosmic dust analogues production in microgravity conditions p 113 N94-10175
Solidification from supercooled melt under microgravity p 113 N94-10176
Scientific specifications for an automated facility for growing large semiconducting crystals from the melt in space p 114 N94-10180
Results of crystal growth experiments by FZM on Zona facilities in microgravity p 116 N94-10193
Effects of a microgravity environment on the crystallization of biological macromolecules p 117 N94-10198
Solidification and metastable phase formation of highly undercooled Fe-Cr-Ni alloy melts p 87 N94-10204
Containerless processing of equiatomic Mn50Bi50 in a drop tube p 118 N94-10205
Liquid phase sintering of tungsten composites under microgravity. Effect of matrix composition p 118 N94-10207
Crystallization of zeolites in the microgravity environment of space p 119 N94-10210
A study of the quasibinary Al-W-Mo system. Part 1: Preliminary investigations and preparation for microgravity experiments p 119 N94-10211
Instability of thermocapillary convection in multiple superposed immiscible liquid layers p 120 N94-10218
Influence of neutral particles concentration on flame propagation in methane-air mixtures at zero and normal gravity conditions p 121 N94-10224
Surface tension and adsorption kinetics in immiscible liquid systems at microgravity p 121 N94-10225
Gravity and electric field effects on pool boiling heat transfer p 121 N94-10226
Chemical pattern formation under microgravity p 121 N94-10227
Transport of heat and mass in near-critical fluids p 122 N94-10230
Study of vapor bubble growth in a supersaturated liquid p 122 N94-10232
Phase separation at gas-liquid critical points p 122 N94-10233
Electrohydrodynamic effects in continuous flow electrophoresis observations on Earth and in microgravity p 122 N94-10234
Interface reactions of (Ni3Al) ribbons/Al-MMC in ground preparation as preliminary test for microgravity experiments p 123 N94-10237
The reaction between titanium carbide and aluminium carbide in liquid aluminium; a microgravity study p 123 N94-10238
Laser cooling and trapping of atoms in microgravity: Ultracold atoms collisions p 124 N94-10241
Single bubble experiments in pool boiling: Results from TEXUS 26 p 124 N94-10243
Some aspects of combustion modelling by low and normal gravity p 124 N94-10244
Photoinitiated radical polymerization of liquid monomers in microgravity p 124 N94-10246
A method for determination of the elongational viscosity of viscoelastic fluids without body forces p 124 N94-10247
Microgravity combustion of dust suspension in a spherical chamber p 80 N94-10248
The International Microgravity Laboratory, a Spacelab for materials and life sciences p 125 N94-10249
Large amplitude shape oscillations in a mercury drop using a drop tower
[DE93-767972] p 125 N94-10730
Effects of CSF hormones and ionic composition on salt/water metabolism
[NASA-CR-193232] p 300 N94-11045
Measuring human performance on NASA's microgravity aircraft p 317 N94-11537
A mechanism for the reduction in risk of decompression sickness in microgravity environment p 312 N94-11545
Comprehensive analysis of airborne contaminants from recent Spacelab missions p 318 N94-11553
Carotid-cardiac baroreflex: Relation with orthostatic hypotension following simulated microgravity and implications for development of countermeasures p 308 N94-11992
Pulmonary function in microgravity: KC-135 experience p 309 N94-11994
Central circulatory hemodynamics as a function of gravitational stress p 309 N94-11995
Autogenic-feedback training: A countermeasure for orthostatic intolerance p 311 N94-12006
REDUCTION (CHEMISTRY)
Effects of microscopic iron metal on the reflectance spectra of glass and minerals p 436 N94-12024
Thermodynamics of lunar ilmenite reduction p 415 N94-12028
The spectral effects of subsolidus reduction of olivine and pyroxene p 81 N94-12110
Oxidation state of the Earth's upper mantle during the last 3800 million years: Implications for the origin of life p 283 N94-12210
REED-SOLOMON CODES
An investigation of error characteristics and coding performance
[NASA-CR-193620] p 324 N94-10932
REENTRY TRAJECTORIES
Aerodynamic and aerothermal challenges for the design of the Hermes spaceplane p 3 N94-10423
REENTRY VEHICLES
Planetary entry vehicle design for planned and potential ESA missions to Titan, Mars, and Earth return (FGE TN 51/92) p 4 N94-10428
Synthesis of the Workshop on Hypersonic Flows for ReEntry Problems p 5 N94-10440
Local aerothermal problems during Hermes re-entry p 10 N94-10464
Progress in modeling hypersonic turbulent boundary layers p 157 N94-12300
REFERENCE SYSTEMS
Toward 10(exp 9) GPS geodesy: Vector baselines, Earth rotation and reference frames
[NASA-CR-193184] p 229 N94-10702
REFINING
Highly anisotropic but nodeless gap from a valence-fluctuation pairing mechanism
[DE93-010738] p 401 N94-11646
REFLECTANCE
Effects of energetic particle events on VLF/LF propagation parameters/1989
[AD-A265266] p 275 N94-11013
An expert system shell for inferring vegetation characteristics: Prototype help system (Task 1)
[NASA-CR-193411] p 231 N94-11236
Needs for super-smooth surfaces
[DE93-012482] p 382 N94-11242
Formulating infrared coatings for defence applications
[MRL-RR-1-93] p 90 N94-11302
On the coupling of electromagnetic radiation into cavities
[DE93-011406] p 137 N94-11621
Feature association without a motion estimate
[AD-A265162] p 138 N94-11891
Effects of microscopic iron metal on the reflectance spectra of glass and minerals p 436 N94-12024
Simulation of possible regolith optical alteration effects on carbonaceous chondrite meteorites p 430 N94-12163
REFLECTED WAVES
Retrieval of radiation budgets in the Arctic from satellite measurements p 229 N94-10714
REFLECTOMETERS
Ocean measuring experiments using optical fiber distributed temperature sensor p 172 N94-11968
REFLECTOR ANTENNAS
PO/PTD diffraction synthesis of array-fed reflector antennas for satellite and radar applications p 137 N94-11636
REFLECTORS
Universal adjustable mould for antenna reflectors p 59 N94-10027
Damage thresholds of fluoride multilayers at 355 nm
[DE93-009523] p 90 N94-11230

Feature association without a motion estimate
[AD-A265162] p 138 N94-11891
Using lunar sounder imagery to distinguish surface from subsurface reflectors in lunar highlands areas
p 464 N94-12179
Spatial light modulator having photosensitive and ferroelectric layers
[AD-D015731] p 404 N94-12400

REFLEXES
Carotid-cardiac baroreflex: Relation with orthostatic hypotension following simulated microgravity and implications for development of countermeasures
p 308 N94-11992

REFRACTIVITY
The sensitivity of an optical fiber holographic interferometer p 107 N94-10117
Demonstration designs for optical-field-ionized plasma x-ray lasers
[DE93-009227] p 175 N94-11266
Laser photoheterodyne interferometers for oceanographic investigations p 177 N94-12732

REFRACTORY MATERIALS
High temperature materials for hypersonic transport
p 56 N94-10003
Distortions and stresses in thin shells due to anisotropic thermal expansion p 57 N94-10014
An ultralight carbon-carbon composite with amorphous matrix p 61 N94-10042
Ceramic matrix composites: High performance materials for space application p 62 N94-10044
Joints between dissimilar metallic and ceramic materials p 63 N94-10052
Advanced methods of permanently joining carbon materials p 63 N94-10057
High temperature composites in Aerospatiale activities
p 64 N94-10062
Structure and properties of an RS Al-Si-Ni-Mn-Zr alloy for high temperature applications p 64 N94-10063
Fibre reinforced structures with glass matrix
p 64 N94-10064
STARDUST: A simulation experiment of cosmic dust analogues production in microgravity conditions
p 113 N94-10175
Space Storable Rocket Technology program (SSRT). Option 1 program
[NASA-CR-191171] p 46 N94-10938
Thermal stability of sealants for military aircraft: Modification of polysulfide prepolymers with ether and thioether monomers
[AD-A264079] p 89 N94-11107
The giant impact produced a precipitated Moon
p 430 N94-12135
Ceramics formed by pyrolysis of either linear or thermosetting carborane (siloxane or silane) acetylene based precursor polymers
[AD-D015747] p 93 N94-12330
Synthesis and polymerization of oligomeric multiple aromatic ether-containing phthalonitriles
[AD-D015729] p 94 N94-12399

REFRACTORY METAL ALLOYS
Structural material, manufacture, and design requirements for high-temperature fasteners for space plane technologies p 63 N94-10055
Constitutive laws for describing the service relevant creep behaviour of metallic materials p 64 N94-10060

REFRACTORY METALS
Chemical Vapor Deposition of Refractory Metals and Ceramics 2. Materials Research Society Symposium proceedings
[AD-A265072] p 92 N94-11866
Isotopic and trace element characteristics of an unusual refractory inclusion from Essebi p 471 N94-12212

REFRIGERANTS
Theoretical evaluation of R22 and R502 alternatives
[DE93-014767] p 411 N94-10853
Measurement of viscosity, density and gas solubility of refrigerant blends
[DE93-014772] p 89 N94-11145
Accelerated screening methods for predicting lubricant performance in refrigerant compressors
[DE93-014773] p 89 N94-11146

REFRIGERATING MACHINERY
Accelerated screening methods for predicting lubricant performance in refrigerant compressors
[DE93-014773] p 89 N94-11146

REFRIGERATORS
The superfluid Stirling refrigerator, a new method for cooling below 0.5 K
[DE93-012672] p 128 N94-11161
The Second Workshop on Refrigerating System Utilization Onboard the JEM
[NASDA-CON-930001] p 129 N94-11831
Summary of the pre-AO of the JEM onboard scientific and engineering experiments for refrigerator utilization
p 129 N94-11832
Development of space refrigerator
p 129 N94-11833
Studies on refrigerator sensors and cooling section interface p 129 N94-11834
Trend of miniature refrigerator utilization in earth observation area p 130 N94-11835
Satellite observation of atmospheric tracer components: JEM/POP p 130 N94-11836
Submillimeter wave observation experiment of Earth atmosphere with SIS mixer p 130 N94-11837
Refrigerator utilization in infrared astronomy
p 130 N94-11838
Study on various cryogenic refrigeration cycles using all purpose refrigerators p 130 N94-11839
Development test on 2 K cooling systems
p 130 N94-11840
Generation of superfluid He by G-M cycle cryogenic refrigerator p 130 N94-11841
Development of 4 K refrigerator using highly efficient heat accumulating reservoir p 130 N94-11842
Utilization of superconductivity in the area of space
p 131 N94-11843

REFUELING
Vehicular fleet operation on natural gas and propane: An overview
[PB93-194603] p 98 N94-10844
Business fleet refueling assessment
[PB93-189892] p 98 N94-11017
On-orbit refueling p 38 N94-11565
On-orbit refueling p 38 N94-11566
Preliminary analysis of the benefits derived to US Air Force spacecraft from on-orbit refueling
p 38 N94-11567

REGENERATION (ENGINEERING)
Regeneration of near-wall turbulence structures
p 158 N94-12308

REGENERATIVE FUEL CELLS
Computation of photovoltaic parameters under lunar temperature variation p 53 N94-11411

REGGE POLES
Model for the pomeron
[DE93-617693] p 362 N94-10552

REGIONAL PLANNING
Summary of implementation and demonstration projects in bays and estuaries
[PB93-194637] p 265 N94-10846

REGISTERS (COMPUTERS)
Simulation of a parallel computer
[NAL-TR-1154] p 335 N94-10368
Wait-free linearization with an assertional proof
[CS-9208] p 323 N94-10878

REGOLITH
Cold press sintering of simulated lunar basalt
p 131 N94-12026
Apollo 16 core 60013/14 as a product of path 1 and path 2 regolith evolution processes p 440 N94-12050
The spectral effects of subsolidus reduction of olivine and pyroxene p 81 N94-12110
Impact comminution of glasses: Implications for lunar regolith evolution p 461 N94-12159
Simulation of possible regolith optical alteration effects on carbonaceous chondrite meteorites
p 430 N94-12163
Porosity and the ecology of icy satellites
p 431 N94-12186

REGRESSION ANALYSIS
Applicability of satellite infrared data for the monitoring of coastal environments p 220 N94-12714

REGULATIONS
Aircraft material fire testing and the creation of an international working group p 21 N94-10790
Development of a hypermedia knowledge base of aircraft fire safety regulations p 21 N94-10793
The future of aircraft cabin fire safety
p 22 N94-10797
Toxic chemical release inventory reporting Form R and instructions. Revised 1992 version. Section 313 of the Emergency Planning and Community Right-to-Know Act
[PB93-194140] p 264 N94-10836

REGULATORY MECHANISMS (BIOLOGY)
The organization of the suprachiasmatic circadian pacemaker of the rat and its regulation by neurotransmitters and modulators
[AD-A266113] p 301 N94-12417

REINFORCED PLASTICS
Advanced Materials for Lightweight Structures
[ESA-SP-336] p 56 N94-10001
Applications of continuous fiber reinforced thermoplastics in aircraft interiors p 18 N94-10775

REINFORCEMENT (PSYCHOLOGY)
Computer software and hardware to determine contrast sensitivity using three methods: Tracking, limits, and constant stimuli
[AD-A265168] p 324 N94-11099

REINFORCEMENT (STRUCTURES)
Three-dimensional finite element analysis of explosive safety facilities: A technology assessment
[AD-A265700] p 35 N94-12562

REINFORCING FIBERS
Design concepts for load-carrying hot structures for reentry bodies p 57 N94-10012
Damping mechanisms in chemically vapor deposited SiC fibers
[NASA-TM-106334] p 66 N94-11135
An analysis of fiber-matrix interface failure stresses for a range of ply stress states
[NASA-TM-108999] p 67 N94-11276
Mechanical interaction between synthetic fiber and cement base matrix in FRC composites
[AD-A265310] p 73 N94-11686
Electronic and total energy properties of ternary and quaternary semiconductor compounds, alloys and superlattices
[NASA-CR-192905] p 405 N94-12570

RELATIVE BIOLOGICAL EFFECTIVENESS (RBE)
Potential health effects of space radiation
p 312 N94-11558

RELATIVISTIC EFFECTS
Efficiency of fast wave current drive for a weakly relativistic plasma
[DE93-012775] p 385 N94-10159
Electron momentum spectroscopy of atoms, molecules and solids
[DE93-610148] p 360 N94-10332
On the relativistic string size at finite temperature
[DE93-617658] p 409 N94-10394
Quasi-relativistic effects in barrier-penetration processes
[DE93-617730] p 410 N94-10721

RELATIVISTIC ELECTRON BEAMS
An experimental program for collective acceleration of ions using intense relativistic electron beams
[DE93-612205] p 371 N94-10316
Scattering of modulated Ultra-Relativistic Electron Beam (UREB) by atmospheric plasma
[DE93-620987] p 387 N94-10558

RELATIVISTIC PARTICLES
Diagnostic complex for the space-time analysis of energy and current of pulsed relativistic particles
[DE93-620980] p 362 N94-10649
Quantized conic sections; quantum gravity
[DE93-010950] p 411 N94-10956
Relativistic heavy-ion collisions
[DE93-014844] p 366 N94-11147
Experimental investigation of wake field excitation in plasma by a periodic succession of relativistic particle clots
[DE93-621655] p 391 N94-11211

RELATIVISTIC PLASMAS
Efficiency of fast wave current drive for a weakly relativistic plasma
[DE93-012775] p 385 N94-10159
Collective acceleration of ions in near-anode plasma of a strong-current relativistic diode
[DE93-620977] p 387 N94-10541
Filamentation instability of hot quark-gluon plasma with hard jet
[DE93-617679] p 388 N94-10882

RELATIVISTIC THEORY
Two fluid plasmas in the vicinity of a Schwarzschild black hole
[DE93-610264] p 385 N94-10284
From the Weyl theory to a theory of locally anisotropic space-time
[DE92-644734] p 410 N94-10535
On the doubling of hydrodynamic theorems in relativistic theory of superfluidity
[DE93-617895] p 148 N94-10717

RELATIVITY
Standard model status (in search of new physics)
[DE93-013288] p 410 N94-10528
From the Weyl theory to a theory of locally anisotropic space-time
[DE92-644734] p 410 N94-10535
The uncertainty principle in resonant gravitational wave antennae and quantum non-demolition measurement schemes p 378 N94-10587
Dimensional transition of the space-time at the minimum action near the planck scale
[DE93-754192] p 410 N94-10718
Explorations in quantum gravity: From one loop effective actions to two-dimensional theories p 413 N94-11822

RELAXATION (MECHANICS)
Viscous relaxation of the Moho under large lunar basins p 452 N94-12113

RELAXATION METHOD (MATHEMATICS)
A new heuristic for set covering problems
[INPE-5471-TDI/502] p 333 N94-12358

Aspects of applying a relaxation method to computing sea surface velocities from sea surface temperature images p 214 N94-12679

RELIABILITY

A reliable stability test for exponential polynomials
[MEMO-COSOR-92-48] p 341 N94-10168

RAMCAD (reliability, availability, and maintainability in computer-aided design)
[AD-A265143] p 331 N94-11679

RELIABILITY ANALYSIS

Bayesian reliability analysis with imprecise prior probabilities
[MEMO-COSOR-92-50] p 183 N94-10170

Investigation of alternate power source for Space Shuttle Orbiter hydraulic system
[NASA-CR-193229] p 46 N94-10911

Applying reliability models to the maintenance of Space Shuttle software p 330 N94-11434

Reliability analysis for FDDI dual homing networks
[AD-A266133] p 337 N94-11475

RELIABILITY ENGINEERING

A Recommended Methodology for Quantifying NDE/NDI Based on Aircraft Engine Experience
[AGARD-LS-190] p 28 N94-11022

RELIEF MAPS

The extraction of bottom characteristics and mapping in Kin Bay, Okinawa Main Island, Japan, using LANDSAT-5/TM and SPOT-1/HRV data
p 197 N94-11931

An ancient inner lake in Maadim Vallis
p 456 N94-12133

RELIEF VALVES

Dual valve plate two-way pressure relief valve
[AD-D015766] p 178 N94-10379

REMOTE CONSOLES

The warm eddy detection from NOAA/AVHRR thermal images using the Hough transformation
p 220 N94-12713

REMOTE CONTROL

Towards real time numerical stimulation of Marangoni convection: A help for telescience microgravity experiments p 102 N94-10087

TOLS (Telescience On-Line Simulator): An essential instrument for micro-gravity interactive experiment
p 39 N94-10134

Analysis of the alignment of a Schlieren system for tele-operation p 111 N94-10140

A portable controller for unmanned ground vehicles
[AD-A264963] p 181 N94-11290

REMOTE MANIPULATOR SYSTEM

Momentum management in redundant manipulators for vibration suppression
[NASA-CR-194112] p 180 N94-10821

REMOTE REGIONS

Space technology in remote health care
p 306 N94-11799

REMOTE SENSING

Space Activities in the Asia Pacific Region
[JTN-93-80421] p 35 N94-10676

Current status of space activities in Asia Pacific region
p 35 N94-10677

Considerations for future regional space cooperation
p 35 N94-10678

Space research and remote sensing programmes in Bangladesh p 35 N94-10679

Space program in Indonesia p 36 N94-10681

Space programme in Malaysia p 36 N94-10685

National space programmes and application of the remote sensing data in Mongolia p 36 N94-10686

Status of remote sensing and Geographic Information System (GIS) applications in the Environment and Natural Resources (ENR) sector p 36 N94-10687

Russian space system for the Earth remote sensing
p 37 N94-10688

Sun-synchronous and geo-synchronous satellite data utilization for environmental studies p 37 N94-10689

Thailand ISY activities p 37 N94-10690

National space program in Australia
p 37 N94-10691

Panel discussion: Role of space program in the Asia Pacific Region p 37 N94-10694

Topex/Poseidon: A United States/France mission. Oceanography from space: The oceans and climate
[NASA-TM-108253] p 43 N94-10699

A browse facility for Earth science remote sensing data: Center director's discretionary fund final report
[NASA-TM-108413] p 419 N94-10723

Meteorological Satellite Center
[MSC-TN-26] p 190 N94-11079

An expert system shell for inferring vegetation characteristics: Prototype help system (Task 1)
[NASA-CR-193411] p 231 N94-11236

Remote surface water monitoring radio based telemetry system
[DE93-009643] p 41 N94-11282

Atmospheric correction of AVIRIS data in ocean waters
[AD-A264931] p 288 N94-11287

Enhancement effects in polarimetric radar returns: Phase difference statistics
[NASA-CR-193408] p 231 N94-11309

Extended ecosystem signatures with application to Eos synergism requirements
[NASA-CR-193398] p 266 N94-11374

Application of the airborne ocean color imager for commercial fishing
[NASA-TM-103986] p 231 N94-11378

Satellite inventory of Minnesota forest resources
[NASA-CR-193565] p 231 N94-11521

Landsat as a commercial enterprise
[INPE-5477-TAE/019] p 232 N94-11524

More sense for less cents: Cost effective servicing of remote sensing satellites p 348 N94-11572

Activities relating to understanding the initiation, organization and structure of moist convection in the Southeast environment
[NASA-CR-193829] p 285 N94-11598

Proceedings of First ERS-1 Symposium on Space at the Service of Our Environment, volume 1
[ESA-SP-359-VOL-1] p 232 N94-11704

Sea ice: A climate component p 232 N94-11705

Calibration and validation of the ERS-1 wind scatterometer p 232 N94-11706

Validation of directional wave spectra from the ERS-1 during the ESA CAL/VAL campaign p 232 N94-11707

The Grand Banks ERS-1 SAR wave spectra validation experiment p 232 N94-11708

ERS-1 scatterometer data characteristics and wind retrieval skill p 233 N94-11709

Validation of ERS-1 wind and wave data by use of operational forecast models p 233 N94-11710

A C-band wind scatterometer model derived from the data obtained during the ERS-1 calibration/validation campaign p 233 N94-11711

ERS-1 studies at the Department of Oceanography from Space, IFREMER/Brest (France) p 233 N94-11712

The activity of the ERS-1 Venice (Italy) group on scatterometry p 233 N94-11713

Use of ERS-1 data at Saclant Undersea Research Centre p 233 N94-11714

A preliminary C-band scatterometer model function for the ERS-1 AMI instrument p 233 N94-11715

Mapping of the East Australian current with the ERS-1 SAR and shipborne studies p 234 N94-11717

Wind and surface features in SAR images: The Canadian program p 234 N94-11718

Preliminary analysis of circulations over the Indian Ocean and adjoining regions using ERS-1 surface winds in the NCMRWF data assimilation system p 234 N94-11719

Coastal ocean studies with ERS-1 SAR during NORCSEX 1991 p 234 N94-11720

SAR imaging of dynamical features in the English Channel p 234 N94-11721

Effects of wave nonlinearity on ERS-1 radar altimeter returns: A preliminary investigation p 235 N94-11722

SAR ocean imaging in the Gulf of Alaska
p 235 N94-11723

Evaluation of two January - June 1992 ERS-1 AMI wind vector data sets p 235 N94-11724

Comparisons of ERS-1 altimeter height data and the Fine Resolution Antarctic Model (FRAM)
p 235 N94-11725

Calibration results for the ERS-1, AIRSAR, and PHARS p 236 N94-11731

Techniques and applications of SAR interferometry for ERS-1: Topographic mapping, change detection, and slope measurement p 236 N94-11734

SAR interferometry experiments with ERS-1
p 237 N94-11735

SAR-interferometry applying ERS-1: Some preliminary test results p 237 N94-11736

Signatures of Antarctic firn by means of ERS-1 AMI and by field measurements p 237 N94-11737

Analysis of ERS-1 altimeter data over the polar ice sheets p 237 N94-11738

Some results of the derivation of ice sheet elevations in Antarctica from ERS-1 altimeter data
p 237 N94-11739

Utilisation of ERS-1 data for mapping of Antarctica
p 237 N94-11740

Monitoring of the Greenland Ice Sheet using ERS-1 synthetic aperture radar imagery p 237 N94-11741

Preliminary evaluation of ERS-1 altimetry over Filchner-Ronne Ice Shelf, Antarctica
p 238 N94-11742

Investigations of Arctic ice-sheets and glaciers using ERS-1 SAR p 238 N94-11743

Spatial patterns in backscatter strength across the Greenland Ice Sheet p 238 N94-11744

Ice studies in the Barents Sea by ERS-1 SAR during SIZEX 92 p 238 N94-11745

Use of ERS-1 SAR to measure ice flux in the East Greenland current p 238 N94-11746

Validation of ERS-1 SAR measurements of sea ice during ARCTIC-1991 p 238 N94-11747

Arctic coastal polynya observations with ERS-1 SAR and DMSP SSM/I p 239 N94-11748

Sea ice deformation observed with ERS-1 SAR
p 239 N94-11749

Finnish ERS-1 Baltic Sea ice experiment in Winter 1992 p 239 N94-11750

Experiences from the Swedish sea ice programme during BEERS-1992 p 239 N94-11751

Greenland Sea observations p 239 N94-11752

Air-sea-ice interactions in the Weddell Sea
p 239 N94-11753

Arctic sea ice microwave signature and geophysical processes study p 240 N94-11754

C-band SAR backscatter from ice on shallow tundra lakes: Observations and modelling p 240 N94-11755

Sea ice radar signatures from ERS-1 SAR during late Summer and Fall in the Beaufort and Chukchi Seas
p 240 N94-11756

Waves and mesoscale features in the marginal ice zone p 240 N94-11757

The seasonal Sea Ice Monitoring and Modelling Site (SIMMS): Using ERS-1 in climate research
p 240 N94-11758

Ocean circulation revealed by ice floe tracking
p 240 N94-11759

Preliminary evaluation of ERS-1 SAR data for operational use in the Canadian sea ice monitoring program
p 241 N94-11760

Sea ice feature and type identification in merged ERS-1 SAR and LANDSAT Thematic Mapper imagery
p 241 N94-11761

Summer Arctic ice concentrations and characteristics from SAR and SSM/I data p 241 N94-11762

Evaluating ERS-1 ice motion and classification products p 241 N94-11763

First results for the simultaneous estimation of the geoid and the sea surface topography by ERS-1 altimeter data
p 241 N94-11765

Quick-look monitoring of the sea surface with ERS-1 fast delivery altimeter data p 243 N94-11777

Satellite, environmental, and medical information applied to epidemiological monitoring p 307 N94-11802

Satellite observation of atmospheric tracer components: JEM/POP p 130 N94-11836

Effects of satellite spectral resolution and atmospheric water vapor on retrieval of near-ground temperatures
[AD-A264920] p 245 N94-11851

Effect of species structure and dielectric constant on C-band forest backscatter
[NASA-TM-109219] p 245 N94-11885

Proceedings of the PORSEC 1992 in Okinawa: Conference for Pacific Ocean Environments and Probing, volume 1
[JTN-93-80418] p 191 N94-11894

Remote sensing and global environment
p 191 N94-11895

Remote sensing and the air-sea boundary layers
p 191 N94-11896

Effects of wind-roughened sea surface on ocean color remote sensing: Noise derived from reflected light and whitecaps p 191 N94-11898

Satellite observations of red tide events: Plans for EESI p 191 N94-11899

An algorithm for the detection of mucilage (green slime) in the Adriatic Sea p 191 N94-11900

Remote sensing of the suspended matter distribution with high concentration in China Sea
p 192 N94-11901

Kuroshio observations by the HF ocean radar
p 192 N94-11904

Statistical study of HF ocean radar echo
p 139 N94-11905

Satellite derived sea surface temperature applications for Indian Ocean resources development
p 193 N94-11907

Exchange of bay water with ocean current monitored by the NOAA satellite p 193 N94-11908

A consideration on principal component analysis of satellite IR data p 193 N94-11909

Current structures in the western equatorial Pacific during JAPACS cruises p 193 N94-11911

Acoustic waveguide characteristics of the Indian Ocean north of equator p 193 N94-11912

Evaporation and thermal/hydrologic balance in the Pacific p 195 N94-11919

The use of remote sensing data for coastal zone management and environment in Indonesia
p 196 N94-11927

Shoreline change detection using remote sensing and GIS in Vietnam p 196 N94-11928

The requirement for global training programmes to meet the new remote sensing technology p 196 N94-11929

Analysis of the characteristic and mechanism of suspended matter transportation in Huanghe delta sea area using remote sensing techniques p 197 N94-11930

The extraction of bottom characteristics and mapping in Kin Bay, Okinawa Main Island, Japan, using LANDSAT-5/TM and SPOT-1/HRV data p 197 N94-11931

Ocean wave detection by SAR p 197 N94-11932

On the determination of the SAR ocean surface scattering patch size p 197 N94-11933

The optical/computer hybrid processing of extracting ocean wave directional spectrum by airborne photograph p 197 N94-11934

Ocean-ice interaction study of waves and mesoscale features p 197 N94-11935

Appearance, behavior, and oceanic structures of warm streamers in the Kuroshio Oyashio frontal region p 198 N94-11937

Warm streamers extended from Warm Core Rings (WCRs) and their role on fish migration and fishing ground formation p 198 N94-11938

The Kyucho events in Sukumo Bay induced by Kuroshio front disturbances p 198 N94-11939

The coherent structure in the oceanic turbulence around Japan Islands Chain forced by an air, sea, and solid Earth interaction p 198 N94-11940

Westward propagation of sea surface anomalies in the western North Pacific as seen by the altimeter and radiometer p 198 N94-11941

Characteristic scales and vortex features of mesoscale vortices observed by the satellites during the winter p 199 N94-11943

The use of CZCS for primary production estimate in the Pacific p 199 N94-11946

CZCS derived chlorophyll distribution in Antarctic water during austral summer p 199 N94-11947

Seasonal changes of phytoplankton distributions in the Northwest Pacific detected by Coastal Zone Color Scanner p 200 N94-11948

Satellite-derived oceanic features p 200 N94-11949

Particle dynamics in the western subarctic Pacific: Implications from CZCS imagery p 200 N94-11950

High-reflectance water mass in Off-Sanriku area observed by CZCS p 200 N94-11951

Physical processes of microwave backscattering from laboratory wind-wave surfaces p 200 N94-11952

Experiment and results of the Italian activity in the field of ocean microwave backscattering p 200 N94-11953

Measurements of ocean cross-section with a side-looking airborne radar p 201 N94-11954

Air-sea interaction: Fluxes, a review p 201 N94-11955

Scatterometer observations: Review p 201 N94-11956

Dependence of oceanic microwave emission on wind direction p 201 N94-11957

Surface roughness variations across the Iceland-Faroes frontal region observed by the GEOSAT altimeter and NOAA AVHRR p 201 N94-11958

The microwave backscattering from wind waves p 201 N94-11959

On the variability of wind speeds in the North Western Pacific observed by altimeter/GEOSAT and SSM/I/DMSP p 201 N94-11960

Observation of wind and waves by GEOSAT altimeter p 202 N94-11961

Wind field estimate by using one hour GMS data p 202 N94-11963

The Pacific responses exhibited by an OGCM to various wind fields p 202 N94-11964

Development of shipboard ocean lidar p 140 N94-11965

Remote sensing of subsurface water temperature profile and backscattering coefficient in the China Sea by Ocean Lidar (OLIDAR) p 203 N94-11970

Bi-directional reflectance by oceanic waters studied via Monte-Carlo simulations p 203 N94-11971

Optical characteristics in Tokyo Bay p 204 N94-11972

Atmospheric correction plans for SeaWiFS p 204 N94-11975

Distribution of mineral aerosols over the North Pacific p 204 N94-11976

Implications of aerosol retrieval and atmospheric correction in remote sensing p 205 N94-11978

Overwater atmospheric dispersion of volcanic smokes from Mt. Sakurajima observed in NOAA-AVHRR data p 205 N94-11979

Incident shortwave and longwave radiations over the western North Pacific and the Sea of Okhotsk derived from GMS-WEFAX images p 205 N94-11982

A study of pollution courses of spilled oil floatation in the outer ocean p 205 N94-11983

Observations of the fractal properties of the Japan sea surface temperature patterns p 205 N94-11984

Flood monitoring in northern part of Central Java by remote sensing technique. Case study: The flooding of Semarang in January, 1990 p 206 N94-11989

Fourier domain target transformation analysis in the thermal infrared p 258 N94-12030

Compositional and textural information from the dual inversion of visible, near and thermal infrared remotely sensed data p 258 N94-12097

Remote sensing x ray fluorescence spectrometry for future lunar exploration missions p 462 N94-12165

Automatic definition of spectral units in the equatorial regions of Mars p 432 N94-12234

Observing and modelling F-region ionospheric dynamics using the (O2) 7320A emission
[AD-A265407] p 279 N94-12419

Sampling and position effects in the Electronically Steered Thinned Array Radiometer (ESTAR)
[NASA-TM-108998] p 245 N94-12432

Interdisciplinary scientist participation in the Phobos mission
[NASA-CR-193715] p 482 N94-12446

Emissions of sulfur gases from marine and freshwater wetlands of the Florida Everglades: Rates and extrapolation using remote sensing p 269 N94-12457

Effects of inorganic sulfur addition on fluxes of volatile sulfur compounds in Sphagnum peatlands p 270 N94-12461

Proceedings of 1st ERS-1 Symposium on Space at the Service of Our Environment, Volume 2
[ESA-SP-359-VOL-2] p 245 N94-12471

ERS-1 altimetry of inland water and land p 246 N94-12475

Combined analysis of ERS-1 SAR and visible/infrared remote sensing data for land cover/land use mapping in a tropical zone: A case study in Guinea p 246 N94-12478

Example of SPOT/ERS-1 complementarity p 247 N94-12479

The use of ERS-1 SAR data to study surface states p 247 N94-12480

Snow and glacier investigations by ERS-1 SAR: First results p 247 N94-12481

Monitoring of snowcover in high mountain terrain with ERS-1 SAR p 247 N94-12482

Application of ERS-1 SAR data to snow mapping p 247 N94-12483

Preliminary ERS-1 assessment for Canadian agriculture and forestry applications p 248 N94-12486

Segmentation and change detection in ERS-1 images over East Anglia p 248 N94-12487

ERS-1 SAR crop monitoring experiment in East Anglia, UK p 248 N94-12488

Geoecological monitoring of an agricultural area p 248 N94-12489

Integration of ERS-1 data into the European project of agriculture statistics p 248 N94-12490

Extraction of plant and soil parameters from multitemporal ERS-1 SLC data of the Freiburg test site p 248 N94-12491

Assessment of ERS-1 SAR data for soil moisture estimation p 249 N94-12492

Temporal monitoring of soil moisture using ERS-1 SAR data p 249 N94-12493

Observations of ERS-1 SAR sensitivities to changes in aboveground biomass in young loblolly pine forests p 249 N94-12494

Seeing the Black Forest by ERS-1 and AIRSAR: A comparison p 249 N94-12495

The TREES project: Pre-processing and generation of terrain data for inclusion in an ERS-1 SAR classification scheme p 249 N94-12496

TREES project: A case study on the use of multi-temporal ERS-1 SAR data and SPOT data for monitoring tropical ecosystems p 249 N94-12497

TREES project: Overview and status of the ERS-1 SAR contribution p 250 N94-12499

Impact of ERS-1 wind/wave/ice data on operational ocean forecasting p 250 N94-12500

A first assessment of the value of ERS-1 scatterometer winds for meteorological studies in the polar regions p 250 N94-12501

Use of SAR-wave, altimeter, and wind-scatterometer data in an operational swell forecasting system p 250 N94-12503

Use of ERS-1 scatterometer winds in Canadian forecast centres p 250 N94-12504

ERS-1 and Almaz SAR ocean wave imaging over the Gulf Stream and the Grand Banks p 251 N94-12505

Real time processing wave spectra from satellite SAR p 251 N94-12506

A statistical analysis of sea state surface ERS-1 SAR-wave mode imagettes p 251 N94-12507

A new model for Synthetic Aperture Radar (SAR) images from ocean scatter p 251 N94-12508

On the extraction of ocean wave spectra from ERS-1 SAR wave mode image spectra p 251 N94-12509

Tide-generated nonlinear internal wave packets in the Strait of Gibraltar observed by the synthetic aperture radar aboard the ERS-1 satellite p 252 N94-12510

Validation of the ATSR/M microwave radiometer data p 252 N94-12511

Multichannel dual angle approach for sea surface temperature retrieval in context of ERS-1 scenario p 252 N94-12512

Estimations of the surface fluxes from satellite observations of boundary layer and the surface p 252 N94-12513

ATSR correlative skin measurements of sea surface temperature p 252 N94-12514

Validation of ATSR-1 using aircraft radiometer measurements over the South Atlantic p 252 N94-12515

A comparison of ATSR and shipboard radiometer SST measurements along transects between the UK and the Antarctic p 253 N94-12518

Artificial oil pollution detection and wave observation in the sea adjacent to Japan by ERS-1 SAR p 253 N94-12520

Ship traffic monitoring using the ERS-1 SAR p 253 N94-12521

Oil spill detection using satellite-based SAR: Experience from a field experiment p 253 N94-12522

Coastal morphodynamics and energetic characteristics of swell studied with ERS-1 SAR p 254 N94-12524

SAR imaging of geology and bathymetry: Kent coastal area - southern North Sea p 254 N94-12527

Proceedings of the PORSEC 1992 in Okinawa: Conference for Pacific Ocean Environments and Probing, volume 2
[JTN-93-80419] p 207 N94-12635

Analysis of GEOSAT wind data p 207 N94-12636

SSMI wind speed variability over the Pacific Ocean p 207 N94-12637

Observation of wave crests by satellite remote sensed data p 207 N94-12638

Observations of eddy fields in the Northwest Pacific by GEOSAT altimetry p 207 N94-12639

Variability of sea level and sea surface temperature anomalies in the equatorial Pacific p 208 N94-12640

Theory and oceanographic applications of satellite altimeter measurements p 208 N94-12641

Analysis of collinear passes of satellite altimeter data p 208 N94-12642

Surface eddy fluxes from the GEOSAT satellite altimeter p 208 N94-12643

Comparison of GEOSAT sea surface height and model-simulated surface dynamic height p 208 N94-12644

Pseudo magnetic anomaly derived from satellite altimetry and its application to the tectonics in the North Fuji Basin p 208 N94-12645

Principal oscillation pattern analysis of sea level variations in the tropical Pacific measured by the GEOSAT altimeter p 209 N94-12646

Measurement of eddy structure and movement in the north-east Pacific with the GEOSAT altimeter p 209 N94-12647

Preliminary results from a satellite altimetric data assimilation using a Kalman filter and smoother p 209 N94-12648

Fluctuations of the Kuroshio extension detected by the GEOSAT altimetry data p 209 N94-12649

Mean flow and variability in the Kuroshio extension from GEOSAT altimetry data p 209 N94-12650

Pacific rim sea ice as observed with the NIMBUS-7 SMMR p 210 N94-12651

Ice studies in the Barents Sea by ERS-1 during SIZEX 1992 p 210 N94-12653

Disintegrating ice front of Shirase Glacier, East Antarctica p 210 N94-12654

Microwave radiometry of ice cover in polar regions p 210 N94-12655

The seasonal change of phytoplankton size distribution using optical fiber sensor p 210 N94-12656

Worldwide map of rainfall amount over the ocean derived from passive microwave radiometer p 211 N94-12663

Study on diffusion phenomena of river effluents issued into sea around Japan with satellite remote sensing data p 212 N94-12664

A basic consideration for remote sensing using microwave radars on a satellite p 212 N94-12665

Migration of operational ice analysis and forecasting to a workstation platform at the Joint Ice Center p 212 N94-12666

Evaluating the spread of red soil with LANDSAT TM data in coral reefs of Okinawa main island, southwestern Japan p 212 N94-12668

Simple and low cost image processing system for satellite remote sensing data p 212 N94-12669

Validation test system for sea surface temperature detected by satellites in Mutsu Bay p 213 N94-12670

Sea surface temperature images of Geostationary Meteorological Satellite (GMS) and sea truth data from ferry boats p 213 N94-12671
Measurement of the sea surface emissivity p 213 N94-12672
Evaluation of the method of geostrophic flow using NOAA-AVHRR data p 213 N94-12673
Further study of the Non-Regression-Coefficient SST retrieval method p 213 N94-12674
Delineation of mesoscale features of ocean on satellite IR image p 214 N94-12675
Observation of warm current at the boundary from north equatorial current to Kuroshio by NOAA/AVHRR p 214 N94-12676
Information capability of NOAA-AVHRR data for monitoring oceanographic and atmospheric pollution p 214 N94-12677
Satellite observations of the northeast monsoon coastal current p 214 N94-12678
Aspects of applying a relaxation method to computing sea surface velocities from sea surface temperature images p 214 N94-12679
Sea surface temperature difference between NOAA/AVHRR and in-situ observation p 215 N94-12680
Application of NOAA AVHRR data to fisheries p 215 N94-12681
Statistical features of mesoscale eddies at the Kuroshio front p 215 N94-12682
Intrusion of Kuroshio warm water into Sagami Bay p 215 N94-12683
A study of front dynamics off northeastern Taiwan based on the NOAA-AVHRR satellite remote sensing data p 215 N94-12684
Satellite thermal variations of Kuroshio in relation to storm floods p 215 N94-12685
ADCP evidence for upper layer circulation in northeast of the South China Sea p 215 N94-12686
Frontal zones in Pacific Ocean: Satellite and ship data analysis p 216 N94-12687
Swordfish (Xiphias gladius) catch distributions relative to environmental features observed from satellites off Coquimbo, Chile (30 deg S) p 216 N94-12688
Observation of cold coastal water with high turbidity around the southwestern tip of Korean Peninsula p 216 N94-12689
On the error characteristics of the sea surface temperature observed by satellite p 216 N94-12690
The WOCE/TOGA Surface Velocity Programme (SVP) p 216 N94-12691
Remote sensing of polluting focal points and coastal disturbances in the Gulf of Arauco and adjacent bays, central Chile p 217 N94-12695
Role of remote sensing and its cost effectiveness in site selection for coastal aquaculture p 217 N94-12697
Seasonal variability of surface ocean color in the Omura Bay using multitemporal LANDSAT-5 TM data p 218 N94-12698
Acoustic estimation of plankton biomass p 218 N94-12699
Properties of spectral reflectance of crown and crown structure of mangrove species in Okinawa p 218 N94-12700
Application of remote sensing for coastal management in the north coast of Java p 218 N94-12701
Study of growing processes of a tombolo using an air photograph p 218 N94-12702
Estimation of areal evapotranspiration using LANDSAT TM data: Kitami City, Hokkaido, Japan p 219 N94-12703
Land use/land cover mapping of central water shed of Iran area based on satellite data interpretation p 219 N94-12704
A method to minimize reference data in classifying satellite remote sensing data into land cover classes p 219 N94-12705
The circulation near Luzon p 219 N94-12707
Current variability on the shelf break northeast of Taiwan p 219 N94-12708
Study on air-sea interactions in the OMLET (Ocean Mixed Layer Experiment) area using satellite remote sensing p 220 N94-12710
Investigation of meso-scale fronts, eddies and upwellings in China Seas with AVHRR data p 220 N94-12711
Coastal upwelling monitored by satellite data: Methodologies and results p 220 N94-12712
Applicability of satellite infrared data for the monitoring of coastal environments p 220 N94-12714
Satellite and moored buoy observations of polar frontal system over the Yamato Rise in the Japan Sea p 221 N94-12715
The relationship between skin and bulk sea surface temperatures p 221 N94-12716
Variability of the Kuroshio observed from satellite thermal imagery p 221 N94-12717
Variability of the mixed layer depth in the North Pacific Ocean as calculated by a 3-D semi-analytical mixed layer remote sensing model p 221 N94-12718
SST assimilation: Eastern Mediterranean case study p 221 N94-12719
Mapping of high density area of benthic diatom in Ariake Sea p 222 N94-12720
Advective surface velocity in the north west Pacific derived from NOAA AVHRR images p 222 N94-12721
Polarisation of backscattering radiation at remote sensing of ocean with impulse laser beam p 177 N94-12722
The method of investigation of the horizontal structure of the thermal fronts p 222 N94-12723
On a nonstationary dynamics of the north-west Pacific Ocean p 222 N94-12724
Optimum selection of spectral channels in the problem of remote sensing of phytoplankton concentration in ocean water p 223 N94-12726
Field research of wind wave spectrum variability p 223 N94-12727
The acoustic arrangement for measuring vertical structure of sea current p 223 N94-12729
Turbulence generation in the Pacific undercurrent by shear p 223 N94-12730
The Pacific Subarctic Frontal Zone: Structure and dynamics p 223 N94-12731
Laser photoheterodyne interferometers for oceanographic investigations p 177 N94-12732
A detailed investigation of the benthic regime in the Clarion-Clipperton province of the Pacific and a forecast of consequences of manganese nodule mining p 224 N94-12733
Bottom currents and possibilities for near bottom layer environmental investigations in the Pacific by means of self contained bottom stations p 224 N94-12734
Remote sensing of light scattering coefficient of sea water vertical distribution by the means of airborne lidar p 224 N94-12736
Influence of the Kuroshio warm-core rings on hydrographic and fishery conditions off southern Kuril Islands p 224 N94-12737
Verification of the atmosphere-ocean radiative transfer parametric models p 225 N94-12738
Spatial variability of the ocean underwater dynamic noise from satellite radar sensing data p 225 N94-12740
Observations of film slicks and internal waves with Ka-band scatterometer p 225 N94-12741
Optical transfer operator of the atmosphere-ocean system p 225 N94-12742
Cloud liquid water content over the Pacific Ocean tropical zone derived from ship microwave radiometric measurement p 225 N94-12743
Variability of spectral reflectance in coastal waters near the river plumes p 226 N94-12744
Wind-wave and foam dynamics from optical and radar airborne observations p 226 N94-12745
Observations of surface signatures in the north-west Pacific Ocean with the spaceborne SAR p 226 N94-12746
Radar observation of internal waves field in the north-west Pacific p 226 N94-12747
Trajectory curving in underwater propagation of light p 226 N94-12748
DISTERM: A shipboard data system for satellite monitoring of ocean and atmosphere p 226 N94-12749
Atmospheric correction for determination of average SST fields based on AVHRR data p 227 N94-12750
Complex (hydrodynamic, satellite) monitoring of dynamic structures in the western Pacific with the aim of forecasting the marine ecosystems behaviour p 227 N94-12753
Mesoscale dynamic structures of the Subarctic Frontal Zone in the Pacific Ocean p 227 N94-12754
Laser fluorescent monitoring of dissolved organic matter in natural water p 177 N94-12755
Ecological application of Surface Enhanced Raman Spectroscopy p 227 N94-12756
A possibility to define the location of epipelagic fish concentrations with assistance of satellite sensing p 228 N94-12757
High biological production of the tidal mixing zones on Japan Sea shelf p 228 N94-12758
Study of the admixture diffusion in the sea using remote techniques p 228 N94-12759
The algorithm of primary production determination p 228 N94-12761
Non-image visible polarization remote sensing of the ocean p 229 N94-12762
Problem of climate change predictability and satellite radiation budget observations p 229 N94-12766

REMOTE SENSORS
Enhanced Damage-Resistant Optics for Spaceflight Laser Systems: Workshop findings and recommendations
[NASA-TM-109243] p 381 N94-11054
Activities relating to understanding the initiation, organization and structure of moist convection in the Southeast environment
[NASA-CR-193829] p 285 N94-11598
Trend of miniature refrigerator utilization in earth observation area p 130 N94-11835
Development test on 2 K cooling systems p 130 N94-11840
HF ocean radar system at Okinawa Radio Observatory p 139 N94-11902
Measurement of wave parameters by HF ocean radar p 192 N94-11903
Groundwave HF ocean surface radar p 139 N94-11906
Trouble areas in the IRT measurement of the Earth surface temperature p 193 N94-11910
Acoustic characteristics of side scan sonar and sub-bottom profiler for 10,000 m class ROV p 172 N94-11916
Atmospheric correction plans for SeaWiFS p 204 N94-11975
Project of an attitude control system (three axis) of a satellite using the LQG/LTR methodology
[INPE-5473-TDI/504] p 44 N94-12356
METEOSAT second generation programme SEVIRI: An enhanced visible and IR radiometer for meteorology p 212 N94-12667
Resistivity and radar void detectors for tunneling machines p 140 N94-12706
Autonomous self contained bottom pop-up stations for study of the benthic layer and seismicity of the ocean's bottom p 224 N94-12735
The structure of hydrophysical measuring systems of vertical sounding and self-contained stations p 227 N94-12751

REMOTELY PILOTED VEHICLES
A portable controller for unmanned ground vehicles
[AD-A264963] p 181 N94-11290

REMOVAL
Environmentally Safe and Effective Processes for Paint Removal
[AGARD-R-791] p 126 N94-10613
Paint removal activities in the US Navy p 126 N94-10614
Paint removal activities in Canada p 126 N94-10615
Procedures without danger to the environment and efficiency (PSDEE) for the removal of paint. Point on the French activities concerning the removal of paint p 126 N94-10616
Paint removal activities in Germany p 126 N94-10617
The development of alternative paint removal techniques in the RAF p 126 N94-10618
Operational aspects of F.16 plastic media blasting, as carried out by Fokker Aircraft Services p 126 N94-10619
Use of robots for aircraft dry stripping via plastic media blasting p 127 N94-10620
German Air Forces experiences with plastic media blasting and future requirements p 127 N94-10621
Plastic media blasting activities at Hill Air Force Base p 127 N94-10622
Large Aircraft Robotic Paint Stripping (LARPS) system and the high pressure water process p 127 N94-10623
Automated Laser Paint Stripping (ALPS) update p 127 N94-10624
Aquastrip (tm): An innovative paint removal technology p 127 N94-10625
Paint removal and surface cleaning using ice particles p 128 N94-10626
Paint removal using wheat starch blast media p 128 N94-10627
IATA taskforce: Paintstripping p 128 N94-10628
Selectively strippable paint schemes p 128 N94-10629

RENAL FUNCTION
Proceedings of the First Joint NASA Cardiopulmonary Workshop
[NASA-CP-10068] p 308 N94-11991
Fluid compartment and renal function alterations in the rat during 7 and 14 day head down tilt p 310 N94-12002
Physiological water model development p 316 N94-12367

RENORMALIZATION GROUP METHODS
On renormalization group flow in matrix model
[DE93-613050] p 409 N94-10413

REPLENISHMENT

The role of the geothermal gradient in the emplacement and replenishment of ground ice on Mars p 463 N94-12169

REPORTS

A comparison of high and low-impact reports of investigation on adjudicators' decision making: A pilot study [AD-A265747] p 416 N94-10298

REPUBLIC OF SOUTH AFRICA

A structural and petrographic investigation of the pretoria saltpan impact structure p 282 N94-12102

Geophysical signature of the Pretoria saltpan impact structure and a possible satellite crater p 282 N94-12103

RESEARCH AIRCRAFT

Measuring human performance on NASA's microgravity aircraft p 317 N94-11537

RESEARCH AND DEVELOPMENT

Advanced Materials for Lightweight Structures [ESA-SP-336] p 56 N94-10001

The EUREKA project portfolio in new materials p 56 N94-10002

Investigations on aluminium-lithium alloys for damage tolerant application p 59 N94-10023

Fibre optic strain and temperature measurement in composite materials: A review of the OSTIC programme p 65 N94-10066

The Netherlands innovation oriented research programme on polymer composites and special polymers 1985-1993 p 65 N94-10067

Protein, glass, aerosol research, containerless processing and diagnostics technology for microgravity application p 106 N94-10112

The NASA Lewis Research Center SBIR program: An assessment [NASA-TM-106205] p 485 N94-10356

Recommendations for future research in hypersonic instrumentation p 4 N94-10433

Future material development trends for commercial airplane interiors p 21 N94-10792

Advanced aircraft materials research and development plan p 22 N94-10796

The future of aircraft cabin fire safety p 22 N94-10797

National patterns of R and D resources, 1992 [NSF-92-330] p 422 N94-11186

NASDA activities in space solar power system research, development and applications p 54 N94-11413

Quality assurance in basic research and R/D [DE93-010825] p 183 N94-11647

The 27th International Applied Military Psychology Symposium: A Focus on Decision Making Research [AD-A265278] p 313 N94-11701

AGARD highlights 92/2, September 1992 [AGARD-HIGHLIGHTS-92/2] p 497 N94-11820

Integrating the services' imagery architectures [AD-A265487] p 171 N94-12335

National SBIR Phase 3 Commercialization Conference [AD-A266083] p 417 N94-12410

Elementary particle physics and high energy phenomena [DE93-013971] p 370 N94-12609

RESEARCH FACILITIES

Proceedings of the 8th European Symposium on Materials and Fluid Sciences in Microgravity, volume 1 [ESA-SP-333-VOL-1] p 99 N94-10070

Description of the liquid structure facility architecture and experimental demonstration of the diagnostic capabilities p 39 N94-10118

The electron beam furnace: A new facility for materials science research p 109 N94-10126

Microgravity Applications Furnace Facility (MAFF) for parabolic flights p 109 N94-10128

Laser beam deflection: A diagnostic tool for vapour growth experiments in microgravity p 111 N94-10135

The advanced fluid physics module: How to achieve scientific goals for Spacelab D2 p 39 N94-10136

Scientific specifications for an automated facility for growing large semiconducting crystals from the melt in space p 114 N94-10180

Crystal growth in the Zone Melting Facility (ZMF) p 119 N94-10213

The critical facility on IML-1 p 44 N94-10250

Numerical wind tunnel project and computational fluid dynamics at National Aerospace Laboratory, Japan [NAL-TM-648T] p 149 N94-10861

Motion and spatial disorientation systems: Special research capabilities [AD-A265155] p 303 N94-11097

Five biomedical experiments flown in an Earth orbiting laboratory: Lessons learned from developing these experiments on the first international microgravity mission from concept to landing p 302 N94-11556

Quality assurance in basic research and R/D [DE93-010825] p 183 N94-11647

RESEARCH MANAGEMENT

Canada's longterm space plan and ISY activities p 37 N94-10692

National Institute of Health Almanac, 1992 [PB93-183556] p 303 N94-10828

Low-expansion ceramics initiative [DE93-011860] p 89 N94-11106

Quality assurance in basic research and R/D [DE93-010825] p 183 N94-11647

The Department of Clinical Investigation, reports control symbol MED-300(R-1) [AD-A264969] p 304 N94-11649

RESEARCH PROJECTS

The EUREKA project portfolio in new materials p 56 N94-10002

The Netherlands innovation oriented research programme on polymer composites and special polymers 1985-1993 p 65 N94-10067

Pakistan Space and Upper Atmosphere Research Commission p 37 N94-10693

Low-expansion ceramics initiative [DE93-011860] p 89 N94-11106

Facts about the US Antarctic program [NSF-92-134] p 279 N94-12568

RESEARCH VEHICLES

Development of a shuttle AUV for oceanographic measurement p 217 N94-12692

RESIDUAL STRESS

Extensions of some guidelines for the mechanical design of coaxial compression pin seals [DE93-012385] p 177 N94-10348

Fracture behavior of surface-modified ceramics [DE93-013707] p 88 N94-10710

Sensitivities of calculated residual stress to separation distances of two simultaneous events [DE92-019571] p 98 N94-10751

Computational simulation of hot composite structures [NASA-TM-106200] p 186 N94-10762

Analytical models for describing the mechanical behavior of fiber reinforced composites [AD-A265906] p 74 N94-12347

RESIDUES

Mineralogy of chondritic interplanetary dust particle impact residues from LDEF p 80 N94-12045

Composition and modal frequencies of hypervelocity particles less than 1 millimeter in diameter in low-Earth orbit p 429 N94-12063

RESIN MATRIX COMPOSITES

Deformation mechanisms of continuous fibre-reinforced thermoplastic composites during manufacturing: A probabilistic approach p 60 N94-10030

Heat analysis of thermoplastic components during the initial stages of manufacturing: A probabilistic approach p 60 N94-10031

Application of advanced thermoplastics p 60 N94-10033

Low cost thermoplastic composites for structural applications: Design concepts using new materials and processes p 60 N94-10034

Tape winding of thermoplastic composites p 60 N94-10035

Silicon-based elementary particle tracking system: Materials science and mechanical engineering design [DE93-012630] p 65 N94-10740

Dry in-line thermoplastic matrix impregnation, phase 1 [AD-A265016] p 67 N94-11221

An analysis of fiber-matrix interface failure stresses for a range of ply stress states [NASA-TM-108999] p 67 N94-11276

RESIN TRANSFER MOLDING

Design and manufacturing of CFRP rings by RTM p 59 N94-10025

RESISTANCE

Photogenerated base in polymer imaging. Synthesis and photopatterning of poly(2-cyano-2-(p-vinylphenyl) butanoic acid) [AD-A265288] p 95 N94-12585

RESISTANCE HEATING

Crystal growth in the Zone Melting Facility (ZMF) p 119 N94-10213

RESONANCE

Progress in zirconium resonance ionization spectroscopy [DE93-011881] p 76 N94-11075

The IR properties of ringed galaxies and the IRAS database [NASA-CR-194286] p 426 N94-11590

Nonlinear resonance: Noise-assisted information processing in physical and neurophysiological systems [AD-A265161] p 313 N94-11890

RESONANCE FLUORESCENCE

Squeezing in phase-conjugated resonance fluorescence p 376 N94-10576

RESONANCE SCATTERING

Linear antenna of an arbitrary orientation and position in cylindric screen [DE93-621353] p 134 N94-11035

RESONANT FREQUENCIES

Laboratory study on the natural modes of a rotating two-phase fluid system subject to axial excitation p 106 N94-10106

Boundary element method for eigenvalue problems of thin plates [ITN-93-85199] p 343 N94-10392

On the stability of stationary regimes in a distributed autovibration system with external feedback [DE93-620979] p 141 N94-10543

Quantum non demolition measurement of cyclotron excitations in a Penning trap p 376 N94-10578

Magnetic Earth Ionosphere Resonant Frequencies (MEIRF) project [NASA-CR-193182] p 276 N94-11355

The laser second threshold: Its exact analytical dependence on detuning and relaxation rates [DE93-619706] p 175 N94-11633

Nonlinear effects in ferrite tuned cavities [DE93-014136] p 374 N94-12785

RESONANT TUNNELING

Effect of effective mass differences on the tunneling current-voltage behaviour of a resonant diode in the presence of space charge build-up [DE93-613817] p 142 N94-10799

RESONATORS

Quantum processes in resonators with moving walls p 380 N94-10612

Dielectric resonator [US-PATENT-4,580,116] p 141 N94-10668

Conversion of the four-strap array in D3-D to a tunable traveling wave antenna [DE93-012085] p 137 N94-11453

RESOURCE ALLOCATION

ACARA user's manual [NASA-TM-106277] p 183 N94-11167

RESOURCES MANAGEMENT

Current status of space activities in Asia Pacific region p 35 N94-10677

Summary of implementation and demonstration projects in bays and estuaries [PB93-194637] p 265 N94-10846

Information resources management long-range plan, FY1994 [DE93-013898] p 420 N94-11588

Data management strategy for the Tampa Bay National Estuary Program: Recommendations and implementation plan [PB93-191633] p 267 N94-11864

The use of remote sensing data for coastal zone management and environment in Indonesia p 196 N94-11927

The requirement for global training programmes to meet the new remote sensing technology p 196 N94-11929

Integrating the services' imagery architectures [AD-A265487] p 171 N94-12335

Quality assurance for environmental chemistry: 1991, volume 2 [DE93-011792] p 272 N94-12780

RESPIRATION

Toxicity study of dimethylethoxysilane (DMSES), the waterproofing agent for the Orbiter heat protective system p 318 N94-11554

RESPIRATORY DISEASES

Allowable exposure limits for carbon dioxide during extravehicular activity [NASA-TM-103832] p 315 N94-11375

RESTORATION

Summary of implementation and demonstration projects in bays and estuaries [PB93-194637] p 265 N94-10846

RESUSCITATION

Evaluation of medical treatments to increase survival of ebullism in guinea pigs p 302 N94-11548

RETINA

Parametric study of diffusion-enhancement networks for spatiotemporal grouping in real-time artificial vision [AD-A265065] p 331 N94-11652

RETINAL IMAGES

Visual psychophysics of egomotion [AD-A265253] p 304 N94-11681

RETRACTABLE EQUIPMENT

In-orbit performance tests and tele-command systems of the umbrella test satellite (DEBUT) [NAL-TR-1165] p 43 N94-10859

RETROREFLECTORS

Galileo EM-2 contributions to the lunar control network p 468 N94-12198

REVENUE

Survey to determine the value of DYNA [DE93-012390] p 321 N94-10267

Federal Aviation Administration aviation forecasts
[AD-A265611] p 2 N94-12578

REVERSE ENGINEERING

Reuse: A knowledge-based approach
p 329 N94-11430

Myths and realities: Defining re-engineering for a large organization p 330 N94-11436

REVERSE FIELD PINCH

Reversed-field pinch studies in the Madison Symmetric Torus
[DE93-013464] p 388 N94-10747

Magnetohydrodynamic computation of feedback stabilization of resistive-shell instabilities in the reversed field pinch
[DE93-013466] p 388 N94-10852

Simulation study of dynamo structure in reversed field pinch
[DE93-771406] p 390 N94-11128

Macroscopic behaviour and discrete dynamo of RFP plasma in high theta discharge
[DE93-771408] p 392 N94-11239

REVIEWING

Research on two phase flow in microgravity
p 162 N94-12554

REYNOLDS NUMBER

Numerical calculation of scramjet inlet flow
[NAL-TR-1174T] p 27 N94-10370

Regeneration of near-wall turbulence structures
p 158 N94-12308

REYNOLDS STRESS

A local dynamic model for large eddy simulation
p 155 N94-12285

Parameterization of subgrid-scale stress by the velocity gradient tensor p 155 N94-12286

A normal stress subgrid-scale eddy viscosity model in large eddy simulation p 155 N94-12288

Application of a dynamic subgrid-scale model to turbulent recirculating flows p 156 N94-12290

Direct numerical simulation of turbulent flow over a backward-facing step p 156 N94-12296

Reynolds stress closure modeling in wall-bounded flows p 157 N94-12298

Application of a Reynolds stress model to separating boundary layers p 157 N94-12299

RHENIUM

Space Storable Rocket Technology program (SSRT). Option 1 program
[NASA-CR-191171] p 46 N94-10938

RHENIUM ISOTOPES

Rhenium-osmium isotope systematics of Group 2A and Group 4A iron meteorites p 431 N94-12182

Re-Os dating of 3AB iron meteorites
p 432 N94-12237

RHEOLOGY

Improving reservoir conformance using gelled polymer systems
[DE93-014532] p 88 N94-10749

A model for the subduction mechanics of flexible lithosphere and its viscous coupling to the mantle using power-law rheologies p 277 N94-11585

Quantifying the effect of rheology on plan-view shapes of lava flows p 282 N94-12116

Numerical simulation of the non-Newtonian mixing layer p 159 N94-12314

RHYOLITE

Stable isotope analyses of the peralkaline volcanics Gregory Rift Valley, Kenya p 281 N94-12072

Th-230 - U-238 series disequilibrium of the Olkaria rhyolites Gregory Rift Valley, Kenya: Petrogenesis
p 281 N94-12075

Th-230 - U-238 series disequilibrium of the Olkaria rhyolites Gregory Rift Valley, Kenya: Residence times
p 281 N94-12076

RHYTHM (BIOLOGY)

The 2nd Annual Meeting of the Society for Research on Biological Rhythms
[AD-A264869] p 303 N94-10872

RIBLETS

Coherent structure in near wall turbulence with riblets
p 165 N94-12628

RIBS (SUPPORTS)

Turbulent drag reduction of a d-type rough wall boundary layer with longitudinal ribs placed within the grooves
p 165 N94-12627

RICCATI EQUATION

A new approach to the I/N-expansion for the Dirac equation
[DE93-617647] p 349 N94-10833

RIDING QUALITY

Active landing gear control for improved ride quality during ground roll p 27 N94-11345

RIEMANN MANIFOLD

From the Weyl theory to a theory of locally anisotropic space-time
[DE92-644734] p 410 N94-10535

RING GALAXIES

The IR properties of ringed galaxies and the IRAS database
[NASA-CR-194286] p 426 N94-11590

RING LASERS

Semiconductor ring lasers
[DE93-012386] p 174 N94-11005

RING STRUCTURES

Design and manufacturing of CFRP rings by RTM
p 59 N94-10025

The ring structure of chiral operators for minimal models coupled to 2D gravity
[DE93-613119] p 409 N94-10500

Morphology of large impact craters and basins on Venus: Implications for ring formation p 436 N94-12023

Yana ring structure, North-Eastern Siberia: A possible counterpart of coronae on Venus p 282 N94-12121

RING WINGS

Simulated wake characteristics of tapered annular wings by a discrete vortex method
[NAL-TR-1156] p 13 N94-10855

Simulated and experimental aerodynamic characteristics of tapered annular wings
[NAL-TR-1157] p 13 N94-10856

RISK

Report on Subgroup on Data Banks for Risk Assessment
[DE93-012150] p 418 N94-10646

RIVER BASINS

Modeling present and future river runoff using global atmospheric models
[AD-A265274] p 285 N94-11685

Simultaneous 3D turbulent large-scale structures in a flood flow by multi-channels measuring system
p 165 N94-12624

RIVERS

Shoreline change detection using remote sensing and GIS in Vietnam p 196 N94-11928

Analysis of the characteristic and mechanism of suspended matter transportation in Huanghe delta sea area using remote sensing techniques
p 197 N94-11930

Methodological considerations for use of ERS-1 imagery for the delineation of river networks in tropical forest areas p 247 N94-12484

Study on diffusion phenomena of river effluents issued into sea around Japan with satellite remote sensing data
p 212 N94-12664

Variability of spectral reflectance in coastal waters near the river plumes p 226 N94-12744

ROBOT ARMS

Payload sensitivity in coupled bending and torsional vibrations in flexible beams
[MEMO-1102] p 184 N94-10161

Force reflection with compliance control
[NASA-CASE-NPO-18668-1-CU] p 179 N94-10654

Telerobot control system
[NASA-CASE-NPO-18116-1-CU] p 179 N94-10670

Momentum management in redundant manipulators for vibration suppression
[NASA-CR-194112] p 180 N94-10821

An adaptive and robust control for motion coordination of two-cooperating robot manipulators
p 340 N94-11825

ROBOT CONTROL

Position and force control of a vehicle with two or more steerable drive wheels
[DE93-012512] p 177 N94-10269

Force reflection with compliance control
[NASA-CASE-NPO-18668-1-CU] p 179 N94-10654

Telerobot control system
[NASA-CASE-NPO-18116-1-CU] p 179 N94-10670

Sensor abstractions to support many-robot systems
[AD-A265907] p 180 N94-10803

Momentum management in redundant manipulators for vibration suppression
[NASA-CR-194112] p 180 N94-10821

The development of an interactive synthesis tool for intelligent controllers of modular, reconfigurable robots
p 339 N94-10898

Basic experiment on an ultrasonic method of localization
[DE93-754295] p 358 N94-11042

Development and evaluation of a predictive algorithm for telerobotic task complexity p 341 N94-11562

The rational behavior model: A multi-paradigm, tri-level software architecture for the control of autonomous vehicles
[AD-A265175] p 332 N94-11874

Derivation of three closed loop kinematic velocity models using normalized quaternion feedback for an autonomous redundant manipulator with application to inverse kinematics
[DE93-012823] p 340 N94-12543

Experiments in mobile robot navigation and range imaging
[DE93-013280] p 341 N94-12598

ROBOT DYNAMICS

The development of an interactive synthesis tool for intelligent controllers of modular, reconfigurable robots
p 339 N94-10898

Trajectory pattern inverse dynamics and control of nonlinear dynamics systems with application to flexible structures p 181 N94-11219

Space Station maintenance studies using plaid graphics p 335 N94-11578

Robotic servicing on Earth orbiting satellites
p 45 N94-11579

An adaptive and robust control for motion coordination of two-cooperating robot manipulators
p 340 N94-11825

Derivation of three closed loop kinematic velocity models using normalized quaternion feedback for an autonomous redundant manipulator with application to inverse kinematics
[DE93-012823] p 340 N94-12543

ROBOT SENSORS

Experiments in mobile robot navigation and range imaging
[DE93-013280] p 341 N94-12598

ROBOTICS

Lightweight CFRP frame structures for a Rotex-derived manipulator system p 56 N94-10005

Position and force control of a vehicle with two or more steerable drive wheels
[DE93-012512] p 177 N94-10269

Preliminary system design of a Three Arm Capture Mechanism (TACM) flight demonstration article
[NASA-CR-192573] p 177 N94-10341

Task planning with uncertainty for robotic systems
[NASA-CR-193253] p 338 N94-10638

Sensor abstractions to support many-robot systems
[AD-A265907] p 180 N94-10803

Mechanical analysis of parallel manipulators with simulation, design, and control applications
[ISBN-0-315-72013-1] p 181 N94-11156

Sixth Annual Workshop on Space Operations Applications and Research (SOAR 1992), volume 2
[NASA-CP-3187-VOL-2] p 486 N94-11527

Space Station maintenance studies using plaid graphics p 335 N94-11578

Robotic servicing on Earth orbiting satellites
p 45 N94-11579

The rational behavior model: A multi-paradigm, tri-level software architecture for the control of autonomous vehicles
[AD-A265175] p 332 N94-11874

ROBOTS

Position and force control of a vehicle with two or more steerable drive wheels
[DE93-012512] p 177 N94-10269

Operational aspects of F.16 plastic media blasting, as carried out by Fokker Aircraft Services
p 126 N94-10619

Use of robots for aircraft dry stripping via plastic media blasting p 127 N94-10620

Plastic media blasting activities at Hill Air Force Base
p 127 N94-10622

Large Aircraft Robotic Paint Stripping (LARPS) system and the high pressure water process
p 127 N94-10623

Telerobot control system
[NASA-CASE-NPO-18116-1-CU] p 179 N94-10670

Sensor abstractions to support many-robot systems
[AD-A265907] p 180 N94-10803

Development and evaluation of a predictive algorithm for telerobotic task complexity p 341 N94-11562

Supervised autonomous control, shared control, and teleoperation for space servicing p 183 N94-11577

Robotic servicing on Earth orbiting satellites
p 45 N94-11579

ROBUSTNESS (MATHEMATICS)

RAMCAD (reliability, availability, and maintainability in computer-aided design)
[AD-A265143] p 331 N94-11679

ROCK INTRUSIONS

Giant radiating dyke swarms on Earth and Venus
p 283 N94-12236

ROCKET ENGINE DESIGN

In-reactor testing of the closed cycle gas core reactor: The Nuclear Light Bulb concept
[DE93-004053] p 370 N94-10149

Space Storable Rocket Technology program (SSRT). Option 1 program
[NASA-CR-191171] p 46 N94-10938

Applying design principles to fusion reactor configurations for propulsion in space
[NASA-TM-108247] p 47 N94-11053

ROCKET ENGINES
Durability of a carbon segmented circumferential seal for a liquid oxygen turbopump
[NAL-TR-1155] p 178 N94-10369
Hot-gas-side heat transfer characteristics of subscale, plug-nozzle rocket calorimeter chamber
[NASA-TP-3380] p 55 N94-12569

ROCKET EXHAUST
Ultraviolet plume instrument description and plume data reduction methodology
[AD-A266141] p 54 N94-11643
The 1991 version of the plume impingement computer program. Volume 2: User's input guide
[NASA-CR-194191] p 166 N94-12774
The 1991 version of the plume impingement computer program. Volume 1: Description
[NASA-CR-194192] p 166 N94-12775

ROCKET NOZZLES
Development of a high specific 1.5 to 5 kW thermal arcjet
[NASA-CR-193133] p 47 N94-11354

ROCKET THRUST
In-reactor testing of the closed cycle gas core reactor: The Nuclear Light Bulb concept
[DE93-004053] p 370 N94-10149

ROCKS
Oxygen isotopes as tracers of tektite source rocks: An example from the Ivory Coast tektites and Lake Bosumtwi Crater p 430 N94-12146

ROCKY MOUNTAINS (NORTH AMERICA)
Large eddy simulations of the atmospheric boundary layer east of the Colorado Rockies p 277 N94-11465

ROTARY WING AIRCRAFT
Smart materials for helicopter rotor active control p 27 N94-11321

ROTARY WINGS
Quantifying disbond area p 61 N94-10038
Determining XV-15 aeroelastic modes from flight data with frequency-domain methods
[NASA-TP-3330] p 25 N94-10935
Performance and rotor loads measurements of the Lynx XZ170 helicopter with rectangular blades
[NASA-TM-104000] p 1 N94-10936
Smart materials for helicopter rotor active control p 27 N94-11321

ROTATING BODIES
Reduced gravity multibody dynamics testing
[NASA-CR-192589] p 125 N94-11483
The magnetic field of rotating bodies
[DE93-619769] p 427 N94-11812
Laboratory studies on the velocity of fragments from impact disruptions p 189 N94-12359
Criteria for onset of boundary-layer transition on spinning bodies p 164 N94-12620

ROTATING FLUIDS
Laboratory study on the natural modes of a rotating two-phase fluid system subject to axial excitation p 106 N94-10106
SWIRL as a means of liquid management in low gravity
[NASA-CR-4545] p 412 N94-11523

ROTATING PLASMAS
Kinetic approach to long wave length modes in rotating plasmas
[DE93-771286] p 388 N94-10807
The role of plasma rotation on MHD instabilities in tokamaks
[DE93-013486] p 393 N94-11512

ROTATION
Effect of rotation on microgravity floating-zone crystal growth p 101 N94-10080
Analytical description of the torsatron Uragan-2M magnetic configuration with account of plasma pressure and external correcting magnetic field
[DE93-620983] p 391 N94-11174
Laboratory studies on the velocity of fragments from impact disruptions p 189 N94-12359

ROTOR AERODYNAMICS
A grid generation method to calculate the flow field in a three-dimensional cascade of blades
[NAL-TR-1158] p 147 N94-10364
Solving the inverse problem for incompressible potential flow through two-dimensional cascades
[NAL-TR-1162] p 147 N94-10365

ROTOR BLADES (TURBOMACHINERY)
A grid generation method to calculate the flow field in a three-dimensional cascade of blades
[NAL-TR-1158] p 147 N94-10364
Solving the inverse problem for incompressible potential flow through two-dimensional cascades
[NAL-TR-1162] p 147 N94-10365
Viscous analysis of three-dimensional rotor flows using a multigrid method
[NASA-TM-106266] p 152 N94-11481

ROTORS
Dynamic tester for rotor seals and bearings
[NASA-CASE-MFS-28493-1] p 33 N94-10669
Development of passive superconducting bearings. Phase 3
[AD-A266050] p 180 N94-10706
A comparison between numerically modelled and experimentally measured loss mechanisms in wave rotors
[NASA-TM-106279] p 29 N94-11255

ROUTES
Federal Aviation Administration aviation forecasts
[AD-A265611] p 2 N94-12578

ROVING VEHICLES
Conceptual studies report on lunar and planetary exploration
[NASDA-TK-SS0438] p 481 N94-12323

RUBIDIUM
Disciplined rubidium oscillator with GPS selective availability p 353 N94-10977

RUN TIME (COMPUTERS)
Massively parallel hydrodynamics on unstructured grids
[DE93-007325] p 153 N94-11601

RUNWAYS
The Memphis Precision Runway Monitor Program Instrument Landing System final approach study
[AD-A266035] p 23 N94-11103

RURAL AREAS
The Canadian experience: Using telemedicine for the support of medical care at remote sites p 305 N94-11789
The revitalization of health and education in Rural America Act of 1992 p 308 N94-11810

RUSSIAN FEDERATION
Space nuclear technology
[DE93-010184] p 45 N94-10299

RUSTING
Effect of surface cleanliness of bearing steel on adhesive strength and tribological properties of sputter-deposited gold films
[DE93-767974] p 82 N94-10732

S

S GLASS
Hydrostatic testing of thick laminated composite cylinders for performance model validation
[DE93-012728] p 184 N94-10264

S WAVES
Wave propagation characteristics of short-period crustal phases near ARCESS and NORESS
[AD-A265959] p 275 N94-11102

S-N DIAGRAMS
Development of a fatigue analysis approach for CFRP structures under acoustic loading p 58 N94-10018

SAFETY
Safety of high speed ground transportation systems: X2000 US demonstration vehicle dynamics trials, preliminary test report, October 1992 - January 1993
[PB93-194645] p 422 N94-10736

SAFETY MANAGEMENT
Achievements and challenges of Space Station Freedom's safety review process
[NASA-TM-106199] p 40 N94-10640
Health and safety issues for aerospace workers in the use of advanced materials p 21 N94-10795
The future of aircraft cabin fire safety p 22 N94-10797

SAGNAC EFFECT
Interferometry with particles of non-zero rest mass
[DE93-613518] p 409 N94-10501

SALINITY
Shear, strain and thermohaline vertical fine structure in the upper ocean
[AD-A265961] p 289 N94-12348

SALMONELLA
Compatibility tests for biological specimens to on-board experiments in the Space Shuttle flight
[NASDA-CNT-930003] p 301 N94-12278

SALTS
Aluminum and membrane channels
[AD-A265241] p 300 N94-11020
Modeling void growth and movement with phase change in thermal energy storage canisters
[NASA-TM-106288] p 163 N94-12576

SAMARIUM ISOTOPES
Radiogenic age and isotopic studies
[DE93-610548] p 274 N94-10407

SAMPLERS
Analytical method for water vapor collection and analysis in aircraft cabin fires
[DOT/FAA/CT-TN93/33] p 22 N94-12575

SAMPLING
Analytical method for water vapor collection and analysis in aircraft cabin fires
[DOT/FAA/CT-TN93/33] p 22 N94-12575
Optimal hemicube sampling
[DE93-010499] p 334 N94-12591

SANDS
Coastal processes due to nearshore current around an upheaving island p 199 N94-11942
A simple model of clastic sediments on Mars p 460 N94-12155

SANDSTONES
Inverting ultrasonic data on solid/fluid mixtures for Biot-Gassmann parameters
[DE93-011952] p 150 N94-11026
In situ secondary ion mass spectrometry analysis
[DE93-012185] p 76 N94-11140
Si-29 NMR spectroscopy of naturally-shocked quartz from Meteor Crater, Arizona: Correlation to Kieffer's classification scheme p 80 N94-12087

SANDWICH STRUCTURES
Low cost and thermally stable sandwich design for FIRST p 57 N94-10009
Design and manufacturing of filament wound thrust cylinder p 57 N94-10010
Development tests for a high stability optical bench p 62 N94-10047
Adaptive structure design employing shape memory actuators p 70 N94-11331

SAPPHIRE
Arcjet exploratory tests of ARC optical window design for the AFE vehicle
[NASA-CR-192655] p 34 N94-10930

SARSAT
Low cost high efficiency GaAs monolithic RF module for SARSAT distress beacons
[NASA-CR-194235] p 146 N94-12773

SATELLITE ALTIMETRY
Topex/Poseidon: A United States/France mission. Oceanography from space: The oceans and climate
[NASA-TM-108253] p 43 N94-10699
Proceedings of First ERS-1 Symposium on Space at the Service of Our Environment, volume 1
[ESA-SP-359-VOL-1] p 232 N94-11704
Calibration of ERS-1 altimetry over the North Sea p 234 N94-11716
Effects of wave nonlinearity on ERS-1 radar altimeter returns: A preliminary investigation p 235 N94-11722
Comparisons of ERS-1 altimeter height data and the Fine Resolution Antarctic Model (FRAM) p 235 N94-11725
Analysis of ERS-1 altimeter data over the polar ice sheets p 237 N94-11738
Some results of the derivation of ice sheet elevations in Antarctica from ERS-1 altimeter data p 237 N94-11739
Preliminary evaluation of ERS-1 altimetry over Filchner-Ronne Ice Shelf, Antarctica p 238 N94-11742
The height calibration of the ERS-1 radar altimeter p 241 N94-11764
First results for the simultaneous estimation of the geoid and the sea surface topography by ERS-1 altimeter data p 241 N94-11765
Separation of geoid and sea surface topography in shallow water regions: A first ERS-1 radar altimeter data evaluation p 242 N94-11766
A stochastic-deterministic approach as an alternative to classical cross-over techniques in small ocean basins p 242 N94-11767
An analysis of the gravity field in the Norwegian Sea and mapping of the ice cap of Greenland using ERS-1 altimeter measurements p 242 N94-11768
Space and time variability of the Gulf Stream using ERS-1 ALT-OPR02 data p 242 N94-11769
ERS-1 radar altimetry over the North Atlantic p 242 N94-11772
The effect of rain on ERS-1 altimeter data p 243 N94-11773
Preliminary geophysical investigation with ERS-1 35-day altimeter data p 243 N94-11775
Arctic geodynamics: Continental shelf and deep ocean geophysics. ERS-1 satellite altimetry: A first look p 243 N94-11776
Quick-look monitoring of the sea surface with ERS-1 fast delivery altimeter data p 243 N94-11777
The Earth's gravity model for the ERS 1 commissioning phase p 243 N94-11778
Global wave height climatologies from ERS-1 altimeter data, and comparisons with those from GEOSAT p 244 N94-11781
The 1992 El Nino viewed by ERS-1 altimetry p 244 N94-11784
Using transponders with the ERS-1 altimeter to measure orbit altitude to +/- 3 cm p 244 N94-11785

Ocean circulation revealed by altimeter data p 245 N94-11786

Westward propagation of sea surface anomalies in the western North Pacific as seen by the altimeter and radiometer p 198 N94-11941

Surface roughness variations across the Iceland-Faroes frontal region observed by the GEOSAT altimeter and NOAA AVHRR p 201 N94-11958

On the variability of wind speeds in the North Western Pacific observed by altimeter/GEOSAT and SSM/I/DMSP p 201 N94-11960

Observation of wind and waves by GEOSAT altimeter p 202 N94-11961

ERS-1 altimetry of inland water and land p 246 N94-12475

Use of ERS-1 wind and wave products in operational meteorology p 250 N94-12502

Comparison of ERS-1 SAR images of the Western Mediterranean to in situ oceanographic data: PRIM-1 Cruise (May 1992) p 255 N94-12529

Topography of the Western Mediterranean from the ERS-1 altimeter p 255 N94-12531

Observations of eddy fields in the Northwest Pacific by GEOSAT altimetry p 207 N94-12639

Variability of sea level and sea surface temperature anomalies in the equatorial Pacific p 208 N94-12640

Theory and oceanographic applications of satellite altimeter measurements p 208 N94-12641

Analysis of collinear passes of satellite altimeter data p 208 N94-12642

Surface eddy fluxes from the GEOSAT satellite altimeter p 208 N94-12643

Comparison of GEOSAT sea surface height and model-simulated surface dynamic height p 208 N94-12644

Pseudo magnetic anomaly derived from satellite altimetry and its application to the tectonics in the North Fuji Basin p 208 N94-12645

Principal oscillation pattern analysis of sea level variations in the tropical Pacific measured by the GEOSAT altimeter p 209 N94-12646

Measurement of eddy structure and movement in the north-east Pacific with the GEOSAT altimeter p 209 N94-12647

Preliminary results from a satellite altimetric data assimilation using a Kalman filter and smoother p 209 N94-12648

Fluctuations of the Kuroshio extension detected by the GEOSAT altimetry data p 209 N94-12649

Mean flow and variability in the Kuroshio extension from GEOSAT altimetry data p 209 N94-12650

SATELLITE ATMOSPHERES

Sources of Na for the Io atmosphere p 455 N94-12127

Geomorphology of Triton's polar materials p 466 N94-12185

SATELLITE ATTITUDE CONTROL

Project of an attitude control system (three axis) of a satellite using the LQG/LTR methodology [INPE-5473-TDI/504] p 44 N94-12356

SATELLITE COMMUNICATION

Potential markets for advanced satellite communications [NASA-CR-191145] p 41 N94-10512

Space Activities in the Asia Pacific Region [JTN-93-80421] p 35 N94-10676

Current status of space activities in Asia Pacific region p 35 N94-10677

Space programme in Malaysia p 36 N94-10685

National space program in Australia p 37 N94-10691

PARTNERS p 38 N94-10695

The 24th Annual Precise Time and Time Interval (PTTI) Applications and Planning Meeting [NASA-CP-3218] p 350 N94-10963

Two way time transfer results at NRL and USNO p 353 N94-10983

New technology applied to telemedicine p 306 N94-11796

Space technology in remote health care p 306 N94-11799

Use of satellite telecommunications for telemedicine p 308 N94-11807

Use of low orbital satellite communications systems for humanitarian programs p 308 N94-11808

SATELLITE CONTROL

Pre-operation analysis of ERS-1 tracking and operation, part 2-A [NASDA-CNT-930001-PT-2-A] p 230 N94-11129

Pre-operation analysis of ERS-1 tracking and operation, part 2-F [NASDA-CNT-930002-PT-2-F] p 230 N94-11130

Flight data analysis of Japanese Earth Resources Satellite-1 (JERS-1) [NASDA-CNT-930004] p 245 N94-12279

SATELLITE DESIGN

Design and development of a CFRP central cylinder for satellites p 56 N94-10007

Japanese space activities p 36 N94-10682

Overview of KITSAT p 36 N94-10683

Korea space program p 36 N94-10684

Space transportation alternatives for large space programs: The International Space University Summer Session, 1992 [NASA-TM-106271] p 40 N94-10811

SATELLITE GROUND SUPPORT

Pre-operation analysis of ERS-1 tracking and operation, part 2-A [NASDA-CNT-930001-PT-2-A] p 230 N94-11129

Pre-operation analysis of ERS-1 tracking and operation, part 2-F [NASDA-CNT-930002-PT-2-F] p 230 N94-11130

SATELLITE GUIDANCE

Pre-operation analysis of ERS-1 tracking and operation, part 2-A [NASDA-CNT-930001-PT-2-A] p 230 N94-11129

Pre-operation analysis of ERS-1 tracking and operation, part 2-F [NASDA-CNT-930002-PT-2-F] p 230 N94-11130

SATELLITE IMAGERY

Space research and remote sensing programmes in Bangladesh p 35 N94-10679

Space program in Indonesia p 36 N94-10681

Panel discussion: Role of space program in the Asia Pacific Region p 37 N94-10694

Statistical study on the regional and seasonal distribution of fog in the far east region by using GMS imagery p 190 N94-11082

TOVS soundings: Impact on the synoptic analysis over the south and southeast regions of Brazil from March 18 to March 19, 1991 [INPE-5497-TDI/512] p 230 N94-11179

Bayesian model for pictorial data fusion of satellite image [INPE-5457-TDI/499] p 345 N94-11193

Satellite inventory of Minnesota forest resources [NASA-CR-193565] p 231 N94-11521

Validation of directional wave spectra from the ERS-1 during the ESA CAL/VAL campaign p 232 N94-11707

Coastal ocean studies with ERS-1 SAR during NORCSEX 1991 p 234 N94-11720

SAR imaging of dynamical features in the English Channel p 234 N94-11721

SAR ocean imaging in the Gulf of Alaska p 235 N94-11723

ERS-1 SAR calibration strategy p 235 N94-11726

Calibration of the ERS-1 SAR fast-delivery images p 236 N94-11730

The use of active devices in the ERS-1 radiometric calibration p 236 N94-11732

An experiment for the radiometric calibration of the ERS-1 SAR p 236 N94-11733

Techniques and applications of SAR interferometry for ERS-1: Topographic mapping, change detection, and slope measurement p 236 N94-11734

SAR interferometry experiments with ERS-1 p 237 N94-11735

SAR-interferometry applying ERS-1: Some preliminary test results p 237 N94-11736

Monitoring of the Greenland Ice Sheet using ERS-1 synthetic aperture radar imagery p 237 N94-11741

Investigations of Arctic ice-sheets and glaciers using ERS-1 SAR p 238 N94-11743

Ice studies in the Barents Sea by ERS-1 SAR during SIZEX 92 p 238 N94-11745

Arctic coastal polynya observations with ERS-1 SAR and DMSP SSM/I p 239 N94-11748

Sea ice deformation observed with ERS-1 SAR p 239 N94-11749

Finnish ERS-1 Baltic Sea ice experiment in Winter 1992 p 239 N94-11750

C-band SAR backscatter from ice on shallow tundra lakes: Observations and modelling p 240 N94-11755

Sea ice radar signatures from ERS-1 SAR during late Summer and Fall in the Beaufort and Chukchi Seas p 240 N94-11756

Sea ice feature and type identification in merged ERS-1 SAR and LANDSAT Thematic Mapper imagery p 241 N94-11761

An analysis of the gravity field in the Norwegian Sea and mapping of the ice cap of Greenland using ERS-1 altimeter measurements p 242 N94-11768

The Earth's gravity model for the ERS-1 commissioning phase p 243 N94-11778

Proceedings of the PORSEC 1992 in Okinawa: Conference for Pacific Ocean Environments and Probing, volume 1 [JTN-93-80418] p 191 N94-11894

A statistical method to determine aerosol path radiance and its application to atmospheric correction for CZCS imagery p 191 N94-11897

Satellite observations of red tide events: Plans for EESI p 191 N94-11899

Satellite derived sea surface temperature applications for Indian Ocean resources development p 193 N94-11907

Exchange of bay water with ocean current monitored by the NOAA satellite p 193 N94-11908

A consideration on principal component analysis of satellite IR data p 193 N94-11909

The use of remote sensing data for coastal zone management and environment in Indonesia p 196 N94-11927

Shoreline change detection using remote sensing and GIS in Vietnam p 196 N94-11928

The requirement for global training programmes to meet the new remote sensing technology p 196 N94-11929

Analysis of the characteristic and mechanism of suspended matter transportation in Huanghe delta sea area using remote sensing techniques p 197 N94-11930

The extraction of bottom characteristics and mapping in Kin Bay, Okinawa Main Island, Japan, using LANDSAT-5/TM and SPOT-1/HRV data p 197 N94-11931

Ocean-ice interaction study of waves and mesoscale features p 197 N94-11935

Warm streamers extended from Warm Core Rings (WCRs) and their role on fish migration and fishing ground formation p 198 N94-11938

The Kyucho events in Sukumo Bay induced by Kuroshio front disturbances p 198 N94-11939

The coherent structure in the oceanic turbulence around Japan Islands Chain forced by an air, sea, and solid Earth interaction p 198 N94-11940

Westward propagation of sea surface anomalies in the western North Pacific as seen by the altimeter and radiometer p 198 N94-11941

Characteristic scales and vortex features of mesoscale vortices observed by the satellites during the winter p 199 N94-11943

The use of CZCS for primary production estimate in the Pacific p 199 N94-11946

CZCS derived chlorophyll distribution in Antarctic water during austral summer p 199 N94-11947

Seasonal changes of phytoplankton distributions in the Northwest Pacific detected by Coastal Zone Color Scanner p 200 N94-11948

Satellite-derived oceanic features p 200 N94-11949

Particle dynamics in the western subarctic Pacific: Implications from CZCS imagery p 200 N94-11950

High-reflectance water mass in Off-Sanriku area observed by CZCS p 200 N94-11951

Dependence of oceanic microwave emission on wind direction p 201 N94-11957

Surface roughness variations across the Iceland-Faroes frontal region observed by the GEOSAT altimeter and NOAA AVHRR p 201 N94-11958

On the variability of wind speeds in the North Western Pacific observed by altimeter/GEOSAT and SSM/I/DMSP p 201 N94-11960

Wind field estimate by using one hour GMS data p 202 N94-11963

Atmospheric correction plans for SeaWiFS p 204 N94-11975

Overwater atmospheric dispersion of volcanic smokes from Mt. Sakurajima observed in NOAA-AVHRR data p 205 N94-11979

Incident shortwave and longwave radiations over the western North Pacific and the Sea of Okhotsk derived from GMS-WEFAX images p 205 N94-11982

Observations of the fractal properties of the Japan sea surface temperature patterns p 205 N94-11984

Flood monitoring in northern part of Central Java by remote sensing technique. Case study: The flooding of Semarang in January, 1990 p 206 N94-11989

Preliminary report of lunar observations by the Near-Infrared Mapping Spectrometer (NIMS) during the second Galileo Earth-Moon encounter p 425 N94-12140

Galileo EM-2 contributions to the lunar control network p 468 N94-12198

Proceedings of 1st ERS-1 Symposium on Space at the Service of Our Environment, Volume 2 [ESA-SP-359-VOL-2] p 245 N94-12471

Methodological considerations for use of ERS-1 imagery for the delineation of river networks in tropical forest areas p 247 N94-12484

Per-field filtering and classification of multitemporal ERS-1 SAR imagery p 247 N94-12485

Preliminary ERS-1 assessment for Canadian agriculture and forestry applications p 248 N94-12486

Segmentation and change detection in ERS-1 images over East Anglia p 248 N94-12487

ERS-1 SAR crop monitoring experiment in East Anglia, UK p 248 N94-12488

The TREES project: Pre-processing and generation of terrain data for inclusion in an ERS-1 SAR classification scheme p 249 N94-12496
ERS-1 and Almaz SAR ocean wave imaging over the Gulf Stream and the Grand Banks p 251 N94-12505
Oil spill detection using satellite-based SAR: Experience from a field experiment p 253 N94-12522
ERS-1 imaging radar over the Waddensea-North Netherlands p 254 N94-12526
Comparison of ERS-1 SAR images of the Western Mediterranean to in situ oceanographic data: PRIM-1 Cruise (May 1992) p 255 N94-12529
Proceedings of the PORSEC 1992 in Okinawa: Conference for Pacific Ocean Environments and Probing, volume 2
[JTN-93-80419] p 207 N94-12635
Analysis of GEOSAT wind data p 207 N94-12636
Observation of wave crests by satellite remote sensed data p 207 N94-12638
Variability of sea level and sea surface temperature anomalies in the equatorial Pacific p 208 N94-12640
Pacific rim sea ice as observed with the NIMBUS-7 SMMR p 210 N94-12651
Disintegrating ice front of Shirase Glacier, East Antarctica p 210 N94-12654
Worldwide map of rainfall amount over the ocean derived from passive microwave radiometer p 211 N94-12663
Study on diffusion phenomena of river effluents issued into sea around Japan with satellite remote sensing data p 212 N94-12664
A basic consideration for remote sensing using microwave radars on a satellite p 212 N94-12665
Migration of operational ice analysis and forecasting to a workstation platform at the Joint Ice Center p 212 N94-12666
Evaluating the spread of red soil with LANDSAT TM data in coral reefs of Okinawa main island, southwestern Japan p 212 N94-12668
Simple and low cost image processing system for satellite remote sensing data p 212 N94-12669
Validation test system for sea surface temperature detected by satellites in Mutsu Bay p 213 N94-12670
Sea surface temperature images of Geostationary Meteorological Satellite (GMS) and sea truth data from ferry boats p 213 N94-12671
Evaluation of the method of geostrophic flow using NOAA-AVHRR data p 213 N94-12673
Further study of the Non-Regression-Coefficient SST retrieval method p 213 N94-12674
Delineation of mesoscale features of ocean on satellite IR image p 214 N94-12675
Observation of warm current at the boundary from north equatorial current to Kuroshio by NOAA/AVHRR p 214 N94-12676
Information capability of NOAA-AVHRR data for monitoring oceanographic and atmospheric pollution p 214 N94-12677
Satellite observations of the northeast monsoon coastal current p 214 N94-12678
Aspects of applying a relaxation method to computing sea surface velocities from sea surface temperature images p 214 N94-12679
Sea surface temperature difference between NOAA/AVHRR and in-situ observation p 215 N94-12680
Application of NOAA AVHRR data to fisheries p 215 N94-12681
Statistical features of mesoscale eddies at the Kuroshio front p 215 N94-12682
Intrusion of Kuroshio warm water into Sagami Bay p 215 N94-12683
A study of front dynamics off northeastern Taiwan based on the NOAA-AVHRR satellite remote sensing data p 215 N94-12684
Satellite thermal variations of Kuroshio in relation to storm floods p 215 N94-12685
Frontal zones in Pacific Ocean: Satellite and ship data analysis p 216 N94-12687
Swordfish (Xiphias gladius) catch distributions relative to environmental features observed from satellites off Coquimbo, Chile (30 deg S) p 216 N94-12688
Observation of cold coastal water with high turbidity around the southwestern tip of Korean Peninsula p 216 N94-12689
On the error characteristics of the sea surface temperature observed by satellite p 216 N94-12690
Remote sensing of polluting focal points and coastal disturbances in the Gulf of Arauco and adjacent bays, central Chile p 217 N94-12695
Role of remote sensing and its cost effectiveness in site selection for coastal aquaculture p 217 N94-12697
Application of remote sensing for coastal management in the north coast of Java p 218 N94-12701
Estimation of areal evapotranspiration using LANDSAT TM data: Kitami City, Hokkaido, Japan p 219 N94-12703
Land use/land cover mapping of central water shed of Iran area based on satellite data interpretation p 219 N94-12704
A method to minimize reference data in classifying satellite remote sensing data into land cover classes p 219 N94-12705
Study on air-sea interactions in the OMLET (Ocean Mixed Layer Experiment) area using satellite remote sensing p 220 N94-12710
Investigation of meso-scale fronts, eddies and upwellings in China Seas with AVHRR data p 220 N94-12711
Coastal upwelling monitored by satellite data: Methodologies and results p 220 N94-12712
The warm eddy detection from NOAA/AVHRR thermal images using the Hough transformation p 220 N94-12713
Applicability of satellite infrared data for the monitoring of coastal environments p 220 N94-12714
Satellite and moored buoy observations of polar frontal system over the Yamato Rise in the Japan Sea p 221 N94-12715
Variability of the Kuroshio observed from satellite thermal imagery p 221 N94-12717
SST assimilation: Eastern Mediterranean case study p 221 N94-12719
Mapping of high density area of benthic diatom in Ariake Sea p 222 N94-12720
Advective surface velocity in the north west Pacific derived from NOAA AVHRR images p 222 N94-12721
On a nonstationary dynamics of the north-west Pacific Ocean p 222 N94-12724
Influence of the Kuroshio warm-core rings on hydrographic and fishery conditions off southern Kuril Islands p 224 N94-12737
Verification of the atmosphere-ocean radiative transfer parametric models p 225 N94-12738
Optical transfer operator of the atmosphere-ocean system p 225 N94-12742
Atmospheric correction for determination of average SST fields based on AVHRR data p 227 N94-12750

SATELLITE NAVIGATION SYSTEMS
Comparison of GPS and GLONASS common-view time transfers p 24 N94-10967

SATELLITE NETWORKS
Use of low orbital satellite communications systems for humanitarian programs p 308 N94-11808

SATELLITE OBSERVATION
Space Activities in the Asia Pacific Region
[JTN-93-80421] p 35 N94-10676
Space research and remote sensing programmes in Bangladesh p 35 N94-10679
Space program in Indonesia p 36 N94-10681
Space programme in Malaysia p 36 N94-10685
National space programmes and application of the remote sensing data in Mongolia p 36 N94-10686
Russian space system for the Earth remote sensing p 37 N94-10688
Sun-synchronous and geo-synchronous satellite data utilization for environmental studies p 37 N94-10689
Thailand ISY activities p 37 N94-10690
National space program in Australia p 37 N94-10691
Panel discussion: Role of space program in the Asia Pacific Region p 37 N94-10694
Retrieval of radiation budgets in the Arctic from satellite measurements p 229 N94-10714
Satellite-derived photosynthetically available and total solar irradiance at the surface during FIFE's intensive field campaigns p 230 N94-10954
Estimating Photosynthetically Available Radiation (PAR) at the Earth's surface from satellite observations p 230 N94-10955
Ultraviolet plume instrument description and plume data reduction methodology
[AD-A266141] p 54 N94-11643
Utilisation of ERS-1 data for mapping of Antarctica p 237 N94-11740
A stochastic-deterministic approach as an alternative to classical cross-over techniques in small ocean basins p 242 N94-11767
The Earth's gravity model for the ERS-1 commissioning phase p 243 N94-11778
Using transponders with the ERS-1 altimeter to measure orbit altitude to +/- 3 cm p 244 N94-11785
Satellite observation of atmospheric tracer components: JEM/POP p 130 N94-11836
Submillimeter wave observation experiment of Earth atmosphere with SIS mixer p 130 N94-11837
Satellite observations of red tide events: Plans for EESI p 191 N94-11899
An algorithm for the detection of mucilage (green slime) in the Adriatic Sea p 191 N94-11900
Remote sensing of the suspended matter distribution with high concentration in China Sea p 192 N94-11901
Scatterometer observations: Review p 201 N94-11956
Overwater atmospheric dispersion of volcanic smokes from Mt. Sakurajima observed in NOAA-AVHRR data p 205 N94-11979
Integration of ERS-1 data into the European project of agriculture statistics p 248 N94-12490
Assessment of ERS-1 SAR data for soil moisture estimation p 249 N94-12492
Temporal monitoring of soil moisture using ERS-1 SAR data p 249 N94-12493
Observations of ERS-1 SAR sensitivities to changes in aboveground biomass in young loblolly pine forests p 249 N94-12494
Seeing the Black Forest by ERS-1 and AIRSAR: A comparison p 249 N94-12495
TREES project: A case study on the use of multi-temporal ERS-1 SAR data and SPOT data for monitoring tropical ecosystems p 249 N94-12497
Studies of dynamical processes affecting the distribution of stratospheric ozone
[NASA-CR-193477] p 279 N94-12560
Proceedings of the PORSEC 1992 in Okinawa: Conference for Pacific Ocean Environments and Probing, volume 2
[JTN-93-80419] p 207 N94-12635
Observations of surface signatures in the north-west Pacific Ocean with the spaceborne SAR p 226 N94-12746
Radar observation of internal waves field in the north-west Pacific p 226 N94-12747
Complex (hydrodynamic, satellite) monitoring of dynamic structures in the western Pacific with the aim of forecasting the marine ecosystems behaviour p 227 N94-12753
Mesoscale dynamic structures of the Subarctic Frontal Zone in the Pacific Ocean p 227 N94-12754
The algorithm of primary production determination p 228 N94-12761
Non-image visible polarization remote sensing of the ocean p 229 N94-12762
Problem of climate change predictability and satellite radiation budget observations p 229 N94-12766
Radiometer offsets and count conversion coefficients for the Earth Radiation Budget Experiment (ERBE) spacecraft for the years 1987, 1988, and 1989
[NASA-CR-191489] p 286 N94-12772

SATELLITE ORBITS
Satellite situation report, volume 32, no. 1
[NASA-TM-109233] p 42 N94-10562
Satellite situation report, volume 32, no. 2
[NASA-TM-109234] p 42 N94-10563
Satellite situation report, volume 31, no. 4
[NASA-TM-109232] p 39 N94-10659
ERS-1 precise orbit determination p 244 N94-11779
Orbital simulations of satellite escape/capture and the origin of satellites such as Triton p 429 N94-12057
Regional orbit precision in the Mediterranean area p 39 N94-12530

SATELLITE ORIENTATION
Estimation of the attitude motion of the small satellite ORIZURU
[NAL-TR-1145] p 42 N94-10366

SATELLITE POWER TRANSMISSION
Space transportation alternatives for large space programs: The International Space University Summer Session, 1992
[NASA-TM-106271] p 40 N94-10811
Construction and testing of a space ready rectenna
[NASA-CR-193310] p 137 N94-11357

SATELLITE SOLAR POWER STATIONS
Space transportation alternatives for large space programs: The International Space University Summer Session, 1992
[NASA-TM-106271] p 40 N94-10811

SATELLITE SOUNDING
Space Activities in the Asia Pacific Region
[JTN-93-80421] p 35 N94-10676
Panel discussion: Role of space program in the Asia Pacific Region p 37 N94-10694
TOVS soundings: Impact on the synoptic analysis over the south and southeast regions of Brazil from March 18 to March 19, 1991
[INPE-5497-TDI/512] p 230 N94-11179
Satellite observation of atmospheric tracer components: JEM/POP p 130 N94-11836
Submillimeter wave observation experiment of Earth atmosphere with SIS mixer p 130 N94-11837
Effects of satellite spectral resolution and atmospheric water vapor on retrieval of near-ground temperatures
[AD-A264920] p 245 N94-11851

The extraction of bottom characteristics and mapping in Kin Bay, Okinawa Main Island, Japan, using LANDSAT-5/TM and SPOT-1/HRV data
p 197 N94-11931

SATELLITE SURFACES

Physical studies of planetary and satellite surfaces
[NASA-CR-193545] p 434 N94-10817

A structural origin for the cantaloupe terrain of Triton
p 449 N94-12095

Sources of Na for the Io atmosphere
p 455 N94-12127

Interdisciplinary scientist participation in the Phobos mission
[NASA-CR-193715] p 482 N94-12446

SATELLITE TRACKING

Toward 10(exp 9) GPS geodesy: Vector baselines, Earth rotation and reference frames
[NASA-CR-193184] p 229 N94-10702

Operational ERS-1 orbit determination at D-PAF
p 243 N94-11774

ERS-1 precise orbit determination
p 244 N94-11779

Regional orbit precision in the Mediterranean area
p 39 N94-12530

SATELLITE-BORNE INSTRUMENTS

Imaging of magnetospheric dynamics using low energy neutral atom detection
[DE93-012656] p 275 N94-10742

Calibration and validation of the ERS-1 wind scatterometer p 232 N94-11706

A preliminary C-band scatterometer model function for the ERS-1 AMI instrument p 233 N94-11715

Calibration of ERS-1 altimetry over the North Sea
p 234 N94-11716

Preliminary results of the experiment I-7
p 235 N94-11728

The ERS-1/CV 580 SAR cross-calibration experiment: Sault Ste Marie, October 26 - November 2, 1991
p 236 N94-11729

Calibration results for the ERS-1, AIRSAR, and PHARS p 236 N94-11731

An experiment for the radiometric calibration of the ERS-1 SAR p 236 N94-11733

SATELLITE-BORNE RADAR

Utilisation of ERS-1 data for mapping of Antarctica
p 237 N94-11740

Monitoring of the Greenland Ice Sheet using ERS-1 synthetic aperture radar imagery p 237 N94-11741

SATURN (PLANET)

Disk-resolved spectral characteristics of Saturn's medium-sized satellites p 471 N94-12213

SATURN SATELLITES

Disk-resolved spectral characteristics of Saturn's medium-sized satellites p 471 N94-12213

SCALARS

The effect of a scalar boson coupled to neutrinos on the behavior of the tritium beta decay spectrum near the end point
[DE93-012655] p 361 N94-10349

Bound states of the N-dimensional Klein-Gordon equation with vector and scalar Coulomb potentials
[DE93-617650] p 349 N94-10547

A new approach to the I/N-expansion for the Dirac equation
[DE93-617647] p 349 N94-10833

Exact solution of the N-dimensional generalized Dirac-Coulomb equation
[DE93-617649] p 411 N94-10834

A theoretical kinematical study of the gradient of any cosmic scalar field
[DE92-644731] p 425 N94-11136

PDF approach for turbulent scalar field: Some recent developments p 160 N94-12315

SCALE EFFECT

Planck scale effects on the Majoron
[DE93-613120] p 410 N94-10545

SCALE MODELS

An experimental investigation of high-speed water-entry for full-size and scale-model pointed nose vehicles
[DE93-008491] p 147 N94-10252

Application of normalized gray-scale correlation
[DE93-013765] p 141 N94-10521

Characterization of a scannerless LADAR system
[DE93-011582] p 174 N94-10959

A four-dimensional, mesoscale, non-gaussian multispectral smoke model. Phase 1: Feasibility study
[AD-A264805] p 152 N94-11519

SCALING LAWS

Dimensional scaling for impact cratering and perforation
[NASA-CR-188259] p 42 N94-10665

Helium transport scaling law studies
[DE93-013487] p 393 N94-11513

Power-law confusion: You say incremental, I say differential p 347 N94-12175

SCANNERS

Calorimetric thermometry of meteoritic troilite: A feasibility study p 428 N94-12025

SCANNING ELECTRON MICROSCOPY

Fractography handbook of spaceflight metals
[NASA-RP-1291] p 81 N94-10504

Measurement of the minority carrier diffusion length and edge surface-recombination velocity in InP
p 49 N94-11388

Atomic-scale imaging of surfaces and interfaces. Materials Research Society Symposium Proceedings, volume 295
[AD-A265674] p 369 N94-12379

SCANNING TUNNELING MICROSCOPY

Site dependence of the apparent shape of a molecule in STM images: Benzene on Pt(111)
[AD-A263488] p 365 N94-11093

Dynamic studies of crystal growth using the AFM
[DE93-009549] p 399 N94-11268

Real-space formation and dissipation dynamics of hexagonal reconstruction on Au(100) in aqueous media as explored by potentiodynamic scanning tunneling microscopy
[AD-A266138] p 368 N94-11658

Adsorption and dissociation of disilane on Si(001) studied by STM
[AD-A265269] p 402 N94-11684

Atomic-scale imaging of surfaces and interfaces. Materials Research Society Symposium Proceedings, volume 295
[AD-A265674] p 369 N94-12379

Electrode potential-induced reconstruction of Au(100): Effect of chemisorption on nanoscale dynamics as probed by the in-situ scanning tunneling microscopy
[AD-A265900] p 404 N94-12388

SCATTERING

Preliminary results on backscattering strength from a wind generated bubbly ocean surface
[AD-A265006] p 287 N94-10490

Coherence effects in radiometry and in spectroscopy
[DE93-013437] p 75 N94-10519

Scattering of modulated Ultra-Relativistic Electron Beam (UREB) by atmospheric plasma
[DE93-620987] p 387 N94-10558

Interstellar scattering and the selection of extragalactic radiosources with highly compact components
p 134 N94-11063

Radiation and scattering by cavity-backed antennas on a circular cylinder
[NASA-CR-193409] p 136 N94-11084

SCATTERING AMPLITUDE

Indication on the existence of the bound state in the p anti p-system
[DE92-641575] p 361 N94-10532

P-matrix description of the two-particle interaction
[DE93-617690] p 361 N94-10549

Crossing-odd spin effects in the dipole model of hadron scattering
[DE93-617692] p 362 N94-10551

Model for the pomeron
[DE93-617693] p 362 N94-10552

Fine structure of the Pomeron and the real part of the elastic scattering amplitude
[DE93-617696] p 362 N94-10555

On the possible unobservability of the Wu-Yang phase factor in curved space
[DE93-617645] p 411 N94-10831

FEFF5: An ab initio multiple scattering XAFS code
[DE93-011000] p 367 N94-11470

Fermion-boson scattering in ladder approximation
[DE93-613111] p 368 N94-11581

SCATTERING COEFFICIENTS

Polarisation of backscattering radiation at remote sensing of ocean with impulse laser beam
p 177 N94-12722

Remote sensing of light scattering coefficient of sea water vertical distribution by the means of airborne lidar
p 224 N94-12736

SCATTERING CROSS SECTIONS

Convergent close-coupling calculations of electron-hydrogen scattering
[DE93-610049] p 360 N94-10328

Distorted-wave calculation of He(e,2e) including core-exchange
[DE93-610072] p 360 N94-10330

Logarithmically rising cross section and the ratio sigma(sub el)/sigma(sub t)
[DE93-617694] p 362 N94-10553

Detecting the odderon
[DE93-617695] p 362 N94-10554

Interpretation of lunar and planetary electromagnetic scattering using the full wave solutions
p 440 N94-12049

Low voltage electron beam lithography
[AD-A265358] p 145 N94-12405

Final state interactions and inclusive nuclear collisions
[NASA-TP-3353] p 373 N94-12435

SCATTEROMETERS

Calibration and validation of the ERS-1 wind scatterometer p 232 N94-11706

ERS-1 scatterometer data characteristics and wind retrieval skill p 233 N94-11709

Validation of ERS-1 wind and wave data by use of operational forecast models p 233 N94-11710

A C-band wind scatterometer model derived from the data obtained during the ERS-1 calibration/validation campaign p 233 N94-11711

ERS-1 studies at the Department of Oceanography from Space, IFREMER/Brest (France) p 233 N94-11712

The activity of the ERS-1 Venice (Italy) group on scatterometry p 233 N94-11713

Use of ERS-1 data at Saclant Undersea Research Centre p 233 N94-11714

A preliminary C-band scatterometer model function for the ERS-1 AMI instrument p 233 N94-11715

Preliminary analysis of circulations over the Indian Ocean and adjoining regions using ERS-1 surface winds in the NCMRWF data assimilation system p 234 N94-11719

Evaluation of two January - June 1992 ERS-1 AMI wind vector data sets p 235 N94-11724

Scatterometer observations: Review
p 201 N94-11956

The microwave backscattering from wind waves
p 201 N94-11959

A first assessment of the value of ERS-1 scatterometer winds for meteorological studies in the polar regions
p 250 N94-12501

Use of ERS-1 wind and wave products in operational meteorology p 250 N94-12502

Use of ERS-1 scatterometer winds in Canadian forecast centres p 250 N94-12504

SCENE ANALYSIS

Retrieval of radiation budgets in the Arctic from satellite measurements p 229 N94-10714

A summary of image segmentation techniques
[NASA-TM-104022] p 327 N94-11274

SCHEDULES

National Aero-Space Plane: A need for program direction and funding decisions
[GAO/NSIAD-93-207] p 416 N94-10910

Avoidance and suppression of compensation code in a trace scheduling compiler
[AD-A265612] p 333 N94-12439

Coordinated Radio, Electron, and Waves Experiment (CREWE) for the NASA Comet Rendezvous and Asteroid Flyby (CRAF) instrument
[NASA-CR-194376] p 427 N94-12566

SCHEDULING

ACARA user's manual
[NASA-TM-106277] p 183 N94-11167

Distributed real-time system design: Theoretical concepts and applications
[AD-A265199] p 337 N94-11881

Avoidance and suppression of compensation code in a trace scheduling compiler
[AD-A265612] p 333 N94-12439

SCHLIEREN PHOTOGRAPHY

Analysis of the alignment of a Schlieren system for tele-operation p 111 N94-10140

Evaluation of dual flow thrust vectored nozzles with exhaust stream impingement
[NASA-CR-193292] p 150 N94-10912

SCHOOLS

A summer program in mathematics and computer science for academically oriented student
[AD-A263467] p 415 N94-11517

Career Information in the Mathematical Sciences (CIMS)
[DE93-013780] p 318 N94-11817

SCHOTTKY DIODES

Activation energy and capture cross section of majority carrier traps in Zn doped InP p 49 N94-11386

SCHROEDINGER EQUATION

P-matrix description of the two-particle interaction
[DE93-617690] p 361 N94-10549

Studies of P-matrix formalism on the basis of the potential description of two-particle interaction
[DE93-617691] p 362 N94-10550

Completeness properties of the minimum uncertainty states p 349 N94-10581

Uncertainty relations, zero point energy and the linear canonical group p 378 N94-10590

Positive phase space distributions and uncertainty relations p 379 N94-10598

Coherent states and uncertainty relations for the damped harmonic oscillator with time-dependent frequency
p 380 N94-10611

Quasi-relativistic effects in barrier-penetration processes
[DE93-617730] p 410 N94-10721

Exact solutions of a many-anyon problem [DE93-617646] p 411 N94-10832

SCIENCE

Project TIMS (Teaching Integrated Math/Science) [NASA-CR-194288] p 416 N94-11599

SCIENTIFIC SATELLITES

ESRO's first scientific satellite programme, 1961 - 1966 [ESA-HSR-2] p 44 N94-11462

SCIENTIFIC VISUALIZATION

The Air Force Interactive Meteorological System: A research tool for satellite meteorology [AD-A265957] p 284 N94-11113

Computing science and statistics, Volume 24: Graphics and visualization [AD-A265181] p 332 N94-11878

SCIENTISTS

The legacy of uncertainty p 376 N94-10577

NASA/DOD Aerospace Knowledge Diffusion Research Project. Report 17: A comparison of the technical communication practices of Dutch and US aerospace engineers and scientists [NASA-TM-108987] p 419 N94-11352

SCINTILLATION

A new data collection system for ionospheric modelling and related topics [AD-A265893] p 278 N94-12277

SCINTILLATION COUNTERS

Experimental efforts and results in finding new heavy scintillators [DE93-010406] p 371 N94-10156

Conceptual design report for the SDC barrel and intermediate muon detectors based on a jet-type drift chamber [DE93-753173] p 367 N94-11510

SCREWS

Self locking set screw [AD-D015774] p 178 N94-10385

SEA BREEZE

A study of the Merritt Island, Florida sea breeze flow regimes and their effect on surface heat and moisture fluxes [NASA-CR-4537] p 286 N94-12580

SEA GRASSES

The role of certain infauna and vascular plants in the mediation of redox reactions in marine sediments p 268 N94-12454

SEA ICE

AMIP: The Atmospheric Model Intercomparison Project [DE93-007400] p 273 N94-10151

AMIP: The Atmospheric Model Intercomparison Project [DE93-007413] p 273 N94-10152

Sea ice: A climate component p 232 N94-11705

Monitoring of the Greenland Ice Sheet using ERS-1 synthetic aperture radar imagery p 237 N94-11741

Investigations of Arctic ice-sheets and glaciers using ERS-1 SAR p 238 N94-11743

Spatial patterns in backscatter strength across the Greenland Ice Sheet p 238 N94-11744

Ice studies in the Barents Sea by ERS-1 SAR during SIZEX 92 p 238 N94-11745

Validation of ERS-1 SAR measurements of sea ice during ARCTIC-1991 p 238 N94-11747

Arctic coastal polynya observations with ERS-1 SAR and DMSP SSM/I p 239 N94-11748

Sea ice deformation observed with ERS-1 SAR p 239 N94-11749

Finnish ERS-1 Baltic Sea ice experiment in Winter 1992 p 239 N94-11750

Experiences from the Swedish sea ice programme during BEERS-1992 p 239 N94-11751

Greenland Sea observations p 239 N94-11752

Arctic sea ice microwave signature and geophysical processes study p 240 N94-11754

Sea ice radar signatures from ERS-1 SAR during late Summer and Fall in the Beaufort and Chukchi Seas p 240 N94-11756

Waves and mesoscale features in the marginal ice zone p 240 N94-11757

The seasonal Sea Ice Monitoring and Modelling Site (SIMMS): Using ERS-1 in climate research p 240 N94-11758

Preliminary evaluation of ERS-1 SAR data for operational use in the Canadian sea ice monitoring program p 241 N94-11760

Sea ice feature and type identification in merged ERS-1 SAR and LANDSAT Thematic Mapper imagery p 241 N94-11761

Summer Arctic ice concentrations and characteristics from SAR and SSM/I data p 241 N94-11762

Evaluating ERS-1 ice motion and classification products p 241 N94-11763

Ocean-ice interaction study of waves and mesoscale features p 197 N94-11935

Impact of ERS-1 wind/wave/ice data on operational ocean forecasting p 250 N94-12500

Pacific rim sea ice as observed with the NIMBUS-7 SMMR p 210 N94-12651

Microwave radiometry of ice cover in polar regions p 210 N94-12655

SEA LEVEL

Topex/Poseidon: A United States/France mission. Oceanography from space: The oceans and climate [NASA-TM-108253] p 43 N94-10699

Hypobaric decompression prebreathe requirements and breathing environment p 317 N94-11541

Spatial scales of wave height p 244 N94-11782

The 1992 El Nino viewed by ERS-1 altimetry p 244 N94-11784

Observation of wind and waves by GEOSAT altimeter p 202 N94-11961

Observations of eddy fields in the Northwest Pacific by GEOSAT altimetry p 207 N94-12639

Variability of sea level and sea surface temperature anomalies in the equatorial Pacific p 208 N94-12640

Theory and oceanographic applications of satellite altimeter measurements p 208 N94-12641

Analysis of collinear passes of satellite altimeter data p 208 N94-12642

Comparison of GEOSAT sea surface height and model-simulated surface dynamic height p 208 N94-12644

Principal oscillation pattern analysis of sea level variations in the tropical Pacific measured by the GEOSAT altimeter p 209 N94-12646

Measurement of eddy structure and movement in the north-east Pacific with the GEOSAT altimeter p 209 N94-12647

Preliminary results from a satellite altimetric data assimilation using a Kalman filter and smoother p 209 N94-12648

Fluctuations of the Kuroshio extension detected by the GEOSAT altimetry data p 209 N94-12649

Mean flow and variability in the Kuroshio extension from GEOSAT altimetry data p 209 N94-12650

SEA OF JAPAN

High biological production of the tidal mixing zones on Japan Sea shelf p 228 N94-12758

Generation of internal waves near the shelf boundary p 229 N94-12763

SEA ROUGHNESS

Proceedings of the PORSEC 1992 in Okinawa: Conference for Pacific Ocean Environments and Probing, volume 1 [JTN-93-80418] p 191 N94-11894

Remote sensing and the air-sea boundary layers p 191 N94-11896

Effects of wind-roughened sea surface on ocean color remote sensing: Noise derived from reflected light and whitecaps p 191 N94-11898

HF ocean radar system at Okinawa Radio Observatory p 139 N94-11902

Measurement of wave parameters by HF ocean radar p 192 N94-11903

The coherent structure in the oceanic turbulence around Japan Islands Chain forced by an air, sea, and solid Earth interaction p 198 N94-11940

Westward propagation of sea surface anomalies in the western North Pacific as seen by the altimeter and radiometer p 198 N94-11941

Surface roughness variations across the Iceland-Faroes frontal region observed by the GEOSAT altimeter and NOAA AVHRR p 201 N94-11958

Proceedings of the PORSEC 1992 in Okinawa: Conference for Pacific Ocean Environments and Probing, volume 2 [JTN-93-80419] p 207 N94-12635

Spatial variability of the ocean underwater dynamic noise from satellite radar sensing data p 225 N94-12740

SEA STATES

Effects of wave nonlinearity on ERS-1 radar altimeter returns: A preliminary investigation p 235 N94-11722

Quick-look monitoring of the sea surface with ERS-1 fast delivery altimeter data p 243 N94-11777

Proceedings of the PORSEC 1992 in Okinawa: Conference for Pacific Ocean Environments and Probing, volume 1 [JTN-93-80418] p 191 N94-11894

Remote sensing and the air-sea boundary layers p 191 N94-11896

Effects of wind-roughened sea surface on ocean color remote sensing: Noise derived from reflected light and whitecaps p 191 N94-11898

Satellite observations of red tide events: Plans for EESI p 191 N94-11899

HF ocean radar system at Okinawa Radio Observatory p 139 N94-11902

Measurement of wave parameters by HF ocean radar p 192 N94-11903

Ocean wave detection by SAR p 197 N94-11932

On the determination of the SAR ocean surface scattering patch size p 197 N94-11933

The coherent structure in the oceanic turbulence around Japan Islands Chain forced by an air, sea, and solid Earth interaction p 198 N94-11940

Westward propagation of sea surface anomalies in the western North Pacific as seen by the altimeter and radiometer p 198 N94-11941

Observations of the fractal properties of the Japan sea surface temperature patterns p 205 N94-11984

Circulation of North Pacific Intermediate Water p 206 N94-11985

SOFAR float tracking in the Shikoku basin p 206 N94-11986

Use of SAR-wave, altimeter, and wind-scatterometer data in an operational swell forecasting system p 250 N94-12503

Proceedings of the PORSEC 1992 in Okinawa: Conference for Pacific Ocean Environments and Probing, volume 2 [JTN-93-80419] p 207 N94-12635

Variability of sea level and sea surface temperature anomalies in the equatorial Pacific p 208 N94-12640

A numerical study of deep convection at high latitudes p 210 N94-12652

The Pacific Subarctic Frontal Zone: Structure and dynamics p 223 N94-12731

Laser photoheterodyne interferometers for oceanographic investigations p 177 N94-12732

Spatial variability of the ocean underwater dynamic noise from satellite radar sensing data p 225 N94-12740

SEA SURFACE TEMPERATURE

AMIP: The Atmospheric Model Intercomparison Project [DE93-007400] p 273 N94-10151

AMIP: The Atmospheric Model Intercomparison Project [DE93-007413] p 273 N94-10152

Preliminary results of the comparison of ATSR measurements with in situ sea temperatures [DE93-013399] p 287 N94-10517

A modeling perspective on cloud radiative forcing [DE93-012383] p 276 N94-11241

Central Equatorial Pacific Experiment (CEPEX) [DE93-011656] p 190 N94-11674

Latent and sensible heat flux estimated from ERS-1 data p 244 N94-11783

The subduction experiment. Cruise report, R/V Oceanus, cruise number 250 legs 1 and 2. Subduction 2 mooring deployment and recovery cruise, 25 January-26 February 1992 [AD-A264922] p 289 N94-11853

Satellite derived sea surface temperature applications for Indian Ocean resources development p 193 N94-11907

Exchange of bay water with ocean current monitored by the NOAA satellite p 193 N94-11908

A consideration on principal component analysis of satellite IR data p 193 N94-11909

Trouble areas in the IRT measurement of the Earth surface temperature p 193 N94-11910

Estimation of solar radiation at the sea surface with geostationary meteorological satellite data p 196 N94-11926

The Kyucho events in Sukumo Bay induced by Kuroshio front disturbances p 198 N94-11939

Satellite-derived oceanic features p 200 N94-11949

Observations of the fractal properties of the Japan sea surface temperature patterns p 205 N94-11984

Sea surface temperature anomalies in the Arabian Sea p 206 N94-11988

Multichannel dual angle approach for sea surface temperature retrieval in context of ERS-1 scenario p 252 N94-12512

ATSR correlative skin measurements of sea surface temperature p 252 N94-12514

Validation of ATSR-1 using aircraft radiometer measurements over the South Atlantic p 252 N94-12515

A user appraisal of ATSR near-real-time products p 252 N94-12516

A comparison of ATSR and shipboard radiometer SST measurements along transects between the UK and the Antarctic p 253 N94-12518

Preliminary validation of ATSR sea surface temperatures near the Faeroes p 253 N94-12519

Comments on possible causes of recent global warming [DE93-010501] p 272 N94-12592

Variability of sea level and sea surface temperature anomalies in the equatorial Pacific p 208 N94-12640

Validation test system for sea surface temperature detected by satellites in Mutsu Bay p 213 N94-12670

Sea surface temperature images of Geostationary Meteorological Satellite (GMS) and sea truth data from ferry boats p 213 N94-12671

Measurement of the sea surface emissivity p 213 N94-12672
Evaluation of the method of geostrophic flow using NOAA-AVHRR data p 213 N94-12673
Further study of the Non-Regression-Coefficient SST retrieval method p 213 N94-12674
Delineation of mesoscale features of ocean on satellite IR image p 214 N94-12675
Observation of warm current at the boundary from north equatorial current to Kuroshio by NOAA/AVHRR p 214 N94-12676
Aspects of applying a relaxation method to computing sea surface velocities from sea surface temperature images p 214 N94-12679
Sea surface temperature difference between NOAA/AVHRR and in-situ observation p 215 N94-12680
Intrusion of Kuroshio warm water into Sagami Bay p 215 N94-12683
Satellite thermal variations of Kuroshio in relation to storm floods p 215 N94-12685
Swordfish (Xiphias gladius) catch distributions relative to environmental features observed from satellites off Coquimbo, Chile (30 deg S) p 216 N94-12688
Observation of cold coastal water with high turbidity around the southwestern tip of Korean Peninsula p 216 N94-12689
On the error characteristics of the sea surface temperature observed by satellite p 216 N94-12690
The WOCE/TOGA Surface Velocity Programme (SVP) p 216 N94-12691
Application of remote sensing for coastal management in the north coast of Java p 218 N94-12701
Investigation of meso-scale fronts, eddies and upwellings in China Seas with AVHRR data p 220 N94-12711
Coastal upwelling monitored by satellite data: Methodologies and results p 220 N94-12712
Applicability of satellite infrared data for the monitoring of coastal environments p 220 N94-12714
Satellite and moored buoy observations of polar frontal system over the Yamato Rise in the Japan Sea p 221 N94-12715
The relationship between skin and bulk sea surface temperatures p 221 N94-12716
Variability of the Kuroshio observed from satellite thermal imagery p 221 N94-12717
SST assimilation: Eastern Mediterranean case study p 221 N94-12719
The method of investigation of the horizontal structure of the thermal fronts p 222 N94-12723
Atmospheric correction for determination of average SST fields based on AVHRR data p 227 N94-12750

SEA TRUTH
A comparison of ATSR and shipboard radiometer SST measurements along transects between the UK and the Antarctic p 253 N94-12518
Preliminary validation of ATSR sea surface temperatures near the Faeroes p 253 N94-12519
Oil spill detection using satellite-based SAR: Experience from a field experiment p 253 N94-12522
Comparison of ERS-1 SAR images of the Western Mediterranean to in situ oceanographic data: PRIM-1 Cruise (May 1992) p 255 N94-12529
A surface water monitoring system: A device for the sea-truth observations p 210 N94-12657
Primary productivity in the Oyashio area in the spring and summer of 1990 p 211 N94-12658
Characterization of dissolved organic matter in the ocean by using the fluorescence excitation-emission matrix p 211 N94-12659
Sea surface temperature images of Geostationary Meteorological Satellite (GMS) and sea truth data from ferry boats p 213 N94-12671
Frontal zones in Pacific Ocean: Satellite and ship data analysis p 216 N94-12687
The WOCE/TOGA Surface Velocity Programme (SVP) p 216 N94-12691
The circulation near Luzon p 219 N94-12707

SEA WATER
A new expression for the production rate of sea water droplets on the sea surface p 195 N94-11920
The flow structure around a cylindrical pier for the flow of transcritical Reynolds number p 169 N94-11944
An application of reduced gravity model to mesoscale eddies p 199 N94-11945
Optical characteristics in Tokyo Bay p 204 N94-11972
Remote sensing for numerical modelling of radiative transfer processes in ocean environment p 204 N94-11973
A development on estimation method of undersea light p 204 N94-11974
A surface water monitoring system: A device for the sea-truth observations p 210 N94-12657
Primary productivity in the Oyashio area in the spring and summer of 1990 p 211 N94-12658
Characterization of dissolved organic matter in the ocean by using the fluorescence excitation-emission matrix p 211 N94-12659
The phytoplankton bloom in the Kinu-ura Bay, Japan in the rainy season p 211 N94-12660
Variation of the photosynthetic products in the regional upwelling area around the Izu Islands, Japan p 211 N94-12661
Propagation of light pulses through a three-layer medium (cloud, pure air, and ocean water) p 222 N94-12725
The Pacific Subarctic Frontal Zone: Structure and dynamics p 223 N94-12731
Laser photoheterodyne interferometers for oceanographic investigations p 177 N94-12732
Remote sensing of light scattering coefficient of sea water vertical distribution by the means of airborne lidar p 224 N94-12736
Convective and dynamic instability in meridional trenches p 225 N94-12739
Variability of spectral reflectance in coastal waters near the river plumes p 226 N94-12744
Ecological application of Surface Enhanced Raman Spectroscopy p 227 N94-12756
Experimental and theoretical investigation of undular bore formation upstream the bank p 229 N94-12764

SEALERS
Thermal stability of sealants for military aircraft: Modification of polysulfide prepolymers with ether and thioether monomers
[AD-A264079] p 89 N94-11107

SEALING
Durability of a carbon segmented circumferential seal for a liquid oxygen turbopump
[NAL-TR-1155] p 178 N94-10369

SEALS (STOPPERS)
Extensions of some guidelines for the mechanical design of coaxial compression pin seals
[DE93-012385] p 177 N94-10348
Check valve with poppet damping mechanism
[NASA-CASE-MSC-21903-1] p 179 N94-10655
Dynamic tester for rotor seals and bearings
[NASA-CASE-MFS-28493-1] p 33 N94-10669

SEAS
An analysis of the gravity field in the Norwegian Sea and mapping of the ice cap of Greenland using ERS-1 altimeter measurements p 242 N94-11768

SEASAT SATELLITES
Variability of wind stress, and sensible and latent heat flux in the North Atlantic during SEASAT p 194 N94-11918

SECONDARY FLOW
Unsteady flow past a NACA 0012 airfoil pitching at constant rates
[AD-A265159] p 16 N94-11889

SECONDARY ION MASS SPECTROMETRY
In situ secondary ion mass spectrometry analysis
[DE93-012185] p 76 N94-11140
Solar wind-induced secondary ions and their relation to lunar surface composition p 474 N94-12232

SECURITY
A comparison of high and low-impact reports of investigation on adjudicators' decision making: A pilot study
[AD-A265747] p 416 N94-10298
Practical authorization in large heterogeneous distributed systems
[DE93-013192] p 335 N94-10324

SEDIMENT TRANSPORT
Application of remote sensing for coastal management in the north coast of Java p 218 N94-12701

SEDIMENTARY ROCKS
Stratigraphy and sedimentology of the K/T boundary deposit in Haiti p 282 N94-12138
A simple model of clastic sediments on Mars p 460 N94-12155

SEDIMENTS
Acoustics of bubbly sediments
[AD-A263726] p 288 N94-11299
Impact mineralogy and chemistry of the cretaceous-tertiary boundary at DSDP site 576 p 282 N94-12091
Minor and trace element composition and age of Yukon probable-microtektites p 429 N94-12094
A simple model of clastic sediments on Mars p 460 N94-12155
Iron and nickel isotopic mass fractionation in deep-sea spherules p 282 N94-12199
The role of certain infauna and vascular plants in the mediation of redox reactions in marine sediments p 268 N94-12454
Acetate concentrations and oxidation in salt marsh sediments p 269 N94-12459
Coastal morphodynamics and energetic characteristics of swell studied with ERS-1 SAR p 254 N94-12524
Application of remote sensing for coastal management in the north coast of Java p 218 N94-12701
Sedimentation rates and particulate fluxes in the slope and deep sea areas off eastern Taiwan p 220 N94-12709

SEISMIC ENERGY
Wave propagation characteristics of short-period crustal phases near ARCESS and NORESS
[AD-A265959] p 275 N94-11102

SEISMIC WAVES
Wave propagation characteristics of short-period crustal phases near ARCESS and NORESS
[AD-A265959] p 275 N94-11102

SEISMOGRAPHS
Preliminary analysis of the FLIP array data from the NOBS experiment
[AD-A265911] p 289 N94-12349

SEISMOLOGY
Inverting ultrasonic data on solid/fluid mixtures for Biot-Gassmann parameters
[DE93-011952] p 150 N94-11026
Wave propagation characteristics of short-period crustal phases near ARCESS and NORESS
[AD-A265959] p 275 N94-11102
Autonomous self contained bottom pop-up stations for study of the benthic layer and seismicity of the ocean's bottom p 224 N94-12735

SELENOLOGY
Mission to the Moon: An ESA study on future exploration p 460 N94-12153
Differential scaling: Implications for central structures in large lunar craters p 461 N94-12158
Exploration planning in the context of human exploration and development of the Moon p 474 N94-12229

SELF ABSORPTION
Time-resolved optical studies of charge relaxation and charge transfer at electrode interfaces
[DE93-013985] p 398 N94-11117

SEMANTICS
Bundle event structures: A non-interleaving semantics for LOTOS
[MEMO-INF-92-73] p 320 N94-10164
Automatic word categorization: An information-theoretic approach
[CS-9209] p 419 N94-10903

SEMICONDUCTOR DEVICES
Continuous-time adaptive learning circuit
[AD-D015773] p 140 N94-10384
Limitation and suppression of hot electron fluctuations in submicron semiconductor structures
[DE93-613911] p 396 N94-10801
Review of betavoltaic energy conversion p 53 N94-11407
GaAs PCSS: High gain switching and device reliability
[DE93-009851] p 401 N94-11605
Multicomponent and multilayered thin films for advanced microtechnologies: Techniques, fundamentals, and devices
[AD-A265685] p 405 N94-12442

SEMICONDUCTOR DIODES
Nonlinear Dynamics in Optical Systems. Postdeadline papers presented at the Optical Society of America Conference
[AD-A264958] p 375 N94-10486
Lecture note on circuit technology for high energy physics experiment
[DE93-771422] p 372 N94-11245

SEMICONDUCTOR JUNCTIONS
InGaAs concentrator cells for laser power converters and tandem cells p 50 N94-11394
Review of betavoltaic energy conversion p 53 N94-11407

SEMICONDUCTOR LASERS
Nonlinear Dynamics in Optical Systems. Postdeadline papers presented at the Optical Society of America Conference
[AD-A264958] p 375 N94-10486
Rapid thermal processing for strained-layer semiconductor devices
[DE93-013754] p 396 N94-10809
Characterization of a scannerless LADAR system
[DE93-011582] p 174 N94-10959
Semiconductor ring lasers
[DE93-012386] p 174 N94-11005
New challenges in optical materials development
[DE93-011889] p 383 N94-11676

SEMICONDUCTORS (MATERIALS)
Measurement of the thermal conductivity of molten InSb in a drop shaft p 105 N94-10102
Scientific specifications for an automated facility for growing large semiconducting crystals from the melt in space p 114 N94-10180
THM-growth of III-V-semiconductors in the magnetic field p 118 N94-10209

Photostimulated attenuation of hypersound in superlattice
[DE93-611231] p 357 N94-10408
Structure of s - p bonded metal clusters with 8, 20 and 40 valence electrons
[DE93-613643] p 361 N94-10503
Method for producing a hybridization of detector array and integrated circuit for readout
[NASA-CASE-NPO-18062-1-CU] p 141 N94-10656
Crack suppression in GaInSb buffer layers initially under tensile stress
[DE93-012839] p 396 N94-10745
Confinement of acoustical modes due to the electron-phonon interaction within 2D-electron gas
[DE93-613910] p 396 N94-10800
Rapid thermal processing for strained-layer semiconductor devices
[DE93-013754] p 396 N94-10809
Electronic characterization of defects in narrow gap semiconductors
[NASA-CR-193568] p 397 N94-10819
Ellipsometry studies of semiconductors surface cleaning
[AD-A265150] p 142 N94-11094
Time-resolved optical studies of charge relaxation and charge transfer at electrode interfaces
[DE93-013985] p 398 N94-11117
Characterization of the Si/SiO2 interfere morphology from quantum oscillations in Fowler-Nordheim tunneling currents
[AD-A265149] p 143 N94-11160
Memory effects in the organometallic chemical beam epitaxy of compound semiconductors
[NASA-CR-193106] p 399 N94-11439
Remote plasma enhanced chemical vapor deposition of GaP with in situ generation of phosphine precursors
p 399 N94-11440
Lattice-matched heteroepitaxy of wide gap ternary compound semiconductors p 400 N94-11441
Development of microstrip gas chambers with multi-chip technology
[DE93-753169] p 367 N94-11509
Wide Band-Gap Semiconductors. 1991 Materials Rese arch Society Symposium proceedings
[AD-A263418] p 401 N94-11515
A thermal ionization model for the sustaining phase of lock-on in GaAs
[DE93-011558] p 144 N94-11624
The additional contribution caused by Coulomb interaction to the exciton dispersion in multiple quantum wells and superlattices for direct band gap cubic semiconductors
[DE93-613538] p 402 N94-11659
On the theory of phonoriton in cubic semiconductors with a degenerate valence band
[DE93-613539] p 402 N94-11660
Adsorption and dissociation of disilane on Si(001) studied by STM
[AD-A265269] p 402 N94-11684
Gallium arsenide dynamic random access memory support circuitry
[AD-A265176] p 320 N94-11875
Production of electronic grade lunar silicon by disproportionation of silicon difluoride
p 435 N94-12017
Development of ultra-low noise, high sensitivity planar metal grating coupled 3 to 5 multiquantum well infrared detectors for focal plane array staring IR sensor systems
[AD-A265599] p 404 N94-12375
Multicomponent and multilayered thin films for advanced microtechnologies: Techniques, fundamentals, and devices
[AD-A265685] p 405 N94-12442
Synthesis and electronic properties of nanophase semiconductor materials
[AD-A265287] p 146 N94-12584
Theoretical investigation of some novel phenomenal in artificially structured semiconductors
[AD-A266142] p 405 N94-12587

SENSITIVITY
Computer software and hardware to determine contrast sensitivity using three methods: Tracking, limits, and constant stimuli
[AD-A265168] p 324 N94-11099

SEPARATED FLOW
A comparative study of full Navier-Stokes and Reduced Navier-Stokes analyses for separating flows within a diffusing inlet S-duct
[NASA-TM-106250] p 39 N94-10764
Unsteady flow past a NACA 0012 airfoil pitching at constant rates
[AD-A265159] p 16 N94-11889

SEPARATION
Convection related radial segregation in an idealized horizontal Bridgman configuration p 115 N94-10185

SEPARATORS
Monochromator SP-017. The results of the first experiments
[DE93-617463] p 372 N94-10849

SERIES (MATHEMATICS)
Detecting non-linearities in stationary time series
[W-9223] p 344 N94-10906

SERIES EXPANSION
Studies of P-matrix formalism on the basis of the potential description of two-particle interaction
[DE93-617691] p 362 N94-10550
A new approach to the I/N-expansion for the Dirac equation
[DE93-617647] p 349 N94-10833

SERVICE LIFE
Characterization of in-flight performance of ion propulsion systems
[NASA-TM-106283] p 46 N94-10761
Fatigue life prediction for wind turbines: A case study on loading spectra and parameter sensitivity
[DE93-011597] p 263 N94-11173
GaAs PCSS: High gain switching and device reliability
[DE93-009851] p 401 N94-11605

SET THEORY
An algebraic approach to incomparable families of formal languages
[MEMO-INF-92-82] p 342 N94-10279
Boundary of Fatou sets of hyperbolic rational maps or degree two
[DE93-613031] p 348 N94-10412
A surrogate heuristic for set covering problems
[INPE-5462-PRE/1770] p 325 N94-11178
A new heuristic for set covering problems
[INPE-5471-TDI/502] p 333 N94-12358

SEWING
Parachute having improved vent line stacking
[NASA-CASE-MFS-28508-1] p 14 N94-11021

SHADOWGRAPH PHOTOGRAPHY
Flowfield structure of swept shock wave/turbulent boundary-layer interactions p 149 N94-10899

SHAFTS (MACHINE ELEMENTS)
Dynamic tester for rotor seals and bearings
[NASA-CASE-MFS-28493-1] p 33 N94-10669

SHALES
Petrography and preliminary interpretations of the crystalline breccias from the Manson M-1 core
p 281 N94-12056
Microtektite-like glass spherules in Late Devonian (367 MA) shales p 461 N94-12160

SHALLOW WATER
SAR imaging of geology and bathymetry: Kent coastal area - southern North Sea p 254 N94-12527
Trajectory curving in underwater propagation of light
p 226 N94-12748
Coupled numerical model for altimetric data assimilation and velocity field analysis p 227 N94-12752

SHAPE MEMORY ALLOYS
On the stability of shape memory materials and their properties in static and dynamic applications
p 69 N94-11329
Adaptive structure design employing shape memory actuators p 70 N94-11331
Structural analysis and optimization of adaptive structures by use of the finite element method
p 71 N94-11339

SHAPES
Stability of liquid bridges between parallel plates
p 101 N94-10078
On shape of single crystals grown by FZM in microgravity p 102 N94-10084
A preliminary study on ice shape tracing with a laser light sheet
[NASA-TM-105964] p 174 N94-11132
Fractal dimensions of rampart impact craters on Mars
p 460 N94-12154

SHEAR
Shear, strain and thermohaline vertical fine structure in the upper ocean
[AD-A265961] p 289 N94-12348

SHEAR FLOW
Transport mechanisms acting in toroidal devices: A theoretician's view
[DE93-013463] p 385 N94-10310
The nonlinear evolution of modes on unstable stratified shear layers
[NASA-CR-191492] p 149 N94-10810
High order accurate solutions of viscous problems
[NASA-TM-106267] p 151 N94-11253
Shear flow control of gas jets in liquids
[AD-A264673] p 152 N94-11448
Modelling quasi-two-dimensional turbulent shear flow
p 153 N94-11616
Vortex-induced forces on oscillating bluff cylinders
[AD-A265056] p 154 N94-11865
Numerical simulation using vorticity-vector potential formulation p 157 N94-12297
Local isotropy in high Reynolds number turbulent shear flows p 157 N94-12302
Probability density distribution of velocity differences at high Reynolds numbers p 158 N94-12304
Mixing in a stratified shear flow: Energetics and sampling p 159 N94-12311
Numerical simulation of the non-Newtonian mixing layer p 159 N94-12314
The thermodynamics of the nonlinear shear flows
p 169 N94-12728
Turbulence generation in the Pacific undercurrent by shear p 223 N94-12730
Study of the admixture diffusion in the sea using remote techniques p 228 N94-12759

SHEAR LAYERS
The nonlinear evolution of modes on unstable stratified shear layers
[NASA-CR-191492] p 149 N94-10810
Application of jet-shear-layer mixing and effervescent atomization to the development of a low-NO(x) combustor
[NASA-TM-105888] p 28 N94-11234
High order accurate solutions of viscous problems
[NASA-TM-106267] p 151 N94-11253
Receptivity in parallel flows: An adjoint approach
p 157 N94-12301
LIF measurements of scalar mixing in turbulent shear layers p 159 N94-12312
Shear, strain and thermohaline vertical fine structure in the upper ocean
[AD-A265961] p 289 N94-12348
Aerodynamic sound due to interaction between a two-dimensional free shear layer and the leading edge of a parallel flat plate p 163 N94-12615

SHEAR STRAIN
Computational procedures for determining parameters in Ramberg-Osgood elastoplastic model based on modulus and damping versus strain
[DE93-013309] p 185 N94-10306
Damping measurements for ultra-high carbon steel/brass laminates
[DE93-011886] p 82 N94-11076

SHEAR STRENGTH
Design of inspection and acceptance test methodology for TIG welded aluminum-alloy bracket for camera housings for IRS-1A space craft and executing it
p 61 N94-10037
Computational procedures for determining parameters in Ramberg-Osgood elastoplastic model based on modulus and damping versus strain
[DE93-013309] p 185 N94-10306

SHEAR STRESS
Design evaluation of GLARE laminate lay-ups
p 63 N94-10051
The effects of successive distortions on a turbulent boundary layer in a supersonic flow p 14 N94-11058
Application of a Reynolds stress model to separating boundary layers p 157 N94-12299

SHERGOTTITES
Moessbauer spectroscopy of the SNC meteorite Zagami p 428 N94-12016
Nitrogen and noble gases in a glass sample from LEW88516 p 80 N94-12051
Noble gases in LEW88516 shergottite: Evidence for exposure age pairing with ALH77005 p 80 N94-12082
LEW88516 and SNC meteorites p 430 N94-12150
Noble gas evidence of an aqueous reservoir near the surface of Mars more recently than 1.3 Ga
p 473 N94-12228

SHIELDING
Linear antenna of an arbitrary orientation and position in cylindric screen
[DE93-621353] p 134 N94-11035

SHIP HULLS
Microstructure-based fatigue life prediction methods for naval steel structures
[AD-A265429] p 85 N94-12426
Advances in low carbon, high strength ferrous alloys
[AD-A265264] p 85 N94-12532

SHIPS
DISTERM: A shipboard data system for satellite monitoring of ocean and atmosphere
p 226 N94-12749

SHOCK HEATING
Impact mineralogy and chemistry of the cretaceous-tertiary boundary at DSDP site 576
p 282 N94-12091
Primordial lightning: Evidence preserved in chondrites
p 432 N94-12230

SHOCK LOADS
Vaporization by shock loading of albite, jadeite, and pyrex glass: Experimental study p 97 N94-12039
Shock transformations in quartzite p 97 N94-12040
Dynamic high-pressure shock compaction of diamond powders
[AD-A266004] p 93 N94-12354

SHOCK SPECTRA
Computational methods for problems in aerodynamics using parallel and vector architectures [AD-A265626] p 16 N94-12377

SHOCK TESTS
Start-up imprinting and shock dynamics in laser-target interaction [DE93-008051] p 172 N94-10150
Theoretical investigation of 3-D shock wave turbulent boundary layer interactions [AD-A265275] p 150 N94-11014
Dynamic loading in manufacturing and service: Australia's shock testing capability p 128 N94-11304

SHOCK TUBES
Comparison of computation and experiment for a high enthalpy, heated-driver, shock-tube environment p 7 N94-10447
New developments in the method of space-time conservation element and solution element: Applications to the Euler and Navier-Stokes equations [NASA-TM-106226] p 150 N94-10939

SHOCK TUNNELS
The high enthalpy facilities HEG and TH 2 in Germany p 4 N94-10430

SHOCK WAVE INTERACTION
Experimental, analytical, and computational methods applied to hypersonic compression ramp flows p 6 N94-10444
Development of a Delaunay-based adaption scheme with applications to complex three-dimensional rotational flows p 149 N94-10824
Flowfield structure of swept shock wave/turbulent boundary-layer interactions p 149 N94-10899
An improved material interface reconstruction algorithm for Eulerian codes [DE93-011679] p 326 N94-11226
Large eddy simulation of shock turbulence interaction p 155 N94-12289

SHOCK WAVE PROPAGATION
Flow visualization of shock propagation in baffle systems [DE93-013312] p 147 N94-10307
Giant impact-induced atmospheric blow-off p 435 N94-12019

SHOCK WAVES
Problems in the validation of CFD codes through comparison with experiment p 6 N94-10441
Aerodynamic characteristics analysis of Garabedian-Korn 75-06-12 airfoil [PAPER-2D-8] p 11 N94-10473
Exergy decrease in shock waves and boundary layers of space launch vehicles [AD-A265272] p 42 N94-10493
Acceleration of positrons in supernova shocks [NASA-CR-193713] p 425 N94-10511
Evaluation of dual flow thrust vectored nozzles with exhaust stream impingement [NASA-CR-193292] p 150 N94-10912
Theoretical investigation of 3-D shock wave turbulent boundary layer interactions [AD-A265275] p 150 N94-11014
A symmetrical form for equations of a nonlinear spiral magnetic [DE93-621350] p 344 N94-11033
Turbulent wall jet in blast wave precursor [DE93-011955] p 151 N94-11144
Nonlinear aspects of transonic aeroelasticity [UTIAS-RN-345] p 15 N94-11857
Chondrule formation by clumpy accretion onto the solar nebula p 448 N94-12089
Initiating solar system formation through stellar shock waves p 448 N94-12090
NMR spectroscopy of experimentally shocked single crystal quartz: A reexamination of the NMR shock barometer p 81 N94-12258
Large eddy simulation of shock turbulence interaction p 155 N94-12289
Analysis of Hopkinson bar pressure gage [AD-A262366] p 171 N94-12362
Computational methods for problems in aerodynamics using parallel and vector architectures [AD-A265626] p 16 N94-12377

SHORELINES
Shoreline change detection using remote sensing and GIS in Vietnam p 196 N94-11928
Coastal processes due to nearshore current around an upheaving island p 199 N94-11942
Study on sea water purification using a substratum of marine organisms p 217 N94-12696
Study of growing processes of a tombolo using an air photograph p 218 N94-12702

SHORT WAVE RADIATION
Studies of the net surface radiative flux from satellite radiances during FIFE [NASA-CR-193150] p 230 N94-10953

SHUTDOWNS
Impact of shutting down en route primary radars within CONUS interior [DOT-VNTSC-FAA-93-1] p 23 N94-11626

SIDE-LOOKING RADAR
Artificial oil pollution detection and wave observation in the sea adjacent to Japan by ERS-1 SAR p 253 N94-12520

SIDEBANDS
Numerical simulation of sidebands in free electron laser oscillators [DE93-612675] p 173 N94-10483

SIDEREAL TIME
A method to determine asteroid poles p 431 N94-12205

SIGNAL ANALYSIS
Signal feature analysis using neural networks and psychoacoustics [AD-A266048] p 340 N94-12398

SIGNAL DETECTION
The theory for, and demonstration of, information theory applied to radar target identification [DE93-006393] p 132 N94-10315
Signal detection theory and methods for evaluating human performance in decision tasks p 314 N94-11531
Comparison of multiresolution techniques for digital signal processing [AD-A265364] p 138 N94-12406

SIGNAL DETECTORS
Observations of optical counterparts of Gamma-Ray bursts [NASA-CR-193573] p 485 N94-12589

SIGNAL DISTORTION
NRL review for 1993 [AD-A265666] p 497 N94-12334

SIGNAL ENCODING
Necessary conditions for the optimality of variable rate residual vector quantizers [NASA-CR-193730] p 326 N94-11197
Flexible high-speed CODEC [NASA-CR-191169] p 146 N94-12433

SIGNAL GENERATORS
Dielectric resonator [US-PATENT-4,580,116] p 141 N94-10668

SIGNAL MEASUREMENT
A new method of time difference measurement: The time difference method by dual phase coincidence points detection p 357 N94-11002
Building penetration loss measurements for DAB signals at 211 MHz [BBC-RD-1992/14] p 133 N94-11024

SIGNAL PROCESSING
Variable rate transfer of optical information [AD-D015758] p 418 N94-10374
Wideband beamforming for a sparse nonuniform spaced sensor array [AD-A265909] p 133 N94-10660
Basic experiment on an ultrasonic method of localization [DE93-754295] p 358 N94-11042
Generalization of Dyson criterion for the amplitude-phase fluctuations case and for the system of interferometers p 135 N94-11067
Necessary conditions for the optimality of variable rate residual vector quantizers [NASA-CR-193730] p 326 N94-11197
Chaotic time series analysis p 31 N94-11490
Limited bandwidth microwave filter [AD-D015744] p 145 N94-12322
Comparison of multiresolution techniques for digital signal processing [AD-A265364] p 138 N94-12406

SIGNAL RECEPTION
Magnetic Earth Ionosphere Resonant Frequencies (MEIRF) project [NASA-CR-193182] p 276 N94-11355

SIGNAL TRANSMISSION
Underwater hydrophone location survey p 290 N94-10975
Adaptive algorithms for use with digital filters in vibration control p 71 N94-11338
NRL review for 1993 [AD-A265666] p 497 N94-12334

SIGNATURES
Geophysical signature of the Pretoria saltpan impact structure and a possible satellite crater p 282 N94-12103

SIGNS AND SYMPTOMS
Effects of CSF hormones and ionic composition on salt/water metabolism [NASA-CR-193232] p 300 N94-11045
Monitoring cognitive function and need with the automated neuropsychological assessment metrics in Decompression Sickness (DCS) research p 314 N94-11533
Risk of decompression sickness in the presence of circulating microbubbles p 312 N94-11546
Promethazine and its use as a treatment for space motion sickness p 312 N94-11550
Update on the incidence and treatment of space motion sickness p 312 N94-11551

SILANES
Toxicity study of dimethylethoxysilane (DMSES), the waterproofing agent for the Orbiter heat protective system p 318 N94-11554
Adsorption and dissociation of disilane on Si(001) studied by STM [AD-A265269] p 402 N94-11684

SILICA GLASS
Material advances for lightweight TPS p 62 N94-10049
Arcjet exploratory tests of ARC optical window design for the AFE vehicle [NASA-CR-192655] p 34 N94-10930

SILICATES
The stability of hibonite and other aluminous phases in silicate melts: Implications for the origin of hibonite-bearing inclusions p 80 N94-12052
Alkali-granitoids as fragments within the ordinary chondrite Adzhi-Bogdo: Evidence for highly fractionated, alkali-granitic liquids on asteroids p 429 N94-12069
The solubility of gold in silicate melts: First results p 87 N94-12086
Unequilibrated, equilibrated, and reduced aggregates in anhydrous interplanetary dust particles p 429 N94-12098
The spectral effects of subsolidus reduction of olivine and pyroxene p 81 N94-12110
Micro-zoning in minerals of a Landes silicate inclusion p 432 N94-12231
In-situ crystallization of silicate glass films deposited on alpha- Al2O3 [DE93-012969] p 95 N94-12596

SILICON
Effect of gravity on the dissolution and liquid phase epitaxial growth processes in a horizontal sandwich system p 118 N94-10208
Journal of Research of the National Institute of Standards and Technology, volume 98, number 2, March - April 1993 [PB93-196228] p 485 N94-10850
Thermal-optical switching of a silicon based interference filter [AD-A265152] p 174 N94-11095
Characterization of the Si/SiO2 interfere morphology from quantum oscillations in Fowler-Nordheim tunneling currents [AD-A265149] p 143 N94-11160
Radiation hardness of Mo/Si multilayers designed for use in a soft x ray projection lithography system [DE93-011879] p 143 N94-11273
Production of electronic grade lunar silicon by disproportionation of silicon difluoride p 435 N94-12017
The correlation of alkalis and aluminum during high-temperature volatilization of albite and nepheline p 81 N94-12214
The adsorption and surface reaction of SiCl4 on Si(100)-(2x1) [AD-A266124] p 79 N94-12538
Synthesis and electronic properties of nanophase semiconductor materials [AD-A265287] p 146 N94-12584

SILICON ALLOYS
Structure and properties of an RS Al-Si-Ni-Mn-Zr alloy for high temperature applications p 64 N94-10063
EUSO-D2-experiment: Unidirectional solidification with quenching of an AlSi11 alloy p 86 N94-10199

SILICON CARBIDES
Design concepts for load-carrying hot structures for reentry bodies p 57 N94-10012
New processes for lightweight ceramic matrix composites p 61 N94-10043
Study of the tribological behavior of SiC and Si3N4 ceramic couples in terms of temperature: The reality p 64 N94-10061
High temperature composites in Aerospatiale activities p 64 N94-10062
Damping mechanisms in chemically vapor deposited SiC fibers [NASA-TM-106334] p 66 N94-11135
The effects of an aggressive environment on the subcritical crack growth of a continuous-fiber ceramic composite [DE93-011690] p 73 N94-11612

SILICON DIOXIDE
Thermal-optical switching of a silicon based interference filter [AD-A265152] p 174 N94-11095

Characterization of the Si/SiO2 interfere morphology from quantum oscillations in Fowler-Nordheim tunneling currents
[AD-A265149] p 143 N94-11160

Radiation-induced aperiodicity in irradiated ceramics
[DE93-013335] p 91 N94-11698

Development of a molecular beam technique to study early solar system silicon reactions p 432 N94-12224

SILICON FILMS

Workshop summary: New silicon cells
p 54 N94-11417

An ellipsometry investigation of nucleation and growth of electron cyclotron resonance plasma deposited silicon films
[AD-A265037] p 401 N94-11651

SILICON ISOTOPES

Si-29 NMR spectroscopy of naturally-shocked quartz from Meteor Crater, Arizona: Correlation to Kieffer's classification scheme p 80 N94-12087

NMR spectroscopy of experimentally shocked single crystal quartz: A reexamination of the NMR shock barometer p 81 N94-12258

SILICON NITRIDES

Study of the tribological behavior of SiC and Si3N4 ceramic couples in terms of temperature: The reality
p 64 N94-10061

Protective coatings for high-temperature polymer matrix composites
[NASA-TM-106276] p 74 N94-12431

SILICON OXIDES

Development of a molecular beam technique to study early solar system silicon reactions p 432 N94-12224

SILICON RADIATION DETECTORS

Silicon-based elementary particle tracking system: Materials science and mechanical engineering design
[DE93-012630] p 65 N94-10740

Fast trigger algorithm for B-events selection
[DE93-621452] p 365 N94-11089

Relativistic heavy ion research
[DE93-013127] p 367 N94-11373

Theory of elementary particles and accelerator theory. Task C: Experimental high energy physics
[DE93-013139] p 368 N94-11696

Experimental particle physics at the University of Pittsburgh
[DE93-013326] p 369 N94-12546

SILOXANES

A non-halogenated, flame retarded polycarbonate
p 19 N94-10781

SILVER

The effects of organic adsorbates on the underpotential deposition of silver on Pt(111) electrodes
[AD-A265623] p 404 N94-12376

Nonlinear optical spectroscopy of Ag(111) in electrolyte and in vacuum
[AD-A265622] p 79 N94-12534

SIMD (COMPUTERS)

Layering techniques for development of parallel systems: An algebraic approach
[MEMO-INF-92-62] p 335 N94-10277

SIMPLEX METHOD

Design of a continuous resistively loaded monopole antenna
[AD-A265852] p 138 N94-12281

SIMULATION

Functional reasoning, explanation, and analysis
[DE92-526832] p 313 N94-10251

Photostimulated attenuation of hypersound in superlattice
[DE93-611231] p 357 N94-10408

The development of an interactive synthesis tool for intelligent controllers of modular, reconfigurable robots
p 339 N94-10898

Simulation of images of water vapor channel and infrared split channel p 190 N94-11081

Gas-Grain Simulation Facility (GGSF). Volume 2: Conceptual design definition
[NASA-CR-177613] p 423 N94-11229

Large eddy simulations of the atmospheric boundary layer east of the Colorado Rockies p 277 N94-11465

Discrete Kalman filtering equations of second-order form for control-structure interaction simulations
[NASA-CR-193723] p 331 N94-11522

SIMULATORS

TOLS (Telescience On-Line Simulator): An essential instrument for micro-gravity interactive experiment
p 39 N94-10134

A flexible modelling software for data acquisition
[DE93-612915] p 322 N94-10484

Telerobot control system
[NASA-CASE-NPO-18116-1-CU] p 179 N94-10670

SINE WAVES

Vortex-induced forces on oscillating bluff cylinders
[AD-A265056] p 154 N94-11865

SINGAPORE

Sun-synchronous and geo-synchronous satellite data utilization for environmental studies p 37 N94-10689

SINGLE CRYSTALS

Use of inert immiscible liquid for crystal separation out of its feeding solution in weightlessness
p 124 N94-10242

Recent developments in piezoelectric and electrostrictive sensors and actuators for smart structures p 70 N94-11332

Investigation of ZnSe-coated silicon substrates for GaAs solar cells p 52 N94-11405

Low energy electron diffraction and cyclic voltammetry studies of flame-annealed platinum single crystals
[AD-A263566] p 401 N94-11518

Polaronic charge separation in mixed-halide MX solids
[AD-A266073] p 403 N94-12345

The effects of organic adsorbates on the underpotential deposition of silver on Pt(111) electrodes
[AD-A265623] p 404 N94-12376

Low voltage electron beam lithography
[AD-A265358] p 145 N94-12405

Fatigue in single crystal nickel superalloys
[AD-A266116] p 85 N94-12418

Deformation mechanisms in tungsten single crystals in ballistic impact experiments
[AD-A265701] p 405 N94-12563

Tin whiskers in electronic circuits
[AD-A265917] p 146 N94-12565

SINGLE EVENT UPSETS

Relationship between IBICC imaging and SEU in CMOS ICs
[DE93-009854] p 143 N94-11285

SINGULAR INTEGRAL EQUATIONS

Integral equation methods for mixed boundary problem of fracture mechanics p 188 N94-11617

SINGULARITY (MATHEMATICS)

Numerical method of singular problems on singular integrals
[DE93-613654] p 343 N94-10546

SINKS

A method of influence regions in the theory of vacancy swelling of metals
[DE93-620579] p 83 N94-11363

SINTERING

Ostwald ripening of solid cobalt particles in liquid copper p 87 N94-10202

Production of reactive sintered nickel aluminide
[DE93-014434] p 83 N94-11127

Creep deformation and mechanical properties of sintered glass and polycrystalline matrix composites
p 67 N94-11315

Effect of powder processing on slip casting parameters and sintering of Si3N4-Y2O3-SiO2
[AD-A264474] p 83 N94-11445

Cold press sintering of simulated lunar basalt
p 131 N94-12026

General overview of an integrated lunar oxygen production/brickmaking system p 131 N94-12027

SIS (SUPERCONDUCTORS)

Submillimeter wave observation experiment of Earth atmosphere with SIS mixer p 130 N94-11837

Utilization of superconductivity in the area of space
p 131 N94-11843

SIZE DETERMINATION

Atomization characteristics of a prefilming airblast atomizer
[NAL-TM-644] p 148 N94-10727

SIZE DISTRIBUTION

The development of phytoplankton sensing system with optical fiber p 203 N94-11967

Venus small volcano classification and description
p 438 N94-12037

Deviations from the straight line: Bumps (and grinds) in the collisionally evolved size distribution of asteroids
p 431 N94-12201

Laboratory studies on the velocity of fragments from impact disruptions p 189 N94-12359

The seasonal change of phytoplankton size distribution using optical fiber sensor p 210 N94-12656

SIZE SEPARATION

The carbon isotopic composition of Novo Urei diamonds p 433 N94-12255

SKIN FRICTION

Experimental and computational comparisons of Mach 6 high Reynolds number heat transfer and skin friction
p 6 N94-10443

Real gas and surface transpiration effects upon swept leading edge high speed flow including transition
p 8 N94-10452

SKIRTS

Stress relaxation forming of Ariane 5 front skirt outer skin panels p 62 N94-10046

SKY SURVEYS (ASTRONOMY)

Preparing for the initial observations of the Targeted Search and the Sky Survey systems
[NASA-CR-193644] p 318 N94-10865

First results of the seven-color asteroid survey
p 430 N94-12162

SLABS

An analytic model for calculating pump-induced wavefront distortions in laser slabs
[DE93-011953] p 174 N94-11126

SLEEP

Noise levels and their effects on Shuttle crewmembers' performance: Operational concerns p 314 N94-11538

SLENDER BODIES

Stability of hypersonic flow over a blunt body
p 7 N94-10450

SLIDING

Properties of interfacial tribo-films
[AD-A265591] p 182 N94-12374

SLIDING CONTACT

Tribological characteristics of sputtered Au/Cr films on alumina substrates at elevated temperatures
[NASA-TM-106078] p 55 N94-11362

SLIDING FRICTION

Effect of surface cleanliness of bearing steel on adhesive strength and tribological properties of sputter-deposited gold films
[DE93-767974] p 82 N94-10732

SLIP CASTING

Effect of powder processing on slip casting parameters and sintering of Si3N4-Y2O3-SiO2
[AD-A264474] p 83 N94-11445

SLOPES

Evolution of steep Martian slopes p 434 N94-11184

Power-law confusion: You say incremental, I say differential p 347 N94-12175

Mapping bathymetric slopes from bathymetry data
[AD-A265923] p 290 N94-12350

SLURRIES

Coprocessing of fossil fuels and biomass for CO2 emission reduction in the transportation sector
[PB93-194165] p 267 N94-11845

SMALL SCIENTIFIC SATELLITES

Estimation of the attitude motion of the small satellite ORIZURU
[NAL-TR-1145] p 42 N94-10366

In-orbit performance tests and tele-command systems of the umbrella test satellite (DEBUT)
[NAL-TR-1165] p 43 N94-10859

SMART STRUCTURES

Smart Structures for Aircraft and Spacecraft
[AGARD-CP-531] p 68 N94-11317

Smart structures: A technology for next generation aircraft p 27 N94-11318

Dynamic tests on the NASA Langley CSI evolutionary model p 45 N94-11320

Smart materials for helicopter rotor active control
p 27 N94-11321

Intelligent structures: A technology overview and assessment p 68 N94-11322

The Satellite Attack Warning and Assessment Flight Experiment (SAWAFE) p 45 N94-11323

Optical fibre techniques for structural monitoring in composites p 69 N94-11324

Smart processing of composite materials for enhanced performance and properties p 69 N94-11325

Smart structures at Aastra Corporation
p 69 N94-11326

Fiber optic sensing for composite smart structures
p 69 N94-11327

On the stability of shape memory materials and their properties in static and dynamic applications
p 69 N94-11329

Smart polymeric system for electromechanical transduction p 70 N94-11330

Recent developments in piezoelectric and electrostrictive sensors and actuators for smart structures p 70 N94-11332

In-flight aircraft structure health monitoring based on smart structures technology p 22 N94-11333

Structural health monitoring using embedded fibre optic sensors p 22 N94-11334

Fault location in structures using neural networks
p 70 N94-11335

Factors affecting the embedding of optical fibre sensors in advanced composite structures p 70 N94-11336

Fiber-optic sensor systems for measuring strain and the detection of acoustic emissions in smart structures
p 71 N94-11337

Structural analysis and optimization of adaptive structures by use of the finite element method
p 71 N94-11339

Fiber-optic interferometric strain gauge for smart structures applications: First flight tests
p 71 N94-11340

On possible applications of smart structures to control of space systems p 45 N94-11342
Aircraft smart structures research in the USAF Wright Laboratory p 72 N94-11343
Advances in adaptive structures at Jet Propulsion Laboratory p 72 N94-11344
Multidimensional intelligent control for superlight air vehicles p 27 N94-11347
Active vibration control of adaptive flexible structures using piezoelectric smart sensors and actuators p 189 N94-11823

SMOKE
New thermoplastic laminating adhesives for the aircraft industry with low heat release and low smoke emission p 17 N94-10767
A new low smoke, low heat release structural foam p 17 N94-10768
A four-dimensional, mesoscale, non-gaussian multispectral smoke model. Phase 1: Feasibility study [AD-A264805] p 152 N94-11519
Information capability of NOAA-AVHRR data for monitoring oceanographic and atmospheric pollution p 214 N94-12677

SMOKE TRAILS
Simulated wake characteristics of tapered annular wings by a discrete vortex method [NAL-TR-1156] p 13 N94-10855

SMOOTHING
Improvement of the flow quality in the ARA transonic tunnel by means of a long cell honeycomb [ARA-MEMO-375] p 34 N94-10894
FFTSCAN: A program for spectral smoothing using Fourier transforms [AD-A264921] p 278 N94-11852

SNOW COVER
Signatures of Antarctic firn by means of ERS-1 AMI and by field measurements p 237 N94-11737
Snow and glacier investigations by ERS-1 SAR: First results p 247 N94-12481
Monitoring of snowcover in high mountain terrain with ERS-1 SAR p 247 N94-12482
Application of ERS-1 SAR data to snow mapping p 247 N94-12483
Disintegrating ice front of Shirase Glacier, East Antarctica p 210 N94-12654

SOBOLEV SPACE
On the Sobolev systems with ellipsoid cavities [DE92-641290] p 148 N94-10530

SODIUM
Laser system design for the generation of a sodium-layer laser guide star [DE93-014127] p 176 N94-12784

SODIUM COMPOUNDS
Vaporization by shock loading of albite, jadeite, and pyrex glass: Experimental study p 97 N94-12039

SODIUM FLUORIDES
Production of electronic grade lunar silicon by disproportionation of silicon difluoride p 435 N94-12017

SOFTENING
Investigation of the reason for the softening behaviour of filled polymers p 63 N94-10058

SOFTWARE ENGINEERING
System engineering concept demonstration, technology assessments, volume 5 [AD-A265471] p 323 N94-10494
System engineering concept demonstration, trade studies, volume 6 [AD-A265472] p 323 N94-10495
The Zipcode message-passing system [DE93-011958] p 336 N94-11027
Development of generic field classes for finite element and finite difference problems [DE93-011678] p 345 N94-11225
Computational mechanics needs study [NASA-CR-193712] p 327 N94-11279
Proceedings of the Seventeenth Annual Software Engineering Workshop [NASA-TM-109245] p 328 N94-11422
Experimental software engineering: Seventeen years of lessons in the SEL p 328 N94-11423
The experience factory: Can it make you a 5? or what is its relationship to other quality and improvement concepts? p 328 N94-11424
Impacts of object-oriented technologies: Seven years of SEL studies p 329 N94-11425
The MERMAID project p 329 N94-11426
Software process assessments p 329 N94-11427
The role of metrics and measurements in a software intensive total quality management environment p 329 N94-11428
Maximizing reuse: Applying common sense and discipline p 329 N94-11429
Reuse: A knowledge-based approach p 329 N94-11430
Large project experiences with object-oriented methods and reuse p 329 N94-11431
Development and application of an acceptance testing model p 330 N94-11432
A recent Cleanroom success story: The Redwing project p 39 N94-11433
Insights into software development in Japan p 330 N94-11435
Myths and realities: Defining re-engineering for a large organization p 330 N94-11436
Development and implementation of a general purpose x-windows display program [AD-A265306] p 332 N94-11860
The instrumentation of the multimodel and multilingual user interface [AD-A265444] p 333 N94-12332

SOFTWARE RELIABILITY
Techniques, processes, and measures for software safety and reliability [DE93-012379] p 322 N94-10347
The experience factory: Can it make you a 5? or what is its relationship to other quality and improvement concepts? p 328 N94-11424
Software process assessments p 329 N94-11427
A recent Cleanroom success story: The Redwing project p 39 N94-11433
Applying reliability models to the maintenance of Space Shuttle software p 330 N94-11434

SOFTWARE REUSE
Effective software reuse in an embedded realtime system [AD-A264993] p 326 N94-11220
The role of metrics and measurements in a software intensive total quality management environment p 329 N94-11428
Maximizing reuse: Applying common sense and discipline p 329 N94-11429
Reuse: A knowledge-based approach p 329 N94-11430
Large project experiences with object-oriented methods and reuse p 329 N94-11431
Analysis and guidelines for reusable Ada software [AD-A264918] p 332 N94-11850

SOFTWARE TOOLS
Propellant management in surface tension tanks p 106 N94-10110
TOLS (Telescience On-Line Simulator): An essential instrument for micro-gravity interactive experiment p 39 N94-10134
The super vectorfield package for REDUCE. Version 1.0 [MEMO-1099] p 321 N94-10265
The INTEGRATOR package for REDUCE, version 1.0 [MEMO-1100] p 322 N94-10418
System engineering concept demonstration, technology assessments, volume 5 [AD-A265471] p 323 N94-10494
A toolkit for building Earth system models [DE93-012147] p 276 N94-11138
A tool for generation of expert system shells [INPE-5493-TDI/510] p 325 N94-11181
The MERMAID project p 329 N94-11426
Large project experiences with object-oriented methods and reuse p 329 N94-11431
System engineering concept demonstration, process model, volume 3 [AD-A265469] p 333 N94-12008
Radarmap of Germany: First mosaic and classification p 246 N94-12477
Use of SAR-wave, altimeter, and wind-scatterometer data in an operational swell forecasting system p 250 N94-12503
Problem specific environments for parallel systems [AD-A266129] p 337 N94-12540

SOIL MOISTURE
Design of a global soil moisture initialization procedure for the simple biosphere model [NASA-TM-104590] p 284 N94-10940
The impact of vegetation on the atmospheric boundary layer and convective storms p 277 N94-11480
The use of ERS-1 SAR data to study surface states p 247 N94-12480
Geoecological monitoring of an agricultural area p 248 N94-12489
Extraction of plant and soil parameters from multitemporal ERS-1 SLC data of the Freiburg test site p 248 N94-12491
Assessment of ERS-1 SAR data for soil moisture estimation p 249 N94-12492
Temporal monitoring of soil moisture using ERS-1 SAR data p 249 N94-12493

SOIL SCIENCE
Sulfate reduction and other sedimentary biogeochemistry in a northern New England salt marsh p 268 N94-12453
Sulfur transformations in the sediments of a New Hampshire salt marsh p 270 N94-12463

SOILS
Immediate response to free product discovery [PB93-182970] p 265 N94-11015
In situ secondary ion mass spectrometry analysis [DE93-012185] p 76 N94-11140
Catalytic oxidation of organics in vapor streams at remediation sites [PB93-182962] p 266 N94-11472
Reflectance spectra of sulfate-and carbonate-bearing Fe(3+)-doped montmorillonites as Mars soil analogs p 445 N94-12070
The effects of atmospheric pressure on infrared reflectance spectra of Martian analogs p 445 N94-12071
A comparison of the visible and near infrared reflectance of hydrovolcanic palagonite tuffs and Martian weathered soils p 477 N94-12245
Elevated acetate concentrations in the rhizosphere of Spartina alterniflora and potential influences on sulfate reduction p 271 N94-12468
Evaluating the spread of red soil with LANDSAT TM data in coral reefs of Okinawa main island, southwestern Japan p 212 N94-12668

SOL-GEL PROCESSES
Fibre reinforced structures with glass matrix p 64 N94-10064
Low temperature synthesis of monolithic transparent Ta2O5 gels from hydrolysis of metal alkoxide [NASA-TM-106246] p 89 N94-11204
Synthesis and thermal evolution of structure in alkoxide-derived niobium pentoxide gels [NASA-TM-106259] p 90 N94-11257
Structural development in ceramic precursor sols and gels [AD-A264354] p 90 N94-11281

SOLAR ACTIVITY
Effects of energetic particle events on VLF/LF propagation parameters/1989 [AD-A265266] p 275 N94-11013
Disturbance Impact Assessment System (DIAS), version 2.0. System design document [AD-A265251] p 138 N94-11883
Yohkoh Bragg Crystal Spectrometer light curves for Ca XIX (3.1631-3.1912A): 1 October 1991 - 30 September 1992 [AD-A266090] p 483 N94-12414

SOLAR ACTIVITY EFFECTS
Radiation considerations for interplanetary missions p 45 N94-11559
Results from a year-long auroral-E measurement campaign [AD-A265059] p 278 N94-11871

SOLAR ARRAYS
Proceedings of the 12th Space Photovoltaic Research and Technology Conference (SPRAT 12) [NASA-CP-3210] p 48 N94-11380
Results of some initial space qualification testing on triple junction a-Si and CuInSe2 thin film solar cells p 50 N94-11392
The efficiency of photovoltaic cells exposed to pulsed laser light p 50 N94-11395
EOL performance comparison of GaAs/Ge and Si BSF/R solar arrays p 51 N94-11398
A high specific power solar array for low to mid-power spacecraft p 51 N94-11399
Results of thermal vacuum tests for the PASP+ flight modules p 53 N94-11410
Computation of photovoltaic parameters under lunar temperature variation p 53 N94-11411
Workshop on Solar Electric Propulsion p 54 N94-11416
Workshop summary: Receivers for laser power beaming p 54 N94-11419
Property changes induced by the space environment in composite materials on LDEF: Solar array materials passive LDEF experiment A0171 (SAMPLE) [NASA-CR-192572] p 73 N94-11484

SOLAR CELLS
Japan's Sunshine Project [DE93-767980] p 262 N94-10498
Proceedings of the 12th Space Photovoltaic Research and Technology Conference (SPRAT 12) [NASA-CP-3210] p 48 N94-11380
A detailed study of the photo-injection annealing of thermally diffused InP solar cells p 48 N94-11381
High temperature annealing of minority carrier traps in irradiated MOCVD n(+)p InP solar cell junctions p 48 N94-11382
Radiation effects in heteroepitaxial InP solar cells p 48 N94-11383
Progress in p(+)n InP solar cells fabricated by thermal diffusion p 48 N94-11384
Effects of solar cell environment on contact integrity p 49 N94-11387

Surface passivation of InP solar cells with InAlAs layers p 49 N94-11389
Polyimide based amorphous silicon solar modules p 49 N94-11390
Investigation of the radiation resistance of triple-junction a-Si:H alloy solar cells irradiated with 1.00 MeV protons p 50 N94-11391
Results of some initial space qualification testing on triple junction a-Si and CuInSe2 thin film solar cells p 50 N94-11392
InGaAs concentrator cells for laser power converters and tandem cells p 50 N94-11394
Response of silicon solar cell to pulsed laser illumination p 51 N94-11396
Approaches to solar cell design for pulsed laser power receivers p 51 N94-11397
A high specific power solar array for low to mid-power spacecraft p 51 N94-11399
TAB interconnects for space concentrator solar cell arrays p 51 N94-11400
New experimental techniques for solar cells p 52 N94-11403
Radiation effects in Ga(0.47)In(0.53)As solar cells p 52 N94-11404
Investigation of ZnSe-coated silicon substrates for GaAs solar cells p 52 N94-11405
Heteroepitaxial InP, and ultrathin, directly glassed, GaAs 3-5 solar cells p 52 N94-11406
UV testing of solar cells: Effects of antireflective coating, prior irradiation, and UV source p 53 N94-11408
The UoSAT-5 solar cell experiment: First year in orbit p 53 N94-11409
Results of thermal vacuum tests for the PASP+ flight modules p 53 N94-11410
An overview of the Defence Research Agency photovoltaic programme p 53 N94-11412
NASDA activities in space solar power system research, development and applications p 54 N94-11413
Workshop on Heteroepitaxial InP Solar Cells p 54 N94-11414
Thin film solar cell workshop p 54 N94-11415
Workshop summary: New silicon cells p 54 N94-11417
Multi-band gap and new solar cell options workshop p 54 N94-11418
Measurement and modeling of the stability of hydrogenated amorphous silicon solar cells and films after intense illumination p 263 N94-11638

SOLAR COLLECTORS
Department of Energy solar process heat program: FY 1991 solar process heat prefeasibility studies activity
[DE93-010010] p 262 N94-10258
Renewable energy sources 1991, part 2
[DE93-605634] p 263 N94-11506

SOLAR CORONA
Why convective heat transport in the solar nebula was inefficient p 458 N94-12143
Are cosmic rays effective for ionization of the solar nebula? p 472 N94-12220

SOLAR COSMIC RAYS
Measurements of cosmogenic nuclides in lunar rock 64455 p 437 N94-12033

SOLAR CYCLES
Radiation considerations for interplanetary missions p 45 N94-11559
Comments on possible causes of recent global warming
[DE93-010501] p 272 N94-12592

SOLAR ELECTRIC PROPULSION
Workshop on Solar Electric Propulsion p 54 N94-11416

SOLAR ENERGY
Department of Energy solar process heat program: FY 1991 solar process heat prefeasibility studies activity
[DE93-010010] p 262 N94-10258
Japan's Sunshine Project
[DE93-767980] p 262 N94-10498
Space Solar Power Program
[DE93-011750] p 55 N94-11675

SOLAR FLARES
Proton transport methods for satellite shield modeling
[DE93-013602] p 42 N94-10520
SMM x ray polychromator
[NASA-CR-193282] p 483 N94-11048
Results from a year-long auroral-E measurement campaign
[AD-A265059] p 278 N94-11871
Disturbance Impact Assessment System (DIAS), version 2.0. System design document
[AD-A265251] p 138 N94-11883
Using solar flare track densities to determine the origin of interplanetary dust particles p 429 N94-12078
Data analysis tasks: BATSE
[NASA-CR-192598] p 483 N94-12427

SOLAR FLUX
The evaluation of radiative process in the atmosphere-ground system by Monte Carlo method p 205 N94-11980

SOLAR GENERATORS
Japan's Sunshine Project
[DE93-767980] p 262 N94-10498

SOLAR GRAVITATION
New tests of the equivalence principle using non-metric couplings of electromagnetism and gravitation p 413 N94-11821

SOLAR HEATING
Department of Energy solar process heat program: FY 1991 solar process heat prefeasibility studies activity
[DE93-010010] p 262 N94-10258

SOLAR INSTRUMENTS
Continued development of an ultra-narrow bandpass filter for solar research
[NASA-CR-194169] p 381 N94-10735
NASA Marshall Space Flight Center solar observatory report, January - June 1993
[NASA-TM-108417] p 423 N94-10866

SOLAR NEUTRINOS
Solar neutrinos with three flavor mixings
[DE93-011006] p 483 N94-11619

SOLAR OBSERVATORIES
NASA Marshall Space Flight Center solar observatory report, January - June 1993
[NASA-TM-108417] p 423 N94-10866

SOLAR ORBITS
Using solar flare track densities to determine the origin of interplanetary dust particles p 429 N94-12078

SOLAR PHYSICS
Solar neutrinos with three flavor mixings
[DE93-011006] p 483 N94-11619

SOLAR POWER SATELLITES
Space transportation alternatives for large space programs: The International Space University Summer Session, 1992
[NASA-TM-106271] p 40 N94-10811
Construction and testing of a space ready rectenna
[NASA-CR-193310] p 137 N94-11357

SOLAR PROTONS
Proton transport methods for satellite shield modeling
[DE93-013602] p 42 N94-10520

SOLAR RADIATION
Estimating Photosynthetically Available Radiation (PAR) at the Earth's surface from satellite observations p 230 N94-10955
A modeling perspective on cloud radiative forcing
[DE93-012383] p 276 N94-11241
Estimation of solar radiation at the sea surface with geostationary meteorological satellite data p 196 N94-11926
The evaluation of radiative process in the atmosphere-ground system by Monte Carlo method p 205 N94-11980
Oxidation state of the Earth's upper mantle during the last 3800 million years: Implications for the origin of life p 283 N94-12210
Comments on possible causes of recent global warming
[DE93-010501] p 272 N94-12592

SOLAR SENSORS
Estimation of the attitude motion of the small satellite ORIZURU
[NAL-TR-1145] p 42 N94-10366

SOLAR SPECTRA
Solar neutrinos with three flavor mixings
[DE93-011006] p 483 N94-11619
Remote sensing x ray fluorescence spectrometry for future lunar exploration missions p 462 N94-12165
Near-infrared spectra of the Martian surface: Reading between the lines p 465 N94-12184

SOLAR SPECTROMETERS
SMM x ray polychromator
[NASA-CR-193282] p 483 N94-11048

SOLAR SYSTEM
Development of a molecular beam technique to study early solar system silicon reactions p 432 N94-12224

SOLAR SYSTEM EVOLUTION
Origins of Solar Systems Workshop: The Origin, Evolution, and Detectability of Short Period Comets
[NASA-CR-194255] p 427 N94-11628
The long-term dynamical behavior of short-period comets p 427 N94-11629
Midplane temperatures in the solar nebula p 448 N94-12088
Chondrule formation by clumpy accretion onto the solar nebula p 448 N94-12089
Initiating solar system formation through stellar shock waves p 448 N94-12090
Studies of the release of radiogenic Xe-129 from Bjurboele: Evidence against simple diffusion models p 430 N94-12125
The giant impact produced a precipitated Moon p 430 N94-12135
Recondensation of chondritic material in the early solar system: Results of thermodynamic simulation p 432 N94-12226

SOLAR WIND
Solar wind channels for MeV particles
[DE93-012648] p 482 N94-10741
SMM x ray polychromator
[NASA-CR-193282] p 483 N94-11048

SOLAR X-RAYS
Remote sensing x ray fluorescence spectrometry for future lunar exploration missions p 462 N94-12165

SOLDERED JOINTS
ENSAFE fireset flex circuit analysis
[DE93-013106] p 144 N94-11478

SOLDERING
Advanced soldering processes
[DE93-009856] p 129 N94-11606

SOLDERS
Advanced soldering processes
[DE93-009856] p 129 N94-11606

SOLENOIDS
High-field conductor testing at the FENIX facility
[DE93-012318] p 387 N94-10737
Spin characteristics of ion beams during the motion of electromagnetic elements
[DE93-617448] p 364 N94-10848

SOLID CRYOGENS
Experiments with energetic (mu)d and (mu)t emitted from solid hydrogen
[DE93-010252] p 373 N94-12542

SOLID ELECTROLYTES
Technical Update: Johnson Space Center system using a solid electrolytic cell in a remote location to measure oxygen fugacities in CO/CO2 controlled-atmosphere furnaces
[NASA-TM-104774] p 423 N94-11183
Polymer electrolyte fuel cells: Potential transportation and stationary applications
[DE93-010734] p 264 N94-11666

SOLID LUBRICANTS
Study of the tribological behavior of SiC and Si3N4 ceramic couples in terms of temperature: The reality p 64 N94-10061
Advanced model of gradual wear of viscoelastic surface film
[AD-A265130] p 90 N94-11222
Properties of interfacial tribo-films
[AD-A265591] p 182 N94-12374

SOLID PROPELLANT COMBUSTION
Combustion-induced crack propagation process in a solid-propellant crack cavity p 98 N94-10901

SOLID PROPELLANT ROCKET ENGINES
Combustion-induced crack propagation process in a solid-propellant crack cavity p 98 N94-10901

SOLID PROPELLANTS
Polymeric nitrogen
[DE93-012600] p 89 N94-11151
Distributed combustion in solid propellants
[AD-A265727] p 99 N94-12564

SOLID SOLUTIONS
Symmetry lowering in crystalline solid solutions: A study of cinnamamide-thienylacrylamide by x ray and neutron diffraction and solid-state photochemistry
[DE93-010871] p 394 N94-10301
Materials for adaptive structural acoustic control, volume 3
[AD-A264621] p 358 N94-11262

SOLID STATE
Solid state ionics 3. Materials Research Society Symposium Proceedings, volume 293
[AD-A265675] p 395 N94-10416
Solid-state structures of guanidinium methane, ethane, and trifluoromethanesulfonate
[AD-A265293] p 402 N94-11654
Hydrogen-bond polymorphs of guanidinium 4-biphenylsulfonate
[AD-A265294] p 402 N94-11827
The 13C and 15N solid-state NMR of copolymers of nylon 6 and 7: Observation of a stable pseudohexagonal phase
[AD-A265799] p 94 N94-12381
Engineering solid-state materials. Strategies for modeling and packing control of molecular assemblies into 3-D networks
[AD-A265291] p 404 N94-12438

SOLID STATE DEVICES
Solid state ionics 3. Materials Research Society Symposium Proceedings, volume 293
[AD-A265675] p 395 N94-10416

SOLID STATE LASERS
Limitations to the quality of optical phase conjugation by stimulated Brillouin scattering
[AD-A266006] p 383 N94-12389

SOLID SURFACES

Application of spin-sensitive electron spectroscopies to investigations of electronic and magnetic properties of solid surfaces and epitaxial systems
[DE93-015079] p 76 N94-10854

SOLID SUSPENSIONS

Remote sensing of the suspended matter distribution with high concentration in China Sea
p 192 N94-11901

Analysis of the characteristic and mechanism of suspended matter transportation in Huanghe delta sea area using remote sensing techniques
p 197 N94-11930

Development of shipboard ocean lidar
p 140 N94-11965

A development on estimation method of undersea light p 204 N94-11974

Proceedings of the PORSEC 1992 in Okinawa: Conference for Pacific Ocean Environments and Probing, volume 2
[JTN-93-80419] p 207 N94-12635

SOLID-SOLID INTERFACES

Effect of experimental procedure on pattern formation and array disorder in cellular solidification
p 117 N94-10203

SOLIDIFICATION

Structure and properties of an RS Al-Si-Ni-Mn-Zr alloy for high temperature applications p 64 N94-10063

Convection related radial segregation in an idealized horizontal Bridgman configuration p 115 N94-10185

Wetting effects on nylon spheres engulfment in ice
p 115 N94-10189

Thermophysical properties of undercooled liquid metals p 86 N94-10190

Solidification of undercooled Ni-32.5 wt percent Sn eutectic alloy p 86 N94-10194

Undercooled W-Re and Mo-Re drops in an ultra high vacuum drop tube p 86 N94-10195

Non-equilibrium solidification in undercooled Ni-B alloys p 86 N94-10196

Ground results of the Mephisto program: Benefits and space experiments orientation p 86 N94-10197

Solidification and metastable phase formation of highly undercooled Fe-Cr-Ni alloy melts p 87 N94-10204

SOLIDS

X ray and gamma ray spectroscopy of solids under pressure
[DE93-014847] p 76 N94-10653

Characterization of an excimer laser-ablated plasma and applications p 392 N94-11450

Corrosion control by vitreous films on aluminum and high T(sub c) superconductors
[AD-A266016] p 85 N94-12393

SOLITARY WAVES

Marangoni-driven solitary waves p 119 N94-10214

Quantum solitons with cylindrical symmetry
[DE93-617659] p 344 N94-10881

Nonlinear excitation in quasi-one-dimensional Peierls dielectrics with charge density waves
[DE93-613827] p 398 N94-11025

Creation and annihilation of solitons in nonlinear integrable systems
[DE93-621379] p 365 N94-11078

Negative viscosity and generation of dissipative solitons and zonal dissipative structures by drift waves
[DE93-621656] p 392 N94-11212

Femtosecond dynamics, photoexcitation, and ESR spectra of MX chain solids
[AD-A264689] p 399 N94-11263

SOLUBILITY

Determination of concentration profiles at interfaces and surfaces of partially miscible polymer blends
[DE93-013140] p 89 N94-11007

Measurement of viscosity, density and gas solubility of refrigerant blends
[DE93-014772] p 89 N94-11145

Joint pain and Doppler-detectable bubbles in altitude (Hypobaric) decompression p 312 N94-11542

The solubility of epsilon-CL-20 in selected materials
[DE93-009304] p 77 N94-11602

Polymer-polymer interactions
[AD-A265304] p 91 N94-11830

The solubility of gold in silicate melts: First results
p 87 N94-12086

Graphite solubility and [illegible] vesiculation in basalt-like melts at one-ATM p 463 N94-12173

SOLUTES

The effect of gravity modulation on thermosolutal convection p 105 N94-10103

The effect of gravitational modulation on convection in vertical Bridgman growth p 113 N94-10178

Experimental studies of the structure of grain boundaries
[DE93-013979] p 402 N94-11700

SOLUTIONS

Synthesis of molecular sieves from clear solution
p 124 N94-10245

SOLVATION

Polar solvation and electron transfer
[DE93-013328] p 365 N94-11010

SOLVENTS

Polar solvation and electron transfer
[DE93-013328] p 365 N94-11010

Dynamics of charge-transfer excited states relevant to photochemical energy conversion
[DE93-013981] p 263 N94-11116

Joint pain and Doppler-detectable bubbles in altitude (Hypobaric) decompression p 312 N94-11542

Solvent dynamical effects in electron transfer: Molecular dynamics simulations of reactions in methanol
[AD-A266061] p 369 N94-12420

SONAR

Acoustic characteristics of side scan sonar and sub-bottom profiler for 10,000 m class ROV
p 172 N94-11916

Mapping bathymetric slopes from bathymetry data
[AD-A265923] p 290 N94-12350

Signal feature analysis using neural networks and psychoacoustics
[AD-A266048] p 340 N94-12398

SORET COEFFICIENT

On the role of Soret effect in concentration distribution in crystals growing from the melt p 112 N94-10173

Marangoni Benard instabilities in liquid mixtures with Soret effect p 119 N94-10215

SOUND FIELDS

Determination of the viscous acoustic field for liquid drop positioning/forcing in an acoustic levitation chamber in microgravity p 110 N94-10131

SOUND GENERATORS

Direct numerical simulation of hot jets
p 156 N94-12295

SOUND TRANSDUCERS

Acoustic characteristics of side scan sonar and sub-bottom profiler for 10,000 m class ROV
p 172 N94-11916

SOUND WAVES

Virtual sound for virtual reality
[DE93-010519] p 321 N94-10291

Sensing glass transitions in thin polymer films on acoustic wave microsensors
[DE93-010805] p 87 N94-10295

Estimation of the direct acoustic radiation from turbulent spots using boundary layer velocity measurements
p 357 N94-10358

Photostimulated attenuation of hypersound in superlattice
[DE93-611231] p 357 N94-10408

Confinement of acoustical modes due to the electron-phonon interaction within 2D-electron gas
[DE93-613910] p 396 N94-10800

Acoustics of bubbly sediments
[AD-A263726] p 288 N94-11299

Near surface ocean processes: Acoustical observations, ambient sound, and Langmuir circulation
p 288 N94-11447

Study on color video pictures transmission by digital acoustic signal p 139 N94-11917

NRL review for 1993
[AD-A265666] p 497 N94-12334

Preliminary analysis of the FLIP array data from the NOBS experiment
[AD-A265911] p 289 N94-12349

SOUNDING ROCKETS

MUZO: The programmable multi zone furnace for gas payloads and sounding rockets p 110 N94-10132

Microgravity experiments using TR-1A rocket
p 112 N94-10142

TEXUS 28 experiment: Convections and crystal growth of Ge:Ga. Analysis of temperature measurements
p 114 N94-10184

AD100/ADSIM, ACSL, and MATLAB output comparisons using frequency-response analysis
[DE93-009640] p 47 N94-11122

SOURCE PROGRAMS

Reuse: A knowledge-based approach
p 329 N94-11430

SOUTH KOREA

Overview of KITSAT p 36 N94-10683

Korea space program p 36 N94-10684

SOUTHERN OSCILLATION

Updated forecast of Atlantic seasonal hurricane activity for 1993 p 285 N94-11194

Current structures in the western equatorial Pacific during JAPACS cruises p 193 N94-11911

Principal oscillation pattern analysis of sea level variations in the tropical Pacific measured by the GEOSAT altimeter p 209 N94-12646

SOVIET SPACECRAFT

Russian space system for the Earth remote sensing
p 37 N94-10688

SPACE ADAPTATION SYNDROME

Cardiovascular dynamics during space sickness and deconditioning p 311 N94-12007

SPACE BASED RADAR

Spaceborne SAR study: LDRD 1992
[DE93-011485] p 232 N94-11623

ERS-1 SAR calibration strategy p 235 N94-11726

ERS-1 preliminary antenna elevation pattern measured by ground-receivers p 235 N94-11727

Preliminary results of the experiment I-7
p 235 N94-11728

The ERS-1/CV 580 SAR cross-calibration experiment: Sault Ste Marie, October 26 - November 2, 1991
p 236 N94-11729

Calibration of the ERS-1 SAR fast-delivery images
p 236 N94-11730

Calibration results for the ERS-1, AIRSAR, and PHARS p 236 N94-11731

An experiment for the radiometric calibration of the ERS-1 SAR p 236 N94-11733

Techniques and applications of SAR interferometry for ERS-1: Topographic mapping, change detection, and slope measurement p 236 N94-11734

SAR interferometry experiments with ERS-1
p 237 N94-11735

SAR-interferometry applying ERS-1: Some preliminary test results p 237 N94-11736

Utilisation of ERS-1 data for mapping of Antarctica
p 237 N94-11740

Observations of surface signatures in the north-west Pacific Ocean with the spaceborne SAR
p 226 N94-12746

SPACE CHARGE

A parallel implementation of particle tracking with space charge effects on an Intel iPSC/860
[DE93-012307] p 335 N94-10340

Nonlinear space charge effect of bunched beam in linac
[DE93-612176] p 371 N94-10409

Effect of effective mass differences on the tunneling current-voltage behaviour of a resonant diode in the presence of space charge build-up
[DE93-613817] p 142 N94-10799

Time-resolved optical studies of charge relaxation and charge transfer at electrode interfaces
[DE93-013985] p 398 N94-11117

SPACE COLONIES

Exploration planning in the context of human exploration and development of the Moon p 474 N94-12229

SPACE COMMERCIALIZATION

Potential markets for advanced satellite communications
[NASA-CR-191145] p 41 N94-10512

Landsat as a commercial enterprise
[INPE-5477-TAE/019] p 232 N94-11524

The guide to Design For On-orbit Spacecraft Servicing (DFOSS) manual: Producing a consensus document
p 421 N94-11575

Special investigation report: Commercial space launch incident, launch procedure anomaly orbital sciences corporation PEGASUS/SCD-1, 80 nautical miles east of Cape Canaveral, Florida, February 9, 1993
[PB93-917003] p 40 N94-11893

SPACE COMMUNICATION

Use of low orbital satellite communications systems for humanitarian programs p 308 N94-11808

SPACE DEBRIS

Satellite situation report, volume 32, no. 1
[NASA-TM-109233] p 42 N94-10562

Satellite situation report, volume 32, no. 2
[NASA-TM-109234] p 42 N94-10563

Satellite situation report, volume 31, no. 4
[NASA-TM-109232] p 39 N94-10659

The magnitude of impact damage on LDEF materials
[NASA-CR-188258] p 43 N94-10666

Modelling hypervelocity impacts into aluminum structures based on LDEF data p 190 N94-12178

Model of optical scatter from microimpacts on the Hubble Telescope p 384 N94-12189

SPACE ERECTABLE STRUCTURES

Advances in adaptive structures at Jet Propulsion Laboratory p 72 N94-11344

On-orbit servicing for USAF space missions: A phased development approach p 348 N94-11571

Definition of spacecraft standard interfaces by the NASA Space Assembly and Servicing Working Group (SASWG) p 348 N94-11574

SPACE EXPLORATION

ESA/ESOC: 25 years
[ESA-BR-90] p 485 N94-11379

Sixth Annual Workshop on Space Operations Applications and Research (SOAR 1992), volume 2
[NASA-CP-3187-VOL-2] p 486 N94-11527

In-space operations for lunar and Mars space transfer vehicles p 348 N94-11568
Terrestrial case studies of ilmenite exploration and lunar implications p 478 N94-12247
Conceptual studies report on lunar and planetary exploration
[NASDA-TK-SS0438] p 481 N94-12323
Mars exploration missions p 482 N94-12327
Technical problems on lunar an planetary exploration mission p 482 N94-12328

SPACE LABORATORIES
Advanced protein, crystallization facility and associated new developments p 39 N94-10119
The International Microgravity Laboratory, a Spacelab for materials and life sciences p 125 N94-10249
The critical facility on IML-1 p 44 N94-10250
Effect of double density caging during Space Shuttle transport of laboratory rats
[NASA-CR-193228] p 300 N94-11180

SPACE LOGISTICS
Definition of spacecraft standard interfaces by the NASA Space Assembly and Servicing Working Group (SASWG) p 348 N94-11574

SPACE MAINTENANCE
On-orbit refueling p 38 N94-11566
Preliminary analysis of the benefits derived to US Air Force spacecraft from on-orbit refueling
p 38 N94-11567
Forecasting the impact of virtual environment technology on maintenance training p 314 N94-11570
On-orbit servicing for USAF space missions: A phased development approach p 348 N94-11571
More sense for less cents: Cost effective servicing of remote sensing satellites p 348 N94-11572
Space Station maintenance studies using plaid graphics p 335 N94-11578
Robotic servicing on Earth orbiting satellites
p 45 N94-11579

SPACE MANUFACTURING
Solidification in immiscible systems: The influence of processing conditions on resulting microstructures
p 112 N94-10174
Space Solar Power Program
[DE93-011750] p 55 N94-11675

SPACE MISSIONS
An analysis of the modes and states for generic avionics
[NASA-CR-188253] p 27 N94-10664
The 1987 RIACS annual report
[NASA-CR-193220] p 324 N94-11046
Analyzing human errors in flight mission operations
p 314 N94-11534
On-orbit servicing for USAF space missions: A phased development approach p 348 N94-11571
Supervised autonomous control, shared control, and teleoperation for space servicing p 183 N94-11577
Summary of the pre-AO of the JEM onboard scientific and engineering experiments for refrigerator utilization
p 129 N94-11832
Moessbauer spectrometer for mineralogical analysis of the Mars surface: Moessbauer source considerations
p 476 N94-12242
Conceptual studies report on lunar and planetary exploration
[NASDA-TK-SS0438] p 481 N94-12323
Significance and scenarios of lunar and planetary exploration missions p 482 N94-12324
Technical problems on lunar an planetary exploration mission p 482 N94-12328
Interdisciplinary scientist participation in the Phobos mission
[NASA-CR-193715] p 482 N94-12446

SPACE NAVIGATION
NASA's first in-space optical gyroscope: A technology experiment on the X ray Timing Explorer spacecraft
[NASA-TM-109242] p 170 N94-10667
Lunar Scout Two spacecraft gravity experiment
p 459 N94-12152

SPACE OBSERVATIONS (FROM EARTH)
The 1.2 to 3.5 microns observations of asteroid 4179 Toutatis p 430 N94-12111

SPACE PLASMAS
Solar wind channels for MeV particles
[DE93-012648] p 482 N94-10741
Imaging of magnetospheric dynamics using low energy neutral atom detection
[DE93-012656] p 275 N94-10742
The influence of the propagation medium on the sensitivity and resolution of meter wavelength aperture synthesis systems p 134 N94-11062

SPACE PLATFORMS
Robotic servicing on Earth orbiting satellites
p 45 N94-11579
Spaceborne SAR study: LDRD 1992
[DE93-011485] p 232 N94-11623

SPACE POWER REACTORS
The 40 kWe S-PRIME Thermionic Design and Technology Demonstration Program
[DE93-004738] p 40 N94-10147
A critical assembly designed to measure neutronic benchmarks in support of the Space Nuclear Thermal Propulsion program
[DE92-040974] p 371 N94-10529
Fully coupled neutronic and hydrodynamic analysis of space nuclear reactor reentry accidents
[DE93-005459] p 372 N94-10890
A facility for testing 10- to 100-kWe space power reactors
[DE92-040420] p 372 N94-11296
Proceedings of the 12th Space Photovoltaic Research and Technology Conference (SPRAT 12)
[NASA-CP-3210] p 48 N94-11380
TFE verification program
[DE93-009609] p 373 N94-11694

SPACE PROBES
Estimation of the attitude motion of the small satellite ORIZURU
[NAL-TR-1145] p 42 N94-10366

SPACE PROCESSING
Proceedings of the 8th European Symposium on Materials and Fluid Sciences in Microgravity, volume 1
[ESA-SP-333-VOL-1] p 99 N94-10070
Gas film levitator for containerless processing of glasses in microgravity conditions: Early concept and technology demonstration p 108 N94-10122
TEMPUS: An electromagnetic levitation facility for containerless processing under micro-g in Spacelab
p 109 N94-10125
Microgravity Applications Furnace Facility (MAFF) for parabolic flights p 109 N94-10128
High temperature processing and diagnostic technologies for microgravity applications
p 110 N94-10130
Determination of the viscous acoustic field for liquid drop positioning/forcing in an acoustic levitation chamber in microgravity p 110 N94-10131
Laser beam deflection: A diagnostic tool for vapour growth experiments in microgravity p 111 N94-10135
Mission support for crystal growth experiments in Russian unmanned carriers p 111 N94-10139
AGF (Automatic Gradient Furnace): A proposed microgravity facility p 112 N94-10141
Microgravity experiments using TR-1A rocket
p 112 N94-10142
Proceedings of the 8th European Symposium on Materials and Fluid Sciences in Microgravity, volume 2
[ESA-SP-333-VOL-2] p 112 N94-10171
Scientific specifications for an automated facility for growing large semiconducting crystals from the melt in space p 114 N94-10180
Variations of the temperature profile in the gradient furnace GFQ within a cylindrical sample used for directional solidification p 114 N94-10181
Numerical simulation of multi-droplet hydrodynamic interactions in liquid dispersions p 114 N94-10182
Convection related radial segregation in an idealized horizontal Bridgman configuration p 115 N94-10185
TEM study of a space processed Al-Al2O3 metallic composite p 75 N94-10186
In situ observation of temperature dependence of concentration field during growth of KB5 crystals by holographic interferometry p 115 N94-10187
Crystal growth from low temperature vapour phase
p 115 N94-10191
Results of crystal growth experiments by FZM on Zona facilities in microgravity p 116 N94-10193
Undercooled W-Re and Mo-Re drops in an ultra high vacuum drop tube p 86 N94-10195
Effects of a microgravity environment on the crystallization of biological macromolecules
p 117 N94-10198
EUSO-D2-experiment: Unidirectional solidification with quenching of an AlSi11 alloy p 86 N94-10199
Liquid phase sintering of tungsten composites under microgravity. Effect of matrix composition
p 118 N94-10207
Crystallization of zeolites in the microgravity environment of space p 119 N94-10210
Crystal growth in the Zone Melting Facility (ZMF)
p 119 N94-10213
Memory effects in the organometallic chemical beam epitaxy of compound semiconductors
[NASA-CR-193106] p 399 N94-11439
Cold press sintering of simulated lunar basalt
p 131 N94-12026
General overview of an integrated lunar oxygen production/brickmaking system p 131 N94-12027
Thermodynamics of lunar ilmenite reduction
p 415 N94-12028

SPACE PROGRAMS
Analysis of the cost evaluation of ESA programmes and comparable national and international programmes
[GTS-92063] p 416 N94-10145
Space Activities in the Asia Pacific Region
[JTN-93-80421] p 35 N94-10676
Current status of space activities in Asia Pacific region
p 35 N94-10677
Considerations for future regional space cooperation
p 35 N94-10678
Space research and remote sensing programmes in Bangladesh p 35 N94-10679
Overview of KITSAT p 36 N94-10683
Korea space program p 36 N94-10684
Space programme in Malaysia p 36 N94-10685
National space programmes and application of the remote sensing data in Mongolia p 36 N94-10686
Thailand ISY activities p 37 N94-10690
Panel discussion: Role of space program in the Asia Pacific Region p 37 N94-10694
Space Solar Power Program
[DE93-011750] p 55 N94-11675
Medical care delivery in the US space program
p 307 N94-11806

SPACE SHUTTLE MAIN ENGINE
Probabilistic evaluation of uncertainties and risks in aerospace components
[NASA-TM-105603] p 185 N94-10361
Application of powder metallurgy techniques to produce improved bearing elements for liquid rocket engines
[NASA-CR-193731] p 82 N94-10804
Enhancements to the Engine Data Interpretation System (EDIS)
[NASA-CR-192593] p 180 N94-10815
A study of strength evaluations of EDNi/EDCu/NARloy-Z bonded joints
[NASA-TM-108418] p 188 N94-11275

SPACE SHUTTLE MISSIONS
Echocardiography in the flight program
p 309 N94-11993

SPACE SHUTTLE ORBITERS
Extraction of stability and control derivatives from orbiter flight data
[NASA-TM-4500] p 13 N94-10707
Space Shuttle hypersonic aerodynamic and aerothermodynamic flight research and the comparison to ground test results
[NASA-TM-4499] p 13 N94-10820
Investigation of alternate power source for Space Shuttle Orbiter hydraulic system
[NASA-CR-193229] p 46 N94-10911
Vigilance problems in orbiter processing
p 314 N94-11536

SPACE SHUTTLE PAYLOADS
Compatibility tests for biological specimens to on-board experiments in the Space Shuttle flight
[NASDA-CNT-930003] p 301 N94-12278

SPACE SHUTTLES
Space Shuttle hypersonic aerodynamic and aerothermodynamic flight research and the comparison to ground test results
[NASA-TM-4499] p 13 N94-10820
Applying reliability models to the maintenance of Space Shuttle software p 330 N94-11434
Microgravity vibration isolation technology: Development to demonstration
[NASA-TM-106320] p 1 N94-11703

SPACE STATION FREEDOM
Microbiological test results using three urine pretreatment regimes with 316L stainless steel
[NASA-CR-192568] p 299 N94-10360
Achievements and challenges of Space Station Freedom's safety review process
[NASA-TM-106199] p 40 N94-10640
Space Station Redesign Team: Final report to the Advisory Committee on the Redesign of the Space Station
[NASA-TM-109241] p 42 N94-10663
Space Station redesign option A: Modular buildup concept
[NASA-TM-108415] p 43 N94-10808
Transportation systems analyses: Volume 1: Executive Summary
[NASA-CR-192583] p 41 N94-10826
Transportation systems analyses. Volume 2: Technical/programmatics
[NASA-CR-192582] p 41 N94-10827
Large project experiences with object-oriented methods and reuse p 329 N94-11431
Sixth Annual Workshop on Space Operations Applications and Research (SOAR 1992), volume 2
[NASA-CP-3187-VOL-2] p 486 N94-11527
Space Station maintenance studies using plaid graphics p 335 N94-11578

Microgravity vibration isolation technology: Development to demonstration
[NASA-TM-106320] p 1 N94-11703

SPACE STATION POWER SUPPLIES
Space Station Freedom advanced photovoltaics and battery technology development planning
p 52 N94-11401

SPACE STATION STRUCTURES
Space Station maintenance studies using plaid graphics p 335 N94-11578

SPACE SUITS
Crew chief p 335 N94-11564

SPACE TECHNOLOGY EXPERIMENTS
The Second Workshop on Refrigerating System Utilization Onboard the JEM
[NASDA-CON-930001] p 129 N94-11831
Summary of the pre-AO of the JEM onboard scientific and engineering experiments for refrigerator utilization
p 129 N94-11832
Submillimeter wave observation experiment of Earth atmosphere with SIS mixer p 130 N94-11837
Utilization of superconductivity in the area of space
p 131 N94-11843
The Third Workshop on Two Phase Fluid Experiment in the Space Environment
[NASDA-CON-930002] p 161 N94-12547
Summary of studies on JEM utilization experiment projects p 161 N94-12548
Compilation of proposals for boiling and evaporation experiments in space environments and proposals concerning experiment projects p 161 N94-12549
Condensation phenomena p 162 N94-12550
Developmental research of thermal control system in space environment p 162 N94-12551
Two phase flow and isopycnic liquid-liquid two phase fluid in reduced gravity field p 162 N94-12552
Research on two phase flow in microgravity
p 162 N94-12554
Organization and management policy for two phase fluid experiment in space environment p 162 N94-12556

SPACE TRANSPORTATION
Space transportation alternatives for large space programs: The International Space University Summer Session, 1992
[NASA-TM-106271] p 40 N94-10811
Transportation systems analyses: Volume 1: Executive Summary
[NASA-CR-192583] p 41 N94-10826
Transportation systems analyses. Volume 2: Technical/programmatics
[NASA-CR-192582] p 41 N94-10827
Space Solar Power Program
[DE93-011750] p 55 N94-11675

SPACE TRANSPORTATION SYSTEM
Transportation systems analyses: Volume 1: Executive Summary
[NASA-CR-192583] p 41 N94-10826
Transportation systems analyses. Volume 2: Technical/programmatics
[NASA-CR-192582] p 41 N94-10827
Visual Earth observation performance in the space environment. Human performance measurement 4: Flight experiments p 314 N94-11539
Toxicity study of dimethylethoxysilane (DMSES), the waterproofing agent for the Orbiter heat protective system p 318 N94-11554

SPACE TRANSPORTATION SYSTEM FLIGHTS
Debris/ice/TPS assessment and integrated photographic analysis for Shuttle Mission STS-57
[NASA-TM-107562] p 40 N94-10805
Echocardiography in the flight program
p 309 N94-11993

SPACE-TIME FUNCTIONS
Discrete space-time symmetries
[DE93-010199] p 341 N94-10259
On the generalized Jordan-Brans-Dicke theory
[DE93-613051] p 409 N94-10499
From the Weyl theory to a theory of locally anisotropic space-time
[DE92-644734] p 410 N94-10535
Wavelets and spacetime squeeze
p 379 N94-10604
Dimensional transition of the space-time at the minimum action near the planck scale
[DE93-754192] p 410 N94-10718
New developments in the method of space-time conservation element and solution element: Applications to the Euler and Navier-Stokes equations
[NASA-TM-106226] p 150 N94-10939
A version of superstring with four space-time dimensions
[DE93-608196] p 412 N94-11163

SPACEBORNE ASTRONOMY
Propagation Effects in Space VLBI
p 134 N94-11060
Yohkoh Bragg Crystal Spectrometer light curves for Ca XIX (3.1631-3.1912A): 1 October 1991 - 30 September 1992
[AD-A266090] p 483 N94-12414

SPACEBORNE EXPERIMENTS
Proceedings of the 8th European Symposium on Materials and Fluid Sciences in Microgravity, volume 1
[ESA-SP-333-VOL-1] p 99 N94-10070
The formation and breakage of liquid bridges under microgravity p 100 N94-10071
Towards real time numerical stimulation of Marangoni convection: A help for telescience microgravity experiments p 102 N94-10087
Marangoni instability induced convection in an evaporating liquid droplet p 104 N94-10094
Bubbles and drops behaviour under low-gravity: A space experiment for the IML-2 mission p 104 N94-10098
Description of the liquid structure facility architecture and experimental demonstration of the diagnostic capabilities
p 39 N94-10118
Advanced protein, crystallization facility and associated new developments p 39 N94-10119
MUZO: The programmable multi zone furnace for gas payloads and sounding rockets p 110 N94-10132
The surface plasmon spectroscopy as diagnostic technique in microgravity experiments
p 110 N94-10133
TOLS (Telescience On-Line Simulator): An essential instrument for micro-gravity interactive experiment
p 39 N94-10134
Laser beam deflection: A diagnostic tool for vapour growth experiments in microgravity p 111 N94-10135
The advanced fluid physics module: How to achieve scientific goals for Spacelab D2 p 39 N94-10136
Results of mission preparation support to microgravity experiments on board of Eureca 1 p 111 N94-10138
Mission support for crystal growth experiments in Russian unmanned carriers p 111 N94-10139
Analysis of the alignment of a Schlieren system for tele-operation p 111 N94-10140
AGF (Automatic Gradient Furnace): A proposed microgravity facility p 112 N94-10141
Microgravity experiments using TR-1A rocket
p 112 N94-10142
Experimental approach to non-contact calorimetry in space p 112 N94-10143
Proceedings of the 8th European Symposium on Materials and Fluid Sciences in Microgravity, volume 2
[ESA-SP-333-VOL-2] p 112 N94-10171
Numerical calculation of the growth of InP by the travelling heater method in the first mission of the Space Flyer Unit p 114 N94-10179
Results of crystal growth experiments by FZM on Zona facilities in microgravity p 116 N94-10193
EUSO-D2-experiment: Unidirectional solidification with quenching of an AlSi11 alloy p 86 N94-10199
Ripening of immiscible liquid droplets in microgravity with constrained Marangoni drift p 117 N94-10200
Liquid phase sintering of tungsten composites under microgravity. Effect of matrix composition
p 118 N94-10207
A study of the quasibinary Al-W-Mo system. Part 1: Preliminary investigations and preparation for microgravity experiments p 119 N94-10211
Transport of heat and mass in near-critical fluids
p 122 N94-10230
Measurements of heat capacity in undercooled metals
p 87 N94-10231
Columbus proto-planetesimal dust aggregation experiment p 123 N94-10236
Use of inert immiscible liquid for crystal separation out of its feeding solution in weightlessness
p 124 N94-10242
Single bubble experiments in pool boiling: Results from TEXUS 26 p 124 N94-10243
The International Microgravity Laboratory, a Spacelab for materials and life sciences p 125 N94-10249
The critical facility on IML-1 p 44 N94-10250
Space Activities in the Asia Pacific Region
[JTN-93-80421] p 35 N94-10676
Space environmental effects on the integrity of chromic acid anodized coatings
[NASA-CR-191468] p 55 N94-10947
Gas-Grain Simulation Facility (GGSF). Volume 2: Conceptual design definition
[NASA-CR-177613] p 423 N94-11229
An overview of the Defence Research Agency photovoltaic programme p 53 N94-11412
Microgravity vibration isolation technology: Development to demonstration
[NASA-TM-106320] p 1 N94-11703
Summary of the pre-AO of the JEM onboard scientific and engineering experiments for refrigerator utilization
p 129 N94-11832
Submillimeter wave observation experiment of Earth atmosphere with SIS mixer p 130 N94-11837
Utilization of superconductivity in the area of space
p 131 N94-11843
Lunar Scout Two spacecraft gravity experiment
p 459 N94-12152
The Third Workshop on Two Phase Fluid Experiment in the Space Environment
[NASDA-CON-930002] p 161 N94-12547
Summary of studies on JEM utilization experiment projects p 161 N94-12548
Compilation of proposals for boiling and evaporation experiments in space environments and proposals concerning experiment projects p 161 N94-12549
Condensation phenomena p 162 N94-12550
Developmental research of thermal control system in space environment p 162 N94-12551
Two phase flow and isopycnic liquid-liquid two phase fluid in reduced gravity field p 162 N94-12552
Research on two phase flow in microgravity
p 162 N94-12554
Organization and management policy for two phase fluid experiment in space environment p 162 N94-12556

SPACEBORNE LASERS
Enhanced Damage-Resistant Optics for Spaceflight Laser Systems: Workshop findings and recommendations
[NASA-TM-109243] p 381 N94-11054

SPACEBORNE PHOTOGRAPHY
Preliminary report of lunar observations by the Near-Infrared Mapping Spectrometer (NIMS) during the second Galileo Earth-Moon encounter
p 425 N94-12140

SPACEBORNE TELESCOPES
An approach to high precision antenna structures by a CFRP core sandwich concept p 57 N94-10008
Zerodur polishing process for high surface quality and high efficiency
[DE93-012596] p 87 N94-10271

SPACECRAFT CHARGING
Experimental measurement of the plasma conductivity of Z93 and Z93P thermal control paint
[NASA-TM-106284] p 43 N94-10756
Analysis of geophysical measurements and spacecraft interactions
[AD-A266064] p 43 N94-10944
NASCAP programmer's reference manual
[NASA-CR-191044] p 278 N94-11702

SPACECRAFT COMPONENTS
Spinforming characteristics of a net shape forming process p 56 N94-10004
Development tests for a high stability optical bench
p 62 N94-10047
Introducing SMaSE: An aide memoire on structural materials and space engineering p 63 N94-10053
The properties of perfluoropolyethers used for space applications
[NASA-TM-106275] p 88 N94-10864
The trial manufacture and test of critical components in docking mechanism
[NASDA-TMR-930005] p 44 N94-12280
Conceptual studies report on lunar and planetary exploration
[NASDA-TK-SS0438] p 481 N94-12323
Manned lunar exploration missions
p 482 N94-12326
Mars exploration missions p 482 N94-12327

SPACECRAFT CONFIGURATIONS
Space Station Redesign Team: Final report to the Advisory Committee on the Redesign of the Space Station
[NASA-TM-109241] p 42 N94-10663

SPACECRAFT CONSTRUCTION MATERIALS
Advanced Materials for Lightweight Structures
[ESA-SP-336] p 56 N94-10001
The EUREKA project portfolio in new materials
p 56 N94-10002
Spinforming characteristics of a net shape forming process p 56 N94-10004
Design and development of a CFRP central cylinder for satellites p 56 N94-10007
Design and manufacturing of filament wound thrust cylinder p 57 N94-10010
Design concepts for load-carrying hot structures for reentry bodies p 57 N94-10012
Hybrid materials for use at elevated temperatures
p 57 N94-10013
Analytical prediction and test verification of the multiaxial behaviour of high-strength steel for lightweight structures
p 58 N94-10016
Aluminium-lithium forgings: Properties and potential satellite applications p 58 N94-10021
Mechanical and fatigue properties of fibre reinforced aluminium-lithium alloy and aluminium-lithium MMC based laminates p 58 N94-10022
Investigations on aluminium-lithium alloys for damage tolerant application p 59 N94-10023

- Design and manufacturing of CFRP rings by RTM p 59 N94-10025
- Aluminum-beryllium alloys for aerospace applications p 60 N94-10029
- Ceramic matrix composites: High performance materials for space application p 62 N94-10044
- Stress relaxation forming of Ariane 5 front skirt outer skin panels p 62 N94-10046
- Vectra insulative support structures within spacecraft p 62 N94-10050
- Introducing SMaSE: An aide memoire on structural materials and space engineering p 63 N94-10053
- Structural material, manufacture, and design requirements for high-temperature fasteners for space plane technologies p 63 N94-10055
- High temperature composites in Aerospatiale activities p 64 N94-10062
- Structure and properties of an RS Al-Si-Ni-Mn-Zr alloy for high temperature applications p 64 N94-10063
- Material characterization and modeling with shear ography [NASA-CR-192576] p 185 N94-10342
- Fractography handbook of spaceflight metals [NASA-RP-1291] p 81 N94-10504
- Failure prediction of thin beryllium sheets used in spacecraft structures [NASA-CR-194164] p 187 N94-11190
- Vacuum stability requirements of polymeric material for spacecraft application [NASA-TM-109216] p 91 N94-11350

SPACECRAFT CONTAMINATION
- Analysis of geophysical measurements and spacecraft interactions [AD-A266064] p 43 N94-10944
- Spacelab J air filter debris analysis [NASA-CR-192569] p 301 N94-11201

SPACECRAFT CONTROL
- An analysis of the modes and states for generic avionics [NASA-CR-188253] p 27 N94-10664
- Stability analysis and aerospace vehicle dynamics p 31 N94-11491
- Technical problems on lunar an planetary exploration mission p 482 N94-12328

SPACECRAFT DESIGN
- High temperature materials for hypersonic transport p 56 N94-10003
- Design and manufacturing of filament wound thrust cylinder p 57 N94-10010
- Aluminium-lithium forgings: Properties and potential satellite applications p 58 N94-10021
- Structural material, manufacture, and design requirements for high-temperature fasteners for space plane technologies p 63 N94-10055
- Planetary entry vehicle design for planned and potential ESA missions to Titan, Mars, and Earth return (FGE TN 51/92) p 4 N94-10428
- A CFD validation roadmap for hypersonic flows p 5 N94-10439
- Space Station Redesign Team: Final report to the Advisory Committee on the Redesign of the Space Station [NASA-TM-109241] p 42 N94-10663
- An analysis of the modes and states for generic avionics [NASA-CR-188253] p 27 N94-10664
- Space Station redesign option A: Modular buildup concept [NASA-TM-108415] p 43 N94-10808
- Progress in multidisciplinary design optimization at NASA Langley [NASA-TM-107754] p 318 N94-10814
- The guide to Design For On-orbit Spacecraft Servicing (DFOSS) manual: Producing a consensus document p 421 N94-11575
- The trial manufacture and test of critical components in docking mechanism [NASDA-TMR-930005] p 44 N94-12280
- Conceptual studies report on lunar and planetary exploration [NASDA-TK-SS0438] p 481 N94-12323
- Unmanned lunar exploration mission p 482 N94-12325
- Manned lunar exploration missions p 482 N94-12326
- Mars exploration missions p 482 N94-12327

SPACECRAFT DOCKING
- Definition of spacecraft standard interfaces by the NASA Space Assembly and Servicing Wnrking Group (SASWG) p 348 N94-11574
- Robotic servicing on Earth orbiting satellites p 45 N94-11579
- The trial manufacture and test of critical components in docking mechanism [NASDA-TMR-930005] p 44 N94-12280

SPACECRAFT ELECTRONIC EQUIPMENT
- Multiplexed and distributed optical fibre sensors p 64 N94-10065
- Satellite observations of red tide events: Plans for EESI p 191 N94-11899
- METEOSAT second generation programme SEVIRI: An enhanced visible and IR radiometer for meteorology p 212 N94-12667

SPACECRAFT EQUIPMENT
- Design of multisample, multistep phase partitioning apparatus for use on Space Shuttle Spacelab, and Spacelab missions p 108 N94-10120
- The Second Workshop on Refrigerating System Utilization Onboard the JEM [NASDA-CON-930001] p 129 N94-11831
- Development of space refrigerator p 129 N94-11833
- Studies on refrigerator sensors and cooling section interface p 129 N94-11834
- Trend of miniature refrigerator utilization in earth observation area p 130 N94-11835
- Satellite observation of atmospheric tracer components: JEM/POP p 130 N94-11836
- Submillimeter wave observation experiment of Earth atmosphere with SIS mixer p 130 N94-11837
- Refrigerator utilization in infrared astronomy p 130 N94-11838
- Study on various cryogenic refrigeration cycles using all purpose refrigerators p 130 N94-11839
- Development test on 2 K cooling systems p 130 N94-11840
- Generation of superfluid He by G-M cycle cryogenic refrigerator p 130 N94-11841
- Development of 4 K refrigerator using highly efficient heat accumulating reservoir p 130 N94-11842
- Utilization of superconductivity in the area of space p 131 N94-11843
- Flight data analysis of Japanese Earth Resources Satellite-1 (JERS-1) [NASDA-CNT-930004] p 245 N94-12279
- The trial manufacture and test of critical components in docking mechanism [NASDA-TMR-930005] p 44 N94-12280
- Conceptual studies report on lunar and planetary exploration [NASDA-TK-SS0438] p 481 N94-12323
- Unmanned lunar exploration mission p 482 N94-12325
- Manned lunar exploration missions p 482 N94-12326
- Mars exploration missions p 482 N94-12327
- The Third Workshop on Two Phase Fluid Experiment in the Space Environment [NASDA-CON-930002] p 161 N94-12547
- Summary of studies on JEM utilization experiment projects p 161 N94-12548
- Devices related for thermal control systems used in microgravity p 162 N94-12553
- Research and development of cold plate for two phase fluid loop thermal control system p 162 N94-12555

SPACECRAFT INSTRUMENTS
- The advanced fluid physics module: How to achieve scientific goals for Spacelab D2 p 39 N94-10136
- Data processing units for eight magnetospheric particle and field sensors [AD-A264403] p 276 N94-11463
- The Los Alamos neutron spectrometer for the Lunar Scout-1 mission p 172 N94-12038
- Flight data analysis of Japanese Earth Resources Satellite-1 (JERS-1) [NASDA-CNT-930004] p 245 N94-12279
- Conceptual studies report on lunar and planetary exploration [NASDA-TK-SS0438] p 481 N94-12323
- Unmanned lunar exploration mission p 482 N94-12325
- Manned lunar exploration missions p 482 N94-12326
- Mars exploration missions p 482 N94-12327

SPACECRAFT LAUNCHING
- Exergy decrease in shock waves and boundary layers of space launch vehicles [AD-A265272] p 42 N94-10493
- Parametric analysis of atmospheric processes [NASA-CR-192523] p 347 N94-10757
- Preliminary analysis of the benefits derived to US Air Force spacecraft from on-orbit refueling p 38 N94-11567
- The National Launch System Advanced Development Program: A brief overview p 40 N94-11576
- Special investigation report: Commercial space launch incident, launch procedure anomaly orbital sciences corporation PEGASUS/SCD-1, 80 nautical miles east of Cape Canaveral, Florida, February 9, 1993 [PB93-917003] p 40 N94-11893
- Flight data analysis of Japanese Earth Resources Satellite-1 (JERS-1) [NASDA-CNT-930004] p 245 N94-12279

SPACECRAFT MAINTENANCE
- Definition of spacecraft standard interfaces by the NASA Space Assembly and Servicing Working Group (SASWG) p 348 N94-11574

SPACECRAFT MODULES
- The advanced fluid physics module: How to achieve scientific goals for Spacelab D2 p 39 N94-10136

SPACECRAFT MOTION
- Lunar Scout Two spacecraft gravity experiment p 459 N94-12152

SPACECRAFT ORBITS
- On-orbit servicing for USAF space missions: A phased development approach p 348 N94-11571
- Lunar Scout Two spacecraft gravity experiment p 459 N94-12152
- Exploration planning in the context of human exploration and development of the Moon p 474 N94-12229

SPACECRAFT PERFORMANCE
- Progress in multidisciplinary design optimization at NASA Langley [NASA-TM-107754] p 318 N94-10814
- Flight data analysis of Japanese Earth Resources Satellite-1 (JERS-1) [NASDA-CNT-930004] p 245 N94-12279

SPACECRAFT POWER SUPPLIES
- Fully coupled neutronic and hydrodynamic analysis of space nuclear reactor reentry accidents [DE93-005459] p 372 N94-10890
- Investigation of alternate power source for Space Shuttle Orbiter hydraulic system [NASA-CR-193229] p 46 N94-10911
- A facility for testing 10- to 100-kWe space power reactors [DE92-040420] p 372 N94-11296
- Experimental and theoretical investigations of Cs-Ba vapor tacitron inverter for power conditioning in space power systems [DE93-012971] p 48 N94-11372
- Polyimide based amorphous silicon solar modules p 49 N94-11390
- Flexible polycrystalline thin-film photovoltaics for space applications p 50 N94-11393
- Recent developments in refractive concentrators for space photovoltaic power systems p 52 N94-11402
- NASDA activities in space solar power system research, development and applications p 54 N94-11413

SPACECRAFT PROPULSION
- Arcjet space thrusters [NASA-CR-193191] p 46 N94-10700
- Space transportation alternatives for large space programs: The International Space University Summer Session, 1992 [NASA-TM-106271] p 40 N94-10811
- Applying design principles to fusion reactor configurations for propulsion in space [NASA-TM-108247] p 47 N94-11053
- The National Launch System Advanced Development Program: A brief overview p 40 N94-11576

SPACECRAFT RECOVERY
- Preliminary system design of a Three Arm Capture Mechanism (TACM) flight demonstration article [NASA-CR-192573] p 177 N94-10341

SPACECRAFT REENTRY
- New hypersonic test methods developed at ONERA: The R5 and F4 wind tunnels p 4 N94-10429
- Local measurement of temperatures and concentrations: A review for hypersonic flows p 4 N94-10434
- Fully coupled neutronic and hydrodynamic analysis of space nuclear reactor reentry accidents [DE93-005459] p 372 N94-10890

SPACECRAFT SHIELDING
- Debris/ice/TPS assessment and integrated photographic analysis for Shuttle Mission STS-57 [NASA-TM-107562] p 40 N94-10805
- Development of deterministic transport methods for low energy neutrons for shielding in space [NASA-CR-194172] p 366 N94-11199

SPACECRAFT STABILITY
- Stability analysis and aerospace vehicle dynamics p 31 N94-11491

SPACECRAFT STRUCTURES
- The EUREKA project portfolio in new materials p 56 N94-10002
- Design and development of a CFRP central cylinder for satellites p 56 N94-10007
- Design and manufacturing of filament wound thrust cylinder p 57 N94-10010
- Special problems of 3-D ultrasonic QNDI techniques and applications to composites aerospace structures p 61 N94-10036
- Stress relaxation forming of Ariane 5 front skirt outer skin panels p 62 N94-10046

Failure prediction of thin beryllium sheets used in spacecraft structures [NASA-CR-194164] p 187 N94-11190

Smart Structures for Aircraft and Spacecraft [AGARD-CP-531] p 68 N94-11317

Modelling hypervelocity impacts into aluminum structures based on LDEF data p 190 N94-12178

Space truss zero gravity dynamics [AD-A266130] p 44 N94-12541

SPACECREWS

Noise levels and their effects on Shuttle crewmembers' performance: Operational concerns p 314 N94-11538

Promethazine and its use as a treatment for space motion sickness p 312 N94-11550

Update on the incidence and treatment of space motion sickness p 312 N94-11551

Baseline characteristics of different strata of astronaut corps p 312 N94-11552

Potential health effects of space radiation p 312 N94-11558

Operational radiological support for the US manned space program p 318 N94-11561

Crew chief p 335 N94-11564

Medical care delivery in the US space program p 307 N94-11806

SPACELAB

Comprehensive analysis of airborne contaminants from recent Spacelab missions p 318 N94-11553

SPACELAB PAYLOADS

Bubbles and drops behaviour under low-gravity: A space experiment for the IML-2 mission p 104 N94-10098

Benard and Marangoni convection in multiple liquid layers p 105 N94-10100

Advanced protein, crystallization facility and associated new developments p 39 N94-10119

TEMPUS: An electromagnetic levitation facility for containerless processing under micro-g in Spacelab p 109 N94-10125

The advanced fluid physics module: How to achieve scientific goals for Spacelab D2 p 39 N94-10136

Marangoni motion during melting of a hypermonotectic alloy: Numerical simulations for the D2 experiment IHF04 p 113 N94-10177

EUSO-D2-experiment: Unidirectional solidification with quenching of an AlSi11 alloy p 86 N94-10199

The International Microgravity Laboratory, a Spacelab for materials and life sciences p 125 N94-10249

The critical facility on IML-1 p 44 N94-10250

Analysis and interpretation of high energy cosmic rays measured on Spacelab-2 [NASA-CR-193586] p 485 N94-12771

SPALLATION

Possibility of a crossed-beam experiment involving slow-neutron capture by unstable nuclei rapid-process-tron [DE93-754288] p 363 N94-10720

Separation of spallation and terrestrial C-14 in chondrites p 431 N94-12183

SPANISH SPACE PROGRAM

Spain: Success story in space [ESA-BR-81] p 38 N94-11461

SPANWISE BLOWING

Navier-Stokes flowfield computation of wing/rotor interaction for a tilt rotor aircraft in hover [NASA-CR-4532] p 13 N94-10758

Turbulent boundary layer interacting with spanwise periodic longitudinal vortex arrays p 165 N94-12626

SPATIAL DISTRIBUTION

Monte Carlo algorithms in simulation of 2beta-decay and penetration of electrons through matter [DE93-617741] p 364 N94-10837

Experimental study of multiple droplet evaporative cooling [PB93-198463] p 149 N94-10851

Visual encoding of spatial relations [AD-A266049] p 313 N94-10909

Evaluation of ECMWF latent heat flux in TOGA CD-ROM p 195 N94-11921

Sea surface heat flux in the beginning of the Kuroshio p 195 N94-11923

Appearance, behavior, and oceanic structures of warm streamers in the Kuroshio Oyashio frontal region p 198 N94-11937

The development of phytoplankton sensing system with optical fiber p 203 N94-11967

Distribution of mineral aerosols over the North Pacific p 204 N94-11976

Implications of aerosol retrieval and atmospheric correction in remote sensing p 205 N94-11978

Overwater atmospheric dispersion of volcanic smokes from Mt. Sakurajima observed in NOAA-AVHRR data p 205 N94-11979

SOFAR float tracking in the Shikoku basin p 206 N94-11986

Spatial variation in the seasonal south polar cap of Mars as observed by Mariner 7 p 456 N94-12134

Mass and spatial distribution of carbonaceous component in Comet Halley p 433 N94-12263

Sea surface temperature difference between NOAA/AVHRR and in-situ observation p 215 N94-12680

Variability of spectral reflectance in coastal waters near the river plumes p 226 N94-12744

Trajectory curving in underwater propagation of light p 226 N94-12748

Mixing of drifter ensemble by mesoscale currents p 228 N94-12760

SPATIAL FILTERING

Presort processor --- optical filtering [AD-A263872] p 382 N94-11300

Per-field filtering and classification of multitemporal ERS-1 SAR imagery p 247 N94-12485

SPATIAL RESOLUTION

Interferometric and optical tests of water window imaging x ray microscopes [NASA-CR-193369] p 375 N94-10506

Characterization of a scannerless LADAR system [DE93-011582] p 174 N94-10959

Numerical simulations of thermal convection in rapidly rotating spherical fluid shells p 153 N94-11635

SPECIFIC HEAT

A new method for hysteresis measurements developed for C(sub v) measurements at the critical point during the D2-mission p 107 N94-10114

The High Precision Thermostat HPT-HYDRA p 109 N94-10124

Thermophysical properties of undercooled liquid metals p 86 N94-10190

Measurements of heat capacity in undercooled metals p 87 N94-10231

Thermodynamic model of air in chemical equilibrium p 7 N94-10448

SPECIFIC IMPULSE

In-reactor testing of the closed cycle gas core reactor: The Nuclear Light Bulb concept [DE93-004053] p 370 N94-10149

SPECIFICATIONS

Test specifications, specimen design and instrumentation test data interpretation [DE93-012338] p 188 N94-11367

METEOSAT second generation programme SEVIRI: An enhanced visible and IR radiometer for meteorology p 212 N94-12667

SPECKLE INTERFEROMETRY

Material characterization and modeling with shear ography [NASA-CR-192576] p 185 N94-10342

SPECTRA

Stationary spectra in a magnetized current-carrying plasma [DE93-617847] p 386 N94-10397

Coherence effects in radiometry and in spectroscopy [DE93-013437] p 75 N94-10519

Stationary spectra in a sheared plasma (linear limit) [DE93-617850] p 387 N94-10540

Polar mesospheric waves and structure [AD-A265360] p 279 N94-12561

SPECTRAL BANDS

Review of SHARC 2.0 O3 kinetics and spectroscopy [AD-A265481] p 274 N94-10496

Thermographic properties of eight blue-emitting phosphors [DE93-011459] p 78 N94-11622

A comparison of telescopic and Phobos-2 ISM spectra of Mars in the short-wave near-infrared (0.76-1.02 microns) p 424 N94-12053

Near-infrared spectra of the Martian surface: Reading between the lines p 465 N94-12184

Computational methods for problems in aerodynamics using parallel and vector architectures [AD-A265626] p 16 N94-12377

SPECTRAL EMISSION

Characterization of dissolved organic matter in the ocean by using the fluorescence excitation-emission matrix p 211 N94-12659

SPECTRAL ENERGY DISTRIBUTION

Comparison of multiresolution techniques for digital signal processing [AD-A265364] p 138 N94-12406

SPECTRAL METHODS

A spectral nodal method for the solution of the Sn equations in x, y geometry for highly absorbing deep penetration problems [DE93-613520] p 349 N94-10636

New developments in the method of space-time conservation element and solution element: Applications to the Euler and Navier-Stokes equations [NASA-TM-106226] p 150 N94-10939

Computational methods for problems in aerodynamics using parallel and vector architectures [AD-A265626] p 16 N94-12377

DNS on control of laminar-turbulent transition in channel flow with suction and blowing p 163 N94-12613

Boundary conditions and bifurcations in plane Poiseuille flow p 166 N94-12634

SPECTRAL REFLECTANCE

High-reflectance water mass in Off-Sanriku area observed by CZCS p 200 N94-11951

A comparison of telescopic and Phobos-2 ISM spectra of Mars in the short-wave near-infrared (0.76-1.02 microns) p 424 N94-12053

Reflectance spectra of sulfate-and carbonate-bearing Fe(3+)-doped montmorillonites as Mars soil analogs p 445 N94-12070

The effects of atmospheric pressure on infrared reflectance spectra of Martian analogs p 445 N94-12071

Spectral and multispectral imaging studies of lunar mantled mare deposits p 446 N94-12079

Compositional and textural information from the dual inversion of visible, near and thermal infrared remotely sensed data p 258 N94-12097

How diverse is the asteroid belt? p 430 N94-12124

Simulation of possible regolith optical alteration effects on carbonaceous chondrite meteorites p 430 N94-12163

Spectral mixing models of S-Type asteroids p 431 N94-12164

Olivine-rich asteroids, pallasitic olivine and olivine-metal mixtures: Comparisons of reflectance spectra p 431 N94-12171

Chondrites, S asteroids, and space weathering: Thumping noises from the coffin? p 433 N94-12244

A comparison of the visible and near infrared reflectance of hydrovolcanic palagonite tuffs and Martian weathered soils p 477 N94-12245

Properties of spectral reflectance of crown and crown structure of mangrove species in Okinawa p 218 N94-12700

Variability of spectral reflectance in coastal waters near the river plumes p 226 N94-12744

Planetary astronomy of Mars. Mars data reduction [NASA-CR-193515] p 424 N94-12768

SPECTRAL RESOLUTION

Effects of satellite spectral resolution and atmospheric water vapor on retrieval of near-ground temperatures [AD-A264920] p 245 N94-11851

Using high spectral resolution spectrophotometry to study broad mineral absorption features on Mars p 446 N94-12077

Near-infrared spectra of the Martian surface: Reading between the lines p 465 N94-12184

SPECTRAL SIGNATURES

Chondrites, S asteroids, and space weathering: Thumping noises from the coffin? p 433 N94-12244

SPECTRAL THEORY

HEAO-1 analysis of Low Energy Detectors (LED) [NASA-CR-194087] p 424 N94-12574

SPECTROMETERS

A new matrix for the ageless 21.6-keV Eu-151 nuclear gamma ray Moessbauer source [DE93-009795] p 75 N94-10338

Strange meson spectroscopy in K(omega) and K(phi) at 11 GeV/c and Cherenkov ring imaging at SLD [DE93-013593] p 363 N94-10748

Implications of aerosol retrieval and atmospheric correction in remote sensing p 205 N94-11978

Remote sensing x ray fluorescence spectrometry for future lunar exploration missions p 462 N94-12165

Moessbauer spectrometer for mineralogical analysis of the Mars surface: Moessbauer source considerations p 476 N94-12242

SPECTROPHOTOMETRY

Using high spectral resolution spectrophotometry to study broad mineral absorption features on Mars p 446 N94-12077

The 1.2 to 3.5 microns observations of asteroid 4179 Toutatis p 430 N94-12111

Disk-resolved spectral characteristics of Saturn's medium-sized satellites p 471 N94-12213

Properties of spectral reflectance of crown and crown structure of mangrove species in Okinawa p 218 N94-12700

Laser fluorescent monitoring of dissolved organic matter in natural water p 177 N94-12755

SPECTRORADIOMETERS

Global monitoring of atmospheric properties by the EOS MODIS [NASA-TM-109237] p 231 N94-11485

SPECTROSCOPIC ANALYSIS

Laser spectroscopy [DE93-009403] p 173 N94-10255

Review of SHARC 2.0 O3 kinetics and spectroscopy [AD-A265481] p 274 N94-10496

The multiplicity spectra of the (169)Tm(n, gamma) reaction [DE93-617733] p 364 N94-10835

Radiation effects in Ga(0.47)In(0.53)As solar cells p 52 N94-11404

Characterization of an excimer laser-ablated plasma and applications p 392 N94-11450

Moessbauer spectroscopy of the SNC meteorite Zagami p 428 N94-12016

Measurements of cosmogenic nuclides in lunar rock 64455 p 437 N94-12033

Mineralogy of chondritic interplanetary dust particle impact residues from LDEF p 80 N94-12045

Disk-resolved spectral characteristics of Saturn's medium-sized satellites p 471 N94-12213

Atmospheric and spectroscopic research in the far infrared [NASA-CR-193551] p 280 N94-12582

Ecological application of Surface Enhanced Raman Spectroscopy p 227 N94-12756

SPECTROSCOPY

The surface plasmon spectroscopy as diagnostic technique in microgravity experiments p 110 N94-10133

Photodetachment studies on few-electron atomic negative ions [DE93-008474] p 358 N94-10154

A new matrix for the ageless 21.6-keV Eu-151 nuclear gamma ray Moessbauer source [DE93-009795] p 75 N94-10338

Coherence effects in radiometry and in spectroscopy [DE93-013437] p 75 N94-10519

Strange meson spectroscopy in K(omega) and K(phi) at 11 GeV/c and Cherenkov ring imaging at SLD [DE93-013593] p 363 N94-10748

Ellipsometry studies of semiconductors surface cleaning [AD-A265150] p 142 N94-11094

Applications of spectroscopic ellipsometry to microelectronics [AD-A265148] p 143 N94-11159

FFTSCAN: A program for spectral smoothing using Fourier transforms [AD-A264921] p 278 N94-11852

Applications of in-situ ellipsometry to microwave electron cyclotron resonance plasma processes [AD-A265197] p 373 N94-11880

Moessbauer spectroscopy of the SNC meteorite Zagami p 428 N94-12016

Reflectance spectra of sulfate-and carbonate-bearing Fe(3+)-doped montmorillonites as Mars soil analogs p 445 N94-12070

Si-29 NMR spectroscopy of naturally-shocked quartz from Meteor Crater, Arizona: Correlation to Kieffer's classification scheme p 80 N94-12087

Nonlinear optical spectroscopy of Ag(111) in electrolyte and in vacuum [AD-A265622] p 79 N94-12534

SPECTRUM ANALYSIS

The multiplicity spectra of the (169)Tm(n, gamma) reaction [DE93-617733] p 364 N94-10835

Measurement methods and algorithms for comparison of local and remote clocks p 354 N94-10987

Study of the surface circulation to the North of Bransfield Strait, Antarctica [INPE-5472-TDI/503] p 266 N94-11200

The IR properties of ringed galaxies and the IRAS database [NASA-CR-194286] p 426 N94-11590

The morphologies of distant radio galaxies p 426 N94-11597

Implementation and use of a computational ray-tracing program for the design and analysis of complex optical systems [AD-A265075] p 382 N94-11653

The Grand Banks ERS-1 SAR wave spectra validation experiment p 232 N94-11708

The optical/computer hybrid processing of extracting ocean wave directional spectrum by airborne photograph p 197 N94-11934

Spectral analysis of resting cardiovascular variables and responses to oscillatory LBNP before and after 6 degree head dowm bedrest p 309 N94-11997

Cardiovascular dynamics during space sickness and deconditioning p 311 N94-12007

Effects of microscopic iron metal on the reflectance spectra of glass and minerals p 436 N94-12024

Fourier domain target transformation analysis in the thermal infrared p 258 N94-12030

A comparison of telescopic and Phobos-2 ISM spectra of Mars in the short-wave near-infrared (0.76-1.02 microns) p 424 N94-12053

Spectral analysis of the gravity and topography of Mars p 444 N94-12065

The spectral effects of subsolidus reduction of olivine and pyroxene p 81 N94-12110

Spectral mixing models of S-Type asteroids p 431 N94-12164

Olivine-rich asteroids, pallasitic olivine and olivine-metal mixtures: Comparisons of reflectance spectra p 431 N94-12171

Composition of the Martian aerosols through near-IR spectroscopy p 475 N94-12235

Chondrites, S asteroids, and space weathering: Thumping noises from the coffin? p 433 N94-12244

Cronstedtite and iron sulfide mineralogy of CM-type carbonaceous chondrites from cryogenic Moessbauer spectra p 433 N94-12257

Comparison of multiresolution techniques for digital signal processing [AD-A265364] p 138 N94-12406

Spectrum analysis in beam diagnostics [DE93-013401] p 373 N94-12601

Characterization of dissolved organic matter in the ocean by using the fluorescence excitation-emission matrix p 211 N94-12659

Field research of wind wave spectrum variability p 223 N94-12727

Observations of film slicks and internal waves with Ka-band scatterometer p 225 N94-12741

Wind-wave and foam dynamics from optical and radar airborne observations p 226 N94-12745

Laser fluorescent monitoring of dissolved organic matter in natural water p 177 N94-12755

Ecological application of Surface Enhanced Raman Spectroscopy p 227 N94-12756

The algorithm of primary production determination p 228 N94-12761

Non-image visible polarization remote sensing of the ocean p 229 N94-12762

SPEECH RECOGNITION

A new HMM learning algorithm for continuous speech recognition [NHK-SERIAL-413] p 132 N94-10560

A real-time spoken-language system for interactive problem solving [AD-A266046] p 324 N94-11104

SPHERES

Wetting effects on nylon spheres engulfment in ice p 115 N94-10189

SPHERICAL SHELLS

Microgravity combustion of dust suspension in a spherical chamber p 80 N94-10248

SPHERULES

The stability of hibonite and other aluminous phases in silicate melts: Implications for the origin of hibonite-bearing inclusions p 80 N94-12052

Arroyo el Mimbral, Mexico, K/T unit: Origin as debris flow/turbidite, not a tsunami deposit p 281 N94-12084

K/T spherules from Haiti and Wyoming: Origin, diagenesis, and similarity to some microtektites p 281 N94-12085

Microtektite-like glass spherules in Late Devonian (367 MA) shales p 461 N94-12160

KT boundary impact glasses from the Gulf of Mexico region p 282 N94-12161

Iron and nickel isotopic mass fractionation in deep-sea spherules p 282 N94-12199

Modelling of dispersal and deposition of impact glass spherules from the Cretaceous-Tertiary boundary deposit p 432 N94-12238

SPIN DYNAMICS

Crossing-odd spin effects in the dipole model of hadron scattering [DE93-617692] p 362 N94-10551

Squeezed spin states: Squeezing the spin uncertainty relations p 377 N94-10585

SPIN GLASS

The peculiarities of the spin glass state in Fe(x)Mn(1-x)TiO3 [DE93-617882] p 395 N94-10525

SPIN-LATTICE RELAXATION

Synthesis and magnetic properties of novel La*2-x*M*x*CuO*4 equals y* compositions (La equals La, Pr, Nd, Sm, Eu, Cd; M equals Ca, Sr, Ba; O (less than or equal) x 0.2; -0.5 (less than or equal) y (less than or equal) 0.5) [DE93-011359] p 403 N94-12363

SPINEL

The stability of hibonite and other aluminous phases in silicate melts: Implications for the origin of hibonite-bearing inclusions p 80 N94-12052

SPLINE FUNCTIONS

Spline approximation for system of n-th order nonlinear ordinary differential equations [DE93-608188] p 346 N94-11507

On convexity and Schoenberg's variation diminishing splines [DE93-619673] p 346 N94-11632

SPOILERS

A determination of the external forces required to move the benchmark active controls testing model in pure plunge and pure pitch [NASA-TM-107743] p 16 N94-12421

SPONTANEOUS EMISSION

Improved super luminescent light source specification [AD-D015746] p 176 N94-12329

SPORADIC E LAYER

Results from a year-long auroral-E measurement campaign [AD-A265059] p 278 N94-11871

SPOT (FRENCH SATELLITE)

Combined analysis of ERS-1 SAR and visible/infrared remote sensing data for land cover/land use mapping in a tropical zone: A case study in Guinea p 246 N94-12478

Example of SPOT/ERS-1 complementarity p 247 N94-12479

TREES project: A case study on the use of multi-temporal ERS-1 SAR data and SPOT data for monitoring tropical ecosystems p 249 N94-12497

SPRAY NOZZLES

Atomization characteristics of a prefilming airblast atomizer [NAL-TM-644] p 148 N94-10727

Performance aspects of de Laval spray-forming nozzles [DE93-013671] p 163 N94-12604

SPRAYED COATINGS

Performance aspects of de Laval spray-forming nozzles [DE93-013671] p 163 N94-12604

SPRAYERS

Atomization characteristics of a prefilming airblast atomizer [NAL-TM-644] p 148 N94-10727

Combustion chamber analysis code [NASA-CR-192585] p 46 N94-10934

On the combustion of a laminar spray [NASA-TM-106210] p 28 N94-11238

KIVA-3: A KIVA program with block-structured mesh for complex geometries [DE93-011986] p 77 N94-11249

Performance aspects of de Laval spray-forming nozzles [DE93-013671] p 163 N94-12604

SPREAD SPECTRUM TRANSMISSION

A fiber optic network system with low crosstalk using code-division multiplexing [AD-D015763] p 374 N94-10376

SPREADING

Spreading of Bimodulated Ultra-relativistic Electron Beam (BUEB) in Atmospheric Plasma Channel (APCh) [DE93-621658] p 392 N94-11213

SPUTTERING

Effect of surface cleanliness of bearing steel on adhesive strength and tribological properties of sputter-deposited gold films [DE93-767974] p 82 N94-10732

Sources of Na for the Io atmosphere p 455 N94-12127

Solar wind-induced secondary ions and their relation to lunar surface composition p 474 N94-12232

Damage threshold study of ion beam sputtered coatings for a visible high-repetition laser at LLNL [DE93-013430] p 95 N94-12602

SQUALLS

The cloud radiative feedback of a midlatitude squall line system and implication for climate study [DE93-010511] p 283 N94-10290

SQUARE WELLS

P-matrix description of the two-particle interaction [DE93-617690] p 361 N94-10549

SQUEEZED STATES (QUANTUM THEORY)

The Second International Workshop on Squeezed States and Uncertainty Relations [NASA-CP-3219] p 375 N94-10564

Smoothly deformed light p 375 N94-10566

Nonclassical states of the second optical harmonic in the presence of self-action p 375 N94-10567

Quantum noise and squeezing in optical parametric oscillator with arbitrary output coupling p 375 N94-10568

One dimensional representations in quantum optics p 375 N94-10570

Harmonic oscillator interaction with squeezed radiation p 376 N94-10571

Photon number amplification/duplication through parametric conversion p 376 N94-10572

An exactly solvable model of an oscillator with nonlinear coupling and zeros of Bessel functions p 349 N94-10573

Non classical effects in planar waveguides p 376 N94-10574

Nonperturbative methods in the problem of multiphoton excitation of atom by squeezed light p 376 N94-10575

Generalised squeezing and information theory approach to quantum entanglement p 377 N94-10580

Completeness properties of the minimum uncertainty states p 349 N94-10581

Dissipation in a squeezed-state environment p 370 N94-10584

Squeezed spin states: Squeezing the spin uncertainty relations p 377 N94-10585

Quantum entropy and uncertainty for two-mode squeezed, coherent and intelligent spin states p 377 N94-10586

The uncertainty principle in resonant gravitational wave antennae and quantum non-demolition measurement schemes p 378 N94-10587

Uncertainty relations, zero point energy and the linear canonical group p 378 N94-10590

Supersqueezed states from squeezed states p 378 N94-10591

Squeezed states of electrons and transitions of the density of states p 370 N94-10593

Quantum mechanical effects of topological origin p 378 N94-10594

Nonunitary and unitary approach to Eigenvalue problem of Boson operators and squeezed coherent states p 350 N94-10595

Collision-induced squeezing in a harmonic oscillator p 379 N94-10597

Squeezed colour states in gluon jet p 379 N94-10599

New squeezed landau states p 379 N94-10601

Wigner functions for nonclassical states of a collection of two-level atoms p 379 N94-10603

Wavelets and spacetime squeeze p 379 N94-10604

Non-stationary and non-linear dispersive medium as external field which generates the squeezed states p 380 N94-10605

Relation of squeezed states between damped harmonic and simple harmonic oscillators p 380 N94-10606

Wave and pseudo-diffusion equations from squeezed states p 347 N94-10607

Infinite-mode squeezed coherent states and non-equilibrium statistical mechanics (phase-space-picture approach)
[LBL-32695] p 380 N94-10608

Coherent states and uncertainty relations for the damped harmonic oscillator with time-dependent frequency p 380 N94-10611

Quantum processes in resonators with moving walls p 380 N94-10612

SQUID (DETECTORS)

Large array SQUID magnetometer for NDE
[AD-A264799] p 304 N94-11449

Superconducting SQUID amplifiers for IR detectors and other applications, phase 2
[AD-A265447] p 145 N94-12333

STABILITY

Granular instability in fluidized beds: A small-over-large instability p 122 N94-10235

Enhanced stability of magic clusters: A case study of icosahedric Al(sub 12)X, X=B, Al, Ga, C, Si, Ge, Ti, As
[DE93-613644] p 395 N94-10386

Stability by linear processes
[NASA-CR-194131] p 323 N94-10862

Vacuum stability requirements of polymeric material for spacecraft application
[NASA-TM-109216] p 91 N94-11350

Analytical details of the instability threshold of the laser-Lorenz model
[DE93-619707] p 175 N94-11634

Resist materials design: Base-catalyzed chemical amplification
[AD-A265286] p 145 N94-11819

Preparation of stable photopatternable polymeric materials for non-linear optics
[AD-A265359] p 95 N94-12577

STABILITY DERIVATIVES

Extraction of stability and control derivatives from orbiter flight data
[NASA-TM-4500] p 13 N94-10707

Nonlinear aspects of transonic aeroelasticity
[UTIAS-RN-345] p 15 N94-11857

STABILITY TESTS

Marangoni instability in a liquid layer with two free surfaces
[NASA-TM-106166] p 152 N94-11376

Stability analysis and aerospace vehicle dynamics p 31 N94-11491

Stability model of the atmosphere p 32 N94-11500

STABILIZATION

Magnetohydrodynamic computation of feedback stabilization of resistive-shell instabilities in the reversed field pinch
[DE93-013466] p 388 N94-10852

STABILIZED PLATFORMS

Development of a balloon-borne stabilized platform for measuring radiative flux profiles in the atmospheric boundary layer
[DE93-013186] p 274 N94-10323

STAGE SEPARATION

Estimation of the attitude motion of the small satellite ORIZURU
[NAL-TR-1145] p 42 N94-10366

STAGNATION FLOW

A model of elementary chemistry and fluid mechanics in the combustion of hydrogen on platinum surfaces
[DE93-012767] p 77 N94-11370

STAINLESS STEELS

Microbiological test results using three urine pretreatment regimes with 316L stainless steel
[NASA-CR-192568] p 299 N94-10360

Welding tritium aged stainless steel
[DE93-011782] p 181 N94-11228

STANDARDIZATION

Progress on GPS standardization p 24 N94-10965

MIL-STDS and PTTI: What's available and what needs to be done p 352 N94-10973

Abbreviations, acronyms, and initialisms frequently used by Martin Marietta Energy Systems, Incorporated
[DE93-012509] p 420 N94-11369

Longitudinal study of astronaut health: Mortality in the years 1959-1991 p 312 N94-11560

The guide to Design For On-orbit Spacecraft Servicing (DFOSS) manual: Producing a consensus document p 421 N94-11575

STANDARDS

An intercomparison of the radium mass standards of the UK and the USSR: 2
[NPL-RSA(EXT)-34] p 359 N94-10266

The 17th Transducer Workshop
[AD-A265526] p 141 N94-10509

Correspondence standards
[NHB-1450.10B] p 420 N94-11589

Analysis and guidelines for reusable Ada software
[AD-A264918] p 332 N94-11850

STANDING WAVES

The x ray standing waves on surfaces
[AD-A265265] p 402 N94-11682

STAR FORMATION

Detection of accreting circumstellar gas around weak emission-line Herbig Ae/Be stars
[NASA-TM-108256] p 424 N94-11306

Analysis of interstellar fragmentation structure based on IRAS images
[NASA-CR-193518] p 428 N94-12767

STARCHES

Paint removal using wheat starch blast media p 128 N94-10627

STATE ESTIMATION

Estimation with multisensor/multiscan detection fusion
[AD-A265673] p 138 N94-12338

STATE VECTORS

Nonlinear and dynamic analysis of flight p 32 N94-11496

STATIC ELECTRICITY

The response of an electron in a biased double well to a strong laser: Delocalization and low frequency generation
[AD-A265169] p 366 N94-11100

STATIC LOADS

Nonlinear response of a clamped-clamped beam with internal resonance under sinusoidal excitation p 186 N94-10897

STATIC PRESSURE

Dynamic tester for rotor seals and bearings
[NASA-CASE-MFS-28493-1] p 33 N94-10669

STATIC STABILITY

X-29: Longitudinal instability at high angle-of-attack p 33 N94-11504

STATISTICAL ANALYSIS

General renormalized statistical approach with finite cross-field correlations
[DE93-617846] p 386 N94-10396

Stationary spectra in a plasma with a shear (renormalized statistical approach with non-zero eigenfrequencies)
[DE93-617851] p 386 N94-10523

A window least squares algorithm for statistical noise smoothing of 2D-ACAR data
[DE93-613828] p 395 N94-10537

The Langevin's approach to the statistical theory of bounded plasma
[DE93-617842] p 388 N94-10839

Stationary spectra of short-wave convective and magnetostatic fluctuations in a finite-pressure plasma and anomalous heat conductivity
[DE93-617852] p 386 N94-10840

Advanced statistical methods for improved data analysis of NASA astrophysics missions
[NASA-CR-193514] p 425 N94-10943

Statistical analysis of environmental variability within the CELSS breadboard project's biomass production chamber
[NASA-TM-109188] p 315 N94-11258

Three-dimensional object recognition using an unsupervised BCM network: The usefulness of distinguishing features
[AD-A264576] p 304 N94-11261

Statistical and optimization methods to expedite neural network training for transient identification
[DE93-009985] p 340 N94-11644

General aviation aircraft-normal acceleration data analysis and collection project
[AD-A265055] p 26 N94-11858

Computing science and statistics, Volume 24: Graphics and visualization
[AD-A265181] p 332 N94-11878

Statistical process control in the hybrid microelectronics manufacturing industry: A Navy view point
[AD-A265164] p 145 N94-11884

A statistical method to determine aerosol path radiance and its application to atmospheric correction for CZCS imagery p 191 N94-11897

Remote sensing of the suspended matter distribution with high concentration in China Sea p 192 N94-11901

Statistical study of HF ocean radar echo p 139 N94-11905

A new expression for the production rate of sea water droplets on the sea surface p 195 N94-11920

Estimation of solar radiation at the sea surface with geostationary meteorological satellite data p 196 N94-11926

Incident shortwave and longwave radiations over the western North Pacific and the Sea of Okhotsk derived from GMS-WEFAX images p 205 N94-11982

A statistical analysis of sea state surface ERS-1 SAR-wave mode imagettes p 251 N94-12507

Further study of the Non-Regression-Coefficient SST retrieval method p 213 N94-12674

Aspects of applying a relaxation method to computing sea surface velocities from sea surface temperature images p 214 N94-12679

Sea surface temperature difference between NOAA/AVHRR and in-situ observation p 215 N94-12680

Coastal upwelling monitored by satellite data: Methodologies and results p 220 N94-12712

Advective surface velocity in the north west Pacific derived from NOAA AVHRR images p 222 N94-12721

Problem of climate change predictability and satellite radiation budget observations p 229 N94-12766

STATISTICAL CORRELATION

Chaos, entropy, and reversibility: A simple example p 31 N94-11495

Analysis of gravity, magnetic, and seismic reflection data from Tibet and neighboring regions of China
[NASA-CR-193405] p 278 N94-11886

The extraction of bottom characteristics and mapping in Kin Bay, Okinawa Main Island, Japan, using LANDSAT-5/TM and SPOT-1/HRV data p 197 N94-11931

STATISTICAL DISTRIBUTIONS

Imprecise highest density regions related to intervals of measures
[MEMO-COSOR-92-54] p 347 N94-10876

A CM chondrite cluster and CM streams p 432 N94-12215

STATISTICAL MECHANICS

Lattice gas hydrodynamics: Theory and simulations
[DE93-013297] p 147 N94-10320

Infinite-mode squeezed coherent states and non-equilibrium statistical mechanics (phase-space-picture approach)
[LBL-32695] p 380 N94-10608

STATISTICAL TESTS

Object recognition in industrial environment by means of tactile sensor
[ITN-93-85200] p 178 N94-10393

STATOR BLADES

Viscous analysis of three-dimensional rotor flows using a multigrid method
[NASA-TM-106266] p 152 N94-11481

STATORS

Laser anemometer measurements and computations for transonic flow conditions in an annular cascade of high turning core turbine vanes
[NASA-TP-3383] p 15 N94-11133

STEADY STATE
Material removal processes: Engineering mechanics consideration
[DE93-010733] p 126 N94-10293
A model for the subduction mechanics of flexible lithosphere and its viscous coupling to the mantle using power-law rheologies p 277 N94-11585

STEEL STRUCTURES
Microstructure-based fatigue life prediction methods for naval steel structures
[AD-A265429] p 85 N94-12426

STEELS
Spinforming characteristics of a net shape forming process p 56 N94-10004
Heavy-section steel technology program
[DE93-009222] p 184 N94-10155
Effect of surface cleanliness of bearing steel on adhesive strength and tribological properties of sputter-deposited gold films
[DE93-767974] p 82 N94-10732
Advanced zinc phosphate conversion and pre-ceramic polymetallosiloxane coatings for corrosion protection of steel and aluminum, and characteristics of polyphenyletheretherketone-based materials
[DE93-008717] p 88 N94-10891
Immediate response to free product discovery
[PB93-182970] p 265 N94-11015

STELLAR COLOR
The controlling parameters of the integrated flux of a stellar population p 426 N94-11187

STELLAR COMPOSITION
The abundances of the elements in sharp-lined early type stars
[NASA-CR-194055] p 424 N94-12573

STELLAR ENVELOPES
Detection of accreting circumstellar gas around weak emission-line Herbig Ae/Be stars
[NASA-TM-108256] p 424 N94-11306
Why convective heat transport in the solar nebula was inefficient p 458 N94-12143

STELLAR EVOLUTION
The controlling parameters of the integrated flux of a stellar population p 426 N94-11187
Carbon and nitrogen in Type 2 supernova diamonds p 431 N94-12166

STELLAR MASS
Carbon and nitrogen in Type 2 supernova diamonds p 431 N94-12166

STELLAR MASS ACCRETION
Detection of accreting circumstellar gas around weak emission-line Herbig Ae/Be stars
[NASA-TM-108256] p 424 N94-11306

STELLAR MASS EJECTION
Nuclear astrophysics
[DE93-010569] p 425 N94-10292

STELLAR OCCULTATION
Wave structure in planetary rings p 434 N94-11185
Submission of Earth-based ring occultation observations to the NASA planetary data system rings discipline node
[NASA-CR-193469] p 427 N94-12557

STELLARATORS
Transport mechanisms acting in toroidal devices: A theoretician's view
[DE93-013463] p 385 N94-10310
Characterization of high-power RF structures using time-domain field codes
[DE93-013416] p 132 N94-10518
Looking beyond ITER: Toroidal concept improvement
[DE93-012762] p 388 N94-10744
Calculation of Mercier stability criterium in stellarators
[DE93-621599] p 389 N94-11091
Possibilities of magnetic diagnostics in stellarators
[DE93-621608] p 389 N94-11092
Charged particle motion in torsatrons, part 1
[DE93-621639] p 389 N94-11119
Particle transport analysis in torsatron configurations
[DE93-621640] p 390 N94-11120
Probability of particle trapping/detrapping in torsatrons
[DE93-621641] p 390 N94-11121
Analytical description of the torsatron Uragan-2M magnetic configuration with account of plasma pressure and external correcting magnetic field
[DE93-620983] p 391 N94-11174
Characteristics of ICR-produced peripheral plasma in the Uragan-3M torsatron
[DE93-621666] p 392 N94-11214
Magnetic island suppression in torsatron configurations
[DE93-621681] p 392 N94-11215

STEREOPHOTOGRAPHY
On resolution of underwater stereo photogrammetry p 172 N94-11966

STEREOSCOPY
Preliminary studies on the application of ERS-1 data to topographic mapping p 246 N94-12476

STIFFNESS
Analytical models for describing the mechanical behavior of fiber reinforced composites
[AD-A265906] p 74 N94-12347

STILBENE
Preparation of stable photopatternable polymeric materials for non-linear optics
[AD-A265359] p 95 N94-12577

STIRLING CYCLE
The superfluid Stirling refrigerator, a new method for cooling below 0.5 K
[DE93-012672] p 128 N94-11161

STIRLING ENGINES
Establishing baseline data for an experimental appratus that measures heat transfer under conditions of oscillating pressure and flow
[NASA-CR-193772] p 413 N94-12343

STISHOVITE
Shock induced reaction in Chicxulub target materials (CaSO4 and SiO2) and their relation to extinctions p 282 N94-12149

STOCHASTIC PROCESSES
Canonical operator formulation of nonequilibrium thermodynamics
[DE93-613028] p 409 N94-10388
A multi-variance analysis in the time domain p 146 N94-10999
Kinetic effects in stochastic topologically nontrivial field
[DE93-621642] p 391 N94-11207
Simple kinetic model for plasma in stochastic helical field
[DE93-621643] p 391 N94-11208
Experimental investigation of wake field excitation in plasma by a periodic succession of relativistic particle clots
[DE93-621655] p 391 N94-11211
Further studies using matched filter theory and stochastic simulation for gust loads prediction
[NASA-TM-109010] p 26 N94-11587
A stochastic-deterministic approach as an alternative to classical cross-over techniques in small ocean basins p 242 N94-11767
Nonlinear resonance: Noise-assisted information processing in physical and neurophysiological systems
[AD-A265161] p 313 N94-11890
Mapping closures for turbulent combustion
[AD-A265671] p 79 N94-12378

STOICHIOMETRY
Synthesis and magnetic properties of novel La*2-x*M*x*CuO*4 equals y* compositions (La equals La, Pr, Nd, Sm, Eu, Cd; M equals Ca, Sr, Ba; O (less than or equal) x 0.2; -0.5 (less than or equal) y (less than or equal) 0.5)
[DE93-011359] p 403 N94-12363

STOKES LAW (FLUID MECHANICS)
Numerical simulation of multi-droplet hydrodynamic interactions in liquid dispersions p 114 N94-10182

STONY-IRON METEORITES
Metal-rich meteorites from the aubrite parent body p 430 N94-12142

STOPPING POWER
Experimental efforts and results in finding new heavy scintillators
[DE93-010406] p 371 N94-10156

STORAGE RINGS (PARTICLE ACCELERATORS)
Radiation hardness of Mo/Si multilayers designed for use in a soft x ray projection lithography system
[DE93-011879] p 143 N94-11273

STORAGE STABILITY
Space Storable Rocket Technology program (SSRT). Option 1 program
[NASA-CR-191171] p 46 N94-10938

STORAGE TANKS
Immediate response to free product discovery
[PB93-182970] p 265 N94-11015

STORMS (METEOROLOGY)
The impact of vegetation on the atmospheric boundary layer and convective storms p 277 N94-11480
Rainfall-runoff estimation using digital radar
[AD-A265390] p 286 N94-12408
A study of the Merritt Island, Florida sea breeze flow regimes and their effect on surface heat and moisture fluxes
[NASA-CR-4537] p 286 N94-12580

STOVL AIRCRAFT
Criteria for design of integrated flight/propulsion control systems for STOVL fighter aircraft
[NASA-TP-3356] p 30 N94-11134
Application of controller partitioning optimization procedure to integrated flight/propulsion control design for a STOVL aircraft
[NASA-TM-106265] p 30 N94-11251
Moving-base simulation evaluation of thrust margins for vertical landing for the NASA YAV-8B Harrier aircraft
[NASA-TM-104008] p 30 N94-11259

STRAIN ENERGY RELEASE RATE
Understanding cracking failures of coatings: A fracture mechanics approach p 187 N94-11218

STRAIN GAGES
Design and development of a miniature column-based interface (MCBI) stress gage
[AD-A266054] p 170 N94-10873
Fiber-optic interferometric strain gauge for smart structures applications: First flight tests p 71 N94-11340
Localized and distributed fiber-optic strain sensors embedded in composite materials
[UTIAS-346] p 73 N94-12013

STRAIN HARDENING
A modeling investigation of thermal and strain induced recovery and nonlinear hardening in potential based viscoplasticity
[NASA-TM-106122] p 188 N94-11482

STRAIN MEASUREMENT
An electro-optical system for the measurement of strains p 186 N94-10900
Smart structures at Aastra Corporation p 69 N94-11326
Fiber optic sensing for composite smart structures p 69 N94-11327
Strain measurement of carbon/epoxy composite with fibre optics white light quasi distributed polarimetric sensor p 69 N94-11328
Structural health monitoring using embedded fibre optic sensors p 22 N94-11334
Factors affecting the embedding of optical fibre sensors in advanced composite structures p 70 N94-11336
Fiber-optic sensor systems for measuring strain and the detection of acoustic emissions in smart structures p 71 N94-11337
Fiber-optic interferometric strain gauge for smart structures applications: First flight tests p 71 N94-11340
Localized and distributed fiber-optic strain sensors embedded in composite materials
[UTIAS-346] p 73 N94-12013

STRAIN RATE
Material removal processes: Engineering mechanics consideration
[DE93-010733] p 126 N94-10293
Facility for stress corrosion cracking test of irradiated material in high temperature water
[DE93-753189] p 84 N94-11593
Parameterization of subgrid-scale stress by the velocity gradient tensor p 155 N94-12286

STRAITS
Tide-generated nonlinear internal wave packets in the Strait of Gibraltar observed by the synthetic aperture radar aboard the ERS-1 satellite p 252 N94-12510

STRAKES
Lift enhancement of a wing/strake using pneumatic blowing
[AD-A265074] p 26 N94-11872

STRANGE ATTRACTORS
Detecting non-linearities in stationary time series
[W-9223] p 344 N94-10906

STRANGENESS
Production of strange clusters in relativistic heavy ion collisions
[DE93-010876] p 359 N94-10303
Strangeness production with protons and pions
[DE93-010879] p 359 N94-10304
A generalized Bethe-Weizsaecker mass formula for strange hadronic matter
[DE93-011010] p 368 N94-11620

STRATA
The nonlinear evolution of modes on unstable stratified shear layers
[NASA-CR-191492] p 149 N94-10810
Post-impact alteration of the Manson impact structure p 282 N94-12188

STRATIFIED FLOW
Similarity states of homogeneous stably-stratified turbulence at infinite Froude number p 156 N94-12292
Mixing in a stratified shear flow: Energetics and sampling p 159 N94-12311

STRATIGRAPHY
The Lathrop Wells Volcanic Center: Status of field and geochronology studies
[DE93-008917] p 273 N94-10285
Twenty-fourth Lunar and Planetary Science Conference. Part 1: A-F
[NASA-CR-193095] p 435 N94-12015
Estimation of age of Dali-Ganis rifting and associated volcanic activity, Venus p 440 N94-12046
Apollo 16 core 60013/14 as a product of path 1 and path 2 regolith evolution processes p 440 N94-12050
The great 8 MA event and the structure of the H-chondrite parent body p 429 N94-12058

Stratigraphy and sedimentology of the K/T boundary deposit in Haiti p 282 N94-12138
Differential scaling: Implications for central structures in large lunar craters p 461 N94-12158
Geomorphology of Triton's polar materials p 466 N94-12185

STRATOSPHERE
Implications of aerosol retrieval and atmospheric correction in remote sensing p 205 N94-11978
Identification of cometary and asteroidal particles in stratospheric IDP collections p 430 N94-12115
Studies of dynamical processes affecting the distribution of stratospheric ozone [NASA-CR-193477] p 279 N94-12560
Stratospheric aircraft exhaust plume and wake chemistry [NASA-CR-191495] p 279 N94-12572

STREAK CAMERAS
Plans to improve the experimental limit in the comparison of the east-west and west-east one-way light propagation times on the rotating earth p 351 N94-10971

STREAMS
An application of reduced gravity model to mesoscale eddies p 199 N94-11945
SOFAR float tracking in the Shikoku basin p 206 N94-11986
On an upwelling front, propagation of upwelling and vertical velocity in the eastern Arabian Sea during monsoon, 1987 p 206 N94-11987
A numerical study of deep convection at high latitudes p 210 N94-12652
Study on diffusion phenomena of river effluents issued into sea around Japan with satellite remote sensing data p 212 N94-12664
Sedimentation rates and particulate fluxes in the slope and deep sea areas off eastern Taiwan p 220 N94-12709
A detailed investigation of the benthic regime in the Clarion-Clipperton province of the Pacific and a forecast of consequences of manganese nodule mining p 224 N94-12733
Bottom currents and possibilities for near bottom layer environmental investigations in the Pacific by means of self contained bottom stations p 224 N94-12734
Convective and dynamic instability in meridional trenches p 225 N94-12739
Coupled numerical model for altimetric data assimilation and velocity field analysis p 227 N94-12752
Complex (hydrodynamic, satellite) monitoring of dynamic structures in the western Pacific with the aim of forecasting the marine ecosystems behaviour p 227 N94-12753
Mesoscale dynamic structures of the Subarctic Frontal Zone in the Pacific Ocean p 227 N94-12754
Mixing of drifter ensemble by mesoscale currents p 228 N94-12760
Generation of internal waves near the shelf boundary p 229 N94-12763
Experimental and theoretical investigation of undular bore formation upstream the bank p 229 N94-12764
Model of Kuroshio region circulation p 229 N94-12765

STRESS (PHYSIOLOGY)
Motion and spatial disorientation systems: Special research capabilities [AD-A265155] p 303 N94-11097
P2NBC2 Heat Strain Decision Aid. User's guide, version 2.1 [AD-A266072] p 304 N94-11224
Central circulatory hemodynamics as a function of gravitational stress p 309 N94-11995

STRESS (PSYCHOLOGY)
Aviators, air combat, and combat stress: An Air F orce commander's primer [AD-A265083] p 313 N94-11867

STRESS ANALYSIS
Design and development of a miniature column-based interface (MCBI) stress gage [AD-A266054] p 170 N94-10873
Imperfection sensitivity of the Brazier effect for orthotropic cylindrical shells [LR-687] p 186 N94-10879
An electro-optical system for the measurement of strains p 186 N94-10900
Computational gearing mechanics [NASA-CR-193666] p 181 N94-11157
Fatigue life prediction for wind turbines: A case study on loading spectra and parameter sensitivity [DE93-011597] p 263 N94-11173
A study of strength evaluations of EDNi/EDCu/NARloy-Z bonded joints [NASA-TM-108418] p 188 N94-11275
An analysis of fiber-matrix interface failure stresses for a range of ply stress states [NASA-TM-108999] p 67 N94-11276
RAMCAD (reliability, availability, and maintainability in computer-aided design) [AD-A265143] p 331 N94-11679
Horizontal stresses induced by vertical processes in planetary lithospheres p 281 N94-12042
A normal stress subgrid-scale eddy viscosity model in large eddy simulation p 155 N94-12288
Application of a Reynolds stress model to separating boundary layers p 157 N94-12299
Analytical models for describing the mechanical behavior of fiber reinforced composites [AD-A265906] p 74 N94-12347
Advances in low carbon, high strength ferrous alloys [AD-A265264] p 85 N94-12532

STRESS CONCENTRATION
Analytical models for describing the mechanical behavior of fiber reinforced composites [AD-A265906] p 74 N94-12347

STRESS CORROSION
Corrosion behavior of metal matrix composites [AD-A265352] p 85 N94-12404

STRESS CORROSION CRACKING
Facility for stress corrosion cracking test of irradiated material in high temperature water [DE93-753189] p 84 N94-11593
Corrosion behavior of metal matrix composites [AD-A265352] p 85 N94-12404

STRESS DISTRIBUTION
Elastic plastic fracture mechanics methodology for surface cracks [NASA-CR-194129] p 185 N94-10712
Parameterization of subgrid-scale stress by the velocity gradient tensor p 155 N94-12286

STRESS INTENSITY FACTORS
The effects of an aggressive environment on the subcritical crack growth of a continuous-fiber ceramic composite [DE93-011690] p 73 N94-11612

STRESS MEASUREMENT
Design and development of a miniature column-based interface (MCBI) stress gage [AD-A266054] p 170 N94-10873

STRESS RATIO
Fatigue-life behavior and matrix fatigue crack spacing in unnotched SCS-6/Timetal 21S metal matrix composites [NASA-CR-191467] p 185 N94-10715

STRESS RELAXATION
Stress relaxation forming of Ariane 5 front skirt outer skin panels p 62 N94-10046
Investigation of the reason for the softening behaviour of filled polymers p 63 N94-10058
Time-temperature shift factors for gun propellants [AD-A264979] p 97 N94-10489
Crack suppression in GaInSb buffer layers initially under tensile stress [DE93-012839] p 396 N94-10745

STRESS TENSORS
A local dynamic model for large eddy simulation p 155 N94-12285

STRESS-STRAIN RELATIONSHIPS
A modeling investigation of thermal and strain induced recovery and nonlinear hardening in potential based viscoplasticity [NASA-TM-106122] p 188 N94-11482

STRESSES
Protective coatings for high-temperature polymer matrix composites [NASA-TM-106276] p 74 N94-12431

STRIATION
Electron runaway in RF discharges [DE93-771407] p 363 N94-10661

STRING THEORY
Some new/old approaches to QCD [DE93-010451] p 408 N94-10261
On renormalization group flow in matrix model [DE93-613050] p 409 N94-10413
Green-Schwarz superstrings in the generalized harmonical Newmann-Penrose formalism [DE93-621422] p 412 N94-11088
A version of superstring with four space-time dimensions [DE93-608196] p 412 N94-11163
The solutions of cosmic string loop equation in expanding universe [DE93-619717] p 427 N94-11692
Divergences in the moduli space integral and accumulating handles in the infinite-genus limit [DE93-619722] p 346 N94-11693

STRINGS
On the relativistic string size at finite temperature [DE93-617658] p 409 N94-10394
Classical gravity coupled to Liouville theory [DE93-613049] p 275 N94-10798

STRIPPING
Environmentally Safe and Effective Processes for Paint Removal [AGARD-R-791] p 126 N94-10613
Paint removal activities in the US Navy p 126 N94-10614
Paint removal activities in Canada p 126 N94-10615
Procedures without danger to the environment and efficiency (PSDEE) for the removal of paint. Point on the French activities concerning the removal of paint p 126 N94-10616
Paint removal activities in Germany p 126 N94-10617
The development of alternative paint removal techniques in the RAF p 126 N94-10618
Operational aspects of F.16 plastic media blasting, as carried out by Fokker Aircraft Services p 126 N94-10619
Use of robots for aircraft dry stripping via plastic media blasting p 127 N94-10620
German Air Forces experiences with plastic media blasting and future requirements p 127 N94-10621
Plastic media blasting activities at Hill Air Force Base p 127 N94-10622
Large Aircraft Robotic Paint Stripping (LARPS) system and the high pressure water process p 127 N94-10623
Automated Laser Paint Stripping (ALPS) update p 127 N94-10624
Aquastrip (tm): An innovative paint removal technology p 127 N94-10625
Paint removal and surface cleaning using ice particles p 128 N94-10626
Paint removal using wheat starch blast media p 128 N94-10627
IATA taskforce: Paintstripping p 128 N94-10628
Selectively strippable paint schemes p 128 N94-10629

STROKE VOLUME
Echocardiography in the flight program p 309 N94-11993

STRONTIUM ISOTOPES
Strontium and oxygen isotope study of M-1, M-3 and M-4 drill core samples from the Manson impact structure, Iowa: Comparison with Haitian K-T impact glasses p 281 N94-12080

STRUCTURAL ANALYSIS
Computational procedures for determining parameters in Ramberg-Osgood elastoplastic model based on modulus and damping versus strain [DE93-013309] p 185 N94-10306
Probabilistic evaluation of uncertainties and risks in aerospace components [NASA-TM-105603] p 185 N94-10361
NASTRAN modeling of flight test components for UH-60A airloads program test configuration [NASA-CR-193614] p 186 N94-10937
Functional approximation using artificial neural networks in structural mechanics [NASA-TM-105820] p 188 N94-11254
Computational mechanics needs study [NASA-CR-193712] p 327 N94-11279
Structural analysis and optimization of adaptive structures by use of the finite element method p 71 N94-11339
A high specific power solar array for low to mid-power spacecraft p 51 N94-11399
A structural and petrographic investigation of the pretoria saltpan impact structure p 282 N94-12102

STRUCTURAL BASINS
Sandia ocean modeling system programmer's guide and user's manual [DE93-007427] p 287 N94-10153
SOFAR float tracking in the Shikoku basin p 206 N94-11986
Morphology of large impact craters and basins on Venus: Implications for ring formation p 436 N94-12023
Viscous relaxation of the Moho under large lunar basins p 452 N94-12113
Do large impact basins in the southern hemisphere of Mars control the distribution of polar structures and deposits? p 481 N94-12266

STRUCTURAL DESIGN
NASTRAN modeling of flight test components for UH-60A airloads program test configuration [NASA-CR-193614] p 186 N94-10937
A study of strength evaluations of EDNi/EDCu/NARloy-Z bonded joints [NASA-TM-108418] p 188 N94-11275
RAMCAD (reliability, availability, and maintainability in computer-aided design) [AD-A265143] p 331 N94-11679
The trial manufacture and test of critical components in docking mechanism [NASDA-TMR-930005] p 44 N94-12280

Fracture behavior of ionomers and ionomeric blends
[AD-A265379] p 94 N94-12407

STRUCTURAL ENGINEERING
Smart Structures for Aircraft and Spacecraft
[AGARD-CP-531] p 68 N94-11317

STRUCTURAL FAILURE
Failure prediction of thin beryllium sheets used in spacecraft structures
[NASA-CR-194164] p 187 N94-11190
Fiber optic sensing for composite smart structures
p 69 N94-11327
Strain concentration assessment of laminates subjected to low velocity impact
[AD-A264497] p 73 N94-11446
Microstructure-based fatigue life prediction methods for naval steel structures
[AD-A265429] p 85 N94-12426
Resistivity and radar void detectors for tunneling machines p 140 N94-12706

STRUCTURAL MEMBERS
Method of recertifying a loaded bearing member using a phase point
[NASA-CASE-LAR-14741-1] p 185 N94-10671

STRUCTURAL PROPERTIES (GEOLOGY)
On the mechanical development of the Flexible External Insulation (FEI) for Hermes spaceplane
p 62 N94-10048
Twenty-fourth Lunar and Planetary Science Conference. Part 1: A-F
[NASA-CR-193095] p 435 N94-12015
Lineament analysis and tectonic interpretation for the Tharsis region p 437 N94-12031
Horizontal stresses induced by vertical processes in planetary lithospheres p 281 N94-12042
A structural origin for the cantaloupe terrain of Triton
p 449 N94-12095
Sources of Na for the Io atmosphere
p 455 N94-12127
Volcanism in southern Guinevere Planitia, Venus: Regional volcanic history and morphology of volcanic domes p 467 N94-12190
Large volcanoes on Venus: Examples of geologic and structural characteristics from different classes
p 467 N94-12195
Characteristics of arachnoids from Magellan data
p 469 N94-12204
Classification of Martian deltas p 470 N94-12207
Giant radiating dyke swarms on Earth and Venus
p 283 N94-12236
Morphotectonics of Venus p 478 N94-12248

STRUCTURAL RELIABILITY
Elastic plastic fracture mechanics methodology for surface cracks
[NASA-CR-194129] p 185 N94-10712

STRUCTURAL STABILITY
The impact of active controls technology on the structural integrity of aeronautical vehicles
p 27 N94-11341

STRUCTURAL STRAIN
Strain concentration assessment of laminates subjected to low velocity impact
[AD-A264497] p 73 N94-11446

STRUCTURAL VIBRATION
Computational gearing mechanics
[NASA-CR-193666] p 181 N94-11157
Active landing gear control for improved ride quality during ground roll p 27 N94-11345
Active vibration control of adaptive flexible structures using piezoelectric smart sensors and actuators
p 189 N94-11823

STRUCTURED PROGRAMMING
Bundle event structures: A non-interleaving semantics for LOTOS
[MEMO-INF-92-73] p 320 N94-10164

STUDENTS
A summer program in mathematics and computer science for academically oriented student
[AD-A263467] p 415 N94-11517
Career Information in the Mathematical Sciences (CIMS)
[DE93-013780] p 318 N94-11817

STUDS (STRUCTURAL MEMBERS)
Instability around an isolated roughness element
p 165 N94-12629

STYPHNATES
Energy transfer dynamics and impact sensitivity
[DE93-009551] p 98 N94-11269

SUBCRITICAL FLOW
A numerical experiment of boundary layer transition at subcritical Reynolds numbers p 165 N94-12625

SUBDUCTION (GEOLOGY)
A model for the subduction mechanics of flexible lithosphere and its viscous coupling to the mantle using power-law rheologies p 277 N94-11585
The subduction experiment. Cruise report, R/V Oceanus, cruise number 250 legs 1 and 2. Subduction 2 mooring deployment and recovery cruise, 25 January-26 February 1992
[AD-A264922] p 289 N94-11853
Flexure and the role of inplane force around coronae on Venus p 452 N94-12112
Buoyant subduction on Venus: Implications for subduction around coronae p 455 N94-12130
Convective and dynamic instability in meridional trenches p 225 N94-12739

SUBMARINES
Submarine internal waves
[MRL-GD-0049] p 98 N94-11303

SUBMILLIMETER WAVES
Investigation of passive atmospheric sounding using millimeter and submillimeter wavelength channels
[NASA-CR-193627] p 274 N94-10726
Submillimeter wave observation experiment of Earth atmosphere with SIS mixer p 130 N94-11837

SUBROUTINES
Subroutine functions for generating animation data
[DE93-767973] p 313 N94-10731

SUBSONIC FLOW
High order accurate solutions of viscous problems
[NASA-TM-106267] p 151 N94-11253

SUBSONIC FLUTTER
Laser velocimeter measurements of the flow field generated by a forward-swept propfan during flutter
[NASA-TM-106195] p 14 N94-10892

SUBSONIC WIND TUNNELS
Wall interference correction based on interface measurements in subsonic wind tunnel testing
p 15 N94-11154

SUBSTRATES
Zerodur polishing process for high surface quality and high efficiency
[DE93-012596] p 87 N94-10271
Rapid thermal processing for strained-layer semiconductor devices
[DE93-013754] p 396 N94-10809
Needs for super-smooth surfaces
[DE93-012482] p 382 N94-11242
Carbon analyses of IDP's sectioned in sulfur and supported on beryllium films p 81 N94-12099
Analysis of the economics of DC arc CVD diamond
[AD-A265688] p 403 N94-12339
Dynamic high-pressure shock compaction of diamond powders
[AD-A266004] p 93 N94-12354
Development of ultra-low noise, high sensitivity planar metal grating coupled 3 to 5 multiquantum well infrared detectors for focal plane array staring IR sensor systems
[AD-A265599] p 404 N94-12375
Corrosion and passivation of high temperature superconductors
[AD-A265402] p 405 N94-12586

SUBSTRUCTURES
Multilevel computer-aided optimum design of structural systems using multiple basis vectors
p 187 N94-11055

SUCTION
DNS on control of laminar-turbulent transition in channel flow with suction and blowing p 163 N94-12613

SULFATES
Second and third order nonlinear optical properties of crystalline inorganic/organic complexes
[DE93-011883] p 173 N94-10755
Sulfate reduction and other sedimentary biogeochemistry in a northern New England salt marsh
p 268 N94-12453
Acetate concentrations and oxidation in salt marsh sediments p 269 N94-12459
The effects of acid deposition on sulfate reduction and methane production in peatlands p 270 N94-12465

SULFIDES
Thermal stability of sealants for military aircraft: Modification of polysulfide prepolymers with ether and thioether monomers
[AD-A264079] p 89 N94-11107
Biogeochemical factors which regulate the formation and fate of sulfide in wetlands p 270 N94-12464

SULFONATES
Solid-state structures of guanidinium methane, ethane, and trifluoromethanesulfonate
[AD-A265293] p 402 N94-11654
Hydrogen-bond polymorphs of guanidinium 4-biphenylsulfonate
[AD-A265294] p 402 N94-11827

SULFONES
New aromatic activated dihalides and bisphenol monomers for the preparation of novel poly(arylene ethers)
[NASA-CR-193190] p 55 N94-10513

SULFUR
Hydrogen partitioning and transport in titanium aluminides
[NASA-CR-194117] p 76 N94-10713
Carbon analyses of IDP's sectioned in sulfur and supported on beryllium films p 81 N94-12099
Sulfur transformations in the sediments of a New Hampshire salt marsh p 270 N94-12463
Emissions of biogenic sulfur gases from northern bogs and fens p 271 N94-12467
Sulfur gas exchange in Sphagnum-dominated wetlands p 271 N94-12470

SULFUR COMPOUNDS
Terminal Decomposition and Gaseous Sulfur Release from Tidal Wetlands
[NASA-CR-193466] p 267 N94-12451
A preliminary study of the variability and magnitude of the flux of biogenic sulfur gases from a New Hampshire salt marsh p 267 N94-12452
Emissions of biogenic sulfur gases from Alaskan tundra p 268 N94-12455
Factors controlling fluxes of volatile sulfur compounds in Sphagnum peatlands p 268 N94-12456
Emissions of sulfur gases from marine and freshwater wetlands of the Florida Everglades: Rates and extrapolation using remote sensing p 269 N94-12457
Emissions of sulfur gases from wetlands
p 269 N94-12458
Application of static and dynamic enclosures in determining DMS and OCS fluxes in Sphagnum peatlands p 269 N94-12460
Effects of inorganic sulfur addition on fluxes of volatile sulfur compounds in Sphagnum peatlands
p 270 N94-12461
Environmental factors controlling fluxes of dimethyl sulfide in a New Hampshire fen p 270 N94-12462
Factors controlling sulfur gas exchange in Sphagnum-dominated wetlands p 271 N94-12469

SULFUR DIOXIDES
Study of climatic effects of cloud-aerosol interaction
p 204 N94-11977

SULFUR FLUORIDES
Studies of critical point phenomena of fluids: Bulk fluids, fluids in pores, and at interfaces p 80 N94-10228

SULFUR HEXAFLUORIDE
Transport of heat and mass in near-critical fluids
p 122 N94-10230

SULFUR OXIDES
User's manual for the plume visibility model PLUVUE 2 (revised)
[PB93-188233] p 265 N94-11016

SUMMER
A summer program in mathematics and computer science for academically oriented student
[AD-A263467] p 415 N94-11517

SUMS
Summation by parts, projections, and stability
[NASA-CR-194290] p 346 N94-12776

SUN
Orbital simulations of satellite escape/capture and the origin of satellites such as Triton p 429 N94-12057

SUNLIGHT
A development on estimation method of undersea light p 204 N94-11974
The evaluation of radiative process in the atmosphere-ground system by Monte Carlo method
p 205 N94-11980
Incident shortwave and longwave radiations over the western North Pacific and the Sea of Okhotsk derived from GMS-WEFAX images p 205 N94-11982

SUPERCOMPUTERS
An account of Sandia's research booth at Supercomputing 1992: A collaborative effort in high-performance computing and networking
[DE93-012397] p 319 N94-10268
Numerical wind tunnel project and computational fluid dynamics at National Aerospace Laboratory, Japan
[NAL-TM-648T] p 149 N94-10861
The DOE Program in High-Performance Computing and Communications (HPCC)
[DE93-013813] p 334 N94-12606

SUPERCONDUCTING CAVITY RESONATORS
Fabrication and test of a superconducting RFQ
[DE93-010860] p 140 N94-10300
Nonlinear effects in ferrite tuned cavities
[DE93-014136] p 374 N94-12785

SUPERCONDUCTING DEVICES
Fabrication and test of a superconducting RFQ
[DE93-010860] p 140 N94-10300
Improvement of azimuthal homogeneity in permanent-magnet bearing rotors
[DE93-009954] p 144 N94-11607
Utilization of superconductivity in the area of space
p 131 N94-11843

SUPERCONDUCTING FILMS

Processing and transport properties of high J(sub c) silver clad Bi-2223 tapes and coils [DE93-010674] p 398 N94-11073

Multicomponent and multilayered thin films for advanced microtechnologies: Techniques, fundamentals, and devices [AD-A265685] p 405 N94-12442

SUPERCONDUCTING MAGNETS

High-field conductor testing at the FENIX facility [DE93-012318] p 387 N94-10737

SUPERCONDUCTING SUPER COLLIDER

Database computing in HEP [DE93-011765] p 419 N94-11105

Nonlinear effects in ferrite tuned cavities [DE93-014136] p 374 N94-12785

SUPERCONDUCTIVITY

Orbital glass in HTSC [DE93-613988] p 395 N94-10415

Power losses of a type 2 superconducting slab of arbitrary thickness in the presence of alternating current conductors [DE93-617892] p 396 N94-10716

Development and testing of a superconducting link for an IR detector [NASA-CR-193674] p 170 N94-10948

Assessment of the impact of HTSC's on superconducting fault-current limiters [DE93-009986] p 143 N94-11454

Fullerene superconductors: Phase stability and anomalously low T(sub c)'s in some ternary compounds [DE93-010687] p 400 N94-11457

Synthesis and magnetic properties of novel La*2-x*M*x*CuO*4 equals y* compositions (La equals La, Pr, Nd, Sm, Eu, Cd; M equals Ca, Sr, Ba; O (less than or equal) x 0.2; -0.5 (less than or equal) y (less than or equal) 0.5) [DE93-011359] p 403 N94-12363

Quark and lepton masses [DE93-012308] p 370 N94-12787

SUPERCONDUCTORS

High-energy density physics at Los Alamos [DE93-010271] p 371 N94-10260

Development of passive superconducting bearings. Phase 3 [AD-A266050] p 180 N94-10706

Power losses of a type 2 superconducting slab of arbitrary thickness in the presence of alternating current conductors [DE93-617892] p 396 N94-10716

High-field conductor testing at the FENIX facility [DE93-012318] p 387 N94-10737

Similarity of the leading contributions to the self-energy and the thermodynamics in two- and three-dimensional Fermi Liquids [DE93-012673] p 412 N94-11162

Fullerene superconductors: Phase stability and anomalously low T(sub c)'s in some ternary compounds [DE93-010687] p 400 N94-11457

SUPERCOOLING

Solidification from supercooled melt under microgravity p 113 N94-10176

Numerical calculation of the growth of InP by the travelling heater method in the first mission of the Space Flyer Unit p 114 N94-10179

Thermophysical properties of undercooled liquid metals p 86 N94-10190

Solidification of undercooled Ni-32.5 wt percent Sn eutectic alloy p 86 N94-10194

Undercooled W-Re and Mo-Re drops in an ultra high vacuum drop tube p 86 N94-10195

Non-equilibrium solidification in undercooled Ni-B alloys p 86 N94-10196

Solidification and metastable phase formation of highly undercooled Fe-Cr-Ni alloy melts p 87 N94-10204

SUPERCRITICAL FLUIDS

Polymer-polymer interactions [AD-A265304] p 91 N94-11830

SUPERCRITICAL WINGS

X-29: Longitudinal instability at high angle-of-attack p 33 N94-11504

SUPERFLUIDITY

On the doubling of hydrodynamic theorems in relativistic theory of superfluidity [DE93-617895] p 148 N94-10717

Quantum dynamics of helium clusters [AD-A266060] p 411 N94-10874

The superfluid Stirling refrigerator, a new method for cooling below 0.5 K [DE93-012672] p 128 N94-11161

Superfluid turbulence p 158 N94-12307

SUPERHIGH FREQUENCIES

Wide band 140 GHz TWTA p 132 N94-10514

Nonlinear analysis of a magnicon output cavity [AD-A265342] p 145 N94-12424

Fundamental studies of radar scattering from water surfaces: The Lake Washington experiment [NASA-CR-194030] p 139 N94-12778

SUPERLATTICES

Photostimulated attenuation of hypersound in superlattice [DE93-611231] p 357 N94-10408

Rapid thermal processing for strained-layer semiconductor devices [DE93-013754] p 396 N94-10809

Organometallic chemical vapor deposition and characterization of ZnGe(1-x)Si(x)P2-Ge alloys on GaP substrates p 400 N94-11443

The additional contribution caused by Coulomb interaction to the exciton dispersion in multiple quantum wells and superlattices for direct band gap cubic semiconductors [DE93-613538] p 402 N94-11659

Electronic and total energy properties of ternary and quaternary semiconductor compounds, alloys and superlattices [NASA-CR-192905] p 405 N94-12570

SUPERNOVA REMNANTS

Acceleration of positrons in supernova shocks [NASA-CR-193713] p 425 N94-10511

VLBI and the detection of interstellar magnetohydrodynamic waves p 135 N94-11066

SUPERNOVA 1987A

Carbon and nitrogen in Type 2 supernova diamonds p 431 N94-12166

SUPERNOVAE

Nuclear astrophysics [DE93-010569] p 425 N94-10292

Acceleration of positrons in supernova shocks [NASA-CR-193713] p 425 N94-10511

Search for effects of a supernova explosion 30 to 40 thousand years ago in chondrites p 428 N94-12022

SUPERPLASTICITY

SPF/DB: A manufacturing technique for lightweight structures p 59 N94-10026

SUPERSATURATION

Study of vapor bubble growth in a supersaturated liquid p 122 N94-10232

SUPERSONIC BOUNDARY LAYERS

The effects of successive distortions on a turbulent boundary layer in a supersonic flow p 14 N94-11058

SUPERSONIC COMBUSTION

Direct simulation of compressible wall-bounded turbulence p 156 N94-12294

Theories of turbulent combustion in high speed flows [AD-A265735] p 79 N94-12403

SUPERSONIC COMBUSTION RAMJET ENGINES

Studies on scramjet nozzles. Part 1: Performance of two dimensional nozzles [NAL-TR-1149] p 27 N94-10367

Numerical calculation of scramjet inlet flow [NAL-TR-1174T] p 27 N94-10370

Numerical simulation of the flow through a scramjet engine p 3 N94-10425

Schlieren photographs and internal pressure distributions for three-dimensional sidewall-compression scramjet inlets at a Mach number of 6 in CF4 [NASA-TM-4479] p 148 N94-10644

An environmental study of the National Aerospace Plane [AD-A266071] p 25 N94-10945

Preprints of the 13th Hydrogen Energy System Symposium [DE93-781115] p 99 N94-11444

SUPERSONIC FLIGHT

Preliminary supersonic flight test evaluation of performance seeking control [NASA-TM-4494] p 28 N94-11205

SUPERSONIC FLOW

Estimation of critical values and vibration characteristics on supersonic delta wings. Part 1: On-line time series analysis of stationary random response [NAL-TR-1153] p 2 N94-10363

Studies on scramjet nozzles. Part 1: Performance of two dimensional nozzles [NAL-TR-1149] p 27 N94-10367

Exergy decrease in shock waves and boundary layers of space launch vehicles [AD-A265272] p 42 N94-10493

Examination of wall functions for a parabolized Navier-Stokes code for supersonic flow [DE93-011590] p 14 N94-11111

SUPERSONIC JET FLOW

Control of jet noise [NASA-CR-193612] p 358 N94-11176

High order accurate solutions of viscous problems [NASA-TM-106267] p 151 N94-11253

SUPERSONIC NOZZLES

Control of jet noise [NASA-CR-193612] p 358 N94-11176

SUPERSONIC TRANSPORTS

Supersonic airplane study and design [NASA-CR-193219] p 25 N94-11150

Stratospheric aircraft exhaust plume and wake chemistry [NASA-CR-191495] p 279 N94-12572

SUPERSYMMETRY

The super vectorfield package for REDUCE. Version 1.0 [MEMO-1099] p 321 N94-10265

The INTEGRATOR package for REDUCE, version 1.0 [MEMO-1100] p 322 N94-10418

The ring structure of chiral operators for minimal models coupled to 2D gravity [DE93-613119] p 409 N94-10500

Supersqueezed states from squeezed states p 378 N94-10591

Superfield description of N = 2 extended one-dimensional supersymmetric quantum mechanics [DE93-621420] p 412 N94-11087

Green-Schwarz superstrings in the generalized harmonical Newmann-Penrose formalism [DE93-621422] p 412 N94-11088

A version of superstring with four space-time dimensions [DE93-608196] p 412 N94-11163

Three-dimensional N = 4 extended supersymmetrical quantum mechanics [DE93-621421] p 412 N94-11164

SUPINE POSITION

Pulmonary function in microgravity: KC-135 experience p 309 N94-11994

SUPPORTS

Vibration isolation mount with locking means [AD-D015769] p 178 N94-10381

SUPPRESSORS

Corner vortex suppressor [AD-D015772] p 147 N94-10383

SURFACE COOLING

A structural origin for the cantaloupe terrain of Triton p 449 N94-12095

Lava flows on Venus: Analysis of motion and cooling p 457 N94-12137

Boiling heat-transfer processes and their application in the cooling of high heat flux devices [AD-A266086] p 413 N94-12535

SURFACE CRACKS

Elastic plastic fracture mechanics methodology for surface cracks [NASA-CR-194129] p 185 N94-10712

SURFACE DEFECTS

Invariance of the mobility edge in anodic titanium oxides [DE92-642136] p 394 N94-10281

Potential change in flaw geometry during pressurized-thermal-shock transients [DE93-009709] p 184 N94-10288

SURFACE DISTORTION

An analytic model for calculating pump-induced wavefront distortions in laser slabs [DE93-011953] p 174 N94-11126

PO/PTD diffraction synthesis of array-fed reflector antennas for satellite and radar applications p 137 N94-11636

SURFACE EMITTING LASERS

Preliminary surface-emitting laser logic device evaluation [AD-A266111] p 383 N94-12416

SURFACE FINISHING

Protective coatings for high-temperature polymer matrix composites [NASA-TM-106276] p 74 N94-12431

SURFACE IONIZATION

Solar wind-induced secondary ions and their relation to lunar surface composition p 474 N94-12232

SURFACE LAYERS

Marangoni flows in open cavities with differentially heated end walls p 104 N94-10097

The surface plasmon spectroscopy as diagnostic technique in microgravity experiments p 110 N94-10133

Remote sensing x ray fluorescence spectrometry for future lunar exploration missions p 462 N94-12165

SURFACE NAVIGATION

Real-time tomography mooring [AD-A264923] p 289 N94-11854

SURFACE PROPERTIES

Wetting effects on nylon spheres engulfment in ice p 115 N94-10189

Hydrogen partitioning and transport in titanium aluminides [NASA-CR-194117] p 76 N94-10713

Evolution of steep Martian slopes p 434 N94-11184

Characterization of gas-aerosol interaction kinetics using morphology dependent stimulated Raman scattering [DE93-012324] p 77 N94-11359

Organometallic chemical vapor deposition and characterization of ZnGeP2/GaP multiple heterostructures on GaP substrates p 400 N94-11442
Property changes induced by the space environment in composite materials on LDEF: Solar array materials passive LDEF experiment A0171 (SAMPLE)
[NASA-CR-192572] p 73 N94-11484
The x ray standing waves on surfaces
[AD-A265265] p 402 N94-11682
Wind and surface features in SAR images: The Canadian program p 234 N94-11718
A comparison of telescopic and Phobos-2 ISM spectra of Mars in the short-wave near-infrared (0.76-1.02 microns) p 424 N94-12053
Thermal-infrared emission spectroscopy of natural surfaces: Application to coated surfaces
p 81 N94-12156
Near-infrared spectra of the Martian surface: Reading between the lines p 465 N94-12184
Examination of the surface second harmonic response at infrared wavelengths
[AD-A265206] p 403 N94-12371
Interdisciplinary scientist participation in the Phobos mission
[NASA-CR-193715] p 482 N94-12446

SURFACE REACTIONS
Electrochemical process and product therefrom
[AD-D015767] p 75 N94-10380
CRESLAF. Version 4.0: A Fortran program for modeling laminar, chemically reacting, boundary-layer flow in cylindrical or planar channels
[DE93-012835] p 152 N94-11371
Wide Band-Gap Semiconductors. 1991 Materials Research Society Symposium proceedings
[AD-A263418] p 401 N94-11515
Real-space formation and dissipation dynamics of hexagonal reconstruction on Au(100) in aqueous media as explored by potentiodynamic scanning tunneling microscopy
[AD-A266138] p 368 N94-11658
The adsorption and surface reaction of SiCl4 on Si(100)-(2x1)
[AD-A266124] p 79 N94-12538

SURFACE ROUGHNESS
Ultrasonic inspection, material noise and surface roughness
[DE93-011560] p 183 N94-11110
Needs for super-smooth surfaces
[DE93-012482] p 382 N94-11242
Plating under reduced pressure
[DE93-011896] p 84 N94-11668
The physics of pattern formation of liquid interfaces
[DE93-013333] p 154 N94-11814
Interpretation of lunar and planetary electromagnetic scattering using the full wave solutions
p 440 N94-12049
Coherent structure in near wall turbulence with riblets
p 165 N94-12628
Instability around an isolated roughness element
p 165 N94-12629

SURFACE ROUGHNESS EFFECTS
Ultrasonic inspection, material noise and surface roughness
[DE93-011560] p 183 N94-11110
Coherent structure in near wall turbulence with riblets
p 165 N94-12628
Instability around an isolated roughness element
p 165 N94-12629

SURFACE STABILITY
Evaporation under microgravity conditions
p 102 N94-10086

SURFACE TEMPERATURE
Design and production of insulated wind tunnel models of the Hermes shuttle for heat transfer measurements at hypersonic speeds p 4 N94-10431
Experimental study of multiple droplet evaporative cooling
[PB93-198463] p 149 N94-10851
Central Equatorial Pacific Experiment (CEPEX)
[DE93-011656] p 190 N94-11674
Effects of satellite spectral resolution and atmospheric water vapor on retrieval of near-ground temperatures
[AD-A264920] p 245 N94-11851
Rates of fluvio-thermal erosion on Mars
p 435 N94-12018
Comments on possible causes of recent global warming
[DE93-010501] p 272 N94-12592

SURFACE TREATMENT
Fracture behavior of surface-modified ceramics
[DE93-013707] p 88 N94-10710
Ellipsometry studies of semiconductors surface cleaning
[AD-A265150] p 142 N94-11094

SURFACE VEHICLES
Safety of high speed ground transportation systems: X2000 US demonstration vehicle dynamics trials, preliminary test report, October 1992 - January 1993
[PB93-194645] p 422 N94-10736

SURFACE WATER
Sandia ocean modeling system programmer's guide and user's manual
[DE93-007427] p 287 N94-10153
Remote surface water monitoring radio based telemetry system
[DE93-009643] p 41 N94-11282
Mars: The initial emplacement of ground ice in response to the thermal evolution of its early crust
p 462 N94-12168
The thermodynamic case for a water-rich Mars
p 463 N94-12170

SURFACE WAVES
Uni-directional waves over slowly varying bottom. Part 1: Derivation of a KdV-type of equation
[MEMO-1098] p 147 N94-10275
Wave propagation characteristics of short-period crustal phases near ARCESS and NORESS
[AD-A265959] p 275 N94-11102
Near surface ocean processes: Acoustical observations, ambient sound, and Langmuir circulation
p 288 N94-11447
Decay interaction of bulk and surface Langmuir waves
[DE93-617843] p 393 N94-11477
Air-sea fluxes and universal constants in weak-turbulence theory of surface gravity waves
p 195 N94-11922
Topics in pattern formation and chaotic systems
[AD-A265922] p 161 N94-12342

SURVEILLANCE
Estimation with multisensor/multiscan detection fusion
[AD-A265673] p 138 N94-12338

SURVEYS
Survey to determine the value of DYNA
[DE93-012390] p 321 N94-10267
Aerosol sampling models survey
[AD-A265903] p 75 N94-10337
Computer models used to support cleanup decision-making at hazardous and radioactive waste sites
[PB93-183333] p 274 N94-10698
National patterns of R and D resources, 1992
[NSF-92-330] p 422 N94-11186
A survey of techniques for corrosion monitoring
[DE93-012131] p 83 N94-11250
NASA/DOD Aerospace Knowledge Diffusion Research Project. Report 17: A comparison of the technical communication practices of Dutch and US aerospace engineers and scientists
[NASA-TM-108987] p 419 N94-11352
Pattern of federal procurement from minority and women-owned small business
[PB93-189355] p 417 N94-11844
Aviators, air combat, and combat stress: An Air Force commander's primer
[AD-A265083] p 313 N94-11867

SURVIVAL
Evaluation of medical treatments to increase survival of ebullism in guinea pigs p 302 N94-11548

SUSPENDING (MIXING)
Separation of gravitational effects on the flow of suspension in tubes by measurements in weightlessness
p 105 N94-10105

SUSPENSIONS
The solubility of epsilon-CL-20 in selected materials
[DE93-009304] p 77 N94-11602

SWEAT
Modifications to an interactive model of the human body during exercise: With special emphasis on thermoregulation p 317 N94-12368

SWEDEN
Experiences from the Swedish sea ice programme during BEERS-1992 p 239 N94-11751

SWELLING
A method of influence regions in the theory of vacancy swelling of metals
[DE93-620579] p 83 N94-11363

SWEPT FORWARD WINGS
X-29: Longitudinal instability at high angle-of-attack
p 33 N94-11504

SWEPT WINGS
Physics of forebody flow control
[NASA-CR-193626] p 15 N94-11195
Modeling nonlinear aerodynamic loads for aircraft stability and control analysis p 32 N94-11499

SWIRLING
SWIRL as a means of liquid management in low gravity
[NASA-CR-4545] p 412 N94-11523

SWITCHES
A picosecond high pressure gas switch
[DE93-011897] p 142 N94-11050
Experimental and theoretical investigations of Cs-Ba vapor tacitron inverter for power conditioning in space power systems
[DE93-012971] p 48 N94-11372
GaAs PCSS: High gain switching and device reliability
[DE93-009851] p 401 N94-11605
A thermal ionization model for the sustaining phase of lock-on in GaAs
[DE93-011558] p 144 N94-11624

SWITCHING
A picosecond high pressure gas switch
[DE93-011897] p 142 N94-11050
Experimental and theoretical investigations of Cs-Ba vapor tacitron inverter for power conditioning in space power systems
[DE93-012971] p 48 N94-11372
Assessment of the impact of HTSC's on superconducting fault-current limiters
[DE93-009986] p 143 N94-11454
GaAs PCSS: High gain switching and device reliability
[DE93-009851] p 401 N94-11605
Ceramic actuators for smart materials
[AD-A265664] p 93 N94-12331

SWITCHING CIRCUITS
A study of DC-DC converters with MCTs for arcjet power supplies
[NASA-CR-193457] p 142 N94-10931

SYMBOLS
Symbolic dynamics and description of complexity
[DE93-613030] p 418 N94-10485

SYMMETRY
Symmetry lowering in crystalline solid solutions: A study of cinnamamide-thienylacrylamide by x ray and neutron diffraction and solid-state photochemistry
[DE93-010871] p 394 N94-10301
Exact solutions of a many-anyon problem
[DE93-617646] p 411 N94-10832
Quantum solitons with cylindrical symmetry
[DE93-617659] p 344 N94-10881
Quenched chiral logarithms
[DE93-010195] p 346 N94-11663
Engineering solid-state materials. Strategies for modeling and packing control of molecular assemblies into 3-D networks
[AD-A265291] p 404 N94-12438

SYMPATHETIC NERVOUS SYSTEM
Valsalva maneuver: Insights into baroreflex modulation of human sympathetic activity p 310 N94-12000
Hormonal regulation of fluid and electrolyte metabolism in zero-g and bedrest p 311 N94-12004

SYNCHRONISM
An object-oriented model for extensible concurrent systems: The composition-filters approach
[MEMO-INF-92-87] p 320 N94-10166
LASSO observations at McDonald and OCA/CERGA: A preliminary analysis p 352 N94-10972
PTTI-aided ephemeris calculation and rapid data link acquisition for manned space flight p 42 N94-10974
Timing in private digital telecommunication networks
p 139 N94-10991
SONET synchronization: What's happening
p 355 N94-10992

SYNCHRONOUS PLATFORMS
Progress in multidisciplinary design optimization at NASA Langley
[NASA-TM-107754] p 318 N94-10814

SYNCHRONOUS SATELLITES
Sun-synchronous and geo-synchronous satellite data utilization for environmental studies p 37 N94-10689

SYNCHROTRON RADIATION
Laser Synchrotron Source (LSS)
[AD-D015755] p 173 N94-10371
Cosmological gamma-ray burst model
[NASA-CR-193368] p 484 N94-10507

SYNCHROTRONS
Upgraded D(O) calorimeter electronics for short Tevatron bunch space and the effect of pile-up on the W mass measurement
[DE93-013566] p 146 N94-12603

SYNOPTIC METEOROLOGY
TOVS soundings: Impact on the synoptic analysis over the south and southeast regions of Brazil from March 18 to March 19, 1991
[INPE-5497-TDI/512] p 230 N94-11179

SYNTAX
Processing proper nouns in machine translation for English news
[NHK-SERIAL-414] p 418 N94-10559

SYNTHESIS (CHEMISTRY)
Synthesis of molecular sieves from clear solution
p 124 N94-10245

New aromatic activated dihalides and bisphenol monomers for the preparation of novel poly(arylene ethers)
[NASA-CR-193190] p 55 N94-10513
Primaset (tm): A safer material for aircraft interior applications p 18 N94-10772
Low temperature synthesis of monolithic transparent Ta2O5 gels from hydrolysis of metal alkoxide
[NASA-TM-106246] p 89 N94-11204
Synthesis and thermal evolution of structure in alkoxide-derived niobium pentoxide gels
[NASA-TM-106259] p 90 N94-11257
Synthesis and electronic properties of nanophase semiconductor materials
[AD-A265287] p 146 N94-12584
Photogenerated base in polymer imaging. Synthesis and photopatterning of poly(2-cyano-2-(p-vinylphenyl) butanoic acid)
[AD-A265288] p 95 N94-12585

SYNTHETIC APERTURE RADAR
Spaceborne SAR study: LDRD 1992
[DE93-011485] p 232 N94-11623
Proceedings of First ERS-1 Symposium on Space at the Service of Our Environment, volume 1
[ESA-SP-359-VOL-1] p 232 N94-11704
Validation of directional wave spectra from the ERS-1 during the ESA CAL/VAL campaign p 232 N94-11707
The Grand Banks ERS-1 SAR wave spectra validation experiment p 232 N94-11708
Use of ERS-1 data at Saclant Undersea Research Centre p 233 N94-11714
Mapping of the East Australian current with the ERS-1 SAR and shipborne studies p 234 N94-11717
Wind and surface features in SAR images: The Canadian program p 234 N94-11718
Coastal ocean studies with ERS-1 SAR during NORCSEX 1991 p 234 N94-11720
SAR imaging of dynamical features in the English Channel p 234 N94-11721
SAR ocean imaging in the Gulf of Alaska
p 235 N94-11723
ERS-1 SAR calibration strategy p 235 N94-11726
ERS-1 preliminary antenna elevation pattern measured by ground-receivers p 235 N94-11727
Preliminary results of the experiment I-7
p 235 N94-11728
The ERS-1/CV 580 SAR cross-calibration experiment: Sault Ste Marie, October 26 - November 2, 1991
p 236 N94-11729
Calibration of the ERS-1 SAR fast-delivery images
p 236 N94-11730
Calibration results for the ERS-1, AIRSAR, and PHARS p 236 N94-11731
The use of active devices in the ERS-1 radiometric calibration p 236 N94-11732
An experiment for the radiometric calibration of the ERS-1 SAR p 236 N94-11733
Techniques and applications of SAR interferometry for ERS-1: Topographic mapping, change detection, and slope measurement p 236 N94-11734
SAR interferometry experiments with ERS-1
p 237 N94-11735
SAR-interferometry applying ERS-1: Some preliminary test results p 237 N94-11736
Monitoring of the Greenland Ice Sheet using ERS-1 synthetic aperture radar imagery p 237 N94-11741
Investigations of Arctic ice-sheets and glaciers using ERS-1 SAR p 238 N94-11743
Spatial patterns in backscatter strength across the Greenland Ice Sheet p 238 N94-11744
Ice studies in the Barents Sea by ERS-1 SAR during SIZEX 92 p 238 N94-11745
Validation of ERS-1 SAR measurements of sea ice during ARCTIC-1991 p 238 N94-11747
Waves and mesoscale features in the marginal ice zone p 240 N94-11757
Ocean circulation revealed by ice floe tracking
p 240 N94-11759
Preliminary evaluation of ERS-1 SAR data for operational use in the Canadian sea ice monitoring program
p 241 N94-11760
Summer Arctic ice concentrations and characteristics from SAR and SSM/I data p 241 N94-11762
Ocean wave detection by SAR p 197 N94-11932
On the determination of the SAR ocean surface scattering patch size p 197 N94-11933
Ocean-ice interaction study of waves and mesoscale features p 197 N94-11935
Characteristics of arachnoids from Magellan data
p 469 N94-12204
ISAR motion compensation using the burst derivative measure as a focal quality indicator
[AD-A265647] p 138 N94-12440
Proceedings of 1st ERS-1 Symposium on Space at the Service of Our Environment, Volume 2
[ESA-SP-359-VOL-2] p 245 N94-12471
Segmented land use classification of multitemporal ERS-1 SAR data using a majority filter
p 245 N94-12472
Land cover monitoring with multi-temporal ERS-1 SAR observations in the Netherlands p 246 N94-12473
Mapping a dynamic playa surface using multitemporal ERS-1 SAR data: First results p 246 N94-12474
Preliminary studies on the application of ERS-1 data to topographic mapping p 246 N94-12476
Radarmap of Germany: First mosaic and classification
p 246 N94-12477
Combined analysis of ERS-1 SAR and visible/infrared remote sensing data for land cover/land use mapping in a tropical zone: A case study in Guinea
p 246 N94-12478
Example of SPOT/ERS-1 complementarity
p 247 N94-12479
The use of ERS-1 SAR data to study surface states
p 247 N94-12480
Snow and glacier investigations by ERS-1 SAR: First results p 247 N94-12481
Monitoring of snowcover in high mountain terrain with ERS-1 SAR p 247 N94-12482
Application of ERS-1 SAR data to snow mapping
p 247 N94-12483
Per-field filtering and classification of multitemporal ERS-1 SAR imagery p 247 N94-12485
Preliminary ERS-1 assessment for Canadian agriculture and forestry applications p 248 N94-12486
Segmentation and change detection in ERS-1 images over East Anglia p 248 N94-12487
ERS-1 SAR crop monitoring experiment in East Anglia, UK p 248 N94-12488
Geoecological monitoring of an agricultural area
p 248 N94-12489
Assessment of ERS-1 SAR data for soil moisture estimation p 249 N94-12492
Temporal monitoring of soil moisture using ERS-1 SAR data p 249 N94-12493
Observations of ERS-1 SAR sensitivities to changes in aboveground biomass in young loblolly pine forests
p 249 N94-12494
Seeing the Black Forest by ERS-1 and AIRSAR: A comparison p 249 N94-12495
The TREES project: Pre-processing and generation of terrain data for inclusion in an ERS-1 SAR classification scheme p 249 N94-12496
TREES project: A case study on the use of multi-temporal ERS-1 SAR data and SPOT data for monitoring tropical ecosystems p 249 N94-12497
TREES project: A suite of tools for information extraction from ERS-1 SAR data p 250 N94-12498
TREES project: Overview and status of the ERS-1 SAR contribution p 250 N94-12499
A statistical analysis of sea state surface ERS-1 SAR-wave mode imagettes p 251 N94-12507
A new model for Synthetic Aperture Radar (SAR) images from ocean scatter p 251 N94-12508
On the extraction of ocean wave spectra from ERS-1 SAR wave mode image spectra p 251 N94-12509
Tide-generated nonlinear internal wave packets in the Strait of Gibraltar observed by the synthetic aperture radar aboard the ERS-1 satellite p 252 N94-12510
Artificial oil pollution detection and wave observation in the sea adjacent to Japan by ERS-1 SAR
p 253 N94-12520
Ship traffic monitoring using the ERS-1 SAR
p 253 N94-12521
Oil spill detection using satellite-based SAR: Experience from a field experiment p 253 N94-12522
Pilot project PPF12. Coastal and fluvial environment in French Guiana: First results of ERS-1 SAR data analysis
p 254 N94-12523
Coastal morphodynamics and energetic characteristics of swell studied with ERS-1 SAR p 254 N94-12524
Mapping of sea bottom topography with ERS-1 C-band SAR p 254 N94-12525
ERS-1 imaging radar over the Waddensea-North Netherlands p 254 N94-12526
SAR imaging of geology and bathymetry: Kent coastal area - southern North Sea p 254 N94-12527
Applications of ERS-1 SAR data for analyzing riverine and coastal processes and geomorphology
p 254 N94-12528
Comparison of ERS-1 SAR images of the Western Mediterranean to in situ oceanographic data: PRIM-1 Cruise (May 1992) p 255 N94-12529
Ice studies in the Barents Sea by ERS-1 during SIZEX 1992 p 210 N94-12653
Observations of surface signatures in the north-west Pacific Ocean with the spaceborne SAR
p 226 N94-12746

SYNTHETIC APERTURES
Sampling and position effects in the Electronically Steered Thinned Array Radiometer (ESTAR)
[NASA-TM-108998] p 245 N94-12432

SYNTHETIC FIBERS
Mechanical interaction between synthetic fiber and cement base matrix in FRC composites
[AD-A265310] p 73 N94-11686

SYNTHETIC RUBBERS
Thermal stability of sealants for military aircraft: Modification of polysulfide prepolymers with ether and thioether monomers
[AD-A264079] p 89 N94-11107

SYSTEMS ANALYSIS
Transportation systems analyses. Volume 2: Technical/programmatics
[NASA-CR-192582] p 41 N94-10827
Design for testability and diagnosis at the system-level
p 184 N94-11563
Space Life Support Engineering Program
[NASA-CR-193474] p 316 N94-12365
Systems analysis of a closed loop ECLSS using the ASPEN simulation tool. Thermodynamic efficiency analysis of ECLSS components p 316 N94-12366
Analysis of the Army's installation support modules with the private sector's open information systems
[AD-A265667] p 421 N94-12579

SYSTEMS ENGINEERING
System engineering concept demonstration, technology assessments, volume 5
[AD-A265471] p 323 N94-10494
System engineering concept demonstration, trade studies, volume 6
[AD-A265472] p 323 N94-10495
System monitoring and diagnosis with qualitative models
[NASA-CR-193812] p 323 N94-10711
Space Station redesign option A: Modular buildup concept
[NASA-TM-108415] p 43 N94-10808
Progress in multidisciplinary design optimization at NASA Langley
[NASA-TM-107754] p 318 N94-10814
Transportation systems analyses: Volume 1: Executive Summary
[NASA-CR-192583] p 41 N94-10826
Transportation systems analyses. Volume 2: Technical/programmatics
[NASA-CR-192582] p 41 N94-10827
National Airspace System operational concept
[DOT/FAA/SE-93/1] p 23 N94-10933
MIL-STDS and PTTI: What's available and what needs to be done p 352 N94-10973
The guide to Design For On-orbit Spacecraft Servicing (DFOSS) manual: Producing a consensus document
p 421 N94-11575
The National Launch System Advanced Development Program: A brief overview p 40 N94-11576
System engineering concept demonstration, process model, volume 3
[AD-A265469] p 333 N94-12008
Integrating the services' imagery architectures
[AD-A265487] p 171 N94-12335
Machine translation technology: A potential key to the information age
[PB93-134336] p 421 N94-12385

SYSTEMS INTEGRATION
STGT program: Ada coding and architecture lessons learned p 330 N94-11437

SYSTEMS MANAGEMENT
Analysis of the Army's installation support modules with the private sector's open information systems
[AD-A265667] p 421 N94-12579

SYSTEMS SIMULATION
System monitoring and diagnosis with qualitative models
[NASA-CR-193812] p 323 N94-10711

SYSTEMS STABILITY
On the stability of stationary regimes in a distributed autovibration system with external feedback
[DE93-620979] p 141 N94-10543

SYSTOLE
Strategies and methodologies to develop techniques for computer-assisted analysis of gas phase formation during altitude decompression p 312 N94-11547

T

T TAURI STARS
Why convective heat transport in the solar nebula was inefficient p 458 N94-12143

TACTILE SENSORS (ROBOTICS)
Object recognition in industrial environment by means of tactile sensor
[ITN-93-85200] p 178 N94-10393

TAIWAN
Sedimentation rates and particulate fluxes in the slope and deep sea areas off eastern Taiwan
p 220 N94-12709

TANDEM MIRRORS
Applying design principles to fusion reactor configurations for propulsion in space
[NASA-TM-108247] p 47 N94-11053
TANTALUM OXIDES
Low temperature synthesis of monolithic transparent Ta2O5 gels from hydrolysis of metal alkoxide
[NASA-TM-106246] p 89 N94-11204
TARGET ACQUISITION
Fuzzification of ASAT's rule based aimpoint selection
[AD-A266068] p 43 N94-11223
Aircraft windscreens enhance visual search disruption produced by laser glare
[AD-A265167] p 26 N94-11892
Estimation with multisensor/multiscan detection fusion
[AD-A265673] p 138 N94-12338
TARGET RECOGNITION
The theory for, and demonstration of, information theory applied to radar target identification
[DE93-006393] p 132 N94-10315
Spatial light rebroadcaster architecture study
[AD-A266102] p 382 N94-11421
Airborne optical tracking control system design study
[DE93-009515] p 382 N94-11662
A hybrid neural network and feature extraction technique for target recognition
[AD-D015732] p 333 N94-12386
ISAR motion compensation using the burst derivative measure as a focal quality indicator
[AD-A265647] p 138 N94-12440
TARGETS
GRAFTED (GRAphical Fault Tree EDitor): A fault tree description program for target vulnerability/survivability analysis
[AD-A264078] p 328 N94-11301
Projectile-target mixing in melted ejecta formed during a hypervelocity impact cratering event
p 432 N94-12241
TASK COMPLEXITY
Vigilance problems in orbiter processing
p 314 N94-11536
Development and evaluation of a predictive algorithm for telerobotic task complexity p 341 N94-11562
TASK PLANNING (ROBOTICS)
Task planning with uncertainty for robotic systems
[NASA-CR-193253] p 338 N94-10638
Development and evaluation of a predictive algorithm for telerobotic task complexity p 341 N94-11562
TASKS
Crew chief p 335 N94-11564
Career Information in the Mathematical Sciences (CIMS)
[DE93-013780] p 318 N94-11817
Locus coeruleus, vigilance, and stress: Brain mechanisms of adaptive behavioral responsiveness
[AD-A265657] p 302 N94-12441
TATB
Temperature effects on failure thickness and deflagration-to-detonation transition in PBX 9502 and TATB
[DE93-010742] p 97 N94-10294
TAXONOMY
How diverse is the asteroid belt? p 430 N94-12124
First results of the seven-color asteroid survey
p 430 N94-12162
TDR SATELLITES
STGT program: Ada coding and architecture lessons learned p 330 N94-11437
TEARING MODES (PLASMAS)
Reversed-field pinch studies in the Madison Symmetric Torus
[DE93-013464] p 388 N94-10747
Simulation study of dynamo structure in reversed field pinch
[DE93-771406] p 390 N94-11128
Macroscopic behaviour and discrete dynamo of RFP plasma in high theta discharge
[DE93-771408] p 392 N94-11239
TECHNOLOGICAL FORECASTING
Space Station Freedom advanced photovoltaics and battery technology development planning
p 52 N94-11401
TECHNOLOGY ASSESSMENT
Protein, glass, aerosol research, containerless processing and diagnostics technology for microgravity application p 106 N94-10112
High temperature processing and diagnostic technologies for microgravity applications
p 110 N94-10130
The 40 kWe S-PRIME Thermionic Design and Technology Demonstration Program
[DE93-004738] p 40 N94-10147
Department of Energy solar process heat program: FY 1991 solar process heat prefeasibility studies activity
[DE93-010010] p 262 N94-10258
System engineering concept demonstration, technology assessments, volume 5
[AD-A265471] p 323 N94-10494
Intelligent structures: A technology overview and assessment p 68 N94-11322
Workshop summary: New silicon cells
p 54 N94-11417
Software process assessments p 329 N94-11427
TFE verification program
[DE93-009609] p 373 N94-11694
TECHNOLOGY TRANSFER
Survey to determine the value of DYNA
[DE93-012390] p 321 N94-10267
Technology transfer at Lawrence Berkeley Laboratory
[DE93-010460] p 423 N94-11059
Tropical medicine: Telecommunications and technology transfer p 305 N94-11793
TECHNOLOGY UTILIZATION
Advanced Materials for Lightweight Structures
[ESA-SP-336] p 56 N94-10001
New technology applied to telemedicine
p 306 N94-11796
Machine translation technology: A potential key to the information age
[PBS3-134336] p 421 N94-12385
TECTONICS
Statistical description of tectonic motions
[NASA-CR-193701] p 275 N94-10950
Analysis of gravity, magnetic, and seismic reflection data from Tibet and neighboring regions of China
[NASA-CR-193405] p 278 N94-11886
Lineament analysis and tectonic interpretation for the Tharsis region p 437 N94-12031
Horizontal stresses induced by vertical processes in planetary lithospheres p 281 N94-12042
Estimation of age of Dali-Ganis rifting and associated volcanic activity, Venus p 440 N94-12046
Global organization of tectonic deformation on Venus
p 444 N94-12066
Buoyant subduction on Venus: Implications for subduction around coronae p 455 N94-12130
Stratigraphy and sedimentology of the K/T boundary deposit in Haiti p 282 N94-12138
Porosity and the ecology of icy satellites
p 431 N94-12186
Tectonics on Triton p 466 N94-12187
Regional mantle upwelling on Venus: The Beta-Atla-Themis anomaly and correlation with global tectonic patterns p 467 N94-12196
Transmantle flux tectonics p 283 N94-12249
Pseudo magnetic anomaly derived from satellite altimetry and its application to the tectonics in the North Fuji Basin p 208 N94-12645
TEFLON (TRADEMARK)
Dimensional scaling for impact cratering and perforation
[NASA-CR-188259] p 42 N94-10665
TEKTITES
Vaporization by shock loading of albite, jadeite, and pyrex glass: Experimental study p 97 N94-12039
K/T spherules from Haiti and Wyoming: Origin, diagenesis, and similarity to some microtektites
p 281 N94-12085
Minor and trace element composition and age of Yukon probable-microtektites p 429 N94-12094
Oxygen isotopes as tracers of tektite source rocks: An example from the Ivory Coast tektites and Lake Bosumtwi Crater p 430 N94-12146
Microtektite-like glass spherules in Late Devonian (367 MA) shales p 461 N94-12160
KT boundary impact glasses from the Gulf of Mexico region p 282 N94-12161
Soret diffusion: A possible cause of compositional heterogeneity within tektites p 432 N94-12211
Modelling of dispersal and deposition of impact glass spherules from the Cretaceous-Tertiary boundary deposit p 432 N94-12238
TELECOMMUNICATION
Potential markets for advanced satellite communications
[NASA-CR-191145] p 41 N94-10512
The 24th Annual Precise Time and Time Interval (PTTI) Applications and Planning Meeting
[NASA-CP-3218] p 350 N94-10963
Synopsis of timing measurement techniques used in telecommunications p 139 N94-10990
Timing in private digital telecommunication networks
p 139 N94-10991
Telescience capability for the Sondre Stromfjord, Greenland, incoherent-scatter radar facility
[NASA-CR-193683] p 136 N94-11206
Telemetering and telecommunications research
[NASA-CR-193235] p 42 N94-11297
International Telemedicine/Disaster Medicine Conference: Papers and Presentations
[NASA-NP-207] p 304 N94-11787
The Canadian experience: Using telemedicine for the support of medical care at remote sites
p 305 N94-11789
Global considerations for implementation of telemedicine p 305 N94-11792
Tropical medicine: Telecommunications and technology transfer p 305 N94-11793
Applications of the INTELSAT system to remote health care p 306 N94-11794
Clinical aspects of telemedicine p 306 N94-11795
Commercial applications of telemedicine
p 306 N94-11798
The use of communication technology in medicine
p 306 N94-11800
A telemedicine health care delivery system
p 307 N94-11803
Communications infrastructure requirements for telemedicine/telehealth in the context of planning for and responding to natural disasters: Considering the need for shared regional networks p 307 N94-11804
International disaster research p 307 N94-11805
Medical care delivery in the US space program
p 307 N94-11806
US-USSR telemedicine consultation spacebridge to Armenia and Ufa p 308 N94-11809
The revitalization of health and education in Rural America Act of 1992 p 308 N94-11810
Asynchronous Transfer Mode (ATM) technology: An overview
[AD-A266087] p 383 N94-12413
TELECONFERENCING
International Telemedicine/Disaster Medicine Conference: Papers and Presentations
[NASA-NP-207] p 304 N94-11787
Telemedicine and international disaster response: Medical consultation to Armenia and Russia via a telemedicine spacebridge p 305 N94-11790
Clinical aspects of telemedicine p 306 N94-11795
TELEMETRY
Telemetering and telecommunications research
[NASA-CR-193235] p 42 N94-11297
A telemedicine health care delivery system
p 307 N94-11803
Real-time tomography mooring
[AD-A264923] p 289 N94-11854
The structure of hydrophysical measuring systems of vertical sounding and self-contained stations
p 227 N94-12751
TELEOPERATORS
TOLS (Telescience On-Line Simulator): An essential instrument for micro-gravity interactive experiment
p 39 N94-10134
Analysis of the alignment of a Schlieren system for tele-operation p 111 N94-10140
Telerobot control system
[NASA-CASE-NPO-18116-1-CU] p 179 N94-10670
A portable controller for unmanned ground vehicles
[AD-A264963] p 181 N94-11290
Sixth Annual Workshop on Space Operations Applications and Research (SOAR 1992), volume 2
[NASA-CP-3187-VOL-2] p 486 N94-11527
Supervised autonomous control, shared control, and teleoperation for space servicing p 183 N94-11577
TELEPHONES
Performances of a date dissemination code on telephone lines using commercial modems
p 139 N94-10984
TELEROBOTICS
Telerobotic control of a mobile coordinated robotic server
[NASA-CR-193465] p 338 N94-10345
Telerobot control system
[NASA-CASE-NPO-18116-1-CU] p 179 N94-10670
Development and evaluation of a predictive algorithm for telerobotic task complexity p 341 N94-11562
In-space operations for lunar and Mars space transfer vehicles p 348 N94-11568
In-space assembly-servicing requirements
p 348 N94-11569
More sense for less cents: Cost effective servicing of remote sensing satellites p 348 N94-11572
Supervised autonomous control, shared control, and teleoperation for space servicing p 183 N94-11577
TELESCOPES
Continued development of an ultra-narrow bandpass filter for solar research
[NASA-CR-194169] p 381 N94-10735
Monochromator SP-017. The results of the first experiments
[DE93-617463] p 372 N94-10849
NASA Marshall Space Flight Center solar observatory report, January - June 1993
[NASA-TM-108417] p 423 N94-10866
Visual Earth observation performance in the space environment. Human performance measurement 4: Flight experiments p 314 N94-11539

A comparison of telescopic and Phobos-2 ISM spectra of Mars in the short-wave near-infrared (0.76-1.02 microns) p 424 N94-12053
Model of optical scatter from microimpacts on the Hubble Telescope p 384 N94-12189
Galileo EM-2 contributions to the lunar control network p 468 N94-12198
Laser system design for the generation of a sodium-layer laser guide star
[DE93-014127] p 176 N94-12784

TELEVISION CAMERAS
A compact, four-way image splitter
[AD-A266107] p 382 N94-11656

TELEVISION EQUIPMENT
Measurement of display transfer characteristics using test pictures
[BBC-RD-1992/13] p 133 N94-11023

TELEVISION SYSTEMS
A compact, four-way image splitter
[AD-A266107] p 382 N94-11656

TEMPERATE REGIONS
The cloud radiative feedback of a midlatitude squall line system and implication for climate study
[DE93-010511] p 283 N94-10290

TEMPERATURE COMPENSATION
Sea surface temperature difference between NOAA/AVHRR and in-situ observation
p 215 N94-12680

TEMPERATURE CONTROL
The Third Workshop on Two Phase Fluid Experiment in the Space Environment
[NASDA-CON-930002] p 161 N94-12547
Summary of studies on JEM utilization experiment projects p 161 N94-12548
Compilation of proposals for boiling and evaporation experiments in space environments and proposals concerning experiment projects p 161 N94-12549
Condensation phenomena p 162 N94-12550
Developmental research of thermal control system in space environment p 162 N94-12551
Two phase flow and isopycnic liquid-liquid two phase fluid in reduced gravity field p 162 N94-12552
Devices related for thermal control systems used in microgravity p 162 N94-12553
Research and development of cold plate for two phase fluid loop thermal control system p 162 N94-12555
Organization and management policy for two phase fluid experiment in space environment p 162 N94-12556

TEMPERATURE DEPENDENCE
On the relativistic string size at finite temperature
[DE93-617658] p 409 N94-10394
Experiments in ultracold collisions
[DE93-012110] p 365 N94-11029
Phase equilibria and volumetric properties for the system NaCl-CaCl2-H2O
[DE93-013590] p 76 N94-11244
Computation of photovoltaic parameters under lunar temperature variation p 53 N94-11411
Apical Cu-O bond in YBa2Cu3O(7-delta) superconductors by XAFS
[DE93-010861] p 400 N94-11458
Thermographic properties of eight blue-emitting phosphors
[DE93-011459] p 78 N94-11622
The role of the geothermal gradient in the emplacement and replenishment of ground ice on Mars
p 463 N94-12169
Environmental factors controlling fluxes of dimethyl sulfide in a New Hampshire fen p 270 N94-12462

TEMPERATURE DISTRIBUTION
Marangoni and buoyant convections in zone melting of GaAs with liquid encapsulation p 101 N94-10081
Simulation of images of water vapor channel and infrared split channel p 190 N94-11081
On temperature distribution in non-participating medium with radiation boundary condition
[DE93-619375] p 153 N94-11604
Observations of the fractal properties of the Japan sea surface temperature patterns p 205 N94-11984
On an upwelling front, propagation of upwelling and vertical velocity in the eastern Arabian Sea during monsoon, 1987 p 206 N94-11987
Roles of the NEC and MC in the formation and evolution of the Equatorial Pacific Warm Pool p 206 N94-11990
Does the thermal wind exist near the Earth's core boundary? p 283 N94-12217
Search for structures in the cosmic microwave background radiation
[INPE-5491-TDI/508] p 484 N94-12357
Observation of cold coastal water with high turbidity around the southwestern tip of Korean Peninsula
p 216 N94-12689
The relationship between skin and bulk sea surface temperatures p 221 N94-12716
Atmospheric correction for determination of average SST fields based on AVHRR data p 227 N94-12750

TEMPERATURE EFFECTS
In situ observation of temperature dependence of concentration field during growth of KB5 crystals by holographic interferometry p 115 N94-10187
Temperature effects on failure thickness and deflagration-to-detonation transition in PBX 9502 and TATB
[DE93-010742] p 97 N94-10294
Kinetics of high concentration arsenic deactivation at moderate to low temperatures
[DE93-013349] p 395 N94-10516
Hydrogen partitioning and transport in titanium aluminides
[NASA-CR-194117] p 76 N94-10713
Computational simulation of hot composite structures
[NASA-TM-106200] p 186 N94-10762
Flammability parameters of materials: Ignition, combustion, and flame spread p 20 N94-10788
Factors that affect OSU thermal performance of aircraft interior materials p 20 N94-10789
The influence of irradiation conditions, type, and concentration of impurities on radiation defects characteristics in indium antimonide under electron irradiation
[DE93-617201] p 397 N94-10843
Time-resolved optical studies of charge relaxation and charge transfer at electrode interfaces
[DE93-013985] p 398 N94-11117
DBTT measurement by use of Small Punch (SP) test
[DE93-753188] p 183 N94-11168
Thermal testing of aluminized Mylar
[NASA-TM-108414] p 89 N94-11175
P2NBC2 Heat Strain Decision Aid. User's guide, version 2.1
[AD-A266072] p 304 N94-11224
Thermographic properties of eight blue-emitting phosphors
[DE93-011459] p 78 N94-11622
Changes in Hawaiian palagonite FE mineralogy associated with thermal alteration: Implications for Mars
p 281 N94-12055
Primordial lightning: Evidence preserved in chondrites
p 432 N94-12230
On the origin of (4)He and (40)Ar in natural gold
p 87 N94-12240
Thermal error compensation feasibility study using artificial intelligence
[AD-A266084] p 340 N94-12411
NiAl alloys for structural uses
[NASA-CR-194113] p 85 N94-12447
Molecular properties of polymeric materials for space applications
[NASA-CR-194370] p 94 N94-12450

TEMPERATURE GRADIENTS
Coupled thermogravitational and thermocapillary convection in a two-layer fluid system
p 105 N94-10101
Boundary layers along horizontal free surfaces due to combined effects of temperature and concentration gradients p 106 N94-10108
A study of the quasibinary Al-Mo-W system. Part 2: A physico-mechanical investigation of the system fabricated under the gravitylessness conditions
p 119 N94-10212
Crystal growth in the Zone Melting Facility (ZMF)
p 119 N94-10213
Numerical investigations on Marangoni-Benard instability in multi layer systems p 120 N94-10217
Convective motion in a multi-layered system with a free surface p 120 N94-10219
Appearance of convective instabilities caused by liquid-liquid phase separation under small buoyancy forces p 120 N94-10221
A theoretical kinematical study of the gradient of any cosmic scalar field
[DE92-644731] p 425 N94-11136
The role of the geothermal gradient in the emplacement and replenishment of ground ice on Mars
p 463 N94-12169
Does the thermal wind exist near the Earth's core boundary? p 283 N94-12217
A user appraisal of ATSR near-real-time products
p 252 N94-12516
Investigation of meso-scale fronts, eddies and upwellings in China Seas with AVHRR data
p 220 N94-12711

TEMPERATURE MEASUREMENT
Low cost and thermally stable sandwich design for FIRST p 57 N94-10009
Experimental analysis of Benard-convection by the combined application of liquid crystals and PIV
p 106 N94-10109
The pyrene laser induced fluorescence technique as a diagnostic tool for combustion thermometry in microgravity p 107 N94-10113
A new method for hysteresis measurements developed for C(sub v) measurements at the critical point during the D2-mission p 107 N94-10114
High temperature processing and diagnostic technologies for microgravity applications
p 110 N94-10130
TEXUS 28 experiment: Convections and crystal growth of Ge:Ga. Analysis of temperature measurements
p 114 N94-10184
Ground results of the Mephisto program: Benefits and space experiments orientation p 86 N94-10197
Local measurement of temperatures and concentrations: A review for hypersonic flows
p 4 N94-10434
Experiments in ultracold collisions
[DE93-012110] p 365 N94-11029
Electron temperature measurements of x ray laser plasmas
[DE93-011874] p 389 N94-11074
A laboratory model of a hydrogen/oxygen engine for combustion and nozzle studies
[NASA-TM-106281] p 47 N94-11252
Heat flux measurements on ceramics with thin film thermocouples
[NASA-TM-106305] p 170 N94-11310
A detailed study of the photo-injection annealing of thermally diffused InP solar cells p 48 N94-11381
The excitation of cyanogen and ionized carbon in interstellar and extragalactic gas clouds
p 426 N94-11582
Overview of the 1989 Wind Tunnel Calibration Workshop
[NASA-TP-3393] p 34 N94-11869
Trouble areas in the IRT measurement of the Earth surface temperature p 193 N94-11910
Ocean measuring experiments using optical fiber distributed temperature sensor p 172 N94-11968
Remote sensing of subsurface water temperature profile and backscattering coefficient in the China Sea by Ocean Lidar (OLIDAR) p 203 N94-11970
Calorimetric thermometry of meteoritic troilite: A feasibility study p 428 N94-12025
Establishing baseline data for an experimental appratus that measures heat transfer under conditions of oscillating pressure and flow
[NASA-CR-193772] p 413 N94-12343
Preliminary validation of ATSR sea surface temperatures near the Faeroes p 253 N94-12519

TEMPERATURE MEASURING INSTRUMENTS
The High Precision Thermostat HPT-HYDRA
p 109 N94-10124
A comparison of ATSR and shipboard radiometer SST measurements along transects between the UK and the Antarctic p 253 N94-12518

TEMPERATURE PROBES
Ocean measuring experiments using optical fiber distributed temperature sensor p 172 N94-11968

TEMPERATURE PROFILES
The electron beam furnace: A new facility for materials science research p 109 N94-10126
Variations of the temperature profile in the gradient furnace GFQ within a cylindrical sample used for directional solidification p 114 N94-10181
Effects of satellite spectral resolution and atmospheric water vapor on retrieval of near-ground temperatures
[AD-A264920] p 245 N94-11851
Remote sensing of subsurface water temperature profile and backscattering coefficient in the China Sea by Ocean Lidar (OLIDAR) p 203 N94-11970

TEMPERATURE SENSORS
A laboratory model of a hydrogen/oxygen engine for combustion and nozzle studies
[NASA-TM-106281] p 47 N94-11252

TEMPORAL DISTRIBUTION
Distribution of mineral aerosols over the North Pacific
p 204 N94-11976

TEMPORAL RESOLUTION
SAR interferometry experiments with ERS-1
p 237 N94-11735
Segmented land use classification of multitemporal ERS-1 SAR data using a majority filter
p 245 N94-12472
Mapping a dynamic playa surface using multitemporal ERS-1 SAR data: First results p 246 N94-12474
Snow and glacier investigations by ERS-1 SAR: First results p 247 N94-12481
Per-field filtering and classification of multitemporal ERS-1 SAR imagery p 247 N94-12485
Extraction of plant and soil parameters from multitemporal ERS-1 SLC data of the Freiburg test site
p 248 N94-12491
Temporal monitoring of soil moisture using ERS-1 SAR data p 249 N94-12493
TREES project: A case study on the use of multi-temporal ERS-1 SAR data and SPOT data for monitoring tropical ecosystems p 249 N94-12497

TENSILE PROPERTIES
Physical properties of injection molded liquid crystal polymers and high temperature engineering polymers [AD-A264912] p 87 N94-10508
The effect of processing on the microstructure and tensile properties of a (gamma)-TiAl based alloy [DE93-013221] p 84 N94-11488
Ceramic technology project database [DE93-012432] p 91 N94-11673

TENSILE STRENGTH
Design with high strength steel: A case of failure and its implications p 58 N94-10017
Mechanical properties of magnesium/carbon composites developed by hot pressing under medium pressure p 59 N94-10024
High temperature stability, interface bonding, and mechanical behavior in (beta)-NiAl and Ni3Al matrix composites with reinforcements modified by ion beam enhanced deposition [DE93-013977] p 398 N94-11115
Thermal testing of aluminized Mylar [NASA-TM-108414] p 89 N94-11175
Interface considerations in Al2O3/NiAl composite [NASA-CR-191167] p 66 N94-11202

TENSILE STRESS
Extensions of some guidelines for the mechanical design of coaxial compression pin seals [DE93-012385] p 177 N94-10348
Crack suppression in GaInSb buffer layers initially under tensile stress [DE93-012839] p 396 N94-10745
High temperature stability, interface bonding, and mechanical behavior in (beta)-NiAl and Ni3Al matrix composites with reinforcements modified by ion beam enhanced deposition [DE93-013977] p 398 N94-11115
Damage thresholds of fluoride multilayers at 355 nm [DE93-009523] p 90 N94-11230

TENSILE TESTS
Mechanical and fatigue properties of fibre reinforced aluminium-lithium alloy and aluminium-lithium MMC based laminates p 58 N94-10022
A method for determination of the elongational viscosity of viscoelastic fluids without body forces p 124 N94-10247

TENSORS
Regular tensor Green functions of the round waveguide [DE93-621354] p 345 N94-11036
Parameterization of subgrid-scale stress by the velocity gradient tensor p 155 N94-12286

TERMINAL BALLISTICS
Deformation mechanisms in tungsten single crystals in ballistic impact experiments [AD-A265701] p 405 N94-12563

TERMINAL GUIDANCE
Evaluation of the capacity and delay benefits of terminal air traffic control automation [AD-A265323] p 24 N94-11863

TERMINOLOGY
Abbreviations, acronyms, and initialisms frequently used by Martin Marietta Energy Systems, Incorporated [DE93-012509] p 420 N94-11369

TERNARY ALLOYS
Lattice-matched heteroepitaxy of wide gap ternary compound semiconductors p 400 N94-11441
Electronic and total energy properties of ternary and quaternary semiconductor compounds, alloys and superlattices [NASA-CR-192905] p 405 N94-12570

TERNARY SYSTEMS
Rapid thermal processing for strained-layer semiconductor devices [DE93-013754] p 396 N94-10809

TERRACES (LANDFORMS)
Descriptions and preliminary interpretations of cores recovered from the Manson Impact Structure (Iowa) p 281 N94-12032

TERRAIN
Measures for simulator evaluation of a helicopter obstacle avoidance system p 35 N94-11535
A structural origin for the cantaloupe terrain of Triton p 449 N94-12095
Venus mountain-top mineralogy: Misconceptions about pyrite as the high radar-reflecting phase p 455 N94-12129
Relation between ages and elevations of Martian channels p 472 N94-12216
Do large impact basins in the southern hemisphere of Mars control the distribution of polar structures and deposits? p 481 N94-12266
Free-air and Bouguer gravity anomalies and the Martian crustal dichotomy p 481 N94-12267

TERRAIN ANALYSIS
Sources of Na for the Io atmosphere p 455 N94-12127
Terrestrial case studies of ilmenite exploration and lunar implications p 478 N94-12247

TERRESTRIAL PLANETS
Giant impact-induced atmospheric blow-off p 435 N94-12019
Differential scaling: Implications for central structures in large lunar craters p 461 N94-12158

TERRESTRIAL RADIATION
A comparison of the visible and near infrared reflectance of hydrovolcanic palagonite tuffs and Martian weathered soils p 477 N94-12245

TEST EQUIPMENT
Dynamic tester for rotor seals and bearings [NASA-CASE-MFS-28493-1] p 33 N94-10669
Programmable logic devices [DE93-013117] p 144 N94-11479
Hot-gas-side heat transfer characteristics of subscale, plug-nozzle rocket calorimeter chamber [NASA-TP-3380] p 55 N94-12569

TEST FACILITIES
High-field conductor testing at the FENIX facility [DE93-012318] p 387 N94-10737
Aircraft material fire testing and the creation of an international working group p 21 N94-10790
Experimental approach to the physics of the high density divertor [DE93-009149] p 391 N94-11170
A facility for testing 10- to 100-kWe space power reactors [DE92-040420] p 372 N94-11296
Development of a high specific 1.5 to 5 kW thermal arcjet [NASA-CR-193133] p 47 N94-11354
An overview of the capabilities of ARA for the measurement of nozzle discharge and thrust [ARA-MEMO-378] p 55 N94-12283

TEST PILOTS
Quantitative EEG patterns of differential in-flight workload p 317 N94-11528

TEST STANDS
Operational characteristics of a 100-mA, 2-MeV radio-frequency quadrupole [DE93-014474] p 374 N94-12786

TETHERED BALLOONS
Development of a balloon-borne stabilized platform for measuring radiative flux profiles in the atmospheric boundary layer [DE93-013186] p 274 N94-10323

TETRACHLORIDES
The adsorption and surface reaction of SiCl4 on Si(100)-(2x1) [AD-A266124] p 79 N94-12538

TEXTILES
New technology for effective control of flammability in polyolefin fiber/textiles p 18 N94-10774

TEXTS
Abbreviations, acronyms, and initialisms frequently used by Martin Marietta Energy Systems, Incorporated [DE93-012509] p 420 N94-11369

TEXTURES
Texture analysis of high Tc superconductors p 399 N94-11314
Compositional and textural information from the dual inversion of visible, near and thermal infrared remotely sensed data p 258 N94-12097
The EET87513 clast N: A CM2 fragment in an HED polymict breccia p 453 N94-12117
Trace element distributions in primitive achondrites p 431 N94-12200

THAILAND
Thailand ISY activities p 37 N94-10690

THALLIUM ALLOYS
Effect of experimental procedure on pattern formation and array disorder in cellular solidification p 117 N94-10203

THEMATIC MAPPERS (LANDSAT)
Combined analysis of ERS-1 SAR and visible/infrared remote sensing data for land cover/land use mapping in a tropical zone: A case study in Guinea p 246 N94-12478

THEMATIC MAPPING
Satellite inventory of Minnesota forest resources [NASA-CR-193565] p 231 N94-11521
Basal scarp, paleoglacier, and fissure flows of Elysium Mons, Mars p 459 N94-12148
Synthesis of global thematic mapping, Venus: Geologic correlations/questions for the Magellan gravity mission p 467 N94-12194
Geoecological monitoring of an agricultural area p 248 N94-12489

THEOREM PROVING
Operator substitution [MEMO-COSOR-92-51] p 343 N94-10867
Wait-free linearization with an assertional proof [CS-9208] p 323 N94-10878

THEOREMS
Convergence theorems for a class of nonlinear maps in uniformly smooth Banach spaces [DE92-641347] p 343 N94-10531
On the doubling of hydrodynamic theorems in relativistic theory of superfluidity [DE93-617895] p 148 N94-10717

THEORETICAL PHYSICS
On parity conservation and the question of the missing, right-handed neutrino [DE93-613092] p 361 N94-10414
A version of superstring with four space-time dimensions [DE93-608196] p 412 N94-11163
Experimental and theoretical high energy physics program [DE93-013336] p 373 N94-12600

THERMAL ANALYSIS
Fire resistance and mechanical properties for phenolic prepregs p 20 N94-10786
A high specific power solar array for low to mid-power spacecraft p 51 N94-11399
Results of thermal vacuum tests for the PASP+ flight modules p 53 N94-11410

THERMAL BOUNDARY LAYER
Boundary layers along horizontal free surfaces due to combined effects of temperature and concentration gradients p 106 N94-10108

THERMAL CONDUCTIVITY
Measurement of the thermal conductivity of molten InSb in a drop shaft p 105 N94-10102
Thermophysical properties of undercooled liquid metals p 86 N94-10190
Stationary spectra of short-wave convective and magnetostatic fluctuations in a finite-pressure plasma and anomalous heat conductivity [DE93-617852] p 388 N94-10840
Experimental study of multiple droplet evaporative cooling [PB93-198463] p 149 N94-10851
Low-expansion ceramics initiative [DE93-011860] p 89 N94-11106
Progress toward atomic layer epitaxy of diamond: Diamond films grown one layer at a time [AD-A265530] p 403 N94-12010
Martian particle size based on thermal inertia corrected for elevation-dependent atmospheric properties p 430 N94-12107
Does the thermal wind exist near the Earth's core boundary? p 283 N94-12217

THERMAL CONTROL COATINGS
Experimental measurement of the plasma conductivity of Z93 and Z93P thermal control paint [NASA-TM-106284] p 43 N94-10756
Vacuum stability requirements of polymeric material for spacecraft application [NASA-TM-109216] p 91 N94-11350

THERMAL CYCLING TESTS
Transport of heat and mass in near-critical fluids p 122 N94-10230
TAB interconnects for space concentrator solar cell arrays p 51 N94-11400

THERMAL DEGRADATION
Advanced diagnostics for in situ measurement of particle formation and deposition in thermally stressed jet fuels [DE93-009798] p 98 N94-11366
Advanced thermally stable coal-derived jet fuels: Compositional factors affecting thermal degradation of jet fuels [AD-A265842] p 99 N94-12282

THERMAL DIFFUSION
Marangoni Benard instabilities in liquid mixtures with Soret effect p 119 N94-10215
Progress in p(+)n InP solar cells fabricated by thermal diffusion p 48 N94-11384
Electrochemical characterization of p(+)n and n(+)p diffused InP structures p 49 N94-11385
Micro-zoning in minerals of a Landes silicate inclusion p 432 N94-12231

THERMAL DISSOCIATION
Tribological characteristics of hot-pressed self-lubricating composites [NAL-TR-1160] p 66 N94-10858

THERMAL EMISSION
Galileo/NIMS near-infrared thermal imagery of the surface of Venus p 457 N94-12139
Thermal-infrared emission spectroscopy of natural surfaces: Application to coated surfaces p 81 N94-12156

THERMAL ENVIRONMENTS
The spectral effects of subsolidus reduction of olivine and pyroxene p 81 N94-12110

THERMAL EXPANSION
Low cost and thermally stable sandwich design for FIRST p 57 N94-10009

Sensing glass transitions in thin polymer films on acoustic wave microsensors
[DE93-010805] p 87 N94-10295
Method for producing a hybridization of detector array and integrated circuit for readout
[NASA-CASE-NPO-18062-1-CU] p 141 N94-10656
Ceramic technology project database
[DE93-012432] p 91 N94-11673

THERMAL INSULATION
Material advances for lightweight TPS
p 62 N94-10049
Vectra insulative support structures within spacecraft
p 62 N94-10050
Polyimide foam insulation systems: A major weight reduction and improvement in fire resistance of sidewall systems p 17 N94-10769
A new FR water resistant acoustic insulation material for aircraft p 18 N94-10773

THERMAL MAPPING
Compositional and textural information from the dual inversion of visible, near and thermal infrared remotely sensed data p 258 N94-12097
Martian particle size based on thermal inertia corrected for elevation-dependent atmospheric properties
p 430 N94-12107
Galileo/NIMS near-infrared thermal imagery of the surface of Venus p 457 N94-12139
A simple model of clastic sediments on Mars
p 460 N94-12155

THERMAL NEUTRONS
Possibility of a crossed-beam experiment involving slow-neutron capture by unstable nuclei rapid-process-tron
[DE93-754288] p 363 N94-10720
The multiplicity spectra of the (169)Tm(n, gamma) reaction
[DE93-617733] p 364 N94-10835
Analytic expression for epithermal neutron spectra amplitudes as a function of water content
p 473 N94-12227

THERMAL PLASMAS
Momentum and heat frictions between fast ions and thermal plasma species
[DE93-771240] p 390 N94-11149
An ellipsometry investigation of nucleation and growth of electron cyclotron resonance plasma deposited silicon films
[AD-A265037] p 401 N94-11651

THERMAL PROTECTION
On the mechanical development of the Flexible External Insulation (FEI) for Hermes spaceplane
p 62 N94-10048
Material advances for lightweight TPS
p 62 N94-10049
Debris/ice/TPS assessment and integrated photographic analysis for Shuttle Mission STS-57
[NASA-TM-107562] p 40 N94-10805
Space Storable Rocket Technology program (SSRT). Option 1 program
[NASA-CR-191171] p 46 N94-10938

THERMAL RADIATION
In-reactor testing of the closed cycle gas core reactor: The Nuclear Light Bulb concept
[DE93-004053] p 370 N94-10149
The heat transfer by radiation between two media
[DE93-617820] p 149 N94-10838
The Langevin's approach to the statistical theory of bounded plasma
[DE93-617842] p 388 N94-10839
Combustion chamber analysis code
[NASA-CR-192585] p 46 N94-10934

THERMAL REACTORS
A critical assembly designed to measure neutronic benchmarks in support of the Space Nuclear Thermal Propulsion program
[DE92-040974] p 371 N94-10529

THERMAL RESISTANCE
Advanced Materials for Lightweight Structures
[ESA-SP-336] p 56 N94-10001
Protective coatings for high-temperature polymer matrix composites
[NASA-TM-106276] p 74 N94-12431

THERMAL SHOCK
Potential change in flaw geometry during pressurized-thermal-shock transients
[DE93-009709] p 184 N94-10288
Assessment of damage in ceramics and ceramic matrix composites using ultrasonic techniques
[NASA-TM-106121] p 67 N94-11237

THERMAL STABILITY
An approach to high precision antenna structures by a CFRP core sandwich concept p 57 N94-10008
A wide-band fiber optic frequency distribution system employing thermally controlled phase compensation
p 355 N94-10995
Thermal stability of sealants for military aircraft: Modification of polysulfide prepolymers with ether and thioether monomers
[AD-A264079] p 89 N94-11107
High temperature stability, interface bonding, and mechanical behavior in (beta)-NiAl and Ni3Al matrix composites with reinforcements modified by ion beam enhanced deposition
[DE93-013977] p 398 N94-11115
Thermal testing of aluminized Mylar
[NASA-TM-108414] p 89 N94-11175
Vacuum stability requirements of polymeric material for spacecraft application
[NASA-TM-109216] p 91 N94-11350
Processing and properties of coated HPZ fiber reinforced glass-ceramic matrix composites
[AD-A265177] p 92 N94-11876
The stability of hibonite and other aluminous phases in silicate melts: Implications for the origin of hibonite-bearing inclusions p 80 N94-12052
A novel test method for fuel thermal stability
[AD-A265853] p 99 N94-12275
Advanced thermally stable coal-derived jet fuels: Compositional factors affecting thermal degradation of jet fuels
[AD-A265842] p 99 N94-12282
Liquid Cooled Heat Sink with through Vias (LCHS)
[AD-A266008] p 73 N94-12344
Photogenerated base in polymer imaging. Synthesis and photopatterning of poly(2-cyano-2-(p-vinylphenyl) butanoic acid)
[AD-A265288] p 95 N94-12585

THERMAL STRESSES
Arcjet exploratory tests of ARC optical window design for the AFE vehicle
[NASA-CR-192655] p 34 N94-10930
Advanced diagnostics for in situ measurement of particle formation and deposition in thermally stressed jet fuels
[DE93-009798] p 98 N94-11366
Instantaneous engine frictional torque: Its components and piston assembly friction
[DE93-011639] p 182 N94-11625
A novel test method for fuel thermal stability
[AD-A265853] p 99 N94-12275
Analytical models for describing the mechanical behavior of fiber reinforced composites
[AD-A265906] p 74 N94-12347

THERMAL VACUUM TESTS
Results of thermal vacuum tests for the PASP+ flight modules p 53 N94-11410

THERMIONIC CONVERTERS
TFE verification program
[DE93-009609] p 373 N94-11694

THERMIONIC DIODES
Collective acceleration of ions in near-anode plasma of a strong-current relativistic diode
[DE93-620977] p 387 N94-10541

THERMIONIC EMITTERS
TFE verification program
[DE93-009609] p 373 N94-11694

THERMIONIC POWER GENERATION
The 40 kWe S-PRIME Thermionic Design and Technology Demonstration Program
[DE93-004738] p 40 N94-10147

THERMOCHEMISTRY
Technical Update: Johnson Space Center system using a solid electrolytic cell in a remote location to measure oxygen fugacities in CO/CO2 controlled-atmosphere furnaces
[NASA-TM-104774] p 423 N94-11183
Chemical Vapor Deposition of Refractory Metals and Ceramics 2. Materials Research Society Symposium proceedings
[AD-A265072] p 92 N94-11866
Crystal-chemistry and partitioning of REE in whitlockite
p 408 N94-12174
The rate of chemical weathering of pyrite on the surface of Venus p 477 N94-12246

THERMOCLINES
The subduction experiment. Cruise report, R/V Oceanus, cruise number 250 legs 1 and 2. Subduction 2 mooring deployment and recovery cruise, 25 January-26 February 1992
[AD-A264922] p 289 N94-11853
On an upwelling front, propagation of upwelling and vertical velocity in the eastern Arabian Sea during monsoon, 1987 p 206 N94-11987
The Pacific Subarctic Frontal Zone: Structure and dynamics p 223 N94-12731
Generation of internal waves near the shelf boundary
p 229 N94-12763

THERMOCOUPLES
High temperature processing and diagnostic technologies for microgravity applications
p 110 N94-10130

THERMODYNAMIC CYCLES
Study on various cryogenic refrigeration cycles using all purpose refrigerators p 130 N94-11839

THERMODYNAMIC EFFICIENCY
Space Life Support Engineering Program
[NASA-CR-193474] p 316 N94-12365
Systems analysis of a closed loop ECLSS using the ASPEN simulation tool. Thermodynamic efficiency analysis of ECLSS components p 316 N94-12366
An estimate of the second law thermodynamic efficiency of the various units comprising an Environmental Control and Life Support System (ECLSS) p 317 N94-12369

THERMODYNAMIC EQUILIBRIUM
Rapid thermal processing for strained-layer semiconductor devices
[DE93-013754] p 396 N94-10809
Stability and dynamics of spatio-temporal structures
[DE93-011374] p 401 N94-11610
Thermodynamics of lunar ilmenite reduction
p 415 N94-12028

THERMODYNAMIC PROPERTIES
LAMINV: A computer code for creating laminates having prescribed properties p 65 N94-10069
Experimental approach to non-contact calorimetry in space p 112 N94-10143
On thermodynamic properties of heavy fermion systems in magnetic field
[DE93-613819] p 409 N94-10403
Thermodynamic model of air in chemical equilibrium
p 7 N94-10448
Exergy decrease in shock waves and boundary layers of space launch vehicles
[AD-A265272] p 42 N94-10493
The effect of pressure and quadrupolar interactions on the nematic-isotropic transition properties: Numerical results for a system of prolate ellipsoids including second and fourth rank orientational order parameters
[DE93-613540] p 410 N94-10536
Primaset (tm): A safer material for aircraft interior applications p 18 N94-10772
Level 3 material characterization of NARC HRPF, HRHU, HRHF, and HRPU
[NASA-CR-192579] p 65 N94-10812
Variability of wind stress, and sensible and latent heat flux in the North Atlantic during SEASAT
p 194 N94-11918
Evaluation of ECMWF latent heat flux in TOGA CD-ROM p 195 N94-11921
Thermodynamics of lunar ilmenite reduction
p 415 N94-12028
Variability of the mixed layer depth in the North Pacific Ocean as calculated by a 3-D semi-analytical mixed layer remote sensing model p 221 N94-12718
Laser photoheterodyne interferometers for oceanographic investigations p 177 N94-12732

THERMODYNAMICS
Coupled thermovibrational and thermocapillary convection in liquid bridge (floating zone system)
p 101 N94-10082
A lattice gas model for enzyme kinetics with next-nearest neighbor interactions
[DE93-613026] p 410 N94-10631
Similarity of the leading contributions to the self-energy and the thermodynamics in two- and three-dimensional Fermi Liquids
[DE93-012673] p 412 N94-11162
A modeling investigation of thermal and strain induced recovery and nonlinear hardening in potential based viscoplasticity
[NASA-TM-106122] p 188 N94-11482
Chaos, entropy, and reversibility: A simple example
p 31 N94-11495
Proposed framework for thermomechanical life modeling of metal matrix composites
[NASA-TP-3320] p 74 N94-12449
The thermodynamics of the nonlinear shear flows
p 169 N94-12728

THERMOELECTRIC POWER GENERATION
High efficiency direct thermal to electric energy conversion from radioisotope decay using selective emitters and spectrally tuned solar cells
[NASA-TM-106227] p 47 N94-11307

THERMOGRAPHY
Thermal flux measurements in hypersonic flows: A review p 5 N94-10438
Experimental study of multiple droplet evaporative cooling
[PB93-198463] p 149 N94-10851
Thermographic properties of eight blue-emitting phosphors
[DE93-011459] p 78 N94-11622

THERMOGRAVIMETRY
Analytical method for water vapor collection and analysis in aircraft cabin fires
[DOT/FAA/CT-TN93/33] p 22 N94-12575

THERMOLUMINESCENCE
Meteorites from recent amor-type orbits p 429 N94-12059
Natural thermoluminescence profiles in lunar cores and implications for meteorites p 443 N94-12060
Diamond thermoluminescence properties of different chondrites p 433 N94-12252

THERMOMETERS
Preliminary results of the comparison of ATSR measurements with in situ sea temperatures [DE93-013399] p 287 N94-10517
Trouble areas in the IRT measurement of the Earth surface temperature p 193 N94-11910

THERMONUCLEAR REACTIONS
High heat flux components and plasma surface interactions [DE93-008786] p 385 N94-10253

THERMOPHILES
Conversion of acetic acid to methane by thermophiles [DE93-014433] p 300 N94-10652

THERMOPLASTIC RESINS
Universal adjustable mould for antenna reflectors p 59 N94-10027
Deformation mechanisms of continuous fibre-reinforced thermoplastic composites during manufacturing: A probabilistic approach p 60 N94-10030
Heat analysis of thermoplastic components during the initial stages of manufacturing: A probabilistic approach p 60 N94-10031
Cost effectiveness of structural applications of fibre reinforced thermoplastics p 60 N94-10032
Application of advanced thermoplastics p 60 N94-10033
Low cost thermoplastic composites for structural applications: Design concepts using new materials and processes p 60 N94-10034
Tape winding of thermoplastic composites p 60 N94-10035
Applications of continuous fiber reinforced thermoplastics in aircraft interiors p 18 N94-10775
Uralane (tm) 5774-A/B: Ciba-Geigy's advanced urethane adhesive for the aircraft industry p 18 N94-10777
Fire-resistant hydrolytically stable poly(arylene phosphine oxide) material systems p 19 N94-10780
Dry in-line thermoplastic matrix impregnation, phase 1 [AD-A265016] p 67 N94-11221

THERMOPLASTICITY
New thermoplastic laminating adhesives for the aircraft industry with low heat release and low smoke emission p 17 N94-10767
Crystallinity and dielectric properties of PEEK, a thermoplastic poly(ether ether ketone) [AD-A266027] p 91 N94-11487

THERMOREGULATION
Modifications to an interactive model of the human body during exercise: With special emphasis on thermoregulation p 317 N94-12368

THERMOSETTING RESINS
Ceramics formed by pyrolysis of either linear or thermosetting carborane (siloxane or silane) acetylene based precursor polymers [AD-D015747] p 93 N94-12330
Synthesis and polymerization of oligomeric multiple aromatic ether-containing phthalonitriles [AD-D015729] p 94 N94-12399

THERMOSTATS
The High Precision Thermostat HPT-HYDRA p 109 N94-10124

THICKNESS
Material removal processes: Engineering mechanics consideration [DE93-010733] p 126 N94-10293
Temperature effects on failure thickness and deflagration-to-detonation transition in PBX 9502 and TATB [DE93-010742] p 97 N94-10294
Radiation considerations for interplanetary missions p 45 N94-11559
Dielectric breakdown and its influence on ignition [AD-A264925] p 78 N94-11855

THIN FILMS
Invariance of the mobility edge in anodic titanium oxides [DE92-642136] p 394 N94-10281
Sensing glass transitions in thin polymer films on acoustic wave microsensors [DE93-010805] p 87 N94-10295
Thin-film edge field emitter device and method of manufacture therefore [AD-D015764] p 140 N94-10377
Crack suppression in GaInSb buffer layers initially under tensile stress [DE93-012839] p 396 N94-10745
Determination of concentration profiles at interfaces and surfaces of partially miscible polymer blends [DE93-013140] p 89 N94-11007
Characterization of the Si/SiO2 interfere morphology from quantum oscillations in Fowler-Nordheim tunneling currents [AD-A265149] p 143 N94-11160
Materials for adaptive structural acoustic control, volume 3 [AD-A264621] p 358 N94-11262
Structural development in ceramic precursor sols and gels [AD-A264354] p 90 N94-11281
Thin film preparation and interfacial reaction study of solid oxide fuel cell materials p 263 N94-11313
Tribological characteristics of sputtered Au/Cr films on alumina substrates at elevated temperatures [NASA-TM-106078] p 55 N94-11362
Investigation of the radiation resistance of triple-junction a-Si:H alloy solar cells irradiated with 1.00 MeV protons p 50 N94-11391
Results of some initial space qualification testing on triple junction a-Si and CuInSe2 thin film solar cells p 50 N94-11392
Flexible polycrystalline thin-film photovoltaics for space applications p 50 N94-11393
Thin film solar cell workshop p 54 N94-11415
Remote plasma enhanced chemical vapor deposition of GaP with in situ generation of phosphine precursors p 399 N94-11440
In situ XANES studies of the passive film on Fe and Fe-26Cr [DE93-010869] p 84 N94-11459
Wide Band-Gap Semiconductors. 1991 Materials Rese arch Society Symposium proceedings [AD-A263418] p 401 N94-11515
Chemical Vapor Deposition of Refractory Metals and Ceramics 2. Materials Research Society Symposium proceedings [AD-A265072] p 92 N94-11866
Applications of in-situ ellipsometry to microwave electron cyclotron resonance plasma processes [AD-A265197] p 373 N94-11880
NRL review for 1993 [AD-A265666] p 497 N94-12334
Ballistic electron transport studies using BEEM [AD-A266029] p 369 N94-12395
Multicomponent and multilayered thin films for advanced microtechnologies: Techniques, fundamentals, and devices [AD-A265685] p 405 N94-12442
In-situ crystallization of silicate glass films deposited on alpha- Al2O3 [DE93-012969] p 95 N94-12596

THIN PLATES
Boundary element method for eigenvalue problems of thin plates [ITN-93-85199] p 343 N94-10392

THIN WALLED SHELLS
Distortions and stresses in thin shells due to anisotropic thermal expansion p 57 N94-10014

THIN WALLS
Perforated plates for thin-walled structures p 63 N94-10056

THIN WINGS
Simulated wake characteristics of tapered annular wings by a discrete vortex method [NAL-TR-1156] p 13 N94-10855
Simulated and experimental aerodynamic characteristics of tapered annular wings [NAL-TR-1157] p 13 N94-10856

THIOUREAS
Second and third order nonlinear optical properties of crystalline inorganic/organic complexes [DE93-011883] p 173 N94-10755

THOMAS-FERMI MODEL
Radiative properties of strongly magnetized plasmas [DE93-014098] p 389 N94-11118

THOMSON SCATTERING
Optimization of a CO2 laser Thomson scattering alpha particle diagnostic [DE93-012782] p 173 N94-10160

THORAX
Hormonal regulation of fluid and electrolyte metabolism during periods of headward fluid shifts p 311 N94-12005

THORIUM
Th-230 - U-238 series disequilibrium of the Olkaria rhyolites Gregory Rift Valley, Kenya: Residence times p 281 N94-12076

THORIUM ISOTOPES
LEW88516 and SNC meteorites p 430 N94-12150
The Th and U abundances in chondritic meteorites p 430 N94-12151

THREE BODY PROBLEM
Three-nucleon problem with phase equivalent potentials [DE93-617731] p 363 N94-10722
On the depletion in the outer asteroid belt and the structure of the 4 to 3 mean motion resonance p 426 N94-11596
Orbital simulations of satellite escape/capture and the origin of satellites such as Triton p 429 N94-12057

THREE DIMENSIONAL BOUNDARY LAYER
On nonlinear Tollmien-Schlichting/vortex interaction in three-dimensional boundary layers [NASA-TM-106184] p 152 N94-11377
Experiments on near-wall structure of three-dimensional boundary layers p 159 N94-12309
Criteria for onset of boundary-layer transition on spinning bodies p 164 N94-12620
Curvature effects in three-dimensional boundary layers p 164 N94-12623

THREE DIMENSIONAL FLOW
Three-dimensional hypersonic rarefied flow calculations using direct simulation Monte Carlo method p 7 N94-10449
Development of a Delaunay-based adaption scheme with applications to complex three-dimensional rotational flows p 149 N94-10824
Theoretical investigation of 3-D shock wave turbulent boundary layer interactions [AD-A265275] p 150 N94-11014
KIVA-3: A KIVA program with block-structured mesh for complex geometries [DE93-011986] p 77 N94-11249
Viscous analysis of three-dimensional rotor flows using a multigrid method [NASA-TM-106266] p 152 N94-11481
The flow structure around a cylindrical pier for the flow of transcritical Reynolds number p 169 N94-11944
Numerical simulation using vorticity-vector potential formulation p 157 N94-12297
Reynolds stress closure modeling in wall-bounded flows p 157 N94-12298
Experiments on near-wall structure of three-dimensional boundary layers p 159 N94-12309
The three-dimensional evolution of a plane wake p 159 N94-12310
Towards a cell-vertex Navier-Stokes algorithm for three-dimensional structured/unstructured meshes [ARA-MEMO-366] p 161 N94-12437
Simultaneous 3D turbulent large-scale structures in a flood flow by multi-channels measuring system p 165 N94-12624
VIB3D: Method for calculating 3-D unsteady flow through turbomachinery blades [CUED/A-TURBO/TR.128] p 166 N94-12777
VIB2D: Quasi 3-D unsteady viscous flow method for blade flutter calculation [CUED/A-TURBO/TR.129] p 166 N94-12779

THREE DIMENSIONAL MODELS
Transient three-dimensional numerical simulation of Marangoni flow in a liquid column under microgravity p 101 N94-10079
Calculation of the effects of magnetic field damping in fluid flow: Comparison of magnetohydrodynamic models of different complexity p 103 N94-10089
Venus resurfacing rates: Constraints provided by 3-D Monte Carlo simulations p 453 N94-12119
Engineering solid-state materials. Strategies for modeling and packing control of molecular assemblies into 3-D networks [AD-A265291] p 404 N94-12438

THRESHOLDS (PERCEPTION)
Computer software and hardware to determine contrast sensitivity using three methods: Tracking, limits, and constant stimuli [AD-A265168] p 324 N94-11099

THRUST BEARINGS
Improvement of azimuthal homogeneity in permanent-magnet bearing rotors [DE93-009954] p 144 N94-11607

THRUST CHAMBERS
Space Storable Rocket Technology program (SSRT). Option 1 program [NASA-CR-191171] p 46 N94-10938

THRUST MEASUREMENT
Characterization of in-flight performance of ion propulsion systems [NASA-TM-106283] p 46 N94-10761
An overview of the capabilities of ARA for the measurement of nozzle discharge and thrust [ARA-MEMO-378] p 55 N94-12283

THRUST REVERSAL
Turbulence modeling for thrust reverser flow field prediction methods [AD-A266139] p 154 N94-11641

THRUST VECTOR CONTROL
Static internal performance of a single expansion ramp nozzle with multiaxis thrust vectoring capability [NASA-TM-4450] p 12 N94-10675
AD100/ADSIM, ACSL, and MATLAB output comparisons using frequency-response analysis [DE93-009640] p 47 N94-11122
Adaptive reconfigurable flight controls for high angle of attack aircraft agility p 32 N94-11502

THRUST-WEIGHT RATIO
Static internal performance of a single expansion ramp nozzle with multiaxis thrust vectoring capability [NASA-TM-4450] p 12 N94-10675

THRUSTORS
Arcjet space thrusters [NASA-CR-193191] p 46 N94-10700
A laboratory model of a hydrogen/oxygen engine for combustion and nozzle studies [NASA-TM-106281] p 47 N94-11252

THULIUM ISOTOPES
The multiplicity spectra of the (169)Tm(n, gamma) reaction [DE93-617733] p 364 N94-10835

THYRISTORS
A study of DC-DC converters with MCTs for arcjet power supplies [NASA-CR-193457] p 142 N94-10931

TIBET
Analysis of gravity, magnetic, and seismic reflection data from Tibet and neighboring regions of China [NASA-CR-193405] p 278 N94-11886

TIDAL WAVES
Generation of internal waves near the shelf boundary p 229 N94-12763
Experimental and theoretical investigation of undular bore formation upstream the bank p 229 N94-12764

TIDES
A stochastic-deterministic approach as an alternative to classical cross-over techniques in small ocean basins p 242 N94-11767
Experimental and theoretical investigation of undular bore formation upstream the bank p 229 N94-12764

TILES
Toxicity study of dimethylethoxysilane (DMSES), the waterproofing agent for the Orbiter heat protective system p 318 N94-11554

TILT ROTOR AIRCRAFT
Navier-Stokes flowfield computation of wing/rotor interaction for a tilt rotor aircraft in hover [NASA-CR-4532] p 13 N94-10758

TILTING ROTORS
Navier-Stokes flowfield computation of wing/rotor interaction for a tilt rotor aircraft in hover [NASA-CR-4532] p 13 N94-10758

TIMBER IDENTIFICATION
Properties of spectral reflectance of crown and crown structure of mangrove species in Okinawa p 218 N94-12700

TIME
The 24th Annual Precise Time and Time Interval (PTTI) Applications and Planning Meeting [NASA-CP-3218] p 350 N94-10963

TIME DEPENDENCE
Coherent states and uncertainty relations for the damped harmonic oscillator with time-dependent frequency p 380 N94-10611
The angular structure of second harmonic emission from laser-produced plasmas irradiated at moderate intensity [DE93-013102] p 389 N94-11114
The effects of an aggressive environment on the subcritical crack growth of a continuous-fiber ceramic composite [DE93-011690] p 73 N94-11612
Parametric study of diffusion-enhancement networks for spatiotemporal grouping in real-time artificial vision [AD-A265065] p 331 N94-11652
Large eddy simulations of time-dependent and buoyancy-driven channel flows p 155 N94-12287

TIME LAG
Plans to improve the experimental limit in the comparison of the east-west and west-east one-way light propagation times on the rotating earth p 351 N94-10971
Performances of a date dissemination code on telephone lines using commercial modems p 139 N94-10984
Time signal distribution in communication networks based on synchronous digital hierarchy p 139 N94-10989
Comments on possible causes of recent global warming [DE93-010501] p 272 N94-12592

TIME MEASUREMENT
The 24th Annual Precise Time and Time Interval (PTTI) Applications and Planning Meeting [NASA-CP-3218] p 350 N94-10963
The time keeping system for GPS block IIR p 24 N94-10964
Progress on GPS standardization p 24 N94-10965
Comparison of GPS and GLONASS common-view time transfers p 24 N94-10967
Pulsar astrometry by using VLBI (PSR0329 between Kashima 26mPhi and Usuda 64mPhi) p 351 N94-10968
An ensemble pulsar time p 351 N94-10969
Experimental comparison of time synchronization techniques by means of light signals and clock transport on the rotating earth p 351 N94-10970
LASSO observations at McDonald and OCA/CERGA: A preliminary analysis p 352 N94-10972
MIL-STDS and PTTI: What's available and what needs to be done p 352 N94-10973
Possible applications of atomic frequency standards with an internal high resolution digital synthesizer p 353 N94-10979
Development of a cryogenic hydrogen maser at the NPL p 176 N94-10982
Performances of a date dissemination code on telephone lines using commercial modems p 139 N94-10984
TimeSet: A computer program that accesses five atomic time services on two continents p 334 N94-10985
RighTime: A real time clock correcting program for MS-DOS-based computer systems p 334 N94-10986
Measurement methods and algorithms for comparison of local and remote clocks p 354 N94-10987
Advances in time-scale algorithms p 334 N94-10988
Time signal distribution in communication networks based on synchronous digital hierarchy p 139 N94-10989
Synopsis of timing measurement techniques used in telecommunications p 139 N94-10990
Analysis of the eastern range multiplexed fiber optic IRIG B120 distribution system p 139 N94-10996
A new method of time difference measurement: The time difference method by dual phase coincidence points detection p 357 N94-11002
Confidence of the three-point estimator of frequency drift p 357 N94-11003
Rhenium-osmium isotope systematics of Group 2A and Group 4A iron meteorites p 431 N94-12182
An optoelectronic graphics display processor [AD-A266011] p 171 N94-12391

TIME MEASURING INSTRUMENTS
A new method of time difference measurement: The time difference method by dual phase coincidence points detection p 357 N94-11002

TIME OF FLIGHT SPECTROMETERS
Measurement of polycyclic aromatic hydrocarbon (PAHs) in interplanetary dust particles p 431 N94-12167

TIME SERIES ANALYSIS
Estimation of critical values and vibration characteristics on supersonic delta wings. Part 1: On-line time series analysis of stationary random response [NAL-TR-1153] p 2 N94-10363
Detecting non-linearities in stationary time series [W-9223] p 344 N94-10906
Chaotic time series analysis p 31 N94-11490
Advective surface velocity in the north west Pacific derived from NOAA AVHRR images p 222 N94-12721
Study of the admixture diffusion in the sea using remote techniques p 228 N94-12759

TIME SIGNALS
A precise GPS-based time and frequency system p 353 N94-10978
TimeSet: A computer program that accesses five atomic time services on two continents p 334 N94-10985
Time signal distribution in communication networks based on synchronous digital hierarchy p 139 N94-10989
Synopsis of timing measurement techniques used in telecommunications p 139 N94-10990
Performance of low-cost commercial fiber-optic transceivers for reference frequency distribution p 355 N94-10993
Analysis of the eastern range multiplexed fiber optic IRIG B120 distribution system p 139 N94-10996
Estimating the instabilities of N clocks by means of comparison measurements p 356 N94-10997

TIME TEMPERATURE PARAMETER
Time-temperature shift factors for gun propellants [AD-A264979] p 97 N94-10489
Advanced diagnostics for in situ measurement of particle formation and deposition in thermally stressed jet fuels [DE93-009798] p 98 N94-11366

TIMING DEVICES
Experimental comparison of time synchronization techniques by means of light signals and clock transport on the rotating earth p 351 N94-10970
Disciplined rubidium oscillator with GPS selective availability p 353 N94-10977

TIMOSHENKO BEAMS
Control of large space structures with varying configuration [AD-A265764] p 44 N94-12387

TIN ALLOYS
Solidification of undercooled Ni-32.5 wt percent Sn eutectic alloy p 86 N94-10194

TIROS N SERIES SATELLITES
TOVS soundings: Impact on the synoptic analysis over the south and southeast regions of Brazil from March 18 to March 19, 1991 [INPE-5497-TDI/512] p 230 N94-11179

TISSUES (BIOLOGY)
Research on acoustic coupling to electromagnetic pulses in tissue [AD-A264764] p 301 N94-11583
Momentum induced by laser-tissue interaction [DE93-010737] p 301 N94-11667

TITANATES
Grain boundaries in complex oxides [DE93-013986] p 398 N94-11012

TITANIUM ALLOYS
Hydrogen partitioning and transport in titanium aluminides [NASA-CR-194117] p 76 N94-10713
Titanium alloys milling assistance by high pressure lubricoolant jet [DE93-013302] p 82 N94-11008

TITANIUM CARBIDES
The reaction between titanium carbide and aluminium carbide in liquid aluminium; a microgravity study p 123 N94-10238

TITANIUM COMPOUNDS
Hydrogen partitioning and transport in titanium aluminides [NASA-CR-194117] p 76 N94-10713

TITANIUM OXIDES
Grain boundaries in complex oxides [DE93-013986] p 398 N94-11012

TOKAMAK DEVICES
Efficiency of fast wave current drive for a weakly relativistic plasma [DE93-012775] p 385 N94-10159
Optimization of a CO2 laser Thomson scattering alpha particle diagnostic [DE93-012782] p 173 N94-10160
Physics and modelling of scrape-off layer transport [DE93-010510] p 385 N94-10289
Transport mechanisms acting in toroidal devices: A theoretician's view [DE93-013463] p 385 N94-10310
Texas experimental tokamak [DE93-013377] p 386 N94-10321
A flexible modelling software for data acquisition [DE93-612915] p 322 N94-10484
Characterization of high-power RF structures using time-domain field codes [DE93-013416] p 132 N94-10518
Optimization of break-down conditions in tokamak TOTUS [DE93-617863] p 386 N94-10524
Looking beyond ITER: Toroidal concept improvement [DE93-012762] p 388 N94-10744
Reversed-field pinch studies in the Madison Symmetric Torus [DE93-013464] p 388 N94-10747
Kinetic approach to long wave length modes in rotating plasmas [DE93-771286] p 388 N94-10807
Possibilities of magnetic diagnostics in stellarators [DE93-621608] p 389 N94-11092
Physics of tokamak scrape-off layer confinement [DE93-011949] p 390 N94-11125
Gyrosheath near the tokamak edge [DE93-012191] p 390 N94-11142
Studies on the parametric decay of waves in fusion plasmas [DE93-621659] p 390 N94-11148
Intense neutron sources for fusion materials studies [DE93-009782] p 391 N94-11171
The role of plasma rotation on MHD instabilities in tokamaks [DE93-013486] p 393 N94-11512
Helium transport scaling law studies [DE93-013487] p 393 N94-11513
Results from the D3-D advanced divertor program [DE93-015472] p 393 N94-11514
Initial assessment of lower hybrid current drive in D3-D [DE93-013310] p 394 N94-12370
An emerging understanding of H-mode discharges in tokamaks [DE93-012829] p 394 N94-12544

Statistical approach to LHCD modeling using the wave kinetic equation [DE93-012831] p 394 N94-12545

TOLLMIEN-SCHLICHTING WAVES

On nonlinear Tollmien-Schlichting/vortex interaction in three-dimensional boundary layers [NASA-TM-106184] p 152 N94-11377

TOMOGRAPHY

Real-time tomography mooring [AD-A264923] p 289 N94-11854

TOPEX

Topex orbit determination using GPS tracking system p 38 N94-10359

Topex/Poseidon: A United States/France mission. Oceanography from space: The oceans and climate [NASA-TM-108253] p 43 N94-10699

TOPOGRAPHY

New x ray scanning topographic approaches to nondestructive evaluation of composites p 61 N94-10039

First results for the simultaneous estimation of the geoid and the sea surface topography by ERS-1 altimeter data p 241 N94-11765

A stochastic-deterministic approach as an alternative to classical cross-over techniques in small ocean basins p 242 N94-11767

Analysis of gravity, magnetic, and seismic reflection data from Tibet and neighboring regions of China [NASA-CR-193405] p 278 N94-11886

Lineament analysis and tectonic interpretation for the Tharsis region p 437 N94-12031

Spectral analysis of the gravity and topography of Mars p 444 N94-12065

Venus' center of mass - center of figure displacement and implications p 444 N94-12067

A structural and petrographic investigation of the pretoria saltpan impact structure p 282 N94-12102

Flexure and the role of inplane force around coronae on Venus p 452 N94-12112

Can weak crust explain the correlation of geoid and topography on Venus? p 453 N94-12118

Landscape and geomorphic survey of Zhamanshin area, Northern Kazakhstan: Preliminary report on 1992 field trip data p 282 N94-12123

An ancient inner lake in Maadim Vallis p 456 N94-12133

Geology and surface characteristics of Bell Regio, Venus p 457 N94-12136

Differential scaling: Implications for central structures in large lunar craters p 461 N94-12158

Using lunar sounder imagery to distinguish surface from subsurface reflectors in lunar highlands areas p 464 N94-12179

Morphotectonics of Venus p 478 N94-12248

Transmantle flux tectonics p 283 N94-12249

New Mars free-air and Bouguer gravity: Correlation with topography, geology and large impact basins p 481 N94-12268

Interdisciplinary scientist participation in the Phobos mission [NASA-CR-193715] p 482 N94-12446

ERS-1 altimetry of inland water and land p 246 N94-12475

Preliminary studies on the application of ERS-1 data to topographic mapping p 246 N94-12476

The TREES project: Pre-processing and generation of terrain data for inclusion in an ERS-1 SAR classification scheme p 249 N94-12496

Topography of the Western Mediterranean from the ERS-1 altimeter p 255 N94-12531

TOPOLOGY

On local frame fields and fermion dynamics in space with nontrivial topologies [DE93-617657] p 349 N94-10548

Quantum mechanical effects of topological origin p 378 N94-10594

On the possible unobservability of the Wu-Yang phase factor in curved space [DE93-617645] p 411 N94-10831

The Lip microbundle representation theorem [DE93-619671] p 346 N94-11348

TOROIDAL PLASMAS

Reversed-field pinch studies in the Madison Symmetric Torus [DE93-013464] p 388 N94-10747

Macroscopic behaviour and discrete dynamo of RFP plasma in high theta discharge [DE93-771408] p 392 N94-11239

Conversion of the four-strap array in D3-D to a tunable traveling wave antenna [DE93-012085] p 137 N94-11453

TORQUE

Instantaneous engine frictional torque: Its components and piston assembly friction [DE93-011639] p 182 N94-11625

TORSION

Damping measurements for ultra-high carbon steel/brass laminates [DE93-011886] p 82 N94-11076

TORSIONAL VIBRATION

Payload sensitivity in coupled bending and torsional vibrations in flexible beams [MEMO-1102] p 184 N94-10161

TOTAL QUALITY MANAGEMENT

The 17th Transducer Workshop [AD-A265526] p 141 N94-10509

Engineering performance metrics [DE93-012084] p 128 N94-11028

The role of metrics and measurements in a software intensive total quality management environment p 329 N94-11428

Development and application of an acceptance testing model p 330 N94-11432

Analyzing human errors in flight mission operations p 314 N94-11534

TOUGHNESS

Damping measurements for ultra-high carbon steel/brass laminates [DE93-011886] p 82 N94-11076

Processing and properties of coated HPZ fiber reinforced glass-ceramic matrix composites [AD-A265177] p 92 N94-11876

TOWING

Calibration of anemometers at low speed by means of towing carriage p 164 N94-12619

TOXICITY

Toxic chemical release inventory reporting Form R and instructions. Revised 1992 version. Section 313 of the Emergency Planning and Community Right-to-Know Act [PB93-194140] p 264 N94-10836

Toxicity study of dimethylethoxysilane (DMSES), the waterproofing agent for the Orbiter heat protective system p 318 N94-11554

A combustion products analyzer for contingency use during thermodegradation events on spacecraft p 318 N94-11555

Wind system documentation [DE93-010381] p 285 N94-11664

TOXICITY AND SAFETY HAZARD

Environmentally Safe and Effective Processes for Paint Removal [AGARD-R-791] p 126 N94-10613

TOXICOLOGY

A combustion products analyzer for contingency use during thermodegradation events on spacecraft p 318 N94-11555

TRACE ELEMENTS

Minor and trace element composition and age of Yukon probable-microtektites p 429 N94-12094

Trace-element abundances in several new ureilites p 80 N94-12096

SXRF determination of trace elements in chondrule rims in the unequilibrated CO3 chondrite, ALH A77307 p 429 N94-12106

Trace element distributions in primitive achondrites p 431 N94-12200

Isotopic and trace element characteristics of an unusual refractory inclusion from Essebi p 471 N94-12212

Trace element content of chondritic cosmic dust: Volatile enrichments, thermal alterations, and the possibility of contamination p 433 N94-12260

New low-Ni (igneous?) particles among the C and C? types of cosmic dust p 433 N94-12262

TRACHYTE

Stable isotope analyses of the peralkaline volcanics Gregory Rift Valley, Kenya p 281 N94-12072

TRACKING (POSITION)

Underwater hydrophone location survey p 290 N94-10975

Quantitative EEG patterns of differential in-flight workload p 317 N94-11528

TRACKING NETWORKS

Analysis of the eastern range multiplexed fiber optic IRIG B120 distribution system p 139 N94-10996

TRACKING PROBLEM

Derivation of three closed loop kinematic velocity models using normalized quaternion feedback for an autonomous redundant manipulator with application to inverse kinematics [DE93-012823] p 340 N94-12543

TRACKING STATIONS

Pre-operation analysis of ERS-1 tracking and operation, part 2-F [NASDA-CNT-930002-PT-2-F] p 230 N94-11130

TRAILING EDGE FLAPS

Control effectiveness at hypersonic speeds p 3 N94-10426

TRAILING EDGES

New aerodynamic information obtained from the solution of the inverse problem for aerofoils [NAL-TR-1172] p 14 N94-10860

TRAINING ANALYSIS

Teaching high-performance skills using above-real-time training [NASA-CR-4528] p 315 N94-11627

SATORI: Situation Assessment Through the Re-creation of Incidents [DOT/FAA/AM-93/12] p 38 N94-12567

TRAINING DEVICES

Quantitative EEG patterns of differential in-flight workload p 317 N94-11528

TRAINING EVALUATION

Teaching high-performance skills using above-real-time training [NASA-CR-4528] p 315 N94-11627

TRAINING SIMULATORS

Teaching high-performance skills using above-real-time training [NASA-CR-4528] p 315 N94-11627

TRAJECTORIES

Feature association without a motion estimate [AD-A265162] p 138 N94-11891

TRAJECTORY ANALYSIS

On renormalization group flow in matrix model [DE93-613050] p 409 N94-10413

Study of the surface circulation to the North of Bransfield Strait, Antarctica [INPE-5472-TDI/503] p 288 N94-11200

Modelling of dispersal and deposition of impact glass spherules from the Cretaceous-Tertiary boundary deposit p 432 N94-12238

TRAJECTORY OPTIMIZATION

Progress in multidisciplinary design optimization at NASA Langley [NASA-TM-107754] p 318 N94-10814

TRAJECTORY PLANNING

Trajectory pattern inverse dynamics and control of nonlinear dynamics systems with application to flexible structures p 181 N94-11219

Experiments in mobile robot navigation and range imaging [DE93-013280] p 341 N94-12598

TRANSATMOSPHERIC VEHICLES

Hypersonic, nonequilibrium flow over a cylindrically blunted 6 deg wedge [NASA-TM-108994] p 162 N94-12571

TRANSDUCERS

The 17th Transducer Workshop [AD-A265526] p 141 N94-10509

Direct current transducer [DE92-644548] p 141 N94-10533

Design of a matching network for dipole antennas [AD-A265115] p 136 N94-11158

Strategies and methodologies to develop techniques for computer-assisted analysis of gas phase formation during altitude decompression p 312 N94-11547

Ceramic actuators for smart materials [AD-A265664] p 93 N94-12331

TRANSFER FUNCTIONS

ERS-1 scatterometer data characteristics and wind retrieval skill p 233 N94-11709

The ideal Kolmogorov inertial range and constant p 158 N94-12305

The helical decomposition and the instability assumption p 158 N94-12306

TRANSFER OF TRAINING

Transfer of training for aerospace operations: How to measure, validate, and improve it p 314 N94-11530

TRANSFER ORBITS

In-space operations for lunar and Mars space transfer vehicles p 348 N94-11568

In-space assembly-servicing requirements p 348 N94-11569

TRANSFORMATIONS (MATHEMATICS)

Subband/transform functions for image processing [NASA-TM-106183] p 323 N94-10639

TRANSFORMERS

Design of a matching network for dipole antennas [AD-A265115] p 136 N94-11158

Characterization of the pulse transformer [AD-A263414] p 143 N94-11298

TRANSIENT HEATING

Primordial lightning: Evidence preserved in chondrites p 432 N94-12230

TRANSIENT LOADS

Response of composite laminates to dynamic surface loads p 66 N94-10902

TRANSIENT RESPONSE

Transient effects in the Benard instabilities: Coupling between capillary and gravity effects p 119 N94-10216

Statistical and optimization methods to expedite neural network training for transient identification [DE93-009985] p 340 N94-11644

TRANSISTORS
Effect of switched-bias bakes on the postirradiation electrical response of MOS devices
[DE93-009629] p 143 N94-11271
TRANSIT TIME
Electron runaway in RF discharges
[DE93-771407] p 363 N94-10661
TRANSITION FLOW
A research program for improving heat transfer prediction for the laminar to turbulent transition region of turbine vanes/blades
[NASA-TM-106278] p 151 N94-11256
Boundary layer transition: Prediction and wind tunnel simulation p 32 N94-11498
DNS on control of laminar-turbulent transition in channel flow with suction and blowing p 163 N94-12613
Criteria for onset of boundary-layer transition on spinning bodies p 164 N94-12620
Turbulent boundary layer interacting with spanwise periodic longitudinal vortex arrays p 165 N94-12626
TRANSITION METALS
Non-empirical interatomic potentials for transition metals
[DE93-013705] p 365 N94-11011
Interatomic interactions in BCC and FCC lattices of transition metals
[DE93-621541] p 398 N94-11090
Polaronic charge separation in mixed-halide MX solids
[AD-A266073] p 403 N94-12345
TRANSITION PRESSURE
Heavy-section steel technology program
[DE93-009222] p 184 N94-10155
TRANSITION PROBABILITIES
Probability of particle trapping/detrapping in torsatrons
[DE93-621641] p 390 N94-11121
TRANSITION TEMPERATURE
Apical Cu-O bond in YBa2Cu3O(7-delta) superconductors by XAFS
[DE93-010861] p 400 N94-11458
X-ray and neutron scattering studies of magnetic critical fluctuations in holmium
[DE93-010873] p 400 N94-11467
TRANSMISSION ELECTRON MICROSCOPY
HRTEM in protein crystallography
[DE93-610322] p 395 N94-10406
Test of a method for phase retrieval in HRTEM
[DE93-612641] p 170 N94-10630
Mineralogy of chondritic interplanetary dust particle impact residues from LDEF p 80 N94-12045
TRANSMISSION LOSS
Building penetration loss measurements for DAB signals at 211 MHz
[BBC-RD-1992/14] p 133 N94-11024
TRANSMITTANCE
A development on estimation method of undersea light p 204 N94-11974
Propagation of light pulses through a three-layer medium (cloud, pure air, and ocean water) p 222 N94-12725
TRANSMITTERS
Galileo EM-2 contributions to the lunar control network p 468 N94-12198
TRANSONIC FLOW
Nonlinear aspects of transonic aeroelasticity
p 2 N94-10357
Flow analysis around ONERA model M5 configuration
[PAPER-3D-2] p 12 N94-10478
Flow analysis around ONERA model M5 configuration
[PAPER-3D-3] p 12 N94-10479
Flow analysis around ONERA model M5 configuration
[PAPER-3D-4] p 12 N94-10480
Laser anemometer measurements and computations for transonic flow conditions in an annular cascade of high turning core turbine vanes
[NASA-TP-3383] p 15 N94-11133
Nonlinear aspects of transonic aeroelasticity
[UTIAS-RN-345] p 15 N94-11857
TRANSONIC SPEED
Aerodynamic characteristics analysis of Garabedian-Korn 75-06-12 airfoil
[PAPER-2D-2] p 10 N94-10468
TRANSONIC WIND TUNNELS
Improvement of the flow quality in the ARA transonic tunnel by means of a long cell honeycomb
[ARA-MEMO-375] p 34 N94-10894
The evolution of whole field optical diagnostics for external transonic testing
[ARA-MEMO-379] p 383 N94-11887
TRANSPIRATION
Real gas and surface transpiration effects upon swept leading edge high speed flow including transition
p 8 N94-10452
TRANSPONDERS
Performance of traffic-alert collision avoidance (TCAS) antennas in the presence of scatterers
[NASA-CR-193569] p 23 N94-11525
Impact of shutting down en route primary radars within CONUS interior
[DOT-VNTSC-FAA-93-1] p 23 N94-11626
TRANSPORT AIRCRAFT
High temperature materials for hypersonic transport
p 56 N94-10003
AGBT advanced counter-rotating gearbox detailed design report
[NASA-CR-180883] p 179 N94-10400
TRANSPORT PROPERTIES
Physics and modelling of scrape-off layer transport
[DE93-010510] p 385 N94-10289
Transport mechanisms acting in toroidal devices: A theoretician's view
[DE93-013463] p 385 N94-10310
Aerosol sampling models survey
[AD-A265903] p 75 N94-10337
Arcjet space thrusters
[NASA-CR-193191] p 46 N94-10700
Hydrogen partitioning and transport in titanium aluminides
[NASA-CR-194117] p 76 N94-10713
Processing and transport properties of high J(sub c) silver clad Bi-2223 tapes and coils
[DE93-010674] p 398 N94-11073
Process modelling for materials preparation experiments
[NASA-CR-193556] p 56 N94-12588
TRANSPORT THEORY
A spectral nodal method for discrete ordinates problems in x,y geometry
[DE93-610128] p 342 N94-10283
Physics and modelling of scrape-off layer transport
[DE93-010510] p 385 N94-10289
A spectral nodal method for the solution of the Sn equations in x, y geometry for highly absorbing deep penetration problems
[DE93-613520] p 349 N94-10636
The searchlight problem for neutrons in a semi-infinite medium
[DE93-010796] p 365 N94-10952
Development of deterministic transport methods for low energy neutrons for shielding in space
[NASA-CR-194172] p 366 N94-11199
Helium transport scaling law studies
[DE93-013487] p 393 N94-11513
Grid optimization and multigrid techniques for fluid flow and transport problems p 154 N94-11824
TRANSPORTATION
Polymer electrolyte fuel cells: Potential transportation and stationary applications
[DE93-010734] p 264 N94-11666
TRANSPUTERS
Application of parallel processing to a surface patch/wire junction EFIE code
[AD-A264965] p 336 N94-10488
TRAPPED PARTICLES
Laser cooling and trapping of atoms in microgravity: Ultracold atoms collisions p 124 N94-10241
Quantum non demolition measurement of cyclotron excitations in a Penning trap p 376 N94-10578
Kinetic approach to long wave length modes in rotating plasmas
[DE93-771286] p 388 N94-10807
Analysis of geophysical measurements and spacecraft interactions
[AD-A266064] p 43 N94-10944
The 24th Annual Precise Time and Time Interval (PTTI) Applications and Planning Meeting
[NASA-CP-3218] p 350 N94-10963
Particle transport analysis in torsatron configurations
[DE93-621640] p 390 N94-11120
Probability of particle trapping/detrapping in torsatrons
[DE93-621641] p 390 N94-11121
TRAPPING
Laser cooling and trapping of atoms in microgravity: Ultracold atoms collisions p 124 N94-10241
Bond distortion and electron trapping in charged C60
[DE93-613642] p 396 N94-10637
Probability of particle trapping/detrapping in torsatrons
[DE93-621641] p 390 N94-11121
TRAVELING SALESMAN PROBLEM
Bibliographic notes on Voronoi diagrams
[PB93-189298] p 343 N94-10825
TRAVELING WAVE AMPLIFIERS
Wide band 140 GHz TWTA p 132 N94-10514
TRAVELING WAVES
Conversion of the four-strap array in D3-D to a tunable traveling wave antenna
[DE93-012085] p 137 N94-11453
The x ray standing waves on surfaces
[AD-A265265] p 402 N94-11682
Traveling disturbances appearing in yawed cylinder boundary layer transition p 166 N94-12632
TREES (MATHEMATICS)
Marginal allocations in the core of minimal chain-games
[MEMO-1103] p 348 N94-10162
Algorithms for the maximum clique problem
[MEMO-1101] p 322 N94-10419
An introduction to chordal graphs and clique trees
[DE93-012508] p 332 N94-11695
TREES (PLANTS)
Satellite inventory of Minnesota forest resources
[NASA-CR-193565] p 231 N94-11521
TRENDS
Potential markets for advanced satellite communications
[NASA-CR-191145] p 41 N94-10512
National patterns of R and D resources, 1992
[NSF-92-330] p 422 N94-11186
TRIANGULATION
Finding a covering triangulation whose maximum angle is provably small
[DE93-010691] p 334 N94-12593
TRIATOMIC MOLECULES
The global potential energy surfaces of the lowest two 1A' states of the ozone molecule: Theoretical determination and analysis p 267 N94-12269
TRIBOLOGY
Study of the tribological behavior of SiC and Si3N4 ceramic couples in terms of temperature: The reality
p 64 N94-10061
Durability of a carbon segmented circumferential seal for a liquid oxygen turbopump
[NAL-TR-1155] p 178 N94-10369
Effect of surface cleanliness of bearing steel on adhesive strength and tribological properties of sputter-deposited gold films
[DE93-767974] p 82 N94-10732
Tribological characteristics of hot-pressed self-lubricating composites
[NAL-TR-1160] p 66 N94-10858
The properties of perfluoropolyethers used for space applications
[NASA-TM-106275] p 88 N94-10864
Advanced model of gradual wear of viscoelastic surface film
[AD-A265130] p 90 N94-11222
Tribological characteristics of sputtered Au/Cr films on alumina substrates at elevated temperatures
[NASA-TM-106078] p 55 N94-11362
Ceramics technology project database
[DE93-012431] p 91 N94-11672
Properties of interfacial tribo-films
[AD-A265591] p 182 N94-12374
TRIGGER CIRCUITS
Upgraded D(O) calorimeter electronics for short Tevatron bunch space and the effect of pile-up on the W mass measurement
[DE93-013566] p 146 N94-12603
TRIMERS
The synthesis of photocrosslinkable chalcone-bearing polyphosphazenes
[AD-A264915] p 92 N94-11849
TRITIUM
High-energy density physics at Los Alamos
[DE93-010271] p 371 N94-10260
The effect of a scalar boson coupled to neutrinos on the behavior of the tritium beta decay spectrum near the end point
[DE93-012655] p 361 N94-10349
Three-nucleon problem with phase equivalent potentials
[DE93-617731] p 363 N94-10722
Welding tritium aged stainless steel
[DE93-011782] p 181 N94-11226
TRITON
Orbital simulations of satellite escape/capture and the origin of satellites such as Triton p 429 N94-12057
A structural origin for the cantaloupe terrain of Triton
p 449 N94-12095
Geomorphology of Triton's polar materials
p 466 N94-12185
Tectonics on Triton p 466 N94-12187
On the unique structure of the magnetic fields of Uranus and Neptune p 472 N94-12221
TROILITE
Calorimetric thermometry of meteoritic troilite: A feasibility study p 428 N94-12025
TROPICAL REGIONS
Technical Conference on Tropical Urban Climates: Extended Abstracts
[WMO/TD-538] p 283 N94-10561
An overview of intertropical convergence and intertropical discontinuity
[DE93-619229] p 277 N94-11603
Central Equatorial Pacific Experiment (CEPEX)
[DE93-011656] p 190 N94-11674

Evaluation of ECMWF latent heat flux in TOGA CD-ROM p 195 N94-11921
Methodological considerations for use of ERS-1 imagery for the delineation of river networks in tropical forest areas p 247 N94-12484
TREES project: A case study on the use of multi-temporal ERS-1 SAR data and SPOT data for monitoring tropical ecosystems p 249 N94-12497
TREES project: Overview and status of the ERS-1 SAR contribution p 250 N94-12499
Principal oscillation pattern analysis of sea level variations in the tropical Pacific measured by the GEOSAT altimeter p 209 N94-12646
Preliminary results from a satellite altimetric data assimilation using a Kalman filter and smoother p 209 N94-12648

TROPICAL STORMS
Updated forecast of Atlantic seasonal hurricane activity for 1993 p 285 N94-11194

TROPOSPHERE
In situ detection of tropospheric OH, HO2, NO2, and NO by laser-induced fluorescence in detection chambers at reduced pressures [NASA-CR-193189] p 274 N94-10701
Preliminary validation of the low frequency variability of tropospheric temperature and circulation simulated for the AMIP by the ECMWF model [DE93-012382] p 284 N94-10739
An overview of intertropical convergence and intertropical discontinuity [DE93-619229] p 277 N94-11603

TROUGHS
Fault geometries and extension in the Valles Marineris, Mars p 458 N94-12144
Shallow crustal discontinuities and graben and scarp formation in the Tharsis region of Mars p 469 N94-12203

TRUNCATION ERRORS
Finite difference schemes for long-time integration [NASA-CR-191471] p 343 N94-10642

TRUSSES
Space truss zero gravity dynamics [AD-A266130] p 44 N94-12541

TUNABLE LASERS
Thermal-optical switching of a silicon based interference filter [AD-A265152] p 174 N94-11095
Laser system design for the generation of a sodium-layer laser guide star [DE93-014127] p 176 N94-12784

TUNDRA
Energy flow in an Arctic aquatic ecosystem [DE93-013178] p 267 N94-11697
Emissions of biogenic sulfur gases from Alaskan tundra p 268 N94-12455
Emissions of sulfur gases from wetlands p 269 N94-12458

TUNGSTEN
Liquid phase sintering of tungsten composites under microgravity. Effect of matrix composition p 118 N94-10207
Deformation mechanisms in tungsten single crystals in ballistic impact experiments [AD-A265701] p 405 N94-12563

TUNGSTEN ALLOYS
A history of tungsten- and molybdenum-base alloys [DE93-010283] p 82 N94-11108

TUNING
Lightweight linear alternators with and without capacitive tuning [NASA-CR-185273] p 140 N94-10505
Fine tuning of stretched-VISSR image mapping p 190 N94-11080
The laser second threshold: Its exact analytical dependence on detuning and relaxation rates [DE93-619706] p 175 N94-11633
Nonlinear effects in ferrite tuned cavities [DE93-014136] p 374 N94-12785

TUNNELING (EXCAVATION)
Resistivity and radar void detectors for tunneling machines p 140 N94-12706

TURBINE BLADES
Comprehensive dynamic analysis of a bladed disk-turborotor-bearing system [ISBN-0-315-73646-1] p 180 N94-11155
Fatigue life prediction for wind turbines: A case study on loading spectra and parameter sensitivity [DE93-011597] p 263 N94-11173
Blading models for TURBAN and CSPAN turbomachine design codes [NASA-CR-191164] p 15 N94-11203
Field evaluation of six protective coatings applied to T-56 turbine blades after 2500 hours of engine use [ARL-TR-27] p 90 N94-11311
VIB3D: Method for calculating 3-D unsteady flow through turbomachinery blades [CUED/A-TURBO/TR.128] p 166 N94-12777
VIB2D: Quasi 3-D unsteady viscous flow method for blade flutter calculation [CUED/A-TURBO/TR.129] p 166 N94-12779

TURBINE ENGINES
Laser anemometer measurements and computations for transonic flow conditions in an annular cascade of high turning core turbine vanes [NASA-TP-3383] p 15 N94-11133
A research program for improving heat transfer prediction for the laminar to turbulent transition region of turbine vanes/blades [NASA-TM-106278] p 151 N94-11256

TURBINE EXHAUST NOZZLES
Studies on scramjet nozzles. Part 1: Performance of two dimensional nozzles [NAL-TR-1149] p 27 N94-10367

TURBINE PUMPS
Durability of a carbon segmented circumferential seal for a liquid oxygen turbopump [NAL-TR-1155] p 178 N94-10369
Application of powder metallurgy techniques to produce improved bearing elements for liquid rocket engines [NASA-CR-193731] p 82 N94-10804

TURBINE WHEELS
Comprehensive dynamic analysis of a bladed disk-turborotor-bearing system [ISBN-0-315-73646-1] p 180 N94-11155

TURBINES
Method of reducing drag in aerodynamic systems [NASA-CASE-LEW-14791-1] p 12 N94-10672

TURBOMACHINE BLADES
Probabilistic evaluation of uncertainties and risks in aerospace components [NASA-TM-105603] p 185 N94-10361

TURBOMACHINERY
VIB3D: Method for calculating 3-D unsteady flow through turbomachinery blades [CUED/A-TURBO/TR.128] p 166 N94-12777
VIB2D: Quasi 3-D unsteady viscous flow method for blade flutter calculation [CUED/A-TURBO/TR.129] p 166 N94-12779

TURBULENCE
An experimental investigation of the sources of propeller noise due to turbulence ingestion p 358 N94-11057
The effects of successive distortions on a turbulent boundary layer in a supersonic flow p 14 N94-11058
Examination of wall functions for a parabolized Navier-Stokes code for supersonic flow [DE93-011590] p 14 N94-11111
Control of jet noise [NASA-CR-193612] p 358 N94-11176
Turbulence modeling for thrust reverser flow field prediction methods [AD-A266139] p 154 N94-11641
The coherent structure in the oceanic turbulence around Japan Islands Chain forced by an air, sea, and solid Earth interaction p 198 N94-11940
Annual Research Briefs, 1992 [NASA-CR-194389] p 155 N94-12284
Local isotropy in high Reynolds number turbulent shear flows p 157 N94-12302
The ideal Kolmogorov inertial range and constant p 158 N94-12305
Plane mixing layer vortical structure kinematics p 159 N94-12313
Numerical simulation of the non-Newtonian mixing layer p 159 N94-12314
Mapping closures for turbulent combustion [AD-A265671] p 79 N94-12378
Fluctuations of longitudinal vortices along a concave wall p 16 N94-12616
Coherent structure in near wall turbulence with riblets p 165 N94-12628
Turbulence generation in the Pacific undercurrent by shear p 223 N94-12730

TURBULENCE EFFECTS
Estimation of the direct acoustic radiation from turbulent spots using boundary layer velocity measurements p 357 N94-10358
Direct simulation of compressible wall-bounded turbulence p 156 N94-12294

TURBULENCE MODELS
Numerical calculation of scramjet inlet flow [NAL-TR-1174T] p 27 N94-10370
Problems in the validation of CFD codes through comparison with experiment p 6 N94-10441
Experimental, analytical, and computational methods applied to hypersonic compression ramp flows p 6 N94-10444
Aerodynamic characteristics analysis of Garabedian-Korn 75-06-12 airfoil: Computation using q-omega 2 equation turbulence model [PAPER-2D-4] p 10 N94-10470
Aerodynamic characteristics analysis of Garabedian-Korn 75-06-12 airfoils: Computation using Baldwin-Lomax turbulence model [PAPER-2D-5] p 11 N94-10471
Aerodynamic characteristics analysis of Garabedian-Korn 75-06-12 aircraft [PAPER-2D-7] p 11 N94-10472
Aerodynamic characteristics analysis of Garabedian-Korn 75-06-12 airfoil [PAPER-2D-8] p 11 N94-10473
Flow analysis around ONERA model M5 configuration [PAPER-3D-1] p 11 N94-10477
Examination of wall functions for a parabolized Navier-Stokes code for supersonic flow [DE93-011590] p 14 N94-11111
A research program for improving heat transfer prediction for the laminar to turbulent transition region of turbine vanes/blades [NASA-TM-106278] p 151 N94-11256
A four-dimensional, mesoscale, non-gaussian multispectral smoke model. Phase 1: Feasibility study [AD-A264805] p 152 N94-11519
Modelling quasi-two-dimensional turbulent shear flow p 153 N94-11616
Turbulence modeling for thrust reverser flow field prediction methods [AD-A266139] p 154 N94-11641
Annual Research Briefs, 1992 [NASA-CR-194389] p 155 N94-12284
Large eddy simulations of time-dependent and buoyancy-driven channel flows p 155 N94-12287
A normal stress subgrid-scale eddy viscosity model in large eddy simulation p 155 N94-12288
Large eddy simulation of shock turbulence interaction p 155 N94-12289
Application of a dynamic subgrid-scale model to turbulent recirculating flows p 156 N94-12290
Large-eddy simulation of turbulent flow with a surface-mounted two-dimensional obstacle p 156 N94-12291
Similarity states of homogeneous stably-stratified turbulence at infinite Froude number p 156 N94-12292
Application of incremental unknowns to the Burgers equation p 156 N94-12293
Direct simulation of compressible wall-bounded turbulence p 156 N94-12294
Application of a Reynolds stress model to separating boundary layers p 157 N94-12299
The ideal Kolmogorov inertial range and constant p 158 N94-12305
PDF approach for turbulent scalar field: Some recent developments p 160 N94-12315
Proceedings of the 9th and 10th NAL Workshop on Investigation and Control of Boundary-Layer Transition [NAL-SP-18] p 163 N94-12611
Turbulence modeling and compressibility p 163 N94-12614

TURBULENT BOUNDARY LAYER
Problems in the validation of CFD codes through comparison with experiment p 6 N94-10441
Aerodynamic characteristics analysis of Garabedian-Korn 75-06-12 airfoil: Compendium of results p 11 N94-10475
Flowfield structure of swept shock wave/turbulent boundary-layer interactions p 149 N94-10899
Theoretical investigation of 3-D shock wave turbulent boundary layer interactions [AD-A265275] p 150 N94-11014
The effects of successive distortions on a turbulent boundary layer in a supersonic flow p 14 N94-11058
Remote sensing and the air-sea boundary layers p 191 N94-11896
Application of a Reynolds stress model to separating boundary layers p 157 N94-12299
Progress in modeling hypersonic turbulent boundary layers p 157 N94-12300
An investigation of small scales of turbulence in a boundary layer at high Reynolds numbers p 157 N94-12303
Experiments on near-wall structure of three-dimensional boundary layers p 159 N94-12309
Suppression of the near wall burst process of a fully developed turbulent pipe flow [AD-A265995] p 161 N94-12352
Experiment on a high Reynolds number turbulent boundary layer p 164 N94-12617
Turbulent boundary layer interacting with spanwise periodic longitudinal vortex arrays p 165 N94-12626
Coherent structure in near wall turbulence with riblets p 165 N94-12628

TURBULENT COMBUSTION
The evolution equation for the flame surface density in turbulent premixed combustion p 81 N94-12316
Study and modeling of finite rate chemistry effects in turbulent non-premixed flames p 81 N94-12317

Generation of two-dimensional vortices in a cross-flow p 160 N94-12318
Why does preferential diffusion strongly affect premixed turbulent combustion? p 81 N94-12319
Mapping closures for turbulent combustion [AD-A265671] p 79 N94-12378
Theories of turbulent combustion in high speed flows [AD-A265735] p 79 N94-12403

TURBULENT DIFFUSION
Aerosol sampling models survey [AD-A265903] p 75 N94-10337
A self-consistent model of non-linear parameterization of turbulent diffusion in atmospheric boundary layer [DE93-011950] p 275 N94-11052
Why does preferential diffusion strongly affect premixed turbulent combustion? p 81 N94-12319
Theories of turbulent combustion in high speed flows [AD-A265735] p 79 N94-12403

TURBULENT FLOW
Combustion chamber analysis code [NASA-CR-192585] p 46 N94-10934
Examination of wall functions for a parabolized Navier-Stokes code for supersonic flow [DE93-011590] p 14 N94-11111
Physics of tokamak scrape-off layer confinement [DE93-011949] p 390 N94-11125
Turbulent wall jet in blast wave precursor [DE93-011955] p 151 N94-11144
A Galilean and tensorial invariant k-epsilon model for near wall turbulence [NASA-TM-106263] p 151 N94-11192
KIVA-3: A KIVA program with block-structured mesh for complex geometries [DE93-011986] p 77 N94-11249
A research program for improving heat transfer prediction for the laminar to turbulent transition region of turbine vanes/blades [NASA-TM-106278] p 151 N94-11256
Dynamics and control of coherent structures in the turbulent wall layer: An overview p 31 N94-11494
Modelling quasi-two-dimensional turbulent shear flow p 153 N94-11616
A two-stage (turbulent-drainage) mechanism for the emplacement of impact crater outflows on Venus p 458 N94-12145
Annual Research Briefs, 1992 [NASA-CR-194389] p 155 N94-12284
A normal stress subgrid-scale eddy viscosity model in large eddy simulation p 155 N94-12288
Large eddy simulation of shock turbulence interaction p 155 N94-12289
Application of a dynamic subgrid-scale model to turbulent recirculating flows p 156 N94-12290
Large-eddy simulation of turbulent flow with a surface-mounted two-dimensional obstacle p 156 N94-12291
Similarity states of homogeneous stably-stratified turbulence at infinite Froude number p 156 N94-12292
Application of incremental unknowns to the Burgers equation p 156 N94-12293
Direct simulation of compressible wall-bounded turbulence p 156 N94-12294
Direct numerical simulation of turbulent flow over a backward-facing step p 156 N94-12296
Numerical simulation using vorticity-vector potential formulation p 157 N94-12297
Local isotropy in high Reynolds number turbulent shear flows p 157 N94-12302
An investigation of small scales of turbulence in a boundary layer at high Reynolds numbers p 157 N94-12303
The helical decomposition and the instability assumption p 158 N94-12306
Superfluid turbulence p 158 N94-12307
Regeneration of near-wall turbulence structures p 158 N94-12308
Mixing in a stratified shear flow: Energetics and sampling p 159 N94-12311
LIF measurements of scalar mixing in turbulent shear layers p 159 N94-12312
The evolution equation for the flame surface density in turbulent premixed combustion p 81 N94-12316
Study and modeling of finite rate chemistry effects in turbulent non-premixed flames p 81 N94-12317
Why does preferential diffusion strongly affect premixed turbulent combustion? p 81 N94-12319
Tensoral: A system for post-processing turbulence simulation data p 75 N94-12320
Topics in pattern formation and chaotic systems [AD-A265922] p 161 N94-12342
Suppression of the near wall burst process of a fully developed turbulent pipe flow [AD-A265995] p 161 N94-12352
Mapping closures for turbulent combustion [AD-A265671] p 79 N94-12378
Theories of turbulent combustion in high speed flows [AD-A265735] p 79 N94-12403
Development of the one-component diode-array velocimeter [AD-A265552] p 171 N94-12533
DNS on control of laminar-turbulent transition in channel flow with suction and blowing p 163 N94-12613
Turbulence modeling and compressibility p 163 N94-12614
Fluctuations of longitudinal vortices along a concave wall p 16 N94-12616
Simultaneous 3D turbulent large-scale structures in a flood flow by multi-channels measuring system p 165 N94-12624
Turbulent boundary layer interacting with spanwise periodic longitudinal vortex arrays p 165 N94-12626
Coherent structure in near wall turbulence with riblets p 165 N94-12628

TURBULENT JETS
Turbulent wall jet in blast wave precursor [DE93-011955] p 151 N94-11144

TURBULENT MIXING
A normal stress subgrid-scale eddy viscosity model in large eddy simulation p 155 N94-12288
LIF measurements of scalar mixing in turbulent shear layers p 159 N94-12312
PDF approach for turbulent scalar field: Some recent developments p 160 N94-12315

TURBULENT WAKES
The three-dimensional evolution of a plane wake p 159 N94-12310
On the wake behind a high speed train p 164 N94-12618

TURING MACHINES
Finite state machine microarchitecture transformations described with relational algebra [MEMO-INF-92-63] p 319 N94-10278

TVD SCHEMES
Large time-step stability of explicit one-dimensional advection schemes [NASA-TM-106203] p 342 N94-10362
Numerical calculation of scramjet inlet flow [NAL-TR-1174T] p 27 N94-10370
Aerodynamic characteristics analysis of Garabedian-Korn 75-06-12 airfoil [PAPER-2D-2] p 10 N94-10468
Aerodynamic characteristics analysis of Garabedian-Korn 75-06-12 aircraft [PAPER-2D-7] p 11 N94-10472
Flow analysis around ONERA model M5 configuration [PAPER-3D-2] p 12 N94-10478
Flow analysis around ONERA model M5 configuration [PAPER-3D-4] p 12 N94-10480
Viscous flow simulation using an upwind method for hexahedral based adaptive meshes [AD-A265901] p 148 N94-10703

TWILIGHT GLOW
Aircraft windscreens enhance visual search disruption produced by laser glare [AD-A265167] p 26 N94-11892

TWO BODY PROBLEM
P-matrix description of the two-particle interaction [DE93-617690] p 361 N94-10549
Studies of P-matrix formalism on the basis of the potential description of two-particle interaction [DE93-617691] p 362 N94-10550
Exact solutions of a many-anyon problem [DE93-617646] p 411 N94-10832

TWO DIMENSIONAL FLOW
Thermocapillary instabilities in cylindrical liquid bridges: Mechanisms and transition boundaries p 101 N94-10077
Solving the inverse problem for incompressible potential flow through two-dimensional cascades [NAL-TR-1162] p 147 N94-10365
Modelling quasi-two-dimensional turbulent shear flow p 153 N94-11616
Aerodynamic sound due to interaction between a two-dimensional free shear layer and the leading edge of a parallel flat plate p 163 N94-12615
Boundary conditions and bifurcations in plane Poiseuille flow p 166 N94-12634

TWO DIMENSIONAL JETS
Direct numerical simulation of hot jets p 156 N94-12295

TWO DIMENSIONAL MODELS
Numerical simulation of Marangoni convection around gas bubbles in a liquid matrix p 106 N94-10107
Flow transitions in a 2D directional solidification model p 114 N94-10183
Marangoni Benard instabilities in liquid mixtures with Soret effect p 119 N94-10215
Simulations of D3-D divertor biasing with the LEDGE code [DE93-010500] p 385 N94-10262
On a class of two-dimensional nearest neighboring random walks [CWI-BS-R9220] p 347 N94-10353
Axisymmetric single shear element combustion instability experiment [NASA-TM-106327] p 46 N94-10763
Classical gravity coupled to Liouville theory [DE93-613049] p 275 N94-10798
Finite element simulation of the 2D collapse of a polyelectrolyte gel disk [DE93-010693] p 91 N94-11665
Explorations in quantum gravity: From one loop effective actions to two-dimensional theories p 413 N94-11822

TWO FLUID MODELS
On the coupling of electromagnetic radiation into cavities [DE93-011406] p 137 N94-11621

TWO PHASE FLOW
Two-phase flow heat transfer and hydrodynamics in an electric field p 103 N94-10093
Separation of gravitational effects on the flow of suspension in tubes by measurements in weightlessness p 105 N94-10105
Laboratory study on the natural modes of a rotating two-phase fluid system subject to axial excitation p 106 N94-10106
FORCE2: A state-of-the-art two-phase code for hydrodynamic calculations [DE93-010661] p 150 N94-11072
KIVA-3: A KIVA program with block-structured mesh for complex geometries [DE93-011986] p 77 N94-11249
The physics of pattern formation of liquid interfaces [DE93-013333] p 154 N94-11814
The Third Workshop on Two Phase Fluid Experiment in the Space Environment [NASDA-CON-930002] p 161 N94-12547
Summary of studies on JEM utilization experiment projects p 161 N94-12548
Compilation of proposals for boiling and evaporation experiments in space environments and proposals concerning experiment projects p 161 N94-12549
Condensation phenomena p 162 N94-12550
Developmental research of thermal control system in space environment p 162 N94-12551
Two phase flow and isopycnic liquid-liquid two phase fluid in reduced gravity field p 162 N94-12552
Devices related for thermal control systems used in microgravity p 162 N94-12553
Research on two phase flow in microgravity p 162 N94-12554
Research and development of cold plate for two phase fluid loop thermal control system p 162 N94-12555
Organization and management policy for two phase fluid experiment in space environment p 162 N94-12556

U

U BENDS
Corrosion behavior of metal matrix composites [AD-A265352] p 85 N94-12404

U.S.S.R. SPACE PROGRAM
Russian space system for the Earth remote sensing p 37 N94-10688

UBV SPECTRA
First results of the seven-color asteroid survey p 430 N94-12162

UH-60A HELICOPTER
A feasibility study regarding the addition of a fifth control to a rotorcraft in-flight simulator [NASA-CR-193240] p 30 N94-10895
Helicopter approach capability using the differential Global Positioning System [NASA-CR-177618] p 24 N94-12355

ULTRASONIC FLAW DETECTION
Ultrasonic inspection, material noise and surface roughness [DE93-011560] p 183 N94-11110
Assessment of damage in ceramics and ceramic matrix composites using ultrasonic techniques [NASA-TM-106121] p 67 N94-11237

ULTRASONIC RADIATION
Nonlinear excitation in quasi-one-dimensional Peierls dielectrics with charge density waves [DE93-613827] p 398 N94-11025
Inverting ultrasonic data on solid/fluid mixtures for Biot-Gassmann parameters [DE93-011952] p 150 N94-11026

ULTRASONIC SCANNERS
Basic experiment on an ultrasonic method of localization [DE93-754295] p 358 N94-11042

ULTRASONIC TESTS

Special problems of 3-D ultrasonic QNDI techniques and applications to composites aerospace structures p 61 N94-10036

High temperature processing and diagnostic technologies for microgravity applications p 110 N94-10130

Method of recertifying a loaded bearing member using a phase point [NASA-CASE-LAR-14741-1] p 185 N94-10671

Ultrasonic inspection, material noise and surface roughness [DE93-011560] p 183 N94-11110

Project ARGO: Gas phase formation in simulated microgravity [NASA-TM-104762] p 125 N94-11235

Assessment of damage in ceramics and ceramic matrix composites using ultrasonic techniques [NASA-TM-106121] p 67 N94-11237

ULTRASONICS

Comparison of Al-Fe alloys produced by PFC and USGA techniques p 58 N94-10019

Use of ultrasound in altitude decompression modeling p 317 N94-11540

Transcranial Doppler ultrasound and the etiology of neurologic decompression sickness during altitude decompression p 312 N94-11544

ULTRAVIOLET ABSORPTION

ADP study of the structure of the IUE halo [NASA-CR-194374] p 428 N94-12595

ULTRAVIOLET DETECTORS

Ultraviolet plume instrument description and plume data reduction methodology [AD-A266141] p 54 N94-11643

ULTRAVIOLET FILTERS

Alkali metal for ultraviolet band-pass filter [NASA-CASE-NPO-18433-1-CU] p 381 N94-10657

ULTRAVIOLET RADIATION

UV testing of solar cells: Effects of antireflective coating, prior irradiation, and UV source p 53 N94-11408

Oxidation state of the Earth's upper mantle during the last 3800 million years: Implications for the origin of life p 283 N94-12210

ULTRAVIOLET SPECTRA

On renormalization group flow in matrix model [DE93-613050] p 409 N94-10413

ULTRAVIOLET SPECTROSCOPY

Detection of accreting circumstellar gas around weak emission-line Herbig Ae/Be stars [NASA-TM-108256] p 424 N94-11306

ULTRAVIOLET TELESCOPES

Lunar-Ultraviolet Telescope Experiment (LUTE) integrated program plan [NASA-CR-193267] p 424 N94-11356

UNDERGROUND EXPLOSIONS

Sensitivities of calculated residual stress to separation distances of two simultaneous events [DE92-019571] p 98 N94-10751

UNDERGROUND STORAGE

Immediate response to free product discovery [PB93-182970] p 265 N94-11015

Catalytic oxidation of organics in vapor streams at remediation sites [PB93-182962] p 266 N94-11472

UNDERGROUND STRUCTURES

Design and development of a miniature column-based interface (MCBI) stress gage [AD-A266054] p 170 N94-10873

Resistivity and radar void detectors for tunneling machines p 140 N94-12706

UNDERWATER ACOUSTICS

Underwater hydrophone location survey p 290 N94-10975

Acoustics of bubbly sediments [AD-A263726] p 288 N94-11299

Use of ERS-1 data at Saclant Undersea Research Centre p 233 N94-11714

Acoustic characteristics of side scan sonar and sub-bottom profiler for 10,000 m class ROV p 172 N94-11916

Study on color video pictures transmission by digital acoustic signal p 139 N94-11917

Signal feature analysis using neural networks and psychoacoustics [AD-A266048] p 340 N94-12398

UNDERWATER COMMUNICATION

Study on color video pictures transmission by digital acoustic signal p 139 N94-11917

UNDERWATER EXPLOSIONS

Dynamic loading in manufacturing and service: Australia's shock testing capability p 128 N94-11304

UNDERWATER OPTICS

Trajectory curving in underwater propagation of light p 226 N94-12748

UNDERWATER PHOTOGRAPHY

On resolution of underwater stereo photogrammetry p 172 N94-11966

UNDERWATER RESOURCES

A detailed investigation of the benthic regime in the Clarion-Clipperton province of the Pacific and a forecast of consequences of manganese nodule mining p 224 N94-12733

UNDERWATER STRUCTURES

Coastal processes due to nearshore current around an upheaving island p 199 N94-11942

The flow structure around a cylindrical pier for the flow of transcritical Reynolds number p 169 N94-11944

Idea of underground airplane p 27 N94-12630

The acoustic arrangement for measuring vertical structure of sea current p 223 N94-12729

UNDERWATER TESTS

Underwater hydrophone location survey p 290 N94-10975

Dynamic loading in manufacturing and service: Australia's shock testing capability p 128 N94-11304

UNDERWATER VEHICLES

Development of a shuttle AUV for oceanographic measurement p 217 N94-12692

UNIFIED FIELD THEORY

The magnetic field of rotating bodies [DE93-619769] p 427 N94-11812

Quark and lepton masses [DE93-012308] p 370 N94-12787

UNITED STATES

National patterns of R and D resources, 1992 [NSF-92-330] p 422 N94-11186

From red tape to results: Creating a government that works better and costs less p 422 N94-11351

From red tape to results: Creating a government that works better and costs less. Executive summary p 422 N94-11353

Insights into software development in Japan p 330 N94-11435

Landsat as a commercial enterprise [INPE-5477-TAE/019] p 232 N94-11524

UNIVERSAL TIME

A precise GPS-based time and frequency system p 353 N94-10978

UNIVERSE

Dimensional transition of the space-time at the minimum action near the planck scale [DE93-754192] p 410 N94-10718

A theoretical kinematical study of the gradient of any cosmic scalar field [DE92-644731] p 425 N94-11136

The solutions of cosmic string loop equation in expanding universe [DE93-619717] p 427 N94-11692

UNIVERSITIES

Flight Dynamics Directorate (FDD) Historically Black Colleges and Universities (HBCU's) database managment system: A user's guide [AD-A264947] p 419 N94-11288

UNIX (OPERATING SYSTEM)

A distributed version of the NASA Engine Performance Program [NASA-TM-106208] p 327 N94-11231

UNSTEADY FLOW

A dynamically adaptive mesh method for internal flows p 149 N94-10896

Unsteady flow past a NACA 0012 airfoil pitching at constant rates [AD-A265159] p 16 N94-11889

VIB3D: Method for calculating 3-D unsteady flow through turbomachinery blades [CUED/A-TURBO/TR.128] p 166 N94-12777

VIB2D: Quasi 3-D unsteady viscous flow method for blade flutter calculation [CUED/A-TURBO/TR.129] p 166 N94-12779

UPPER ATMOSPHERE

Pakistan Space and Upper Atmosphere Research Commission p 37 N94-10693

Selected upper-air wind speed distributions [AD-A264822] p 284 N94-10871

The Air Force Interactive Meteorological System: A research tool for satellite meteorology [AD-A265957] p 284 N94-11113

The upwelling radiation at the top of the atmosphere in coastal region p 205 N94-11981

UPSTREAM

Experimental and theoretical investigation of undular bore formation upstream the bank p 229 N94-12764

UPWELLING WATER

Ocean-ice interaction study of waves and mesoscale features p 197 N94-11935

On an upwelling front, propagation of upwelling and vertical velocity in the eastern Arabian Sea during monsoon, 1987 p 206 N94-11987

Variation of the photosynthetic products in the regional upwelling area around the Izu Islands, Japan p 211 N94-12661

Swordfish (Xiphias gladius) catch distributions relative to environmental features observed from satellites off Coquimbo, Chile (30 deg S) p 216 N94-12688

Investigation of meso-scale fronts, eddies and upwellings in China Seas with AVHRR data p 220 N94-12711

Coastal upwelling monitored by satellite data: Methodologies and results p 220 N94-12712

A possibility to define the location of epipelagic fish concentrations with assistance of satellite sensing p 228 N94-12757

High biological production of the tidal mixing zones on Japan Sea shelf p 228 N94-12758

URANIUM

Th-230 - U-238 series disequilibrium of the Olkaria rhyolites Gregory Rift Valley, Kenya: Residence times p 281 N94-12076

URANIUM ISOTOPES

Radiogenic age and isotopic studies [DE93-610548] p 274 N94-10407

Spin characteristics of ion beams during the motion of electromagnetic elements [DE93-617448] p 364 N94-10848

LEW88516 and SNC meteorites p 430 N94-12150

The Th and U abundances in chondritic meteorites p 430 N94-12151

URANUS (PLANET)

On the unique structure of the magnetic fields of Uranus and Neptune p 472 N94-12221

Precession of Uranus and Neptune and their magnetic field p 473 N94-12222

URBAN PLANNING

Technical Conference on Tropical Urban Climates: Extended Abstracts [WMO/TD-538] p 283 N94-10561

UREAS

Engineering solid-state materials. Strategies for modeling and packing control of molecular assemblies into 3-D networks [AD-A265291] p 404 N94-12438

UREILITES

Trace-element abundances in several new ureilites p 80 N94-12096

URETHANES

Uralane (tm) 5774-A/B: Ciba-Geigy's advanced urethane adhesive for the aircraft industry p 18 N94-10777

URINE

Microbiological test results using three urine pretreatment regimes with 316L stainless steel [NASA-CR-192568] p 299 N94-10360

A prototype urine collection device for female aircrew p 317 N94-11549

USER MANUALS (COMPUTER PROGRAMS)

Sandia ocean modeling system programmer's guide and user's manual [DE93-007427] p 287 N94-10153

PANACEA user's manual for PANACEA version 2.0 [DE93-012502] p 321 N94-10263

User's manual for the plume visibility model PLUVUE 2 (revised) [PB93-188233] p 265 N94-11016

Landing Craft Air Cushion (LCAC) crew selection system manual [AD-A265158] p 313 N94-11098

User's manual for the DAD-1 data acquisition daughter board for the SuperCard-2 [DE93-012153] p 325 N94-11139

ACARA user's manual [NASA-TM-106277] p 183 N94-11167

P2NBC2 Heat Strain Decision Aid. User's guide, version 2.1 [AD-A266072] p 304 N94-11224

Flight Dynamics Directorate (FDD) Historically Black Colleges and Universities (HBCU's) database managment system: A user's guide [AD-A264947] p 419 N94-11288

GRAFTED (GRAphical Fault Tree EDitor): A fault tree description program for target vulnerability/survivability analysis [AD-A264078] p 328 N94-11301

Software management guide [DE93-012034] p 330 N94-11452

NASCAP programmer's reference manual [NASA-CR-191044] p 278 N94-11702

The 1991 version of the plume impingement computer program. Volume 2: User's input guide [NASA-CR-194191] p 166 N94-12774

VIB3D: Method for calculating 3-D unsteady flow through turbomachinery blades [CUED/A-TURBO/TR.128] p 166 N94-12777

VIB2D: Quasi 3-D unsteady viscous flow method for blade flutter calculation
[CUED/A-TURBO/TR.129] p 166 N94-12779

USER REQUIREMENTS
Studies on refrigerator sensors and cooling section interface p 129 N94-11834
Data management strategy for the Tampa Bay National Estuary Program: Recommendations and implementation plan
[PB93-191633] p 267 N94-11864
Devices related for thermal control systems used in microgravity p 162 N94-12553

UTILITIES
Intergovernmental decisionmaking for environmental protection and public works
[PB93-176824] p 266 N94-11584

UTILITY AIRCRAFT
Idea of underground airplane p 27 N94-12630

V

V/STOL AIRCRAFT
Moving-base simulation evaluation of thrust margins for vertical landing for the NASA YAV-8B Harrier aircraft
[NASA-TM-104008] p 30 N94-11259

VACANCIES (CRYSTAL DEFECTS)
Invariance of the mobility edge in anodic titanium oxides
[DE92-642136] p 394 N94-10281
Electronic characterization of defects in narrow gap semiconductors
[NASA-CR-193568] p 397 N94-10819
Adsorption and dissociation of disilane on Si(001) studied by STM
[AD-A265269] p 402 N94-11684

VACUUM
Vacuum stability requirements of polymeric material for spacecraft application
[NASA-TM-109216] p 91 N94-11350
Evaluation of medical treatments to increase survival of ebullism in guinea pigs p 302 N94-11548
The 1991 version of the plume impingement computer program. Volume 1: Description
[NASA-CR-194192] p 166 N94-12775

VACUUM TESTS
An investigation of conducted and radiated emissions from a hollow-cathode plasma contactor
[NASA-CR-191172] p 386 N94-10346

VALENCE
Enhanced stability of magic clusters: A case study of icosahedric Al(sub 12)X, X=B, Al, Ga, C, Si, Ge, Ti, As
[DE93-613644] p 395 N94-10386
X ray and gamma ray spectroscopy of solids under pressure
[DE93-014847] p 76 N94-10653

VALLEYS
Thermal studies of Martian channels and valleys using Termoskan data p 443 N94-12064
Mars: The initial emplacement of ground ice in response to the thermal evolution of its early crust
p 462 N94-12168

VALSALVA EXERCISE
Valsalva maneuver: Insights into baroreflex modulation of human sympathetic activity p 310 N94-12000

VALVES
Check valve with poppet damping mechanism
[NASA-CASE-MSC-21903-1] p 179 N94-10655
Check valve with poppet dashpot/frictional damping mechanism
[NASA-CASE-MSC-21950-1] p 179 N94-10658

VANES
Laser anemometer measurements and computations for transonic flow conditions in an annular cascade of high turning core turbine vanes
[NASA-TP-3383] p 15 N94-11133
A research program for improving heat transfer prediction for the laminar to turbulent transition region of turbine vanes/blades
[NASA-TM-106278] p 151 N94-11256
Performance characteristics of the INS 25.5-MHz split coaxial RFQ
[DE93-753168] p 144 N94-11508

VAPOR DEPOSITION
Design of a CVD reactor for the deposition of diamond in a microgravity environment p 109 N94-10127
Alkali metal for ultraviolet band-pass filter
[NASA-CASE-NPO-18433-1-CU] p 381 N94-10657
Thermal-optical switching of a silicon based interference filter
[AD-A265152] p 174 N94-11095
Damping mechanisms in chemically vapor deposited SiC fibers
[NASA-TM-106334] p 66 N94-11135
Wide Band-Gap Semiconductors. 1991 Materials Research Society Symposium proceedings
[AD-A263418] p 401 N94-11515
An ellipsometry investigation of nucleation and growth of electron cyclotron resonance plasma deposited silicon films
[AD-A265037] p 401 N94-11651
Chemical Vapor Deposition of Refractory Metals and Ceramics 2. Materials Research Society Symposium proceedings
[AD-A265072] p 92 N94-11866
Progress toward atomic layer epitaxy of diamond: Diamond films grown one layer at a time
[AD-A265530] p 403 N94-12010
Analysis of the economics of DC arc CVD diamond
[AD-A265688] p 403 N94-12339
Protective coatings for high-temperature polymer matrix composites
[NASA-TM-106276] p 74 N94-12431

VAPOR PHASES
Laser beam deflection: A diagnostic tool for vapour growth experiments in microgravity p 111 N94-10135
STARDUST: A simulation experiment of cosmic dust analogues production in microgravity conditions
p 113 N94-10175
Crystal growth from low temperature vapour phase
p 115 N94-10191
Project ARGO: Gas phase formation in simulated microgravity
[NASA-TM-104762] p 125 N94-11235
Size dependence of chemical reactivity of gaseous metal clusters: A new mechanistic probe
[AD-A264690] p 77 N94-11264
Characterization of gas-aerosol interaction kinetics using morphology dependent stimulated Raman scattering
[DE93-012324] p 77 N94-11359
A model of elementary chemistry and fluid mechanics in the combustion of hydrogen on platinum surfaces
[DE93-012767] p 77 N94-11370
CRESLAF. Version 4.0: A Fortran program for modeling laminar, chemically reacting, boundary-layer flow in cylindrical or planar channels
[DE93-012835] p 152 N94-11371
Risk of decompression sickness in the presence of circulating microbubbles p 312 N94-11546
Strategies and methodologies to develop techniques for computer-assisted analysis of gas phase formation during altitude decompression p 312 N94-11547
Resist materials design: Base-catalyzed chemical amplification
[AD-A265286] p 145 N94-11819
Graphite solubility and co-vesiculation in basalt-like melts at one-ATM p 463 N94-12173
Development of a molecular beam technique to study early solar system silicon reactions p 432 N94-12224

VAPOR PRESSURE
Evaluation of medical treatments to increase survival of ebullism in guinea pigs p 302 N94-11548
The role of the geothermal gradient in the emplacement and replenishment of ground ice on Mars
p 463 N94-12169

VAPORIZING
Evaluation of medical treatments to increase survival of ebullism in guinea pigs p 302 N94-11548
Vaporization by shock loading of albite, jadeite, and pyrex glass: Experimental study p 97 N94-12039
The correlation of alkalis and aluminum during high-temperature volatilization of albite and nepheline
p 81 N94-12214

VAPORS
Hygroscopic absorption to falling films: The effects of the concentration level
[ITN-93-85198] p 148 N94-10391
Catalytic oxidation of organics in vapor streams at remediation sites
[PB93-182962] p 266 N94-11472
Toxicity study of dimethylethoxysilane (DMSES), the waterproofing agent for the Orbiter heat protective system p 318 N94-11554

VARIABILITY
Intraday variability and the compactness of extragalactic radio sources p 135 N94-11064
Statistical analysis of environmental variability within the CELSS breadboard project's biomass production chamber
[NASA-TM-109188] p 315 N94-11258
Variability of wind stress, and sensible and latent heat flux in the North Atlantic during SEASAT
p 194 N94-11918
A preliminary study of the variability and magnitude of the flux of biogenic sulfur gases from a New Hampshire salt marsh p 267 N94-12452
Mean flow and variability in the Kuroshio extension from GEOSAT altimetry data p 209 N94-12650
Field research of wind wave spectrum variability
p 223 N94-12727

VARIATIONS
Time evolution of cross-stream exchange associated with the variations in the Kuroshio p 197 N94-11936
Fluctuations of the Kuroshio extension detected by the GEOSAT altimetry data p 209 N94-12649

VECTOR ANALYSIS
Multilevel computer-aided optimum design of structural systems using multiple basis vectors
p 187 N94-11055
Evaluation of two January - June 1992 ERS-1 AMI wind vector data sets p 235 N94-11724

VECTOR PROCESSING (COMPUTERS)
A molecular dynamics simulation code ISIS
[DE93-753187] p 368 N94-11592

VECTOR QUANTIZATION
Necessary conditions for the optimality of variable rate residual vector quantizers
[NASA-CR-193730] p 326 N94-11197

VECTOR SPACES
The super vectorfield package for REDUCE. Version 1.0
[MEMO-1099] p 321 N94-10265
The ring structure of chiral operators for minimal models coupled to 2D gravity
[DE93-613119] p 409 N94-10500
Bound states of the N-dimensional Klein-Gordon equation with vector and scalar Coulomb potentials
[DE93-617650] p 349 N94-10547
Exact solution of the N-dimensional generalized Dirac-Coulomb equation
[DE93-617649] p 411 N94-10834
Homoclinic intermittency
[W-9302] p 344 N94-10908

VECTORS (MATHEMATICS)
Evaluation of two January - June 1992 ERS-1 AMI wind vector data sets p 235 N94-11724

VEGA PROJECT
Regional geology of the Vega landing sites: Tentative results of photogeologic mapping p 440 N94-12047

VEGETATION
An expert system shell for inferring vegetation characteristics: Prototype help system (Task 1)
[NASA-CR-193411] p 231 N94-11236
Enhancement effects in polarimetric radar returns: Phase difference statistics
[NASA-CR-193408] p 231 N94-11309
The impact of vegetation on the atmospheric boundary layer and convective storms p 277 N94-11480
Emissions of biogenic sulfur gases from Alaskan tundra p 268 N94-12455
Emissions of sulfur gases from marine and freshwater wetlands of the Florida Everglades: Rates and extrapolation using remote sensing p 269 N94-12457
Emissions of sulfur gases from wetlands
p 269 N94-12458
Effects of inorganic sulfur addition on fluxes of volatile sulfur compounds in Sphagnum peatlands
p 270 N94-12461
Information capability of NOAA-AVHRR data for monitoring oceanographic and atmospheric pollution
p 214 N94-12677

VEGETATION GROWTH
Sulfur transformations in the sediments of a New Hampshire salt marsh p 270 N94-12463
Elevated acetate concentrations in the rhizosphere of Spartina alterniflora and potential influences on sulfate reduction p 271 N94-12468
Plant architecture, growth and radiative transfer for terrestrial and space environments
[NASA-CR-193476] p 302 N94-12559
Application of remote sensing for coastal management in the north coast of Java p 218 N94-12701

VEGETATIVE INDEX
Design of a global soil moisture initialization procedure for the simple biosphere model
[NASA-TM-104590] p 284 N94-10940
Assessment of ERS-1 SAR data for soil moisture estimation p 249 N94-12492
Properties of spectral reflectance of crown and crown structure of mangrove species in Okinawa
p 218 N94-12700

VELOCITY DISTRIBUTION
Experimental study of axisymmetric thermocapillary flows p 100 N94-10072
Marangoni and buoyant convections in zone melting of GaAs with liquid encapsulation p 101 N94-10081
Comparison of hydrodynamic and semi-kinetic treatments for plasma flow along closed field lines
[NASA-CR-193589] p 387 N94-10641
Examination of wall functions for a parabolized Navier-Stokes code for supersonic flow
[DE93-011590] p 14 N94-11111
CRESLAF. Version 4.0: A Fortran program for modeling laminar, chemically reacting, boundary-layer flow in cylindrical or planar channels
[DE93-012835] p 152 N94-11371

Dynamics and control of coherent structures in the turbulent wall layer: An overview p 31 N94-11494

A four-dimensional, mesoscale, non-gaussian multispectral smoke model. Phase 1: Feasibility study [AD-A264805] p 152 N94-11519

Use of ERS-1 data at Saclant Undersea Research Centre p 233 N94-11714

Parameterization of subgrid-scale stress by the velocity gradient tensor p 155 N94-12286

Similarity states of homogeneous stably-stratified turbulence at infinite Froude number p 156 N94-12292

Numerical simulation using vorticity-vector potential formulation p 157 N94-12297

Laboratory studies on the velocity of fragments from impact disruptions p 189 N94-12359

On the wake behind a high speed train p 164 N94-12618

Spatial variability of the ocean underwater dynamic noise from satellite radar sensing data p 225 N94-12740

VELOCITY MEASUREMENT

Experimental analysis of Benard-convection by the combined application of liquid crystals and PIV p 106 N94-10109

Particle image velocimetry technique: Calibration tests p 111 N94-10137

Estimation of the direct acoustic radiation from turbulent spots using boundary layer velocity measurements p 357 N94-10358

Velocity measurements in hypersonic flows: A review p 5 N94-10436

Perpendicular blade vortex interaction and its implications for helicopter noise prediction: Wave-number frequency spectra in a trailing vortex for BWI noise prediction [NASA-CR-193623] p 357 N94-10752

Laser velocimeter measurements of the flow field generated by a forward-swept propfan during flutter [NASA-TM-106195] p 14 N94-10892

Wall interference correction based on interface measurements in subsonic wind tunnel testing p 15 N94-11154

Measurement of the minority carrier diffusion length and edge surface-recombination velocity in InP p 49 N94-11388

The subduction experiment. Cruise report, R/V Oceanus, cruise number 250 legs 1 and 2. Subduction 2 mooring deployment and recovery cruise, 25 January-26 February 1992 [AD-A264922] p 289 N94-11853

The evolution of whole field optical diagnostics for external transonic testing [ARA-MEMO-379] p 383 N94-11887

Statistical study of HF ocean radar echo p 139 N94-11905

An investigation of small scales of turbulence in a boundary layer at high Reynolds numbers p 157 N94-12303

Probability density distribution of velocity differences at high Reynolds numbers p 158 N94-12304

Development of the one-component diode-array velocimeter [AD-A265552] p 171 N94-12533

VENERA SATELLITES

Regional geology of the Venera landing sites: Tentative results of photogeologic mapping p 440 N94-12048

VENEZIANO MODEL

One-loop quantum gravity on de Sitter space [DE92-641349] p 425 N94-11152

VENTILATION

Icing of turbine intake louvers [AD-A265714] p 29 N94-12274

VENTING

Analysis of geophysical measurements and spacecraft interactions [AD-A266064] p 43 N94-10944

VENTS

Parachute having improved vent line stacking [NASA-CASE-MFS-28508-1] p 14 N94-11021

VENUS (PLANET)

Giant impact-induced atmospheric blow-off p 435 N94-12019

Morphology of large impact craters and basins on Venus: Implications for ring formation p 436 N94-12023

Venus small volcano classification and description p 438 N94-12037

Estimation of age of Dali-Ganis rifting and associated volcanic activity, Venus p 440 N94-12046

Regional geology of the Vega landing sites: Tentative results of photogeologic mapping p 440 N94-12047

Regional geology of the Venera landing sites: Tentative results of photogeologic mapping p 440 N94-12048

Global organization of tectonic deformation on Venus p 444 N94-12066

Venus' center of mass - center of figure displacement and implications p 444 N94-12067

Flexure and the role of inplane force around coronae on Venus p 452 N94-12112

Can weak crust explain the correlation of geoid and topography on Venus? p 453 N94-12118

Yana ring structure, North-Eastern Siberia: A possible counterpart of coronae on Venus p 282 N94-12121

Russia's contribution to regional geologic mapping of Venus p 454 N94-12122

The origin of Venusian channels: Modelling of thermal erosion by lava p 456 N94-12131

Volcanism in southern Guinevere Planitia, Venus: Regional volcanic history and morphology of volcanic domes p 467 N94-12190

Large volcanoes on Venus: Examples of geologic and structural characteristics from different classes p 467 N94-12195

Regional mantle upwelling on Venus: The Beta-Atla-Themis anomaly and correlation with global tectonic patterns p 467 N94-12196

Characteristics of arachnoids from Magellan data p 469 N94-12204

Vulcanian explosive eruptions: A mechanism for localised pyroclast dispersal on Venus p 477 N94-12243

Morphotectonics of Venus p 478 N94-12248

VENUS ATMOSPHERE

Photochemical modelling of Venus clouds using Pioneer Venus data [NASA-CR-194108] p 434 N94-10823

VENUS CLOUDS

Photochemical modelling of Venus clouds using Pioneer Venus data [NASA-CR-194108] p 434 N94-10823

VENUS RADAR ECHOES

Venus mountain-top mineralogy: Misconceptions about pyrite as the high radar-reflecting phase p 455 N94-12129

VENUS SURFACE

Morphology of large impact craters and basins on Venus: Implications for ring formation p 436 N94-12023

Estimation of age of Dali-Ganis rifting and associated volcanic activity, Venus p 440 N94-12046

Regional geology of the Vega landing sites: Tentative results of photogeologic mapping p 440 N94-12047

Global organization of tectonic deformation on Venus p 444 N94-12066

Venus' center of mass - center of figure displacement and implications p 444 N94-12067

Venus resurfacing rates: Constraints provided by 3-D Monte Carlo simulations p 453 N94-12119

A pattern recognition system for locating small volvanoes in Magellan SAR images of Venus p 455 N94-12126

Venus mountain-top mineralogy: Misconceptions about pyrite as the high radar-reflecting phase p 455 N94-12129

Buoyant subduction on Venus: Implications for subduction around coronae p 455 N94-12130

The origin of Venusian channels: Modelling of thermal erosion by lava p 456 N94-12131

Geology and surface characteristics of Bell Regio, Venus p 457 N94-12136

Lava flows on Venus: Analysis of motion and cooling p 457 N94-12137

Galileo/NIMS near-infrared thermal imagery of the surface of Venus p 457 N94-12139

A two-stage (turbulent-drainage) mechanism for the emplacement of impact crater outflows on Venus p 458 N94-12145

Volcanism in southern Guinevere Planitia, Venus: Regional volcanic history and morphology of volcanic domes p 467 N94-12190

Comparison of the distribution of large magmatic centers on Earth, Venus, and Mars p 467 N94-12192

The Magellan volcanic and magmatic feature catalog p 467 N94-12193

Synthesis of global thematic mapping, Venus: Geologic correlations/questions for the Magellan gravity mission p 467 N94-12194

Giant radiating dyke swarms on Earth and Venus p 283 N94-12236

The rate of chemical weathering of pyrite on the surface of Venus p 477 N94-12246

Morphotectonics of Venus p 478 N94-12248

VERBAL COMMUNICATION

Noise levels and their effects on Shuttle crewmembers' performance: Operational concerns p 314 N94-11538

Correspondence standards [NHB-1450.10B] p 420 N94-11589

VERTICAL AIR CURRENTS

Dynamics and control of coherent structures in the turbulent wall layer: An overview p 31 N94-11494

VERTICAL DISTRIBUTION

An investigation using empirical orthogonal functions and objective analysis to analyse the vertical temperature structure of a gulf stream meander [AD-A265116] p 289 N94-11868

The acoustic arrangement for measuring vertical structure of sea current p 223 N94-12729

Remote sensing of light scattering coefficient of sea water vertical distribution by the means of airborne lidar p 224 N94-12736

VERTICAL LANDING

Moving-base simulation evaluation of thrust margins for vertical landing for the NASA YAV-8B Harrier aircraft [NASA-TM-104008] p 30 N94-11259

VERTICAL MOTION SIMULATORS

Moving-base simulation evaluation of thrust margins for vertical landing for the NASA YAV-8B Harrier aircraft [NASA-TM-104008] p 30 N94-11259

VERY HIGH FREQUENCIES

Groundwave HF ocean surface radar p 139 N94-11906

VERY LONG BASE INTERFEROMETRY

Pulsar astrometry by using VLBI (PSR0329 between Kashima 26mPhi and Usuda 64mPhi) p 351 N94-10968

Propagation Effects in Space VLBI p 134 N94-11060

Interstellar scattering and the selection of extragalactic radiosources with highly compact components p 134 N94-11063

Intraday variability and the compactness of extragalactic radio sources p 135 N94-11064

Interstellar scattering and the pulsar studies with space VLBI p 135 N94-11065

VLBI and the detection of interstellar magnetohydrodynamic waves p 135 N94-11066

Generalization of Dyson criterion for the amplitude-phase fluctuations case and for the system of interferometers p 135 N94-11067

The possibility of image restoration under observation in a regime of strong scattering p 136 N94-11068

The superresolution effect observed through a random medium p 136 N94-11069

Tropospheric and ionospheric effects on differential astrometry with a ground-space based VLBI array p 136 N94-11070

Elimination of the influence of the atmosphere on the accuracy of solutions to astrometric problems by means of a ground-space VLBI network p 136 N94-11071

VERY LOW FREQUENCIES

Effects of energetic particle events on VLF/LF propagation parameters/1989 [AD-A265266] p 275 N94-11013

VESTA ASTEROID

Ejecting basaltic achondrites from Vesta: Hydrodynamical impact models p 429 N94-12036

The asteroid-meteorite connection: Forging a new link to Vesta as the parent body of basaltic achondrite (HED) meteorites p 429 N94-12068

VESTIBULAR TESTS

Motion and spatial disorientation systems: Special research capabilities [AD-A265155] p 303 N94-11097

VESTIBULES

Motion and spatial disorientation systems: Special research capabilities [AD-A265155] p 303 N94-11097

VIBRATION

Review of SHARC 2.0 O3 kinetics and spectroscopy [AD-A265481] p 274 N94-10496

On the stability of stationary regimes in a distributed autovibration system with external feedback [DE93-620979] p 141 N94-10543

Dynamic tester for rotor seals and bearings [NASA-CASE-MFS-28493-1] p 33 N94-10669

Sine and random vibration program evaluation on vibration control systems [DE93-011974] p 188 N94-11460

Vortex-induced forces on oscillating bluff cylinders [AD-A265056] p 154 N94-11865

Absorption spectrum calculations using mixed quantum-gaussian wave packet dynamics [AD-A265179] p 413 N94-11877

Thermal-infrared emission spectroscopy of natural surfaces: Application to coated surfaces p 81 N94-12156

A vibrational spectroscopic study of the structure of electroactive self-assembled monolayers of viologen derivatives [AD-A265705] p 78 N94-12273

Vibrational overtone activation of methylcyclopropene [AD-A265588] p 79 N94-12373

VIBRATION DAMPING

Coupled thermovibrational and thermocapillary convection in liquid bridge (floating zone system) p 101 N94-10082

Vibration isolation mount with locking means [AD-D015769] p 178 N94-10381
Dynamic tester for rotor seals and bearings [NASA-CASE-MFS-28493-1] p 33 N94-10669
Momentum management in redundant manipulators for vibration suppression [NASA-CR-194112] p 180 N94-10821
Damping measurements for ultra-high carbon steel/brass laminates [DE93-011886] p 82 N94-11076
Damping mechanisms in chemically vapor deposited SiC fibers [NASA-TM-106334] p 66 N94-11135
Ground vibration and flight flutter tests of the single-seat F-16XL aircraft with a modified wing [NASA-TM-104269] p 26 N94-11233
Adaptive structures for spacecraft: A USAF perspective p 45 N94-11319
Smart structures at Aastra Corporation p 69 N94-11326
On the stability of shape memory materials and their properties in static and dynamic applications p 69 N94-11329
Adaptive algorithms for use with digital filters in vibration control p 71 N94-11338
Structural analysis and optimization of adaptive structures by use of the finite element method p 71 N94-11339
Active landing gear control for improved ride quality during ground roll p 27 N94-11345
Active damping augmentation of elastomechanical systems using piezoelectric sensors and actuators p 72 N94-11346
Multidimensional intelligent control for superlight air vehicles p 27 N94-11347
Sine and random vibration program evaluation on vibration control systems [DE93-011974] p 188 N94-11460
Microgravity vibration isolation technology: Development to demonstration [NASA-TM-106320] p 1 N94-11703
Active vibration control of adaptive flexible structures using piezoelectric smart sensors and actuators p 189 N94-11823

VIBRATION EFFECTS
Vibrational-thermocapillary parallel flows and stability p 120 N94-10220
Comprehensive dynamic analysis of a bladed disk-turborotor-bearing system [ISBN-0-315-73646-1] p 180 N94-11155

VIBRATION ISOLATORS
Vibration isolation mount with locking means [AD-D015769] p 178 N94-10381
Microgravity vibration isolation technology: Development to demonstration [NASA-TM-106320] p 1 N94-11703

VIBRATION MODE
Estimation of critical values and vibration characteristics on supersonic delta wings. Part 1: On-line time series analysis of stationary random response [NAL-TR-1153] p 2 N94-10363
NASTRAN modeling of flight test components for UH-60A airloads program test configuration [NASA-CR-193614] p 186 N94-10937

VIBRATION TESTS
Damping mechanisms in chemically vapor deposited SiC fibers [NASA-TM-106334] p 66 N94-11135
Ground vibration and flight flutter tests of the single-seat F-16XL aircraft with a modified wing [NASA-TM-104269] p 26 N94-11233

VIBRATIONAL SPECTRA
A vibrational spectroscopic study of the structure of electroactive self-assembled monolayers of viologen derivatives [AD-A265705] p 78 N94-12273
Vibrational overtone activation of methylcyclopropene [AD-A265588] p 79 N94-12373

VIBRATORY LOADS
Performance and rotor loads measurements of the Lynx XZ170 helicopter with rectangular blades [NASA-TM-104000] p 1 N94-10936

VIDEO COMMUNICATION
Studies and simulations of the DigiCipher system [NASA-CR-193470] p 321 N94-10343
New technology applied to telemedicine p 306 N94-11796
Study on color video pictures transmission by digital acoustic signal p 139 N94-11917

VIDEO DATA
Study on color video pictures transmission by digital acoustic signal p 139 N94-11917

VIDEO SIGNALS
GaAs sigma-delta modulator modeling for Analog to Digital Converters (ADC's) [AD-A263419] p 144 N94-11516
Observations of optical counterparts of Gamma-Ray bursts [NASA-CR-193573] p 485 N94-12589

VIETNAM
Shoreline change detection using remote sensing and GIS in Vietnam p 196 N94-11928

VIGNETTING
Interferometric and optical tests of water window imaging x ray microscopes [NASA-CR-193369] p 375 N94-10506

VIKING LANDER SPACECRAFT
Geologic history of central Chryse Planitia and the Viking 1 landing site, Mars p 465 N94-12180

VIRIAL COEFFICIENTS
Phase equilibria and volumetric properties for the system NaCl-CaCl2-H2O [DE93-013590] p 76 N94-11244

VIRTUAL REALITY
Virtual sound for virtual reality [DE93-010519] p 321 N94-10291
Forecasting the impact of virtual environment technology on maintenance training p 314 N94-11570

VISCOELASTIC DAMPING
Computational algorithms or identification of distributed parameter systems [AD-A265252] p 331 N94-11680

VISCOELASTICITY
A method for determination of the elongational viscosity of viscoelastic fluids without body forces p 124 N94-10247
Advanced model of gradual wear of viscoelastic surface film [AD-A265130] p 90 N94-11222
Stability of viscoelastic flow: Physical and numerical considerations p 31 N94-11493
On temperature distribution in non-participating medium with radiation boundary condition [DE93-619375] p 153 N94-11604
Numerical simulation of the non-Newtonian mixing layer p 159 N94-12314

VISCOPLASTICITY
A modeling investigation of thermal and strain induced recovery and nonlinear hardening in potential based viscoplasticity [NASA-TM-106122] p 188 N94-11482

VISCOSITY
Determination of the viscous acoustic field for liquid drop positioning/forcing in an acoustic levitation chamber in microgravity p 110 N94-10131
Thermophysical properties of undercooled liquid metals p 86 N94-10190
A method for determination of the elongational viscosity of viscoelastic fluids without body forces p 124 N94-10247
Measurement of viscosity, density and gas solubility of refrigerant blends [DE93-014772] p 89 N94-11145
Negative viscosity and generation of dissipative solitons and zonal dissipative structures by drift waves [DE93-621656] p 392 N94-11212
Viscous relaxation of the Moho under large lunar basins p 452 N94-12113

VISCOUS DAMPING
A numerical experiment of boundary layer transition at subcritical Reynolds numbers p 165 N94-12625

VISCOUS FLOW
Studies of hypersonic viscous flows p 8 N94-10454
Calculations of viscous nonequilibrium flows in nozzles p 8 N94-10455
On the accuracy and efficiency of CFD methods in real gas hypersonics p 9 N94-10462
Thermal and chemical non equilibrium hypersonic flow computations p 10 N94-10465
Viscous flow simulation using an upwind method for hexahedral based adaptive meshes [AD-A265901] p 148 N94-10703
High order accurate solutions of viscous problems [NASA-TM-106267] p 151 N94-11253
Viscous analysis of three-dimensional rotor flows using a multigrid method [NASA-TM-106266] p 152 N94-11481
Numerical simulation using vorticity-vector potential formulation p 157 N94-12297
VIB2D: Quasi 3-D unsteady viscous flow method for blade flutter calculation [CUED/A-TURBO/TR.129] p 166 N94-12779

VISCOUS FLUIDS
Deformation mechanisms of continuous fibre-reinforced thermoplastic composites during manufacturing: A probabilistic approach p 60 N94-10030
A method for determination of the elongational viscosity of viscoelastic fluids without body forces p 124 N94-10247
The physics of pattern formation of liquid interfaces [DE93-013333] p 154 N94-11814

VISIBILITY
User's manual for the plume visibility model PLUVUE 2 (revised) [PB93-188233] p 265 N94-11016
On resolution of underwater stereo photogrammetry p 172 N94-11966

VISIBLE INFRARED SPIN SCAN RADIOMETER
Effects of satellite spectral resolution and atmospheric water vapor on retrieval of near-ground temperatures [AD-A264920] p 245 N94-11851

VISIBLE SPECTRUM
Continued development of an ultra-narrow bandpass filter for solar research [NASA-CR-194169] p 381 N94-10735
Compositional and textural information from the dual inversion of visible, near and thermal infrared remotely sensed data p 258 N94-12097

VISION
Aviation accident risk for airmen with aphakia and artificial lens implants [DOT/FAA/AM-93/11] p 303 N94-10813

VISUAL AIDS
Animating engineering science results using AVS [DE93-011591] p 325 N94-11123

VISUAL OBSERVATION
Visual Earth observation performance in the space environment. Human performance measurement 4: Flight experiments p 314 N94-11539

VISUAL PERCEPTION
Automaticity of processing location versus identity information in brief visual displays [AD-A265013] p 418 N94-10491
Visual encoding of spatial relations [AD-A266049] p 313 N94-10909
Computer software and hardware to determine contrast sensitivity using three methods: Tracking, limits, and constant stimuli [AD-A265168] p 324 N94-11099
Three-dimensional object recognition using an unsupervised BCM network: The usefulness of distinguishing features [AD-A264576] p 304 N94-11261
Perceptual response to visual noise and display media [NASA-CR-193406] p 313 N94-11511
Visual psychophysics of egomotion [AD-A265253] p 304 N94-11681

VISUAL STIMULI
Computer software and hardware to determine contrast sensitivity using three methods: Tracking, limits, and constant stimuli [AD-A265168] p 324 N94-11099

VITRIFICATION
Radiation-induced aperiodicity in irradiated ceramics [DE93-013335] p 91 N94-11698

VLASOV EQUATIONS
Dynamics of ion acceleration in electron flux by a virtual cathode potential [DE93-620978] p 371 N94-10542

VOICE DATA PROCESSING
Necessary conditions for the optimality of variable rate residual vector quantizers [NASA-CR-193730] p 326 N94-11197

VOIDS
A method of influence regions in the theory of vacancy swelling of metals [DE93-620579] p 83 N94-11363
Modeling void growth and movement with phase change in thermal energy storage canisters [NASA-TM-106288] p 163 N94-12576

VOLATILITY
Vaporization by shock loading of albite, jadeite, and pyrex glass: Experimental study p 97 N94-12039
Shock induced reaction in Chicxulub target materials (CaSO4 and SiO2) and their relation to extinctions p 282 N94-12149
The correlation of alkalis and aluminum during high-temperature volatilization of albite and nepheline p 81 N94-12214

VOLCANOES
The Lathrop Wells Volcanic Center: Status of field and geochronology studies [DE93-008917] p 273 N94-10285
Overwater atmospheric dispersion of volcanic smokes from Mt. Sakurajima observed in NOAA-AVHRR data p 205 N94-11979
Venus small volcano classification and description p 438 N94-12037
Reconstruction of the dynamics of the 1800-1801 Hualalai eruption: Implications for planetary lava flows p 281 N94-12041
Horizontal stresses induced by vertical processes in planetary lithospheres p 281 N94-12042
Estimation of age of Dali-Ganis rifting and associated volcanic activity, Venus p 440 N94-12046
Regional geology of the Vega landing sites: Tentative results of photogeologic mapping p 440 N94-12047

A pattern recognition system for locating small volvanoes in Magellan SAR images of Venus p 455 N94-12126
Lava flows on Venus: Analysis of motion and cooling p 457 N94-12137
Graphite solubility and co-vesiculation in basalt-like melts at one-ATM p 463 N94-12173
Volcanism in southern Guinevere Planitia, Venus: Regional volcanic history and morphology of volcanic domes p 467 N94-12190
Comparison of the distribution of large magmatic centers on Earth, Venus, and Mars p 467 N94-12192
The Magellan volcanic and magmatic feature catalog p 467 N94-12193
Large volcanoes on Venus: Examples of geologic and structural characteristics from different classes p 467 N94-12195
Regional mantle upwelling on Venus: The Beta-Atla-Themis anomaly and correlation with global tectonic patterns p 467 N94-12196
Small volcanoes in Tempe Terra, Mars: Their detailed morphometry and inferred geologic significance p 469 N94-12202
Oxidation state of the Earth's upper mantle during the last 3800 million years: Implications for the origin of life p 283 N94-12210
Giant radiating dyke swarms on Earth and Venus p 283 N94-12236

VOLCANOLOGY
Twenty-fourth Lunar and Planetary Science Conference. Part 1: A-F
[NASA-CR-193095] p 435 N94-12015
Venus small volcano classification and description p 438 N94-12037
Reconstruction of the dynamics of the 1800-1801 Hualalai eruption: Implications for planetary lava flows p 281 N94-12041
Estimation of age of Dali-Ganis rifting and associated volcanic activity, Venus p 440 N94-12046
Regional geology of the Vega landing sites: Tentative results of photogeologic mapping p 440 N94-12047
Stable isotope analyses of the peralkaline volcanics Gregory Rift Valley, Kenya p 281 N94-12072
Th-230 - U-238 series disequilibrium of the Olkaria basalts Gregory Rift Valley, Kenya p 281 N94-12073
Th-230 - U-238 series disequilibrium of the Olkaria rhyolites Gregory Rift Valley, Kenya: Residence times p 281 N94-12076
Geology and surface characteristics of Bell Regio, Venus p 457 N94-12136
Volcanism in southern Guinevere Planitia, Venus: Regional volcanic history and morphology of volcanic domes p 467 N94-12190
Comparison of the distribution of large magmatic centers on Earth, Venus, and Mars p 467 N94-12192
Characteristics of arachnoids from Magellan data p 469 N94-12204
Compositional heterogeneity within a dumbbell-shaped Apollo 15 green glass: Evidence for simultaneous eruption of different magmas p 470 N94-12209
Vulcanian explosive eruptions: A mechanism for localised pyroclast dispersal on Venus p 477 N94-12243
A comparison of the visible and near infrared reflectance of hydrovolcanic palagonite tuffs and Martian weathered soils p 477 N94-12245

VOLTAGE CONVERTERS (DC TO DC)
A study of DC-DC converters with MCTs for arcjet power supplies
[NASA-CR-193457] p 142 N94-10931

VOLUMETRIC ANALYSIS
Studies of critical point phenomena of fluids: Bulk fluids, fluids in pores, and at interfaces p 80 N94-10228

VORTEX ALLEVIATION
Corner vortex suppressor
[AD-D015772] p 147 N94-10383
Underwing compression vortex attenuation device
[NASA-CASE-LAR-14744-1] p 12 N94-10673

VORTEX BREAKDOWN
Underwing compression vortex attenuation device
[NASA-CASE-LAR-14744-1] p 12 N94-10673
Growth and breakdown of Taylor-Goertler vortices in rotating Blasius boundary layer p 165 N94-12631

VORTEX FLAPS
Underwing compression vortex attenuation device
[NASA-CASE-LAR-14744-1] p 12 N94-10673

VORTEX GENERATORS
Generation of two-dimensional vortices in a cross-flow p 160 N94-12318
Topics in pattern formation and chaotic systems
[AD-A265922] p 161 N94-12342
Growth and breakdown of Taylor-Goertler vortices in rotating Blasius boundary layer p 165 N94-12631

VORTEX SHEDDING
Perpendicular blade vortex interaction and its implications for helicopter noise prediction: Wave-number frequency spectra in a trailing vortex for BWI noise prediction
[NASA-CR-193623] p 357 N94-10752
Vortex-induced forces on oscillating bluff cylinders
[AD-A265056] p 154 N94-11865
On the wake behind a high speed train p 164 N94-12618

VORTICES
Underwing compression vortex attenuation device
[NASA-CASE-LAR-14744-1] p 12 N94-10673
Simulation study of dynamo structure in reversed field pinch
[DE93-771406] p 390 N94-11128
Control of jet noise
[NASA-CR-193612] p 358 N94-11176
Physics of forebody flow control
[NASA-CR-193626] p 15 N94-11195
On nonlinear Tollmien-Schlichting/vortex interaction in three-dimensional boundary layers
[NASA-TM-106184] p 152 N94-11377
Discrete vortex representation of magnetohydrodynamics
[DE93-012190] p 393 N94-11669
Vortex-induced forces on oscillating bluff cylinders
[AD-A265056] p 154 N94-11865
An investigation using empirical orthogonal functions and objective analysis to analyse the vertical temperature structure of a gulf stream meander
[AD-A265116] p 289 N94-11868
Time evolution of cross-stream exchange associated with the variations in the Kuroshio p 197 N94-11936
Characteristic scales and vortex features of mesoscale vortices observed by the satellites during the winter p 199 N94-11943
An application of reduced gravity model to mesoscale eddies p 199 N94-11945
Behavior of vortices generated by an advancing ejecta curtain in theory, in the laboratory, and on Mars p 169 N94-12044
A local dynamic model for large eddy simulation p 155 N94-12285
Large eddy simulations of time-dependent and buoyancy-driven channel flows p 155 N94-12287
A normal stress subgrid-scale eddy viscosity model in large eddy simulation p 155 N94-12288
Large eddy simulation of shock turbulence interaction p 155 N94-12289
Application of a dynamic subgrid-scale model to turbulent recirculating flows p 156 N94-12290
Large-eddy simulation of turbulent flow with a surface-mounted two-dimensional obstacle p 156 N94-12291
Similarity states of homogeneous stably-stratified turbulence at infinite Froude number p 156 N94-12292
Application of incremental unknowns to the Burgers equation p 156 N94-12293
Numerical simulation using vorticity-vector potential formulation p 157 N94-12297
Local isotropy in high Reynolds number turbulent shear flows p 157 N94-12302
Plane mixing layer vortical structure kinematics p 159 N94-12313
Generation of two-dimensional vortices in a cross-flow p 160 N94-12318
Suppression of the near wall burst process of a fully developed turbulent pipe flow
[AD-A265995] p 161 N94-12352
Proceedings of the 9th and 10th NAL Workshop on Investigation and Control of Boundary-Layer Transition
[NAL-SP-18] p 163 N94-12611
Fluctuations of longitudinal vortices along a concave wall p 16 N94-12616
On the formation process of Karman vortex street p 16 N94-12621
Turbulent boundary layer interacting with spanwise periodic longitudinal vortex arrays p 165 N94-12626
Observations of eddy fields in the Northwest Pacific by GEOSAT altimetry p 207 N94-12639
Surface eddy fluxes from the GEOSAT satellite altimeter p 208 N94-12643
Measurement of eddy structure and movement in the north-east Pacific with the GEOSAT altimeter p 209 N94-12647
Fluctuations of the Kuroshio extension detected by the GEOSAT altimetry data p 209 N94-12649
Aspects of applying a relaxation method to computing sea surface velocities from sea surface temperature images p 214 N94-12679
Statistical features of mesoscale eddies at the Kuroshio front p 215 N94-12682
The WOCE/TOGA Surface Velocity Programme (SVP) p 216 N94-12691
Investigation of meso-scale fronts, eddies and upwellings in China Seas with AVHRR data p 220 N94-12711
The warm eddy detection from NOAA/AVHRR thermal images using the Hough transformation p 220 N94-12713
Satellite and moored buoy observations of polar frontal system over the Yamato Rise in the Japan Sea p 221 N94-12715
On a nonstationary dynamics of the north-west Pacific Ocean p 222 N94-12724
Mixing of drifter ensemble by mesoscale currents p 228 N94-12760

VORTICITY
On the importance of mesoscale potential vorticity anomalies and topographic forcing during cyclone redevelopment across the Appalachians: A GALE case study p 284 N94-10822
Near surface ocean processes: Acoustical observations, ambient sound, and Langmuir circulation p 288 N94-11447
Unsteady flow past a NACA 0012 airfoil pitching at constant rates
[AD-A265159] p 16 N94-11889
Parameterization of subgrid-scale stress by the velocity gradient tensor p 155 N94-12286
The three-dimensional evolution of a plane wake p 159 N94-12310
Plane mixing layer vortical structure kinematics p 159 N94-12313

VSAT (NETWORK)
Two way time transfer results at NRL and USNO p 353 N94-10983

VULCANIZING
Vulcanian explosive eruptions: A mechanism for localised pyroclast dispersal on Venus p 477 N94-12243

VULNERABILITY
GRAFTED (GRAphical Fault Tree EDitor): A fault tree description program for target vulnerability/survivability analysis
[AD-A264078] p 328 N94-11301

W

WAFERS
RF vacuum microelectronics
[AD-A266066] p 142 N94-10818
An ellipsometry investigation of nucleation and growth of electron cyclotron resonance plasma deposited silicon films
[AD-A265037] p 401 N94-11651
Radiation-induced modifications of allylamino-substituted polyphosphazenes
[AD-A264914] p 92 N94-11848
Analysis of the economics of DC arc CVD diamond
[AD-A265688] p 403 N94-12339

WAKES
Submarine internal waves
[MRL-GD-0049] p 98 N94-11303
Topics in pattern formation and chaotic systems
[AD-A265922] p 161 N94-12342

WALKING
Robotic servicing on Earth orbiting satellites p 45 N94-11579

WALL FLOW
Wall interference correction based on interface measurements in subsonic wind tunnel testing p 15 N94-11154
A Galilean and tensorial invariant k-epsilon model for near wall turbulence
[NASA-TM-106263] p 151 N94-11192
Dynamics and control of coherent structures in the turbulent wall layer: An overview p 31 N94-11494
Reynolds stress closure modeling in wall-bounded flows p 157 N94-12298
Application of a Reynolds stress model to separating boundary layers p 157 N94-12299
Regeneration of near-wall turbulence structures p 158 N94-12308
Suppression of the near wall burst process of a fully developed turbulent pipe flow
[AD-A265995] p 161 N94-12352
Fluctuations of longitudinal vortices along a concave wall p 16 N94-12616
A numerical experiment of boundary layer transition at subcritical Reynolds numbers p 165 N94-12625
Turbulent drag reduction of a d-type rough wall boundary layer with longitudinal ribs placed within the grooves p 165 N94-12627

WALL JETS
Turbulent wall jet in blast wave precursor
[DE93-011955] p 151 N94-11144

WALL TEMPERATURE
Establishing baseline data for an experimental appratus that measures heat transfer under conditions of oscillating pressure and flow
[NASA-CR-193772] p 413 N94-12343
WALLS
Potential change in flaw geometry during pressurized-thermal-shock transients
[DE93-009709] p 184 N94-10288
Application of a Reynolds stress model to separating boundary layers p 157 N94-12299
WARFARE
Aviators, air combat, and combat stress: An Air F orce commander's primer
[AD-A265083] p 313 N94-11867
WARNING SYSTEMS
The Satellite Attack Warning and Assessment Flight Experiment (SAWAFE) p 45 N94-11323
WASTE DISPOSAL
Environmental Sciences Division
[DE93-013865] p 264 N94-10650
Computer models used to support cleanup decision-making at hazardous and radioactive waste sites
[PB93-183333] p 274 N94-10698
WASTE TREATMENT
Toxic chemical release inventory reporting Form R and instructions. Revised 1992 version. Section 313 of the Emergency Planning and Community Right-to-Know Act
[PB93-194140] p 264 N94-10836
Some environmental aspects of the application of fibre reinforced plastics in structures
[LM-998] p 88 N94-10877
Catalytic oxidation of organics in vapor streams at remediation sites
[PB93-182962] p 266 N94-11472
An estimate of the second law thermodynamic efficiency of the various units comprising an Environmental Control and Life Support System (ECLSS) p 317 N94-12369
Novel mass spectrometric instrument for gaseous and particulate characterization and monitoring
[DE93-014093] p 272 N94-12783
WASTE UTILIZATION
Some environmental aspects of the application of fibre reinforced plastics in structures
[LM-998] p 88 N94-10877
Coprocessing of fossil fuels and biomass for CO2 emission reduction in the transportation sector
[PB93-194165] p 267 N94-11845
WATER
Atomic and molecular data for H2O, CO and CO2 relevant to edge plasma impurities
[DE93-771423] p 387 N94-10662
Experimental study of multiple droplet evaporative cooling
[PB93-198463] p 149 N94-10851
Structural development in ceramic precursor sols and gels
[AD-A264354] p 90 N94-11281
An observational search for CO2 ice clouds on Mars p 441 N94-12054
Noble gas evidence of an aqueous reservoir near the surface of Mars more recently than 1.3 Ga p 473 N94-12228
Primitive SNC parent magmas and crystallization: Low PH2O experiments p 433 N94-12264
Space Life Support Engineering Program
[NASA-CR-193474] p 316 N94-12365
Physiological water model development p 316 N94-12367
Fundamental studies of radar scattering from water surfaces: The Lake Washington experiment
[NASA-CR-194030] p 139 N94-12778
WATER BALANCE
Flood monitoring in northern part of Central Java by remote sensing technique. Case study: The flooding of Semarang in January, 1990 p 206 N94-11989
WATER COLOR
Atmospheric correction of AVIRIS data in ocean waters
[AD-A264931] p 288 N94-11287
Effects of wind-roughened sea surface on ocean color remote sensing: Noise derived from reflected light and whitecaps p 191 N94-11898
Satellite-derived oceanic features p 200 N94-11949
Bi-directional reflectance by oceanic waters studied via Monte-Carlo simulations p 203 N94-11971
Optical characteristics in Tokyo Bay p 204 N94-11972
Remote sensing for numerical modelling of radiative transfer processes in ocean environment p 204 N94-11973
Seasonal variability of surface ocean color in the Omura Bay using multitemporal LANDSAT-5 TM data p 218 N94-12698
WATER COOLED REACTORS
Facility for stress corrosion cracking test of irradiated material in high temperature water
[DE93-753189] p 84 N94-11593
WATER CURRENTS
Sandia ocean modeling system programmer's guide and user's manual
[DE93-007427] p 287 N94-10153
WATER DEPTH
The extraction of bottom characteristics and mapping in Kin Bay, Okinawa Main Island, Japan, using LANDSAT-5/TM and SPOT-1/HRV data p 197 N94-11931
WATER EROSION
Rates of fluvio-thermal erosion on Mars p 435 N94-12018
WATER FLOW
The flow structure around a cylindrical pier for the flow of transcritical Reynolds number p 169 N94-11944
Rates of fluvio-thermal erosion on Mars p 435 N94-12018
Rainfall-runoff estimation using digital radar
[AD-A265390] p 286 N94-12408
Simultaneous 3D turbulent large-scale structures in a flood flow by multi-channels measuring system p 165 N94-12624
Turbulence generation in the Pacific undercurrent by shear p 223 N94-12730
WATER HEATING
Department of Energy solar process heat program: FY 1991 solar process heat prefeasibility studies activity
[DE93-010010] p 262 N94-10258
WATER IMMERSION
Development and analysis of insulation constructions for aerospace wiring applications p 21 N94-10791
WATER LOSS
Modifications to an interactive model of the human body during exercise: With special emphasis on thermoregulation p 317 N94-12368
WATER MANAGEMENT
Space Activities in the Asia Pacific Region
[JTN-93-80421] p 35 N94-10676
International Space Year in China p 36 N94-10680
An algorithm for the detection of mucilage (green slime) in the Adriatic Sea p 191 N94-11900
WATER POLLUTION
Immediate response to free product discovery
[PB93-182970] p 265 N94-11015
Gulf of Mexico sales 147 and 150: Central and western planning areas. Draft environmental impact statement. Volume 1: Sections 1 through 4.C
[PB93-190304] p 265 N94-11018
Gulf of Mexico sales 147 and 150: Central and western planning areas. Draft environmental impact statement. Volume 2: Sections 4.D through 9
[PB93-190312] p 265 N94-11019
Biscayne bay: A bibliography of the marine environment
[PB93-184802] p 266 N94-11451
An algorithm for the detection of mucilage (green slime) in the Adriatic Sea p 191 N94-11900
A study of pollution courses of spilled oil floatation in the outer ocean p 205 N94-11983
Remote sensing of polluting focal points and coastal disturbances in the Gulf of Arauco and adjacent bays, central Chile p 217 N94-12695
Laser fluorescent monitoring of dissolved organic matter in natural water p 177 N94-12755
Study of the admixture diffusion in the sea using remote techniques p 228 N94-12759
WATER QUALITY
Summary of implementation and demonstration projects in bays and estuaries
[PB93-194637] p 265 N94-10846
Remote surface water monitoring radio based telemetry system
[DE93-009643] p 41 N94-11282
Optical characteristics in Tokyo Bay p 204 N94-11972
WATER RECLAMATION
Microbiological test results using three urine pretreatment regimes with 316L stainless steel
[NASA-CR-192568] p 299 N94-10360
Systems analysis of a closed loop ECLSS using the ASPEN simulation tool. Thermodynamic efficiency analysis of ECLSS components p 316 N94-12366
WATER RESOURCES
Land use/land cover mapping of central water shed of Iran area based on satellite data interpretation p 219 N94-12704
WATER TREATMENT
Space Life Support Engineering Program
[NASA-CR-193474] p 316 N94-12365
WATER TUNNEL TESTS
Unsteady flow past a NACA 0012 airfoil pitching at constant rates
[AD-A265159] p 16 N94-11889
WATER VAPOR
The impact of horizontal resolution on moist processes in the ECMWF model
[DE93-011718] p 276 N94-11227
Central Equatorial Pacific Experiment (CEPEX)
[DE93-011656] p 190 N94-11674
Evaporation and thermal/hydrologic balance in the Pacific p 195 N94-11919
Evaluation of ECMWF latent heat flux in TOGA CD-ROM p 195 N94-11921
Validation of the ATSR/M microwave radiometer data p 252 N94-12511
Multichannel dual angle approach for sea surface temperature retrieval in context of ERS-1 scenario p 252 N94-12512
Analytical method for water vapor collection and analysis in aircraft cabin fires
[DOT/FAA/CT-TN93/33] p 22 N94-12575
Worldwide map of rainfall amount over the ocean derived from passive microwave radiometer p 211 N94-12663
Cloud liquid water content over the Pacific Ocean tropical zone derived from ship microwave radiometric measurement p 225 N94-12743
WATER WAVES
Preliminary results on backscattering strength from a wind generated bubbly ocean surface
[AD-A265006] p 287 N94-10490
Validation of directional wave spectra from the ERS-1 during the ESA CAL/VAL campaign p 232 N94-11707
The Grand Banks ERS-1 SAR wave spectra validation experiment p 232 N94-11708
Validation of ERS-1 wind and wave data by use of operational forecast models p 233 N94-11710
The activity of the ERS-1 Venice (Italy) group on scatterometry p 233 N94-11713
Waves and mesoscale features in the marginal ice zone p 240 N94-11757
Global wave height climatologies from ERS-1 altimeter data, and comparisons with those from GEOSAT p 244 N94-11781
Spatial scales of wave height p 244 N94-11782
Proceedings of the PORSEC 1992 in Okinawa: Conference for Pacific Ocean Environments and Probing, volume 1
[JTN-93-80418] p 191 N94-11894
Remote sensing and the air-sea boundary layers p 191 N94-11896
HF ocean radar system at Okinawa Radio Observatory p 139 N94-11902
Measurement of wave parameters by HF ocean radar p 192 N94-11903
Statistical study of HF ocean radar echo p 139 N94-11905
Groundwave HF ocean surface radar p 139 N94-11906
A new expression for the production rate of sea water droplets on the sea surface p 195 N94-11920
Air-sea fluxes and universal constants in weak-turbulence theory of surface gravity waves p 195 N94-11922
Ocean wave detection by SAR p 197 N94-11932
On the determination of the SAR ocean surface scattering patch size p 197 N94-11933
The optical/computer hybrid processing of extracting ocean wave directional spectrum by airborne photograph p 197 N94-11934
Ocean-ice interaction study of waves and mesoscale features p 197 N94-11935
Coastal processes due to nearshore current around an upheaving island p 199 N94-11942
Physical processes of microwave backscattering from laboratory wind-wave surfaces p 200 N94-11952
Dependence of oceanic microwave emission on wind direction p 201 N94-11957
Surface roughness variations across the Iceland-Faroes frontal region observed by the GEOSAT altimeter and NOAA AVHRR p 201 N94-11958
The microwave backscattering from wind waves p 201 N94-11959
Observation of wind and waves by GEOSAT altimeter p 202 N94-11961
Impact of ERS-1 wind/wave/ice data on operational ocean forecasting p 250 N94-12500
Real time processing wave spectra from satellite SAR p 251 N94-12506
On the extraction of ocean wave spectra from ERS-1 SAR wave mode image spectra p 251 N94-12509
Tide-generated nonlinear internal wave packets in the Strait of Gibraltar observed by the synthetic aperture radar aboard the ERS-1 satellite p 252 N94-12510

Artificial oil pollution detection and wave observation in the sea adjacent to Japan by ERS-1 SAR p 253 N94-12520
Proceedings of the PORSEC 1992 in Okinawa: Conference for Pacific Ocean Environments and Probing, volume 2 [JTN-93-80419] p 207 N94-12635
Observation of wave crests by satellite remote sensed data p 207 N94-12638
Field research of wind wave spectrum variability p 223 N94-12727
Observations of film slicks and internal waves with Ka-band scatterometer p 225 N94-12741
Wind-wave and foam dynamics from optical and radar airborne observations p 226 N94-12745
Observations of surface signatures in the north-west Pacific Ocean with the spaceborne SAR p 226 N94-12746
Radar observation of internal waves field in the north-west Pacific p 226 N94-12747

WATERPROOFING
Toxicity study of dimethylethoxysilane (DMSES), the waterproofing agent for the Orbiter heat protective system p 318 N94-11554

WATERSHEDS
Energy flow in an Arctic aquatic ecosystem [DE93-013178] p 267 N94-11697

WAVE ATTENUATION
Photostimulated attenuation of hypersound in superlattice [DE93-611231] p 357 N94-10408

WAVE DISPERSION
Nonlinear MHD-waves in a dissipative plasma with hall currents [DE93-617844] p 386 N94-10395
General renormalized statistical approach with finite cross-field correlations [DE93-617846] p 386 N94-10396
Studies of P-matrix formalism on the basis of the potential description of two-particle interaction [DE93-617691] p 362 N94-10550
On the doubling of hydrodynamic theorems in relativistic theory of superfluidity [DE93-617895] p 148 N94-10717
Wave propagation characteristics of short-period crustal phases near ARCESS and NORESS [AD-A265959] p 275 N94-11102
Dispersion of plasma waves in a finite magnetic field (omega(sub H) greater than omega(sub p)) [DE93-621654] p 391 N94-11210
Negative viscosity and generation of dissipative solitons and zonal dissipative structures by drift waves [DE93-621656] p 392 N94-11212
One-dimensional calculation of high-power microwave pulse compression by the earth's ionosphere [DE93-009517] p 137 N94-11466

WAVE EQUATIONS
Wave and pseudo-diffusion equations from squeezed states p 347 N94-10607

WAVE EXCITATION
Wave generation by contaminant ions [NASA-CR-193558] p 364 N94-10946

WAVE FRONTS
An analytic model for calculating pump-induced wavefront distortions in laser slabs [DE93-011953] p 174 N94-11126
Multiple laser beam combining and phasing using closed-loop control [DE93-009830] p 175 N94-11283

WAVE FUNCTIONS
Satellite structure of the xenon valence shell by electron momentum spectroscopy [DE93-609993] p 360 N94-10327
Distorted-wave calculation of He(e,2e) including core-exchange [DE93-610072] p 360 N94-10330
Electron momentum spectroscopy of atoms, molecules and solids [DE93-610148] p 360 N94-10332
Recent advances in electron momentum spectroscopy [DE93-610149] p 361 N94-10333
Wave function collapse: An unnecessary condition for the dynamical description of the Zeno and partial Zeno effect [DE93-612970] p 132 N94-10401
P-matrix description of the two-particle interaction [DE93-617690] p 361 N94-10549
Studies of P-matrix formalism on the basis of the potential description of two-particle interaction [DE93-617691] p 362 N94-10550
The uncertainty principle and quantum chaos p 379 N94-10602
Wavelets and spacetime squeeze p 379 N94-10604
Coherent states and uncertainty relations for the damped harmonic oscillator with time-dependent frequency p 380 N94-10611
Test of a method for phase retrieval in HRTEM [DE93-612641] p 170 N94-10630
Quasi-relativistic effects in barrier-penetration processes [DE93-617730] p 410 N94-10721
On the possible unobservability of the Wu-Yang phase factor in curved space [DE93-617645] p 411 N94-10831
Exact solutions of a many-anyon problem [DE93-617646] p 411 N94-10832

WAVE GENERATION
Wave generation by contaminant ions [NASA-CR-193558] p 364 N94-10946

WAVE INTERACTION
Evaluation of dual flow thrust vectored nozzles with exhaust stream impingement [NASA-CR-193292] p 150 N94-10912
Theoretical investigation of 3-D shock wave turbulent boundary layer interactions [AD-A265275] p 150 N94-11014
Wave structure in planetary rings p 434 N94-11185
On nonlinear Tollmien-Schlichting/vortex interaction in three-dimensional boundary layers [NASA-TM-106184] p 152 N94-11377
Ultrasonic wave interaction with advanced complex materials for nondestructive evaluation applications [AD-A265704] p 74 N94-12401

WAVE PACKETS
On a Lagrange-Hamilton formalism describing position and momentum uncertainties p 349 N94-10583
Correlated states of a quantum oscillator acted by short pulses p 380 N94-10609
Absorption spectrum calculations using mixed quantum-gaussian wave packet dynamics [AD-A265179] p 413 N94-11877

WAVE PROPAGATION
Nonlinear MHD-waves in a dissipative plasma with hall currents [DE93-617844] p 386 N94-10395
Wideband beamforming for a sparse nonuniform spaced sensor array [AD-A265909] p 133 N94-10660
Spatial helicon-wave echo in an inhomogeneous magnetized plasma [DE93-617845] p 389 N94-10885
Inverting ultrasonic data on solid/fluid mixtures for Biot-Gassmann parameters [DE93-011952] p 150 N94-11026
A symmetrical form for equations of a nonlinear spiral magnetic [DE93-621350] p 344 N94-11033
The influence of the propagation medium on the sensitivity and resolution of meter wavelength aperture synthesis systems p 134 N94-11062
The superresolution effect observed through a random medium p 136 N94-11069
Wave propagation characteristics of short-period crustal phases near ARCESS and NORESS [AD-A265959] p 275 N94-11102
Studies on the parametric decay of waves in fusion plasmas [DE93-621659] p 390 N94-11148
One-dimensional calculation of high-power microwave pulse compression by the earth's ionosphere [DE93-009517] p 137 N94-11466
Decay interaction of bulk and surface Langmuir waves [DE93-617843] p 393 N94-11477
Stability and dynamics of spatio-temporal structures [DE93-011374] p 401 N94-11610
Spaceborne SAR study: LDRD 1992 [DE93-011485] p 232 N94-11623
Results from a year-long auroral-E measurement campaign [AD-A265059] p 278 N94-11871
Propagation of light pulses through a three-layer medium (cloud, pure air, and ocean water) p 222 N94-12725
Trajectory curving in underwater propagation of light p 226 N94-12748

WAVE REFLECTION
Preliminary results on backscattering strength from a wind generated bubbly ocean surface [AD-A265006] p 287 N94-10490
Effects of energetic particle events on VLF/LF propagation parameters/1989 [AD-A265266] p 275 N94-11013
Acoustics of bubbly sediments [AD-A263726] p 288 N94-11299

WAVE SCATTERING
On the possible unobservability of the Wu-Yang phase factor in curved space [DE93-617645] p 411 N94-10831
Radiowaves propagation through inhomogeneous interstellar plasma p 134 N94-11061

WAVE-PARTICLE INTERACTIONS
Nonlinear analysis of a magnicon output cavity [AD-A265342] p 145 N94-12424

WAVEFORMS
On the coupling of electromagnetic radiation into cavities [DE93-011406] p 137 N94-11621

WAVEGUIDES
Nonlinear space charge effect of bunched beam in linac [DE93-612176] p 371 N94-10409
Non classical effects in planar waveguides p 376 N94-10574
About excitation of round waveguide by a point current source [DE93-621352] p 133 N94-11034
Linear antenna of an arbitrary orientation and position in cylindric screen [DE93-621353] p 134 N94-11035
Regular tensor Green functions of the round waveguide [DE93-621354] p 345 N94-11036
Asymptotic expressions for regular Green functions of a round cylindrical screen [DE93-621356] p 134 N94-11038
Dispersion of plasma waves in a finite magnetic field (omega(sub H) greater than omega(sub p)) [DE93-621654] p 391 N94-11210
Non-linear dynamics of automodulation processes in coupled distributed autovibration systems with delay [DE93-620976] p 143 N94-11365
Acoustic waveguide characteristics of the Indian Ocean north of equator p 193 N94-11912

WAVELENGTH DIVISION MULTIPLEXING
An efficient medium access control strategy for high speed WDM multiaccess networks [MEMO-INF-92-74] p 131 N94-10165

WAVELENGTHS
Interference photocathode [AD-D015770] p 132 N94-10382

WAVES
FEFF5: An ab initio multiple scattering XAFS code [DE93-011000] p 367 N94-11470

WEAK INTERACTIONS (FIELD THEORY)
Discrete space-time symmetries [DE93-010199] p 341 N94-10259
Effective action in the gauged Nambu-Jona-Lasinio model [DE93-617654] p 409 N94-10405
Future high precision experiments and new physics beyond Standard Model [DE93-011004] p 373 N94-11618

WEAPON SYSTEMS
Selected upper-air wind speed distributions [AD-A264822] p 284 N94-10871

WEAR
Report of the IAEA Consultants' Meeting on Real-Time Nondestructive Monitoring of Wear and Corrosion Using the Thin Layer Activation Technique [DE93-617422] p 183 N94-10847
Titanium alloys milling assistance by high pressure lubricoolant jet [DE93-013302] p 82 N94-11008
Advanced model of gradual wear of viscoelastic surface film [AD-A265130] p 90 N94-11222
Properties of interfacial tribo-films [AD-A265591] p 182 N94-12374

WEAR RESISTANCE
Processing, properties, and wear resistance of aluminides [DE93-012186] p 83 N94-11141
Weld overlay coatings for erosion control [DE93-013592] p 84 N94-11816

WEAR TESTS
Report of the IAEA Consultants' Meeting on Real-Time Nondestructive Monitoring of Wear and Corrosion Using the Thin Layer Activation Technique [DE93-617422] p 183 N94-10847

WEATHER
A toolkit for building Earth system models [DE93-012147] p 276 N94-11138
Development of a graphical user interface and graphics display for the WIND system [DE93-011780] p 285 N94-11614
Wind system documentation [DE93-010381] p 285 N94-11664

WEATHER FORECASTING
Updated forecast of Atlantic seasonal hurricane activity for 1993 p 285 N94-11194
Rainfall-runoff estimation using digital radar [AD-A265390] p 286 N94-12408
Use of ERS-1 wind and wave products in operational meteorology p 250 N94-12502

Use of SAR-wave, altimeter, and wind-scatterometer data in an operational swell forecasting system p 250 N94-12503

Use of ERS-1 scatterometer winds in Canadian forecast centres p 250 N94-12504

WEATHERING

Carbon in weathered ordinary chondrites from Roosevelt County p 428 N94-12035

Chemical weathering on Mars: Rate of oxidation of iron dissolved in brines p 455 N94-12128

The rate of chemical weathering of pyrite on the surface of Venus p 477 N94-12246

Measuring and distinguishing compositional and maturity properties of lunar soils by remote VIS-NIR spectroscopy p 478 N94-12251

WEIBULL DENSITY FUNCTIONS

Selected upper-air wind speed distributions [AD-A264822] p 284 N94-10871

WEIGHTLESSNESS

Coupled thermovibrational and thermocapillary convection in liquid bridge (floating zone system) p 101 N94-10082

Separation of gravitational effects on the flow of suspension in tubes by measurements in weightlessness p 105 N94-10105

A study of the quasibinary Al-Mo-W system. Part 2: A physico-mechanical investigation of the system fabricated under the gravitylessness conditions p 119 N94-10212

Use of inert immiscible liquid for crystal separation out of its feeding solution in weightlessness p 124 N94-10242

Physiologic mechanisms of circulatory and body fluid losses in weightlessness identified by mathematical modeling p 312 N94-11557

Proceedings of the First Joint NASA Cardiopulmonary Workshop [NASA-CP-10068] p 308 N94-11991

Pulmonary function in microgravity: KC-135 experience p 309 N94-11994

Central circulatory hemodynamics as a function of gravitational stress p 309 N94-11995

Spectral analysis of resting cardiovascular variables and responses to oscillatory LBNP before and after 6 degree head dowm bedrest p 309 N94-11997

Effect of prolonged LBNP and saline ingestion on plasma volume and orthostatic responses during bed rest p 310 N94-11998

Fitness, autonomic regulation and orthostatic tolerance p 310 N94-11999

Hormonal regulation of fluid and electrolyte metabolism in zero-g and bedrest p 311 N94-12004

WEIGHTLESSNESS SIMULATION

Exercise countermeasures for bed-rest deconditioning [NASA-TM-103987] p 300 N94-11191

Project ARGO: Gas phase formation in simulated microgravity [NASA-TM-104762] p 125 N94-11235

Physiologic mechanisms of circulatory and body fluid losses in weightlessness identified by mathematical modeling p 312 N94-11557

Mechanistic studies on reduced exercise performance and cardiac deconditioning with simulated zero gravity p 310 N94-12001

Fluid compartment and renal function alterations in the rat during 7 and 14 day head down tilt p 310 N94-12002

Local fluid shifts and edema in humans during simulated microgravity p 311 N94-12003

WELDABILITY

Weldability of maraging steels p 59 N94-10028

WELDED JOINTS

Heavy-section steel technology program [DE93-009222] p 184 N94-10155

Advances in low carbon, high strength ferrous alloys [AD-A265264] p 85 N94-12532

WELDING

Weldability of maraging steels p 59 N94-10028

Weld overlay coatings for erosion control [DE93-013592] p 84 N94-11816

WETLANDS

Emissions of biogenic sulfur gases from Alaskan tundra p 268 N94-12455

Emissions of sulfur gases from wetlands p 269 N94-12458

Biogeochemical factors which regulate the formation and fate of sulfide in wetlands p 270 N94-12464

DMS emissions from Sphagnum-dominated wetlands p 271 N94-12466

Emissions of biogenic sulfur gases from northern bogs and fens p 271 N94-12467

Factors controlling sulfur gas exchange in Sphagnum-dominated wetlands p 271 N94-12469

Sulfur gas exchange in Sphagnum-dominated wetlands p 271 N94-12470

WETTABILITY

Determination of concentration profiles at interfaces and surfaces of partially miscible polymer blends [DE93-013140] p 89 N94-11007

WETTING

Wetting effects on nylon spheres engulfment in ice p 115 N94-10189

Studies of critical point phenomena of fluids: Bulk fluids, fluids in pores, and at interfaces p 80 N94-10228

Determination of concentration profiles at interfaces and surfaces of partially miscible polymer blends [DE93-013140] p 89 N94-11007

Advanced soldering processes [DE93-009856] p 129 N94-11606

WHARVES

The flow structure around a cylindrical pier for the flow of transcritical Reynolds number p 169 N94-11944

WHEAT

Paint removal using wheat starch blast media p 128 N94-10627

WHEELS

Position and force control of a vehicle with two or more steerable drive wheels [DE93-012512] p 177 N94-10269

WHISKERS (CRYSTALS)

Tin whiskers in electronic circuits [AD-A265917] p 146 N94-12565

WHITE NOISE

DILUTE: A code for studying beam evolution under RF noise [DE93-011605] p 133 N94-10960

The limit of frequency estimation p 356 N94-11001

WIGNER COEFFICIENT

Wigner functions for nonclassical states of a collection of two-level atoms p 379 N94-10603

WIND (METEOROLOGY)

Stability model of the atmosphere p 32 N94-11500

ERS-1 scatterometer data characteristics and wind retrieval skill p 233 N94-11709

Validation of ERS-1 wind and wave data by use of operational forecast models p 233 N94-11710

A C-band wind scatterometer model derived from the data obtained during the ERS-1 calibration/validation campaign p 233 N94-11711

Availability of wind field over the North Pacific derived from data on ships-of-opportunity and analysis of long-term variabilities p 202 N94-11962

Impact of ERS-1 wind/wave/ice data on operational ocean forecasting p 250 N94-12500

A first assessment of the value of ERS-1 scatterometer winds for meteorological studies in the polar regions p 250 N94-12501

Field research of wind wave spectrum variability p 223 N94-12727

Observations of film slicks and internal waves with Ka-band scatterometer p 225 N94-12741

WIND DIRECTION

Dependence of oceanic microwave emission on wind direction p 201 N94-11957

WIND EFFECTS

Effects of wind-roughened sea surface on ocean color remote sensing: Noise derived from reflected light and whitecaps p 191 N94-11898

Variability of wind stress, and sensible and latent heat flux in the North Atlantic during SEASAT p 194 N94-11918

A new expression for the production rate of sea water droplets on the sea surface p 195 N94-11920

Field research of wind wave spectrum variability p 223 N94-12727

WIND MEASUREMENT

US areal wind resource assessment [DE93-011905] p 262 N94-11051

Calibration and validation of the ERS-1 wind scatterometer p 232 N94-11706

The Grand Banks ERS-1 SAR wave spectra validation experiment p 232 N94-11708

ERS-1 scatterometer data characteristics and wind retrieval skill p 233 N94-11709

A C-band wind scatterometer model derived from the data obtained during the ERS-1 calibration/validation campaign p 233 N94-11711

The activity of the ERS-1 Venice (Italy) group on scatterometry p 233 N94-11713

Wind and surface features in SAR images: The Canadian program p 234 N94-11718

Preliminary analysis of circulations over the Indian Ocean and adjoining regions using ERS-1 surface winds in the NCMRWF data assimilation system p 234 N94-11719

Spatial scales of wave height p 244 N94-11782

Analysis of GEOSAT wind data p 207 N94-12636

WIND PROFILES

HF ocean radar system at Okinawa Radio Observatory p 139 N94-11902

Groundwave HF ocean surface radar p 139 N94-11906

Current structures in the western equatorial Pacific during JAPACS cruises p 193 N94-11911

Availability of wind field over the North Pacific derived from data on ships-of-opportunity and analysis of long-term variabilities p 202 N94-11962

Wind field estimate by using one hour GMS data p 202 N94-11963

The Pacific responses exhibited by an OGCM to various wind fields p 202 N94-11964

On an upwelling front, propagation of upwelling and vertical velocity in the eastern Arabian Sea during monsoon, 1987 p 206 N94-11987

Analysis of GEOSAT wind data p 207 N94-12636

SSMI wind speed variability over the Pacific Ocean p 207 N94-12637

Spatial variability of the ocean underwater dynamic noise from satellite radar sensing data p 225 N94-12740

WIND SHEAR

On non-linear longitudinal stability of an aircraft in a dive in the presence of atmospheric disturbances p 31 N94-11492

WIND TUNNEL CALIBRATION

Overview of the 1989 Wind Tunnel Calibration Workshop [NASA-TP-3393] p 34 N94-11869

WIND TUNNEL MODELS

A unique facility to support cryogenic wind tunnel operations [ARA-MEMO-377] p 34 N94-12436

WIND TUNNEL NOZZLES

A CFD-based aerodynamic design procedure for hypersonic wind-tunnel nozzles p 9 N94-10458

WIND TUNNEL TESTS

An investigation on the effectiveness of the piping interference removal system for STOL aircraft wind tunnel tests [NAL-TM-647] p 2 N94-10350

Experimental results in aerodynamic stability and control of a TSTO configuration p 3 N94-10424

New hypersonic test methods developed at ONERA: The R5 and F4 wind tunnels p 4 N94-10429

Design and production of insulated wind tunnel models of the Hermes shuttle for heat transfer measurements at hypersonic speeds p 4 N94-10431

Experimental and computational comparisons of Mach 6 high Reynolds number heat transfer and skin friction p 6 N94-10443

Joint computational and experimental aerodynamic research on a hypersonic vehicle p 6 N94-10445

Some experimental study and numerical simulation in wind tunnel flow p 8 N94-10457

Simulated wake characteristics of tapered annular wings by a discrete vortex method [NAL-TR-1156] p 13 N94-10855

Simulated and experimental aerodynamic characteristics of tapered annular wings [NAL-TR-1157] p 13 N94-10856

An experimental investigation of the sources of propeller noise due to turbulence ingestion p 358 N94-11057

A preliminary study on ice shape tracing with a laser light sheet [NASA-TM-105964] p 174 N94-11132

Supersonic airplane study and design [NASA-CR-193219] p 25 N94-11150

Boundary layer transition: Prediction and wind tunnel simulation p 32 N94-11498

Modeling nonlinear aerodynamic loads for aircraft stability and control analysis p 32 N94-11499

Computation of hypersonic nosetip heat transfer rates for an M829-like projectile [AD-A263226] p 16 N94-11870

Lift enhancement of a wing/strake using pneumatic blowing [AD-A265074] p 26 N94-11872

An investigation of small scales of turbulence in a boundary layer at high Reynolds numbers p 157 N94-12303

Plane mixing layer vortical structure kinematics p 159 N94-12313

A unique facility to support cryogenic wind tunnel operations [ARA-MEMO-377] p 34 N94-12436

WIND TUNNELS

Estimation of critical values and vibration characteristics on supersonic delta wings. Part 1: On-line time series analysis of stationary random response [NAL-TR-1153] p 2 N94-10363

The upgrading of the arc heated wind tunnel of the DLR (LBK) with respect to its effects on the material testing p 4 N94-10432

New aerodynamic information obtained from the solution of the inverse problem for aerofoils [NAL-TR-1172] p 14 N94-10860

Numerical wind tunnel project and computational fluid dynamics at National Aerospace Laboratory, Japan [NAL-TM-648T] p 149 N94-10861

Overview of the 1989 Wind Tunnel Calibration Workshop
[NASA-TP-3393] p 34 N94-11869
Superfluid turbulence p 158 N94-12307

WIND TURBINES
US areal wind resource assessment
[DE93-011905] p 262 N94-11051
Fatigue life prediction for wind turbines: A case study on loading spectra and parameter sensitivity
[DE93-011597] p 263 N94-11173

WIND VELOCITY
Preliminary results on backscattering strength from a wind generated bubbly ocean surface
[AD-A265006] p 287 N94-10490
Selected upper-air wind speed distributions
[AD-A264822] p 284 N94-10871
US areal wind resource assessment
[DE93-011905] p 262 N94-11051
A preliminary C-band scatterometer model function for the ERS-1 AMI instrument p 233 N94-11715
Wind and surface features in SAR images: The Canadian program p 234 N94-11718
Evaluation of two January - June 1992 ERS-1 AMI wind vector data sets p 235 N94-11724
Spatial scales of wave height p 244 N94-11782
Current structures in the western equatorial Pacific during JAPACS cruises p 193 N94-11911
The microwave backscattering from wind waves
p 201 N94-11959
On the variability of wind speeds in the North Western Pacific observed by altimeter/GEOSAT and SSM/I/DMSP p 201 N94-11960
Observation of wind and waves by GEOSAT altimeter
p 202 N94-11961
Availability of wind field over the North Pacific derived from data on ships-of-opportunity and analysis of long-term variabilities p 202 N94-11962
Analysis of GEOSAT wind data p 207 N94-12636
SSMI wind speed variability over the Pacific Ocean
p 207 N94-12637
Theory and oceanographic applications of satellite altimeter measurements p 208 N94-12641
Spatial variability of the ocean underwater dynamic noise from satellite radar sensing data p 225 N94-12740

WIND VELOCITY MEASUREMENT
Evaluation of two January - June 1992 ERS-1 AMI wind vector data sets p 235 N94-11724

WINDING
Tape winding of thermoplastic composites
p 60 N94-10035

WINDOWS (APERTURES)
Arcjet exploratory tests of ARC optical window design for the AFE vehicle
[NASA-CR-192655] p 34 N94-10930

WINDOWS (COMPUTER PROGRAMS)
An expert system shell for inferring vegetation characteristics: Prototype help system (Task 1)
[NASA-CR-193411] p 231 N94-11236
Development and implementation of a general purpose x-windows display program
[AD-A265306] p 332 N94-11860

WINDPOWER UTILIZATION
US areal wind resource assessment
[DE93-011905] p 262 N94-11051
Renewable energy sources 1991, part 2
[DE93-605634] p 263 N94-11506

WINDPOWERED GENERATORS
US areal wind resource assessment
[DE93-011905] p 262 N94-11051

WINDPOWERED PUMPS
Renewable energy sources 1991, part 3
[DE93-605594] p 263 N94-11505

WINDSHIELDS
Aircraft windscreens enhance visual search disruption produced by laser glare
[AD-A265167] p 26 N94-11892

WING NACELLE CONFIGURATIONS
Supersonic airplane study and design
[NASA-CR-193219] p 25 N94-11150

WING PANELS
Underwing compression vortex attenuation device
[NASA-CASE-LAR-14744-1] p 12 N94-10673

WING PLANFORMS
Ground vibration and flight flutter tests of the single-seat F-16XL aircraft with a modified wing
[NASA-TM-104269] p 26 N94-11233

WING PROFILES
New aerodynamic information obtained from the solution of the inverse problem for aerofoils
[NAL-TR-1172] p 14 N94-10860

WING SPAN
Simulated and experimental aerodynamic characteristics of tapered annular wings
[NAL-TR-1157] p 13 N94-10856

WING TIP VORTICES
Simulated and experimental aerodynamic characteristics of tapered annular wings
[NAL-TR-1157] p 13 N94-10856

WINGS
Navier-Stokes flowfield computation of wing/rotor interaction for a tilt rotor aircraft in hover
[NASA-CR-4532] p 13 N94-10758

WIRING
Specification and testing for power by wire aircraft
[NASA-TM-106232] p 46 N94-10765
Development and analysis of insulation constructions for aerospace wiring applications p 21 N94-10791

WORK CAPACITY
Glycerol-induced hyperhydration p 309 N94-11996

WORK FUNCTIONS
Squeezed states of electrons and transitions of the density of states p 370 N94-10593

WORKLOADS (PSYCHOPHYSIOLOGY)
Quantitative EEG patterns of differential in-flight workload p 317 N94-11528
Psychophysiological measures of cognitive workload in laboratory and flight p 317 N94-11529

WORKSTATIONS
System engineering concept demonstration, technology assessments, volume 5
[AD-A265471] p 323 N94-10494
A distributed version of the NASA Engine Performance Program
[NASA-TM-106208] p 327 N94-11231
RAMCAD (reliability, availability, and maintainability in computer-aided design)
[AD-A265143] p 331 N94-11679

X

X RAY ABSORPTION
X ray absorption spectroscopy of electrochemically generated species
[AD-A264749] p 77 N94-11265
Apical Cu-O bond in YBa2Cu3O(7-delta) superconductors by XAFS
[DE93-010861] p 400 N94-11458
In situ XANES studies of the passive film on Fe and Fe-26Cr
[DE93-010869] p 84 N94-11459

X RAY ANALYSIS
New x ray scanning topographic approaches to nondestructive evaluation of composites
p 61 N94-10039
Interferometric and optical tests of water window imaging x ray microscopes
[NASA-CR-193369] p 375 N94-10506
High resolution time- and 2-dimensional space-resolved x ray imaging of plasmas at NOVA
[DE93-011892] p 393 N94-11677

X RAY APPARATUS
Interferometric and optical tests of water window imaging x ray microscopes
[NASA-CR-193369] p 375 N94-10506

X RAY DIFFRACTION
Symmetry lowering in crystalline solid solutions: A study of cinnamamide-thienylacrylamide by x ray and neutron diffraction and solid-state photochemistry
[DE93-010871] p 394 N94-10301
Tribological characteristics of hot-pressed self-lubricating composites
[NAL-TR-1160] p 66 N94-10858
The x ray standing waves on surfaces
[AD-A265265] p 402 N94-11682

X RAY FLUORESCENCE
Remote sensing x ray fluorescence spectrometry for future lunar exploration missions p 462 N94-12165

X RAY IMAGERY
Development of microstrip gas chamber and application to imaging gamma-ray detector
[DE93-754294] p 34 N94-11041

X RAY LASERS
High power z pinches as x ray laser photopumps
[DE93-012842] p 173 N94-10746
High-order harmonic conversion efficiency in helium
[DE93-011714] p 364 N94-10753
Electron temperature measurements of x ray laser plasmas
[DE93-011874] p 389 N94-11074
Demonstration designs for optical-field-ionized plasma x-ray lasers
[DE93-009227] p 175 N94-11266
LCLS optics: Selected technological issues and scientific opportunities
[DE93-010953] p 175 N94-11468
Inexpensive capillary discharge x-ray laser driver
[AD-A265932] p 176 N94-12382
Spatial coherence of soft x ray lasers
[DE93-012497] p 176 N94-12590

X RAY SCATTERING
X-ray and neutron scattering studies of magnetic critical fluctuations in holmium
[DE93-010873] p 400 N94-11467
FEFF5: An ab initio multiple scattering XAFS code
[DE93-011000] p 367 N94-11470

X RAY SOURCES
X ray production (approximately)130 (Angstrom) from laser-produced plasmas for projection x ray lithography applications
[DE93-009256] p 385 N94-10286
Physical optics modelling of Soft X ray Projection Lithography (SXPL) imaging experiments
[DE93-011556] p 374 N94-10339
Wavelength considerations in soft x ray projection lithography
[DE93-014115] p 381 N94-10651
Radiation hardness of Mo/Si multilayers designed for use in a soft x ray projection lithography system
[DE93-011879] p 143 N94-11273
Submicrosecond, synchronizable x ray source
[AD-D015745] p 176 N94-12337
HEAO-1 analysis of Low Energy Detectors (LED)
[NASA-CR-194087] p 424 N94-12574

X RAY SPECTRA
Source to detector spectrum transformation and its inverse for the Pegasus Z-pinch
[DE93-012674] p 384 N94-10157
X ray production (approximately)130 (Angstrom) from laser-produced plasmas for projection x ray lithography applications
[DE93-009256] p 385 N94-10286

X RAY SPECTROSCOPY
Microanalysis of directionally solidified cobalt oxide-zirconia eutectic
[DE93-013207] p 88 N94-10527
X ray and gamma ray spectroscopy of solids under pressure
[DE93-014847] p 76 N94-10653
Effect of surface cleanliness of bearing steel on adhesive strength and tribological properties of sputter-deposited gold films
[DE93-767974] p 82 N94-10732
Tribological characteristics of hot-pressed self-lubricating composites
[NAL-TR-1160] p 66 N94-10858
X ray absorption spectroscopy of electrochemically generated species
[AD-A264749] p 77 N94-11265
High resolution time- and 2-dimensional space-resolved x ray imaging of plasmas at NOVA
[DE93-011892] p 393 N94-11677
Remote sensing x ray fluorescence spectrometry for future lunar exploration missions p 462 N94-12165
Yohkoh Bragg Crystal Spectrometer light curves for Ca XIX (3.1631-3.1912A): 1 October 1991 - 30 September 1992
[AD-A266090] p 483 N94-12414

X RAY TUBES
Laser Synchrotron Source (LSS)
[AD-D015755] p 173 N94-10371

X RAYS
X ray production (approximately)130 (Angstrom) from laser-produced plasmas for projection x ray lithography applications
[DE93-009256] p 385 N94-10286
Needs for super-smooth surfaces
[DE93-012482] p 382 N94-11242
The x ray standing waves on surfaces
[AD-A265265] p 402 N94-11682

X-29 AIRCRAFT
X-29: Longitudinal instability at high angle-of-attack
p 33 N94-11504

X-30 VEHICLE
An environmental study of the National Aerospace Plane
[AD-A266071] p 25 N94-10945

XENON
Satellite structure of the xenon valence shell by electron momentum spectroscopy
[DE93-609993] p 360 N94-10327

XENON ISOTOPES
Nitrogen and noble gases in a glass sample from LEW88516 p 80 N94-12051
The Xe-Q in Iodranites and a hint for Xe-L. FRO90011 another Iodranite? p 432 N94-12239

XENON 129
Noble gases in LEW88516 shergottite: Evidence for exposure age pairing with ALH77005 p 80 N94-12082
Studies of the release of radiogenic Xe-129 from Bjurboele: Evidence against simple diffusion models
p 430 N94-12125

XI HYPERONS
Double-lambda compound nucleus and the formation of double hypernuclei
[DE93-754289] p 365 N94-11040

A generalized Bethe-Weizsaecker mass formula for strange hadronic matter
[DE93-011010] p 368 N94-11620

XV-15 AIRCRAFT
Determining XV-15 aeroelastic modes from flight data with frequency-domain methods
[NASA-TP-3330] p 25 N94-10935

Y

YAG LASERS
Nonlinear Dynamics in Optical Systems. Postdeadline papers presented at the Optical Society of America Conference
[AD-A264958] p 375 N94-10486
Thermal-optical switching of a silicon based interference filter
[AD-A265152] p 174 N94-11095
Short wavelength crystal fiber devices
[AD-A265716] p 176 N94-12402

YAW
Static internal performance of a single expansion ramp nozzle with multiaxis thrust vectoring capability
[NASA-TM-4450] p 12 N94-10675
Traveling disturbances appearing in yawed cylinder boundary layer transition p 166 N94-12632

YBCO SUPERCONDUCTORS
Microstructure and associated properties of YB2Cu3O(x) superconductors prepared by melt processing techniques
[DE93-010675] p 398 N94-11004
Texture analysis of high Tc superconductors
p 399 N94-11314
Apical Cu-O bond in YBa2Cu3O(7-delta) superconductors by XAFS
[DE93-010861] p 400 N94-11458
Synthesis and magnetic properties of novel La*2-x*M*x*CuO*4 equals y* compositions (La equals La, Pr, Nd, Sm, Eu, Cd; M equals Ca, Sr, Ba; O (less than or equal) x 0.2; -0.5 (less than or equal) y (less than or equal) 0.5)
[DE93-011359] p 403 N94-12363
Corrosion and passivation of high temperature superconductors
[AD-A265402] p 405 N94-12586

YIELD
Integration of ERS-1 data into the European project of agriculture statistics p 248 N94-12490

YIELD POINT
Damage thresholds of fluoride multilayers at 355 nm
[DE93-009523] p 90 N94-11230

YIELD STRENGTH
Collisions of small Spacewatch asteroids with the Earth p 430 N94-12157

YLF LASERS
A 1.94 micron laser apparatus, system, and method using a thulium-doped yttrium-lithium-fluoride laser crystal pumped with a diode laser
[AD-D015740] p 176 N94-12321

YUKON TERRITORY
Minor and trace element composition and age of Yukon probable-microtektites p 429 N94-12094

Z

ZEOLITES
Crystallization of zeolites in the microgravity environment of space p 119 N94-10210
Synthesis of molecular sieves from clear solution
p 124 N94-10245

ZERO POINT ENERGY
Uncertainty relations, zero point energy and the linear canonical group p 378 N94-10590

ZETA PINCH
Source to detector spectrum transformation and its inverse for the Pegasus Z-pinch
[DE93-012674] p 384 N94-10157
High power z pinches as x ray laser photopumps
[DE93-012842] p 173 N94-10746
Advanced concepts theory annual report 1992
[AD-A266132] p 393 N94-11474

ZINC COATINGS
Advanced zinc phosphate conversion and pre-ceramic polymetallosiloxane coatings for corrosion protection of steel and aluminum, and characteristics of polyphenyletheretherketone-based materials
[DE93-008717] p 88 N94-10891

ZINC COMPOUNDS
Second and third order nonlinear optical properties of crystalline inorganic/organic complexes
[DE93-011883] p 173 N94-10755
Advanced zinc phosphate conversion and pre-ceramic polymetallosiloxane coatings for corrosion protection of steel and aluminum, and characteristics of polyphenyletheretherketone-based materials
[DE93-008717] p 88 N94-10891

ZINC SELENIDES
Investigation of ZnSe-coated silicon substrates for GaAs solar cells p 52 N94-11405

ZIRCONIUM ALLOYS
Structure and properties of an RS Al-Si-Ni-Mn-Zr alloy for high temperature applications p 64 N94-10063

ZIRCONIUM ISOTOPES
Progress in zirconium resonance ionization spectroscopy
[DE93-011881] p 76 N94-11075

ZIRCONIUM OXIDES
Microanalysis of directionally solidified cobalt oxide-zirconia eutectic
[DE93-013207] p 88 N94-10527

ZONAL FLOW (METEOROLOGY)
Updated forecast of Atlantic seasonal hurricane activity for 1993 p 285 N94-11194
Numerical simulations of thermal convection in rapidly rotating spherical fluid shells p 153 N94-11635

ZONE MELTING
Marangoni and buoyant convections in zone melting of GaAs with liquid encapsulation p 101 N94-10081
On shape of single crystals grown by FZM in microgravity p 102 N94-10084
Calculation of the effects of magnetic field damping in fluid flow: Comparison of magnetohydrodynamic models of different complexity p 103 N94-10089
Mission support for crystal growth experiments in Russian unmanned carriers p 111 N94-10139
Crystal growth in the Zone Melting Facility (ZMF)
p 119 N94-10213

ZOOPLANKTON
Automatic classification system for zooplankton
p 203 N94-11969
The seasonal change of phytoplankton size distribution using optical fiber sensor p 210 N94-12656

PERSONAL AUTHOR INDEX

SCIENTIFIC AND TECHNICAL AEROSPACE REPORTS VOLUME 32 NUMBER 1

Typical Personal Author Index Listing

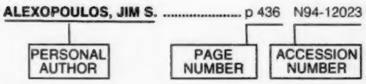

Listings in this index are arranged alphabetically by personal author. The page number helps you locate the citation in the abstract section. The accession number denotes the number by which the citation is identified.

A

AARTS, E. H. L. p 338 N94-10169
AARTS, HARRY F. M. p 348 N94-10162
ABAKSHIN, E. V. p 97 N94-12040
ABARBANEL, H. D. p 161 N94-12342
ABATE, J. E. p 139 N94-10991
ABDEL-SALAM, F. A. p 346 N94-11507
ABE, SUMIYOSHI p 349 N94-10588
ABE, T. p 140 N94-12706
ABGRALL, REMI p 5 N94-10440
ABIVEN, H. p 59 N94-10024
ABOUEL-ELA, M. N. p 346 N94-11507
ABRAHAM, N. B. p 175 N94-11633
p 175 N94-11634
ABRUNA, H. D. p 404 N94-12376
ABRUNA, HECTOR D. p 402 N94-11682
ABUDAGGA, KHALED p 49 N94-11390
ACREE, C. W., JR. p 25 N94-10935
ADACHI, SATOSHI p 107 N94-10115
p 114 N94-10179
ADAM, G. p 395 N94-10537
ADAM, P. p 375 N94-10570
ADAM, S. p 395 N94-10537
ADAM, SUSAN C. p 314 N94-11538
ADAMEDES, ZOE p 140 N94-10390
ADAMS, D. p 319 N94-10146
ADAMS, JOHN B. p 281 N94-12055
ADAMSON, STEVEN p 41 N94-10512
ADDIS, F. WILLIAM p 52 N94-11405
ADELBERG, L. K. p 274 N94-10726
ADELMAN, SAUL J. p 424 N94-12573
ADIBE, E. C. p 277 N94-11603
ADJEPONG, S. K. p 357 N94-10408
p 84 N94-12361
ADOLF, D. p 91 N94-11665
AESCHLIMAN, DANIEL P. p 6 N94-10445
AFANEH, ABDUL-HAFIZ AHMED p 186 N94-10897
AFTOSMIS, MICHAEL J. p 148 N94-10703
AGARWAL, G. S. p 379 N94-10603
AGARWAL, VIJAY K. p 252 N94-12512
p 252 N94-12513
AGATANOVIC, P. p 63 N94-10055
AGATONOVIC, P. p 58 N94-10016
p 64 N94-10060
AGERKVIST, D. P. p 428 N94-12016
AGNES, GREGORY S. p 72 N94-11343
AGNEW, B. W. p 351 N94-10970
AGNEW, DUNCAN CARR p 275 N94-10950
AGOSTO, WILLIAM N. p 435 N94-12017
AGUIRRE-PUENTE, J. p 435 N94-12018
AHERN, F. p 248 N94-12486
AHLBORN, H. p 113 N94-10177
AHMADI, D. p 348 N94-10412
AHRENS, THOMAS J. p 435 N94-12019
p 282 N94-12149
p 432 N94-12241
AIELLO, ROSARIO p 124 N94-10245
AIT-KACI, HASSAN p 320 N94-10167
AIZAWA, TERUAKI p 418 N94-10559
AJZATSKIJ, N. I. p 141 N94-10543
p 392 N94-11213
AKER, P. M. p 77 N94-11359
AKHMEDOV, E. KH. p 410 N94-10545
AKHUNDOVA, E. A. p 350 N94-10600
AKIMOTO, KAZUNORI p 197 N94-11936
AKINSHIN, D. V. p 484 N94-10534
AKITOMO, KAZUNORI p 210 N94-12652
AKIYAMA, HIDEKI p 198 N94-11939
AKIYAMA, MASATOSHI p 196 N94-11925
p 213 N94-12673
p 222 N94-12721
AKKELIN, S. V. p 362 N94-10551
AKSAY, I. A. p 82 N94-10957
AKSEL, N. p 63 N94-10058
AKSIT, MEHMET p 320 N94-10166
AKTSIPETROV, O. A. p 227 N94-12756
AL-RAMADHAN, F. A. p 78 N94-11855
ALAM, JAVED p 188 N94-11254
ALBANESE, CARLO p 124 N94-10241
ALBERY, CHRISTOPHER p 316 N94-12346
ALDWORTH, E. p 238 N94-11746
ALEXANDER, D. p 51 N94-11396
ALEXANDER, J. IWAN D. p 114 N94-10183
p 56 N94-12588
ALEXEEV, V. A. p 136 N94-11071
p 428 N94-12020
p 428 N94-12021
p 428 N94-12022
ALEXOPOULOS, JIM S. p 436 N94-12023
ALI, M. M. p 242 N94-11770
ALLAIN, C. p 115 N94-10189
ALLAN, T. D. p 196 N94-11929
ALLBROOKS, M. K. p 190 N94-12178
ALLBROOKS, MARTHA p 43 N94-10666
ALLCOCK, H. R. p 92 N94-11848
ALLCOCK, HARRY R. p 90 N94-11292
p 92 N94-11847
p 92 N94-11849
ALLEN, C. C. p 436 N94-12024
ALLEN, C. T. p 232 N94-11623
ALLEN, S. L. p 385 N94-10289
ALLEN, WILLIAM p 92 N94-11876
ALLENDORF, M. D. p 77 N94-11370
ALLEY, C. O. p 351 N94-10970
p 351 N94-10971
ALLINGHAM, M. p 232 N94-11708
ALLISON, S. W. p 78 N94-11622
ALLOTEY, F. K. p 357 N94-10408
ALLTON, J. H. p 428 N94-12025
ALMAGRI, A. p 388 N94-10747
ALONSO, A. p 57 N94-10008
ALPERS, W. p 252 N94-12510
ALSBROOKS, T. H. p 14 N94-11111
ALTEMIR, D. A. p 131 N94-12026
p 131 N94-12027
ALTENBERG, B. H. p 415 N94-12028
ALVAREZ, WALTER p 282 N94-12161
ALVI, FARRUKH SABBAH p 149 N94-10899
ALVIN, K. F. p 331 N94-11522
ALZHEIMER, J. M. p 274 N94-10323
AMADOU, I. p 197 N94-11933
p 251 N94-12508
AMALDI, A. p 58 N94-10015
AMANO, T. p 390 N94-11128
AMARI, SACHIKO p 97 N94-12029
AMBROSE, CATHERINE GLAUBER
p 339 N94-10898
AMBROSIUS, B. A. C. p 242 N94-11772
p 244 N94-11779
AMENDT, P. A. p 175 N94-11266
AMITANI, YASUTAKA p 172 N94-11916
p 139 N94-11917
AMSDEN, A. A. p 77 N94-11249
ANASTASI, ROBERT F. p 73 N94-11446
ANCHISHKIN, D. V. p 410 N94-10721
ANCIANT, M. p 345 N94-11217
ANDERMAN, ALFRED p 42 N94-10974
ANDERSEN, C. S. p 341 N94-12598
ANDERSEN, O. BALTAZAR p 242 N94-11768
ANDERSON, ALLEN JOEL p 243 N94-11776
ANDERSON, B. H. p 39 N94-10764
ANDERSON, C. A. p 126 N94-10293
ANDERSON, CHRISTOPHER p 331 N94-11657
ANDERSON, D. L. p 258 N94-12030
ANDERSON, DAVID L. T. p 233 N94-11709
ANDERSON, G. A. p 274 N94-10323
ANDERSON, R. J. p 232 N94-11708
ANDERSON, R. R. p 281 N94-12032
p 281 N94-12056
ANDERSON, ROBERT p 437 N94-12031
ANDERSON, ROBERT C. p 170 N94-11310
ANDERSON, STEVE P. p 289 N94-12348
ANDERSON, W. W. p 432 N94-12241
ANDERSSEN, TOM p 253 N94-12522
ANDO, AKIO p 132 N94-10560
ANDO, T. p 392 N94-11239
ANDOU, K. p 208 N94-12640
ANDOU, KENTAROU p 193 N94-11911
ANDOU, YASUKATSU p 2 N94-10363
ANDREWS, J. BARRY p 112 N94-10174
ANDREWS, PAUL G. p 421 N94-12579
ANDRISANI, DOMINICK, II p 30 N94-10895
ANGELI, ROBERT J. p 178 N94-10379
ANGELL, D. p 382 N94-11421
ANGHILERI, M. p 61 N94-10036
ANIKIN, L. T. p 63 N94-10057
ANNIS, CHARLES p 85 N94-12418
ANSPAUGH, BRUCE E. p 50 N94-11392
ANTHES, J. p 174 N94-10959
ANTONIAZZI, A. p 61 N94-10036
ANTONY, M. K. p 206 N94-11987
ANZENHOFER, M. p 243 N94-11777
AOKI, ICHIROU p 218 N94-12699
AOKI, SHIGERU p 198 N94-11941
p 209 N94-12649
AOYAMA, ISAO p 372 N94-11591
APPAJI, SUDESH p 87 N94-10508
APPENDINO, P. p 123 N94-10237
APPLEHANS, A. D. p 76 N94-11140
ARAGONE, C. p 377 N94-10586
p 379 N94-10601
ARAI, S. p 144 N94-11508
ARAI, Y. p 367 N94-11510
ARBOCZ, JOHANN p 186 N94-10879
ARCHER, D. J. p 246 N94-12474
ARENT, N. p 241 N94-11765
AREVALO, F. p 62 N94-10047
ARHENS, T. J. p 93 N94-12354
ARIF, HUMAYUN p 55 N94-11675
ARIGANE, KENJI p 372 N94-11591
ARIMOTO, H. p 392 N94-11239
ARITOMI, MASANORI p 162 N94-12551
ARMAND, MICHEL p 395 N94-10416
ARMAND, NEON A. p 37 N94-10688
ARMONE, ROBERT p 288 N94-11287
ARMSTRONG, J. H. p 50 N94-11393
ARMSTRONG, JOE p 54 N94-11415
ARNAL, D. p 32 N94-11498
ARNOLD, J. R. p 437 N94-12033
p 452 N94-12109
ARNOLD, LANA p 348 N94-11574
ARNOLD, S. M. p 188 N94-11482
ARNOLDS-MAYER, G. p 126 N94-10617
ARNOLDUS, HENK F. p 376 N94-10576
ARNONE, A. p 152 N94-11481
ARPACI, V. S. p 104 N94-10094
ARRINGTON, LYNN A. p 47 N94-11252
ARVIDSON, R. E. p 438 N94-12034
ARVIDSON, RAYMOND E. p 258 N94-12097
ASAI, MAKOTO p 165 N94-12625
ASAI, TOMIO p 195 N94-11924
ASANUMA, ICHIROU p 208 N94-12640
ASANUMA, ICHIO p 140 N94-11965
ASAY, B. W. p 97 N94-10294
ASH, R. D. p 428 N94-12035
ASHIDA, H. p 390 N94-11128
ASHLEY, NORM p 42 N94-11297
ASHURST, A. N. p 60 N94-10029
ASHWILL, T. D. p 263 N94-11173
ASKINS, CHARLES p 374 N94-10373
ASKNE, J. p 238 N94-11747
ASLAM, MIAN SUHAIL p 37 N94-10693
ASPHAUG, E. p 429 N94-12036
p 429 N94-12062

ASVELD, PETER R. J. p 342 N94-10279
ATANASOVA, V. p 119 N94-10211
p 119 N94-10212
ATCHITY, GREGORY JOHN p 267 N94-12269
ATCLIFFE, P. A. p 3 N94-10426
ATKINSON, D. R. p 190 N94-12178
ATKINSON, DALE p 42 N94-10665
p 43 N94-10666
ATKINSON, JAMES D., IV p 382 N94-11653
ATTEMA, E. P. W. p 232 N94-11706
ATWELL, WILLIAM p 318 N94-11561
AUBELE, J. C. p 438 N94-12037
p 455 N94-12126
p 467 N94-12194
p 467 N94-12195
AUBELE, JAYNE C. p 465 N94-12180
p 467 N94-12193
p 467 N94-12196
AUCHAMPAUGH, GEORGE p 172 N94-12038
AUCIELLO, ORLANDO p 405 N94-12442
AUGUSTINE, B. H. p 174 N94-11095
AUSTIN, EDWARD p 27 N94-11341
AUTIO, M. p 63 N94-10054
p 65 N94-10069
AUVIL, LORETTA S. p 337 N94-12540
AUWETER-KURTZ, M. p 47 N94-11354
AVANCINI, S. S. p 349 N94-10633
AVARA, ELTON P. p 284 N94-10871
AVERY, J. p 51 N94-11400
AVVA, R. K. p 46 N94-10934
AWAJI, TOSHIYUKI p 197 N94-11936
p 210 N94-12652
AYENSU, A. p 84 N94-12361
AYUSO, A. p 59 N94-10025
p 62 N94-10047
AZAIEZ, JALEL p 159 N94-12314
AZOUNI, M. A. p 115 N94-10189
AZU, CHARLES C., JR. p 145 N94-11884
AZUMA, HISAO p 125 N94-10730
AZUMI, MASAFUMI p 390 N94-11149

B

BAAKLINI, G. Y. p 67 N94-11237
BABANIN, A. V. p 223 N94-12727
BABARUTSI, SOFIA p 153 N94-11616
BABENKO, V. A. p 361 N94-10549
p 362 N94-10550
BABINSKY, H. p 3 N94-10426
BACA, A. G. p 144 N94-11624
BACHMANN, KLAUS J. p 399 N94-11439
p 399 N94-11440
p 400 N94-11441
p 400 N94-11442
p 400 N94-11443
BACKES, PAUL G. p 179 N94-10670
p 183 N94-11577
BADA, J. L. p 452 N94-12109
BADARCH, MENDBAYARIIN p 36 N94-10686
BADAVI, FRANCIS F. p 484 N94-10759
p 485 N94-12434
BADEAU, ALBERT p 317 N94-11529
BADEN, A. p 419 N94-11105
BADINI, C. p 123 N94-10237
BADJUKOV, D. D. p 97 N94-12039
p 97 N94-12040
BADWAR, GAUTAM D. p 45 N94-11559
BAE, DONG-JAE p 370 N94-10579
BAEHR, G. p 114 N94-10184
BAGATIN, A. C. p 431 N94-12201
BAGIAN, JAMES P. p 312 N94-11550
BAHAR, E. p 440 N94-12049
BAILEY, J. L. p 79 N94-12415
BAILEY, J. M. p 373 N94-12542
BAILEY, SHEILA G. p 49 N94-11388
p 404 N94-12430
BAINES, K. H. p 457 N94-12139
p 425 N94-12140
BAJT, S. p 433 N94-12260
p 433 N94-12261
p 433 N94-12262
BAJT, SASA p 429 N94-12106
BAKASOV, A. A. p 175 N94-11633
p 175 N94-11634
BAKER, K. L. p 389 N94-11114
BAKER, S. G. p 246 N94-12475
BAKER, V. R. p 478 N94-12248
p 283 N94-12249
BAKTASH, C. p 358 N94-10254
BALACHANDRAN, U. p 142 N94-10951
p 398 N94-11004
p 398 N94-11073
BALAGEAS, D. p 5 N94-10438
BALDWIN, S. L. p 430 N94-12125
BALINT, J.-L. p 157 N94-12303
BALL, A. D. p 70 N94-11335
BALL, R. M. p 371 N94-10529
BALLANCE, JOHN p 401 N94-11515
BALLATO, ARTHUR p 141 N94-10668
BALMINO, G. p 243 N94-11778
BALOGA, STEPHEN p 281 N94-12041
BALTENSPERGER, W. p 350 N94-10313
BALTZ, A. J. p 359 N94-10303
BAMBER, J. L. p 237 N94-11738
BAME, S. J. p 482 N94-10741
BANCILLON, J. p 108 N94-10122
BANDOS, I. A. p 412 N94-11088
BANDOU, TOSHIO p 25 N94-10728
BANDYOPADHYAY, PROMODE R. p 147 N94-10383
BANERDT, W. B. p 281 N94-12042
BANHART, J. p 64 N94-10059
BANNOV, V. A. p 223 N94-12729
BANSAL, INDAR p 29 N94-12271
BANSAL, NAROTTAM P. p 89 N94-11204
p 90 N94-11257
BANSAL, R. K. p 234 N94-11719
BANTA, G. T. p 271 N94-12468
BARAT, C. p 114 N94-10180
BARBAUX, Y. p 59 N94-10023
BARBER, DAVID G. p 240 N94-11758
BARBER, J. F. p 309 N94-11995
BARBERA, PAUL p 81 N94-12156
BARBIERI, ENRIQUE p 180 N94-10821
BARBOSA, HUGO p 55 N94-11675
BARCLAY, REBECCA O. p 419 N94-11352
BARDET, CHRISTOPHE p 55 N94-11675
BARDSLEY, J. N. p 181 N94-11247
BARDWELL, J. A. p 84 N94-11459
BARKER, A. R. p 370 N94-12609
BARKER, TREVOR p 220 N94-12712
BARLIER, F. p 39 N94-12530
BARLIN, B. p 326 N94-11220
BARLOW, N. G. p 439 N94-12043
BARMIN, I. V. p 106 N94-10111
p 107 N94-10116
p 111 N94-10139
p 116 N94-10193
BARNABA, JAMES M. p 316 N94-11642
BARNES, BERNIS p 415 N94-11517
BARNES, CHRISTOPHER F. p 326 N94-11197
BARNES, E. J. p 214 N94-12679
BARNES, G. MICHAEL p 314 N94-11534
BARNOUIN, O. S. p 169 N94-12044
BAROUD, MICHEL p 55 N94-11675
BARRACLOUGH, BRUCE p 172 N94-12038
BARRETT, R. A. p 80 N94-12045
p 453 N94-12117
BARTEL, NORBERT p 136 N94-11070
BARTH, TIMOTHY S. p 314 N94-11536
BARTON, J. J. p 169 N94-10526
BARUCH, MENAHEM p 186 N94-10879
BARUT, A. O. p 361 N94-10414
BASHFORD, DAVID P. p 63 N94-10052
BASILEVSKY, A. T. p 440 N94-12046
p 440 N94-12047
p 440 N94-12048
BASILI, VICTOR R. p 328 N94-11424
BASOL, B. M. p 50 N94-11393
BASS, B. R. p 184 N94-10288
BASS, J. N. p 43 N94-10944
BASU, A. p 440 N94-12050
BATCHELOR, D. B. p 131 N94-10270
BATISTIC, L. p 399 N94-11263
BATMANOVA, E. G. p 141 N94-10533
BATON, S. p 389 N94-11114
BATTENBURG, J. A. p 40 N94-11576
BATURIN, GLEB N. p 224 N94-12733
BAUER, B. S. p 389 N94-11114
BAUER, MARVIN E. p 231 N94-11521
BAUMAN, J. S. p 51 N94-11400
BAUMEISTER, J. p 64 N94-10059
BAUMGARTL, JOHANNES p 100 N94-10073
p 103 N94-10089
BAVLI, RAANAN p 366 N94-11100
BAXTER, D. p 41 N94-11282
BAYLESS, W. R. p 400 N94-11457
BAYLEY, SUZANNE E. p 270 N94-12461
p 270 N94-12465
p 271 N94-12466
p 271 N94-12467
p 271 N94-12469
BAYLOT, JAMES T. p 171 N94-12362
BEAL, ROBERT CARL p 251 N94-12505
BEARE, STEVEN D. p 20 N94-10789
BEAT, T. G. p 84 N94-11668
BECK, BRADLEY G. p 312 N94-11550
p 312 N94-11551
BECK, STEVE W. p 318 N94-11555
BECKER, G. THOMAS p 334 N94-10986
BECKER, K. J. p 425 N94-12140
BECKER, R. H. p 80 N94-12051
BECKETT, J. R. p 80 N94-12052
BECKSTEAD, M. W. p 99 N94-12564
BEDARIDA, F. p 107 N94-10117
BEDDO, M. E. p 368 N94-11613
BEDELL, K. S. p 412 N94-11162
BEDFORD, A. p 288 N94-11299
BEECHER, JODY E. p 95 N94-12577
BEECHING, M. J. p 170 N94-10630
BEER, G. A. p 373 N94-12542
BEFORT, WILLIAM p 231 N94-11521
BEHAR, ALBERTO p 55 N94-11675
BEIGHTOL, LARRY A. p 310 N94-12000
BEIN, W. W. p 343 N94-10708
BEITEL, G. R. p 413 N94-12535
BEKAERT, G. p 39 N94-10118
BELL, G. E. C. p 84 N94-11593
BELL, J. F. p 430 N94-12111
BELL, J. F., III p 446 N94-12079
p 465 N94-12184
BELL, JAMES F., III p 424 N94-12053
p 441 N94-12054
p 281 N94-12055
BELL, JEFFREY F. p 430 N94-12124
p 430 N94-12162
p 431 N94-12164
BELL, M. S. p 281 N94-12056
BELL, R. L. p 326 N94-11226
BELL, STUART p 250 N94-12502
BELLSHAW, D. p 321 N94-10267
BELLUCCI, V. p 10 N94-10465
BELOKHVOSTIKOV, ANDREY V. p 225 N94-12738
BELOUSOV, A. V. p 376 N94-10575
BELTON, M. J. S. p 468 N94-12198
BELTON, MICHAEL p 459 N94-12147
BELVIN, W. KEITH p 331 N94-11522
BEN-ZVI, I. p 140 N94-10300
BENDER, ROBERT L. p 166 N94-12774
p 166 N94-12775
BENDER, W. p 116 N94-10192
p 87 N94-10202
BENHADID, H. p 119 N94-10215
BENKO, STEPHEN E. p 47 N94-11252
BENNER, LANCE A. M. p 429 N94-12057
BENNER, R. E. p 335 N94-10257
BENNETT, MARVIN E. p 429 N94-12061
BENNETT, VICTORIA p 432 N94-12237
BENOIT, P. H. p 429 N94-12058
p 429 N94-12059
p 443 N94-12060
BENOY, P. A. p 55 N94-11362
BENTAMY, ABDERRAHIM p 233 N94-11712
BENTILLO, ISRAEL p 219 N94-12707
BENTLEY, J. p 88 N94-10527
p 95 N94-12596
BENTLEY, R. D. p 483 N94-12414
BENTS, DAVID p 54 N94-11416
BENZ, K. W. p 106 N94-10111
p 107 N94-10116
p 118 N94-10209
p 119 N94-10213
BENZ, W. p 429 N94-12062
BERESTOV, A. L. p 227 N94-12752
BEREZHIANI, Z. G. p 410 N94-10545
BEREZIN, A. K. p 391 N94-11211
BEREZOVOJ, V. P. p 412 N94-11087
p 412 N94-11164
BERG, HANS-DIETER p 21 N94-10794
BERG, S. p 124 N94-10247
BERGAMASCO, A. p 221 N94-12719
BERGLUND, R. p 239 N94-11750
BERGMAN, C. M. p 9 N94-10460
BERGMANS, LODEWIJK p 320 N94-10166
BERGSTROEM, L. p 82 N94-10957
BERKE, LASZLO p 188 N94-11254
BERKOOZ, GAL p 31 N94-11494
BERN, TOM-IVAR p 253 N94-12522
BERNAL, J. p 343 N94-10825
BERNHARD, R. p 80 N94-12045
BERNHARD, R. P. p 429 N94-12063
BERNHARDT, H.-G. p 109 N94-10124
BERNICOT, N. p 59 N94-10023
BERRIER, KEITH p 55 N94-11675
BERRYMAN, J. G. p 150 N94-11026
p 327 N94-11240
BERTHE, PHILLIPPE p 55 N94-11675
BERTHIER, Y. p 64 N94-10061
BERTOLOTTI, M. p 376 N94-10574
BERTRAND, REINHOLD p 55 N94-11675
BESEDIN, N. T. p 392 N94-11214
BESMANN, THEODORE M. p 92 N94-11866
BETTERTON, W. J. p 281 N94-12085
BETTERTON, WILLIAM J. p 281 N94-12084
BETTI, F. p 45 N94-11342
BETTS, B. H. p 443 N94-12064
BETTS, R. R. p 372 N94-11124
BETZ, JOHANN p 106 N94-10107

BEUKENS, R. P. p 431 N94-12183
BEVERIDGE, J. L. p 373 N94-12542
BEWERSDORFF, A. p 87 N94-10231
BEWERSDORFF, AXEL p 121 N94-10227
BEYER, J. p 69 N94-11329
BEYSENS, DANIEL p 122 N94-10230
BEZRUKOV, A. M. p 301 N94-11648
BHAT, GOPALAKRISHNA K. p 186 N94-10900
BHAVNANI, K. H. p 43 N94-10944
BHUIYAN, A. K. M. FARIDUDDIN p 35 N94-10679
BIANCALE, R. p 243 N94-11778
BIANCHINI, RICARDO p 320 N94-11294
BIBYK, IRENE p 55 N94-11675
BICKEL, D. L. p 232 N94-11623
BIDDISCOMBE, J. p 244 N94-11785
BIEGELSEN, DAVID K. p 369 N94-12379
BILGEN, M. p 183 N94-11110
BILLIA, B. p 117 N94-10203
p 118 N94-10206
BILLS, BRUCE G. p 444 N94-12065
p 481 N94-12267
p 481 N94-12268
BILOTTI, FRANK p 444 N94-12066
BINDSCHADLER, D. L. p 444 N94-12067
BINDSCHADLER, ROBERT p 237 N94-11741
BINZEL, R. P. p 429 N94-12068
BIONDO, ANTHONY CHARLES p 399 N94-11314
BIRD, P. J. p 236 N94-11733
p 248 N94-12488
p 249 N94-12493
BIRIKH, R. p 120 N94-10220
BIRJMOHAN, S. R. p 57 N94-10010
BIRKELAND, D. p 238 N94-11747
BIRKETT, C. M. p 246 N94-12475
BIRKS, A. R. p 244 N94-11785
BISCHOF, OSCAR p 485 N94-11379
BISCHOFF, A. p 429 N94-12069
BISCHOPINK, G. p 119 N94-10213
BISHOP, A. R. p 399 N94-11263
p 403 N94-12345
BISHOP, GLADE M. p 321 N94-10335
BISHOP, JANICE L. p 445 N94-12070
p 445 N94-12071
BISHOP, R. p 319 N94-10146
BISSON, JOEL p 55 N94-11675
BISSON, ROGER U. p 317 N94-11549
BITTEN, E. J. p 372 N94-11296
BLACK, S. p 281 N94-12072
p 281 N94-12073
p 281 N94-12074
p 281 N94-12075
p 281 N94-12076
BLACKABY, NICHOLAS p 149 N94-10810
BLACKFORD, ROGER W. p 128 N94-10629
BLAHA, F. A. p 71 N94-11337
BLAIR, J. R. S. p 332 N94-11695
BLAKE, H. W. p 184 N94-10264
BLANEY, D. L. p 446 N94-12077
BLANFORD, GEORGE E. p 429 N94-12078
BLATTNER, MEERA M. p 321 N94-10291
BLECH, RICHARD A. p 327 N94-11232
BLETRY, J. p 86 N94-10195
BLEWETT, D. T. p 446 N94-12079
BLOM, J. G. p 342 N94-10351
BLOOM, E. E. p 391 N94-11171
BLUM, J. p 123 N94-10236
BLUM, JOEL D. p 281 N94-12080
p 430 N94-12146
BOATWRIGHT, D. W. p 185 N94-10712
BOBINA, N. N. p 454 N94-12122
BOCCACCIO, E. p 8 N94-10456
BOCKER, RICHARD P. p 138 N94-12440
BODART, C. p 31 N94-11493
BODE, A. p 243 N94-11778
BOELMAN, E. p 162 N94-12553
BOERS, H. p 416 N94-10868
BOESENBERG, JOSEPH S. p 281 N94-12081
p 432 N94-12208
BOFILIOS, DIMITRI A. p 60 N94-10030
p 60 N94-10031
BOGARD, D. D. p 80 N94-12082
p 281 N94-12083
BOGATYREVA, L. G. p 103 N94-10092
BOGOSLOVSKY, G. Y. p 410 N94-10535
BOHIGAS, A. p 148 N94-10530
BOHOR, B. F. p 281 N94-12085
BOHOR, BRUCE F. p 281 N94-12084
BOLDEN, WILLIAM p 286 N94-12772
BOLLE-MEAD, PAULINE p 485 N94-11379
BOLLER, C. p 27 N94-11318
p 22 N94-11333
BOLME, G. O. p 374 N94-12786
BOLOGA, M. K. p 103 N94-10093
BOLSHEVA, L. N. p 433 N94-12254
BOLZ, J. p 62 N94-10048
BOMAN, DUANE p 314 N94-11570
BONET, A. p 57 N94-10008
p 62 N94-10047
BONITO, N. A. p 43 N94-10944
BONNEFOND, P. p 39 N94-12530
BONNER, B. P. p 82 N94-11076
BORGWARDT, ROBERT H. p 267 N94-11845
BORISOV, A. p 87 N94-12086
BORRELLI, S. p 8 N94-10457
BOSCH, R. p 39 N94-10119
BOSCH, W. p 243 N94-11777
BOSLOUGH, M. B. p 80 N94-12087
BOSS, A. P. p 448 N94-12088
p 448 N94-12089
p 448 N94-12090
BOSTWICK, JENNIFER A. p 282 N94-12091
BOSWELL, STEVEN B. p 24 N94-11863
BOTHWELL, WILLIAM W. p 417 N94-11856
BOTTKE, W. F., JR. p 429 N94-12092
BOTTOMLEY, R. J. p 282 N94-12093
BOUDON, Y. p 352 N94-10972
p 39 N94-12530
BOUGH, R. M. p 29 N94-12272
BOULANGER, J.-S. p 356 N94-10998
BOUNAR, K. H. p 43 N94-10944
BOUNDY-SANDERS, S. Q. p 429 N94-12094
BOURGEAU-CHAVEZ, L. L. p 249 N94-12494
BOURGEOIS, PAUL A. p 333 N94-12332
BOURIANOFF, G. p 335 N94-10340
BOURNE, WILLIAM p 321 N94-10335
BOUTIER, ALAIN p 5 N94-10436
BOWEN, BARRY C. p 40 N94-10805
BOWMAN, KENNETH P. p 279 N94-12560
BOYAR, R. E. p 169 N94-10326
BOYCE, JOSEPH M. p 449 N94-12095
BOYD, J. F. p 318 N94-11553
BOYLE, J. S. p 284 N94-10739
BOYNTON, WILLIAM V. p 80 N94-12096
BOZOKI, E. p 374 N94-12782
BRACKETT, ROBERT A. p 258 N94-12097
BRADDY, D. p 321 N94-10263
BRADFORD, W. J. p 244 N94-11785
BRADLEY, B. D. p 174 N94-10959
BRADLEY, J. P. p 429 N94-12098
p 81 N94-12099
p 430 N94-12115
BRADLEY, R. p 79 N94-12534
BRADSHAW, PETER p 154 N94-11641
BRADY, R. F. p 90 N94-11302
BRAIDWOOD, S. p 360 N94-10327
BRAINERD, J. J. p 484 N94-10507
BRAJLOVSKIJ, E. Y. p 397 N94-10845
BRAKENRIDGE, G. R. p 450 N94-12100
BRANDOW, B. H. p 401 N94-11646
BRANDSTAETTER, F. p 429 N94-12101
BRANDSTATTER, F. p 432 N94-12233
BRANDT, D. p 282 N94-12102
p 282 N94-12103
BRANKA, A. C. p 361 N94-10502
BRATTKUS, K. p 115 N94-10188
BRAU, J. E. p 368 N94-11696
BRAUN, MICHAEL p 109 N94-10126
p 111 N94-10135
BRAUN, RICHARD J. p 115 N94-10188
BRAY, I. p 359 N94-10312
p 360 N94-10331
BRAY, IGOR p 360 N94-10328
p 360 N94-10329
BREARLEY, ADRIAN J. p 282 N94-12104
p 429 N94-12105
p 429 N94-12106
BRECKENRIDGE, A. p 319 N94-10268
BREISACHER, KEVIN J. p 46 N94-10763
BREIVIK, LARS-ANDERS p 233 N94-11710
BRENDER, KAREN D. p 52 N94-11401
BRENNAN, G. M. p 37 N94-10691
BRENNAN, JOHN p 92 N94-11876
BRENNEIS, A. p 9 N94-10459
BREWER, DENNIS W. p 331 N94-11680
BREWER, J. H. p 373 N94-12542
BRIDGES, N. T. p 430 N94-12107
BRIGGS, D. A. p 159 N94-12311
BRILES, S. D. p 132 N94-10315
BRILLIANT, D. R. p 451 N94-12108
BRINK, NANCY J. p 289 N94-11853
BRINKER, D. J. p 48 N94-11383
p 48 N94-11384
BRINTON, K. L. F. p 452 N94-12109
BRISCO, B. p 248 N94-12486
BRISKMAN, VLADIMIR p 120 N94-10220
BRISKMAN, VLADIMIR A. p 103 N94-10092
BRISSON, J. G. p 128 N94-11161
BRITT, D. T. p 81 N94-12110
p 430 N94-12111
BROCK, B. C. p 232 N94-11623
BRODEN, G. p 59 N94-10026
BROERSMA, H. J. p 341 N94-10274
BRONIKOWSKI, M. p 402 N94-11684
BROOKS, G. H. p 272 N94-12780
BROOKS, K. P. p 99 N94-12564
BROOKS, N. H. p 393 N94-11514
BROOKS, PETER S. p 417 N94-11856
BROSSIER, C. p 242 N94-11769
BROUSSAUD, P. p 4 N94-10429
BROWN, A. E. p 82 N94-11076
BROWN, ALAN M. p 137 N94-11357
BROWN, C. DAVID p 452 N94-12112
p 452 N94-12113
BROWN, CHARLES p 25 N94-10945
BROWN, JAMES E. p 19 N94-10779
BROWN, LAURIE M. p 376 N94-10577
BROWN, LAWRENCE E. p 431 N94-12166
BROWN, R. C. p 279 N94-12572
BROWN, R. J. p 248 N94-12486
BROWN, ROBERT A. p 201 N94-11955
p 201 N94-11956
BROWN, S. A. p 321 N94-10263
BROWN, V. R. p 361 N94-10334
BROWNING, LAUREN B. p 430 N94-12114
BROWNING, R. p 145 N94-12405
BROWNLEE, D. E. p 81 N94-12099
p 430 N94-12115
BROWNLEE, DONALD E. p 282 N94-12199
BROZ, J. S. p 350 N94-10313
BRUCHEY, W. J., JR. p 405 N94-12563
BRUCKART, JAMES E. p 315 N94-11291
BRUCKENSTEIN, STANLEY p 405 N94-12586
BRUENING, C. p 251 N94-12509
BRUENING, J. p 48 N94-11381
BRUN, R. p 8 N94-10456
BRUNE, WILLIAM H. p 274 N94-10701
BRUNGER, M. p 360 N94-10327
BRUNO, B. C. p 282 N94-12116
BRUNO, BARBARA C. p 460 N94-12154
BRUNO, KRISTIN J. p 314 N94-11534
BRYANSTON-CROSS, P. p 383 N94-11887
BRYSON, J. W. p 184 N94-10288
BUCHANAN, P. C. p 453 N94-12117
BUCHHOLTZ, BRETT W. p 386 N94-10346
BUCK, W. ROGER p 453 N94-12118
BUCKEY, JAY C. p 310 N94-11999
BUCKLEY, J. R. p 232 N94-11708
BUDGE, K. G. p 345 N94-11225
BUGEAT, J. P. p 108 N94-10122
BUKSA, J. J. p 372 N94-10890
BULATOV, N. V. p 224 N94-12737
BULATOV, NAFANAIL V. p 228 N94-12757
BULLOCK, M. A. p 453 N94-12119
BULMER, M. H. p 454 N94-12120
BULSARA, ADI p 313 N94-11890
BULZAN, DANIEL L. p 28 N94-11238
BUNGO, MICHAEL W. p 309 N94-11993
BUNIMOVICH, LEONID A. p 205 N94-11984
BURBA, G. A. p 282 N94-12121
p 454 N94-12122
BURBA, G. G., JR. p 282 N94-12123
BURBECK, CHRISTINA A. p 313 N94-10909
BURBINE, THOMAS H. p 430 N94-12124
BURCHETT, S. N. p 177 N94-10348
BURENKOV, VLADIMIR I. p 226 N94-12744
BURGE, S. W. p 150 N94-11072
BURK, THOMAS E. p 231 N94-11521
BURKE, W. R. p 56 N94-10001
BURKLAND, M. K. p 430 N94-12125
BURL, M. C. p 455 N94-12126
BURMAN, NORBERT M. p 328 N94-11301
BURNETT, D. S. p 455 N94-12127
BURNS, I. F. p 55 N94-12283
BURNS, J. BRIAN p 418 N94-10515
BURNS, ROGER G. p 445 N94-12070
p 455 N94-12128
p 455 N94-12129
p 433 N94-12257
BURNS, WILLIAM K. p 176 N94-12329
BURNSIDE, W. D. p 23 N94-11525
BURT, J. D. p 455 N94-12130
BUSECK, P. R. p 432 N94-12230
p 432 N94-12231
BUSH, D. p 139 N94-12778
BUSSDESOUZA, RONALD p 288 N94-11200
BUSSEY, D. B. J. p 456 N94-12131
BUSSOLETTI, E. p 113 N94-10175
BUSTIN, R. p 430 N94-12132
BUTA, RONALD J. p 426 N94-11590
BUTS, V. A. p 134 N94-11037
BUTTRAM, M. T. p 144 N94-11624
BUTTRY, DANIEL A. p 78 N94-12273
BUZZI, V. p 385 N94-10284
BYKOVSKIJ, B. V. p 361 N94-10532
BYRD, ROGER p 172 N94-12038
BYRNES, P. p 371 N94-10260
BYRNES, RONALD B., JR. p 332 N94-11874

C

CABOT, WILLIAM H. p 155 N94-12287
CABROL, N. A. p 456 N94-12133
CAFFEE, M. W. p 437 N94-12033
CAFFORIO, C. p 235 N94-11728
CAHAN, B. D. p 401 N94-11518
CAI, S. X. p 94 N94-12396
CAI, SUI X. p 93 N94-12353
CAIRNS, SARA p 267 N94-11864
CALHOUN, MALCOLM p 355 N94-10994
p 355 N94-10995
CALKINS, D. J. p 254 N94-12528
CALLAHAN, P. X. p 302 N94-11556
CALLAHAN, VIRGINIA p 185 N94-10342
CALLEN, J. D. p 390 N94-11149
CALVIN, WENDY M. p 441 N94-12054
p 456 N94-12134
CAMACHO, A. p 59 N94-10023
CAMBON, G. p 114 N94-10180
CAMERON, A. G. W. p 430 N94-12135
CAMERON, CHARLES G. p 92 N94-11849
CAMERON, J. F. p 145 N94-11819
CAMERON, JAMES F. p 95 N94-12585
CAMERON, WILFRID L. p 21 N94-10795
CAMPBELL, BRUCE A. p 457 N94-12136
p 457 N94-12137
CAMPBELL, WALTON B. p 211 N94-12662
CAMPBELL, WILLIAM J. p 238 N94-11745
p 210 N94-12651
CAMPOS, L. M. B. C. p 31 N94-11492
CANESSA, E. p 348 N94-10404
CANFIELD, D. J. p 340 N94-12411
CAO, TIEHUA p 338 N94-10638
CAPONE, FRANCIS J. p 12 N94-10675
CARCIELLO, N. R. p 88 N94-10891
CARDON, J. G. p 54 N94-11643
CAREY, P. G. p 395 N94-10516
CAREY, S. p 282 N94-12138
p 432 N94-12238
CARLBERG, TORBJORN p 110 N94-10132
CARLSON, R. W. p 457 N94-12139
p 425 N94-12140
CARLSON, W. F. p 372 N94-11296
CARLSTROEM, A. p 238 N94-11747
CARLSTROM, ANDERS p 239 N94-11751
CAROTENUTO, L. p 113 N94-10175
CARPENTER, BERNIE p 70 N94-11331
CARPENTER, SCOTT A. p 47 N94-11053
CARPENTER, THOMAS W. p 150 N94-10912
CARR, P. W. p 369 N94-11826
CARR, STEPHEN S. p 279 N94-12419
CARRERAS, B. A. p 385 N94-10310
CARRETTA, THOMAS R. p 314 N94-12276
CARSON, GREGORY D. p 332 N94-11860
CARTER, C. B. p 88 N94-10527
p 95 N94-12596
CARTER, D. J. T. p 244 N94-11781
CARTER, JAMES L. p 464 N94-12179
CARTER, M. D. p 131 N94-10270
CARTER, W. p 423 N94-11183
CARTWRIGHT, S. p 382 N94-11421
CASANOVA, I. p 282 N94-12141
p 430 N94-12142
CASH, BERNARD L. p 318 N94-11561
CASIER, JEAN-GEORGES p 461 N94-12160
CASSEN, P. p 458 N94-12143
CASTAGNOLO, DARIO p 104 N94-10097
CASTELLANOS, ANTONIO p 100 N94-10075
CASTELLON, A. p 255 N94-12529
CATON, R. p 170 N94-10948
CATT, TYRONE F. p 27 N94-11345
CATTOLICA, R. p 4 N94-10434
CAUNEAU, F. p 250 N94-12503
CAUTRU, J. P. p 254 N94-12523
CAVALIERI, D. J. p 239 N94-11748
CAVALIERI, DONALD J. p 210 N94-12651
CAVANIE, ALAIN p 233 N94-11712
CAVES, R. G. p 248 N94-12487
CAVESTRI, R. C. p 89 N94-11145
CAZENAVE, A. p 243 N94-11775
CECIL, JACK B. p 290 N94-10975
CEDERQUIST, J. p 382 N94-11421
CEFUS, G. R. p 327 N94-11246
CEGLIO, N. M. p 381 N94-10651
p 143 N94-11273
CEKIC, M. p 388 N94-10747
CELENLIGIL, M. CEVDET p 7 N94-10449
CELLINO, A. p 431 N94-12201
CERBONE, R. J. p 371 N94-10529
CERDEIRA, H. A. p 132 N94-10401
CERJAN, C. J. p 389 N94-11074
CERRONI, PRISCILLA p 432 N94-12234
p 475 N94-12235
CESPEDOSA, F. p 56 N94-10007
CHACHO, E. F. p 254 N94-12528
CHADWICK, D. J. p 458 N94-12144
p 458 N94-12145
CHAEN, MASAAKI p 195 N94-11920
p 215 N94-12680
CHAI, AN-TI p 104 N94-10094
CHALLENOR, P. G. p 253 N94-12519
CHALLENOR, PETER G. p 244 N94-11782
CHAMBERLAIN, C. PAGE p 281 N94-12080
p 430 N94-12146
CHAMBERS, R. S. p 177 N94-10348
CHAMIS, C. C. p 185 N94-10361
p 186 N94-10762
CHAN, K. S. p 85 N94-12426
CHAN, YIN-WEN p 73 N94-11686
CHANDRASEKARAN, M. p 69 N94-11329
CHANETZ, B. p 4 N94-10429
CHANG, K.-T. p 112 N94-10172
CHANG, L. C. p 335 N94-10340
CHANG, S. p 433 N94-12263
CHANG, SIN-CHUNG p 150 N94-10939
CHAO, Y. p 208 N94-12644
CHAPLIN, M. R. p 387 N94-10737
CHAPMAN, B. p 388 N94-10747
CHAPMAN, CLARK R. p 459 N94-12147
CHAPMAN, DAVID p 418 N94-10515
CHAPMAN, MARY G. p 459 N94-12148
CHAPRON, B. p 251 N94-12507
CHAPRON, BERTRAND p 233 N94-11712
CHARLES, J. B. p 312 N94-11557
CHARLES, JOHN B. p 309 N94-11993
p 309 N94-11997
CHARNOTSKII, M. I. p 136 N94-11069
CHARRIEZ, P. p 250 N94-12503
CHARRON, CHRISTOPHE p 254 N94-12523
CHASNOV, JEFFREY R. p 156 N94-12292
CHATTERJEE, SHARMISTA p 316 N94-12366
p 317 N94-12369
CHAUDHRI, M. M. p 78 N94-11855
CHAUDIER, A. p 98 N94-11017
CHAUHAN, N. p 245 N94-11885
CHAZEN, MELVIN L. p 46 N94-10938
CHECHKIN, A. V. p 391 N94-11207
p 391 N94-11208
p 392 N94-11212
CHECHKIN, V. V. p 392 N94-11214
CHELTON, DUDLEY p 208 N94-12643
CHEN, CHIEH-CHENG p 263 N94-11313
CHEN, CHUN p 409 N94-10403
CHEN, D. p 402 N94-11684
CHEN, F. F. p 363 N94-10661
CHEN, G. p 101 N94-10076
p 105 N94-10101
CHEN, GE p 197 N94-11930
p 220 N94-12711
CHEN, GUANGQING p 282 N94-12149
CHEN, H. p 325 N94-11109
CHEN, J. H. p 430 N94-12150
p 430 N94-12151
CHEN, J. I. p 93 N94-12380
CHEN, JEN-PING p 265 N94-11189
CHEN, JIAN-CHU p 185 N94-10306
CHEN, W. C. p 115 N94-10187
CHEN, WEN-ZHONG p 203 N94-11970
CHEN, X. C. p 86 N94-10194
CHEN, X. S. p 86 N94-10194
CHEN, XIMING p 405 N94-12587
CHEN, Y. C. p 321 N94-10343
CHEN, Y. M. p 93 N94-12380
CHEN, YANHUI p 322 N94-10484
CHEN, YINBAO p 371 N94-10409
CHEN, Z. p 243 N94-11778
CHENEY, ROBERT p 244 N94-11784
CHENG, ANDREW F. p 459 N94-12152
CHENG, C. C. p 79 N94-12538
CHEPILKO, N. M. p 344 N94-10881
CHERENKOV, G. T. p 24 N94-10967
CHERN, R. T. p 92 N94-11848
CHESLOW, RICHARD p 417 N94-11856
CHETIRKIN, P. V. p 315 N94-11258
CHEUNG, SAMSON p 25 N94-11150
CHIANG, YET-MING p 398 N94-11012
CHIARELLI, P. p 70 N94-11330
CHIBA, KOUICHI p 161 N94-12549
CHICARRO, A. F. p 460 N94-12153
CHIDUME, C. E. p 343 N94-10531
CHILDS, P. N. p 324 N94-10893
p 154 N94-11859
CHILDS, ROBERT E. p 154 N94-11641
CHIN, H. N. S. p 283 N94-10290
CHING, DELWYN p 460 N94-12154
CHINO, TSUTOMU p 213 N94-12671
CHIRIKOV, BORIS V. p 379 N94-10602
CHIRKIN, A. S. p 375 N94-10567
CHISHOLM, JEAN p 417 N94-12360
CHIU, S. C. p 385 N94-10159
CHMELYNSKI, H. J. p 417 N94-11844
CHO, JIN HYUNG p 403 N94-12363
CHO, KYEHYUN p 83 N94-11316
CHOI, HAECHEON p 156 N94-12293
CHOI, HYEUNG-SIK p 340 N94-11825
CHOI, S. W. p 399 N94-11440
CHOLEWA, M. p 143 N94-11285
CHONG, YEAN-JOO p 37 N94-10689
CHOO, HYO SANG p 215 N94-12683
CHOU, KOHEI p 210 N94-12654
CHOW, R. p 90 N94-11230
CHOW, WENG W. p 374 N94-10339
CHOYKE, W. J. p 79 N94-12538
CHRISTENSEN, J. D. p 127 N94-10622
CHRISTENSEN, N. L., JR. p 249 N94-12494
CHRISTENSEN, PHILIP R. p 460 N94-12155
p 81 N94-12156
CHRISTMAS, P p 359 N94-10266
CHU, STEVEN p 352 N94-10976
CHU, TAK-KIN p 404 N94-12400
CHU, Y. C. p 67 N94-11237
CHUBAROV, VASILY V. p 177 N94-12755
CHUBB, DONALD L. p 47 N94-11307
CHUCHKALOV, S. I. p 103 N94-10093
CHUKWUMAH, G. C. p 409 N94-10402
CHUN, SANG Y. p 485 N94-12434
CHUNG, Y. p 220 N94-12709
CHURCH, J. M. p 64 N94-10060
CHURCH, JOHN p 208 N94-12643
CHYBA, C. F. p 430 N94-12157
CIMOLINO, MARC p 381 N94-11054
CINI, E. p 86 N94-10195
CINTALA, M. J. p 461 N94-12158
CINTALA, MARK J. p 461 N94-12159
CLAEYS, PHILIPPE p 461 N94-12160
p 282 N94-12161
CLARK, B. E. p 433 N94-12244
CLARK, BETH E. p 430 N94-12162
p 430 N94-12163
p 431 N94-12164
CLARK, EDWIN C. p 18 N94-10777
CLARK, PAMELA E. p 462 N94-12165
CLARKE, FREDERIC B. p 20 N94-10785
CLARKSON, J. E. p 77 N94-11602
CLAYTON, DONALD D. p 431 N94-12166
CLAYTON, JOSEPH P. p 166 N94-12774
p 166 N94-12775
CLEARY, THOMAS G. p 19 N94-10781
CLELAND, W. E. p 369 N94-12546
CLEMETT, S. J. p 431 N94-12167
CLEMMER, TERRY P. p 305 N94-11788
p 305 N94-11790
CLIFFORD, STEPHEN M. p 462 N94-12168
p 463 N94-12169
p 463 N94-12170
CLIFTON, MICHAEL J. p 122 N94-10234
CLORMANN, U. p 58 N94-10016
CLOUGH, ROGER L. p 183 N94-11586
CLOUGH, S. A. p 278 N94-11852
CLOUTIS, E. A. p 431 N94-12171
COCHRANE, R. F. p 86 N94-10196
COCKRELL, CHARLES E. p 348 N94-11569
COET, M.-C. p 4 N94-10429
COFFEY, D. p 412 N94-11162
COGGIOLA, M. J. p 272 N94-12783
COHEN, J. W. p 342 N94-10352
p 347 N94-10353
COHEN, MALCOLM M. p 314 N94-11530
COHEN, MARSHALL J. p 401 N94-11476
COHEN, MARTIN I. p 17 N94-10768
COHEN, R. H. p 385 N94-10289
p 390 N94-11125
COLANGELI, L. p 113 N94-10175
COLANTONIO, RENATO OLAF p 28 N94-11234
COLE, B. p 335 N94-10340
COLE, GARY L. p 327 N94-11232
COLE, J. K. p 147 N94-10252
COLEMAN, GARY N. p 156 N94-12294
COLEMAN, M. M. p 99 N94-12282
COLEMAN, RICHARD p 208 N94-12642
p 208 N94-12643
COLINET, P. p 121 N94-10223
COLINET, PIERRE p 119 N94-10216
COLLINSON, D. W. p 431 N94-12172
COLLYER, STANLEY C. p 313 N94-11701
COLOMBINI, M. p 300 N94-11020
COLSON, R. O. p 463 N94-12173
p 408 N94-12174
COLTRIN, M. E. p 77 N94-11370
p 152 N94-11371
COLVIN, T. R. p 468 N94-12198
COLWELL, JOSHUA E. p 347 N94-12175
COMER, EDWARD p 323 N94-10495
COMERA, J. p 86 N94-10197
COMHAIRE, A. L. p 254 N94-12524
COMISO, JOEY C. p 241 N94-11762

COMISO, JOSEFINO C. p 210 N94-12651
CONNOLLY, HAROLD C., JR. p 431 N94-12176
p 431 N94-12177
CONNORS, CHRIS p 444 N94-12066
CONRAD, K. p 401 N94-11651
CONSTABLE, STEFAN H. p 301 N94-11861
CONTAMIN, P. p 86 N94-10197
CONTOGURIS, A. P. p 362 N94-10554
CONVERTINO, VICTOR A. p 308 N94-11992
CONWAY, J. p 249 N94-12497
CONWAY, J. A. p 250 N94-12498
p 250 N94-12499
COOK, H. F. p 146 N94-12773
COOLEN, F. P. A. p 183 N94-10170
COOMBS, C. R. p 190 N94-12178
COOPER, BONNIE L. p 464 N94-12179
COOPER, H. J. p 286 N94-12580
COOPER, R. M. p 83 N94-11127
COPPEE, J. L. p 61 N94-10040
COPPIN, POL R. p 231 N94-11521
COQUEL, F. p 8 N94-10455
CORADINI, A. p 433 N94-12265
CORADINI, ANGIOLETTA p 432 N94-12234
p 475 N94-12235
CORDARA, F. p 139 N94-10984
CORDES, JAMES M. p 135 N94-11065
CORDEY, R. A. p 248 N94-12488
CORIELL, S. R. p 105 N94-10103
p 113 N94-10178
CORK, M. p 44 N94-10250
CORNET, Y. p 254 N94-12524
CORRY, GLEN p 146 N94-12433
CORSETTI, L. p 276 N94-11241
CORSETTI, L. C. p 276 N94-11227
CORSON, M. R. p 54 N94-11643
CORTELLA, L. p 86 N94-10195
COSTANTINI, S. p 58 N94-10018
COSTARD, FRANCOIS M. p 435 N94-12018
COSTEN, ROBERT C. p 484 N94-10759
COSTIGAN, KEELEY ROCHELLE p 277 N94-11465
COTTINGAME, W. B. p 374 N94-12786
COUEDOR, C. p 4 N94-10431
COURS, JEFFREY T. p 327 N94-11231
COVINGTON, AL p 34 N94-10930
COVINGTON, P. A. p 318 N94-11553
COWART, J. S. p 177 N94-10322
COWDEN, W. C. p 84 N94-11668
COWDEROY, A. J. C. p 329 N94-11426
COWINGS, PATRICIA S. p 311 N94-12006
COWLING, DAVID p 27 N94-11345
COX, SPRUCE M. p 52 N94-11401
CRADDOCK, ROBERT A. p 465 N94-12180
CRAFT, D. C. p 174 N94-11005
CRAIG, J. W. p 91 N94-11350
CRAIG, ROGER A. p 34 N94-10930
CRAISE, LAURIE M. p 312 N94-11558
CRANE, J. K. p 364 N94-10753
CRAVEY, W. R. p 142 N94-11050
CRAWFORD, D. A. p 431 N94-12181
CRAWLEY, EDWARD F. p 68 N94-11322
CREASER, R. A. p 431 N94-12182
CRESPO, A. p 104 N94-10095
CRESPO, G. p 132 N94-10401
CRESSWELL, R. G. p 431 N94-12183
CREWS, J. H. p 67 N94-11276
CRILL, PATRICK M. p 269 N94-12457
CRISP, D. p 446 N94-12077
p 465 N94-12184
CRISP, DAVID p 441 N94-12054
CROCHET, M. J. p 31 N94-11493
CROCKER, DEBORAH A. p 426 N94-11590
CROCKER, N. p 388 N94-10747
CROELL, A. p 102 N94-10085
CROFT, STEVEN K. p 466 N94-12185
p 431 N94-12186
p 466 N94-12187
CROSS, L. E. p 358 N94-11262
p 93 N94-12331
CROSS, L. ERIC p 70 N94-11332
CROSS, P. p 359 N94-10266
CROSS, T. A. p 52 N94-11406
CROSSEY, L. J. p 282 N94-12188
CROTINGER, J. A. p 385 N94-10289
CROVELLA, MARK E. p 320 N94-11294
CROWE, B. p 273 N94-10285
CROWELL, L. B. p 384 N94-12189
CROWLEY, W. P. p 151 N94-11272
CROWN, DAVID A. p 467 N94-12190
CROZAZ, GHISLAINE p 431 N94-12191
CRUMPLER, L. S. p 455 N94-12126
p 465 N94-12180
p 467 N94-12192
p 467 N94-12193
p 467 N94-12194
p 467 N94-12195
p 467 N94-12196
p 469 N94-12204
CRUTCHFIELD, W. Y. p 325 N94-11112
CUADRADO, A. p 57 N94-10008
CUBBAGE, ROBERT W. p 355 N94-10992
CUCINELLI, G. p 3 N94-10424
CUCINOTTA, FRANCIS A. p 484 N94-11278
p 45 N94-11559
p 373 N94-12435
CULOSI, SALVATORE J. p 417 N94-11856
CULSHAW, B. p 69 N94-11324
CULSHAW, BRIAN p 65 N94-10066
CUMALAT, J. P. p 370 N94-12609
CUNDY, S. p 356 N94-10998
CUNNINGHAM, D. M. p 78 N94-11622
CUNNINGHAM, GLENN p 240 N94-11756
CUNNINGHAM, ROBERT K. p 331 N94-11652
CURLETT, BRIAN P. p 327 N94-11231
CURRAN, M. J. p 57 N94-10011
p 70 N94-11336
CURRAN, MARY ANN p 265 N94-10841
CURRY, ROBERT E. p 3 N94-10427
CURTAIN, R. F. p 344 N94-10905
CURTIN, W. J. p 185 N94-10712
CURTIS, H. B. p 48 N94-11383
CURTIS, HENRY p 53 N94-11410
CUSANO, C. p 89 N94-11146
CUSHING, J. A. p 282 N94-12197
CYGAN, R. T. p 80 N94-12087
CZYRYCA, E. J. p 85 N94-12532

D

DABOUL, JAMIL p 347 N94-10607
DAGOSTINO, PAUL A. p 78 N94-12009
DAHL, D. A. p 76 N94-11140
DAKHNOVSKII, YURI p 366 N94-11100
DAKIN, J. P. p 64 N94-10065
p 70 N94-11336
DALLAGLIO, GIAN ANTONIO p 107 N94-10117
DALLEMAND, J. F. p 246 N94-12478
DALLMANN, UWE p 8 N94-10453
DANDO, ANDREW p 149 N94-10810
DANDREA, J. A. p 26 N94-11892
DANDREA, JOHN A. p 324 N94-11099
DANDRIDGE, A. p 374 N94-10376
DANG, CHUANGYIN p 322 N94-10355
DANIEL, M. p 108 N94-10122
DANIELS, CHARLES B. p 329 N94-11428
DANIELSON, G. E. p 425 N94-12140
DANILEWSKY, A. N. p 118 N94-10209
p 119 N94-10213
DANKERT, C. p 4 N94-10434
DARIANO, G. M. p 376 N94-10572
DARLING, DOUGLAS p 163 N94-12576
DAS, ALOK p 45 N94-11319
DAS, D. K. p 249 N94-12492
DAS, SAJAL p 18 N94-10772
DASILVA, X. A. p 395 N94-10314
DASILVAVELLOSOFERREIRA, CLAUDIA ALVARES
p 325 N94-11166
DATTA, A. p 283 N94-10725
DAUBY, PIERRE C. p 103 N94-10090
DAUMER, MARTIN p 378 N94-10589
DAUNCEY, S. R. p 416 N94-10145
DAUTREBANDE, SYLVIA p 247 N94-12480
DAUX, J. C. p 59 N94-10024
DAVENPORT, A. J. p 84 N94-11459
DAVIDSON, D. L. p 187 N94-11096
DAVIDSON, J. L. p 109 N94-10127
DAVIDSON, K. p 234 N94-11720
DAVIES, M. A. H. p 53 N94-11412
DAVIES, M. E. p 468 N94-12198
DAVIS, ANDREW M. p 282 N94-12199
p 431 N94-12200
DAVIS, D. R. p 431 N94-12201
DAVIS, DOMINIC A. R. p 152 N94-11377
DAVIS, G. C. p 177 N94-10322
DAVIS, GARY C. p 19 N94-10781
DAVIS, H. p 302 N94-11548
DAVIS, J. BRADLEY p 40 N94-10805
DAVIS, J. E. p 399 N94-11243
DAVIS, L. E. p 173 N94-10755
DAVIS, MICHAEL M. p 318 N94-10865
DAVIS, P. A. p 469 N94-12202
p 469 N94-12203
DAVIS, R. H. p 114 N94-10182
DAVIS, ROBERT F. p 19 N94-10778
DAVIS, S. p 346 N94-11693
DAVIS, S. H. p 115 N94-10188
DAVISON, C. p 246 N94-12476
DAWIDOWICZ, G. p 456 N94-12133
DAWSON, C. B. p 469 N94-12204
DAWSON, H. p 149 N94-10851
DAWSON, WILLIAM J. p 331 N94-11679
DAY, C. T. p 419 N94-11105
DCRUZ, JONATHAN p 16 N94-12421
DEALWIS, S. P. p 370 N94-12609
DEAN, CHARLES E. p 413 N94-12343
DEANGELIS, G. p 431 N94-12205
DEBAGGIS, AMELIA p 17 N94-10770
DEBARROS, R. C. p 342 N94-10283
p 349 N94-10636
DEBY, ROLF A. p 320 N94-10167
DECAROLIS, G. p 235 N94-11728
DECH, STEFAN WERNER p 214 N94-12677
DECHAMBRE, M. p 254 N94-12523
DECONINCK, H. p 10 N94-10463
DEEKSHATULU, B. L. p 193 N94-11907
DEFFONTAINES, B. p 254 N94-12523
DEFLORE, THOMAS p 26 N94-11858
DEFORD, J. F. p 132 N94-10518
DEGRAND, T. A. p 370 N94-12609
DEGROOF, H. p 249 N94-12496
p 249 N94-12497
p 250 N94-12498
p 250 N94-12499
DEHART, JOHN M. p 432 N94-12206
DEHON, R. A. p 470 N94-12207
DEISSLER, ROBERT J. p 152 N94-11376
DEIWERT, GEORGE S. p 7 N94-10446
DEKNECHT, J. p 246 N94-12476
DELAEY, L. p 75 N94-10186
DELANEY, JEREMY S. p 281 N94-12081
p 432 N94-12208
DELANO, J. W. p 470 N94-12209
p 283 N94-12210
p 432 N94-12211
DELGADO, A. p 124 N94-10247
DELGER, KARLYNA L. p 317 N94-11549
DELLACORTE, C. p 55 N94-11362
DELLAVERSANA, P. p 113 N94-10175
DELMORE, J. E. p 76 N94-11140
DELOULE, E. p 471 N94-12212
DELOZIER, R. p 128 N94-11028
DELUCA, DANIEL P. p 85 N94-12418
DEMAIO, JOE p 35 N94-11535
DEMARCO, STEVEN J. p 301 N94-12417
DEMARIA, M. p 44 N94-11462
DEMELLO, WILLIAM ZAMBONI p 268 N94-12456
p 269 N94-12460
p 270 N94-12461
p 270 N94-12462
p 271 N94-12466
p 271 N94-12467
p 271 N94-12469
p 271 N94-12470
DEMIDOVA, TATIANA A. p 224 N94-12733
p 224 N94-12734
DEMIN, A. V. p 63 N94-10057
DEMIRCAN, A. p 248 N94-12491
DEMORAES, OSMAR p 218 N94-12700
DEMOUSTIER, CHRISTIAN p 290 N94-12350
DEMUYNCK, WILLEM M. p 375 N94-10569
DENHARTOG, D. J. p 388 N94-10747
DENISON, G. J. p 401 N94-11605
DENK, TILMANN p 471 N94-12213
DENNISON, BRIAN p 134 N94-11063
DENNY, SAMUEL A. p 21 N94-10793
DENTON, J. D. p 166 N94-12777
DEOLIVEIRACOSTA, ANGELICA p 484 N94-12357
DER, S. W. p 138 N94-11655
DERENZO, S. E. p 371 N94-10156
DERION, TONIANN p 302 N94-11548
DERMOTT, S. F. p 483 N94-10949
DEROIN, J. P. p 254 N94-12523
DEROSSI, D. p 70 N94-11330
DERRO, REBECCA J. p 81 N94-10504
DERUYTTERE, A. p 75 N94-10186
DERVIEUX, ALAIN p 345 N94-11277
DESAI, P. D. p 81 N94-10297
DESCHAMBAULT, R. L. p 6 N94-10442
DESIDERI, JEAN-ANTOINE p 5 N94-10440
DESIDERIO, GIANFRANCO p 102 N94-10087
DESOUZAALMEIDA, FABIO p 306 N94-11797
DETHOMAS, ANTHONY p 27 N94-11347
DETOMA, E. p 353 N94-10979
DEUSER, MARK S. p 108 N94-10120
DEUTSCH, S. p 161 N94-12352
DEVELYN, MARK P. p 403 N94-12010
DEVENPORT, WILLIAM J. p 357 N94-10752
DEVENY, MARC E. p 47 N94-11053
DEVIETTI, TERRY L. p 324 N94-11099
DEVOTO, J. A. p 346 N94-11631
DEWANDRE, T. p 44 N94-10250
DEWANTI, RATIH p 206 N94-11989
DEWEY, WAYNE P. p 353 N94-10977
DEWEZ, ARNAUD p 247 N94-12480
DEZA, MICHEL p 347 N94-10354
DHERE, NEELKANTH G. p 53 N94-11411
DHONDT, S. p 282 N94-12138
DIAMENT, A. p 248 N94-12488
DIAMENT, A. D. p 238 N94-11743

DIAZ, V. p 56 N94-10007
DICARLO, JAMES A. p 66 N94-11135
DICKERMAN, C. E. p 169 N94-10326
DICKEY, F. M. p 141 N94-10521
DICKINSON, STUART C. p 178 N94-10381
DICKSON, T. L. p 184 N94-10288
DIDION, D. A. p 411 N94-10853
DIDYK, A. Y. p 484 N94-10534
DIECKMANN, MATTHIAS p 106 N94-10112
p 110 N94-10130
DIEFENBACH, ANGELIKA p 112 N94-10143
DIEFENBACH, S. p 113 N94-10177
p 114 N94-10182
DIEHL, ROBERT G. p 18 N94-10775
DIENER, WILLIAM p 139 N94-11000
DIERKING, W. p 239 N94-11753
DIETRICH, DAVID p 287 N94-10153
DIGRANES, G. p 234 N94-11720
DIKOV, YU. P. p 81 N94-12214
DILGER, R. p 22 N94-11333
DIMARCO, PAOLO p 121 N94-10226
DIMARZO, M. p 149 N94-10851
DIMAURO, L. F. p 173 N94-10287
DING, JIAN M. p 301 N94-12417
DING, JIANMIN p 150 N94-11072
DINGUS, R. S. p 301 N94-11667
DINI, J. W. p 84 N94-11668
DIRENZO, F. p 119 N94-10210
DIRGAHAYU, DEDE p 206 N94-11989
DITTUS, HANSJORG p 108 N94-10121
DJEU, N. p 176 N94-12402
DJILALI, N. p 118 N94-10208
DOAKE, CHRISTOPHER p 238 N94-11742
DOBSON, F. W. p 232 N94-11708
DOBSON, M. CRAIG p 266 N94-11374
DODD, DAROL p 318 N94-11554
DODD, R. T. p 432 N94-12215
DODONOV, V. V. p 376 N94-10571
p 349 N94-10573
p 350 N94-10600
p 380 N94-10612
DOGIGLI, M. p 63 N94-10055
DOHERTY, JOSEPH p 284 N94-11113
DOHM, JAMES M. p 472 N94-12216
DOHNALEK, Z. p 79 N94-12538
DOI, D. A. p 35 N94-12562
DOI, T. p 105 N94-10100
DOLD, P. p 118 N94-10209
DOLGIN, DANIEL L. p 313 N94-11098
DOLGINOV, A. Z. p 283 N94-12217
p 472 N94-12218
p 283 N94-12219
p 472 N94-12220
p 478 N94-12248
p 283 N94-12249
DOLGINOV, SH. SH. p 472 N94-12221
p 473 N94-12222
DOLGOPOLOV, V. V. p 371 N94-10542
DOLIER, B. p 254 N94-12527
DOLLFUS, A. p 456 N94-12133
p 473 N94-12223
DOLLING, DAVID S. p 6 N94-10441
DOMANSKI, P. A. p 411 N94-10853
DOMASH, V. R. p 171 N94-11420
DOMINH, K. p 243 N94-11775
DONG, Q. W. p 432 N94-12224
DONG, YUAN-JI p 267 N94-11845
DONLEY, SHAWN p 27 N94-11341
DONN, B. p 123 N94-10236
DOROFEYEVA, V. A. p 432 N94-12225
p 432 N94-12226
DORUM, O. H. p 341 N94-12598
DOST, SADIK p 118 N94-10208
DOTSENKO, I. S. p 362 N94-10557
DOTY, SUSAN p 316 N94-12367
DOUGLAS, R. J. p 356 N94-10998
DOUGLASS, JOHN K. p 313 N94-11890
DOVER, C. B. p 359 N94-10303
p 359 N94-10304
p 368 N94-11620
DOW, J. M. p 242 N94-11771
DOWDESWELL, J. A. p 238 N94-11743
DOWLING, JONATHAN P. p 379 N94-10603
DOWMAN, I. p 246 N94-12476
DOYLE, B. L. p 143 N94-11285
DRAGONETTE, RICHARD p 355 N94-10993
DRAKE, DARRELL p 172 N94-12038
p 473 N94-12227
DRAKE, MICHAEL J. p 473 N94-12228
DRAKE, R. P. p 389 N94-11114
DRDACKY, M. p 63 N94-10056
DREIER, W. p 109 N94-10125
DRESSELHAUS, ELIOT p 75 N94-12320
DRESSENDORFER, P. p 174 N94-10959
DRIEMAN, J. p 248 N94-12486
DRIKAKIS, D. p 9 N94-10462
DROBYAZIN, V. N. p 82 N94-10842
DROPINSKI, S. C. p 76 N94-11075
DROSSART, P. p 457 N94-12139
DRUGUET, M. C. p 8 N94-10456
DRUMM, C. R. p 42 N94-10520
DRUMMOND, T. J. p 396 N94-10745
DSPAIN, G. L. p 289 N94-12349
DU, YUHUA p 396 N94-10705
DUAN, DAH-WEIH p 137 N94-11636
DUBEY, RAJENDRA R. p 373 N94-12435
DUC, DAO VONG p 412 N94-11163
DUCRET, ERIC p 106 N94-10110
DUECKER, GREGORY T. p 25 N94-10945
DUFFAR, THIERRY p 114 N94-10180
p 115 N94-10185
DUFFY, P. B. p 272 N94-12592
DUFNER, K. p 266 N94-11471
DUH, J. C. p 152 N94-11376
DUKE, DUANE A. p 38 N94-12567
DUKE, MICHAEL B. p 474 N94-12229
DULING, IRL N. p 374 N94-10372
DUNBAR, R. S. p 233 N94-11715
p 235 N94-11724
DUNCAN, L. S. p 67 N94-11221
DUNCAN, MARTIN J. p 427 N94-11629
DUNCAN, MICHAEL J. p 139 N94-10996
DUNHAM, GLEN p 52 N94-11405
DUNN, DONALD E. p 381 N94-10657
DUNNING, F. B. p 76 N94-10854
DUPONT, J. N. p 84 N94-11816
DUPONT, OLIVIER p 39 N94-10118
p 119 N94-10216
DUPOUY, C. p 199 N94-11946
DUQUE, P. p 242 N94-11771
DURANT, W. S. p 418 N94-10646
DURBIN, PAUL A. p 157 N94-12298
DURGIN, FRANK H. p 313 N94-11511
DUROX, DANIEL p 123 N94-10240
DURRHEIM, R. J. p 282 N94-12103
DURST, TONY p 95 N94-12577
DURU, I. H. p 378 N94-10594
DUSAN, RYBAN p 59 N94-10028
DUSSACK, LARRY p 310 N94-11998
DUTARTRE, R. p 119 N94-10210
DUTTON, ROLLIE EUGENE p 67 N94-11315
DUVA, ANTHONY W. p 178 N94-10375
p 178 N94-10378
DUVAL, WALTER M. B. p 123 N94-10239
DUVALL, LORRAINE M. p 330 N94-11435
DYSON, P. W. p 395 N94-10406

E

EASTERLY, JILL p 335 N94-11564
EATON, N. C. p 57 N94-10011
p 70 N94-11336
EBEL, WILLIAM J. p 324 N94-10932
EBERLE, A. p 9 N94-10459
EBISAWA, S. p 473 N94-12223
EBISU, N. p 219 N94-12705
EBUCHI, NAOTO p 200 N94-11952
p 202 N94-11961
p 220 N94-12710
ECK, JUERGEN p 237 N94-11739
ECKBERG, DWAIN L. p 310 N94-12000
ECKELMANN, HELMUT p 105 N94-10104
ECKLER, KLAUS p 86 N94-10196
EDENS, GREGORY J. p 368 N94-11658
EDER, D. C. p 175 N94-11266
EDGE, T. p 51 N94-11396
EDLUND, MAURICE E. p 417 N94-11856
EDMUNDS, R. S. p 47 N94-11122
EDWARDS, D. L. p 89 N94-11175
EDWARDS, K. p 425 N94-12140
EDWARDS, LEO, JR. p 416 N94-11599
EDWARDS, T. A. p 2 N94-10422
EERENS, HERMAN p 247 N94-12485
EFIMOV, V. V. p 223 N94-12727
EGAMI, KOUICHI p 10 N94-10470
p 11 N94-10471
EGOROV, A. V. p 106 N94-10111
p 107 N94-10116
p 111 N94-10139
p 116 N94-10193
EGRY, IVAN p 86 N94-10190
EICHELBERGER, CHARLES W. p 73 N94-12344
EID, A. M. p 427 N94-11812
EIGLER, D. M. p 365 N94-11093
EISENHOUR, D. p 432 N94-12230
EISENHOUR, D. D. p 432 N94-12231
EISLER, G. R. p 175 N94-11283
EITELBERG, G. p 4 N94-10430
EITELBERG, GEORG p 5 N94-10437
EJIRI, HIROSHI p 2 N94-10363
EK, ALAN R. p 231 N94-11521
EKBOM, LARS p 109 N94-10128
EKBOM, LARS B. p 118 N94-10207
EKHOLM, S. p 242 N94-11768
EKLUND, THOR p 17 N94-10766
p 22 N94-10796
EL-GENK, M. p 48 N94-11372
EL-SAYED, M. A. p 77 N94-11264
ELANGOVAN, P. T. p 63 N94-10051
ELDER, RICHARD C. p 77 N94-11265
ELDHUSET, KNUT p 253 N94-12521
ELDRIDGE, A. p 270 N94-12463
ELEID, MOUNIB p 431 N94-12166
ELGORESY, A. p 123 N94-10236
p 471 N94-12212
ELIASSON, A. p 109 N94-10128
p 118 N94-10207
ELISCHER, P. p 128 N94-11304
ELLENBOGEN, KENNETH A. p 310 N94-12000
ELLIOTT, D. L. p 262 N94-11051
ELLIOTT, K. B. p 45 N94-11320
ELLIOTT, M. p 55 N94-12283
ELLIS, SUSAN B. p 455 N94-12127
ELLISON, DONALD C. p 425 N94-10511
ELLISON, J. p 133 N94-10960
ELPHIC, R. C. p 474 N94-12232
ELSHAMY, M. p 347 N94-10757
ELSON, J. S. p 372 N94-10890
EMERY, M. H. p 172 N94-10150
EMERY, W. J. p 221 N94-12716
ENCRENAZ, T. p 457 N94-12139
ENDOU, YOSHIHARU p 198 N94-11937
ENEGREN, T. p 374 N94-12785
ENGELS, E., JR. p 369 N94-12546
ENGELSBERGER, J. p 108 N94-10123
ENGEN, G. p 251 N94-12507
ENGLISH, GLENN p 308 N94-11810
ENGQUIST, BJORN p 331 N94-11657
ENGRAND, C. p 432 N94-12233
EPSTEIN, M. A. p 24 N94-10964
EPSTEIN, S. p 455 N94-12127
ERARD, STEPHANE p 432 N94-12234
p 475 N94-12235
ERBAY, H. A. p 118 N94-10208
ERBAY, S. p 118 N94-10208
ERLANDSON, A. C. p 174 N94-11126
ERMAKOV, M. K. p 102 N94-10087
p 104 N94-10099
ERMAKOV, S. A. p 225 N94-12741
ERNST, HUGO A. p 185 N94-10712
ERNST, RICHARD E. p 283 N94-12236
ESAREY, ERIC p 173 N94-10371
ESAT, TEZER M. p 432 N94-12237
ESER, S. p 99 N94-12282
ESFAHANIAN, VAHID p 7 N94-10450
ESHLEMAN, VON R. p 434 N94-11361
ESMAN, RONALD D. p 374 N94-10372
ESPIAU, P. p 119 N94-10210
ESPINDOLA, J. M. p 282 N94-12138
p 432 N94-12238
ESPINO, J. L. p 111 N94-10137
ESPOSITO, G. p 412 N94-11047
ESSEN, H.-H. p 233 N94-11714
ESTABROOK, K. p 389 N94-11114
ESTEROWITZ, LEON p 176 N94-12321
ETKIN, V. S. p 226 N94-12745
ETKIN, VALENTIN S. p 226 N94-12746
p 226 N94-12747
ETO, MOTOKUNI p 183 N94-11168
ETTER, M C. p 402 N94-11654
p 404 N94-12438
ETTER, M. C. p 369 N94-11826
p 402 N94-11827
EUGSTER, O. p 432 N94-12239
p 87 N94-12240
EURITT, MARK A. p 98 N94-10844
EVANS, DAVID R. p 423 N94-11305
EVANS, I. K. p 174 N94-10959
EVANS, J. M. p 309 N94-11997
EVANS, LARRY G. p 462 N94-12165
EVANS, NOREEN JOYCE p 432 N94-12241
EVANS, R. p 249 N94-12493
EVANS, T. E. p 393 N94-11514
EVLANOV, E. N. p 476 N94-12242
EXERTIER, P. p 39 N94-12530
EXNER, M. p 111 N94-10138
EYLER, JOHN R. p 67 N94-11260
EYMARD, LAURENCE p 252 N94-12511
EZRATY, ROBERT p 233 N94-11712

F

FADEEV, VICTOR V. p 177 N94-12755
FAGENTS, S. A. p 477 N94-12243
FAHNESTOCK, MARK p 237 N94-11741
FAIMAN, LIA E. p 301 N94-12417

FAINSTEIN, MICHAEL p 178 N94-10393
FAJNBERG, Y. B. p 391 N94-11209
p 391 N94-11211
FAJULA, F. p 119 N94-10210
FALCIANI, P. G. p 110 N94-10133
FALKINGHAM, JOHN C. p 241 N94-11760
FALLICK, A. E. p 281 N94-12072
FALOUTSOS, CHRISTOS p 420 N94-11520
FANALE, F. P. p 425 N94-12140
p 433 N94-12244
FANALE, FRASER P. p 430 N94-12162
p 430 N94-12163
p 431 N94-12164
FANG, HUI p 197 N94-11934
FANTON, J. W. p 302 N94-11548
p 309 N94-11995
FAR, B. H. p 313 N94-10251
FARCY, PATRICK p 233 N94-11712
FARINELLA, P. p 431 N94-12201
FARRAND, W. H. p 477 N94-12245
FARSAIE, ALI p 333 N94-12386
FAST, J. D. p 285 N94-11614
FATEMI, N. S. p 48 N94-11384
FATEMI, NAVID S. p 49 N94-11387
FAUR, MARIA p 48 N94-11384
p 49 N94-11385
FAUR, MIRCEA p 48 N94-11384
p 49 N94-11385
FAVIER, JEAN-JACQUES p 114 N94-10180
p 115 N94-10185
p 86 N94-10197
FAYYAD, U. M. p 455 N94-12126
FECHT, HANS-JORG p 112 N94-10143
FECHTIG, H. p 123 N94-10236
FEDDRIX, F. H. p 401 N94-11518
FEDERER, J. I. p 72 N94-11368
FEDERICO, C. p 433 N94-12265
FEDOSEYEV, A. p 117 N94-10201
FEDUTENKO, E. A. p 389 N94-10885
FEGLEY, B., JR. p 477 N94-12246
FEIGELSON, ERIC D. p 425 N94-10943
FEJTEK, IAN G. p 13 N94-10758
FELDMAN, EVAN M. p 314 N94-11531
FELDMAN, S. C. p 478 N94-12247
FELDMAN, WILLIAM p 172 N94-12038
FELIPE, R. p 148 N94-10530
FELKER, B. p 387 N94-10737
FENG, GUOHUI p 329 N94-11430
FENG, MING p 206 N94-11990
FENG, S. T. p 174 N94-11095
FENG, YUYU p 346 N94-11632
FENOGLIO, L. p 242 N94-11767
FENSTERMACHER, M. E. p 394 N94-12370
FERAUDY, D. p 352 N94-10972
FERGUSON, FRANK p 113 N94-10175
FERMIGIER, M. p 121 N94-10229
FERRARIO, M. T. p 147 N94-10252
FERRARIS, M. p 123 N94-10237
FERRON, J. R. p 325 N94-11139
FERZIGER, J. H. p 159 N94-12311
FERZIGER, JOEL H. p 156 N94-12291
FETTERER, F. p 241 N94-11763
FEUERBACHER, BERNDT p 113 N94-10177
p 86 N94-10190
p 116 N94-10192
p 86 N94-10196
p 87 N94-10202
p 122 N94-10233
p 123 N94-10236
FEULNER, T. p 100 N94-10073
FIEDLER, R. L. p 134 N94-11063
FIKSEL, G. p 388 N94-10747
FILATOV, G. p 107 N94-10116
FILIPPOVA, ELENA M. p 177 N94-12755
FINDENEGG, GERHARD H. p 80 N94-10228
FINKEL, R. C. p 437 N94-12033
FINLEY, J. p 373 N94-12600
FINN, V. J. p 478 N94-12248
p 283 N94-12249
FINNILA, A. B. p 478 N94-12250
FIRAGO, S. A. p 379 N94-10599
FISCHER, ERICH M. p 478 N94-12251
FISCHER, J. E. p 400 N94-11457
FISENKO, A. V. p 433 N94-12252
p 433 N94-12253
p 433 N94-12254
p 433 N94-12255
p 81 N94-12256
FISHER, AMON p 173 N94-10371
FISHER, DUNCAN S. p 433 N94-12257
FISHER, M. J. p 76 N94-11216
FISKE, P. S. p 81 N94-12258
FLACK, KAREN A. p 159 N94-12309
FLEETWOOD, D. M. p 143 N94-11271
FLEISCHAUER, MICHAEL p 375 N94-10565
FLEISCHER, C. A. p 93 N94-12340
FLETCHER, J. G. p 335 N94-10324
FLOOD, D. J. p 48 N94-11384
FLOOD, DENNIS J. p 47 N94-11307
p 49 N94-11389
FLORYAN, J. M. p 163 N94-12613
FLYNN, G. J. p 480 N94-12259
p 433 N94-12260
p 433 N94-12261
p 433 N94-12262
FOLDESI, I. p 375 N94-10570
FOLTZ, M. F. p 77 N94-11602
FOMENKOVA, M. p 433 N94-12263
FOMIN, I. P. p 66 N94-11143
p 392 N94-11214
FOMIN, P. I. p 349 N94-10548
p 148 N94-10717
FONSECA, A. A. p 31 N94-11492
FONT, GABRIEL I. p 15 N94-11195
FONT, J. p 255 N94-12529
FONTAINE, A. A. p 161 N94-12352
FONTAINE, J.-P. p 104 N94-10096
FORBUS, KENNETH D. p 340 N94-12537
FORD, D. J. p 433 N94-12264
FORD, W. T. p 370 N94-12609
FORNARI, B. p 69 N94-11328
FORNI, O. p 433 N94-12265
FORREST, LARRY p 424 N94-11356
FORRESTER, T. N. p 253 N94-12519
FORSTER, B. M. p 373 N94-12542
FORSYTHE, J. p 425 N94-12140
FORTEZZA, RAIMOND p 124 N94-10241
FORTEZZA, RAIMONDO p 102 N94-10087
p 104 N94-10098
p 39 N94-10134
FORTGANG, C. M. p 374 N94-12786
FORTINI, PIERLUIGI p 378 N94-10587
FORTNEY, SUZANNE M. p 308 N94-11991
p 310 N94-11998
FORTSON, R. E. p 315 N94-11258
FOSSLER, EARL p 353 N94-10978
FOSSUM, ERIC R. p 141 N94-10656
FOSTER, C. T., JR. p 281 N94-12056
FOSTER, I. p 276 N94-11138
FOSTER, JOHN C. p 280 N94-12583
FOSTER, TERRY p 126 N94-10615
p 128 N94-10626
p 128 N94-10627
FOUST, M. J. p 152 N94-11526
FOWELL, ANDREW J. p 20 N94-10787
FRANCHI, I. A. p 451 N94-12108
FRANCIS, C. R. p 241 N94-11764
FRANCOIS, G. p 4 N94-10429
FRANKLIN, H. A. p 415 N94-12028
p 478 N94-12247
FRANKLIN, JAMES A. p 30 N94-11134
p 30 N94-11259
FRASCHETTI, GEORGE A. p 381 N94-10657
FREAR, D. R. p 129 N94-11606
FRECHET, J. M. p 145 N94-11819
FRECHET, JEAN M. p 95 N94-12577
p 95 N94-12585
FREDRIKSSON, HASSE p 123 N94-10238
FREEMAN, W. R. p 144 N94-11478
FREILICH, M. H. p 233 N94-11715
p 235 N94-11724
FRENCH, RICHARD G. p 427 N94-12557
FRENKEL, D. p 361 N94-10502
FRETTE, O. p 234 N94-11720
FREUDENBERGER, S. M. p 333 N94-12439
FREUND, FRIEDEMANN p 78 N94-11699
FREUND, R. F. p 336 N94-11293
FREY, HERBERT p 481 N94-12266
p 481 N94-12267
p 481 N94-12268
FREY, HERBERT V. p 444 N94-12065
FREYMANN, RAYMOND p 72 N94-11346
FREYTAG, E. K. p 181 N94-11247
FRIDELANCE, P. p 352 N94-10972
FRIEBELE, EDWARD p 374 N94-10373
FRIED, L. E. p 98 N94-11269
FRIEDMAN, H. W. p 176 N94-12784
FRIEDMAN, LOUIS D. p 438 N94-12034
FRIEMAN, JOSHUA A. p 425 N94-11153
FRITSCH, JANICE M. p 310 N94-12000
FROEVEL, MALTE p 64 N94-10064
FROGGATT, J. R. p 285 N94-11664
FROLOV, V. A. p 476 N94-12242
FROLOW, F. p 394 N94-10301
FROUIN, ROBERT p 230 N94-10953
p 230 N94-10954
p 230 N94-10955
FROYEN, L. p 75 N94-10186
FRY, K. A. p 383 N94-11887
FRYE, DANIEL p 289 N94-11854
FU, LEE-LUENG p 209 N94-12648
FU, R. L. p 396 N94-10637
FU, R. T. p 396 N94-10637
FUCHS, B. p 87 N94-10271
FUCHS, G. E. p 84 N94-11488
FUERSTENAU, N. p 71 N94-11340
FUJII, GENSHIROU p 130 N94-11640
FUJII, TERUSHIGE p 162 N94-12551
p 162 N94-12552
FUJII, YOSHIO p 358 N94-11042
FUJIMORI, YOSHINORI p 129 N94-11832
FUJIMOTO, T. p 393 N94-11594
FUJINAWA, YUKIO p 172 N94-11968
FUJISAWA, K. p 351 N94-10968
FUJITA, D. p 105 N94-10100
FUJITA, MASAHARU p 253 N94-12520
FUJITA, SHIN p 215 N94-12681
FUKASAWA, MASAO p 206 N94-11985
FUKAYA, KIYOSHI p 183 N94-11168
FUKUCHI, MITSUO p 210 N94-12657
FUKUDA, MASAAKI p 204 N94-11974
FUKUDA, TAMIO p 129 N94-11833
FUKUHARA, MICHIKAZU p 212 N94-12668
FUKUMORI, ICHIROU p 209 N94-12648
FUKUNISHI, YUU p 164 N94-12617
FUKUSHIMA, CHIHARU p 165 N94-12626
FUKUSHIMA, HAJIME p 200 N94-11951
FUKUTOMI, YASUYUKI p 16 N94-12616
FULLENBAUM, R. F. p 416 N94-11473
FULLER, JOSEPH J. p 333 N94-12386
FUNAHASHI, Y. p 367 N94-11510
FUNSTEN, H. O. p 275 N94-10742
FUNSTEN, H. O, III p 474 N94-12232
FURUKAWA, MASAO p 162 N94-12556
FUXIN, ZHOU p 107 N94-10113

G

GAALMAN, A. E. p 60 N94-10034
GABRIEL, EDWARD A. p 26 N94-11858
GADDIS, L. R. p 425 N94-12140
GADOLIN, R. E. p 303 N94-11097
GAGE, DOUGLAS W. p 180 N94-10803
GAGNON, E. p 50 N94-11394
GAIDOS, J. A. p 373 N94-12600
GAINES, D. P. p 143 N94-11273
GAL, A. p 368 N94-11620
GALASSI, LELLO p 6 N94-10443
GALLAGHER, P. p 51 N94-11400
GALLERY, W. O. p 278 N94-11852
GALLET, R. p 59 N94-10025
GALLMAN, EVE A. p 301 N94-12417
GALLOIS, BERNARD M. p 92 N94-11866
GALYSH, IVAN J. p 353 N94-10983
GAMBLE, M. T. p 65 N94-10740
GAMMAGE, R. B. p 264 N94-10256
GAMMEL, J. T. p 399 N94-11263
p 403 N94-12345
GANAPOL, B. D. p 365 N94-10952
GANAPOL, BARRY p 366 N94-11199
GANN, V. V. p 398 N94-11090
GAO, FENG p 160 N94-12315
GAO, H. B. p 409 N94-10413
GAO, XIAOPING p 368 N94-11658
p 404 N94-12388
GAPONENKO, N. I. p 387 N94-10541
GARANDET, J. P. p 115 N94-10185
GARAZO, ALFREDO N. p 119 N94-10214
GARBA, JOHN A. p 72 N94-11344
GARCIA, E. p 255 N94-12529
GARCIA, P. p 174 N94-10959
GARCIAPRIETO, RAFAEL p 59 N94-10027
GARDINER, P. p 69 N94-11325
GARELLO, R. p 251 N94-12507
GARFIELD, DONALD E. p 29 N94-12274
GARG, SANJAY p 30 N94-11251
GARNER, DAVID P. p 417 N94-11856
GARRABOS, YVES p 122 N94-10230
GARRISON, D. H. p 80 N94-12082
p 281 N94-12083
GASBARRI, P. p 45 N94-11342
GASHI, A. p 410 N94-10631
GASIEWSKI, A. J. p 274 N94-10726
GAT, ROY p 403 N94-12010
GATES, MARK T. p 52 N94-11401
GATES, W. L. p 273 N94-10151
p 273 N94-10152
GATTI, L. p 107 N94-10117
GATTO, L. W. p 254 N94-12528
GAUDENZI, P. p 45 N94-11342
GAUDETTE, H. E. p 270 N94-12464
GAUNTT, R. O. p 370 N94-10149
GAUTHIER, PIERRE p 126 N94-10616
GAUTIER, C. p 244 N94-11783
GAUTIER, M. A. p 272 N94-12780
GAVRILOV, V. P. p 275 N94-11052
GAZTANAGA, ENRIQUE p 425 N94-11153

GAZZA, GEORGE p 83 N94-11445
GEIGER, H. p 70 N94-11336
GEISSMAN, J. p 273 N94-10285
GELFGAT, J. M. p 107 N94-10116
GELFGAT, Y. M. p 106 N94-10111
GENNERO, M. C. p 243 N94-11775
GENNERO, M.-C. p 242 N94-11769
GENTILI, BERNARD p 203 N94-11971
GEO, Q. p 79 N94-12538
GEORGALA, J. M. p 154 N94-11859
GEORGE, THOMAS F. p 380 N94-10606
p 380 N94-10611
GEORGIADIS, R. p 79 N94-12534
GEORIS, PHILIPPE p 119 N94-10216
p 120 N94-10217
GERASIMOV, M. V. p 81 N94-12214
GERASIMOV, O. I. p 366 N94-11349
GERASKO, V. N. p 324 N94-11031
GERLING, T. p 251 N94-12509
GERNHARDT, M. L. p 341 N94-11562
GERSHUNI, GRIGORY Z. p 101 N94-10082
GHERBEK, E. E. p 226 N94-12749
GHOSAL, SANDIP p 155 N94-12285
GIANINONI, IVA p 107 N94-10113
GIANNUZZI, M. p 58 N94-10015
GIANTS, THOMAS W. p 91 N94-11487
GIBBLE, KURT p 352 N94-10976
GIBBS, D. p 400 N94-11467
GIBLIN, A. E. p 271 N94-12468
GIBSON, E. K., JR. p 430 N94-12132
GIBSON, M. ALAN p 286 N94-12772
GIBSON, R. T. p 416 N94-10145
GIERAS, M. M. p 121 N94-10224
GIESE, R. F. p 143 N94-11454
GILDE, GARY p 83 N94-11445
GILLARD, E. p 127 N94-10620
GILLEN, KENNETH T. p 183 N94-11586
GILLETTE, MARTHA U. p 301 N94-12417
GILP, B. F. p 81 N94-10297
GILYARD, GLENN B. p 28 N94-11205
GINERIS, D. p 241 N94-11763
GINZBURG, A. I. p 222 N94-12724
GIORDANO, D. p 7 N94-10448
GIRARD, M. p 457 N94-12139
GIRARDY, HENRI p 59 N94-10025
GIRIDHARAN, M. G. p 46 N94-10934
GLADNEY, E. S. p 272 N94-12780
GLASER, RUEDIGER p 214 N94-12677
GLASS, B. P. p 281 N94-12085
GLASSMAN, ARTHUR J. p 15 N94-11203
GLAZMAN, ROMAN E. p 195 N94-11922
p 208 N94-12641
GLEGG, STEWART A. L. p 357 N94-10752
GLINSKY, M. p 369 N94-11815
GLOCKER, B. p 47 N94-11354
GLOERSEN, PER p 210 N94-12651
GLOR, PETER J. p 331 N94-11679
GLOVER, DANIEL p 323 N94-10639
GNOFFO, PETER A. p 162 N94-12571
GODT, ADELHEID p 95 N94-12577
GOEL, NARENDRA S. p 302 N94-12559
GOER, D. B. p 397 N94-10845
GOERLER, G. P. p 87 N94-10231
GOFF, O. T. p 309 N94-11995
GOGINENI, S. p 139 N94-12778
GOHIN, FRANCIS p 233 N94-11712
GOLD, JOSHUS I. p 304 N94-11261
GOLD, S. H. p 145 N94-12424
GOLDBERG, P. p 331 N94-11611
GOLDBERGER, ARY L. p 311 N94-12007
GOLDEN, J. p 129 N94-11606
GOLDIN, YURI A. p 224 N94-12736
GOLDMAN, LOUIS J. p 15 N94-11133
GOLDSBY, JON C. p 66 N94-11135
GOLDSTEIN, B. G. p 482 N94-10741
GOLDSTEIN, RICHARD M. p 236 N94-11734
GOLDSTEIN, SHELDON p 378 N94-10589
GOLDSTEIN, W. H. p 389 N94-11074
GOLDSTONE, J. A. p 363 N94-10743
GOLEMINOV, N. G. p 484 N94-10534
GOLIA, C. p 104 N94-10097
p 104 N94-10098
GOLIGHTLY, MICHAEL J. p 318 N94-11561
GOLOMBEK, M. P. p 469 N94-12203
GOLUBEVA, E. N. p 229 N94-12765
GOMBEER, ROLAND p 247 N94-12485
GOMEZ, M. p 102 N94-10083
GONFALONE, ALAIN p 39 N94-10118
p 44 N94-10250
GONG, X. G. p 395 N94-10386
GONYOU, H. W. p 300 N94-11180
GONZALEZ, FRANCOIS p 100 N94-10075
GONZALEZ, I. p 59 N94-10025
GOODBODY, C. p 53 N94-11409
p 53 N94-11412
GOODING, J. L. p 428 N94-12025
GOODMAN, S. p 117 N94-10200
GOODWIN, W. L. p 41 N94-11282
GOPALKRISHNAN, RAMNARAYAN
p 154 N94-11865
GORADIA, C. p 48 N94-11384
GORADIA, M. p 48 N94-11384
p 49 N94-11385
GORBACHEV, V. V. p 227 N94-12751
GORDON, HOWARD R. p 204 N94-11975
GORE, ALBERT, JR. p 422 N94-11351
p 422 N94-11353
GOREN, Y. p 374 N94-12785
GORIN, I. I. p 226 N94-12749
GORKOVOY, VLADIMIR p 308 N94-11808
GORMAN, M. R. p 248 N94-12488
GORRIZ, E. G. p 255 N94-12529
GORYUNOV, O. Y. p 372 N94-10849
GOTO, ICHIRO p 84 N94-11593
GOTOU, KEINOSUKE p 197 N94-11931
p 218 N94-12698
GOTTESFELD, S. p 264 N94-11666
GOTTLIEB, DAVID p 16 N94-12377
GOTTMANN, T. p 3 N94-10424
GOUDA, NORIAKI p 194 N94-11913
p 194 N94-11914
GOULD, GEOFF p 18 N94-10773
GOULD, P. L. p 365 N94-11029
GOULDING, R. H. p 137 N94-11453
GOUVEIA, A. D. p 214 N94-12678
GOWER, J. F. R. p 234 N94-11718
p 191 N94-11899
p 209 N94-12647
GOZHENKO, S. V. p 66 N94-11143
GRACHJOVA, T. V. p 433 N94-12254
GRADY, C. A. p 424 N94-11306
GRADY, P. L. p 43 N94-10944
GRAF, MARTIN p 375 N94-10565
GRAFAREND, ERIK W. p 242 N94-11766
GRAHAM, GEORGE p 27 N94-11341
GRAHAM, J. A. p 448 N94-12089
GRANAHAN, J. C. p 425 N94-12140
GRANATSTEIN, V. L. p 145 N94-11645
GRANIER, JEAN p 108 N94-10122
GRANT, B. K. p 336 N94-11248
GRASSI, W. p 121 N94-10226
GRASSO, F. p 10 N94-10465
GRATE, J. W. p 87 N94-10295
GRATZ, A. J. p 399 N94-11268
p 81 N94-12258
GRAY, HENRY F. p 140 N94-10377
GRAY, WILLIAM M. p 285 N94-11194
GREBE, A. p 93 N94-12354
GREELEY, R. p 468 N94-12198
GREEN, D. J. p 88 N94-10710
GREEN, D. W. p 88 N94-10749
GREEN, J. A. p 133 N94-11024
GREEN, J. E. p 34 N94-10894
GREENBERG, D. S. p 336 N94-10738
GREENBERG, JAMES p 92 N94-11862
GREENBERG, R. p 429 N94-12092
GREENLEAF, JOHN p 300 N94-11191
GREGSON, P. J. p 58 N94-10022
GREIDANUS, H. p 232 N94-11707
GRENSING, F. C. p 60 N94-10029
GREVSTAD, KURT p 27 N94-11347
GREYSUKH, V. M. p 222 N94-12725
GRIAZNOV, VLADIMIR p 104 N94-10099
GRIAZNOV, VLADIMIR L. p 102 N94-10087
GRIEVE, R. A. F. p 282 N94-12093
p 461 N94-12158
GRIFFIN, O. HAYDEN, JR. p 327 N94-11279
GRIFFIN, P. B. p 395 N94-10516
GRIFFITHS, G. H. p 249 N94-12493
GRIFFITHS, NICHOLAS p 1 N94-10936
GRILLET, ANNICK p 247 N94-12485
GRIMES, HUBERT H. p 485 N94-10356
GRIMES, R. p 59 N94-10023
GRIMM, ROBERT E. p 452 N94-12112
p 452 N94-12113
GRIMMER, DERRICK P. p 49 N94-11390
GRIN, E. A. p 456 N94-12133
GRINSPOON, D. H. p 453 N94-12119
GRODSINSKY, CARLOS M. p 1 N94-11703
GROEBNER, R. J. p 393 N94-11514
p 394 N94-12544
GROENEWOLD, G. S. p 76 N94-11140
GROOM, STEPHEN B. p 201 N94-11958
GROOT, J. S. p 236 N94-11731
GROSFILS, ERIC p 283 N94-12236
GROSS, D. J. p 408 N94-10261
GROSS, T. R. p 333 N94-12439
GROSSMAN, L. p 282 N94-12141
GROSSMAN, R. p 319 N94-10318
GROTCH, S. L. p 276 N94-11227
GROTEN, E. p 242 N94-11767
GROVER, K. D. p 248 N94-12487
GRUBBS, H. J. p 19 N94-10780
GRUBER, T. p 243 N94-11777
GRUCZA, DAVID p 382 N94-11300
GRUEN, E. p 123 N94-10236
GRUMMON, D. S. p 398 N94-11115
GRUNE, G. L. p 92 N94-11848
GRUNER, S. M. p 301 N94-11648
GRUNTHANER, FRANK J. p 141 N94-10656
GU, QUANCHENG p 61 N94-10042
GUARD, PETER S. p 21 N94-10792
GUBAREV, S. P. p 362 N94-10649
GUBKIN, E. S. p 359 N94-10266
GUCKENBERGER, DUTCH p 315 N94-11627
GUDDAL, JOHANNES p 250 N94-12500
GUDIKSEN, P. H. p 275 N94-11052
GUDMANDSEN, P. p 232 N94-11705
p 239 N94-11752
GUELHAN, A. p 4 N94-10432
GUENOUN, P. p 122 N94-10230
GUENTER, M. p 87 N94-10231
GUENTHER, ARTHUR p 381 N94-11054
GUENTHER, B. p 64 N94-10059
GUERIN, J. J. p 69 N94-11328
GUEST, J. E. p 454 N94-12120
p 456 N94-12131
GUICHETEAU, P. p 32 N94-11496
GUIDICE, DON p 53 N94-11410
GUIDOS, BERNARD J. p 16 N94-11870
GUIGNARD, JEAN PIERRE p 235 N94-11726
GUIMARAES, A. P. p 395 N94-10314
GULSEREN, O. p 396 N94-10800
GUNGOR, A. p 19 N94-10780
GUO, JING-MEI p 346 N94-11348
GUO, JUNPENG p 393 N94-11513
GUO, WEI p 356 N94-11001
GUPTA, HERMAN p 18 N94-10776
GUREEV, BORIS A. p 224 N94-12736
GURIN, A. A. p 386 N94-10524
GURVITS, LEONID I. p 134 N94-11060
GUSTAFSON, GARY B. p 284 N94-11113
GUSYNIN, V. P. p 409 N94-10405
GUTICH, Y. I. p 397 N94-10845
GUTIERREZ, W. T. p 147 N94-10252
GUY, HAROLD J. p 309 N94-11994
GUYMER, T. H. p 243 N94-11773
p 253 N94-12519
p 255 N94-12531
GUZHVA, O. I. p 395 N94-10525

H

HA, NGUYEN HONG p 412 N94-11163
HAAKANSSON, BERTIL p 239 N94-11751
HAASE, W. p 6 N94-10444
HABE, HIROAKI p 42 N94-10366
HABETS, L. C. G. J. M. p 341 N94-10168
HACKMAN, CHRISTINE p 357 N94-11003
HADJIEV, S. A. p 368 N94-11581
HADLEY, G. R. p 174 N94-11005
HAEFNER, HAROLD p 247 N94-12482
HAFIZI, B. p 145 N94-12424
HAGERTY, M. T. p 289 N94-12349
HAGHOOIE, M. p 177 N94-10322
HAGIWARA, NAOKI p 206 N94-11985
HAILEY, C. E. p 147 N94-10252
HAJJI, H. p 250 N94-12503
HAKIMZADEH, ROSHANAK p 49 N94-11388
p 404 N94-12430
HALD, HERMANN p 56 N94-10005
HALDAR, P. p 142 N94-10951
p 398 N94-11073
HALE, K. K. p 266 N94-11451
HALFORD, GARY R. p 74 N94-12449
HALL, CLIFF T. M. p 19 N94-10782
HALL, I. M. p 7 N94-10447
HALL, KENNETH R. p 330 N94-11432
HALL, PHILIP p 149 N94-10810
HALL, W. A. p 312 N94-11547
HALLEY, J. W. p 394 N94-10281
HALLIKAINEN, M. p 239 N94-11750
p 247 N94-12483
HALPERN, D. p 235 N94-11724
p 208 N94-12644
HALPERN, DAVID p 207 N94-12637
HAMA, JUNKO p 211 N94-12660
HAMA, S. p 351 N94-10968
HAMA, TAKEO p 211 N94-12661
HAMELIN, ANTOINETTE p 368 N94-11658
HAMERS, R. J. p 402 N94-11684
HAMILTON, JAMES M. p 158 N94-12308
HAMLETT, NEIL A. p 138 N94-12406
HAMLEY, JOHN A. p 180 N94-10760
HAMM, PEGGY B. p 312 N94-11552
HAMMER, J. H. p 369 N94-11815
HAMMOND, J. K. p 345 N94-11217

HAMON, ROB p 348 N94-11573
HAN, D. p 375 N94-10564
p 379 N94-10604
HAN, KWANG S. p 76 N94-10713
HANADO, Y. p 351 N94-10968
HANDA, NOBUHIKO p 211 N94-12660
HANDRICK, K. p 61 N94-10043
HANEY, E. p 249 N94-12494
HANHELA, P. J. p 89 N94-11107
HANLON, J. A. p 65 N94-10740
HANNA, S. R. p 279 N94-12422
HANSEN, C. FREDERICK p 366 N94-11360
HANSEN, GARY B. p 456 N94-12134
HANSEN, IRVING G. p 46 N94-10765
HANSMA, P. K. p 399 N94-11268
HANSON, K. M. p 347 N94-11006
HAO, BAILIN p 418 N94-10485
HAQ, I. U. p 78 N94-11855
HARA, MASANORI p 94 N94-12407
HARADA, KOUICHI p 335 N94-10368
HARAS, ZIGO p 343 N94-10642
HARBAUGH, DARCY p 127 N94-10623
HARBER, K. S. p 340 N94-12428
HARBICH, W. p 61 N94-10039
HARDING, DAVID R. p 74 N94-12431
HARDINGHAM, C. M. p 52 N94-11406
HARDY, ALVA C. p 318 N94-11561
HARGENS, ALAN R. p 308 N94-11991
p 311 N94-12003
HARLEY, D. p 483 N94-11619
HARMAN, DONNA K. p 419 N94-10829
HARMS, G. A. p 370 N94-10149
HARMS, JOCHEN p 248 N94-12490
HARRIES, WYNFORD L. p 94 N94-12450
HARRIS, ELFRIEDA p 333 N94-12448
HARRIS, TERRY p 27 N94-11341
HARRISON, DAWN L. p 252 N94-12516
HARRISON, P. C. p 300 N94-11180
HARRISON, STEPHANIE T. p 81 N94-12156
HARTL, P. p 237 N94-11736
HARTLEY, M. p 126 N94-10618
HARTMANN, R. p 237 N94-11740
HARTOKO, A. p 218 N94-12701
HARTUNG, J. B. p 281 N94-12032
HARVEY, PAUL p 75 N94-10337
HARVEY, T. JEFFERY p 51 N94-11399
HASHIGUCHI, D. p 60 N94-10029
HASHIMA, MASAHIRO p 199 N94-11942
p 218 N94-12702
HASHIMOTO, HIROMASA p 99 N94-11444
HASHIMOTO, N. p 193 N94-11908
HASHOLDER, J. M. p 10 N94-10464
HASSELMANN, K. p 251 N94-12509
HASSELMANN, S. p 251 N94-12509
HASSENZAHL, W. V. p 387 N94-10737
HASSLACHER, B. p 147 N94-10320
HASSOON, SALAH p 79 N94-12373
HASSOUN, JOHN A. p 316 N94-11642
p 24 N94-11879
HASYIM, BIDAWI p 196 N94-11927
HATAKEYAMA, A. p 205 N94-11980
HATAKEYAMA, YUUJI p 198 N94-11940
HATANAKA, MASAHIKO p 212 N94-12665
HATCHER, DONALD J. p 324 N94-11099
HATCHER, P. G. p 99 N94-12282
HATTORI, HIROSHI p 210 N94-12657
HAUG, K. p 413 N94-11877
HAUGLAND, M. p 440 N94-12049
HAUPT, AXEL p 107 N94-10114
p 109 N94-10124
HAUSLER, PHILIP A. p 39 N94-11433
HAUSTEIN, P. E. p 75 N94-10338
HAUTUS, M. L. J. p 343 N94-10867
HAWKE, B. R. p 446 N94-12079
HAWKER, JOHN E. p 314 N94-11539
HAWKINS, J. A. p 288 N94-11299
HAWRYLUK, A. M. p 381 N94-10651
HAXTON, W. C. p 425 N94-10292
HAYAFUJI, HIDETOSHI p 164 N94-12618
HAYASHI, SHIGERU p 148 N94-10727
HAYASHI, YUUJIROU p 162 N94-12550
HAYDER, M. EHTESHAM p 151 N94-11253
HAYNES, GERALD p 19 N94-10783
HAYNES, TIMOTHY S. p 7 N94-10451
HAYT, D. W. p 235 N94-11723
HAZELTINE, R. D. p 390 N94-11142
HE, LI p 166 N94-12777
p 166 N94-12779
HE, MING XIA p 197 N94-11934
p 213 N94-12674
p 220 N94-12711
HE, MINGXIA p 197 N94-11930
HE, Z. p 6 N94-10442
HEAD, J. W. p 453 N94-12119
p 455 N94-12130
p 467 N94-12193
p 467 N94-12194
p 467 N94-12195
p 467 N94-12196
HEAD, JAMES W. p 283 N94-12236
HEALD, S. M. p 400 N94-11458
HEDGECOCK, J. C. p 341 N94-11562
HEERD, STEFAN p 333 N94-12383
HEESTAND, R. L. p 82 N94-11108
HEFFELFINGER, G. p 366 N94-11284
HEILEMAN, G. L. p 345 N94-11225
HEINEMAN, WILLIAM R. p 77 N94-11265
HEINRICHS, J. p 241 N94-11761
HEINZEN, DAVID F. p 231 N94-11521
HEISS, S. p 9 N94-10459
HEITZER, JOERG p 57 N94-10012
HELGESEN, G. p 400 N94-11467
HELGESON, W. D. p 401 N94-11605
HELLER, ADAM p 87 N94-10510
p 94 N94-12425
HELM, MARY E. p 335 N94-11578
HELMAN, J. A. S. p 350 N94-10313
HELMINCK, A. G. p 348 N94-10272
HELMINCK, G. F. p 348 N94-10272
HELTON, KATHLEEN T. p 313 N94-11098
HELWIG, G. p 57 N94-10009
HENAGER, C. H., JR. p 73 N94-11612
HENDERSON, ARTHUR, JR. p 34 N94-11869
HENDRICKS, E. W. p 152 N94-11448
HENDRICKSON, B. p 366 N94-11284
HENDRICKSON, B. A. p 367 N94-11455
HENEIN, N. A. p 182 N94-11625
HENGEL, JOHN E. p 14 N94-11021
HENLEY, E. M. p 341 N94-10259
HENNENBERG, MARCEL p 112 N94-10173
p 120 N94-10217
HENNESSY, C. J. p 190 N94-12178
HENRY, DANIEL p 119 N94-10215
HENRY, J. p 388 N94-10747
HENSLEY, SCOTT p 236 N94-11734
HENSON, T. J. p 72 N94-11368
HENTSCHEL, M. P. p 61 N94-10039
HERBERT, THORWALD p 7 N94-10450
HERLACH, D. M. p 86 N94-10196
HERLACH, DIETER M. p 87 N94-10204
HERLAND, E.-A. p 239 N94-11750
p 247 N94-12483
HERON, M. L. p 139 N94-11906
p 197 N94-11933
p 251 N94-12508
HERREN, K. p 51 N94-11396
HERRING, R. N. p 405 N94-12563
HERRMANN, D. J. p 185 N94-10715
HERRMANN, F. M. p 100 N94-10073
HERTEL, E. S. p 326 N94-11226
HERVIG, R. L. p 429 N94-12094
p 474 N94-12232
HESS, P. C. p 478 N94-12250
HESSELINK, WIM H. p 323 N94-10878
HETTENA, E. p 8 N94-10457
HEURING, VINCENT P. p 171 N94-12391
HEWETT, R. p 262 N94-10258
HEWINS, ROGER H. p 431 N94-12176
p 431 N94-12177
HEWITT, W. B. p 84 N94-11668
HEYMAN, JOSEPH S. p 185 N94-10671
HIBBS-BRENNER, MARY p 383 N94-12444
HIBIYA, TAKETOSHI p 105 N94-10102
HIESINGER, H. p 446 N94-12079
HIGAKI, KYOKO p 10 N94-10469
p 11 N94-10477
HIGASHI, Y. p 367 N94-11510
HIKICHI, MASAYUKI p 212 N94-12665
HILDEBRAND, A. R. p 282 N94-12161
HILDMANN, B. O. p 114 N94-10184
HILL, D. CHRISTOPHER p 157 N94-12301
HILL, DOLORES H. p 80 N94-12096
HILL, J. P. p 400 N94-11467
HILL, RICHARD G. p 17 N94-10766
p 21 N94-10790
p 22 N94-10797
HILLARD, G. BARRY p 43 N94-10756
HILLBERRY, B. M. p 185 N94-10715
HILLIER, R. p 8 N94-10454
HILLNER, P. E. p 399 N94-11268
HINDMAN, D. L. p 72 N94-11368
HINES, K. C. p 385 N94-10284
HINES, MARK E. p 267 N94-12451
p 268 N94-12453
p 268 N94-12454
p 268 N94-12455
p 269 N94-12457
p 269 N94-12458
p 269 N94-12460
p 270 N94-12461
p 270 N94-12462
p 270 N94-12463
p 270 N94-12464
p 270 N94-12465
p 271 N94-12466
p 271 N94-12467
p 271 N94-12468
p 271 N94-12469
p 271 N94-12470
HINGSTON, MICHAEL P. p 281 N94-12080
HINO, MIKIO p 165 N94-12624
HINTON, F. L. p 393 N94-11514
HIRABAYASHI, H. p 351 N94-10968
HIRAIWA, TETSUO p 27 N94-10367
HIROSE, NAOKI p 10 N94-10467
p 11 N94-10475
p 149 N94-10861
HIRUMA, MASARU p 99 N94-11444
HISAKI, YUKIHARU p 139 N94-11902
p 192 N94-11903
HISANO, I. p 198 N94-11940
HISHIDA, MASATAKA p 214 N94-12676
HISHIKI, MANABU p 148 N94-10727
HJALMARSON, H. P. p 144 N94-11624
HNDERSON, LESLIE J. p 93 N94-12330
HO, C. Y. p 81 N94-10297
HOBBIE, J. E. p 271 N94-12468
HOBBS, L. W. p 91 N94-11698
HOCKADAY, R. p 384 N94-10157
HODGKISS, W. S. p 289 N94-12349
HODGKISS, WILLIAM S. p 170 N94-10704
HOEHN, J. G., JR. p 398 N94-11073
HOERZ, F. p 429 N94-12063
HOERZ, FRIEDRICH p 461 N94-12159
HOFACKER, SCOTT A. p 127 N94-10623
HOFFMAN, D. J. p 137 N94-11453
HOFFMANN, K. p 118 N94-10205
HOFMANN, B. p 87 N94-12240
HOFMANN, MARTIN O. p 180 N94-10815
HOFMANN, PETER p 107 N94-10116
p 108 N94-10123
p 111 N94-10139
HOGAN, B. p 145 N94-11645
HOHIMER, J. P. p 174 N94-11005
HOKE, P. B. p 183 N94-11647
HOKIN, S. p 388 N94-10747
HOLANDA, RAYMOND p 170 N94-11310
HOLBEIN, R. p 126 N94-10617
HOLBROUCK, P. p 39 N94-10118
HOLDEN, DAN p 45 N94-11323
HOLECZ, FRANCESCO p 247 N94-12482
HOLLAND, SCOTT D. p 148 N94-10644
HOLLAND, T. J. p 35 N94-12562
HOLLERBACH, M. A. p 393 N94-11514
HOLLIER, P. p 212 N94-12667
HOLLOWAY, HARRY C. p 305 N94-11790
HOLMES, M. G. p 248 N94-12488
HOLMES, PHILIP p 31 N94-11494
HOLSHEIMER, MARCEL p 320 N94-10167
HOLT, BENJAMIN p 240 N94-11756
HOLT, MARTIN p 250 N94-12502
HOLZ, ANDREA p 214 N94-12677
HOMBURG, ALE JAN p 344 N94-10908
HOMSY, G. M. p 159 N94-12314
HONG, SUK-YOON p 189 N94-11823
HOOVER, JAMES R. p 20 N94-10785
HOOVLER, G. S. p 371 N94-10529
HOPKE, P. K. p 266 N94-11671
HORAN, D. M. p 54 N94-11643
HORIE, HIROAKI p 201 N94-11954
p 253 N94-12520
HORIGUCHI, FUMIO p 210 N94-12656
HORIUTI, K. p 155 N94-12288
HORN, K. M. p 143 N94-11285
HORN, LINDA JOYCE p 434 N94-11185
HORNER, APRIL p 17 N94-10766
HORWATH, E. J. p 405 N94-12563
HORWITZ, J. L. p 387 N94-10641
HOSHI, TAKASHI p 218 N94-12700
HOSHINO, HIDEO p 2 N94-10350
HOSKING, F. M. p 129 N94-11606
HOSOKAWA, S. p 113 N94-10176
HOSONO, YASUHARU p 99 N94-11444
HOSOYAMADA, S. p 205 N94-11979
HOUPIS, CONSTANTINE H. p 32 N94-11501
HOURY, S. p 242 N94-11769
p 243 N94-11775
HOUSE, MAXWELL p 305 N94-11789
HOUTCHENS, BRUCE A. p 305 N94-11790
HOWE, CARL D. p 337 N94-11829
HOWE, D. C. p 179 N94-10400
HOWE, J. p 128 N94-11304
HOWELL, E. S. p 430 N94-12111
HOWELL, J. R. p 26 N94-11464
HOWELL, NORMAN E. p 26 N94-11464
HRACH, FRANK J. p 12 N94-10672
HSIUNG, A. p 188 N94-11460
HSU, DAVID S. p 140 N94-10377
HSU, WEIBIAO p 431 N94-12191
HU, DUNXIN p 206 N94-11990

HU, Y. Z. p 142 N94-11094
p 401 N94-11651
p 373 N94-11880
HUANG-TAO p 212 N94-12669
HUANG, MIN p 153 N94-11615
HUANG, WEI p 197 N94-11930
p 213 N94-12674
HUANG, X. Z. p 403 N94-12345
HUANG, XIAO-SHENG p 192 N94-11901
p 203 N94-11970
HUBER, DANIEL A. p 52 N94-11405
HUBER, T. M. p 373 N94-12542
HUBERT, R. R. p 188 N94-11460
HUDNALL, J. M. p 138 N94-11655
HUDYNTZEV, N. N. p 366 N94-11349
HUEBNER, C. p 63 N94-10058
HUECKELHEIM, G. p 241 N94-11765
HUFF, TIMOTHY L. p 299 N94-10360
HUGHES, MICHEAL p 35 N94-11535
HUGHES, R. S., JR. p 399 N94-11243
HUGHES, T. W. p 181 N94-11290
HUGHES, THOMAS C. p 316 N94-11642
HUKKA, TERTTU I. p 403 N94-12010
HULL, J. R. p 144 N94-11607
HULSEY, G. p 374 N94-12785
HUMANIC, T. J. p 369 N94-12546
HUNG, G. W. p 220 N94-12709
HUNSUCKER, R. D. p 278 N94-11871
HUNT, E. P. p 58 N94-10022
HUNTER, R. C. p 341 N94-11562
HUNTER, WILLIAM R. p 132 N94-10382
HUNTOON, CAROLYN L. p 305 N94-11791
HUONG, NGUYEN THI QUE p 402 N94-11659
p 402 N94-11660
HURST, R. p 64 N94-10060
HUSTON, RONALD L. p 181 N94-11157
HUTCHBY, J. p 54 N94-11418
HUTCHEON, I. D. p 471 N94-12212
HUTCHINSON, D. P. p 173 N94-10160
HUTCHINSON, I. H. p 391 N94-11170
HUTH, JOHN F. p 314 N94-11539
HWA, R. C. p 366 N94-11147
HYATT, A. W. p 393 N94-11514
HYDE, ANDREW R. p 62 N94-10044

I

IACOBELLIS, S. F. p 244 N94-11783
IANNARELLA, L. p 395 N94-10314
ICHIHARA, M. p 203 N94-11967
ICHIKAWA, HIROSHI p 215 N94-12680
ICHIKAWA, KAORU p 198 N94-11941
p 201 N94-11958
p 209 N94-12649
ICHIKAWA, MASAFUMI p 217 N94-12694
p 221 N94-12715
IDOSOR, FLORENTINO R. p 186 N94-10937
IFTI, M. p 410 N94-10631
IGNATENKO, K. I. p 433 N94-12253
IHDE, JOHANNES p 237 N94-11739
IIDA, NORIKO p 195 N94-11920
IITAKA, HIROSHI p 172 N94-11968
IKEDA, HIROKAZU p 372 N94-11245
IKEDA, M. p 240 N94-11759
p 245 N94-11786
IKEGAMI, Y. p 107 N94-10115
p 114 N94-10179
IKEZOE, HIROSHI p 372 N94-11043
IKUSHIMA, TAKAJI p 300 N94-10888
ILANTHIRAYAN, S. p 252 N94-12513
ILES, P. A. p 54 N94-11417
ILIFF, KENNETH W. p 13 N94-10707
p 13 N94-10820
ILIN, S. V. p 397 N94-10883
IMAE, M. p 351 N94-10968
IMAGAWA, TOSHIAKI p 212 N94-12668
IMAI, TORU p 132 N94-10560
IMAMURA, F. p 193 N94-11908
IMANISHI, A. p 144 N94-11508
IMAOKA, ATSUSHI p 139 N94-10989
IMASATO, NORIHISA p 197 N94-11936
p 210 N94-12652
p 213 N94-12672
p 221 N94-12717
IMAWAKI, SHIROU p 198 N94-11941
p 209 N94-12649
IMBERT, M. p 8 N94-10456
IMMAMOTO, S. S. p 276 N94-11463
INAGAKI, TADASHI p 218 N94-12699
INAGAKI, TOSHIHARU p 30 N94-10734
INAGUCHI, TAKASHI p 130 N94-11841
INATANI, JUNJI p 130 N94-11837
INDEIKINA, A. E. p 120 N94-10219
INGALLS, R. L. p 76 N94-10653
INGALLS, W. B. p 374 N94-12786
INGELS, FRANK M. p 324 N94-10932
INGRAM, J. C. p 76 N94-11140
INGUSCIO, M. p 124 N94-10241
INOMATA, SHINJI p 358 N94-11042
INOUE, F. p 193 N94-11909
INOUE, FUMIO p 220 N94-12713
INOUE, KENJI p 147 N94-10364
p 147 N94-10365
INOUE, S. p 219 N94-12705
INOUE, TAKASHI p 2 N94-10350
INSLEY, E. M. p 152 N94-11519
INTRATOR, NATHAN p 338 N94-10487
p 304 N94-11261
IOLTUKHOVSKI, ANDREY A. p 225 N94-12738
IP, W.-H. p 123 N94-10236
IRENE, E. A. p 142 N94-11094
p 174 N94-11095
p 143 N94-11159
p 143 N94-11160
p 401 N94-11651
p 373 N94-11880
ISAACS, H. S. p 84 N94-11459
ISCOE, NEIL p 329 N94-11430
ISHIBASHI, M. p 201 N94-11959
ISHIDA, KIYOMICHI p 2 N94-10363
ISHIGURO, TOMIKO p 27 N94-10370
ISHII, KAZUTO p 42 N94-10366
ISHII, TAKEO p 218 N94-12699
ISHIJIMA, SUGURU p 193 N94-11910
ISHIKAWA, MASAMICHI p 113 N94-10176
ISHIMARU, TAKASHI p 17 N94-12633
ISHIMINE, ANSHIN p 205 N94-11983
ISHIMORI, SHIGEKI p 207 N94-12638
ISHINO, KAZUO p 169 N94-11944
ISHIZAKA, J. p 200 N94-11948
ISODA, YUTAKA p 221 N94-12715
ITIKAWA, Y. p 367 N94-11580
ITO, AKIRA p 16 N94-12616
ITOH, NOBUTAKE p 163 N94-12612
ITOH, RYOZO p 12 N94-10480
ITOU, A. p 193 N94-11909
ITOU, AKIYOSHI p 220 N94-12713
ITOU, KATSUHIRO p 27 N94-10367
IVALDI, CHARLES F., JR. p 284 N94-11113
IVANCHENKO, E. A. p 344 N94-11033
IVANOV, A. V. p 429 N94-12101
IVEY, G. N. p 159 N94-12311
IVIE, GUY p 323 N94-10494
IWAKUMA, YUKIFUMI p 216 N94-12690
IWAMOTO, AKIRA p 372 N94-11043
IWASAKI, A. p 113 N94-10176
IWATA, TSUTOMU p 482 N94-12324
p 482 N94-12328
IYENGAR, S. K. p 371 N94-10316
IZUMIKAWA, MUNEO p 27 N94-10367

J

JACINTO, GIL p 219 N94-12707
JACKSON, D. M. p 274 N94-10726
JACKSON, G. L. p 393 N94-11514
JACKSON, MICHAEL G. p 417 N94-11856
JACOB, MARC C. p 156 N94-12295
JACOBS, J. L. p 144 N94-11479
JACOBSEN, S. V. p 341 N94-12598
JACQUES, C. p 356 N94-10998
JACUNSKI, M. p 319 N94-10146
JAEAESKELAEINEN, V. p 247 N94-12483
JAEGER, E. F. p 131 N94-10270
JAFAROV, R. G. p 368 N94-11581
JAHSHAN, S. N. p 365 N94-10952
JAIN, A. p 140 N94-10300
JAIN, RAJ K. p 49 N94-11389
p 51 N94-11397
JAKUBCZAK, J. p 319 N94-10146
JALINAUD, T. p 389 N94-11114
JAMES, J. T. p 318 N94-11553
JAMES, JOHN T. p 318 N94-11554
p 318 N94-11555
JAMGOTCHIAN, HAIK p 117 N94-10203
p 118 N94-10206
JANASWAMY, RAMAKRISHNA p 138 N94-12281
JANKOWSKI, D. F. p 112 N94-10172
JANKOWSKI, JOHN E., JR. p 422 N94-11186
JANNING, N. p 39 N94-10136
JANSKY, J. p 376 N94-10574
JANSZKY, J. p 375 N94-10570
JANZEN, D. D. p 71 N94-11340
JARFORS, ANDERS E. W. p 109 N94-10128
p 123 N94-10238
JARMON, DAVID p 92 N94-11876
JARVELA, P. p 60 N94-10035
JAUMANN, R. p 446 N94-12079
JAUMANN, RALF p 471 N94-12213
JEFFREY, FRANK p 54 N94-11415
JEFFREY, FRANK R. p 49 N94-11390
JEFFRIES, M. O. p 240 N94-11755
JELLISON, J. L. p 129 N94-11606
JENFFER, P. p 121 N94-10229
JENKINS, JERRY E. p 32 N94-11499
JENKINS, JOHN O. p 329 N94-11426
JENKINS, P. p 50 N94-11395
JENKOVSZKY, L. L. p 362 N94-10552
p 362 N94-10553
p 362 N94-10554
p 362 N94-10555
JENSEN, B. p 64 N94-10063
JENSEN, M. S. p 341 N94-12598
JENSRUD, O. p 64 N94-10063
JERRUM, M. p 331 N94-11611
JEWELL, NICK p 220 N94-12712
JEWELL, TANYA E. p 374 N94-10339
JEZEK, K. C. p 238 N94-11744
JI, H. p 388 N94-10747
JI, WENGUI p 173 N94-10483
JIANG, GUANGSHAN p 345 N94-11280
JIANG, SONGNIAN p 215 N94-12686
JIANG, YI-TSANN p 28 N94-10816
JIMENEZ-FERNANDEZ, J. p 104 N94-10095
JIMENEZ, A. p 56 N94-10007
p 59 N94-10025
JOHANNESSEN, J. A. p 234 N94-11720
JOHANNESSEN, O. M. p 234 N94-11720
JOHANNESSEN, OLA M. p 238 N94-11745
p 210 N94-12653
JOHANSEN, I. p 64 N94-10063
JOHN, SARAH p 485 N94-12434
JOHNSON, A. W. S. p 395 N94-10406
JOHNSON, B. R. p 383 N94-12341
JOHNSON, C. G. p 94 N94-12381
JOHNSON, D. p 423 N94-11059
JOHNSON, DEAN p 355 N94-10995
JOHNSON, JAMES R. p 419 N94-11288
JOHNSON, K. F. p 374 N94-12786
JOHNSON, R. BARRY p 375 N94-10506
JOHNSTON, J. P. p 159 N94-12309
JOHNSTON, K. J. p 134 N94-11063
JOHNSTON, RICHARD K. p 420 N94-11846
JOLLIFF, B. L. p 408 N94-12174
JOLY, V. p 8 N94-10455
JONES, C. H. p 415 N94-12028
JONES, CLIVE P. p 252 N94-12516
JONES, E. A. p 272 N94-12780
JONES, GARY A. p 302 N94-12441
JONES, IAN S. F. p 197 N94-11932
p 251 N94-12506
JONES, J. P. p 341 N94-12598
JONES, P. ALAN p 51 N94-11399
JONES, R. H. p 73 N94-11612
JONES, RHIAN H. p 429 N94-12105
JONES, SCOTT A. p 138 N94-12440
JONES, WILLIAM R., JR. p 88 N94-10864
JOSEPH, J. p 373 N94-11880
JOSHI, P. C. p 234 N94-11719
JOSHI, V. S. p 93 N94-12354
JOSWIAK, D. J. p 430 N94-12115
JOUAN, J. p 212 N94-12667
JOYCE, TERRENCE M. p 209 N94-12650
JULIA, A. p 255 N94-12529
JUN, BYUNGDUG p 197 N94-11931
JUREWICZ, A. J. G. p 423 N94-11183
JURISCH, M. p 86 N94-10196
JUSTH, ERIC A. p 140 N94-10384

K

KACZMARCZIK, U. p 108 N94-10121
KADOTA, HIROSHI p 163 N94-12612
KAELBLING, LESLIE P. p 418 N94-10515
KAHANA, D. E. p 359 N94-10302
KAHANA, S. H. p 359 N94-10302
p 359 N94-10303
KAHN, PHILIP p 418 N94-10515
KAIDEN, TAKESHI p 11 N94-10474
p 12 N94-10481
KAISER, D. A. p 317 N94-11528
KAISER, T. B. p 385 N94-10289
KAKUI, Y. p 203 N94-11967
KALDEICH, BRIGITTE p 99 N94-10070
p 112 N94-10171
p 232 N94-11704
p 245 N94-12471
KALEPS, INTS p 316 N94-12346
KALINICHENKO, V. V. p 141 N94-10533
KAMBAYASHI, SHAW p 368 N94-11592
KAMEI, S. p 113 N94-10176
KAMINAGA, HUMITO p 161 N94-12549
KAMIYA, JOE p 311 N94-12006
KAMP, L. W. p 457 N94-12139
KAMPMANN, L. p 62 N94-10049

KANEKO, ARATA p 194 N94-11913
p 194 N94-11914
KANEKO, FUMIO p 217 N94-12696
KANEKO, YUTAKA p 482 N94-12325
p 482 N94-12328
KANNE, W. R., JR. p 181 N94-11228
KANNO, SUSUMU p 191 N94-11898
KANTHA, L. p 221 N94-12716
KANTZ, MELVIN R. p 17 N94-10768
p 17 N94-10771
KANZAKI, TADASHI p 217 N94-12693
KAPOOR, K. p 39 N94-10764
KAPUR, V. K. p 50 N94-11393
KARAMANOS, GAYLE M. p 305 N94-11791
KARASSO, PARIS S. p 159 N94-12312
KARNEY, C. F. F. p 385 N94-10159
KARPENKO, A. Y. p 397 N94-10843
KARSTETTER, KENT M. p 311 N94-12364
KASAPI, STEVEN p 352 N94-10976
KASCHMITTER, J. L. p 140 N94-10309
KASHIWAGI, TAKASHI p 19 N94-10781
KASHKAROV, L. L. p 433 N94-12252
KASILINGAM, D. P. p 235 N94-11723
KASISCHKE, E. S. p 249 N94-12494
KAST, B. A. p 141 N94-10521
KATAKURA, NORIO p 217 N94-12696
KATAOKA, H. p 411 N94-10880
KATAYAMA, I. p 363 N94-10720
KATNIK, GREGORY N. p 40 N94-10805
KATO, T. p 367 N94-11580
p 393 N94-11594
KATOH, NAOTO p 418 N94-10559
KATSAROS, KRISTINA B. p 233 N94-11712
KATZ, I. p 278 N94-11702
KATZ, N. p 276 N94-11463
KATZBERG, STEPHEN J. p 245 N94-12432
KAUFFMAN, R. L. p 385 N94-10286
KAUFMAN, DAVID M. p 170 N94-10667
KAUFMANN, DAVID N. p 24 N94-12355
KAUFMANN, V. p 246 N94-12478
KAUSHAL, ASHOK p 180 N94-11155
KAWAGUCHI, KATSUYOSHI p 217 N94-12692
KAWAGUCHI, KENTAROU p 130 N94-11837
KAWAHARA, HIROYASU p 33 N94-10733
KAWAI, HIROYASU p 212 N94-12664
KAWAI, MASASHI p 207 N94-12638
KAWAMURA, HIROSHI p 200 N94-11952
p 201 N94-11960
p 202 N94-11961
p 220 N94-12710
KAWANO, T. p 199 N94-11945
KAWASAKI, K. p 393 N94-11594
KAWASAKI, KIYOSHI p 215 N94-12682
KAWATA, YOSHIYUKI p 205 N94-11980
KAWATATE, KAZUO p 194 N94-11913
p 194 N94-11914
KAWAZOE, TAKESHI p 482 N94-12325
p 482 N94-12328
KAYNES, IAN p 27 N94-11341
KAZAKOVA, G. G. p 141 N94-10533
KAZANSKY, ALEXANDER V. p 227 N94-12750
KAZMIN, A. S. p 216 N94-12687
p 220 N94-12711
KEANA, J. F. p 94 N94-12396
KEANA, JOHN F. p 93 N94-12353
KEE, R. J. p 77 N94-11370
p 152 N94-11371
KEEFER, DENNIS p 46 N94-10700
KEENEY-WALKER, J. p 184 N94-10288
KEICHER, D. M. p 129 N94-11606
KEIL, K. p 281 N94-12083
p 430 N94-12142
p 282 N94-12197
KEIL, LANNY C. p 311 N94-12005
KEISER, J. R. p 72 N94-11368
KEITEL, C. H. p 378 N94-10592
KELL, GENEVIEVE p 87 N94-10231
KELLER, H. U. p 123 N94-10236
KELLER, L. p 81 N94-12099
KELLER, L. P. p 433 N94-12261
KELLER, S. L. p 301 N94-11648
KELLER, TEDDY M. p 93 N94-12330
p 94 N94-12399
KELLEY, K. W. p 300 N94-11180
KELLNDORFER, J. p 245 N94-12472
KELLY, KATHRYN A. p 209 N94-12650
KELLY, M. p 281 N94-12072
p 281 N94-12073
p 281 N94-12074
p 281 N94-12075
p 281 N94-12076
KEMMERLE, K. p 111 N94-10139
KEMMERLE, KURT p 107 N94-10114
p 109 N94-10124
KEMP, DAVID VANDYKE p 277 N94-11585
KEMPEL, LEO C. p 136 N94-11084
KEMPER, C. A. L. p 57 N94-10010
KEMPER, G. B. p 302 N94-11548
KENNAUGH, A. p 7 N94-10447
KENNEDY, A. K. p 471 N94-12212
KENNEDY, DAVID p 35 N94-11535
KENNEDY, DAVID B. p 314 N94-11536
KENNEDY, JOHN M. p 419 N94-11352
KENNEY, BARBARA H. p 46 N94-10765
KENNINGTON, JEFFERY L. p 322 N94-10492
KENWARD, D. R. D. p 236 N94-11733
p 248 N94-12488
p 249 N94-12493
KER, H. L. p 82 N94-10957
KERN, JOHN p 318 N94-11561
KERN, KRISTEN T. p 94 N94-12450
KERSEY, ALAN D. p 374 N94-10376
KERSHAW, MARY ANN p 318 N94-11554
KERSTEN, P. H. M. p 341 N94-10163
KERSTETER, S. L. p 266 N94-11471
KERY, SEAN p 289 N94-11854
KESHARI, ASHOK K. p 210 N94-12655
KESLER, J. K. p 422 N94-10736
KETTUNEN, P. p 58 N94-10019
KETTUNEN, PENTTI O. p 61 N94-10042
KEVAN, S. D. p 79 N94-12534
KEY, J. p 241 N94-11761
KEY, J. F. p 163 N94-12604
KEYES, B. L. P. p 91 N94-11672
p 91 N94-11673
KEYTE, G. E. p 236 N94-11733
p 248 N94-12488
p 249 N94-12493
KHADR, N. p 231 N94-11309
p 245 N94-11885
KHALIL, H. S. p 346 N94-11608
KHALIL, S. M. p 386 N94-10387
KHAN, A. p 140 N94-12706
KHANDEKAR, M. p 232 N94-11708
KHILCHENKO, A. D. p 336 N94-10544
KHIZHNYAK, N. A. p 133 N94-11034
p 134 N94-11035
p 345 N94-11036
p 134 N94-11038
KHOLNOVA, E. A. p 359 N94-10266
KIEFER, WALTER S. p 444 N94-12065
p 481 N94-12267
p 481 N94-12268
KIEFFER, H. H. p 425 N94-12140
KIERKEBY, N. O. S. p 341 N94-12598
KIESS, T. E. p 351 N94-10971
KIGAWA, SEIICHIRO p 190 N94-11080
KIHARA, MASAMI p 139 N94-10989
KIKUCHI, MASATAKA p 178 N94-10369
KILIC, O. p 245 N94-11885
KILIN, S. YA. p 379 N94-10599
KILLMAN, R. J. p 82 N94-10804
KILMATOV, T. R. p 223 N94-12731
KIM, JOHN J. p 155 N94-12288
p 158 N94-12308
KIM, JONG-JEAN p 370 N94-10579
KIM, SUNG-RYONG p 187 N94-11218
KIM, WALTER S. p 485 N94-10356
KIM, WON S. p 179 N94-10654
KIM, Y. S. p 375 N94-10564
p 379 N94-10604
KIM, YOUNG B. p 92 N94-11847
KIM, YOUNG SEUP p 196 N94-11926
KIMURA, M. p 203 N94-11967
KIMURA, RYUUJI p 196 N94-11926
KINDLER, K. p 4 N94-10432
KING, MICHAEL D. p 231 N94-11485
KING, PATRICK p 250 N94-12504
KING, ROGER J. p 142 N94-10931
KINGMAN, P. W. p 405 N94-12563
KINNEY, R. p 393 N94-11669
KINOSHITA, K. p 205 N94-11979
KINTNER, PAUL M. p 278 N94-12392
KIPP, G. p 321 N94-10343
KIRICHENKO, Y. V. p 371 N94-10542
KIRK, ALBERT p 139 N94-11000
KIRK, D. C. p 8 N94-10454
KIRKPATRICK, R. J. p 80 N94-12087
KISELEV, ALEXANDER A. p 305 N94-11790
KISELEV, V. A. p 391 N94-11211
KISHIHARA, N. p 219 N94-12705
KISHIMOTO, TAKUJI p 12 N94-10478
KISHINO, MOTOAKI p 140 N94-11965
p 204 N94-11972
KISHIYAMA, K. I. p 387 N94-10737
KITAGAWA, MASAHIRO p 377 N94-10585
KITAGAWA, SHOUJI p 206 N94-11986
KIUCHI, H. p 351 N94-10968
KIVSHAR, YU. S. p 398 N94-11025
KIZAKI, MINORU p 84 N94-11593
KIZU, SHOUICHI p 220 N94-12710
KLAVETTER, E. A. p 98 N94-11366
KLEIJWEG, J. C. M. p 232 N94-11707
KLEIN, H. p 122 N94-10233
KLEMENT, MARY A. p 331 N94-11679
KLEMETTI, W. I. p 275 N94-11013
KLEPIKOVA, N. V. p 275 N94-11052
KLETT, R. p 111 N94-10139
KLEVTSOV, A. M. p 227 N94-12756
KLIMA, B. p 370 N94-12781
KLIMOV, A. B. p 349 N94-10573
p 380 N94-10612
KLIMOV, S. M. p 103 N94-10093
KLINGELHOEFER, G. p 476 N94-12242
KLINGSPORN, P. E. p 381 N94-10647
KLINKHAMER, F. p 39 N94-10136
KLOECK, W. p 433 N94-12261
p 433 N94-12262
KNAPP, CHARLES F. p 309 N94-11997
KNAUF, RICHARD p 109 N94-10125
KNAUSS, WILLIAM p 207 N94-12637
KNEPTON, J. C., JR. p 26 N94-11892
KNIAZ, K. p 400 N94-11457
KNIGHT, DOYLE D. p 150 N94-11014
KNIGHT, FREDERICK K. p 485 N94-12589
KNIGHT, KIM S. p 99 N94-12275
KNISKERN, FRANKLIN E. p 212 N94-12666
KNOLLMEYER, S. L. p 270 N94-12463
KNOLLMEYER, STEPHEN L. p 268 N94-12453
KNOWLES, P. E. p 373 N94-12542
KNUDSEN, P. p 242 N94-11768
KNUEPPEL, ANDREAS p 32 N94-11500
KNUTH, KURT V. p 29 N94-12274
KNYSTAUTAS, ROM p 80 N94-10248
KO, M. K. W. p 279 N94-12572
KO, SUNG HO p 157 N94-12299
KOBAYASHI, H. p 351 N94-10968
KOBAYASHI, HEIHACHIROU p 217 N94-12692
KOBAYASHI, RYOUJI p 164 N94-12617
KOBAYASHI, T. p 367 N94-11509
KOBERSTEIN, J. T. p 93 N94-12340
KOBLENTZ-MISHKE, OLGA J. p 228 N94-12761
KOBUSHKIN, A. P. p 344 N94-10881
KOC, U. V. p 145 N94-11645
KOCH, K. R. p 241 N94-11765
KOCHAN, H. p 123 N94-10236
KOCHELAP, V. A. p 396 N94-10800
p 396 N94-10801
KOCHENDOERFER, R. p 56 N94-10003
KODAMA, YASUMASA p 205 N94-11982
KOEBERL, CHRISTIAN p 281 N94-12080
p 430 N94-12146
KOEBERLE, H. p 61 N94-10043
KOENIG, H. p 118 N94-10205
KOENIG, MANFRED p 57 N94-10014
KOENIG, R. p 243 N94-11774
KOERVER, W. p 111 N94-10138
KOFLER, R. R. p 364 N94-10754
KOGA, MOMOKI p 195 N94-11923
KOGA, R. p 276 N94-11463
KOGAN, V. YA. p 223 N94-12729
p 229 N94-12764
KOHAMA, YASUAKI p 164 N94-12617
p 164 N94-12620
p 166 N94-12632
KOHL, C. P. p 437 N94-12033
KOIKE, F. p 393 N94-11594
KOITO, ATSUSHI p 148 N94-10727
KOLB, C. E. p 279 N94-12572
KOLOMENSKIJ, G. A. p 365 N94-11089
KONDA, M. p 213 N94-12670
KONDA, MASANORI p 213 N94-12672
KONDOU, JIROU p 191 N94-11895
KONDRANIN, TIMOTHY V. p 177 N94-12722
KONDRANIN, TYMOTHY V. p 229 N94-12762
KONO, AYAHIKO p 122 N94-10232
KONOTOP, Y. F. p 66 N94-11143
KONOVALOV, D. A. p 359 N94-10311
p 360 N94-10330
KONTAR, EVGENY A. p 224 N94-12733
p 224 N94-12734
p 224 N94-12735
KONTOTHANASSIS, LEONIDAS I. p 320 N94-11294
p 337 N94-11650
KONTROS, J. E. p 362 N94-10555
KONYUKHOV, V. V. p 336 N94-10544
KOO, JE-HWAN p 370 N94-10579
KOOLISH, RICHARD p 337 N94-11829
KOONEN, A. M. J. p 131 N94-10165
KOOPMANS, B. N. p 254 N94-12526
KOPP, BRIAN p 42 N94-11297
KOPROVA, L. I. p 222 N94-12723
KORCHINSKIJ, G. M. p 389 N94-10886
KOROLKOVA, N. V. p 375 N94-10567
KOROS, ANTON S. p 314 N94-11538
KOROTENKO, KONSTANTIN A. p 223 N94-12730
KORSUNSKIJ, S. V. p 386 N94-10395
KORTE, JOHN J. p 9 N94-10458

KOSEFF, J. R. .... p 156 N94-12290
p 159 N94-12311
KOSHELYAEVSKY, N. B. .... p 24 N94-10967
KOSHIOKA, YASUHIRO .... p 10 N94-10469
p 11 N94-10477
KOSKI, N. L. .... p 272 N94-12780
KOSKINEN, J. .... p 247 N94-12483
KOSLOV, E. A. .... p 97 N94-12040
KOSMANN, D. .... p 237 N94-11740
p 246 N94-12477
KOSS, D. A. .... p 85 N94-12447
KOSSENTINI, FAOUZI .... p 326 N94-11197
KOSSEY, P. A. .... p 275 N94-11013
KOSTAREV, K. G. .... p 103 N94-10092
KOSTER, JEAN N. .... p 105 N94-10100
KOSTIKOV, V. I. .... p 63 N94-10057
KOTHE, D. B. .... p 372 N94-10890
KOTNOUR, T. G. .... p 417 N94-11661
KOTSUBO, V. .... p 128 N94-11161
KOU, SINDO .... p 101 N94-10080
KOVARSKY, V. A. .... p 376 N94-10575
KOYAMATUSU, A. H. .... p 181 N94-11290
KOZAK, J. .... p 346 N94-11632
KOZLOV, V. P. .... p 223 N94-12726
KOZLOWSKI, M. R. .... p 90 N94-11230
KOZODEROV, VLADIMIR V. .... p 229 N94-12766
KOZOL, JOSEPH .... p 126 N94-10614
KRAINAK, MICHAEL .... p 170 N94-10667
KRAMER, A. J. .... p 111 N94-10140
KRAMER, S. L. .... p 374 N94-12782
KRANE, MICHAEL H. .... p 357 N94-10358
KRASILSHCHIK, I. S. .... p 341 N94-10163
KRASS, C. .... p 109 N94-10126
KRAVETSKIY, G. A. .... p 63 N94-10057
KREMER, HARRO .... p 131 N94-10280
KRIGE, J. .... p 44 N94-11462
KRISHEN, KUMAR .... p 486 N94-11527
KRISHNAN, A. .... p 46 N94-10934
KRISS, JORDAN R. .... p 24 N94-11879
KRISTENSEN, S. .... p 341 N94-12598
KRIVE, I. V. .... p 412 N94-11039
KROEGER, R. .... p 124 N94-10247
KROLIK, JEFFREY .... p 133 N94-10660
KROO, ERIK .... p 99 N94-12275
KROTHAPALLI, A. .... p 16 N94-11889
KROTKOV, NIKOLAY A. .... p 229 N94-12762
KRUER, W. .... p 369 N94-11815
KRUG, C. .... p 111 N94-10138
KRUGER, JAN .... p 379 N94-10598
KRUMREY, M. .... p 143 N94-11273
KRUPAR, MARTIN J. .... p 14 N94-10892
KRUPKE, W. F. .... p 383 N94-11676
KUB, FRANCIS J. .... p 140 N94-10384
KUBOTA, MASAHISA .... p 207 N94-12636
KUBOTA, S. .... p 392 N94-11239
KUDO, I. .... p 113 N94-10176
KUEHL, DANIEL T. .... p 132 N94-10497
KUHL, A. L. .... p 147 N94-10307
p 151 N94-11144
KUHL, R. .... p 87 N94-10231
KUHLMANN-WILSDORF, D. .... p 182 N94-12374
KUHLMANN, HENDRIK C. .... p 101 N94-10077
KUHNKE, B. CARL .... p 37 N94-10692
KUHNLE, PAUL .... p 355 N94-10994
p 139 N94-11000
KUIPERS, BENJAMIN .... p 323 N94-10711
KUKUSHKIN, A. V. .... p 134 N94-11062
KUMAGAI, M. .... p 203 N94-11967
KUMAGAI, TAKAO .... p 43 N94-10859
KUMAR, D. .... p 3 N94-10426
KUMAR, J. .... p 93 N94-12380
KUMAR, K. VASANTHA .... p 125 N94-11235
p 312 N94-11544
p 312 N94-11546
KUMAR, M. R. RAMESH .... p 206 N94-11988
KUMAR, S. PRASANNA .... p 193 N94-11912
KUMAR, V. .... p 395 N94-10386
p 361 N94-10503
KUMSHAEV, S. B. .... p 324 N94-11031
KUNKEE, D. B. .... p 274 N94-10726
KUNKLE .... p 212 N94-12667
KUO, EDWARD Y. .... p 287 N94-10490
KUO, T. K. .... p 483 N94-11619
KUPFER, K. .... p 394 N94-12545
KURAT, G. .... p 429 N94-12101
p 432 N94-12233
KURIBAYASHI, M. .... p 107 N94-10115
p 114 N94-10179
KURODA, YOSHIFUMI .... p 193 N94-11911
KUROIWA, HIROSHI .... p 139 N94-11902
KURSTEDT, H. A. .... p 417 N94-11600
KURTZ, H. .... p 47 N94-11354
KURVONEN, L. .... p 247 N94-12483
KUSABA, T. .... p 201 N94-11959
KUSAKA, KAZUO .... p 27 N94-10367
KUSIOR, J. PATRICK .... p 73 N94-12344
KUSMARTSEV, F. V. .... p 408 N94-10148
p 395 N94-10415
KUTSUWADA, KUNIO .... p 202 N94-11962
KUTZMAN, RUSSELL A. .... p 286 N94-12408
KUVSHINOV, V. I. .... p 379 N94-10599
KUZIN, V. I. .... p 229 N94-12765
KUZMIN, V. A. .... p 223 N94-12731
KUZNETSOV, VADIM R. .... p 81 N94-12319
KUZNETSOV, Y. K. .... p 391 N94-11174
KVASHNIN, A. N. .... p 336 N94-10544
KWAN, T. J. T. .... p 137 N94-11621
KWOK, RON .... p 237 N94-11741
p 240 N94-11756
p 241 N94-11762
KWON, YOUNGJOON .... p 363 N94-10748
KYTE, FRANK T. .... p 282 N94-12091

L

LAAKMANN, J. .... p 118 N94-10205
LAARHUIS, J. H. .... p 131 N94-10165
LABAUNE, C. .... p 389 N94-11114
LADANYI, BRANKA M. .... p 369 N94-12420
LAFONTAINE, J. R. C. .... p 236 N94-11729
LAGASSE, R. R. .... p 89 N94-10958
LAHAV, M. .... p 394 N94-10301
LAHTEENKORVA, K. .... p 60 N94-10035
LAHTINEN, H. .... p 63 N94-10054
LAI, K. .... p 32 N94-11502
LAI, Y. G. .... p 46 N94-10934
LAIRD, J. S. .... p 143 N94-11285
LAITINEN, M. .... p 65 N94-10069
LALBEHARRY, R. .... p 232 N94-11708
LALLEMANT, M. .... p 102 N94-10086
LAM, C. W. .... p 234 N94-11716
LAM, CHIU-WING .... p 318 N94-11554
LAM, H. F. .... p 356 N94-10998
LAMBERT, D. M. .... p 185 N94-10712
LAMBERT, D. R. .... p 138 N94-11883
LAMBRECHT, WALTER R. L. .... p 405 N94-12570
LAMMERING, R. .... p 71 N94-11339
LAMOTTE, B. .... p 59 N94-10025
LAN, C. W. .... p 101 N94-10080
LANDEAU-CONSTANTIN, JOCELYNE
p 485 N94-11379
LANDEN, O. L. .... p 393 N94-11677
LANDIS, G. A. .... p 50 N94-11395
LANDIS, G. PAUL .... p 353 N94-10983
LANDIS, GEOFFREY A. .... p 49 N94-11389
p 51 N94-11397
p 54 N94-11419
LANDRY, R. .... p 245 N94-11885
LANE, NORMAN E. .... p 315 N94-11627
LANG, HEINZ .... p 105 N94-10104
LANG, R. H. .... p 231 N94-11309
p 245 N94-11885
LANG, VALERIE I. .... p 274 N94-10496
LANGBEIN, DIETER .... p 101 N94-10078
LANGE, A. .... p 61 N94-10039
LANGE, CHARLES .... p 331 N94-11657
LANGERAK, ROM .... p 320 N94-10164
LANGSTON, CHARLES A. .... p 275 N94-11102
LANGSTON, JAMES .... p 329 N94-11429
LANGUELL, MICHAEL L. .... p 109 N94-10127
LANIER, A. .... p 423 N94-11183
LANKHORST, MARC M. .... p 419 N94-10903
LANNING, B. R. .... p 50 N94-11393
LAPIANO-SMITH, D. A. .... p 169 N94-10526
LAPITAN, R. .... p 219 N94-12705
LAPSHIN, V. I. .... p 389 N94-10885
LAPSHINA, VALENTINA I. .... p 228 N94-12757
LAREO, S. .... p 62 N94-10047
LARMORE, L. L. .... p 343 N94-10708
LARROUDE, PHILIPPE .... p 114 N94-10183
LARSEN, E. W. .... p 342 N94-10283
LARSON, A. C. .... p 363 N94-10743
LASHBROOK, J. J. .... p 302 N94-11556
LASNIER, P. .... p 250 N94-12503
LATHAM, P. E. .... p 145 N94-11645
LATHAM, RICK D. .... p 309 N94-11995
LATHAM, T. S. .... p 370 N94-10149
LATINSKIJ, S. M. .... p 412 N94-11039
p 412 N94-11086
LAU, BENTON H. .... p 1 N94-10936
LAUER, H. V., JR. .... p 436 N94-12024
LAURENT, MONIQUE .... p 347 N94-10354
LAUTENSCHLAGER, P. .... p 39 N94-10119
LAUTISSIER, P. .... p 64 N94-10062
LAVALLE, CARLO .... p 236 N94-11732
p 249 N94-12495
LAVIOLETTE, P. E. .... p 252 N94-12510
LAW, C. C. .... p 112 N94-10172
LAWLER, J. M. .... p 326 N94-11220
LAWRENCE, GEORGE N. .... p 374 N94-10339
LAWSON, A. C. .... p 363 N94-10743
LAWSON, D. E. .... p 254 N94-12528
LAWSON, W. .... p 145 N94-11645
LAXON, S. W. .... p 237 N94-11738
p 246 N94-12475
LE, HUNG .... p 156 N94-12296
LE, L. .... p 423 N94-11183
LEADORE, MICHAEL G. .... p 97 N94-10489
LEANO, H. J. .... p 318 N94-11553
LEBLANC, THOMAS J. .... p 320 N94-11294
LEBOEUF, RICHARD L. .... p 159 N94-12313
LEBOFSKY, L. A. .... p 430 N94-12111
LEBON, G. .... p 103 N94-10090
LEBOUTEILLER, A. .... p 199 N94-11946
LECAVALIER, M. M. .... p 174 N94-10959
LECHAT, M. F. .... p 305 N94-11792
LECKIE, D. .... p 245 N94-11885
LECOMTE, P. .... p 232 N94-11706
LECORNEC, ALAIN .... p 252 N94-12511
LEDREW, ELLSWORTH F. .... p 240 N94-11758
LEE, BEN .... p 27 N94-11341
LEE, CHEN-CHUNG .... p 409 N94-10403
LEE, D. .... p 219 N94-12708
LEE, GORDON .... p 338 N94-10345
LEE, H. W. H. .... p 399 N94-11243
LEE, HAI-WOONG .... p 379 N94-10597
LEE, HUAN .... p 384 N94-10157
LEE, J. C. .... p 340 N94-11644
LEE, JEANNIE .... p 348 N94-11572
LEE, JOHN H. S. .... p 80 N94-10248
LEE, S. R. .... p 396 N94-10745
LEE, SANGSAN .... p 155 N94-12289
LEE, SEUNG JOO .... p 370 N94-10593
LEE, SING H. .... p 382 N94-11286
LEE, TSENGDAR JOHN .... p 277 N94-11480
LEE, WEON S. .... p 76 N94-10713
LEE, YONG-ILL .... p 392 N94-11450
LEFORT, A. .... p 58 N94-10020
LEGGE, G. J.F. .... p 143 N94-11285
LEGLER, DAVID M. .... p 194 N94-11918
LEGROS, J. C. .... p 39 N94-10118
p 112 N94-10173
p 124 N94-10242
LEGROS, J.-C. .... p 119 N94-10215
p 119 N94-10216
p 120 N94-10217
p 121 N94-10223
LEGTERS, LLEWELLYN J. .... p 305 N94-11793
p 307 N94-11802
LEHNER, S. .... p 251 N94-12509
LEISEROWITZ, L. .... p 394 N94-10301
LEMKE, P. .... p 239 N94-11753
LEMOINE, J. M. .... p 243 N94-11778
LEMOS, MARIA CARMEN DEMELLO
p 232 N94-11524
LEMOULLEC, L. .... p 106 N94-10110
LENDEL, A. I. .... p 362 N94-10553
p 362 N94-10555
LENEINDRE, B. .... p 122 N94-10230
LENK, R. .... p 52 N94-11403
LENSKI, H. .... p 109 N94-10126
LENSU, M. .... p 239 N94-11750
LENTZ, HARALD .... p 235 N94-11727
LEONARD, A. W. .... p 393 N94-11514
LEONARD, B. P. .... p 342 N94-10362
LEONTYEV, V. B. .... p 103 N94-10092
LEPISTO, T. K. .... p 58 N94-10019
LEPISTO, TOIVO K. .... p 61 N94-10042
LEPPARANTA, M. .... p 239 N94-11750
LEQUIME, M. .... p 69 N94-11328
LERCH, BRADLEY A. .... p 74 N94-12449
LESAK, J. .... p 63 N94-10056
LESUER, D. R. .... p 82 N94-11076
LEUNG, A. P. .... p 336 N94-11027
LEUNG, MAN-KIT .... p 95 N94-12585
LEVCHUK, L. G. .... p 364 N94-10875
LEVENHAGEN, D. .... p 309 N94-11997
LEVER, A. B. .... p 78 N94-11873
LEVIN, B. .... p 84 N94-11816
LEVIN, I. M. .... p 222 N94-12725
LEVIN, J. M. .... p 223 N94-12726
LEVINE, JUDAH .... p 354 N94-10987
LEVINE, M. W. .... p 353 N94-10981
LEVISON, HAROLD F. .... p 427 N94-11629
LEVKOVICH, M. G. .... p 103 N94-10092
LEVY, YESHAYAHOU .... p 28 N94-11238
LEWANDOWSKI, W. .... p 24 N94-10967
LEWIS, ROY S. .... p 97 N94-12029
LEWKOWSKI, B. E. .... p 309 N94-11995
LEXOW, B. .... p 106 N94-10111
p 107 N94-10116
LHEUREUX, JACQUES .... p 485 N94-12771
LI, C. P. .... p 10 N94-10463
LI, JIANHUA .... p 188 N94-11617
LI, JING .... p 101 N94-10081
LI, JUN .... p 214 N94-12675
LI, M. .... p 401 N94-11651

LI, SHANG S. p 404 N94-12375
LI, VICTOR C. p 73 N94-11686
LI, XIAO-RUI p 263 N94-11638
LI, XINZHOU p 427 N94-11692
LI, YONGXIANG p 206 N94-11990
LI, ZHANQING p 229 N94-10714
LIAO, B. C. p 101 N94-10080
LIBBY, P. A. p 79 N94-12403
LIBBY, S. I. p 383 N94-12416
LIBERATORE, STEPHEN p 289 N94-11854
LICHTENEGGER, J. p 246 N94-12478
LICKISS, REBECCA p 321 N94-10335
LIE, HEUNG-JAE p 216 N94-12689
LIEB, ROBERT J. p 97 N94-10489
LIEBERT, CURT H. p 170 N94-11310
LIFKA, D. p 319 N94-10318
p 419 N94-11105
LIGGIERI, LIBERO p 121 N94-10225
LIH, SHYH-SHIUH p 66 N94-10902
LILLELEHT, LEMBIT U. p 113 N94-10175
LILLIBRIDGE, JOHN p 244 N94-11784
LIM, E. C. p 263 N94-11116
LIMAT, L. p 121 N94-10229
LIME, STEPHEN D. p 231 N94-11521
LIMERO, T. F. p 318 N94-11553
LIMERO, THOMAS F. p 318 N94-11555
LIN-LIU, Y. R. p 385 N94-10159
LIN, CHI-YUAN p 215 N94-12684
LIN, QUAN p 36 N94-10680
LIN, R.-S. p 164 N94-12623
LIN, ROBERT P. p 428 N94-12770
LINCOLN, PATRICK p 326 N94-11188
LINDBERG, C. p 111 N94-10138
LINDEMUTH, I. R. p 384 N94-10158
LINNIK, A. F. p 391 N94-11211
LIPPMANN, S. I. p 393 N94-11514
LIPSCHUTZ, M. E. p 432 N94-12215
LIPSKIKH, S. I. p 409 N94-10394
LIPTAK, S. C. p 19 N94-10780
LIPTON, ALAN E. p 245 N94-11851
LISTON, G. E. p 284 N94-10940
LITAUDON, X. p 394 N94-12545
LITOVCHENKO, KONSTANTIN T. p 226 N94-12746
LITOVCHENKO, P. G. p 397 N94-10843
LIU, ANTONY K. p 240 N94-11757
p 197 N94-11935
LIU, CHO-TENG p 219 N94-12707
LIU, GENCHEN p 322 N94-10484
LIU, Q. S. p 105 N94-10101
p 120 N94-10218
LIU, W. TIMOTHY p 195 N94-11919
p 202 N94-11964
LIU, Y.-G. p 432 N94-12211
LIU, YONG p 339 N94-11289
LIU, ZHENG-YANG p 329 N94-11430
LIU, ZHI-SHEN p 192 N94-11901
p 203 N94-11970
LIU, ZHI-SHENG p 212 N94-12669
LIVINGSTONE, C. E. p 236 N94-11729
LJUL, A. YU. p 433 N94-12253
LOBANOV, V. B. p 224 N94-12737
LOBASHOV, A. A. p 380 N94-10605
LOCKE, JAMES E. p 26 N94-11858
LOCKOWANDT, CHRISTIAN p 109 N94-10128
LODDERS, K. p 477 N94-12246
LOEFFLER, F. J. p 373 N94-12600
LOESER, W. p 87 N94-10204
LOETH, K. p 109 N94-10128
LOFGREN, G. p 423 N94-11183
LOFGREN, GARY E. p 431 N94-12177
p 432 N94-12206
LOGAN, JAMES S. p 305 N94-11790
LOHOEFER, GEORG p 110 N94-10129
LOINTIER, MARC p 254 N94-12523
LOKEN, S. p 419 N94-11105
LOKOS, S. p 146 N94-12603
LOMBARDI, A. p 140 N94-10300
LONDON, R. A. p 175 N94-11266
LONG, R. p 221 N94-12719
LONGDON, NORMAN p 485 N94-11379
p 38 N94-11461
LOOMIS, G. E. p 90 N94-11230
LOPES-GAUTIER, R. M. C. p 282 N94-12116
LOPES, FABIO BELO p 325 N94-11178
p 333 N94-12358
LOPEZ-DIEZ, JESUS p 100 N94-10072
LORD, KENNETH R., II p 50 N94-11391
LORENA, LUIZ ANTONIO N. p 325 N94-11178
LOTT, GUS K. p 278 N94-11871
LOTZ-IWEN, HANS-JOACHIM p 214 N94-12677
LOUBRIEL, G. M. p 401 N94-11605
p 144 N94-11624
LOUIE, ALEXANDER W. p 1 N94-10936
LOURENCO, LUIZ M. p 16 N94-11869
LOVE, S. G. p 430 N94-12115
LOVE, WENDELL p 34 N94-10930
LOVOI, PAUL p 127 N94-10624
LOWDEN, D. W. p 61 N94-10038
LOWE, D. L., II p 89 N94-11175
LOWE, R. A. p 50 N94-11395
LOWE, ROLAND A. p 47 N94-11307
LOWNEY, P. G. p 333 N94-12439
LU, M. p 341 N94-10274
LU, YEU-CHERNG p 98 N94-10901
LUBJAKO, L. V. p 225 N94-12741
LUBOWINSKI, S. J. p 67 N94-11276
LUCCHITTA, B. K. p 458 N94-12144
LUCEY, P. G. p 446 N94-12079
LUCEY, PAUL G. p 430 N94-12162
p 431 N94-12164
LUCIABEZERRACANDEIAS, ANA p 345 N94-11193
LUCOVSKY, G. p 399 N94-11440
LUKEN, D. p 270 N94-12463
LUMLEY, D. E. p 150 N94-11026
LUMLEY, JOHN p 31 N94-11494
LUND, THOMAS S. p 155 N94-12285
p 155 N94-12286
LUNDQUIST, CHARLES A. p 108 N94-10120
LUNDSTROEM, A. p 107 N94-10113
p 110 N94-10130
LUNING, S. p 395 N94-10516
LUO, MING-XING p 373 N94-11618
LUONG, PHAM TRUNG p 196 N94-11928
LUPINSKI, JOHN H. p 19 N94-10781
LUSK, E. p 419 N94-11105
LUTES, GEORGE p 355 N94-10995
LYCZKOWSKI, R. W. p 150 N94-11072
LYELL, MARGARET J. p 110 N94-10131
LYNCH, JAMES p 289 N94-11854
LYNN, CHARLES p 337 N94-11829
LYNN, N. p 254 N94-12527
LYON, RICHARD p 22 N94-10796
LYONS, TIMOTHY P. p 309 N94-11996
LYONS, W. BERRY p 270 N94-12463
p 270 N94-12464
LYUBIMOV, D. V. p 101 N94-10082
LYUBIMOVA, TATIANA P. p 101 N94-10082
p 103 N94-10092

M

MA, C. H. p 173 N94-10160
MA, E. p 10 N94-10463
MA, JUN p 192 N94-11901
p 203 N94-11970
MA, M. Y. p 115 N94-10187
MA, OU p 181 N94-11156
MAA, SCOTT p 34 N94-10930
MACCHIAVELLO, C. p 376 N94-10572
MACDONALD, R. p 281 N94-12072
p 281 N94-12073
p 281 N94-12074
p 281 N94-12075
p 281 N94-12076
MACDONALD, S. A. p 145 N94-11819
MACDOUGALL, B. p 84 N94-11459
MACFARLANE, J. F. p 419 N94-11105
MACHIDA, S. p 335 N94-10340
MACKAMAN, JOHN R. p 44 N94-12541
MACKOWIAK, C. L. p 315 N94-11258
MACLEAN, BRIAN p 70 N94-11331
MACRET, J. L. p 64 N94-10062
MACZYNSKI, JACEK F. p 326 N94-11182
MADER, JOHN F. p 171 N94-12335
MAECHLING, C. R. p 431 N94-12167
MAEDA, H. p 400 N94-11458
MAEDA, KOREHIRO p 482 N94-12328
p 213 N94-12670
MAEDA, TOSHIHIDE p 482 N94-12327
MAEJIMA, HIRONORI p 213 N94-12670
MAEKAWA, H. p 159 N94-12310
MAGAL, M. I. p 364 N94-10848
MAGALHAESFARESSABA, MARCELO
p 276 N94-11165
MAHALE, N. p 374 N94-12785
MAHANTHAPPA, K. T. p 370 N94-12609
MAHAPATRA, KEDARNATH p 199 N94-11947
MAHMASSANI, HANI p 98 N94-10844
MAHMOOD, NIK NASRUDDIN p 36 N94-10685
MAHURIN, ERIC p 144 N94-11516
MAIDAN, RUBEN p 87 N94-10510
MAILHIOT, C. p 89 N94-11151
MAIN, W. p 145 N94-11645
MAJUMDAR, BHASKAR S. p 74 N94-12594
MAKALKIN, A. B. p 432 N94-12225
p 432 N94-12226
MAKASHIN, V. P. p 227 N94-12754
MAKEL, D. D. p 182 N94-12374
MAKHALDIANI, N. p 345 N94-11077
MAKINO, MITSUO p 13 N94-10855
p 13 N94-10856
MAKSIMENKO, NIKOLAY A. p 228 N94-12760
MALARET, E. R. p 54 N94-11643
MALETER, ANDREA p 306 N94-11794
MALIN, MICHAEL C. p 460 N94-12155
MALLAMACI, M. P. p 95 N94-12596
MALLET, M. p 10 N94-10464
MALLET, MICHEL p 5 N94-10440
MALMSTROEM, HENRIK p 110 N94-10132
MALVAR, L. J. p 35 N94-12562
MANDELKER, D. R. p 266 N94-11584
MANDELL, D. A. p 95 N94-12610
MANDELL, M. J. p 278 N94-11702
MANGLIK, V. K. p 61 N94-10037
MANHEIMER, W. M. p 145 N94-12424
MANKO, O. V. p 380 N94-10609
MANKO, V. I. p 375 N94-10564
p 350 N94-10600
p 380 N94-10610
MANN, C. A. p 317 N94-11528
MANN, I. p 123 N94-10236
MANNA, M. p 6 N94-10444
p 10 N94-10463
MANNE, S. p 399 N94-11268
MANNINEN, T. p 239 N94-11750
MANRIQUEZ, M. p 255 N94-12529
MANSLEY, J. A. D. p 237 N94-11738
MANSOUR, N. N. p 155 N94-12288
p 159 N94-12310
MANTRIPP, D. p 237 N94-11738
MANTRIPP, D. R. p 244 N94-11780
MANTRIPP, DAVID p 238 N94-11742
MARACHYKE, MICHAEL J. p 75 N94-10380
MARCHAL, C. p 31 N94-11495
MARCHETTI, M. p 58 N94-10015
MARCHUK, N. D. p 395 N94-10525
MARCIANO, W. J. p 410 N94-10528
MARCY, H. O. p 173 N94-10755
MARDASHKINA, NATALYA M. p 228 N94-12760
MARDER, A. R. p 84 N94-11816
MARDER, J. M. p 60 N94-10029
MARDESICH, NICK p 381 N94-10657
MAREDA, J. F. p 325 N94-11123
MAREK, RUDI p 101 N94-10079
p 106 N94-10107
MARENGONI, MAURICIO p 325 N94-11181
MARGHERI, G. p 110 N94-10133
MARINO, F. p 123 N94-10237
MARISKA, JOHN T. p 483 N94-12414
MARISSEN, R. p 60 N94-10034
p 88 N94-10877
MARK, LEO p 420 N94-11520
MARKOWITZ, SID E. p 331 N94-11679
MARMIGNON, C. p 8 N94-10455
MARQUARDT, J. p 374 N94-12786
MARQUART, GABRIELE p 243 N94-11776
MARRAFFA, L. p 7 N94-10448
MARSHALL, G. M. p 373 N94-12542
MARTADIWIRYA, SUHARSO p 196 N94-11927
MARTELL, JOHN S. p 139 N94-10996
MARTENS, DANIEL p 32 N94-11500
MARTENS, HANS p 375 N94-10569
MARTENS, STEVEN A. p 49 N94-11390
MARTIN, S. J. p 98 N94-11366
MARTIN, TERRY Z. p 456 N94-12134
MARTINEZ-SANCHEZ, M. p 279 N94-12572
MARTINEZ, A. p 255 N94-12529
MARTINEZ, I. p 102 N94-10083
p 102 N94-10085
MARTURUNKAKUL, S. p 93 N94-12380
MARTYNOV, A. V. p 229 N94-12765
MARTYNOV, E. S. p 362 N94-10551
p 362 N94-10554
MARUBAYASHI, K. p 201 N94-11959
MARUSHKEVICH, A. D. p 227 N94-12752
MARUYAMA, TSUYOSHI p 36 N94-10682
MARVIN, DEAN p 54 N94-11416
MARVIN, JOSEPH G. p 5 N94-10439
MARZOLI, IRENE p 376 N94-10578
MASAMUNE, S. p 392 N94-11239
MASCORRO, EDWARD p 187 N94-11190
MASHINSKY, A. L. p 103 N94-10092
MASHKEVICH, S. V. p 411 N94-10832
MASLANIK, J. p 241 N94-11761
MASON, G. R. p 373 N94-12542
MASON, KEVIN T. p 315 N94-11291
MASSA, DERCK p 428 N94-12595
MASSERANT, BRIAN J. p 142 N94-10931
MASSMANN, F.-H. p 243 N94-11774
p 243 N94-11778
MASSON, A. p 4 N94-10429
MASUDA, KAZUHIKO p 205 N94-11981
MASUDA, SHIGEAKI p 165 N94-12631
MASUKO, HARUNOBU p 130 N94-11837
p 253 N94-12520
MASUZAWA, HIDEO p 33 N94-10733
MATHIAS, L. J. p 94 N94-12381

MATHUR, ALOKE K. p 252 N94-12512
p 252 N94-12513
MATIOUKHIN, D. G. p 106 N94-10111
p 111 N94-10139
MATNEY, M. L. p 318 N94-11553
MATSUBARA, MASAHARU p 165 N94-12631
MATSUBARA, YOUICHI p 130 N94-11839
MATSUDA, SUMIO p 54 N94-11413
MATSUI, AKIHIKO p 82 N94-10732
MATSUI, TAKAYUKI p 364 N94-10889
MATSUI, TATSUYA p 164 N94-12618
MATSUMOTO, KOUTAROU p 33 N94-10733
MATSUMOTO, TAKESHI p 208 N94-12645
MATSUMOTO, TOSHIO p 130 N94-11838
MATSUMURA, SATSUKI p 211 N94-12658
MATSUSHIMA, KISA p 11 N94-10473
MATSUSHITA, TADASHI p 161 N94-12548
MATSUZAKI, YUUJI p 2 N94-10363
MATTERN, DUANE L. p 319 N94-10724
MATTHEWS, H. W. p 145 N94-11645
MATTHEWS, JOHN P. p 201 N94-11958
MATTIA, F. p 235 N94-11728
MATTISON, E. M. p 353 N94-10981
MATTOR, N. p 385 N94-10289
MATTSON, BENGT p 183 N94-11586
MATUKAWA, MOTOI p 190 N94-11082
MATUSKA, W. p 384 N94-10157
MAURETTE, M. p 432 N94-12233
MAUSER, W. p 245 N94-12472
p 248 N94-12491
MAX, N. p 334 N94-12591
MAXWELL, D. p 236 N94-11729
MAY, E. p 419 N94-11105
MAY, HOWARD p 311 N94-12364
MAYALL, SHERWOOD D. p 381 N94-10657
MAYER, H.-G. p 109 N94-10126
MAYER, S. T. p 140 N94-10309
MAYHALL, D. J. p 137 N94-11466
MAZUREK, W. p 89 N94-11107
MAZURKIEWICZ, M. p 82 N94-11008
MAZZITELLI, F. D. p 275 N94-10798
MCAFEE, J. B. p 97 N94-10294
MCBRIDE, K. p 440 N94-12050
MCBRIDE, S. L. p 71 N94-11337
MCCABE, D. E. p 184 N94-10155
MCCABE, MICKEY p 18 N94-10776
MCCANN, TIMOTHY A. p 381 N94-10657
MCCARTHY, I. E. p 359 N94-10311
p 360 N94-10330
p 360 N94-10331
MCCARVILLE, P. p 282 N94-12188
MCCLUNG, R. C. p 85 N94-12426
MCCLUSKEY, PHILIP p 92 N94-11876
MCCOMAS, D. J. p 275 N94-10742
MCCOY, T. J. p 281 N94-12083
p 430 N94-12142
MCCRACKEN, R. W. p 174 N94-11126
MCCREARY, JULIA p 330 N94-11436
MCCURLEY, K. S. p 336 N94-10738
MCDONACH, A. p 69 N94-11325
MCDONALD, E. p 273 N94-10285
MCELLISTREM, M. p 402 N94-11684
MCELROY, MICHAEL B. p 434 N94-10823
MCFADDEN, G. B. p 105 N94-10103
p 113 N94-10178
MCFADDEN, L. p 273 N94-10285
MCGAREL, W. p 56 N94-10006
MCGARRY, FRANK E. p 328 N94-11423
MCGHEE, J. M. p 372 N94-10890
MCGRATH, JAMES E. p 19 N94-10780
MCHUGH, C. A. p 34 N94-10894
MCHUGH, K. M. p 163 N94-12604
MCILWAIN, R. L. p 373 N94-12600
MCKAY, D. S. p 436 N94-12024
p 440 N94-12050
MCKAY, K. K. p 143 N94-11160
MCKERNAN, S. p 88 N94-10527
MCKIBBON, A. H. p 179 N94-10400
MCKINNEY, L. WAYNE p 34 N94-11869
MCKINNON, WILLIAM B. p 436 N94-12023
p 429 N94-12057
MCLAREN, N. R. p 139 N94-11906
MCLAUGHLIN, D. L. p 401 N94-11605
MCLEAN, WILLIAM E. p 315 N94-11291
MCMAHAN, A. K. p 89 N94-11151
MCMANUS, JAMES C. p 331 N94-11679
MCMINN, TED p 381 N94-11054
MCMULLAN, R. K. p 394 N94-10301
MCNABB, JACK p 353 N94-10978
MCNAMARA, M. COLLEEN p 309 N94-11996
MCNEIL, M. A. p 416 N94-11473
MCNIDER, RICHARD T. p 285 N94-11598
MCNUTT, MARCIA p 278 N94-11886
MCPHADEN, MICHAEL J. p 193 N94-11911
MCPHAIL, ANDREW T. p 78 N94-11683
MCPHEE, NEIL p 289 N94-11853
MCPHERSON, ALEXANDER p 117 N94-10198
MCPHERSON, J. p 230 N94-10954
MCSWEEN, HARRY Y., JR. p 429 N94-12061
p 430 N94-12114
MCWILLIAMS, J. C. p 393 N94-11669
MEADE, PERRY p 35 N94-11535
MEASURES, RAYMOND M. p 69 N94-11327
MECARTNEY, MARTHA L. p 90 N94-11281
MEGELA, I. G. p 397 N94-10843
p 397 N94-10845
MEHRAFARIN, M. p 409 N94-10388
MEHTA, N. S. p 249 N94-12492
MEHTA, R. L. p 249 N94-12492
MEIER, ERICH p 247 N94-12482
MEIROVITCH, LEONARD p 44 N94-12387
MEISEL, L. V. p 347 N94-12390
MEJDANI, R. p 395 N94-10411
p 410 N94-10631
MELE, F. p 113 N94-10175
MELEK, M. p 425 N94-11136
MELLOH, R. A. p 254 N94-12528
MELNIKOV, V. K. p 365 N94-11078
MELOSH, H. J. p 429 N94-12036
MENDENHALL, MICHAEL R. p 3 N94-10427
MENEZES, D. P. p 349 N94-10633
MENG, CHING I. p 278 N94-11828
MENG, YANG p 165 N94-12624
MENNELLA, V. p 113 N94-10175
MENSAH, S. Y. p 357 N94-10408
p 142 N94-10799
MERCER, CAROLYN R. p 174 N94-11132
MERCHANT, G. J. p 115 N94-10188
MERKLE, J. G. p 184 N94-10288
MERKLE, K. L. p 363 N94-10750
MERRELL, RONALD C. p 305 N94-11790
p 306 N94-11795
MERRICK, R. A. p 112 N94-10174
MERTE, H. p 122 N94-10232
MESHCHERSKAYA, V. A. p 282 N94-12123
MESHCHERYAKOV, D. V. p 361 N94-10532
MESHCHERYAKOV, V. A. p 361 N94-10532
MESHKOV, S. p 370 N94-12787
MESSENGER, S. R. p 48 N94-11382
p 52 N94-11404
METIU, H. p 413 N94-11877
METIU, HORIA p 366 N94-11100
METS, G. J. p 244 N94-11779
METZ, DENNIS p 75 N94-10337
METZGER, MARIE E. p 485 N94-10356
METZNER, MARGITTA p 242 N94-11766
MEULENBERG, A. p 53 N94-11408
p 54 N94-11417
MEVREL, R. p 59 N94-10024
MEYER, OLAF p 56 N94-10002
MEYER, P. J. p 419 N94-10723
MEYER, PETER p 485 N94-12771
MEYERSON, GENICK p 148 N94-10391
MEYWERK, JENS p 252 N94-12514
MIAKE-LYE, R. C. p 279 N94-12572
MICHAELS, G. p 454 N94-12120
MICHALICKA, L. p 263 N94-11505
p 263 N94-11506
MICHALSKI, T. p 80 N94-10228
MICHIE, CRAIG p 65 N94-10066
MICHIE, W. CRAIG p 69 N94-11324
MICKALONIS, J. I. p 83 N94-11250
MIELE, G. p 412 N94-11047
MIKHAIL, F. I. p 427 N94-11812
MILEY, G. H. p 393 N94-11512
p 393 N94-11513
MILIOZZI, A. p 58 N94-10015
MILLER, CHARLES G. p 5 N94-10435
MILLER, D. H. p 373 N94-12600
MILLER, EDWARD F. p 306 N94-11796
MILLER, GEORGE P. p 279 N94-12581
MILLER, H. p 237 N94-11737
MILLER, J. T. p 420 N94-11369
MILLER, NEAL E. p 311 N94-12006
MILLER, ROBERT N. p 209 N94-12648
MILLER, SHARON E. p 329 N94-11427
MILLER, W. O. p 65 N94-10740
MILLINGTON, A. C. p 246 N94-12474
MILOVICH, J. p 385 N94-10262
MILOVICH, J. L. p 385 N94-10289
MIN, J. B. p 188 N94-11275
MINAMI, S. p 34 N94-11041
MINDERHOUD, P. p 63 N94-10051
MINEGISHI, MASAKATSU p 2 N94-10363
MINNETT, P. p 239 N94-11752
MINNETT, P. J. p 287 N94-10517
MINSTER, J.-F. p 242 N94-11769
MIRANSKIJ, V. A. p 409 N94-10405
MIRONENKO, M. V. p 432 N94-12226
MIROSHNICHENKO, G. A. p 362 N94-10649
p 392 N94-11213
MIROSHNICHENKO, V. I. p 391 N94-11209
MISENCIK, TOM p 348 N94-11572
MISRA, AJAY K. p 66 N94-11202
MISRA, M. S. p 50 N94-11393
MISRA, MOHAN S. p 70 N94-11331
MITANI, TOORU p 27 N94-10367
MITCHELL, CHRISTINE M. p 320 N94-12558
MITCHELL, G. W. p 45 N94-10282
MITCHELL, S. A. p 334 N94-12593
MITNIK, L. M. p 225 N94-12740
p 225 N94-12743
MITNIK, M. L. p 225 N94-12740
p 225 N94-12743
MITSUYASU, H. p 201 N94-11959
MITTELMANN, H. D. p 112 N94-10172
MITTY, TODD JAY p 149 N94-10824
MIURA, YUUICHI p 199 N94-11943
MIYAGI, T. p 34 N94-11041
p 367 N94-11509
MIYAJIMA, HIROSHI p 27 N94-10367
MIYAZAKI, YOSHIROU p 129 N94-11834
MIZUNO, K. p 389 N94-11114
MIZUNO, SHINJIROU p 194 N94-11913
p 194 N94-11914
MIZUTORI, MASAFUMI p 220 N94-12714
MOCCIA, A. p 235 N94-11728
MOCHIZUKI, SHINSUKE p 165 N94-12627
MODDEMEIJER, RUDY p 419 N94-10903
MODEN, JAMES R. p 140 N94-10390
MOELLER, C. P. p 137 N94-11453
MOELLER, ROBERT P. p 176 N94-12329
MOELLER, UWE p 114 N94-10184
MOFFAT, H. K. p 152 N94-11371
MOFFETT, RAYMOND J. p 321 N94-10335
MOGILEVSKIJ, O. A. p 397 N94-10883
MOHAMED, B. F. p 386 N94-10387
MOHAMED, DARWISH A. p 138 N94-12281
MOHAMMEDI, N. p 275 N94-10798
MOHAN, S. p 249 N94-12492
MOHAPATRA, R. N. p 410 N94-10545
MOHLER, R. R. p 25 N94-10344
MOIN, PARVIZ p 155 N94-12285
p 156 N94-12296
MOISEYEV, V. M. p 229 N94-12765
MOLINA, R. C. p 9 N94-10461
MONTANARI, ALESSANDRO p 282 N94-12161
MONTI, RODOLFO p 102 N94-10087
p 39 N94-10134
MONTIGUARNIERI, A. p 237 N94-11735
MOORE, DOUG p 27 N94-11347
MOORE, JAMES S. p 38 N94-11566
MOORE, JOHN THOMAS p 137 N94-11639
MOORE, K. R. p 275 N94-10742
MOORE, P. p 234 N94-11716
MOORE, ROBERT C. p 324 N94-11104
MOORE, THOMAS R. p 383 N94-12389
MOORHOUSE, DAVID J. p 32 N94-11497
MOOY, THOMAS p 128 N94-10628
MORACZ, D. J. p 82 N94-10804
MORALES, A. R. p 93 N94-12340
MORANO, ERIC p 345 N94-11277
MORARI, M. p 336 N94-11027
MORCRETTE, J. J. p 276 N94-11241
MORDEN, S. J. p 431 N94-12172
MOREAU, D. p 394 N94-12545
MOREL, ANDRE p 203 N94-11971
MOREL, J. E. p 372 N94-10890
MORETON, R. p 58 N94-10022
MORGAN, K. p 9 N94-10461
MORI, NOBORU p 11 N94-10472
MORIMATSU, HIDEHARU p 172 N94-11916
MORIMOTO, T. p 144 N94-11508
MORINAGA, KENJI p 198 N94-11937
MORIYAMA, TAKASHI p 130 N94-11835
MORLEY, J. G. p 237 N94-11738
MORLEY, R. p 273 N94-10285
MORREN, SYBIL HUANG p 47 N94-11252
MORRIS, BRIAN G. p 179 N94-10655
p 179 N94-10658
p 179 N94-10674
MORRIS, D. p 356 N94-10998
MORRIS, MICHAEL A. p 320 N94-11875
MORRIS, R. V. p 436 N94-12024
MORRIS, RANDY B. p 317 N94-11537
MORRIS, RICHARD V. p 281 N94-12055
MORRISON, DONALD A. p 474 N94-12229
MORRISON, MICHAEL C. p 268 N94-12455
MORRISON, MICHAEL COPE p 267 N94-12452
MORROW, DENNIS p 288 N94-11358
MORROW, ROSEMARY p 208 N94-12642
p 208 N94-12643
MORSE, JAMES S. p 29 N94-12274
MORTENSEN, H. BUCH p 239 N94-11752
MOSCATI, NEY RICARDO p 44 N94-12356
MOSER, M. D. p 152 N94-11526
MOSER, R. D. p 159 N94-12310
MOSES, HARRY p 301 N94-11583

MOSES, W. W. p 371 N94-10156
MOSS, CALVIN p 45 N94-11323
p 172 N94-12038
MOSS, FRANK p 313 N94-11890
MOSS, JAMES N. p 7 N94-10449
MOSS, W. C. p 98 N94-10751
MOSS, W. D. p 272 N94-12780
MOSSAVATI, R. p 176 N94-10982
MOSTEPANENKO, V. M. p 380 N94-10605
MOSTERDIJK, W. H. p 143 N94-11298
MOTOHASHI, TATSUO p 165 N94-12629
MOTOWIDLO, L. R. p 142 N94-10951
p 398 N94-11073
MOU, ZONGZE p 343 N94-10546
MOUGINIS-MARK, PETER p 460 N94-12154
MOULTON, BRYAN p 3 N94-10427
MOUROU, GERALD p 173 N94-10371
MOWRER, FREDERICK W. p 21 N94-10793
MOXSON, V. S. p 82 N94-10804
MOYNOT, B. p 243 N94-11778
MUEHLRATZER, A. p 61 N94-10043
MUELLER-WIESNER, D. p 56 N94-10004
MUELLER, DIETRICH p 485 N94-12771
MUELLER, GEORG p 100 N94-10073
p 103 N94-10089
MUELLER, R. p 124 N94-10246
MUELLER, ROBERT L. p 50 N94-11392
MUELLER, STEFAN C. p 121 N94-10227
MUELLER, THOMAS p 46 N94-10938
MUKAI, SONOYO p 200 N94-11949
p 205 N94-11978
MUKAIDA, AKIRA p 207 N94-12639
MULCAHY, T. M. p 144 N94-11607
MULHERIN, NATHAN D. p 29 N94-12274
MULVAGH, SHARON L. p 309 N94-11993
MUNAKATA, H. p 411 N94-10880
MUNDARAIN, D. p 377 N94-10586
MUNEYAMA, KEI p 193 N94-11911
MUNEYAMA, KEI p 199 N94-11945
p 140 N94-11965
p 208 N94-12640
MUNGAL, M. G. p 159 N94-12312
MUNK, J. p 89 N94-11145
MUNSON, H. E. p 82 N94-10804
MURALIKRISHNA, I. V. p 204 N94-11973
MURASE, TAKEO p 163 N94-12613
MURATA, YOSHIKAZU p 172 N94-11968
MURATOV, L. F. p 225 N94-12739
MURAYAMA, NOBUYOSHI p 165 N94-12624
MURPHY, D. P. p 382 N94-11656
MURPHY, D. W. p 400 N94-11457
MURRAY, B. C. p 443 N94-12064
MURRAY, BRUCE T. p 105 N94-10103
p 113 N94-10178
MURRAY, C. p 48 N94-11372
MURRAY, GEORGIA L. p 270 N94-12465
MURRAY, HUGH S. p 45 N94-11323
MURRAY, J. p 319 N94-10146
MURRAY, JAMES A. p 352 N94-10973
MURTHY, P. L. N. p 186 N94-10762
MURTHY, SUNIL KESHAVA p 40 N94-11637
MURTY, C. S. p 193 N94-11912
MURTY, HEMA SANDHYARANI p 2 N94-10357
p 15 N94-11857
MURTY, T. V. RAMANA p 193 N94-11912
MUSAZZI, SERGIO p 111 N94-10135
MUSGRAVE, JEFFREY L. p 319 N94-10724
MUSSELWHITE, DONALD p 473 N94-12228
MUSTARD, JOHN F. p 424 N94-12053
MYAKININ, V. A. p 136 N94-11069
MYASNIKOV, YEGENY V. p 177 N94-12722
MYATT, JAMES H. p 32 N94-11499
MYERS, D. R. p 396 N94-10809
MYERS, ROGER M. p 47 N94-11252
MYHILL, E. A. p 448 N94-12090
MYZNIKOV, V. p 120 N94-10220

N

NABOT, J. P. p 114 N94-10180
NADAI, AKITSUGU p 139 N94-11902
p 139 N94-11905
NAEGLE, J. H. p 325 N94-11109
NAEIJE, M. C. p 242 N94-11772
NAEYMI-RAD, FRANK p 306 N94-11797
NAGAE, T. p 34 N94-11041
p 367 N94-11509
NAGAME, YUICHIRO p 372 N94-11043
NAGAO, MASASHI p 130 N94-11841
NAGAO, MASAYUKI p 193 N94-11908
NAGATA, A. p 390 N94-11128
p 392 N94-11239
NAGATA, HIROSHI p 17 N94-12633
NAGATSU, M. p 392 N94-11239
NAGLER, TH. p 247 N94-12481
NAGPAL, V. K. p 185 N94-10361
NAGUCHEV, O. Y. p 387 N94-10558
NAGURNEY, DON p 330 N94-11437
NAGY, P. B. p 183 N94-11110
NAIK, R. A. p 67 N94-11276
NAIM, A. p 10 N94-10464
NAKA, MASAO p 193 N94-11909
p 220 N94-12713
NAKAGAWA, YOSHITAKA p 169 N94-11944
NAKAGAWARA, VAN B. p 303 N94-10813
NAKAGOME, HIDEKI p 130 N94-11842
NAKAI, MASAO p 253 N94-12520
NAKAJIMA, ATSUSHI p 42 N94-10366
p 43 N94-10859
NAKAJIMA, HAJIME p 84 N94-11593
NAKAJIMA, HIDEO p 194 N94-11913
NAKAJIMA, TERUYUKI p 204 N94-11977
NAKAMICHI, JIRO p 11 N94-10476
p 12 N94-10482
NAKAMOTO, S. p 199 N94-11945
NAKAMURA, A. p 392 N94-11239
NAKAMURA, AKIKO M. p 189 N94-12359
NAKAMURA, KENJI p 201 N94-11954
p 253 N94-12520
NAKAMURA, KINUYO p 335 N94-10368
NAKAMURA, SHIGEHISA p 215 N94-12685
NAKAMURA, SHIN p 105 N94-10102
NAKAMURA, T. p 112 N94-10142
NAKAMURA, TATSUSABUROU p 162 N94-12555
NAKAMURA, TOSHIAKI p 172 N94-11916
NAKAMURA, YOSHIAKI p 10 N94-10468
NAKANE, TOORU p 210 N94-12656
NAKANO, H. p 203 N94-11969
NAKASHIKI, NORIKAZU p 220 N94-12714
NAKATA, K. p 200 N94-11948
NAKATA, KISABUROU p 210 N94-12656
NAKAYA, TERUOMI p 2 N94-10350
NAKAZAWA, TETSUO p 202 N94-11963
NAMKOONG, DAVID p 163 N94-12576
NARAYANAN, M. S. p 234 N94-11719
NASEEM, A. p 153 N94-11604
NASH, T. J. p 173 N94-10746
NASRTO, ALFONSO p 124 N94-10245
NATH, A. NARENDRA p 193 N94-11907
NATIELLO, THOMAS A. p 306 N94-11798
NAUENBERG, U. p 370 N94-12609
NAUMKIN, JU. V. p 226 N94-12749
NAUTA, JANET p 417 N94-11856
NAVROTSKY, V. V. p 229 N94-12763
NAYFEH, ADNAN H. p 74 N94-12401
NAYLER, G. H. F. p 62 N94-10050
NAZRI, GHOLAM A. p 395 N94-10416
NEAL, D. R. p 175 N94-11283
NEALY, JOHN E. p 484 N94-11278
NEAR, C. D. p 139 N94-10991
NECHITAILO, G. S. p 103 N94-10092
NEDOVBA, V. I. p 386 N94-10524
NEDZWETSKIJ, A. V. p 398 N94-11025
NEGISHI, SATORU p 139 N94-11917
NEITZEL, G. P. p 112 N94-10172
NELLIS, W. J. p 81 N94-12258
NELSON, P. A. p 345 N94-11217
NELSON, R. A. p 351 N94-10970
p 351 N94-10971
NEMOV, V. V. p 389 N94-11091
NEPOMNYASHCHY, ALEXANDER A.
p 121 N94-10223
NEREM, R. STEVEN p 444 N94-12065
p 481 N94-12267
p 481 N94-12268
NESSETT, D. M. p 335 N94-10324
NESTHUS, THOMAS E. p 314 N94-11533
NEUHAUSEN, T. p 111 N94-10138
NEUKUM, G. p 446 N94-12079
NEUKUM, GERHARD p 459 N94-12147
p 471 N94-12213
NEUMANN, R. D. p 5 N94-10438
NEVINS, W. M. p 385 N94-10289
NEWAZ, GOLAM M. p 74 N94-12594
NEWBY, M. J. p 183 N94-10170
NEWMAN, C. E. p 177 N94-10322
NEWTON, N. J. p 332 N94-11878
NGUYEN, GAM D. p 337 N94-11475
NICHOLS, FRED A. p 182 N94-11625
NICHOLSON, P. D. p 483 N94-10949
NICOGOSSIAN, ARNAULD E. p 305 N94-11790
NICOLLE, M. A. p 119 N94-10210
NICOUT, D. p 4 N94-10429
NIEDERMANN, S. p 87 N94-12240
NIEDRA, JANIS M. p 140 N94-10505
NIENN, ROBERT E. p 87 N94-10508
NIER, A. O. p 430 N94-12115
NIESERT, C. P. p 145 N94-11819
NIETO, MICHAEL MARTIN p 378 N94-10591
NIEUWENHUIS, G. J. A. p 246 N94-12473
NIGG, D. W. p 365 N94-10952
NIILER, PEARN P. p 216 N94-12691
NIJMEIJER, HENK p 341 N94-10276
NIKITIN, S. A. p 102 N94-10087
p 104 N94-10099
NIKOGOSSIAN, HAIK A. p 305 N94-11790
NIKOLOVA, I. PETROVA p 124 N94-10244
NIKONOV, D. E. p 376 N94-10571
NILSSON, C. S. p 234 N94-11717
NISHI, KATSUYA p 213 N94-12672
NISHIHARA, H. KEITH p 418 N94-10515
NISHIIZUMI, K. p 437 N94-12033
NISHIKAWA, NOBUHIDE p 11 N94-10472
NISHIMOTO, A. p 203 N94-11967
NISHIMURA, HIDEAKI p 343 N94-10729
NISHIMURA, KATSUTOSHI p 215 N94-12680
NISHIMURA, MAKOTO p 82 N94-10732
p 66 N94-10858
NISHIMURA, TSUKASA p 198 N94-11940
p 214 N94-12676
NISHIO, FUMIHIKO p 210 N94-12654
NISHIOKA, MICHIO p 16 N94-12621
NISHITSUJI, AKIRA p 212 N94-12665
NISHIYAMA, YUTAKA p 183 N94-11168
NISSIM, E. p 33 N94-12769
NITSCHE, K. p 107 N94-10114
p 109 N94-10124
NOAK, MAX p 49 N94-11390
NOBUNAGA, B. N. p 181 N94-11290
NODA, JUNICHI p 2 N94-10363
NODA, TADAHIKO p 217 N94-12694
NOE, J. W. p 140 N94-10300
NOEVER, DAVID A. p 122 N94-10235
NOGUCHI, SUGURU p 130 N94-11837
NOGUCHI, YOSHIO p 65 N94-10857
NOGUTI, MASAYOSHI p 2 N94-10350
NOJIRI, SHIN-ICHI p 411 N94-10887
NOLAN, M. C. p 429 N94-12092
NOLL, THOMAS E. p 27 N94-11341
NOMURA, TAMIYA p 37 N94-10694
NONAKA, OSAMU p 2 N94-10350
NONTASAK, TATREE p 313 N94-11098
NOOMEN, R. p 244 N94-11779
NOONAN, CAROLINE H. p 330 N94-11432
NORFLEET, W. T. p 312 N94-11544
NORFLEET, WILLIAM T. p 125 N94-11235
NORMAN, JOHN M. p 302 N94-12559
NORMAN, M. D. p 282 N94-12197
NOSAKA, MASATAKA p 178 N94-10369
NOUSEK, JOHN A. p 424 N94-12574
NOVIKOV, E. A. p 155 N94-12286
NOWIK, I. p 75 N94-10338
NOYES, H. P. p 411 N94-10956
NOZ, MARILYN E. p 379 N94-10604
NUEESCH, DANIEL p 247 N94-12482
NUSINOVICH, G. S. p 145 N94-11645
NUTH, J. p 113 N94-10175
NYDEN, MARC R. p 19 N94-10779
NYKJAER, LEO p 220 N94-12712
NYMAN, JANICE p 421 N94-11575

O

OAKES, CHARLES STEGER p 76 N94-11244
OANH, NGUYEN LAN p 412 N94-11163
OBAL, MICHAEL p 45 N94-11319
p 45 N94-11323
OBENHUBER, DONALD C. p 301 N94-11201
OBERKAMPF, WILLIAM L. p 6 N94-10445
OBRANT, G. Z. p 365 N94-11089
OBRIEN, B. p 58 N94-10021
OBRIEN, JAMES J. p 194 N94-11918
OBRIEN, KEVIN p 314 N94-11531
OCHELTREE, S. L. p 4 N94-10433
OCHI, HIROSHI p 139 N94-11917
OCHIAI, J. p 107 N94-10115
p 114 N94-10179
OCHIAI, SATOSHI p 130 N94-11837
p 253 N94-12520
OCONNELL, R. F. p 370 N94-10584
ODA, T. p 393 N94-11594
ODONNELL, MICHAEL D. p 17 N94-10769
OESTMAN, ERIK p 183 N94-11586
OESTREICH, JOHN p 128 N94-10627
OFFRINGA, ARNT R. p 60 N94-10033
OGAWA, S. p 219 N94-12705
OGAWA, SATORU p 27 N94-10370
p 12 N94-10479
OGDEN, T. G. p 152 N94-11448
OGINO, JUN p 11 N94-10474
p 12 N94-10481
OHANDLEY, CHRISTOPHER p 284 N94-10822
OHARA, H. p 219 N94-12705
OHARA, TIMOTHY J. p 94 N94-12425
OHERN, T. J. p 98 N94-11366
OHMI, MASAO p 84 N94-11593

OIKE, MAMORU p 178 N94-10369
OIRY, H. p 199 N94-11946
OKADA, KOUZOU p 217 N94-12694
p 221 N94-12715
OKADA, RYOUTA p 169 N94-11944
OKADA, Y. p 196 N94-11925
p 222 N94-12721
OKADA, YOSHIHIRO p 199 N94-11947
OKAMOTO, A. p 140 N94-12706
OKAMOTO, KATSUO p 212 N94-12668
OKAMOTO, KENICHI p 253 N94-12520
OKASAKA, R. p 393 N94-11594
OKBEL-BAB, A. S. p 342 N94-10325
OKUBO, AKIRA p 221 N94-12718
OKUDAIRA, TOSHIAKI p 130 N94-11840
OKUDE, MUNESHIGE p 164 N94-12618
OKUYAMA, MASAHIRO p 13 N94-10855
p 13 N94-10856
OLBRIGHT, G. R. p 383 N94-12416
OLDENBURG, JOHN R. p 174 N94-11132
OLIN, A. p 373 N94-12542
OLIVIER, H. p 4 N94-10430
OLLENDORF, STANFORD p 45 N94-11579
OLSEN, GREGORY H. p 401 N94-11476
OLSEN, LARRY C. p 52 N94-11405
p 53 N94-11407
OLSEN, RICHARD p 253 N94-12522
OLSON, J. M. p 54 N94-11418
OLSON, ROBERT M. p 317 N94-11540
p 312 N94-11543
OLSSON, PELLE p 346 N94-12776
OMALLEY, B. T. p 272 N94-12780
OMALLEY, M. W. p 401 N94-11605
ONEILL, MARK J. p 52 N94-11402
ONEILL, PATRICK M. p 45 N94-11559
ONG, L. p 157 N94-12303
ONISHCHENKO, I. N. p 391 N94-11210
p 391 N94-11211
ONOFRIO, ROBERTO p 378 N94-10587
ONSTOTT, R. G. p 239 N94-11748
ONSTOTT, ROBERT G. p 240 N94-11754
OOGUSHI, TETSUROU p 162 N94-12553
OOIDA, KIYOSHI p 38 N94-10695
OONARI, HIROFUMI p 165 N94-12628
OONISHI, SOTOAKI p 212 N94-12664
OONO, YUUICHI p 139 N94-11902
p 192 N94-11904
OONUMA, KAZUHIKO p 191 N94-11897
OOSAKA, HIDEO p 165 N94-12626
p 165 N94-12627
OOTA, JUNICHI p 162 N94-12552
OOTA, KAZUO p 482 N94-12324
p 482 N94-12325
p 482 N94-12327
p 482 N94-12328
OOTANI, HIDEO p 169 N94-11944
OPAT, G. I. p 409 N94-10501
ORASANU, JUDITH p 314 N94-11532
ORGILL, MONTIE M. p 286 N94-12539
ORLOV, VLADIMIR M. p 225 N94-12738
ORMBREK, GLENN p 45 N94-11319
ORME, JOHN S. p 28 N94-11205
ORMESHER, R. C. p 334 N94-12608
ORNELLAS, D. p 77 N94-11602
ORON, ALXANDER p 152 N94-11376
ORRELL, S. p 419 N94-11137
ORTIZ, ALBERTO p 333 N94-12008
OSBORNE, WILLIAM p 42 N94-11297
OSHER, STANLEY p 331 N94-11657
OSHIMA, MASUMI p 372 N94-11043
OSILIKE, M. O. p 343 N94-10531
OSINGA, H. M. p 344 N94-10907
OSTAPCHUK, P. N. p 83 N94-11363
OSTASHKO, V. V. p 372 N94-10849
OSTEEN, B. L. p 285 N94-11614
OSTERHELD, A. L. p 389 N94-11074
OSTERMAN, DAVID p 145 N94-12333
OSTERTAG, R. p 61 N94-10041
OSTROVSKII, ALEXANDER G. p 205 N94-11984
OSTROVSKIJ, A. O. p 141 N94-10543
p 133 N94-11030
p 143 N94-11365
OTOBE, HIROTAKA p 195 N94-11924
OUAZZANI, JALIL p 114 N94-10183
OVERMYER, D. L. p 400 N94-11457
OWEN, A. D. p 337 N94-11829
OWEN, MARTHA R. p 23 N94-11103
OWEN, TOBY p 473 N94-12228
OWENS, R. W. p 309 N94-11995
OWENS, SHELBY L. p 38 N94-11566
OZER, A. p 254 N94-12524
OZMIDOV, ROSTISLAV V. p 228 N94-12759
OZORES, E. p 62 N94-10047

P

PACIESAS, WILLIAM S. p 483 N94-12427
PACQUETTE, STEVEN P. p 315 N94-11291
PADDAY, JOHN F. p 100 N94-10071
PADEN, JACK p 286 N94-12772
PADULA, SHARON L. p 318 N94-10814
PAETTIKANGAS, T. p 390 N94-11148
PAETZ, B. p 111 N94-10138
PAGE, D. E. p 482 N94-10741
PAGE, R. H. p 76 N94-11075
PAI, SU-CHENG p 219 N94-12707
PAIRMAN, D. p 214 N94-12679
PAL, S. p 152 N94-11526
PALASZEWSKI, BRYAN A. p 40 N94-10811
PALFREY, T. R. p 373 N94-12600
PALLASCHKE, SIEGMAR p 485 N94-11379
PALME, H. p 87 N94-12086
p 429 N94-12101
p 432 N94-12231
PALMER, JODY HUPTON p 413 N94-11821
PAMPALONI, C. p 217 N94-12695
PAMPERIN, OLAF p 103 N94-10091
PANDEY, DHIRENDRA K. p 286 N94-12772
PANDEY, LAKSHMI N. p 380 N94-10606
p 380 N94-10611
PANG, YANG p 359 N94-10303
PANIN, ALEXANDER M. p 176 N94-12382
PANTALEONE, J. p 483 N94-11619
PANTALONI, J. p 102 N94-10086
PANTELAKIS, S. p 59 N94-10023
PAOLICCHI, P. p 431 N94-12201
PAORICI, CARLO p 115 N94-10191
PAPADOPOULOS, DEMETRIOS S. p 74 N94-12431
PAPADOS, PHOTIOS p 187 N94-11190
PAPANASTASSIOU, D. A. p 430 N94-12151
p 431 N94-12182
PAPIKE, J. J. p 282 N94-12104
p 429 N94-12105
p 429 N94-12106
PAPKOVICH, V. G. p 133 N94-11034
p 134 N94-11035
p 345 N94-11036
PAPP, ALBERT L., III p 321 N94-10291
PARAYRE, C. p 108 N94-10122
PARDHANANI, ANAND L. p 154 N94-11824
PARFITT, ELISABETH p 283 N94-12236
PARIS, M. p 376 N94-10572
PARK, J. K. p 343 N94-10708
p 344 N94-10961
p 334 N94-12593
PARK, JENNIFER p 136 N94-11158
PARK, K. C. p 331 N94-11522
PARK, KWANGJAI p 280 N94-12582
PARKER, J. M. p 387 N94-10737
PARKER, M. A. p 383 N94-12416
PARKINSON, CLAIRE L. p 210 N94-12651
PARMA, E. J. p 371 N94-10529
PARMIGGIANI, F. p 238 N94-11746
PARNELL, L. A. p 152 N94-11448
PASCH, HANS p 131 N94-10280
PASHNEV, A. I. p 412 N94-11087
p 412 N94-11164
PASHNEV, V. K. p 389 N94-11092
PASSERONE, ALBERTO p 121 N94-10225
PASTERNAK, A. F. p 227 N94-12756
PASTERNAK, F. p 212 N94-12667
PATEL, PARUL p 249 N94-12492
PATSAYEVA, SVETLANA V. p 177 N94-12755
PATTERSON, JAMES C., JR. p 12 N94-10673
PATTERSON, JAMES D. p 397 N94-10819
PATTERSON, WILLIAM p 445 N94-12071
PATWARDHAN, A. p 309 N94-11997
PAUDYAL, D. p 246 N94-12478
PAUL, A. K. p 275 N94-11101
PAUL, DONALD R. p 91 N94-11830
PAUL, P. p 140 N94-10300
PAULSON, DOUGLAS N. p 304 N94-11449
PAVESE, PIERO p 233 N94-11713
PAVLAKOS, C. p 325 N94-11109
PAVLENKO, E. A. p 364 N94-10835
PAVLENKO, N. G. p 362 N94-10649
p 392 N94-11213
PAVLENKO, O. P. p 388 N94-10882
PAVLICHENKO, R. O. p 66 N94-11143
PAVLOVSKY, D. S. p 102 N94-10087
p 104 N94-10099
PAXSON, DANIEL E. p 29 N94-11255
PAZ, ROBERT p 42 N94-11297
PEACE, A. J. p 154 N94-11859
p 16 N94-11888
p 161 N94-12437
PEAL, KENNETH p 289 N94-11854
PEARSON, JACQUELYN Y. p 418 N94-10491
PEASE, R. F. p 145 N94-12405
PECHACEK, R. E. p 362 N94-11656
PEDERSEN, L. TOUDAL p 239 N94-11752
PEEL, C. J. p 58 N94-10022
PEETZ, K. p 61 N94-10043
PEGG, D. J. p 358 N94-10154
PEIRO, J. p 9 N94-10461
PEKALA, R. W. p 140 N94-10309
PELEVIN, VADIM N. p 228 N94-12761
PELLETIER, RAMONA E. p 269 N94-12457
PELTIER, J. F. p 59 N94-10024
PELTONEN, P. p 60 N94-10035
PENDLEY, REX D. p 330 N94-11432
PENDUS, A. I. p 63 N94-10051
PENETRANTE, B. M. p 175 N94-11266
PENG, CHIH Y. p 240 N94-11757
p 197 N94-11935
PEPIN, R. O. p 80 N94-12051
PEPPER, L. J. p 312 N94-11552
PERAELAE, J. p 247 N94-12483
PERAIRE, J. p 9 N94-10461
PERALDI, OLIVIER p 80 N94-10248
PERALES, J. M. p 102 N94-10083
PERERA, U. p 369 N94-12546
PEREZ, JAMES p 175 N94-12012
PEREZ, M. R. p 424 N94-11306
PERIAUX, JACQUES p 5 N94-10440
PERINA, J. p 376 N94-10574
PERINI, U. p 107 N94-10113
PERL, M. L. p 367 N94-11469
PERLANT, FREDERIC P. p 247 N94-12479
PERNOVA, V. p 376 N94-10574
PERONE, MICHAEL P. p 338 N94-10487
PERREAU, M. p 432 N94-12233
PERRIER, PIERRE p 3 N94-10423
p 5 N94-10440
PERROT, F. p 122 N94-10230
PERRY, BOYD III p 26 N94-11587
PERRY, F. p 273 N94-10285
PERRY, R. T. p 372 N94-10890
PERSIANI, F. p 45 N94-11342
PERSSON, P. A. p 93 N94-12354
PETERSEN, W. C. p 146 N94-12773
PETERSON, D. p 384 N94-10157
PETERSON, J. p 234 N94-11717
PETERSON, JAMES M. p 21 N94-10792
p 21 N94-10795
PETERSON, LEIF E. p 312 N94-11560
PETHRICK, R. p 69 N94-11325
PETIT, G. p 24 N94-10967
PETIT, GERARD p 351 N94-10969
PETRAKIS, P. L. p 334 N94-10985
PETRE, G. p 115 N94-10189
PETROV, N. M. p 361 N94-10549
p 362 N94-10550
PETROV, V. p 374 N94-12785
PETROVA, T. L. p 97 N94-12039
PETROVA, Y. V. p 223 N94-12729
PETTITI, V. p 139 N94-10984
PETTY, C. C. p 137 N94-11453
PETVIASHVILI, N. p 393 N94-11669
PEYSER, T. A. p 382 N94-11656
PEYTON, B. W. p 332 N94-11695
PFEIFFER, J. R. p 340 N94-12411
PHELPS, D. A. p 137 N94-11453
PHELPS, DONALD K. p 369 N94-12420
PHILLION, D. W. p 385 N94-10286
PHILLIPS, C. A. p 344 N94-10961
PHILLIPS, T. J. p 276 N94-11227
PHUVAN, SONLINK N. p 418 N94-10374
PIANTANIDA, TOM p 314 N94-11570
PICKER, G. p 122 N94-10232
PICKERELL, THOMAS p 23 N94-10933
PICKERING, THOMAS G. p 311 N94-12006
PIERCE, J. T. p 174 N94-10959
PIERSON, D. L. p 318 N94-11553
PIETERS, CARLE M. p 445 N94-12070
p 445 N94-12071
p 478 N94-12251
PIKE, C. D. p 483 N94-12414
PILE, P. H. p 359 N94-10308
PILLER, J. p 109 N94-10125
PILLINGER, C. T. p 428 N94-12035
p 451 N94-12108
p 433 N94-12252
p 433 N94-12255
PILMANIS, ANDREW A. p 317 N94-11540
p 317 N94-11541
p 312 N94-11543
p 302 N94-11548
PINCOSY, P. A. p 142 N94-11050
PINDZOLA, M. S. p 366 N94-11172
PINELLI, THOMAS E. p 419 N94-11352
PINES, DAVID S. p 99 N94-12275
PINKERTON, S. D. p 276 N94-11463
PINOS, I. B. p 391 N94-11174
PINSKER, R. I. p 137 N94-11453

PIRIZ, R. p 242 N94-11771
PISZCZOR, MICHAEL p 53 N94-11410
PISZCZOR, MICHAEL F. p 52 N94-11402
PITZ, W. J. p 177 N94-10322
PLAGEMANN, W. L. p 55 N94-10947
PLATON, F. p 64 N94-10061
PLAUT, JEFFREY J. p 467 N94-12190
PLETSER, V. p 39 N94-10136
PLIMPTON, S. p 366 N94-11284
PLIMPTON, S. J. p 367 N94-11455
PLUMMER, J. D. p 395 N94-10516
PODBOY, GARY G. p 14 N94-10892
PODZIREJ, Y. S. p 82 N94-10842
POEL, MANNES p 335 N94-10277
POEPPEL, R. B. p 398 N94-11004
POKHODYASHCHIJ, V. I. p 398 N94-11090
POLER, J. C. p 143 N94-11160
POLEZHAEV, V. I. p 102 N94-10087
p 104 N94-10099
POLL, D. I. A. p 7 N94-10447
p 8 N94-10452
POLLACK, JAMES B. p 441 N94-12054
POLOVNEVA, S. P. p 82 N94-10842
POLUEHKTOV, Y. M. p 188 N94-11364
PONTE, S. p 235 N94-11728
POOL, SAM L. p 306 N94-11799
POOLE, A. B. p 187 N94-11169
POPE, STEPHEN B. p 79 N94-12378
PORKOLAB, M. p 394 N94-12370
PORTER, CAROLYN A. p 271 N94-12470
PORTER, G. D. p 385 N94-10289
PORTER, R. p 34 N94-12436
POSA, F. p 235 N94-11728
POSADO-CANO, R. p 435 N94-12018
POSPISIL p 38 N94-11565
POST, R. F. p 142 N94-11009
POSTHILL, J. B. p 400 N94-11443
POT, FRANK p 126 N94-10619
POT, T. p 4 N94-10429
POTOTZKY, ANTHONY S. p 26 N94-11587
POTTER, G. L. p 276 N94-11241
POTTHAST, LOTHAR p 39 N94-10119
POULSEN, P. P. p 142 N94-11050
POULYMENAKOU, A p 329 N94-11426
POVEY, NICK J. p 22 N94-10797
POWELL, M. R. p 312 N94-11544
POWELL, MICHAEL R. p 125 N94-11235
p 312 N94-11542
p 312 N94-11545
p 312 N94-11546
p 312 N94-11547
POWELL, R. J. p 244 N94-11785
POWERS, ROBERT K. p 331 N94-11680
POZZI, R. p 107 N94-10113
PRADIER, A. p 58 N94-10021
p 62 N94-10047
PRAGER, S. p 388 N94-10747
PRAKASH, A. p 105 N94-10100
PRAMILA, A. p 63 N94-10054
p 65 N94-10069
PRASAD, SUDHAKAR p 375 N94-10568
PRASKOVSKY, ALEXANDER A. p 158 N94-12304
PRATI, C. p 237 N94-11735
PRATT, STEPHEN F. p 445 N94-12071
PREMOLI, AMEDEO p 356 N94-10997
PRENDERGAST, MAURICE J. p 166 N94-12774
p 166 N94-12775
PRICE, H. p 59 N94-10023
PRICE, L. E. p 419 N94-11105
PRICE, PATTI J. p 324 N94-11104
PRIETZSCH, CORINNA p 248 N94-12489
PRIJMENKO, S. D. p 133 N94-11034
p 134 N94-11035
p 345 N94-11036
p 134 N94-11038
PRILUTSKII, O. F. p 476 N94-12242
PRINSENBERG, S. p 240 N94-11759
PRINZ, B. p 113 N94-10177
PRINZ, MARTIN p 431 N94-12200
PRISK, G. K. p 309 N94-11994
PROFFITT, DENNIS R. p 313 N94-11511
PROSHYANTS, JU. G. p 226 N94-12749
PROST, M. T. p 254 N94-12523
PROTO, A. N. p 132 N94-10401
PROVOST, LIONEL R. p 78 N94-12009
PRZEKWAS, A. J. p 46 N94-10934
PU, SHUZHEN p 215 N94-12686
PUDJAPRASETYA, S. R. p 147 N94-10275
PUKHNACHOV, V. V. p 103 N94-10088
PUSHKASH, O. M. p 363 N94-10722
PUSHKIN, S. B. p 24 N94-10967

Q

QI, HUA p 191 N94-11897
QIAN, M. p 400 N94-11458
QIN, XIAO p 319 N94-10318
QIU, BO p 209 N94-12650
QUAINOO, G. K. p 84 N94-12361
QUARTLY, G. D. p 235 N94-11722
p 243 N94-11773
QUASSO, R. p 139 N94-10984
QUEALY, ANGELA p 327 N94-11232
QUEECKERS, PATRICK p 124 N94-10242
QUEFFEULOU, PIERRE p 233 N94-11712
QUEGAN, S. p 248 N94-12487
QUENTMEYER, RICHARD J. p 55 N94-12569
QUILFEN, YVES p 233 N94-11712
QUINTIERE, JAMES G. p 19 N94-10783
QUIRRENBACH, A. p 135 N94-11064
QURESHI, SHAHID P. p 20 N94-10786

R

RAAKE, DIETER p 106 N94-10106
RABIN, B. H. p 83 N94-11141
RABINOVITCH, M. p 59 N94-10024
RADAVICH, J. F. p 81 N94-10297
RADOSTITZ, JAMES V. p 280 N94-12582
RADTKE, ROBERT p 348 N94-11574
RADTKE, W. p 62 N94-10045
p 62 N94-10046
RAFAILOVICH, M. p 89 N94-11007
RAHKA, KLAUS p 58 N94-10017
RAHMAN, MIFTA p 87 N94-10508
RAIMONDO, J. C. p 243 N94-11774
p 243 N94-11778
RAINER, F. p 90 N94-11230
RAINER, FRANK p 381 N94-11054
RAIZER, V. YU. p 226 N94-12745
RAJAK, D. p 249 N94-12492
RAJAN, J. A. p 24 N94-10964
RAJASENAN, C. p 243 N94-11774
RALPH, J. A. p 29 N94-12270
RALSTIN, S. p 419 N94-11137
RAMADAN, W. p 266 N94-11471
RAMAKER, DAVID E. p 85 N94-12393
RAMANATHAN, RAGULAN p 67 N94-11260
RAMBO, J. T. p 98 N94-10751
RAMOS, ANTONIO p 100 N94-10075
RAMSAY, BRUCE p 241 N94-11760
RAMSAY, D. J. p 311 N94-12005
RAMSEY, J. M. p 173 N94-10255
RANDJBARDAEMI, S. p 410 N94-10802
RANKIN, P. p 370 N94-12609
RAO, C. R. p 347 N94-11882
RAO, DANTAM K. p 180 N94-10706
RAO, L. V. G. p 214 N94-12678
RAO, M. V. p 193 N94-11907
RAO, R. p 91 N94-11665
RAPER, JAMES L., SR. p 348 N94-11568
RAPLEY, C. G. p 237 N94-11738
p 246 N94-12475
RAPP, H. p 27 N94-11321
RAPUC, MARC p 5 N94-10437
RASHIDNIA, N. p 104 N94-10094
RASMUSSEN, J. E. p 275 N94-11013
RASTOGI, ANUPMA p 210 N94-12655
RATH, HANS J. p 103 N94-10091
p 105 N94-10105
p 108 N94-10121
p 124 N94-10247
RATH, HANS-J. p 124 N94-10246
RATKE, L. p 113 N94-10177
p 114 N94-10182
p 116 N94-10192
p 87 N94-10202
RAUSCHER, CHRISTEN p 140 N94-10389
p 145 N94-12322
RAUTIOLA, J. p 58 N94-10019
RAVERA, FRANCESCA p 121 N94-10225
RAVIART, J. L. p 59 N94-10024
RAWICZ, H. C. p 24 N94-10964
RAWLES, ROBIN E. p 403 N94-12010
RAWLIN, VINCENT K. p 46 N94-10761
RAYCHOWDHURY, P. p 371 N94-10316
RAYMAN, RUSSELL B. p 305 N94-11790
RAYMOND, D. p 254 N94-12523
RAYNER, J. D. p 351 N94-10970
REAGAN, M. K. p 281 N94-12056
REDA, HELMUT p 25 N94-10945
REDDY, D. R. p 39 N94-10764
REE, MALCOLM J. p 314 N94-12276
REED, BRIAN D. p 47 N94-11252
REED, H. L. p 164 N94-12623
REED, HELEN L. p 7 N94-10451
REEDY, ROBERT p 172 N94-12038
REES, W. G. p 238 N94-11743
REGIER, LLOYD p 289 N94-11853
REGIS, J. P. p 169 N94-10326
REHBEIN, TRACY p 310 N94-11998
REHR, J. J. p 367 N94-11470
REICH, M. p 237 N94-11736
REICHENBACH, H. p 147 N94-10307
REICHERT, P. p 246 N94-12478
REID, A. M. p 453 N94-12117
REID, BILL p 417 N94-12360
REIDY, ANNE-MARIE p 481 N94-12266
REIFER, DONALD J. p 329 N94-11431
REIFMAN, J. p 340 N94-11644
REIGBER, C. p 243 N94-11774
p 243 N94-11778
REIMOLD, W. U. p 282 N94-12102
p 282 N94-12103
REINHARD, L. p 81 N94-10522
REINHOLD, A. p 237 N94-11740
REINHOLD, ANDREAS p 237 N94-11739
REIS, HOWARD P. p 306 N94-11800
REISS, H. R. p 378 N94-10596
REISTAD, MAGNAR p 233 N94-11710
REISTER, D. B. p 177 N94-10269
REMIZOVICH, V. S. p 226 N94-12748
RENSINK, M. E. p 385 N94-10262
p 385 N94-10289
REUTERSHAN, THOMAS P. p 307 N94-11801
REVCOLEVSCHI, A. p 88 N94-10527
REX, S. p 114 N94-10181
RHODES, BRIAN T. p 19 N94-10783
RHODES, ROBERT p 46 N94-10700
RICE, A. p 455 N94-12127
RICE, C. I. p 253 N94-12517
RICHARDS, R. K. p 173 N94-10160
RICHERSON, D. W. p 89 N94-11106
RICHMOND, G. L. p 403 N94-12371
p 79 N94-12534
RICKLEFS, R. L. p 352 N94-10972
RICKMAN, DENIS D. p 170 N94-10873
RICKS, R. L. p 138 N94-11891
RIDER, W. J. p 372 N94-10890
RIDLEY, J. K. p 237 N94-11738
p 244 N94-11780
p 246 N94-12475
RIECK, U. p 62 N94-10049
RIECKE, H. p 401 N94-11610
RIECO, STEVE p 42 N94-10665
RIEDESEL, MARVIN L. p 309 N94-11996
RIEHLE, M. p 47 N94-11354
RIES, JUDIT GYOERGYEY p 426 N94-11596
RIEWE, L. C. p 143 N94-11271
RIGHETTI, P. G. p 103 N94-10092
RIGLER, MICHAEL ANTHONY p 426 N94-11597
RIGNEY, DAVID R. p 311 N94-12007
RIM, HYUNG JIN p 38 N94-10359
RIOLI, ALESSANDRO p 378 N94-10587
RISKOWSKI, G. L. p 300 N94-11180
RITS, W. p 57 N94-10010
RITS, W. J. p 56 N94-10007
RIZVI, S. R. H. p 234 N94-11719
RIZZI, A. W. p 9 N94-10460
RIZZOLI, P. MALANOTTE p 221 N94-12719
ROARK, JAMES H. p 481 N94-12267
p 481 N94-12268
ROBERTS, A. p 133 N94-11023
ROBERTS, DAVID p 41 N94-10512
ROBERTS, DONALD R. p 307 N94-11802
ROBERTS, PAUL p 331 N94-11657
ROBERTSON, BILL p 348 N94-11572
ROBINSON, A. C. p 345 N94-11225
ROBINSON, DAVID W. p 40 N94-10640
ROBINSON, G. N. p 279 N94-12572
ROBINSON, IAN S. p 234 N94-11721
ROBINSON, MARK S. p 430 N94-12163
ROBINSON, R. A. p 363 N94-10743
ROCCA, F. p 237 N94-11735
ROCKWAY, J. W. p 336 N94-10488
RODDY, D. J. p 281 N94-12032
RODEAN, H. C. p 275 N94-11052
RODGERS, MARK D. p 38 N94-12567
RODGERS, R. J. p 370 N94-10149
RODIER, M. p 199 N94-11946
RODIN, A. M. p 476 N94-12242
RODMAN, LAURA C. p 154 N94-11641
RODRIGUES, LOUIS J. p 416 N94-10910
RODRIGUEZ, J. p 319 N94-10146
RODRIGUEZ, J. M. p 279 N94-12572
RODRIGUEZ, P. p 59 N94-10025
ROELOFS, G. H. MARCEL p 321 N94-10265
p 322 N94-10418
ROERDINK, J. B. T. M. p 174 N94-10904
ROESCH, RAIMUND p 112 N94-10141
p 86 N94-10199
ROESTEL, R. p 87 N94-10231
ROGERS, PATRICIA G. p 457 N94-12136
ROGNLIEN, T. p 385 N94-10262
ROGNLIEN, T. D. p 385 N94-10289
ROGOZKIN, D. B. p 226 N94-12748

ROHDE, SHARON p 323 N94-10494
p 323 N94-10495
ROJAS, R. G. p 23 N94-11525
ROKHLIN, S.I. p 67 N94-11237
ROMAN, W. C. p 370 N94-10149
ROMANO, S. p 182 N94-12605
ROMANOV, JU. A. p 222 N94-12723
ROMANOV, S. S. p 371 N94-10542
ROMAY-MERINO, M. p 242 N94-11771
ROMBACH, M. p 248 N94-12491
ROMEO, G. p 69 N94-11328
ROMERO, L. A. p 144 N94-11624
RONCACE, ELIZABETH A. p 55 N94-12569
ROPER, BENJAMIN F. p 42 N94-10493
ROSA, L. p 412 N94-11047
ROSCHKE, PAUL N. p 187 N94-11190
ROSE, J. H. p 183 N94-11110
ROSE, R. B. p 138 N94-11883
ROSE, ROBERT B. p 278 N94-11871
ROSEN, M. D. p 389 N94-11074
p 175 N94-11266
ROSEN, PAUL A. p 236 N94-11734
ROSENBERGER, FRANZ p 56 N94-12588
ROSENCHEIN, STANLEY J. p 418 N94-10515
ROSENTHAL, R. R. p 175 N94-11283
ROSHKO, A. p 423 N94-11183
ROSING, MATTHEW p 323 N94-10643
p 326 N94-11196
ROSS, MICHAEL p 42 N94-11297
ROSSEINSKY, M. J. p 400 N94-11457
ROSSING, T. D. p 144 N94-11607
ROSTAND, P. p 10 N94-10464
ROSU, H. p 410 N94-10635
ROTH, KATHERINE CAROL p 426 N94-11582
ROTHENBERG, SIMON p 318 N94-11554
ROTHROCK, D. A. p 239 N94-11749
ROTT, H. p 237 N94-11737
p 247 N94-12481
ROTTER, M. D. p 174 N94-11126
ROUFF, CHRIS p 333 N94-12448
ROUSSEAU, P. M. p 395 N94-10516
ROUSSELLE, OLIVIER p 39 N94-10118
ROUSSOPOULOS, NICK p 420 N94-11520
ROUX-DEBALMANN, H. p 122 N94-10234
ROUX, A. p 117 N94-10201
ROUX, BERNARD p 101 N94-10076
p 101 N94-10082
p 105 N94-10101
p 117 N94-10201
p 119 N94-10215
p 120 N94-10218
p 120 N94-10220
ROUZAUD, ANDRE p 86 N94-10197
ROVEN, H. J. p 64 N94-10063
ROZHAVSKIJ, A. S. p 398 N94-11025
RUBENCHIK, A. M. p 389 N94-11114
RUBES, M. T. p 286 N94-12580
RUBIN, K. I. p 266 N94-11584
RUBIN, M. H. p 370 N94-10582
RUBINO, M. C. p 266 N94-11584
RUBIOLA, E. p 139 N94-10984
RUCKLIDGE, J. C. p 431 N94-12183
RUDANT, JEAN-PAUL p 254 N94-12523
RUDMIK, ANDRES p 323 N94-10495
RUEB, JUSTIN D. p 24 N94-11879
RUELLENRATH, S. p 118 N94-10205
RUFF, STEVE p 81 N94-12156
RUGGIERO, A. J. p 98 N94-11269
RUGGIERO, S. T. p 396 N94-10648
RUGGLES, L. p 173 N94-10746
RUNDE, M. p 143 N94-11454
RUPERT, A. H. p 303 N94-11097
RUPLEY, F. M. p 152 N94-11371
RUSHBY, JOHN p 326 N94-11188
RUSSELL, L. C. p 336 N94-10488
RUSSELL, S. S. p 433 N94-12255
RUSSELL, V. A. p 402 N94-11654
p 402 N94-11827
RUSSO, ARTURO p 44 N94-11462
RUSSO, M. S. p 139 N94-10991
RUSSO, S. G. p 90 N94-11311
RUST, DAVID M. p 381 N94-10735
RUST, THOMAS p 46 N94-10938
RUSTHOI, D. P. p 374 N94-12786
RUTHERFORD, M. J. p 478 N94-12250
p 433 N94-12264
RYAN, E. p 429 N94-12036
RYAN, H. M. p 152 N94-11526
RYAN, L. E. p 84 N94-11668
RYAN, P. M. p 137 N94-11453
RYBICKI, GEORGE p 49 N94-11386
RYOO, JANG-SOO p 36 N94-10684

S

SABA, J. L. R. p 483 N94-11048
SACKOS, J. T. p 174 N94-10959
SADDOUGHI, SEYED G. p 157 N94-12302
SADEGHI, T. p 32 N94-11502
SADO, KIMITERU p 219 N94-12703
SAFFORD, ROBERT R. p 314 N94-11536
SAGGIANI, G. M. p 45 N94-11342
SAGHIR, M. ZIAD p 101 N94-10081
SAHOTA, M. S. p 153 N94-11601
SAIF, A. G. p 396 N94-10716
SAILOR, MICHAEL J. p 146 N94-12584
SAINO, TOSHIROU p 200 N94-11950
SAINT, A. p 143 N94-11285
SAITO, M. p 112 N94-10142
SAITO, T. T. p 382 N94-11242
SAITOU, IKUHIRO p 129 N94-11833
SAITOU, KATSUYA p 215 N94-12681
SAITOU, MASAKI p 162 N94-12554
SAITOU, SEI-ICHI p 198 N94-11939
p 204 N94-11976
p 205 N94-11979
SAITOU, SEIICHI p 221 N94-12715
SAITOU, T. p 203 N94-11967
SAKAI, H. p 107 N94-10115
p 114 N94-10179
SAKAI, SHINICHI p 220 N94-12714
SAKAIDA, FUTOKI p 220 N94-12710
SAKAKIBARA, SEIZOU p 2 N94-10363
SAKANISHI, S. p 140 N94-12706
SAKAO, FUJIHIKO p 163 N94-12615
SAKIMOTO, K. p 367 N94-11580
p 393 N94-11594
SAKURAGI, JOJHY p 230 N94-11179
SAKURAI, YOSHIO p 43 N94-10859
SAKYA, ANDI EKA p 10 N94-10468
SALA, G. p 61 N94-10036
SALAM, A. p 410 N94-10802
p 139 N94-12778
SALASHIN, S. G. p 225 N94-12741
SALAZAR, CLAUDIO p 216 N94-12688
SALAZAR, JOSE p 18 N94-10777
SALE, R. S. p 55 N94-12283
SALEEB, A. F. p 188 N94-11482
SALERNO, LOUIS J. p 34 N94-10930
SALK, MANFRED p 106 N94-10111
p 107 N94-10116
p 111 N94-10139
SALTMARSH, M. J. p 391 N94-11171
SALTSMAN, JAMES F. p 74 N94-12449
SALTZ, JOEL p 323 N94-10643
SAMANIEGO, JEAN-MICHEL p 160 N94-12318
SAMARAKOON, L. p 219 N94-12705
SAMPATH, K. S. p 23 N94-11525
SAMUELS, DAVID C. p 158 N94-12307
SANCHEZ, BRAULIO V. p 288 N94-11358
SANCHEZ, ISAAC C. p 91 N94-11830
SANCHEZ, V. p 122 N94-10234
SANDER, O. R. p 374 N94-12786
SANDERS, GLENN p 170 N94-10667
SANDERS, JAY H. p 307 N94-11803
SANDVEN, STEIN p 238 N94-11745
p 210 N94-12653
SANDWELL, DAVID T. p 243 N94-11776
SANFELD, A. p 102 N94-10086
SANI, R. L. p 104 N94-10096
SANKOVIC, JOHN M. p 180 N94-10760
SANO, ITARU p 200 N94-11949
p 205 N94-11978
SANSONETTI, P. p 69 N94-11328
SANTIAGO, JAMES V. p 53 N94-11411
SANTINI, P. p 45 N94-11342
SANTORO, R. J. p 152 N94-11526
SANTOSA, FADIL p 138 N94-12338
SANZ, A. p 59 N94-10025
p 111 N94-10137
SARABANDI, KAMAL p 266 N94-11374
SARATHY, SRIPRAKASH PARTHA p 25 N94-11056
SARKISIAN, ASHOT E. p 305 N94-11790
SARKOS, CONSTANTINE P. p 17 N94-10766
SARMADI, M. H. p 409 N94-10500
SARVER, GEORGE L., III p 34 N94-10930
SASAKI, KATSUYUKI p 211 N94-12658
SASAKI, T. p 203 N94-11969
SASS, S. L. p 402 N94-11700
SATHAYE, SHIRISH S. p 337 N94-11881
SATO, H. p 411 N94-10880
SATO, K. I. p 390 N94-11128
p 392 N94-11239
SATOU, HIROSHI p 27 N94-12630
SATOU, KAZUHIRO p 218 N94-12700
SATOU, SHIGERU p 27 N94-10367
SATOU, SOUJUN p 172 N94-11968
SAUNDERS, BONITA V. p 105 N94-10103
SAUNDERS, R. W. p 252 N94-12515
SAUNDERS, S. p 454 N94-12120
SAUZE, MARTIN J. p 289 N94-11868
SAVINO, R. p 106 N94-10108
SAWYER, CONSTANCE p 484 N94-11312
SAXENA, A. p 399 N94-11263
p 403 N94-12345
SAXENA, C. M. p 249 N94-12492
SAYLOR, BILL p 45 N94-11323
SAYOOD, K. p 321 N94-10343
SAZHINA, TATYANA G. p 228 N94-12760
SCAGGS, NORMAN E. p 6 N94-10443
SCALO, JOHN M. p 428 N94-12767
SCHABER, G. G. p 458 N94-12145
SCHADT, R. p 245 N94-12472
SCHAEFER, MARTIN p 105 N94-10104
SCHAEFER, OTTO p 177 N94-10341
SCHAEFER, R. L. p 302 N94-11556
SCHAFFER, M. J. p 393 N94-11514
SCHARPF, DANIEL FRANCIS p 358 N94-11057
SCHARROO, R. p 242 N94-11772
p 244 N94-11779
SCHELL, D. M. p 267 N94-11697
SCHENA, V. D. p 235 N94-11728
SCHERB, MEGAN KAY p 317 N94-12368
SCHERNECK, HANS-GEORG p 243 N94-11776
SCHERPEN, J. M. A. p 341 N94-10273
SCHIEBER, W. M. p 152 N94-11448
SCHIESSER, W. p 133 N94-10960
SCHIFLETT, SAMMUEL G. p 314 N94-11533
SCHILLING, C. H. p 82 N94-10957
SCHIRBER, J. E. p 400 N94-11457
SCHIRMER, ALBERTO W. p 12 N94-10675
SCHIRMER, UWE p 237 N94-11739
SCHLAGEL, T. J. p 359 N94-10303
SCHLAGER, MARK S. p 314 N94-11570
SCHLEICH, WOLFGANG P. p 379 N94-10603
SCHLENKER, E. p 65 N94-10068
SCHLICKER, INGE p 485 N94-11379
SCHLUESSEL, PETER p 252 N94-12514
p 221 N94-12716
SCHLUTTER, D. J. p 430 N94-12115
SCHMALE, A. L. p 112 N94-10174
SCHMID, ANSGAR p 381 N94-11054
SCHMID, G. p 69 N94-11326
SCHMIDT-GROETTRUP, M. p 239 N94-11753
SCHMIDT, H. P. p 111 N94-10138
SCHMIDT, PHILLIP H. p 30 N94-11251
SCHMIDT, W. p 27 N94-11318
p 71 N94-11340
SCHMITT, R. A. p 432 N94-12211
SCHMITZ, GERD p 122 N94-10233
SCHNABEL, ROBERT p 326 N94-11196
SCHNEIDER, G. M. p 120 N94-10221
SCHNEIDER, HOWARD J. p 305 N94-11791
SCHNEIDER, THOMAS p 78 N94-12273
SCHNEIDEWIND, NORMAN F. p 330 N94-11434
SCHOBERT, H. H. p 99 N94-12282
SCHOLAERT, H. p 69 N94-11326
SCHOTT, ROBERT R. p 87 N94-10508
SCHOTTEN, C. G. J. p 246 N94-12473
SCHOWALTER, LEO J. p 369 N94-12395
SCHRECK, STEFAN p 358 N94-11176
SCHRODER, KENNETH J. p 337 N94-11829
SCHUBERT, G. p 444 N94-12067
SCHUBERT, LEROY p 41 N94-10512
SCHUCH, DIETER p 349 N94-10583
SCHUETZ, G. p 346 N94-11811
SCHULKES, R. M. S. M. p 100 N94-10074
SCHULTE, KARL p 66 N94-11085
SCHULTZ, P. H. p 169 N94-12044
p 431 N94-12181
SCHULZ, B.-S. p 246 N94-12477
SCHULZE, NORMAN p 381 N94-11054
SCHULZE, NORMAN R. p 170 N94-10667
p 47 N94-11053
SCHUTZ, BOB E. p 229 N94-10702
SCHWANTES, S. p 59 N94-10023
SCHWARK-WERWACH, BERNHARD
p 105 N94-10105
SCHWARTZ, M. N. p 262 N94-11051
SCHWARZ, RALF p 119 N94-10213
SCHWINDT, PETER C. p 79 N94-12351
SCHWINTZER, P. p 243 N94-11778
SCIME, E. E. p 275 N94-10742
SCIRE, J. S. p 152 N94-11519
p 279 N94-12422
SCOGGINS, TERRELL E. p 302 N94-11548
SCOON, ALISON p 234 N94-11721
SCOTT, DAVID H. p 472 N94-12216
SCOTT, JOHN CARVER p 307 N94-11804
SCOTT, MICHAEL L. p 337 N94-11650
SCOTT, R. F. p 246 N94-12475
SCOTT, ROBERT C. p 26 N94-11587
SCUDDER, JACK D. p 427 N94-12566
SCULLY, MARLAN O. p 375 N94-10565

SEAGRAVE, RICHARD C. p 316 N94-12365
p 317 N94-12369
SEARS, D. W. G. p 429 N94-12058
p 429 N94-12059
p 443 N94-12060
SEE, DAVID W. p 127 N94-10623
SEE, T. H. p 429 N94-12063
SEELY, JOHN F. p 132 N94-10382
SEGALLIS, GREG P. p 146 N94-12433
SEGALMAN, D. p 91 N94-11665
SEGUCHI, TADAO p 372 N94-11591
SEIBLE, FRIEDER p 186 N94-10937
SEIDEL, A. p 109 N94-10125
SEIDMAN, D. N. p 363 N94-10750
SEIFERT, PEDRO p 235 N94-11727
SEITEL, STEVEN C. p 381 N94-11054
SELCOW, E. C. p 371 N94-10529
SELF, BRIAN P. p 316 N94-12346
SELF, MARK F. p 78 N94-11683
SELIM, R. p 170 N94-10948
SELL, M. p 8 N94-10454
SELLERS, W. p 4 N94-10434
SELLIS, TIMOS p 420 N94-11520
SELMIN, V. p 3 N94-10425
SEMJENOVA, L. F. p 433 N94-12255
SEMJONOVA, L. F. p 433 N94-12252
p 433 N94-12253
p 433 N94-12254
p 81 N94-12256
SEMMES, P. B. p 368 N94-11813
SENCHENKO, T. A. p 364 N94-10835
SENCHENKOV, ALEXANDER S. p 102 N94-10084
p 106 N94-10111
p 107 N94-10116
p 111 N94-10139
p 116 N94-10193
SENGA, YASUHIRO p 211 N94-12659
SENJANOVIC, G. p 410 N94-10545
SEOMUN, KANG-SEON p 187 N94-11055
SERABIAN, STEVEN M. p 73 N94-11446
SERGI, R. p 235 N94-11728
SERGIENKO, A. V. p 370 N94-10582
p 351 N94-10971
SERIO, MICHAEL A. p 99 N94-12275
SERNA, OSCAR R. p 187 N94-11190
SETER, ANDREW J. p 315 N94-11375
SETYONO, DWI p 218 N94-12700
SEVERANCE, PAUL p 53 N94-11410
SEVERCAN, M. p 322 N94-10410
SEVERS, W. B. p 311 N94-12005
SEVERS, WALTER B. p 300 N94-11045
SEXTON, F. W. p 143 N94-11285
SHA, LUI p 337 N94-11881
SHAFER, MARY F. p 13 N94-10707
p 13 N94-10820
SHAH, A. K. p 61 N94-10037
SHAH, A. R. p 185 N94-10361
SHAHINPOOR, M. p 91 N94-11665
p 432 N94-12241
SHAHPAR, S. p 7 N94-10447
SHALABY, M. A. p 339 N94-11630
SHANE, H. p 405 N94-12599
SHANEYFELT, M. R. p 143 N94-11271
SHANG, C. C. p 132 N94-10518
SHANNEY, BILL p 348 N94-11571
SHANNON, SAMUEL G. p 315 N94-11291
SHAPLEY, JOHN R. p 396 N94-10705
SHAPOVAL, D. V. p 363 N94-10722
SHARAF, F. p 386 N94-10387
SHARKEY, THOMAS J. p 35 N94-11535
SHARMA, RASHMI p 242 N94-11770
SHARMA, SUNDER p 249 N94-12492
SHARMAN, R. D. p 283 N94-10725
SHARPE, S. R. p 346 N94-11663
SHASHKINA, V. P. p 454 N94-12122
SHAW, G. J. p 52 N94-11404
SHAW, J. A. p 324 N94-10893
p 154 N94-11859
p 16 N94-11888
SHAW, W. J. p 274 N94-10323
SHCHEPKIN, Y. G. p 364 N94-10835
SHEEHAN, ROBERT E. p 278 N94-12277
SHEEHEY, P. p 384 N94-10153
SHEFFIELD, J. p 388 N94-10744
SHEKHMAMETYEV, SH. A. p 226 N94-12748
SHELUS, P. J. p 352 N94-10972
SHEMDIN, O. H. p 235 N94-11723
SHEN, S. S. p 387 N94-10737
SHEN, Y. p 112 N94-10172
SHEN, Y. X. p 115 N94-10187
SHENOI, S. S. C. p 214 N94-12678
SHEPARD, P. F. p 369 N94-12546
SHEPHERD, ALAN p 27 N94-11345
SHEPHERD, R. L. p 389 N94-11074
SHEPPARD, JOHN W. p 184 N94-11563
SHERBY, O. D. p 82 N94-11076
SHERIF, JOSEF p 314 N94-11534
SHERMAN, RICHARD A. p 311 N94-12364
SHERSHENKOV, SERGEY YU. p 228 N94-12757
SHETYE, S. R. p 214 N94-12678
SHEVTSOVA, VALENTINA M. p 120 N94-10219
SHI, MAO-CHONG p 192 N94-11901
SHI, MAOCHONG p 197 N94-11930
SHIA, R-L. p 279 N94-12572
SHIAO, M. C. p 185 N94-10361
SHIBA, KIYOYUKI p 84 N94-11593
SHIBATA, AKIRA p 253 N94-12520
p 211 N94-12663
SHIBATA, E. I. p 373 N94-12600
SHIBATANI, K. p 140 N94-12706
SHIBUYA, S. p 144 N94-11508
SHIDA, SHIGEO p 372 N94-11591
SHIGEMI, MASASHI p 14 N94-10860
SHIH, C. p 16 N94-11889
SHIH, H. J. p 133 N94-10960
SHIH, T. H. p 151 N94-11192
SHIH, WEN-HUNG p 215 N94-12684
SHIH, Y. H. p 370 N94-10582
p 351 N94-10970
p 351 N94-10971
SHIMA, EIJI p 10 N94-10470
p 11 N94-10471
SHIMADA, MASANOBU p 253 N94-12520
SHIMANUKI, MAMORU p 217 N94-12694
SHIMKAVEG, G. M. p 389 N94-11074
SHIMODA, TOORU p 211 N94-12658
SHIMON, L. J. W. p 394 N94-10301
SHINBO, T. p 140 N94-12706
SHINN, JUDY L. p 484 N94-10759
p 484 N94-11278
SHINOHARA, NOBUO p 372 N94-11043
SHINOHARA, YOSHIKUNI p 358 N94-11042
SHINOMIYA, H. p 193 N94-11909
SHINOMIYA, HIROSHI p 220 N94-12713
SHIOMOTO, AKIHIRO p 211 N94-12658
SHIPLEY, R. J. p 82 N94-10804
SHIPSEY, I. P. p 373 N94-12600
SHIRANE, G. p 400 N94-11467
SHIRASAWA, AZUMI p 205 N94-11979
SHISHKIN, A. A. p 389 N94-11119
p 392 N94-11215
SHISHOV, V. I. p 134 N94-11061
SHMYROV, N. A. p 227 N94-12751
SHOEMAKER, E. M. p 281 N94-12032
SHOKR, MOHAMMED E. p 241 N94-11760
SHOOM, M. YU. p 225 N94-12743
SHORE, H. B. p 394 N94-10281
SHU, CHI-WANG p 345 N94-11280
SHU, XIAOJIAN p 173 N94-10483
SHU, YANTAI p 322 N94-10484
SHUCHMAN, R. A. p 234 N94-11720
SHUCHMAN, ROBERT A. p 240 N94-11754
SHUCHMANN, ROBERT p 238 N94-11745
SHUGAR, T. A. p 35 N94-12562
SHUKOLYUKOV, YU. A. p 433 N94-12254
p 81 N94-12256
SHULL, R. N. p 26 N94-11892
SHUM, D. K. M. p 184 N94-10288
SHUTOU, N. p 193 N94-11908
SHVEDOV, A. A. p 372 N94-10849
SHYU, CHUNG-ZEN p 215 N94-12684
SIBILIA, C. p 376 N94-10574
SICKINGER, PETER p 106 N94-10111
p 107 N94-10116
p 111 N94-10139
SIDDIQUI, M. S. p 217 N94-12697
SIDDIQUI, SARFRAZ A. p 17 N94-10767
SIDORENKO, I. N. p 390 N94-11121
SIEBER, A. J. p 249 N94-12496
p 249 N94-12497
p 250 N94-12498
p 250 N94-12499
SIEBER, ALOIS J. p 249 N94-12495
SIEGEL, R. W. p 397 N94-10962
SIEGER, E. p 56 N94-10004
SIEGER, G. E. p 137 N94-11466
SIEKMANN, JULIUS p 106 N94-10106
SIEMER, ANDREAS p 32 N94-11500
SIEVERS, J. p 237 N94-11740
SIEVERS, JOERN p 238 N94-11742
SIFORD, RAY p 144 N94-11516
SIGALO, F. B. p 142 N94-10799
SIGURDSSON, H. p 282 N94-12138
p 432 N94-12238
SILLANPAA, MEIJA p 125 N94-11483
SILVA, KEVIN p 72 N94-11343
SILVERSTEIN, MARTIN ELLIOT p 307 N94-11805
SIMANONOK, K. E. p 312 N94-11557
SIMANOVSKII, ILLYA B. p 120 N94-10217
p 121 N94-10223
SIMEN, MARTIN p 8 N94-10453
SIMENOG, I. V. p 363 N94-10722
SIMEONIDES, G. p 6 N94-10444
SIMILA, M. p 239 N94-11750
SIMON, B. p 234 N94-11719
SIMON, DONALD L. p 319 N94-10724
SIMON, FREDERICK F. p 151 N94-11256
SIMON, R. L. p 134 N94-11063
SIMON, WILLIAM E. p 46 N94-10911
SIMONENKO, S. V. p 169 N94-12728
p 229 N94-12763
p 229 N94-12764
SIMONS, A. p 32 N94-11502
SIMPSON, WILLIAM R. p 184 N94-11563
SINGER, R. B. p 477 N94-12245
SINGER, ROBERT B. p 424 N94-12768
SINGH, K. p 410 N94-10536
SINGH, N. p 364 N94-10946
SINGH, NAGENDRA p 387 N94-10641
SINGH, RAMESH P. p 210 N94-12655
SINGHAL, S. N. p 186 N94-10762
SINK, D. S. p 417 N94-11600
SINKE, J. p 57 N94-10013
SINYUGIN, A. V. p 387 N94-10558
SINYUKOV, YU. M. p 349 N94-10556
SIPPEL, R. p 57 N94-10009
SIRIPONG, A. p 196 N94-11925
SISLIAN, J. P. p 6 N94-10442
SISSON, T. R. p 340 N94-12411
SITENKO, A. G. p 361 N94-10549
SITENKO, Y. A. p 411 N94-10831
SIU, D. P. p 146 N94-12773
SJOLIND, S.-G. p 63 N94-10054
SKALOZUB, V. V. p 397 N94-10884
SKARDA, J. RAYMOND LEE p 163 N94-12576
SKIBENKO, A. I. p 66 N94-11143
SKJELLUM, A. p 336 N94-11027
p 336 N94-11248
SKOEELV, AAGE p 253 N94-12521
SKOLNIK, J. p 417 N94-11844
SKRIVER, H. p 239 N94-11752
SKURATOV, V. A. p 484 N94-10534
SLAD, L. M. p 362 N94-10634
SLATER, JOHN WILLIAM p 149 N94-10896
SLEAFORD, B. p 389 N94-11114
SLENSKI, GEORGE A. p 21 N94-10791
SLEVA, S. p 266 N94-11471
SLEZOV, V. V. p 83 N94-11363
SLINEY, JACK p 348 N94-11572
SLINGO, J. M. p 276 N94-11241
SLUTZ, S. A. p 370 N94-10149
SMACCHIA, P. p 235 N94-11728
SMATHERS, H. W. p 54 N94-11643
SMEETS, GUNTER p 5 N94-10436
SMIRNOV, A. I. p 365 N94-11089
SMIRNOV, ANDRE V. p 226 N94-12746
p 226 N94-12747
SMIRNOV, G. V. p 227 N94-12751
SMIRNOVA, I. G. p 102 N94-10084
SMIRNOVA, M. S. p 389 N94-11119
p 390 N94-11120
SMIT, JAN p 282 N94-12161
SMITCHENS, AIVARS p 27 N94-11347
SMITH, A. H. p 252 N94-12515
SMITH, ARTHUR p 4 N94-10428
SMITH, BRIAN p 41 N94-10512
SMITH, BRIAN S. p 51 N94-11399
SMITH, C. D. p 19 N94-10780
SMITH, D. B. p 78 N94-11622
SMITH, DAVID J. p 369 N94-12379
SMITH, DOUGLAS F. p 17 N94-10771
SMITH, DOUGLAS ROBERT p 14 N94-11058
SMITH, E. A. p 286 N94-12580
SMITH, FRANK T. p 152 N94-11377
SMITH, HOWARD W. p 26 N94-11858
SMITH, J. E. p 423 N94-10866
SMITH, J. G. p 370 N94-12609
SMITH, JANICE F. p 424 N94-11356
SMITH, M. p 374 N94-12786
SMITH, MARK J. T. p 326 N94-11197
SMITH, MICHAEL L. p 310 N94-12000
SMITH, NOVIS p 18 N94-10773
SMITH, REGINALD W. p 117 N94-10200
SMITH, S. D. p 232 N94-11708
SMITH, S. G. p 336 N94-11027
SMITH, SCOTT p 38 N94-11567
SMITH, SHEILA p 461 N94-12159
SMITH, SHELDON D. p 166 N94-12774
p 166 N94-12775
SMITH, T. G. p 175 N94-11283
SMITH, WILLIAM HAYDEN p 482 N94-12429
SMOLYANSKIJ, S. A. p 397 N94-10883
SMYTH, P. p 455 N94-12126
SNAITH, H. M. p 235 N94-11725
SNAVELY, D. L. p 79 N94-12373
SNAVELY, GEOFF p 79 N94-12373
SNEAD, L. L. p 385 N94-10253
SNELL, MARK p 19 N94-10782

SNITZER, ELIAS p 176 N94-12329
SNOW, S. p 266 N94-11471
SNYDER, N. p 128 N94-11028
SNYDER, ROBERT S. p 125 N94-10249
SOBECK, CHARLES K. p 34 N94-10930
SOEKELAND, A. p 250 N94-12499
SOEKELAND, A. D. p 249 N94-12497
SOFAIR, ISAAC p 229 N94-10417
SOGEGIAN, ROBERT p 41 N94-10512
SOILEAU, M. J. p 381 N94-11054
SOKOLOV, J. p 89 N94-11007
SOKOLOV, V. N. p 396 N94-10801
SOLDATENKO, G. A. p 82 N94-10842
SOLITRO, F. p 107 N94-10117
SOLOMON, PETER R. p 99 N94-12275
SOLOMON, S. I. p 247 N94-12484
SOLTANI, S. p 8 N94-10454
SOM, SUKHAMOY p 142 N94-11131
SOMAYAJULU, Y. K. p 193 N94-11912
SOMBARDIER, LAURENCE p 216 N94-12691
SOMERS, RICHARD E. p 166 N94-12774
p 166 N94-12775
SONG, C. p 99 N94-12282
SONG, Q. W. p 381 N94-10697
SOON, DAL CHOI p 36 N94-10683
SORENSEN, S-A. p 456 N94-12131
SORKIN, M. Z. p 106 N94-10111
SOROUSH, KIADOKHI AHMADI p 219 N94-12704
SOSOV, YU. V. p 362 N94-10557
SOTIRIOU, COSTANTINOS P. p 1 N94-10936
SOTNIKOV, G. V. p 391 N94-11210
p 391 N94-11211
SOUMA, T. p 213 N94-12670
SOUMA, TAKASHI p 216 N94-12690
SOUTHON, J. R. p 437 N94-12033
SOVEY, JAMES S. p 46 N94-10761
SOWTER, A. p 249 N94-12496
p 250 N94-12499
SOZZI, V. p 235 N94-11728
SPAAN, F. H. P. p 111 N94-10140
SPANGLER, STEVEN R. p 135 N94-11066
SPANIOL, CRAIG p 276 N94-11355
SPANYER, K. L. p 188 N94-11275
SPARGO, A. E. C. p 395 N94-10406
p 170 N94-10630
SPARKMAN, D. p 322 N94-10347
SPARROW, JAMES p 27 N94-11341
SPEITEL, LOUISE C. p 22 N94-12575
SPEKTOROVSKIJ, A. P. p 324 N94-11031
SPETTEL, B. p 87 N94-12086
p 429 N94-12101
SPEZIA, PAUL p 311 N94-12364
SPIELMAN, R. B. p 173 N94-10746
SPIJKERMAN, J. J. p 75 N94-10338
SPINKA, H. p 368 N94-11613
SPINKS, DEBRA p 155 N94-12284
SPIRKOVSKA, LILLY p 327 N94-11274
SPITTLE, ERIC K. p 316 N94-12346
SPITZER, R. C. p 385 N94-10286
p 143 N94-11273
SPOECKER, T. p 243 N94-11777
SPRAGUE, R. A. p 275 N94-11101
SPRANGLE, P. p 145 N94-12424
SPRANGLE, PHILIP p 173 N94-10371
SPUDIS, P. D. p 446 N94-12079
SPUDIS, PAUL p 281 N94-12041
SRINIVASAN, R. S. p 312 N94-11557
SRIVASTAVA, HARI SHANKER p 249 N94-12492
SROKOSZ, M. A. p 235 N94-11722
STADELMAIER, H. p 75 N94-10338
STADUM, C. J. p 438 N94-12034
STALKER, K. T. p 141 N94-10521
STALNAKER, DALE K. p 183 N94-11167
STANCIL, PHILLIP C. p 94 N94-12450
STANDLEY, HILDA M. p 324 N94-10942
STANNARD, P. R. p 278 N94-11702
STANNETT, V. T. p 92 N94-11848
STANNILAND, D. R. p 34 N94-10894
STAPELMANN, J. p 39 N94-10119
STARBUCK, J. M. p 184 N94-10264
STARIKOV, A. G. p 227 N94-12751
STARK, H. p 57 N94-10008
p 57 N94-10009
STARK, JAROSLAV p 31 N94-11490
STARK, MICHAEL p 329 N94-11425
STARNS, JOHN F. p 417 N94-11856
STASI, BILL p 177 N94-10341
STASSI, JOSEPH C. p 286 N94-12772
STAVREV, STAVRI p 119 N94-10211
p 119 N94-10212
STEFFEN, K. p 241 N94-11761
STEGGERDA, C. A. p 351 N94-10970
STEGMANN, BARBARA J. p 302 N94-11548
STEHLE, MARTIN p 114 N94-10181
STEIN, R. p 128 N94-10629
STEIN, S. R. p 334 N94-10988
STEINBERG, MEYER p 267 N94-11845
STEINBICHLER, HANS p 108 N94-10123
STEINCHEN, A. p 102 N94-10086
STEINCHEN, ANNIE p 121 N94-10225
STEINMANN, LAURA p 310 N94-11998
STELBOVICS, A. T. p 359 N94-10312
p 360 N94-10328
STENBERG, BENGT p 183 N94-11586
STENGEL, ROBERT F. p 33 N94-11503
STENHOLM, STIG p 375 N94-10566
STENZEL, CHRISTIAN p 109 N94-10126
STEPANOV, S. S. p 349 N94-10833
STEPHENS, J. R. p 113 N94-10175
STEPHENS, ROBERT L. p 418 N94-10491
STEPHENSON, A. G. p 341 N94-11562
STEPHENSON, G. J., JR. p 361 N94-10349
STEPHENSON, ROBERT p 314 N94-11570
STEPINSKI, T. F. p 472 N94-12220
STERMAN, M. B. p 317 N94-11528
STERN, A. p 353 N94-10979
STERN, E. A. p 400 N94-11458
STERN, H. L. p 239 N94-11749
STERN, S. ALAN p 427 N94-11628
STERRETT, ANDREW p 318 N94-11817
STEWARD, W. GENE p 412 N94-11523
STEWART, DONALD F. p 307 N94-11806
STEWART, R. E. p 389 N94-11074
STIES, M. p 246 N94-12477
STILL, C. H. p 336 N94-11027
STINTON, D. P. p 89 N94-11106
STOCKDALE, J. A. D. p 76 N94-11075
STOERMER, MATTHIAS p 127 N94-10621
STOFAN, ELLEN R. p 467 N94-12190
STOFFELEN, AD p 233 N94-11709
STOLLERY, J. L. p 3 N94-10426
STOLPER, E. p 80 N94-12052
STOLZ, C. J. p 95 N94-12602
STONE, E. C. p 484 N94-11486
STONE, LEWIS W. p 311 N94-12423
STONE, M. ANTHONY p 127 N94-10623
STONEMAN, ROBERT C. p 176 N94-12321
STOORVOGEL, A. A. p 339 N94-10869
STORTZ, MICHAEL W. p 30 N94-11259
STOUFFLET, BRUNO p 5 N94-10440
STOWERS, DAVID p 139 N94-11000
STOYTCHEV, O. p 349 N94-10632
STRATHDEE, J. p 410 N94-10802
STRAUB, DARCY W. p 455 N94-12129
STRAUB, JOHANNES p 101 N94-10079
p 106 N94-10107
p 107 N94-10114
p 109 N94-10124
p 122 N94-10232
p 124 N94-10243
STRAUCH, K. p 111 N94-10138
STRAUSS, A. M. p 109 N94-10127
STRAWBRIDGE, F. p 246 N94-12475
STREET, R. L. p 156 N94-12290
STREHLOW, H. p 27 N94-11321
STRELNITSKIJ, V. E. p 66 N94-11143
STRIFFLER, C. D. p 145 N94-11645
STRIMAITIS, D. G. p 152 N94-11519
STRYMINSKY, B. V. p 362 N94-10554
STUARDO, J. p 217 N94-12695
STUART, BRUCE p 318 N94-11554
STUART, THOMAS A. p 142 N94-10931
STUCKERT, GREGORY K. p 7 N94-10451
STUCKEY, WAYNE K. p 44 N94-12394
STUEMPER, EDMOND p 72 N94-11346
STUERGA, D. p 102 N94-10086
STUPIAN, GARY W. p 146 N94-12565
STUREK, WALTER B. p 16 N94-11870
STURM, DIETER p 124 N94-10246
STURM, K. p 237 N94-11737
STUTTE, G. W. p 315 N94-11258
SUBOTIC, N. p 382 N94-11421
SUCHAN, JAMES E. p 416 N94-10298
SUCHKEVICH, T. A. p 225 N94-12742
SUD, Y. C. p 284 N94-10940
SUDARSHAN, E. C. G. p 378 N94-10590
SUDARSHANA, R. p 217 N94-12697
SUDO, KENJI p 84 N94-11593
SUEMATSU, KAZUYO p 313 N94-10731
SUGAMA, T. p 88 N94-10891
SUGAWARA, SATOSHI p 129 N94-11833
SUGIHARA, SHIGEHIKO p 204 N94-11972
SUGIMORI, YASUHIRO p 196 N94-11925
p 199 N94-11942
p 199 N94-11947
p 206 N94-11985
p 207 N94-12639
p 213 N94-12673
p 218 N94-12702
p 222 N94-12721
SUGIMOTO, TAKASHIGE p 198 N94-11937
p 198 N94-11938
p 215 N94-12683
SUGIMURA, TOSHIROU p 198 N94-11940
p 214 N94-12676
SUIRE, B. S. p 285 N94-11614
SULLIVAN, ROBERT JOHN, JR. p 434 N94-11184
SUMARDJO p 206 N94-11989
SUMI, AKIMASA p 195 N94-11921
p 202 N94-11963
SUMMERS, G. P. p 48 N94-11381
p 48 N94-11382
p 52 N94-11404
SUN, X. p 396 N94-10637
SUN, XIAN-HE p 337 N94-11308
SUN, Y. p 238 N94-11747
SUN, ZI-PING p 153 N94-11635
SUNDT, C. V. p 179 N94-10400
SUPPE, JOHN p 444 N94-12066
SUPRAPTO, D. p 218 N94-12701
SUTER, JOSEPH J. p 355 N94-10993
SUTHERLAND, H. J. p 263 N94-11173
SUTRODHAR, A. K. p 249 N94-12492
SUTTER, JAMES K. p 74 N94-12431
SUTTON, S. R. p 433 N94-12260
p 433 N94-12261
p 433 N94-12262
SUTTON, STEVE R. p 429 N94-12106
SUWA, JUN p 196 N94-11925
p 207 N94-12639
SUZUDO, TOMOAKI p 358 N94-11042
SUZUKI, AKIKO p 35 N94-10677
p 35 N94-10678
SUZUKI, K. p 203 N94-11967
SUZUKI, KATSUO p 358 N94-11042
SUZUKI, MAKOTO p 130 N94-11836
SUZUKI, MASAHIDE p 183 N94-11168
SUZUKI, MICHIYA p 139 N94-11917
SUZUKI, MINEO p 66 N94-10858
SWAN, P. D. p 431 N94-12167
SWANSON, ANDREW D. p 44 N94-12541
SWANSON, P. D. p 383 N94-12416
SWART, WILLIAM W. p 314 N94-11536
SWARTZ, C. K. p 48 N94-11383
SWARTZ, K. L. p 133 N94-10709
SWATLOSKI, T. L. p 132 N94-10518
SWEATT, WILLIAM C. p 374 N94-10339
SWEET, MARTIN R. p 45 N94-11323
SWIFT, G. W. p 128 N94-11161
SWINDLE, T. D. p 430 N94-12125
SWINDLE, TIMOTHY p 473 N94-12228
SWORDY, SIMON p 485 N94-12771
SYAMTOMOV, A. I. p 344 N94-10881
SYBRANDY, ANDREW p 216 N94-12691
SYDNOR, RICHARD p 355 N94-10995
p 139 N94-11000
SYDNOR, RICHARD L. p 350 N94-10963
SYMKO, OREST G. p 403 N94-12336
SYMON, C. J. p 253 N94-12518
SYN, C. K. p 82 N94-11076
SZE, J. S. p 170 N94-11267
SZOSTAK, ROSEMARIE p 124 N94-10245

T

TAASAN, SHLOMO p 343 N94-10642
TABAK, M. p 369 N94-11815
TABARY, LUC p 252 N94-12511
TABATA, S. p 209 N94-12647
TACCONI, MATTEO p 110 N94-10133
TACHIBANA, MASAKAZU p 12 N94-10480
TADRIST, L. p 102 N94-10086
TAGUCHI, HARUO p 190 N94-11083
TAI, A. p 382 N94-11421
TAIRA, KEISUKE p 194 N94-11915
p 195 N94-11924
p 206 N94-11986
TAIWO, T. A. p 346 N94-11608
TAJIMA, T. p 393 N94-11669
TAKAHASHI, HIDETAKE p 372 N94-11591
TAKAHASHI, HITOSHI p 2 N94-10350
TAKAHASHI, K. p 107 N94-10115
p 114 N94-10179
TAKAHASHI, T. p 34 N94-11041
TAKAHASHI, Y. p 351 N94-10968
TAKAKURA, YOKO p 12 N94-10479
TAKAKUSAKI, TSUNEHIKO p 129 N94-11833
TAKAMATSU, KUNIO p 363 N94-10696
TAKANASHI, SUSUMU p 11 N94-10473
p 12 N94-10480
TAKANO, YUTAKA p 482 N94-12326
p 482 N94-12328
TAKASHIMA, TSUTOMU p 205 N94-11981
TAKEDA, ATSUSHI p 221 N94-12717
TAKENS, F. p 344 N94-10906
TAKEUCHI, TOMOYOSHI p 194 N94-11915
TAKIYAMA, K. p 393 N94-11594
TAKRITI, SALAHEDDIN p 397 N94-10830

TAM, RICKY YIN JUN p 339 N94-11640
TAMEISHI, HIDEO p 193 N94-11909
p 198 N94-11938
p 215 N94-12681
p 215 N94-12683
p 220 N94-12713
TAMKOVICH, GENNADY p 308 N94-11807
TAMURA, HIROKAZU p 365 N94-11040
TANABASHI, YOSHIHIKO p 197 N94-11931
TANAKA, ATSUSHIGE p 27 N94-10367
TANAKA, K. L. p 469 N94-12202
p 469 N94-12203
TANAKA, KEIJI p 33 N94-10733
TANAKA, KOHEI p 10 N94-10469
p 11 N94-10477
TANAKA, S. p 411 N94-10880
TANAKA, SOUTAROU p 198 N94-11940
p 214 N94-12676
TANAKA, TASUKU p 35 N94-10677
p 35 N94-10678
TANBA, S. p 213 N94-12670
TANBA, SUMIO p 216 N94-12690
TANG, T. Y. p 219 N94-12708
TANG, WENQING p 202 N94-11964
TANG, XIAOYAN p 78 N94-12273
TANI, KEIJI p 390 N94-11149
TANI, KOUICHIROU p 27 N94-10367
TANIMORI, T. p 34 N94-11041
p 367 N94-11509
TANIMOTO, M. p 113 N94-10176
TANTAWI, S. p 145 N94-11645
TARABROVA, L. I. p 397 N94-10843
TARASCON, JEAN M. p 395 N94-10416
TARASOFF, LEV p 413 N94-11822
TARTAKOVSKIJ, V. K. p 362 N94-10557
TASCILLO, M. p 32 N94-11502
TASSA, O. p 58 N94-10020
TASSAN, STELVIO p 191 N94-11900
TATARSKII, V. I. p 135 N94-11067
TATCHYN, R. p 175 N94-11468
TATE, M. W. p 301 N94-11648
TATEM, P. A. p 79 N94-12415
TATSUMI, TOMOMASA p 164 N94-12622
TATUM, C. P. p 285 N94-11664
TAVELLA, PATRIZIA p 351 N94-10969
p 356 N94-10997
TAWARA, HIRO p 387 N94-10662
TAYLOR, BILL p 170 N94-10667
TAYLOR, D. L. p 404 N94-12376
TAYLOR, DEAN B. p 98 N94-10844
TAYLOR, F. W. p 457 N94-12139
TAYLOR, G. J. p 282 N94-12116
p 282 N94-12197
TAYLOR, G. JEFFREY p 460 N94-12154
TAYLOR, J. J. p 327 N94-11246
TAYLOR, J. R. p 95 N94-12602
TAYLOR, STEPHEN p 328 N94-11295
TAZUKE, M. p 198 N94-11940
TCHON, KRZYSZTOF p 341 N94-10276
TEMAM, ROGER p 156 N94-12293
TENBERG, A. J. W. M. p 319 N94-10278
TENSI, HANS M. p 112 N94-10141
p 86 N94-10199
TERAKUBO, SATOSHI p 172 N94-11968
TERAO, YOSHIYA p 164 N94-12619
TERAZAWA, HIDEZUMI p 410 N94-10718
TERMINELLO, L. J. p 169 N94-10526
TERRAZAS-SALINAS, IMELDA p 34 N94-10930
TERRIE, GREGORY p 288 N94-11287
TERUI, FUYUTO p 42 N94-10366
TESAR, A. p 87 N94-10271
TESTA, FLAVIANO p 124 N94-10245
TESTANI, C. p 58 N94-10020
TESTI, N. p 325 N94-11109
TEWARSON, A. p 20 N94-10788
THACKER, W. p 221 N94-12719
THADATHIL, PANKAJAKSHAN p 196 N94-11925
p 222 N94-12721
THADHANI, N. N. p 93 N94-12354
THALMANN, CH. p 87 N94-12240
THE, P. S. p 424 N94-11306
THEISS, T. J. p 188 N94-11367
THEON, JOHN S. p 381 N94-11054
THI, HENRI NGUYEN p 117 N94-10203
THIEL, K.-H. p 237 N94-11736
p 237 N94-11740
THIEMENS, M. H. p 432 N94-12224
THILAGAR, A. p 318 N94-11554
THINH, TO QUANG p 196 N94-11928
THIRSK, ROBERT p 80 N94-10248
THOMAS, C. p 24 N94-10965
p 24 N94-10967
THOMAS, CLAUDINE p 351 N94-10969
THOMAS, J. P. p 250 N94-12501
p 253 N94-12518
THOMAS, K. L. p 81 N94-12099
p 433 N94-12261
THOMAS, MICHAEL L. p 49 N94-11390
THOMAS, SUSAN p 286 N94-12772
THOMASON, JAMES S. p 417 N94-11856
THOMMES, M. p 80 N94-10228
THOMPSON, J. A. p 369 N94-12546
THOMPSON, T. C. p 65 N94-10740
THOMPSON, THOMAS p 239 N94-11751
THONG, LE QUI p 402 N94-11659
p 402 N94-11660
THORNTON, JEFFREY M. p 315 N94-10296
THORPE, A. p 75 N94-10338
THRASHER, T. p 311 N94-12005
THUMM, D. p 128 N94-10629
THURSTON, T. R. p 400 N94-11467
THYSSEN, FRANZ p 238 N94-11742
TILDESLEY, P. p 234 N94-11717
TILLEY, DAVID GEORGE p 251 N94-12505
TIMMONS, M. p 54 N94-11418
TIMMONS, M. L. p 400 N94-11443
TING, ANTONIO p 173 N94-10371
TINO, G. M. p 124 N94-10241
TIPTON, CHARLES M. p 310 N94-12001
TIRILLY, L. p 59 N94-10023
TISCHLER, MARK B. p 25 N94-10935
TIT, N. p 394 N94-10281
TKACH, Y. N. p 371 N94-10542
TKACH, Y. V. p 387 N94-10541
p 362 N94-10649
p 133 N94-11030
p 392 N94-11213
p 143 N94-11365
TKACHENKO, E. V. p 324 N94-11031
TKACHENKO, V. I. p 387 N94-10558
p 392 N94-11213
TKALCEVIC, FRANK J. p 328 N94-11301
TOBA, YOSHIAKI p 191 N94-11896
p 195 N94-11920
p 200 N94-11952
p 202 N94-11961
p 220 N94-12710
TOBIAS, MARK E. p 65 N94-10812
TODA, TAKASHI p 213 N94-12672
p 221 N94-12717
TOIKKA, M. p 239 N94-11750
TOJYO, E. p 144 N94-11508
TOKMAKIAN, R. T. p 255 N94-12531
TOKUDA, MASAYUKI p 192 N94-11903
p 192 N94-11904
TOKUDA, N. p 144 N94-11508
TOKUNAGA, HIROSHI p 157 N94-12297
TOKUNO, MASAMI p 190 N94-11081
TOLSTOLUZHSKIJ, A. P. p 134 N94-11037
p 391 N94-11209
TOLSTYKH, A. YU. p 349 N94-10556
TOMBESI, PAOLO p 376 N94-10578
TOMII, NAOYA p 211 N94-12659
TOMLINSON, G. R. p 70 N94-11335
TOMODA, YOSHIBUMI p 217 N94-12692
TONG, S. Y. p 369 N94-12379
TORINESI, A. p 111 N94-10135
TORMALA, P. p 60 N94-10035
TORNG, T. Y. p 85 N94-12426
TOSCANO, WILLIAM B. p 311 N94-12006
TOURNADRE, JEAN p 233 N94-11712
TRABANDT, U. p 61 N94-10041
TRABANDT, ULRICH p 57 N94-10012
p 59 N94-10027
TRACE, DAVID p 306 N94-11797
TRASK, RICHARD P. p 289 N94-11853
TRAUGER, JOHN T. p 381 N94-10657
TRAVIS, D. J. p 169 N94-10326
TREASE, H. E. p 153 N94-11601
TREBES, J. p 176 N94-12590
TREHIN, YVES p 485 N94-11379
TREMBLEY, NANCY p 22 N94-12397
TRENT, WILLIAM p 23 N94-10933
TRENTELMAN, H. L. p 339 N94-10869
TRESPIDI, F. p 111 N94-10135
TRETYAK, V. I. p 364 N94-10837
TREUMANN, R. A. p 385 N94-10284
TRIFONOV, D. A. p 349 N94-10581
TRIPATHY, S. K. p 93 N94-12380
TRIVEDI, R. p 118 N94-10206
TRIVERO, PAOLO p 200 N94-11953
TROIDL, H. p 45 N94-11320
TROLINGER, JAMES p 5 N94-10437
TROMBKA, JACOB I. p 462 N94-12165
TROTT, W. M. p 98 N94-11366
TROUVE, ARNAUD p 81 N94-12316
TSANGARIS, S. p 9 N94-10462
TSCHERNING, C. C. p 242 N94-11768
TSO, KAM S. p 179 N94-10670
TSUCHIYA, TOSHIO p 172 N94-11916
p 139 N94-11917
TSUCHIYA, YOSHIO p 20 N94-10784
TSUDA, R. p 203 N94-11967
TSUIKI, ATSUO p 131 N94-11843
TSUKADA, TAKASHI p 84 N94-11593
TSUKANO, YUUKICHI p 30 N94-10734
TSUKISHIMA, T. p 392 N94-11239
TSURIKOV, V. A. p 362 N94-10649
TSURU, TSUNEAKI p 363 N94-10696
TU, QING p 181 N94-11219
TUCCHIO, MICHAEL A. p 178 N94-10385
TUCK, E. O. p 98 N94-11303
TUCKER, BRYAN J. p 310 N94-12002
TUCKER, GEORGE T. p 329 N94-11427
TUGEL, JOYCE B. p 268 N94-12453
p 270 N94-12463
p 271 N94-12468
TULLOCH, P. A. p 395 N94-10406
TUMBLESON, M. E. p 300 N94-11180
TUR, A. V. p 391 N94-11207
p 391 N94-11208
p 392 N94-11212
TURANO, KATHLEEN p 304 N94-11681
TURCHI, P. E. A. p 81 N94-10522
TUREK, FRED W. p 303 N94-10872
TURK, MATTHEW p 418 N94-10515
TURKEL, ELI p 151 N94-11253
TURNER, J. p 250 N94-12501
p 253 N94-12518
TURNER, SIMON p 30 N94-10895
TUTIK, R. S. p 349 N94-10547
p 349 N94-10833
p 411 N94-10834
TUTTON, P. A. p 22 N94-11334
TYUPA, V. I. p 391 N94-11174

U

UEDA, MASAHITO p 377 N94-10585
UEDA, SHUUICHI p 27 N94-10367
UEMATSU, MITSUO p 204 N94-11976
UENG, TZOU-SHIN p 185 N94-10306
UESUGI, MASATO p 54 N94-11413
UFFELMANN, DIRK p 116 N94-10192
UFFEN, D. R. p 69 N94-11326
UHERKA, K. L. p 144 N94-11607
ULABY, FAWWAZ T. p 266 N94-11374
ULANDER, L. M. H. p 236 N94-11730
p 238 N94-11747
ULANDER, LARS p 239 N94-11751
ULBRICH, NORBERT MANFRED HERMANN
p 15 N94-11154
ULIANO, KEVIN C. p 315 N94-11627
ULM, G. p 143 N94-11273
ULWICK, JAMES C. p 279 N94-12561
UM, CHUNG IN p 370 N94-10593
UM, CHUNG-IN p 380 N94-10606
p 380 N94-10611
UMALI, RICARDO M. p 36 N94-10687
UMATANI, SHIN-ICHIROU p 205 N94-11984
UMEDA, A. Y. p 181 N94-11290
UMEKI, MAKOTO p 166 N94-12634
UMEZAWA, KAYO p 70 N94-11330
UNDERWOOD, D. G. p 368 N94-11613
UNDERWOOD, F. M. p 22 N94-11334
UNGER, GLENN p 170 N94-10667
UNNIKRISHNAN, A. S. p 206 N94-11987
UNO, SHIROU p 218 N94-12698
p 222 N94-12720
UNSEREN, M. A. p 177 N94-10269
p 340 N94-12543
UPTON, M. p 246 N94-12476
URA, TAMAKI p 217 N94-12692
URATANI, NORIYOSHI p 418 N94-10559
URATSUKA, SEIHO p 253 N94-12520
URIBE, EDUARDO p 216 N94-12688
USAVAGE, PAUL p 330 N94-11437
USENKO, A. S. p 149 N94-10838
p 388 N94-10839
USKOV, V. V. p 391 N94-11211
USTINOVA, G. K. p 428 N94-12022
UTTAMCHANDANI, D. p 69 N94-11324
UWAMINO, Y. p 363 N94-10720
UZUNALIOGLU, H. p 322 N94-10410

V

VACHON, P. W. p 232 N94-11708
VAESSEN, G. p 59 N94-10023
VAGHMARE, RAJEEV p 61 N94-10037
VAHDATI, M. p 9 N94-10461
VAHLE, M. O. p 319 N94-10268
VAIDA, M. p 394 N94-10301
VAJTA, M. p 184 N94-10161
VAKULENKO, M. O. p 386 N94-10396
p 386 N94-10397
p 386 N94-10523
p 387 N94-10538

p 387 N94-10539
p 387 N94-10540
p 388 N94-10840
VALANJU, P. M. p 390 N94-11142
VALDOVINOS, C. p 217 N94-12695
VALIS, TOMAS p 73 N94-12013
VANALSTINE, JAMES M. p 108 N94-10120
VANBLARCUM, SCOTT C. p 285 N94-11685
VANCAMP, LIEVE p 220 N94-12712
VANDEMARK, D. p 232 N94-11708
VANDENBERG, J. P. p 322 N94-10419
VANDENBROEK, A. C. p 236 N94-11731
VANDENENDE, C. A. M. p 60 N94-10030
VANDERBURG, G. p 254 N94-12525
VANDERHAEGHE, O. p 254 N94-12523
VANDERKOOIJ, M. W. A. p 254 N94-12525
VANDERSCHAFT, A. J. p 341 N94-10273
VANDERWOOD, T. B. p 81 N94-12099
VANDOMMELEN, L. p 16 N94-11889
VANECK, J. L. p 39 N94-10118
VANGAALEN, W. J. p 244 N94-11779
VANGROESEN, E. W. C. p 147 N94-10275
VANGYSEN, HERMAN p 208 N94-12642
VANHALEN, C. J. G. p 65 N94-10067
VANHEERDE, JAN WILLEM p 131 N94-10280
VANLOCHEM, J. H. p 60 N94-10031
VANMAAREN, HANS p 322 N94-10355
VANTOOREN, M. J. L. p 57 N94-10013
VANVAERENBERGH, STEFAN p 112 N94-10173
p 119 N94-10215
p 120 N94-10217
p 121 N94-10223
VARADARAJAN, V. p 393 N94-11512
VARGAS-ABURTO, C. p 48 N94-11383
VARGAS-ABURTO, CARLOS p 49 N94-11385
p 404 N94-12430
VARGAS, C. p 48 N94-11384
VARGAS, M. p 173 N94-10746
VARGAS, MARIO p 174 N94-11132
VARGO, RICK C. p 348 N94-11568
VASILEV, V. V. p 66 N94-11143
VASILIEV, A. S. p 227 N94-12753
p 227 N94-12754
VASILKOV, ALEXANDER P. p 177 N94-12722
p 224 N94-12736
p 226 N94-12744
p 229 N94-12762
VASSILAROS, M. G. p 85 N94-12532
VASSILEVICH, D. V. p 425 N94-11152
VAUGHAN, DAVID p 238 N94-11742
VAWTER, G. A. p 174 N94-11005
VEDERNIKOV, A. A. p 124 N94-10242
VEERS, P. S. p 263 N94-11173
VEILLET, CH. p 352 N94-10972
VELARDE, MANUEL G. p 119 N94-10214
p 120 N94-10220
VELLINGER, JOHN C. p 108 N94-10120
VELSKO, S. P. p 173 N94-10755
VENEMA, W. Z. p 416 N94-10868
VENNEMANN, D. p 4 N94-10429
VERCHOVSKY, A. B. p 433 N94-12254
p 433 N94-12255
p 81 N94-12256
VERDUCCI, ANTHONY J., JR. p 329 N94-11427
VERGA, A. p 39 N94-10118
p 39 N94-10136
VERMEEREN, C. A. J. R. p 57 N94-10013
VERNER, D. A. p 345 N94-11225
VERNIKOS, JOAN p 311 N94-12004
VERNON, S. p 50 N94-11394
VERVISCH, LUC p 81 N94-12317
VERWER, J. G. p 342 N94-10351
VERZWYVELT, SCOTT A. p 52 N94-11401
VESELOVA, G. V. p 476 N94-12242
VESSOT, R. F. C. p 353 N94-10981
VEVERKA, JOSEPH p 434 N94-10817
p 459 N94-12147
VIBULSRESTH, SUVIT p 37 N94-10690
VICAR, MAC p 68 N94-11322
VIDAL-SETIF, M. H. p 59 N94-10024
VIDENOVA-ADRABINSKA, V. p 404 N94-12438
VIDZIGOVSKIJ, V. B. p 386 N94-10524
VIEHOFF, T. p 239 N94-11753
VIET, NGUYEN AI p 402 N94-11659
p 402 N94-11660
VIJAYAN, T. p 371 N94-10316
VIKHLIJ, G. A. p 397 N94-10843
VILCANS, JANIS p 23 N94-11626
VILCHINSKIJ, S. I. p 148 N94-10717
VILLERMAUX, E. p 123 N94-10240
VINCENT, P. p 242 N94-11769
VINDUSKA, M. p 344 N94-11032
VINET, B. p 86 N94-10195
VINOGRADOV, AN. V. p 375 N94-10570
VISAISOUK, S. p 128 N94-10626
VISINTINI, L. p 4 N94-10431
VISSER, BASTIAAN p 57 N94-10010
VISSER, P. N. A. M. p 242 N94-11772
VISTISEN, L. p 428 N94-12016
VITELA, E. J. p 340 N94-11644
VITRIA, M. R. p 255 N94-12529
VITYAZEV, A. V. p 432 N94-12225
p 432 N94-12226
VIUDEZ, A. p 255 N94-12529
VIVIANI, ANTONIO p 104 N94-10097
p 104 N94-10098
p 106 N94-10108
VLASOV, VLADIMIR N. p 308 N94-11808
VLASSOV, V. L. p 177 N94-12732
VODYANOY, I. p 301 N94-11648
VOGEL, BERND p 124 N94-10243
VOGELZANG, J. p 254 N94-12525
VOGFJORD, KRISTIN S. p 275 N94-11102
VOGTLIN, G. E. p 181 N94-11247
VOJTSENYA, V. S. p 66 N94-11143
VOLAKIS, JOHN L. p 136 N94-11084
VOLKMANN, T. p 87 N94-10204
VOLKMAR, J. p 127 N94-10625
VOLKOV, A. E. p 391 N94-11209
VONDREELE, R. B. p 363 N94-10743
VONHOLTZ, E. p 77 N94-11602
VONPRAGENAU, GEORGE L. p 33 N94-10669
VORACEK, DAVID F. p 26 N94-11233
VOROBEV, V. G. p 82 N94-10842
VORONIN, A. A. p 223 N94-12729
VOS, J. B. p 9 N94-10460
VOURDAS, A. p 377 N94-10580

W

WADA, BEN K. p 72 N94-11344
WADA, YASUHIRO p 27 N94-10370
p 12 N94-10479
WADGE, G. p 246 N94-12474
WADHAMS, P. p 238 N94-11746
WAGNER, J. R. p 190 N94-12178
WAGSTAFF, J. p 423 N94-11183
WAHL, TERJE p 253 N94-12521
p 253 N94-12522
WAKABAYASHI, H. p 240 N94-11755
WAKE, L. V. p 90 N94-11302
WAKITA, KEN p 320 N94-10166
WAKKER, K. F. p 242 N94-11772
p 244 N94-11779
WALCHLI, LAWRENCE A. p 33 N94-11504
WALEFFE, FABIAN A. p 158 N94-12306
p 158 N94-12308
WALIGORA, J. p 312 N94-11544
WALIGORA, JAMES M. p 125 N94-11235
WALIGORA, SHARON p 329 N94-11429
WALKER, G. K. p 284 N94-10940
WALKER, J. V. p 45 N94-10299
WALKER, MARY MCWHERTER p 6 N94-10445
WALKER, R. M. p 431 N94-12167
WALL, J. p 401 N94-11651
WALLACE, JAMES M. p 157 N94-12303
WALLING, L. p 374 N94-12785
WALLING, R. S. p 389 N94-11074
WALLMAN, H. p 181 N94-11247
WALSH, E. J. p 232 N94-11708
WALSH, MICHAEL R. p 29 N94-12274
WALSH, TERESE A. p 231 N94-11521
WALSWORTH, R. L. p 353 N94-10981
WALTER, J. W. p 321 N94-10267
WALTER, TODD p 146 N94-10999
WALTERS, DANIEL p 41 N94-10512
WALTERS, DAVID K. p 231 N94-11521
WALTERS, G. K. p 76 N94-10854
WALTERS, MICHAEL R. p 50 N94-11391
WALTERS, R. J. p 48 N94-11381
p 48 N94-11382
p 52 N94-11404
WALTERS, R. W. p 54 N94-11414
WALTERS, THOMAS J. p 301 N94-11861
WALZ, WILLIAM p 381 N94-11054
WANAS, M. I. p 427 N94-11812
WANG, B. C. p 351 N94-10970
p 351 N94-10971
WANG, DAN-LI p 87 N94-10510
WANG, H. p 140 N94-10300
WANG, JIANPING p 390 N94-11149
WANG, M. p 309 N94-11997
WANG, TAICHUN p 173 N94-10483
WANG, XU p 409 N94-10403
WANG, Y. p 402 N94-11684
WANIE, K. M. p 9 N94-10459
WANKE, R. p 369 N94-11826
WARAGAI, HEITA p 372 N94-11591
WARD, G. T. p 185 N94-10715
WARD, M D. p 402 N94-11654
WARD, M. D. p 402 N94-11827
p 404 N94-12438
WARNATZ, J. p 77 N94-11370
WARNER, ROBERT ANDREW p 212 N94-12666
WARREN, JAMES W. p 92 N94-11866
WARREN, L. F. p 173 N94-10755
WASSERBURG, G. J. p 430 N94-12150
p 430 N94-12151
p 431 N94-12182
WATANABE, M. p 107 N94-10115
p 114 N94-10179
WATANABE, T. p 213 N94-12670
WATANABE, TAKASHI p 216 N94-12690
WATANABE, YOSHIAKI p 178 N94-10369
WATERS, MARSHALL P. p 211 N94-12662
WATTS, A. J. p 190 N94-12178
WATTS, ALAN p 42 N94-10665
WAXMAN, ALLEN M. p 331 N94-11652
WEAVER, MICHAEL J. p 396 N94-10705
p 368 N94-11658
p 404 N94-12388
p 369 N94-12420
WEBB, D. J. p 235 N94-11725
WEBB, JAMES T. p 317 N94-11541
WEBB, M. S. p 173 N94-10755
WEBER, M. p 64 N94-10059
WEBSTER, JAMES R. p 383 N94-12413
WEEDING, M. p 126 N94-10618
WEEKS, W. F. p 240 N94-11755
WEIGEL, A. p 432 N94-12239
WEIGHT, THOMAS H. p 43 N94-11223
WEIGOLD, E. p 360 N94-10327
p 360 N94-10332
p 361 N94-10333
WEINBERG, I. p 48 N94-11383
p 48 N94-11384
p 54 N94-11414
WEINER, BRAD R. p 175 N94-12012
WEISBERG, MICHAEL K. p 431 N94-12200
WEISHEIT, J. C. p 389 N94-11118
WEISS, MARC A. p 357 N94-11003
WEISS, OFER p 343 N94-10392
WEISS, P. S. p 365 N94-11093
WEISSINGER-LEWIN, Y. p 394 N94-10301
WEITZ, C. M. p 440 N94-12047
p 440 N94-12048
WEIZER, VICTOR G. p 49 N94-11387
WELCOME, M. L. p 325 N94-11112
WELKER, M. F. p 92 N94-11848
WELLER, DAVID p 329 N94-11431
WELLS, MARK K. p 313 N94-11867
WELLS, RICHARD L. p 78 N94-11683
WELLS, S. p 273 N94-10285
WELZ, LINDA L. p 314 N94-11534
WEMPLE, C. A. p 365 N94-10952
WENDT, J. F. p 5 N94-10438
WENG, W. T. p 373 N94-12601
WENMAKERS, L. E. P. p 60 N94-10034
WENSINK, G. J. p 254 N94-12525
WENTWORTH, S. J. p 440 N94-12050
p 430 N94-12132
WENTZ, FRANK J. p 201 N94-11957
WERNER, CHARLES L. p 236 N94-11734
WERNER, WINFRIED p 60 N94-10032
WERNLUND, JIM V. p 146 N94-12433
WERNSMAN, B. p 48 N94-11372
WERTGEIM, I. p 120 N94-10217
WESCOTT, J. p 19 N94-10780
WESFREID, J. E. p 121 N94-10229
WESSALE, WILLIAM p 329 N94-11431
WESSELS, J. p 338 N94-10169
p 416 N94-10868
WESSLING, FRANCIS C. p 108 N94-10120
WESTBROOK, C. K. p 177 N94-10322
WEYLAND, MARK D. p 318 N94-11561
WHALEY, K. B. p 411 N94-10874
WHEAT, HAROVEL G. p 85 N94-12404
WHEELER, A. A. p 105 N94-10103
p 113 N94-10178
WHEELER, DAVID A. p 332 N94-11850
WHEELWRIGHT, CHARLES D. p 314 N94-11538
WHITE, C. D. p 309 N94-11995
WHITE, JOSEPH D. p 352 N94-10973
WHITE, L. P. p 416 N94-10145
WHITE, NEIL p 208 N94-12642
p 208 N94-12643
WHITE, R. G. p 248 N94-12487
WHITE, STEPHEN F. p 51 N94-11399
WHITELEY, JAMES D. p 314 N94-11539
WHITEMAN, C. D. p 274 N94-10323
WHITING, ELLIS E. p 34 N94-10930
WHITLOCK, ROBERT p 176 N94-12337
WHITMORE, MIHRIBAN p 317 N94-11537
WHITNEY, JAMES M. p 74 N94-12347
WHITTEN, B. T. p 422 N94-10736
WIANT, J. R. p 352 N94-10972
WICK, G. A. p 221 N94-12716
WIERZBANOWSKI, TED p 25 N94-10945

WIGGENHAGEN, M. p 246 N94-12477
WILBUR, PAUL J. p 386 N94-10346
WILCOXEN, J. L. p 175 N94-11283
WILKS, S. p 369 N94-11815
WILLAND, JAMES H. p 283 N94-10336
WILLEMS, PIERRE Y. p 31 N94-11491
WILLHITE, G. P. p 88 N94-10749
WILLIAMS, D. p 319 N94-10146
WILLIAMS, F. A. p 79 N94-12403
WILLIAMS, F. W. p 79 N94-12415
WILLIAMS, R. J. p 423 N94-11183
WILLIAMS, WENDELL p 49 N94-11386
p 404 N94-12430
WILLIAMSON, E. J. p 253 N94-12517
WILLNECKER, RAINER p 112 N94-10143
p 87 N94-10231
WILLOWBY, D. p 51 N94-11396
WILLSON, C. G. p 145 N94-11819
p 95 N94-12585
WILSON, G. R. p 387 N94-10641
WILSON, GLENN F. p 317 N94-11529
WILSON, JOHN W. p 484 N94-10759
p 484 N94-11278
p 485 N94-12434
WILSON, JOSEPHINE p 63 N94-10053
WILSON, L. p 477 N94-12243
WILSON, LIONEL p 283 N94-12236
WILSON, ROBERT p 286 N94-12772
WILSON, S. K. p 120 N94-10222
WILSON, STEVE p 318 N94-11555
WILT, DAVID M. p 49 N94-11385
WILT, T. E. p 188 N94-11482
WIMMEL, R. p 71 N94-11338
WIMMER, R. p 182 N94-12605
WINGET, C. M. p 302 N94-11556
WINGHAM, D. J. p 237 N94-11738
WINKLER, JEFFREY D. p 55 N94-12011
WINOKUR, P. S. p 143 N94-11271
WINTER, J. p 108 N94-10123
p 122 N94-10232
WINTER, R. p 246 N94-12477
WIRYOSUMARTO, I. H. p 36 N94-10681
WISMANN, VOLKMAR p 233 N94-11711
WISNIA, JEFFRY A. p 353 N94-10980
WISNIEWSKI, ROBERT W. p 337 N94-11650
WISSE, E. p 242 N94-11772
WITKOWSKI, W. p 91 N94-11665
WITTMANN, KLAUS p 87 N94-10231
WITZEL, A. p 135 N94-11064
WITZKE, B. J. p 281 N94-12032
WLOTZKA, F. p 81 N94-12214
WODKIEWICZ, K. p 378 N94-10592
WOERMANN, D. p 122 N94-10233
WOIKE, THOMAS J. p 51 N94-11398
WOJCIECHOWSKI, K. W. p 361 N94-10502
WOJTCZUK, S. p 50 N94-11394
WOLF, E. p 75 N94-10519
WOLF, E. G. p 302 N94-11548
WOLF, K. L. p 373 N94-12607
WOLFE, JAMES F. p 55 N94-10513
WONG, E. K. p 403 N94-12371
WONG, EDMOND p 319 N94-10724
WOOD, J. S. p 484 N94-11278
WOOD, KATHRYN J. p 303 N94-10813
WOOD, MARGIE p 310 N94-11998
WOOD, P. A. p 19 N94-10780
WOODFORD, LYNN M. p 21 N94-10791
WOODING, M. p 248 N94-12488
WOODING, M. G. p 249 N94-12493
WOODS, S. A. p 359 N94-10266
WOODWORTH, J. p 369 N94-11815
WOODWORTH, P. L. p 234 N94-11716
WOODYARD, JAMES R. p 50 N94-11391
WOOLLEY, CHARLES p 348 N94-11574
WOOTTON, A. J. p 386 N94-10321
WORDEN, E. F., JR. p 76 N94-11075
WORDEN, K. p 70 N94-11335
WORKMAN, GARY L. p 185 N94-10342
WORSNOP, D. R. p 279 N94-12572
WORTH, G. T. p 374 N94-12786
WORTHEY, GUY p 426 N94-11187
WOUTHUYZEN, SAM p 197 N94-11931
p 218 N94-12698
WOZNIAK, BOGDAN p 228 N94-12761
WOZNIAK, G. p 106 N94-10109
WOZNIAK, KLAUS p 106 N94-10109
WRAY, RICHARD B. p 27 N94-10664
WRENCH, C. L. p 244 N94-11785
WRIGHT, J. K. p 83 N94-11141
WRIGHT, JAMES L. p 139 N94-10996
WRIGHT, JOHN R. p 94 N94-12536
WRIGHT, P. A. p 248 N94-12488
WRIGHT, R. N. p 83 N94-11141
WRIGLEY, ROBERT C. p 231 N94-11378
WU, JIANGUO p 172 N94-11966
WU, JIE p 337 N94-11308
WU, Q. X. p 214 N94-12679
WULF, E. p 111 N94-10139
WUNDERLICH, RAINER K. p 112 N94-10143
WUNSCHE, A. p 350 N94-10595
WURTELE, M. G. p 283 N94-10725
WYBOURNE, M. N. p 93 N94-12353
p 94 N94-12396
WYNTER, C. I. p 75 N94-10338

X

XIA, XIAOGUONG p 405 N94-12587
XIA, Y. p 237 N94-11736
XIAO, H. p 390 N94-11142
XING, G. C. p 400 N94-11442
p 400 N94-11443
XING, L. Q. p 86 N94-10194

Y

YABE, AKIRA p 162 N94-12550
YACOBY, Y. p 400 N94-11458
YACOMENI, CHARLES W. p 18 N94-10774
YADI, BERT A. p 314 N94-11536
YAGURA, TETSUO p 217 N94-12696
YAKIMENKO, I. P. p 149 N94-10838
p 388 N94-10839
p 389 N94-10886
YAKOVIEV, V. p 374 N94-12785
YAKOVLEV, O. I. p 81 N94-12214
YAMADA, HARUMI p 217 N94-12694
YAMADA, HIROFUMI p 396 N94-10645
YAMADA, HIROYUKI p 162 N94-12555
YAMADA, ICHIROU p 212 N94-12668
YAMADA, K. K. p 181 N94-11290
YAMAGISHI, T. p 388 N94-10807
YAMAGUCHI, H. p 140 N94-12706
YAMAGUCHI, MASAYOSHI p 172 N94-11968
YAMAMOTO, HIROMICHI p 193 N94-11909
p 220 N94-12713
YAMAMOTO, KIYOSHI p 163 N94-12613
YAMAMOTO, YASUNARI p 54 N94-11413
YAMANE, RIKO p 195 N94-11921
YAMARTINO, R. J. p 152 N94-11519
YAMAZAKI, K. p 203 N94-11967
YAMAZAKI, T. p 363 N94-10720
YAMAZAKI, TETSUO p 11 N94-10477
YAMAZAKI, TOSHIMITSU p 365 N94-11040
YAN, XIAO-HAI p 221 N94-12718
YANAGIHARA, MASAAKI p 25 N94-10728
YANAGIMOTO, DAIGO p 206 N94-11986
YANAGISAWA, ATSUHIRO p 210 N94-12657
YANG, B. p 173 N94-10287
YANG, CHUI-HSU p 312 N94-11558
YANG, F. M. p 351 N94-10971
YANG, G. C. p 86 N94-10194
YANG, KYUNG-SOO p 156 N94-12291
YANG, L. H. p 89 N94-11151
YANG, SONGQI p 322 N94-10484
YANG, W. S. p 346 N94-11608
YANG, Y. J. p 219 N94-12708
YANG, Z. p 151 N94-11192
YANOVSKIJ, V. V. p 391 N94-11207
p 392 N94-11212
YANOVSKY, V. V. p 391 N94-11208
YANTA, WILLIAM J. p 5 N94-10436
YARMAK, V. G. p 362 N94-10649
YASUDA, YOSHIZUMI p 191 N94-11897
YATABE, S. p 248 N94-12486
YATES, J. T., JR. p 79 N94-12538
YATES, R. K. p 338 N94-12597
YE, H. J. p 396 N94-10637
YEAGER, ARLEEN p 333 N94-12448
YEAGER, E. B. p 401 N94-11518
YEE, J. H. p 137 N94-11466
YEE, M. p 141 N94-10521
YEH, LEEHWA p 380 N94-10608
YEMMOU, M. p 115 N94-10189
YEON, KYU-HWANG p 380 N94-10606
p 380 N94-10611
YERKES, J. W. p 51 N94-11400
YIMAN, WANG p 254 N94-12526
YIN, SANDRA p 330 N94-11436
YODA, SCHINICHI p 112 N94-10142
YOKOYAMA, R. p 213 N94-12670
YOKOYAMA, RYUUZOU p 216 N94-12690
YONEYAMA, K. p 208 N94-12640
YONEZAWA, AKINORI p 320 N94-10166
YOO, HONG-RHYONG p 216 N94-12689
YOSHIDA, I. p 213 N94-12670
YOSHIDA, ISAO p 216 N94-12690
YOSHIDA, MASAHIRO p 335 N94-10368
YOSHIHARA, SHOUICHI p 125 N94-10730
YOSHIMURA, HIDETO p 130 N94-11841
YOSHIMURA, TAKAHIRO p 164 N94-12622
YOSHITOMI, S. p 112 N94-10142
YOSHIZAWA, AKIRA p 163 N94-12614
YOST, F. G. p 129 N94-11606
YOUNG, B. K. F. p 389 N94-11074
YOUNG, FRED M. p 46 N94-10911
YOUNG, JOSEPH W. p 315 N94-10806
YOUNGDAHL, C. A. p 142 N94-10951
p 398 N94-11004
YU, HUILING p 215 N94-12686
YU, YUN YUE p 213 N94-12674
YUAN, TAO p 123 N94-10240
YUDIN, M. F. p 359 N94-10266
YUEN, WAYNE p 44 N94-12541
YUK, SANG SUP p 216 N94-12689
YUZHAKOV, VICTOR I. p 177 N94-12755

Z

ZABINSKY, S. I. p 367 N94-11470
ZABOROWSKI, DAVID J. p 315 N94-10296
ZAGORODNIJ, A. G. p 149 N94-10838
p 388 N94-10839
p 389 N94-10885
p 389 N94-10886
p 366 N94-11349
ZAHLENIUK, N. A. p 396 N94-10801
ZAHNISER, M. S. p 279 N94-12572
ZAIDE, A. p 139 N94-12778
ZAIKA, N. I. p 364 N94-10848
ZAMBRE, YADUNATH B. p 136 N94-11206
ZAMEL, JAMES M. p 423 N94-11229
ZAMPETTI, GEORGE p 139 N94-10990
ZANDBERGEN, R. p 242 N94-11771
ZANDER, ROLAND p 120 N94-10221
ZANG, Y. p 156 N94-12290
ZAPPALA, E. p 431 N94-12201
ZARE, R. N. p 431 N94-12167
ZASENKO, V. I. p 393 N94-11477
ZAVOROTNY, V. U. p 136 N94-11068
p 136 N94-11069
ZDEBLICK, W. J. p 340 N94-12411
ZEBKER, HOWARD A. p 236 N94-11734
ZECCHETTO, STEFANO p 233 N94-11713
p 200 N94-11953
ZEDEL, LEN p 288 N94-11447
ZEITOUN, D. p 8 N94-10456
ZEJDLITS, V. P. p 387 N94-10558
p 362 N94-10649
p 392 N94-11213
ZEMAN, OTTO p 157 N94-12300
ZEMLYAKOV, A. T. p 349 N94-10548
ZEMLYANSKIJ, N. M. p 134 N94-11037
ZGRAGGEN, CRAIG J. p 26 N94-11872
ZHANG, G. Q. p 186 N94-10879
ZHANG, JIANZU p 427 N94-11692
ZHANG, JIN-LONG p 203 N94-11970
ZHANG, S. Y. p 373 N94-12601
ZHANG, TING-LU p 212 N94-12669
ZHANG, X. p 114 N94-10182
ZHANG, XIAO DONG p 197 N94-11934
ZHANG, YUANZHONG p 409 N94-10499
ZHANG, YUN p 396 N94-10705
ZHAO, CHAO FANG p 197 N94-11934
ZHAO, D. Q. p 86 N94-10194
ZHAO, HUAIGUO p 343 N94-10546
ZHELTUKHIN, A. A. p 412 N94-11088
ZHONG, W. p 398 N94-11004
ZHOU, FENGXIAN p 214 N94-12675
ZHOU, O. p 400 N94-11457
ZHOU, WEI p 357 N94-11002
ZHOU, Y. H. p 86 N94-10194
ZHOU, YE p 158 N94-12305
ZHU, Q. p 400 N94-11457
ZHU, XIAODONG p 405 N94-12587
ZHU, YUN p 405 N94-12587
ZHUGIN, YU. N. p 97 N94-12040
ZIINO, G. p 361 N94-10414
ZIMBELMAN, JAMES R. p 457 N94-12137
ZIMMERMAN, JEFFREY A. p 67 N94-11260
ZINDER, S. H. p 300 N94-10652
ZINK, MANFRED p 235 N94-11727
ZINK, W. p 59 N94-10023
ZINNER, ERNST p 97 N94-12029
ZINOVEV, G. M. p 397 N94-10883
ZIPFEL, J. p 432 N94-12231
ZITA, E. J. p 388 N94-10852
ZIZAK, G. p 107 N94-10113
ZOLENSKY, M. E. p 80 N94-12045
p 453 N94-12117
ZOLENSKY, MICHAEL p 430 N94-12114
ZOLESI, V. p 39 N94-10118
ZOLOTUKHIN, A. V. p 392 N94-11215
ZOLOTUKHIN, L. V. p 223 N94-12726
ZOLPER, J. C. p 396 N94-10809

ZOU, H. .... p 75 N94-10186
ZOU, JIANSHENG .... p 209 N94-12646
ZUBER, MARIA T. .... p 444 N94-12065
p 481 N94-12267
p 481 N94-12268
ZUENKO, YURY I. .... p 228 N94-12757
p 228 N94-12758
ZUTAVERN, F. J. .... p 401 N94-11605
p 144 N94-11624
ZWALLY, H. JAY .... p 210 N94-12651
ZWART, H. J. .... p 344 N94-10905
ZWIERS, JOB .... p 335 N94-10277
ZWIETERING, P. J. .... p 338 N94-10169

CORPORATE SOURCE INDEX

SCIENTIFIC AND TECHNICAL AEROSPACE REPORTS VOLUME 32 NUMBER 1

Typical Corporate Source Index Listing

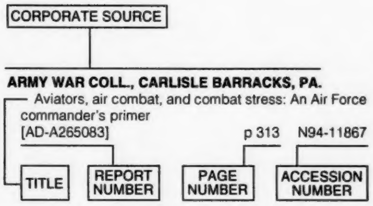

ARMY WAR COLL., CARLISLE BARRACKS, PA.
Aviators, air combat, and combat stress: An Air Force commander's primer
[AD-A265083] p 313 N94-11867

Listings in this index are arranged alphabetically by corporate source. The title of the document provides the user with a brief description of the subject matter. The report number helps to indicate the type of document cited (e.g., NASA report, translation, NASA contractor report). The accession number denotes the number by which the citation is identified. The page number helps you locate the citation in the abstract section. The titles are arranged under each corporate source in ascending accession number order.

A

AACHENER CENTRUM FUER ERSTARRUNG UNTER SCHWERELOSIGKEIT E.V. (GERMANY).
Variations of the temperature profile in the gradient furnace GFQ within a cylindrical sample used for directional solidification p 114 N94-10181
Containerless processing of equiatomic Mn50Bi50 in a drop tube p 118 N94-10205

AASTRA AEROSPACE, INC., DOWNSVIEW (ONTARIO).
Smart structures at Aastra Corporation p 69 N94-11326

ACADEMIA SINICA, BEIJING (CHINA).
In situ observation of temperature dependence of concentration field during growth of KB5 crystals by holographic interferometry p 115 N94-10187
Solidification of undercooled Ni-32.5 wt percent Sn eutectic alloy p 86 N94-10194
Roles of the NEC and MC in the formation and evolution of the Equatorial Pacific Warm Pool p 206 N94-11990
Delineation of mesoscale features of ocean on satellite IR image p 214 N94-12675

ACADEMY OF SCIENCES, POTSDAM (GERMAN D.R.).
Operational ERS-1 orbit determination at D-PAF p 243 N94-11774
Quick-look monitoring of the sea surface with ERS-1 fast delivery altimeter data p 243 N94-11777
The Earth's gravity model for the ERS-1 commissioning phase p 243 N94-11778

ACADEMY OF SCIENCES OF THE AZERBAIJAN SSR, BAKU.
Exact and quasi-classical density matrix and Wigner functions for a particle in the box and half space p 350 N94-10600

ACADEMY OF SCIENCES OF THE MOLDAVIAN SSR, KISHINEV.
Two-phase flow heat transfer and hydrodynamics in an electric field p 103 N94-10093
Nonperturbative methods in the problem of multiphoton excitation of atom by squeezed light p 376 N94-10575

ACADEMY OF SCIENCES OF THE UKRAINE, KHARKOV.
Collective acceleration of ions in near-anode plasma of a strong-current relativistic diode [DE93-620977] p 387 N94-10541
Dynamics of ion acceleration in electron flux by a virtual cathode potential [DE93-620978] p 371 N94-10542
On the stability of stationary regimes in a distributed autovibration system with external feedback [DE93-620979] p 141 N94-10543
Scattering of modulated Ultra-Relativistic Electron Beam (UREB) by atmospheric plasma [DE93-620987] p 387 N94-10558
The intra-atomic motion of bound electrons as a possible source of a systematic error in electron beam polarization measurements by means of a Moeller polarimeter [DE93-620984] p 364 N94-10875
Nonlinear excitation in quasi-one-dimensional Peierls dielectrics with charge density waves [DE93-613827] p 398 N94-11025
Regular tensor Green functions of the round waveguide [DE93-621354] p 345 N94-11036
To the complexity of dynamic system problem [DE93-621355] p 134 N94-11037
Asymptotic expressions for regular Green functions of a round cylindrical screen [DE93-621356] p 134 N94-11038
Dissipative phase transitions in field theory models with spontaneous symmetry violation [DE93-621382] p 412 N94-11039
The influence of the propagation medium on the sensitivity and resolution of meter wavelength aperture synthesis systems p 134 N94-11062
Non-barrier tunneling in presence of dissipations [DE93-621381] p 412 N94-11086
Green-Schwarz superstrings in the generalized harmonical Newmann-Penrose formalism [DE93-621422] p 412 N94-11088
Calculation of Mercier stability criterium in stellarators [DE93-621599] p 389 N94-11091
Probability of particle trapping/detrapping in torsatrons [DE93-621641] p 390 N94-11121
The possibility of using carbon-graphite materials for microwave plasma diagnostics in large fusion devices [DE93-621609] p 66 N94-11143
Analytical description of the torsatron Uragan-2M magnetic configuration with account of plasma pressure and external correcting magnetic field [DE93-620983] p 391 N94-11174
Kinetic effects in stochastic topologically nontrivial field [DE93-621642] p 391 N94-11207
Simple kinetic model for plasma in stochastic helical field [DE93-621643] p 391 N94-11208
Elementary mechanism of electron beam dissipative instability development [DE93-621653] p 391 N94-11209
Dispersion of plasma waves in a finite magnetic field (omega(sub H) greater than omega(sub p)) [DE93-621654] p 391 N94-11210
Experimental investigation of wake field excitation in plasma by a periodic succession of relativistic particle clots [DE93-621655] p 391 N94-11211
Negative viscosity and generation of dissipative solitons and zonal dissipative structures by drift waves [DE93-621656] p 392 N94-11212
Spreading of Bimodulated Ultra-relativistic Electron Beam (BUEB) in Atmospheric Plasma Channel (APCh) [DE93-621658] p 392 N94-11213
Magnetic island suppression in torsatron configurations [DE93-621681] p 392 N94-11215
A method of influence regions in the theory of vacancy swelling of metals [DE93-620579] p 83 N94-11363
Non-linear dynamics of automodulation processes in coupled distributed autovibration systems with delay [DE93-620976] p 143 N94-11365

ACADEMY OF SCIENCES OF THE UKRAINE, KIEV.
On the relativistic string size at finite temperature [DE93-617658] p 409 N94-10394
Nonlinear MHD-waves in a dissipative plasma with hall currents [DE93-617844] p 386 N94-10395
General renormalized statistical approach with finite cross-field correlations [DE93-617846] p 386 N94-10396
Stationary spectra in a magnetized current-carrying plasma [DE93-617847] p 386 N94-10397
Effective action in the gauged Nambu-Jona-Lasinio model [DE93-617654] p 409 N94-10405
Stationary spectra in a plasma with a shear (renormalized statistical approach with non-zero eigenfrequencies) [DE93-617851] p 386 N94-10523
Optimization of break-down conditions in tokamak TOTUS [DE93-617863] p 386 N94-10524
The peculiarities of the spin glass state in Fe(x)Mn(1-x)TiO3 [DE93-617882] p 395 N94-10525
Stationary spectra in a finite-pressure current-carrying plasma [DE93-617848] p 387 N94-10538
Stationary spectra in a quasi neutral current-carrying plasma [DE93-617849] p 387 N94-10539
Stationary spectra in a sheared plasma (linear limit) [DE93-617850] p 387 N94-10540
Bound states of the N-dimensional Klein-Gordon equation with vector and scalar Coulomb potentials [DE93-617650] p 349 N94-10547
On local frame fields and fermion dynamics in space with nontrivial topologies [DE93-617657] p 349 N94-10548
P-matrix description of the two-particle interaction [DE93-617690] p 361 N94-10549
Studies of P-matrix formalism on the basis of the potential description of two-particle interaction [DE93-617691] p 362 N94-10550
Crossing-odd spin effects in the dipole model of hadron scattering [DE93-617692] p 362 N94-10551
Model for the pomeron [DE93-617693] p 362 N94-10552
Logarithmically rising cross section and the ratio sigma(sub el)/sigma(sub t) [DE93-617694] p 362 N94-10553
Detecting the odderon [DE93-617695] p 362 N94-10554
Fine structure of the Pomeron and the real part of the elastic scattering amplitude [DE93-617696] p 362 N94-10555
Coherence influence on the intensity of Bose-Einstein correlations and visible size of a source [DE93-617697] p 349 N94-10556
The determination of nucleon-nucleon scattering phases by the phase functions method [DE93-617729] p 362 N94-10557
On the doubling of hydrodynamic theorems in relativistic theory of superfluidity [DE93-617895] p 148 N94-10717
Quasi-relativistic effects in barrier-penetration processes [DE93-617730] p 410 N94-10721
Three-nucleon problem with phase equivalent potentials [DE93-617731] p 363 N94-10722
On the possible unobservability of the Wu-Yang phase factor in curved space [DE93-617645] p 411 N94-10831
Exact solutions of a many-anyon problem [DE93-617646] p 411 N94-10832
A new approach to the I/N-expansion for the Dirac equation [DE93-617647] p 349 N94-10833

Exact solution of the N-dimensional generalized Dirac-Coulomb equation
[DE93-617649] p 411 N94-10834
The multiplicity spectra of the (169)Tm(n, gamma) reaction
[DE93-617733] p 364 N94-10835
Monte Carlo algorithms in simulation of 2beta-decay and penetration of electrons through matter
[DE93-617741] p 364 N94-10837
The heat transfer by radiation between two media
[DE93-617820] p 149 N94-10838
The Langevin's approach to the statistical theory of bounded plasma
[DE93-617842] p 388 N94-10839
Stationary spectra of short-wave convective and magnetostatic fluctuations in a finite-pressure plasma and anomalous heat conductivity
[DE93-617852] p 388 N94-10840
On problem about nature of Portevin-Le Chatelier effect in irradiated aluminium alloys
[DE93-617200] p 82 N94-10842
The influence of irradiation conditions, type, and concentration of impurities on radiation defects characteristics in indium antimonide under electron irradiation
[DE93-617201] p 397 N94-10843
Radiation defect production in InAs crystals under electron irradiation
[DE93-617202] p 397 N94-10845
Spin characteristics of ion beams during the motion of electromagnetic elements
[DE93-617448] p 364 N94-10848
Monochromator SP-017. The results of the first experiments
[DE93-617463] p 372 N94-10849
All possible electroweak models from Z orbifold
[DE93-617656] p 411 N94-10880
Quantum solitons with cylindrical symmetry
[DE93-617659] p 344 N94-10881
Filamentation instability of hot quark-gluon plasma with hard jet
[DE93-617679] p 388 N94-10882
Gluon gas viscosity in nonperturbative region
[DE93-617680] p 397 N94-10883
Gauge independence of the A(sub 0)-condensate
[DE93-617681] p 397 N94-10884
Spatial helicon-wave echo in an inhomogeneous magnetized plasma
[DE93-617845] p 389 N94-10885
Distribution of charged particles near the plasma boundary in the presence of external electric field
[DE93-617862] p 389 N94-10886
The graphical library for technological process automatization
[DE93-621316] p 324 N94-11031
Structural and electronic properties of atomic chains
[DE93-617758] p 366 N94-11349
Decay interaction of bulk and surface Langmuir waves
[DE93-617843] p 393 N94-11477

ACADEMY OF SCIENCES (USSR), LENINGRAD.
Fast trigger algorithm for B-events selection
[DE93-621452] p 365 N94-11089

ACADEMY OF SCIENCES (USSR), MOSCOW.
Space and temporal behavior and control of the residual convection in microgravity p 104 N94-10099
Convective motion in a multi-layered system with a free surface p 120 N94-10219
Use of inert immiscible liquid for crystal separation out of its feeding solution in weightlessness
p 124 N94-10242
Harmonic oscillator interaction with squeezed radiation
p 376 N94-10571
An exactly solvable model of an oscillator with nonlinear coupling and zeros of Bessel functions
p 349 N94-10573
Correlated states of a quantum oscillator acted by short pulses p 380 N94-10609
Floquet operator as integral of motion
p 380 N94-10610
Quantum processes in resonators with moving walls
p 380 N94-10612
Russian space system for the Earth remote sensing
p 37 N94-10688
Radiowaves propagation through inhomogeneous interstellar plasma p 134 N94-11061
Generalization of Dyson criterion for the amplitude-phase fluctuations case and for the system of interferometers p 135 N94-11067
The possibility of image restoration under observation in a regime of strong scattering p 136 N94-11068
The superresolution effect observed through a random medium p 136 N94-11069
Use of satellite telecommunications for telemedicine
p 308 N94-11807
Observations of the fractal properties of the Japan sea surface temperature patterns p 205 N94-11984
Dispersion of the ratios of cosmogenic isotopes of noble gases in chondrites of different cosmic-ray exposure ages p 428 N94-12020
Peculiarities of distributions of the cosmic-ray exposure ages of H chondrite falls and finds p 428 N94-12021
Search for effects of a supernova explosion 30 to 40 thousand years ago in chondrites p 428 N94-12022
Vaporization by shock loading of albite, jadeite, and pyrex glass: Experimental study p 97 N94-12039
Shock transformations in quartzite p 97 N94-12040
Yana ring structure, North-Eastern Siberia: A possible counterpart of coronae on Venus p 282 N94-12121
Russia's contribution to regional geologic mapping of Venus p 454 N94-12122
Landscape and geomorphic survey of Zhamanshin area, Northern Kazakhstan: Preliminary report on 1992 field trip data p 282 N94-12123
The correlation of alkalis and aluminum during high-temperature volatilization of albite and nepheline
p 81 N94-12214
On the unique structure of the magnetic fields of Uranus and Neptune p 472 N94-12221
Precession of Uranus and Neptune and their magnetic field p 473 N94-12222
On high-temperature formation of iron-rich olivine in the early solar system p 432 N94-12225
Recondensation of chondritic material in the early solar system: Results of thermodynamic simulation
p 432 N94-12226
Moessbauer spectrometer for mineralogical analysis of the Mars surface: Moessbauer source considerations
p 476 N94-12242
Diamond thermoluminescence properties of different chondrites p 433 N94-12252
The unusual metallic particles in Krymka LL3.0 chondrite p 433 N94-12253
On possibility of diamond formations in radiation process p 433 N94-12254
The carbon isotopic composition of Novo Urei diamonds p 433 N94-12255
The fractionation of noble gases in diamonds of CV3 Efremovka chondrite p 81 N94-12256
Frontal zones in Pacific Ocean: Satellite and ship data analysis p 216 N94-12687
Polarisation of backscattering radiation at remote sensing of ocean with impulse laser beam
p 177 N94-12722
The method of investigation of the horizontal structure of the thermal fronts p 222 N94-12723
On a nonstationary dynamics of the north-west Pacific Ocean p 222 N94-12724
Turbulence generation in the Pacific undercurrent by shear p 223 N94-12730
A detailed investigation of the benthic regime in the Clarion-Clipperton province of the Pacific and a forecast of consequences of manganese nodule mining
p 224 N94-12733
Bottom currents and possibilities for near bottom layer environmental investigations in the Pacific by means of self contained bottom stations p 224 N94-12734
Autonomous self contained bottom pop-up stations for study of the benthic layer and seismicity of the ocean's bottom p 224 N94-12735
Remote sensing of light scattering coefficient of sea water vertical distribution by the means of airborne lidar
p 224 N94-12736
Verification of the atmosphere-ocean radiative transfer parametric models p 225 N94-12738
Optical transfer operator of the atmosphere-ocean system p 225 N94-12742
Variability of spectral reflectance in coastal waters near the river plumes p 226 N94-12744
Wind-wave and foam dynamics from optical and radar airborne observations p 226 N94-12745
Observations of surface signatures in the north-west Pacific Ocean with the spaceborne SAR
p 226 N94-12746
Radar observation of internal waves field in the north-west Pacific p 226 N94-12747
Coupled numerical model for altimetric data assimilation and velocity field analysis p 227 N94-12752
Study of the admixture diffusion in the sea using remote techniques p 228 N94-12759
Mixing of drifter ensemble by mesoscale currents
p 228 N94-12760
The algorithm of primary production determination
p 228 N94-12761
Problem of climate change predictability and satellite radiation budget observations p 229 N94-12766

ACADEMY OF SCIENCES (USSR), NIZHNY NOVGOROD.
Observations of film slicks and internal waves with Ka-band scatterometer p 225 N94-12741

ACADEMY OF SCIENCES (USSR), NOVOSIBIRSK.
Model of convective motion under low gravity
p 103 N94-10088
Controller of serial multiplex communication channel
[DE92-641157] p 336 N94-10544
The uncertainty principle and quantum chaos
p 379 N94-10602
Model of Kuroshio region circulation
p 229 N94-12765

ACADEMY OF SCIENCES (USSR), PERM.
Heat and mass transfer mechanisms of the polymerization under terrestrial and microgravity conditions p 103 N94-10092

ACADEMY OF SCIENCES (USSR), SAINT PETERSBURG.
Propagation of light pulses through a three-layer medium (cloud, pure air, and ocean water) p 222 N94-12725
Optimum selection of spectral channels in the problem of remote sensing of phytoplankton concentration in ocean water p 223 N94-12726

ACADEMY OF SCIENCES (USSR), VLADIVOSTOK.
The thermodynamics of the nonlinear shear flows
p 169 N94-12728
The acoustic arrangement for measuring vertical structure of sea current p 223 N94-12729
The Pacific Subarctic Frontal Zone: Structure and dynamics p 223 N94-12731
Laser photoheterodyne interferometers for oceanographic investigations p 177 N94-12732
Influence of the Kuroshio warm-core rings on hydrographic and fishery conditions off southern Kuril Islands p 224 N94-12737
Convective and dynamic instability in meridional trenches p 225 N94-12739
Spatial variability of the ocean underwater dynamic noise from satellite radar sensing data p 225 N94-12740
Cloud liquid water content over the Pacific Ocean tropical zone derived from ship microwave radiometric measurement p 225 N94-12743
DISTERM: A shipboard data system for satellite monitoring of ocean and atmosphere
p 226 N94-12749
Atmospheric correction for determination of average SST fields based on AVHRR data p 227 N94-12750
The structure of hydrophysical measuring systems of vertical sounding and self-contained stations
p 227 N94-12751
Complex (hydrodynamic, satellite) monitoring of dynamic structures in the western Pacific with the aim of forecasting the marine ecosystems behaviour p 227 N94-12753
Mesoscale dynamic structures of the Subarctic Frontal Zone in the Pacific Ocean p 227 N94-12754
A possibility to define the location of epipelagic fish concentrations with assistance of satellite sensing
p 228 N94-12757
High biological production of the tidal mixing zones on Japan Sea shelf p 228 N94-12758
Generation of internal waves near the shelf boundary
p 229 N94-12763
Experimental and theoretical investigation of undular bore formation upstream the bank p 229 N94-12764

ADVANCED FUEL RESEARCH, INC., EAST HARTFORD, CT.
A novel test method for fuel thermal stability
[AD-A265853] p 99 N94-12275

ADVANCED RESOURCE DEVELOPMENT CORP., COLUMBIA, MD.
Signal feature analysis using neural networks and psychoacoustics
[AD-A266048] p 340 N94-12398

ADVISORY COMMISSION ON INTERGOVERNMENTAL RELATIONS, WASHINGTON, DC.
Intergovernmental decisionmaking for environmental protection and public works
[PB93-176824] p 266 N94-11584

ADVISORY GROUP FOR AEROSPACE RESEARCH AND DEVELOPMENT, NEUILLY-SUR-SEINE (FRANCE).
Theoretical and Experimental Methods in Hypersonic Flows
[AGARD-CP-514] p 2 N94-10421
Environmentally Safe and Effective Processes for Paint Removal
[AGARD-R-791] p 126 N94-10613
A Recommended Methodology for Quantifying NDE/NDI Based on Aircraft Engine Experience
[AGARD-LS-190] p 28 N94-11022
Smart Structures for Aircraft and Spacecraft
[AGARD-CP-531] p 68 N94-11317
Stability in Aerospace Systems
[AGARD-R-789] p 31 N94-11489
AGARD highlights 92/2, September 1992
[AGARD-HIGHLIGHTS-92/2] p 497 N94-11820

AEC-ABLE ENGINEERING CO., INC., GOLETA, CA.
A high specific power solar array for low to mid-power spacecraft p 51 N94-11399

AERODYNE RESEARCH, INC., BILLERICA, MA.
Stratospheric aircraft exhaust plume and wake chemistry
[NASA-CR-191495] p 279 N94-12572

AERONAUTICA MACCHI S.P.A., VARESE (ITALY).
Design and production of insulated wind tunnel models of the Hermes shuttle for heat transfer measurements at hypersonic speeds p 4 N94-10431
AERONAUTICAL RADIO, INC., ANNAPOLIS, MD.
Design for testability and diagnosis at the system-level p 184 N94-11563
AERONAUTICAL RESEARCH LABS., MELBOURNE (AUSTRALIA).
Field evaluation of six protective coatings applied to T-56 turbine blades after 2500 hours of engine use
[ARL-TR-27] p 90 N94-11311
AERONAUTICAL SYSTEMS DIV., WRIGHT-PATTERSON AFB, OH.
An environmental study of the National Aerospace Plane
[AD-A266071] p 25 N94-10945
A comparison of head-up and head-down display formats during instrument flying tasks
[AD-A266140] p 316 N94-11642
Evaluation of the C/EC/KC-135 ground collision avoidance system (GCAS), Study 2
[AD-A265193] p 24 N94-11879
AEROSPACE CORP., EL SEGUNDO, CA.
Review of SHARC 2.0 O3 kinetics and spectroscopy
[AD-A265481] p 274 N94-10496
Data processing units for eight magnetospheric particle and field sensors
[AD-A264403] p 276 N94-11463
Crystallinity and dielectric properties of PEEK, a thermoplastic poly(ether ether ketone)
[AD-A266027] p 91 N94-11487
Light scattering from a spherical particle on a conducting plane. Part 1: Normal incidence
[AD-A265920] p 383 N94-12341
Lessons learned from the Long Duration Exposure Facility
[AD-A266026] p 44 N94-12394
Tin whiskers in electronic circuits
[AD-A265917] p 146 N94-12565
AEROSPACE CORP., SUNNYVALE, CA.
On-orbit servicing for USAF space missions: A phased development approach p 348 N94-11571
AEROSPACE MEDICAL RESEARCH LABS., BROOKS AFB, TX.
Arterial gas emboli in altitude-induced decompression sickness p 312 N94-11543
A prototype urine collection device for female aircrew p 317 N94-11549
Effect of intermittent cold exposure on the fiber-type composition of selected skeletal muscles in rats
[AD-A265309] p 301 N94-11861
AEROSPACE MEDICAL RESEARCH LABS., WRIGHT-PATTERSON AFB, OH.
Psychophysiological measures of cognitive workload in laboratory and flight p 317 N94-11529
Visual Earth observation performance in the space environment. Human performance measurement 4: Flight experiments p 314 N94-11539
AEROSPATIALE, TOULOUSE (FRANCE).
Use of robots for aircraft dry stripping via plastic media blasting p 127 N94-10620
AEROSPATIALE AQUITAINE, SAINT-MEDARD EN JALLES (FRANCE).
High temperature composites in Aerospatiale activities p 64 N94-10062
AGENCY OF INDUSTRIAL SCIENCE AND TECHNOLOGY, TOKYO (JAPAN).
Japan's Sunshine Project
[DE93-767980] p 262 N94-10498
AIR-CONDITIONING AND REFRIGERATION TECHNOLOGY INST., INC., ARLINGTON, VA.
Theoretical evaluation of R22 and R502 alternatives
[DE93-014767] p 411 N94-10853
Measurement of viscosity, density and gas solubility of refrigerant blends
[DE93-014772] p 89 N94-11145
Accelerated screening methods for predicting lubricant performance in refrigerant compressors
[DE93-014773] p 89 N94-11146
AIR FORCE HUMAN RESOURCES LAB., WRIGHT-PATTERSON AFB, OH.
Crew chief p 335 N94-11564
On-orbit refueling p 38 N94-11565
AIR FORCE INST. OF TECH., WRIGHT-PATTERSON AFB, OH.
The radar eye blinded: The USAF and electronic warfare, 1945-1955
[AD-A265494] p 132 N94-10497
Utilizing quantitative feedback theory design technique for flight control system p 32 N94-11501
Modeling present and future river runoff using global atmospheric models
[AD-A265274] p 285 N94-11685
Development and implementation of a general purpose x-windows display program
[AD-A265306] p 332 N94-11860
Rainfall-runoff estimation using digital radar
[AD-A265390] p 286 N94-12408
AIR FORCE LOGISTICS COMMAND, HILL AFB, UT.
Plastic media blasting activities at Hill Air Force Base p 127 N94-10622
AIR FORCE LOGISTICS COMMAND, KELLY AFB, TX.
Preliminary analysis of the benefits derived to US Air Force spacecraft from on-orbit refueling p 38 N94-11567
AIR FORCE SYSTEMS COMMAND, BROOKS AFB, TX.
Central circulatory hemodynamics as a function of gravitational stress p 309 N94-11995
Basic attributes test (BAT): Operational pre-implementation analysis and score equating
[AD-A265885] p 314 N94-12276
AIR FORCE SYSTEMS COMMAND, NORTON AFB, CA.
The National Launch System Advanced Development Program: A brief overview p 40 N94-11576
AIR FORCE SYSTEMS COMMAND, WRIGHT-PATTERSON AFB, OH.
Accuracy and repeatability of the standard automated mass properties measurement system
[AD-A265897] p 316 N94-12346
AIR SYSTEM TECHNOLOGIES, INC., DALLAS, TX.
RighTime: A real time clock correcting program for MS-DOS-based computer systems p 334 N94-10986
AIRCRAFT RESEARCH ASSOCIATION LTD., BEDFORD (ENGLAND).
Generation and analysis of hybrid structured/unstructured grids
[ARA-MEMO-365] p 324 N94-10893
Improvement of the flow quality in the ARA transonic tunnel by means of a long cell honeycomb
[ARA-MEMO-375] p 34 N94-10894
SAUNA: A system for grid generation and flow simulation using hybrid structured/unstructured grids
[ARA-MEMO-370] p 154 N94-11859
The evolution of whole field optical diagnostics for external transonic testing
[ARA-MEMO-379] p 383 N94-11887
The modelling of aerodynamic flows by solution of the Euler equations on mixed polyhedral grids
[ARA-84] p 16 N94-11888
An overview of the capabilities of ARA for the measurement of nozzle discharge and thrust
[ARA-MEMO-378] p 55 N94-12283
A unique facility to support cryogenic wind tunnel operations
[ARA-MEMO-377] p 34 N94-12436
Towards a cell-vertex Navier-Stokes algorithm for three-dimensional structured/unstructured meshes
[ARA-MEMO-366] p 161 N94-12437
AIX-MARSEILLES UNIV. (FRANCE).
Instability of thermocapillary convection in floating zones p 101 N94-10076
Evaporation under microgravity conditions p 102 N94-10086
Coupled thermogravitational and thermocapillary convection in a two-layer fluid system p 105 N94-10101
Flow transitions in a 2D directional solidification model p 114 N94-10183
Conductive-radiative model for predicting the shape of Hgl2 crystal grown in the LTVG furnace p 117 N94-10201
Effect of experimental procedure on pattern formation and array disorder in cellular solidification p 117 N94-10203
Instability of thermocapillary convection in multiple superposed immiscible liquid layers p 120 N94-10218
AKADEMIYA NAUK BSSR, MINSK.
Squeezed colour states in gluon jet p 379 N94-10599
AKRON UNIV., OH.
Dynamics of charge-transfer excited states relevant to photochemical energy conversion
[DE93-013981] p 263 N94-11116
ALABAMA UNIV., BIRMINGHAM.
Solidification in immiscible systems: The influence of processing conditions on resulting microstructures p 112 N94-10174
ALABAMA UNIV., HUNTSVILLE.
Material characterization and modeling with shear ography
[NASA-CR-192576] p 185 N94-10342
Interferometric and optical tests of water window imaging x ray microscopes
[NASA-CR-193369] p 375 N94-10506
Cosmological gamma-ray burst model
[NASA-CR-193368] p 484 N94-10507
Comparison of hydrodynamic and semi-kinetic treatments for plasma flow along closed field lines
[NASA-CR-193589] p 387 N94-10641
Parametric analysis of atmospheric processes
[NASA-CR-192523] p 347 N94-10757
Enhancements to the Engine Data Interpretation System (EDIS)
[NASA-CR-192593] p 180 N94-10815
Activities relating to understanding the initiation, organization and structure of moist convection in the Southeast environment
[NASA-CR-193829] p 285 N94-11598
Data analysis tasks: BATSE
[NASA-CR-192598] p 483 N94-12427
Chemical release and radiation effects (CRRES) data directory
[NASA-CR-192551] p 279 N94-12581
Process modelling for materials preparation experiments
[NASA-CR-193556] p 56 N94-12588
ALABAMA UNIV., TUSCALOOSA.
The IR properties of ringed galaxies and the IRAS database
[NASA-CR-194286] p 426 N94-11590
ALASKA UNIV., FAIRBANKS.
A study of the magnetic field annihilation process in the magnetosphere and some geotechnical applications
[DE93-013249] p 273 N94-10305
A study of the magnetic field annihilation process in the magnetosphere and some geotechnical applications
[DE93-013248] p 273 N94-10319
Energy flow in an Arctic aquatic ecosystem
[DE93-013178] p 267 N94-11697
ALBERTA UNIV., CALGARY.
Olivine-rich asteroids, pallasitic olivine and olivine-metal mixtures: Comparisons of reflectance spectra p 431 N94-12171
ALBRIGHT COLL., READING, PA.
Remote sensing x ray fluorescence spectrometry for future lunar exploration missions p 462 N94-12165
ALCATEL NETWORK SYSTEMS, INC., RICHARDSON, TX.
SONET synchronization: What's happening p 355 N94-10992
ALENIA AERONAUTICA, TORINO (ITALY).
Numerical simulation of the flow through a scramjet engine p 3 N94-10425
ALENIA SPAZIO S.P.A., TURIN (ITALY).
Strain measurement of carbon/epoxy composite with fibre optics white light quasi distributed polarimetric sensor p 69 N94-11328
ALFRED-WEGENER-INST. FOR POLAR RESEARCH, BREMERHAVEN (GERMANY).
Air-sea-ice interactions in the Weddell Sea p 239 N94-11753
ALLAN (T. D.) ASSOCIATES, GODALMING (ENGLAND).
The requirement for global training programmes to meet the new remote sensing technology p 196 N94-11929
ALLIED-SIGNAL AEROSPACE CO., KANSAS CITY, MO.
Fabrication and analysis of a special optical connector containing a 1/4-inch-long optical fiber for DOI tests
[DE93-013115] p 381 N94-10647
Sine and random vibration program evaluation on vibration control systems
[DE93-011974] p 188 N94-11460
ENSAFE fireset flex circuit analysis
[DE93-013106] p 144 N94-11478
Programmable logic devices
[DE93-013117] p 144 N94-11479
ALLIED-SIGNAL CORP., MORRISTOWN, NJ.
Primaset (tm): A safer material for aircraft interior applications p 18 N94-10772
AMERICAN SYSTEMS, INC., CHANTILLY, VA.
Software usability assessment guide
[AD-A265017] p 321 N94-10335
AMERICAN TECHNOLOGIES INTERNATIONAL, CLEARWATER, FL.
New thermoplastic laminating adhesives for the aircraft industry with low heat release and low smoke emission p 17 N94-10767
AMERICAN UNIV., WASHINGTON, DC.
Non-gauge phase transformations in quantum transition amplitudes p 378 N94-10596
AMES LAB., IA.
Coupled growth of cells and bubbles in directional solidification of succinonitrile-acetone alloys p 118 N94-10206
Particle attraction effects on the centrifugal casting and extrusion of alumina
[DE93-011559] p 82 N94-10957
Ultrasonic inspection, material noise and surface roughness
[DE93-011560] p 183 N94-11110
Synthesis and magnetic properties of novel La*2-x*M*x*CuO*4 equals y* compositions (La equals La, Pr, Nd, Sm, Eu, Cd; M equals Ca, Sr, Ba; O (less than or equal) x 0.2; -0.5 (less than or equal) y (less than or equal) 0.5)
[DE93-011359] p 403 N94-12363

Low temperature pathways to Chevrel phases via reduced molybdenum sulfide cluster complexes
[DE93-013282] p 405 N94-12599

ANALYTIC SCIENCES CORP., ARLINGTON, VA.
Assessing the adequacy of the industrial base
[AD-A264954] p 417 N94-11856

APPLIED RESEARCH CORP., LANDOVER, MD.
ADP study of the structure of the IUE halo
[NASA-CR-194374] p 428 N94-12595

APPLIED SOLAR ENERGY CORP., CITY OF INDUSTRY, CA.
EOL performance comparison of GaAs/Ge and Si BSF/R solar arrays p 51 N94-11398

APPLIMATH CO., BROOKLINE, MA.
Research on acoustic coupling to electromagnetic pulses in tissue
[AD-A264764] p 301 N94-11583

ARGONNE NATIONAL LAB., IL.
A proof-of-concept implementation of persistence in a hierarchical storage system
[DE93-009959] p 319 N94-10318
Demonstration prototype gamma-ray hodoscope alternative to CARGOSCAN for rocket stage monitoring
[DE93-006908] p 169 N94-10326
Development of commercially viable high-T(sub c) Bi-2223 superconductor tapes
[DE93-009966] p 142 N94-10951
Synthesis and properties of nanophase materials
[DE93-011757] p 397 N94-10962
Microstructure and associated properties of YB2Cu3O(x) superconductors prepared by melt processing techniques
[DE93-010675] p 398 N94-11004
FORCE2: A state-of-the-art two-phase code for hydrodynamic calculations
[DE93-010661] p 150 N94-11072
Processing and transport properties of high J(sub c) silver clad Bi-2223 tapes and coils
[DE93-010674] p 398 N94-11073
Database computing in HEP
[DE93-011765] p 419 N94-11105
Heavy ion fusion at sub-barrier energies: Progress and questions
[DE93-011764] p 372 N94-11124
A toolkit for building Earth system models
[DE93-012147] p 276 N94-11138
Assessment of the impact of HTSC's on superconducting fault-current limiters
[DE93-009986] p 143 N94-11454
Improvement of azimuthal homogeneity in permanent-magnet bearing rotors
[DE93-009954] p 144 N94-11607
Direct solution of the mathematical adjoint equations for an interface current nodal formulation
[DE93-009961] p 346 N94-11608
Experiments to measure the gluon helicity distribution in protons
[DE93-011756] p 368 N94-11613
Instantaneous engine frictional torque: Its components and piston assembly friction
[DE93-011639] p 182 N94-11625
Statistical and optimization methods to expedite neural network training for transient identification
[DE93-009985] p 340 N94-11644

ARIZONA STATE UNIV., FLAGSTAFF.
Curvature effects in three-dimensional boundary layers
p 164 N94-12623

ARIZONA STATE UNIV., TEMPE.
Stability of hypersonic boundary-layer flows with chemistry p 7 N94-10451
Evolution of steep Martian slopes p 434 N94-11184
Fourier domain target transformation analysis in the thermal infrared p 258 N94-12030
Flexure and the role of inplane force around coronae on Venus p 452 N94-12112
Viscous relaxation of the Moho under large lunar basins p 452 N94-12113
A simple model of clastic sediments on Mars
p 460 N94-12155
Thermal-infrared emission spectroscopy of natural surfaces: Application to coated surfaces
p 81 N94-12156
Galileo EM-2 contributions to the lunar control network p 468 N94-12198
Primordial lightning: Evidence preserved in chondrites
p 432 N94-12230
Micro-zoning in minerals of a Landes silicate inclusion
p 432 N94-12231

ARIZONA UNIV., TUCSON.
Mechanistic studies on reduced exercise performance and cardiac deconditioning with simulated zero gravity
p 310 N94-12001
Ejecting basaltic achondrites from Vesta: Hydrodynamical impact models p 429 N94-12036
Explicit 3D continuum fracture modeling with smooth particle hydrodynamics p 429 N94-12062
Collision lifetimes and impact statistics of near-Earth asteroids p 429 N94-12092
Trace-element abundances in several new ureilites
p 80 N94-12096
The spectral effects of subsolidus reduction of olivine and pyroxene p 81 N94-12110
The 1.2 to 3.5 microns observations of asteroid 4179 Toutatis p 430 N94-12111
Studies of the release of radiogenic Xe-129 from Bjurboele: Evidence against simple diffusion models
p 430 N94-12125
Geomorphology of Triton's polar materials
p 466 N94-12185
Porosity and the ecology of icy satellites
p 431 N94-12186
Tectonics on Triton p 466 N94-12187
Noble gas evidence of an aqueous reservoir near the surface of Mars more recently than 1.3 Ga
p 473 N94-12228
Morphotectonics of Venus p 478 N94-12248
Transmantle flux tectonics p 283 N94-12249
Planetary astronomy of Mars. Mars data reduction
[NASA-CR-193515] p 424 N94-12768

ARIZONA WATER RESOURCES RESEARCH CENTER, TUCSON.
Development of deterministic transport methods for low energy neutrons for shielding in space
[NASA-CR-194172] p 366 N94-11199

ARKANSAS COLL., BATESVILLE.
Volatiles in fourteen interplanetary dust particles: A comparison with CI and CM chondrites
p 430 N94-12132

ARKANSAS UNIV., FAYETTEVILLE.
Computational algorithms or identification of distributed parameter systems
[AD-A265252] p 331 N94-11680
The great 8 MA event and the structure of the H-chondrite parent body p 429 N94-12058
Meteorites from recent amor-type orbits
p 429 N94-12059
Natural thermoluminescence profiles in lunar cores and implications for meteorites p 443 N94-12060
Cathodoluminescence properties of components in enstatite chondrites p 432 N94-12206

ARMY AEROMEDICAL RESEARCH LAB., FORT RUCKER, AL.
Automaticity of processing location versus identity information in brief visual displays
[AD-A265013] p 418 N94-10491
Correlation of HGU-56/P aircrew helmet fitting with head anthropometric measurements
[AD-A264988] p 315 N94-11291
The aging military aviator: A review and annotated bibliography
[AD-A265341] p 311 N94-12423

ARMY ARMAMENT RESEARCH, DEVELOPMENT AND ENGINEERING CENTER, WATERVLIET, NY.
Generalized Mandelbrot rule for fractal sections
[AD-A266010] p 347 N94-12390

ARMY AVIATION SYSTEMS COMMAND, MOFFETT FIELD, CA.
Determining XV-15 aeroelastic modes from flight data with frequency-domain methods
[NASA-TP-3330] p 25 N94-10935

ARMY COLD REGIONS RESEARCH AND ENGINEERING LAB., HANOVER, NH.
Icing of turbine intake louvers
[AD-A265714] p 29 N94-12274
Applications of ERS-1 SAR data for analyzing riverine and coastal processes and geomorphology
p 254 N94-12528

ARMY ELECTRONIC PROVING GROUND, FORT HUACHUCA, AZ.
FR/GE/US radar receiver pulse compression ratio
[AD-A265391] p 138 N94-12409

ARMY ENGINEER WATERWAYS EXPERIMENT STATION, VICKSBURG, MS.
Design and development of a miniature column-based interface (MCBI) stress gage
[AD-A266054] p 170 N94-10873
Analysis of Hopkinson bar pressure gage
[AD-A262366] p 171 N94-12362

ARMY LOGISTICS EVALUATION AGENCY, CUMBERLAND, PA.
Assessing the adequacy of the industrial base
[AD-A264954] p 417 N94-11856

ARMY MEDICAL CENTER, AURORA, CO.
Pilot trial of potentiating normal healing of stress fractures using pulsing electromagnetic fields
[AD-A264251] p 311 N94-12364

ARMY MEDICAL RESEARCH AND DEVELOPMENT COMMAND, FORT DETRICK, MD.
Pilot trial of potentiating normal healing of stress fractures using pulsing electromagnetic fields
[AD-A264251] p 311 N94-12364

ARMY RESEARCH LAB., ABERDEEN PROVING GROUND, MD.
Time-temperature shift factors for gun propellants
[AD-A264979] p 97 N94-10489
Computation of hypersonic nosetip heat transfer rates for an M829-like projectile
[AD-A263226] p 16 N94-11870
Deformation mechanisms in tungsten single crystals in ballistic impact experiments
[AD-A265701] p 405 N94-12563

ARMY RESEARCH LAB., WATERTOWN, MA.
Effect of powder processing on slip casting parameters and sintering of Si3N4-Y2O3-SiO2
[AD-A264474] p 83 N94-11445
Strain concentration assessment of laminates subjected to low velocity impact
[AD-A264497] p 73 N94-11446

ARMY RESEARCH LAB., WHITE SANDS MISSLE RANGE, NM.
Selected upper-air wind speed distributions
[AD-A264822] p 284 N94-10871

ARMY RESEARCH OFFICE, RESEARCH TRIANGLE PARK, NC.
Advanced zinc phosphate conversion and pre-ceramic polymetallosiloxane coatings for corrosion protection of steel and aluminum, and characteristics of polyphenyletheretherketone-based materials
[DE93-008717] p 88 N94-10891
Transactions of the 10th Army Conference on Applied Mathematics and Computing
[AD-A265098] p 318 N94-11678

ARMY WAR COLL., CARLISLE BARRACKS, PA.
Aviators, air combat, and combat stress: An Air F orce commander's primer
[AD-A265083] p 313 N94-11867
Integrating the services' imagery architectures
[AD-A265487] p 171 N94-12335

ARNOLD ENGINEERING DEVELOPMENT CENTER, ARNOLD AFS, TN.
Boiling heat-transfer processes and their application in the cooling of high heat flux devices
[AD-A266086] p 413 N94-12535

ASTON UNIV., BIRMINGHAM (ENGLAND).
Calibration of ERS-1 altimetry over the North Sea
p 234 N94-11716

AT AND T INFORMATION SYSTEMS LABS., DENVER, CO.
Software process assessments p 329 N94-11427

ATMOSPHERIC AND ENVIRONMENTAL RESEARCH, INC., CAMBRIDGE, MA.
The Air Force Interactive Meteorological System: A research tool for satellite meteorology
[AD-A265957] p 284 N94-11113
FFTSCAN: A program for spectral smoothing using Fourier transforms
[AD-A264921] p 278 N94-11852

ATMOSPHERIC ENVIRONMENT SERVICE, DOWNSVIEW (ONTARIO).
Preliminary evaluation of ERS-1 SAR data for operational use in the Canadian sea ice monitoring program
p 241 N94-11760

ATMOSPHERIC ENVIRONMENT SERVICE, TORONTO (ONTARIO).
Use of ERS-1 scatterometer winds in Canadian forecast centres p 250 N94-12504

ATOMIC ENERGY COMMISSION, DAMASCUS (SYRIA).
Szilard-Chalmers effect in solid HIO4.2H2O by neutron irradiation
[DE93-617173] p 397 N94-10830

AUBURN UNIV., AL.
Theoretical atomic physics for fusion
[DE93-013872] p 366 N94-11172
Reduced gravity multibody dynamics testing
[NASA-CR-192589] p 125 N94-11483

AUGSBURG UNIV. (GERMANY).
Experimental approach to non-contact calorimetry in space p 112 N94-10143

AUSTRALIAN NATIONAL UNIV., CANBERRA.
Re-Os dating of 3AB iron meteorites
p 432 N94-12237

AVIONS MARCEL DASSAULT, SAINT-CLOUD (FRANCE).
Aerodynamic and aerothermal challenges for the design of the Hermes spaceplane p 3 N94-10423
Local aerothermal problems during Hermes re-entry
p 10 N94-10464

B

BANGLADESH SPACE RESEARCH AND REMOTE SENSING ORGANIZATION, DHAKA.
Space research and remote sensing programmes in Bangladesh p 35 N94-10679

BARI UNIV. (ITALY).

Preliminary results of the experiment I-7 p 235 N94-11728

BATTELLE INST., FRANKFURT AM MAIN (GERMANY).

Stability of liquid bridges between parallel plates p 101 N94-10078

BATTELLE MEMORIAL INST., COLUMBUS, OH.

Isothermal fatigue mechanisms in Ti-based metal matrix composites [NASA-CR-191181] p 74 N94-12594

BECHTEL CORP., SAN FRANCISCO, CA.

Thermodynamics of lunar ilmenite reduction p 415 N94-12028

Terrestrial case studies of ilmenite exploration and lunar implications p 478 N94-12247

BEDFORD INST. OF OCEANOGRAPHY, DARTMOUTH (NOVA SCOTIA).

Ocean circulation revealed by ice floe tracking p 240 N94-11759

Ocean circulation revealed by altimeter data p 245 N94-11786

BELL TELEPHONE LABS., INC., HOLMDEL, NJ.

Timing in private digital telecommunication networks p 139 N94-10991

BENJAMIN/CLARKE ASSOCIATES, INC., KENSINGTON, MD.

Practical hazard assessment: An approach to the fire safety p 20 N94-10785

BERN UNIV. (SWITZERLAND).

The Xe-Q in lodranites and a hint for Xe-L. FRO90011 another lodranite? p 432 N94-12239

On the origin of (4)He and (40)Ar in natural gold p 87 N94-12240

BHABHA ATOMIC RESEARCH CENTRE, BOMBAY (INDIA).

An experimental program for collective acceleration of ions using intense relativistic electron beams [DE93-612205] p 371 N94-10316

BHP LABS. LTD., LIMERICK (IRELAND).

Aluminium-lithium forgings: Properties and potential satellite applications p 58 N94-10021

BIOELASTICS RESEARCH LTD., BIRMINGHAM, AL.

Development of bioelastic materials for the prevention of adhesions: Polypenta- and polytetrapeptides [AD-A264851] p 88 N94-10863

BIONETICS CORP., COCOA BEACH, FL.

Statistical analysis of environmental variability within the CELSS breadboard project's biomass production chamber [NASA-TM-109188] p 315 N94-11258

BNF-FULMER, WANTAGE (ENGLAND).

Joints between dissimilar metallic and ceramic materials p 63 N94-10052

Introducing SMaSE: An aide memoire on structural materials and space engineering p 63 N94-10053

BOEING CO., SEATTLE, WA.

Health and safety issues for aerospace workers in the use of advanced materials p 21 N94-10795

BOEING COMMERCIAL AIRPLANE CO., SEATTLE, WA.

Future material development trends for commercial airplane interiors p 21 N94-10792

BOEING DEFENSE AND SPACE GROUP, HUNTSVILLE, AL.

Lunar campsite concept: Space transfer concepts and analysis for exploration missions [NASA-CR-192602] p 433 N94-10144

BOEING DEFENSE AND SPACE GROUP, SEATTLE, WA.

Space environmental effects on the integrity of chromic acid anodized coatings [NASA-CR-191468] p 55 N94-10947

TAB interconnects for space concentrator solar cell arrays p 51 N94-11400

BOLT, BERANEK, AND NEWMAN, INC., CAMBRIDGE, MA.

High-performance distributed systems architecture [AD-A265297] p 337 N94-11829

BONN UNIV. (GERMANY).

First results for the simultaneous estimation of the geoid and the sea surface topography by ERS-1 altimeter data p 241 N94-11765

BOOZ-ALLEN AND HAMILTON, INC., MCLEAN, VA.

Potential markets for advanced satellite communications [NASA-CR-191145] p 41 N94-10512

BOSTON COLL., CHESTNUT HILL, MA.

A new data collection system for ionospheric modelling and related topics [AD-A265893] p 278 N94-12277

BOWLING GREEN STATE UNIV., OH.

Vibrational overtone activation of methylcyclopropene [AD-A265588] p 79 N94-12373

BREMEN UNIV. (GERMANY).

Thermocapillary instabilities in cylindrical liquid bridges: Mechanisms and transition boundaries p 101 N94-10077

Gas-liquid jets under reduced gravity conditions p 103 N94-10091

Separation of gravitational effects on the flow of suspension in tubes by measurements in weightlessness p 105 N94-10105

Calibration of accelerometers on drop tower Bremen p 108 N94-10121

Photoinitiated radical polymerization of liquid monomers in microgravity p 124 N94-10246

A method for determination of the elongational viscosity of viscoelastic fluids without body forces p 124 N94-10247

BRIGHAM YOUNG UNIV., PROVO, UT.

Distributed combustion in solid propellants [AD-A265727] p 99 N94-12564

BRITISH AEROSPACE AIRCRAFT GROUP, KINGSTON-UPON-THAMES (ENGLAND).

Structural health monitoring using embedded fibre optic sensors p 22 N94-11334

BRITISH AEROSPACE PUBLIC LTD. CO., BRISTOL (ENGLAND).

Vectra insulative support structures within spacecraft p 62 N94-10050

BRITISH ANTARCTIC SURVEY, CAMBRIDGE (ENGLAND).

Preliminary evaluation of ERS-1 altimetry over Filchner-Ronne Ice Shelf, Antarctica p 238 N94-11742

A first assessment of the value of ERS-1 scatterometer winds for meteorological studies in the polar regions p 250 N94-12501

A comparison of ATSR and shipboard radiometer SST measurements along transects between the UK and the Antarctic p 253 N94-12518

BRITISH BROADCASTING CORP., KINGSWOOD (ENGLAND).

Measurement of display transfer characteristics using test pictures [BBC-RD-1992/13] p 133 N94-11023

Building penetration loss measurements for DAB signals at 211 MHz [BBC-RD-1992/14] p 133 N94-11024

BRITISH COLUMBIA UNIV., VANCOUVER.

Near surface ocean processes: Acoustical observations, ambient sound, and Langmuir circulation p 288 N94-11447

BROOKHAVEN NATIONAL LAB., UPTON, NY.

Dynamics of dissociation versus ionization in strong laser fields [DE93-009261] p 173 N94-10287

Fabrication and test of a superconducting RFQ [DE93-010860] p 140 N94-10300

Symmetry lowering in crystalline solid solutions: A study of cinnamamide-thienylacrylamide by x ray and neutron diffraction and solid-state photochemistry [DE93-010871] p 394 N94-10301

Top and Higgs masses in a composite boson model [DE93-010874] p 359 N94-10302

Production of strange clusters in relativistic heavy ion collisions [DE93-010876] p 359 N94-10303

Strangeness production with protons and pions [DE93-010879] p 359 N94-10304

Searches for strangelets and other exotics at the AGS [DE93-013341] p 359 N94-10308

A new matrix for the ageless 21.6-keV Eu-151 nuclear gamma ray Moessbauer source [DE93-009795] p 75 N94-10338

Preliminary results of the comparison of ATSR measurements with in situ sea temperatures [DE93-013399] p 287 N94-10517

Standard model status (in search of new physics) [DE93-013288] p 410 N94-10528

Advanced zinc phosphate conversion and pre-ceramic polymetallosiloxane coatings for corrosion protection of steel and aluminum, and characteristics of polyphenyletheretherketone-based materials [DE93-008717] p 88 N94-10891

Apical Cu-O bond in YBa2Cu3O(7-delta) superconductors by XAFS [DE93-010861] p 400 N94-11458

In situ XANES studies of the passive film on Fe and Fe-26Cr [DE93-010869] p 84 N94-11459

X-ray and neutron scattering studies of magnetic critical fluctuations in holmium [DE93-010873] p 400 N94-11467

Coprocessing of fossil fuels and biomass for CO2 emission reduction in the transportation sector [PB93-194165] p 267 N94-11845

Spectrum analysis in beam diagnostics [DE93-013401] p 373 N94-12601

Ion shaking in the 200 MeV XLS-ring [DE93-014057] p 374 N94-12782

BROWN UNIV., PROVIDENCE, RI.

Unsupervised splitting rules for neural tree classifiers [AD-A264961] p 338 N94-10487

Three-dimensional object recognition using an unsupervised BCM network: The usefulness of distinguishing features [AD-A264576] p 304 N94-11261

Neural network model selection using asymptotic jackknife estimator and cross-validation method [AD-A264960] p 339 N94-11289

Venus small volcano classification and description p 438 N94-12037

Behavior of vortices generated by an advancing ejecta curtain in theory, in the laboratory, and on Mars p 169 N94-12044

Estimation of age of Dali-Ganis rifting and associated volcanic activity, Venus p 440 N94-12046

Regional geology of the Vega landing sites: Tentative results of photogeologic mapping p 440 N94-12047

Regional geology of the Venera landing sites: Tentative results of photogeologic mapping p 440 N94-12048

Reflectance spectra of sulfate-and carbonate-bearing Fe(3+)-doped montmorillonites as Mars soil analogs p 445 N94-12070

The effects of atmospheric pressure on infrared reflectance spectra of Martian analogs p 445 N94-12071

Buoyant subduction on Venus: Implications for subduction around coronae p 455 N94-12130

Macroscopic electric charge separation during hypervelocity impacts: Potential implications for planetary paleomagnetism p 431 N94-12181

Comparison of the distribution of large magmatic centers on Earth, Venus, and Mars p 467 N94-12192

The Magellan volcanic and magmatic feature catalog p 467 N94-12193

Synthesis of global thematic mapping, Venus: Geologic correlations/questions for the Magellan gravity mission p 467 N94-12194

Large volcanoes on Venus: Examples of geologic and structural characteristics from different classes p 467 N94-12195

Regional mantle upwelling on Venus: The Beta-Atla-Themis anomaly and correlation with global tectonic patterns p 467 N94-12196

Characteristics of arachnoids from Magellan data p 469 N94-12204

Assimilation in lunar basalts and volcanic glasses: Implications for a heterogenous mantle source region p 478 N94-12250

Measuring and distinguishing compositional and maturity properties of lunar soils by remote VIS-NIR spectroscopy p 478 N94-12251

Primitive SNC parent magmas and crystallization: Low PH2O experiments p 433 N94-12264

Computational methods for problems in aerodynamics using parallel and vector architectures [AD-A265626] p 16 N94-12377

Interdisciplinary scientist participation in the Phobos mission [NASA-CR-193715] p 482 N94-12446

BRUSH WELLMAN, INC., CLEVELAND, OH.

Aluminum-beryllium alloys for aerospace applications p 60 N94-10029

BRUSSELS UNIV. (BELGIUM).

On the role of Soret effect in concentration distribution in crystals growing from the melt p 112 N94-10173

Transient effects in the Benard instabilities: Coupling between capillary and gravity effects p 119 N94-10216

BUDAPEST SCIENCE UNIV. (HUNGARY).

One dimensional representations in quantum optics p 375 N94-10570

BULGARIAN ACADEMY OF SCIENCES, SOFIA.

A study of the quasibinary Al-W-Mo system. Part 1: Preliminary investigations and preparation for microgravity experiments p 119 N94-10211

A study of the quasibinary Al-Mo-W system. Part 2: A physico-mechanical investigation of the system fabricated under the gravitylessness conditions p 119 N94-10212

Some aspects of combustion modelling by low and normal gravity p 124 N94-10244

Completeness properties of the minimum uncertainty states p 349 N94-10581

BUNDESANSTALT FUER MATERIALPRUEFUNG, BERLIN (GERMANY).

New x ray scanning topographic approaches to nondestructive evaluation of composites p 61 N94-10039

BUREAU INTERNATIONAL DES POIDS ET MESURES, SEVRES (FRANCE).

Progress on GPS standardization p 24 N94-10965

Comparison of GPS and GLONASS common-view time transfers p 24 N94-10967

An ensemble pulsar time p 351 N94-10969

C

CAE-FEM ENGINEERING, STUTTGART (GERMANY).
Solving the essentials of an innovative tennis racket product: Functionality, simplicity, and super-lightweight technology p 65 N94-10068

CALIFORNIA INST. OF TECH., PASADENA.
Scalable concurrent programming project [AD-A266097] p 328 N94-11295
Post-launch analysis of data from the High Energy Astrophysical Observatory Heavy Nuclei Experiment (HEAO-C3) [NASA-CR-193513] p 484 N94-11486
Giant impact-induced atmospheric blow-off p 435 N94-12019
The stability of hibonite and other aluminous phases in silicate melts: Implications for the origin of hibonite-bearing inclusions p 80 N94-12052
Thermal studies of Martian channels and valleys using Termoskan data p 443 N94-12064
Shock induced reaction in Chicxulub target materials (CaSO4 and SiO2) and their relation to extinctions p 282 N94-12149
LEW88516 and SNC meteorites p 430 N94-12150
The Th and U abundances in chondritic meteorites p 430 N94-12151
Projectile-target mixing in melted ejecta formed during a hypervelocity impact cratering event p 432 N94-12241

CALIFORNIA POLYTECHNIC STATE UNIV., SAN LUIS OBISPO.
Evaluation of dual flow thrust vectored nozzles with exhaust stream impingement [NASA-CR-193292] p 150 N94-10912
Helicopter approach capability using the differential Global Positioning System [NASA-CR-177618] p 24 N94-12355

CALIFORNIA UNIV., BERKELEY.
Quantum dynamics of helium clusters [AD-A266060] p 411 N94-10874
Minor and trace element composition and age of Yukon probable-microtektites p 429 N94-12094
Giotto data analysis: Electron plasma and heavy ion composition measurements at Comet Halley [NASA-CR-193587] p 428 N94-12770

CALIFORNIA UNIV., BERKELEY. LAWRENCE BERKELEY LAB.
Experimental efforts and results in finding new heavy scintillators [DE93-010406] p 371 N94-10156
Some new/old approaches to QCD [DE93-010451] p 408 N94-10261
Infinite-mode squeezed coherent states and non-equilibrium statistical mechanics (phase-space-picture approach) [LBL-32695] p 380 N94-10608
Technology transfer at Lawrence Berkeley Laboratory [DE93-010460] p 423 N94-11059

CALIFORNIA UNIV., DAVIS.
Microtektite-like glass spherules in Late Devonian (367 MA) shales p 461 N94-12160
KT boundary impact glasses from the Gulf of Mexico region p 282 N94-12161

CALIFORNIA UNIV., LOS ANGELES.
Lee waves: Benign and malignant [NASA-CR-186024] p 283 N94-10725
Response of composite laminates to dynamic surface loads p 66 N94-10902
Multilevel computer-aided optimum design of structural systems using multiple basis vectors p 187 N94-11055
Wave structure in planetary rings p 434 N94-11185
Size dependence of chemical reactivity of gaseous metal clusters: A new mechanistic probe [AD-A264690] p 77 N94-11264
Quantitative EEG patterns of differential in-flight workload p 317 N94-11528
A model for the subduction mechanics of flexible lithosphere and its viscous coupling to the mantle using power-law rheologies p 277 N94-11585
Numerical simulations of thermal convection in rapidly rotating spherical fluid shells p 153 N94-11635
PO/PTD diffraction synthesis of array-fed reflector antennas for satellite and radar applications p 137 N94-11636
Research in computing and applied mathematics [AD-A266137] p 331 N94-11657
Venus' center of mass - center of figure displacement and implications p 444 N94-12067
Impact mineralogy and chemistry of the cretaceous-tertiary boundary at DSDP site 576 p 282 N94-12091

CALIFORNIA UNIV., RIVERSIDE.
Effects of a microgravity environment on the crystallization of biological macromolecules p 117 N94-10198

CALIFORNIA UNIV., SAN DIEGO.
Lattice gas hydrodynamics: Theory and simulations [DE93-013297] p 147 N94-10320
Pulmonary function in microgravity: KC-135 experience p 309 N94-11994

CALIFORNIA UNIV., SAN DIEGO, LA JOLLA.
NASTRAN modeling of flight test components for UH-60A airloads program test configuration [NASA-CR-193614] p 186 N94-10937
Smart spatial light modulator research and development [AD-A264928] p 382 N94-11286
Central Equatorial Pacific Experiment (CEPEX) [DE93-011656] p 190 N94-11674
Fluid compartment and renal function alterations in the rat during 7 and 14 day head down tilt p 310 N94-12002
Measurements of cosmogenic nuclides in lunar rock 64455 p 437 N94-12033
Development of a molecular beam technique to study early solar system silicon reactions p 432 N94-12224
Mass and spatial distribution of carbonaceous component in Comet Halley p 433 N94-12263
Theories of turbulent combustion in high speed flows [AD-A265735] p 79 N94-12403
Synthesis and electronic properties of nanophase semiconductor materials [AD-A265287] p 146 N94-12584

CALIFORNIA UNIV., SANTA BARBARA.
The response of an electron in a biased double well to a strong laser: Delocalization and low frequency generation [AD-A265169] p 366 N94-11100
Arctic geodynamics: Continental shelf and deep ocean geophysics. ERS-1 satellite altimetry: A first look p 243 N94-11776
Absorption spectrum calculations using mixed quantum-gaussian wave packet dynamics [AD-A265179] p 413 N94-11877

CALIFORNIA UNIV., SANTA CRUZ.
The controlling parameters of the integrated flux of a stellar population p 426 N94-11187

CAMBER CORP., HUNTSVILLE, AL.
Property changes induced by the space environment in composite materials on LDEF: Solar array materials passive LDEF experiment A0171 (SAMPLE) [NASA-CR-192572] p 73 N94-11484

CAMBRIDGE UNIV. (ENGLAND).
Non-linear liquid bridge dynamics p 100 N94-10074
Dielectric breakdown and its influence on ignition [AD-A264925] p 78 N94-11855
VIB3D: Method for calculating 3-D unsteady flow through turbomachinery blades [CUED/A-TURBO/TR.128] p 166 N94-12777
VIB2D: Quasi 3-D unsteady viscous flow method for blade flutter calculation [CUED/A-TURBO/TR.129] p 166 N94-12779

CAMERINO UNIV. (ITALY).
Quantum non demolition measurement of cyclotron excitations in a Penning trap p 376 N94-10578

CANADA CENTRE FOR REMOTE SENSING, OTTAWA (ONTARIO).
The ERS-1/CV 580 SAR cross-calibration experiment: Sault Ste Marie, October 26 - November 2, 1991 p 236 N94-11729
Preliminary ERS-1 assessment for Canadian agriculture and forestry applications p 248 N94-12486

CANADIAN MARCONI CO. LTD., MONTREAL (QUEBEC).
Fiber-optic sensor systems for measuring strain and the detection of acoustic emissions in smart structures p 71 N94-11337

CANADIAN SPACE AGENCY, OTTAWA (ONTARIO).
Marangoni and buoyant convections in zone melting of GaAs with liquid encapsulation p 101 N94-10081

CARNEGIE INSTITUTION OF WASHINGTON, DC.
Midplane temperatures in the solar nebula p 448 N94-12088
Chondrule formation by clumpy accretion onto the solar nebula p 448 N94-12089
Initiating solar system formation through stellar shock waves p 448 N94-12090

CARNEGIE-MELLON UNIV., PITTSBURGH, PA.
Distributed real-time system design: Theoretical concepts and applications [AD-A265199] p 337 N94-11881
Avoidance and suppression of compensation code in a trace scheduling compiler [AD-A265612] p 333 N94-12439

CASE WESTERN RESERVE UNIV., CLEVELAND, OH.
Low energy electron diffraction and cyclic voltammetry studies of flame-annealed platinum single crystals [AD-A263566] p 401 N94-11518
Electronic and total energy properties of ternary and quaternary semiconductor compounds, alloys and superlattices [NASA-CR-192905] p 405 N94-12570

CENTER FOR MATHEMATICS AND COMPUTER SCIENCE, AMSTERDAM (NETHERLANDS).
Vectorizing matrix operations arising from PDE discretization on 9-point stencils [CWI-NM-R9221] p 342 N94-10351
Complex functions in queueing theory [CWI-BS-R9219] p 342 N94-10352
On a class of two-dimensional nearest neighboring random walks [CWI-BS-R9220] p 347 N94-10353
Applications of cut polyhedra [CWI-BS-R9221] p 347 N94-10354

CENTER FOR OCEANOLOGY RESEARCH AND DEVELOPMENT, JAKARTA (INDONESIA).
Seasonal variability of surface ocean color in the Omura Bay using multitemporal LANDSAT-5 TM data p 218 N94-12698

CENTER FOR PUBLIC SERVICE COMMUNICATIONS, ARLINGTON, VA.
Communications infrastructure requirements for telemedicine/telehealth in the context of planning for and responding to natural disasters: Considering the need for shared regional networks p 307 N94-11804

CENTRAL AEROLOGICAL OBSERVATORY, MOSCOW (USSR).
Non-image visible polarization remote sensing of the ocean p 229 N94-12762

CENTRAL RESEARCH INST. OF ELECTRIC POWER INDUSTRY, TOKYO (JAPAN).
Applicability of satellite infrared data for the monitoring of coastal environments p 220 N94-12714

CENTRE D'ETUDES ET DE RECHERCHES, TOULOUSE (FRANCE).
Boundary layer transition: Prediction and wind tunnel simulation p 32 N94-11498

CENTRE D'ETUDES ET DE RECHERCHES GEODYNAMIQUES ET ASTRONOMIQUES, GRASSE (FRANCE).
LASSO observations at McDonald and OCA/CERGA: A preliminary analysis p 352 N94-10972

CENTRE DE RECHERCHES EN PHYSIQUE DE L'ENVIRONNEMENT, VELIZY (FRANCE).
Validation of the ATSR/M microwave radiometer data p 252 N94-12511

CENTRE DE SPECTROMETRIE NUCLEAIRE ET DE SPECTROMETRIE DE MASSE DU CNRS, ORSAY (FRANCE).
A new carbon-rich phase (COPS) in Antarctic micrometeorites p 432 N94-12233

CENTRE NATIONAL D'ETUDES SPATIALES, TOULOUSE (FRANCE).
Space and time variability of the Gulf Stream using ERS-1 ALT-OPR02 data p 242 N94-11769
Preliminary geophysical investigation with ERS-1 35-day altimeter data p 243 N94-11775

CENTRE NATIONAL DE LA RECHERCHE SCIENTIFIQUE, MEUDON-BELLEVUE (FRANCE).
Wetting effects on nylon spheres engulfment in ice p 115 N94-10189
Influence of gravity and ambient pressure variations on the behavior of buoyant laminar diffusion flames p 123 N94-10240
Rates of fluvio-thermal erosion on Mars p 435 N94-12018

CENTRO BRASILEIRO DE PESQUISAS FISICAS, RIO DE JANEIRO.
Magnetization reversal by nucleation [DE93-610313] p 350 N94-10313
Effect of a distribution of exchange parameters within a simple localized-itinerant model [DE93-610314] p 395 N94-10314

CENTRO INFORMAZIONI STUDI ESPERIENZE, MILAN (ITALY).
The pyrene laser induced fluorescence technique as a diagnostic tool for combustion thermometry in microgravity p 107 N94-10113
Laser beam deflection: A diagnostic tool for vapour growth experiments in microgravity p 111 N94-10135

CENTRO ITALIANO RICERCHE AEROSPAZIALI, NAPLES.
Some experimental study and numerical simulation in wind tunnel flow p 8 N94-10457

CENTRO SVILUPPO MATERIALI S.P.A., ROME (ITALY).
The microstructure and mechanical properties of hot worked FeAl intermetallic alloys p 58 N94-10020

CESKOSLOVENSKA AKADEMIE VED, PRAGUE.
Perforated plates for thin-walled structures p 63 N94-10056

CHALMERS UNIV. OF TECHNOLOGY, GOETEBORG (SWEDEN).
Calibration of the ERS-1 SAR fast-delivery images p 236 N94-11730
Validation of ERS-1 SAR measurements of sea ice during ARCTIC-1991 p 238 N94-11747

CHIBA UNIV. (JAPAN).
Aerodynamic characteristics analysis of Garabedian-Korn 75-06-12 aircraft [PAPER-2D-7] p 11 N94-10472
A statistical method to determine aerosol path radiance and its application to atmospheric correction for CZCS imagery p 191 N94-11897

CHICAGO MEDICAL SCHOOL, IL.
Linking medical records to an expert system p 306 N94-11797

CHICAGO UNIV., IL.
Iron and nickel isotopic mass fractionation in deep-sea spherules p 282 N94-12199
Trace element distributions in primitive achondrites p 431 N94-12200
Analysis and interpretation of high energy cosmic rays measured on Spacelab-2 [NASA-CR-193586] p 485 N94-12771

CHILWORTH RESEARCH CENTRE, SOUTHAMPTON (ENGLAND).
Effects of wave nonlinearity on ERS-1 radar altimeter returns: A preliminary investigation p 235 N94-11722
Comparisons of ERS-1 altimeter height data and the Fine Resolution Antarctic Model (FRAM) p 235 N94-11725
The effect of rain on ERS-1 altimeter data p 243 N94-11773
Spatial scales of wave height p 244 N94-11782
Preliminary validation of ATSR sea surface temperatures near the Faeroes p 253 N94-12519
Topography of the Western Mediterranean from the ERS-1 altimeter p 255 N94-12531

CHINA NUCLEAR INFORMATION CENTRE, BEIJING.
Nonlinear space charge effect of bunched beam in linac [DE93-612176] p 371 N94-10409
Numerical simulation of sidebands in free electron laser oscillators [DE93-612675] p 173 N94-10483
A flexible modelling software for data acquisition [DE93-612915] p 322 N94-10484
Numerical method of singular problems on singular integrals [DE93-613654] p 343 N94-10546

CHRISTOPHER NEWPORT COLL., NEWPORT NEWS, VA.
Development and testing of a superconducting link for an IR detector [NASA-CR-193674] p 170 N94-10948

CHUNGBUK NATIONAL UNIV. (REPUBLIC OF KOREA).
Coherent states and uncertainty relations for the damped harmonic oscillator with time-dependent frequency p 380 N94-10611

CINCINNATI UNIV., OH.
Computational gearing mechanics [NASA-CR-193666] p 181 N94-11157
X ray absorption spectroscopy of electrochemically generated species [AD-A264749] p 77 N94-11265
Ultrasonic wave interaction with advanced complex materials for nondestructive evaluation applications [AD-A265704] p 74 N94-12401

CITADEL COLL., CHARLESTON, SC.
The abundances of the elements in sharp-lined early type stars [NASA-CR-194055] p 424 N94-12573

CITY OF LONDON POLYTECHNIC (ENGLAND).
SAR imaging of geology and bathymetry: Kent coastal area - southern North Sea p 254 N94-12527

CITY UNIV., LONDON (ENGLAND).
The MERMAID project p 329 N94-11426

CLARKSON UNIV., POTSDAM, NY.
Study of the atmospheric chemistry of radon progeny in laboratory and real indoor atmospheres [DE93-012236] p 266 N94-11671

CLEMSON UNIV., SC.
Carbon and nitrogen in Type 2 supernova diamonds p 431 N94-12166

CLEVELAND STATE UNIV., OH.
The efficiency of photovoltaic cells exposed to pulsed laser light p 50 N94-11395

COAST GUARD, WASHINGTON, DC.
US Coast Guard GPS Information Center (GPSIC) and its function within the Civil GPS Service (CGS) p 24 N94-10966

COASTAL ENVIRONMENTAL SERVICES, INC., LINTHICUM, MD.
Data management strategy for the Tampa Bay National Estuary Program: Recommendations and implementation plan [PB93-191633] p 267 N94-11864

COLORADO STATE UNIV., FORT COLLINS.
An investigation of conducted and radiated emissions from a hollow-cathode plasma contactor [NASA-CR-191172] p 386 N94-10346
Updated forecast of Atlantic seasonal hurricane activity for 1993 p 285 N94-11194
Large eddy simulations of the atmospheric boundary layer east of the Colorado Rockies p 277 N94-11465
The impact of vegetation on the atmospheric boundary layer and convective storms p 277 N94-11480

COLORADO UNIV., BOULDER.
High Prandtl number fluids in a multilayered system under 1-g or micro-g environment p 104 N94-10096
Benard and Marangoni convection in multiple liquid layers p 105 N94-10100
Sea ice feature and type identification in merged ERS-1 SAR and LANDSAT Thematic Mapper imagery p 241 N94-11761
Venus resurfacing rates: Constraints provided by 3-D Monte Carlo simulations p 453 N94-12119
Power-law confusion: You say incremental, I say differential p 347 N94-12175
An optoelectronic graphics display processor [AD-A266011] p 171 N94-12391
Elementary particle physics and high energy phenomena [DE93-013971] p 370 N94-12609
The relationship between skin and bulk sea surface temperatures p 221 N94-12716

COLUMBIA UNIV., PALISADES, NY.
Can weak crust explain the correlation of geoid and topography on Venus? p 453 N94-12118

COMMERCE DEPT., WASHINGTON, DC.
Information resources management plan of the Federal Government [ISBN-0-16-037895-8] p 421 N94-12014

COMMISSARIAT A L'ENERGIE ATOMIQUE, GRENOBLE (FRANCE).
Gas film levitator for containerless processing of glasses in microgravity conditions: Early concept and technology demonstration p 108 N94-10122
Scientific specifications for an automated facility for growing large semiconducting crystals from the melt in space p 114 N94-10180
Convection related radial segregation in an idealized horizontal Bridgman configuration p 115 N94-10185
Undercooled W-Re and Mo-Re drops in an ultra high vacuum drop tube p 86 N94-10195
Ground results of the Mephisto program: Benefits and space experiments orientation p 86 N94-10197

COMMISSION OF THE EUROPEAN COMMUNITIES, ISPRA (ITALY).
An algorithm for the detection of mucilage (green slime) in the Adriatic Sea p 191 N94-11900

COMMITTEE ON GOVERNMENT OPERATIONS (U.S. HOUSE).
The revitalization of health and education in Rural America Act of 1992 p 308 N94-11810

COMMONWEALTH SCIENTIFIC AND INDUSTRIAL RESEARCH ORGANIZATION, HOBART (AUSTRALIA).
Mapping of the East Australian current with the ERS-1 SAR and shipborne studies p 234 N94-11717

COMMUNICATIONS SATELLITE CORP., CLARKSBURG, MD.
UV testing of solar cells: Effects of antireflective coating, prior irradiation, and UV source p 53 N94-11408
Workshop summary: New silicon cells p 54 N94-11417

COMPRESSOR COMPONENTS TEXTRON, INC., CLEVELAND, OH.
Application of powder metallurgy techniques to produce improved bearing elements for liquid rocket engines [NASA-CR-193731] p 82 N94-10804

COMPUTATIONAL FLUID DYNAMICS RESEARCH CORP., HUNTSVILLE, AL.
Combustion chamber analysis code [NASA-CR-192585] p 46 N94-10934

COMPUTER RESOURCE MANAGEMENT, INC., HERNDON, VA.
National Airspace System operational concept [DOT/FAA/SE-93/1] p 23 N94-10933

COMPUTER SCIENCES CORP., LANHAM, MD.
Maximizing reuse: Applying common sense and discipline p 329 N94-11429
Development and application of an acceptance testing model p 330 N94-11432

COMPUTER SCIENCES CORP., PATRICK AFB, FL.
Analysis of the eastern range multiplexed fiber optic IRIG B120 distribution system p 139 N94-10996

COMPUTER SOFTWARE MANAGEMENT AND INFORMATION CENTER, ATHENS, GA.
COSMIC monthly progress report [NASA-CR-194400] p 332 N94-11688

COMPUTER TECHNOLOGY ASSOCIATES, INC., HAMPTON, VA.
Node assignment in heterogeneous computing [NASA-CR-4534] p 142 N94-11131

CONCEPCION UNIV. (CHILE).
Remote sensing of polluting focal points and coastal disturbances in the Gulf of Arauco and adjacent bays, central Chile p 217 N94-12695

CONCORDIA UNIV., MONTREAL (QUEBEC).
Comprehensive dynamic analysis of a bladed disk-turborotor-bearing system [ISBN-0-315-73646-1] p 180 N94-11155

CONNECTICUT UNIV., STORRS.
Experiments in ultracold collisions [DE93-012110] p 365 N94-11029
Estimation with multisensor/multiscan detection fusion [AD-A265673] p 138 N94-12338
Interfacial modification through end group complexation in polymer blends [AD-A265887] p 93 N94-12340

CONSEJO SUPERIOR DE INVESTIGACIONES CIENTIFICAS, BARCELONA (SPAIN).
Comparison of ERS-1 SAR images of the Western Mediterranean to in situ oceanographic data: PRIM-1 Cruise (May 1992) p 255 N94-12529

CONSIGLIO NAZIONALE DELLE RICERCHE, GENOA (ITALY).
Surface tension and adsorption kinetics in immiscible liquid systems at microgravity p 121 N94-10225

CONSIGLIO NAZIONALE DELLE RICERCHE, VENICE (ITALY).
The activity of the ERS-1 Venice (Italy) group on scatterometry p 233 N94-11713
Experiment and results of the Italian activity in the field of ocean microwave backscattering p 200 N94-11953
SST assimilation: Eastern Mediterranean case study p 221 N94-12719

CONSTRUCCIONES AERONAUTICAS S.A., MADRID (SPAIN).
Design and development of a CFRP central cylinder for satellites p 56 N94-10007
An approach to high precision antenna structures by a CFRP core sandwich concept p 57 N94-10008
Design and manufacturing of CFRP rings by RTM p 59 N94-10025
Development tests for a high stability optical bench p 62 N94-10047

COPENHAGEN UNIV. (DENMARK).
An analysis of the gravity field in the Norwegian Sea and mapping of the ice cap of Greenland using ERS-1 altimeter measurements p 242 N94-11768

CORNELL UNIV., ITHACA, NY.
Conversion of acetic acid to methane by thermophiles [DE93-014433] p 300 N94-10652
Physical studies of planetary and satellite surfaces [NASA-CR-193545] p 434 N94-10817
Preparing for the initial observations of the Targeted Search and the Sky Survey systems [NASA-CR-193644] p 318 N94-10865
Analysis of IRAS solar system dust data [NASA-CR-193704] p 483 N94-10949
Interstellar scattering and the pulsar studies with space VLBI p 135 N94-11065
Dynamics and control of coherent structures in the turbulent wall layer: An overview p 31 N94-11494
The x ray standing waves on surfaces [AD-A265265] p 402 N94-11682
Experimental studies of the structure of grain boundaries [DE93-013979] p 402 N94-11700
Resist materials design: Base-catalyzed chemical amplification [AD-A265286] p 145 N94-11819
The effects of organic adsorbates on the underpotential deposition of silver on Pt(111) electrodes [AD-A265623] p 404 N94-12376
Mapping closures for turbulent combustion [AD-A265671] p 79 N94-12378
Studies of electrostatic waves and VLF-wave particle interaction in the ionosphere [AD-A266013] p 278 N94-12392
Preparation of stable photopatternable polymeric materials for non-linear optics [AD-A265359] p 95 N94-12577
Photogenerated base in polymer imaging. Synthesis and photopatterning of poly(2-cyano-2-(p-vinylphenyl) butanoic acid) [AD-A265288] p 95 N94-12585

CRANFIELD INST. OF TECH., BEDFORD (ENGLAND).
Control effectiveness at hypersonic speeds p 3 N94-10426

CSA ENGINEERING, INC., PALO ALTO, CA.

Flight Dynamics Directorate (FDD) Historically Black Colleges and Universities (HBCU's) database managment system: A user's guide [AD-A264947] p 419 N94-11288

CZECHOSLOVAK SOLAR ENERGY SOCIETY, PRAGUE.

Renewable energy sources 1991, part 3 [DE93-605594] p 263 N94-11505

Renewable energy sources 1991, part 2 [DE93-605634] p 263 N94-11506

D

DARCHEM ENGINEERING, STILLINGTON (ENGLAND).

An investigation into aircraft fuselage fire hardening p 19 N94-10782

DARTMOUTH COLL., HANOVER, NH.

Strontium and oxygen isotope study of M-1, M-3 and M-4 drill core samples from the Manson impact structure, Iowa: Comparison with Haitian K-T impact glasses p 281 N94-12080

Modern shelf ice, equatorial Aeolis Quadrangle, Mars p 450 N94-12100

Oxygen isotopes as tracers of tektite source rocks: An example from the Ivory Coast tektites and Lake Bosumtwi Crater p 430 N94-12146

DEFENCE RESEARCH AGENCY, FARNBOROUGH (ENGLAND).

The UoSAT-5 solar cell experiment: First year in orbit p 53 N94-11409

An overview of the Defence Research Agency photovoltaic programme p 53 N94-11412

An experiment for the radiometric calibration of the ERS-1 SAR p 236 N94-11733

ERS-1 SAR crop monitoring experiment in East Anglia, UK p 248 N94-12488

DEFENCE RESEARCH ESTABLISHMENT PACIFIC, VICTORIA (BRITISH COLUMBIA).

Paint removal activities in Canada p 126 N94-10615

Paint removal and surface cleaning using ice particles p 128 N94-10626

Paint removal using wheat starch blast media p 128 N94-10627

DEFENCE RESEARCH ESTABLISHMENT SUFFIELD, RALSTON (ALBERTA).

Tandem mass spectrometric analysis of phosphate esters [AD-A265483] p 78 N94-12009

DEFENSE PERSONNEL SECURITY RESEARCH CENTRE, MONTEREY, CA.

A comparison of high and low-impact reports of investigation on adjudicators' decision making: A pilot study [AD-A265747] p 416 N94-10298

DELAWARE UNIV., NEWARK.

Variability of the mixed layer depth in the North Pacific Ocean as calculated by a 3-D semi-analytical mixed layer remote sensing model p 221 N94-12718

DELEGATION GENERALE DE L'ARMEMENT, TOULOUSE (FRANCE).

Procedures without danger to the environment and efficiency (PSDEE) for the removal of paint. Point on the French activities concerning the removal of paint p 126 N94-10616

DEPARTMENT OF DEFENSE, WASHINGTON, DC.

Department of Energy fundamentals handbook: Engineering symbology, prints, and drawings [DE93-012220] p 129 N94-11670

DEPARTMENT OF EDUCATION, WASHINGTON, DC.

Software management guide [DE93-012034] p 330 N94-11452

DEPARTMENT OF ENERGY, WASHINGTON, DC.

Computer models used to support cleanup decision-making at hazardous and radioactive waste sites [PB93-183333] p 274 N94-10698

Information resources management long-range plan, FY1994 [DE93-013898] p 420 N94-11588

The DOE Program in High-Performance Computing and Communications (HPCC) [DE93-013813] p 334 N94-12606

DEPARTMENT OF ENVIRONMENT AND NATURAL RESOURCES, QUEZON CITY (PHILIPPINES).

Status of remote sensing and Geographic Information System (GIS) applications in the Environment and Natural Resources (ENR) sector p 36 N94-10687

DEPARTMENT OF SCIENTIFIC AND INDUSTRIAL RESEARCH, LOWER HUTT (NEW ZEALAND).

Aspects of applying a relaxation method to computing sea surface velocities from sea surface temperature images p 214 N94-12679

DEPARTMENT OF THE ARMY, WASHINGTON, DC.

Dielectric resonator [US-PATENT-4,580,116] p 141 N94-10668

DEPARTMENT OF THE NAVY, WASHINGTON, DC.

Laser Synchrotron Source (LSS) [AD-D015755] p 173 N94-10371

Method and apparatus for polarization-maintaining fiber optical amplification with orthogonal polarization output [AD-D015756] p 374 N94-10372

Technique to prepare high-reflectance optical fiber bragg gratings with single exposure in-line on fiber draw tower [AD-D015757] p 374 N94-10373

Variable rate transfer of optical information [AD-D015758] p 418 N94-10374

External combustion engine having a combustion expansion chamber [AD-D015761] p 178 N94-10375

A fiber optic network system with low crosstalk using code-division multiplexing [AD-D015763] p 374 N94-10376

Thin-film edge field emitter device and method of manufacture therefore [AD-D015764] p 140 N94-10377

Heat regenerative external combustion engine [AD-D015765] p 178 N94-10378

Dual valve plate two-way pressure relief valve [AD-D015766] p 178 N94-10379

Electrochemical process and product therefrom [AD-D015767] p 75 N94-10380

Vibration isolation mount with locking means [AD-D015769] p 178 N94-10381

Interference photocathode [AD-D015770] p 132 N94-10382

Corner vortex suppressor [AD-D015772] p 147 N94-10383

Continuous-time adaptive learning circuit [AD-D015773] p 140 N94-10384

Self locking set screw [AD-D015774] p 178 N94-10385

Microwave multiplexer with channels of varying fractional bandwidths [AD-D015754] p 140 N94-10389

Aluminum based alkaline battery [AD-D015775] p 140 N94-10390

A 1.94 micron laser apparatus, system, and method using a thulium-doped yttrium-lithium-fluoride laser crystal pumped with a diode laser [AD-D015740] p 176 N94-12321

Limited bandwidth microwave filter [AD-D015744] p 145 N94-12322

Improved super luminescent light source specification [AD-D015746] p 176 N94-12329

Ceramics formed by pyrolysis of either linear or thermosetting carborane (siloxane or silane) acetylene based precursor polymers [AD-D015747] p 93 N94-12330

Submicrosecond, synchronizable x ray source [AD-D015745] p 176 N94-12337

A hybrid neural network and feature extraction technique for target recognition [AD-D015732] p 333 N94-12386

Synthesis and polymerization of oligomeric multiple aromatic ether-containing phthalonitriles [AD-D015729] p 94 N94-12399

Spatial light modulator having photosensitive and ferroelectric layers [AD-D015731] p 404 N94-12400

DEPARTMENT OF TRANSPORTATION, CAMBRIDGE, MA.

Impact of shutting down en route primary radars within CONUS interior [DOT-VNTSC-FAA-93-1] p 23 N94-11626

DEUTSCHE AIRBUS G.M.B.H., BREMEN (GERMANY).

Investigations on aluminium-lithium alloys for damage tolerant application p 59 N94-10023

Future needs in the development of materials for aircraft interiors and equipment p 21 N94-10794

DEUTSCHE FORSCHUNGS- UND VERSUCHSANSTALT FUER LUFT- UND RAUMFAHRT, BRUNSWICK (GERMANY).

Fiber-optic interferometric strain gauge for smart structures applications: First flight tests p 71 N94-11340

DEUTSCHE FORSCHUNGS- UND VERSUCHSANSTALT FUER LUFT- UND RAUMFAHRT, COLOGNE (GERMANY).

The upgrading of the arc heated wind tunnel of the DLR (LBK) with respect to its effects on the material testing p 4 N94-10432

DEUTSCHE FORSCHUNGS- UND VERSUCHSANSTALT FUER LUFT- UND RAUMFAHRT, GOETTINGEN (GERMANY).

The high enthalpy facilities HEG and TH 2 in Germany p 4 N94-10430

DEUTSCHE FORSCHUNGS- UND VERSUCHSANSTALT FUER LUFT- UND RAUMFAHRT, MUNICH (GERMANY).

Smart structures: A technology for next generation aircraft p 27 N94-11318

In-flight aircraft structure health monitoring based on smart structures technology p 22 N94-11333

Adaptive algorithms for use with digital filters in vibration control p 71 N94-11338

Structural analysis and optimization of adaptive structures by use of the finite element method p 71 N94-11339

DEUTSCHE FORSCHUNGSANSTALT FUER LUFT- UND RAUMFAHRT, BERLIN (GERMANY).

Disk-resolved spectral characteristics of Saturn's medium-sized satellites p 471 N94-12213

DEUTSCHE FORSCHUNGSANSTALT FUER LUFT- UND RAUMFAHRT, BRUNSWICK (GERMANY).

Fibre reinforced structures with glass matrix p 64 N94-10064

DEUTSCHE FORSCHUNGSANSTALT FUER LUFT- UND RAUMFAHRT, COLOGNE (GERMANY).

Force and power efficiency of micro-g electromagnetic levitation coils p 110 N94-10129

Results of mission preparation support to microgravity experiments on board of Eureca 1 p 111 N94-10138

Marangoni motion during melting of a hypermonotectic alloy: Numerical simulations for the D2 experiment IHF04 p 113 N94-10177

Numerical simulation of multi-droplet hydrodynamic interactions in liquid dispersions p 114 N94-10182

TEXUS 28 experiment: Convections and crystal growth of Ge:Ga. Analysis of temperature measurements p 114 N94-10184

Thermophysical properties of undercooled liquid metals p 86 N94-10190

New mechanism of Ostwald ripening in Lorentz-force stabilized Cu-Pb dispersions p 116 N94-10192

Non-equilibrium solidification in undercooled Ni-B alloys p 86 N94-10196

Ostwald ripening of solid cobalt particles in liquid copper p 87 N94-10202

Measurements of heat capacity in undercooled metals p 87 N94-10231

Phase separation at gas-liquid critical points p 122 N94-10233

Fibre reinforced polymer matrix composites: Microstructure and mechanical properties [DLR-FB-92-28] p 66 N94-11085

DEUTSCHE FORSCHUNGSANSTALT FUER LUFT- UND RAUMFAHRT, GOETTINGEN (GERMANY).

On the instability of hypersonic flow past a pointed cone: Comparison of theoretical and experimental results at Mach 8 p 8 N94-10453

DEUTSCHE FORSCHUNGSANSTALT FUER LUFT- UND RAUMFAHRT, OBERPFAFFENHOFEN (GERMANY).

ERS-1 preliminary antenna elevation pattern measured by ground-receivers p 235 N94-11727

Operational ERS-1 orbit determination at D-PAF p 243 N94-11774

Quick-look monitoring of the sea surface with ERS-1 fast delivery altimeter data p 243 N94-11777

The Earth's gravity model for the ERS-1 commissioning phase p 243 N94-11778

Radarmap of Germany: First mosaic and classification p 246 N94-12477

Information capability of NOAA-AVHRR data for monitoring oceanographic and atmospheric pollution p 214 N94-12677

DEUTSCHE FORSCHUNGSANSTALT FUER LUFT- UND RAUMFAHRT, STUTTGART (GERMANY).

High temperature materials for hypersonic transport p 56 N94-10003

Lightweight CFRP frame structures for a Rotex-derived manipulator system p 56 N94-10005

DEUTSCHE LUFTHANSA A.G., HAMBURG (GERMANY).

Aquastrip (tm): An innovative paint removal technology p 127 N94-10625

DIPONEGORO UNIV., JEPARA (INDONESIA).

Application of remote sensing for coastal management in the north coast of Java p 218 N94-12701

DISTRICT OF COLUMBIA UNIV., WASHINGTON, DC.

A summer program in mathematics and computer science for academically oriented student [AD-A263467] p 415 N94-11517

DORNIER LUFTFAHRT G.M.B.H., FRIEDRICHSHAFEN (GERMANY).

SPF/DB: A manufacturing technique for lightweight structures p 59 N94-10026

Universal adjustable mould for antenna reflectors p 59 N94-10027

Cost effectiveness of structural applications of fibre reinforced thermoplastics p 60 N94-10032

Paint removal activities in Germany p 126 N94-10617

DORNIER SYSTEM G.M.B.H., FRIEDRICHSHAFEN (GERMANY).
Low cost and thermally stable sandwich design for FIRST p 57 N94-10009
Design concepts for load-carrying hot structures for reentry bodies p 57 N94-10012
Fibre-reinforced ceramic components by filament winding for intermediate temperature applications p 61 N94-10041
Advanced protein, crystallization facility and associated new developments p 39 N94-10119
TEMPUS: An electromagnetic levitation facility for containerless processing under micro-g in Spacelab p 109 N94-10125

DSM/NV NEDERLANDSE STAATSMIJNEN, GELEEN.
Low cost thermoplastic composites for structural applications: Design concepts using new materials and processes p 60 N94-10034

DU PONT DE NEMOURS (E. I.) AND CO., WILMINGTON, DE.
Factors that affect OSU thermal performance of aircraft interior materials p 20 N94-10789

DUKE UNIV., DURHAM, NC.
Aluminum-phosphorus chemistry: Preparation and structural characterization of (Et2AlP(SiMe3)2)2, Et(Cl)2Al(dot)P(SiMe3)3, and i-Bu2(Cl)Al(dot)P(SiMe3)3
[AD-A265268] p 78 N94-11683

DYNAMICS RESEARCH CORP., ARLINGTON, VA.
More sense for less cents: Cost effective servicing of remote sensing satellites p 348 N94-11572

E

ECC INTERNATIONAL CORP., ORLANDO, FL.
Teaching high-performance skills using above-real-time training
[NASA-CR-4528] p 315 N94-11627

ECOLE CENTRALE DE LYON (FRANCE).
Marangoni Benard instabilities in liquid mixtures with Soret effect p 119 N94-10215

ECOLE NATIONALE SUPERIEURE DE CERAMIQUE INDUSTRIELLE, LIMOGES (FRANCE).
Study of the tribological behavior of SiC and Si3N4 ceramic couples in terms of temperature: The reality p 64 N94-10061

ECOLE NATIONALE SUPERIEURE DE CHIMIE, MONTPELLIER (FRANCE).
Crystallization of zeolites in the microgravity environment of space p 119 N94-10210

ECOLE POLYTECHNIQUE FEDERALE DE LAUSANNE (SWITZERLAND).
Hypersonic multi block flow simulations around space vehicles including non-equilibrium chemistry p 9 N94-10460

ECOLE SUPERIEURE DE PHYSIQUE ET DE CHIMIE INDUSTRIELLES, PARIS (FRANCE).
Fluid-fluid interfacial instabilities induced by gravity p 121 N94-10229

EDGERTON, GERMESHAUSEN AND GRIER, INC., IDAHO FALLS, ID.
The searchlight problem for neutrons in a semi-infinite medium
[DE93-010796] p 365 N94-10952
In situ secondary ion mass spectrometry analysis
[DE93-012185] p 76 N94-11140
Processing, properties, and wear resistance of aluminides
[DE93-012186] p 83 N94-11141
Performance aspects of de Laval spray-forming nozzles
[DE93-013671] p 163 N94-12604

EG AND G ENERGY MEASUREMENTS, INC., ALBUQUERQUE, NM.
An alternative to sneakernet
[DE93-012130] p 419 N94-11137

EG AND G ROCKY FLATS, INC., GOLDEN, CO.
Remote surface water monitoring radio based telemetry system
[DE93-009643] p 41 N94-11282

EHIME UNIV., MATSUYAMA (JAPAN).
The Kyucho events in Sukumo Bay induced by Kuroshio front disturbances p 198 N94-11939

ELECTROTECHNICAL LAB., IBARAKI (JAPAN).
The development of phytoplankton sensing system with optical fiber p 203 N94-11967
Ocean measuring experiments using optical fiber distributed temperature sensor p 172 N94-11968
Automatic classification system for zooplankton p 203 N94-11969

EMBASSY OF AUSTRALIA, TOKYO (JAPAN).
National space program in Australia p 37 N94-10691

EMBASSY OF CANADA, TOKYO (JAPAN).
Canada's longterm space plan and ISY activities p 37 N94-10692

EMBASSY OF PAKISTAN, TOKYO (JAPAN).
Pakistan Space and Upper Atmosphere Research Commission p 37 N94-10693

ENGINEERING SYSTEMS MANAGEMENT, INC., GAITHERSBURG, MD.
Life-cycle cost analysis of conventional and fuel cell/battery powered urban passenger vehicles
[DE93-010770] p 182 N94-11438

ENGLISH ELECTRIC VALVE CO. LTD., CHELMSFORD (ENGLAND).
Heteroepitaxial InP, and ultrathin, directly glassed, GaAs 3-5 solar cells p 52 N94-11406

ENSCO, INC., SPRINGFIELD, VA.
Safety of high speed ground transportation systems: X2000 US demonstration vehicle dynamics trials, preliminary test report, October 1992 - January 1993
[PB93-194645] p 422 N94-10736

ENVIRONMENTAL PROTECTION AGENCY, CINCINNATI, OH.
Environmental Protection Agency's life cycle methodology: Guidelines for use in development of packaging
[PB93-194199] p 265 N94-10841

ENVIRONMENTAL PROTECTION AGENCY, WASHINGTON, DC.
Computer models used to support cleanup decision-making at hazardous and radioactive waste sites
[PB93-183333] p 274 N94-10698
Toxic chemical release inventory reporting Form R and instructions. Revised 1992 version. Section 313 of the Emergency Planning and Community Right-to-Know Act
[PB93-194140] p 264 N94-10836
Summary of implementation and demonstration projects in bays and estuaries
[PB93-194637] p 265 N94-10846
Gulf of Mexico sales 147 and 150: Central and western planning areas. Draft environmental impact statement. Volume 1: Sections 1 through 4.C
[PB93-190304] p 265 N94-11018

ENVIRONMENTAL RESEARCH INST. OF MICHIGAN, ANN ARBOR.
Spatial light rebroadcaster architecture study
[AD-A266102] p 382 N94-11421
The guide to Design For On-orbit Spacecraft Servicing (DFOSS) manual: Producing a consensus document p 421 N94-11575
Arctic sea ice microwave signature and geophysical processes study p 240 N94-11754
Observations of ERS-1 SAR sensitivities to changes in aboveground biomass in young loblolly pine forests p 249 N94-12494

ERLANGEN-NUREMBERG UNIV. (GERMANY).
The use of magnetic fields for damping unsteady Marangoni convection in GaAs floating zones under microgravity p 100 N94-10073
Calculation of the effects of magnetic field damping in fluid flow: Comparison of magnetohydrodynamic models of different complexity p 103 N94-10089
On the accuracy and efficiency of CFD methods in real gas hypersonics p 9 N94-10462
Geometric aspects of uncertainty and correlation p 349 N94-10588

ERNO RAUMFAHRTTECHNIK G.M.B.H., BREMEN (GERMANY).
On the mechanical development of the Flexible External Insulation (FEI) for Hermes spaceplane p 62 N94-10048
Material advances for lightweight TPS p 62 N94-10049

ESCUELA TECNICA SUPERIOR DE INGENIEROS AERONAUTICOS, MADRID (SPAIN).
Experimental study of axisymmetric thermocapillary flows p 100 N94-10072
Particle image velocimetry technique: Calibration tests p 111 N94-10137

ESCUELA TECNICA SUPERIOR DE INGENIEROS INDUSTRIALES, MADRID (SPAIN).
Thermocapillary migration of bubbles: A semi-analytical solution for large Marangoni numbers p 104 N94-10095

EUROCOPTER DEUTSCHLAND G.M.B.H., MUNICH (GERMANY).
Smart materials for helicopter rotor active control p 27 N94-11321

EUROPEAN CENTRE FOR MEDIUM-RANGE WEATHER FORECASTS, READING (ENGLAND).
ERS-1 scatterometer data characteristics and wind retrieval skill p 233 N94-11709

EUROPEAN RESEARCH COORDINATION AGENCY, BRUSSELS (BELGIUM).
The EUREKA project portfolio in new materials p 56 N94-10002

EUROPEAN SPACE AGENCY, PARIS (FRANCE).
Advanced Materials for Lightweight Structures
[ESA-SP-336] p 56 N94-10001
Proceedings of the 8th European Symposium on Materials and Fluid Sciences in Microgravity, volume 1
[ESA-SP-333-VOL-1] p 99 N94-10070
Proceedings of the 8th European Symposium on Materials and Fluid Sciences in Microgravity, volume 2
[ESA-SP-333-VOL-2] p 112 N94-10171
Proceedings of First ERS-1 Symposium on Space at the Service of Our Environment, volume 1
[ESA-SP-359-VOL-1] p 232 N94-11704
Calibration and validation of the ERS-1 wind scatterometer p 232 N94-11706
Proceedings of 1st ERS-1 Symposium on Space at the Service of Our Environment, Volume 2
[ESA-SP-359-VOL-2] p 245 N94-12471

EUROPEAN SPACE AGENCY. EUROPEAN SPACE OPERATIONS CENTER, DARMSTADT (GERMANY).
ERS-1 precise orbits and altimetry analysis p 242 N94-11771

EUROPEAN SPACE AGENCY. EUROPEAN SPACE RESEARCH AND TECHNOLOGY CENTER, ESTEC, NOORDWIJK (NETHERLANDS).
Protein, glass, aerosol research, containerless processing and diagnostics technology for microgravity application p 106 N94-10112
High temperature processing and diagnostic technologies for microgravity applications p 110 N94-10130
The advanced fluid physics module: How to achieve scientific goals for Spacelab D2 p 39 N94-10136
The critical facility on IML-1 p 44 N94-10250
Thermodynamic model of air in chemical equilibrium p 7 N94-10448
ESA/ESOC: 25 years
[ESA-BR-90] p 485 N94-11379
Spain: Success story in space
[ESA-BR-81] p 38 N94-11461
ESRO's first scientific satellite programme, 1961 - 1966
[ESA-HSR-2] p 44 N94-11462
ERS-1 SAR calibration strategy p 235 N94-11726
The height calibration of the ERS-1 radar altimeter p 241 N94-11764
ESA Costing Software (ECOS) introduction
[ESA-F-28] p 333 N94-12383

EUROPEAN SPACE RESEARCH LAB., NOORDWIJK (NETHERLANDS).
Mission to the Moon: An ESA study on future exploration p 460 N94-12153

EUROPEAN SPACE RESEARCH ORGANIZATION, NOORDWIKJ (NETHERLANDS).
A method to determine asteroid poles p 431 N94-12205

EXECUTIVE OFFICE OF THE PRESIDENT, WASHINGTON, DC.
From red tape to results: Creating a government that works better and costs less p 422 N94-11351
From red tape to results: Creating a government that works better and costs less. Executive summary p 422 N94-11353

F

FACTORY MUTUAL RESEARCH CORP., NORWOOD, MA.
Flammability parameters of materials: Ignition, combustion, and flame spread p 20 N94-10788

FACULTE DES SCIENCES AGRONOMIQUES DE L'ETAT, GEMBLOUX (BELGIUM).
The use of ERS-1 SAR data to study surface states p 247 N94-12480

FAUCETT (JACK) ASSOCIATES, INC., BETHESDA, MD.
Pattern of federal procurement from minority and women-owned small business
[PB93-189355] p 417 N94-11844

FAYETTEVILLE STATE UNIV., NC.
Project TIMS (Teaching Integrated Math/Science)
[NASA-CR-194288] p 416 N94-11599

FEDERAL AVIATION ADMINISTRATION, ATLANTA, GA.
Proceedings of the International Conference for the Promotion of Advanced Fire Resistant Aircraft Interior Materials
[DOT/FAA/CT-93/3] p 17 N94-10766
Aircraft material fire testing and the creation of an international working group p 21 N94-10790
Advanced aircraft materials research and development plan p 22 N94-10796
The future of aircraft cabin fire safety p 22 N94-10797

FEDERAL AVIATION ADMINISTRATION, ATLANTIC CITY, NJ.
Proceedings of the International Conference for the Promotion of Advanced Fire Resistant Aircraft Interior Materials
[AD-A266057] p 22 N94-12384

Analytical method for water vapor collection and analysis in aircraft cabin fires
[DOT/FAA/CT-TN93/33] p 22 N94-12575

FEDERAL AVIATION ADMINISTRATION, OKLAHOMA CITY, OK.
Head and face anthropometry of adult US civilians
[DOT/FAA/AM-93/10] p 315 N94-10806
SATORI: Situation Assessment Through the Re-creation of Incidents
[DOT/FAA/AM-93/12] p 38 N94-12567

FEDERAL AVIATION ADMINISTRATION, WASHINGTON, DC.
FAA air traffic activity
[AD-A266043] p 22 N94-12397
US civil airmen statistics for calendar year 1991
[AD-A266085] p 2 N94-12412
Federal Aviation Administration aviation forecasts
[AD-A265611] p 2 N94-12578

FEDERAL AVIATION AGENCY, OKLAHOMA CITY, OK.
Aviation accident risk for airmen with aphakia and artificial lens implants
[DOT/FAA/AM-93/11] p 303 N94-10813

FEDERAL COORDINATING COUNCIL FOR SCIENCE, ENGINEERING AND TECHNOLOGY, WASHINGTON, DC.
Machine translation technology: A potential key to the information age
[PB93-134336] p 421 N94-12385

FERMI NATIONAL ACCELERATOR LAB., BATAVIA, IL.
The three-point function as a probe of models for large-scale structure
[NASA-CR-193249] p 425 N94-11153
Upgraded D(O) calorimeter electronics for short Tevatron bunch space and the effect of pile-up on the W mass measurement
[DE93-013566] p 146 N94-12603
Top quark search in D(O) from the lepton + jets mode
[DE93-014027] p 370 N94-12781

FERRARA UNIV. (ITALY).
The uncertainty principle in resonant gravitational wave antennae and quantum non-demolition measurement schemes p 378 N94-10587

FIAT RESEARCH CENTER, ORBASSANO, TURIN (ITALY).
Possible applications of atomic frequency standards with an internal high resolution digital synthesizer
p 353 N94-10979

FIELD MUSEUM OF NATURAL HISTORY, CHICAGO, IL.
Distribution of vanadium and melting of opaque assemblages in Efremovka CAI's p 282 N94-12141
Metal-rich meteorites from the aubrite parent body
p 430 N94-12142

FIRST INST. OF OCEANOGRAPHY, QINGDAO (CHINA).
ADCP evidence for upper layer circulation in northeast of the South China Sea p 215 N94-12686

FLINDERS UNIV., ADELAIDE (AUSTRALIA).
Integrated cross sections for the ionisation of atomic hydrogen by electron impact
[DE93-610179] p 359 N94-10311
Calculation of the total ionization cross section and spin asymmetry in electron-hydrogen scattering from threshold to 500 eV
[DE93-610180] p 359 N94-10312
Satellite structure of the xenon valence shell by electron momentum spectroscopy
[DE93-609993] p 360 N94-10327
Convergent close-coupling calculations of electron-hydrogen scattering
[DE93-610049] p 360 N94-10328
Calculation of spin-dependent observables in electron-sodium scattering using the coupled-channel optical method
[DE93-610050] p 360 N94-10329
Distorted-wave calculation of He(e,2e) including core-exchange
[DE93-610072] p 360 N94-10330
Spin-dependent observables in electron-sodium scattering calculated using the coupled-channel optical method
[DE93-610073] p 360 N94-10331
Electron momentum spectroscopy of atoms, molecules and solids
[DE93-610148] p 360 N94-10332
Recent advances in electron momentum spectroscopy
[DE93-610149] p 361 N94-10333

FLORIDA AGRICULTURAL AND MECHANICAL UNIV., TALLAHASSEE.
Unsteady flow past a NACA 0012 airfoil pitching at constant rates
[AD-A265159] p 16 N94-11889

FLORIDA INST. OF TECH., MELBOURNE.
Electronic characterization of defects in narrow gap semiconductors
[NASA-CR-193568] p 397 N94-10819

FLORIDA SOLAR ENERGY CENTER, CAPE CANAVERAL.
Computation of photovoltaic parameters under lunar temperature variation p 53 N94-11411

FLORIDA STATE UNIV., TALLAHASSEE.
Variability of wind stress, and sensible and latent heat flux in the North Atlantic during SEASAT
p 194 N94-11918
A study of the Merritt Island, Florida sea breeze flow regimes and their effect on surface heat and moisture fluxes
[NASA-CR-4537] p 286 N94-12580

FLORIDA UNIV., GAINESVILLE.
Ionization potentials of small carbon clusters
[AD-A264379] p 67 N94-11260
Development of ultra-low noise, high sensitivity planar metal grating coupled 3 to 5 multiquantum well infrared detectors for focal plane array staring IR sensor systems
[AD-A265599] p 404 N94-12375

FLUID GRAVITY ENGINEERING LTD., WITLEY (ENGLAND).
Planetary entry vehicle design for planned and potential ESA missions to Titan, Mars, and Earth return (FGE TN 51/92) p 4 N94-10428

FLUIDTHERM ENGINEERING, BOULDER, CO.
SWIRL as a means of liquid management in low gravity
[NASA-CR-4545] p 412 N94-11523

FOKKER B.V., AMSTERDAM (NETHERLANDS).
Operational aspects of F.16 plastic media blasting, as carried out by Fokker Aircraft Services
p 126 N94-10619
Applications of continuous fiber reinforced thermoplastics in aircraft interiors p 18 N94-10775

FOKKER B.V., SCHIPOL-OOST (NETHERLANDS).
Design evaluation of GLARE laminate lay-ups
p 63 N94-10051

FOKKER SPECIAL PRODUCTS B.V., HOOGEVEEN (NETHERLANDS).
Application of advanced thermoplastics
p 60 N94-10033

FOOD AND AGRICULTURE ORGANIZATION OF THE UNITED NATIONS, ROME (ITALY).
Combined analysis of ERS-1 SAR and visible/infrared remote sensing data for land cover/land use mapping in a tropical zone: A case study in Guinea
p 246 N94-12478

FOSTER-MILLER ASSOCIATES, INC., WALTHAM, MA.
Holographic multiplexing for 3D optical memory
[AD-A266099] p 171 N94-11420

FRAUNHOFER-INST. FUER ANGEWANDTE MATERIAL FORSCHUNG, BREMEN (GERMANY).
PM technology and mechanical properties of metallic foams p 64 N94-10059

FRAUNHOFER-INST. FUER CHEMISCHE TECHNOLOGIE, PFINZTAL (GERMANY).
Investigation of the reason for the softening behaviour of filled polymers p 63 N94-10058

FREIBURG UNIV. (GERMANY).
CdTe crystal growth in the Soviet facility zona 4
p 106 N94-10111
THM-growth of III-V-semiconductors in the magnetic field p 118 N94-10209
Crystal growth in the Zone Melting Facility (ZMF)
p 119 N94-10213

FUJI HEAVY INDUSTRIES LTD., UTSUNOMIYA (JAPAN).
Aerodynamic characteristics analysis of Garabedian-Korn 75-06-12 airfoil
[PAPER-2D-3] p 10 N94-10469
Flow analysis around ONERA model M5 configuration
[PAPER-3D-1] p 11 N94-10477

FUJITSU LTD., TOKYO (JAPAN).
Aerodynamic characteristics analysis of Garabedian-Korn 75-06-12 airfoil
[PAPER-2D-8] p 11 N94-10473
Flow analysis around ONERA model M5 configuration
[PAPER-3D-3] p 12 N94-10479

FURANE PLASTICS, INC., LOS ANGELES, CA.
Uralane (tm) 5774-A/B: Ciba-Geigy's advanced urethane adhesive for the aircraft industry
p 18 N94-10777

FUYO OCEAN DEVELOPMENT AND ENGINEERING CO. LTD., TOKYO (JAPAN).
Effects of wind-roughened sea surface on ocean color remote sensing: Noise derived from reflected light and whitecaps p 191 N94-11898

G

GEC ALSTHOM, STAFFORD (ENGLAND).
Ceramic matrix composites: High performance materials for space application p 62 N94-10044

GEC HIRST RESEARCH CENTRE, WEMBLEY (ENGLAND).
Chaotic time series analysis p 31 N94-11490

GENERAL ACCOUNTING OFFICE, WASHINGTON, DC.
National Aero-Space Plane: A need for program direction and funding decisions
[GAO/NSIAD-93-207] p 416 N94-10910
NASA procurement: Proposed changes to the Jet Propulsion Laboratory contract. Report to Congressional Requesters
[GAO/NSIAD-93-178] p 416 N94-10941
Financial management: NASA's financial reports are based on unreliable data
[AD-A265690] p 418 N94-12443
Defense: Health care
[AD-A265914] p 421 N94-12445

GENERAL ATOMIC CO., SAN DIEGO, CA.
Efficiency of fast wave current drive for a weakly relativistic plasma
[DE93-012775] p 385 N94-10159
User's manual for the DAD-1 data acquisition daughter board for the SuperCard-2
[DE93-012153] p 325 N94-11139
Conversion of the four-strap array in D3-D to a tunable traveling wave antenna
[DE93-012085] p 137 N94-11453
Results from the D3-D advanced divertor program
[DE93-015472] p 393 N94-11514
TFE verification program
[DE93-009609] p 373 N94-11694
An emerging understanding of H-mode discharges in tokamaks
[DE93-012829] p 394 N94-12544
Statistical approach to LHCD modeling using the wave kinetic equation
[DE93-012831] p 394 N94-12545

GENERAL DYNAMICS/ASTRONAUTICS, SAN DIEGO, CA.
Transportation systems analyses: Volume 1: Executive Summary
[NASA-CR-192583] p 41 N94-10826

GENERAL DYNAMICS/CONVAIR, SAN DIEGO, CA.
RAMCAD (reliability, availability, and maintainability in computer-aided design)
[AD-A265143] p 331 N94-11679

GENERAL DYNAMICS CORP., SAN DIEGO, CA.
Transportation systems analyses. Volume 2: Technical/programmatics
[NASA-CR-192582] p 41 N94-10827

GENERAL ELECTRIC CO., CINCINNATI, OH.
Advanced control for airbreathing engines, volume 2: General Electric aircraft engines
[NASA-CR-189204] p 29 N94-12271

GENERAL ELECTRIC CO., PHILADELPHIA, PA.
STGT program: Ada coding and architecture lessons learned p 330 N94-11437

GENERAL ELECTRIC CO., SCHENECTADY, NY.
The effect of processing on the microstructure and tensile properties of a (gamma)-TiAl based alloy
[DE93-013221] p 84 N94-11488

GENERAL MANAGEMENT ASSOCIATES, ABINGDON, MD.
Aerosol sampling models survey
[AD-A265903] p 75 N94-10337

GENERAL MOTORS CORP., INDIANAPOLIS, IN.
Advanced controls for airbreathing engines, volume 3: Allison gas turbine
[NASA-CR-189205] p 29 N94-12272

GENERAL SERVICES ADMINISTRATION, WASHINGTON, DC.
Information resources management plan of the Federal Government
[ISBN-0-16-037895-8] p 421 N94-12014

GENERAL TECHNOLOGY SYSTEMS LTD., UXBRIDGE (ENGLAND).
Analysis of the cost evaluation of ESA programmes and comparable national and international programmes
[GTS-92063] p 416 N94-10145

GENOA UNIV. (ITALY).
The sensitivity of an optical fiber holographic interferometer p 107 N94-10117

GEOLOGICAL SURVEY, DENVER, CO.
Arroyo el Mimbral, Mexico, K/T unit: Origin as debris flow/turbidite, not a tsunami deposit
p 281 N94-12084
K/T spherules from Haiti and Wyoming: Origin, diagenesis, and similarity to some microtektites
p 281 N94-12085

GEOLOGICAL SURVEY, FLAGSTAFF, AZ.
Spatial variation in the seasonal south polar cap of Mars as observed by Mariner 7 p 456 N94-12134
Fault geometries and extension in the Valles Marineris, Mars p 458 N94-12144
A two-stage (turbulent-drainage) mechanism for the emplacement of impact crater outflows on Venus
p 458 N94-12145

Basal scarp, paleoglacier, and fissure flows of Elysium Mons, Mars p 459 N94-12148
Small volcanoes in Tempe Terra, Mars: Their detailed morphometry and inferred geologic significance p 469 N94-12202
Shallow crustal discontinuities and graben and scarp formation in the Tharsis region of Mars p 469 N94-12203
Relation between ages and elevations of Martian channels p 472 N94-12216

GEOLOGICAL SURVEY, MENLO PARK, CA.
Martian particle size based on thermal inertia corrected for elevation-dependent atmospheric properties p 430 N94-12107

GEOLOGICAL SURVEY OF CANADA, OTTAWA (ONTARIO).
Radiogenic age and isotopic studies
[DE93-610548] p 274 N94-10407

GEORGE WASHINGTON UNIV., WASHINGTON, DC.
Enhancement effects in polarimetric radar returns: Phase difference statistics
[NASA-CR-193408] p 231 N94-11309
Corrosion control by vitreous films on aluminum and high T(sub c) superconductors
[AD-A266016] p 85 N94-12393

GEORGETOWN UNIV., WASHINGTON, DC.
Research development and demonstration of a fuel cell/battery powered bus system
[DE93-013778] p 182 N94-12605

GEORGIA INST. OF TECH., ATLANTA.
Thermocapillary convection instability in microgravity crystal growth p 112 N94-10172
Elastic plastic fracture mechanics methodology for surface cracks
[NASA-CR-194129] p 185 N94-10712
Investigation of passive atmospheric sounding using millimeter and submillimeter wavelength channels
[NASA-CR-193627] p 274 N94-10726
Necessary conditions for the optimality of variable rate residual vector quantizers
[NASA-CR-193730] p 326 N94-11197
Cognitive engineering models: A prerequisite to the design of human-computer interaction in complex dynamic systems
[NASA-CR-193472] p 320 N94-12558

GEORGIA-PACIFIC CORP., DECATUR, GA.
Fire resistance and mechanical properties for phenolic prepregs p 20 N94-10786

GEORGIA TECH RESEARCH INST., ATLANTA.
Synthesis of molecular sieves from clear solution p 124 N94-10245

GERMAN AIR FORCE, COLOGNE (GERMANY).
German Air Forces experiences with plastic media blasting and future requirements p 127 N94-10621

GESAMTHOCHSCHULE, ESSEN (GERMANY).
Laboratory study on the natural modes of a rotating two-phase fluid system subject to axial excitation p 106 N94-10106
Experimental analysis of Benard-convection by the combined application of liquid crystals and PIV p 106 N94-10109

GHENT UNIV. (BELGIUM).
Positive phase space distributions and uncertainty relations p 379 N94-10598

GIFU UNIV. (JAPAN).
Visual structure of Karman vortex streets in a route to chaotic states excited by oscillation of a circular cylinder p 17 N94-12633

GILL (M. C.) CORP., EL MONTE, CA.
A new low smoke, low heat release structural foam p 17 N94-10768
A repair patching system for aircraft cargo liners p 17 N94-10771

GOETTINGEN UNIV. (GERMANY).
Thermocapillary slug flow in a capillary tube p 105 N94-10104

GOSUDARSTVENNYI KOMITET PO ISPOLZOVANIYU ATOMNOI ENERGII, MOSCOW (USSR).
Diagnostic complex for the space-time analysis of energy and current of pulsed relativistic particles
[DE93-620980] p 362 N94-10649
To the theory of irregular auto modulation in electron beam-backward electromagnetic wave dynamic system
[DE93-620982] p 133 N94-11030
A symmetrical form for equations of a nonlinear spiral magnetic
[DE93-621350] p 344 N94-11033
About excitation of round waveguide by a point current source
[DE93-621352] p 133 N94-11034
Linear antenna of an arbitrary orientation and position in cylindric screen
[DE93-621353] p 134 N94-11035
Superfield description of N = 2 extended one-dimensional supersymmetric quantum mechanics
[DE93-621420] p 412 N94-11087
Interatomic interactions in BCC and FCC lattices of transition metals
[DE93-621541] p 398 N94-11090
Possibilities of magnetic diagnostics in stellarators
[DE93-621608] p 389 N94-11092
Charged particle motion in torsatrons, part 1
[DE93-621639] p 389 N94-11119
Particle transport analysis in torsatron configurations
[DE93-621640] p 390 N94-11120
Three-dimensional N = 4 extended supersymmetrical quantum mechanics
[DE93-621421] p 412 N94-11164
Characteristics of ICR-produced peripheral plasma in the Uragan-3M torsatron
[DE93-621666] p 392 N94-11214
Elastic deformations and sound in anisotrope superconductors near critical temperature
[DE93-620636] p 188 N94-11364

GREAT LAKES CHEMICAL CORP., WEST LAFAYETTE, IN.
New technology for effective control of flammability in polyolefin fiber/textiles p 18 N94-10774

GRONINGEN RIJKSUNIV. (NETHERLANDS).
Wait-free linearization with an assertional proof
[CS-9208] p 323 N94-10878
Automatic word categorization: An information-theoretic approach
[CS-9209] p 419 N94-10903
FFT-based methods for nonlinear image restoration in confocal microscopy
[CS-9301] p 174 N94-10904
The Nehari problem for the Pritchard-Salamon class of infinite-dimensional linear systems: A direct approach
[CS-9216] p 344 N94-10905
Detecting non-linearities in stationary time series
[W-9223] p 344 N94-10906
Intermittency following a Hopf bifurcation
[W-9301] p 344 N94-10907
Homoclinic intermittency
[W-9302] p 344 N94-10908

GRUMMAN AEROSPACE CORP., BETHPAGE, NY.
Preliminary system design of a Three Arm Capture Mechanism (TACM) flight demonstration article
[NASA-CR-192573] p 177 N94-10341

H

HAHNEMANN MEDICAL COLL. AND HOSPITAL, PHILADELPHIA, PA.
Locus coeruleus, vigilance, and stress: Brain mechanisms of adaptive behavioral responsiveness
[AD-A265657] p 302 N94-12441

HAMBURG UNIV. (GERMANY).
A C-band wind scatterometer model derived from the data obtained during the ERS-1 calibration/validation campaign p 233 N94-11711
On the extraction of ocean wave spectra from ERS-1 SAR wave mode image spectra p 251 N94-12509
Tide-generated nonlinear internal wave packets in the Strait of Gibraltar observed by the synthetic aperture radar aboard the ERS-1 satellite p 252 N94-12510
ATSR correlative skin measurements of sea surface temperature p 252 N94-12514
Principal oscillation pattern analysis of sea level variations in the tropical Pacific measured by the GEOSAT altimeter p 209 N94-12646

HAMPTON UNIV., VA.
Hydrogen partitioning and transport in titanium aluminides
[NASA-CR-194117] p 76 N94-10713

HARRIS CORP., MELBOURNE, FL.
Flexible high-speed CODEC
[NASA-CR-191169] p 146 N94-12433

HARVARD MEDICAL SCHOOL, BOSTON, MA.
Cardiovascular dynamics during space sickness and deconditioning p 311 N94-12007

HARVARD-SMITHSONIAN CENTER FOR ASTROPHYSICS, CAMBRIDGE, MA.
Tropospheric and ionospheric effects on differential astrometry with a ground-space based VLBI array p 136 N94-11070

HARVARD UNIV., CAMBRIDGE, MA.
Photochemical modelling of Venus clouds using Pioneer Venus data
[NASA-CR-194108] p 434 N94-10823

HAWAII UNIV., HONOLULU.
The morphologies of distant radio galaxies p 426 N94-11597
Spectral and multispectral imaging studies of lunar mantled mare deposits p 446 N94-12079
Quantifying the effect of rheology on plan-view shapes of lava flows p 282 N94-12116
Fractal dimensions of rampart impact craters on Mars p 460 N94-12154
First results of the seven-color asteroid survey p 430 N94-12162
Simulation of possible regolith optical alteration effects on carbonaceous chondrite meteorites p 430 N94-12163
Spectral mixing models of S-Type asteroids p 431 N94-12164
The granulite suite: Impact melts and metamorphic breccias of the early lunar crust p 282 N94-12197

HAWAII UNIV., MANOA.
Chondrites, S asteroids, and space weathering: Thumping noises from the coffin? p 433 N94-12244

HELSINKI UNIV. (FINLAND).
Smoothly deformed light p 375 N94-10566
Finnish ERS-1 Baltic Sea ice experiment in Winter 1992 p 239 N94-11750

HELSINKI UNIV. OF TECHNOLOGY, ESPOO (FINLAND).
Application of ERS-1 SAR data to snow mapping p 247 N94-12483

HELSINKI UNIV. OF TECHNOLOGY, OTANIEMI (FINLAND).
Studies on the parametric decay of waves in fusion plasmas
[DE93-621659] p 390 N94-11148

HIROSAKI UNIV. (JAPAN).
Incident shortwave and longwave radiations over the western North Pacific and the Sea of Okhotsk derived from GMS-WEFAX images p 205 N94-11982

HIROSHIMA UNIV. (JAPAN).
One-year mooring of an ADCP in the central region of the Kuroshio west of Okinawa p 194 N94-11913
Acoustic Doppler current profiling of the Kuroshio over the East China Sea shelf slope p 194 N94-11914
Aerodynamic sound due to interaction between a two-dimensional free shear layer and the leading edge of a parallel flat plate p 163 N94-12615

HITACHI LTD., TOKYO (JAPAN).
Development of space refrigerator p 129 N94-11833
Boundary conditions and bifurcations in plane Poiseuille flow p 166 N94-12634

HOKKAIDO TOKAI UNIV., TOKYO (JAPAN).
A surface water monitoring system: A device for the sea-truth observations p 210 N94-12657

HOKKAIDO UNIV., SAPPORO (JAPAN).
A development on estimation method of undersea light p 204 N94-11974
Distribution of mineral aerosols over the North Pacific p 204 N94-11976

HOKKAIDO UNIV. OF EDUCATION, KUSHIRO (JAPAN).
Disintegrating ice front of Shirase Glacier, East Antarctica p 210 N94-12654

HONEYWELL, INC., MINNEAPOLIS, MN.
Optoelectronic technology consortium
[AD-A265691] p 383 N94-12444

HOUSTON UNIV., CLEAR LAKE, TX.
Using solar flare track densities to determine the origin of interplanetary dust particles p 429 N94-12078

HOUSTON UNIV., TX.
The EET87513 clast N: A CM2 fragment in an HED polymict breccia p 453 N94-12117

HOWELL (J. R.), BRADENTON, FL.
Comparing aircraft agility using mahalanobis distances
[PB93-175446] p 26 N94-11464

HUGHES AIRCRAFT CO., TORRANCE, CA.
RF vacuum microelectronics
[AD-A266066] p 142 N94-10818

HUGHES STX, INC., LEXINGTON, MA.
Database blending for the climatology of cloud statistics program
[AD-A265034] p 283 N94-10336

HUMBOLDT UNIV., BERLIN (GERMAN D.R.).
Nonunitary and unitary approach to Eigenvalue problem of Boson operators and squeezed coherent states p 350 N94-10595

HYDERABAD UNIV. (INDIA).
Wigner functions for nonclassical states of a collection of two-level atoms p 379 N94-10603

HYPERBARIC MEDICINE, SAN ANTONIO, TX.
Evaluation of medical treatments to increase survival of ebullism in guinea pigs p 302 N94-11548

HYPRESS, INC., ELMSFORD, NY.
Superconducting SQUID amplifiers for IR detectors and other applications, phase 2
[AD-A265447] p 145 N94-12333

I

IBARAKI UNIV., HITACHI (JAPAN).
Compilation of proposals for boiling and evaporation experiments in space environments and proposals concerning experiment projects p 161 N94-12549

IBIS ASSOCIATES, INC., WELLESLEY, MA.
Analysis of the economics of DC arc CVD diamond
[AD-A265688] p 403 N94-12339

IBM FEDERAL SYSTEMS DIV., GAITHERSBURG, MD.
A recent Cleanroom success story: The Redwing project p 39 N94-11433

IFLYSIB, LA PLATA (ARGENTINA).
Marangoni-driven solitary waves p 119 N94-10214

ILLBRUCK, INC., MINNEAPOLIS, MN.
A polyimide foam for advanced fire resistant aircraft applications p 17 N94-10770

ILLINOIS INST. OF TECH., CHICAGO.
An electro-optical system for the measurement of strains p 186 N94-10900
Texture analysis of high Tc superconductors
p 399 N94-11314

ILLINOIS UNIV., URBANA.
The role of plasma rotation on MHD instabilities in tokamaks
[DE93-013486] p 393 N94-11512
Helium transport scaling law studies
[DE93-013487] p 393 N94-11513
The organization of the suprachiasmatic circadian pacemaker of the rat and its regulation by neurotransmitters and modulators
[AD-A266113] p 301 N94-12417
Qualitative reasoning about the physical world
[AD-A266117] p 340 N94-12537

ILLINOIS UNIV., URBANA-CHAMPAIGN.
Accelerated screening methods for predicting lubricant performance in refrigerant compressors
[DE93-014773] p 89 N94-11146
Effect of double density caging during Space Shuttle transport of laboratory rats
[NASA-CR-193228] p 300 N94-11180

IMAGINATION RESOURCES, INC., DUBLIN, OH.
Measurement of viscosity, density and gas solubility of refrigerant blends
[DE93-014772] p 89 N94-11145

IMITECH, INC., ELK GROVE VILLAGE, IL.
Polyimide foam insulation systems: A major weight reduction and improvement in fire resistance of sidewall systems p 17 N94-10769

IMPERIAL CHEMICAL INDUSTRIES LTD., DUESSELDORF (GERMANY).
Selectively strippable paint schemes
p 128 N94-10629

IMPERIAL COLL. OF SCIENCE AND TECHNOLOGY, LONDON (ENGLAND).
Studies of hypersonic viscous flows p 8 N94-10454
Hypersonic flow computations around re-entry vehicles p 9 N94-10461
Information entrophy via Glauber's Q-representation
p 378 N94-10592

INDIAN INST. OF REMOTE SENSING, DEHRA DUN.
Role of remote sensing and its cost effectiveness in site selection for coastal aquaculture
p 217 N94-12697

INDIAN INST. OF TECH., KANPUR.
Microwave radiometry of ice cover in polar regions
p 210 N94-12655

INDIAN SPACE RESEARCH ORGANIZATION, AHMEDABAD.
Design of inspection and acceptance test methodology for TIG welded aluminum-alloy bracket for camera housings for IRS-1A space craft and executing it
p 61 N94-10037
Preliminary analysis of circulations over the Indian Ocean and adjoining regions using ERS-1 surface winds in the NCMRWF data assimilation system p 234 N94-11719
Removal of orbital error and the local geoid effects from ERS-1 altimeter data p 242 N94-11770
Assessment of ERS-1 SAR data for soil moisture estimation p 249 N94-12492
Multichannel dual angle approach for sea surface temperature retrieval in context of ERS-1 scenario
p 252 N94-12512
Estimations of the surface fluxes from satellite observations of boundary layer and the surface
p 252 N94-12513

INDIANA UNIV., BLOOMINGTON.
Apollo 16 core 60013/14 as a product of path 1 and path 2 regolith evolution processes p 440 N94-12050

INDONESIAN NATIONAL INST. OF AERONAUTICS AND SPACE, JAKARTA.
Space program in Indonesia p 36 N94-10681

INNSBRUCK UNIV. (AUSTRIA).
Signatures of Antarctic firn by means of ERS-1 AMI and by field measurements p 237 N94-11737
Snow and glacier investigations by ERS-1 SAR: First results p 247 N94-12481

INSTITUT FRANCAIS DE RECHERCHE POUR L'EXPLOITATION DE LA MER, BREST.
ERS-1 studies at the Department of Oceanography from Space, IFREMER/Brest (France) p 233 N94-11712
A statistical analysis of sea state surface ERS-1 SAR-wave mode imagettes p 251 N94-12507

INSTITUT FUER ANGEWANDTE GEODAESIE, FRANKFURT AM MAIN (GERMANY).
Utilisation of ERS-1 data for mapping of Antarctica
p 237 N94-11740

INSTITUT FUER ANGEWANDTE GEODAESIE, LEIPZIG (GERMANY).
Some results of the derivation of ice sheet elevations in Antarctica from ERS-1 altimeter data
p 237 N94-11739

INSTITUT NATIONAL DE RECHERCHE D'INFORMATIQUE ET D'AUTOMATIQUE, VALBONNE (FRANCE).
Synthesis of the Workshop on Hypersonic Flows for ReEntry Problems p 5 N94-10440

INSTITUT SUPERIEUR DE TECHNOLOGIE (LUXEMBOURG).
Active damping augmentation of elastomechanical systems using piezoelectric sensors and actuators
p 72 N94-11346

INSTITUTE FOR COMPUTER APPLICATIONS IN SCIENCE AND ENGINEERING, HAMPTON, VA.
Finite difference schemes for long-time integration
[NASA-CR-191471] p 343 N94-10642
Low latency messages on distributed memory multiprocessors
[NASA-CR-191479] p 323 N94-10643
The nonlinear evolution of modes on unstable stratified shear layers
[NASA-CR-191492] p 149 N94-10810
Flexible language constructs for large parallel programs
[NASA-CR-191478] p 326 N94-11196
Summary of research in progress at ICASE
[NASA-CR-191481] p 318 N94-11198
Looking for O(N) Navier-Stokes solutions on non-structured meshes
[NASA-CR-191472] p 345 N94-11277
On cell entropy inequality for discontinuous Galerkin methods
[NASA-CR-191493] p 345 N94-11280
Optimal cube-connected cube multiprocessors
[NASA-CR-191463] p 337 N94-11308

INSTITUTE FOR DEFENSE ANALYSES, ALEXANDRIA, VA.
Analysis and guidelines for reusable Ada software
[AD-A264918] p 332 N94-11850
Assessing the adequacy of the industrial base
[AD-A264954] p 417 N94-11856

INSTITUTE FOR PRODUCTIVITY RESEARCH, NEW YORK, NY.
Advanced model of gradual wear of viscoelastic surface film
[AD-A265130] p 90 N94-11222

INSTITUTE OF DISASTER AND EARTH SCIENCES, IBARAKI (JAPAN).
Variability of the Kuroshio observed from satellite thermal imagery p 221 N94-12717

INSTITUTE OF FLOW RESEARCH, TOKYO (JAPAN).
Idea of underground airplane p 27 N94-12630

INSTITUTE OF OCEAN SCIENCES, SIDNEY (BRITISH COLUMBIA).
Wind and surface features in SAR images: The Canadian program p 234 N94-11718
Satellite observations of red tide events: Plans for EESI p 191 N94-11899
Measurement of eddy structure and movement in the north-east Pacific with the GEOSAT altimeter
p 209 N94-12647

INSTITUTE OF OCEANOGRAPHIC SCIENCES, WORMLEY (ENGLAND).
Global wave height climatologies from ERS-1 altimeter data, and comparisons with those from GEOSAT
p 244 N94-11781

INSTITUTE OF PHYSICAL AND CHEMICAL RESEARCH, SAITAMA (JAPAN).
Optical characteristics in Tokyo Bay
p 204 N94-11972

INSTITUTE OF SOUND AND VIBRATION RESEARCH, SOUTHAMPTON (ENGLAND).
A theory of membrane absorbers
[ISVR-TR-217] p 76 N94-11216
Optimisation methods for solving separable nonlinear least squares problems
[ISVR-TR-219] p 345 N94-11217

INSTITUTO DE ENGENHARIA NUCLEAR, RIO DE JANEIRO (BRAZIL).
A spectral nodal method for the solution of the Sn equations in x, y geometry for highly absorbing deep penetration problems
[DE93-613520] p 349 N94-10636

INSTITUTO DE FISICA TEORICA, SAO PAULO (BRAZIL).
Generating function for Clebsch-Gordan coefficients of the SU(sub q)(2) quantum algebra
[DE93-613093] p 349 N94-10633

INSTITUTO DE PESQUISAS ENERGETICAS E NUCLEARES, SAO PAULO (BRAZIL).
The theory for, and demonstration of, information theory applied to radar target identification
[DE93-006393] p 132 N94-10315

INSTITUTO DE PESQUISAS ESPACIAIS, SAO JOSE DOS CAMPOS (BRAZIL).
A study on the magnetospheric activity using the AE, ap, and Dst geomagnetic indices
[INPE-5470-TDI/501] p 276 N94-11165
Visualization and simulation of a real physical problem based on physical modeling with the use of computer animation
[INPE-5492-TDI/509] p 325 N94-11166
A surrogate heuristic for set covering problems
[INPE-5462-PRE/1770] p 325 N94-11178
TOVS soundings: Impact on the synoptic analysis over the south and southeast regions of Brazil from March 18 to March 19, 1991
[INPE-5497-TDI/512] p 230 N94-11179
A tool for generation of expert system shells
[INPE-5493-TDI/510] p 325 N94-11181
Bayesian model for pictorial data fusion of satellite image
[INPE-5457-TDI/499] p 345 N94-11193
Study of the surface circulation to the North of Bransfield Strait, Antarctica
[INPE-5472-TDI/503] p 288 N94-11200
Landsat as a commercial enterprise
[INPE-5477-TAE/019] p 232 N94-11524
Project of an attitude control system (three axis) of a satellite using the LQG/LTR methodology
[INPE-5473-TDI/504] p 44 N94-12356
Search for structures in the cosmic microwave background radiation
[INPE-5491-TDI/508] p 484 N94-12357
A new heuristic for set covering problems
[INPE-5471-TDI/502] p 333 N94-12358

INSTITUTO ELETTROTECNICO NAZIONALE, GALILEO FERRARIS, TURIN (ITALY).
Performances of a date dissemination code on telephone lines using commercial modems
p 139 N94-10984

INTEGRATED AEROSPACE SCIENCES CORP., ATHENS (GREECE).
Deformation mechanisms of continuous fibre-reinforced thermoplastic composites during manufacturing: A probabilistic approach p 60 N94-10030
Heat analysis of thermoplastic components during the initial stages of manufacturing: A probabilistic approach
p 60 N94-10031

INTEGRATED SYSTEM ASSEMBLIES CORP., WOBURN, MA.
Liquid Cooled Heat Sink with through Vias (LCHS)
[AD-A266008] p 73 N94-12344

INTELLIGENT REASONING SYSTEMS, INC., LAS CRUCES, NM.
A high-speed object recognition chip based on biologically-realistic hybrid temporal processing element
[AD-A265490] p 339 N94-11049

INTERACTIVE TELEMEDICAL SYSTEMS, CORAL GABLES, FL.
A telemedicine health care delivery system
p 307 N94-11803

INTERFACE FOUNDATION OF NORTH AMERICA, INC., FAIRFAX STATION, VA.
Computing science and statistics, Volume 24: Graphics and visualization
[AD-A265181] p 332 N94-11878

INTERNAL REVENUE SERVICE, SILVER SPRING, MD.
Myths and realities: Defining re-engineering for a large organization p 330 N94-11436

INTERNATIONAL ATOMIC ENERGY AGENCY, VIENNA (AUSTRIA).
Report of the IAEA Consultants' Meeting on Real-Time Nondestructive Monitoring of Wear and Corrosion Using the Thin Layer Activation Technique
[DE93-617422] p 183 N94-10847
Directory of IAEA databases
[DE93-622837] p 420 N94-11818

INTERNATIONAL CENTRE FOR THEORETICAL PHYSICS, TRIESTE (ITALY).
Aharonov-Bohm effect in Luttinger liquid
[DE93-613818] p 408 N94-10148
Invariance of the mobility edge in anodic titanium oxides
[DE92-642136] p 394 N94-10281
Convergence of exponentially convex functions on foundation semigroups
[DE93-619665] p 342 N94-10325
Enhanced stability of magic clusters: A case study of icosahedric Al(sub 12)X, X=B, Al, Ga, C, Si, Ge, Ti, As
[DE93-613644] p 395 N94-10386
Nonlinear second harmonic generation by light wave-plasma interaction in oscillating magnetic field
[DE93-613723] p 386 N94-10387

Canonical operator formulation of nonequilibrium thermodynamics
[DE93-613028] p 409 N94-10388
Wave function collapse: An unnecessary condition for the dynamical description of the Zeno and partial Zeno effect
[DE93-612970] p 132 N94-10401
A group-theoretic approach to the study of small oscillations of a dynamical system with a known symmetry
[DE93-612971] p 409 N94-10402
On thermodynamic properties of heavy fermion systems in magnetic field
[DE93-613819] p 409 N94-10403
Singularity spectrum of self-organized criticality
[DE93-613820] p 348 N94-10404
Photostimulated attenuation of hypersound in superlattice
[DE93-611231] p 357 N94-10408
Model-based recognition of 3-D objects by geometric hashing technique
[DE93-612916] p 322 N94-10410
A lattice gas model for enzyme kinetics with alternate interactions
[DE93-613027] p 395 N94-10411
Boundary of Fatou sets of hyperbolic rational maps or degree two
[DE93-613031] p 348 N94-10412
On renormalization group flow in matrix model
[DE93-613050] p 409 N94-10413
On parity conservation and the question of the missing, right-handed neutrino
[DE93-613092] p 361 N94-10414
Orbital glass in HTSC
[DE93-613988] p 395 N94-10415
Symbolic dynamics and description of complexity
[DE93-613030] p 418 N94-10485
On the generalized Jordan-Brans-Dicke theory
[DE93-613051] p 409 N94-10499
The ring structure of chiral operators for minimal models coupled to 2D gravity
[DE93-613119] p 409 N94-10500
Monte Carlo simulations of a two-dimensional hard dimer system
[DE93-613535] p 361 N94-10502
Structure of s - p bonded metal clusters with 8, 20 and 40 valence electrons
[DE93-613643] p 361 N94-10503
On the Sobolev systems with ellipsoid cavities
[DE92-641290] p 148 N94-10530
Convergence theorems for a class of nonlinear maps in uniformly smooth Banach spaces
[DE92-641347] p 343 N94-10531
The effect of pressure and quadrupolar interactions on the nematic-isotropic transition properties: Numerical results for a system of prolate ellipsoids including second and fourth rank orientational order parameters
[DE93-613540] p 410 N94-10536
A window least squares algorithm for statistical noise smoothing of 2D-ACAR data
[DE93-613828] p 395 N94-10537
Planck scale effects on the Majoron
[DE93-613120] p 410 N94-10545
A lattice gas model for enzyme kinetics with next-nearest neighbor interactions
[DE93-613026] p 410 N94-10631
The modular group and super-KMS functionals
[DE93-613029] p 349 N94-10632
S(sup 1) x S(sup 2) as a bag membrane and its Einstein-Weyl geometry
[DE93-613149] p 410 N94-10635
Bond distortion and electron trapping in charged C60
[DE93-613642] p 396 N94-10637
Power losses of a type 2 superconducting slab of arbitrary thickness in the presence of alternating current conductors
[DE93-617892] p 396 N94-10716
Classical gravity coupled to Liouville theory
[DE93-613049] p 275 N94-10798
Effect of effective mass differences on the tunneling current-voltage behaviour of a resonant diode in the presence of space charge build-up
[DE93-613817] p 142 N94-10799
Confinement of acoustical modes due to the electron-phonon interaction within 2D-electron gas
[DE93-613910] p 396 N94-10800
Limitation and suppression of hot electron fluctuations in submicron semiconductor structures
[DE93-613911] p 396 N94-10801
Generalized spin systems and sigma-models
[DE93-613981] p 410 N94-10802
Cosmological restrictions on conformally-invariant SU(5) GUT models
[DE93-619770] p 412 N94-11047
A theoretical kinematical study of the gradient of any cosmic scalar field
[DE92-644731] p 425 N94-11136
One-loop quantum gravity on de Sitter space
[DE92-641349] p 425 N94-11152
A version of superstring with four space-time dimensions
[DE93-608196] p 412 N94-11163
The Lip microbundle representation theorem
[DE93-619671] p 346 N94-11348
Spline approximation for system of n-th order nonlinear ordinary differential equations
[DE93-608188] p 346 N94-11507
Fermion-boson scattering in ladder approximation
[DE93-613111] p 368 N94-11581
An overview of intertropical convergence and intertropical discontinuity
[DE93-619229] p 277 N94-11603
On temperature distribution in non-participating medium with radiation boundary condition
[DE93-619375] p 153 N94-11604
A regional inverse eigenvalue problem: Solution with application in control theory
[DE93-619666] p 339 N94-11630
The completion homomorphism in equivariant elliptic cohomology
[DE93-619672] p 346 N94-11631
On convexity and Schoenberg's variation diminishing splines
[DE93-619673] p 346 N94-11632
The laser second threshold: Its exact analytical dependence on detuning and relaxation rates
[DE93-619706] p 175 N94-11633
Analytical details of the instability threshold of the laser-Lorenz model
[DE93-619707] p 175 N94-11634
The additional contribution caused by Coulomb interaction to the exciton dispersion in multiple quantum wells and superlattices for direct band gap cubic semiconductors
[DE93-613538] p 402 N94-11659
On the theory of phonoriton in cubic semiconductors with a degenerate valence band
[DE93-613539] p 402 N94-11660
The solutions of cosmic string loop equation in expanding universe
[DE93-619717] p 427 N94-11692
Divergences in the moduli space integral and accumulating handles in the infinite-genus limit
[DE93-619722] p 346 N94-11693
The magnetic field of rotating bodies
[DE93-619769] p 427 N94-11812
Grain boundary creep in copper
[DE93-610974] p 84 N94-12361

INTERNATIONAL INST. FOR AEROSPACE SURVEY AND EARTH SCIENCES, ENSCHEDE (NETHERLANDS).
ERS-1 imaging radar over the Waddensea-North Netherlands p 254 N94-12526

INTERNATIONAL SPACE UNIV., INC., KITAKYUSHU (JAPAN).
Space Solar Power Program
[DE93-011750] p 55 N94-11675

INTERNATIONAL SPACE YEAR ASSOCIATION, TOKYO (JAPAN).
Space Activities in the Asia Pacific Region
[JTN-93-80421] p 35 N94-10676

INTERNATIONAL TECHNICAL ASSOCIATES, INC., SANTA CLARA, CA.
Automated Laser Paint Stripping (ALPS) update
p 127 N94-10624

INTERNATIONAL TELECOMMUNICATIONS SATELLITE ORGANIZATION, WASHINGTON, DC.
Applications of the INTELSAT system to remote health care p 306 N94-11794

IOWA GEOLOGICAL SURVEY, IOWA CITY.
Descriptions and preliminary interpretations of cores recovered from the Manson Impact Structure (Iowa)
p 281 N94-12032

IOWA STATE UNIV. OF SCIENCE AND TECHNOLOGY, AMES.
A dynamically adaptive mesh method for internal flows
p 149 N94-10896
The global potential energy surfaces of the lowest two 1A' states of the ozone molecule: Theoretical determination and analysis p 267 N94-12269
Space Life Support Engineering Program
[NASA-CR-193474] p 316 N94-12365
Systems analysis of a closed loop ECLSS using the ASPEN simulation tool. Thermodynamic efficiency analysis of ECLSS components p 316 N94-12366
Physiological water model development
p 316 N94-12367
Modifications to an interactive model of the human body during exercise: With special emphasis on thermoregulation p 317 N94-12368
An estimate of the second law thermodynamic efficiency of the various units comprising an Environmental Control and Life Support System (ECLSS) p 317 N94-12369

IOWA THIN FILM TECHNOLOGIES, INC., AMES.
Polyimide based amorphous silicon solar modules
p 49 N94-11390

IOWA UNIV., IOWA CITY.
VLBI and the detection of interstellar magnetohydrodynamic waves p 135 N94-11066
Petrography and preliminary interpretations of the crystalline breccias from the Manson M-1 core
p 281 N94-12056

ISHIKAWAJIMA-HARIMA HEAVY INDUSTRIES CO. LTD., TOKYO (JAPAN).
Concept and design of ampoule for melt growth of gallium arsenide in first mission of space flyer unit
p 107 N94-10115
Numerical calculation of the growth of InP by the travelling heater method in the first mission of the Space Flyer Unit p 114 N94-10179

ISTAR, VALBONNE (FRANCE).
Example of SPOT/ERS-1 complementarity
p 247 N94-12479

ITT AEROSPACE/COMMUNICATIONS DIV., CLIFTON, NJ.
The time keeping system for GPS block IIR
p 24 N94-10964

IWATE UNIV., MORIOKA (JAPAN).
Validation test system for sea surface temperature detected by satellites in Mutsu Bay p 213 N94-12670
On the error characteristics of the sea surface temperature observed by satellite p 216 N94-12690

J

JAMES COOK UNIV. OF NORTH QUEENSLAND, TOWNSVILLE (AUSTRALIA).
Groundwave HF ocean surface radar
p 139 N94-11906
On the determination of the SAR ocean surface scattering patch size p 197 N94-11933
A new model for Synthetic Aperture Radar (SAR) images from ocean scatter p 251 N94-12508

JAPAN ATOMIC ENERGY RESEARCH INST., TOKYO.
Functional reasoning, explanation, and analysis
[DE92-526832] p 313 N94-10251
Proceedings of the Second Technical Meeting on High Temperature Gas-Cooled Reactors
[DE93-754285] p 371 N94-10719
Basic experiment on an ultrasonic method of localization
[DE93-754295] p 358 N94-11042
Report of the third Seminar on Nuclear Physics at the Energy Region of the JAERI Tandem-Booster Accelerator
[DE93-754330] p 372 N94-11043
Momentum and heat frictions between fast ions and thermal plasma species
[DE93-771240] p 390 N94-11149
DBTT measurement by use of Small Punch (SP) test
[DE93-753188] p 183 N94-11168
Development of plastic capsule for research reactor irradiation
[DE93-753186] p 372 N94-11591
A molecular dynamics simulation code ISIS
[DE93-753187] p 368 N94-11592
Facility for stress corrosion cracking test of irradiated material in high temperature water
[DE93-753189] p 84 N94-11593

JAPAN BROADCASTING CORP., TOKYO.
Processing proper nouns in machine translation for English news
[NHK-SERIAL-414] p 418 N94-10559
A new HMM learning algorithm for continuous speech recognition
[NHK-SERIAL-413] p 132 N94-10560

JAPAN CONSULTING ENGINEERS ASSOCIATION.
A study of pollution courses of spilled oil floatation in the outer ocean p 205 N94-11983

JAPAN FISHERIES INFORMATION SERVICE CENTER, TOKYO.
Warm streamers extended from Warm Core Rings (WCRs) and their role on fish migration and fishing ground formation p 198 N94-11938
Application of NOAA AVHRR data to fisheries
p 215 N94-12681

JAPAN MARINE SCIENCE AND TECHNOLOGY CENTER, TOKYO.
Current structures in the western equatorial Pacific during JAPACS cruises p 193 N94-11911
Acoustic characteristics of side scan sonar and sub-bottom profiler for 10,000 m class ROV
p 172 N94-11916
Study on color video pictures transmission by digital acoustic signal p 139 N94-11917

An application of reduced gravity model to mesoscale eddies p 199 N94-11945
Development of shipboard ocean lidar p 140 N94-11965
Variability of sea level and sea surface temperature anomalies in the equatorial Pacific p 208 N94-12640
Pseudo magnetic anomaly derived from satellite altimetry and its application to the tectonics in the North Fuji Basin p 208 N94-12645

JAPAN WEATHER ASSOCIATION, TOKYO.
Development of a buoy system for monitoring marine weather and marine life abundance p 217 N94-12694
Satellite and moored buoy observations of polar frontal system over the Yamato Rise in the Japan Sea p 221 N94-12715

JAWAHARLAL NEHRU TECHNOLOGICAL UNIV., HYDERABAD (INDIA).
Remote sensing for numerical modelling of radiative transfer processes in ocean environment p 204 N94-11973

JET PROPULSION LAB., CALIFORNIA INST. OF TECH., PASADENA.
Force reflection with compliance control [NASA-CASE-NPO-18668-1-CU] p 179 N94-10654
Method for producing a hybridization of detector array and integrated circuit for readout [NASA-CASE-NPO-18062-1-CU] p 141 N94-10656
Alkali metal for ultraviolet band-pass filter [NASA-CASE-NPO-18433-1-CU] p 381 N94-10657
Telerobot control system [NASA-CASE-NPO-18116-1-CU] p 179 N94-10670
Ultrastable reference frequency distribution utilizing a fiber optic link p 355 N94-10994
A wide-band fiber optic frequency distribution system employing thermally controlled phase compensation p 355 N94-10995
Spacecraft signal sources portable test system p 139 N94-11000
Advances in adaptive structures at Jet Propulsion Laboratory p 72 N94-11344
Results of some initial space qualification testing on triple junction a-Si and CuInSe2 thin film solar cells p 50 N94-11392
Analyzing human errors in flight mission operations p 314 N94-11534
Supervised autonomous control, shared control, and teleoperation for space servicing p 183 N94-11577
Evaluation of two January - June 1992 ERS-1 AMI wind vector data sets p 235 N94-11724
Sea ice radar signatures from ERS-1 SAR during late Summer and Fall in the Beaufort and Chukchi Seas p 240 N94-11756
Evaporation and thermal/hydrologic balance in the Pacific p 195 N94-11919
Air-sea fluxes and universal constants in weak-turbulence theory of surface gravity waves p 195 N94-11922
The Pacific responses exhibited by an OGCM to various wind fields p 202 N94-11964
Horizontal stresses induced by vertical processes in planetary lithospheres p 281 N94-12042
Using high spectral resolution spectrophotometry to study broad mineral absorption features on Mars p 446 N94-12077
A pattern recognition system for locating small volvanoes in Magellan SAR images of Venus p 455 N94-12126
Galileo/NIMS near-infrared thermal imagery of the surface of Venus p 457 N94-12139
Preliminary report of lunar observations by the Near-Infrared Mapping Spectrometer (NIMS) during the second Galileo Earth-Moon encounter p 425 N94-12140
Near-infrared spectra of the Martian surface: Reading between the lines p 465 N94-12184
Volcanism in southern Guinevere Planitia, Venus: Regional volcanic history and morphology of volcanic domes p 467 N94-12190
SSMI wind speed variability over the Pacific Ocean p 207 N94-12637
Theory and oceanographic applications of satellite altimeter measurements p 208 N94-12641
Comparison of GEOSAT sea surface height and model-simulated surface dynamic height p 208 N94-12644
Preliminary results from a satellite altimetric data assimilation using a Kalman filter and smoother p 209 N94-12648

JJM SYSTEMS, INC., ARLINGTON, VA.
An expert system shell for inferring vegetation characteristics: Prototype help system (Task 1) [NASA-CR-193411] p 231 N94-11236

JOHANN-WOLFGANG-GOETHE-UNIV., FRANKFURT AM MAIN (GERMANY).
On a Lagrange-Hamilton formalism describing position and momentum uncertainties p 349 N94-10583

JOHNS HOPKINS UNIV., BALTIMORE, MD.
Visual psychophysics of egomotion [AD-A265253] p 304 N94-11681

JOHNS HOPKINS UNIV., LAUREL, MD.
Continued development of an ultra-narrow bandpass filter for solar research [NASA-CR-194169] p 381 N94-10735
Performance of low-cost commercial fiber-optic transceivers for reference frequency distribution p 355 N94-10993
An investigation of the near Earth space environments [AD-A265295] p 278 N94-11828
Lunar Scout Two spacecraft gravity experiment p 459 N94-12152
ERS-1 and Almaz SAR ocean wave imaging over the Gulf Stream and the Grand Banks p 251 N94-12505

JOINT INST. FOR NUCLEAR RESEARCH, DUBNA (USSR).
Indication on the existence of the bound state in the p anti p-system [DE92-641575] p 361 N94-10532
Direct current transducer [DE92-644548] p 141 N94-10533
Investigation of soft errors in MOS RAM under influence of heavy ions [DE92-644554] p 484 N94-10534
Non-Euclidean space for local hidden variables [DE93-621341] p 344 N94-11032
On a p-adic metrical dimension of space [DE93-621374] p 345 N94-11077
Creation and annihilation of solitons in nonlinear integrable systems [DE93-621379] p 365 N94-11078

JOINT RESEARCH CENTRE OF THE EUROPEAN COMMUNITIES, ISPRA (ITALY).
The use of active devices in the ERS-1 radiometric calibration p 236 N94-11732
Seeing the Black Forest by ERS-1 and AIRSAR: A comparison p 249 N94-12495
TREES project: A case study on the use of multi-temporal ERS-1 SAR data and SPOT data for monitoring tropical ecosystems p 249 N94-12497
TREES project: Overview and status of the ERS-1 SAR contribution p 250 N94-12499
Coastal upwelling monitored by satellite data: Methodologies and results p 220 N94-12712

K

KAGOSHIMA UNIV. (JAPAN).
Overwater atmospheric dispersion of volcanic smokes from Mt. Sakurajima observed in NOAA-AVHRR data p 205 N94-11979
Sea surface temperature difference between NOAA/AVHRR and in-situ observation p 215 N94-12680

KAMAN AEROSPACE CORP., TUCSON, AZ.
Airborne optical tracking control system design study [DE93-009515] p 382 N94-11662

KANAZAWA INST. OF TECH. (JAPAN).
The evaluation of radiative process in the atmosphere-ground system by Monte Carlo method p 205 N94-11980

KANSAS STATE UNIV., MANHATTAN.
Electric and hybrid vehicle site operators program: Thinking of the future [DE93-011231] p 144 N94-11609

KANSAS UNIV., LAWRENCE.
Improving reservoir conformance using gelled polymer systems [DE93-014532] p 88 N94-10749
General aviation aircraft-normal acceleration data analysis and collection project [AD-A265055] p 26 N94-11858

KANSAS UNIV. CENTER FOR RESEARCH, INC., LAWRENCE.
Fundamental studies of radar scattering from water surfaces: The Lake Washington experiment [NASA-CR-194030] p 139 N94-12778

KATHOLIEKE UNIV. TE LEUVEN (BELGIUM).
TEM study of a space processed Al-Al2O3 metallic composite p 75 N94-10186
Per-field filtering and classification of multitemporal ERS-1 SAR imagery p 247 N94-12485

KAWASAKI HEAVY INDUSTRIES LTD., GIFU (JAPAN).
Aerodynamic characteristics analysis of Garabedian-Korn 75-06-12 airfoil: Computation using q-omega 2 equation turbulence model [PAPER-2D-4] p 10 N94-10470
Aerodynamic characteristics analysis of Garabedian-Korn 75-06-12 airfoils: Computation using Baldwin-Lomax turbulence model [PAPER-2D-5] p 11 N94-10471
Flow analysis around ONERA model M5 configuration [PAPER-3D-2] p 12 N94-10478

KAWASAKI HEAVY INDUSTRIES LTD., KOBE (JAPAN).
Research and development of cold plate for two phase fluid loop thermal control system p 162 N94-12555

KAYSER THREDE G.M.B.H., MUNICH (GERMANY).
Holographic interferometry for microgravity applications p 108 N94-10123
The High Precision Thermostat HPT-HYDRA p 109 N94-10124
Mission support for crystal growth experiments in Russian unmanned carriers p 111 N94-10139

KEIO UNIV., YOKAHAMA (JAPAN).
Growth and breakdown of Taylor-Goertler vortices in rotating Blasius boundary layer p 165 N94-12631

KELSEY SEYBOLD CLINIC, P.A., HOUSTON, TX.
Longitudinal study of astronaut health: Mortality in the years 1959-1991 p 312 N94-11560

KENTUCKY UNIV., LEXINGTON.
Spectral analysis of resting cardiovascular variables and responses to oscillatory LBNP before and after 6 degree head dowm bedrest p 309 N94-11997

KERNCO, INC., DANVERS, MA.
CAFS: A Cesium Atomic Frequency Standard for GPS block IIR p 353 N94-10980

KINKI UNIV., OSAKA (JAPAN).
Satellite-derived oceanic features p 200 N94-11949
Implications of aerosol retrieval and atmospheric correction in remote sensing p 205 N94-11978

KITAMI INST. OF TECH., HOKKAIDO (JAPAN).
Estimation of areal evapotranspiration using LANDSAT TM data: Kitami City, Hokkaido, Japan p 219 N94-12703

KLM AEROCARTO, SCHIPHOL (NETHERLANDS).
IATA taskforce: Paintstripping p 128 N94-10628

KOBE UNIV. (JAPAN).
Two phase flow and isopycnic liquid-liquid two phase fluid in reduced gravity field p 162 N94-12552

KODAK LTD., HARROW (ENGLAND).
The formation and breakage of liquid bridges under microgravity p 100 N94-10071

KOMATSU LTD. (JAPAN).
Resistivity and radar void detectors for tunneling machines p 140 N94-12706

KOREA ADVANCED INST. OF SCIENCE AND TECHNOLOGY, SEOUL (REPUBLIC OF KOREA).
Overview of KITSAT p 36 N94-10683

KOREA AEROSPACE RESEARCH INST., TAEJON (REPUBLIC OF KOREA).
Korea space program p 36 N94-10684

KOREA INST. OF TECH., TAE-JON (REPUBLIC OF KOREA).
Phasing operator for two oscillators in classical field p 370 N94-10579
Collision-induced squeezing in a harmonic oscillator p 379 N94-10597

KOREA OCEAN RESEARCH AND DEVELOPMENT INST., SEOUL (REPUBLIC OF KOREA).
Observation of cold coastal water with high turbidity around the southwestern tip of Korean Peninsula p 216 N94-12689

KOREA UNIV., SEOUL (REPUBLIC OF KOREA).
Relation of squeezed states between damped harmonic and simple harmonic oscillators p 380 N94-10606

KOREAN AIR FORCE, SEOUL (REPUBLIC OF KOREA).
Squeezed states of electrons and transitions of the density of states p 370 N94-10593

KRUG LIFE SCIENCES, INC., HOUSTON, TX.
Proceedings of the First Joint NASA Cardiopulmonary Workshop [NASA-CP-10068] p 308 N94-11991

KRUG LIFE SCIENCES, INC., SAN ANTONIO, TX.
Monitoring cognitive function and need with the automated neuropsychological assessment metrics in Decompression Sickness (DCS) research p 314 N94-11533
Use of ultrasound in altitude decompression modeling p 317 N94-11540
Hypobaric decompression prebreathe requirements and breathing environment p 317 N94-11541

KUNSAN NATIONAL FISHERIES JUNIOR COLL. (REPUBLIC OF KOREA).
Estimation of solar radiation at the sea surface with geostationary meteorological satellite data p 196 N94-11926

KYOTO INST. OF TECH. (JAPAN).
Nonlinear instability of a laminar flow in a rectangular duct and generation of the turbulent secondary flow p 164 N94-12622

KYOTO UNIV., KUMATORI (JAPAN).
Proceedings of the Symposium on Radiation Research in Life Science [DE93-754137] p 300 N94-10888

KYOTO UNIV., SAKYOKU (JAPAN).
Time evolution of cross-stream exchange associated with the variations in the Kuroshio p 197 N94-11936

Surface roughness variations across the Iceland-Faroes frontal region observed by the GEOSAT altimeter and NOAA AVHRR p 201 N94-11958
A numerical study of deep convection at high latitudes p 210 N94-12652
Measurement of the sea surface emissivity p 213 N94-12672
Satellite thermal variations of Kuroshio in relation to storm floods p 215 N94-12685

KYUSHU UNIV., FUKUOKA (JAPAN).
Westward propagation of sea surface anomalies in the western North Pacific as seen by the altimeter and radiometer p 198 N94-11941
The microwave backscattering from wind waves p 201 N94-11959
Fluctuations of the Kuroshio extension detected by the GEOSAT altimetry data p 209 N94-12649

L

LAMAR UNIV., BEAUMONT, TX.
Investigation of alternate power source for Space Shuttle Orbiter hydraulic system
[NASA-CR-193229] p 46 N94-10911

LANCASTER UNIV. (ENGLAND).
Stable isotope analyses of the peralkaline volcanics Gregory Rift Valley, Kenya p 281 N94-12072
Th-230 - U-238 series disequilibrium of the Olkaria basalts Gregory Rift Valley, Kenya p 281 N94-12073
Th-230 - U-238 series disequilibrium of the Olkaria basalts Gregory Rift Valley, Kenya: Petrogenesis p 281 N94-12074
Th-230 - U-238 series disequilibrium of the Olkaria rhyolites Gregory Rift Valley, Kenya: Petrogenesis p 281 N94-12075
Th-230 - U-238 series disequilibrium of the Olkaria rhyolites Gregory Rift Valley, Kenya: Residence times p 281 N94-12076
Vulcanian explosive eruptions: A mechanism for localised pyroclast dispersal on Venus p 477 N94-12243

LAWRENCE ASSOCIATES, INC., DAYTON, OH.
Thermal error compensation feasibility study using artificial intelligence
[AD-A266084] p 340 N94-12411

LAWRENCE LIVERMORE NATIONAL LAB., CA.
AMIP: The Atmospheric Model Intercomparison Project
[DE93-007400] p 273 N94-10151
AMIP: The Atmospheric Model Intercomparison Project
[DE93-007413] p 273 N94-10152
Simulations of D3-D divertor biasing with the LEDGE code
[DE93-010500] p 385 N94-10262
PANACEA user's manual for PANACEA version 2.0
[DE93-012502] p 321 N94-10263
Survey to determine the value of DYNA
[DE93-012390] p 321 N94-10267
Zerodur polishing process for high surface quality and high efficiency
[DE93-012596] p 87 N94-10271
X ray production (approximately)130 (Angstrom) from laser-produced plasmas for projection x ray lithography applications
[DE93-009256] p 385 N94-10286
Physics and modelling of scrape-off layer transport
[DE93-010510] p 385 N94-10289
The cloud radiative feedback of a midlatitude squall line system and implication for climate study
[DE93-010511] p 283 N94-10290
Virtual sound for virtual reality
[DE93-010519] p 321 N94-10291
Computational procedures for determining parameters in Ramberg-Osgood elastoplastic model based on modulus and damping versus strain
[DE93-013309] p 185 N94-10306
Flow visualization of shock propagation in baffle systems
[DE93-013312] p 147 N94-10307
Effects of aqueous solution compositions on Aerocapacitor energy density
[DE93-013431] p 140 N94-10309
The intensity of knock in an internal combustion engine: An experimental and modeling study
[DE93-013089] p 177 N94-10322
Practical authorization in large heterogeneous distributed systems
[DE93-013192] p 335 N94-10324
Workshop on NN Bremsstrahlung and Polarization Observables
[DE93-010181] p 361 N94-10334
Techniques, processes, and measures for software safety and reliability
[DE93-012379] p 322 N94-10347
Kinetics of high concentration arsenic deactivation at moderate to low temperatures
[DE93-013349] p 395 N94-10516
Characterization of high-power RF structures using time-domain field codes
[DE93-013416] p 132 N94-10518
Monte Carlo simulations of phase transformations in Fe-Cr alloys
[DE93-013847] p 81 N94-10522
Surface and near-surface atom imaging with photoelectron holography
[DE93-013197] p 169 N94-10526
Wavelength considerations in soft x ray projection lithography
[DE93-014115] p 381 N94-10651
High-field conductor testing at the FENIX facility
[DE93-012318] p 387 N94-10737
Preliminary validation of the low frequency variability of tropospheric temperature and circulation simulated for the AMIP by the ECMWF model
[DE93-012382] p 284 N94-10739
Sensitivities of calculated residual stress to separation distances of two simultaneous events
[DE92-019571] p 98 N94-10751
High-order harmonic conversion efficiency in helium
[DE93-011714] p 364 N94-10753
Second and third order nonlinear optical properties of crystalline inorganic/organic complexes
[DE93-011883] p 173 N94-10755
Electromechanical batteries and the electric locomotive
[DE93-013311] p 142 N94-11009
Inverting ultrasonic data on solid/fluid mixtures for Biot-Gassmann parameters
[DE93-011952] p 150 N94-11026
The Zipcode message-passing system
[DE93-011958] p 336 N94-11027
A picosecond high pressure gas switch
[DE93-011897] p 142 N94-11050
A self-consistent model of non-linear parameterization of turbulent diffusion in atmospheric boundary layer
[DE93-011950] p 275 N94-11052
Electron temperature measurements of x ray laser plasmas
[DE93-011874] p 389 N94-11074
Progress in zirconium resonance ionization spectroscopy
[DE93-011881] p 76 N94-11075
Damping measurements for ultra-high carbon steel/brass laminates
[DE93-011886] p 82 N94-11076
Object oriented implementation of adaptive mesh refinement algorithms
[DE93-011885] p 325 N94-11112
The angular structure of second harmonic emission from laser-produced plasmas irradiated at moderate intensity
[DE93-013102] p 389 N94-11114
Physics of tokamak scrape-off layer confinement
[DE93-011949] p 390 N94-11125
An analytic model for calculating pump-induced wavefront distortions in laser slabs
[DE93-011953] p 174 N94-11126
Turbulent wall jet in blast wave precursor
[DE93-011955] p 151 N94-11144
Polymeric nitrogen
[DE93-012600] p 89 N94-11151
The impact of horizontal resolution on moist processes in the ECMWF model
[DE93-011718] p 276 N94-11227
Damage thresholds of fluoride multilayers at 355 nm
[DE93-009523] p 90 N94-11230
Resolution for Lanczos and Paige-Saunders inverses in tomography
[DE93-012312] p 327 N94-11240
A modeling perspective on cloud radiative forcing
[DE93-012383] p 276 N94-11241
Needs for super-smooth surfaces
[DE93-012482] p 382 N94-11242
Investigation of optically generated electronic defects and protonic transport in hydrogen-bonded molecular solids: Isomorphs of potassium dihydrogen phosphate
[DE93-012498] p 399 N94-11243
Pulsed plasma processing for control of diesel engine emissions
[DE93-011884] p 181 N94-11247
The PVM systems: An in-depth analysis and documenting study. Concise edition
[DE93-011959] p 336 N94-11248
Demonstration designs for optical-field-ionized plasma x-ray lasers
[DE93-009227] p 175 N94-11266
Design of CCD camera system for use inside electron beam furnace
[DE93-009525] p 170 N94-11267
Dynamic studies of crystal growth using the AFM
[DE93-009549] p 399 N94-11268
Energy transfer dynamics and impact sensitivity
[DE93-009551] p 98 N94-11269
Quality factors and local adaption (with applications in Eulerian hydrodynamics)
[DE93-010502] p 151 N94-11272
Radiation hardness of Mo/Si multilayers designed for use in a soft x ray projection lithography system
[DE93-011879] p 143 N94-11273
One-dimensional calculation of high-power microwave pulse compression by the earth's ionosphere
[DE93-009517] p 137 N94-11466
The solubility of epsilon-CL-20 in selected materials
[DE93-009304] p 77 N94-11602
Airborne optical tracking control system design study
[DE93-009515] p 382 N94-11662
Plating under reduced pressure
[DE93-011896] p 84 N94-11668
New challenges in optical materials development
[DE93-011889] p 383 N94-11676
High resolution time- and 2-dimensional space-resolved x ray imaging of plasmas at NOVA
[DE93-011892] p 393 N94-11677
Short pulse lasers for generation of fields exceeding 100 MG
[DE93-013346] p 369 N94-11815
Initial assessment of lower hybrid current drive in D3-D
[DE93-013310] p 394 N94-12370
Spatial coherence of soft x ray lasers
[DE93-012497] p 176 N94-12590
Optimal hemicube sampling
[DE93-010499] p 334 N94-12591
Comments on possible causes of recent global warming
[DE93-010501] p 272 N94-12592
Networks of real-time processes
[DE93-013049] p 338 N94-12597
Damage threshold study of ion beam sputtered coatings for a visible high-repetition laser at LLNL
[DE93-013430] p 95 N94-12602
Laser system design for the generation of a sodium-layer laser guide star
[DE93-014127] p 176 N94-12784

LEHIGH UNIV., BETHLEHEM, PA.
Weld overlay coatings for erosion control
[DE93-013592] p 84 N94-11816

LIEGE UNIV. (BELGIUM).
Surface-tension driven convection in finite-size containers p 103 N94-10090
Coastal morphodynamics and energetic characteristics of swell studied with ERS-1 SAR p 254 N94-12524

LIFE SCIENCES SOFTWARE, CAMANO ISLAND, WA.
TimeSet: A computer program that accesses five atomic time services on two continents p 334 N94-10985

LIVERPOOL UNIV. (ENGLAND).
Generalised squeezing and information theory approach to quantum entanglement p 377 N94-10580

LOCKHEED ENGINEERING AND SCIENCES CO., HOUSTON, TX.
An analysis of the modes and states for generic avionics
[NASA-CR-188253] p 27 N94-10664
Measuring human performance on NASA's microgravity aircraft p 317 N94-11537
Space Station maintenance studies using plaid graphics p 335 N94-11578
Effects of microscopic iron metal on the reflectance spectra of glass and minerals p 436 N94-12024
Calorimetric thermometry of meteoritic troilite: A feasibility study p 428 N94-12025
Mineralogy of chondritic interplanetary dust particle impact residues from LDEF p 80 N94-12045
Composition and modal frequencies of hypervelocity particles less than 1 millimeter in diameter in low-Earth orbit p 429 N94-12063

LOCKHEED MISSILES AND SPACE CO., PALO ALTO, CA.
SMM x ray polychromator
[NASA-CR-193282] p 483 N94-11048

LOGISTICS MANAGEMENT INST., BETHESDA, MD.
Assessing the adequacy of the industrial base
[AD-A264954] p 417 N94-11856

LONDON UNIV. OBSERVATORY (ENGLAND).
Scalloped margin domes: What are the processes responsible and how do they operate? p 454 N94-12120
The origin of Venusian channels: Modelling of thermal erosion by lava p 456 N94-12131

LOS ALAMOS NATIONAL LAB., NM.
Source to detector spectrum transformation and its inverse for the Pegasus Z-pinch
[DE93-012674] p 384 N94-10157
MHD simulation of deuterium-fiber-initiated Z-pinches with two-fluid effects
[DE93-012682] p 384 N94-10158

High-energy density physics at Los Alamos
[DE93-010271] p 371 N94-10260
The Lathrop Wells Volcanic Center: Status of field and geochronology studies
[DE93-008917] p 273 N94-10285
Material removal processes: Engineering mechanics consideration
[DE93-010733] p 126 N94-10293
Temperature effects on failure thickness and deflagration-to-detonation transition in PBX 9502 and TATB
[DE93-010742] p 97 N94-10294
The effect of a scalar boson coupled to neutrinos on the behavior of the tritium beta decay spectrum near the end point
[DE93-012655] p 361 N94-10349
Supersqueezed states from squeezed states
p 378 N94-10591
Silicon-based elementary particle tracking system: Materials science and mechanical engineering design
[DE93-012630] p 65 N94-10740
Solar wind channels for MeV particles
[DE93-012648] p 482 N94-10741
Imaging of magnetospheric dynamics using low energy neutral atom detection
[DE93-012656] p 275 N94-10742
Rietveld refinement of magnetic structures from pulsed-neutron-source powder-diffraction data
[DE93-012740] p 363 N94-10743
Fully coupled neutronic and hydrodynamic analysis of space nuclear reactor reentry accidents
[DE93-005459] p 372 N94-10890
Introduction to Bayesian image analysis
[DE93-012628] p 347 N94-11006
The superfluid Stirling refrigerator, a new method for cooling below 0.5 K
[DE93-012672] p 128 N94-11161
Similarity of the leading contributions to the self-energy and the thermodynamics in two- and three-dimensional Fermi Liquids
[DE93-012673] p 412 N94-11162
KIVA-3: A KIVA program with block-structured mesh for complex geometries
[DE93-011986] p 77 N94-11249
Massively parallel hydrodynamics on unstructured grids
[DE93-007325] p 153 N94-11601
On the coupling of electromagnetic radiation into cavities
[DE93-011406] p 137 N94-11621
Highly anisotropic but nodeless gap from a valence-fluctuation pairing mechanism
[DE93-010738] p 401 N94-11646
Polymer electrolyte fuel cells: Potential transportation and stationary applications
[DE93-010734] p 264 N94-11666
Momentum induced by laser-tissue interaction
[DE93-010737] p 301 N94-11667
The Los Alamos neutron spectrometer for the Lunar Scout-1 mission p 172 N94-12038
Analytic expression for epithermal neutron spectra amplitudes as a function of water content
p 473 N94-12227
Solar wind-induced secondary ions and their relation to lunar surface composition p 474 N94-12232
Prediction of alumina penetration
[DE93-014017] p 95 N94-12610
Quality assurance for environmental chemistry: 1991, volume 2
[DE93-011792] p 272 N94-12780
Operational characteristics of a 100-mA, 2-MeV radio-frequency quadrupole
[DE93-014474] p 374 N94-12786

LOUISIANA STATE UNIV., BATON ROUGE.
Dissipation in a squeezed-state environment
p 370 N94-10584

LUNAR AND PLANETARY INST., HOUSTON, TX.
Twenty-fourth Lunar and Planetary Science Conference. Part 1: A-F
[NASA-CR-193095] p 435 N94-12015
Increased depth-diameter ratios in the Medusae Fossae Formation deposits of Mars p 439 N94-12043
Cratering on Gaspra p 459 N94-12147
Mars: The initial emplacement of ground ice in response to the thermal evolution of its early crust
p 462 N94-12168
The role of the geothermal gradient in the emplacement and replenishment of ground ice on Mars
p 463 N94-12169
The thermodynamic case for a water-rich Mars
p 463 N94-12170
Using lunar sounder imagery to distinguish surface from subsurface reflectors in lunar highlands areas
p 464 N94-12179
Does the thermal wind exist near the Earth's core boundary? p 283 N94-12217
Magnetic fields and nonuniform structures of the Moon p 472 N94-12218
Polarity reversals and tilt of the Earth's magnetic dipole p 283 N94-12219
Are cosmic rays effective for ionization of the solar nebula? p 472 N94-12220

LUNAR INDUSTRIES, INC., HOUSTON, TX.
Production of electronic grade lunar silicon by disproportionation of silicon difluoride
p 435 N94-12017

M

M AND R ASSOCIATES, ROCKVILLE, MD.
Federal contractors in appalachia
[PB93-188779] p 416 N94-11473

MALAYAN CENTRE FOR REMOTE SENSING, KUALA-LAMPUR.
Space programme in Malaysia p 36 N94-10685

MANCHESTER UNIV. (ENGLAND).
Comparison of computation and experiment for a high enthalpy, heated-driver, shock-tube environment
p 7 N94-10447
Real gas and surface transpiration effects upon swept leading edge high speed flow including transition
p 8 N94-10452
Fault location in structures using neural networks
p 70 N94-11335
Carbon in weathered ordinary chondrites from Roosevelt County p 428 N94-12035

MARINE HYDROPHYSICAL INST., SEVASTOPOL (USSR).
Field research of wind wave spectrum variability
p 223 N94-12727

MARTIN MARIETTA AEROSPACE, DENVER, CO.
Flexible polycrystalline thin-film photovoltaics for space applications p 50 N94-11393
Thin film solar cell workshop p 54 N94-11415

MARTIN MARIETTA CORP., DENVER, CO.
Adaptive structure design employing shape memory actuators p 70 N94-11331

MARTIN MARIETTA ENERGY SYSTEMS, INC., PIKETON, OH.
Engineering performance metrics
[DE93-012084] p 128 N94-11028

MARYLAND UNIV., BALTIMORE.
A simple model of melt fracture
[AD-A265311] p 92 N94-11862

MARYLAND UNIV., COLLEGE PARK.
Applications of a model to predict flame spread over interior finish materials in a compartment
p 19 N94-10783
Development of a hypermedia knowledge base of aircraft fire safety regulations p 21 N94-10793
Experimental study of multiple droplet evaporative cooling
[PB93-198463] p 149 N94-10851
Experimental comparison of time synchronization techniques by means of light signals and clock transport on the rotating earth p 351 N94-10970
Plans to improve the experimental limit in the comparison of the east-west and west-east one-way light propagation times on the rotating earth p 351 N94-10971
Aluminum and membrane channels
[AD-A265241] p 300 N94-11020
The experience factory: Can it make you a 5? or what is its relationship to other quality and improvement concepts? p 328 N94-11424
Design issues for high performance engineering information systems
[AD-A264839] p 420 N94-11520
Three-cavity circuit studies of the Maryland gyroklystron
[DE93-010173] p 145 N94-11645
Analysis of the Army's installation support modules with the private sector's open information systems
[AD-A265667] p 421 N94-12579

MARYLAND UNIV. BALTIMORE COUNTY, CATONSVILLE.
Study of Einstein-Podolsky-Rosen state for space-time variables in a two photon interference experiment
p 370 N94-10582

MASCHINENFABRIK AUGSBURG-NUERNBERG A.G., MUNICH (GERMANY).
Analytical prediction and test verification of the multiaxial behaviour of high-strength steel for lightweight structures
p 58 N94-10016
New processes for lightweight ceramic matrix composites p 61 N94-10043
Spin-rolling, welding, and heat treatment of aluminium 2219 for Ariane 5 GAM high pressure vessel liners
p 62 N94-10045
Stress relaxation forming of Ariane 5 front skirt outer skin panels p 62 N94-10046
Structural material, manufacture, and design requirements for high-temperature fasteners for space plane technologies p 63 N94-10055
Constitutive laws for describing the service relevant creep behaviour of metallic materials p 64 N94-10060

MASSACHUSETTS INST. OF TECH., CAMBRIDGE.
Grain boundaries in complex oxides
[DE93-013986] p 398 N94-11012
The Memphis Precision Runway Monitor Program Instrument Landing System final approach study
[AD-A266035] p 23 N94-11103
Experimental approach to the physics of the high density divertor
[DE93-009149] p 391 N94-11170
Intelligent structures: A technology overview and assessment p 68 N94-11322
Radiation-induced aperiodicity in irradiated ceramics
[DE93-013335] p 91 N94-11698
Analysis of gravity, magnetic, and seismic reflection data from Tibet and neighboring regions of China
[NASA-CR-193405] p 278 N94-11886
The asteroid-meteorite connection: Forging a new link to Vesta as the parent body of basaltic achondrite (HED) meteorites p 429 N94-12068
Chemical weathering on Mars: Rate of oxidation of iron dissolved in brines p 455 N94-12128
Venus mountain-top mineralogy: Misconceptions about pyrite as the high radar-reflecting phase
p 455 N94-12129
The giant impact produced a precipitated Moon
p 430 N94-12135
Cronstedtite and iron sulfide mineralogy of CM-type carbonaceous chondrites from cryogenic Moessbauer spectra p 433 N94-12257
Establishing baseline data for an experimental appratus that measures heat transfer under conditions of oscillating pressure and flow
[NASA-CR-193772] p 413 N94-12343

MASSACHUSETTS INST. OF TECH., LEXINGTON.
Parametric study of diffusion-enhancement networks for spatiotemporal grouping in real-time artificial vision
[AD-A265065] p 331 N94-11652
Evaluation of the capacity and delay benefits of terminal air traffic control automation
[AD-A265323] p 24 N94-11863
Observations of optical counterparts of Gamma-Ray bursts
[NASA-CR-193573] p 485 N94-12589

MASSACHUSETTS INST. OF TECH., WESTFORD.
Mid-latitude ionospheric response to active experiments
[NASA-CR-193549] p 280 N94-12583

MASSACHUSETTS UNIV., AMHERST.
A review of two photon production of jets at PEP and PETRA energies
[DE93-011742] p 364 N94-10754

MASSACHUSETTS UNIV., LOWELL.
Physical properties of injection molded liquid crystal polymers and high temperature engineering polymers
[AD-A264912] p 87 N94-10508
Characterization of an excimer laser-ablated plasma and applications p 392 N94-11450
A relaxation study of poled nonlinear optical polymers by infrared reflection-absorption spectroscopy
[AD-A265797] p 93 N94-12380

MATERIALS RESEARCH LABS., ASCOT VALE (AUSTRALIA).
Thermal stability of sealants for military aircraft: Modification of polysulfide prepolymers with ether and thioether monomers
[AD-A264079] p 89 N94-11107
GRAFTED (GRAphical Fault Tree EDitor): A fault tree description program for target vulnerability/survivability analysis
[AD-A264078] p 328 N94-11301
Formulating infrared coatings for defence applications
[MRL-RR-1-93] p 90 N94-11302

MATERIALS RESEARCH LABS., MARIBYRNONG (AUSTRALIA).
Submarine internal waves
[MRL-GD-0049] p 98 N94-11303

MATERIALS RESEARCH LABS., MELBOURNE (AUSTRALIA).
Dynamic loading in manufacturing and service: Australia's shock testing capability p 128 N94-11304

MATERIALS RESEARCH SOCIETY, PITTSBURG, PA.
Solid state ionics 3. Materials Research Society Symposium Proceedings, volume 293
[AD-A265675] p 395 N94-10416
Wide Band-Gap Semiconductors. 1991 Materials Research Society Symposium proceedings
[AD-A263418] p 401 N94-11515
Chemical Vapor Deposition of Refractory Metals and Ceramics 2. Materials Research Society Symposium proceedings
[AD-A265072] p 92 N94-11866

Atomic-scale imaging of surfaces and interfaces. Materials Research Society Symposium Proceedings, volume 295
[AD-A265674] p 369 N94-12379

MATHEMATICAL ASSOCIATION OF AMERICA, INC., WASHINGTON, DC.
Career Information in the Mathematical Sciences (CIMS)
[DE93-013780] p 318 N94-11817

MATRA MARCONI SPACE, TOULOUSE (FRANCE).
Propellant management in surface tension tanks
p 106 N94-10110
METEOSAT second generation programme SEVIRI: An enhanced visible and IR radiometer for meteorology
p 212 N94-12667

MAX-PLANCK-INST. FUER AERONOMIE, KATLENBURG-LINDAU (GERMANY).
On non-linear longitudinal stability of an aircraft in a dive in the presence of atmospheric disturbances
p 31 N94-11492

MAX-PLANCK-INST. FUER CHEMIE, MAINZ (GERMANY).
The solubility of gold in silicate melts: First results
p 87 N94-12086

MAX-PLANCK-INST. FUER ERNAEHRUNGSPHYSIOLOGIE, DORTMUND (GERMANY).
Chemical pattern formation under microgravity
p 121 N94-10227

MAX-PLANCK-INST. FUER RADIOASTRONOMIE, BONN (GERMANY).
Intraday variability and the compactness of extragalactic radio sources p 135 N94-11064

MAXWELL LABS., INC., LA JOLLA, CA.
NASCAP programmer's reference manual
[NASA-CR-191044] p 278 N94-11702

MCAT INST., SAN JOSE, CA.
Supersonic airplane study and design
[NASA-CR-193219] p 25 N94-11150
Physics of forebody flow control
[NASA-CR-193626] p 15 N94-11195

MCGILL UNIV., MONTREAL (QUEBEC).
Microgravity combustion of dust suspension in a spherical chamber p 80 N94-10248
Retrieval of radiation budgets in the Arctic from satellite measurements p 229 N94-10714
Mechanical analysis of parallel manipulators with simulation, design, and control applications
[ISBN-0-315-72013-1] p 181 N94-11156
Modelling quasi-two-dimensional turbulent shear flow
p 153 N94-11616

MECHANICAL ENGINEERING LAB., TSUKUBA (JAPAN).
Condensation phenomena p 162 N94-12550

MECHANICAL TECHNOLOGY, INC., LATHAM, NY.
Development of passive superconducting bearings. Phase 3
[AD-A266050] p 180 N94-10706

MEDICAL COLL. OF VIRGINIA, RICHMOND.
Valsalva maneuver: Insights into baroreflex modulation of human sympathetic activity p 310 N94-12000

MEIJI UNIV., KAWASAKI (JAPAN).
Fluctuations of longitudinal vortices along a concave wall p 16 N94-12616

MEIJO UNIV., NAGOYA (JAPAN).
On the wake behind a high speed train
p 164 N94-12618

MELBOURNE UNIV., PARKVILLE (AUSTRALIA).
Two fluid plasmas in the vicinity of a Schwarzschild black hole
[DE93-610264] p 385 N94-10284
HRTEM in protein crystallography
[DE93-610322] p 395 N94-10406
Interferometry with particles of non-zero rest mass
[DE93-613518] p 409 N94-10501
Test of a method for phase retrieval in HRTEM
[DE93-612641] p 170 N94-10630

MEMORIAL UNIV. OF NEWFOUNDLAND, SAINT JOHNS.
The Canadian experience: Using telemedicine for the support of medical care at remote sites
p 305 N94-11789

MESSERSCHMITT-BOELKOW-BLOHM G.M.B.H., BREMEN (GERMANY).
Spinforming characteristics of a net shape forming process p 56 N94-10004

MESSERSCHMITT-BOELKOW-BLOHM G.M.B.H., MUNICH (GERMANY).
Experimental results in aerodynamic stability and control of a TSTO configuration p 3 N94-10424
Numerical methods for aerothermodynamic design of hypersonic space transport vehicles p 9 N94-10459

METALS INFORMATION ANALYSIS CENTER, WEST LAFAYETTE, IN.
Bibliography on Hot Isostatic Pressing (HIP) technology
[AD-A265668] p 81 N94-10297

METEORMER, PUGET SUR ARGENS (FRANCE).
Use of SAR-wave, altimeter, and wind-scatterometer data in an operational swell forecasting system
p 250 N94-12503

METEOROLOGICAL OFFICE, BRACKNELL (ENGLAND).
Use of ERS-1 wind and wave products in operational meteorology p 250 N94-12502
A user appraisal of ATSR near-real-time products
p 252 N94-12516

METEOROLOGICAL OFFICE, FARNBOROUGH (ENGLAND).
Validation of ATSR-1 using aircraft radiometer measurements over the South Atlantic
p 252 N94-12515

METEOROLOGICAL RESEARCH INST., TSUKUBA (JAPAN).
The upwelling radiation at the top of the atmosphere in coastal region p 205 N94-11981
Worldwide map of rainfall amount over the ocean derived from passive microwave radiometer p 211 N94-12663

METEOROLOGICAL SATELLITE CENTER, TOKYO (JAPAN).
Meteorological Satellite Center
[MSC-TN-26] p 190 N94-11079
Fine tuning of stretched-VISSR image mapping
p 190 N94-11080
Simulation of images of water vapor channel and infrared split channel p 190 N94-11081
Statistical study on the regional and seasonal distribution of fog in the far east region by using GMS imagery
p 190 N94-11082
Overview of training seminar for the use of Japanese Earth Resources Satellite-1 (JERS-1) data
p 190 N94-11083

METROLASER, IRVINE, CA.
Flow visualization and spectroscopy in hypersonic flows: New trends p 5 N94-10437

MIAMI UNIV., CORAL GABLES, FL.
Atmospheric correction plans for SeaWiFS
p 204 N94-11975

MIAMI UNIV., FL.
Biscayne bay: A bibliography of the marine environment
[PB93-184802] p 266 N94-11451

MICHIGAN STATE UNIV., EAST LANSING.
High temperature stability, interface bonding, and mechanical behavior in (beta)-NiAl and Ni3Al matrix composites with reinforcements modified by ion beam enhanced deposition
[DE93-013977] p 398 N94-11115

MICHIGAN UNIV., ANN ARBOR.
Radiation and scattering by cavity-backed antennas on a circular cylinder
[NASA-CR-193409] p 136 N94-11084
Extended ecosystem signatures with application to Eos synergism requirements
[NASA-CR-193398] p 266 N94-11374
Mechanical interaction between synthetic fiber and cement base matrix in FRC composites
[AD-A265310] p 73 N94-11686
Observing and modelling F-region ionospheric dynamics using the (O2) 7320A emission
[AD-A265407] p 279 N94-12419

MICROELECTRONICS AND COMPUTER TECHNOLOGY CORP., AUSTIN, TX.
Reuse: A knowledge-based approach
p 329 N94-11430

MICROELECTRONICS CENTER OF NORTH CAROLINA, RESEARCH TRIANGLE PARK.
Multicomponent and multilayered thin films for advanced microtechnologies: Techniques, fundamentals, and devices
[AD-A265685] p 405 N94-12442

MICROGRAVITY ADVANCED RESEARCH AND SUPPORT CENTER, NAPLES (ITALY).
TOLS (Telescience On-Line Simulator): An essential instrument for micro-gravity interactive experiment
p 39 N94-10134
Laser cooling and trapping of atoms in microgravity: Ultracold atoms collisions p 124 N94-10241

MICROWAVE MONOLITHICS, INC., SIMI VALLEY, CA.
Low cost high efficiency GaAs monolithic RF module for SARSAT distress beacons
[NASA-CR-194235] p 146 N94-12773

MIDWEST RESEARCH INST., GOLDEN, CO.
Department of Energy solar process heat program: FY 1991 solar process heat prefeasibility studies activity
[DE93-010010] p 262 N94-10258

MINERALS MANAGEMENT SERVICE, NEW ORLEANS, LA.
Gulf of Mexico sales 147 and 150: Central and western planning areas. Draft environmental impact statement. Volume 2: Sections 4.D through 9
[PB93-190312] p 265 N94-11019

MINISTRY OF ECONOMIC AFFAIRS, THE HAGUE (NETHERLANDS).
The Netherlands innovation oriented research programme on polymer composites and special polymers 1985-1993 p 65 N94-10067

MINISTRY OF POSTS AND TELECOMMUNICATIONS, KASHIMA (JAPAN).
Pulsar astrometry by using VLBI (PSR0329 between Kashima 26mPhi and Usuda 64mPhi)
p 351 N94-10968
Measurements of ocean cross-section with a side-looking airborne radar p 201 N94-11954

MINISTRY OF POSTS AND TELECOMMUNICATIONS, OKINAWA (JAPAN).
HF ocean radar system at Okinawa Radio Observatory p 139 N94-11902
Measurement of wave parameters by HF ocean radar
p 192 N94-11903
Kuroshio observations by the HF ocean radar
p 192 N94-11904
Statistical study of HF ocean radar echo
p 139 N94-11905

MINISTRY OF POSTS AND TELECOMMUNICATIONS, TOKYO (JAPAN).
PARTNERS p 38 N94-10695
Artificial oil pollution detection and wave observation in the sea adjacent to Japan by ERS-1 SAR
p 253 N94-12520

MINNESOTA UNIV., MINNEAPOLIS.
Structural development in ceramic precursor sols and gels
[AD-A264354] p 90 N94-11281
Solid-state structures of guanidinium methane, ethane, and trifluoromethanesulfonate
[AD-A265293] p 402 N94-11654
Chromatographic assessment of hydrogen-bond donating ability
[AD-A265292] p 369 N94-11826
Hydrogen-bond polymorphs of guanidinium 4-biphenylsulfonate
[AD-A265294] p 402 N94-11827
Nitrogen and noble gases in a glass sample from LEW88516 p 80 N94-12051
Engineering solid-state materials. Strategies for modeling and packing control of molecular assemblies into 3-D networks
[AD-A265291] p 404 N94-12438
Coordinated Radio, Electron, and Waves Experiment (CREWE) for the NASA Comet Rendezvous and Asteroid Flyby (CRAF) instrument
[NASA-CR-194376] p 427 N94-12566

MINNESOTA UNIV., SAINT PAUL.
Satellite inventory of Minnesota forest resources
[NASA-CR-193565] p 231 N94-11521

MISSISSIPPI STATE UNIV., MISSISSIPPI STATE.
An investigation of error characteristics and coding performance
[NASA-CR-193620] p 324 N94-10932

MISSOURI UNIV., ROLLA.
Titanium alloys milling assistance by high pressure lubricoolant jet
[DE93-013302] p 82 N94-11008
Thin film preparation and interfacial reaction study of solid oxide fuel cell materials p 263 N94-11313
Creep deformation and mechanical properties of sintered glass and polycrystalline matrix composites
p 67 N94-11315

MITSUBISHI ELECTRIC CORP., AMAGASAKI (JAPAN).
Generation of superfluid He by G-M cycle cryogenic refrigerator p 130 N94-11841

MITSUBISHI ELECTRIC CORP., TOKYO (JAPAN).
Pre-operation analysis of ERS-1 tracking and operation, part 2-A
[NASDA-CNT-930001-PT-2-A] p 230 N94-11129
Flight data analysis of Japanese Earth Resources Satellite-1 (JERS-1)
[NASDA-CNT-930004] p 245 N94-12279

MITSUBISHI HEAVY INDUSTRIES LTD., TOKYO (JAPAN).
Aerodynamic characteristics analysis of Garabedian-Korn 75-06-12 airfoil
[PAPER-2D-9] p 11 N94-10474
Flow analysis around ONERA model M5 configuration
[PAPER-3D-5] p 12 N94-10481
Compatibility tests for biological specimens to on-board experiments in the Space Shuttle flight
[NASDA-CNT-930003] p 301 N94-12278

MITSUBISHI RESEARCH INST., INC., TOKYO (JAPAN).
Solidification from supercooled melt under microgravity p 113 N94-10176

MITSUBISHI SPACE SOFTWARE CORP. (JAPAN).
Pre-operation analysis of ERS-1 tracking and operation, part 2-F
[NASDA-CNT-930002-PT-2-F] p 230 N94-11130

MOSCOW PHYSICAL-ENGINEERING INST. (RUSSIA).

Trajectory curving in underwater propagation of light p 226 N94-12748

MOSCOW STATE UNIV. (RUSSIA).

From the Weyl theory to a theory of locally anisotropic space-time [DE92-644734] p 410 N94-10535

Nonclassical states of the second optical harmonic in the presence of self-action p 375 N94-10567

Principles of gauge theory of real hadrons [DE93-613094] p 362 N94-10634

Laser fluorescent monitoring of dissolved organic matter in natural water p 177 N94-12755

Ecological application of Surface Enhanced Raman Spectroscopy p 227 N94-12756

MUENSTER UNIV. (GERMANY).

Alkali-granitoids as fragments within the ordinary chondrite Adzhi-Bogdo: Evidence for highly fractionated, alkali-granitic liquids on asteroids p 429 N94-12069

MULLARD SPACE SCIENCE LAB., DORKING (ENGLAND).

Analysis of ERS-1 altimeter data over the polar ice sheets p 237 N94-11738

Validating the UK-PAF land ice product surface elevation p 244 N94-11780

ERS-1 altimetry of inland water and land p 246 N94-12475

MULTILAYER OPTICS AND X-RAY TECHNOLOGY, INC., OREM, UT.

Inexpensive capillary discharge x-ray laser driver [AD-A265932] p 176 N94-12382

MURORAN INST. OF TECH., MIZUMOTO (JAPAN).

A basic consideration for remote sensing using microwave radars on a satellite p 212 N94-12665

MUSASHI INST. OF TECH., TOKYO (JAPAN).

Preprints of the 13th Hydrogen Energy System Symposium [DE93-781115] p 99 N94-11444

MVA, INC., NORCROSS, GA.

Unequilibrated, equilibrated, and reduced aggregates in anhydrous interplanetary dust particles p 429 N94-12098

Carbon analyses of IDP's sectioned in sulfur and supported on beryllium films p 81 N94-12099

N

NAGASAKI UNIV., BUNKYO (JAPAN).

The extraction of bottom characteristics and mapping in Kin Bay, Okinawa Main Island, Japan, using LANDSAT-5/TM and SPOT-1/HRV data p 197 N94-11931

NAGOYA UNIV. (JAPAN).

Aerodynamic characteristics analysis of Garabedian-Korn 75-06-12 airfoil [PAPER-2D-2] p 10 N94-10468

Electron runaway in RF discharges [DE93-771407] p 363 N94-10661

Simulation study of dynamo structure in reversed field pinch [DE93-771406] p 390 N94-11128

Macroscopic behaviour and discrete dynamo of RFP plasma in high theta discharge [DE93-771408] p 392 N94-11239

Refrigerator utilization in infrared astronomy p 130 N94-11838

The phytoplankton bloom in the Kinu-ura Bay, Japan in the rainy season p 211 N94-12660

Variation of the photosynthetic products in the regional upwelling area around the Izu Islands, Japan p 211 N94-12661

NANSEN ENVIRONMENTAL AND REMOTE SENSING CENTER, SOLHEIMSVIK (NORWAY).

Ice studies in the Barents Sea by ERS-1 during SIZEX 1992 p 210 N94-12653

NANSEN OCEAN AND REMOTE SENSING CENTER, SOLHEIMSVIK (NORWAY).

Ice studies in the Barents Sea by ERS-1 SAR during SIZEX 92 p 238 N94-11745

NANSEN REMOTE SENSING CENTER, BERGEN (NORWAY).

Coastal ocean studies with ERS-1 SAR during NORCSEX 1991 p 234 N94-11720

NAPLES UNIV. (ITALY).

Towards real time numerical stimulation of Marangoni convection: A help for telescience microgravity experiments p 102 N94-10087

Marangoni flows in open cavities with differentially heated end walls p 104 N94-10097

Bubbles and drops behaviour under low-gravity: A space experiment for the IML-2 mission p 104 N94-10098

Boundary layers along horizontal free surfaces due to combined effects of temperature and concentration gradients p 106 N94-10108

NATIONAL AERONAUTICS AND SPACE ADMINISTRATION, WASHINGTON, DC.

Aerospace medicine and biology: A continuing bibliography with indexes (supplement 375) [NASA-SP-7011(375)] p 303 N94-10398

Aerospace medicine and biology: A continuing bibliography with indexes (supplement 376) [NASA-SP-7011(376)] p 303 N94-10399

Aeronautical engineering: A continuing bibliography with indexes (supplement 293) [NASA-SP-7037(293)] p 1 N94-10420

Space Station Redesign Team: Final report to the Advisory Committee on the Redesign of the Space Station [NASA-TM-109241] p 42 N94-10663

Topex/Poseidon: A United States/France mission. Oceanography from space: The oceans and climate [NASA-TM-108253] p 43 N94-10699

Applying design principles to fusion reactor configurations for propulsion in space [NASA-TM-108247] p 47 N94-11053

Enhanced Damage-Resistant Optics for Spaceflight Laser Systems: Workshop findings and recommendations [NASA-TM-109243] p 381 N94-11054

Correspondence standards [NHB-1450.10B] p 420 N94-11589

Aeronautical engineering: A continuing bibliography with indexes (supplement 289) [NASA-SP-7037(289)] p 1 N94-11687

Aerospace medicine and biology: A continuing bibliography with indexes (supplement 374) [NASA-SP-7011(374)] p 304 N94-11689

Aeronautical engineering: A continuing bibliography with indexes (supplement 291) [NASA-SP-7037(291)] p 1 N94-11690

Aeronautical engineering: A continuing bibliography with indexes (supplement 290) [NASA-SP-7037(290)] p 1 N94-11691

International Telemedicine/Disaster Medicine Conference: Papers and Presentations [NASA-NP-207] p 304 N94-11787

Telemedicine and international disaster response: Medical consultation to Armenia and Russia via a telemedicine spacebridge p 305 N94-11790

Medical care delivery in the US space program p 307 N94-11806

US-USSR telemedicine consultation spacebridge to Armenia and Ufa p 308 N94-11809

Overview of the 1989 Wind Tunnel Calibration Workshop [NASA-TP-3393] p 34 N94-11869

Reconstruction of the dynamics of the 1800-1801 Hualalai eruption: Implications for planetary lava flows p 281 N94-12041

A structural origin for the cantaloupe terrain of Triton p 449 N94-12095

NATIONAL AERONAUTICS AND SPACE ADMINISTRATION. AMES RESEARCH CENTER, MOFFETT FIELD, CA.

CFD analysis of hypersonic, chemically reacting flow fields p 2 N94-10422

A CFD validation roadmap for hypersonic flows p 5 N94-10439

Issues and approach to develop validated analysis tools for hypersonic flows: One perspective p 7 N94-10446

Arcjet exploratory tests of ARC optical window design for the AFE vehicle [NASA-CR-192655] p 34 N94-10930

Determining XV-15 aeroelastic modes from flight data with frequency-domain methods [NASA-TP-3330] p 25 N94-10935

Performance and rotor loads measurements of the Lynx XZ170 helicopter with rectangular blades [NASA-TM-104000] p 1 N94-10936

Criteria for design of integrated flight/propulsion control systems for STOVL fighter aircraft [NASA-TP-3356] p 30 N94-11134

Exercise countermeasures for bed-rest deconditioning [NASA-TM-103987] p 300 N94-11191

Moving-base simulation evaluation of thrust margins for vertical landing for the NASA YAV-8B Harrier aircraft [NASA-TM-104008] p 30 N94-11259

A summary of image segmentation techniques [NASA-TM-104022] p 327 N94-11274

Allowable exposure limits for carbon dioxide during extravehicular activity [NASA-TM-103832] p 315 N94-11375

Application of the airborne ocean color imager for commercial fishing [NASA-TM-103986] p 231 N94-11378

Transfer of training for aerospace operations: How to measure, validate, and improve it p 314 N94-11530

Criteria for assessing problem solving and decision making in complex environments p 314 N94-11532

Measures for simulator evaluation of a helicopter obstacle avoidance system p 35 N94-11535

Five biomedical experiments flown in an Earth orbiting laboratory: Lessons learned from developing these experiments on the first international microgravity mission from concept to landing p 302 N94-11556

Local fluid shifts and edema in humans during simulated microgravity p 311 N94-12003

Hormonal regulation of fluid and electrolyte metabolism in zero-g and bedrest p 311 N94-12004

Hormonal regulation of fluid and electrolyte metabolism during periods of headward fluid shifts p 311 N94-12005

Autogenic-feedback training: A countermeasure for orthostatic intolerance p 311 N94-12006

A comparison of telescopic and Phobos-2 ISM spectra of Mars in the short-wave near-infrared (0.76-1.02 microns) p 424 N94-12053

An observational search for CO2 ice clouds on Mars p 441 N94-12054

Changes in Hawaiian palagonite FE mineralogy associated with thermal alteration: Implications for Mars p 281 N94-12055

Why convective heat transport in the solar nebula was inefficient p 458 N94-12143

A normal stress subgrid-scale eddy viscosity model in large eddy simulation p 155 N94-12288

The three-dimensional evolution of a plane wake p 159 N94-12310

NATIONAL AERONAUTICS AND SPACE ADMINISTRATION. GODDARD SPACE FLIGHT CENTER, ALBUQUERQUE, NM.

Do large impact basins in the southern hemisphere of Mars control the distribution of polar structures and deposits? p 481 N94-12266

NATIONAL AERONAUTICS AND SPACE ADMINISTRATION. GODDARD SPACE FLIGHT CENTER, GREENBELT, MD.

STARDUST: A simulation experiment of cosmic dust analogues production in microgravity conditions p 113 N94-10175

Columbus proto-planetesimal dust aggregation experiment p 123 N94-10236

Fractography handbook of spaceflight metals [NASA-RP-1291] p 81 N94-10504

Satellite situation report, volume 32, no. 1 [NASA-TM-109233] p 42 N94-10562

Satellite situation report, volume 32, no. 2 [NASA-TM-109234] p 42 N94-10563

The Second International Workshop on Squeezed States and Uncertainty Relations [NASA-CP-3219] p 375 N94-10564

Wavelets and spacetime squeeze p 379 N94-10604

Satellite situation report, volume 31, no. 4 [NASA-TM-109232] p 39 N94-10659

NASA's first in-space optical gyroscope: A technology experiment on the X ray Timing Explorer spacecraft [NASA-TM-109242] p 170 N94-10667

Design of a global soil moisture initialization procedure for the simple biosphere model [NASA-TM-104590] p 284 N94-10940

The 24th Annual Precise Time and Time Interval (PTTI) Applications and Planning Meeting [NASA-CP-3218] p 350 N94-10963

Detection of accreting circumstellar gas around weak emission-line Herbig Ae/Be stars [NASA-TM-108256] p 424 N94-11306

Normal modes of the world's oceans: A numerical investigation using Proudman functions [NASA-TM-104587] p 288 N94-11358

Proceedings of the Seventeenth Annual Software Engineering Workshop [NASA-TM-109245] p 328 N94-11422

Experimental software engineering: Seventeen years of lessons in the SEL p 328 N94-11423

Impacts of object-oriented technologies: Seven years of SEL studies p 329 N94-11425

Large project experiences with object-oriented methods and reuse p 329 N94-11431

Global monitoring of atmospheric properties by the EOS MODIS [NASA-TM-109237] p 231 N94-11485

Robotic servicing on Earth orbiting satellites p 45 N94-11579

Monitoring of the Greenland Ice Sheet using ERS-1 synthetic aperture radar imagery p 237 N94-11741

Arctic coastal polynya observations with ERS-1 SAR and DMSP SSM/I p 239 N94-11748

Waves and mesoscale features in the marginal ice zone p 240 N94-11757

Summer Arctic ice concentrations and characteristics from SAR and SSM/I data p 241 N94-11762

Effect of species structure and dielectric constant on C-band forest backscatter [NASA-TM-109219] p 245 N94-11885

Ocean-ice interaction study of waves and mesoscale features p 197 N94-11935

Spectral analysis of the gravity and topography of Mars p 444 N94-12065

Collisions of small Spacewatch asteroids with the Earth p 430 N94-12157

Free-air and Bouguer gravity anomalies and the Martian crustal dichotomy p 481 N94-12267

New Mars free-air and Bouguer gravity: Correlation with topography, geology and large impact basins p 481 N94-12268

Transportable Applications Environment (TAE) Tenth Users' Conference [NASA-CP-3225] p 333 N94-12448

Pacific rim sea ice as observed with the NIMBUS-7 SMMR p 210 N94-12651

NATIONAL AERONAUTICS AND SPACE ADMINISTRATION. HUGH L. DRYDEN FLIGHT RESEARCH FACILITY, EDWARDS, CA.

In-flight evaluation of aerodynamic predictions of an air-launched space booster p 3 N94-10427

Extraction of stability and control derivatives from orbiter flight data [NASA-TM-4500] p 13 N94-10707

Space Shuttle hypersonic aerodynamic and aerothermodynamic flight research and the comparison to ground test results [NASA-TM-4499] p 13 N94-10820

Technical Update: Johnson Space Center system using a solid electrolytic cell in a remote location to measure oxygen fugacities in CO/CO2 controlled-atmosphere furnaces [NASA-TM-104774] p 423 N94-11183

Preliminary supersonic flight test evaluation of performance seeking control [NASA-TM-4494] p 28 N94-11205

Ground vibration and flight flutter tests of the single-seat F-16XL aircraft with a modified wing [NASA-TM-104269] p 26 N94-11233

NATIONAL AERONAUTICS AND SPACE ADMINISTRATION. JOHN C. STENNIS SPACE CENTER, BAY SAINT LOUIS, MS.

Emissions of sulfur gases from marine and freshwater wetlands of the Florida Everglades: Rates and extrapolation using remote sensing p 269 N94-12457

NATIONAL AERONAUTICS AND SPACE ADMINISTRATION. JOHN F. KENNEDY SPACE CENTER, COCOA BEACH, FL.

Debris/ice/TPS assessment and integrated photographic analysis for Shuttle Mission STS-57 [NASA-TM-107562] p 40 N94-10805

Vigilance problems in orbiter processing p 314 N94-11536

NATIONAL AERONAUTICS AND SPACE ADMINISTRATION. JOHN F. KENNEDY SPACE CENTER, LOMPOC, CA.

Carotid-cardiac baroreflex: Relation with orthostatic hypotension following simulated microgravity and implications for development of countermeasures p 308 N94-11992

NATIONAL AERONAUTICS AND SPACE ADMINISTRATION. LYNDON B. JOHNSON SPACE CENTER, HOUSTON, TX.

A comparison of high resolution upwind solvers on 3-D inviscid hypersonic flows p 10 N94-10463

Check valve with poppet damping mechanism [NASA-CASE-MSC-21903-1] p 179 N94-10655

Check valve with poppet dashpot/frictional damping mechanism [NASA-CASE-MSC-21950-1] p 179 N94-10658

Cooled spool piston compressor [NASA-CASE-MSC-22020-1] p 179 N94-10674

Project ARGO: Gas phase formation in simulated microgravity [NASA-TM-104762] p 125 N94-11235

Vacuum stability requirements of polymeric material for spacecraft application [NASA-TM-109216] p 91 N94-11350

Sixth Annual Workshop on Space Operations Applications and Research (SOAR 1992), volume 2 [NASA-CP-3187-VOL-2] p 486 N94-11527

Signal detection theory and methods for evaluating human performance in decision tasks p 314 N94-11531

Noise levels and their effects on Shuttle crewmembers' performance: Operational concerns p 314 N94-11538

Risk of decompression sickness in the presence of circulating microbubbles p 312 N94-11546

Promethazine and its use as a treatment for space motion sickness p 312 N94-11550

Update on the incidence and treatment of space motion sickness p 312 N94-11551

Baseline characteristics of different strata of astronaut corps p 312 N94-11552

Comprehensive analysis of airborne contaminants from recent Spacelab missions p 318 N94-11553

Toxicity study of dimethylethoxysilane (DMSES), the waterproofing agent for the Orbiter heat protective system p 318 N94-11554

A combustion products analyzer for contingency use during thermodegradation events on spacecraft p 318 N94-11555

Potential health effects of space radiation p 312 N94-11558

Radiation considerations for interplanetary missions p 45 N94-11559

Operational radiological support for the US manned space program p 318 N94-11561

On-orbit refueling p 38 N94-11566

Definition of spacecraft standard interfaces by the NASA Space Assembly and Servicing Working Group (SASWG) p 348 N94-11574

Use of telescience for biomedical research during space flight p 305 N94-11791

Space technology in remote health care p 306 N94-11799

Echocardiography in the flight program p 309 N94-11993

Effect of prolonged LBNP and saline ingestion on plasma volume and orthostatic responses during bed rest p 310 N94-11998

Cold press sintering of simulated lunar basalt p 131 N94-12026

General overview of an integrated lunar oxygen production/brickmaking system p 131 N94-12027

Noble gases in LEW88516 shergottite: Evidence for exposure age pairing with ALH77005 p 80 N94-12082

Ar-39 - Ar-40 ages of acapulcoites and lodranites: Evidence for early parent body heating p 281 N94-12083

Differential scaling: Implications for central structures in large lunar craters p 461 N94-12158

Impact comminution of glasses: Implications for lunar regolith evolution p 461 N94-12159

Exploration planning in the context of human exploration and development of the Moon p 474 N94-12229

NATIONAL AERONAUTICS AND SPACE ADMINISTRATION. LANGLEY RESEARCH CENTER, HAMPTON, VA.

Recommendations for future research in hypersonic instrumentation p 4 N94-10433

Local measurement of temperatures and concentrations: A review for hypersonic flows p 4 N94-10434

Pressure and force measurements on models set in hypersonic flows: A review p 5 N94-10435

Three-dimensional hypersonic rarefied flow calculations using direct simulation Monte Carlo method p 7 N94-10449

A CFD-based aerodynamic design procedure for hypersonic wind-tunnel nozzles p 9 N94-10458

Schlieren photographs and internal pressure distributions for three-dimensional sidewall-compression scramjet inlets at a Mach number of 6 in CF4 [NASA-TM-4479] p 148 N94-10644

Method of recertifying a loaded bearing member using a phase point [NASA-CASE-LAR-14741-1] p 185 N94-10671

Underwing compression vortex attenuation device [NASA-CASE-LAR-14744-1] p 12 N94-10673

Static internal performance of a single expansion ramp nozzle with multiaxis thrust vectoring capability [NASA-TM-4450] p 12 N94-10675

Nonperturbative methods in HZE ion transport [NASA-TP-3363] p 484 N94-10759

Progress in multidisciplinary design optimization at NASA Langley [NASA-TM-107754] p 318 N94-10814

An analysis of fiber-matrix interface failure stresses for a range of ply stress states [NASA-TM-108999] p 67 N94-11276

A proposed performance index for galactic cosmic ray shielding materials [NASA-TM-4444] p 484 N94-11278

Dynamic tests on the NASA Langley CSI evolutionary model p 45 N94-11320

The impact of active controls technology on the structural integrity of aeronautical vehicles p 27 N94-11341

NASA/DOD Aerospace Knowledge Diffusion Research Project. Report 17: A comparison of the technical communication practices of Dutch and US aerospace engineers and scientists [NASA-TM-108987] p 419 N94-11352

Space Station Freedom advanced photovoltaics and battery technology development planning p 52 N94-11401

Discrete Kalman filtering equations of second-order form for control-structure interaction simulations [NASA-CR-193723] p 331 N94-11522

In-space operations for lunar and Mars space transfer vehicles p 348 N94-11568

In-space assembly-servicing requirements p 348 N94-11569

Further studies using matched filter theory and stochastic simulation for gust loads prediction [NASA-TM-109010] p 26 N94-11587

A determination of the external forces required to move the benchmark active controls testing model in pure plunge and pure pitch [NASA-TM-107743] p 16 N94-12421

Sampling and position effects in the Electronically Steered Thinned Array Radiometer (ESTAR) [NASA-TM-108998] p 245 N94-12432

Coulomb effects in low-energy nuclear fragmentation [NASA-TP-3352] p 485 N94-12434

Final state interactions and inclusive nuclear collisions [NASA-TP-3353] p 373 N94-12435

Hypersonic, nonequilibrium flow over a cylindrically blunted 6 deg wedge [NASA-TM-108994] p 162 N94-12571

NATIONAL AERONAUTICS AND SPACE ADMINISTRATION. LEWIS RESEARCH CENTER, CLEVELAND, OH.

Marangoni instability induced convection in an evaporating liquid droplet p 104 N94-10094

The kinematics of buoyancy induced mixing p 123 N94-10239

The NASA Lewis Research Center SBIR program: An assessment [NASA-TM-106205] p 485 N94-10356

Probabilistic evaluation of uncertainties and risks in aerospace components [NASA-TM-105603] p 185 N94-10361

Large time-step stability of explicit one-dimensional advection schemes [NASA-TM-106203] p 342 N94-10362

Subband/transform functions for image processing [NASA-TM-106183] p 323 N94-10639

Achievements and challenges of Space Station Freedom's safety review process [NASA-TM-106199] p 40 N94-10640

Method of reducing drag in aerodynamic systems [NASA-CASE-LEW-14791-1] p 12 N94-10672

Distributed simulation using a real-time shared memory network [NASA-TM-106239] p 319 N94-10724

Experimental measurement of the plasma conductivity of Z93 and Z93P thermal control paint [NASA-TM-106284] p 43 N94-10756

A soft-start circuit for arcjet ignition [NASA-TM-106287] p 180 N94-10760

Characterization of in-flight performance of ion propulsion systems [NASA-TM-106283] p 46 N94-10761

Computational simulation of hot composite structures [NASA-TM-106200] p 186 N94-10762

Axisymmetric single shear element combustion instability experiment [NASA-TM-106327] p 46 N94-10763

A comparative study of full Navier-Stokes and Reduced Navier-Stokes analyses for separating flows within a diffusing inlet S-duct [NASA-TM-106250] p 39 N94-10764

Specification and testing for power by wire aircraft [NASA-TM-106232] p 46 N94-10765

Space transportation alternatives for large space programs: The International Space University Summer Session, 1992 [NASA-TM-106271] p 40 N94-10811

The properties of perfluoropolyethers used for space applications [NASA-TM-106275] p 88 N94-10864

Laser velocimeter measurements of the flow field generated by a forward-swept propfan during flutter [NASA-TM-106195] p 14 N94-10892

New developments in the method of space-time conservation element and solution element: Applications to the Euler and Navier-Stokes equations [NASA-TM-106226] p 150 N94-10939

A preliminary study on ice shape tracing with a laser light sheet [NASA-TM-105964] p 174 N94-11132

Laser anemometer measurements and computations for transonic flow conditions in an annular cascade of high turning core turbine vanes [NASA-TP-3383] p 15 N94-11133

Damping mechanisms in chemically vapor deposited SiC fibers [NASA-TM-106334] p 66 N94-11135

ACARA user's manual [NASA-TM-106277] p 183 N94-11167

A Galilean and tensorial invariant k-epsilon model for near wall turbulence [NASA-TM-106263] p 151 N94-11192

Low temperature synthesis of monolithic transparent Ta2O5 gels from hydrolysis of metal alkoxide [NASA-TM-106246] p 89 N94-11204

A distributed version of the NASA Engine Performance Program
[NASA-TM-106208] p 327 N94-11231

Portable programming on parallel/networked computers using the Application Portable Parallel Library (APPL)
[NASA-TM-106238] p 327 N94-11232

Application of jet-shear-layer mixing and effervescent atomization to the development of a low-NO(x) combustor
[NASA-TM-105888] p 28 N94-11234

Assessment of damage in ceramics and ceramic matrix composites using ultrasonic techniques
[NASA-TM-106121] p 67 N94-11237

On the combustion of a laminar spray
[NASA-TM-106210] p 28 N94-11238

Application of controller partitioning optimization procedure to integrated flight/propulsion control design for a STOVL aircraft
[NASA-TM-106265] p 30 N94-11251

A laboratory model of a hydrogen/oxygen engine for combustion and nozzle studies
[NASA-TM-106281] p 47 N94-11252

High order accurate solutions of viscous problems
[NASA-TM-106267] p 151 N94-11253

Functional approximation using artificial neural networks in structural mechanics
[NASA-TM-105820] p 188 N94-11254

A comparison between numerically modelled and experimentally measured loss mechanisms in wave rotors
[NASA-TM-106279] p 29 N94-11255

A research program for improving heat transfer prediction for the laminar to turbulent transition region of turbine vanes/blades
[NASA-TM-106278] p 151 N94-11256

Synthesis and thermal evolution of structure in alkoxide-derived niobium pentoxide gels
[NASA-TM-106259] p 90 N94-11257

High efficiency direct thermal to electric energy conversion from radioisotope decay using selective emitters and spectrally tuned solar cells
[NASA-TM-106227] p 47 N94-11307

Heat flux measurements on ceramics with thin film thermocouples
[NASA-TM-106305] p 170 N94-11310

Tribological characteristics of sputtered Au/Cr films on alumina substrates at elevated temperatures
[NASA-TM-106078] p 55 N94-11362

Marangoni instability in a liquid layer with two free surfaces
[NASA-TM-106166] p 152 N94-11376

On nonlinear Tollmien-Schlichting/vortex interaction in three-dimensional boundary layers
[NASA-TM-106184] p 152 N94-11377

Proceedings of the 12th Space Photovoltaic Research and Technology Conference (SPRAT 12)
[NASA-CP-3210] p 48 N94-11380

Radiation effects in heteroepitaxial InP solar cells
p 48 N94-11383

Progress in p(+)n InP solar cells fabricated by thermal diffusion p 48 N94-11384

Electrochemical characterization of p(+)n and n(+)p diffused InP structures p 49 N94-11385

Activation energy and capture cross section of majority carrier traps in Zn doped InP p 49 N94-11386

Effects of solar cell environment on contact integrity
p 49 N94-11387

Measurement of the minority carrier diffusion length and edge surface-recombination velocity in InP
p 49 N94-11388

Surface passivation of InP solar cells with InAlAs layers p 49 N94-11389

Approaches to solar cell design for pulsed laser power receivers p 51 N94-11397

Recent developments in refractive concentrators for space photovoltaic power systems p 52 N94-11402

Results of thermal vacuum tests for the PASP+ flight modules p 53 N94-11410

Workshop on Heteroepitaxial InP Solar Cells
p 54 N94-11414

Workshop on Solar Electric Propulsion
p 54 N94-11416

Viscous analysis of three-dimensional rotor flows using a multigrid method
[NASA-TM-106266] p 152 N94-11481

A modeling investigation of thermal and strain induced recovery and nonlinear hardening in potential based viscoplasticity
[NASA-TM-106122] p 188 N94-11482

Microgravity vibration isolation technology: Development to demonstration
[NASA-TM-106320] p 1 N94-11703

New technology applied to telemedicine
p 306 N94-11796

Diffusion length damage coefficient and annealing studies in proton-irradiated InP
[NASA-TM-106262] p 404 N94-12430

Protective coatings for high-temperature polymer matrix composites
[NASA-TM-106276] p 74 N94-12431

Proposed framework for thermomechanical life modeling of metal matrix composites
[NASA-TP-3320] p 74 N94-12449

Hot-gas-side heat transfer characteristics of subscale, plug-nozzle rocket calorimeter chamber
[NASA-TP-3380] p 55 N94-12569

Modeling void growth and movement with phase change in thermal energy storage canisters
[NASA-TM-106288] p 163 N94-12576

NATIONAL AERONAUTICS AND SPACE ADMINISTRATION. MARSHALL SPACE FLIGHT CENTER, HUNTSVILLE, AL.

Granular instability in fluidized beds: A small-over-large instability p 122 N94-10235

The International Microgravity Laboratory, a Spacelab for materials and life sciences p 125 N94-10249

Dynamic tester for rotor seals and bearings
[NASA-CASE-MFS-28493-1] p 33 N94-10669

A browse facility for Earth science remote sensing data: Center director's discretionary fund final report
[NASA-TM-108413] p 419 N94-10723

Space Station redesign option A: Modular buildup concept
[NASA-TM-108415] p 43 N94-10808

NASA Marshall Space Flight Center solar observatory report, January - June 1993
[NASA-TM-108417] p 423 N94-10866

Parachute having improved vent line stacking
[NASA-CASE-MFS-28508-1] p 14 N94-11021

Thermal testing of aluminized Mylar
[NASA-TM-108414] p 89 N94-11175

A study of strength evaluations of EDNi/EDCu/NARloy-Z bonded joints
[NASA-TM-108418] p 188 N94-11275

Response of silicon solar cell to pulsed laser illumination p 51 N94-11396

NATIONAL AERONAUTICS AND SPACE ADMINISTRATION. PASADENA OFFICE, CA.

Force reflection with compliance control
[NASA-CASE-NPO-18668-1-CU] p 179 N94-10654

Method for producing a hybridization of detector array and integrated circuit for readout
[NASA-CASE-NPO-18062-1-CU] p 141 N94-10656

Alkali metal for ultraviolet band-pass filter
[NASA-CASE-NPO-18433-1-CU] p 381 N94-10657

Telerobot control system
[NASA-CASE-NPO-18116-1-CU] p 179 N94-10670

NATIONAL AERONAUTICS AND SPACE ADMINISTRATION. WALLOPS FLIGHT CENTER, WALLOPS ISLAND, VA.

The Grand Banks ERS-1 SAR wave spectra validation experiment p 232 N94-11708

NATIONAL AERONAUTICS AND SPACE INST., BANDUNG (INDONESIA).

The use of remote sensing data for coastal zone management and environment in Indonesia
p 196 N94-11927

NATIONAL AEROSPACE LAB., EMMELOORD (NETHERLANDS).

Analysis of the alignment of a Schlieren system for tele-operation p 111 N94-10140

NATIONAL AEROSPACE LAB., KAKUDA (JAPAN).

Studies on scramjet nozzles. Part 1: Performance of two dimensional nozzles
[NAL-TR-1149] p 27 N94-10367

Durability of a carbon segmented circumferential seal for a liquid oxygen turbopump
[NAL-TR-1155] p 178 N94-10369

NATIONAL AEROSPACE LAB., TOKYO (JAPAN).

An investigation on the effectiveness of the piping interference removal system for STOL aircraft wind tunnel tests
[NAL-TM-647] p 2 N94-10350

Estimation of critical values and vibration characteristics on supersonic delta wings. Part 1: On-line time series analysis of stationary random response
[NAL-TR-1153] p 2 N94-10363

A grid generation method to calculate the flow field in a three-dimensional cascade of blades
[NAL-TR-1158] p 147 N94-10364

Solving the inverse problem for incompressible potential flow through two-dimensional cascades
[NAL-TR-1162] p 147 N94-10365

Estimation of the attitude motion of the small satellite ORIZURU
[NAL-TR-1145] p 42 N94-10366

Simulation of a parallel computer
[NAL-TR-1154] p 335 N94-10368

Numerical calculation of scramjet inlet flow
[NAL-TR-1174T] p 27 N94-10370

Proceedings of the 10th NAL Symposium on Aircraft Computational Aerodynamics: CFD Workshop on GK Airfoil and ONERA M5 Geometry
[NAL-SP-20] p 10 N94-10466

Description of 2D problem: Aerodynamic analysis of Garabedian-Korn 75-06-12 airfoil p 10 N94-10467

Aerodynamic characteristics analysis of Garabedian-Korn 75-06-12 airfoil: Compendium of results p 11 N94-10475

Description of 3D problem: Flow analysis around ONERA model M5 configuration p 11 N94-10476

Flow analysis around ONERA model M5 configuration
[PAPER-3D-4] p 12 N94-10480

Flow analysis around ONERA model M5 configuration: Compendium of results p 12 N94-10482

Atomization characteristics of a prefilming airblast atomizer
[NAL-TM-644] p 148 N94-10727

Aerodynamic model identification of quiet STOL experimental aircraft ASKA from dynamic flight test data
[DE93-767967] p 25 N94-10728

Improvements for obtaining iterative solutions of large linear systems
[DE93-767968] p 343 N94-10729

Large amplitude shape oscillations in a mercury drop using a drop tower
[DE93-767972] p 125 N94-10730

Subroutine functions for generating animation data
[DE93-767973] p 313 N94-10731

Effect of surface cleanliness of bearing steel on adhesive strength and tribological properties of sputter-deposited gold films
[DE93-767974] p 82 N94-10732

Flight simulator experiment of the cockpit advisory system
[NAL-TR-1151] p 33 N94-10733

In-flight simulation of backside operating models using direct lift controller
[NAL-TR-1152] p 30 N94-10734

Simulated wake characteristics of tapered annular wings by a discrete vortex method
[NAL-TR-1156] p 13 N94-10855

Simulated and experimental aerodynamic characteristics of tapered annular wings
[NAL-TR-1157] p 13 N94-10856

Evaluation of test specimen shape effects on the flexural fatigue of CFRP laminates
[NAL-TR-1159] p 65 N94-10857

Tribological characteristics of hot-pressed self-lubricating composites
[NAL-TR-1160] p 66 N94-10858

In-orbit performance tests and tele-command systems of the umbrella test satellite (DEBUT)
[NAL-TR-1165] p 43 N94-10859

New aerodynamic information obtained from the solution of the inverse problem for aerofoils
[NAL-TR-1172] p 14 N94-10860

Numerical wind tunnel project and computational fluid dynamics at National Aerospace Laboratory, Japan
[NAL-TM-648T] p 149 N94-10861

Proceedings of the 9th and 10th NAL Workshop on Investigation and Control of Boundary-Layer Transition
[NAL-SP-18] p 163 N94-12611

Nonlinear stability calculations of pipe flow
p 163 N94-12612

DNS on control of laminar-turbulent transition in channel flow with suction and blowing p 163 N94-12613

NATIONAL AIR AND SPACE MUSEUM, WASHINGTON, DC.

Geology and surface characteristics of Bell Regio, Venus p 457 N94-12136

Lava flows on Venus: Analysis of motion and cooling
p 457 N94-12137

Geologic history of central Chryse Planitia and the Viking 1 landing site, Mars p 465 N94-12180

NATIONAL ASTRONOMY AND IONOSPHERE CENTER, ARECIBO, PUERTO RICO.

Propagation Effects in Space VLBI
p 134 N94-11060

NATIONAL CENTER FOR SCIENTIFIC RESEARCH OF VIETNAM, HANOI.

Shoreline change detection using remote sensing and GIS in Vietnam p 196 N94-11928

NATIONAL CENTRE FOR SCIENCE INFORMATION SYSTEMS, TOKYO (JAPAN).

A new expression for the production rate of sea water droplets on the sea surface p 195 N94-11920

NATIONAL DEFENSE MEDICAL COLL., SAITAMA (JAPAN).

Coastal processes due to nearshore current around an upheaving island p 199 N94-11942

Study of growing processes of a tombolo using an air photograph p 218 N94-12702

NATIONAL INST. FOR ENVIRONMENTAL STUDIES, TSUKUBA (JAPAN).
Satellite observation of atmospheric tracer components: JEM/POP p 130 N94-11836

NATIONAL INST. FOR FUSION SCIENCE, NAGOYA (JAPAN).
Atomic and molecular data for H2O, CO and CO2 relevant to edge plasma impurities
[DE93-771423] p 387 N94-10662
Kinetic approach to long wave length modes in rotating plasmas
[DE93-771286] p 388 N94-10807
Compilation of excitation cross sections for He atoms by electron impact
[DE93-753246] p 367 N94-11580
Atomic processes relevant to polarization plasma spectroscopy
[DE93-753240] p 393 N94-11594

NATIONAL INST. FOR RESOURCES AND ENVIRONMENT, IBARAKI (JAPAN).
Seasonal changes of phytoplankton distributions in the Northwest Pacific detected by Coastal Zone Color Scanner p 200 N94-11948
The seasonal change of phytoplankton size distribution using optical fiber sensor p 210 N94-12656

NATIONAL INST. OF AGRO-ENVIRONMENTAL SCIENCE, IBARAKI (JAPAN).
Evaluating the spread of red soil with LANDSAT TM data in coral reefs of Okinawa main island, southwestern Japan p 212 N94-12668

NATIONAL INST. OF HEALTH, BETHESDA, MD.
National Institute of Health Almanac, 1992
[PB93-183556] p 303 N94-10828

NATIONAL INST. OF OCEANOGRAPHY, GOA (INDIA).
Acoustic waveguide characteristics of the Indian Ocean north of equator p 193 N94-11912
On an upwelling front, propagation of upwelling and vertical velocity in the eastern Arabian Sea during monsoon, 1987 p 206 N94-11987
Sea surface temperature anomalies in the Arabian Sea p 206 N94-11988
Satellite observations of the northeast monsoon coastal current p 214 N94-12678
Advective surface velocity in the north west Pacific derived from NOAA AVHRR images
p 222 N94-12721

NATIONAL INST. OF STANDARDS AND TECHNOLOGY, BOULDER, CO.
Measurement methods and algorithms for comparison of local and remote clocks p 354 N94-10987
Confidence of the three-point estimator of frequency drift p 357 N94-11003

NATIONAL INST. OF STANDARDS AND TECHNOLOGY, GAITHERSBURG, MD.
The effect of gravity modulation on thermosolutal convection p 105 N94-10103
The effect of gravitational modulation on convection in vertical Bridgman growth p 113 N94-10178
Pulsatile instability in rapid directional solidification: Strongly-nonlinear analysis p 115 N94-10188
Computer-aided molecular design of fire resistant aircraft materials p 19 N94-10779
A non-halogenated, flame retarded polycarbonate
p 19 N94-10781
Developments needed to expand the role of fire modeling in material fire hazard assessment
p 20 N94-10787
Bibliographic notes on Voronoi diagrams
[PB93-189298] p 343 N94-10825
The First Text Retrieval Conference (TREC-1)
[PB93-191641] p 419 N94-10829
Journal of Research of the National Institute of Standards and Technology, volume 98, number 2, March - April 1993
[PB93-196228] p 485 N94-10850
Theoretical evaluation of R22 and R502 alternatives
[DE93-014767] p 411 N94-10853

NATIONAL LAB. FOR HIGH ENERGY PHYSICS, IBARAKI (JAPAN).
Proceedings of the third workshop on light quark meson spectroscopy
[DE93-754138] p 363 N94-10696
Proceedings of the Second KEK Topical Conference on e(sup +)e(sup -) collision physics
[DE93-754139] p 364 N94-10889

NATIONAL LAB. FOR HIGH ENERGY PHYSICS, TSUKUBA (JAPAN).
Lecture note on circuit technology for high energy physics experiment
[DE93-771422] p 372 N94-11245
Conceptual design report for the SDC barrel and intermediate muon detectors based on a jet-type drift chamber
[DE93-753173] p 367 N94-11510

NATIONAL OCEAN SURVEY, ROCKVILLE, MD.
The 1992 El Nino viewed by ERS-1 altimetry
p 244 N94-11784

NATIONAL OCEANIC AND ATMOSPHERIC ADMINISTRATION, CAMP SPRINGS, MD.
An integrated approach to total end-to-end quality control of ocean data in the real-time environment
p 211 N94-12662

NATIONAL OCEANIC AND ATMOSPHERIC ADMINISTRATION, WASHINGTON, DC.
Migration of operational ice analysis and forecasting to a workstation platform at the Joint Ice Center
p 212 N94-12666

NATIONAL PHYSICAL LAB., TEDDINGTON (ENGLAND).
An intercomparison of the radium mass standards of the UK and the USSR: 2
[NPL-RSA(EXT)-34] p 359 N94-10266
Development of a cryogenic hydrogen maser at the NPL p 176 N94-10982

NATIONAL REMOTE SENSING AGENCY, HYDERABAD (INDIA).
Satellite derived sea surface temperature applications for Indian Ocean resources development
p 193 N94-11907

NATIONAL REMOTE SENSING CENTRE, FARNBOROUGH (ENGLAND).
TREES project: A suite of tools for information extraction from ERS-1 SAR data p 250 N94-12498

NATIONAL REMOTE SENSING CENTRE, ULAANBAATAR (MONGOLIA).
National space programmes and application of the remote sensing data in Mongolia p 36 N94-10686

NATIONAL RESEARCH COUNCIL, BANGKOK (THAILAND).
Thailand ISY activities p 37 N94-10690

NATIONAL RESEARCH COUNCIL OF CANADA, OTTAWA (ONTARIO).
The OSU heat release rate test using the oxygen consumption principle p 20 N94-10784
Time scale algorithms for an inhomogeneous group of atomic clocks p 356 N94-10998

NATIONAL RESEARCH INST. OF FAR SEAS FISHERIES, SHIZUOKA (JAPAN).
Primary productivity in the Oyashio area in the spring and summer of 1990 p 211 N94-12658
Statistical features of mesoscale eddies at the Kuroshio front p 215 N94-12682

NATIONAL RESEARCH LAB. OF METROLOGY, TOKYO (JAPAN).
Calibration of anemometers at low speed by means of towing carriage p 164 N94-12619

NATIONAL SCIENCE FOUNDATION, WASHINGTON, DC.
National patterns of R and D resources, 1992
[NSF-92-330] p 422 N94-11186
Facts about the US Antarctic program
[NSF-92-134] p 279 N94-12568

NATIONAL SPACE ACTIVITIES COUNCIL, TOKYO (JAPAN).
Panel discussion: Role of space program in the Asia Pacific Region p 37 N94-10694

NATIONAL SPACE DEVELOPMENT AGENCY, IBARAKI (JAPAN).
The Second Workshop on Refrigerating System Utilization Onboard the JEM
[NASDA-CON-930001] p 129 N94-11831
The trial manufacture and test of critical components in docking mechanism
[NASDA-TMR-930005] p 44 N94-12280
Conceptual studies report on lunar and planetary exploration
[NASDA-TK-SS0438] p 481 N94-12323
Significance and scenarios of lunar and planetary exploration missions p 482 N94-12324
Unmanned lunar exploration mission
p 482 N94-12325
Manned lunar exploration missions
p 482 N94-12326
Mars exploration missions p 482 N94-12327
Technical problems on lunar an planetary exploration mission p 482 N94-12328
The Third Workshop on Two Phase Fluid Experiment in the Space Environment
[NASDA-CON-930002] p 161 N94-12547
Organization and management policy for two phase fluid experiment in space environment p 162 N94-12556

NATIONAL SPACE DEVELOPMENT AGENCY, SAITAMA (JAPAN).
C-band SAR backscatter from ice on shallow tundra lakes: Observations and modelling p 240 N94-11755

NATIONAL SPACE DEVELOPMENT AGENCY, TOKYO (JAPAN).
Microgravity experiments using TR-1A rocket
p 112 N94-10142
Space Activities in the Asia Pacific Region
[JTN-93-80421] p 35 N94-10676
Current status of space activities in Asia Pacific region
p 35 N94-10677
Considerations for future regional space cooperation
p 35 N94-10678
Summary of the pre-AO of the JEM onboard scientific and engineering experiments for refrigerator utilization
p 129 N94-11832
Studies on refrigerator sensors and cooling section interface p 129 N94-11834
Trend of miniature refrigerator utilization in earth observation area p 130 N94-11835
Utilization of superconductivity in the area of space
p 131 N94-11843
Summary of studies on JEM utilization experiment projects p 161 N94-12548
Validation test system for sea surface temperature detected by satellites in Mutsu Bay p 213 N94-12670

NATIONAL SUN YAT-SEN UNIV., KAOHSIUNG (CHINA).
Sedimentation rates and particulate fluxes in the slope and deep sea areas off eastern Taiwan
p 220 N94-12709

NATIONAL TAIWAN UNIV., TAIPEI.
The circulation near Luzon p 219 N94-12707
Current variability on the shelf break northeast of Taiwan p 219 N94-12708

NATIONAL TRANSPORTATION SAFETY BOARD, WASHINGTON, DC.
Aircraft Accident/Incident Summary Report: Loss of control. Business Express, Inc., Beechcraft 1900C N811BE near Block Island, Rhode Island, December 28, 1991
[PB93-910405] p 22 N94-11044
Special investigation report: Commercial space launch incident, launch procedure anomaly orbital sciences corporation PEGASUS/SCD-1, 80 nautical miles east of Cape Canaveral, Florida, February 9, 1993
[PB93-917003] p 40 N94-11893

NATIONAL UNIV. OF SINGAPORE.
Sun-synchronous and geo-synchronous satellite data utilization for environmental studies p 37 N94-10689

NATURHISTORISCHES MUSEUM, VIENNA (AUSTRIA).
Mineralogy versus bulk composition of the carbonaceous chondrite clast Kaidun 2
p 429 N94-12101

NAUCHNO-ISSLEDOVATELSKII INST. GRAFIT, MOSCOW (RUSSIA).
Advanced methods of permanently joining carbon materials p 63 N94-10057

NAUCHNO-ISSLEDOVATELSKII INST. GRAFIT-EUROPA G.M.B.H. (GERMANY).
Advanced methods of permanently joining carbon materials p 63 N94-10057

NAUCHNO-ISSLEDOVATELSKII INST. GRAFIT USA CORP.
Advanced methods of permanently joining carbon materials p 63 N94-10057

NAUCHNO-PROIZVODSTVENNOE OBEDINENIE PRECISION INSTRUMENTS, MOSCOW (RUSSIA).
Use of low orbital satellite communications systems for humanitarian programs p 308 N94-11808

NAUCHNO-PROIZVODSTVENNOE OBEDINENIE SOYUZ MEDINFORM, MOSCOW (RUSSIA).
US-USSR telemedicine consultation spacebridge to Armenia and Ufa p 308 N94-11809

NAVAL AEROSPACE MEDICAL RESEARCH LAB., PENSACOLA, FL.
Motion and spatial disorientation systems: Special research capabilities
[AD-A265155] p 303 N94-11097
Landing Craft Air Cushion (LCAC) crew selection system manual
[AD-A265158] p 313 N94-11098
Computer software and hardware to determine contrast sensitivity using three methods: Tracking, limits, and constant stimuli
[AD-A265168] p 324 N94-11099
Aircraft windscreens enhance visual search disruption produced by laser glare
[AD-A265167] p 26 N94-11892

NAVAL AIR WARFARE CENTER, WARMINSTER, PA.
Mass properties test procedure for manikin headforms and helmet systems
[AD-A265654] p 315 N94-10296
Paint removal activities in the US Navy
p 126 N94-10614

NAVAL CIVIL ENGINEERING LAB., PORT HUENEME, CA.
Three-dimensional finite element analysis of explosive safety facilities: A technology assessment
[AD-A265700] p 35 N94-12562

NAVAL COMMAND, CONTROL AND OCEAN SURVEILLANCE CENTER, SAN DIEGO, CA.
Application of parallel processing to a surface patch/wire junction EFIE code
[AD-A264965] p 336 N94-10488
Sensor abstractions to support many-robot systems
[AD-A265907] p 180 N94-10803

Some results with the new digital ionosonde in San Diego
[AD-A265178] p 275 N94-11101
Effective software reuse in an embedded realtime system
[AD-A264993] p 326 N94-11220
Femtosecond dynamics, photoexcitation, and ESR spectra of MX chain solids
[AD-A264689] p 399 N94-11263
A portable controller for unmanned ground vehicles
[AD-A264963] p 181 N94-11290
Heterogeneous SuperConcurrent Parallelism (HeSCP)
[AD-A265004] p 336 N94-11293
Shear flow control of gas jets in liquids
[AD-A264673] p 152 N94-11448
Results from a year-long auroral-E measurement campaign
[AD-A265059] p 278 N94-11871
Disturbance Impact Assessment System (DIAS), version 2.0. System design document
[AD-A265251] p 138 N94-11883
Statistical process control in the hybrid microelectronics manufacturing industry: A Navy view point
[AD-A265164] p 145 N94-11884
Nonlinear resonance: Noise-assisted information processing in physical and neurophysiological systems
[AD-A265161] p 313 N94-11890
Feature association without a motion estimate
[AD-A265162] p 138 N94-11891
Polaronic charge separation in mixed-halide MX solids
[AD-A266073] p 403 N94-12345
ISAR motion compensation using the burst derivative measure as a focal quality indicator
[AD-A265647] p 138 N94-12440

NAVAL ENERGY AND ENVIRONMENTAL SUPPORT ACTIVITY, PORT HUENEME, CA.
Immediate response to free product discovery
[PB93-182970] p 265 N94-11015
Catalytic oxidation of organics in vapor streams at remediation sites
[PB93-182962] p 266 N94-11472

NAVAL OCEAN RESEARCH AND DEVELOPMENT ACTIVITY, BAY SAINT LOUIS, MS.
Evaluating ERS-1 ice motion and classification products p 241 N94-11763

NAVAL POSTGRADUATE SCHOOL, MONTEREY, CA.
Exergy decrease in shock waves and boundary layers of space launch vehicles
[AD-A265272] p 42 N94-10493
Design of a matching network for dipole antennas
[AD-A265115] p 136 N94-11158
Applying reliability models to the maintenance of Space Shuttle software p 330 N94-11434
Implementation and use of a computational ray-tracing program for the design and analysis of complex optical systems
[AD-A265075] p 382 N94-11653
The relational-to-object-oriented cross-model accessing capability in a multi-model and multi-lingual database system
[AD-A264911] p 420 N94-11846
An investigation using empirical orthogonal functions and objective analysis to analyse the vertical temperature structure of a gulf stream meander
[AD-A265116] p 289 N94-11868
Lift enhancement of a wing/strake using pneumatic blowing
[AD-A265074] p 26 N94-11872
The rational behavior model: A multi-paradigm, tri-level software architecture for the control of autonomous vehicles
[AD-A265175] p 332 N94-11874
Gallium arsenide dynamic random access memory support circuitry
[AD-A265176] p 320 N94-11875
Design of a continuous resistively loaded monopole antenna
[AD-A265852] p 138 N94-12281
The instrumentation of the multimodel and multilingual user interface
[AD-A265444] p 333 N94-12332
Comparison of multiresolution techniques for digital signal processing
[AD-A265364] p 138 N94-12406

NAVAL RESEARCH LAB., BAY SAINT LOUIS, MS.
Atmospheric correction of AVIRIS data in ocean waters
[AD-A264931] p 288 N94-11287

NAVAL RESEARCH LAB., WASHINGTON, DC.
Start-up imprinting and shock dynamics in laser-target interaction
[DE93-008051] p 172 N94-10150
Two way time transfer results at NRL and USNO
p 353 N94-10983
A detailed study of the photo-injection annealing of thermally diffused InP solar cells p 48 N94-11381
Radiation effects in Ga(0.47)In(0.53)As solar cells
p 52 N94-11404
Advanced concepts theory annual report 1992
[AD-A266132] p 393 N94-11474
Reliability analysis for FDDI dual homing networks
[AD-A266133] p 337 N94-11475
Ultraviolet plume instrument description and plume data reduction methodology
[AD-A266141] p 54 N94-11643
HF-OTH radar performance results
[AD-A266106] p 138 N94-11655
A compact, four-way image splitter
[AD-A266107] p 382 N94-11656
NRL review for 1993
[AD-A265666] p 497 N94-12334
Asynchronous Transfer Mode (ATM) technology: An overview
[AD-A266087] p 383 N94-12413
Yohkoh Bragg Crystal Spectrometer light curves for Ca XIX (3.1631-3.1912A): 1 October 1991 - 30 September 1992
[AD-A266090] p 483 N94-12414
Methanol pan fires in an enclosed space: Effect of pressure and oxygen concentration
[AD-A266108] p 79 N94-12415
Nonlinear analysis of a magnicon output cavity
[AD-A265342] p 145 N94-12424

NAVAL SURFACE WARFARE CENTER, BETHESDA, MD.
Advances in low carbon, high strength ferrous alloys
[AD-A265264] p 85 N94-12532

NAVAL SURFACE WARFARE CENTER, SILVER SPRING, MD.
A method for calculating exact geodetic latitude and altitude
[AD-A265783] p 229 N94-10417

NAVAL UNDERSEA WARFARE CENTER, NEW LONDON, CT.
Preliminary results on backscattering strength from a wind generated bubbly ocean surface
[AD-A265006] p 287 N94-10490

NAVAL UNDERSEA WARFARE CENTER, WEST PALM BEACH, FL.
Underwater hydrophone location survey
p 290 N94-10975

NEBRASKA UNIV., LINCOLN.
Studies and simulations of the DigiCipher system
[NASA-CR-193470] p 321 N94-10343
Interpretation of lunar and planetary electromagnetic scattering using the full wave solutions
p 440 N94-12049

NEGEV UNIV., BEERSHEVA (ISRAEL).
Wave and pseudo-diffusion equations from squeezed states p 347 N94-10607

NEW HAMPSHIRE UNIV., DURHAM.
Terminal Decomposition and Gaseous Sulfur Release from Tidal Wetlands
[NASA-CR-193466] p 267 N94-12451
A preliminary study of the variability and magnitude of the flux of biogenic sulfur gases from a New Hampshire salt marsh p 267 N94-12452
Sulfate reduction and other sedimentary biogeochemistry in a northern New England salt marsh
p 268 N94-12453
The role of certain infauna and vascular plants in the mediation of redox reactions in marine sediments
p 268 N94-12454
Emissions of biogenic sulfur gases from Alaskan tundra p 268 N94-12455
Factors controlling fluxes of volatile sulfur compounds in Sphagnum peatlands p 268 N94-12456
Emissions of sulfur gases from wetlands
p 269 N94-12458
Acetate concentrations and oxidation in salt marsh sediments p 269 N94-12459
Application of static and dynamic enclosures in determining DMS and OCS fluxes in Sphagnum peatlands p 269 N94-12460
Effects of inorganic sulfur addition on fluxes of volatile sulfur compounds in Sphagnum peatlands
p 270 N94-12461
Environmental factors controlling fluxes of dimethyl sulfide in a New Hampshire fen p 270 N94-12462
Sulfur transformations in the sediments of a New Hampshire salt marsh p 270 N94-12463
Biogeochemical factors which regulate the formation and fate of sulfide in wetlands p 270 N94-12464
The effects of acid deposition on sulfate reduction and methane production in peatlands p 270 N94-12465
DMS emissions from Sphagnum-dominated wetlands
p 271 N94-12466
Emissions of biogenic sulfur gases from northern bogs and fens p 271 N94-12467
Elevated acetate concentrations in the rhizosphere of Spartina alterniflora and potential influences on sulfate reduction p 271 N94-12468
Factors controlling sulfur gas exchange in Sphagnum-dominated wetlands p 271 N94-12469
Sulfur gas exchange in Sphagnum-dominated wetlands p 271 N94-12470

NEW MEXICO INST. OF MINING AND TECHNOLOGY, SOCORRO.
Dynamic high-pressure shock compaction of diamond powders
[AD-A266004] p 93 N94-12354

NEW MEXICO STATE UNIV., LAS CRUCES.
Telemetering and telecommunications research
[NASA-CR-193235] p 42 N94-11297

NEW MEXICO UNIV., ALBUQUERQUE.
Experimental and theoretical investigations of Cs-Ba vapor tacitron inverter for power conditioning in space power systems
[DE93-012971] p 48 N94-11372
Glycerol-induced hyperhydration p 309 N94-11996
Carbonaceous chondrite clasts in the Kapoeta howardite p 282 N94-12104
Chondrite thermal histories from Low-CA pyroxene microstructures: Autometamorphism versus prograde metamorphism revisited p 429 N94-12105
SXRF determination of trace elements in chondrule rims in the unequilibrated CO3 chondrite, ALH A77307
p 429 N94-12106
Post-impact alteration of the Manson impact structure
p 282 N94-12188

NEWCASTLE-UPON-TYNE UNIV. (ENGLAND).
Remanent magnetism of HED meteorites: Implications for their evolution and ancient magnetic fields
p 431 N94-12172

NIELS BOHR INST., COPENHAGEN (DENMARK).
Moessbauer spectroscopy of the SNC meteorite Zagami p 428 N94-12016

NIELSEN ENGINEERING AND RESEARCH, INC., MOUNTAIN VIEW, CA.
Turbulence modeling for thrust reverser flow field prediction methods
[AD-A266139] p 154 N94-11641

NIHON UNIV., FUNABASHI (JAPAN).
Study on various cryogenic refrigeration cycles using all purpose refrigerators p 130 N94-11839
The warm eddy detection from NOAA/AVHRR thermal images using the Hough transformation
p 220 N94-12713

NIHON UNIV., TOKYO (JAPAN).
A consideration on principal component analysis of satellite IR data p 193 N94-11909
Instability around an isolated roughness element
p 165 N94-12629

NIPPON ELECTRIC CO. LTD., YOKOHAMA (JAPAN).
Development test on 2 K cooling systems
p 130 N94-11840

NIPPON KOEI CO. LTD., TOKYO (JAPAN).
A method to minimize reference data in classifying satellite remote sensing data into land cover classes
p 219 N94-12705

NIPPON TELEGRAPH AND TELEPHONE PUBLIC CORP., TOKYO (JAPAN).
Squeezed spin states: Squeezing the spin uncertainty relations p 377 N94-10585

NIPPON TELEGRAPH AND TELEPHONE PUBLIC CORP., YOKOSUKA (JAPAN).
Time signal distribution in communication networks based on synchronous digital hierarchy
p 139 N94-10989

NOBEYEMA SOLAR RADIO OBSERVATORY (JAPAN).
Submillimeter wave observation experiment of Earth atmosphere with SIS mixer p 130 N94-11837

NORFOLK STATE UNIV., VA.
Wave generation by contaminant ions
[NASA-CR-193558] p 364 N94-10946

NORGES TEKNISKE HOEGSKOLE, TRONDHEIM.
Structure and properties of an RS Al-Si-Ni-Mn-Zr alloy for high temperature applications p 64 N94-10063

NORTH CAROLINA STATE UNIV., RALEIGH.
Telerobotic control of a mobile coordinated robotic server
[NASA-CR-193465] p 338 N94-10345
Acceleration of positrons in supernova shocks
[NASA-CR-193713] p 425 N94-10511
Memory effects in the organometallic chemical beam epitaxy of compound semiconductors
[NASA-CR-193106] p 399 N94-11439
Remote plasma enhanced chemical vapor deposition of GaP with in situ generation of phosphine precursors
p 399 N94-11440
Lattice-matched heteroepitaxy of wide gap ternary compound semiconductors p 400 N94-11441
Organometallic chemical vapor deposition and characterization of ZnGeP2/GaP multiple heterostructures on GaP substrates p 400 N94-11442
Organometallic chemical vapor deposition and characterization of ZnGe(1-x)Si(x)P2-Ge alloys on GaP substrates p 400 N94-11443

An adaptive and robust control for motion coordination of two-cooperating robot manipulators
p 340 N94-11825

NORTH CAROLINA UNIV., CHAPEL HILL.
Visual encoding of spatial relations
[AD-A266049] p 313 N94-10909
Ellipsometry studies of semiconductors surface cleaning
[AD-A265150] p 142 N94-11094
Thermal-optical switching of a silicon based interference filter
[AD-A265152] p 174 N94-11095
Applications of spectroscopic ellipsometry to microelectronics
[AD-A265148] p 143 N94-11159
Characterization of the Si/SiO2 interfere morphology from quantum oscillations in Fowler-Nordheim tunneling currents
[AD-A265149] p 143 N94-11160
An ellipsometry investigation of nucleation and growth of electron cyclotron resonance plasma deposited silicon films
[AD-A265037] p 401 N94-11651
Applications of in-situ ellipsometry to microwave electron cyclotron resonance plasma processes
[AD-A265197] p 373 N94-11880

NORTH COAST INNOVATION, INC., CLEVELAND, OH.
Dry in-line thermoplastic matrix impregnation, phase 1
[AD-A265016] p 67 N94-11221

NORTH TEXAS RESEARCH AND DEVELOPMENT INST., DENTON.
Controlling chaotic behavior in CO2 and other lasers
[AD-A264811] p 174 N94-10870
Controlling chaotic behavior in a CO2 and other lasers
[AD-A265458] p 176 N94-12372

NORTHEAST LOUISIANA STATE COLL., MONROE.
Classification of Martian deltas p 470 N94-12207

NORTHWESTERN UNIV., EVANSTON, IL.
The legacy of uncertainty p 376 N94-10577
Atomic structures and compositions of internal interfaces
[DE93-014840] p 363 N94-10750
The excitation of cyanogen and ionized carbon in interstellar and extragalactic gas clouds
p 426 N94-11582
Stability and dynamics of spatio-temporal structures
[DE93-011374] p 401 N94-11610

NORWEGIAN DEFENCE RESEARCH ESTABLISHMENT, KJELLER.
Ship traffic monitoring using the ERS-1 SAR
p 253 N94-12521

NORWEGIAN METEOROLOGICAL INST., BLINDERN.
Validation of ERS-1 wind and wave data by use of operational forecast models p 233 N94-11710
Impact of ERS-1 wind/wave/ice data on operational ocean forecasting p 250 N94-12500

NOTRE DAME UNIV., IN.
Single-electron tunneling
[DE93-013337] p 396 N94-10648
An experimental investigation of the sources of propeller noise due to turbulence ingestion p 358 N94-11057

NUCLEAR REGULATORY COMMISSION, WASHINGTON, DC.
Computer models used to support cleanup decision-making at hazardous and radioactive waste sites
[PB93-183333] p 274 N94-10698

NYNEX SCIENCE AND TECHNOLOGY, INC., WHITE PLAINS, NY.
The use of communication technology in medicine
p 306 N94-11800

O

OAK RIDGE ASSOCIATED UNIVERSITIES, INC., WASHINGTON, DC.
Department of Energy fundamentals handbook: Engineering symbology, prints, and drawings
[DE93-012181] p 129 N94-11456

OAK RIDGE NATIONAL LAB., TN.
Heavy-section steel technology program
[DE93-009222] p 184 N94-10155
Optimization of a CO2 laser Thomson scattering alpha particle diagnostic
[DE93-012782] p 173 N94-10160
High heat flux components and plasma surface interactions
[DE93-008786] p 385 N94-10253
High spin properties of nuclei
[DE93-008788] p 358 N94-10254
Laser spectroscopy
[DE93-009403] p 173 N94-10255
Presentations to the Mexican Physics Society on Environmental Contamination
[DE93-009565] p 264 N94-10256
Hydrostatic testing of thick laminated composite cylinders for performance model validation
[DE93-012728] p 184 N94-10264
Position and force control of a vehicle with two or more steerable drive wheels
[DE93-012512] p 177 N94-10269
Multiple Antenna Implementation System (MAntIS)
[DE93-012515] p 131 N94-10270
Potential change in flaw geometry during pressurized-thermal-shock transients
[DE93-009709] p 184 N94-10288
Transport mechanisms acting in toroidal devices: A theoretician's view
[DE93-013463] p 385 N94-10310
Microanalysis of directionally solidified cobalt oxide-zirconia eutectic
[DE93-013207] p 88 N94-10527
Environmental Sciences Division
[DE93-013865] p 264 N94-10650
Looking beyond ITER: Toroidal concept improvement
[DE93-012762] p 388 N94-10744
Low-expansion ceramics initiative
[DE93-011860] p 89 N94-11106
A history of tungsten- and molybdenum-base alloys
[DE93-010283] p 82 N94-11108
Fracture mechanics and full scale pipe break testing for the Department of Environment's New Production Reactor-Heavy Water Reactor
[DE93-005428] p 187 N94-11169
Intense neutron sources for fusion materials studies
[DE93-009782] p 391 N94-11171
Test specifications, specimen design and instrumentation test data interpretation
[DE93-012338] p 188 N94-11367
High-temperature corrosion of ceramic-ceramic composites in a waste incinerator environment
[DE93-012430] p 72 N94-11368
Abbreviations, acronyms, and initialisms frequently used by Martin Marietta Energy Systems, Incorporated
[DE93-012509] p 420 N94-11369
Thermographic properties of eight blue-emitting phosphors
[DE93-011459] p 78 N94-11622
Quality assurance in basic research and R/D
[DE93-010825] p 183 N94-11647
Ceramics technology project database
[DE93-012431] p 91 N94-11672
Ceramic technology project database
[DE93-012432] p 91 N94-11673
An introduction to chordal graphs and clique trees
[DE93-012508] p 332 N94-11695
Proceedings of the Seventh International Symposium on Methodologies for Intelligent Systems (poster session)
[DE93-013470] p 340 N94-12428
Derivation of three closed loop kinematic velocity models using normalized quaternion feedback for an autonomous redundant manipulator with application to inverse kinematics
[DE93-012823] p 340 N94-12543
In-situ crystallization of silicate glass films deposited on alpha- Al2O3
[DE93-012969] p 95 N94-12596
Experiments in mobile robot navigation and range imaging
[DE93-013280] p 341 N94-12598

OBSERVATOIRE DE LA COTE D'AZUR, NICE (FRANCE).
Regional orbit precision in the Mediterranean area
p 39 N94-12530

OBSERVATOIRE DE PARIS-MEUDON (FRANCE).
An ancient inner lake in Maadim Vallis
p 456 N94-12133
Dust in the Martian atmosphere: Polarimetric sensing
p 473 N94-12223

OCEAN RESEARCH AND ENGINEERING, PASADENA, CA.
SAR ocean imaging in the Gulf of Alaska
p 235 N94-11723

OCEANEERING SPACE SYSTEMS, WEBSTER, TX.
Development and evaluation of a predictive algorithm for telerobotic task complexity p 341 N94-11562

OCEANOR, TRONDHEIM (NORWAY).
Oil spill detection using satellite-based SAR: Experience from a field experiment p 253 N94-12522

OFFICE DE LA RECHERCHE SCIENTIFIQUE ET TECHNIQUE OUTRE-MER, NOUMEA (NEW CALEDONIA).
The use of CZCS for primary production estimate in the Pacific p 199 N94-11946

OFFICE NATIONAL D'ETUDES ET DE RECHERCHES AEROSPATIALES, PARIS (FRANCE).
Mechanical properties of magnesium/carbon composites developed by hot pressing under medium pressure p 59 N94-10024
Velocity measurements in hypersonic flows: A review
p 5 N94-10436
Calculations of viscous nonequilibrium flows in nozzles
p 8 N94-10455
Nonequilibrium hypersonic flow in a wind-tunnel nozzle
p 8 N94-10456
Chaos, entropy, and reversibility: A simple example
p 31 N94-11495
Nonlinear and dynamic analysis of flight
p 32 N94-11496

OFFICE NATIONAL D'ETUDES ET DE RECHERCHES AEROSPATIALES, TOULOUSE (FRANCE).
New hypersonic test methods developed at ONERA: The R5 and F4 wind tunnels p 4 N94-10429

OFFICE OF EMERGENCY PREPAREDNESS, ROCKVILLE, MD.
The National Disaster Medical System
p 307 N94-11801

OFFICE OF MANAGEMENT AND BUDGET, WASHINGTON, DC.
Information resources management plan of the Federal Government
[ISBN-0-16-037895-8] p 421 N94-12014

OFFICE OF NAVAL RESEARCH EUROPEAN OFFICE, FPO NEW YORK, NY.
The 27th International Applied Military Psychology Symposium: A Focus on Decision Making Research
[AD-A265278] p 313 N94-11701

OFFICE OF THE SECRETARY OF DEFENSE, WASHINGTON, DC.
National SBIR Phase 3 Commercialization Conference
[AD-A266083] p 417 N94-12410

OFFICINE GALILEO S.P.A., FLORENCE (ITALY).
The surface plasmon spectroscopy as diagnostic technique in microgravity experiments
p 110 N94-10133

OHIO STATE UNIV., COLUMBUS.
Stability of hypersonic flow over a blunt body
p 7 N94-10450
Performance of traffic-alert collision avoidance (TCAS) antennas in the presence of scatterers
[NASA-CR-193569] p 23 N94-11525
Spatial patterns in backscatter strength across the Greenland Ice Sheet p 238 N94-11744

OKINAWA PREFECTURAL OFFICE (JAPAN).
Evaluating the spread of red soil with LANDSAT TM data in coral reefs of Okinawa main island, southwestern *Japan p 212 N94-12668*

OLD DOMINION UNIV., NORFOLK, VA.
Molecular properties of polymeric materials for space applications
[NASA-CR-194370] p 94 N94-12450

OPEN UNIV., MILTON (ENGLAND).
Multiple nitrogen components in lunar soil sample 12023 p 451 N94-12108

OPTICAL SOCIETY OF AMERICA, WASHINGTON, DC.
Nonlinear Dynamics in Optical Systems. Postdeadline papers presented at the Optical Society of America Conference
[AD-A264958] p 375 N94-10486

OREGON STATE UNIV., CORVALLIS.
Nonlinear stability and control study of highly maneuverable high performance aircraft
[NASA-CR-193480] p 25 N94-10344
A preliminary C-band scatterometer model function for the ERS-1 AMI instrument p 233 N94-11715

OREGON UNIV., EUGENE.
Relativistic heavy-ion collisions
[DE93-014844] p 366 N94-11147
Electronic excitation of ground state atoms by collision with heavy gas particles
[NASA-CR-193364] p 366 N94-11360
Theory of elementary particles and accelerator theory. Task C: Experimental high energy physics
[DE93-013139] p 368 N94-11696
A novel photosensitive polyimide resist consisting of a soluble polyimide and a bis(perfluorophenyl azide) as a cross-linker
[AD-A265998] p 93 N94-12353
Examination of the surface second harmonic response at infrared wavelengths
[AD-A265206] p 403 N94-12371
Polymers for microelectronics
[AD-A266036] p 94 N94-12396
Nonlinear optical spectroscopy of Ag(111) in electrolyte and in vacuum
[AD-A265622] p 79 N94-12534
Atmospheric and spectroscopic research in the far infrared
[NASA-CR-193551] p 280 N94-12582

OSAKA PREFECTURE UNIV., SAKAI (JAPAN).
On the formation process of Karman vortex street
p 16 N94-12621
A numerical experiment of boundary layer transition at subcritical Reynolds numbers p 165 N94-12625

OSAKA UNIV., IBARAKI (JAPAN).
Report of the Workshop on Light Particle-Induced Reactions
[DE93-752300] p 360 N94-10317

OSAKA UNIV., SUITA (JAPAN).
Research on two phase flow in microgravity
p 162 N94-12554

OTTAWA UNIV. (ONTARIO).
Giant radiating dyke swarms on Earth and Venus
p 283 N94-12236

OULU UNIV. (FINLAND).
A new and efficient way to join composite pipes
p 63 N94-10054
LAMINV: A computer code for creating laminates having prescribed properties p 65 N94-10069

OXFORD UNIV. (ENGLAND).
Cloud studies using ATSR data p 253 N94-12517

P

PACIFIC NORTHWEST LAB., RICHLAND, WA.
Sensing glass transitions in thin polymer films on acoustic wave microsensors
[DE93-010805] p 87 N94-10295
Development of a balloon-borne stabilized platform for measuring radiative flux profiles in the atmospheric boundary layer
[DE93-013186] p 274 N94-10323
US areal wind resource assessment
[DE93-011905] p 262 N94-11051
The effects of an aggressive environment on the subcritical crack growth of a continuous-fiber ceramic composite
[DE93-011690] p 73 N94-11612

PARAMAX SYSTEMS CORP., HOUSTON, TX.
The role of metrics and measurements in a software intensive total quality management environment
p 329 N94-11428

PARIS VI UNIV. (FRANCE).
Pilot project PPF12. Coastal and fluvial environment in French Guiana: First results of ERS-1 SAR data analysis
p 254 N94-12523

PARIS VI UNIV., VILLEFRANCHE-SUR-MER (FRANCE).
Bi-directional reflectance by oceanic waters studied via Monte-Carlo simulations p 203 N94-11971

PARIS VIII UNIV., VILLETANEUSE (FRANCE).
Transport of heat and mass in near-critical fluids
p 122 N94-10230

PARIS XI UNIV., ORSAY (FRANCE).
Phase transitions and 2D spherical convection in a large icy satellite p 433 N94-12265

PARMA UNIV. (ITALY).
Crystal growth from low temperature vapour phase
p 115 N94-10191

PAVIA UNIV. (ITALY).
Photon number amplification/duplication through parametric conversion p 376 N94-10572

PENNSYLVANIA STATE UNIV., HERSHEY.
Effects of CSF hormones and ionic composition on salt/water metabolism
[NASA-CR-193232] p 300 N94-11045

PENNSYLVANIA STATE UNIV., UNIVERSITY PARK.
Estimation of the direct acoustic radiation from turbulent spots using boundary layer velocity measurements
p 357 N94-10358
In situ detection of tropospheric OH, HO2, NO2, and NO by laser-induced fluorescence in detection chambers at reduced pressures
[NASA-CR-193189] p 274 N94-10701
Fracture behavior of surface-modified ceramics
[DE93-013707] p 88 N94-10710
Flowfield structure of swept shock wave/turbulent boundary-layer interactions p 149 N94-10899
Combustion-induced crack propagation process in a solid-propellant crack cavity p 98 N94-10901
Advanced statistical methods for improved data analysis of NASA astrophysics missions
[NASA-CR-193514] p 425 N94-10943
Polar solvation and electron transfer
[DE93-013328] p 365 N94-11010
Site dependence of the apparent shape of a molecule in STM images: Benzene on Pt(111)
[AD-A263488] p 365 N94-11093
Wave propagation characteristics of short-period crustal phases near ARCESS and NORESS
[AD-A265959] p 275 N94-11102
Numerical simulations on the redistribution of atmospheric trace chemicals through cloud processes
p 265 N94-11189
Materials for adaptive structural acoustic control, volume 3
[AD-A264621] p 358 N94-11262
Ring-opening polymerization of phosphazenes
[AD-A265000] p 90 N94-11292
Experimental proof of the new IR-induced mechanism of crevice corrosion and its consequences regarding protection schemes p 83 N94-11316
Recent developments in piezoelectric and electrostrictive sensors and actuators for smart structures p 70 N94-11332
Shear coaxial injector atomization phenomena for combusting and non-combusting conditions
[NASA-CR-193339] p 152 N94-11526
Active vibration control of adaptive flexible structures using piezoelectric smart sensors and actuators
p 189 N94-11823
Synthesis, characterization, and modification of poly(organophosphazenes), that bear both 2,2,2-trifluoroethoxy and phenoxy groups
[AD-A264913] p 92 N94-11847
Radiation-induced modifications of allylamino-substituted polyphosphazenes
[AD-A264914] p 92 N94-11848
The synthesis of photocrosslinkable chalcone-bearing polyphosphazenes
[AD-A264915] p 92 N94-11849
Applications of multivariate analysis
[AD-A265250] p 347 N94-11882
Advanced thermally stable coal-derived jet fuels: Compositional factors affecting thermal degradation of jet fuels
[AD-A265842] p 99 N94-12282
Ceramic actuators for smart materials
[AD-A265664] p 93 N94-12331
Suppression of the near wall burst process of a fully developed turbulent pipe flow
[AD-A265995] p 161 N94-12352
NiAl alloys for structural uses
[NASA-CR-194113] p 85 N94-12447
HEAO-1 analysis of Low Energy Detectors (LED)
[NASA-CR-194087] p 424 N94-12574

PENNSYLVANIA UNIV., PHILADELPHIA.
Studies in bioorganic chemistry
[AD-A265532] p 55 N94-12011

PERM STATE UNIV. (RUSSIA).
Coupled thermovibrational and thermocapillary convection in liquid bridge (floating zone system)
p 101 N94-10082
Numerical investigations on Marangoni-Benard instability in multi layer systems p 120 N94-10217
Vibrational-thermocapillary parallel flows and stability
p 120 N94-10220
The combined influence of anticonvective and thermocapillary mechanisms on the stability of systems with interface p 121 N94-10223

PHILLIPS LAB., EDWARDS AFB, CA.
Adaptive structures for spacecraft: A USAF perspective p 45 N94-11319

PHILLIPS LAB., HANSCOM AFB, MA.
Effects of energetic particle events on VLF/LF propagation parameters/1989
[AD-A265266] p 275 N94-11013
Effects of satellite spectral resolution and atmospheric water vapor on retrieval of near-ground temperatures
[AD-A264920] p 245 N94-11851
Guidelines for the establishment and operation of an RFP (Request for proposal) library
[AD-A265894] p 417 N94-12360

PHYSICS AND ELECTRONICS LAB. TNO, THE HAGUE (NETHERLANDS).
Validation of directional wave spectra from the ERS-1 during the ESA CAL/VAL campaign p 232 N94-11707
Calibration results for the ERS-1, AIRSAR, and PHARS p 236 N94-11731

PISA UNIV. (ITALY).
Gravity and electric field effects on pool boiling heat transfer p 121 N94-10226
Smart polymeric system for electromechanical transduction p 70 N94-11330

PITTSBURGH UNIV., PA.
Time-resolved optical studies of charge relaxation and charge transfer at electrode interfaces
[DE93-013985] p 398 N94-11117
Characterization of gas-aerosol interaction kinetics using morphology dependent stimulated Raman scattering
[DE93-012324] p 77 N94-11359
The physics of pattern formation of liquid interfaces
[DE93-013333] p 154 N94-11814
Lineament analysis and tectonic interpretation for the Tharsis region p 437 N94-12031
The adsorption and surface reaction of SiCl4 on Si(100)-(2x1)
[AD-A266124] p 79 N94-12538
Experimental particle physics at the University of Pittsburgh
[DE93-013326] p 369 N94-12546

PLAN AND BUDGET ORGANIZATION, TEHERAN (IRAN).
Land use/land cover mapping of central water shed of Iran area based on satellite data interpretation
p 219 N94-12704

PLANETARY SCIENCE INST., TUCSON, AZ.
Deviations from the straight line: Bumps (and grinds) in the collisionally evolved size distribution of asteroids
p 431 N94-12201

PLANNING RESEARCH CORP., ALEXANDRIA, VA.
Software usability assessment guide
[AD-A265017] p 321 N94-10335

POD ASSOCIATES, INC., ALBUQUERQUE, NM.
Dimensional scaling for impact cratering and perforation
[NASA-CR-188259] p 42 N94-10665
The magnitude of impact damage on LDEF materials
[NASA-CR-188258] p 43 N94-10666
Modelling hypervelocity impacts into aluminum structures based on LDEF data p 190 N94-12178
Model of optical scatter from microimpacts on the Hubble Telescope p 384 N94-12189

POLISH ACADEMY OF SCIENCES, WARSAW.
The solving of equations by the method of boundary elements p 326 N94-11182

POLITECNICO DI MILANO (ITALY).
Special problems of 3-D ultrasonic QNDI techniques and applications to composites aerospace structures
p 61 N94-10036
SAR interferometry experiments with ERS-1
p 237 N94-11735

POLITECNICO DI TORINO (ITALY).
Interface reactions of (Ni3Al) ribbons/Al-MMC in ground preparation as preliminary test for microgravity experiments p 123 N94-10237

PRATT AND WHITNEY AIRCRAFT, EAST HARTFORD, CT.
AGBT advanced counter-rotating gearbox detailed design report
[NASA-CR-180883] p 179 N94-10400

PRINCETON UNIV., NJ.
Development of a Delaunay-based adaption scheme with applications to complex three-dimensional rotational flows p 149 N94-10824
The effects of successive distortions on a turbulent boundary layer in a supersonic flow p 14 N94-11058
Toward intelligent flight control p 33 N94-11503
Measurement and modeling of the stability of hydrogenated amorphous silicon solar cells and films after intense illumination p 263 N94-11638
Probability of alamethicin conductance states varies with nonlamellar tendency of bilayer phospholipids
[AD-A264957] p 301 N94-11648
Global organization of tectonic deformation on Venus
p 444 N94-12066

PRINS MAURITS LAB. TNO, RIJSWIJK (NETHERLANDS).
Characterization of the pulse transformer
[AD-A263414] p 143 N94-11298

PUERTO RICO UNIV., RIO PIEDRAS.
The laser ablation of gold films at the electrode surface of a quartz crystal microbalance
[AD-A265535] p 175 N94-12012

PURDUE UNIV., WEST LAFAYETTE, IN.
Surface-enhanced raman spectroscopy of electroactive films of C60 and an Ir-C60 complex on gold: Symmetry lowering, electron localization, and counteraction effects
[AD-A265934] p 396 N94-10705
Fatigue-life behavior and matrix fatigue crack spacing in unnotched SCS-6/Timetal 21S metal matrix composites
[NASA-CR-191467] p 185 N94-10715
Development of an unstructured solution adaptive method for the quasi-three-dimensional Euler and Navier-Stokes equations
[NASA-CR-191161] p 28 N94-10816
A feasibility study regarding the addition of a fifth control to a rotorcraft in-flight simulator
[NASA-CR-193240] p 30 N94-10895
Real-space formation and dissipation dynamics of hexagonal reconstruction on Au(100) in aqueous media as explored by potentiodynamic scanning tunneling microscopy
[AD-A266138] p 368 N94-11658
Electrode potential-induced reconstruction of Au(100): Effect of chemisorption on nanoscale dynamics as probed by the in-situ scanning tunneling microscopy
[AD-A265900] p 404 N94-12388
Solvent dynamical effects in electron transfer: Molecular dynamics simulations of reactions in methanol
[AD-A266061] p 369 N94-12420
Experimental and theoretical high energy physics program
[DE93-013336] p 373 N94-12600

Q

QINGDAO INST. OF OCEANOLOGY (CHINA).
Remote sensing of the suspended matter distribution with high concentration in China Sea p 192 N94-11901
Analysis of the characteristic and mechanism of suspended matter transportation in Huanghe delta sea area using remote sensing techniques p 197 N94-11930
The optical/computer hybrid processing of extracting ocean wave directional spectrum by airborne photograph p 197 N94-11934
Remote sensing of subsurface water temperature profile and backscattering coefficient in the China Sea by Ocean Lidar (OLIDAR) p 203 N94-11970
Simple and low cost image processing system for satellite remote sensing data p 212 N94-12669
Further study of the Non-Regression-Coefficient SST retrieval method p 213 N94-12674
Investigation of meso-scale fronts, eddies and upwellings in China Seas with AVHRR data p 220 N94-12711

QUEENS UNIV., KINGSTON (ONTARIO).
Ripening of immiscible liquid droplets in microgravity with constrained Marangoni drift p 117 N94-10200

R

RADEX, INC., BEDFORD, MA.
Analysis of geophysical measurements and spacecraft interactions
[AD-A266064] p 43 N94-10944

RADIO RESEARCH INST. (USSR).
Elimination of the influence of the atmosphere on the accuracy of solutions to astrometric problems by means of a ground-space VLBI network p 136 N94-11071

RADIOPHYSICS, INC., BOULDER, CO.
Detection of dust impacts by the Voyager planetary radio astronomy experiment
[NASA-CR-193281] p 423 N94-11305
Models of Neptune's smooth recurrent radio emission
[NASA-CR-193283] p 484 N94-11312

RANGE COMMANDERS COUNCIL, WHITE SANDS MISSILE RANGE, NM.
The 17th Transducer Workshop
[AD-A265526] p 141 N94-10509

READING UNIV. (ENGLAND).
Mapping a dynamic playa surface using multitemporal ERS-1 SAR data: First results p 246 N94-12474

REMOTE SENSING APPLICATIONS CENTRE, JAKARTA (INDONESIA).
Flood monitoring in northern part of Central Java by remote sensing technique. Case study: The flooding of Semarang in January, 1990 p 206 N94-11989

REMOTE SENSING APPLICATIONS CONSULTANTS, FARNBOROUGH (ENGLAND).
Temporal monitoring of soil moisture using ERS-1 SAR data p 249 N94-12493

REMOTE SENSING SYSTEMS, INC., SANTA ROSA, CA.
Dependence of oceanic microwave emission on wind direction p 201 N94-11957

REMOTE SENSING TECHNOLOGY CENTER, TOKYO (JAPAN).
Observation of warm current at the boundary from north equatorial current to Kuroshio by NOAA/AVHRR p 214 N94-12676

REMTECH, INC., HUNTSVILLE, AL.
The 1991 version of the plume impingement computer program. Volume 2: User's input guide
[NASA-CR-194191] p 166 N94-12774
The 1991 version of the plume impingement computer program. Volume 1: Description
[NASA-CR-194192] p 166 N94-12775

RENSSELAER POLYTECHNIC INST., TROY, NY.
Task planning with uncertainty for robotic systems
[NASA-CR-193253] p 338 N94-10638
Ballistic electron transport studies using BEEM
[AD-A266029] p 369 N94-12395

RESEARCH INST. FOR ADVANCED COMPUTER SCIENCE, MOFFETT FIELD, CA.
The 1987 RIACS annual report
[NASA-CR-193220] p 324 N94-11046
Summation by parts, projections, and stability
[NASA-CR-194290] p 346 N94-12776

RESEARCH TRIANGLE INST., RESEARCH TRIANGLE PARK, NC.
Multi-band gap and new solar cell options workshop p 54 N94-11418

RHODE ISLAND UNIV., NARRAGANSETT.
Stratigraphy and sedimentology of the K/T boundary deposit in Haiti p 282 N94-12138

RICE UNIV., HOUSTON, TX.
Application of spin-sensitive electron spectroscopies to investigations of electronic and magnetic properties of solid surfaces and epitaxial systems
[DE93-015079] p 76 N94-10854
Radiative properties of strongly magnetized plasmas
[DE93-014098] p 389 N94-11118
Progress toward atomic layer epitaxy of diamond: Diamond films grown one layer at a time
[AD-A265530] p 403 N94-12010

RIJKSWATERSTAAT, RIJSWIJK (NETHERLANDS).
Mapping of sea bottom topography with ERS-1 C-band SAR p 254 N94-12525

RK CARBON FIBERS, INC., PHILADELPHIA, PA.
A new FR water resistant acoustic insulation material for aircraft p 18 N94-10773

ROBERT GORDON'S INST. OF TECH., ABERDEEN (SCOTLAND).
Quantifying disbond area p 61 N94-10038

ROCHESTER UNIV., NY.
Coherence effects in radiometry and in spectroscopy
[DE93-013437] p 75 N94-10519
Quantum noise and squeezing in optical parametric oscillator with arbitrary output coupling p 375 N94-10568
Alleviating memory contention in matrix computations on large-scale shared-memory multiprocessors
[AD-A265009] p 320 N94-11294
Scalable spin locks for multiprogrammed systems
[AD-A265007] p 337 N94-11650
Limitations to the quality of optical phase conjugation by stimulated Brillouin scattering
[AD-A266006] p 383 N94-12389

ROCKWELL INTERNATIONAL CORP., CANOGA PARK, CA.
The 40 kWe S-PRIME Thermionic Design and Technology Demonstration Program
[DE93-004738] p 40 N94-10147

ROCKWELL INTERNATIONAL CORP., DOWNEY, CA.
PTTI-aided ephemeris calculation and rapid data link acquisition for manned space flight p 42 N94-10974

ROME LAB., GRIFFISS AFB, NY.
Presort processor
[AD-A263872] p 382 N94-11300
Preliminary surface-emitting laser logic device evaluation
[AD-A266111] p 383 N94-12416
Problem specific environments for parallel systems
[AD-A266129] p 337 N94-12540

ROME UNIV. (ITALY).
Numerical simulation and experimental results of filament wound CFRP tubes tested under biaxial load p 58 N94-10015
Thermal and chemical non equilibrium hypersonic flow computations p 10 N94-10465
Non classical effects in planar waveguides p 376 N94-10574
On possible applications of smart structures to control of space systems p 45 N94-11342

ROYAL AIR FORCE, HARROGATE (ENGLAND).
The development of alternative paint removal techniques in the RAF p 126 N94-10618

ROYAL INST. OF TECH., STOCKHOLM (SWEDEN).
Liquid phase sintering of tungsten composites under microgravity. Effect of matrix composition p 118 N94-10207
The reaction between titanium carbide and aluminium carbide in liquid aluminium; a microgravity study p 123 N94-10238

RUNZHEIMER INTERNATIONAL, ROCHESTER, WI.
Business fleet refueling assessment
[PB93-189892] p 98 N94-11017

RYUKYU UNIV., OKINAWA (JAPAN).
Trouble areas in the IRT measurement of the Earth surface temperature p 193 N94-11910
Sea surface heat flux in the beginning of the Kuroshio p 195 N94-11923
Properties of spectral reflectance of crown and crown structure of mangrove species in Okinawa p 218 N94-12700

RUHR UNIV., BOCHUM (GERMANY).
Appearance of convective instabilities caused by liquid-liquid phase separation under small buoyancy forces p 120 N94-10221

RUTGERS - THE STATE UNIV., NEW BRUNSWICK, NJ.
Theoretical investigation of 3-D shock wave turbulent boundary layer interactions
[AD-A265275] p 150 N94-11014

RUTGERS - THE STATE UNIV., PISCATAWAY, NJ.
Fracture behavior of ionomers and ionomeric blends
[AD-A265379] p 94 N94-12407

RUTGERS UNIV., NEW BRUNSWICK, NJ.
Observables, measurements and phase operators from a Bohmian perspective p 378 N94-10589
Preliminary results of Mn partitioning experiments on Murchison analogues p 281 N94-12081
The experimental production of matrix lumps within chondrules: Evidence of post-formational processes p 431 N94-12176
Flash melting of chondrule precursors in excess of 1600 C. Series 1: Type 2 (B1) chondrule composition experiments p 431 N94-12177
The Fe/Mn constraint on precursors of basaltic achondrites p 432 N94-12208

RUTHERFORD APPLETON LAB., CHILTON (ENGLAND).
Using transponders with the ERS-1 altimeter to measure orbit altitude to +/- 3 cm p 244 N94-11785

S

SACLANT ASW RESEARCH CENTER, LA SPEZIA (ITALY).
Use of ERS-1 data at Saclant Undersea Research Centre p 233 N94-11714

SANDIA NATIONAL LABS., ALBUQUERQUE, NM.
Radiation hardened nonvolatile memory for space and strategic applications
[DE93-000746] p 319 N94-10146
In-reactor testing of the closed cycle gas core reactor: The Nuclear Light Bulb concept
[DE93-004053] p 370 N94-10149
Sandia ocean modeling system programmer's guide and user's manual
[DE93-007427] p 287 N94-10153
An experimental investigation of high-speed water-entry for full-size and scale-model pointed nose vehicles
[DE93-008491] p 147 N94-10252
Massively parallel multifrontal methods for finite element analysis on MIMD computer systems
[DE93-009838] p 335 N94-10257
An account of Sandia's research booth at Supercomputing 1992: A collaborative effort in high-performance computing and networking
[DE93-012397] p 319 N94-10268
Space nuclear thermal propulsion nuclear element tests at Sandia National Laboratories
[DE93-002301] p 45 N94-10282
Space nuclear technology
[DE93-010184] p 45 N94-10299
Physical optics modelling of Soft X ray Projection Lithography (SXPL) imaging experiments
[DE93-011556] p 374 N94-10339
Extensions of some guidelines for the mechanical design of coaxial compression pin seals
[DE93-012385] p 177 N94-10348
Joint computational and experimental aerodynamic research on a hypersonic vehicle p 6 N94-10445
Proton transport methods for satellite shield modeling
[DE93-013602] p 42 N94-10520
Application of normalized gray-scale correlation
[DE93-013765] p 141 N94-10521
A critical assembly designed to measure neutronic benchmarks in support of the Space Nuclear Thermal Propulsion program
[DE92-040974] p 371 N94-10529
The d-edge shortest-path problem for a Monge graph
[DE93-009828] p 343 N94-10708
Bringing theory to practice: The reality of interprocessor communication
[DE93-012346] p 336 N94-10738
Crack suppression in GaInSb buffer layers initially under tensile stress
[DE93-012839] p 396 N94-10745
High power z pinches as x ray laser photopumps
[DE93-012842] p 173 N94-10746
Rapid thermal processing for strained-layer semiconductor devices
[DE93-013754] p 396 N94-10809
Preparation of carbon monoliths having tailored pore structure from porous polymer precursors
[DE93-011576] p 89 N94-10958
Characterization of a scannerless LADAR system
[DE93-011582] p 174 N94-10959
Finding minimum-quotient cuts in planar graphs
[DE93-011675] p 344 N94-10961
Semiconductor ring lasers
[DE93-012386] p 174 N94-11005
Using a private SMDS/ATM network to provide long-haul supercomputing visualization services
[DE93-010692] p 325 N94-11109
Examination of wall functions for a parabolized Navier-Stokes code for supersonic flow
[DE93-011590] p 14 N94-11111
AD100/ADSIM, ACSL, and MATLAB output comparisons using frequency-response analysis
[DE93-009640] p 47 N94-11122
Animating engineering science results using AVS
[DE93-011591] p 325 N94-11123
Fatigue life prediction for wind turbines: A case study on loading spectra and parameter sensitivity
[DE93-011597] p 263 N94-11173

Development of generic field classes for finite element and finite difference problems
[DE93-011678] p 345 N94-11225

An improved material interface reconstruction algorithm for Eulerian codes
[DE93-011679] p 326 N94-11226

A heterogeneous graphics procedure for visualization of massively parallel solutions
[DE93-009628] p 336 N94-11270

Effect of switched-bias bakes on the postirradiation electrical response of MOS devices
[DE93-009629] p 143 N94-11271

Multiple laser beam combining and phasing using closed-loop control
[DE93-009830] p 175 N94-11283

A new decomposition strategy for parallel bonded molecular dynamics
[DE93-009839] p 366 N94-11284

Relationship between IBICC imaging and SEU in CMOS ICs
[DE93-009854] p 143 N94-11285

Advanced diagnostics for in situ measurement of particle formation and deposition in thermally stressed jet fuels
[DE93-009798] p 98 N94-11366

A model of elementary chemistry and fluid mechanics in the combustion of hydrogen on platinum surfaces
[DE93-012767] p 77 N94-11370

CRESLAF. Version 4.0: A Fortran program for modeling laminar, chemically reacting, boundary-layer flow in cylindrical or planar channels
[DE93-012835] p 152 N94-11371

Parallel molecular dynamics with the embedded atom method
[DE93-010683] p 367 N94-11455

Fullerene superconductors: Phase stability and anomalously low T(sub c)'s in some ternary compounds
[DE93-010687] p 400 N94-11457

Potential techniques for non-destructive evaluation of cable materials
[DE93-008350] p 183 N94-11586

GaAs PCSS: High gain switching and device reliability
[DE93-009851] p 401 N94-11605

Advanced soldering processes
[DE93-009856] p 129 N94-11606

Bounding the Vapnik-Chervonenkis dimension of concept classes parameterized by real numbers
[DE93-011600] p 331 N94-11611

Spaceborne SAR study: LDRD 1992
[DE93-011485] p 232 N94-11623

A thermal ionization model for the sustaining phase of lock-on in GaAs
[DE93-011558] p 144 N94-11624

Finite element simulation of the 2D collapse of a polyelectrolyte gel disk
[DE93-010693] p 91 N94-11665

Si-29 NMR spectroscopy of naturally-shocked quartz from Meteor Crater, Arizona: Correlation to Kieffer's classification scheme p 80 N94-12087

Finding a covering triangulation whose maximum angle is provably small
[DE93-010691] p 334 N94-12593

Improved Many-On-Many ROUTE software description
[DE93-013961] p 334 N94-12608

SCIENCE AND TECHNOLOGY AGENCY, TOKYO (JAPAN).

Space Activities in the Asia Pacific Region
[JTN-93-80421] p 35 N94-10676

Japanese space activities p 36 N94-10682

SCIENCE AND TECHNOLOGY CORP., LAS CRUCES, NM.

An examination of the evolution of radiation and advection fogs
[AD-A266127] p 286 N94-12539

SCIENCE APPLICATIONS INTERNATIONAL CORP., DURHAM, NC.

Methodologies for estimating air emissions from three non-traditional source categories: Oil spills, petroleum vessel loading and unloading, and cooling towers
[PB93-181592] p 266 N94-11471

SCIENCE APPLICATIONS INTERNATIONAL CORP., FALLS CHURCH, VA.

A comparison of the visible and near infrared reflectance of hydrovolcanic palagonite tuffs and Martian weathered soils p 477 N94-12245

SCIENCE APPLICATIONS INTERNATIONAL CORP., HAMPTON, VA.

Radiometer offsets and count conversion coefficients for the Earth Radiation Budget Experiment (ERBE) spacecraft for the years 1987, 1988, and 1989
[NASA-CR-191489] p 286 N94-12772

SCIENCE APPLICATIONS INTERNATIONAL CORP., JOPPA, MD.

P2NBC2 Heat Strain Decision Aid. User's guide, version 2.1
[AD-A266072] p 304 N94-11224

SCIENCE COUNCIL OF JAPAN, TOKYO.

Remote sensing and global environment
p 191 N94-11895

SCIENCE UNIV. OF TOKYO, CHIBA (JAPAN).

The coherent structure in the oceanic turbulence around Japan Islands Chain forced by an air, sea, and solid Earth interaction p 198 N94-11940

Characteristic scales and vortex features of mesoscale vortices observed by the satellites during the winter
p 199 N94-11943

Study on diffusion phenomena of river effluents issued into sea around Japan with satellite remote sensing data
p 212 N94-12664

SCIENTIFIC ORGANIZING COMMITTEE OF PORSEC, SHIZUOKA (JAPAN).

Proceedings of the PORSEC 1992 in Okinawa: Conference for Pacific Ocean Environments and Probing, volume 1
[JTN-93-80418] p 191 N94-11894

Proceedings of the PORSEC 1992 in Okinawa: Conference for Pacific Ocean Environments and Probing, volume 2
[JTN-93-80419] p 207 N94-12635

SCOT CONSEIL, RAMONVILLE (FRANCE).

Integration of ERS-1 data into the European project of agriculture statistics p 248 N94-12490

SCOTT POLAR RESEARCH INST., CAMBRIDGE (ENGLAND).

Investigations of Arctic ice-sheets and glaciers using ERS-1 SAR p 238 N94-11743

Use of ERS-1 SAR to measure ice flux in the East Greenland current p 238 N94-11746

SCRIPPS INSTITUTION OF OCEANOGRAPHY, LA JOLLA, CA.

Wideband beamforming for a sparse nonuniform spaced sensor array
[AD-A265909] p 133 N94-10660

Low power digital recorder development
[AD-A265921] p 170 N94-10704

Statistical description of tectonic motions
[NASA-CR-193701] p 275 N94-10950

Studies of the net surface radiative flux from satellite radiances during FIFE
[NASA-CR-193150] p 230 N94-10953

Satellite-derived photosynthetically available and total solar irradiance at the surface during FIFE's intensive field campaigns p 230 N94-10954

Estimating Photosynthetically Available Radiation (PAR) at the Earth's surface from satellite observations
p 230 N94-10955

Latent and sensible heat flux estimated from ERS-1 data p 244 N94-11783

A reexamination of amino acids in lunar soil
p 452 N94-12109

Topics in pattern formation and chaotic systems
[AD-A265922] p 161 N94-12342

Shear, strain and thermohaline vertical fine structure in the upper ocean
[AD-A265961] p 289 N94-12348

Preliminary analysis of the FLIP array data from the NOBS experiment
[AD-A265911] p 289 N94-12349

Mapping bathymetric slopes from bathymetry data
[AD-A265923] p 290 N94-12350

The WOCE/TOGA Surface Velocity Programme (SVP)
p 216 N94-12691

SEIKAI REGIONAL FISHERIES RESEARCH LAB., NAGASAKI (JAPAN).

Mapping of high density area of benthic diatom in Ariake Sea p 222 N94-12720

SENSORS UNLTD., INC., PRINCETON, NJ.

An indium gallium arsenide charge-coupled device (CCD) for 1-3 micron imaging
[AD-A266134] p 401 N94-11476

SERVICE DE LA PROGRAMMATION DE LA POLITIQUE SCIENTIFIQUE, BRUSSELS (BELGIUM).

Per-field filtering and classification of multitemporal ERS-1 SAR imagery p 247 N94-12485

SEVILLE UNIV. (SPAIN).

Dielectric liquid bridge stabilization in microgravity by means of electric fields p 100 N94-10075

SFA, INC., LANDOVER, MD.

MIL-STDS and PTTI: What's available and what needs to be done p 352 N94-10973

High temperature annealing of minority carrier traps in irradiated MOCVD n(+)p InP solar cell junctions
p 48 N94-11382

SHAANXI ASTRONOMICAL OBSERVATORY, LINTONG (CHINA).

The limit of frequency estimation p 356 N94-11001

SHEFFIELD UNIV. (ENGLAND).

Segmentation and change detection in ERS-1 images over East Anglia p 248 N94-12487

SHORT BROS. AND HARLAND LTD., BELFAST (NORTHERN IRELAND).

Application of composite materials for production nacelle structures p 56 N94-10006

SIGMA RESEARCH, INC., CONCORD, MA.

User's manual for the plume visibility model PLUVUE 2 (revised)
[PB93-188233] p 265 N94-11016

An atmospheric boundary layer stability estimator for urban areas
[AD-A265189] p 279 N94-12422

SIGMA RESEARCH, INC., WESTFORD, MA.

A four-dimensional, mesoscale, non-gaussian multispectral smoke model. Phase 1: Feasibility study
[AD-A264805] p 152 N94-11519

SLOVAK TECHNICAL UNIV., TRNAVA (CZECHOSLOVAKIA).

Weldability of maraging steels p 59 N94-10028

SMITHSONIAN ASTROPHYSICAL OBSERVATORY, CAMBRIDGE, MA.

Status of local oscillators for operating ultra-high resolution frequency discriminators as frequency standards p 353 N94-10981

How diverse is the asteroid belt? p 430 N94-12124

SOCIETE ANONYME BELGE DE CONSTRUCTIONS AERONAUTIQUES, BRUSSELS.

Description of the liquid structure facility architecture and experimental demonstration of the diagnostic capabilities
p 39 N94-10118

SOCIETE NATIONALE DE CONSTRUCTION AERONAUTIQUE, GOSSELIES (BELGIUM).

Development of a fatigue analysis approach for CFRP structures under acoustic loading p 58 N94-10018

Application of the infrared photoacoustic spectroscopy to the study of the cure mechanisms of structural epoxy adhesives p 61 N94-10040

SOCIETY FOR RESEARCH ON BIOLOGICAL RHYTHMS, CHARLOTTESVILLE, VA.

The 2nd Annual Meeting of the Society for Research on Biological Rhythms
[AD-A264869] p 303 N94-10872

SOFTWARE PRODUCTIVITY SOLUTIONS, INC., INDIALANTIC, FL.

System engineering concept demonstration, technology assessments, volume 5
[AD-A265471] p 323 N94-10494

System engineering concept demonstration, trade studies, volume 6
[AD-A265472] p 323 N94-10495

System engineering concept demonstration, process model, volume 3
[AD-A265469] p 333 N94-12008

SOUTHAMPTON UNIV. (ENGLAND).

Mechanical and fatigue properties of fibre reinforced aluminium-lithium alloy and aluminium-lithium MMC based laminates p 58 N94-10022

Multiplexed and distributed optical fibre sensors
p 64 N94-10065

SAR imaging of dynamical features in the English Channel p 234 N94-11721

SOUTHEASTERN OKLAHOMA STATE UNIV., DURANT.

NMR characterization of polymers formed in diazotizing mixtures of luminol and 3-amino-L-tyrosine
[AD-A266093] p 94 N94-12536

SOUTHERN METHODIST UNIV., DALLAS, TX.

Optimization algorithms for integer networks with side constraints for application in routing and scheduling
[AD-A265254] p 322 N94-10492

SOUTHWEST RESEARCH INST., SAN ANTONIO, TX.

Micromechanisms of fatigue crack growth and fracture toughness in metal matrix composites
[AD-A265153] p 187 N94-11096

Origins of Solar Systems Workshop: The Origin, Evolution, and Detectability of Short Period Comets
[NASA-CR-194255] p 427 N94-11628

The long-term dynamical behavior of short-period comets p 427 N94-11629

Microstructure-based fatigue life prediction methods for naval steel structures
[AD-A265429] p 85 N94-12426

SP SYSTEMS, LOS ANGELES, CA.

Advanced phenolic systems for aircraft interiors
p 18 N94-1[illegible]

SPACE BIOMEDICAL RESEARCH INST., HOUSTON, TX.

Joint pain and Doppler-detectable bubbles in altitude (Hypobaric) decompression p 312 N94-11542

Transcranial Doppler ultrasound and the etiology of neurologic decompression sickness during altitude decompression p 312 N94-11544

A mechanism for the reduction in risk of decompression sickness in microgravity environment
p 312 N94-11545

Strategies and methodologies to develop techniques for computer-assisted analysis of gas phase formation during altitude decompression p 312 N94-11547

SPACE COMMAND, PETERSON AFB, CO.
Assured Mission Support Space Architecture (AMSSA) study p 348 N94-11573
SPACE HARDWARE OPTIMIZATION TECHNOLOGY, INC., FLOYDS KNOBS, IN.
Design of multisample, multistep phase partitioning apparatus for use on Space Shuttle Spacelab, and Spacelab missions p 108 N94-10120
SPACE SYSTEMS/LORAL, PALO ALTO, CA.
New experimental techniques for solar cells p 52 N94-11403
SPACE TECHNOLOGY CORP., TOKYO (JAPAN).
Measurement of the thermal conductivity of molten InSb in a drop shaft p 105 N94-10102
SPIRE CORP., BEDFORD, MA.
InGaAs concentrator cells for laser power converters and tandem cells p 50 N94-11394
SPLAV TECHNICAL CENTER, MOSCOW (RUSSIA).
On shape of single crystals grown by FZM in microgravity p 102 N94-10084
CdTe crystal growth by THM with a rotating magnetic field p 107 N94-10116
Results of crystal growth experiments by FZM on Zona facilities in microgravity p 116 N94-10193
SRI INTERNATIONAL CORP., MENLO PARK, CA.
A real-time spoken-language system for interactive problem solving
[AD-A266046] p 324 N94-11104
A formally verified algorithm for interactive consistency under a hybrid fault model
[NASA-CR-4527] p 326 N94-11188
Telescience capability for the Sondre Stromfjord, Greenland, incoherent-scatter radar facility
[NASA-CR-193683] p 136 N94-11206
Forecasting the impact of virtual environment technology on maintenance training p 314 N94-11570
Novel mass spectrometric instrument for gaseous and particulate characterization and monitoring
[DE93-014093] p 272 N94-12783
STANFORD LINEAR ACCELERATOR CENTER, CA.
Optimal routing of IP packets to multi-homed servers
[DE93-010949] p 133 N94-10709
Strange meson spectroscopy in K(omega) and K(phi) at 11 GeV/c and Cherenkov ring imaging at SLD
[DE93-013593] p 363 N94-10748
Quantized conic sections; quantum gravity
[DE93-010950] p 411 N94-10956
LCLS optics: Selected technological issues and scientific opportunities
[DE93-010953] p 175 N94-11468
Tau physics
[DE93-010956] p 367 N94-11469
STANFORD UNIV., CA.
Navier-Stokes flowfield computation of wing/rotor interaction for a tilt rotor aircraft in hover
[NASA-CR-4532] p 13 N94-10758
A laser-cooled cesium fountain frequency standard and a measurement of the frequency shift due to ultra-cold collisions p 352 N94-10976
A multi-variance analysis in the time domain p 146 N94-10999
Theoretical studies of the radar properties of the icy Galilean moons of Jupiter
[NASA-CR-193407] p 434 N94-11361
Measurement of polycyclic aromatic hydrocarbon (PAHs) in interplanetary dust particles p 431 N94-12167
NMR spectroscopy of experimentally shocked single crystal quartz: A reexamination of the NMR shock barometer p 81 N94-12258
Annual Research Briefs, 1992
[NASA-CR-194389] p 155 N94-12284
A local dynamic model for large eddy simulation p 155 N94-12285
Parameterization of subgrid-scale stress by the velocity gradient tensor p 155 N94-12286
Large eddy simulations of time-dependent and buoyancy-driven channel flows p 155 N94-12287
Large eddy simulation of shock turbulence interaction p 155 N94-12289
Application of a dynamic subgrid-scale model to turbulent recirculating flows p 156 N94-12290
Large-eddy simulation of turbulent flow with a surface-mounted two-dimensional obstacle p 156 N94-12291
Similarity states of homogeneous stably-stratified turbulence at infinite Froude number p 156 N94-12292
Application of incremental unknowns to the Burgers equation p 156 N94-12293
Direct simulation of compressible wall-bounded turbulence p 156 N94-12294
Direct numerical simulation of hot jets p 156 N94-12295
Direct numerical simulation of turbulent flow over a backward-facing step p 156 N94-12296
Numerical simulation using vorticity-vector potential formulation p 157 N94-12297
Reynolds stress closure modeling in wall-bounded flows p 157 N94-12298
Application of a Reynolds stress model to separating boundary layers p 157 N94-12299
Progress in modeling hypersonic turbulent boundary layers p 157 N94-12300
Receptivity in parallel flows: An adjoint approach p 157 N94-12301
Local isotropy in high Reynolds number turbulent shear flows p 157 N94-12302
An investigation of small scales of turbulence in a boundary layer at high Reynolds numbers p 157 N94-12303
Probability density distribution of velocity differences at high Reynolds numbers p 158 N94-12304
The ideal Kolmogorov inertial range and constant p 158 N94-12305
The helical decomposition and the instability assumption p 158 N94-12306
Superfluid turbulence p 158 N94-12307
Regeneration of near-wall turbulence structures p 158 N94-12308
Experiments on near-wall structure of three-dimensional boundary layers p 159 N94-12309
Mixing in a stratified shear flow: Energetics and sampling p 159 N94-12311
LIF measurements of scalar mixing in turbulent shear layers p 159 N94-12312
Plane mixing layer vortical structure kinematics p 159 N94-12313
Numerical simulation of the non-Newtonian mixing layer p 159 N94-12314
PDF approach for turbulent scalar field: Some recent developments p 160 N94-12315
The evolution equation for the flame surface density in turbulent premixed combustion p 81 N94-12316
Study and modeling of finite rate chemistry effects in turbulent non-premixed flames p 81 N94-12317
Generation of two-dimensional vortices in a cross-flow p 160 N94-12318
Why does preferential diffusion strongly affect premixed turbulent combustion? p 81 N94-12319
Tensoral: A system for post-processing turbulence simulation data p 75 N94-12320
Low voltage electron beam lithography
[AD-A265358] p 145 N94-12405
STATE DEPT. FOR GEODESY AND CARTOGRAPHY (VIETNAM).
Shoreline change detection using remote sensing and GIS in Vietnam p 196 N94-11928
STATE METEOROLOGICAL INST., SAINT PETERSBURG (RUSSIA).
Non-stationary and non-linear dispersive medium as external field which generates the squeezed states p 380 N94-10605
STATE SCIENCE AND TECHNOLOGY COMMISSION, BEIJING (CHINA).
International Space Year in China p 36 N94-10680
STATE UNIV. OF NEW YORK, ALBANY.
On the importance of mesoscale potential vorticity anomalies and topographic forcing during cyclone redevelopment across the Appalachians: A GALE case study p 284 N94-10822
Compositional heterogeneity within a dumbbell-shaped Apollo 15 green glass: Evidence for simultaneous eruption of different magmas p 470 N94-12209
Oxidation state of the Earth's upper mantle during the last 3800 million years: Implications for the origin of life p 283 N94-12210
Soret diffusion: A possible cause of compositional heterogeneity within tektites p 432 N94-12211
STATE UNIV. OF NEW YORK, BINGHAMTON.
Adaptive reconfigurable flight controls for high angle of attack aircraft agility p 32 N94-11502
STATE UNIV. OF NEW YORK, BUFFALO.
Corrosion and passivation of high temperature superconductors
[AD-A265402] p 405 N94-12586
STATE UNIV. OF NEW YORK, PLATTSBURGH.
Organic matter on the early surface of Mars: An assessment of the contribution by interplanetary dust p 480 N94-12259
Trace element content of chondritic cosmic dust: Volatile enrichments, thermal alterations, and the possibility of contamination p 433 N94-12260
Depletions of sulfur and/or zinc in IDPs: Are they reliable indicators of atmospheric entry heating? p 433 N94-12261
New low-Ni (igneous?) particles among the C and C? types of cosmic dust p 433 N94-12262
STATE UNIV. OF NEW YORK, STONY BROOK.
Determination of concentration profiles at interfaces and surfaces of partially miscible polymer blends
[DE93-013140] p 89 N94-11007
Trajectory pattern inverse dynamics and control of nonlinear dynamics systems with application to flexible structures p 181 N94-11219
Integral equation methods for mixed boundary problem of fracture mechanics p 188 N94-11617
A CM chondrite cluster and CM streams p 432 N94-12215
STIRLING DYNAMICS LTD., BRISTOL (ENGLAND).
Active landing gear control for improved ride quality during ground roll p 27 N94-11345
STORK PRODUCT ENGINEERING, AMSTERDAM (NETHERLANDS).
Design and manufacturing of filament wound thrust cylinder p 57 N94-10010
STRATEGIC DEFENSE INITIATIVE ORGANIZATION, WASHINGTON, DC.
The Satellite Attack Warning and Assessment Flight Experiment (SAWAFE) p 45 N94-11323
STRATHCLYDE UNIV., GLASGOW (SCOTLAND).
Fibre optic strain and temperature measurement in composite materials: A review of the OSTIC programme p 65 N94-10066
The effect of a uniform magnetic field on the onset of steady Marangoni convection in a layer of conducting fluid p 120 N94-10222
Optical fibre techniques for structural monitoring in composites p 69 N94-11324
Smart processing of composite materials for enhanced performance and properties p 69 N94-11325
STUTTGART UNIV. (GERMANY).
Distortions and stresses in thin shells due to anisotropic thermal expansion p 57 N94-10014
The electron beam furnace: A new facility for materials science research p 109 N94-10126
Development of a high specific 1.5 to 5 kW thermal arcjet
[NASA-CR-193133] p 47 N94-11354
SAR-interferometry applying ERS-1: Some preliminary test results p 237 N94-11736
Separation of geoid and sea surface topography in shallow water regions: A first ERS-1 radar altimeter data evaluation p 242 N94-11766
SUPERCONDUCTING SUPER COLLIDER LAB., DALLAS, TX.
A parallel implementation of particle tracking with space charge effects on an Intel iPSC/860
[DE93-012307] p 335 N94-10340
DILUTE: A code for studying beam evolution under RF noise
[DE93-011605] p 133 N94-10960
Nonlinear effects in ferrite tuned cavities
[DE93-014136] p 374 N94-12785
Quark and lepton masses
[DE93-012308] p 370 N94-12787
SURFACE/INTERFACE, INC., MOUNTAIN VIEW, CA.
Charge distribution analysis of catalysts under simulated reaction conditions
[DE93-013604] p 78 N94-11699
SVERDRUP TECHNOLOGY, INC., BROOK PARK, OH.
Lightweight linear alternators with and without capacitive tuning
[NASA-CR-185273] p 140 N94-10505
Interface considerations in Al2O3/NiAl composite
[NASA-CR-191167] p 66 N94-11202
Workshop summary: Receivers for laser power beaming p 54 N94-11419
SVERDRUP TECHNOLOGY, INC., HUNTSVILLE, AL.
Microbiological test results using three urine pretreatment regimes with 316L stainless steel
[NASA-CR-192568] p 299 N94-10360
Spacelab J air filter debris analysis
[NASA-CR-192569] p 301 N94-11201
SWEDISH METEOROLOGICAL AND HYDROLOGICAL INST., NORKOEPING.
Experiences from the Swedish sea ice programme during BEERS-1992 p 239 N94-11751
SWEDISH SPACE CORP., SOLNA.
Microgravity Applications Furnace Facility (MAFF) for parabolic flights p 109 N94-10128
MUZO: The programmable multi zone furnace for gas payloads and sounding rockets p 110 N94-10132
SYDNEY UNIV. (AUSTRALIA).
Ocean wave detection by SAR p 197 N94-11932
Real time processing wave spectra from satellite SAR p 251 N94-12506
Analysis of collinear passes of satellite altimeter data p 208 N94-12642
Surface eddy fluxes from the GEOSAT satellite altimeter p 208 N94-12643
SYRACUSE UNIV., NY.
Design and analysis of an optical interface message processor
[AD-A266079] p 381 N94-10697
Advanced rotorcraft flight simulation: Model development, validation and parallel implementation p 25 N94-11056

Insights into software development in Japan p 330 N94-11435

SYSTEM STUDIES AND SIMULATION, INC., HUNTSVILLE, AL.

Lunar-Ultraviolet Telescope Experiment (LUTE) integrated program plan [NASA-CR-193267] p 424 N94-11356

T

TAISEI CORP., NARASHINO (JAPAN).

Study on sea water purification using a substratum of marine organisms p 217 N94-12696

TAISEI CORP., TOKYO (JAPAN).

Integrated marine survey system p 217 N94-12693

TAISEI CORP., YOKOHAMA (JAPAN).

The flow structure around a cylindrical pier for the flow of transcritical Reynolds number p 169 N94-11944

TAIWAN FISHERIES RESEARCH INST., TUNGKANG.

A study of front dynamics off northeastern Taiwan based on the NOAA-AVHRR satellite remote sensing data p 215 N94-12684

TAMPERE UNIV. OF TECHNOLOGY (FINLAND).

Comparison of Al-Fe alloys produced by PFC and USGA techniques p 58 N94-10019

Tape winding of thermoplastic composites p 60 N94-10035

An ultralight carbon-carbon composite with amorphous matrix p 61 N94-10042

TECHNICAL RESEARCH CENTRE OF FINLAND, ESPOO.

Design with high strength steel: A case of failure and its implications p 58 N94-10017

Studies on the parametric decay of waves in fusion plasmas [DE93-621659] p 390 N94-11148

TECHNICAL UNIV. OF DENMARK, LYNGBY.

Sea ice: A climate component p 232 N94-11705

Greenland Sea observations p 239 N94-11752

TECHNICAL UNIV. OF PRAGUE (CZECHOSLOVAKIA).

Renewable energy sources 1991, part 3 [DE93-605594] p 263 N94-11505

Renewable energy sources 1991, part 2 [DE93-605634] p 263 N94-11506

TECHNION RESEARCH AND DEVELOPMENT FOUNDATION LTD., HAIFA (ISRAEL).

Improvement of method for experimental determination of flutter speed by parameter identification [NASA-CR-193555] p 33 N94-12769

TECHNISCHE HOCHSCHULE, DARMSTADT (GERMANY).

A stochastic-deterministic approach as an alternative to classical cross-over techniques in small ocean basins p 242 N94-11767

TECHNISCHE HOGESCHOOL, EINDHOVEN (NETHERLANDS).

Disturbance, the uncertainty principle and quantum optics p 375 N94-10569

TECHNISCHE HOGESCHOOL, TWENTE (NETHERLANDS).

On the stability of shape memory materials and their properties in static and dynamic applications p 69 N94-11329

TECHNISCHE UNIV., BERLIN (GERMANY).

Studies of critical point phenomena of fluids: Bulk fluids, fluids in pores, and at interfaces p 80 N94-10228

Geoecological monitoring of an agricultural area p 248 N94-12489

TECHNISCHE UNIV., BRUNSWICK (GERMANY).

Stability model of the atmosphere p 32 N94-11500

TECHNISCHE UNIV., DELFT (NETHERLANDS).

Hybrid materials for use at elevated temperatures p 57 N94-10013

A simplicial approach to integer programming [REPT-93-06] p 322 N94-10355

Some environmental aspects of the application of fibre reinforced plastics in structures [LM-998] p 88 N94-10877

Imperfection sensitivity of the Brazier effect for orthotropic cylindrical shells [LR-687] p 186 N94-10879

ERS-1 radar altimetry over the North Atlantic p 242 N94-11772

ERS-1 precise orbit determination p 244 N94-11779

TECHNISCHE UNIV., EINDHOVEN (NETHERLANDS).

A reliable stability test for exponential polynomials [MEMO-COSOR-92-48] p 341 N94-10168

The applicability of neural nets for decision support [MEMO-COSOR-92-49] p 338 N94-10169

Bayesian reliability analysis with imprecise prior probabilities [MEMO-COSOR-92-50] p 183 N94-10170

Operator substitution [MEMO-COSOR-92-51] p 343 N94-10867

An advisor module for tactical and strategic state-oriented planning systems with an application in manpower planning [MEMO-COSOR-92-57] p 416 N94-10868

Sample-data and discrete-time H2 optimal control [MEMO-COSOR-92-53] p 339 N94-10869

Imprecise highest density regions related to intervals of measures [MEMO-COSOR-92-54] p 347 N94-10876

TECHNISCHE UNIV., MUNICH (GERMANY).

Transient three-dimensional numerical simulation of Marangoni flow in a liquid column under microgravity p 101 N94-10079

Numerical simulation of Marangoni convection around gas bubbles in a liquid matrix p 106 N94-10107

A new method for hysteresis measurements developed for C(sub v) measurements at the critical point during the D2-mission p 107 N94-10114

AGF (Automatic Gradient Furnace): A proposed microgravity facility p 112 N94-10141

EUSO-D2-experiment: Unidirectional solidification with quenching of an AlSi11 alloy p 86 N94-10199

Study of vapor bubble growth in a supersaturated liquid p 122 N94-10232

Single bubble experiments in pool boiling: Results from TEXUS 26 p 124 N94-10243

Segmented land use classification of multitemporal ERS-1 SAR data using a majority filter p 245 N94-12472

Extraction of plant and soil parameters from multitemporal ERS-1 SLC data of the Freiburg test site p 248 N94-12491

TEL-AVIV UNIV. (ISRAEL).

Hygroscopic absorption to falling films: The effects of the concentration level [ITN-93-85198] p 148 N94-10391

Boundary element method for eigenvalue problems of thin plates [ITN-93-85199] p 343 N94-10392

Object recognition in industrial environment by means of tactile sensor [ITN-93-85200] p 178 N94-10393

TELECOM SOLUTIONS LTD., SAN JOSE, CA.

Synopsis of timing measurement techniques used in telecommunications p 139 N94-10990

TELEMEDICINE SYSTEMS CORP., MIAMI, FL.

Commercial applications of telemedicine p 306 N94-11798

TELEOS RESEARCH, PALO ALTO, CA.

Acting to gain information [NASA-CR-193399] p 418 N94-10515

TENNESSEE TECHNOLOGICAL UNIV., COOKEVILLE.

Nuclear structure models: Applications and development [DE93-012934] p 368 N94-11813

TENNESSEE UNIV., KNOXVILLE.

Photodetachment studies on few-electron atomic negative ions [DE93-008474] p 358 N94-10154

Wall interference correction based on interface measurements in subsonic wind tunnel testing p 15 N94-11154

Metallographic cooling rates of L-group ordinary chondrites p 429 N94-12061

Determining the relative extent of alteration in CM chondrites p 430 N94-12114

Theoretical investigation of some novel phenomenal in artificially structured semiconductors [AD-A266142] p 405 N94-12587

TENNESSEE UNIV. SPACE INST., TULLAHOMA.

Arcjet space thrusters [NASA-CR-193191] p 46 N94-10700

TEXAS A&M UNIV., COLLEGE STATION.

A phaseonium magnetometer: A new optical magnetometer based on index enhanced media p 375 N94-10565

Failure prediction of thin beryllium sheets used in spacecraft structures [NASA-CR-194164] p 187 N94-11190

Construction and testing of a space ready rectenna [NASA-CR-193310] p 137 N94-11357

Studies of dynamical processes affecting the distribution of stratospheric ozone [NASA-CR-193477] p 279 N94-12560

Pion correlations and calorimeter design for high energy heavy ion collisions [DE93-013861] p 373 N94-12607

TEXAS UNIV., AUSTIN.

Texas experimental tokamak [DE93-013377] p 386 N94-10321

Topex orbit determination using GPS tracking system p 38 N94-10359

Problems in the validation of CFD codes through comparison with experiment p 6 N94-10441

Amperometric biosensors based on 3-dimensional hydrogel-forming epoxy networks [AD-A265528] p 87 N94-10510

Uncertainty relations, zero point energy and the linear canonical group p 378 N94-10590

Toward 10(exp 9) GPS geodesy: Vector baselines, Earth rotation and reference frames [NASA-CR-193184] p 229 N94-10702

System monitoring and diagnosis with qualitative models [NASA-CR-193812] p 323 N94-10711

Vehicular fleet operation on natural gas and propane: An overview [PB93-194603] p 98 N94-10844

The development of an interactive synthesis tool for intelligent controllers of modular, reconfigurable robots p 339 N94-10898

Gyrosheath near the tokamak edge [DE93-012191] p 390 N94-11142

Precision GPS ephemerides and baselines [NASA-CR-194171] p 23 N94-11177

Acoustics of bubbly sediments [AD-A263726] p 288 N94-11299

On the depletion in the outer asteroid belt and the structure of the 4 to 3 mean motion resonance p 426 N94-11596

Accretion disk viscosity and internal waves in disks p 153 N94-11615

Investigation of multiphase railgun systems p 40 N94-11637

Boundary integral solution to the electromagnetic scattering from coated surfaces containing edges, gaps, and periodic gratings p 137 N94-11639

Discrete vortex representation of magnetohydrodynamics [DE93-012190] p 393 N94-11669

Grid optimization and multigrid techniques for fluid flow and transport problems p 154 N94-11824

Polymer-polymer interactions [AD-A265304] p 91 N94-11830

Corrosion behavior of metal matrix composites [AD-A265352] p 85 N94-12404

Glucose electrodes based on cross-linked (Os(bpy)2Cl)(sup +/2+) complexed poly(1-vinylimidazole) films [AD-A265404] p 94 N94-12425

Analysis of interstellar fragmentation structure based on IRAS images [NASA-CR-193518] p 428 N94-12767

TEXAS UNIV., BROWNSVILLE.

Stability by linear processes [NASA-CR-194131] p 323 N94-10862

TEXAS UNIV., DALLAS.

Fitness, autonomic regulation and orthostatic tolerance p 310 N94-11999

TEXAS UNIV., HOUSTON.

Clinical aspects of telemedicine p 306 N94-11795

THIOKOL CORP., BRIGHAM CITY, UT.

Level 3 material characterization of NARC HRPF, HRHU, HRHF, and HRPU [NASA-CR-192579] p 65 N94-10812

TIMING SOLUTIONS CORP., BOULDER, CO.

Advances in time-scale algorithms p 334 N94-10988

TOHOKU UNIV., SENDAI (JAPAN).

Remote sensing and the air-sea boundary layers p 191 N94-11896

Exchange of bay water with ocean current monitored by the NOAA satellite p 193 N94-11908

Physical processes of microwave backscattering from laboratory wind-wave surfaces p 200 N94-11952

On the variability of wind speeds in the North Western Pacific observed by altimeter/GEOSAT and SSM/I/DMSP p 201 N94-11960

Observation of wind and waves by GEOSAT altimeter p 202 N94-11961

Experiment on a high Reynolds number turbulent boundary layer p 164 N94-12617

Criteria for onset of boundary-layer transition on spinning bodies p 164 N94-12620

Traveling disturbances appearing in yawed cylinder boundary layer transition p 166 N94-12632

Study on air-sea interactions in the OMLET (Ocean Mixed Layer Experiment) area using satellite remote sensing p 220 N94-12710

TOKAI UNIV., SHIZUOKA (JAPAN).

Mixed layer heat budget of Kuroshio-Tango triangle using satellite and ship observations p 196 N94-11925

CZCS derived chlorophyll distribution in Antarctic water during austral summer p 199 N94-11947

High-reflectance water mass in Off-Sanriku area observed by CZCS p 200 N94-11951

Availability of wind field over the North Pacific derived from data on ships-of-opportunity and analysis of long-term variabilities p 202 N94-11962

Circulation of North Pacific Intermediate Water p 206 N94-11985
Analysis of GEOSAT wind data p 207 N94-12636
Observations of eddy fields in the Northwest Pacific by GEOSAT altimetry p 207 N94-12639
Characterization of dissolved organic matter in the ocean by using the fluorescence excitation-emission matrix p 211 N94-12659
Evaluation of the method of geostrophic flow using NOAA-AVHRR data p 213 N94-12673
Development of a shuttle AUV for oceanographic measurement p 217 N94-12692

TOKUYAMA COLL. OF TECHNOLOGY (JAPAN).
Coherent structure in near wall turbulence with riblets p 165 N94-12628

TOKYO INST. OF TECH. (JAPAN).
Developmental research of thermal control system in space environment p 162 N94-12551
Simultaneous 3D turbulent large-scale structures in a flood flow by multi-channels measuring system p 165 N94-12624

TOKYO METROPOLITAN FISHERIES EXPERIMENT STATION (JAPAN).
Sea surface temperature images of Geostationary Meteorological Satellite (GMS) and sea truth data from ferry boats p 213 N94-12671

TOKYO UNIV. (JAPAN).
Space Activities in the Asia Pacific Region [JTN-93-80421] p 35 N94-10676
Research results [DE93-753403] p 372 N94-11595
Evaluation of ECMWF latent heat flux in TOGA CD-ROM p 195 N94-11921
Seasonal variation of the surface mixed layer in the subtropical re-circulation area of the North Pacific during OMLET p 195 N94-11924
Appearance, behavior, and oceanic structures of warm streamers in the Kuroshio Oyashio frontal region p 198 N94-11937
Particle dynamics in the western subarctic Pacific: Implications from CZCS imagery p 200 N94-11950
Wind field estimate by using one hour GMS data p 202 N94-11963
Study of climatic effects of cloud-aerosol interaction p 204 N94-11977
SOFAR float tracking in the Shikoku basin p 206 N94-11986
Turbulence modeling and compressibility p 163 N94-12614
Boundary conditions and bifurcations in plane Poiseuille flow p 166 N94-12634
Acoustic estimation of plankton biomass p 218 N94-12699

TOKYO UNIV., SAGAMIHARA (JAPAN).
Laboratory studies on the velocity of fragments from impact disruptions p 189 N94-12359

TOKYO UNIV., TANASHI (JAPAN).
Spontaneous symmetry breaking in QCD [DE93-753080] p 396 N94-10645
Dimensional transition of the space-time at the minimum action near the planck scale [DE93-754192] p 410 N94-10718
Possibility of a crossed-beam experiment involving slow-neutron capture by unstable nuclei rapid-process-tron [DE93-754288] p 363 N94-10720
Proceedings of the Workshop on New Aspects of Quantum Field Theories [DE93-754136] p 411 N94-10887
Double-lambda compound nucleus and the formation of double hypernuclei [DE93-754289] p 365 N94-11040
Development of microstrip gas chamber and application to imaging gamma-ray detector [DE93-754294] p 34 N94-11041
Performance characteristics of the INS 25.5-MHz split coaxial RFQ [DE93-753168] p 144 N94-11508
Development of microstrip gas chambers with multi-chip technology [DE93-753169] p 367 N94-11509

TOKYO UNIV. OF AGRICULTURE AND TECHNOLOGY (JAPAN).
Devices related for thermal control systems used in microgravity p 162 N94-12553

TOLEDO UNIV., OH.
A study of DC-DC converters with MCTs for arcjet power supplies [NASA-CR-193457] p 142 N94-10931
Efficient partitioning and assignment on programs for multiprocessor execution [NASA-CR-193458] p 324 N94-10942
Blading models for TURBAN and CSPAN turbomachine design codes [NASA-CR-191164] p 15 N94-11203

TOMARK INDUSTRIES, INC., WILMINGTON, DE.
The fire properties of insulation bags, as installed and after aircraft operations p 19 N94-10778

TORONTO UNIV., DOWNSVIEW (ONTARIO).
Flow development in a circular pipe in the UTIAS/RPI M = 8.3 gun tunnel p 6 N94-10442
Fiber optic sensing for composite smart structures p 69 N94-11327
Nonlinear aspects of transonic aeroelasticity [UTIAS-RN-345] p 15 N94-11857

TORONTO UNIV. (ONTARIO).
Nonlinear aspects of transonic aeroelasticity p 2 N94-10357
Explorations in quantum gravity: From one loop effective actions to two-dimensional theories p 413 N94-11822
Localized and distributed fiber-optic strain sensors embedded in composite materials [UTIAS-346] p 73 N94-12013
Age of Popigai impact event using the Ar-40 - Ar-39 method p 282 N94-12093
Separation of spallation and terrestrial C-14 in chondrites p 431 N94-12183

TOSHIBA CORP., KAWASAKI (JAPAN).
Development of 4 K refrigerator using highly efficient heat accumulating reservoir p 130 N94-11842

TOULOUSE UNIV. (FRANCE).
Electrohydrodynamic effects in continuous flow electrophoresis observations on Earth and in microgravity p 122 N94-10234

TOYAMA NATIONAL COLL. OF MARITIME TECHNOLOGY, SHINMINATO (JAPAN).
Observation of wave crests by satellite remote sensed data p 207 N94-12638

TRAK MICROWAVE CORP., TAMPA, FL.
A precise GPS-based time and frequency system p 353 N94-10978

TRAKYA UNIV., EDIRNE (TURKEY).
Quantum mechanical effects of topological origin p 378 N94-10594

TRIESTE UNIV. (ITALY).
Estimating the instabilities of N clocks by means of comparison measurements p 356 N94-10997

TRIPLER ARMY MEDICAL CENTER, HONOLULU, HI.
The Department of Clinical Investigation, reports control symbol MED-300(R-1) [AD-A264969] p 304 N94-11649

TRISTAN TECHNOLOGIES, INC., SAN DIEGO, CA.
Large array SQUID magnetometer for NDE [AD-A264799] p 304 N94-11449

TRUETIME, INC., SANTA ROSA, CA.
Disciplined rubidium oscillator with GPS selective availability p 353 N94-10977

TRW SPACE TECHNOLOGY LABS., REDONDO BEACH, CA.
Space Storable Rocket Technology program (SSRT). Option 1 program [NASA-CR-191171] p 46 N94-10938
Gas-Grain Simulation Facility (GGSF). Volume 2: Conceptual design definition [NASA-CR-177613] p 423 N94-11229

TSUKUBA SPACE CENTER (JAPAN).
NASDA activities in space solar power system research, development and applications p 54 N94-11413

TULANE UNIV., NEW ORLEANS, LA.
Momentum management in redundant manipulators for vibration suppression [NASA-CR-194112] p 180 N94-10821

U

UNIFORMED SERVICES UNIV. OF THE HEALTH SCIENCES, BETHESDA, MD.
Tropical medicine: Telecommunications and technology transfer p 305 N94-11793
Satellite, environmental, and medical information applied to epidemiological monitoring p 307 N94-11802

UNIFORMED SERVICES UNIV. OF THE HEALTH SCIENCES, TUSCON, AZ.
International disaster research p 307 N94-11805

UNITED TECHNOLOGIES CORP., WEST PALM BEACH, FL.
Advanced control for airbreathing engines, volume 1: Pratt and Whitney [NASA-CR-189203] p 29 N94-12270
Fatigue in single crystal nickel superalloys [AD-A266116] p 85 N94-12418

UNITED TECHNOLOGIES RESEARCH CENTER, EAST HARTFORD, CT.
Processing and properties of coated HPZ fiber reinforced glass-ceramic matrix composites [AD-A265177] p 92 N94-11876

UNIVERSAL TECHNOLOGY CORP., DAYTON, OH.
Analytical models for describing the mechanical behavior of fiber reinforced composites [AD-A265906] p 74 N94-12347

UNIVERSIDAD BOLIVIANA MAYOR DE SAN SIMON, COCHABAMBA.
Quantum entropy and uncertainty for two-mode squeezed, coherent and intelligent spin states p 377 N94-10586
New squeezed landau states p 379 N94-10601

UNIVERSIDAD CATOLICA DEL NORTE, COQUIMBO (CHILE).
Swordfish (Xiphias gladius) catch distributions relative to environmental features observed from satellites off Coquimbo, Chile (30 deg S) p 216 N94-12688

UNIVERSIDAD NACIONAL AUTONOMA DE MEXICO, MEXICO CITY.
Modelling of dispersal and deposition of impact glass spherules from the Cretaceous-Tertiary boundary deposit p 432 N94-12238

UNIVERSIDAD POLITECNICA DE MADRID (SPAIN).
Effects of axial and centrifugal forces on the stability of liquid bridges p 102 N94-10083
Liquid bridges and floating zones p 102 N94-10085

UNIVERSIDADE DO ESTADO DO RIO DE JANEIRO (BRAZIL).
A spectral nodal method for discrete ordinates problems in x,y geometry [DE93-610128] p 342 N94-10283

UNIVERSITE CATHOLIQUE DE LOUVAIN (BELGIUM).
Stability analysis and aerospace vehicle dynamics p 31 N94-11491
Stability of viscoelastic flow: Physical and numerical considerations p 31 N94-11493
Global considerations for implementation of telemedicine p 305 N94-11792

UNIVERSITEIT TWENTE, ENSCHEDE (NETHERLANDS).
Payload sensitivity in coupled bending and torsional vibrations in flexible beams [MEMO-1102] p 184 N94-10161
Marginal allocations in the core of minimal chain-games [MEMO-1103] p 348 N94-10162
Deformations and recursion operators for evolution equations [MEMO-1104] p 341 N94-10163
Bundle event structures: A non-interleaving semantics for LOTOS [MEMO-INF-92-73] p 320 N94-10164
An efficient medium access control strategy for high speed WDM multiaccess networks [MEMO-INF-92-74] p 131 N94-10165
An object-oriented model for extensible concurrent systems: The composition-filters approach [MEMO-INF-92-87] p 320 N94-10166
A correct and efficient interface for logical query languages with complex objects [MEMO-INF-93-01] p 320 N94-10167
The super vectorfield package for REDUCE. Version 1.0 [MEMO-1099] p 321 N94-10265
The structure of Hilbert flag varieties [MEMO-1095] p 348 N94-10272
Balancing of the normalized right coprime factorization of a nonlinear system [MEMO-1096] p 341 N94-10273
Cycles through particular subgraphs of claw-free graphs [MEMO-1097] p 341 N94-10274
Uni-directional waves over slowly varying bottom. Part 1: Derivation of a KdV-type of equation [MEMO-1098] p 147 N94-10275
On output linearization of observable dynamics [MEMO-1105] p 341 N94-10276
Layering techniques for development of parallel systems: An algebraic approach [MEMO-INF-92-62] p 335 N94-10277
Finite state machine microarchitecture transformations described with relational algebra [MEMO-INF-92-63] p 319 N94-10278
An algebraic approach to incomparable families of formal languages [MEMO-INF-92-82] p 342 N94-10279
Formal specification of the plain UCN layer in LOTOS [MEMO-INF-92-83] p 131 N94-10280
The INTEGRATOR package for REDUCE, version 1.0 [MEMO-1100] p 322 N94-10418
Algorithms for the maximum clique problem [MEMO-1101] p 322 N94-10419

UNIVERSITIES SPACE RESEARCH ASSOCIATION, HOUSTON, TX.
Physiologic mechanisms of circulatory and body fluid losses in weightlessness identified by mathematical modeling p 312 N94-11557

UNIVERSITY COLL., LONDON (ENGLAND).
Preliminary studies on the application of ERS-1 data to topographic mapping p 246 N94-12476

UNIVERSITY OF ELECTRO-COMMUNICATIONS, CHOFU (JAPAN).
Measurement of the surface layer current averaged vertically using Multipaths Inverted Echosounder
p 194 N94-11915
UNIVERSITY OF SOUTH FLORIDA, TAMPA.
Short wavelength crystal fiber devices
[AD-A265716] p 176 N94-12402
UNIVERSITY OF SOUTHERN CALIFORNIA, LOS ANGELES.
Control of jet noise
[NASA-CR-193612] p 358 N94-11176
UNIVERSITY OF SOUTHERN CALIFORNIA, PASADENA.
Sources of Na for the Io atmosphere
p 455 N94-12127
Rhenium-osmium isotope systematics of Group 2A and Group 4A iron meteorites p 431 N94-12182
Isotopic and trace element characteristics of an unusual refractory inclusion from Essebi p 471 N94-12212
UNIVERSITY OF SOUTHERN ILLINOIS, CARBONDALE.
Model reference adaptive control (MRAC) with applications to robotics p 339 N94-11640
UNIVERSITY OF SOUTHERN MISSISSIPPI, HATTIESBURG.
The 13C and 15N solid-state NMR of copolymers of nylon 6 and 7: Observation of a stable pseudohexagonal phase
[AD-A265799] p 94 N94-12381
UTAH STATE UNIV., LOGAN.
Polar mesospheric waves and structure
[AD-A265360] p 279 N94-12561
UTAH UNIV., SALT LAKE CITY.
Understanding cracking failures of coatings: A fracture mechanics approach p 187 N94-11218
Medical informatics and telemedicine: A vision
p 305 N94-11788
High frequency behavior of long and small junctions
[AD-A265670] p 403 N94-12336

V

VANDERBILT UNIV., NASHVILLE, TN.
Design of a CVD reactor for the deposition of diamond in a microgravity environment p 109 N94-10127
VARIAN ASSOCIATES OF CANADA LTD., GEORGETOWN (ONTARIO).
Wide band 140 GHz TWTA p 132 N94-10514
VEGA SPACE SYSTEMS ENGINEERING LTD., HARPENDEN (ENGLAND).
The TREES project: Pre-processing and generation of terrain data for inclusion in an ERS-1 SAR classification scheme p 249 N94-12496
VETERANS ADMINISTRATION HOSPITAL, SEPULVEDA, CA.
Quantitative EEG patterns of differential in-flight workload p 317 N94-11528
VIALE UNIV., ROME (ITALY).
Automatic definition of spectral units in the equatorial regions of Mars p 432 N94-12234
Composition of the Martian aerosols through near-IR spectroscopy p 475 N94-12235
VICTORIA UNIV. (BRITISH COLUMBIA).
Effect of gravity on the dissolution and liquid phase epitaxial growth processes in a horizontal sandwich system p 118 N94-10208
VILLANOVA UNIV., PA.
Squeezing in phase-conjugated resonance fluorescence p 376 N94-10576
VIRGINIA POLYTECHNIC INST. AND STATE UNIV., BLACKSBURG.
New aromatic activated dihalides and bisphenol monomers for the preparation of novel poly(arylene ethers)
[NASA-CR-193190] p 55 N94-10513
Perpendicular blade vortex interaction and its implications for helicopter noise prediction: Wave-number frequency spectra in a trailing vortex for BWI noise prediction
[NASA-CR-193623] p 357 N94-10752
Fire-resistant hydrolytically stable poly(arylene phosphine oxide) material systems p 19 N94-10780
Interstellar scattering and the selection of extragalactic radiosources with highly compact components
p 134 N94-11063
Phase equilibria and volumetric properties for the system NaCl-CaCl2-H2O
[DE93-013590] p 76 N94-11244
Computational mechanics needs study
[NASA-CR-193712] p 327 N94-11279
Research and development of post-classical management tools for government program offices, volume 2
[DE93-010236] p 417 N94-11600
Design, development, and testing of an automated knowledge-acquisition tool to aid problem solving, decision making, and planning
[DE93-010239] p 417 N94-11661
Control of large space structures with varying configuration
[AD-A265764] p 44 N94-12387
Development of the one-component diode-array velocimeter
[AD-A265552] p 171 N94-12533
VIRGINIA UNIV., CHARLOTTESVILLE.
Perceptual response to visual noise and display media
[NASA-CR-193406] p 313 N94-11511
Properties of interfacial tribo-films
[AD-A265591] p 182 N94-12374
VON KARMAN INST. FOR FLUID DYNAMICS, RHODE-SAINT-GENESE (BELGIUM).
Thermal flux measurements in hypersonic flows: A review p 5 N94-10438
Experimental, analytical, and computational methods applied to hypersonic compression ramp flows
p 6 N94-10444

W

WARSAW TECHNICAL UNIV. (POLAND).
Influence of neutral particles concentration on flame propagation in methane-air mixtures at zero and normal gravity conditions p 121 N94-10224
WASHINGTON STATE UNIV., RICHLAND.
Investigation of ZnSe-coated silicon substrates for GaAs solar cells p 52 N94-11405
Review of betavoltaic energy conversion
p 53 N94-11407
WASHINGTON UNIV., SAINT LOUIS, MO.
Non-empirical interatomic potentials for transition metals
[DE93-013705] p 365 N94-11011
Morphology of large impact craters and basins on Venus: Implications for ring formation p 436 N94-12023
Interstellar graphite in Murchison: Continued search for isotopically distinct components p 97 N94-12029
Marslink p 438 N94-12034
Orbital simulations of satellite escape/capture and the origin of satellites such as Triton p 429 N94-12057
Compositional and textural information from the dual inversion of visible, near and thermal infrared remotely sensed data p 258 N94-12097
Graphite solubility and co-vesiculation in basalt-like melts at one-ATM p 463 N94-12173
Crystal-chemistry and partitioning of REE in whitlockite
p 408 N94-12174
Anomalous REE patterns in unequilibrated enstatite chondrites: Evidence and implications
p 431 N94-12191
The rate of chemical weathering of pyrite on the surface of Venus p 477 N94-12246
An interferometric spectral mapper for the Cassini mission to Saturn and Titan
[NASA-CR-193805] p 482 N94-12429
WASHINGTON UNIV., SEATTLE.
Discrete space-time symmetries
[DE93-010199] p 341 N94-10259
Nuclear astrophysics
[DE93-010569] p 425 N94-10292
X ray and gamma ray spectroscopy of solids under pressure
[DE93-014847] p 76 N94-10653
FEFF5: An ab initio multiple scattering XAFS code
[DE93-011000] p 367 N94-11470
Future high precision experiments and new physics beyond Standard Model
[DE93-011004] p 373 N94-11618
Solar neutrinos with three flavor mixings
[DE93-011006] p 483 N94-11619
A generalized Bethe-Weizsaecker mass formula for strange hadronic matter
[DE93-011010] p 368 N94-11620
Quenched chiral logarithms
[DE93-010195] p 346 N94-11663
Sea ice deformation observed with ERS-1 SAR
p 239 N94-11749
Air-sea interaction: Fluxes, a review
p 201 N94-11955
Scatterometer observations: Review
p 201 N94-11956
Identification of cometary and asteroidal particles in stratospheric IDP collections p 430 N94-12115
Role of spatially distributed ion channels in single neuron computation
[AD-A265972] p 79 N94-12351
WATERLOO UNIV. (ONTARIO).
The seasonal Sea Ice Monitoring and Modelling Site (SIMMS): Using ERS-1 in climate research
p 240 N94-11758
New tests of the equivalence principle using non-metric couplings of electromagnetism and gravitation
p 413 N94-11821
Methodological considerations for use of ERS-1 imagery for the delineation of river networks in tropical forest areas p 247 N94-12484
WAYNE STATE UNIV., DETROIT, MI.
Nonlinear response of a clamped-clamped beam with internal resonance under sinusoidal excitation
p 186 N94-10897
Relativistic heavy ion research
[DE93-013127] p 367 N94-11373
Investigation of the radiation resistance of triple-junction a-Si:H alloy solar cells irradiated with 1.00 MeV protons
p 50 N94-11391
WEIGHT (THOMAS H.) AND ASSOCIATES, LONG BEACH, CA.
Fuzzification of ASAT's rule based aimpoint selection
[AD-A266068] p 43 N94-11223
WEIZMANN INST. OF SCIENCE, REHOVOTH (ISRAEL).
Duality twisted boundary conditions in n-sta te Potts models
[DE93-619724] p 346 N94-11811
WELLESLEY COLL., MA.
Submission of Earth-based ring occultation observations to the NASA planetary data system rings discipline node
[NASA-CR-193469] p 427 N94-12557
WEST VIRGINIA STATE COLL., CHARLESTON.
Magnetic Earth Ionosphere Resonant Frequencies (MEIRF) project
[NASA-CR-193182] p 276 N94-11355
WEST VIRGINIA UNIV., MORGANTOWN.
Determination of the viscous acoustic field for liquid drop positioning/forcing in an acoustic levitation chamber in microgravity p 110 N94-10131
WESTINGHOUSE HANFORD CO., RICHLAND, WA.
A facility for testing 10- to 100-kWe space power reactors
[DE92-040420] p 372 N94-11296
WESTINGHOUSE SAVANNAH RIVER CO., AIKEN, SC.
Report on Subgroup on Data Banks for Risk Assessment
[DE93-012150] p 418 N94-10646
Welding tritium aged stainless steel
[DE93-011782] p 181 N94-11228
GRISET certification package
[DE93-011783] p 327 N94-11246
A survey of techniques for corrosion monitoring
[DE93-012131] p 83 N94-11250
Development of a graphical user interface and graphics display for the WIND system
[DE93-011780] p 285 N94-11614
Wind system documentation
[DE93-010381] p 285 N94-11664
WESTLAND AEROSTRUCTURES LTD., EAST COWES (ENGLAND).
The application of advanced materials to aircraft nacelle structures p 57 N94-10011
Factors affecting the embedding of optical fibre sensors in advanced composite structures p 70 N94-11336
WINAND STARING CENTRE, WAGENINGEN (NETHERLANDS).
Land cover monitoring with multi-temporal ERS-1 SAR observations in the Netherlands p 246 N94-12473
WISCONSIN UNIV., MADISON.
Effect of rotation on microgravity floating-zone crystal growth p 101 N94-10080
Reversed-field pinch studies in the Madison Symmetric Torus
[DE93-013464] p 388 N94-10747
Magnetohydrodynamic computation of feedback stabilization of resistive-shell instabilities in the reversed field pinch
[DE93-013466] p 388 N94-10852
Adsorption and dissociation of disilane on Si(001) studied by STM
[AD-A265269] p 402 N94-11684
Plant architecture, growth and radiative transfer for terrestrial and space environments
[NASA-CR-193476] p 302 N94-12559
WITWATERSRAND UNIV., JOHANNESBURG (SOUTH AFRICA).
A structural and petrographic investigation of the pretoria saltpan impact structure p 282 N94-12102
Geophysical signature of the Pretoria saltpan impact structure and a possible satellite crater
p 282 N94-12103
WOODS HOLE OCEANOGRAPHIC INST., MA.
The subduction experiment. Cruise report, R/V Oceanus, cruise number 250 legs 1 and 2. Subduction 2 mooring deployment and recovery cruise, 25 January-26 February 1992
[AD-A264922] p 289 N94-11853
Real-time tomography mooring
[AD-A264923] p 289 N94-11854

Vortex-induced forces on oscillating bluff cylinders
[AD-A265056] p 154 N94-11865
Mean flow and variability in the Kuroshio extension from GEOSAT altimetry data p 209 N94-12650

WORLD METEOROLOGICAL ORGANIZATION, GENEVA (SWITZERLAND).
Technical Conference on Tropical Urban Climates: Extended Abstracts
[WMO/TD-538] p 283 N94-10561

WRIGHT LAB., EGLIN AFB, FL.
Large Aircraft Robotic Paint Stripping (LARPS) system and the high pressure water process
p 127 N94-10623

WRIGHT LAB., WRIGHT-PATTERSON AFB, OH.
Experimental and computational comparisons of Mach 6 high Reynolds number heat transfer and skin friction
p 6 N94-10443
Viscous flow simulation using an upwind method for hexahedral based adaptive meshes
[AD-A265901] p 148 N94-10703
Development and analysis of insulation constructions for aerospace wiring applications p 21 N94-10791
Aircraft smart structures research in the USAF Wright Laboratory p 72 N94-11343
Multidimensional intelligent control for superlight air vehicles p 27 N94-11347
Decoupling of aircraft responses p 32 N94-11497
Modeling nonlinear aerodynamic loads for aircraft stability and control analysis p 32 N94-11499
X-29: Longitudinal instability at high angle-of-attack
p 33 N94-11504
Space truss zero gravity dynamics
[AD-A266130] p 44 N94-12541

WRIGHT STATE UNIV., DAYTON, OH.
GaAs sigma-delta modulator modeling for Analog to Digital Converters (ADC's)
[AD-A263419] p 144 N94-11516

WYOMING UNIV., LARAMIE.
A vibrational spectroscopic study of the structure of electroactive self-assembled monolayers of viologen derivatives
[AD-A265705] p 78 N94-12273
Experiments with energetic (mu)d and (mu)t emitted from solid hydrogen
[DE93-010252] p 373 N94-12542

X

XFORM, INC., COHOES, NY.
Production of reactive sintered nickel aluminide
[DE93-014434] p 83 N94-11127

XIAN INST. OF OPTICS AND PRECISION MECHANICS (CHINA).
On resolution of underwater stereo photogrammetry
p 172 N94-11966

XIAN JIAOTONG UNIV. (CHINA).
A new method of time difference measurement: The time difference method by dual phase coincidence points detection p 357 N94-11002

Y

YAMAGUCHI UNIV., UBE (JAPAN).
Turbulent boundary layer interacting with spanwise periodic longitudinal vortex arrays p 165 N94-12626
Turbulent drag reduction of a d-type rough wall boundary layer with longitudinal ribs placed within the grooves
p 165 N94-12627

YORK UNIV. (ONTARIO).
Publications/Patents/Presentations/Honors/Student eport
[AD-A265136] p 78 N94-11873

YOSU NATIONAL FISHERIES COLL. (REPUBLIC OF KOREA).
Intrusion of Kuroshio warm water into Sagami Bay
p 215 N94-12683

Z

ZENTRALINSTITUT FUER FESTKOERPERPHYSIK UND WERKSTOFFORSCHUNG, DRESDEN (GERMAN D.R.).
Solidification and metastable phase formation of highly undercooled Fe-Cr-Ni alloy melts p 87 N94-10204

ZURICH UNIV. (SWITZERLAND).
Techniques and applications of SAR interferometry for ERS-1: Topographic mapping, change detection, and slope measurement p 236 N94-11734
Monitoring of snowcover in high mountain terrain with ERS-1 SAR p 247 N94-12482

CONTRACT NUMBER INDEX

Typical Contract Number Index Listing

AF PROJ. 2306 .... p 92 N94-11866

CONTRACT NUMBER | PAGE NUMBER | ACCESSION NUMBER

Listings in this index are arranged alphanumerically by contract number. Under each contract number the accession numbers denoting documents that have been produced as a result of research done under that contract are arranged in ascending order. The page number helps to locate the citation in the abstract section. The accession number denotes the number by which the citation is identified.

AF PROJ. RM3-3-F-60 .... p 35 N94-12562
AF PROJ. 2306 .... p 92 N94-11866
AF PROJ. 2312 .... p 94 N94-12536
AF PROJ. 2401 .... p 44 N94-12541
AF PROJ. 2404 .... p 148 N94-10703
AF PROJ. 3048 .... p 99 N94-12282
AF PROJ. 4600 .... p 382 N94-11300
AF PROJ. 5581 .... p 337 N94-12540
AF PROJ. 7231 .... p 316 N94-12346
AF PROJ. 7719 .... p 314 N94-12276
AF PROJ. 9993 .... p 417 N94-12360
AF-AFOSR-0077-87 .... p 381 N94-10735
AF-AFOSR-0080-90 .... p 112 N94-10172
AF-AFOSR-0089-88 .... p 77 N94-11265
AF-AFOSR-0090-93 .... p 345 N94-11280
AF-AFOSR-0093-90 .... p 16 N94-12377
AF-AFOSR-0102-90 .... p 381 N94-10735
AF-AFOSR-0147-90 .... p 302 N94-12441
AF-AFOSR-0149-89 .... p 403 N94-12336
AF-AFOSR-0152-91 .... p 99 N94-12564
AF-AFOSR-0154-91 .... p 304 N94-11681
AF-AFOSR-0177-89 .... p 74 N94-12401
AF-AFOSR-0184-91 .... p 79 N94-12378
AF-AFOSR-0205-90 .... p 301 N94-12417
AF-AFOSR-0242-91 .... p 347 N94-11882
AF-AFOSR-0263-89 .... p 176 N94-12402
AF-AFOSR-0266-86 .... p 150 N94-11014
AF-AFOSR-0303-89 .... p 420 N94-11520
AF-AFOSR-0328-90 .... p 73 N94-11686
AF-AFOSR-0352-91 .... p 92 N94-11862
AF-AFOSR-0411-91 .... p 401 N94-11515
AF-AFOSR-0472-89 .... p 331 N94-11680
AF-AFOSR-0479-89 .... p 91 N94-11830
ARC-91-132-CO-10783-91-I-302-0 .. p 416 N94-11473
ARPA ORDER 8021 .... p 73 N94-12344
ARPA ORDER 8162 .... p 142 N94-10818
ARPA ORDER 8930 .... p 320 N94-11294
p 337 N94-11650
ASI-91-RS-63 .... p 235 N94-11728
ASI-91-RS-70 .... p 235 N94-11728
B/SC1-900617 .... p 100 N94-10074
BE-3062-89/BREU-268 .... p 60 N94-10030
p 60 N94-10031
BMFT-01-QC-85229 .... p 103 N94-10089
BMFT-01-QS-8901 .... p 241 N94-11765
BMFT-01-QS-90144 .... p 233 N94-11711
BMFT-01-QS-9014 .... p 251 N94-12509
p 252 N94-12510
BMFT-01-QV-8873 .... p 109 N94-10124
BRITE/EURAM-0173 .... p 69 N94-11328
CICYT-ESP88-0586-C02-02 .... p 104 N94-10095
CICYT-PB86-651 .... p 119 N94-10214
CICYT-PB90-264 .... p 119 N94-10214
CRG-92.05 .... p 342 N94-10351
CSA-9F007-1-80-22 .... p 80 N94-10248
DA PROJ. 1L1-61102-AH-43 .... p 97 N94-10489
DA PROJ. 1L1-61102-AH-45 .... p 319 N94-10724
DA PROJ. 1L1-62618-AH-80 .... p 16 N94-11870
p 405 N94-12563
DA PROJ. 3M1-62787-A-874 .... p 311 N94-12364
DA PROJ. 3M1-62787-A-879 .... p 315 N94-11291
p 311 N94-12423
DA PROJ. 3M2-63002-D-995 .... p 418 N94-10491
DAAA15-87-D-0021 .... p 75 N94-10337
DAAD07-89-C-0035 .... p 286 N94-12539
DAAD07-91-C-0133 .... p 152 N94-11519
DAAD07-91-C-0135 .... p 279 N94-12422
DAAL01-92-C-0217 .... p 132 N94-10514
DAAL02-90-C-0071 .... p 304 N94-11224
DAAL03-89-K-0044 .... p 94 N94-12407
DAAL03-89-K-0092 .... p 33 N94-11503
DAAL03-91-G-0123 .... p 345 N94-11280
DAAL03-92-C-0039 .... p 401 N94-11476
DAAL03-92-G-0418 .... p 395 N94-10416
DAAL04-92-C-0011 .... p 67 N94-11221
DARA-FKZ-50-EE-9115/22 .... p 248 N94-12489
DARA-50-QV-9101 .... p 112 N94-10143
DARA-50-WM-9110-5 .... p 112 N94-10143
DASG60-93-C-0005 .... p 43 N94-11223
DE-AC02-76CH-00016 .... p 173 N94-10287
p 140 N94-10300
p 394 N94-10301
p 359 N94-10302
p 359 N94-10303
p 359 N94-10304
p 359 N94-10308
p 75 N94-10338
p 287 N94-10517
p 169 N94-10526
p 410 N94-10528
p 88 N94-10891
p 400 N94-11457
p 400 N94-11458
p 84 N94-11459
p 400 N94-11467
p 368 N94-11620
p 373 N94-12601
p 374 N94-12782
DE-AC02-76CH-03000 .... p 146 N94-12603
p 370 N94-12781
DE-AC02-76CH-03073 .... p 385 N94-10159
DE-AC02-78ET-51013 .... p 391 N94-11170
DE-AC02-83CH-10093 .... p 262 N94-10258
DE-AC02-85ER-40194 .... p 364 N94-10754
DE-AC02-87NV-10649 .... p 182 N94-12605
DE-AC02-91CH-10491 .... p 182 N94-11438
DE-AC03-76SF-00098 .... p 371 N94-10156
p 408 N94-10261
p 380 N94-10608
p 423 N94-11059
DE-AC03-76SF-00515 .... p 133 N94-10709
p 363 N94-10748
p 411 N94-10956
p 175 N94-11468
p 367 N94-11469
DE-AC03-86SF-16298 .... p 373 N94-11694
DE-AC03-89ER-51114 .... p 385 N94-10159
p 385 N94-10289
p 325 N94-11139
p 137 N94-11453
p 393 N94-11514
p 394 N94-12544
p 394 N94-12545
DE-AC03-89ER-53277 .... p 393 N94-11514
DE-AC03-92SF-19138 .... p 40 N94-10147
DE-AC04-76DP-00613 .... p 381 N94-10647
p 188 N94-11460
p 144 N94-11478
p 144 N94-11479
DE-AC04-76DP-00789 .... p 319 N94-10146
p 370 N94-10149
p 287 N94-10153
p 147 N94-10252
p 335 N94-10257
p 319 N94-10268
p 45 N94-10282
p 385 N94-10289
p 45 N94-10299
p 374 N94-10339
p 177 N94-10348
p 6 N94-10445
p 42 N94-10520
p 141 N94-10521
p 371 N94-10529
p 343 N94-10708
p 336 N94-10738
p 396 N94-10745
p 173 N94-10746
p 396 N94-10809
p 89 N94-10958
p 174 N94-10959
p 344 N94-10961
p 174 N94-11005
p 325 N94-11109
p 14 N94-11111
p 47 N94-11122
p 325 N94-11123
p 263 N94-11173
p 345 N94-11225
p 326 N94-11226
p 336 N94-11270
p 143 N94-11271
p 175 N94-11283
p 366 N94-11284
p 143 N94-11285
p 98 N94-11366
p 77 N94-11370
p 152 N94-11371
p 367 N94-11455
p 400 N94-11457
p 393 N94-11514
p 183 N94-11586
p 401 N94-11605
p 129 N94-11606
p 331 N94-11611
p 232 N94-11623
p 144 N94-11624
p 91 N94-11665
p 334 N94-12593
p 334 N94-12608
DE-AC05-76OR-00001 .... p 128 N94-11028
DE-AC05-76OR-00033 .... p 88 N94-10527
p 95 N94-12596
DE-AC05-84ER-40150 .... p 346 N94-11663
DE-AC05-84OR-21400 .... p 184 N94-10155
p 173 N94-10160
p 385 N94-10253
p 358 N94-10254
p 173 N94-10255
p 264 N94-10256
p 184 N94-10264
p 177 N94-10269
p 131 N94-10270
p 184 N94-10288
p 385 N94-10310
p 88 N94-10527
p 264 N94-10650
p 388 N94-10744
p 89 N94-11106
p 82 N94-11108
p 187 N94-11169
p 76 N94-11244
p 188 N94-11367
p 72 N94-11368
p 420 N94-11369
p 137 N94-11453
p 393 N94-11514
p 78 N94-11622
p 183 N94-11647
p 91 N94-11672
p 91 N94-11673
p 332 N94-11695
p 340 N94-12428
p 340 N94-12543
p 95 N94-12596
p 341 N94-12598
DE-AC06-76RL-01830 .... p 87 N94-10295
p 274 N94-10323
p 262 N94-11051
p 73 N94-11612
DE-AC06-87RL-10930 .... p 372 N94-11296
DE-AC07-76ID-01570 .... p 365 N94-10952
p 76 N94-11140
p 83 N94-11141
p 163 N94-12604
DE-AC08-88NV-10617 .... p 419 N94-11137
DE-AC09-89SR-18035 .... p 418 N94-10646

p 181 N94-11228
p 327 N94-11246
p 83 N94-11250
p 285 N94-11614
p 285 N94-11664
DE-AC12-76SN-00052 .... p 84 N94-11488
DE-AC21-92MC-29116 .... p 272 N94-12783
DE-AC22-92BC-14881 .... p 88 N94-10749
DE-AC22-92PC-92106 .... p 78 N94-11699
DE-AC34-90DP-62349 .... p 41 N94-11282
DE-AC35-89ER-40486 .... p 335 N94-10340
p 133 N94-10960
p 374 N94-12785
p 370 N94-12787
DE-AI01-91CE-50306 .... p 55 N94-11362
DE-AI03-79DP-40092 .... p 172 N94-10150
DE-FC07-91ID-13074 .... p 144 N94-11609
DE-FG01-90CE-15467 .... p 82 N94-11008
DE-FG01-91CE-15492 .... p 83 N94-11127
DE-FG02-84ER-45130 .... p 365 N94-11011
DE-FG02-84ER-45131 .... p 154 N94-11814
DE-FG02-85ER-13370 .... p 300 N94-10652
DE-FG02-85ER-45205 .... p 398 N94-11115
DE-FG02-85ER-45211 .... p 402 N94-11700
DE-FG02-85ER-53198 .... p 388 N94-10747
DE-FG02-85ER-53212 .... p 388 N94-10852
DE-FG02-86ER-45252 .... p 88 N94-10710
DE-FG02-86ER-45254 .... p 400 N94-11457
DE-FG02-87ER-40333 .... p 373 N94-12542
DE-FG02-87ER-45307 .... p 398 N94-11012
DE-FG02-87ER-60522 .... p 301 N94-11648
DE-FG02-88ER-45373 .... p 396 N94-10648
DE-FG02-89ER-14020 .... p 365 N94-11010
DE-FG02-89ER-14024 .... p 263 N94-11116
DE-FG02-89ER-14062 .... p 398 N94-11117
DE-FG02-89ER-45396 .... p 91 N94-11698
DE-FG02-89ER-45403 .... p 363 N94-10750
DE-FG02-90ER-14119 .... p 75 N94-10519
p 375 N94-10568
DE-FG02-90ER-45437 .... p 89 N94-11007
DE-FG02-90ER-54092 .... p 393 N94-11512
p 393 N94-11513
DE-FG02-90ER-61029 .... p 266 N94-11671
DE-FG02-91CE-23810 .... p 411 N94-10853
p 89 N94-11145
p 89 N94-11146
DE-FG02-91ER-40646 .... p 369 N94-12546
DE-FG02-91ER-40672 .... p 370 N94-12609
DE-FG02-91ER-40681 .... p 373 N94-12600
DE-FG02-91NP-00119 .... p 417 N94-11600
p 417 N94-11661
DE-FG02-92ER-14263 .... p 365 N94-11029
DE-FG02-92ER-14303 .... p 401 N94-11610
DE-FG02-92ER-40713 .... p 367 N94-11373
DE-FG02-92ER-45465 .... p 95 N94-12596
DE-FG02-92ER-61480 .... p 77 N94-11359
DE-FG02-92ER-75708 .... p 48 N94-11372
DE-FG02-92ER-75839 .... p 55 N94-11675
DE-FG02-93ER-75840 .... p 318 N94-11817
DE-FG03-88ER-53275 .... p 385 N94-10289
DE-FG03-89ER-13991 .... p 147 N94-10320
DE-FG03-89ER-51121 .... p 393 N94-11514
DE-FG03-91ER-61198 .... p 190 N94-11674
DE-FG05-80ET-53088 .... p 385 N94-10289
p 390 N94-11142
p 393 N94-11669
DE-FG05-85ER-13456 .... p 358 N94-10154
DE-FG05-85ER-40200 .... p 378 N94-10590
DE-FG05-86ER-45233 .... p 76 N94-10854
DE-FG05-86ER-53217 .... p 366 N94-11172
DE-FG05-88ER-40437 .... p 373 N94-12607
DE-FG05-88ER-53267 .... p 386 N94-10321
DE-FG05-89ER-14065 .... p 76 N94-11244
DE-FG05-90ER-75596 .... p 400 N94-11457
DE-FG05-91ER-14213 .... p 389 N94-11118
DE-FG05-91ER-40642 .... p 145 N94-11645
DE-FG05-92ER-40694 .... p 368 N94-11813
DE-FG06-84ER-45163 .... p 76 N94-10653
DE-FG06-84ER-60265 .... p 267 N94-11697
DE-FG06-85ER-40224 .... p 368 N94-11696
DE-FG06-86ER-13530 .... p 273 N94-10305
p 273 N94-10319
DE-FG06-88ER-40427 .... p 341 N94-10259
DE-FG06-90ER-40561 .... p 425 N94-10292
p 373 N94-11618
p 483 N94-11619
p 368 N94-11620
DE-FG06-90ER-45415 .... p 367 N94-11470
DE-FG06-90ER-45425 .... p 400 N94-11458
DE-FG06-91ER-40614 .... p 346 N94-11663
DE-FG06-91ER-40637 .... p 366 N94-11147
DE-FG22-92PC-92542 .... p 84 N94-11816
DFG-GR-361/30-1 .... p 242 N94-11767
DFG-STR-117/29-1 .... p 106 N94-10107
DGICYT-PB-90-0905 .... p 100 N94-10075
DGICYT-PS-90-0011 .... p 104 N94-10095
DLA900-90-D-0305 .... p 81 N94-10297
DNA-MIPR-88-503 .... p 170 N94-10873
DTFA01-88-Z-0200 .... p 24 N94-11863
DTFA01-91-Y-01004 .... p 23 N94-10933
DTFA01-93-Z-02012 .... p 23 N94-11103
DTFR53-90-C-00025 .... p 422 N94-10736
EPA-IAG-DW-89934598 .... p 267 N94-11845
EPA-68-D9-0067 .... p 265 N94-11016
EPA-68-D9-0173 .... p 266 N94-11471
ESA-9915/92/F/EM .... p 416 N94-10145
ESTEC-7337/87/NL/PB(SC) .... p 109 N94-10126
p 111 N94-10135
ESTEC-7337/87/NL/PB .... p 111 N94-10137
ESTEC-8431/89/F/BZ .... p 117 N94-10201
ESTEC-8822/90/NL/PB(SC) .... p 107 N94-10117
ESTEC-9638/91/NL/JSC .... p 86 N94-10195
FWF-P8476 .... p 237 N94-11737
F04611-91-M-0149 .... p 87 N94-10508
F04701-88-C-0089 .... p 274 N94-10496
p 276 N94-11463
p 91 N94-11487
p 383 N94-12341
p 44 N94-12394
p 146 N94-12565
F19628-88-C-0089 .... p 283 N94-10336
F19628-89-C-0068 .... p 43 N94-10944
F19628-89-C-0150 .... p 278 N94-11852
F19628-89-K-0001 .... p 278 N94-12277
F19628-90-C-0002 .... p 23 N94-11103
p 331 N94-11652
p 24 N94-11863
F19628-90-C-0003 .... p 337 N94-11881
F19628-90-K-0044 .... p 275 N94-11102
F19628-91-C-0011 .... p 284 N94-11113
F30602-90-C-0021 .... p 323 N94-10494
p 323 N94-10495
p 333 N94-12008
F30602-90-C-0036 .... p 337 N94-11829
F30602-91-C-0048 .... p 381 N94-10697
F33615-87-C-0003 .... p 331 N94-11679
F33615-87-C-2748 .... p 6 N94-10442
F33615-89-C-5605 .... p 21 N94-10791
F33615-89-C-5609 .... p 74 N94-12347
F33615-89-C-5708 .... p 340 N94-12411
F33615-90-C-1405 .... p 144 N94-11516
F33615-90-C-1437 .... p 382 N94-11421
F33615-90-C-3002 .... p 154 N94-11641
F33615-90-C-3211 .... p 419 N94-11288
F33615-91-C-5708 .... p 127 N94-10623
F33615-92-C-2213 .... p 99 N94-12275
F49620-87-K-0005 .... p 7 N94-10450
F49620-88-C-0062 .... p 92 N94-11876
F49620-88-C-0070 .... p 301 N94-11583
F49620-88-C-0076 .... p 7 N94-10451
F49620-88-C-0082 .... p 7 N94-10450
F49620-89-C-0045 .... p 44 N94-12387
F49620-89-C-0050 .... p 90 N94-11281
F49620-92-C-0026 .... p 304 N94-11449
F49620-92-C-0077 .... p 171 N94-11420
F49620-92-J-0003 .... p 155 N94-12286
F49620-92-J-0032 .... p 322 N94-10492
F49620-92-J-0114 .... p 313 N94-10909
F49620-92-J-0150 .... p 138 N94-12338
F49620-92-J-0181 .... p 303 N94-10872
F49620-92-J-0184 .... p 79 N94-12403
F49620-92-J-0196 .... p 278 N94-11828
F49620-92-J-0467 .... p 382 N94-11286
F49629-89-C-0014 .... p 16 N94-11889
GM-32614 .... p 301 N94-11648
GRI-5092-810-2365 .... p 98 N94-11017
JPL-958003 .... p 428 N94-12767
JPL-959294 .... p 233 N94-11715
p 235 N94-11724
JPL-959351 .... p 233 N94-11715
p 235 N94-11724
KSOEF-91-08-00-05 .... p 380 N94-10611
MDA903-88-D-0019 .... p 321 N94-10335
MDA903-89-C-0003 .... p 332 N94-11850
MDA903-90-C-0006 .... p 417 N94-11856
MDA972-92-C-0034 .... p 142 N94-10818
MDA972-92-C-0071 .... p 383 N94-12444
MIPR-FY1455-91N-0638 .... p 99 N94-12282
MIPR-91MM1519 .... p 311 N94-12364
MOD-D/ER1/9/4/2029/RARDE .... p 78 N94-11855
MOE-01646010 .... p 197 N94-11936
MOE-03248216 .... p 200 N94-11951
NA-89-AA-D-SG053 .... p 266 N94-11451
NAGW-0512 .... p 267 N94-12451
p 270 N94-12462
NAGW-1101 .... p 266 N94-11374
NAGW-1168 .... p 485 N94-12589
NAGW-1196 .... p 108 N94-10120
NAGW-1278 .... p 139 N94-12778
NAGW-1298 .... p 428 N94-12770
NAGW-1311 .... p 485 N94-12771
NAGW-1333 .... p 338 N94-10638
NAGW-1356 .... p 152 N94-11526
NAGW-1408 .... p 424 N94-12768
NAGW-1431 .... p 231 N94-11521
NAGW-1575 .... p 302 N94-12559
NAGW-1736 .... p 47 N94-11354
NAGW-1801 .... p 482 N94-12429
NAGW-1809 .... p 9 N94-10461
NAGW-1868 .... p 482 N94-12446
NAGW-1913 .... p 424 N94-12768
NAGW-1917 .... p 425 N94-10943
NAGW-1930 .... p 484 N94-11486
NAGW-1934 .... p 484 N94-11486
NAGW-1954 .... p 484 N94-11486
NAGW-1964 .... p 434 N94-11361
NAGW-2049 .... p 433 N94-12257
NAGW-2128 .... p 387 N94-10641
NAGW-2220 .... p 445 N94-12070
p 433 N94-12257
NAGW-2381 .... p 425 N94-11153
NAGW-2416 .... p 381 N94-10735
NAGW-2540 .... p 109 N94-10127
NAGW-2598 .... p 241 N94-11761
NAGW-2629 .... p 278 N94-11886
NAGW-2717 .... p 23 N94-11177
NAGW-273 .... p 204 N94-11975
NAGW-2771 .... p 269 N94-12457
NAGW-28 .... p 445 N94-12070
p 445 N94-12071
p 478 N94-12251
NAGW-3062 .... p 233 N94-11715
p 235 N94-11724
NAGW-3083 .... p 416 N94-11599
NAGW-3201 .... p 33 N94-12769
NAGW-512 .... p 268 N94-12453
p 268 N94-12454
p 268 N94-12455
p 269 N94-12457
p 269 N94-12459
NAGW-748 .... p 445 N94-12070
p 445 N94-12071
NAGW-812 .... p 108 N94-10120
NAGW-992 .... p 279 N94-12560
NAG1-1041 .... p 366 N94-11199
NAG1-1042 .... p 170 N94-10948
NAG1-1057 .... p 274 N94-10701
NAG1-1058 .... p 23 N94-11525
NAG1-1081 .... p 25 N94-10344
NAG1-1096 .... p 358 N94-11176
NAG1-1100 .... p 399 N94-11439
NAG1-1110 .... p 76 N94-10713
NAG1-1119 .... p 357 N94-10752
NAG1-1145 .... p 345 N94-11280
NAG1-1250 .... p 55 N94-10513
NAG1-1270 .... p 180 N94-10821
NAG1-1283 .... p 338 N94-10345
NAG1-1316 .... p 185 N94-10715
NAG1-1427 .... p 366 N94-11360
NAG1-1478 .... p 136 N94-11084
NAG1-675 .... p 327 N94-11279
NAG1-963 .... p 280 N94-12582
NAG2-264 .... p 434 N94-10823
NAG2-392 .... p 310 N94-12001
NAG2-507 .... p 323 N94-10711
NAG2-514 .... p 311 N94-12007
NAG2-543 .... p 240 N94-11754
NAG2-659 .... p 310 N94-12002
NAG2-696 .... p 318 N94-10865
NAG2-722 .... p 316 N94-12365
NAG2-736 .... p 300 N94-11180
NAG2-750 .... p 315 N94-11627
NAG2-814 .... p 313 N94-11511
p 427 N94-12557
NAG3-1005 .... p 110 N94-10131
NAG3-1076 .... p 413 N94-12343
NAG3-1094 .... p 105 N94-10100
NAG3-1102 .... p 142 N94-10931
NAG3-1127 .... p 28 N94-10816
NAG3-1159 .... p 46 N94-10700
NAG3-1165 .... p 15 N94-11203
NAG3-1221 .... p 112 N94-10172
NAG3-1368 .... p 137 N94-11357
NAG3-1371 .... p 364 N94-10946
NAG3-776 .... p 386 N94-10346
NAG3-827 .... p 85 N94-12447
NAG3-833 .... p 50 N94-11391
NAG3-954 .... p 405 N94-12570
NAG3-975 .... p 324 N94-10942
NAG5-1131 .... p 425 N94-10511
NAG5-1261 .... p 483 N94-10949
NAG5-1267 .... p 276 N94-11355
NAG5-1402 .... p 424 N94-12573
NAG5-1490 .... p 274 N94-10726
NAG5-1491 .... p 42 N94-11297
NAG5-1612 .... p 321 N94-10343
NAG5-1643 .... p 426 N94-11590
NAG5-1728 .... p 136 N94-11206

NAG5-1807 p 231 N94-11309
NAG5-1936 p 229 N94-10702
NAG5-2006 p 324 N94-10932
NAG5-2056 p 484 N94-10507
NAG5-2187 p 326 N94-11197
NAG5-2210 p 323 N94-10862
NAG5-669 p 280 N94-12583
NAG5-900 p 230 N94-10953
NAG5-905 p 275 N94-10950
NAG5-941 p 424 N94-12574
NAG5-983 p 427 N94-12566
NAG8-243 p 185 N94-10712
NAG8-790 p 56 N94-12588
NAG8-916 p 286 N94-12580
NAG8-941 p 397 N94-10819
NAG9-106 p 429 N94-12106
NAG9-280 p 187 N94-11190
NAG9-422 p 320 N94-12558
NAG9-437 p 429 N94-12106
NAG9-43 p 431 N94-12182
NAG9-497 p 282 N94-12104
p 429 N94-12105
NAG9-56 p 408 N94-12174
NAG9-574 p 331 N94-11522
NAG9-626 p 46 N94-10911
NAG9-81 p 429 N94-12058
p 429 N94-12059
p 443 N94-12060
NANB1H1173 p 149 N94-10851
NASA ORDER A-41524-C p 412 N94-11523
NASA ORDER H-13030-D p 375 N94-10506
NASA ORDER H-20750-D p 424 N94-11356
NASA ORDER T-9297-R p 312 N94-11558
NASW-4574 p 435 N94-12015
NASW-4617 p 423 N94-11305
NASW-4670 p 332 N94-11688
NASW-4697 p 484 N94-11312
NAS1-18224 p 55 N94-10947
NAS1-18605 p 343 N94-10642
p 323 N94-10643
p 326 N94-11196
NAS1-18936 p 142 N94-11131
NAS1-18969 p 326 N94-11188
NAS1-19161 p 279 N94-12572
NAS1-19247 p 55 N94-10947
p 52 N94-11401
NAS1-19258 p 50 N94-11394
NAS1-19480 p 343 N94-10642
p 323 N94-10643
p 149 N94-10810
p 326 N94-11196
p 318 N94-11198
p 345 N94-11277
p 337 N94-11308
NAS1-19570 p 286 N94-12772
NAS1-19592 p 50 N94-11394
NAS10-11400 p 348 N94-11568
NAS10-11624 p 315 N94-11258
NAS2-13326 p 418 N94-10515
NAS2-13408 p 423 N94-11229
NAS2-13721 p 346 N94-12776
NAS3-22826 p 278 N94-11702
NAS3-24342 p 179 N94-10400
NAS3-25087 p 146 N94-12433
NAS3-25266 p 140 N94-10505
p 66 N94-11202
p 51 N94-11397
NAS3-25459 p 29 N94-12272
NAS3-25712 p 146 N94-12773
NAS3-25951 p 29 N94-12271
NAS3-25952 p 29 N94-12270
NAS3-26244 p 49 N94-11390
NAS3-26246 p 46 N94-10938
NAS3-26387 p 41 N94-10512
NAS3-26494 p 74 N94-12594
NAS5-30127 p 231 N94-11236
NAS5-30376 p 375 N94-10564
NAS5-30431 p 483 N94-11048
NAS5-30788 p 428 N94-12595
NAS5-30911 p 204 N94-11975
NAS5-31000 p 350 N94-10963
NAS5-31363 p 204 N94-11975
NAS5-31734 p 204 N94-11975
NAS8-34763 p 82 N94-10804
NAS8-36479 p 285 N94-11598
NAS8-36641 p 177 N94-10341
NAS8-36955 p 347 N94-10757
NAS8-37814 p 299 N94-10360
p 301 N94-11201
NAS8-37824 p 46 N94-10934
NAS8-37857 p 433 N94-10144
NAS8-38100 p 65 N94-10812
NAS8-38423 p 166 N94-12774
p 166 N94-12775
NAS8-38609 p 185 N94-10342
p 180 N94-10815
p 483 N94-12427
p 279 N94-12581
NAS8-38862 p 152 N94-11526
NAS8-38978 p 73 N94-11484
NAS8-39131 p 125 N94-11483
NAS8-39209 p 41 N94-10826
p 41 N94-10827
NAS9-11410 p 423 N94-11183
NAS9-17720 p 308 N94-11991
NAS9-17900 p 27 N94-10664
p 43 N94-10666
p 314 N94-11538
NA90AA-D-SG424 p 154 N94-11865
NCC1-139 p 94 N94-12450
NCC2-0374 p 283 N94-10725
NCC2-127 p 300 N94-11045
NCC2-387 p 324 N94-11046
NCC2-460 p 155 N94-12284
NCC2-55 p 13 N94-10758
NCC2-617 p 25 N94-11150
NCC2-653 p 34 N94-10930
NCC2-671 p 30 N94-10895
NCC2-686 p 150 N94-10912
NCC2-712 p 186 N94-10937
NCC2-729 p 15 N94-11195
NCC2-775 p 24 N94-12355
NCC3-233 p 342 N94-10362
p 151 N94-11192
p 152 N94-11376
p 152 N94-11377
p 152 N94-11481
NCS-81-0209-M-002A-08 p 219 N94-12708
NERC-GR3/ERS-1/1-3 p 238 N94-11743
NERC-GR3/8507 p 238 N94-11743
NGL-31-001-252 p 33 N94-11503
NGT-50836 p 431 N94-12176
p 431 N94-12177
NIVR-02905N p 111 N94-10140
NRFH-1444 p 375 N94-10570
NSC-80-0209-M056-01 p 215 N94-12684
NSF AST-89-02087 p 136 N94-11070
NSF CCR-90-05633 p 337 N94-11650
NSF CDA-88-227240 p 337 N94-11650
NSF CDS-88-22724 p 320 N94-11294
NSF CHE-91-96214 p 380 N94-10606
p 380 N94-10611
NSF CTS-87-19509 p 156 N94-12290
NSF CTS-90-15217 p 101 N94-10080
NSF CTS-92-17505 p 157 N94-12303
NSF DMR-92-02210 p 400 N94-11442
NSF DMS-91-05661 p 378 N94-10589
NSF DMS-92-11820 p 345 N94-11280
NSF DPP-91-13962 p 239 N94-11752
NSF DPP-91-15521 p 443 N94-12060
NSF INT-91-00685 p 379 N94-10603
NSF MIP-91-16113 p 326 N94-11197
NSF OCE-80-18460 p 268 N94-12454
NSF OCE-82-14863 p 268 N94-12454
NSF OCE-84-15687 p 269 N94-12459
NSF OCE-85-11431 p 154 N94-11865
NSF OCE-85-15639 p 268 N94-12454
NSF OCE-85-18491 p 269 N94-12459
NSF OCE-86-15055 p 269 N94-12459
NSF OCE-91-16020 p 221 N94-12718
NSF PHY-90-21139 p 380 N94-10608
NSG-3188 p 181 N94-11157
NSG-7156 p 434 N94-10817
NWO-62-58 p 342 N94-10279
N00014-C-90-0098 p 289 N94-11854
N00014-82-0280 p 79 N94-12538
N00014-83-K-4130 p 79 N94-12373
N00014-85-C-0206 p 187 N94-11096
N00014-85-K-0225 p 340 N94-12537
N00014-86-K-0691 p 331 N94-11657
N00014-87-J-1248 p 67 N94-11260
N00014-88-K-0207 p 221 N94-12718
N00014-88-K-0621 p 405 N94-12586
N00014-89-C-0179 p 154 N94-11865
N00014-89-C-0282 p 88 N94-10863
N00014-89-D-0142 p 133 N94-10660
p 170 N94-10704
p 161 N94-12342
p 289 N94-12349
N00014-89-J-1178 p 142 N94-11094
p 174 N94-11095
p 143 N94-11159
p 143 N94-11160
p 401 N94-11651
p 373 N94-11880
N00014-89-J-1225 p 94 N94-12381
N00014-89-J-1261 p 403 N94-12371
p 79 N94-12534
N00014-89-J-1301 p 402 N94-11654
p 369 N94-11826
p 402 N94-11827
p 404 N94-12438
N00014-89-J-1343 p 156 N94-12291
N00014-89-J-1350 p 77 N94-11264
N00014-89-J-1545 p 78 N94-11683
N00014-89-J-1755 p 411 N94-10874
N00014-89-J-1829 p 175 N94-12012
N00014-89-J-3116 p 85 N94-12404
N00014-89-J-3174 p 290 N94-12350
N00014-90-C-0003 p 278 N94-12392
N00014-90-C-0085 p 324 N94-11104
N00014-90-C-0148 p 240 N94-11754
N00014-90-C-0228 p 340 N94-12398
N00014-90-J-1024 p 300 N94-11020
N00014-90-J-1099 p 289 N94-12348
N00014-90-J-1124 p 370 N94-10584
N00014-90-J-1148 p 93 N94-12380
N00014-90-J-1167 p 78 N94-12273
N00014-90-J-1209 p 366 N94-11100
p 413 N94-11877
N00014-90-J-1212 p 401 N94-11518
N00014-90-J-1490 p 289 N94-11853
N00014-90-J-1627 p 79 N94-12351
N00014-90-J-1702 p 301 N94-11648
N00014-90-J-1915 p 405 N94-12587
N00014-91-C-0124 p 85 N94-12418
N00014-91-C-0214 p 85 N94-12426
N00014-91-C-0219 p 73 N94-12344
N00014-91-C-0264 p 145 N94-12333
N00014-91-C-2173 p 93 N94-12354
N00014-91-F-0201 p 301 N94-11648
N00014-91-J-1052 p 221 N94-12718
N00014-91-J-1064 p 161 N94-12352
N00014-91-J-1194 p 90 N94-11292
p 92 N94-11847
p 92 N94-11848
p 92 N94-11849
N00014-91-J-1316 p 338 N94-10487
p 304 N94-11261
p 339 N94-11289
N00014-91-J-1338 p 145 N94-11819
p 95 N94-12577
p 95 N94-12585
N00014-91-J-1409 p 396 N94-10705
p 368 N94-11658
p 404 N94-12388
p 369 N94-12420
N00014-91-J-1550 p 403 N94-12010
N00014-91-J-1608 p 161 N94-12352
N00014-91-J-1629 p 402 N94-11684
N00014-91-J-1630 p 365 N94-11093
N00014-91-J-1786 p 93 N94-12340
N00014-91-J-1809 p 288 N94-11299
N00014-91-J-1883 p 279 N94-12561
N00014-91-J-1886 p 55 N94-12011
N00014-91-J-1896 p 85 N94-12393
N00014-91-J-1910 p 78 N94-11873
N00014-91-J-1922 p 93 N94-12331
N00014-91-J-1976 p 404 N94-12375
N00014-91-J-4072 p 155 N94-12286
N00014-92-C-0101 p 90 N94-11222
N00014-92-C-0140 p 240 N94-11754
N00014-92-C-2218 p 176 N94-12382
N00014-92-J-1015 p 405 N94-12442
N00014-92-J-1277 p 369 N94-12395
N00014-92-J-1292 p 171 N94-12533
N00014-92-J-1412 p 93 N94-12353
p 94 N94-12396
N00014-92-J-1459 p 332 N94-11878
N00014-92-J-1505 p 182 N94-12374
N00014-92-J-1510 p 358 N94-11262
N00014-92-J-1611 p 159 N94-12311
N00014-92-J-1726 p 154 N94-11865
N00014-92-J-1801 p 320 N94-11294
p 337 N94-11650
N00014-92-J-1810 p 146 N94-12584
N00014-93-C-0051 p 174 N94-10870
p 176 N94-12372
N00014-93-C-0118 p 339 N94-11049
N00014-93-C-2044 p 403 N94-12339
N00014-93-J-0023 p 369 N94-12379
N00014-93-1-0215 p 395 N94-10416
N00014-93-1-0419 p 171 N94-12391
PHYS-9113926 p 378 N94-10596
POD PROJ. 960-12-171 p 43 N94-10666
PROJ. 91-09 p 419 N94-10723
RTOP 039-09-01-25 p 284 N94-10940
RTOP 142-20-37 p 231 N94-11378
RTOP 144-10-10 p 323 N94-10639
RTOP 144-50-50 p 41 N94-10512
RTOP 199-14-11-13 p 310 N94-11998
RTOP 199-14-12-03 p 311 N94-12004
RTOP 199-14-12-04 p 311 N94-12003
RTOP 199-21-12-07 p 300 N94-11191
RTOP 199-45-16-11 p 484 N94-10759
p 485 N94-12434
p 373 N94-12435
RTOP 324-89-00 p 485 N94-10356

RTOP 474-12-10 ..... p 183 N94-11167
RTOP 474-17-10 ..... p 40 N94-10640
RTOP 476-14-15-01 ..... p 245 N94-12432
RTOP 505-53-1A ..... p 88 N94-10864
RTOP 505-59-36 ..... p 1 N94-10936
p 30 N94-11259
RTOP 505-61-51 ..... p 25 N94-10935
RTOP 505-62-10 ..... p 28 N94-10816
RTOP 505-62-11 ..... p 28 N94-11238
RTOP 505-62-21 ..... p 151 N94-11192
p 151 N94-11253
p 152 N94-11377
RTOP 505-62-30-01 ..... p 12 N94-10675
RTOP 505-62-41 ..... p 29 N94-12271
p 29 N94-12272
RTOP 505-62-50 ..... p 319 N94-10724
p 30 N94-11251
p 29 N94-11255
p 170 N94-11310
RTOP 505-62-52 ..... p 39 N94-10764
p 150 N94-10939
p 15 N94-11133
p 327 N94-11232
p 151 N94-11256
RTOP 505-62-61 ..... p 29 N94-12270
RTOP 505-63-1A ..... p 55 N94-11362
RTOP 505-63-36-06 ..... p 318 N94-10814
RTOP 505-63-5B ..... p 188 N94-11254
RTOP 505-63-50-04 ..... p 67 N94-11276
RTOP 505-63-50-15 ..... p 26 N94-11587
p 16 N94-12421
RTOP 505-63-52 ..... p 74 N94-12449
RTOP 505-63-53 ..... p 185 N94-10361
RTOP 505-64-10-13 ..... p 326 N94-11188
RTOP 505-68-00 ..... p 315 N94-11627
RTOP 505-68-10 ..... p 174 N94-11132
RTOP 505-68-50 ..... p 13 N94-10707
p 283 N94-10725
RTOP 505-69-50 ..... p 15 N94-11203
p 327 N94-11231
RTOP 505-90-00 ..... p 419 N94-11352
RTOP 505-90-5K ..... p 342 N94-10362
p 152 N94-11376
p 152 N94-11481
RTOP 505-90-52-01 ..... p 343 N94-10642
p 323 N94-10643
p 149 N94-10810
p 326 N94-11196
p 318 N94-11198
p 345 N94-11277
p 345 N94-11280
p 337 N94-11308
RTOP 506-40-41-02 ..... p 148 N94-10644
RTOP 506-40-91-02 ..... p 162 N94-12571
RTOP 506-41-11 ..... p 47 N94-11307
p 48 N94-11380
p 404 N94-12430
RTOP 506-41-31 ..... p 163 N94-12576
RTOP 506-41-52 ..... p 43 N94-10756
p 278 N94-11702
RTOP 506-42-31 ..... p 180 N94-10760
p 46 N94-10761
p 47 N94-11252
RTOP 506-42-72 ..... p 40 N94-10811
RTOP 506-43-61-02 ..... p 55 N94-10947
RTOP 506-59-31 ..... p 327 N94-11274
RTOP 506-69-50 ..... p 13 N94-10820
RTOP 506-71-00 ..... p 315 N94-11375
RTOP 506-72-21 ..... p 146 N94-12433
RTOP 510-01-50 ..... p 186 N94-10762
p 66 N94-11135
p 66 N94-11202
p 89 N94-11204
p 67 N94-11237
p 90 N94-11257
p 188 N94-11482
p 74 N94-12431
p 74 N94-12594
RTOP 533-02-34 ..... p 28 N94-11205
RTOP 533-02-35 ..... p 26 N94-11233
RTOP 533-02-37 ..... p 30 N94-11134
RTOP 535-03-10 ..... p 14 N94-10892
RTOP 535-03-22 ..... p 179 N94-10400
RTOP 535-05-10 ..... p 28 N94-11234
RTOP 537-01-20-01 ..... p 279 N94-12572
RTOP 538-01-11 ..... p 46 N94-10765
RTOP 578-22-26-40 ..... p 235 N94-11724
p 207 N94-12637
RTOP 578-22-29-40 ..... p 207 N94-12637
RTOP 578-35-02-20 ..... p 237 N94-11741
RTOP 583-02-21 ..... p 140 N94-10505
RTOP 584-03-11 ..... p 46 N94-10763
p 55 N94-12569
RTOP 586-03-11 ..... p 142 N94-11131
RTOP 592-43-21-01 ..... p 484 N94-11278
RTOP 665-45-20-01 ..... p 286 N94-12772
RTOP 694-03-03 ..... p 1 N94-11703
RTOP 763-23-45-85 ..... p 185 N94-10715
RTOP 926-00-00 ..... p 288 N94-11358
SBA-5645-OA-90 ..... p 417 N94-11844
SBIR-02.08-8581A ..... p 166 N94-12774
p 166 N94-12775
SBIR-14.03-6642 ..... p 146 N94-12773
SC-02N0165768 ..... p 43 N94-10666
SDIO84-89-C-0043 ..... p 180 N94-10706
SLS41B/2437 ..... p 324 N94-10893
p 154 N94-11859
p 16 N94-11888
p 161 N94-12437
SRC-GR/G/57277 ..... p 8 N94-10454
SRI PROJ. 2724 ..... p 136 N94-11206
SSTC-75760605 ..... p 203 N94-11970
SWRI PROJ. 15-5296 ..... p 427 N94-11628
T-91-11 ..... p 267 N94-11864
W-31-109-ENG-38 ..... p 319 N94-10318
p 169 N94-10326
p 142 N94-10951
p 397 N94-10962
p 398 N94-11004
p 150 N94-11072
p 398 N94-11073
p 419 N94-11105
p 372 N94-11124
p 276 N94-11138
p 143 N94-11454
p 144 N94-11607
p 346 N94-11608
p 368 N94-11613
p 182 N94-11625
p 340 N94-11644
W-7405-ENG-36 ..... p 384 N94-10157
p 384 N94-10158
p 371 N94-10260
p 273 N94-10285
p 126 N94-10293
p 97 N94-10294
p 132 N94-10315
p 361 N94-10349
p 65 N94-10740
p 482 N94-10741
p 275 N94-10742
p 363 N94-10743
p 372 N94-10890
p 347 N94-11006
p 128 N94-11161
p 412 N94-11162
p 77 N94-11249
p 153 N94-11601
p 137 N94-11621
p 401 N94-11646
p 264 N94-11666
p 301 N94-11667
p 95 N94-12610
p 272 N94-12780
p 374 N94-12786
W-7405-ENG-48 ..... p 273 N94-10151
p 273 N94-10152
p 385 N94-10262
p 321 N94-10263
p 321 N94-10267
p 87 N94-10271
p 385 N94-10286
p 385 N94-10289
p 283 N94-10290
p 321 N94-10291
p 185 N94-10306
p 147 N94-10307
p 140 N94-10309
p 177 N94-10322
p 335 N94-10324
p 361 N94-10334
p 322 N94-10347
p 395 N94-10516
p 132 N94-10518
p 81 N94-10522
p 169 N94-10526
p 381 N94-10651
p 387 N94-10737
p 284 N94-10739
p 98 N94-10751
p 364 N94-10753
p 173 N94-10755
p 142 N94-11009
p 150 N94-11026
p 336 N94-11027
p 142 N94-11050
p 275 N94-11052
p 389 N94-11074
p 76 N94-11075
p 82 N94-11076
p 325 N94-11112
p 389 N94-11114
p 390 N94-11125
p 174 N94-11126
p 151 N94-11144
p 89 N94-11151
p 276 N94-11227
p 90 N94-11230
p 327 N94-11240
p 276 N94-11241
p 382 N94-11242
p 399 N94-11243
p 181 N94-11247
p 336 N94-11248
p 175 N94-11266
p 170 N94-11267
p 399 N94-11268
p 98 N94-11269
p 151 N94-11272
p 143 N94-11273
p 137 N94-11466
p 393 N94-11514
p 77 N94-11602
p 382 N94-11662
p 84 N94-11668
p 383 N94-11676
p 393 N94-11677
p 369 N94-11815
p 394 N94-12370
p 176 N94-12590
p 334 N94-12591
p 272 N94-12592
p 338 N94-12597
p 95 N94-12602
p 176 N94-12784
W-7405-ENG-82 ..... p 82 N94-10957
p 183 N94-11110
p 403 N94-12363
p 405 N94-12599
293/62 ..... p 45 N94-11342

REPORT NUMBER INDEX

SCIENTIFIC AND TECHNICAL AEROSPACE REPORTS VOLUME 32 NUMBER 1

Typical Report Number Index Listing

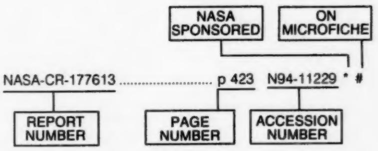

Listings in this index are arranged alphanumerically by report number. The accession number denotes the number by which the citation is identified. The page number helps to locate the citation in the abstract section. An asterisk (*) indicates that the item is a NASA report. A pound sign (#) indicates that the item is available on microfiche.

A-122 .... p 266 N94-11584 #
A-91002 .... p 25 N94-10935 * #
A-91045 .... p 315 N94-11375 * #
A-93005 .... p 231 N94-11378 * #
A-93008 .... p 300 N94-11191 * #
A-93038 .... p 30 N94-11134 * #
A-93039 .... p 1 N94-10936 * #
A-93051 .... p 30 N94-11259 * #
A-93082 .... p 327 N94-11274 * #
A-93096 .... p 13 N94-10758 * #
A-93101-VOL-2 .... p 423 N94-11229 * #
A-93110 .... p 24 N94-12355 * #
A-93116 .... p 412 N94-11523 * #

AD-A262366 .... p 171 N94-12362 #
AD-A263226 .... p 16 N94-11870 #
AD-A263414 .... p 143 N94-11298
AD-A263418 .... p 401 N94-11515
AD-A263419 .... p 144 N94-11516
AD-A263467 .... p 415 N94-11517
AD-A263488 .... p 365 N94-11093 #
AD-A263566 .... p 401 N94-11518
AD-A263726 .... p 288 N94-11299
AD-A263872 .... p 382 N94-11300
AD-A264078 .... p 328 N94-11301
AD-A264079 .... p 89 N94-11107
AD-A264251 .... p 311 N94-12364 #
AD-A264354 .... p 90 N94-11281
AD-A264379 .... p 67 N94-11260
AD-A264403 .... p 276 N94-11463
AD-A264474 .... p 83 N94-11445 #
AD-A264497 .... p 73 N94-11446 #
AD-A264576 .... p 304 N94-11261 #
AD-A264621 .... p 358 N94-11262 #
AD-A264673 .... p 152 N94-11448 #
AD-A264689 .... p 399 N94-11263 #
AD-A264690 .... p 77 N94-11264 #
AD-A264749 .... p 77 N94-11265 #
AD-A264764 .... p 301 N94-11583 #
AD-A264799 .... p 304 N94-11449 #
AD-A264805 .... p 152 N94-11519 #
AD-A264811 .... p 174 N94-10870 #
AD-A264822 .... p 284 N94-10871 #
AD-A264839 .... p 420 N94-11520
AD-A264851 .... p 88 N94-10863 #
AD-A264869 .... p 303 N94-10872 #
AD-A264911 .... p 420 N94-11846 #
AD-A264912 .... p 87 N94-10508 #
AD-A264913 .... p 92 N94-11847 #
AD-A264914 .... p 92 N94-11848 #
AD-A264915 .... p 92 N94-11849 #
AD-A264918 .... p 332 N94-11850 #
AD-A264920 .... p 245 N94-11851 #
AD-A264921 .... p 278 N94-11852 #
AD-A264922 .... p 289 N94-11853 #
AD-A264923 .... p 289 N94-11854 #
AD-A264925 .... p 78 N94-11855 #
AD-A264928 .... p 382 N94-11286 #
AD-A264931 .... p 288 N94-11287 #
AD-A264947 .... p 419 N94-11288 #
AD-A264954 .... p 417 N94-11856 #
AD-A264957 .... p 301 N94-11648
AD-A264958 .... p 375 N94-10486 #
AD-A264960 .... p 339 N94-11289 #
AD-A264961 .... p 338 N94-10487 #
AD-A264963 .... p 181 N94-11290 #
AD-A264965 .... p 336 N94-10488 #
AD-A264969 .... p 304 N94-11649
AD-A264979 .... p 97 N94-10489 #
AD-A264988 .... p 315 N94-11291 #
AD-A264993 .... p 326 N94-11220 #
AD-A265000 .... p 90 N94-11292 #
AD-A265004 .... p 336 N94-11293 #
AD-A265006 .... p 287 N94-10490 #
AD-A265007 .... p 337 N94-11650
AD-A265009 .... p 320 N94-11294 #
AD-A265013 .... p 418 N94-10491 #
AD-A265016 .... p 67 N94-11221 #
AD-A265017 .... p 321 N94-10335 #
AD-A265034 .... p 283 N94-10336 #
AD-A265037 .... p 401 N94-11651
AD-A265055 .... p 26 N94-11858 #
AD-A265056 .... p 154 N94-11865 #
AD-A265059 .... p 278 N94-11871 #
AD-A265065 .... p 331 N94-11652
AD-A265072 .... p 92 N94-11866 #
AD-A265074 .... p 26 N94-11872 #
AD-A265075 .... p 382 N94-11653
AD-A265083 .... p 313 N94-11867 #
AD-A265098 .... p 318 N94-11678
AD-A265115 .... p 136 N94-11158 #
AD-A265116 .... p 289 N94-11868 #
AD-A265130 .... p 90 N94-11222 #
AD-A265136 .... p 78 N94-11873 #
AD-A265143 .... p 331 N94-11679
AD-A265148 .... p 143 N94-11159 #
AD-A265149 .... p 143 N94-11160 #
AD-A265150 .... p 142 N94-11094 #
AD-A265152 .... p 174 N94-11095 #
AD-A265153 .... p 187 N94-11096 #
AD-A265155 .... p 303 N94-11097 #
AD-A265158 .... p 313 N94-11098 #
AD-A265159 .... p 16 N94-11889 #
AD-A265161 .... p 313 N94-11890 #
AD-A265162 .... p 138 N94-11891 #
AD-A265164 .... p 145 N94-11884 #
AD-A265167 .... p 26 N94-11892 #
AD-A265168 .... p 324 N94-11099 #
AD-A265169 .... p 366 N94-11100 #
AD-A265175 .... p 332 N94-11874 #
AD-A265176 .... p 320 N94-11875 #
AD-A265177 .... p 92 N94-11876 #
AD-A265178 .... p 275 N94-11101 #
AD-A265179 .... p 413 N94-11877 #
AD-A265181 .... p 332 N94-11878 #
AD-A265189 .... p 279 N94-12422 #
AD-A265193 .... p 24 N94-11879 #
AD-A265197 .... p 373 N94-11880 #
AD-A265199 .... p 337 N94-11881 #
AD-A265206 .... p 403 N94-12371
AD-A265241 .... p 300 N94-11020 #
AD-A265250 .... p 347 N94-11882 #
AD-A265251 .... p 138 N94-11883 #
AD-A265252 .... p 331 N94-11680 #
AD-A265253 .... p 304 N94-11681 #
AD-A265254 .... p 322 N94-10492 #
AD-A265264 .... p 85 N94-12532 #
AD-A265265 .... p 402 N94-11682 #
AD-A265266 .... p 275 N94-11013 #
AD-A265268 .... p 78 N94-11683 #
AD-A265269 .... p 402 N94-11684 #
AD-A265272 .... p 42 N94-10493 #
AD-A265274 .... p 285 N94-11685 #
AD-A265275 .... p 150 N94-11014 #
AD-A265278 .... p 313 N94-11701 #
AD-A265286 .... p 145 N94-11819 #
AD-A265287 .... p 146 N94-12584 #
AD-A265288 .... p 95 N94-12585 #
AD-A265291 .... p 404 N94-12438 #
AD-A265292 .... p 369 N94-11826 #
AD-A265293 .... p 402 N94-11654 #
AD-A265294 .... p 402 N94-11827 #
AD-A265295 .... p 278 N94-11828 #
AD-A265297 .... p 337 N94-11829 #
AD-A265304 .... p 91 N94-11830 #
AD-A265306 .... p 332 N94-11860 #
AD-A265309 .... p 301 N94-11861 #
AD-A265310 .... p 73 N94-11686
AD-A265311 .... p 92 N94-11862 #
AD-A265323 .... p 24 N94-11863 #
AD-A265341 .... p 311 N94-12423 #
AD-A265342 .... p 145 N94-12424 #
AD-A265352 .... p 85 N94-12404 #
AD-A265358 .... p 145 N94-12405 #
AD-A265359 .... p 95 N94-12577 #
AD-A265360 .... p 279 N94-12561 #
AD-A265364 .... p 138 N94-12406 #
AD-A265379 .... p 94 N94-12407 #
AD-A265390 .... p 286 N94-12408 #
AD-A265391 .... p 138 N94-12409 #
AD-A265402 .... p 405 N94-12586 #
AD-A265404 .... p 94 N94-12425 #
AD-A265407 .... p 279 N94-12419 #
AD-A265429 .... p 85 N94-12426
AD-A265444 .... p 333 N94-12332
AD-A265447 .... p 145 N94-12333
AD-A265458 .... p 176 N94-12372 #
AD-A265469 .... p 333 N94-12008
AD-A265471 .... p 323 N94-10494
AD-A265472 .... p 323 N94-10495
AD-A265481 .... p 274 N94-10496
AD-A265483 .... p 78 N94-12009
AD-A265487 .... p 171 N94-12335
AD-A265490 .... p 339 N94-11049 #
AD-A265494 .... p 132 N94-10497
AD-A265526 .... p 141 N94-10509
AD-A265528 .... p 87 N94-10510
AD-A265530 .... p 403 N94-12010
AD-A265532 .... p 55 N94-12011
AD-A265535 .... p 175 N94-12012
AD-A265552 .... p 171 N94-12533
AD-A265588 .... p 79 N94-12373 #
AD-A265591 .... p 182 N94-12374 #
AD-A265599 .... p 404 N94-12375 #
AD-A265611 .... p 2 N94-12578 #
AD-A265612 .... p 333 N94-12439 #
AD-A265622 .... p 79 N94-12534 #
AD-A265623 .... p 404 N94-12376 #
AD-A265626 .... p 16 N94-12377 #
AD-A265647 .... p 138 N94-12440
AD-A265654 .... p 315 N94-10296 #
AD-A265657 .... p 302 N94-12441 #
AD-A265664 .... p 93 N94-12331
AD-A265666 .... p 497 N94-12334
AD-A265667 .... p 421 N94-12579 #
AD-A265668 .... p 81 N94-10297 #
AD-A265670 .... p 403 N94-12336
AD-A265671 .... p 79 N94-12378 #
AD-A265673 .... p 138 N94-12338 #
AD-A265674 .... p 369 N94-12379 #
AD-A265675 .... p 395 N94-10416 #
AD-A265685 .... p 405 N94-12442 #
AD-A265688 .... p 403 N94-12339 #
AD-A265690 .... p 418 N94-12443 #
AD-A265691 .... p 383 N94-12444 #
AD-A265700 .... p 35 N94-12562 #
AD-A265701 .... p 405 N94-12563 #
AD-A265704 .... p 74 N94-12401 #
AD-A265705 .... p 78 N94-12273 #
AD-A265714 .... p 29 N94-12274 #
AD-A265716 .... p 176 N94-12402 #
AD-A265727 .... p 99 N94-12564 #
AD-A265735 .... p 79 N94-12403 #
AD-A265747 .... p 416 N94-10298 #
AD-A265764 .... p 44 N94-12387 #
AD-A265783 .... p 229 N94-10417 #
AD-A265797 .... p 93 N94-12380 #
AD-A265799 .... p 94 N94-12381 #
AD-A265842 .... p 99 N94-12282 #
AD-A265852 .... p 138 N94-12281 #
AD-A265853 .... p 99 N94-12275 #

AD-A265885 .... p 314 N94-12276 #
AD-A265887 .... p 93 N94-12340 #
AD-A265893 .... p 278 N94-12277 #
AD-A265894 .... p 417 N94-12360 #
AD-A265897 .... p 316 N94-12346 #
AD-A265900 .... p 404 N94-12388
AD-A265901 .... p 148 N94-10703
AD-A265903 .... p 75 N94-10337 #
AD-A265906 .... p 74 N94-12347 #
AD-A265907 .... p 180 N94-10803
AD-A265909 .... p 133 N94-10660
AD-A265911 .... p 289 N94-12349 #
AD-A265914 .... p 421 N94-12445 #
AD-A265917 .... p 146 N94-12565 #
AD-A265920 .... p 383 N94-12341 #
AD-A265921 .... p 170 N94-10704
AD-A265922 .... p 161 N94-12342 #
AD-A265923 .... p 290 N94-12350 #
AD-A265925 .... p 413 N94-12343 * #
AD-A265932 .... p 176 N94-12382
AD-A265934 .... p 396 N94-10705
AD-A265957 .... p 284 N94-11113
AD-A265959 .... p 275 N94-11102
AD-A265961 .... p 289 N94-12348 #
AD-A265972 .... p 79 N94-12351 #
AD-A265995 .... p 161 N94-12352 #
AD-A265998 .... p 93 N94-12353 #
AD-A266004 .... p 93 N94-12354 #
AD-A266006 .... p 383 N94-12389 #
AD-A266008 .... p 73 N94-12344 #
AD-A266010 .... p 347 N94-12390 #
AD-A266011 .... p 171 N94-12391 #
AD-A266013 .... p 278 N94-12392 #
AD-A266016 .... p 85 N94-12393 #
AD-A266026 .... p 44 N94-12394 #
AD-A266027 .... p 91 N94-11487 #
AD-A266029 .... p 369 N94-12395 #
AD-A266035 .... p 23 N94-11103
AD-A266036 .... p 94 N94-12396 #
AD-A266043 .... p 22 N94-12397 #
AD-A266046 .... p 324 N94-11104
AD-A266048 .... p 340 N94-12398 #
AD-A266049 .... p 313 N94-10909
AD-A266050 .... p 180 N94-10706
AD-A266054 .... p 170 N94-10873
AD-A266057 .... p 22 N94-12384 #
AD-A266060 .... p 411 N94-10874
AD-A266061 .... p 369 N94-12420 #
AD-A266064 .... p 43 N94-10944
AD-A266066 .... p 142 N94-10818
AD-A266068 .... p 43 N94-11223 #
AD-A266071 .... p 25 N94-10945
AD-A266072 .... p 304 N94-11224 #
AD-A266073 .... p 403 N94-12345 #
AD-A266079 .... p 381 N94-10697
AD-A266083 .... p 417 N94-12410 #
AD-A266084 .... p 340 N94-12411 #
AD-A266085 .... p 2 N94-12412 #
AD-A266086 .... p 413 N94-12535 #
AD-A266087 .... p 383 N94-12413 #
AD-A266090 .... p 483 N94-12414 #
AD-A266093 .... p 94 N94-12536 #
AD-A266097 .... p 328 N94-11295 #
AD-A266099 .... p 171 N94-11420 #
AD-A266102 .... p 382 N94-11421 #
AD-A266106 .... p 138 N94-11655 #
AD-A266107 .... p 382 N94-11656 #
AD-A266108 .... p 79 N94-12415 #
AD-A266111 .... p 383 N94-12416 #
AD-A266113 .... p 301 N94-12417 #
AD-A266116 .... p 65 N94-12418 #
AD-A266117 .... p 340 N94-12537 #
AD-A266124 .... p 79 N94-12538 #
AD-A266127 .... p 286 N94-12539 #
AD-A266129 .... p 337 N94-12540 #
AD-A266130 .... p 44 N94-12541 #
AD-A266132 .... p 393 N94-11474 #
AD-A266133 .... p 337 N94-11475 #
AD-A266134 .... p 401 N94-11476 #
AD-A266137 .... p 331 N94-11657 #
AD-A266138 .... p 368 N94-11658 #
AD-A266139 .... p 154 N94-11641 #
AD-A266140 .... p 316 N94-11642 #
AD-A266141 .... p 54 N94-11643 #
AD-A266142 .... p 405 N94-12587 #

AD-B172623L .... p 73 N94-12013

AD-D015729 .... p 94 N94-12399 #
AD-D015731 .... p 404 N94-12400 #
AD-D015732 .... p 333 N94-12386 #
AD-D015740 .... p 176 N94-12321 #
AD-D015744 .... p 145 N94-12322 #
AD-D015745 .... p 176 N94-12337 #
AD-D015746 .... p 176 N94-12329 #
AD-D015747 .... p 93 N94-12330 #
AD-D015754 .... p 140 N94-10389 #
AD-D015755 .... p 173 N94-10371 #
AD-D015756 .... p 374 N94-10372 #
AD-D015757 .... p 374 N94-10373 #
AD-D015758 .... p 418 N94-10374 #
AD-D015761 .... p 178 N94-10375 #
AD-D015763 .... p 374 N94-10376 #
AD-D015764 .... p 140 N94-10377 #
AD-D015765 .... p 178 N94-10378 #
AD-D015766 .... p 178 N94-10379 #
AD-D015767 .... p 75 N94-10380 #
AD-D015769 .... p 178 N94-10381 #
AD-D015770 .... p 132 N94-10382 #
AD-D015772 .... p 147 N94-10383 #
AD-D015773 .... p 140 N94-10384 #
AD-D015774 .... p 178 N94-10385 #
AD-D015775 .... p 140 N94-10390 #

AD-E201466 .... p 417 N94-12360 #
AD-E201507 .... p 87 N94-10508 #
AD-E201523 .... p 245 N94-11851 #
AD-E201529 .... p 278 N94-11852 #
AD-E201543 .... p 275 N94-11013 #
AD-E501655 .... p 332 N94-11850 #

AECS-C/FRSR-59 .... p 397 N94-10830

AEDC-TR-93-3 .... p 413 N94-12535 #

AFB-0077-FM-9566-624 .... p 171 N94-11420 #

AFE-9004-003 .... p 34 N94-10930 * #

AFIT/CI/CIA-92-031D .... p 279 N94-12419 #
AFIT/CI/CIA-92-033D .... p 132 N94-10497
AFIT/CI/CIA-92-114 .... p 286 N94-12408 #
AFIT/CI/CIA-92-128 .... p 332 N94-11860 #
AFIT/CI/CIA-92115 .... p 285 N94-11685 #

AFOSR-93-0180TR .... p 401 N94-11515
AFOSR-93-0209TR .... p 77 N94-11265 #
AFOSR-93-0210TR .... p 420 N94-11520
AFOSR-93-0218TR .... p 90 N94-11281
AFOSR-93-0259TR .... p 304 N94-11681 #
AFOSR-93-0261TR .... p 278 N94-11828 #
AFOSR-93-0267TR .... p 92 N94-11866 #
AFOSR-93-0295TR .... p 322 N94-10492 #
AFOSR-93-0323TR .... p 92 N94-11862 #
AFOSR-93-0334TR .... p 301 N94-11583 #
AFOSR-93-0345TR .... p 303 N94-10872 #
AFOSR-93-0348TR .... p 304 N94-11449 #
AFOSR-93-0353TR .... p 382 N94-11286 #
AFOSR-93-0357TR .... p 150 N94-11014 #
AFOSR-93-0358TR .... p 91 N94-11830 #
AFOSR-93-0359TR .... p 347 N94-11882 #
AFOSR-93-0361TR .... p 331 N94-11680 #
AFOSR-93-0362TR .... p 92 N94-11876 #
AFOSR-93-0363TR .... p 16 N94-11889 #
AFOSR-93-0364TR .... p 73 N94-11686
AFOSR-93-0380TR .... p 79 N94-12378 #
AFOSR-93-0382TR .... p 79 N94-12403 #
AFOSR-93-0387TR .... p 44 N94-12387 #
AFOSR-93-0391TR .... p 138 N94-12338 #
AFOSR-93-0393TR .... p 403 N94-12336
AFOSR-93-0394TR .... p 74 N94-12401 #
AFOSR-93-0396TR .... p 176 N94-12402 #
AFOSR-93-0399TR .... p 302 N94-12441 #
AFOSR-93-0401TR .... p 99 N94-12564 #
AFOSR-93-0404TR .... p 16 N94-12377 #
AFOSR-93-0414TR .... p 171 N94-11420 #
AFOSR-93-0418TR .... p 94 N94-12536 #
AFOSR-93-0420TR .... p 313 N94-10909
AFOSR-93-0423TR .... p 301 N94-12417 #

AFR-526021 .... p 99 N94-12275 #

AGARD-CP-514 .... p 2 N94-10421 #
AGARD-CP-531 .... p 68 N94-11317 #

AGARD-HIGHLIGHTS-92/2 .... p 497 N94-11820 #

AGARD-LS-190 .... p 28 N94-11022 #

AGARD-R-789 .... p 31 N94-11489 #
AGARD-R-791 .... p 126 N94-10613 #

AGILITY-1 .... p 26 N94-11464 #

AIAA PAPER 90-3387 .... p 331 N94-11522 * #
AIAA PAPER 92-3988 .... p 13 N94-10820 * #
AIAA PAPER 93-0363 .... p 98 N94-11366 #
AIAA PAPER 93-1821 .... p 28 N94-11205 * #
AIAA PAPER 93-1825 .... p 47 N94-11252 * #
AIAA PAPER 93-1953 .... p 46 N94-10763 * #
AIAA PAPER 93-2027 .... p 47 N94-11053 * #
AIAA PAPER 93-2154 .... p 39 N94-10764 * #
AIAA PAPER 93-2217 .... p 46 N94-10761 * #
AIAA PAPER 93-2278 .... p 40 N94-10811 * #
AIAA PAPER 93-2396 .... p 180 N94-10760 * #
AIAA PAPER 93-2522 .... p 29 N94-11255 * #
AIAA PAPER 93-2832 .... p 163 N94-12576 * #
AIAA PAPER 93-2919 .... p 14 N94-10892 * #
AIAA PAPER 93-3074 .... p 151 N94-11253 * #
AIAA PAPER 93-3105 .... p 151 N94-11192 * #
AIAA PAPER 93-3766 .... p 30 N94-11251 * #

AL-TP-1993-0015 .... p 314 N94-12276 #

AL-TR-1992-0058 .... p 331 N94-11679
AL-TR-1992-0099 .... p 301 N94-11861 #
AL-TR-1992-0137 .... p 316 N94-12346 #

ANL-HEP-CP-92-100 .... p 319 N94-10318 #
ANL-HEP-CP-93-23 .... p 368 N94-11613 #

ANL-HEP-TR-92-129 .... p 419 N94-11105 #

ANL/ACTV-92/2 .... p 169 N94-10326 #

ANL/ES/CP-78917 .... p 143 N94-11454 #

ANL/MCS-TM-171 .... p 276 N94-11138 #

ANL/MCT/CP-76429 .... p 150 N94-11072 #
ANL/MCT/CP-76965 .... p 398 N94-11004 #
ANL/MCT/CP-77835 .... p 144 N94-11607 #
ANL/MCT/CP-78926 .... p 142 N94-10951
ANL/MCT/CP-79135 .... p 398 N94-11073 #

ANL/MSD/CP-76872 .... p 397 N94-10962 #

ANL/OTM/CR-1 .... p 182 N94-11625 #

ANL/PHY/CP-79433 .... p 372 N94-11124 #

ANL/RA/CP-76759 .... p 346 N94-11608 #
ANL/RA/CP-77255 .... p 340 N94-11644 #

AR-008-254 .... p 90 N94-11302 #
AR-008-256 .... p 98 N94-11303 #
AR-008-336 .... p 90 N94-11311

ARA-MEMO-365 .... p 324 N94-10893 #
ARA-MEMO-366 .... p 161 N94-12437 #
ARA-MEMO-370 .... p 154 N94-11859 #
ARA-MEMO-375 .... p 34 N94-10894 #
ARA-MEMO-377 .... p 34 N94-12436 #
ARA-MEMO-378 .... p 55 N94-12283 #
ARA-MEMO-379 .... p 383 N94-11887 #

ARA-84 .... p 16 N94-11888 #

ARCCB-TR-93016 .... p 347 N94-12390 #

ARI-RR-1006 .... p 279 N94-12572 * #

ARL-CR-10 .... p 279 N94-12422 #
ARL-CR-15 .... p 152 N94-11519 #
ARL-CR-24 .... p 286 N94-12539 #
ARL-CR-55-PHASE-1 .... p 67 N94-11221 #

ARL-MR-52 .... p 16 N94-11870 #

ARL-TR-131 .... p 97 N94-10489 #
ARL-TR-133 .... p 405 N94-12563 #
ARL-TR-27 .... p 90 N94-11311
ARL-TR-38 .... p 284 N94-10871 #
ARL-TR-91 .... p 73 N94-11446 #
ARL-TR-93 .... p 83 N94-11445 #

ARO-25424.15-MS .... p 94 N94-12407 #
ARO-30480.1-EL-SBI .... p 401 N94-11476 #

ASC-TR-93-5003 .... p 316 N94-11642 #
ASC-TR-93-5004 .... p 24 N94-11879 #
ASC-TR-93-5007 .... p 25 N94-10945

ASIAC-TR-92-10 .... p 419 N94-11288 #

ASIPP-0031 .... p 322 N94-10484 #

ATC-192 .... p 24 N94-11863 #
ATC-194 .... p 23 N94-11103

ATS-92-2 .... p 177 N94-10341 * #

AVSCOM-TR-92-C-020 .... p 319 N94-10724 * #

B-235387 .... p 416 N94-10910 #
B-253238 .... p 416 N94-10941 #

BARC-1992/E/008 .... p 371 N94-10316

BBC-RD-1992/13 .... p 133 N94-11023
BBC-RD-1992/14 .... p 133 N94-11024

BBNI-7711 .... p 337 N94-11829 #

BNL-48106 .... p 88 N94-10891 #
BNL-48568 .... p 400 N94-11458 #
BNL-48570 .... p 140 N94-10300 #
BNL-48594 .... p 359 N94-10303 #
BNL-48595 .... p 359 N94-10304 #
BNL-48605 .... p 359 N94-10302 #
BNL-48610 .... p 400 N94-11467 #
BNL-48611 .... p 173 N94-10287 #
BNL-48620 .... p 84 N94-11459 #
BNL-48628 .... p 75 N94-10338 #
BNL-48645 .... p 394 N94-10301 #
BNL-48679 .... p 374 N94-12782 #
BNL-48736 .... p 359 N94-10308 #
BNL-48760 .... p 410 N94-10528 #
BNL-48858 .... p 287 N94-10517 #
BNL-48907 .... p 373 N94-12601 #

CBPF-NF-033/91 .... p 350 N94-10313 #
CBPF-NF-034/91 .... p 395 N94-10314 #

CDNSWC/SME-92/64 .... p 85 N94-12532 #

CFDRC-4105/6 .... p 46 N94-10934 * #

CIRSSE-137 .... p 338 N94-10638 * #

CMOTT-93-10 .... p 151 N94-11192 * #

CMU-CS-93-145 .... p 333 N94-12439 #

CMU/SEI-93-TR-02 .... p 337 N94-11881 #

CNIC-00582 .... p 343 N94-10546 #
CNIC-00592 .... p 371 N94-10409
CNIC-00599 .... p 322 N94-10484 #
CNIC-00605 .... p 173 N94-10483 #

COLO-HEP-314/2 .... p 370 N94-12609 #

CONF-9005440 .... p 183 N94-10847
CONF-9105418-1 .... p 173 N94-10755
CONF-9107237 .... p 263 N94-11505 #
CONF-9107237 .... p 263 N94-11506 #
CONF-9109114-12 .... p 98 N94-10751 #
CONF-9111189 .... p 364 N94-10889
CONF-9112148 .... p 360 N94-10317 #
CONF-9201125 .... p 300 N94-10888
CONF-9201148-1 .... p 272 N94-12592 #
CONF-920124-29 .... p 399 N94-11268 #
CONF-920142-4 .... p 390 N94-11125 #
CONF-920144-6 .... p 73 N94-11612 #
CONF-9202146 .... p 411 N94-10887
CONF-9202147 .... p 363 N94-10696
CONF-920315-47 .... p 374 N94-12782 #
CONF-9203159-9 .... p 364 N94-10754
CONF-9203213 .... p 371 N94-10719
CONF-920362-46 .... p 393 N94-11677 #
CONF-9204120-5 .... p 385 N94-10286 #
CONF-9204120-6 .... p 143 N94-11273 #
CONF-9204120-8 .... p 381 N94-10651 #
CONF-9204235-2-REV-1 .... p 89 N94-11151 #
CONF-9205147-5 .... p 75 N94-10519 #
CONF-920523-11 .... p 176 N94-12590 #
CONF-920523-9 .... p 389 N94-11074 #
CONF-920604-4 .... p 84 N94-11488 #
CONF-9206129-4 .... p 84 N94-11668 #
CONF-9206185-12 .... p 151 N94-11272 #
CONF-9206276-5 .... p 373 N94-12542 #
CONF-9206297-2 .... p 382 N94-11242 #
CONF-920671-14 .... p 142 N94-11050 #
CONF-920672-4 .... p 187 N94-11169 #
CONF-920708-7 .... p 425 N94-10292 #
CONF-9207140-6 .... p 367 N94-11469 #
CONF-920735-6 .... p 169 N94-10526 #
CONF-920799-7 .... p 183 N94-11110 #
CONF-9208109-80 .... p 145 N94-11645 #
CONF-9208109-82 .... p 132 N94-10518 #
CONF-9208127-7 .... p 137 N94-11466 #
CONF-9208150 .... p 170 N94-10630
CONF-920881-2 .... p 283 N94-10290 #
CONF-9209158-12 .... p 275 N94-11052 #
CONF-9209181-7 .... p 385 N94-10262 #
CONF-9209253-4 .... p 371 N94-10156 #
CONF-9209290-8 .... p 385 N94-10289 #
CONF-9209326-1 .... p 77 N94-11602
CONF-9209332-1 .... p 341 N94-10259 #
CONF-9209333-1 .... p 408 N94-10261 #
CONF-9210140-2-REV-1 .... p 177 N94-10322 #
CONF-9210278-1 .... p 175 N94-11468 #
CONF-9210282-2 .... p 170 N94-11267 #
CONF-9210331-2 .... p 133 N94-10709 #
CONF-9210337-1 .... p 140 N94-10300 #
CONF-9210339-1 .... p 358 N94-10154 #
CONF-921047-1 .... p 90 N94-11230 #
CONF-921047-2 .... p 383 N94-11676 #
CONF-921047-4 .... p 95 N94-12602 #
CONF-921101-101 .... p 98 N94-11269 #
CONF-921101-110 .... p 367 N94-11455 #
CONF-921101-117 .... p 81 N94-10522 #
CONF-921103-10 .... p 394 N94-12544 #
CONF-921103-11-APP-B .... p 393 N94-11513 #
CONF-9211101-8 .... p 181 N94-11247 #
CONF-9211101-9 .... p 89 N94-11106 #
CONF-9211104-8 .... p 87 N94-10271 #
CONF-9211117-6 .... p 82 N94-11076 #
CONF-9211128-7 .... p 326 N94-11226 #
CONF-921121-2 .... p 397 N94-10962 #
CONF-921122-48 .... p 359 N94-10302 #
CONF-921122-56 .... p 146 N94-12603 #
CONF-921122-58 .... p 370 N94-12781 #
CONF-921133-19 .... p 369 N94-11815 #
CONF-921188-1 .... p 319 N94-10146 #
CONF-921204-2 .... p 395 N94-10516 #
CONF-921244 .... p 40 N94-10147 #
CONF-921267-1 .... p 188 N94-11367 #
CONF-921268-1 .... p 174 N94-11126 #
CONF-930103-12 .... p 371 N94-10529
CONF-930103-13 .... p 45 N94-10282 #
CONF-930103-24 .... p 370 N94-10149 #
CONF-930103-9 .... p 372 N94-11296
CONF-930107-1 .... p 400 N94-11458 #
CONF-930108-6 .... p 98 N94-11366 #
CONF-9301100-1 .... p 151 N94-11144 #
CONF-9301101-1 .... p 400 N94-11467 #
CONF-9301103-2 .... p 370 N94-12787 #
CONF-9301106-1 .... p 388 N94-10744
CONF-930159-22 .... p 301 N94-11667 #
CONF-930159-23 .... p 401 N94-11605
CONF-930159-24 .... p 175 N94-11266 #
CONF-930159-25 .... p 76 N94-11075 #
CONF-930159-28 .... p 144 N94-11624 #
CONF-930159-32 .... p 176 N94-12784 #
CONF-930171-2 .... p 175 N94-11283 #
CONF-930171-3 .... p 91 N94-11665 #
CONF-930173-5 .... p 359 N94-10303 #
CONF-930173-6 .... p 359 N94-10308 #
CONF-930184-2 .... p 173 N94-10287 #
CONF-930187-2 .... p 361 N94-10349 #
CONF-930194-1 .... p 343 N94-10708 #
CONF-930195-1 .... p 75 N94-10338 #
CONF-930202-6 .... p 398 N94-11004 #
CONF-930202-7 .... p 398 N94-11073 #
CONF-930202-8 .... p 82 N94-11108 #
CONF-9302101-1 .... p 129 N94-11606 #
CONF-9302102-1 .... p 411 N94-10956 #
CONF-9302108-1 .... p 347 N94-11006 #
CONF-9302115-1 .... p 275 N94-10742
CONF-930235-1 .... p 142 N94-10951
CONF-930239-1 .... p 359 N94-10304 #
CONF-930245-1 .... p 335 N94-10324 #
CONF-930254-3 .... p 183 N94-11586 #
CONF-930269-12 .... p 133 N94-10960 #
CONF-930271-2 .... p 84 N94-11459 #
CONF-930275-2 .... p 372 N94-11124 #
CONF-930281-7 .... p 393 N94-11512 #
CONF-9303111-3 .... p 183 N94-11647 #
CONF-9303121-1 .... p 41 N94-11282 #
CONF-9303122-2 .... p 274 N94-10323 #
CONF-9303127-1 .... p 321 N94-10291 #
CONF-9303130-1 .... p 137 N94-11453 #
CONF-9303131-1 .... p 325 N94-11109 #
CONF-9303133-1 .... p 262 N94-11051 #
CONF-9303157-1 .... p 387 N94-10737
CONF-9303167-1 .... p 287 N94-10517 #
CONF-930331-8 .... p 366 N94-11284 #
CONF-930331-9 .... p 336 N94-11027 #
CONF-930367-1 .... p 401 N94-11646 #
CONF-930367-4 .... p 412 N94-11162 #
CONF-930372-2 .... p 372 N94-10890 #
CONF-930372-4 .... p 153 N94-11601 #
CONF-930389-2 .... p 368 N94-11613 #
CONF-930389-3 .... p 410 N94-10528 #
CONF-930398-2 .... p 87 N94-10295 #
CONF-930401-12 .... p 340 N94-11644 #
CONF-930404-10 .... p 346 N94-11608 #
CONF-930404-14 .... p 365 N94-10952
CONF-930405-2 .... p 396 N94-10745
CONF-930405-6 .... p 396 N94-10809 #
CONF-9304103-5 .... p 181 N94-11228 #
CONF-9304106-2 .... p 126 N94-10293 #
CONF-9304108-1 .... p 264 N94-11666 #
CONF-9304112-4 .... p 385 N94-10159 #
CONF-9304112-5 .... p 394 N94-12545 #
CONF-9304113-1 .... p 394 N94-10301 #
CONF-9304114-1 .... p 325 N94-11112 #
CONF-9304114-4 .... p 345 N94-11225 #
CONF-9304118-1 .... p 14 N94-11111 #
CONF-9304126-1 .... p 384 N94-10158 #
CONF-9304126-2 .... p 384 N94-10157 #
CONF-9304126-6 .... p 173 N94-10746
CONF-9304140-1 .... p 336 N94-10738
CONF-930416-2 .... p 144 N94-11607 #
CONF-930433-4 .... p 143 N94-11454 #
CONF-930435-8 .... p 262 N94-10258 #
CONF-930438-4 .... p 82 N94-10957 #
CONF-930445-12 .... p 141 N94-10521 #
CONF-930445-5 .... p 174 N94-10959 #
CONF-930461-2 .... p 319 N94-10318 #
CONF-930511-34 .... p 374 N94-12785 #
CONF-930511-47 .... p 374 N94-12786 #
CONF-9305151-1 .... p 419 N94-11137 #
CONF-9305153-3 .... p 344 N94-10961 #
CONF-9305159-2 .... p 374 N94-10339 #
CONF-9305168-1 .... p 325 N94-11123 #
CONF-9305169-1 .... p 327 N94-11240 #
CONF-9305177-2 .... p 363 N94-10743
CONF-9305198-1 .... p 341 N94-12598 #
CONF-930521-5 .... p 150 N94-11072 #
CONF-9305210-1 .... p 393 N94-11514 #
CONF-930532-2 .... p 263 N94-11173 #
CONF-930537-5 .... p 370 N94-12787 #
CONF-930537-8-REV-1 .... p 335 N94-10340 #
CONF-930571-12 .... p 140 N94-10309 #
CONF-930586-5 .... p 399 N94-11243 #
CONF-9306142-1 .... p 150 N94-11026 #
CONF-9306143-1 .... p 418 N94-10646
CONF-9306144-1 .... p 400 N94-11457 #
CONF-9306145-1 .... p 335 N94-10257 #
CONF-930615-1 .... p 89 N94-10958 #
CONF-9306151 .... p 340 N94-12428 #
CONF-9306165-1 .... p 163 N94-12604 #
CONF-930621-3 .... p 336 N94-11270 #
CONF-930702-12 .... p 184 N94-10288 #
CONF-930704-7 .... p 143 N94-11271 #
CONF-930704-8 .... p 143 N94-11285 #
CONF-930713-6 .... p 97 N94-10294 #
CONF-930758-1 .... p 65 N94-10740
CONF-930765-1 .... p 47 N94-11122 #
CONF-930768-1 .... p 128 N94-11028 #
CONF-930772-1 .... p 331 N94-11611 #
CONF-930773-1 .... p 336 N94-11248 #
CONF-930779-8 .... p 482 N94-10741
CONF-930783-1 .... p 88 N94-10527 #
CONF-930801-1 .... p 128 N94-11161 #
CONF-930822-4 .... p 95 N94-12596 #
CONF-930881-1 .... p 334 N94-12591 #
CONF-930884-2 .... p 334 N94-12593 #
CONF-930898-1 .... p 338 N94-12597 #

CRREL-SR-93-4 .... p 29 N94-12274 #

CS-9208 .... p 323 N94-10878 #
CS-9209 .... p 419 N94-10903 #
CS-9216 .... p 344 N94-10905 #
CS-9301 .... p 174 N94-10904 #

CTR-3-4-90/2-983-5F .... p 98 N94-10844

CUED/A-TURBO/TR.128 .... p 166 N94-12777 #
CUED/A-TURBO/TR.129 .... p 166 N94-12779 #

CWI-BS-R9219 .... p 342 N94-10352 #
CWI-BS-R9220 .... p 347 N94-10353 #
CWI-BS-R9221 .... p 347 N94-10354 #

CWI-NM-R9221 .... p 342 N94-10351 #

C931032-U-2R08 .... p 231 N94-11236 * #

DE92-019571 .... p 98 N94-10751 #
DE92-040420 .... p 372 N94-11296
DE92-040974 .... p 371 N94-10529
DE92-526832 .... p 313 N94-10251 #
DE92-641157 .... p 336 N94-10544
DE92-641290 .... p 148 N94-10530
DE92-641347 .... p 343 N94-10531
DE92-641349 .... p 425 N94-11152 #
DE92-641575 .... p 361 N94-10532
DE92-642136 .... p 394 N94-10281 #
DE92-644548 .... p 141 N94-10533
DE92-644554 .... p 484 N94-10534
DE92-644731 .... p 425 N94-11136 #
DE92-644734 .... p 410 N94-10535
DE93-000746 .... p 319 N94-10146 #
DE93-002301 .... p 45 N94-10282 #
DE93-004053 .... p 370 N94-10149 #
DE93-004738 .... p 40 N94-10147 #
DE93-005428 .... p 187 N94-11169 #
DE93-005459 .... p 372 N94-10890 #
DE93-006393 .... p 132 N94-10315 #
DE93-006908 .... p 169 N94-10326 #
DE93-007325 .... p 153 N94-11601 #
DE93-007400 .... p 273 N94-10151 #

DE93-007413 .... p 273 N94-10152 #
DE93-007427 .... p 287 N94-10153 #
DE93-008051 .... p 172 N94-10150 #
DE93-008350 .... p 183 N94-11586 #
DE93-008474 .... p 358 N94-10154 #
DE93-008491 .... p 147 N94-10252 #
DE93-008717 .... p 88 N94-10891 #
DE93-008786 .... p 385 N94-10253 #
DE93-008788 .... p 358 N94-10254 #
DE93-008917 .... p 273 N94-10285 #
DE93-009149 .... p 391 N94-11170 #
DE93-009222 .... p 184 N94-10155 #
DE93-009227 .... p 175 N94-11266 #
DE93-009256 .... p 385 N94-10286 #
DE93-009261 .... p 173 N94-10287 #
DE93-009304 .... p 77 N94-11602
DE93-009403 .... p 173 N94-10255 #
DE93-009515 .... p 382 N94-11662 #
DE93-009517 .... p 137 N94-11466 #
DE93-009523 .... p 90 N94-11230 #
DE93-009525 .... p 170 N94-11267 #
DE93-009549 .... p 399 N94-11268 #
DE93-009551 .... p 98 N94-11269 #
DE93-009565 .... p 264 N94-10256 #
DE93-009609 .... p 373 N94-11694 #
DE93-009628 .... p 336 N94-11270 #
DE93-009629 .... p 143 N94-11271 #
DE93-009640 .... p 47 N94-11122 #
DE93-009643 .... p 41 N94-11282 #
DE93-009709 .... p 184 N94-10288 #
DE93-009782 .... p 391 N94-11171 #
DE93-009795 .... p 75 N94-10338 #
DE93-009796 .... p 98 N94-11366 #
DE93-009828 .... p 343 N94-10708 #
DE93-009830 .... p 175 N94-11283 #
DE93-009838 .... p 335 N94-10257 #
DE93-009839 .... p 366 N94-11284 #
DE93-009851 .... p 401 N94-11605
DE93-009854 .... p 143 N94-11285 #
DE93-009856 .... p 129 N94-11606 #
DE93-009954 .... p 144 N94-11607 #
DE93-009959 .... p 319 N94-10318 #
DE93-009961 .... p 346 N94-11608 #
DE93-009966 .... p 142 N94-10951
DE93-009985 .... p 340 N94-11644 #
DE93-009986 .... p 143 N94-11454 #
DE93-010010 .... p 262 N94-10258 #
DE93-010173 .... p 145 N94-11645 #
DE93-010181 .... p 361 N94-10334 #
DE93-010184 .... p 45 N94-10299 #
DE93-010195 .... p 346 N94-11663 #
DE93-010199 .... p 341 N94-10259 #
DE93-010236 .... p 417 N94-11600 #
DE93-010239 .... p 417 N94-11661 #
DE93-010252 .... p 373 N94-12542 #
DE93-010271 .... p 371 N94-10260 #
DE93-010283 .... p 82 N94-11108 #
DE93-010381 .... p 285 N94-11664 #
DE93-010406 .... p 371 N94-10156 #
DE93-010451 .... p 408 N94-10261 #
DE93-010460 .... p 423 N94-11059 #
DE93-010499 .... p 334 N94-12591 #
DE93-010500 .... p 385 N94-10262 #
DE93-010501 .... p 272 N94-12592 #
DE93-010502 .... p 151 N94-11272 #
DE93-010510 .... p 385 N94-10289 #
DE93-010511 .... p 283 N94-10290 #
DE93-010519 .... p 321 N94-10291 #
DE93-010569 .... p 425 N94-10292 #
DE93-010661 .... p 150 N94-11072 #
DE93-010674 .... p 398 N94-11073 #
DE93-010675 .... p 398 N94-11004 #
DE93-010683 .... p 367 N94-11455 #
DE93-010687 .... p 400 N94-11457 #
DE93-010691 .... p 334 N94-12593 #
DE93-010692 .... p 325 N94-11109 #
DE93-010693 .... p 91 N94-11665 #
DE93-010733 .... p 126 N94-10293 #
DE93-010734 .... p 264 N94-11666 #
DE93-010737 .... p 301 N94-11667 #
DE93-010738 .... p 401 N94-11646 #
DE93-010742 .... p 97 N94-10294 #
DE93-010770 .... p 182 N94-11438 #
DE93-010796 .... p 365 N94-10952
DE93-010805 .... p 87 N94-10295 #
DE93-010825 .... p 183 N94-11647 #
DE93-010860 .... p 140 N94-10300 #
DE93-010861 .... p 400 N94-11458 #
DE93-010869 .... p 84 N94-11459 #
DE93-010871 .... p 394 N94-10301 #
DE93-010873 .... p 400 N94-11467 #
DE93-010874 .... p 359 N94-10302 #
DE93-010876 .... p 359 N94-10303 #
DE93-010879 .... p 359 N94-10304 #
DE93-010949 .... p 133 N94-10709 #
DE93-010950 .... p 411 N94-10956 #
DE93-010953 .... p 175 N94-11468 #
DE93-010956 .... p 367 N94-11469 #
DE93-011000 .... p 367 N94-11470 #
DE93-011004 .... p 373 N94-11618 #
DE93-011006 .... p 463 N94-11619 #
DE93-011010 .... p 368 N94-11620 #
DE93-011231 .... p 144 N94-11609 #
DE93-011359 .... p 403 N94-12363 #
DE93-011374 .... p 401 N94-11610 #
DE93-011406 .... p 137 N94-11621 #
DE93-011459 .... p 78 N94-11622 #
DE93-011485 .... p 232 N94-11623 #
DE93-011556 .... p 374 N94-10339 #
DE93-011558 .... p 144 N94-11624 #
DE93-011559 .... p 82 N94-10957 #
DE93-011560 .... p 183 N94-11110 #
DE93-011576 .... p 89 N94-10958 #
DE93-011582 .... p 174 N94-10959 #
DE93-011590 .... p 14 N94-11111 #
DE93-011591 .... p 325 N94-11123 #
DE93-011597 .... p 263 N94-11173 #
DE93-011600 .... p 331 N94-11611 #
DE93-011605 .... p 133 N94-10960 #
DE93-011639 .... p 182 N94-11625 #
DE93-011656 .... p 190 N94-11674 #
DE93-011675 .... p 344 N94-10961 #
DE93-011678 .... p 345 N94-11225 #
DE93-011679 .... p 326 N94-11226 #
DE93-011690 .... p 73 N94-11612 #
DE93-011714 .... p 364 N94-10753
DE93-011718 .... p 276 N94-11227 #
DE93-011742 .... p 364 N94-10754
DE93-011750 .... p 55 N94-11675 #
DE93-011756 .... p 368 N94-11613 #
DE93-011757 .... p 397 N94-10962 #
DE93-011764 .... p 372 N94-11124 #
DE93-011765 .... p 419 N94-11105 #
DE93-011780 .... p 285 N94-11614 #
DE93-011782 .... p 181 N94-11228 #
DE93-011783 .... p 327 N94-11246 #
DE93-011792 .... p 272 N94-12780 #
DE93-011860 .... p 89 N94-11106 #
DE93-011874 .... p 389 N94-11074 #
DE93-011879 .... p 143 N94-11273 #
DE93-011881 .... p 76 N94-11075 #
DE93-011883 .... p 173 N94-10755
DE93-011884 .... p 181 N94-11247 #
DE93-011885 .... p 325 N94-11112 #
DE93-011886 .... p 82 N94-11076 #
DE93-011889 .... p 383 N94-11676 #
DE93-011892 .... p 393 N94-11677 #
DE93-011896 .... p 84 N94-11668 #
DE93-011897 .... p 142 N94-11050 #
DE93-011905 .... p 262 N94-11051 #
DE93-011949 .... p 390 N94-11125 #
DE93-011950 .... p 275 N94-11052 #
DE93-011952 .... p 150 N94-11026 #
DE93-011953 .... p 174 N94-11126 #
DE93-011955 .... p 151 N94-11144 #
DE93-011958 .... p 336 N94-11027 #
DE93-011959 .... p 336 N94-11248 #
DE93-011974 .... p 188 N94-11460 #
DE93-011986 .... p 77 N94-11249 #
DE93-012034 .... p 330 N94-11452 #
DE93-012084 .... p 128 N94-11028 #
DE93-012085 .... p 137 N94-11453 #
DE93-012110 .... p 365 N94-11029 #
DE93-012130 .... p 419 N94-11137 #
DE93-012131 .... p 83 N94-11250 #
DE93-012147 .... p 276 N94-11138 #
DE93-012150 .... p 418 N94-10646
DE93-012153 .... p 325 N94-11139 #
DE93-012181 .... p 129 N94-11456 #
DE93-012185 .... p 76 N94-11140 #
DE93-012186 .... p 83 N94-11141 #
DE93-012190 .... p 393 N94-11669 #
DE93-012191 .... p 390 N94-11142 #
DE93-012220 .... p 129 N94-11670 #
DE93-012236 .... p 266 N94-11671 #
DE93-012307 .... p 335 N94-10340 #
DE93-012308 .... p 370 N94-12787 #
DE93-012312 .... p 327 N94-11240 #
DE93-012318 .... p 387 N94-10737
DE93-012324 .... p 77 N94-11359 #
DE93-012338 .... p 188 N94-11367 #
DE93-012346 .... p 336 N94-10738
DE93-012379 .... p 322 N94-10347 #
DE93-012382 .... p 284 N94-10739
DE93-012383 .... p 276 N94-11241 #
DE93-012385 .... p 177 N94-10348 #
DE93-012386 .... p 174 N94-11005 #
DE93-012390 .... p 321 N94-10267 #
DE93-012397 .... p 319 N94-10268 #
DE93-012430 .... p 72 N94-11368 #
DE93-012431 .... p 91 N94-11672 #
DE93-012432 .... p 91 N94-11673 #
DE93-012482 .... p 382 N94-11242 #
DE93-012497 .... p 176 N94-12590 #
DE93-012498 .... p 399 N94-11243 #
DE93-012502 .... p 321 N94-10263 #
DE93-012508 .... p 332 N94-11695 #
DE93-012509 .... p 420 N94-11369 #
DE93-012512 .... p 177 N94-10269 #
DE93-012515 .... p 131 N94-10270 #
DE93-012596 .... p 87 N94-10271 #
DE93-012600 .... p 89 N94-11151 #
DE93-012628 .... p 347 N94-11006 #
DE93-012630 .... p 65 N94-10740
DE93-012648 .... p 482 N94-10741
DE93-012655 .... p 361 N94-10349 #
DE93-012656 .... p 275 N94-10742
DE93-012672 .... p 128 N94-11161 #
DE93-012673 .... p 412 N94-11162 #
DE93-012674 .... p 384 N94-10157 #
DE93-012682 .... p 384 N94-10158 #
DE93-012728 .... p 184 N94-10264 #
DE93-012740 .... p 363 N94-10743
DE93-012762 .... p 388 N94-10744
DE93-012767 .... p 77 N94-11370 #
DE93-012775 .... p 385 N94-10159 #
DE93-012782 .... p 173 N94-10160 #
DE93-012823 .... p 340 N94-12543 #
DE93-012829 .... p 394 N94-12544 #
DE93-012831 .... p 394 N94-12545 #
DE93-012835 .... p 152 N94-11371 #
DE93-012839 .... p 396 N94-10745
DE93-012842 .... p 173 N94-10746
DE93-012934 .... p 368 N94-11813 #
DE93-012969 .... p 95 N94-12596 #
DE93-012971 .... p 48 N94-11372 #
DE93-013049 .... p 338 N94-12597 #
DE93-013089 .... p 177 N94-10322 #
DE93-013102 .... p 389 N94-11114 #
DE93-013106 .... p 144 N94-11478 #
DE93-013115 .... p 381 N94-10647
DE93-013117 .... p 144 N94-11479 #
DE93-013127 .... p 367 N94-11373 #
DE93-013139 .... p 368 N94-11696 #
DE93-013140 .... p 89 N94-11007 #
DE93-013178 .... p 267 N94-11697 #
DE93-013186 .... p 274 N94-10323 #
DE93-013192 .... p 335 N94-10324 #
DE93-013197 .... p 169 N94-10526 #
DE93-013207 .... p 88 N94-10527 #
DE93-013221 .... p 84 N94-11488 #
DE93-013248 .... p 273 N94-10319 #
DE93-013249 .... p 273 N94-10305 #
DE93-013280 .... p 341 N94-12598 #
DE93-013282 .... p 405 N94-12599 #
DE93-013288 .... p 410 N94-10528 #
DE93-013297 .... p 147 N94-10320 #
DE93-013302 .... p 82 N94-11008 #
DE93-013309 .... p 185 N94-10306 #
DE93-013310 .... p 394 N94-12370 #
DE93-013311 .... p 142 N94-11009 #
DE93-013312 .... p 147 N94-10307 #
DE93-013326 .... p 369 N94-12546 #
DE93-013328 .... p 365 N94-11010 #
DE93-013333 .... p 154 N94-11814 #
DE93-013335 .... p 91 N94-11698 #
DE93-013336 .... p 373 N94-12600 #
DE93-013337 .... p 396 N94-10648
DE93-013341 .... p 359 N94-10308 #
DE93-013346 .... p 369 N94-11815 #
DE93-013349 .... p 395 N94-10516 #
DE93-013377 .... p 386 N94-10321 #
DE93-013399 .... p 287 N94-10517 #
DE93-013401 .... p 373 N94-12601 #
DE93-013416 .... p 132 N94-10518 #
DE93-013430 .... p 95 N94-12602 #
DE93-013431 .... p 140 N94-10309 #
DE93-013437 .... p 75 N94-10519 #
DE93-013463 .... p 385 N94-10310 #
DE93-013464 .... p 388 N94-10747 #
DE93-013466 .... p 388 N94-10852 #
DE93-013470 .... p 340 N94-12428 #
DE93-013486 .... p 393 N94-11512 #
DE93-013487 .... p 393 N94-11513 #
DE93-013566 .... p 146 N94-12603 #
DE93-013590 .... p 76 N94-11244 #
DE93-013592 .... p 84 N94-11816 #
DE93-013593 .... p 363 N94-10748 #
DE93-013602 .... p 42 N94-10520 #
DE93-013604 .... p 78 N94-11699 #
DE93-013671 .... p 163 N94-12604 #
DE93-013705 .... p 365 N94-11011 #
DE93-013707 .... p 88 N94-10710
DE93-013754 .... p 396 N94-10809 #
DE93-013765 .... p 141 N94-10521 #
DE93-013778 .... p 182 N94-12605 #
DE93-013780 .... p 318 N94-11817 #
DE93-013813 .... p 334 N94-12606 #

DE93-013847 .... p 81 N94-10522 #
DE93-013861 .... p 373 N94-12607 #
DE93-013865 .... p 264 N94-10650 #
DE93-013872 .... p 366 N94-11172 #
DE93-013898 .... p 420 N94-11588 #
DE93-013961 .... p 334 N94-12608 #
DE93-013971 .... p 370 N94-12609 #
DE93-013977 .... p 398 N94-11115 #
DE93-013979 .... p 402 N94-11700 #
DE93-013981 .... p 263 N94-11116 #
DE93-013985 .... p 398 N94-11117 #
DE93-013986 .... p 398 N94-11012 #
DE93-014017 .... p 95 N94-12610 #
DE93-014027 .... p 370 N94-12781 #
DE93-014057 .... p 374 N94-12782 #
DE93-014093 .... p 272 N94-12783 #
DE93-014098 .... p 389 N94-11118 #
DE93-014115 .... p 381 N94-10651 #
DE93-014127 .... p 176 N94-12784 #
DE93-014136 .... p 374 N94-12785 #
DE93-014433 .... p 300 N94-10652 #
DE93-014434 .... p 83 N94-11127 #
DE93-014474 .... p 374 N94-12786 #
DE93-014532 .... p 88 N94-10749 #
DE93-014767 .... p 411 N94-10853 #
DE93-014772 .... p 89 N94-11145 #
DE93-014773 .... p 89 N94-11146 #
DE93-014840 .... p 363 N94-10750 #
DE93-014844 .... p 366 N94-11147 #
DE93-014847 .... p 76 N94-10653 #
DE93-015079 .... p 76 N94-10854 #
DE93-015472 .... p 393 N94-11514 #
DE93-605594 .... p 263 N94-11505 #
DE93-605634 .... p 263 N94-11506 #
DE93-608188 .... p 346 N94-11507 #
DE93-608196 .... p 412 N94-11163 #
DE93-609993 .... p 360 N94-10327 #
DE93-610049 .... p 360 N94-10328 #
DE93-610050 .... p 360 N94-10329 #
DE93-610072 .... p 360 N94-10330 #
DE93-610073 .... p 360 N94-10331 #
DE93-610128 .... p 342 N94-10283 #
DE93-610148 .... p 360 N94-10332 #
DE93-610149 .... p 361 N94-10333 #
DE93-610179 .... p 359 N94-10311 #
DE93-610180 .... p 359 N94-10312 #
DE93-610264 .... p 385 N94-10284
DE93-610313 .... p 350 N94-10313 #
DE93-610314 .... p 395 N94-10314 #
DE93-610322 .... p 395 N94-10406 #
DE93-610548 .... p 274 N94-10407 #
DE93-610974 .... p 84 N94-12361
DE93-611231 .... p 357 N94-10408 #
DE93-612176 .... p 371 N94-10409
DE93-612205 .... p 371 N94-10316
DE93-612641 .... p 170 N94-10630
DE93-612675 .... p 173 N94-10483 #
DE93-612915 .... p 322 N94-10484 #
DE93-612916 .... p 322 N94-10410
DE93-612970 .... p 132 N94-10401
DE93-612971 .... p 409 N94-10402
DE93-613026 .... p 410 N94-10631 #
DE93-613027 .... p 395 N94-10411 #
DE93-613028 .... p 409 N94-10388
DE93-613029 .... p 349 N94-10632
DE93-613030 .... p 418 N94-10485 #
DE93-613031 .... p 348 N94-10412 #
DE93-613049 .... p 275 N94-10798
DE93-613050 .... p 409 N94-10413 #
DE93-613051 .... p 409 N94-10499
DE93-613092 .... p 361 N94-10414 #
DE93-613093 .... p 349 N94-10633 #
DE93-613094 .... p 362 N94-10634
DE93-613111 .... p 368 N94-11581
DE93-613119 .... p 409 N94-10500
DE93-613120 .... p 410 N94-10545 #
DE93-613149 .... p 410 N94-10635
DE93-613518 .... p 409 N94-10501
DE93-613520 .... p 349 N94-10636 #
DE93-613535 .... p 361 N94-10502
DE93-613538 .... p 402 N94-11659
DE93-613539 .... p 402 N94-11660
DE93-613540 .... p 410 N94-10536 #
DE93-613642 .... p 396 N94-10637
DE93-613643 .... p 361 N94-10503
DE93-613644 .... p 395 N94-10386
DE93-613654 .... p 343 N94-10546 #
DE93-613723 .... p 386 N94-10387
DE93-613817 .... p 142 N94-10799
DE93-613818 .... p 408 N94-10148 #
DE93-613819 .... p 409 N94-10403
DE93-613820 .... p 348 N94-10404
DE93-613827 .... p 398 N94-11025
DE93-613828 .... p 395 N94-10537
DE93-613910 .... p 396 N94-10800
DE93-613911 .... p 396 N94-10801
DE93-613981 .... p 410 N94-10802
DE93-613988 .... p 395 N94-10415
DE93-617173 .... p 397 N94-10830
DE93-617200 .... p 82 N94-10842
DE93-617201 .... p 397 N94-10843
DE93-617202 .... p 397 N94-10845
DE93-617422 .... p 183 N94-10847
DE93-617448 .... p 364 N94-10848
DE93-617463 .... p 372 N94-10849
DE93-617645 .... p 411 N94-10831
DE93-617646 .... p 411 N94-10832
DE93-617647 .... p 349 N94-10833
DE93-617649 .... p 411 N94-10834
DE93-617650 .... p 349 N94-10547
DE93-617654 .... p 409 N94-10405
DE93-617656 .... p 411 N94-10880
DE93-617657 .... p 349 N94-10548
DE93-617658 .... p 409 N94-10394
DE93-617659 .... p 344 N94-10881
DE93-617679 .... p 388 N94-10882
DE93-617680 .... p 397 N94-10883
DE93-617681 .... p 397 N94-10884
DE93-617690 .... p 361 N94-10549
DE93-617691 .... p 362 N94-10550
DE93-617692 .... p 362 N94-10551
DE93-617693 .... p 362 N94-10552
DE93-617694 .... p 362 N94-10553
DE93-617695 .... p 362 N94-10554
DE93-617696 .... p 362 N94-10555
DE93-617697 .... p 349 N94-10556
DE93-617729 .... p 362 N94-10557
DE93-617730 .... p 410 N94-10721
DE93-617731 .... p 363 N94-10722
DE93-617733 .... p 364 N94-10835
DE93-617741 .... p 364 N94-10837
DE93-617758 .... p 366 N94-11349
DE93-617820 .... p 149 N94-10838
DE93-617842 .... p 388 N94-10839
DE93-617843 .... p 393 N94-11477
DE93-617844 .... p 386 N94-10395
DE93-617845 .... p 389 N94-10885
DE93-617846 .... p 386 N94-10396
DE93-617847 .... p 386 N94-10397
DE93-617848 .... p 387 N94-10538
DE93-617849 .... p 387 N94-10539
DE93-617850 .... p 387 N94-10540
DE93-617851 .... p 386 N94-10523
DE93-617852 .... p 388 N94-10840
DE93-617862 .... p 389 N94-10886
DE93-617863 .... p 386 N94-10524
DE93-617882 .... p 395 N94-10525
DE93-617892 .... p 396 N94-10716
DE93-617895 .... p 148 N94-10717
DE93-619229 .... p 277 N94-11603
DE93-619375 .... p 153 N94-11604
DE93-619665 .... p 342 N94-10325 #
DE93-619666 .... p 339 N94-11630
DE93-619671 .... p 346 N94-11348
DE93-619672 .... p 346 N94-11631 #
DE93-619673 .... p 346 N94-11632 #
DE93-619706 .... p 175 N94-11633 #
DE93-619707 .... p 175 N94-11634
DE93-619717 .... p 427 N94-11692 #
DE93-619722 .... p 346 N94-11693
DE93-619724 .... p 346 N94-11811
DE93-619769 .... p 427 N94-11812
DE93-619770 .... p 412 N94-11047 #
DE93-620579 .... p 83 N94-11363
DE93-620636 .... p 188 N94-11364
DE93-620976 .... p 143 N94-11365
DE93-620977 .... p 387 N94-10541
DE93-620978 .... p 371 N94-10542
DE93-620979 .... p 141 N94-10543
DE93-620980 .... p 362 N94-10649
DE93-620982 .... p 133 N94-11030
DE93-620983 .... p 391 N94-11174
DE93-620984 .... p 364 N94-10875
DE93-620987 .... p 387 N94-10558
DE93-621316 .... p 324 N94-11031
DE93-621341 .... p 344 N94-11032
DE93-621350 .... p 344 N94-11033
DE93-621352 .... p 133 N94-11034
DE93-621353 .... p 134 N94-11035
DE93-621354 .... p 345 N94-11036
DE93-621355 .... p 134 N94-11037
DE93-621356 .... p 134 N94-11038
DE93-621374 .... p 345 N94-11077
DE93-621379 .... p 365 N94-11078
DE93-621381 .... p 412 N94-11086
DE93-621382 .... p 412 N94-11039
DE93-621420 .... p 412 N94-11087
DE93-621421 .... p 412 N94-11164
DE93-621422 .... p 412 N94-11088
DE93-621452 .... p 365 N94-11089
DE93-621541 .... p 398 N94-11090
DE93-621599 .... p 389 N94-11091
DE93-621608 .... p 389 N94-11092
DE93-621609 .... p 66 N94-11143
DE93-621639 .... p 389 N94-11119
DE93-621640 .... p 390 N94-11120
DE93-621641 .... p 390 N94-11121
DE93-621642 .... p 391 N94-11207
DE93-621643 .... p 391 N94-11208
DE93-621653 .... p 391 N94-11209
DE93-621654 .... p 391 N94-11210
DE93-621655 .... p 391 N94-11211
DE93-621656 .... p 392 N94-11212
DE93-621658 .... p 392 N94-11213
DE93-621659 .... p 390 N94-11148 #
DE93-621666 .... p 392 N94-11214
DE93-621681 .... p 392 N94-11215
DE93-622837 .... p 420 N94-11818 #
DE93-752300 .... p 360 N94-10317 #
DE93-753080 .... p 396 N94-10645
DE93-753168 .... p 144 N94-11508
DE93-753169 .... p 367 N94-11509
DE93-753173 .... p 367 N94-11510
DE93-753186 .... p 372 N94-11591
DE93-753187 .... p 368 N94-11592
DE93-753188 .... p 183 N94-11168
DE93-753189 .... p 84 N94-11593
DE93-753240 .... p 393 N94-11594
DE93-753246 .... p 367 N94-11580
DE93-753403 .... p 372 N94-11595
DE93-754136 .... p 411 N94-10887
DE93-754137 .... p 300 N94-10888
DE93-754138 .... p 363 N94-10696
DE93-754139 .... p 364 N94-10889
DE93-754192 .... p 410 N94-10718
DE93-754285 .... p 371 N94-10719
DE93-754288 .... p 363 N94-10720
DE93-754289 .... p 365 N94-11040
DE93-754294 .... p 34 N94-11041
DE93-754295 .... p 358 N94-11042
DE93-754330 .... p 372 N94-11043
DE93-767967 .... p 25 N94-10728 #
DE93-767968 .... p 343 N94-10729 #
DE93-767972 .... p 125 N94-10730 #
DE93-767973 .... p 313 N94-10731 #
DE93-767974 .... p 82 N94-10732 #
DE93-767975 .... p 33 N94-10733 #
DE93-767976 .... p 30 N94-10734 #
DE93-767977 .... p 2 N94-10363 #
DE93-767978 .... p 147 N94-10364 #
DE93-767979 .... p 147 N94-10365 #
DE93-767980 .... p 262 N94-10498 #
DE93-771240 .... p 390 N94-11149 #
DE93-771286 .... p 388 N94-10807
DE93-771406 .... p 390 N94-11128 #
DE93-771407 .... p 363 N94-10661
DE93-771408 .... p 392 N94-11239 #
DE93-771422 .... p 372 N94-11245 #
DE93-771423 .... p 387 N94-10662
DE93-781115 .... p 99 N94-11444 #
DE93-793615 .... p 149 N94-10861 #
DE93-793617 .... p 27 N94-10367 #
DE93-793618 .... p 335 N94-10368 #
DE93-793619 .... p 178 N94-10369 #
DE93-793622 .... p 65 N94-10857 #
DE93-793623 .... p 66 N94-10858 #
DE93-793626 .... p 27 N94-10370 #

DLR-FB-92-28 .... p 66 N94-11085 #

DODA-AR-006-864 .... p 89 N94-11107
DODA-AR-006-911 .... p 328 N94-11301

DOE-HDBK-1016/1-93 .... p 129 N94-11670 #
DOE-HDBK-1016/2-93 .... p 129 N94-11456 #

DOE/AD-0028 .... p 330 N94-11452 #
DOE/AD-0043 .... p 420 N94-11588 #

DOE/BC-14881/2 .... p 88 N94-10749 #

DOE/CE-15467/T1 .... p 82 N94-11008 #
DOE/CE-15492/T4 .... p 83 N94-11127 #
DOE/CE-23810/11B .... p 89 N94-11145 #
DOE/CE-23810/11C .... p 89 N94-11146 #
DOE/CE-23810/7 .... p 411 N94-10853 #

DOE/CH-10491/1 .... p 182 N94-11438 #

DOE/ER-0536 .... p 334 N94-12606 #
DOE/ER-13370/T2 .... p 300 N94-10652 #
DOE/ER-13456/50 .... p 358 N94-10154 #
DOE/ER-13530/5 .... p 273 N94-10305 #
DOE/ER-13530/6 .... p 273 N94-10319 #
DOE/ER-13991/2 .... p 147 N94-10320 #
DOE/ER-14020/4 .... p 365 N94-11010 #
DOE/ER-14024/4 .... p 263 N94-11116 #
DOE/ER-14062/3 .... p 398 N94-11117 #

DOE/ER-14065/T1 ..... p 76 N94-11244 #
DOE/ER-14213/1 ..... p 389 N94-11118 #
DOE/ER-14263/1 ..... p 365 N94-11029 #
DOE/ER-14303/1 ..... p 401 N94-11610 #
DOE/ER-40224/247 ..... p 368 N94-11696 #
DOE/ER-40333/136 ..... p 373 N94-12542 #
DOE/ER-40427/32-N92 ..... p 341 N94-10259 #
DOE/ER-40437/4 ..... p 373 N94-12607 #
DOE/ER-40561/077 ..... p 483 N94-11619 #
DOE/ER-40561/080 ..... p 425 N94-10292 #
DOE/ER-40561/095 ..... p 373 N94-11618 #
DOE/ER-40561/096 ..... p 368 N94-11620 #
DOE/ER-40614/25 ..... p 346 N94-11663 #
DOE/ER-40637/6 ..... p 366 N94-11147 #
DOE/ER-40646/3 ..... p 369 N94-12546 #
DOE/ER-40672/2 ..... p 370 N94-12609 #
DOE/ER-40681/2 ..... p 373 N94-12600 #
DOE/ER-40694/2 ..... p 368 N94-11813 #
DOE/ER-40713/1 ..... p 367 N94-11373 #
DOE/ER-45130/8 ..... p 365 N94-11011 #
DOE/ER-45131/T2 ..... p 154 N94-11814 #
DOE/ER-45163/33 ..... p 76 N94-10653 #
DOE/ER-45205/8 ..... p 398 N94-11115 #
DOE/ER-45211/22 ..... p 402 N94-11700 #
DOE/ER-45233/8 ..... p 76 N94-10854 #
DOE/ER-45252/6 ..... p 88 N94-10710
DOE/ER-45307/5 ..... p 398 N94-11012 #
DOE/ER-45373/5 ..... p 396 N94-10648
DOE/ER-45396/4 ..... p 91 N94-11698 #
DOE/ER-45403/4 ..... p 363 N94-10750 #
DOE/ER-45415/7 ..... p 367 N94-11470 #
DOE/ER-45437/2 ..... p 89 N94-11007 #
DOE/ER-53198/218 ..... p 388 N94-10747 #
DOE/ER-53212/212 ..... p 388 N94-10852 #
DOE/ER-53217/T1 ..... p 366 N94-11172 #
DOE/ER-53267/6 ..... p 386 N94-10321 #
DOE/ER-60265/T1 ..... p 267 N94-11697 #
DOE/ER-61029/13 ..... p 266 N94-11671 #
DOE/ER-61198/T2 ..... p 190 N94-11674 #
DOE/ER-61480/1 ..... p 77 N94-11359 #
DOE/ER-75708/T1 ..... p 48 N94-11372 #
DOE/ER-75839/1 ..... p 55 N94-11675 #
DOE/ER-75840/1 ..... p 318 N94-11817 #

DOE/ET-53088/592 ..... p 393 N94-11669 #
DOE/ET-53088/599 ..... p 390 N94-11142 #

DOE/FTR-93009149 ..... p 391 N94-11170 #
DOE/FTR-93010181 ..... p 361 N94-10334 #
DOE/FTR-93010184 ..... p 45 N94-10299 #

DOE/ID-13074/T7 ..... p 144 N94-11609 #

DOE/MC-29116/3355 ..... p 272 N94-12783 #

DOE/NASA/50306-3 ..... p 55 N94-11362 * #

DOE/NP-00119/T4 ..... p 417 N94-11661 #
DOE/NP-00119/3-VOL-2 ..... p 417 N94-11600 #

DOE/NV-10649/T1 ..... p 182 N94-12605 #

DOE/OR-21400/T474 ..... p 420 N94-11369 #

DOE/PC-92106/T1 ..... p 78 N94-11699 #
DOE/PC-92542/T1 ..... p 84 N94-11816 #

DOT-VNTSC-FAA-93-1 ..... p 23 N94-11626 #

DOT/FAA/AM-93/10 ..... p 315 N94-10806 #
DOT/FAA/AM-93/11 ..... p 303 N94-10813 #
DOT/FAA/AM-93/12 ..... p 38 N94-12567 #

DOT/FAA/CT-TN93/33 ..... p 22 N94-12575 #

DOT/FAA/CT-91/20 ..... p 26 N94-11858 #
DOT/FAA/CT-93/3 ..... p 17 N94-10766 #

DOT/FAA/NR-92/11 ..... p 23 N94-11103
DOT/FAA/NR-93-1 ..... p 23 N94-11626 #

DOT/FAA/SE-93/1 ..... p 23 N94-10933 #

DOT/FAA/93/3 ..... p 22 N94-12384 #

DOT/FRA/ORD-93/13 ..... p 422 N94-10736

DRES-SR-581 ..... p 78 N94-12009

DU/DC/TR-35 ..... p 78 N94-11683 #

E-6240 ..... p 185 N94-10361 * #
E-7251 ..... p 188 N94-11254 * #
E-7353 ..... p 28 N94-11234 * #
E-7375-1 ..... p 174 N94-11132 * #
E-7483 ..... p 74 N94-12449 * #
E-7551 ..... p 48 N94-11380 * #
E-7614 ..... p 55 N94-12569 * #
E-7662 ..... p 15 N94-11133 * #
E-7692 ..... p 55 N94-11362 * #
E-7697 ..... p 66 N94-11135 * #
E-7785 ..... p 67 N94-11237 * #
E-7786 ..... p 188 N94-11482 * #
E-7813 ..... p 47 N94-11252 * #
E-7850 ..... p 278 N94-11702 * #
E-7862 ..... p 152 N94-11376 * #
E-7867 ..... p 342 N94-10362 * #
E-7888 ..... p 323 N94-10639 * #
E-7889 ..... p 152 N94-11377 * #
E-7903 ..... p 14 N94-10892 * #
E-7908 ..... p 186 N94-10762 * #
E-7914 ..... p 485 N94-10356 * #
E-7918 ..... p 327 N94-11231 * #
E-7920 ..... p 28 N94-11238 * #
E-7929 ..... p 140 N94-10505 * #
E-7943 ..... p 150 N94-10939 * #
E-7945 ..... p 47 N94-11307 * #
E-7951 ..... p 46 N94-10765 * #
E-7959 ..... p 40 N94-10640 * #
E-7960 ..... p 327 N94-11232 * #
E-7963 ..... p 170 N94-11310 * #
E-7966 ..... p 89 N94-11204 * #
E-7967 ..... p 28 N94-10816 * #
E-7969 ..... p 319 N94-10724 * #
E-7972 ..... p 39 N94-10764 * #
E-7984 ..... p 90 N94-11257 * #
E-7988 ..... p 404 N94-12430 * #
E-7990 ..... p 151 N94-11192 * #
E-7992 ..... p 30 N94-11251 * #
E-7993 ..... p 152 N94-11481 * #
E-7994 ..... p 151 N94-11253 * #
E-7997 ..... p 15 N94-11203 * #
E-7999 ..... p 40 N94-10811 * #
E-8005 ..... p 29 N94-12271 * #
E-8006 ..... p 29 N94-12270 * #
E-8007 ..... p 29 N94-12272 * #
E-8010 ..... p 88 N94-10864 * #
E-8013 ..... p 74 N94-12431 * #
E-8014 ..... p 183 N94-11167 * #
E-8015 ..... p 151 N94-11256 * #
E-8018 ..... p 29 N94-11255 * #
E-8021 ..... p 46 N94-10761 * #
E-8022 ..... p 43 N94-10756 * #
E-8025 ..... p 180 N94-10760 * #
E-8026 ..... p 163 N94-12576 * #
E-8032 ..... p 66 N94-11202 * #
E-8041 ..... p 146 N94-12433 * #
E-8067 ..... p 1 N94-11703 * #
E-8082 ..... p 46 N94-10763 * #
E-8086 ..... p 74 N94-12594 * #

EER-1041 ..... p 82 N94-10804 * #

EGG-M-92469 ..... p 365 N94-10952
EGG-M-92696 ..... p 163 N94-12604 #

EGG-MS-10441 ..... p 83 N94-11141 #

EGG-WTD-10507 ..... p 76 N94-11140 #

EGG-10617-6097 ..... p 419 N94-11137 #

EMRTC-FR-93-12 ..... p 93 N94-12354 #

ENSCO-ATE-93-02 ..... p 422 N94-10736

EPA/402/R-92/005 ..... p 274 N94-10698
EPA/454/B-92/008 ..... p 265 N94-11016 #
EPA/600/A-93/109 ..... p 267 N94-11845 #
EPA/600/A-93/112 ..... p 265 N94-10841
EPA/600/R-93/063 ..... p 266 N94-11471 #
EPA/745/K-93/001 ..... p 264 N94-10836
EPA/842/B-92/009 ..... p 265 N94-10846

ERDEC-CR-019 ..... p 75 N94-10337 #

ERIM-226800-27-F ..... p 382 N94-11421 #

ERP-1112 ..... p 275 N94-11013 #

ES/IRA-1 ..... p 420 N94-11369 #

ESA-BR-81 ..... p 38 N94-11461 #
ESA-BR-90 ..... p 485 N94-11379 #

ESA-F-28 ..... p 333 N94-12383 #

ESA-HSR-2 ..... p 44 N94-11462 #

ESA-SP-333-VOL-1 ..... p 99 N94-10070 #
ESA-SP-333-VOL-2 ..... p 112 N94-10171 #
ESA-SP-336 ..... p 56 N94-10001 #
ESA-SP-359-VOL-1 ..... p 232 N94-11704 #
ESA-SP-359-VOL-2 ..... p 245 N94-12471 #

ESC-TR-92-207 ..... p 331 N94-11652
ESC-TR-93-179 ..... p 337 N94-11881 #

ESDP-4034 ..... p 264 N94-10650 #

ESM-38 ..... p 360 N94-10332 #
ESM-39 ..... p 361 N94-10333 #
ESM-40 ..... p 360 N94-10330 #
ESM-41 ..... p 360 N94-10328 #
ESM-42 ..... p 360 N94-10329 #
ESM-43 ..... p 360 N94-10327 #
ESM-44 ..... p 359 N94-10311 #
ESM-45 ..... p 360 N94-10331 #
ESM-47 ..... p 359 N94-10312 #

ETDE/JP-MF-93767980 ..... p 262 N94-10498 #
ETDE/JP-MF-93781115 ..... p 99 N94-11444 #

ETN-93-93747 ..... p 359 N94-10266
ETN-93-93943 ..... p 56 N94-10001 #
ETN-93-93949 ..... p 99 N94-10070 #
ETN-93-93950 ..... p 112 N94-10171 #
ETN-93-93959 ..... p 66 N94-11085 #
ETN-93-94149 ..... p 342 N94-10351 #
ETN-93-94150 ..... p 342 N94-10352 #
ETN-93-94151 ..... p 347 N94-10353 #
ETN-93-94152 ..... p 347 N94-10354 #
ETN-93-94301 ..... p 322 N94-10355 #
ETN-93-94308 ..... p 348 N94-10272 #
ETN-93-94309 ..... p 341 N94-10273 #
ETN-93-94310 ..... p 341 N94-10274 #
ETN-93-94311 ..... p 147 N94-10275 #
ETN-93-94312 ..... p 321 N94-10265 #
ETN-93-94313 ..... p 322 N94-10418 #
ETN-93-94314 ..... p 322 N94-10419 #
ETN-93-94315 ..... p 184 N94-10161 #
ETN-93-94316 ..... p 348 N94-10162 #
ETN-93-94317 ..... p 341 N94-10163 #
ETN-93-94318 ..... p 341 N94-10276 #
ETN-93-94319 ..... p 335 N94-10277 #
ETN-93-94320 ..... p 319 N94-10278 #
ETN-93-94321 ..... p 320 N94-10164 #
ETN-93-94322 ..... p 131 N94-10165 #
ETN-93-94323 ..... p 342 N94-10279 #
ETN-93-94324 ..... p 131 N94-10280 #
ETN-93-94325 ..... p 320 N94-10166 #
ETN-93-94326 ..... p 320 N94-10167 #
ETN-93-94327 ..... p 341 N94-10168 #
ETN-93-94328 ..... p 338 N94-10169 #
ETN-93-94329 ..... p 183 N94-10170 #
ETN-93-94330 ..... p 343 N94-10867 #
ETN-93-94331 ..... p 416 N94-10868 #
ETN-93-94332 ..... p 339 N94-10869 #
ETN-93-94333 ..... p 347 N94-10876 #
ETN-93-94334 ..... p 88 N94-10877 #
ETN-93-94346 ..... p 323 N94-10878 #
ETN-93-94347 ..... p 419 N94-10903 #
ETN-93-94348 ..... p 174 N94-10904 #
ETN-93-94349 ..... p 344 N94-10905 #
ETN-93-94350 ..... p 344 N94-10906 #
ETN-93-94351 ..... p 344 N94-10907 #
ETN-93-94352 ..... p 344 N94-10908 #
ETN-93-94415 ..... p 186 N94-10879 #
ETN-93-94634 ..... p 232 N94-11704 #
ETN-93-94635 ..... p 245 N94-12471 #

FAA-APO-93-1 ..... p 2 N94-12578 #

FERMILAB-PUB-93/140-A ..... p 425 N94-11153 * #

FMRL-TR-8 ..... p 16 N94-11889 #

FNAL/C-93/051-E ..... p 370 N94-12781 #
FNAL/C-93/053-E ..... p 146 N94-12603 #

FTINT-27-89 ..... p 398 N94-11025

GA-A-21128 ..... p 394 N94-12544 #
GA-A-21210 ..... p 373 N94-11694 #
GA-A-21236 ..... p 325 N94-11139 #
GA-A-21254 ..... p 385 N94-10159 #
GA-A-21258 ..... p 394 N94-12545 #
GA-A-21264 ..... p 137 N94-11453 #
GA-A-21281 ..... p 393 N94-11514 #

GAO/AFMD-93-3 ..... p 418 N94-12443 #

GAO/IMTEC-93-29R ..... p 421 N94-12445 #

GAO/NSIAD-93-178 ..... p 416 N94-10941 #
GAO/NSIAD-93-207 ..... p 416 N94-10910 #

GDC-RAMCAD-91-019 ..... p 331 N94-11679

GI-91-75A .... p 273 N94-10319 #
GI-91-75 .... p 273 N94-10305 #

GRI-93/0026 .... p 98 N94-11017 #

GSCAN-P-91-2 .... p 274 N94-10407 #

GTS-92063 .... p 416 N94-10145 #

H-1890 .... p 283 N94-10725 * #
H-1894 .... p 13 N94-10820 * #
H-1906 .... p 26 N94-11233 * #
H-1909 .... p 28 N94-11205 * #
H-1912 .... p 13 N94-10707 * #
H-1919 .... p 315 N94-11627 * #

IAE-0100 .... p 371 N94-10409

IAPCM-0020 .... p 173 N94-10483 #

IC-91/253 .... p 427 N94-11812
IC-92/220 .... p 412 N94-11163 #
IC-92/259 .... p 346 N94-11507 #
IC-92/278 .... p 361 N94-10502
IC-92/279 .... p 361 N94-10414 #
IC-92/280 .... p 410 N94-10631 #
IC-92/281 .... p 395 N94-10411 #
IC-92/282 .... p 396 N94-10800
IC-92/283 .... p 396 N94-10801
IC-92/285 .... p 427 N94-11692 #
IC-92/286 .... p 277 N94-11603
IC-92/290 .... p 386 N94-10387
IC-92/292 .... p 275 N94-10798
IC-92/294 .... p 410 N94-10802
IC-92/295 .... p 322 N94-10410
IC-92/296 .... p 342 N94-10325 #
IC-92/297 .... p 409 N94-10388
IC-92/298 .... p 132 N94-10401
IC-92/300 .... p 142 N94-10799
IC-92/301 .... p 409 N94-10500
IC-92/302 .... p 409 N94-10413 #
IC-92/303 .... p 395 N94-10537
IC-92/304 .... p 409 N94-10402
IC-92/305 .... p 357 N94-10408 #
IC-92/307 .... p 349 N94-10632
IC-92/308 .... p 418 N94-10485 #
IC-92/309 .... p 395 N94-10415
IC-92/310 .... p 396 N94-10637
IC-92/311 .... p 408 N94-10148 #
IC-92/313 .... p 361 N94-10503
IC-92/314 .... p 395 N94-10386
IC-92/316 .... p 410 N94-10635
IC-92/318 .... p 402 N94-11659
IC-92/320 .... p 402 N94-11660
IC-92/321 .... p 410 N94-10536 #
IC-92/322 .... p 348 N94-10412 #
IC-92/323 .... p 339 N94-11630
IC-92/326 .... p 368 N94-11581
IC-92/327 .... p 84 N94-12361
IC-92/328 .... p 410 N94-10545 #
IC-92/329 .... p 409 N94-10403
IC-92/330 .... p 409 N94-10499
IC-92/334 .... p 348 N94-10404
IC-92/359 .... p 396 N94-10716
IC-92/374 .... p 153 N94-11604
IC-92/386 .... p 346 N94-11348
IC-92/387 .... p 412 N94-11047 #
IC-92/388 .... p 346 N94-11631 #
IC-92/389 .... p 346 N94-11632 #
IC-92/390 .... p 175 N94-11633 #
IC-92/391 .... p 175 N94-11634
IC-92/431 .... p 346 N94-11693
IC-92/85 .... p 394 N94-10281 #
IC-92/91 .... p 343 N94-10531
IC-92/94 .... p 148 N94-10530
IC-92/95 .... p 425 N94-11136 #
IC-92/99 .... p 425 N94-11152 #

ICASE-93-23 .... p 337 N94-11308 * #
ICASE-93-25 .... p 343 N94-10642 * #
ICASE-93-26 .... p 345 N94-11277 * #
ICASE-93-29 .... p 326 N94-11196 * #
ICASE-93-30 .... p 323 N94-10643 * #
ICASE-93-36 .... p 149 N94-10810 * #
ICASE-93-37 .... p 345 N94-11280 * #

ICOMP-93-14 .... p 342 N94-10362 * #
ICOMP-93-15 .... p 152 N94-11376 * #
ICOMP-93-17 .... p 152 N94-11377 * #
ICOMP-93-24 .... p 151 N94-11192 * #
ICOMP-93-25 .... p 152 N94-11481 * #
ICOMP-93-26 .... p 151 N94-11253 * #

IDA-P-2765 .... p 332 N94-11850 #

IDA/HQ-92-042441 .... p 332 N94-11850 #

IEN-23/91 .... p 342 N94-10283 #
IEN-24/91 .... p 349 N94-10636 #

IFSR-592 .... p 393 N94-11669 #

IFT-P-016/92 .... p 349 N94-10633 #

INIS-MF-13362-PT-2 .... p 263 N94-11506 #
INIS-MF-13363-PT-3 .... p 263 N94-11505 #
INIS-MF-13441 .... p 183 N94-10847
INIS-MF-13507 .... p 420 N94-11818 #

INP-MSU-91-15-219 .... p 410 N94-10535
INP-MSU-92-13-262 .... p 362 N94-10634

INPE-5457-TDI/499 .... p 345 N94-11193 #
INPE-5462-PRE/1770 .... p 325 N94-11178 #
INPE-5470-TDI/501 .... p 276 N94-11165 #
INPE-5471-TDI/502 .... p 333 N94-12358 #
INPE-5472-TDI/503 .... p 288 N94-11200 #
INPE-5473-TDI/504 .... p 44 N94-12356 #
INPE-5477-TAE/019 .... p 232 N94-11524 #
INPE-5491-TDI/508 .... p 484 N94-12357 #
INPE-5492-TDI/509 .... p 325 N94-11166 #
INPE-5493-TDI/510 .... p 325 N94-11181 #
INPE-5497-TDI/512 .... p 230 N94-11179 #

INS-T-513 .... p 411 N94-10887

INS-918 .... p 396 N94-10645
INS-919 .... p 367 N94-11509
INS-920 .... p 144 N94-11508
INS-932 .... p 410 N94-10718
INS-939 .... p 34 N94-11041
INS-940 .... p 363 N94-10720
INS-941 .... p 365 N94-11040

INT-PATENT-CLASS-B64C-21/04 p 12 N94-10672 * #
INT-PATENT-CLASS-B64C-23/06 p 12 N94-10673 *

INT-PATENT-CLASS-F04B-35/00 p 179 N94-10674 *
INT-PATENT-CLASS-F16K-15/06 p 179 N94-10655 *
INT-PATENT-CLASS-F16K-15/06 p 179 N94-10658 *

INT-PATENT-CLASS-G01H-1/00 . p 185 N94-10671 *
INT-PATENT-CLASS-G01M-15/00 p 33 N94-10669 *
INT-PATENT-CLASS-G01N-19/00 p 33 N94-10669 *
INT-PATENT-CLASS-G01N-29/16 p 185 N94-10671 *
INT-PATENT-CLASS-G02B-1/10 . p 381 N94-10657 *
INT-PATENT-CLASS-G02B-5/20 . p 381 N94-10657 *
INT-PATENT-CLASS-G05B-19/24 p 179 N94-10670 *
INT-PATENT-CLASS-G06F-15/00 p 179 N94-10670 *
INT-PATENT-CLASS-G06F-15/46 p 179 N94-10670 *

INT-PATENT-CLASS-H01L-21/44 p 141 N94-10656 *
INT-PATENT-CLASS-H01P-7/10 . p 141 N94-10668

IRS-93-P7 .... p 47 N94-11354 * #

IS-M-741 .... p 183 N94-11110 #
IS-M-744 .... p 82 N94-10957 #

IS-T-1536 .... p 403 N94-12363 #
IS-T-1609 .... p 405 N94-12599 #

ISBN-0-16-037895-8 .... p 421 N94-12014 #
ISBN-0-315-72013-1 .... p 181 N94-11156
ISBN-0-315-73646-1 .... p 180 N94-11155
ISBN-92-835-0694-4 .... p 2 N94-10421 #
ISBN-92-835-0701-X .... p 68 N94-11317 #
ISBN-92-835-0702-9 .... p 31 N94-11489 #
ISBN-92-835-0705-3 .... p 126 N94-10613 #
ISBN-92-835-0707-X .... p 28 N94-11022 #
ISBN-92-9092-103-X .... p 38 N94-11461 #
ISBN-92-9092-139-0 .... p 485 N94-11379 #
ISBN-92-9092-174-9 .... p 99 N94-10070 #
ISBN-92-9092-174-9 .... p 112 N94-10171 #
ISBN-92-9092-186-2 .... p 56 N94-10001 #
ISBN-92-9092-278-8 .... p 232 N94-11704 #
ISBN-92-9092-278-8 .... p 245 N94-12471 #
ISBN-951-38-4228-2 .... p 390 N94-11148 #

ISL-PML-1992-73 .... p 143 N94-11298

ISVR-TR-217 .... p 76 N94-11216
ISVR-TR-219 .... p 345 N94-11217

ITF-91-50 .... p 409 N94-10405
ITF-91-71 .... p 388 N94-10839
ITF-91-73 .... p 393 N94-11477
ITF-91-74 .... p 148 N94-10717
ITF-91-75 .... p 149 N94-10838
ITF-92-2 .... p 362 N94-10557
ITF-92-6 .... p 411 N94-10831

ITN-93-85198 .... p 148 N94-10391
ITN-93-85199 .... p 343 N94-10392
ITN-93-85200 .... p 178 N94-10393

ITOP-6-2-531 .... p 138 N94-12409 #

ITP-91-103 .... p 388 N94-10882
ITP-91-106 .... p 411 N94-10832
ITP-91-107 .... p 411 N94-10834
ITP-91-18 .... p 410 N94-10721
ITP-91-49 .... p 363 N94-10722
ITP-91-58 .... p 389 N94-10886
ITP-91-71 .... p 386 N94-10395
ITP-91-78 .... p 411 N94-10880
ITP-91-85 .... p 349 N94-10548
ITP-91-87 .... p 361 N94-10549
ITP-91-93 .... p 362 N94-10550
ITP-91-94 .... p 349 N94-10833
ITP-91-95 .... p 366 N94-11349
ITP-91-98 .... p 409 N94-10394
ITP-92-10 .... p 397 N94-10883
ITP-92-11 .... p 362 N94-10551
ITP-92-12 .... p 397 N94-10884
ITP-92-13 .... p 349 N94-10547
ITP-92-1 .... p 389 N94-10885
ITP-92-22 .... p 386 N94-10396
ITP-92-23 .... p 386 N94-10397
ITP-92-24 .... p 387 N94-10538
ITP-92-25 .... p 387 N94-10539
ITP-92-26 .... p 387 N94-10540
ITP-92-27 .... p 386 N94-10523
ITP-92-28 .... p 344 N94-10881
ITP-92-29 .... p 362 N94-10552
ITP-92-30 .... p 388 N94-10840
ITP-92-31 .... p 362 N94-10554
ITP-92-3 .... p 362 N94-10553
ITP-92-41 .... p 362 N94-10555
ITP-92-5 .... p 349 N94-10556

IYAF-91-37 .... p 336 N94-10544

JACKFAU-92-414 .... p 417 N94-11844

JAERI-M-91-225 .... p 313 N94-10251 #
JAERI-M-92-078 .... p 372 N94-11591
JAERI-M-92-080 .... p 368 N94-11592
JAERI-M-92-081 .... p 84 N94-11593
JAERI-M-92-086 .... p 183 N94-11168
JAERI-M-92-087 .... p 390 N94-11149 #
JAERI-M-92-090 .... p 371 N94-10719
JAERI-M-92-112 .... p 358 N94-11042
JAERI-M-92-138 .... p 372 N94-11043

JINR-E-2-91-573 .... p 345 N94-11077
JINR-E-5-91-534 .... p 344 N94-11032

JINR-R-13-91-201 .... p 484 N94-10534
JINR-R-13-91-282 .... p 141 N94-10533
JINR-R-2-90-311 .... p 361 N94-10532
JINR-R-2-91-473 .... p 365 N94-11078

JTN-93-80418 .... p 191 N94-11894
JTN-93-80419 .... p 207 N94-12635
JTN-93-80421 .... p 35 N94-10676 #
JTN-93-80422 .... p 148 N94-10727 #
JTN-93-80424 .... p 25 N94-10728 #
JTN-93-80425 .... p 343 N94-10729 #
JTN-93-80429 .... p 125 N94-10730 #
JTN-93-80430 .... p 313 N94-10731 #
JTN-93-80431 .... p 82 N94-10732 #
JTN-93-80432 .... p 33 N94-10733 #
JTN-93-80433 .... p 30 N94-10734 #
JTN-93-80434 .... p 2 N94-10363 #
JTN-93-80435 .... p 147 N94-10364 #
JTN-93-80436 .... p 147 N94-10365 #
JTN-93-80437 .... p 42 N94-10366 #
JTN-93-80438 .... p 27 N94-10367 #
JTN-93-80439 .... p 335 N94-10368 #
JTN-93-80440 .... p 178 N94-10369 #
JTN-93-80441 .... p 13 N94-10855 #
JTN-93-80442 .... p 13 N94-10856 #
JTN-93-80443 .... p 65 N94-10857 #
JTN-93-80444 .... p 66 N94-10858 #
JTN-93-80445 .... p 43 N94-10859 #
JTN-93-80446 .... p 14 N94-10860 #
JTN-93-80447 .... p 27 N94-10370 #
JTN-93-80448 .... p 2 N94-10350 #
JTN-93-80449 .... p 149 N94-10861 #
JTN-93-80451 .... p 481 N94-12323 #
JTN-93-80455 .... p 230 N94-11129 #
JTN-93-80456 .... p 230 N94-11130 #
JTN-93-80457 .... p 301 N94-12278 #
JTN-93-80458 .... p 245 N94-12279 #
JTN-93-80473 .... p 129 N94-11831 #
JTN-93-80474 .... p 161 N94-12547 #
JTN-93-80480 .... p 44 N94-12280 #
JTN-93-80498 .... p 163 N94-12611 #

KAPL-4737 .... p 84 N94-11488 #

KCP-613-5039 .... p 381 N94-10647
KCP-613-5040 .... p 188 N94-11460 #
KCP-613-5042 .... p 144 N94-11479 #
KCP-613-5113 .... p 144 N94-11478 #

KEK-PROC-92-8 .... p 363 N94-10696
KEK-PROC-92-9 .... p 364 N94-10889

KEK-92-1 .... p 367 N94-11510
KEK-92-9 .... p 372 N94-11245 #

KFTI-91-13 .... p 398 N94-11090
KFTI-91-14 .... p 344 N94-11033
KFTI-91-17 .... p 188 N94-11364
KFTI-91-20 .... p 412 N94-11087
KFTI-91-21 .... p 412 N94-11164
KFTI-91-23-PT-1 .... p 389 N94-11119
KFTI-91-24 .... p 390 N94-11120
KFTI-91-26 .... p 392 N94-11214
KFTI-91-27 .... p 133 N94-11034
KFTI-91-29 .... p 134 N94-11035
KFTI-91-30 .... p 143 N94-11365
KFTI-91-33 .... p 387 N94-10541
KFTI-91-35 .... p 389 N94-11092
KFTI-91-36 .... p 390 N94-11121
KFTI-91-37 .... p 371 N94-10542
KFTI-91-38 .... p 391 N94-11209
KFTI-91-39 .... p 141 N94-10543
KFTI-91-41 .... p 391 N94-11210
KFTI-91-42 .... p 345 N94-11036
KFTI-91-44 .... p 389 N94-11091
KFTI-91-45 .... p 391 N94-11211
KFTI-91-46 .... p 412 N94-11088
KFTI-91-47 .... p 392 N94-11215
KFTI-91-49 .... p 362 N94-10649
KFTI-91-50 .... p 392 N94-11212
KFTI-91-51 .... p 134 N94-11037
KFTI-91-7 .... p 133 N94-11030
KFTI-92-14 .... p 83 N94-11363
KFTI-92-25 .... p 391 N94-11207
KFTI-92-31 .... p 391 N94-11174
KFTI-92-32 .... p 364 N94-10875
KFTI-92-40 .... p 66 N94-11143
KFTI-92-41 .... p 392 N94-11213
KFTI-92-43 .... p 391 N94-11208
KFTI-92-4 .... p 134 N94-11038
KFTI-92-5 .... p 387 N94-10558
KFTI-92-6 .... p 412 N94-11086
KFTI-92-7 .... p 412 N94-11039

KIYAI-91-14 .... p 82 N94-10842
KIYAI-91-15 .... p 386 N94-10524
KIYAI-91-24 .... p 397 N94-10843
KIYAI-91-27 .... p 364 N94-10848
KIYAI-91-29 .... p 397 N94-10845
KIYAI-91-41 .... p 364 N94-10835
KIYAI-92-3 .... p 395 N94-10525
KIYAI-92-7 .... p 372 N94-10849
KIYAI-92-8 .... p 364 N94-10837
KIYAI-92-9 .... p 324 N94-11031

KR-FRL-926-1 .... p 26 N94-11858 #

KURRI-TR-363 .... p 300 N94-10888

L-17163 .... p 12 N94-10675 * #
L-17199 .... p 484 N94-11278 * #
L-17206 .... p 148 N94-10644 * #
L-17226 .... p 485 N94-12434 * #
L-17240 .... p 373 N94-12435 * #
L-17241 .... p 484 N94-10759 * #

LA-SUB-93-51 .... p 273 N94-10285 #

LA-UR-92-4382 .... p 372 N94-10890 #
LA-UR-93-1018 .... p 264 N94-11666 #
LA-UR-93-1025 .... p 126 N94-10293 #
LA-UR-93-1088 .... p 401 N94-11646 #
LA-UR-93-1099 .... p 301 N94-11667 #
LA-UR-93-1119 .... p 97 N94-10294 #
LA-UR-93-1162 .... p 65 N94-10740
LA-UR-93-1179 .... p 347 N94-11006 #
LA-UR-93-1241 .... p 275 N94-10742
LA-UR-93-1243 .... p 361 N94-10349 #
LA-UR-93-1286 .... p 482 N94-10741
LA-UR-93-1382 .... p 384 N94-10158 #
LA-UR-93-1408 .... p 384 N94-10157 #
LA-UR-93-1414 .... p 412 N94-11162 #
LA-UR-93-1420 .... p 128 N94-11161 #
LA-UR-93-1519 .... p 363 N94-10743
LA-UR-93-1873 .... p 374 N94-12786 #
LA-UR-93-435 .... p 153 N94-11601 #

LA-12436-MS-VOL-2 .... p 272 N94-12780 #

LA-12480-T .... p 132 N94-10315 #
LA-12493-MS .... p 137 N94-11621 #
LA-12503-MS .... p 77 N94-11249 #
LA-12520 .... p 95 N94-12610 #

LALP-93-17 .... p 371 N94-10260 #

LBL-PUB-671 .... p 423 N94-11059 #

LBL-32695 .... p 380 N94-10608 * #
LBL-33232 .... p 408 N94-10261 #
LBL-33295 .... p 371 N94-10156 #

LESC-30749 .... p 27 N94-10664 * #

LIYAF-1699 .... p 365 N94-11089

LLNL-M-276-REV-2 .... p 321 N94-10263 #

LM-998 .... p 88 N94-10877 #

LMU-12/92 .... p 410 N94-10545 #

LR-687 .... p 186 N94-10879 #

M-727 .... p 286 N94-12580 * #

MCAT-93-10 .... p 25 N94-11150 * #
MCAT-93-12 .... p 15 N94-11195 * #

MEMO-COSOR-92-48 .... p 341 N94-10168 #
MEMO-COSOR-92-49 .... p 338 N94-10169 #
MEMO-COSOR-92-50 .... p 183 N94-10170 #
MEMO-COSOR-92-51 .... p 343 N94-10867 #
MEMO-COSOR-92-53 .... p 339 N94-10869 #
MEMO-COSOR-92-54 .... p 347 N94-10876 #
MEMO-COSOR-92-57 .... p 416 N94-10868 #

MEMO-INF-92-62 .... p 335 N94-10277 #
MEMO-INF-92-63 .... p 319 N94-10278 #
MEMO-INF-92-73 .... p 320 N94-10164 #
MEMO-INF-92-74 .... p 131 N94-10165 #
MEMO-INF-92-82 .... p 342 N94-10279 #
MEMO-INF-92-83 .... p 131 N94-10280 #
MEMO-INF-92-87 .... p 320 N94-10166 #
MEMO-INF-93-01 .... p 320 N94-10167 #

MEMO-1095 .... p 348 N94-10272 #
MEMO-1096 .... p 341 N94-10273 #
MEMO-1097 .... p 341 N94-10274 #
MEMO-1098 .... p 147 N94-10275 #
MEMO-1099 .... p 321 N94-10265 #
MEMO-1100 .... p 322 N94-10418 #
MEMO-1101 .... p 322 N94-10419 #
MEMO-1102 .... p 184 N94-10161 #
MEMO-1103 .... p 348 N94-10162 #
MEMO-1104 .... p 341 N94-10163 #
MEMO-1105 .... p 341 N94-10276 #

MIAC-1 .... p 81 N94-10297 #

MPL-TM-429 .... p 289 N94-12349 #

MPL-U-20/93 .... p 133 N94-10660
MPL-U-24/93 .... p 161 N94-12342 #
MPL-U-26/93 .... p 290 N94-12350 #
MPL-U-4/93 .... p 289 N94-12348 #
MPL-U-42/92 .... p 289 N94-12349 #
MPL-U-5/93 .... p 170 N94-10704

MRL-GD-0043 .... p 328 N94-11301
MRL-GD-0049 .... p 98 N94-11303 #

MRL-RR-1-93 .... p 90 N94-11302 #

MRL-TR-92-2 .... p 89 N94-11107

MSC-TN-26 .... p 190 N94-11079 #

MTI-93TR26 .... p 180 N94-10706

NAL-SP-18 .... p 163 N94-12611 #
NAL-SP-20 .... p 10 N94-10466 #

NAL-TM-644 .... p 148 N94-10727 #
NAL-TM-647 .... p 2 N94-10350 #
NAL-TM-648T .... p 149 N94-10861 #

NAL-TR-1138 .... p 25 N94-10728 #
NAL-TR-1139 .... p 343 N94-10729 #
NAL-TR-1143 .... p 125 N94-10730 #
NAL-TR-1145 .... p 42 N94-10366 #
NAL-TR-1147 .... p 313 N94-10731 #
NAL-TR-1148 .... p 82 N94-10732 #
NAL-TR-1149 .... p 27 N94-10367 #
NAL-TR-1151 .... p 33 N94-10733 #
NAL-TR-1152 .... p 30 N94-10734 #
NAL-TR-1153 .... p 2 N94-10363 #
NAL-TR-1154 .... p 335 N94-10368 #
NAL-TR-1155 .... p 178 N94-10369 #
NAL-TR-1156 .... p 13 N94-10855 #
NAL-TR-1157 .... p 13 N94-10856 #
NAL-TR-1158 .... p 147 N94-10364 #
NAL-TR-1159 .... p 65 N94-10857 #
NAL-TR-1160 .... p 66 N94-10858 #
NAL-TR-1162 .... p 147 N94-10365 #
NAL-TR-1165 .... p 43 N94-10859 #
NAL-TR-1172 .... p 14 N94-10860 #
NAL-TR-1174T .... p 27 N94-10370 #

NAMRL-SR-92-4 .... p 313 N94-11098 #

NAMRL-SR93-1 .... p 303 N94-11097 #

NAMRL-TM-92-4 .... p 324 N94-11099 #

NAMRL-1380 .... p 26 N94-11892 #

NAS 1.15:103832 .... p 315 N94-11375 * #
NAS 1.15:103986 .... p 231 N94-11378 * #
NAS 1.15:103987 .... p 300 N94-11191 * #
NAS 1.15:104000 .... p 1 N94-10936 * #
NAS 1.15:104008 .... p 30 N94-11259 * #
NAS 1.15:104022 .... p 327 N94-11274 * #
NAS 1.15:104269 .... p 26 N94-11233 * #
NAS 1.15:104587 .... p 288 N94-11358 * #
NAS 1.15:104590 .... p 284 N94-10940 * #
NAS 1.15:104762 .... p 125 N94-11235 * #
NAS 1.15:104774 .... p 423 N94-11183 * #
NAS 1.15:105603 .... p 185 N94-10361 * #
NAS 1.15:105820 .... p 188 N94-11254 * #
NAS 1.15:105888 .... p 28 N94-11234 * #
NAS 1.15:105964 .... p 174 N94-11132 * #
NAS 1.15:106078 .... p 55 N94-11362 * #
NAS 1.15:106121 .... p 67 N94-11237 * #
NAS 1.15:106122 .... p 188 N94-11482 * #
NAS 1.15:106166 .... p 152 N94-11376 * #
NAS 1.15:106183 .... p 323 N94-10639 * #
NAS 1.15:106184 .... p 152 N94-11377 * #
NAS 1.15:106195 .... p 14 N94-10892 * #
NAS 1.15:106199 .... p 40 N94-10640 * #
NAS 1.15:106200 .... p 186 N94-10762 * #
NAS 1.15:106203 .... p 342 N94-10362 * #
NAS 1.15:106205 .... p 485 N94-10356 * #
NAS 1.15:106208 .... p 327 N94-11231 * #
NAS 1.15:106210 .... p 28 N94-11238 * #
NAS 1.15:106226 .... p 150 N94-10939 * #
NAS 1.15:106227 .... p 47 N94-11307 * #
NAS 1.15:106232 .... p 46 N94-10765 * #
NAS 1.15:106238 .... p 327 N94-11232 * #
NAS 1.15:106239 .... p 319 N94-10724 * #
NAS 1.15:106246 .... p 89 N94-11204 * #
NAS 1.15:106250 .... p 39 N94-10764 * #
NAS 1.15:106259 .... p 90 N94-11257 * #
NAS 1.15:106262 .... p 404 N94-12430 * #
NAS 1.15:106263 .... p 151 N94-11192 * #
NAS 1.15:106265 .... p 30 N94-11251 * #
NAS 1.15:106266 .... p 152 N94-11481 * #
NAS 1.15:106267 .... p 151 N94-11253 * #
NAS 1.15:106271 .... p 40 N94-10811 * #
NAS 1.15:106275 .... p 88 N94-10864 * #
NAS 1.15:106276 .... p 74 N94-12431 * #
NAS 1.15:106277 .... p 183 N94-11167 * #
NAS 1.15:106278 .... p 151 N94-11256 * #
NAS 1.15:106279 .... p 29 N94-11255 * #
NAS 1.15:106281 .... p 47 N94-11252 * #
NAS 1.15:106283 .... p 46 N94-10761 * #
NAS 1.15:106284 .... p 43 N94-10756 * #
NAS 1.15:106287 .... p 180 N94-10760 * #
NAS 1.15:106288 .... p 163 N94-12576 * #
NAS 1.15:106305 .... p 170 N94-11310 * #
NAS 1.15:106320 .... p 1 N94-11703 * #
NAS 1.15:106327 .... p 46 N94-10763 * #
NAS 1.15:106334 .... p 66 N94-11135 * #
NAS 1.15:107562 .... p 40 N94-10805 * #
NAS 1.15:107743 .... p 16 N94-12421 * #
NAS 1.15:107754 .... p 318 N94-10814 * #
NAS 1.15:108247 .... p 47 N94-11053 * #
NAS 1.15:108253 .... p 43 N94-10699 * #
NAS 1.15:108256 .... p 424 N94-11306 * #
NAS 1.15:108413 .... p 419 N94-10723 * #
NAS 1.15:108414 .... p 89 N94-11175 * #
NAS 1.15:108415 .... p 43 N94-10808 * #
NAS 1.15:108417 .... p 423 N94-10866 * #
NAS 1.15:108418 .... p 188 N94-11275 * #
NAS 1.15:108987 .... p 419 N94-11352 * #
NAS 1.15:108994 .... p 162 N94-12571 * #
NAS 1.15:108998 .... p 245 N94-12432 * #
NAS 1.15:108999 .... p 67 N94-11276 * #
NAS 1.15:109010 .... p 26 N94-11587 * #
NAS 1.15:109188 .... p 315 N94-11258 * #
NAS 1.15:109216 .... p 91 N94-11350 * #

NAS 1.15:109219 p 245 N94-11885 * #
NAS 1.15:109232 p 39 N94-10659 * #
NAS 1.15:109233 p 42 N94-10562 * #
NAS 1.15:109234 p 42 N94-10563 * #
NAS 1.15:109237 p 231 N94-11485 * #
NAS 1.15:109241 p 42 N94-10663 * #
NAS 1.15:109242 p 170 N94-10667 * #
NAS 1.15:109243 p 381 N94-11054 * #
NAS 1.15:109245 p 328 N94-11422 * #
NAS 1.15:4444 p 484 N94-11278 * #
NAS 1.15:4450 p 12 N94-10675 * #
NAS 1.15:4479 p 148 N94-10644 * #
NAS 1.15:4494 p 28 N94-11205 * #
NAS 1.15:4499 p 13 N94-10820 * #
NAS 1.15:4500 p 13 N94-10707 * #
NAS 1.18:1450.10B p 420 N94-11589 * #
NAS 1.21:7011(374) p 304 N94-11689 *
NAS 1.21:7011(375) p 303 N94-10398 *
NAS 1.21:7011(376) p 303 N94-10399 *
NAS 1.21:7037(289) p 1 N94-11687 *
NAS 1.21:7037(290) p 1 N94-11691 *
NAS 1.21:7037(291) p 1 N94-11690 *
NAS 1.21:7037(293) p 1 N94-10420 *
NAS 1.26:177613 p 423 N94-11229 * #
NAS 1.26:177618 p 24 N94-12355 * #
NAS 1.26:180883 p 179 N94-10400 * #
NAS 1.26:185273 p 140 N94-10505 * #
NAS 1.26:186024 p 283 N94-10725 * #
NAS 1.26:188253 p 27 N94-10664 * #
NAS 1.26:188258 p 43 N94-10666 * #
NAS 1.26:188259 p 42 N94-10665 * #
NAS 1.26:189203 p 29 N94-12270 * #
NAS 1.26:189204 p 29 N94-12271 * #
NAS 1.26:189205 p 29 N94-12272 * #
NAS 1.26:191044 p 278 N94-11702 * #
NAS 1.26:191145 p 41 N94-10512 * #
NAS 1.26:191161 p 28 N94-10816 * #
NAS 1.26:191164 p 15 N94-11203 * #
NAS 1.26:191167 p 66 N94-11202 * #
NAS 1.26:191169 p 146 N94-12433 * #
NAS 1.26:191171 p 46 N94-10938 * #
NAS 1.26:191172 p 386 N94-10346 * #
NAS 1.26:191181 p 74 N94-12594 * #
NAS 1.26:191463 p 337 N94-11308 * #
NAS 1.26:191467 p 185 N94-10715 * #
NAS 1.26:191468 p 55 N94-10947 * #
NAS 1.26:191471 p 343 N94-10642 * #
NAS 1.26:191472 p 345 N94-11277 * #
NAS 1.26:191478 p 326 N94-11196 * #
NAS 1.26:191479 p 323 N94-10643 * #
NAS 1.26:191481 p 318 N94-11198 * #
NAS 1.26:191489 p 286 N94-12772 * #
NAS 1.26:191492 p 149 N94-10810 * #
NAS 1.26:191493 p 345 N94-11280 * #
NAS 1.26:191495 p 279 N94-12572 * #
NAS 1.26:192523 p 347 N94-10757 * #
NAS 1.26:192551 p 279 N94-12581 * #
NAS 1.26:192568 p 299 N94-10360 * #
NAS 1.26:192569 p 301 N94-11201 * #
NAS 1.26:192572 p 73 N94-11484 * #
NAS 1.26:192573 p 177 N94-10341 * #
NAS 1.26:192576 p 185 N94-10342 * #
NAS 1.26:192579 p 65 N94-10812 * #
NAS 1.26:192582 p 41 N94-10827 * #
NAS 1.26:192583 p 41 N94-10826 * #
NAS 1.26:192585 p 46 N94-10934 * #
NAS 1.26:192589 p 125 N94-11483 * #
NAS 1.26:192593 p 180 N94-10815 * #
NAS 1.26:192598 p 483 N94-12427 * #
NAS 1.26:192602 p 433 N94-10144 * #
NAS 1.26:192655 p 34 N94-10930 * #
NAS 1.26:192905 p 405 N94-12570 * #
NAS 1.26:193095 p 435 N94-12015 * #
NAS 1.26:193106 p 399 N94-11439 *
NAS 1.26:193133 p 47 N94-11354 * #
NAS 1.26:193150 p 230 N94-10953 * #
NAS 1.26:193182 p 276 N94-11355 * #
NAS 1.26:193184 p 229 N94-10702 * #
NAS 1.26:193189 p 274 N94-10701 * #
NAS 1.26:193190 p 55 N94-10513 * #
NAS 1.26:193191 p 46 N94-10700 * #
NAS 1.26:193219 p 25 N94-11150 * #
NAS 1.26:193220 p 324 N94-11046 * #
NAS 1.26:193228 p 300 N94-11180 * #
NAS 1.26:193229 p 46 N94-10911 * #
NAS 1.26:193232 p 300 N94-11045 * #
NAS 1.26:193235 p 42 N94-11297 * #
NAS 1.26:193240 p 30 N94-10895 * #
NAS 1.26:193249 p 425 N94-11153 * #
NAS 1.26:193253 p 338 N94-10638 * #
NAS 1.26:193267 p 424 N94-11356 * #
NAS 1.26:193281 p 423 N94-11305 * #
NAS 1.26:193282 p 483 N94-11048 * #
NAS 1.26:193283 p 484 N94-11312 * #
NAS 1.26:193292 p 150 N94-10912 * #
NAS 1.26:193310 p 137 N94-11357 * #
NAS 1.26:193339 p 152 N94-11526 * #
NAS 1.26:193364 p 366 N94-11360 * #
NAS 1.26:193368 p 484 N94-10507 * #
NAS 1.26:193369 p 375 N94-10506 * #
NAS 1.26:193398 p 266 N94-11374 * #
NAS 1.26:193399 p 418 N94-10515 * #
NAS 1.26:193405 p 278 N94-11886 * #
NAS 1.26:193406 p 313 N94-11511 * #
NAS 1.26:193407 p 434 N94-11361 * #
NAS 1.26:193408 p 231 N94-11309 * #
NAS 1.26:193409 p 136 N94-11084 * #
NAS 1.26:193411 p 231 N94-11236 * #
NAS 1.26:193457 p 142 N94-10931 * #
NAS 1.26:193458 p 324 N94-10942 * #
NAS 1.26:193465 p 338 N94-10345 * #
NAS 1.26:193466 p 267 N94-12451 * #
NAS 1.26:193469 p 427 N94-12557 * #
NAS 1.26:193470 p 321 N94-10343 * #
NAS 1.26:193472 p 320 N94-12558 * #
NAS 1.26:193474 p 316 N94-12365 * #
NAS 1.26:193476 p 302 N94-12559 * #
NAS 1.26:193477 p 279 N94-12560 * #
NAS 1.26:193480 p 25 N94-10344 * #
NAS 1.26:193513 p 484 N94-11486 * #
NAS 1.26:193514 p 425 N94-10943 * #
NAS 1.26:193515 p 424 N94-12768 * #
NAS 1.26:193518 p 428 N94-12767 * #
NAS 1.26:193545 p 434 N94-10817 * #
NAS 1.26:193549 p 280 N94-12583 * #
NAS 1.26:193551 p 280 N94-12582 * #
NAS 1.26:193555 p 33 N94-12769 * #
NAS 1.26:193556 p 56 N94-12588 * #
NAS 1.26:193558 p 364 N94-10946 * #
NAS 1.26:193565 p 231 N94-11521 * #
NAS 1.26:193568 p 397 N94-10819 * #
NAS 1.26:193569 p 23 N94-11525 * #
NAS 1.26:193573 p 485 N94-12589 * #
NAS 1.26:193586 p 485 N94-12771 * #
NAS 1.26:193587 p 428 N94-12770 * #
NAS 1.26:193589 p 387 N94-10641 * #
NAS 1.26:193612 p 358 N94-11176 * #
NAS 1.26:193614 p 186 N94-10937 * #
NAS 1.26:193620 p 324 N94-10932 * #
NAS 1.26:193623 p 357 N94-10752 * #
NAS 1.26:193626 p 15 N94-11195 * #
NAS 1.26:193627 p 274 N94-10726 * #
NAS 1.26:193644 p 318 N94-10865 * #
NAS 1.26:193666 p 181 N94-11157 * #
NAS 1.26:193674 p 170 N94-10948 * #
NAS 1.26:193683 p 136 N94-11206 * #
NAS 1.26:193701 p 275 N94-10950 * #
NAS 1.26:193704 p 483 N94-10949 * #
NAS 1.26:193712 p 327 N94-11279 * #
NAS 1.26:193713 p 425 N94-10511 * #
NAS 1.26:193715 p 482 N94-12446 * #
NAS 1.26:193723 p 331 N94-11522 * #
NAS 1.26:193730 p 326 N94-11197 * #
NAS 1.26:193731 p 82 N94-10804 * #
NAS 1.26:193772 p 413 N94-12343 * #
NAS 1.26:193805 p 482 N94-12429 * #
NAS 1.26:193812 p 323 N94-10711 * #
NAS 1.26:193829 p 285 N94-11598 * #
NAS 1.26:194030 p 139 N94-12778 * #
NAS 1.26:194055 p 424 N94-12573 * #
NAS 1.26:194087 p 424 N94-12574 * #
NAS 1.26:194108 p 434 N94-10823 * #
NAS 1.26:194112 p 180 N94-10821 * #
NAS 1.26:194113 p 85 N94-12447 * #
NAS 1.26:194117 p 76 N94-10713 * #
NAS 1.26:194129 p 185 N94-10712 * #
NAS 1.26:194131 p 323 N94-10862 * #
NAS 1.26:194164 p 187 N94-11190 * #
NAS 1.26:194169 p 381 N94-10735 * #
NAS 1.26:194171 p 23 N94-11177 * #
NAS 1.26:194172 p 366 N94-11199 * #
NAS 1.26:194191 p 166 N94-12774 * #
NAS 1.26:194192 p 166 N94-12775 * #
NAS 1.26:194235 p 146 N94-12773 * #
NAS 1.26:194255 p 427 N94-11628 * #
NAS 1.26:194286 p 426 N94-11590 * #
NAS 1.26:194288 p 416 N94-11599 * #
NAS 1.26:194290 p 346 N94-12776 * #
NAS 1.26:194370 p 94 N94-12450 * #
NAS 1.26:194374 p 428 N94-12595 * #
NAS 1.26:194376 p 427 N94-12566 * #
NAS 1.26:194389 p 155 N94-12284 * #
NAS 1.26:194400 p 332 N94-11688 * #
NAS 1.26:4527 p 326 N94-11188 * #
NAS 1.26:4528 p 315 N94-11627 * #
NAS 1.26:4532 p 13 N94-10758 * #
NAS 1.26:4534 p 142 N94-11131 * #
NAS 1.26:4537 p 286 N94-12580 * #
NAS 1.26:4545 p 412 N94-11523 * #
NAS 1.55:10068 p 308 N94-11991 * #
NAS 1.55:3187-VOL-2 p 486 N94-11527 * #
NAS 1.55:3210 p 48 N94-11380 * #
NAS 1.55:3218 p 350 N94-10963 * #
NAS 1.55:3219 p 375 N94-10564 * #
NAS 1.55:3225 p 333 N94-12448 * #
NAS 1.60:3320 p 74 N94-12449 * #
NAS 1.60:3330 p 25 N94-10935 * #
NAS 1.60:3352 p 485 N94-12434 * #
NAS 1.60:3353 p 373 N94-12435 * #
NAS 1.60:3356 p 30 N94-11134 * #
NAS 1.60:3363 p 484 N94-10759 * #
NAS 1.60:3380 p 55 N94-12569 * #
NAS 1.60:3383 p 15 N94-11133 * #
NAS 1.60:3393 p 34 N94-11869 * #
NAS 1.61:1291 p 81 N94-10504 * #
NAS 1.71:MFS-28508-1 p 14 N94-11021 * #
NAS 1.83:207 p 304 N94-11787 * #

NAS-SR-130 p 23 N94-10933 #

NASA-CASE-LAR-14741-1 p 185 N94-10671 *
NASA-CASE-LAR-14744-1 p 12 N94-10673 *

NASA-CASE-LEW-14791-1 p 12 N94-10672 * #

NASA-CASE-MFS-28493-1 p 33 N94-10669 *
NASA-CASE-MFS-28508-1 p 14 N94-11021 * #

NASA-CASE-MSC-21903-1 p 179 N94-10655 *
NASA-CASE-MSC-21950-1 p 179 N94-10658 *
NASA-CASE-MSC-22020-1 p 179 N94-10674 *

NASA-CASE-NPO-18062-1-CU p 141 N94-10656 *
NASA-CASE-NPO-18116-1-CU p 179 N94-10670 *
NASA-CASE-NPO-18433-1-CU p 381 N94-10657 *
NASA-CASE-NPO-18668-1-CU p 179 N94-10654 *

NASA-CP-10068 p 308 N94-11991 * #
NASA-CP-3187-VOL-2 p 486 N94-11527 * #
NASA-CP-3210 p 48 N94-11380 * #
NASA-CP-3218 p 350 N94-10963 * #
NASA-CP-3219 p 375 N94-10564 * #
NASA-CP-3225 p 333 N94-12448 * #

NASA-CR-177613 p 423 N94-11229 * #
NASA-CR-177618 p 24 N94-12355 * #
NASA-CR-180883 p 179 N94-10400 * #
NASA-CR-185273 p 140 N94-10505 * #
NASA-CR-186024 p 283 N94-10725 * #
NASA-CR-188253 p 27 N94-10664 * #
NASA-CR-188258 p 43 N94-10666 * #
NASA-CR-188259 p 42 N94-10665 * #
NASA-CR-189203 p 29 N94-12270 * #
NASA-CR-189204 p 29 N94-12271 * #
NASA-CR-189205 p 29 N94-12272 * #
NASA-CR-191044 p 278 N94-11702 * #
NASA-CR-191145 p 41 N94-10512 * #
NASA-CR-191161 p 28 N94-10816 * #
NASA-CR-191164 p 15 N94-11203 * #
NASA-CR-191167 p 66 N94-11202 * #
NASA-CR-191169 p 146 N94-12433 * #
NASA-CR-191171 p 46 N94-10938 * #
NASA-CR-191172 p 386 N94-10346 * #
NASA-CR-191181 p 74 N94-12594 * #
NASA-CR-191463 p 337 N94-11308 * #
NASA-CR-191467 p 185 N94-10715 * #
NASA-CR-191468 p 55 N94-10947 * #
NASA-CR-191471 p 343 N94-10642 * #
NASA-CR-191472 p 345 N94-11277 * #
NASA-CR-191478 p 326 N94-11196 * #
NASA-CR-191479 p 323 N94-10643 * #
NASA-CR-191481 p 318 N94-11198 * #
NASA-CR-191489 p 286 N94-12772 * #
NASA-CR-191492 p 149 N94-10810 * #
NASA-CR-191493 p 345 N94-11280 * #
NASA-CR-191495 p 279 N94-12572 * #
NASA-CR-192523 p 347 N94-10757 * #
NASA-CR-192551 p 279 N94-12581 * #
NASA-CR-192568 p 299 N94-10360 * #
NASA-CR-192569 p 301 N94-11201 * #
NASA-CR-192572 p 73 N94-11484 * #
NASA-CR-192573 p 177 N94-10341 * #
NASA-CR-192576 p 185 N94-10342 * #
NASA-CR-192579 p 65 N94-10812 * #
NASA-CR-192582 p 41 N94-10827 * #
NASA-CR-192583 p 41 N94-10826 * #
NASA-CR-192585 p 46 N94-10934 * #
NASA-CR-192589 p 125 N94-11483 * #
NASA-CR-192593 p 180 N94-10815 * #
NASA-CR-192598 p 483 N94-12427 * #
NASA-CR-192602 p 433 N94-10144 * #
NASA-CR-192655 p 34 N94-10930 * #
NASA-CR-192905 p 405 N94-12570 * #
NASA-CR-193095 p 435 N94-12015 * #
NASA-CR-193106 p 399 N94-11439 *
NASA-CR-193133 p 47 N94-11354 * #
NASA-CR-193150 p 230 N94-10953 * #
NASA-CR-193182 p 276 N94-11355 * #

NASA-CR-193184 .... p 229 N94-10702 * #
NASA-CR-193189 .... p 274 N94-10701 * #
NASA-CR-193190 .... p 55 N94-10513 * #
NASA-CR-193191 .... p 46 N94-10700 * #
NASA-CR-193219 .... p 25 N94-11150 * #
NASA-CR-193220 .... p 324 N94-11046 * #
NASA-CR-193228 .... p 300 N94-11180 * #
NASA-CR-193229 .... p 46 N94-10911 * #
NASA-CR-193232 .... p 300 N94-11045 * #
NASA-CR-193235 .... p 42 N94-11297 * #
NASA-CR-193240 .... p 30 N94-10895 * #
NASA-CR-193249 .... p 425 N94-11153 * #
NASA-CR-193253 .... p 338 N94-10638 * #
NASA-CR-193267 .... p 424 N94-11356 * #
NASA-CR-193281 .... p 423 N94-11305 * #
NASA-CR-193282 .... p 483 N94-11048 * #
NASA-CR-193283 .... p 484 N94-11312 * #
NASA-CR-193292 .... p 150 N94-10912 * #
NASA-CR-193310 .... p 137 N94-11357 * #
NASA-CR-193339 .... p 152 N94-11526 * #
NASA-CR-193364 .... p 366 N94-11360 * #
NASA-CR-193368 .... p 484 N94-10507 * #
NASA-CR-193369 .... p 375 N94-10506 * #
NASA-CR-193398 .... p 266 N94-11374 * #
NASA-CR-193399 .... p 418 N94-10515 * #
NASA-CR-193405 .... p 278 N94-11886 * #
NASA-CR-193406 .... p 313 N94-11511 * #
NASA-CR-193407 .... p 434 N94-11361 * #
NASA-CR-193408 .... p 231 N94-11309 * #
NASA-CR-193409 .... p 136 N94-11084 * #
NASA-CR-193411 .... p 231 N94-11236 * #
NASA-CR-193457 .... p 142 N94-10931 * #
NASA-CR-193458 .... p 324 N94-10942 * #
NASA-CR-193465 .... p 338 N94-10345 * #
NASA-CR-193466 .... p 267 N94-12451 * #
NASA-CR-193469 .... p 427 N94-12557 * #
NASA-CR-193470 .... p 321 N94-10343 * #
NASA-CR-193472 .... p 320 N94-12558 * #
NASA-CR-193474 .... p 316 N94-12365 * #
NASA-CR-193476 .... p 302 N94-12559 * #
NASA-CR-193477 .... p 279 N94-12560 * #
NASA-CR-193480 .... p 25 N94-10344 * #
NASA-CR-193513 .... p 484 N94-11486 * #
NASA-CR-193514 .... p 425 N94-10943 * #
NASA-CR-193515 .... p 424 N94-12768 * #
NASA-CR-193518 .... p 428 N94-12767 * #
NASA-CR-193545 .... p 434 N94-10817 * #
NASA-CR-193549 .... p 280 N94-12583 * #
NASA-CR-193551 .... p 280 N94-12582 * #
NASA-CR-193555 .... p 33 N94-12769 * #
NASA-CR-193556 .... p 56 N94-12588 * #
NASA-CR-193558 .... p 364 N94-10946 * #
NASA-CR-193565 .... p 231 N94-11521 * #
NASA-CR-193568 .... p 397 N94-10819 * #
NASA-CR-193569 .... p 23 N94-11525 * #
NASA-CR-193573 .... p 485 N94-12589 * #
NASA-CR-193586 .... p 485 N94-12771 * #
NASA-CR-193587 .... p 428 N94-12770 * #
NASA-CR-193589 .... p 387 N94-10641 * #
NASA-CR-193612 .... p 358 N94-11176 * #
NASA-CR-193614 .... p 186 N94-10937 * #
NASA-CR-193620 .... p 324 N94-10932 * #
NASA-CR-193623 .... p 357 N94-10752 * #
NASA-CR-193626 .... p 15 N94-11195 * #
NASA-CR-193627 .... p 274 N94-10726 * #
NASA-CR-193644 .... p 318 N94-10865 * #
NASA-CR-193666 .... p 181 N94-11157 * #
NASA-CR-193674 .... p 170 N94-10948 * #
NASA-CR-193683 .... p 136 N94-11206 * #
NASA-CR-193701 .... p 275 N94-10950 * #
NASA-CR-193704 .... p 483 N94-10949 * #
NASA-CR-193712 .... p 327 N94-11279 * #
NASA-CR-193713 .... p 425 N94-10511 * #
NASA-CR-193715 .... p 482 N94-12446 * #
NASA-CR-193723 .... p 331 N94-11522 * #
NASA-CR-193730 .... p 326 N94-11197 * #
NASA-CR-193731 .... p 82 N94-10804 * #
NASA-CR-193772 .... p 413 N94-12343 * #
NASA-CR-193805 .... p 482 N94-12429 * #
NASA-CR-193812 .... p 323 N94-10711 * #
NASA-CR-193829 .... p 285 N94-11598 * #
NASA-CR-194030 .... p 139 N94-12778 * #
NASA-CR-194055 .... p 424 N94-12573 * #
NASA-CR-194087 .... p 424 N94-12574 * #
NASA-CR-194108 .... p 434 N94-10823 * #
NASA-CR-194112 .... p 180 N94-10821 * #
NASA-CR-194113 .... p 85 N94-12447 * #
NASA-CR-194117 .... p 76 N94-10713 * #
NASA-CR-194129 .... p 185 N94-10712 * #
NASA-CR-194131 .... p 323 N94-10862 * #
NASA-CR-194164 .... p 187 N94-11190 * #
NASA-CR-194169 .... p 381 N94-10735 * #
NASA-CR-194171 .... p 23 N94-11177 * #
NASA-CR-194172 .... p 366 N94-11199 * #
NASA-CR-194191 .... p 166 N94-12774 * #
NASA-CR-194192 .... p 166 N94-12775 * #
NASA-CR-194235 .... p 146 N94-12773 * #
NASA-CR-194255 .... p 427 N94-11628 * #
NASA-CR-194286 .... p 426 N94-11590 * #
NASA-CR-194288 .... p 416 N94-11599 * #
NASA-CR-194290 .... p 346 N94-12776 * #
NASA-CR-194370 .... p 94 N94-12450 * #
NASA-CR-194374 .... p 428 N94-12595 * #
NASA-CR-194376 .... p 427 N94-12566 * #
NASA-CR-194389 .... p 155 N94-12284 * #
NASA-CR-194400 .... p 332 N94-11688 * #
NASA-CR-4527 .... p 326 N94-11188 * #
NASA-CR-4528 .... p 315 N94-11627 * #
NASA-CR-4532 .... p 13 N94-10758 * #
NASA-CR-4534 .... p 142 N94-11131 * #
NASA-CR-4537 .... p 286 N94-12580 * #
NASA-CR-4545 .... p 412 N94-11523 * #

NASA-NP-207 .... p 304 N94-11787 * #

NASA-RP-1291 .... p 81 N94-10504 * #

NASA-SP-7011(374) .... p 304 N94-11689 *
NASA-SP-7011(375) .... p 303 N94-10398 *
NASA-SP-7011(376) .... p 303 N94-10399 *
NASA-SP-7037(289) .... p 1 N94-11687 *
NASA-SP-7037(290) .... p 1 N94-11691 *
NASA-SP-7037(291) .... p 1 N94-11690 *
NASA-SP-7037(293) .... p 1 N94-10420 *

NASA-TM-103832 .... p 315 N94-11375 * #
NASA-TM-103986 .... p 231 N94-11378 * #
NASA-TM-103987 .... p 300 N94-11191 * #
NASA-TM-104000 .... p 1 N94-10936 * #
NASA-TM-104008 .... p 30 N94-11259 * #
NASA-TM-104022 .... p 327 N94-11274 * #
NASA-TM-104269 .... p 26 N94-11233 * #
NASA-TM-104587 .... p 288 N94-11358 * #
NASA-TM-104590 .... p 284 N94-10940 * #
NASA-TM-104762 .... p 125 N94-11235 * #
NASA-TM-104774 .... p 423 N94-11183 * #
NASA-TM-105603 .... p 185 N94-10361 * #
NASA-TM-105820 .... p 188 N94-11254 * #
NASA-TM-105888 .... p 28 N94-11234 * #
NASA-TM-105964 .... p 174 N94-11132 * #
NASA-TM-106078 .... p 55 N94-11362 * #
NASA-TM-106121 .... p 67 N94-11237 * #
NASA-TM-106122 .... p 188 N94-11482 * #
NASA-TM-106166 .... p 152 N94-11376 * #
NASA-TM-106183 .... p 323 N94-10639 * #
NASA-TM-106184 .... p 152 N94-11377 * #
NASA-TM-106195 .... p 14 N94-10892 * #
NASA-TM-106199 .... p 40 N94-10640 * #
NASA-TM-106200 .... p 186 N94-10762 * #
NASA-TM-106203 .... p 342 N94-10362 * #
NASA-TM-106205 .... p 485 N94-10356 * #
NASA-TM-106208 .... p 327 N94-11231 * #
NASA-TM-106210 .... p 28 N94-11238 * #
NASA-TM-106226 .... p 150 N94-10939 * #
NASA-TM-106227 .... p 47 N94-11307 * #
NASA-TM-106232 .... p 46 N94-10765 * #
NASA-TM-106238 .... p 327 N94-11232 * #
NASA-TM-106239 .... p 319 N94-10724 * #
NASA-TM-106246 .... p 89 N94-11204 * #
NASA-TM-106250 .... p 39 N94-10764 * #
NASA-TM-106259 .... p 90 N94-11257 * #
NASA-TM-106262 .... p 404 N94-12430 * #
NASA-TM-106263 .... p 151 N94-11192 * #
NASA-TM-106265 .... p 30 N94-11251 * #
NASA-TM-106266 .... p 152 N94-11481 * #
NASA-TM-106267 .... p 151 N94-11253 * #
NASA-TM-106271 .... p 40 N94-10811 * #
NASA-TM-106275 .... p 88 N94-10864 * #
NASA-TM-106276 .... p 74 N94-12431 * #
NASA-TM-106277 .... p 183 N94-11167 * #
NASA-TM-106278 .... p 151 N94-11256 * #
NASA-TM-106279 .... p 29 N94-11255 * #
NASA-TM-106281 .... p 47 N94-11252 * #
NASA-TM-106283 .... p 46 N94-10761 * #
NASA-TM-106284 .... p 43 N94-10756 * #
NASA-TM-106287 .... p 180 N94-10760 * #
NASA-TM-106288 .... p 163 N94-12576 * #
NASA-TM-106305 .... p 170 N94-11310 * #
NASA-TM-106320 .... p 1 N94-11703 * #
NASA-TM-106327 .... p 46 N94-10763 * #
NASA-TM-106334 .... p 66 N94-11135 * #
NASA-TM-107562 .... p 40 N94-10805 * #
NASA-TM-107743 .... p 16 N94-12421 * #
NASA-TM-107754 .... p 318 N94-10814 * #
NASA-TM-108247 .... p 47 N94-11053 * #
NASA-TM-108253 .... p 43 N94-10699 * #
NASA-TM-108256 .... p 424 N94-11306 * #
NASA-TM-108413 .... p 419 N94-10723 * #
NASA-TM-108414 .... p 89 N94-11175 * #
NASA-TM-108415 .... p 43 N94-10808 * #
NASA-TM-108417 .... p 423 N94-10866 * #
NASA-TM-108418 .... p 188 N94-11275 * #
NASA-TM-108987 .... p 419 N94-11352 * #
NASA-TM-108994 .... p 162 N94-12571 * #
NASA-TM-108998 .... p 245 N94-12432 * #
NASA-TM-108999 .... p 67 N94-11276 * #
NASA-TM-109010 .... p 26 N94-11587 * #
NASA-TM-109188 .... p 315 N94-11258 * #
NASA-TM-109216 .... p 91 N94-11350 * #
NASA-TM-109219 .... p 245 N94-11885 * #
NASA-TM-109232 .... p 39 N94-10659 * #
NASA-TM-109233 .... p 42 N94-10562 * #
NASA-TM-109234 .... p 42 N94-10563 * #
NASA-TM-109237 .... p 231 N94-11485 * #
NASA-TM-109241 .... p 42 N94-10663 * #
NASA-TM-109242 .... p 170 N94-10667 * #
NASA-TM-109243 .... p 381 N94-11054 * #
NASA-TM-109245 .... p 328 N94-11422 * #
NASA-TM-4444 .... p 484 N94-11278 * #
NASA-TM-4450 .... p 12 N94-10675 * #
NASA-TM-4479 .... p 148 N94-10644 * #
NASA-TM-4494 .... p 28 N94-11205 * #
NASA-TM-4499 .... p 13 N94-10820 * #
NASA-TM-4500 .... p 13 N94-10707 * #

NASA-TP-3320 .... p 74 N94-12449 * #
NASA-TP-3330 .... p 25 N94-10935 * #
NASA-TP-3352 .... p 485 N94-12434 * #
NASA-TP-3353 .... p 373 N94-12435 * #
NASA-TP-3356 .... p 30 N94-11134 * #
NASA-TP-3363 .... p 484 N94-10759 * #
NASA-TP-3380 .... p 55 N94-12569 * #
NASA-TP-3383 .... p 15 N94-11133 * #
NASA-TP-3393 .... p 34 N94-11869 * #

NASDA-CNT-930001-PT-2-A .... p 230 N94-11129 #
NASDA-CNT-930002-PT-2-F .... p 230 N94-11130 #
NASDA-CNT-930003 .... p 301 N94-12278 #
NASDA-CNT-930004 .... p 245 N94-12279 #

NASDA-CON-930001 .... p 129 N94-11831 #
NASDA-CON-930002 .... p 161 N94-12547 #

NASDA-TK-SS0438 .... p 481 N94-12323 #

NASDA-TMR-930005 .... p 44 N94-12280 #

NAVY-CASE-72490 .... p 176 N94-12321 #
NAVY-CASE-73258 .... p 94 N94-12399 #
NAVY-CASE-73675 .... p 176 N94-12329 #
NAVY-CASE-74067 .... p 145 N94-12322 #
NAVY-CASE-74171 .... p 333 N94-12386 #
NAVY-CASE-74582 .... p 176 N94-12337 #
NAVY-CASE-74662 .... p 404 N94-12400 #
NAVY-CASE-75190 .... p 93 N94-12330 #

NAWCADWAR-92092-60 .... p 315 N94-10296 #

NCCOSC/RDT/E-TD-2452 .... p 138 N94-11883 #

NCEL-TN-1856 .... p 35 N94-12562 #

NCI/93-07-PHASE-1 .... p 67 N94-11221 #

NEAR-TR-457 .... p 154 N94-11641 #

NEESA-20.2-051.4 .... p 265 N94-11015 #
NEESA-20.2-051.5 .... p 266 N94-11472 #

NHB-1450.10B .... p 420 N94-11589 * #

NHK-SERIAL-413 .... p 132 N94-10560
NHK-SERIAL-414 .... p 418 N94-10559

NIFS-DATA-15 .... p 367 N94-11580
NIFS-DATA-16 .... p 393 N94-11594
NIFS-DATA-19 .... p 387 N94-10662

NIFS-138 .... p 388 N94-10807

NIH-PUB-92-5 .... p 303 N94-10828

NIIYAF-MGU-91-15-219 .... p 410 N94-10535
NIIYAF-MGU-92-13-262 .... p 362 N94-10634

NIST/GCR-93/624 .... p 149 N94-10851

NIST/SP-500/207 .... p 419 N94-10829

NISTIR-5164 .... p 343 N94-10825

NPL-RSA(EXT)-34 .... p 359 N94-10266

NPSEC-93-011 .... p 138 N94-12281 #

NRA-87-106 .... p 231 N94-11521 * #

NREL/TP-432-5068 .... p 262 N94-10258 #

NRL/FR/5862-93-9552 ..... p 337 N94-11475 #
NRL/FR/8121-93-9531 ..... p 54 N94-11643 #

NRL/MR-6440-92-7174 ..... p 172 N94-10150 #

NRL/MR/5325-93-7326 ..... p 138 N94-11655 #
NRL/MR/6180-93-7310 ..... p 79 N94-12415 #
NRL/MR/6722-93-7301 ..... p 393 N94-11474 #
NRL/MR/6754-93-7322 ..... p 382 N94-11656 #
NRL/MR/6790-93-7300 ..... p 145 N94-12424 #
NRL/MR/7673-93-7313 ..... p 483 N94-12414 #
NRL/MR/8143-93-7337 ..... p 383 N94-12413 #

NRL/PU/5230-92-235 ..... p 497 N94-12334

NRLD-PR92-075-352 ..... p 288 N94-11287 #

NSF-92-134 ..... p 279 N94-12568 #
NSF-92-330 ..... p 422 N94-11186 #

NSWC-TR-85-85-REV ..... p 229 N94-10417 #

NTSB/AAR-93/01/SUM ..... p 22 N94-11044 #

NTSB/SIR-93/02 ..... p 40 N94-11893 #

NUWC-NL-TM-921240 ..... p 287 N94-10490 #

OCS/EIS/EA/MMS-93-0012-VOL-1 p 265 N94-11018 #
OCS/EIS/EA/MMS-93-0012-VOL-2 p 265 N94-11019 #

ODU-TR-PTR-92-1 ..... p 94 N94-12450 * #

ONREUR-92-4-W ..... p 313 N94-11701 #

ORNL-6733 ..... p 264 N94-10650 #

ORNL/ATD-67 ..... p 184 N94-10264 #
ORNL/ATD-70 ..... p 78 N94-11622 #

ORNL/FTR-4398 ..... p 184 N94-10155 #
ORNL/FTR-4444 ..... p 391 N94-11171 #
ORNL/FTR-4469 ..... p 358 N94-10254 #
ORNL/FTR-4479 ..... p 264 N94-10256 #
ORNL/FTR-4495 ..... p 385 N94-10253 #
ORNL/FTR-4513 ..... p 173 N94-10255 #

ORNL/M-12212 ..... p 72 N94-11368 #
ORNL/M-1860 ..... p 91 N94-11673 #
ORNL/M-1862 ..... p 91 N94-11672 #

ORNL/TM-12193 ..... p 177 N94-10269 #
ORNL/TM-12203 ..... p 332 N94-11695 #
ORNL/TM-12209 ..... p 385 N94-10310 #
ORNL/TM-12219 ..... p 173 N94-10160 #
ORNL/TM-12264 ..... p 131 N94-10270 #
ORNL/TM-12288 ..... p 340 N94-12543 #
ORNL/TM-12375 ..... p 340 N94-12428 #

OSU-ECE-NASA-93-03 ..... p 25 N94-10344 * #

PAPER-2D-2 ..... p 10 N94-10468 #
PAPER-2D-3 ..... p 10 N94-10469 #
PAPER-2D-4 ..... p 10 N94-10470 #
PAPER-2D-5 ..... p 11 N94-10471 #
PAPER-2D-7 ..... p 11 N94-10472 #
PAPER-2D-8 ..... p 11 N94-10473 #
PAPER-2D-9 ..... p 11 N94-10474 #
PAPER-3D-1 ..... p 11 N94-10477 #
PAPER-3D-2 ..... p 12 N94-10478 #
PAPER-3D-3 ..... p 12 N94-10479 #
PAPER-3D-4 ..... p 12 N94-10480 #
PAPER-3D-5 ..... p 12 N94-10481 #

PB93-134336 ..... p 421 N94-12385 #
PB93-175446 ..... p 26 N94-11464 #
PB93-176824 ..... p 266 N94-11584 #
PB93-181592 ..... p 266 N94-11471 #
PB93-182962 ..... p 266 N94-11472 #
PB93-182970 ..... p 265 N94-11015 #
PB93-183333 ..... p 274 N94-10698
PB93-183556 ..... p 303 N94-10828
PB93-184802 ..... p 266 N94-11451
PB93-188233 ..... p 265 N94-11016 #
PB93-188779 ..... p 416 N94-11473 #
PB93-189298 ..... p 343 N94-10825
PB93-189355 ..... p 417 N94-11844
PB93-189892 ..... p 98 N94-11017 #
PB93-190304 ..... p 265 N94-11018 #
PB93-190312 ..... p 265 N94-11019 #
PB93-191633 ..... p 267 N94-11864 #
PB93-191641 ..... p 419 N94-10829
PB93-194140 ..... p 264 N94-10836
PB93-194165 ..... p 267 N94-11845 #
PB93-194199 ..... p 265 N94-10841
PB93-194603 ..... p 98 N94-10844
PB93-194637 ..... p 265 N94-10846
PB93-194645 ..... p 422 N94-10736
PB93-196228 ..... p 485 N94-10850
PB93-198463 ..... p 149 N94-10851
PB93-910405 ..... p 22 N94-11044 #
PB93-917003 ..... p 40 N94-11893 #

PCMDI-11 ..... p 284 N94-10739
PCMDI-7 ..... p 273 N94-10151 #
PCMDI-8 ..... p 276 N94-11227 #
PCMDI-9 ..... p 276 N94-11241 #

PERS-93-002 ..... p 416 N94-10298 #

PL-TR-92-2131 ..... p 278 N94-11852 #
PL-TR-92-2263 ..... p 278 N94-12277 #
PL-TR-92-2327 ..... p 284 N94-11113
PL-TR-92-2329 ..... p 275 N94-11013 #
PL-TR-92-2344 ..... p 283 N94-10336 #
PL-TR-92-3056 ..... p 87 N94-10508 #
PL-TR-93-2031 ..... p 43 N94-10944
PL-TR-93-2034 ..... p 275 N94-11102
PL-TR-93-2090 ..... p 417 N94-12360 #
PL-TR-93-2101 ..... p 245 N94-11851 #

PNL-SA-19958 ..... p 73 N94-11612 #
PNL-SA-21606 ..... p 262 N94-11051 #
PNL-SA-21812 ..... p 87 N94-10295 #
PNL-SA-21966 ..... p 274 N94-10323 #

POEF-T-3605 ..... p 128 N94-11028 #

PSC-24 ..... p 390 N94-11128 #
PSC-25 ..... p 363 N94-10661
PSC-26 ..... p 392 N94-11239 #

PUBL-931333 ..... p 65 N94-10812 * #

PW/GESP-FR21998-18 ..... p 85 N94-12418 #

RCNP-P-120 ..... p 360 N94-10317 #

REPT-038-3524-150-93-1 ..... p 142 N94-11131 * #
REPT-1953-09 ..... p 170 N94-10667 * #
REPT-5307-00-9307-F ..... p 424 N94-11356 * #
REPT-92-1 ..... p 149 N94-10851
REPT-93-06 ..... p 322 N94-10355 #
REPT-93B00019 ..... p 81 N94-10504 * #
REPT-93B00078 ..... p 288 N94-11358 * #
REPT-93B00087 ..... p 350 N94-10963 * #
REPT-93B00088 ..... p 375 N94-10564 * #
REPT-93B00092 ..... p 284 N94-10940 * #
REPT-93B00098 ..... p 333 N94-12448 * #
REPT-93H-C-009-0-VOL-2 ..... p 41 N94-10827 * #

REV-399 ..... p 315 N94-11258 * #

RFP-4718 ..... p 41 N94-11282 #

RIACS-TR-93-04 ..... p 346 N94-12776 * #

RL-TR-92-338 ..... p 382 N94-11300
RL-TR-92-345-VOL-3 ..... p 333 N94-12008
RL-TR-92-345-VOL-5 ..... p 323 N94-10494
RL-TR-92-345-VOL-6 ..... p 323 N94-10495
RL-TR-93-19 ..... p 381 N94-10697
RL-TR-93-35 ..... p 383 N94-12416 #
RL-TR-93-43 ..... p 337 N94-12540 #

RSL-TR-7970-2 ..... p 139 N94-12778 * #

RTR-214-01-VOL-1 ..... p 166 N94-12775 * #
RTR-214-01-VOL-2 ..... p 166 N94-12774 * #

RU-TR-MAE-184-F ..... p 150 N94-11014 #

RXR-93011 ..... p 43 N94-10944

R93-970104-2 ..... p 92 N94-11876 #

S-706-VOL-2 ..... p 486 N94-11527 * #
S-711 ..... p 125 N94-11235 * #
S-727 ..... p 423 N94-11183 * #

SAIC(EARTH)-92/01 ..... p 286 N94-12772 * #

SAND-91-2016C ..... p 335 N94-10257 #
SAND-92-0259C ..... p 366 N94-11284 #
SAND-92-0501C ..... p 263 N94-11173 #
SAND-92-1168C ..... p 98 N94-11366 #
SAND-92-1350C ..... p 45 N94-10282 #
SAND-92-1407C ..... p 371 N94-10529
SAND-92-1462C ..... p 370 N94-10149 #
SAND-92-1636C ..... p 401 N94-11605
SAND-92-1716C ..... p 326 N94-11226 #
SAND-92-1724C ..... p 343 N94-10708 #
SAND-92-1896C ..... p 175 N94-11283 #
SAND-92-2029C ..... p 129 N94-11606 #
SAND-92-2043C ..... p 319 N94-10146 #
SAND-92-2239C ..... p 91 N94-11665 #
SAND-92-2498C ..... p 396 N94-10745
SAND-92-2526C ..... p 47 N94-11122 #
SAND-92-2579 ..... p 147 N94-10252 #
SAND-92-2585C ..... p 344 N94-10961 #
SAND-92-2760 ..... p 174 N94-11005 #
SAND-92-2804C ..... p 173 N94-10746
SAND-92-2857C ..... p 144 N94-11624 #
SAND-92-7286 ..... p 287 N94-10153 #
SAND-93-0200 ..... p 42 N94-10520 #
SAND-93-0224 ..... p 319 N94-10268 #
SAND-93-0227C ..... p 336 N94-11270 #
SAND-93-0260C ..... p 367 N94-11455 #
SAND-93-0306 ..... p 177 N94-10348 #
SAND-93-0308C ..... p 183 N94-11586 #
SAND-93-0346C ..... p 143 N94-11271 #
SAND-93-0478 ..... p 152 N94-11371 #
SAND-93-0483C ..... p 331 N94-11611 #
SAND-93-0539C ..... p 141 N94-10521 #
SAND-93-0595C ..... p 143 N94-11285 #
SAND-93-0690C ..... p 334 N94-12593 #
SAND-93-0731 ..... p 232 N94-11623 #
SAND-93-0744C ..... p 400 N94-11457 #
SAND-93-0767C ..... p 345 N94-11225 #
SAND-93-0825C ..... p 89 N94-10958 #
SAND-93-0858 ..... p 334 N94-12608 #
SAND-93-0878C ..... p 14 N94-11111 #
SAND-93-0892C ..... p 325 N94-11109 #
SAND-93-0901C ..... p 374 N94-10339 #
SAND-93-0921C ..... p 325 N94-11123 #
SAND-93-0937C ..... p 174 N94-10959 #
SAND-93-0955 ..... p 336 N94-10738
SAND-93-1020C ..... p 396 N94-10809 #
SAND-93-8228 ..... p 77 N94-11370 #

SDL/93-039 ..... p 279 N94-12561 #

SEL-92-004 ..... p 328 N94-11422 * #

SIO-REF-93-3 ..... p 289 N94-12348 #

SIP-0047 ..... p 343 N94-10546 #

SISSA-149/92/EP ..... p 410 N94-10545 #

SMC-TR-93-18 ..... p 146 N94-12565 #
SMC-TR-93-20 ..... p 276 N94-11463
SMC-TR-93-23 ..... p 44 N94-12394 #
SMC-TR-93-29 ..... p 91 N94-11487 #
SMC-TR-93-30-PT-1 ..... p 383 N94-12341 #

SP-R-0022A ..... p 91 N94-11350 * #

SR-272 ..... p 417 N94-12360 #
SR-2 ..... p 284 N94-11113

SSCL-PREPRINT-149-REV-1 ..... p 335 N94-10340 #
SSCL-PREPRINT-220 ..... p 133 N94-10960 #
SSCL-PREPRINT-241 ..... p 370 N94-12787 #
SSCL-PREPRINT-355 ..... p 374 N94-12785 #

SSRP-93/03 ..... p 186 N94-10937 * #

STS-49-SLJ ..... p 301 N94-11201 * #

SU-SLAC-PUB-5895 ..... p 133 N94-10709 #
SU-SLAC-PUB-6057 ..... p 411 N94-10956 #
SU-SLAC-PUB-6064 ..... p 175 N94-11468 #
SU-SLAC-PUB-6071 ..... p 367 N94-11469 #

SU-SLAC-409 ..... p 363 N94-10748 #

SU-SLAC/SSRL-0010 ..... p 175 N94-11468 #

SWRI-06-8602/8 ..... p 187 N94-11096 #

TBNEP-08-92 ..... p 267 N94-11864 #

TIOS-92/30 ..... p 320 N94-10164 #
TIOS-92/31 ..... p 131 N94-10165 #
TIOS-92/32 ..... p 131 N94-10280 #

TK-ST0467 ..... p 44 N94-12280 #

TOR-93(3078)-1 ..... p 274 N94-10496

TP-67 ..... p 266 N94-11451

TR-004 ..... p 87 N94-10510
TR-0091(6940-05)-05 ..... p 276 N94-11463
TR-0091(6945-08)-PT-1 ..... p 383 N94-12341 #
TR-10-ONR ..... p 95 N94-12585 #
TR-11-ONR ..... p 145 N94-11819 #

TR-12 p 92 N94-11847 #
TR-12 p 79 N94-12373 #
TR-12 p 95 N94-12577 #
TR-136 p 396 N94-10705
TR-139 p 369 N94-12420 #
TR-13 p 92 N94-11849 #
TR-140 p 368 N94-11658 #
TR-16-ONR p 403 N94-12010
TR-1 p 93 N94-12340 #
TR-1 p 403 N94-12371
TR-20-ONR p 402 N94-11654 #
TR-20 p 78 N94-12273 #
TR-21-ONR p 369 N94-11826 #
TR-22-ONR p 404 N94-12438 #
TR-23-0NR p 402 N94-11827 #
TR-40 p 67 N94-11260
TR-449 p 320 N94-11294 #
TR-454 p 337 N94-11650
TR-4 p 175 N94-12012
TR-52 p 143 N94-11160 #
TR-54 p 174 N94-11095 #
TR-54 p 94 N94-12381 #
TR-55 p 142 N94-11094 #
TR-57 p 373 N94-11880 #
TR-58 p 401 N94-11651
TR-6-ONR p 366 N94-11100 #
TR-65-ONR p 304 N94-11261 #
TR-6 p 365 N94-11093 #
TR-722792-5 p 23 N94-11525 * #
TR-75 p 77 N94-11264 #
TR-8-ONR p 90 N94-11292 #
TR-90-ONR p 401 N94-11518
TR-92(2925)-7 p 146 N94-12565 #
TR-93(3935)-10 p 91 N94-11487 #
TR-93(3935)-7 p 44 N94-12394 #
TR-93-01 p 93 N94-12380 #
TR-93-03 p 418 N94-10515 * #
TR-93-06 p 161 N94-12352 #
TR-93-1 p 337 N94-11829 #
TR-9 p 92 N94-11848 #

TWR-60736 p 65 N94-10812 * #

TX-93+983-5F p 98 N94-10844

UAH-5-33018 p 375 N94-10506 * #
UAH-5-33180 p 279 N94-12581 * #

UCB-PTH-92/25 p 380 N94-10608 * #

UCID-113435 p 389 N94-11114 #

UCRL-CR-113095 p 382 N94-11662 #

UCRL-ID-108158 p 276 N94-11241 #
UCRL-ID-108725 p 322 N94-10347 #
UCRL-ID-111487 p 185 N94-10306 #
UCRL-ID-111532-REV-1 p 273 N94-10151 #
UCRL-ID-111532 p 273 N94-10152 #
UCRL-ID-111838 p 394 N94-12370 #
UCRL-ID-111855 p 142 N94-11009 #
UCRL-ID-111898 p 147 N94-10307 #
UCRL-ID-112296 p 364 N94-10753
UCRL-ID-112607 p 321 N94-10267 #
UCRL-ID-112719 p 276 N94-11227 #
UCRL-ID-113623 p 284 N94-10739

UCRL-JC-105732 p 173 N94-10755
UCRL-JC-109094 p 393 N94-11677 #
UCRL-JC-109333 p 390 N94-11125 #
UCRL-JC-109645 p 98 N94-10751 #
UCRL-JC-109782 p 84 N94-11668 #
UCRL-JC-109804 p 389 N94-11074 #
UCRL-JC-110-843 p 385 N94-10262 #
UCRL-JC-110049-REV-1 p 89 N94-11151 #
UCRL-JC-110069-REV-1 p 177 N94-10322 #
UCRL-JC-110117 p 137 N94-11466 #
UCRL-JC-110202 p 132 N94-10518 #
UCRL-JC-110217 p 385 N94-10286 #
UCRL-JC-110274 p 382 N94-11242 #
UCRL-JC-110334 p 82 N94-11076 #
UCRL-JC-110398 p 385 N94-10289 #
UCRL-JC-110400 p 283 N94-10290 #
UCRL-JC-110510 p 399 N94-11268 #
UCRL-JC-110558 p 275 N94-11052 #
UCRL-JC-110846 p 272 N94-12592 #
UCRL-JC-110862 p 151 N94-11272 #
UCRL-JC-110977 p 142 N94-11050 #
UCRL-JC-111004 p 81 N94-10522 #
UCRL-JC-111005 p 77 N94-11602
UCRL-JC-111173 p 176 N94-12784 #
UCRL-JC-111193 p 174 N94-11126 #
UCRL-JC-111388 p 95 N94-12602 #
UCRL-JC-111392 p 176 N94-12590 #
UCRL-JC-111396 p 87 N94-10271 #
UCRL-JC-111482 p 90 N94-11230 #
UCRL-JC-111540 p 369 N94-11815 #
UCRL-JC-111555 p 181 N94-11247 #
UCRL-JC-111578 p 170 N94-11267 #
UCRL-JC-111627 p 169 N94-10526 #
UCRL-JC-111712 p 381 N94-10651 #
UCRL-JC-111725 p 143 N94-11273 #
UCRL-JC-111945 p 395 N94-10516 #
UCRL-JC-111995 p 98 N94-11269 #
UCRL-JC-112016 p 336 N94-11248 #
UCRL-JC-112022 p 336 N94-11027 #
UCRL-JC-112052 p 150 N94-11026 #
UCRL-JC-112177 p 140 N94-10309 #
UCRL-JC-112301 p 335 N94-10324 #
UCRL-JC-112312 p 399 N94-11243 #
UCRL-JC-112518 p 76 N94-11075 #
UCRL-JC-112597 p 334 N94-12591 #
UCRL-JC-112713 p 151 N94-11144 #
UCRL-JC-112806 p 321 N94-10291 #
UCRL-JC-112924 p 175 N94-11266 #
UCRL-JC-113188 p 383 N94-11676 #
UCRL-JC-113199 p 387 N94-10737
UCRL-JC-113380 p 327 N94-11240 #
UCRL-JC-113502 p 325 N94-11112 #
UCRL-JC-113531 p 338 N94-12597 #

UM-P-92/15 p 395 N94-10406 #
UM-P-92/19 p 385 N94-10284
UM-P-92/21 p 170 N94-10630
UM-P-92/57 p 409 N94-10501

UM-030601-1-T p 136 N94-11084 * #

UMDHEP-93-020 p 410 N94-10545 #

UMICH-024557-1-F p 266 N94-11374 * #

UNM-ISNPS-1-1993 p 48 N94-11372 #

UO-JFWK-MNW-02 p 94 N94-12396 #
UO-JFWK-MNW-04 p 93 N94-12353 #

UOP-TR-93-2 p 289 N94-11853 #

US-PATENT-APPL-SN-006544 p 374 N94-10373 #
US-PATENT-APPL-SN-007884 p 404 N94-12400 #
US-PATENT-APPL-SN-010252 p 374 N94-10376 #
US-PATENT-APPL-SN-010253 p 176 N94-12321 #
US-PATENT-APPL-SN-010944 p 176 N94-12329 #
US-PATENT-APPL-SN-010948 p 140 N94-10389 #
US-PATENT-APPL-SN-012837 p 178 N94-10385 #
US-PATENT-APPL-SN-014928 p 93 N94-12330 #
US-PATENT-APPL-SN-017918 p 140 N94-10390 #
US-PATENT-APPL-SN-019373 p 94 N94-12399 #
US-PATENT-APPL-SN-020158 p 173 N94-10371 #
US-PATENT-APPL-SN-020940 p 147 N94-10383 #
US-PATENT-APPL-SN-023426 p 178 N94-10379 #
US-PATENT-APPL-SN-025210 p 145 N94-12322 #
US-PATENT-APPL-SN-028012 p 333 N94-12386 #
US-PATENT-APPL-SN-031251 p 374 N94-10372 #
US-PATENT-APPL-SN-035862 p 178 N94-10375 #
US-PATENT-APPL-SN-035867 p 178 N94-10378 #
US-PATENT-APPL-SN-037877 p 14 N94-11021 * #
US-PATENT-APPL-SN-037878 p 178 N94-10381 #
US-PATENT-APPL-SN-040944 p 140 N94-10377 #
US-PATENT-APPL-SN-041388 p 176 N94-12337 #
US-PATENT-APPL-SN-046254 p 418 N94-10374 #
US-PATENT-APPL-SN-678780 p 33 N94-10669 *
US-PATENT-APPL-SN-699299 p 179 N94-10670 *
US-PATENT-APPL-SN-699990 p 141 N94-10668
US-PATENT-APPL-SN-720153 p 185 N94-10671 *
US-PATENT-APPL-SN-877966 p 141 N94-10656 *
US-PATENT-APPL-SN-886998 p 12 N94-10673 *
US-PATENT-APPL-SN-888083 p 132 N94-10382 #
US-PATENT-APPL-SN-902265 p 179 N94-10658 *
US-PATENT-APPL-SN-902266 p 179 N94-10655 *
US-PATENT-APPL-SN-912955 p 179 N94-10654 *
US-PATENT-APPL-SN-936417 p 381 N94-10657 *
US-PATENT-APPL-SN-943659 p 12 N94-10672 * #
US-PATENT-APPL-SN-984111 p 140 N94-10384 #
US-PATENT-APPL-SN-998062 p 179 N94-10674 *
US-PATENT-APPL-SN-999629 p 75 N94-10380 #

US-PATENT-CLASS-137-514.7 p 179 N94-10655 *
US-PATENT-CLASS-137-514.7 p 179 N94-10658 *
US-PATENT-CLASS-137-514 p 179 N94-10658 *
US-PATENT-CLASS-148-DIG.80 p 141 N94-10656 *
US-PATENT-CLASS-244-130 p 12 N94-10672 * #
US-PATENT-CLASS-244-198 p 12 N94-10673 *
US-PATENT-CLASS-244-199 p 12 N94-10673 *
US-PATENT-CLASS-244-208 p 12 N94-10672 * #
US-PATENT-CLASS-244-209 p 12 N94-10672 * #
US-PATENT-CLASS-318-560 p 179 N94-10654 *
US-PATENT-CLASS-318-568.11 p 179 N94-10654 *
US-PATENT-CLASS-318-568.12 p 179 N94-10654 *
US-PATENT-CLASS-318-568.17 p 179 N94-10654 *
US-PATENT-CLASS-318-568.1 p 179 N94-10670 *
US-PATENT-CLASS-318-568.21 p 179 N94-10654 *
US-PATENT-CLASS-333-219 p 141 N94-10668
US-PATENT-CLASS-333-234 p 141 N94-10668
US-PATENT-CLASS-333-235 p 141 N94-10668
US-PATENT-CLASS-359-359 p 381 N94-10657 *
US-PATENT-CLASS-359-360 p 381 N94-10657 *
US-PATENT-CLASS-359-582 p 381 N94-10657 *
US-PATENT-CLASS-359-585 p 381 N94-10657 *
US-PATENT-CLASS-359-892 p 381 N94-10657 *
US-PATENT-CLASS-364-508 p 185 N94-10671 *
US-PATENT-CLASS-364-571.03 p 185 N94-10671 *
US-PATENT-CLASS-395-84 p 179 N94-10670 *
US-PATENT-CLASS-395-905 p 179 N94-10670 *
US-PATENT-CLASS-395-99 p 179 N94-10670 *
US-PATENT-CLASS-417-393 p 179 N94-10674 *
US-PATENT-CLASS-417-404 p 179 N94-10674 *
US-PATENT-CLASS-437-195 p 141 N94-10656 *
US-PATENT-CLASS-437-203 p 141 N94-10656 *
US-PATENT-CLASS-437-234 p 141 N94-10656 *
US-PATENT-CLASS-437-3 p 141 N94-10656 *
US-PATENT-CLASS-437-5 p 141 N94-10656 *
US-PATENT-CLASS-73-118.1 p 33 N94-10669 *
US-PATENT-CLASS-73-119R p 33 N94-10669 *
US-PATENT-CLASS-73-761 p 185 N94-10671 *
US-PATENT-CLASS-73-862.59 p 185 N94-10671 *
US-PATENT-CLASS-73-865.9 p 33 N94-10669 *
US-PATENT-CLASS-901-19 p 179 N94-10654 *
US-PATENT-CLASS-901-9 p 179 N94-10654 *

US-PATENT-4,580,116 p 141 N94-10668
US-PATENT-5,230,486 p 12 N94-10673 *
US-PATENT-5,231,693 p 179 N94-10670 *
US-PATENT-5,232,013 p 179 N94-10655 *
US-PATENT-5,236,155 p 12 N94-10672 * #
US-PATENT-5,236,871 p 141 N94-10656 *
US-PATENT-5,237,447 p 381 N94-10657 *
US-PATENT-5,237,516 p 185 N94-10671 *
US-PATENT-5,238,372 p 179 N94-10674 *
US-PATENT-5,239,246 p 179 N94-10654 *
US-PATENT-5,239,864 p 33 N94-10669 *
US-PATENT-5,240,036 p 179 N94-10658 *

USAARL-93-11 p 311 N94-12423 #
USAARL-93-14 p 315 N94-11291 #
USAARL-93-17 p 418 N94-10491 #

USAATCOM-TR-93-A-004 p 25 N94-10935 * #

UTIAS-RN-345 p 15 N94-11857

UTIAS-346 p 73 N94-12013

UTNL-R-0280 p 372 N94-11595

UVA/525755/MSE93/101 p 182 N94-12374 #

VPI-AOE-201 p 171 N94-12533

VTT-PUB-110 p 390 N94-11148 #

W-9223 p 344 N94-10906 #
W-9301 p 344 N94-10907 #
W-9302 p 344 N94-10908 #

WCASP-24 p 283 N94-10561 #

WES/TR/SL-93-1 p 171 N94-12362 #
WES/TR/SL-93-3 p 170 N94-10873

WHC-SA-1536 p 372 N94-11296

WHH-139-0 p 323 N94-10878 #

WHOI-92-29 p 289 N94-11854 #
WHOI-92-38 p 154 N94-11865 #
WHOI-93-13 p 289 N94-11853 #

WIS-PH-92-86 p 346 N94-11811

WL-TR-92-3030 p 44 N94-12541 #
WL-TR-92-3109 p 419 N94-11288 #
WL-TR-92-3121 p 154 N94-11641 #
WL-TR-93-2007 p 99 N94-12282 #
WL-TR-93-2032 p 99 N94-12275 #
WL-TR-93-3015 p 148 N94-10703
WL-TR-93-4060 p 74 N94-12347 #
WL-TR-93-5004 p 382 N94-11421 #
WL-TR-93-5006 p 144 N94-11516
WL-TR-93-8020 p 340 N94-12411 #

WMO/TD-538 p 283 N94-10561 #

WSRC-MS-93-090 p 181 N94-11228 #
WSRC-MS-93-146 p 418 N94-10646

WSRC-RP-92-1425 p 285 N94-11614 #

WSRC-RP-93-778 .... p 285 N94-11664 #

WSRC-TR-92-472 .... p 83 N94-11250 #
WSRC-TR-92-547 .... p 327 N94-11246 #

XC-PL/HANSCOM .... p 417 N94-12360 #

ZIMP-92-18 .... p 409 N94-10413 #

APPENDIX

NASA SCIENTIFIC AND TECHNICAL INFORMATION PROGRAM PRODUCTS AND SERVICES

The NASA Scientific and Technical Information (STI) Program provides for the collection and announcement of aerospace-related reports and literature obtained worldwide through agreements and exchanges. The result of the collection is the comprehensive NASA STI Database that covers aeronautics, space, and supporting disciplines.

The STI Database, documents generated or obtained by NASA, and products and services derived from or supporting the database are made available to the NASA research community and to the public. Descriptions and sources of these items are presented in the following pages.

Scientific and Technical Aerospace Reports (STAR) is an abstract journal, listing citations with abstracts for aerospace-related reports obtained from worldwide sources. *STAR* is issued on the first of each month, and announces current documents that have been entered into the NASA STI Database during the previous month. The reports are of the following types:

- NASA, NASA contractor, and NASA grantee reports;
- Reports issued by other U.S. Government agencies, domestic and foreign institutions, universities, and private firms;
- Translations in report form;
- NASA-owned patents and patent applications
- Other U.S. Government agency and foreign patents and patent applications
- Domestic and foreign dissertations and theses.

Journal, book, and conference literature, journal translations, and certain foreign dissertations having the same subject scope as *STAR* are announced in a companion journal, *International Aerospace Abstracts (IAA). IAA* is issued on the 1st and 15th of each month and is available from the American Institute of Aeronautics and Astronautics, Technical Information Service, 555 West 57th Street, 12th Floor, New York, NY 10019.

ELIGIBILITY AND REGISTRATION FOR NASA STI PRODUCTS AND SERVICES

Organizations of the type listed below that have registered with NASA can receive products and services.

- NASA offices and installations, contractors, subcontractors, grantees, and consultants;
- Other U.S. Government agencies and their contractors;
- Libraries in the United States that have arrangements with NASA to maintain collections of NASA documents for public reference;
- Other organizations in the United States having a need for NASA documents in work related to aeronautics and space research;
- Organizations abroad that have established reciprocal documents exchange arrangements with NASA.

The central service points—central points of document acquisition and control within qualified organizations—or individuals are eligible to register for NASA STI products and services. Domestic organizations or individuals may be eligible to receive various classes of NASA publications and services and should address their requests for registration or further information to:

ATTN: Registration Services
NASA Center for AeroSpace Information
800 Elkridge Landing Road
Linthicum Heights, MD 21090-2934
301-621-0390

Organizations abroad should direct requests to:

National Aeronautics and Space Administration
Scientific and Technical Information Program (JTT)
International STI Program
Washington, DC 20546-0001
USA
703-271-5640

SUBJECT SCOPE

The subject scope of *STAR* and *IAA* includes all aspects of aeronautics and space research and development, supporting basic and applied research, and applications. Aerospace aspects of Earth resources, energy development, conservation, oceanography, environmental protection, urban transportation, and other topics of high national priority are also covered.

HOW TO USE *STAR* SUBJECT CATEGORIES

Abstracts in *STAR* are categorized by 10 major subject divisions that are divided further into 76 specific subject categories. The subject divisions and categories are listed in the Table of Contents together with a note for each that defines its scope and provides any cross-references. For example:

> **16 SPACE TRANSPORTATION**
>
> Includes passenger and cargo space transportation, e.g., shuttle operations; and space rescue techniques. For related information see also *03 Air Transportation and Safety* and *18 Spacecraft Design, Testing and Performance*. For space suits see *54 Man/System Technology and Life Support*.

CROSS-REFERENCES

Individual *STAR* abstracts are not ordinarily cross-referenced, except for certain conference reports or book translations that have had separate abstracts written for their component papers or chapters. Citations and abstracts of the components follow immediately after those of the parent document. When the subject content of a component differs sufficiently from the general content of the parent, a cross-reference citation also is printed at the end of the category to which it normally would have been assigned if it were independent.

DOCUMENTS ON MICROFICHE

Documents available on microfiche are designated by a pound sign (#) following the accession number.

LIMITED REPRODUCIBILITY

A note of limited reproducibility appears in the citation, if there are factors affecting the reproducibility of more than 20% of the document. These factors include faint or broken type, color photographs, black and white photographs, foldouts, dot matrix print, or some other factor that limits the reproducibility of the document. This notation also appears on the microfiche header.

COLOR COPIES

An increasing number of NASA scientific and technical reports are being produced with color graphs, charts, illustrations, and photographs. An indication that a document has color pages follows the source and pricing (SAP) information in the *STAR* citation.

Registered users of the NASA Scientific and Technical Information Program will receive ordered documents with color at no additional cost, as long as stock copies of the document are available. Otherwise, an additional fee of $2.00 per color page will be charged. The NASA Center for AeroSpace Information staff will contact registered users to determine individual user's needs.

NASA PATENTS AND PATENT APPLICATIONS

Patents and patent applications owned by NASA are announced in *STAR* under appropriate subject categories and are referenced in the *STAR* indexes. In the Report Number Index, patents are indexed by the NASA Case Number, and the U.S. Patent Class. Patent applications are indexed by the NASA Case Number and the U.S. Patent Application Serial Number.

Printed copies of patents (which are not microfiched) are available for purchase from the U.S. Patent and Trademark Office.

When ordering patents, the U.S. Patent Number should be used, and payment must be remitted in advance, by money order or check payable to the Commissioner of Patents and Trademarks. Prepaid purchase coupons for ordering are also available from the U.S. Patent and Trademark Office.

NASA patent application specifications are sold in both paper copy and microfiche by the NASA Center for AeroSpace Information (CASI). The N accession number should be used in ordering either paper copy or microfiche from CASI.

The patents and patent applications announced in *STAR* are owned by NASA and are available for royalty-free licensing. Requests for licensing terms and further information should be addressed to:

National Aeronautics and Space Administration
Associate General Counsel for Intellectual Property
Code GP
Washington, DC 20546-0001

SOURCES FOR DOCUMENTS

One or more sources from which a document announced in *STAR* is available to the public is ordinarily given on the last line of the citation. The most commonly indicated sources and their acronyms or abbreviations are listed below, and their addresses are listed on page A-6. If the publication is available from a source other than those listed, the publisher and his address will be displayed on the availability line or in combination with the corporate source line.

Avail: CASI. Sold by the NASA Center for AeroSpace Information. Prices for hard copy (HC) and microfiche (MF) are indicated by a price code following the letters HC or MF in the *STAR* citation. Current values for the price codes are given in the tables on page A-7.

NOTE ON ORDERING DOCUMENTS: When ordering publications from CASI, use the N accession number or other report number. It is also advisable to cite the title and other bibliographic identification.

Avail: SOD (or GPO). Sold by the Superintendent of Documents, U.S. Government Printing Office, in hard copy.

Avail: BLL (formerly NLL): British Library Lending Division, Boston Spa, Wetherby, Yorkshire, England. Photocopies available from this organization at the price shown. (If none is given, inquiry should be addressed to the BLL.)

Avail: DOE Depository Libraries. Organizations in U.S. cities and abroad that maintain collections of Department of Energy reports, usually in microfiche form, are listed in *Energy Research Abstracts*. Services available from the DOE and its depositories are described in a booklet, *DOE Technical Information Center - Its Functions and Services* (TID-4660), which may be obtained without charge from the DOE Technical Information Center.

Avail: ESDU. Pricing information on specific data, computer programs, and details on Engineering Sciences Data Unit (ESDU) topic categories can be obtained from ESDU International Ltd. Requesters in North America should use the Virginia address while all other requesters should use the London address, both of which are on page A-6.

Avail: Fachinformationszentrum, Karlsruhe. Gesellschaft für wissenschaftlich-technische Information mbH 7514 Eggenstein-Leopoldshafen 2, Germany.

Avail: HMSO. Publications of Her Majesty's Stationery Office are sold in the U.S. by Pendragon House, Inc. (PHI), Redwood City, CA. The U.S. price (including a service and mailing charge) is given, or a conversion table may be obtained from PHI.

Avail: Issuing Activity, or Corporate Author, or no indication of availability. Inquiries as to the availability of these documents should be addressed to the organization shown in the citation as the corporate author of the document.

Avail: NASA Public Document Rooms. Documents so indicated may be examined at or purchased from the National Aeronautics and Space Administration (JBD-4), Public Documents Room (Room 1H23), Washington, DC 20546-0001, or public document rooms located at NASA installations, and the NASA Pasadena Office at the Jet Propulsion Laboratory.

Avail: NTIS. Sold by the National Technical Information Service. Initially distributed microfiche under the NTIS SRIM (Selected Research in Microfiche) are available. For information concerning this service, consult the NTIS Subscription Section, Springfield, VA 22161.

Avail: Univ. Microfilms. Documents so indicated are dissertations selected from *Dissertation Abstracts* and are sold by University Microfilms as xerographic copy (HC) and microfilm. All requests should cite the author and the Order Number as they appear in the citation.

Avail: US Patent and Trademark Office. Sold by Commissioner of Patents and Trademarks, U.S. Patent and Trademark Office, at the standard price of $1.50 each, postage free. (See discussion of NASA patents and patent applications on page A-3.)

Avail: (US Sales Only). These foreign documents are available to users within the United States from the National Technical Information Service (NTIS). They are available to users outside the United States through the International Nuclear Information Service (INIS) representative in their country, or by applying directly to the issuing organization.

Avail: USGS. Originals of many reports from the U.S. Geological Survey, which may contain color illustrations, or otherwise may not have the quality of illustrations preserved in the microfiche or facsimile reproduction, may be examined by the public at the libraries of the USGS field offices whose addresses are listed on page A-6. The libraries may be queried concerning the availability of specific documents and the possible utilization of local copying services, such as color reproduction.

FEDERAL DEPOSITORY LIBRARY PROGRAM

In order to provide the general public with greater access to U.S. Government publications, Congress established the Federal Depository Library Program under the Government Printing Office (GPO), with 53 regional depositories responsible for permanent retention of material, inter-library loan, and reference services. At least one copy of nearly every NASA and NASA-sponsored publication, either in printed or microfiche format, is received and retained by the 53 regional depositories. A list of the regional GPO libraries, arranged alphabetically by state, appears on page A-8. These libraries are *not* sales outlets. A local library can contact a regional depository to help locate specific reports, or direct contact may be made by an individual.

PUBLIC COLLECTION OF NASA DOCUMENTS

An extensive collection of NASA and NASA-sponsored publications is maintained by the British Library Lending Division, Boston Spa, Wetherby, Yorkshire, England for public access. The British Library Lending Division also has available many of the non-NASA publications cited in *STAR*. European requesters may purchase facsimile copy or microfiche of NASA and NASA-sponsored documents, those identified by both the symbols # and * from ESA — Information Retrieval Service European Space Agency, 8-10 rue Mario-Nikis, 75738 CEDEX 15, France.

SUBMITTING DOCUMENTS

All users of this abstract service are urged to forward reports to be considered for announcement in *STAR*. This will aid NASA in its efforts to provide the fullest possible coverage of all scientific and technical publications that might support aeronautics and space research and development. If you have prepared relevant reports (other than those you will transmit to NASA, DOD, or DOE through the usual contract- or grant-reporting channels), please send them for consideration to the NASA Center for AeroSpace Information, 800 Elkridge Landing Road, Linthicum Heights, MD 21090-2934.

Reprints of journal articles, book chapters, and conference papers are also welcome. These will be considered for announcement in *STAR's* companion journal, *IAA*.

You may specify a particular source to be included in a report announcement if you wish; otherwise the report will be placed on a public sale at the NASA Center for AeroSpace Information. Copyrighted publications will be announced but not distributed or sold.

PURCHASE OF *STAR*

STAR is publicly available on annual subscription from the NASA Center for AeroSpace Information (CASI) at $94.00/domestic, $117.00/foreign. Single copy prices: $33.00/domestic, $41.00/foreign.

An annual, cumulative *STAR Index* is also available at $54.00/domestic, $65.00/foreign.

STAR is available to registered users on annual subscription from the NASA Center for AeroSpace Information, ATTN: Registration Services, 800 Elkridge Landing Road, Linthicum Heights, MD 21090-2934.

ADDRESSES OF ORGANIZATIONS

American Institute of Aeonautics
and Astronautics
Technical Information Service
555 West 57th Street, 12th Floor
New York, NY 10019

British Library Lending Division
Boston Spa, Wetherby, Yorkshire
England

Commissioner of Patents and Trademarks
U.S. Patent and Trademark Office
Washington, DC 20231

Department of Energy
Technical Information Center
P.O. Box 62
Oak Ridge, TN 37830

European Space Agency-
Information Retrieval Service ESRIN
Via Galileo Galilei
00044 Frascati (Rome) Italy

Engineering Sciences Data Unit International
P.O. Box 1633
Manassas, VA 22110

Engineering Sciences Data Unit
International, Ltd.
251-259 Regent Street
London, W1R 7AD, England

Fachinformationszentrum Karlsruhe
Gesellschaft für wissenschaftlich-technische
Information mbH
7514 Eggenstein-Leopoldshafen 2, Germany

Her Majesty's Stationery Office
P.O. Box 569, S.E. 1
London, England

NASA Center for AeroSpace Information
800 Elkridge Landing Road
Linthicum Heights, MD 21090-2934

National Aeronautics and Space Administration
Scientific and Technical Information Program
(JTT)
Washington, DC 20546-0001

National Technical Information Service
5285 Port Royal Road
Springfield, VA 22161

Pendragon House, Inc.
899 Broadway Avenue
Redwood City, CA 94063

Superintendent of Documents
U.S. Government Printing Office
Washington, DC 20402

University Microfilms
A Xerox Company
300 North Zeeb Road
Ann Arbor, MI 48106

University Microfilms, Ltd.
Tylers Green
London, England

U.S. Geological Survey Library National Center
MS 950
12201 Sunrise Valley Drive
Reston, VA 22092

U.S. Geological Survey Library
2255 North Gemini Drive
Flagstaff, AZ 86001

U.S. Geological Survey
345 Middlefield Road
Menlo Park, CA 94025

U.S. Geological Survey Library
Box 25046
Denver Federal Center, MS914
Denver, CO 80225

CASI PRICE TABLES

(Effective August 1, 1993)

STANDARD PRICE DOCUMENTS

PRICE CODE	NORTH AMERICAN PRICE	FOREIGN PRICE
A01	$ 9.00	$ 18.00
A02	12.50	25.00
A03	17.50	35.00
A04-A05	19.50	39.00
A06-A09	27.00	54.00
A10-A13	36.50	73.00
A14-A17	44.50	89.00
A18-A21	52.00	104.00
A22-A25	61.00	122.00
A99	Call For Price	Call For Price

MICROFICHE

PRICE CODE	NORTH AMERICAN PRICE	FOREIGN PRICE
A01	$ 9.00	$ 18.00
A02	12.50	25.00
A03	17.50	35.00
A04	19.50	39.00
A06	27.00	54.00
A10	36.50	73.00

IMPORTANT NOTICE

CASI Shipping and Handling Charges
U.S.—ADD $3.00 per TOTAL ORDER
Canada and Mexico—ADD $3.50 per TOTAL ORDER
All Other Countries—ADD $7.50 per TOTAL ORDER
Does NOT apply to orders
requesting CASI RUSH HANDLING.
CASI accepts charges to American Express, Diners Club, MasterCard and VISA.

FEDERAL REGIONAL DEPOSITORY LIBRARIES

ALABAMA
AUBURN UNIV. AT MONTGOMERY LIBRARY
Documents Dept.
7300 University Dr.
Montgomery, AL 36117-3596
(205) 244-3650 Fax: (205) 244-0678

UNIV. OF ALABAMA
Amelia Gayle Gorgas Library
Govt. Documents
Box 870266
Tuscaloosa, AL 35487-0266
(205) 348-6046 Fax: (205) 348-8833

ARIZONA
DEPT. OF LIBRARY, ARCHIVES, AND PUBLIC RECORDS
Federal Documents
Third Floor State Capitol
1700 West Washington
Phoenix, AZ 85007
(602) 542-4121 Fax: (602) 542-4400, 542-4500

ARKANSAS
ARKANSAS STATE LIBRARY
State Library Services
One Capitol Mall
Little Rock, AR 72201
(501) 682-2869

CALIFORNIA
CALIFORNIA STATE LIBRARY
Govt. Publications Section
914 Capitol Mall - P.O. Box 942837
Sacramento, CA 94237-0001
(916) 322-4572 Fax: (916) 324-8120

COLORADO
UNIV. OF COLORADO - BOULDER
Norlin Library
Govt. Publications
Campus Box 184
Boulder, CO 83309-0184
(303) 492-8834 Fax: (303) 492-2185

DENVER PUBLIC LIBRARY
Govt. Publications Dept. BS/GPD
1357 Broadway
Denver, CO 80203
(303) 571-2135

CONNECTICUT
CONNECTICUT STATE LIBRARY
231 Capitol Avenue
Hartford, CT 06106
(203) 566-4971 Fax: (203) 566-3322

FLORIDA
UNIV. OF FLORIDA LIBRARIES
Documents Dept.
Library West
Gainesville, FL 32611-2048
(904) 392-0366 Fax: (904) 392-7251

GEORGIA
UNIV. OF GEORGIA LIBRARIES
Govt. Documents Dept.
Jackson Street
Athens, GA 30602
(404) 542-8949 Fax: (404) 542-6522

HAWAII
UNIV. OF HAWAII
Hamilton Library
Govt. Documents Collection
2550 The Mall
Honolulu, HI 96822
(808) 948-8230 Fax: (808) 956-5968

IDAHO
UNIV. OF IDAHO LIBRARY
Documents Section
Moscow, ID 83843
(208) 885-6344 Fax: (208) 885-6817

ILLINOIS
ILLINOIS STATE LIBRARY
Reference Dept.
300 South Second
Springfield, IL 62701-1796
(217) 782-7596 Fax: (217) 524-0041

INDIANA
INDIANA STATE LIBRARY
Serials/Documents Section
140 North Senate Avenue
Indianapolis, IN 46204
(317) 232-3678 Fax: (317) 232-3728

IOWA
UNIV. OF IOWA LIBRARIES
Govt. Publications Dept.
Washington & Madison Streets
Iowa City, IA 52242
(319) 335-5926 Fax: (319) 335-5830

KANSAS
UNIV. OF KANSAS
Govt. Documents & Map Library
6001 Malatt Hall
Lawrence, KS 66045-2800
(913) 864-4660 Fax: (913) 864-5380

KENTUCKY
UNIV. OF KENTUCKY LIBRARIES
Govt. Publications/Maps Dept.
Lexington, KY 40506-0039
(606) 257-3139 Fax: (606) 257-1563, 257-8379

LOUISIANA
LOUISIANA STATE UNIV.
Middleton Library
Govt. Documents Dept.
Baton Rouge, LA 70803
(504) 388-2570 Fax: (504) 388-6992

LOUISIANA TECHNICAL UNIV.
Prescott Memorial Library
Govt. Documents Dept.
305 Wisteria Street
Ruston, LA 71270-9985
(318) 257-4962 Fax: (318) 257-2447

MAINE
TRI-STATE DOCUMENTS DEPOS.
Raymond H. Fogler Library
Govt. Documents & Microforms Dept.
Univ. of Maine
Orono, ME 04469
(207) 581-1680

MARYLAND
UNIV. OF MARYLAND
Hornbake Library
Govt. Documents/Maps Unit
College Park, MD 20742
(301) 454-3034 Fax: (301) 454-4985

MASSACHUSETTS
BOSTON PUBLIC LIBRARY
Govt. Documents Dept.
666 Boylston Street
Boston, MA 02117
(617) 536-5400 ext. 226
Fax: (617) 267-8273, 267-8248

MICHIGAN
DETROIT PUBLIC LIBRARY
5201 Woodward Avenue
Detroit, MI 48202-4093
(313) 833-1440, 833-1409
Fax: (313) 833-5039

LIBRARY OF MICHIGAN
Govt. Documents Unit
P.O. Box 30007
Lansing, MI 48909
(517) 373-0640 Fax: (517) 373-3381

MINNESOTA
UNIV. OF MINNESOTA
Wilson Library
Govt. Publications Library
309 19th Avenue South
Minneapolis, MN 55455
(612) 624-5073 Fax: (612) 626-9353

MISSISSIPPI
UNIV. OF MISSISSIPPI
J.D. Williams Library
Federal Documents Dept.
106 Old Gym Bldg.
University, MS 38677
(601) 232-5857 Fax: (601) 232-5453

MISSOURI
UNIV. OF MISSOURI - COLUMBIA
Ellis Library
Govt. Documents
Columbia, MO 65201
(314) 882-6733 Fax: (314) 882-8044

MONTANA
UNIV. OF MONTANA
Maureen & Mike Mansfield Library
Documents Div.
Missoula, MT 59812-1195
(406)243-6700 Fax: (406) 243-2060

NEBRASKA
UNIV. OF NEBRASKA - LINCOLN
D.L. Love Memorial Library
Documents Dept.
Lincoln, NE 68588
(402) 472-2562

NEVADA
UNIV. OF NEVADA
Reno Library
Govt. Publications Dept.
Reno, NV 89557
(702) 784-6579 Fax: (702) 784-1751

NEW JERSEY
NEWARK PUBLIC LIBRARY
U.S. Documents Div.
5 Washington Street - P.O. Box 630
Newark, NJ 07101-0630
(201) 733-7812 Fax: (201) 733-5648

NEW MEXICO
UNIV. OF NEW MEXICO
General Library
Govt. Publications Dept.
Albuquerque, NM 87131-1466
(505) 277-5441 Fax: (505) 277-6019

NEW MEXICO STATE LIBRARY
325 Don Gaspar Avenue
Santa Fe, NM 87503
(505) 827-3826 Fax: (505) 827-3820

NEW YORK
NEW YORK STATE LIBRARY
Documents/Gift & Exchange Section
Federal Depository Program
Cultural Education Center
Albany, NY 12230
(518) 474-5563 Fax: (518) 474-5786

NORTH CAROLINA
UNIV. OF NORTH CAROLINA - CHAPEL HILL
CB#3912, Davis Library
BA/SS Dept. - Documents
Chapel Hill, NC 27599
(919) 962-1151 Fax: (919) 962-0484

NORTH DAKOTA
NORTH DAKOTA STATE UNIV. LIB.
Documents Office
Fargo, ND 58105
(701) 237-8886 Fax: (701) 237-7138
In cooperation with Univ. of North Dakota, Chester Fritz Library Grand Forks

OHIO
STATE LIBRARY OF OHIO
Documents Dept.
65 South Front Street
Columbus, OH 43266
(614) 644-7051 Fax: (614) 752-9178

OKLAHOMA
OKLAHOMA DEPT. OF LIBRARIES
U.S. Govt. Information Div.
200 NE 18th Street
Oklahoma City, OK 73105-3298
(405) 521-2502, ext. 252, 253
Fax: (405) 525-7804

OKLAHOMA STATE UNIV.
Edmon Low Library
Documents Dept.
Stillwater, OK 74078
(405) 744-6546 Fax: (405) 744-5183

OREGON
PORTLAND STATE UNIV.
Millar Library
934 SW Harrison - P.O. Box 1151
Portland, OR 97207
(503) 725-3673 Fax: (503) 725-4527

PENNSYLVANIA
STATE LIBRARY OF PENN.
Govt. Publications Section
Walnut St. & Commonwealth Ave. - P.O. Box 1601
Harrisburg, PA 17105
(717) 787-3752

SOUTH CAROLINA
CLEMSON UNIV.
Cooper Library
Public Documents Unit
Clemson, SC 29634-3001
(803) 656-5174 Fax: (803) 656-3025
In cooperation with Univ. of South Carolina, Thomas Cooper Library, Columbia

TENNESSEE
MEMPHIS STATE UNIV. LIBRARIES
Govt. Documents
Memphis, TN 38152
(901) 678-2586 Fax: (901) 678-2511

TEXAS
TEXAS STATE LIBRARY
United States Documents
P.O. Box 12927 - 1201 Brazos
Austin, TX 78711
(512) 463-5455 Fax: (512) 463-5436

TEXAS TECH. UNIV. LIBRARY
Documents Dept.
Lubbock, TX 79409
(806) 742-2268 Fax: (806) 742-1920

UTAH
UTAH STATE UNIV.
Merrill Library & Learning Resources Center, UMC-3000
Documents Dept.
Logan, UT 84322-3000
(801) 750-2684 Fax: (801) 750-2677

VIRGINIA
UNIV. OF VIRGINIA
Aldermman Library
Govt. Documents
Charlottesville, VA 22903-2498
(804) 824-3133 Fax: (804) 924-4337

WASHINGTON
WASHINGTON STATE LIBRARY
Document Section
MS AJ-11
Olympia, WA 98504-0111
(206) 753-4027 Fax: (206) 753-3546

WEST VIRGINIA
WEST VIRGINIA UNIV. LIBRARY
Govt. Documents Section
P.O. Box 6069
Morgantown, WV 26506
(304) 293-3640

WISCONSIN
ST. HIST. SOC. OF WISCONSIN LIBRARY
Govt. Publications Section
816 State Street
Madison, WI 53706
(608) 262-2781 Fax: (608) 262-4711
In cooperation with Univ. of Wisconsin - Madison, Memorial Library

MILWAUKEE PUBLIC LIBRARY
Documents Div.
814 West Wisconsin Avenue
Milwaukee, WI 53233
(414) 278-2167 Fax: (414) 278-2137

POSTMASTER
Address Correction Requested
(Sections 137 and 159 Post Manual)

National Aeronautics and
Space Administration
Code JTT
Washington, DC 20546-0001

Official Business
Penalty for Private Use, $300

BULK RATE
POSTAGE & FEES PAID
NASA
PERMIT No. G-27

NASA

POSTMASTER: If Undeliverable (Section 158
Postal Manual) Do Not Return

Please circulate this publication to other colleagues within your organization.

NASA
STI PROGRAM
SCIENTIFIC &
TECHNICAL
INFORMATION

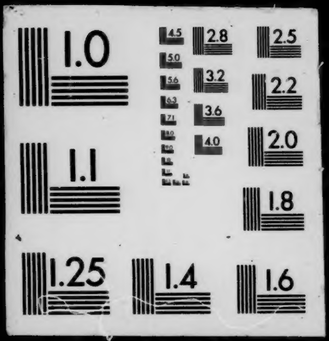
1.0
4.5
5.0
5.6
6.3
7.1
8.0
9.0
2.8
3.2
3.6
4.0
2.5
2.2
2.0
1.1
1.8
1.25
1.4
1.6